1 GENERAL

This alloy is a delta ferrite-free compositional modification of 17-4PH precipitation-hardening martensitic stainless steel containing less chromium and slightly higher nickel. Vacuum arc remelting lowers the alloy's gas content, reduces and disperses inclusions, and minimizes alloy segregation during solidification. These factors, coupled with the elimination of delta ferrite, result in superior transverse toughness compared to 17-4PH.

The alloy transforms to martensite on cooling to room temperature from the solution treatment. Hardening results from the precipitation of a copper-rich phase at temperatures of only 900 to 1150F, depending on the properties desired.

The corrosion resistance of this alloy is comparable to Type 304 in most media. Its oxidation resistance is superior to Type 410 but inferior to Type 430. The alloy is available as billet, plate, bar, and wire. It is forgeable, castable, weldable, and machinable.

Many physical and mechanical properties of this alloy are the same as for 17-4PH. Consequently, some of the data presented here were determined for 17-4PH and are noted as such. For properties which are independent of melting practice (air melt versus consumable electrode vacuum arc remelt), the melting method is usually not specified and the reader is to assume the data apply to either method.

1.1 Commercial Designation - 15-5PH precipitation-hardening stainless steel

1.2 Alternate Designations - UNS S15500; UNS J92110; AISI S15500

1.3 Specifications

1.3.1 *[Table]* AMS specifications for wrought products.

1.3.2 *[Table]* ASTM specifications for wrought products.

1.3.3 *[Table]* AMS specifications for investment castings.

1.3.4 *[Table]* AMS specifications for tubular centrifugal castings.

1.4 Composition

1.4.1 *[Table]* Specified composition for wrought products.

1.4.2 *[Table]* Producer's specified composition for castings.

1.4.3 *[Table]* AMS specified composition for investment castings.

1.4.4 *[Table]* AMS specified composition for tubular centrifugal castings.

1.4.5 *[Table]* AMS specified composition for weld electrodes and wire.

Fe	
15.0	Cr
4.50	Ni
0.30	Cb
3.5	Cu

1.5 Heat Treatment

1.5.1 Solution treat to Condition A, 1900 + 25F, 30 to 60 minutes, oil quench or air cool to below 90F (Refs. 1, 27).

1.5.2 *[Table]* Age Condition A to H Conditions (Precipitation hardening heat treatment schedules).

1.5.2.1 Precipitation in this alloy is complex. The formation and growth mechanisms of the several types of precipitates have been recently studied and described in detail in reference 54.

Aging produces a hardness peak at around 850F, followed by softening and then a second hardening beginning at about 1200F (see Figures 1.6.3 to 1.6.5). TEM observations reveal the successive formation (between 850 and 1200F) of two types of coherent precipitate, one type subsequently becoming partialy coherent rods with selective growth direction, the other partialy incoherent globules. All of the precipitates are enriched in copper. Aging beyond 1200F produces new precipitates which are coherent at first, and then become partially incoherent within the range 1350 to 1550F.

An earlier study (Ref. 53) also found the initial peak hardening on direct aging from the solution treatment, evidenced by resistivity (Figures 2.2.2.1 and 2.2.2.2) and hardness (Figure 1.6.6) measurements. A hardening peak was also observed during aging at a relatively lower temperature range (Between 780 and 890F) after higher temperature aging (1040 to 1110F) (see Figure 2.2.2.3). That peak corresponded to a severe drop in notch tensile strength (see Figure 3.2.7.1.3). The investigators attributed the hardening and attendant notch embrittlement to formation of a Ni-rich zone.

1.5.2.2 Precipitation hardening alloys are generally susceptible to hydrogen embrittlement. This susceptibility can be minimized by overaging or other treatments, or both, that alter the microstructure. One possible explanation of the beneficial effect of overaging is the development of incoherent precipitates, the interfaces of which act as hydrogen traps and alter the stress or strain induced localization of hydrogen.

Due to the fact that hydrogen diffusion is rapid compared to other interstitial atoms, and hydrogen is known to interact with defects and segregate to regions of localized lattice dilation, one may expect the aging kinetics and the resulting properties to be

This section produced with the support of NASA-Lewis Research Center.

© 1997 by Purdue Research Foundation, West Lafayette, Indiana 47907. All Rights Reserved. U.S. Government License. This material may be used, duplicated or disclosed by United States Government agencies without the payment of any royalty.

altered if the process takes place in a hydrogen environment. These are demonstrated in Figures 1.5.2.2.1 through 1.5.2.2.6, which show two hardening reactions, one of which only develops during higher temperature aging at 900F and above. The presence of hydrogen increases peak hardness and decreases time to achieve peak hardness. Outgassing at room temperature of material aged in hydrogen increases hardness in most cases.

1.5.2.2.1 *[Figure]* Influence of hydrogen aging treatment environment on age hardening at 700F.

1.5.2.2.2 *[Figure]* Influence of hydrogen aging treatment environment on age hardening at 800F.

1.5.2.2.3 *[Figure]* Influence of hydrogen aging treatment environment on age hardening at 900F.

1.5.2.2.4 *[Figure]* Influence of hydrogen aging treatment environment on age hardening at 1000F.

1.5.2.2.5 *[Figure]* Influence of hydrogen aging treatment environment on age hardening at 1100F.

1.5.2.2.6 *[Figure]* Influence of hydrogen aging treatment environment on 900F aged tensile properties.

1.5.2.3 A dimensional change takes place on precipitation hardening.

1.5.2.3.1 *[Table]* Dimensional change (contraction) from hardening heat treatment.

1.6 Hardness

1.6.1 Producer's specified acceptable hardness and strength for Condition A, see Table 3.2.1.7.

1.6.2 Producer's specified acceptable hardness and strength for H Conditions, see Table 3.2.1.8.

1.6.3 *[Figure]* Effect of aging temperature on hardness of bar.

1.6.4 *[Figure]* Effect of aging time on hardness of bar.

1.6.5 *[Figure]* Effect of aging time on hardness of bar.

1.6.6 *[Figure]* Effect of aging temperature on hardness of bar.

1.6.7 *[Figure]* Effect of holding time at the aging temperature on hardness and notch tensile strength of bar.

1.6.8 *[Figure]* Effect of aging time on hardness and notch tensile strength for specimens aged at a lower temperature subsequent to pre-aging for 2 hours at a higher temperature.

1.6.9 *[Figure]* Effect of aging time at 752F and 842F on hardness of base and weld metal.

1.7 Forms and Conditions Available

The alloy is produced in the forms of billets, plate, bar, and wire. It is usually supplied solution treated to Condition A, ready for fabrication and subsequent hardening by the user. However, it can be supplied in hardened conditions, if desired. Recommended conditions for certain fabrication processes are discussed in Section 4. (Fabrication).

1.8 Melting and Casting

1.8.1 Melting. The alloy is produced by electric arc melting in air or by consumable electrode vacuum arc or electroslag remelting. Vacuum arc remelting lowers gas content, reduces and disperses inclusions, and minimizes alloy segregation during solidification. These factors, coupled with the elimination of delta ferrite (as a result of its basic compositional difference from 17-4PH which is not delta ferrite-free), results in superior transverse mechanical properties in all locations within the product compared to 17-4PH.

1.8.2 Casting. The alloy is readily castable and is used for castings in jet engines and aircraft, processing equipment, and nuclear reactors. It is also used for cast parts in valves, controls, compressors and intricately shaped parts requiring high strength plus corrosion resistance. To meet the specified mechanical properties for 15-5PH alloy, the composition of castings should be within the limits shown in Table 1.4.2. The lower copper range for sand castings is necessary so that they can be welded without danger of underbead cracking in the presence of copper and copper compounds which precipitate during slow cooling of these generally large sections. Being usually much smaller sections which cool rapidly, investment castings can tolerate more copper without the danger of underbead cracking.

Where welding is not a factor, higher levels of copper in the range 3.0 to 5.0 percent can be used. However, such castings with copper outside the specified range will not meet property specifications. Higher copper content generaly results in higher yield strength but lower ductility castings

The composition of castings must be "in balance" to achieve maximum hardening. The alloy producer suggests that castings not be rejected on composition alone since variations in analysis may be self compensating so that balance is maintained. Hardness measurements after heat treatment are suggested as a means of determining hardening capacity.

It is suggested (Ref. 46) that castings be solution treated at 1900 to 1925F for best refinement of the cast structure. If the analysis is improperly balanced and castings are non-magnetic, or fail to harden upon aging, solution treatment at a lower temperature (1700F, 1500F, or 1400F) may correct the difficulty. The lower temperature restricts carbide solution, lowers the stability of the resulting austenite, and induces considerable transformation to martensite.

If the 1900F solution treatment is not applied to castings of recommended analysis, maximum tensile and yield strengths, ductility, and hardness may not be obtained.

A double solution treatment at 1900F is effective in refining grain size and improving ductility and impact strength.

Castings should be soaked 15 minutes to an hour at 1900 to 1925F, then air or oil cooled to 70F or lower. If reheating for the aging treatment begins before 70F has been reached, full hardening may not be achieved. After solution treatment, the alloy is age hardened in the range 925 to 1150F. For maximum strength, it is recommended that the casting be precipitation hardened at 925F for 90 minutes followed by air cooling to room temperature.

To minimize distortion in large or intricate castings, a lower solution treatment (1700) may be advisable. Slightly lower tensile and yield strengths usually result from this treatment, but may be adequate for the application.

1.8.2.1 Room temperature axial-load high-cycle fatigue strength of machined and as-cast specimens from welded and unwelded vacuum casting. (See Figure 3.5.1.8)

1.8.2.2 Room temperature tension-compression high-cycle fatigue strength of specimens machined from cast cylinders and from a lag damper casting. (See Figure 3.5.1.9)

1.8.2.3 Room temperature axial-load high-cycle fatigue strength of specimens machined from bars vacuum cast into either production or high thermal conductivity shell molds, and subsequently HIP'd or not HIP'd. (See Figure 3.5.1.10)

1.8.2.4 Room temperature axial-load high-cycle fatigue strength of HIP'd and not HIP'd notched ($K_t = 3.0$) specimens machined from shell mold castings and notched ($K_t = 3.0$) specimens machined from HIP'd lag damper casting. (See Figure 3.5.1.11)

1.9 Special Considerations

1.9.1 Directional ductility. Precipitation-hardening stainless steel alloys are used in many applications requiring large and medium size sections. In many cases, loading transverse to the fiber is involved. It has been demonstrated (Ref. 3) that certain structural characteristics, particularly delta ferrite and some precipitates, cause substantial reductions in transverse ductility, and presumably fracture toughness, for many of these alloys. For compositions in which delta ferrite is present, vacuum remelting does not improve this situation.

15-5PH is a delta ferrite-free compositional modification of 17-4PH alloy containing less chromium and slightly higher nickel. Its short-transverse ductility at edge and intermediate locations is superior to 17-4PH in heavy sections. However, in products made from air cast ingots of 15-5PH, the short-transverse ductility at the center location may be lower than at edge or intermediate locations (See Table 3.2.1.11). This nonuniformity of ductility is evidently the result of gross segregation (Ref. 3) which may be reduced by vacuum remelting (Table 3.2.1.11).

1.9.2 Embrittlement. Martensitic and precipitation-hardening stainless steels are subject to an embrittling reaction when heated in the approximate temperature range 500 to 900F. This is evidenced by an increase in yield strength and a reduction in the resistance to crack propagation. Its magnitude depends on a number of factors including the exposure time, composition, and previous treatment.

Insufficient data are available to quantitatively define the effects of these variables for any of the commercial steels subject to this embrittlement. However, on the basis of the information available for the PH steels (alloy codes 1501 through 1510), it would be expected that long time exposures at temperatures in the lower portion of the embrittling range would produce the maximum embrittling effects.

It has been reported (Refs. 11, 35) that the embrittlement is associated with the formation of a copper-rich alpha prime ferrite phase and that the following factors are important in establishing its magnitude:

1. Increased amounts of chromium, silicon and columbium increase the rate of embrittlement at 800F. When silicon and columbium are low, chromium becomes the sole controlling factor, except that the nickel content as related to the chromium influences the result (Cr-Ni balance influences the martensite reaction). The highest nickel content which can be used at a given level of chromium without inhibiting martensite transformation is best from the standpoint of embrittlement.

2. Aluminum and apparently titanium increase the rate of embrittlement at 800F.

3. The embrittlement is completely reversible by reapplying the initial precipitation-hardening temperature, if that temperature is 1025F or higher.

4. Lowering the solution-treating temperature, at least down to 1650F, slightly lessens the tendency toward embrittlement at 800F.

1.9.3 Composition limits. Consumers have sometimes complained that the composition limits of precipitation-hardenable semi-austenitic steels are too wide to permit uniform response to heat treatment (Ref. 8). The impact strength of 17-4PH type precipitation-hardening stainless steel both before and after exposure at 800F are affected by variations in chemistry within the recommended composition range (Ref. 11). It would be expected that 15-5PH would be similarly affected.

1.9.4 Solution treated material. For many applications, 15-5PH should not be used in Condition A. The structure is untempered martensite that has low ductility and poor resistance to stress corrosion cracking (See Figure 2.3.2.6).

1.9.5 Mechanical hysteresis. Force transducers made from this alloy can give erroneous indications of strain due to a nonlinear, anelastic stress-strain relationship known as mechanical hysteresis. The amount of mechanical hysteresis is mainly controlled by heat treatment. A specially developed heat treatment process can substantially reduce hysteresis error, and thus improve force transducer accuracy (Ref. 31).

1.9.5.1 *[Table]* Effect of heat treatment on shear beam force transducer mechanical hysteresis.

1.9.6 Hydrogen embrittlement. (See section 4.4.6)

2 PHYSICAL PROPERTIES AND ENVIRONMENTAL EFFECTS

2.1 Thermal Properties

2.1.1 Melting range.

2.1.2 Phase changes. This is a martensitic alloy which undergoes transformation from austenite to martensite above room temperature, upon cooling from an austenitizing temperature of about 1900F. During austenitizing (also a solution treatment), all of the copper (the precipitation-hardening agent) is dissolved in the austenite. On cooling from this treatment, martensite transformation (Ms) starts normally at about 250F and is virtually complete at 90F. After cooling, the structure consists of a "soft martensite" supersaturated with copper. During subsequent hardening treatment a copper-rich phase is precipitated in the martensite matrix and, at the same time, the matrix is stress relieved or tempered.

2.1.3 *[Figure]* Thermal conductivity.

2.1.4 *[Figure]* Thermal expansion.

2.1.5 *[Table]* Specific heat.

2.1.6 Thermal diffusivity.

2.2 Other Physical Properties

2.2.1 *[Table]* Density.

2.2.2 *[Table]* Electrical resistivity.

2.2.2.1 *[Figure]* Effect of 10-minute aging temperature on change in electrical resistivity and its temperature derivative.

2.2.2.2 *[Figure]* Effect of aging time on change in electrical resistivity over a range of aging temperatures.

2.2.2.3 *[Figure]* Effect of 2-hour aging temperature on electrical resistivity and its temperature derivative for specimens pre-aged at 1040F for 2 hours.

2.2.2.4 *[Figure]* Effect of aging time on electrical resistivity for specimens aged at various temperatures subsequent to 1040F, 2 hour pre-age.

2.2.3 Magnetic properties.

2.2.3.1 *[Figure]* Induction curves.

2.2.3.2 *[Figure]* Hysteresis curves.

2.2.4 Emittance.

2.2.5 Damping capacity.

2.3 Chemical Properties.

2.3.1 Corrosion resistance. The general level of corrosion resistance of this alloy exceeds that of Types 410 and 431 stainless steels (Ref. 27). It is comparable to Type 304 stainless steel in most media and similar to that of 17-4PH (Refs. 1, 4, 7). In boiling 65 percent $HN0_3$ and in 1 percent HCl, 15-5PH and 17-4PH exhibit about the same resistance. In salt fog and chloride pitting solutions, 15-5PH exhibits somewhat superior resistance as shown in Table 2.3.1.1.

In all heat treated conditions, 15-5PH exhibits very little rusting during 500 hours' exposure to 5-percent salt fog at 95F (Ref. 27). When exposed to seacoast atmospheres for long periods of time, it gradually develops a superficial layer of rustlike other precipitation-hardening stainless steels (Ref. 27). The general level of corrosion resistance is best in the fully hardened condition, and decreases slightly as the aging temperature is increased (Ref. 27).

2.3.1.1 *[Table]* Corrosion of consumable electrode vacuum arc remelted 15-5PH and air melted 17-4PH in several corrosive media.

2.3.2 Stress corrosion cracking. The stress corrosion cracking resistance of 15-5PH is reported to be superior to 17-4PH in boiling 42 percent $MgCl_2$ solutions but slightly inferior to 17-4PH in H_2S-NaCl-Acetic Acid solutions (Ref. 1).

The results in Table 2.3.2.1 show the alloy to be highly resistant to stress corrosion cracking in aqueous salt environments in conditions H 1000 and H 1050 in that no failures were encountered even when the material was stressed to 100 percent of F_{ty}. Failures did occur, however, in the fully hardened H 900 condition but only at very high stress; i.e., 100 percent F_{ty}. As with 17-4PH, 15-5PH has the greatest degree of resistance to stress-corrosion cracking when heat treated at the highest aging temperature (1100F being preferred) (Ref. 1).

2.3.2.1 *[Table]* Stress corrosion cracking behavior of bar in three salt media.

2.3.2.2 *[Table]* Stress corrosion cracking of strip in marine atmosphere.

2.3.2.3 *[Table]* Effect of aqueous salt environment and specimen orientation on stress corrosion cracking, K_{Iscc}.

2.3.2.4 *[Table]* Tensile, plane strain fracture toughness, and stress corrosion stress intensity factor in 3.5 percent aqueous salt solution for air melted and CVM billet in H 900 and H 1000 conditions.

2.3.2.5 GTA welded stress-corrosion specimens of 1/8 inch thick 15-5PH plate in the H 1025 and H 1100 conditions have shown no evidence of cracking in 283 days exposure at the Kure Beach, North Carolina, 80-foot lot while stressed as bent beams to 90 percent of the room temperature yield strengths (Refs. 1, 7, 12).

2.3.2.6 *[Figure]* Sulfide stress corrosion cracking of rod.

2.3.3 Oxidation resistance. The oxidation resistance of this alloy is superior to Type 410 but inferior to Type 430.

2.4 Nuclear Environments

3 MECHANICAL PROPERTIES

3.1 Specified Mechanical Properties

3.1.1 *[Table]* Producer's guaranteed mechanical properties.

3.1.2 *[Table]* AMS specified mechanical properties for air melted alloy products.

3.1.3 *[Table]* AMS specified mechanical properties for consumable electrode vacuum arc remelted alloy products.

3.1.4 *[Table]* AMS and ASTM specified strength, hardness, and bendability of solution heat treated sheet, strip, and plate.

3.1.5 *[Table]* AMS and ASTM specified tensile strength and hardness for solution heat treated bars, forgings, flash welded rings, and wire.

3.1.6 *[Table]* AMS and ASTM specified tensile properties and hardness for precipitation hardened sheet, strip, and plate.

3.1.7 *[Table]* AMS and ASTM specified tensile properties and hardness for precipitation hardened bars, forgings, flash welded rings, extrusions, and stock for forging, flash welded rings, or extruding.

3.1.8 *[Table]* AMS specified tensile properties and hardness for precipitation hardened investment castings.

3.1.9 *[Table]* AMS specified tensile properties and hardness for precipitation hardened tubular centrifugal castings.

3.1.10 *[Table]* Producer's specified acceptable tensile properties and hardness for Condition A.

3.1.11 *[Table]* Producer's specified acceptable tensile properties and hardness for sheet and strip in H Conditions.

3.2 Mechanical Properties at Room Temperature

3.2.1 Tension Stress-Strain Diagrams and Tensile Properties.

3.2.1.1 *[Table]* Typical mechanical properties for bar.

3.2.1.2 *[Table]* Typical mechanical properties for sheet and strip.

3.2.1.3 *[Table]* Effects of section size, specimen location and specimen direction on tensile properties of arc melted and vacuum remelted stock in H 900 condition.

3.2.1.4 *[Table]* Room temperature tension, compression, shear, and bearing properties of plate in H 1025 condition, for which fatigue properties appear in Figures 3.5.1.6 and 3.5.1.7.

3.2.2 Compression Stress-Strain Diagrams and Compression Properties. (See also Table 3.2.1.4)

3.2.3 Impact (see also Section 3.3.3).

3.2.4 Bending.

3.2.5 Torsion and shear. (See also Table 3.2.1.4)

3.2.5.1 *[Table]* Shear strength in torsion.

3.2.5.2 *[Table]* Shear strength in double shear for H 900 condition.

3.2.5.3 *[Figure]* Effect of aging temperature (H Condition) on shear strength in double shear.

3.2.6 Bearing. (See also Table 3.2.1.4)

3.2.6.1 *[Table]* Bearing strength of plate in H 1025 condition.

3.2.6.2 *[Table]* Bearing strength of bar in H 1150 condition.

3.2.7 Stress concentration.

3.2.7.1 Notch properties.

3.2.7.1.1 Effect of holding time at the aging temperature on hardness and notch tensile strength of bar. (See Figure 1.6.7)

3.2.7.1.2 Effect of aging time on hardness and notch tensile strength for specimens aged at a lower temperature subsequent to pre-aging for 2 hours at a higher temperature. (See Figure 1.6.8)

3.2.7.2.2 *[Figure]* Effect of aging temperature on notch tensile strength of bar.

3.2.7.2 Fracture toughness.

3.2.7.2.1 *[Figure]* Effect of age (H condition) temperature on tensile properties and plane strain fracture toughness.

3.2.7.2.2 Influence of final forge temperature on tensile properties and plane strain fracture toughness. (See Figure 4.1.1.1)

3.2.7.2.3 Tensile, plane strain fracture toughness, and stress corrosion stress intensity factor in 3.5 percent aqueous salt solution for air melted and CVM billet in H 900 and H 1000 conditions. (See Table 2.3.2.4)

3.2.7.2.4 *[Table]* J-integral fracture toughness of plate and weldment.

3.2.8 Combined Loading.

3.3 Mechanical Properties at Various Temperatures (see also Section 3.2)

3.3.1 Tension Stress-Strain Diagrams and Tensile Properties.

3.3.1.1 *[Figure]* Effect of test temperature on tensile properties of bar in H 925 condition.

3.3.1.2 *[Figure]* Effect of test temperature on tensile properties of bar in H 1025 condition.

3.3.1.3 *[Figure]* Effect of test temperature on tensile properties of bar in H 1100 condition.

3.3.1.4 *[Figure]* Effect of test temperature on tensile properties of bar in H 1150-M condition.

3.3.2 Compression Stress-Strain Diagrams and Compression Properties.

3.3.2.1 *[Figure]* Typical compressive stress-strain and tangent-modulus curves at selected temperatures for bar in H 1025 condition.

3.3.2.2 *[Figure]* Typical compressive stress-strain and tangent-modulus curves at selected temperatures for bar in H 1150 condition.

3.3.2.3 *[Figure]* Effect of test temperature on compressive yield strength of bar in H 1025 condition.

3.3.2.4 *[Figure]* Effect of test temperature on compressive yield strength of bar in H 1150 condition.

3.3.3 Impact.

3.3.3.1 *[Table]* Charpy-V impact energy for sheet at room temperature and -65F.

3.3.3.2 *[Figure]* Effect of temperature on Charpy-V impact energy for Condition H 1150-M.

3.3.4 Bending.

3.3.5 Torsion and shear.

3.3.6 Bearing.

3.3.7 Stress concentration.

3.3.7.1 Notch properties.

3.3.7.2 Fracture toughness.

3.2.7.2.1 *[Figure]* Effect of test temperature in the range -4 to +72F on the tensile properties and plane strain fracture toughness.

3.2.7.2.2 *[Table]* Effect of aged condition, test temperature, and specimen orientation on strength and plane strain fracture toughness.

3.3.8 Combined properties.

3.4 Creep and Creep Rupture Properties

3.4.1 *[Figure]* Creep deformation and rupture curves at selected temperatures for forged bar in H 1025 condition.

3.5 Fatigue Properties

3.5.1 Conventional high-cycle fatigue.

3.5.1.1 *[Figure]* Room temperature axial-load fatigue strength of CVM billet in H 925 and H 1075 conditions.

3.5.1.2 *[Figure]* Room temperature longitudinal unnotched axial-load constant-life fatigue diagram for bar.

3.5.1.3 *[Figure]* Room temperature transverse unnotched axial-load constant-life fatigue diagram for bar.

3.5.1.4 *[Figure]* Room temperature londitudinal and transverse notched (K_t = 3.0) axial-load constant-life fatigue diagram for bar.

3.5.1.5 *[Figure]* Mild-notch axial-load fatigue strength of bar in H 1025 condition at stress ratios, R = 0.5, 0.1, -1.0.

3.5.1.6 *[Figure]* Room temperature axial-load fatigue strength of plate in H 1025 condition.

3.5.1.7 *[Figure]* Room temperature axial-load notched (K_t = 3.0) fatigue strength of plate in H 1025 condition.

3.5.1.8 *[Figure]* Room temperature axial-load high-cycle fatigue strength of machined and as-cast specimens from welded and unwelded vacuum castings.

3.5.1.9 *[Figure]* Room temperature tension-compression high-cycle fatigue strength of specimens machined from cast cylinders and from a lag damper casting.

3.5.1.10 *[Figure]* Room temperature axial-load high-cycle fatigue strength of specimens machined from bars vacuum cast into either production or high thermal conductivity shell molds, and subsequently HIP'd or not HIP'd.

3.5.1.11 *[Figure]* Room temperature axial-load high-cycle fatigue strength of HIP'd and not HIP'd notched (K_t = 3.0) specimens machined from shell mold castings and notched (K_t = 3.0) specimens machined from HIP'd lag damper casting.

3.5.1.12 *[Figure]* Elevated temperature transverse unnotched axial-load fatigue strength of forged bar.

3.5.1.13 *[Figure]* Elevated temperature transverse notched (K_t = 3.0) axial-load fatigue strength of forged bar.

3.5.2 Low-cycle Fatigue

3.5.3 Fatigue Crack Propagation.

3.5.3.1 *[Figure]* Room temperature fatigue crack growth rate at 10 Hz, R = 0.05 for plate in H 1050 condition.

3.5.3.2 *[Figure]* Room temperature fatigue crack growth rate at R = 0.67, trapezoidal load wave form (1-minute hold times), for plate in H 1050 condition.

3.5.3.3 *[Figure]* Room temperature fatigue crack growth rate at 10 Hz, R = 0.05 for plate in H 1100 condition.

3.5.3.4 *[Figure]* Room temperature fatigue crack growth rate at R = 0.05, trapezoidal load wave form (1-minute hold times), for plate in H 1100 condition.

3.5.3.5 *[Figure]* Room temperature fatigue crack growth rate in 3.5-percent NaCl solution at R = 0.05, trapezoidal load wave form (1-minute hold times), for plate in H 1100 condition.

3.5.3.6 *[Figure]* Room temperature fatigue crack growth rate at R = 0.67, trapezoidal load wave form (1-minute hold times), for plate in H 1100 condition.

3.5.3.7 *[Figure]* Room temperature fatigue crack growth rate in 3.5-percent NaCl solution at R = 0.67, trapezoidal load wave form (1-minute hold times), for plate in H 1100 condition.

3.5.3.8 *[Figure]* Effects of load ratio (R) and environment (air versus salt water) on room temperature fatigue crack growth rate for plate in H 1100 condition.

3.5.3.9 *[Figure]* Effects of load wave form (sinusoidal versus trapezoidal), load ratio (R), and heat treated condition (H) on room temperature fatigue crack growth rate for plate.

3.5.3.10 *[Figure]* Fatigue crack growth rate in air and 3.5 percent aqueous NaCl solution for the H 1025 and H 1100 conditions.

3.6 Elastic Properties

3.6.1 Poisson's Ratio, 0.272 in all hardened conditions (Ref. 27).

3.6.2 Modulus of Elasticity.

3.6.2.1 *[Table]* Elastic moduli in tension and in torsion.

3.6.2.2 *[Figure]* Effect of temperature on modulus of elasticity.

3.6.2.3 *[Figure]* Effect of temperature on modulus of elasticity in compression of bar in H 1025 condition.

3.6.2.4 *[Figure]* Effect of temperature on modulus of elasticity in compression of bar in H 1150 condition.

3.6.3 Modulus of Rigidity.

3.6.4 Tangent Modulus.

3.6.5 Secant Modulus.

4 FABRICATION

4.1 Forming

4.1.1 Forging. Elimination of delta ferrite gives this alloy improved forging properties over 17-4PH in critical upset forgings and hot flattening operations (Refs. 1, 2, 4). Materials for forging should be ordered "overaged for forging," a condition which also allows cold sawing of large sections without cracking (Ref. 1).

Forging blanks less than 3/4 inch diameter or thickness should be heated uniformly to 2150 to 2200F and held at temperature at least 15 minutes before forging. For sections over 3/4 inch, material should be heated 1/2 hour per inch of thickness at 2150 to 2200F and held one hour at temperature prior to forging. Heating above 2200F may cause undesirable grain coarsening.

Temperature during forging should not be allowed to drop below 1850F (Ref. 1).

After forging, material should be cooled below 90F to assure complete transformation to martensite. For better toughness in hardened condition, forged parts must first be treated to Condition A (Ref. 1).

4.1.1.1 *[Figure]* Influence of final forge temperature on tensile properties and plane strain fracture toughness.

4.1.2 Cold-forming. Forming should be limited to mild operations for Condition A. Fabrication is greatly improved by heat treating (Ref. 27). If severe cold forming is required, use Conditions H 1150 and H 1150-M (Ref. 1).

4.1.3 Cold-heading. Wire for cold heading should be ordered overaged, copper coated and cold drawn.

4.1.4 *[Table]* Minimum room temperature bend radii.

4.1.5 Primary and secondary fabrication methods, including equipment and tooling, are discussed in detail in Reference 50. Primary fabrication includes rolling, extruding, forging, and drawing of tube, rod, and wire. Secondary fabrication produces finished or semifinished parts from sheet, bar, or tube using additional metalforming operations. Secondary forming processes include brake bending, deep drawing, spinning and shear forming, drop hammer, trapped rubber, stretch, roll forming, dimpling, joggling, and sizing.

4.2 Machining and Grinding

4.2.1 The alloy can be machined in any heat treated condition. Parts machined in Condition A may be subsequently hardened with no harmful scaling or distortion. Design allowances can be made for the predictable contraction on hardening (Ref. 1). Machining rates for the alloy in Condition A are

similar to those for Type 302 or Type 304 (Ref. 1). The relative machinability of Condition H 1150-M is comparable to Type 303 (Ref. 4). Condition H 900 material should be machined at 60 percent of the rate used for Condition A.

4.3 Joining

4.3.1 Welding procedures are similar to those for austenitic stainless steel, even though the composition and structure of this alloy more closely resemble those of a martensitic type. Any arc or resistance welding process for regular grades of stainless are applicable (Refs. 1, 2). The usual weld filler employed is AWS A5.9 Classification ER 630. Resolution annealing is unnecessary (Ref. 7).

Autogenous welding (no filler) methods such as LW and EBW should be used with caution since the lack of ferrite forming potential can lead to hot cracking if stresses are sufficiently high. Autogenous CO_2 laser beam welds between 15-5PH and HP 9-4-20 exhibited hot-cracking, attributed to the formation of a NbC-austenite eutectic constituent (Ref. 34).

Although the alloy can be welded in any condition, the overaged conditions are preferred for highly constrained joints. If welded in condition A, or in the condition of use, or in a lower temperature aged condition than that intended for component use, then a simple post-weld aging at the desired H condition will impart weld properties comparable to those of the base metal, but possibly with somewhat less ductility and toughness. If the material is overaged (e.g. H 1150) for welding and a high final strength is desired (e.g. H 900 condition), then subsequent to welding, the component must be re-solution treated prior to aging. Otherwise, as-welded strength will be similar to that of the H 1150 condition.

The alloy's low carbon content restricts the hardness of rapidly cooled material and avoids the formation of cracks in the weld metal and heat-affected zone. This eliminates the need for preheating (Refs. 1, 2). While the alloy shows no susceptibility to spontaneous underbead cracking from weld hardening, it does not possess the high ductility and toughness of austenitic Cr-Ni steels. Therefore it should not be subjected to high levels of biaxial or triaxial stress from severely restrained weldments or exposed to notched conditions (Ref. 1).

With W-17-4PH electrodes and welding rods [specifications AMS 5827D (Ref. 22) and AMS 5825EA (Ref. 20) respectively], or 15-5PH welding wire [specification AMS 5826B (Ref. 21)], mechanical properties of the weld are equivalent to those of the base metal. Likewise , where weld deposits need to have the strength of the base metal, an E308 stainless steel electrode may be used (Ref. 2). For selected applications, the use of ER308L filler metal for the first and second passes and a 17-4PH or PH13-8Mo filler for subsequent passes has proven successful. Types 309 or 309-Cb electrodes are recommended for joining 15-5PH with dissimilar metals.

State-of-the-art welding of precipitation-hardening stainless steels is reviewed in Reference 30. Welding preparation, specific welding processes, and joint quality are exhaustively discussed. A systematic study of weld filler metal compositions, with the goal of developing a weld chemistry for the 15-5PH/17-4PH alloy system joint that would exhibit comparable properties regardless of whether it was solution treated and aged or aged only after welding, is described in Reference 43. General guidelines for weld wire composition are presented, but no specific composition is recommended.

4.3.2 *[Table]* Weld electrode and wire compositions.

4.4 Surface Treating

4.4.1 Air is a satisfactory furnace atmosphere for heat treating this alloy. Fuel-fired furnaces, where c ombustion products might contaminate the work-piece surfaces, should be avoided (Ref. 7).

4.4.2 Hardening treatments produce only a light heat tint on surfaces. It is easily removed by pickling 3 to 5 minutes in 10 percent nitric-2 percent hydrofluoric acid (by volume) at 110 to 140F. This treatment also passivates or cleans the surfaces for maximum corrosion resistance. Where pickling is undesirable, heat tint may be removed by electropolishing (Refs. 1, 2, 7).

4.4.3 A two-step procedure will remove scale formed by forging or solution treating. First, the part is immersed in caustic permanganate at 160 to 18OF for one hour. After a water rinse, it is pickled in the HNO_3-HF solution used for removing tint. A hot water rinse, high pressure water or a brush scrubbing completes descaling.

4.4.4 Nitriding. There are three methods for nitrogen penetration into the alloy, corresponding to three energy levels of implantation: (1) low energy liquid and gas nitriding; (2) medium energy ion nitriding; (3) high energy ion implantation. The first method is widely used; the second and third are newer and therefore less widely used.

The results of a study (Ref. 47) of nitriding parameters on "white" and "diffusion" layers are presented in Figures 4.4.4.1 through 4.4.4.5. Nitriding temperature, time, gas pressure and flow rate were systematically varied. Composition of the gas mixture [40 vol.%N_2, 40 vol. % Ar, and 20 vol. % H_2] and the distance between cathode and anode were held constant. The study concluded the optimum conditions for ion nitriding aged 15-5PH to be one hour at 840F at gas pressure of 8 Torr and flow rate of 2.93 in^3/min. Under these conditions a "diffusion " layer free of a

"white" layer is produced. It is possible to select other parameters to produce a thicker "diffusion" layer, while the thickness of the "white" layer remains below specified limits (Ref. 47).

4.4.4.1 *[Figure]* Effect of nitriding treatment time on "white" layer thickness.

4.4.4.2 *[Figure]* Effect of nitriding treatment time and temperature on "diffusion" layer thickness.

4.4.4.3 *[Figure]* Effect of nitriding reactor pressure on "white" and "diffusion" layer thicknesses.

4.4.4.4 *Figure]* Effect of nitriding treatment temperature on thicknesses of "white" and "diffusion" layers.

4.4.4.5 *[Figure]* Effect of nitriding gas flow rate on "white" and "diffusion" layer thicknesses.

4.4.4.6 A nitrided surface adds resistance to galling and wear. The gas-phase method of nitriding produces case hardnesses of approximately R_c 67 to a depth of 0.004 to 0.006 inch. It employs a temperature of about 1050F and produces a tough core with a hardness of about R_c 36. Nitriding slightly decreases the corrosion resistance of this alloy as it does with any stainless steel (Ref. 2).

4.4.4.7 Nitriding by the proprietary Malcomizing process raises the smooth fatigue endurance limit for the H 1100 condition in reversed bending by 15 percent.

4.4.4.8 *[Figure]* Effect of nitriding (proprietary Malcomizing) on smooth and mild notch rotating beam fatigue strength of bar in H 1100 condition.

4.4.4.9 Ion nitriding (also called glow discharge or plasma nitriding), relatively new, has the advantages of short heat treatment time, low treatment temperature, minimal product distortion, cleanliness and low energy consumption. It is especially well suited to this alloy in that removal of oxide layer is unnecessary and the aging and nitriding treatments can be combined into a single-step operation. An additional advantage is that the thicknes of the diffusion zone and the "white" layer and their microstructure and composition can be controlled by the nitriding treatment parameters: composition, pressure, and flow rate of the gas as well as the temperature, voltage, and current.

4.4.5 Friction and wear of 15-5PH are reduced substantially by ion implantation of Ti and C. Results (Ref. 36) for polished samples implanted to fluences of $5x10^{14}$ Ti/mm^2 at 180, 150, 120, and 90 keV, in that order, and $2x10^{15}$ C/mm^2 at 30 keV are shown in Figures 4.4.5.1 and 4.4.5.2. Ti concentration based on previous work in Fe were estimated to range from approximately 20 atomic percent over a depth of 2 μ-in., to approximately 10 atomic percent at 3 μ-in., and to zero at approximately 6 μ-in. C concentration profiles were estimated to be nearly identical to Ti concentration profiles.

The friction coefficient (Figure 4.4.5.1) is reduced about 50 percent by ion implantation for all loads studied, seemingly independent of pin material, and due to the production of an amorphous surface layer by the implanted ions (Ref. 37). For all tests in Figure 4.4.5.1, the coefficient of friction initiated at a value between 0.2 to 0.7 gradually increased 20 to 100 percent over 100 to 250 cycles, and then remained essentially constant over the balance of 1000 cycles. Only the final coefficient of friction after 1000 cycles is shown in Figure 4.4.5.1.

Maximum wear depth results after 1000 cycles of unlubricated wear are shown in Figure 4.4.5.2. Wear increased with load at rates somewhat independent of pin material. At the lowest loads, the mean maximum wear depth ($\overline{MWD}$) was decreased by ion implantation to 5 percent of the value of the unimplanted samples. For the 440C pins, this beneficial reduction in wear completely disappeared at loads > 30 g, whereas for the 304 pins a reduced wear depth corresponding to 66 percent of the unimplanted value persisted to the highest load studied (50 g).

Wear scar diameter on the harder 440C pins was less than 0.001 in for both ion implanted and unimplanted plates at all Hertzian stress levels. Wear scar diameters on the softer 304 pins varied with stress and plate condition (See Table 4.4.5.3), and were significantly less when mating was with an ion implanted plate. The 304 pins were shortened by wear a maximum of 0.001-in when mated with unimplanted plates and by a maximum of 0.0002-in when mated with implanted plates.

Wear tracks topography was characterized by fine parallel grooves at low Hertzian stress levels, changing to galling and debris generation which increased with increasing stress at the higher stress levels. The change in wear track topography occured at the stress level where reduction in wear due to implantation disappeared.

Implanted plates had no titanium in the wear tracks after 1000 cycles at stresses > 146 ksi, but significant amounts remained at lesser stresses. Wear scars on the pins evidenced transfer films containing titanium, in larger amounts for the 304 pins than for the 440C pins.

The above study was repeated (Ref. 38) using N^+ ion implantation as the variable affecting dry friction and wear behavior. Polished samples were implanted to fluences of $4.0x10^{17}$ N^+/cm^2 at 50keV. Peak concentration was 45 atomic percent at a depth of 2.8 μ-in. dropping to about 10 atomic percent at 4.7 μ-in. The implanted alloy exhibited reduced wear at low Hertzian stresses but no significant reduction in the friction coefficient (Figures 4.4.5.5 and 4.4.5.4, respectively). At the lowest normal load studied

(12.3g = 123 ksi Hertzian stress), the average maximum wear depth of the N^+ implanted alloy (about 0.04 μ-in.) was only about 10 percent of the unimplanted value; but at normal loads of 50g (236 ksi) or above, the benefit of implantation disappears (see Figure 4.4.5.5). With the exception of 304 pin wear, implantation with Ti and C ions reduced friction and wear twice as effectively as N^+ ion implantation (see Figure 4.4.5.6).

4.4.5.1 *[Figure]* Influence of titanium and carbon ion implantation on unlubricated friction coefficient after 1000 pin-on-disc revolutions.

4.4.5.2 *[Figure]* Influence of titanium and carbon ion implantation on unlubricated wear depth after 1000 pin-on-disc revolutions.

4.4.5.3 *[Table]* 304 stainless steel pin wear in pin-on-disc tests of Ti and C ion implanted plates and of unimplanted plates.

4.4.5.4 *[Figure]* Influence of N^+ implantation on unlubricated friction coefficient after 1000 pin-on-disc revolutions.

4.4.5.5 *[Figure]* Influence of N^+ implantation on unlubricated wear depth after 1000 pin-on-disc revolutions.

4.4.5.6 *[Figure]* Influence of ion implantation (Ti and C or N^+) on unlubricated friction coefficient and mean maximum wear depth at 173 ksi Hertzian stress, expressed as ratios of unimplanted to implanted values.

4.4.6 One of the chief drawbacks of PH stainles steels is their susceptibility to hydrogen embrittlement. General sensitivity to hydrogen embrittlement is demonstrated in Figure 4.4.6.1, where the ductility of electrochemically charged and uncharged tension specimens is compared over a broad range of tensile strength for a typical PH stainless steel. Ductility loss for 15-5PH alloy in two aged conditions, cathodically charged by immersion in a 10 percent H_2SO_4 solution containing 10 mg/l of AS_2O_3 as a poison, at a current density of 90 A/m^2 for times ranging from 0.5 to 24 hours, is shown in Figure 4.4.6.2 for time up to 8 hours. Yield strengths of charged and uncharged specimens were nearly the same. The higher strength H 1025 condition shows a significantly greater susceptibility to hydrogen embrittlement than does the H 1050 treatment. Only 8 hours of charging time is required for complete loss of ductility compared to 16 hours for the H 1050 condition (not shown). The hydrogen embrittlement appears somewhat reversible. One specimen in the H 1050 condition was charged for 8 hours and then allowed to stand at ambient room temperature for 63 hours. The subsequent tensile test showed that the ductility recovered to a significant extent, being 36 percent RA compared to 4 percent for an 8-hour charge.

Via strong binding energy to the alloy, certain additives (inhibitors) to liquid or gasious media can occupy atom sites on the alloy's surfaces, thus preventing a metal-hydrogen bond and thereby inhibiting the entry of hydrogen. These inhibiting films imposed on the surface offer protection through alteration of surface adsorption characteristics, as described in Reference 33.

In a review of the literature (Ref. 33), borax nitrite is claimed to be the most effective amongst a large number of candidate inhibitors, including phosphates, chromates, nitrates, amines, and alcohols. The effectiveness of the borax-nitrite inhibitor system was observed in both sustained-load and cyclic-load experiments.

Metallic and nonmetallic thin surface films prevent (or at least reduce) hydrogen entry if the film has a lesser binding energy for hydrogen than for the alloy, and a low hydrogen solubility and/or diffusivity. "Thin" in the context used here means coatings from a monolayer of atoms to something on the order of 10^{-6} micrometers (4×10^{-5} μ-in) in thickness; not paint, spray, or clad coatings and the like where entry of hydrogen is prevented essentially by mechanical screening barriers. "Thin" films retard hydrogen entry either through a surface adsorption effect or by possessing a low diffusivity and/or a low solubility for hydrogen. The literature review cited above (Ref. 33) offers several candidate metallic and nonmetallic surface coatings. Tungsten has the lowest hydrogen permeability of the metals studied, while TiO_2 and Al_2O_3 nonmetallic coatings are protective in thin layers of the order of 2 μ-in. TiO_2 film protection is demonstrated in Figure 4.4.6.3. Reduction in area is plotted against coating thickness for specimens hydrogen charged for four hours. The reduction in area for uncoated and uncharged specimens averaged 69 percent. That for 2 μ-in thick coated specimens was approximately 60 percent; that for 20 μ-in thick casting about 67 percent. Both casting thicknesses were effective in preventing hydrogen embrittlement.

The influence of hydrogen charging time on ductility for 20 μ-in thick TiO_2 coated specimens is shown in Figure 4.4.6.4. There is some loss in ductility for 40-hour charged specimens, but those specimens are still considerably more ductile that 4-hour charged uncoated specimens (for which the reduction in area is about 15 percent; see Figure 4.4.6.3). The literature (Ref. 33) suggests that nonmetallic films appear to be superior to metallic thin films for preventing hydrogen entry and subsequent embrittlement.

For stainless steels it is possible to thermally grow adherent oxide films of hundreds of nanometers thickness at temperatures in the vicinity of 1800F.

These films offer extensive protection and appear to be abrasion proof.

4.4.6.1 *[Figure]* Effect of strength on ductility loss for typical PH steel specimens hydrogen charged at $90A/m^2$ and tensile tested at room temperature.

4.4.6.2 *[Figure]* Effect of hydrogen charging on ductility of rod in H 1025 and H 1050 conditions.

4.4.6.3 *[Figure]* Effect of TiO_2 film thickness on ductility of specimens hydrogen charged four hours at $90A/m^2$ and tensile tested at room temperature.

4.4.6.4 *[Figure]* Effect of hydrogen charging time on ductility of TiO_2 coated (20 m-in. thick) specimens (H 1025 condition) tensile tested at room temperature after charging.

Table 1.3.1 AMS specifications for wrought products (Refs. 5, 6, 19)

Alloy	15-5PH	
Alloy Grade	Multiple Melted Using Consumable Electrode Practice During Remelting or Using Electroslag Process in the Final Melting Cycle	
Condition	A and H 900 through H 1150	
Form	Bars, Wire, Forgings, Flash Welded Rings, Extrusions, and Stock for Forging, Flash Welded Rings or Extrusions	Sheet, Strip, and Plate
AMS (Reference)	5658C (5) 5659H (6)	5862D (19)

Table 1.3.2 ASTM specifications for wrought products (Refs. 23-25)

Alloy	15-5PH		
Condition	A and H 900 through H 1150		
Form	Plate, Sheet, and Strip	Hot-rolled and Cold-finished Bars and Shapes	Forgings
ASTM Specification [Reference]	A 693-93 (XM-12) [23]	A 564/A 564M-5 (XM-12) [24]	A 705/A 705M-95 (XM-12) [25]

Table 1.3.3 AMS specifications for investment castings (Refs. 13-17)

Alloy	15-5PH
Form	Investment Castings
AMS Specification (Reference)	Condition
5346A (13)	H 925 (F_{tu} = 180 ksi)
5400 (17)	H 935 (F_{tu} = 170 ksi)
5347 (14)	H 1000 (F_{tu} = 150 ksi)
5356 (15)	H 1100 (F_{tu} = 130 ksi)
5357 (16)	A (Hardness R_C 31 max)

Table 1.3.4 AMS specifications for tubular centrifugal castings (Ref. 18)

Alloy	15-5PH
Form	Tubular Centrifugal Castings
Condition	A (Hardness BHN 363 max)
AMS Specification	5348A

Table 1.4.1 Specified composition for wrought products (Refs. 1, 5, 6, 19, 23-25, 27)

Alloy	15-5PH					
Source	Armco (1, 27) ASTM (23-25)		AMS (19)		AMS (5, 6)	
Form	All Wrought Products		Sheet, Strip, and Plate		Bars, Wire, Forgings, Flash Welded Rings, Extrusions, and Stock for Forging, Flash Welded Rings or Extruding	
Grade	Air melt or consumable electrode vacuum arc remelt		Multiple melted using vacuum-arc consumable electrode or electroslag processes in the final melt		Multiple melted using vacuum arc consumable electrode practice during remelting or electroslag process in the final melting cycle	
	Weight Percent					
	Minimum	Maximum	Minimum	Maximum	Minimum	Maximum
Carbon	—	0.07	—	0.07	—	0.07
Manganese	—	1.00	—	1.00	—	1.00
Silicon	—	1.00	—	1.00	—	1.00
Phosphorous	—	0.040	—	0.030	—	0.030
Sulfur	—	0.030	—	0.015	—	0.015
Chromium	14.00	15.50	14.00	15.50	14.00	15.50
Nickel	3.50	5.50	3.50	5.50	3.50	5.50
Copper	2.50	4.50	2.50	4.50	2.50	4.50
Columbium + Tantalum	0.15	0.45	5xC	0.45	—	—
Columbium	—	—	—	—	5xC	0.45
Tantalum	—	—	—	—	—	0.05
Molybdenum	—	—	—	0.50	—	0.50
Iron	Balance		Balance		Balance	

Table 1.4.2 Producer's specified composition for castings (Ref. 9)

Alloy	15-5PH			
Form	Castings			
Type of Casting	Investment		Sand and Centrifugal	
	Weight Percent			
	Minimum	Maximum	Minimum	Maximum
Carbon	—	0.05	—	0.05
Manganese	—	0.60	—	0.60
Phosphorous	—	0.03	—	0.03
Sulfur	—	0.03	—	0.03
Silicon	0.50	1.00	0.50	1.00
Chromium	14.5	15.5	14.5	15.5
Nickel	4.2	5.0	4.2	5.0
Copper	2.8	3.5	2.5	3.2
Columbium + Tantalum	0.15	0.30	0.15	0.30
Nitrogen	—	0.05	—	0.05
Iron	Balance		Balance	

Table 1.4.3 AMS specified composition for investment castings (Refs. 13-17)

Alloy	15-5PH			
Source	AMS (13)		AMS (14-17)	
Form	Investment Castings			
Condition/ Grade	H 925 / F_{tu} = 180 ksi		H 935 / F_{tu} = 170 ksi H 1000 / F_{tu} = 150 ksi H 1100 / F_{tu} = 130 ksi and A / Hardness = R_C 31 max	
	Weight Percent			
	Minimum	Maximum	Minimum	Maximum
Carbon	—	0.05	—	0.05
Manganese	—	0.60	—	0.60
Silicon	0.50	1.00	0.50	1.00
Sulfur	—	0.025	—	0.025
Phosphorous	—	0.025	—	0.025
Chromium	14.00	15.50	14.00	15.50
Nickel	4.20	5.00	4.20	5.50
Copper	2.50	3.20	2.50	3.20
Columbium + Tantalum	0.15	0.30	0.15	0.30
Tantalum	—	0.10	—	—
Nitrogen	—	0.05	—	0.05
Iron	Balance		Balance	

Table 1.4.4 AMS specified composition for tubular centrifugal castings (Ref. 18)

Alloy	15-5PH	
Form	Tubular Centrigugal Castings	
Condition/Grade	H 925 / F_{tu} = 180 ksi	
	Weight Percent	
	Minimum	Maximum
Carbon	—	0.05
Manganese	—	0.60
Silicon	0.50	1.00
Phosphorous	—	0.025
Sulfur	—	0.025
Chromium	14.00	15.50
Nickel	4.20	5.00
Copper	2.50	3.20
Columbium + Tantalum	0.15	0.30
Aluminum	—	0.05
Tin	—	0.02
Nitrogen	—	0.05
Iron	Balance	

Table 1.4.5 AMS specified compostition for weld electrodes and wire (Refs. 20-22)

Alloy	17-4PH		15-5PH		17-4PH	
Source	AMS (20)		AMS (21)		AMS (22)	
Form	Weld Wire		Weld Wire		Weld Electrode	
	Weight Percent					
	Minimum	Maximum	Minimum	Maximum	Minimum	Maximum
Carbon	—	0.05	0.025	0.050	—	0.05
Manganese	0.25	0.75	0.25	0.75	0.25	0.75
Silicon	—	0.75	—	0.60	—	0.75
Phosphorous	—	0.025	—	0.020	—	0.04
Sulfur	—	0.025	—	0.010	—	0.03
Chromium	16.00	16.75	14.40	15.30	16.00	16.75
Nickel	4.50	5.00	4.75	5.50	4.50	5.00
Columbium	0.15	0.30	5xC	0.40	0.15	0.30
Copper	3.25	4.00	3.00	3.50	3.25	4.00
Molybdenum	—	0.75	—	0.30	—	0.75
Tantalum	—	—	—	0.05	—	—
Aluminum	—	—	—	0.025	—	—
Oxygen	—	—	—	0.01	—	—
Nitrogen	—	—	—	0.040	—	—
Hydrogen	—	—	—	0.0006	—	—
Iron	Balance		Balance		Balance	

Table 1.5.2 Age condition A to H Conditions
(Precipitation hardening heat treatment schedules)
(Refs. 1, 2, 5, 6, 27)

Alloy	15-5PH		
Condition	Age		
	Temperature ± 15F[a]	Time (hr)	Cool
H 900	900	1	Air
H 925	925	4	Air
H 1025	1025	4	Air
H 1075	1075	4	Air
H 1100	1100	4	Air
H 1150	1150	4	Air
H 1150 + H 1150	1150 1150	4 followed by 4	Air Air
H 1150-M	1400 1150	2 followed by 4	Air Air

[a] AMS (5, 6): Temperature ± 10F, Time ± 0.3 hour.

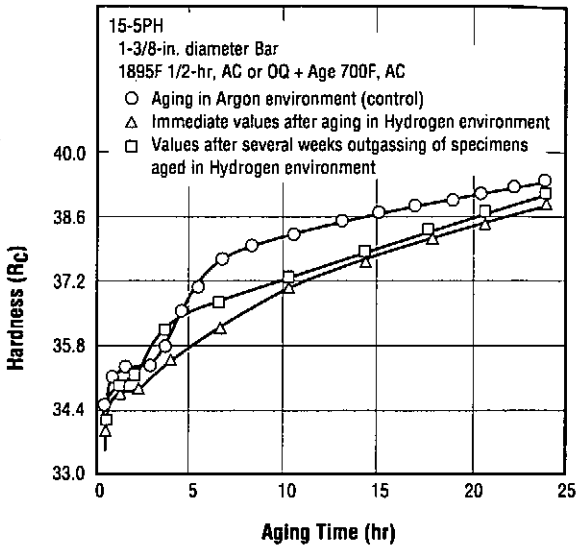


Figure 1.5.2.2.1 Influence of hydrogen aging treatment environment on age hardening at 700F (Ref. 59)

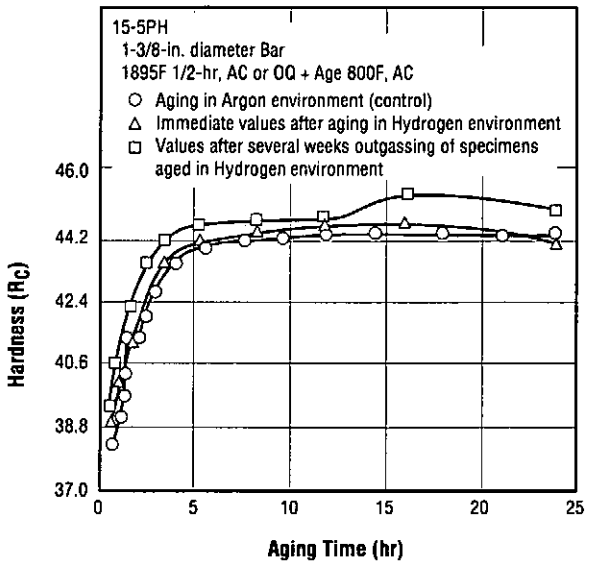


Figure 1.5.2.2.2 Influence of hydrogen aging treatment environment on age hardening at 800F (Ref. 59)

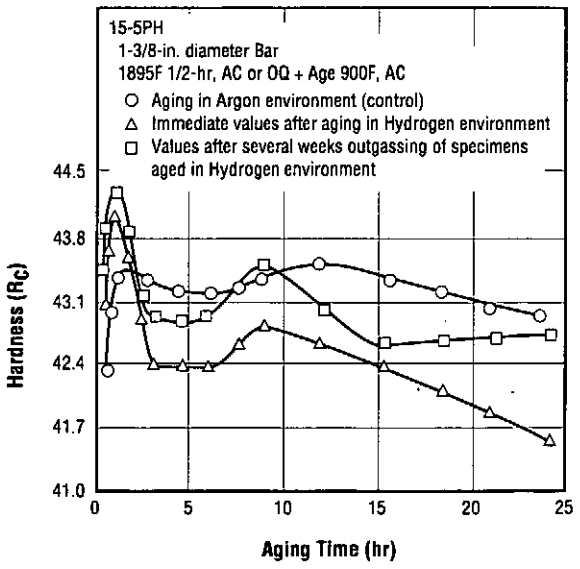


Figure 1.5.2.2.3 Influence of hydrogen aging treatment environment on age hardening at 900F (Ref. 59)

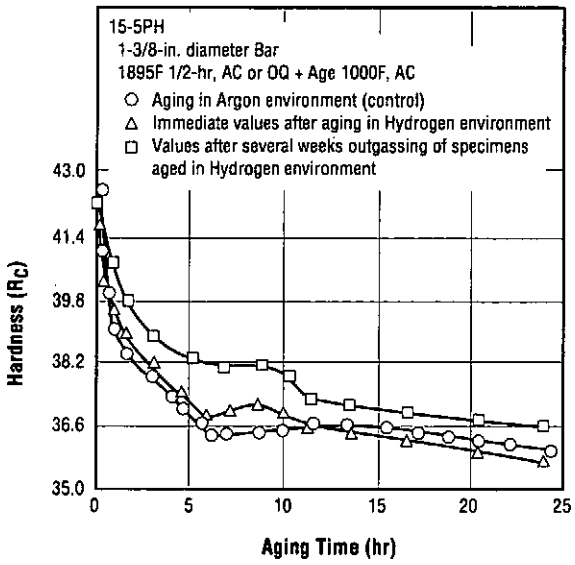


Figure 1.5.2.2.4 Influence of hydrogen aging treatment environment on age hardening at 1000F (Ref. 59)

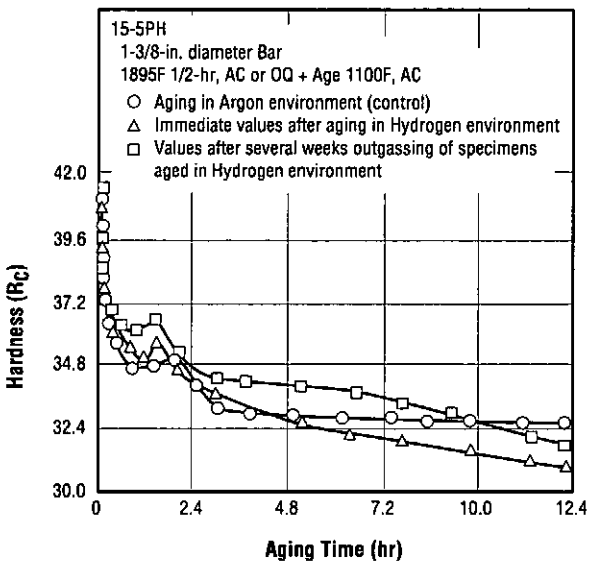


Figure 1.5.2.2.5 Influence of hydrogen aging treatment environment on age hardening at 1100F (Ref. 59)

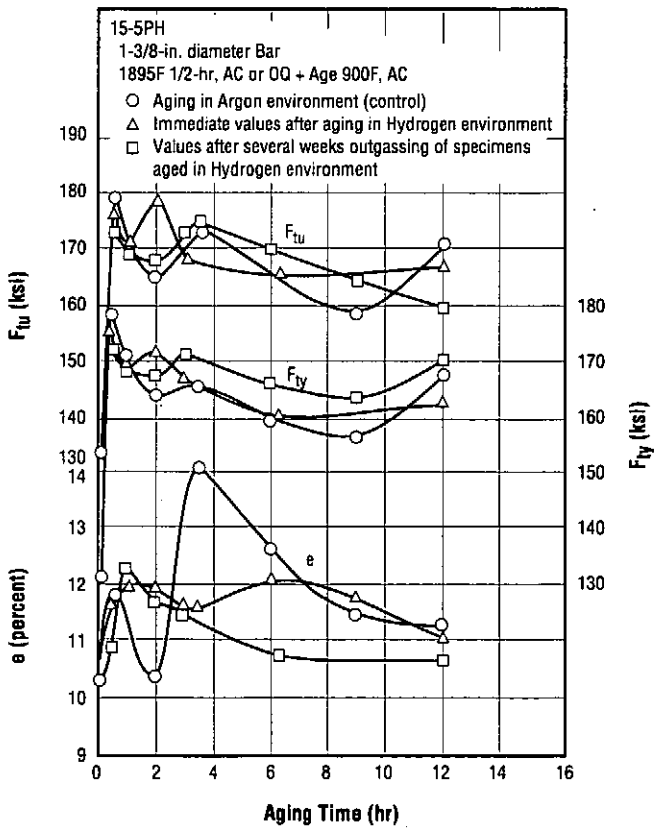


Figure 1.5.2.2.6 Influence of hydrogen aging treatment environment on 900F aged tensile properties (Ref. 59)

Table 1.5.2.3.1 Dimensional change (contraction) from hardening heat treatment (Ref. 27)

Alloy	15-5PH
Form	Sheet and Strip
Condition	Dimensional Contraction (in./in.)
H 900	0.00045
H 925	0.00051
H 1025	0.00053
H 1100	0.0009
H 1150	0.0022
H 1150M 1400 =	0.00037
1150 =	0.00206
therefore, 1400 + 1150 =	0.00243

Each value single test from single heat; can vary from heat to heat.

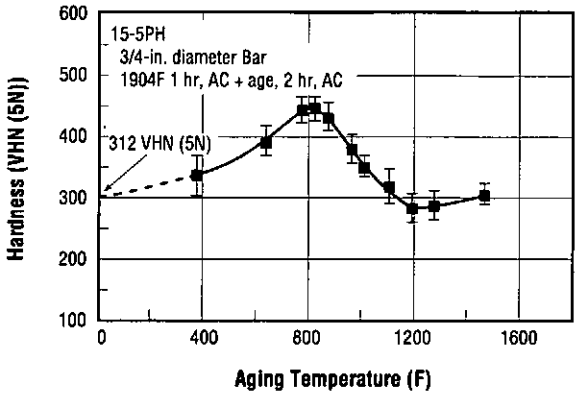


Figure 1.6.3 Effect of aging temperature on hardness of bar (Ref. 54)

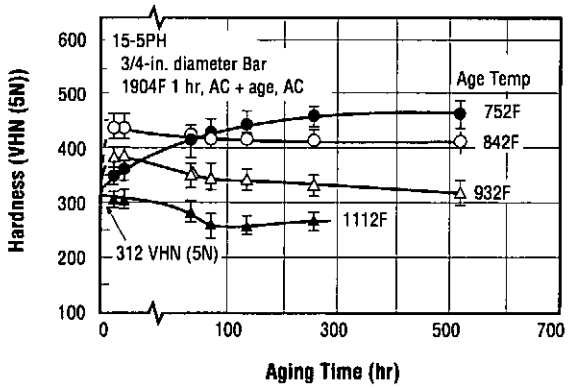


Figure 1.6.4 Effect of aging time on hardness of bar (Ref. 54)

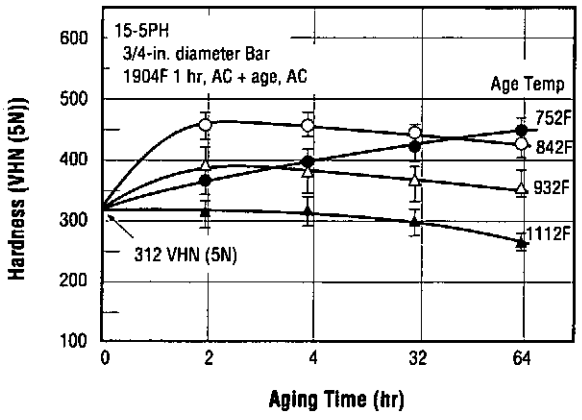


Figure 1.6.5 Effect of aging time on hardness of bar (Ref. 53)

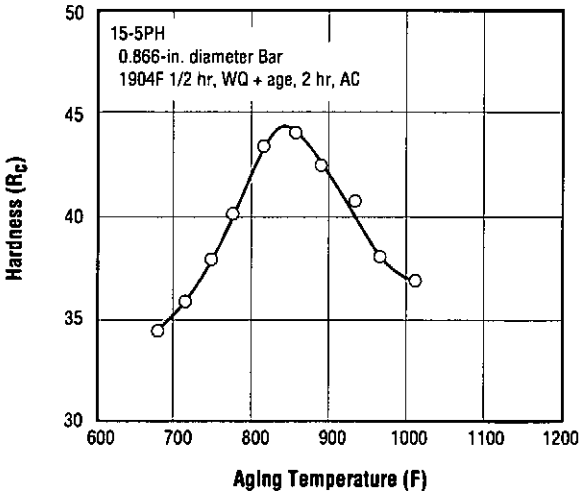


Figure 1.6.6 Effect of aging temperature on hardness of bar (Ref. 53)

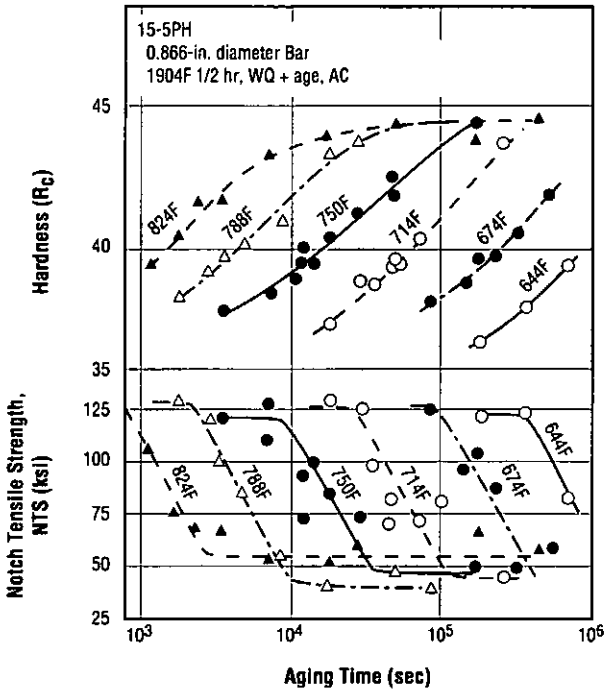


Figure 1.6.7 Effect of holding time at the aging temperature on hardness and notch tensile strength of bar (Ref. 53)

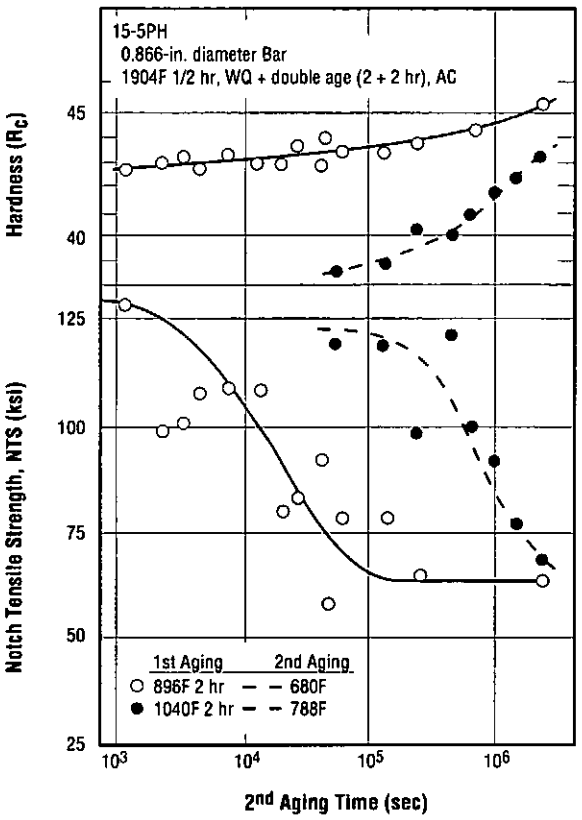


Figure 1.6.8 Effect of aging time on hardness and notch tensile strength for specimens aged at a lower temperature subsequent to pre-aging for 2 hours at a higher temperature (Ref. 53)

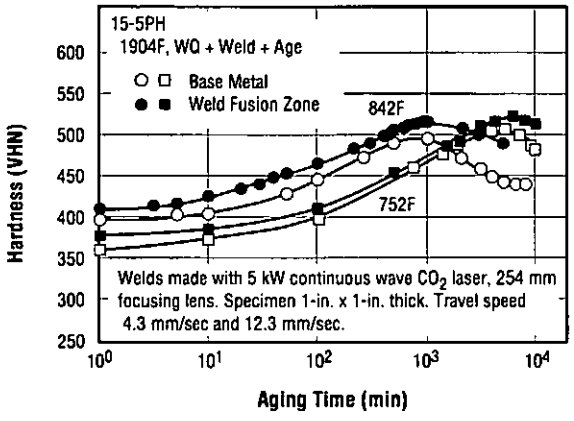


Figure 1.6.9 Effect of aging time at 752F and 842F on hardness of base and weld metal (Ref. 58)

Table 1.9.5.1 Effect of heat treatment on shear beam force transducer mechanical hysteresis (Ref. 31)

Alloy	15-5PH
Heat Treatment (Condition)	Hysteresis (μV)
H 900	7.0
Special Temperature Profile[a]	2.5
Special Temperature Profile above, but Higher Cooling Rate	2.6

[a] Proprietary; however, it is suspected that solution temperature plays a significant role and should not be too high if good hysteresis performance is to be achieved.

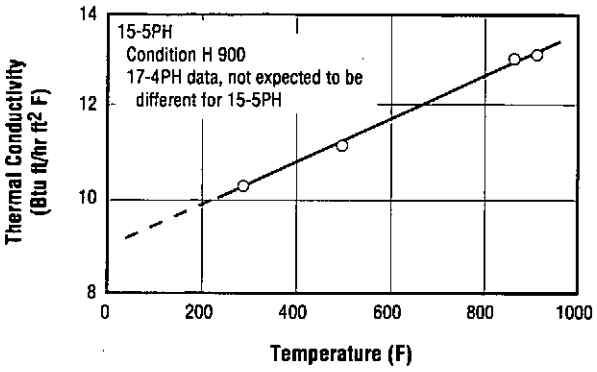


Figure 2.1.3 Thermal conductivity (Refs. 1, 7, 27)

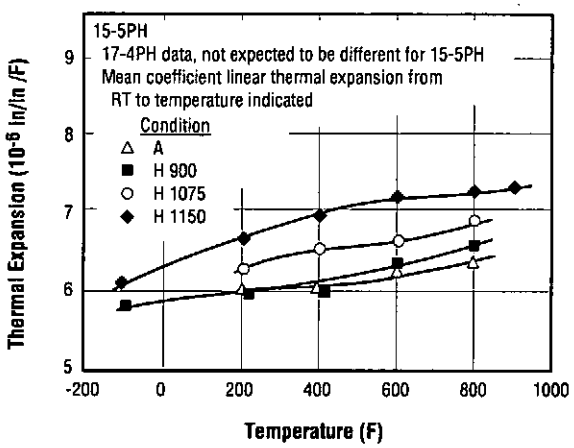


Figure 2.1.4 Thermal expansion (Refs. 1, 7, 27)

Table 2.1.5 Specific heat (Refs. 1, 7, 27)

Alloy	15-5PH[a]	
Condition	A	H 900
Specific Heat (32/212F) Btu/lb F	0.11	0.10

[a] 17-4PH data, not expected to be different for 15-5PH.

Table 2.2.1 Density (Refs. 1, 7, 27)

Alloy	15-5PH[a]			
Condition	A	H 900	H 1075	H 1150
Density (lb/cu in.) (gr/cu cm)	0.280 7.78	0.282 7.80	0.283 7.81	0.284 7.82

[a] 17-4PH data, not expected to be different for 15-5PH.

Table 2.2.2 Electrical resistivity (Refs. 1, 7, 27)

Alloy	15-5PH[a]	
Condition	A	H 900
Electrical Resistivity (microhm-inch)	38.5	30.3

[a] 17-4PH data, not expected to be different for 15-5PH.

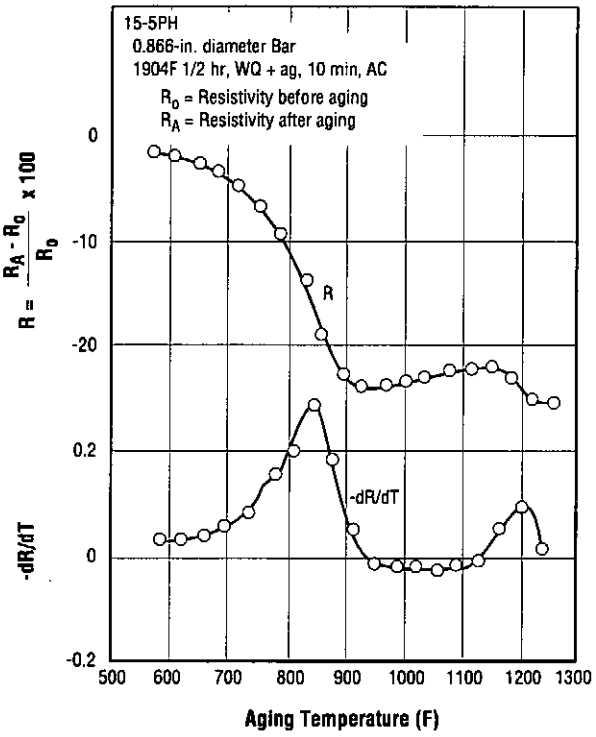


Figure 2.2.2.1 Effect of 10-minute aging temperature on change in electrical resistivity and its temperature derivative (Ref. 53)

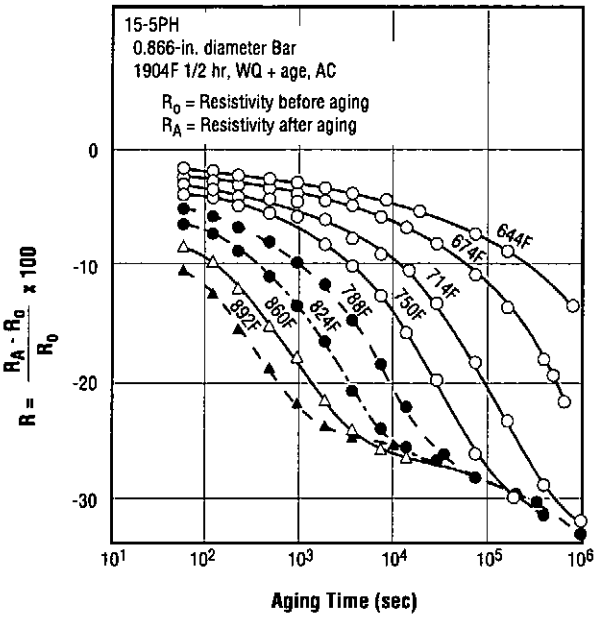


Figure 2.2.2.2 Effect of aging time on change in electrical resistivity over a range of aging temperatures (Ref. 53)

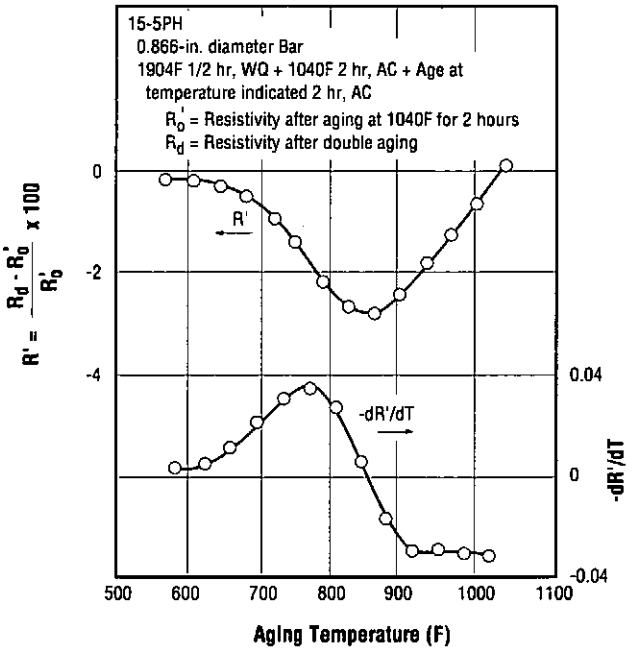


Figure 2.2.2.3 Effect of 2-hour aging temperature on electrical resistivity and its temperature derivative for specimens pre-aged at 1040F for 2 hours (Ref. 53)

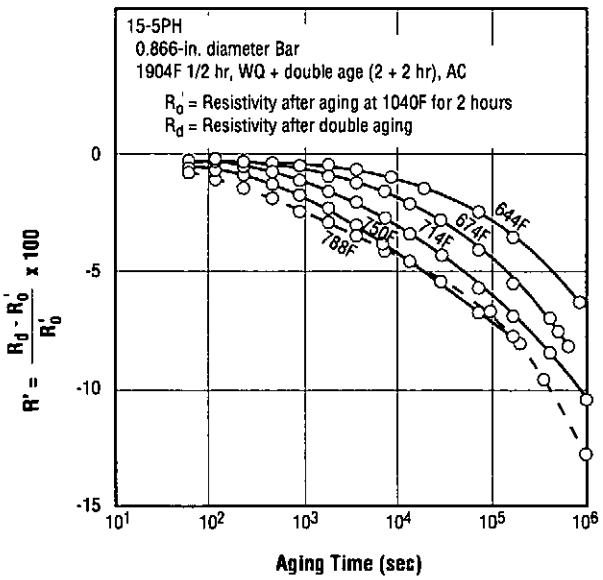


Figure 2.2.2.4 Effect of aging time on electrical resistivity for specimens aged at various temperatures subsequent to 1040F, 2 hour pre-age (Ref. 53)

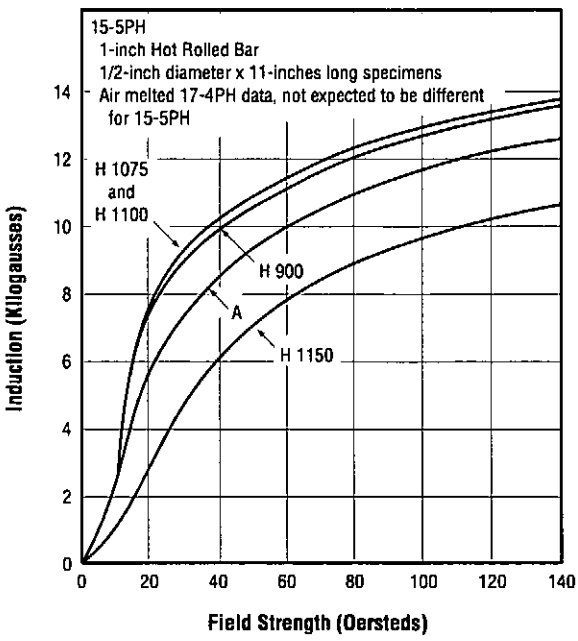


Figure 2.2.3.1 Induction curves (Ref. 10)

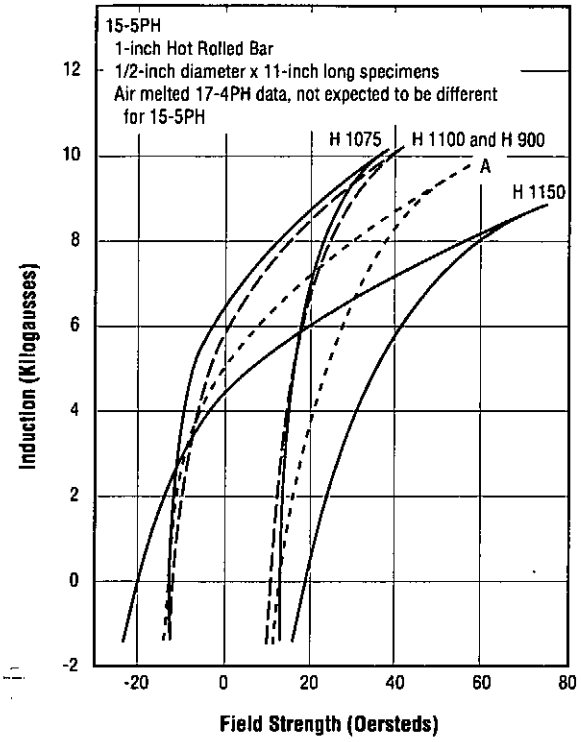


Figure 2.2.3.2 Hysteresis curves (Ref. 10)

Table 2.3.1.1 Corrosion of consumable electrode vacuum arc remelted 15-5PH and air melted 17-4PH in several corrosive media (Refs. 1, 12, 27)

Alloy	15-5PH	17-4PH
Form	1-inch Round Bar	
Condition	CVM	Air Melt
Boiling 65 percent HNO_3 - Average of five 48-hour periods[d]		
H 900	0.0083 IPM[a]	0.014 IPM
H 1025	0.0106 IPM	0.007 IPM
H 1150	0.0083 IPM	0.0065 IPM
1 percent HC1 at 95F - Average of five 48-hour periods[e]		
H 900	0.025 IPY[b]	0.035 IPY
H 1025	0.085 IPY	0.174 IPY
H 1150	0.730 IPY	0.650 IPY
Commercial Bleach - 7 days at 95F[e]		
H 900	0.0016 IPY	0.03 IPY
H 1025	0.013 IPY	0.03 IPY
H 1150	0.0083 IPY	0.03 IPY
5 percent Salt Fog at 95F - 10 days[f]		
H 900	No rust	5 - 10 percent rust
H 1025	0 - 5 percent rust[c]	10 - 25 percent rust
H 1150	0 - 5 percent rust	5 - 10 percent rust

[a] IPM = Inches per month.

[b] IPY = Inches per year.

[c] Percentage of total exposed area that rusted during test period.

[d] Tested according to ASTM Standard A 262.

[e] Tested according to ASTM Standard A 279.

[f] Tested according to ASTM Standard B 117.

Table 2.3.2.1 Stress corrosion cracking behavior of bar in three salt media (Refs. 60, 61)

a. Conventional tensile properties and salt spray and sea coast continuous exposure

Alloy	15-5PH					
Conventional Tensile Properties						
Heat (Reference)	Form	Condition	Test Direction	F_{tu} (ksi)	F_{ty} (ksi)	e (percent)
A (60)	3-in x 6-in Bar	H 1000 H 1050 H 1000 H 1050	ST ST LT LT	165 160 158 156	160 158 158 156	9 10 9 9
B (60)	3-in Diameter Bar	H 1000 H 1050	T T	169 162	164 158	14 16
C (60)	2 1/4-in x 6-in Bar	H 900 H 1000	ST ST	191 166	170 154	20 19
D (61)	2-in Diameter Bar	H 900 H 925 H 1025	L L L	189 187 164	173 163 156	11 11 9

Continuous Exposure[b]									
Heat (Reference)	Form	Condition	Test Direction	Applied Stress		5% Salt Spray		Sea Coast[a]	
				(ksi)	(% F_{ty})	F/N[c]	Exposure Time	F/N[c]	Exposure Time
A (60)	3-in x 6-in Bar	H 1000 H 1000 H 1000 H 1050 H 1050 H 1050 H 1000 H 1000 H 1000 H 1050 H 1050 H 1050	ST ST ST ST ST ST LT LT LT LT LT LT	80 120 160 79 119 158 79 119 158 78 117 156	50 75 100 50 75 100 50 75 100 50 75 100	0/4 0/3 0/3 0/3 0/3 0/3 0/3 0/3 0/3 0/3 0/3 0/3	6 mos	0/5	14 mos
B (60)	3-in Diameter Bar	H 1000 H 1000 H 1000 H 1050 H 1050 H 1050	T T T T T T	82 123 164 79 119 158	50 75 100 50 75 100	0/3	6 mos	0/5 0/4 0/4 0/5 0/4 0/4	14 mos
C (60)	2 1/4-in x 6-in Bar	H 900 H 900 H 1000 H 1000	ST ST ST ST	128 170 116 154	75 100 75 100	1/2 0/4	< 180 days 6 mos	0/5 2/5 0/5 0/5	14 mos 366, 384 days 14 mos 14 mos

Table 2.3.2.1 (cont'd) Stress corrosion cracking behavior of bar in three salt media (Refs. 60, 61)

b. Salt water alternate immersion

Alternate Immersion Exposure[d]							
Heat (Reference)	Form	Condition	Test Direction	Applied Stress		3.5% Salt Water Alternate Immersion[e]	
				(ksi)	(% F_{ty})	F/N[c]	Exposure Time
C (60)	2 1/4-in x 6-in Bar	H 900 H 1000	ST ST	170 154	100 100	2/2 0/4	156, 158 days 6 mos
D (61)	2-in Diameter Bar	H 900 H 900 H 925 H 925 H 1025 H 1025	L L L L L L	130 173 123 163 117 156	75 100 75 100 75 100	0/3	6 mos

[a] Kennedy Space Center.

[b] 1/8-inch diameter tensile specimens.

[c] F/N = ratio of failures to total number of specimens exposed.

[d] C-ring specimen.

[e] 10 minutes in solution; 50 minutes out of solution.

Table 2.3.2.2 Stress corrosion cracking of strip in marine atmosphere (Ref. 63)

Alloy		15-5PH				
Heat	Condition	F_{tu} (ksi)	F_{ty} (ksi)	Hardness (R_c)	Time (days) to Failure at	
					100% F_{ty} [a]	75% F_{ty} [a]
A	H 900	201	180	44.5	22, 22, 22	22, 22, 22
	H 925	187	172	42.5	22[b], 22[b], 266[b]	22[b], 22[b], 109[b]
	H 975	173	163	38.5	NF, NF, NF	NF, NF, NF
	H 1025	165	159	37.5	NF, NF, NF	NF, NF, NF
B	A	158	133	43.0	NF, NF, NF	NF, NF, NF
	H 900	196	173	44.5	21, 21, 21	21, 21, 26
	H 925	190	166	41.5	23[b], 23[b], 23[b]	23[b], 23[b], 23[b]
	H 975	170	159	39.5	NF, NF, NF	NF, NF, NF

[a] 1-inch x 8-inch x approximately 0.060-inch thick bent strip specimens exposed to a marine atmosphere on test racks facing the turf, tilted 30 degrees to the horizontal, located nominally 80 feet from the Atlantic Ocean at Kure Beach, North Carolina.

[b] Failure at stamped identification number near end of specimen.

[c] NF, no failures.

Table 2.3.2.3 Effect of aqueous salt environment and specimen orientation on stress corrosion cracking threshold, K_{Iscc} (Ref. 51)

Alloy-	15-5PH		
Condition	Environment	Orientation	K_{Iscc} (ksi $\sqrt{in.}$)
H 900	3.5% NaCl	LT	56
	20% NaCl	TL	33

Table 2.3.2.4 Tensile, plane strain fracture toughness, and stress corrosion cracking stress intensity factor in 3.5 percent aqueous salt solution for air melted and CVM billet in H 900 and H 1000 conditions (Ref. 64)

Alloy	15-5PH						
Form	Condition	F_{tu}[a] (ksi)	F_{ty}[a] (ksi)	e[a] (percent)	K_{Ic}[b] (ksi $\sqrt{in.}$)	K_{Iscc}[b,c] (ksi $\sqrt{in.}$)
3-in Sq Billet (Air Melt)	H 900 H1000	195.7 161.6	175.0 157.9	16 16	96.8[d] 114.0[d]	80.0 ± 2.0 114.0[e]
4 1/2-in Sq Billet (CVM)	H 900 H 1000	191.5 162.9	174.9 157.6	14 15	74.5 120.0[d]	55.8 ± 3.8 120.0

[a] L direction.

[b] LT crack plane orientation.

[c] In 3.5 NaCl aqueous solution.

[d] Not valid acording to ASTM E 399.

[e] No stress corrosion crack growth at stress intensity factor levels below approximately 85% K_Q.

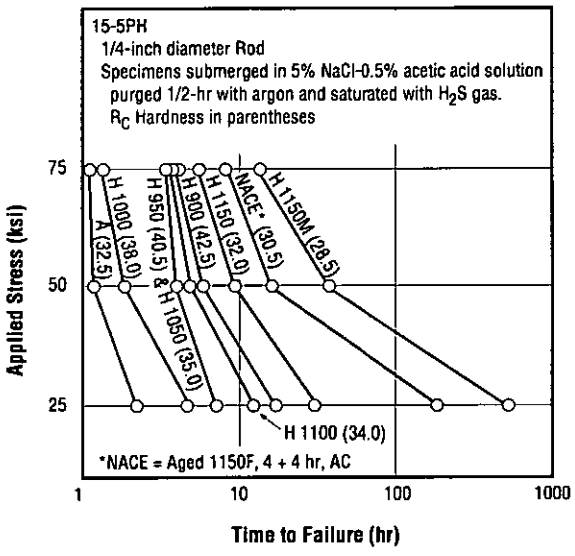


Figure 2.3.2.6 Sulfide stress corrosion cracking of rod (Ref. 62)

Table 3.1.1 Producer's guaranteed mechanical properties (Refs. 1, 2)

Alloy	15-5PH						
Form	See footnotes						
Condition	H 900	H 925	H 1025	H 1075	H 1100	H 1150	H 1150-M
Longitudinal Direction [a,b]							
F_{tu}, min (ksi)	190	170	155	145	140	135	115
F_{ty}, min (ksi)	170	155	145	125	115	105	75
e (2-in. or 4D) min (percent)	10	10	12	13	14	16	18
RA, min (percent)	35	38	45	45	45	50	55
Hardness, range, min (R_C)	40 - 47	38 - 45	35 - 42	31 - 39	32 - 38	28 - 37	24 - 30
Charpy-V Impact Energy, min (ft-lbs)	c	5	15	20	25	30	55
Transverse Direction[d]							
F_{tu}, min (ksi)	190	170	155	145	140	135	115
F_{ty}, min (ksi)	170	155	145	125	115	105	75
e (2-in. or 4D) min (percent)	6	7	8	9	10	11	14
RA, min (percent)	15	20	27	28	29	30	35
Hardness, range, min (R_C)	40 - 47	38 - 45	35 - 42	31 - 39	32 - 38	28 - 37	24 - 30
Charpy-V Impact Energy, min (ft-lbs)	c	c	10	15	15	20	35

[a] Intermediate location, (midway between center and edge).

[b] Air melted (up to 8-inch sections) or consumable electrode vacuum arc remelted (up to 12-inch sections).

[c] Minimum impact properties are not guaranteed in this condition.

[d] Consumable electrode vacuum arc remelted (up to 12-inch sections).

Table 3.1.2 AMS specified mechanical properties for air melted alloy products (Ref. 5)[a]

Alloy	15-5PH
Form	Bars, Wire, Forgings, Flash Welded Rings, and Stock for Forgings or Flash Welded Rings[b]
Condition	H 900
F_{tu}, min (ksi)	190
F_{ty}[c], min (ksi)	170
e (2-in. or 4D), min (percent)	10
RA, min (percent)	35
Hardness (BHN or equivalent)	388 - 448

[a] Reference 5 has been superseded by Reference 6.

[b] Up to 8-inch in section.

[c] 0.2 percent offset or 0.0159-inch extension in 2-inch gage length with $E = 28.5 \times 10^6$ psi.

Specimens taken in the longitudinal direction from bars and wire, from forgings with specimen axis approximately parallel to the forging flow lines, and in the circumferential direction from parent metal of flash welded rings.

Table 3.1.3 AMS specified mechanical properties for consumable electrode vacuum arc remelted alloy products (Ref. 6)

Alloy	15-5PH	
Form	Bars, Wire, Forgings, Flash Welded Rings, and Stock for Forgings or Flash Welded Rings[a]	
Condition	H 900	
	Longitudinal	Transverse
F_{tu}, min (ksi)	190	190
F_{ty}[b], min (ksi)	170	170
e (2-in. or 4D), min (percent)	10	6
RA, min (percent)	35	15
Hardness (BHN or equivalent)	388 - 444	

[a] Up to 12 inch in section.

[b] 0.2 percent offset or 0.0159-inch extension in 2-inch gage length with $E = 28.5 \times 10^6$ psi.

Longitudinal test requirements apply to specimens taken in the longitudinal direction from bars and wire, specimens taken from forgings with axis approximately parallel to the flow lines, and specimens taken in the circumferential direction from parent metal of flash welded rings; transverse test requirements apply to all other specimens.

Table 3.1.4 AMS and ASTM specified strength, hardness, and bendability of solution treated sheet, strip, and plate (Refs. 19, 23)

Alloy	15-5PH
Form	Sheet, Strip and Plate
Condition	A
Nominal Thickness (in.)	0.015 - 0.1875
F_{tu}, max (ksi)	185
F_{ty}, max (ksi)	160
e (2-in.), min (percent)	3
Hardness[a], max - R_C BHN	38 363
180 degree Bend Radius	18 x nominal thickness[b]

[a] Section thickness 0.0015 to 4.00 inch.

[b] Product nominal thickness 0.109-inch maximum.

Table 3.1.5 AMS and ASTM specified tensile strength and hardness for solution heat treated bars, forgings, flash welded rings, and wire (Refs. 6, 24, 25)

Alloy	15-5PH	
Form	Wire	Bars, Forgings, Flash Welded Rings, and Wire
Condition	A	
F_{tu}, max (ksi)	175	
Hardness[a], max R_C BHN or equivalent		38[b] 363[b]

[a] Hardness conversions are provided in ASTM E 140.

[b] For bars, determined at mid-radius or quarter thickness.

Table 3.1.6 AMS and ASTM specified tensile properties and hardness for precipitation hardened sheet, strip, and plate (Refs. 19, 23)

Alloy	15-5PH[a]					
Form	Sheet, Strip, and Plate[b]					
Condition	Nominal Thickness (in.)	F_{tu}, min (ksi)	F_{ty}, min (ksi)	e (2-in. or 4D), min (percent)	RA, min (percent)	Hardness, range [BHN (R_C)]
H 900	< 0.1875 0.1875 - 0.625 > 0.625 - 4.000	190	170	5 8 10	— 30 35	375-444 (40-47)
H 925	< 0.1875 0.1875 - 0.625 > 0.625 - 4.000	170	155	5 8 10	— 30 35	352-415 (38-45)
H 1025	< 0.1875 0.1875 - 0.625 > 0.625 - 4.000	155	145	5 8 12	— 35 40	331-388 (35-42)
H 1075	< 0.1875 0.1875 - 0.625 > 0.625 - 4.000	145	125	5 9 13	— 35 45	311-363 (33-39)
H 1100	< 0.1875 0.1875 - 0.625 > 0.625 - 4.000	140	115	5 10 14	— 35 45	302-352 (32-38)
H 1150	< 0.1875 0.1875 - 0.625 > 0.625 - 4.000	135	105	8 10 16	— 40 50	269-341 (28-37)

[a] Multiple melted using vacuum-arc consumable electrode or electroslag processes in the final melting cycle.

[b] Products thickness 4.0 inch maximum.

Table 3.1.7 AMS and ASTM specified tensile properties and hardness for precipitation hardened bars, forgings, flash welded rings extrusions, and stock for forging, flash welded rings, or extruding (Refs. 6, 24, 25)

Alloy	15-5PH[a]					
Form	Bars, Forgings, Flash Welded Rings, Extrusions, and Stock[b] for Forging, Flash Welded Rings, or Extruding					
Condition	H 900	H 925	H 1025	H 1075	H 1100	H 1150
Longitudinal						
F_{tu}, min (ksi)	190	170	155	145	140	135
F_{ty}, min (ksi)	170	155	145	125	115	105
e (2-in. or 4D), min (percent)	10	10	12	13	14	16
RA, min (percent)	35	38	45	45	45	50
Hardness, range (BHN)	388 - 444	375 - 429	331 - 401	311 - 375	302 - 363	277 - 352
Transverse[c]						
F_{tu}, min (ksi)	190	170	155	145	140	135
F_{ty}, min (ksi)	170	155	145	125	115	105
e (2-in. or 4D), min (percent)	6	10	8	9	10	11
RA, min (percent)	20[d]	25[e]	32[f]	33[g]	34[h]	35
Hardness, range (BHN)	388 - 444	375 - 429	331 - 401	311 - 375	302 - 363	277 - 352

[a] Multiple melted using vacuum consumable electrode practice during remelting or multiple melted using electroslag process in the final melting cycle.

[b] Property specification applies to stock forged to a test coupon and heat treated. Tests on coupons taken from forged stock after heat treatment shall be accepted as equivalent to tests of a heat treated forged coupon.

[c] Transverse tensile property requirements apply only to products from which a test specimen not less than 2-1/2 inch long or 1/2-inch x 1/2-inch cross-section can be extracted.

[d] ASTM (25) specifies RA, min = 15 percent.

[e] ASTM (25) specifies RA, min = 20 percent.

[f] ASTM (25) specifies RA, min = 27 percent.

[g] ASTM (25) specifies RA, min = 28 percent.

[h] ASTM (25) specifies RA, min = 30 percent.

Table 3.1.8 AMS specified tensile properties and hardness for precipitation hardened investment castings (Refs. 13 - 17)

Alloy	15-5PH			
Form	Investment Castings			
Source	AMS (13, 16)	AMS (16, 17)	AMS (14, 16)	AMS (15, 16)
Condition	H 925	H 935	H 1000	H 1100
Separately Cast Specimens				
F_{tu}, min (ksi)	180	170	150	130
F_{ty}, min (ksi)	160	150	130	120
e (4D), min (percent)	6	7	8	8
RA, min (percent)	15	16	18	20
Hardness, range (R_C)	40 - 44	38 - 47	35 - 42	33 - 40
Integrally Cast Specimens or Specimens Machined From Castings				
F_{tu}, min (ksi)	180	170	150	130
F_{ty}, min (ksi)	160	150	130	120
e (4D), min (percent)	5	6	8	6
RA, min (percent)	12	14	15	18
Hardness, range (R_C)	40 - 44	38 - 47	35 - 42	33 - 40

Separately cast and integrally cast tensile specimens may be either cast to size, or cast oversize and subsequently machined to required 0.250-inch diameter.

Table 3.1.9 AMS specified tensile properties and hardness for precipitation hardened tubular centrifugal castings (Ref. 18)

Alloy	15-5PH
Form	Tubular Centrifugal Castings
Condition	H 925
F_{tu}, min (ksi)	180
F_{ty}, min (ksi)	150
e (4D), min (percent)	6
RA, min (percent)	15
Hardness, range (R_C)	40 - 45

Table 3.1.10 Producer's specified acceptable tensile properties and hardness for Condition A (Refs. 1, 27)

Alloy	15-5PH				
Form	Rounds, Hexagons, and Squares			Flats	Sheet and Strip
Condition	A				
Size	≤ 1/8 inch	> 1/8 inch to 1/2 inch	> 1/2 inch	> 1/2 inch	all
F_{tu} (ksi)	175 max	—	—	—	185 max
F_{ty} (ksi)	—	—	—	—	160 max
e (2-in.), (percent)	—	—	—	—	3 min
Hardness	—	R_C 38 max	BHN 363 max	BHN 363 max	R_C 38 max

Note: See Section 1.9.4.

Table 3.1.11 Producer's specified acceptable tensile properties and hardness for sheet and strip in H Conditions (Ref. 27)

Alloy	15-5PH					
Form	Sheet and Strip					
Condition	H 900	H 925	H 1025	H 1075	H 1100	H 1150
F_{tu}, min (ksi)	190	170	155	145	140	135
F_{ty}, min (ksi)	170	155	145	125	115	105
e (2-in.), min (percent)	5	5	5	5	5	8
Hardness, range (R_C)	40 - 48	38 - 46	35 - 43	31 - 40	31 - 40	28 - 38

Table 3.2.1.1 Typical mechanical properties for bar (Refs. 1, 7)

Alloy	15-5PH						
Form	Up to 12-inch Sections						
Condition	H 900	H 925	H 1025	H 1075	H 1100	H 1150	H 1150-M
Longitudinal Direction - Intermediate Location Air Melted or Consumable Electrode Vacuum Arc Remelted							
F_{tu} (ksi)	200	190	170	165	150	145	125
F_{ty} (ksi)	185[a]	175	165	150	135	125	85
e (2-in. or 4D), (percent)	14	14	15	16	17	19	22
RA (percent)	50	54	56	58	58	60	68
Hardness (BHN) (R_C)	420 44	409 42	352 38	341 36	332 34	311 33	277 27
Charpy-V Impact Energy (ft-lbs) RW or RT Direction	15	25	35	40	45	50	100
Transverse Direction - Intermediate or Center Location Consumable Electrode Vacuum Arc Remelted							
F_{tu} (ksi)	200	190	170	165	150	145	125
F_{ty} (ksi)	185	175	165	150	135	125	85
e (2-in. or 4D), (percent)	10	11	12	13	14	15	18
RA (percent)	30	35	42	43	44	45	50
Hardness (BHN) (R_C)	420 44	409 42	352 38	341 36	332 34	311 33	277 27
Charpy-V Impact Energy[b] (ft-lbs) TW or WT Direction TR or WR Direction	7 8	17 12	27 25	30 25	30 25	50 45	100 70

[a] For condition H 900, F_{cy} = 178 ksi.

[b] For intermediate location only.

Table 3.2.1.2 Typical mechanical properties for sheet and strip (Ref. 27)

Alloy	15-5PH						
Form	Sheet and Strip - Cold Flattened						
Condition	A	H 900	H 925	H 1025	H 1075	H 1150	H 1150-M
Longitudinal							
F_{tu} (ksi)	161	209	181	174	162	150	136
F_{ty} (ksi)	140	201	175	171	160	140	111
e (2-in.), (percent)	8.4	10.1	12.2	12.2	12.8	14.6	18.8
Hardness (R_C)	35	46	41	40	38	36	31
Transverse							
F_{tu} (ksi)	162	213	184	175	162	152	137
F_{ty} (ksi)	143	202	177	171	161	146	111
e (2-in.), (percent)	7.6	9.4	9.8	9.3	11.4	13.1	17.8
Hardness (R_C)	35	46	42	39	38	36	0.

Average of two heats.

0.090-inch gage.

Table 3.2.1.3 Effects of section size, specimen location and specimen direction on tensile properties of arc melted and vacuum remelted stock in H 900 Condition (Ref. 3)

Alloy	15-5PH						
Form	Large Rectangular Forged Sections						
Condition	H 900						
Melting Method	Section Size (in)	Direction	Location[a]	F_{tu} (ksi)	F_{ty} (ksi)	e (4D), (percent)	RA (percent)
Arc Air	12 x 14	ST	E	188	172	11	36
			I				32
			C	186	176	4	9
Vacuum Remelted	12 x 14	ST	E	186	172	11	34
			I		174		35
			C		170		32
	3 x 5 1/2	L	I	188	187	15	54
		ST	C	189	—	14	46
	3 1/2 x 12	L	I	187	185	15	50
		ST	C	190	—	14	48
	3 1/2 x 15 1/2	L	I	193	190	11	40
		ST	C		192	8	28
	4 x 24	L	I	194	189	12	40
		ST	C				36

[a] E = edge; I = intermediate; C = center.

Table 3.2.1.4 Room temperature tension, compression, shear, and bearing properties of plate in H 1025 condition, for which fatigue properties appear in Figures 3.5.1.6 and 3.5.1.7 (Ref. 32)

Alloy	15-5PH		
Form	0.215 - 2.579-in. Plate		
Condition	H 1025[a]		
Direction	L	T	ST
F_{tu} (ksi)	171.0	171.4	—
F_{ty} (ksi)	165.6	166.0	—
RA (percent)	58.5	57.6	—
e (2-in.) (percent)	15.0	14.8	—
E_t (1000 ksi)	28.66	28.72	—
F_{cy} (ksi)	175.6	175.3	174.9[b]
E_c (1000 ksi)	29.85	29.84	30.03[b]
F_{su}[c] (ksi)	114.3	113.2	—
F_{su}[d] (ksi)	108.1	109.0	—
e/D = 1.5			
F_{bru} (ksi)	287.3	287.2	—
F_{bry} (ksi)	246.1	246.3	—
e/D = 2.0			
F_{bru} (ksi)	368.4	367.8	—
F_{bry} (ksi)	286.7	289.1	—

[a] Values average of triplicate tests.

[b] Results from two heats, plate thickness > 1.5 inch.

[c] Full thickness tests from three heats (plates), for which plate thickness < 3.0 inch.

[d] 0.25-inch diameter double pin shear tests from seven heats (plates), for which plate thickness > 3.0 inch.

Table 3.2.5.1 Shear strength in torsion (Refs. 1, 7)

Alloy	15-5PH[a]			
Condition	H 900	H 1025	H 1075	H 1150
Torsional Shear Strength at Elastic Limit (ksi)	98.0	86.2	67.5	42.5
Ultimate Torsional Shear Strength (Modulus of Rupture) (ksi)	171.0	141.0	135.0	124.0

[a] 17-4PH data, not expected to be different for 15-5PH.

Table 3.2.5.2 Shear strength in double shear for H 900 condition (Ref. 1)

Alloy	15-5PH	
Condition	H 900	
Specimen Size	F_{su} (ksi)	F_{tu} (ksi)
5/8-inch round	133.0	192.0
1/2-inch round	130.0	
1/4-inch round	133.5	

17-4PH data, not expected to be different for 15-5PH.

Tests conducted in accordance with the National Aircraft Standard No. 498.

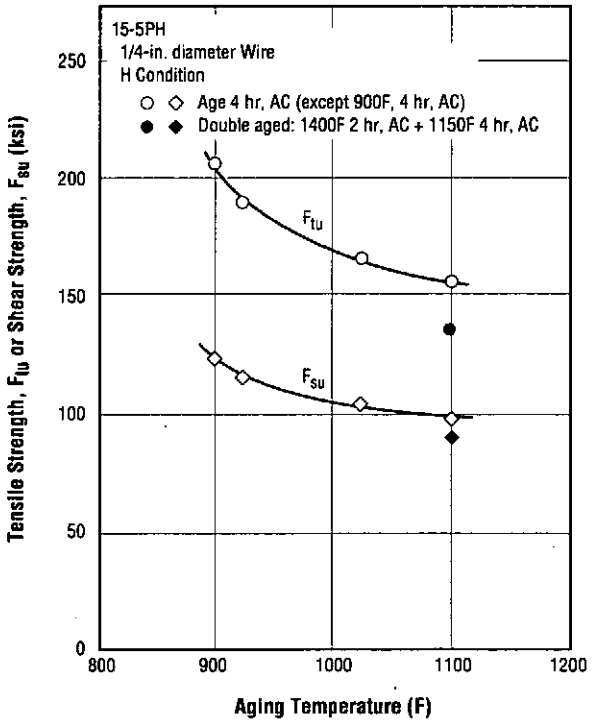


Figure 3.2.5.3 Effect of aging temperature (H condition) on shear strength in double shear (Ref. 49)

Table 3.2.6.1 Bearing strength of plate in H 1025 condition (Refs. 32, 65)

Alloy	15-5PH					
Condition	H 1025					
	Ratio of Edge Distance to Hole Diameter		e/D = 1.5		e/D = 2.0	
Source	Heat/Form	Test Direction	F_{bru} (ksi)	F_{bry} (ksi)	F_{bru} (ksi)	F_{bry} (ksi)
Ref. 32	0.215 - 2.579-in. Plate	L	287.3	246.1	368.4	286.7
		T	287.2	246.3	367.8	289.1
Ref. 65	A/ 1 1/2 x 5-in Flat Bar	L	280.5	234.1	364.7	281.7
	B/ 5/8 x 2-in. Flat Bar	L	274.1	229.0	355.4	275.8
	C/ 5/8 x 2-in. Flat Bar	L	281.1	238.3	363.1	276.9

Table 3.2.6.2 Bearing strength of bar in H 1150 condition (Ref. 65)

Alloy		15-5PH			
Condition		H 1025			
Ratio of Edge Distance to Hole Diameter		e/D = 1.5		e/D = 2.0	
Heat/Form	Test Direction	F_{bru} (ksi)	F_{bry} (ksi)	F_{bru} (ksi)	F_{bry} (ksi)
A/ 5 1/2-in. Dia Cylindrical Bar	L	228.9	179.6	294.8	221.1
	T	227.1	178.7	292.3	215.2
B/ 1 1/2 x 5-in Flat Bar	L	233.9	186.4	297.6	224.6
	T	231.3	180.6	290.9	220.8
C/ 1 1/2 x 7.7-in. Flat Bar	L	235.6	190.0	301.5	224.0
	T	237.9	185.8	301.6	226.6
D/ 1 1/2 x 3-in. Flat Bar	L	231.6	182.6	295.9	222.3
E/ 5/8 x 2-in. Flat Bar	L	230.9	177.0	296.4	213.8
F/ 5/8 x 2-in. Flat Bar	L	238.1	188.2	298.4	224.6

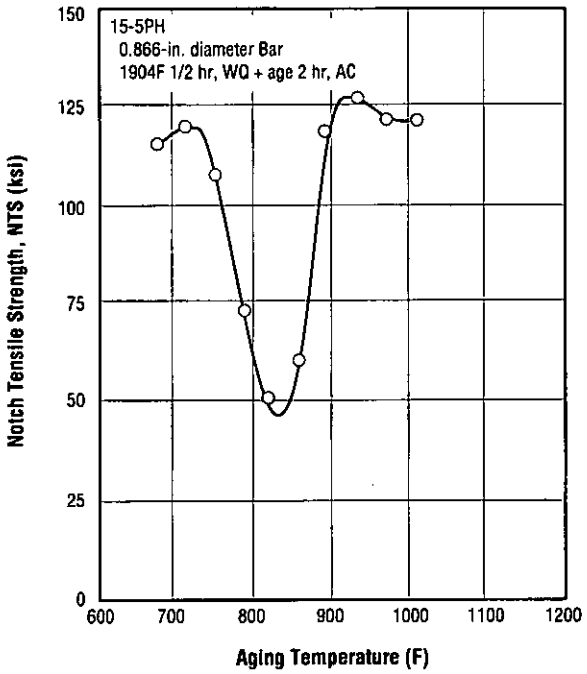


Figure 3.2.7.1.3 Effect of aging temperature on notch tensile strength of bar (Ref. 53)

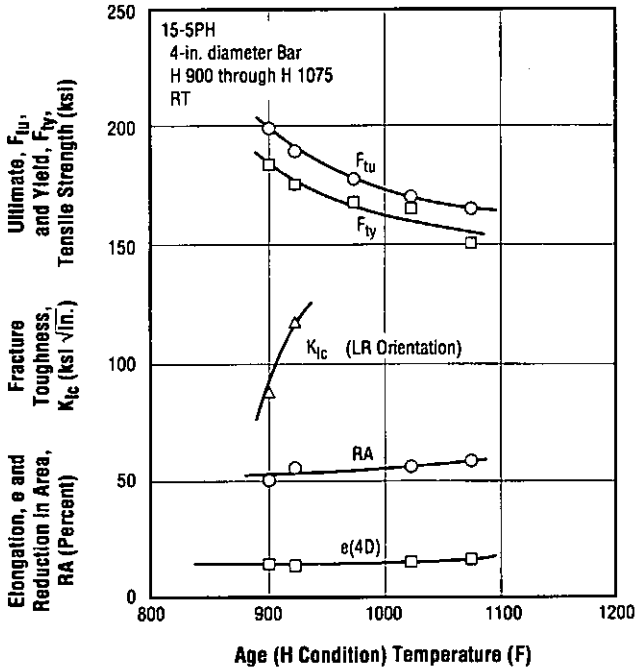


Figure 3.2.7.2.1 Effect of age (H condition) temperature on tensile properties and plane strain fracture toughness (Ref. 40)

Table 3.2.7.2.4 J-integral fracture toughness of plate and weldment (Ref. 48)

Alloy		15-5PH		
Form	Condition	Crack Plane Orientation	J_{Ic} (kN/m)	Effective[a] F_{ty} (MPa)
Plate	ST + Age	TL	192 - 238	1100
Weld[b]	As-welded	—	107 - 124	1050
	Weld + Age	—	76 - 156	1220
	Weld + ST + Age	—	157 - 157	1200

[a] $(F_{ty} + F_{tu})/2$

[b] AMS 5826.

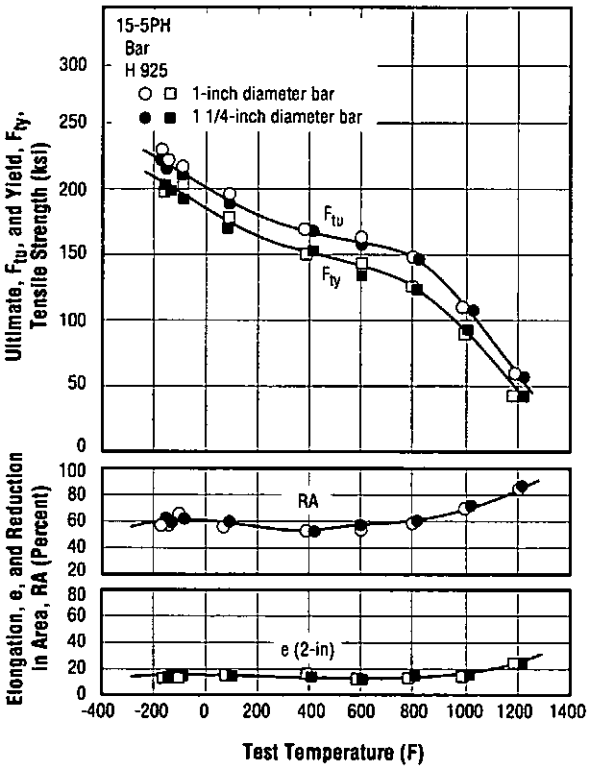


Figure 3.3.1.1 Effect of test temperature on tensile properties of bar in H 925 condition (Ref. 29)

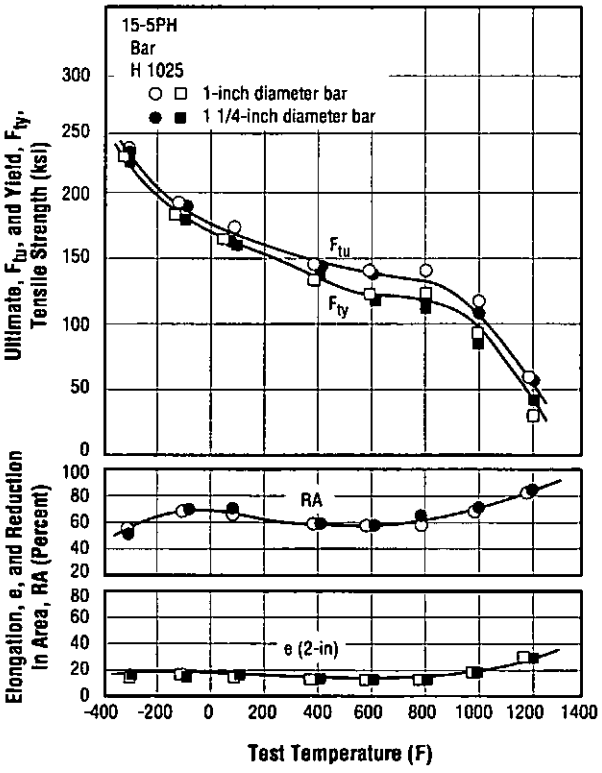


Figure 3.3.1.2 Effect of test temperature on tensile properties of bar in H 1025 condition (Ref. 29)

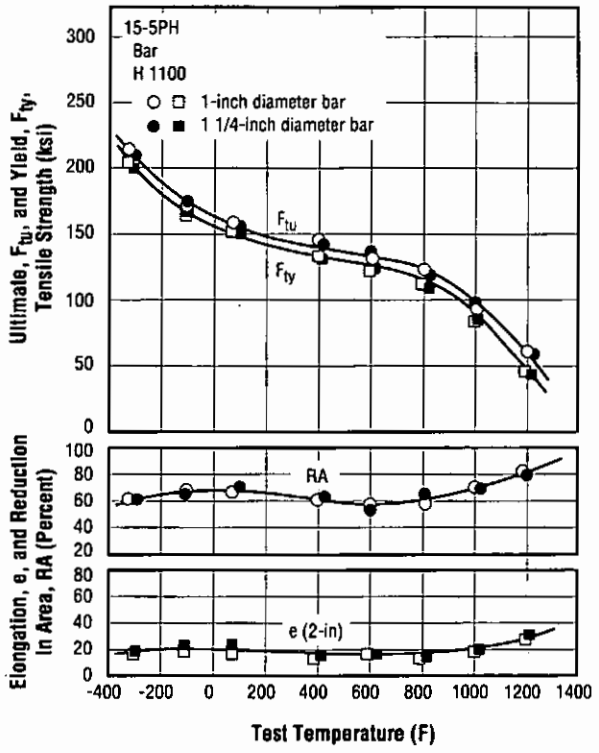


Figure 3.3.1.3 Effect of test temperature on tensile properties of bar in H 1100 condition (Ref. 29)

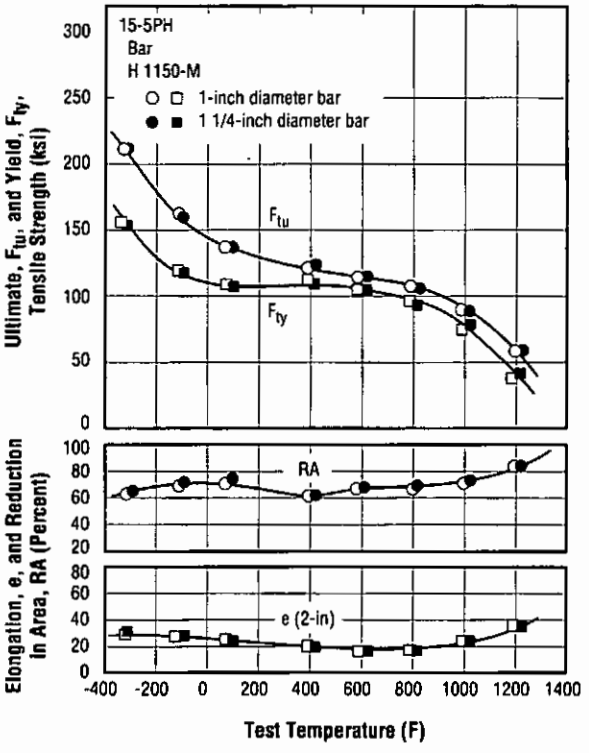


Figure 3.3.1.4 Effect of test temperature on tensile properties of bar in H 1150-M condition (Ref. 29)

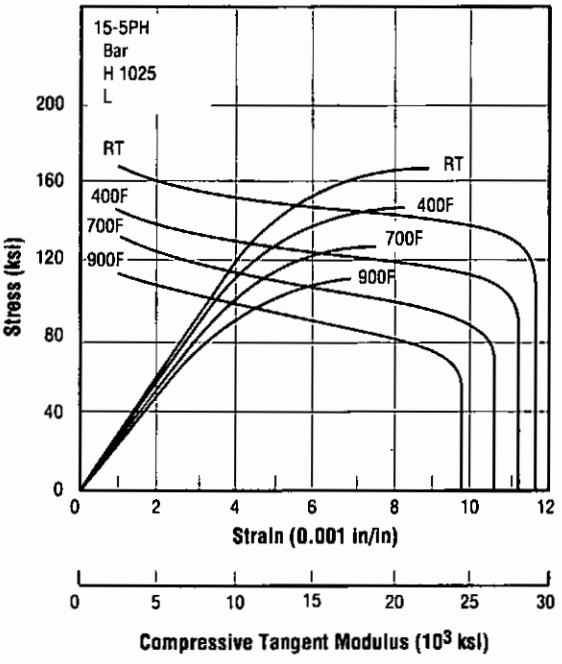


Figure 3.3.2.1 Typical compressive stress-strain and tangent-modulus curves at selected temperatures for bar in H 1025 condition (Ref. 65)

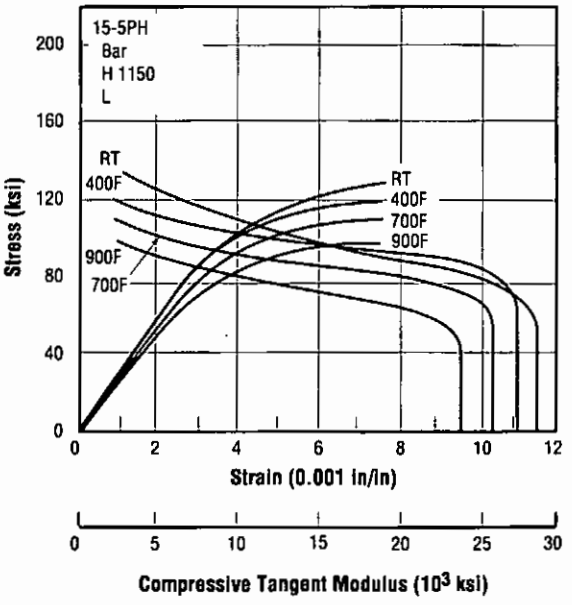


Figure 3.3.2.2 Typical compressive stress-strain and tangent-modulus curves at selected temperatures for bar in H 1150 condition (Ref. 65)

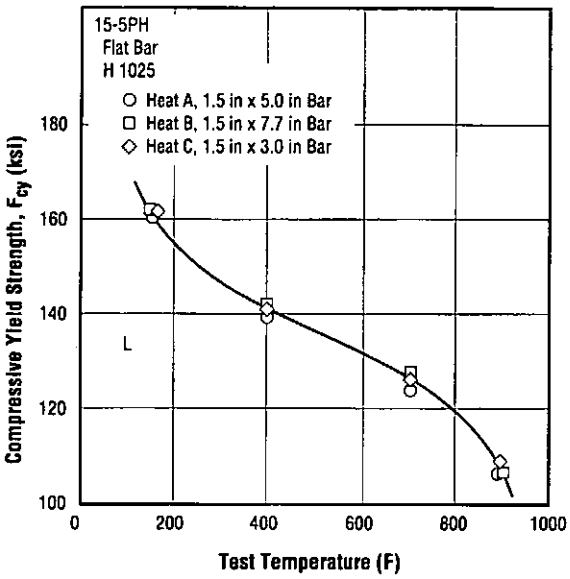


Figure 3.3.2.3 Effect of test temperature on compressive yield strength of bar in H 1025 condition (Ref. 65)

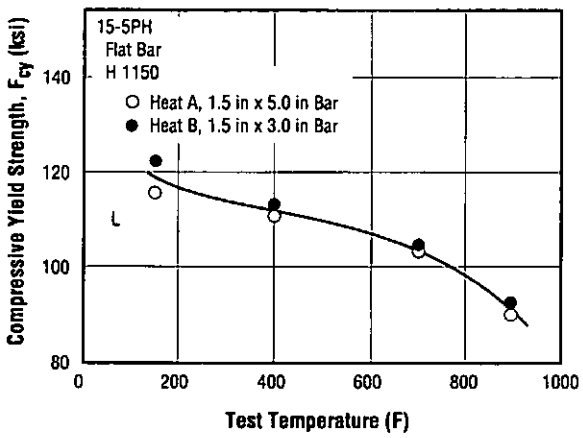


Figure 3.3.2.4 Effect of test temperature on compressive yield strength of bar in H 1150 condition (Ref. 65)

Table 3.3.3.1 Charpy-V impact energy for sheet at room temperature and -65F (Ref. 27)

Alloy	15-5PH	
Form	0.093-inch thick	
Condition	Charpy-V Impact Energy[a,b] (in-lbs)	
	RT	-65F
A	3265	2669
H 900	2857	2361
H 1025	3974	3378
H 1150	4626	4248
H 1150-M	5616	5049

[a] Each value average triplicate tests for two heats.

[b] Charpy-V specimens: B = 0.093 inch, (W-a) = 0.314 Inch.

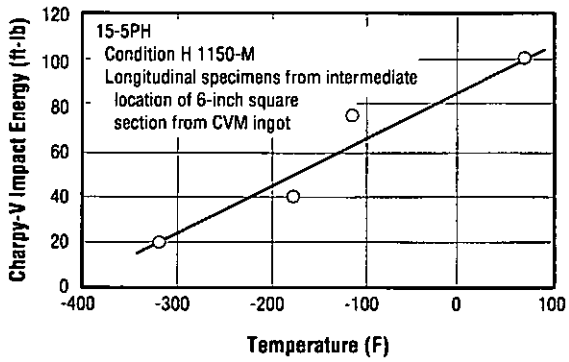


Figure 3.3.3.2 Effect of temperature on Charpy-V impact energy for Condition H 1150-M (Refs. 1, 2)

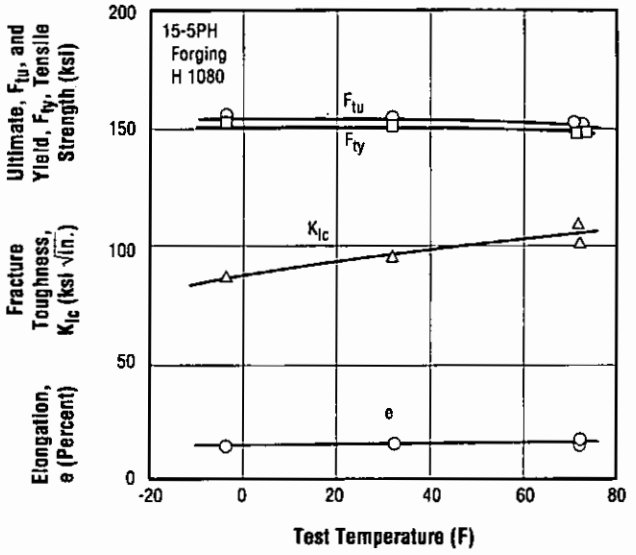


Figure 3.3.7.2.1 Effect of test temperature in the range -4 to 72F on the tensile properties and plane strain fracture toughness (Ref. 44)

Table 3.3.7.2.2 Effect of aged condition, test temperature, and specimen orientation on strength and plane strain fracture toughness (Ref. 51)

Alloy	15-5PH				
Condition	Test Temperature (F)	Orientation	F_{tu} (ksi)	F_{ty} (ksi)	K_{Ic} (ksi $\sqrt{in.}$)
H 900	RT	LT	200	185	87
		—	192	175	74
		TL	193	171	74
H 1080	72	Random	151	149	104 - 111
	32		152	151	87 - 104
	-4		153	151	81 - 92

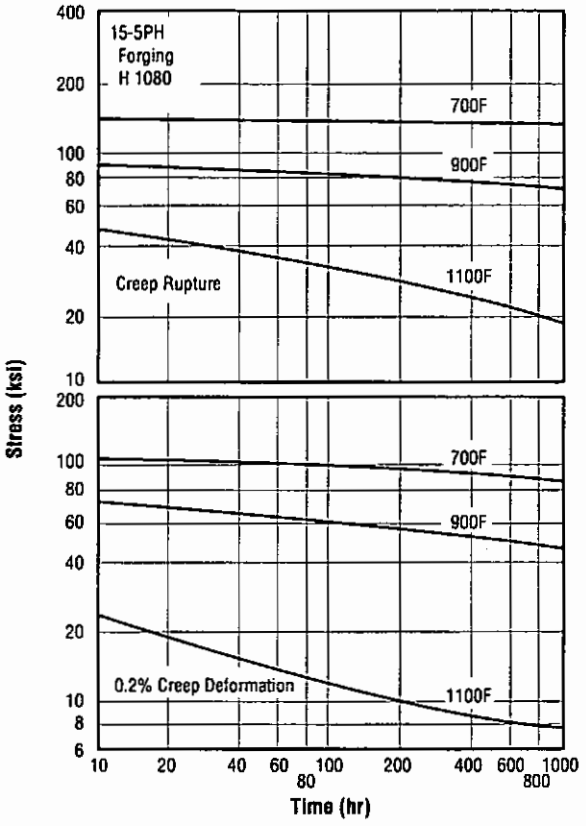


Figure 3.4.1 Creep deformation and rupture curves at selected temperatures for forged bar in the H 1025 condition (Ref. 66)

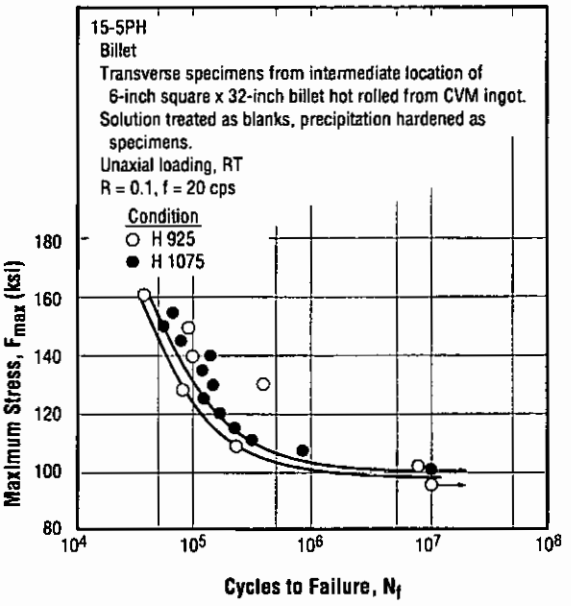


Figure 3.5.1.1 Room temperature axial-load fatigue strength of CVM billet in H 925 and H 1075 (Ref. 1)

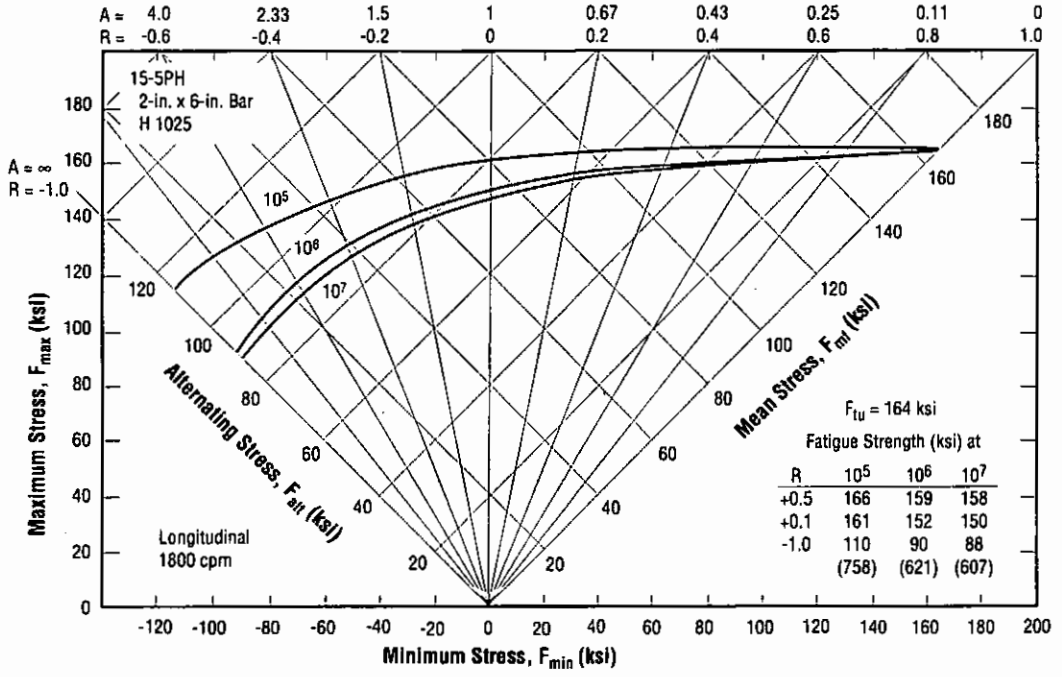


Figure 3.5.1.2 Room temperature longitudinal unnotched axial-load constant-life fatigue diagram for bar (Ref. 56)

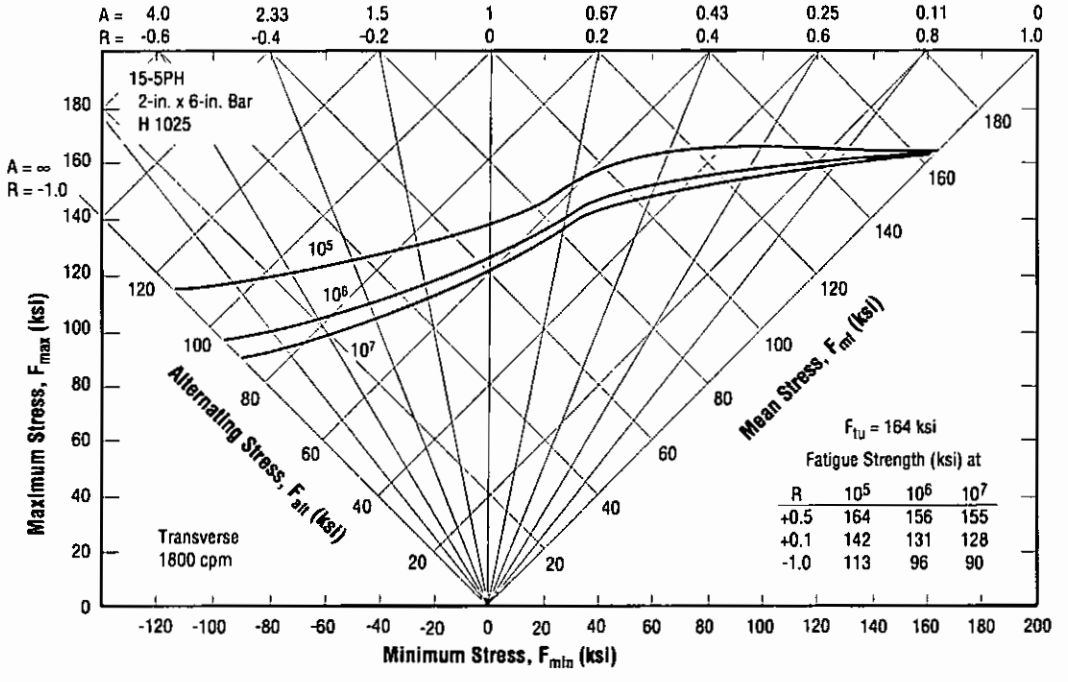


Figure 3.5.1.3 Room temperature transverse unnotched axial-load constant-life fatigue diagram for bar (Ref. 56)

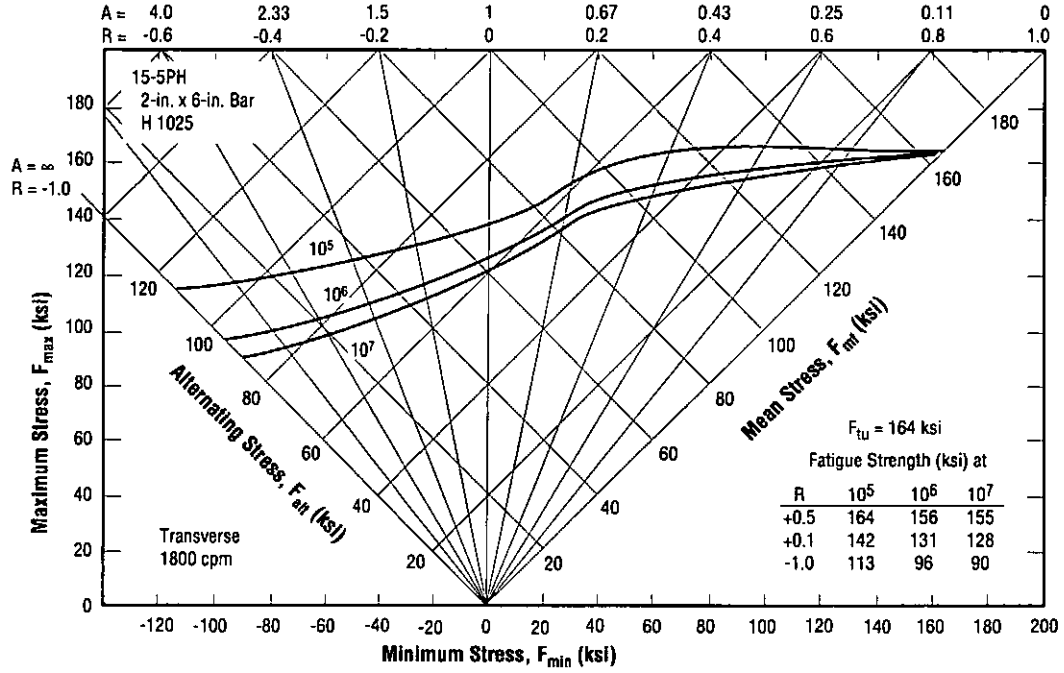


Figure 3.5.1.3 Room temperature transverse unnotched axial-load constant-life fatigue diagram for bar (Ref. 56)

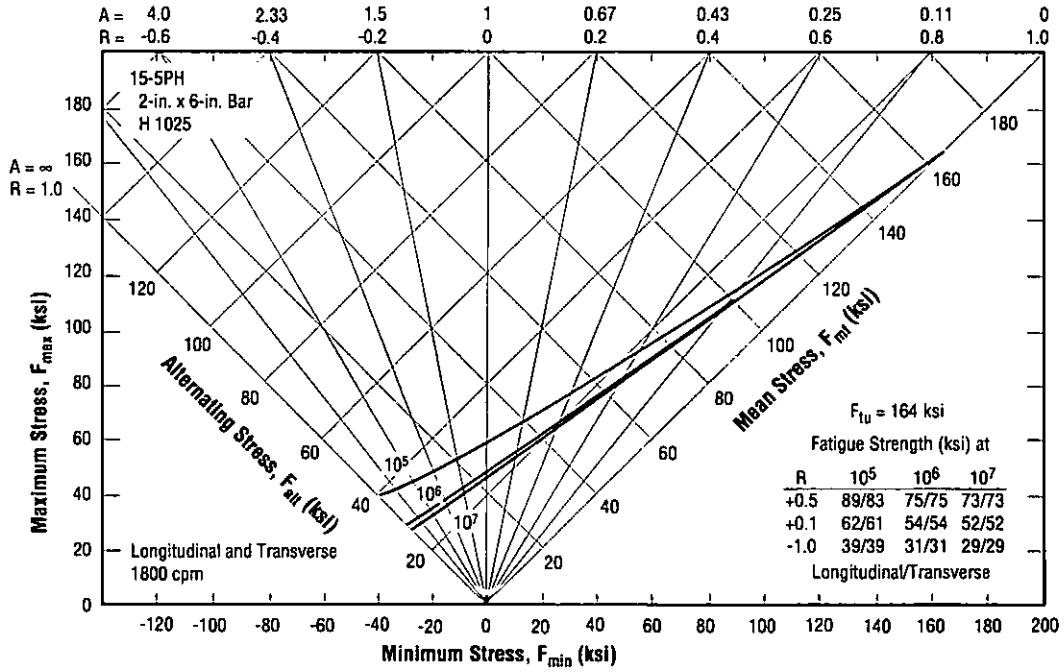


Figure 3.5.1.4 Room temperature longitudinal and transverse notched (K_t = 3.0) axial-load constant-life fatigue diagram for bar (Ref. 56)

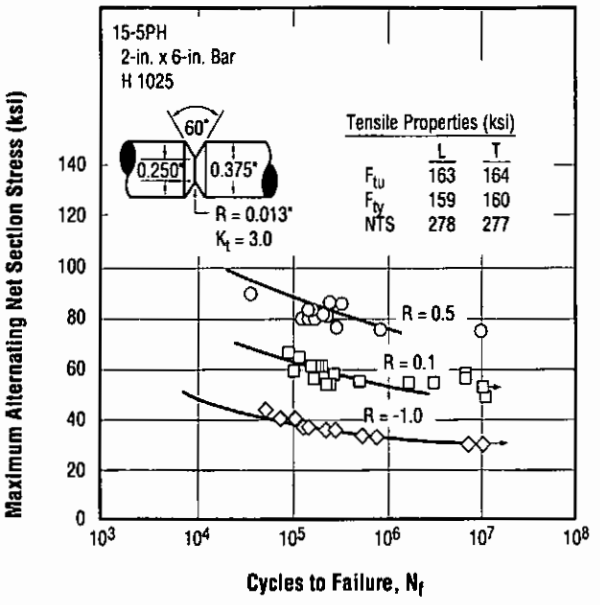


Figure 3.5.1.5 Mild-notch axial-load fatigue strength of bar in H 1025 condition at stress ratios, R = 0.5, 0.1, and -1.0 (Ref. 55)

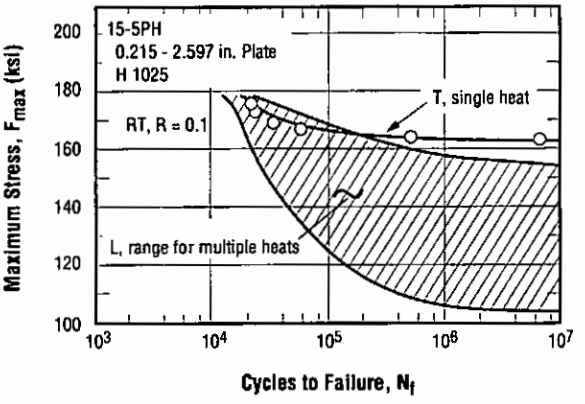


Figure 3.5.1.6 Room temperature axial-load fatigue strength of plate in H 1025 condition (Ref. 32)

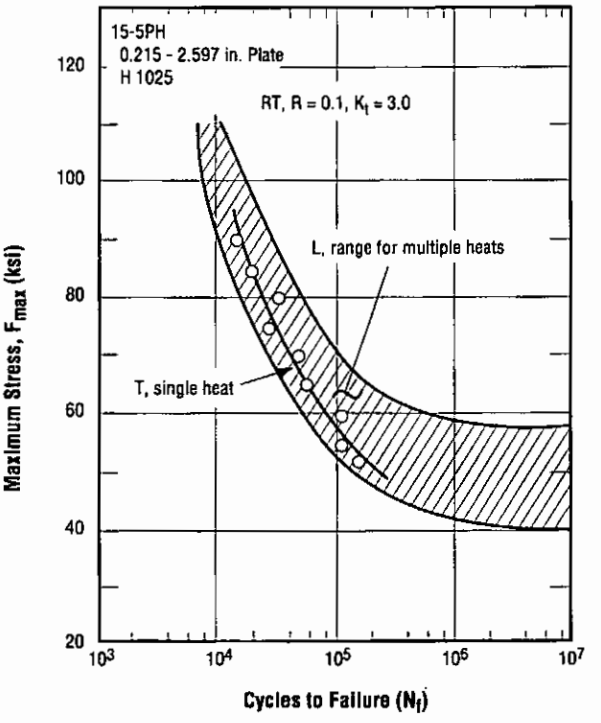


Figure 3.5.1.7 Room temperature axial-load notched (K_t = 3.0) fatigue strength of plate in H 1025 condition (Ref. 32)

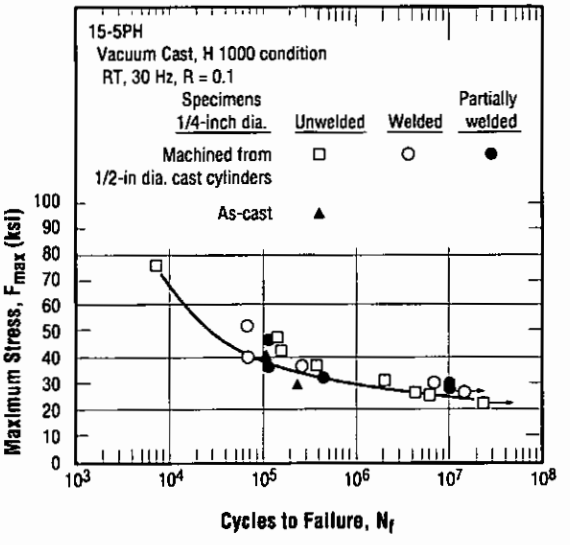


Figure 3.5.1.8 Room temperature axial-load high-cycle fatigue strength of machined and as-cast specimens from welded and unwelded vacuum castings (Ref. 26)

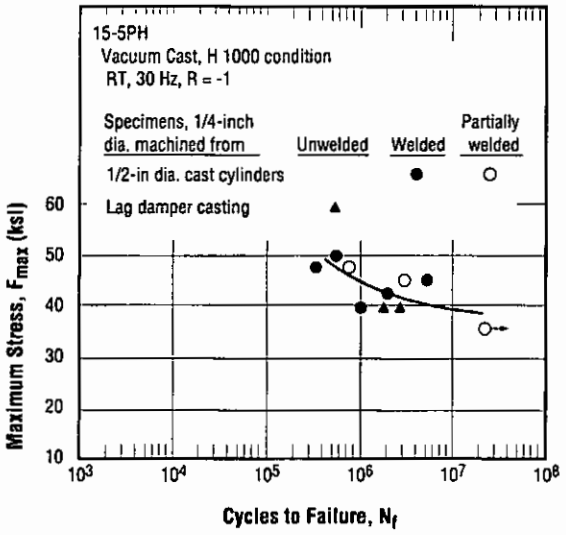


Figure 3.5.1.9 Room temperature tension-compression high-cycle fatigue strength of specimens machined from cast cylinders and from a lag damper casting (Ref. 26)

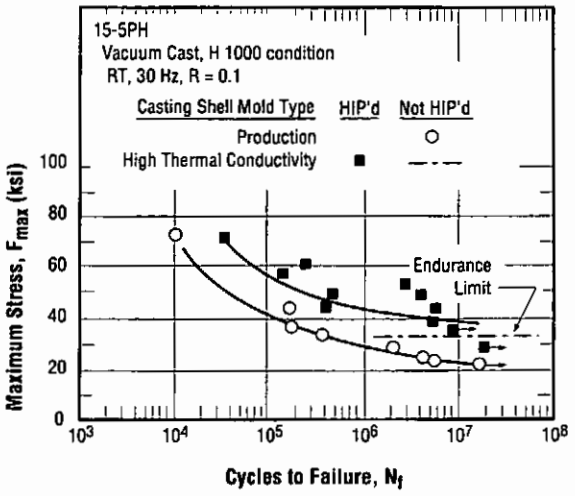


Figure 3.5.1.10 Room temperature axial-load high-cycle fatigue strength of specimens machined from bars vacuum cast into either production or high thermal conductivity shell molds, and subsequently HIP'd or not HIP'd (Ref. 26)

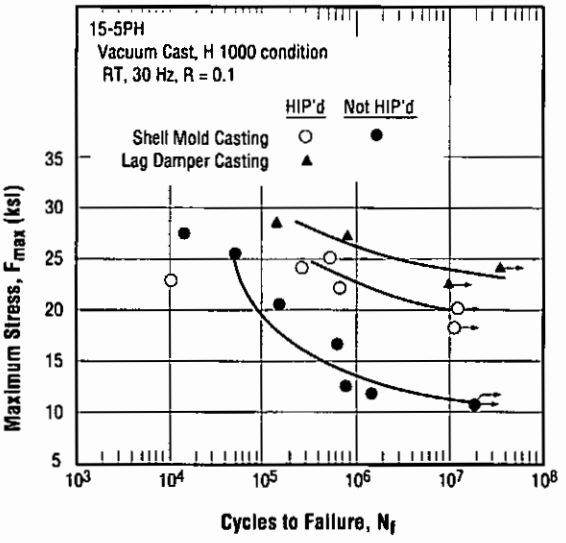


Figure 3.5.1.11 Room temperature axial-load high-cycle fatigue strength of HIP'd and not HIP'd notched (K_t = 3.0) specimens machined from shell mold castings and notched (K_t = 3.0) specimens machined from HIP'd lag damper casting (Ref. 26)

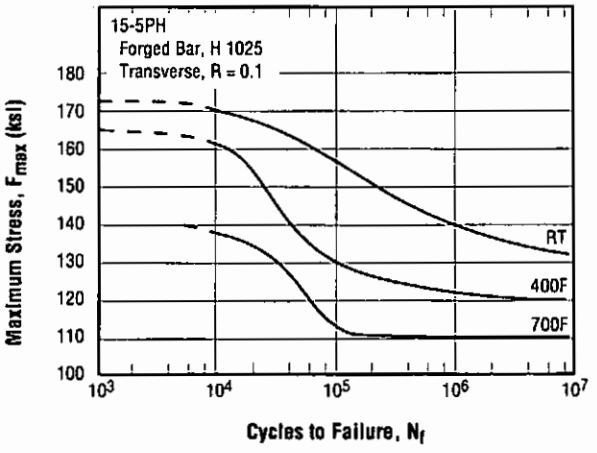


Figure 3.5.1.12 Elevated temperature transverse unnotched axial-load fatigue strength of forged bar (Ref. 56)

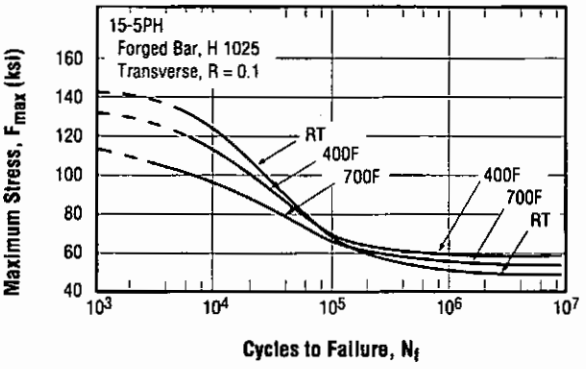


Figure 3.5.1.13 Elevated temperature transverse notched (K_t = 3.0) axial-load fatigue strength of forged bar (Ref. 56)

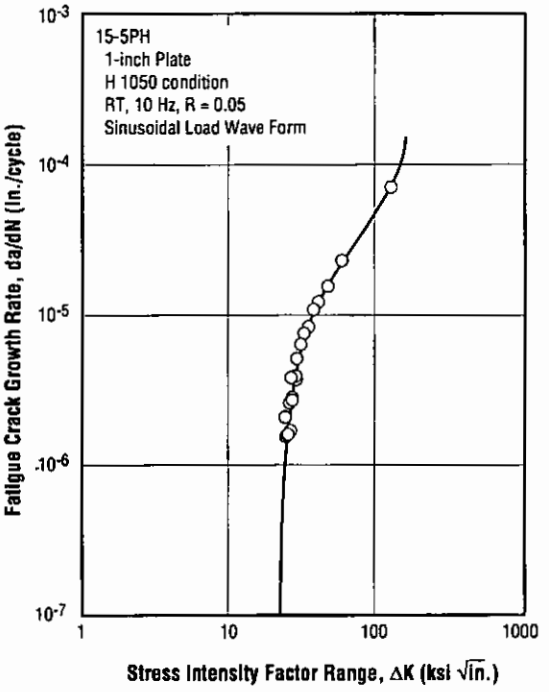


Figure 3.5.3.1 Room temperature fatigue crack growth rate at 10 Hz, R = 0.05 for plate in H 1050 condition (Ref. 28)

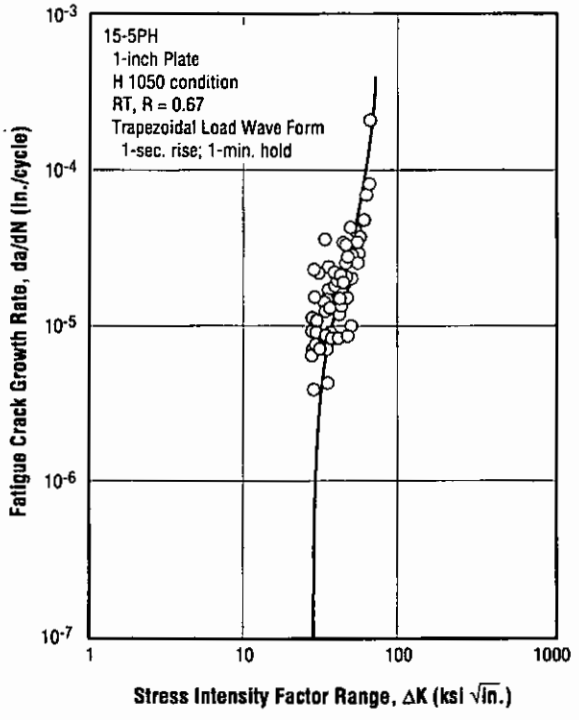


Figure 3.5.3.2 Room temperature fatigue crack growth rate at R = 0.67, trapezoidal load wave form (1-minute hold time), for plate in H 1050 condition (Ref. 28)

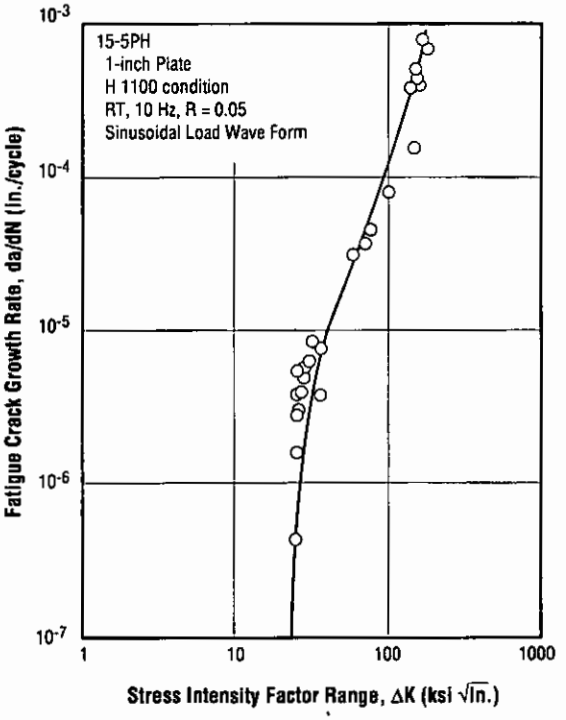


Figure 3.5.3.3 Room temperature fatigue crack growth rate at 10 Hz, R = 0.05, for plate in H 1100 condition (Ref. 28)

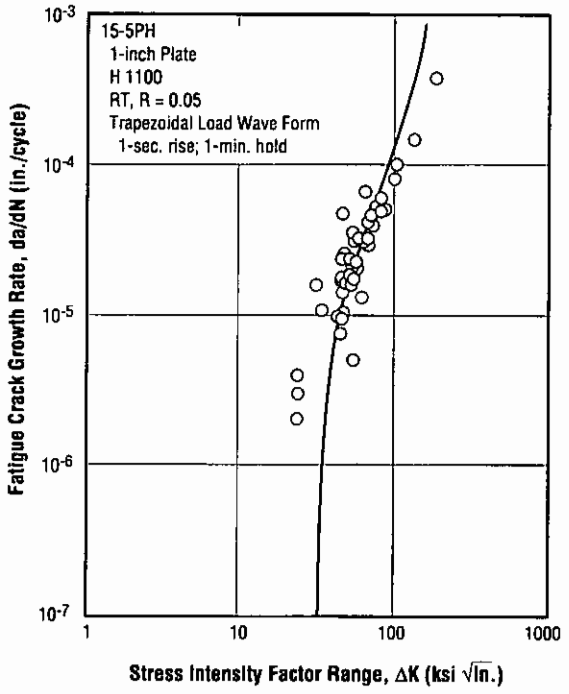


Figure 3.5.3.4 Room temperature fatigue crack growth rate at R = 0.05, trapezoidal load wave form (1-minute hold time), for plate in H 1100 condition (Ref. 28)

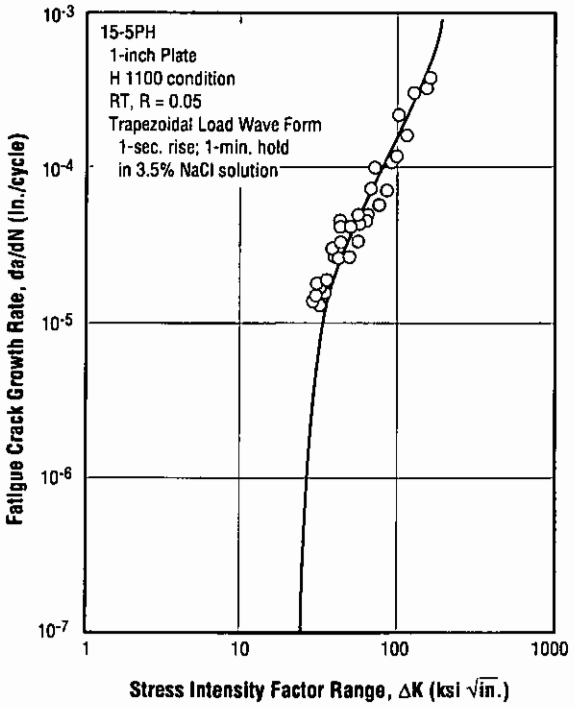


Figure 3.5.3.5 Room temperature fatigue crack growth rate in 3.5 percent NaCl solution at R = 0.05, trapezoidal load wave form (1-minute hold time), for plate in H 1100 condition (Ref. 28)

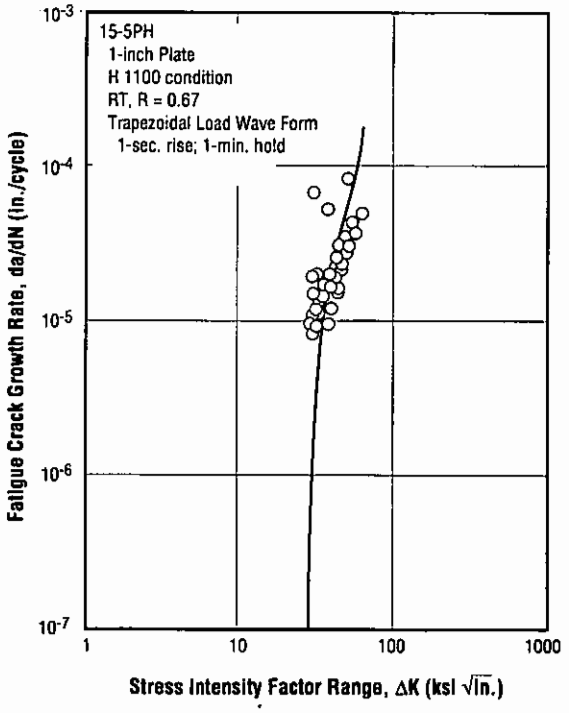


Figure 3.5.3.6 Room temperature fatigue crack growth rate at R = 0.67, trapezoidal load wave form (1-minute hold time), for plate in H 1100 condition (Ref. 28)

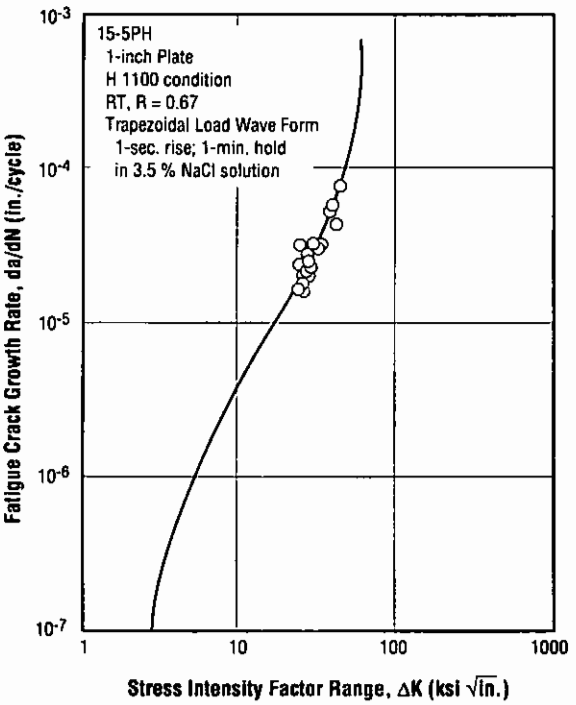


Figure 3.5.3.7 Room temperature fatigue crack growth rate in 3.5 percent NaCl solution at R = 0.67, trapezoidal load wave form (1-minute hold time), for plate in H 1100 condition (Ref. 28)

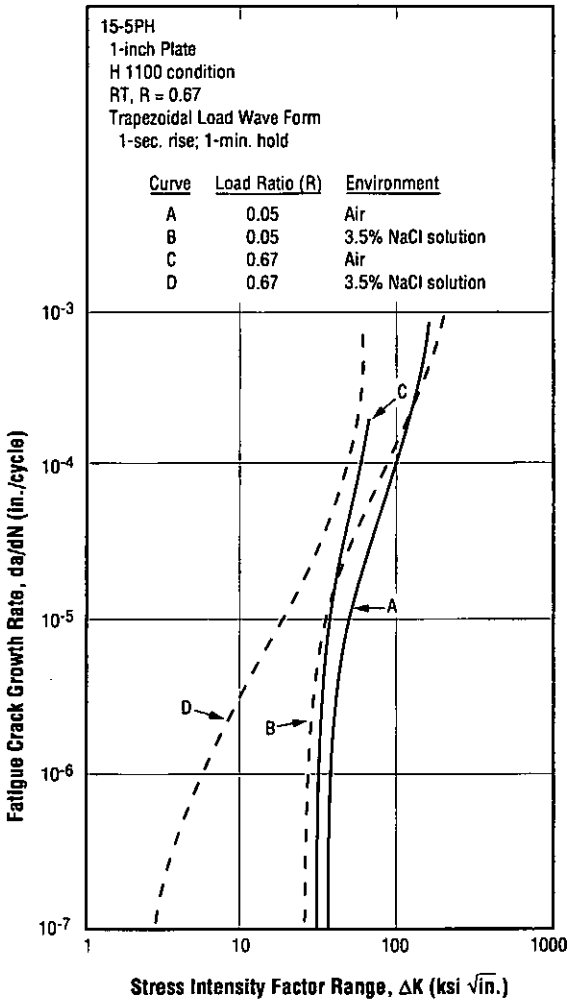


Figure 3.5.3.8 Effects of load ratio (R) and environment (air versus salt water) on room temperature fatigue crack growth rate for plate in H 1100 condition (Ref. 28)

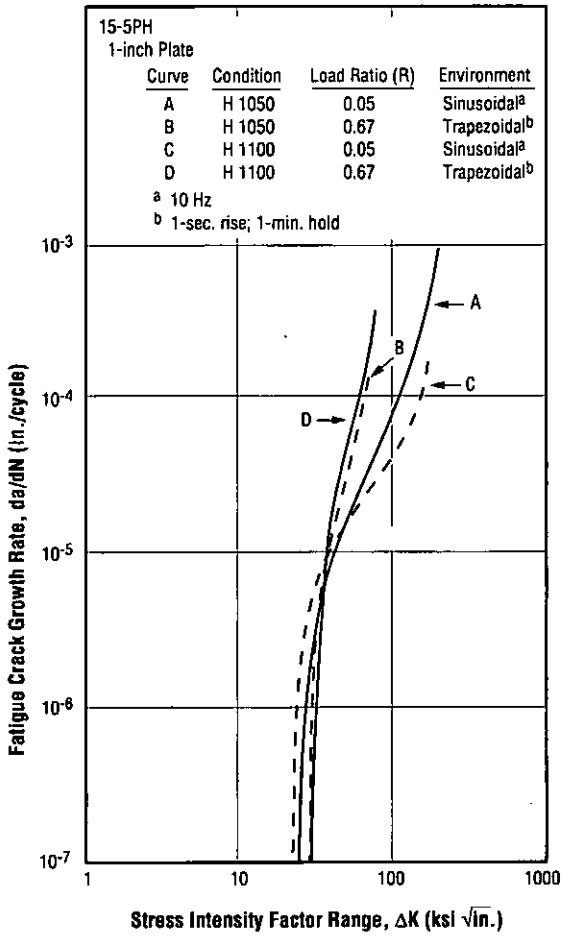


Figure 3.5.3.9 Effects of load wave form (sinusoidal versus trapezoidal), load ratio (R), and heat treated condition (H) on room temperature fatigue crack growth rate for plate (Ref. 28)

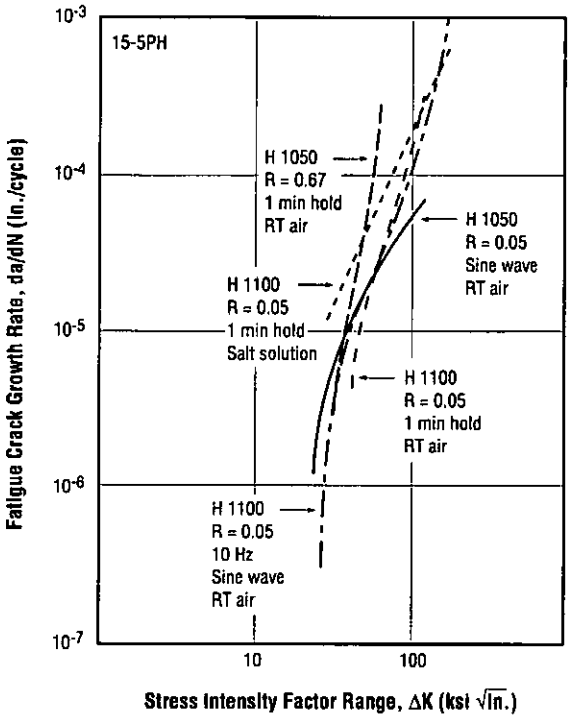


Figure 3.5.3.10 Fatigue crack growth rate in air and 3.5 percent aqueous NaCl solution for the H 1050 and H 1100 conditions (Ref. 51)

Table 3.6.2.1 Elastic moduli in tension and in torsion (Refs. 1, 7, 27)

Alloy	15-5PH			
Condition	H 900	H 1025	H 1075	H 1150
E (10^6 psi)	28.5	—	—	—
G[a] (10^6 psi)	11.2	11.0	10.0	10.0

[a] 17-4PH data, not expected to be different for 15-5PH.

Each value average duplicate tests from single heat.

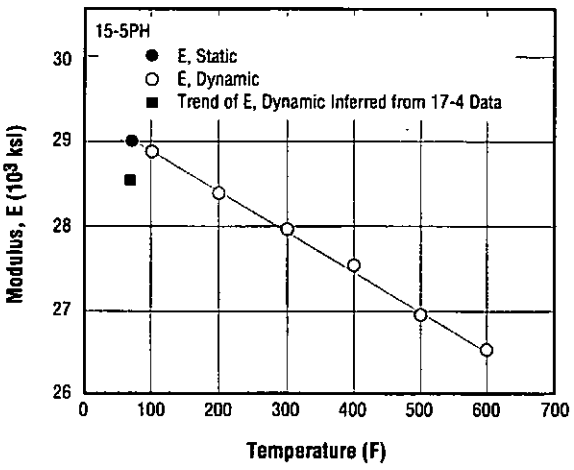


Figure 3.6.2.2 Effect of temperature on modulus of elasticity (Ref. 1)

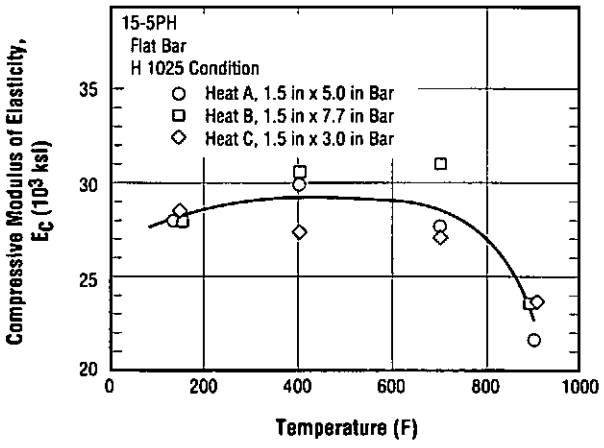


Figure 3.6.2.3 Effect of temperature on modulus of elasticity in compression of bar in H 1025 condition (Ref. 65)

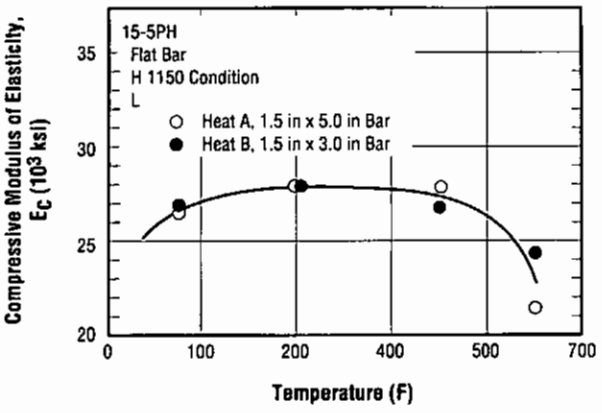


Figure 3.6.2.4 Effect of temperature on modulus of elasticity in compression of bar in H 1150 condition (Ref. 65)

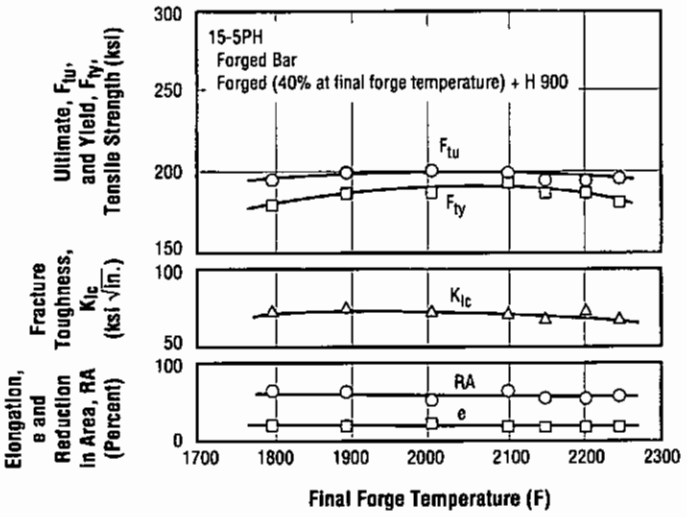


Figure 4.1.1.1 Influence of final forge temperature on tensile properties and plane strain fracture toughness (Ref. 39)

Table 4.1.4 Minimum room temperature bend radii (Ref. 27)

Alloy	15-5PH	
Form	0.090-inch Sheet	
Condition	Direction	Minimum Bend Radii
A	L	2t
	T	4t
H 900	L	3t
	T	5t
H 925	L	3t
	T	—
H 1025	L	3t
	T	
H 1150	L	2t
	T	
H 1150-M	L	2t
	T	

Average two heats.

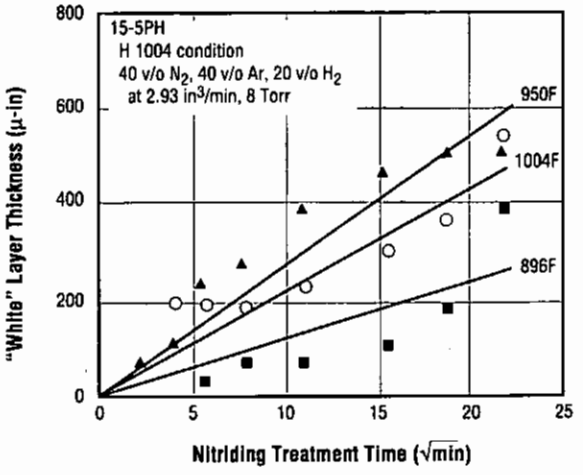


Figure 4.4.4.1 Effect of nitriding treatment time on "white" layer thickness (Ref. 47)

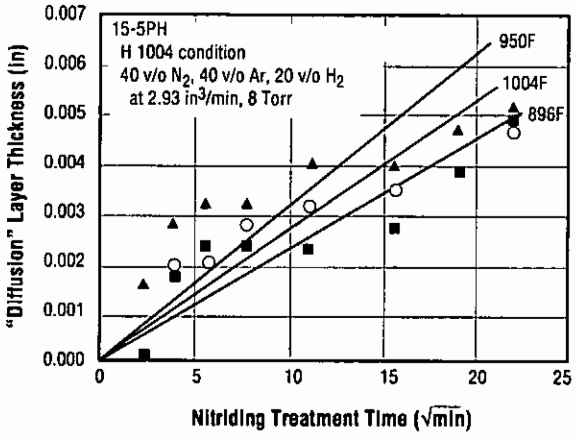


Figure 4.4.4.2 Effect of nitriding treatment time and temperature on "diffusion" layer thickness (Ref. 47)

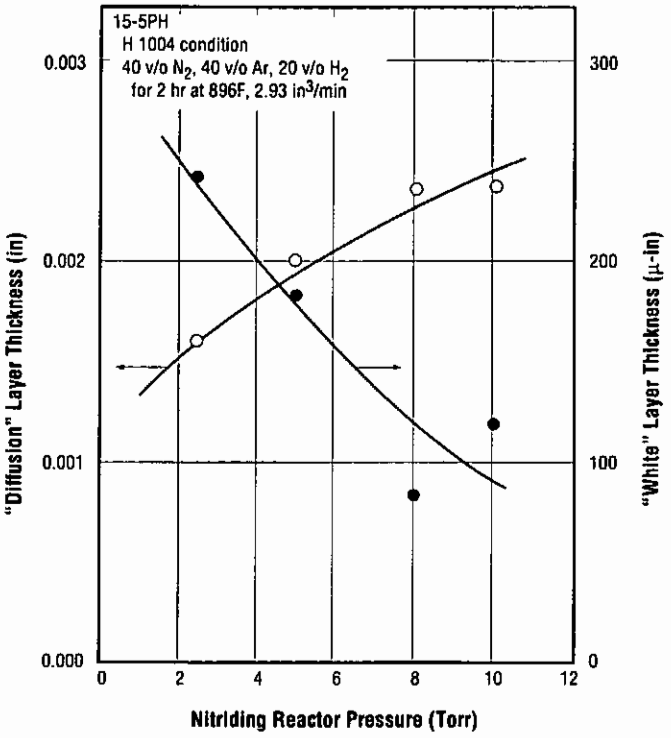


Figure 4.4.4.3 Effect of nitriding reactor pressure on "white" and "diffusion" layer thicknesses (Ref. 47)

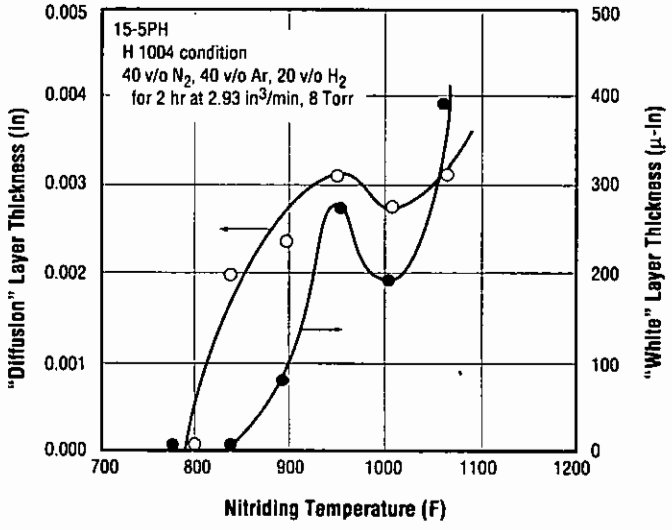


Figure 4.4.4.4 Effect of nitriding treatment temperature on thicknesses of "white" and "diffusion" layers (Ref. 47)

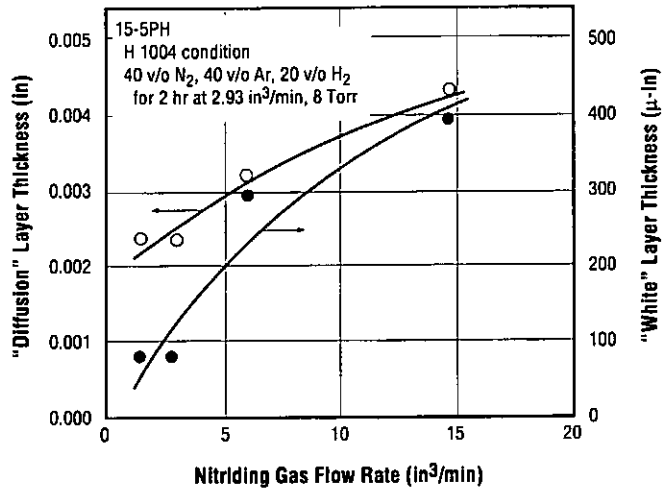


Figure 4.4.4.5 Effect of nitriding gas flow rate on "white" and "diffusion" layer thicknesses (Ref. 47)

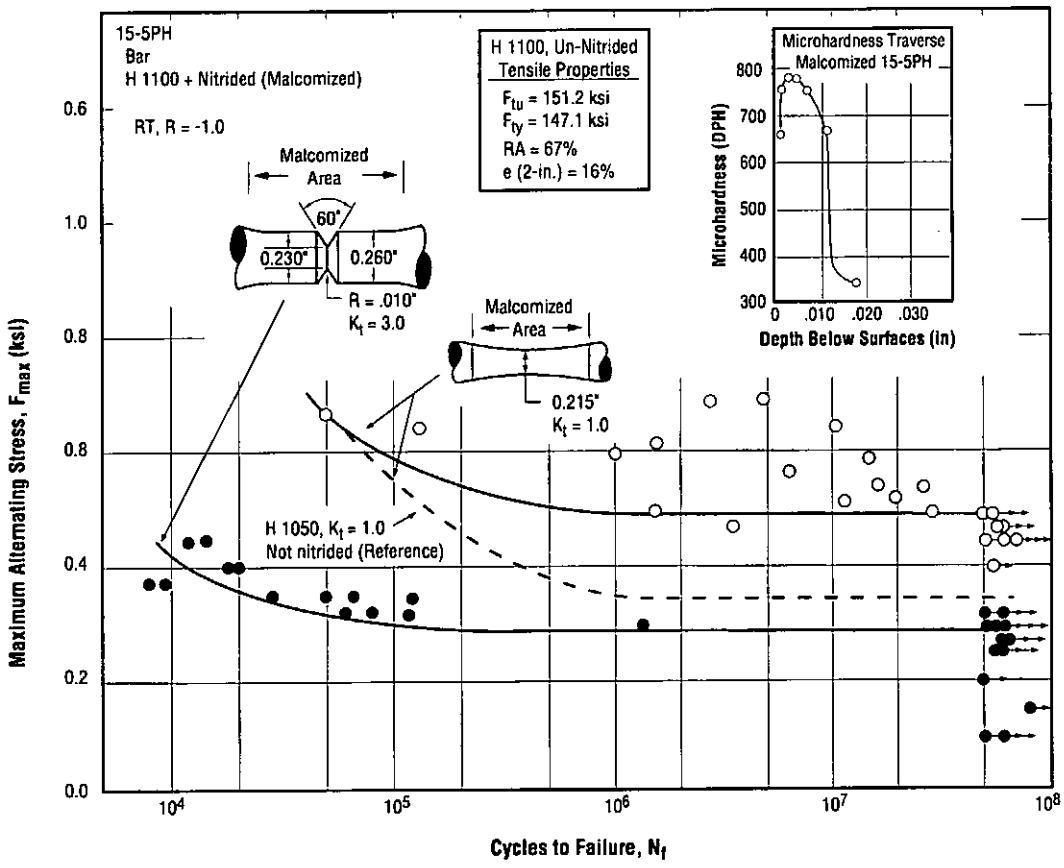


Figure 4.4.4.8 Smooth and mild-notch rotating beam fatigue strength of (proprietary Malcomizing) nitrided bar in H 1100 condition, with reference to smooth fatigue strength of bar not nitrided (Ref. 45)

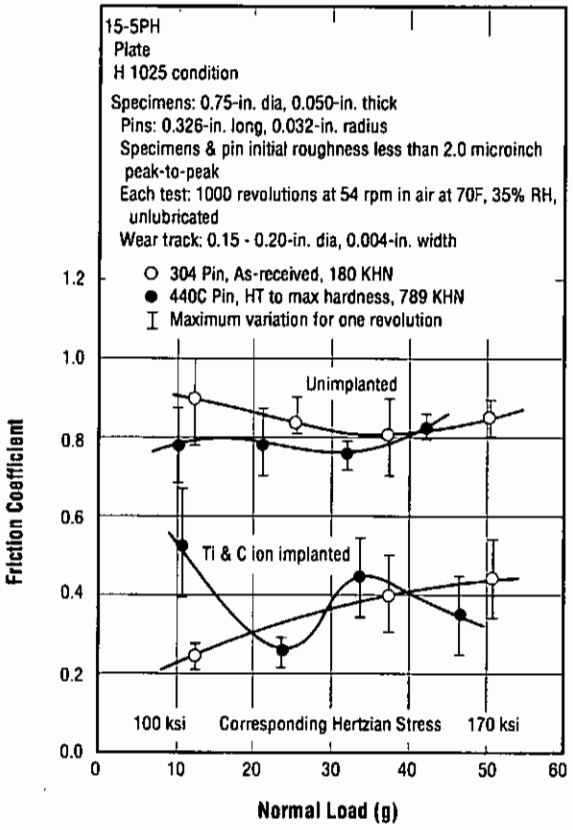


Figure 4.4.5.1 Influence of titanium and carbon ion implantation on unlubricated friction after 1000 pin-on-disc revolutions (Ref. 36)

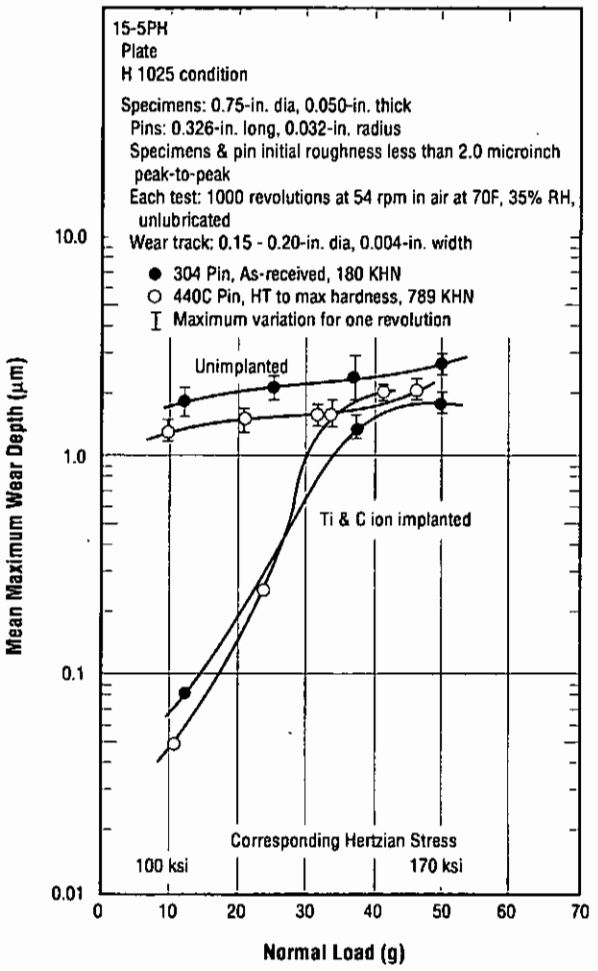


Figure 4.4.5.2 Influence of titanium and carbon ion implantation on unlubricated wear depth after 1000 pin-on-disc revolutions (Ref. 36)

[See ASTM Test Standard G 99-90 for Pin-on-Disk Wear Test Procedure]

Table 4.4.5.3 304 stainless steel pin wear in pin-on-disc tests of Ti and C ion implanted plates and of unimplanted plates (Ref. 36)

Alloy	15-5PH		
Form	Plate		
Condition	H 1025 + Ti & C Ion Implanted		
Pin Wear Scar Diameter (in)			
Normal Load (g)	Hertzian Stress (ksi)	Unimplanted	Ion Implanted
12.3	106	0.0066	< 0.0008
25.5	134	0.0115	< 0.0008
37.5	152	0.0123	0.0049
50.4	169	0.0094	0.0059

Specimens: 0.75-inch diameter, 0.050-inch thick.

Pins: 0.326-inch long, 0.032-inch radius.

Specimen and pin initial roughness < 2.0 μ-inch peak-to-peak.

Each test: 1000 revolutions @ 54 rpm in air at 70F, 33% RH, unlubricated.

Wear track: 0.15 - 0.20-inch diameter, 0.004-inch width.

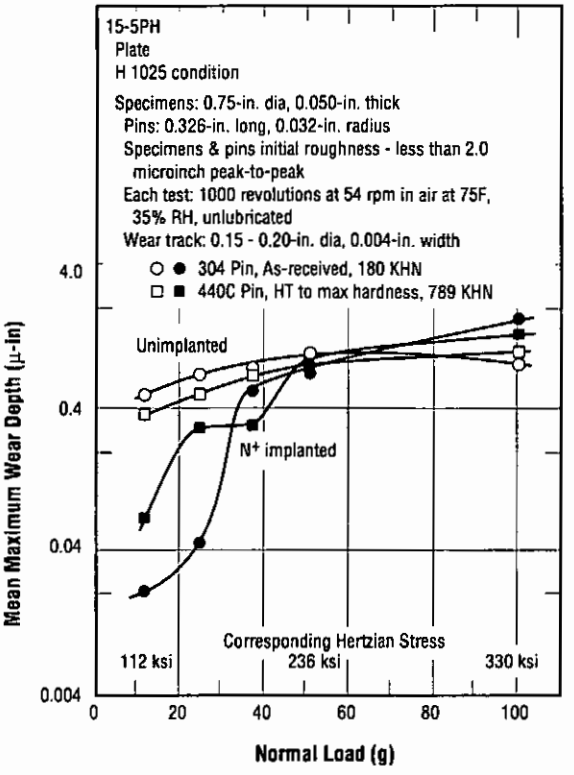


Figure 4.4.5.4 Influence of N^+ implantation on unlubricated wear depth after 1000 pin-on-disc revolutions (Ref. 38)

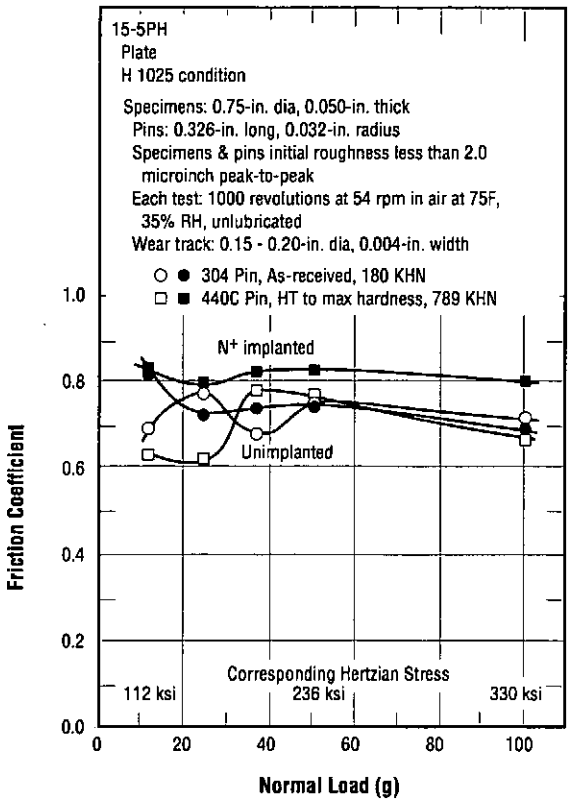
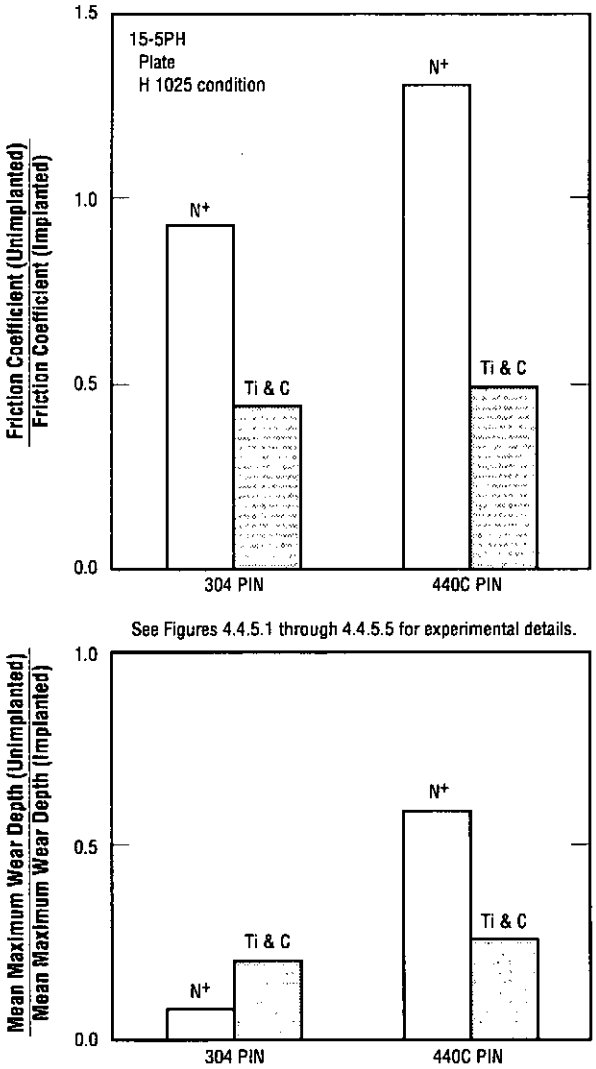


Figure 4.4.5.5 Influence of N^+ implantation on unlubricated friction after 1000 pin-on-disc revolutions (Ref. 38)



See Figures 4.4.5.1 through 4.4.5.5 for experimental details.

Figure 4.4.5.6 Influence on ion implantation (Ti and C or N^+) on unlubricated friction coefficient and mean maximum wear depth at 173 ksi Hertzian stress, expressed as ratios of unimplanted to implanted values (Ref. 38)

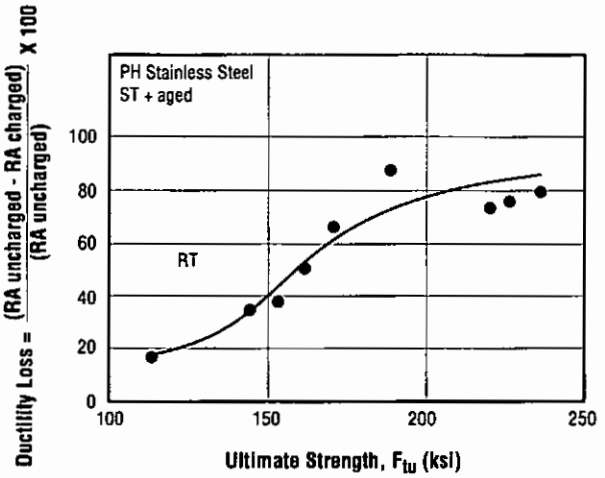


Figure 4.4.6.1 Effect of strength on ductility loss for typical PH steel specimens hydrogen charged at 90A/m^2 and tensile tested at room temperature (Ref. 33)

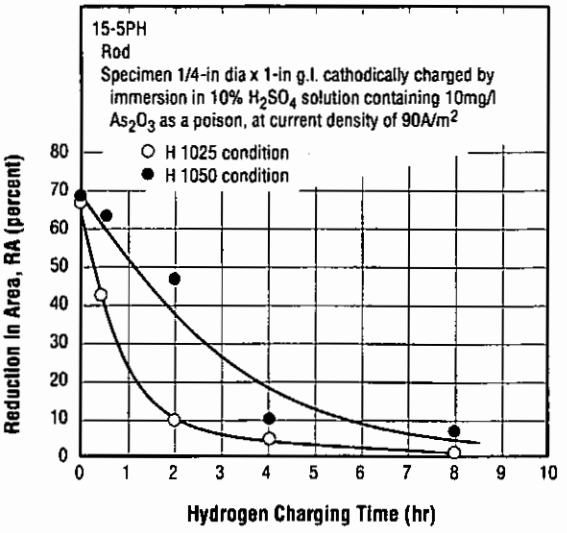


Figure 4.4.6.2 Effect of hydrogen charging on ductility of rod in H 1025 and H 1050 conditions (Ref. 57)

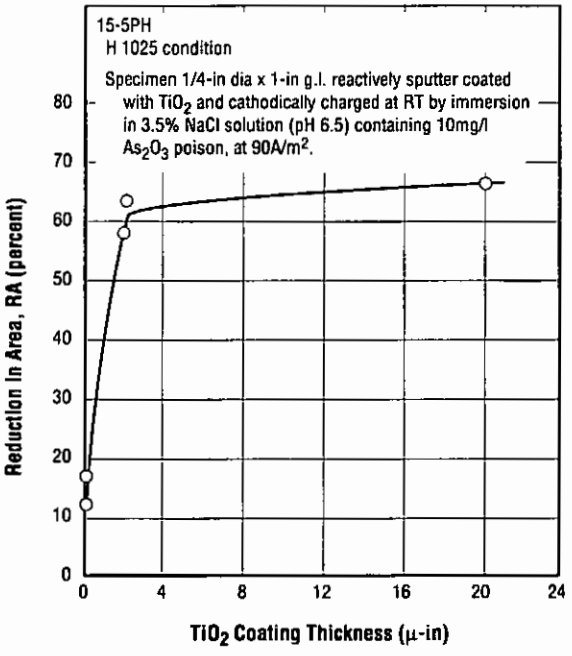


Figure 4.4.6.3 Effect of TiO_2 film thickness on ductility of specimens hydrogen charged for four hours at 90A/m^2 and tensile tested at room temperature (Ref. 52)

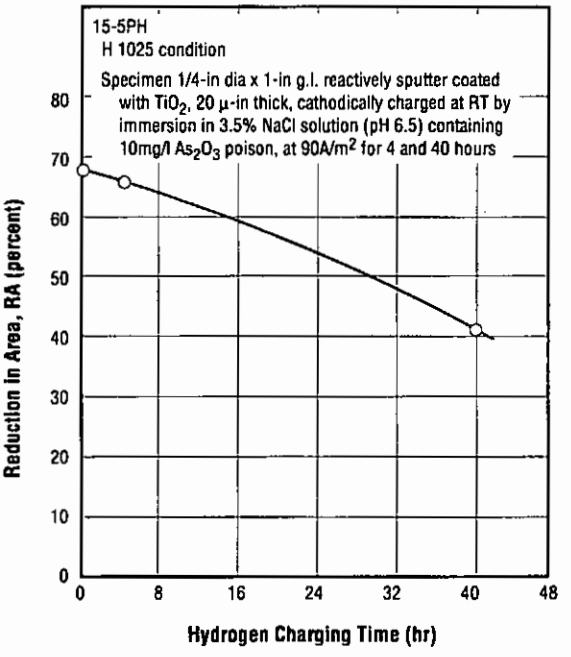


Figure 4.4.6.4 Effect of hydrogen charging time on ductility of TiO_2 coated (20 μ-in thick) specimens (H 1025 condition) tensile tested at room temperature after charging. (Ref. 52)

REFERENCES

1. Armco 15-5PH Precipitation-Hardening Stainless Steel Bar and Wire, *Armco Product Data Bulletin S-21a*, Armco Steel Corporation, Middletown, Ohio, (March 1968).
2. W.C. Clarke, Jr., "Applications and Properties of 15-5PH," *Metal Progress*, pp. 93 to 96, (August 1967).
3. W.C. Clarke, Jr. and H.W. Garvin, "Effect of Composition and Section Size on Mechanical Properties of Some Precipitation-Hardening Stainless Steels," American Society for Testing and Materials, *Special Technical Publication No. 369* (1965).
4. "Selection Guide - Armco Precipitation-Hardening Stainless Steel," Armco Steel Corporation, Middletown, OH.
5. Aerospace Material Specification, AMS 5658C, (July 1, 1976). (Superceded by Ref. 6)
6. Aerospace Material Specification, AMS 5659H, (March, 1995).
7. A.F. Hoenie and D.B. Roach, "New Developments in High Strength Stainless Steels," *DMIC Report 223*, Defense Metals Information Center, Battelle Memorial Institute, Columbus, OH (January 3, 1966).
8. R.J. Nekervis, C.H. Lund and A.M. Hall, "Status of High-Strength Steels for the Aircraft Industry," TML Report No. 91, Titanium Metallurgical Laboratory, Battelle Memorial Institute, Columbus, OH (January 3, 1958).
9. "Casting Armco 17-4PH and 15-5PH Precipitation-Hardening Stainless Steels," *Armco Products Data Bulletin SF-3*, Armco Steel Corporation, Middletown, Ohio (November, 1967)
10. R.E. Palmer and E.G. Takacs, "Magnetic Properties of Armco 17-4PH," Armco Steel Corporation, Baltimore, MD (October 31, 1967)
11. W. C. Clark, Jr., "A Study of Embrittlement of a Precipitation-Hardening Stainless Steel and Some Related Materials," Armco Steel Corporation, Baltimore, MD.
12. Private Communication with H. W. Garvin, Senior Research Engineer, Armco Steel Corporation, Baltimore, MD.
13. Aerospace Material Specification, AMS 5346A, (01 April 1993).
14. Aerospace Material Specification, AMS 5347, (16 October 1978).
15. Aerospace Material Specification, AMS 5356 (16 October 1978).
16. Aerospace Material Specification, AMS 5357 (16 October 1978).
17. Aerospace Material Specification, AMS 5400 (15 January 1979).
18. Aerospace Material Specification, AMS 5348A (01 January 1985).
19. Aerospace Material Specification, AMS 5862D (01 January 1991).
20. Aerospace Material Specification, AMS 5825E (01 October 1992).
21. Aerospace Material Specification, AMS 5826D (April 1994).
22. Aerospace Material Specification, AMS 5827D (01 October 1992).
23. American Society for Testing and Materials, ASTM A 693-93(XM-12) (15 July 1993).
24. American Society for Testing and Materials, ASTM A 564/A 564M-95(XM-12) (15 January 1995).
25. American Society for Testing and Materials, ASTM A 705/A 705M-95(XM-12) (15 January 1995).
26. R.M. Nagan and R.J. Cunningham, "Optimizing Fatigue Properties of Cast 15-5PH Steel," *Metal Progress*, Vol. 119, No. 4, pp 72-77 (March 1981).
27. "Armco 15-5PH Precipitation-Hardening Stainless Steel Sheet and Strip," *Armco Product Data Bulletin S-21a*, Armco Steel Corporation, Middletown, OH (1994).
28. K.R. Kondas, "Influence of Microstructure and Load Wave Form Control on Fatigue Crack Growth Behavior of Precipitation Hardening Stainless Steels," PhD Thesis, University of Missouri-Columbia (July 1976).
29. G.V. Smith, "Evaluation of the Elevated Temperature Tensile and Creep Rupture Properties of 12 to 27 Percent Chromium Steels," ASTM Data Series Publication DS 59.
30. J.E. Mortland, R.M. Evans, and R.E. Monroe, "Welding and Brazing of Precipitation-Hardening Stainless Steels," Prepared for NASA by Battelle Memorial Institute under Contract No. NASW-1948 (30 April 1970).
31. T. Allgeier and W.T. Evans, "Mechanical Hysteresis in Force Transducers Manufactured From Precipitation-Hardened Stainless Steel," Proceedings of the Institution of Mechanical Engineers, Part C: *Journal of Mechanical Engineering Science*, Vol. 209, No. C2 (1995).
32. "Mechanical Property Data - 15-5PH (H 1025) Stainless Steel Alloy: Hot-Rolled Plate," University of Dayton Report UDR-TM-84-14 on Contract No. F33615-82-C-5102 (May 1984).

33. G.T. Murray, "Prevention of Hydrogen Embrittlement by Surface Films," *Hydrogen Embrittlement: Prevention and Control*, ASTM STP 962, pp. 304-317 (1988).

34. M.J. Cieslak, "Hot-Cracking Mechanism in CO_2 Laser Beam Welds of Dissimilar Metals Involving PH Martensitic Stainless Steels," *Welding Research Supplement*, pp. 57s-60s (February 1987).

35. W.C. Clark, Jr., "A Study of Embrittlement of a Precipitation-Hardening Stainless Steel and Some Related Materials," *Transactions of the Metallurgical Society of AIME*, Vol. 245, pp. 2135-2140 (October 1969).

36. L.E. Pope, F.G. Yost, D.M. Follstaedt, J.A. Knapp, and S.T. Picraux, "Effects of Ion Implantation on Friction and Wear of Stainless Steels," Sandia National Labs Report No. SAND-82-0979C/CONF-820483-1, presented at Wear of Materials Conference, Reston, VA (11 April 1982).

37. D.M. Follstaedt, F.G. Yost, and L.E. Pope, "Microstructure of Stainless Steels Exhibiting Reduced Friction and Wear After Implantation with Ti and C," Sandia National Labs Report No. SAND-83-1234C/CONF-820483-13, presented at Materials Research Society Annual Meeting, Boston, MA (14 November 1983).

38. F.G. Yost, S.T. Picraux, D.M. Follstaedt, L.E. Pope, and J.A. Knapp, "The Effects of N^+ Implantation on the Wear and Friction of Type 304 and 15-5PH Stainless Steels," *Thin Solid Films*, Vol. 107:3, pp. 287-295 (23 September 1983).

39. G.W. Kuhlman, R. Pishko, W.S. Darden, and W.L. Krubsack, "Optimizing Mechanical Properties of Specialty, Stainless, and Heat-Resistant Alloy Steel Forgings by Thermomechanical Procesing," ASTM STP No. 903, *Steel Forgings*; Conference held Williamsburg, VA (28-30 November 1984).

40. Private communication between E.G. Takacs of Armco Steel Corporation, Baltimore, MD and J.E. Campbell, Battelle Memorial Institute, Columbus, OH (18 October 1972).

41. H. Espy, "Welding the PH Grades," Armoco Steel Corporation, Middletown, OH.

42. R.L. Rice, "Fracture Toughness and Fatigue Crack Propagation in 15-5PH Stainless Steel Bar," Memorandum from R.L. Rice to J.E. Campbell, Battelle Memorial Institute, Columbus, OH (31 January 1975).

43. T.J. Bosworth and A.J. Zvanut, "Development of a Direct Aging Filler Metal for Welding 15-5PH/17-4PH Steel," *Welding Research Supplement* (Supplement to the Welding Journal), pp. 159s-170s (June 1977).

44. C. Calabrese, "Fracture Mode and Toughness vs Temperature (-20 - 22C) for UNS-S15500 (15-5PH) Stainless Steel," *Engineering Fracture Mechanics*, Vol. 11:3, pp. 537-546 (1979).

45. M. Raefsky, "Metalurgical and Fatigue Evaluation of Malcomized 15-5PH Steel (AMS 5659B)," Boeing Company Engineering Materials Laboratory Report No. 69-378 (February 1970).

46. H. Garvin, "Casting 15-5PH and 17-4PH Stainless Steels," Armco Steel Corporation.

47. A. Cohen, M. Boas, and A. Rosen, "The Influence of Ion Nitriding Parameters on the Hardness Layer of 15-5PH Stainless Steel," *Thin Solid Films*, Vol. 141, No. 1, pp. 53-58 (15 July 1986).

48. J.H. Underwood, R.A. Farrara, G.P. O-Hara, J.J. Zalinka, and J.R. Senick, "Fracture Toughness and Fatigue Crack Initiation of Welded Precipitation-Hardening Stainless Steel," *Elastic-Plastic Fracture Test Methods: The User's Experience* (Second Volume), ASTM STP 1114, pp. 197-212 (1991).

49. C.W. Marschall and A.M. Hall, "Thermal and Mechanical Treatment for Precipitation-Hardening Stainless Steels," NASA Special Report on Contact NASW-1948 with Battelle Memorial Institute, Columbus, OH (30 April 1970).

50. D.E. Strohecker, A.F. Gerds, C.T. Olofsen, and F.W. Boulger, "Deformation Processing of Precipitation-Hardenable Stainless Steel," NASA Special Report on Contact NASW-1948 with Battelle Memorial Institute, Columbus, OH (01 May 1970).

51. J.E. Campbell, *Applications of Fracture Mechanics for Selection of Metallic Structural Materials*, Chapter 5: Fracture Properties of Wrought Stainless Steels, pp. 105-167, American Society for Metals, Metals Park, OH (1982).

52. J.G. Nelson and G.T. Murray, "Prevention of Hydrogen Embrittlement by a TiO_2 Surface Layer, *Metallurgical Transactions A*, Vol. 15A, pp. 597-600 (March 1984).

53. Y. Asayama, "Precipitation Processes and Notch Tensile Strengths of Precipitation Hardening Stainless Steels," *Journal of the Institute of Metals*, Vol. 45:7, pp. 731-739 (July 1981).

54. H.R. Habibi Bajuirani, C. Servant, and G. Cizron, "TEM Investigation of Precipitation Phenomena Occuring in PH 15-5 Alloy," *Acta Metall. Mater.*, Vol. 45(5), pp. 1613-1623 (1993).

55. *Military Handbook: Metallic Materials and Elements for Aerospace Vehicle Structures*, MIL-HDBK-5F, pp. 2-149 - 2-162 (01 November 1990).

56. *Products Bulletin S-6*, Armco Steel Corporation, Middletown, OH furnished by private communication with Kirk W. Olsen, Lord Corporation, Erie, PA (17 January 1997).

57. G.T. Murray, "Hydrogen Embrittlement of 15-5PH Stainles Steels," *Metallurgical Transactions A*, Vol. 12A, pp. 2138-2141 (December 1981).

58. K. Ozybaysal and O.T. Inal, "Thermodynamics and Structure of Solidification in the Fusion Zone of CO_2 Laser Welds of 15-5PH Stainless Steel," *Materials Science and Engineering*, A130, pp. 205-217 (1990).

59. J. Murali, M.R. Louthan, Jr. and R.P. McNitt, "Influence of Hydrogen on Age-Hardening Processes in 15-5 Precipitation Hardened Stainless Steel," Proceedings of Symposium MICON 78: *Optimization of Processing, Properties, and Service Performance Through Microstructural Control*, Houston, TX, published by ASTM, pp. 382-392 (April 1978).

60. T.S. Humphries and E.E. Nelson, "Stress Corrosion Cracking Evaluation of Martensitic Precipitation Hardening Stainless Steels," NASA TM-78257, NASA George C. Marshall Space Flight Center, Huntsville, AL (January 1980).

61. T.S. Humphries and E.E. Nelson, "Stress Corrosion Cracking Evaluation of Martensitic Precipitation Hardening Stainless Steels," NASA TM-53910, NASA George C. Marshall Space Flight Center, Huntsville, AL (12 September 1969).

62. R.R. Gaugh, "Sulfide Stress Cracking of Precipitation Hardening Stainless Steels," *Materials Performance*, Vol. 16:9, pp. 24-29 (September 1977).

63. R.R. Gaugh, "Stress Corrosion Cracking of Precipitation-Hardening Stainless Steels," *Materials Performance*, pp. 29-34 (February 1987).

64. C.S. Carter, D.G. Farwick, A.M. Ross and J.M. Uchida, "Stress Corrosion Properties of High Strength Precipitation Hardening Stainless Steels," *Corrosion*, Vol. 27:5, pp. 190-197 (May 1971).

65. P.E. Ruff and S.H. Smith,"Development of MIL-HNBK-5 Design Allowable Properties and Fatigue-Crack-Propagation Data for Several Aerospace Materials," AFML-TR-77-162 (October 1977).

66. *Structural Alloys Handbook*, published by CINDAS/ Purdue University, 1293 Potter Engineering Center, Room 316B, West Lafayette, IN 47907-1293 (1995).

Reference not used:

F. Bellucci, "Galvanic Corrosion Between Nonmetallic Composites and Metals: 1 - Effect of Metal and of Temperature," *Corrosion*, Vol. 47, No.10 (October 1991).

1. General

17-4PH, a martensitic stainless steel, is produced in the form of wrought, cast, and powder-metal products. It offers a good combination of high strength, toughness, corrosion resistance, and weldability. In addition, it can be fabricated in the relatively soft solution-treated condition and then precipitation hardened to a wide range of mechanical properties by an aging treatment in the range of 900F to 1150F. Strengthening is achieved by martensitic transformation (when air-cooled from its solution temperature of 1900F) and subsequent aging at 900F to 1075F, which induces the precipitation of small coherent copper-rich particles. At higher aging temperatures overaging occurs by the precipitation of incoherent larger copper-rich particles resulting in lower strength and hardness. The alloy retains useful strength at temperatures up to about 900F; like other martensitic steels, it undergoes a ductile-brittle transition at subzero temperatures. Some typical applications are aircraft and missile fittings, fasteners, gears, jet engine parts, valve parts, turbine blades, pump shafts, chemical process equipment, nuclear reactor components, and paper mill equipment. (Refs. 2, 4, 22, 23, 73)

1.1 Commercial Designation

17-4PH

1.2 Alternate Designations

AISI Type 630, CB-7Cu-1 (ACI designation for castings), UNS S17400 (wrought), UNS J92200 (castings), UNS S17480 (welding wire), UNS W37410 (covered welding electrodes).

1.3 Specifications

1.3.1 *[Table]* AMS, ASTM, and MIL specifications.

1.4 Composition

1.4.1 *[Table]* AMS specified compositions.

1.5 Heat Treatment

1.5.1 For optimum properties, 17-4PH should be precipitation hardened, which requires a solution treatment at 1900F plus aging at a temperature in the range 900 to 1150F. Generally, maximum strength and hardness are obtained with a 900F aging treatment (identified as Condition H900), but ductility, toughness, machinability, and resistance to stress corrosion increase as strength and hardness decrease with increasing aging temperature up to a maximum of 1150F. Wrought products are usually supplied by the manufacturer in the solution-treated condition (Condition A), and precipitation hardened (aged) to the desired properties by the fabricator or user. Exceptions to this practice can be made for material to be cold worked, which may be supplied in the overaged condition (H1150 or H1150-M) for ease of forming; for such products as well as for those that are hot worked, welded, or brazed, it is necessary to fully solution treat and age harden in order to obtain optimum properties in the final product. Although the solution-treated (Condition A) alloy has performed satisfactorily in a number of applications, precipitation hardening is recommended for critical applications because it provides optimum combinations of strength, toughness, and resistance to stress corrosion cracking. For castings, a homogenization treatment at 2100F and air cool to below 90F prior to the solution treatment can significantly benefit mechanical properties, particularly ductility and toughness, and can help to ensure compliance with minimum specification requirements. (Refs. 2-4, 49, 51, 52, 70)

Fe
17. Cr
4.0 Ni
4.0 Cu

1.5.1.1 *[Table]* Heat treatments for 17-4PH.

1.5.2 During the aging treatment a predictable dimensional change occurs, ranging from contractions of 0.0004-0.0006 in./in. for the H900 treatment to 0.0008-0.0010 in./in. for the H1150 treatment. (Refs. 20, 21, 23)

1.5.3 Electric furnaces or gas-fired radiant-tube furnaces are generally used for heat treating 17-4PH. Air has proved to be a satisfactory furnace atmosphere for solution treating and age hardening. Controlled reducing atmospheres such as dissociated ammonia or bright annealing gas introduce the hazard of nitriding and carburizing or decarburizing. Bright solution treating may be accomplished in hydrogen, argon, or helium atmosphere (dew-point approximately -65F), but these atmospheres, generally, are not useful at the aging temperatures because of the extremely low dew-point required. Heat treating in a vacuum can provide freedom from scale and heat discoloration. Solution treatment in molten salts is not recommended because of the danger of carburization and intergranular penetration. However, age hardening (900 to 1150F) has been successfully accomplished in a few of the hydride or nitrate salts. (Ref. 23)

1.5.4 Thorough cleaning prior to heat treatment facilitates scale removal and prevents carburization from surface contamination such as oils or other lubricants. The following procedure has proved to be effective: first, vapor degrease or solvent clean to remove oil, grease, and drawing lubricants; second, mechanically scrub with mild abrasive cleaners to remove dirt and other insoluble materials; finally, warm-water rinse to remove the remains of the cleaners. (Ref. 23)

This section produced with the support of NASA-Lewis Research Center.

© 1995 by Purdue Research Foundation, West Lafayette, Indiana 47907. All Rights Reserved. U.S. Government License. This material may be used, duplicated or disclosed by United States Government agencies without the payment of any royalty.

1.6 Hardness

(See also Table 1.7.3.1)

1.6.1 *[Table]* Hardness of wrought products and castings in various heat-treated conditions.

1.6.2 *[Figure]* Effects of long-time exposures at 700F and 900F on room-temperature hardness of bar in three heat-treated conditions.

1.7 Forms and Conditions Available

1.7.1 Wrought Products. The alloy is available in the form of sheet, strip, plate, billets, bars, wire, forgings, tube, and welding wires and electrodes. Wrought forms are normally supplied by the mills in the solution-treated condition (Condition A), ready for fabrication and subsequent hardening by the user. For other conditions, special arrangements may be made with the mills. (Refs. 49, 50, 55)

1.7.2 Castings. Available as sand castings, investment castings, and centrifugal castings, which can be supplied in Condition A or in one of the hardened or overaged conditions as specified by the user. (Ref. 51)

1.7.3 Powder-Metal Products. Powder-metal products of 17-4PH are produced by both the conventional press-and-sinter method and the more recently developed metal-injection-molding process. These processes are attractive for certain types of parts (normally relatively small and intricate), which can be made to final or nearly final shapes, thus eliminating or reducing scrap metal and secondary machining and assembly operations. On the other hand, they normally retain a certain amount of porosity, which results in somewhat lower density and mechanical properties than wrought and cast products. (See Table 1.7.3.1)

In the conventional process, suitable powder is mixed or blended along with a lubricant such as zinc stearate or stearic acid. The mixture is then compacted in a steel die under controlled pressure into the desired shape with sufficient "green" strength to avoid damage during ejection from the die and during normal handling between compacting and sintering. Prior to sintering, the lubricant is burned off at about 800-1000F, after which the compact is sintered in a protective atmosphere, normally at a temperature in the range of 2100 to 2300F. After the sintering operation, the desired heat treatment is applied. The mechanical properties of the product tend to increase with increasing sintered (final) density; the density increases with increasing compacting pressure and increasing sintering temperature. (Refs. 56, 57, 59)

With injection molding much finer powders are used; particle size is about 10 microns rather than 100 microns as in the conventional process. Large quantities of thermoplastic binders are used to permit injection molding into dies by means of conventional plastic molding equipment, which molds the feedstock material into the desired shape. Before sintering, the binder is removed by one of two methods: one consists of two stages in which the part is first processed in a solvent extraction unit, which removes a portion of the binder; subsequently, the remainder of the binder is burned out in an oven; the second method employs an evaporative technique in which the binder is designed to provide reasonable rheology and stability in molding yet can be rapidly evaporated from the green body under proper thermal conditions. Sintering is carried out at temperatures and controlled atmospheres similar to those used for conventional powder-metal parts, after which the desired heat treatment is applied. Injection molding permits production of denser, stronger, more uniform, and more complex powder-metal parts than conventional press and sinter. (Refs. 54, 58)

In both powder-metal processes, the parts shrink in proportion to the increase in density that occurs during sintering. The molds are sized to compensate for this shrinkage. If necessary and practical, the density and mechanical properties of powder-metal parts, in general, can be increased by a hot isostatic pressure (HIP) treatment applied to the as-sintered parts, that is prior to heat treatment. (See Fig. 3.5.1.9) (Refs. 58, 60)

1.7.3.1 *[Table]* Comparison of properties of wrought, cast, and powder-metal (P/M) products.

1.8 Melting and Casting Practice

Although 17-4PH is generally air-melted in electric-arc furnaces, consumable-electrode vacuum arc remelted (VAC CE) material is also available for aerospace and other applications requiring optimum mechanical properties. Induction melting in air or vacuum is also used, primarily in the production of castings. (Ref. 21)

1.9 Special Considerations

1.9.1 In common with most high-strength steels, the ductility of wrought products in the transverse and short-transverse orientations is significantly inferior to that in the longitudinal orientation, the differences being more pronounced in conjunction with the lower aging temperatures. (See Table 3.1.1 and 3.2.1.8) (Refs. 23, 35)

1.9.2 The transverse orientation of bar and the short-transverse orientation of plate are lower in fatigue strength than the longitudinal orientation. (Ref. 24)

1.9.3 In all age-hardened conditions, long-time exposure at temperatures of 700 to 900F cause sharp decreases in room-temperature impact strength. (See Table 3.2.3.2) (Ref. 23)

1.9.4 Material in the solution-treated condition (Condition A) is generally not recommended for critical applications since the microstructure consists of untempered martensite, which is relatively low in ductility and in resistance to stress corrosion and hydrogen embrittle-

ment. Heat treating to any of the age-hardened conditions (H conditions) has a dual effect: the martensite is tempered at the same time that precipitation hardening occurs. Thus, the combination of strength, ductility, toughness, hardness, and resistance to stress corrosion and hydrogen embrittlement is improved. (Refs. 24, 55)

1.9.5 Whereas the mechanical properties of the cast and powder-metal products are generally inferior to wrought material, they can be improved by hot isostatic pressing. (See Figures 3.5.1.7 and 3.5.1.9) (Refs. 60, 61)

1.9.6 17-4PH is susceptible to hydrogen embrittlement by galvanically introduced hydrogen or by exposure to pressurized hydrogen gas. (See Section 2.3.3)

1.9.7 Close control of temperature is important in solution treatment. Below 1900F, copper (the hardening element) is not completely dissolved, which results in less-than-optimum strength after the age-hardening treatment. Solution treatment at temperatures appreciably above 1900F causes excessive grain growth, resulting in deficiencies in ductility and toughness in the aged condition. (Ref. 23)

1.9.8 The AMS specifications on castings require that "castings shall not be peened, plugged, welded, or repaired by other methods without written permission from purchaser." (Refs. 27-31)

2. Physical Properties and Environmental Effects

2.1 Thermal Properties

2.1.1 Melting Range, 2550 to 2625F. (Ref. 5)

2.1.2 Phase Changes.

2.1.2.1 Time-temperature-transformation diagrams

2.1.2.2 When 17-4PH is heated, the martensite microstructure, which is stable at low temperatures, begins to transform to austenite at about 1160F and transformation is complete at 1300F. With further increases in temperatures, the copper dispersed in the matrix goes into solution in the austenite, the solution becoming complete at 1900F. Upon cooling from 1900F, transformation from austenite to martensite starts at approximately 270F and is complete when 90F is reached. This martensite is supersaturated with copper. Aging at 900F to about 1075F precipitates an extremely fine coherent copper-rich phase within the martensite resulting in excellent combinations of strength and toughness. At 1100F to 1160F overaging occurs, which is characterized by the precipitation of larger incoherent copper-rich particles and decreased strength and hardness but increased ductility. (Refs. 18, 23, 73)

2.1.3 Thermal Conductivity.

2.1.3.1 *[Figure]* Thermal conductivity from 200F to 2500F.

2.1.4 Thermal Expansion.

2.1.4.1 *[Figure]* Thermal expansion from -100F to 900F.

2.1.5 Specific Heat. 0.11 Btu per (lb-F) from 32F to 212F. (Refs. 21, 49, 51)

2.1.6 Thermal Diffusivity.

2.2 Other Physical Properties

2.2.1 Density.

2.2.1.1 *[Table]* Density in various heat-treated conditions.

2.2.2 Electrical Properties.

2.2.2.1 *[Table]* Electrical properties of sheet and bar in various heat-treated conditions.

2.2.3 Magnetic Properties. The alloy is magnetic.

2.2.3.1 *[Table]* Magnetic permeability in various heat-treated conditions.

2.2.4 Emittance.

2.2.5 Damping Capacity.

2.3 Chemical Environments

2.3.1 General Corrosion. In rural and mild industrial atmospheres, 17-4PH in all heat-treated conditions has excellent resistance to general corrosion, equivalent to Type 304 stainless steel. When exposed to seacoast atmospheres it gradually develops over-all light rusting and pitting, its resistance under such conditions being slightly inferior to Type 304 but much better than the standard hardenable (martensitic) stainless steels. It is well suited for many dynamic marine applications such as valve parts and pump and propeller shafting. However, like other stainless steels, 17-4PH is subject to crevice attack in stagnant seawater; if equipment exposed to seawater is not operated continuously, cathodic protection is desirable to prevent such attack. (Refs. 6, 36, 37, 47, 49)

Welds are subject to heat-affected-zone corrosion unless a postweld full solution and aging treatment is carried out. (Ref. 36)

In pressurized water at temperatures from 500 to 600F, 17-4PH corrodes at a rate comparable to other martensitic and ferritic stainless steels, which is about five times faster than austenitic stainless steels but only one tenth as fast as low-carbon and low-alloy steels. (Ref. 10)

In aerospace application, Type 17-4PH has been used for tanks, thrust chambers, fins, fuel-line elements, control shafts, and other components exposed to various fuels and oxidizers. These include oxygen, hydro-

gen, nitrogen tetroxide, red fuming nitric acid, anhydrous ammonia, hydrogen peroxide, hydrazine, and unsymetrical dimethyl hydrazine (UDMH). Except for long-time containment of hydrogen peroxide, the alloy is suitable for storage as well as short-time usage in conjunction with these substances. (Ref. 23)

Whereas the overall corrosion resistance of 17-4PH and Type 304 stainless steels are generally considered to be comparable, their resistances to certain specific chemical media can vary significantly depending upon concentration and temperature.

2.3.1.1 *[Table]* Comparison of typical corrosion rates for Types 17-4PH and 304 stainless steels in several chemical media.

2.3.2 Stress Corrosion. In salt-water and marine environments, 17-4PH in Condition H900 is susceptible to stress corrosion cracking; but when hardened at temperatures of 1025F and above, the alloy is much more resistant. For maximum resistance to chloride stress corrosion cracking, 17-4PH should be hardened at the highest aging temperature that will yield required properties, but not less than 1025F. (Refs. 2, 23, 38, 40-42, 49)

2.3.2.1 *[Table]* Effects of heat-treat condition and applied stress on time to stress corrosion failure of bent-beam strip specimens exposed to marine environment at Kure Beach, NC.

2.3.2.2 *[Table]* Comparison of tensile properties for various heat-treated conditions with critical stress intensity levels for stress corrosion cracking in salt water.

In a study of the effects of welding, bent-beam specimens consisting of 17-4PH base and weld metals were stressed at 90 percent of F_{ty} and exposed to a marine atmosphere at Kure Beach, NC. The test samples were divided into three groups, each in Conditions H900, H1025, H1075, and H1150:

a. Not welded (solution treated + aged)

b. Solution treated + welded + aged

c. Welded + solution treated + aged

All specimens in Condition H900 cracked due to stress corrosion in 68 days or less, regardless of whether welded or not. None of the others failed after more that 25 years in test. (Ref. 49) In addition, welded specimens were made by fusing 2-in.-diameter 17-4PH circular weld beads onto one face of 1/4-in.-thick plate. After welding and final heat treatment, the surfaces were ground to a smooth finish. The residual stresses caused by welding can approach or exceed the yield strength of the steel. These specimens were exposed to quiet sea water. The welding and heat-treat conditions were as follows:

a. Solution treated + aged to Conditions H1025, H1075, H1150 + welded

b. Welded + solution treated + aged to Conditions H1025, H1075, H1150

c. Solution treated + welded + aged to Conditions H1025, H1075, H1100

Careful examination showed no evidence of stress corrosion cracking in any of the test specimens after one year in test. (Ref. 49)

Laboratory tests in synthetic sour well solution (5 percent sodium chloride + 0.5 percent acetic acid saturated with hydrogen sulfide) in accordance with NACE Test Method TM-01-77 show that for best resistance to this aggressive medium, 17-4PH should be either in Condition H1150-M or aged at 1150F for two four-hour periods. In either of these heat-treated conditions, it is considered acceptable for use in sour (sulfide) service. (Ref. 49)

2.3.3 Hydrogen Effects. Hydrogen embrittlement is a potential threat to 17-4PH, as well as to all other high-strength martensitic steels, wherever the reduction of hydrogen ions to atomic hydrogen may occur. Common examples are acid pickling, aqueous corrosion, electroplating, and galvanic coupling with less noble metals. Table 2.3.2.2 shows the deleterious effects of galvanic coupling with less noble metals on K_{Iscc} in salt water. The adverse effect of the coupling on resistance to stress-corrosion cracking is due to the galvanic formation and absorption of atomic hydrogen at the surface of the 17-4PH, which functions as the cathode while the less noble metal functions as the anode. Practical experience indicates that, for most conditions of use, 17-4PH has adequate resistance to hydrogen embrittlement. Where the problem is acute and strength requirements permit, it should be aged at temperatures of 1100F or higher to obtain optimum resistance. (Refs. 16, 36, 39, 40, 49)

In one investigation of hydrogen embrittlement (Ref. 53), tensile and impact specimens that had been machined from 17-4PH Condition A bar were aged to several hardened conditions and then cathodically charged with hydrogen for up to 24 hours in a solution of sulfuric acid and arsenic trioxide at a current density of 58 mA/sq. in. When tested immediately after charging, the specimens showed marked decreases in tensile strength and ductility (reduction of area) for the higher-strength conditions but much less significant effects for the lower-strength conditions. Except for Condition A, the notch-impact properties were not significantly affected by hydrogen charging, probably because of the very high strain rate. The adverse effect on the notch-impact properties of the Condition A material is attributed to the fact that its microstructure of untempered martensite is highly sensitive to hydrogen embrittlement.

2.3.3.1 *[Figure]* Impact energy of specimens machined from bar, heat treated to various con-

ditions, and tested as-heat-treated and also tested immediately after cathodic hydrogen charging for 16 hours.

2.3.3.2 *[Figure]* Ultimate tensile strength of specimens machined from bar, heat-treated to various conditions, and tested immediately after cathodic hydrogen charging for various lengths of time.

2.3.3.3 *[Figure]* Tensile ductility (percent reduction of area) of specimens machined from bar, heat treated to various conditions, and tested immediately after cathodic hydrogen charging for various lengths of time.

In order to evaluate the reversibility of hydrogen charging, additional charged tensile specimens were tested after they had been held for various periods of time rather that tested immediately after charging. In these tests a 40-hour holding period at room temperature resulted in recovery of about 50 percent from the embrittling effects of a 16-hour charging time; the effects of longer holding periods were not reported. However, baking at 400F for four hours produced full recovery. These test results suggest that the damaging effects of hydrogen absorbed into 17-4PH during production operations, such as pickling and electroplating, may be ameliorated naturally during the time period prior to service installation or may be completely eliminated by a mild baking treatment. However, hydrogen absorbed during service, for example due to aqueous corrosion, galvanic coupling to a less noble metal, or simply exposure to pressurized hydrogen may create more serious problems; under these conditions hydrogen damage tends to decrease as the aging temperature, applied during prior heat treatment, increases within the normal range. (Refs. 53, 64)

Solution treatment at 1900F in air creates a tight oxide surface skin about 0.0001-in. thick plus a loose flaky outer scale. If the outer scale is removed, for example by a mild abrasive, the intact inner skin provides effective mitigation of hydrogen absorption and resulting embrittlement. Of course, this benefit of an oxide skin is obviated if non-oxidizing solution atmospheres are used or if the skin is removed by full surface cleaning (Section 4.4.1) or by machining. The much lighter oxide skin developed during aging treatments has little or no effect on hydrogen absorption. Sputtered surface films of aluminum oxide, less that 0.00001-in. thick, also provide effective protection against hydrogen absorption and embrittlement. (Ref. 74)

2.4 Nuclear Environments

Nuclear irradiation described as "water loop at 450F, 3 months at 4×10^{19} and 3×10^{19} NVT (thermal)" produced no changes in the density or dimensions of 17-4PH in Conditions A and H900; it produced a 4 percent increase in the magnetic permeability of the material in Condition H900. The 4×10^{19} NVT exposure increased the hardness from 34 to 50 R_C for Condition A and from 43 to 46 for Condition H900. (Ref. 44)

3. Mechanical Properties

3.1 Specified Mechanical Properties

3.1.1 *[Table]* AMS specified mechanical properties for wrought products.

3.1.2 *[Table]* AMS specified mechanical properties for investment, sand, and centrifugal castings.

3.2 Mechanical Properties at Room Temperature

3.2.1 Tension Stress-Strain Diagrams and Tensile Properties.

3.2.1.1 *[Figure]* Stress-strain curves for bar in three heat-treated conditions.

3.2.1.2 *[Figure]* Effect of aging treatment on tensile properties of wrought products at room temperature.

3.2.1.3 *[Figure]* Effect of aging treatment on tensile properties of castings at room temperature.

3.2.1.4 *[Figure]* Effects of long-time exposure at 700F on room-temperature tensile properties of bar in three heat-treated conditions.

3.2.1.5 *[Figure]* Effects of long-time exposure at 900F on room-temperature properties of bar in three heat-treated conditions.

3.2.1.6 *[Figure]* Effects of short exposure times at high temperatures on room-temperature tensile properties of sheet in Condition H900.

3.2.1.7 *[Figure]* Effects of 30-second exposures at temperatures from 1000F to 2000F on room-temperature properties of sheet in Condition H1150.

3.2.1.8 *[Table]* Comparison of longitudinal and transverse tensile properties of plate and bar.

3.2.1.9 Tensile properties of powder-metal products. (See Table 1.7.3.1 and Figures 3.5.1.8 and 3.5.1.9)

3.2.2 Compression Stress-Strain Diagrams and Compression Properties. (See Figures 3.3.2.1 and 3.3.2.2)

3.2.3 Impact.

3.2.3.1 *[Figure]* Effects of aging temperature on room-temperature Charpy V-notch impact properties of wrought bar and castings.

3.2.3.2 *[Table]* Effects of exposures of 1000 and 2000 hours at 700F, 800F, and 900F on room-temperature Izod impact properties.

3.2.4 Bending

3.2.5 Torsion and Shear.

3.2.5.1 *[Figure]* Effects of aging temperature on room-temperature shear strength determined on pin-type double-shear specimens.

3.2.5.2 *[Table]* Torsional strength of bar in various heat-treated conditions.

3.2.6 Bearing.

3.2.6.1 *[Figure]* Effects of aging treatment on bearing properties at room temperature.

3.2.7 Stress Concentration.

3.2.7.1 Notch Properties.

3.2.7.1.1 *[Table]* Comparison of smooth and notched tensile properties.

3.2.7.2 Fracture toughness.

3.2.7.2.1 *[Table]* Fracture toughness of bar in several heat-treated conditions.

3.2.8 Combined Loading.

3.3 Mechanical Properties at Various Temperatures

3.3.1 Tension Stress-Strain Diagrams and Tensile Properties.

3.3.1.1 *[Figure]* Tensile stress-strain curves for bar at room and elevated temperatures.

3.3.1.2 *[Figure]* Complete tensile stress-strain curves for bar at room and cryogenic temperatures.

3.3.1.3 *[Figure]* Effects of elevated temperatures on tensile properties of bar in five heat-treated conditions.

3.3.1.4 *[Figure]* Effects of elevated temperatures on tensile properties of bar in Condition H900.

3.3.1.5 *[Figure]* Effects of elevated temperatures on tensile properties of plate.

3.3.1.6 *[Figure]* Effects of long-time exposures at 700F on tensile properties at 700F of bar in three heat-treated conditions.

3.3.1.7 *[Figure]* Effects of long-time exposures at 900F on tensile properties at 900F of bar in three heat-treated conditions.

3.3.1.8 *[Figure]* Tensile properties at room and elevated temperatures after exposures up to 7000 hours at 600F and 750F of sheet initially in Condition H1150.

3.3.1.9 *[Figure]* Tensile properties of sheet at temperatures from 1000F to 2000F after exposures of 30 seconds at test temperature.

3.3.1.10 *[Figure]* Low-temperature tensile properties of bar in various heat-treated conditions.

3.3.1.11 *[Figure]* Low-temperature tensile properties of investment castings in Condition H1150-M.

3.3.2 Compression Stress-Strain Diagrams - Compression Properties.

3.3.2.1 *[Figure]* Compressive stress-strain curves for bar at room temperature and elevated temperatures.

3.3.2.2 *[Figure]* Effect of elevated temperatures on compressive strength of bar.

3.3.3 Impact.

3.3.3.1 *[Figure]* Low-temperature impact properties of bar and forgings in several overaged conditions.

3.3.3.2 *[Figure]* Low-temperature impact properties of bar in various heat-treated conditions.

3.3.3.3 *[Figure]* Low-temperature impact properties of castings in an overaged condition.

3.3.3.4 Injection-molded powder products. (See Figure 3.5.1.9)

3.3.4 Bending.

3.3.5 Torsion and Shear.

3.3.6 Bearing.

3.3.6.1 *[Figure]* Effect of elevated temperatures on bearing properties.

3.3.7 Stress Concentration.

3.3.7.1 Notch properties.

3.3.7.1.1 *[Figure]* Comparison of low-temperature notch tensile strength with ultimate tensile strength of bar in two overaged conditions.

3.3.7.1.2 *[Figure]* Comparison of low-temperature notch tensile strength with ultimate tensile strength of investment casting in Condition H1150-M.

3.3.7.2 Fracture toughness.

3.3.7.2.1 *[Figure]* Comparison of low-temperature tensile and fracture-toughness properties of plate in Condition H900.

3.3.8 Combined Properties.

3.4 Creep and Creep Rupture

3.4.1 *[Figure]* Creep and rupture curves for bar at 700F, 900F, and 1100F.

3.4.2 *[Figure]* Effects of temperature on stress to cause creep rupture in 100 and 1000 hours for bar in various heat-treated conditions.

3.4.3 *[Figure]* Creep-rupture curves at 600 to 800F for smooth and notched bars in Condition H1000.

3.4.4 *[Figure]* Creep-rupture curves at 300 to 800F for smooth and notched bars in Condition H1100.

3.5 Fatigue Properties

3.5.1 Conventional High-Cycle Fatigue.

3.5.1.1 *[Figure]* Fatigue properties of smooth and notched bars at room temperature and elevated temperatures.

3.5.1.2 *[Figure]* Fatigue properties of bar in Conditions H900 and H1050 at room temperature.

3.5.1.3 *[Figure]* Effects of stress ratio (R) on fatigue properties of forged bar in longitudinal and transverse orientations at room temperature.

3.5.1.4 *[Table]* Rotating beam fatigue strength at 10^7 and 10^8 cycles of bar in various heat-treated conditions.

3.5.1.5 *[Figure]* Fatigue properties of smooth and notched specimens in air and brackish water at room temperature.

3.5.1.6 *[Figure]* Effects of chloride environment and shot peening on the fatigue properties of bar.

3.5.1.7 *[Figure]* Effect of hot isostatic pressing (HIP), 4-hr. at 2050F in 15,000 psi argon, on fatigue and tensile properties of investment castings.

3.5.1.8 *[Figure]* Bending fatigue and other properties of powder-metal products made by injection-molding process.

3.5.1.9 *[Figure]* Effect of hot isostatic pressing (HIP), 2-hr. at 2125F in 15,000 psi argon, on fatigue and other properties of powder products made by injection molding.

3.5.2 Low-Cycle Fatigue.

3.5.3 Fatigue Crack Propagation.

3.5.3.1 *[Figure]* Fatigue-crack growth rate as a function of stress-intensity-factor range in atmospheres of dry argon and humid argon.

3.5.3.2 *[Figure]* Fatigue-crack growth rate as a function of stress-intensity-factor range with variations in melting practice, heat-treatment, and stress ratio (R).

3.5.3.3 *[Figure]* Fatigue-crack growth rate as a function of stress-intensity-factor range in air and in flowing sea water with different applied negative electrochemical potentials and with variations in melting practice and heat treatment.

3.5.3.4 *[Figure]* Effects of stress ratio (R) on fatigue-crack growth rate at low (near threshold) stress-intensity levels.

3.6 Elastic Properties

3.6.1 Poisson's Ratio, 0.291 at room temperature for all heat-treated conditions. (Ref. 45)

3.6.1.1 *[Figure]* Poisson's Ratio of overaged casting determined by ultrasonic technique at temperatures from -45 to 1465F.

3.6.2 Modulus of Elasticity.

3.6.2.1 *[Figure]* Effects of elevated temperatures on static modulus of elasticity in both tension and compression.

3.6.2.2 *[Figure]* Dynamic modulus of elasticity of overaged casting at temperatures from -45 to 1465F.

3.6.3 Modulus of Rigidity.

3.6.3.1 *[Table]* Modulus of rigidity for various heat-treated conditions.

3.6.3.2 *[Figure]* Dynamic modulus of rigidity of overaged casting at temperatures from -45 to 1465F.

3.6.4 Tangent Modulus.

3.6.4.1 *[Figure]* Tangent modulus curves in compression at room and elevated temperatures.

3.6.5 Secant Modulus.

4. Fabrication

4.1 Forming

4.1.1 Cold Forming. Because of its relatively high yield strength, cold forming of 17-4PH is normally limited to mild operations. Test results indicate that for stretch forming and similar uniaxial methods an overaged condition such as H1150 or H1150-M is preferable. In biaxial operations such as drawing, however, Condition A may be just as satisfactory as an overaged condition. After cold forming, full solution-and-aging heat treatment is recommended to develop the higher strength levels. However, if an overaged condition (H1150 or H1150-M) is desired in the final product and the forming stock is initially in that condition, the formed part may simply be re-aged to relieve residual stresses and restore toughness. (Ref. 49)

4.1.1.1 *[Table]* Minimum radius to make indicated cold bend with no fissuring when viewed under 10x magnification.

4.1.2 Warm Forming. Type 17-4PH sheet and strip can be warm formed by first solution treating at 1900F and then forming during cooling from this temperature while it is still austenitic. The preferred temperature range for such forming is 650 to 900F. After subsequent aging (hardening), the mechanical properties are comparable to those obtained by standard heat treatments. (Ref. 20, 49)

4.1.2.1 *[Table]* Tensile properties of sheet and strip warm stretch formed during cooling from solution-treatment temperature (1900F) and subsequently aged.

4.1.3 Hot Forming. The alloy can be readily hot forged, headed, and upset within the temperature range 2200 to 1850F. For optimum grain size and mechanical properties, hot-worked material should be cooled in air to below 90F before further processing. For proper hardening it must then be solution treated prior to the aging treatment. (Refs. 2, 21-23, 50)

4.2 Machining and Grinding

Type 17-4PH can be machined in both the solution-treated and age-hardened conditions. In the solution-treated condition (Condition A), it machines similarly to Type 302 and 304 stainless steels. After machining to final dimensions in this condition, one of the standard aging treatments can be applied, for which temperatures are low enough to obviate scaling and distortion. However, on large sections, allowance should be made for the predictable contraction on hardening (See Section 1.5.2). Generally, cutting rates vary inversely with hardness, Condition H1150-M providing optimum machinability. If material in this condition is used for best machinability, subsequent full solution and aging heat treatment is required to obtain higher mechanical properties. (Refs. 21, 50)

4.2.1 *[Table]* Relative machinability of 17-4PH bar in various heat-treated conditions.

4.3 Joining

4.3.1 Type 17-4PH has excellent weldability. It can be welded with any of the usual electric-arc, resistance-welding, and electron-beam processes. For optimum strength, 17-4PH filler metal is recommended in conjunction with the electric-arc processes; when high weld strength is not needed, a standard austenitic filler such as 308L can be used. No preheat is required for thicknesses up to about 4-in.; for thicker sections, preheat and interpass temperatures of 200 to 500F are recommended. Condition A is a satisfactory condition prior to welding, but for heavy sections and highly restrained joints an overaged condition (H1100 or H1150) is preferred. After welding, a full solution and aging treatment is required to obtain optimum mechanical properties. When material in Condition A is welded, however, postweld aging at 900 to 1150F without solution treatment produces properties approaching those obtained by full postweld heat treatment in sections less than 1/2-in. thick but not in heavier sections. When postweld solution treatment is not feasible in weldments 1/2-in. and greater in thickness, precipitation hardening at 1025F or less is suggested. The use of 17-4PH weldments in the as-welded condition is not recommended. Oxyacetylene welding is not advisable because of possible impairment of both corrosion resistance and mechanical properties caused by carbon pickup. For castings that are intended to be welded, copper content below 3.0 percent is desirable since higher copper levels have been associated with under-bead cracking. (Refs. 22, 23, 50, 51, 55, 65, 66, 75)

4.3.1.1 *[Table]* Variations in tensile properties with section size and postweld treatment for butt welds made by the manual-shielded-metal-arc technique with 17-4PH electrodes.

4.3.1.2 *[Table]* Comparison of tensile properties of sheet with those of sheet containing a transverse butt weld made by automatic GTA technique with 17-4PH weld wire.

4.3.1.3 *[Table]* Tensile properties of sheet containing a transverse butt weld made by the GMA technique with 17-4PH weld wire.

4.3.1.4 *[Figure]* Comparison of fatigue properties of base metal and shielded-metal-arc weldments fully heat treated after welding.

4.3.1.5 *[Table]* Tensile properties of flash-butt welds in bars.

4.3.2 Satisfactory furnace-brazed joints in 17-4PH parts can be made with nickel-base, copper-base, and silver-base brazing alloys. Where feasible, a brazing alloy should be selected that permits the use of a procedure that fits into the heat-treating cycle. (Ref. 23)

4.4 Surface Treating

4.4.1 Cleaning. Scale from hot-working or solution-treating operations can be removed by wet grit blasting or by a duplex pickling procedure. One effective pickling method requires 60 minutes in a caustic permanganate bath at 160 to 180F, water rinse, and then 2 to 3 minutes in 10 percent nitric-2 percent hydrofluoric acid solution at 110 to 140F, followed by hot-water rinse with high pressure or brush scrub. Light discoloration or heat tint produced by aging treatments can be removed by mechanical means such as wet grit blasting or with a short pickle in 10 percent nitric-2 percent hydrofluoric acid (by volume) at 110-140F followed be water rinse. Alternatively, heat tint may be removed by a light electropolishing operation. Both the short pickling and the electropolishing treatments also passivate the surfaces for maximum corrosion resistance. (Refs. 23, 49, 50)

4.4.2 Nitriding. Whereas nitriding decreases the corrosion resistance of any stainless steel, it can be used when increased resistance to galling and wear is required. For example, nitriding has been used to case harden 17-4PH jet engine fuel pump shafts. Using the gas-phase method, case hardness of approximately R_C67 can be obtained to a depth of about 0.005 in. This method of nitriding utilizes a temperature of about 1050F which, when applied to material initially in Condition A, results in a strong core with good toughness. (Refs. 21, 23)

Table 1.3.1 AMS, ASTM, and MIL specifications (Refs. 26-35, 49, 51, 55)

Alloy	17-4PH
Specification	Form
AMS 5643N	Bars, Wire, Forgings, Tubing, and Rings
AMS 5604C	Plate, Sheet, and Strip
AMS 5622B	Wrought, Consumable Electrode Melted
AMS 5398D	Sand and Centrifugal Castings
AMS 5355E	Investment Castings
AMS 5342D	Investment Castings, 130 ksi
AMS 5343D	Investment Castings, 150 ksi
AMS 5344D	Investment Castings, 180 ksi
AMS 5825E	Welding Wire
AMS 5827D	Covered Welding Electrodes
ASTM A 564	Bars and Shapes
ASTM A 693	Plate, Sheet, and Strip
ASTM A 705	Forgings
ASTM A 747	Castings
MIL-C-24111	Bars, Rod, and Forgings
MIL-S-81591	Castings

Table 1.4.1 AMS specified compositions (Refs. 26-35)

Alloy	17-4PH					
AMS Specifications	5344D, 5342D, 5343D, 5355E		5604C, 5643N, 5622B[a]		5827D[a], 5825E	
Form	Investment Cast[b]		Wrought		Weld Filler Metal	
Percent	Min.	Max.	Min.	Mx.	Min.	Max.
Carbon	–	0.06	–	0.07	–	0.05
Manganese	–	0.70	–	1.00	0.25	0.75
Silicon	0.50	1.00	–	1.00	–	0.75
Phosphorus	–	0.025	–	0.040	–	0.04
Sulfur	–	0.025	–	0.030	–	0.03
Chromium	15.50	16.70	15.00	17.50	16.00	16.75
Nickel	3.60	4.60	3.00	5.00	4.50	5.00
Columbium	0.15	0.40	5XC	0.45[c]	0.15	0.30
Copper	2.80	3.50	3.00	5.00	3.25	4.00
Tantalum	–	0.05	–	–	–	–
Aluminum	–	0.05	–	–	–	–
Tin	–	0.02	–	–	–	–
Nitrogen	–	0.05	–	–	–	–
Molybdenum	–	–	–	0.05	–	0.75
Iron	Remainder		Remainder		Remainder	

[a] AMS 5622B and 5827D specify 0.025 percent maximum sulfur and phosphorus.

[b] AMS 5398D (Sand and Centrifugal Castings) is similar with the following minor exceptions: 0.04 maximum phosphorus, 0.03 maximum sulfur, 2.50 to 3.20 copper, and 0.10 to 0.35 columbium plus tantalum.

[c] Columbium plus tantalum.

Table 1.5.1.1 Heat treatments for 17-4PH (Refs. 5, 8, 21, 23, 49-52)

Alloy	17-4 PH		
Form	Wrought and Cast		
Solution Treatment[a]	Condition[d]	Age[b]	
		Temperature (F)	Time (Hour)
For all conditions, 1900F is the most common solution temperature, but some sources use 1925 or 1950F. A minimum of 30 minutes at solution temperature is recommended; longer times may be appropriate for large sections. Cooling to below 90F is required before aging. Air cooling is widely used, but oil quench is acceptable for simple sections less than 3 in.	A	–	–
	H900	900	1[c]
	H925	925	4[c]
	H1025	1025	4
	H1075	1075	
	H1100	1100	
	H1150	1150	
	H1150-M	1400 + 1150	2 4
	H1150 DBL	1150 + 1150	4 4

[a] For optimum properties in castings, a homogenization treatment at 2100F for 90 minutes or more followed by air cool to below 90F prior to solution treatment is sometimes applied. Also for castings, after the specified solution treatment, it is occasionally necessary to cool in dry ice to ensure complete transformation of the austenite. (Ref. 52)

[b] Air cool from aging temperature.

[c] For castings, 1.5 hours aging time is recommended for conditions H900 and H925. (Ref. 52)

[d] Occasionally, other conditions such as H975 or H1050 are used, indicative of other aging temperatures.

Table 1.6.1 Hardness of wrought products and castings in various heat-treated conditions (Refs. 21, 49-51, 72)

Alloy	17-4PH		
Form	Sheet	Bar	Castings
Condition	Hardness, R_C		
A	35	36	34
H900	45	44	
H925	43	42	44
H1025	38		
H1075	37	36	34
H1100	–	35	31
H1150	35	33	29
H1150-M	33	28	–

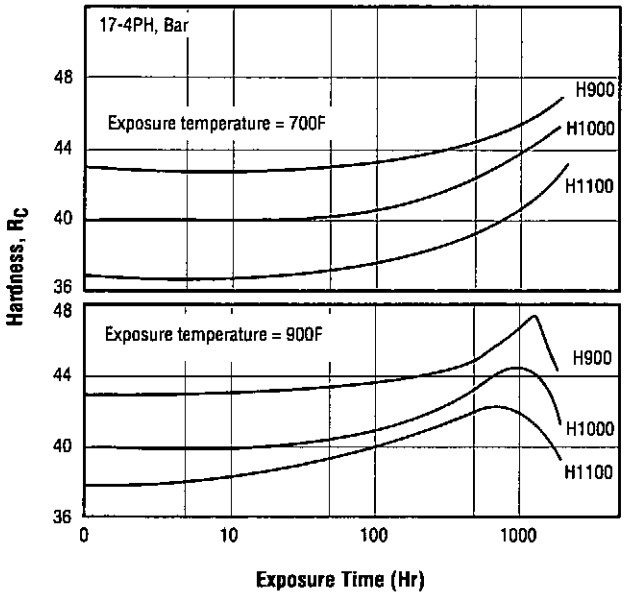


Fig. 1.6.2 Effects of long-time exposures at 700F and 900F on room-temperature hardness of bar in three heat-treated conditions (Ref. 23)

Table 1.7.3.1 Comparison of properties of wrought, cast, and powder-metal (P/M) products (Refs 49-51, 54, 57)

Alloy	17-4PH			
Form	Conventional P/M	MIM[a] P/M	Wrought	Castings
Condition	H900			
F_{tu} (ksi)	140.0	140.5	195.6	187.0
F_{ty} (ksi)	122.0	133.9	177.0	161.0
e, 4D (percent)	2	7	14	10
Hardness, R_C	24[b]	34[b]	44	44
Density, (g/cm^3)	7.15	7.48	7.81	7.76

[a] Metal injection molded.

[b] Apparent hardness, that is an integrated hardness representing the combination of metal and pores inherent in powder-metal products.

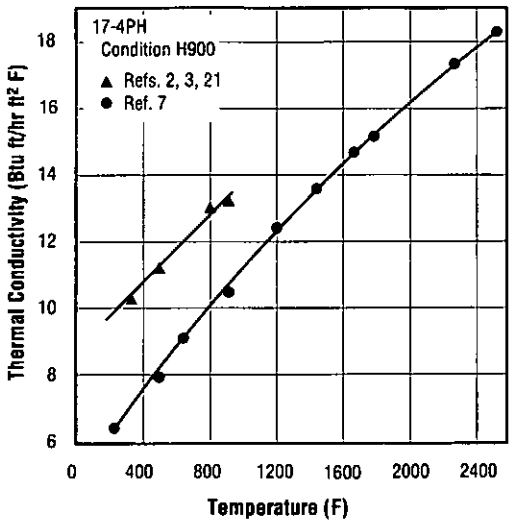


Fig. 2.1.3.1 Thermal conductivity from 200F to 2500F (Refs. 2, 3, 7, 21)

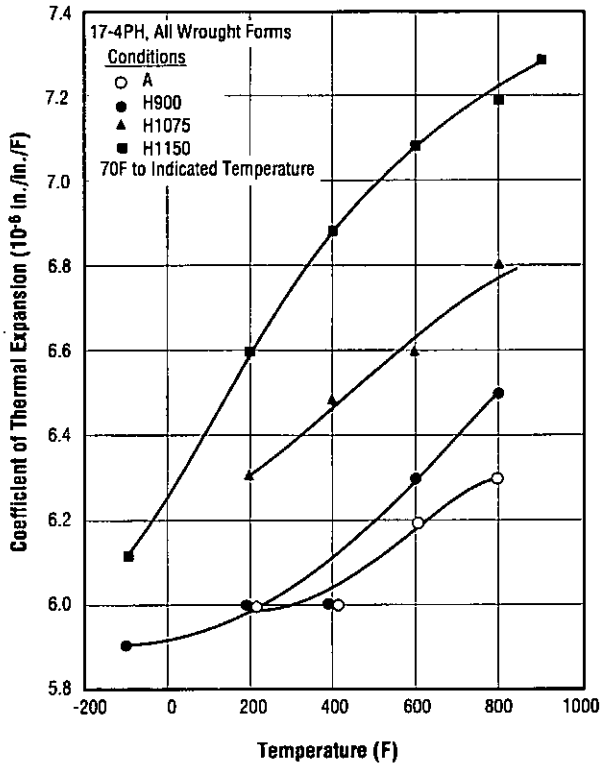


Fig. 2.1.4.1 Thermal expansion from -100F to 900F (Refs. 20, 21)

Table 2.2.1.1 Density in various heat-treated conditions (Refs. 20-22)

Alloy	17-4PH	
Form	All Wrought Forms	
	Density	
Condition	($lb./in.^3$)	(g/cm^3)
A	0.280	7.75
H900	0.282	7.81
H1075	0.283	7.84
H1150	0.284	7.87

Table 2.2.2.1 Electrical properties of sheet and bar in various heat-treated conditions (Refs. 20, 21, 49)

Alloy	17-4PH			
Form	Condition	Electrical Conductivity		Electrical Resistivity
		(percent IACS)	(megohms per cu in.)	(microhm-in.)
Sheet	A	1.76	0.0259	38.6
	H900	2.24	0.0330	30.3
Bar	A	1.73	0.0254	39.4
	H900	2.16	0.0317	31.5
	H1075			

Table 2.2.3.1 Magnetic permeability in various heat-treated conditions (Ref. 3)

Alloy	17-4PH		
Form	All Wrought Forms		
Condition	Magnetic Permeability		
	at 100 oersteds	at 200 oersteds	Maximum
A	74	48	95
H900	90	56	135
H1075	88	52	136
H1150	59	38	71

Table 2.3.1.1 Comparison of typical corrosion rates for Types 17-4PH and 304 stainless steels in several chemical media (Ref. 49)

Alloy			17-4PH				Type 304
Form			Sheet				
Condition			H925	H1025	H1075	H1150	Annealed
Medium	Concentration (percent)	Temperature (F)	Corrosion Rate[a] (mils per year)				
Sulfuric Acid	2	95	< 1				57
	5		4	7	11	9	240
	1	176	1				350
	2		8	9	13	17	480
Hydrochloric Acid	1/2	95	2		3	16	33
	1		35	174	518	650	240
Nitric Acid	25	Boiling	14	6	7	8	2
	50		70	35	47	31	4
10% Nitric + 1% Hydroflouric Acid	–	95	1500				380
Formic Acid	10	176	2	3		5	100
Acetic Acid	33	Boiling	6	6	4	4	300
Phosphoric Acid	20		1			2	
	70		86	57	60	119	32
Sodium Hydroxide	50	176	3		4	5	1
		Boiling	480	450	560		80
Ammonium Hydroxide	10		< 1				
Salt-Sugar-Vinegar	–						

[a] Rates determined after total immersion, in most instances, for five 48-hour periods. Chemically pure reagents were used. These data should be used only as guide to comparative performance.

Table 2.3.2.1 Effects of heat-treat condition and applied stress on time to stress corrosion failure of bent-beam strip specimens exposed to marine environment at Kure Beach, NC (Ref. 49)

Alloy	17-4PH	
Form	Strip	
Condition	Applied Stress (ksi)	Time to Failure[a]
A	124 - 100% F_{ty}	NF
	93 - 75% F_{ty}	
H900	187 - 100% F_{ty}	26 days
	140 - 75% F_{ty}	28 days
H925	173 - 100% F_{ty}	100 months + 1 NF
	130 - 75% F_{ty}	52 months + 1 NF
H975	168 - 100% F_{ty}	NF
	126- 75% F_{ty}	78 months + 2 NF
H1025	140 - 90% F_{ty}	NF
	116- 75% F_{ty}	
H1075	135 - 90% F_{ty}	
	113- 75% F_{ty}	
H1150	102 - 90% F_{ty}	
	85- 75% F_{ty}	

[a] The results are based upon the average of three or five tests for each test condition. NF signifies no failure after more than 15 years of exposure.

Table 2.3.2.2 Comparison of tensile properties for various heat-treated conditions with critical stress intensity levels for stress corrosion cracking in salt water (Ref. 10)

Alloy	17-4PH				
Form	1.0 in. Plate				
	Conditions				
Properties	H900	H975	H1075	H1150	H1150-M
F_{ty} (ksi)	177.0	161.7	150.9	120.3	91.0
F_{tu} (ksi)	195.6	170.8	156.5	141.6	124.6
e, 2 in. (percent)	14	15	17	19	22
RA (percent)	50	55		61	64
K_{Iscc}, (ksi $\sqrt{in.}$)[a,b]					
Open circuit	45	82	117	124	97
Al coupled	36	73	103	105	93
Zn coupled	30	45	59	74	88
Mg coupled	17	20	49	52	90

[a] Stress corrosion tests for Condition H900 carried out in natural seawater; for all other conditions, stress-corrosion tests were done in 3.5 percent sodium chloride in distilled water.

[b] K_{Iscc} is the stress intensity level below which no evident crack extension will occur.

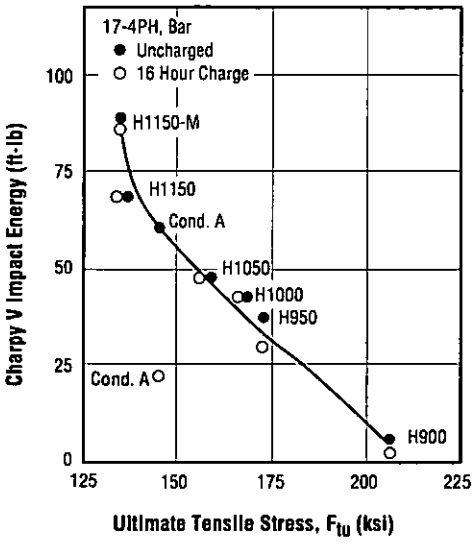


Fig. 2.3.3.1 Impact energy of specimens machined from bar, heat-treated to various conditions, and tested as-heat-treated and also tested immediately after cathodic hydrogen charging for 16 hours (Ref. 53)

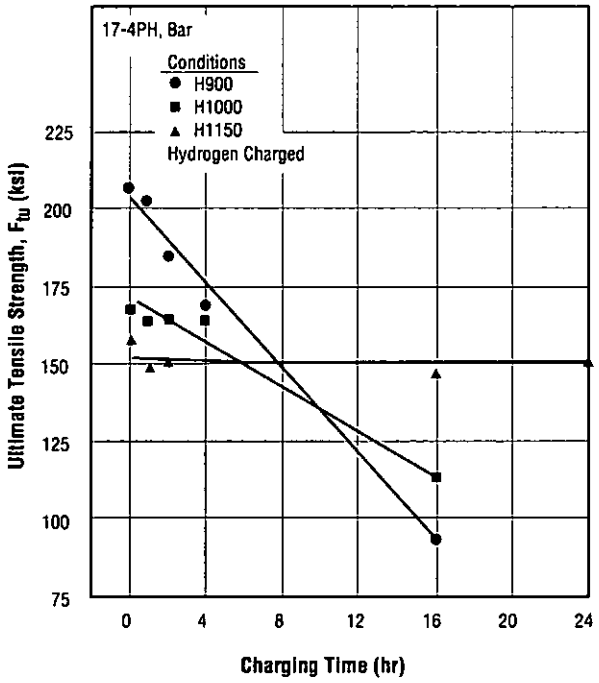


Fig. 2.3.3.2 Ultimate tensile strength of specimens machined from bar, heat-treated to various conditions, and tested immediately after cathodic hydrogen charging for various lengths of time (Ref. 53)

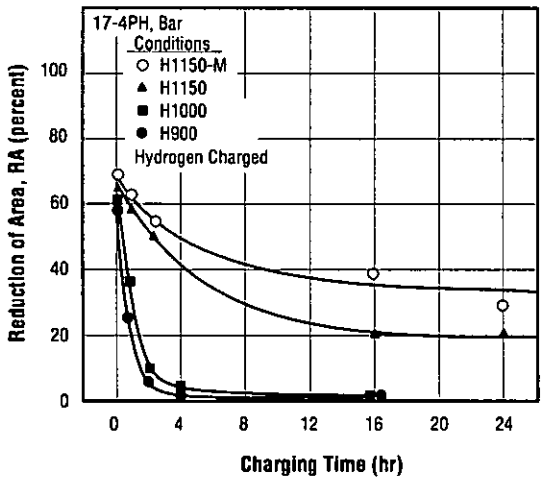


Fig. 2.3.3.3 Tensile ductility (percent reduction of area) of specimens machined from bar, heat-treated to various conditions, and tested immediately after cathodic hydrogen charging for various lengths of time (Ref. 53)

Table 3.1.1 AMS specified mechanical properties for wrought products (Refs. 26, 34, 35)

Alloy	17-4PH							
Specs.	Form	Condition	F_{ty}, min (ksi)	F_{tu}, min (ksi)	e, 4D[a], min (percent)	RA[a], min (percent)	Hardness	
							min	max
AMS 5604C	Sheet, Strip, Plate up to 4.0 in. thick	A	160[b]	185[b]	3	–	–	38 R_C
		H900	170	190	5, 8, 10	–, 30, 35	40 R_C	47 R_C
		H925	155	170	5, 8, 10	–, 30, 35	38 R_C	45 R_C
		H1025	145	155	5, 8, 12	–, 35, 40	35 R_C	42 R_C
		H1075	125	145	5, 9, 13	–, 35, 45	33 R_C	39 R_C
		H1100	115	140	5, 10, 14	–, 35, 45	32 R_C	38 R_C
		H1150	105	135	8, 10, 16	–, 40, 50	28 R_C	37 R_C
AMS 5622B	Bars, Wire, Forgings, Tubing, Rings up to 8.0 in. in diameter or thickness. (Consumable-electrode melted.)	A	–	175[b]	–	–	–	363 BHN
		H900	170	190	10(L), 5(T)	35(L), 15(T)	388 BHN	444 BHN
		H925	155	170	10(L), 6(T)	38(L), 20(T)	375 BHN	429 BHN
		H1025	145	155	12(L), 7(T)	45(L), 27(T)	331 BHN	401 BHN
		H1075	125	145	13(L), 8(T)	45(L), 28(T)	311 BHN	375 BHN
		H1100	115	140	14(L), 9(T)	45(L), 29(T)	302 BHN	363 BHN
		H1150	105	135	16(L), 10(T)	50(L), 30(T)	277 BHN	352 BHN
AMS 5643N	Bars, Wire, Forgings, Tubing, Rings up to 8.0 in. in diameter or thickness.	A	–	175[b]	–	–	–	363 BHN
		H900	170	190	10	40[c]	388 BHN	444 BHN
		H925	155	170	10	44[c]	375 BHN	425 BHN
		H1025	145	155	12	45	331 BHN	401 BHN
		H1075	125	145	13	45	311 BHN	375 BHN
		H1100	115	140	14	45	302 BHN	363 BHN
		H1150	105	135	16	50	277 BHN	352 BHN

[a] The series of e (4D) and RA numbers for AMS 5604C apply to the following thicknesses respectively: up to 0.1875 in., 0.1875 to 0.625 in., and 0.625 to 4,000 in.; the F_{ty} and F_{tu} values do not vary with thickness. For AMS 5622B, the two numbers for both e (4D) and RA refer to longitudinal (L) and transverse(T) orientations; the F_{ty} and F_{tu} values are the same for L and T.

[b] This particular value is maximum rather than minimum.

[c] For sizes over 3 in. these values are reduced to 35 and 38 percent respectively.

Table 3.1.2 AMS specified mechanical properties for investment, sand, and centrifugal castings (Refs. 27-31)

Alloy	17-4PH							
Refs.	Form	Condition	F_{ty}, min (ksi)	F_{tu}, min (ksi)	e, 4D, min (percent)	RA, min (percent)	Hardness	
							min	max
(27)	Investment castings	A	–	–	–	–	–	36 R_C
(27)(28)	Investment castings test bar	H900	160	180	6	15	40 R_C	–
(28)	Investment castings				4	12	40 R_C	46 R_C
(27)	Investment castings test bar	H925	150	180	6	15	40 R_C	–
(27)(30)	Investment castings test bar	H1000	130	150	8	20	34 R_C	–
(30)	Investment castings				4	12	34 R_C	42 R_C
(27)	Investment castings test bar	H1025	130	150	10	20	34 R_C	–
(27)(29)	Investment castings test bar	H1100	120	130	10	25	30 R_C	–
(29)	Investment castings				6	15	30 R_C	38 R_C
(27)	Investment castings test bar	H1150	110	125	12	25	28 R_C	–
(31)	Sand & Centrifugal castings	–	–	–	–	–	–	363 BHN
	Test bars	H925	150	180	6	12	375 BHN	–

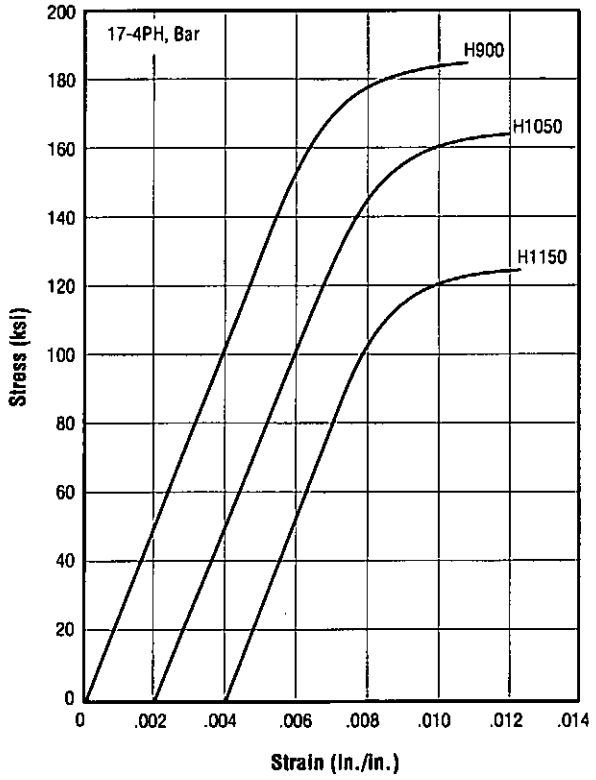


Fig. 3.2.1.1 Stress-strain curves for bar in three heat-treated conditions (Ref. 23)

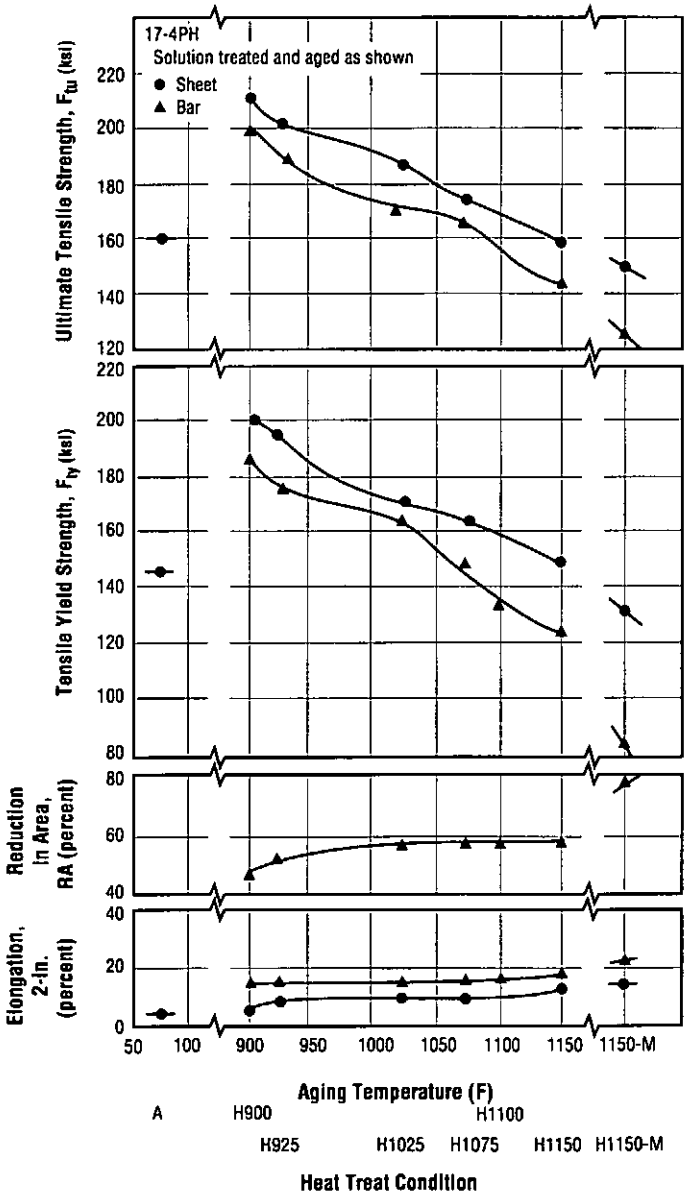


Figure 3.2.1.2 Effect of aging treatment on tensile properties of wrought products at room temperature (Ref. 20, 21)

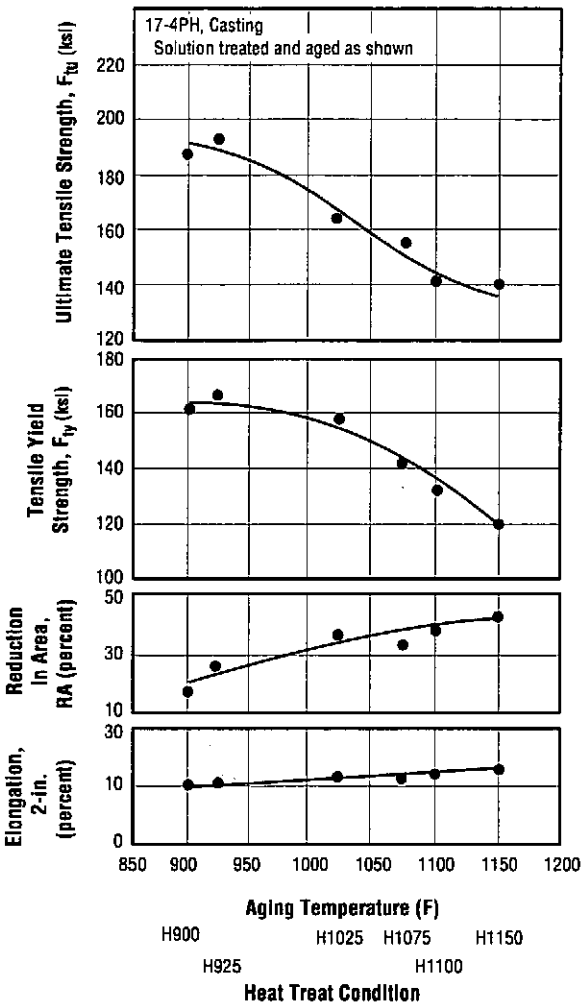


Figure 3.2.1.3 Effect of aging treatment on tensile properties of castings at room temperature (Ref. 20, 21)

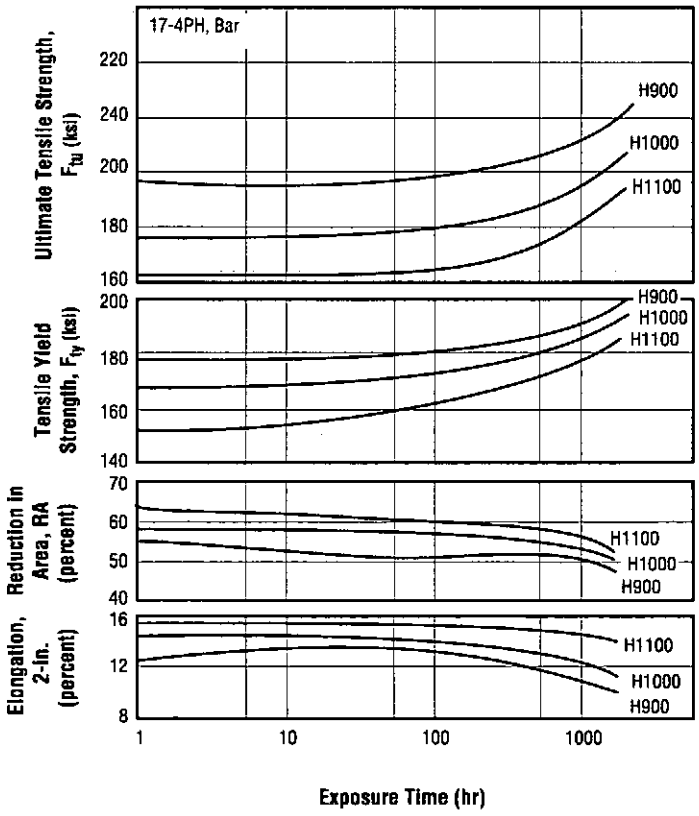


Figure 3.2.1.4 Effects of long-time exposures at 700F on room-temperature tensile properties of bar in three heat-treated conditions (Ref. 23)

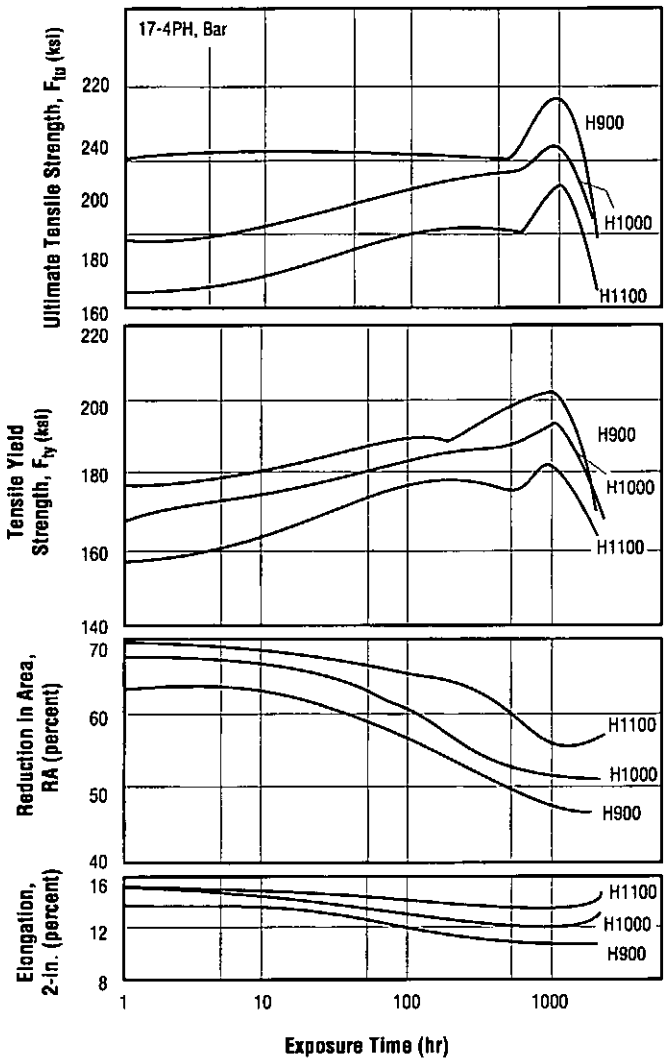


Figure 3.2.1.5 Effects of long-time exposure at 900F on room-temperature tensile properties of bar in three heat-treated conditions (Ref. 23)

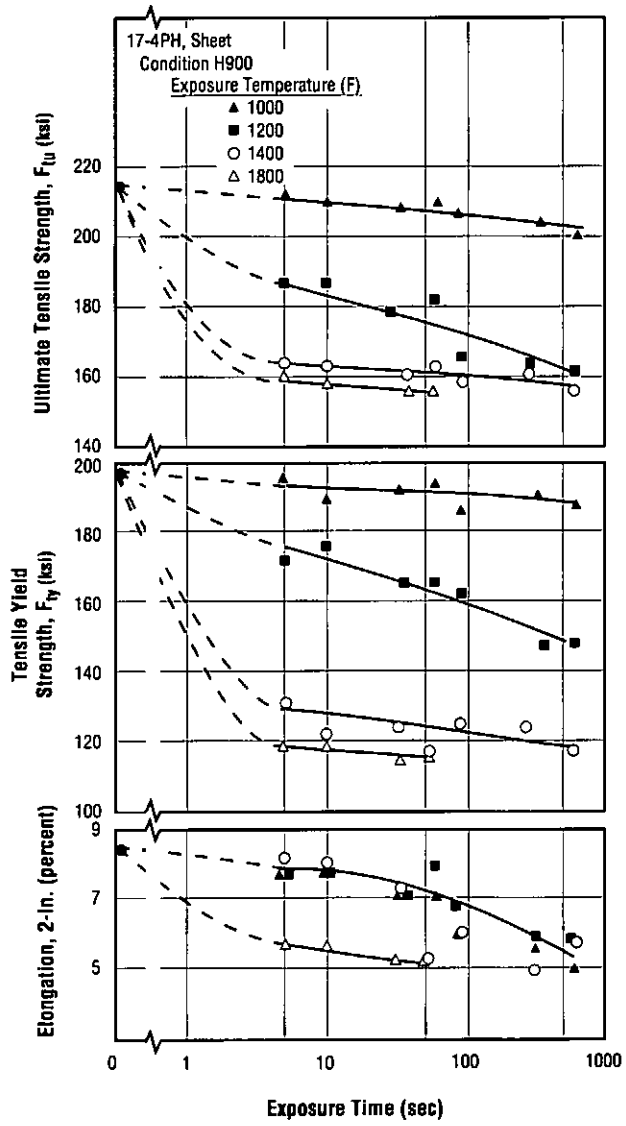


Figure 3.2.1.6 Effects of short exposure times at high temperatures on room-temperature tensile properties of sheet in condition H900 (Ref. 20)

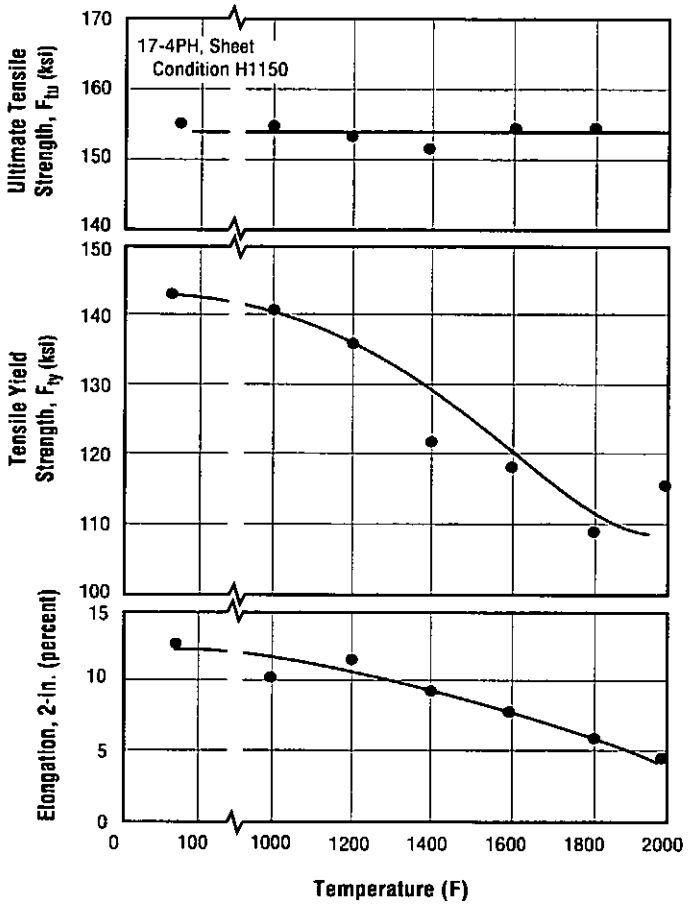


Figure 3.2.1.7 Effects of 30-second exposures at temperatures from 1000 to 2000F on room-temperature properties of sheet in Condition H1150 (Ref. 20)

Table 3.2.1.8 Comparison of longitudinal and transverse tensile properties of plate and bar (Ref. 23)

Alloy	17-4PH					
Form	Condition	Orientation[a]	F_{ty} (ksi)	F_{tu} (ksi)	e, 2 in. (percent)	RA (percent)
4-in. plate	H925	L	–	195	17.0	53.5
		ST			4.5	5.0
	H1025	L	160	163	17.0	58.0
		ST	159	162	13.0	32.0
	H1075	L	144	155	18.0	61.0
		ST	147	154	12.0	27.0
6-in. square bar	H1075	L	157	160	17.5	62.0
		T	155	158	14.0	40.0
	H1150	L	139	147	20.0	63.0
		T	136		15.0	44.0

[a] L = longitudinal, ST = short transverse, T=transverse.

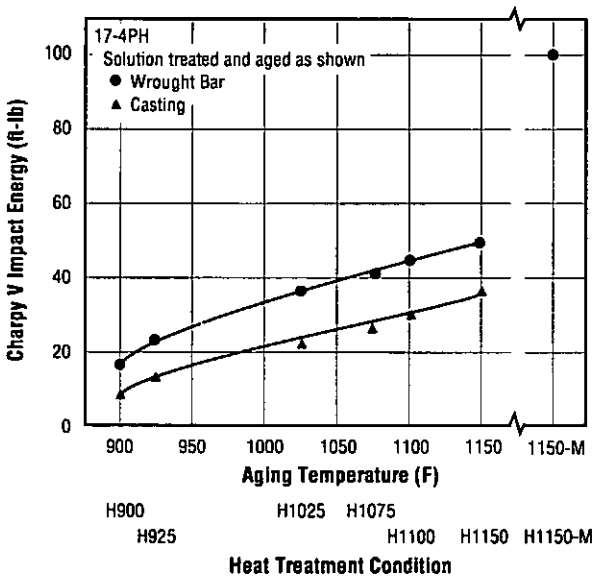


Figure 3.2.3.1 Effects of aging temperature on room-temperature Charpy V-notch impact properties of wrought bar and castings (Refs. 21, 51)

Table 3.2.3.2 Effects of exposures of 1000 and 2000 hours at 700F, 800F, and 900F on room-temperature Izod impact properties (Ref. 23)

Alloy		17-4PH		
Form		Bar		
Exposure		Izod Impact (ft-lb)		
		Condition		
Temperature (F)	Time (Hr)	H900	H1000	H1100
75	–	14	45	56
700	1000	7		
	2000	4	3	4
800	1000	2		3
	2000	2		
900	1000	3	4	6
	2000	6	8	11

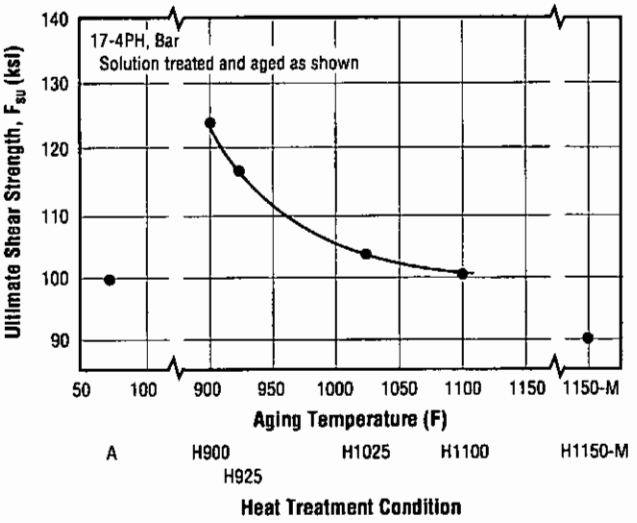


Figure 3.2.5.1 Effects of aging treatment on room-temperature shear strength determined on pin-type double-shear-specimens (Ref. 21)

Table 3.2.5.2 Torsional strength of bar in various heat-treated conditions (Ref. 25)

Alloy	17-4PH	
Form	Bar	
Condition	Yield Strength, F_{sty} (ksi)	Modulus of Rupture, F_{st} (ksi)
A	83.5	125.0
H900	119.8	171.4
H925	119.3	161.8
H1025	109.8	141.1
H1100	103.4	134.3
H1150	91.4	130.2
H1150-M	62.9	116.8

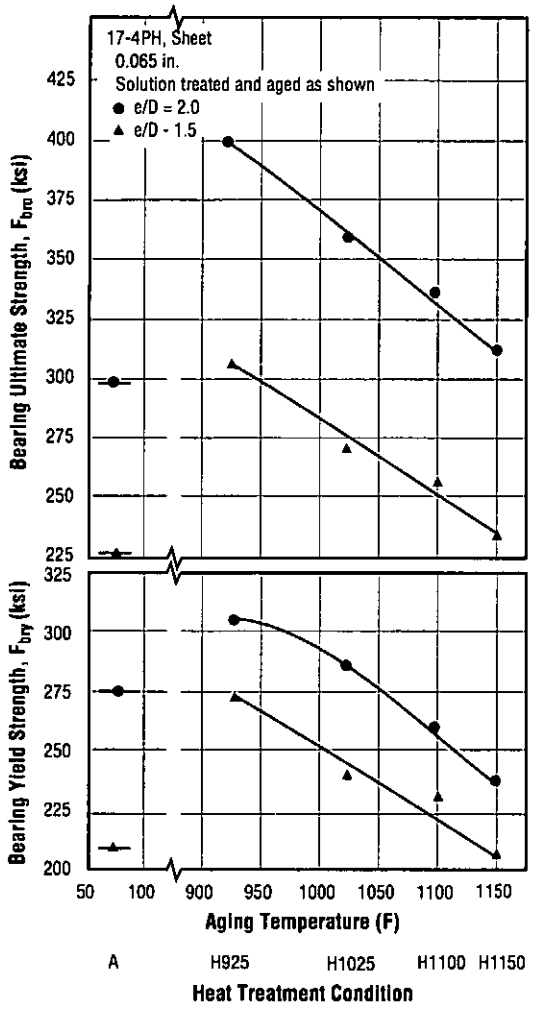


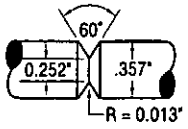
Figure 3.2.6.1 Effects of aging treatment on bearing properties at room-temperature (Ref. 24)

Table 3.2.7.1.1 Comparison of smooth and notched tensile properties (Ref. 9)

Alloy			17-4PH		
Form			Bar		
Condition			H900		
Smooth[a]			Notched		
F_{ty} (ksi)	F_{tu} (ksi)	e, 2 in. (percent)	K_t	NTS[b] (ksi)	NTS[c] (ksi)
195	201	15.4	3	318	324

[a] Average of 9 tests.

[b] Average of 3 tests.



[c] Average of 3 tests.

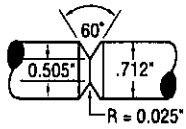


Table 3.2.7.2.1 Fracture toughness of bar in several heat-treated conditions (Ref. 24)

Alloy	17-4PH
Form	Bar
Condition	K_{Ic} (ksi $\sqrt{in.}$)
A	62.4
H900	54.8
H925	100.8
H975	84.6

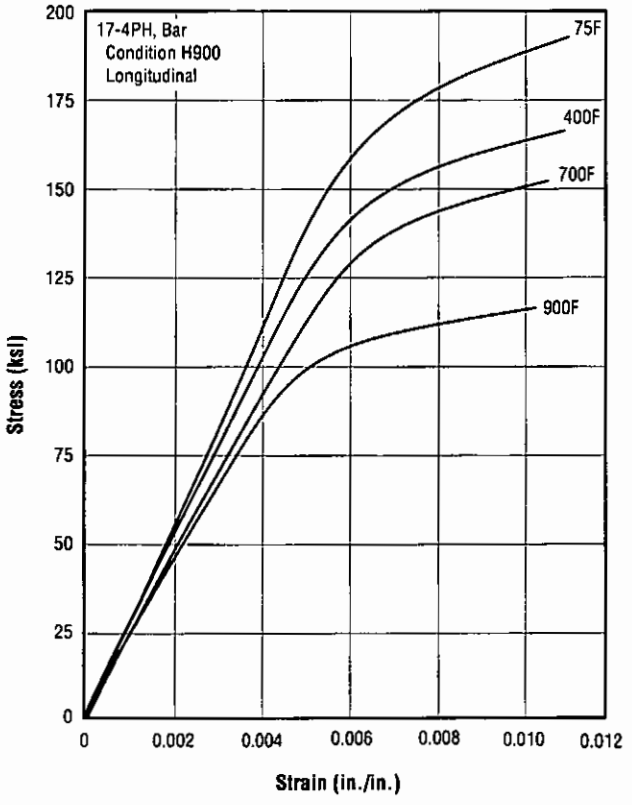


Figure 3.3.1.1 Tensile stress-strain curves for bar at room and elevated temperatures (Ref. 11)

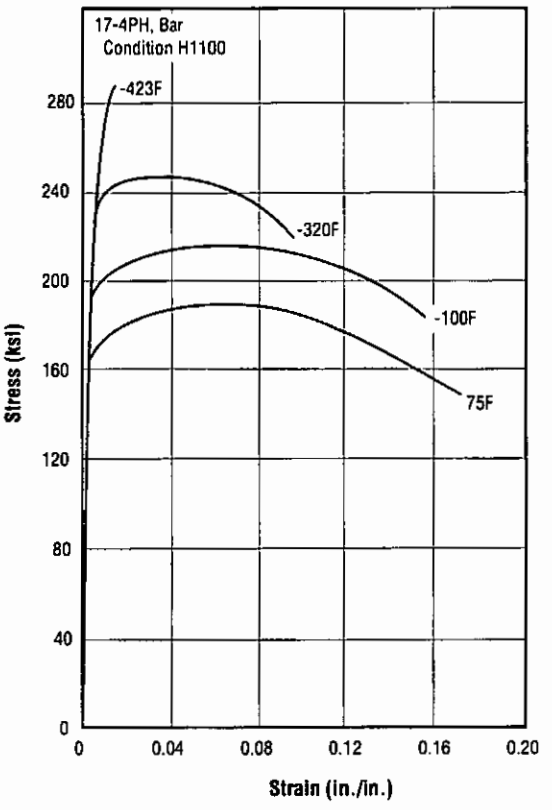


Figure 3.3.1.2 Complete tensile stress-strain curves for bar at room and cryogenic temperatures (Ref. 17)

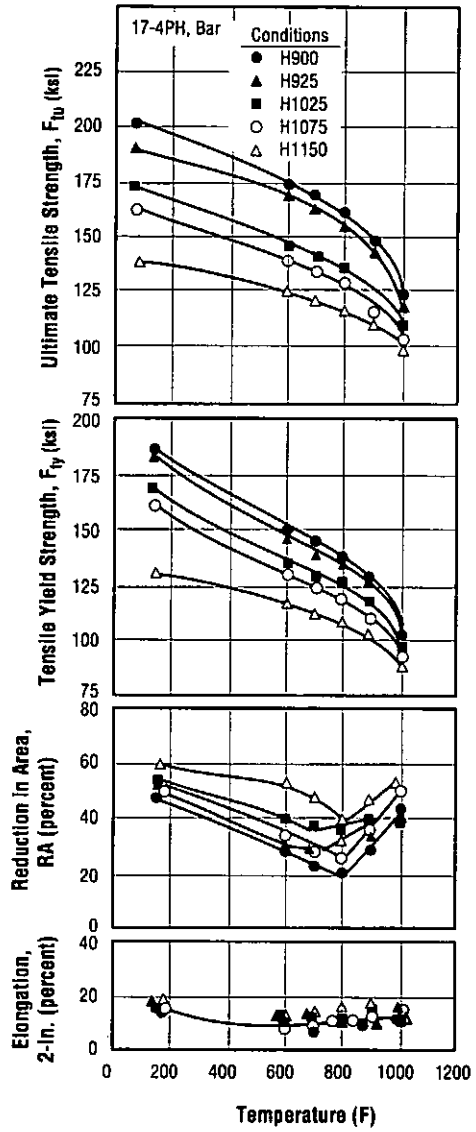


Figure 3.3.1.3 Effects of elevated temperatures on tensile properties of bar in five heat-treated conditions (Ref. 21)

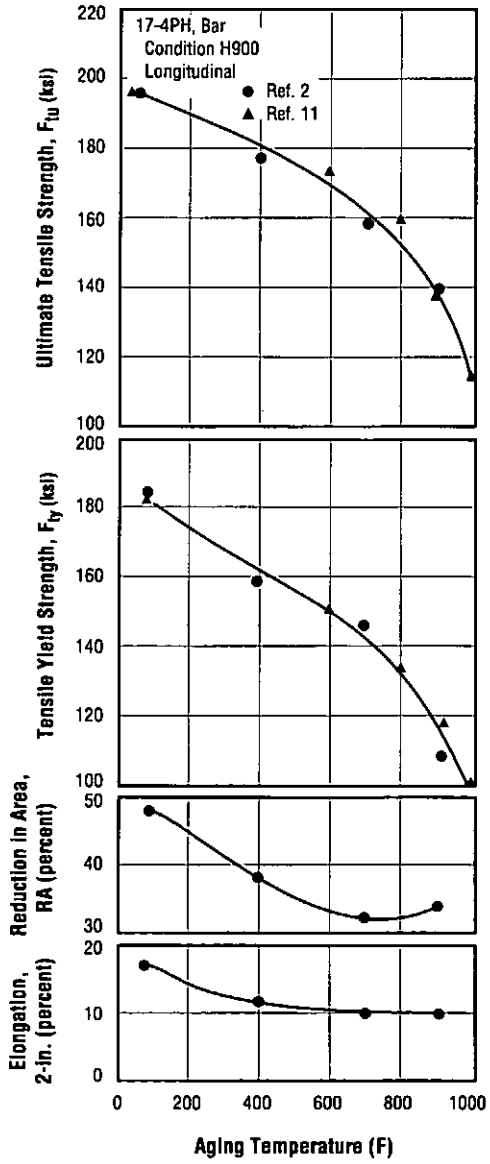


Figure 3.3.1.4 Effect of elevated temperatures on tensile properties of bar in Condition H900 (Ref. 2, 11)

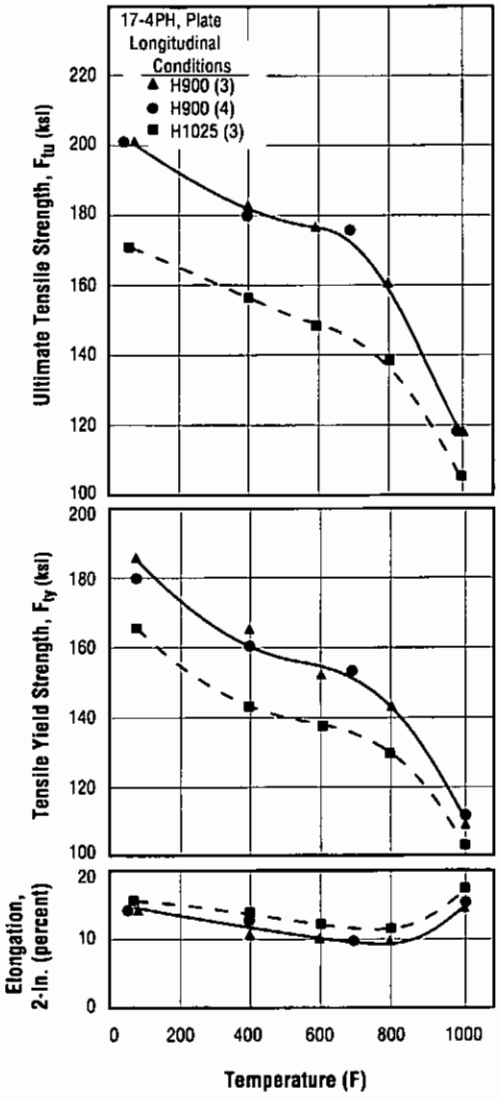


Figure 3.3.1.5 Effects of elevated temperatures on tensile properties of plate (Refs. 3, 4)

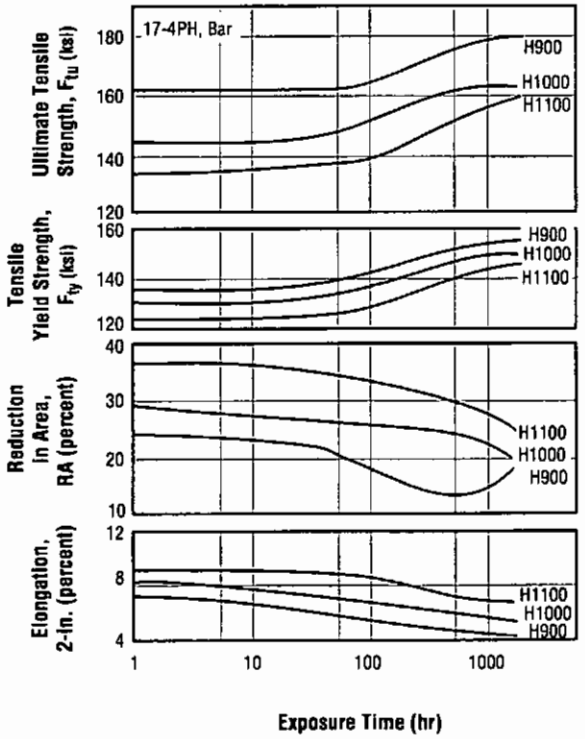


Figure 3.3.1.6 Effects of long-time exposures at 700F on tensile properties at 700F of bar in three heat-treated conditions (Ref. 23)

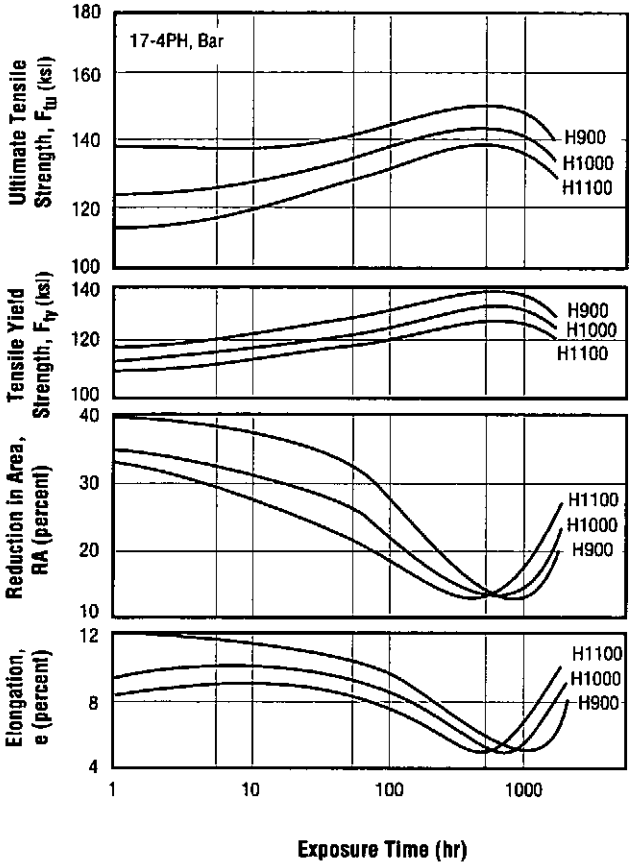


Figure 3.3.1.7 Effects of long-time exposures at 900F on tensile properties at 900F of bar in three heat-treated conditions (Ref. 23)

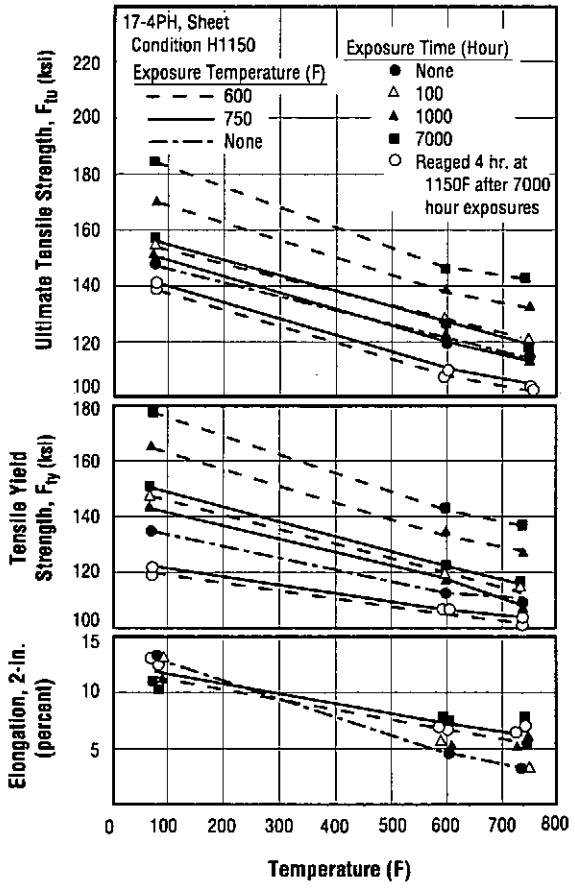


Figure 3.3.1.8 Tensile properties at room and elevated temperatures after exposures up to 7000 hours at 600F and 750F of sheet initially in Condition H1150 (Ref. 20)

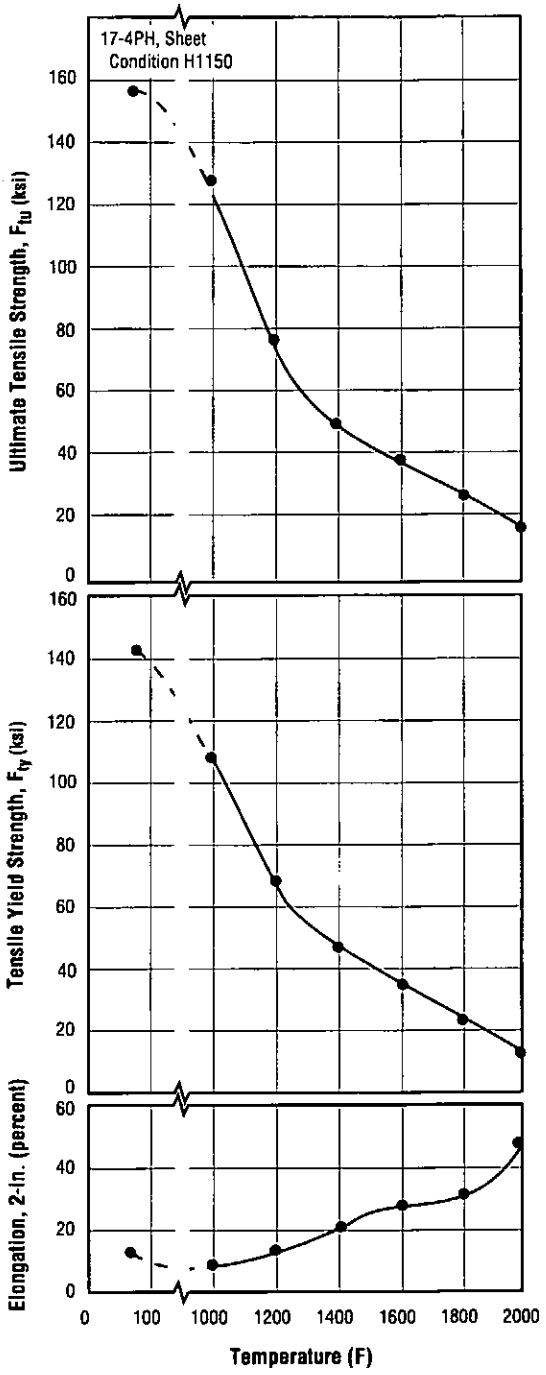


Figure 3.3.1.9 Tensile properties of sheet at temperatures from 1000F and 2000F after exposures of 30 seconds at test temperature (Ref. 20)

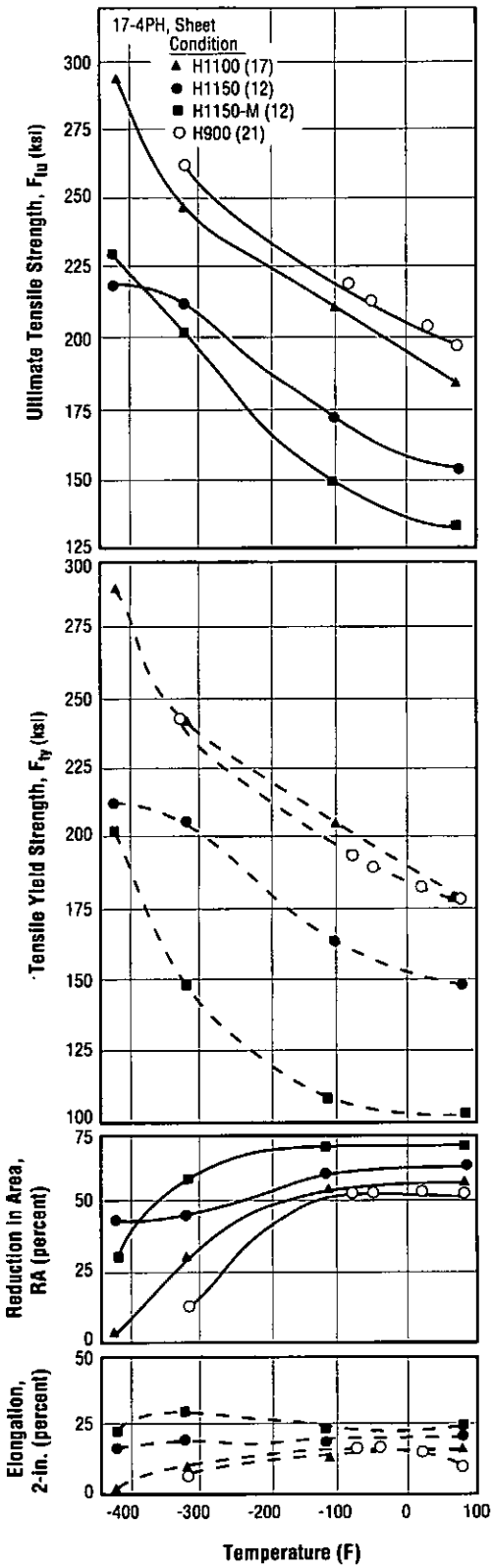


Figure 3.3.1.10 Low-temperature tensile properties of bar in various heat-treated conditions (Refs. 12, 17, 21)

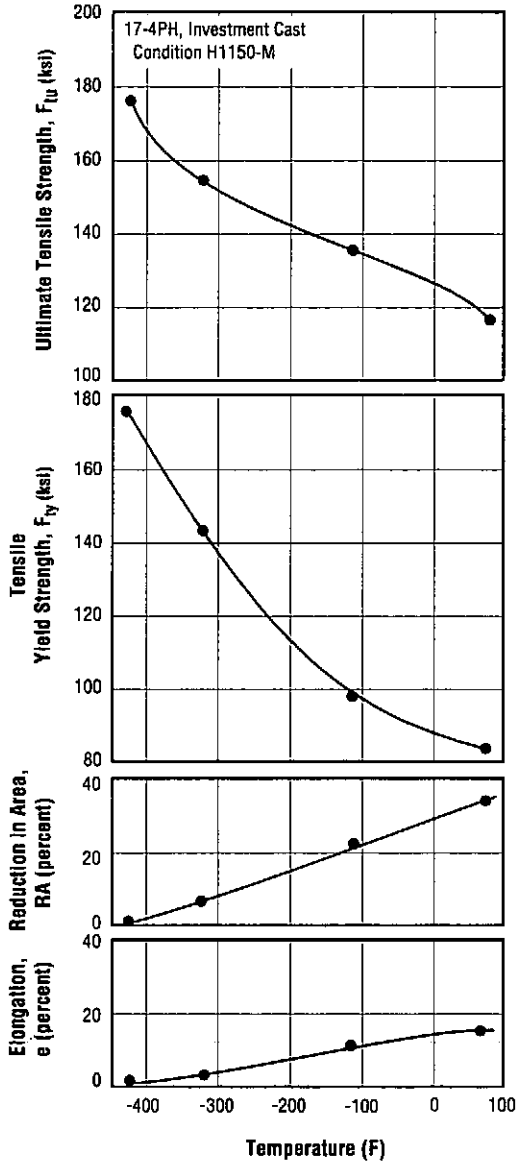


Figure 3.3.1.11 Low-temperature tensile properties of investment castings in Condition H1150-M (Ref. 13)

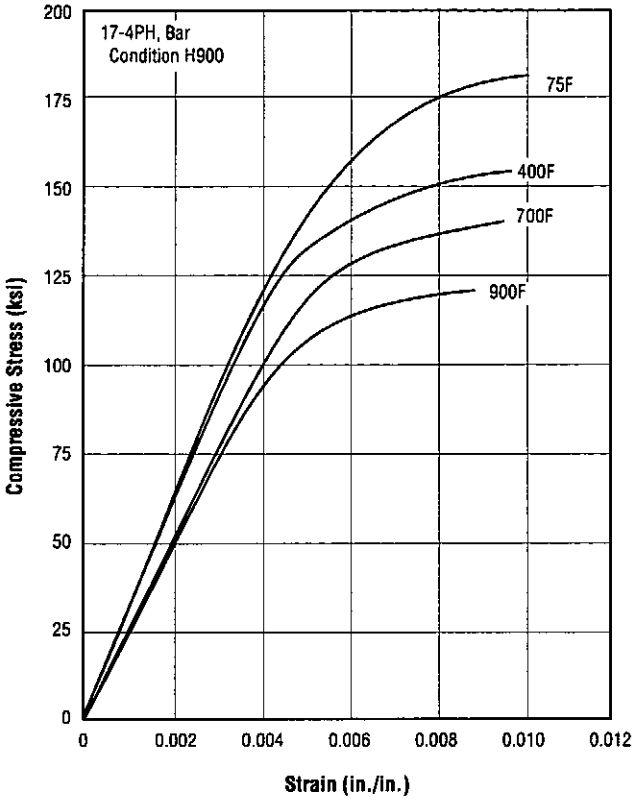


Fig. 3.3.2.1 Compressive stress-strain curves for bar at room and elevated temperatures (Ref. 11)

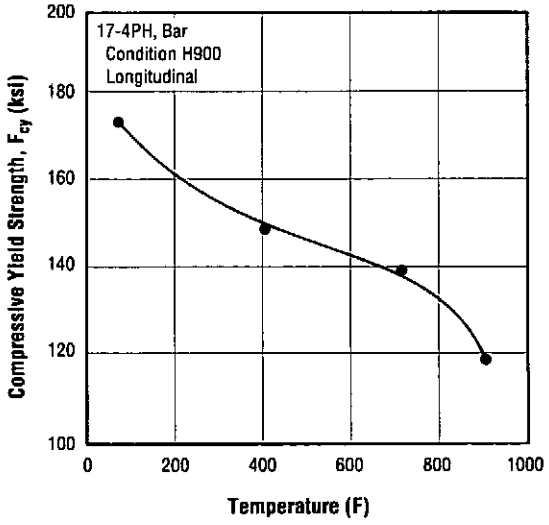


Fig. 3.3.2.2 Effect of elevated temperatures on compressive strength of bar (Ref. 11)

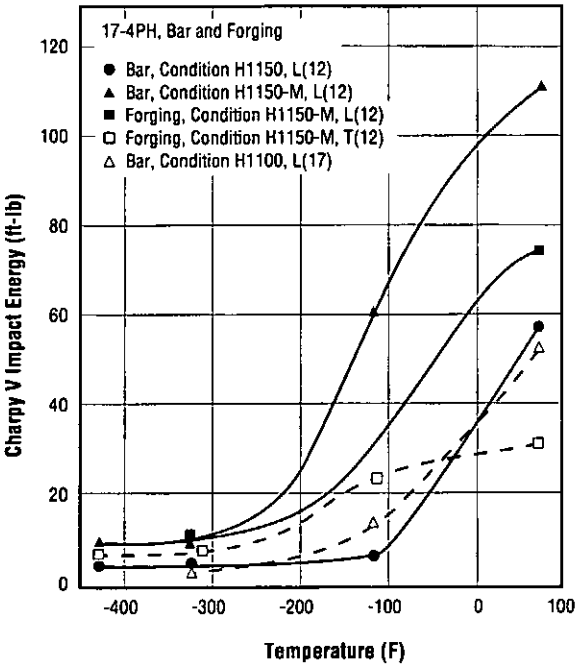


Fig. 3.3.3.1 Low-temperature impact properties of bar and forgings in several overaged conditions (Refs. 12, 17)

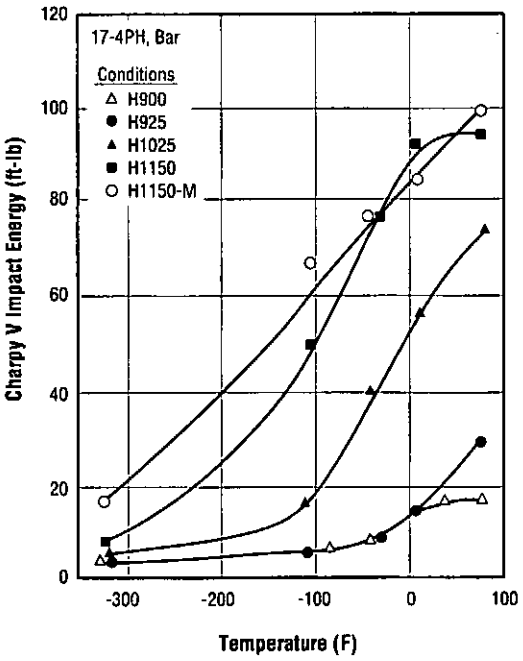


Fig. 3.3.3.2 Low-temperature impact properties of bar in various heat-treated conditions (Ref. 21)

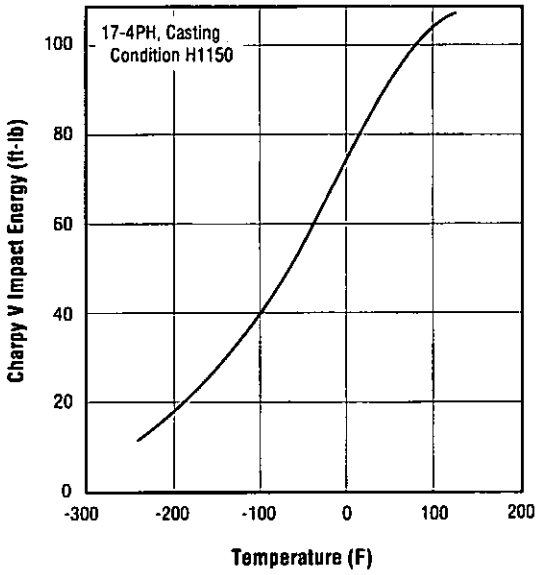


Fig. 3.3.3.3 Low-temperature impact properties of castings in an overaged condition (Ref. 71)

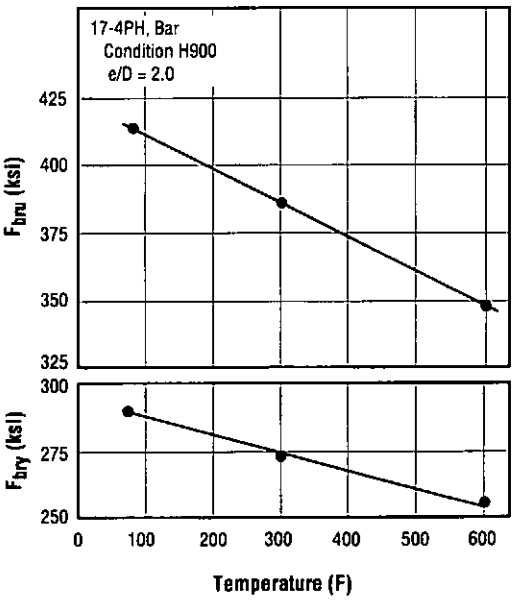


Fig. 3.3.6.1 Effect of elevated temperatures on bearing properties (Ref. 1)

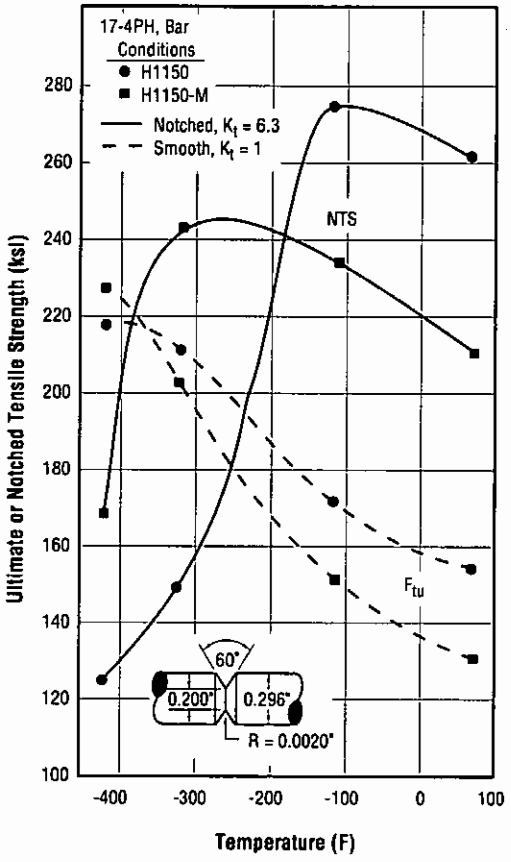


Fig. 3.3.7.1.1 Comparison of low-temperature notch tensile strength with ultimate tensile strength of bar in two overaged conditions (Ref. 12)

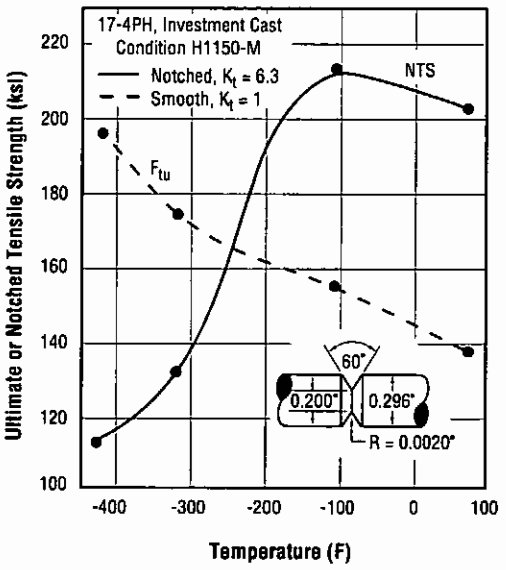


Fig. 3.3.7.1.2 Comparison of low-temperature notch tensile strength with ultimate tensile strength of investment casting in Condition H1150-M (Ref. 13)

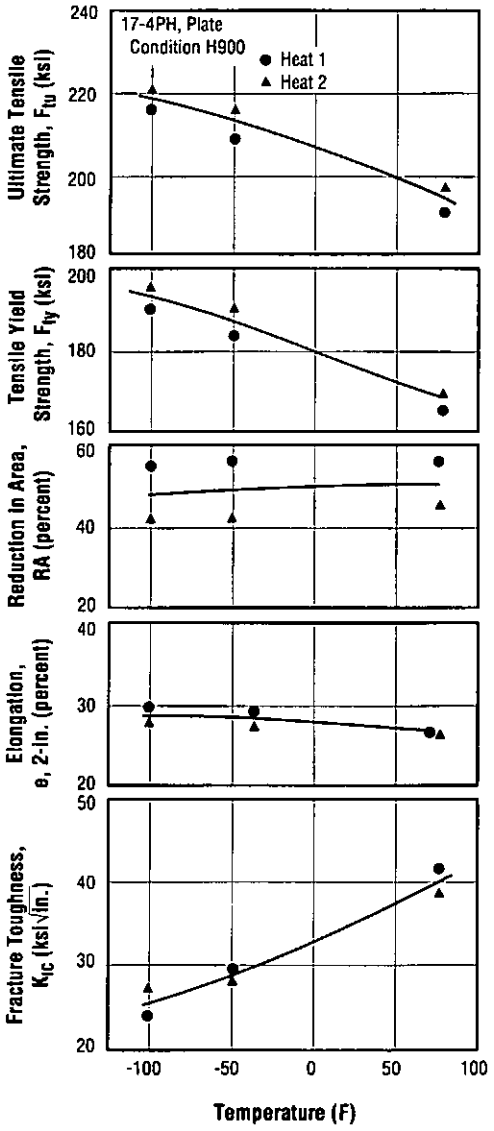


Fig. 3.3.7.2.1 Comparison of low-temperature tensile and fracture-toughness properties of plate in Condition H900 (Ref. 19)

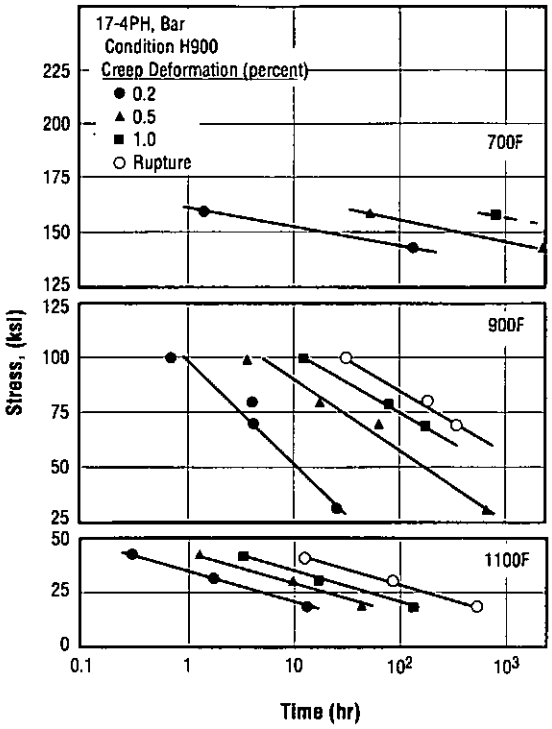


Fig. 3.4.1 Creep and rupture curves for bar at 700F, 900F, and 1100F (Ref. 11)

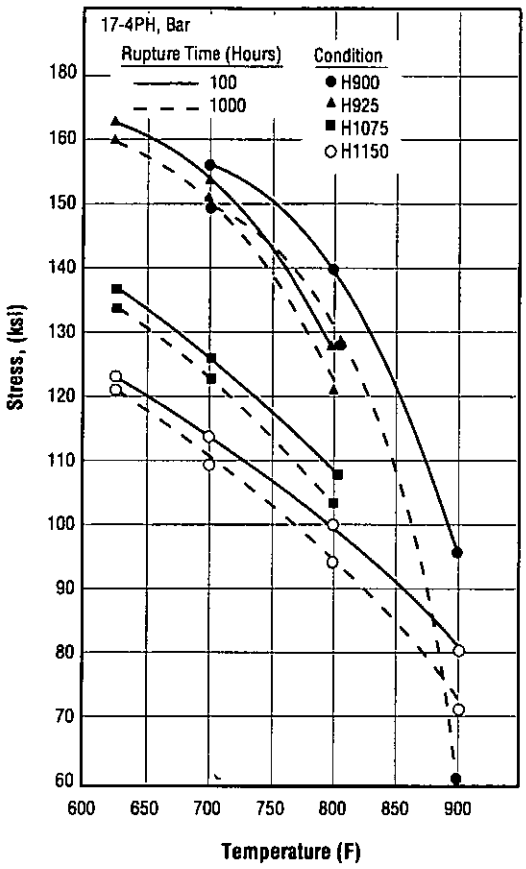


Fig. 3.4.2 Effects of temperature on stress to cause creep rupture in 100 and 1000 hours for bar in various heat-treated conditions (Ref. 21)

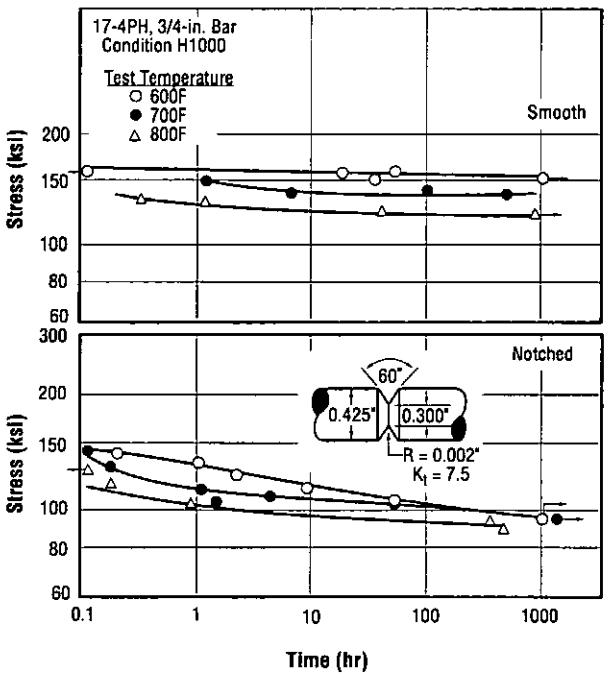


Fig. 3.4.3 Creep-rupture curves at 600 to 800F for smooth and notched bars in Condition H1000 (Ref. 43)

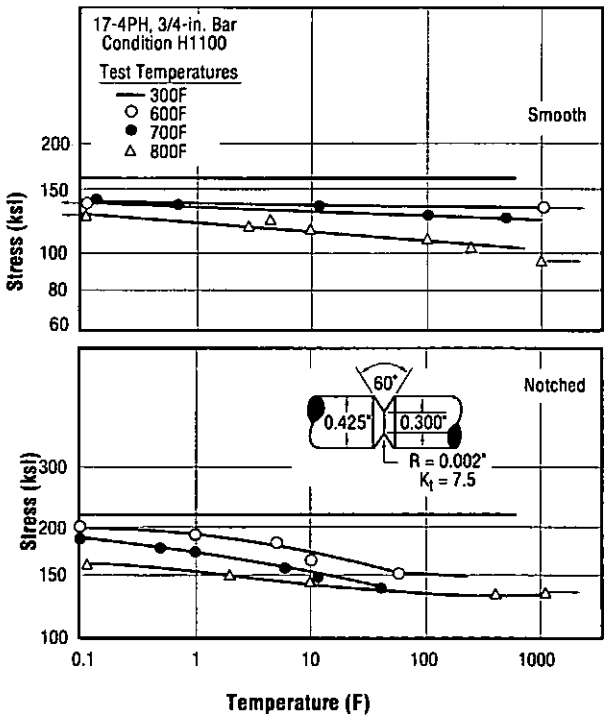


Fig. 3.4.4 Creep-rupture curves at 300 to 800F for smooth and notched bars in Condition H1100 (Ref. 43)

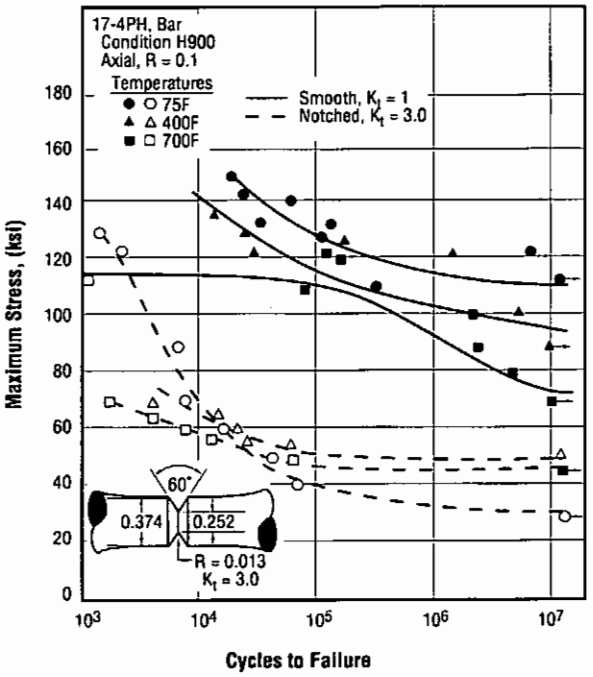


Fig. 3.5.1.1 Fatigue properties of smooth and notched bars at room and elevated temperatures (Ref. 11)

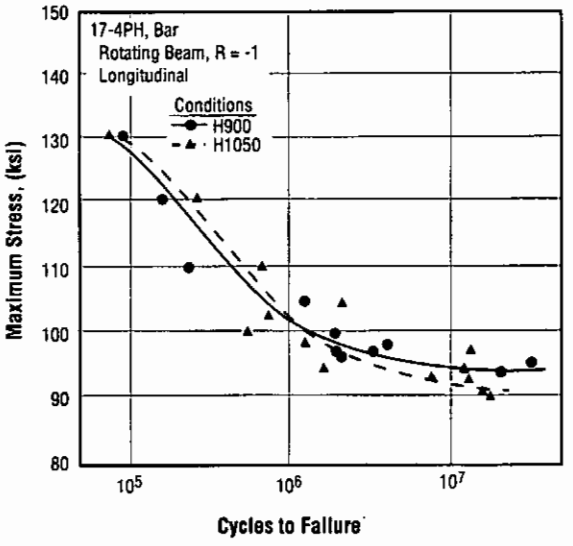


Fig. 3.5.1.2 Fatigue properties of bar in Conditions H900 and H1050 at room temperature (Ref. 14)

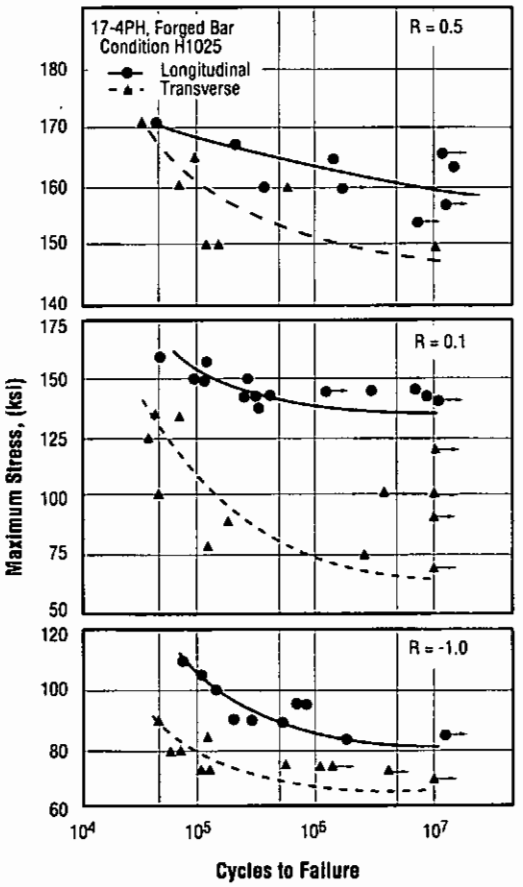


Fig. 3.5.1.3 Effects of stress ratio (R) on fatigue properties of forged bar in longitudinal and transverse orientations at room temperature (Ref. 24)

Table 3.5.1.4 Rotating beam fatigue strength at 10^7 and 10^8 cycles of bar in various heat-treated conditions (Ref. 21)

Alloy	17-4PH		
Form	Bar		
Condition	Temperature (F)	Fatigue Strength[a] (ksi) at	
		10^7 cycles	10^8 cycles
H900	75	90	73
H925		88	74
H1025		83	78
H1150		90	
H900	600	77	62
H1025		75	65

[a] Rotating Beam, R = -1.

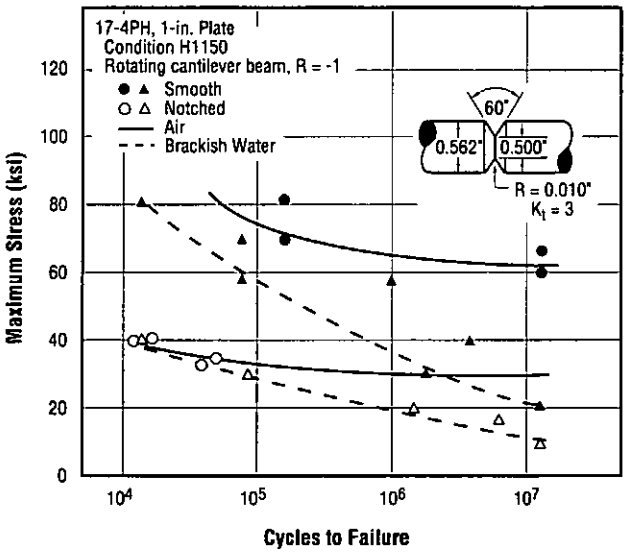


Fig. 3.5.1.5 Fatigue properties of smooth and notched specimens in air and brackish water at room temperature (Ref. 15)

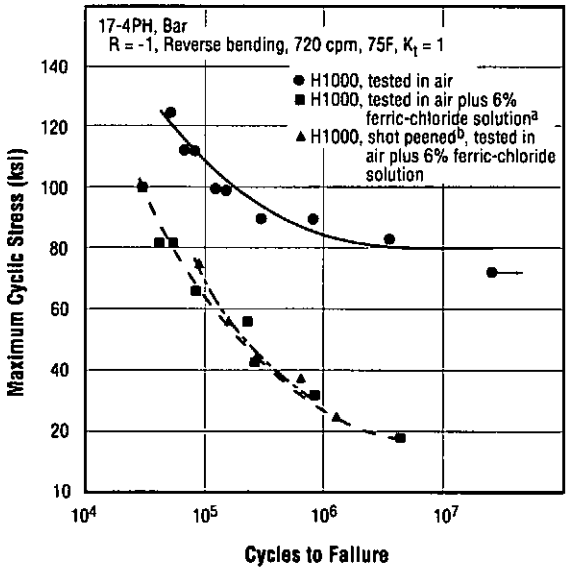


Fig. 3.5.1.6 Effects of chloride environment and shot peening on the fatigue properties of bar (Ref. 24)

Notes:

[a] 6% water solution of ferric chloride dripped onto specimens at a controlled rate during testing.

[b] Peened with steel shot, size S230 to a Almen intensity of 0.004 to 0.008 inch.

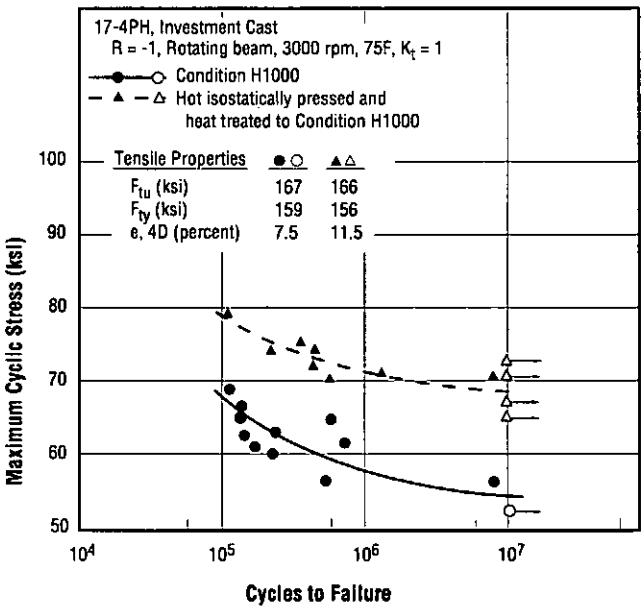


Fig. 3.5.1.7 Effects of hot isostatic pressing (HIP), 4 hr. at 2050F in 15,000 psi argon, on fatigue and tensile properties of investment castings (Ref. 61)

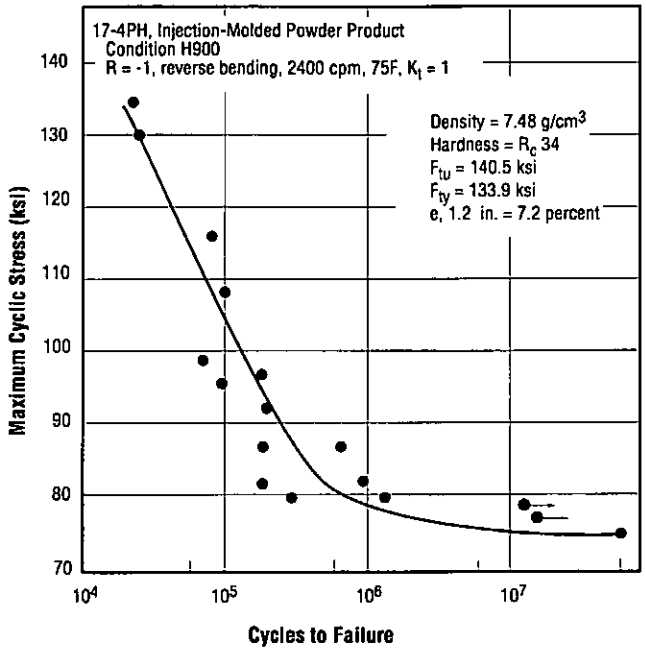


Fig. 3.5.1.8 Bending fatigue and other properties of powder-metal products made by injection-molding process (Ref. 54)

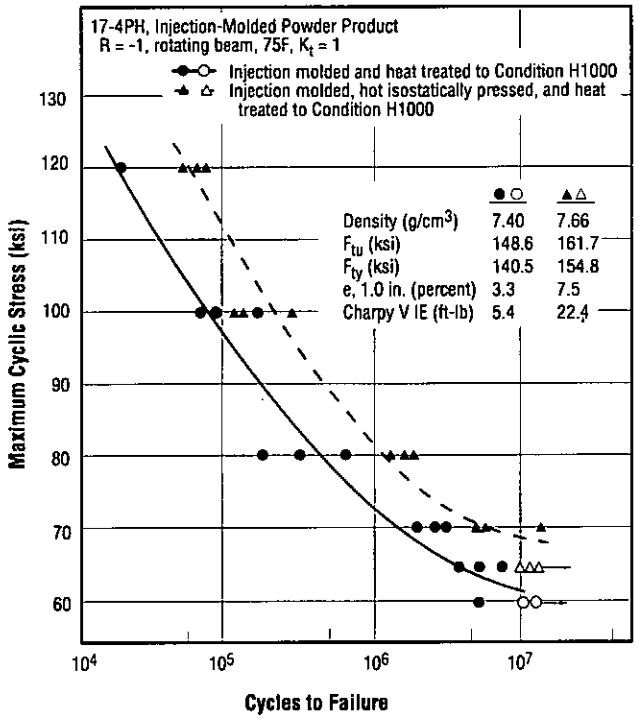


Fig. 3.5.1.9 Effect of hot isostatic pressing (HIP), 2 hours at 2125F in 15,000 psi argon, on fatigue and other properties of powder products made by injection molding (Ref. 60)

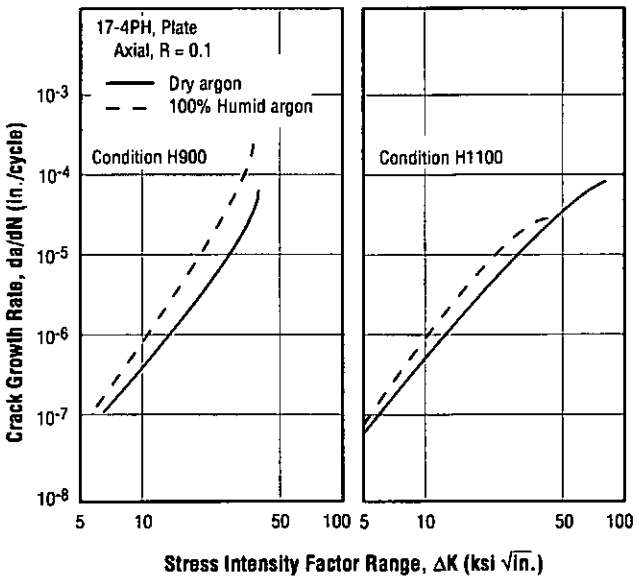


Fig. 3.5.3.1 Fatigue-crack growth rate as a function of stress-intensity-factor range in atmospheres of dry argon and humid argon (Ref. 18)

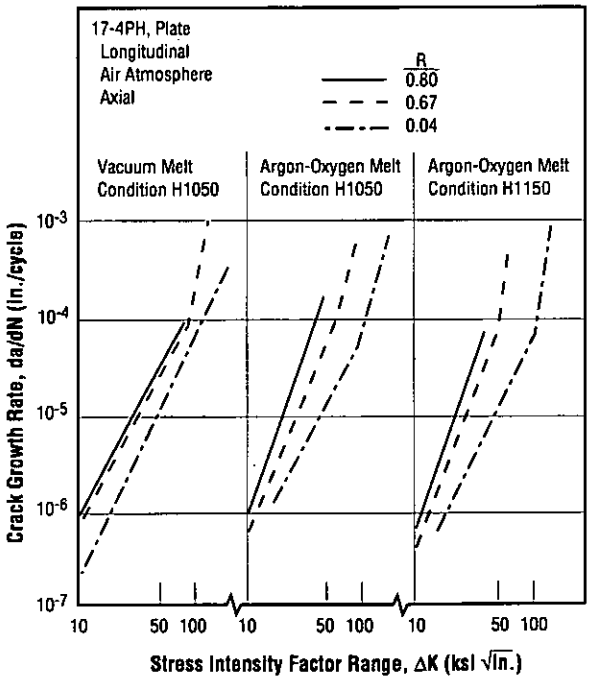


Fig. 3.5.3.2 Fatigue-crack growth rate as a function of stress-intensity-factor range with variations in melting practice, heat-treatment, and stress ratio (R) (Ref. 48)

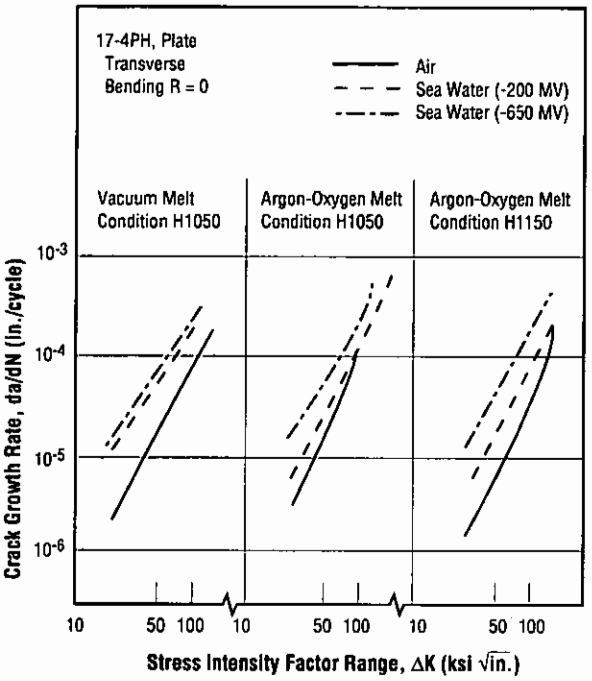


Fig. 3.5.3.3 Fatigue-crack growth rate as a function of stress-intensity-factor range in air and in flowing sea water with different applied negative electrochemical potentials and with variations in melting practice and heat-treatment (Ref. 48)

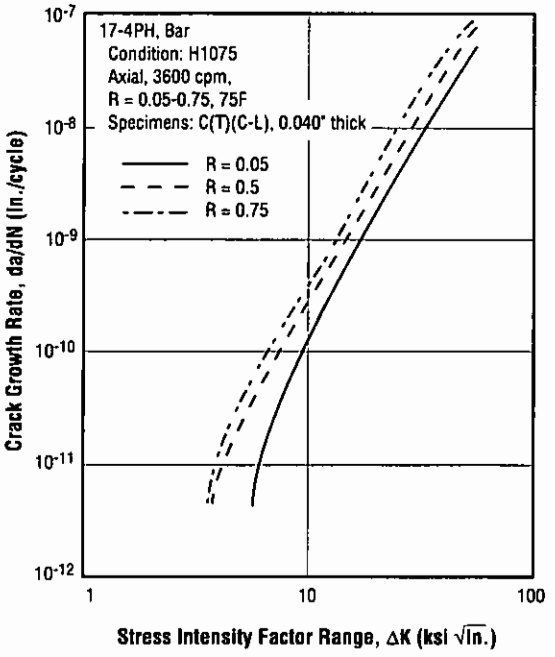


Fig. 3.5.3.4 Effects of stress ratio (R) on fatigue-crack growth rates at low (near threshold) stress-intensity levels (Ref. 62)

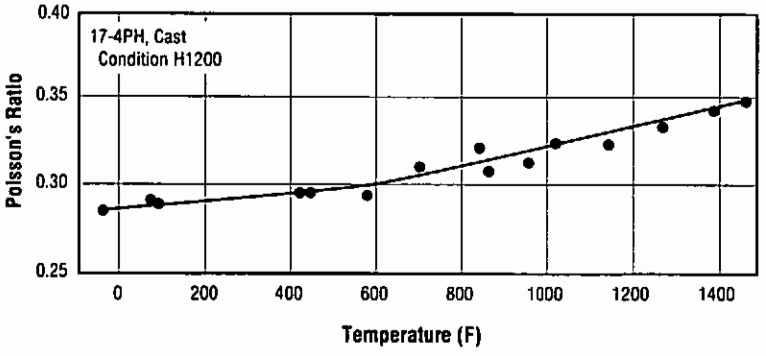


Fig. 3.6.1.1 Poisson's ratio of overaged casting determined by ultrasonic techniques at temperatures from -45 to 1465F (Refs. 67, 68)

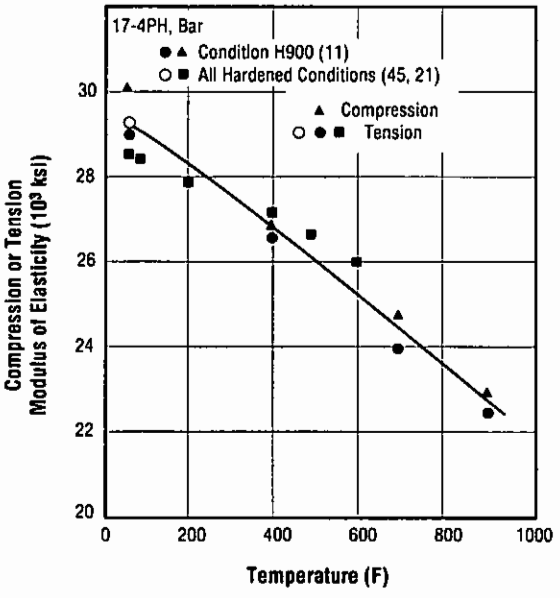


Fig. 3.6.2.1 Effects of elevated temperatures on static modulus of elasticity in both tension and compression (Refs. 11, 21, 45)

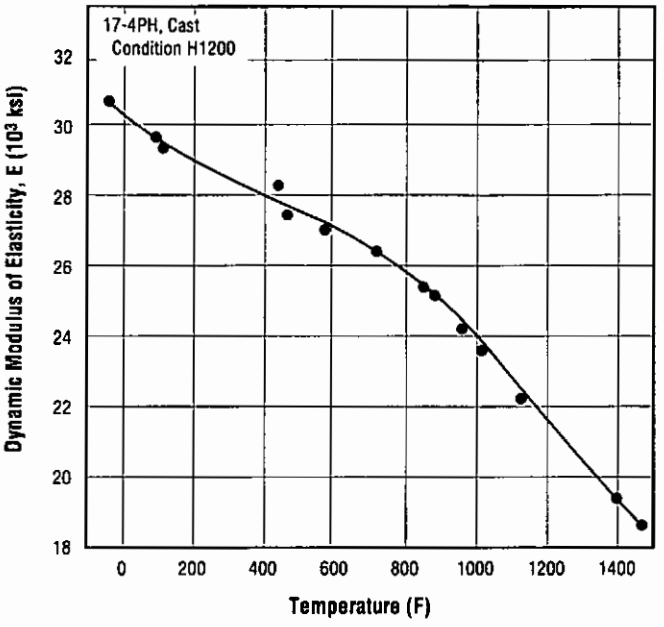


Fig. 3.6.2.2 Dynamic modulus of elasticity of overaged casting at temperatures from -45 to 1465F (Refs. 67, 68)

Table 3.6.3.1 Modulus of rigidity for various heat-treated conditions (Ref. 25)

Alloy	17-4PH
Form	Bar
Condition	G (10^3 ksi)
A	9.68
H900	11.00
H925	10.70
H1025	10.70
H1100	10.80
H1150	10.10
H1150-M	9.50

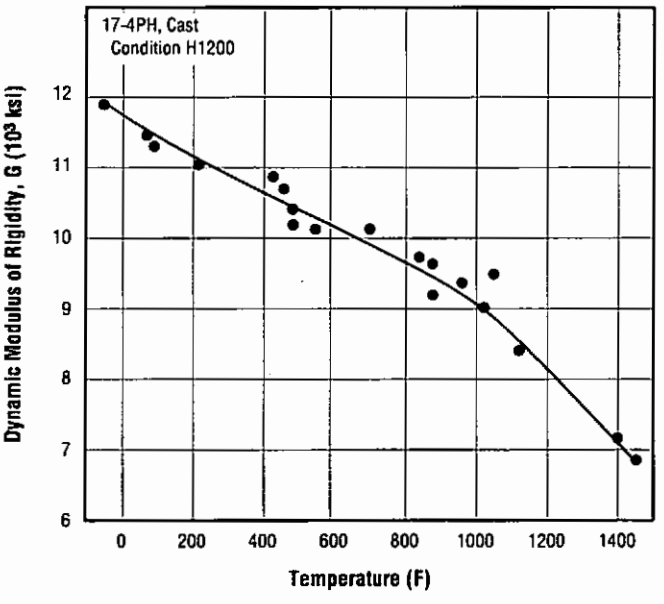


Fig. 3.6.3.2 Dynamic modulus of rigidity of overaged casting at temperatures from -45 to 1465F (Refs. 67, 68)

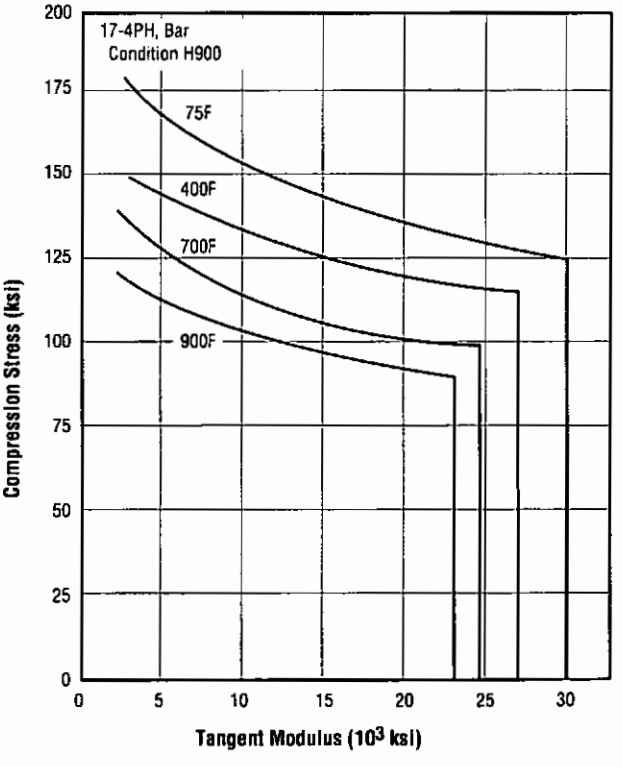


Fig. 3.6.4.1 Tangent modulus curves in compression at room and elevated temperatures (Ref. 11)

Table 4.1.1.1 Minimum radius to make indicated cold bend with no fissuring when viewed under 10X magnification (Refs. 23, 49)

Alloy	17-4PH					
Form	Sheet and Strip, 0.015 to 0.109 in. thick					
Condition	90° Bend		135° Bend		180° Bend	
	L	T	L	T	L	T
A	3T	4T	3T	5T	6T	9T
H900	3T	4T	3T	6T	5T	9T
H925	2T	4T	3T	6T	5T	9T
H1025	2T	4T	3T	6T	4T	7T
H1075	2T	4T	3T	4T	4T	7T
H1150	2T	2T	2T	3T	4T	6T

Table 4.1.2.1 Tensile properties of sheet and strip warm stretch formed during cooling from solution-treatment temperature (1900F) and subsequently aged (Ref. 49)

Alloy		17-4PH			
Form		Sheet and Strip			
Warm Forming Temperature (F)	% Stretch in 2 in.	Aging Temp., 4 hr. (F)	F_{ty} (ksi)	F_{tu} (ksi)	e, 2 in. (percent)
a	a	900	173.8	195.0	11.0
500	9.0		198.0	202.2	9.0
650	33.5	none	133.6	162.4	6.0
	16.0	900	168.7	190.8	9.0
	20.0		171.8	190.5	
	35.0		181.4	194.6	7.5
		1050	155.0	160.0	
800	42.0	none	116.0	155.8	7.0
	22.0	900	166.6	178.4	11.0
	47.5		176.0	190.0	8.0

[a] Standard H900, not stretch formed.

Table 4.2.1 Relative machinability of 17-4PH bar in various heat-treated conditions (Ref. 21)

Alloy	17-4PH		
Form	Bar		
Condition	Hardness, Rockwell C	Cutting Rate, SF/M[a] (Automatics)	Comments
H1150-M	27	100-130	Best cutting rate. Surface not as good as other heat-treated conditions.
H1150	33	80-100	Machinability improves as hardening temperature increases. Higher cutting rates obtained with some sacrifice in surface finish.
H1100	34	75-95	
H1075	36	70-90	
A (Solution Treated)	34	60-80	Machinability, cutting rate, and surface finish comparable to Types 302 and 304.
H1025	38	50-70	Machinability improves as hardening temperature increases.
H925	42	30-50	
H900	44	20-30	High hardness and strength limit machinability. Carbide cutters needed for maximum production.

[a] SF/M = surface feet per minute.

Table 4.3.1.1 Variations in tensile properties with section size and postweld treatment for butt welds made by the manual-shielded-metal-arc technique with 17-4PH electrodes (Ref. 23)

Alloy	17-4PH					
Condition	A (Before Welding)					
Form	Postweld Treatment	F_{ty} (ksi)	F_{tu} (ksi)	e, 2 in. (percent)	RA (percent)	Fracture Location
1-in. thick flat bars[a]	900F age	118	158	8.0	21.0	Weld
	1000F age	108	155	9.5	27.0	
	1100F age	111	158	7.5	18.5	
	H900	163	186	9.5	36.0	
	H1000	146	167		39.0	
	H1100	129	158	11.0	38.0	
3/4-in. thick flat bars[b]	900F age	154	178	10.0	32.0	Base
	1000F age	136	160	11.0	29.0	Weld
	1100F age	112	159	13.5	50.0	Base
	H900	172	187	11.0	48.0	Weld
	H1000	161	170	12.0		
	H1100	134	158		54.0	

[a] Standard 0.505-inch tensile specimens taken transverse to weld axis.

[b] Subsize 0.200-inch tensile specimens taken transverse to weld axis.

Table 4.3.1.2 Comparison of tensile properties of sheet with those of sheet containing a transverse butt weld made by the automatic GTA technique with 17-4PH weld wire (Ref. 8)

Alloy	17-4PH			
Condition	H900			
Form	0.090-in Sheet			
Specimens	Orientation	F_{ty} (ksi)	F_{tu} (ksi)	e, 2 in. (percent)
Base Metal	L	178	199	8.4
	T	181	202	7.6
Welded[a,b]	L	178	201	9.5

[a] Failed in base metal.

[b] Fully solution treated and aged to Condition H900 after welding; no preheat.

4.3.1.3 Tensile properties of sheet containing a transverse butt weld made by the GMA technique with 17-4PH weld wire (Ref. 23)

Alloy	17-4PH		
Condition	A (Before Welding)		
Form	0.188-in. Sheet		
Postweld Treatment	F_{ty} (ksi)	F_{tu} (ksi)	e, 2 in. (percent)
H900	181	203	7.0
H950	174	185	7.5
H1025	163	173	

Tensile-test fractures occured in the welds.

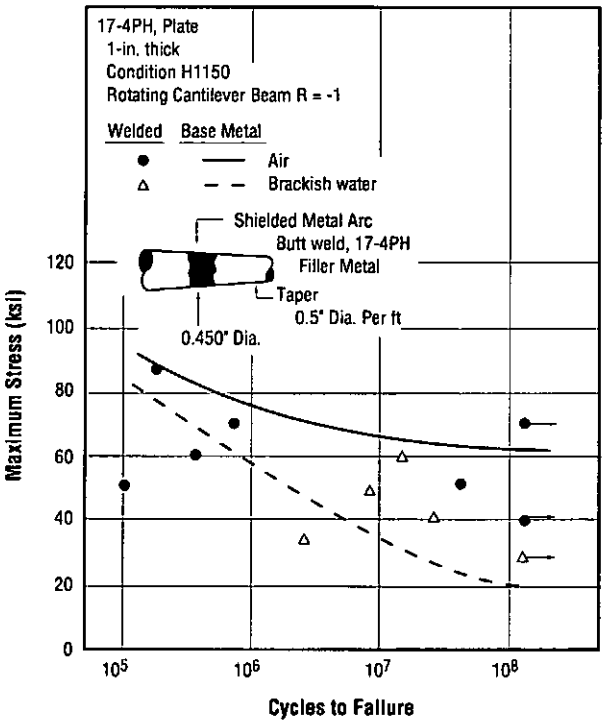


Fig. 4.3.1.4 Comparison of fatigue properties of base metal and shielded-metal-arc weldments fully heat treated after welding (Ref. 15)

4.3.1.5 Tensile properties of flash-butt welds in bars (Ref. 23)

Alloy	17-4PH				
Condition	A (Before Welding)				
Form	Bars[a]				
Postweld Treatment	F_{ty} (ksi)	F_{tu} (ksi)	e, 2 in. (percent)	RA (percent)	Fracture Location
900F age	b	182	14.2	b	Base Metal
H900	184	203	8.0	37.0	Weld

[a] Standard 0.505-in. tensile test bars used.

[b] Not reported.

References

1. Keller, G., "Compilation of NAA Inc. Unpublished Materials Data," North American Aviation Inc., Report No. NA61-588-6 (November 1961).
2. "Carpenter Custom 630 (17Cr - 4Ni) Precipitation Hardening Stainless Steel," Carpenter Technology Corp. (1969).
3. Precipitation Hardenable Stainless Steels, Republic Steel Corp. (1975).
4. 17Cr - 4Ni Alloy, Technical Data, Allegheny - Ludlum Steel Corp.
5. Metals Handbook, Tenth Edition, Vol. 1, ASM (1990).
6. Reinhart, F.M., "Corrosion of Materials in Hydrospace," TR R-544, U.S. Naval Civil Engineering Laboratory (December 1966).
7. Fieldhouse, I.B. and Lang, J.I., "Measurements of Thermal Properties," WADD TR60-904, Armour Research Foundation (January 1961).
8. Hamilton, C.H. and Meredith, R., "Evaluation of 17-4PH Stainless Steel Sheet for Welded Pressure Applications," Report No. SDL 301, North American Aviation, Inc. (28 June 1961).
9. Wolanski, Z.R., "Material Evaluation - 17-4 PH CRES, H900 Condition, Fatigue Characteristics," General Dynamics, FTDM - 3287 (June 1964).
10. Beaver, R.J. and Leitten, C.F. Jr., "A Survey of the Corrosion of Martensitic and Ferritic Stainless Steels in Pressurized Water," ORNL-TM 539, Oak Ridge National Lab (July 16, 1963).
11. Deel, O.L. and Mindlin, H., "Engineering Data on New Aerospace Structural Materials," AFML - TR-72-196, Volume 1, Battelle Columbus Labs (September 1972).
12. Malin, C.O., "Low-Temperature Properties of 17-4PH Alloy," Rocketdyne Div. North American Rockwell Corp., NAR 80010 (August 8, 1968).
13. Malin, C.O., "Low-Temperature Properties of 17-4PH, Condition H1150M," Rocketdyne Div. North American Rockwell Corp., NAR 80005 (July. 10, 1968).
14. "Fatigue Properties of 17-4PH and 15-5PH Steel in the H900 and H1050 Conditions," The Boeing Corp., Vertol Div., Report No. D8 - 1038 (July 1, 1968).
15. Ferrara, R.J., and Vreeland, D.C., "Flexural Fatigue Behavior of Welded and Unwelded 17-4PH Stainless Steel and Titanium Alloy Ti-6Al-2Cb-1Ta-0.8Mo," Naval Ship Research and Development Center, Report 8-570 (November 1970).
16. Judy, R.W., Fujii, C.T., and Goode, R.J., "Properties of 17-4PH Steel," Naval Research Laboratory Report 7639 (December 18, 1973).
17. Warren, K.A., and Reed, R.P., "Tensile and Impact Properties of Selected Materials from 20 to 300°K," National Bureau of Standards Monograph 63 (June 28, 1963).
18. Rack, H.J., and Kalish, D., "The Strength, Fracture Toughness, and Low-Cycle Fatigue Behavior of 17-4PH Stainless Steel," *Metallurgical Transactions*, Vol. 5 (July 1974).
19. Steigerwald, E.A., "Plane Strain Fracture Toughness Data for Handbook Presentation," TRW Inc., AF 33-615-5001 (June 1967).
20. "Armco 17-4PH Precipitation-Hardening Stainless Steel Sheets and Strip," Armco Steel Corp., S-96, LA-6772 (August 1972).
21. "Armco 17-4PH Precipitation-Hardening Stainless Steel Bar and Wire," Armco Steel Corp., S-6c, LA-10273 (January 1974).
22. "Carpenter Custom 630 (17Cr-4Ni)," Carpenter Technology Corp. (1977).
23. "Armco 17-4PH Stainless Steel Bar and Wire," Armco Steel Corp., LA-3575 (April 1975).
24. Data furnished by E.G. Takocs, Armco Steel Corp. (March 15, 1977).
25. Lanning, W.J., "Torsion Properties of 17-4PH and 15-5PH Stainless Steel Bars," Advanced Materials Division, Armco Steel Corp. (March 16, 1972).
26. AMS 5604C, Society of Automotive Engineers, Inc. (October 1, 1988).
27. AMS 5355E, Society of Automotive Engineers, Inc. (November 1994).
28. AMS 5344D, Society of Automotive Engineers, Inc. (November 1994).
29. AMS 5342D, Society of Automotive Engineers, Inc. (November 1994).
30. AMS 5343D, Society of Automotive Engineers, Inc. (November 1994).
31. AMS 5398D, Society of Automotive Engineers, Inc. (October 1, 1989).
32. AMS 5825E, Society of Automotive Engineers, Inc. (October 1, 1992).
33. AMS 5827D, Society of Automotive Engineers, Inc. (October 1, 1992).
34. AMS 5643N, Society of Automotive Engineers, Inc. (January 1, 1992).
35. AMS 5622B, Society of Automotive Engineers, Inc. (January 1, 1990).

36. Hack, H., "A Summary of Corrosion and Corrosion Fatigue of 17-4PH and 15-5PH Stainless Steels," Naval Ship Research and Development Center, Report 4277 (May 1974).

37. McClure, A.H., "Results of 197-Day Exposure to Deep Ocean Environment on Structural Materials and Coatings," The Boeing Co., Report No. D2-125376-1 (March 12, 1967).

38. Humphries, T.S., and Nelson E.E., "Stress-Corrosion Cracking of Several Precipitation-Hardening Stainless Steels," NASA, MSFC, MFS-20667 (1970).

39. Raymond, L., and Kendall, E.G., "Hydrogen Stress Cracking of 17-4PH Stainless," Aerospace Corp., Report TR-0158 (3250-10)-6 (August 1967).

40. Ferrara, R.J., and Vreeland, D.C., "Stress-Corrosion Cracking and Galvanic Couple Tests of 17-4PH Stainless Steel in Sea Water," Naval Ship Research and Development Center, Report 8-881 (October 1971).

41. "Material - Stress Corrosion Resistance, AISI 4340 and 17-4PH Stainless Steel, Evaluation of," General Dynamics Fort Worth Texas, Report FTDM-2979 (August 5, 1963).

42. Dreyer, G.A., and Gallaugher, W.C., "Investigation of the Effects of Stress Corrosion of High-Strength Steel Alloys," AFML TDR ML-TDR-64-3, Boeing Co. (February 1964).

43. Sessler, J.G. and Manzari, N.J., "Summary and General Evaluation of Stress-Rupture Test Data on Various High-Temperature Alloys at 600F to 800F," SWRI Final Report No. 9, Acct. No. 1620.812818 (July 1954).

44. Suss, H., "Type 17-4PH Steel," Knolls Atomic Power Laboratory Manual, Section XVIII (August 1, 1956).

45. Takacs, E.G., "Armco 17-4PH, Type 410 - Young's Modulus and Poisson's Ratio," Advanced Materials Div., Armco Steel Corp. (October 7, 1976).

46. Crooker, T.W., Hasson, D.F., and Yoder, G.R., "A Fracture Mechanics and Fractographic Study of Fatigue-Crack Propagation Resistance in 17-4PH Stainless Steel," Naval Research Laboratory Report 7910 (July 17, 1975).

47. Davis, J.A., and Gehring, G.A., Jr., "The Effect of Velocity on The Sea Water Corrosion Behavior of High Performance Ship Materials," Bell Aerospace Co. (March 1974).

48. Crooker, T.W., Bogar, F.D., and Cares, W.R., "Effects of Flowing Natural Seawater and Electrochemical Potential on Fatigue-Crack Growth in Several High-Strength Marine Alloys," Naval Research Laboratory Report 8042 (August 30, 1976).

49. "Armco 17-4PH Precipitation-Hardening Stainless Steel Sheet and Strip," Armco Advanced Materials Co., Product Data Bulletin No. FS-11 (1993).

50. "Carpenter Custom 630 (17Cr-4Ni)," Carpenter Technology Corp. (1990).

51. "Corrosion Resistant Type CB-7Cu," Bulletin furnished by Steel Founders Society of America.

52. ASTM A 747-86, ASTM Annual Book of Standards (1990).

53. Hayes, K.R., "Hydrogen Embrittlement in 17-4PH Stainless Steel," NWC TP6343, Naval Weapons Center, China Lake, California (August 1982).

54. Bulger, M.K., and Erickson, A.R., "Fatigue Properties of MIM Fe-7%Ni and 17-4PH," Powder Injection Molding Symposium, Metal Powder Industries Federation (June 1992).

55. "Stainless Steel AL 17-4PH Precipitation Hardening Alloy," Technical Data Blue Sheet, Allegheny Ludlum Corp. (1987).

56. Metals Handbook, Ninth Edition, Vol. 1, American Society for Metals (1978).

57. Sanderow, H.I., Ruhkamp, J.D., and Rodrigues, H.A., "Precipitation Hardening P/M Material for Aerospace Applications," International Powder Metal Conference, Metal Powder Industries Federation and American Powder Metal Institute, Vol. 16, pp. 167-180 (June 1984).

58. Metals Handbook, Ninth Edition, Vol. 7, American Society for Metals (1984).

59. Reinshagen, J.H., and Witsberger, J.C., "Properties of Precipitation Hardening Stainless Steel Processed by Conventional Powder Metallurgy Techniques," Conference: Advances in Powder Metallurgy and Particulate Materials, Vol. 7, Metal Powder Industries Federation (May 1994).

60. Marshall, T.P., "Injection Molding of 17-4PH Stainless Steel," SAE Technical Paper Series, Report No. 841516 (October 1984).

61. Crane, L.W., and Potter, A., "Improvement of the Fatigue Properties of Investment-Cast Steels as a Result of HIPing," *Cast Metals*, Vol. 5, No. 2, pp. 92-94 (1992).

62. Blom, A.F., "Near-Threshold Fatigue Crack Growth and Crack Closure in 17-4PH Steel and 2024-T3 Aluminum Alloy," Conference: Fatigue Crack Growth Threshold Concepts, The Metallurgical Society/AIME (October 1983).

63. Viswanathan, R., Wittig, J.E., and Syrett, B.C., "Corrosive Fatigue of 17-4PH Turbine Blade Steel in Chloride Environments," Conference: Corrosion Fatigue of Steam Turbine Blade Materials, Palo Alto, CA (September 21-24, 1981).

64. Capeletti, T.L., "Effect of Hydrogen on the Fracture Toughness of 17-4PH Stainless Steel," Conference: Mechanical Behavior of Materials, Federation of Materials Societies (August 1976).

65. "Welding the PH Grades," Armco Steel Corp. (1978).

66. Weymueller, C.R., "The PH Stainless - Simple to Weld But Touchy," *Welding Design and Fabrication*, Vol. 53:5, pp. 68-71 (May 1980).

67. Gieske, J.H., "Ultrasonic Measurement of Elastic Moduli of 17-4PH Stainless Steel and Uranium - 2 Molybdenum from -40 to 800C," Sandia National Labs, Report No. SAND80-1121, TTC-0125 (October 1980).

68. Rack, H.J., "Physical and Mechanical Properties of Cast 17-4PH Stainless Steel," Sandia National Labs, Report No. SAND80-2302, TTC-0161 (February 1981).

69. Syrett, B.C., Viswanathan, R., Wing, S.S., and Wittig, J.E., "Effect of Microstructure on Pitting and Corrosion Fatigue of 17-4 PH Turbine Blade Steel in Chloride Environments," International Corrosion Forum, NACE (March 1982).

70. Woulds, M., and Lloyd, A., "Correctly Heat Treating 17-4PH Investment Castings," *Precision Metals*, pp. 62-65, (April 1982).

71. Pichard, C., and Nectoux, G., "Recent Results Concerning Properties of High-Performance Cast Martensitic Stainless Steels: The 17Cr-4Ni Low-Carbon Steels," ASTM STP 756, pp. 201-221 (1982).

72. Hicho, A.E., and Smith, J.H., "Metallurgical Evaluation of 17-4PH Stainless Steel Castings," National Institute of Standards and Technology, Report No. NISTIR 89-4075 (May 1989).

73. Raja, K.S., and Rao, K.P., "On the Hardness Criterion for Stress Corrosion Cracking Resistance of 17-4PH Stainless Steel," *Journal of Materials Science Letters*, Vol. 12, pp. 963-966 (1993).

74. Murray, G.T., Bouffard, J.P., and Briggs, D., "Retardation of Hydrogen Embrittlement of 17-4PH Stainless Steels by Nonmetallic Surface Layers," *Metallurgical Transactions*, Vol. 18A, pp. 162-164 (January 1987).

75. Turner, A.J., "Electron Beam Welding Thick Section Precipitation Hardening Stainless Steel," *Welding Journal*, Vol. 60, pp. 18-26 (January 1981).

This page is blank.

1 General

17-7PH is a semiaustenitic grade of precipitation-hardening stainless steel, which can be readily formed and welded in the annealed condition and subsequently heat treated with minimum distortion to tensile strength levels exceeding 200 ksi. It retains good strength at temperatures up to 900F, but its notched impact resistance is reduced at subzero temperatures. Its corrosion resistance is superior to that of the hardenable martensitic "400-series" stainless steels and in some environments approaches that of the austenitic "300-series" grades. Because of its good combination of strength and corrosion resistance, the alloy has a wide variety of uses ranging from aircraft structural parts to surgical instruments. With excellent spring properties at temperatures up to 600F, hard-drawn 17-7PH is used in many types of springs made of both flat and round wire for aircraft instruments and controls, processing equipment, and automotive and appliance components (Refs. 14, 15, 17, 19).

1.1 Commercial Designation

17-7PH.

1.2 Alternate Designations

AISI Type 631, UNS S17700.

1.3 Specifications

1.3.1 *[Table]* Specifications.

1.4 Composition

1.4.1 *[Table]* Composition.

1.5 Heat Treatment

1.5.1 General. Type 17-7PH is most often supplied by the producing mills in the solution-treated condition (Condition A), in which it is relatively soft, ductile, and readily fabricated. Following fabrication, it is normally strengthened by one of two alternative precipitation-hardening treatments resulting in Condition RH950 or TH1050 (Refs. 7, 8, 9, 14, 15, 20, 45, 46, 47).

1.5.1.1 Condition A, solution-treated (also annealed): 1900-1950F, cool to room temperature. Specifications recommend 1900F and water quench for bars, shapes, and forgings (Refs. 8, 9). For sheet, plate, strip, and tubing, they generally recommend 1950F and air cool or faster, which presumably implies liquid quench for heavy sections and air cool for thin sections (Refs. 7, 45, 46, 47).

1.5.1.2 Condition RH950, precipitation-hardened: 1750F 10 minutes, air cool to room temperature (results in Condition A1750), cool within 24 hours to -100F, hold 8 hours, warm in air to room temperature (results in Condition R100), age 1 hour at 950F, air cool (results in Condition RH950).

1.5.1.3 Condition TH1050, precipitation-hardened: 1400F 90 minutes, cool to 50-60F within one hour, hold 30 minutes (results in Condition T), age 90 minutes at 1050F, air cool (results in Condition TH1050).

Fe
17 Cr
7 Ni
1 Al

1.5.1.4 For improved ductility and notch toughness but lower strength in wrought products and weldments (see also Section 4.3.1 and Table 4.3.1.2), overaging, that is, higher final aging temperatures, may be employed, for example 1100F, resulting in Condition RH1100 or TH1100.

1.5.1.4.1 *[Figure]* Effect of RH aging temperature (1 hr) on tensile properties of sheet after prior treatment to Condition R100.

1.5.1.4.2 *[Figure]* Effect of RH aging treatment (1 hr) on tensile strength and sharp-notch strength of sheet after prior treatment to Condition R100.

1.5.2 In-process anneals, equivalent to Condition A solution treatment, may be required to restore the ductility of cold-worked material so that it can take additional drawing or forming. In order to develop full strength, severely cold-worked material requires an anneal prior to heat treatment to Condition TH1050; no anneal or cold-worked material is necessary prior to RH-type treatments (Ref. 19).

1.5.2.1 *[Figure]* Effect of cold work introduced in Condition A on tensile properties of sheet subsequently heat treated to Condition TH1050 without an intermediate anneal.

1.5.2.2 *[Figure]* Effect of cold work introduced in Condition A1750 on tensile properties of the alloy after subsequent completion of the RH950 heat treatment.

1.5.3 Strip and wire can be provided by the mills after 60 percent cold reduction, resulting in Condition C. Condition C is usually aged (precipitation hardened) at 900F, 1 hour, and air cooled, resulting in Condition CH900. Springs, for example, are normally fabricated in Condition C, and then aged to Condition CH900 to provide an optimum combination of high strength and elasticity, corrosion resistance, and dimensional stability (Refs. 7, 14, 15, 17).

If somewhat lower strength is acceptable, springs can be treated at 1000 to 1050F to eliminate residual forming stresses while still maintaining good spring properties for room-temperature applications. This treatment results in a constant spring rate (Ref. 17).

1.5.4 When the alloy is heat treated from Condition A to Condition RH950 or TH1050, dimensional changes

© 1992 by Purdue Research Foundation, West Lafayette, Indiana 47907.
All Rights Reserved.

occur consisting of an expansion of 0.0045 in. per in. during the low-temperature exposure and a contraction of 0.0005 in. per in. during the elevated-temperature aging treatment, resulting in a net expansion of 0.0040 in. per in. When the cold-worked material (Condition C) is aged at 900F to produce Condition CH900, only the 0.0005 in. per in. contraction occurs (Refs. 15, 17, 19).

1.5.5 Air is often a satisfactory furnace atmosphere for heat treating and annealing operations. Controlled reducing atmospheres such as dissociated ammonia or bright-annealing gas introduce the hazards of nitriding and carburizing, which can be detrimental to mechanical properties. For treatments at 1750F and above, essentially scale-free surfaces can be obtained with atmospheres of dry hydrogen, argon, or helium (dew point -75F), but these atmospheres tend to be less effective at lower temperatures because of the extremely low dew point required. For complete freedom from scale or heat discoloration, a vacuum furnace is required. Solution treating (1900F) or austenite conditioning (1750 or 1400F) in molten salts is not recommended because of the danger of carburization or intergranular penetration. Hardening in the 900-1200F range can be done successfully in certain hydride or nitrate salts. The -100F temperature requirement during the RH heat treatment can be achieved with suitable commercial refrigeration equipment or with a saturated bath of dry ice in alcohol or acetone (Refs. 17, 19).

1.5.6 The alloy should be thoroughly cleaned prior to heat treatment to facilitate scale removal and to prevent carburization from organic contamination such as oils and lubricants. Cleaning can be accomplished, first by means of solvents or vapor degreasing, followed by mechanical scrubbing with mild abrasive cleaners to remove insoluble contaminants, and, finally, thorough water rinsing (Ref. 19).

1.6 Hardness

1.6.1 *[Table]* Hardness in various heat-treated conditions at room temperature.

1.6.2 *[Figure]* Effects of exposures up to 1000 hours at 600, 800, and 1000F on the room-temperature hardness of sheet in Condition RH950.

1.7 Forms and Conditions Available

1.7.1 In Condition A, the alloy is available in the form of sheet, strip, plate, bar, rod, wire, tubing, billets, shapes, and forgings (Refs. 7, 8, 9, 14, 15, 16).

1.7.2 In Condition C, sheet and strip (0.050 in. and thinner) and wire are also available (Refs. 15, 19).

1.8 Melting and Casting Practice

1.8.1 The alloy is normally produced in conventional electric-arc furnaces. For optimum quality, vacuum consumable-electrode or electroslag remelt can be employed.

1.9 Special Considerations

1.9.1 In heavy sections, the alloy tends to have inferior mechanical properties, particularly ductility and notch strength, in the transverse orientations (see Figures 3.3.7.1.4 and 3.3.7.1.5). For this reason, most applications involve relatively thin sections. In many instances, however, forgings can be successfully applied where the configurations permit directional flow to be developed in the direction of load application (Ref. 41).

1.9.1.1 *[Table]* Effect of section size and orientation on tensile strength and ductility.

1.9.2 Long-time exposures to temperatures in the range 600 to 900F tend to have a strengthening but embrittling effect on the room-temperature properties of 17-7PH as well as on other semiaustenitic and martensitic precipitation-hardening stainless steels (see Figure 3.2.1.4 and Table 3.2.1.5). The embrittlement is reversible by reapplying the precipitation-hardening (final aging) temperature if it is 1025F or higher (Ref. 4). Elevated-temperature strength in the same temperature range is also increased by long exposures at temperature prior to testing (see Figures 3.3.1.13, 3.3.1.14, 3.3.2.6, 3.3.5.3, 3.3.6.1, and 3.3.6.2).

1.9.3 In Conditions RH950 and TH1050, the notched-impact resistance of 17-7PH is generally low at subzero temperatures. The impact values can be improved, while strength properties are decreased, by overaging; that is, by final aging temperatures of 1100F and above (see Figures 3.3.3.1, 3.3.3.2).

1.9.4 Radial cracks running parallel to the wire axis have been observed to form occasionally in spring wire during the cold-drawing process or after a certain incubation period. This phenomenon appears to be an effect of the formation of strain-induced martensite in combination with a high content of aluminum-oxide inclusions. Since martensite formation is essential to the development of the desired spring properties, the cracking tendency should be minimized by the use of clean steel (low content of nonmetallic inclusions). The cracking tendency also appears to decrease with smoother surfaces on the rods from which the wire is drawn (Ref. 44).

2 Physical Properties and Environmental Effects

2.1 Thermal Properties

2.1.1 Melting Range, 2560 to 2620F (Ref. 23).

2.1.2 Phase Changes.

2.1.2.1 Time-temperature-transformation diagrams.

2.1.2.2 The microstructure of the alloy is mostly austenite, normally with 10 to 15 percent ferrite, in the solution-treated condition (Condition A). Heating to temperatures of 1400 or 1750F

destabilizes the austenite by rejecting carbon, greater destabilization occurring at the lower temperature. As a result, austenite conditioned at 1400F and 1750F, respectively, transforms to martensite when cooled to about 55F and -100F. Subsequent heating to temperatures in the range 900 to 1150F causes the precipitation of nickel-aluminum compounds from the martensite (Refs. 10, 14, 15, 21).

2.1.2.3 Cold working of the solution-treated alloy (Condition A) also causes transformation of the austenite to martensite (resulting in Condition C) and subsequent heating at 900F effects precipitation of nickel-aluminum compounds (resulting in Condition CH900) (Refs. 17, 19).

2.1.3 Thermal Conductivity.

2.1.3.1 *[Figure]* Effects of temperatures from 300 to 900F on thermal conductivity.

2.1.4 Thermal Expansion.

2.1.4.1 *[Figure]* Effects of temperatures from 200 to 800F on thermal expansion.

2.1.5 Specific Heat.

2.1.5.1 *[Figure]* Effects of temperatures up to 2000F on specific heat.

2.1.6 Thermal Diffusivity.

2.2 Other Physical Properties

2.2.1 Density.

2.2.1.1 *[Table]* Density in various heat-treated conditions at room temperature.

2.2.2 Electrical Properties.

2.2.2.1 *[Table]* Electrical properties in various heat-treated conditions at room temperature.

2.2.3 Magnetic Properties.

2.2.3.1 *[Table]* Magnetic permeability in various heat-treated conditions at room temperature.

2.2.4 Emittance.

2.2.4.1 *[Table]* Total normal emittance at temperatures from 400 to 900F.

2.2.5 Damping Capacity.

2.3 Chemical Environments

2.3.1 General Corrosion. The corrosion resistance of 17-7PH in Conditions TH1050 and RH950 in many chemical and atmospheric environments is generally superior to that of the standard hardenable chromium types of stainless steels such as Types 410, 420, and 431, but, overall, not quite as good as chrome-nickel austenitic grades such as Type 304 (Ref. 19).

2.3.1.1 *[Table]* Comparison of typical corrosion rates for 17-7PH and Type 304 stainless steels in seven common chemical reagents.

2.3.2 Stress Corrosion. When immersed in seawater, 17-7PH is susceptible to pitting, tunneling, and crevis types of corrosive attack, and also to stress-corrosion cracking in areas where appreciable applied or residual stresses exist (Ref. 1).

2.3.3 The alloy is resistant to corrosion in liquid oxygen, ammonia, and both liquid and gaseous hydrogen at low temperatures. At high pressures, however, hydrogen tends to cause embrittlement (Refs. 19, 28, 54).

2.3.3.1 *[Table]* Effects of high-pressure hydrogen atmosphere on tensile properties at room temperature.

2.3.4 The alloy is susceptible to stress-corrosion cracking in environments containing hydrogen sulfide (Refs. 17, 19).

2.3.5 Like other high-strength martensitic steels, hardened 17-7PH is susceptible to stress-corrosion cracking when subjected to tensile stresses in moist environments. This tendency is related to the level of tensile stress, the corrosiveness of the environment, and the heat-treated condition of the steel. Tests on 17-7PH sheet in marine environments have indicated that Condition CH900 provides the greatest resistance to stress-corrosion cracking; Condition TH1050, although somewhat less resistant than Condition CH900, appears to be more resistant than Condition RH950 (Ref. 19).

2.3.5.1 *[Table]* Threshold stress intensity factor (K_{Iscc}) for stress-corrosion cracking of bar in aerated 3.5 percent aqueous sodium-chloride solution.

2.4 Nuclear Environments

3 Mechanical Properties

3.1 Specified Mechanical Properties

3.1.1 *[Table]* AMS specified mechanical properties for plate, sheet, and strip.

3.1.2 *[Table]* ASTM specified properties for plate, sheet, and strip.

3.1.3 *[Table]* AMS specified mechanical properties for tubing.

3.1.4 *[Table]* AMS specified tensile strength for spring wire.

3.1.5 *[Table]* ASTM specified tensile strength for spring wire.

3.1.6 *[Table]* ASTM specified mechanical properties for longitudinal orientation in bars, shapes, and forgings.

3.2 Mechanical Properties at Room Temperature

3.2.1 Tension Stress-strain Diagrams and Tensile Properties.

3.2.1.1 *[Figure]* Tensile stress-strain curves for spring wire at room temperature.

3.2.1.2 *[Figure]* Tensile stress-strain curves for sheet in longitudinal and transverse orientations for Conditions TH1050 and RH950.

3.2.1.3 *[Table]* Tensile properties in various heat-treated conditions at room temperature.

3.2.1.4 *[Figure]* Effects of 500-hour exposures at elevated temperatures up to 900F on tensile properties at room temperature of sheet in Conditions TH1050 and CH900.

3.2.1.5 *[Table]* Effects of 1000-hour exposures to elevated temperatures with load on tensile properties at room temperature of sheet in Conditions TH1050 and RH950.

3.2.2 Compression Stress-strain Diagrams and Compression Properties.

3.2.2.1 *[Figure]* Compression stress-strain curves for sheet in longitudinal and transverse orientations for Conditions TH1050 and RH950 at room temperature.

3.2.2.2 *[Table]* Typical compressive yield strengths at room temperature for various heat-treat conditions.

3.2.3 Impact, see Figures 3.3.3.1 and 3.3.3.2.

3.2.4 Bending.

3.2.5 Torsion and Shear, see Figures 3.3.5.1, 3.3.5.2, 3.3.5.3.

3.2.6 Bearing, see Figures 3.3.6.1 and 3.3.6.2.

3.2.6.1 *[Table]* Bearing properties of sheet at room temperature in Conditions TH1050 and RH950.

3.2.7 Stress Concentration.

3.2.7.1 Notch properties, see Figures 3.3.7.1.1 through 3.3.7.1.5.

3.2.7.1.1 *[Table]* Crack strength of plate at room temperature in Condition RH1050.

3.2.7.2 Fracture toughness, see Table 2.3.5.1.

3.2.8 Combined Properties.

3.3 Mechanical Properties at Various Temperatures

3.3.1 Tension Stress-strain Diagrams and Tensile Properties.

3.3.1.1 *[Figure]* Tensile stress-strain curves at temperatures from -423F to 1000F for sheet in Condition TH1050.

3.3.1.2 *[Figure]* Tensile stress-strain curves at temperatures from 75F to 1000F for sheet in Condition RH950.

3.3.1.3 *[Figure]* Tensile stress-strain curves for sheet in Condition CH900 at temperatures up to 1200F under conditions of rapid heating, rapid loading, and short time at temperature.

3.3.1.4 *[Figure]* Tensile stress-strain curves at temperatures up to 2000F for sheet in Condition TH1050 loaded at a strain rate of 0.0002 in. per in. per second.

3.3.1.5 *[Figure]* Tensile stress-strain curves at temperatures up to 2000F for sheet in Condition TH1050 loaded at a strain rate of 0.002 in. per in. per second.

3.3.1.6 *[Figure]* Tensile stress-strain curves at temperatures up to 2000F for sheet in Condition TH1050 loaded at a strain rate of 0.02 in. per in. per second.

3.3.1.7 *[Figure]* Tensile stress-strain curves for sheet in Condition TH1050 when simultaneously loaded at a strain rate of 0.0002 in. per in. per second and heated at rates of 2.5 to 19.5F per second.

3.3.1.8 *[Figure]* Tensile stress-strain curves for sheet in Condition TH1050 when simultaneously loaded at a strain rate of 0.002 in. per in. per second and heated at rates of 20 to 220F per second.

3.3.1.9 *[Figure]* Tensile stress-strain curves for sheet in Condition TH1050 when simultaneously loaded at a strain rate of 0.02 in. per in. per second and heated at rates of 400 to 2000F per second.

3.3.1.10 *[Figure]* Effects of temperature up to 1000F on tensile properties of sheet in Conditions TH1050 and RH950.

3.3.1.11 *[Figure]* Effects of low temperatures down to -423F on tensile properties of sheet in Condition TH1050.

3.3.1.12 *[Figure]* Tensile properties of sheet in Condition TH1050 for various rates of loading at temperatures up to 1200F after rapid heating and holding times of 10 seconds and 1/2 hour at temperature.

3.3.1.13 *[Figure]* Tensile properties of sheet in Condition RH950 at temperatures up to 1000F after holding times of 1/2 and 1000 hours at test temperature.

3.3.1.14 *[Figure]* Effects of test temperatures up to 1000F and of exposure time at temperature on tensile properties of sheet in Condition CH900.

3.3.2 Compression Stress-strain Diagrams and Compression Properties.

3.3.2.1 *[Figure]* Compressive stress-strain curves for sheet in Condition TH1050 at temperatures up to 1200F.

3.3.2.2 *[Figure]* Compressive stress-strain curves for sheet in Condition RH950 at temperatures up to 1000F.

3.3.2.3 *[Figure]* Compressive stress-strain curves for sheet in Condition TH1050 at 800 and 900F after two different exposure times at temperature.

3.3.2.4 *[Figure]* Effects of temperatures up to 1200F on the compressive yield strength of sheet in both

the TH1050 and annealed (solution-treated) conditions.

3.3.2.5 *[Figure]* Effects of elevated temperatures and of exposure time at temperature on the compressive yield strength of sheet in Conditions TH1050 and RH950.

3.3.2.6 *[Figure]* Compressive yield strength of sheet in Condition RH950 at temperatures up to 1000F after holding times of 1/2, 100, and 1000 hours at temperature.

3.3.3 Impact.

3.3.3.1 *[Figure]* Effects of low temperatures on impact resistance in Conditions TH1050 and TH1150.

3.3.3.2 *[Figure]* Impact resistance over a wide range of temperature of bar in various conditions.

3.3.4 Bending.

3.3.5 Torsion and Shear.

3.3.5.1 *[Figure]* Ultimate shear strength of sheet in Conditions TH1050 and RH950 at temperatures up to 1000F.

3.3.5.2 *[Figure]* Ultimate shear strength of plate in Condition RH950 at temperatures up to 1000F after holding times of 1/2, 100, and 1000 hours at test temperature.

3.3.5.3 *[Figure]* Ultimate shear strength of sheet in Condition TH1050 at temperatures up to 900F after holding times of 1/2, 100, and 1000 hours at test temperature.

3.3.6 Bearing.

3.3.6.1 *[Figure]* Bearing properties (e/D = 1.5) of sheet in Condition RH950 at temperatures up to 1000F after holding times of 1/2 and 1000 hours at test temperature.

3.3.6.2 *[Figure]* Bearing properties (e/D = 2.0) of sheet in Condition RH950 at temperatures up to 1000F after holding times of 1/2 and 1000 hours at test temperature.

3.3.7 Stress Concentration.

3.3.7.1 Notch properties.

3.3.7.1.1 *[Figure]* Notch strength and tensile strength of sheet in Condition TH1050 at temperatures down to -423F.

3.3.7.1.2 *[Figure]* Comparison of tensile and notch tensile properties at temperatures up to 800F for sheet in Condition RH950.

3.3.7.1.3 *[Figure]* Comparison of tensile and notch tensile properties at temperatures up to 800F for sheet in Condition TH1050.

3.3.7.1.4 *[Figure]* Comparison of tensile and notch tensile properties at temperatures up to 800F for forging in Condition RH950.

3.3.7.1.5 *[Figure]* Comparison of tensile and notch tensile properties at temperatures up to 800F for forging in Condition TH1050.

3.3.7.2 Fracture toughness.

3.3.7.2.1 *[Figure]* Fracture toughness, tensile strength, and yield strength of plate in Condition TH1050 at various temperatures.

3.3.8 Combined Properties.

3.4 Creep and Creep Rupture Properties

3.4.1 *[Figure]* Creep properties of sheet in Condition TH1050 at temperatures from 600 to 900F.

3.4.2 *[Figure]* Effect of temperature on tensile stress required to cause creep rupture in 100 and 1000 hours for sheet in various heat-treated conditions.

3.4.3 *[Figure]* Effect of temperature on tensile stress required to cause 0.1 and 0.2 percent creep deformation in 1000 hours for sheet in two heat-treated conditions.

3.4.4 *[Figure]* Isochronous stress-strain curves at 600 to 900F for sheet in Condition RH950.

3.4.5 *[Figure]* Isochronous stress-strain curves at 600 to 900F for sheet in Condition TH1050.

3.4.6 *[Figure]* Short-time creep and rupture properties of sheet in Condition TH1050 at temperatures from 800 to 1200F.

3.4.7 *[Figure]* Short-time creep and rupture properties of sheet in Condition CH900 at temperatures from 800 to 1200F.

3.4.8 *[Figure]* Short-time total strain curves at 600 to 900F for sheet in Condition TH1050.

3.4.9 *[Figure]* Creep-rupture curves at 600 to 900F for smooth and notched sheet in Condition TH1050.

3.4.10 *[Figure]* Loss of load due to stress relaxation of helical compression springs held at constant length and at temperatures from 450 to 750F for 96 hours.

3.4.11 *[Table]* Effects of wire diameter, preset stress, and initial stress on stress relaxation of helical extension springs held at constant extension at room temperature for 100 hours.

3.5 Fatigue Properties

3.5.1 *[Figure]* Flexural fatigue properties at room and low temperatures for sheet in Condition TH1050.

3.5.2 *[Figure]* Flexural fatigue properties at room and low temperatures for notched sheet (K_t=3.0) in Condition RH950.

3.5.3 *[Figure]* Flexural strain-cycling fatigue curves at room and low temperatures for sheet in Condition RH950.

3.5.4 *[Figure]* Constant-life fatigue curves at room temperature for smooth and notched sheet in Condition RH950.

3.5.5 *[Figure]* Constant-life fatigue curves at 600F for smooth and notched sheet in Condition RH950.

3.5.6 *[Figure]* Constant-life fatigue curves at 800F for smooth and notched sheet in Condition RH950.

3.5.7 *[Figure]* Constant-life fatigue curves at room temperature for smooth and notched sheet in Condition TH1050.

3.5.8 *[Figure]* Constant-life fatigue curves at 600F for smooth and notched sheet in Condition TH1050.

3.5.9 *[Figure]* Constant-life fatigue curves at 800F for smooth and notched sheet in Condition TH1050.

3.5.10 *[Figure]* Constant-life fatigue curves at room temperature for smooth and notched forging in Condition RH950.

3.5.11 *[Figure]* Constant-life fatigue curves at 600F for smooth and notched forging in Condition RH950.

3.5.12 *[Figure]* Constant-life fatigue curves at 800F for smooth and notched forging in Condition RH950.

3.5.13 *[Figure]* Constant-life fatigue curves at room temperature for smooth and notched forging in Condition TH1050.

3.5.14 *[Figure]* Constant-life fatigue curves at 600F for smooth and notched forging in Condition TH1050.

3.5.15 *[Figure]* Constant-life fatigue curves at 800F for smooth and notched forging in Condition TH1050.

3.5.16 *[Table]* Effects of wire diameter and surface condition on the fatigue endurance limit of helical compression springs at room temperature.

3.5.17 *[Table]* Effect of surface protection with dodecyl alcohol on fatigue crack initiation and propagation of notched bar.

3.6 Elastic Properties

3.6.1 Poisson's Ratio.

3.6.2 Modulus of Elasticity.

3.6.2.1 *[Figure]* Modulus of elasticity at various temperatures.

3.6.2.2 *[Figure]* Effects of temperatures up to 1200F on the modulus of elasticity in compression of sheet.

3.6.3 Modulus of Rigidity.

3.6.3.1 *[Figure]* Modulus of rigidity at room and elevated temperatures.

3.6.3.2 *[Figure]* Effects of temperatures from -105 to 750F on modulus of rigidity of spring wire.

3.6.4 Tangent Modulus.

3.6.4.1 *[Figure]* Tangent-modulus curves in tension at room temperature for sheet in Conditions TH1050 and RH950.

3.6.4.2 *[Figure]* Tangent-modulus curves in compression for sheet in Condition TH1050 at temperature up to 1200F.

3.6.4.3 *[Figure]* Tangent-modulus curves in compression for sheet in Condition RH950 at room temperature and 600F, showing effects of prior exposure at 600F.

3.6.4.4 *[Figure]* Tangent-modulus curves in compression for sheet in Condition RH950 at 800 and 1000F, showing effects of prior exposure to test temperature.

3.6.5 Secant Modulus.

4 Fabrication

4.1 Forming

4.1.1 Cold Forming.

4.1.1.1 Type 17-7PH in Condition A has cold-forming characteristics similar to those of Type 301 austenitic stainless steel (Code 1301). Because of its high rate of work hardening, which leads to large spring back, intermediate annealing (Condition A) may be required in deep drawing or forming intricate parts. When Condition TH1050 is desired in the final product, severely cold-worked material should be fully heat treated starting with the Condition A anneal; but when Condition RH950 is desired, the 1750F conditioning treatment serves the purpose of an anneal (Ref. 19, see also Sections 1.5.1.1, 1.5.1.2, 1.5.1.3 and Figures 1.5.2.1, 1.5.2.2, and 4.1.1.6.2).

4.1.1.2 *[Figure]* Effect of cold work on tensile properties of sheet given less cold reduction than required for Condition C (see Section 1.5.3).

4.1.1.3 *[Figure]* Effect of cold work on tensile properties of sheet given less cold reduction than required for Conditions C and CH900 and then aged for one hour at 900F (see Section 1.5.3).

4.1.1.4 *[Figure]* Effect of cold work on hardness of sheet given less cold reduction than required for Conditions C and CH900 (see Section 1.5.3).

4.1.1.5 Parts that are to be used in the hardened condition but are fabricated in Condition A should be made undersize by the proper amount to compensate for the dimensional changes that occur during heat treatment (see Section 1.5.4).

4.1.1.6 Shear forming (Ref. 26).

4.1.1.6.1 *[Figure]* Effect of percent reduction by shear forming on tensile properties.

4.1.1.6.2 *[Figure]* Effects of shear forming and subsequent heat treatment on hardness (see Sections 1.5.2 and 4.1.1.1).

4.1.2 Hot Forming.

4.1.2.1 Forging practices are similar to those used for austenitic stainless steels such as Type 302. Forging temperature should not exceed 2250F, but scale loss will be lessened with lower forging temperatures of 2150F or less. There is no critical temperature range in which the alloy may not be worked. The alloy may be charged into either a hot or cold furnace, and air cooling or oil or water quenching may be employed (Ref. 17).

4.2 Machining and Grinding

4.2.1 The alloy is normally machined in Condition A, T, or R100 (see Sections 1.5.1.1, 1.5.1.2, and 1.5.1.3) with characteristics somewhat similar to those of Type 302 austenitic stainless steel (Code 1301), requiring maximum feed at low speeds. Machining in Condition T or R100 results in minimum dimensional changes during subsequent precipitation-hardening treatment. One comparative classification rates the machinability of Type 17-7PH and Type 302 as 33 percent and 50 percent respectively, based on 100 percent for AISI B1112 using high-speed steel cutting tools (Refs. 15, 17, 25).

4.3 Joining

4.3.1 Whereas 17-7PH can be welded by most of the arc and resistance processes used for stainless steel, the gas-tungsten-arc (GTA) process is the preferred method. The heat of welding effectively solution treats the zone immediately adjacent to the weld. Therefore, regardless of the condition of the base metal prior to welding, the as-deposited welds and heat-affected zones are normally relatively soft with strength comparable to that of the alloy in Condition A. The steel, therefore, may be welded in any condition of heat treatment without preheat and without critical control of interpass temperature or postweld cooling rate. When matching filler metal is used, which responds to heat treatment similarly to the base metal, improved weld strength can be obtained by full postweld RH or TH type heat treatment. Because they enhance weld ductility, either TH1100 or RH1100 is frequently the preferred postweld treatment, although TH1050 and RH950 provide higher strength. Conditions C and CH900, which require cold work, are not normally obtainable in welds. Filler metals consisting of standard grades of austenitic stainless steels, such as Type 308L, can be employed, but they do not respond to precipitation-hardening heat treatment; consequently the joints are relatively tough and ductile, but strength levels are less than those obtainable with the matching precipitation-hardenable grade. To achieve best ductility, welders should use helium shielding, stringer-bead practice, slow weld travel speeds, and low current (Refs. 6, 21).

4.3.1.1 Fusion weld deposits of 17-7PH tend to form more ferrite in their microstructures than is normally present in wrought products. Excessive amounts of ferrite in the deposits can result in hot cracking or embrittlement. Susceptibility to these weld deficiencies is governed, largely, by the composition balance of the deposit and the amount of ferrite that the composition retains in the weld microstructure. In addition, susceptibility tends to become more pronounced with thicker weld beads, higher welding current, and faster welding speed. Fusion welds in light-gage sheet up to 0.037 in. made single pass with square-butt edges generally have low ferrite contents resulting in reasonably good toughness over a range of heat-treated strengths. Welds in intermediate-gage sheets (0.037-0.093 in.) are best used in an overaged condition, that is, TH1100 or RH1100. For weldments in heavy material where single-pass weld deposits may have excessive ferrite contents, multipass weld practice should be considered (Ref. 21).

4.3.1.2 *[Table]* Tensile properties determined on sheet with butt welds across the gage length of the test specimens.

4.3.1.3 *[Table]* Comparison of tensile properties at both room and elevated temperatures of sheets in Condition TH1075 with the same sheets containing butt welds (as-welded) across the gage length of the test specimens.

4.3.2 Resistance spot and seam welding can be performed on 17-7PH with good results that satisfy the requirements of NIL-W-6858B. Normally, best results are obtained by welding just before or after the final hardening treatment, which leaves the nugget in a tough, but relatively soft, austenitic condition (Ref. 21).

4.3.2.1 *[Table]* Shear strength of spot-welded joints.

4.3.3 Type 17-7PH can be brazed with either torch- or furnace-brazing methods. In torch brazing and in furnace brazing in an air atmosphere, fluxes are necessary. However, by using a controlled atmosphere, for which argon or helium is preferred, bright furnace brazing can be done without flux. Atmospheres containing either carbonaceous materials or dissociated ammonia should not be used since carburizing and nitriding impair mechanical properties. Typical brazing alloys that are suitable for high-temperature brazing (above 1500F) are the silver-base alloys containing manganese or copper, sometimes with additions of lithium, which provides a fluxing action. A typical alloy for low-temperature brazing (below 1500F) is one containing about 50 percent silver with additions of copper, zinc, nickel, and cadmium. Other common brazing alloys such as copper, nickel-base alloys, and alloys containing silicon or boron have a high penetration rate into the base metal, which can cause embrittlement.

Type 17-7PH is usually brazed in Condition A and then transformed and aged (see Sections 1.5.1.2 and 1.5.1.3); brazing after transformation is not recommended. If an entire RH or TH type transformation-and-age cycle is to be carried out after brazing, the melting point of the brazing alloy must be high enough to hold the joints together during the 1750 or 1400F stage of the cycle. On the other hand, it is often possible to combine the brazing and heat-treat cycles producing base-metal mechanical properties similar to those of the standard heat treatments. For example, if the brazing can be carried out at about 1750F (high-temperature) or 1400F (low-temperature) the brazing operation can also be the first step in a standard RH or TH cycle, with subsequent steps to be carried out as given in Sections 1.5.1.2 or 1.5.1.3. If the brazing temperature must differ from the recommended austenite-conditioning temperatures, properly modified heat-treat procedures are capable of providing base-metal mechanical properties approaching those of the standard TH1050 and RH950 heat treatments (Ref. 21).

4.4 Surface Treating

4.4.1 Wet grit blasting is the preferred method of scale removal because it avoids the hazard of intergranular attack from acid pickling, and it provides possible advantages of better fatigue resistance and corrosion resistance. For parts that have been thoroughly cleaned prior to heat treatment (see Section 1.5.5), acid pickling with 10 percent nitric acid plus 2 percent hydrofluoric acid, if properly controlled, can be effective particularly for the removal of light discoloration or heat tint produced by final hardening treatment at 900-1200F. An alternative descaling method, particularly effective for heavy scales and poorly cleaned parts, is the use of one of the commercially available salt-bath conditioning treatments followed by the nitric-plus-hydrofluoric acid pickle. However, fused-salt conditioning should not be used on material in Condition A1750 since it will inhibit maximum transformation upon subsequent refrigeration. In such instances a boiling aqueous solution of 10 percent sodium hydroxide plus 3 percent potassium permanganate may be substituted for the fused salt. If the effective operating temperature range for the conditioning salt bath, as recommended by the manufacturer, is compatible with the final precipitation-hardening temperature, the two operations may be combined (Refs. 17, 19).

4.4.2 Certain military applications require dark, nonreflective finishes. One study showed the following effects of various blackening processes on the corrosion resistance of 17-7PH and other precipitation-hardening stainless steels: (1) black chromium plating improves corrosion resistance; (2) zinc phosphate coatings improve corrosion resistance but form a gray-colored surface; (3) alkaline-oxidizing treatments slightly reduce corrosion resistance; and (4) molten dichromate coatings significantly reduce corrosion resistance (Ref. 43).

Table 1.3.1 Specifications (Refs. 17, 19, 27, 45-49)

Alloy: 17-7PH	
Specification	Form
AMS 5528E	Sheet, strip, and plate, solution treated
AMS 5529D	Sheet and strip, cold rolled
AMS 5568C	Welded tubing
AMS 5644	Bars and forgings (non-current)
AMS 5678B	Wire, spring temper
AMS 5824B	Welding wire
ASTM A 313	Spring wire, Type 631
ASTM A 564	Bars and shapes, Type 631
ASTM A 579	Forgings, Grade 62
ASTM A 693	Plate, sheet, and strip, Type 631
ASTM A 705	Forgings, Type 631
MIL-S-25043	Plate, sheet, strip
QQ-S-766	Plate, sheet, strip

Table 1.4.1 Composition (Refs. 45-49)

Alloy: 17-7PH						
Specification	**AMS (45, 46, 47)**		**AMS (48)**		**AMS (49)**	
Form	**Sheet, Strip, Plate, Tubing**		**Wire, Spring Temper**		**Welding Wire**	
Element	**Percent**		**Percent**		**Percent**	
	Min	**Max**	**Min**	**Max**	**Min**	**Max**
Carbon	-	0.09	-	0.09	-	0.09
Manganese	-	1.00	-	1.00	-	1.00
Silicon	-	1.00	-	1.00	-	0.50
Phosphorus	-	0.040	-	0.040	-	0.025
Sulfur	-	0.030	-	0.030	-	0.025
Chromium	16.00	18.00	16.00	18.00	16.00	18.00
Nickel	6.50	7.75	6.50	7.75	6.50	7.75
Aluminum	0.75	1.50	0.75	1.50	0.75	1.25
Molybdenum	-	-	-	0.75	-	-
Copper	-	-	-	0.50	-	-

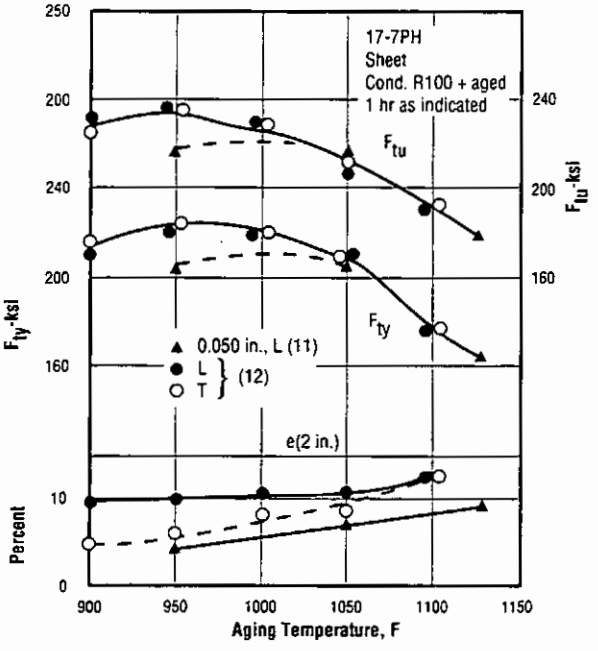


Fig. 1.5.1.4.1 Effect of RH aging temperatures (1 hr) on tensile properties of sheet after prior treatment to Condition R100 (Refs. 11, 12)

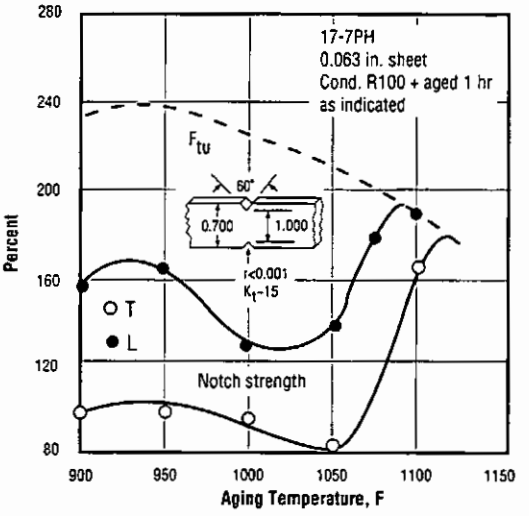


Fig. 1.5.1.4.2 Effect of RH aging temperatures (1 hr) on tensile strength and sharp-notch strength of sheet after prior treatment to Condition R100 (Ref. 12)

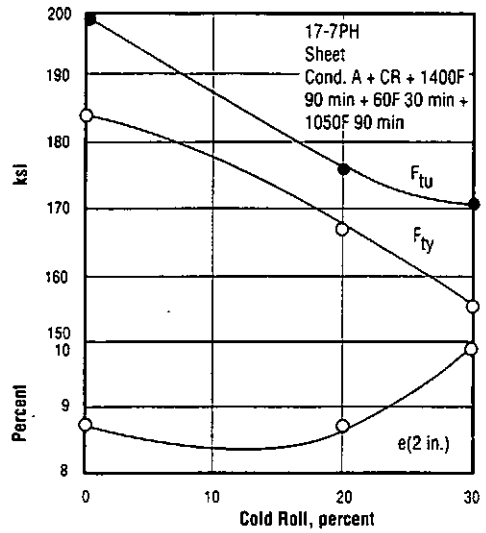


Fig. 1.5.2.1 Effect of cold work introduced in Condition A on tensile properties of sheet subsequently heat treated to Condition TH1050 without an intermediate anneal (Ref. 13)

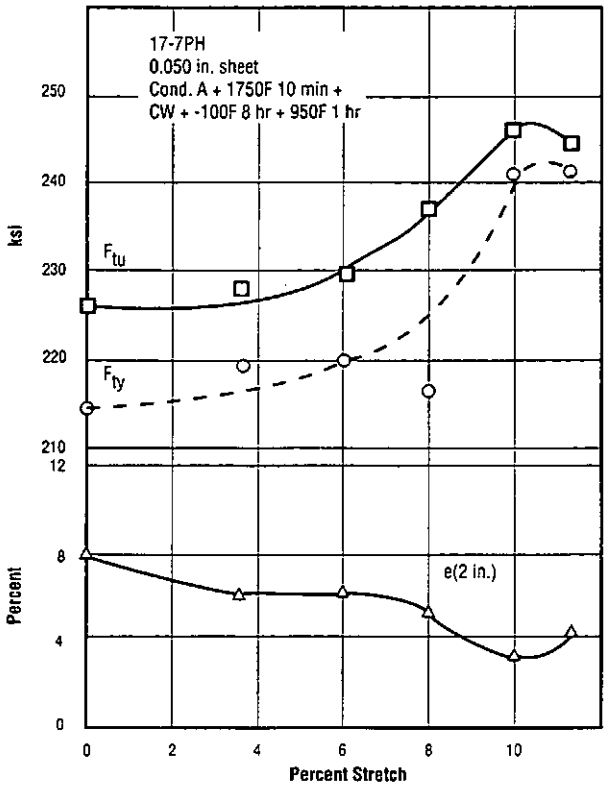


Fig. 1.5.2.2 Effect of cold work introduced in Condition A1750 on tensile properties of the alloy after subsequent completion of the RH950 heat treatment (Ref. 13)

Table 1.6.1 Hardness in various heat-treated conditions at room temperature (Refs. 17, 19)

Alloy: 17-7PH		
Condition	**Hardness, Rockwell**	
	Sheet & Strip	**Bar, Rod, Wire**
A	B 85	B 90
T	C 31	C 32
TH1050	C 43	C 42
A1750	B 85	-
R100	C 36.5	C 34
RH950	C 48	C 44
C	C 43	C 44 min
CH900	C 49	C 48 min

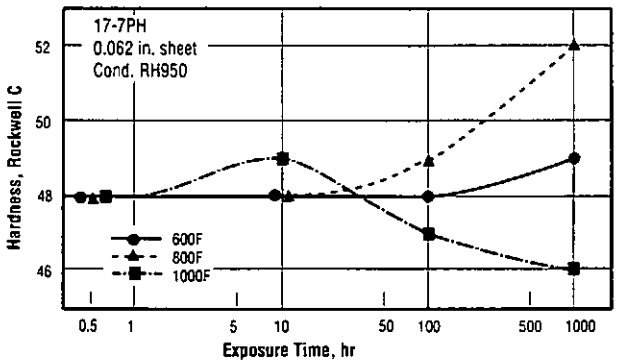


Fig. 1.6.2 Effects of exposures up to 1000 hours at 600, 800, and 1000F on the room-temperature hardness of sheet in Condition RH950 (Ref. 35)

Table 1.9.1.1 Effect of section size and orientation on tensile strength and ductility (Ref. 41)

Alloy: 17-7PH						
Condition	**Form, in.**	**Melting**	**Orientation**	**F_{tu}, ksi**	**e(2 in.) percent**	**RA percent**
TH1050	6 x 6 forging	arc air	L	169	2.0	2.0
			T	140	0	0
TH1050	6 x 6 forging	vac. melt	L	179	8.0	14.0
			T	150	1.0	0
RH950	3 5/8 dia. forg.	arc air	L	205	3.0	6.0
			T	185	1.0	0
RH950	3 5/8 dia. forg.	vac. melt	L	216	7.0	11.0
			T	188	3.0	2.0
TH1050	4 plate	arc air	L	195	10.0	25.0
			T	186	1.0	0.5
			ST	112	0	0
TH1050	2 1/4 plate	arc air	L	179	12.0	1.0
			T	178	10.0	26.0
			ST	113	0	0
TH1050	0.050 sheet	arc air	L	193	182	10.0
			T	193	182	10.0

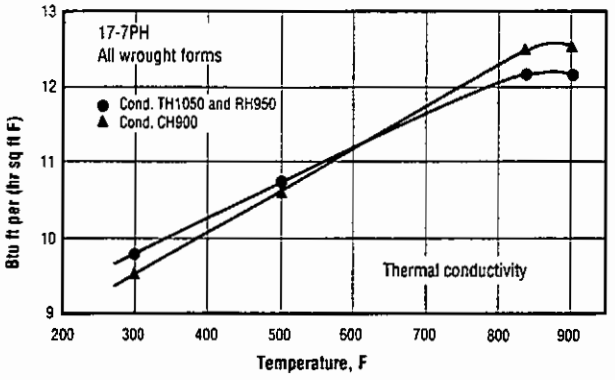


Fig. 2.1.3.1 Effects of temperatures from 300 of 900F on thermal conductivity (Refs. 17, 19)

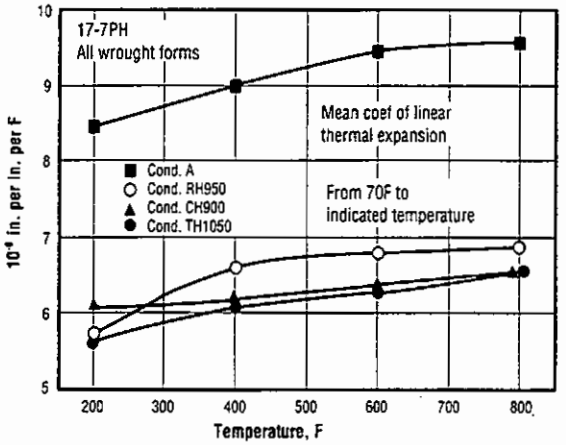


Fig. 2.1.4.1 Effects of temperatures from 200 to 800F on thermal expansion (Refs. 17, 19)

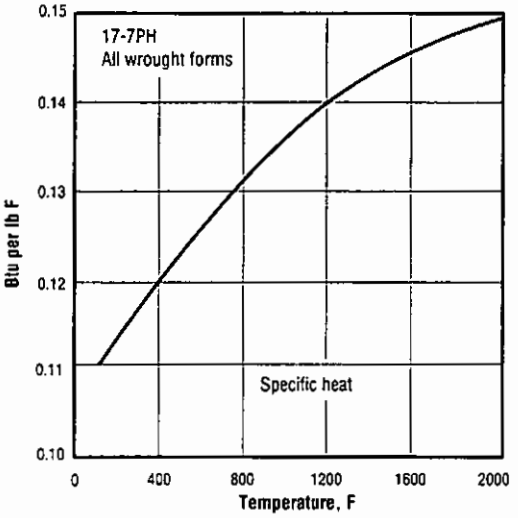


Fig. 2.1.5.1 Effect of temperatures up to 2000F on specific heat (Refs. 22, 60)

Table 2.2.1.1 Density in various heat-treated conditions at room temperature (Refs. 17, 19)

Alloy: 17-7PH				
Condition	**A**	**TH1050**	**RH950**	**CH900**
lb per cu in.	0.282	0.276	0.276	0.277
gr per cu cm	7.81	7.65	7.65	7.67

Table 2.2.2.1 Electrical properties in various heat-treated conditions at room temperature (Refs. 17, 19)

Alloy: 17-7PH				
Condition	**A**	**TH1050**	**RH950**	**CH900**
Electrical Resistivity, microohm - in.	31.5	32.3	32.7	33.0
Electrical Conductivity, megmhos per in.	.0317	.0310	.0306	.0303
Electrical Conductivity, % IACS	2.16	2.11	2.08	2.06

Table 2.2.3.1 Magnetic permeability in various heat-treated conditions at room temperature (Refs. 17, 19)

Alloy: 17-7PH				
Condition	**A**	**TH1050**	**RH950**	**CH900**
25 oersteds	1.4 - 3.4	132 - 194	82 - 88	-
50 oersteds	1.4 - 3.6	120 - 167	113 - 130	-
100 oersteds	1.4 - 3.5	80 - 99	75 - 87	70
200 oersteds	1.4 - 3.2	46 - 55	44 - 52	43.5
maximum	1.4 - 3.6	134 - 208	119 - 135	125

Table 2.2.4.1 Total normal emittance at temperatures from 400 to 900F (Ref. 2)

Alloy: 17-7PH	
Condition	**TH1050, Pickled**
Temperature, F	**Total Normal Emittance**
400	0.54
500	0.72
600	0.63
700	0.61
750	0.62
800	0.63
900	0.60

Table 2.3.1.1 Comparison of typical corrosion rates for 17-7PH and Type 304 stainless steels in seven common reagents (Refs. 17, 19)

Alloy: 17-7PH					Type 304
Form			Sheet		Sheet
Condition			TH1050	RH950	Annealed
Medium	Concentration percent	Temp. F	Corrosion Rate mils per year (a)		
Sulfuric Acid	1	95	0.5	0.2	0.4
	2	95	0.9	0.7	1.3
	5	95	124	132	7.7
Sulfuric Acid	1	176	50	297	22.2
	2	176	374	884	65
Hydrochloric Acid	0.5	95	65	4	7.1
	1	95	695	447	17.3
Nitric Acid	25	Boiling	19	20.4	1.2
	50	Boiling	70	81	3.0
	65	Boiling	128	136	7.2
Formic Acid	5	176	2.7	4.3	4.1
	10	176	5.5	5.7	18.0
Acetic Acid	33	Boiling	3.1	5.6	2.6
	60	Boiling	12.3	3.0	10.9
Phosphoric Acid	20	Boiling	7.0	18	1.6
	50	Boiling	24	46	8.5
	70	Boiling	104	315	39
Sodium Hydroxide	30	76	13.1	3.7	0.9
	30	Boiling	67	58	17.5

(a) Rates determined after total immersion, in most instances for five 48-hour periods. Chemically pure laboratory reagents were used. The data should be used only as guide to comparative performance.

Table 2.3.3.1 Effects of high-pressure hydrogen atmosphere on tensile properties at room temperature (Ref. 54)

Alloy: 17-7PH		
Form	Bar	
Condition	TH1050	
Environment	Air zero psig	Hydrogen 10,000 psig
F_{tu}, ksi	174	151
F_{ty}, ksi	163	148
e(1.25 in.) percent	17.0	1.7
RA, percent	45.0	2.5

Table 2.3.5.1 Threshold stress intensity factor (Klscc) for stress-corrosion cracking of bar in aerated 3.5 percent aqueous sodium-chloride solution (Ref. 5)

Alloy: 17-7PH					
Form		1 3/4-in. Square Bar			
Condition	F_{ty}, ksi	F_{tu}, ksi	e(2 in.)	K_{Ic}, ksi $\sqrt{in.}$	K_{Iscc}, ksi $\sqrt{in.}$
RH950	171.3	186.5	11	32.3	<19.0
TH1050	-	197.2	9	38.7	15.8

Notes
1. K_{Ic} specimens: SE (B)(L-T), 1/2 in. thick
2. K_{Iscc} specimens: SE (B Cantilever)(L-T), 1/2 in. thick

Table 3.1.1 AMS specified mechanical properties for plate, sheet, and strip (Refs. 45, 46)

Alloy: 17-7PH					
Form		Plate, Sheet, Strip			
Condition	Thickness, in.	F_{ty}, ksi min	F_{tu}, ksi	e(2 in.) percent min	Hardness, Rockwell
A	0.005 to 0.010	65	150 min	20	B 92 max
A	>0.010	55	150 min	20	B 92 max
TH1050	0.005 to 0.010	150	180 - 210	4	C 38 - 46
TH1050	>0.010 to 0.019	150	180 - 210	5	C 38 - 46
TH1050	>0.019 to 1.000	150	180 - 210	6	C 38 - 46
C	0.0015 to 0.050	175	200 min	1	C 41 min
CH900	0.0015 to 0.050	230	240 min	1	C 46 min

Table 3.1.2 ASTM specified mechanical properties for plate, sheet, and strip (Ref. 7)

Alloy: 17-7PH						
Form		Plate, Sheet, Strip				
Condition	Thickness, in.	F_{ty}, ksi min	F_{tu}, ksi min	e(2 in.) (T) percent min	RA (T) percent min	Hardness, Rockwell
A	0.010 in. and under	65	150	-	-	-
A	>0.010 in. to 4.0 in.	55	150	20	-	B 92 max
TH1050	0.0015 to 0.0049	150	180	3	-	C 38 min
TH1050	0.0050 to 0.0099	150	180	4	-	C 38 min
TH1050	0.010 to 0.0199	150	180	5	-	C 38 min
TH1050	0.020 to 0.1874	150	180	6	-	C 38 min
TH1050	0.1875 to 0.625	140	170	7	20	C 38 min
RH950	0.0015 to 0.0049	190	210	1	-	C 44 min
RH950	0.0050 to 0.0099	190	210	2	-	C 44 min
RH950	0.010 to 0.0199	190	210	3	-	C 44 min
RH950	0.020 to 0.1874	190	210	4	-	C 44 min
RH950	0.1875 to 0.625	180	200	6	20	C 43 min
C	0.0015 to 0.050	175	200	1	-	C 41 min
CH900	0.0015 to 0.050	230	240	1	-	C 46 min

Table 3.1.3 AMS specified mechanical properties for tubing (Ref. 47)

Alloy: 17-7PH				
Form	Tubing			
Condition	F_{ty}, ksi	F_{tu}, ksi	e(2 in.) percent	Hardness, Rockwell
A	55 max	150 max	20 min	C 92 max
TH1050	150 min	180 min	6 min	C 38 min

Table 3.1.4 AMS specified tensile strength for spring wire (Ref. 48)

Alloy: 17-7PH				
Form	Wire, Spring Temper			
Condition	C		CH900	
Diameter, in.	F_{tu}, ksi		F_{tu}, ksi	
	min	max	min	max
0.016 to 0.020	248	305	335	365
over 0.020 to 0.025	243	300	330	360
over 0.025 to 0.029	239	295	325	355
over 0.029 to 0.041	234	290	320	350
over 0.041 to 0.051	230	285	310	340
over 0.051 to 0.061	225	280	305	335
over 0.061 to 0.071	218	272	297	327
over 0.071 to 0.086	216	270	292	322
over 0.086 to 0.090	207	260	282	312
over 0.090 to 0.100	204	257	279	309
over 0.100 to 0.106	201	253	274	304
over 0.106 to 0.130	199	251	272	302
over 0.130 to 0.138	194	245	260	290
over 0.138 to 0.146	192	243	258	288
over 0.146 to 0.162	190	241	256	286
over 0.162 to 0.180	188	239	254	284
over 0.180 to 0.207	186	237	252	282
over 0.207 to 0.225	183	233	248	278
over 0.225 to 0.306	178	228	242	272
over 0.306 to 0.440	173	222	235	265

Note: Armco specifies minimum hardness of RC 44 for Condition C and RC 48 for Condition CH900 regardless of diameter (17).

Table 3.1.5 ASTM specified tensile strength for spring wire (Ref. 18)

Alloy: 17-7PH			
Form	Spring Wire		
Condition	C	CH900	
Diameter, in.	F_{tu}, ksi	F_{tu}, ksi	
	nominal	min	max
0.010 to 0.015	295	335	365
over 0.015 to 0.020	290	330	360
over 0.020 to 0.029	285	325	355
over 0.029 to 0.041	275	320	350
over 0.041 to 0.051	270	310	340
over 0.051 to 0.061	265	305	335
over 0.061 to 0.071	257	297	327
over 0.071 to 0.086	255	292	322
over 0.086 to 0.090	245	282	312
over 0.090 to 0.100	242	279	309
over 0.100 to 0.106	238	274	304
over 0.106 to 0.130	236	272	302
over 0.130 to 0.138	230	260	290
over 0.138 to 0.146	228	258	288
over 0.146 to 0.162	226	256	286
over 0.162 to 0.180	224	254	284
over 0.180 to 0.207	222	252	282
over 0.207 to 0.225	218	248	278
over 0.225 to 0.306	213	242	272
over 3.306 to 0.440	207	235	265
over 0.440 to 0.625	203	230	260

Notes:
1. When wire is specified in straightened and cut lengths minimum tensile strength (F_{tu}) shall be 90 percent of the values listed in the table.
2. For hardness, Armco specifies a minimum of Rockwell C 44 for Condition C and C 48 for Condition CH900 regardless of diameter (17).

Table 3.1.6 ASTM specified mechanical properties for longitudinal specimens from bars, shapes, and forgings (Refs. 8, 9)

Alloy: 17-7PH						
Form		Bars, Shapes, and Forgings				
Condition	Thickness, or Diameter, in.	F_{ty}, ksi min	F_{tu}, ksi min	e(2 in.) min	RA, percent min	Hardness, Rockwell
A	-	-	-	-	-	(a)
TH1050	up to 6 in.	140	170	6	25	C 38 min
RH950	up to 4 in.	150	185	6	10	C 41 min

(a) Rockwell B 98 max for bars and shapes (8) and B 89 max for forgings (9).

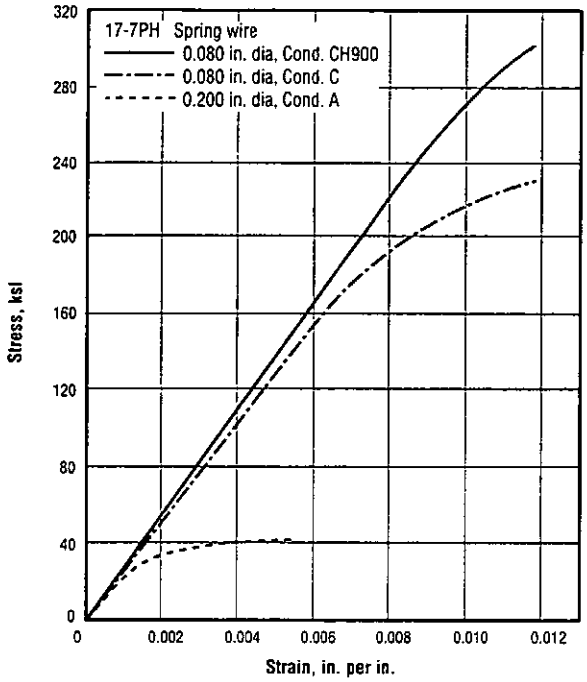


Fig. 3.2.1.1 Tensile stress-strain curves for spring wire at room temperature (Ref. 17)

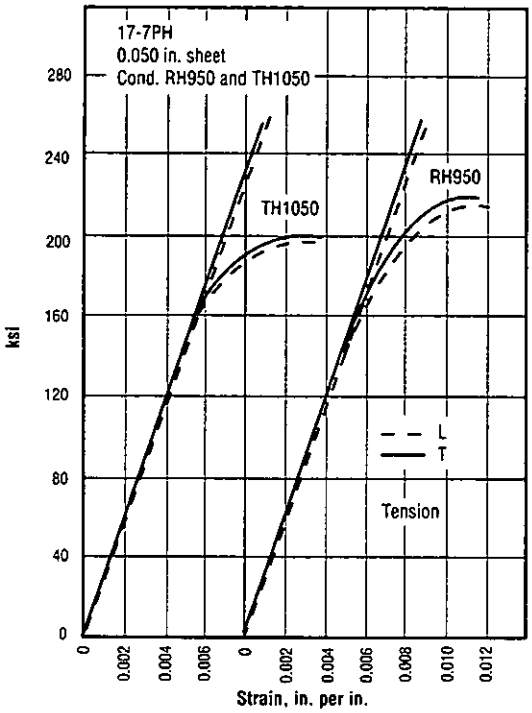


Fig. 3.2.1.2 Tensile stress-strain curves for sheet in longitudinal and transverse orientations for Conditions TH1050 and RH950 (Ref. 13)

Table 3.2.1.3 Tensile properties in various heat-treated conditions at room temperature (Refs. 17, 19)

Alloy: 17-7PH					
Form	Condition	Tensile Properties			
		F_{ty}, ksi	F_{tu}, ksi	e(2 in.) percent	RA percent
(1)	A	40	130	35	-
(1)	T	100	145	9	-
(1)	TH1050	185	200	9	-
(2)	TH1050	155	175	12	34
(1)	A1750	42	133	19	-
(1)	R100	115	175	9	-
(1)	RH950	220	235	5	-
(2)	RH950	175	200	10	30
(1)	C	190	220	5	-
(1)	CH900	260	265	2	-

(1) Sheet and strip, (2) Bar, rod, and wire

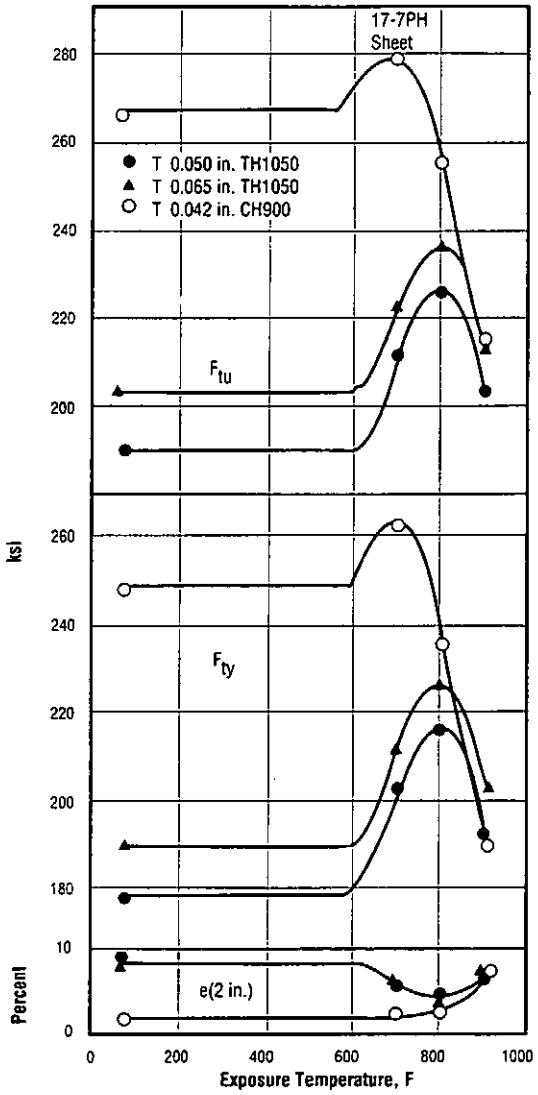


Fig. 3.2.1.4 Effects of 500-hour exposures at elevated temperatures up to 900F on tensile properties at room temperature of sheet in Conditions TH1050 and CH900 (Ref. 29)

Table 3.2.1.5 Effects of 1000-hour exposure to elevated temperatures with load on tensile properties at room temperature of sheet in Conditions TH1050 and RH950 (Ref. 29)

Alloy: 17-7PH					
Form		0.050-in. Sheet, T			
Condition		TH1050			
1000-hr Exposure at		Tensile Properties after Exposure			
		F_{tu}, ksi		e(2 in.) Percent	
Temp, F	Load, ksi	Heat A	Heat B	Heat A	Heat B
RT	-	201.5	188.8	8.0	11.0
600	80.0	206.2	190.0	7.5	10.0
	120.0	209.8	192.6	7.0	7.5
700	50.0	221.0	207.0	6.0	7.5
	90.0	228.4	210.0	4.5	7.0
800	50.0	235.7	220.0	4.5	3.5
	80.0	245.0	227.0	4.0	3.5
900	15.0	208.0	190.6	5.5	5.5
	35.0	210.0	192.8	5.0	5.0
Condition		RH950			
1000-hr Exposure at		Tensile Properties after Exposure			
Temp, F	Load, ksi	F_{tu}, ksi		e(2 in.) Percent	
RT	-	232.6		7.5	
600	40.0	236.0		7.5	
	170.0	270.1		2.3	
700	40.0	253.0		5.5	
	115.0	263.2		3.0	
800	30.0	255.7		2.0	
	70.0	263.0		1.0	
900	10.0	224.5		5.5	
	30.0	227.0		4.5	

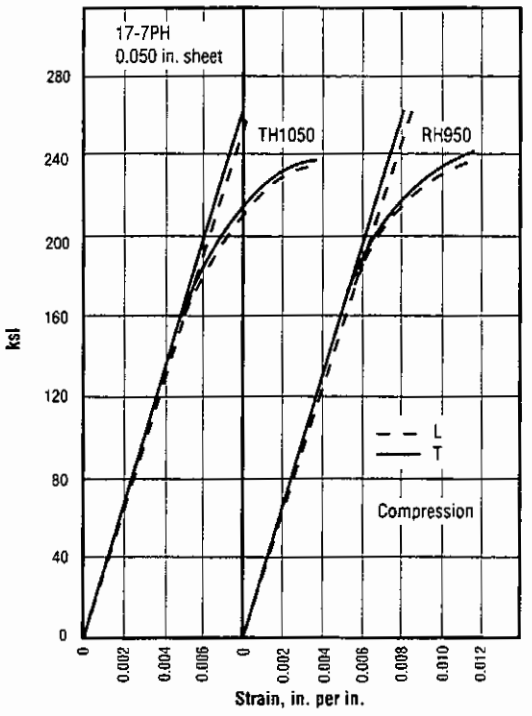


Fig. 3.2.2.1 Compression stress-strain curves for sheet in longitudinal and transverse orientations for Conditions TH1050 and RH950 at room temperature (Ref. 13)

Table 3.2.2.2 Typical compressive yield strengths at room temperature for various heat-treat conditions (Ref. 19)

Alloy: 17-7PH	
Form	**Sheet**
Condition	**F_{cy}, ksi**
TH1050	203
RH950	240
C	218
CH900	300

Table 3.2.6.1 Bearing properties of sheet at room temperature in Conditions TH1050 and RH950 (Refs. 56, 57, 58)

Alloy: 17-7PH					
Form	**0.048 to 0.065 in. Sheet**				
Condition	**TH1050**		**RH950**		
Orientation	-	-	T	L	T
(e/D = 1.5)					
F_{bru}, ksi	-	-	-	358	358
F_{bry}, ksi	-	-	-	300	296
F_{bru}/F_{tu}	-	-	-	1.62	1.63
F_{bry}/F_{tu}	-	-	-	1.47	1.45
(e/D = 2.0)					
F_{bru}, ksi	313	365	463	-	-
F_{bry}, ksi	273	270	379	-	-
F_{bru}/F_{tu}	1.60	1.93	-	-	-
F_{bry}/F_{tu}	1.42	1.47	-	-	-

Table 3.2.7.1.1 Crack strength of plate at room temperature in Condition RH1050 (Ref. 55)

Alloy: 17-7PH		
Form	**0.36-in. Plate**	
Specimen	**Full plate thickness by 3.0 in. wide with 1.0 in. fatigue crack**	
Condition	**RH1050**	
	Longitudinal	**Transverse**
F_{ty}, ksi	186.6	185.4
Crack strength, ksi	149.2	122.8
Ratio, crack strength/F_{ty}	0.80	0.66
Percent shear fracture	85 - 90	30 - 40

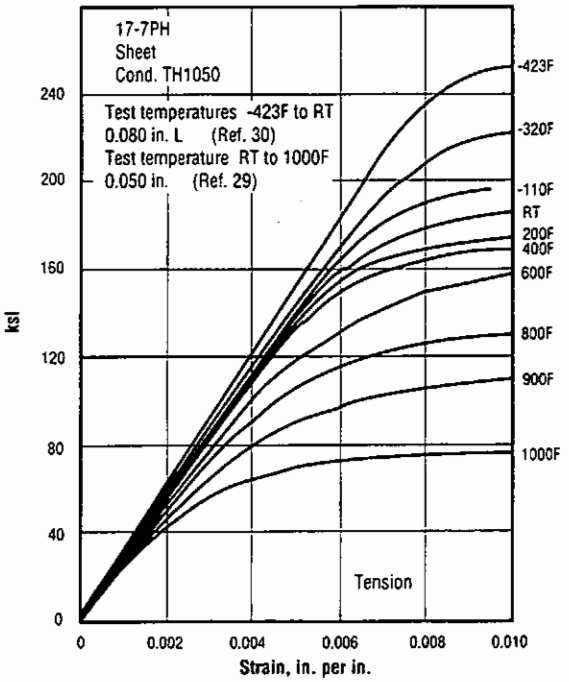


Fig. 3.3.1.1 Tensile stress-strain curves at temperatures from -423F to 1000F for sheet in Condition TH1050 (Refs. 29, 30)

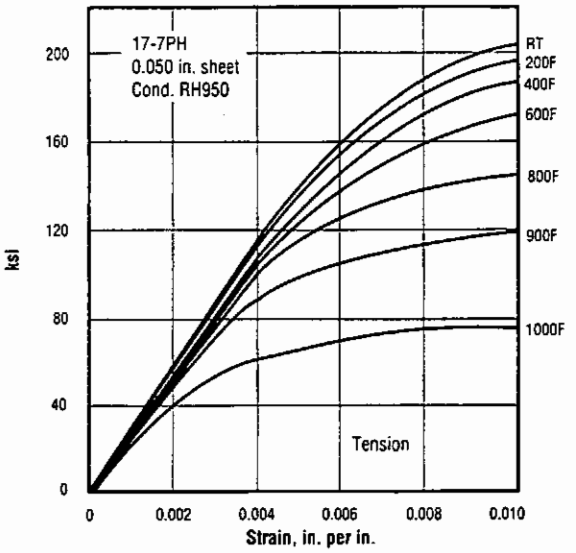


Fig. 3.3.1.2 Tensile stress-strain curves at temperatures from 75F to 1000F for sheet in Condition RH950 (Ref. 29)

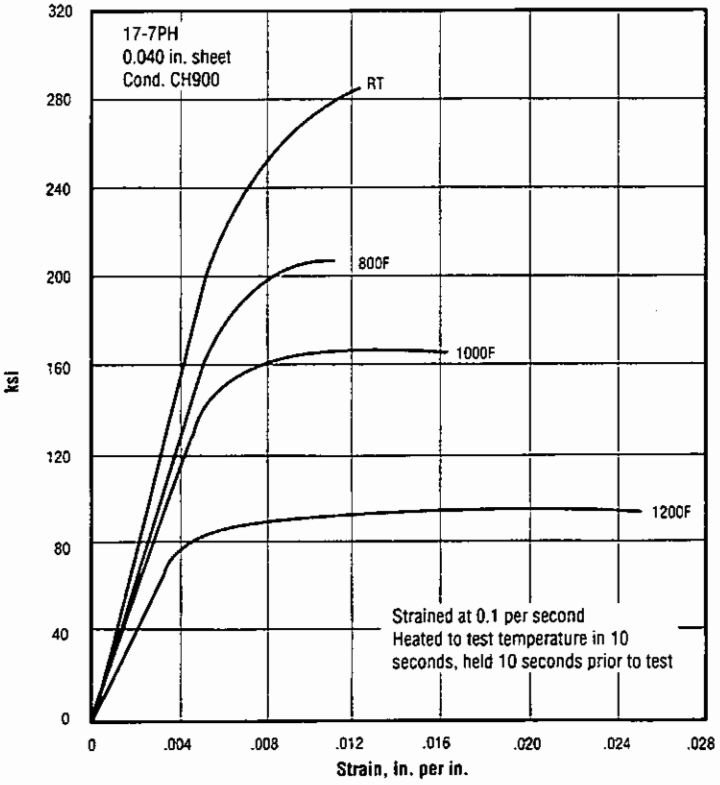


Fig. 3.3.1.3 Tensile stress-strain curves for sheet in Condition CH900 at temperatures up to 1200F under conditions of rapid heating, rapid loading, and short time at temperature (Ref. 31)

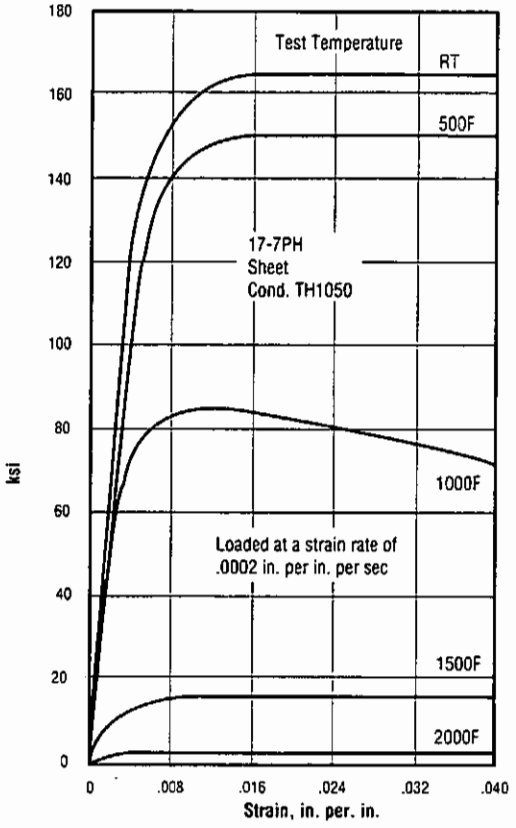


Fig. 3.3.1.4 Tensile stress-strain curves at temperatures up to 2000F for sheet in Condition TH1050 loaded at a strain rate of 0.0002 in. per in. per second (Ref. 32)

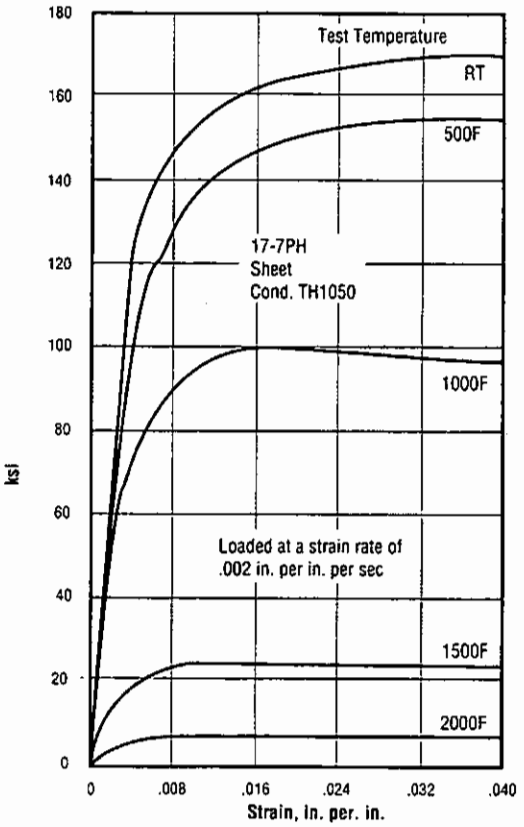


Fig. 3.3.1.5 Tensile stress-strain curves at temperatures up to 2000F for sheet in Condition TH1050 loaded at a strain rate of 0.002 in. per in. per second (Ref. 32)

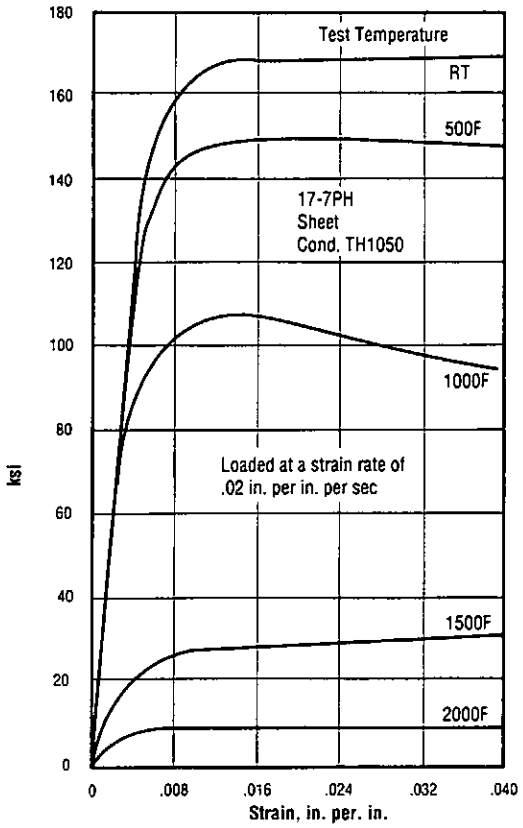


Fig. 3.3.1.6 Tensile stress-strain curves at temperatures up to 2000F for sheet in Condition TH1050 loaded at a strain rate of 0.02 in. per in. per second (Ref. 32)

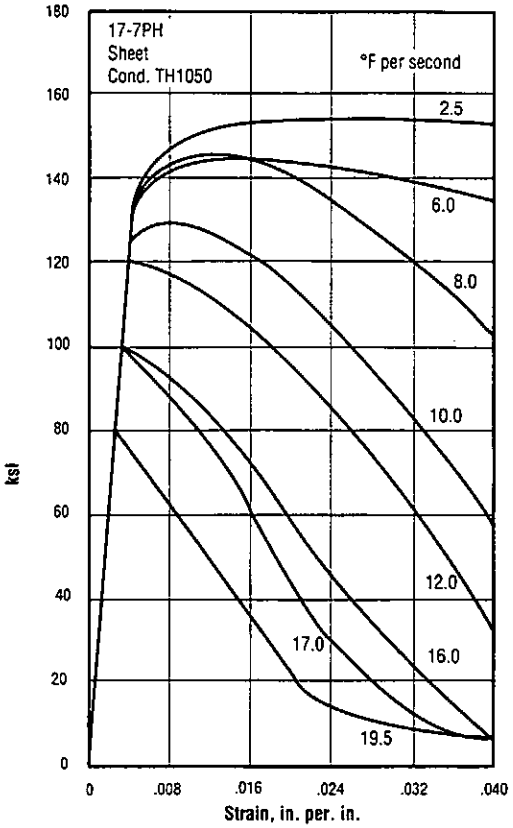


Fig. 3.3.1.7 Tensile stress-strain curves for sheet in Condition TH1050 when simultaneously loaded at a strain rate of 0.0002 in. per in. per second and heated at rates of 2.5 to 19.5F per second (Ref. 32)

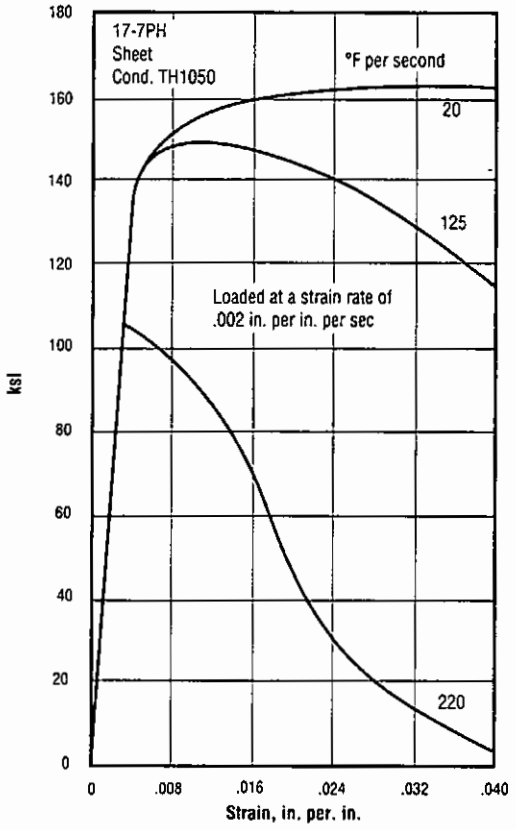


Fig. 3.3.1.8 Tensile stress-strain curves for sheet in Condition TH1050 when simultaneously loaded at a strain rate of 0.002 in. per in. per second and heated at rates of 20 to 220F per second (Ref. 32)

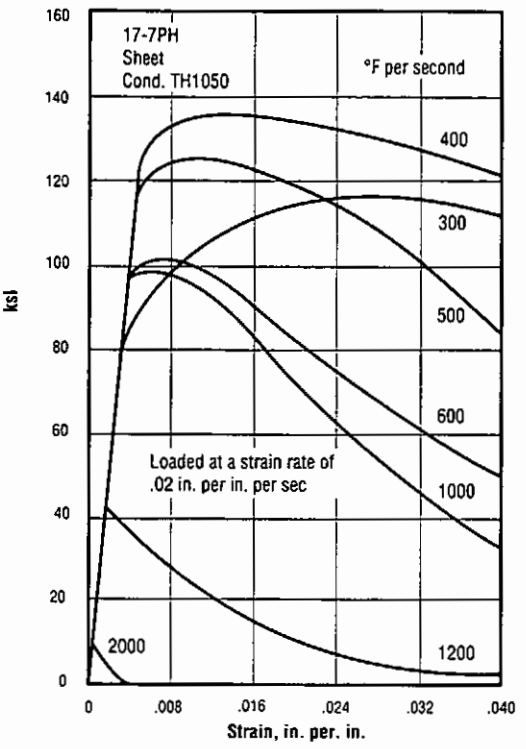


Fig. 3.3.1.9 Tensile stress-strain curves for sheet in Condition TH1050 when simultaneously loaded at a strain rate of 0.02 in. per in. per second and heated at rates of 400 to 2000F per second (Ref. 32)

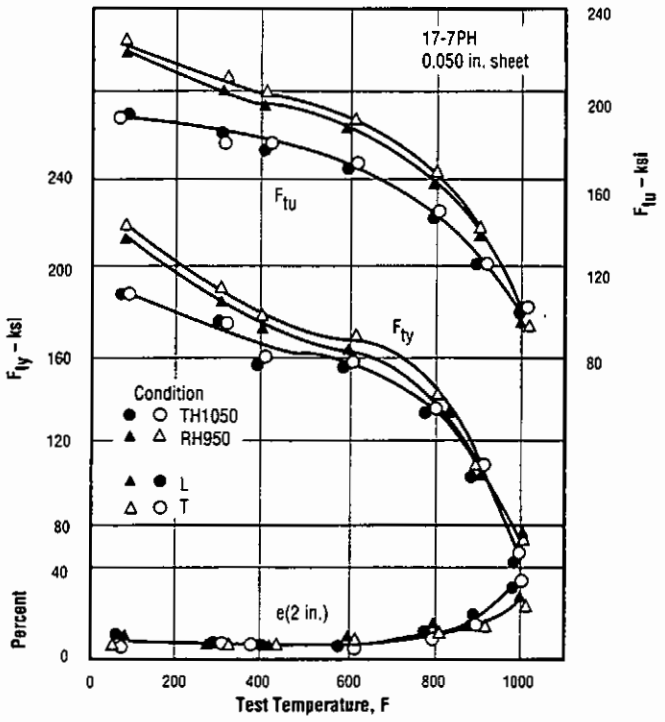


Fig. 3.3.1.10 Effects of temperatures up to 1000F on tensile properties of sheet in Conditions TH1050 and RH950 (Ref. 29)

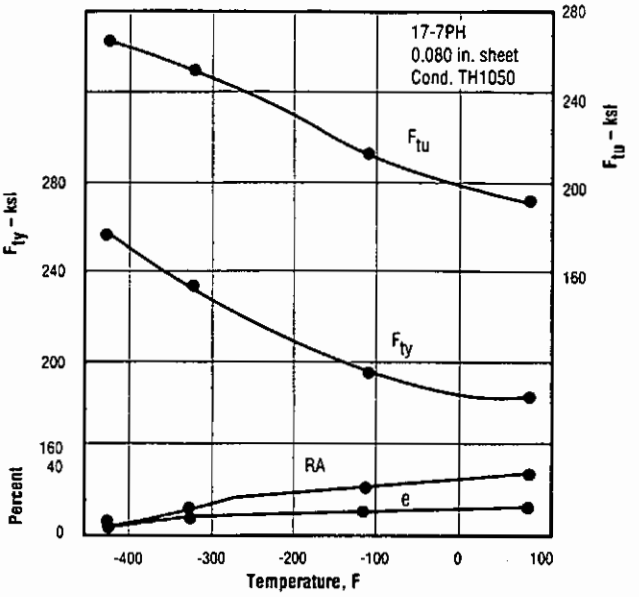


Fig. 3.3.1.11 Effects of low temperatures down to -423F on tensile properties of sheet in Condition TH1050 (Ref. 30)

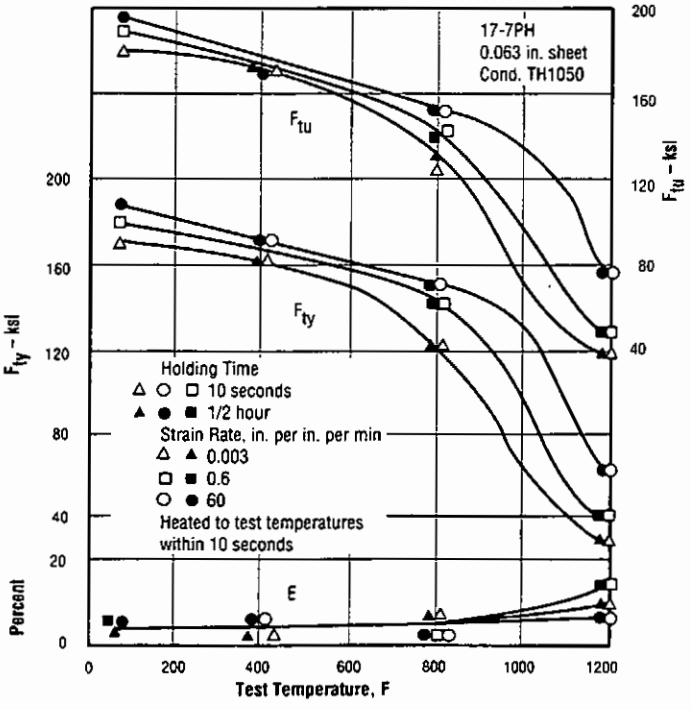


Fig. 3.3.1.12 Tensile properties of sheet in Condition TH1050 for various rates of loading at temperatures up to 1200F after rapid heating and holding times of 10 seconds and 1/2 hour at temperature (Ref. 33)

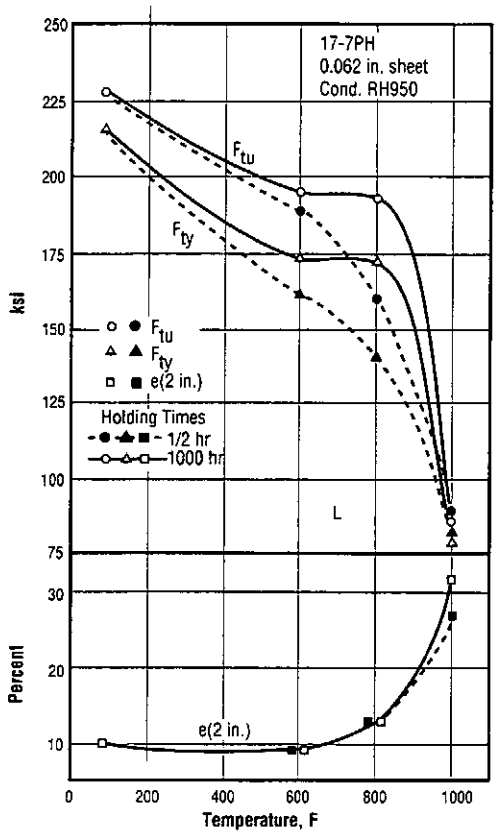


Fig. 3.3.1.13 Tensile properties of sheet in Condition RH950 at temperatures up to 1000F after holding times of 1/2 and 1000 hours at test temperatures (Ref. 35)

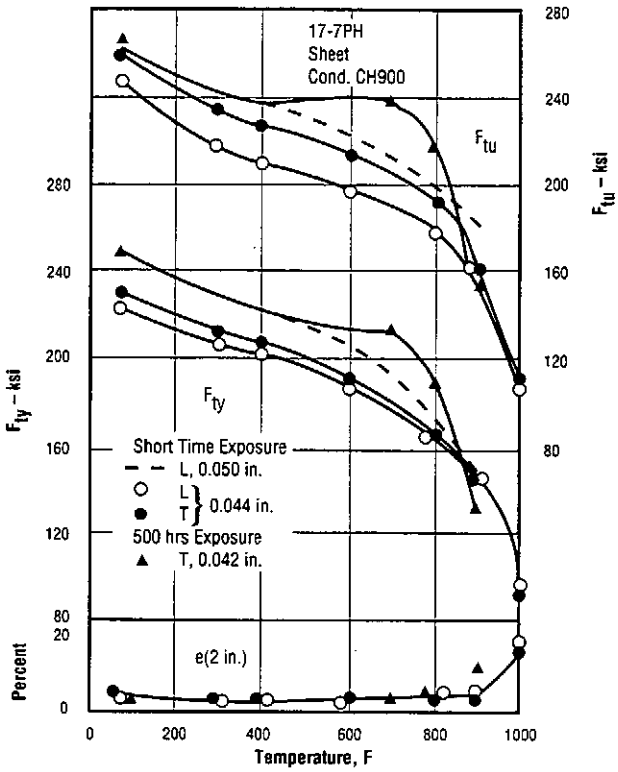


Fig. 3.3.1.14 Effects of test temperatures up to 1000F and of exposure time at temperature on tensile properties of sheet in Condition CH900 (Ref. 29)

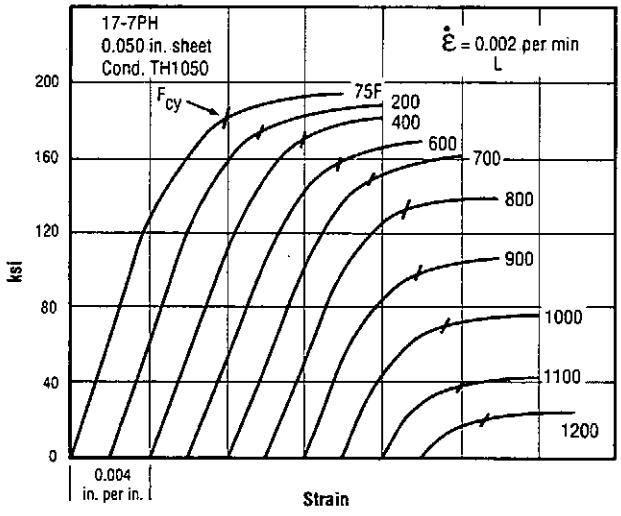


Fig. 3.3.2.1 Compressive stress-strain curves for sheet in Condition TH1050 at temperatures up to 1200F (Ref. 3)

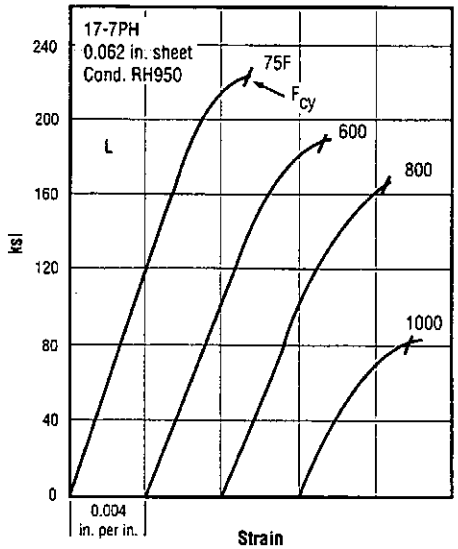


Fig. 3.3.2.2 Compressive stress-strain curves for sheet in Condition RH950 at temperatures up to 1000F (Ref. 35)

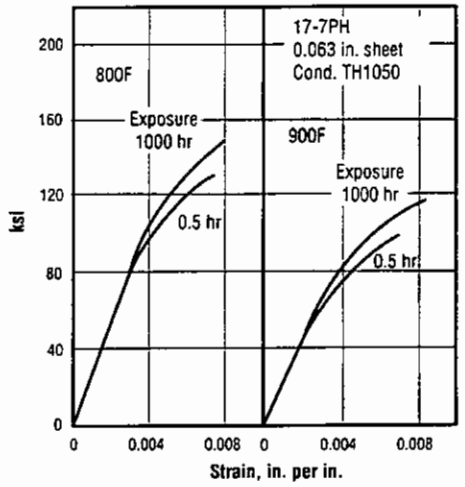


Fig. 3.3.2.3 Compressive stress-strain curves for sheet in Condition TH1050 at 800 and 900F after two different exposure times at temperature (Ref. 34)

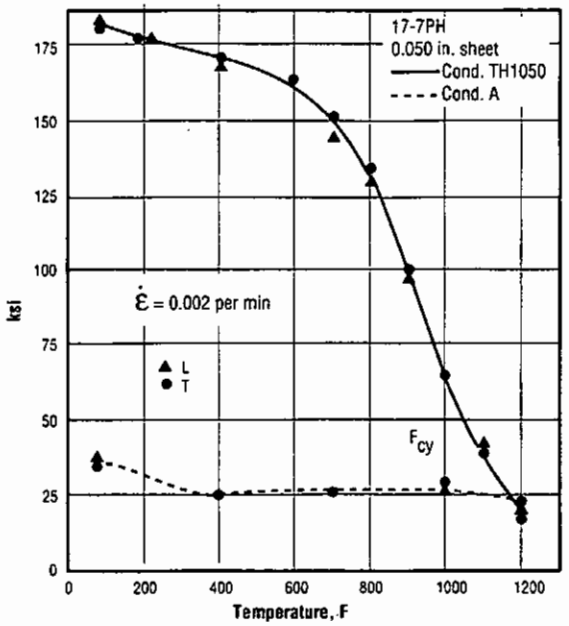


Fig. 3.3.2.4 Effects of temperatures up to 1200F on the compressive yield strength of sheet in both the TH1050 and annealed (solution-treated) conditions (Ref. 3)

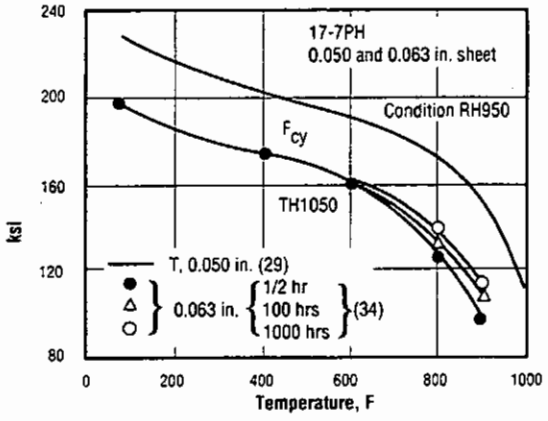


Fig. 3.3.2.5 Effects of elevated temperatures and of exposure time at temperature on the compressive yield strength of sheet in Conditions TH1050 and RH950 (Refs. 29, 34)

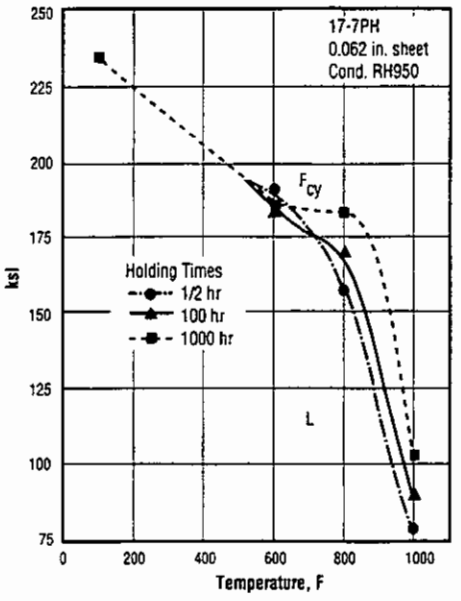


Fig. 3.3.2.6 Compressive yield strength of sheet in Condition RH950 at temperatures up to 1000F after holding times of 1/2, 100, and 1000 hours at temperature (Ref. 35)

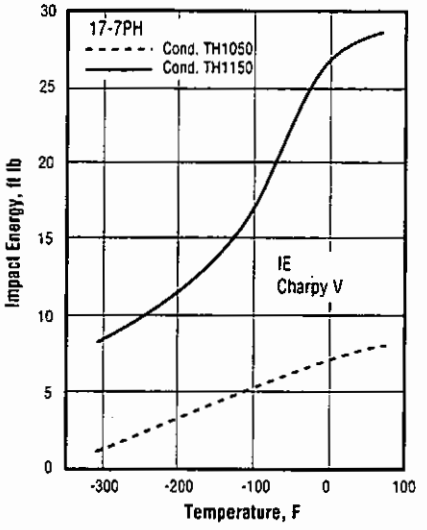


Fig. 3.3.3.1 Effects of low temperatures on impact resistance in Conditions TH1050 and TH1150 (Ref. 10)

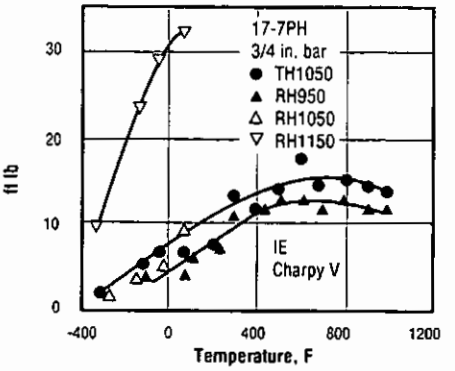


Fig. 3.3.3.2 Impact resistance over a wide range of temperature of bar in various conditions (Ref. 53)

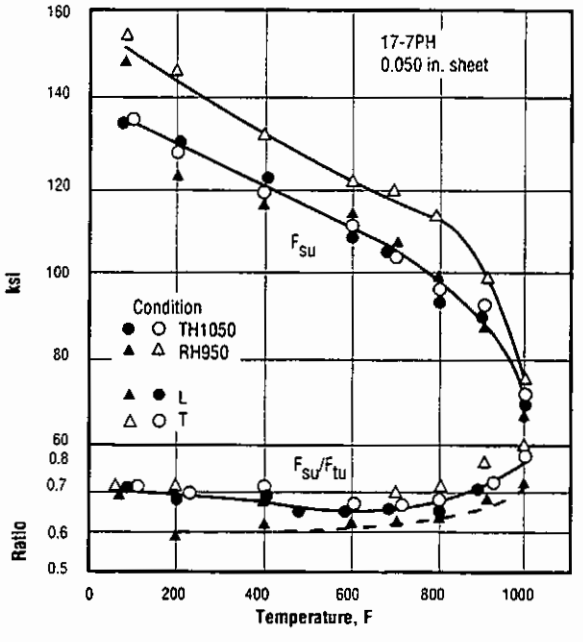


Fig. 3.3.5.1 Ultimate shear strength of sheet in Conditions TH1050 and RH950 at temperatures up to 1000F (Ref. 29)

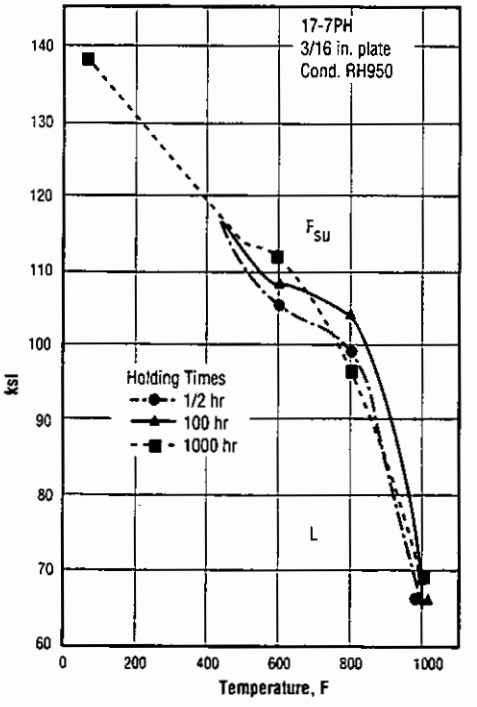


Fig. 3.3.5.2 Ultimate sheer strength of plate in Condition RH950 at temperatures up to 1000F after holding times of 1/2, 100, and 1000 hours at test temperature (Ref. 35)

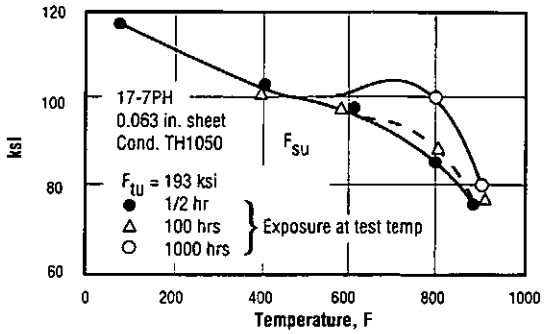


Fig. 3.3.5.3 Ultimate shear strength of sheet in Condition TH1050 at temperatures up to 900F after holding times of 1/2, 100, and 1000 hours at test temperatures (Ref. 34)

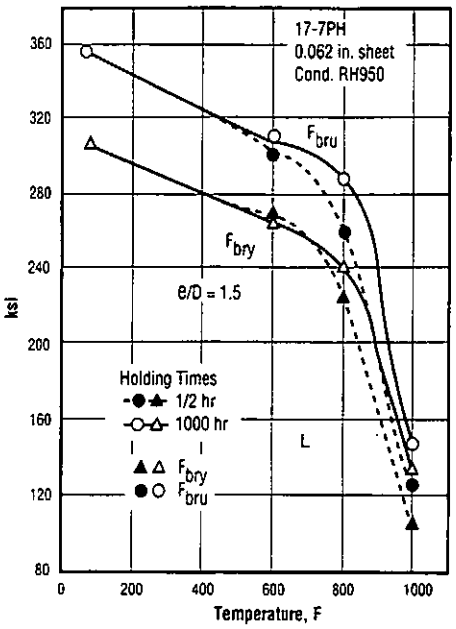


Fig. 3.3.6.1 Bearing properties (e/D = 1.5) of sheet in Condition RH950 at temperatures up to 1000F after holding times of 1/2 and 1000 hours at test temperature (Ref. 35)

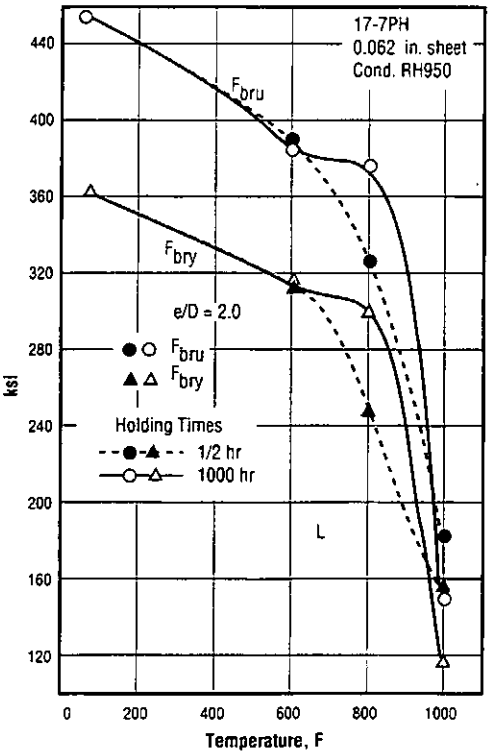


Fig. 3.3.6.2 Bearing properties (e/D = 2.0) of sheet in Condition RH950 at temperatures up to 1000F after holding times of 1/2 and 1000 hours at test temperature (Ref. 35)

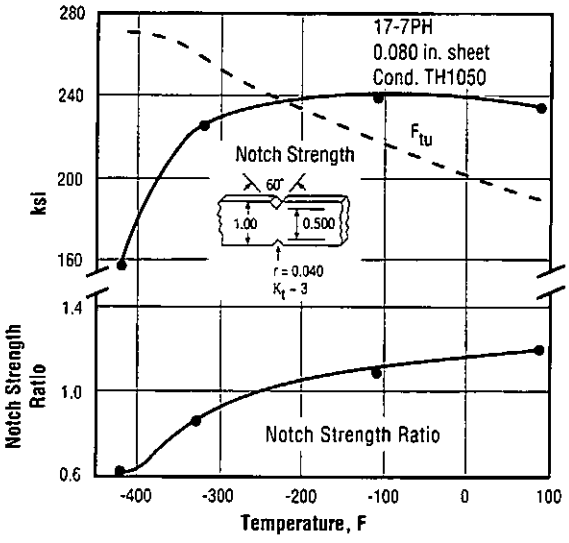


Fig. 3.3.7.1.1 Notch strength and tensile strength of sheet in Condition TH1050 at temperatures down to -423F (Ref. 30)

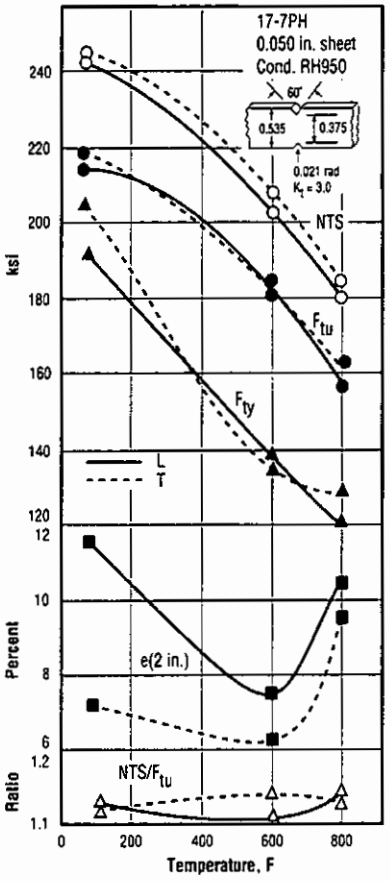


Fig. 3.3.7.1.2 Comparison of tensile and notch tensile properties at temperatures up to 800F for sheet in Condition RH950 (Ref. 39)

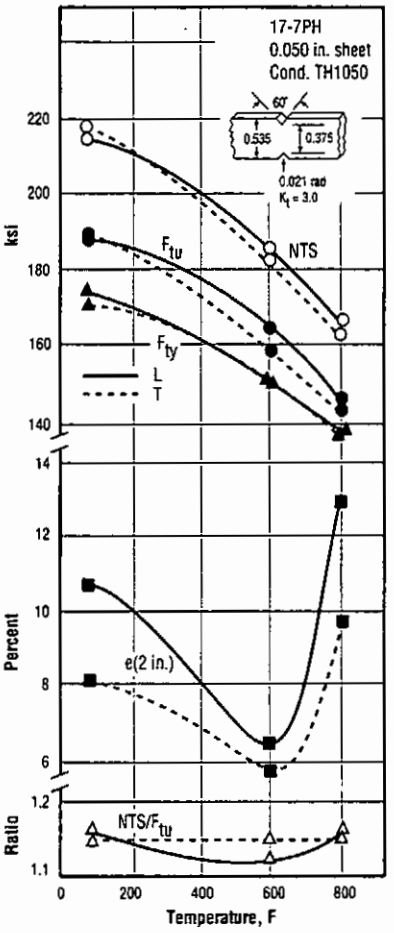


Fig. 3.3.7.1.3 Comparison of tensile and notch tensile properties at temperatures up to 800F for sheet in Condition TH1050 (Ref. 38)

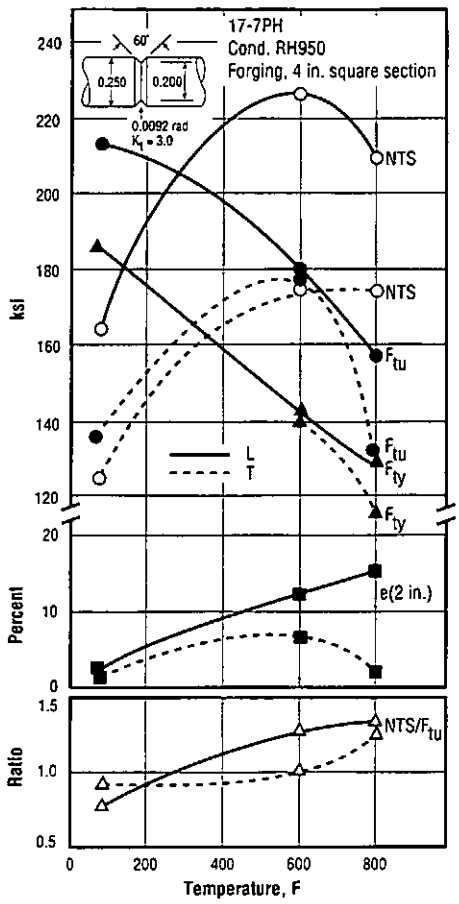


Fig. 3.3.7.1.4 Comparison of tensile and notch tensile properties at temperatures up to 800F for forging in Condition RH950 (Ref. 39)

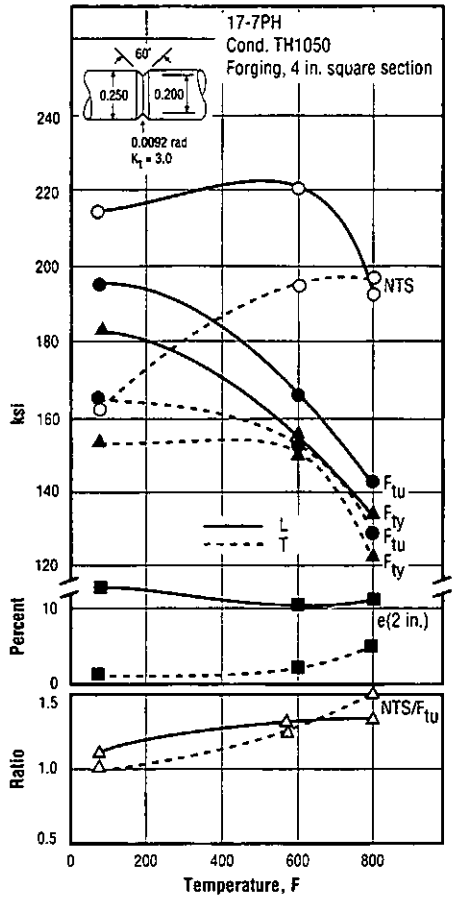


Fig. 3.3.7.1.5 Comparison of tensile and notch tensile properties at temperatures up to 800F for forging in Condition TH1050 (Ref. 39)

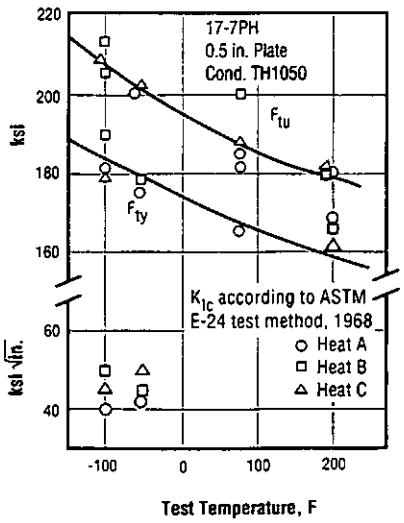


Fig. 3.3.7.2.1 Fracture toughness, tensile strength, and yield strength of plate in Condition TH1050 at various temperatures (Ref. 36)

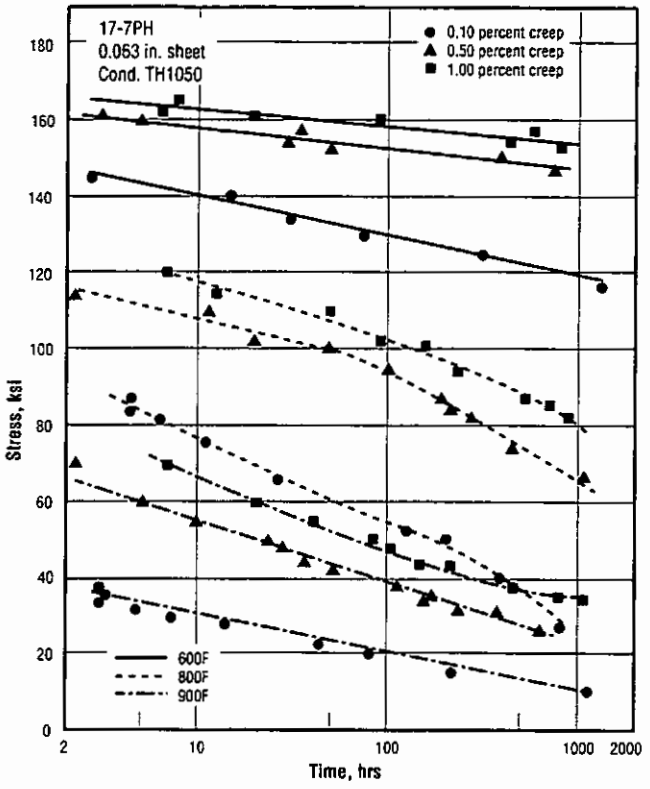


Fig. 3.4.1 Creep properties of sheet in Condition TH1050 at temperatures from 600 to 900F (Ref. 40)

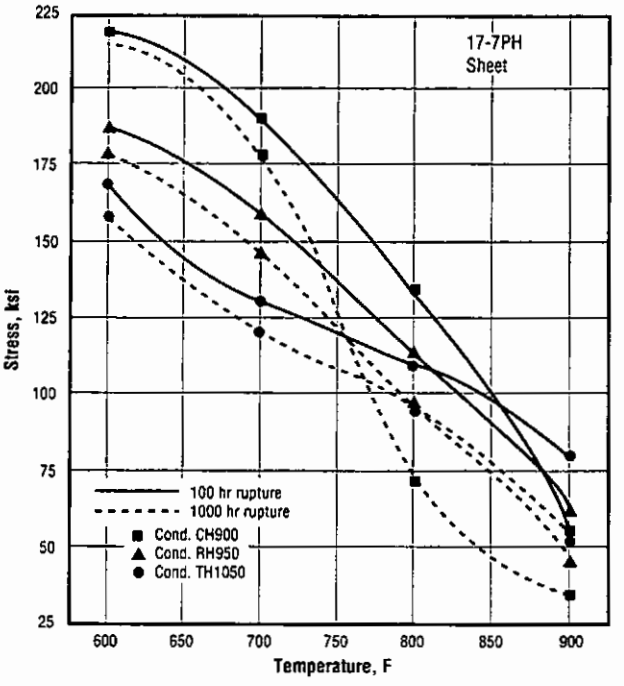


Fig. 3.4.2 Effect of temperature on tensile stress required to cause creep rupture in 100 and 1000 hours for sheet in various heat-treated conditions (Ref. 19)

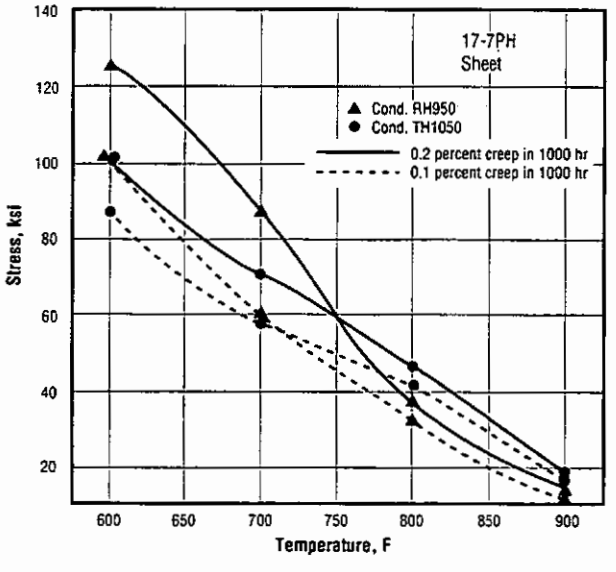


Fig. 3.4.3 Effect of temperature on tensile stress required to cause 0.1 and 0.2 percent creep deformation in 1000 hours for sheet in two heat-treated conditions (Ref. 19)

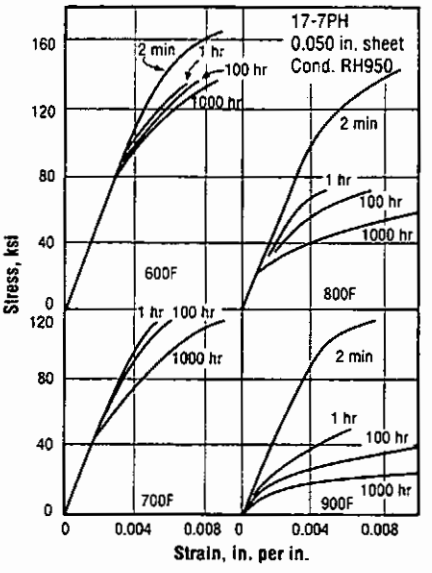


Fig. 3.4.4 Isochronous stress-strain curves at 600 to 900F for sheet in Condition RH950 (Ref. 29)

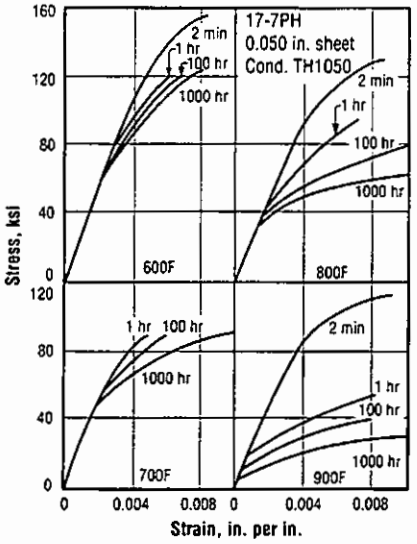


Fig. 3.4.5 Isochronous stress-strain curves at 600 to 900F for sheet in Condition TH1050 (Ref. 29)

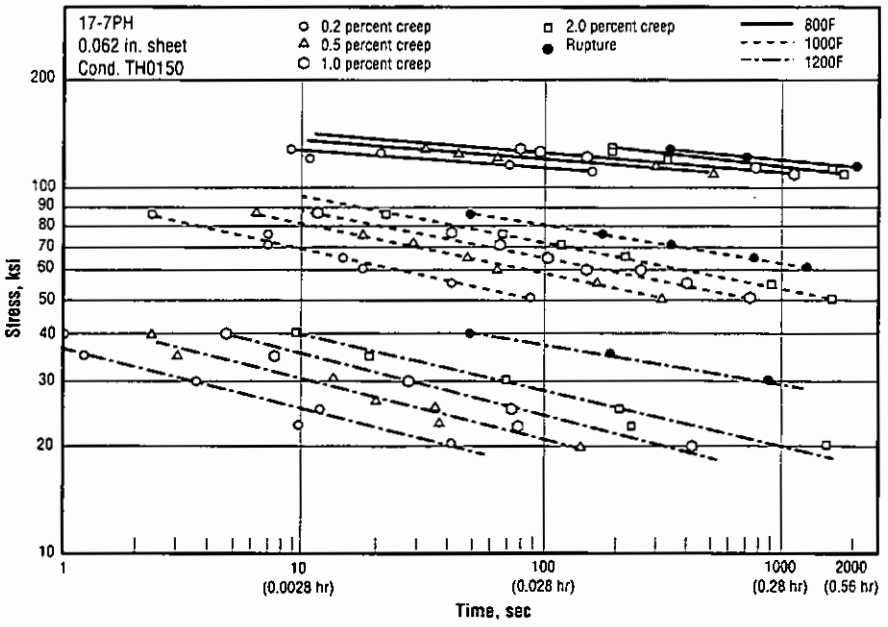


Fig. 3.4.6 Short-time creep and rupture properties of sheet in Condition TH1050 at temperatures from 800 to 1200F (Ref. 31) Note: Specimens were loaded at room temperature, heated rapidly to test temperature, and then creep measurements were started.

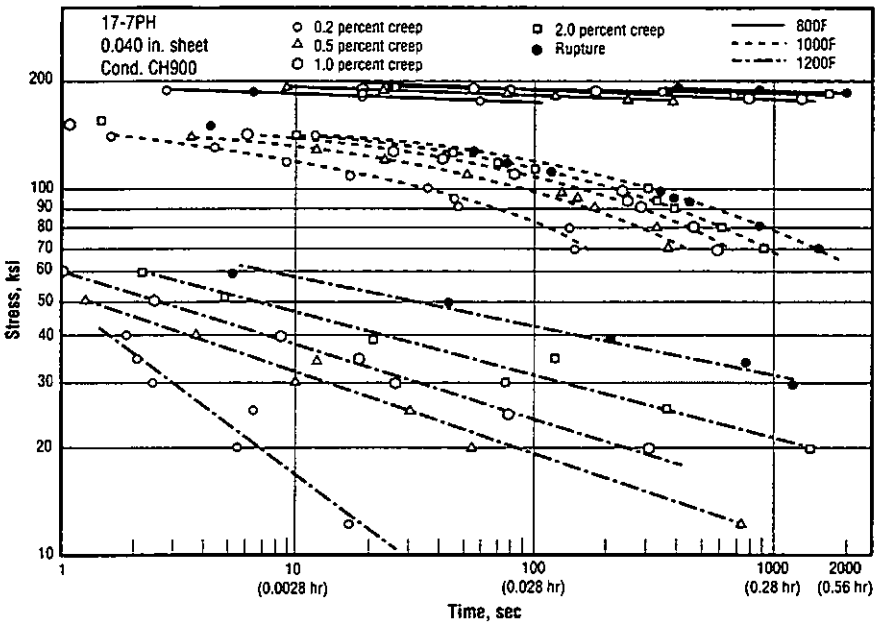


Fig. 3.4.7 Short-time creep and rupture properties of sheet in Condition CH900 at temperatures from 800 to 1200F (Ref. 31) Note: Specimens were loaded at room temperature, heated rapidly to test temperature, and then creep measurements were started.

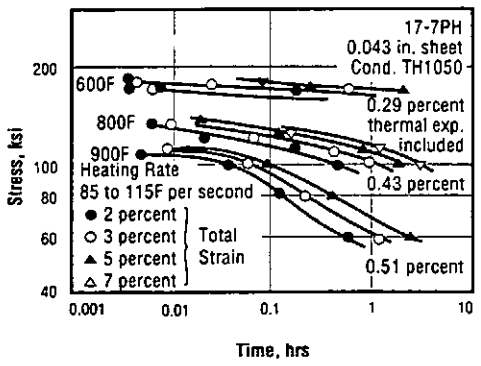


Fig. 3.4.8 Short-time total strain curves at 600 to 900F for sheet in Condition TH1050 (Ref. 37)

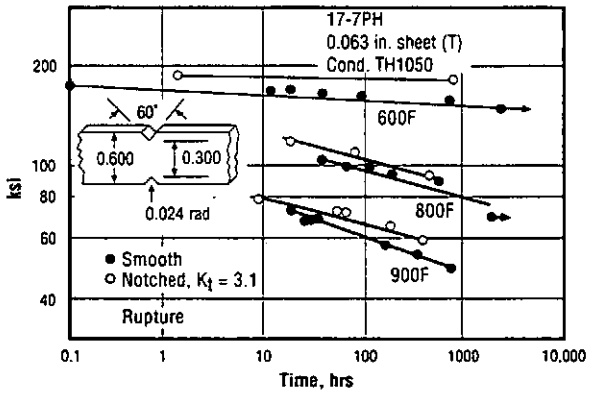


Fig. 3.4.9 Creep-rupture curves at 600 to 900F for smooth and notched sheet in Condition TH1050 (Ref. 50)

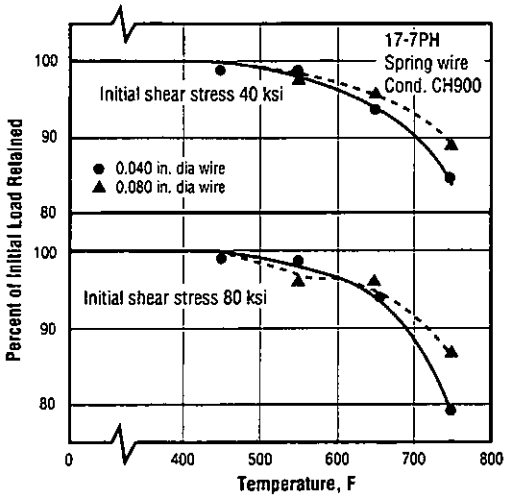


Fig. 3.4.10 Loss of load due to stress relaxation of helical compression springs held at constant length and at temperatures from 450 to 750F for 96 hours (Ref. 17)

Table 3.4.11 Effects of wire diameter, preset stress, and initial stress on stress relaxation of helical extension springs held at constant extension at room temperature for 100 hours (Ref. 42)
Note: The constant extension is the elastic strain associated with the initial shear stress

Alloy: 17-7PH					
Form		**Helical Extension Springs**			
Condition		**CH900**			
Wire Dia, in.	**F_{ty}, ksi**	**F_{sty}, ksi**	**Preset (1) ksi**	**Initial Shear Stress, ksi**	**Stress Relaxation in 100 hr., percent (2)**
0.040	318	223	191	145	1.2
				174	2.2
				203	7.7
0.040	318	223	223	145	1.7
				174	3.9
				203	4.3
0.080	293	181	178	145	1.4
				174	1.5
0.080	293	181	181	145	2.0
				174	2.5

Notes:
(1) Preset refers to cycling of the springs to the indicated shear stresses five times prior to the application of the initial stress.
(2) Percentage loss of initial shear stress.

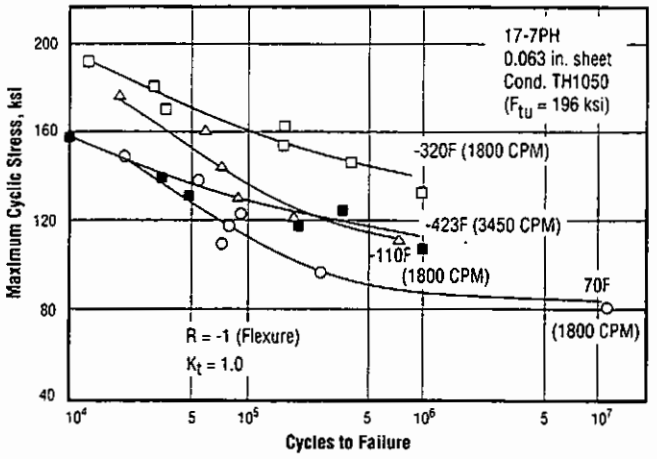


Fig. 3.5.1 Flexural fatigue properties at room and low temperatures for sheet in Condition TH1050 (Ref. 51)

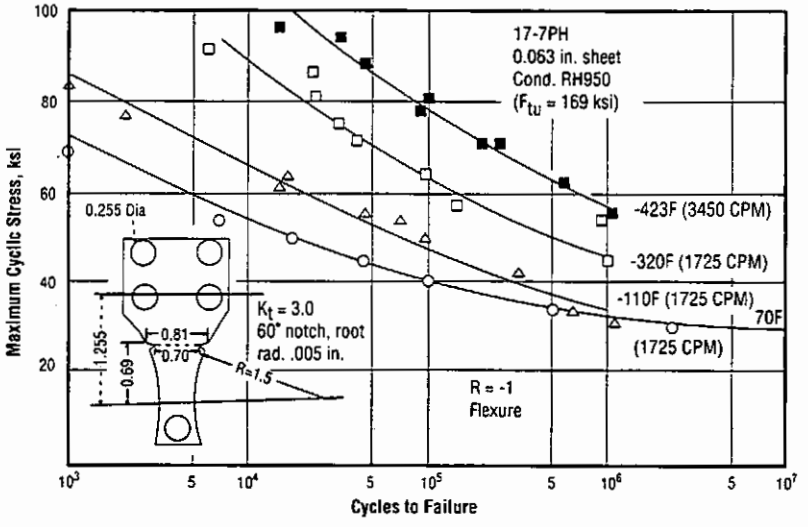


Fig. 3.5.2 Flexural fatigue properties at room and low temperatures for notched sheet (K_t = 3.0) in Condition RH950 (Ref. 51)

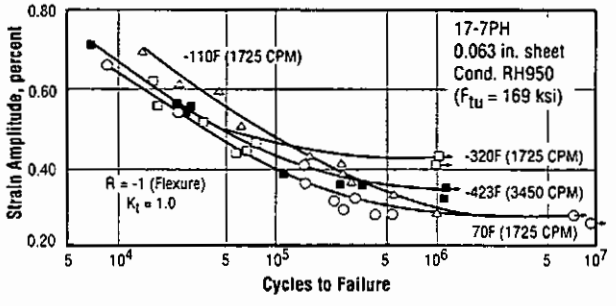


Fig. 3.5.3 Flexural strain-cycling fatigue curves at room and low temperatures for sheet in Condition RH950 (Ref. 51)

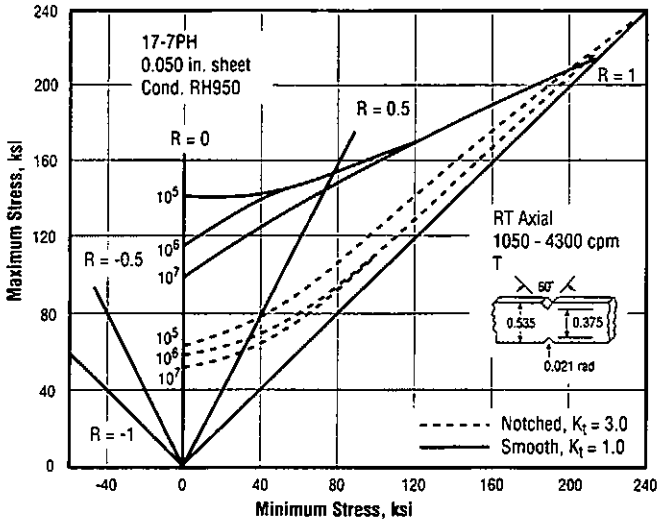


Fig. 3.5.4 Constant-life fatigue curves at room temperature for smooth and notched sheet in Condition RH950 (Ref. 39)

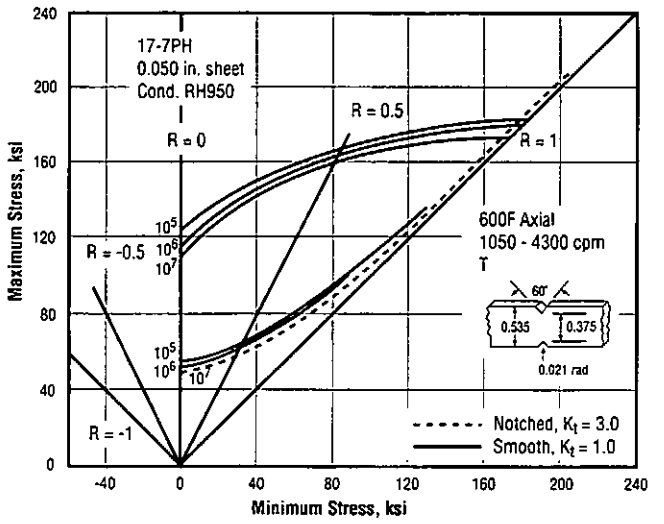


Fig. 3.5.5 Constant-life fatigue curves at 600F for smooth and notched sheet in Condition RH950 (Ref. 39)

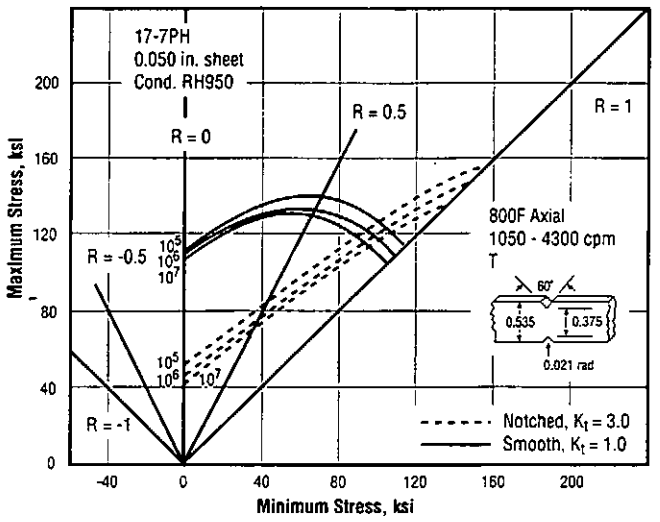


Fig. 3.5.6 Constant-life fatigue curves at 800F for smooth and notched sheet in Condition RH950 (Ref. 39)

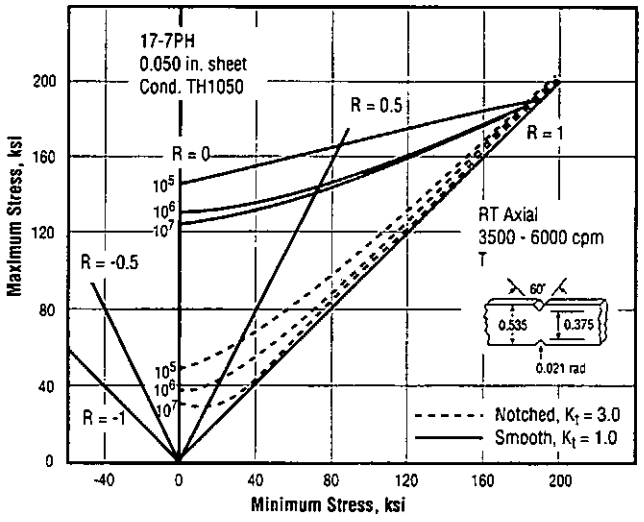


Fig. 3.5.7 Constant-life fatigue curves at room temperature for smooth and notched sheet in Condition TH1050 (Ref. 38)

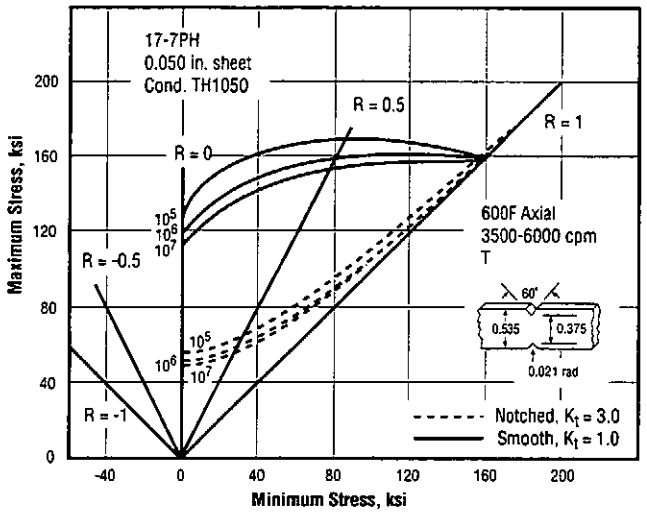


Fig. 3.5.8 Constant-life fatigue curves at 600F for smooth and notched sheet in Condition TH1050 (Ref. 38)

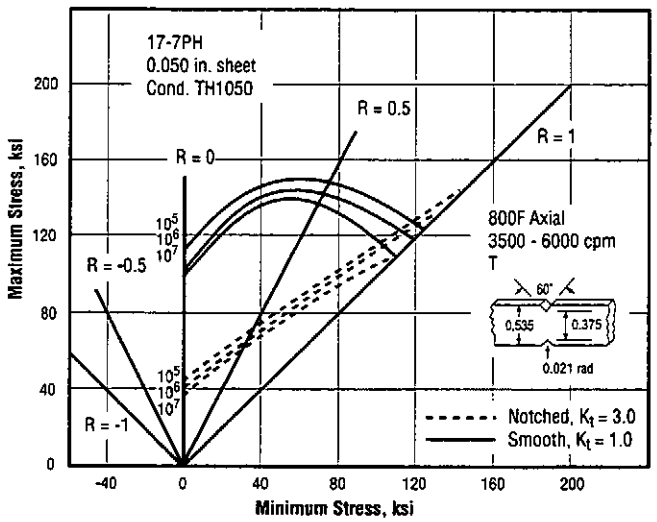


Fig. 3.5.9 Constant-life fatigue curves at 800F for smooth and notched sheet in Condition TH1050 (Ref. 38)

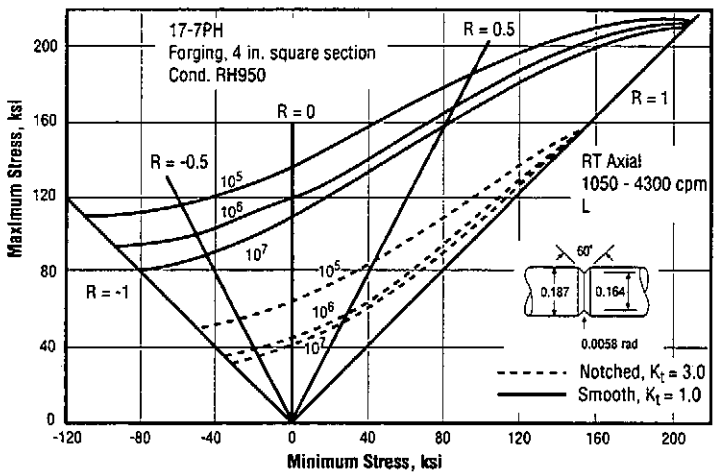


Fig. 3.5.10 Constant-life fatigue curves at room temperature for smooth and notched forging in Condition RH950 (Ref. 39)

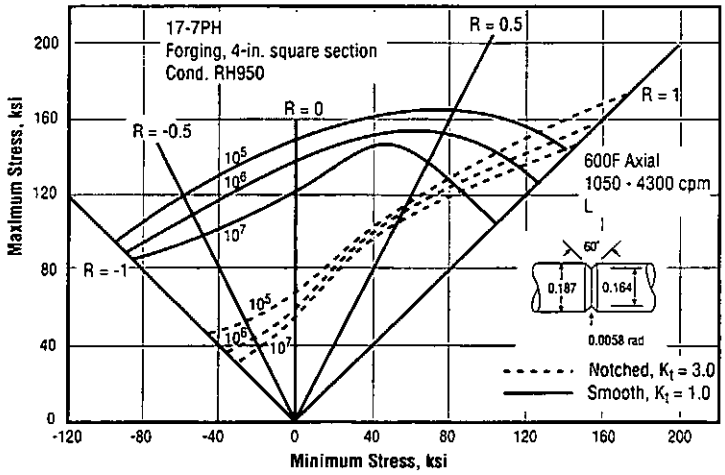


Fig. 3.5.11 Constant-life fatigue curves at 600F for smooth and notched forging in Condition RH950 (Ref. 39)

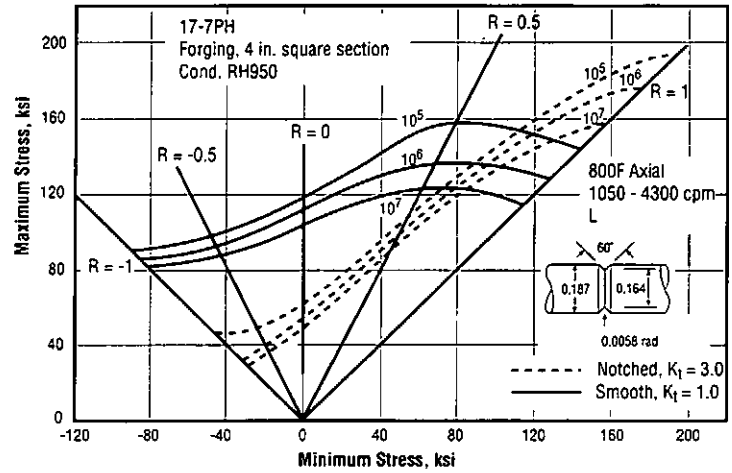


Fig. 3.5.12 Constant-life fatigue curves at 800F for smooth and notched forging in Condition RH950 (Ref. 39)

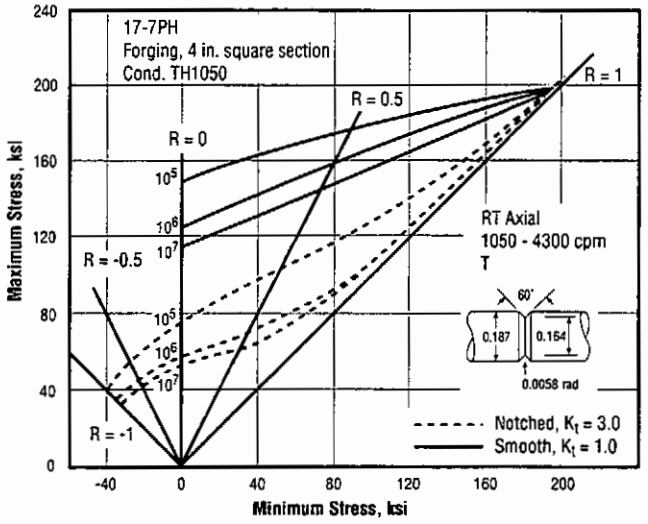


Fig. 3.5.13 Constant-life fatigue curves at room temperature for smooth and notched forging in Condition TH1050 (Ref. 39)

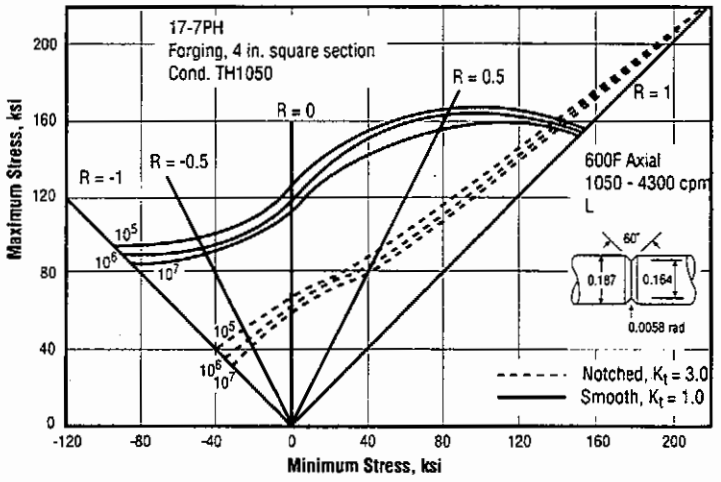


Fig. 3.5.14 Constant-life fatigue curves at 600F for smooth and notched forging in Condition TH1050 (Ref. 39)

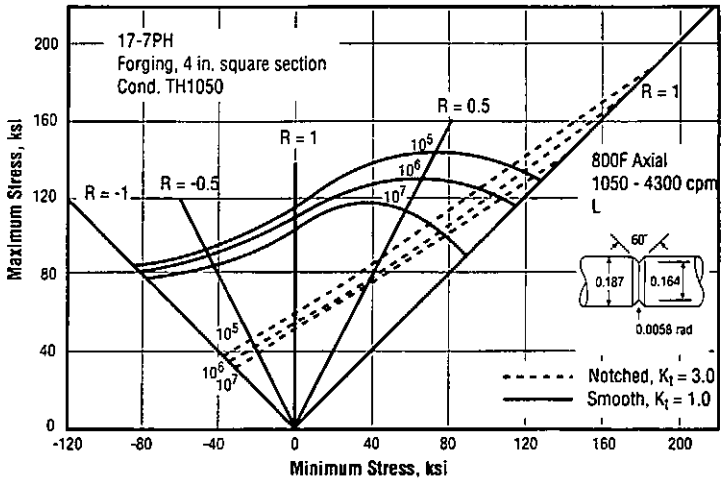


Fig. 3.5.15 Constant-life fatigue curves at 800F for smooth and notched forging in Condition TH1050 (Ref. 39)

Table 3.5.16 Effects of wire diameter and surface condition on the fatigue endurance limit of helical compression springs at room temperature (Ref. 17)

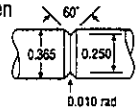
Alloy: 17-7PH			
Form		**Helical Compression Springs**	
Condition		**CH900**	
Wire Dia., in.	**Surface Condition**	**F_{tu}, ksi**	**Fatigue Endurance Limit (Shear Stress) at 10^7 cycles, ksi (a)**
0.067	Cold Drawn	297 - 327	85
0.067	Electropolish	297 - 327	105
0.085	Cold Drawn	292 - 322	85
0.105	Cold Drawn	274 - 304	85
0.105	Shot Peen	274 - 304	120
0.105	Electropolish & Shot Peen	274 - 304	130
0.125	Cold Drawn	272 - 302	73
0.125	Electropolish	272 - 302	85

(a) 10 ksi minimum cyclic stress

Table 3.5.17 Effect of surface protection with dodecyl alcohol on fatigue crack initiation and propagation of notched bar (Ref. 59)

Alloy: 17-7PH							
Form	**0.365-in. Bar (a)**						
Condition	**TH1050 (45 RC)**						
Rotating Beam R = -1 3000 rpm	**Thousands of cycles of stress (b)**						
	Clean Surface			**Surface coated with dodecyl alcohol**			
Max Cyclic Stress, ksi	**N_c (c)**	**N_p (d)**	**N_f (e)**	**N_c (c)**	**N_p (d)**	**N_f (e)**	**R (f)**
42.5	40	75	115	40	285	325	3.8
52.5	12	20	32	12	27	39	1.4

(a) Notched specimen



(b) Median value, 5-7 specimens
(c) Cycles to cause detectable crack at notch root
(d) Cycles to propagate crack to failure
(e) Total cycles to failure
(f) Ratio of cycles to propagate crack, coated: clean

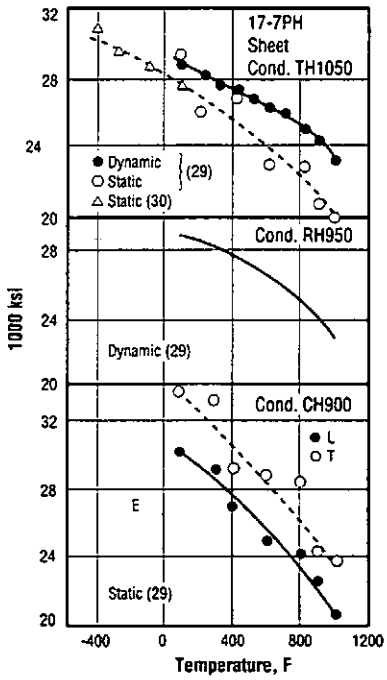


Fig. 3.6.2.1 Modulus of elasticity at various temperatures (Refs. 29, 30)

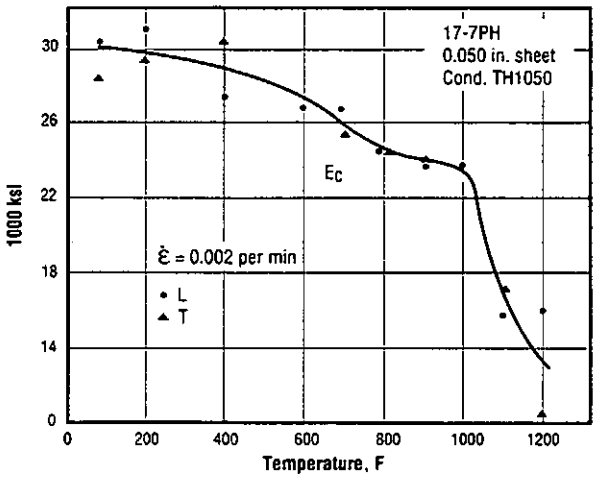


Fig. 3.6.2.2 Effects of temperatures up to 1200F on the modulus of elasticity in compression of sheet (Ref. 3)

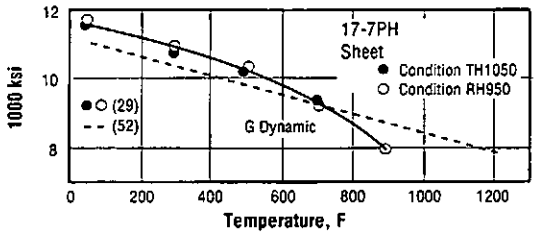


Fig. 3.6.3.1 Modulus of rigidity at room and elevated temperatures (Refs. 29, 52)

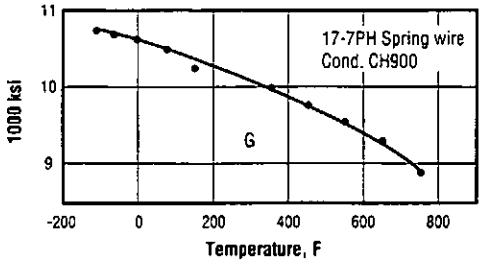


Fig. 3.6.3.2 Effects of temperatures from -105 to 750F on modulus of rigidity of spring wire (Ref. 17)

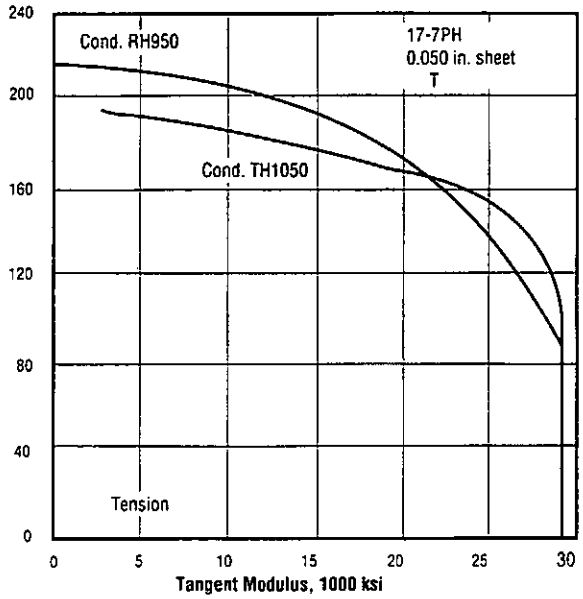


Fig. 3.6.4.1 Tangent-modulus curves in tension at room temperature for sheet in Conditions TH1050 and RH950 (Ref. 29)

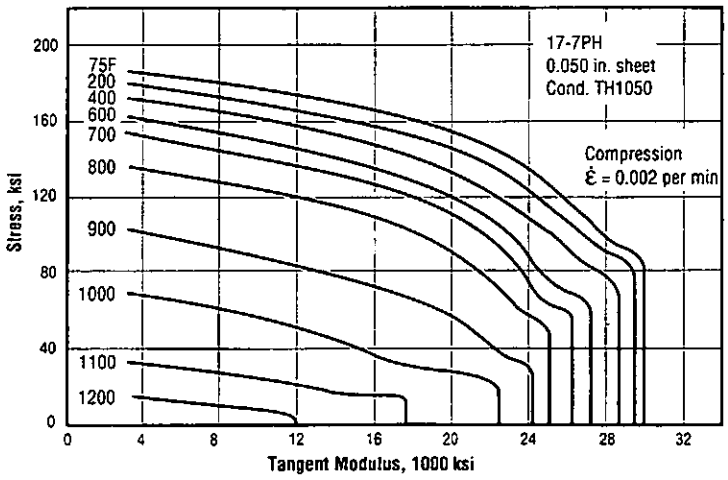


Fig. 3.6.4.2 Tangent-modulus curves in compression for sheet in Condition TH1050 at temperatures up to 1200F (Ref. 3)

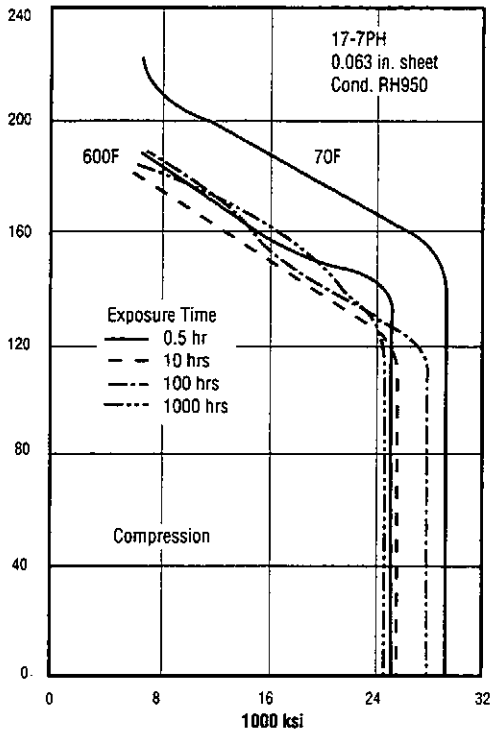


Fig. 3.6.4.3 Tangent-modulus curves in compression for sheet in Condition RH950 at room temperature and 600F, showing effects of prior exposure at 600F (Ref. 35)

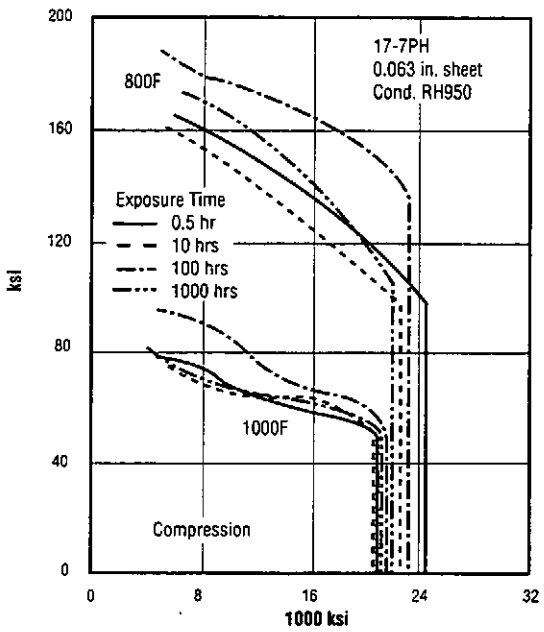


Fig. 3.6.4.4 Tangent-modulus curves in compression for sheet in Condition RH950 at 800 and 1000F, showing effects of prior exposure at test temperature (Ref. 35)

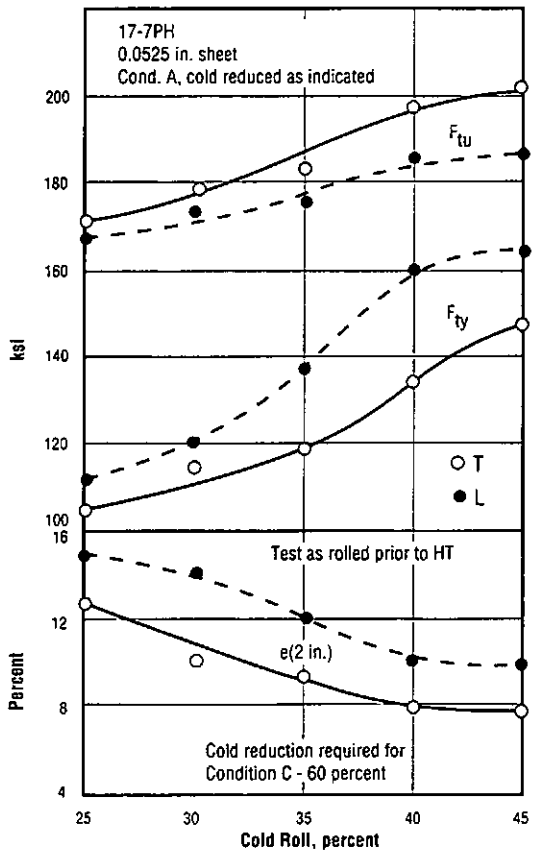


Fig. 4.1.1.2 Effect of cold work on tensile properties of sheet given less cold reduction than required for Condition C (Ref. 13)

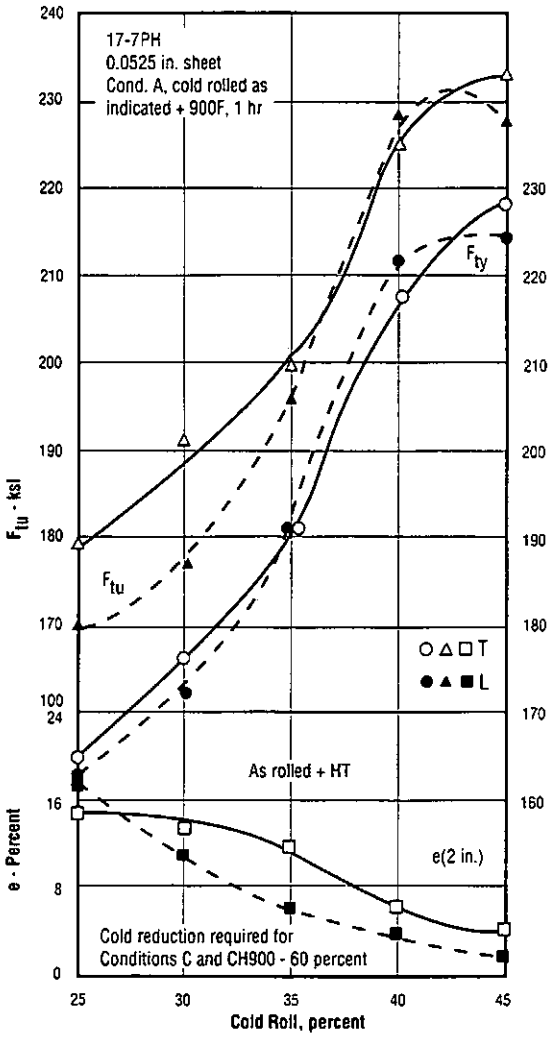


Fig. 4.1.1.3 Effect of cold work on tensile properties of sheet given less cold reduction than required for Conditions C and CH900 and then aged for one hour at 900F (Ref. 13)

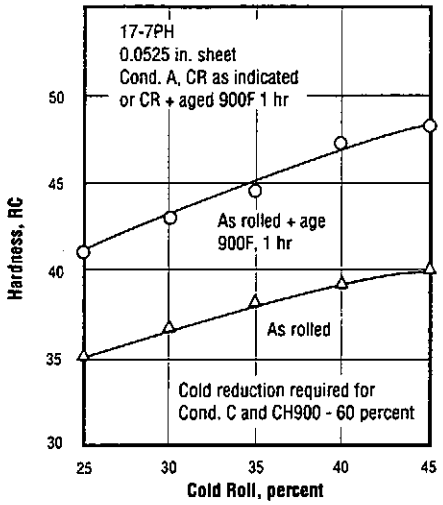


Fig. 4.1.1.4 Effect of cold work on hardness of sheet given less cold reduction than required for Conditions C and CH900 (Ref. 13)

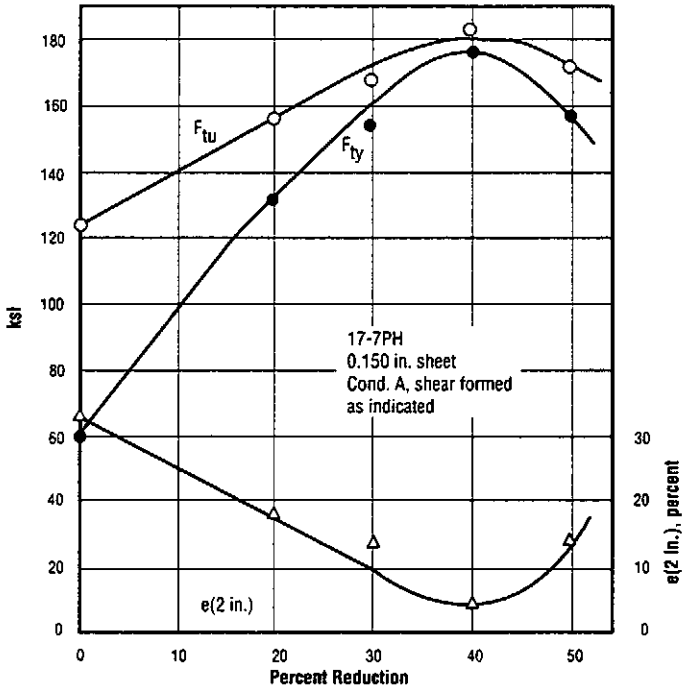


Fig. 4.1.1.6.1 Effect of percent reduction by shear forming on tensile properties at room temperature (Ref. 26)

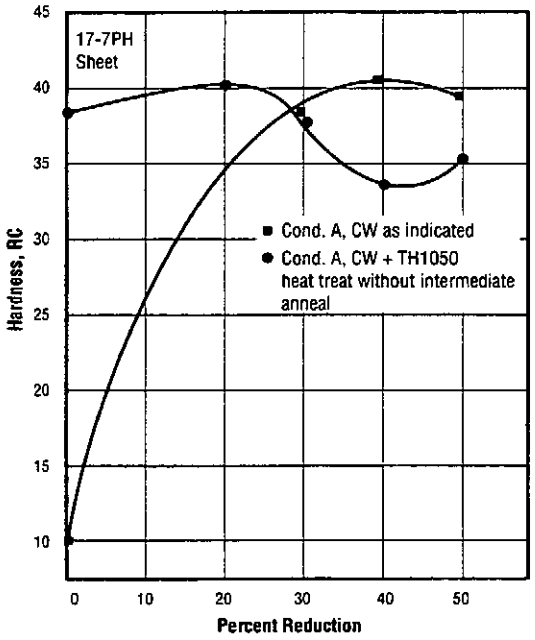


Fig. 4.1.1.6.2 Effects of sheer forming and subsequent heat treatment on hardness (Ref. 26)

Table 4.3.1.2 Tensile properties determined on sheet with butt welds across the gage length of the test specimens (Refs. 6, 10, 21)

Alloy: 17-7PH			
Form	**0.062-in. Sheet, Butt Welded (a)**		
Condition (b)	**F_{ty}, ksi**	**F_{tu}, ksi**	**El(2 in.), percent**
RH950	205	220	2.0
RH1100	132	165	6.0
TH1050	195	205	1.5
TH1100	130	160	6.0
A, TH1050	195	208	2.5
A, TH1100	132	160	6.0

(a) GATW (helium shielding at 60 in. ft. per hr.) at 15 in. per min., d-c s-p, with 1/16-in.-dia. 17-7PH filler added at 28 in. per min.

(b) Sheet was in Condition A when welded and was heat treated to conditions shown after welding. The last two samples were given an intermediate treatment to Condition A after welding but prior to the final treatments.

Table 4.3.1.3 Comparison of tensile properties at both room and elevated temperatures of sheets in Condition TH1075 with the same sheets containing butt welds (as-welded) across the gage length of the test specimens (Ref. 21)

Alloy: 17-7PH						
Form			Sheet			
Location			Base Metal		Weld Joint (a)	
Condition (b)			TH1075		As-Welded (c)	
Sheet Thickness, in.	Orientation	Temp., F	F_{tu}, ksi	e(2 in.) percent	F_{tu}, ksi	e(2 in.) percent
0.018	T	75	182.6	10.8	143.9	2.1
0.050	T	75	177.7	10.4	140.5	3.8
0.080	T	75	187.5	9.0	156.7	4.7
0.050	L	75	184.2	-	151.4	4.0
0.078	L	75	189.0	-	145.8	5.6
0.078	L	300	175.8	9.1	96.0	4.9
0.050	L	500	161.3	4.7	90.1	2.8
0.050	L	700	152.4	6.5	92.3	3.0
0.050	L	900	116.7	22.0	81.2	3.2

(a) GTAW with 17-7PH filler wire.
(b) The sheet was in Condition TH1075 prior to welding and no postweld heat treatment was applied.
(c) Specimens fractured in the welds.

Table 4.3.2.1 Shear strength of spot-welded joints (Ref. 21)

Alloy: 17-7PH			
Form	0.050-in. Sheet		
Condition in Which Welded (a)	Condition in Which Tested	Shear Breaking Load lb/weld	
		Low Test	20 Test Avg.
A	TH1050 (b)	2720	2790 (d)
T	TH1050 (b)	2950	2970 (d)
TH1050	TH1050 (c)	2250	2610 (d)
A	RH950 (b)	2300	2556
R100	RH950 (b)	2582	2882
RH950	RH950 (c)	2380	2660
MIL-W-6858B, minimums		2125	2620

(a) Spot welding conditions: welding pressure 120 lb., current 1500 amps, electrode dome radius 3 in., time 10 cycles, sheet vapor blasted prior to welding.
(b) Postweld heat treatment completed from condition in which welded; no intermediate solution treatment.
(c) No postweld heat treatment.
(d) Average of three tests.

References

1. Reinhart, F. N., "Corrosion of Materials in Hydrospace—Part VI—Stainless Steels," Naval Civil Engineering Laboratory, Technical Note N-1172 (Sept. 1971).
2. "Emissivity of Metals at Elevated Temperatures," McDonnell Aircraft Corp., Report No. 9096 (Oct. 10, 1962).
3. Stein, B. A., "Compressive Stress-Strain Properties of 17-7 PH and AM 350 Stainless-Steel Sheet at Elevated Temperatures," NACA TN 4074 (Aug. 19, 1957).
4. Clarke, W. C., Jr., "A Study of Embrittlement of a Precipitation Hardening Stainless Steel and Some Related Materials," *Trans. of the Metallurgical Society of AIME*, Vol. 245, pp. 2135-2140 (Oct. 1969).
5. Carter, C. S.; Farwick, D. G.; Ross, A. M.; and Uchida, J. M., "Stress Corrosion Properties of High Strength Precipitation Hardening Stainless Steels," *Corrosion*, Vol. 27, pp. 190-197 (May 1971).
6. Weymueller, C. R., "The PH Stainlesses—Simple to Weld but Touchy," *Welding Design and Fabrication*, Vol. 53, pp. 68-72 (May 1980).
7. ASTM A 693, *ASTM Annual Book of Standards*, Vol. 1.03.
8. ASTM A 564, *ASTM Annual Book of Standards*, Vol. 1.05.
9. ASTM A 705, *ASTM Annual Book of Standards*, Vol. 1.05.
10. "Precipitation-Hardenable Stainless Steels," The International Nickel Co., Inc., Bulletin D (1963).
11. "Stability of Armco 17-7 PH Steel in the RH Condition on Exposure to Elevated Temperatures," The Martin Co., ER-9582-5 (Oct. 10, 1957).
12. NASA (1959).
13. "Armco 17-7 PH and PH 15-7Mo," Armco Steel Corp. (1966).
14. "Armco Precipitation Hardening Stainless Steels," Armco Stainless Steel Division (Nov. 1983).
15. "Precipitation Hardenable Stainless Steels," Republic Steel Corp. (1975).
16. "Armco Stainless Steels," Armco Specialty Steels Division (Feb. 1985).
17. "Armco 17-7 PH Precipitation-Hardening Stainless Steel, Bar, Rod and Wire," Armco Stainless Steel Division, Bulletin No. S-29e (April 1983).
18. ASTM A 313, *ASTM Annual Book of Standards*, Vol. 1.03.
19. "Armco 17-7 PH Precipitation-Hardening Stainless Steel Sheet and Strip," Armco Product Data Bulletin No. FS-2 (1987).
20. "Heat Treating Armco Stainless Steels," Armco Fabricating Data Bulletin No. SF-56 (1984).
21. "Welding and Brazing Armco 17-7 PH and PH 15-7Mo Precipitation Hardening Stainless Steels," Armco Bulletin SF-5 (1967).
22. "Armco Stainless Steels," Armco Publication LA172 (1972).
23. *Metals Handbook*, Ninth Edition, Vol. 3, ASM International (1980).
24. Campbell, J. E.; Gerberich, W. W.; and Underwood, J. H., "Application of Fracture Mechanics for Selection of Metallic Structural Materials," American Society for Metals (1982).
25. *Metals Handbook*, Tenth Edition, Vol. 1, ASM International (1990).
26. Jacobs, Frank, "Mechanical Properties of Materials Fabricated by Shear Forming," ASD-TDR-62-830 (Feb. 1963).
27. "Stainless Steel, AL 17-7 Precipitation-Hardening Alloy," Allegheny Ludlum Steel Corp., Bulletin B-158-Ed1-3M-186 BPA (1985).
28. Thompson, A. W., "How High-Pressure Hydrogen Affects Stainless Steel," *Metal Progress*, Vol. 110, pp. 30-33 (July 1976).
29. "Armco Precipitation Hardening Stainless Steels Technical Data Manual," Armco Steel Corp. (Nov. 1, 1957).
30. McGee, A. L.; Campbell, J. E.; Carlson, R. L.; and Manning, G. K., "The Mechanical Properties of Certain Aircraft Structural Metals at Very Low Temperatures," WADC TR 58-386 (Nov. 1958).
31. Kattus, J. R., "Tensile and Creep Rupture Properties of Structural Alloys Under Conditions of Rapid Heating, Rapid Loading, and Short Times at Temperature," Southern Research Institute Report 3962-867-2-I to International Nickel Co. (April 10, 1959).
32. Willhelm, A. C., and Kattus, J. R., "Determination of the Mechanical Properties of Aircraft Structural Materials at Very High Temperatures After Rapid Heating"; Part 3, "The Effects of Simultaneous Heating and Loading on the Tensile Properties of Typical Structural Alloys," WADC TR 57-647, Part 3 (Nov. 1960).
33. Morrison, J. D., and Kattus, J. R., "Tensile Properties of Aircraft Structural Metals at Various Rates of Loading After Rapid Heating," WADC TR 55-199, Part 2 (Nov. 1956).
34. Miller, E. D., "Determination of the Physical Properties of Ferrous and Nonferrous Structural Sheet Materials at Elevated Temperatures," AF TR No. 6517, Part 4 (Dec. 1954).

35. Kattus, J. R.; Preston, J. B.; and Lessley, H. L., "Determination of Tensile, Compressive, Bearing, and Shear Properties of Sheet Steels at Elevated Temperatures," WADC Technical Report 58-365 (Nov. 1958).

36. Steigerwald, E. A., "Plane Strain Fracture Toughness for Handbook Presentation," AFML-TR-67-187 (July 1967).

37. AFTR 6731, Part 3 (1955).

38. Bass, C. D., and Harmsworth, C. L., "Fatigue, Tensile, and Creep Properties of 17-7 PH TH1050 and AM 350 SCT Sheet," AFML-TR-69-331 (March 1970).

39. Roach, T. A., "Development of Fatigue Data for Several Alloys for Use in Aerospace Design," AFML-TR-69-175 (June 1969).

40. Fritz, L. J.; Koster, W. P.; and Field, M., "Low-Stress Creep Testing of 17-7 PH Stainless Steel," Metcut Research Associates Report No. 363-1536, Air Material Command Contract No. AF 33(600)-36430 (April 14, 1960).

41. Armco Materials and Processing Update, "The Effect of Composition and Section Size on Transverse Properties of Precipitation Hardening of Stainless Steels" (1981).

42. Idermark, S. U. V., and Johansson, E. R., "Room Temperature Stress Relaxation of High-Strength Strip and Wire Spring Steels—Procedures and Data," *Stress-Relaxation Testing*, ASTM STP 676, pp. 61-77 (1979).

43. Menke, Joseph T., "An Evaluation of Processes for the Blackening of Precipitation-Hardening Stainless Steels," Rock Island Arsenal Technical Report No. EN-79-01 (June 1979).

44. Angel, Stefan, and Solly, Barry, "Factors Controlling the Reliability of 17-7 PH Spring Wire," *Wire Journal International*, Vol. 15, No. 8, pp. 78-81 (Aug. 1982).

45. AMS 5528E, Society of Automotive Engineers (Oct. 1988).

46. AMS 5529D, Society of Automotive Engineers (Oct. 1989).

47. AMS 5568C, Society of Automotive Engineers (Jan. 1988).

48. AMS 5678B, Society of Automotive Engineers (Oct. 1987).

49. AMS 5824B, Society of Automotive Engineers (Jan. 1987).

50. Voorhees, H. R., and Freeman, J. W., "Notch Sensitivity of Aircraft Structural and Engine Alloys," WADC TR 57-58, Part 1 (May 1957).

51. Gideon, D. N.; Favor, R. J.; Koppenhafer, A.; Grover, H. J.; and McClure, G. M., "Investigation of Notch Fatigue Behavior of Certain Alloys in the Temperature Range of Room Temperature to -423F," ASD-TDR-62-351 (Aug. 1962).

52. General Electric Co., "G. E. Spec." (Dec. 17, 1957).

53. AMS 5673C, Society of Automotive Engineers (1974), [Superseded by AMS 5678 (July 1982)].

54. Walter, R. J., and Chandler, W. T., "Effects of High-Pressure Hydrogen," Reports to NASA by Rocketdyne Corp. under Contract NAS8-19, Part I, R-7234-1 (Sept. 1967); Part II, R-7234-2 (March 1968); Part III, R-7234-3 (Sept. 1968).

55. Davis, S. O.; Tupper, N. G.; Lagrone, D. C.; and Niemi, R. M., "Center-Notch Plane-Strain KIc Fracture Toughness Properties of Several High-Strength Steel Alloys," AFML-TR-65-214 (Oct. 1965).

56. Brisbane, A. W., "Mechanical Properties of 17-7 PH and PH 15-7Mo Stainless Steel," WADC TR 58-400 (Jan. 1959).

57. Armco Steel Corp., Private communication (April 9, 1959).

58. WADC TR 6517, Part 4 (1954).

59. Holhauser, W. L., and Utech, H. P., "Effect of Oleophobic Films on Crack Propagation," ASTM *Proceedings*, Vol. 61, pp. 749-54 (1961).

60. Lewis, J. R., "Physical Properties of Stainless Steels," *Handbook of Stainless Steels*, Chapter 19, McGraw-Hill (1977).

This page is blank.

REVISED: MARCH 1975
AUTHOR: J.R. KATTUS

FERROUS ALLOYS

1. GENERAL

These low-alloy steels are useful in aerospace applications, primarily because of their excellent mechanical properties at elevated temperatures in the hardened-and-tempered condition. Type 17-22A(S) is recommended for long-time service at temperatures up to 1000F; type 17-22A(V), because of its better resistance to tempering imparted by the increased vanadium content, can be used for extended periods to a maximum temperature of 1100F. They can also be used in applications requiring short-time exposures to much higher temperatures. Type 17-22A(S), for example, because of its outstanding resistance to thermal cracking, is used for disc-and drum-type aircraft brakes where skin temperatures up to 1700F and higher are reached. It is also used in various jet-engine applications, such as outer combustion chamber and tail-cone assembly, and compressor wheels and blading. Both modifications should be considered for turbine rotors and for missile and space-vehicle components that may be exposed to high skin temperatures for short periods of time. Since the alloys are susceptible to rusting in moist atmospheres and to scaling at temperatures of 800F and above, surface protection should be provided when such conditions are encountered for long times. Both versions of the alloy can be readily hot worked and can be welded by any of the common electric-arc methods. They can be readily machined in the annealed condition (14)(17). Both 17-22A(S) and 17-22A(V) are subject to a time-temperature dependent creep embrittlement (see 1.09).

1.01 Commercial Designations

17-22A(S) and 17-22A(V).

1.02 Alternate Designation

Unilloy 14 MV (Universal Cyclops designation for 17-22A(S))

1.03 Specifications

Table 1.03.

1.04 Composition

Table 1.04.

1.05 Heat Treatment

1.051 Anneal: 1450F 1 hour per inch of thickness, cool 20F per hour to 1100F, air cool. Resulting hardness is about 180 to 200 BHN (17).

1.052 Hardening: Because of their high hardenability both alloy modifications can be hardened by normalizing (air cooling) or oil-quenching from the austenitizing temperature. Normalizing results in superior high temperature creep and rupture properties, but greater impact resistance is obtained by oil-quenching (17).

1.0521 Normalizing: 1700 to 1750F for 17-22A(S) and 1800 to 1850F for 17-22A(V) 1 hour per inch of thickness, air cool (17).

1.0522 Oil-quench: 1650F for 17-22A(S) and 1750F for 17-22A (V) 1 hour per inch of thickness, oil quench (17).

1.053 Temper: 800F to 1300F, preferably 1000 to 1300F, exact temperature and time depending on hardness and strength levels desired (17).

1.054 Isothermal anneal for 17-22A(S): 1700 to 1750F, cool to 1300 to 1320F, hold 4 hours. Resulting hardness is about 212 BHN (17).

1.055 Marquench for 17-22A(S): 1650F, quench to 525F to 600F. Resulting hardness is 47-48 R_C (17).

1.06 Hardness

1.061 End-quench hardenability, Figure 1.061.

1.062 Effect of tempering temperature on hardness in the normalized and oil-quenched conditions, Figure 1.062.

1.063 Effect of normalizing temperature and time on hardness and grain size of subsequently tempered alloy, Figure 1.063.

1.064 Effect of normalizing temperature on hardness, Figure 1.064.

1.065 Effect of tempering time and temperature on hardness of bar, Figure 1.065.

1.066 Effect of temperature on hardness, Figure 1.066.

1.07 Forms and Conditions Available

1.071 Available in the form of bars, billets, tubes, sheet and plate, and forgings in the hot-rolled, cold-drawn, annealed, or heat-treated conditions. Type 17-22A(S) is also available in the form of welding wire (17)(4).

1.08 Melting and Casting Practice

1.081 These alloys are generally melted in basic electric furnaces. For applications requiring exceptional quality, they are induction or consumable-electrode-remelted in vacuum.

1.09 Special Considerations

1.091 Bainitic structures in these alloys, which are generally produced by air cooling from the austenitizing temperature, have elevated-temperature creep strengths superior to those of martensitic structures, which are produced by oil-quenching from the austenitizing temperature. However, the martensitic structures have superior toughness and ductility.

1.092 Both 17-22A(S) and 17-22A(V) are subject to a time-temperature dependent embrittlement under creep conditions. This is apparent from the tests on sharply notched cylindrical specimens (see Figure 3.0411 and 3.0413) The embrittlement tendency increases with a decrease in the temperature (see Figure 3.0412). When used in conditions producing high creep resistance, particular attention should be given to the possibility of a significant decrease in fracture toughness with continued exposure to load and temperature.

Fe	
0.3	C
1.3	Cr
0.5	Mo
0.25	V

17-22A(S)

Fe	
0.28	C
1.3	Cr
0.5	Mo
0.85	V

17-22A(V)

2. PHYSICAL AND CHEMICAL PROPERTIES

2.01 Thermal Properties

2.011 Melting range. 2800 to 2900F.

2.012 Phase changes.

2.0121 Time-temperature-transformation diagrams.

2.01211 Time-temperature-transformation diagram for 17-22A (S), Figure 2.01211.

2.01212 Time-temperature-transformation diagram for 17-22A (V), Figure 2.01212.

2.0122 The critical temperatures for 17-22A(S) are as follows: A_{c1} = 1440F, A_{c3} = 1600F, A_{r3} = 1460F, A_{r1} = 1280F, M_s = 632F (17).

2.0123 The critical temperatures for 17-22A(V) are as follows: A_{c1} = 1435F, A_{c3} = 1700F, A_{r3} = 1525F, A_{r1} = 1230F, M_s = 589F (17).

2.013 Thermal conductivity. Figure 2.013.

2.014 Thermal expansion.

2.0141 Thermal expansion of 17-22A(S), Figure 2.0141.

2.0142 Thermal expansion of 17-22A(V), Figure 2.0142.

2.015 Specific heat.

2.016 Thermal diffusivity.

2.02 Other Physical Properties

2.021 Density. 0.284 lb per cu in; 7.85 grams per cu cm (17).

2.022 Electrical properties.

2.023 Magnetic properties. Ferromagnetic.

2.024 Emittance, Figure 2.024.

2.025 Damping capacity.

2.03 Chemical Properties

2.031 Since these alloys are susceptible to rusting in moist environments and to scaling at elevated temperatures, surface protection is required for most applications. Hot-dip aluminizing and nickel electroplating are two protective methods that are effective (17).

2.032 Both alloys are susceptible to stress corrosion in the presence of chlorides and of various types of fuels. Nickel plating protects them against stress corrosion by chloride salts and by JP-4 fuel or fuel residues at temperatures up to at least 600F (11).

2.04 Nuclear Properties

Fe
0.3 C
1.3 Cr
0.5 Mo
0.25 V

17-22A(S)

Fe
0.28 C
1.3 Cr
0.5 Mo
0.85 V

17-22A(V)

3. MECHANICAL PROPERTIES

3.01 Specified Mechanical Properties
Table 3.01.

3.02 Mechanical Properties at Room Temperature
3.021 Tension-stress/strain diagrams - tension properties.
3.0211 Stress-strain curve (see Figure 3.0311).
3.0212 Effect of tempering temperature on tensile properties of 17-22A(S), Figure 3.0212.
3.0213 Effect of tempering temperature on tensile properties of 17-22A(V), Figure 3.0213.
3.0214 Tensile properties of forgings, Table 3.0214.
3.0215 Tensile properties of annealed bar, Table 3.0215.
3.0216 Effects of exposures to stresses at elevated temperatures on room-temperature tensile properties of 17-22A (S), Table 3.0216.
3.0217 Effects of exposures to stresses at elevated temperatures on room-temperature tensile properties of 17-22A (V), Table 3.0217.
3.022 Compression-stress/strain diagrams - compression properties.
3.0221 Stress-strain curve (see Figure 3.0321).
3.0222 Compressive yield strength (see Figure 3.0322).
3.023 Impact.
3.0231 Effect of normalizing temperature on impact strength of 17-22A(S), Figure 3.0231.
3.0232 Effect of normalizing temperature on impact strength of 17-22A(V), Figure 3.0232.
3.0233 Effect of tempering temperature on the impact resistance of 17-22A(S), Figure 3.0233.
3.024 Bending.
3.025 Torsion and shear (see Figure 3.0351).
3.026 Bearing (see Figure 3.0361).
3.027 Stress concentration.
3.0271 Notch properties.
3.0272 Fracture toughness.
3.028 Combined properties.

3.03 Mechanical Properties at Various Temperatures
3.031 Tension-stress/strain diagrams - tension properties.
3.0311 Tensile stress-strain curves for sheet at room and elevated temperatures, Figure 3.0311.
3.0312 Effects of temperature on tensile properties of sheet of different thicknesses in various heat-treated conditions, Figure 3.0312.
3.0313 Effects of temperature on tensile properties of 17-22A(S) 1 in. diameter bar in normalized-and-tempered conditions, Figure 3.0313.
3.0314 Effects of temperature on tensile properties of 17-22A (V) 1 in. diameter bar in various heat-treated conditions, Figure 3.0314.
3.0315 Effect of temperatures up to 800F on tensile properties of 4 in. diameter bar in oil-quenched and tempered condition, Figure 3.0315.
3.0316 Effects of repeated cycling to various elevated temperatures on tensile properties at room temperature and 800F, Figure 3.0316.
3.032 Compression-stress/strain diagrams-compression properties.
3.0321 Compressive stress-strain curves for sheet at room and elevated temperatures, Figure 3.0321.
3.0322 Effect of temperature on compressive yield strength of sheet, Figure 3.0322.
3.033 Impact.
3.0331 Effects of temperature on impact resistance of 17-22A (S) bar in various heat-treated conditions, Figure 3.0331
3.0332 Effects of temperature on impact resistance of normalized and of oil-quenched 17-22A(V), Figure 3.0332.
3.034 Bending.
3.035 Torsion and shear.
3.0351 Effect of temperature on shear strength after two different exposure times at temperature, Figure 3.0351.
3.036 Bearing.
3.0361 Effects of temperature on bearing properties, Figure 3.0361.
3.037 Stress concentration.
3.0371 Notch properties.
3.0372 Fracture toughness.
3.038 Combined properties.

3.04 Creep and Creep-Rupture Properties
3.041 Creep curves for sheet at 800, 1000, and 1050F, Figure 3.041.
3.042 Short-time total strain curves for sheet at 1000, 1200, and 1500F, Figure 3.042.
3.043 Creep-rupture curves for 17-22A(S) bar at 600 to 1350F, Figure 3.043.
3.044 Creep-rupture curves for 17-22A(S) bar at different temperatures and in various heat-treated conditions, Figure 3.044.
3.045 Creep-rupture curves for 17-22A(V) bar at different temperatures and in various heat-treated conditions, Figure 3.045.
3.046 Creep-rupture curves at 1100F for 17-22A(V) bar in various conditions of heat-treatment and hot work, Figure 3.046.
3.047 Creep-rupture properties of forging at 1100F, Figure 3.047.
3.048 Effect of temperature on creep-rupture strength of bar, Figure 3.048.
3.049 Effect of stress on creep rate at 1000 and 1100F, Figure 3.049.
3.0410 Creep-rupture curves for 17-22A(S)notched bar at 600 to 1350F, Figure 3.0410.
3.0411 Corresponding variations in notch creep-rupture strength ratio and unnotched creep-rupture ductility as functions of temperature and rupture time, Figure 3.0411.
3.0412 Effects of normalizing and tempering temperatures on creep-rupture strength of smooth and notched bars of 17-22A(S) at 1000F for 10 hour and 100 hour rupture times, Figure 3.0412.
3.0413 Creep-rupture curves for smooth and notched specimens of 17-22A(V) at 1100F, Figure 3.0413.
3.0414 Comparison of creep-rupture properties in shear and tension at 1100F, Figure 3.0414.

3.05 Fatigue Properties

3.06 Elastic Properties
3.061 Poisson's ratio.
3.0611 Effect of temperature on Poisson's ratio, Figure 3.0611
3.062 Modulus of elasticity.
3.0621 Effect of temperature on dynamic modulus of elasticity, Figure 3.0621.
3.0622 Effect of temperature on static modulus of elasticity of sheet in tension and compression, Figure 3.0622.
3.0623 Tangent modulus curves in compression for sheet at various temperatures, Figure 3.0623.
3.063 Modulus of rigidity.
3.0631 Effect of temperature on modulus of rigidity, Figure 3.0631.

4. FABRICATION

4.01 Formability
4.011 Types 17-22A(S) and (V) have formability similar to that of Type 4130 steel; that is, limited cold formability in the annealed condition and excellent hot formability. (See Type 4130, Code 1201, Sections 4.011 and 4.012.) The maximum recommended hot-forming temperature is 2300F (17).

4.02 Machining and Grinding
4.021 Machinability of Types 17-22A(S) and (V) is good in the annealed condition, being about 57 percent of that of B1112 screw machine stock (14).

4.03 Welding
4.031 Both 17-22A(S) and 17-22A(V) can be welded by any of the commercial electric-arc processes. Filler metal corresponding to the composition of 17-22A(S), which is commercially available, is recommended. Preheating to 600F prior to welding is recommended, particularly for large parts and irregular shapes. For maximum

uniformity of properties, a full hardening and tempering treatment should be carried out after welding. When a full heat treatment is not feasible, a tempering treatment in the range 1100 to 1200F is recommended (17).

4.032 Comparison of tensile properties of base metal and welded joints in plates of various thicknesses. Weld beads not machined or ground, Table 4.032.

4.033 Comparison of fatigue life of base metal and welded joints, Figure 4.033.

4.04 Surface Treatment

4.041 For elevated-temperature applications, surface protection by hot-dip aluminizing or nickel electroplating are recommended. Although the aluminizing temperature is normally 1300F, the properties of parts tempered at lower temperatures are not appreciably affected because of the short aluminizing time of a few minutes (17).

4.042 For long-time exposures to ordinary temperatures, paint provides suitable surface protection.

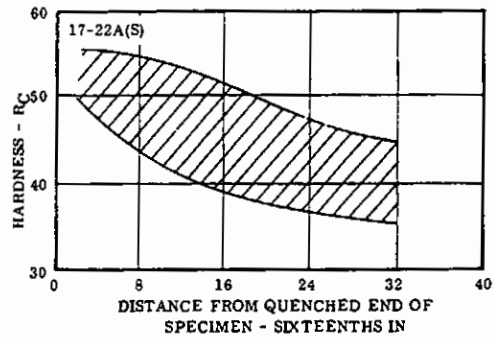


FIG. 1.061 END-QUENCH HARDENABILITY. (17)

Fe
0.3 C
1.3 Cr
0.5 Mo
0.25 V

17-22A(S)

Fe
0.28 C
1.3 Cr
0.5 Mo
0.85 V

17-22A(V)

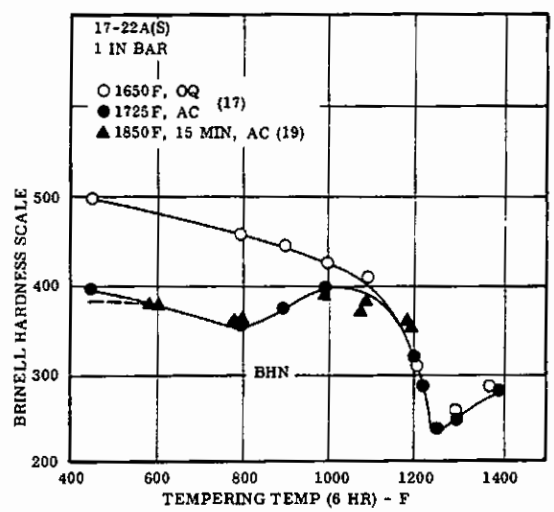


FIG. 1.062 EFFECT OF TEMPERING TEMPERATURE ON HARDNESS IN THE NORMALIZED AND OIL-QUENCHED CONDITIONS. (17)(19)

Alloy	Form	Specification
17-22A(S)	Bars, forgings	AMS 6302B
	Sheet, strip, plate	AMS 6385B
	Welding wire	AMS 6458D
	Bolting	ASTM 193
17-22A(V)	Bars, forgings	AMS 6303B
	Sheet, strip, plate	AMS 6436A

TABLE 1.03 SPECIFICATIONS

Alloy	17-22A(V)		17-22A(S)			
Source	AMS 6303B(2)		AMS 6302B(1)		AMS 6458D (5) Vacuum melt	
	Percent		Percent		Percent	
	min.	max.	min.	max.	min.	max.
Carbon	0.25	0.30(a)	0.28	0.33(b)	0.28	0.33
Manganese	0.60	0.90	0.45	0.65	0.45	0.65
Silicon	0.55	0.75	0.55	0.75	0.55	0.75
Phosphorus	-	0.025	-	0.025	-	0.008
Sulfur	-	0.025	-	0.025	-	0.008
Chromium	1.00	1.50	1.00	1.50	1.15	1.35
Molybdenum	0.40	0.60	0.40	0.60	0.40	0.60
Vanadium	0.75	0.95	0.20	0.30	0.20	0.40
Nickel	-	0.50	-	0.25	-	0.25
Copper	-	0.50	-	0.35	-	0.35
Oxygen	-	-	-	-	-	0.0025
Hydrogen	-	-	-	-	-	0.0025
Nitrogen	-	-	-	-	-	0.005

(a) AMS 6436A (4): C, 0.20 min - 0.25 max.
(b) AMS 6585B (3): C, 0.27 min - 0.33 max.

TABLE 1.04 COMPOSITION

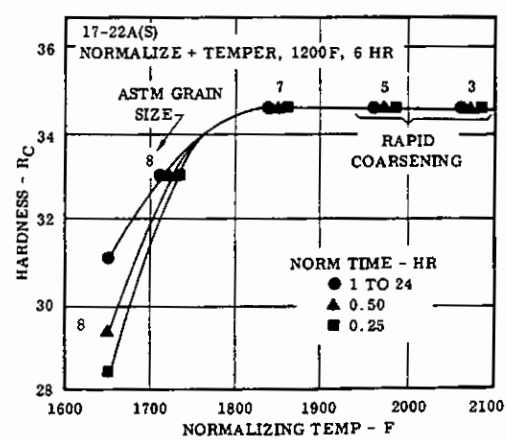


FIG. 1.063 EFFECT OF NORMALIZING TEMPERATURE AND TIME ON HARDNESS AND GRAIN SIZE OF SUBSEQUENTLY TEMPERED ALLOY. (19)

Fe	
0.3	C
1.3	Cr
0.5	Mo
0.25	V

17-22A(S)

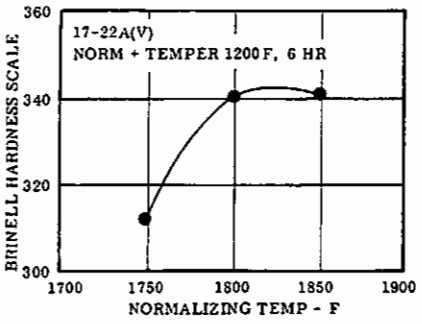


FIG. 1.064 EFFECT OF NORMALIZING TEMPERATURE ON HARDNESS. (17)

Fe	
0.28	C
1.3	Cr
0.5	Mo
0.85	V

17-22A(V)

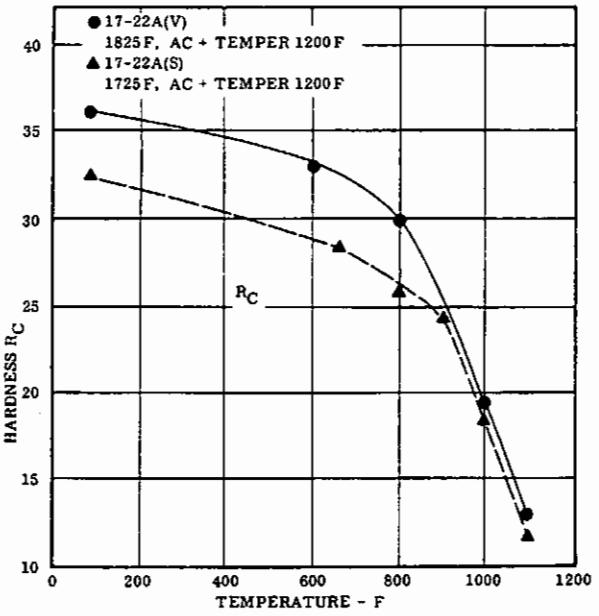


FIG. 1.066 EFFECT OF TEMPERATURE ON HARDNESS. (17)

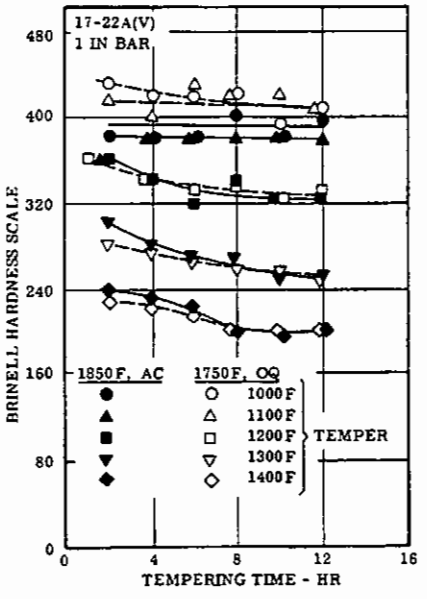


FIG. 1.065 EFFECT OF TEMPERING TIME AND TEMPERATURE ON HARDNESS OF BAR. (17)

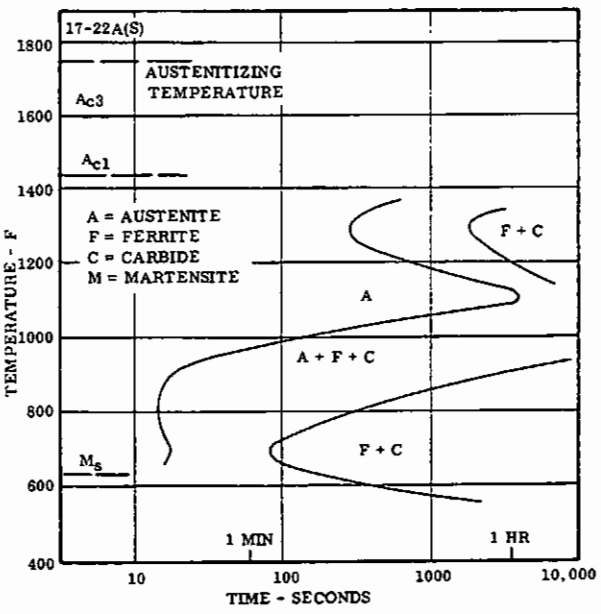


FIG. 2.01211 TIME-TEMPERATURE-TRANSFORMATION DIAGRAM FOR 17-22A(S). (17)

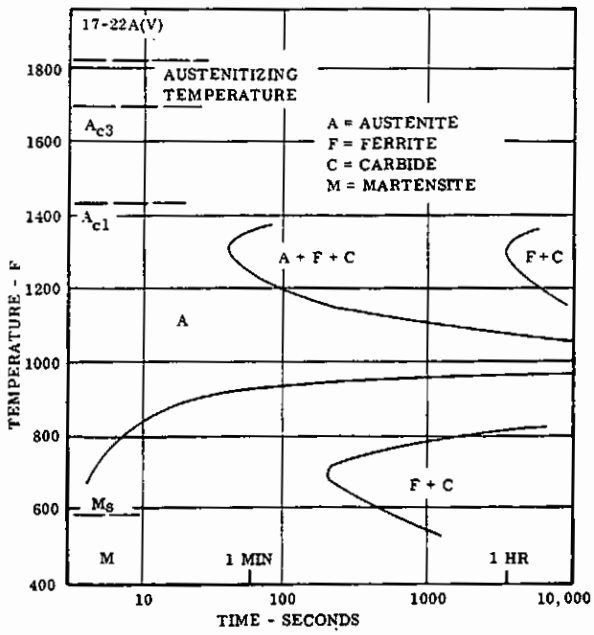


FIG. 2.01212 TIME-TEMPERATURE-TRANSFORMATION DIAGRAM FOR 17-22A(V). (17)

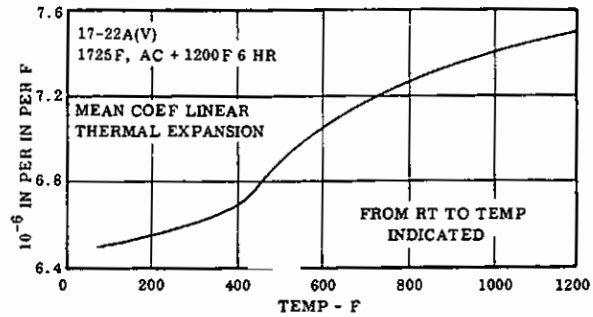


FIG. 2.0142 THERMAL EXPANSION OF 17-22A(V). (17)

Fe	
0.3	C
1.3	Cr
0.5	Mo
0.25	V

17-22A(S)

Fe	
0.28	C
1.3	Cr
0.5	Mo
0.85	V

17-22A(V)

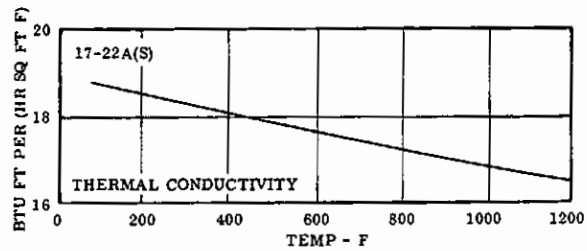


FIG. 2.013 THERMAL CONDUCTIVITY. (20)

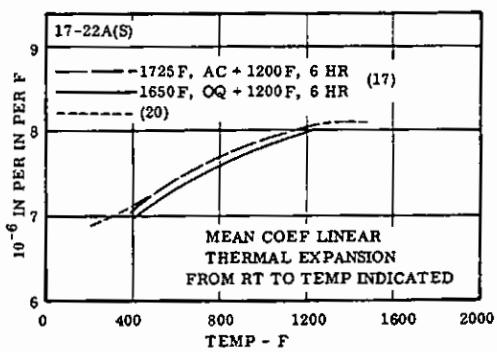


FIG. 2.0141 THERMAL EXPANSION OF 17-22A(S). (17)(20)

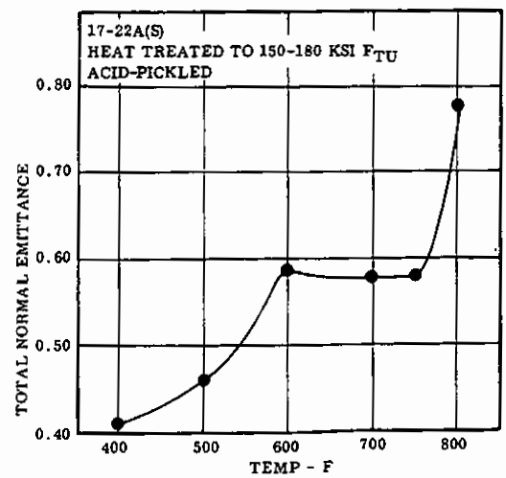


FIG. 2.024 EMITTANCE. (13)

Fe	
0.3	C
1.3	Cr
0.5	Mo
0.25	V

17-22A(S)

Fe	
0.28	C
1.3	Cr
0.5	Mo
0.85	V

17-22A(V)

AMS Spec.	Alloy	Form	Condition	Hardness	F_{ty} (ksi)	F_{tu} (ksi)	e (2 in.)
6303B (2)	17-22A(V)	Bar					
		up to 0.50 in. dia.	Cold finished	-	-	125 max.	-
		over 0.50 in. dia.	Cold finished	248 BHN max.	-	-	-
		over 0.50 in. dia.	Hot finished	241 BHN max.	-	-	-
6436A (4)	17-22A(V)	Sheet, strip, plate	Annealed	98 R_b max.	-	-	-
6302B (1)	17-22A(S)	Bars & forgings	1750F AC + 1100F, 6 hr.				
		up to 2 in. thick		331 BHN max.	-	-	-
		over 2 in. thick		302 BHN max.	-	-	-
6385B (3)	17-22A(S)	Sheet, strip, plate	Annealed	98 R_b max.	-	-	-
			1750F, AC + temper				
			test at RT	27 R_c min.	115 min.	135 min.	8 min.
			test at 1000F	-	70 min.	85 min.	8 min.

TABLE 3.01 SPECIFIED MECHANICAL PROPERTIES

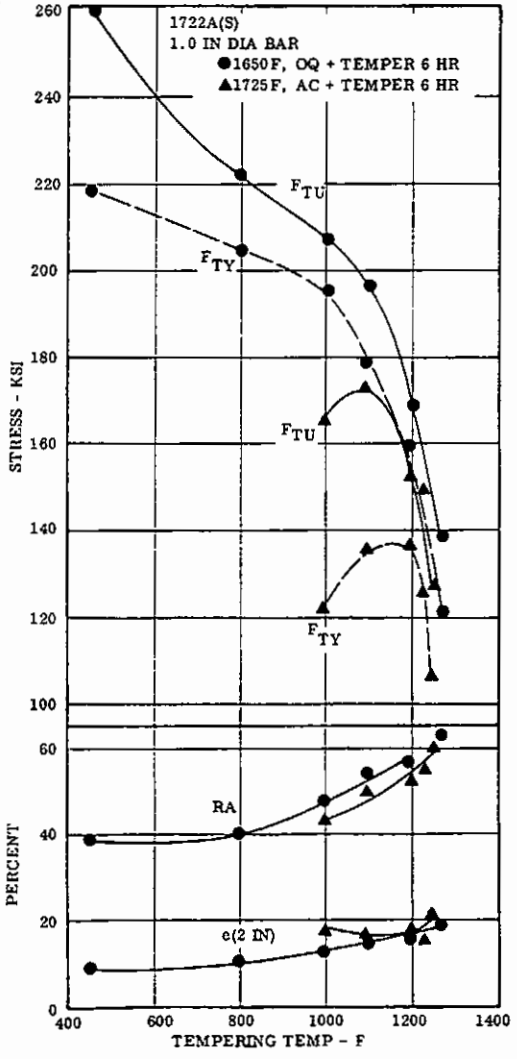


FIG. 3.0212 EFFECT OF TEMPERING TEMPERATURE ON TENSILE PROPERTIES OF 17-22A(S). (17)

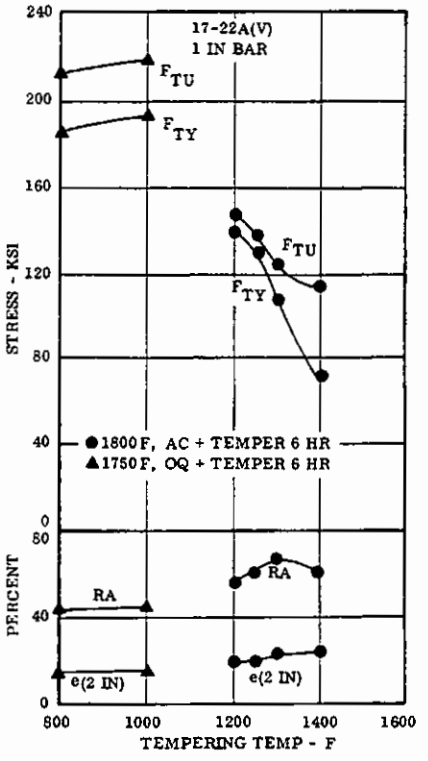


FIG. 3.0213 EFFECT OF TEMPERING TEMPERATURE ON TENSILE PROPERTIES OF 17-22A(V). (17)

Form	Pancake forgings - 22 in dia x 2 in.							
Source	(17)							
Alloy	17-22A(S)				17-22A(V)			
Condition	1725F, AC + 1200F, 6 hr.				1800F, AC + 1225F, 6 hr.			
Specimen Orientation	F_{ty} (ksi)	F_{tu} (ksi)	e(2 in) (percent)	RA (percent)	F_{ty} (ksi)	F_{tu} (ksi)	e(2 in) (percent)	RA (percent)
Radial	130	147	16	48	126	142	18	52
Tangential	129	146	15	37	132	146	18	53

TABLE 3.0214 TENSILE PROPERTIES OF FORGINGS

Form	1 in. dia. bar				
Condition	Annealed				
Source	(17)				
Alloy	F_{ty} (ksi)	F_{tu} (ksi)	e (2 in.) (percent)	RA (percent)	BHN
17-22A(S)	68	88	27	59	187
17-22A(V)	68	88	27	59	197

TABLE 3.0215 TENSILE PROPERTIES OF ANNEALED BAR

Fe
0.3 C
1.3 Cr
0.5 Mo
0.25 V

17-22A(S)

Fe
0.28 C
1.3 Cr
0.5 Mo
0.85 V

17-22A(V)

Alloy	17-22A(S)					
Form	Bar					
Source	(17)					
Exposure						
Temp. (F)	Stress (ksi)	Time (hr)	F_{tu} (ksi)	F_{ty} (ksi)	e (2 in) (percent)	RA (percent)
Condition	1725F, AC + temper 1250F, 6 hr.					
-	-	-	128	108	21	61
900	32.5	1096	132	111	19	58
950	20	1174	118	92	20	60
1000	15	1270	113	85	22	60
Condition	1725F, AC + temper 1225F, 6 hr.					
-	-	-	148	128	16.5	56
900	32.5	1280	150	130	15.5	54
950	37.5	1104	146	130	17	54
1000	23	1273	144	126	16	54
Condition	1725F, AC + temper 1200F, 6 hr.					
-	-	-	155	142	16	51
900	60	2012	151	136	16	50
1100	5	1314	129	111	19	55
Condition	1650F, OQ + temper 1275F, 6 hr.					
-	-	-	135	132	21	65
900	25	1010	135	122	21	61
950	17.5	1053	138	123	19	61
1000	10	1356	132	118	21	61

TABLE 3.0216 EFFECTS OF EXPOSURES TO STRESSES AT ELEVATED TEMPERATURES ON ROOM TEMPERATURE TENSILE PROPERTIES OF 17-22A(S).

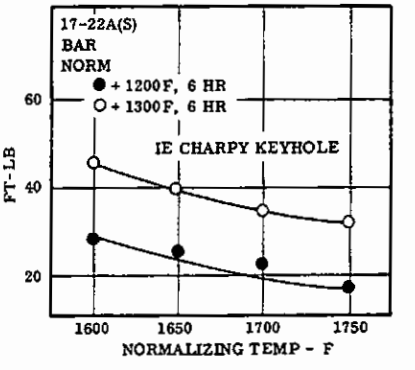


FIG. 3.0231 EFFECT OF NORMALIZING TEMPERATURE ON IMPACT STRENGTH OF 17-22A(S). (17)

Alloy	17-22A(V)					
Form	Bar					
Condition	1800F, AC + temper 1200F					
Source	(14)					
Exposure						
Temp. (F)	Stress (ksi)	Time (hr)	F_{ty} (ksi)	F_{tu} (ksi)	e (2 in) (percent)	RA (percent)
-	-	-	146	157	17	54
1000	23	2197	144	151	17	53
1000	20	4003	132	144	17	53
1100	7	2470	106	118	20	60
1100	12	2198	112	120	19	61

TABLE 3.0217 EFFECTS OF EXPOSURES TO STRESSES AT ELEVATED TEMPERATURES ON ROOM TEMPERATURE TENSILE PROPERTIES OF 17-22A(V).

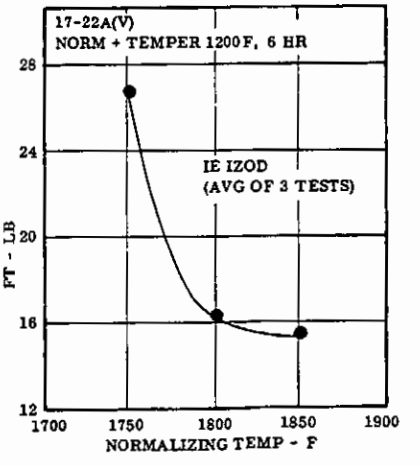


FIG. 3.0232 EFFECT OF NORMALIZING TEMPERATURE ON IMPACT STRENGTH OF 17-22A(V). (17)

Fe
0.3 C
1.3 Cr
0.5 Mo
0.25 V

17-22A(S)

Fe
0.28 C
1.3 Cr
0.5 Mo
0.85 V

17-22A(V)

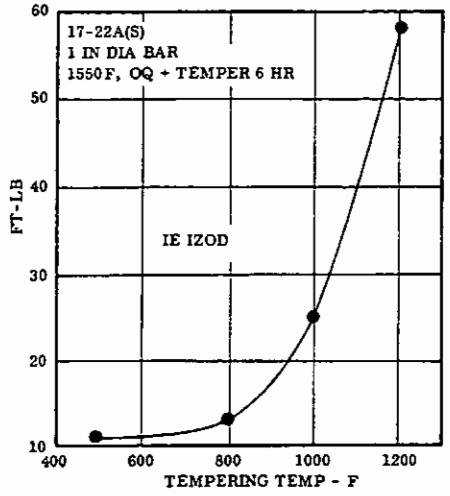


FIG. 3.0233 EFFECT OF TEMPERING TEMPERATURE ON THE IMPACT RESISTANCE OF 17-22A(S). (17)

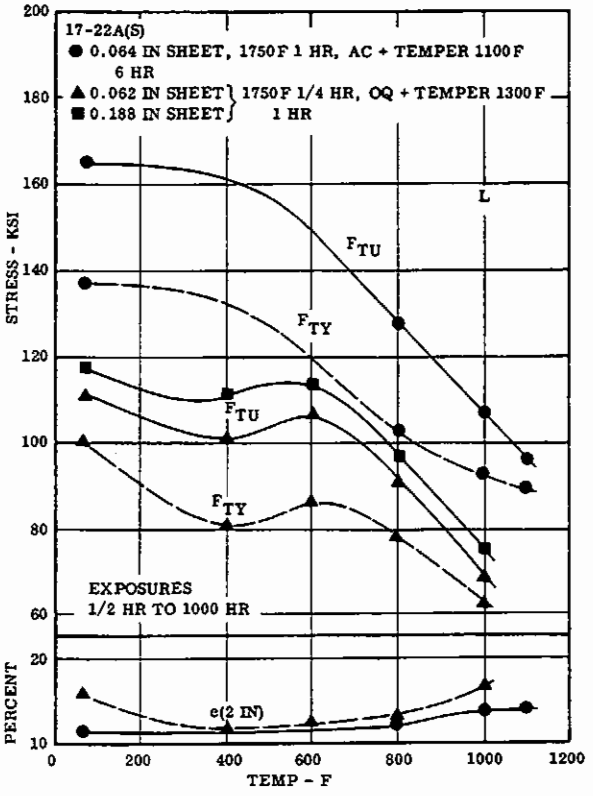


FIG. 3.0312 EFFECTS OF TEMPERATURE ON TENSILE PROPERTIES OF SHEET OF DIFFERENT THICKNESSES IN VARIOUS HEAT-TREATED CONDITIONS. (6)(7)

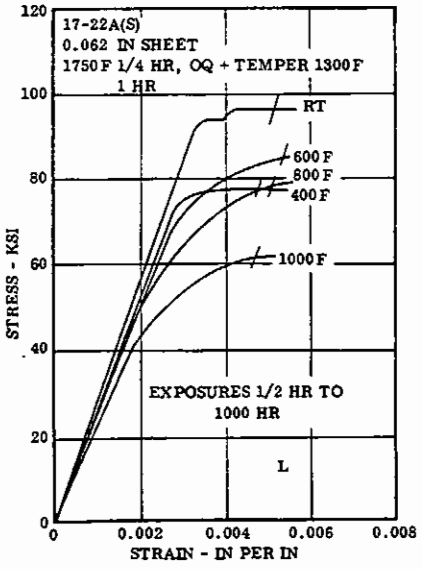


FIG. 3.0311 TENSILE STRESS-STRAIN CURVES FOR SHEET AT ROOM AND ELEVATED TEMPERATURES. (6)

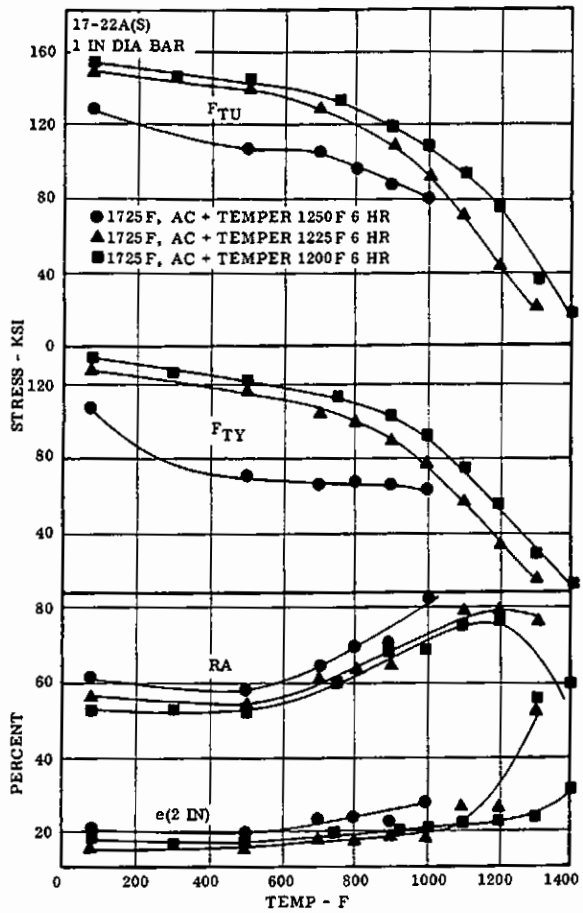


FIG. 3.0313 EFFECTS OF TEMPERATURE ON TENSILE PROPERTIES OF 17-22A(S) 1 IN DIAMETER BAR IN NORMALIZED AND TEMPERED CONDITIONS. (17)

	Fe
0.3	C
1.3	Cr
0.5	Mo
0.25	V

17-22A(S)

	Fe
0.28	C
1.3	Cr
0.5	Mo
0.85	V

17-22A(V)

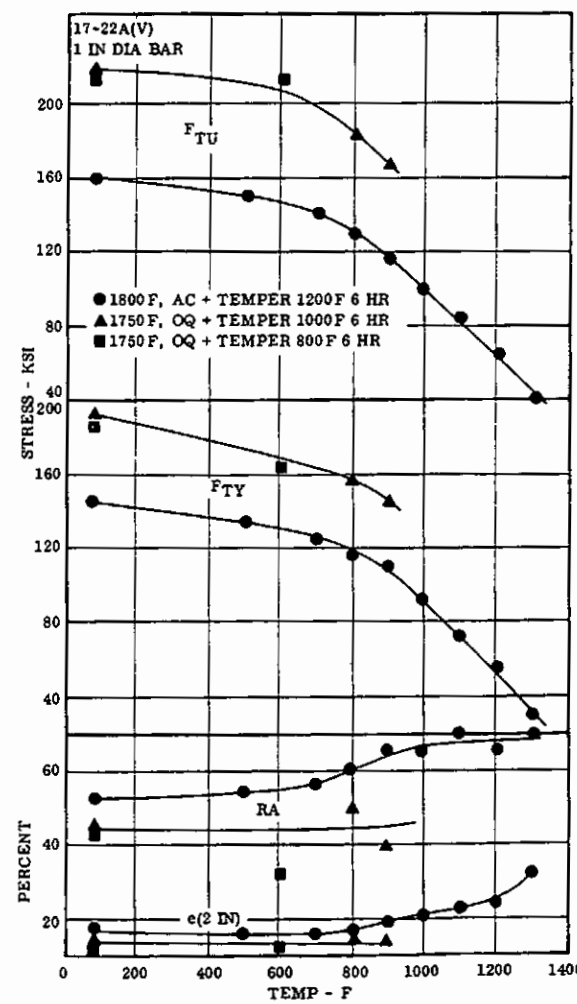


FIG. 3.0314 EFFECTS OF TEMPERATURE ON TENSILE PROPERTIES OF 17-22A(V) 1 IN DIAMETER BAR IN VARIOUS HEAT-TREATED CONDITIONS. (17)

	Fe
0.3	C
1.3	Cr
0.5	Mo
0.25	V

17-22A(S)

	Fe
0.28	C
1.3	Cr
0.5	Mo
0.85	V

17-22A(V)

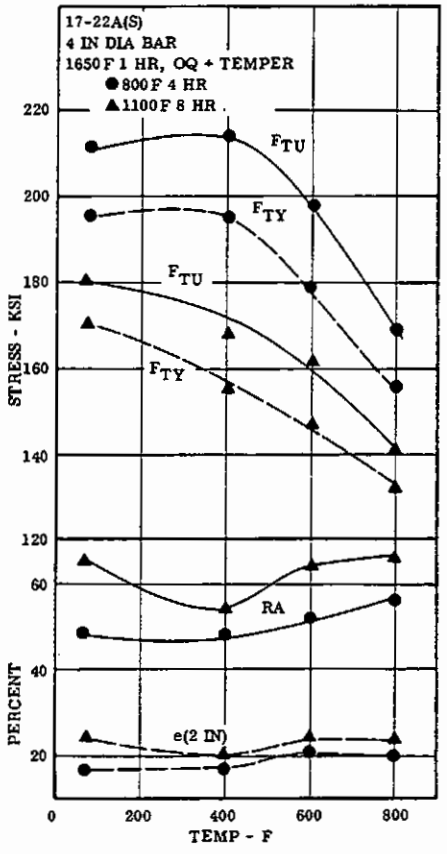


FIG. 3.0315 EFFECT OF TEMPERATURES UP TO 800 F ON TENSILE PROPERTIES OF 4 IN DIAMETER BAR IN OIL-QUENCHED AND TEMPERED CONDITION. (8)

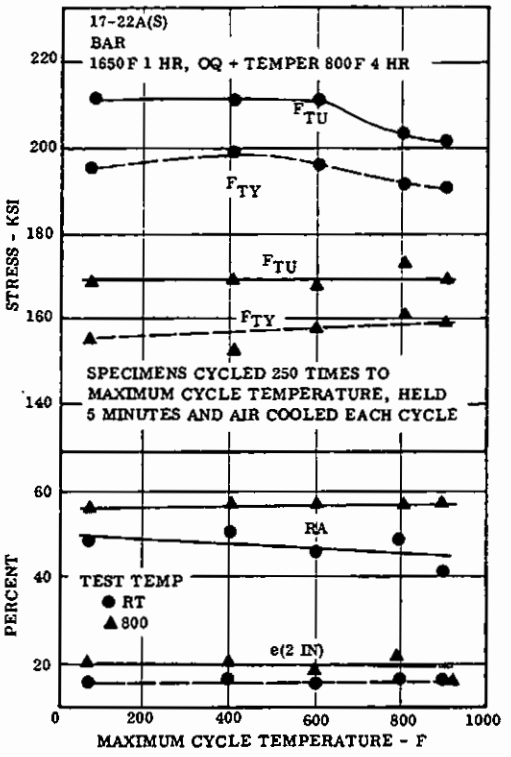


FIG. 3.0316 EFFECTS OF REPEATED CYCLING TO VARIOUS ELEVATED TEMPERATURES ON TENSILE PROPERTIES AT ROOM TEMPERATURE AND 800 F. (8)

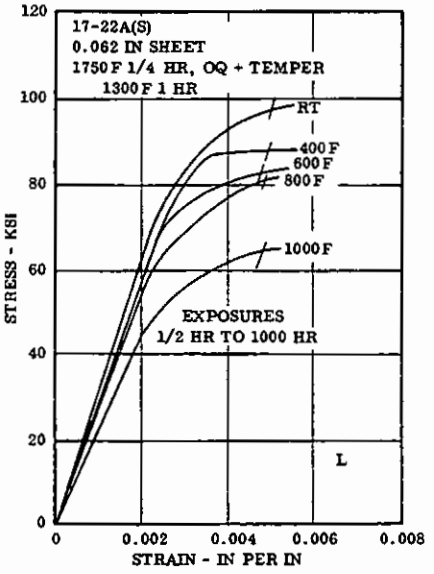


FIG. 3.0321 COMPRESSIVE STRESS-STRAIN CURVES FOR SHEET AT ROOM AND ELEVATED TEMPERATURES. (6)

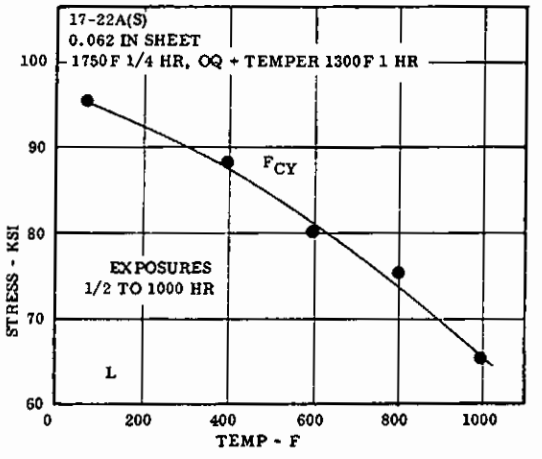
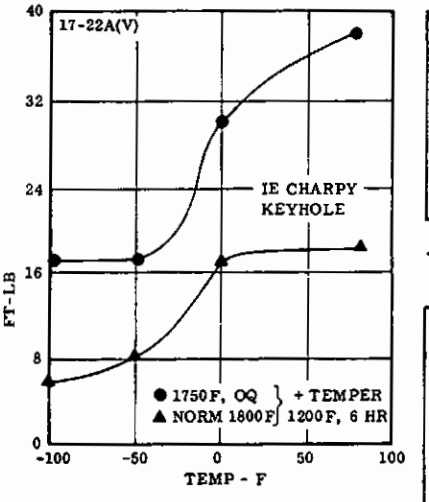


FIG. 3.0322 EFFECT OF TEMPERATURE ON COMPRESSIVE YIELD STRENGTH OF SHEET. (6)



Fe	
0.3	C
1.3	Cr
0.5	Mo
0.25	V

17-22A(S)

Fe	
0.28	C
1.3	Cr
0.5	Mo
0.85	V

17-22A(V)

FIG. 3.0332 EFFECTS OF TEMPERATURE ON IMPACT RESISTANCE OF NORMALIZED AND OF OIL QUENCHED 17-22A(V). (17)

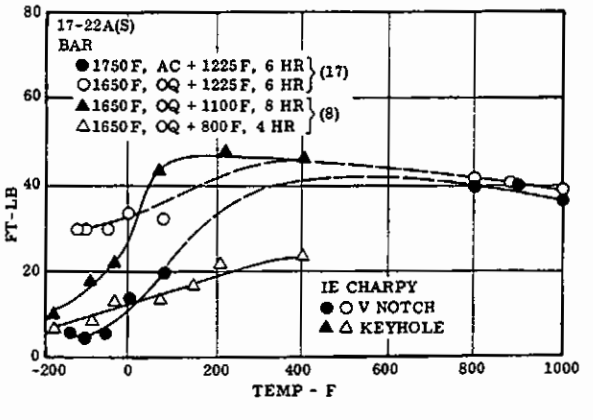


FIG. 3.0331 EFFECTS OF TEMPERATURE ON IMPACT RESISTANCE OF 17-22A(S) BAR IN VARIOUS HEAT-TREATED CONDITIONS. (17)(8)

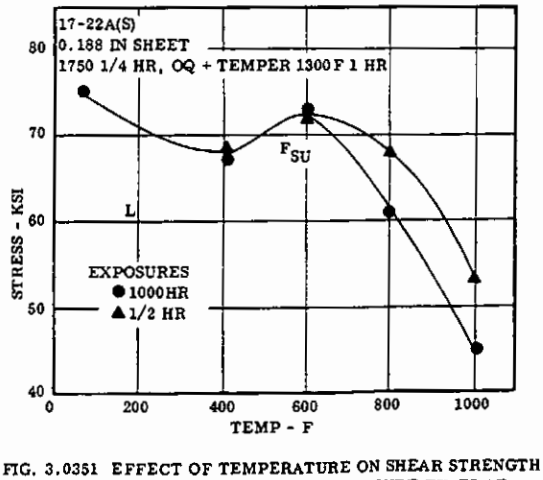


FIG. 3.0351 EFFECT OF TEMPERATURE ON SHEAR STRENGTH AFTER TWO DIFFERENT EXPOSURE TIMES AT TEMPERATURE. (6)

Fe	
0.3	C
1.3	Cr
0.5	Mo
0.25	V

17-22A(S)

Fe	
0.28	C
1.3	Cr
0.5	Mo
0.85	V

17-22A(V)

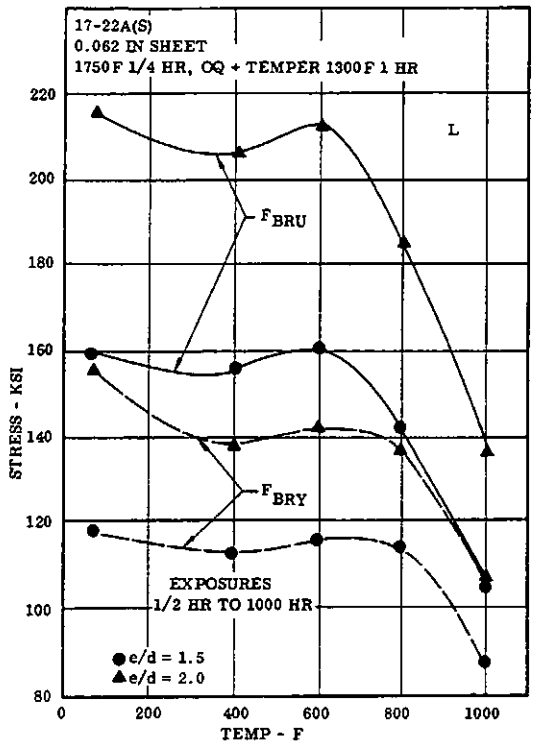


FIG. 3.0361 EFFECTS OF TEMPERATURE ON BEARING PROPERTIES. (6)

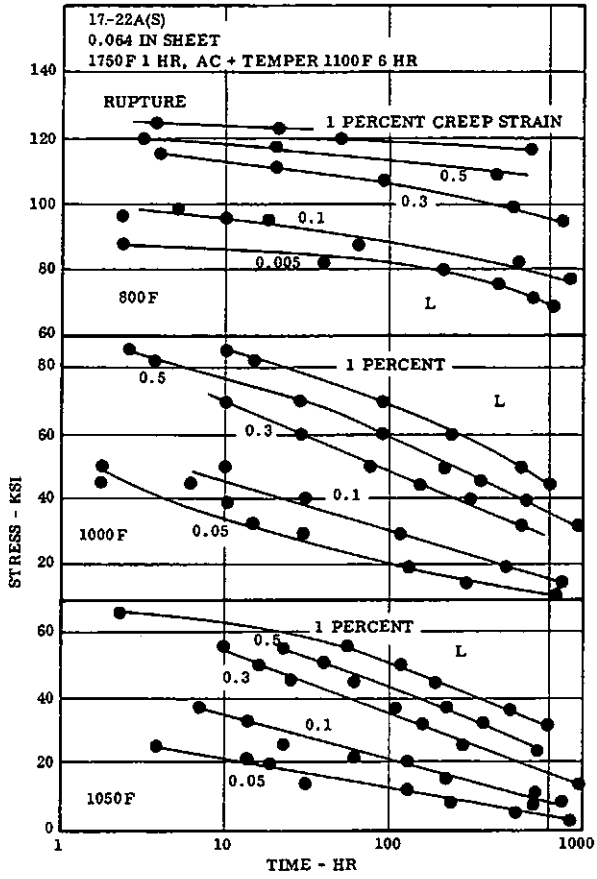


FIG. 3.041 CREEP CURVES FOR SHEET AT 800, 1000 AND 1050 F. (7)

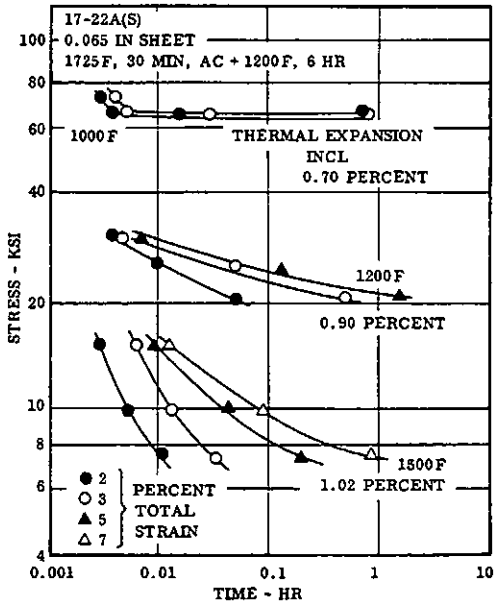


FIG. 3.042 SHORT TIME TOTAL STRAIN CURVES FOR SHEET AT 1000, 1200 AND 1500 F. (21)

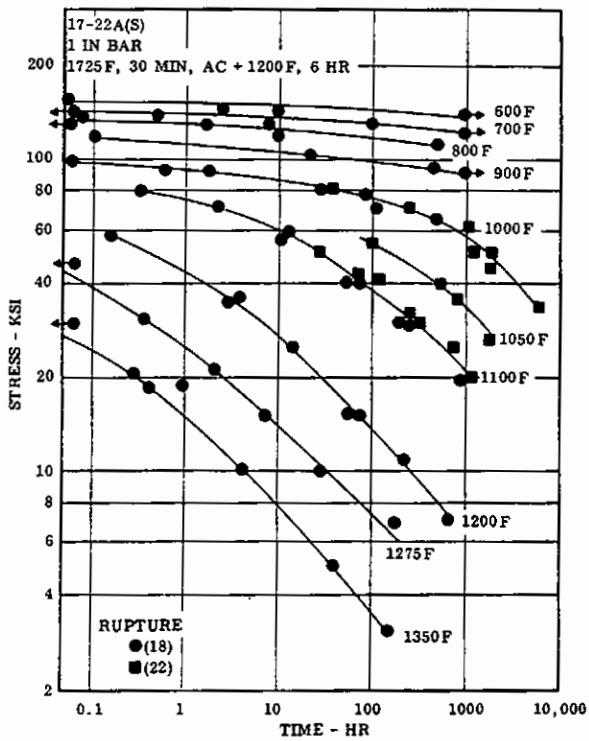


FIG. 3.043 CREEP RUPTURE CURVES FOR 17-22A(S) BAR AT 600 TO 1350F. (18)(22)

	Fe
0.3	C
1.3	Cr
0.5	Mo
0.25	V

17-22A(S)

	Fe
0.28	C
1.3	Cr
0.5	Mo
0.85	V

17-22A(V)

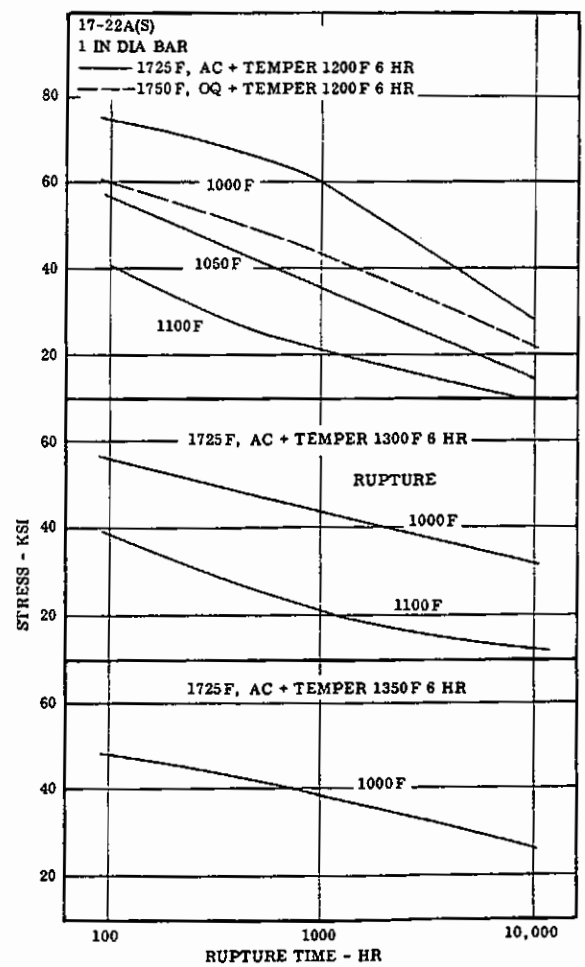


FIG. 3.044 CREEP-RUPTURE CURVES FOR 17-22A(S) BAR AT DIFFERENT TEMPERATURES AND IN VARIOUS HEAT-TREATED CONDITIONS. (17)

Fe
0.3 C
1.3 Cr
0.5 Mo
0.25 V

17-22A(S)

Fe
0.28 C
1.3 Cr
0.5 Mo
0.85 V

17-22A(V)

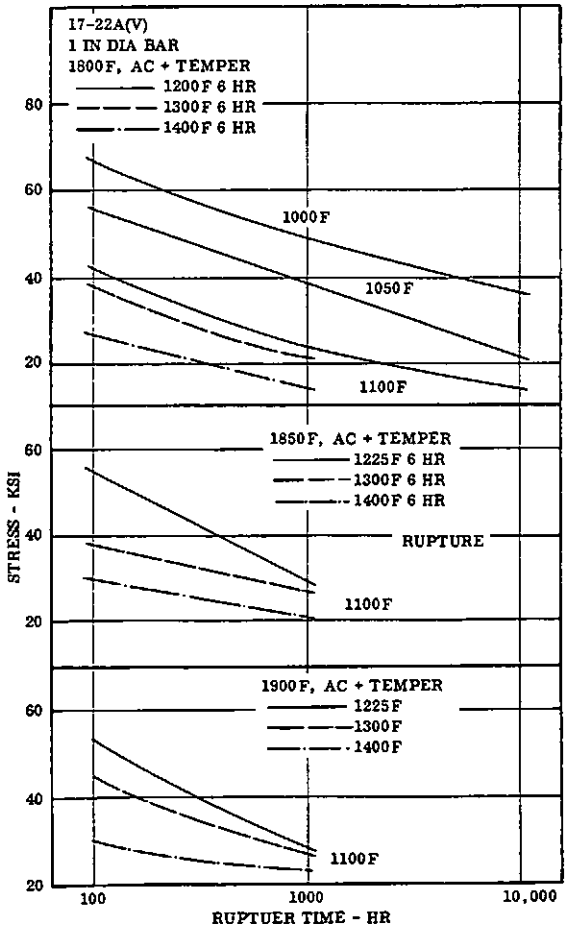


FIG. 3.045 CREEP-RUPTURE CURVES FOR 17-22A(V) BAR AT DIFFERENT TEMPERATURES AND IN VARIOUS HEAT-TREATED CONDITIONS. (17)

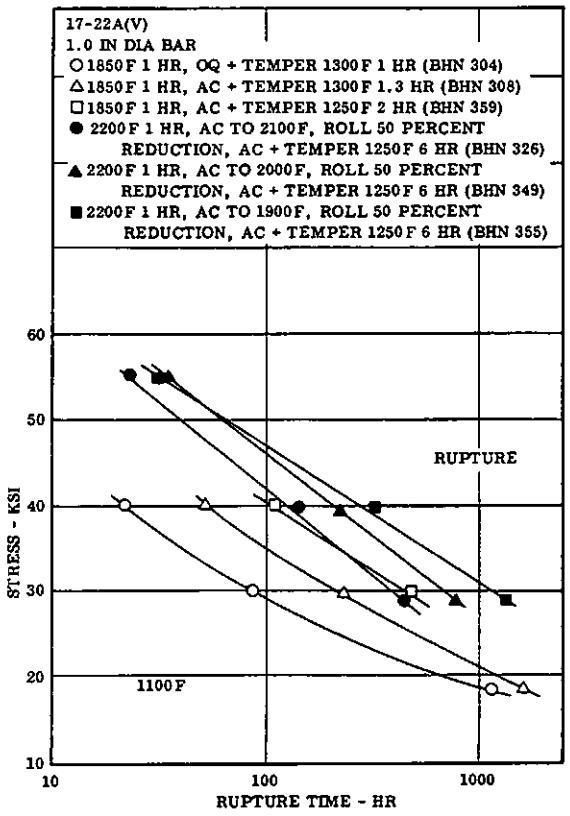


FIG. 3.046 CREEP-RUPTURE CURVES AT 1100F FOR 17-22A(V) BAR IN VARIOUS CONDITIONS OF HEAT TREATMENT AND HOT WORK. (9)

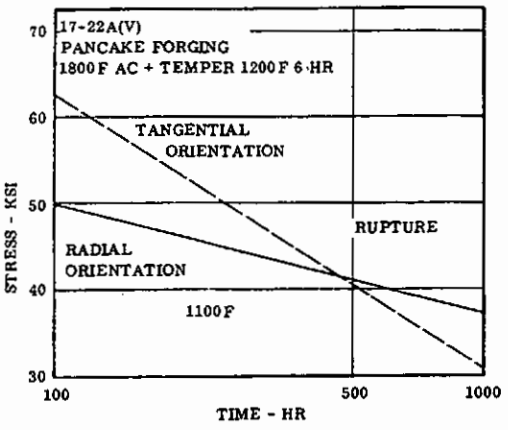


FIG. 3.047 CREEP-RUPTURE PROPERTIES OF FORGING AT 1100 F. (13)

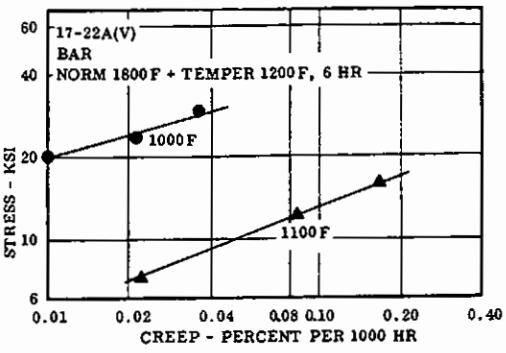


FIG. 3.049 EFFECT OF STRESS ON CREEP RATE AT 1000 AND 1100 F. (17)

Fe	
0.3	C
1.3	Cr
0.5	Mo
0.25	V

17-22A(S)

Fe	
0.28	C
1.3	Cr
0.5	Mo
0.85	V

17-22A(V)

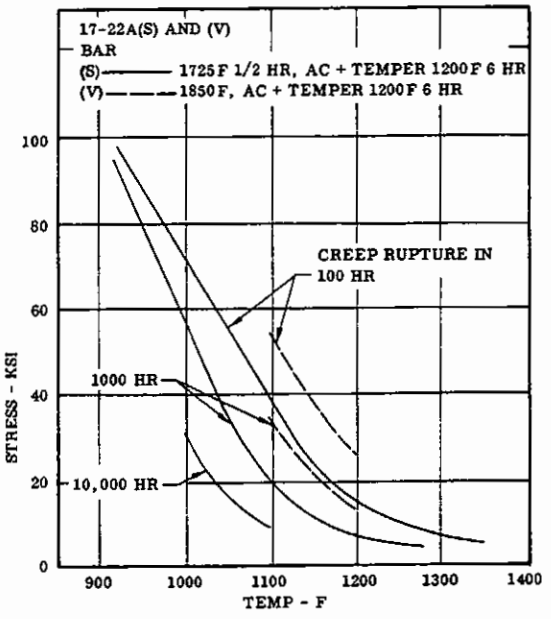


FIG. 3.048 EFFECT OF TEMPERATURE ON CREEP-RUPTURE STRENGTH OF BAR. (16)

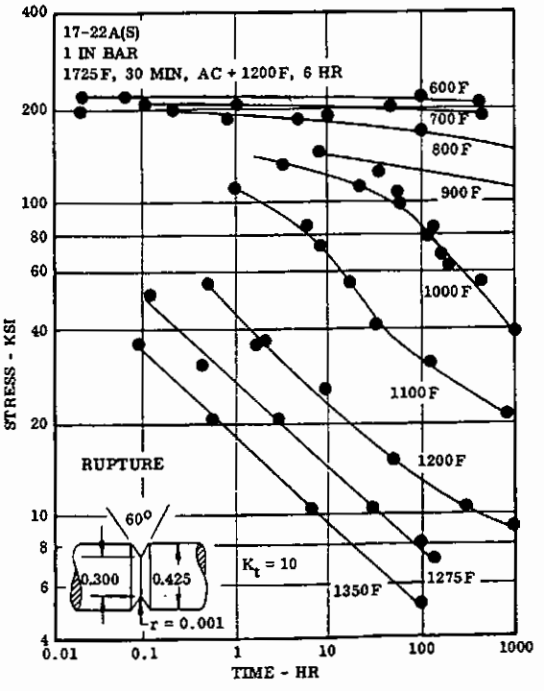


FIG. 3.0410 CREEP-RUPTURE CURVES FOR 17-22A(S) NOTCHED BAR AT 600 TO 1350 F. (18)

Fe	
0.3	C
1.3	Cr
0.5	Mo
0.25	V

17-22A(S)

Fe	
0.28	C
1.3	Cr
0.5	Mo
0.85	V

17-22A(V)

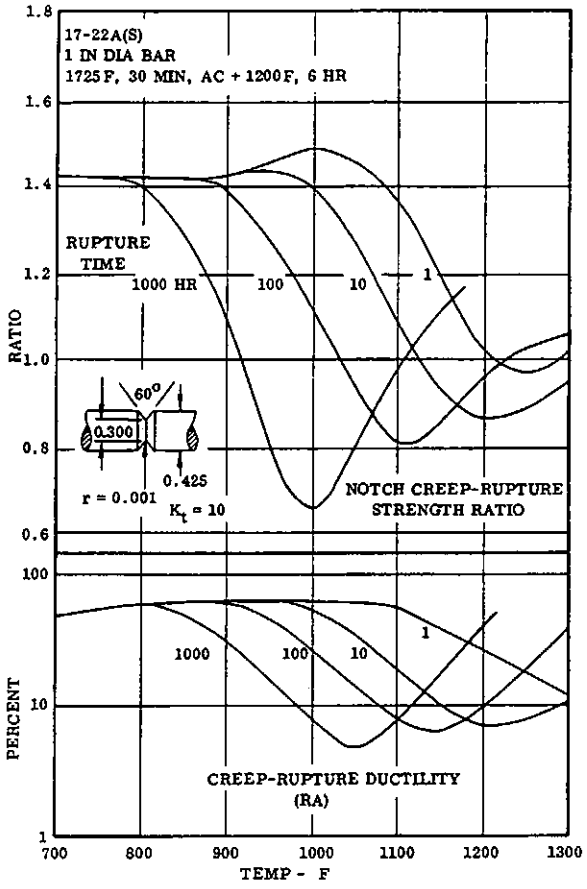


FIG. 3.0411 CORRESPONDING VARIATIONS IN NOTCH CREEP-RUPTURE STRENGTH RATIO AND UNNOTCHED CREEP-RUPTURE DUCTILITY AS FUNCTIONS OF TEMPERATURE AND RUPTURE TIME. (18)

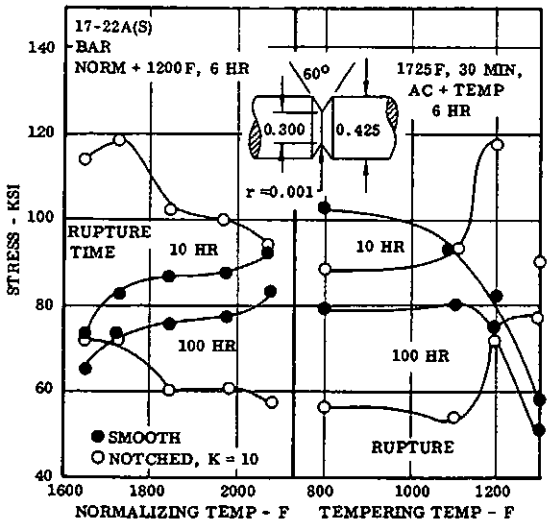


FIG. 3.0412 EFFECTS OF NORMALIZING AND TEMPERING TEMPERATURES ON CREEP-RUPTURE STRENGTH OF SMOOTH AND NOTCHED BARS OF 17-22A(S) AT 1000 F FOR 10 HOUR AND 100 HOUR RUPTURE TIMES. (18)

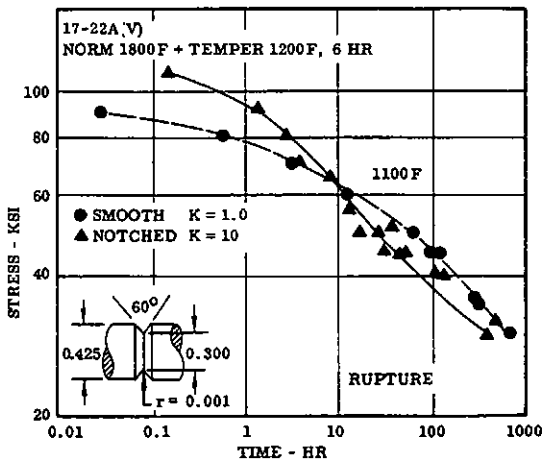


FIG. 3.0413 CREEP-RUPTURE CURVES FOR SMOOTH AND NOTCHED SPECIMENS OF 17-22A(V) AT 1100 F. (23)

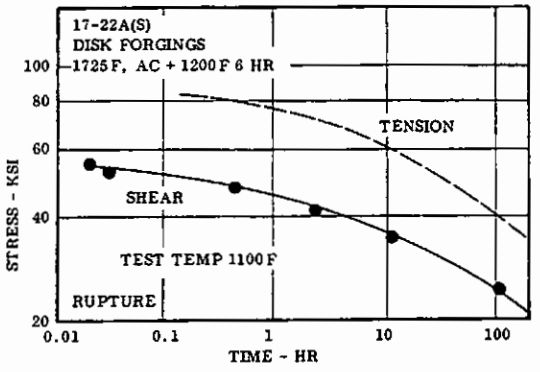
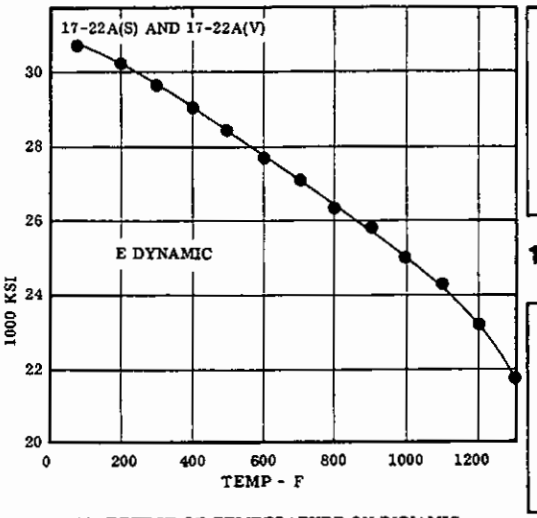


FIG. 3.0414 COMPARISON OF CREEP-RUPTURE PROPERTIES IN SHEAR AND TENSION AT 1100 F. (24)



Fe	
0.3	C
1.3	Cr
0.5	Mo
0.25	V

17-22A(S)

Fe	
0.28	C
1.3	Cr
0.5	Mo
0.85	V

17-22A(V)

FIG. 3.0621 EFFECT OF TEMPERATURE ON DYNAMIC MODULUS OF ELASTICITY. (17)

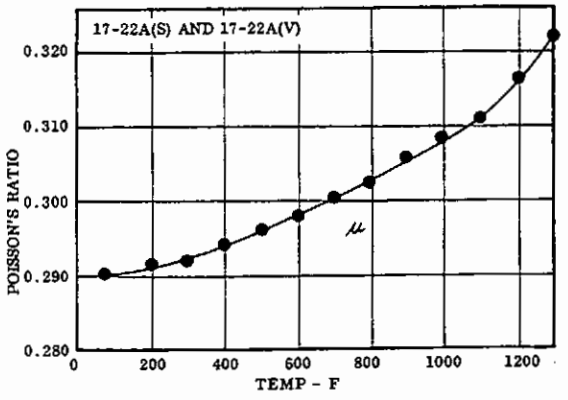


FIG. 3.0611 EFFECT OF TEMPERATURE ON POISSON'S RATIO. (17)

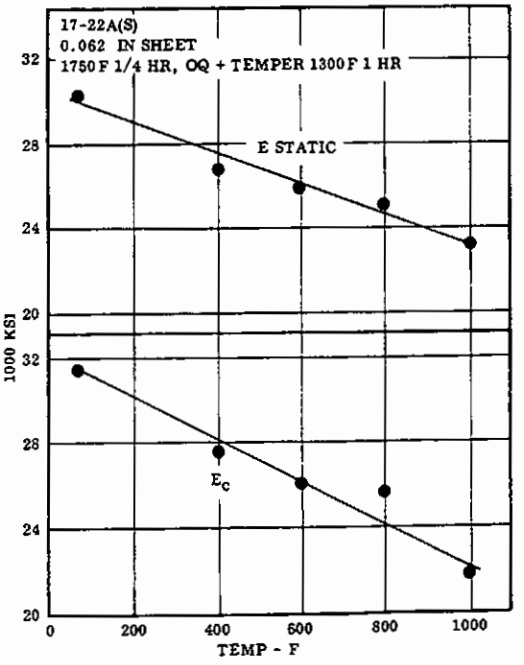


FIG. 3.0622 EFFECT OF TEMPERATURE ON STATIC MODULUS OF ELASTICITY OF SHEET IN TENSION AND COMPRESSION. (6)

Fe	
0.3	C
1.3	Cr
0.5	Mo
0.25	V

17-22A(S)

Fe	
0.28	C
1.3	Cr
0.5	Mo
0.85	V

17-22A(V)

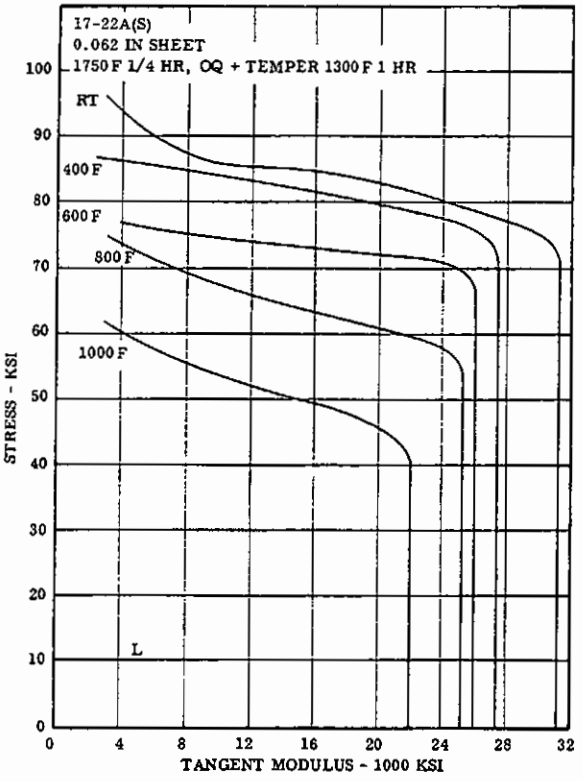


FIG. 3.0623 TANGENT MODULUS CURVES IN COMPRESSION FOR SHEET AT VARIOUS TEMPERATURES. (6)

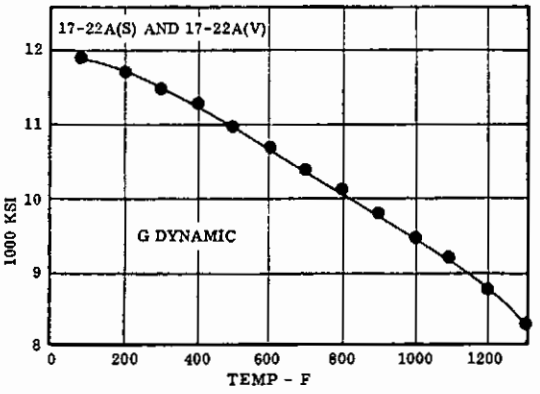


FIG. 3.0631 EFFECT OF TEMPERATURE ON MODULUS OF RIGIDITY. (17)

Alloy	17-22A(S)										
Source	(10)										
Form	Base-metal plate				Plate butt welded across test section						
Condition	1750F 2 hr, AC + temper 1165F 6 hr.				1750F 2 hr, AC + temper 1165F 6 hr, preheat to 600F, weld with 17-22A(S) filler by inert-gas shielded-arc process, stress relieve 1165F 6 hr.						
Plate thickness (in.)	F_{ty} (ksi)	F_{tu} (ksi)	e (2 in.) (percent)	R_C	F_{ty} (ksi)	F_{tu} (ksi)	e (2 in.) (percent)	Hardness, R_C Weld	HAZ(a)	BM(b)	Failure Location
0.125	165	180	9	40	141	156	5	38	37	36	HAZ
0.160	166	181	6.5	40	123	140	11.5	31	31	32	BM
0.190	165	184	10	40	-	-	-	-	-	-	-
0.250	155	175	12.5	41	139	156	5.5	38	32	37	BM
0.500	143	168	15.5	38	135	150	8.5	39	31	36	HAZ

(a) HAZ = heat affected zone.
(b) BM = base metal.

TABLE 4.032 COMPARISON OF TENSILE PROPERTIES OF BASE METAL AND WELDED JOINTS IN PLATES OF VARIOUS THICKNESS. WELD BEADS NOT MACHINED OR GROUND.

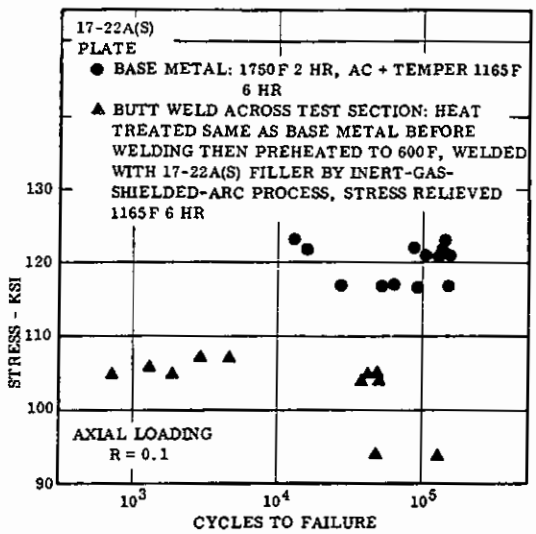


FIG. 4.033 COMPARISON OF FATIGUE LIFE OF BASE METAL AND WELDED JOINTS. WELD BEADS NOT MACHINED OR GROUND. (10)

REFERENCES

1. AMS 6302B (November 1, 1967).
2. AMS 6303B (May 15, 1972).
3. AMS 6385B (November 1, 1967).
4. AMS 6436A (May 1, 1969).
5. AMS 6458D (November 15, 1971).
6. Kattus, J.R., Preston, J.B., Lessley, H.L., "Determination of Tensile, Compressive, Bearing, and Shear Properties of Sheet Steels at Elevated Temperatures", WADC Technical Report 58-365 (November 1958).
7. Fritz, L.J. and Koster, W.P., "Low-Stress Creep Testing of 17-22A(S) Low Alloy Steel", by Metcut Research Associates for Air Material Command, Report No. 363-1740 (April 15, 1960).
8. Manzari, N.J. and Sachs, G., "Tension and Impact Properties of Steels Heat-Treated to 160,000 - 190,000 PSI Yield Strength at Temperatures Between Minus 40F (Impact) and 800F (Tension)", by Syracuse University for Watertown Arsenal, WAL 310/210 (August 1956).
9. Coldren, A.P., White, J.E., Bowen, R.K. and Freeman, J.W., "Studies of Heat-Resistant Alloys", WADC Technical Report 59-606 (February 1960).
10. Jones, R.L., "Process Welding - 17-22A(S) Steel - Mechanical Properties - Determination Of", Convair, Fort Worth, Texas, Report FGT-1961 (17 July 1958).
11. Crossley, F.A., Reichel, C.J. and Simicoe, C.R., "The Determination of the Effects of Elevated Temperatures on the Stress Corrosion Behavior of Structural Materials", WADD Technical Report 60-191 (May 1960).
12. MacKay, K.P., Coldren, A.P., Rush, A.I. and Freeman, J.W., "A Survey of the Effect of Austenitizing Temperature and Rate of Continuous Cooling on the Structure and 700F to 1200F Properties of Three Low-Alloy Steels", WADC Technical Report 55-388 (January 1956).
13. "Emissivity of Metals at Elevated Temperatures", Mc Donnell-Douglas Corp., St. Louis, Mo., Report 9096, Serial No. 28 (10 October 1962).
14. "Timken 17-22A(V)", Alloy Digest, Filing Code SA-82 (April 1959).
15. "Cross-Index of Chemically Similar Specifications and Identification Code", MIL-HDBK-H1D (22 June 1970).
16. Simmons, W.F. and Cross, H.C., "Elevated-Temperature Properties of Wrought Medium Carbon Steels", ASTM STP No. 199 (1957).
17. "17-22-A Type Steels for High Temperature Applications", Timken Technical Bulletin No. 36B (1956).
18. Brown, W.F. Jr., Manson, S.S., Sachs, G. and Sessler, J.G., "Literature Surveys on Influence of Stress Concentrations at Elevated Temperatures and the Effects of Non-Steady Load and Temperature Conditions on the Creep of Metals", ASTM STP No. 260 (December 1959).
19. Brown, W.F. Jr., "Strength Limitations of High-Strength Steels at Moderately High Temperatures", Lewis Flight Propulsion Lab, NACA No. 4025.
20. "High-Temperature Metals", Universal Cyclops Steel Corp. (1959).
21. VanEcho, J.A., Page, L.C., Simmons, W.S. and Cross, H.C., "Short-Time Creep Properties of Structural Sheet Materials for Aircraft", AF TR No. 6731, Part 1 (December 1951).
22. "Digest of Steels for High-Temperature Service", 6th Edition, Timken Company (1957).
23. Brown, W.F. Jr., Jones, M.H. and Newman, D.F., "Influence of Sharp Notches on the Stress-Rupture Characteristics of Heat-Resisting Alloy, Part II", Proceedings ASTM, Vol. 53 (1953).
24. Holms, A.G. and Repko, A.J., "Correllation of Fir-Tree-Type-Turbine-Blade-Fastening Strength With Mechanical Properties of Materials", Transactions ASME, Vol. 78 (1956).

Fe
0.3 C
1.3 Cr
0.5 Mo
0.25 V

17-22A(S)

Fe
0.28 C
1.3 Cr
0.5 Mo
0.85 V

17-22A(V)

Fe
18 Ni
8.5 Co
Mo
Ti
Al

18 Ni (200) Maraging

GENERAL

(See also FeUH Maraging, Code 1220).

This steel is one of the 18Ni maraging types in which a relatively low yield strength of approximately 200 ksi is chosen because of its accompanying high ductility and exceptional toughness. The alloy differs from the other higher strength 18Ni maraging grades primarily in its lower molybdenum and titanium content.

Mechanical properties can be varied over a wide range by heat treatment and processing, and by variations in composition within the specified limits, while still falling within the general designation of "200 Grade".

The major experience to date has been obtained with the material in two major yield strength ranges; from 175 to 200 ksi, developed principally for deep submergence submarine applications, and from 200 to 235 ksi used principally for solid propellant rocket motor casing applications.

As with other 18Ni maraging steels, the resistance to hydrogen embrittlement is much superior to that of conventional low alloy steels, and its corrosion characteristics are somewhat better than 4340 steel. Because of its good corrosion resistance and outstanding fracture toughness it is currently under intensive investigation for such high performance applications as deep submergence submarines, special aircraft forgings, and large solid rocket motor casings. Data in this section are drawn extensively from characterization evaluations for the rocket motor casing applications, and must be qualitively regarded as "typical" results obtained thus far in a program of rapidly developing material technology. Despite its apparent desirable features, care is still required in choice of composition, heat treatment and processing variables. As with other high strength steels, special attention must be given to the possibility of reduced fracture properties in the short transverse direction of forgings. Welding may also require special precautions since the toughness of the weld deposit may not be as high as that of the parent metal, although this difficulty has been overcome to a greater extent with the 200 grade of the alloy than with those of higher yield strength.

1.01 Commercial Designations

18Ni Maraging Steel, 18NiCo-Mo, 18Ni (200) Maraging, 18-8-3, Vascomax 200 CVM, RSM 200, Almar 18.

1.02 Alternate Designations

1.03 Specifications

1.031 Producer heat treatment specification.

1.0311 Aerojet solution treatment specifications for plate and forging. 1475-1525F for not less than 1 hour. For plates or forgings greater than 1 inch, hold at solution temperature for 1 hour per inch of thickness, (16)(17).

1.0312 Lockheed solution treatment specifications for plate, 1650-1700F for not less than 1 hour. For plates greater than 1 inch, hold at solution temperature for 1 hour per inch of thickness, (19).

1.032 Grain size specifications, ≥ ASTM 5, occasional grains may be as large as ASTM 3, (16)(17)(19).

1.033 Grain flow in highly stressed areas of forgings shall be parallel to principal stresses specified in applicable drawings. Grain flow pattern shall be free from reentrant and sharply folded lines, (17).

1.034 Inclusion rating, determined by comparison of the worst area of inclusions found in test specimens with Plate I of ASTM E 45 maximum permissible inclusion ratings, Table 1.034.

TABLE 1.034

Source	(16)(17)		(19)	
Alloy	Fe-18Ni-8.5Co-Mo-Ti-Al(200)		Fe-18Ni-7.5Co-Mo-Ti-Al	
Inclusion Type	Thin Series	Heavy Series	Thin Series	Heavy Series
A	2	1 1/2	1 1/2	1
B	2 1/2	1 1/2	2 1/2	1
C	2	1 1/2	1 1/2	1
D	2 1/2	2	2	1 1/2
E	-	-	2 1/2	1 1/2

1.035 Specified mechanical properties

1.0351 Aerojet specified mechanical properties for plate and forgings; F_{ty} shall range from 200 to 235 ksi after following heat treatment: 1475 to 1525F, 30 minutes, air cool + 880 to 900F, 2 to 8 hours. (See also ASTM Spec. A-538-65).

1.0352 Lockheed specified mechanical properties for plate: 175 ksi < F_{ty} < 200 ksi, e(2 inch) ≥ 6%, RA ≥ 40%, Charpy V-notch impact energy at 70F > 35 ft-lb.

1.04 Composition

1.041 Developer's specifications for alloy composition, Table 1.041.

TABLE 1.041

Source	Inco (2)	
Alloy	Fe-18Ni-8.5Co-Mo-Ti-Al (200 Grade)	
	Percent	
	Min	Max
Aluminum	0.05	0.15
Boron (b)	-	-
Calcium (d)	-	-
Carbon	-	0.03
Cobalt	8	9
Manganese (a)	-	0.12
Molybdenum	3	3.5
Nickel	17	19
Phosphorus	-	0.01
Silicon	-	0.12
Sulfur	-	0.01
Titanium	0.15	0.25
Zirconium (c)	-	-
Iron	Balance	

(a) Si plus Mn combined shall be less than 0.20 maximum
(b) 0.003 added
(c) 0.02 added
(d) 0.05 added

1.042 Typical producer's composition specification, Table 1.042.

TABLE 1.042

Source	Vasco(1)
Alloy	Fe-18Ni-8.5Co-Mo-Ti-Al(200) 200 CVM
	Percent desired
Aluminum	0.10
Boron	0.003
Carbon	0.03 max
Cobalt	8.50
Manganese	0.10 max
Molybdenum	3.25
Nickel	18.50
Phosphorus	0.01 max
Silicon	0.10 max
Sulfur	0.01 max
Titanium	0.20
Zirconium	0.02

1.043 User composition specifications, Table 1.043.

TABLE 1.043

Source	Aerojet (16)		Aerojet (17)		Aerojet (18)	
Alloy	Fe-18Ni-8.5Co-Mo-Ti-Al(200)					
Form	Plate		Forgings		Wire, filler	
	Percent		Percent		Percent	
	Min	Max	Min	Max	Min	Max
Aluminum	0.05	0.15	0.05	0.15	(a)	(a)
Carbon	-	0.03	-	0.03	-	0.03
Cobalt	7.0	8.0	7.0	8.0	7.5	8.0
Manganese		0.10	-	0.10	-	0.10
Nickel	17.5	19.0	17.5	19.0	17.5	18.5
Molybdenum	4.0	4.5	4.0	4.5	3.6	3.8
Phosphorus	-	0.025	-	0.025	-	0.01
Silicon	-	0.10	-	0.10	-	0.10
Sulfur	-	0.01	-	0.01	-	0.01
Titanium	0.05	0.25	0.05	0.25	0.26	0.36

(a) 0.10 added

Fe
18 Ni
8.5 Co
Mo
Ti
Al

18 Ni (200) Maraging

1.044 User composition specification, Table 1.044.

TABLE 1.044

Source	Lockheed(19)		
Alloy	Fe-18Ni-7.5Co-Mo-Ti-Al(a)		
Form	Plate(200 Ksi max Fcy)		
	Percent Min	Percent Max	Percent desired
Aluminum	0.05	0.15	0.10
Arsenic	-	nil	-
Bismuth	-	nil	-
Carbon	-	0.02	0.01
Chromium	-	0.20	-
Cobalt	7.0	8.0	7.5
Copper	-	0.20	-
Hydrogen	-	5 ppm	-
Lead	-	nil	-
Manganese	-	0.10(b)	-
Molybdenum	3.5	4.5	3.8
Nickel	17.5	18.5	18.0
Nitrogen	-	35 ppm	-
Oxygen	-	20 ppm	-
Phosphorus	-	0.012	0.01
Silicon	-	0.10(b)	-
Sulfur	-	0.008	0.005
Tin	-	nil	-
Titanium	0.05	0.15	0.10

(a) For optimizing fracture toughness and stress corrosion for deep submergance submarine applications
(b) Manganese plus Silicon shall not exceed 0.18

1.045 Typical compositions for rocket motor casing applications, Table 1.045.

TABLE 1.045

Source	(12)		(10)		(11)		(6)
Alloy	Fe-18Ni-8.5Co-Mo-Ti-Al(200)						
Form	Plate XA Cameron Iron Works plate --50234-1		Forward y ring		Weld wire Heat No. 08950		Plate Lukens Heat No. R-559
	Mill(a)	Sun Ship(b)	Ladish	Sun Ship(b)	Armetco	Sun Ship	
Aluminum	0.08	0.095	0.12	0.104	0.065	0.075	0.07
Carbon	0.022	0.021	0.02	0.024	0.01	0.016	0.02
Cobalt	7.51	7.49	7.68	7.51	7.80	7.88	7.82
Hydrogen	-	-	-	-	2.5*	1.3*	-
Manganese	0.05**	0.029	0.08	0.052	0.02	0.007	0.07
Molybdenum	4.25	4.38	4.36	4.29	3.68	3.74	4.25
Nickel	18.37	18.23	17.99	18.14	17.88	17.82	18.11
Nitrogen	-	-	-	-	35*	51*	-
Oxygen	-	-	-	-	15*	37*	-
Phosphorus	0.006	0.005	0.009	0.003	0.002	0.007	0.008
Silicon	0.05**	0.021	0.07	0.014	0.01	0.008	0.08
Sulfur	0.009	0.008	0.005	0.004	0.007	0.003	0.007
Titanium	0.16	0.21	0.23	0.22	0.29	0.28	0.17

(a) Average of 4 locations on the plate pattern
(b) Worst field
* ppm
** maximum

1.05 Heat Treatment

1.051 Anneal. 1450 to 1550F, 1 hour, air cool, generally recommended. Selection of an optimium annealing temperature in terms of strength and toughness will depend on the prior thermal mechanical history. In some cases heating to temperatures of 1650 to 1700F is desirable in order to recrystallize the material (but annealing above 1800F should be avoided). When a high temperature anneal is used, it is desirable to follow it by a second anneal at 1450F in order to remove any deleterious effect on the fatigue properties that the high temperature might produce.

1.052 Age. 700 to 950F, air cool. Full age is generally recommended, 875 to 925F, 3 hours, air cool. Structures which are badly segregated may not age in a normal manner and austenite reversion may be encountered. Aging after severe cold working should be avoided.

1.06 Hardness

1.061 Effect of solution annealing temperature on hardness of bar in 200 ksi CVM condition, Fig. 1.061. (See, however, section 1.061 for recommended double anneal when high temperature anneal is included).

1.062 Effect of aging temperature on hardness of bar in 200 ksi CVM condition, Fig. 1.062.

1.063 Effect of aging time on hardness of bar in 200 ksi CVM condition, Fig. 1.063.

1.07 Forms and Conditions Available

This steel is available in bar, sheet, plate, tubing, and forging stock in the hot worked or annealed condition. Sheet is also available in the annealed and cold worked condition.

1.08 Melting and Casting Practice

Electric furnace air melting with or without vacuum degassing, induction vacuum melting, consumable electrode vacuum remelting. Low carbon content and residual element content requires high quality raw material.

1.09 Special Considerations

1.091 General. The heat to heat variability of this steel within the composition limits given in Tables 1.041, 1.042, 1.043, 1.044, and 1.045 is higher than that normally encountered for low alloy heat treated steels such as 4340. Special consideration should also be given to directionality of mechanical properties, the possibility of high temperature embrittlement and the very high tolerance for hydrogen. Weldments present special problems which are discussed under 4.03.

1.092 Variability of properties. The yield strength and toughness of aged material will vary from heat to heat within the composition limits of a given grade. This variation in aging response is only in part caused by differences in content of the hardening elements but also arises from differences in the melting and processing history. Generally the toughness will decrease with those factors tending to increase the yield strength, such as cold work retained after annealing, increased titanium content or reduced testing temperature. The influence of melting practice on the mechanical properties is poorly understood, however, toughness is improved with a reduction in the residual element content and segregation appears to increase with increasing processed size. At this time it is recommended that for critical applications the aging response both regarding tensile strength and toughness be determined separately for each heat.

Uniformity of response is often enhanced by a double anneal, see section 1.051.

1.093 Directionality. Heavy sections of this alloy and other high strength steels can exhibit a banded structure which is associated with alloy segregation. If the bands contain a high concentration on non-metallic inclusions, (possibly titanium carbonitrides or oxides)the short transverse ductility and toughness may be considerably lower than the corresponding longitudinal properties. Under these circumstances the banding can result in delaminations or splitting in the plane of the bands. In severe cases splitting may occur during forming operations or result from thermal stresses induced by flame cutting or welding. Effects similar to those produced by banding are associated with an excess of directional sulphide inclusions. It should be noted that in banded structures the fracture toughness for cracks propagating in a plane perpendicular to the bands will be higher than for an identical structure without banding because the banded regions absorb energy by splitting. The degree of banding and its influence on the mechanical properties is related to the melting and processing practices employed. By very careful control of the melting and processing techniques it is possible to either reduce the amount of banding or to greatly minimize the deleterious effects on the transverse properties of heavy sections, (64)(55).

	Fe
18	Ni
8.5	Co
	Mo
	Ti
	Al

18 Ni (200) Maraging

1.094 Isothermal embrittlement. Embrittlement associated with the prior austenite grain boundaries has been observed after prolonged exposure in the temperature range between 1400 and 1800F. This is particularly evident when the alloy is allowed to cool very slowly through this temperature range following prior hot working at some higher temperature. For this reason hot working should be followed by as rapid an air cool as possible.

1.095 Hydrogen embrittlement. Alloy has much greater tolerance to hydrogen than does 4340 steel. Residual hydrogen can also be baked out readily.

2. PHYSICAL AND CHEMICAL PROPERTIES

2.01 Thermal Properties

2.011 Melting range. 2600 to 2650F, (4).

2.012 Phase changes. Alloy transforms to martensite on slow cooling from annealing temperature. M_s = 400F, M_f = 300F, A_s = 850F (possibly higher depending on heating rate), (4).

2.0121 Dimensional and phase changes during maraging treatment, Fig. 2.0121.

2.013 Thermal conductivity, Table 2.013.

TABLE 2.013

Source	Inco (4)
Alloy	Fe-18Ni-8.5Co-Mo-Ti-Al (200)
Temp - F	Thermal conductivity B_{tu} ft per (hr sq ft F)
68	11.3
122	11.6
212	12.1

2.014 Thermal expansion.
75 to 900F, 5.6 x 10^{-6} in per in per F, (4).

2.015 Specific heat, Table 2.015.

TABLE 2.015

Source	Inco(North American Aviation Data)
Alloy	Fe-18Ni-8.5Co-Mo-Ti-Al (200)
Temp - F	Specific heat B_{tu} per (lb F)
200	0.10 (estimated)
250	0.107
300	0.115

2.016 Thermal diffusivity

2.02 Other Physical Properties

2.021 0.289 lbs per cu in, 8 gr per cu cm, (2).

2.022 Electrical resistivity, 23.6 to 27.6 microhm-in solution annealed condition; 19 to 23.6 microhm-in when maraged 900F, 3 hours. Electrical resistivity within range indicated depends primarily on titanium level.

2.023 Magnetic properties. Permeability at 200 oersteds = 77.5. Saturation induction equals 21.2 kilogauss at 1300 oersteds. Nominal coercive force (H_c) in solution annealed condition equals 22-34 oersteds; in maraged condition 21-54 oersteds, (2).

2.024 Emissivity

2.025 Damping capacity

2.03 Chemical Properties

2.031 General. Corrosion resistance of this alloy is better than that of normal low alloy steels heat treated to correspondingly high strength levels. Since the corrosion resistance of this class of alloys increases somewhat with decreasing strength level, the 200 grade alloy can be expected to be better than the higher strength 18 Ni maraging steels which have been more extensively investigated. The alloy also exhibits greater tolerance for hydrogen than other high strength steels such as 4340 after exposure to H_2 and exhibit fast recovery by baking at 400-600F, (4).

2.032 Corrosion by liquids. Static immersion tests in quiet sea water show average corrosion rate of 0.003 inch per year, tests in flowing sea water; 0.005-0.007 inch per year. The alloy is susceptible to corrosion pitting in tap water, some neutral salt solutions, and some inorganic and organic acids. However, corrosion rate is lower than that of low alloy steels heat treated to correspondingly high strength. Inco (4) recommends protection from corrosive solutions by some means such as suitable coating. In general, the alloy requires the same type of surface protection as usually used for the ultra high strength alloy steels.

2.033 Corrosion by gases. Atmospheric environments such as the industrial atmosphere at Kure Beach, N. C., corrode maraging steels 0.0005-0.001 inch per year, approximately half that of other normal high strength low alloy steels. Oxidation resistance is substantially better than that of a 5 percent chromium tool steel used for comparison.

2.034 Stress corrosion. Resistance to stress corrosion is superior to that of high strength low alloy steels, although Inco (4) recommends a suitable protective coating. Two point loaded seam-type specimens stressed to yield point required more than 240 days to develop first significant stress corrosion cracking in the Bayonne industrial atmosphere and more than 240 days in the marine atmosphere at Kure Beach. Many specimens passed 500 days without failing, whereas the control 4340 steel specimens failed between 1 and 99 days. The sea water U-bend specimens required 355 days to develop first failure, whereas all 4340 specimens failed in less than 6 days.

2.04 Nuclear Properties

3. MECHANICAL PROPERTIES

3.01 Specified Mechanical Properties

See 1.035, 3.0214.

3.02 Mechanical Properties at Room Temperature

3.021 Tension. See also 3.03.

3.0211 True stress-strain curve, Fig. 3.0211.

3.0212 Effect of melting practice and test direction on ranges of tensile properties of various forms of alloy, Table 3.0212.

TABLE 3.0212

Source	(3)						
Alloy	Fe-18Ni-8.5Co-Mo-Ti-Al (200)						
Heat treat	1500F, AC + Age 900F, 3 or 4 hr						
Form	Sheet	Plate				Heavy sections	
Dimensions - in	0.070-0.187	0.375 to 1.75				1/2 x 1/2 to 4 x 16	
Condition	Vac arc remelt	Air melt		Vac arc remelt		Air melt	Vac arc remelt
Test direction	T	L	T	L	T	L	T
F_{tu}, min-ksi	217	230	234	214	204	241	210
max-ksi	229	246	252	230	233	243	230
overall avg-ksi	223	239	241	223	223	242	220
F_{ty}, min-ksi	206	223	226	208	200	238	200
max-ksi	221	241	245	225	228	238	222
overall avg-ksi	215	231	235	216	219	238	211
e, min-%	5	7.5	6	11	8	12	7
max-%	11	12.5	9.5	12	16	12	10
overall avg-%	7.5	10	8	11.5	11.5	12	8.5
No. of values used in determination	6	4	4	3	9	2	5

Fe
18 Ni
8.5 Co
Mo
Ti
Al

18 Ni (200) Maraging

3.0213 Producers typical mechanical properties, Table 3.0213.

TABLE 3.0213

Source		Vasco (1)			
Material		Fe-18Ni-8.5Co-Mo-Ti-Al (200)			
Condition		Ann	1500F, 1 hr + 900F, 3 hr Round 5/8 in, L	1 1/4 in, L	Sheet 1/4 in, T
F_{tu},	ksi	140	212	214.3	218.1
F_{ty},	ksi	110	207.7	208.5	213.0
e,	%	18	12.5	12	11
RA,	%	72	61.7	60.6	45

3.0214 Alloy developers ranges of mechanical properties, Table 3.0214.

TABLE 3.0214

Source		Inco (2)			
Alloy		Fe-18Ni-8.5Co-Mo-Ti-Al (200)			
Condition		Ann 1500F, 1hr	1500F, 1hr + 900F, 8 hr		
F_{tu},	ksi	145	195	220	
F_{ty},	ksi	117	190	225	
e(2 in),	%	17	6 (a)	12 (b)	
e(1 in),	%	-	11	15	
RA,	%	79	35	67	

(a) Minimum
(b) Maximum

3.0215 Mechanical properties for bar
3.02151 Effect of solution annealing temperature on tensile properties of bar in 200 ksi CVM Condition, Fig. 3.02151.
3.02152 Effect of aging temperature on tensile properties of bar in 200 ksi CVM Condition, Fig. 3.02152.
3.02153 Effect of aging time on tensile properties of bar in 200 ksi CVM Condition, Fig. 3.02153.
3.0216 Mechanical properties for plate in longitudinal direction
3.02161 Effect of aging time and temperature on longitudinal tensile properties of plate, Fig. 3.02161.
3.02162 Effect of aging temperature on scatterband of longitudinal tensile properties of four plates used in fabrication of solid propellent rocket motor casing "A", solution treated at 1500F, Fig. 3.02162.
3.02163 Effect of aging temperature on scatterband of longitudinal tensile properties of thirteen large plates used in fabrication of solid propellent rocket motor casing "A" solution treated at 1675F, Fig. 3.02163.
3.02164 Effect of aging temperature on scatterband of longitudinal tensile properties of four plates used in fabrication of solid propellent rocket motor casing "A", solution treated at 1500F and 1650F, Fig. 3.02164.
3.02165 Effect of aging temperature on scatterband of longitudinal tensile properties of seventeen large plates used in fabrication of solid propellent rocket motor casing "B", Fig. 3.02165.
3.0217 Mechanical properties for plate in transverse direction
3.02171 Effect of aging time and temperature on transverse tensile properties of plate, Fig. 3.02171.
3.02172 Effect of aging temperature on scatterband of transverse tensile properties of three plates used in fabrication of solid propellent rocket motor casing "A", solution treated at 1500F, Fig. 3.02172.
3.02173 Effect of aging temperature on scatterband of transverse tensile properties of 3 plates used in fabrication of solid propellent rocket motor casing "A", double solution treated at 1500F and 1650F, Fig. 3.02173.
3.02174 Effect of aging temperature on scatterband of transverse tensile properties of thirteen large plates used in fabrication of solid propellent rocket motor casing "A", solution treated at 1675F, Fig. 3.02174.
3.0218 Mechanical properties for plate
3.02181 Effect of aging temperature and time on tensile properties of hot rolled 200 ksi plate, Fig. 3.02181.
3.02182 Effect of aging time and temperature on yield strength of plate, Fig. 3.02182.
3.02183 Overall ranges in tensile properties, orientation effect and location effect within plate for seventeen plates used in fabrication of solid propellent rocket motor casing "B", Table 3.02183.

TABLE 3.02183

Source	Sun Ship (10)											
Alloy	Fe-18Ni-7.5Co-4.2Mo-0.2Ti-0.09Al (200)											
Condition	1675F, 1 hr, WQ + age 850F to 950F, 4 - 16 hr											
Form	Plate approx 430 x 100 x 0.6 in (17 sheets)											
F_{ty} - ksi		F_{tu} - ksi		e - %		RA - %		Orientation (a) effect - ksi		Location (b) effect - ksi	
Min	Max	Min	Max	Min	Max	Min	Max	Min	Max	Min	Max
193	226	204	244	9	15	46	62	0	9	0	7

(a) Difference between transverse and longitudinal.
(b) Maximum difference in F_{tu} or F_{ty} within a plate.

3.022 Compression
3.0221 Stress-strain diagrams
3.023 Impact, see also 3.033.
3.0231 Range of Charpy V-notch impact values at room temperature, 26-50 ft-lbs, (2).
Effect of specimen location (in thickness direction of 1.05 inch plate) on energy absorption in precracked Charpy impact test, Fig. 3.0231.
3.0232 Effect of fatigue crack depth on energy absorption in precracked Charpy impact test on specimens of variable width cut from 1 inch plate, Fig. 3.0232.
3.0233 Effect of specimen width and plate thickness on energy absorption in precracked Charpy impact specimens cut from plate of various thicknesses, Fig. 3.0233.
3.0234 Effect of specimen width on energy absorption in precracked Charpy impact, Fig. 3.0234.
3.0235 Effect of various solution treatments and aging temperatures on energy absorption in precracked Charpy impact tests of plate at room temperature, Fig. 3.0235.
3.024 Bending
3.025 Torsion and shear
3.026 Bearing
3.027 Stress concentration
3.0271 Notch properties
3.02711 Effect of stress concentration factor on notch tensile strength ratio of 200 ksi CVM bar, Fig. 3.02711.

3.0272 Fracture toughness

3.02721 General. Although extensive data are available on edge cracked bend specimens and attempts have been made to apply these data to the determination of fracture toughness parameters (eg. (13)(14)), care must be exercised in applying cited values of K_{Ic} from tests conducted to date. The specimens in general have been too small for such determination and gave no distinct pop-in indications. The toughness of the alloy can best be judged from a series of surface crack specimen tests on 0.4 and 0.6 inch plate aged to F_{ty} = 225 to 230 ksi. High toughness is indicated in that the ratio of net stress to yield stress is above 0.8 at a value of a/Q = 0.14, (Fig. 3.02722) Similar tests on TIG welded plates indicate that somewhat lower toughness may exist at weld center line (compare Fig. 3.02723 to 3.02722), although the limited amount of data available makes such a conclusion tentative. Flow sizes in the surface crack tests were not sufficiently large to permit valid K_{Ic} calculation; the values given for K_{Ic} are most likely too high.
The fracture toughness of the alloy is probably affected by cold work and thermal history in a manner similar to that described for 250 and 300 grade (See Code 1220 section 1.09).

3.02722 Effect of defect geometry on net fracture stress for plate; computations show expected relation for several selected values of K_{Ic}, Fig. 3.02722.

3.02723 Effect of defect geometry on net fracture stress for weld sections, repaired defects, and heat affected zone for plate; computations show expected relation for several selected values of K_{Ic}, Fig. 3.02723.

3.02724 Effect of humidity and applied stress intensity factor on time required to cause fracture of GTA welded plate, Fig. 3.02724.

3.03 Mechanical Properties at Various Temperatures

3.031 Tension

3.0311 Stress-strain diagrams

3.0312 Effect of test temperature on tensile properties of 200 ksi CVM bar, Fig. 3.0312.

3.0313 Effect of test temperature on yield strength of 18Ni maraging steels aged at 900F for 3 hours, and showing relation of 200 CVM steel within scatterband of other maraging steels, Fig. 3.0313.

3.0314 Effect of test temperature on ultimate tensile strength of 18Ni maraging steels aged at 900F for 3 hours, and showing relation of 200 CVM steel within scatterband of other maraging steels.

3.032 Compression

3.0321 Stress-strain diagrams

3.033 Impact

3.0331 Effect of test temperature on Charpy V-notch impact strength of bar in 200 CVM Condition, Fig. 3.0331.

3.0332 Effect of various solution treatments and aging temperature on energy absorption in precracked Charpy impact tests at -40F, Fig. 3.0332.

3.0333 Effect of various solution treatments and aging temperatures on energy absorption in precracked Charpy impact tests at 200F, Fig. 3.0333.

3.0334 Effect of maraging temperature, test temperature, and specimen orientation on energy absorption in impact test of precracked Charpy specimen, Fig. 3.0334.

3.0335 Effect of test temperature on energy absorption in precracked Charpy impact specimens from heavy forging including parent metal, weld area, and heat affected zone, Fig. 3.0335.

3.034 Bending

3.035 Torsion and shear

3.036 Bearing

3.037 Stress concentration. See 3.033.

3.0371 Notch properties. See 3.033.

3.0372 Fracture toughness, See 3.033.

3.038 Combined properties

3.04 Creep and Creep Rupture Properties

3.05 Fatigue Properties (See also Section 1.051)

3.051 Fatigue strength in rotating beam bending, Fig. 3.051.

3.06 Elastic Properties

3.061 Poisson's ratio, 0.264, (2).

3.062 Modulus of elasticity, 26.2 x 10^3 ksi, (2).

3.0621 Effect of cold work, resolution treatment after cold work, and direction relative to cold work on dynamic modulus, Fig. 3.0621.

3.063 Modulus of rigidity

4. FABRICATION

4.01 Formability

4.011 General. This alloy is a member of the 18Ni maraging steel series, and its machining characteristics are similar to other compositions in this series. (See 4.01 Code 1220 and Ref. (2) for details.)

4.02 Machining and Grinding

4.021 General. See 4.021, Code 1220 and Ref. (2).

4.03 Welding

4.031 General. (See 4.031, Code 1220 for additional general comments.) Steel is weldable without preheat in both fully heat treated and solution annealed conditions. Post weld heat treatment is accomplished by the normal aging procedure. Gas tungsten-arc welding involves virtually no problems. Gas metal-arc welding occasionally produces porosity which can be eliminated by closer control of welding technique or filler composition. Short-arc welding requires use of pure helium shielding for best mechanical properties and equipment operability, (2).

4.032 Filler wire. Toughness of weld may be improved by reduction of filler wire cobalt or molybdenum and titanium alloy. Developer's recommended weld wire compositions, Table 4.032.

Fe
18 Ni
8.5 Co
Mo
Ti
Al

18 Ni (200) Maraging

TABLE 4.032

Source	Inco (2)						
Alloy	Fe-18Ni-8.5Co-Mo-Ti-Al (200)						
Nominal F_{ty} of weld - ksi	Composition, percent						PPM H_2
	Ni	Co	Mo	Al	Ti	Fe	
175-185	18	1.0	3.5	0.15	0.45	Bal	5
190-200	18	4.0	3.5	0.15	0.45	Bal	5
200-210	18	8	4.5	0.2	0.5	Bal	5

4.0321 User's recommended filler wire composition, Table 4.0321.

TABLE 4.0321

Source	Aerojet (9)	
Alloy	Fe-18Ni-8.5Co-Mo-Ti-Al (200)	
	Percent	
	Min	Max
Aluminum	(a)	(a)
Carbon	-	0.03
Cobalt	7.5	8.0
Manganese	-	0.1
Molybdenum	3.6	3.8
Nickel	17.5	18.5
Phosphorus	-	0.01
Silicon	-	0.01
Sulfur	-	0.01
Titanium	0.26	0.30

(a) 0.10 added

4.033 Welding parameters recommended by alloy developer, Table 4.033.

TABLE 4.033

Source	Inco (2)					
Alloy	Fe-18Ni-8.5Co-Mo-Ti-Al (200)					
Nominal F_{ty} of weld - ksi	Process	Plate Thick-in	Amps	Volts	Passes	ipm
175-185	MIG	1/2	300	29	4	10
190-200	MIG	1/2	320	32	4	10
200-210	MIG	1	300	29	13	10

Fe
18 Ni
8.5 Co
Mo
Ti
Al

18 Ni (200) Maraging

4.0331 User's recommended welding procedure for 0.6 inch plate Table 4.0331.

TABLE 4.0331

Source	Aerojet (9)
Alloy	Fe-18Ni-8.5Co-Mo-Ti-Al (200)
Form	0.6 in plate
Melting practice	Vac-arc remelt or induction melt
Welding process	TIG
Joint design	Single U or double V
Maximum root gap	0.70 inch
Maximum interpass temp	200F

4.034 Average weld properties of plate, Table 4.034. (See Tables 4.032 and 4.033 for corresponding filler wire composition and welding parameters).

TABLE 4.034

Source	Inco (2)				
Alloy	Fe-18Ni-8.5Co-Mo-Ti-Al (200)				
Condition	Weld + age 900F, 3 hr				
Form	Plate				
Nominal F_{ty} of weld - ksi	F_{ty}, ksi	F_{tu}, ksi	e, %	RA, %	Charpy V- ft-lb
175-185	191	198	8	35	22.5
190-200	197	207	8	30	10
200-210	215	220	7	30	18

4.035 Mechanical properties of parent metal and electron beam weldment with and without post-weld age, Table 4.035.

TABLE 4.035

Source	(8)			
Alloy	Fe-18Ni-8.5Co-3.1Mo-Ti-Al (200) 1/2 in plate			
Form	Parent metal		Weld	
Condition, 1500F, 1 hr, AC + age or weld	900F, 3 hr	900F, 3 hr + 900F, 3 hr	900F, 3 hr + weld	900F, 3hr + weld 900F, 3hr
F_{tu}, ksi	214 (a)	219	169 (a)	218 (a)
F_{ty}, ksi	208 (a)	216	161 (a)	215 (a)
RA, %	56 (a)	55	30 (a)	14 (a)
e(1/4 in), %	41 (a)	40	19 (a)	11 (a)
e(1/2in), %	23 (a)	24	10 (a)	6 (a)

(a) Average of 3 tests.

4.04 Heat Treatment

4.041 General. Before heating remove grease and oil (see 4.05). Furnace fuel oil should not contain more than 0.75 percent sulfur by weight. Fuel gas not more than 100 grains sulfur per 100 cu ft. Furnace atmosphere of about 5 percent CO_2 is recommended, (2). Maraging may be done in air.

4.05 Surface Treatment

4.051 General. Sand blasting removes oxide scale effectively. Pickling solution 18 percent H_2SO_4 at 150 to 160F is recommended. Sodium hydride and other high temperature (> 700F) descaling treatments should be avoided.

4.052 Nitriding. Nitriding at 850F for 20 hours or 800F for 44 hours recommended and will give case hardness of about 66 Rockwell C. Higher temperatures give lower case hardness. Longer times will increase case depths but very long times may require a drop in temperature to maintain case hardness, (56).

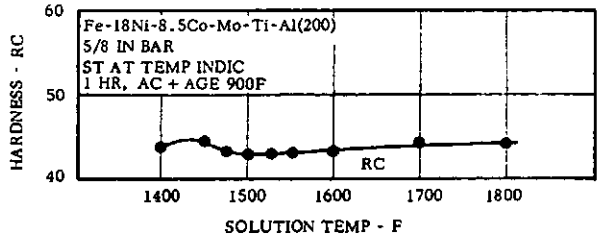


FIG. 1.061 EFFECT OF SOLUTION ANNEALING TEMPERATURE ON HARDNESS OF BAR IN 200 KSI CVM CONDITION (1, p. 6)

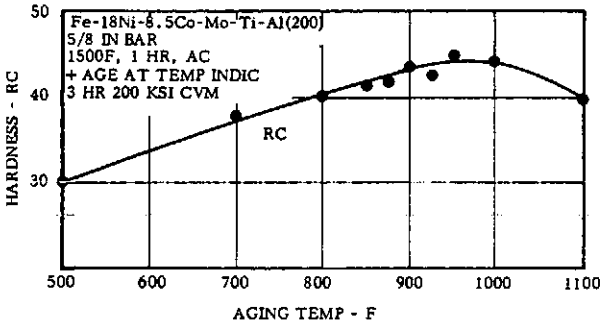


FIG. 1.062 EFFECT OF AGING TEMPERATURE ON HARDNESS OF BAR IN 200 KSI CVM CONDITION (1, p. 5)

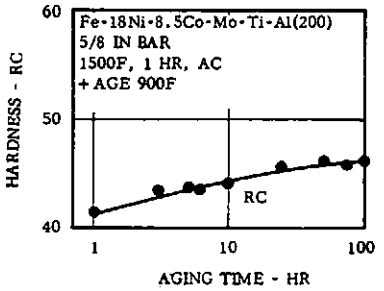


FIG. 1.063 EFFECT OF AGING TIME ON HARDNESS OF BAR IN 200 KSI CVM CONDITION (1, p. 7)

	Fe
18	Ni
8.5	Co
	Mo
	Ti
	Al

18 Ni (200)
Maraging

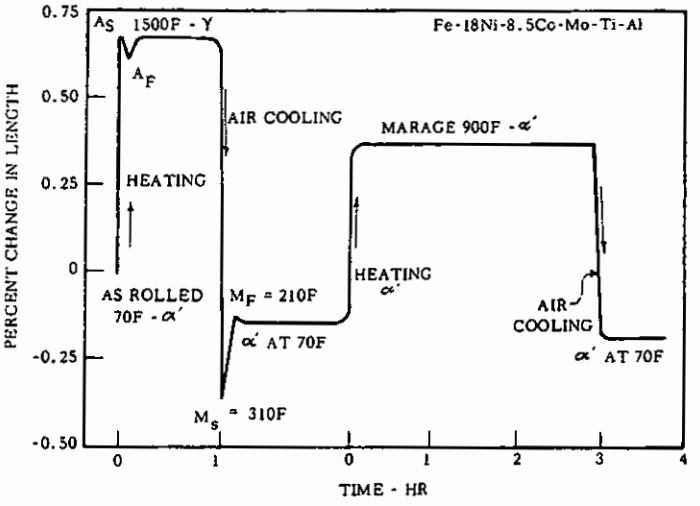


FIG. 2.0121 DIMENSIONAL AND PHASE CHANGES DURING MARAGING TREATMENT OF 18Ni MARAGING STEEL (2, p. 25)

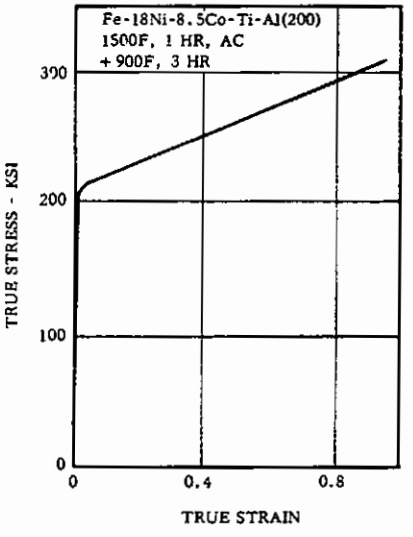


FIG. 3.0211 TRUE STRESS-STRAIN CURVE (2, p.11)

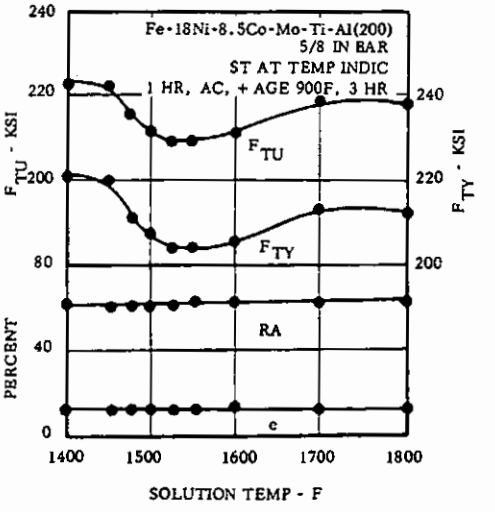


FIG. 3.02151 EFFECT OF SOLUTION ANNEALING TEMPERATURE ON TENSILE PROPERTIES OF BAR IN 200 KSI CVM CONDITION (1, p.6)

Fe
18 Ni
8.5 Co
Mo
Ti
Al

18 Ni (200)
Maraging

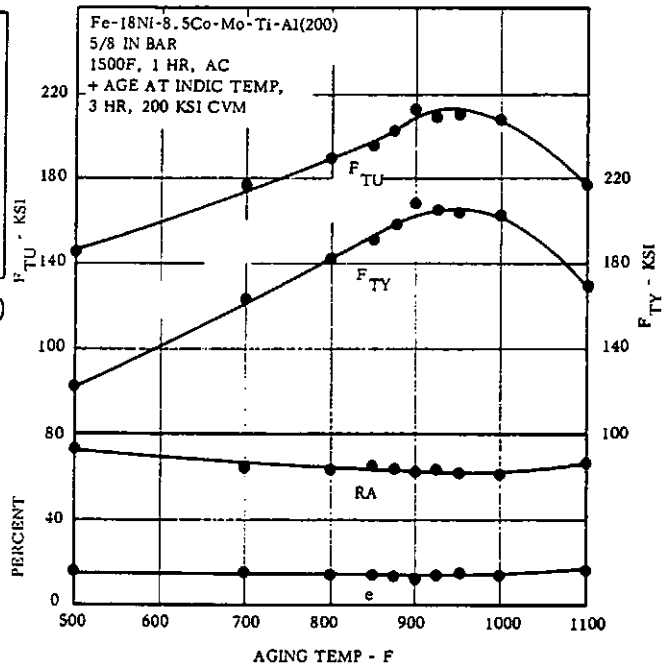


FIG. 3.02152 EFFECT OF AGING TEMPERATURE ON TENSILE PROPERTIES OF BAR IN 200 KSI CVM CONDITION (1, p. 5)

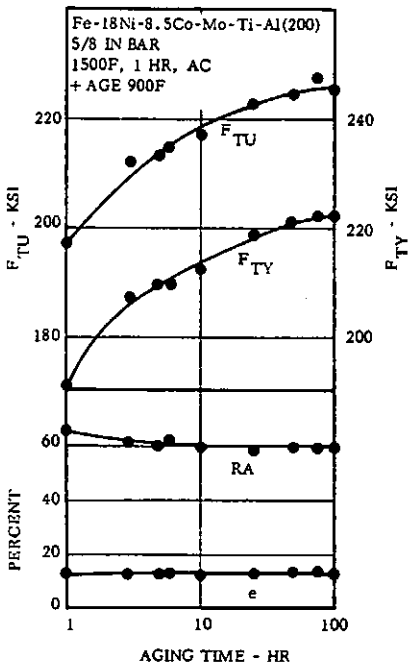


FIG. 3.02153 EFFECT OF AGING TIME ON TENSILE PROPERTIES OF BAR IN 200 KSI CVM CONDITION (1, p. 7)

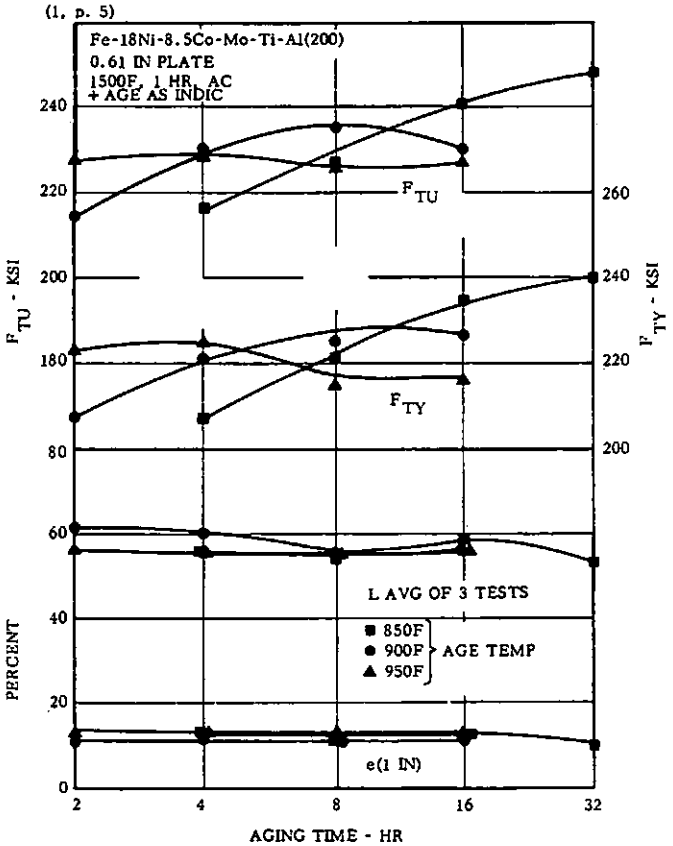


FIG. 3.02161 EFFECT OF AGING TIME AND TEMPERATURE ON LONGITUDINAL TENSILE PROPERTIES OF PLATE (5, Tbl. II)

	Fe
18	Ni
8.5	Co
	Mo
	Ti
	Al

18 Ni (200)
Maraging

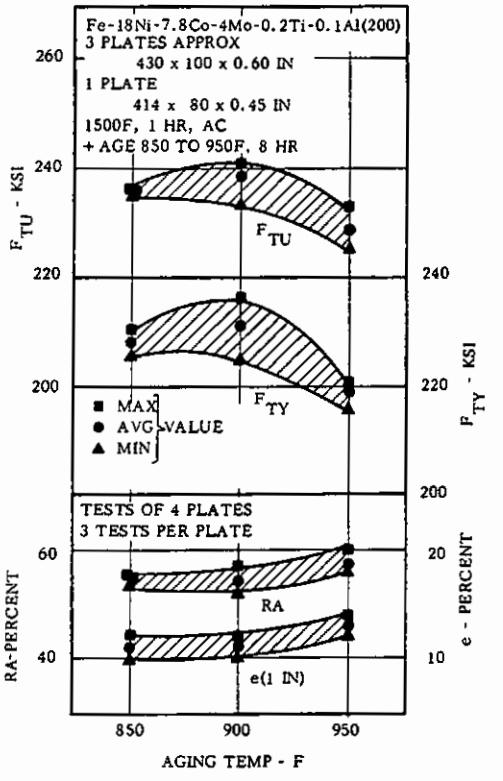


FIG. 3.02162 EFFECT OF AGING TEMPERATURE ON SCATTERBAND OF LONGITUDINAL TENSILE PROPERTIES OF FOUR PLATES USED IN FABRICATION OF SOLID PROPELLENT ROCKET MOTOR CASING "A", SOLUTION TREATED AT 1500F (11) -

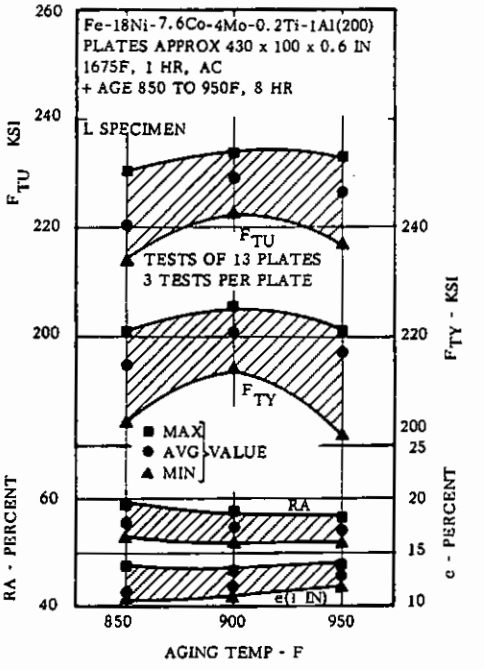


FIG. 3.02163 EFFECT OF AGING TEMPERATURE ON SCATTERBAND OF LONGITUDINAL TENSILE PROPERTIES OF THIRTEEN LARGE PLATES USED IN FABRICATION OF SOLID PROPELLENT ROCKET MOTOR CASING "A" SOLUTION TREATED AT 1675F (11)

	Fe
18	Ni
8.5	Co
	Mo
	Ti
	Al

18 Ni (200) Maraging

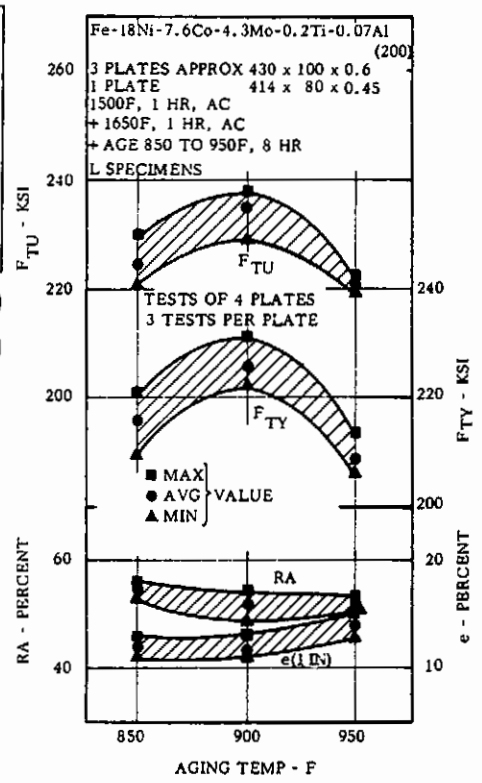


FIG. 3.02164 EFFECT OF AGING TEMPERATURE ON SCATTERBAND OF LONGITUDINAL TENSILE PROPERTIES OF FOUR PLATES USED IN FABRICATION OF SOLID PROPELLENT ROCKET MOTOR CASING "A" DOUBLE SOLUTION TREATED AT 1500 AND 1650F (11)

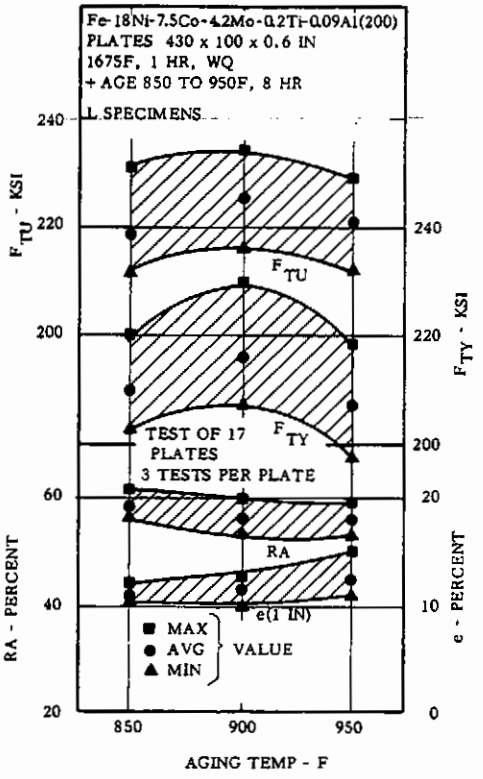


FIG. 3.02165 EFFECT OF AGING TEMPERATURE ON SCATTERBAND OF LONGITUDINAL TENSILE PROPERTIES OF SEVENTEEN LARGE PLATES USED IN FABRICATION OF SOLID PROPELLENT ROCKET MOTOR CASING "B" (10)

	Fe
18	Ni
8.5	Co
	Mo
	Ti
	Al

18 Ni (200)
Maraging

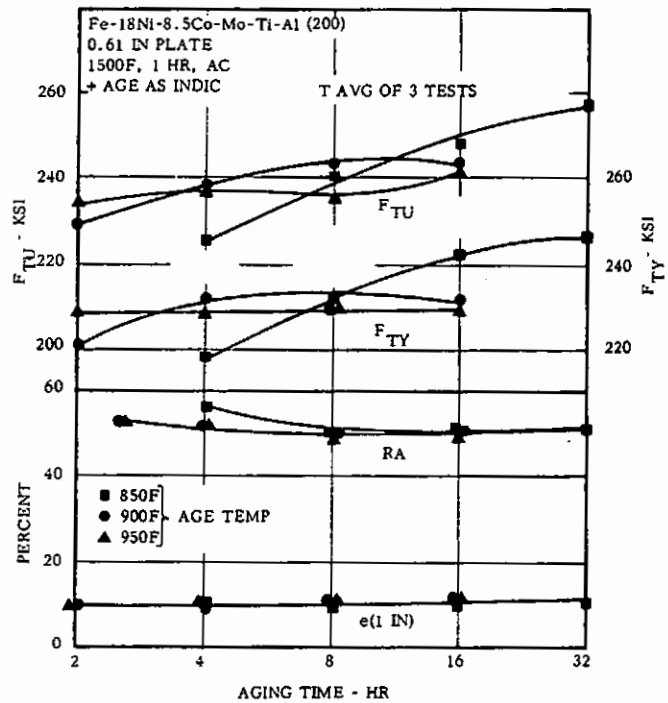


FIG. 3.02171 EFFECT OF AGING TIME AND TEMPERATURE ON TRANSVERSE TENSILE PROPERTIES OF PLATE (5, Tbl. 2)

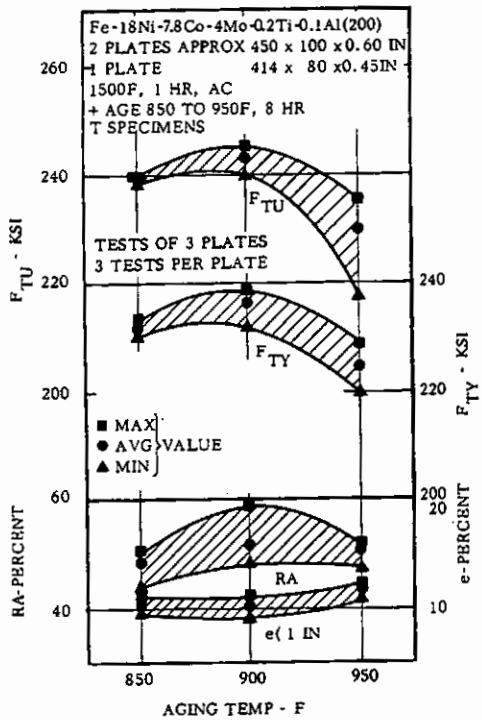


FIG. 3.02172 EFFECT OF AGING TEMPERATURE ON SCATTERBAND OF TRANSVERSE TENSILE PROPERTIES OF THREE PLATES USED IN FABRICATION OF SOLID PROPELLENT ROCKET MOTOR CASING "A" SOLUTION TREATED AT 1500F (11)

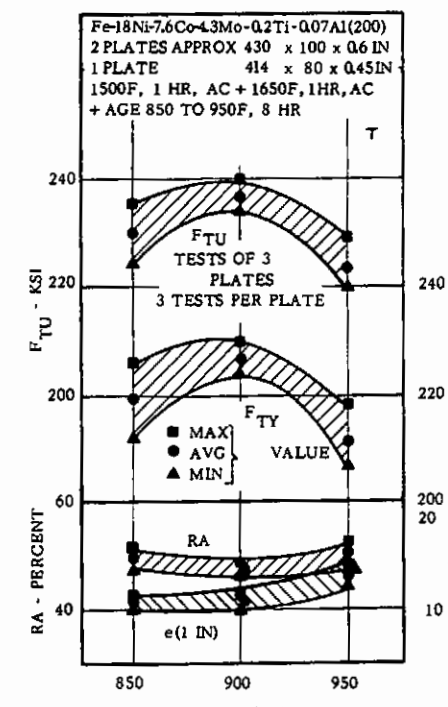


FIG. 3.02173 EFFECT OF AGING TEMPERATURE ON SCATTERBAND OF TRANSVERSE TENSILE PROPERTIES OF 3 PLATES USED IN FABRICATION OF SOLID PROPELLENT ROCKET MOTOR CASING "A" DOUBLE SOLUTION TREATED AT 1500 AND 1650F (11)

Fe
18 Ni
8.5 Co
Mo
Ti
Al

18Ni (200)
Maraging

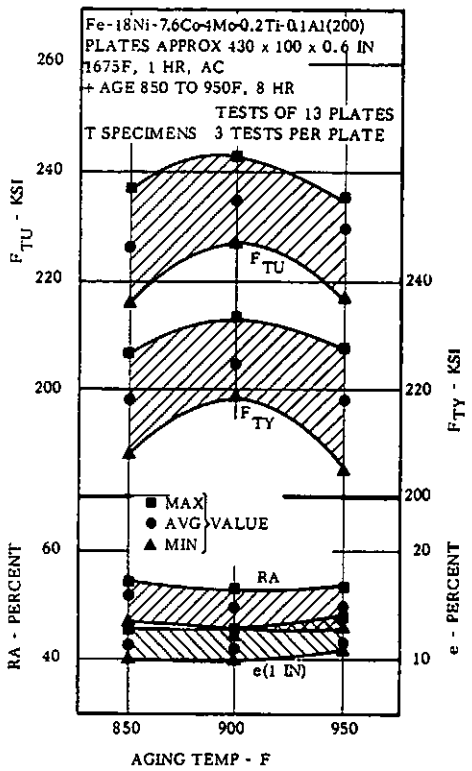


FIG. 3.02174 EFFECT OF AGING TEMPERATURE ON SCATTERBAND OF TRANSVERSE TENSILE PROPERTIES OF THIRTEEN LARGE PLATES USED IN FABRICATION OF SOLID PROPELLENT ROCKET MOTOR CASING "A" SOLUTION TREATED AT 1675F (11

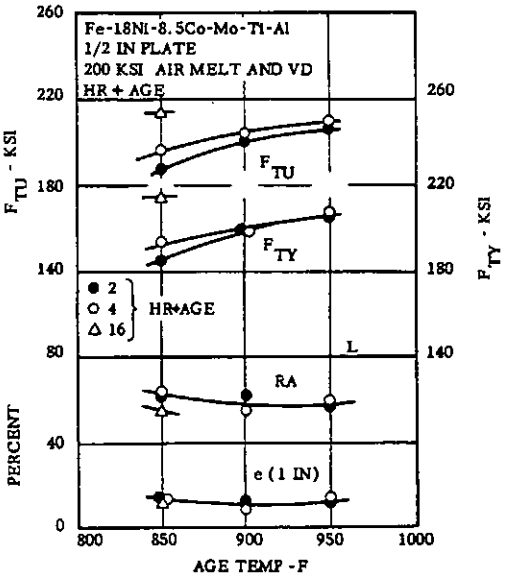


FIG. 3.02181 EFFECT OF AGING TEMPERATURE AND TIME ON TENSILE PROPERTIES OF HOT ROLLED 200 KSI PLATE (20)

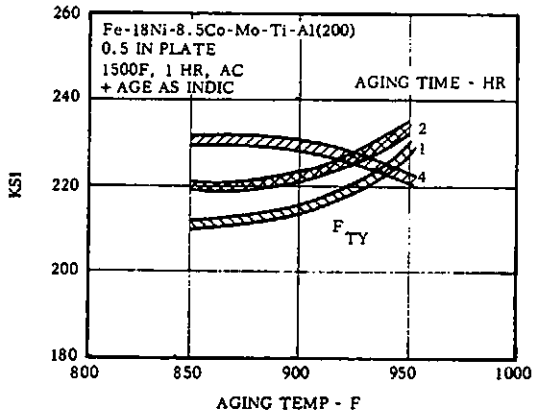


FIG. 3.02182 EFFECT OF AGING TIME AND TEMPERATURE ON YIELD STRENGTH OF PLATE (2, p. 25)

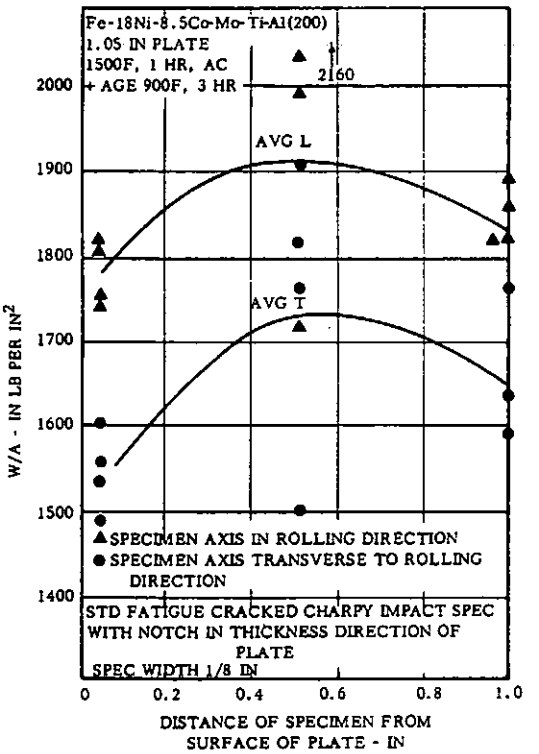


FIG. 3.0231 EFFECT OF SPECIMEN LOCATION (IN THICKNESS DIRECTION OF 1.05 IN PLATE) ON ENERGY ABSORPTION IN PRECRACKED CHARPY IMPACT TEST (8, p. 394)

	Fe
18	Ni
8.5	Co
	Mo
	Ti
	Al

18 Ni (200)
Maraging

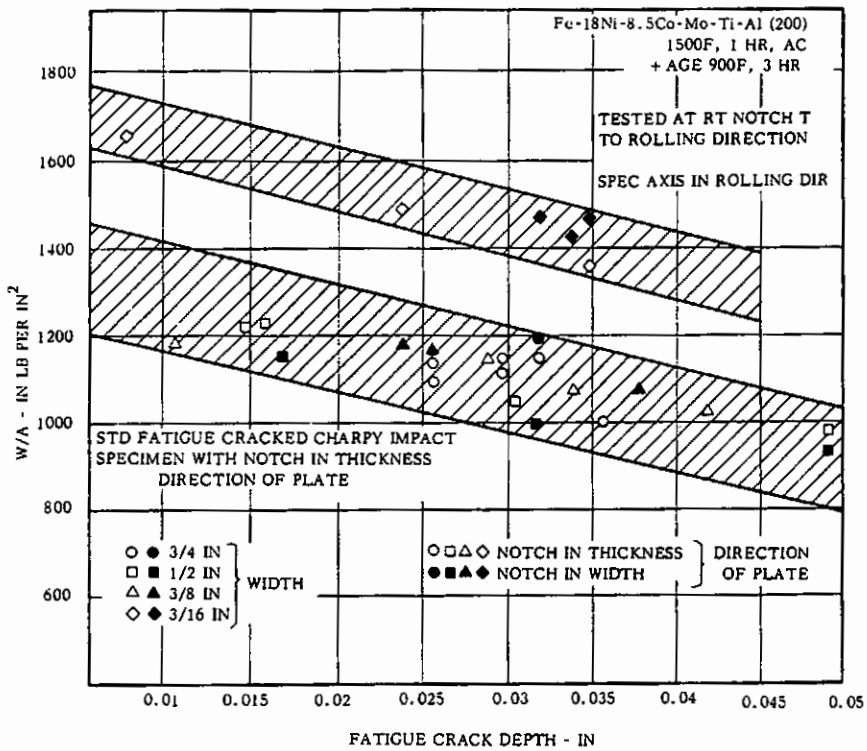


FIG. 3.0232 EFFECT OF FATIGUE CRACK DEPTH ON ENERGY ABSORPTION IN PRECRACKED CHARPY IMPACT TEST ON SPECIMENS OF VARIABLE WIDTH CUT FROM 1 INCH PLATE (8, p. 402)

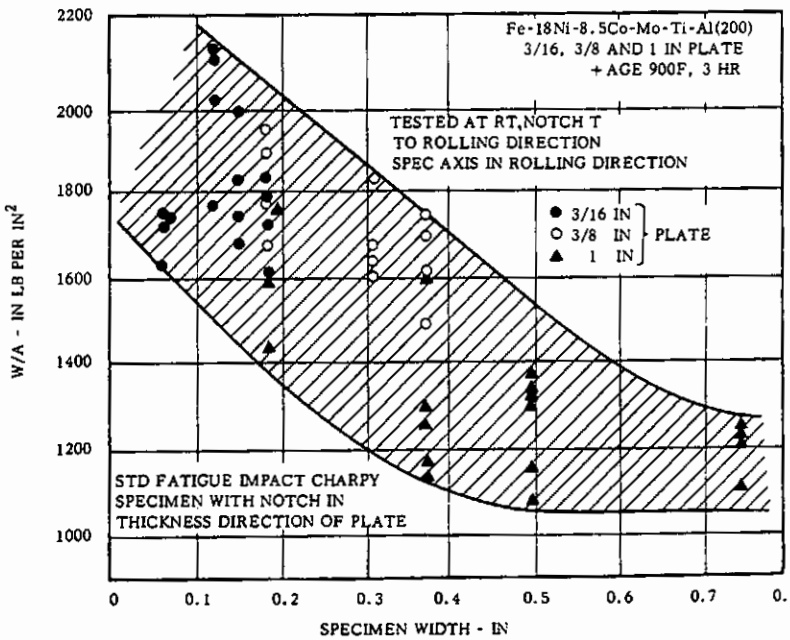


FIG. 3.0233 EFFECT OF SPECIMEN WIDTH AND PLATE THICKNESS ON ENERGY ABSORPTION IN PRECRACKED CHARPY IMPACT TEST ON SPECIMENS CUT FROM PLATE OF VARIOUS THICKNESSES (8, p. 399)

	Fe
18	Ni
8.5	Co
	Mo
	Ti
	Al

18Ni (200)
Maraging

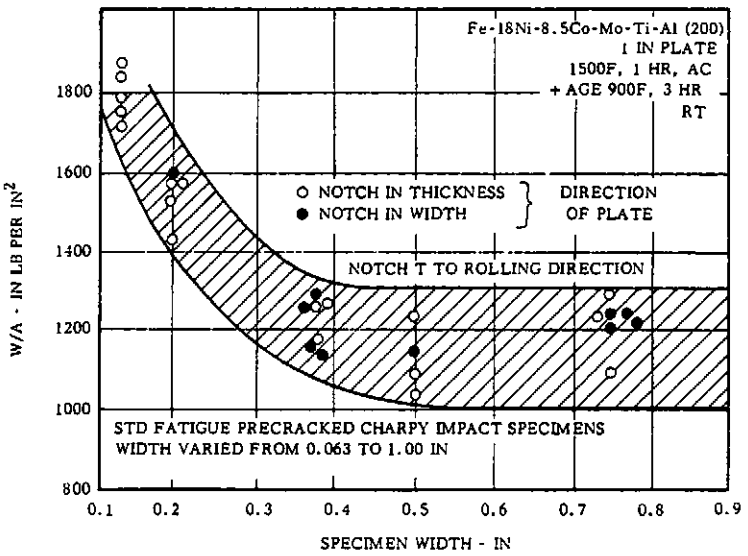


FIG. 3.0234 EFFECT OF SPECIMEN WIDTH ON ENERGY ABSORPTION IN PRECRACKED CHARPY IMPACT (8, p. 397)

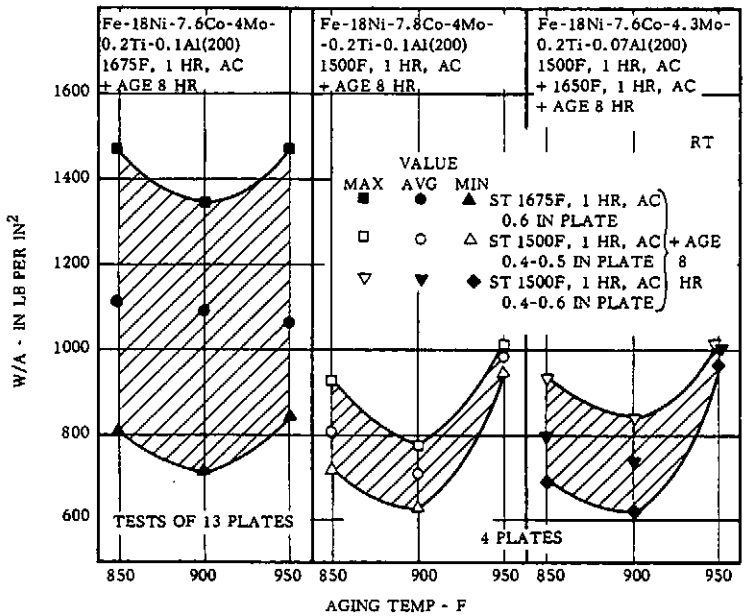


FIG. 3.0235 EFFECT OF VARIOUS SOLUTION TREATMENTS AND AGING TEMPERATURES ON ENERGY ABSORPTION IN PRECRACKED CHARPY IMPACT TESTS OF PLATE AT ROOM TEMPERATURE (11)

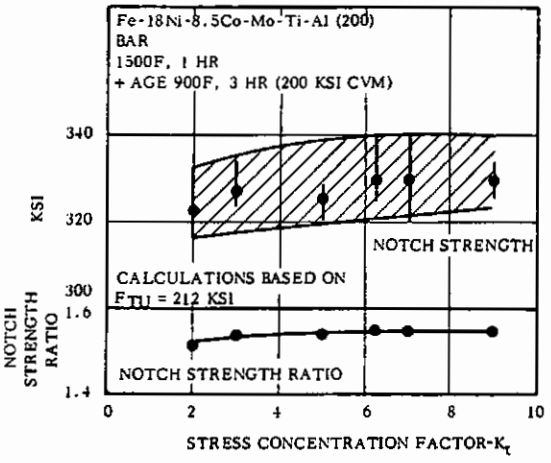


FIG. 3.02711 EFFECT OF STRESS CONCENTRATION FACTOR ON NOTCH TENSILE STRENGTH AND NOTCH STRENGTH RATIO OF 200 KSI CVM BAR (2, p. 2)

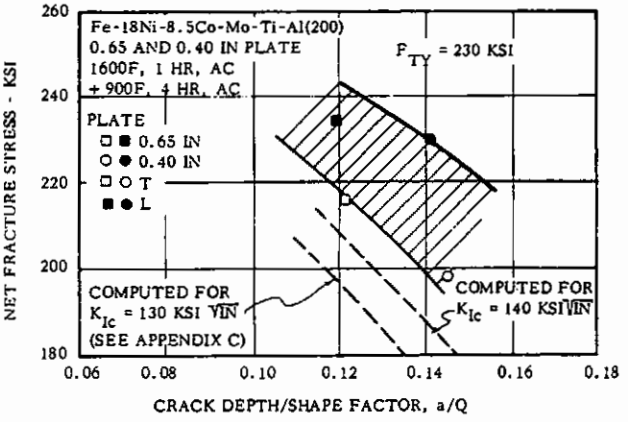


FIG. 3.02722 EFFECT OF DEFECT GEOMETRY ON NET FRACTURE STRESS FOR PLATE. COMPUTATIONS SHOW EXPECTED RELATION FOR SEVERAL SELECTED VALUES OF K_{Ic} (23)

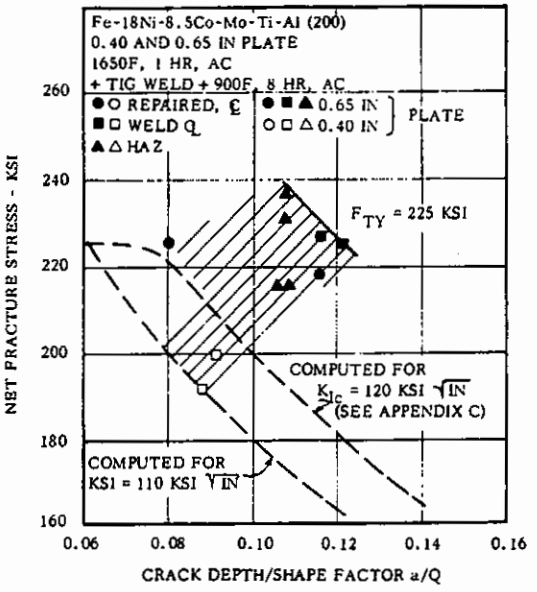


FIG. 3.02723 EFFECT OF DEFECT GEOMETRY ON NET FRACTURE STRESS FOR WELD SECTIONS, REPAIRED DEFECTS, AND HEAT-AFFECTED ZONE FOR PLATE. COMPUTATIONS SHOW EXPECTED RELATION FOR SEVERAL SELECTED VALUES OF K_{Ic} (24)

	Fe
18	Ni
8.5	Co
	Mo
	Ti
	Al

18 Ni (200)
Maraging

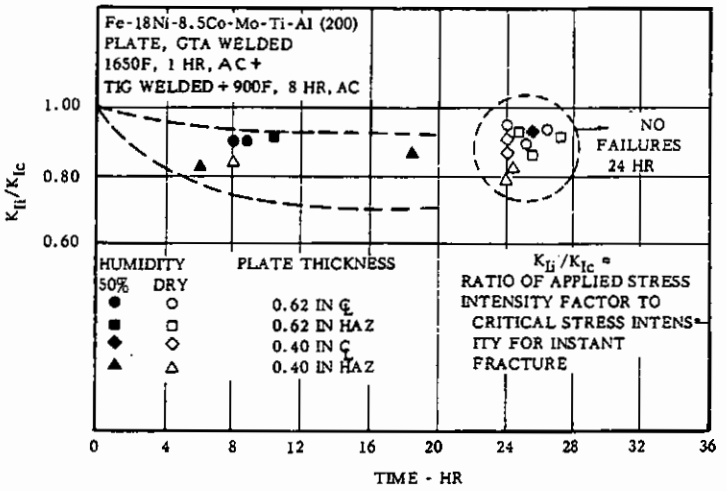


FIG. 3.02724 EFFECT OF HUMIDITY AND APPLIED STRESS INTENSITY FACTOR ON TIME REQUIRED TO CAUSE FRACTURE OF TIG WELDED PLATE (12, p. 40)

	Fe
18	Ni
8.5	Co
	Mo
	Ti
	Al

18 Ni (200) Maraging

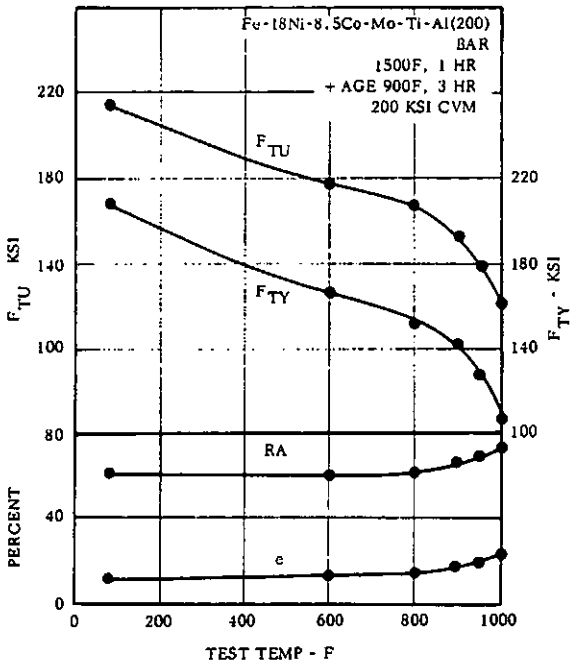


FIG. 3.0312 EFFECT OF TEST TEMPERATURE ON TENSILE PROPERTIES OF 200 KSI CVM BAR (1, p. 1, 2)

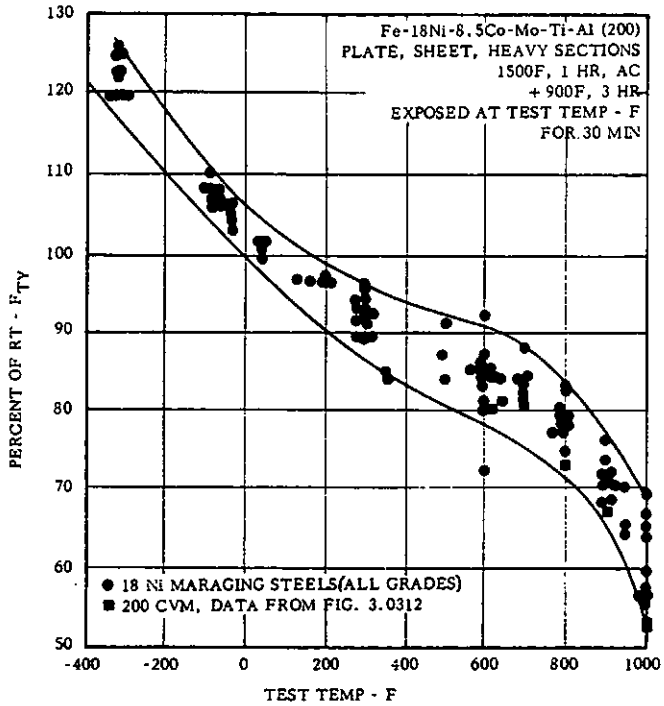


FIG. 3.0313 EFFECT OF TEST TEMPERATURE ON YIELD STRENGTH OF 18 Ni MARAGING STEELS AGED AT 900F FOR 3 HR AND SHOWING RELATION OF 200 CVM STEEL WITHIN SCATTERBAND OF OTHER MARAGING STEELS (3, p. 30)

	Fe
18	Ni
8.5	Co
	Mo
	Ti
	Al

18 Ni (200)
Maraging

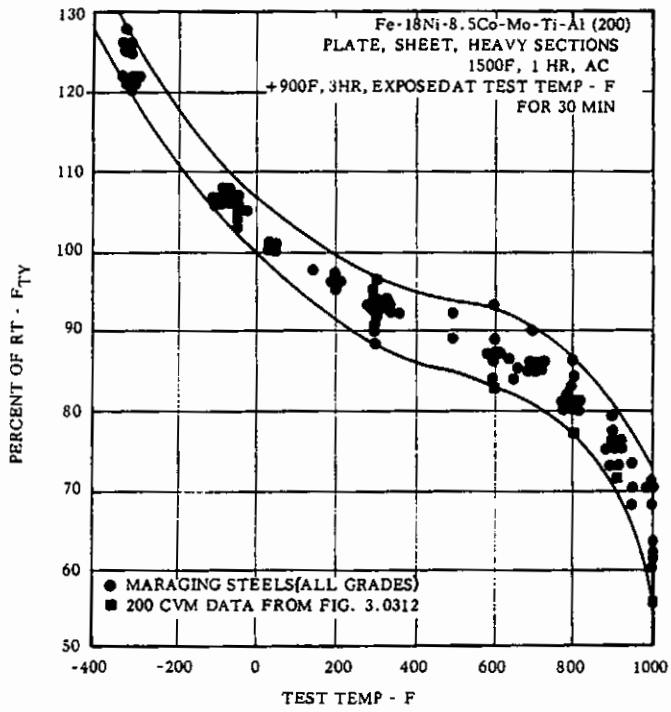


FIG. 3.0314 EFFECT OF TEST TEMPERATURE ON ULTIMATE TENSILE STRENGTH OF 18 Ni MARAGING STEELS AGED AT 900F FOR 3 HR, AND SHOWING RELATION OF 200 CVM STEEL WITHIN SCATTERBAND OF OTHER MARAGING STEELS (3, p. 29)

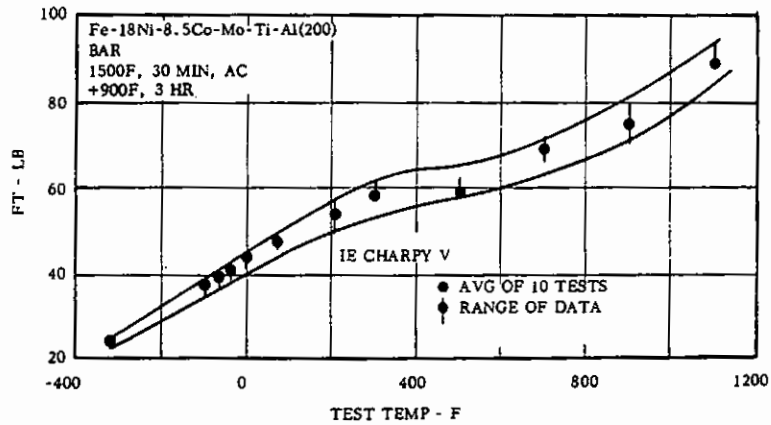


FIG. 3.0331 EFFECT OF TEST TEMPERATURE ON CHARPY V-NOTCH IMPACT STRENGTH OF BAR IN 200 CVM CONDITION (1, p. 11)

	Fe
18	Ni
8.5	Co
	Mo
	Ti
	Al

18 Ni (200) Maraging

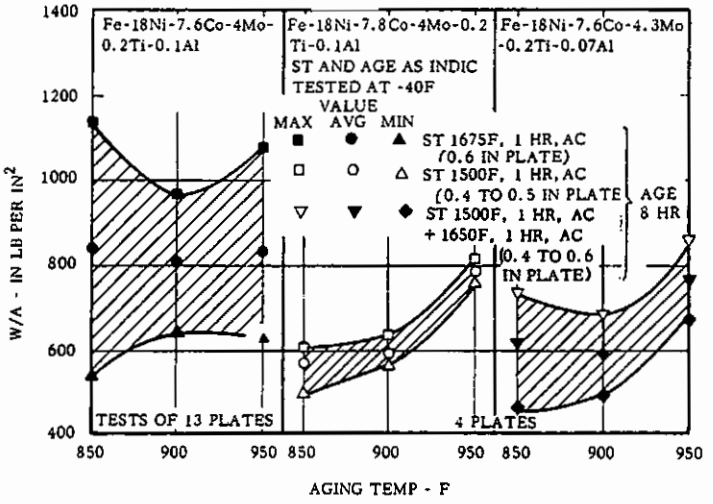


FIG. 3.0332 EFFECT OF VARIOUS SOLUTION TREATMENTS AND AGING TEMPERATURE ON ENERGY ABSORPTION IN PRECRACKED CHARPY IMPACT TESTS AT -40F (11)

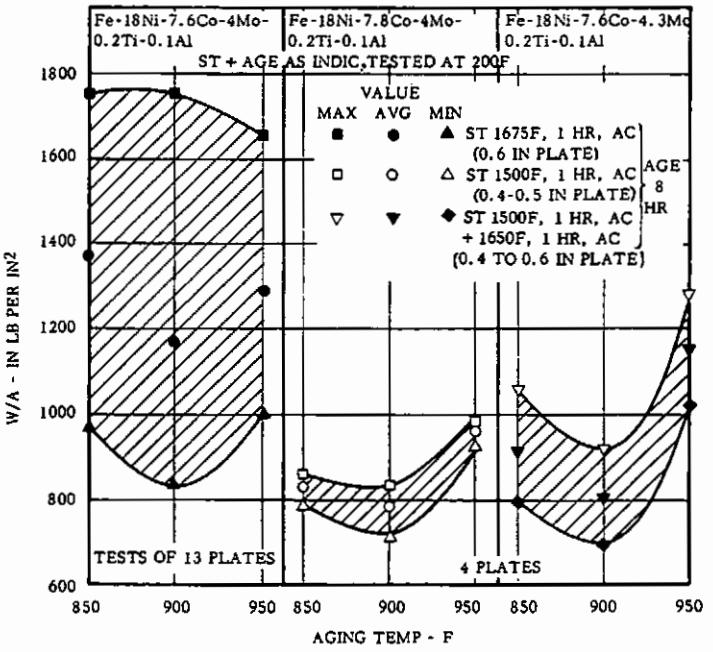


FIG. 3.0333 EFFECT OF VARIOUS SOLUTION TREATMENTS AND AGING TEMPERATURES ON ENERGY ABSORPTION IN PRECRACKED CHARPY IMPACT TESTS AT 200F (11)

	Fe
18	Ni
8.5	Co
	Mo
	Ti
	Al

18 Ni (200)
Maraging

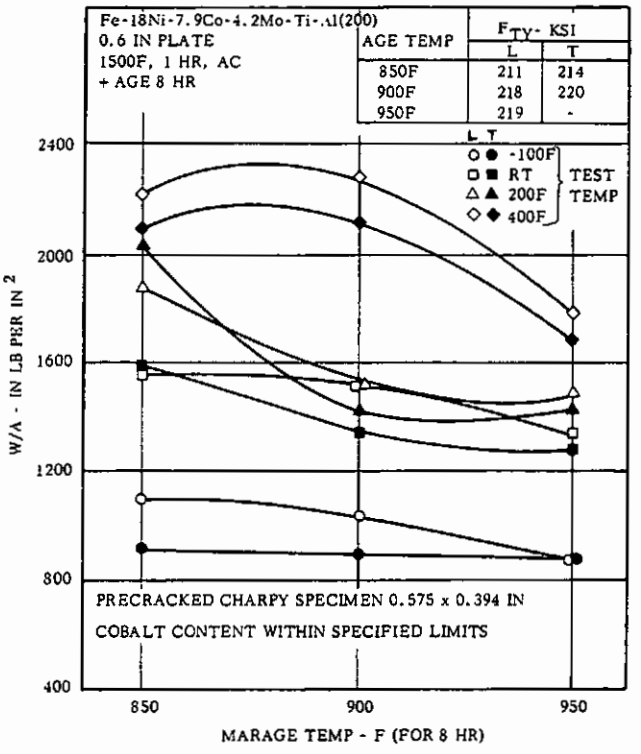


FIG. 3.0334 EFFECT OF MARAGING TEMPERATURE, TEST TEMPERATURE AND SPECIMEN ORIENTATION ON ENERGY ABSORPTION IN IMPACT TEST OF PRECRACKED CHARPY SPECIMEN (9, Tbl. 9)

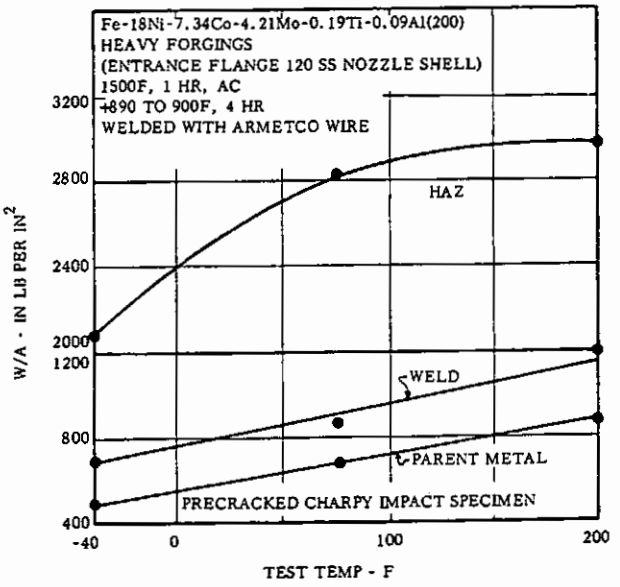


FIG. 3.0335 EFFECT OF TEST TEMPERATURE ON ENERGY ABSORPTION IN PRECRACKED CHARPY IMPACT SPECIMENS FROM HEAVY FORGING INCLUDING PARENT METAL, WELD AREA AND HEAT-AFFECTED ZONE (6, p.55)

	Fe
18	Ni
8.5	Co
	Mo
	Ti
	Al

18 Ni (200) Maraging

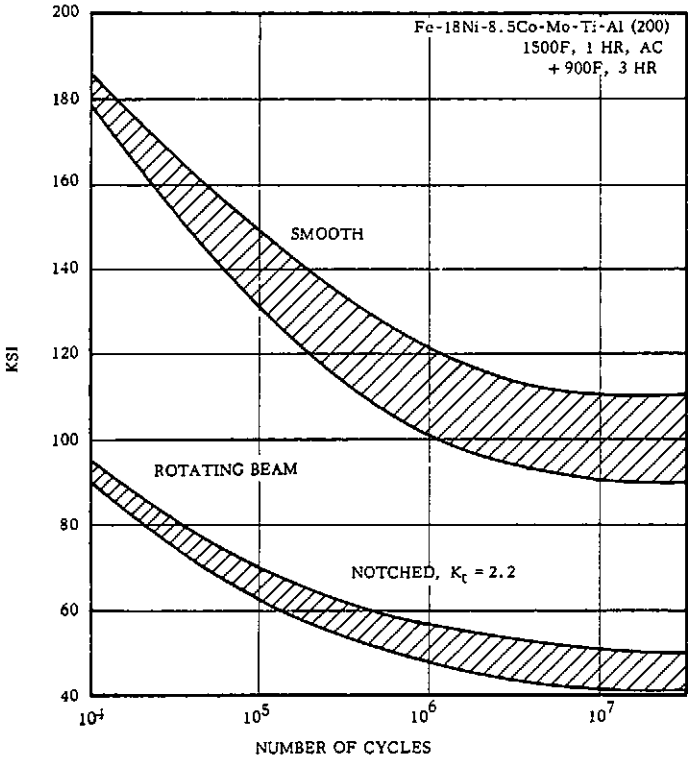


FIG. 3.051 FATIGUE STRENGTH IN ROTATING BEAM BENDING (4, p. 3)

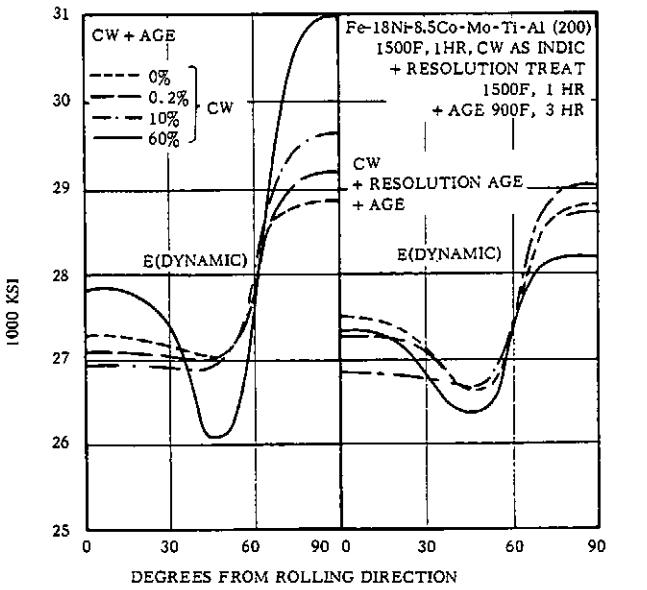


FIG. 3.0621 EFFECT OF COLD WORK, RESOLUTION TREATMENT AFTER COLD WORK, AND DIRECTION RELATIVE TO COLD WORK ON DYNAMIC MODULUS (12, p. 378-383)

	Fe
18	Ni
8.5	Co
	Mo
	Ti
	Al

18 Ni (200) Maraging

REFERENCES

1. Vanadium Alloys Steel Co., "Vascomax 200 CVM," Ready Reference Data Sheets, (1965)
2. International Nickel Co., "18% Nickel Maraging Steels, Data Bulletin," (Nov. 1964)
3. Campbell, J. E., Barone, F. J. and Moon, D. P., "The Mechanical Properties of the 18 Percent Nickel Maraging Steels," DMIC Report 198, (Feb. 1964)
4. International Nickel Co., "18% Nickel Maraging Steels, Summary Data," (March 30, 1965)
5. Sun Shipbuilding and Dry Dock Co., "260 Inch Diameter Motor Fabrication Program; Materials and Process Evaluation Program Subtask II," Phases I and II, Lukens Plate R-599-1, Document No. 40-4, (May 1964)
6. Sun Shipbuilding and Dry Dock Co., "260 Inch Diameter Motor Fabrication Program; Evaluation of the Forged Components for the 120-SS Nozzle Shell," Document No. 40-10, (July 1964)
7. Sun Shipbuilding and Dry Dock Co., "260 Inch Diameter Motor Fabrication Program; Evaluation of Solutions Annealing Temperatures for 260-SL-1 Plate," Document No. 40-11, (Aug. 1964)
8. Lewis, R. E., "Fracture Toughness in Plate Thicknesses of 18 Nickel Maraging Steels," Third Maraging Steel Project Review, RTD-TDR-63-4048, p. 388, (1963)
9. Aerojet General Corporation, "Informal Final Report, Process Evaluation Program 623A," (1964)
10. Sun Shipbuilding and Dry Dock Co., "Material Characterization Report, Second 260 Inch Chamber and Nozzle Shell," (March 1965)
11. Sun Shipbuilding and Dry Dock Co., "Material Characterization Reports, First 260-SL Chamber and Nozzle Shell," (Nov. 1964)
12. Lewis, R. E., "Anisotropy of Young's Modulus in 18 Ni Maraging Steel," Third Maraging Steel Project Review, RTD-TDR-63-4048, p. 369, (1963)
13. Romine, H. E., "Plane Strain Fracture Toughness of 18 Ni (250) and 18 Ni (200) Maraging Welded Steel Plate," U. S. Naval Weapons Laboratory Report No. 1959, (Jan. 1965)
14. Crimmins, P. P., "Evaluation of High Nickel Maraging Steel for Application in Large Booster Motor Applications," Third Maraging Project Review, RTD-TDR-63-4048, pp. 96-184, (Nov. 1963)
15. Boeing Co., Aero-Space Division, "Large Motor Case Technology Evaluation," First Year Summary Progress Report, Vol. I, (June 1965)
16. Aerojet General Corp. Specification AGC 34315, Amendment 1, (April 3, 1964)
17. Aerojet General Corp. Specification AGC 34316, Amendment 1, (April 3, 1964)
18. Aerojet General Corp. Specification AGC 34326 (Supersedes Amendment 1, Dec. 27, 1963), (March 19, 1964)
19. Lockheed Missiles and Space Co., "Material Specification LMSC 5050026, (Sept. 27, 1965)
20. Audener, R. E. and Tenner, W. S., "Evaluation of High Nickel Steel for Application in Large Booster Motor Application, ASD Contract AF 33(657)-8740, Aerojet General Corp., Sacramento, California, Report 0705-82Q-2, (Dec. 1962)
21. Clark, C. C., International Nickel Co., "Personal Communication with W. F. Brown, Jr.," (1962)
22. Tiffany, C. F. and Masters, J. N., "Large Motor Case Technology Evaluation," Progress Report, Boeing Co. Contract AF 33(615)-1623, (Dec. 1964)
23. Tiffany, C. F. and Masters, J. N., "Large Motor Case Technology Evaluation," Progress Report, Boeing Co. Contract AF 33(615)-1623, (March 1965)

	Fe
18	Ni
7.5	Co
5	Mo
	Ti
	Al

18Ni(250) Maraging

GENERAL

This steel is one of a series of wrought high-nickel alloys developed in 1959 to combine superior toughness and resistance to crack propagation with high strength. This attractive property combination is achieved by aging to promote complex precipitation reactions in a low carbon iron-nickel martensite. In these 18Ni maraging steels, the transformation from austenite to martensite occurs just above room temperature (200 to 400 F). In the martensitic condition, the steels are soft and ductile. They can be easily fabricated and subsequently strengthened by age-hardening at 900 F. A high degree of dimensional stability is maintained throughout heat treatment.

Four compositions have been specified according to their approximate yield strengths in ksi. These are grades 200, 250, 300, and 350, with the 250 grade being most widely used. The nominal amounts of cobalt, molybdenum, and titanium vary in these four grades. For optimum strength and toughness, carbon, silicon, manganese, sulfur, and phosphorus are held at low levels.

The actual strength level and toughness of 18Ni(250) maraging steel can vary considerably with composition variations within the specified limits and also depend strongly on processing history. Properly processed sheet product has higher fracture toughness than standard low alloy quenched and tempered steels. The toughness and impact properties of heavy sections are also superior to those of conventional medium carbon low alloy high strength steels heat treated to comparable strength levels. However, the fracture properties of heavy sections can be directional and are lowest in the short transverse direction. This directionality is influenced by melting and processing conditions. Some early heats of maraging steel were air melted and data from such heats are included in this chapter. However, modern practice requires vacuum induction melting (VIM) plus consumable vacuum arc (CVM) remelting.

Although maraging steels are more resistant to rusting than most of the non-corrosion resistant steels, some form of protective coating is normally used for prolonged service life. Resistance to environmentally enhanced crack propagation is better than that of 4340 steel at an equivalent level of tensile strength. The maraging steels are embrittled by hydrogen but less so than conventional low alloy steels. Welding requires special precautions and the toughness of the weld metal is generally below that of the parent metal. Maraging steel can be surface hardened by nitriding.

The use of 18Ni(250) maraging steel is limited by high cost compared with lower alloyed steels of comparable strength. It is particularly suited to specialized applications where heat treat distortions and dimensional changes must be minimized and high fracture toughness is required. These applications include casings for small solid rockets, light aircraft landing gear, helicopter power shafts and rotor joints, permanent molds, and dies for injection molds.

1.01 **Commercial Designation**
18Ni 250 grade maraging steel.

1.02 **Alternate Designations**
UNS K92890, UNS K92940, Almar 18 250, Marvac 250, Nimark 250, Udimar B-250, and Vasco max 250.

1.03 **Specifications**
1.031 AMS specifications, Table 1.031.
1.032 Other specifications: ASTM A538 (Grade B); ASTM A579 (Grade 72); MIL-S-46850.

1.04 **Composition**
1.041 Composition, Table 1.041.
1.042 Precipitates formed during aging include Ni_3Ti and Ni_3Mo. Carbon in excess of 0.03 percent adversely affects notch toughness by removing titanium and molybdenum from the matrix to form carbides. Aluminum is added for deoxidation and improved impact strength. Amounts over 0.15 percent increase strength but decrease toughness. Grain boundary precipitation is retarded by small additions of boron and zirconium, thereby improving the toughness and resistance to stress corrosion cracking. Phosphorus, antimony, arsenic, and tin can cause isothermal embrittlement in the temperature range 600 to 1100 F (82).

1.05 **Heat Treatment**
1.051 General. Although the 18Ni maraging steels are fully austenitic above 1350 F, higher annealing temperatures are generally used to ensure that the precipitates go into solution and that any residual fabrication stresses are removed. On cooling, the austenite transforms to low carbon iron-nickel martensite that has a body-centered cubic structure with no evidence of tetragonality. The structure is untwinned but with dense tangles of dislocations. This type of martensite is relatively soft (approximately HRC 30) and tough. Since the austenite to martensite transformation takes place at low temperatures (see Figure 2.0122) where diffusion controlled processes are not favored, the martensite forms by diffusionless shear.

An important practical aspect of maraging steels is that martensite is formed at all cooling rates and thus in all section sizes. The usual concepts of hardenability do not apply to maraging steels. Although it forms at low temperatures, the iron-nickel martensite must be reheated to about 1100 F before it transforms back into austenite for short heating times. Reheat times on the order of tens of hours cause austenite to form at lower temperatures. The heat treatment of maraging steels makes use of this hysteresis to age-harden the martensite below the austenite transformation temperature. The strength of annealed 18Ni(250) grade more than doubles on aging at 900 F for 3 hours.

Although the strengthening precipitates are small and not easily identifiable, they are thought to be primarily Ni_3Mo with a secondary titanium-containing precipitate, possibly Ni_3Ti. Cobalt is believed to reduce the solubility of molybdenum in the iron-nickel matrix, thereby producing a

	Fe
18	Ni
7.5	Co
5	Mo
	Ti
	Al

18Ni(250) Maraging

larger amount of finely dispersed precipitate which increases the strength of the alloy. The cobalt-molybdenum combination in maraging steels is unique and allows retention of good toughness at strength levels up to about 300 ksi.

The standard aging heat treatment of 3 hours at 900 F is near the peak hardness achievable in a reasonable time period. Softening at times over 20 hours at 900 F is caused by a combination of classical overaging and the formation of soft, stable austenite. The diffusion-controlled formation of austenite is called "austenite reversion". At temperatures in the two-phase region of the phase diagram, martensite breaks down into ferrite and austenite after sufficiently long heating times. Partitioning of the alloying elements occurs, with the reverted austenite having a slightly different composition than that formed by solution annealing in the single phase austenite field. Austenite reversion is promoted by local changes in composition, such as by overaging, which causes local compositional changes. Austenite, being soft, lowers the strength and should be avoided. This is accomplished by solution annealing at temperatures well above the two-phase region and aging at time-temperature conditions under which the precipitate is stable (83).

1.052 Annealing treatment, 1450 to 1650 F, 1 hour per inch of thickness, 15 to 30 minutes minimum, and air cool is generally recommended. Double annealing treatment of 1650 to 1700 F, 1 hour, air cool, plus 1500 to 1550 F, 1 hour, air cool, is also recommended. Selection of an optimum annealing temperature in terms of strength and toughness will depend on the prior thermal-mechanical history. Generally, annealing temperature should be kept below 1800 F to prevent excessive grain coarsening and to avoid thermal embrittlement (see Section 1.094).

1.053 Aging treatment, 700 to 950 F, air cool. Full age is generally recommended, 875 to 925 F, 3 hours, air cool. Broad latitude in aging treatment is available through proper combinations of aging time and temperature. Structures that are badly segregated may not age in a normal manner and austenite reversion may be encountered. Structures that have undergone austenite reversion may be restored to strength by reannealing and aging. Duplex aging treatments may be used to provide some increase in strength (see Table 3.02178). Aging after severe cold working should be avoided (see Section 3.02181c).

1.054 Special considerations. Decarburization limits are not applicable to this steel because of the low carbon content. Care should be taken, however, to avoid surface carburization, sulfurization, and excessive oxidation. The use of cracked ammonia as a protective atmosphere during annealing treatments can introduce hydrogen into this steel and produce embrittlement under certain conditions. This hydrogen embrittlement is less severe for air cooling from annealing temperature than for water quenching, and is eliminated by the standard aging treatment (see Section 1.095).

Before heating remove grease and oil. Furnace fuel oil should not contain more than 0.75 percent sulfur by weight; fuel gas not more than 100 total grains of sulfur per 100 ft^3. Furnace atmosphere should not be carburizing; atmosphere containing 5 percent CO_2 is suggested (6). Aging is normally done in air.

1.055 Effect of solution anneal temperature on prior austenite grain size, Figure 1.055.

1.06 **Hardness**

1.061 Typical hardness for annealed condition, 28 to 35 HRC (4–6).

1.062 Typical hardness for fully aged material, 48 to 52 HRC (4–6).

1.063 Effect of aging temperature and time on hardness, Figure 1.063.

1.064 Hardenability. Air cooling from anneal followed by aging produces full hardness in heavy section (4–6).

1.07 **Forms and Conditions Available**

This steel is available in bar, rod, wire, sheet, strip, plate, tubing, shapes, extrusions, and forgings in the hot worked or annealed condition. Sheet is also available in the annealed and cold worked condition.

1.08 **Melting and Casting Practice**

Electric furnace air melting with or without vacuum degassing, induction vacuum melting, consumable electrode vacuum remelting. Low carbon content and low residual element content require high quality raw materials. Vacuum melting is recommended. For improved fracture toughness, carbon should be kept well below the specified 0.03 percent maximum (see Table 1.082 and Section 3.0339).

1.081 Room temperature tensile properties of air and vacuum melted slab, Table 1.081.

1.082 Influence of carbon content on the room temperature properties of laboratory vacuum melted plate, Table 1.082.

1.09 **Special Considerations**

1.091 General. The heat to heat variability of this steel within the composition limits given in Table 1.041 is higher than that normally encountered for low alloy heat treated steels such as 4340. Special consideration should also be given to directionality of mechanical properties, the possibility of high temperature embrittlement, and the high tolerance for hydrogen. Weldments present special problems which are discussed in Section 4.03.

1.092 Variability of properties. The yield strength and toughness of aged material will vary from heat to heat within the specified composition limits (e.g., see Figures 1.0921, 3.0234, 3.02717, 3.0315, 3.0318, 3.0331, 3.03391, and 3.03392). The variation in strength is caused primarily by differences in the content of strengthening elements, and also arises from differences in the melting and processing history (11–13). Generally the toughness will decrease with those factors that tend to increase the yield strength, such as cold work retained after annealing, increased titanium content (see Figure 3.02712, FeUH 1225) or cryogenic testing temperature (see Table 3.03711). The influence of melting practice on the mechanical properties is not well understood; however, toughness is improved with a reduction in the carbon content (see Table 1.082) and is affected by processing history

(see Section 1.094). It is recommended that for critical applications the aging response regarding strength and toughness be determined for each heat.

1.0921 Effect of titanium content on tensile properties of annealed and aged sheets from laboratory and production heats, Figure 1.0921.

1.093 Directionality. Heavy sections of this alloy and other high strength steels can exhibit a banded structure which is associated with alloy segregation. If the bands contain a high concentration of nonmetallic inclusions (titanium carbides/nitrides, titanium sulfides or oxides), the short transverse ductility and toughness may be considerably lower than the corresponding longitudinal properties (see Table 3.02156 and Table 3.02724). Under these circumstances, the banding can result in delaminations or splitting in the plane of the bands. In severe cases, splitting may occur during shearing or forming operations, or may be produced by thermal stresses induced by flame (or plasma-arc) cutting or welding.

It should be noted that in banded structures, the apparent fracture toughness for cracks propagating in a direction perpendicular to the bands (TS and LS orientation) will be higher than that for cracks propagating in the other directions because of momentary crack arrest and reinitiation at the delaminations (see Tables 3.02723 and 3.02724) (14, 15).

The presence of these inclusions reduces the general level of ductility and toughness in the other directions (10). The degree of banding and its influence on the mechanical properties is related to the melting and processing practices employed. In this respect particular attention should be given to Sections 1.08, 1.094, and 4.011. By very careful control of the melting and processing techniques, it is possible to reduce the amount of banding and to minimize its deleterious effects on the transverse properties of heavy sections (10, 16, 17).

1.094 Isothermal embrittlement. This steel may be severely embrittled by certain high temperature thermal treatments involved in processing and fabrication. The most severe embrittlement results from prolonged exposure in the temperature range 1500 to 1800 F following heating to 2200 to 2400 F, and is caused by the precipitation of TiC,N at austenite boundaries and the marked coarsening of the austenite grains during high temperature heating (10). This condition would be encountered if the alloy is allowed to cool very slowly following prior hot working (see Figure 3.02725). For this reason hot working should be followed by as rapid an air cool as possible (10, 18). Heavy sections welded by high heat input processes may also exhibit this embrittlement (10).

1.0941 Effect of combined annealing treatments on impact strength of annealed plate, Figure 1.0941.

1.0942 Effect of combined annealing treatments on impact strength of annealed and aged plate, Figure 1.0942.

1.0943 Effect of combined annealing treatments on strength and crack toughness of plate, Table 1.0943.

1.095 Hydrogen embrittlement. Hydrogen embrittles this alloy but it exhibits a greater tolerance for hydrogen than other high-strength steels such as 4340 at lower strength levels. This has been demonstrated by both tensile tests and static fatigue tests. Charging conditions (0.02 amps per square inch for 5 minutes) that severely reduce the reduction of area of 4340 (F_{tu} = 230 ksi) have no effect on this grade of maraging steel. Sufficiently severe charging conditions will reduce the ductility of this steel. Recovery by baking is much more rapid than observed for 4340; a bake of 24 hours at 400 to 600 F usually restores their full mechanical properties (4, 19, 20).

	Fe
18	Ni
7.5	Co
5	Mo
	Ti
	Al

18Ni(250) Maraging

Hydrogen embrittlement may result from high temperature treatment in certain atmospheres, such as cracked ammonia. The embrittlement effect is completely removed by the standard aging treatment (3 hours at 900 F) (10). Electroplating and acid chemical contouring do not appear to embrittle this steel; however, specific processes should be checked by control tests before adoption (21, 22). Dry hydrogen at 1 atmosphere causes rapid crack extension in this steel under both static and fatigue loads (see Figures 2.0332 and 3.0523) (24). This effect is eliminated by the introduction of moisture into the hydrogen atmosphere (23) (see also Section 2.033).

2 PHYSICAL PROPERTIES AND ENVIRONMENTAL EFFECTS

2.01 Thermal Properties

2.011 Melting range approximately 2600 to 2650 F.

2.012 Phase changes. Alloy transforms to martensite on slow cooling from annealing temperature. M_s = 450 F and M_f = 300 F approximately (see Figure 2.0122); these temperatures depend on the alloy composition, M_s being lowered by molybdenum (8, 9). Austenite reversion occurs on overaging which depends on time and temperature and on composition (8, 14). Austenite content after aging for 80 hours at 900 F is about 12 percent (8). Length changes from maraging, which vary with processing history, are approximately 0.06 to 0.08 percent (4, 85).

2.0121 Time-temperature-transformation diagrams.

2.0122 Austenite to martensite transformation curve, Figure 2.0122.

2.013 Thermal conductivity, Figure 2.013.

2.014 Thermal expansion (75 to 900 F, 5.6 x 10^{-6} inch per inch per F), Figure 2.014.

2.015 Specific heat at constant pressure, Figure 2.015.

2.016 Thermal diffusivity (see Figures 2.013 and 2.015, and Section 2.021).

2.02 Other Physical Properties

2.021 Density, 0.29 lb/in.^{3}, 8.0 gm/cm^3 (3–5).

2.022 Electrical resistivity, increases within the indicated ranges primarily with titanium content (see also Section 2.022, FeUH 1225) (4).

As annealed at 1500 F	23.6 to 27.5 microhm-in. 60 to 70 microhm-cm
Maraged, 3 hr – 900 F	13.8 to 23.6 microhm-in. 35 to 60 microhm-cm.

2.023 Magnetic properties (see Section 2.023, FeUH 1225).

2.0231 D. C. magnetic properties. Permeability at 200 oersteds = 77.5. Saturation induction equals 21.2 kilogauss at 1300 oersteds (26).

2.024 Emittance.

2.025 Damping capacity.

	Fe
18	Ni
7.5	Co
5	Mo
	Ti
	Al

18Ni(250) Maraging

2.03 Chemical Environments

2.031 Corrosion resistance. Atmospheric environments, such as industrial and marine atmospheres, corrode the maraging steels 0.0005 to 0.001 inch per year, about half that of normal high strength low alloy steels. Static immersion tests show the average corrosion rate to be 0.003 inch per year in quiet seawater (0.5 ft per second), and 0.007 to 0.011 inch per year in flowing seawater (at 2 ft per second) and 0.09 to 0.11 inch per year (at 130 ft per second), these rates being comparable to those for control samples of 4340 and HY-80 steels. The maraging steels corrode substantially in tap water, some neutral salt solutions, and in some inorganic and organic acids. Their corrosion rate is lower than those of low-alloy steels heat treated to high strength levels. In general, the maraging steels should be protected from exposure to corrosive solutions by some means, such as by a suitable coating. Conventional cathodic protection, as with zinc anodes, is not recommended because of the danger of hydrogen embrittlement (4, 19, 27, 28).

2.032 Stress corrosion.

2.0321 This maraging steel exhibits better stress corrosion resistance than 18Ni(300) maraging steel (FeUH 1225 – Fe-18Ni-9Co-5Mo-Ti-Al) and other low alloy high strength steels, such as 4340 heat treated to high strength levels; however, a suitable coating is recommended (4, 27, 29, 30). Delayed failure can occur in water environment. The sensitivity to water- or moisture-enhanced crack growth is less than that for 18Ni(300) maraging steel and 4340 (28, 31, 32). Moisture has only a slight effect on the rate of fatigue crack growth in this alloy (23, 33).

2.0322 Delayed failure characteristics of air-melted and CVM sheets in 3 percent NaCl solution at room temperature, Figure 2.0322.

2.0323 Delayed failure characteristics of air-melted and CVM plates in 3 percent NaCl solution at room temperature, Figure 2.0323.

2.0324 Delayed failure characteristics of air-melted plate in synthetic seawater at room temperature, Figure 2.0324.

2.0325 Prior heat treatment has a moderate effect on the time to failure under constant load stress corrosion in humid air, as shown in Figure 2.0326. This effect is related to a grain boundary precipitate of Ti(C,N) which is present in the high temperature annealed, austenitized, and aged material (Lot B) but absent in the high temperature annealed and aged material (Lot A). The precipitate-free material has high fracture toughness (K value at zero time to failure) compared to the precipitate-containing material, but the threshold stress intensities are similar (about 30 ksi $\sqrt{in.}$) for both materials (86).

2.0326 Effects of heat treatment on sustained load failure time in 100 percent relative humidity at room temperature, Figure 2.0326.

2.0327 The threshold stress intensity factor for stress-corrosion cracking in salt air is reduced by welding (see Table 4.0365).

2.033 Hydrogen environment effects.

2.0331 This maraging steel is susceptible to embrittlement and sustained-load cracking in gaseous hydrogen. Crack growth is characterized by an apparent threshold stress intensity, a region where the growth rate increases sharply with the stress intensity factor K (Stage I), and a range where the growth rate is little changed with increasing K (Stage II). The crack growth behavior in dry hydrogen at room temperature is shown in Figure 2.0332. Cracking proceeds on load application (above the threshold stress intensity factor) with little or no detectable incubation period and is continuous with time. The rate-limited Stage II crack growth exhibits three distinct regions of temperature dependency, with a different isothermal pressure dependence in each region, as shown in Figures 2.0333 and 2.0334.

In the low temperature region (below about 0 F), the Stage II crack growth rate is thermally activated with an activation energy of 4.4 kcal/mole. This activation energy relates to a hydrogen transport process and is independent of hydrogen pressure and alloy yield strength. The crack-growth rates are proportional to $P_{H_2}^{1/2}$. In the intermediate temperature range, Stage II crack-growth rates deviate from the low temperature thermally activated behavior, pass through a maximum, and then decrease with increasing temperature. The apparent threshold stress intensity factor increases gradually with increasing temperature in the low temperature region but increases sharply in the intermediate temperature region, as shown in Figure 2.0335.

Above a "transition" temperature, the 18Ni maraging steels become essentially immune to gaseous hydrogen embrittlement. The transition temperature is strongly dependent on hydrogen pressure and varies also with yield strength among the various grades of maraging steel (87, 88). (See also Figure 3.0523.)

2.0332 Influence of stress intensity factor K on the rate of crack growth under sustained load in dry hydrogen at 1 atmosphere and room temperature, Figure 2.0332.

2.0333 Effect of temperature on Stage II (rate limited) sustained load crack-growth rate in high purity hydrogen at several pressures, Figure 2.0333.

2.0334 Effects of hydrogen pressure on Stage II sustained load crack-growth rates at -49 to 68 F, Figure 2.0334.

2.0335 Effects of temperature on apparent threshold stress intensity factor for sustained load crack growth in high purity hydrogen, Figure 2.0335.

2.0336 The threshold stress intensity for sustained load cracking in hydrogen is substantially increased by preloading in an inert atmosphere, as shown in Figure 2.0337. Thus, an increase in the load capacity of a structure with cracks, to be utilized under hydrogen cracking conditions, can be achieved by preloading under the proper conditions (89).

2.0337 Effects of static preloading on threshold stress intensity factor for sustained load cracking in dry hydrogen, Figure 2.0337.

2.0338 Tensile embrittlement of 18Ni(250) maraging occurs at room temperature when tested in gaseous hydrogen at strain rates of less than about 10^{-1} min.$^{-1}$, as shown in Figure 2.0339. Alloy tested in vacuum is ductile, while alloy that has

	Fe
18	Ni
7.5	Co
5	Mo
	Ti
	Al

18Ni(250) Maraging

been cathodically charged with hydrogen is embrittled at strain rates from 4×10^{-3} to 2 $min.^{-1}$. These strain rate effects are attributed to the necessity for hydrogen diffusion to support brittle decohesion at the stress levels involved. It is of interest to note that the critical ductile-to-brittle strain rate of 10^{-1} $min.^{-1}$ in tensile testing is almost identical to the sustained load crack-growth rate in hydrogen at room temperature shown in Figure 2.0333, suggesting that the same hydrogen embrittlement reaction is rate-controlling under both sets of conditions. Tensile embrittlement of aged alloy in hydrogen is affected by the prior solution annealing temperature. As shown in Figure 2.03310, annealing temperatures above 1600 F promote embrittlement during subsequent tensile testing in hydrogen, while annealing at 1400 F decreases susceptibility to hydrogen embrittlement. It has been suggested that this annealing effect is attributable to banding, which is intensified by the low temperature heat treatment. In the soft (unaged) solution annealed condition, the alloy is not susceptible to hydrogen embrittlement (90).

2.0339 Effects of strain rate on tensile reduction in area at room temperature for specimens tested in vacuum, in hydrogen, and in vacuum immediately after cathodically charging, Figure 2.0339.

2.03310 Effects of solution anneal temperature on tensile ductility of aged bar tested in vacuum and in hydrogen (1 atmosphere), Figure 2.03310.

3 MECHANICAL PROPERTIES

3.01 Specified Mechanical Properties

3.011 AMS specified mechanical properties for sheet, strip, and plate, Table 3.01.

3.012 AMS specified mechanical properties for bars, forgings, tubing, and rings, Table 3.012.

3.02 Mechanical Properties at Room Temperature

3.021 Tension – stress-strain diagrams – tension properties.

3.0211 Stress-strain diagrams. Cyclic softening occurs in solution annealed and aged 18Ni(250) maraging steel, Figures 3.0212b and c, while mixed behavior is observed in solution annealed material, as shown in Figure 3.0212a. Cyclic softening results in a 13 to 15 percent decrease in the 0.2 percent yield strength under cyclic as compared to monotonic conditions for the aged material. This reduction in yield strength can occur during design life as a result of cyclic loading and should be considered during component design. The yield strength reduction is mild as compared to the 50 to 60 percent softening which has been observed in 4340 and in 300-grade maraging steel. Cyclic softening has been related to the monotonic work hardening exponent n, with small values indicating a tendency toward cyclic softening. Low n values reflect minimal work hardening and a starting microstructure which is optimally strengthened. The value of n for the two aged conditions shown in Figures 3.0212b and c is 0.05 and is consistent with the observed cyclic softening. The value of n for the solution annealed material shown in Figure 3.0212a is about 0.16. Strength differential effects are also observed in 18Ni(250) maraging, with the yield and flow stresses being greater in compression than in tension. The strength differential effect is greater under monotonic than under cyclic loading conditions and is smaller than the cyclic softening effect (91).

3.0212 Monotonic and cyclic stress-strain curves [(a) solution annealed, (b) solution annealed plus 4-hour age, and (c) solution annealed plus 8-hour age], Figure 3.0212.

3.0213 Stress-strain curve for annealed and aged bar, Figure 3.0213.

3.0214 Producers' typical range of tensile properties, Table 3.0214.

3.0215 Typical tensile properties.

3.02151 Typical tensile properties of sheet, plate, and bar, Table 3.02151.

3.02152 Typical tensile properties of annealed and aged billets, Table 3.02152.

3.02153 Typical tensile properties of annealed and forged billets, Table 3.02153.

3.02154 Typical tensile properties of air and vacuum melted slab, Table 3.02154.

3.02155 Typical tensile properties of sheet and plate from an air melted heat, Table 3.02155.

3.02156 Typical tensile properties of sheet and plate from a CVM heat, Table 3.02156.

3.0216 Effect of annealing. Solution annealing temperatures (1 hour) from 1500 to 2400 F have little effect on the tensile properties of CVM plate tested in the annealed condition, as shown in Figure 3.02161. The yield and ultimate strengths in this condition are quite low. The effects of a single anneal at various temperatures on the tensile properties of aged stock are not consistent. Thus, in the annealing temperature range between 1400 and 1800 F, the tensile ultimate and yield strength of CVM sheet (see Figure 3.02162) is reduced with increasing annealing temperature while corresponding elongation changes are relatively small. In contrast, the tensile properties of CVM bar (Figure 3.02163) and air melted plate (Figure 3.02164) change relatively little in the annealing temperature range between 1400 and 1800 F. Very high annealing temperatures (1800 to 2400 F) reduce the ultimate and yield strength of CVM plate substantially but have little effect on the elongation (Figure 3.02165). The tensile ultimate and yield strengths of double annealed plate are essentially unaffected by reannealing at temperatures between 1500 and 2400 F (Figure 3.02166), while the elongation and reduction in area are substantially reduced by reannealing at temperatures above 2100 F.

3.02161 Influence of high temperature annealing treatment on tensile properties of annealed CVM plate, Figure 3.02161.

3.02162 Effect of annealing temperature on the tensile properties of annealed and aged sheet, Figure 3.02162.

3.02163 Influence of annealing temperature on tensile properties of bar, Figure 3.02163.

3.02164 Influence of annealing temperature on the tensile properties of plate, Figure 3.02164.

3.02165 Influence of high temperature annealing treatment on tensile properties of aged CVM plate, Figure 3.02165.

3.02166 Influence of high temperature annealing treatment on tensile properties of air melted plate, Figure 3.02166.

Fe
18 Ni
7.5 Co
5 Mo
Ti
Al

18Ni(250) Maraging

3.0217 Effect of aging. The available data support the recommended aging temperature of 900 F for high values of tensile ultimate and yield strength. Aging is time-dependent (see Figure 3.02173) and is also influenced by composition (see Figure 3.02176). Aging for very long times at temperatures below 900 F can produce higher tensile strengths than the conventional 900 F/3 hour age (e.g., Figures 3.02173 and 3.02175).

3.02171 Effects of solution annealing temperature and aging time on the tensile properties of VIM + CVM plate, Figure 3.02171.

3.02172 Effect of aging temperature and time on the tensile properties of sheet, Figure 3.02172.

3.02173 Effect of aging temperature and time on the tensile properties of air melted plate, Figure 3.02173.

3.02174 Effect of aging temperature and time on the tensile properties of VIM + CVM plate, Figure 3.02174.

3.02175 Effect of aging temperature and time on the tensile properties of hot rolled and aged plate, Figure 3.02175.

3.02176 Effect of aging temperature on the tensile properties of annealed plate from three heats, Figure 3.02176.

3.02177 Effect of aging temperature on the tensile properties of hot rolled and annealed plate from two heats, Figure 3.02177.

3.02178 Effect of duplex aging treatments on the tensile properties of 300 lb laboratory vacuum melted plate, Table 3.02178.

3.02179 Effect of aging temperature on the tensile properties of 1.8 inch thick CVM plate, Figure 3.02179.

3.021710 Effect of aging temperature on tensile properties of bar, Figure 3.021710.

3.021711 Effect of aging time on tensile properties of bar, Figure 3.021711.

3.0218 Thermomechanical processing. Cold rolling prior to aging produces a significant increase in tensile strength, as shown in Figure 3.02181. The strength increases with increasing amount of reduction in both the cold rolled and cold rolled plus aged condition. Aging increases strength by about 100 ksi. This improvement is the result of changes in precipitate distribution and morphology caused by the cold work. Aging kinetics are changed to the extent that material with more than about 40 percent cold work is overaged by the standard aging treatment of 3 hours at 900 F (92). The effects of hot rolling finishing temperature and subsequent cooling rate, shown in Figures 3.02183 and 3.02184, are for practical purposes insignificant on the tensile ultimate and yield strengths for several conventional heat treated conditions. In general, the corresponding elongations and reductions in area tend to decrease at the highest finishing temperature (1980 F). A substantial reduction in fracture toughness is also noted for slowly cooled material at the higher finishing temperatures (see Figure 3.02725).

3.02181 Effects of cold rolling and cold rolling plus aging on tensile properties of sheet [(a) yield strength, (b) ultimate strength, and (c) elongation], Figure 3.02181.

3.02182 Effect of rolling temperature on the tensile properties of annealed, rolled, and aged sheet, Figure 3.02182.

3.02183 Effect of hot rolling finishing temperature and cooling rate on properties of laboratory air induction melted plate aged at 900 F, Figure 3.02183.

3.02184 Effect of hot rolling finishing temperature and cooling rate on tensile properties of laboratory air induction melted plate aged at 850 F, Figure 3.02184.

3.02185 Effect of rolling temperature on tensile properties of plate, Figure 3.02185.

3.02186 Effect of forging temperature on tensile properties of 5:1 upset forged pancakes, Figure 3.02186.

3.022 Compression – stress-strain diagrams – compression properties.

3.0221 Stress-strain diagrams. (See Sections 3.0211 and 3.0321.)

3.0222 Compressive yield strength of annealed and aged bar, Table 3.0222.

3.0223 Typical compressive yield strength of sheet, plate, and bar, Table 3.0223.

3.023 Impact (see also Sections 1.094 and 3.033).

3.0231 Effect of aging temperature and time on the impact properties of air melted plate, Figure 3.0231.

3.0232 Effect of yield strength on impact properties of 300 lb laboratory vacuum melted plate, Figure 3.0232.

3.0233 Effect of aging temperature on the impact energy of annealed plate, Figure 3.0233.

3.0234 Effect of sulfur content on room temperature impact energy, Figure 3.0234.

3.0235 Impact energy variation with intermediate annealing temperature after high temperature heat treatment at 2400 F, Figure 3.0235.

3.0236 Impact energy variation with annealing time at 1600 F after high temperature heat treatment at 2400 F, Figure 3.0236.

3.024 Bending.

3.025 Torsion and shear. (See also Section 3.035.)

3.0251 Typical ultimate shear strength of sheet, plate, and bar, Table 3.0251.

3.026 Bearings. (See also Section 3.036.)

3.0261 Typical bearing strengths of sheet and plate, Table 3.0261.

3.0262 Effect of 1000 hour elevated temperature exposure on bearing strength of sheet, Figure 3.0262.

3.027 Stress concentration.

3.0271 Notch properties (see also Sections 3.0371, 3.0372, and FeUH 1225).

3.02711 Effect of aging time on crack strength of 250 ksi annealed sheet, Figure 3.02711.

3.02712 Effect of aging temperature on crack strength of air melted and CVM plate, Figure 3.02712.

3.02713 Effect of cold rolling prior to aging on crack strength of sheet, Figure 3.02713.

3.02714 Effect of thickness on the sharp notch properties of air melted plate, Figure 3.02714.

3.02715 Effect of thickness on crack strength of air melted and CVM sheet, Table 3.02715.

3.02716 Effect of surface crack length on the crack strength of air melted plate aged at two temperatures, Figure 3.02716.

3.02717 Effect of surface crack length on crack strength of plate from two air melted heats, Figure 3.02717.

3.0272 Fracture toughness.

3.02721 Plane strain fracture toughness of CVM plate, Table 2.02721.

3.02722 Effect of aging temperature on plane strain fracture toughness of 1.8 inch thick CVM plate, Figure 3.02722.

3.02723	Plane strain fracture toughness of air melted and vacuum degassed plate, Table 3.02723.
3.02724	Plane strain fracture toughness for annealed and aged laboratory air melt plate, Table 3.02724.
3.02725	Effect of finishing temperature for hot rolling and cooling rate on plane strain crack toughness of laboratory air induction melted plate, Figure 3.02725.
3.028	Combined properties.
3.03	**Mechanical Properties at Various Temperatures**
3.031	Tension – stress-strain diagrams – tension properties.
3.0311	Stress-strain curves at room and elevated temperatures for air melted, annealed, and aged bar, Figure 3.0311.
3.0312	Stress-strain curves at room and elevated temperatures for CVM bar, Figure 3.0312.
3.0313	Typical stress-strain curves for tension at cryogenic, room, and elevated temperatures, Figure 3.0313.
3.0314	Effect of test temperature on the tensile properties of sheet, Figure 3.0314.
3.0315	Effect of test temperature on tensile properties of two heats of CVM sheet, Figure 3.0315.
3.0316	Influence of test temperature on tensile properties of cold rolled and aged sheet, Figure 3.0316.
3.0317	Effect of test temperature on the tensile properties of plate, Figure 3.0317.
3.0318	Effect of cryogenic temperatures on the tensile properties of plate at two titanium levels, Figure 3.0318.
3.0319	Effect of test temperature on tensile properties of annealed and aged bar, Figure 3.0319.
3.03110	Effect of test temperature on the tensile properties of bar, Figure 3.03110.
3.03111	Effect of test temperature on CVM bar after holding 30 minutes and 200 hours at test temperature, Figure 3.03111.
3.03112	Effect of 1000 hour elevated temperature exposure on the tensile properties of sheet at room temperature and test temperature, Table 3.03112.
3.032	Compression – stress-strain diagrams – compression properties.
3.0321	Typical stress-strain curves for compression at room and elevated temperatures, Figure 3.0321.
3.0322	Effect of test temperature on the compressive properties of sheet, Figure 3.0322.
3.0323	Effect of test temperature on the compressive properties of plate, Figure 3.0323.
3.0324	Effect of test temperature on the compressive properties of bar, Figure 3.0324.
3.0325	Effect of 1000 hour elevated temperature exposure on the compressive properties of sheet at room temperature, Table 3.0325.
3.033	Impact.
3.0331	Effect of test temperature on impact energy of plate from several heats, Figure 3.0331.
3.0332	Effect of low test temperature on impact energy of annealed and aged plate, Figure 3.0332.
3.0333	Effect of test temperature on impact energy of bar and forging from several heats, Figure 3.0333.
3.0334	Effect of test temperature on the impact energy of annealed and aged bar, Figure 3.0334.
3.0335	Effect of test temperature on the impact energy of bar, billet, and plate from several heats, Figure 3.0335.
3.0336	Impact energy of castings at room and low temperatures, Table 3.0336.
3.0337	Effect of solution annealing temperature and aging time on the impact properties of VIM + CVM plate at +30 F, Figure 3.0337.
3.0338	Effect of aging temperature and time on the impact properties of VIM + CVM plate at +30 F, Figure 3.0338.
3.0339	Effect of purity on impact energy. Toughness properties are more sensitive to purity levels than are strength properties, as shown in Figure 3.03391. The toughness of high purity alloy increases sharply with temperature; and at room temperature, it is about five times greater than that of normal purity alloy. Figure 3.03392 illustrates that for the same strength level after aging, the impact energy of the high purity alloy is three to six times greater than that of the normal purity material.
3.03391	Effects of purity and temperature on the impact energy of annealed and aged plate, Figure 3.03391.
3.03392	Effects of purity on the relation between impact energy and yield strength at room temperature, Figure 3.03392.
3.034	Bending.
3.035	Torsion and shear.
3.0351	Effect of test temperature on the shear ultimate strength of sheet, Figure 3.0351.
3.0352	Effect of test temperature on the shear ultimate strength of plate, Figure 3.0352.
3.0353	Effect of test temperature on the shear ultimate strength of bar, Figure 3.0353.
3.0354	Effect of 1000 hour elevated temperature exposure on the shear ultimate strength of sheet at room temperature, Table 3.0354.
3.036	Bearing.
3.0361	Effect of test temperature on the bearing strength of sheet, Figure 3.0361.
3.0362	Effect of test temperature on the bearing strength of plate, Figure 3.0362.
3.0363	Effect of test temperature on the bearing strength of sheet after holding 1000 hours at test temperature, Figure 3.0363.
3.037	Stress concentration.
3.0371	Notch properties.
3.03711	Room and low temperature smooth and sharp notch tensile properties of annealed and aged sheet, Table 3.03711.
3.03712	Effect of test temperature and strain rate on crack strength of annealed and aged sheet, Figure 3.03712.
3.03713	Effect of test temperature on crack strength of CVM sheet, Figure 3.03713.
3.03714	Effect of test temperature on crack strength of CVM sheet and plate, Figure 3.03714.
3.03715	Effect of test temperature on crack strength of CVM bar, Table 3.03715.
3.0372	Fracture toughness.
3.038	Combined properties.
3.04	**Creep and Creep-Rupture Properties**
3.041	Creep properties of 0.07 inch thick CVM sheet at 600 and 800 F, Table 3.041.
3.05	**Fatigue Properties**
3.051	Smooth and notched fatigue strength. It should be noted that the fatigue life (i.e., number of cycles to failure) for high strength metal alloys exhibits considerable scatter. The fatigue strengths are based on a limited number of tests. These values should

	Fe
18	Ni
7.5	Co
5	Mo
	Ti
	Al

18Ni(250) Maraging

Fe
18 Ni
7.5 Co
5 Mo
Ti
Al

18Ni(250) Maraging

be considered only as guides and not be used for design (71, 72). The fatigue life of 18Ni(250) maraging steel is improved by finish machining and/or shot peening subsequent to final aging. Compressive stresses are introduced at the surface which are beneficial to smooth and notched fatigue properties (85).

3.0511 Smooth fatigue strength of air melted and vacuum degassed plate, Table 3.0511.

3.0512 Smooth and notched fatigue strength of air melted plate, Table 3.0512.

3.0513 Smooth and notched fatigue strength of annealed and aged bar, Table 3.0513.

3.0514 Smooth and notched axial-load fatigue strength of 0.07 inch thick sheet at room and elevated temperatures, Table 3.0514.

3.0515 Smooth fatigue strength of mill-annealed and annealed-and-aged plate, Table 3.0515.

3.052 Fatigue crack propagation.

3.0521 Influence of stress intensity factor (ΔK) and test environment on fatigue crack propagation of sheet and plate at room temperature, Figure 3.0521.

3.0522 Fatigue crack propagation at room temperature in sheet aged at 1100 F, Figure 3.0522.

3.0523 Influence of test frequency on fatigue crack propagation in dry hydrogen (at room temperature and 1 atmosphere pressure), Figure 3.0523.

3.06 Elastic Properties

3.061 Poisson's ratio.

3.0611 Effect of cold rolling prior to aging on Poisson's ratio, Figure 3.0611.

3.062 Modulus of elasticity.

3.0621 Static and dynamic moduli for tension at cryogenic, room, and elevated temperatures, Figure 3.0621.

3.0622 Static moduli for compression at room and elevated temperatures, Figure 3.0622.

3.063 Modulus of rigidity, 10.7×10^3 ksi (95); 10.35×10^3 ksi (85).

3.064 Tangent modulus.

3.0641 Tangent modulus curves at room and elevated temperatures for air melt, annealed and aged bar, Figure 3.0641.

3.0642 Tangent modulus curves at room and elevated temperatures for CVM annealed and aged bar, Figure 3.0642.

3.065 Secant modulus.

3.0651 Secant modulus curves at room and elevated temperatures for air melt, annealed and aged bar, Figure 3.0651.

3.0652 Secant modulus curves at room and elevated temperatures for CVM annealed, and aged bar, Figure 3.0652.

4 FABRICATION

4.01 Forming

4.011 General. This alloy is hot worked readily by conventional rolling and forging operations, and is easily cold worked by conventional procedures in the annealed condition. A preliminary soak at 2300 F (homogenizing treatment) is recommended. Provision should be made for adequate work to break up the as-cast structure and to minimize directionality. For optimum properties, a maximum reheating temperature of 2000 F is suggested prior to the final hot working operation; however, this temperature will depend on the degree and method of hot working. Finishing should be in the range of 1500 to 1800 F, accompanied by about 25 percent reduction. Attention to cooling should be given to avoid isothermal embrittlement (see Section 1.094). Hot forming and bending should be performed at temperatures under 1800 F to prevent grain coarsening. Because of its low work hardening characteristics, this alloy may be cold reduced by substantial amounts before intermediate annealing is required (reannealing will essentially remove the effects of cold work). Cold work prior to aging will increase the aged strengths but will reduce fracture toughness. Severely cold worked parts should be reannealed (4–6, 73, 74).

4.012 Forging. Preliminary soak at 2300 F for homogenization. Starting temperature of 2000 F maximum is preferred. Preheat for sections greater than 6 inch square 1700 to 1800 F, approximately 15 minutes per inch of thickness. Finish temperature 1500 to 1700 F. Reheat at 1800 F. Do not delay cooling (see Section 1.094).

4.013 Rolling.

4.0131 Sheet bar, start 2000 F maximum.

4.0132 Plate. Start at 2000 F maximum and roll straight away to finish at 1600 F, or start at 1750 to 2000 F with reheats at the same temperature and finish rolling at 1500 to 1600 F. Cooling to room temperature should not be delayed (see Section 1.094 and Figures 3.02162 and 3.027215).

4.0133 Sheet. Start 1800 to 1900 F, and finish 1500 to 1600 F.

4.014 Powder metallurgy.

4.0141 This alloy has been produced by powder metallurgy techniques on an experimental basis. Tables 4.0142 and 4.0143 give some mechanical properties of compacts hot isostatically pressed (HIP) from rotating electrode process (REP) powder and from inert gas atomized (IGA) powder, respectively. Material compacted from the spherical REP powder exhibited good tensile strength and ductility in the double solution annealed condition but had poor ductility after aging at 900 or 950 F. A pre-age heat treatment at 975 to 1040 F substantially improved ductility, although it remained below that of similarly processed wrought alloy. The ductility loss in the HIP material was caused by titanium segregation to particle surfaces during powder production (96).

Material compacted from the IGA powder, which consisted of spherical particles plus fines, was more sensitive to HIP temperature than material compacted from REP powder. At HIP temperatures below about 2060 F, incomplete densification resulted in poor mechanical properties. At a HIP temperature of 2200 F, optimum properties were obtained, with slight additional benefit being derived from an aging cycle which included a 980 F pre-age. The strength, ductility, and toughness approached those of wrought material (97).

4.0142 Tensile properties of alloy consolidated from rotating electrode process powder, Table 4.0142.

4.0143 Tensile and impact properties of alloy consolidated from inert gas atomized powder, Table 4.0143.

	Fe
18	Ni
7.5	Co
5	Mo
	Ti
	Al

18Ni(250) Maraging

4.02 **Machining and Grinding**

4.021 General. This alloy is machined most easily in the solution annealed condition. After aging its machinability is comparable to AISI 4340 at equal hardness levels. Reduced surface speeds are helpful. Carbide cutters with ample water soluble coolants are recommended (4, 6, 77). However, because of its dimensional stability, machining prior to aging should be considered.

4.03 **Joining**

4.031 General. This alloy is weldable in both the solution annealed and fully heat treated conditions. Gas shielded processes (GMA and GTA) are suitable for this alloy. Using proper techniques, joint efficiencies from 90 to 100 percent are obtainable for aged (900 F, 3 hours) welds in sheet and heavy sections. Submerged arc welding is not recommended due to a pronounced tendency for hot cracking, low fracture toughness, and severe embrittlement in the heat affected zone (HAZ) (78, 79). The weld metal deposit is segregated in such a way that stable austenite may be present in some areas and that austenite reversion can occur in others (including the HAZ) on aging. The result is that the aging response of the weldment will be different from that of the base metal and that of the weld wire.

Heat input to the weld area should be minimized in order to minimize the amount of reverted austenite in the HAZ (83). The micro-segregation of the weld deposit and the amount and morphology of the retained/reverted austenite are of great importance in determining the strength and toughness of the weldment. The presence of austenite can prevent achieving 100 percent joint efficiency. Segregation of nonmetallics, such as titanium carbide, reduces weld toughness. Resistance to hot cracking without preheat is considerably superior to quenched and tempered steels when using the proper filler wire compositions.

The weld HAZ will contain regions with stable reverted austenite where the peak temperatures had reached the neighborhood of 1200 F. These soft regions may be removed by subsequent annealing and aging; however, in most cases, their influence on strength is relatively small and the toughness is higher than that of the parent metal.

General recommendations concerning welding techniques include: avoid prolonged time at elevated temperature; do not preheat; keep interpass temperature below 250 F; use minimum possible weld energy input; and avoid conditions causing low cooling rates (16, 17, 78, 83).

Electron beam welding techniques have been developed, particularly for the thinner gauges. The very close fit-ups required to assure satisfactory joints are a disadvantage. Other joining methods, including resistance welding, inertia welding, and brazing have all been explored but are not widely used (83).

4.032 Filler wire. A minimum of 0.35 percent titanium in the filler wire is necessary to prevent objectionable porosity in GMA welds. Titanium in excess of 0.70 percent with GMA and about 1.0 percent with GTA tends to produce a sensitivity to hot cracking and a weld deposit of decreased toughness. The residual element content of the filler should be as low as possible with the following recommended maximums: 0.03C, 0.05Si, and 0.05Mn (carbon should preferrably be kept well below this maximum). Sulfur and phosphorus also promote hot cracking and their contents should be minimized. Vacuum melting and vacuum annealing of wire are recommended. Argon is recommended for use with either GMA or GTA process.

4.033 Sheet metal welds. Welds in thin sections are subject to high dilution effects and are markedly influenced by the welding procedure. Recommended wire compositions are given in Table 4.0351. Improved strength with only a small loss in toughness can be obtained by a double pass procedure (see Table 4.035, FeUH 1225).

4.034 Plate weld. Attempts to increase weld strength by the use of high hardener filler wire have been unsuccessful in the gas shielded processes because of the formation of coarse pools of austenite in the weld metal which do not respond to subsequent aging treatment. Using proper procedures and filler wire in multi-pass GTA or GMA process (see Table 4.0351), weldments with joint efficiencies of better than 90 percent and with fracture toughness comparable to the base metal may be obtained (see Table 4.0372). Local aging after welding is often used, however the effectiveness of this treatment in achieving desired strengths and toughness should be carefully checked (78).

4.035 Tensile and impact properties of weldments.

4.0351 Typical tensile and impact properties and recommended wire compositions for welding sheet and plate, Table 4.0351.

4.0352 Typical tensile and impact properties of GTA and submerged arc (SA) plate weldments, Figure 4.0352.

4.036 Crack toughness properties.

4.0361 Effect of surface crack length on the crack strength of GTA welds in CVM plate, Figure 4.0361.

4.0362 Effect of surface crack depth on the crack strength of various weld deposits in air melt plate, Figure 4.0362.

4.0363 Effect of surface crack depth on the sharp notch strength of weld deposits in 250 ksi air melt plate aged after welding or annealed and aged after welding, Figure 4.0363.

4.0364 Plane strain fracture toughness of GTA and SA welds in air melt plate, Table 4.0364.

4.0365 Effects of welding on fracture toughness and threshold stress intensity factor for stress corrosion, Table 4.0365.

4.04 **Surface Treating**

4.041 General. Sand blasting removes oxide scales effectively. Pickling solution 18 percent sulfuric acid at 150 to 160 F is recommended. Sodium hydride and other high temperature (>700 F) descaling treatments should be avoided (6).

4.042 Nitriding. Nitriding at 850 F for 20 hours or 800 F for 44 hours is recommended and will give case hardness of about 66 HRC. Higher temperature gives lower case hardness. Longer times will increase case depth but very long times may require a drop in temperature to maintain case hardness (77).

4.043 This maraging steel can also be surface hardened by pack aluminizing, siliconizing, or boronizing. The fatigue strength of experimentally coated

Fe
18 Ni
7.5 Co
5 Mo
Ti
Al

18Ni(250) Maraging

material, shown in Figure 4.044, was degraded relative to that of uncoated material (see Tables 3.0511, 3.0512, and 3.0513). However, all three coated materials had good bend ductility (60° bend at room temperature without fracturing) and good thermal fatigue resistance. The coatings consisted of a 1-mil-thick intermetallic zone plus, for the boron coating only, a 2-mil-thick interdiffusion zone (99).

4.044 Effects of coatings on rotating beam fatigue behavior, Figure 4.044.

REFERENCES

1 ASTM A 538-65-Grade B, ASTM Standards, Part 4 (January 1967).

2 AMS 6520A (April 1, 1982).

3 VASCO, Latrobe, Pennsylvania, Spec. Nos. MB-250 CVM and MS-250 CVM (November 15, 1967).

4 International Nickel Company, "Summary Data" (March 30, 1965).

5 U. S. Steel Corporation, "USS Maraging Steel", ADUSS 94034 (1964).

6 VASCO, Latrobe, Pennsylvania, "Vascomax 18 Percent Nickel Ultrahigh Strength Maraging Steels" (1966).

7 Curtiss-Wright Corporation, "Research on Binary Iron-Nickel Alloys With 20–25 Percent Nickel", Contract AF33(616)-8018, Progress Report No. 3 (November 30, 1961).

8 Reisdorf, B. G. and Baker, A. J., "The Kinetics and Mechanisms of the Strengthening of Maraging Steels", AFML-TR-64-390 (January 1965).

9 DeVries, R. P., "Effect of Processing Factors and Size on the Properties of Commercially Produced 18Ni-Co-Mo Maraging Steel", Symposium on Maraging Steels at Wright-Patterson Air Force Base (May 14, 1962).

10 Barton, C. J., Reisdorf, B. G., Salmon Cox, P. H., Chilton, J. M., and Oskin, C. E., Jr., "Investigation of Thermal Embrittlement in 18Ni(250) Maraging Steel", AFML-TR-67-34 (March 1967).

11 Hamaker, J. C., Jr., "Effect of Primary Processing on Ultrahigh-Strength Steels", in DMIC Report 210 (October 26–28, 1964), p 32.

12 Republic Steel Corporation, "Manufacturing Process Development for High Strength Steels, Forging Survey 18Ni-Co-Mo Maraging and 9Ni-4Co Quench and Temper High Strength Steels", Interim Engineering Progress Report IR-8-157-L, ASD Contract AF 33(657)-11277 (September 1963).

13 Ibid, Plate and Sheet Survey.

14 Pellissier, G. E., "Some Microstructural Aspects of Maraging (250) Steel in Relation to Strength and Toughness", Proceedings of the Third Maraging Steel Project Review, RTD-TDR-63-4048 (November 1963), pp 408–437.

15 Wei, R. P., "Fracture Toughness Testing in Alloy Development", ASTM STP 381 (1965), p 279.

16 Yates, D. H., Vanadium Alloy Steel Company, Personal Communications with W. F. Brown, Jr. (1963).

17 Witherel, C. E., International Nickel Company, Personal Communications with W. F. Brown, Jr. (1963).

18 Decker, R. F., International Nickel Company, Personal Communications with W. F. Brown, Jr. (1963).

19 Peterson, W. A., Dean, S. W., Scott, T. E., and DiBari, G. A., "Review of Current Work on Maraging Steels", ASD-TDR-63-262 (May 1963), p 309.

20 Troiano, A. K., "Hydrogen in Maraging Steel, Type 18Ni-9Co-5Mo (300 Grade)", 3rd Maraging Steel Project Review, ASD Project 7381 (July 1963).

21 McDonnell Aircraft Corporation, "Static Fatigue Strength of Diffused Nickel Cadmium Plated VascoMax 250 and VascoMax 300", Report A733, Serial No. 19 (July 1963) (AD441111).

22 Bristol Aerojet Ltd. and Westland Aircraft Ltd., "The Chemical Contouring of 18 Percent Nickel Maraging Steel Sheet", D. Mat. Rept. No. 143 (April 1967).

23 Spitzig, W. A., Talda, P. M., and Wei, R. P., "Fatigue Crack Propagation and Fractographic Analysis of 18Ni(250) Maraging Steel Tested in Argon and Hydrogen Environments", *Journal of Engineering Fracture Mechanics*, Vol. 1 (1968), p 155.

24 Wei, R. P. and Landes, J. D., "Correlation Between Sustained Load and Fatigue Crack Growth in High Strength Steels", Materials Research and Standards, ASTM, Vol. 9, No. 7 (1969), p 25.

25 Hoenie, A. F., Lumm, J. A., Shelton, R. J., and Wallace, R. A., "Determination of Mechanical Property Design Values for 18NiCoMo 250 and 300 Grade Maraging Steels", AFML-TR-65-197 (July 1965).

26 International Nickel Company, "Preliminary Data Sheet" (1962).

27 Dean, S. W. and Copson, H. R., "Stress Corrosion Behavior of Maraging Nickel Steels in Natural Environments", *Corrosion*, Vol. 21 (March 1965), pp 95–103.

28 Rubin, A., "Stress Corrosion Cracking of Maraging Steels", Proceedings of the Fourth Maraging Steel Project Review (July 1964).

29 Kirk, W. W., Covert, R. A., and May, T. P., "Corrosion Behavior of High Strength Steels in Marine Environments", ASM Metals Engineering Quarterly, Vol. 8 (November 1968), pp 31–38.

30 Wacher, G. A., "Stress Corrosion Cracking Studies of 10-, 12-, and 18-Percent Ni Maraging Steel Alloys in Seawater", U.S. Navy, Marine Engineering Laboratory, MEL R&D Phase Report 73166 (March 1966).

31 Aerojet-General Corporation, "Stress Corrosion Cracking of High Strength Alloys", Report No. 0414-02-2 (Quarterly), Contract DA-04-495-ORD-3069 (January 1964).

32 Aerojet-General Corporation, "Stress Corrosion Cracking of High Strength Alloys", Report No. 0414-02-3 (Quarterly), Contract DA-04-495-ORD-3069 (April 1964).

33 Wei, R. P., Talda, P. M., and Li, Che-Yu, "Fatigue Crack Propagation in Some Ultrahigh Strength Steels", ASTM STP 415 (1967), pp 460–485.

34 Novak, S. R. and Rolfe, S. T., "Comparison of Fracture-Mechanics and Nominal Stress Analyses in Stress Corrosion Testing", *Corrosion* (1969) (to be published).

35 Republic Steel Corporation, "Special Property Steels", Adv. 1868-10M-468 (1968), p 31.

36 Republic Steel Corporation, "Manufacturing Process Development for High Strength Steels", Interim Engineering Progress Report IR-8-157 (VIII) (May 1, 1965–August 1, 1965).

37 Spaeder, G. J. and Murphy, W. J., "An Investigation of the Effect of Heat Treating Variables on the Strength and Fracture Toughness of 18Ni-Co-Mo Maraging Steel", U. S. Steel Corporation, Applied Research Laboratory Report 40.002-070(8) (December 24, 1963).

38 Puzak, P. P., et al., "Metallurgical Characteristics of High Strength Structural Materials", Eleventh Quarterly Report, NRL Report 6513 (August 1966).

39 Curtiss-Wright Corporation, "Research on Binary Iron-Nickel Alloys with 20–25 Percent Nickel", Contract AF33(616)-8018, Progress Report No. 4 (February 28, 1962).

40 U. S. Steel Corporation, Applied Research Laboratory, "Unpublished Data", Communication to R. P. Wei (1969).

41 Audener, R. E. and Tenner, W. S., "Evaluation of High Nickel Steel for Application in Large Booster Motor Application", ASD Contract AF33(657)-8740, Aerojet-General Corporation, Sacramento, California, Report 0705-82Q-2 (December 1962).

42 Zaperstein, Z. P. and Mixon, W. V., "Evaluation of Maraging Steel for Application to Space Launch Vehicles", NASA Contract NAS 7-214, Douglas Report SM43105 (July 8, 1963).

43 Crimmins, P. P. and Tenner, W. S., "Informal Monthly Report for the Investigation of Maraging Steel Covering the Period (May 1 Through May 30, 1963), ASD Contract AF33(657)-8740, Aerojet-General Corporation, Sacramento, California (May 1963).

44 Spitzig, W. A., "The Effect of Duplex Aging Treatment on the Mechanical Properties of 18Ni-Co-Mo-Ti Maraging Steels", U. S. Steel Corporation, preprint of paper to be published in *Trans. ASM* (1969).

45 Srawley, J. E., "Plane Strain Fracture Toughness Tests on Two Inch Thick Maraging Steel Plate at Various Strength Levels", FRACTURE 1969, Proceedings of the Second International Conference on Fracture, Brighton (April 1969), Chapman and Hall, Ltd. (1969).

46 Glasgal, B. M., Looby, G. T., and Traymor, M. T., Republic Steel Corporation, "Unpublished Data" (1962).

47 Curtiss-Wright Corporation, "Research on Binary Iron-Nickel Alloys with 20–25 Percent Nickel", Contract AF33(616)-8018, Progress Report No. 5 (May 30, 1962).

48 Spaeder, G. J., Brown, R. M., and Murphy, W. J., "The Effect of Hot Rolling Variables on the Fracture Toughness of 18Ni Maraging Steel", *Trans. ASM*, Vol. 60 (1967), p 418.

49 Aggen, G. N., Allegheny-Ludlum Steel Corporation, Personal Communication with W. F. Brown, Jr. (1962).

50 Aerojet-General Corporation, "Evaluation of High Nickel Maraging Alloy Steels", Contract AF33(657)-8890, Task No. 738103, Phase I (October 1 through December 31, 1962) (January 15, 1963) (AD 295680).

51 Grotke, G. E., "Some Aspects of Weldability of 18 Percent Ni-Co-Mo Maraging Steel", Maraging Steel Project Review, ASD-TDR 63-262 (November 1962), p 47.

52 Hughes, W., Thiokol Chemical Company, Personal Communication with W. F. Brown, Jr. (1962).

53 Bhat, G. K., "Metallurgical Research in Support of the Construction and Testing of a 10-Foot-Diameter Prototype Pressure Vessel Using Maraging 18 Percent Nickel Steel Plates", AFO Contract 4 (611)-8525, Mellon Institute, Pittsburgh, Pennsylvania (April 22, 1963).

54 Decker, R. F., Eash, J. T., and Goldman, A. J., "Maraging Nickel Molybdenum Steels", *ASM Trans. Quarterly* (1962).

55 Zaperstein, Z. P. and Mixon, W. V., "Evaluation of Maraging Steel for Application to Space Launch Vehicles", NASA Contract NAS 7-214, Douglas Report SM 13105 (October 4, 1963).

56 Zaperstein, Z. P. and Whiteson, B. V., "The Properties of Welded 18Ni-7Co-5Mo Plate", Engineering Paper No. 1696, Douglas Missile and Space Systems Division (July 1963).

57 Shimmin, J. P., et al., Republic Steel Corporation, "Manufacturing Process Development for High Strength Steels", Interim Engineering Progress Report IR-8-157(V) (July 1, 1964–October 1, 1964).

58 Brown, W. F., Jr. and Srawley, J. E., "Plane Strain Crack Toughness Testing of High Strength Metallic Materials", ASTM STP 410 (1967).

59 Crimmins, P. P. and Tenner, W. S., "Informal Monthly Report for the Investigation of Maraging Steels", (July 1, 1963–July 30, 1963), ASD Contract AF33(657)-8740, Aerojet-General Corporation, Sacramento, California (July 1963).

60 Sampson, H. B., "Preliminary Investigation of 250 and 300 Maraging Steel Sheets (18Ni-Co-Mo)", Maraging Steel Project Review, ASD TDR 63-262 (November 1962), p 271.

61 Hanna, G. L. and Steigerwald, E. A., "Fracture Characteristics of Structural Metals", Bureau of Naval Weapons Contract No. N600 (19)-58831, Final Report ER 5426, TAPCO, Cleveland, Ohio (June 1963).

62 Kula, E. B. and Hickey, C. F., Jr., "Evaluation of Maraging Steel at U. S. Army Materials Research Agency", 3rd Maraging Steel Project Review, ASD Project 7381 (July 1963).

63 Vanadium Alloy Steel Company, Personal Communication between J. G. Hamaker and S. S. Manson (NASA Lewis) (1963).

64 Boeing Company, "Evaluation of Cold Rolled Sheet and Hot Rolled and Forged Bar of the 18, 20, and 25 Percent Ni Maraging Steels", Boeing Document No. D2-35109 (1963) (AD443891).

65 DMIC, "The Mechanical Properties of Maraging Steels", DMIC Memorandum Draft (July 22, 1963).

66 Clark, C. C., International Nickel Company, Personal Communication to W. F. Brown, Jr. (1962).

67 Steigerwald, E. A., TAPCO Group, Thompson-Ramo-Wooldridge, Inc., Personal Communication to W. F. Brown, Jr. (September 24, 1962).

68 Tuffnell, G. W., Pasquine, D. L., and Olson, J. H., "An Investigation of the Fatigue Behavior of 18 Percent Nickel Maraging Steel", *Trans. ASM*, Vol. 59 (1966), p 769.

69 Cicci, F., "An Investigation of the Statistical Distribution of Constant Amplitude Fatigue Endurance for a Maraging Steel", UTIAS Note No. 73 (July 1964) (AD448046).

	Fe
18	Ni
7.5	Co
5	Mo
	Ti
	Al

18Ni(250) Maraging

	Fe
18	Ni
7.5	Co
5	Mo
	Ti
	Al

18Ni(250) Maraging

70 Swanson, S. R., "A Survey of the Fatigue Aspects of the Application of Ultrahigh Strength Steels", in DMIC Report 210 (October 26–28, 1964), p 136.

71 Spaeder, G. J. and Murphy, W. J., "Properties of Cold Reduced 300 Grade 18Ni Maraging Steel", *Journal of Materials*, Vol. 3, No. 1 (1968), p 116.

72 Campbell, J. E., "Review of Alloys and Fabricating Methods for Tactical Missile Motor Cases", DMIC Memorandum 224 (August 15, 1967).

73 Carman, C. M. and Katlin, J. M., "Low Cycle Fatigue Crack Propagation of High Strength Steels", 66-MET-3-ASME (April 1966).

74 Miller, G. A., "The Dependence of Fatigue Crack Growth Rate on Stress Intensity Factor and the Mechanical Properties of Some High Strength Steels", *Trans. ASM*, Vol. 61 (1968).

75 Seabrook, J. B., "Working with Maraging Steels – Nitriding", Metal Progress (July 1963).

76 Reisdorf, B. G., Birkle, A. J., and Salmon Cox, P. H., "An Investigation of the Mechanical Properties and Microstructures of 18Ni(250) Maraging Steel Weldments", AFML-TR-65-364 (November 1965).

77 Srawley, J. E. and Esgar, J. B., "Investigation of Hydrotest Failure of Thiokol Chemical Corporation 260-Inch-Diameter SL-1 Motor Case", NASA TM-1194 (January 1966).

78 Sippel, G. R. and Vonnegut, G. L., "Evaluation of 18 Percent Ni-Co-Mo Maraging Steel for Heavy and Thin Wall Rocket Motor Case Applications", Allison Division General Motors Corporation, Engineering Department Report No. 3448 (July 12, 1963).

79 Proposed Method of Test for Plane Strain Fracture Toughness of Metallic Materials, ASTM Book of Standards, Pt. 31 (1969), p 1099.

80 AMS 6512B (July 1, 1985).

81 AMS 6501 (October 1, 1984).

82 Ghosh, P. C. and Roy, L. C., "Maraging Steel", *Iron and Steel Engineer*, Vol. 52, No. 4 (April 1975), pp 100–101.

83 Lang, F. H. and Kenyon, N., "Welding in Maraging Steels", Welding Research Council, New York, WRC Bulletin No. 159 (February 1971).

84 Rack, H. J., "Age Hardening-Grain Size Relationships in 18Ni Maraging Steels", *Materials Science and Engineering*, Vol. 34, No. 3 (August 1978), pp 263–270.

85 Anon., "Nickel Maraging Steels in the Aerospace Industry", International Nickel Company, Inc., New York, Trade Literature (1974).

86 Rack, H. J., "The Relationship Between Thermal Embrittlement and Hydrogen Cracking in 18Ni(250) Maraging Steel", Sandia Labs, Albuquerque, New Mexico, SAND-75-5159 (1975).

87 Gangloff, R. P. and Wei, R. P., "Gaseous Hydrogen Assisted Crack Growth in 18 Nickel Maraging Steels", *Scripta Metallurgica*, Vol. 8, No. 6 (June 1974), pp 661–667.

88 Gangloff, R. P. and Wei, R. P., "Gaseous Hydrogen Embrittlement of High Strength Steels", *Metallurgical Transactions*, Vol. 8A, No. 7 (July 1977), pp 1043–1053.

89 Jonas, O., "Influence of Preloading on the Sustained Load Cracking Behavior of Maraging Steels in Hydrogen", *Corrosion*, Vol. 29, No. 8 (August 1973), pp 299–304.

90 Hardie, D. and Murray, T. I., "The Effect of Hydrogen Upon the Tensile Ductility of a High Strength Maraging Steel", Proceedings of International Conference on Mechanisms of Environment Sensitive Cracking of Materials, University of Surrey, Guildford, England (April 4–7, 1977), pp 459–470.

91 Jones, W. B. and Swearengen, J. C., "Mechanical Stability of Ultrahigh Strength Steels", *Materials Science and Engineering*, Vol. 41, No. 2 (December 1979), pp 225–235.

92 Adair, A. M. and Roberson, J. A., "The Influence of Thermomechanical Processing on the Structure and Properties of Maraging Steel", Air Force Materials Lab, Wright-Patterson AFB, Ohio, AFML-TR-69-222 (January 1970).

93 Johnson, W. C. and Stein, D. F., "A Study of Grain Boundary Segregants in Thermally Embrittled Maraging Steel", *Metal Science and Heat Treatment*, Vol. 15, No. 9-10 (September–October 1973), pp 842–846.

94 Spaeder, G. J., "Impact Transition Behavior of High-Purity 18Ni Maraging Steel", *Metallurgical Transactions*, Vol. 1, No. 7 (July 1970), pp 2011–2014.

95 Prado, M. E. and Cordill, C. A., "Static, Dynamic Toughness, and High Strain Rate Properties of Maraging 250, HY-180, and HP 9-4-20 Steels", University of California Lawrence Livermore Laboratory, Livermore, California, UCRL-52017 (February 11, 1976).

96 German, R. M. and Smugeresky, J. E., "Ductility in Hot Isostatically Pressed 250-Grade Maraging Steel", *Metallurgical Transactions*, Vol. 9A, No. 3 (March 1978), pp 405–412.

97 German, R. M. and Smugeresky, J. E., "Effect of Hot Isostatic Pressing Temperature on the Properties of Inert Gas Atomized Maraging Steel", *Materials Science and Engineering*, Vol. 36, No. 2 (December 1978), pp 223–230.

98 Freedman, A. H., "An Accelerated Stress Corrosion Test for High Strength Ferrous Alloys", *ASTM Journal of Materials*, Vol. 5, No. 2 (June 1970), pp 431–466.

99 Chase, J. J. and Crump, D. N., "A Study and Evaluation of the Effects of Various New Surface Diffusion Treatments", TRW, Inc., Cleveland, Ohio, AMSWE-RE 71-50 (August 1971).

Alloy	18Ni(250) Maraging
AMS Specification	Product Form
6512B	Bars, Forgings, Tubing, Rings, Vacuum Consumable Electrode Melted
6520A	Sheet, Strip, Plate, Consumable Electrode Melted
6501	Welding Wire, Vacuum Melted

TABLE 1.031. AMS SPECIFICATIONS (2, 80, 81)

Alloy	18Ni(250) Maraging					
AMS Specification	6512B[a]		6520A[a]		6501	
	Percent		Percent		Percent	
Element	Min	Max	Min	Max	Min	Max
Nickel	17.00	19.00	17.00	19.00	17.00	19.00
Cobalt	7.00	8.50	7.00	8.50	7.50	8.50
Molybdenum	4.60	5.20	4.60	5.20	4.60	5.20
Titanium	0.30	0.50	0.30	0.50	0.30	0.50
Aluminum	0.05	0.15	0.05	0.15	0.05	0.15
Chromium	–	0.50	–	–	–	–
Copper	–	0.50	–	–	–	–
Manganese	–	0.10	–	0.10	–	0.10
Silicon	–	0.10	–	0.10	–	0.10
Carbon	–	0.03	–	0.03	–	0.03
Phosphorus	–	0.010	–	0.010	–	0.010
Sulfur	–	0.010	–	0.010	–	0.010
Zirconium	–	–	–	–	–	0.010
Boron	–	–	–	–	–	0.003
Oxygen	–	–	–	–	–	0.0025
Nitrogen	–	–	–	–	–	0.0050
Hydrogen	–	–	–	–	–	0.0010

(a) Prior to pouring, up to 0.05 percent calcium, 0.02 percent zirconium, and 0.003 percent boron shall be added to the air-melted heat; analyses for these elements need not be made.

TABLE 1.041. COMPOSITION (2, 80, 81)

Fe
18 Ni
7.5 Co
5 Mo
Ti
Al

18Ni(250) Maraging

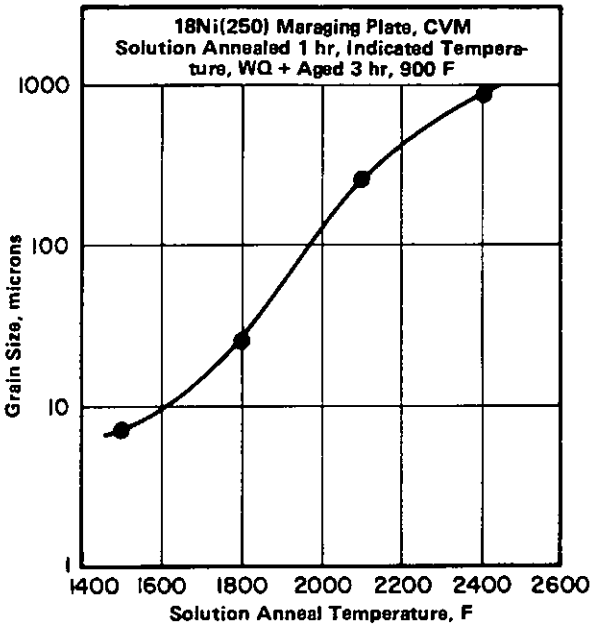


FIGURE 1.055. EFFECT OF SOLUTION ANNEAL TEMPERATURE ON PRIOR AUSTENITE GRAIN SIZE (84)

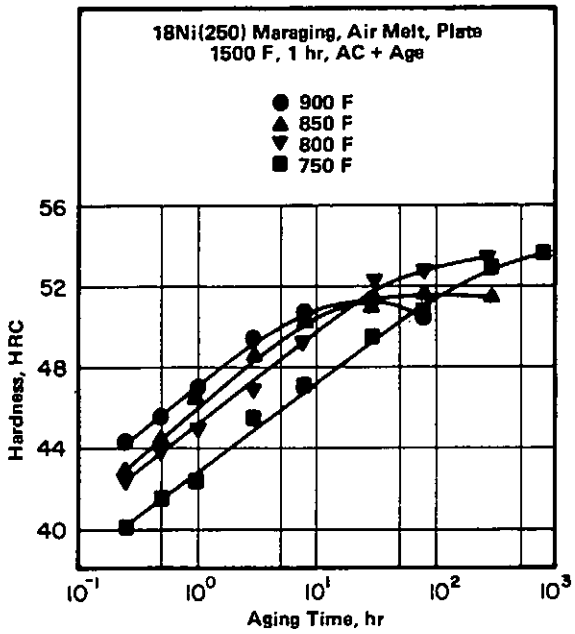


FIGURE 1.063. EFFECT OF AGING TEMPERATURE AND TIME ON HARDNESS (8)

Alloy	18Ni(250) Maraging	
Form	2-1/2 to 2-3/4 inch Thick Slabs, Short Transverse	
Melting Practice	Air Melt	CVM
F_{tu}, ksi	275	280
F_{ty}, ksi	260	268
e (2 in.), percent	3	10
RA, percent	25	35

TABLE 1.081. ROOM TEMPERATURE TENSILE PROPERTIES OF AIR AND VACUUM MELTED SLAB (9)

Alloy	18Ni(250) Maraging			
Form	Lab Vacuum Melted Plate, L			
Condition	1500 F, 1 hr, AC		1500 F, 1 hr, AC +900 F, 3 hr, AC	
Carbon Content, percent	0.027	0.004	0.027	0.004
F_{tu}, ksi	144	137	245	240
F_{ty}, ksi	107	109	239	230
e (1 in.), percent	17	18	11	13
RA, percent	74	82	53	65
IE Charpy V, ft-lb	78	173	20	39

TABLE 1.082. INFLUENCE OF CARBON CONTENT ON THE ROOM TEMPERATURE PROPERTIES OF LABORATORY VACUUM MELTED PLATE (10)

	Fe
18	Ni
7.5	Co
5	Mo
	Ti
	Al

18Ni(250) Maraging

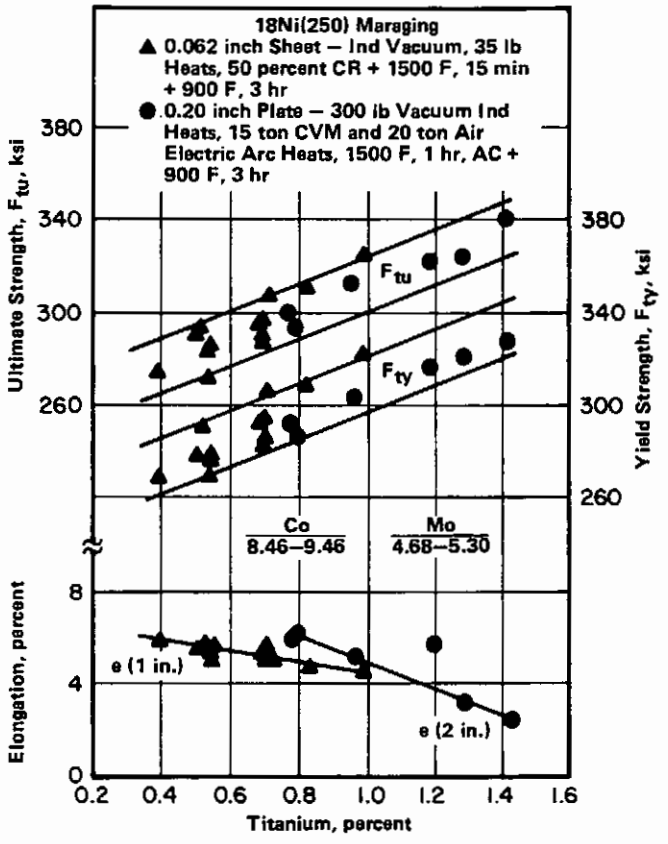


FIGURE 1.0921. EFFECT OF TITANIUM CONTENT ON TENSILE PROPERTIES OF ANNEALED AND AGED SHEETS FROM LABORATORY AND PRODUCTION HEATS (40, 49, 50)

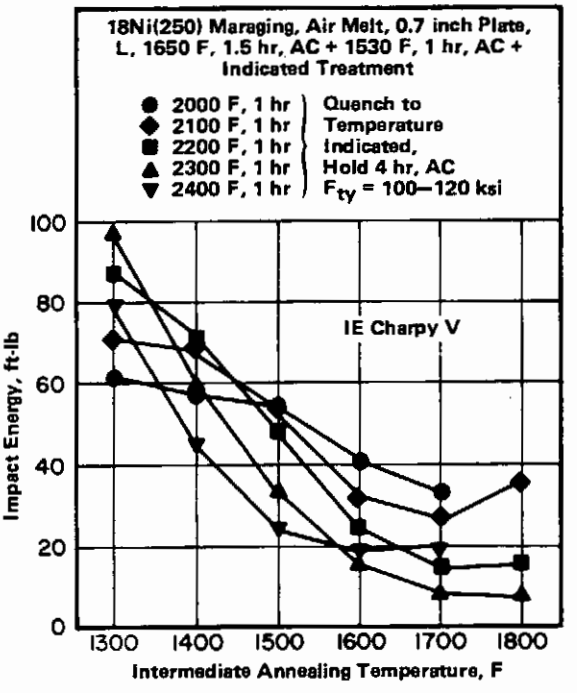


FIGURE 1.0941. EFFECT OF COMBINED ANNEALING TREATMENTS ON IMPACT STRENGTH OF ANNEALED PLATE (10)

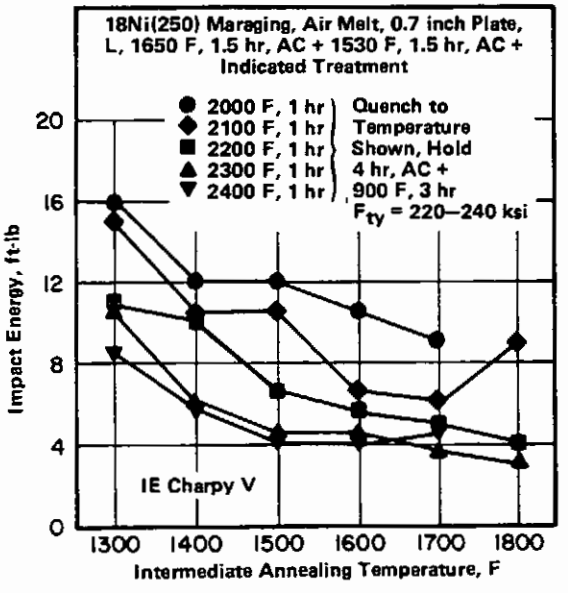


FIGURE 1.0942. EFFECT OF COMBINED ANNEALING TREATMENTS ON IMPACT STRENGTH OF ANNEALED AND AGED PLATE (10)

Alloy	18Ni(250) Maraging					
Form	Air Melt, 0.7 inch Plate, L					
Condition	1650 F, 1.5 hr, AC + 1530 F, 1.5 hr, AC + Indicated Treatment					
Additional Heat Treatment	F_{tu}, ksi	F_{ty}, ksi	e (1.4 in.), percent	RA, percent	IE Charpy V, ft-lb(a)	K_{Ic}, ksi $\sqrt{in.}$
None (Mill Annealed)	148	133	17	70	61	–
2300 F, 1 hr, AC	150	115	16	63	75	–
2300 F, 1 hr, AC + 900 F, 3 hr, AC	246	223	7	24	13	75
2300 F, 1 hr, Quench to 1700 F, Hold 4 hr, AC	144	115	9	28	8	46
2300 F, 1 hr, Quench to 1700 F, Hold 4 hr, AC + 900 F, 3 hr, AC	236	232	1.4	1	3.5	32
2400 F, 1 hr, AC	149	108	11	69	81	–
2400 F, 1 hr, AC + 900 F, 3 hr, AC	252	234	2	3	11	60
2400 F, 1 hr, Quench to 1700 F, Hold 4 hr, AC	142	110	–	–	6	43
2400 F, 1 hr, Quench to 1700 F, Hold 4 hr, AC + 900 F, 3 hr, AC	256	237	1.4	2	5.5	36

(a) At +80 F.

TABLE 1.0943. EFFECT OF COMBINED ANNEALING TREATMENTS ON STRENGTH AND CRACK TOUGHNESS OF PLATE (10)

Fe
18 Ni
7.5 Co
5 Mo
Ti
Al

18Ni(250) Maraging

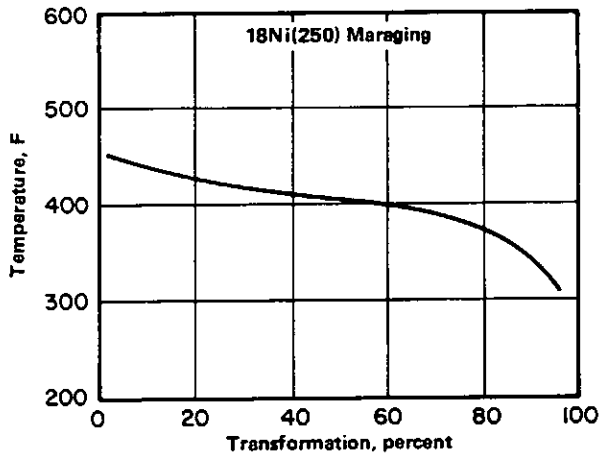


FIGURE 2.0122. AUSTENITE TO MARTENSITE TRANSFORMATION CURVE (8)

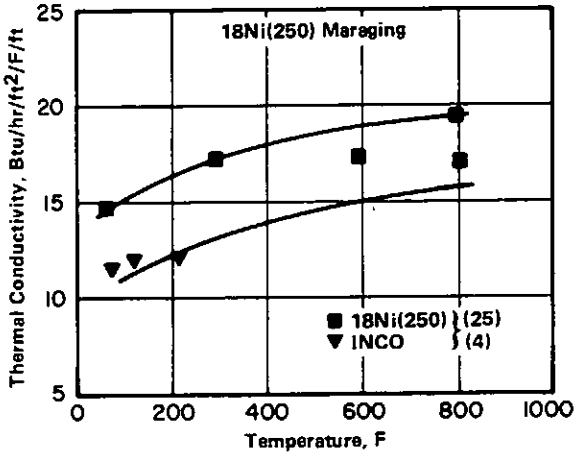


FIGURE 2.013. THERMAL CONDUCTIVITY (4, 25)

	Fe
18	Ni
7.5	Co
5	Mo
	Ti
	Al

18Ni(250) Maraging

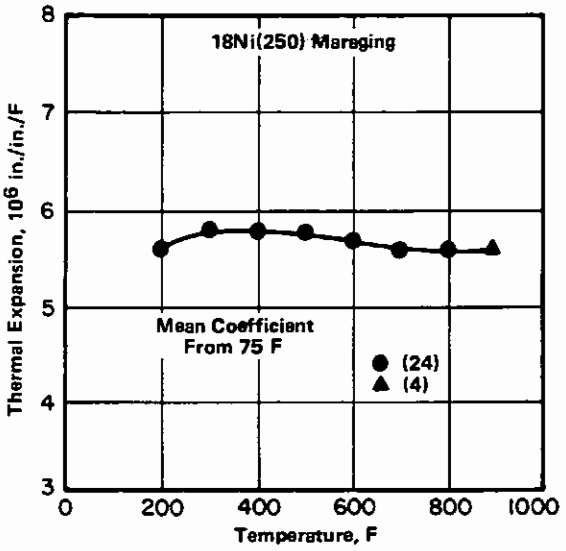


FIGURE 2.014. THERMAL EXPANSION (4, 25)

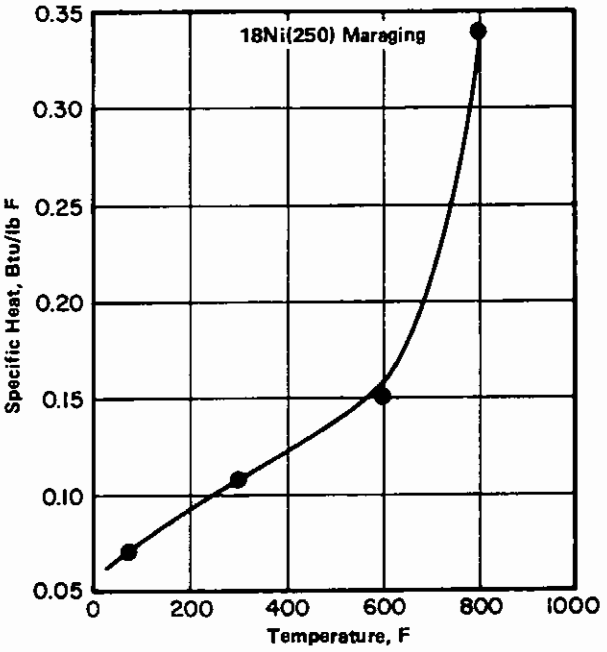


FIGURE 2.015. SPECIFIC HEAT AT CONSTANT PRESSURE AS A FUNCTION OF TEMPERATURE (1 ATM) (25)

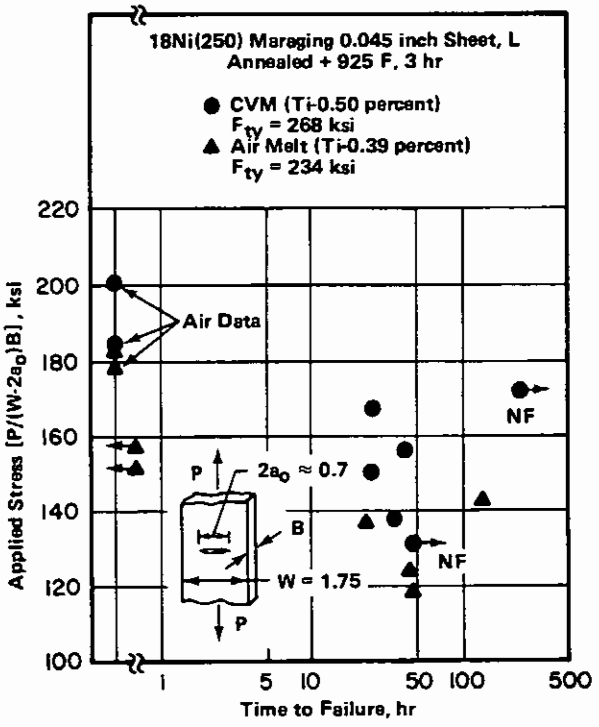


FIGURE 2.0322. DELAYED FAILURE CHARACTERISTICS OF AIR-MELTED AND CVM SHEETS IN 3 PERCENT NaCl SOLUTION AT ROOM TEMPERATURE (36)

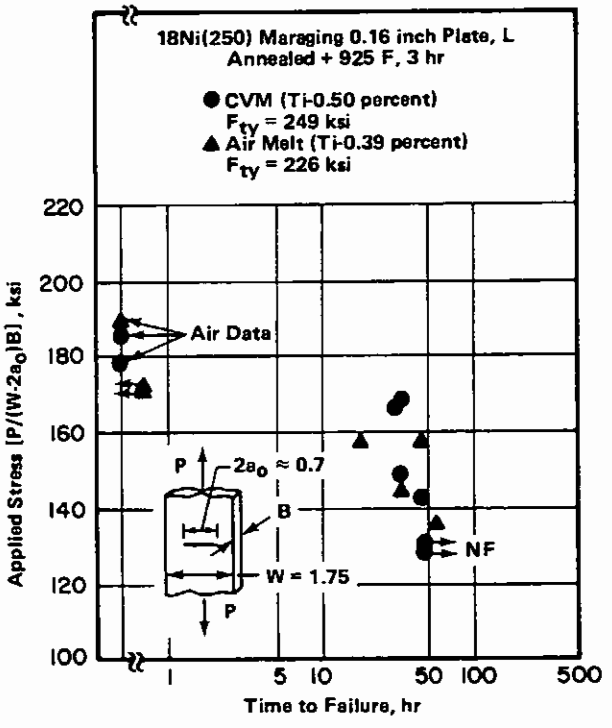


FIGURE 2.0323. DELAYED FAILURE CHARACTERISTICS OF AIR-MELTED AND CVM PLATES IN 3 PERCENT NaCl SOLUTION AT ROOM TEMPERATURE (36)

Fe
18 Ni
7.5 Co
5 Mo
Ti
Al

18Ni(250) Maraging

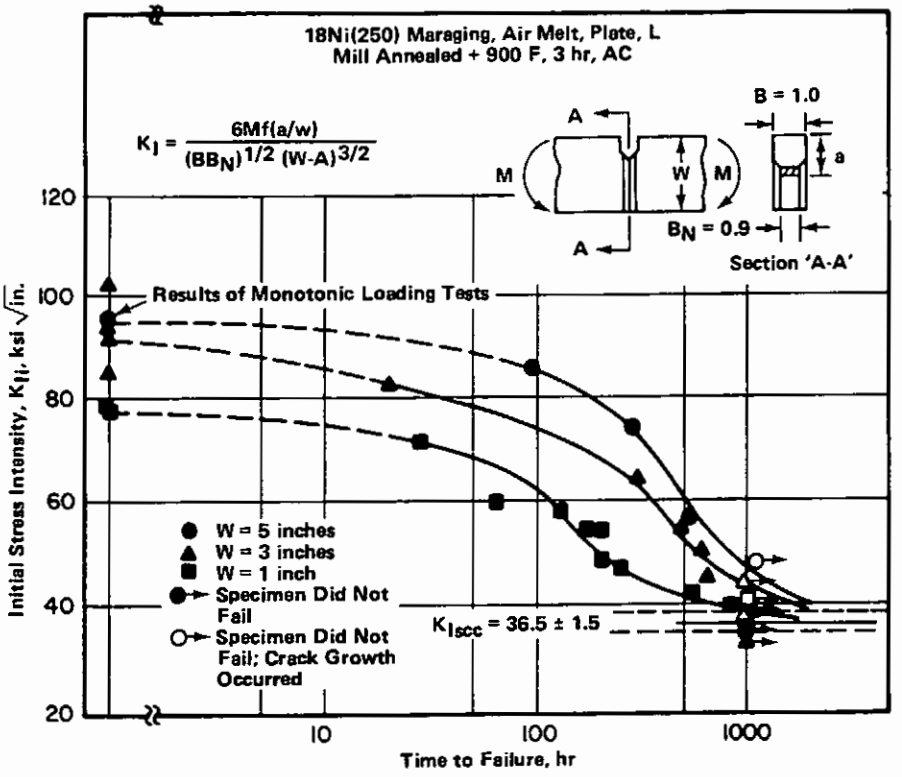


FIGURE 2.0324. DELAYED FAILURE CHARACTERISTICS OF AIR-MELTED PLATE IN SYNTHETIC SEAWATER AT ROOM TEMPERATURE (34)

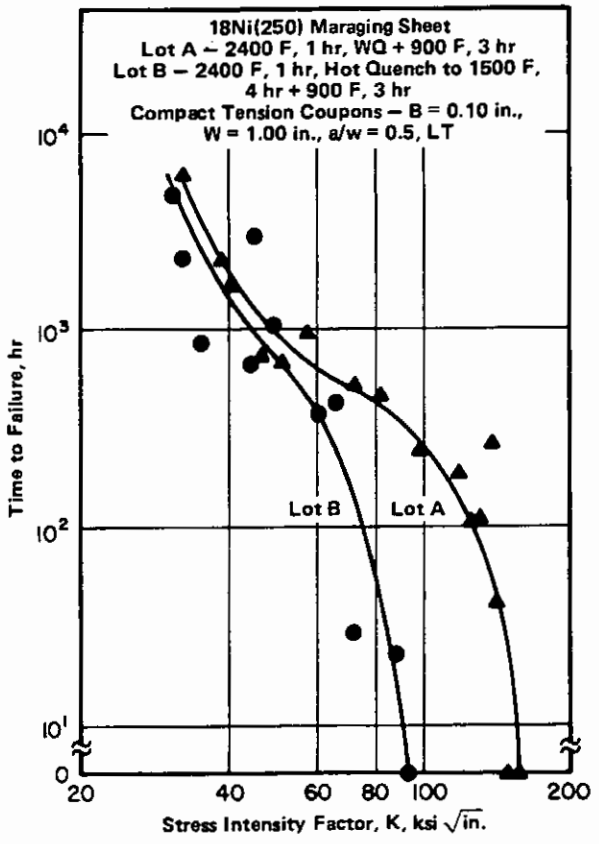


FIGURE 2.0326. EFFECTS OF HEAT TREATMENT ON SUSTAINED LOAD FAILURE TIME IN 100 PERCENT RELATIVE HUMIDITY AT ROOM TEMPERATURE (86)

	Fe
18	Ni
7.5	Co
5	Mo
	Ti
	Al

18Ni(250) Maraging

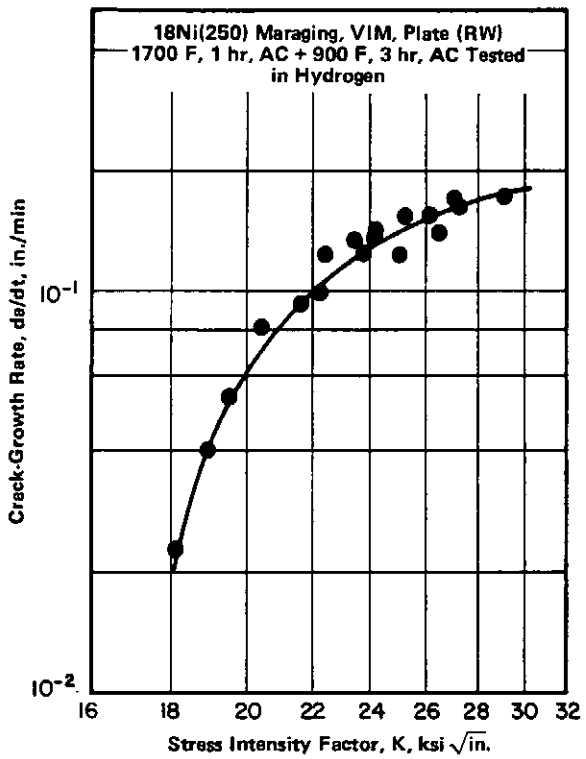


FIGURE 2.0332. INFLUENCE OF STRESS INTENSITY FACTOR K ON THE RATE OF CRACK GROWTH UNDER SUSTAINED LOAD IN DRY HYDROGEN AT 1 ATMOSPHERE AND ROOM TEMPERATURE (24)

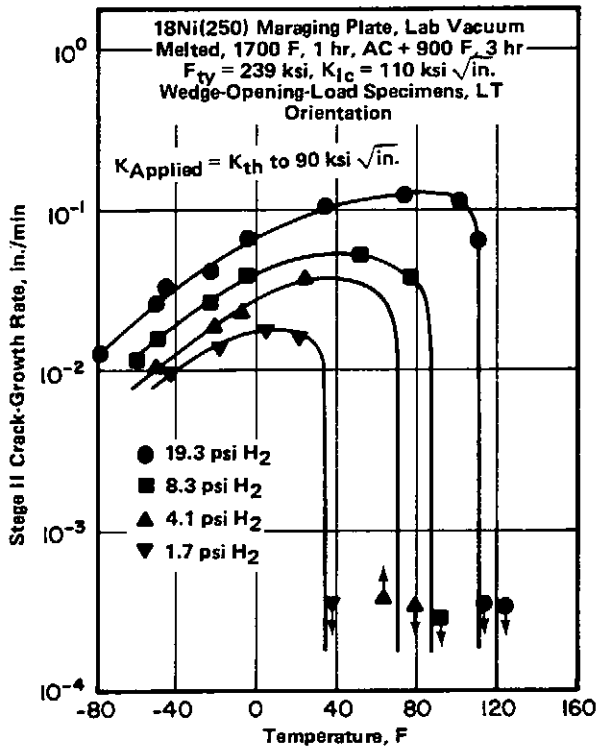


FIGURE 2.0333. EFFECT OF TEMPERATURE ON STAGE II (RATE LIMITED) SUSTAINED LOAD CRACK-GROWTH RATE IN HIGH PURITY HYDROGEN AT SEVERAL PRESSURES (87, 88)

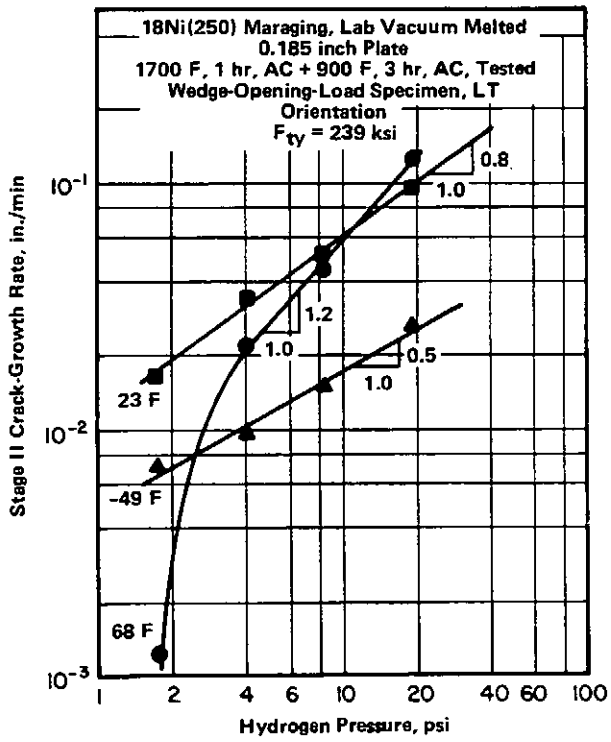


FIGURE 2.0334. EFFECTS OF HYDROGEN PRESSURE ON STAGE II SUSTAINED LOAD CRACK-GROWTH RATES AT -49 TO 68 F (88)

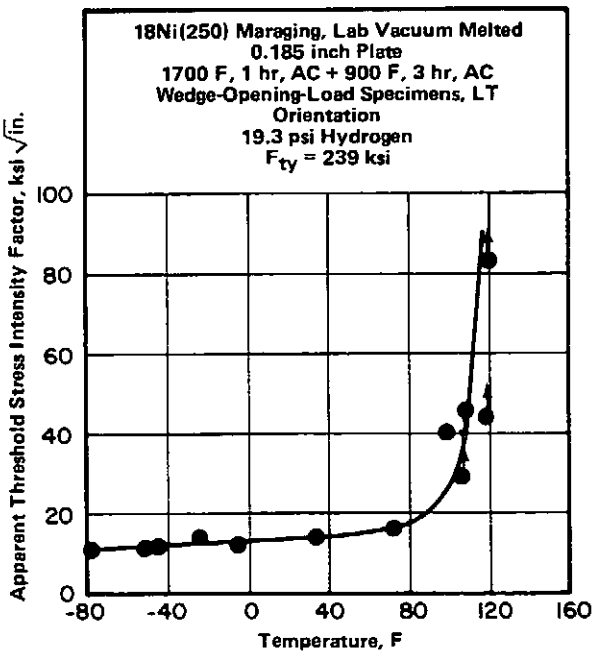


FIGURE 2.0335. EFFECTS OF TEMPERATURE ON APPARENT THRESHOLD STRESS INTENSITY FACTOR FOR SUSTAINED LOAD CRACK GROWTH IN HIGH PURITY HYDROGEN (88)

	Fe
18	Ni
7.5	Co
5	Mo
	Ti
	Al

18Ni(250) Maraging

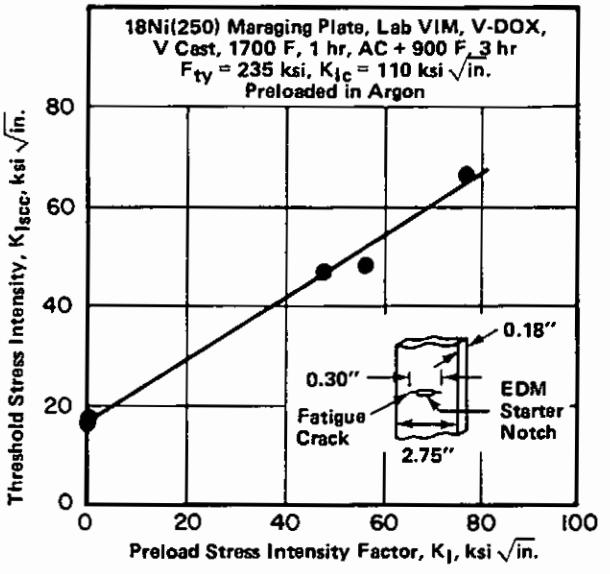


FIGURE 2.0337. EFFECTS OF STATIC PRELOADING ON THRESHOLD STRESS INTENSITY FACTOR FOR SUSTAINED LOAD CRACKING IN DRY HYDROGEN (89)

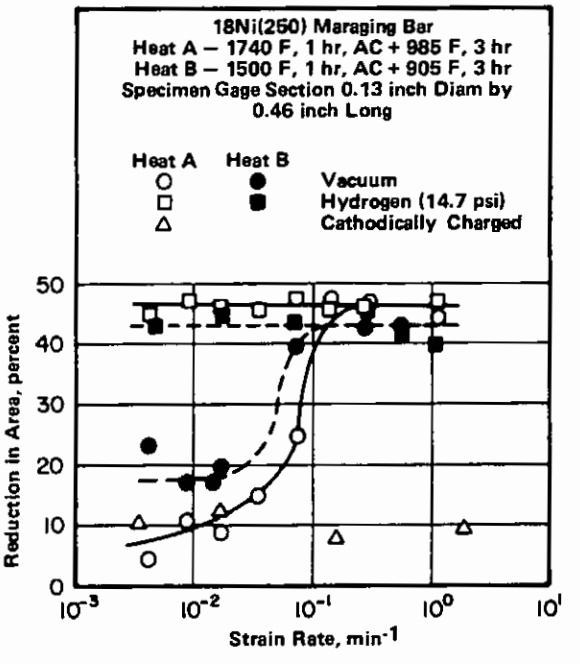


FIGURE 2.0339. EFFECTS OF STRAIN RATE ON TENSILE REDUCTION IN AREA AT ROOM TEMPERATURE FOR SPECIMENS TESTED IN VACUUM, IN HYDROGEN, AND IN VACUUM IMMEDIATELY AFTER CATHODICALLY CHARGING (90)

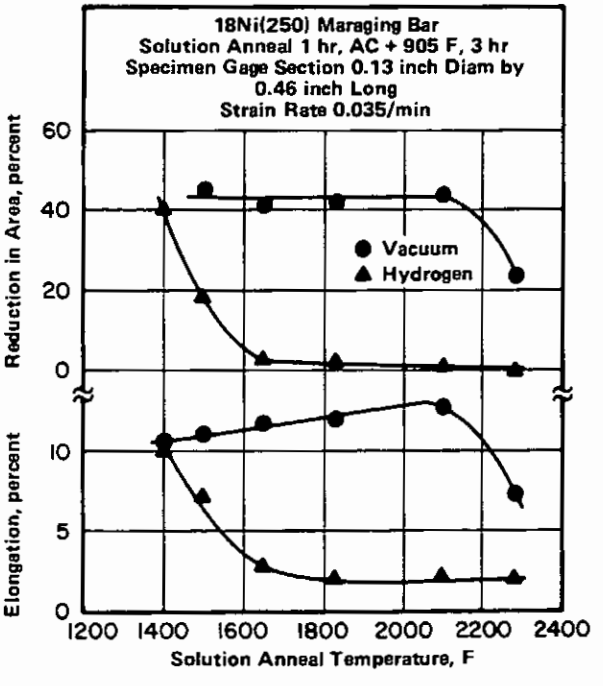


FIGURE 2.03310. EFFECTS OF SOLUTION ANNEAL TEMPERATURE ON TENSILE DUCTILITY OF AGED BAR TESTED IN VACUUM AND IN HYDROGEN (1 ATMOSPHERE) (90)

Fe
18 Ni
7.5 Co
5 Mo
Ti
Al

18Ni(250) Maraging

Alloy	18Ni(250) Maraging							
Condition	Anneal 1500 F ± 25, AC + Age 900 F ± 10, 3 to 5 hr, AC							
Form	CVM, Sheet, Strip, and Plate							
Thickness, in.	Under 0.030	0.030 Thru 0.045	0.046 Thru 0.065	0.066 Thru 0.090	0.091 Thru 0.125	0.126 Thru 0.250	0.251 to 0.375	0.375 or Over
F_{tu}, Min, ksi	255	255	255	255	255	255	255	255
F_{ty}, Min, ksi	245	245	245	245	245	245	245	245
e, Min, percent								
(0.5 in.)	1.0	2.0	–	–	–	–	–	–
(1.0 in.)	–	–	2.0	5.0	6.0	8.0	–	–
(2.0 in. or 4D)	–	–	–	2.5	3.0	4.0	5.0	6.0

Note: The original AMS document should be consulted for complete specification details.

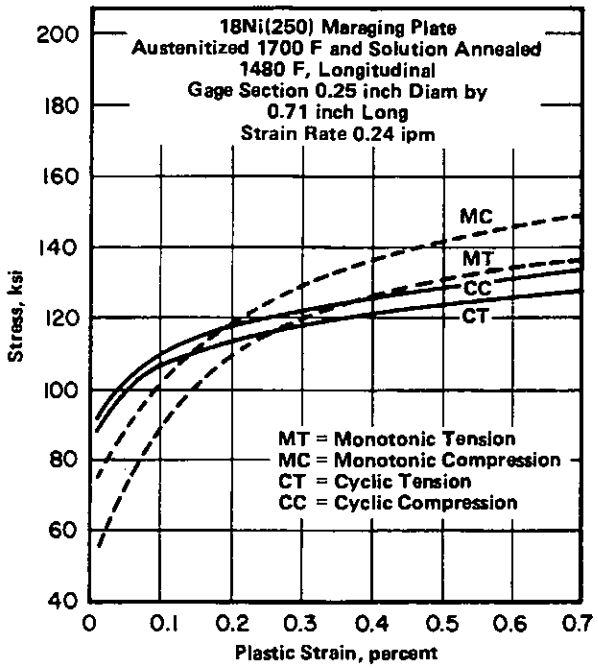
TABLE 3.011. AMS SPECIFIED MECHANICAL PROPERTIES FOR SHEET, STRIP, AND PLATE (2)

Alloy	18Ni(250) Maraging								
Nominal Section Thickness, in.	Condition[a]	Specimen Orientation[b]	F_{tu}, ksi Min	F_{tu}, ksi Max	F_{ty}, ksi, Min	Elongation, percent, Min	RA, percent, Min	Hardness Min	Hardness Max
Up to 0.500	Annealed	–	–	160	–	–	–	–	–
Over 0.500	Annealed	–	–	–	–	–	–	–	321 HB
Under 4.000	Annealed	L	255	–	250	6	45	48 HRC[c]	–
	Plus Aged	T	255	–	250	4	35	48 HRC[c]	–
4.000 thru 10.000	Annealed	L	245	–	240	5	30	48 HRC[c]	–
	Plus Aged	T	245	–	240	3	20	48 HRC[c]	–

Note: The original AMS document should be consulted for complete specification details.

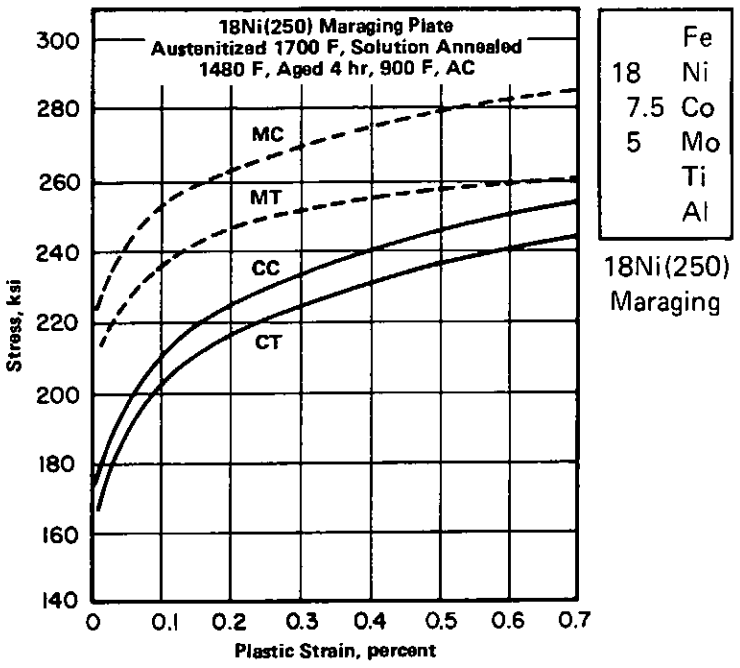
(a) Annealing treatment: 1500–1700 F for 1–2 hr, AC.
Aging treatment: 900 ± 10 F for 6 hr AC.
(b) Transverse tensile specimens must not be less than 2.50 inch in length. Tensile properties in the longitudinal direction need not be determined on product tested in the transverse direction.
(c) Product shall not be rejected on the basis of hardness if the tensile requirements are met.

TABLE 3.012. AMS SPECIFIED MECHANICAL PROPERTIES FOR BARS, FORGINGS, TUBING, AND RINGS



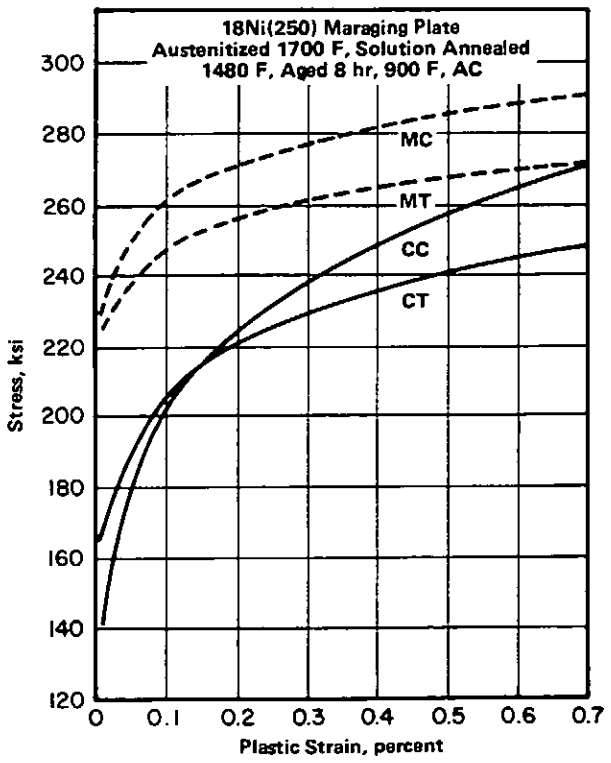
(a) Solution Annealed

FIGURE 3.0212. MONOTONIC AND CYCLIC STRESS-STRAIN CURVES (91)



(b) Solution Annealed Plus 4-Hour Age

FIGURE 3.0212. MONOTONIC AND CYCLIC STRESS-STRAIN CURVES (91)



(c) Solution Annealed Plus 8-Hour Age

FIGURE 3.0212. MONOTONIC AND CYCLIC STRESS-STRAIN CURVES (91)

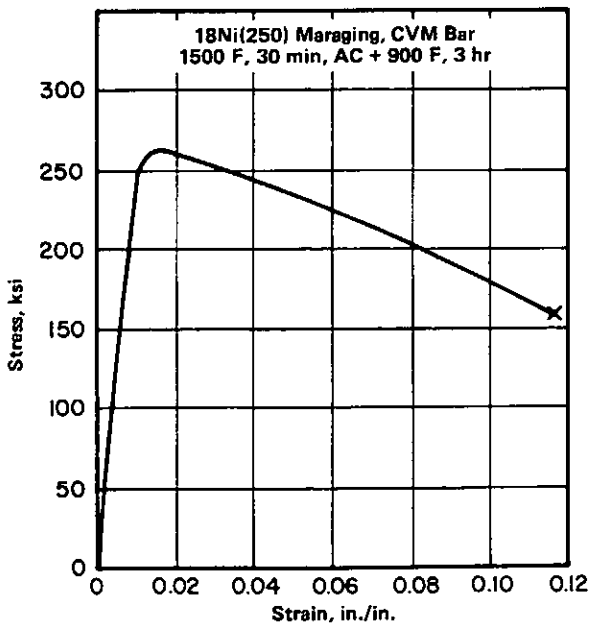


FIGURE 3.0213. STRESS-STRAIN CURVE FOR ANNEALED AND AGED BAR (6)

Fe
18 Ni
7.5 Co
5 Mo
Ti
Al

18Ni(250) Maraging

Alloy	18Ni(250) Maraging	
Condition	Annealed 1500 F, 1 hr	Annealed 1500 F, 1 hr + Age 900 F, 3 hr
F_{tu}, ksi	145–165	240–270
F_{ty}, ksi	105–130	230–265
e (2 in.), percent	8–16	4–10
e (1 in.), percent	–	10–12
RA, percent	55–70	30–60
Hardness, HRC	28–35	48–52

TABLE 3.0214. PRODUCERS' TYPICAL RANGE OF TENSILE PROPERTIES (4, 5, 35)

Alloy	18Ni(250) Maraging				
Condition	CVM, Mill Anneal 1500 F + 900 F, 3 hr				
Form	0.7 in. Thick Sheet		0.25 in. Thick Plate		7/8-in.-Diam Bar
Direction	L	T	L	T	L
No. of Tests[a]	30	30	30	30	30
F_{tu}, ksi					
Mean	263	269	253	248	261
Minimum	242	248	246	241	256
Maximum	285	292	262	253	266
Standard Dev	16.0	16.2	4.8	3.0	3.0
F_{ty}, ksi					
Mean	257	263	244	238[c]	252
Minimum	232	237	235	232	242
Maximum	282	288	254	244	257
Standard Dev	17.7	18.7	5.7	3.1	3.7
e (2 in.), percent	3.7 (3.0–4.5)	3.1[b] (3.0–5.0)	7.4 (6.0–9.0)	7.5 (6.0–8.0)	9.7 (9.0–10.0)
RA, percent	– –	– –	– –	– –	46 (43–48)

(a) From three production heats, 10 specimens per heat.
(b) Average of 28 tests.
(c) Average of 29 tests.

TABLE 3.02151. TYPICAL TENSILE PROPERTIES OF SHEET, PLATE, AND BAR (25)

Alloy	18Ni(250) Maraging					
Condition	1500 F, 1/2 to 1 hr, AC + 900 F, 3 hr					
Form	CVM Forged Billets, T					
Size	6 in. Square		9 in. Square		12 in. Square	
Location	MR	C	MR	C	MR	C
F_{tu}, ksi	260	262	253	252	251	253
F_{ty}, ksi	254	260	248	248	246	248
RA, percent	9	9	8.5	8.0	7.0	8.0
e (4D), percent	47	46	41	36	28	34

TABLE 3.02152. TYPICAL TENSILE PROPERTIES OF ANNEALED AND AGED BILLETS (16)

Alloy	18Ni(250) Maraging			
Condition	Annealed 1600–1650 F + Age 900 F, 3 hr			
Form	CVM Forged Billets, T			
Size	3 in. Round	4 in. Round	5 in. Round	7-1/2 in. Round
F_{tu}, ksi	247	251	248	248
F_{ty}, ksi	238	243	235	237
RA, percent	33	36	37	34
e (4D), percent	8	8	6	7

TABLE 3.02153. TYPICAL TENSILE PROPERTIES OF ANNEALED AND FORGED BILLETS (46)

Fe
18 Ni
7.5 Co
5 Mo
Ti
Al

18Ni(250) Maraging

Alloy	18Ni(250) Maraging	
Form	2-1/2 to 2-3/4 in. Thick Slab, ST	
Melting Practice	Air Melt	CVM
F_{tu}, ksi	275	280
F_{ty}, ksi	260	268
RA, percent	25	35
e (2 in.), percent	3	10

TABLE 3.02154. TYPICAL TENSILE PROPERTIES OF AIR AND VACUUM MELTED SLAB (9)

Alloy	18Ni(250) Maraging							
Condition	Mill Annealed + Age 925 F, 3 hr							
Form	Air Melt, Sheet and Plate							
Thickness	0.045 in.		0.160 in.		0.375 in.		0.750 in.	
Direction	L	T	L	T	L	T	L	T
F_{tu}, ksi	234	247	239	242	240	240	244	237
F_{ty}, ksi	234	246	226	230	233	231	226	227
e (1 in.), percent	1.3	1.8	12	11	18	18	–	–
e (2 in.), percent	–	–	–	–	–	–	10	12
RA, percent	–	–	–	–	–	–	38	49

TABLE 3.02155. TYPICAL TENSILE PROPERTIES OF SHEET AND PLATE FROM AN AIR MELTED HEAT (36)

Alloy	18Ni(250) Maraging										
Condition	Mill Annealed + Age 925 F, 3 hr										
Form	CVM, Sheet and Plate										
Thickness	0.045 in.		0.160 in.		0.375 in.		0.750 in.		3.0 in.		
Direction	L	T	L	T	L	T	L	T	L	T	ST
F_{tu}, ksi	268	271	261	263	263	264	248	252	244	242	241
F_{ty}, ksi	268	270	249	251	254	254	225	237	234	231	233
e (1 in.), percent	1.2	1.5	10	10	20	18	–	–	–	–	5
e (2 in.), percent	–	–	–	–	–	–	12	10	12	9	–
RA, percent	–	–	–	–	–	–	54	44	54	40	14

TABLE 3.02156. TYPICAL TENSILE PROPERTIES OF SHEET AND PLATE FROM A CVM HEAT (36)

	Fe
18	Ni
7.5	Co
5	Mo
	Ti
	Al

18Ni(250) Maraging

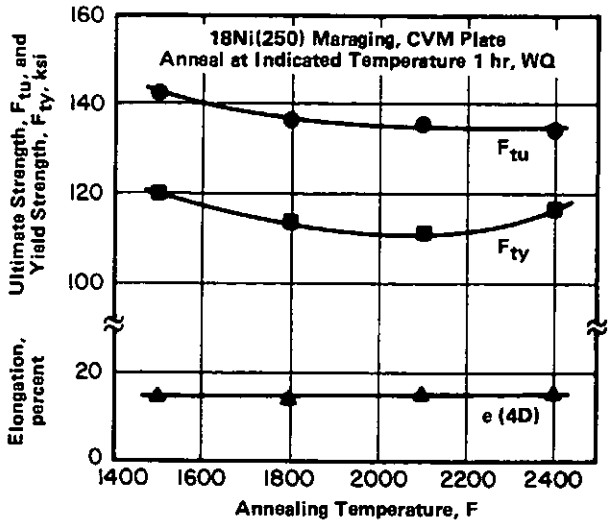


FIGURE 3.02161. INFLUENCE OF HIGH TEMPERATURE ANNEALING TREATMENT ON TENSILE PROPERTIES OF ANNEALED CVM PLATE (84)

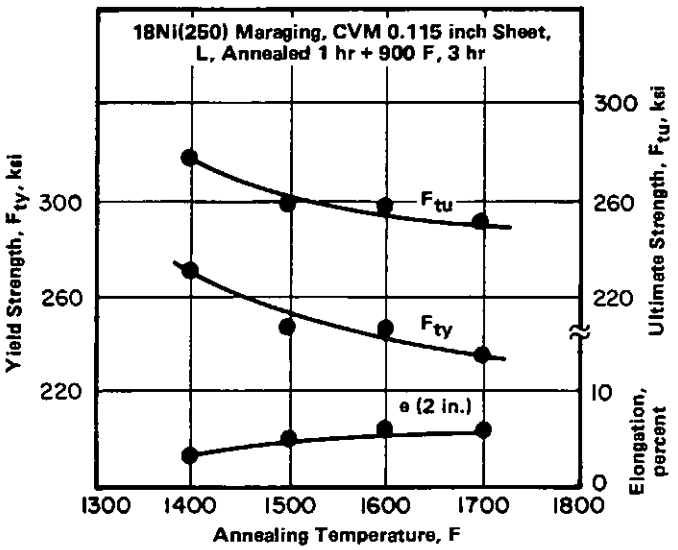


FIGURE 3.02162. EFFECT OF ANNEALING TEMPERATURE ON THE TENSILE PROPERTIES OF ANNEALED AND AGED SHEET (39)

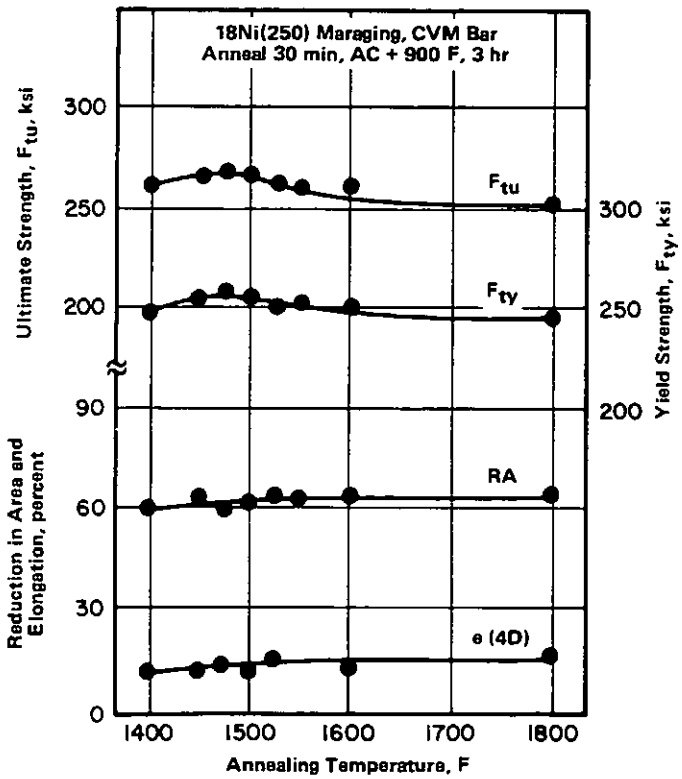


FIGURE 3.02163. INFLUENCE OF ANNEALING TEMPERATURE ON TENSILE PROPERTIES OF BAR (6)

	Fe
18	Ni
7.5	Co
5	Mo
	Ti
	Al

18Ni(250) Maraging

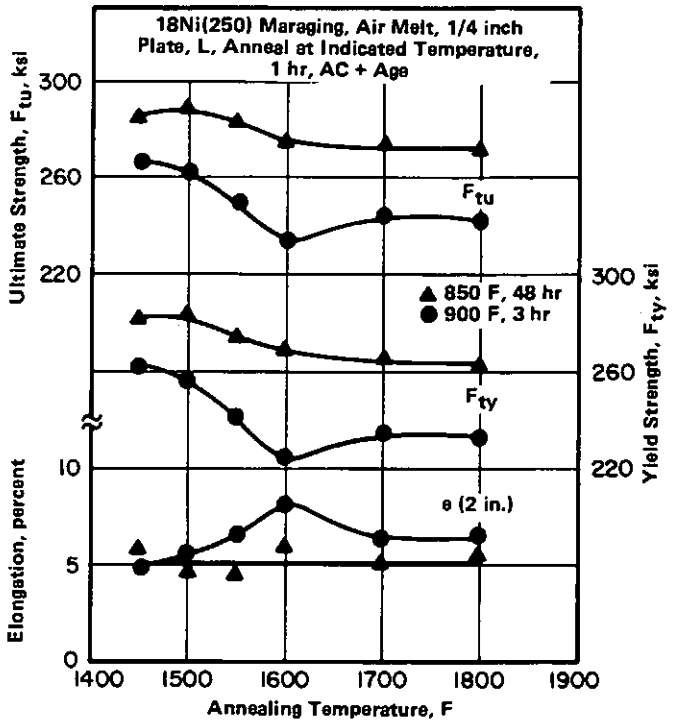


FIGURE 3.02164. INFLUENCE OF ANNEALING TEMPERATURE ON THE TENSILE PROPERTIES OF PLATE (5, 37)

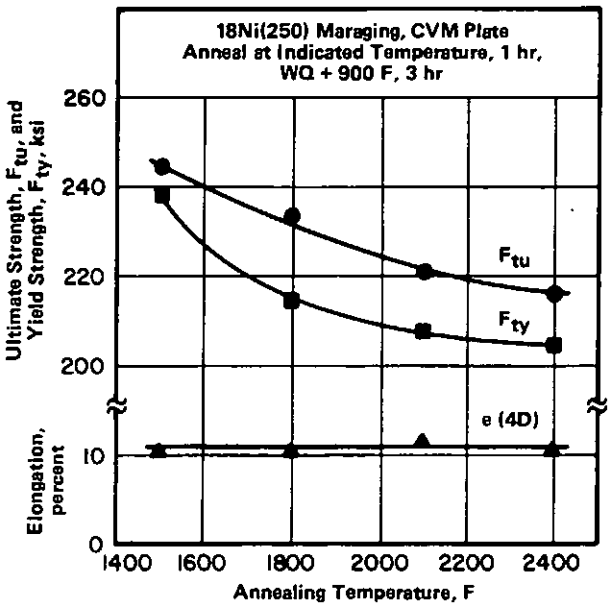


FIGURE 3.02165. INFLUENCE OF HIGH TEMPERATURE ANNEALING TREATMENT ON TENSILE PROPERTIES OF AGED CVM PLATE (84)

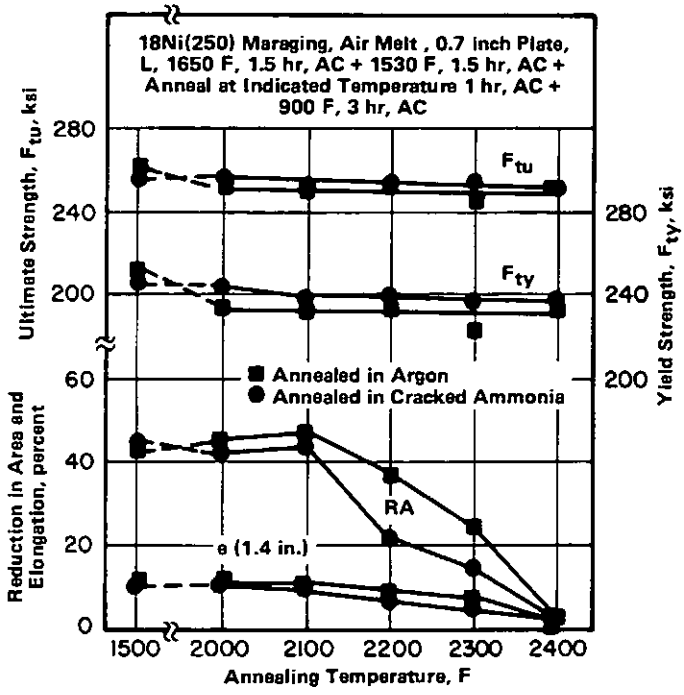


FIGURE 3.02166. INFLUENCE OF HIGH TEMPERATURE ANNEALING TREATMENT ON TENSILE PROPERTIES OF AIR MELTED PLATE (10)

	Fe
18	Ni
7.5	Co
5	Mo
	Ti
	Al

18Ni(250) Maraging

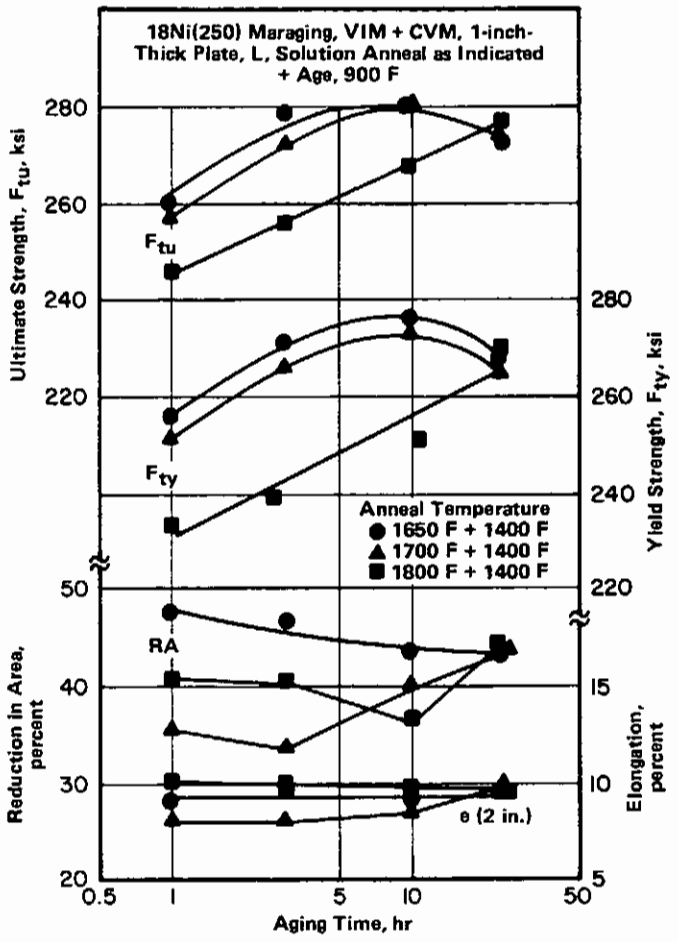


FIGURE 3.02171. EFFECTS OF SOLUTION ANNEALING TEMPERATURE AND AGING TIME ON THE TENSILE PROPERTIES OF VIM + CVM PLATE (38)

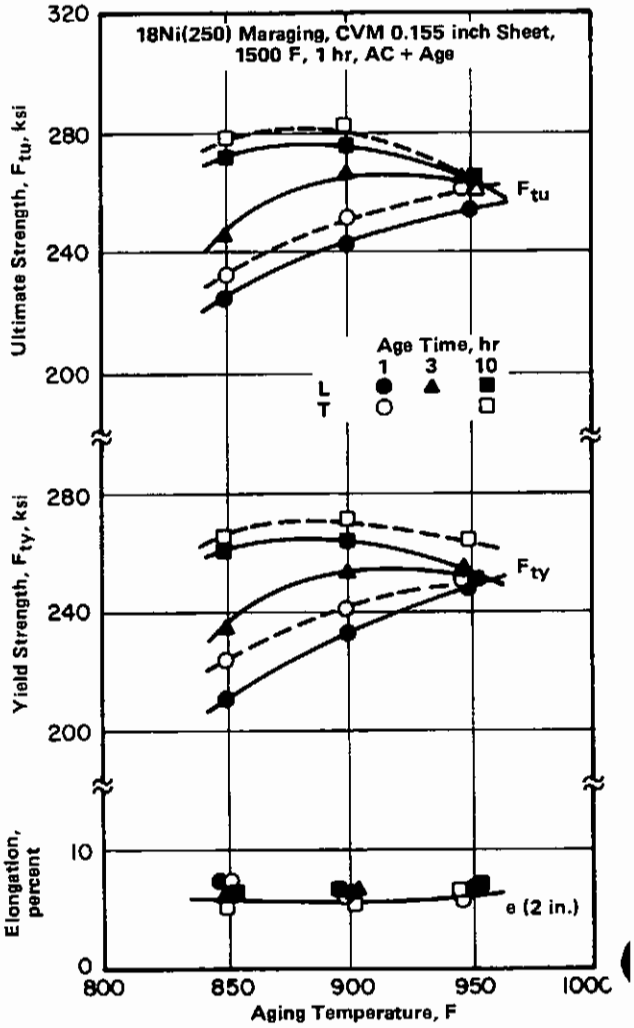


FIGURE 3.02172. EFFECT OF AGING TEMPERATURE AND TIME ON THE TENSILE PROPERTIES OF SHEET (39)

	Fe
18	Ni
7.5	Co
5	Mo
	Ti
	Al

18Ni(250) Maraging

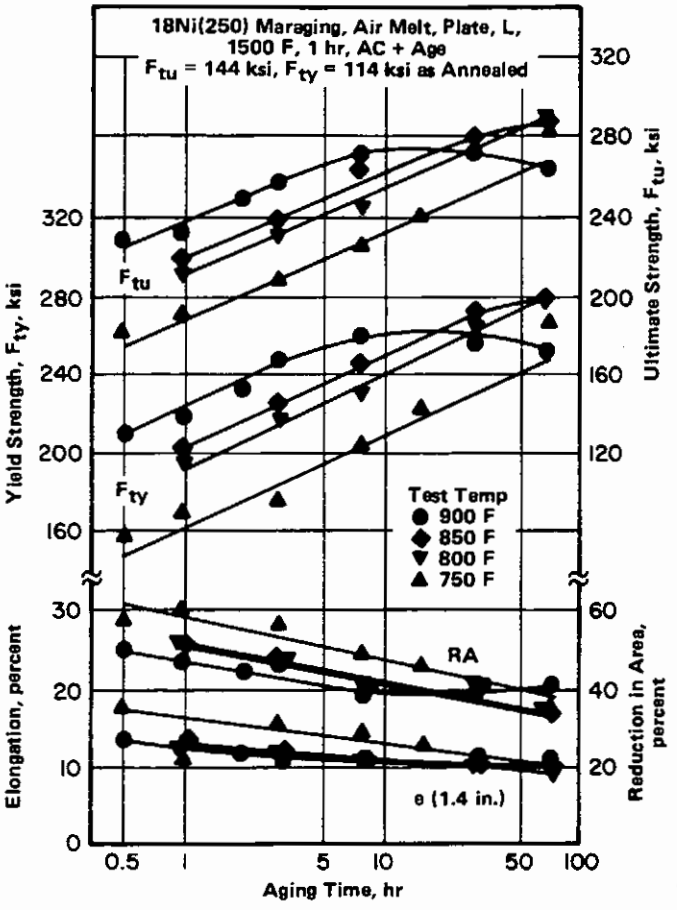


FIGURE 3.02173. EFFECT OF AGING TEMPERATURE AND TIME ON THE TENSILE PROPERTIES OF AIR MELTED PLATE (40)

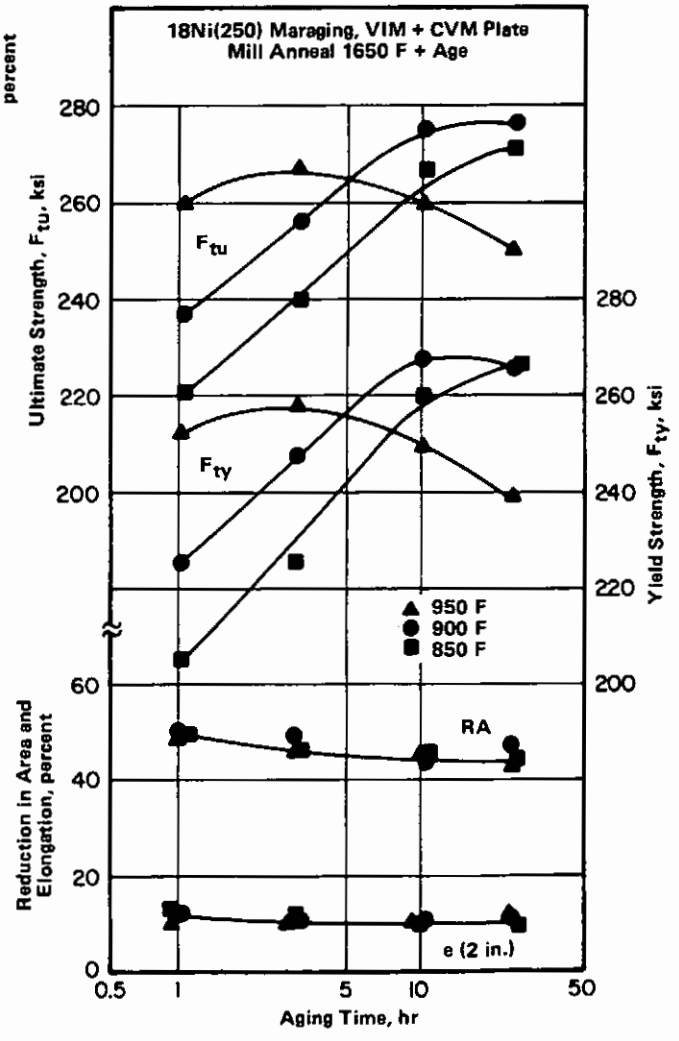


FIGURE 3.02174. EFFECT OF AGING TEMPERATURE AND TIME ON THE TENSILE PROPERTIES OF VIM + CVM PLATE (38)

	Fe
18	Ni
7.5	Co
5	Mo
	Ti
	Al

18Ni(250) Maraging

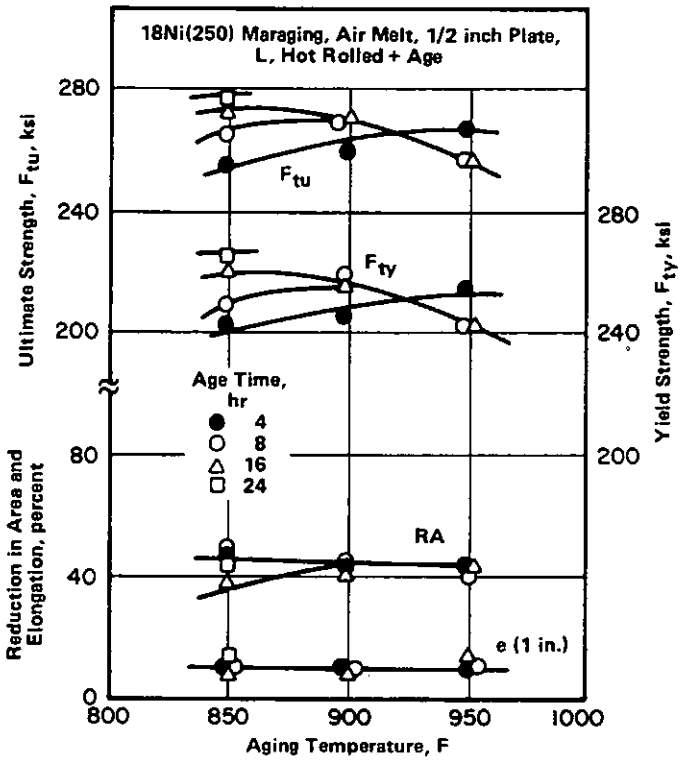


FIGURE 3.02175. EFFECT OF AGING TEMPERATURE AND TIME ON THE TENSILE PROPERTIES OF HOT ROLLED AND AGED PLATE (41)

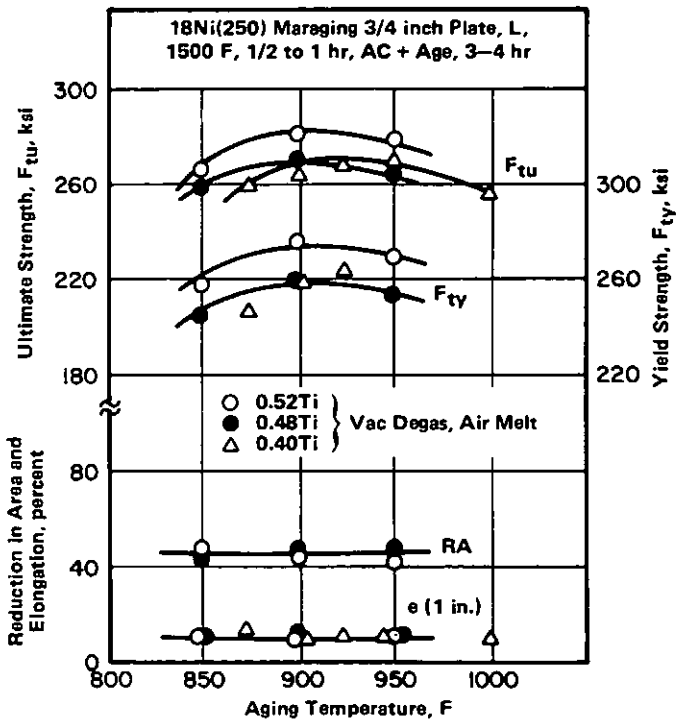


FIGURE 3.02176. EFFECT OF AGING TEMPERATURE ON TENSILE PROPERTIES OF ANNEALED PLATE FROM THREE HEATS (41–43)

	Fe
18	Ni
7.5	Co
5	Mo
	Ti
	Al

18Ni(250) Maraging

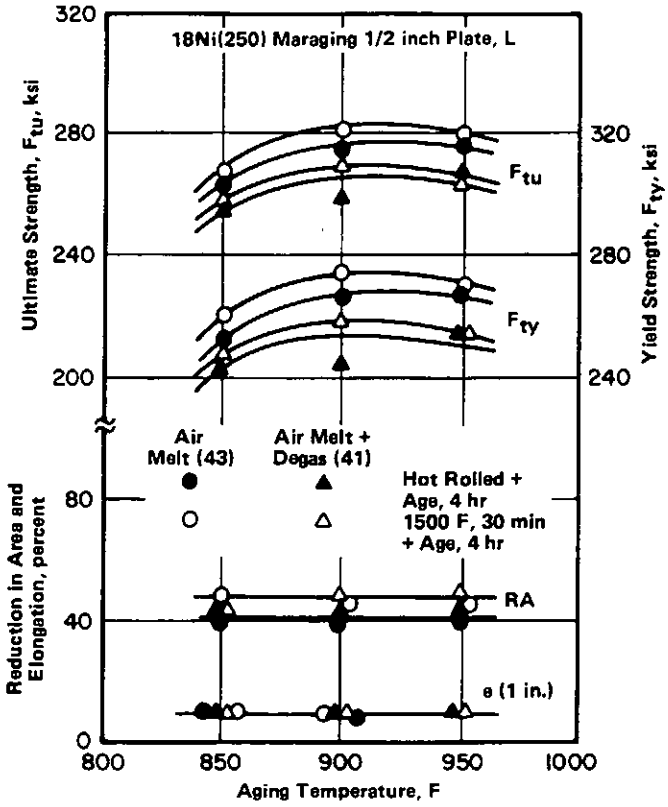


FIGURE 3.02177. EFFECT OF AGING TEMPERATURE ON THE TENSILE PROPERTIES OF HOT ROLLED AND ANNEALED PLATE FROM TWO HEATS (41, 43)

Alloy	18Ni(250) Maraging				
Form	300 lb Lab Vac Melted Heat, 1/2 in. Plate, L				
Condition	1500 F, 1 hr, AC + Age as Indicated				
Aging Treatment	F_{ty}, ksi	F_{tu}, ksi	e (1 in.), percent	RA, percent	IE Charpy-V, ft-lb
None (Annealed)	130	150	18	80	119
900 F, 3 hr[a]	251	254	12	62	35
900 F, 1-1/2 hr, AC + 900 F, 1-1/2 hr	256	260	12	60	34
900 F, 6 hr	266	270	12	62	31
900 F, 3 hr, AC + 900 F, 3 hr	266	270	12	58	29
900 F, 3 hr, AC + 600 F, 24 hr	255	257	13	61	32
900 F, 3 hr, AC + 600 F, 48 hr	254	257	13	62	33
700 F, 48 hr	261	264	12	61	30
700 F, 48 hr, AC + 900 F, 3 hr	270	277	12	61	23
900 F, 3 hr, AC + 700 F, 48 hr	260	264	13	61	27
800 F, 48 hr	289	290	12	55	23
800 F, 48 hr, AC + 900 F, 3 hr	277	280	11	58	25
900 F, 3 hr, AC + 800 F, 24 hr	271	275	12	56	24
900 F, 3 hr, AC + 800 F, 48 hr	287	290	11	58	23
900 F, 3 hr, AC + 800 F, 72 hr	293	294	11	67	21

(a) Standard aging treatment.

TABLE 3.02178. EFFECT OF DUPLEX AGING TREATMENTS ON THE TENSILE PROPERTIES OF 300 LB LABORATORY VACUUM MELTED PLATE (44)

	Fe
18	Ni
7.5	Co
5	Mo
	Ti
	Al

18Ni(250) Maraging

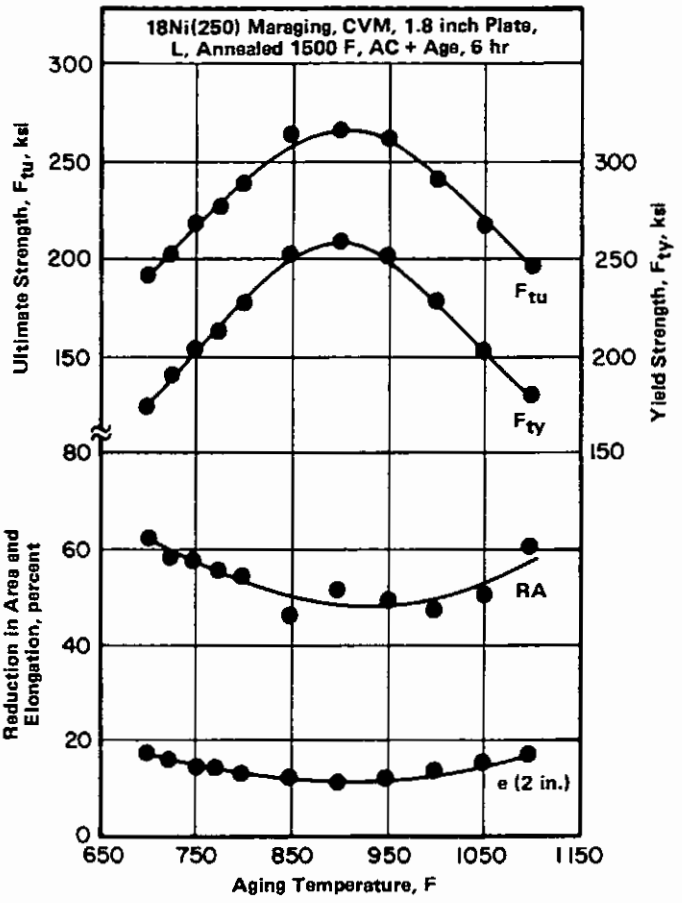


FIGURE 3.02179. EFFECT OF AGING TEMPERATURE ON THE TENSILE PROPERTIES OF 1.8 INCH THICK CVM PLATE (45)

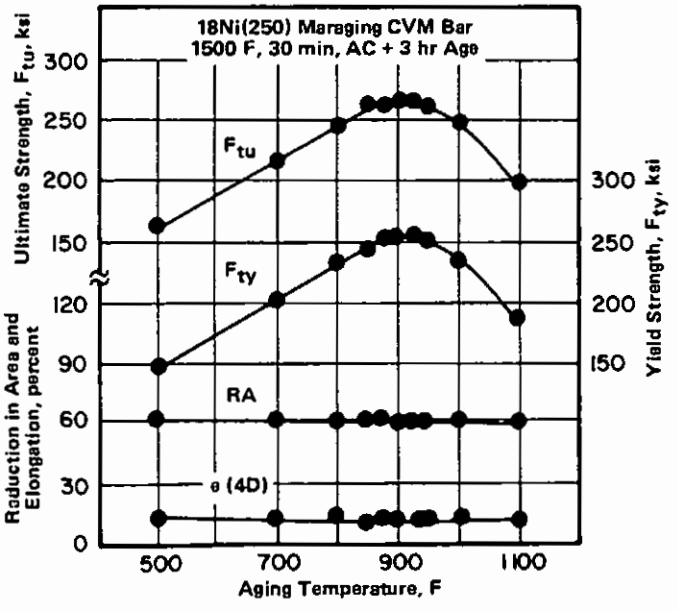


FIGURE 3.021710. EFFECT OF AGING TEMPERATURE ON TENSILE PROPERTIES OF BAR (6)

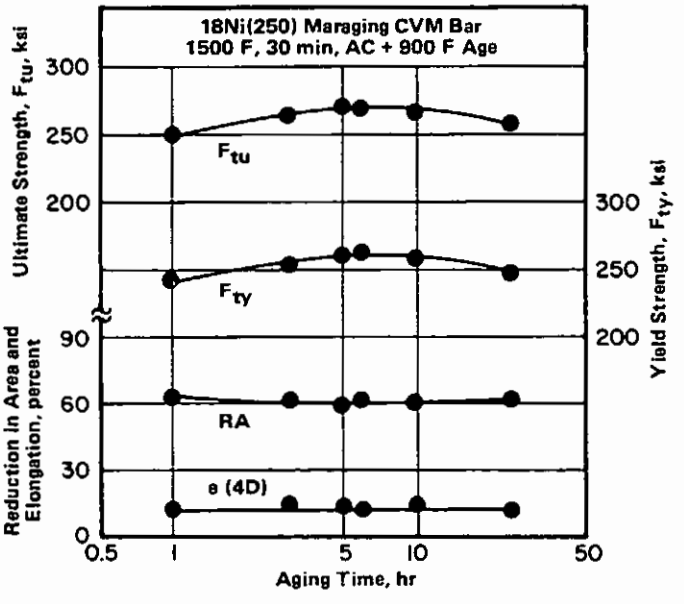
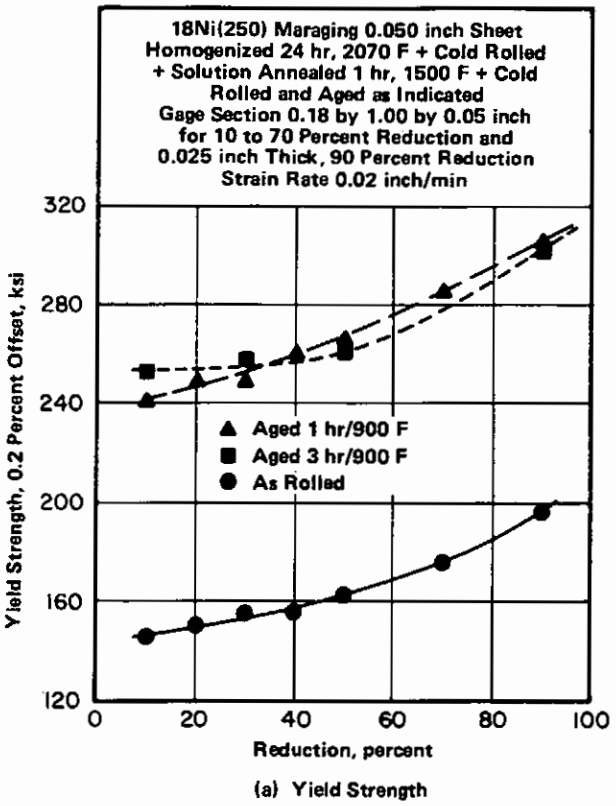
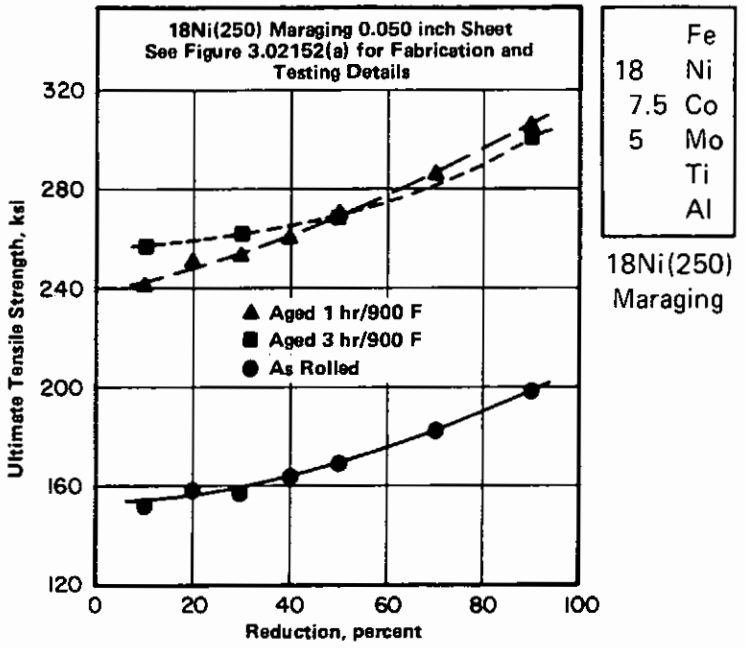


FIGURE 3.021711. EFFECT OF AGING TIME ON TENSILE PROPERTIES OF BAR (6)



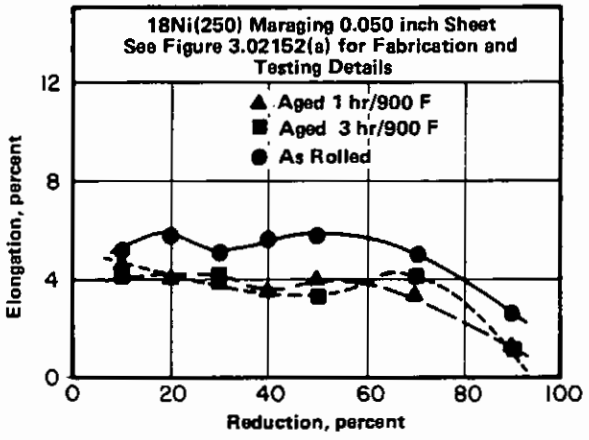
(a) Yield Strength

FIGURE 3.02181. EFFECTS OF COLD ROLLING AND COLD ROLLING PLUS AGING ON TENSILE PROPERTIES OF SHEET (92)



(b) Ultimate Tensile Strength

FIGURE 3.02181. EFFECTS OF COLD ROLLING AND COLD ROLLING PLUS AGING ON TENSILE PROPERTIES OF SHEET (92)



(c) Elongation

FIGURE 3.02181. EFFECTS OF COLD ROLLING AND COLD ROLLING PLUS AGING ON TENSILE PROPERTIES OF SHEET (92)

	Fe
18	Ni
7.5	Co
5	Mo
	Ti
	Al

18Ni(250) Maraging

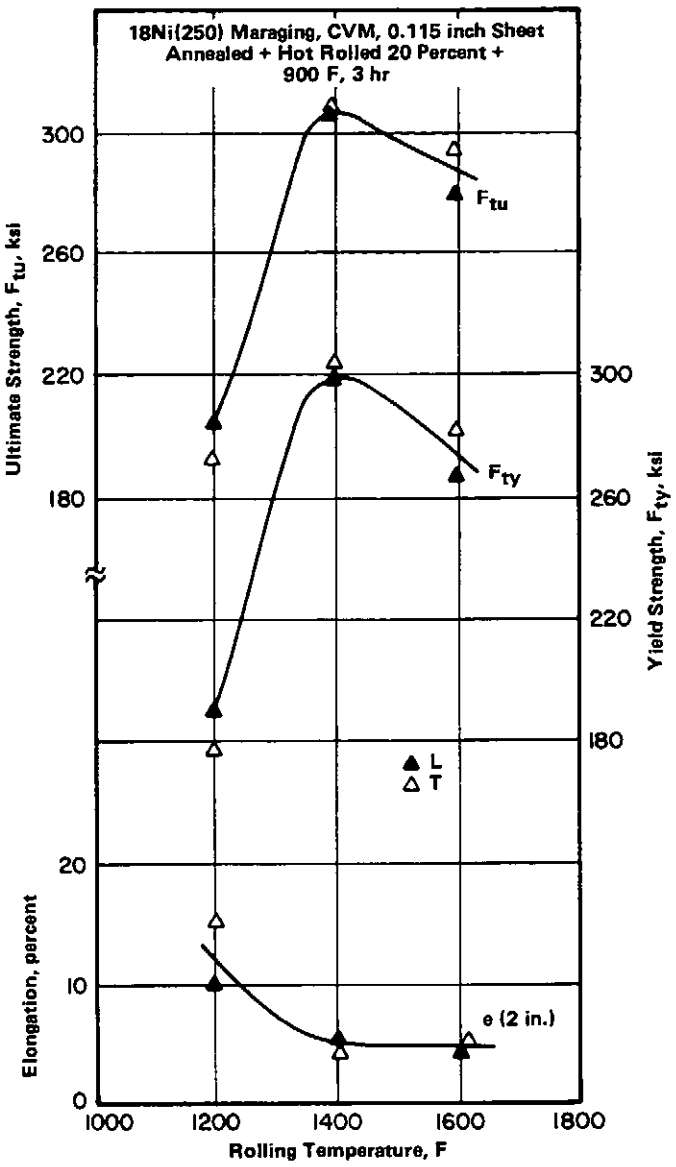


FIGURE 3.02182. EFFECT OF ROLLING TEMPERATURE ON THE TENSILE PROPERTIES OF ANNEALED, ROLLED, AND AGED SHEET (47)

	Fe
18	Ni
7.5	Co
5	Mo
	Ti
	Al

18Ni(250)
Maraging

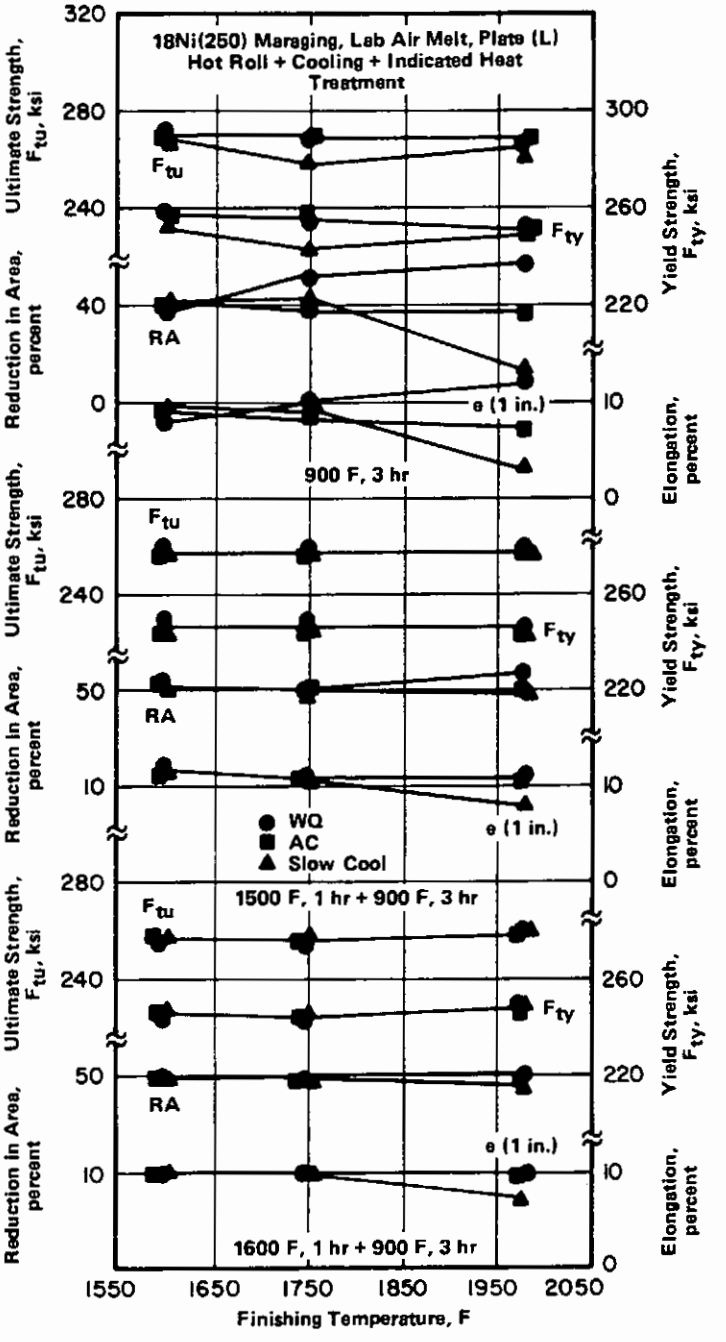


FIGURE 3.02183. EFFECT OF HOT ROLLING FINISHING TEMPERATURE AND COOLING RATE ON PROPERTIES OF LABORATORY AIR-INDUCTION-MELTED PLATE AGED AT 900 F (40, 48)

	Fe
18	Ni
7.5	Co
5	Mo
	Ti
	Al

18Ni(250)
Maraging

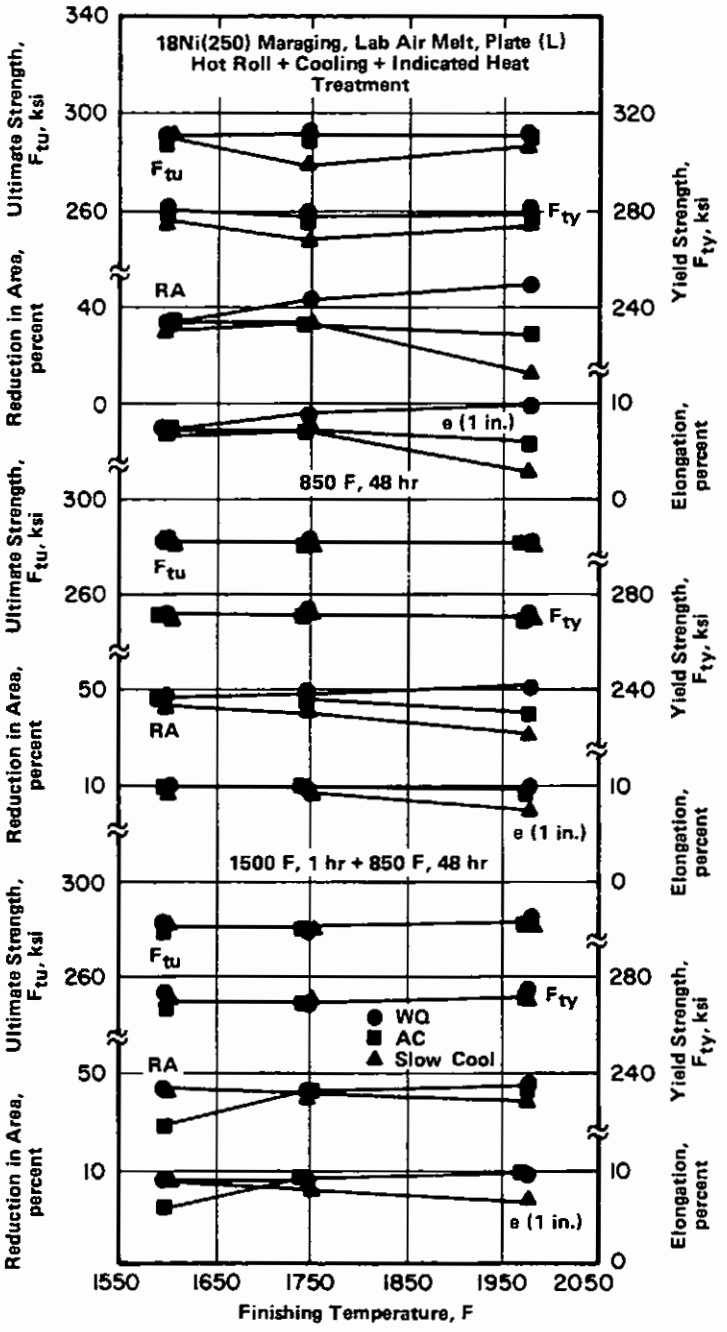


FIGURE 3.02184. EFFECT OF HOT ROLLING FINISHING TEMPERATURE AND COOLING RATE ON TENSILE PROPERTIES OF LABORATORY AIR-INDUCTION-MELTED PLATE AGED AT 850 F (40, 48)

	Fe
18	Ni
7.5	Co
5	Mo
	Ti
	Al

18Ni(250)
Maraging

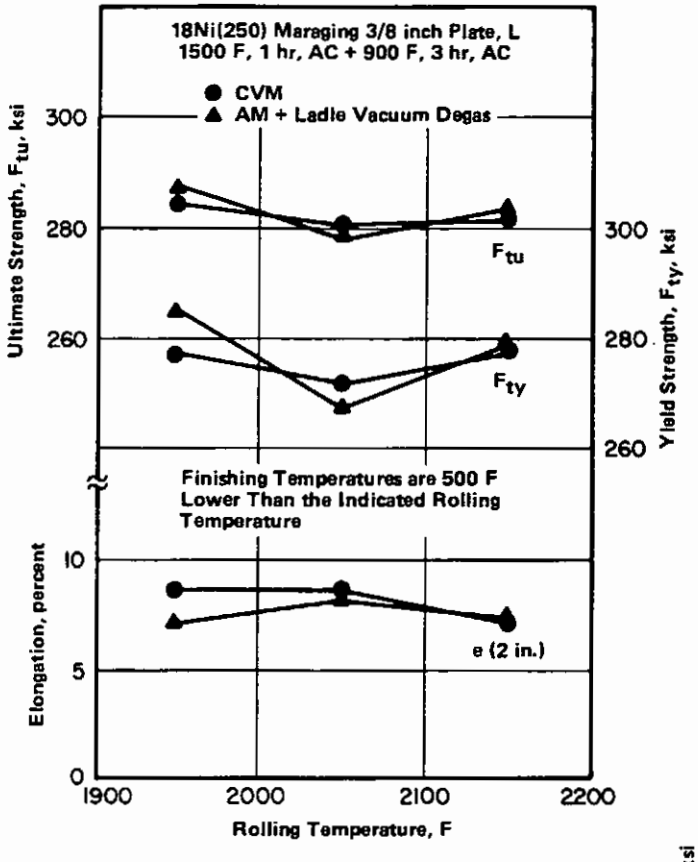


FIGURE 3.02185. EFFECT OF ROLLING TEMPERATURE ON TENSILE PROPERTIES OF PLATE (57)

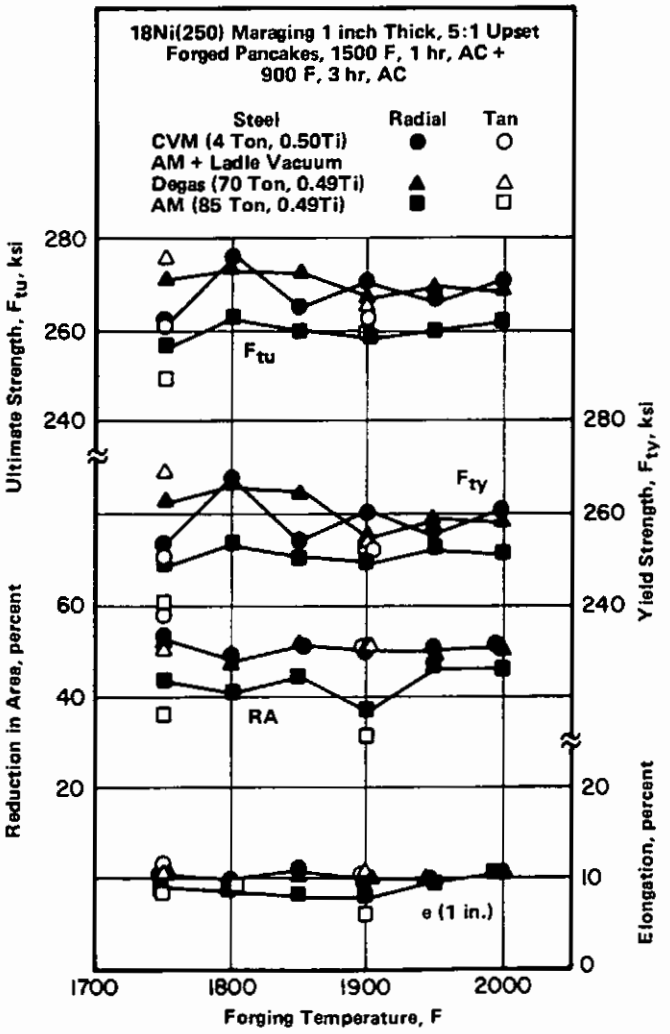


FIGURE 3.02186. EFFECT OF FORGING TEMPERATURE ON TENSILE PROPERTIES OF 5:1 UPSET FORGED PANCAKES (57)

	Fe
18	Ni
7.5	Co
5	Mo
	Ti
	Al

18Ni(250) Maraging

Alloy	18Ni(250) Maraging			
Form	Bar			
Condition	Annealed 1500 F, 1/2 hr, AC		Annealed + Aged 1500 F, 1/2 hr, AC + 900 F, 3 hr	
Melting Practice	Air Melt	CVM	Air Melt	CVM
F_{cy}[(a)], ksi	150	149	283	280

(a) Averages of three tests.

TABLE 3.0222. COMPRESSIVE YIELD STRENGTH OF ANNEALED AND AGED BAR (6)

Alloy	18Ni(250) Maraging			
Condition	CVM, Mill Anneal 1500 F + Age 900 F, 3 hr			
Form	0.07 in. Sheet		0.25 in. Plate	1.5-in.-Diam Bar
Direction	L	T	T	L
F_{cy}[(a)], ksi				
Mean	248	239	264	262
Minimum	222	194	252	246
Maximum	265	276	277	267

(a) From three production heats, ten specimens per heat.

TABLE 3.0223. TYPICAL COMPRESSIVE YIELD STRENGTH OF SHEET, PLATE, AND BAR (25)

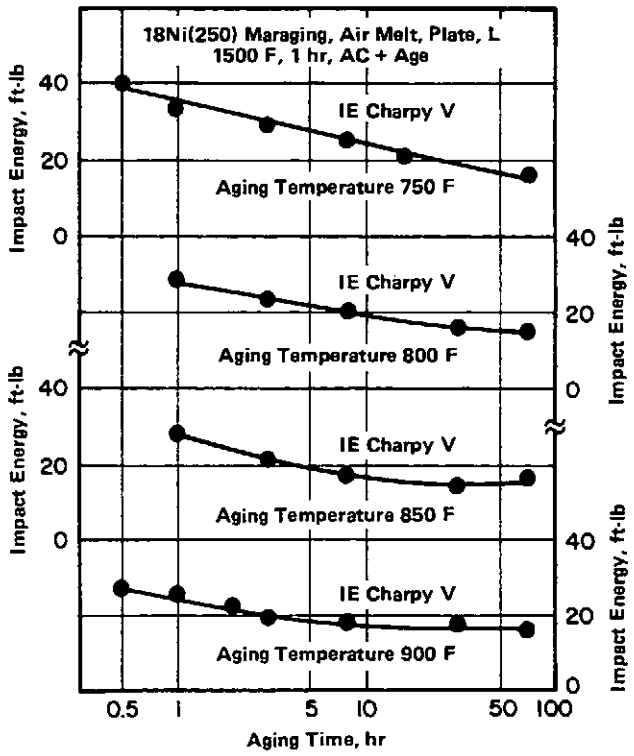


FIGURE 3.0231. EFFECT OF AGING TEMPERATURE AND TIME ON THE IMPACT PROPERTIES OF AIR MELTED PLATE (40)

(See Figure 3.02173 for Corresponding Tensile Properties)

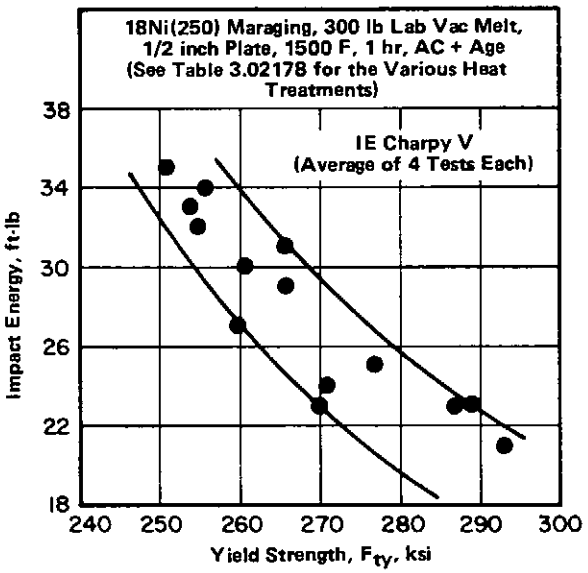


FIGURE 3.0232. YIELD STRENGTH VERSUS IMPACT PROPERTIES FOR A 300 LB LABORATORY VACUUM MELTED PLATE (44)

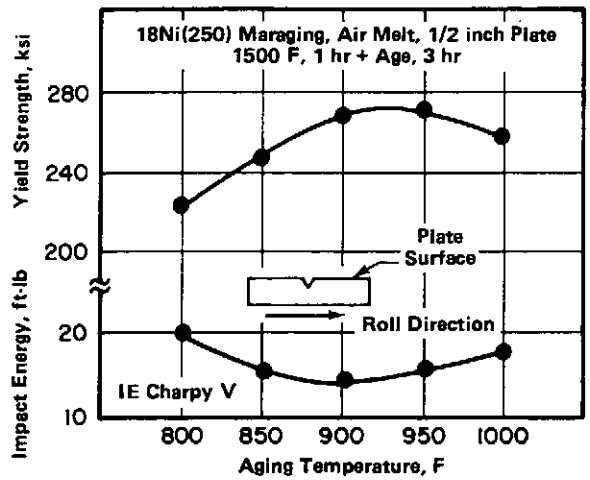


FIGURE 3.0233. EFFECT OF AGING TEMPERATURE ON THE IMPACT ENERGY OF ANNEALED PLATE (51)

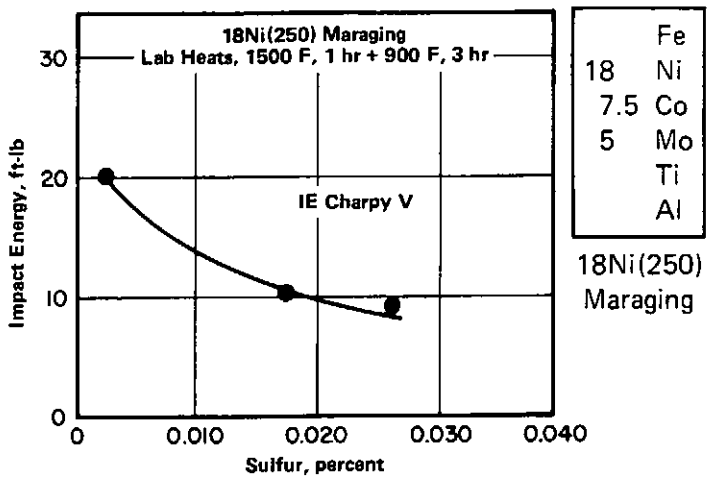


FIGURE 3.0234. EFFECT OF SULFUR CONTENT ON ROOM TEMPERATURE IMPACT ENERGY (67)

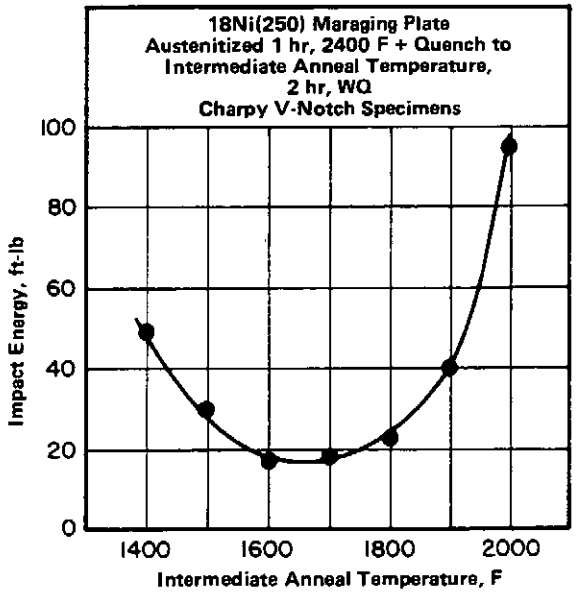


FIGURE 3.0235. IMPACT ENERGY VARIATION WITH INTERMEDIATE ANNEALING TEMPERATURE AFTER HIGH TEMPERATURE HEAT TREATMENT AT 2400 F (93)

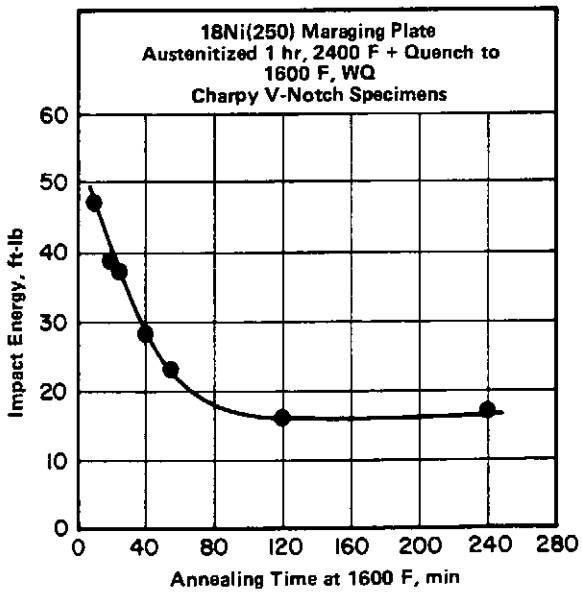


FIGURE 3.0236. IMPACT ENERGY VARIATION WITH ANNEALING TIME AT 1600 F AFTER HIGH TEMPERATURE HEAT TREATMENT AT 2400 F (93)

Fe
18 Ni
7.5 Co
5 Mo
Ti
Al

18Ni(250) Maraging

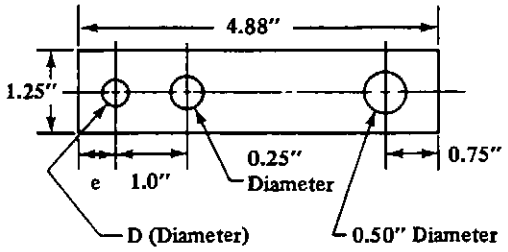
Alloy	18Ni(250) Maraging			
Condition	CVM, Mill Annealed 1500 F + Age 900 F, 3 hr			
Form	0.07 in. Sheet		0.25 in. Plate	7/8-in.-Diam Bar
Direction	L	T	T	L
F_{su}[(a)], ksi				
Mean	158	160	159	163
Minimum	144	149	151	157
Maximum	177	176	176	171

(a) From three production heats, 10 specimens per heat.

TABLE 3.0251. TYPICAL ULTIMATE SHEAR STRENGTH OF SHEET, PLATE, AND BAR (25)

Alloy	18Ni(250) Maraging					
Condition	CVM, Mill Annealed 1500 F + Age 900 F, 3 hr					
e/D	1.5			2.0		
Form[(a)]	0.07 in. Sheet		0.25 in. Plate	0.07 in. Sheet		0.25 in. Plate
Direction	L	T	T	L	T	T
F_{bru}[(b)], ksi						
Mean	350[(c)]	352	357	472	480	460
Minimum	–	–	341	430	446	439
Maximum	–	–	376	519	528	494
F_{bry}[(b)], ksi						
Mean	319[(c)]	323	339	387	390	378
Minimum	–	–	320	342	326	335
Maximum	–	–	367	451	471	447

(a) 0.07 inch sheet tested in full thickness; 0.25 inch plate tested in 0.1 inch thickness.
(b) From three production heats, 10 specimens per heat except as noted.
(c) For 10 specimens from a single heat.



e	D	e/D
0.375	0.25	1.5
0.50	0.25	2.0

TABLE 3.0261. TYPICAL BEARING STRENGTHS OF SHEET AND PLATE (25)

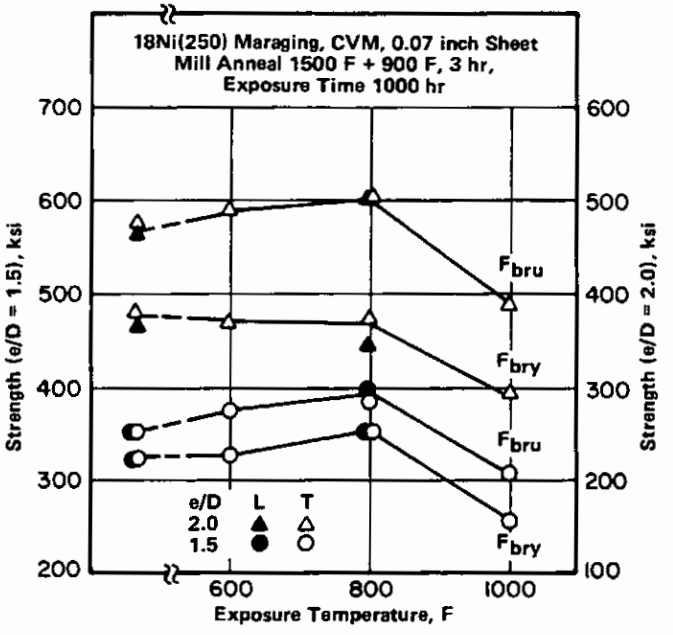


FIGURE 3.0262. EFFECT OF 1000 HOUR ELEVATED TEMPERATURE EXPOSURE ON THE BEARING STRENGTH OF SHEET (25)

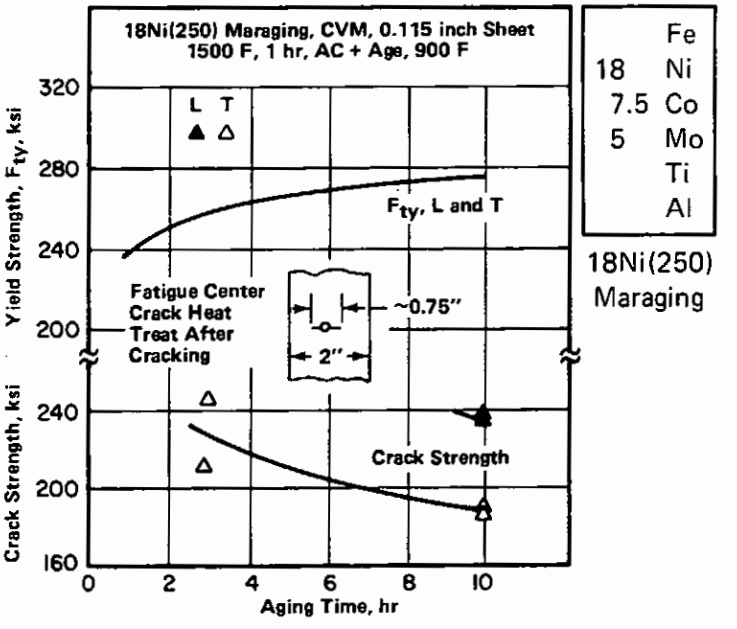


FIGURE 3.02711. EFFECT OF AGING TIME ON CRACK STRENGTH OF 250 KSI ANNEALED SHEET (39)

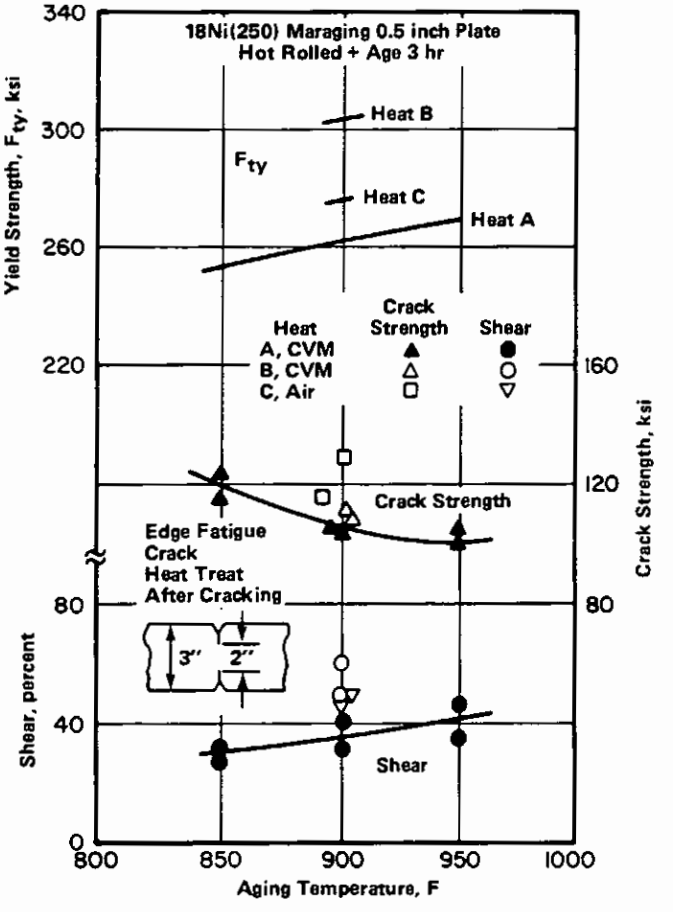


FIGURE 3.02712. EFFECT OF AGING TEMPERATURE ON CRACK STRENGTH OF AIR AND CVM PLATE (52)

	Fe
18	Ni
7.5	Co
5	Mo
	Ti
	Al

18Ni(250) Maraging

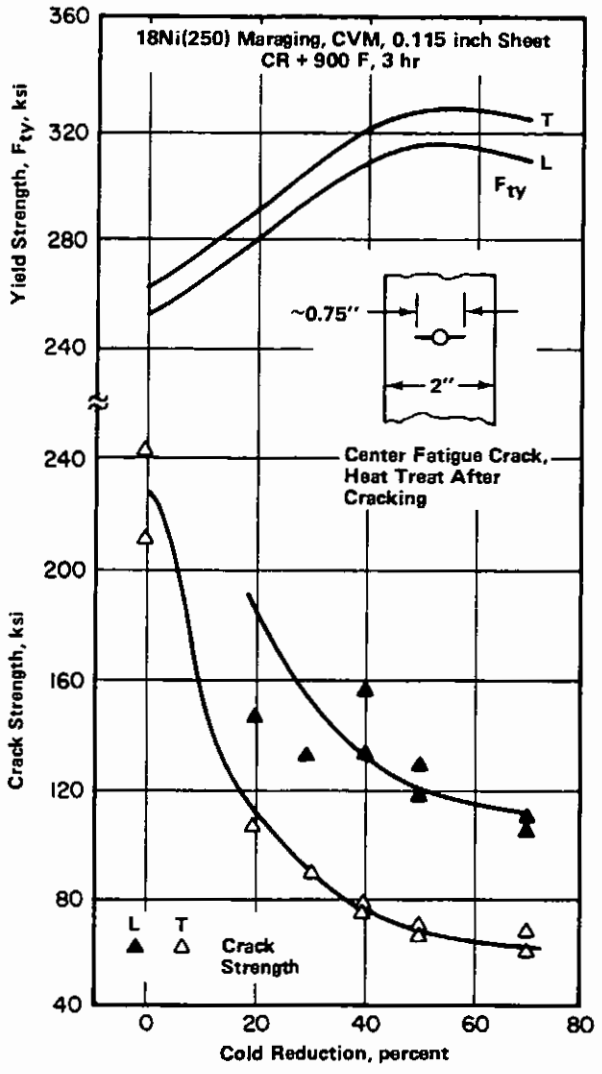


FIGURE 3.02713. EFFECT OF COLD ROLLING PRIOR TO AGING ON CRACK STRENGTH OF SHEET (47)

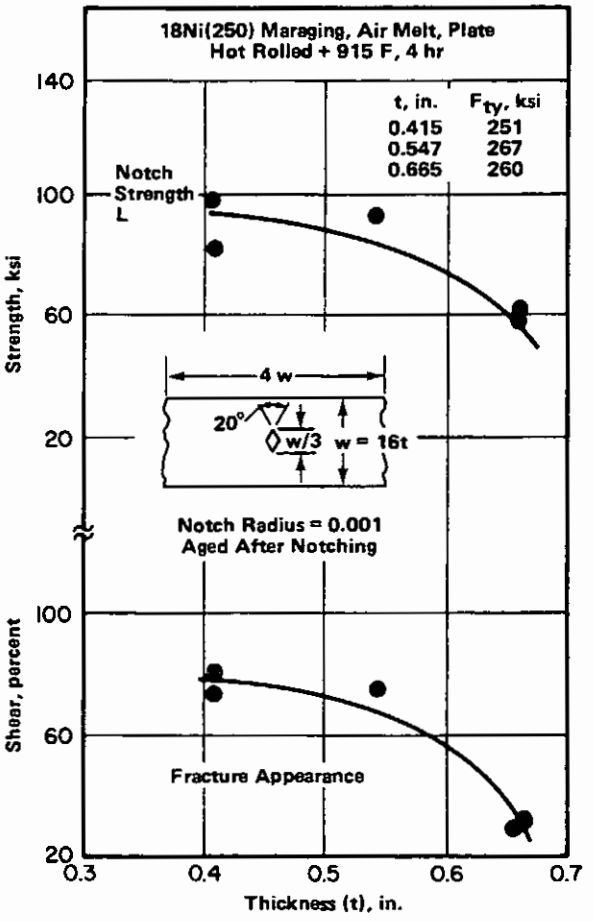


FIGURE 3.03714. EFFECT OF THICKNESS ON THE SHARP NOTCH PROPERTIES OF AIR MELTED PLATE (53)

Alloy	18Ni(250) Maraging							
Condition	Mill Annealed + 925 F, 3 hr							
Melting Practice	Air Melt				CVM			
Thickness	0.045 in.		0.16 in.		0.045 in.		0.16 in.	
Direction	L	T	L	T	L	T	L	T
F_{ty}, ksi	234	246	226	230	268	270	249	251
Crack Strength, ksi	173	167	167	162	159	164	177	160

TABLE 3.02715. EFFECT OF THICKNESS ON CRACK STRENGTH OF AIR MELTED AND CVM SHEET (36)

Fe
18 Ni
7.5 Co
5 Mo
Ti
Al

18Ni(250) Maraging

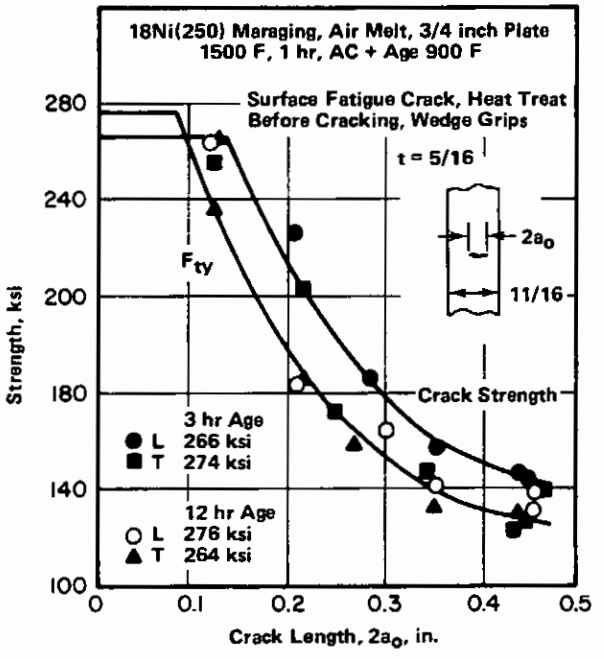


FIGURE 3.02716. EFFECT OF SURFACE CRACK LENGTH ON THE CRACK STRENGTH OF AIR MELTED PLATE AGED AT TWO TEMPERATURES (55)

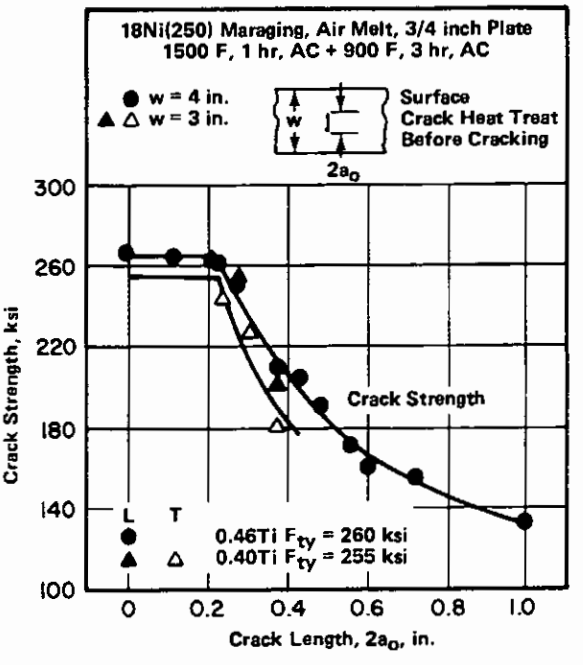


FIGURE 3.02717. EFFECT OF SURFACE CRACK LENGTH ON CRACK STRENGTH OF PLATE FROM TWO AIR MELTED HEATS (42)

	Fe
18	Ni
7.5	Co
5	Mo
	Ti
	Al

18Ni(250) Maraging

Alloy	18Ni(250) Maraging
Form	CVM, 1 inch Plate, LT
Condition	Mill Anneal + 900 F, 3 hr
F_{ty}, ksi	259
K_{Ic} (Mean), ksi $\sqrt{in.}$	68.4(a)
Standard Deviation	
σ, ksi $\sqrt{in.}$	3.51
σ/Mean K_{Ic}	0.0515

(a) 23 tests.

TABLE 3.02721. PLANE STRAIN FRACTURE TOUGHNESS OF CVM PLATE (58)

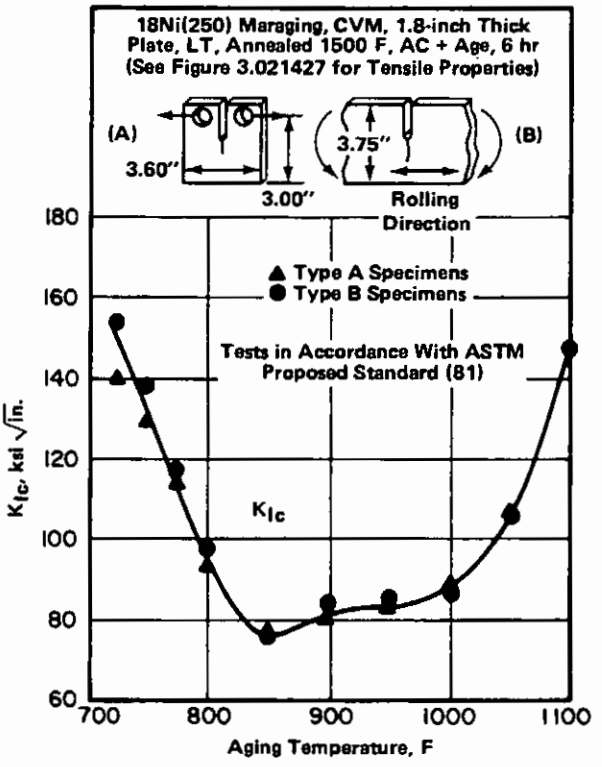


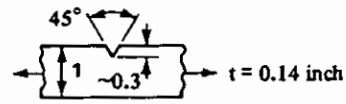
FIGURE 3.02722. EFFECT OF AGING TEMPERATURE ON PLANE STRAIN CRACK TOUGHNESS OF 1.8 INCH CVM PLATE (45)

Alloy	18Ni(250) Maraging			
Form	Air Melt + Vacuum Degas, 1/2 inch Plate			
Condition	1500 F, 1/2 hr, AC + 900 F, 4 hr(a) (F_{ty} = 258 ksi, L and 265 ksi, T)			
Direction	LT	TL	LS	TS
K_{Ic}(b), ksi $\sqrt{in.}$	74	81	81	84

(a) All specimens heat treated before cracking.
(b) Precracked bend specimens.

TABLE 3.02723. PLANE STRAIN FRACTURE TOUGHNESS OF AIR MELTED AND VACUUM DEGASSED PLATE (59)

Alloy	18Ni(250) Maraging			
Form	Lab Air Melt (300 lb Heat), 1 inch Plate			
Condition	1500 F, 1 hr, AC + 900 F, 3 hr (F_{ty} = 230 ksi), L, T			
Direction(b)	LT	TL	LS	ST
K_{Ic}, ksi $\sqrt{in.}$(a)	85	83	96	68



Fatigue cracked single edge notch specimen.
Heat treat before cracking.

	Fe
18	Ni
7.5	Co
5	Mo
	Ti
	Al

18Ni(250) Maraging

(a) K_{Ic} from displacement gage pop-in load.
(b) First letter indicates direction normal to crack and second letter direction of propagation. R in rolling direction, W perpendicular to rolling direction, and T in thickness direction.

TABLE 3.02724. PLANE STRAIN FRACTURE TOUGHNESS FOR ANNEALED AND AGED LABORATORY AIR MELT PLATE (15)

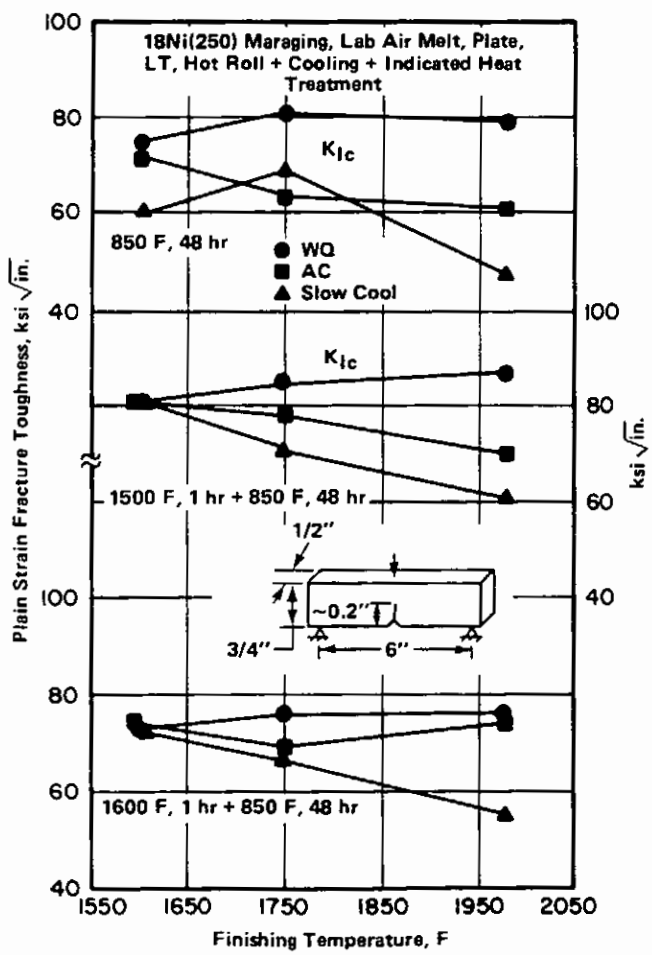


FIGURE 3.02725. EFFECT OF FINISHING TEMPERATURE FOR HOT ROLLING AND COOLING RATE ON PLANE STRAIN CRACK TOUGHNESS OF LABORATORY AIR INDUCTION MELTED PLATE (SEE FIGURE 3.02184 FOR TENSILE PROPERTIES) (40, 48)

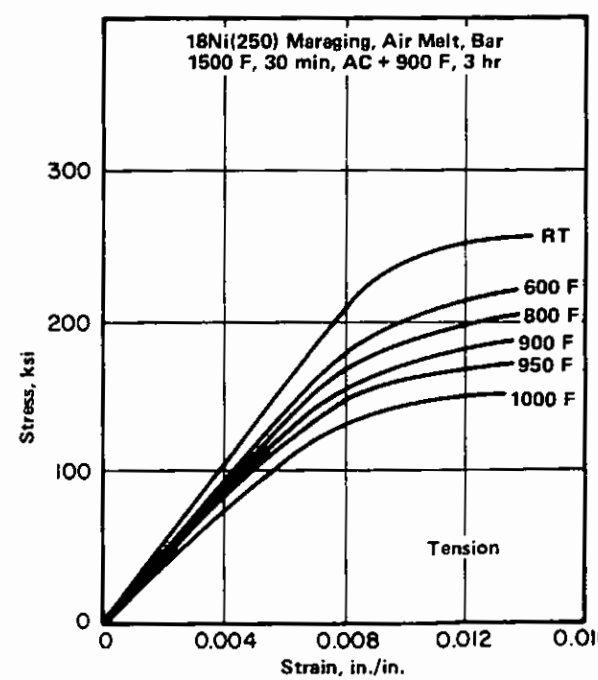


FIGURE 3.0311. STRESS-STRAIN CURVES AT ROOM AND ELEVATED TEMPERATURES FOR AIR MELTED, ANNEALED, AND AGED BAR (6)

	Fe
18	Ni
7.5	Co
5	Mo
	Ti
	Al

18Ni(250) Maraging

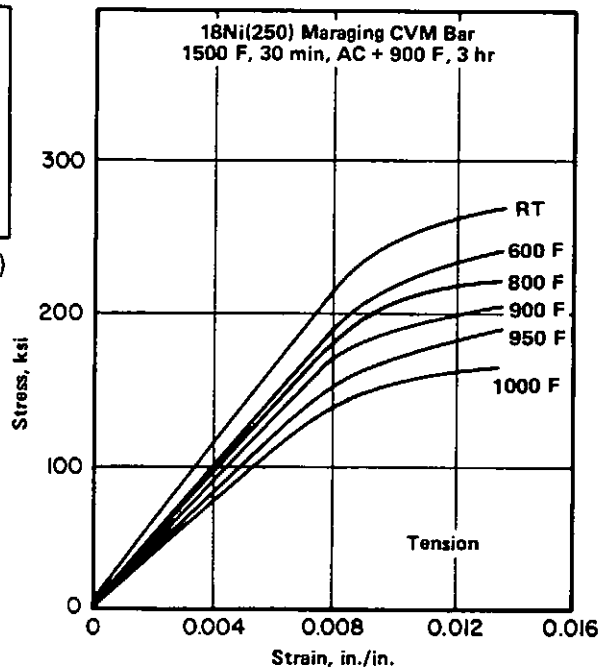


FIGURE 3.0312. STRESS-STRAIN CURVES AT ROOM AND ELEVATED TEMPERATURES FOR CVM BAR (6)

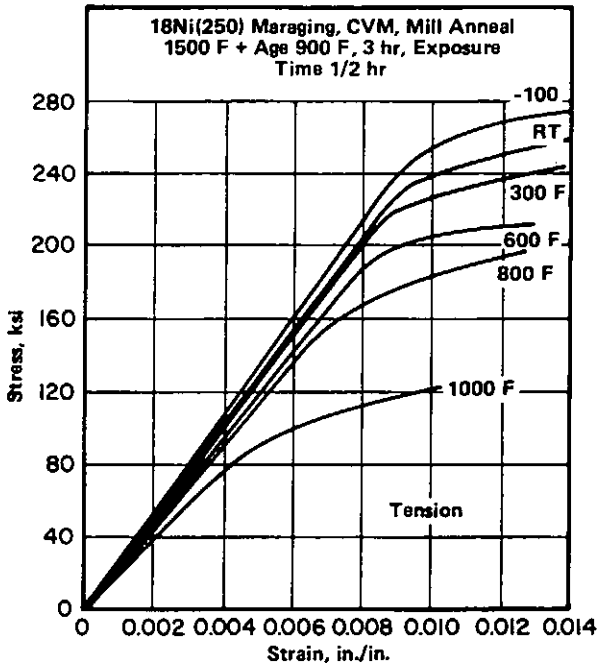


FIGURE 3.0313. TYPICAL STRESS-STRAIN CURVES FOR TENSION AT CRYOGENIC, ROOM, AND ELEVATED TEMPERATURES (25)

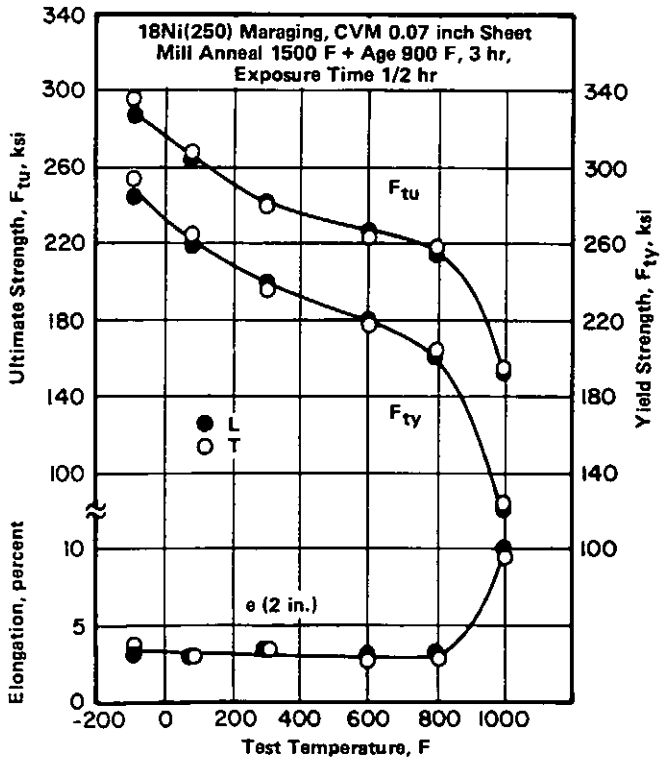


FIGURE 3.0314. EFFECT OF TEST TEMPERATURE ON THE TENSILE PROPERTIES OF SHEET (25)

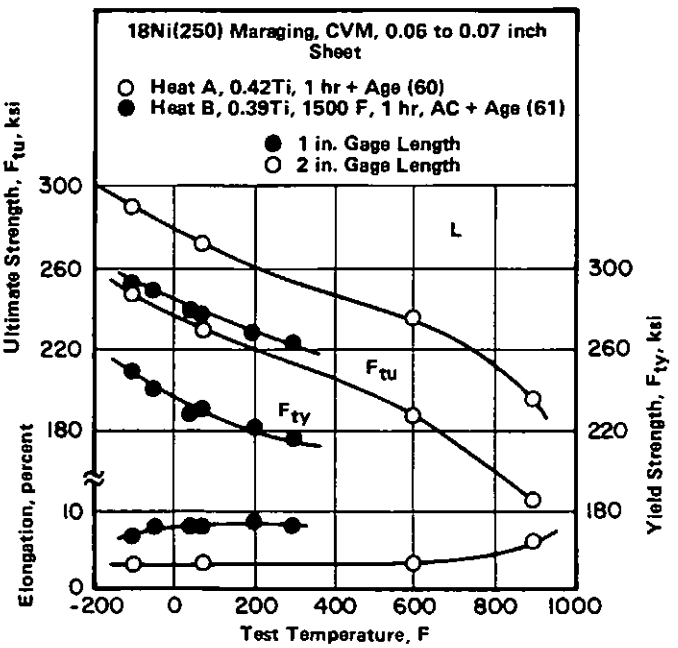


FIGURE 3.0315. EFFECT OF TEST TEMPERATURE ON THE TENSILE PROPERTIES OF TWO HEATS OF CVM SHEET (60, 61)

	Fe
18	Ni
7.5	Co
5	Mo
	Ti
	Al

18Ni(250) Maraging

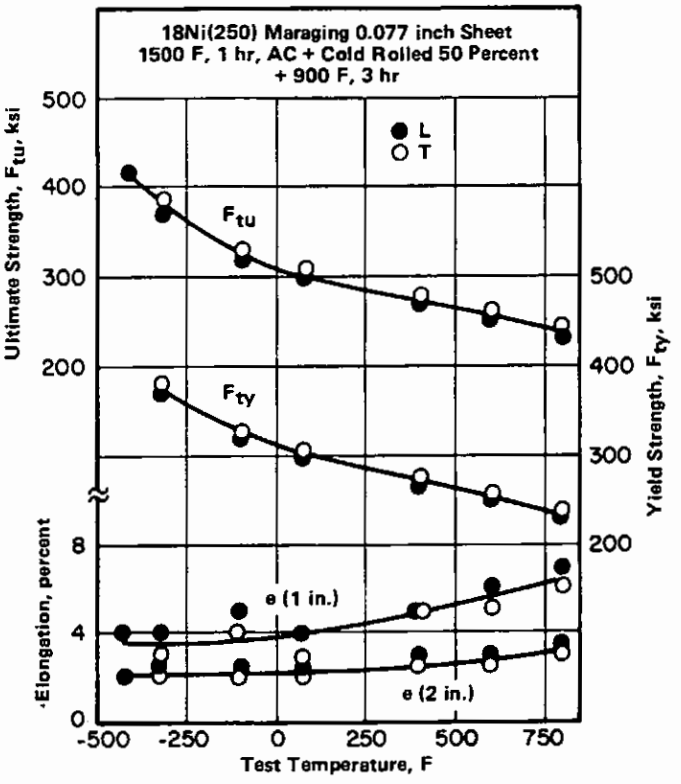


FIGURE 3.0316. INFLUENCE OF TEST TEMPERATURE ON TENSILE PROPERTIES OF COLD ROLLED AND AGED SHEET (65)

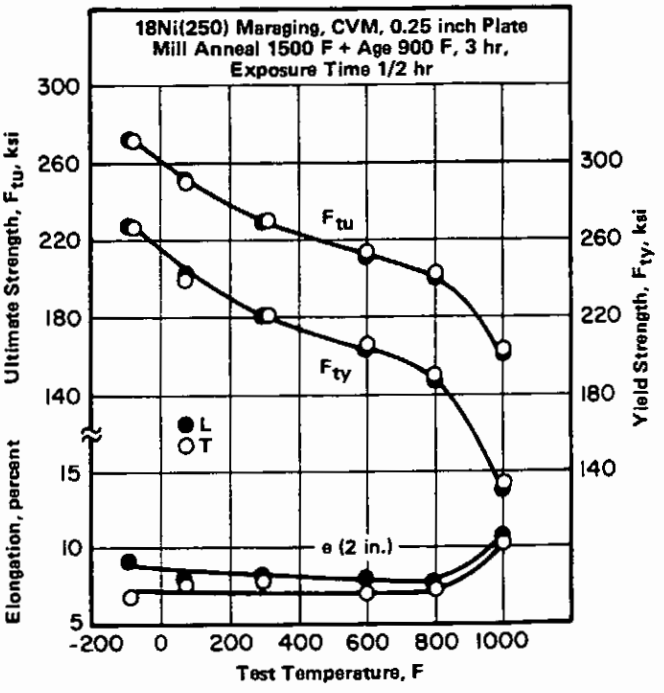


FIGURE 3.0317. EFFECT OF TEST TEMPERATURE ON THE TENSILE PROPERTIES OF PLATE (25)

	Fe
18	Ni
7.5	Co
5	Mo
	Ti
	Al

18Ni(250) Maraging

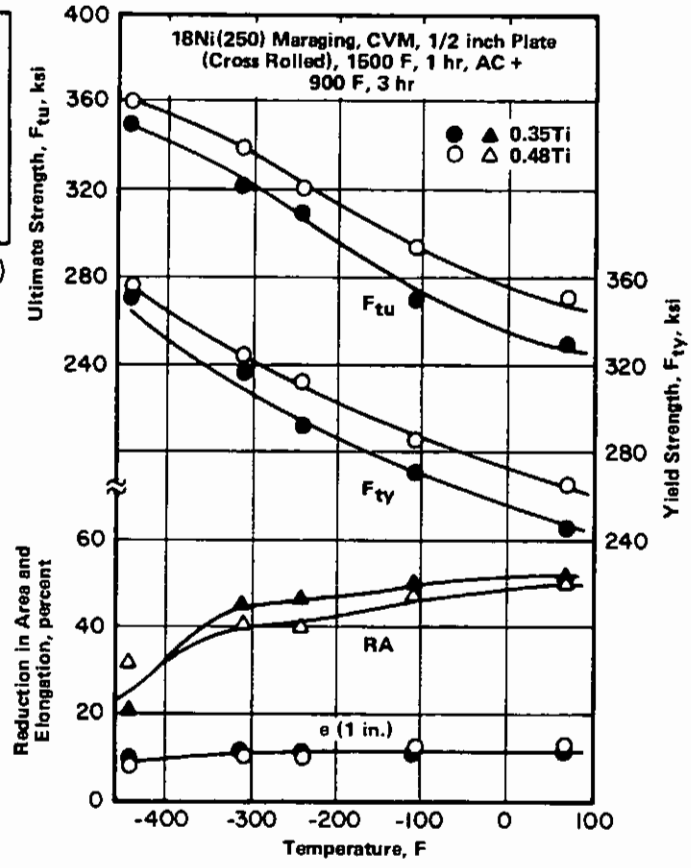


FIGURE 3.0318. EFFECT OF CRYOGENIC TEMPERATURES ON THE TENSILE PROPERTIES OF PLATE AT TWO TITANIUM LEVELS (63)

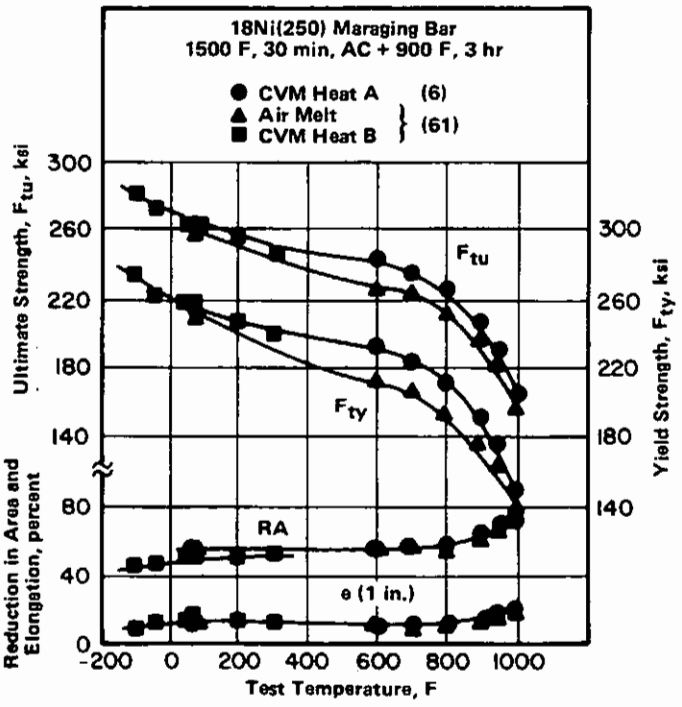


FIGURE 3.0319. EFFECT OF TEST TEMPERATURE ON TENSILE PROPERTIES OF ANNEALED AND AGED BAR (6, 61)

	Fe
18	Ni
7.5	Co
5	Mo
	Ti
	Al

18Ni(250) Maraging

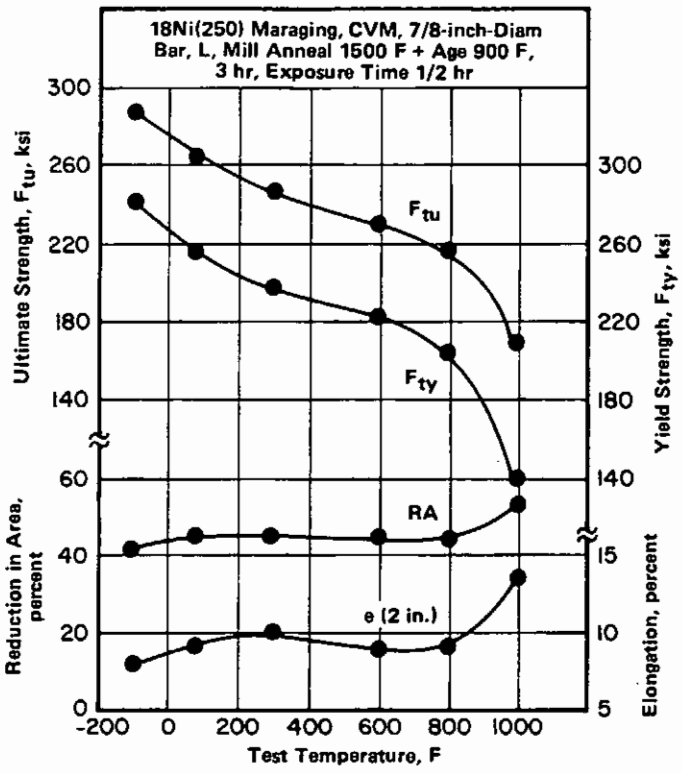


FIGURE 3.03110. EFFECT OF TEST TEMPERATURE ON THE TENSILE PROPERTIES OF BAR (25)

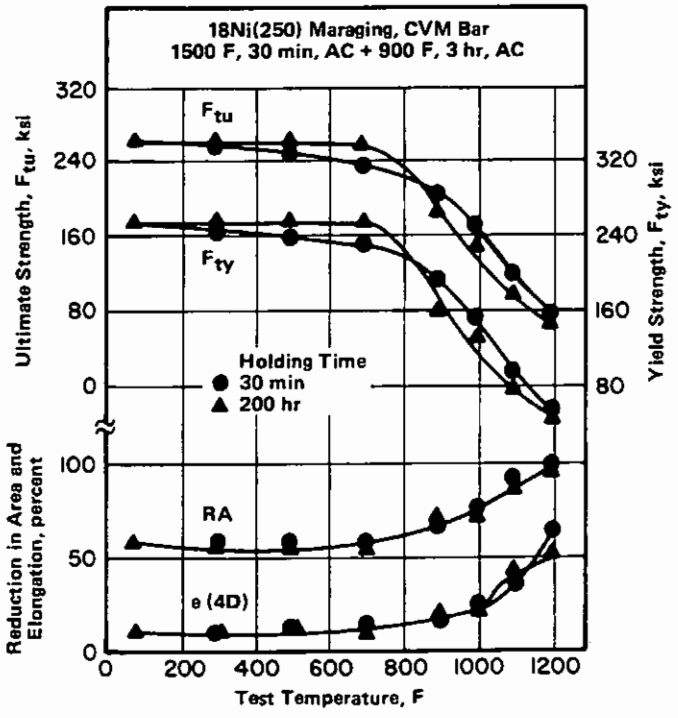


FIGURE 3.03111. EFFECT OF TEST TEMPERATURE ON CVM BAR AFTER HOLDING 30 MINUTES AND 200 HOURS AT TEST TEMPERATURE (64)

Fe
18 Ni
7.5 Co
5 Mo
Ti
Al

18Ni(250) Maraging

Alloy	18Ni(250) Maraging							
Form	CVM, 0.07 inch Sheet							
Condition	Mill Anneal 1500 F + Age, 900 F, 3 hr (RT: F_{tu} = 264 ksi, F_{ty} = 259 ksi, L; F_{tu} = 269 ksi, F_{ty} = 265 ksi, T)							
1000 hour Exposure Temp	600 F		800 F				1000 F	
Test Temp	RT	600 F	RT		800 F		RT	1000 F
Direction	T	T	L	T	L	T	T	T
F_{tu}, ksi	285	243	277	287	218	227	187	130
F_{ty}, ksi	281	234	271	281	198	207	176	97
e (2 in.), percent	3	3	3	3	5	5	8	12

TABLE 3.03112. EFFECT OF 1000 HOUR ELEVATED TEMPERATURE EXPOSURE ON THE TENSILE PROPERTIES OF SHEET AT ROOM TEMPERATURE AND TEST TEMPERATURE (25)

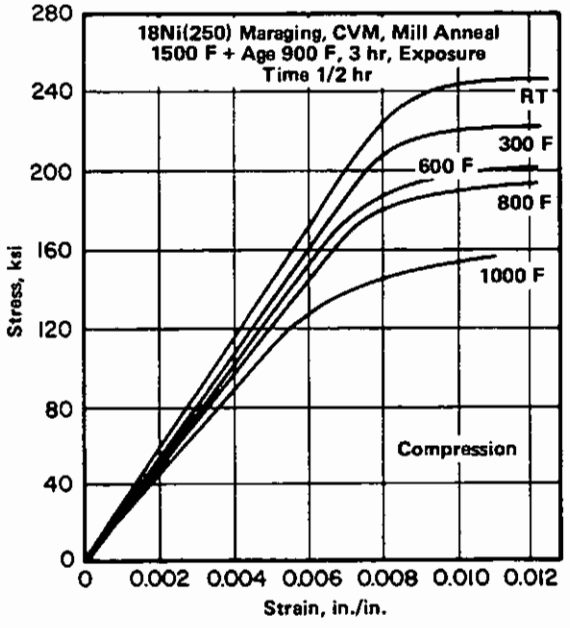


FIGURE 3.0321. TYPICAL STRESS-STRAIN CURVES FOR COMPRESSION AT ROOM AND ELEVATED TEMPERATURES (25)

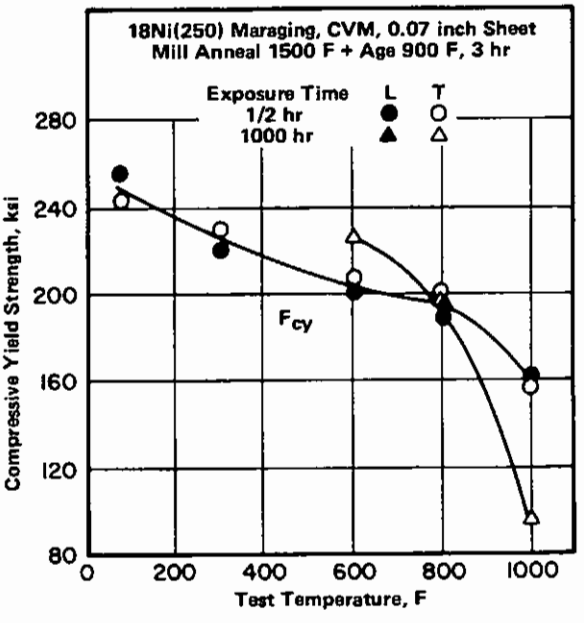


FIGURE 3.0322. EFFECT OF TEST TEMPERATURE ON THE COMPRESSIVE PROPERTIES OF SHEET (25)

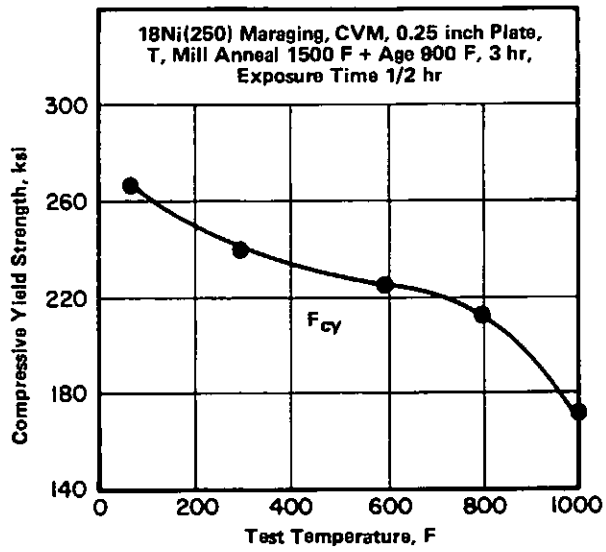


FIGURE 3.0323. EFFECT OF TEST TEMPERATURE ON THE COMPRESSIVE PROPERTIES OF PLATE (25)

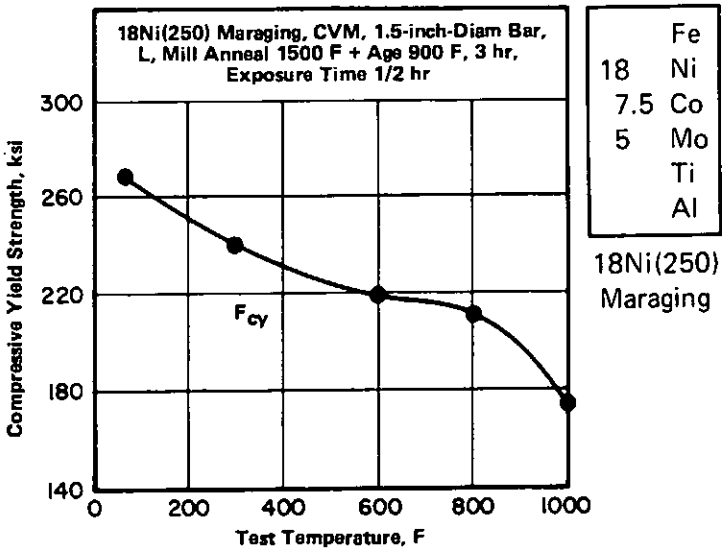


FIGURE 3.0324. EFFECT OF TEST TEMPERATURE ON THE COMPRESSIVE PROPERTIES OF BAR (25)

Alloy	18Ni(250) Maraging					
Form	CVM, 0.07 inch Sheet					
Condition	Mill Anneal 1500 F + Age 900 F, 3 hr					
1000 hour Exposure Temp	(RT Reference)		600 F	800 F		1000 F
Direction	L	T	T	L	T	T
F_{cy}, ksi	255	243	259	254	252	162

TABLE 3.0325. EFFECT OF 1000 HOUR ELEVATED TEMPERATURE EXPOSURE ON THE COMPRESSIVE PROPERTIES OF SHEET AT ROOM TEMPERATURE (25)

	Fe
18	Ni
7.5	Co
5	Mo
	Ti
	Al

18Ni(250) Maraging

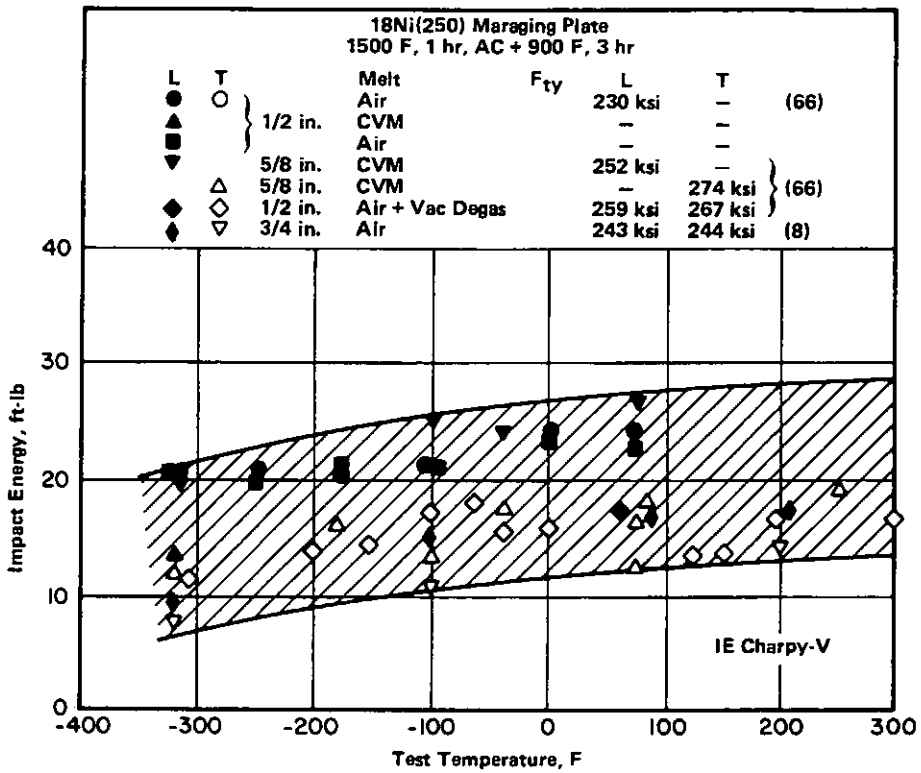


FIGURE 3.0331. EFFECT OF TEST TEMPERATURE ON IMPACT ENERGY OF PLATE FROM SEVERAL HEATS (8, 66)

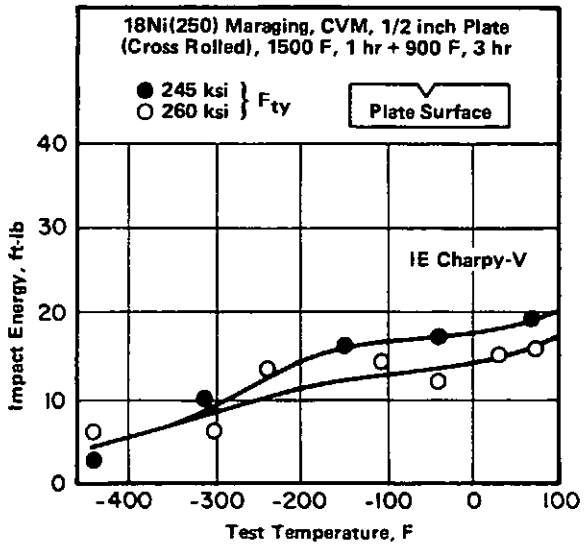


FIGURE 3.0332. EFFECT OF LOW TEST TEMPERATURE ON IMPACT ENERGY OF ANNEALED AND AGED PLATE (63)

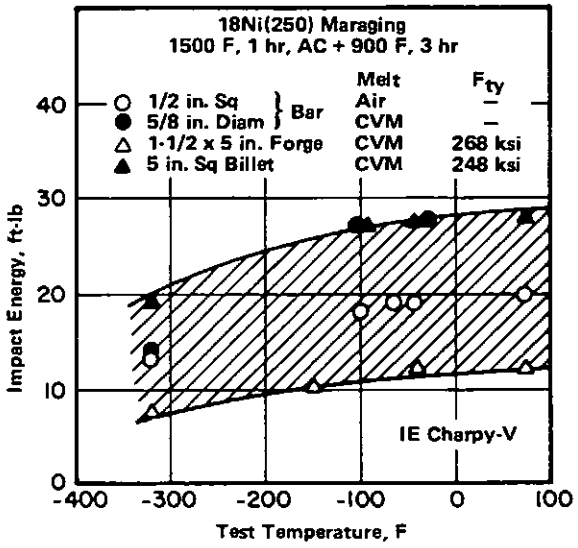


FIGURE 3.0333. EFFECT OF TEST TEMPERATURE ON IMPACT ENERGY OF BAR AND FORGING FROM SEVERAL HEATS (66)

	Fe
18	Ni
7.5	Co
5	Mo
	Ti
	Al

18Ni(250) Maraging

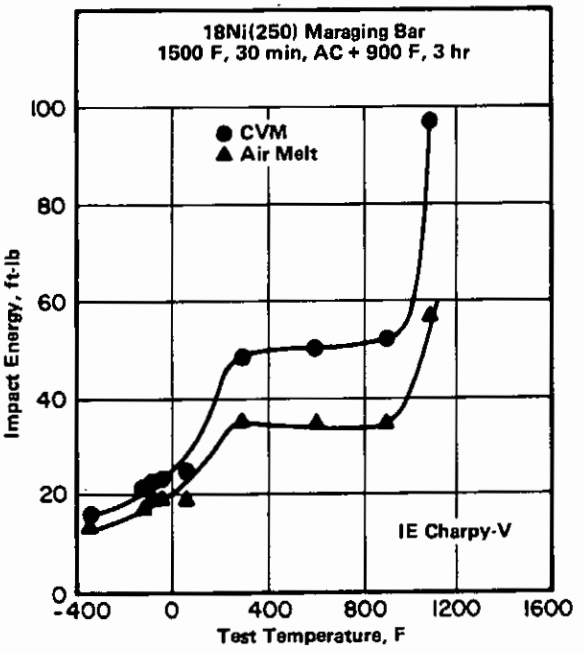


FIGURE 3.0334. EFFECT OF TEST TEMPERATURE ON THE IMPACT ENERGY OF ANNEALED AND AGED BAR (6)

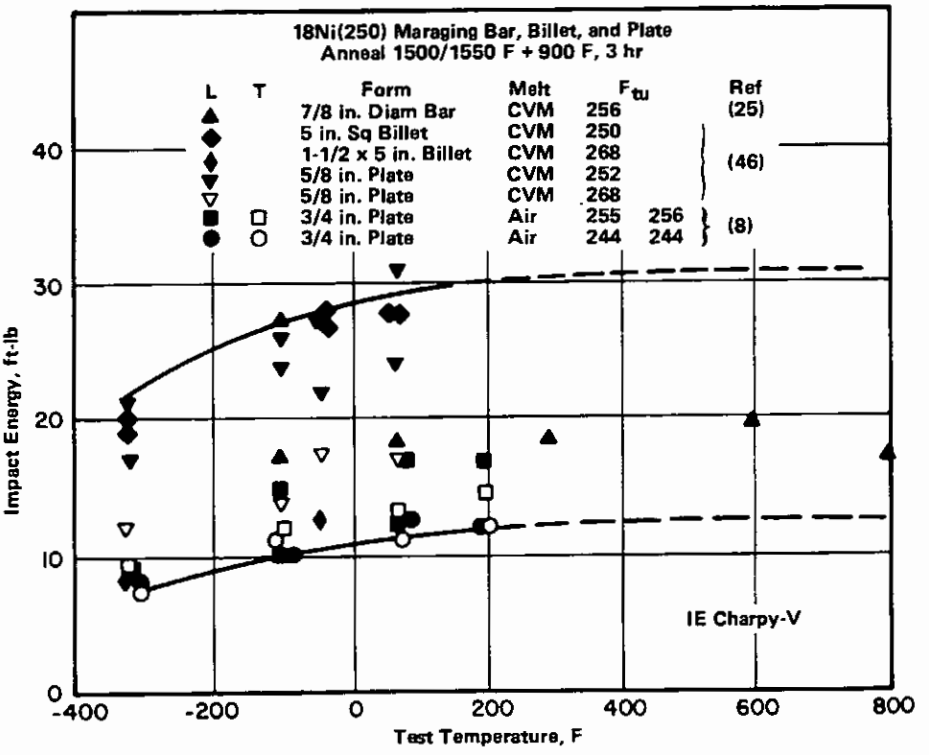


FIGURE 3.0335. EFFECT OF TEST TEMPERATURE ON THE IMPACT ENERGY OF BAR, BILLET, AND PLATE FROM SEVERAL HEATS (8, 25, 46)

18	Fe
7.5	Ni
5	Co
	Mo
	Ti
	Al

18Ni(250) Maraging

Alloy	18Ni(250) Maraging					
Form	Cast					
Condition	2100 F, 4 hr, AC + 900 F, 3 hr					
Thickness, in.	1		2		3	
F_{ty}, ksi	230	250	230	250	230	250
Charpy-V, ft-lb						
RT	13	17	10	16	10	16
-40 F	12	17	8	14	8	10

TABLE 3.0336. IMPACT ENERGY OF CASTINGS AT ROOM AND LOW TEMPERATURES (66)

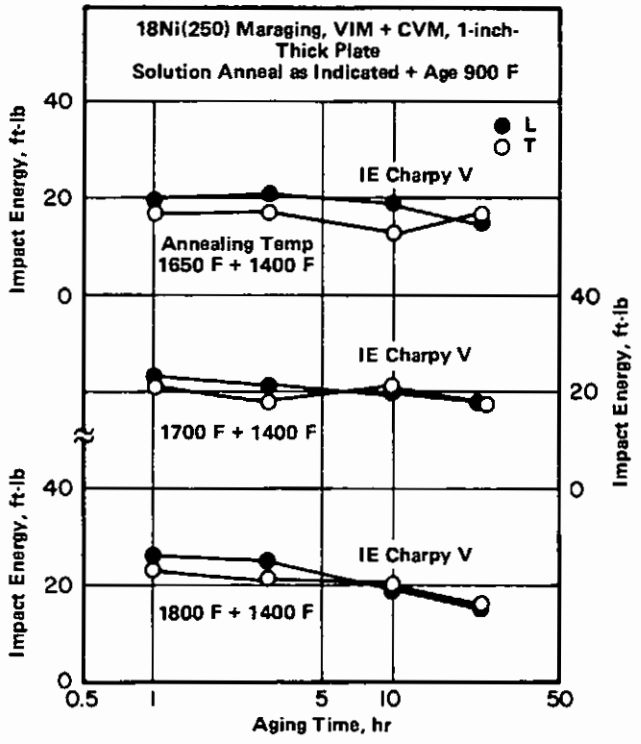


FIGURE 3.0337. EFFECTS OF SOLUTION ANNEALING TEMPERATURE AND AGING TIME ON THE IMPACT PROPERTIES OF VIM + CVM PLATE AT +30 F (38) (SEE FIGURE 3.02171 FOR ROOM TEMPERATURE TENSILE PROPERTIES)

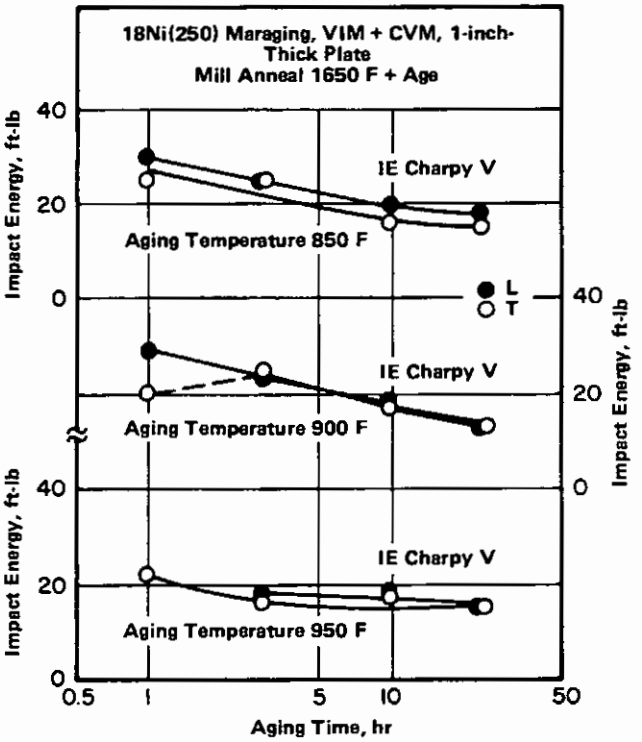


FIGURE 3.0338. EFFECT OF AGING TEMPERATURE AND TIME ON THE IMPACT PROPERTIES OF VIM + CVM PLATE AT +30 F (38)

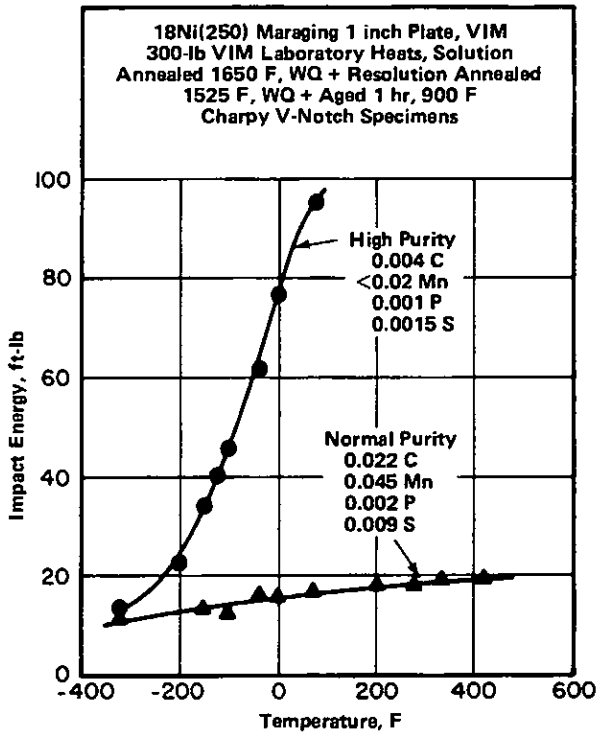
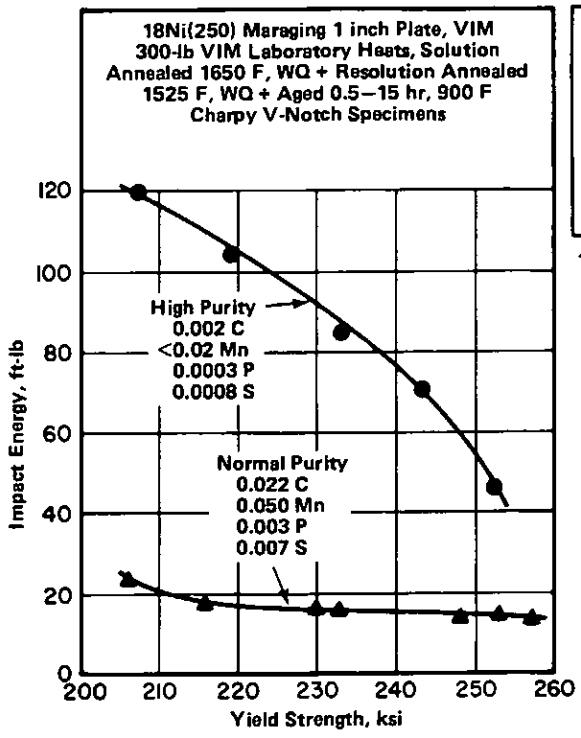


FIGURE 3.03391. EFFECTS OF PURITY AND TEMPERATURE ON THE IMPACT ENERGY OF ANNEALED AND AGED PLATE (94)



Fe
18 Ni
7.5 Co
5 Mo
Ti
Al

18Ni(250) Maraging

FIGURE 3.03392. EFFECT OF PURITY ON THE RELATION BETWEEN IMPACT ENERGY AND YIELD STRENGTH AT ROOM TEMPERATURE (94)

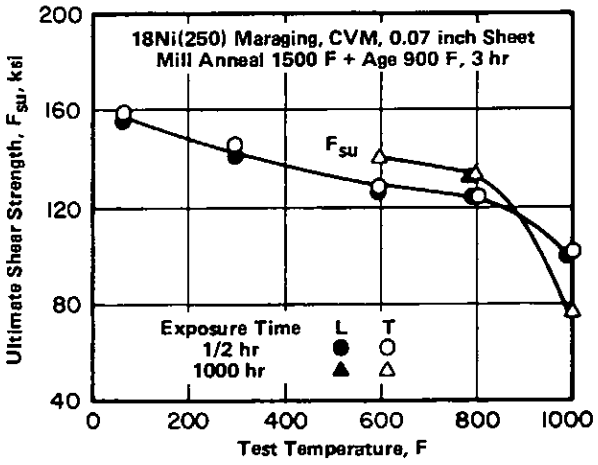


FIGURE 3.0351. EFFECT OF TEST TEMPERATURE ON THE SHEAR ULTIMATE STRENGTH OF SHEET (25)

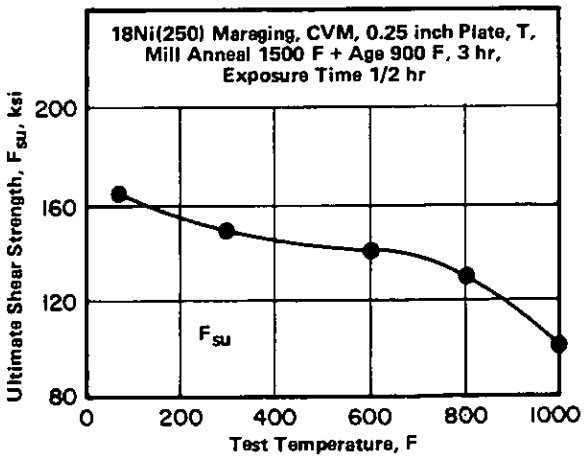


FIGURE 3.0352. EFFECT OF TEST TEMPERATURE ON THE SHEAR ULTIMATE STRENGTH OF PLATE (25)

	Fe
18	Ni
7.5	Co
5	Mo
	Ti
	Al

18Ni(250) Maraging

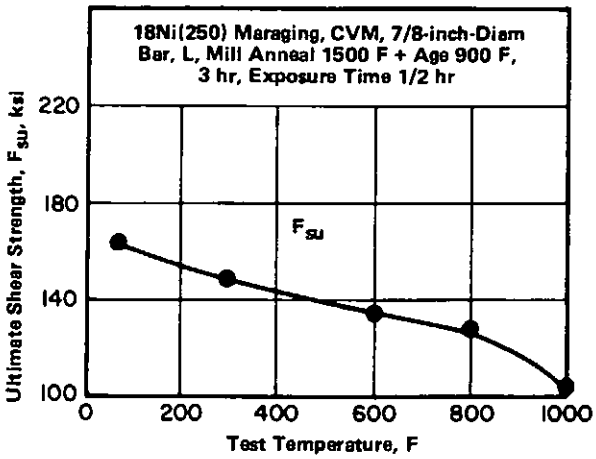


FIGURE 3.0353. EFFECT OF TEST TEMPERATURE ON THE SHEAR ULTIMATE STRENGTH OF BAR (25)

Alloy	18Ni(250) Maraging					
Form	CVM, 0.07 inch Sheet					
Condition	Mill Anneal 1500 F + Age 900 F, 3 hr					
1000 hour Exposure Temp	(RT Reference)		600 F	800 F		1000 F
Direction	L	T	T	L	T	T
F_{su}, ksi	155	158	169	175	170	121

TABLE 3.0354. EFFECT OF 1000 HOUR ELEVATED TEMPERATURE EXPOSURE ON THE SHEAR ULTIMATE STRENGTH OF SHEET AT ROOM TEMPERATURE (25)

	Fe
18	Ni
7.5	Co
5	Mo
	Ti
	Al

18Ni(250)
Maraging

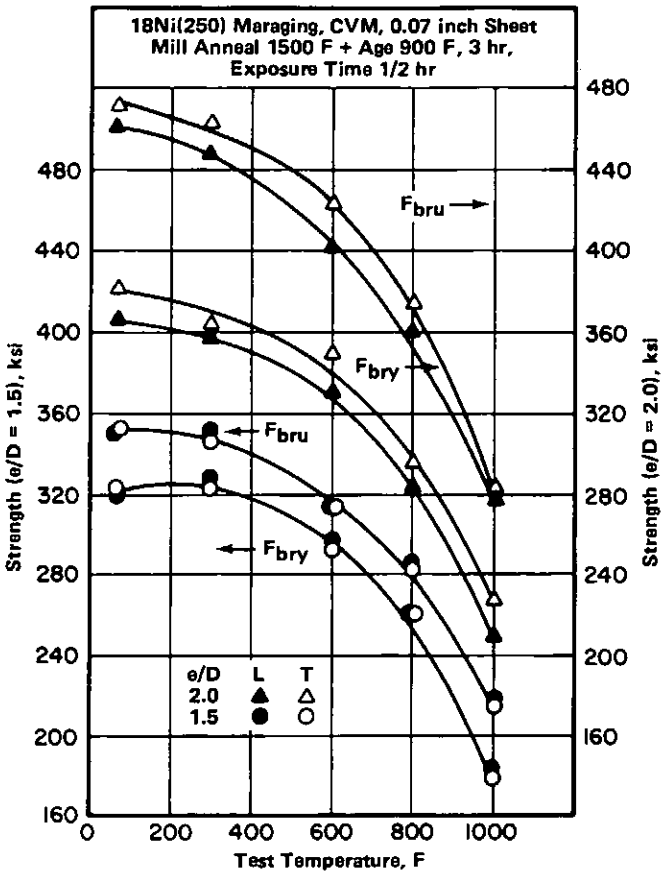


FIGURE 3.0361. EFFECT OF TEST TEMPERATURE ON THE BEARING STRENGTH OF SHEET (25)

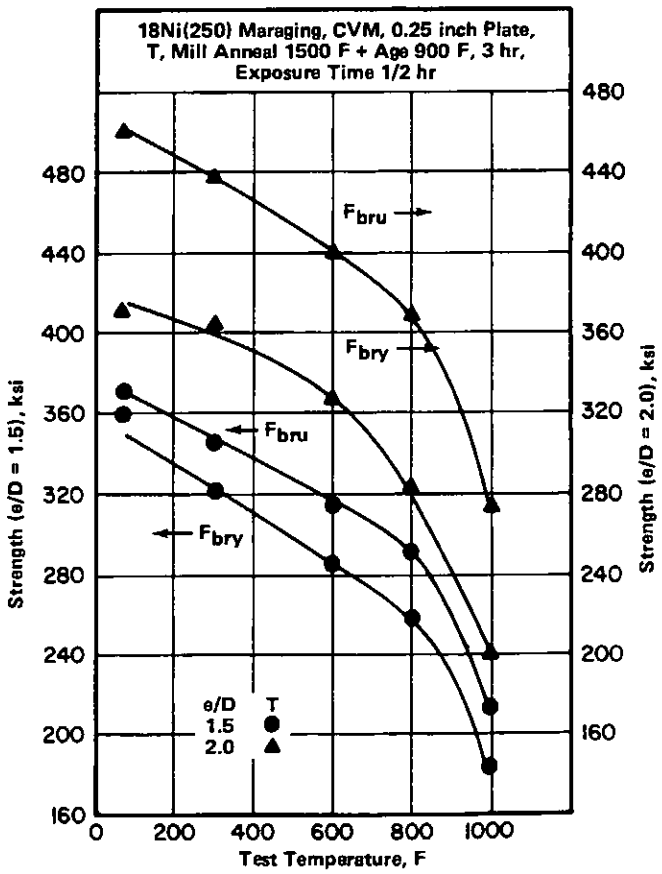


FIGURE 3.0362. EFFECT OF TEST TEMPERATURE ON THE BEARING STRENGTH OF PLATE (25)

	Fe
18	Ni
7.5	Co
5	Mo
	Ti
	Al

18Ni(250) Maraging

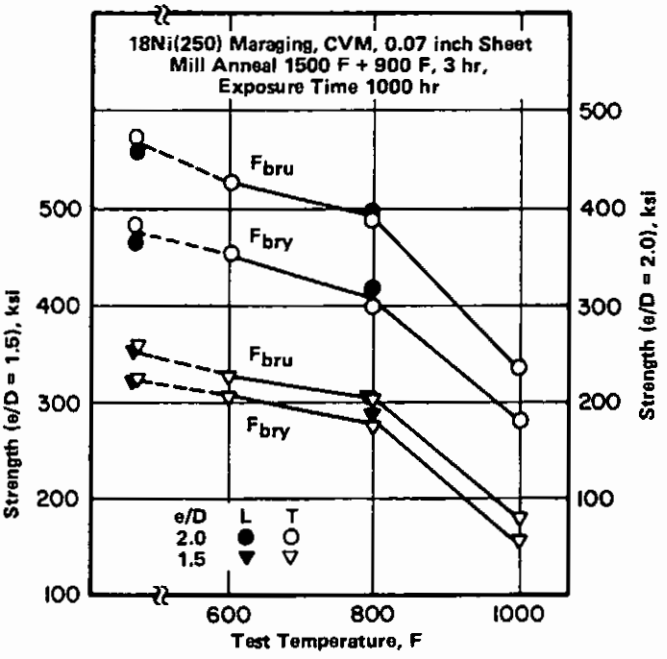


FIGURE 3.0363. EFFECT OF TEST TEMPERATURE ON THE BEARING STRENGTH OF SHEET AFTER HOLDING 1000 HOURS AT TEST TEMPERATURE (25)

Alloy	18Ni(250) Maraging							
Form	0.063 inch Sheet							
Condition	1500 F, 15 min + 900 F, 3 hr							
Test Temp	Room Temperature				-320 F			
Melting Practice	Air Melt		CVM		Air Melt		CVM	
Direction	L	T	L	T	L	T	L	T
F_{tu}, ksi	267	278	273	–	336	348	333	339
F_{ty}, ksi	262	273	267	–	322	336	322	334
e (1 in.), percent	4	3	3.5	–	3	1.5	–	–
Sharp Notch Strength[a], ksi	250	247	257	250	229	238	234	225

(a) Notch tensile specimens, 1 inch wide, with 60° edge notches, notch radii ≈ 0.0006 inch.

TABLE 3.03711. ROOM AND LOW TEMPERATURE SMOOTH AND SHARP NOTCH TENSILE PROPERTIES OF ANNEALED AND AGED SHEET (6)

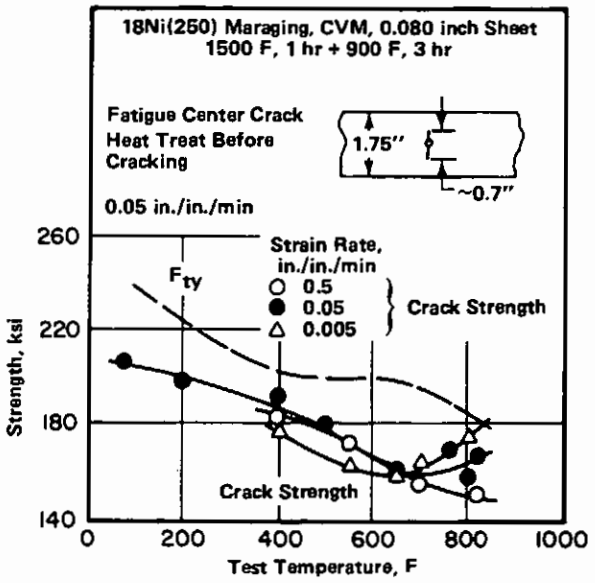


FIGURE 3.03712. EFFECT OF TEST TEMPERATURE AND STRAIN RATE ON CRACK STRENGTH OF ANNEALED AND AGED SHEET (69)

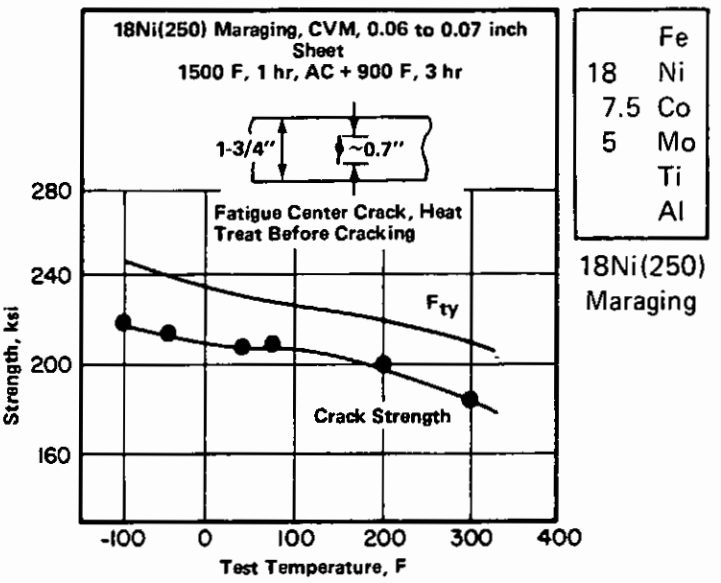


FIGURE 3.03713. EFFECT OF TEST TEMPERATURE ON CRACK STRENGTH OF CVM SHEET (61)

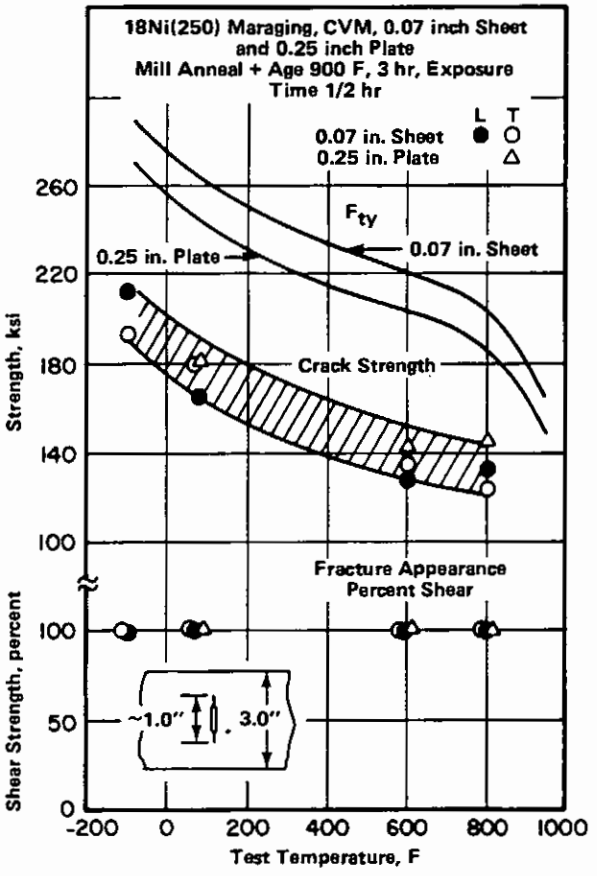


FIGURE 3.03714. EFFECT OF TEST TEMPERATURE ON CRACK STRENGTH OF CVM SHEET AND PLATE (25)

Fe
18 Ni
7.5 Co
5 Mo
Ti
Al

18Ni(250) Maraging

Alloy	18Ni(250) Maraging			
Form	CVM, 1-1/2-inch Diameter Bar, L			
Condition	Mill Anneal + 900 F, 3 hr			
Test Temperature	-100 F	RT	600 F	800 F
F_{ty}[a], ksi	282	256	223	204
Crack Strength, ksi	200	227	202	184

(a) 7/8-inch diameter bar data.

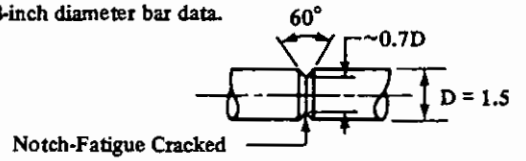


TABLE 3.03715. EFFECT OF TEST TEMPERATURE ON CRACK STRENGTH OF CVM BAR (25)

Alloy	18Ni(250) Maraging					
Form	CVM, 0.07 inch Sheet (T)					
Condition	Mill Anneal 1500 F + Age 900 F, 3 hr (F_{ty} = 265 ksi)					
Temperature	600 F[a]			800 F[a]		
	Time, hr					
Stress, ksi	10	100	1000	10	100	1000
0.05 Percent Creep	205	(195)[b]	–	115	–	–
0.10 Percent Creep	215	205	(195)	130	(105)	–
0.50 Percent Creep	233	230	–	165	140	(110)
1.0 Percent Creep	236	233	(225)	175	150	115

(a) See Figure 3.0314 for tensile properties at these temperatures.
(b) Values in parentheses extrapolated.

TABLE 3.041. CREEP PROPERTIES OF 0.07-INCH-THICK CVM SHEET AT 600 AND 800 F (25)

Alloy	18Ni(250) Maraging						
Form	Air Melt + Vacuum Degas, 1/2 inch Plate (T)						
Condition	Mill Anneal + 900 F, 3 hr (F_{tu} = 274 ksi)						
	Stress Ratio			Stress	Fatigue Life[a] Cycles		
Method	A	R	Stress Concentration	Amplitude, ksi	Medium	Minimum	Maximum
Rotating Beam	∞	-1	K_t = 1 Smooth	120	2.8×10^5	7.5×10^4	2.4×10^6
				115	6.5×10^5	1.2×10^5	8.1×10^6
				110	2.5×10^6	1.3×10^5	1.2×10^7
				105	9.2×10^6	3.2×10^5	2.4×10^7
				102	1.1×10^7	2.5×10^5	2.6×10^7

(a) Forty-eight tests at each stress. Medium represent 50 percent survival.

TABLE 3.0511. SMOOTH FATIGUE STRENGTH OF AIR MELTED AND VACUUM DEGASSED PLATE (71)

Fe
18 Ni
7.5 Co
5 Mo
Ti
Al

18Ni(250) Maraging

Alloy	18Ni(250) Maraging						
Form	Air Melt, 1/2 and 3/4 inch Plates (L)						
Condition	1650 F, 1 hr, WQ + 1510/1530 F, 1 hr, WQ + Indicated Age						
Method	Material[a] and Aging Treatment	Stress Ratio A	Stress Ratio R	Stress Concentration	Fatigue Strength, ksi, at Cycles 10^5	10^6	10^7
Rotating Beam	Steel A			$K_t = 1$			
	900 F, 3 hr, AC	∞	-1	Smooth	141	105	100
	850 F, 48 hr, AC				136	111	103
	Steel B						
	900 F, 3 hr, AC				134	108	103
	850 F, 48 hr, AC				143	114	108
	Steel A			Notched			
	900 F, 3 hr, AC			$K_t = 3$	56	46	45
	850 F, 48 hr, AC				70	65	63
	Steel B						
	900 F, 3 hr, AC				58	55	54
	850 F, 48 hr, AC				56	46	45

(a) Steel A – 0.35 percent Ti, F_{tu} = 261 ksi, F_{ty} = 251 ksi for 900 F, 3 hr, AC.
F_{tu} = 288 ksi, F_{ty} = 276 ksi for 850 F, 48 hr, AC.
Steel B – 0.42 percent Ti, F_{tu} = 264 ksi, F_{ty} = 256 ksi for 900 F, 3 hr, AC.
F_{tu} = 281 ksi, F_{ty} = 274 ksi for 850 F, 48 hr, AC.

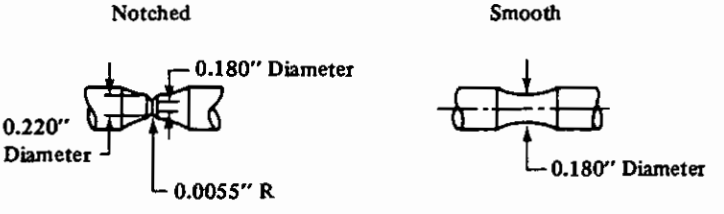


TABLE 3.0512. SMOOTH AND NOTCHED FATIGUE STRENGTH OF AIR MELTED PLATE (40)

Alloy	18Ni(250) Maraging									
Form	5/8-inch-Diameter Bar (L)									
Condition	1500 F, 1 hr, AC + 900 F, 3 hr, AC									
Method	Melting Practice	Stress Ratio A	Stress Ratio R	Stress Concentration	Fatigue Strength, ksi, at Cycles 10^3	10^4	10^5	10^6	10^7	10^8
Rotating Beam	Air Melt[a]	∞	-1	$K_t = 1$	(210)[b]	170	140	125	116	113
	CVM[a]			Smooth	200	160	135	120	115	110
	Air Melt	∞	-1	$K_t = 2.2$	–	100	70	57	55	55
	CVM			Notched	–	100	70	57	55	55

(a) Air melt = 0.43 percent Ti, F_{tu} = 270 ksi, F_{ty} = 263 ksi
CVM = 0.35 percent Ti, F_{tu} = 250 ksi, F_{ty} = 246 ksi.
(b) Values in parentheses extrapolated.

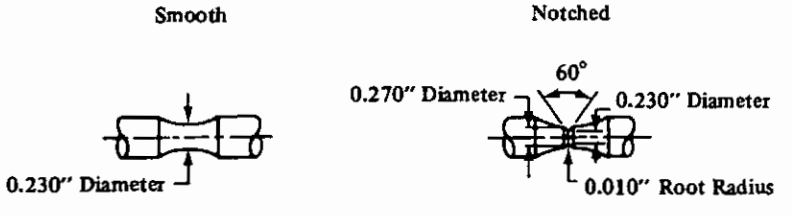


TABLE 3.0513. SMOOTH AND NOTCHED FATIGUE STRENGTH OF ANNEALED AND AGED BAR (70)

Fe
18 Ni
7.5 Co
5 Mo
Ti
Al

18Ni(250) Maraging

Alloy		18Ni(250) Maraging						
Form		CVM, 0.07 inch Sheet						
Condition		Mill Anneal 1500 F + Age 900 F, 3 hr						
Method		Axial Load (Smooth and Double Edge Notch Specimens)						
Stress Ratio		Test Temp,	Stress		Fatigue Strength[a], ksi, at Cycles			
A	R	F	Concentration	Direction	10^4	10^5	10^6	10^7
∞	-1	RT	Smooth[c]	L	125	85	55	45
				T	126	84	48	40
			Notched[d]	L and T	60	36	25	22
		600	Smooth[c]	L	90	60	50	46
				T	86	64	61	60
			Notched[d]	L and T	53	35	25	23
		800	Smooth[c]	L	83	68	64	(64)[b]
				T	80	64	60	(58)
			Notched[d]	L and T	52	34	28	26
0.98	0.01	RT	Smooth[c]	T	150	72	52	50
			Notched[d]	T	70	36	24	20
		600	Smooth[c]	T	120	80	72	70
			Notched[d]	T	70	38	28	26
		800	Smooth[c]	T	120	87	84	81
			Notched[d]	T	65	46	43	41
0.67	0.20	RT	Smooth[c]	T	165	84	58	52
			Notched[d]	T	86	42	30	30
		600	Smooth[c]	T	(135)	90	66	60
			Notched[d]	T	74	43	40	40
		800	Smooth[c]	T	143	125	110	93
			Notched[d]	T	67	44	34	30

(a) Based on limited number of tests.
(b) Values in parentheses extrapolated.
(c) $K_t = 1$.
(d) $K_t = 3$.

TABLE 3.0514. SMOOTH AND NOTCHED AXIAL-LOAD FATIGUE STRENGTH OF 0.07-INCH-THICK SHEET AT ROOM AND ELEVATED TEMPERATURES (25)

Alloy	18Ni(250) Maraging				
Form	CVM, 3/4 inch Plate (L)				
Method	Axial Load (Smooth, $K_t = 1$)				
	Mean Stress,	Fatigue Strength, ksi, at Cycles			
Condition	ksi	10^4	10^5	10^6	10^7
Mill Annealed					
F_{tu} = 140 ksi	50	100	65	45	40
Mill Anneal + 900 F,					
3 hr	0	150	120	96	–
F_{tu} = 250 ksi	50	150	100	80	–

TABLE 3.0515. SMOOTH FATIGUE STRENGTH OF MILL-ANNEALED AND ANNEALED-AND-AGED PLATE (72)

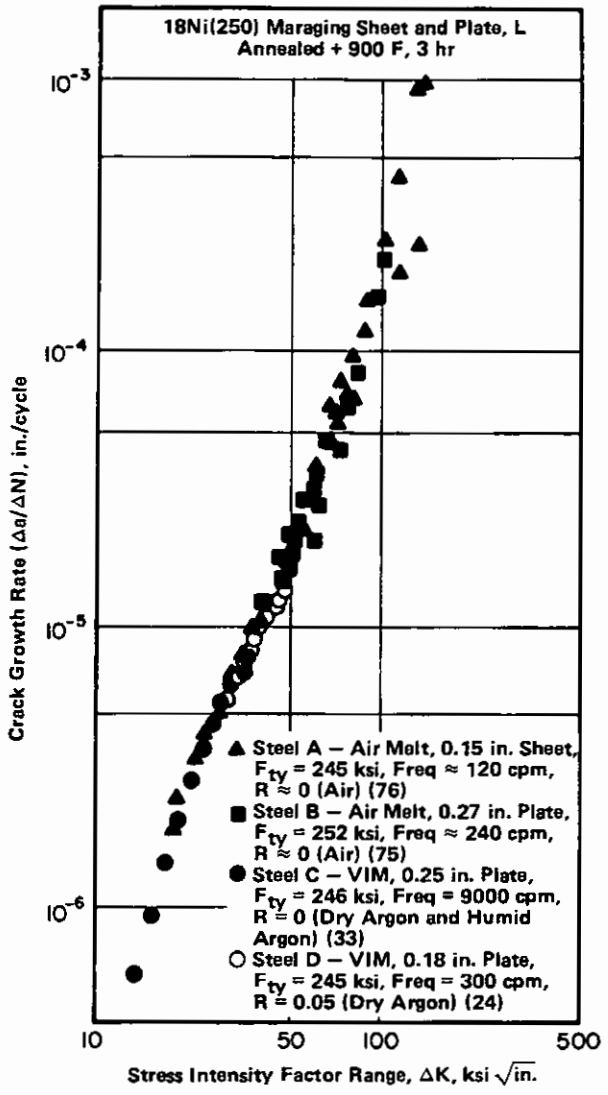


FIGURE 3.0521. INFLUENCE OF STRESS INTENSITY FACTOR (ΔK) AND TEST ENVIRONMENT ON FATIGUE CRACK PROPAGATION OF SHEET AND PLATE AT ROOM TEMPERATURE (24, 33, 75, 76)

	Fe
18	Ni
7.5	Co
5	Mo
	Ti
	Al

18Ni(250) Maraging

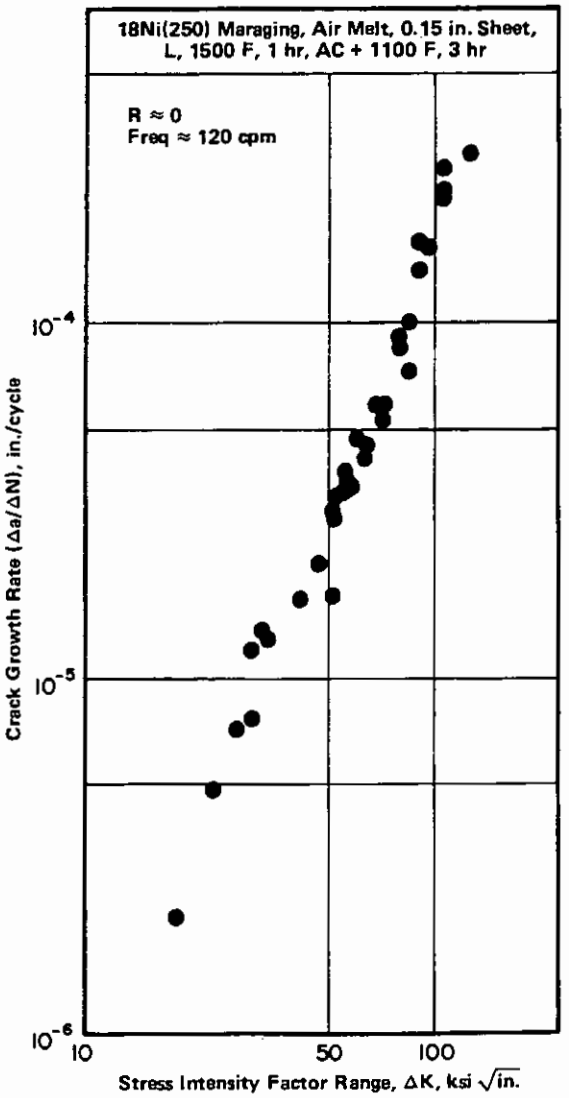


FIGURE 3.0522. FATIGUE CRACK PROPAGATION AT ROOM TEMPERATURE IN SHEET AGED AT 1100 F (76)

	Fe
18	Ni
7.5	Co
5	Mo
	Ti
	Al

18Ni(250) Maraging

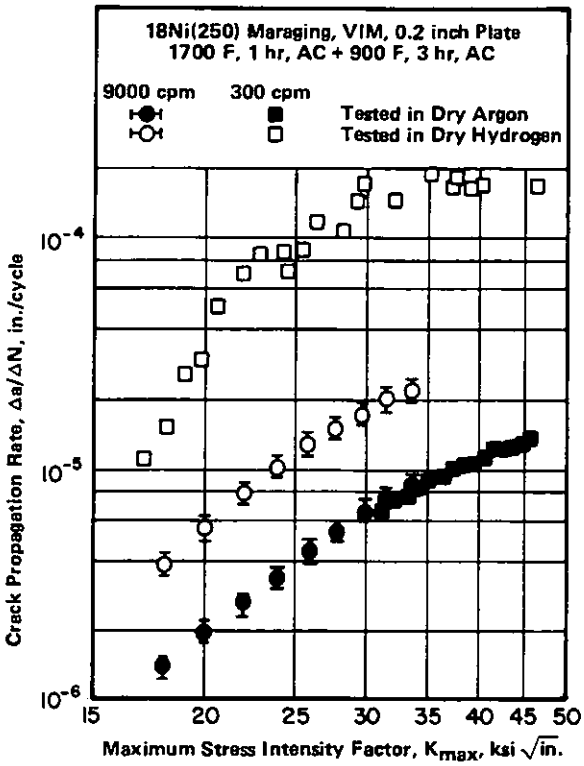


FIGURE 3.0523. INFLUENCE OF TEST FREQUENCY ON FATIGUE CRACK PROPAGATION IN DRY HYDROGEN (AT ROOM TEMPERATURE AND 1 ATMOSPHERE PRESSURE) (23, 24)

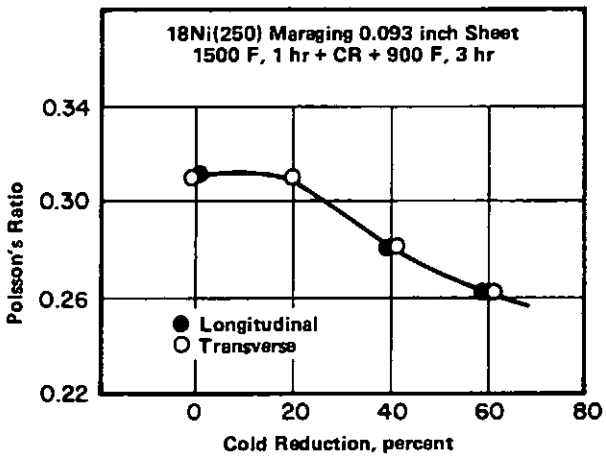


FIGURE 3.0611. EFFECT OF COLD ROLLING PRIOR TO AGING ON POISSON'S RATIO (63)

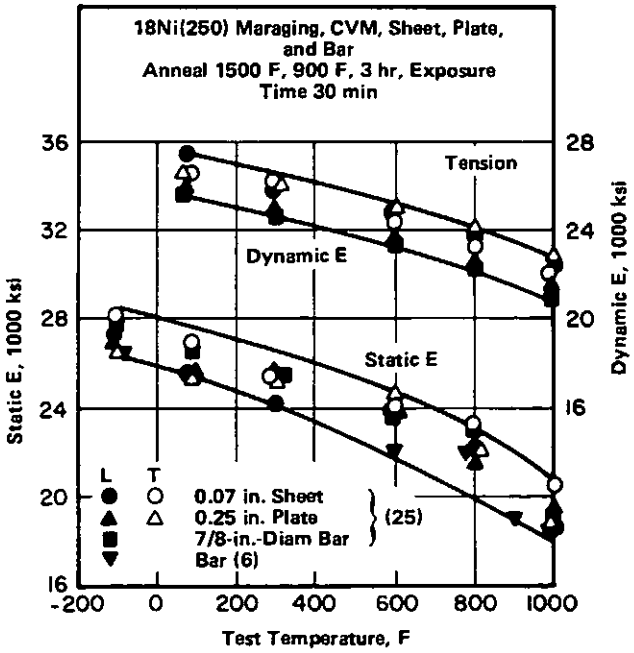


FIGURE 3.0621. STATIC AND DYNAMIC MODULI FOR TENSION AT CRYOGENIC, ROOM, AND ELEVATED TEMPERATURES (6, 25)

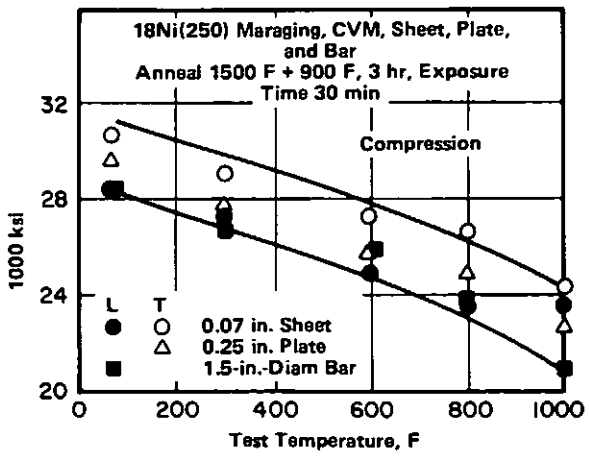


FIGURE 3.0622. STATIC MODULI FOR COMPRESSION AT ROOM AND ELEVATED TEMPERATURES (25)

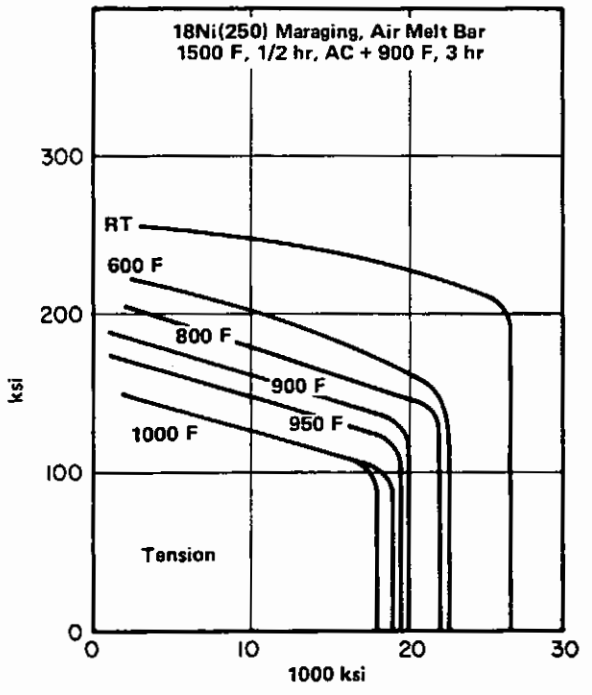
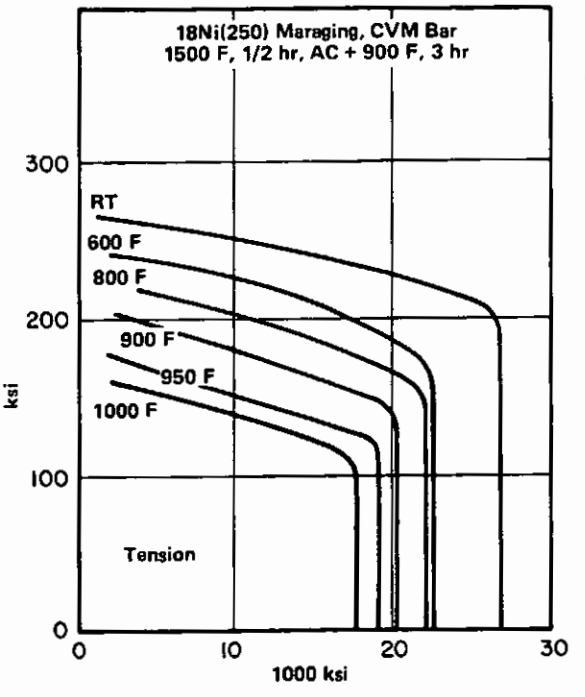


FIGURE 3.0641. TANGENT MODULUS CURVES AT ROOM AND ELEVATED TEMPERATURES FOR AIR MELT, ANNEALED, AND AGED BAR (6)



	Fe
18	Ni
7.5	Co
5	Mo
	Ti
	Al

18Ni(250) Maraging

FIGURE 3.0642. TANGENT MODULUS CURVES AT ROOM AND ELEVATED TEMPERATURES FOR CVM ANNEALED AND AGED BAR (6)

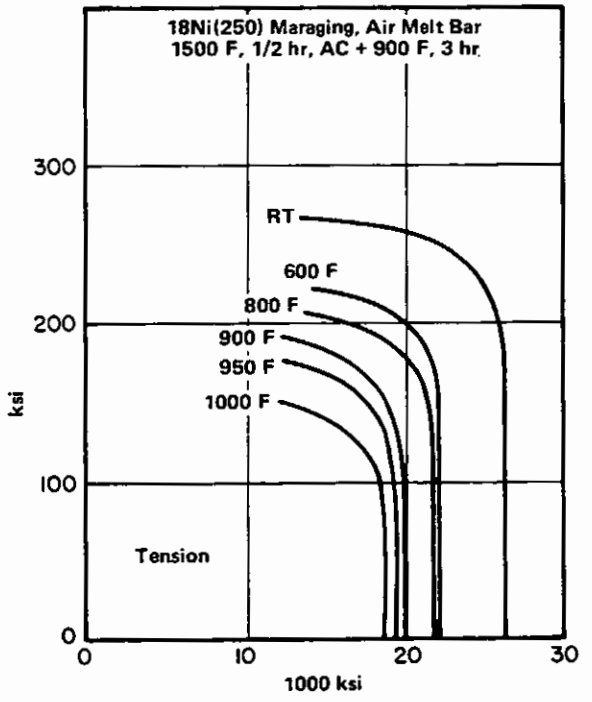


FIGURE 3.0651. SECANT MODULUS CURVES AT ROOM AND ELEVATED TEMPERATURES FOR AIR MELT, ANNEALED, AND AGED BAR (6)

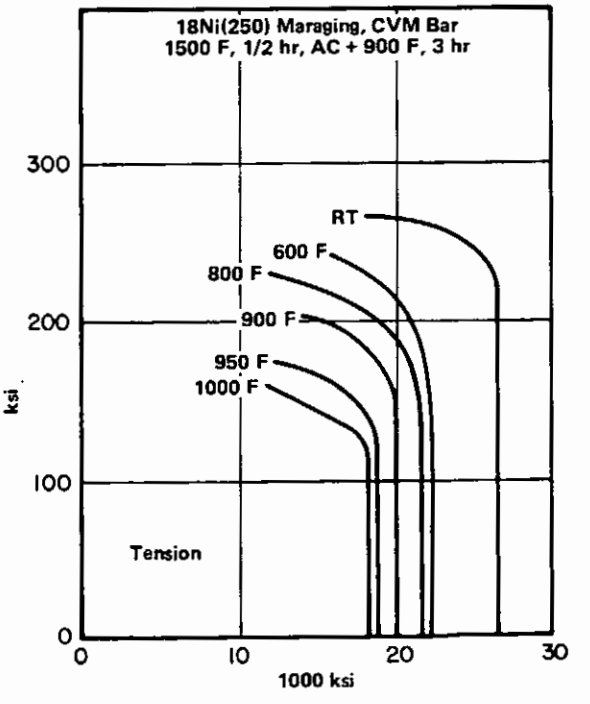


FIGURE 3.0652. SECANT MODULUS CURVES AT ROOM AND ELEVATED TEMPERATURES FOR CVM ANNEALED AND AGED BAR (6)

Fe
18 Ni
7.5 Co
5 Mo
Ti
Al

18Ni(250) Maraging

Alloy	18Ni(250) Maraging			
	Wrought[a]		PM-HIP[b]	
Heat Treatment	F_{ty}, ksi	Reduction in Area, percent	F_{ty}, ksi	Reduction in Area, percent
Solution Annealed (S) 1 hr, 1700 F, AC + 1 hr, 1500 F, AC	115	85	113	80
S + 3 hr, 900 F	244	62	247	0.2
S + 3 hr, 950 F	240	53	256	1
S + 10 min, 930 F + 3 hr, 900 F	238	62	220	40
S + 10 min, 975 F + 3 hr, 900 F	236	67	240	47
S + 10 min, 1005 F + 3 hr, 900 F	223	69	232	40
S + 10 min, 1040 F + 3 hr, 900 F	236	59	240	27

(a) Commercial bar stock.
(b) Prealloyed powder, hot isostatically pressed 3 hr, 2012 or 2192 F at 30 ksi argon pressure. Compacts were approximately 0.8 inch diameter by 4.0 inch long.

TABLE 4.0142. TENSILE PROPERTIES OF ALLOY CONSOLIDATED FROM ROTATING ELECTRODE PROCESS POWDER (96)

Alloy	18Ni(250) Maraging			
Hot Isostatic Pressing Temperature, F[a]	Tensile Properties			Charpy Impact Energy, ft-lb
	F_{tu}, ksi	F_{ty}, ksi	Reduction in Area, percent	
Solution Annealed 1 hr, 1700 F + 1 hr, 1500 F				
(b)	139	140	85	16
1850	139	140	62	1
2000	142	144	74	14
2100	138	139	76	12
2200	137	138	76	15
2300	139	140	77	15
Solution Annealed + Aged 3 hr, 900 F				
(b)	252	254	57	5
1850	188	188	0	1
2000	234	237	42	3
2100	241	242	51	3
2200	248	250	52	4
2300	242	245	54	4
Solution Annealed + Aged 10 min, 980 F + 3 hr, 900 F				
(b)	251	256	58	4
1850	214	214	3	1
2000	247	252	38	2
2100	245	250	52	4
2200	242	246	55	4
2300	248	261	50	4

(a) Hot isostatically pressed at gas pressure of 15 ksi for 3 hours. Compacts were approximately 1.0 inch diameter by 18 inch long.
(b) Commercial wrought bar stock.

TABLE 4.0143. TENSILE AND IMPACT PROPERTIES OF ALLOY CONSOLIDATED FROM INERT GAS ATOMIZED POWDER (97)

Fe
18 Ni
7.5 Co
5 Mo
Ti
Al

18Ni(250) Maraging

Alloy	18Ni(250) Maraging		
Form	1/2 inch Plate		0.07 inch Sheet
Condition	1500 F, 1 hr, AC + 900 F, 3 hr + Weld + 900 F, 3 hr		1500 F, 1 hr, AC + Weld + 900 F, 3 hr
Process	Coated Electrode[a]	GMA	GTA
Wire	Fe-18Ni-8Co-4.5Mo-2.2Ti-0.2Al	Fe-18Ni-8Co-4.5Mo-0.5Ti-0.2Al	Fe-18Ni-7.5Co-4.9Mo-0.5Ti
F_{tu}[b], ksi	242	235	241
F_{ty}, ksi	228	220	232
e (1.4 in.), percent	9	7	3.6 (2 in.)
RA, percent	39	30	–
RT Charpy-V[c], ft-lb	10	15	–

(a) Coating – calcium carbonate and cryolite bonded with sodium silicate.
(b) Specimens transverse to weld.
(c) Notch at weld centerline and perpendicular to plate surface.

TABLE 4.0351. TYPICAL TENSILE AND IMPACT PROPERTIES AND RECOMMENDED WIRE COMPOSITIONS FOR WELDING SHEET AND PLATE (17)

Alloy	18Ni(250) Maraging			
Form	Air Melt, 3/4 inch Plate			
Condition	1650 F, 1 hr, WQ + 1530 F, 1 hr, WQ + Weld + 900 F, 3 hr			
Process	GTA[b]		SA[c]	
Wire	Fe-18Ni-8Co-5Mo-0.5Ti-0.1Al (0.004C)		Fe-18Ni-9Co-4.5Mo-0.7Ti-0.15Al (0.02C)	
Weld Orientation	Parallel to Plate Rolling Direction	Perpendicular to Plate Rolling Direction	Parallel to Plate Rolling Direction	Perpendicular to Plate Rolling Direction
F_{tu}[a], ksi	242	245	249	246
F_{ty}, ksi	237	242	238	235
e (2 in.), percent	6	6.5	3.5	4.0
RA, percent	32	32	20	21
IE Charpy-V[d] at +80 F, ft-lb	11	–	6	5

(a) Transverse to weld.
(b) Specimens failed in weld metal.
(c) Specimens failed in HAZ of base plate.
(d) Notch at weld centerline and perpendicular to plate surface.

Note: Base plate properties: Longitudinal – F_{tu} = 262 ksi, F_{ty} = 254 ksi, e (2 in.) = 9.5 percent, RA = 45 percent, and IE Charpy-V (+80 F) = 15 ft-lb. Transverse – F_{tu} = 265 ksi, F_{ty} = 257 ksi, e (2 in.) = 8.8 percent, RA = 41 percent, and IE Charpy-V (+80 F) = 14 ft-lb.

TABLE 4.0352. TYPICAL TENSILE AND IMPACT PROPERTIES OF GTA AND SUBMERGED ARC (SA) PLATE WELDMENTS (78)

	Fe
18	Ni
7.5	Co
5	Mo
	Ti
	Al

18Ni(250) Maraging

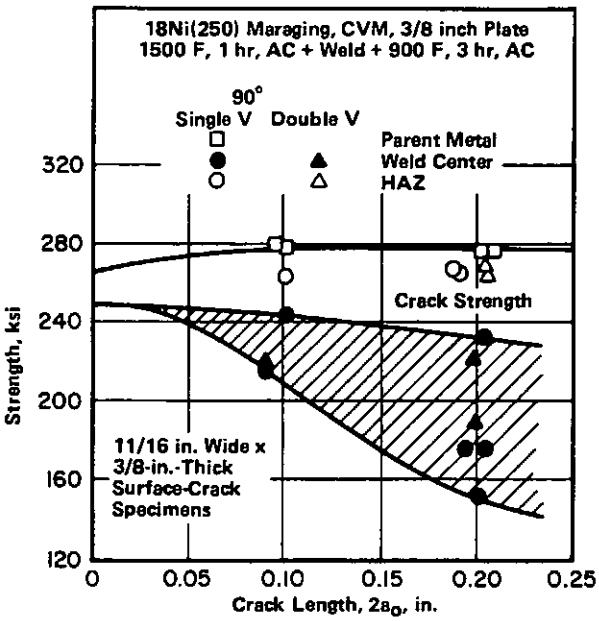


FIGURE 4.0361. EFFECT OF SURFACE CRACK LENGTH ON THE CRACK STRENGTH OF GTA WELDS IN CVM PLATE (80)

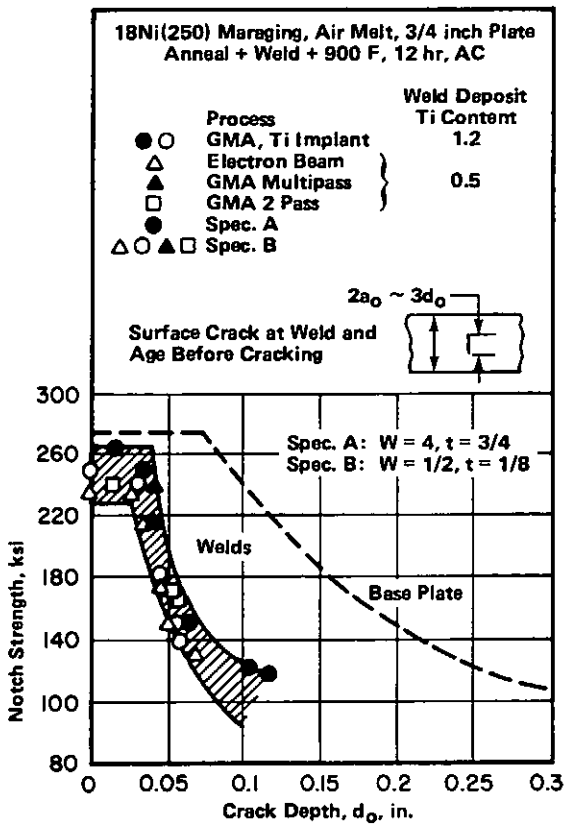


FIGURE 4.0362. EFFECT OF SURFACE CRACK DEPTH ON THE CRACK STRENGTH OF VARIOUS WELD DEPOSITS IN AIR MELT PLATE (56)

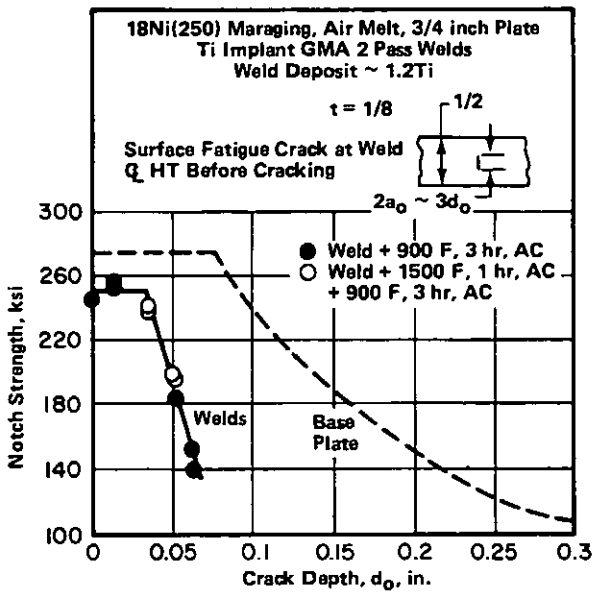


FIGURE 4.0363. EFFECT OF SURFACE CRACK DEPTH ON THE SHARP NOTCH STRENGTH OF WELD DEPOSITS IN 250 KSI AIR MELT PLATE AGED AFTER WELDING OR ANNEALED AND AGED AFTER WELDING (56)

Fe
18 Ni
7.5 Co
5 Mo
Ti
Al

18Ni(250) Maraging

Alloy		18Ni(250) Maraging							
Form		Air Melt, 3/4 inch Plate							
Condition		1650 F, 1 hr, WQ + 1530 F, 1 hr, WQ + Weld + 900 F, 3 hr							
Weld Orientation		Parallel to Plate Rolling Direction				Perpendicular to Plate Rolling Direction			
Notch Location[a]		WRC	WRE	WTC	RWC	RWC	RWE	RTC	WRC
K_{Ic}[b], ksi $\sqrt{in.}$	Process								
	GTA	63	86	86	58	61	92	75	64
	SA	36	87	44	–	44	86	37	43

(a) First letter gives direction of normal to crack plane, second letter gives direction of propagation (R – rolling direction, W – width direction, and T – thickness direction), third letter gives crack location with respect to weld (C – at weld centerline and E – at weld edge near fusion line).

(b) Base plate K_{Ic} = 80 ksi $\sqrt{in.}$, L; 77 ksi $\sqrt{in.}$, T. (See Table 4.0352 for tensile properties.)

TABLE 4.0364. PLANE STRAIN FRACTURE TOUGHNESS OF GTA AND SA WELDS IN AIR MELT PLATE (78)

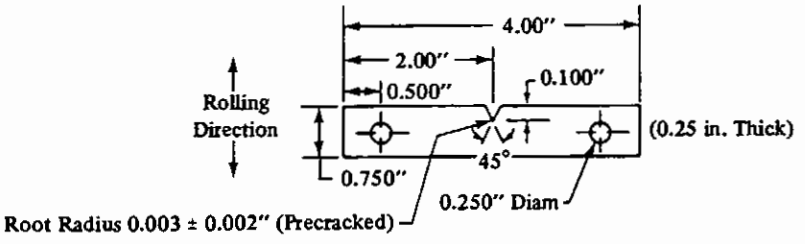
Alloy	18Ni(250) Maraging 0.25 inch Plate[e]	
Material	K_{Ic}, ksi $\sqrt{in.}$	K_{Iscc}, ksi $\sqrt{in.}$[d]
Base[a]	105.0	55.6 ± 7.6
Weld Fusion Zone[b]	54.0	27.8 ± 7.3
Weld HAZ, 1200 F Max[c]	113.2	<54.1
Weld HAZ, 1400 F Max[c]	91.3	–
Weld HAZ, 2400 F Max[c]	114.8	–

(a) Solution annealed plus aged 3 hr, 900 F.

(b) GTA welded in solution annealed condition plus aged 3 hr, 900 F.

(c) Synthetic weld heat-affected zones; solution annealed specimens exposed to various thermal cycles, then aged 3 hr, 900 F.

(d) Threshold stress-intensity factor for stress corrosion determined by exposure in natural seacoast atmosphere.



(e) Base plate tensile properties: F_{tu}, 269.5 ksi; F_{ty}, 267.0 ksi; and elongation, 6.5 percent.

TABLE 4.0365. EFFECTS OF WELDING ON FRACTURE TOUGHNESS AND THRESHOLD STRESS INTENSITY FACTOR FOR STRESS CORROSION (98)

	Fe
18	Ni
7.5	Co
5	Mo
	Ti
	Al

18Ni(250)
Maraging

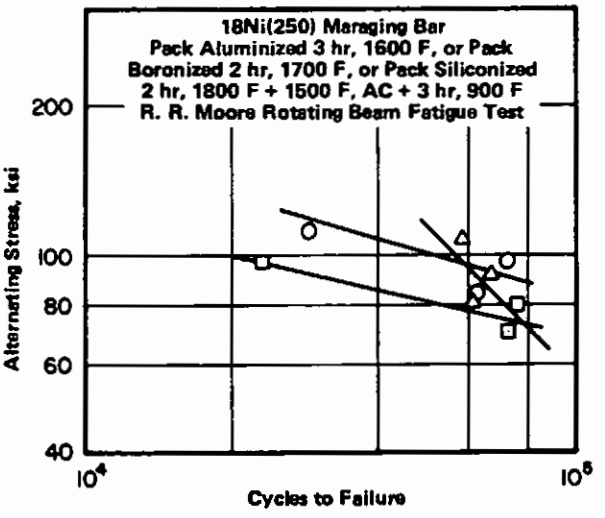


FIGURE 4.044. EFFECTS OF COATINGS ON ROTATING BEAM FATIGUE BEHAVIOR (99)

REVISED: SEPTEMBER, 1969

FERROUS ALLOYS

ROBERT P WEI

Fe
18 Ni
9 Co
5 Mo
Ti
Al

18 Ni Maraging (300)

1. GENERAL

This steel is one of a class of maraging types that developes yield strengths up to 350 ksi primarily as a result of complex precipitation reactions in a very low carbon Fe-Ni martensite. The maraging steels were designed to have superior resistance to crack propagation at high strength levels. In the 18Ni maraging steels, transformation from austenite to martensite occurs above room temperature (200 to 400F). High strength is then developed by aging. Three composition ranges have been specified corresponding to typical yield strength grades of 200, 250 and 280 ksi; the latter grade, considered here, being more frequently designated as 300 ksi. The various yield strength grades differ principally in the amounts of titanium, molybdenum and cobalt in the composition. (material with yield strength up to 350 ksi may be obtained from some producers through further adjustments in composition). The nominal composition of the 300 - grade is Fe-18Ni-9Co-5Mo, with titanium in the range 0.5 to 0.8 percent. The actual strength level and toughness will vary considerably within the composition limits and can also depend strongly on the processing history. High fracture toughness, compared with other types of quenched and tempered steels, characterizes a properly processed sheet product. The toughness and impact properties of heavy sections are superior to those of conventional medium-carbon, low-alloy ultrahigh-strength steels heat treated to tensile strength levels in excess of 250 ksi. However, the fracture properties of heavy sections can be directional and are lowest in the short transverse direction. This directionability is influenced by the melting and processing conditions. Corrosion and oxidation resistance are somewhat better than 4340 steel. Resistance to environment-assisted crack propagation is better than 4340 steel at an equivalent level of tensile strength. Hydrogen embrittles the maraging steels, but they exhibit a greater tolerance for hydrogen than conventional low-alloy steels. Formability is excellent in the annealed condition. The steel is readily machined in the annealed condition and can be machined in the fully aged condition. A high degree of dimensional stability is maintained throughout heat treatment. Welding requires special precautions and the toughness of the weld deposit is generally below that of the parent metal.

1.01 Commercial Designation

18Ni Maraging Steel, 18Ni Co Mo, 18-9-5, Vasco Max 300 CVM, RSM 300, Almar 18, Marvac 300.

1.02 Alternate Designations

18 Ni- (300) maraging steel, 300 grade maraging steel, 18 percent nickel precipitation-hardening steel, Grade C - MAR - 18 - 300

1.03 Specifications

1.031 ASTM A538 - 65, Grade C for plates (1, pp. 818 - 821)

1.032 SAE - AMD Specification for wrought products, Table 1.032.

TABLE 1.032

AMD	Form	Condition
64BR-1	Bars, forgings tubing, and rings, CVM	Annealed

1.033 AMS 6521 for CVM sheet, strip, and plate.

1.04 Composition

1.041 Specified composition.

1.0411 ASTM specified composition. Table 1.0411.

TABLE 1.0411

Source	ASTM (1)		
Form	Plates		
Type of Analysis	Ladle		Check
	Percent		Permissible Variations
	Min	Max	Percent
Carbon	-	0.03	+ 0.005
Manganese	-	0.10	+ 0.03
Phosphorus	-	0.010	+ 0.002
Sulfur	-	0.010	+ 0.002
Silicon	-	0.10	+ 0.02
Nickel	18.0	19.0	± 0.20
Cobalt	8.0	9.5	± 0.20
Molybdenum	4.6	5.2	± 0.10
Titanium	0.55	0.80	± 0.05
Aluminum	0.05	0.15	± 0.03
Boron*	0.003		
Zirconium*	0.02		
Calcium*	0.05		
Iron	Balance		

*Additions

1.0412 AMS, specified composition. Table 1.0412.

TABLE 1.0412

Source	AMS(70)	
Alloy	Fe-18Ni-9Co-5Mo-Ti-Al	
Form	CVM, sheet, strip, plate	
	Percent	
	Minimum	Maximum
Carbon	----	0.03
Manganese	----	0.10
Phosphorus	----	0.010
Sulfur	----	0.010
Silicon	----	0.10
Nickel	18.00	19.00
Cobalt	8.50	9.50
Molybdenum	4.60	5.20
Titanium	0.50	0.80
Aluminum	0.05	0.15
Boron*	0.003	
Zirconium*	0.02	
Calcium*	0.05	
Iron	Balance	

*Additions

Fe
18 Ni
9 Co
5 Mo
Ti
Al

18 Ni Maraging (300)

1.042 Producer's specified composition. Table 1.042.

TABLE 1.042

Source	VASCO (2)			
Type of Analysis	Ladle		Check	
	Percent		Percent	
	Min	Max	under Min	over Max
Carbon	-	0.02	-	0.01
Manganese	-	0.10	-	0.01
Phosphorus	-	0.010	-	0.003
Sulfur	-	0.010	-	0.003
Silicon	-	0.10	-	0.01
Nickel	18.00	19.00	0.20	0.20
Cobalt	8.50	9.50	0.15	0.15
Molybdenum	4.60	5.00	0.10	0.10
Titanium	0.50	0.70	0.04	0.04
Aluminum	0.05	0.15	0.02	0.01
Boron	-	0.006	-	0.003
Zirconium*	0.02			
Calcium*	0.05			
Iron	Balance			

*Additions

1.043 Modifications. Steels containing greater amounts of titanium, but conforming otherwise to ASTM A538-65, Grade C, specification, are produced to meet strength specifications. Refrigeration after annealing may be necessary to minimize the amount of retained austenite in the steel prior to aging (45)

1.05 Heat Treatment

1.051 Anneal. 1450 to 1650F, 1 hour per inch of thickness, 15 to 30 minutes minimum, air cool, generally is recommended. Double annealing treatment of 1650 - 1700F, 1 hour, air cool, plus 1500 - 1550F, 1 hour, air cool, is also recommended. Selection of an optimum annealing temperature in terms of strength and toughness will depend on the prior thermal-mechanical history. Generally, annealing temperature should be kept below 1800F to prevent excessive grain coarsening and to avoid thermal embrittlement (see 1.043, 1.094, and 18Ni (250) maraging steel).

1.052 Age. 700 to 950F, air cool. Full age is generally recommended, 875 to 925F, 3 hours, air cool. Broad latitude in aging treatment is available through proper combinations of aging time and temperature. Structures that are badly segregated may not age in a normal manner and austenite reversion may be encountered. Structures that have undergone austenite reversion may be restored to strength by re-annealing and aging. Aging after severe cold working should be avoided (see 1.09).

1.053 Special Consideration. Decarburization limits are not applicable to this steel because of the low carbon content. Care should be taken, however, to avoid surface carburization, sulfurization, and excessive oxidation.

1.06 Hardness

1.061 Typical hardness for annealed condition, 30 to 37 Rockwell C (3)(4)(5).

1.062 Typical hardness for fully aged material, 51 to 56 Rockwell C (3)(4)(5).

1.063 Effect of annealing temperature and aging on hardness. Figure 1.063.

1.064 Effect of aging temperature and time on hardness.

1.0641 Effect of aging temperature and time on hardness of plate. Figure 1.0641.

1.0642 Effect of aging temperature and time on hardness of cold rolled and annealed sheet. Figure 1.0642.

1.065 Hardenability. Air cooling from anneal followed by aging produces full hardness in heavy sections (3)(4)(5).

1.07 Forms and Conditions Available

1.071 This steel is available in bars, rods, wires, sheets, plates, tubing, shapes, extrusions and forging stock in the hot-worked or annealed condition. Sheet is also available in the annealed and cold-worked condition

1.08 Melting and Casting Practice

1.081 Electric furnace air melting with or without vacuum degassing, induction vacuum melting, consumable electrode vacuum remelting. Low carbon content and residual element content require high quality raw materials. Vacuum melting is recommended (2). Carbon should be kept well below the specified 0.03 percent maximum (see 18 Ni (250) maraging steel).

1.082 Room temperature tensile properties of air and vacuum melted slab. Table 1.082.

TABLE 1.082

Source	(5)	
Alloy	Fe-18Ni-9Co-5Mo-Ti-Al	
Form	2 1/2 to 2 3/4 inch thick slabs, short transverse (ST)	
Melting Practice	Air Melt	CVM
Ftu, ksi	290	290
Fty, ksi	280	273
e(2 In), percent	3	10
RA, percent	7	25

1.09 Special Considerations

1.091 General. The heat-to-heat variability of this steel within the composition limits given in Table 1.04 is higher than that normally encountered for low-alloy, heat-treated steels such as 4340. Special consideration should also be given to directionality of mechanical properties, the possibility of high temperature embrittlement, and high tolerance for hydrogen. Weldments present special problems which are discussed under 4.03.

1.092 Variability of properties. The yield strength and toughness of aged material will vary from heat to heat within the specified composition limits (e.g. see Figure 3.0217 and Table 3.027231). The variation in strength is caused primarily by differences in the content of strengthening elements, and also arises from differences in the melting and processing history (9)(10)(11). Generally the toughness will decrease with those factors that tend to increase the yield strength, such as cold work retained after annealing (see Figure 3.027151), increased titanium content (see Figure 3.0217), or reduced testing temperature (see 3.0371 and 3.0372). The influence of melting practice on the mechanical properties is not well understood; however, toughness is improved with a reduction in the residual element content (see 18 Ni (250) maraging steel) and is affected by processing history (see 1.094). At this time it is recommended that for critical applications the aging response regarding strength and toughness be determined for each heat.

1.093 Directionality. Heavy sections of this alloy and other high-strength steels can exhibit a banded structure which is associated with alloy segregation. If the bands contain a high concentration of non-metallic inclusions (titanium carbonitrides, titanium sulfides or oxides), the short transverse ductility and toughness may be considerably lower than the corresponding longitudinal properties (see Figure 3.021443 and 18 Ni (250) maraging steel). Under those circumstances the banding can result in delaminations or splitting in the plane of the bands. In severe cases splitting may occur during shearing or forming operations, or may be produced by thermal stresses induced by flame (or plasma arc) cutting or welding. It should be noted that in banded structures the apparent fracture toughness for cracks propagating in a direction perpendicular to the bands will be higher than that for crack propagation in the other directions because of momentary crack arrest and reinitiation at the delaminations. The presence of these inclusions,

	Fe
18	Ni
9	Co
5	Mo
	Ti
	Al

18 Ni Maraging (300)

however, reduces the general level of ductility and toughness in the other directions. The degree of banding and its influence on the mechanical properties is related to the melting and processing practices employed. In this respect particular attention should be given to Sections 1.05, 1.094 and 4.01. By very careful control of the melting and processing techniques it is possible to reduce the amount of banding and to minimize its deleterious effects on the transverse properties of heavy sections (12)(13).

1.094 Isothermal embrittlement. This steel may be severely embrittled by certain high temperature thermal treatments involved in processing and fabrication. The most severe embrittlement results from prolonged exposure in the temperature range 1500 to 1800F following heating to 2200 to 2400F and is caused by the precipitation of TiCN particles at austenite boundaries and the marked coarsening of the austenite grains during high temperature heating (14). This condition would be encountered if the alloy is allowed to cool very slowly following prior hot-working. For this reason hot-working should be followed by as rapid an air cool as possible.(14)(15). Heavy sections welded by high heat input process may also exhibit this embrittlement.

1.095 Hydrogen embrittlement. Hydrogen embrittles this alloy but it exhibits a greater tolerance for hydrogen than other high strength steels, such as 4340, at considerably lower strength levels. This has been demonstrated by both tensile tests and static fatigue tests. Charging conditions (0.02 amps per square inch for 5 minutes) that severely reduce the reduction of area of 4340(F_{tu} = 230 ksi) have no effect on this grade of maraging steel. Sufficiently severe charging conditions will reduce the ductility of this steel; however, recovery by baking is much more rapid than observed for 4340 (3)(16)(17). A bake of 24 hours at 400-600F usually restores their full mechanical properties (3). Electroplating and acid chemical contouring do not appear to embrittle this steel (18)(19), though specific processes should be checked by control tests before adoption.

2. PHYSICAL AND CHEMICAL PROPERTIES

2.01 Thermal Properties

2.011 Melting range approximately 2600 to 2650F.

2.012 Phase changes. Alloy transforms to martensite on slow cooling from annealing temperature. M_s = 300F and M_f = 200F approximately: these temperatures depend on the alloy composition (7). Austenite reversion occurs on overaging which depends on time and temperature (20)(see 18 Ni (250) maraging steel). Length change from maraging, which varies with processing history, is approximately 0.08 percent (3).

2.0121 Time-temperature-transformation diagrams.

2.0122 Austenite-to-martensite transformation curve, Figure 2.0122.

2.013 Thermal conductivity, Figure 2.013.

2.014 Thermal expansion. 75 to 900F, 5.6×10^{-6} inch per inch per degree F (3).

2.0141 Mean coefficient of thermal expansion from 75F, Figure 2.0141.

2.015 Specific heat, Figure 2.015.

2.016 Thermal diffusivity.

2.02 Other Physical Properties

2.021 Density. 0.29 lb per cu in, 8.0 gm per cu cm (2)(3)(4).

2.022 Electrical resistivity. Electrical resistivity increases within the indicated ranges primarily with titanium content (3).

As annealed at 1500F,	23.6 - 27.5 microhm - in 60 - 70 microhm - cm
Maraged, 3 hours - 900F,	13.8 - 23.6 microhm - in 35 - 60 microhm - cm
(Typical value at 72F, 0.62 Ti)	15.0 microhm - in 38.0 microhm - cm (22)

2.023 Magnetic properties.

2.0231 D.C. magnetic properties. Permeability at 200 oersteds - 77.5. Saturation induction equals 21.2 kilogauss at 1300 oersteds (32)

2.02311 D.C. magnetic properties of forging at different temperatures, Table 2.02311.

TABLE 2.02311

Source	(22, p. 118)*	
Alloy	Fe-18Ni-9Co-5Mo-Ti-Al	
Condition	CVM, 1500F, 1 hr, WQ + 900F 3 hrs, Rc=51-53	
	*Induction (B_{tip}) for H=250 oersteds - kilogauss	
Test Temp - F	Solid Ring	0.014 inch Thick Laminations
72	17.6	18.1
300	17.4	----
500	16.8	----
800	15.1	15.0
*Tested in accordance with ASTM A341-64 for solid and laminated Rowland ring samples.		

2.02312 D.C. magnetization curves for forging tested in air, Figure 2.02312.

2.02313 Room temperature d.c. magnetization curves for forging before and after aging at 800F (tested in air), Figure 2.02313.

2.0232 A.C. magnetic properties.

2.02321 A.C. magnetic properties of forging at different temperatures, Table 2.02321.

TABLE 2.02321

Source	(22, p. 118)*	
Alloy	Fe-18Ni-9Co-5Mo-Ti-Al	
Condition	CVM, 1500F, 1 hr, WQ + 900F, 3 hrs, Rc=51-53	
Form	Forging (tested as 0.014 inch thick laminations)	
Test Temperature F	Exciting Volt-Ampere (For B=10 kilogauss, @ 500cps) volt-amp/lb	Core Loss watts/lb
72	285	116
300	294	118
500	308	119
800	336	118
* Tested in accordance with ASTM A343-60 T wattmeter method except that ring samples were used.		

2.024 Emissivity

2.025 Damping capacity.

2.03 Chemical Properties

2.031 Corrosion resistance.

2.0311 General. Atmospheric environments, such as industrial and marine atmospheres, corrode the maraging steels 0.0005 to 0.001 inch per year, about half that of normal high strength low alloy steels. Static immersion tests show the average corrosion rate to be 0.003 inch per year in quiet sea water and 0.005 to 0.007 inch per year in flowing sea water, both rates being essentially the same as control samples of 4340 and HY-80 steels. The maraging steels corrode substantially in tap water, some neutral salt solutions, and some inorganic and organic acids; however, their corrosion rate is lower than that of low alloy steels heat treated to high strength levels. In general, the maraging steels should be protected from exposure to corrosive solutions by some means such as a suitable coating. Conventional cathodic protection, as with zinc anodes, is not recommended because of the danger of hydrogen embrittlement (3)(16)(23)(24).

Fe
18 Ni
9 Co
5 Mo
Ti
Al

18 Ni Maraging (300)

2.0312 Stress corrosion cracking. This maraging steel exhibits better stress corrosion resistance than other low alloy high strength steels, such as 4340 heat treated to high strength levels; however, a suitable coating is recommended (3)(23)(25). Two point loaded beam type specimens and U-bend specimens tested in industrial and marine atmospheres, and in sea water, gave widely varying results (21)(23)(25) which may be caused in part by differences in processing history. Delayed failure and increase in the rate of fatigue crack growth occur in water environment; however, the sensitivity to moisture enhanced crack growth is less than that for 4340 (24)(26)(27)(28).

2.03121 Effect of aging treatment on delayed failure of sheet in distilled water at 70F. Figure 2.03121.

2.03122 Delayed failure characteristics of plate in distilled water at room temperature. Figure 2.03122.

2.03123 Delayed failure characteristics of sheet and plate in 3 percent salt solution at room temperature. Figure 2.03123.

2.03124 Delayed failure characteristics of plate in several environments. Figure 2.03124.

3. MECHANICAL PROPERTIES

3.01 Specified Mechanical Properties

3.011 ASTM specified mechanical properties for plate, Table 3.011.

TABLE 3.011

Source	ASTM (1)
Alloy	Fe-18Ni-9Co-5Mo-Ti-Al
Condition	1500-1750F, 1 hr per in, 1 hr minimum AC or WQ + 900 ± 25F, 4 hrs
Form	Plate, L and T
Ftu, minimum - ksi	250
Fty, minimum - ksi	275 to 305
e(2 in), minimum - percent	6
RA (2 in), minimum - percent	
Round cross section specimens	30
Rectangular cross section specimens	25

3.012 AMS specified mechanical properties for CVM sheet, strip, and plate, Table 3.012.

3.013 Producer guaranteed mechanical properties for CVM sheet, strip, and plate, Table 3.013.

TABLE 3.013

Source	(2)					
Alloy	Fe-18Ni-9Co-5Mo-Ti-Al					
Condition	Mill annealed + 900 + 10F, 6 hrs					
Form	CVM sheet, strip, and plate, L and T					
Thickness - inch	Under 0.045	0.045-0.064	0.065-0.089	0.090-0.124	0.125-0.249	0.250- or over
Ftu, minimum - ksi	285	285	285	285	285	285
Fty, minimum - ksi	275	275	275	275	275	275
e(0.5 in) minimum-percent	-	4.0	-	-	-	-
e(1 in) minimum-percent	-	2.0	5.0	6.0	8.0	9.0
e(2 in) minimum-percent	-	-	2.5	3.0	4.0	5.0

3.014 Producer guaranteed mechanical properties for CVM billets, bars, rods, wires, shapes, and extrusions, Table 3.014.

TABLE 3.014

Source	(2)				
Alloy	Fe-18Ni-9Co-5Mo-Ti-Al				
Condition	1700F, 1 hr minimum, AC + 1500F, 1 hr minimum, AC + 900 ± 10F, 6 hrs				
Form	CVM billets, bars, rod, wire, shapes and extrusions				
Cross Section Dimension Thickness or Diameter - inches	< 3	< 3		> 2	
Width - inches	< 3	> 3		> 3	
Direction	L	L	LT	L	T
Ftu, minimum - ksi	280	280	280	275	275
Fty, minimum - ksi	270	270	270	270	270
e(4D), minimum - percent	8.0	8.0	5.0	8.0	4.0
RA, minimum - percent	40.0	40.0	25.0	40.0	20.0

TABLE 3.012

Source	AMS (70)							
Alloy	Fe-18Ni-9Co-5Mo-Ti-Al							
Condition	1500F ± 25, AC + 900F ± 10, 3 to 5 hrs, AC							
Form	CVM, sheet, strip, plate, L or T*							
Thickness, inch	under 0.030	0.030-0.045	0.046-0.065	0.066-0.090	0.091-0.125	0.126-0.250	0.251-0.375	0.376 or over
F_{tu}, minimum, ksi	280	280	280	280	280	280	280	280
F_{ty}, minimum, ksi	270	270	270	270	270	270	270	270
e, minimum, percent								
(0.5 inch)	1.0	2.0	---	---	---	---	---	---
(1.0 inch)	---	---	2.0	5.0	6.0	8.0	---	---
(2.0 inches or 4D)	---	---	---	2.5	3.0	4.0	5.0	6.0

*T: for widths 9 inches and over; L: for widths less than 9 inches.

3.02 Mechanical Properties at Room Temperatures
3.021 Tension (see also 3.027).
3.0211 Stress-strain diagrams (see also 3.0311).
3.02111 Stress-strain curve for annealed and aged bar, Figure 3.02111.
3.0212 Typical tensile properties.
3.02121 Producer's typical range of tensile properties, Table 3.02121.

TABLE 3.02121

Source	(3)(4)(29)	
Alloy	Fe-18Ni-9Co-5Mo-Ti-Al	
Condition	Annealed 1500F, 1 hr	Annealed + Age 900F, 3 hrs
F_{tu} - ksi	145-170	265-305
F_{ty} - ksi	110-130	260-300
e(2 in) - percent	6-15	5-10
e(1 in) - percent	-	7-11
RA - percent	45-60	30-50
Hardness RC	30-37	50-55

3.02122 Producer's typical tensile properties for bars, Table 3.02122.

TABLE 3.02122

Source	(30)					
Alloy	Fe-18Ni-9Co-5Mo-Ti-Al (Aim Ti 0.68 weight percent)					
Form	CVM, 1/2 to 2 inch diameter rolled round bars*, L					
Condition	1500F, 1 hr, AC + 900F, 3 hrs					
	Specified Minimum	Mean	Standard Deviation	Skewness	Kurtosis	Number of Tests
F_{tu} - ksi	274	292	6.2	+0.24	-0.25	57
F_{ty} - ksi	265	285	7.1	+0.24	-0.25	57
e(1 in) - percent	9.5	12	0.9	+0.02	-0.30	57
RA - percent	46	54	3	-0.27	-0.40	55
Hardness RC	50.5	53.4	1.0	-0.91	+0.40	55

* From 6 to 8 production heats. 0.252 inch diameter tensile test specimens taken from center to mid radius locations

3.02123 Typical tensile properties of sheet, plate, and bar, Table 3.02123.

TABLE 3.02123

Source	(21, pp. 33-35, 162-171)				
Alloy	Fe-18Ni-9Co-5Mo-(0.67 - 0.70) Ti-Al				
Condition	CVM, Mill Anneal, 1500F, + Age 900F - 3 hrs				
Form	0.07 inch thick sheet		0.25 inch thick plate		7/8 inch diameter bar
Direction	L	T	L	T	L
Number of tests*	30	30	30	30	30
F_{tu} - ksi					
Mean	280	284	288	287	282
Minimum	271	267	264	269	272
Maximum	305	297	303	305	291
Standard Deviation	7.2	7.6	13.0	12.9	5.5
F_{tu} - ksi					
Mean	272	272	279	277	272
Minimum	261	261	258	257	259
Maximum	300	291	301	294	285
Standard Deviation	8.7	9.8	14.4	13.7	6.2
e(2 in) - percent	3.6 (2.0-5.0)	3.5 (2.0-4.0)	7.0 (6.0-8.0)	6.7 (5.0-6.0)	9.3 (8.0-10.0)
RA - percent	-	-	-	-	41.5 (38.6-45.1)

*From 3 production heats, ten specimens per heat

3.0213 Effect of annealing treatment on tensile properties.
3.02131 Influence of annealing temperature on the tensile properties of annealed and aged forgings. Figure 3.02131.
3.02132 Influence of annealing temperature on the tensile properties of bar, Figure 3.02132.
3.02133 Effect of annealing temperature on the tensile properties of annealed and aged sheet. Figure 3.02133.
3.02134 Effect of annealing temperature and time on the tensile properties of annealed and aged sheet. Figure 3.02134.
3.02135 Effect of re-solution annealing and aging on the tensile properties of sheet subjected to prior austenite reversion treatment. Figure 3.02135.
3.02136 Effect of resolution annealing time on the tensile properties of sheet subjected to prior austenite reversion treatment, Figure 3.02136.

Fe
18 Ni
9 Co
5 Mo
Ti
Al

18 Ni Maraging (300)

Fe
18 Ni
9 Co
5 Mo
Ti
Al

18 Ni Maraging (300)

3.02137 Influence of annealing temperature on tensile properties of annealed and aged billets. Table 3.02137.

TABLE 3.02137

Source	(42)							
Alloy	Fe-18Ni-9Co-5Mo-Ti-Al							
Form	CVM Billets							
Condition	1650F Anneal + 900F, 3 hrs				1500F Anneal + 900F, 3hrs			
Size	14 inches sq		10 in x 7 in		14 inches sq		10 in x 7 in	
Direction	L	T	L	T	L	T	L	T
F_{tu} - ksi	304	306	304	302	325	316	310	308
F_{ty} - ksi	297	297	297	293	317	306	302	299
RA - percent	49	19	49	24	49	16	46	15
e(4D) - percent	11	4	9	6	8	3	9	3

3.0214 Effect of aging on tensile properties.
3.02141 Effect of aging on tensile properties of sheet.
3.021411 Effect of aging time and temperature on the tensile properties of sheet. Figure 3.021411.
3.021412 Effect of aging temperature and time on tensile properties of annealed sheet. Figure 3.021412.
3.021413 Effect of aging time on tensile properties of air-melted and vacuum-melted sheets, Figure 3.021413.
3.02142 Effect of aging on tensile properties of plate.
3.021421 Effect of aging temperature on tensile properties of plate, Figure 3.021421.
3.021422 Effect of aging temperature on tensile properties of hot rolled plate from three heats. Figure 3.021422.
3.021423 Effect of aging temperature and time on tensile properties of laboratory vacuum induction melted plate. Figure 3.021423.

TABLE 3.021424

Source	(62)				
Alloy	Fe-18Ni-9Co-5Mo-Ti-Al				
Form	300 lb Lab Vac Melted Heat 1/2 inch Plate, L				
Condition	1500F, 1 hr, AC + age as indicated				
Aging Treatment	F_{ty} ksi	F_{tu} ksi	e(1 in) percent	RA percent	IE Charpy V ft - lb
None (annealed)	135	151	19	50	119
900F, 3 hrs	272	278	12	60	24
900F, 1 1/2 hrs, AC + 900F, 1 1/2 hrs	280	284	10	50	21
900F, 6 hrs	285	296	12	58	24
900F, 3 hrs, AC + 900F, 3 hrs	291	299	11	56	18
900F, 3 hrs, AC + 600F, 24 hrs	275	279	12	57	20
900F, 3 hrs, AC + 600F, 48 hrs	276	280	12	61	20
700F, 48 hrs	289	295	12	58	17
700F, 48 hrs, AC + 900F, 3 hrs	312	312	12	54	16
900F, 3 hrs, AC + 700F, 48 hrs	284	298	12	57	19
800F, 48 hrs	295	304	11	49	19
800F, 48 hrs, AC + 900F, 3 hrs	309	311	11	52	19
900F, 3hrs, AC + 800F, 24 hrs	310	311	10	48	16
900F, 3 hrs, AC + 800F, 48 hrs	313	315	11	54	16
900F, 3 hrs, AC + 800F, 72 hrs	310	312	10	65	15

3.02143 Effect of aging on tensile properties of bar.
3.021431 Effect of aging temperature on the tensile properties of bar. Figure 3.021431.
3.021432 Effect of aging time on tensile properties of annealed bar, Figure 3.021432.
3.021433 Tensile properties of annealed and aged bars. Table 3.021433.

TABLE 3.021433

Source	(42)			
Alloy	Fe-18Ni-9Co-5Mo-Ti-Al			
Form	CVM Bars, L			
Condition and Ti content	1500F Anneal + 900F, 3 hrs, Ti = 0.63 percent	1650F Anneal + 900F, 3 hrs, Ti = 0.76 percent		1650F Anneal + 900F, 8 hrs, Ti=0.76 percent
Size	1 1/2 inch diameter	1 1/4 inch diameter	1 inch diameter	1 3/16 inch diameter
F_{tu} - ksi	298	302	286	302
F_{ty} - ksi	294	295	276	292
RA- percent	42	43	41	39
e(4D)- percent	9	8	9	8

3.021424 Effect of duplex aging treatments on the tensile properties of 300 lb laboratory vacuum melted plate. Table 3.021424.

3.02144 Effect of aging on tensile properties of forgings, billets and slabs.
3.021441 Effect of aging temperature and maximum forging temperature on tensile properties of forgings. Figure 3.021441.
3.021442 Effect of aging temperature and time on tensile properties of forgings, Figure 3.021442.
3.021443 Effect of aging temperature on the tensile properties of forgings, Figure 3.021443.

Fe
18 Ni
9 Co
5 Mo
Ti
Al

18 Ni Maraging (300)

3.021444 Tensile properties of annealed and aged billets. Table 3.021444.

TABLE 3.021444

Source	(5)(43)									
Alloy	Fe-18Ni-9Co-5Mo-Ti-Al									
Condition	1500F, 1/2 to 1 hr, AC + 900F, 3 hrs									
Form	CVM Forged Billets, T									
Size	10 inches square		6 inches square		5 inches square		6 inches round		4 inches round	
Location	MR	C	MR	C	MR	C	MR	C	MR	C
F_{tu} - ksi	286	284	282	283	281	279	278	278	279	282
F_{ty} - ksi	277	275	278	279	276	272	273	271	274	272
RA - percent	38	40	41	48	43	44	48	44	37	37
e(4D) percent	8.5	8.5	8.0	10.0	8.0	8.0	9.0	9.0	7.0	7.0

3.021445 Tensile properties of air and vacuum melted slabs. Table 3.021445.

TABLE 3.021445

Source	(8)	
Alloy	Fe-18Ni-9Co-5Mo-Ti-Al	
Form	2 1/2 to 2 3/4 inch thick slab, ST	
Condition	Air Melt	CVM
F_{tu} - ksi	290	290
F_{ty} - ksi	280	273
RA - percent	7	25
e(2 in) - percent	3	10

3.0215 Effect of cold work on tensile properties.

3.02151 Effect of cold work prior to aging on the tensile properties of annealed sheet. Figure 3.02151.

3.02152 Effect of cold work prior to aging on the tensile properties of annealed sheet. Figure 3.02152.

3.02153 Effect of cold reduction before aging on tensile properties of sheet. Figure 3.02153.

3.0216 Effect of hot working on tensile properties.

3.02161 Effect of rolling temperature on the tensile properties of annealed, rolled and aged sheet. Figure 3.02161.

3.02162 Effect of forging temperature on the tensile properties of 5 : 1 upset-forged-pancakes. Figure 3.02162.

3.0217 Effect of titanium on room temperature tensile properties of annealed and aged sheets from laboratory and production heats, Figure 3.0217.

3.022 Compression. See also 3.032.

3.0221 Stress-strain diagrams, see Figure 3.0321.

3.0222 Room temperature compressive yield strength.

3.02221 Room temperature compressive yield strength of annealed and aged bar, Table 3.02221.

TABLE 3.02221

Source	(5)	
Alloy	Fe-18Ni-9Co-5Mo-Ti-Al	
Form	CVM Bar	
Condition	Anneal 1500F, 30 minutes	Anneal 1500F, 30 minutes + 900F, 3 hours
F_{cy} - ksi	150	318

3.02222 Typical room temperature compressive yield strength of sheet, plate, and bar, Table 3.02222

TABLE 3.02222

Source	(21, p. 172-178)			
Alloy	Fe-18Ni-9Co-5Mo-Ti-Al			
Condition	CVM, Mill Anneal 1500F + Age 900F, 3 Hours			
Form	0.07 inch Sheet		0.25 inch Plate	1.5 inch Diameter Bar
Direction	L	T	T	L
F_{cy}* - ksi				
Mean	261	270	290	287
Minimum	240	252	275	281
Maximum	280	289	315	291

*From three production heats, ten specimens per heat.

3.023 Impact (see also 3.033).

3.0231 Producers typical impact properties for bars, Table 3.0231.

TABLE 3.0231

Source	(30)					
Alloy	Fe-18Ni-9Co-5Mo-Ti-Al (Aim Ti-0.68 weight percent)					
Form	CVM, 1/2 to 2 inches diameter rolled round bars*, L					
Condition	1500F, 1 hr, AC + 900F, 3 hrs (mean F_{ty}= 285 ksi)**					
	Specified Minimum	Mean	Standard Deviation	Skewness	Kurtosis	Number of Tests
IE Charpy V; ft-lbs	12	18.4	2.2	-38.6	-0.40	36

* From 6 to 8 production heats
** See Table 3.02122.

3.0232 Effect of yield strength on impact properties of 300 lb laboratory vacuum melted plate, Figure 3.0232.

3.024 Bending.

3.025 Torsion and shear (see also 3.035).

3.0251 Typical room temperature ultimate shear strength of sheet, plate and bar, Table 3.0251.

TABLE 3.0251

Source	(21, p. 179 - 185)			
Alloy	Fe-18Ni-9Co-5Mo-Ti-Al			
Condition	Mill Anneal 1500F + Age 900F, 3 hrs, CVM			
Form	0.07 inch Sheet		0.25 inch Plate	7/8 inch Diameter Bar
Direction	L	T	T	L
F_{su}* - ksi				
Mean	173	172	178	181
Minimum	164	161	156	174
Maximum	180	181	189	186

* From three production heats, ten specimens per heat.

Fe
18 Ni
9 Co
5 Mo
Ti
Al

18 Ni Maraging (300)

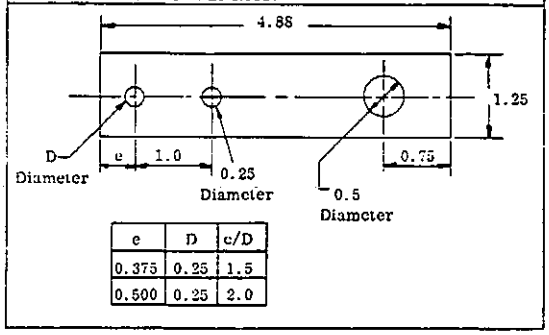
3.026 Bearing.

3.0261 Typical room temperature bearing strengths of sheet and plate. Table 3.0261.

TABLE 3.0261

Source	(21, p. 186 - 195)					
Alloy	Fe-18Ni-9Co-5Mo-Ti-Al					
Condition	CVM, Mill Anneal 1500F + Age 900F, 3 hrs					
e/D	1.5			2.0		
Form***	0.07 inch Sheet		0.25 in Plate	0.07 inch Sheet		0.25 in Plate
Direction	L	T	T	L	T	T
*F_{bru} - ksi						
Mean	392	390	403	507	517	514
Min	378	369	378	480	492	491
Max	403	399	425	524	533	544
*F_{bry} - ksi						
Mean	356	358	373	432**	423	406
Min	338	332	320	377	376	373
Max	387	383	399	505	468	489

* From 3 production heats, ten specimens per heat.
** Mean of 29 specimens.
*** 0.07 inch sheet tested in full thickness, 0.25 inch plate tested in 0.1 inch thickness.



e	D	e/D
0.375	0.25	1.5
0.500	0.25	2.0

3.0262 Bearing strength of sheet, 1500F, 12 minutes + 900F, 3 hours (48).
Longitudinal - F_{bru} = 505 ksi. F_{bry} = 406 ksi.
Transverse - F_{bru} = 479 ksi. F_{bry} = 384 ksi.

3.0263 Bearing strength of bar, see Figure 3.03613.

3.027 Stress concentration.

3.0271 Notch properties, see also 3.0272, 3.0371 and 3.0372.

3.02711 Room temperature tensile properties and crack strength for high and low chemistry heats, Table 3.02711.

3.02712 Effect of titanium on sharp notch properties of annealed and aged sheet from laboratory heats. Figure 3.02712.

3.02713 Effect of annealing temperature on sharp notch properties.

3.027131 Effect of annealing temperature on the sharp notch properties of 0.035 - inch aged sheet. Figure 3.027131.

3.02714 Effect of aging on sharp notch properties, see also 3.0371.

3.027141 Effect of aging time on the crack strength of air melt and CVM 0.04 - inch sheet. Figure 3.027141.

3.027142 Effect of aging time on the sharp notch properties of 0.115 inch sheet. Figure 3.027142.

3.027143 Effect of aging temperature on the sharp notch properties of forged CVM slab, Figure 3.027143.

3.02715 Effect of cold work on sharp notch properties.

3.027151 Effect of cold rolling prior to aging on crack strength of sheet. Figure 3.02751.

3.02716 Effect of thickness on sharp notch properties.

3.027161 Effect of thickness on the crack strength of CVM plate. Figure 3.027161.

3.02717 Effect of surface crack size on crack strength.

3.027171 Effect of surface crack size on the crack strength of sheet and plate, Figure 3.027171.

3.027172 Effect of surface crack length on crack strength of CVM plate at two titanium levels. Figure 3.027172.

3.027173 Effect of surface crack size and specimen size on the crack strength of CVM plate. Figure 3.027173.

3.0272 Fracture toughness (see also 3.0372).

3.02721 Plane-strain fracture toughness of plate at two strength levels, Table 3.02721.

TABLE 3.02721

Source	(60, p. 26)	
Alloy	Fe-18Ni-9Co-5Mo-Ti-Al	
Form	CVM, 1/2 inch plate	CVM, 1 - inch plate
Condition	1600F, 1 hr, AC + 850F, 3 hrs	Mill Anneal + Age 900F, 3 hrs
F_{ty} - ksi	242	285
K_{Ic} (mean)- ksi$\sqrt{in}$	84.5(a)	51.8(b)
Standard Deviation σ - ksi$\sqrt{in}$	4.67	2.47
σ/ mean K_{Ic}	0.0555	0.0478
(a) 44 tests (b) 38 tests		

3.028 Combined properties.

TABLE 3.02711

Source	(6)							
Alloy	Fe-18Ni-9Co-5Mo-Ti-Al, 60 lb Vacuum Melts							
Condition	Low Chemistry (a)				High Chemistry (b)			
	HR + 900F, 3 hrs		1500F, 15 Min + 900F, 3 hrs		HR + 900F, 3 hrs		1500F, 15 Min + 900F, 3 hrs	
Form	Bar	Sheet	Bar	Sheet	Bar	Sheet	Bar	Sheet
F_{tu} - ksi	270	272	275	266	317	312	318	314
F_{ty} - ksi	267	264	270	262	314	305	314	308
e(4 D) - percent	10	-	14	-	11	-	11	-
e (2 In) - percent	-	6	-	6	-	5	-	5
RA	59	-	62	-	56	30	56	28
Crack strength - ksi (c)	-	205	-	209	-	159	-	138

(a) 8.57 Co, 4.67 Mo, 0.50 Ti, 0.12 Al
(b) 9.40 Co, 5.17 Mo, 0.81 Ti, 0.071 Al
(c) See Figure 3.027141 for specimen.

3.03 Mechanical Properties at Various Temperatures

3.031 Tension

3.0311 Stress-strain diagrams.

3.03111 Typical stress-strain curves for tension at cryogenic, room and elevated temperatures. Figure 3.03111.

3.0312 Effect of test temperature on tensile properties.

3.03121 Effect of test temperature on the tensile properties of sheet. Figure 3.03121.

3.03122 Effect of test temperature on the tensile properties of sheets from several heats. Figure 3.03122.

3.03123 Effect of test temperature on the tensile properties of plate, Figure 3.03123.

3.03124 Effect of test temperature on the tensile properties of bar. Figure 3.03124.

3.03125 Effect of test temperature on the tensile properties of bar, Figure 3.03125.

3.0313 Effect of aging treatment and test temperature on tensile properties.

3.03131 Effect of aging treatment and test temperature on the tensile properties of cold-rolled and annealed sheet, Figure 3.03131.

3.0314 Effect of time of exposure at elevated temperatures on tensile properties.

3.03141 Effect of 1000 hour elevated temperature exposure on the tensile properties of sheet at room temperature, Table 3.03141.

TABLE 3.03141

Source	(21, p. 196)					
Alloy	Fe-18Ni-9Co-5Mo-Ti-Al					
Form	CVM, 0.07 inch sheet					
Condition	Mill Anneal 1500F + Age 900F, 3 hrs.					
Exposure temperature	(RT Ref)		600F	800F		1000F
Direction	L	T	T	L	T	T
F_{tu} - ksi	280	284	293	310	311	203
F_{ty} - ksi	272	272	286	302	305	179
e(2 in) - percent	3.6	3.5	3.8	4.0	2.6	8.5

3.03142 Effect of test temperature on the tensile properties of sheet after holding 30 minutes and 1000 hours at test temperature, Figure 3.03142.

3.03143 Effect of test temperature on the tensile properties of CVM bar after holding 30 minutes and 200 hours at test temperature, Figure 3.03143.

3.032 Compression.

3.0321 Stress-strain diagrams.

3.03211 Typical stress-strain curves for compression at room and elevated temperatures, Figure 3.03211.

3.0322 Effect of test temperature on compressive properties.

3.03221 Effect of test temperature on the compressive properties of sheet, Figure 3.03221.

3.03222 Effect of test temperature on the compressive properties of plate, Figure 3.03222.

3.03223 Effect of test temperature on the compressive properties of bar, Figure 3.03223.

3.0322 Effect of time of exposure at elevated temperatures on compressive properties.

3.03231 Effect of 1000 hour elevated temperature exposure on the compressive properties of sheet at room temperature, Table 3.03231.

TABLE 3.03231

Source	(21, p. 197)					
Alloy	Fe-18Ni-9Co-5Mo-Ti-Al					
Form	CVM, 0.07 inch sheet					
Condition	Mill Anneal 1500F + Age 900F, 3 hrs					
1000 Hours Exposure Temp	(RT Ref)		600F	800F		1000F
Direction	L	T	T	L	T	T
F_{cy} - ksi	272	276	278	299	316	174

3.03232 Effect of test temperature on the compressive properties of sheet after holding 30 minutes and 1000 hours at test temperature, see Figure 3.03221.

3.033 Impact.

3.0331 Effect of test temperature on the impact strength of bar, billet, and plates from several heats. Figure 3.0331.

3.034 Bending.

3.035 Torsion and shear.

3.0351 Effect of test temperature on shear properties.

3.03511 Effect of test temperature on shear ultimate strength of sheet, Figure 3.03511.

3.03512 Effect of test temperature on shear ultimate strength of plate, Figure 3.03512.

3.03513 Effect of test temperature on shear ultimate strength of bar, Figure 3.03513.

3.0352 Effect of time of exposure at elevated temperature on shear properties.

3.03521 Effect of 1000 hour elevated temperature exposure on the shear ultimate strength of sheet at room temperature, Table 3.03521.

TABLE 3.03521

Source	(21, p. 198)					
Alloy	Fe-18Ni-9Co-5Mo-Ti-Al					
Form	CVM, 0.07 inch sheet					
Condition	Mill Anneal 1500F + Age 900F, 3 hrs					
1000 hrs exposure temperature	(RT Ref)		600F	800F		1000F
Direction	L	T	T	L	T	T
F_{su} - ksi	172	175	171	186	187	124

3.03522. Effect of test temperature on the shear ultimate strength of sheet after holding 30 minutes and 1000 hours at test temperature, see Figure 3.03511.

3.036 Bearing.

3.0361 Effect of test temperature on bearing strength.

3.03611 Effect of test temperature on bearing strength of sheet, Figure 3.03611.

3.03612 Effect of test temperature on bearing strength of plate, Figure 3.03612.

3.03613 Effect of test temperature on bearing strength of bar, Figure 3.03613.

3.0362 Effect of time of exposure at elevated temperature on bearing strength.

3.03621. Effect of 1000 hour elevated temperature exposure on the bearing strength of sheet at room temperature. Figure 3.03621.

3.03622 Effect of test temperature on the bearing strength of sheet after holding 30 minutes and 1000 hours at test temperature. Figure 3.03622.

3.037 Stress concentration.

3.0371. Notch properties (see also 3.0372).

3.03711 Room and low temperature smooth and sharp notch tensile properties of annealed and aged sheet, Table 3.03711.

TABLE 3.03711

Source	(5)			
Alloy	Fe-18Ni-9Co-5Mo-Ti-Al			
Form	0.063 inch sheet			
Condition	1500F, 15 min, AC + 900F, 3 hrs			
Test Temperature	RT		-320F	
Direction	L	T	L	T
F_{tu} - ksi	299	306	362	374
F_{ty} - ksi	293	301	352	362
e - percent	4	3	0.5	0.5
Notch strength* - ksi	244	227	215	210

*Notch tensile specimens 1 inch wide, with 60° edge notches, 0.0005/0.0006 inch root radii

	Fe
18	Ni
9	Co
5	Mo
	Ti
	Al

18 Ni Maraging (300)

Fe
18 Ni
9 Co
5 Mo
Ti
Al

18 Ni Maraging (300)

3.03712 Effect of test temperature on the strength of sheet aged at three temperatures. Figure 3.03712.

3.03713 Effect of test temperature on sharp notch properties of CVM plate aged at three temperatures, Figure 3.03713.

3.0372 Fracture toughness, see also 3.0272 and 3.0371.

3.03721 Effect of test temperature on the crack strength of sheet. Figure 3.03721.

3.03722 Effect of test temperature on the fracture toughness of plate and bar. Figure 3.03722.

3.038 Combined properties.

3.04 Creep and Creep Rupture Properties

3.041 Creep properties of 0.07 inch sheet at 600 and 800F, Table 3.041.

TABLE 3.041

Source	(21, p. 89 - 90, 207)					
Alloy	Fe-18Ni-9Co-5Mo-Ti-Al					
Form	CVM, 0.07 Inch Sheet (T)					
Condition	Mill Anneal 1500F + Age 900F, 3 hrs (F_{ty}=272ksi)					
Temperature	600F*			800F*		
Stress - ksi	Time - Hours					
	10	100	1000	10	100	1000
0.05 percent creep	230	220	210**	130	-	-
0.10 percent creep	240 **	230	220	155	125	95**
0.50 percent creep	-	-	-	200	165	125
1.0 percent creep	-	-	-	210	195	135

* See Fig. 3.03142 for tensile properties at these temperatures.
** Values extrapolated

3.042 Creep properties of bar at 650 and 800F, Table 3.042.

TABLE 3.042

Source	(63)					
Alloy	Fe-18Ni-9Co-5Mo-Ti-Al					
Form	Bar					
Condition	1500F, 1hr, AC+900F, 3hrs(F_{ty}=272 ksi)					
Temperature - F	650F			800F		
	Time-hr					
Stress - ksi	10	100	1000	10	100	1000
0.1 percent creep	220*	204	185	150	110	---
0.2 percent creep	---	---	---	175	135	95*
1 percent creep	---	---	---	---	180	110

* Values extrapolated

3.043 Creep properties of CVM forgings at 800F and 900F, Table 3.043.

TABLE 3.043

Source	(22)			
Alloy	Fe-18Ni-9Co-5Mo-Ti-Al			
Form	CVM Forging			
Condition	1500F, 1 Hr, WQ + 900F, 3 Hrs			
Temperature	800F		900F	
Direction	L	T	L	T
Stress - ksi	130	130	100	100
Average creep strain at 100 hours - percent	0.85	0.22	3.5	2.8

3.05 Fatigue Properties

3.051 Smooth and notched fatigue strength.

3.0511 Smooth fatigue strength of annealed and aged bar. Table 3.0511.

TABLE 3.0511

Source	(5)(65)							
Alloy	Fe-18Ni-9Co-5Mo-Ti-Al							
Form	CVM Bar							
Condition	1500F, 30 Min + 900F, 3 Hrs							
Method	Stress Ratio		Stress Concentration	Fatigue Strength at Cycles - ksi				
	A	R		10^4	10^5	10^6	10^7	10^8
Rotating Beam	∞	-1	K_t = 1 Smooth	170	145	130	120	110
			K_t = 2.2 Notch	110	70	57	55	55

3.0512 Smooth and notched axial load fatigue strength of CVM bar, Table 3.0512.

TABLE 3.0512

Source	(63)								
Alloy	Fe-18Ni-9Co-5Mo-Ti-Al								
Form	Bar								
Condition	1500F, 1 hr, AC + 900F, 3 hrs (F_{tu} = 281 ksi)								
Direction	Method	Stress Ratio		Stress Concentration	Fatigue Strength - ksi at cycles				
		A	R		10^3	10^4	10^5	10^6	10^7
Longitudinal	Axial Load	0.82	0.1	Smooth K_t = 1	-	230	95	84	84
				Notched K_t = 2.4	-	110	67	53	50
				K_t = 3.3	-	84	42	22	14
Short Transverse	Axial Load	0.82	0.1	Smooth K_t = 1	-	190	93	84	84
				K_t = 3.3	-	79	39	22	14

3.0513 Smooth and notch axial fatigue strength of CVM forgings. Table 3.0513.

TABLE 3.0513

Source	(54)(66)								
Alloy	Fe-18Ni-9Co-5Mo-Ti-Al								
Form	CVM Forgings								
Condition	1500F, 1 to 4 hrs, AC + 900F, 3 hrs								
	Method	Stress Ratio		Stress Concentration	Fatigue Strength at Cycles - ksi (a)					
		A	R		10^2	10^3	10^4	10^5	10^6	10^7
Longitudinal	Axial Load	0.82	0.1	Smooth K_t = 1	-	-	-	165	130	115
				Notched K_t = 2	360	250	150	85	70	65
Short Transverse	Axial Load	0.82	0.1	Smooth K_t = 1	-	-	220	145	110	95
				Notched K_t = 2	250	200	130	75	65	60

(a) Values exhibit large scatter

3.0514 Smooth and notched axial load fatigue strength of 0.07 inch sheet at room and elevated temperatures. Table 3.0514.

3.06 Elastic Properties

3.061 Poisson's ratio(see 18 Ni (250) maraging steel).

3.062 Modulus of elasticity.

	Fe
18	Ni
9	Co
5	Mo
	Ti
	Al

18 Ni Maraging (300)

TABLE 3.0514

Source	(21, p. 74 - 80, 203 - 206)						
Alloy	Fe-18Ni-9Co-5Mo-Ti-Al						
Form	CVM, 0.07 Inch Sheet						
Condition	Mill Anneal 1500F + Age 900F, 3 Hours						
Method	Axial Load (Smooth and Double Edge - Notch)						
Stress Ratio		Test Temperature F	Stress Concentration	Direction	Fatigue Strength* at Cycles - ksi			
A	R				10^4	10^5	10^6	10^7
∞	-1.0	RT	Smooth	L	150	50	42	40
			K_t = 1	T	140 **	65	48	40
			Notch K_t = 3	L and T	55	30	26	25
		600	Smooth	L	90	75	68	65
			K_t = 1	T	100	65	57	56
			Notch K_t = 3	L and T	60	40	35	32
		800	Smooth	L	85	75	72	70
			K_t = 1	T	105	82	64	62
			Notch K_t = 3	L and T	54	37	31	28
0.98	0.01	RT	Smooth K_t = 1	T	155	80	58	57
			Notch K_t = 3	T	72	38	29	27
		600	Smooth K_t = 1	T	130	85	82	82
			Notch K_t = 3	T	74	34	27	26
		800	Smooth K_t = 1	T	140	100	87	85**
			Notch K_t = 3	T	72	51	42	36
0.67	0.20	RT	Smooth K_t = 1	T	168	72	63	60
			Notch K_t = 3	T	88	39	31	30
		600	Smooth K_t =1	T	140	92	91	90
			Notch K_t = 3	T	77	42	40	40
		800	Smooth K_t = 1	T	165**	105	97	95
			Notch K_t = 3	T	82	54	44	42

* Based on limited number of tests

** Values extrapolated

3.0515 Elevated temperature (650F) smooth and notch axial load fatigue strength of CVM bar. Table 3.0515.

TABLE 3.0515

Source	(63)								
Alloy	Fe-18Ni-9Co-5Mo-Ti-Al								
Form	CVM Bar								
Condition	1500F, 1 hr, AC + 900F, 3 hrs (F_{tu} = 281 ksi)								
Direction	Method	Stress Ratio		Stress Concentration	650F Fatigue Strength - ksi				
		A	R		10^3	10^4	10^5	10^6	10^7
Longitudinal	Axial Load	0.82	0.1	Smooth K_t = 1	-	177	151	130	107
				Notched K_t = 3.3	110	67	42	39	39
Short Transverse	Axial Load	0.82	0.1	Smooth K_t = 1	-	157	135	107	79
				Notched K_t = 3.3	92	56	42	39	39

3.052 Fatigue crack propagation.

3.0521 Influence of stress intensity factor K and test environment on fatigue crack propagation in sheet and plate at room temperature. Figure 3.0521.

3.0621 Static and dynamic moduli for tension at cryogenic, room and elevated temperatures. Figure 3.0621.

3.0622 Static moduli for compression at room and elevated temperatures. Figure 3.0622.

3.0623 Effect of cold work on static moduli at room temperature. Figure 3.0623.

3.063 Modulus of rigidity.

3.064 Tangent modulus.

3.0641 Tangent modulus curves at room and elevated temperature for annealed and aged bar. Figure 3.0641.

3.065 Secant modulus.

3.0651 Secant modulus curves at room and elevated temperatures for annealed and aged bar. Figure 3.0651

4. FABRICATION

4.01 Formability

4.011 General. This alloy is hot-worked readily by conventional rolling and forging operations, and is easily cold-worked by conventional procedures in the annealed condition. A preliminary soak at 2300F (homogenizing treatment) is recommended. Provision should be made for adequate work to break up the as-cast structure and to minimize directionality. For optimum properties, a maximum reheating temperature of 2000F is suggested prior to final hot-working operation; however, this temperature will depend on the degree and method of hot-working. Finishing should be in the range 1500 to 1800F, accompanied by about 25 percent reduction. Attention to cooling should be given to avoid isothermal

Fe
18 Ni
9 Co
5 Mo
Ti
Al

18 Ni Maraging (300)

embrittlement (see 1.094). Hot forming and bending should be performed at temperatures under 1600F to prevent grain coarsening. Because of its low work hardening characteristics, this alloy may be cold reduced by substantial amounts before intermediate annealing is required (re-annealing will essentially remove the effects of cold work). Cold work prior to aging will increase the aged strengths but will reduce fracture toughness. Severely cold-worked parts should be re-annealed (3)(4)(5)(53)(56)(57).

4.012 Forging. Preliminary soak at 2300F for homogenization. Starting temperature of 2000F maximum is preferred. Preheat for sections greater than 6 inches square 1700 to 1800F, approximately 15 minutes per inch of thickness. Finish temperature 1500 to 1700F. Reheat at 1900F. Do not delay cooling (see 1.094).

4.013 Rolling.

4.0131 Bar, Start 2000F maximum.

4.0132 Plate. Start at 2000F, maximum preferably, and finish at 1600F, or start at 1750 to 2000F with reheats at the same temperature and finish rolling at 1500 to 1600F. Cooling to room temperature should not be delayed (see 1.094).

4.0133 Sheet. Start 1800 to 1900F and finish 1500 to 1600F

4.014 Extruding.

4.015 Drawing.

4.02 Machining and Grinding

4.021 General. This alloy is machined most easily in the solution annealed condition. After aging its machinability is comparable to AISI 4340, at equal hardness levels. Reduced surface speeds are helpful. Carbide cutters with ample water soluble coolants are recommended (68) (see also (3)(5)). However, because of its dimensional stability, machining prior to aging should be considered.

4.03 Welding

4.031 General. This alloy is weldable in both the solution annealed and fully heat treated conditions. Gas shielded processes (GMA and GTA) are suitable for this alloy. Using proper techniques, joint efficiences from 90 to 100 percent are obtainable for aged (900F, 3 hours) welds in sheet and heavy sections. Submerged arc welding is not recommended due to a pronounced tendency for hot cracking, low fracture toughness, and severe embrittlement in the heat affected zone (HAZ). For a more detailed discussion see 18 Ni (250 ksi) maraging steel.

4.032 Filler wire. A minimum of 0.35 percent titanium in the filler wire is necessary to prevent objectionable porosity in GMA welds. Titanium in excess of about 0.7 percent with GMA and about 1.0 percent with GTA tends to produce a sensitivity to hot cracking and a weld deposit of decreased toughness. The residual element content of the filler should be as low as possible with the following recommended maximums: 0.03C, 0.05 Si and 0.05 Mn (carbon should preferably be kept well below this maximum). Vacuum melting of wire is recommended. Argon is recommended for use with either GMA or GTA process.

4.033 Sheet metal welds. Welds in thin sections are subject to high dilution effects and are markedly influenced by the welding procedure. Recommended wire compositions are given in Table 4.035. Improved strength with only a small loss in toughness can be obtained by a double pass procedure (see Table 4.035).

4.034 Plate weld. Attempts to increase weld strength by the use of high hardener filler wire have been unsuccessful in the gas shielded processes because of the formation of coarse pools of austenite in the weld metal which do not respond to subsequent aging treatment. Using proper procedures and filler wire in multi-pass GTA or GMA process, weldments with joint efficiences of better than 90 percent and with fracture toughness comparable to the base metal may be obtained. Local aging after welding is often used; however, the effectiveness of this treatment in achieving desired strengths and toughness should be carefully checked (34)(see also 18 Ni (250) maraging steel).

4.035 Typical mechanical properties and recommended wire compositions for sheet and plate. Table 4.035.

TABLE 4.035

Source	(13)				
Alloy	Fe-18Ni-9Co-5Mo-Ti-Al (280 ksi)				
Condition	Weld + 900F, 3 hrs				
Form	1/2 in plate	0.072 in sheet			
Process	GMA	GTA			
Wire	18Ni-8.5Co-5Mo-0.60Ti-0.2Al	17.5Ni-9Co-5Mo-0.8Ti-0.2Al		17.5Ni-9Co-5Mo-1.1Ti-0.2Al	
Procedure (b)	-	A	B	A	B
F_{tu} - ksi (a)	243	265	285	261	283
F_{ty} - ksi	241	261	280	259	278
e(1.4 in) percent	6	-	-	-	-
RA - percent	21	-	-	-	-

(a) Specimen transverse to weld.
(b) A = 100 amps, 10 volts, 8 in/min, one pass filler added.
B = Two passes. First pass - A; second pass no filler 80 amps, 9 volts 8 in/min over first pass.

4.04 Heat Treatment

4.041 General. Before heating remove grease and oil (see 4.05). Furnace fuel oil should not contain more than 0.75 percent sulfur by weight; fuel gas not more than 100 total grains of sulfur per 100 cu ft. Furnace atmosphere should not be carburizing. Atmosphere containing 5 percent CO_2 is suggested (5). Aging is normally done in air.

4.05 Surface Treatment

4.051 General. Sand blasting removes oxide scale effectively. Pickling solution 18 percent sulfuric acid at 150 - 160F is recommended. Sodium hydride and other high temperature (> 700F) descaling treatments should be avoided (5).

4.052 Nitriding. Nitriding at 850F for 20 hours or 800F for 44 hours is recommended and will give case hardness of about 66 Rockwell C. Higher temperature gives lower case hardness. Longer times will increase case depths but very long times may require a drop in temperature to maintain case hardness (68).

	Fe
18	Ni
9	Co
5	Mo
	Ti
	Al

18 Ni Maraging (300)

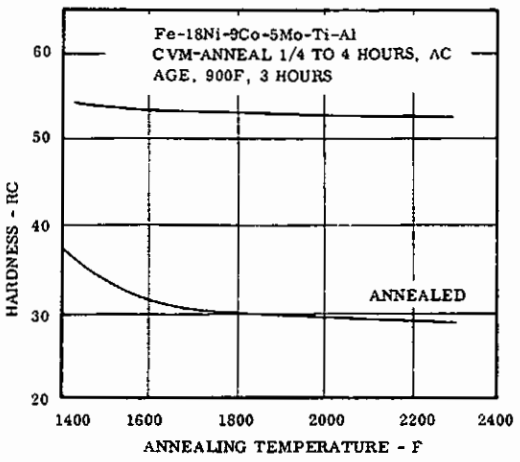


FIG. 1.063 EFFECT OF ANNEALING TEMPERATURE AND AGING ON HARDNESS. (57)

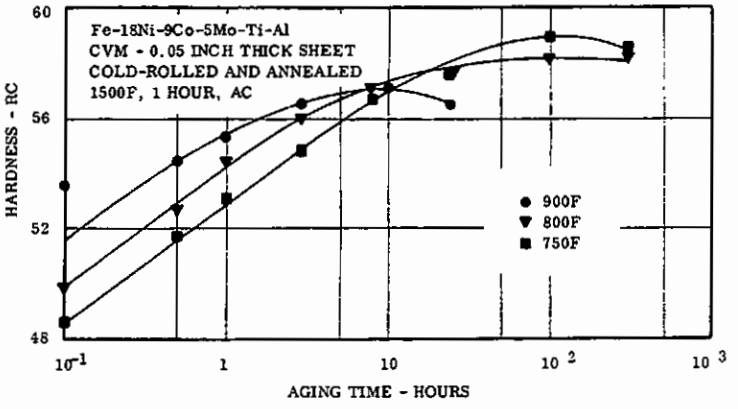


FIG. 1.0642 EFFECT OF AGING TEMPERATURE AND TIME ON HARDNESS OF COLD-ROLLED AND ANNEALED SHEET. (27, p. 397)

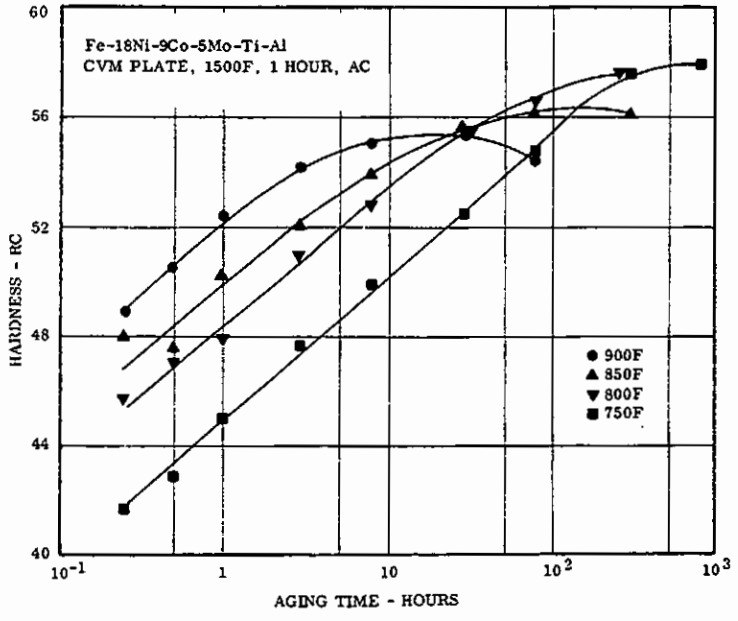


FIG. 1.0641 EFFECT OF AGING TEMPERATURE AND TIME ON HARDNESS OF PLATE. (7, p. 23)

	Fe
18	Ni
9	Co
5	Mo
	Ti
	Al

18 Ni Maraging (300)

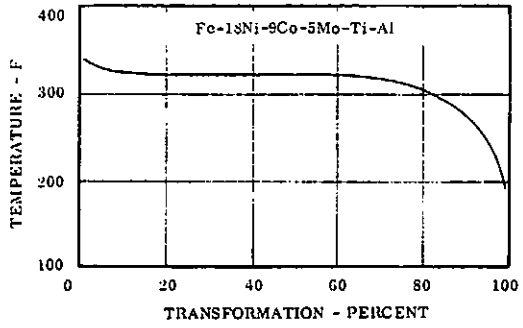


FIG. 2.0122 AUSTENITE - TO - MARTENSITE TRANSFORMATION CURVE (7, p. 21)

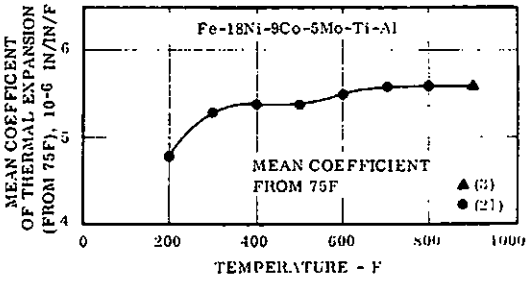


FIG. 2.0141 MEAN COEFFICIENT OF THERMAL EXPANSION FROM 75F. (3)(21, pp. 109 and 214)

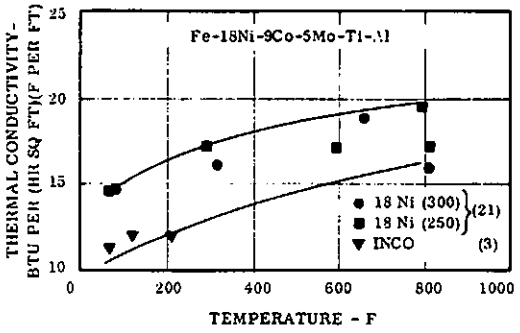


FIG. 2.013 THERMAL CONDUCTIVITY. (3)(21, p. 107)

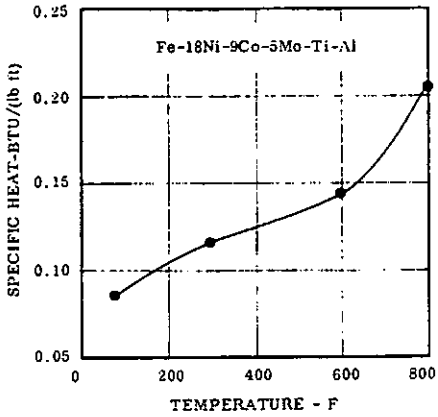


FIG. 2.015 SPECIFIC HEAT AT CONSTANT PRESSURE (1 ATM.) (21, pp. 106 and 209)

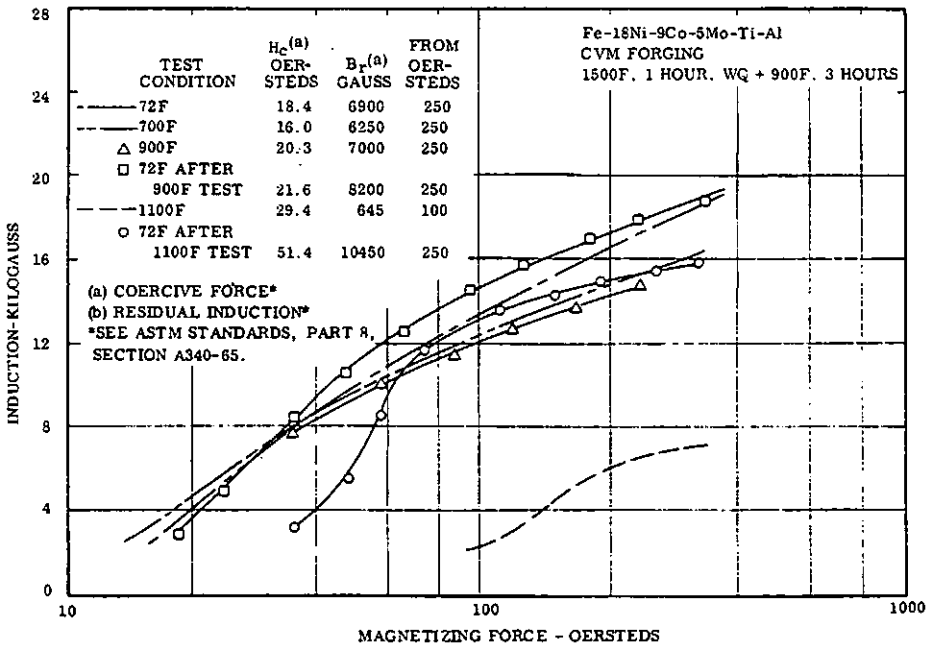
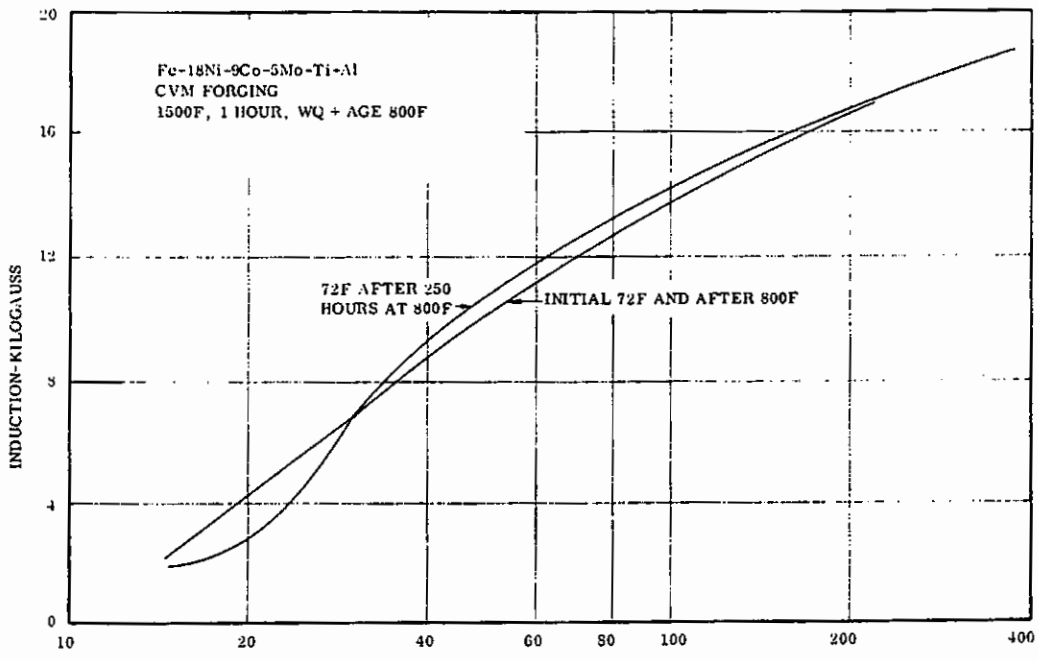


FIG. 2.02312 D.C. MAGNETIZATION CURVES FOR FORGING TESTED IN AIR. (22, p. 121)



	Fe
18	Ni
9	Co
5	Mo
	Ti
	Al

18 Ni Maraging (300)

FIG. 2.02313 ROOM TEMPERATURE D.C. MAGNETIZATION CURVES FOR FORGING BEFORE AND AFTER AGING AT 800F (TESTED IN AIR). (22, p. 123)

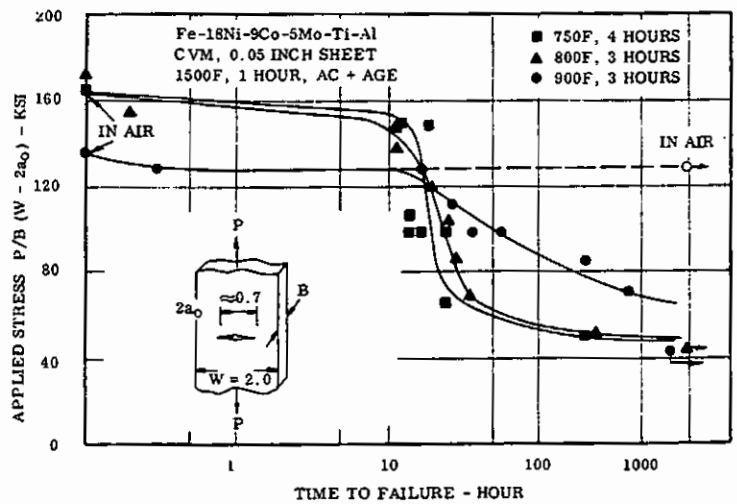


FIG. 2.03121 EFFECT OF AGING TREATMENT ON DELAYED FAILURE OF SHEET IN DISTILLED WATER AT 70F. (27, p. 404)

	Fe
18	Ni
9	Co
5	Mo
	Ti
	Al

18 Ni Maraging (300)

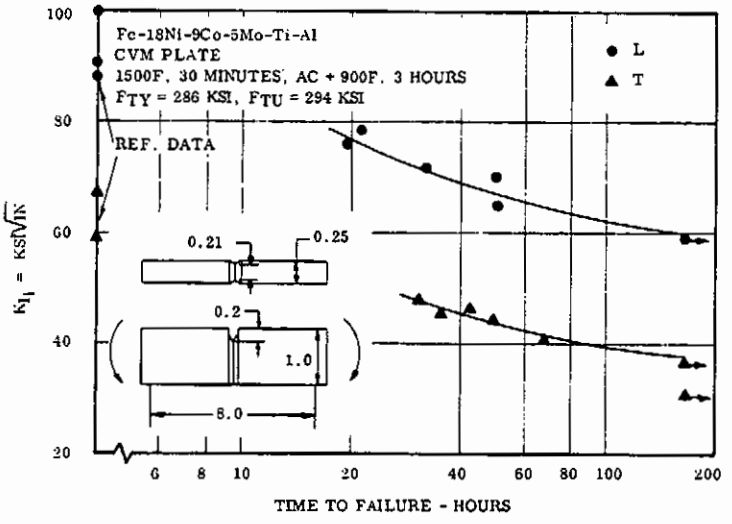


FIG. 2.03122 DELAYED FAILURE CHARACTERISTICS OF PLATE IN DISTILLED WATER AT ROOM TEMPERATURE. (26)

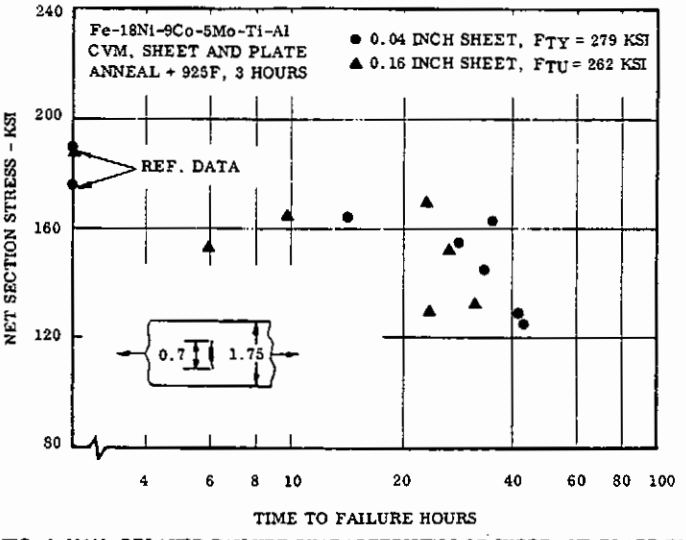


FIG. 2.03123 DELAYED FAILURE CHARACTERISTICS OF SHEET AND PLATE IN 3 PERCENT SALT SOLUTION AT ROOM TEMPERATURE. (33, p. A121)

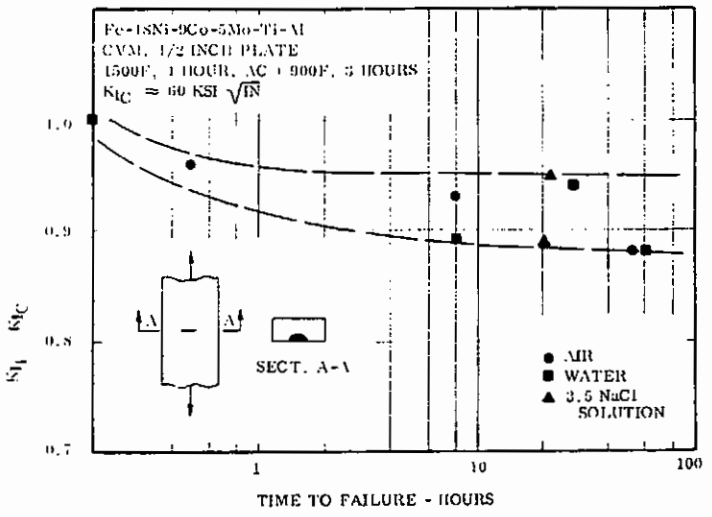


FIG. 2.03124 DELAYED FAILURE CHARACTERISTICS OF PLATE IN SEVERAL ENVIRONMENTS. (34, p. 40)

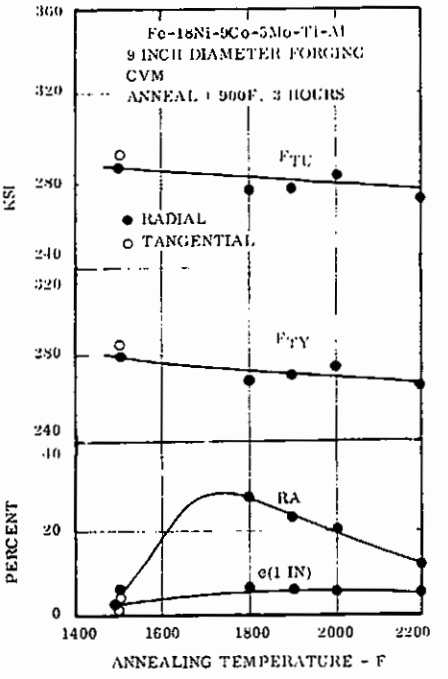


FIG. 3.02131 INFLUENCE OF ANNEALING TEMPERATURE ON THE ROOM TEMPERATURE TENSILE PROPERTIES OF ANNEALED AND AGED FORGINGS. (9)

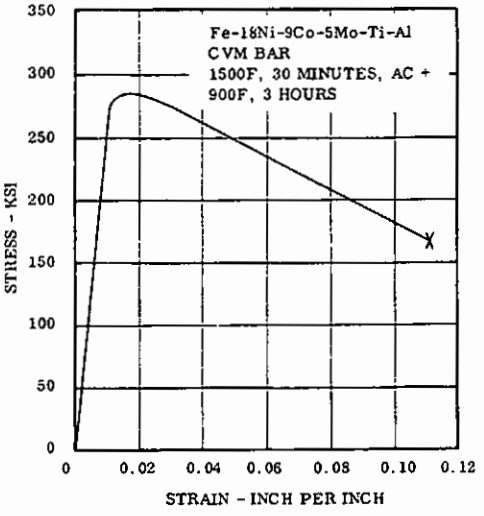


FIG. 3.02111 STRESS - STRAIN CURVE FOR ANNEALED AND AGED BAR. (5)

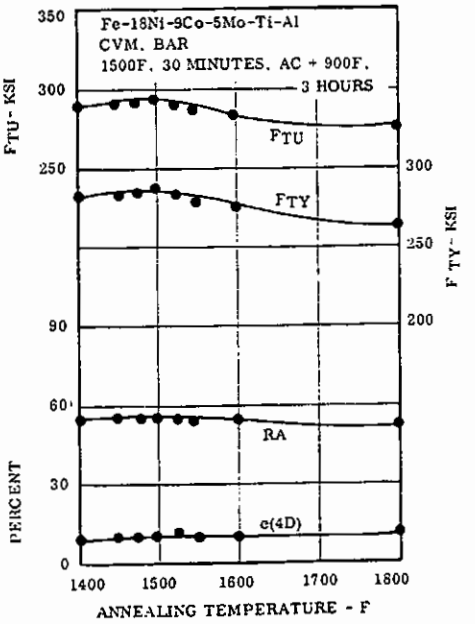


FIG. 3.02132 INFLUENCE OF ANNEALING TEMPERATURE ON THE TENSILE PROPERTIES OF BAR. (5, p. 11)

	Fe
18	Ni
9	Co
5	Mo
	Ti
	Al

18 Ni Maraging (300)

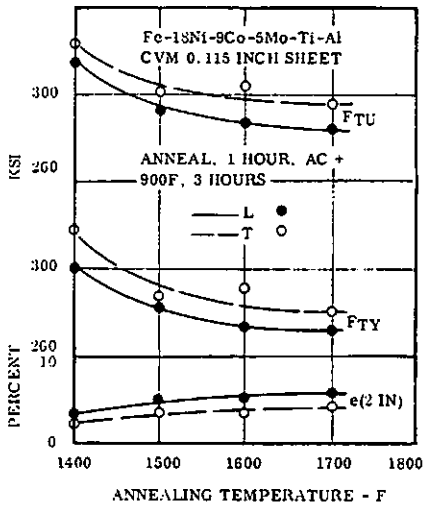


FIG. 3.02133 EFFECT OF ANNEALING TEMPERATURE ON THE TENSILE PROPERTIES OF ANNEALED AND AGED SHEET. (57)

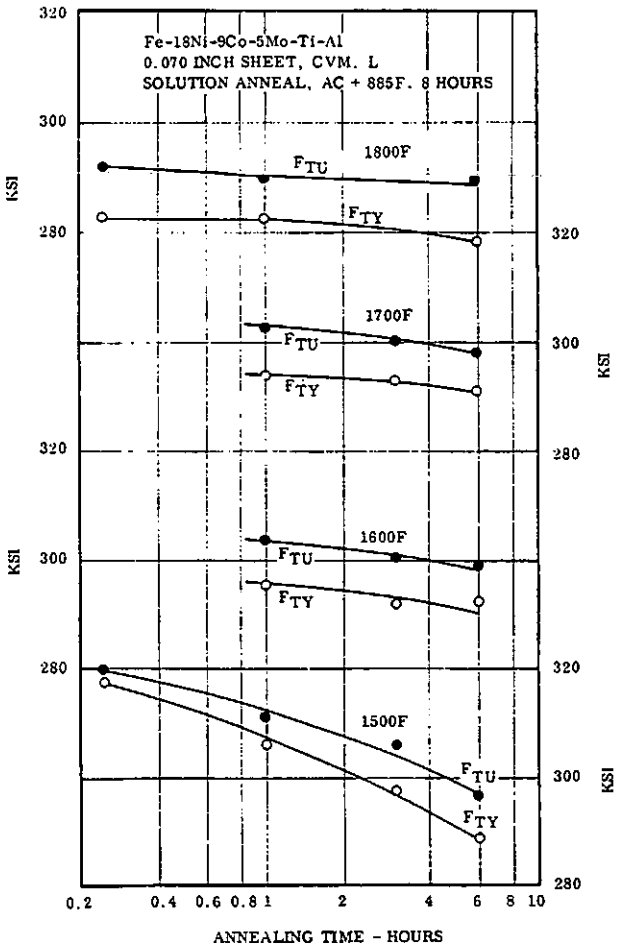


FIG. 3.02134 EFFECT OF ANNEALING TEMPERATURE AND TIME ON THE TENSILE PROPERTIES OF ANNEALED AND AGED SHEET. (31, p. 59 - 61)

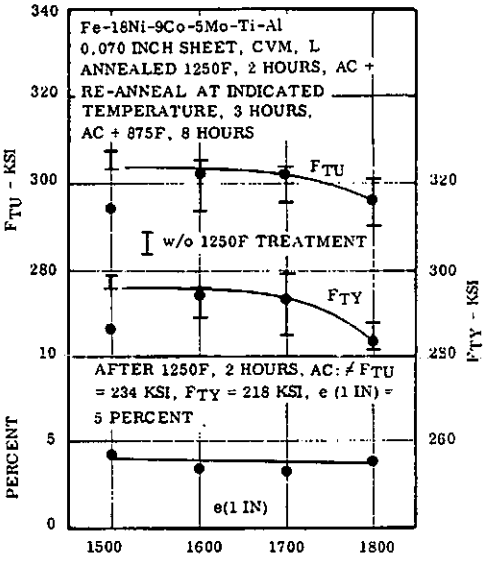


FIG. 3.02135 EFFECT OF RE-SOLUTION ANNEALING AND AGING ON THE TENSILE PROPERTIES OF SHEET SUBJECTED TO PRIOR AUSTENITE - REVERSION TREATMENT. (31, p. 59 and 62)

	Fe
18	Ni
9	Co
5	Mo
	Ti
	Al

18 Ni Maraging (300)

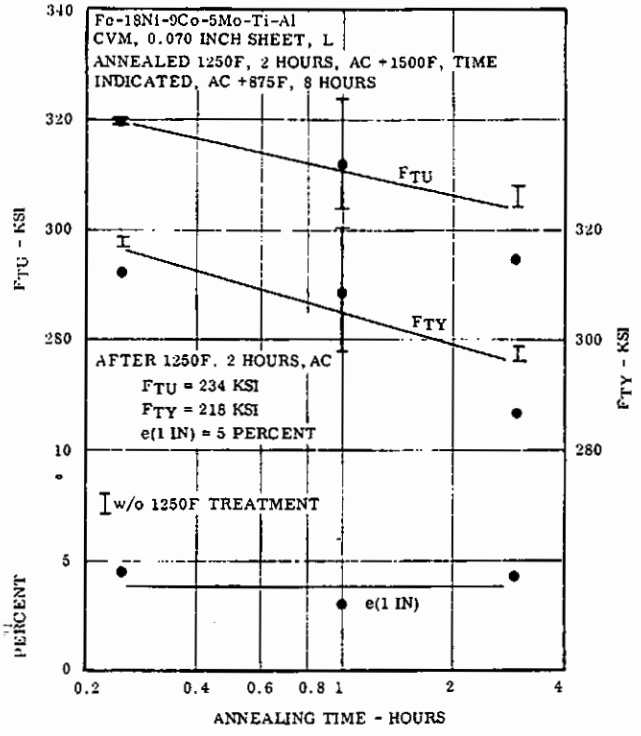


FIG. 3.02136 EFFECT OF RESOLUTION ANNEALING TIME ON THE TENSILE PROPERTIES OF SHEET SUBJECTED TO PRIOR AUSTENITE - REVERSION TREATMENT. (31, p. 59 & 62)

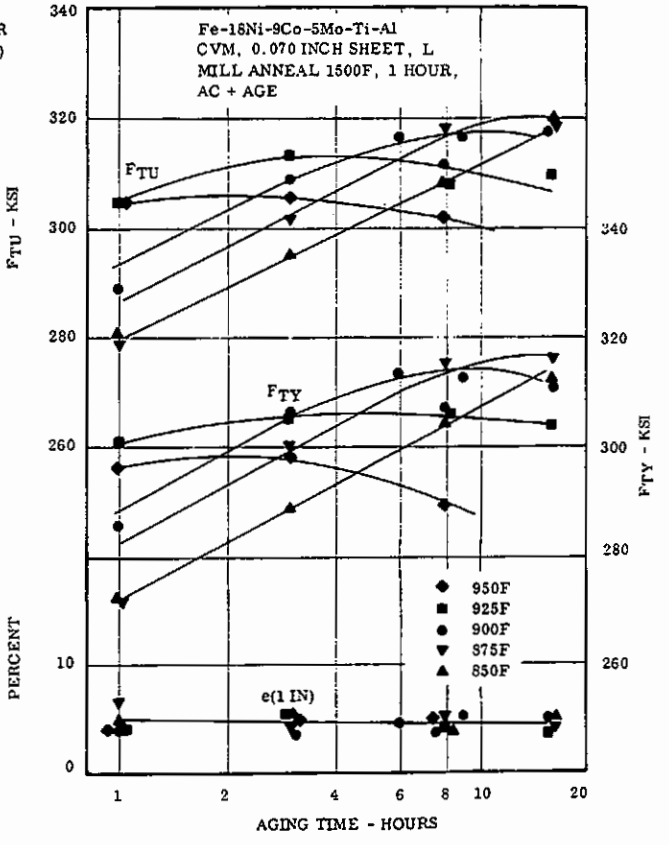


FIG. 3.021411 EFFECT OF AGING TEMPERATURE AND TIME ON THE TENSILE PROPERTIES OF SHEET. (31, p. 52 - 56)

	Fe
18	Ni
9	Co
5	Mo
	Ti
	Al

18 Ni Maraging (300)

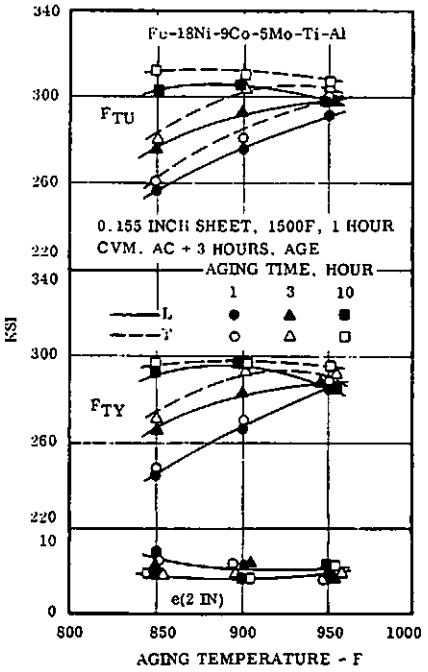


FIG. 3.021412 EFFECT OF AGING TEMPERATURE AND TIME ON THE TENSILE PROPERTIES OF ANNEALED SHEET. (35)

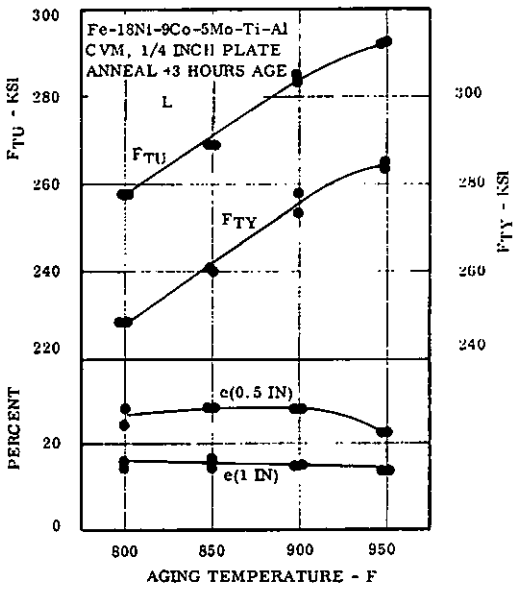


FIG. 3.021421 EFFECT OF AGING TEMPERATURE ON TENSILE PROPERTIES OF PLATE. (37, p. A-8)

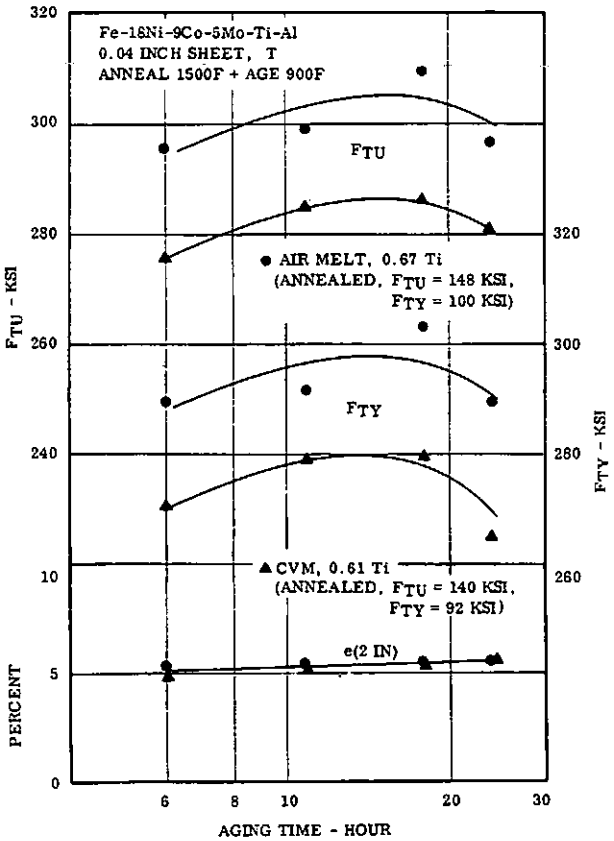


FIG. 3.021413 EFFECT OF AGING TIME ON TENSILE PROPERTIES OF AIR-MELTED AND CVM SHEET. (36)

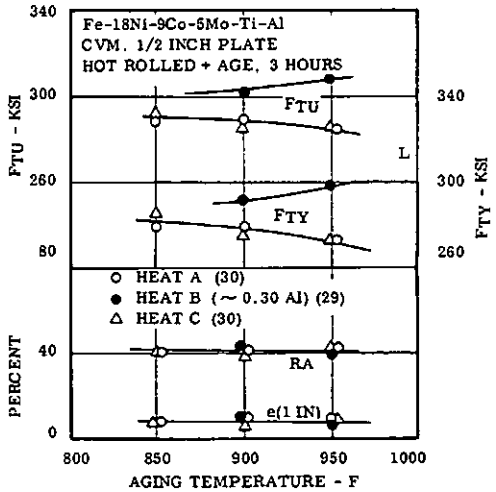


FIG. 3.021422 EFFECT OF AGING TEMPERATURE ON TENSILE PROPERTIES OF HOT ROLLED PLATE FROM THREE HEATS. (38)(39)

	Fe
18	Ni
9	Co
5	Mo
	Ti
	Al

18 Ni Maraging (300)

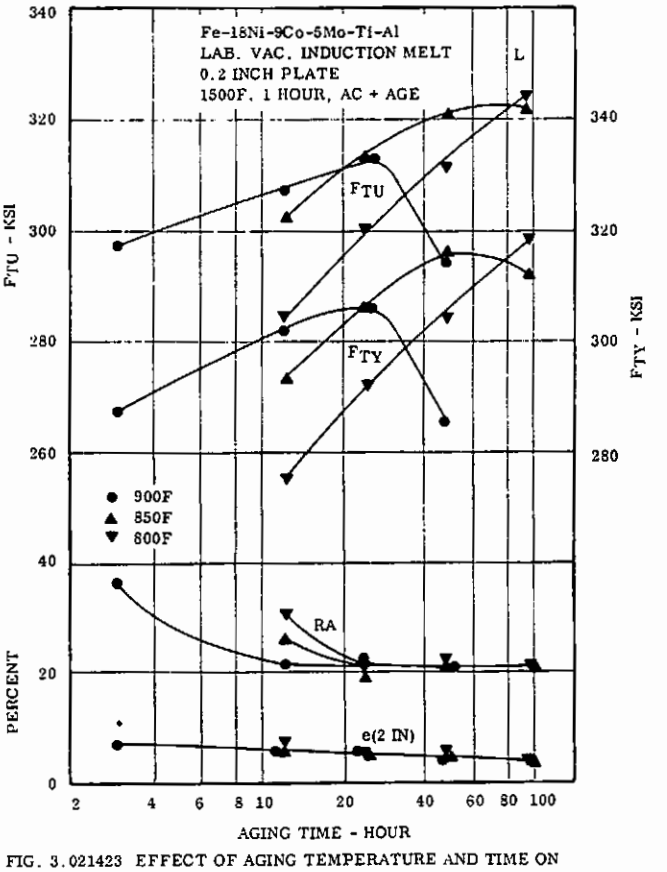


FIG. 3.021423 EFFECT OF AGING TEMPERATURE AND TIME ON TENSILE PROPERTIES OF LABORATORY VACUUM - INDUCTION MELTED PLATE. (45)

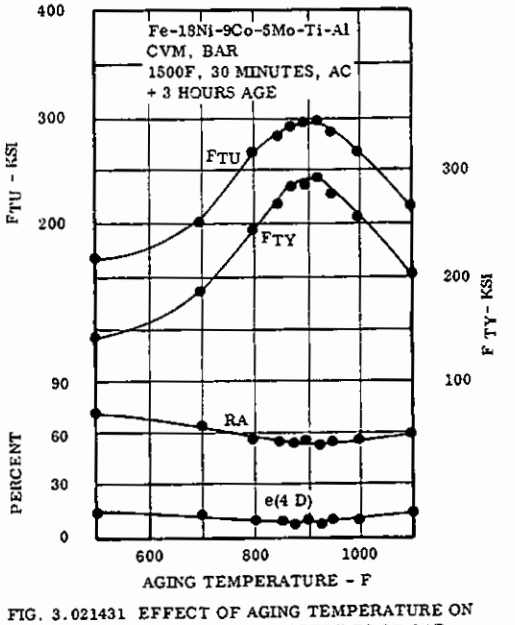


FIG. 3.021431 EFFECT OF AGING TEMPERATURE ON THE TENSILE PROPERTIES OF BAR. (5, p. 12)

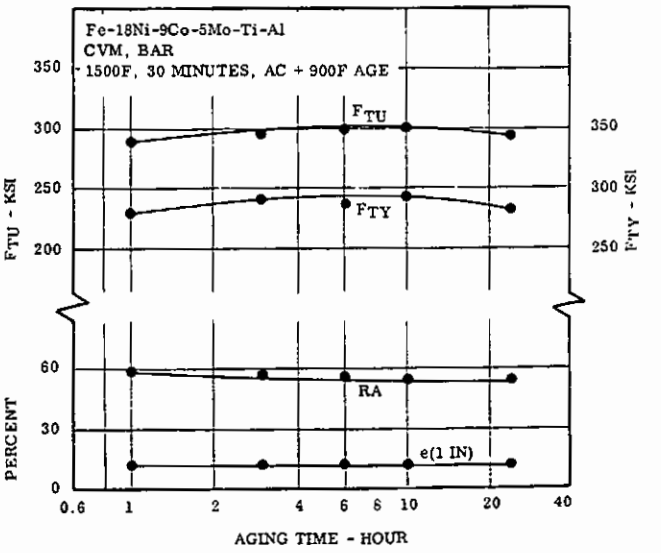


FIG. 3.021432 EFFECT OF AGING TIME ON TENSILE PROPERTIES OF ANNEALED BAR. (5, p. 12)

Fe
18 Ni
9 Co
5 Mo
Ti
Al

18 Ni Maraging (300)

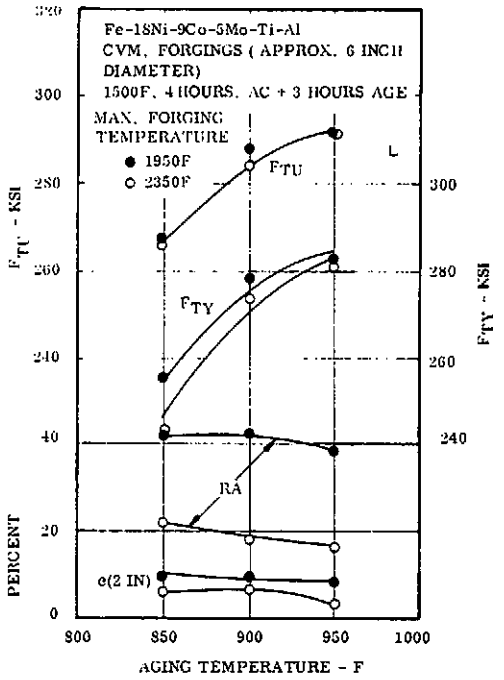


FIG. 3.021441 EFFECT OF AGING TEMPERATURE AND MAXIMUM FORGING TEMPERATURE ON TENSILE PROPERTIES OF FORGINGS. (40, p. 8 and 9)

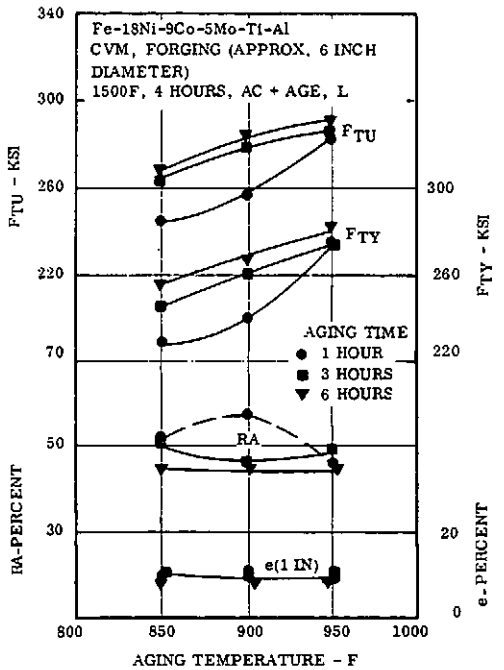


FIG. 3.021442 EFFECT OF AGING TEMPERATURE AND TIME ON TENSILE PROPERTIES OF FORGINGS (40, p. 8)

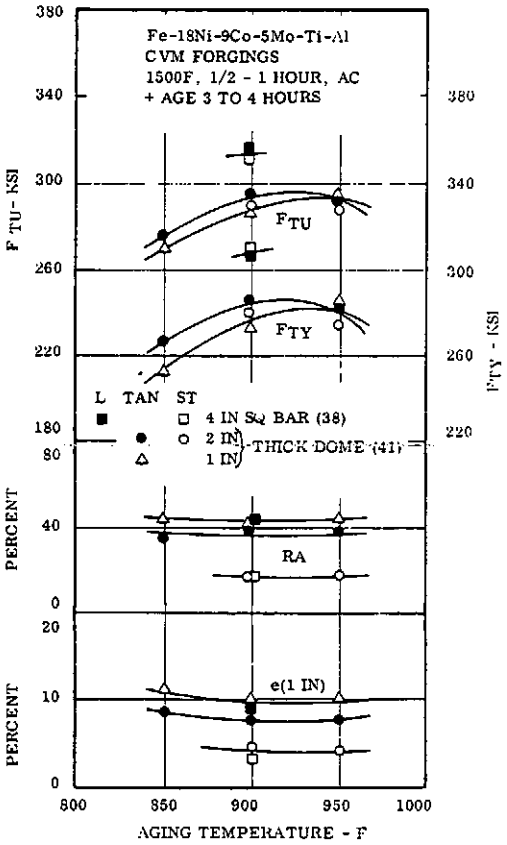


FIG. 3.021443 EFFECT OF AGING TEMPERATURE ON THE TENSILE PROPERTIES OF FORGINGS. (38)(41)

	Fe
18	Ni
9	Co
5	Mo
	Ti
	Al

18 Ni Maraging (300)

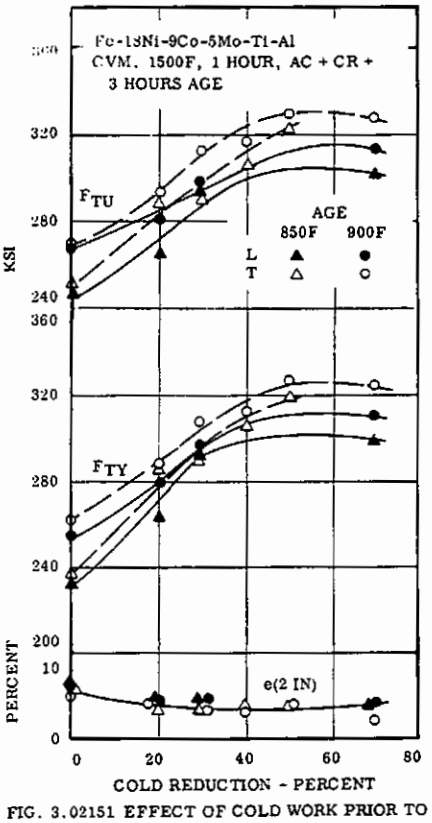


FIG. 3.02151 EFFECT OF COLD WORK PRIOR TO AGING ON TENSILE PROPERTIES OF ANNEALED SHEET. (35)

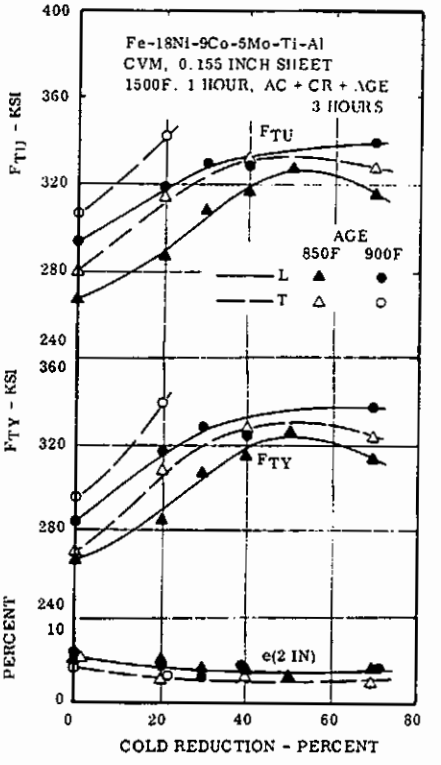


FIG. 3.02152 EFFECT OF COLD WORK PRIOR TO AGING ON TENSILE PROPERTIES OF ANNEALED SHEET. (35)

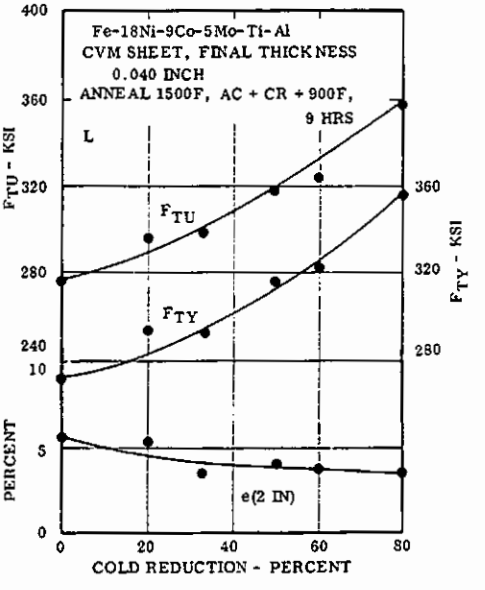


FIG. 3.02153 EFFECT OF COLD REDUCTION BEFORE AGING ON TENSILE PROPERTIES OF SHEET. (36)

	Fe
18	Ni
9	Co
5	Mo
	Ti
	Al

18 Ni Maraging (300)

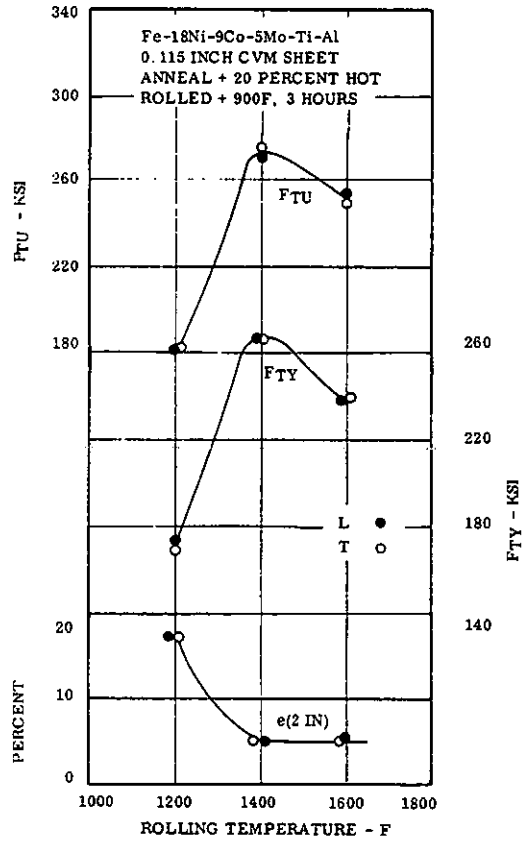


FIG. 3.02161 EFFECT OF ROLLING TEMPERATURE ON THE TENSILE PROPERTIES OF ANNEALED, ROLLED, AND AGED SHEET. (35)

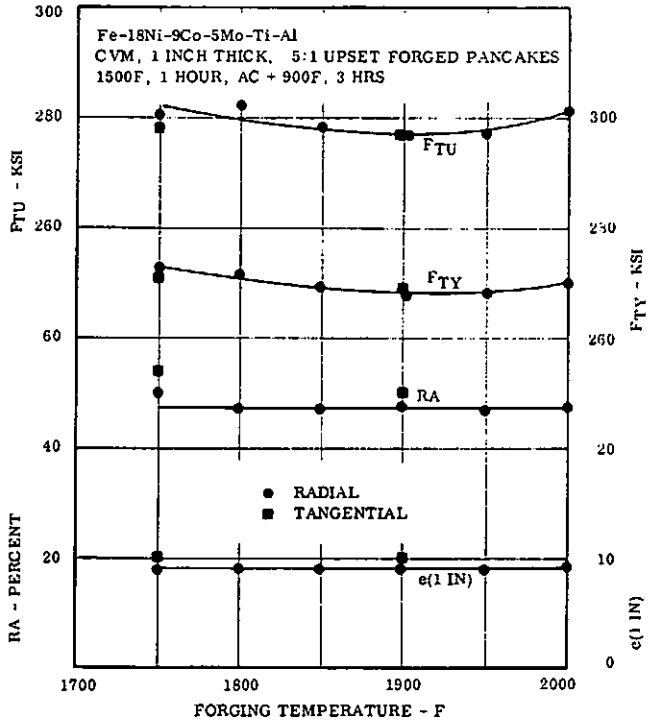


FIG. 3.02162 EFFECT OF FORGING TEMPERATURE ON THE TENSILE PROPERTIES OF 5 : 1 UPSET FORGED PANCAKES.
(44, p. 42 and 94)

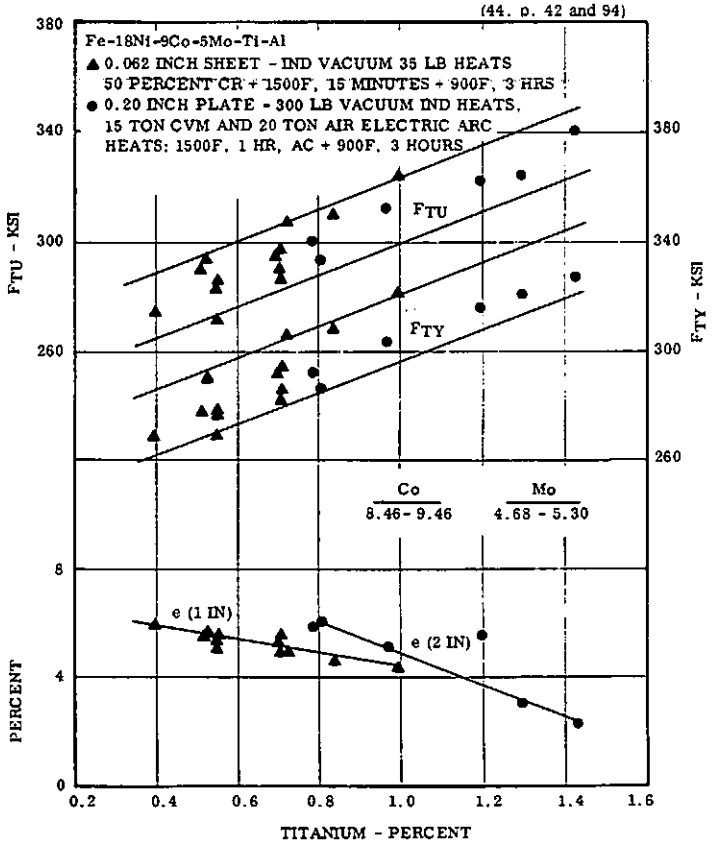


FIG. 3.0217 EFFECT OF TITANIUM ON ROOM TEMPERATURE TENSILE PROPERTIES OF ANNEALED AND AGED SHEETS FROM LABORATORY AND PRODUCTION HEATS (45)(46)(47)

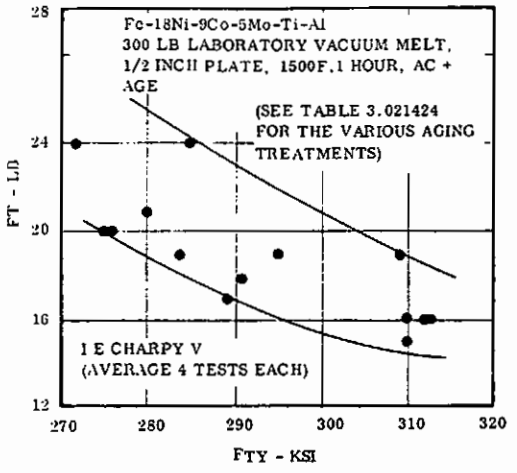


FIG. 3.0232 EFFECT OF YIELD STRENGTH ON IMPACT PROPERTIES OF 300 LB LABORATORY VACUUM MELTED PLATE. (62)

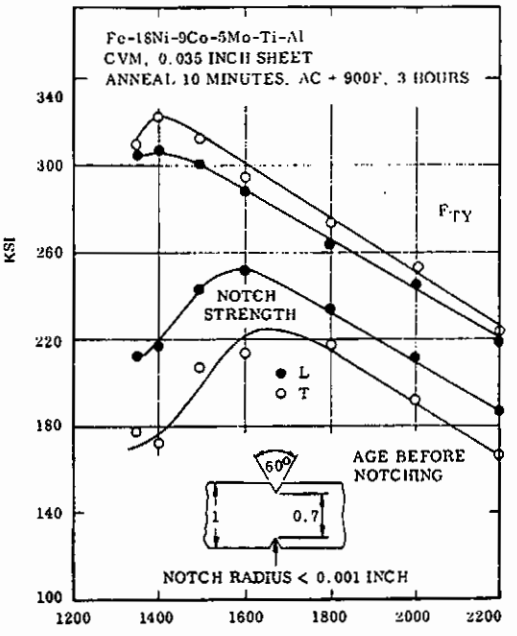


FIG. 3.027131 EFFECT OF ANNEALING TEMPERATURE ON THE SHARP NOTCH PROPERTIES OF 0.035 IN AGED SHEET. (52)

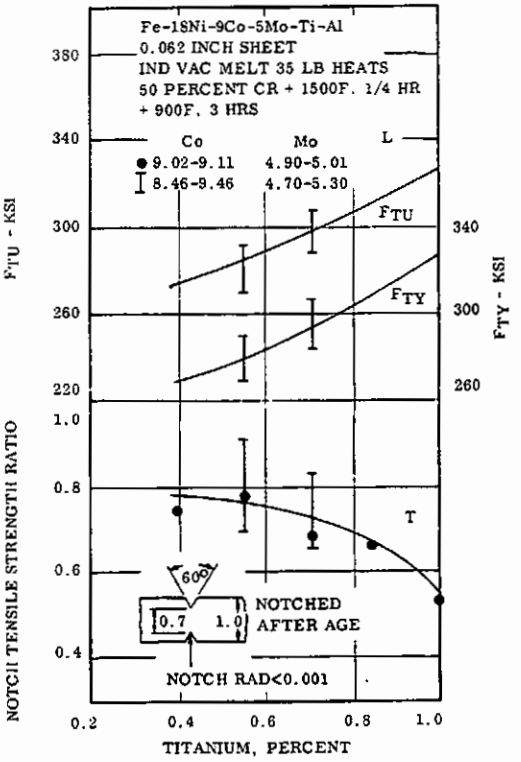


FIG. 3.02712 EFFECT OF TITANIUM ON SHARP NOTCH PROPERTIES OF ANNEALED AND AGED SHEET FROM LABORATORY HEATS. (46)

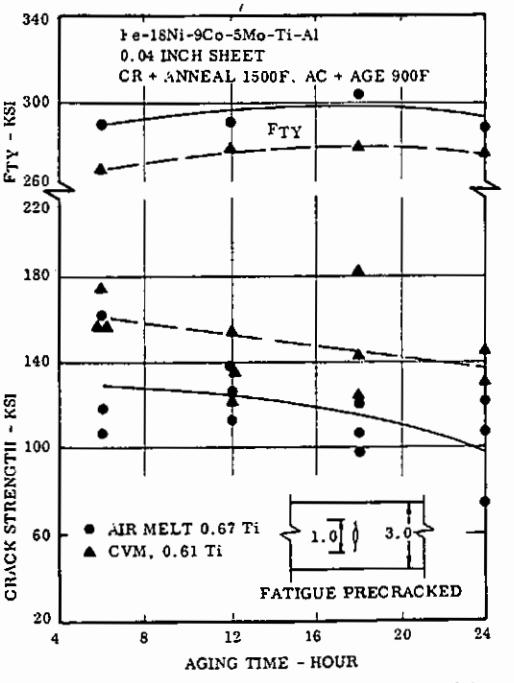


FIG. 3.027141 EFFECT OF AGING TIME ON THE CRACK STRENGTH OF AIR-MELT AND CVM 0.04 INCH SHEET. (36)

	Fe
18	Ni
9	Co
5	Mo
	Ti
	Al

18 Ni Maraging (300)

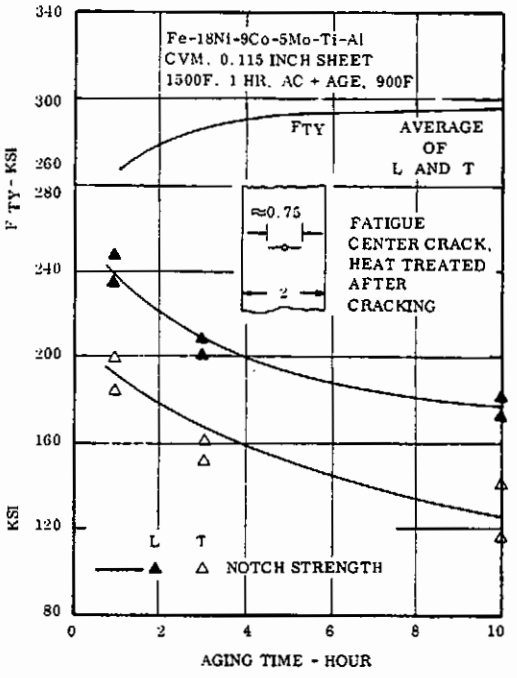


FIG. 3.027142 EFFECT OF AGING TIME ON SHARP NOTCH PROPERTIES 0.115 INCH SHEET. (57)

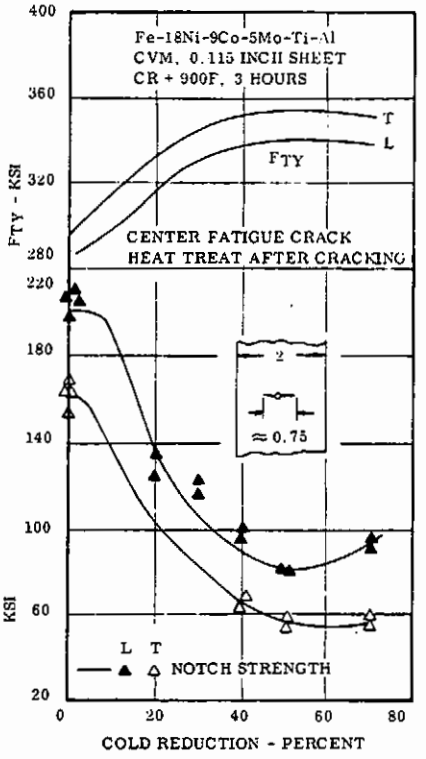


FIG. 3.027151 EFFECT OF COLD ROLLING PRIOR TO AGING ON CRACK STRENGTH OF SHEET (35)

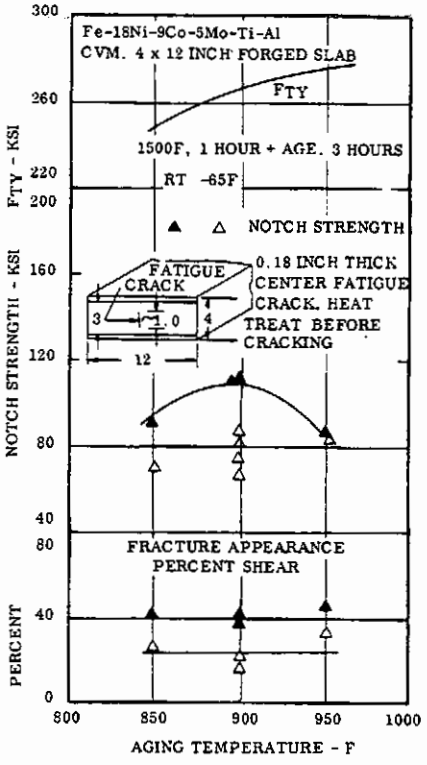


FIG. 3.027143 EFFECT OF AGING TEMPERATURE ON SHARP NOTCH PROPERTIES OF FORGED CVM SLAB. (54) (14)

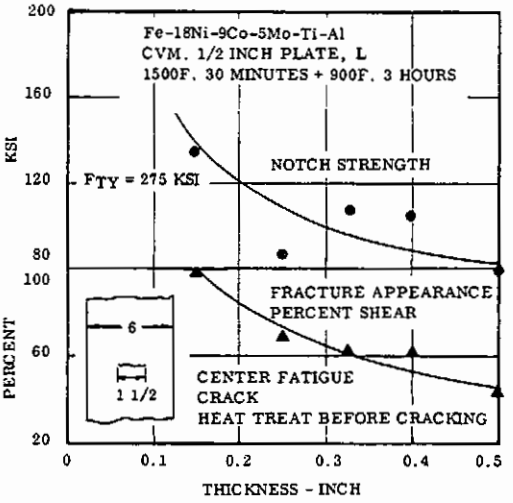


FIG. 3.027161 EFFECT OF THICKNESS ON CRACK STRENGTH OF CVM PLATE. (58)

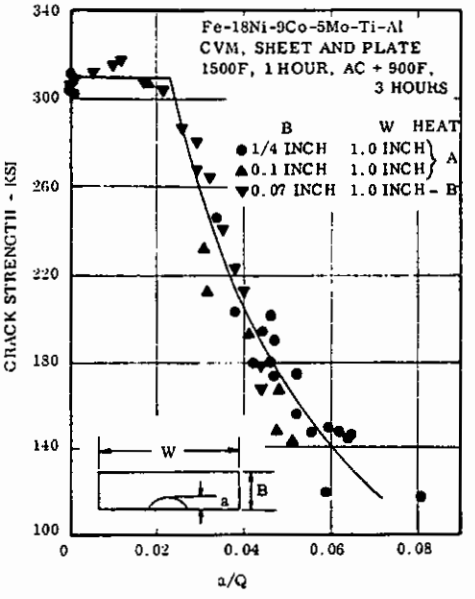


FIG. 3.027171 EFFECT OF SURFACE CRACK SIZE ON CRACK STRENGTH OF SHEET AND PLATE. (64)

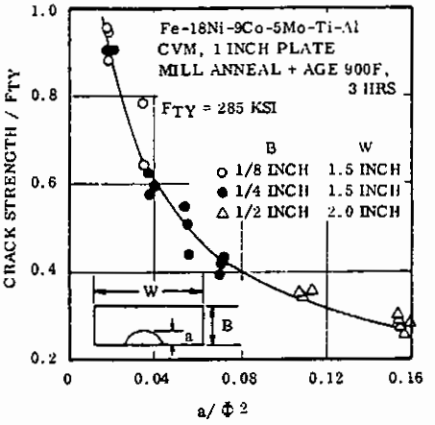


FIG. 3.027173 EFFECT OF SURFACE CRACK SIZE AND SPECIMEN SIZE ON THE CRACK STRENGTH OF CVM PLATE. (60, p. 31)

	Fe
18	Ni
9	Co
5	Mo
	Ti
	Al

18 Ni Maraging (300)

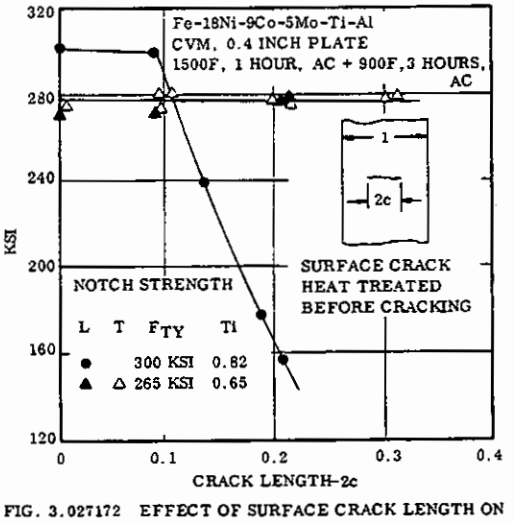


FIG. 3.027172 EFFECT OF SURFACE CRACK LENGTH ON CRACK STRENGTH OF CVM PLATE AT TWO Ti LEVELS. (59)

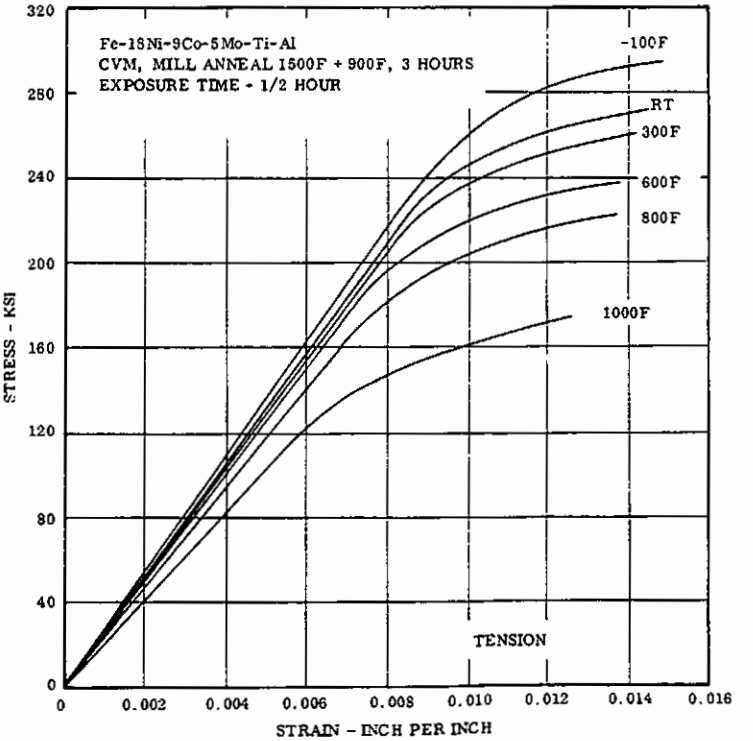


FIG. 3.03111 TYPICAL STRESS - STRAIN CURVES FOR TENSION AT CRYOGENIC, ROOM AND ELEVATED TEMPERATURES. (21, p. 65)

	Fe
18	Ni
9	Co
5	Mo
	Ti
	Al

18 Ni Maraging (300)

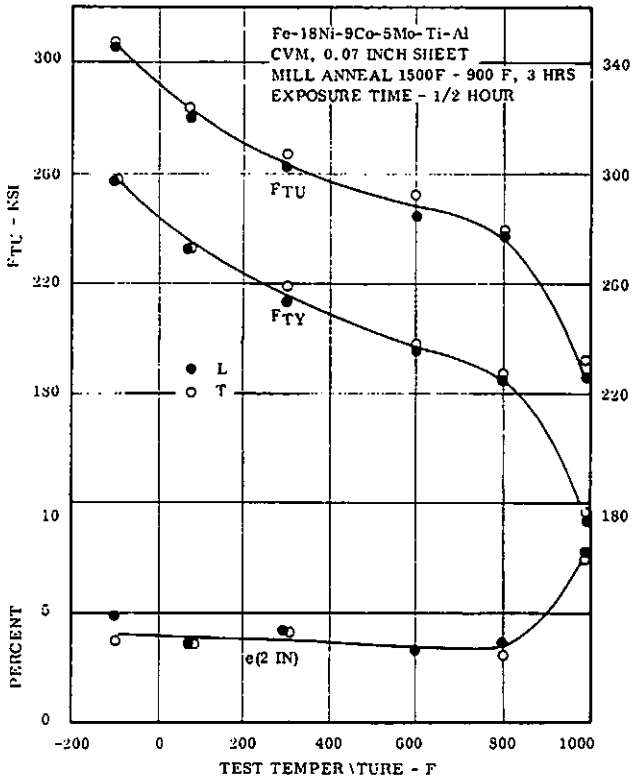


FIG. 3.03121 EFFECT OF TEST TEMPERATURE ON THE TENSILE PROPERTIES OF SHEET. (21, p. 162 - 165)

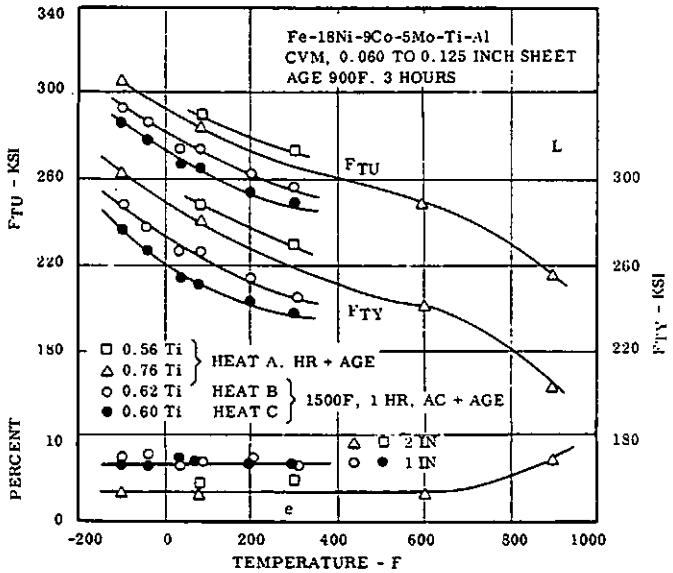


FIG. 3.03122 EFFECT OF TEST TEMPERATURE ON THE TENSILE PROPERTIES OF SHEETS FROM SEVERAL HEATS. (49)(50)(51)

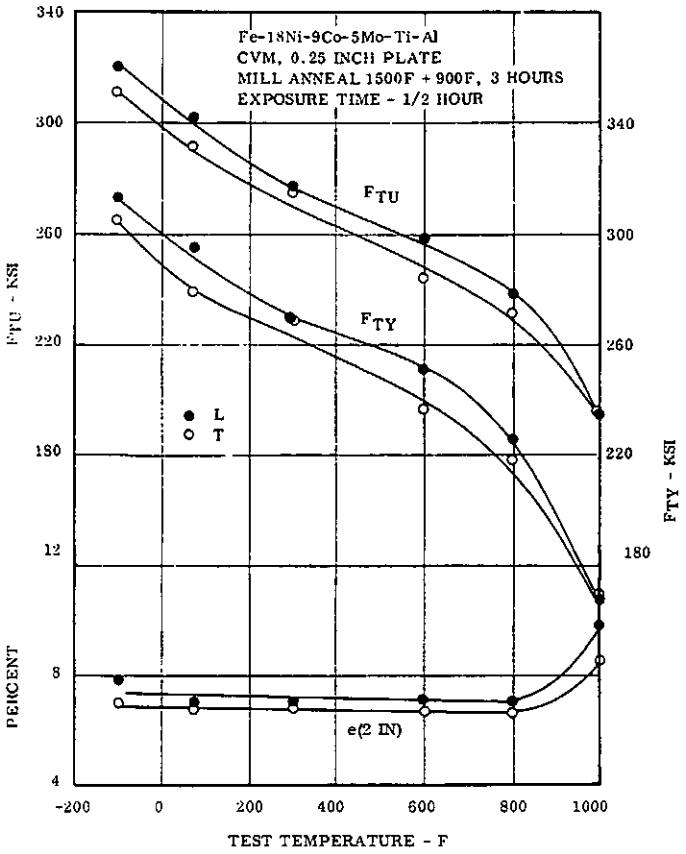


FIG. 3.03123 EFFECT OF TEST TEMPERATURE ON THE TENSILE PROPERTIES OF PLATE. (21, p.166 - 169)

	Fe
18	Ni
9	Co
5	Mo
	Ti
	Al

18 Ni Maraging (300)

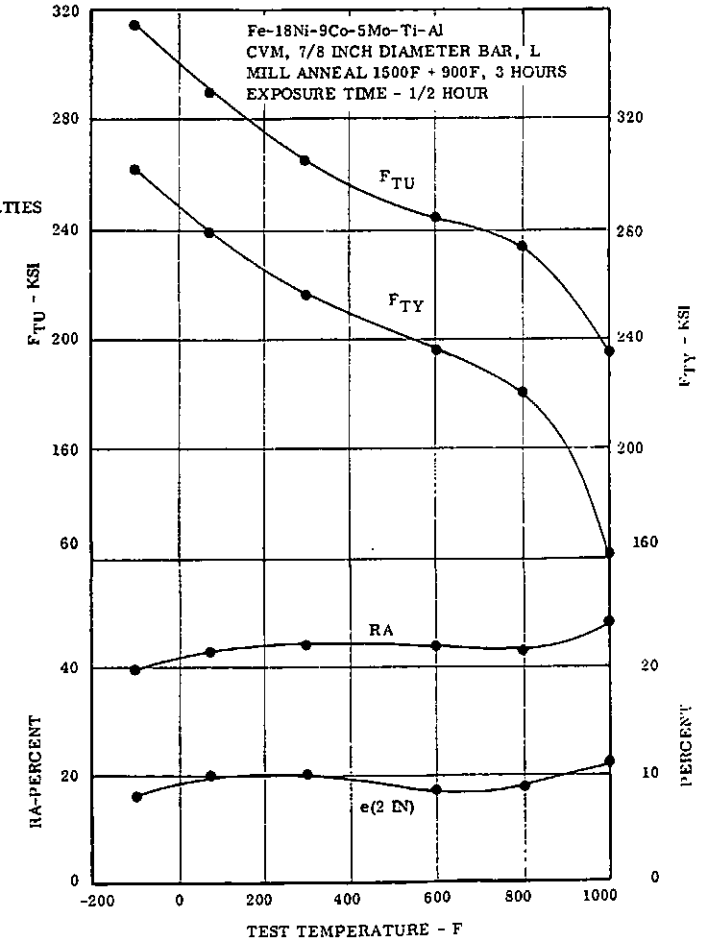


FIG. 3.03124 EFFECT OF TEST TEMPERATURE ON THE TENSILE PROPERTIES OF BAR. (21, p. 170 - 171)

	Fe
18	Ni
9	Co
5	Mo
	Ti
	Al

18 Ni Maraging (300)

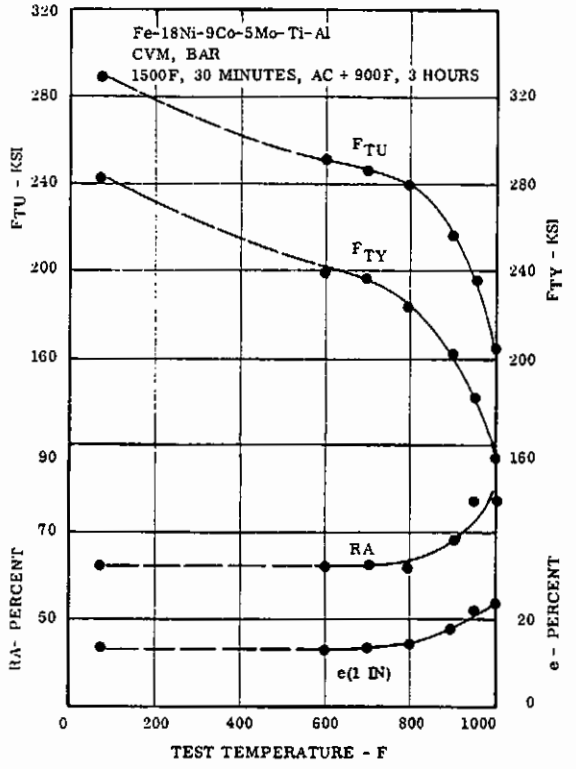


FIG. 3.03125 EFFECT OF TEST TEMPERATURE ON THE TENSILE PROPERTIES OF BAR. (5)

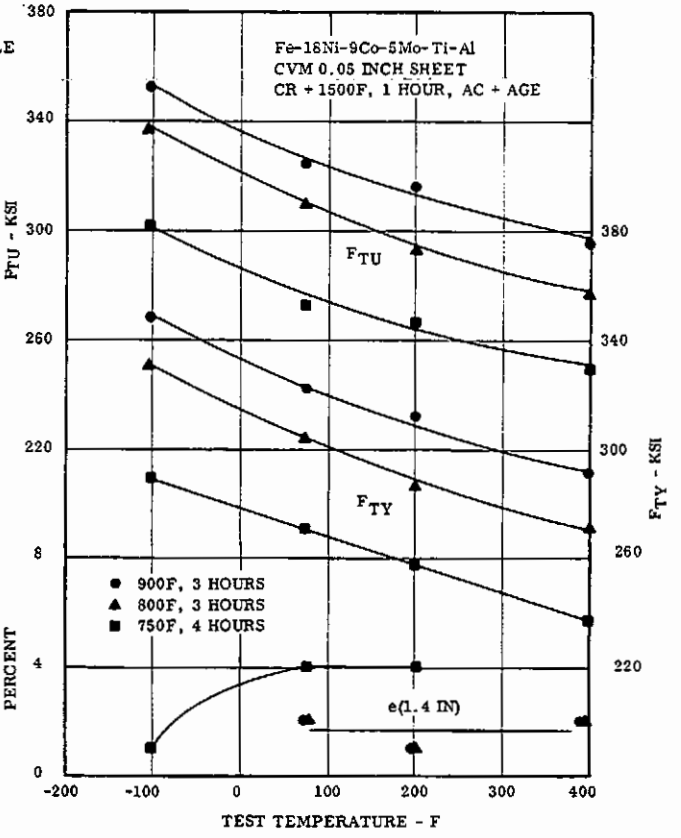


FIG. 3.03131 EFFECT OF AGING TREATMENT AND TEST TEMPERATURE ON THE TENSILE PROPERTIES OF COLD-ROLLED AND ANNEALED SHEET. (27)

	Fe
18	Ni
9	Co
5	Mo
	Ti
	Al

18 Ni Maraging (300)

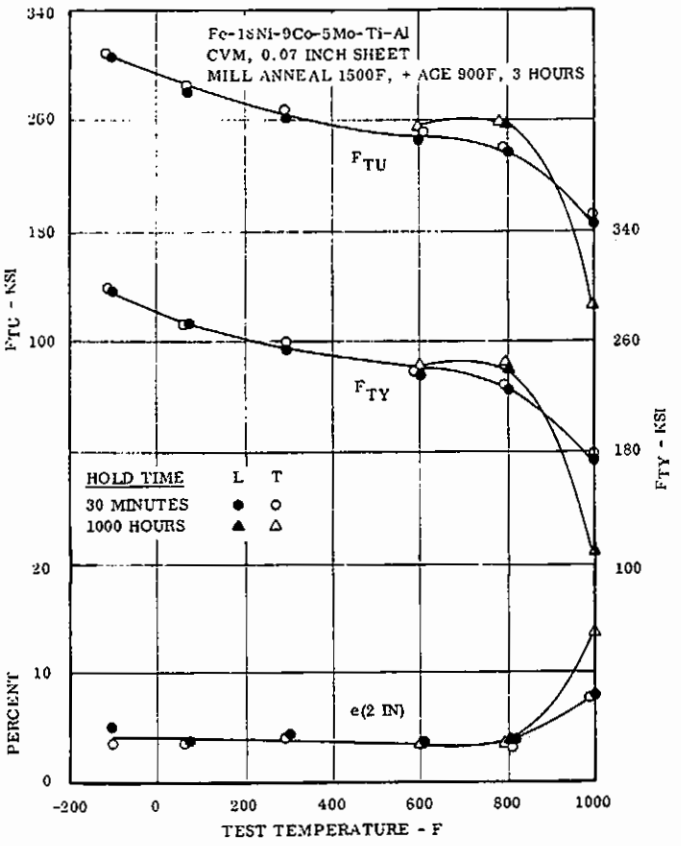


FIG. 3.03142 EFFECT OF TEST TEMPERATURE ON THE TENSILE PROPERTIES OF SHEET AFTER HOLDING 30 MINUTES AND 1000 HOURS AT TEST TEMPERATURE (21, p. 162 - 165, 196)

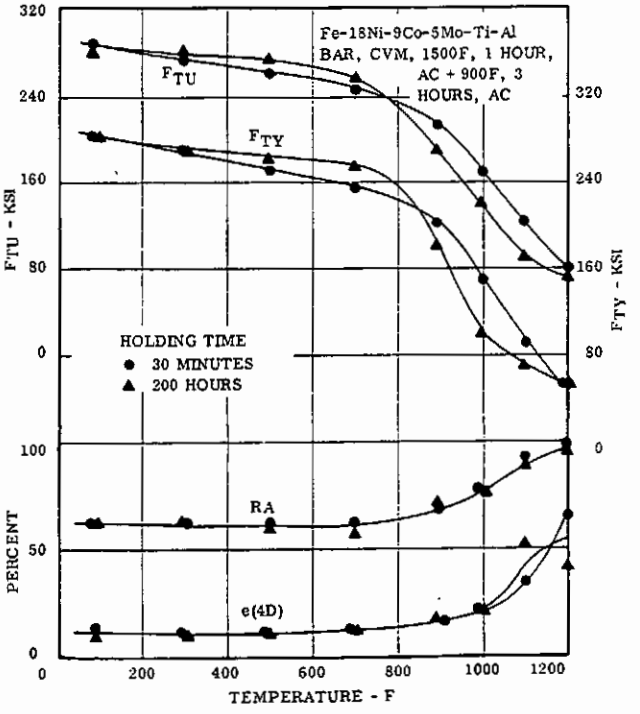


FIG. 3.03143 EFFECT OF TEST TEMPERATURE ON THE TENSILE PROPERTIES OF CVM BAR AFTER HOLDING 30 MINUTES AND 200 HOURS AT TEST TEMPERATURE.(51)

	Fe
18	Ni
9	Co
5	Mo
	Ti
	Al

18 Ni Maraging (300)

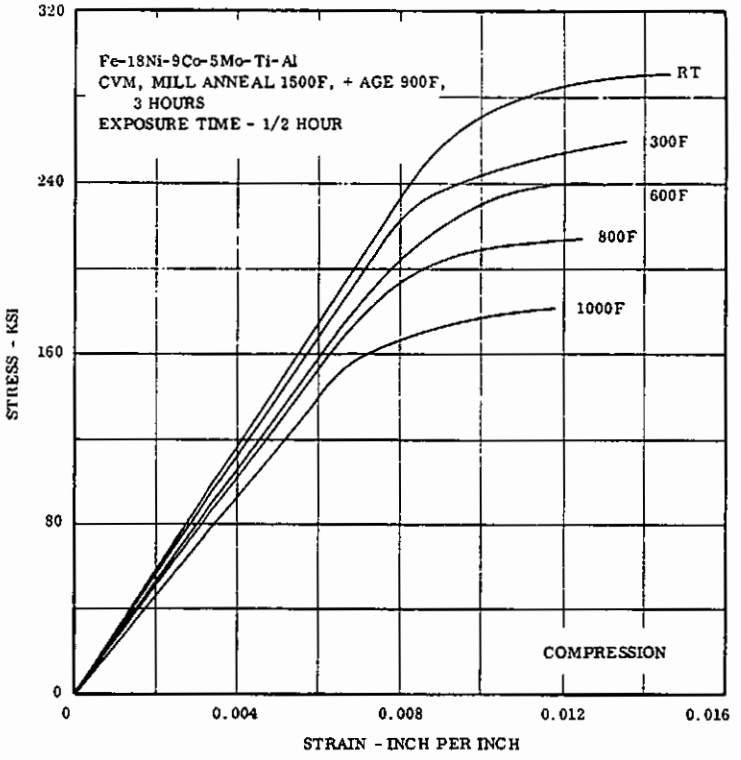


FIG. 3.03211 TYPICAL STRESS - STRAIN CURVES FOR COMPRESSION AT ROOM AND ELEVATED TEMPERATURES.(21. p. 66)

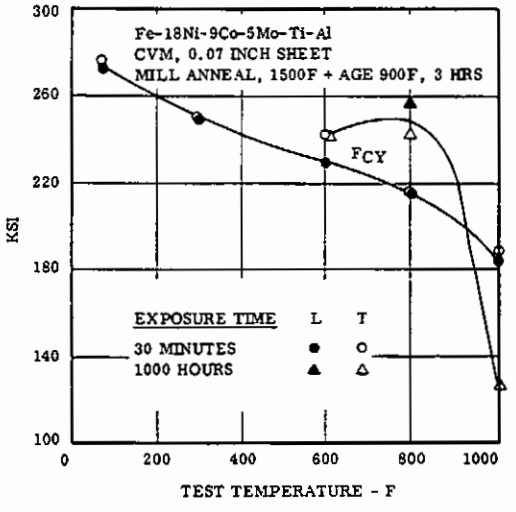


FIG. 3.03221 EFFECT OF TEST TEMPERATURE ON THE COMPRESSIVE PROPERTIES OF SHEET. (21, p. 172 - 174, 197)

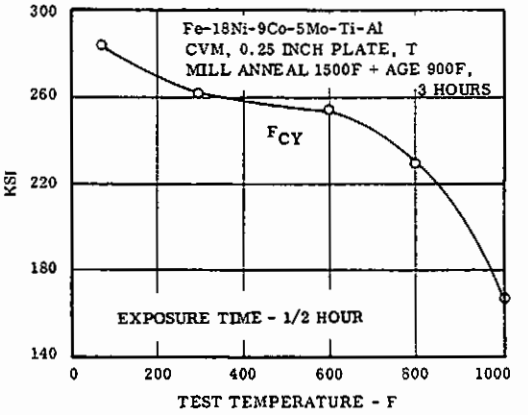


FIG. 3.03222 EFFECT OF TEST TEMPERATURE ON THE COMPRESSIVE PROPERTIES OF PLATE. (21, p. 175 - 176)

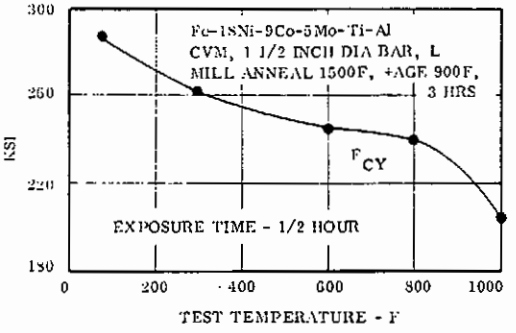


FIG. 3.03223 EFFECT OF TEST TEMPERATURE ON THE COMPRESSIVE PROPERTIES OF BAR. (21, p. 177 - 178)

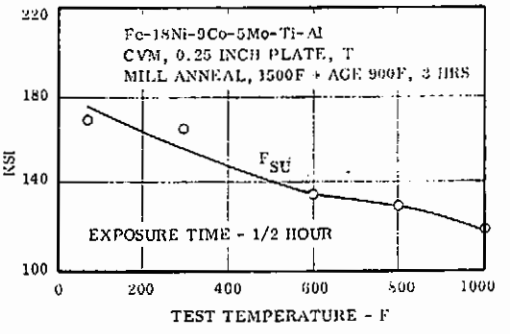


FIG. 3.03512 EFFECT OF TEST TEMPERATURE ON SHEAR ULTIMATE STRENGTH OF PLATE (21, p. 182-183)

	Fe
18	Ni
9	Co
5	Mo
	Ti
	Al

18 Ni Maraging (300)

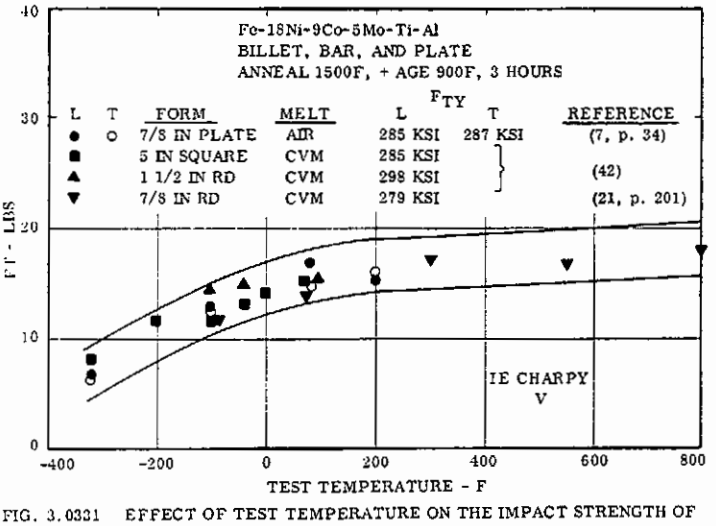


FIG. 3.0331 EFFECT OF TEST TEMPERATURE ON THE IMPACT STRENGTH OF BAR, BILLET AND PLATE FROM SEVERAL HEATS. (7)(21)(42)

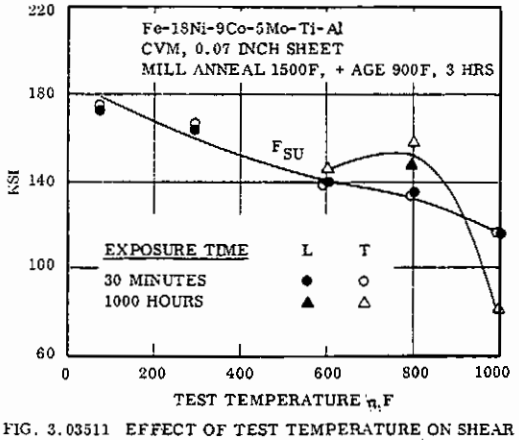


FIG. 3.03511 EFFECT OF TEST TEMPERATURE ON SHEAR ULTIMATE STRENGTH OF SHEET. (21, p. 179-180, 198)

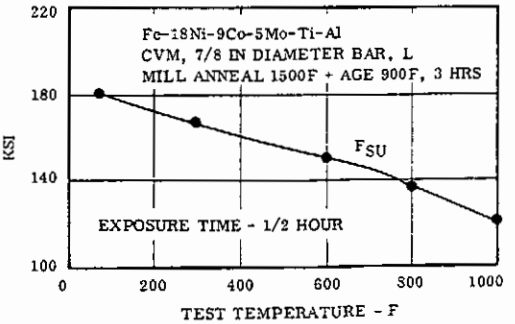


FIG. 3.03513 EFFECT OF TEST TEMPERATURE ON SHEAR ULTIMATE STRENGTH OF BAR. (21, p. 184-185)

	Fe
18	Ni
9	Co
5	Mo
	Ti
	Al

18 Ni Maraging (300)

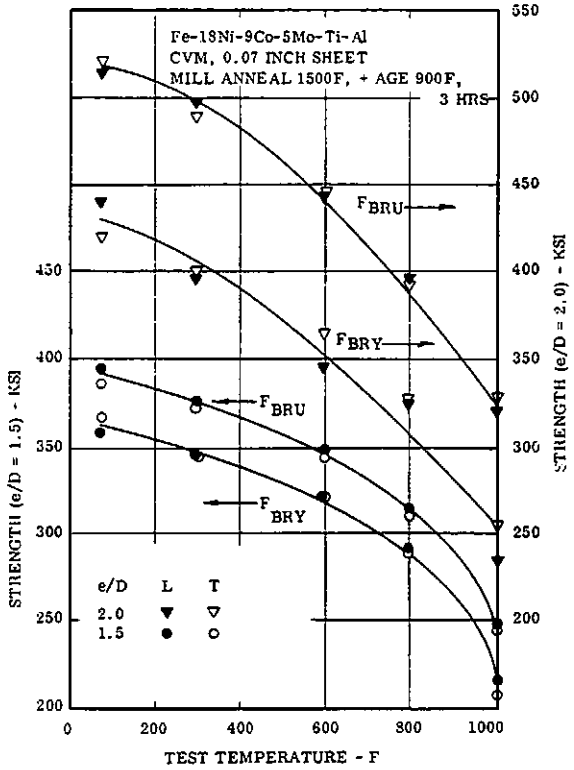


FIG. 3.03611 EFFECT OF TEST TEMPERATURE ON BEARING STRENGTH OF SHEET. (21, p. 186 - 190)

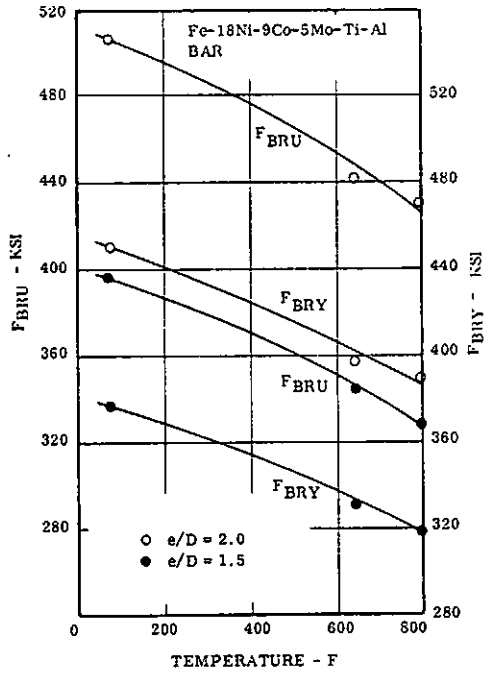


FIG. 3.03613 EFFECT OF TEST TEMPERATURE ON BEARING STRENGTH OF BAR. (52)

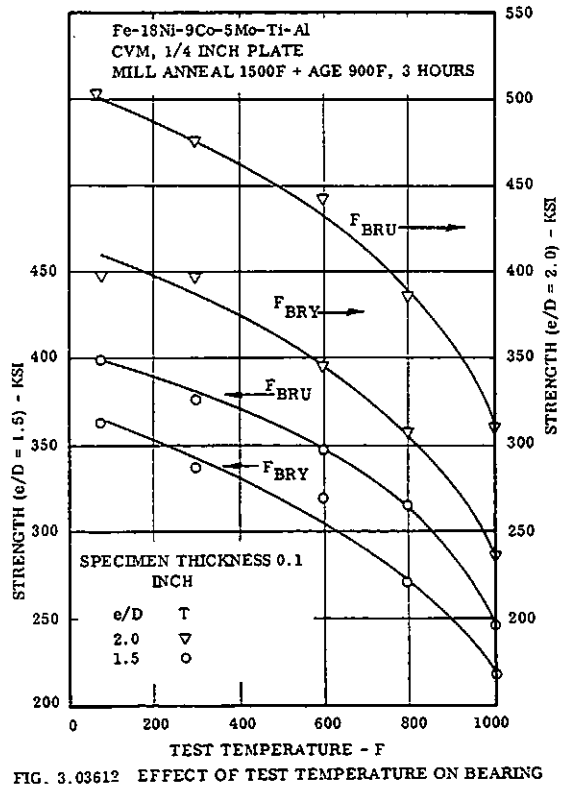


FIG. 3.03612 EFFECT OF TEST TEMPERATURE ON BEARING STRENGTH OF PLATE. (21, p. 192 - 194)

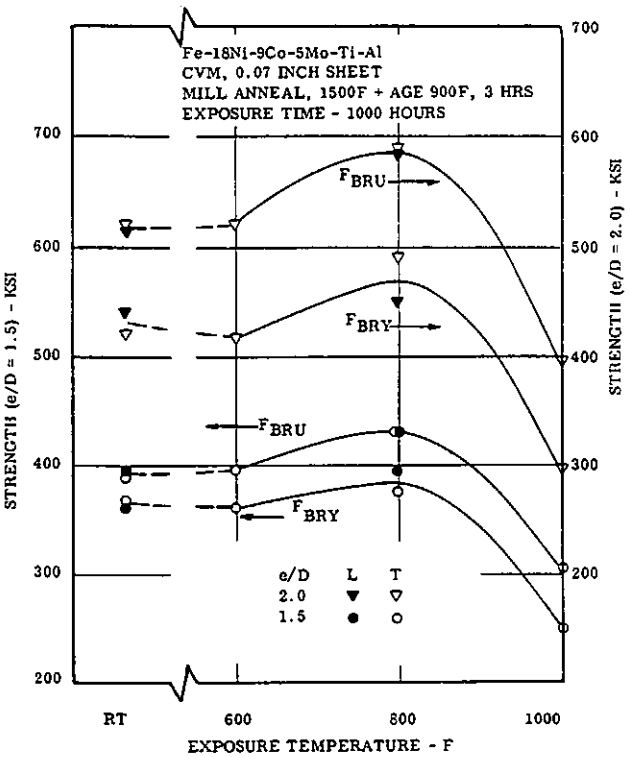


FIG. 3.03621 EFFECT OF 1000 HOUR ELEVATED TEMPERATURE EXPOSURE ON THE BEARING STRENGTH OF SHEET AT ROOM TEMPERATURE (21, p. 199 - 200)

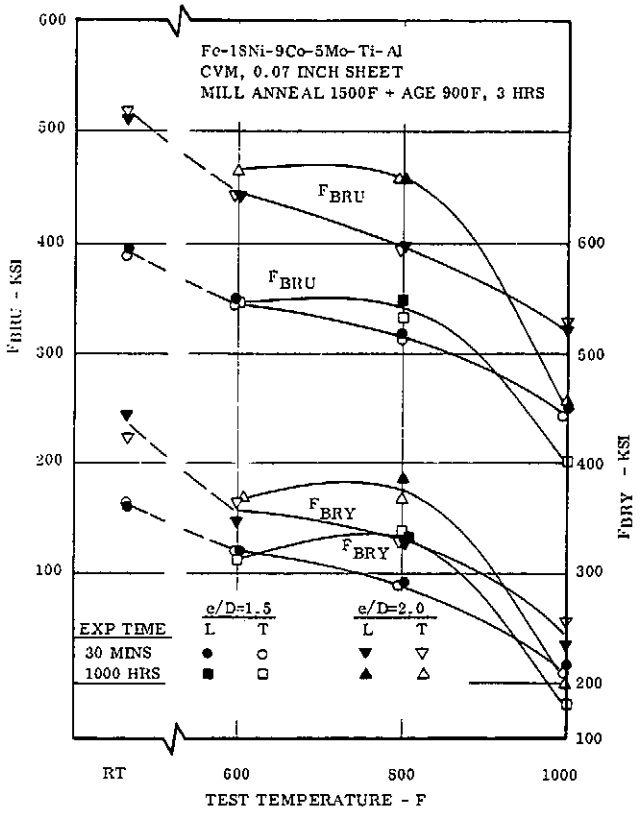


FIG. 3.03622 EFFECT OF TEST TEMPERATURE ON THE BEARING STRENGTH OF SHEET AFTER HOLDING 30 MINUTES AND 1000 HOURS AT TEST TEMPERATURE. (21. p. 186 - 191. 199-200)

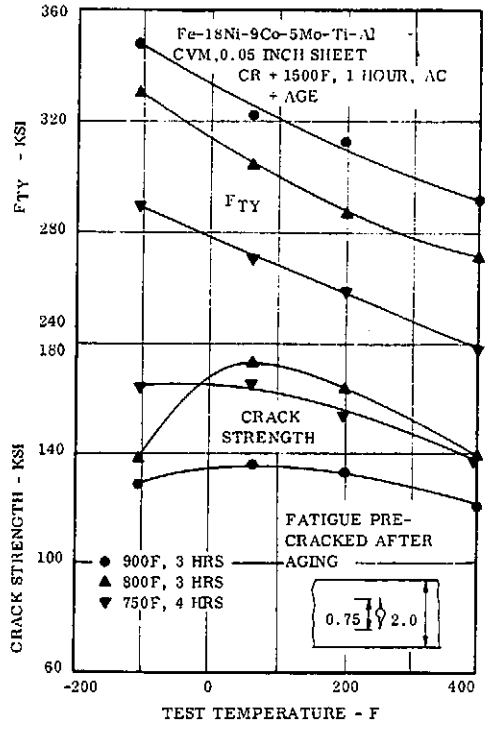


FIG. 3.03712 EFFECT OF TEST TEMPERATURE ON THE CRACK STRENGTH OF SHEET AGED AT THREE TEMPERATURES. (27)

	Fe
18	Ni
9	Co
5	Mo
	Ti
	Al

18 Ni Maraging (300)

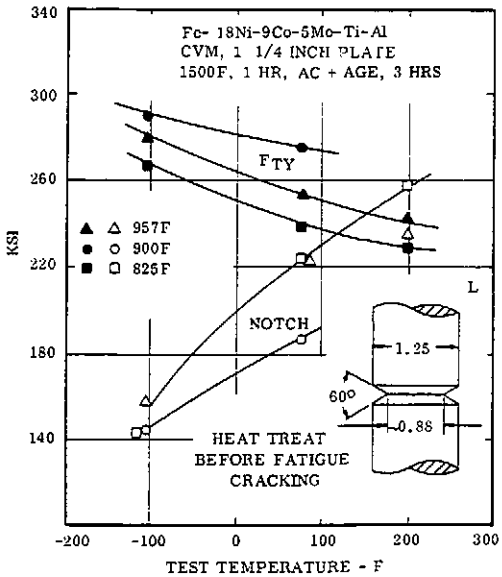


FIG. 3.03713 EFFECT OF TEST TEMPERATURE ON THE SHARP NOTCH PROPERTIES OF CVM PLATE AGED AT THREE TEMPERATURES. (58)

	Fe
18	Ni
9	Co
5	Mo
	Ti
	Al

18 Ni Maraging (300)

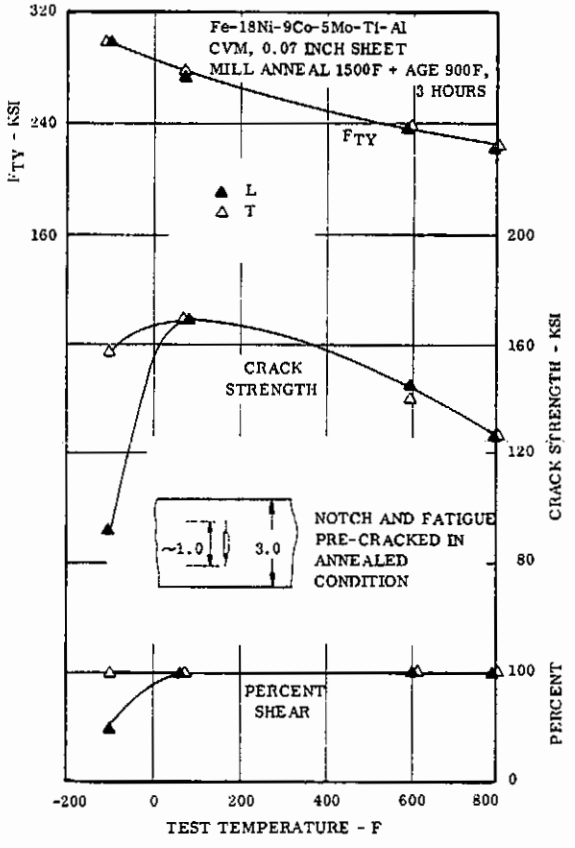


FIG. 3.03721 EFFECT OF TEST TEMPERATURE ON THE CRACK STRENGTH OF SHEET. (21, p. 211)

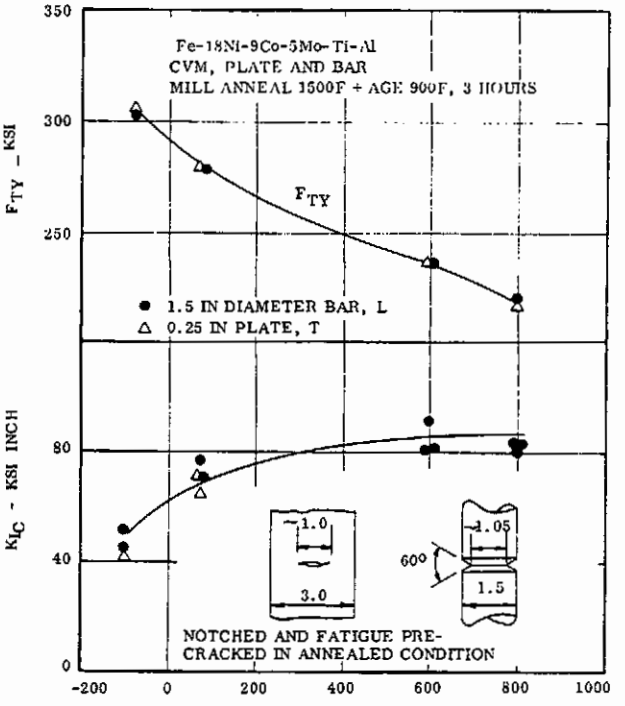


FIG. 3.03722 EFFECT OF TEST TEMPERATURE ON THE FRACTURE TOUGHNESS OF PLATE AND BAR. (21, p. 212-213)

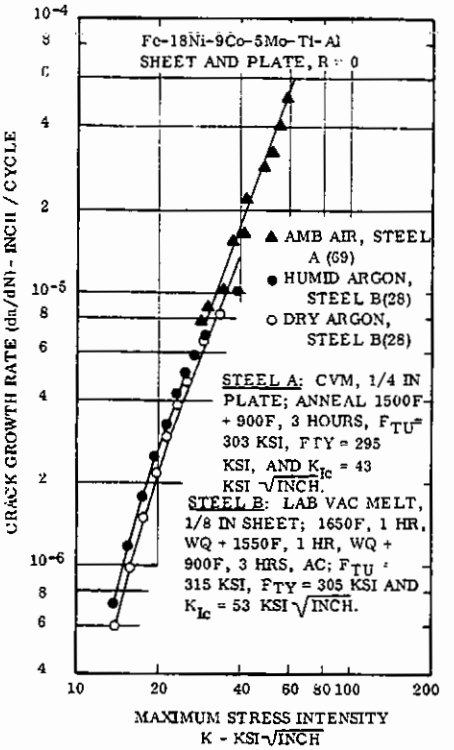


FIG. 3.0521 INFLUENCE OF STRESS INTENSITY FACTOR K AND TEST ENVIRONMENT ON FATIGUE - CRACK PROPAGATION IN SHEET AND PLATE AT ROOM TEMPERATURE. (28)(69)

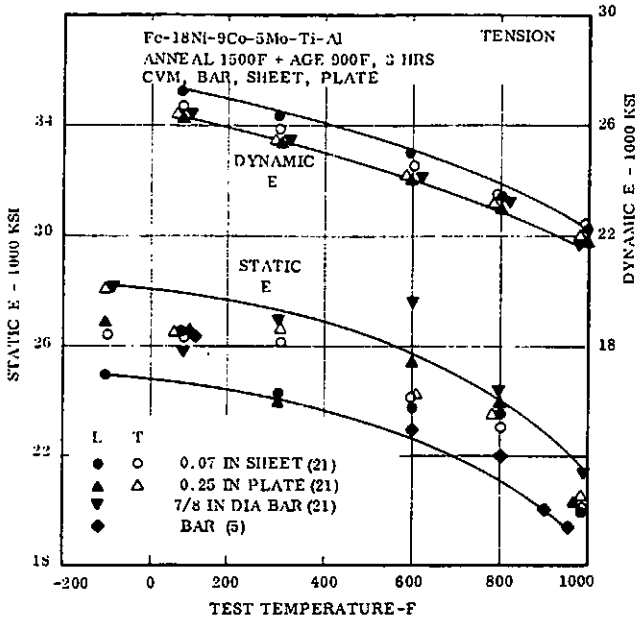


FIG. 3.0621 STATIC AND DYNAMIC MODULI FOR TENSION AT CRYOGENIC. ROOM AND ELEVATED TEMPERATURES. (5)(21, p. 162 - 171. 202)

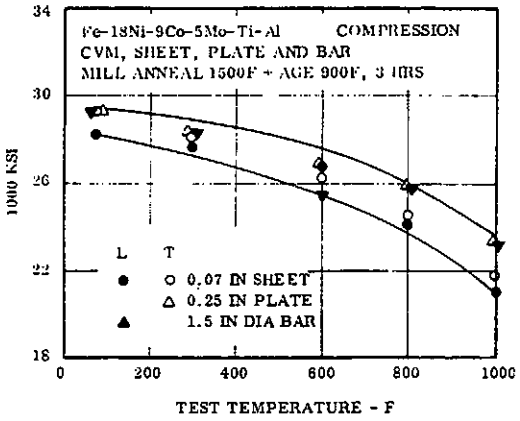


FIG. 3.0622 STATIC MODULI FOR COMPRESSION AT ROOM AND ELEVATED TEMPERATURES. (21, p. 172-181)

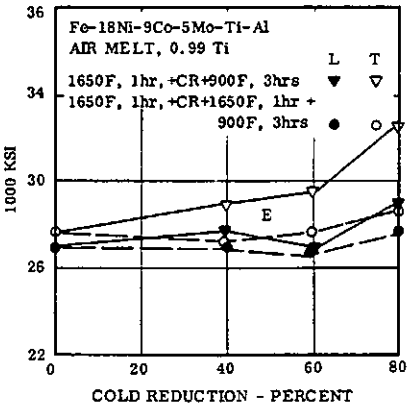


FIG. 3.0623 EFFECT OF COLD WORK ON STATIC MODULI AT ROOM TEMPERATURE. (53)

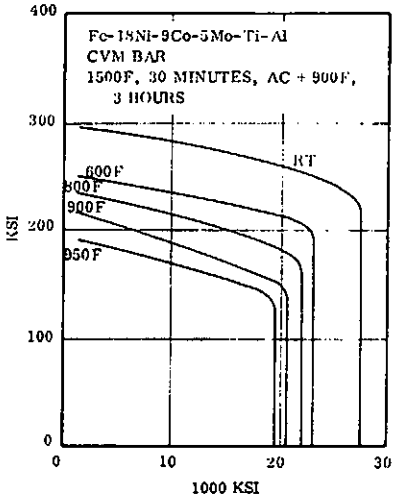


FIG. 3.0641 TANGENT MODULUS CURVES AT ROOM AND ELEVATED TEMPERATURE FOR ANNEALED AND AGED BAR. (5)

	Fe
18	Ni
9	Co
5	Mo
	Ti
	Al

18 Ni Maraging (300)

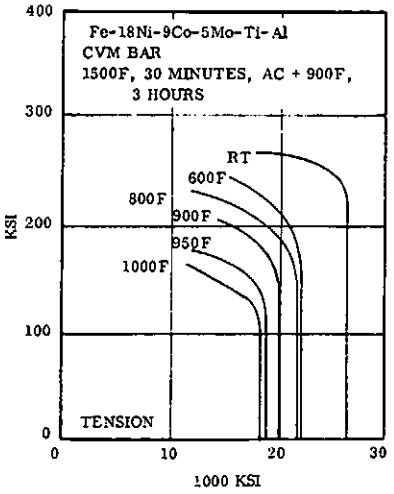


FIG. 3.0651 SECANT MODULUS CURVES AT ROOM AND ELEVATED TEMPERATURES FOR ANNEALED AND AGED BAR. (5)

	Fe
18	Ni
9	Co
5	Mo
	Ti
	Al

18 Ni Maraging (300)

REFERENCES

1. ASTM A-538-65-Grade C, ASTM Standards, Part 4, (January, 1967).
2. VASCO, Latrobe, Penna. Spec. Nos. MB-300 CVM and MS-300 CVM (November 15, 1967).
3. International Nickel Company, "Summary Data". (March 30, 1965).
4. U. S. Steel Corporation, "USS Maraging Steel". ADUSS-94034 (1964).
5. VASCO, Latrobe, Penna. "Vascomax 18 Percent Nickel Ultra High Strength Maraging Steels" (1966)
6. Curtiss-Wright Corporation, "Research on Binary Iron-Nickel Alloys with 20 - 25 Percent Nickel", AF33(616) 8018, Progress Report No. 3 (November 30, 1962).
7. Reisdorf, B. G. and Baker, A. J., "The Kinetics and Mechanisms of the Strengthening of Maraging Steels", AFML-TR-64-390 (January, 1965)
8. DeVries, R. P., "Effect of Processing Factors and Size on the Properties of Commercially Produced 18Ni-Co-Mo-Maraging Steel," Symposium on Maraging Steels at Wright-Patterson Air Force Base (May 14, 1962).
9. Hamaker, J. C. Jr., "Effect of Primary Processing on Ultrahigh-strength Steels", in DMIC Report 210, page 32 (October 26-28 , 1964).
10. Republic Steel Corporation, "Manufacturing Process Development for High Strength Steels, Forging Survey 18Ni-Co-Mo-Maraging and 9Ni-4Co Quench and Temper High Strength Steels", Interim Engineering Progress Report IR-8-157-L, ASD Contract AF33(657) 11277 (September, 1963).
11. Ibid, Plate and Sheet Survey.
12. Yates, D. H., Vanadium Alloys Steel Company. "Personal Communications with W. F. Brown Jr." (1963).
13. Witherel, E. E., International Nickel Company, "Personal Communications with W. F. Brown Jr." (1963)
14. Barton, C.J., Reisdorf, B.G., Salmon Cox, P.H., Chilton, J.M. and Oskin, C.E. Jr., "Investigation of Thermal Embrittlement in 18 Ni (250) Maraging Steel". AFML-TR-67-34 (March, 1967).
15. Decker, R. F., International Nickel Company, "Personal Communications with W. F. Brown Jr." (1963).
16. Peterson, W.A., Dean, S.W., Scott, T.E. and DiBari, G.A., "Review of Current Work on Maraging Steels", ASD-TDR-63-262, Page 309 (May, 1963)
17. Troiano, A.K., "Hydrogen in Maraging Steel, Type 18Ni-9Co-5Mo (300) Grade) presented at the 3rd Maraging Steel Project Review, ASD Project 7381 (July, 1963).
18. McDonnell Aircraft Corporation, "Static Fatigue Strength of Diffused Nickel Cadmium Plated Vascomax 250 and Vascomax 300". Report A733, Serial No. 19 (AD 441111) (July, 1963).
19. Bristol Aerojet Ltd., and Westland Aircraft Ltd. The Chemical Contouring of 18 Percent Nickel Maraging Steel Sheet. D. Mat. Rept. No. 143 (April, 1967).
20. Pellissier, G.E., "Some Microstructural Aspects of Maraging (250) Steel in Relation to Strength and Toughness", in the Proc. of the Third Maraging Steel Project Review, RTD-TDR-63-4048 (November, 1963) pp. 403 - 437.
21. Hoenie, A.F., Lumm, J.A., Shelton, R.J., and Wallace, R.A., "Determination of Mechanical Property Design Values for 18Ni-Co-Mo 250 and 300 Grade Maraging Steels". AFML-TR-65-197 (July, 1965).
22. Lane, D.H., Frost, R.M., and Krause, A.J., "AC Generator Rotor Materials", AFAPL-TR-66-127 (March, 1967)
23. Dean, S.W., and Copson, H.R., "Stress Corrosion Behavior of Maraging Nickel Steels in Natural Environments," Corrosion, Volume 21, pp. 95 - 103 (March, 1965).
24. Rubin, A., "Stress Corrosion Cracking of Maraging Steels," in Proceedings of the Fourth Maraging Steel Project Review
25. Wacker, G.A., "Stress Corrosion Cracking Studies of 10, 12, and 18 percent Ni Maraging Steel Alloys in Sea Water", U.S. Navy, Marine Engineering Lab., MEL R & D Phase Report, 73/66 (March, 1966).
26. Mulherin, J.H., "Stress Corrosion Susceptibility of High Strength Steel, in Relation to Fracture Toughness" ASME Paper No 66-Met-5 (1966).
27. Brisbane, A.W., Hawn, J.M., and Ault, R.T., "Fracture Toughness and Delayed Failure Behavior of 18 Percent Nickel Maraging Steel", Materials Research and Standards, ASTM, pp. 395-405 (August, 1965).
28. Wei, R. P., Talda P.M., and Li, Chi-Yu, "Fatigue Crack Propagation in Some Ultrahigh-Strength Steels", ASTM STP 415 , pp. 460 - 485 (1967)
29. Republic Steel Corporation, "Special Property Steels", Adv. 1868-10M-468, p. 31.
30. Latrobe Steel Company, "Unpublished Data - Personal Communication," R.A. Woodall with R. P. Wei (December, 1968).
31. Corn, D.L., "Evaluation of 18Ni-9Co-5Mo (300 ksi) Maraging Steel Sheet. Part 1: Mechanical Properties" Report No. SM-43110, Douglas Aircraft Company (November 27, 1963).
32. International Nickel Company, "Preliminary Data Sheet" (1962).
33. Shimmin, J.T., and Odar, J.A., "Manufacturing Process Development of High Strength Steels. Phase II". Interim Engineering Progress Report VIII. Republic Steel Corporation, ASD AF33(657)-11277 (August 1965).
34. Lovell, D.T., and Uchida, J.M., "Investigation of Vacuum Melted 18Ni (300) Maraging Steel", Boeing Document No. D2-20256-1 (January 1965).
35. Curtiss-Wright Corporation, Wright Aeronautical Division, "Research on Binary Iron-Nickel Alloys with 20-25 Percent Nickel", AF33(616)-8018, Progress Report No. 5 (May 30, 1962).
36. Maynor, H.W. Jr., and Busch, C.C., "Effects of Melting Practice, Thickness and Thermal and Mechanical Treatments on K_{IC} of Nickel Maraging Steel", Final Technical Report No. 4, Army Missile Command, No. DA-01-009-ORD-889 (June 30, 1965)
37. The Boeing Company Aero-Space Division, "Investigation of Low-Cycle Fatigue Failures Using Applied Fracture Mechanics", Progress Report. AF33(657)-10251 (October, 1963).
38. Crimmins, P.P. and Tenner, W.S., "Informal Monthly Report for the Investigation of Maraging Steel Covering the period 1 May through 30 May 1963", ASD Contract AF33 (657)-8740, Aerojet-General Corporation, Sacramento, California (May, 1963).
39. Ibid, Period from 1 June to 30 June, 1963.
40. General Dynamics Corporation, Fort Worth, Texas, "An Investigation of 18Ni-Co-Mo (300) Maraging Steel Forgings", Report No. FZM-2608 (May 10, 1964).
41. Sparks, R.B., "Properties of Maraging Steel Press Forgings", Maraging Steel Project Review, ASD-TDR-63-262, p. 195 (November, 1962).
42. Glasgal, B.M., Looby, G.T., and Traynor, M.T., Republic Steel Corporation, "Unpublished Data" (1962).
43. Yates, D.H., Vanadium Alloys Steel Company, "Personal Communication with W.F. Brown, Jr." (1963)
44. Shimmin, J.T., et al, Republic Steel Corporation "Manufacturing Progress Development for High Strength Steels", Interim Engineering Progress Report IR-8-157 (V) (1 July 1964 - 1 October 1964).
45. U.S. Steel Corporation, Applied Research Laboratory "Unpublished Data," Communication to R.P. Wei(1969)
46. Aggen, G.N., Allegheny-Ludlum Steel Corporation, "Personal Communication with W.F. Brown, Jr." (1962).
47. Aerojet General Corporation, "Evaluation of High-Nickel Maraging Alloy Steels", AF33(657)-8890, Task No. 738103, Phase I, (AD295680) (1 October

through 31 December 1962 - 15 January 1963).
48. Allegheny Ludlum Steel Corporation. "Research Center Data Sheet 166-73062 BB (1963).
49. Sampson, H.B., "Preliminary Investigation of 250 and 300 Nickel Maraging Steel Sheets (18Ni-Co-Mo)", Maraging Steel Project Review, ASD-TDR 63-262, p. 271 (November, 1962).
50. Hanna, G.L., and Steigerwald, E.A., "Fracture Characteristics of Structural Metals", Bureau of Naval Weapons contract no. N600(19)-58831, Final Report ER 5426, TAPCO, Cleveland, Ohio (June, 1963).
51. Vanadium Alloy Steel Company, "Personal Communication between J.G. Hamaker, and S.S. Manson (1963).
52. Allegheny Ludlum Steel Corporation", Research Center Data Sheet 163-73062-AA (1963).
53. Spaeder, G.J., and Murphy, W.J., "Properties of Cold Reduced 300 Grade 18 Ni Maraging Steel", Journal of Materials, Volume 3, No. 1, p. 116 (1968).
54. Nordquist, F.C., "An Investigation of 18Ni-Co-Mo (300) Maraging Steel Forgings", General Dynamics, Report No. FZM-2608 (May 10, 1962).
55. Matas, S., Republic Steel Research Center, "Personal Communication with W.F. Brown, Jr.," (1962).
56. Maynor, H.W., Jr., et al, "K_{IC} of a 300 Grade 18 Nickel Maraging Steel as Influenced by Specimen Type and Thermal and Mechanical Treatment".
57. Curtiss-Wright Corporation, Wright Aeronautical Division, "Research on Binary Iron-Nickel Alloys with 20-25 Percent Nickel", AF33(616)-8018, Progress Report No. 4 (February 28, 1962).
58. Hoese, W.P., and Master J.N., "An Evaluation of Large Diameter Solid Propellant Motor Case Materials", Boeing Airplane Company, Report D2-22314 (May 1963).
59. Sippel, G.R., and Vonnegut, G.L., "Evaluation of 18 Percent Ni-Co-Mo-Maraging Steel for Heavy and Thin Wall Rocket Motor Case Applications", Allison Division, General Motors Corporation, Engineering Department, Report No. 3448 (July 12, 1963).
60. Brown, W.F., Jr., and Srawley, J.E., "Plane Strain Crack Toughness Testing of High Strength Metallic Materials, ASTM STP 410 (1967).
61. Smith, H.L., and Romine, H.E., "Fracture Toughness Studies of Maraging Steels", Maraging Steel Project Review, ASD-TDR 63-262 (November, 1962), page 1.
62. Spitzig, W.A., "The Effect of Duplex Aging Treatment on the Mechanical Properties of 18Ni-Co-Mo-Ti Maraging Steels", U.S. Steel Corporation, preprint of paper to be published in Trans., ASM (1969).
63. "The Mechanical Properties of Maraging Steels", DMIC Memorandum Draft (July 22, 1963).
64. Corn, D.L., and Mixon, W.V., "Interim Report on the Effect of Crack Shape on Fracture Toughness, Report SM-44671, Douglas Aircraft Company (April 27, 1964).
65. Tuffnell, G.W., Pasquine, D.L., and Olson, J.H., "An Investigation of the Fatigue Behavior of 18 Percent Nickel Maraging Steel", Trans. ASM, Volume 59, p. 769 (1966).
66. Jones, R.L., and Nordquist, F.C., "An Evaluation of High Strength Steel Forgings", RTD-TDR-63-4050 (May, 1964).
67. Campbell, J.E., "Review of Alloys and Fabrication Methods Used for Tactical Missile Motor Cases", DMIC Memo 224 (August 15, 1967).
68. Seabrook, J.B., "Working with Maraging Steels - Nitriding", Metal Progress (July, 1963).
69. Carman, C.M., and Katlin, J.M., "Low Cycle Fatigue Crack Propagation of High Strength Steels", 66-MET-3, ASME (April, 1966).
70. AMS 6521 (May 1, 1969).

	Fe
18	Ni
9	Co
5	Mo
	Ti
	Al

18 Ni Maraging (300)

	Fe
20	Cr
10	Ni
1.5	Mo
1.5	W

19-9 DL

1 **GENERAL**

The 19-9 DL is a high carbon modification of the well-known 18-8 stainless steels. It contains small amounts of molybdenum, tungsten, titanium, and columbium for additional solid solution strengthening. The alloy is intended for high-strength applications up to 1200 F. Above 1200 F, it offers a modest strength advantage over regular austenitic stainless steels. The 19-9 DL is not normally heat treated but is usually strengthened by cold working or by hot-cold working. Aircraft engine applications include rotors, buckets, fasteners, manifolds, ducting, and casings. The 19-9 DL alloy is also used in chemical processing and oil refining equipment and in high temperature steam service. Modified compositions are available for welding.

1.01 **Commercial Designation**

19-9 DL.

1.02 **Alternate Designations**

AISI 651, UNS K63198, UNS J92843 (castings); 19-9 WX and UNS K63199. (welding wire and covered welding electrodes).

1.03 **Specifications,** Table 1.03.

1.04 **Composition,** Table 1.04.

1.05 **Heat Treatment**

1.051 Castings are solution heat treated at 2000 F for at least 30 minutes and air cooled, followed by a precipitation heat treatment at 1600 F for at least 8 hours and air cooled (1).

1.052 Sheet, strip, and plate are solution heat treated at 1800 F for a time commensurate with thickness and air cooled (2).

1.053 Stress relief anneal is 1 hour at 1200 F.

1.054 Strength can be increased by aging for 16 hours at 1290 F after 10 percent cold reduction.

1.055 Heating should be accomplished in a neutral or slightly oxidizing atmosphere.

1.06 **Hardness**

1.061 The alloy is normally hardened by cold work or by hot-cold working. The alloy can also be hardened by cold work followed by aging at 1290 F.

1.062 Hardness of bar and forgings varies between 185 and 320 BHN, depending on processing and annealing history. Hardness of sheet may vary between 90 HRB and 30 HRC.

1.07 **Forms and Conditions Available**

1.071 The alloy is normally hardened by cold work or by hot-cold working. The alloy can also be hardened forgings, and tubing. The alloy is also available in the form of sand castings.

1.072 All products are available in the annealed, hot worked, hot-cold worked, or cold worked, and stress relieved conditions.

1.08 **Melting and Casting Practice**

Electric arc furnace melt.

1.09 **Special Considerations**

1.091 Alloy is susceptible to stress cracking after forming unless stress relieved or annealed.

1.092 Heating at temperatures in the vicinity of 1100 to 1200 F sensitizes the alloy, i.e., develops susceptibility to intergranular attack in acid.

1.093 Alloy may crack after cold work or welding unless annealed or stress relieved.

2 **PHYSICAL PROPERTIES AND ENVIRONMENTAL EFFECTS**

2.01 **Thermal Properties**

2.011 Melting range, 2590 to 2615 F.

2.012 Phase changes.

2.0121 Time-temperature-transformation diagrams.

2.013 Thermal conductivity, Figure 2.013.

2.014 Thermal expansion, Figure 2.014.

2.015 Specific heat, 0.10 Btu/lb F.

2.016 Thermal diffusivity.

2.02 **Other Physical Properties**

2.021 Density, 0.287 lb/in.^{3}, 7.94 g/cm^3.

2.022 Electrical properties.

2.0221 Electrical resistivity, 30.6 microhm-inches.

2.023 Magnetic properties, alloy is nonmagnetic.

2.0231 Permeability, Table 2.0231.

2.024 Emittance.

2.025 Damping capacity.

2.03 **Chemical Environments**

2.031 Corrosion resistance.

2.0311 General corrosion resistance is very similar to that of austenitic stainless steels with a correspondingly high carbon content.

2.0312 Intergranular corrosion may occur in acid environments unless annealed at 1800 F, followed by rapid cooling. Heating to temperatures between 1100 and 1200 F will again sensitize this steel.

2.0313 To avoid stress cracking after cold working or welding, the steel should be immediately stress relieved or annealed.

2.032 Oxidation resistance is good up to 1750 F for continuous service and up to 1450 F for intermittent service.

2.033 Reactions with hydrogen.

2.0331 The hydrogen diffusivity in 19-9 DL at 1200 at 1500 F is expressed by $D = 3.2 \times 10^{-2}$ $e^{-14100/[460 + T(F)]}$cm^2/sec (9). The permeability of hydrogen through 19-9 DL at 1400 to 1500 F, which is of interest for hot hydrogen containment applications such as the Stirling engine, is reduced by a factor of 2 to 3 by doping the hydrogen with an oxygen-containing impurity such as CO or CO_2 at levels up to 5 volume percent. This causes formation of an oxide layer on the surface of the alloy which has low permeability for hydrogen. The permeability reduction obtained with 19-9 DL in doped hydrogen is less than that observed for other high temperature alloys (such as N-155, Incoloy 800, Inconel 718) because of the low content of strong oxide forming constitutents in 19-9 DL (10). Modified 19-9 DL alloys containing 2.5Ni plus 0.5Al, 2.0Cb, or 0.3 misch metal have significantly lower permeabilities to hydrogen at 1300 to 1600 F (11).

2.0332 The hydrogen solubility in 19-9 DL at 1200 to 1500 F is expressed by $S = 14.9$ $e^{-3250/[460+T(F)]}$wt ppm (atm)$^{1/2}$ (9).

	Fe
20	Cr
10	Ni
1.5	Mo
1.5	W

19-9 DL

3 **MECHANICAL PROPERTIES**

3.01 **Specified Mechanical Properties**

3.011 AMS specified mechanical properties at room temperature, Table 3.011.

3.02 **Mechanical Properties at Room Temperature**

3.021 Tension—stress-strain diagrams—tension properties.

3.0211 Tensile properties depend upon processing. F_{tu} may vary between about 100 and 150 ksi, F_{ty} between 40 and 120 ksi, and e betwen 60 and 15 percent.

3.022 Compression—stress-strain diagrams—compression properties.

3.023 Impact.

3.024 Bending.

3.025 Torsion and shear.

3.026 Bearing.

3.027 Stress concentration.

3.0271 Notch properties.

3.0272 Fracture toughness.

3.028 Combined properties.

3.03 **Mechanical Properties at Various Temperatures**

3.031 Tension—stress-strain diagrams—tension properties.

3.0311 Effect of test temperature on tensile properties of stress relieved sheet, plate, and bar, Figure 3.0311.

3.0312 Effect of test temperature on tensile properties of annealed sheet and plate, Figure 3.0312.

3.0313 The effects of various thermal-mechanical processing treatments on the tensile properties of 19-9 DL at 1200 F are shown in Table 3.0314. The ultimate tensile strengths and reductions in area are comparable for the various treatments with exception of those materials aged at 1290 F and those final annealed åt 2100 F to grain sizes of 19-21 microns. There are, however, significant differences in the elongations resulting from the different treatments. The more ductile materials, based on elongation, result from double annealing at 1900 F and 1540 F or from 30 percent reduction at −320 F plus annealing at 1800 F. Material aged at 1290 F displays high strength but low elongation. The large grained material annealed at 2100 F also has high strength but low ductility as measured both by elongation and by reduction in area (12).

3.0314 Tensile properties of 19-9 DL at 1200 F in argon, Table 3.0314.

3.032 Compression—stress-strain diagrams—compression properties.

3.0321 Effect of test temperature on compressive yield strength of sheet, Figure 3.0321.

3.0333 Impact.

3.0331 Effect of test temperature on impact strength of bar, Figure 3.0331.

3.034 Bending.

3.035 Torsion and shear.

3.036 Bearing.

3.0361 Effect of test temperature on bearing properties of sheet, Figure 3.0361.

3.037 Stress concentration.

3.0372 Fracture toughness.

3.038 Combined properties.

3.04 **Creep and Creep-Rupture Properties**

3.041 Creep-rupture curves for bar at 1000 to 1500 F, Figure 3.041.

3.042 The creep and creep-rupture of 19-9 DL sheet are shown in Figures 3.043 and 3.044, respectively. The rupture strength is significantly affected by grain size, with coarse grained material being stronger than fine grained material, as shown in Figure 3.045 (13, 14). Prior exposure for 3500 hours at 1400 F slightly reduces the rupture strength (not shown), with the effect being more noticeable in large grained than in fine grained material (13). For optimum creep and rupture properties at temperatures above 1200 F, solution heat treat at 1800 F to 2150 F and age for stability at 1200 F to 1400 F (15).

3.043 Creep properties of 19-9 DL sheet, Figure 3.043.

3.044 Creep-rupture properties of 19-9 DL sheet [(a) heat treated at 1800 F, and (b) heat treated at 2200 F] Figure 3.044.

3.045 Effects of temperature and grain size on 100-hour and 1000-hour rupture strengths of 19-9 DL, Figure 3.045.

3.046 Stress relaxation data for times up to 8760 hours are shown in Figure 3.047. These data indicate that 19-9 DL does not relax significantly at 1020 F for times up to 8760 hours. At 1110 F, relaxation occurs after about 1000 hours and at 1200 F and higher, after about 100 hours (16).

3.047 Stress relaxation of 19-9 DL at elevated temperatures [(a) 1020 F, (b) 1110 F, (c) 1200 F, (d) 1290 F, and (e) 1380 F] Figure 3.047.

3.05 **Fatigue Properties**

3.051 Fatigue properties of bar, Figure 3.051.

3.06 **Elastic Properties**

3.061 Poisson's ratio, Figure 3.061.

3.062 Modulus of elasticity, Figure 3.062.

3.063 Modulus of rigidity, Figure 3.063.

3.064 Tangent modulus.

3.065 Secant modulus.

4 **FABRICATION**

4.01 **Forming**

4.011 General forming properties of sheet, strip, and plate, annealed at 1800 F, are similar to those of the austenitic stainless steels. The alloys consume greater power, strain harden more rapidly and require more frequent intermediate anneals when forming parts in several operations. Severe cold forming should be followed immediately by a full anneal or a stress relief at 1200 F, to avoid stress cracking.

4.012 Forging. Starting temperature for parts ranging from 5 to 1000 lb, 2020 F maximum, finishing temperature 1500 F minimum. When the hot-cold worked condition is desired, forging temperature may be as low as 1200 F effecting 20 to 40 percent reductions between 1500 and 1200 F.

4.02 **Machining and Grinding**

4.021 Recommendations for obtaining the best machinability of bar include annealing, 15 to 20 percent cold drawing, and stress relieving at 1200 F with a hardness of 200 to 240 BHN. Hot-cold worked and stress relieved material possesses similar machining characteristics. Where such material is not available, annealing at 1650 F to a hardness of 185 to 200 BHN is recommended.

4.022 Alloy can be machined by all common techniques used for austenitic stainless steels. The tool wear will be higher than the 300 series steels. Heavy sulfur base lubricants are recommended.

4.03 **Joining**

4.031 The alloy is readily weldable by all common techniques.

4.032 For fusion welding 19-9 DL special grades of bare wire and coated electrodes have been developed. Stress relieving of welded parts at 1200 F minimum and, preferably, full annealing at 1800 F, followed by air cooling, are recommended.

4.04 **Surface Treating**

Pickling of this alloy should be performed in a molten salt bath, such as sodium hydride. This should be followed by pickling for a few minutes in an 8 to 15 percent sulfuric acid solution at 130 to 140 F, rinsing and dipping in 8 to 12 percent nitric acid, 1 percent hydrofluoric acid at 110 F. If acid pickling is to be performed, the material should be first annealed at 1650 F or higher.

	Fe
20	Cr
10	Ni
1.5	Mo
1.5	W

19-9 DL

REFERENCES

1 AMS 5369C (January 1, 1984).

2 AMS 5526F (July 1, 1984).

3 AMS 5579A (January 15, 1979).

4 AMS 5782B (July 16, 1979).

5 AMS 5783C (July 16, 1979).

6 Universal Cyclops Steel Corporation, "Uniloy 19-9 DL and Uniloy 19-9 DX", Technical Bulletin (July 1956).

7 North American Aviation, Inc., Materials Research, "Materials Property Manual and Summary Report" (October 30, 1957).

8 Favor, Ronald J., Archbach, William P., and Hyler, Walter, S., "Materials Property Design Criteria for Metals", WADC TR 55-150, Pt. 5. (October 1957).

9 Bhattacharyya, S., Veseley, E. J., Jr., and Hill, V. L., "High Pressure/High Temperature Hydrogen Permeability in Candidate Stirling Engine Alloys", *Journal of Materials for Energy Systems*, Vol. 3, No. 4 (March 1982), pp 12-21.

10 Misencik, J. A., "Evaluation of Dopants in Hydrogen to Reduce Hydrogen Permeation in Candidate Stirling Engine Heater Head Tube Alloys at 760 and 820 C", National Aeronautics and Space Administration, Cleveland, Ohio, NASA TM-82920 (October 1982).

11 Bhattacharyya, S. and Petermen, W., "Determination of Hydrogen Permeability in Commercial and Modified Superalloys", IIT Research Institute, Chicago, Illinois, NASA CR-168195 (May 1983).

12 Collins, C. G. and Bohlander, K. M., "Physical Metallurgy of Fast Breeder Reactor Cladding Materials and Refractory Metals", General Electric Company, Cincinnati, Ohio, GEMP-1012 Part II (March 31, 1969).

13 Witzke, W. R. and Stephens, J. R., "Creep-Rupture Behavior of Seven Iron-Base Alloys after Long Term Aging at 750 Deg in Low Pressure Hydrogen", National Aeronautics and Space Administration, Cleveland, Ohio, NASA TM-81534 (August 1980).

14 Bhattacharyya, S., "Creep-Rupture Behavior of Six Candidate Stirling Engine Iron-Base Superalloys in High-Pressure Hydrogen—Volume I—Air Creep-Rupture Behavior", IIT Research Institute, Chicago, Illinois, NASA CR-168071 (December 1982).

15 "19-9 DL Iron Base Alloys for High Temperatures", Allegheny Ludlum Steel Corporation, Pittsburgh, Pennsylvania, Trade Literature (1961).

16 Tanaka, C. and Ohba, T., "Stress Relaxation Data of 1Cr-0.5Mo-0.25V, 12Cr-1Mo-1W-0.25V, and 19Cr-9Ni-1.4Mo-1.4W-Nb Bolting Steels", *Transactions of National Research Institute for Metals*, Vol. 20, No. 2 (March 1978), pp 138-153.

19-9 DL			
Form	AMS Specification	Military Specification	ASTM Standards
Bolts			A453
Castings	5369C		
Sheet, Strip, Plate	5526F		A457
Tubing, Welded	5579A		
Welding Wire	5782B	MIL-R-5031, Comp 6	
Welding Electrode	5783C	MIL-E-6844, Cl 6	
Bar & Forgings			A458, A477

TABLE 1.03. SPECIFICATIONS

	Fe
20	Cr
10	Ni
1.5	Mo
1.5	W

19-9 DL

19-9 DL								
Specification	AMS 5369C		AMS 5526F AMS 5579A		AMS 5782B		AMS 5783C	
	Percent		Percent		Percent		Percent	
Element	Min	Max	Min	Max	Min	Max	Min	Max
Chromium	18.00	21.00	18.00	21.00	19.00	22.00	18.00	21.00
Nickel	8.00	11.00	8.00	11.00	8.00	9.50	8.00	9.50
Molybdenum	1.00	1.75	1.00	1.75	0.35	0.65	0.35	0.65
Tungsten	1.00	1.75	1.00	1.75	1.25	1.75	1.25	1.75
Manganese	0.75	1.50	0.75	1.50	1.00	2.00	1.00	2.50
Columbium plus Tantalum	0.30	0.70	0.25	0.60	1.00	1.40	0.75	1.20
Titanium	0.15	0.50	0.10	0.35	0.10	0.30	—	0.15
Carbon	0.28	0.35	0.28	0.35	0.07	0.13	0.07	0.13
Silicon	—	1.00	0.30	0.80	0.25	1.00	—	1.00
Copper	—	0.50	—	0.50	—	0.50	—	0.50
Phosphorus	—	0.04	—	0.04	—	0.04	—	0.04
Sulfur	—	0.04	—	0.03	—	0.03	—	0.03

TABLE 1.04. COMPOSITION (1, 2, 3, 4, 5)

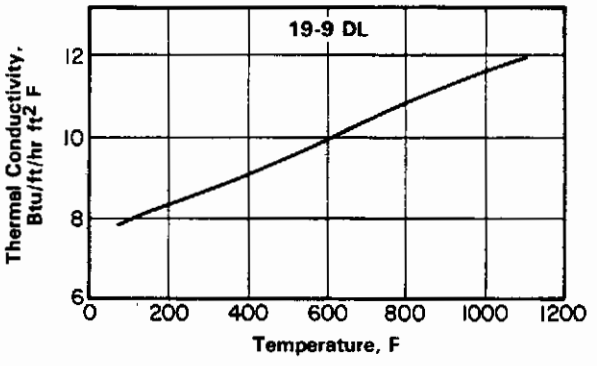


FIGURE 2.013. THERMAL CONDUCTIVITY (6)

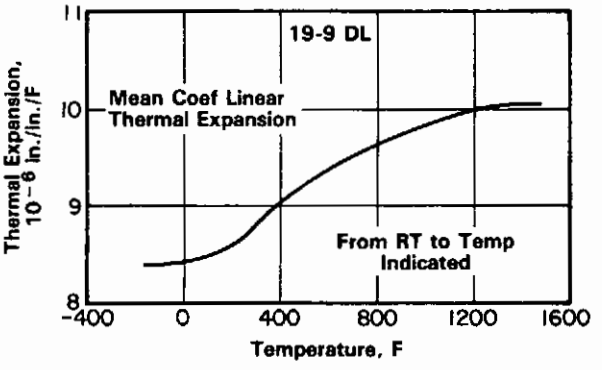


FIGURE 2.014. THERMAL EXPANSION (6)

19-9 DL	
Condition	Magnetic Permeability at 20 Oersteds
ST (1800 F), AC	1.005
ST (1800 F), WQ	1.030
ST + 1500 F	1.014 to 1.018
HW + 1200 F	1.090

TABLE 2.0231. PERMEABILITY (6)

	Fe
20	Cr
10	Ni
1.5	Mo
1.5	W

19-9 DL

19-9 DL											
AMS Spec	Product Form	Metallurgical Condition[a]	Thickness, in.	F_{tu}, ksi Min	F_{tu}, ksi Max	F_{ty}, ksi, Min	Elongation, percent Min	Hardness, Max	Bending Type of Bend	Bending Angle, deg, Min	Bending Bend Factor
5369C	Castings	SHT + PHT	—	—	—	—	—	229 BHN	—	—	—
5526F	Sheet, Strip, and Plate	SHT	All	95	120	45	30	—	—	—	—
			<0.050	—	—	—	—	—	Free Bend	180	2
			<0.050	—	—	—	—	—	V-Block	135	2
			0.050-0.749	—	—	—	—	—	Free Bend	90	2
			0.050-0.749	—	—	—	—	—	V-Block	135	4
5579A	Tubing	SHT + Welded	≲2% OD	95	125	45	30[b] 35[c]	—	—	180	2
5782B	Welding Wire	Cold Drawn	—	110	150	—	—	—	—	—	—

Note: The original AMS documents should be consulted for complete specification details.
(a) SHT = solution heat treated; PHT = precipitation heat treated.
(b) Specification for strip.
(c) Specification for full section.

TABLE 3.011. AMS SPECIFIED MECHANICAL PROPERTIES AT ROOM TEMPERATURE (1, 2, 3, 4)

	Fe
20	Cr
10	Ni
1.5	Mo
1.5	W

19-9 DL

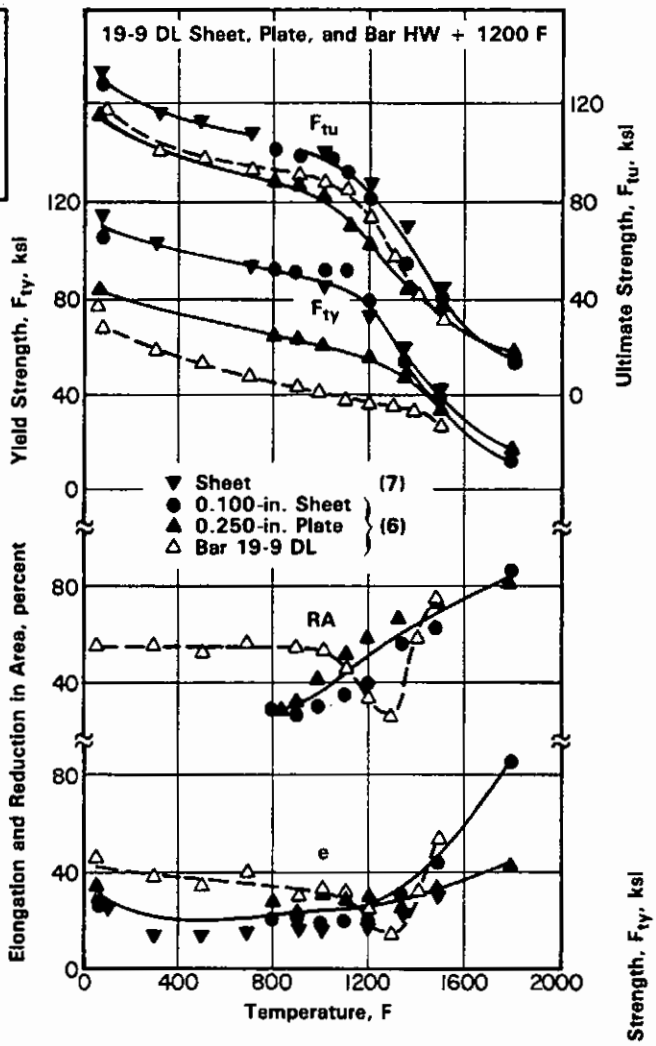


FIGURE 3.0311. EFFECT OF TEST TEMPERATURE ON TENSILE PROPERTIES OF STRESS RELIEVED SHEET, PLATE, AND BAR (6, 7)

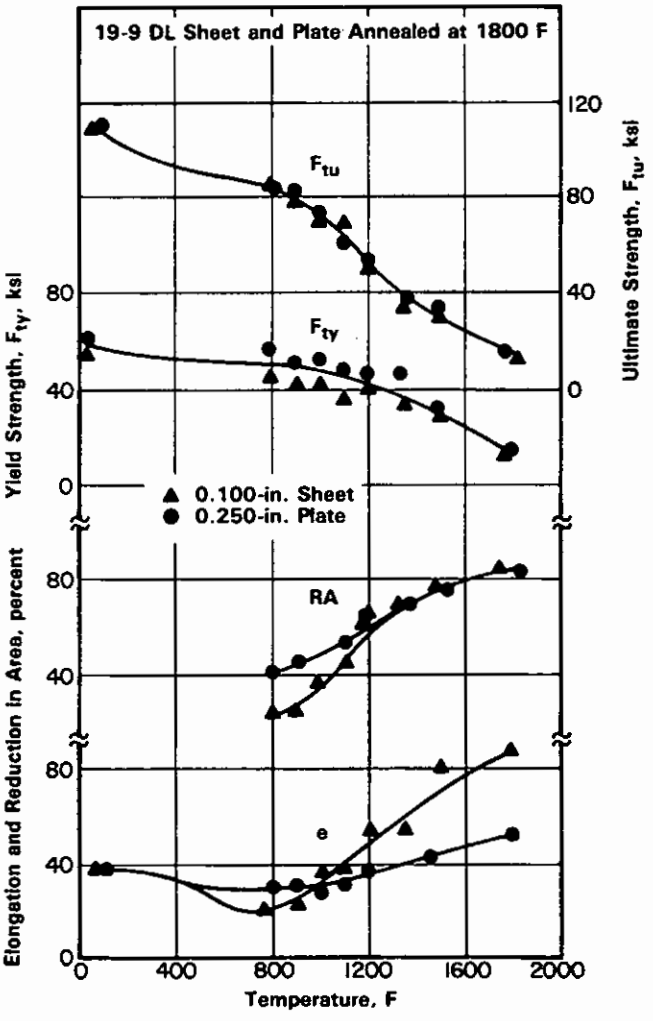


FIGURE 3.0312. EFFECT OF TEST TEMPERATURE ON TENSILE PROPERTIES OF ANNEALED SHEET AND PLATE (6)

Fe
20 Cr
10 Ni
1.5 Mo
1.5 W

19-9 DL

19-9 DL						
Thermal-Mechanical Treatment[b]	Grain Size, microns	Strain Rate, min^{-1}	F_{ty}, ksi	F_{tu}, ksi	Elongation (1 in.), percent	Reduction in Area, percent
Annealed 1800 F,	5	1×10^{-2}	28.0	44.2	36	53
reduced 80 percent,		1×10^{-3}	29.3	36.0	50	71
annealed 1800 F		2×10^{-4}	20.0	27.3	45	72
Annealed 2300 F,	6	1×10^{-2}	38.0	45.7	41	54
reduced 80 percent,		1×10^{-3}	30.0	37.4	31	62
annealed 1800 F		2×10^{-4}	22.0	29.1	43	71
Annealed 1800 F,	6	1×10^{-2}	25.3	41.7	53	59
reduced 80 percent,		1×10^{-3}	25.3	34.8	62	69
annealed 1900 F		2×10^{-4}	20.1	27.9	59	72
and 1540 F						
Annealed 2300 F,	6	1×10^{-2}	54.0	58.2	27	53
reduced 80 percent,		1×10^{-3}	42.0	45.9	32	62
annealed 1800 F		2×10^{-4}	42.0	44.7	16	53
reduced 10 percent,						
aged 16 hr 1290 F						
Annealed 1800 F,	8	1×10^{-2}	21.3	47.6	45	50
reduced 80 percent,		2×10^{-4}	18.7	27.3	53	61
annealed 1800 F						
plus 2 hr 1900 F						
Annealed 1800 F,	8	1×10^{-2}	25.3	49.5	41	45
reduced 50 percent,		2×10^{-4}	21.3	32.3	49	59
at −320 F, annealed						
1800 F plus 2 hr						
1900 F in H_2						
Annealed 1800 F,	8	1×10^{-2}	29.3	44.4	46	57
reduced 50 percent,		1×10^{-3}	23.3	33.2	65	71
at −320 F, annealed		2×10^{-4}	20.0	27.1	49	68
1800 F						
Annealed 1800 F,	10	1×10^{-2}	31.3	47.7	50	63
reduced 30 percent,		1×10^{-3}	18.7	31.9	60	72
at −320 F, annealed		2×10^{-4}	19.3	28.5	57	72
1800 F						
Annealed 1800 F,	19	1×10^{-2}	18.0	55.6	11	15
reduced 80 percent,		2×10^{-4}	18.7	41.1	6	10
annealed 1800 F						
plus 2100 F						
Annealed 1800 F,	21	1×10^{-2}	19.3	60.9	14	13
reduced 50 percent,		2×10^{-4}	18.0	48.1	8	7
at −320 F,						
annealed 1800 F						
plus 2100 F in H_2						

(a) Specimens were 0.030 in. thick with 0.25-in.-wide reduced section and 1.00-in. gage length. Tested in longitudinal direction.
(b) All annealing treatments were 1 hr unless noted otherwise.

TABLE 3.0314. TENSILE PROPERTIES OF 19-9 DL AT 1200 F IN ARGON[a] (12)

	Fe
20	Cr
10	Ni
1.5	Mo
1.5	W

19-9 DL

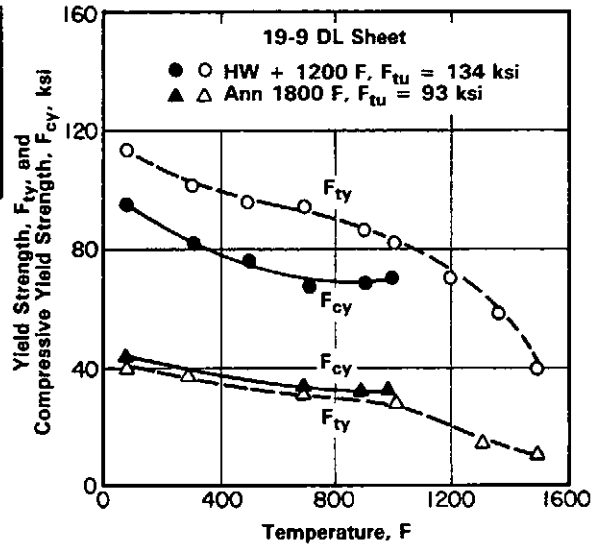


FIGURE 3.0321. EFFECT OF TEST TEMPERATURE ON COMPRESSIVE YIELD STRENGTH OF SHEET (7)

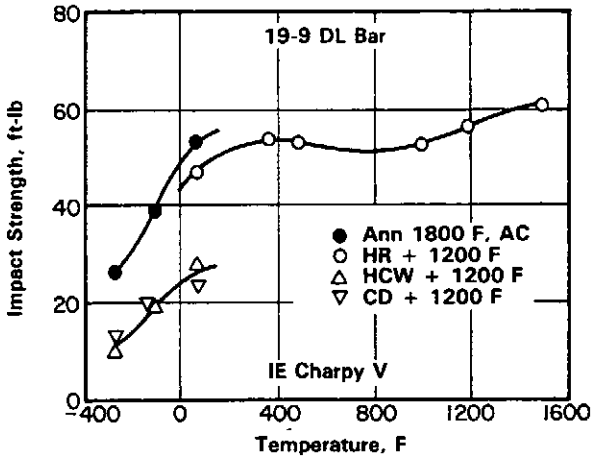


FIGURE 3.0331. EFFECT OF TEST TEMPERATURE ON IMPACT STRENGTH OF BAR (6)

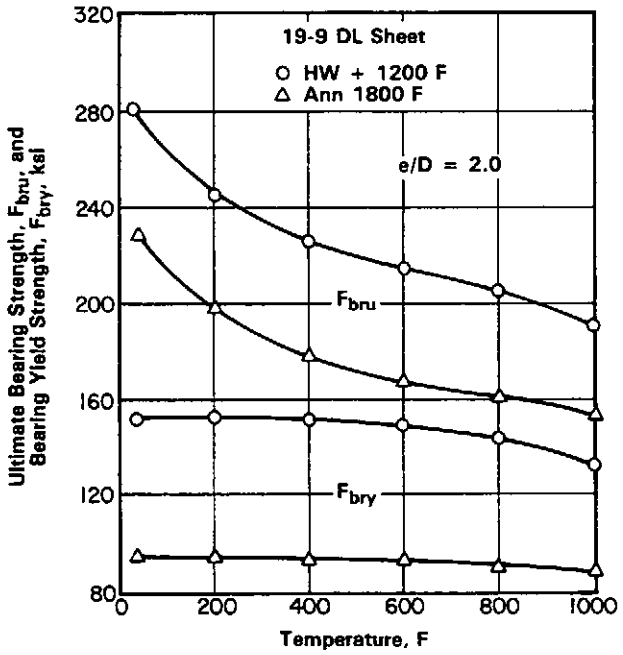


FIGURE 3.0361. EFFECT OF TEST TEMPERATURE ON BEARING PROPERTIES OF SHEET (8)

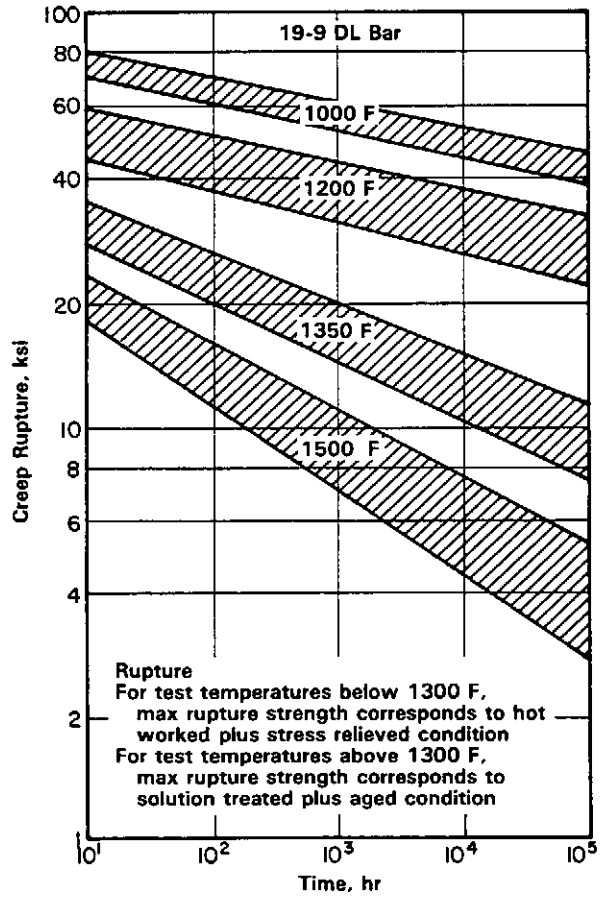


FIGURE 3.041. CREEP-RUPTURE CURVES FOR BAR AT 1000 TO 1500 F (6)

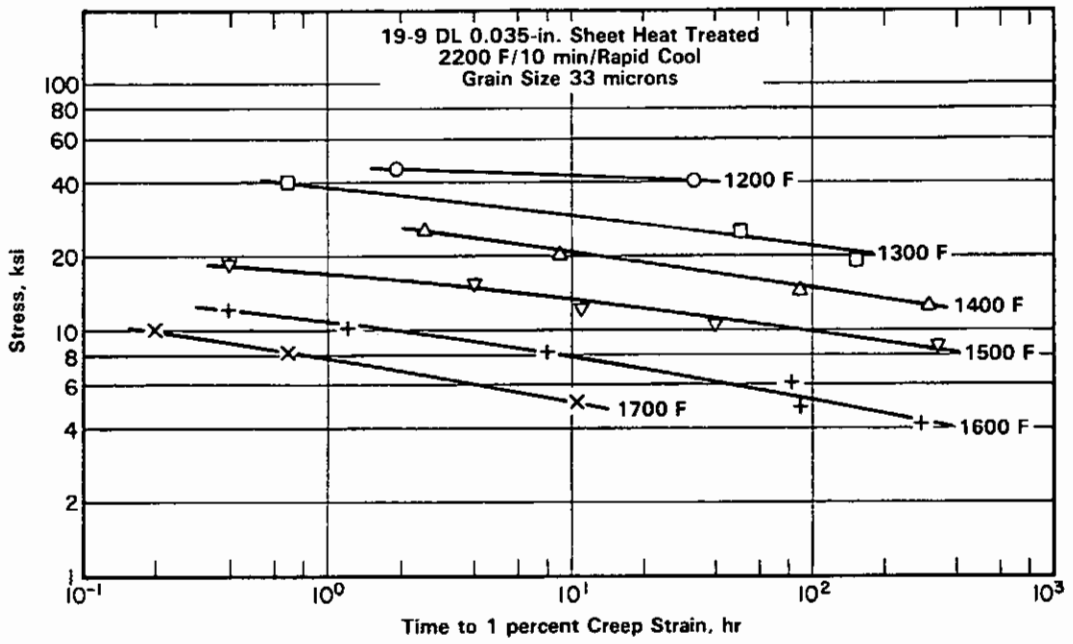
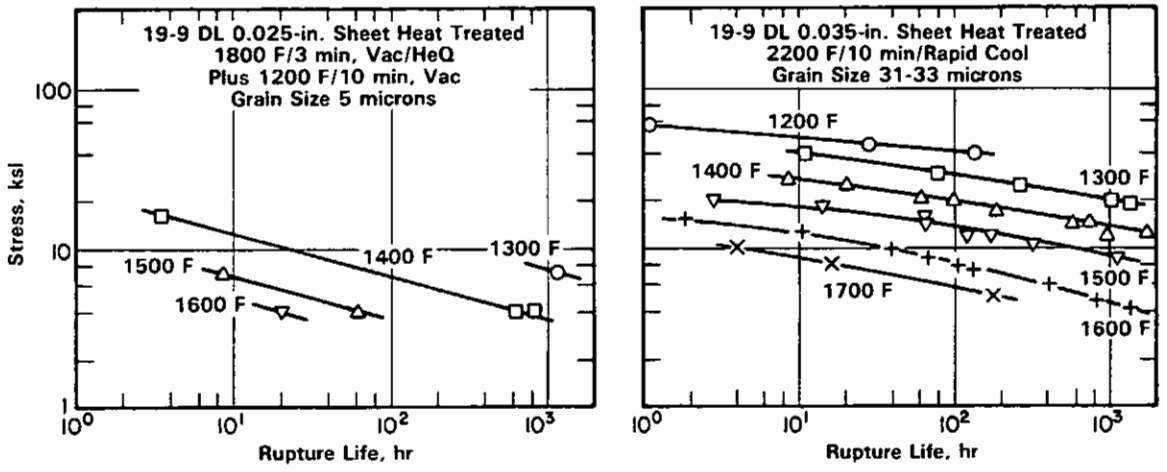


FIGURE 3.043. CREEP PROPERTIES OF 19-9 DL SHEET (14)



(a) Heat Treated at 1800 F

(b) Heat Treated at 2200 F

FIGURE 3.044. CREEP-RUPTURE PROPERTIES OF 19-9 DL SHEET (13, 14)

	Fe
20	Cr
10	Ni
1.5	Mo
1.5	W

19-9 DL

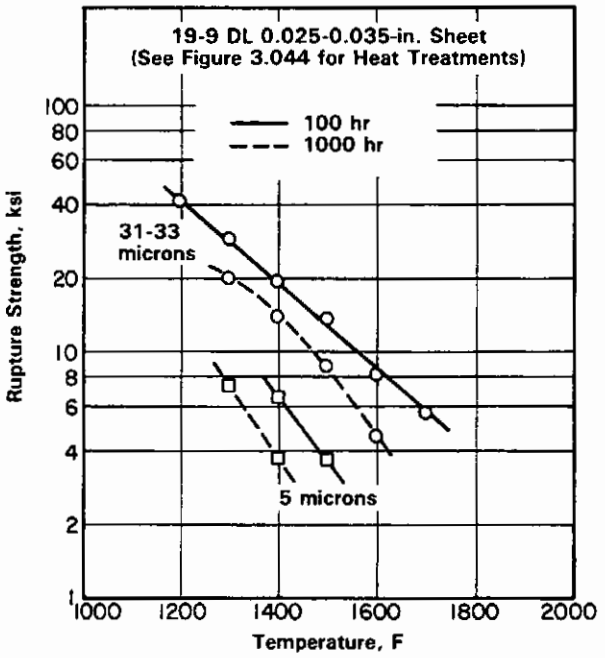


FIGURE 3.045. EFFECTS OF TEMPERATURE AND GRAIN SIZE ON 100-HOUR AND 1000-HOUR RUPTURE STRENGTHS OF 19-9 DL (13, 14)

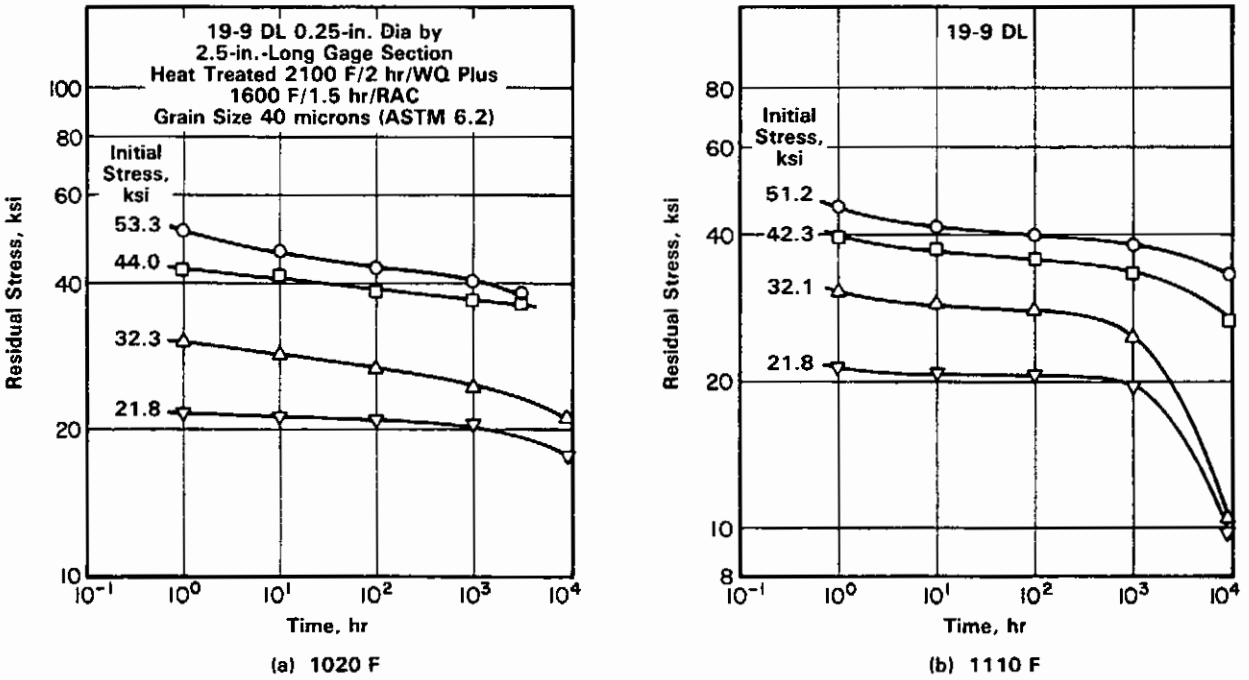
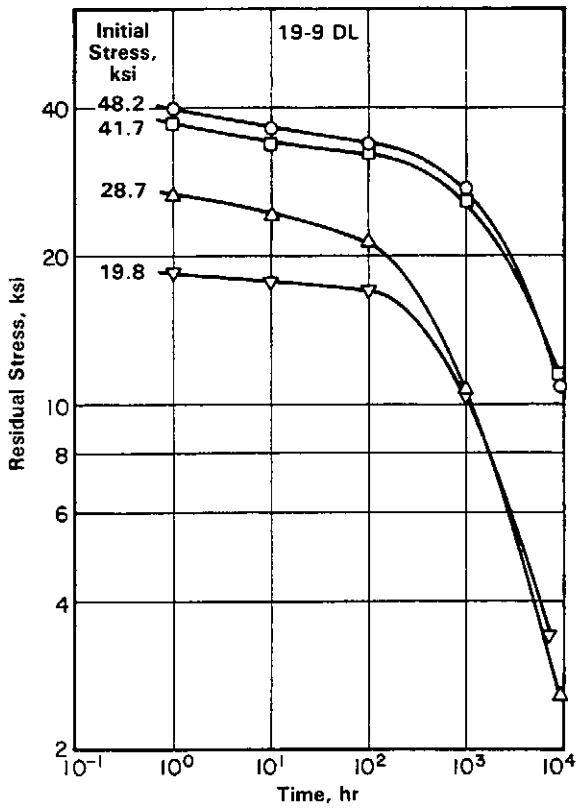
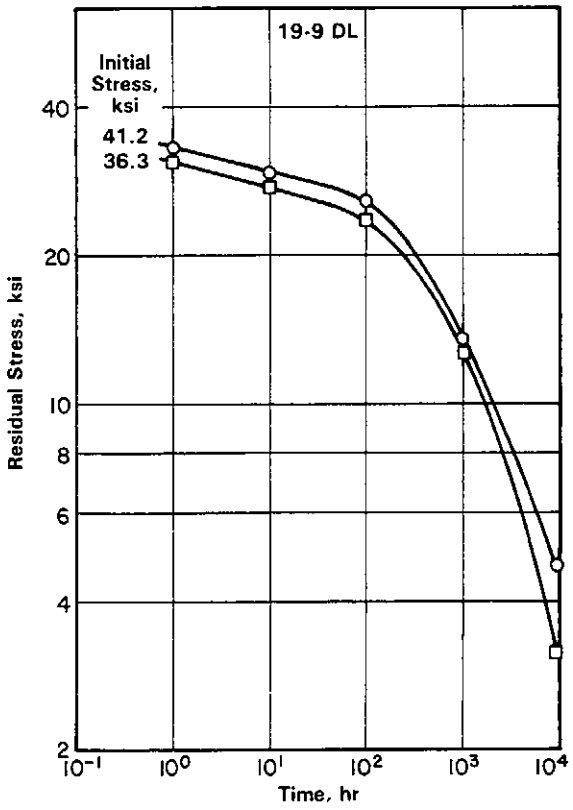


FIGURE 3.047 (a,b). STRESS RELAXATION OF 19-9 DL AT ELEVATED TEMPERATURES (16)



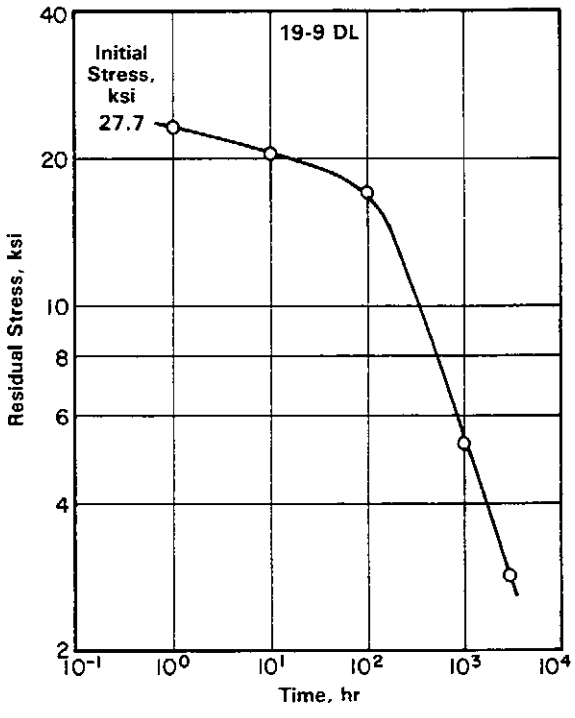
(c) 1200 F



(d) 1290 F

	Fe
20	Cr
10	Ni
1.5	Mo
1.5	W

19-9 DL



(e) 1380 F

FIGURE 3.047 (c,d,e). STRESS RELAXATION OF 19-9 DL AT ELEVATED TEMPERATURES (16)

	Fe
20	Cr
10	Ni
1.5	Mo
1.5	W

19-9 DL

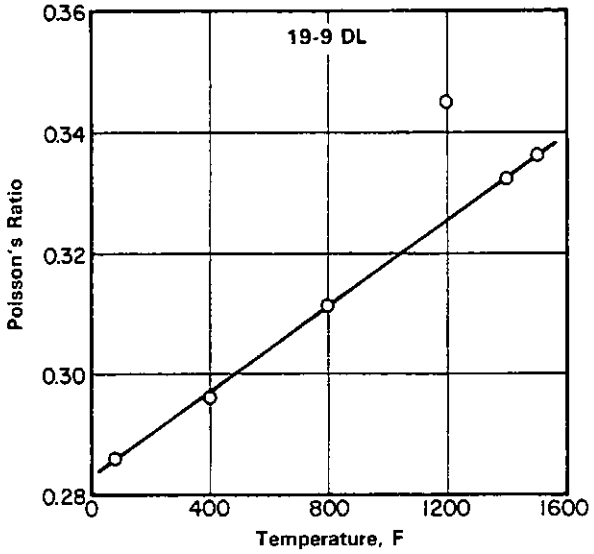


FIGURE 3.061. POISSON'S RATIO (15)

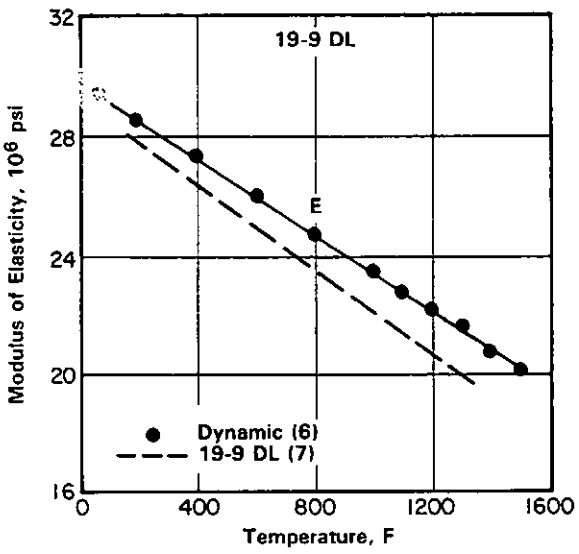


FIGURE 3.062. MODULUS OF ELASTICITY (6, 7)

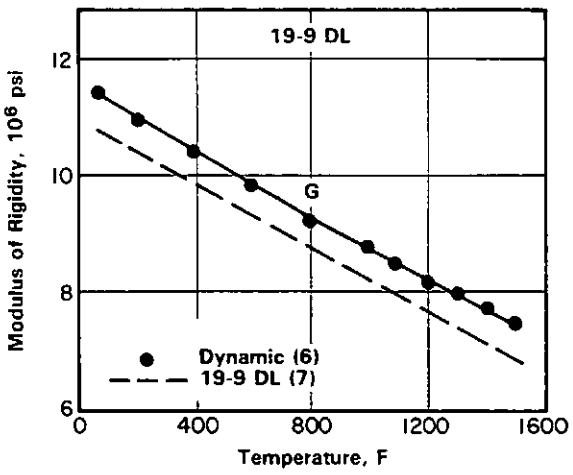


FIGURE 3.063. MODULUS OF RIGIDITY (6, 7)

1. General

Alloy 21-6-9 was introduced in the 1970's as an improved austenitic stainless steel offering excellent corrosion resistance, stability of the austenite phase, and greater room temperature strength and toughness as compared to the basic 18Cr-8Ni AISI Series 300 stainless steels. The improved corrosion resistance is gained by the increase in chromium content from 18 to 21 percent. The addition of 9 percent manganese promotes good stability of the austenite phase even though the nickel content is reduced from 8 to 6 percent. The stable austenitic structure makes 21-6-9 attractive for cryogenic applications. Nitrogen, rather than carbon, is employed as a strengthener in order to reduce corrosion sensitization associated with grain boundary precipitation of chromium carbides. As a result of the higher nitrogen content (0.3 percent), the room temperature yield strength of 21-6-9 is almost twice those of Types 304, 321, and 347 stainless steel. Nitrogen is also an effective strengthener at cryogenic temperatures. The alloy can be further strengthened only by cold work. It can be formed using similar techniques to those used for 300 Series stainless steels and it can be welded using conventional methods. It is easily rolled or forged into a variety of product forms. Severely cold worked material retains low magnetic permeability, reflecting its high austenite stability. Prolonged heating in the range 1000 to 1600F should be avoided in order to prevent formation of grain boundary carbide phases (sensitization) and sigma phase. Alloy 21-6-9 has found applications in chemical process and pollution-control equipment and steam and autoclave applications. It is also used extensively in a variety of aerospace and cryogenic applications such as ducting and bellows systems, exhaust systems, clamps, flanges, and hydraulic line tubing (Refs. 18-22).

1.1 Commercial Designation

21-6-9.

1.2 Alternate Designations

Nitronic 40, ASTM XM-11, UNS S21904 [The grade designated ASTM XM-10 (UNS S21900), which contained 0.08 percent carbon, is no longer produced (Ref. 9).]

1.3 Specifications

1.3.1 *[Table]* Specifications.

1.4 Composition

1.4.1 *[Table]* Specified compositions.

1.5 Heat Treatment

Annealing is performed in the temperature range 1920 to 2100F followed by quenching or rapid cooling. Liquid nitrogen quenching is appropriate for thicker sections. This heat treatment allows all of the carbon to be dissolved and retained in solid solution, thus alleviating any sensitization which might have occurred previously. Slow cooling through or subsequent reheating in the temperature range 1000 to 1600F causes carbides and possibly sigma phase to nucleate at the austenite grain boundaries and should be avoided. The carbides are predominantly $(FeCr)_{23}C_6$. Carbide precipitation and associated reduction of chromium content at the grain boundary regions causes sensitization, which is manifested in both greatly reduced local corrosion resistance and embrittlement (see Section 2.1.2) (Refs. 19, 20).

Fe
Low C
20 Cr
6.5 Ni
9 Mn
0.28N

Stress relief annealing can be performed in the temperature range 900 to 1300F.

Alloy 21-6-9, along with all other austenitic stainless steels, can be bright annealed in either pure hydrogen or dissociated ammonia. The dew point of the atmosphere must be less than -60F and both the workpieces and the furnace must be dry and clean (Ref. 20).

1.6 Hardness

(See Figures 3.2.1.3 and 3.3.1.6 and Tables 3.2.1.2, 3.2.1.4, 3.2.1.5, 3.2.1.6, 3.2.2.1, and 3.2.2.2.)

Hardness can be increased to about Rockwell C 40 to 44 by 60 percent cold reduction.

1.7 Forms and Conditions Available

Alloy 21-6-9 is available as forging billets, bars, wire, forgings, sheet, strip, plate, and tubing in a wide range of commercial sizes in the annealed condition. Sheet, strip and tubing are also available in the high tensile temper condition. The alloy can be cast or extruded as well (Refs. 1, 10).

1.8 Melting and Casting Practice

Standard practice includes electric furnace air melt. Electroslag remelting can also be employed to produce cleaner, more homogeneous ingots (Ref. 23).

1.9 Special Considerations

1.9.1 Alloy 21-6-9 is particularly useful in applications requiring good corrosion resistance and high toughness at cryogenic temperatures.

1.9.2 Alloy 21-6-9 is affected only slightly by hydrogen (see Section 2.3.3).

1.9.3 Prolonged heating or slow cooling through the temperature range 1600 to 1900F promotes formation of deleterious grain boundary precipitates of sigma

© 1994 by Purdue Research Foundation, West Lafayette, Indiana 47907. All Rights Reserved. U.S. Government License. This material may be used, duplicated or disclosed by United States Government agencies without the payment of any royalty.

phase and carbide (sensitization). These reactions cause reduced corrosion resistance and decreased toughness and should be avoided (see Sections 1.5 and 2.1.2).

1.9.4 Alloy 21-6-9 is stable with respect to transformation of austenite to martensite at ambient and elevated temperatures. However, martensite can form during deformation at cryogenic temperatures (see Sections 2.1.2.1 and 3.4.1).

1.9.5 Heating in vacuum at high temperatures causes vaporization of manganese and should be avoided (see Section 2.1.2).

1.9.6 Welds should be heat treated after joining to eliminate sensitization in the heat-affected zone (see Sections 2.3.1, 3.3.3, and 4.3.1).

1.9.7 Alloy 21-6-9 is embrittled by copper contamination during welding or brazing (see Sections 4.3.1 and 4.3.3).

1.9.8 Inconel 625 filler metal should be used for welds intended for cryogenic service to avoid reduced toughness in thick welds joined with W 21-6-9 filler (see Section 4.3.1).

2. Physical Properties and Environmental Effects

2.1 Thermal Properties

2.1.1 Melting Range. Solidus temperature, 2470F (Ref. 24).

2.1.2 Phase Changes. (See Tables 3.3.3.2 and 3.3.7.1.2 for effects of sigma phase on mechanical properties.)

2.1.2.1 Time-temperature-transformation diagrams. Sigma phase forms at the grain boundaries during prolonged heating in the temperature range 1000 to 1600F, with deleterious effects on mechanical properties. Sigma phase causes decreased tensile ductility and decreased impact energies, depending on the amount present. The amount of sigma phase which forms is dependent on heat treatment (or thermal exposure) and on the amount of delta ferrite originally present, which in turn varies with composition and processing. Delta ferrite is a body-centered-cubic phase which is normally stable at temperatures above about 2550F in iron-chromium-nickel alloys but which can also be retained to lower temperatures by high concentrations of ferrite stabilizing elements such as chromium. Delta ferrite is undesirable as it causes low temperature embrittlement and promotes sigma phase formation. The stability of various phases, including delta ferrite, in stainless steels is indicated by the Schaeffler diagram, shown in Figure 2.1.2.1.1. The chromium and nickel equivalents are calculated from the formulae:

$$\text{Cr eq.} = (\text{Cr}) + 2(\text{Si}) + 1.5(\text{Mo}) + 5(\text{V}) + 5.5(\text{Al}) + 1.75(\text{Cb}) + 1.5(\text{Ti}) + 0.75(\text{N})$$

$$\text{Ni eq.} = (\text{Ni}) + (\text{Co}) + 0.5(\text{Mn}) + 0.3(\text{Cu}) + 25(\text{N}) + 30(\text{C})$$

The location of the equivalent composition range corresponding to that specified for 21-6-9, as indicated in Figure 2.1.2.1.1, is seen to overlap the delta ferrite region, although several representative analysed compositions are within the fully austenitic region. It has been suggested that the calculation of nickel equivalents may need to be modified for use with alloys such as 21-6-9 which have much higher nitrogen and manganese contents than normally found in those steels on which the Schaeffler diagram was originally based (Ref. 21). However, even in material whose average composition is austenitic, delta ferrite can sometimes form due to local enrichment of ferrite stabilizing elements resulting from solidification segregation (Ref. 19).

2.1.2.1.1 *[Figure]* Schaeffler diagram showing locations of 21-6-9 equivalent compositions.

In as-rolled plate, the heat treatment temperature producing the maximum amount of sigma phase from delta ferrite is 1500F. Lesser amounts of sigma are formed at 1600 and 1400F. The transformation of delta ferrite to sigma begins within 15 minutes at 1500F and is almost complete after 24 hours at this temperature (Ref. 25). The relative amounts of sigma phase observed after heating for various times and temperatures from a second study are given in Table 2.1.2.1.2 (Ref. 19).

2.1.2.1.2 *[Table]* Effect of elevated temperature exposure on sigma phase formation.

Carbides also form at the grain boundaries during prolonged heating in the temperature range 1000 to 1600F, and, like sigma phase, are deleterious to ductility. The relative amounts of carbide phase observed after heating for various times and temperatures are given in Table 2.1.2.1.3 (Ref. 19).

2.1.2.1.3 *[Table]* Effect of elevated temperature exposure on the precipitation of grain boundary carbides.

Approximate time-temperature curves for formation of precipitates at grain boundaries and at deformation bands of initially cold-worked

material are presented in Figure 2.1.2.1.4. Some of the precipitates were identified as $M_{23}C_6$ (Ref. 26).

2.1.2.1.4 *[Figure]* Time-temperature curves for carbide precipitation.

Transformation of austenite phase to martensite does not occur during cold rolling up to at least 60 percent at room temperature (Ref. 27). Martensite does form, however, on deformation at -321 and -423F (Ref. 22).

The hydrogen solubility in 21-6-9 at 387F and 10 ksi hydrogen pressure is 118 to 127 ppm for both annealed and cold-worked material (Ref. 28).

The diffusivity and permeability of hydrogen in 21-6-9 are shown in Figure 2.1.2.1.5. The rates are not significantly affected by cold working or heat treatment (Ref. 29). The permeability of deuterium/tritium (of interest for potential fusion reactor applications), shown in Figure 2.1.2.1.6, is similar to that of hydrogen when the alloy is sputter-coated with palladium but 2 to 3 orders of magnitude lower when the metal surface is oxidized (Ref. 30). Another study indicated that the permeability of tritium, shown in Figure 2.1.2.1.7, is similar to that of hydrogen when the alloy is in the cold-worked condition. However, for alloy in the annealed condition, the tritium permeability is greater at temperatures below about 750F compared to that observed for cold-worked alloy. This difference in rates is attributed to microstructural changes in the alloy related to slow cooling rather than quenching after heat treatment (Ref. 31).

2.1.2.1.5 *[Figure]* Hydrogen diffusivity and permeability.

2.1.2.1.6 *[Figure]* Permeability of deuterium/tritium through palladium-coated and oxidized alloy.

2.1.2.1.7 *[Figure]* Tritium permeability in cold worked and annealed alloy.

For applications such as the Stirling automotive engine where reduced hydrogen permeability is desired, dopants can be added to the gas phase to promote formation of thin, adherent surface oxide films which have low hydrogen permeability. The permeability of 21-6-9 can be reduced, for example, by a factor of 10 to 50 at 1400 and 1508F by the addition of 1 volume percent CO_2 to the hydrogen (Ref. 32).

Boron cosegregates with nitrogen to the surface during heating at about 1300F or higher where it forms boron nitride. This film uniformly covers the surface after 1 hour of heating and is stable down to room temperature (Ref. 33).

Manganese segregation to the surface has also been observed for 21-6-9. Vacuum annealing at temperatures on the order of 2200F cause vaporization of manganese from grain boundaries with consequent formation of intergranular porosity and deterioration of mechanical properties (Ref. 34).

2.1.3 Thermal Conductivity.

2.1.3.1 *[Figure]* Thermal conductivity.

2.1.4 Thermal Expansion.

2.1.4.1 *[Figure]* Effect of temperature on the mean coefficient of thermal expansion.

2.1.5 Specific Heat.

2.1.5.1 *[Figure]* Specific heat.

2.1.6 Thermal Diffusivity.

2.2 Other Physical Properties

2.2.1 Density 0.283 lb/cu inch, 7.83 g/cc (Ref. 1).

2.2.2 Electrical Properties. Electrical resistivity at room temperature is 29 microhm-inch (Ref. 35).

2.2.3 Magnetic Properties.

2.2.3.1 *[Table]* Effect of cold-working on magnetic permeability at various field strengths.

2.2.3.2 *[Table]* Effect of exposure at cryogenic temperatures on magnetic permeability of 21-6-9 and Type 310 stainless steel.

2.2.4 Emittance.

2.2.5 Damping Capacity.

2.3 Chemical Environments

2.3.1 General Corrosion. The general corrosion resistance of 21-6-9 is very good, approximately equivalent to that of Type 304. Resistance to rusting in marine atmospheres is better than that of Type 304. The reduction in carbon diffusivity effected by nitrogen tends to reduce sensitization in non-heat-treated weldments of 21-6-9 as compared to that which occurs with Type 304 (Ref. 21).

Weldments show complete freedom from accelerated corrosion in the heat-affected zone. However, like Type 304L, even 21-6-9 with its low carbon content of 0.04 percent is susceptible to intergranular corrosion after long exposure in the carbide precipitation temperature range (see Table 2.1.2.1.3) (Refs. 1, 11).

The resistance of 21-6-9 to cracking in hot chloride-containing media is approximately equal to that of Type 304 stainless steel (Ref. 11).

2.3.2 Stress Corrosion. Specimens in both the annealed and high tensile temper conditions stressed to between 40 and 90 percent of yield strength showed good resistance to corrosion in salt fog and aqueous saline solution (Ref. 1).

Welded specimens exposed in marine atmospheres have excellent resistance to stress-corrosion cracking (Ref. 1).

2.3.3 Hydrogen Effects. (See Figures 3.3.1.1 and 4.3.1.4 and Table 2.4.1.) Several different studies agree that hydrogen has only minor effects on tensile properties at near-ambient temperatures but disagree on details. In one study, smooth and notched specimens showed higher ultimate strengths when tensile tested in helium or hydrogen than when tested in air, but yield strength and ductility were essentially unaffected by test environment, as seen in Figure 2.3.3.1. Prior exposure under stress in hydrogen produced an increase in yield strength, but ultimate strength and ductility were similar to those of the unexposed material, as shown in Table 2.3.3.2. No effects of notches were apparent. In a second study, exposure of plate material to 10 ksi hydrogen for 340 hours at 572F resulted in slight increases in room temperature flow stress and about 25 percent loss in reduction in area (RA) as compared to uncharged material. A greater ductility loss occured for notched specimens similarly charged with hydrogen (Ref. 36). A third study reported that 21-6-9 is insensitive to hydrogen damage at slightly elevated temperatures and slow strain rates. These data, shown in Figure 2.3.3.3, indicate that the notched tensile strength was reduced slightly in hydrogen as compared to air, but the elongation to fracture was not significantly affected. Hydrogen did not affect the fracture mode (Ref. 27).

2.3.3.1 *[Figure]* Smooth and notched tensile properties of sheet in air and high-pressure helium and hydrogen.

2.3.3.2 *[Table]* Smooth and notched tensile properties of sheet before and after combined static loading and exposure to high-pressure hydrogen.

2.3.3.3 *[Figure]* Effects of hydrogen on notched tensile properties at slow strain rate.

These differing details on hydrogen effects may reflect minor microstructural differences among the various lots of 21-6-9 studied. Hydrogen has been observed to reduce strength and promote cracking at grain boundaries, slip bands, and other interfaces. These hydrogen-induced effects, which occur primarily at high stresses, are dependent on the metallurgical condition of the alloy and the concentration of available hydrogen (Ref. 37). In high-energy-rate-forged (HERF) alloy, the effect of hydrogen on room temperature toughness has been related to the microstructure. Those microstructures least susceptible to hydrogen-induced intergranular fracture contain patches of recrystallized grains which act as barriers to crack propagation (Ref. 38).

The effects of hydrogen charging pressure and temperature on impact energy are shown in Figure 2.3.3.4. The impact energy is slightly reduced with increasing hydrogen content. The reduction in toughness with decreasing temperature is associated with strain localization and formation of large microvoids. Hydrogen does not change the fracture mode but does enhance the embrittlement mechanisms promoted by low temperature (Ref. 39).

2.3.3.4 *[Figure]* Effect of hydrogen on impact energy at room temperature and -321F.

Stable austenitic steels such as 21-6-9 exhibit mild sensitivity to sustained-load cracking in gaseous hydrogen. In hydrogen at 14.5- and 28-ksi pressure, sustained-load cracking occurs above a threshold stress intensity which has not been accurately measured because of the high toughness of the alloy. The threshold stress intensities are not a function of hydrogen pressure but are similar in magnitude to those exhibited by Types 304L and 316 stainless steel (Ref. 40). At a much lower hydrogen pressure of 15.7 psi, no sustained-load cracking is observed at room temperature (Ref. 27).

Hydrogen causes minor reductions in the ductility of weld metal. As shown in Table 2.3.3.5, testing in a hydrogen environment has little effect on the tensile properties of uncharged welds. However, charging in hydrogen for 10 days at 392F increases the hydrogen content throughout the thickness and decreases tensile reduction in area by about one-fourth. The tensile strengths and uniform elongations are essentially unaffected. Fractures occur at the boundaries between the austenite matrix and ferrite phase which forms in the weld metal during solidification (Refs. 41, 42).

2.3.3.5 *[Table]* Effects of hydrogen on tensile properties of gas-tungsten-arc welds.

2.3.4 Oxidation. The high temperature oxidation resistance of 21-6-9 in air is good, approximately equivalent to that of Type 304 at 1600F but better at 1800F, shown in Table 2.3.4.1.

2.3.4.1 *[Table]* Oxidation resistance in air of 21-6-9 and Type 304 stainless steel.

Exposure in air at 1675F produces a scale which is partially adherent. The loose, nonprotective portion of the scale consists of $MnCr_2O_4$, $FeCr_2O_4$, $(Cr,Fe)_2O_3$, and Mn_3O_4. The composition of the adherent portion of the scale varies with silicon content of the alloy. It is composed primarily of $MnFe_2O_4$ and $MnCr_2O_4$ in 21-6-9 which is high in silicon and $MnFe_2O_4$ alone in low silicon alloy. Low silicon content promotes higher rates of oxidation and greater amounts of spalling (Ref. 43).

In a diesel-fueled atmosphere simulating the combustion environment of a Stirling cycle automotive engine,

the oxidation resistance of 21-6-9 is much less than that exhibited in air. Considerable spalling occurs over long exposures, resulting in weight losses as shown in Figure 2.3.4.2. The surface oxide consists of spinel (Ref. 44).

2.3.4.2 *[Figure]* Oxidation-corrosion behavior at 1508F under simulated Stirling automotive engine combustion conditions.

The ignition temperature in oxygen at ambient pressure appears to be at or just below the alloy melting point. Once ignited, the alloy will generally burn to completion. The temperatures generated during combustion range from 3990 to 4360F (Ref. 45).

2.4 Nuclear Environments

Exposure to high-pressure hydrogen or tritium causes a decrease in total elongation and plastic strain to fracture but does not affect yield or ultimate strengths, as shown in Table 2.4.1. Although low temperature storage has no additional effect on hydrogen-charged alloy, the tritium-charged material is embrittled. The further embrittlement of the tritium-charged material is attributed to porosity produced by tritium decay into helium (Ref. 46).

2.4.1 *[Table]* Effects of long-term hydrogen and tritium exposure and aging on tensile properties.

3. Mechanical Properties

3.1 Specified Mechanical Properties

3.1.1 *[Table]* AMS and ASTM specified mechanical properties.

3.2 Mechanical Properties at Room Temperature

3.2.1 Tension Stress-strain Diagrams and Tensile Properties. Representative stress-strain curves are shown in Figure 3.2.1.1. Typical mechanical properties are presented in Table 3.2.1.2. The effects of cold work and stress relief annealing are shown in Figure 3.2.1.3 and Tables 3.2.1.4 and 3.2.1.5. Test direction has no significant effect on the room temperature tensile properties of annealed sheet, as seen in Table 3.2.1.6.

3.2.1.1 *[Figure]* Stress-strain diagram.

3.2.1.2 *[Table]* Typical mechanical properties for bar and sheet.

3.2.1.3 *[Figure]* Effect of cold working on mechanical properties of sheet.

3.2.1.4 *[Table]* Effect of cold rolling and stress relieving on mechanical properties of sheet.

3.2.1.5 *[Table]* Effect of cold drawing and stress relieving on mechanical properties of wire.

3.2.1.6 *[Table]* Effect of test direction on mechanical properties of sheet for two heats.

The variations of yield strength with strain rate for sheet and bar are shown in Table 3.2.1.7 and Figure 3.2.1.8, respectively. The linearity of the relationship for the bar material indicates absence of any change in mechanism over the eight magnitude range of strain rates covered. The strain rate sensitivity exponent, N, equivalent to the slope of the double-log plot, is determined as 26 (Ref. 47).

3.2.1.7 *[Table]* Effect of strain rate on the yield strength of sheet.

3.2.1.8 *[Figure]* Effect of strain rate on the yield strength of annealed bar at room temperature.

3.2.2 Compression Stress-strain Diagrams and Compression Properties.

3.2.2.1 *[Table]* Compressive yield strength and modulus of elasticity of sheet for two heats.

3.2.2.2 *[Table]* Relaxation characteristics of compression springs exposed at 850F under stress.

3.2.3 Impact. (See Figure 2.3.3.4 and Section 3.3.3.)

3.2.4 Bending.

3.2.5 Torsion and Shear. The shear strength of annealed sheet and strip is approximately 105 ksi in single shear in both the longitudinal and transverse directions. The ratio of shear strength to ultimate strength is about 0.90 (Ref. 1).

3.2.6 Bearing.

3.2.6.1 *[Table]* Bearing strength of sheet for two heats.

3.2.7 Stress Concentration.

3.2.7.1 Notch properties. (See Figures 2.3.3.1 and 4.3.1.4 and Table 2.3.3.2.)

3.2.7.2 Fracture toughness.

3.2.8 Combined Loading.

3.3 Mechanical Properties at Various Temperatures

3.3.1 Tension Stress-strain Diagrams and Tensile Properties. Stress-strain curves at room temperature to -321F, shown in Figure 3.3.1.1, indicate a monotonic reduction in ductility with decreasing temperature, in both the uncharged and hydrogen-charged conditions. The fracture mode was ductile rupture at all temperatures but tended increasingly toward intergranular fracture at lower temperatures (Ref. 48).

3.3.1.1 *[Figure]* Stress-strain behavior of uncharged and hydrogen-charged alloy.

Tensile properties of annealed sheet, plate, and cast alloy are presented in Figures 3.3.1.2 to 3.3.1.5.

3.3.1.2 *[Figure]* Tensile properties of annealed sheet at -423 to 1200F.

3.3.1.3 *[Figure]* Effect of test temperature on tensile properties of annealed sheet.

3.3.1.4 *[Figure]* Effect of cryogenic test temperature on tensile properties of plate.

3.3.1.5 *[Figure]* Tensile properties of cast alloy at -423 to 1200F.

Tensile properties of cold rolled sheet are presented in Figures 3.3.1.6 and 3.3.1.7.

3.3.1.6 *[Figure]* Effect of test temperature on tensile properties of cold rolled sheet.

3.3.1.7 *[Figure]* Effect of cryogenic test temperature on tensile properties of 21-6-9 verses Type 310 stainless cold rolled sheet.

The change in yield strength with strain rate over the temperature range -58 to 167F is shown in Figure 3.3.1.8. The average value of the strain rate sensitivity (slope of plot of log yield stress versus log strain rate) over this temperature range is 24.6, similar to the value of 26 measured at room temperature (see Table 3.2.1.7) (Ref. 49). The increase in yield strength with increasing strain rate remains consistent from room temperature to at least 1400F, as shown in Figure 3.3.1.9 (Ref. 47).

3.3.1.8 *[Figure]* Effect of strain rate on yield strength of annealed bar at -58 to 167F.

3.3.1.9 *[Figure]* Effects of temperature and strain rate on yield strength of annealed bar.

The effects of melting process at room temperature to -321F are shown in Figure 3.3.1.10. The strenth of air-melted material is consistently higher than that of the higher purity electroslag-remelted and vacuum-arc-remelted materials. Ductilities are unaffected by the melting process (Ref. 50).

3.3.1.10 *[Figure]* Effects of melting process on tensile properties at room and cryogenic temperatures.

3.3.2 Compression Stress-strain Diagrams and Compression Properties.

3.3.3 Impact. (See Figure 2.3.3.4.) The Charpy impact energy of plate is greater in the longitudinal than in the transverse orientation, as shown in Figure 3.3.3.1.

3.3.3.1 *[Figure]* Effect of cryogenic test temperature and orientation on impact energy of plate.

The presence of grain boundary carbides causes intergranular fracture and a significant reduction in impact toughness at low temperatures (Ref. 19). Data from another study also illustrates this point, with impact energies for sensitized material being much lower than those for non-sensitized material at -100 and -320F, shown in Table 3.3.3.2.

3.3.3.2 *[Table]* Effect of cryogenic test temperature on impact energy of annealed and sensitized bar.

The low temperature impact energies for materials melted by three processes are shown in Figure 3.3.3.3. The air-induction-melted material has highest impact energy at room temperature and -58F but lower than both electroslag-remelted and vacuum-arc-remelted materials at -148 to -321F. The impact energies decrease with decreasing temperature but remain at a high level (Ref. 50).

3.3.3.3 *[Figure]* Effects of melting process on impact energy at room and cryogenic temperatures.

3.3.4 Bending.

3.3.5 Torsion and Shear.

3.3.6 Bearing.

3.3.7 Stress Concentration.

3.3.7.1 Notch properties. (See Figure 2.3.3.3.) Double edge notch tensile properties from room temperature to -321F are presented in Figure 3.3.7.1.1. The ratio of crack strength to yield strength is above unity even at cryogenic temperatures, indicating that the alloy is crack-tough. However, the value of K_{max} will be dependent on specimen size and type. The results indicate only that the material has good toughness. No effect of melting process is evident on low temperature crack toughness (Ref. 50).

3.3.7.1.1 *[Figure]* Effects of melting process on double edge notch tensile properties at room and cryogenic temperatures.

Heat treatment which simulates sensitization has no significant effect on tensile properties of smooth or notched alloy at room temperature or -320F. Similar behavior is exhibited by Type 304L, as seen in Table 3.3.7.1.2.

3.3.7.1.2 *[Table]* Effect of cryogenic test temperature on smooth and notched tensile properties of annealed and sensitized 21-6-9 and Type 304L stainless steel.

3.3.7.2 Fracture toughness. (See Table 4.3.1.3.) Alloy 21-6-9 has exceptionally high toughness at cryogenic temperatures. Fracture toughness is measured indirectly, since the specimen size required for valid plane strain fracture toughness tests would be larger than that which is practical. The equivalent energy fracture toughness, K_{Icd}, at -275F has been measured as 390.7 ksi$\sqrt{in.}$ for plate annealed for 2 hours at 2000F. This value is independent of orientation (TS or TL) and temperature of precracking (RT or -275F) (Ref. 51). Values for the estimated plane strain fracture toughness parameter $K_{Ic}(J)$ are calculated as 239 and 161 ksi$\sqrt{in.}$ at -321 and -452F, respectively (Ref. 22). Values for K_Q at -452F have been reported as 144 and 151 ksi$\sqrt{in.}$ (Ref. 52).

3.3.8 Combined Loading.

3.4 Creep and Creep Rupture Properties

3.4.1 *[Figure]* Creep rupture behavior at 1200 to 1500F for annealed bar and sheet.

3.4.2 *[Table]* Creep strength of annealed bar.

3.5 Fatigue Properties

3.5.1 Conventional High-cycle Fatigue. The fatigue strength of annealed bar is approximately 49 ksi at 10^8 cycles (based on R.R. Moore tests on specimens from 1-inch diameter bar) (Refs. 1, 11).

3.5.2 Low-cycle Fatigue.

3.5.3 Fatigue Crack Propagation. At stress intensity factor range values less than 25 ksi$\sqrt{\text{in.}}$, crack growth occurs more rapidly at -275F than at room temperature, as shown in Figure 3.5.3.1. Above this value, crack growth rates are comparable at both temperatures (Ref. 51).

3.5.3.1 *[Figure]* Fatigue crack growth behavior of annealed plate at room temperature and -275F.

Crack propagation rates at room temperature to -452F are presented in Figure 3.5.3.2. The alloy undergoes partial transformation to martensite during fatigue at -321 and -452F but not at room temperature. The rates at room temperature and -321F are essentially equivalent, while those at -452F are faster. Formation of martensite during fatigue thus appears to increase the crack propagation rates (Ref. 53).

3.5.3.2 *[Figure]* Fatigue crack growth behavior at room temperature, -321 and -452F.

3.6 Elastic Properties

3.6.1 Poisson's Ratio, 0.285 (Ref. 35).

3.6.2 Modulus of Elasticity. Values for the dynamic modulus of elasticity at room temperature have been reported as 28,500 ksi (Ref. 1) and 28,210 ksi (Ref. 54).

3.6.3 Modulus of Rigidity. (See Table 3.2.2.1.) The dynamic modulus of rigidity (shear modulus) at room temperature is 10,950 ksi (Ref. 54).

3.6.4 Tangent Modulus.

3.6.5 Secant Modulus.

3.6.5.1 *[Figure]* Secant modulus for annealed plate at room and cryogenic temperatures.

4. Fabrication

4.1 Forming

4.1.1 Cold Forming. The same cold forming equipment and techniques are utilized as those for Type 300 series stainless steels. However, 21-6-9 has a higher yield strength and work-hardening rate than the Cr-Ni austenitic steels and this must be taken into consideration in choosing equipment with the proper capacity. Intermediate annealing between operations may be required (see Section 1.5) (Ref. 1).

4.1.2 Forging. 21-6-9 is readily forged with standard procedures using initial forging temperatures of 2100 to 2200F and finishing temperatures of 1700 to 1800F. Large sections should be charged into furnaces operating at or below 1600F, followed by equalizing at 2000F and soaking at 2100 to 2200F for 20 minutes per inch of thickness. Sections under 4 inches in diameter or thickness can be charged directly into furnaces at 2000 to 2200F. After forging, air cooling or water quenching may be used (Ref. 1).

High energy rate forging (HERF) is used to produce complex forgings of 21-6-9 which are required to meet high strength and ductility standards. Since 21-6-9 is not capable of being strengthened by precipitation reactions, such mechanical property requirements must be imparted by fabrication. The high strain rates of HERF, about 800 sec^{-1}, extend the transition from cold working to hot working from the normal values of 0.4 to 0.5 T_m (where T_m is the absolute melting point) to at least 0.6 T_m. Strengths in HERF processed parts are thus higher than those in press formed (PF) parts formed at the same temperatures. A further advantage is that the duplex substructures in HERF forgings result in significantly increased ductility at equivalent strength as compared to PF forgings. The range of HERF processing parameters in one study on 21-6-9 included starting temperatures of 1850 to 1900F (0.79 to 0.81 T_m) and finishing temperatures of 1400 to 1700F (0.63 to 0.74 T_m). Variation in properties and structure can occur between different forgings and also between different locations within an individual forging. These variations relate to finishing temperature of the last forming stage and/or to the forming sequence (Ref. 24).

4.2 Machining and Grinding

Cutting speeds are somewhat lower for 21-6-9 than those for other Cr-Ni austenitic stainless grades due to the higher work hardening rates of 21-6-9. Cutting speeds for single point turning of 21-6-9 are about 20 percent lower than for Types 304 and 316 stainless when carbide tools are used, and about 33 percent lower with high speed steel tooling (Ref. 1).

4.3 Joining

4.3.1 Fusion Welding. (See Table 2.3.3.5.) Alloy 21-6-9 can be welded by most conventional techniques. Welding processes and techniques normally used in joining the Cr-Ni austentic stainless steels, such as gas-tungsten-arc (GTA), gas-metal-arc (GMA), shielded-metal-arc (SMA), and electron-beam (EB), may be used on 21-6-9 with few exceptions.

Alloy 21-6-9 is particularly sensitive to copper contamination. Small amounts of copper on the metal surface cause cracking in the heat-affected zone after GTA welding and should be avoided (Ref. 55). Copper back-up and hold-down fixtures should be chromium plated to avoid copper contamination. Alternatively, fixtures made from steel, aluminum, or the ferrite chromium stainless steels can be used satisfactorily (Refs. 1, 11).

Particular attention must be paid to cleanliness and welding procedures to ensure good welds and maintenance of corrosion resistance in the weld areas. Welded parts should receive a post-weld heat treatment to alleviate residual stresses which can cause cracking in the heat affected zone. Welded parts should also be descaled and passivated in order to remove contaminants which can reduce corrosion resistance during subsequent service (Ref. 56).

For the GTA and GMA methods, W 21-6-9 weld wire should be used. Alternate filler materials are Type 309, 312, and 347 stainless steels or nickel-base alloys. The selection of alternate fillers should be based on the corrosion, strength, or cryogenic requirements of the application.

Welded joints in the as-welded condition have strengths almost equivalent to the unwelded base metal, as shown in Table 4.3.1.1 and Figure 4.3.1.2 (Refs. 1, 12).

4.3.1.1 *[Table]* Typical tensile properties of GTA- and GMA-welded sheet and plate at room temperature.

4.3.1.2 *[Figure]* Typical tensile properties of GMA-welded sheet and strip at room and elevated temperatures.

For cryogenic applications, weldments of 0.250 inch or less in thickness made with W 21-6-9 filler metal exhibit good toughness while those greater than 0.250 inch require special weld filler metals (Refs. 1, 2, 11). Reduced fracture properties at cryogenic temperatures of fusion welds made with 21-6-9 filler metal are possibly related to the presence of delta ferrite in the weld metal (Ref. 21). The use of Inconel 625 filler metal, however, allows retention of good strength, ductility, and toughness at -452F by a variety of standard welding processes, as shown in Table 4.3.1.3. Ductile fracture mode was observed in all tensile tests (Ref. 57).

4.3.1.3 *[Table]* Mechanical properties at -452F for 21-6-9 plate welded with Inconel 625 filler metal.

Weld penetration during autogenous fusion joining of 21-6-9, which is reduced as compared to Type 304 stainless because of higher manganese content, can be substantially improved by the presence of surface-active trace elements such as selenium and sulfur. The addition of 140 ppm selenium to the base metal increased the depth/width ratio of GTA welds by 180 percent (Ref. 58).

Additions of 77 ppm selenium also substantially improved the penetrations for laser and electron-beam welds (Ref. 60). Alternatively, the addition of 500 to 1400 ppm SO_2 to the torch gas allowed a similar increase in depth/width ratio. The increase in sulfur content at the weld bead was less than 30 ppm with 700 ppm SO_2 in the torch gas. It should be noted that SO_2 is toxic and appropriate safety measures are required for its use (Ref. 60).

Specific welding parameters for the GTA and GMA processes are given in References 1, 2, and 10.

High joint efficiencies can be attained in 21-6-9 by electron-beam welding. Tensile strengths approach 100 percent although elongations are less than those of unwelded base metal. The tensile properties of EB-welded sheet are similar to those of GTA-welded sheet. Ductilities are slightly reduced and yield strengths slightly increased in notched specimens. The presence of a 10 ksi hydrogen environment has no significant effect, as shown in Figure 4.3.1.4. The alloy does not exhibit increased sensitivity to intergranular corrosion (sensitization) as a result of welding, although Type 304 is sensitized by electron-beam welding and requires post-weld heat treatment (Ref. 61).

4.3.1.4 *[Figure]* Smooth and notched tensile properties of GTA- and EB-welded sheet at room temperature in air and in high-pressure gases.

Two-pass techniques are generally required in EB welds to eliminate porosity (Refs. 1, 11). Specific parameters for EB welding are given in Reference 12.

4.3.2 Resistance Welding. High quality joints can be made in 21-6-9 using upset resistance welding techniques (Ref. 62). Specific parameters for conventional resistance spot welding are given in Reference 16.

4.3.3 Brazing. Alloy 21-6-9 can be joined satisfactorily with a number of commercially available brazes. However, the alloy is sensitive to liquid metal embrittlement and grain boundary penetration by copper and copper-containing braze alloys. Tin and possibly gold in high copper content brazes contribute to embrittlement. Braze alloys containing copper are not recommend for use with 21-6-9 (Refs. 55, 63).

4.4 Surface Treating

Procedures for cleaning, pickling, descaling, and passivating are the same as those for Types 302 and 304 stainless steels (Ref. 17).

Table 1.3.1 Specifications (Refs. 3-9)

Alloy	21-6-9	
Specifications	**Product Form**	**UNS**
AMS 5595E	Sheet, strip and plate	S21904
5656B	Bars, wire, forgings, extrusions and flash-welded rings	S21904
5561B	Welded and drawn tubing	S21900
5562B	Seamless tubing	S21904
ASTM A 276-91a	Bars and shapes (XM-10) (XM-11)	S21900 S21904
A 580-91a	Wire (XM-10) (XM-11)	S21900 S21904
A 666-91	Sheet, strip, plate, flat bar (XM-11)	S21904

Table 1.4.1 Specified compositions (Refs. 3-9)

Alloy	21-6-9					
Specification	**AMS 5595E, 5656B**		**ASTM A 276, A 580**		**ASTM A 666**	
Element	**Percent**		**Percent**		**Percent**	
	Minimum	**Maximum**	**Minimum**	**Maximum**	**Minimum**	**Maximum**
Carbon	—	0.04	—	0.04	—	0.04
Nitrogen	0.15	0.40	0.15	0.40	0.15	0.40
Chromium	19.00	21.50	19.00	21.50	19.00	21.50
Nickel	5.50	7.50	5.50	7.50	5.50	7.50
Manganese	8.00	10.00	8.00	10.00	8.00	10.00
Silicon	—	1.00	—	1.00	—	0.75
Phosphorus	—	0.060	—	0.060	—	0.060
Sulfur	—	0.030	—	0.030	—	0.030
Molybdenum	—	0.75	—	—	—	—
Copper	—	0.75	—	—	—	—

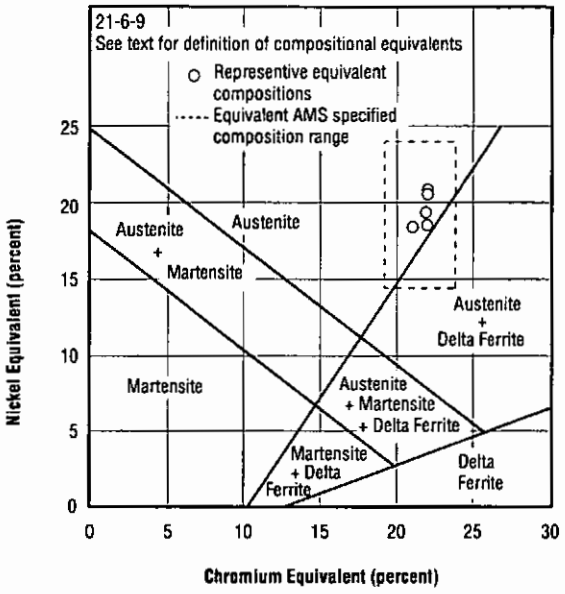


Fig. 2.1.2.1.1 Schaeffler diagram showing locations of 21-6-9 equivalent compositions (Ref. 19)

Table 2.1.2.1.3 Effect of elevated temperature exposure on the precipitation of grain boundary carbides (Ref. 1)

Alloy	21-6-9			
	Carbide Formation Rating [a]			
Exposure Time (hr)	1	9	25	100
Exposure Temperature (F)				
600	1	1	1	1
800	1	1	1	1
1000	1	1	1	1.4
1100	1	1.6	3.2	5
1200	1.6	3.6	4.8	5.6
1400	3	3	3.8	3.8
1600	1.6	2	2	2.5

Note: Ratings are averages of 5 heats containing 0.04 percent carbon maximum.

[a] Solar carbide rating code:
None = 1 - 1.4 Medium = 3.5 - 4.5
Trace = 1.5 - 2.5 Heavy = 4.6 - 5
Light = 2.6 - 3.4 Very heavy = 5.5 - 6

Table 2.1.2.1.2 Effect of elevated temperature exposure on sigma phase formation (Ref. 1)

Alloy	21-6-9			
	Sigma Formation Rating [a]			
Exposure Time (hr)	1	9	25	100
Exposure Temperature (F)				
600	1	1	1	1
800	1	1	1	1
1000	1	1	1	1.2
1100	1.2	1.2	1.2	1.6
1200	1.2	1.2	2	2.6
1400	1.4	2.8	3.4	3.6
1600	1.6	2.4	3	3.4

Note: Ratings are averages of 5 heats containing 0.04 percent carbon maximum.

[a] Sigma rating code:
None = 1 - 1.4 Medium = 3.5 - 4.5
Trace = 1.5 - 2.5 Heavy = 4.6 - 5
Light = 2.6 - 3.4

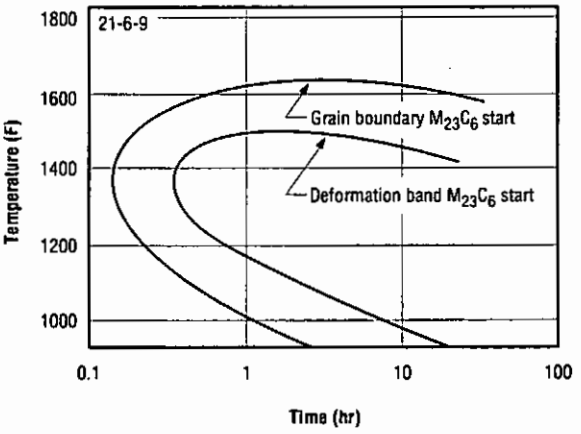


Fig. 2.1.2.1.4 Time-temperature curves for carbide precipitation (Ref. 26)

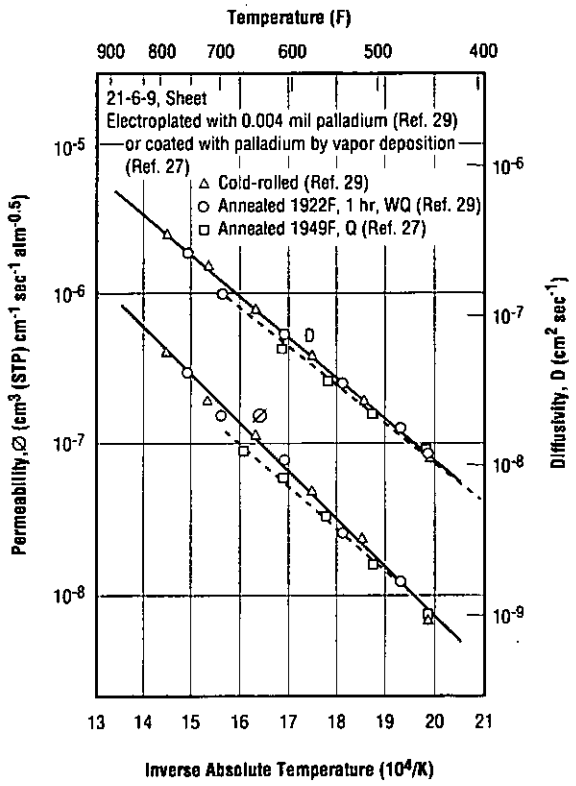


Fig. 2.1.2.1.5 Hydrogen diffusivity and permeability (Refs. 27, 29)

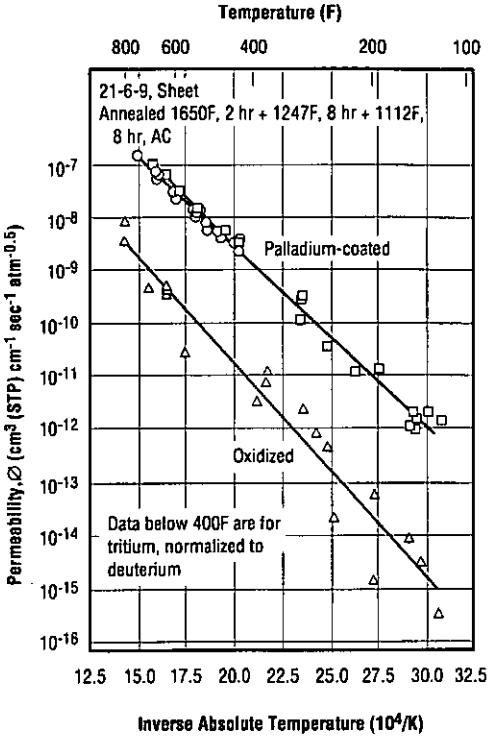


Fig. 2.1.2.1.6 Permeability of deuterium/tritium through palladium-coated and oxidized alloy (Ref. 30)

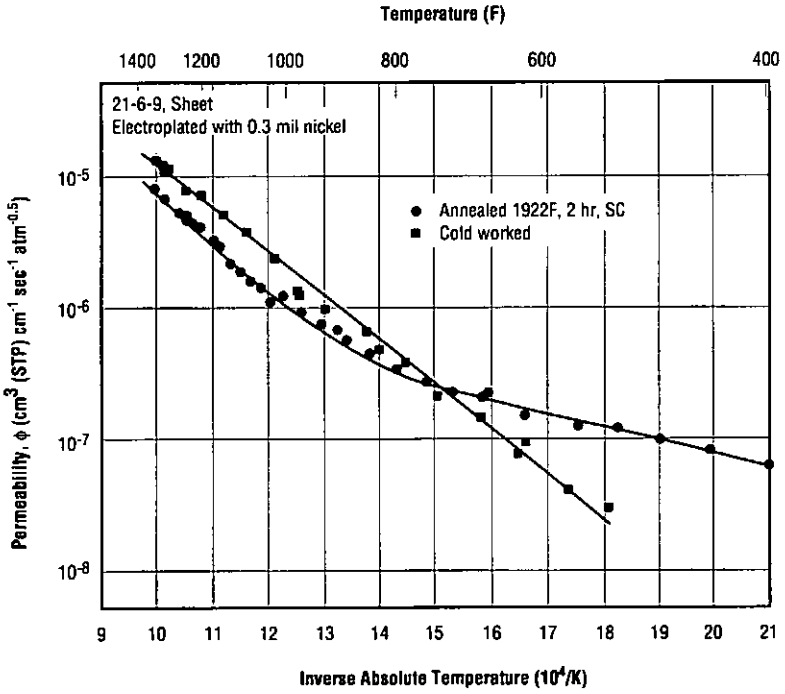


Fig. 2.1.2.1.7 Tritium permeability in cold worked and annealed alloy (Ref. 31)

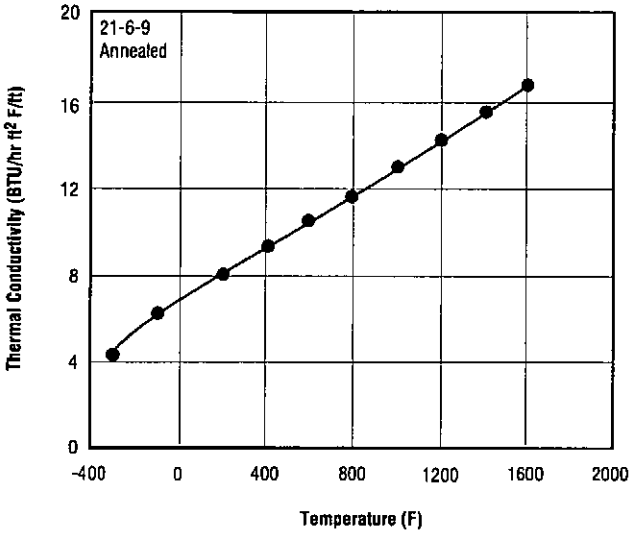


Fig. 2.1.3.1 Thermal conductivity (Ref. 1)

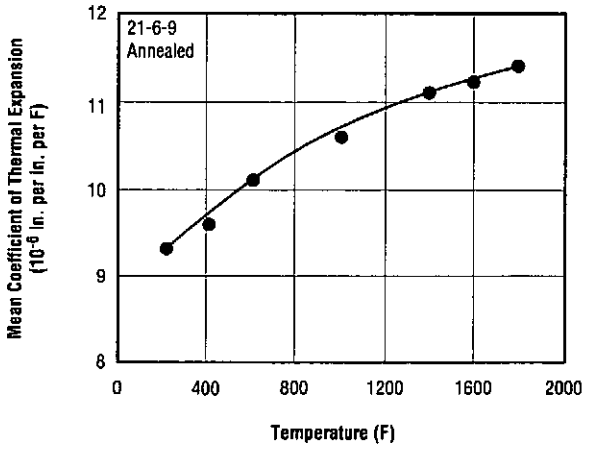


Fig. 2.1.4.1 Effect of temperature on the mean coefficient of thermal expansion (Ref. 1)

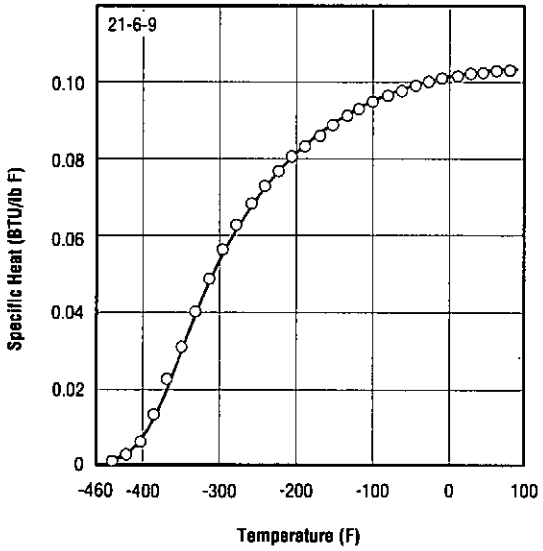


Fig. 2.1.5.1 Specific heat (Ref. 64)

Table 2.2.3.1 Effect of cold-working on magnetic permeability at various field strengths (Ref. 1)

Alloy	21-6-9			
Condition	Magnetic Permeability			
Field Strength (oersteds)	**50**	**100**	**200**	**500**
Annealed	1.005	1.004	1.004	1.002
Cold reduced 15 percent	1.004	1.004	1.003	—
35 percent	1.005	1.005	1.005	—
60 percent	1.010	1.010	1.012	<1.02

Table 2.2.3.2 Effect of exposure at cryogenic temperatures on magnetic permeability of 21-6-9 and Type 310 stainless steel (Ref. 1)

Alloy	21-6-9	310
Condition	Annealed	
Test Temperature (F)	**Magnetic permeability at 500 oersteds**	
75	1.002	1.002
-320	1.005	1.007
75	1.002	1.003

Note: Specimens tested at 75F, at -320F and retested at 75F to measure effects of low temperature exposure on room temperature permeability.

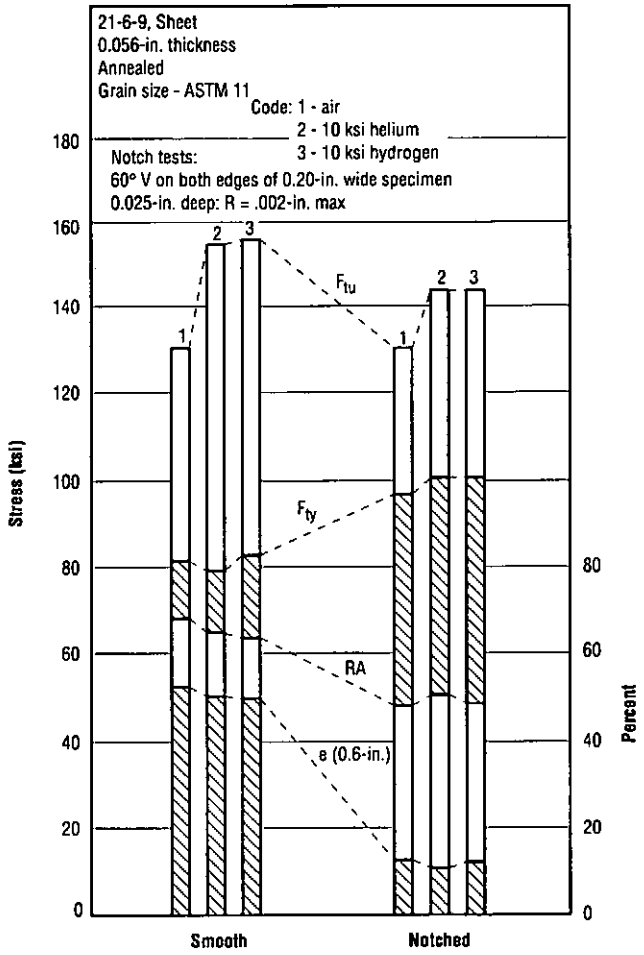


Fig. 2.3.3.1 Smooth and notched tensile properties of sheet in air and in high-pressure helium and hydrogen (Ref. 12)

Table 2.3.3.2 Smooth and notched tensile properties of sheet before and after combined static loading and exposure to high-pressure hydrogen (Ref. 12)

Alloy	21-6-9			
Condition	Annealed			
Thickness (in.)	0.056			
Type of Test	**Smooth**		**Notched[a]**	
Exposure to 10,000 psi hydrogen	**None**	**Exposed[b]**	**None**	**Exposed[b]**
F_{tu} (ksi)	129	137	131	133
F_{ty} (ksi)	81	105	97	122
e, in 0.60-in. (percent)	52	49	11	10
RA (percent)	68	67	48	50

a 60° V-notch at mid-point gage section; 0.025-inch depth; R = 0.002-inch max: K_t = 6.

b Specimens were exposed to 10,000 psi hydrogen for 300 hours at a static stress of 80 ksi to ensure some plastic deformation during exposure. No failures occurred during 300 hour period and specimens were immediately tested in air after removal from autoclave in same manner as unexposed specimens.

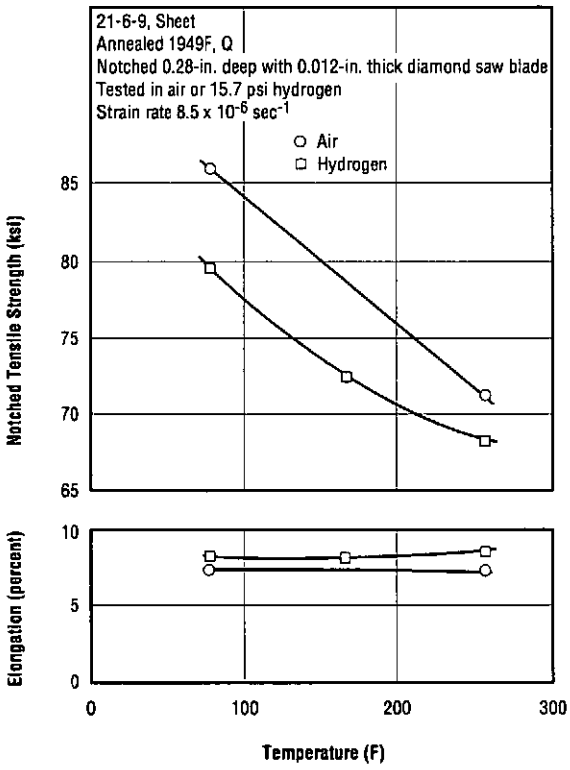


Fig. 2.3.3.3 Effects of hydrogen on notched tensile properties at slow strain rate (Ref. 27)

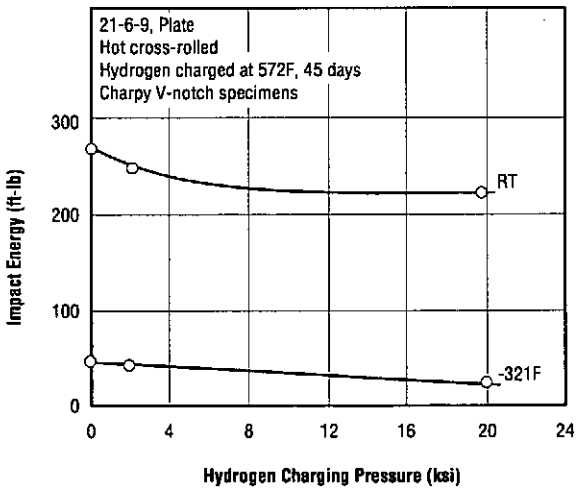


Fig. 2.3.3.4 Effect of hydrogen on impact energy at room temperature and -321F (Ref. 39)

Table 2.3.3.5 Effects of hydrogen on tensile properties of gas-tungsten-arc welds (Ref. 42)

Alloy	21-6-9						
Weld Filler Metal	Hydrogen Charging Pressure (ksi)	Test Environment	Tensile Properties [a]				
			F_{ty} (ksi)	F_{tu} (ksi)	Elongation		Reduction in Area (percent)
					Uniform (percent)	Total (percent)	
Type 308L [b]	—	air	78.2	108.2	9.7	14.3	54
	—	10 ksi H_2	77.5	107.0	10.2	13.8	57
	—	25 ksi H_2	83.1	114.0	10.8	14.6	61
	3.5	air	80.2	109.8	8.8	11.6	49
	3.5	10 ksi H_2	—	109.6	—	—	43
	10	air	84.0	112.5	10.2	11.9	44
	10	25 ksi H_2	88.0	123.1	9.7	10.4	44
21-6-9	—	air	76.9	112.1	11.8	19.0	60
	—	10 ksi H_2	72.2	109.4	13.6	22.1	75
	—	25 ksi H_2	78.8	115.3	11.7	19.8	69
	3.5	air	74.5	111.5	12.9	17.7	56
	3.5	10 ksi H_2	88.8	119.9	—	—	50
	10	air	78.8	114.4	12.5	15.6	50
	10	25 ksi H_2	85.4	122.1	13.8	17.2	49

[a] Tensile specimens contained transverse regions of weld metal, heat affected zone, and base metal. Fractures occurred in weld metal. Strain rate 0.02 min^{-1}. Gage length 1-inch.

[b] Nominal composition: Fe - (19-21)Cr - (10-12)Ni - 0.03C - 2Mn - 1Si.

[c] Charged for 10 days at 392F.

Table 2.3.4.1 Oxidation resistance in air of 21-6-9 and Type 304 stainless steel (Ref. 1)

Alloy	21-6-9	304	21-6-9	304
Test Time (hrs)	**400**		**1000**	
Test Temperature (F)	**Oxidation Loss (grams/sq in.)**			
1600	—	—	.06	.05
1800	.11	.30	—	—

Note: Tests run in an electric muffle furnace with a small amount of saturated air introduced to prevent stagnant atmosphere from occurring during exposure.

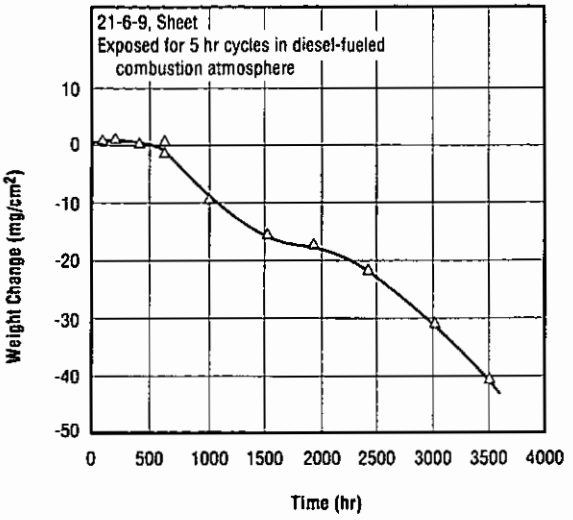


Fig. 2.3.4.2 Oxidation-corrosion behavior at 1508F under simulated Stirling automotive engine combustion conditions (Ref. 44)

Table 2.4.1 Effects of long-term hydrogen and tritium exposure and aging on tensile properties (Ref. 46)

Alloy	21-6-9				
Form	Forged Bar				
Exposure Condition	**Aging Conditions**	**Tensile Properties**			
		F_{ty} (ksi)	**F_{tu} (ksi)**	**Total Elongation (percent)**	**Plastic Strain to Fracture**
(None)	(None)	116	135	70	0.34
4.4 ksi, H_2, 386F, 56 days	-10F, 7 years	123	144	53	0.34
10 ksi, T_2, 386F, 60 days	(None)	120	136	52	0.38
10 ksi, T_2, 386F, 17 months	-10F, 5 years	126	134	10	0.06

Table 3.1.1 AMS and ASTM specified mechanical properties (Refs. 3, 4, and 7-9)

Alloy	21-6-9								
Specification	Form	Condition[a]	Thickness (in.)	Minimum Tensile Properties				Hardness, max (HRB)	Bend Diameter, min (t)
				F_{tu} (ksi)	F_{ty} (ksi)	e[b], (pct)	RA (pct)		
AMS 5595E	Sheet, strip, and plate	SHT 1900F, ≥RAC	<0.1875	100	60	40			
			≥0.1875	90	50	40			
			≤0.249						1[c,e]
			>0.249 ≤0.749						1[d], 2[e]
			—					100	
5656B	Bars, wire, forgings, extrusions, and rings	SHT 1950F, forced air cool or faster	—	90	50	40	60	100	
ASTM A 276	Bars and shapes	Annealed	—	90	50	45	60		
A 580	Wire	Annealed	—	90	50	45	60		
A 666	Sheet, strip, plate and flat bar	1/4 hard	≤0.030	130	115	15			
			>0.030	130	115				
		1/16, 1/8 hard	≤0.1874						1[c]

Note — The original AMS and ASTM documents should be consulted for complete specification details.

a SHT — solution heat treated; RAC — rapid air cool.

b Elongation in 4D or 2-inch.

c Free bend, 180 degrees minimum.

d Free bend, 90 degrees minimum.

e V-block, 135 degrees minimum.

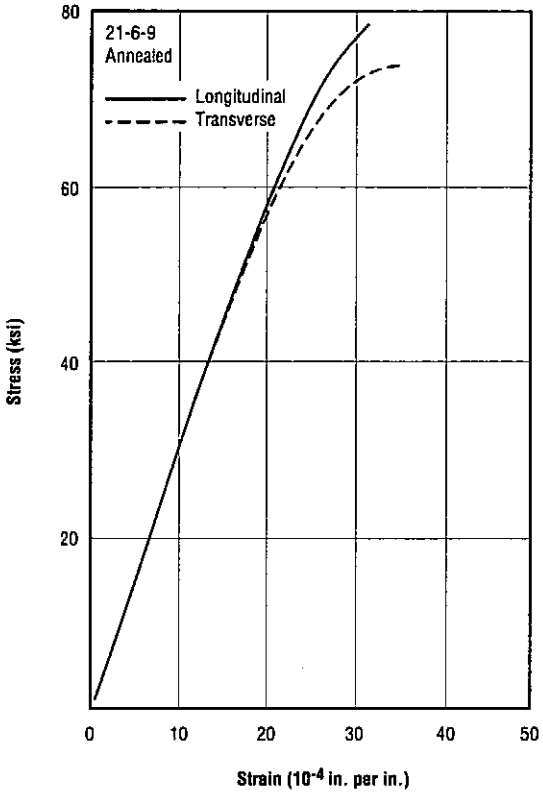


Fig. 3.2.1.1 Stress-strain diagram (Ref. 1)

ıble 3.2.1.2 Typical mechanical properties for bar and sheet (Ref. 1)

Alloy	21-6-9					
Form	Bar				Sheet	
Condition	**Annealed 1950F, WQ**				**Annealed**	**High Tensile Temper**
Size (in.)	**6 x 6**	**4 x 4**	**2.5 x 4.5**	**1 diameter**	—	—
F_{tu} (ksi)	99	98	100	100	112	145
F_{ty} (ksi)	65	58	68	57	68	130
e, 2-in. (percent)	48	55	48	53	44	20
RA (percent)	70	75	70	75	—	—
Hardness - Rockwell	—	—	—	—	B96	C34

Note: Longitudinal Tests

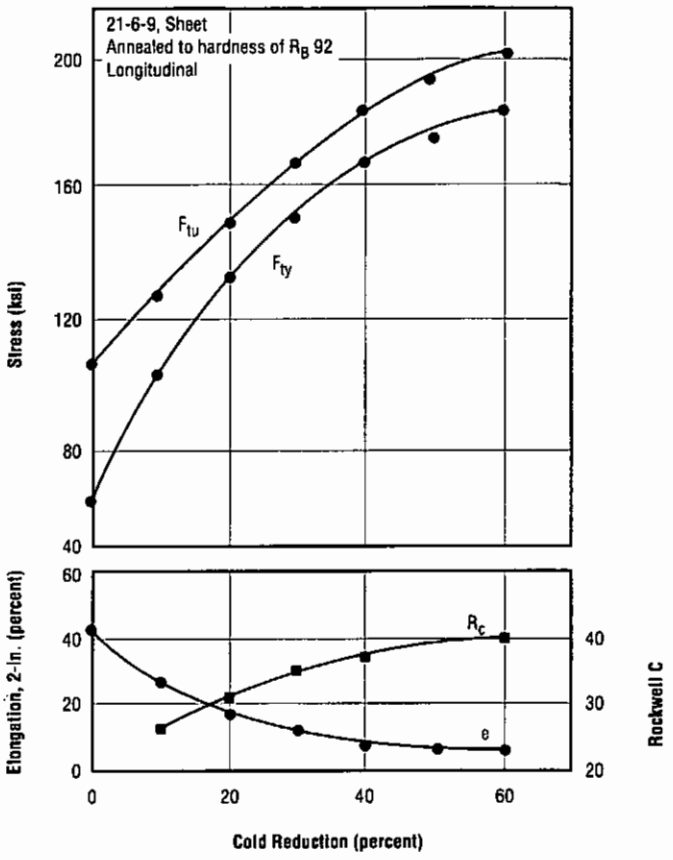


Fig. 3.2.1.3 Effect of cold working on mechanical properties of sheet (Ref. 1)

Table 3.2.1.4 Effect of cold rolling and stress relieving on mechanical properties of sheet (Ref. 1)

Alloy	21-6-9								
Cold Reduction (percent)	**0**			**15**			**30**		
Stress Relief Temperature (F)	**None**	**900**	**1250**	**None**	**900**	**1250**	**None**	**900**	**1250**
F_{tu} (ksi)	115	116	116	142	146	142	177	185	167
F_{ty} (ksi)	70	71	71	131	132	118	159	178	154
e, 2-in. (percent)	44	44	44	23	23	26	12	11	19
Hardness (R_C)	B94	B94	B94	34	34	32	40	42	39

Note: Stress relieving was for 1 hour at indicated temperatures.

Table 3.2.1.5 Effect of cold drawing and stress relieving on mechanical properties of wire (Ref. 1)

Alloy	21-6-9							
Cold Reduction (percent)	**15**				**30**			
Stress Relief Temperature (F)	**None**	**1000**	**1150**	**1300**	**None**	**1000**	**1150**	**1300**
F_{tu} (ksi)	128	128	125	122	179	179	166	159
F_{ty} (ksi)	108	102	92	93	162	162	149	140
e, 4D (percent)	56	56	45	60	28	28	28	40
RA (percent)	70	68	67	65	57	57	54	57
Hardness (R_C)	—	21	20	20	40	39	33	30

Note: Stress relieving was for 2 hours at indicated temperatures followed by air cooling.

Table 3.2.1.6 Effect of test direction on mechanical properties of sheet for two heats (Ref. 1)

Alloy	21-6-9			
Condition	Annealed 1950F			
Heat Designation	**A**		**B**	
Test Direction	**Long.**	**Trans.**	**Long.**	**Trans.**
F_{tu} (ksi)	119.1	117.1	111.7	110.6
F_{ty} (ksi)	75.4	75.0	65.0	63.9
e, 2-in. (percent)	43	43	45	43
Hardness (R_B)	95.5	95.5	93.5	93.5

Table 3.2.1.7 Effect of strain rate on the yield strength of sheet (Ref. 1)

Alloy	21-6-9				
Cross-head Speed to F_{ty} - actual (in. per in. per min.)	**.0017**	**.0254**	**.0515**	**.123**	**.319**
F_{ty} (ksi)	69.2	72.6	74.4	74.9	78.2

Note: F_{ty} are averages of duplicate transverse tests.

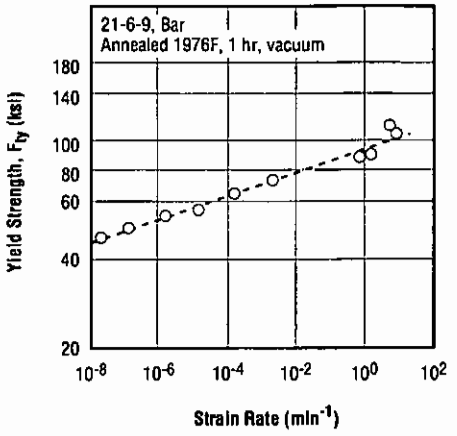


Fig. 3.2.1.8 Effect of strain rate on the yield strength of annealed bar at room temperature (Ref. 47)

Table 3.2.2.1 Compressive yield strength and modulus of elasticity of sheet for two heats (Ref. 1)

Alloy	21-6-9			
Condition	Annealed 1950F			
Heat Designation	**A**		**B**	
Test Direction	**Long.**	**Trans.**	**Long.**	**Trans.**
F_{cy} (ksi)	75.1	73.6	64.6	62.7
Modulus of Elasticity (psi x 10^6)	29.3	28.6	29.4	28.4
Hardness (R_B)	95.5	95.5	93.5	93.5

Table 3.2.2.2 Relaxation characteristics of compression springs exposed at 850F under stress (Ref. 1)

Alloy	21-6-9							
Cold Reduction (percent)	**15**				**30**			
Stress Relief Temperature (F)	**None**	**1000**	**1150**	**1300**	**None**	**1000**	**1150**	**1300**
Relaxation [a], loss in load (percent)	—	10.2	10.0	6.8	—	9.1	6.8	7.3
F_{ty} (ksi)	108	102	92	93	162	162	149	140
Hardness (R_C)	—	21	20	20	40	39	33	30

Note: F_{ty} and hardness shown are properties of original wire.

[a] Compression springs stressed at 40 ksi at room temperature and exposed at 850F for 5 days.

Table 3.2.6.1 Bearing strength of sheet for two heats (Ref. 1)

Alloy	21-6-9			
Condition	Annealed 1950F			
Heat Designation	**A**		**B**	
Test Direction	**Long.**	**Trans.**	**Long.**	**Trans.**
F_{bru} (ksi)	264.0	264.8	251.2	255.2
F_{bry} (ksi) 2.0 percent offset	163.5	141.1	127.5	117.5

Note: e/D = 2.0; hole diameter 0.375-inch.

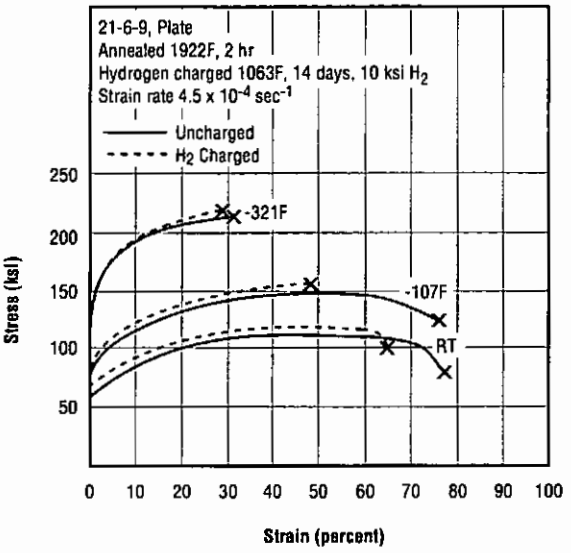


Fig. 3.3.1.1 Stress-strain behavior of uncharged and hydrogen-charged alloy (Ref. 48)

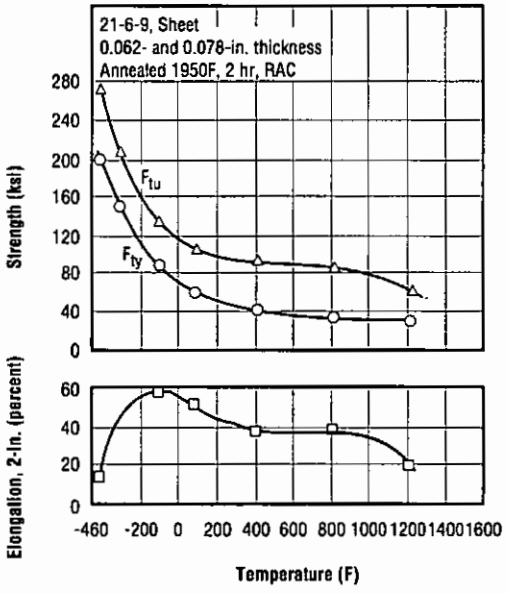


Fig. 3.3.1.2 Tensile properties of annealed sheet at -423 to 1200F (Ref. 65)

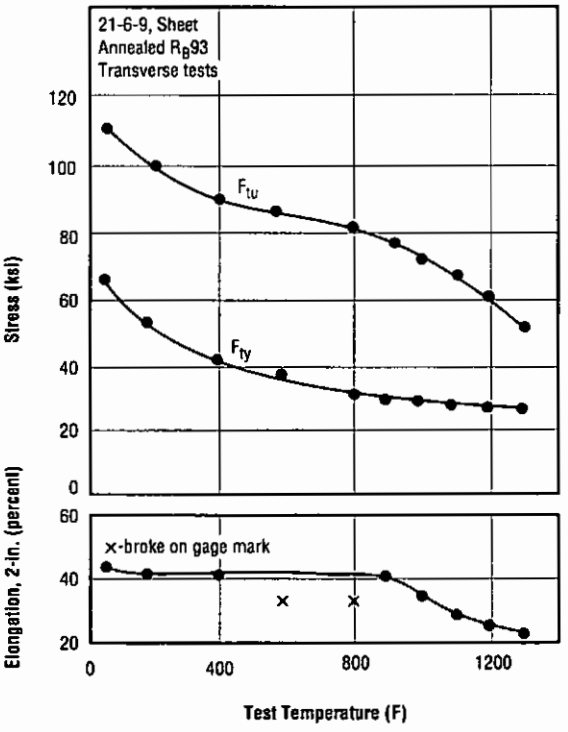


Fig. 3.3.1.3 Effect of test temperature on tensile properties of annealed sheet (Ref. 1)

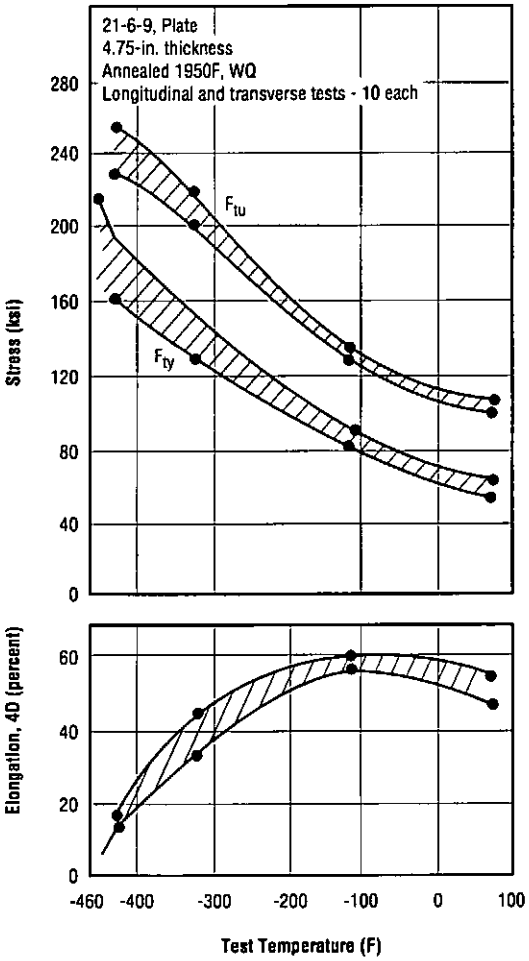


Fig. 3.3.1.4 Effect of cryogenic test temperature on tensile properties of plate (Refs. 13, 14)

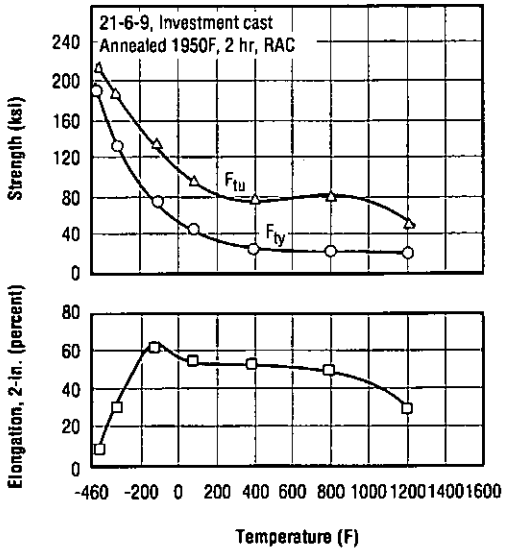


Fig. 3.3.1.5 Tensile properties of cast alloy at -423 to 1200F (Ref. 65)

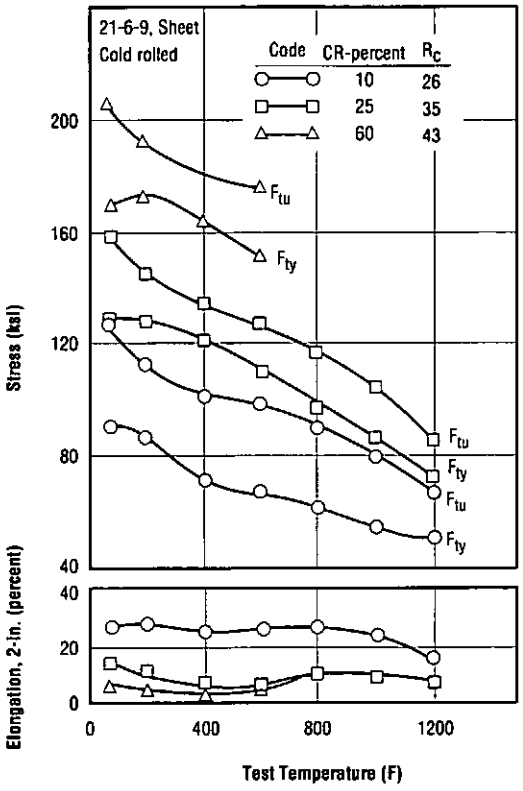


Fig. 3.3.1.6 Effect of test temperature on tensile properties of cold rolled sheet (Ref. 1)

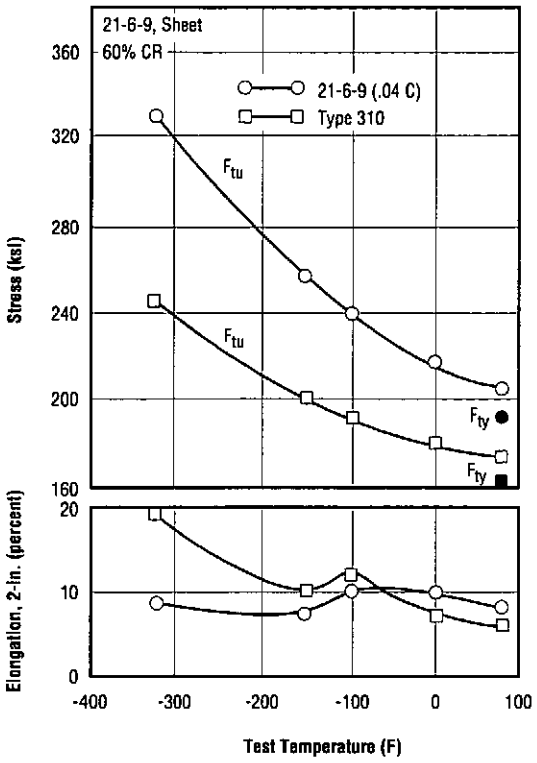


Fig. 3.3.1.7 Effect of cryogenic test temperature on tensile properties of 21-6-9 versus Type 310 stainless cold rolled sheet (Ref. 1)

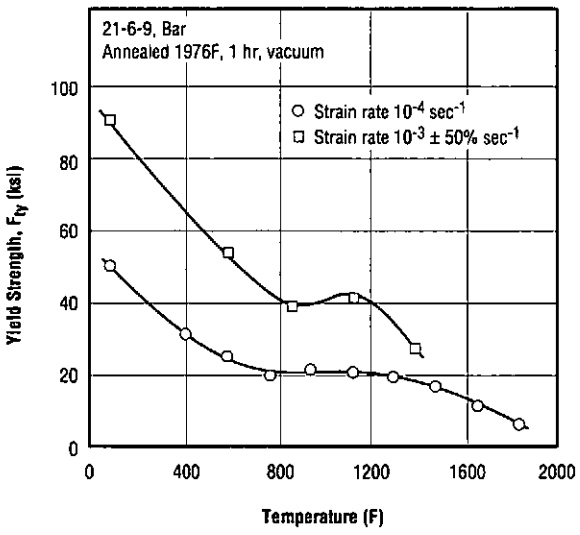


Fig. 3.3.1.9 Effects of temperature and strain rate on yield strength of annealed bar (Ref. 47)

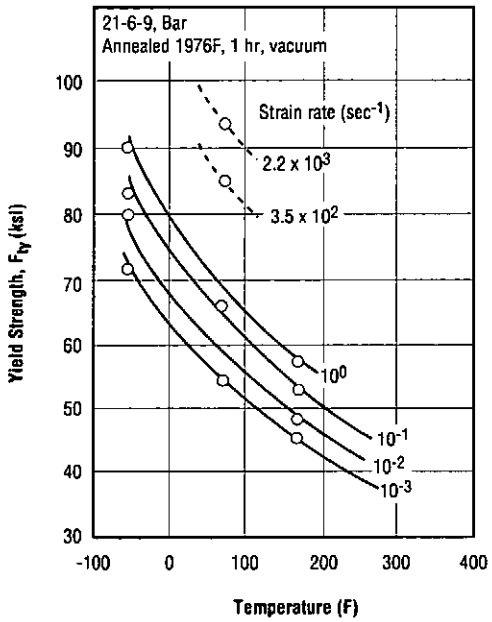


Fig. 3.3.1.8 Effect of strain rate on yield strength of annealed bar at -58 to 167F (Ref. 49)

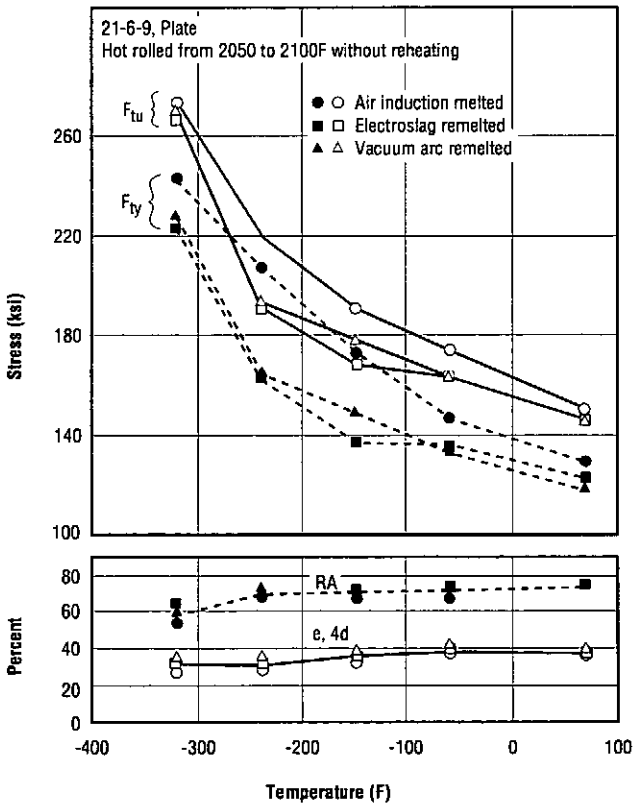


Fig. 3.3.1.10 Effects of melting process on tensile properties at room and cryogenic temperatures (Ref. 50)

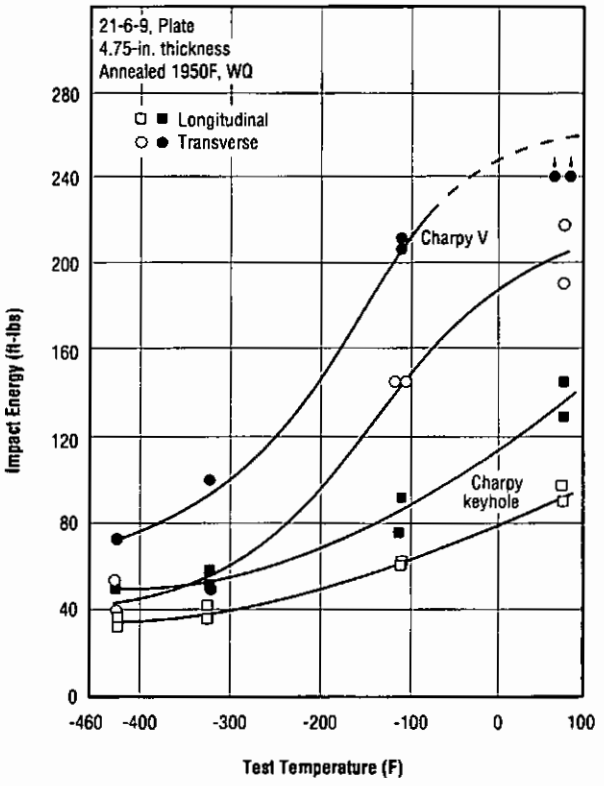


Fig. 3.3.3.1 Effect of cryogenic test temperature and orientation on impact energy of plate (Ref. 13)

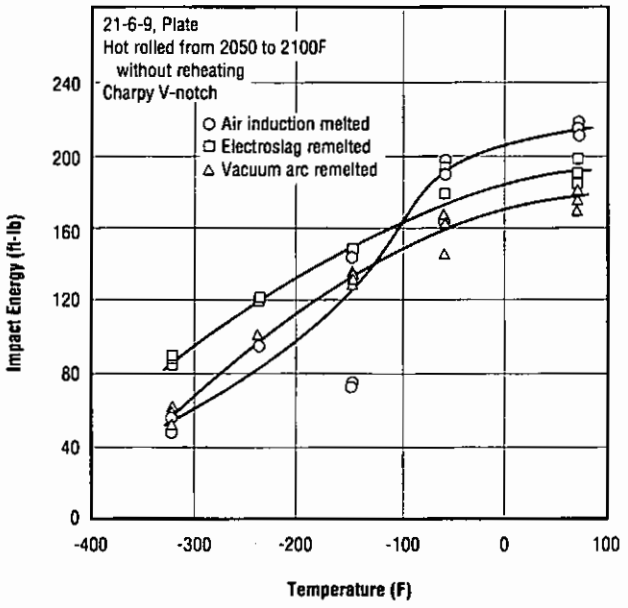


Fig. 3.3.3.3 Effects of melting process on impact energy at room and cryogenic temperatures (Ref. 50)

Table 3.3.3.2 Effect of cryogenic test temperature on impact energy of annealed and sensitized bar (Ref. 1)

Alloy[a]	21-6-9					
Thickness	1-inch diameter					
Condition[b]	Annealed			Sensitized		
Test Temperature (F)	**Room**	**-100**	**-320**	**Room**	**-100**	**-320**
Impact energy, Charpy V-notch (ft/lbs)	>240	>230	115	>240	181	21

a 0.04 C maximum.

b Annealed 1950F; sensitized at 1250F for 2 hours to simulate heat affected zones of weldments.

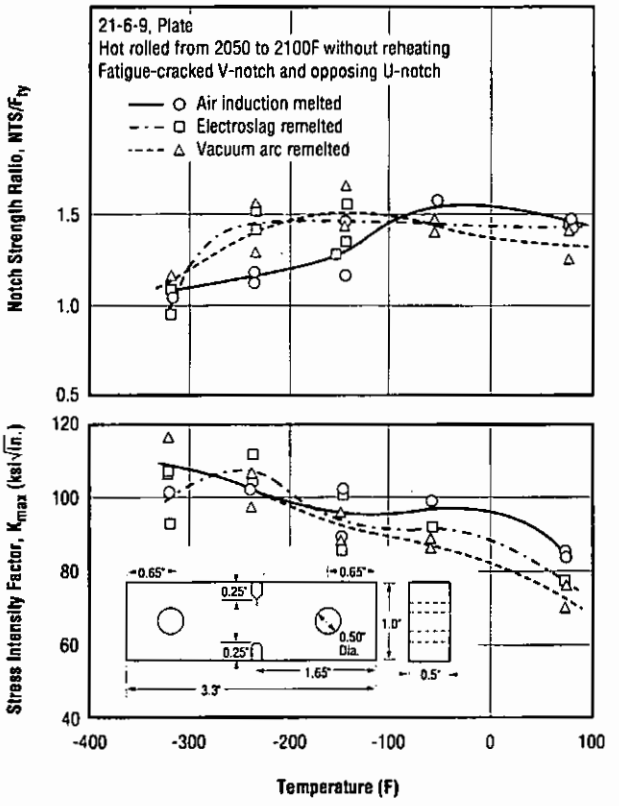


Fig. 3.3.7.1.1 Effects of melting process on double edge notch tensile properties at room and cryogenic temperatures (Ref. 50)

Table 3.3.7.1.2 Effect of cryogenic test temperature on smooth and notched tensile properties of annealed and sensitized 21-6-9 and Type 304L stainless steel (Ref. 1)

Alloy	21-6-9[a]		304L		21-6-9[a]		304L	
Test Temperature	**Room**				**-320F**			
Condition[b]	**Annealed**	**Sensitized**	**Annealed**	**Sensitized**	**Annealed**	**Sensitized**	**Annealed**	**Sensitized**
F_{tu} (ksi)	114	117	89	90	231	230	225	223
F_{ty} (ksi)	71	73	37	36	173	—	74	—
e, 2-in. (percent)	43	43	63	63	57	30	40	40
NTS (ksi)	93	93	61	61	193	185	101	93
NTS/F_{tu}	0.80	0.79	0.69	0.68	0.83	0.80	0.45	0.42

Note: All tests in transverse direction; 0.050-inch thick sheet. Notched strength determined on NASA edge notch specimen. 1-inch wide with 60° notch and 0.0007-inch maximum root radius.

[a] 21-6-9 with 0.08 C maximum.

[b] Annealed at 1950F; sensitized at 1250F for 1 hour.

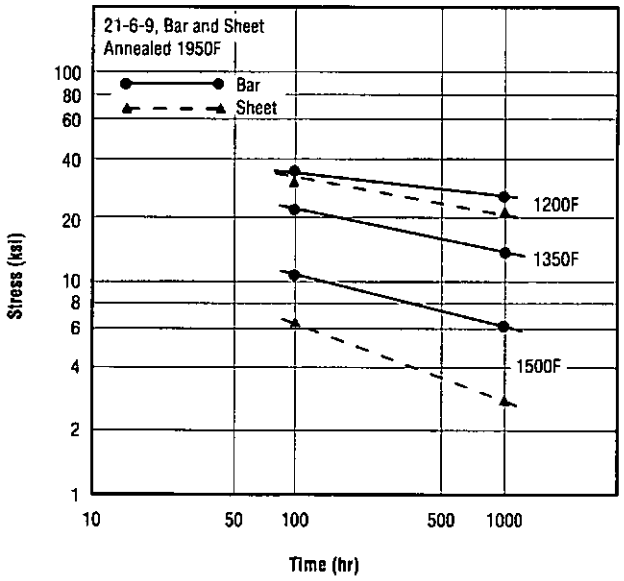


Fig. 3.4.1 Creep rupture behavior at 1200 to 1500F for annealed bar and sheet (Ref. 1)

Table 3.4.2 Creep strength of annealed bar (Ref. 35)

Alloy	21-6-9	
Form	Annealed Bar	
Temperature (F)	**Stress (ksi) for Creep Rate**	
	1×10^{-4} percent/hr	**1×10^{-5} percent/hr**
1200	14.4	10.2
1350	6.3	4

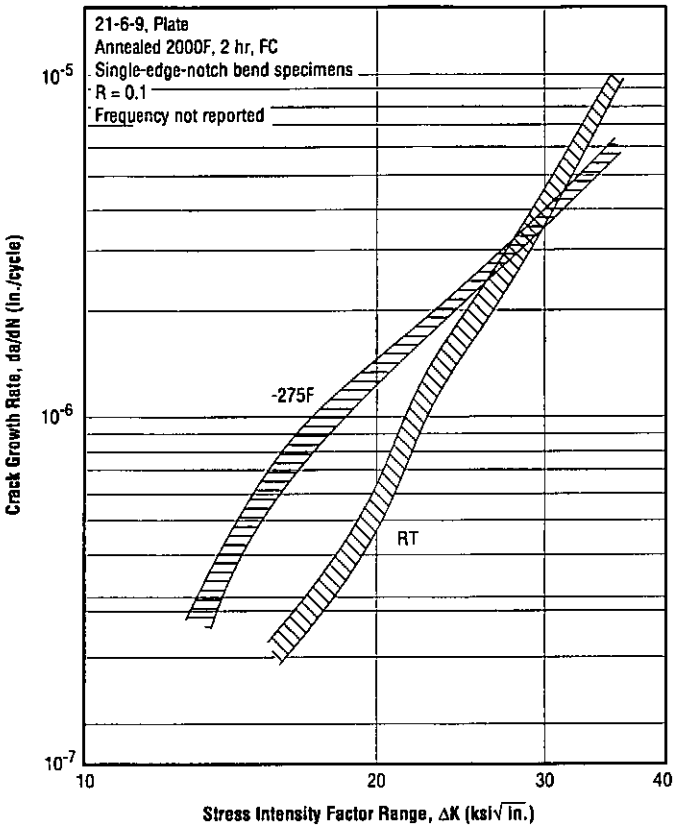


Fig. 3.5.3.1 Fatigue crack growth behavior of annealed plate at room temperature and -275F (Ref. 51)

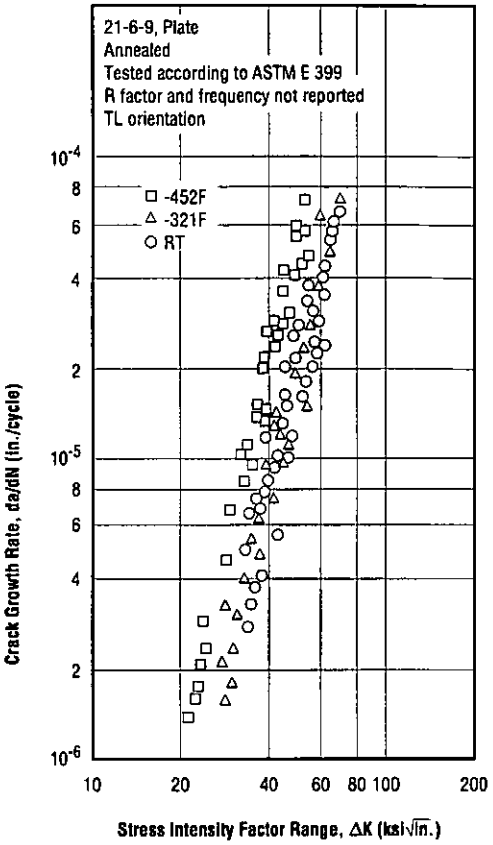


Fig. 3.5.3.2 Fatigue crack growth behavior at room temperature, -321 and -452F (Ref. 53)

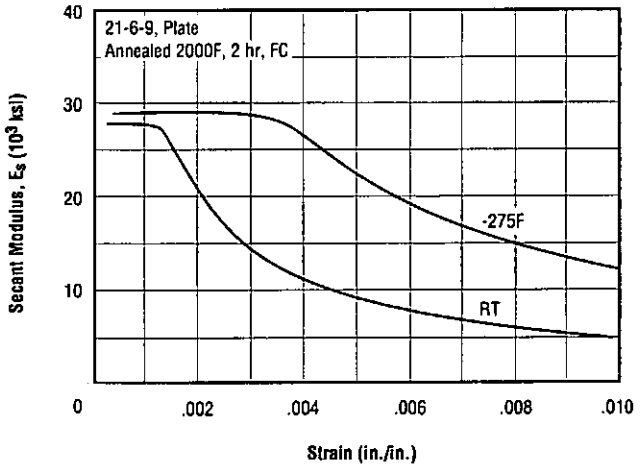


Fig. 3.6.5.1 Secant modulus for annealed plate at room and cryogenic temperatures (Ref. 51)

Table 4.3.1.1 Typical tensile properties of GTA- and GMA - welded sheet and plate at room temperature (Ref. 1)

Alloy	21-6-9	
Condition	Annealed	
Welding Process	**GTA**	**GMA[a]**
Thickness (in.)	**0.062**	**2.0**
F_{tu} (ksi)	109	106
F_{ty} (ksi)	68	65
e, 2-in. (percent)	22	39
Lateral contraction (percent)	17	—
Failure	Weld	Base Metal

[a] Covered electrodes.

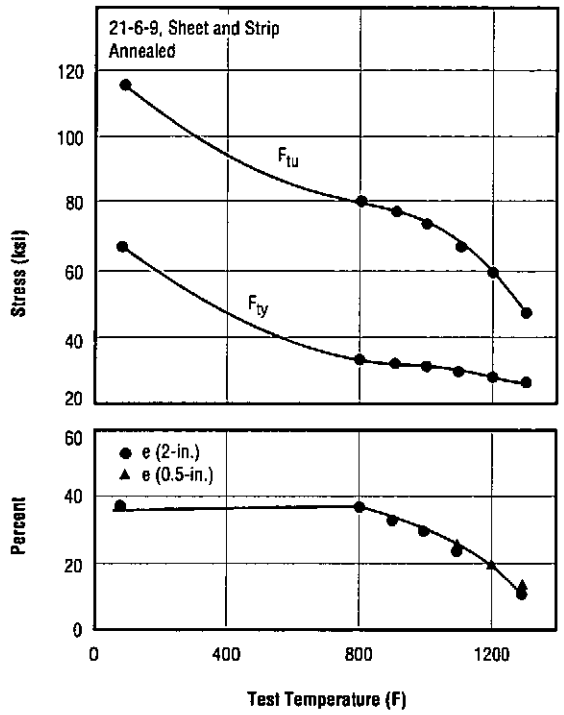


Fig. 4.3.1.2 Typical tensile properties of GMA-welded sheet and strip at room and elevated temperatures (Ref. 1)

Table 4.3.1.3 Mechanical properties at -452F for 21-6-9 plate welded with Inconel 625 filler metal (Ref. 55)

Alloy	21-6-9					
Condition	Annealed Plate					
Weld Process [a]	Specimen Type	Tensile Properties				Apparent Fracture Toughness [b], K_Q (ksi$\sqrt{in.}$)
		F_{ty} (ksi)	F_{tu} (ksi)	e (percent)	RA (percent)	
—	Base metal	196	247	23	30	132
SMA	Weld	127	183	31	27	123
SMA	HAZ[c]	251	272	21	33	105
GTA	Weld	138	177	18	20	121
GTA	HAZ	252	279	17	37	108
GMA	Weld	121	158	19	27	136
GMA	HAZ	245	271	15	27	118

[a] SMA — Shielded metal arc process.
GTA — Gas tungsten arc process.
GMA — Gas metal arc process.

[b] Fracture toughness tests were conducted according to ASTM E 399 but did not meet requirements for plane strain fracture toughness, K_{IC}.

[c] All HAZ specimens contained varying amounts of weld, HAZ, and base metal.

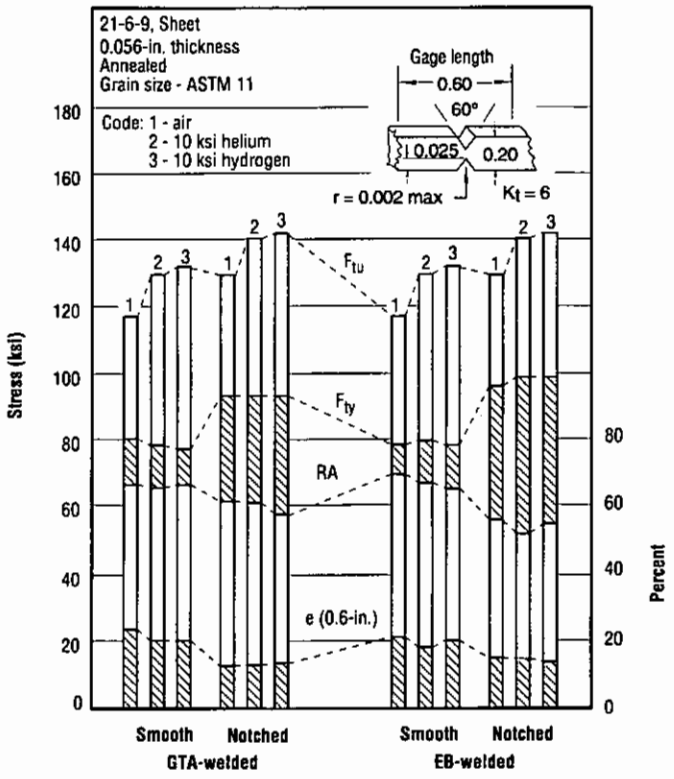


Fig. 4.3.1.4 Smooth and notched tensile properties of GTA- and EB-welded sheet at room temperature in air and in high pressure gases (Ref. 12)

References

1. Product Data Brochure S-26c, "Armco 21-6-9 Stainless Steel," Armco Steel Corp., Baltimore, MD (April 1969).
2. Padian, W. D.; Brubaker, D.; Rohrberg, R.; et al., "Permanent Tube Joint Technology," Technical Report AFRPL-TR-68-206, Air Force Rocket Propulsion Laboratory, Edwards, CA (November 1968).
3. AMS 5595E, Society of Automotive Engineers (April 1992).
4. AMS 5656B, Society of Automotive Engineers (April 1992).
5. AMS 5561B, Society of Automotive Engineers (January 1990).
6. AMS 5562B, Society of Automotive Engineers (July 1989).
7. ASTM A 276-91a, American Society for Testing and Materials (1991).
8. ASTM A 580-91a, American Society for Testing and Materials (1991).
9. ASTM A 666-91, American Society for Testing and Materials (1991).
10. Braun, W. H., "21-6-9: A High Strength Grade for Tubing," *Metal Progress*, Vol. 101, No. 2, p. 64 (February 1972).
11. Denhard, E. E., and Espy, R. H., "Austenitic Stainlesses with Unusual Mechanical and Corrosion Properties," *Metals Engineering Quarterly*, Vol. 12, No. 4 (November 1972).
12. Vandervoort, R. R., "Tensile and Fracture Properties of Austenitic Stainless Steel 21-6-9 in High-Pressure Hydrogen Gas," *Metals Engineering Quarterly*, Vol. 12, No. 1 (February 1972).
13. Malin, C. O., "Low Temperature Properties of Armco 21-6-9 Alloy (Cr-Ni-Mn)," Report NAR 80011, Rocketdyne Div., North American Rockwell Corp., Canoga Park, CA (May 27, 1968).
14. "Low Temperature Mechanical Properties of Various Alloys," Report No. NASA SP-5921(01), Technology Utilization Office, NASA, Washington, D.C. (1970).
15. Masteller, R. D.; Brown, H. J.; Herzog, R. G.; and Osgood, S. H., "Properties of Cyrogenically Worked Materials," Report No. NASA CR-72638, Martin Marietta Corporation, Denver, CO, NASA Lewis Research Center Contract NAS3-12028 (May 1, 1970).
16. "Welding Armco Stainless Steels," Brochure No. LE-4267, Armco Steel Corporation, Baltimore, MD (December 1967).

17. Personal Communication with H. W. Garvin, Sr., Research Engineer, Armco Steel Corporation, Baltimore, MD (February 1, 1973).

18. Brown, R. S., "Higher Strength, Corrosion Resistance with Nitrogen-Strengthened Stainless Steels," *Machine Design*, Vol. 52, No. 9, pp. 56-59 (April 24, 1980).

19. Wigley, D. A., "The Metallurgical Structure and Mechanical Properties at Low Temperatures of Nitronic 40, With Particular Reference to its Use in the Construction of Models for Cryogenic Wind Tunnels," NASA CR-165907, Southampton University, Southampton, England (April 1982).

20. *Metals Handbook*, 10th Edition, Vol. 4, American Society for Metals, pp. 771-772 (1991).

21. Espy, R. H., "Weldability of Nitrogen-Strengthened Stainless Steels," *Welding Journal*, Vol. 61, No. 5, pp. 149-s to 156-s (May 1982).

22. Tobler, R. L., and Reed, R. P., "Tensile and Fracture Behavior of a Nitrogen-Strengthened, Chromium-Nickel-Manganese Stainless Steel at Cryogenic Temperatures," *Proceedings of the Second International Conference on Mechanical Behavior of Materials*, held in Boston, MA, August 16-20, 1976, Federation of Materials Societies (1976).

23. Timmons, W. W., and Bailey, R. E., "Jessop's Experience in Producing Nickel Base Alloys and Stainless Steels by a 12 x 42 in. ESR Ingot Process," *Proceedings of the 1986 Vacuum Metallurgy Conference on Specialty Metals Melting and Processing*, held in Pittsburgh, PA, June 9-11, 1986, Iron and Steel Society of AIME, pp. 131-139 (1987).

24. Mataya, M. C.; Carr, M. J.; Krenzer, R. W.; and Kraus, G., "Processing and Structure of High-Energy-Rate-Forged 21-6-9 and 304L Forgings," DE82000409, Atomics International (August 10, 1981).

25. Packard, C. L.; Mataya, M. C.; and Edstrom, C. M., "Study of the Formation and Effects of Sigma Phase in 21-6-9 Stainless Steel," DE82-004574, Rockwell International, Golden, CO (November 1981).

26. Krenzer, R. W, and Sanderson, E. C., "Microstructural Stability of 21-6-9 Stainless Steel," RFP-2668, Rockwell International, Golden, CO (May 1978).

27. Perng, T. P., and Altstetter, C. J., "Hydrogen Effects in Austenitic Stainless Steels," *Materials Science and Engineering A*, Vol. A129, No. 1, pp. 99-107 (1990).

28. Caskey, G. R., Jr., and Sisson, R. D., Jr., "Hydrogen Solubility in Austenitic Stainless Steels," *Scripta Metallurgica*, Vol. 15, No. 11, pp. 1187-1190 (November 1981).

29. Xuikui, S.; Jian, S.; and Yiyi, L., "Hydrogen Permeation Behavior in Austenitic Stainless Steels," *Materials Science and Engineering A*, Vol. 114, No. 1/2, pp. 179-187 (July 15, 1989).

30. Swansiger, W. A., and Bastasz, R., "Tritium and Deuterium Permeation in Stainless Steels: Influence of Thin Oxide Films," *Journal of Nuclear Materials*, Vols. 85 & 86 (A), pp. 335-339 (December 11, 1979).

31. Bell, J. T., and Redman, J. D., "Tritium Permeability of Nickel-Plated Stainless Steel 21-6-9 and of Gold-Plated Aluminum," *Journal of Materials for Energy Systems*, Vol. 4, No. 4, pp. 217-221 (March 1983).

32. Misencik, J. A., "Evaluation of Dopants in Hydrogen to Reduce Hydrogen Permeation in Candidate Stirling Engine Heater Head Tube Alloys at 760 and 820C," NASA-TM-82920, NASA Lewis Research Center (October 1982).

33. Stulen, R. H., and Bastasz, R., "Surface Segregation of Boron in Nitrogen-Strengthened Stainless Steel," *Journal of Vacuum Science and Technology*, Vol. 16, No. 3, pp. 940-945 (May/June 1979).

34. German, R. M., and Odegard, B. C., "Thermally Induced Segregation in High-Manganese Stainless Steels," *Materials Science and Engineering*, Vol. 35, No. 2, pp. 299-301 (October 1978).

35. "Armco Nitronic 40 Stainless Steel Bar and Wire," Trade Literature, Armco Stainless Steel Division, Baltimore, MD (1981).

36. West, A. J., and Holbrook, J. H., "Hydrogen in Austenitic Stainless Steels: Effects of Phase Transformations and Stress State," *Proceedings of Hydrogen Effects in Metals*, held at Moran, WY, August 26-31, 1980, TMS/AIME, pp. 607-618 (1981).

37. West, A. J., Jr., and Louthan, M. R., Jr., "Hydrogen Effects on the Tensile Properties of 21-6-9 Stainless Steel," *Metallurgical Transactions A*, Vol. 13A, No. 11, pp. 2049-2058 (November 1982).

38. Morgan, M. J., and Tosten, M. H., "Microstructure and Yield Strength Effects on Hydrogen and Tritium Induced Cracking in HERF Stainless Steel," *Proceedings of Hydrogen Effects on Material Behavior*, held in Moran, WY, September 12-15, 1989, The Materials, Metals and Minerals Society, pp. 447-458 (1990).

39. Place, T. A.; Sudarshan, T. S.; Waters, C. K.; and Louthan, M. R., "Fractographic Studies of the Ductile-to-Brittle Transition in Austenitic Stainless Steels," *Proceedings of Fractography of Modern Engineering Materials: Composites and Metals*, held in Nashville, TN, November 18-19, 1985, pp. 350-365 (1987).

40. Perra, M. W., "Sustainer-Load Cracking of Austenitic Steels in Gaseous Hydrogen," *Proceedings of Degradation of Engineering Materials in Hydrogen*, held in Blacksburg, VA, September 21-23, 1981, Virginia Polytechnic Institute, pp. 321-333 (1981).

41. Brooks, J. A., and West, A. J., "Hydrogen Induced Ductility Losses in Austenitic Stainless Steel Welds,"

Metallurgical Transactions A, Vol. 12A, No. 2, pp. 213-223 (February 1981).

42. Brooks, J. A.; West, A. J.; and Thompson, A. W., "Effect of Weld Composition and Microstructure on Hydrogen-Assisted Fracture of Austenitic Stainless Steels," *Metallurgical Transactions A*, Vol. 14A, No. 1, pp. 75-84 (January 1983).

43. Slonaker, R. O., and Powell, G. W., "Oxidation of 21Cr-6Ni-9Mn Stainless Steel in Molten Lead Oxide and Static Air," *Corrosion*, Vol. 26, No. 9, pp. 363-370 (September 1970).

44. Stephens, J. R., and Barrett, C. A., "Oxidation and Corrosion Resistance of Candidate Stirling Engine Heater-Head-Tube Alloys," NASA-TM-83609, NASA Lewis Research Center (May 1984).

45. Bransford, J. W., and Clark, A. F., "Laser-Initiated Combustion Studies of Selected Aluminum, Copper, Iron, and Nickel Alloys," NBSIR-81-1647, National Bureau of Standards, Boulder, CO (April 1981).

46. Rawl, D. E., Jr.; Caskey, G. R., Jr.; and Donovan, J. A., "Low-Temperature Helium Embrittlement of Tritium-Charged Stainless Steel," presented at 109th Annual AIME Meeting, Las Vegas, NV, February 24-28, 1980.

47. Kassner, M. E., and Breithaupt, R. D., "The Yield Stress of Type 21-6-9 Stainless Steel over a Wide Range of Strain Rate (10^{-5} to 10^{4} s^{-1}) and Temperature," *Proceedings of Mechanical Properties at High Rates of Strain, 1984*, held at Oxford, U.K., April 9-12, 1984, The Institute of Physics, pp. 47-54 (1984).

48. Holbrook, J. H., and West, A. J., "The Effect of Temperature and Strain Rate on the Tensile Properties of Hydrogen-Charged 304L, 21-6-9, and JBK 75," *Proceedings of Hydrogen Effects in Metals*, held in Moran, WY, August 26-31, 1980, TMS/AIME, pp. 655-663 (1981).

49. Kassner, M. E., "A Simple Constitutive Equation to Model the Low-Temperature Yield Strength of Type 21-6-9 Stainless Steel," *Journal of Engineering Materials and Technology*, Vol. 105, No. 3, pp. 231-233 (July 1983).

50. Bhat, G. K., "Evaluation of the Mechanical Properties of Electroslag Refined Iron Alloys," NASA CR-135044, Carnegie-Mellon University, Pittsburgh, PA (December 1976).

51. Domack, M. S., "Fracture Toughness and Flaw Growth in Nitronic 40 at Cryogenic Temperatures," NASA TP-2312, NASA Langley Research Center (May 1984).

52. Tobler, R. L.; Reed, R. P.; and Purtscher, P. T., "Linear-Elastic Fracture of High-Nitrogen Austenitic Stainless Steels at Liquid Helium Temperature," *Journal of Testing and Evaluation*, Vol. 17, No. 1, pp. 54-59 (January 1989).

53. Tobler, R. L., "Effects of Cryogenic Temperatures on the Fatigue Crack Propagation Resistance of Austenitic Stainless Steels," *Proceedings of the Second International Conference on Mechanical Behavior of Materials*, held in Boston, MA, August 16-20, 1976, American Society for Metals (1976).

54. Ledbetter, H. M., "Room-Temperature Elastic Constants and Low-Temperature Sound Velocities for Six Nitrogen-Alloyed Austenitic Stainless Steels," *Metallurgical Transactions*, Vol. 11A, No. 6, pp. 1067-1069 (June 1980).

55. Heiple, C.; Bennett, W.; and Rising, T., "Embrittlement of Several Stainless Steels by Liquid Copper and Liquid Braze Alloys," *Materials Science and Engineering*, Vol. 52, No. 3, pp. 277-289 (March 1982).

56. Oliver, M. P., "The Results of Improper Manufacturing Techniques on 21-6-9 Stainless Steel Tubing," *Proceedings of Focus on Mechanical Failures: Mechanism and Detection*, held at Annapolis, MD, April 9-11, 1991, Vibration Institute, pp. 217-226 (1991).

57. Vandervoort, R. R., "Mechanical Properties of Inconel 625 Welds in 21-6-9 Stainless Steel at 4 deg. K," *Cryogenics*, Vol. 19, No. 8, pp. 448-452 (August 1979).

58. Heiple, C. R., and Roper, J. R., "Effect of Selenium and GTAW Fusion Zone Geometry," *Welding Journal*, Vol. 60, No. 8, pp. 143-s to 145-s (August 1981).

59. Heiple, C. R.; Roper, J. R.; Stagner, R. T.; and Aden, R. J., "Surface Active Element Effects on the Shape of GTA, Laser, and Electron Beam Welds," *Welding Journal*, Vol. 62, No. 3, pp. 72-s to 77-s (March 1983).

60. Heiple, C. R., and Burgardt, P., "Effects of SO_2 Shielding Gas Additions on GTA Weld Shape," *Welding Journal*, Vol. 64, No. 6, pp. 159-s to 162-s (June 1985).

61. Raasch, G. D., and Munir, Z. A., "The Effect of Electron Beam Welding on Various Properties of Three Austenitic Stainless Steels," *Journal of Materials Science*, Vol. 13, No. 5, pp. 1061-1074 (May 1978).

62. Kanne, W. R., Jr., "Solid-State Resistance Welding of Cylinders and Spheres," *Welding Journal*, Vol. 65, No. 5, pp. 33-38 (May 1986).

63. Keller, D. L.; McDonald, M. M.; Heiple, C. R.; Johns, W. L.; and Hofmann, W. E., "Wettability of Brazing Filler Metals," *Welding Journal*, Vol. 69, No. 10, pp. 31-34 (October 1990).

64. Tsiovkin, Yu. N., and Sukhanov, V. D., "Specific Heat of Some Steels and Alloys at 10-300°K," *Metal Science Heat Treatment Metals*, No. 9, pp. 702-703 (1967).

65. Cook, E. F., and Greene, E. F., "Comparison of Wrought and Cast Mechanical Properties of Annealed 21-6-9 Alloy from -423 to 1200F," Invention, MSF-18936, NAR-81058, Rockwell International, Canoga Park, CA (January 1970).

This page is blank.

	Fe
17	Cr
6.5	Mn
4.5	Ni

Type 201

1 GENERAL

The 200 series of austenitic stainless steels was developed during and after World War II to provide inexpensive, low-nickel substitutes for the 300 series stainless steels. Type 201 is a substitute for Type 301; the nickel in Type 301 is partially replaced with alternate austenite-stabilizing elements manganese and nitrogen. Mechanical properties and corrosion behaviors are very similar for the two grades. Type 201 is metastable and forms martensite on cold deformation, increasing the work-hardening rate. Type 201 is used in transit and railway cars, large truck trailers, moderately drawn utensils such as cookware lids, roll-formed and stretch bent automotive trim and wheel covers, household appliances, flat conveyor chain, architectural panels, and welded fire extinguisher tanks.

1.01 **Commercial Designation**

Type 201.

1.02 **Alternate Designations**

AISI 201, UNS S20100, and SAE 30201.

1.03 **Specifications**

AMS 5762, ASME SA412, ASTM A412, ASTM A581, ASTM A666, QQ-5-766, and SAE J405.

1.04 **Composition**

Composition, Table 1.04.

1.05 **Heat Treatment**

1.051 Annealing temperature range is 1850 to 2050 F. The alloy must be rapidly cooled or water quenched, depending on section size, in order to prevent carbide precipitation. For maximum corrosion resistance, parts should be full annealed at 1900 F or higher.

1.052 Stress relief, 800 F, 2 hours (5).

1.06 **Hardness**

1.061 The alloy is hardenable only by cold working (6).

1.062 Effect of temper on hardness, Figure 1.062.

1.07 **Forms and Conditions Available**

1.071 Sheet, strip, plate, bar, rod (7).

1.08 **Melting and Casting Practice**

1.09 **Special Considerations**

1.091 Type 201 is subject to intergranular corrosion when sensitized due to precipitation of complex chromium-rich carbides at the grain boundaries. See paragraph 2.0321.

2 PHYSICAL PROPERTIES AND ENVIRONMENTAL EFFECTS

2.01 **Thermal Properties**

2.011 Melting range is 2550 to 2650 F (9).

2.012 Phase changes.

2.0121 Time-temperature-transformation diagrams.

2.013 Thermal conductivity, 212 F, 9.4 Btu/ft/hr/ft^2/F.

2.014 Thermal expansion, Figure 2.014.

2.015 Specific heat, 32 to 212 F, 0.12 Btu/lb/F (3).

2.016 Thermal diffusivity.

2.02 **Other Physical Properties**

2.021 Density is 0.287 lb/in.^{3}, 7.94 g/cc (8).

2.022 Electrical properties.

2.0221 Electrical resistivity, 69 microhm-cm at room temperature (7).

2.023 Magnetic properties.

2.0231 Type 201 is nonmagnetic in the annealed condition and magnetic when cold worked (2).

2.0232 Effect of cold reduction on magnetic permeability, Table 2.0232.

2.024 Emissivity.

2.025 Damping capacity.

2.03 **Chemical Environments**

2.031 General corrosion.

2.0311 Type 201 has good corrosion resistance to a wide variety of media and can be used in most applications where Type 301 is used.

2.0312 The corrosion rate of Type 201 in 10 percent formic acid at room temperature is 0.4 mpy (11).

2.032 Intergranular corrosion.

2.0321 Type 201, like Type 301 and most of the unstabilized austenitic stainless steels, is subject to intergranular corrosion in the sensitized condition. Sensitization occurs when the chromium content of the matrix is reduced by precipitation of chromium-rich carbides in the grain boundary regions. Sensitization is caused by heating in the 800 to 1500 F temperature range. In particular, slow cooling through the critical temperature range after heat treating at a higher temperature or after welding can cause sensitization. Corrosion resistance can be restored by full annealing to redissolve the precipitated carbides.

2.033 Stress corrosion cracking.

2.0331 Type 201 is subject to stress corrosion cracking in chloride solutions. Cracking can be either transgranular or intergranular depending on the composition and temperature of the solution.

2.034 Oxidation.

2.0341 The oxidation resistance of Type 201 is good up to about 1550 F, comparable to that of Type 301. Above this temperature, however, Type 201 scales more rapidly due to its higher manganese content.

2.0342 Alloy is resistant to scaling up to 1550 F for continuous service and up to 1400 F for intermittent service (9).

2.0343 Effect of cold work on long time corrosion in steam at 1000 F, Figure 2.0343.

2.04 **Nuclear Environments**

3 MECHANICAL PROPERTIES

3.01 **Specified Mechanical Properties**

3.02 **Mechanical Properties at Room Temperature**

3.021 Tension – stress-strain diagrams – tension properties.

3.0211 Type 201 is hardened by the strain-induced transformation of austenite to alpha-prime martensite. As shown in Figure 3.0212, the maximum in rate of work hardening occurs simultaneously with the

Fe
17 Cr
6.5 Mn
4.5 Ni

Type 201

maximum rate of formation of alpha-prime martensite. The high degree of metastability of Type 201 with respect to cold deformation is indicated by the very large volume fraction, 85 percent, of martensite forming during tensile straining.

3.0212 Stress-strain curve and martensite content as a function of strain, Figure 3.0212.

3.0213 Effect of temper on mechanical properties at room temperature, Figure 3.0213.

3.0214 Effects of cold working on tensile properties, Figure 3.0214.

3.0215 Effects of cold rolling and stress relief on tensile yield strength, Figure 3.0215.

3.022 Compression – stress-strain diagrams – compression properties.

3.0221 Effect of cold work on compressive yield strength, Figure 3.0221.

3.0222 Effects of cold rolling and stress relief on compressive yield strength, Figure 3.0222.

3.023 Impact.

3.024 Bending.

3.025 Torsion and shear.

3.026 Bearing.

3.027 Stress concentration.

3.0271 Notch properties.

3.0272 Fracture toughness.

3.028 Combined properties.

3.03 **Mechanical Properties at Various Temperatures**

3.031 Tension – stress-strain diagrams – tension properties.

3.0311 Tensile properties of annealed alloy at elevated temperatures, Figure 3.0311.

3.0312 Tensile properties of full hard alloy at elevated temperatures, Figure 3.0312.

3.032 Compression – stress-strain diagrams – compression properties.

3.033 Impact.

3.0331 Effect of low and elevated temperatures on Charpy V impact strength of alloy, Figure 3.0331.

3.034 Bending.

3.035 Torsion and shear.

3.036 Bearing.

3.037 Stress concentration.

3.0371 Notch properties.

3.0372 Fracture toughness.

3.038 Combined properties.

3.04 **Creep and Creep-Rupture Properties**

3.041 Typical stress-rupture properties, Figure 3.041.

3.05 **Fatigue Properties**

3.051 The fatigue behavior of Type 201 in terms of total strain amplitude as a function of fatigue life is shown in Figure 3.052. The stress-strain hysterisis loops for this alloy progressively change with deformation and do not allow separation of total strain into plastic and elastic components. The change in behavior during fatigue life results from the continued formation of martensite. The rate of formation of martensite during cyclic straining, shown in Figure 3.053, is similar to that during monotonic straining, shown earlier in Figure 3.0212. The cyclic stress-strain curve exhibits hardening at much lower strains than the monotonic curve, as shown in Figure 3.054.

3.052 Axial fatigue behavior of smooth alloy at room temperature, Figure 3.052.

3.053 Effect of cyclic straining on martensite content of annealed alloy, Figure 3.053.

3.054 True stress-true strain curves for monotonic and cyclic deformation, Figure 3.054.

3.06 **Elastic Properties**

3.061 Poisson's ratio.

3.062 Modulus of elasticity.

3.0621 Modulus of elasticity for stress-relieved and cold rolled alloy, Figure 3.0621.

3.0622 Modulus of elasticity in compression for stress relieved and cold rolled alloy, Figure 3.0622.

3.063 Modulus of rigidity, 12,500 ksi (8).

3.064 Tangent modulus.

3.065 Secant modulus.

4 FABRICATION

4.01 **Forming**

4.011 Type 201 has good formability and is widely used in press-forming operations. Type 201 was developed as a less costly substitute for Type 301 but does not equal it in press forming characteristics in many applications. The true stress-true strain curves, shown in Figure 4.012, indicate high work-hardening rates for both 201 and 301, which effectively retard localized reduction, or necking, and permit significant stretching during forming operations. By holding nickel on the high side and nitrogen on the low side of the specification, the formability of Type 201 is improved to that of Type 301 (15).

4.012 Work hardening characteristics of Types 201 and 301, Figure 4.012.

4.013 General. 180-degree bending of 2 T radius of Type 201 (1/2 hard) longitudinal and transverse specimens can be successfully done without cracking (6).

4.014 Forging. Starting temperature 2100 to 2250 F, finishing temperature 1700 F or above (7).

4.02 **Machining and Grinding**

4.021 Type 201 has fair to good machinability. The machinability rating is 49 percent, based on 100 percent machinability for an AISI B1112 carbon steel. Maximum cutting speed with high-speed steel tools is 80 surface feet per minute. Cutting speed can be increased with carbide tools.

4.022 Type 201 work hardens during machining so work piece and tool must be rigid for best results. Tools must be kept sharp.

4.023 Apply good cutting fluids, such as sulfurized-chlorinated petroleum oil. This is particularly important in making heavy cuts at relatively slow feeds. Thinning the fluid with paraffin oil helps in making finishing cuts at higher speeds. The blend improves the cooling effect on the work piece and tool.

4.024 Take positive cuts and avoid dwelling to minimize work hardening and glazing (8, 16).

4.03 **Joining**

4.031 Type 201 can be welded by all conventional techniques employed for the standard 18-8 stainless steels. Shielded-arc methods, arc welding, and spot

welding produce good welds with excellent mechanical properties. Weld ductility is good. Type 201 is somewhat less sensitive to intergranular corrosion in the weld heat-affected zone than 300-series compositions with comparable carbon content (8).

4.04 **Surface Treating**

4.041 Scale from heat treating operations can be removed by pickling in a bath of 20 percent hydrochloric acid at 120 to 140 F or in a solution of 10 percent sulfuric acid plus 6 to 12 percent rock salt. After pickling, rinse thoroughly, dip in a warm bath of 15 to 30 percent nitric acid, and wash in water (8).

REFERENCES

1 Nekervis, R. J., Lund, C. H., and Hall, A. M., "Status of High-Strength Steels for the Aircraft Industry", TML, Battelle Memorial Institute, Report No. 91 (January 3, 1958).

2 "Stainless and Heat Resisting Steels", Steel Products Manual, AISI (June 1957).

3 Mangone, F. J., Roach, D. B., and Hall, A. M., "Properties of Certain Cold-Rolled Austenitic Stainless Sheet Steels", Battelle Memorial Institute, DMIC Report No. 113 (May 15, 1959).

4 "Trends in Metals, Stainless Steels", Electro Metallurgical Company, Division of Union Carbide, Report from STEEL (November 4, 1957).

5 Sumsion, H. T., "High-Strength Steels for the Missile Industry", ASM, Proceedings of the Golden Gate Metals Conference (February 4–6, 1960).

6 "Mechanical Properties of Some Engineering Materials – Unpublished Data From Company Sponsored Programs", Third Quarter Report, Vol. II, Phase I (September 1 to November 30, 1961).

7 Materials in Design Engineering, "Materials Selector Issue", Reinhold Publishing Corp., Vol. 56, No. 5, Mag. (mid-October 1962).

8 "AISI Type 201", Alloy Digest, Filing Code: SS-174 (November 1965).

9 "Properties of 200 – 300 – 400 Series", Trade Literature, Republic Steel Corporation, Cleveland, Ohio (May 1964).

10 "Metals Handbook, Vol. 1, 8th Edition", edited by T. Lyman, American Society for Metals, Metals Park, Ohio (1961).

11 Lackey, J. Q. and Degnan, T. F., "Formic Acid Corrosion of Common Materials of Construction", *Materials Performance*, Vol. 13, No. 7 (July 1974) pp 13–18.

12 McCoy, H. E. and McNabb, B., "Corrosion of Several Iron- and Nickel-Base Alloys in Supercritical Steam at 1000 F", ORNL-TM-4552 (August 1974).

13 Franke, G. and Altstetter, C., "Low-Cycle Behavior of Mn/N Stainless Steels", *Metallurgical Transactions*, Vol. 7A (November 1976) pp 1719–1727.

14 "Mechanical and Physical Properties of Austenitic Chromium-Nickel Stainless Steels at Ambient Temperatures", The International Nickel Company, Inc., New York, N.Y., Trade Literature (October 1966).

15 Cunningham, E. R., "Cold Forming Stainless Steels and Other Specialty Grades", *Metals Engineering Quarterly*, Vol. 13, No. 2 (May 1973) pp 7–12.

16 Blott, D. M., "How to Cut the Standard Grades", *Metal Progress*, Vol. 93, No. 2 (February 1968) pp 77–83.

Fe
17 Cr
6.5 Mn
4.5 Ni

Type 201

Source	AISI (2)		(7)	
	Percent		Percent	
	Min	Max	Min	Max
Carbon	–	0.15	–	0.15
Chromium	16.0	18.0	16.0	19.0
Manganese	5.5	7.5	5.5	10.0
Nickel	3.5	5.5	3.5	6.0
Nitrogen	–	0.25	–	–
Silicon	–	1.0	–	–
Sulfur	–	0.03	–	–
Iron	Balance		Balance	

TABLE 1.04. COMPOSITION (2, 7)

	Fe
17	Cr
6.5	Mn
4.5	Ni

Type 201

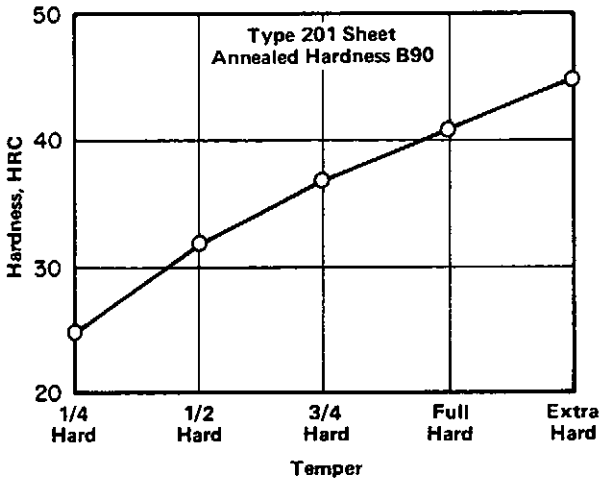


FIGURE 1.062. EFFECT OF TEMPER ON HARDNESS (8)

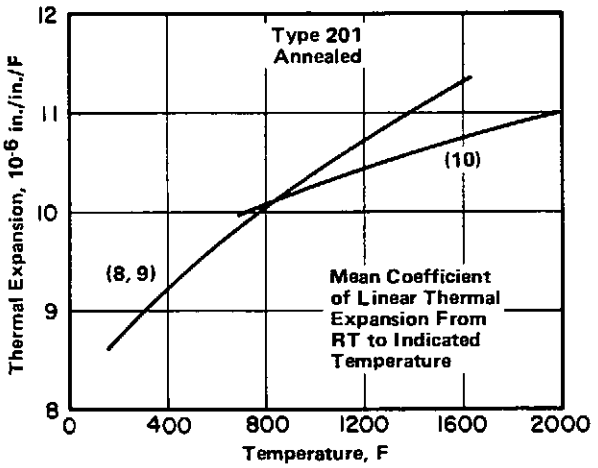


FIGURE 2.014. THERMAL EXPANSION (8, 9, 10)

Alloy	Type 201
Cold Reduction, percent	Normal Magnetic Permeability at 200 Oersteds
Anneal	1.003
5	1.016
10	1.147
20	2.738
30	7.006
50	15.395

TABLE 2.0232. EFFECT OF COLD REDUCTION ON MAGNETIC PERMEABILITY (3)

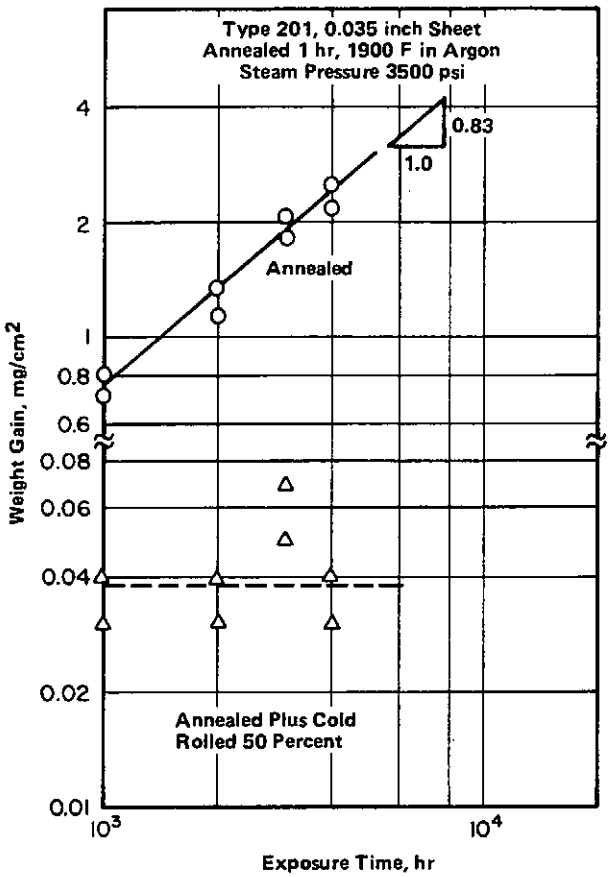


FIGURE 2.0343. EFFECT OF COLD WORK ON LONG-TIME CORROSION IN STEAM AT 1000 F (12)

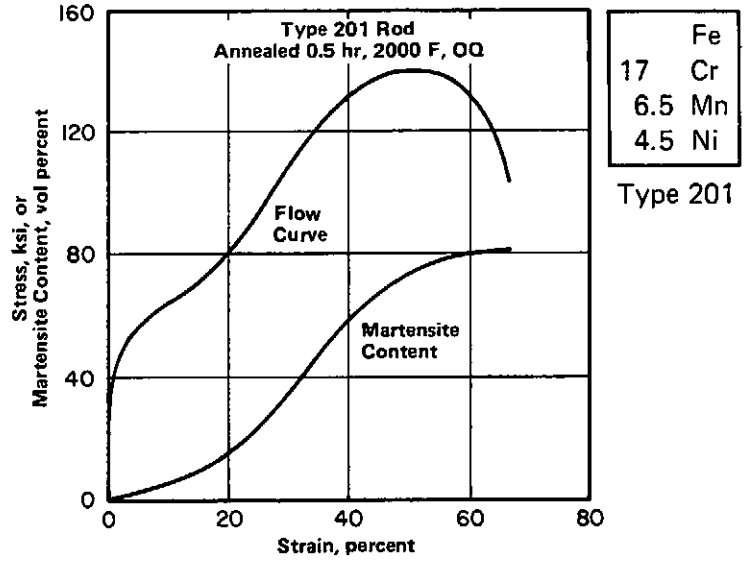


FIGURE 3.0212. STRESS-STRAIN CURVE AND MARTENSITE CONTENT AS A FUNCTION OF STRAIN (13)

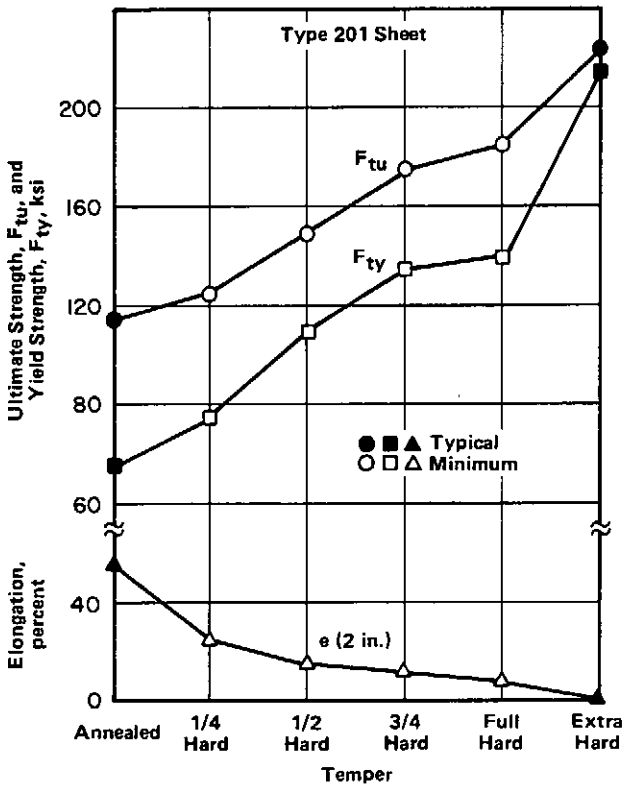


FIGURE 3.0213. EFFECT OF TEMPER ON MECHANICAL PROPERTIES AT ROOM TEMPERATURE (8)

	Fe
17	Cr
6.5	Mn
4.5	Ni

Type 201

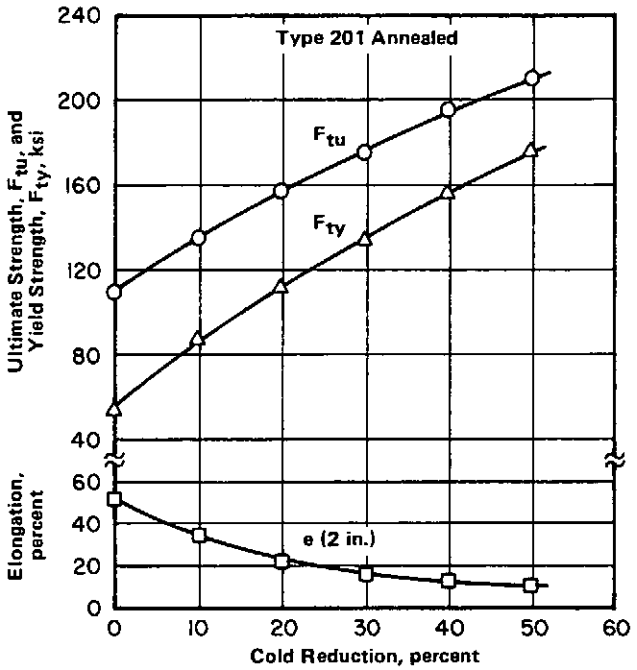


FIGURE 3.0214. EFFECTS OF COLD WORKING ON TENSILE PROPERTIES (8)

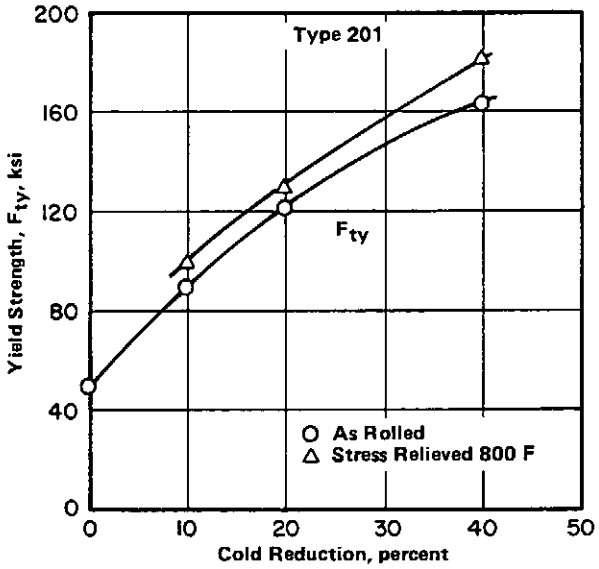


FIGURE 3.0215. EFFECTS OF COLD ROLLING AND STRESS RELIEF ON TENSILE YIELD STRENGTH (8)

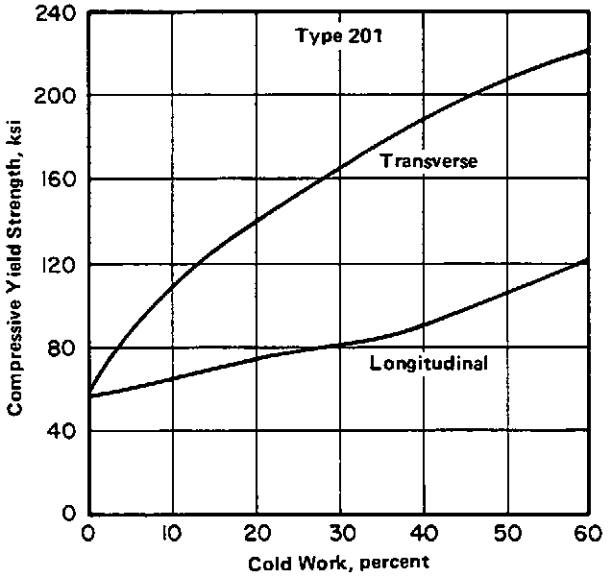


FIGURE 3.0221. EFFECT OF COLD WORK ON COMPRESSIVE YIELD STRENGTH (14)

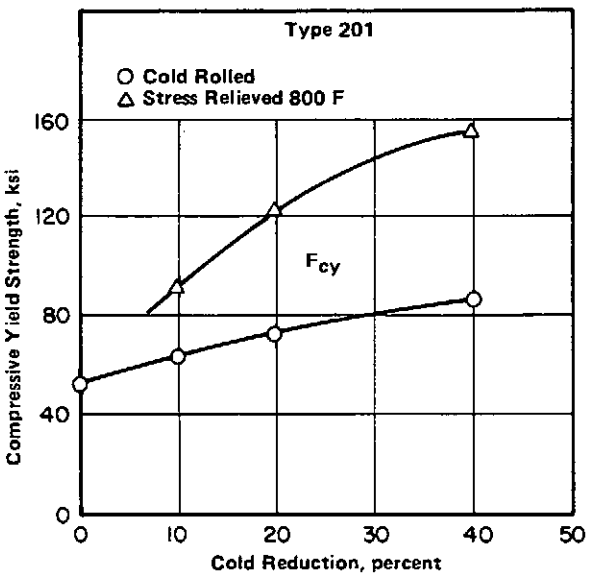


FIGURE 3.0222. EFFECTS OF COLD ROLLING AND STRESS RELIEF ON COMPRESSIVE YIELD STRENGTH (8)

	Fe
17	Cr
6.5	Mn
4.5	Ni

Type 201

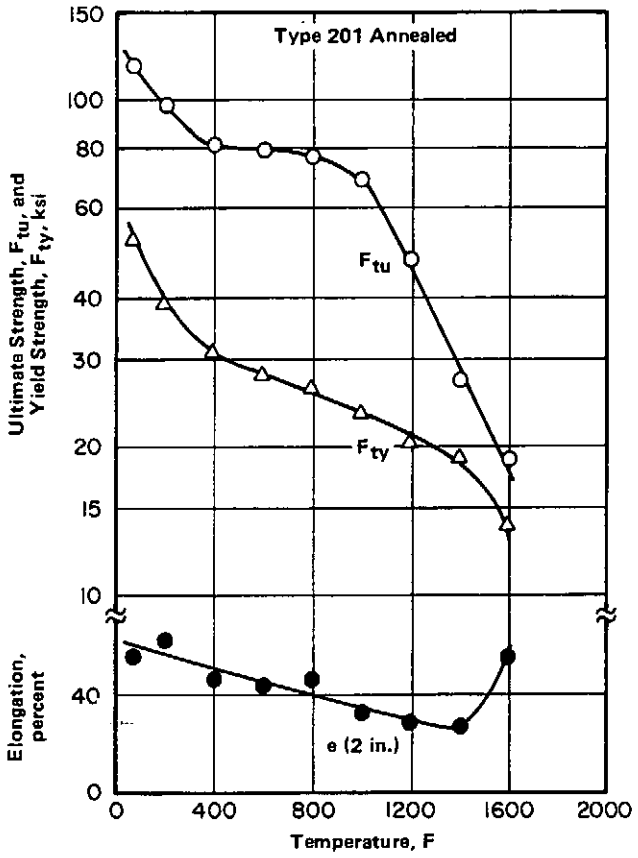


FIGURE 3.0311. TENSILE PROPERTIES OF ANNEALED ALLOY AT ELEVATED TEMPERATURES (8)

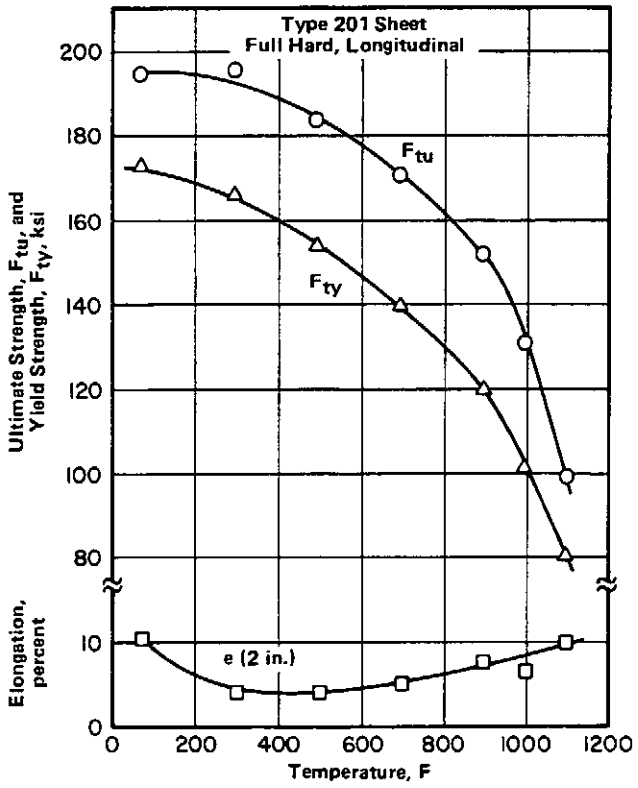


FIGURE 3.0312. TENSILE PROPERTIES OF FULL HARD ALLOY AT ELEVATED TEMPERATURES (8)

	Fe
17	Cr
6.5	Mn
4.5	Ni

Type 201

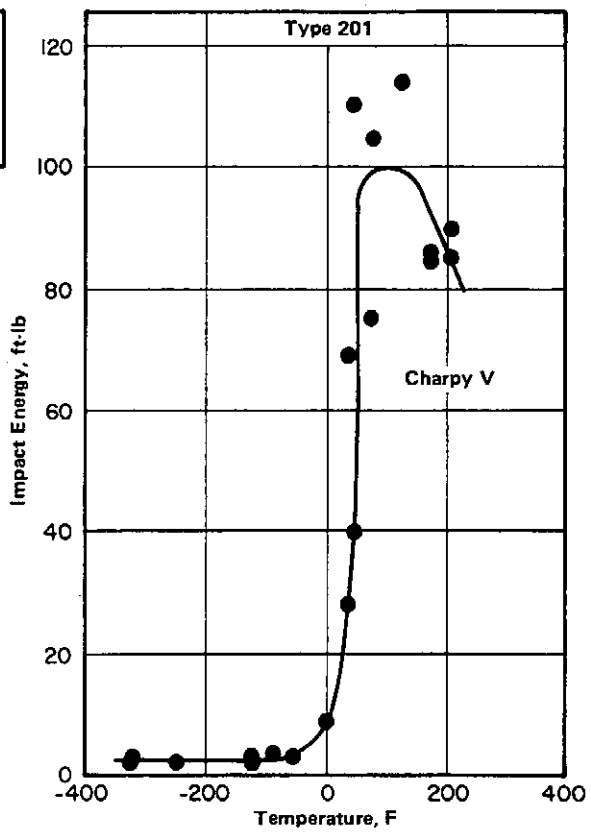


FIGURE 3.0331. EFFECT OF LOW AND ELEVATED TEMPERATURES ON CHARPY V IMPACT STRENGTH OF ALLOY (2)

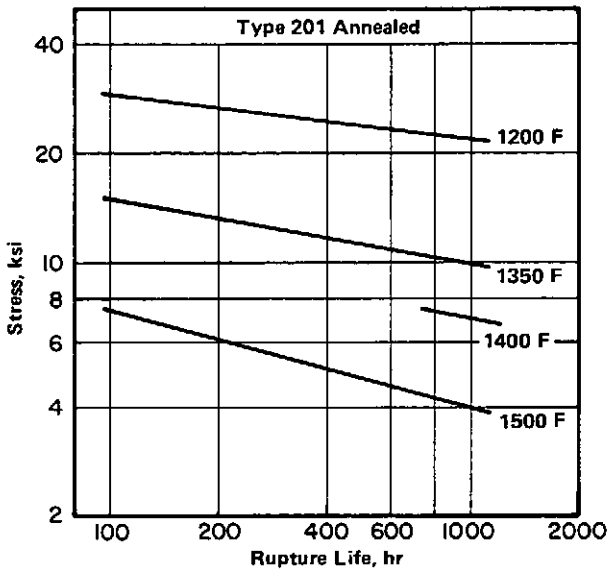


FIGURE 3.041. TYPICAL STRESS-RUPTURE PROPERTIES (8)

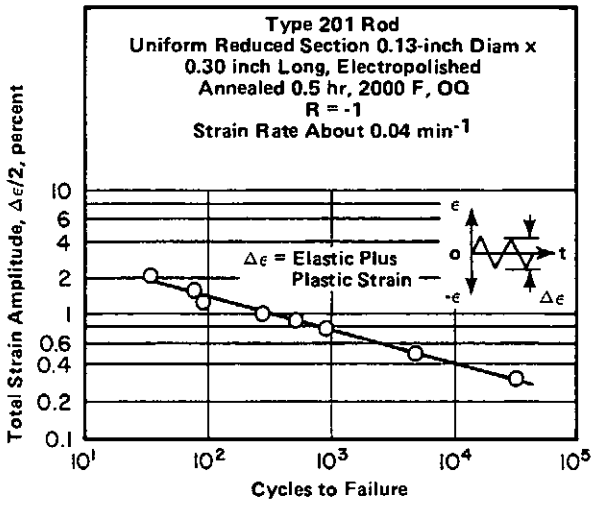


FIGURE 3.052. AXIAL FATIGUE BEHAVIOR OF SMOOTH ALLOY AT ROOM TEMPERATURE (13)

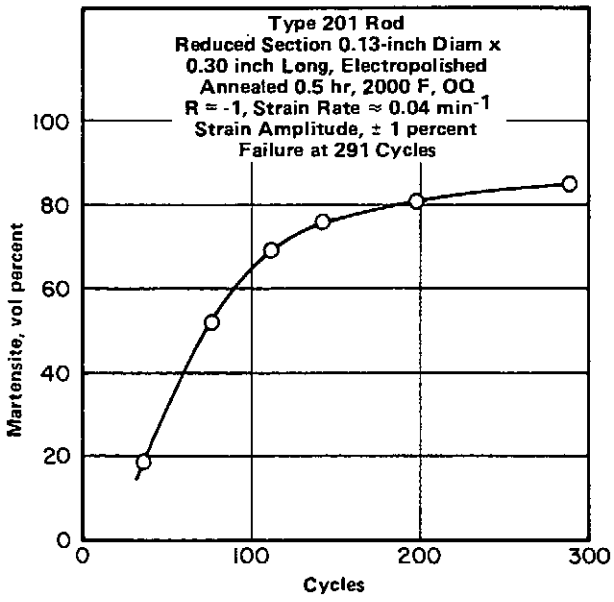


FIGURE 3.053. EFFECT OF CYCLIC STRAINING ON MARTENSITE CONTENT OF ANNEALED ALLOY (13)

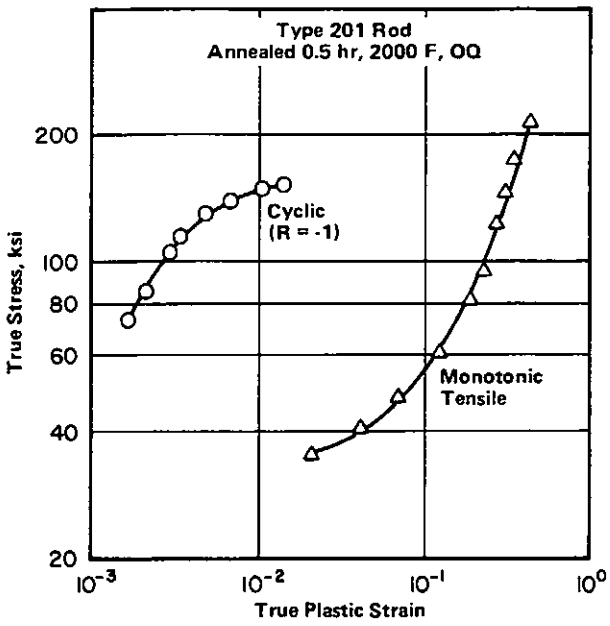


FIGURE 3.054. TRUE STRESS-TRUE STRAIN CURVES FOR MONOTONIC AND CYCLIC DEFORMATION (13)

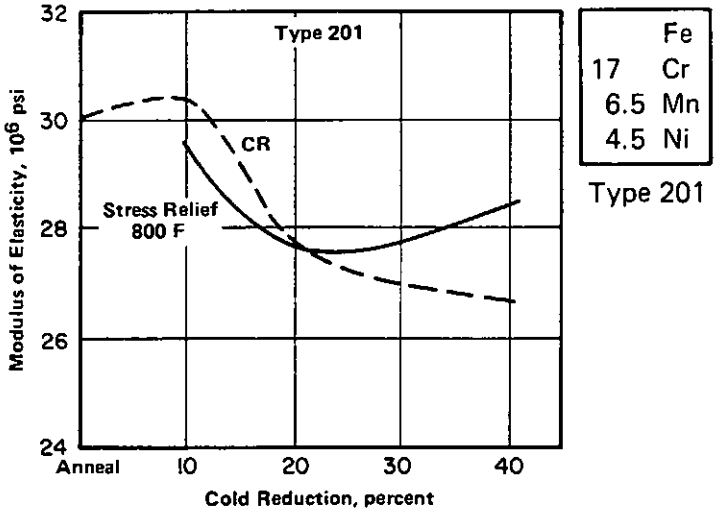


FIGURE 3.0621. MODULUS OF ELASTICITY FOR STRESS RELIEVED AND COLD ROLLED ALLOY (3)

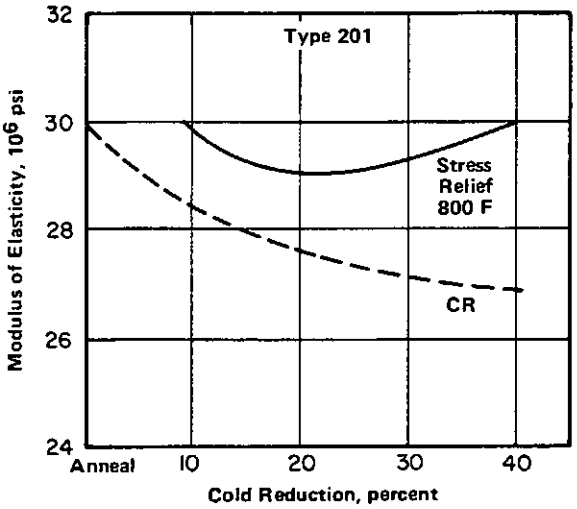


FIGURE 3.0622. MODULUS OF ELASTICITY IN COMPRESSION FOR STRESS RELIEVED AND COLD ROLLED ALLOY (3)

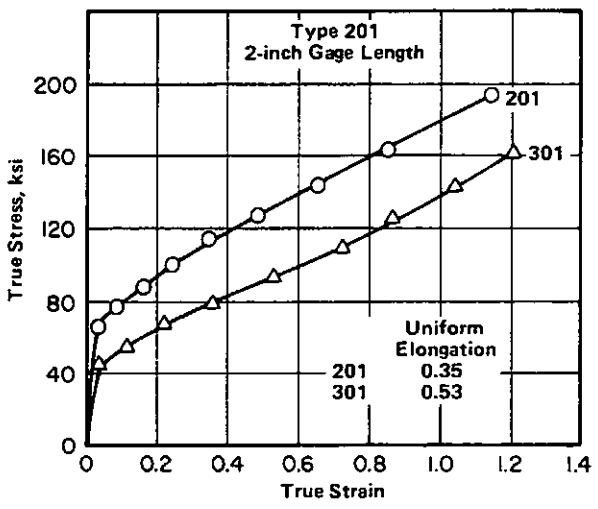


FIGURE 4.012. WORK HARDENING CHARACTERISTICS OF TYPES 201 AND 301 (15)

RELEASED: MARCH 1971
AUTHOR: W. W. DYRKACZ

FERROUS ALLOYS

	Fe
17	Cr
6	Ni
6	Mn
2	Cu
+	S

203 EZ

1. GENERAL

This is an austenitic, sulfur-containing, free-machining chromium-nickel-manganese-copper stainless steel, which was developed as an alternate material for Type 303 applications. It is a low nickel substitute for Type 303 and 303Se with equivalent mechanical and physical properties and comparable corrosion resistance, but with superior machining characteristics. This alloy is available as hot rolled and cold finished bars, rod, and wire; extruded hollow bars; billets; and forgings. It is non-magnetic in the annealed condition.

1.01 Commercial Designation
203 EZ

1.02 Alternate Designations
XM-1

1.03 Specifications
Table 1.03.

TABLE 1.03

AMS	Form	Military	Federal	ASTM
-	Wire, annealed or cold worked	MIL-W-52263B(MR)		
-	Wire, cold finished			A581-67
-	Bar, annealed or cold worked		QQ-S-764a	
-	Bar, hot finished or cold finished			A582-67

1.04 Composition
Table 1.04.

TABLE 1.04

Source	Military(1), Federal(2), ASTM (3, 4)		(5)	
	Percent		Percent	
Element	Minimum	Maximum	Minimum	Maximum
Carbon	-	.08	-	.08
Manganese	5.00	6.50	5.50	6.50
Silicon	-	1.00	-	1.00
Phosphorus	-	.04	-	.04
Sulfur	.18	.35	.15	-
Chromium	16.00	18.00	16.00	17.00
Nickel	5.00	6.50	5.00	6.00
Molybdenum	-	.50	-	-
Copper	1.75	2.25	1.75	2.15
Iron	Balance		Balance	

1.05 Heat Treatment
1.051 Anneal at 1900-2050F followed by water quenching to obtain maximum corrosion resistance and ductility(6).

1.06 Hardness
Alloy can be hardened only by cold work which increases both the strength and hardness. A typical annealed hardness range of 81-98 Rockwell B can be increased by cold drawing to 24-45 Rockwell C (6).

1.07 Forms and Conditions Available
1.071 The steel is available in a wide commercial range of sizes for bars, rod, wire, billets, forgings, and extruded hollows (6).
1.072 All wrought products are available in the annealed condition. Smaller size bars, rod, and wire are also available cold drawn to various strength and hardness levels (5).

1.08 Melting and Casting Practice
Electric furnace air melt.

1.09 Special Considerations
1.091 Alloy must be annealed after hot working. Annealing should be followed by rapid cooling to prevent harmful carbide precipitation, and thereby obtain maximum corrosion resistance. For the same reason, heating within the 800-1600F range should be avoided unless the material can be subsequently annealed.
1.092 Because the free machining austenitic grades have a slightly reduced corrosion resistance in comparison with the non sulfur-bearing types of stainless steel, bright machined parts may be susceptible to surface dulling or etching by final treatment with nitric acid solutions. Several alternate solutions with milder pickling actions are recommended (5).

2. PHYSICAL AND CHEMICAL PROPERTIES

2.01 Thermal Properties
2.011 Melting range. 2550-2630F (7).
2.012 Phase changes.
2.0121 The steel is subject to carbide precipitation at 800 to 1600F.
2.0122 Cold work may transform a small amount of austenite to ferrite (martensite).
2.013 Thermal conductivity. 212F, 9.5 Btu ft per (hr sq ft F) (5).
2.014 Thermal expansion, Figure 2.014.
2.015 Specific heat.
2.016 Thermal diffusivity.

2.02 Other Physical Properties
2.021 Density. 0.284 lb per cu in, 7.87 gr per cu cm (6).
2.022 Electrical properties, resistivity, Figure 2.022.
2.023 Magnetic properties. This steel is non-magnetic in the annealed condition. Permeability of annealed material is less than 1.02 (5, p. 3). It becomes slightly magnetic when severely cold worked.
2.024 Emittance.
2.025 Damping capacity.

2.03 Chemical Properties
2.031 Corrosion resistance.
2.0311 The corrosion resistance of austenitic, free-machining stainless steels, in general, has been sacrificed somewhat in order to enhance machinability. They are comparable to Type 302 in many of the milder corrodants, and are satisfactory for atmosphere service, for most foodstuffs, and for most organic chemicals. However, the sulfur-containing grades are inferior to their non free-machining counterparts in severe corrodants, such as reducing acids and chlorides (8, p. 53)(9, p. 116). The corrosion resistance of 203 EZ is equivalent to that of Type 303 (10, p. 3)(5, p. 2).
2.032 This steel, like Type 303, is susceptible to stress cracking if cold worked.
2.033 203 EZ has good resistance to oxidation at temperatures up to 1700F. In extreme oxidizing atmospheres, irregular scaling may be encountered, particularly above 1400F (5, p. 2).

2.04 Nuclear Properties

3. MECHANICAL PROPERTIES

3.01 Specified Mechanical Properties
3.011 Mechanical properties as specified by military and ASTM specifications, Table 3.011.

TABLE 3.011

Source	Military (1)		ASTM (3)		ASTM(4)
Form	Wire		Wire		Bar
Condition	Ann	CD	Ann	CD	Ann
Thickness - in	-	-	-	≤.500	≥.250
F_{tu}, min - ksi	-	-	85	115	-
max - ksi	115	130	125	145	-
Hardness					
BHN - min	-	-	-	-	-
- max	-	-	-	-	262

	Fe
17	Cr
6	Ni
6	Mn
2	Cu
+	S

203 EZ

3.02 Mechanical Properties at Room Temperature

3.021 Typical and minimum properties for bars, Table 3.021.

TABLE 3.021

Source	(11)(6)		(5)					(6)
Condition	Annealed		CD					CD Full Hard
Diameter - inches	3	1	>3.00	≧1.50 to 3.00	≧ 1.25 to 1.50	≧ 1.00 to 1.25	≧ .75 to 1.00	≧ .125 to .75
F_{tu}, typical - ksi	80	87	-	-	-	-	-	130-210
minimum - ksi	-	-	80	95	100	105	115	-
F_{ty}, typical - ksi	37	45	-	-	-	-	-	100-185
minimum - ksi	-	-	35	45	50	65	80	-
e(2 in), typical - percent	60	53	-	-	-	-	-	10-25
minimum - percent	-	-	28	28	28	20	15	-
RA, typical - percent	65	63	-	-	-	-	-	40-55
minimum - percent	-	-	45	45	45	35	35	-
Hardness - typical								
BHN	141-158	158-171	-	-	-	-	-	248-430
Rockwell B	77-83	84-87	-	-	-	-	-	-
Rockwell C	-	-	-	-	-	-	-	24-45
Impact strength - typical								
Izod ft-lb	-	85	-	-	-	-	-	-

3.03 Mechanical Properties at Various Temperatures

3.031 Effect of test temperature on tensile properties, Figure 3.031.

3.0311 Stress-strain diagrams, Figure 3.0311.

3.033 Effect of test temperature on impact properties, Table 3.033.

TABLE 3.033

Source	(11)							
Form	Bar							
Condition	Annealed							
Diameter - in	1				3			
Test Temp - F	-100	-65	RT	212	-100	-65	RT	212
Impact strength, Charpy V-notch ft-lb								
long - avg	(207)	(197)	(184)	(198)	67	65	75	75
trans - avg	-	-	-	-	14	13	16	15

( ) Tests indicated by parentheses did not fracture completely through. Other tests showed normal fractures.

3.04 Creep and Creep Rupture Properties

3.05 Fatigue Properties

3.051 Fatigue strength in annealed condition is approximately 50 percent of tensile strength (5, p. 4).

3.06 Elastic Properties

3.062 Modulus of elasticity in tension, 29.0×10^3 ksi (5, p. 4).

4. FABRICATION

4.01 Formability

4.011 Forging. Normal practice consists of preheating at 1500-1600F then raising the temperature rapidly to within the range of 2050-2300F. The finishing temperature should be maintained above 1700F. After forging, annealing at 1900-2050F followed by rapid cooling is recommended (6).

4.012 Cold forming is possible to a limited extent and 203 EZ behaves similarly to Type 303 in operations such as upsetting, coining, staking, etc. (12). Material with sulfur on the low side of the chemistry range (.18-.25) exhibits better cold formability and is equivalent to that of Type 303Se (14). The 203 EZ material should be annealed after severe forming to prevent stress cracking

4.02 Machining and Grinding

4.021 The machinability of 203 EZ is superior to that of Type 303, and it can be machined at higher speeds with equal or better tool life(15)It is recommended that speeds be increased on the order of 20-50 percent over those used for Type 303, approaching the speeds used for Type 416, while maintaining the same feed. An improvement in surface finish is also obtained at the higher cutting speeds (5, pp. 1, 5, 6)(12, p. 3). As with other austenitic steels, very sharp tools, low feeds, deep cuts and heavy equipment are required. Machining speeds between 75 and 85 percent of those used for mild carbon steels are suitable.(14).

4.03 Welding

4.031 Welding of these steels is not generally recommended. Fusion welding with Type 310 electrodes is possible to a very limited extent, and post weld annealing is necessary

4.032 203 EZ can be successfully brazed using proprietary techniques. (14)

4.04 Surface Treatment

4.041 Machined parts should be thoroughly cleaned prior to service. Passivation is recommended for certain applications in which case precautions may have to be taken as given under 1.092 Special Considerations.

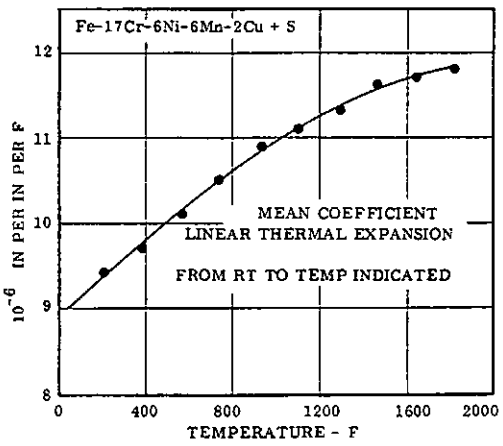


FIG. 2.014 THERMAL EXPANSION. (6, p. 5)

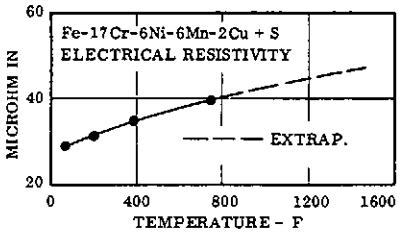
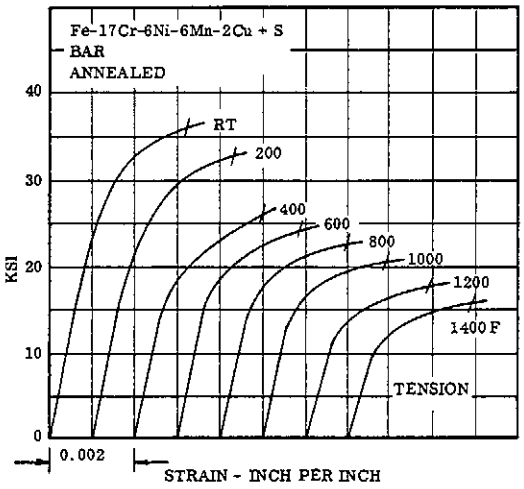


FIG. 2.022 ELECTRICAL RESISTIVITY.. (5, p. 3)



	Fe
17	Cr
6	Ni
6	Mn
2	Cu
+	S

203 EZ

FIG. 3.0311 STRESS-STRAIN CURVES AT ROOM AND ELEVATED TEMPERATURES FOR BAR. (13)

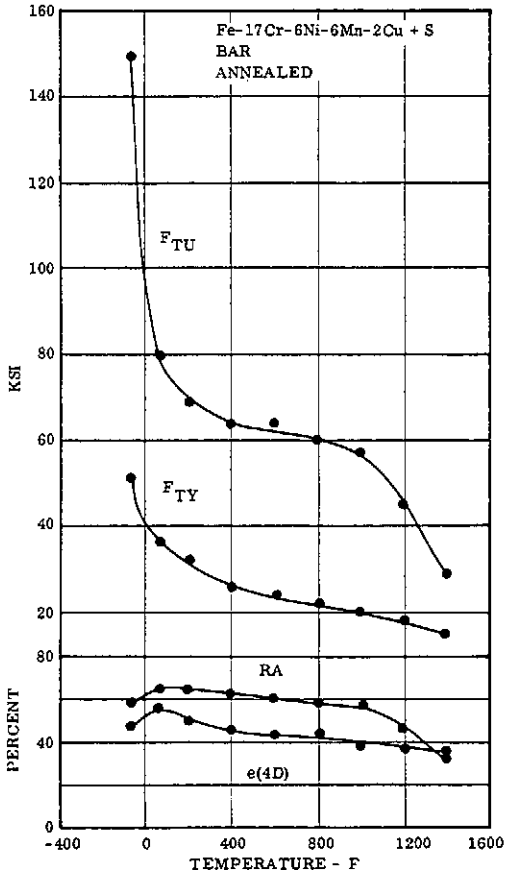


FIG. 3.031 EFFECT OF TEST TEMPERATURE ON TENSILE PROPERTIES. (5, p. 4)(11)(13)

REFERENCES

1. MIL-W-52263B (MR) (9 December 1965).
2. QQ-S-764a (January 3, 1966).
3. ASTM Designation: A-581-67 (December 12, 1967).
4. ASTM Designation: A-582-67 (December 12, 1967).
5. Allegheny Ludlum Steel Corporation, "Stainless Steel --Allegheny Ludlum Free Machining Grades Types 203EZ, 303EZ, 416EZ, and 430F," A-L Blue Sheet (1970).
6. Allegheny Ludlum Steel Corporation, "Allegheny Type 203EZ Machining Stainless," Technical Horizons (1966).
7. Allegheny Ludlum Steel Corporation, Research Center Memorandum, by Paul Lange (June 24, 1969).
8. Universal Cyclops Specialty Steel Division, "Stainless Steels Handbook," (1965).
9. Carpenter Steel Company, "Carpenter Stainless and Heat Resisting Steels--Selection, Description, Fabrication," Working Data (1962).
10. Allegheny Ludlum Steel Corporation, Research Center Memorandum, "Comparison of Corrosion Properties of Types 203EZ, 303, 202, and 304," by W. G. Renshaw (August 13, 1965).
11. Ibid., "Properties of 203EZ compared to 303EZ," by J. A. Ferree (July 6, 1965).
12. Ibid., "Allegheny Ludlum 203EZ, Austenitic Free-Machining Stainless Steel," by J. A. Ferree (February 2, 1966).
13. Ibid., Research Center Test Report, Project No. 70-1137, 203EZ (September 29, 1969).
14. Frederick, P. H., Allegheny Ludlum Steel Corporation, Personal Communication (November 27, 1970).
15. "Free-Machining Stainless Alternative for Type 303," Metal Progress, Volume 98, No. 5 (November 1970).

	Fe
0.43	C
1.8	Ni
1.6	Si
0.8	Cr
0.4	Mo
+	V

300 M

GENERAL

Alloy 300 M is a modified 4340 (Code 1206) high-strength low-alloy steel, which is capable of providing somewhat higher strength than 4340 alloy along with good toughness. The modifications, which consist of higher contents of silicon, molybdenum, and carbon plus a small addition of vanadium, provide improved hardenability and resistance to softening during tempering; furthermore, they increase to above 600 F the tempering-temperature range for tempered-martensite embrittlement (also known as 500 F embrittlement). Consequently, 300 M is generally used after it has been oil quenched and then tempered at approximately 600 F, which provides tensile strength of 270–300 ksi and good toughness. It is normally not recommended for use at temperatures above 600 F. For aerospace applications requiring optimum properties, the vacuum-arc remelted alloy is generally used, but relatively recent investigations have shown that electroslag remelting also provides excellent quality. Although it is not recommended for applications in which high-efficiency weld joints are critical, it can be welded with conventional techniques and proper preheat and post-heat treatments. The alloy is most suitable for applications requiring a combination of ultrahigh strength and good toughness in heavy sections at moderate temperatures. Typical applications include aircraft landing gear, airframe parts, fasteners, gears, and shafts. (14,18,27,28,37)

1.01 **Commercial Designation**

300 M.

1.02 **Alternate Designations**

Tricent (obsolete), 4340 M (obsolete), UNS K44220 (standard grade covered by AMS 6419B; see Table 1.04), UNS K44540 (slightly lower carbon grade covered by AMS 6417C; see Table 1.04).

1.03 **Specifications**

Table 1.03.

1.04 **Composition**

Table 1.04.

1.05 **Heat Treatment**

1.051 Normalize, 1650 to 1725 F, air cool. In section sizes up to at least 1.0 in., the alloy is air hardening, which results in normalized properties quite similar to oil quenched (see Figure 3.0212).(13,26,27)

1.052 Temper after normalizing for improved machinability 1200 to 1250 F, 1 hour minimum, air cool. Charging into tempering furnace should be done before the steel reaches room temperature. (26)

1.053 Spheroidize anneal, 1430 F, cool to 1200 F at a rate no faster than 10 F per hour, cool to 900 F no faster than 20 F per hour, air cool. (26–28)

1.054 Harden. Traditionally the alloy has been hardened by austenitizing at 1575 to 1625 F and oil quenching to below 160 F; AMS specifications (29,30), for example, require austenitization at 1600 F. For minimum distortion, 300 M parts are sometimes quenched from the austenitizing temperature into salt at about 400 F, held 10 minutes, and then air cooled. Recent investigations have shown that fracture toughness can be improved with increased austenitizing temperatures up to 2200 F when subsequent tempering temperatures are below 700 F. (See Figures 3.02722, 3.02723, 3.02726, and Table 3.02727.) On the other hand, increased austenitizing temperatures tend to cause decreases in tensile ductility and notch impact resistance. (See Figures 3.0215, 3.0233, 3.0335, and Tables 3.0217 and 3.0234.) (26–28)

1.055 Temper after hardening, 525–625 F, 2 hours minimum, air cool; double temper is recommended. Tempering within this range provides the optimum combination of high strength and toughness; consequently, tempering at other temperatures is not normally recommended. The AMS specifications (29,30) require double tempering at 575 F. Like other heat-treatable low-alloy steels, tensile strength and hardness decrease continuously with increasing tempering temperatures up to about 1200 F while corresponding increases occur in ductility and toughness except in the tempered-martensite-embrittlement (TEM) range, which is about 700 to 900 F for 300 M alloy. Tempering within that range should be especially avoided. (22, 26–28)

1.056 The time required for complete austenitization during normalizing and hardening treatments increases with increasing section size.

1.0561 Times recommended for austenitization of various section sizes in gaseous and salt-bath environments during normalizing and hardening treatments, Figure 1.0561.

1.057 At elevated temperatures, the alloy is highly susceptible to decarburization, which is detrimental to mechanical properties, particularly fatigue resistance. Consequently, austenitizing should be carried out in controlled endothermic atmosphere, salt bath, or vacuum. (26,37)

1.06 **Hardness**

1.061 Effect of tempering temperature on hardness, Figure 1.061.

1.062 End-quench hardenability, Figure 1.062.

1.063 Hardness of spheroidize-annealed alloy: RB 96, BHN 215 (28).

1.07 **Forms and Conditions Available**

1.071 It is available mostly in relatively heavy wrought forms such as bars, forging billets, forgings, and tubing; it has also been produced in the form of plate, sheet, wire, and castings. (26–28,37)

1.072 The different wrought products are furnished by the mills in various conditions including cold-finished, hot-finished, spheroidize annealed, and normalized and tempered. (29,30)

1.08 **Melting and Casting Practice**

1.081 Although the alloy has been produced by the conventional electric-furnace method, for aerospace applications vacuum-arc remelting has been the most common melting practice; but electroslag remelting has also been shown to provide excellent results (see Tables 3.0213 and 3.0235 and Figures 3.0214, 3.0232, and 3.02721).

	Fe
0.43	C
1.8	Ni
1.6	Si
0.8	Cr
0.4	Mo
+	V

300 M

1.09 **Special Considerations**

1.091 Like other high-strength low-alloy steels, 300 M is susceptible to hydrogen embrittlement as a result of acid pickling or plating operations; generally, the higher the strength, the greater the susceptibility. Baking for about 2 to 6 hours at temperatures of 375 to 550 F is generally recommended for relieving the embrittlement, although longer baking times up to as much as 100 hours have been found necessary to eliminate hydrogen completely from certain types of electroplated samples. (28,40)

1.092 In moist environments, fully heat-treated 300 M is susceptible to stress-corrosion cracking, which is believed to be a result of cathodically released hydrogen. This phenomenon is common to high-strength martensitic steels. For 300 M. in various aqueous environments at room temperature, K_{Iscc} values ranging from about 10 to 18 have been reported. For smooth specimens, uniform tensile stresses above 115 ksi in the short-transverse orientation are capable of inducing stress-corrosion cracking. See Section 2.032 for more details. (14,16)

1.093 The fatigue-crack growth rate of 300 M is markedly increased by aqueous environments and by decreasing cyclic frequency. (See Figures 3.057 and 3.059.) These effects are also believed to be a result of cathodically released hydrogen. (1,16)

1.094 After the alloy has been quenched and tempered to obtain optimum properties, any heating above the tempering range (525–625 F) causes a deterioration of mechanical properties.

1.095 Like other high-strength martensitic steels the notch strength and toughness generally decrease with decreasing temperature. The severity of the decrease in these properties and the temperature range in which it occurs vary with heat treatment, notch sharpness, and section size and configuration. (See Figures 3.0331–3.0335, 3.03711, 3.03712, and 3.03721.)

2 PHYSICAL AND ENVIRONMENTAL EFFECTS

2.01 **Thermal Properties**

Only a limited amount of specific data has been published on the thermal and other physical properties of 300 M. Because of their similarity of chemical composition and metallurgical characteristics, 300 M and 4340 (Code 1206) are believed to be quite similar in these properties.

2.011 Melting range.

2.012 Phase changes.

2.0121 Time-temperature-transformation diagram, Figure 2.0121.

2.0122 Above 1500 F, the steel consists of stable austenite; upon very slow cooling the austenite transforms to ferrite and carbide, but upon rapid cooling it transforms to martensite.

2.0123 The critical points for heating and cooling rates of 400 F per hour are as follows: (28)

Ac1 1400 F (start of transformation during heating)

Ac3 1480 F (completion of transformation during heating)

Ar3 785 F (start of transformation during cooling)

Ar1 650 F (completion of transformation during cooling)

2.013 Thermal conductivity, 21.7 Btu/ft/hr ft^2 F at RT. (27) (See Figure 2.013, Code 1206.)

2.014 Thermal expansion, 6.3×10^{-6} in./in./F at RT. (27) (See Figure 2.014, Code 1206.)

2.015 Specific heat, 0.107 Btu/lb/F at RT. (27)

2.016 Thermal diffusivity.

2.02 **Other Physical Properties**

2.021 Density, 0.283 lb/$in.^3$ at RT. (27)

2.022 Electrical properties (see Figure 2.0221, Code 1206).

2.023 Magnetic properties. Alloy is ferromagnetic.

2.024 Emittance.

2.025 Damping capacity.

2.03 **Chemical Environment**

2.031 Like most other steels, 300 M is susceptible to rusting under most atmospheric conditions. For long exposures, protective measures such as paint or certain types of electroplate are desirable. However, cathodic protection (use of sacrificial anodes) or an anodic electroplate can be detrimental to high-strength steels of this type because of their possible accelerating effect on stress-corrosion cracking as discussed in the following section.

2.032 When heat-treated to its usual high strength level, 300 M is susceptible to stress-corrosion cracking in moist environments. Certain inhibitors, piperazine and piperidine for example, have been shown to be effective in preventing or retarding the cracking. Cathodic protection, however, or any other type of galvanic coupling to an anodic metal (zinc or cadmium electroplating, for example) may result in the release of hydrogen at the surface of the steel, which is believed to induce or accelerate the cracking.

2.0321 Effect of stress intensity on time to stress-corrosion failure of vacuum-arc remelted bar in a 1.0 molar aqueous sodium chloride solution at room temperature, Figure 2.0321.

2.0322 Effects of variations in tempering temperature and environment on stress-corrosion crack-growth rate of forging under constant load at room temperature, Figure 2.0322.

2.0323 Effect of variations in temperature on stress-corrosion crack-growth rate in deionized water, Figure 2.0323.

2.0324 Effects of organic inhibitors, piperazine and piperidine, on resistance to stress-corrosion cracking in an 0.1 molar solution of sodium chloride in distilled water at room temperature, Table 2.0324.

2.0325 Resistance to stress corrosion in a 3.5 percent aqueous solution of sodium chloride at room temperature, Table 2.0325.

2.0326 Uniform threshold tensile stresses (K_I = 1) above which 300 M is susceptible to stress-corrosion cracking in a 3.5 percent aqueous sodium chloride solution at room temperature, Table 2.0326.

2.04 **Nuclear Environment**

3	**MECHANICAL PROPERTIES**
3.01	**Specified Mechanical Properties**
3.011	AMS specified properties for products and conditions furnished by steel mills, Table 3.011.
3.012	Specified tensile properties for fully heat-treated products, Table 3.012.
3.02	**Mechanical Properties at Room Temperature**
3.021	Tension – stress-strain diagrams – tension properties.
3.0211	Effect of tempering temperature on the transverse tensile properties of a vacuum-arc melted billet, Figure 3.0211.
3.0212	Effects of tempering temperature on tensile properties of oil-quenched plate and of normalized plate (air cooled from austenitizing temperature) of two thicknesses, Figure 3.0212.
3.0213	Tensile properties in different orientations of forging produced from electroslag remelted ingot originally 20 in. in diameter, Table 3.0213.
3.0214	Effect of tempering temperature on the longitudinal tensile properties of electroslag remelted and vacuum-arc remelted forged plate, Figure 3.0214.
3.0215	Effect of austenitizing temperature on the tensile properties of vacuum-arc remelted bar, Figure 3.0215.
3.0216	Effect of tempering temperature on the tensile properties of vacuum-arc remelted plate after several different austenitizing treatments, Figure 3.0216.
3.0217	Effects of various austenitizing treatments on tensile properties and on grain size, Table 3.0217.
3.0218	Effect on transverse tensile properties of very fine austenite grain size obtained by short cyclic austenitization at relatively low temperature, Table 3.0218.
3.0219	Effects of austenitizing temperature and tempering temperature on the longitudinal tensile properties of vacuum-arc remelted plate austempered at 600 F, Table 3.0219.
3.02110	Tensile properties of spheroidize-annealed alloy, Table 3.02110.
3.02111	Effect of tempering temperature on the tensile properties of sheet, Figure 3.02111.
3.02112	Effect of tempering temperature on the tensile properties of bar of various diameters heat treated in full size, Figure 3.02112.
3.022	Compression – stress-strain diagrams – compression properties (see Figures 3.0321 and 3.0322).
3.023	Impact.
3.0231	Effect of tempering temperature on the Charpy V-notch impact resistance of oil-quenched plate and of normalized plate (air cooled from austenitizing temperature) of two thicknesses, Figure 3.0231.
3.0232	Effect of tempering temperature on the Charpy V-notch impact resistance of electroslag remelted and vacuum-arc remelted forged plate, Figure 3.0232.
3.0233	Effect of austenitizing temperature on the Izod impact resistance of vacuum-arc remelted bar, Figure 3.0233.
3.0234	Effects of various austenitizing treatments on Charpy V-notch impact resistance and on grain size, Table 3.0234.
3.0235	Room-temperature Charpy V-notch impact properties in different orientations of forging produced from electroslag remelted ingot, originally 20 in. in diameter, Table 3.0235.
3.024	Bending.
3.025	Torsion and shear.
3.0251	Shear strength determined on double-shear pin type specimens machined from a forging and then heat treated at 1600 F 1 hr, OQ + 575 F 2 + 2 hr, AC: (L) F_{su} = 179.0 ksi (T) F_{su} = 179.2 ksi.
3.026	Bearing.
3.027	Stress concentration.
3.0271	Notch properties.
3.02711	Effect of tempering temperature on the sharp notch strength of sheet, Figure 3.02711.
3.02712	Effects of stress concentration and melting practice on the notch strength of sheet, Figure 3.02712.
3.02713	Effects of stress concentration and specimen size and orientation on notch-strength ratio of bar, Figure 3.02713.
3.02714	Effect of surface crack size on crack strength of vacuum-arc melted 1/2 in. plate (F_{tu} = 290 ksi), Figure 3.02714.
3.02715	Effect of surface crack size on crack strength of vacuum-arc melted 1/2 in. plate (F_{tu} = 270 ksi), Figure 3.02715.
3.02716	Effect of surface crack size on crack strength of vacuum-arc melted 1/2 in. plate (F_{tu} = 220 ksi), Figure 3.02716.
3.02717	Effect of surface crack size on crack strength of vacuum-arc melted 7/8 in. plate (F_{tu} = 290 ksi), Figure 3.02717.
3.02718	Effect of surface crack size on crack strength of vacuum-arc melted forging heat treated to three different strength levels, Figure 3.02718.
3.02719	Effect of surface crack size on crack strength of two vacuum-arc melted billets with different carbon contents, Figure 3.02719.
3.027110	Notch tensile strength of vacuum-arc remelted billets, Table 3.027110.
3.0272	Fracture toughness.
3.02721	Effect of tempering temperature on the fracture toughness of electroslag remelted and vacuum-arc remelted forged plate, Figure 3.02721.
3.02722	Effect of tempering temperature on the fracture toughness of vacuum-melted plate after several different austenitizing treatments, Figure 3.02722.
3.02723	Effects of austenitizing temperature and tempering temperature on the fracture toughness and corresponding tensile properties of vacuum-arc melted bar, Figure 3.02723.
3.02724	Effect on fracture toughness of tempering temperature and of very fine austenite grain size obtained by short cyclic austenitization at relatively low temperatures, Figure 3.02724.
3.02725	Effect of tempering temperature on the fracture toughness of oil-quenched plate and of normalized plate (air cooled from austenitizing temperature) of two thicknesses, Figure 3.02725.
3.02726	Effect of austenitizing temperature on the fracture toughness of vacuum-arc remelted bar, Figure 3.02726.
3.02727	Effects of various austenitizing treatments on fracture toughness and grain size, Table 3.02727.

	Fe
0.43	C
1.8	Ni
1.6	Si
0.8	Cr
0.4	Mo
+	V

300 M

	Fe
0.43	C
1.8	Ni
1.6	Si
0.8	Cr
0.4	Mo
+	V

300 M

3.02728 Effects of austenitizing temperature and tempering temperature on the fracture toughness of vacuum-arc remelted plate austempered at 600 F, Table 3.02728.

3.028 Combined properties.

3.03 **Mechanical Properties at Various Temperatures**

3.031 Tension – stress-strain diagrams – tension properties.

3.0311 Tensile stress-strain curves at room and cryogenic temperatures, Figure 3.0311.

3.0312 Effect of temperatures from -423 to 700 F on tensile properties of bar, Figure 3.0312.

3.0313 Effect of elevated temperatures on the tensile properties of a large forging oil quenched and tempered at 575 F, Figure 3.0313.

3.0314 Effect of elevated temperatures on the tensile properties of vacuum-arc melted billet oil quenched and tempered at 750 F, Figure 3.0314.

3.0315 Effects of a rapid strain rate (6 in./in./min) and a short holding time (10 sec) at temperature on tensile properties of sheet in the temperature range 800 to 1200 F, Figure 3.0315.

3.032 Compression – stress-strain diagrams – compression properties.

3.0321 Effect of elevated temperatures on the compressive yield strength of a large forging oil quenched and tempered at 575 F, Figure 3.0321.

3.0322 Effect of elevated temperature on the compressive yield strength of vacuum-arc melted billet oil quenched and tempered at 750 F, Figure 3.0322.

3.033 Impact.

3.0331 Effect of low temperatures down to -423 F on notch impact properties of bars with two carbon contents, Figure 3.0331.

3.0332 Effects of low temperatures and different orientations on the impact resistance of bar of various diameters, Figure 3.0332.

3.0333 Effect of low temperatures on the notch impact resistance of a forging, Figure 3.0333.

3.0334 Effect of test temperatures from -60 to 340 F and of tempering temperatures up to 1200 F on the Charpy V-notch impact resistance of normalized 1.0-in. thick plate (air cooled from austenitizing temperature), Figure 3.0334.

3.0335 Effects of variations in austenitizing treatment on notch-impact-transition curves of vacuum-arc remelted bar, Figure 3.0335.

3.034 Bending.

3.035 Torsion and shear.

3.036 Bearing.

3.037 Stress concentration.

3.0371 Notch properties.

3.03711 Effect of low temperatures on notch strength of bar, Figure 3.03711.

3.03712 Effect of temperatures from 400 to -320 F on tensile (K_t = 1), sharp notch (K_t = 12), and crack (K_t = 17) strength of sheet, Figure 3.03712.

3.0372 Fracture toughness.

3.03721 Effect of low temperatures on the fracture toughness and corresponding tensile properties of vacuum-arc remelted bar, Figure 3.03721.

3.03722 Effect of low temperatures on fracture toughness of plate, Table 3.03722.

3.038 Combined properties.

3.04 **Creep and Creep Rupture**

3.05 **Fatigue Properties**

3.051 Fatigue life of longitudinally ground and shot-peened specimens from forged billet heat treated to high strength level, Figure 3.051.

3.052 Fatigue life of notched specimens from forged billet heat treated to high strength level, Figure 3.052.

3.053 Fatigue life of smooth and notched bar, Figure 3.053.

3.054 Effect of elevated temperatures on fatigue life of smooth and notched specimens from large forging oil quenched and tempered at 575 F, Figure 3.054.

3.055 Effect of variations in tempering temperature and associated strength levels on fatigue-crack growth rate of vacuum-arc remelted plate in an air environment, Figure 3.055.

3.056 Effects of variations in austenitizing temperature and stress ratio (R) on fatigue-crack growth rate of vacuum-arc remelted plate in an air environment, Figure 3.056.

3.057 Effects of variations in frequency and environment on fatigue-crack growth rate, Figure 3.057.

3.058 Fatigue-crack growth rate of vacuum-arc remelted plate in environments of air and of dry hydrogen at frequencies of 5 and 50 cps, Figure 3.058.

3.059 Effects of various environments and a sodium borate, sodium nitrite inhibitor on fatigue-crack growth rate of plate heat treated to a high strength level, Figure 3.059.

3.06 **Elastic Properties**

3.061 Poisson's ratio, 0.32 at RT (3).

3.062 Modulus of elasticity.

3.0621 Effect of elevated temperatures on modulus of elasticity in tension and compression of a large forging oil quenched and tempered at 575 F, Figure 3.0621.

3.0622 Effect of elevated temperatures on modulus of elasticity determined in both tension and compression on a vacuum-arc melted billet oil quenched and tempered at 750 F, Figure 3.0622.

3.0623 Effect of low temperatures on modulus of elasticity of bar, Figure 3.0623.

3.063 Modulus of rigidity, 11.0 – 11.4 x 10^3 ksi at RT. (3,25)

3.064 Tangent modulus.

3.065 Secant modulus.

4 **FABRICATION**

4.01 **Forming**

4.011 Cold forming. (See Section 4.011, 4340, Code 1206.)

4.012 Forging and other hot-working characteristics are similar to those of 4340, Code 1206. The optimum temperature range for these operations is 2250 to 1950 F; 1700 F should be the absolute minimum for hot working. (27,28,37)

4.02 **Machining and Grinding**

300 M can best be machined when its hardness is in the range Brinell 200 to 250, which requires a spheroidizing heat treatment. Under these

conditions its machinability rating is 45 percent based on a 100 percent rating for cold-rolled B1112 steel. In the hardened-and-tempered condition (Rockwell C52–55), machining is possible using heavy equipment, rigid tool support, carbide tooling, and suitable cutting fluids. The speeds and feeds must be carefully controlled to prevent excessive surface heating and the formation of untempered martensite on the machined surface. A flood of coolant is recommended for most machining operations. (27,37)

4.03 **Joining**

4.031 Welding is generally not recommended for critical applications. Because of its alloy content and associated hardenability, fusion welds are susceptible to underbead cracking, heat-affected-zone embrittlement, and thermal-stress cracking. Nevertheless, weld strength approaching that of the base metal can be obtained with proper welding techniques such as the use of low-hydrogen electrodes, adequate preheat and interpass temperatures, and full postweld quench-and-temper heat treatment. (27,28,37)

4.032 Comparison of tensile properties of parent metal and flash-butt weld joint (no filler metal) in tubing, Table 4.032.

4.04 **Surface Treatment**
(See 4140, Code 1203.)

4.041 Nitriding would not normally be desirable because nitriding temperatures, which are above the optimum tempering temperature range, would be detrimental to base-metal properties.

REFERENCES

1 Lynch, C. T., Vahldick, F. W., and Thornton, F., "Comparison of Environmentally Enhanced Crack-Growth Rates of 1410 and Other High-Strength Steels", Proceedings of the 1978 Tri-Service Conference on Corrosion (October 1978).

2 Isothermal Transformation Diagrams of Nickel Alloy Steels, The International Nickel Co., Inc. (1965).

3 Mil-Handbook-5D, Change Notice 1 (January 1, 1984).

4 Verink, E. D., Jr. and Das, K. B., "Research on Inhibition for Corrosion Fatigue of High Strength Alloys", AFML-TR-78-178 (December 15, 1978).

5 Wood, W. E., "Mechanism of Enhanced Toughness in Martensitic Alloys", Naval Air Systems Command, Contract No. N00019-76-C-0149 (April 20, 1977).

6 Wood, W. E., "Mechanism of Enhanced Toughness in Martensitic Alloys", Naval Air Systems Command, Contract No. N00019-77-C-0135 (February 1978).

7 Olsen, G. B., Anctil, A. A., et al, "Anisotropic Embrittlement in High-Hardness ESR 4340 Steel Forgings", AMMRC TR82-1 (January 1982).

8 McDarmaid, D. S., "Effect of Austenite Grain Refinement on the Plane Strain Fracture Toughness and Other Mechanical Properties of 300 M Steel", Royal Aircraft Establishment Technical Report 74025 (April 1974).

9 McDarmaid, D. S., "Effect of Bending and Tempering Temperatures on the Plane Strain Fracture Toughness of 300 M Steel Bar", Royal Aircraft Establishment, Technical Report 75083 (July 1975).

10 Anctil, A. A., "Mechanical Properties and Fractography of Electroslag Remelted 300 M Steel", AMMRC TR83-13 (March 1983).

11 McDarmaid, D. S., "Effects of High Austenitization Treatments Upon the Plane Strain Fracture Toughness and Other Mechanical Properties of 300 M Bar", Royal Aircraft Establishment, Technical Report 76104 (August 1976).

12 Langley, A. E., "A Study of the Properties of 1850 MPa Alloy Steels in Bar Form", Rolls Royce Ltd., DRIC-BR-40333, S&T-MEMO-3-74 (March 1974).

13 Horn, R. M., "The Influence of Retained Austenite on the Thick Section Mechanical Properties of a Commercial Low Alloy Ultra-High Strength Steel", Thesis, University of California, Berkeley (December 1976).

14 McEowen, L. J., "High-Strength Steels", Proceedings of the 1976 Tri-Service Conference on Corrosion (October 1976).

15 Ritchie, R. O., "Effects of Strength and Grain Size on Near-Threshold Fatigue Crack Growth in Ultra-High Strength Steel", Proceedings of the Fourth International Conference on Fracture (June 1977).

16 Carter, C. S., "Application of Fracture Mechanics to Stress Corrosion Cracking", AGARD-AG-257 (1980).

17 Campbell, J. E., "Fracture Toughness of High-Strength Alloys at Low Temperature – A Review", ASTM STP 556 (1974).

18 Lechtenberg, T. A., "A Comparison of the Microstructure and Mechanical Properties of 300 M Steel Manufactured by the Vacuum Arc Remelt and the Electroslag Remelt Processes", ERDA Summary Report (September 1977).

19 Ritchie, R. O., Suresh, S., and Toplosky, J., "Influence of Gaseous Environment on Low Growth Rate Fatigue Crack Propagation in Steels", DOE Contract No. DE-ACO2-79ER10389, A000, Annual Report No. 1 (January 1980) and Final Report (September 1981).

20 Deel, O., "Mechanical-Property Data 300 M Steel", AFML F33615-69-C-1115 (December 1969).

21 Cedeno, M.H.C., "The Effect of Silicon on the Environmental Cracking Behavior of a High Strength Steel", ERDA Summary Report (May 1977).

22 Youngblood, J. L. and Raghavan, M., "Influence of Heat Treatment on Mechanical Properties of 300 M Steel". NASA TSP-75-10271 (October 1975).

23 Youngblood, J. L. and Raghavan, M., "Microstructure and Mechanical Properties of Quenched and Tempered 300 M Steel", NASA Technical Paper 1288 (August 1978).

24 Thrash, C. V., "Evaluation of High-Strength Steels for DC-10", Douglas Aircraft Co., ETR-DAC-67520 (May 27, 1969).

25 Gibson, D. L., "High-Strength Torsion Bar Development for Army Applications", AMMRC TR 79-5 (January 1979).

26 Metals Handbook, Ninth Edition, Vol. 4, Heat Treating, American Society for Metals (1981).

	Fe
0.43	C
1.8	Ni
1.6	Si
0.8	Cr
0.4	Mo
+	V

300 M

	Fe
0.43	C
1.8	Ni
1.6	Si
0.8	Cr
0.4	Mo
+	V

300 M

27 Tricent. Alloy Digest, Filing Code: SA-193 (April 1966).

28 300 M Ultra-High Strength Steel, The International Nickel Co., Inc., A-258 (September 1959).

29 AMS 6417C (April 1, 1985).

30 AMS 6419B (January 15, 1976).

31 MIL-S-8844C (May 25, 1971).

32 ASTM A579-77, Book of Standards, Vol. 1.05 (1984).

33 Padmanabhan, R. and Wood, W. E., "Hydrogen Induced Cracking in Low-Alloy Steel", Metallurgical Transactions, Vol. 14A, pp 2347–2356 (November 1983).

34 Sastry, C. N., Padmanabhan, R., Delepkumar, D., and Wood, W. E., "Achieving Optimum Properties in Ultrahigh-Strength Low-Alloy Steel", Metals Technology, Vol. 8, pp 454–457 (December 1981).

35 Horn, R. M. and Ritchie, R. O., "Mechanisms of Tempered Martensite Embrittlement in Low-Alloy Steels", Metallurgical Transactions, Vol. 9A, pp 1039–1053 (August 1978).

36 Ryder, J. T. and Pickel, F. M., "Effect of Temperature on Stress Corrosion Cracking of 300 M Steel", Journal of Testing and Evaluation, Vol. 6, pp 129–133 (March 1978).

37 Metals Handbook, Ninth Edition, Vol. 1, Properties and Selection: Iron and Steel, American Society for Metals (1978).

38 Bendix Aviation Corporation, Products Division, "Heat Treatment of Tricent Steel to 270,000–300,000 psi", Process Specification P.S. 6004 (September 10, 1958).

39 ASTM, "End Quench Test for Hardenability of Steel", Data Sheet CR 6892.1 (May 1, 1962).

40 Berman, D. A., "The Effect of Baking and Stress on the Hydrogen Content of Cadmium Plated High Strength Steels", Materials Performance, Vol. 24, pp 36–41 (November 1985).

41 Espey, G. B., Jones, H. M., and Brown, W. F., Jr., "The Sharp Edge-Notch Tensile Strength of Several High-Strength Steel Alloys", Proc. ASTM, Vol. 59 (1959).

42 Sands, J. W., "300-M Ultra-High Strength Steel", International Nickel Co., Inc. (November 1958).

43 Sachs, G. and Sessler, J. G., "Effect of Stress Concentration on Tensile Strength of Titanium and Steel Alloy Sheet at Various Temperatures", ASTM STP 287 (1960).

44 Muvdi, B. B., Klier, E. P., and Sachs, G., "Design Properties of High-Strength Steels in the Presence of Stress Concentrations and Hydrogen Embrittlement", WADC TR-55-103, Supplement 1 (January 1956).

45 Pendleberry, S. L., Simeng, R. F., and Walker, E. K., "Fracture Toughness and Crack Propagation of 300M Steel", Technical Report DS-68-18, Contract FA67-WA-1812, Lockheed-California Co. (August 1968).

46 International Nickel Co., Inc. (1958).

47 Srawley, J. E. and Beachem, C. D., "Crack Propagation Tests of Some High-Strength Sheet Steels", Naval Research Laboratory Report 5263 (January 10, 1959).

48 Muvdi, B. B., Sachs, G., and Klier, E. P., "Design Properties of High Strength Steels in the Presence of Stress Concentrations", WADC TR-56-395, Pt. 2 (August 1956).

Alloy	300 M
Specification	Forms
AMS 6417C	Bars, Forgings, Tubing, Consumable-Electrode Melted
AMS 6419B	Bars, Forgings, Tubing, Premium Quality, Consumable-Electrode Melted
MIL-S-8844C, Class 3	Bars, Reforging Stock, Mechanical Tubing, Premium Quality, Vacuum Melted
ASTM A579, Grade 32	Superstrength Alloy Steel Forgings

TABLE 1.03. SPECIFICATIONS (29–32)

Alloy	300 M					
Specification	AMS 6417C		AMS 6419B		MIL-S-8844C	
	Percent		Percent		Percent	
Element	Min	Max	Min	Max	Min	Max
Carbon	0.38	0.43	0.40	0.45	0.40	0.45
Manganese	0.60	0.90	0.60	0.90	0.65	0.90
Silicon	1.45	1.80	1.45	1.80	1.45	1.80
Phosphorus	–	0.010	–	0.010	–	0.010
Sulfur	–	0.010	–	0.010	–	0.010
Chromium	0.70	0.95	0.70	0.95	0.70	0.95
Nickel	1.65	2.00	1.65	2.00	1.65	2.00
Molybdenum	0.30	0.50	0.30	0.50	0.35	0.45
Vanadium	0.05	0.10	0.05	0.10	0.05	–
Copper	–	0.35	–	0.35	–	–

TABLE 1.04. COMPOSITION (29–31)

	Fe
0.43	C
1.8	Ni
1.6	Si
0.8	Cr
0.4	Mo
+	V

300 M

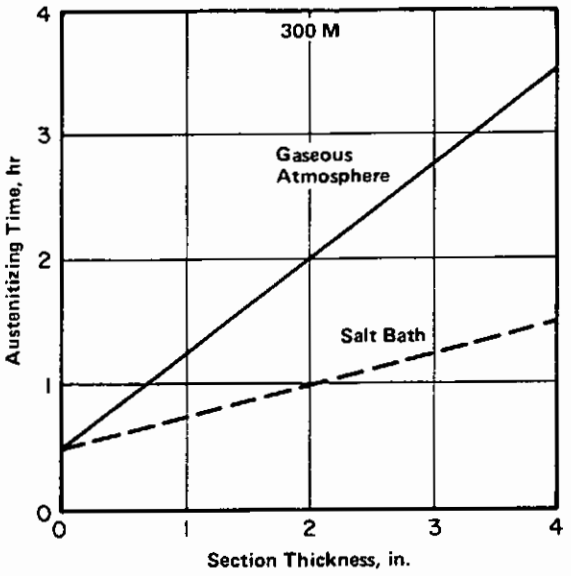


FIGURE 1.0561. TIMES RECOMMENDED FOR AUSTENITIZATION OF VARIOUS SECTION SIZES IN GASEOUS AND SALT-BATH ENVIRONMENTS DURING NORMALIZING AND HARDENING TREATMENTS (38)

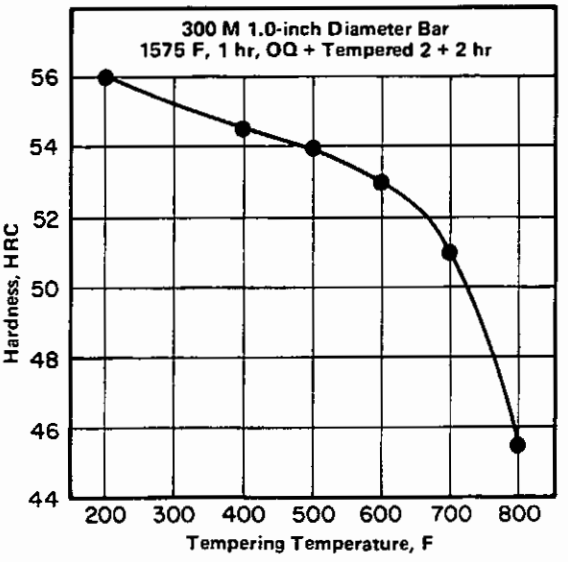


FIGURE 1.061. EFFECT OF TEMPERING TEMPERATURE ON HARDNESS (26)

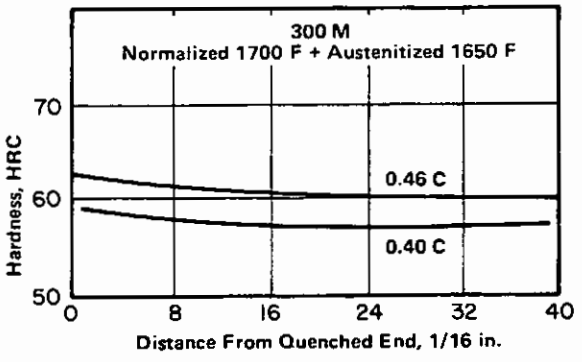


FIGURE 1.062. END-QUENCH HARDENABILITY (39)

	Fe
0.43	C
1.8	Ni
1.6	Si
0.8	Cr
0.4	Mo
+	V

300 M

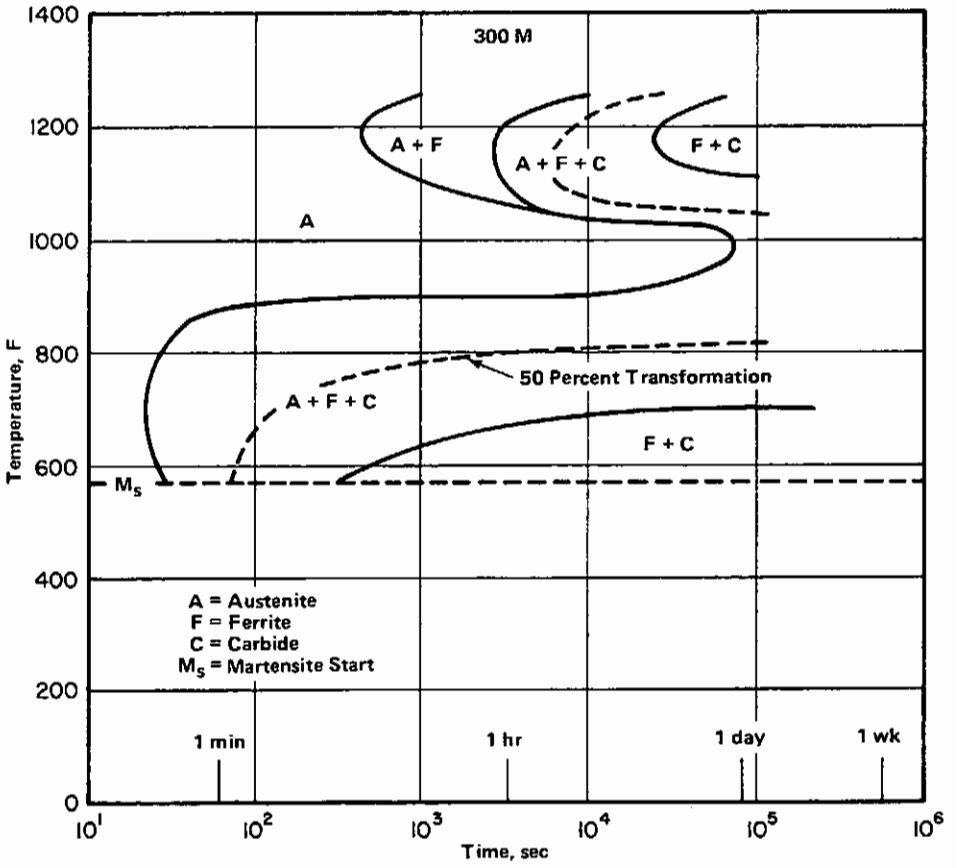


FIGURE 2.0121. TIME-TEMPERATURE-TRANSFORMATION DIAGRAM (2)

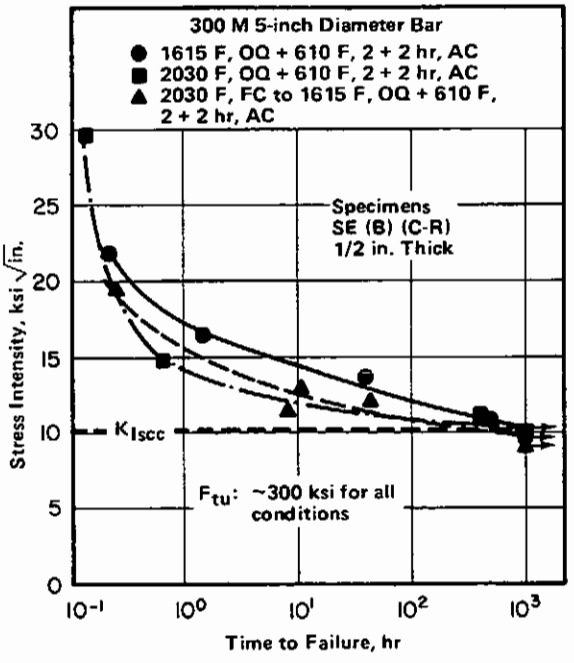


FIGURE 2.0321. EFFECT OF STRESS INTENSITY ON TIME TO STRESS-CORROSION FAILURE OF VACUUM-ARC REMELTED BAR IN A 1.0 MOLAR AQUEOUS SODIUM CHLORIDE SOLUTION AT ROOM TEMPERATURE (11)

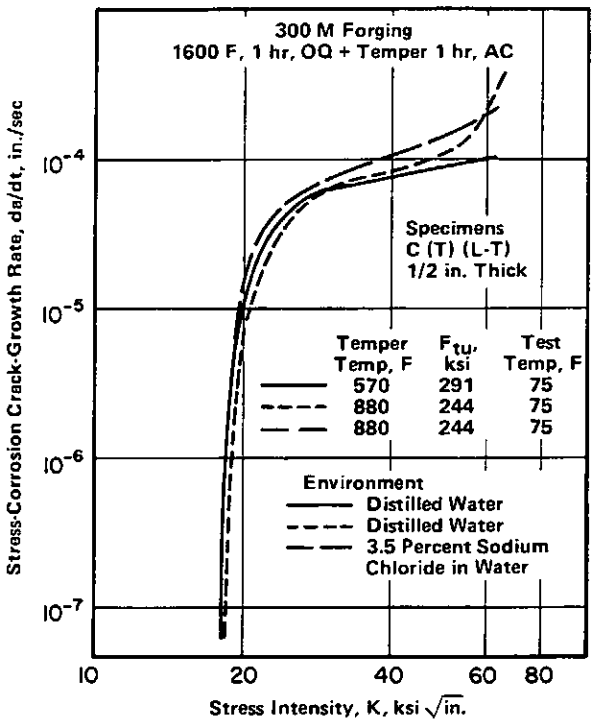


FIGURE 2.0322. EFFECTS OF VARIATIONS IN TEMPERING TEMPERATURE AND ENVIRONMENT ON STRESS-CORROSION CRACK-GROWTH RATE OF FORGING UNDER CONSTANT LOAD AT ROOM TEMPERATURE (21)

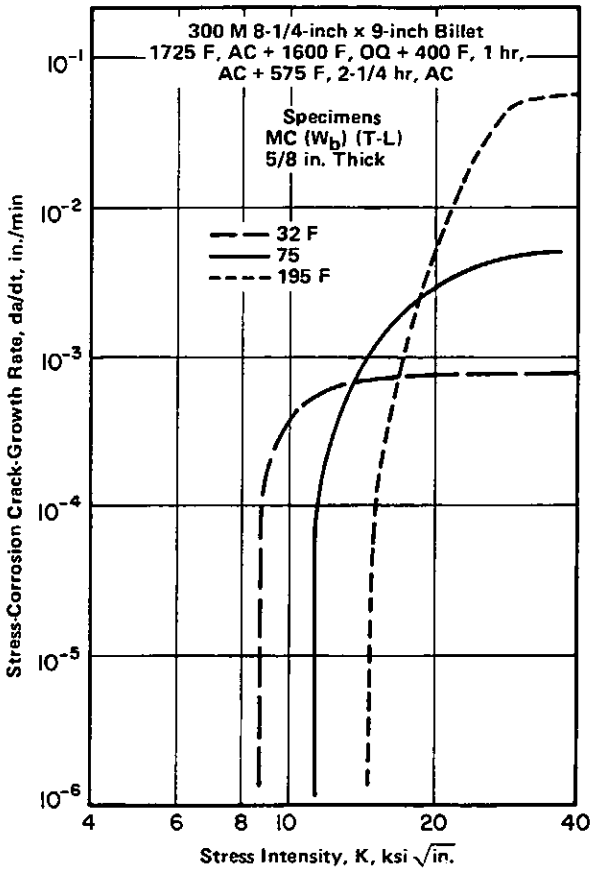


FIGURE 2.0323. EFFECT OF VARIATIONS IN TEMPERATURE ON STRESS-CORROSION CRACK-GROWTH RATE IN DE-IONIZED WATER (36)

Alloy	300 M	
Form	1 Inch x 2 Inch Bar	
Condition	1600 F, 1 hr, OQ + 575 F, 2 + 2 hr, AC	
Environment		K_{Iscc}, ksi √in.
Aqueous Solution, 0.1 molar sodium chloride		16
Aqueous Solution, 0.1 molar sodium chloride plus 1.0 molar piperazine		55
Aqueous Solution, 0.1 molar sodium chloride plus 1.0 molar piperidine		60

Notes: K_{Iscc} specimens, C(T)(T-L) 0.75 inch thick.
F_{tu}, 270–300 ksi.
Both greater and smaller concentrations of inhibitors were less effective in increasing K_{Iscc}.

TABLE 2.0324. EFFECTS OF ORGANIC INHIBITORS, PIPERAZINE AND PIPERIDINE, ON RESISTANCE TO STRESS-CORROSION CRACKING IN AN 0.1 MOLAR SOLUTION OF SODIUM CHLORIDE IN DISTILLED WATER AT ROOM TEMPERATURE (4)

	Fe
0.43	C
1.8	Ni
1.6	Si
0.8	Cr
0.4	Mo
+	V

300 M

Alloy	300 M	
Form	4-Inch x 6-Inch x 6-Inch Forging	
Condition	1700 F, AC + 1600 F, OQ + 570 F, 2 + 2 hr, AC	
Specimen	K_{Iscc}, ksi $\sqrt{in.}$	F_{tu}, ksi
SE (T) (L-T), 0.2 in. thick	11	291
SE (T) (S-T), 0.2 in. thick	11	293

TABLE 2.0325. RESISTANCE TO STRESS CORROSION IN A 3.5 PERCENT AQUEOUS SOLUTION OF SODIUM CHLORIDE AT ROOM TEMPERATURE (10)

Alloy	300 M
Form	Plate
Condition	Quenched and Tempered to F_{tu} 280–300 ksi
Orientation	Threshold Stress, ksi
L	170
T	136
ST	115

TABLE 2.0326. UNIFORM THRESHOLD TENSILE STRESSES (K_t = 1) ABOVE WHICH 300 M IS SUSCEPTIBLE TO STRESS-CORROSION CRACKING IN 3.5 PERCENT AQUEOUS SODIUM CHLORIDE SOLUTION AT ROOM TEMPERATURE (16)

Alloy	300 M			
Source	Form	Condition	F_{tu}, ksi (Max)	Hardness (Max)
AMS 6417C and AMS 6419B	Bars			
	<0.501 in.(a)	Cold Finished	130	–
	>0.500 in.(a)	Hot Finished		241 BHN
		Cold Finished		262 BHN
	Forgings	Normalized and Tempered		248 BHN
	Tubing	Cold Finished		25 HRC
		Hot Finished and Annealed		99 HRB

(a) Nominal diameter or distance between parallel sides.

TABLE 3.011. AMS SPECIFIED PROPERTIES FOR PRODUCTS AND CONDITIONS FURNISHED BY STEEL MILLS (29,30)

Alloy	300 M						
Form	Bars, Forgings, Tubing						
Condition	1700 F, 1 hr, AC + 1600 F, 1 hr, OQ + 575 F, 2 + 2 hr, AC						
Source	Nominal Cross Sectional Area, $in.^2$	Orientation(a)	F_{ty}, ksi (Min)	F_{tu}, ksi (Min)	e (4D), percent (Min)	RA, percent (Min) Average	RA, percent (Min) Single
AMS 6417C	All	L	220	270	8	–	30
	Up to 100 incl.	T	220	270	–	30	25
	Over 100 to 144 incl.	T	220	270	–	25	20
	Over 144 to 225 incl.	T	220	270	–	20	15
	Over 225	T	220	270	–	15	10
AMS 6419B	All	L	230	280	7	–	25
	Up to 100 incl.	T	230	280	–	30	25
	Over 100 to 144 incl.	T	230	280	–	25	20
	Over 144 to 225 incl.	T	230	280	–	20	15
	Over 225	T	230	280	–	15	10
MIL-S-8844C	Up to 100 incl.	T	230	280	6	30	25
	Over 100 to 144 incl.	T	230	280	5	25	20
	Over 144	T	230	280	4	20	15

(a) The AMS transverse tensile property requirements apply only to products from which tensile specimens not less than 2.50 inch in length can be taken. The AMS specifications state that testing in the longitudinal orientation is not required on products tested in the transverse orientation.

TABLE 3.012. SPECIFIED TENSILE PROPERTIES FOR FULLY HEAT-TREATED PRODUCTS (29–31)

	Fe
0.43	C
1.8	Ni
1.6	Si
0.8	Cr
0.4	Mo
+	V

300 M

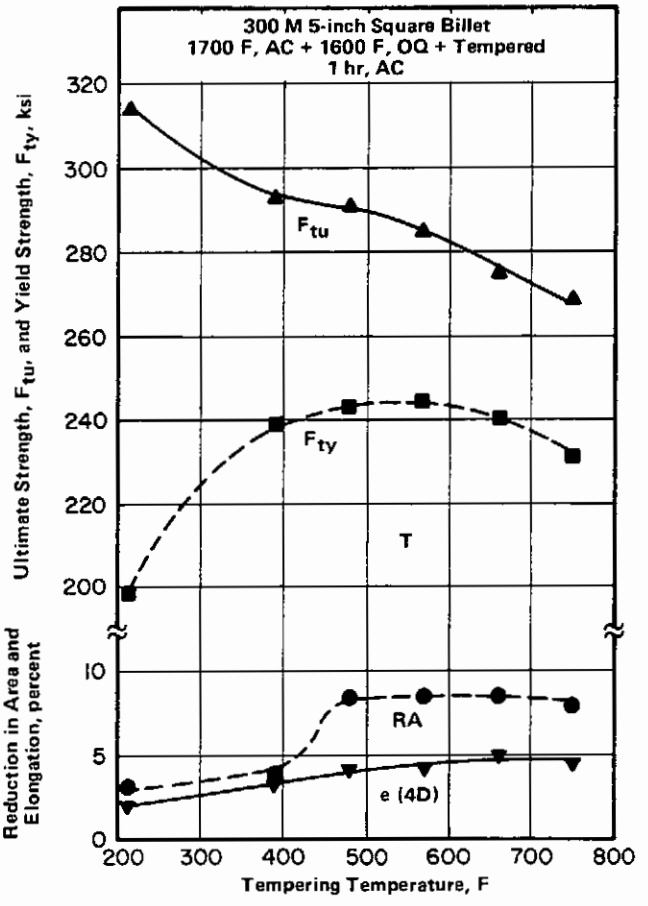


FIGURE 3.0211. EFFECT OF TEMPERING TEMPERATURE ON THE TRANSVERSE TENSILE PROPERTIES OF A VACUUM-ARC MELTED BILLET (12)

	Fe
0.43	C
1.8	Ni
1.6	Si
0.8	Cr
0.4	Mo
+	V

300 M

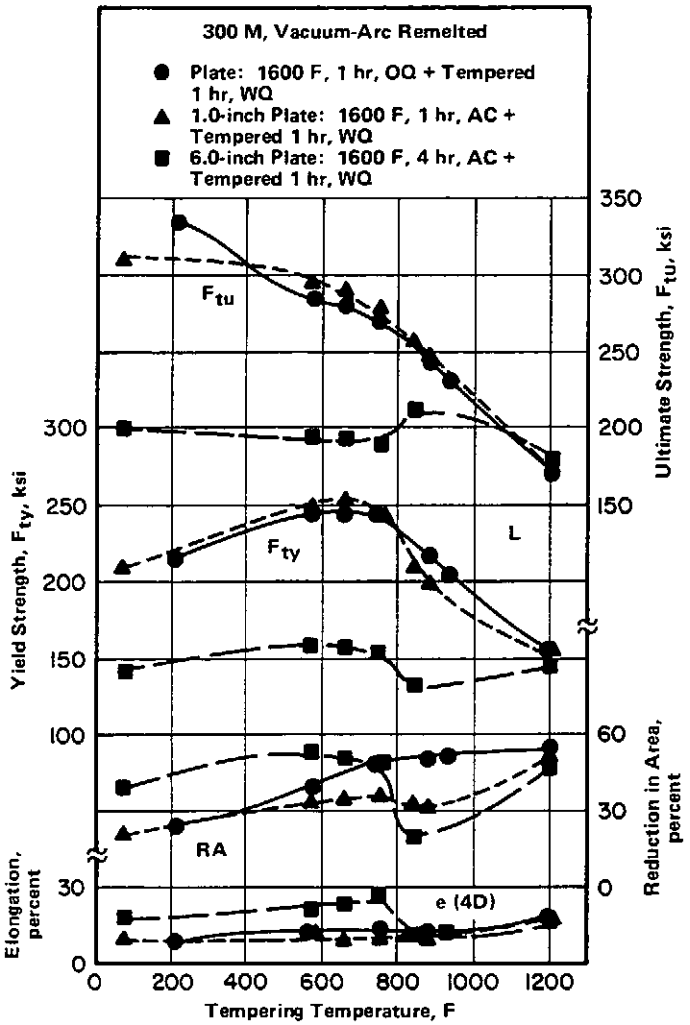


FIGURE 3.0212. EFFECTS OF TEMPERING TEMPERATURE ON TENSILE PROPERTIES OF OIL-QUENCHED PLATE AND OF NORMALIZED PLATE (AIR-COOLED FROM AUSTENITIZING TEMPERATURE) OF TWO THICKNESSES (13)

Alloy	300 M				
Form	4-Inch x 6-Inch x 6-Inch Forging				
Condition	1700 F, AC + 1600 F, OQ + 570 F, 2 + 2 hr, AC				
Orientation	F_{ty}, ksi	F_{tu}, ksi	e (4D), percent	RA, percent	Hardness, HRC
L	245	291	10.6	44.2	55
LT	252	295	7.8	30.2	55
ST	246	293	5.9	19.9	55

TABLE 3.0213. TENSILE PROPERTIES IN DIFFERENT ORIENTATIONS OF FORGING PRODUCED FROM ELECTROSLAG REMELTED INGOT ORIGINALLY 20 INCH IN DIAMETER (7,10)

	Fe
0.43	C
1.8	Ni
1.6	Si
0.8	Cr
0.4	Mo
+	V

300 M

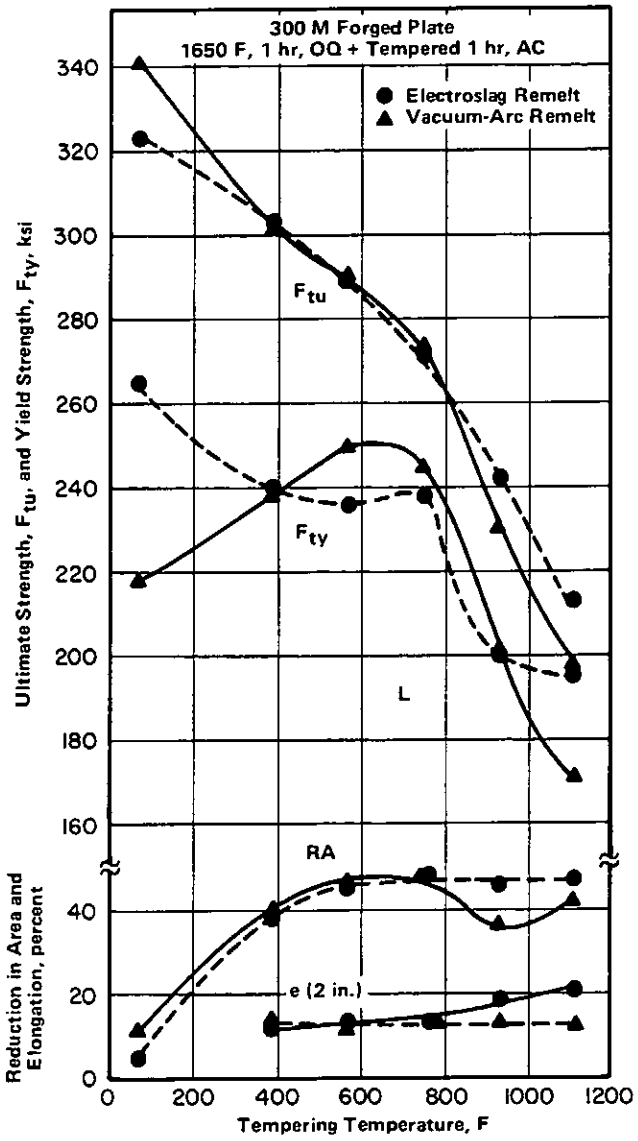


FIGURE 3.0214. EFFECT OF TEMPERING TEMPERATURE ON THE LONGITUDINAL TENSILE PROPERTIES OF ELECTROSLAG REMELTED AND VACUUM-ARC REMELTED FORGED PLATE (18)

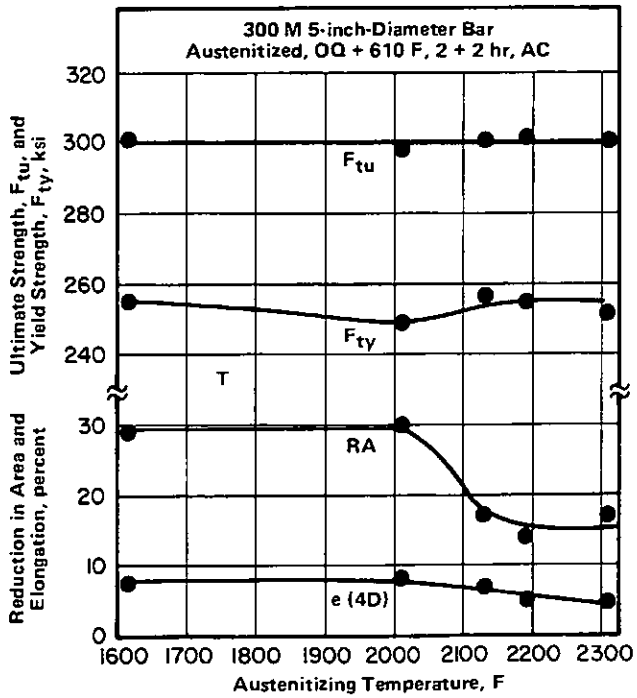


FIGURE 3.0215. EFFECT OF AUSTENITIZING TEMPERATURE ON THE TENSILE PROPERTIES OF VACUUM-ARC REMELTED BAR (11)

	Fe
0.43	C
1.8	Ni
1.6	Si
0.8	Cr
0.4	Mo
+	V

300 M

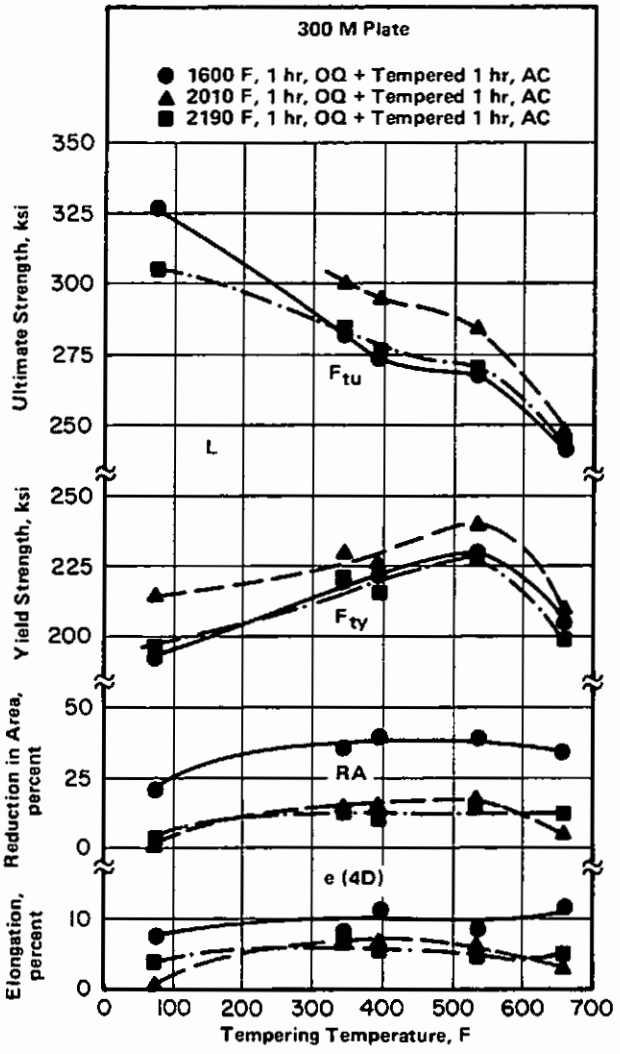


FIGURE 3.0216. EFFECT OF TEMPERING TEMPERATURE ON THE TENSILE PROPERTIES OF VACUUM-ARC REMELTED PLATE AFTER SEVERAL DIFFERENT AUSTENITIZING TREATMENTS (6)

Alloy	300 M			
Form	Bar			
Condition	F_{ty}, ksi	F_{tu}, ksi	e (4D), percent	ASTM Grain Size No.(a)
1600 F, 1 hr, OQ + 535 F, 1 hr, WQ	228	268	8.4	8
1600 F, 1 hr, OQ + 1200 F, 1 hr, Heat to 1570 F, 2 min, OQ + 535 F, 1 hr, WQ	251	282	10.0	9
1600 F, 1 hr, OQ + 1570 F, 3 min, OQ (4 Cycles) + 535 F, 1 hr, WQ	256	291	12.0	10
2190 F, 1 hr, OQ + 535 F, 1 hr, WQ	254	270	4.6	2
2190 F, 1 hr, FC to 1600 F, 5 min, OQ + 1200 F, 1 hr, Heat to 1570 F, 2 min, OQ + 535 F, 1 hr, WQ	236	268	11.0	4

(a) Austenitic grain size.

TABLE 3.0217. EFFECTS OF VARIOUS AUSTENITIZING TREATMENTS ON TENSILE PROPERTIES AND ON GRAIN SIZE (34)

Alloy	300 M				
Form	5-Inch Diameter Bar, Vacuum-Arc Remelted				
Condition	Austenitized + Tempered at 610 F, 2 + 2 hr, AC				
Austenitizing Treatment[a]	ASTM Grain Size No.	F_{ty}, ksi	F_{tu}, ksi	e (4D), percent	RA, percent
1615 F, 1 hr, OQ	7.5	253	302	6.5	26
1570 F, 2-1/2 min, OQ (Repeated 4 Times)	11.0	269	314	7.5	29

(a) Heat treatment carried out on specimen blanks approximately 1/2 inch thick.

	Fe
0.43	C
1.8	Ni
1.6	Si
0.8	Cr
0.4	Mo
+	V

300 M

TABLE 3.0218. EFFECT ON TRANSVERSE TENSILE PROPERTIES OF VERY FINE AUSTENITE GRAIN SIZE OBTAINED BY SHORT CYCLIC AUSTENITIZATION AT RELATIVELY LOW TEMPERATURE (8)

Alloy	300 M				
Form	Plate				
Austemper Treatment	Temper, F	F_{ty}, ksi	F_{tu}, ksi	e (4D), percent	RA, percent
1600 F, 1 hr, SQ to 600 F, 1 hr, OQ	None	102	220	16.9	12.0
	345 (1 hr)	112	214	17.5	30.2
	535 (1 hr)	133	192	24.0	40.8
2190 F, 1 hr, SQ to 600 F, 1 hr, OQ	None	96	201	10.7	13.2
	345 (1 hr)	114	183	13.8	26.5
	535 (1 hr)	132	166	12.5	43.6

TABLE 3.0219. EFFECTS OF AUSTENITIZING TEMPERATURE AND TEMPERING TEMPERATURE ON THE LONGITUDINAL TENSILE PROPERTIES OF VACUUM-REMELTED PLATE AUSTEMPERED AT 600 F (6)

Alloy	300 M
Form	All Wrought Forms
Condition	Spheroidize Annealed (Sect. 1.053)
F_{ty}, ksi	71
F_{tu}, ksi	111
e (2 in.), percent	28.3
RA, percent	56

TABLE 3.02110. TENSILE PROPERTIES FOR SPHEROIDIZE-ANNEALED ALLOY (28)

	Fe
0.43	C
1.8	Ni
1.6	Si
0.8	Cr
0.4	Mo
+	V

300 M

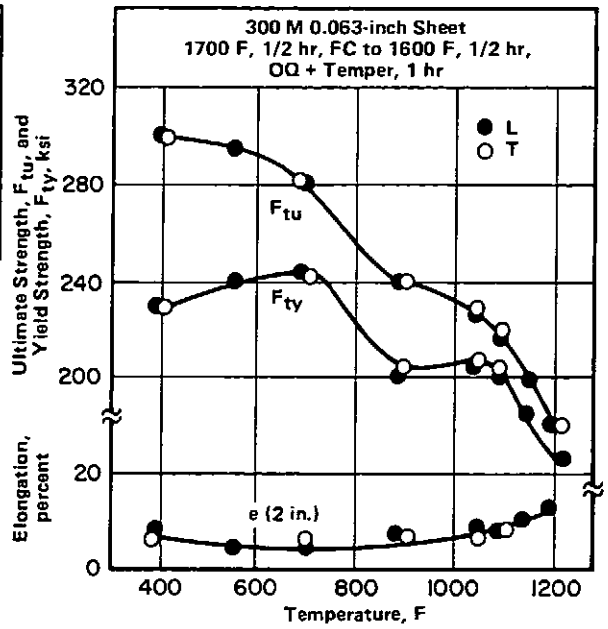


FIGURE 3.02111. EFFECT OF TEMPERING TEMPERATURE ON THE TENSILE PROPERTIES OF SHEET (41)

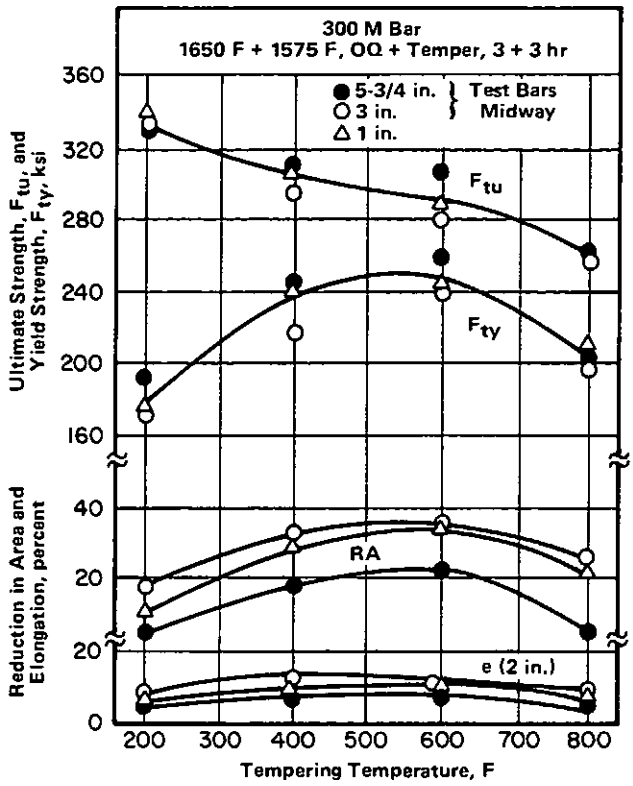


FIGURE 3.02112. EFFECT OF TEMPERING TEMPERATURE ON THE TENSILE PROPERTIES OF BAR OF VARIOUS DIAMETERS HEAT TREATED IN FULL SIZE (42)

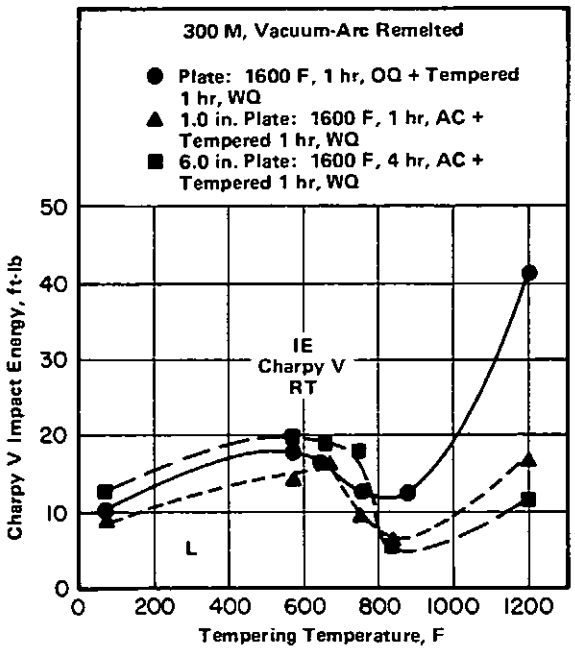


FIGURE 3.0231. EFFECT OF TEMPERING TEMPERATURE ON THE CHARPY V-NOTCH IMPACT RESISTANCE OF OIL-QUENCHED PLATE AND OF NORMALIZED PLATE (AIR COOLED FROM AUSTENITIZING TEMPERATURE) OF TWO THICKNESSES (13,35)

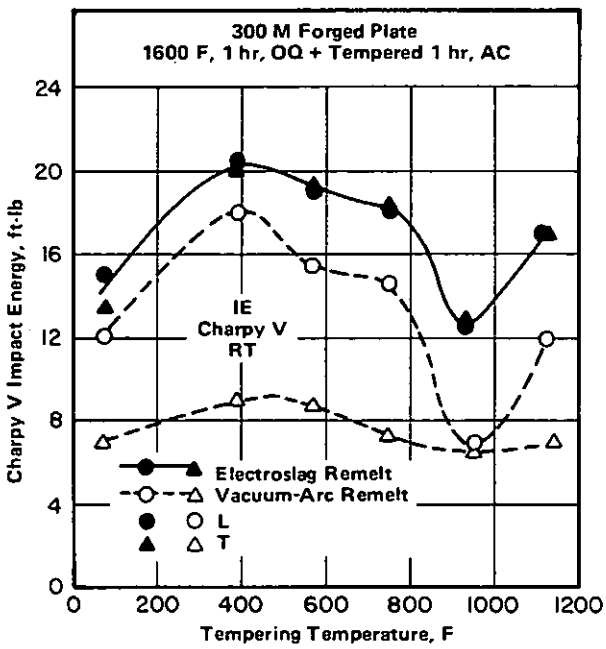


FIGURE 3.0232. EFFECT OF TEMPERING TEMPERATURE ON THE CHARPY V-NOTCH IMPACT RESISTANCE OF ELECTROSLAG REMELTED AND VACUUM-ARC REMELTED FORGED PLATE (18)

	Fe
0.43	C
1.8	Ni
1.6	Si
0.8	Cr
0.4	Mo
+	V

300 M

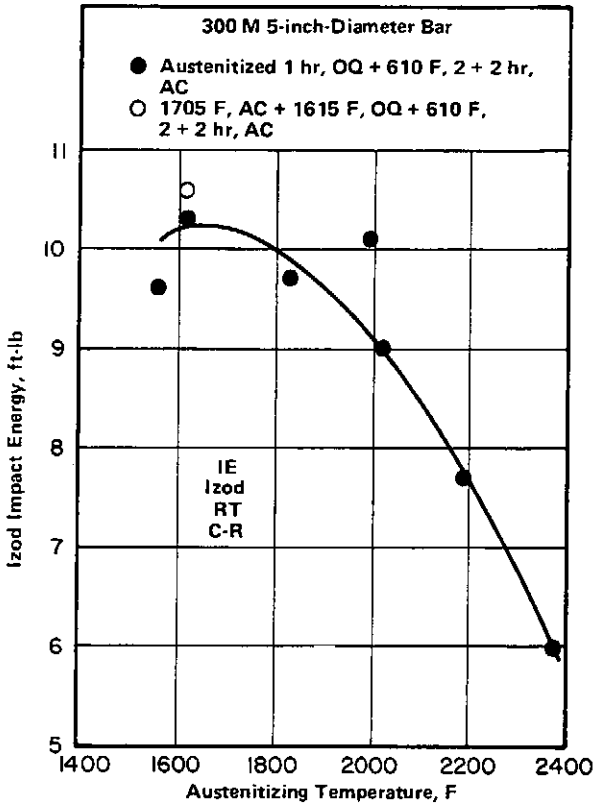


FIGURE 3.0233. EFFECT OF AUSTENITIZING TEMPERATURE ON THE IZOD IMPACT RESISTANCE OF VACUUM-ARC REMELTED BAR (11)

Alloy	300 M	
Form	Bar	
Condition	ASTM Grain Size No.(a)	IE Charpy V, ft-lb
1600 F, 1 hr, OQ + 535 F, 1 hr, WQ	8	20.0
1600 F, 1 hr, OQ + 1200 F, 1 hr, Heat to 1570 F, 2 min, OQ + 535 F, 1 hr, WQ	9	20.0
1600 F, 1 hr, OQ + 1570 F, 3 min, OQ (4 Cycles) + 535 F, 1 hr, WQ	10	22.2
2190 F, 1 hr, OQ + 535 F, 1 hr, WQ	2	13.0
2190 F, 1 hr, FC to 1600 F, 5 min, OQ + 1200 F, 1 hr, Heat to 1570 F, 2 min, OQ + 535 F, 1 hr, WQ	4	18.5

(a) Austenite grain size.

TABLE 3.0234. EFFECTS OF VARIOUS AUSTENITIZING TREATMENTS ON CHARPY V-NOTCH IMPACT RESISTANCE AND ON GRAIN SIZE (33,34)

	Fe
0.43	C
1.8	Ni
1.6	Si
0.8	Cr
0.4	Mo
+	V

300 M

Alloy	300 M	
Form	4-Inch x 6-Inch x 6-Inch Forging	
Condition	1700 F, AC + 1600 F, OQ + 570 F, 2 + 2 hr, AC	
Orientation	Charpy-V Impact Energy, ft-lb	Hardness, HRC
L	19.7	55
LT	14.7	55
ST	11.2	55

Note: See Table 3.012 for comparable tensile properties.

TABLE 3.0235. ROOM-TEMPERATURE CHARPY V-NOTCH IMPACT PROPERTIES IN DIFFERENT ORIENTATIONS OF FORGING PRODUCED FROM ELECTROSLAG REMELTED INGOT, ORIGINALLY 20 INCH IN DIAMETER (7,10)

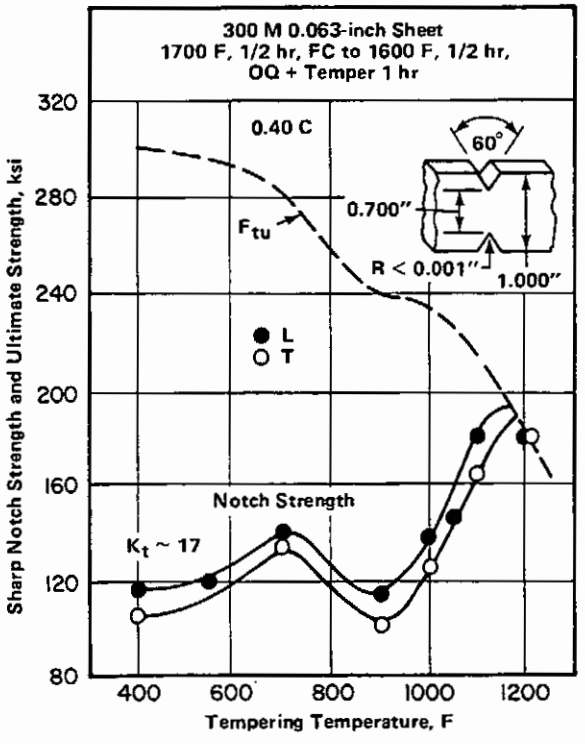


FIGURE 3.02711. EFFECT OF TEMPERING TEMPERATURE ON THE SHARP NOTCH STRENGTH OF SHEET (41)

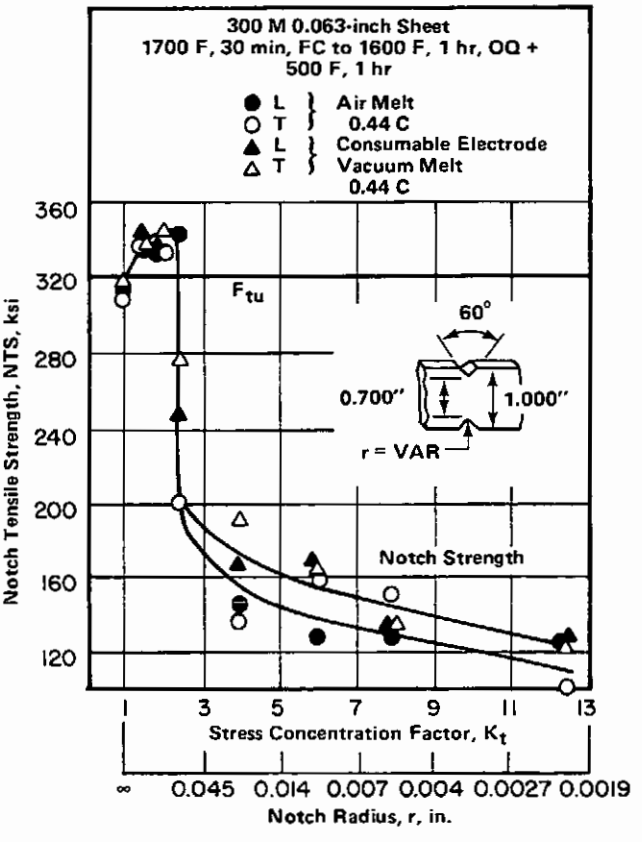


FIGURE 3.02712. EFFECTS OF STRESS CONCENTRATION AND MELTING PRACTICE ON THE NOTCH STRENGTH OF SHEET (43)

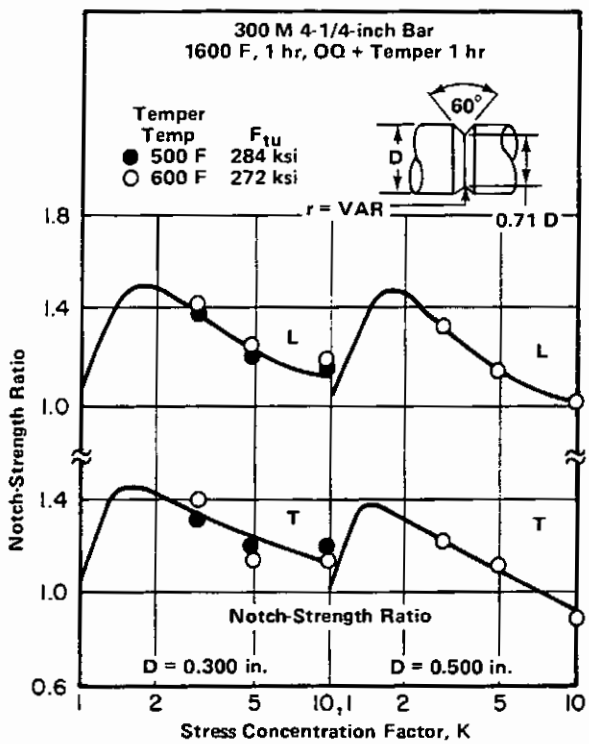


FIGURE 3.02713. EFFECTS OF STRESS CONCENTRATION AND SPECIMEN SIZE AND ORIENTATION ON NOTCH-STRENGTH RATIO OF BAR (44)

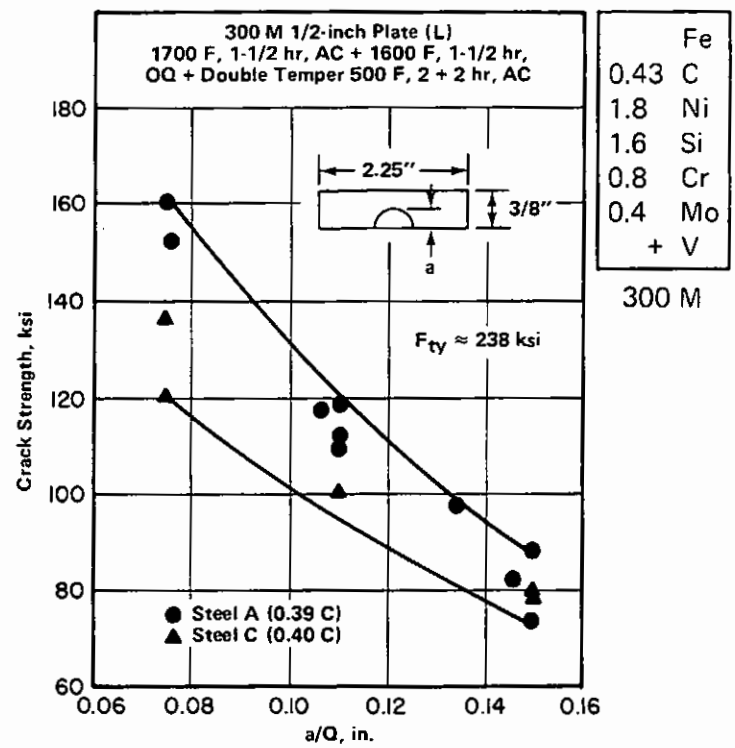


FIGURE 3.02714. EFFECT OF SURFACE CRACK SIZE ON CRACK STRENGTH OF VACUUM-ARC MELTED 1/2-INCH PLATE (F_{tu} = 290 KSI) (45)

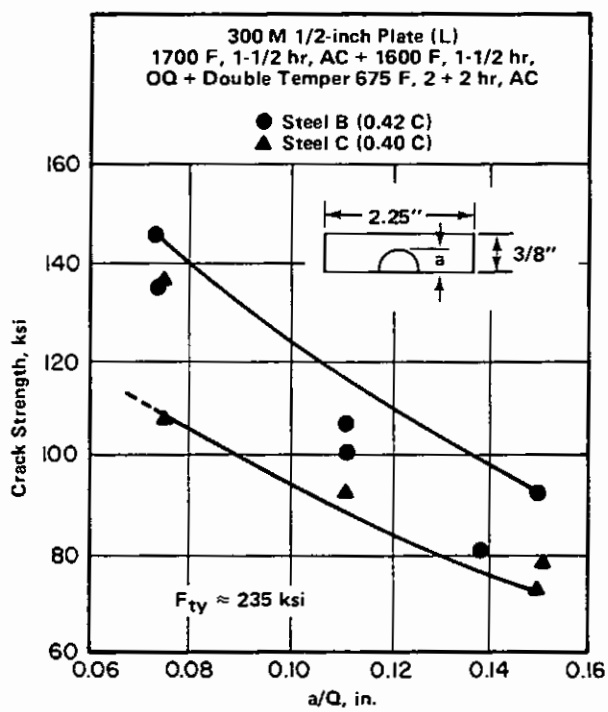


FIGURE 3.02715. EFFECT OF SURFACE CRACK SIZE ON CRACK STRENGTH OF VACUUM-ARC MELTED 1/2-INCH PLATE (F_{tu} = 270 KSI) (45)

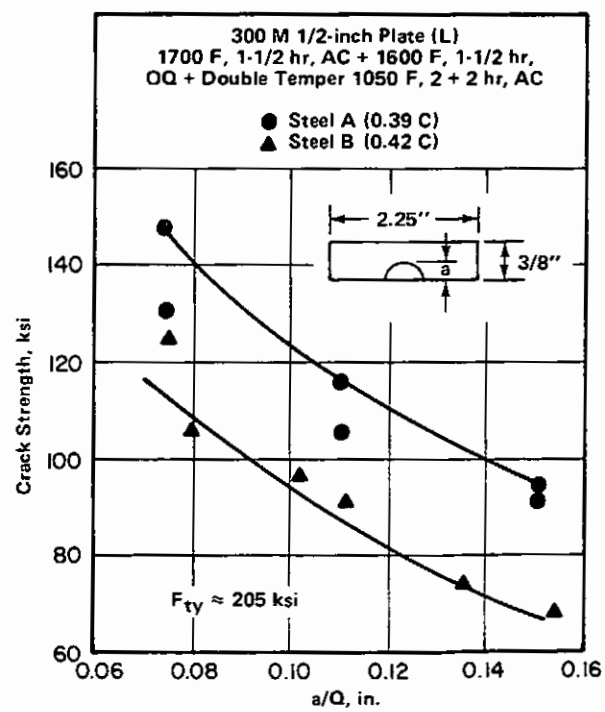


FIGURE 3.02716. EFFECT OF SURFACE CRACK SIZE ON CRACK STRENGTH OF VACUUM-ARC MELTED 1/2-INCH PLATE (F_{tu} = 220 KSI) (45)

	Fe
0.43	C
1.8	Ni
1.6	Si
0.8	Cr
0.4	Mo
+	V

300 M

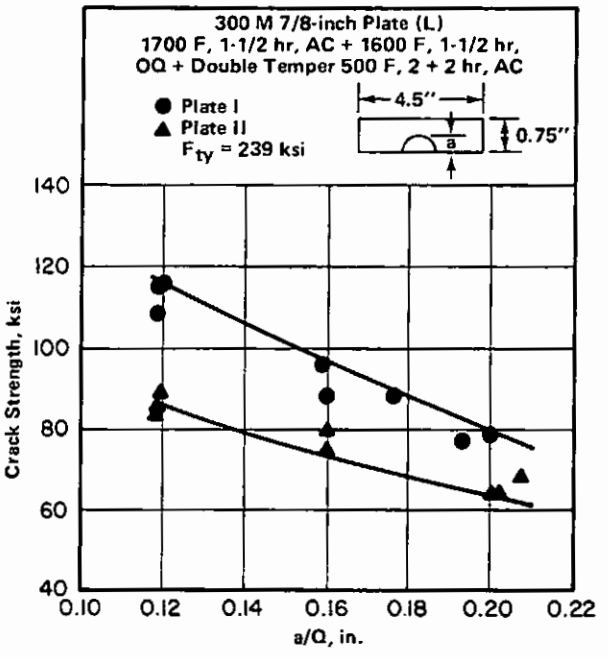


FIGURE 3.02717. EFFECT OF SURFACE CRACK SIZE ON CRACK STRENGTH OF VACUUM-ARC MELTED 7/8 INCH PLATE (F_{tu} = 290 KSI) (45)

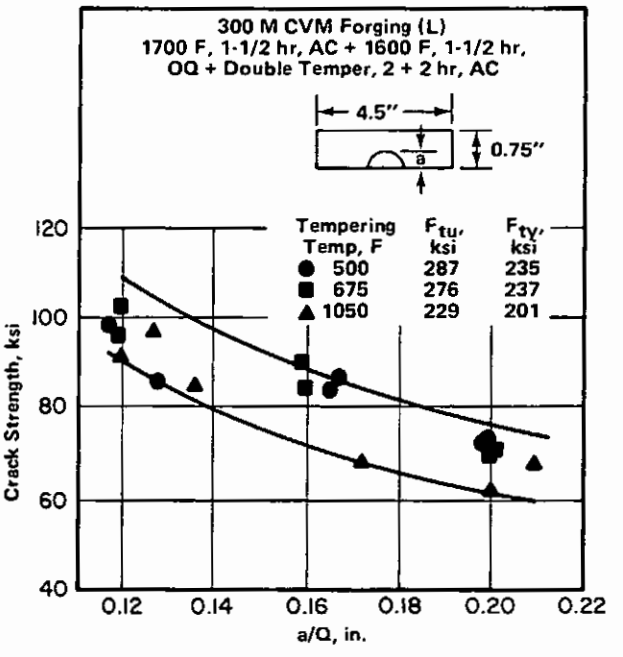


FIGURE 3.02718. EFFECT OF SURFACE CRACK SIZE ON CRACK STRENGTH OF VACUUM-ARC MELTED FORGING HEAT TREATED TO THREE DIFFERENT STRENGTH LEVELS (45)

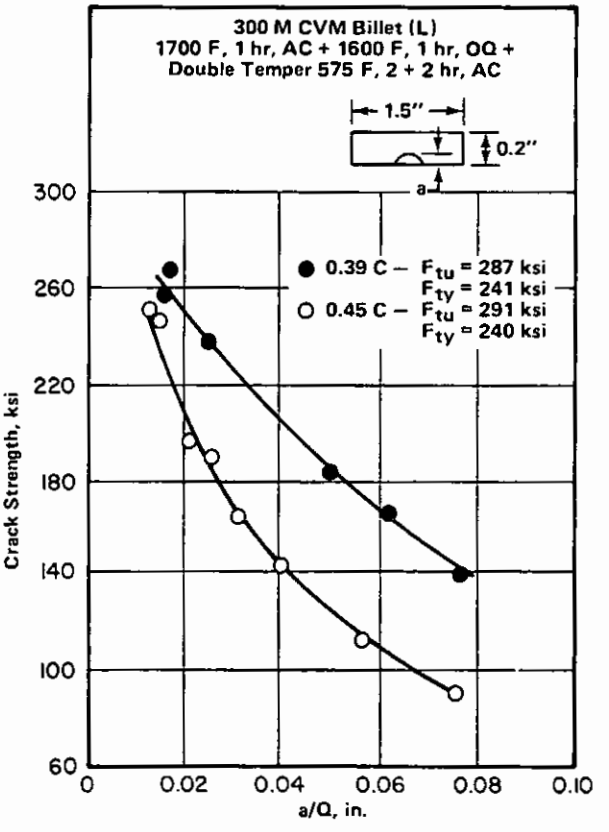
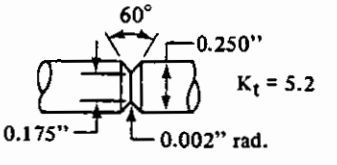


FIGURE 3.02719. EFFECT OF SURFACE CRACK SIZE ON CRACK STRENGTH OF TWO VACUUM-ARC MELTED BILLETS WITH DIFFERENT CARBON CONTENTS (45)

Alloy	300 M			
Form	6-Inch Diameter Billets			
Condition	1600 F, OQ + Temper 2 + 2 hr, AC			
Tempering Temperature, F	Orientation	NTS, ksi	F_{tu}, ksi	NSR
550	L	425	288	1.75
	T	401	291	1.65
575	L	363	272	1.60
	T	395	274	1.74

Note 1: Notch specimen configuration



Note 2: The 550 F and 575 F tempers represent two different heats of steel; minor variations in composition, as well as the difference in tempering temperature, could account for some of the variations in strength.

TABLE 3.027110. NOTCH TENSILE STRENGTH OF VACUUM-ARC REMELTED BILLETS (24)

	Fe
0.43	C
1.8	Ni
1.6	Si
0.8	Cr
0.4	Mo
+	V

300 M

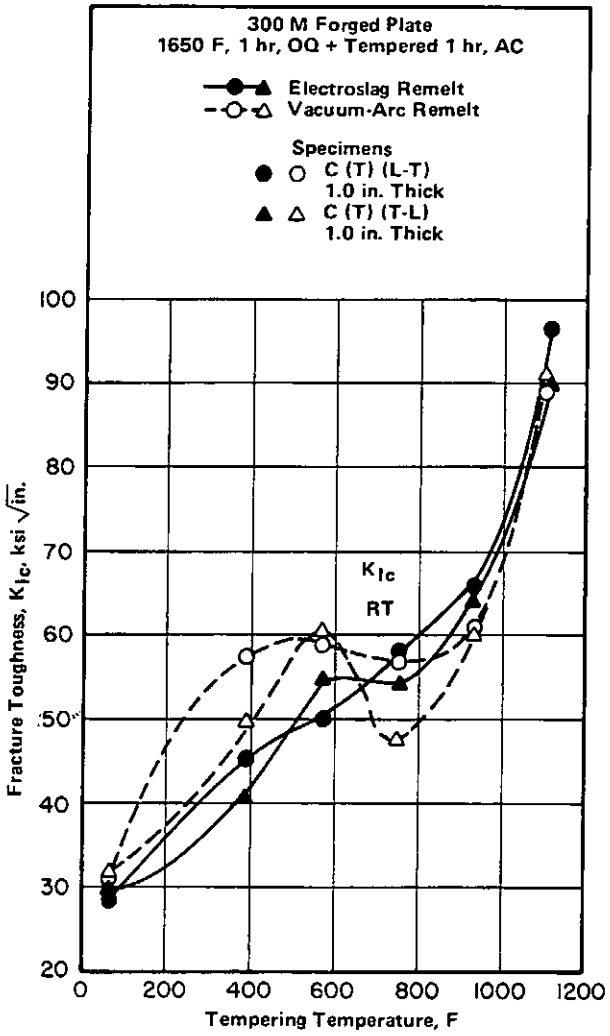


FIGURE 3.02721. EFFECT OF TEMPERING TEMPERATURE ON THE FRACTURE TOUGHNESS OF ELECTROSLAG REMELTED AND VACUUM-ARC REMELTED FORGED PLATE (18)

Note: See Figure 3.0214 for comparable longitudinal tensile properties.

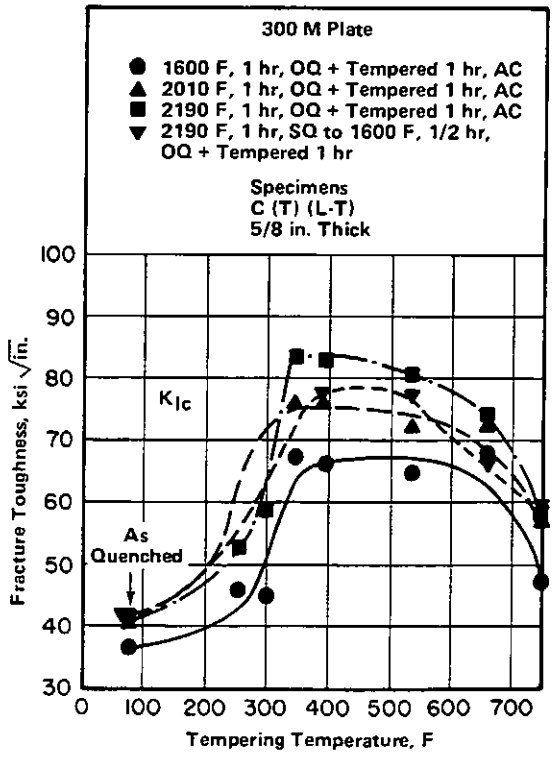


FIGURE 3.02722. EFFECT OF TEMPERING TEMPERATURE ON THE FRACTURE TOUGHNESS OF VACUUM-REMELTED PLATE AFTER SEVERAL DIFFERENT AUSTENITIZING TREATMENTS (5,6)

Note: Figure 3.0216 shows comparable tensile properties for most test conditions.

	Fe
0.43	C
1.8	Ni
1.6	Si
0.8	Cr
0.4	Mo
+	V

300 M

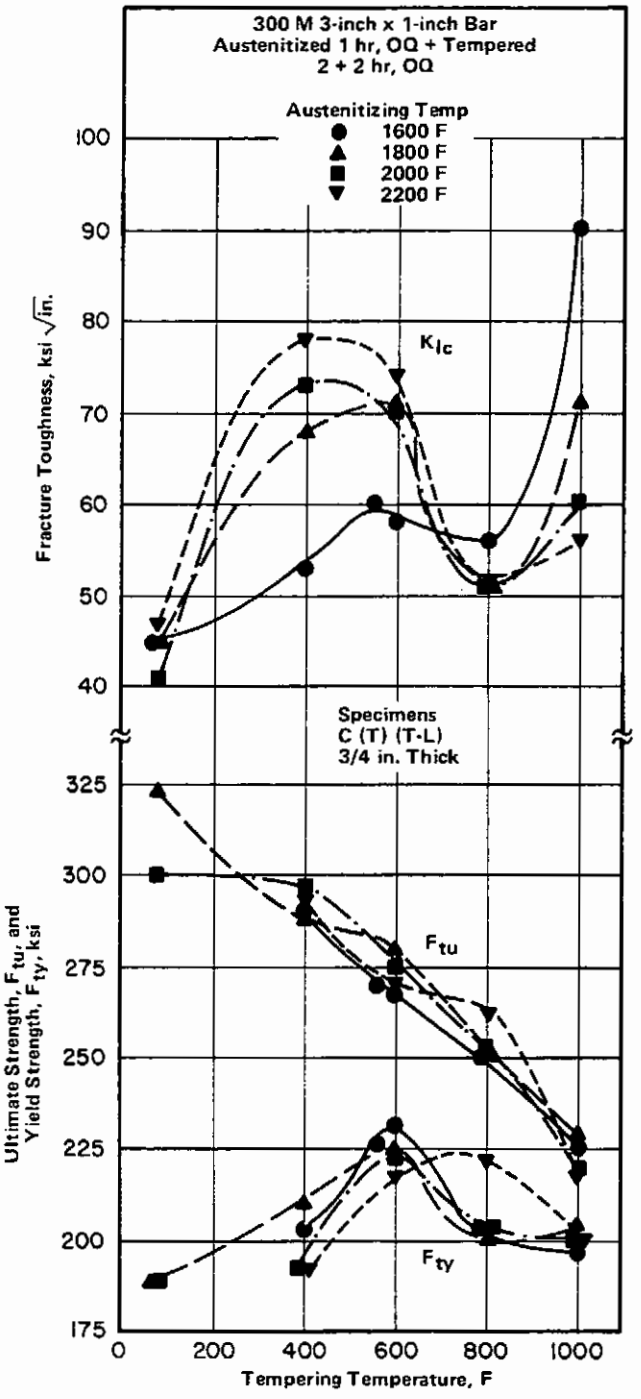


FIGURE 3.02723. EFFECTS OF AUSTENITIZING TEMPERATURE AND TEMPERING TEMPERATURE ON THE FRACTURE TOUGHNESS AND CORRESPONDING TENSILE PROPERTIES OF VACUUM-ARC MELTED BAR (23)

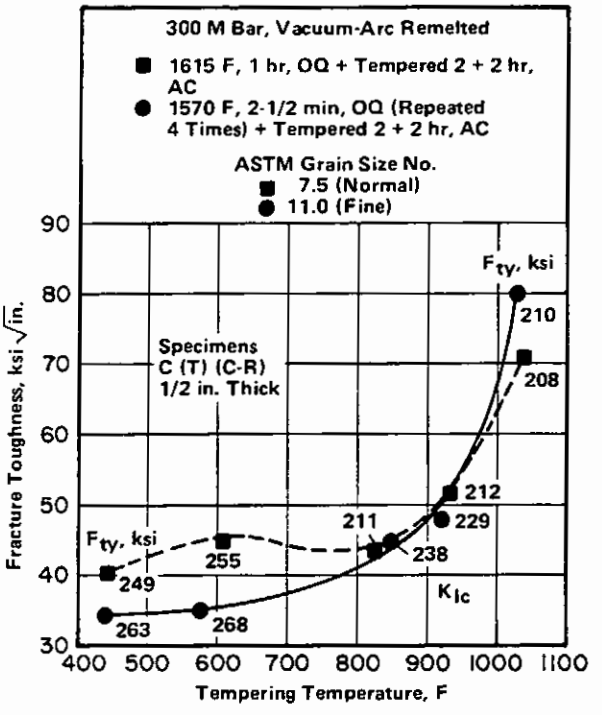


FIGURE 3.02724. EFFECT ON FRACTURE TOUGHNESS OF TEMPERING TEMPERATURE AND OF VERY FINE AUSTENITE GRAIN SIZE OBTAINED BY SHORT CYCLIC AUSTENITIZATION AT RELATIVELY LOW TEMPERATURES (8,9)

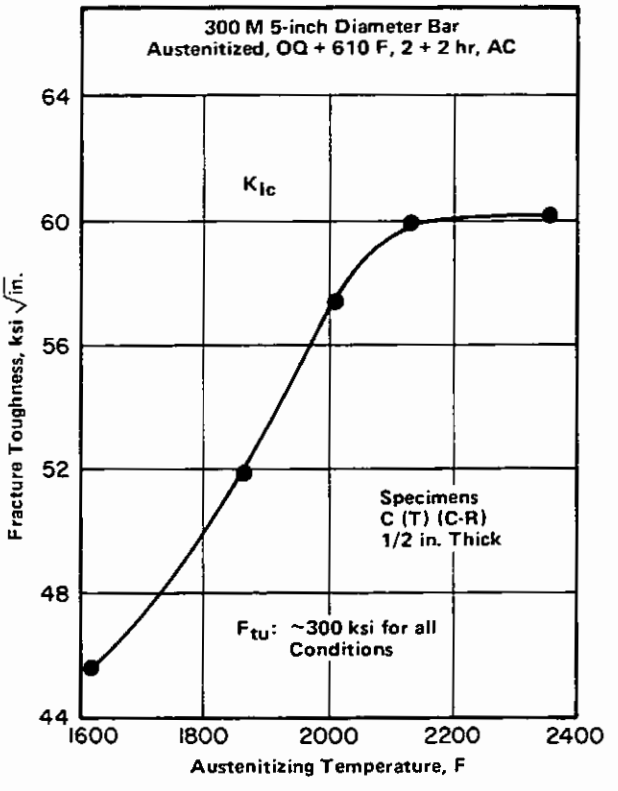


FIGURE 3.02726. EFFECT OF AUSTENITIZING TEMPERATURE ON THE FRACTURE TOUGHNESS OF VACUUM-ARC REMELTED BAR (11)

	Fe
0.43	C
1.8	Ni
1.6	Si
0.8	Cr
0.4	Mo
	+ V

300 M

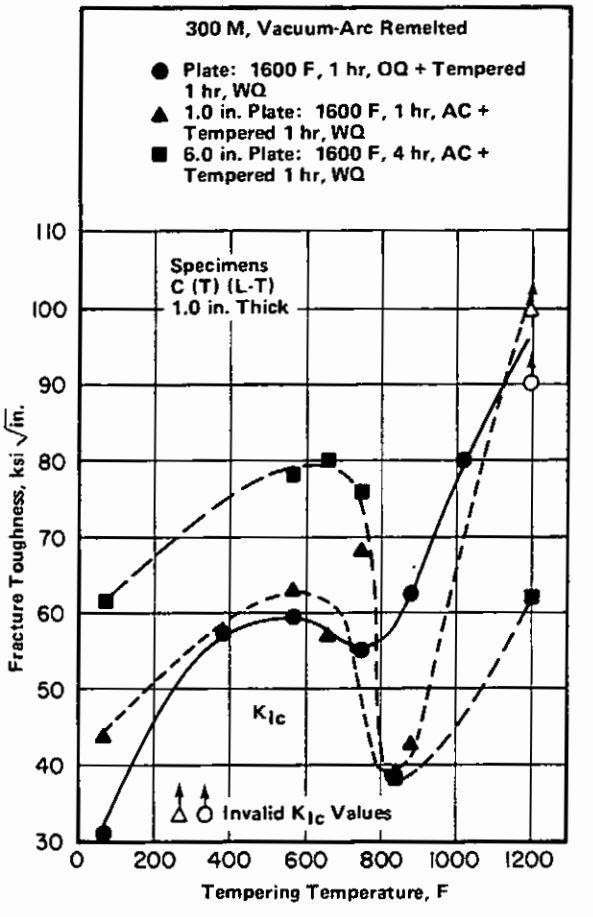


FIGURE 3.02725. EFFECT OF TEMPERING TEMPERATURE ON THE FRACTURE TOUGHNESS OF OIL-QUENCHED PLATE AND OF NORMALIZED PLATE (AIR COOLED FROM AUSTENITIZING TEMPERATURE) OF TWO THICKNESSES (13,35)

Note: Comparable tensile properties given in Figure 3.0212.

	Fe
0.43	C
1.8	Ni
1.6	Si
0.8	Cr
0.4	Mo
+	V

300 M

Alloy	300 M	
Form	Bar	
Condition	ASTM Grain Size No.(a)	K_{Ic}, ksi $\sqrt{in.}$(b,c)
1600 F, 1 hr, OQ + 535 F, 1 hr, WQ	8	51.0
1600 F, 1 hr, OQ + 1200 F, 1 hr, Heat to 1570 F, 1 min, OQ + 535 F, 1 hr, WQ	9	80.1
1600 F, 1 hr, OQ + 1570 F, 3 min, OQ (4 Cycles) + 535 F, 1 hr, WQ	10	49.1
2190 F, 1 hr, OQ + 535 F, 1 hr, WQ	2	82.8
2190 F, 1 hr, FC to 1600 F, 5 min, OQ + 1200 F, 1 hr, Heat to 1570 F, 2 min, OQ + 535 F, 1 hr, WQ	4	90.1

(a) Austenitic grain size.
(b) Specimens, C (T) (L-R), 5/8 inch thick.
(c) See Tables 3.0217 and 3.0234 for comparable tensile and impact properties.

TABLE 3.02727. EFFECTS OF VARIOUS AUSTENITIZING TREATMENTS ON FRACTURE TOUGHNESS AND GRAIN SIZE (33,34)

Alloy	300 M	
Form	Plate	
Austemper Treatment	Temper, F	K_{Ic}, ksi $\sqrt{in.}$
1600 F, 1 hr, SQ to 600 F, 1 hr, OQ	None	43.2
	390 (1 hr)	60.7
2190 F, 1 hr, SQ to 600 F, 1 hr, OQ	660 (1 hr)	54.7
	750 (1 hr)	39.5

Notes: K_{Ic} specimens, C (T) (L-T), 5/8 inch thick.
See Table 3.0219 for some information on tensile properties of austempered plate, although tempering temperatures are different.

TABLE 3.02728. EFFECTS OF AUSTENITIZING TEMPERATURE AND TEMPERING TEMPERATURE ON THE FRACTURE TOUGHNESS OF VACUUM-ARC REMELTED PLATE AUSTEMPERED AT 600 F (6)

	Fe
0.43	C
1.8	Ni
1.6	Si
0.8	Cr
0.4	Mo
+	V

300 M

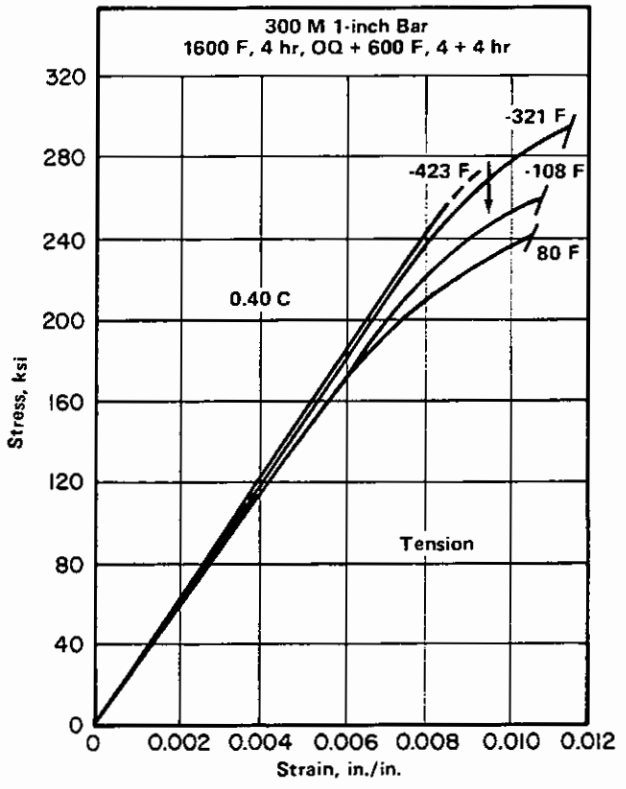


FIGURE 3.0311. TENSILE STRESS-STRAIN CURVES AT ROOM AND CRYOGENIC TEMPERATURES (45)

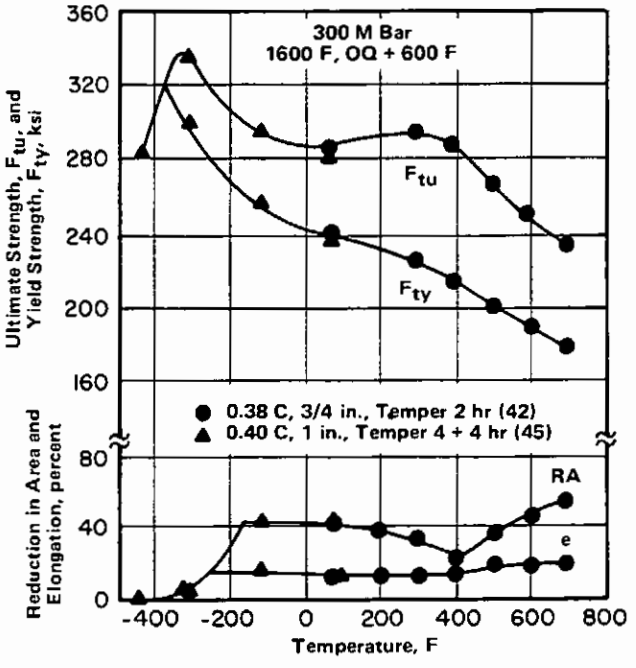


FIGURE 3.0312. EFFECT OF TEMPERATURES FROM -423 TO 700 F ON TENSILE PROPERTIES OF BAR (42,45)

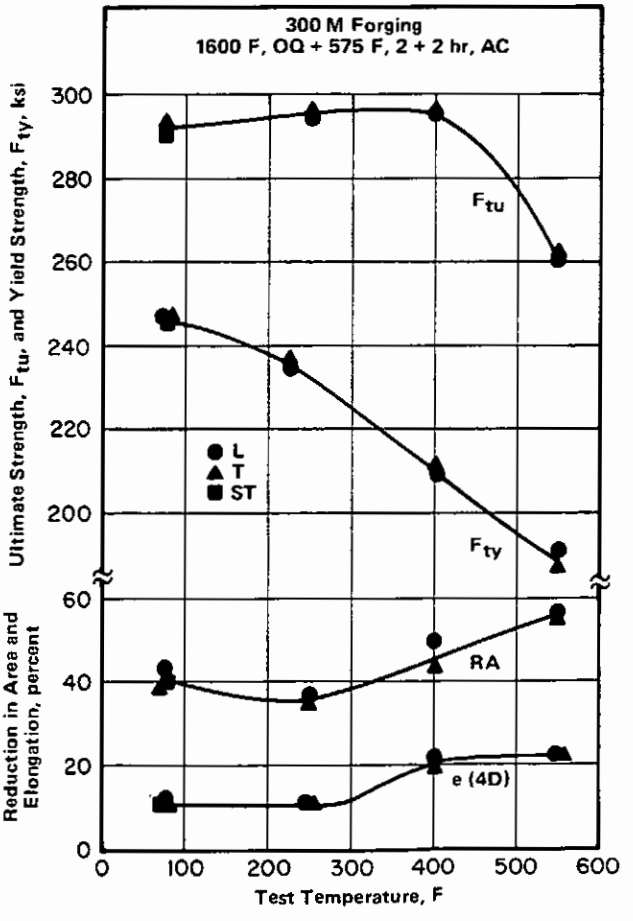


FIGURE 3.0313. EFFECT OF ELEVATED TEMPERATURES ON THE TENSILE PROPERTIES OF A LARGE FORGING OIL QUENCHED AND TEMPERED AT 575 F (20)

	Fe
0.43	C
1.8	Ni
1.6	Si
0.8	Cr
0.4	Mo
+	V

300 M

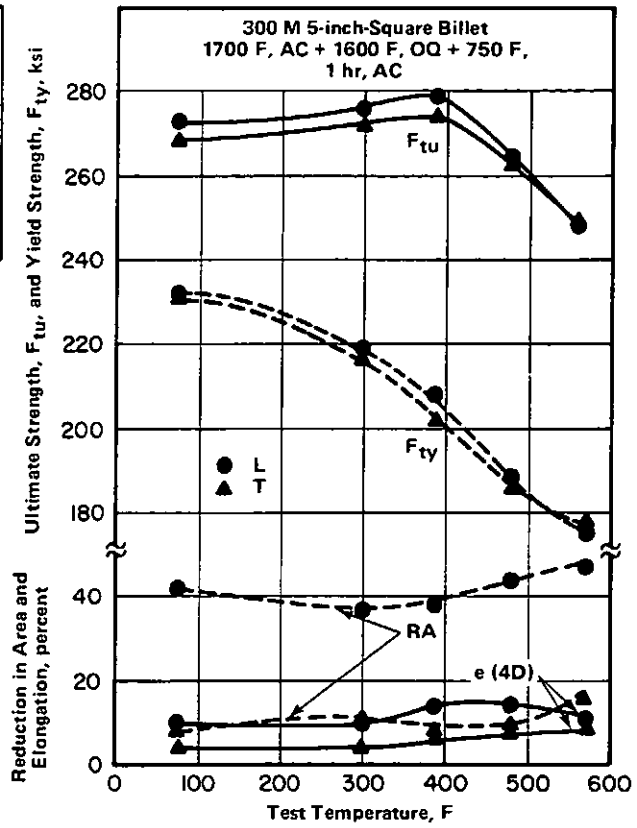


FIGURE 3.0314. EFFECT OF ELEVATED TEMPERATURES ON THE TENSILE PROPERTIES OF VACUUM-ARC MELTED BILLET OIL QUENCHED AND TEMPERED AT 750 F (12)

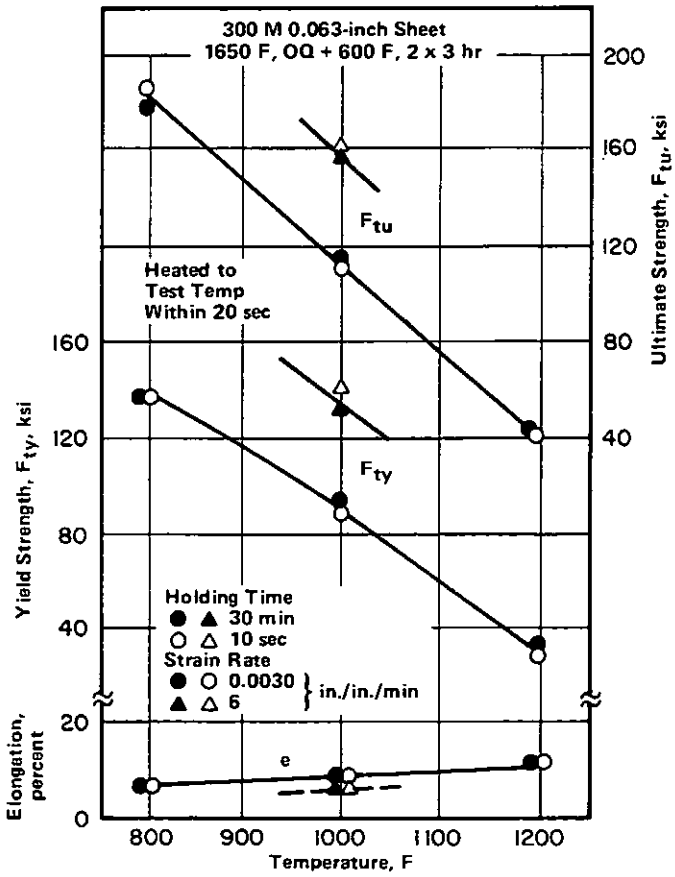


FIGURE 3.0315. EFFECTS OF A RAPID STRAIN RATE (6 IN./IN./MIN) AND A SHORT HOLDING TIME (10 SEC) AT TEMPERATURE ON TENSILE PROPERTIES IN THE TEMPERATURE RANGE 800 TO 1200 F (46)

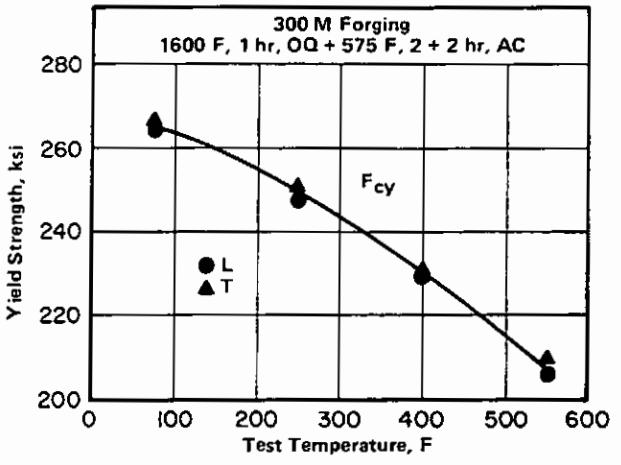


FIGURE 3.0321. EFFECT OF ELEVATED TEMPERATURES ON THE COMPRESSIVE YIELD STRENGTH OF A LARGE FORGING OIL QUENCHED AND TEMPERED AT 575 F (20)

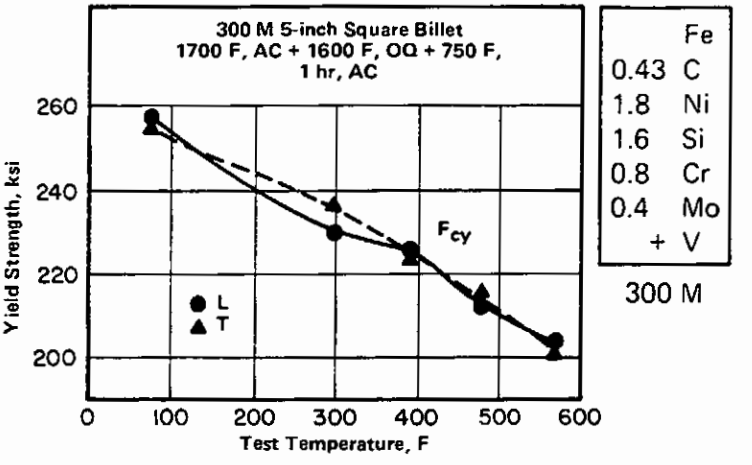


FIGURE 3.0322. EFFECT OF ELEVATED TEMPERATURES ON THE COMPRESSIVE YIELD STRENGTH OF VACUUM-ARC MELTED BILLET OIL QUENCHED AND TEMPERED AT 750 F (12)

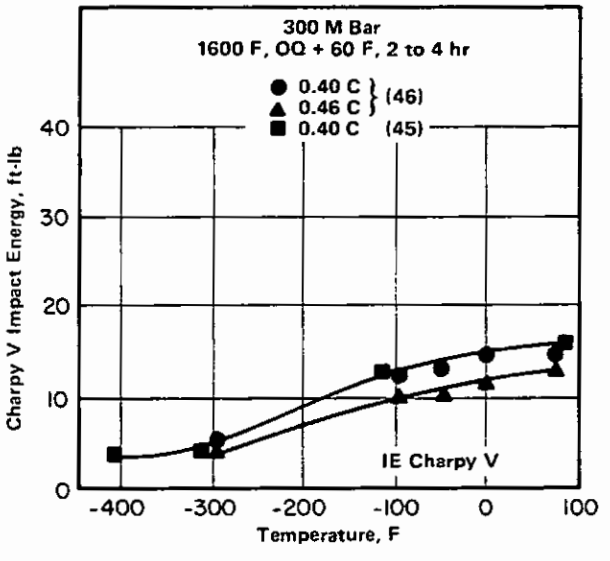


FIGURE 3.0331. EFFECT OF LOW TEMPERATURES DOWN TO -423 F ON NOTCH IMPACT PROPERTIES OF BARS WITH TWO CARBON CONTENTS (45,46)

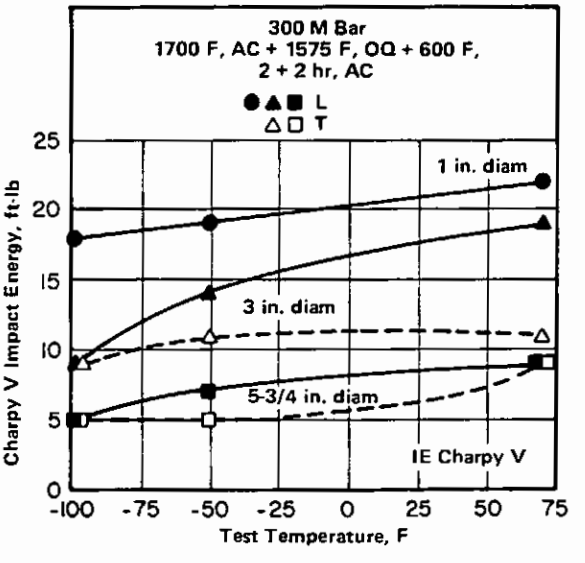


FIGURE 3.0332. EFFECTS OF LOW TEMPERATURES AND DIFFERENT ORIENTATIONS ON THE IMPACT RESISTANCE OF BAR OF VARIOUS DIAMETERS (28)

Note: The specimens were machined after heat treatment from the center of the 1.0-inch-diameter bar and from the mid-radius of the larger bars.

	Fe
0.43	C
1.8	Ni
1.6	Si
0.8	Cr
0.4	Mo
+	V

300 M

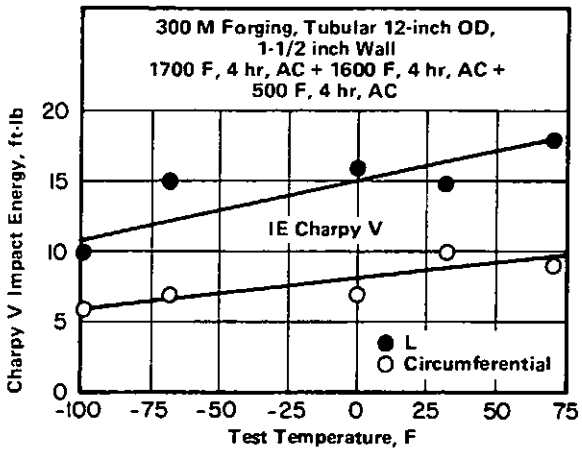


FIGURE 3.0333. EFFECT OF LOW TEMPERATURES ON THE NOTCH IMPACT RESISTANCE OF A FORGING (28)

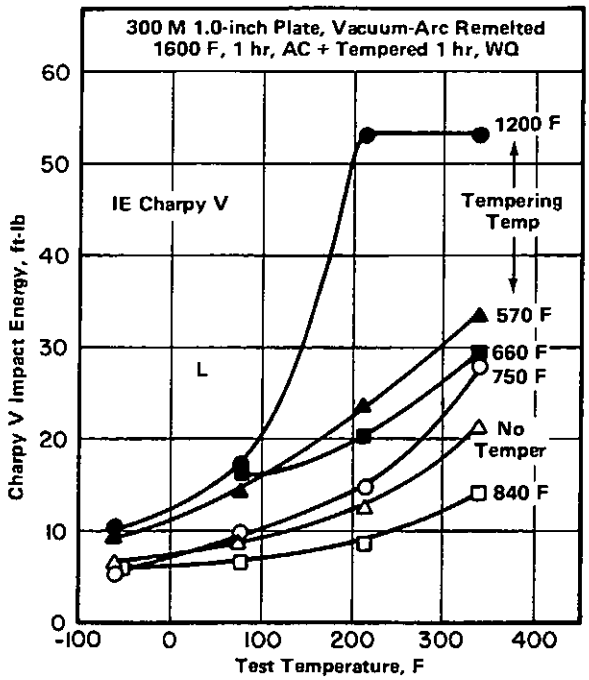


FIGURE 3.0334. EFFECTS OF TEST TEMPERATURES FROM -60 F TO 340 F AND OF TEMPERING TEMPERATURES UP TO 1200 F ON THE CHARPY V-NOTCH IMPACT RESISTANCE OF NORMALIZED 1.0-INCH-THICK PLATE (AIR-COOLED FROM AUSTENITIZING TEMPERATURE) (13)

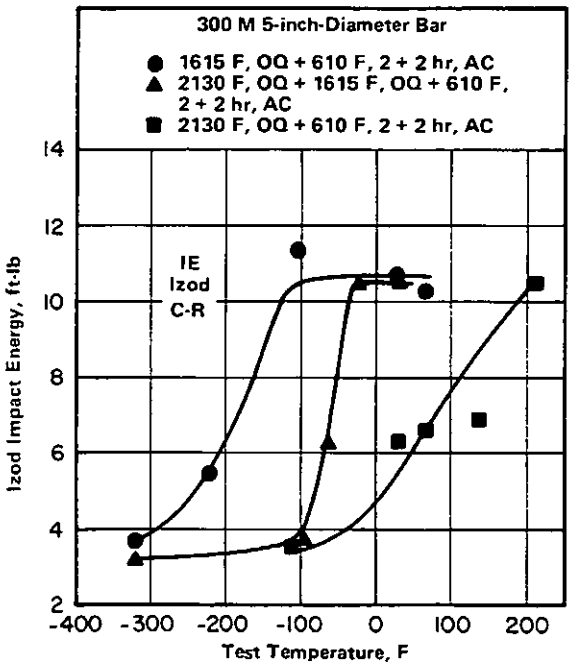


FIGURE 3.0335. EFFECTS OF VARIATIONS IN AUSTENITIZING TREATMENT ON NOTCH-IMPACT-TRANSITION CURVES OF VACUUM-ARC RE-MELTED BAR (11)

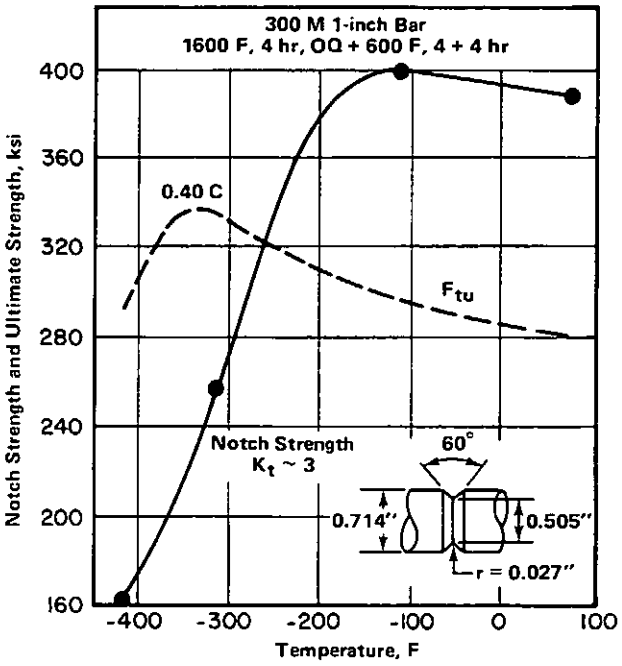


FIGURE 3.03711. EFFECT OF LOW TEMPERATURES ON NOTCH STRENGTH OF BAR (45)

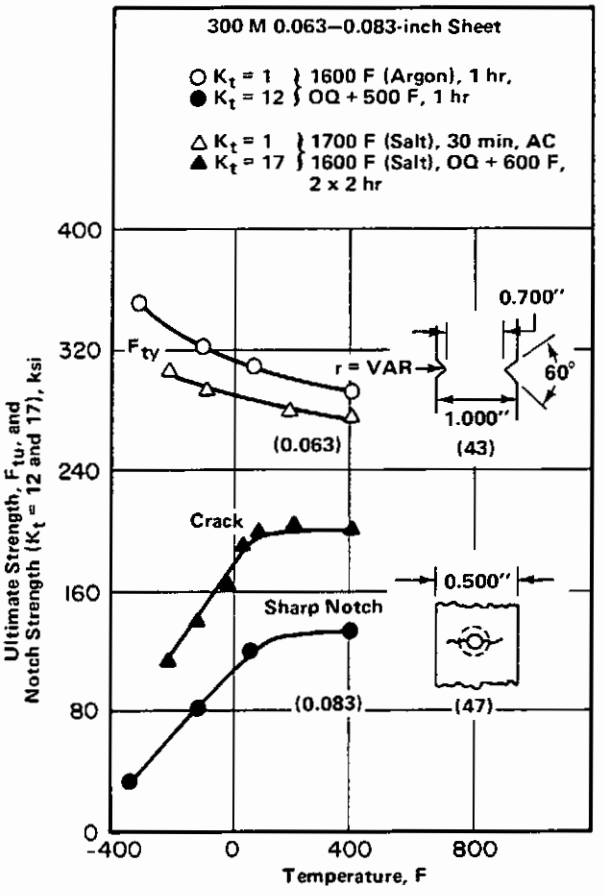


FIGURE 3.03712. EFFECT OF TEMPERATURES FROM 400 TO -320 F ON TENSILE (K_t = 1), SHARP-NOTCH (K_t = 12), AND CRACK (K_t = 17) STRENGTH OF SHEET (43,47)

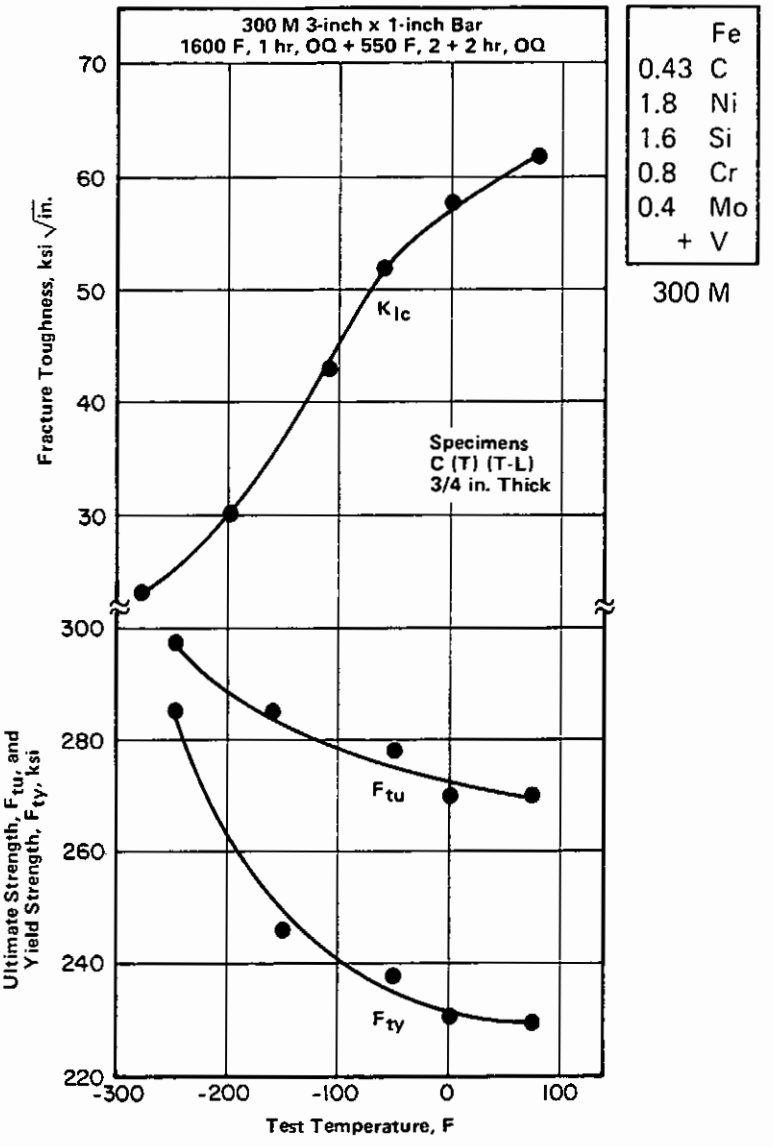


FIGURE 3.03721. EFFECT OF LOW TEMPERATURES ON THE FRACTURE TOUGHNESS AND CORRESPONDING TENSILE PROPERTIES OF VACUUM-ARC REMELTED BAR (23)

Alloy	300 M	
Form	Plate	
Condition	1600 F, 1 hr, OQ + 575 F, 2 + 2 hr, AC	
Temperature, F	K_{Ic}, ksi √in.	F_{ty}, ksi
70	62	230
0	58	231
-65	43	245

Note: Specimen C (T) (L-T), 3/4 inch thick.

TABLE 3.03722. EFFECT OF LOW TEMPERATURES ON FRACTURE TOUGHNESS OF PLATE (17)

	Fe
0.43	C
1.8	Ni
1.6	Si
0.8	Cr
0.4	Mo
+	V

300 M

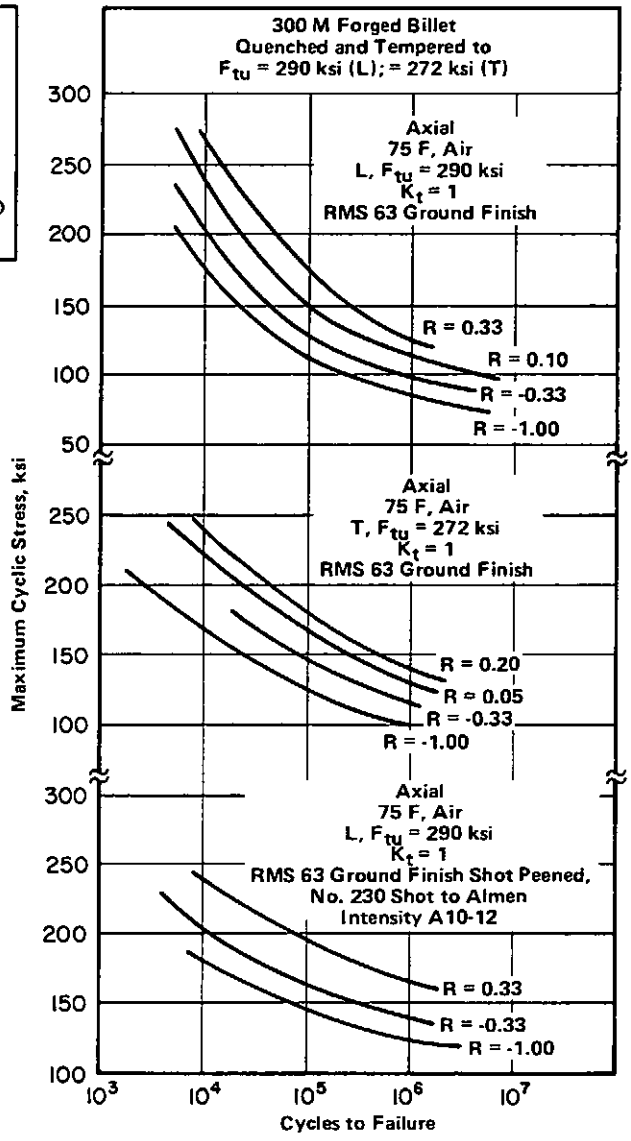


FIGURE 3.051. FATIGUE LIFE OF LONGITUDINALLY GROUND AND SHOT-PEENED SPECIMENS FROM FORGED BILLET HEAT TREATED TO HIGH STRENGTH LEVEL (3)

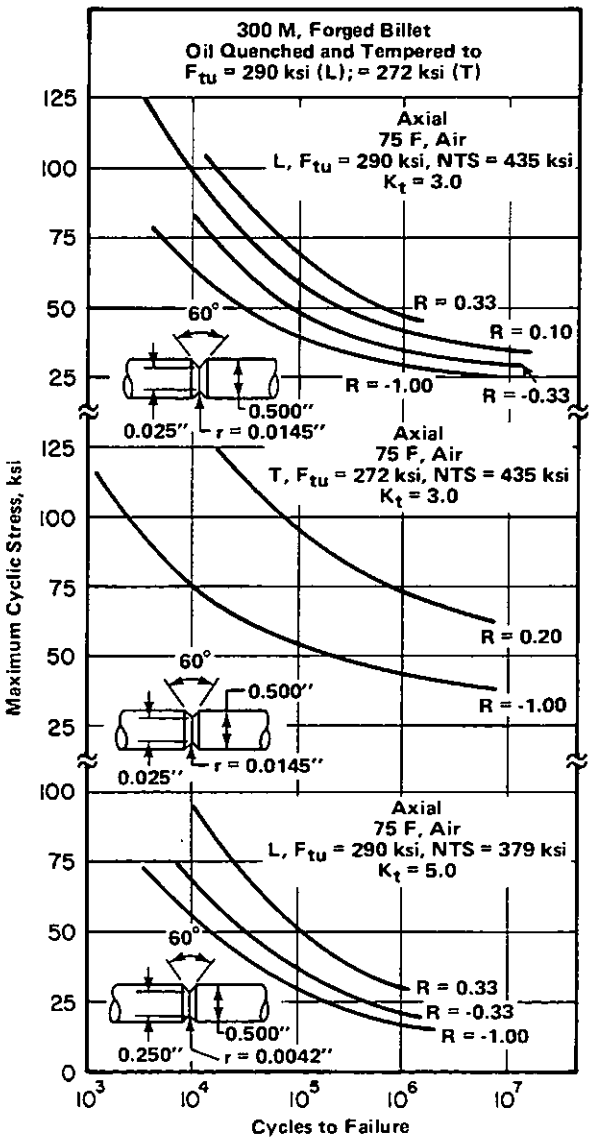


FIGURE 3.052. FATIGUE LIFE OF NOTCHED SPECIMENS FROM FORGED BILLET HEAT TREATED TO HIGH STRENGTH LEVEL (3)

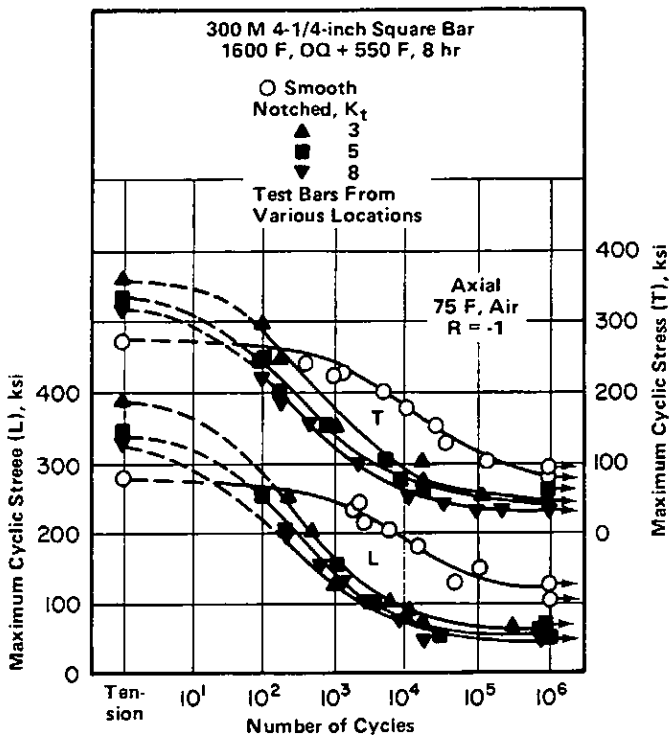


FIGURE 3.053. FATIGUE LIFE OF SMOOTH AND NOTCHED BAR (48)

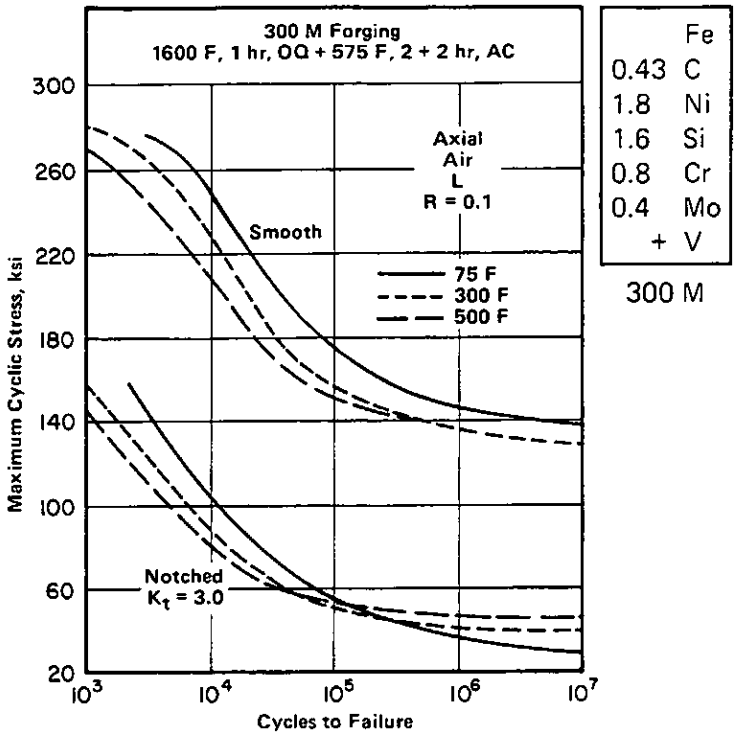


FIGURE 3.054. EFFECT OF ELEVATED TEMPERATURES ON FATIGUE LIFE OF SMOOTH AND NOTCHED SPECIMENS FROM LARGE FORGING OIL QUENCHED AND TEMPERED AT 575 F (20)

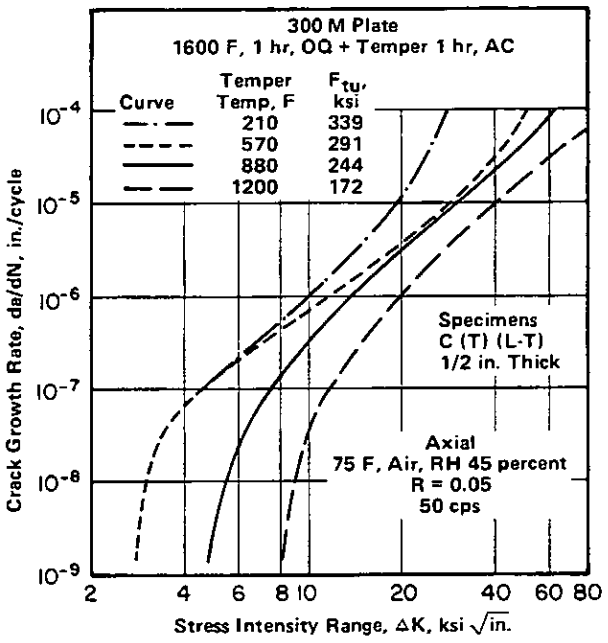


FIGURE 3.055. EFFECT OF VARIATIONS IN TEMPERING TEMPERATURE AND ASSOCIATED STRENGTH LEVELS ON FATIGUE-CRACK GROWTH RATE OF VACUUM-ARC REMELTED PLATE IN AN AIR ENVIRONMENT (15)

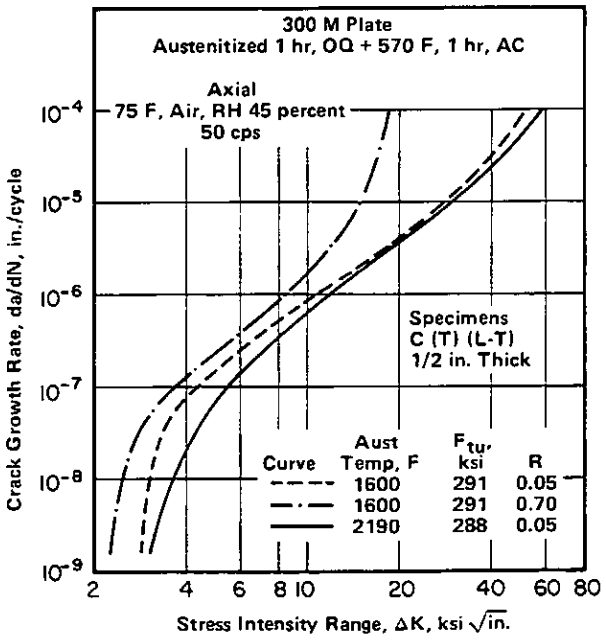


FIGURE 3.056. EFFECTS OF VARIATIONS IN AUSTENITIZING TEMPERATURE AND STRESS RATIO (R) ON FATIGUE-CRACK GROWTH RATE OF VACUUM-ARC REMELTED PLATE IN AN AIR ENVIRONMENT (15)

	Fe
0.43	C
1.8	Ni
1.6	Si
0.8	Cr
0.4	Mo
+	V

300 M

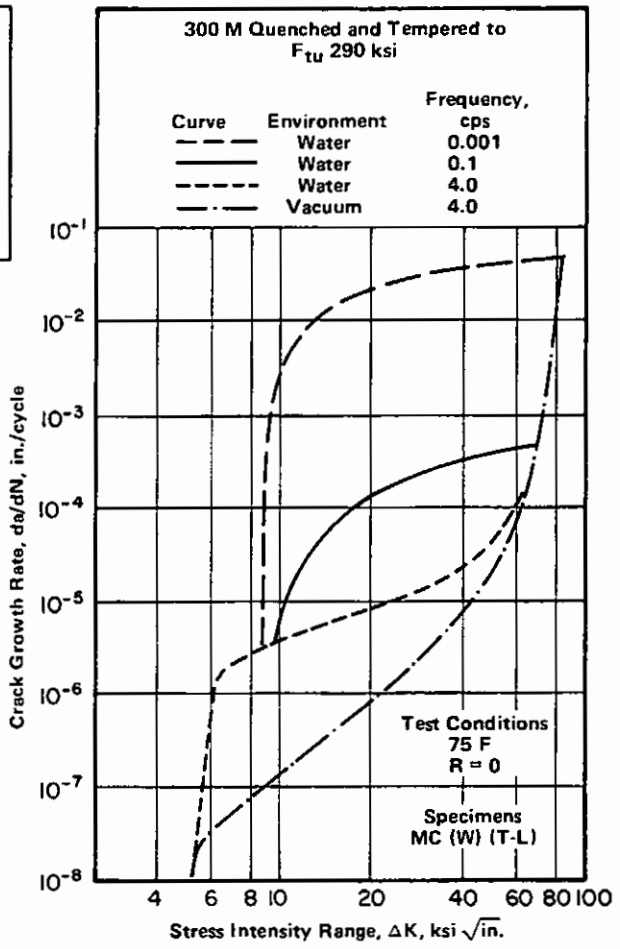


FIGURE 3.057. EFFECTS OF VARIATIONS IN FREQUENCY AND ENVIRONMENT ON FATIGUE-CRACK GROWTH RATE (16)

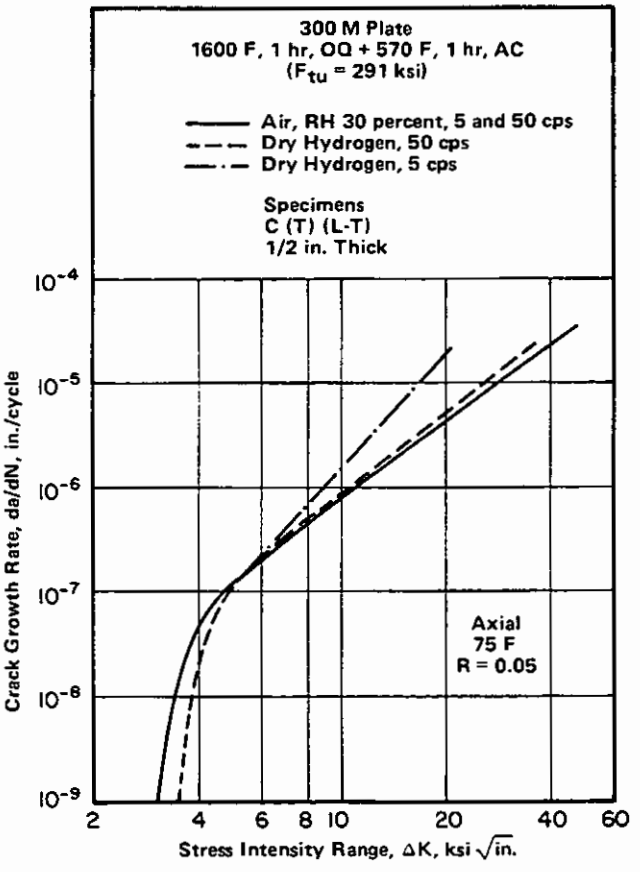


FIGURE 3.058. FATIGUE-CRACK GROWTH RATE OF VACUUM-ARC REMELTED PLATE IN ENVIRONMENTS OF AIR AND OF DRY HYDROGEN AT FREQUENCIES OF 5 AND 50 CPS (20)

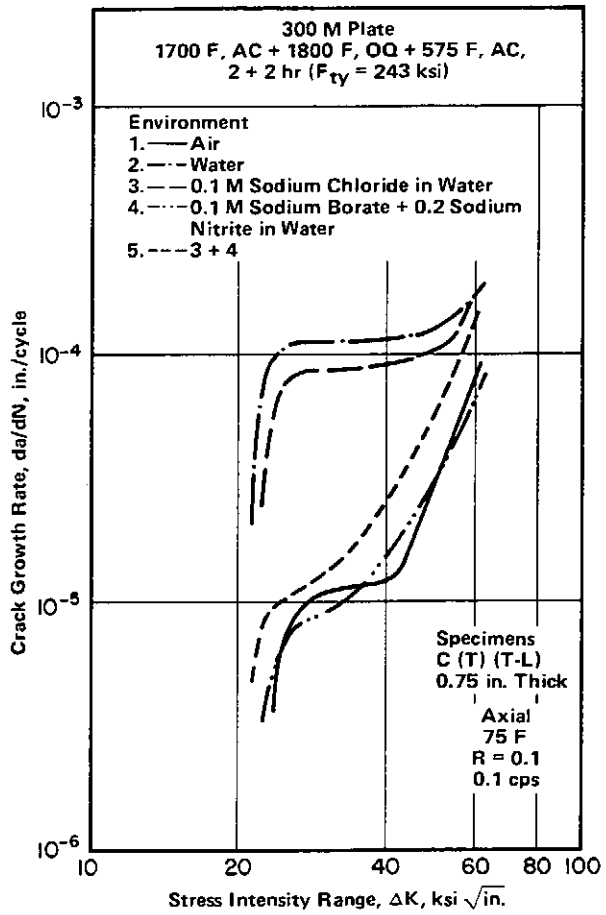


FIGURE 3.059. EFFECTS OF VARIOUS ENVIRONMENTS AND A SODIUM BORATE, SODIUM NITRITE INHIBITOR ON FATIGUE-CRACK GROWTH RATE OF PLATE HEAT TREATED TO A HIGH STRENGTH LEVEL (1)

	Fe
0.43	C
1.8	Ni
1.6	Si
0.8	Cr
0.4	Mo
+	V

300 M

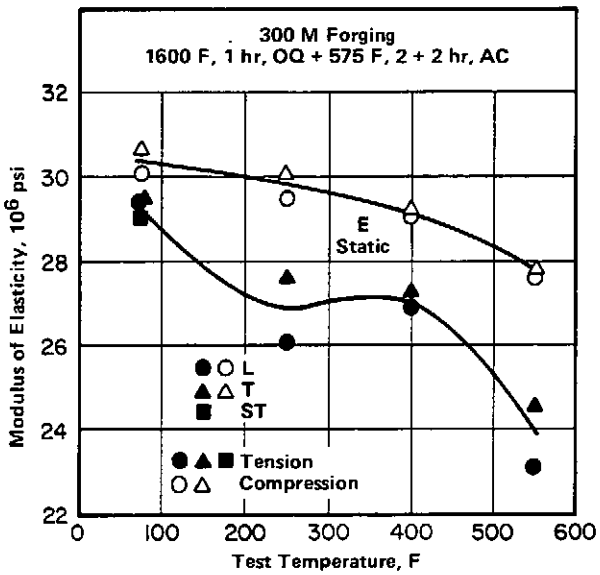


FIGURE 3.0621. EFFECT OF ELEVATED TEMPERATURES ON MODULUS OF ELASTICITY IN TENSION AND COMPRESSION OF A LARGE FORGING OIL QUENCHED AND TEMPERED AT 575 F (20)

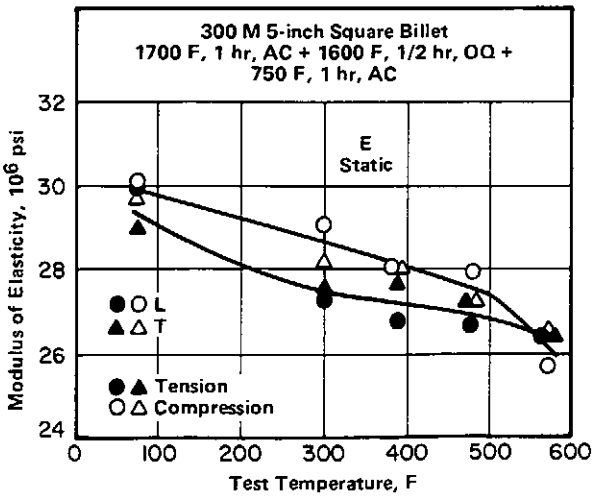


FIGURE 3.0622. EFFECT OF ELEVATED TEMPERATURES ON MODULUS OF ELASTICITY DETERMINED IN BOTH TENSION AND COMPRESSION ON A VACUUM-ARC MELTED BILLET OIL QUENCHED AND TEMPERED AT 750 F (12)

	Fe
0.43	C
1.8	Ni
1.6	Si
0.8	Cr
0.4	Mo
+	V

300 M

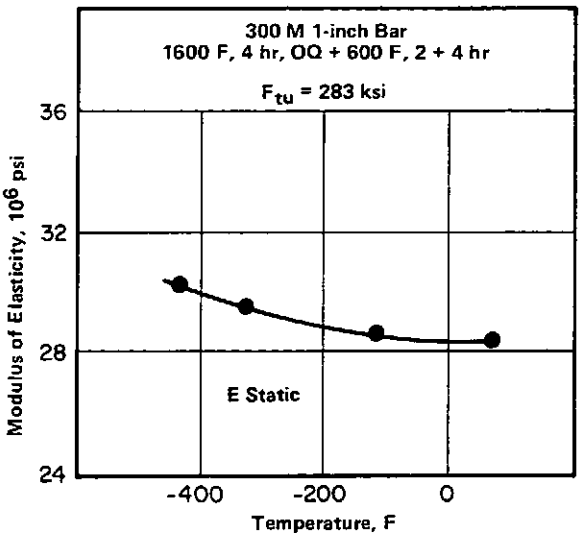


FIGURE 3.0623. EFFECT OF LOW TEMPERATURES ON MODULUS OF ELASTICITY OF BAR (44)

Alloy	300 M			
Form	Tube, 5-1/2 Inch OD x 3/4 Inch Wall			
Condition	Oil Quench and Temper (400 F) After Welding			
	F_{ty}, ksi	F_{tu}, ksi	e (4D), percent	RA, percent
Parent Metal	270.0	302.5	9	18
Across Weld	246.0	285.6	3	7

TABLE 4.032. COMPARISON OF TENSILE PROPERTIES OF PARENT METAL AND FLASH-BUTT WELD JOINT (NO FILLER METAL) IN TUBING (28)

Fe
18 Cr
8 Ni

Type 301
Type 302

1.061 Substantial hardening can be produced in metastable austenitic steels such as Types 301 and 302 by deformation below the M_d temperature (highest temperature for deformation-induced martensitic transformation) to produce alpha-prime martensite. Type 301 is less stable than Type 302 and produces more martensite and greater hardening, as shown in Figures 1.062 and 1.063. Essentially no martensite is produced in either steel on deformation at 330 F, but martensite is produced in both steels by deformation at or below room temperature. Cooling to liquid-nitrogen temperature (-320 F) without deformation produces about 12 percent alpha-prime martensite in Type 301 and 4 percent in Type 302. For a given degree of deformation applied at various temperatures, the hardness is linearly related to the content of strain-induced alpha-prime martensite, as shown in Figure 1.064. Short-time (2 minute) annealing at elevated temperatures causes reductions in both amount of martensite and hardness, as shown in Figures 1.065 and 1.066. It is concluded from these data that the A_{c1} temperature for both steels is in the range 1020 to 1110 F. The A_{c3} temperature for Type 301 is 1380 to 1470 F and for Type 302 is 1290 to 1380 F (55).

1.062 Hardness and martensite contents of Type 301 after rolling to various reductions at 330 F to -320 F, Figure 1.062.

1.063 Hardness and martensite contents of Type 302 after rolling to various reductions at 330 F to -320 F, Figure 1.063.

1.064 Effect of strain-induced martensite content on hardness, Figure 1.064.

1.065 Hardness and martensite contents of Type 301 after cold rolling followed by heat treatment at 1020 to 1560 F, Figure 1.065.

1.066 Hardness and martensite contents of Type 302 after rolling followed by heat treatment at 1020 to 1560 F, Figure 1.066.

1.067 Effect of extrusion temperature on hardness, Figure 1.067.

1.068 AISI typical values for hardness, Table 1.068.

1.069 Effect of low test temperature on hardness of extra-hard cold-rolled sheet, Figure 1.069.

1.0610 Effect of aging temperature on hardness of 67 percent cold-rolled sheet, Figure 1.0610.

1.0611 Effect of hydrogen environment at elevated temperature on surface hardness of half-hard sheet, Figure 1.0611.

1.07 **Forms and Conditions Available**

1.071 Alloy is available in the full commercial range of sizes and conditions for various forms as follows:

1.0711 Type 301 sheet with strip, annealed, 1/4 H, 1/2 H, 3/4 H, full H, extra H, and stress-relieved tempers.

1.0712 Type 302 bar, annealed and two standard tempers.

1.0713 Type 302 wire, annealed and three standard tempers.

1.08 **Melting and Casting Practice**

Electric furnace air melt. Induction and consumable-electrode vacuum melts and remelts are also available. Vacuum-arc and electroslag consumable-electrode remelting are used where high cleanliness and low gas content are required (57).

1.09 **Special Considerations**

1.091 Types 301 and 302 become subject to severe intergranular corrosion after heating in the temperature range 800 to 1500 F. This sensitization, which also occurs after welding, is attributed to precipitation of chromium carbide at the grain boundaries which causes depletion of chromium from the matrix in the intergranular regions. Corrosion resistance can be restored by annealing to re-solution the chromium carbides. See 2.032.

1.092 Improved strength properties can be obtained by cold working at cryogenic temperatures rather than at room temperature. (See Section 3.0217.)

1.093 Increased tensile ductility and drawing properties can be achieved in Type 301 by deforming at 130 to 140 F, just below the M_d temperature. The improved ductility is related to the strain-induced martensitic transformation, which increases work hardening and resistance to necking. (See Section 3.03154.)

1.094 Although these steels are generally considered to have good resistance to hydrogen embrittlement, the notch strength of Type 301 is decreased considerably in hydrogen as compared to air. Further, high contents of dissolved hydrogen in Type 301, such as obtainable by electrolytic charging, can cause crack growth under constant load. (See Section 2.034.)

1.095 The 300-grade stainless steels, including Types 301 and 302, are subject to salt-water corrosion in crevices or under deposits. Corrosion is reduced or eliminated in turbulent seawater or when cathodic protection is present. (See Section 2.0312.)

2 PHYSICAL AND CHEMICAL PROPERTIES

2.01 **Thermal Properties**

2.011 Melting ranges are 2250 to 2590 F for Type 301 and 2550 to 2590 F for Type 302 (51).

2.012 Phase changes.

2.0121 Time-temperature-transformation diagrams.

2.0122 Transformation temperatures, Table 2.0122.

2.013 Thermal conductivity, Figure 2.013.

2.014 Thermal expansion: (a) Type 301, (b) Type 302, Figure 2.014.

2.015 Specific heat, Figure 2.015.

2.016 Thermal diffusivity, Figure 2.016.

2.02 **Other Physical Properties**

2.021 Density, Figure 2.021.

2.022 Electrical properties.

2.0221 Electrical resistivity, Figure 2.0221.

2.023 Magnetic properties.

2.0231 These alloys are nonmagnetic in the annealed (fully austenitic) condition. However, the alloys become magnetic on cold working due to the deformation-induced transformation from nonmagnetic austenite to magnetic alpha-prime martensite. The extent of magnetization on cold working decreases with increasing nickel content in Series 300 stainless steels, as shown in Figure

Fe
18 Cr
8 Ni

Type 301
Type 302

2.0232. This is a result of nickel stabilization of the austenite phase.

2.0232 Effect of composition and reduction on magnetic permeability and tensile strength of 300 series sheet, Figure 2.0232.

2.024 Emittance, Figure 2.024.

2.025 Damping capacity.

2.03 **Chemical Environments**

2.031 General corrosion.

2.0311 General corrosion resistance of Type 301, like that of all austenitic stainless steels, is very high, but it is at the lower end of the corrosion scale for 18-8 steels; Type 302 is slightly superior to Type 301.

2.0312 The 300 series stainless steels can undergo deep localized crevice corrosion in mechanical crevices or under deposits in quiescent seawater. The differences in performance of the various grades of 300 stainless steels under these conditions are not of practical significance. Cathodic protection can be effectively accomplished with iron, zinc, aluminum, or magnesium anodes or by an impressed electrical current system. Multi-component assemblies containing different alloys frequently offer built-in cathodic protection. Turbulent seawater with sufficient agitation to keep austenitic stainless steels free of deposits, either biological or inorganic, permits stainless steel to remain passive and corrosion-free. Chloride stress-corrosion cracking is not a problem in ambient-temperature seawater (64).

2.0313 Corrosion in tropical environments for times up to 16 years, Table 2.0313.

2.0314 Based on galvanic current data and corrosion rates, Type 301 is considered compatible with graphite-epoxy composite materials in aerated neutral 3.5 percent NaCl solution at room temperature (66).

2.032 Intergranular corrosion.

2.0321 A potentially serious problem against which precautions should be taken is intergranular corrosion of "sensitized" alloy. Sensitization occurs when these steels are heated in the temperature range 800 to 1500 F. The sensitization time depends primarily on temperature but is also influenced by the chemical and metallurgical characteristics of the alloy, such as carbon content and grain size. Sensitization is most generally attributed to depletion of chromium from regions adjacent to the grain boundaries because of precipitation of chromium-rich $(Fe,Cr)_{23}C_6$ carbides. During welding, the heat-affected zone reaches the critical temperature range for a short time, promoting nucleation of chromium-rich carbides at the grain boundaries. If a welded component operates below the temperature range for normal sensitization (for example, 600 to 800 F), the previously nucleated carbides grow, but the low temperature prevents further nucleation and restricts chromium diffusion from the grain interiors. However, after extended time periods, such as 10 years, low-temperature sensitization occurs and increases the probability of intergranular stress-corrosion cracking. If material has been sensitized either by welding or by exposure, it should be fully annealed to re-solution the precipitated chromium-rich carbides. This anneal will restore the original corrosion resistance. Self-healing and restoration of corrosion resistance can also occur on heating for very long times in the sensitization temperature range. Self-healing occurs by diffusion of chromium from the grain interiors into the depleted zones. The time-temperature conditions for sensitization of Type 302 are shown in Figure 2.0322 (67).

2.0322 Effects of heat treatment on susceptibility to intergranular stress-corrosion cracking in polythionic acid and in acid copper sulfate, Figure 2.0322.

2.0323 Effect of prior exposure temperature and time on average corrosion rate in boiling nitric acid of cold-rolled sheet, Figure 2.0323.

2.033 Stress-corrosion cracking.

2.0331 Stress cracking may be pronounced in these steels in the formed condition, if high residual stresses are present. The tendency to stress cracking depends primarily on the value of tensile strength developed. Severely formed parts, particularly in the harder tempers of Type 301, should be immediately annealed or stress relieved to prevent cracking.

The susceptibility of cold-worked material to stress corrosion cracking may be related in part to the presence of deformation-induced martensite. The hcp epsilon martensite phase corrodes more rapidly than the matrix austenite phase (69,70).

2.0332 Stress-corrosion cracking may occur in certain media, primarily in hot chlorides, if residual stresses are present. Under normal atmospheric conditions no stress corrosion is observed, even in extra hard sheet. Stress-corrosion cracking can result, for example, from surface contamination with zinc chloride from solder flux (71,72).

2.0333 Effects of cold reduction on yield stress in air and on threshold corrosion stress in boiling 0.5N NaCl + 0.1N $NaNO_2$ aqueous solution, Figure 2.0333.

2.034 Hydrogen embrittlement.

2.0341 Although austenitic stainless steels are generally considered to have good resistance to hydrogen embrittlement, the notch tensile strength of Type 301 is reduced considerably when tested in hydrogen rather than in air. The detrimental effect is lessened when oxygen is present as an impurity in the hydrogen atmosphere, as shown in Figure 2.0342. Oxygen reacts with surface adsorption sites and, if in sufficient quantity, will completely inhibit the adsorption of hydrogen and thus prevent embrittlement (74).

2.0342 Effects of oxygen impurity in hydrogen on notch strength of Type 301, Figure 2.0342.

2.0343 Sustained-load crack growth is observed in material charged to 13 wt ppm hydrogen or more, as shown in Figure 2.0344. The crack-growth rate at a given stress intensity factor increases strongly with increasing hydrogen content. The fracture surface of material which has failed by slow crack growth exhibits brittle transgranular cleavage. Material containing less than 3 wt ppm hydrogen exhibits ductile fracture upon reaching a critical load and

Fe
18 Cr
8 Ni

Type 301
Type 302

does not exhibit slow crack growth. Although the levels of dissolved hydrogen which cause sustained-load crack growth are higher than would normally be encountered in service, it is evident that some reduction of ductility in Type 301 can be affected by hydrogen (73).

2.0344 Sustained-load crack-growth rate of hydrogen-charged Type 301, Figure 2.0344.

2.035 Oxidation.

2.0351 Air oxidation of Type 302 is slight at 1202 and 1292 F, as shown in Figure 2.0352. There is no subsurface oxide penetration at these temperatures. At 1382 F oxide penetration occurs but the surface oxide is still quite protective. Oxidation begins to increase sharply with temperature above 1472 F and the time dependence on an arithmetic basis approaches linearity at 1562 F, indicating a nonprotective scale. Type 302 is considered suitable for continuous service at temperatures up to 1600 F and for intermittent service up to 1700 F (75).

2.0352 Time dependence of oxidation of Type 302 in air at elevated temperatures, Figure 2.0352.

2.04 **Nuclear Environments**

2.041 Effect of irradiation exposure on tensile properties and hardness of alloy, Table 2.041.

3 **MECHANICAL PROPERTIES**

3.01 **Specified Mechanical Properties**

3.011 AMS-specified mechanical properties, Table 3.011.

3.02 **Mechanical Properties at Room Temperature**

3.021 Tension – stress-strain diagrams – tension properties.

3.0211 Stress-strain curves for sheet and strip cold rolled to different temper, Figure 3.0211.

3.0212 Stress-strain curves for sheet and strip cold rolled to full-hard and extra-hard tempers, Figure 3.0212.

3.0213 Percentage cold reduction and corresponding tensile strength for various tempers of Type 301 and Type 302, Table 3.0213.

3.0214 Effect of rolling reduction and composition on tensile properties of 300 series steels, Figure 3.0214.

3.0215 Effect of cold reduction on tensile properties of Type 301, Figure 3.0215.

3.0216 Effects of cold work on tensile properties of Type 302, Figure 3.0216.

3.0217 Cold working at cryogenic temperatures increases the tensile strength to a greater degree than equivalent working at room temperature. The ductility of material cryogenically rolled to a given strength is higher than that of material rolled at room temperature to the same strength, as shown in Figures 3.0218 and 3.0219. The effects of cold rolling on tensile properties are primarily through the amount of martensite produced. The amount of cold work introduced into the matrix has an additional strengthening effect, as shown in Figures 3.02110 and 3.02111. Heat treating cold-worked material at 550 F further increases the yield strength, as shown in Figures 3.02112 and 3.02113.

3.0218 Effect of cold reduction at room and cryogenic temperatures on tensile properties of Type 301, Figure 3.0218.

3.0219 Effect of cold reduction at room and cryogenic temperatures on tensile properties of Type 302, Figure 3.0219.

3.02110 Relationship between tensile properties and martensite content for Type 301, Figure 3.02110.

3.02111 Relationship between tensile properties and martensite content for Type 302, Figure 3.02111.

3.02112 Effect of cold reduction at room and cryogenic temperatures plus heat treatment on tensile properties of Type 301, Figure 3.02112.

3.02113 Effect of cold reduction at room and cryogenic temperatures plus heat treatment on tensile properties of Type 302, Figure 3.02113.

3.02114 Effect of stress-relief temperature on tensile properties of 60 percent reduced sheet, Figure 3.02114.

3.02115 Effect of cyclic exposure stress on room-temperature tensile properties of 60 percent reduced sheet exposed at 600 and 900 F, Figure 3.02115.

3.02116 Effect of exposure at low temperature on room-temperature tensile properties of extra-hard cold-rolled sheet, Figure 3.02116.

3.02117 Effects of extrusion temperature on longitudinal tensile properties of Type 301, Figure 3.02117.

3.02118 Effects of extrusion temperature on longitudinal tensile properties of Type 302, Figure 3.02118.

3.02119 Effect of stretching on tensile yield strength of Type 302, Figure 3.02119.

3.022 Compression – stress-strain curves – compression properties.

3.0221 Effect of stretching on compressive yield strength of Type 302, Figure 3.0221.

3.023 Impact.

3.0231 Impact properties at room temperature, Table 3.0231.

3.0232 Relation between impact energy and tensile strength for cold-rolled Type 302, Figure 3.0232.

3.0233 Effects of exposure time in air at elevated temperatures on impact energy, Figure 3.0233.

3.024 Bending.

3.025 Torsion and shear.

3.026 Bearing.

3.027 Stress concentration.

3.0271 Notch properties.

3.02711 Effect of cold rolling and test direction on notch strength of sheet, Figure 3.02711.

3.02712 Effect of exposure at low temperature on room-temperature notch strength of extra-hard cold-rolled sheet, Figure 3.02712.

3.02713 Effect of test direction in relation to rolling direction on tensile properties and notch strength of 60 percent cold-reduced sheet, Figure 3.02713.

3.0272 Fracture toughness.

3.028 Combined properties.

3.03 **Mechanical Properties at Various Temperatures**

3.031 Tension – stress-strain curves – tension properties.

3.0311 Stress-strain curves.

3.03111 The stress-strain curves for Types 301 and 302 are influenced by the deformation-induced transformation of austenite to martensite. The work-hardening rate (slope of the stress-strain curve) for Type 302

Fe
18 Cr
8 Ni

Type 301
Type 302

at -112 F is compared to that of the structurally stable Type 310 alloy in Figure 3.03112. Type 302 is metastable at this temperature and exhibits an increase in work-hardening rate between about 4 and 20 percent strain due to the martensitic transformation. The Type 310 alloy shows a continuous decrease in work-hardening rate with increasing strain. Stress-strain curves for annealed Types 301 and 302 at temperatures near and below M_d are shown in Figures 3.03113 and 3.03114, respectively. Both stable (continuously decreasing work-hardening rate) and metastable (decreasing and increasing work-hardening rate) curves are seen, depending on test temperature. Type 301 shows increasing work hardening due to martensite formation at 68 F and lower, while Type 302 exhibits martensitic hardening up to at least 77 F (77,78).

3.03112 Tensile work-hardening rates for Types 302 and 310 at -112 F, Figure 3.03112.

3.03113 Stress-strain curves for annealed Type 301, Figure 3.03113.

3.03114 True stress-strain curves for annealed Type 302 at room and cryogenic temperatures, Figure 3.03114.

3.03115 Stress-strain curves for Type 301 full-hard and full-hard stress-relieved sheet at room and elevated temperatures, Figure 3.03115.

3.03116 Stress-strain curves in tension for various temperatures and exposure times for 60 percent cold-reduced sheet, Figure 3.03116.

3.03117 Stress-strain curves in tension at low temperatures of extra-hard cold-rolled sheet, Figure 3.03117.

3.03118 Stress-strain curves for Type 301 extra-hard and extra-hard stress-relieved sheet at room and elevated temperatures, Figure 3.03118.

3.0312 Rolling effects on tension properties.

3.03121 Effect of cold rolling on tensile properties of Type 301 sheet at room temperature and -320 F, Figure 3.03121.

3.03122 Effect of percent reduction on tensile properties of sheet tested at room temperature and -423 F, Figure 3.03122.

3.03123 Effect of low temperature and percent cold reduction on tensile properties of sheet, Figure 3.03123.

3.03124 Effect of low rolling temperature on tensile properties at room temperature and -320 F of reduced sheet, Figure 3.03124.

3.03125 Effect of low rolling temperature on tensile properties at room temperature and -423 F of 10 percent reduced sheet, Figure 3.03125.

3.03126 Effect of rolling temperature on tensile properties at room temperature and -423 F of 65 percent reduced sheet, Figure 3.03126.

3.03127 Effect of test direction on tensile strength of cold-rolled sheet at room and cryogenic temperatures, Figure 3.03127.

3.0313 Prior exposure and strain-rate effects on tension properties.

3.03131 Tensile ductility of Types 301 and 302 is affected by strain rate, temperature, and phase stability, as well as microstructure. For constant microstructure, Type 302 exhibits a minimum in elongation at room temperature at a strain rate of about 200 min^{-1}. A similar but less pronounced minimum is noted for uniform reduction in area, as shown in Figure 3.03132. The ductility at all strain rates from 0.02 to 19,000 min^{-1} is good, ranging from 40 to 80 percent elongation. Similar behavior is exhibited at liquid-nitrogen temperature, with the ductility values being slightly less than those at room temperature, as shown in Figure 3.03133. Type 301 is less stable than Type 302 with respect to martensite formation during deformation and has slightly less ductility at room temperature, as shown in Figure 3.03134 (80).

3.03132 Effects of strain rate on tensile ductility of Type 302 at room temperature, Figure 3.03132.

3.03133 Effects of strain rate on tensile ductility of Type 302 at -321 F, Figure 3.03133.

3.03134 Effects of strain rate on tensile ductility of Type 301 at room temperature, Figure 3.03134.

3.03135 Effect of test temperature, strain rate, and holding time on tensile properties of Type 301 1/2-hard sheet, Figure 3.03135.

3.03136 Effect of test temperature, strain rate, and holding time on tensile properties of Type 301 3/4-hard sheet, Figure 3.03136.

3.03137 Effect of test temperature, strain rate, and holding time on tensile properties of 45 percent reduced sheet, Figure 3.03137.

3.03138 Effect of test temperature, strain rate, and holding time on tensile properties of 60 percent reduced sheet, Figure 3.03138.

3.03139 Effect of test temperature and exposure time on tensile properties of 60 percent cold-reduced sheet, Figure 3.03139.

3.031310 Effect of test temperature and prior exposure on tensile properties of 34 percent cold-reduced sheet, Figure 3.031310.

3.031311 Effect of test temperature and prior exposure on tensile properties of 51 percent cold-reduced sheet, Figure 3.031311.

3.031312 Effect of test temperature and prior exposure on tensile properties of 60 percent cold-reduced sheet, Figure 3.031312.

3.0314 Stress-relief effects on tension properties.

3.03141 Effect of test temperature, test direction, and stress relief on tensile properties of Type 301 full-hard sheet, Figure 3.03141.

3.03142 Effect of test temperature, test direction, and stress relief on tensile properties of Type 301 extra-hard sheet, Figure 3.03142.

3.03143 Effect of stress relief and test temperature on tensile properties of cold-rolled sheet, Figure 3.03143.

3.0315 Elevated-test-temperature effects on tension properties.

3.03151 Effect of test temperature on tensile strength of annealed Type 302 sheet, Figure 3.03151.

3.03152 Effect of test temperature on tensile properties of Type 301 1/2-hard sheet, Figure 3.03152.

3.03153 Effect of test temperature on tensile properties of 60 percent reduced sheet, Figure 3.03153.

3.03154 Type 301 shows a tensile elongation peak at about 130 F, as shown in Figure 3.03155. The maximum elongation is slightly greater for small-grain-size material and slower deformation rate, but the temperature effect remains unchanged. As shown in Figure 3.03156, the temperature for maximum

Fe
18 Cr
8 Ni

Type 301
Type 302

elongation appears to be slightly higher in biaxial straining as compared to uniaxial straining. The elongation peak is related to the strain-induced transformation of austenite to cubic alpha-martensite, which occurs through an intermediate hexagonal epsilon-martensite phase. The volume fraction of epsilon compared to alpha is negligible above about 15 percent strain. The strain-induced martensitic transformation increases the rate of work hardening so that the material is better able to resist necking during straining. The occurrence of a sharp elongation peak at a temperature just below M_d apparently indicates that the distribution of strain-induced martensite is most uniform at this temperature. The temperature dependence of martensite content for Type 301 is shown in Figure 3.03157. The strain dependence of martensite content for Types 301 and 302 is sigmoidal, as shown in Figures 3.03158 and 3.03159. The amount of martensite formed, for example, at 32 F is much greater for Type 301 than for Type 302, reflecting the lower phase stability of Type 301.

3.03155 Effects of grain size, strain rate, and temperature on tensile elongation of Type 301, Figure 3.03155

3.03156 Effects of temperature on failure strain for several types of deformation, Figure 3.03156.

3.03157 Effects of grain size, strain rate, and temperature on martensite content of fractured tensile specimens of Type 301, Figure 3.03157.

3.03158 Effects of grain size, test temperature, and tensile strain on martensite content of Type 301, Figure 3.03158.

3.03159 Effects of test temperature and true tensile strain on martensite content of Type 302, Figure 3.03159.

3.031510 Effects of temperature on tensile properties of cast Type 302, Figure 3.031510.

3.0316 Effects of cryogenic temperatures on tensile properties.

3.03161 Effect of cryogenic temperatures on nominal tensile properties of annealed Type 301 sheet, strip, plate, and bar, Figure 3.03161.

3.03162 Effect of cryogenic temperatures on nominal tensile properties of annealed Type 302 sheet, strip, plate, and bar, Figure 3.03162.

3.03163 Effect of cryogenic temperatures on the tensile properties of annealed bar, Figure 3.03163.

3.03164 Effect of cryogenic temperatures on tensile properties of 40 percent reduced sheet, Figure 3.03164.

3.03165 Effect of cryogenic temperatures on tensile properties of 50 percent reduced sheet, Figure 3.03165.

3.03166 Effect of cryogenic temperatures on tensile properties of 40 and 60 percent reduced sheet, Figure 3.03166.

3.03167 Effect of cryogenic temperatures on tensile properties of 60 percent cold-reduced sheet, Figure 3.03167.

3.03168 Effects of cryogenic temperatures and thickness on tensile properties of 60 percent reduced sheet, Figure 3.03168.

3.03169 Effect of cryogenic temperatures on tensile properties of extra-hard cold-rolled sheet, Figure 3.03169.

3.031610 Effects of cryogenic temperatures and melt method on tensile properties of 70 percent reduced sheet, Figure 3.031610.

3.032 Compression – stress-strain diagrams – compression properties.

3.0321 Stress-strain diagrams.

3.03211 Stress-strain curves in compression for Type 301 annealed sheet at elevated temperatures, Figure 3.03211.

3.03212 Stress-strain curves in compression for Type 301 full-hard and full-hard stress-relieved sheet at room and elevated temperatures, Figure 3.03212.

3.03213 Stress-strain curves in compression for Type 301 extra-hard and extra-hard stress-relieved sheet at room and elevated temperatures, Figure 3.03213.

3.0322 Effect of test temperature on compressive yield strength of Type 301 annealed sheet, Figure 3.0322.

3.0323 Effect of test temperature and test direction on compressive yield strength of Type 301 1/2-hard sheet, Figure 3.0323.

3.0324 Effect of test temperature on compressive yield strength of 45 and 60 percent reduced sheet, Figure 3.0324.

3.0325 Effect of test temperature and exposure time on compressive yield strength of 60 percent cold-reduced sheet, Figure 3.0325.

3.0326 Effect of test temperature, test direction, and stress relief on compressive yield strength of Type 301 full-hard and extra-hard sheet, Figure 3.0326.

3.0327 Effect of test temperature on compressive strength of annealed Type 302 sheet, Figure 3.0327.

3.033 Impact.

3.0331 Impact energy of Type 301 plate at room and cryogenic temperatures, Figure 3.0331.

3.0332 Impact energy of Type 301 bar at room and cryogenic temperatures, Figure 3.0332.

3.0333 The impact energy of heat-treated cast Type 302 (CF-20) decreases with decreasing test temperature, as shown in Figure 3.0334. Carbide precipitation, caused by heat treating in the sensitizing temperature range, lowers the impact energy at cryogenic temperatures (83).

3.0334 Effect of sensitizing heat treatments on the impact energy of cast Type 302 at cryogenic temperatures, Figure 3.0334.

3.034 Bending.

3.035 Torsion and shear.

3.0351 Effect of test temperature on shear strength of Types 301 and 302, Figure 3.0351.

3.0352 Effect of test temperature and exposure time on shear strength of 60 percent cold-reduced sheet, Figure 3.0352.

3.036 Bearing.

3.0361 Effect of test temperature on bearing properties of Types 301 and 302 sheet, Figure 3.0361.

3.0362 Effect of test temperature and exposure time on bearing properties of 60 percent cold-reduced sheet, Figure 3.0362.

3.037 Stress concentration.

3.0371 Notch properties.

3.03711 Rolling effects on notch properties.

3.037111 Effect of rolling temperature on notch strength at room temperature and -423 F of 10 percent reduced sheet, Figure 3.037111.

Fe
18 Cr
8 Ni

Type 301
Type 302

3.037112 Effect of low rolling temperature on notch strength at room temperature and -423 F of 10 percent reduced sheet, Figure 3.037112.

3.037113 Effect of low temperature and percent cold reduction on notch strength of sheet, Figure 3.037113.

3.037114 Effect of low temperature and percent cold reduction on notch strength of various percent reduced sheet, Figure 3.037114.

3.037115 Effect of percent cold reduction on notch strength of sheet tested at room temperature and -320 F, Figure 3.037115.

3.037116 Effect of percent cold reduction on notch strength of sheet tested at room temperature and -423 F, Figure 3.037116.

3.03712 Prior exposure and rate of loading effects on notch strength.

3.037121 Effect of test temperature and prior exposure on notch properties of 60 percent cold-reduced sheet, Figure 3.037121.

3.037122 Effect of test temperature and exposure time on notch strength of 60 percent cold-reduced sheet, Figure 3.037122.

3.037123 Effect of test temperature and prior exposure on notch properties of 34 percent cold-reduced sheet, Figure 3.037123.

3.037124 Effect of stress concentration factor, temperature, and loading rate on notch strength of extra-hard cold-rolled sheet, Figure 3.037124.

3.03713 Stress-relief effects on notch strength.

3.037131 Effect of stress relief and low test temperature on notch strength of Type 301 sheet, Figure 3.037131.

3.03714 Crack effects on notch strength.

3.037141 Effect of test temperature on net fracture stress of full-hard sheet, Figure 3.037141.

3.037142 Effect of percent cold reduction on edge-cracked properties of sheet at room temperature and -110 F, Figure 3.037142.

3.03715 Low-test-temperature effects on notch strength.

3.037151 Effect of low test temperature on notch strength of 60 percent cold-reduced sheet, Figure 3.037151.

3.037152 Effect of low temperature on notch strength of extra-hard cold-rolled sheet, Figure 3.037152.

3.037153 Effect of low test temperature on notch strength of 40 and 60 percent reduced Type 302 sheet, Figure 3.037153.

3.037154 Effect of low test temperature on notch strength of 50 percent reduced sheet, Figure 3.037154.

3.037155 Effect of low test temperature on notch strength of 40 percent reduced sheet, Figure 3.037155.

3.037156 Effect of low test temperature and thickness on notch strength of 60 percent reduced sheet, Figure 3.037156.

3.037157 Effect of low test temperature on notch strength of 70 percent reduced vacuum-melt sheet, Figure 3.037157.

3.037158 Effect of low test temperature on notch strength of 70 percent reduced air-melt sheet, Figure 3.037158.

3.0372 Fracture toughness.

3.03721 Effect of low test temperature on fracture toughness of 60 percent cold-reduced sheet, Figure 3.03721.

3.03722 Effect of initial notch length on fracture toughness of 60 percent cold-reduced sheet at room temperature, -320, and -423 F, Figure 3.03722.

3.03723 The crack strength of Type 302 sheet is significantly affected by orientation with respect to the rolling direction, as shown in Figure 3.03724. At an angle of 90 degrees to the rolling direction, or transverse, the crack strength is about 10 percent less at room temperature and 34 percent less at -320 and -423 F than at 0 degrees to the rolling direction. However, the crack strength at an angle of 11 degrees to the rolling direction is not degraded. The 11-degree angle equals the helix angle at which some liquid-propellant rocket tanks have been spiral welded (79).

3.03724 Effects of center crack and test direction on tensile strength of cold-rolled sheet at room and cryogenic temperatures, Figure 3.03724.

3.04 **Creep and Creep Rupture Properties**

3.041 Creep curves for Type 302 annealed sheet at 1200 to 1600 F, Figure 3.041.

3.042 Short-time total strain curves for annealed Type 302 at 1200 to 1800 F, Figure 3.042.

3.043 Creep and creep-rupture curves for Type 301 1/2-hard sheet at 1200 to 1500 F, Figure 3.043.

3.044 Creep-rupture curves for Type 301 full-hard and stress-relieved sheet at 800 to 1200 F, Figure 3.044.

3.045 Creep-rupture curves for Type 301 extra-hard and stress-relieved sheet at 800 to 1200 F, Figure 3.045.

3.046 Creep curves for Type 301 60 percent reduced sheet under cyclic load at 600 and 900 F, Figure 3.046.

3.047 Creep and creep rupture curves for Type 301 60 percent reduced sheet at 600 and 900 F, Figure 3.047.

3.048 Creep and creep-rupture curves for 80 percent cold-reduced sheet at 1000, 1200, and 1400 F, Figure 3.048.

3.049 Creep-rupture properties of cast Type 302, Figure 3.049.

3.0410 Stress relaxation at room and slightly elevated temperatures, Figure 3.0410.

3.05 **Fatigue Properties**

3.051 Cyclic stress-strain curves for annealed Type 301 at temperatures between M_s and M_d, Figure 3.051.

3.052 Strain-controlled fatigue behavior of annealed rod at room temperature, Figure 3.052.

3.053 Bending fatigue behavior of cold-worked and of annealed sheet at room temperature, Figure 3.053.

3.054 S-N curves in flexure for extra-full-hard sheet at low temperatures, Figure 3.054.

3.055 Axial tension fatigue behavior of smooth and notched sheet at room and cryogenic temperatures, Figure 3.055.

3.056 Aging for up to 26,300 hours at 550 F has little effect on the room-temperature fatigue behavior of smooth or notched Type 301, as seen by comparison of Figures 3.057 and 3.058 (89,90).

3.057 Effects of notches on fatigue behavior of sheet, Figure 3.057.

3.058 Fatigue behavior of smooth and notched sheet at room temperature after aging for 26,300 hours at 550 F, Figure 3.058.

3.059 Low cycle S-N curves for complex welded joints of 60 percent cold-rolled sheet, Figure 3.059.

Fe
18 Cr
8 Ni

Type 301
Type 302

3.0510 S-N curves for uniaxial and biaxial sheet for R = 0.50, Figure 3.0510.

3.0511 S-N curves for uniaxial and biaxial sheet for R = 0.10, Figure 3.0511.

3.0512 Effects of fusion and spot welding on fatigue behavior of sheet, Figure 3.0512.

3.0513 Fatigue behavior of welded sheet at room temperature after aging for 26,300 hours at 550 F, Figure 3.0513.

3.0514 Type 301 alloy is unstable under stress, with the austenite phase transforming martensitically to alpha-prime to a much greater extent than the more stable Type 302 alloy. This stress-induced martensitic phase transformation can lead to remarkable work hardening. The effect of martensite formation on the fatigue crack-growth rate (FCGR) is shown in Figure 3.0515. For annealed material cycled to a maximum stress of 10.9 ksi, the FCGR of Type 301 is only about one-half that of Type 302. However, at a higher maximum stress of 21.5 ksi or in the 19 percent cold-worked condition (shown in Figure 3.0516), the two alloys have similar FCGR's. The difference in FCGR's for the annealed materials at low stress is related to alloy stability. The less stable Type 301 alloy forms more martensite during loading, resulting in greater work hardening and a lower FCGR. Cold rolling of annealed strip from 0.060 in. thick to reductions of 20, 27, and 40 percent resulted in formation of 10, 20, and 30 vol percent alpha-prime martensite in Type 301 and 0.5 to 2.5 vol percent in Type 302, as determined by magnetic measurements (59).

3.0515 Fatigue crack-growth behavior at room temperature for Types 301 and 302 annealed sheet tested at two different stress levels, Figure 3.0515.

3.0516 Fatigue crack-growth behavior at room temperature for Types 301 and 302 cold-rolled sheet tested at two different stress levels, Figure 3.0516.

3.0517 Fatigue crack-growth rates in hydrogen are more rapid than those in argon or in air. The enhancement is greater in Type 301 than in Type 302 because of hydrogen embrittlement of the alpha-prime martensite phase, which forms to a greater extent in Type 301. At a maximum stress of 18.3 ksi, the FCGR for Type 301 is higher by a factor of about six in hydrogen as compared to air, while the factor for the more stable Type 302 alloy is about three. At a slightly higher maximum stress of 19.8 ksi, rates for the two alloys are almost identical in argon but Type 301 is inferior to Type 302 in hydrogen, as shown in Figures 3.0518 and 3.0519. The FCGR's are decreased by cold work in both argon and hydrogen, but cold-worked alloys are more degraded by hydrogen than annealed alloys (90). The FCGR in hydrogen is thought to be controlled by the rate of supply of hydrogen to the highly stressed region ahead of the crack. Hydrogen permeability has been shown to be greater in Type 301 than Type 302 in the temperature range 400 to 600 F. Also, the permeability of hydrogen is increased under stress for Type 302. These factors are consistent with the above observation on enhancement of FCGR's by hydrogen (91,92).

3.0518 Fatigue crack-growth behavior at room temperature for Types 301 and 302 annealed sheet tested in dry hydrogen, dry argon, and air, Figure 3.0518.

3.0519 Fatigue crack-growth behavior at room temperature for annealed and cold-worked sheet tested in argon and in hydrogen, Figure 3.0519.

3.06 **Elastic Properties**

3.061 Poisson's ratio.

3.062 Modulus of elasticity.

3.0621 Modulus of elasticity for Type 301 1/2-hard sheet at room and elevated temperatures, Figure 3.0621.

3.0622 Modulus of elasticity in tension for Type 301 full-hard and extra-hard sheet, Figure 3.0622.

3.0623 Effect of low test temperature on modulus of elasticity for 60 percent reduced sheet, Figure 3.0623.

3.0624 Effect of test temperature, strain rate, and holding time on modulus of elasticity in tension of 45 and 60 percent reduced sheet, Figure 3.0624.

3.0625 Effect of temper on modulus of elasticity in tension and compression for Type 301 sheet, Figure 3.0625.

3.0626 Modulus of elasticity in compression for Type 301 full-hard and extra-hard sheet, Figure 3.0626.

3.0627 Effect of test temperature on modulus of elasticity in compression of 45 and 60 percent reduced sheet, Figure 3.0627.

3.063 Modulus of rigidity.

3.0631 Modulus of rigidity, Figure 3.0631.

3.0632 Effects of cold reduction and temperature on modulus of rigidity, Figure 3.0632.

3.064 Tangent modulus.

3.0641 Tangent modulus curves in compression for Type 301 sheet in various conditions, Figure 3.0641.

3.0642 Tangent modulus curves for 60 percent cold-reduced sheet for various exposure times and temperatures, Figure 3.0642.

4 FABRICATION

4.01 Forming

4.011 General. Although Types 301 and 302 in annealed condition possess a tensile strength relatively high compared to that of other ductile metals, they are readily formable because of their low yield strength. In fact, the high elongation of Type 301 permits particularly severe forming in certain operations, such as bending, stretch forming, and deep drawing. On the other hand, their high rate of strain hardening leads to a large springback which increases with increasing temper conditions, to a pronounced tendency to buckle and wrinkle under compressive strains, and to considerable difficulties in removing distortions. These characteristics call for forming techniques which differ slightly from those used for other metals. The forming of sheet becomes necessarily more difficult with increasing temper; 1/4-hard sheet can still be fabricated readily by many forming techniques, while the forming of 3/4-hard and full-hard sheet is restricted primarily to straight bending.

Stress cracking of deep drawn and spun sheet parts occurs if the resulting local hardening and residual

stresses are high. Such parts require immediate stress relief by full annealing.

4.012 Bending and stretching.

4.0121 Practical bend factors for sheet, Table 4.0121.

4.0122 For effect of stretching on yield strength, see Figures 3.02119 and 3.0221.

4.013 Forging. Starting temperature 2300 F maximum, finishing temperature 1500 F, minimum.

4.014 Deep drawing is enhanced under thermal conditions depressing the amount of strain-induced martensite formed (see Figure 3.03156).

4.015 Extrusion. For effect of extrusion temperature on tensile properties, see Figures 3.02117 and 3.02118.

4.02 **Machining and Grinding**

Because of their high rate of strain hardening, 18-8 stainless steels require maximum feed at relatively low sulface speeds during machining operations. Their high strength necessitates the use of rigid supports of both the tools and the work and very sharp tools. Their turning speeds are approximately 50 percent of those for mild carbon steels. A highly concentrated sulfur-base oil in ample quantity should be used as a coolant.

4.03 **Joining**

4.031 These steels can be readily welded by all techniques, but the weld and heat-affected zone becomes susceptible to intergranular corrosion, unless annealed after welding. For fusion welding, Type 308 electrodes or filler rod are generally used.

4.032 Hard tempers of Type 301 sheet are generally unsuitable for fusion welding and brazing. However, spot welding is possible in hard tempers. Cracking in spot welds can be greatly reduced by the introduction of nickel foil between the faying surfaces. The effect of nickel is to reduce martensite formation in the spot-weld region.

4.05 **Surface Treatment**

4.051 Cleaning. These steels exhibit maximum corrosion resistance only when thoroughly clean, as the corrosion resistance depends on maintaining a thin dense film of chromium oxide. Both preventive measures and removal of all foreign matter from the surfaces by conventional cleaning methods prior to any heating are particularly important.

4.052 Descaling is generally done in a solution of nitric and hydrofluoric acids. Molten caustic soda baths are also widely used for descaling. For removing heavy scale, sand or vapor blasting should precede pickling.

REFERENCES

1 AMS 5515H (April 1, 1985).

2 AMS 5516J (April 1, 1985).

3 AMS 5517G (July 1, 1984).

4 AMS 5518F (July 1, 1984).

5 AMS 5519H (October 1, 1984).

6 AMS 5536C (October 1, 1981).

7 AMS 5637D (October 1, 1981).

8 AMS 5688G (January 15, 1981).

9 AMS 5358 (January 1, 1984).

10 American Iron and Steel Institute, "Stainless and Heat Resisting Steels", Steel Products Manual, pp 22–23 (June 1957).

11 Allegheny Ludlum Steel Corporation, "High Strength Cold Rolled Stainless Steels", Data Sheet (1958).

12 North American Aviation, Inc., "Stainless Steel – Type 301", Data Sheet AL-2604 (1957).

13 American Casting Institute, "Corrosion Resistant Type CF-20", Data Sheet (June 1954).

14 Lucks, C. F., and Deem, H. W., "Thermal Properties of Thirteen Metals", ASTM STP No. 227 (February 1958).

15 Favor, R. J., Achbach, W. P., and Hyler, W. S., "Materials – Property – Design Criteria for Metals, The Conventional Short-Time Elevated-Temperature Properties of Selected Stainless Steels and Super Alloys", WADC TR 55-150, Pt. 5, ASTIA Doc. No. AD 142069 (October 1957).

16 Miller, J., Smith, L. W., and Porter, P. K., "Utilization of Low Alloy Materials for High Temperature Service Applications", AF TR No. 5929 (June 1959).

17 Roe, W. P., and Kattus, J. R., "Tensile Properties of Aircraft Structural Metals at Various Rates of Loading After Rapid Heating", WADC TR 55-199, Pt. III, ASTIA Doc. No. AD 142003 (September 1957).

18 NASA, E-502 (1959).

19 Miller, D. E., "Determination of the Tensile, Compressive and Bearing Properties of Ferrous and Non-Ferrous Structural Sheet Materials at Elevated Temperatures", Armour Research Foundation, AF TR No. 6517, Pt. V (December 1957).

20 Watter, M., and Lincoln, R. A., "Strength of Stainless Steel Structural Members as Function of Design", Allegheny Ludlum Steel Corporation (1950).

21 Goldsmith, A., Hirschhorn, H. J., and Waterman, T. E., "Thermophysical Properties of Solid Materials", Vol II – Alloys, WADC TR 58-476 (November 1960).

22 International Nickel Co. (1949).

23 "Compilation of Materials Research Data", MRG-307, General Dynamics Astronautics (April 4, 1962).

24 "Compilation of Materials Research Data", MRG-244, General Dynamics Astronautics (February 12, 1962).

25 "Compilation of Materials Research Data", MRG-298, General Dynamics Astronautics (March 12, 1962).

26 "Compilation of Materials Research Data", MRG-247, General Dynamics Astronautics (August 14, 1961).

27 "Compilation of Materials Research Data", MRG-269, General Dynamics Astronautics (October 31, 1961).

28 "USS 301: A Standard AISI Type Stainless Steel Cold-Reduced to Higher Properties for Aircraft and Missiles", United States Steel Corp. (June 1959).

29 Steir, H., Turner, H. C., and Sutherland, W. M., "Material – Aluminum, Columbium, Magnesium, Nickel Base, Stainless Steel and Titanium Alloys – Effect of Hydrogen Environment at 400 to

Fe
18 Cr
8 Ni

Type 301
Type 302

Fe
18 Cr
8 Ni

Type 301
Type 302

2400 F", General Dynamics, Report No. 8926-010 (January 23, 1961).

30 Morrison, J. D., and Kattus, J. R., "An Investigation of Methods for Determining the Crack Propagation Resistance of High Strength Alloys", Southern Research Institute (January 1961).

31 Watson, J. R., and Christian, J. L., "Low-Temperature Properties of Cold-Rolled AISI Types 301, 302", presented at ASTM Annual Meeting, Atlantic City (June 1960).

32 Rue, L. P., Campbell, J. E., and Simmons, W. F., "The Evaluation and the Effects of Very Low Temperatures on the Properties of Aircraft and Missile Metals", WADD-TR-60-254 (February 1960).

33 DiSisto, T. S., and Carr. F. L., "Low Temperature Mechanical Properties of 300 Series Stainless Steels and Titanium", Watertown Arsenal Laboratories (December 1961).

34 Hanson, M. P., "Smooth and Sharp-Notch Tensile Properties of Cold-Reduced AISI 301 and 304L Stainless Steel Sheet at 75°, -320° and -423°F", NASA TN D-592 (February 1961).

35 Shober, F. R., "The Effect of Nuclear Radiation on Structural Metals", DMIC Report 166 (September 15, 1961).

36 Christian, J. L., "Physical and Mechanical Properties of Pressure Vessel Materials for Application in a Cryogenic Environment", ASD-TDR-62-258 (March 1962).

37 Christian, J. L., and Hurlich, A., "Physical and Mechanical Properties of Pressure Vessel Materials for Application in a Cryogenic Environment", ASD-TDR 62-258, Part II (April 1963).

38 Lemcoe, M. M., and Trevim, A., Jr., "Determination of the Effects of Elevated Temperature Materials Properties of Several High Temperature Alloys", ASD-TDR-61-529 (June 1962).

39 Favor, R. J., et al., "Investigation of Fatigue Behavior of Certain Alloys in the Temperature Range Room Temperature to -423 F", WADD TR 61-132 (June 1961).

40 Wood, W. D., Deem, H. W., and Lucks, C. F., "The Emittance of Stainless Steels", DMIC Memo 111 (June 12, 1961).

41 Slunder, C. J., "Stress Corrosion Cracking of High-Strength Stainless Steels in Atmospheric Environment", DMIC Report 158 (September 15, 1961).

42 Gideon, D. N., Favor, R. J., Koppenhofer, A., Grover, H. J., and McClure, G. M., "Investigation of Notch Behavior of Certain Alloys in the Temperature Range of Room Temperature to -423 F", ASD-TDR-62-351 (August 1962).

43 Banerjee, B. R., and Hauser, J. J., "Research and Application Engineering to Determine the Effect of Processing Variables on Crack Propagation of High-Strength Steels and Titanium", ASD-TDR-62-1034, Part I (1962).

44 Brisbane, A. W., "The Investigation of the Effects of Cooling Rate and Stress Concentration Factors on the Notch Properties of Three Sheet Alloys at Subzero Temperatures", ASD-TDR-62-930 (1962).

45 Raring, R. H., Freeman, J. W., Schultz, J. W., and Voorhees, H. C., "Progress Report of the NASA Special Committee on Materials Research for Supersonic Transports", NASA TR D-1798 (May 1963).

46 McClaren, S. W., and Best, J. H., "Low Cycle Fatigue Design Data on Materials in Multi-Axial Stress Field", RTD-TDR-63-4094 (November 1963).

47 Kattus, J. R., and McDonell, D. W., Jr., "Strength of Structural Alloys Under Rapid Heating and Loading", Proceedings from American Society for Testing Materials, Vol 60, p 928 (1960).

48 Christian, J. L., "Effects of Chemistry and Processing on the Mechanical Properties of Engineering Alloys at Cryogenic Temperatures", Metals Engineering Quarterly of ASM, Vol 4, No. 3 (August 1964).

49 Personal Communication, B. Wasil with R. L. Cook of Allegheny Ludlum Steel Corporation Research Center (October 15, 1964).

50 "Metals Handbook", Vol 1, Properties and Selection of Metals, Am. Soc. Metals, 8th Edition (1961).

51 Anonymous, "Typical Properties of Wrought Stainless Steel", *Metal Progress*, Vol 92, No. 2 (August 1967), pp 106–109, 112–115.

52 AMS 5500B (July 16, 1979).

53 AMS 5600B (October 1, 1981).

54 AMS 5693 (July 1, 1982).

55 Laptev, D. V., and West, D.R.F., "Structure and Strength of Certain Austenitic Stainless Steels After Plastic Deformation and Subsequent Annealing", *Metals Technology*, Vol 4, No. 3 (March 1977), pp 128–135.

56 McCallum, R., and Cockcroft, M. G., "The Structure and Properties of Warm Extruded Austenitic Stainless Steels", National Engineering Laboratory, East Kilbride, Scotland, NEL 517 (June 1972).

57 Bishop, H. L., Jr., "Melting and Refining Specialty Steels at Allegheny Ludlum Industries", *Metal Progress*, Vol 106, No. 3 (August 1974), pp 53–59.

58 Pineau, A. G., Van Swam, L. F., and Pelloux, R. M., "Cyclic Stress-Strain Curves of a Stainless Austenitic Steel in the M_S-M_d Range", Scripta Metallurgica, Vol 7, No. 6 (June 1973), pp 657–660.

59 Schuster, G., and Altstetter, C., "Fatigue of Annealed and Cold Worked Stable and Unstable Stainless Steels", *Metallurgical Transactions*, Vol 14A, No. 10 (October 1983), pp 2077–2084.

60 Papadakis, E. P., "Tabulation of the Coefficients of a Quadratic Function for the Thermal Expansion of Various Alloys and Other Engineering Materials", *Materials Science and Engineering*, Vol 10 (1972), pp 195–203.

61 Williams, L. R., Young, J. D., and Schmidt, E. H., "Design and Development Engineering Handbook of Thermal Expansion Properties of Aerospace Materials at Cryogenic and Elevated Temperatures", NAS 8-19 (March 30, 1967).

62 International Nickel Company, Inc., "Mechanical and Physical Properties of the Austenitic Chromium-Nickel Stainless Steels at Elevated Temperatures", Trade Literature (March 1964).

63 Clark, A. F., Childs, G. E., and Wallace, G. H., "Electrical Resistivity of Some Engineering Alloys at Low Temperatures", *Cryogenics*, Vol 10, No. 4 (August 1970), pp 295–305.

64 Moller, G. E., "The Successful Use of Austenitic Stainless Steels in Sea Water", *Society of Petroleum Engineers Journal*, Vol 17, No. 2 (April 1977), pp 101–110.

65 Southwell, C. R., and Bultman, J. D., "Corrosion of Metals in Tropical Environments: Part 10 – Final Report of Sixteen-Year Exposures", NRL-7834 (January 2, 1975).

66 Miller, B. A., and Lee, S. G., "The Effect of Graphite-Epoxy Composites on the Galvanic Corrosion of Aerospace Alloys", AFML-TR-76-121 (September 1976).

67 Sinigaglia, D., Fassina, P., Wenger, D., and Re, G., "Experimental Evaluation of a Metallurgical Model for Austenitic Stainless Steels Sensitization", *Corrosion*, Vol 38, No. 2 (February 1982), pp 92–97.

68 Cowan, R. L., II, and Gordon, G. M., "Intergranular Stress Corrosion Cracking and Grain Boundary Composition of Fe-Ni-Cr Alloys", Proceedings, International Corrosion Conference, Stress Corrosion Cracking and Hydrogen Embrittlement of Iron Base Alloys, held at Unieux-Firminy, France (June 12–16, 1973).

69 Vermilyea, D. A., "Susceptibility of Iron- and Nickel-Base Alloys to SCC in pH 2.5 H_2SO_4 at 289 C", *Corrosion*, Vol 31, No. 12 (December 1975), pp 421–424.

70 De, P. K., and Elayaperumal, K., "Preferential Corrosion of Epsilon-Martensite in Austenitic Stainless Steel", *Transactions of the Indian Institute of Metals*, Vol 28, No. 5 (October 1975), pp 380–384 and 451.

71 Truman, J. E., and Pirk, K. R., "A Note on the Corrosion Produced Under Deposits of Chlorides on Austenitic Stainless Steel", *Corrosion Science*, Vol 17, No. 1 (1977), pp 71–74.

72 Logan, H. L., and McBee, M. J., "Stress-Corrosion Cracking of Cold-Reduced Austenitic Stainless Steels", *Materials Research and Standards*, Vol 7, No. 4 (April 1967), pp 137–145.

73 Singh, S., and Altstetter, C., "Effects of Hydrogen Concentration on Slow Crack Growth in Stainless Steels", *Metallurgical Transactions*, Vol 13A, No. 10 (October 1982), pp 1799–1808.

74 Kesterson, R. L., "Effects of Irradiation and Oxygen on Hydrogen Environment Embrittlement of Selected Alloys", Paper presented at the 75th Annual Meeting of the American Society for Testing Materials, Los Angeles, California (June 25–30, 1972).

75 Edwards, A. M., and Nicholson, A., "Some Effects of Reheating Stainless Steels", *Journal of the Iron and Steel Institute*, Vol 207, No. 8 (August 1969), pp 1067–1081.

76 The International Nickel Company, Inc., "Mechanical and Physical Properties of Austenitic Chromium-Nickel Stainless Steels at Ambient Temperatures", trade literature (October 1966).

77 Rosen, A., Jago, R., and Kjer, T., "Tensile Properties of Metastable Stainless Steels", *Journal of Materials Science*, Vol 7 (1972), pp 870–876.

78 Monteiro, S. N., and Fonseca, H., "The Effect of Phase Transformation on the Tensile Fracture of Austenitic Stainless Steel", Proceedings of the Fourth International Conference on Fracture, University of Waterloo, Ontario, Canada (June 1977), pp 135–140.

79 Calfo, F. D., "Cryogenic Fracture Properties of Thin AISI 301 60-Percent Cold-Reduced Sheet at Various Angles to the Rolling Direction", NASA TN D-5413 (September 1969).

80 Neff, D. V., Mitchell, T. E., and Troiano, A. R., "The Influence of Temperature, Transformation, and Strain Rate on the Ductility Properties of Austenitic Stainless Steels", *ASM Transactions Quarterly*, Vol 62, No. 4 (December 1969), pp 858–868.

81 Livitsanos, C. P., and Thomson, P. F., "The Effect of Temperature and Deformation Rate on Transformation-Dependent Ductility of a Metastable Austenitic Stainless Steel", *Materials Science and Engineering*, Vol 30, No. 2 (October 1977), pp 93–98.

82 Muraca, R. F., and Whittick, J. S., "Materials Data Handbook – Stainless Steel Type 301 (Second Edition)", NASA CR-123780 (April 1972).

83 The International Nickel Company, Inc., "Cast Stainless Steels", trade literature (July 1964).

84 Fox, A., "Stress Relaxation in Bending of AISI 301 Type Corrosion-Resistant Steel Strip", Proceedings of ASTM Symposium on Stress Relaxation Testing held in Kansas City, Missouri (May 24–25, 1978), pp 78–88.

85 Hennessy, D., Steckel, G., and Altstetter, C., "Phase Transformation of Stainless Steel During Fatigue", *Metallurgical Transactions*, Vol 7A, No. 3 (March 1976), pp 415–424.

86 Wright, R. N., "The High Cycle Fatigue Strength of Commercial Stainless Steel Strip", *Materials Science and Engineering*, Vol 22, No. 3 (March 1976), pp 223–230.

87 Nachtigall, A. J., Klima, S. J., and Freche, J. C., "Fatigue of Liquid Rocket Engine Metals at Cryogenic Temperatures to -452 F (4 K)", NASA TN D-4274 (December 1967).

88 Illg, W., and Imig, L. A., "Fatigue of Four Stainless Steels, Four Titanium Alloys, and Two Aluminum Alloys Before and After Exposure to Elevated Temperatures for Up to Three Years", NASA TN D-6145 (April 1971).

89 Illg, W., and Castle, C. B., "Fatigue of Four Stainless Steels and Three Titanium Alloys Before and After Exposure to 550 F (561 K) Up to 8800 Hours", NASA TN D-2899 (July 1965).

90 Schuster, G., and Altstetter, C., "Fatigue of Stainless Steel in Hydrogen", *Metallurgical Transactions*, Vol 14A, No. 10 (October 1983), pp 2085–2090.

91 Perng, T. P., and Altstetter, C. J., "Hydrogen Permeation and Diffusion in Cryoformed AISI 301 Stainless Steel", *Scripta Metallurgica*, Vol 18, No. 1 (January 1984), pp 67–70.

Fe
18 Cr
8 Ni

Type 301
Type 302

Fe
18 Cr
8 Ni

Type 301
Type 302

92 Studebaker, P., Altstetter, C., and Conley, W., "Hydrogen Permeation of Stainless Steel Under Stress", Proceedings of 3rd International Conference on Effect of Hydrogen on Behavior of Materials, Hydrogen Effects in Metals held in Moran, Wyoming (August 26–31, 1980), pp 169–175.

93 Mikesell, R. P., and Reed, R. P., "Magnetic Transformation and the Influence of Plastic Strain on the Shear Modulus of Fe-Cr-Ni Alloys", *Journal of Research*, Vol 70C, No. 3 (July–September 1966), pp 207–210.

Alloy Type	AMS Specification	Form
301	5517G	Sheet, strip, 125 ksi
	5518F	Sheet, strip, 150 ksi
	5519H	Sheet, strip, 185 ksi
302	5358B	Investment castings
	5500B	Sheet, laminated
	5515H	Sheet, strip, plate, ST
	5516J	Sheet, strip, plate, ST
	5600B	Sheet, laminated
	5636C	Bar, 100 ksi
	5637D	Bar, 125 ksi
	5688G	Wire, spring temper
	5693	Wire, cryogenically drawn

TABLE 1.03. SPECIFICATIONS (1–9, 52–54)

Alloy	Type 301				Type 302					
AMS Specification	5517G		5518F, 5519H		5358B		5500B, 5516J, 5600B, 5636C, 5637D, 5688G, 5693		5515H	
	Percent		Percent		Percent		Percent		Percent	
Element	Min	Max	Min	Max	Min	Max	Min	Max	Min	Max
Chromium	17.00	–	16.00	18.00	17.00	19.00	17.00	19.00	17.00	19.00
Nickel	7.00	–	6.00	8.00	8.00	10.00	8.00	10.00	7.00	10.00
Manganese	–	2.00	–	2.00	–	1.50	–	2.00	–	2.00
Silicon	–	1.00	–	1.00	–	2.00	–	1.00	–	1.00
Carbon	–	0.15	–	0.15	–	0.25	–	0.15	0.08	0.15
Molybdenum	–	0.75	–	0.75	–	0.75	–	0.75(a)	–	0.75
Copper	–	0.75	–	0.75	–	0.75	–	0.75(a)	–	0.75
Phosphorus	–	0.040	–	0.040	–	0.04	–	0.040	–	0.040
Sulfur	–	0.030	–	0.030	–	0.03	–	0.030	–	0.030

(a) AMS 5500B specifies 0.50 max molybdenum and 0.50 max copper.

TABLE 1.04. COMPOSITION (1–9, 52–54)

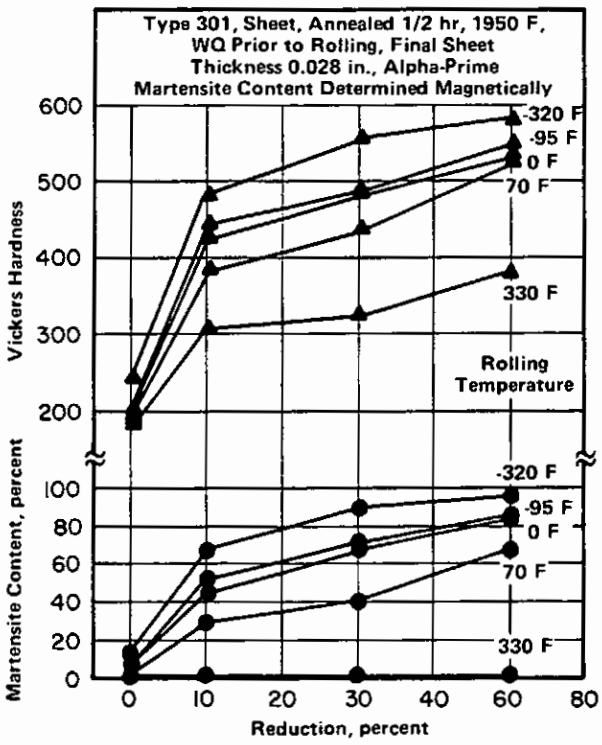
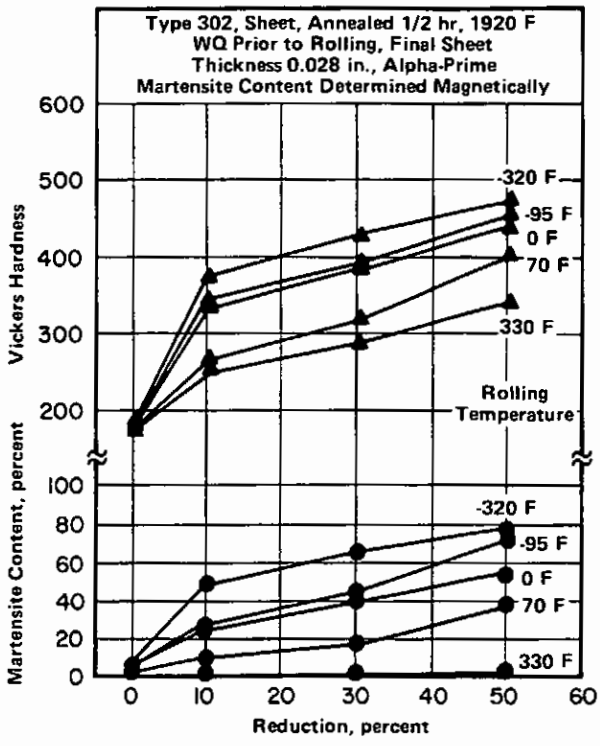


FIGURE 1.062. HARDNESS AND MARTENSITE CONTENTS OF TYPE 301 AFTER ROLLING TO VARIOUS REDUCTIONS AT 330 F TO -320 F (55)



Fe
18 Cr
8 Ni

Type 301
Type 302

FIGURE 1.063. HARDNESS AND MARTENSITE CONTENTS OF TYPE 302 AFTER ROLLING TO VARIOUS REDUCTIONS AT 330 F TO -320 F (55)

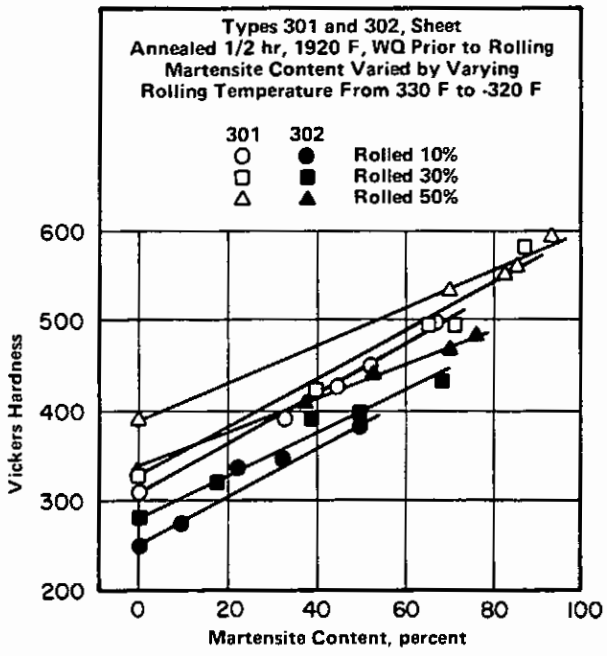


FIGURE 1.064. EFFECT OF STRAIN-INDUCED MARTENSITE CONTENT ON HARDNESS (55)

Fe
18 Cr
8 Ni

Type 301
Type 302

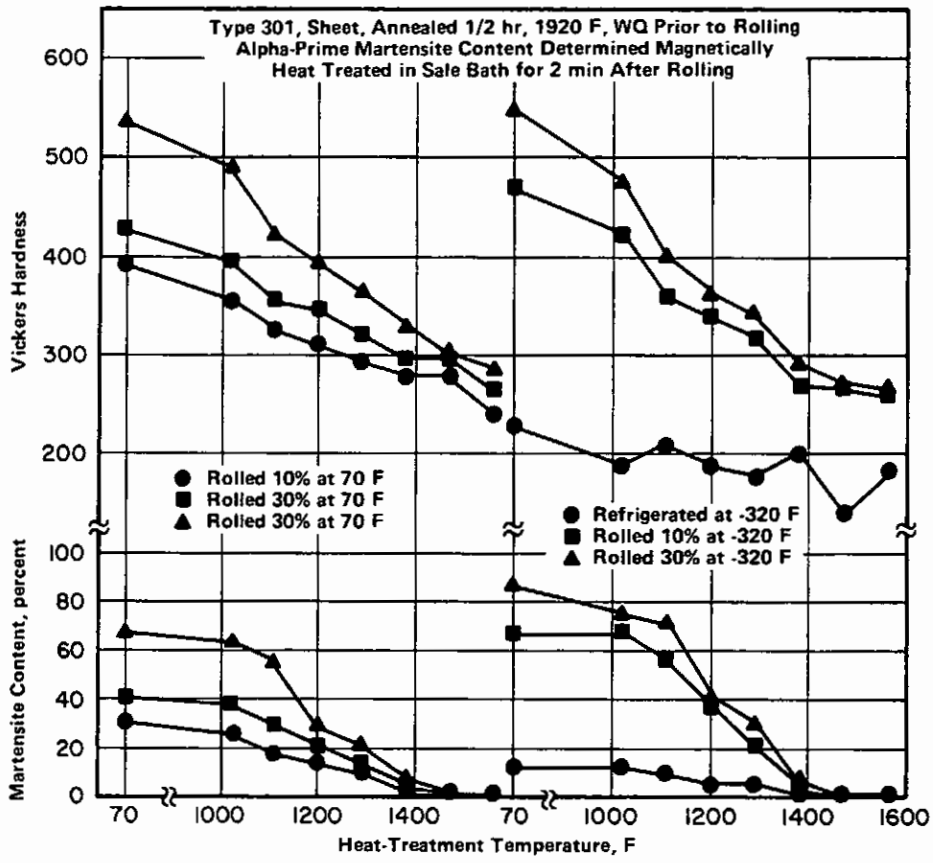


FIGURE 1.065. HARDNESS AND MARTENSITE CONTENTS OF TYPE 301 AFTER COLD ROLLING FOLLOWED BY HEAT TREATMENT AT 1020 TO 1560 F (55)

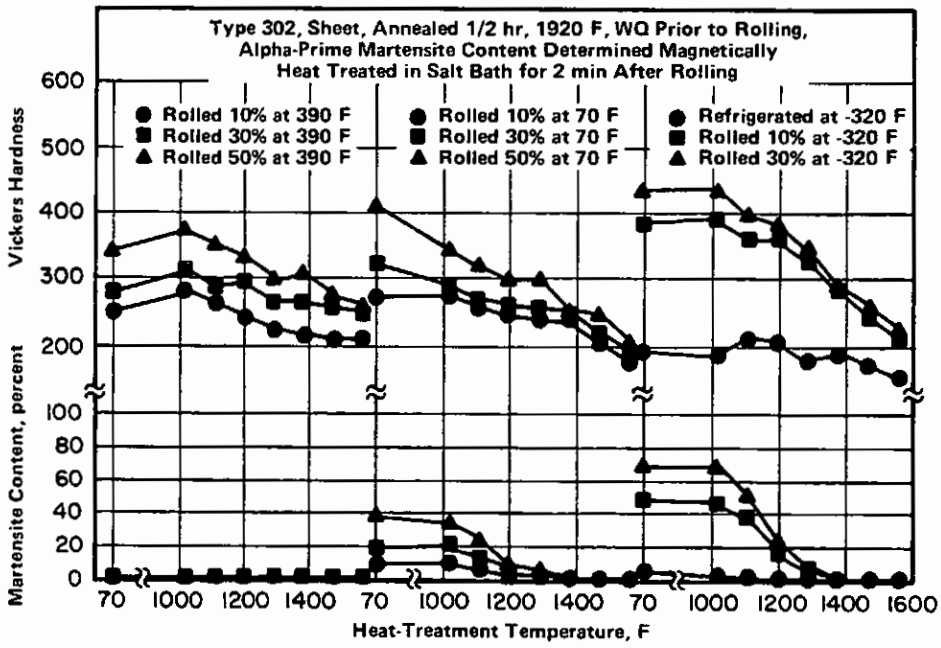


FIGURE 1.066. HARDNESS AND MARTENSITE CONTENTS OF TYPE 302 AFTER ROLLING FOLLOWED BY HEAT TREATMENT AT 1020 TO 1560 F (55)

Fe
18 Cr
8 Ni

Type 301
Type 302

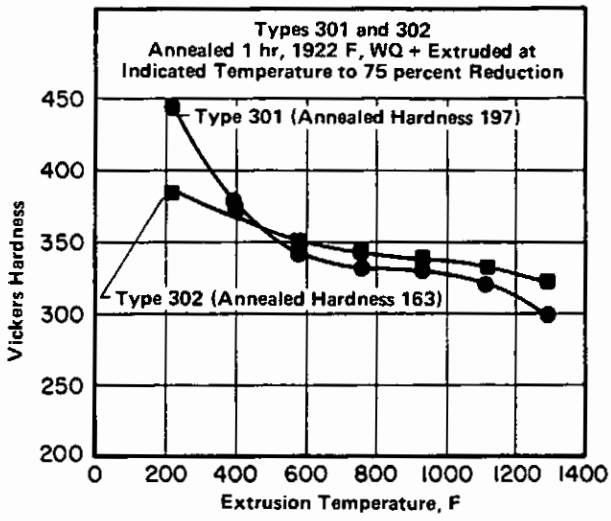


FIGURE 1.067. EFFECT OF EXTRUSION TEMPERATURE ON HARDNESS (56)

Form	Sheet, Strip					Plate
Condition	Anneal	1/4 H	1/2 H	3/4 H	Full H	Anneal
Hardness						
Type 301	85 RB	25 RC	32 RC	37 RC	41 RC	165 BHN
Type 302	85 RB	25 RC	–	–	–	80 RB
Form	Bar			Wire		
Condition	Anneal	CD	High Tension	Anneal	Soft	Hard
Hardness						
Type 301	–	–	–	–	–	–
Type 302	150 BHN	212 BHN	240–277 BHN	83 RB	95 RB	33 RC

TABLE 1.068. AISI TYPICAL VALUES FOR HARDNESS (10)

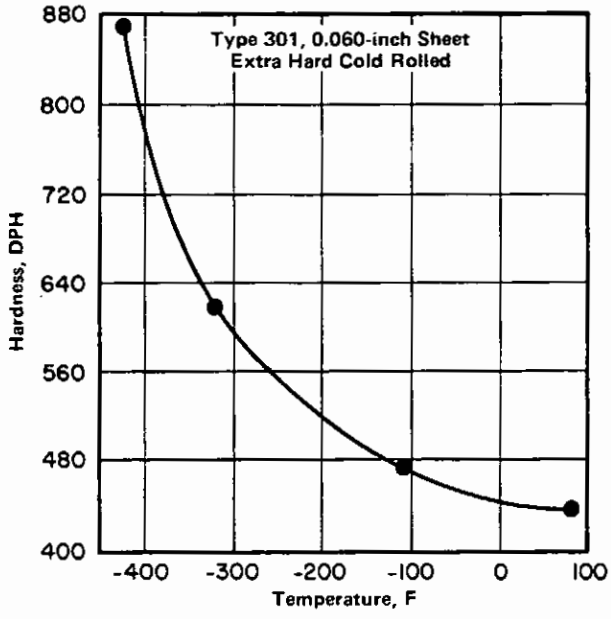


FIGURE 1.069. EFFECT OF LOW TEST TEMPERATURE ON HARDNESS OF EXTRA-HARD COLD-ROLLED SHEET (32)

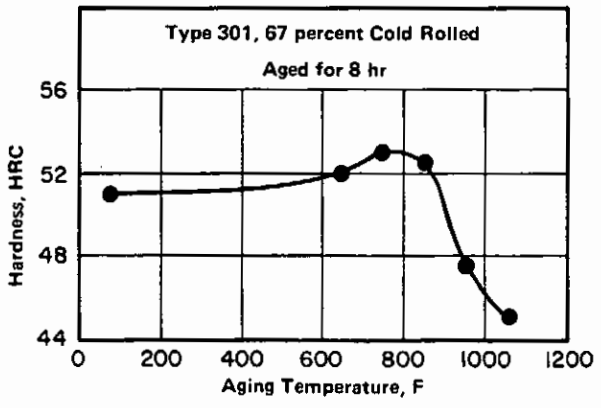


FIGURE 1.0610. EFFECT OF AGING TEMPERATURE ON HARDNESS OF 67 PERCENT COLD-ROLLED SHEET (43)

Fe
18 Cr
8 Ni

Type 301
Type 302

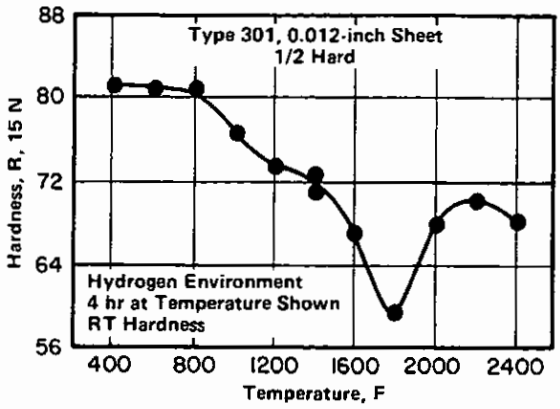


FIGURE 1.0611. EFFECT OF HYDROGEN ENVIRONMENT AT ELEVATED TEMPERATURE ON SURFACE HARDNESS OF HALF-HARD SHEET (29)

Phase Change	Temperature, F	
	Type 301	Type 302
M_s	-35 to -112	-251
M_d	135 to 194	-8
A_{c1}	1020 to 1110	1020 to 1110
A_{c3}	1380 to 1470	1290 to 1380

TABLE 2.0122. TRANSFORMATION TEMPERATURES (55,58,59)

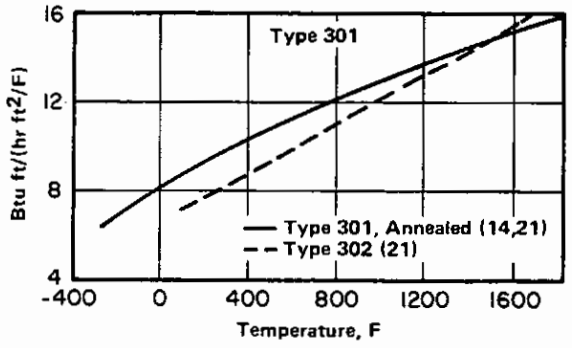
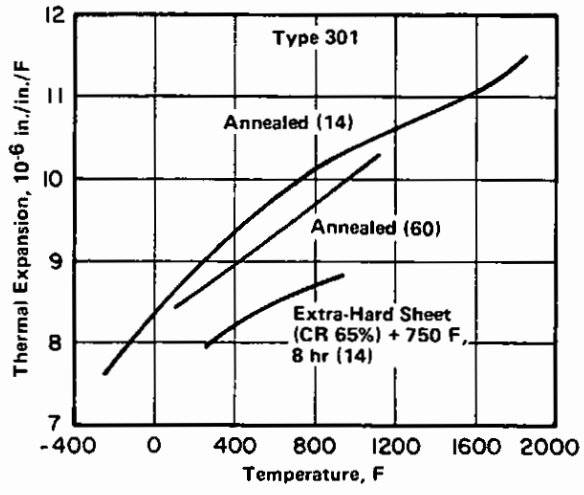
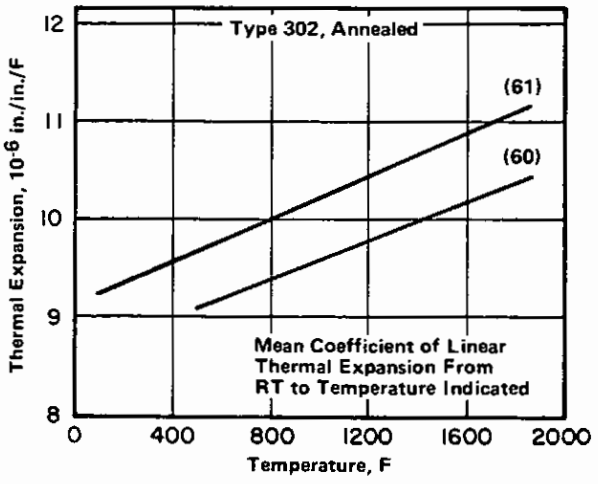


FIGURE 2.013. THERMAL CONDUCTIVITY (14,21)



(a) Type 301



(b) Type 302

FIGURE 2.014. THERMAL EXPANSION (60,61)

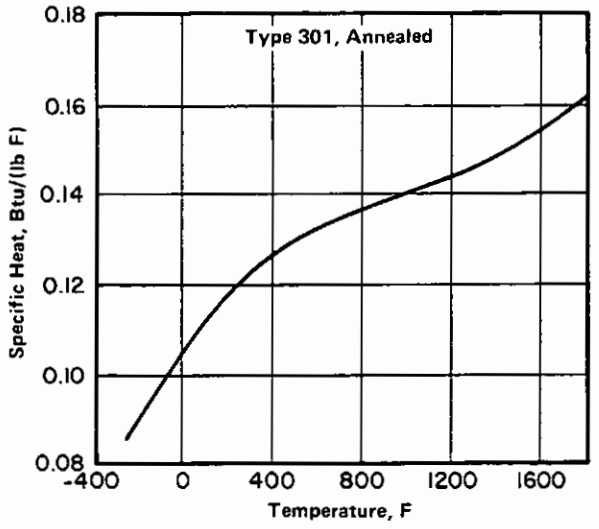
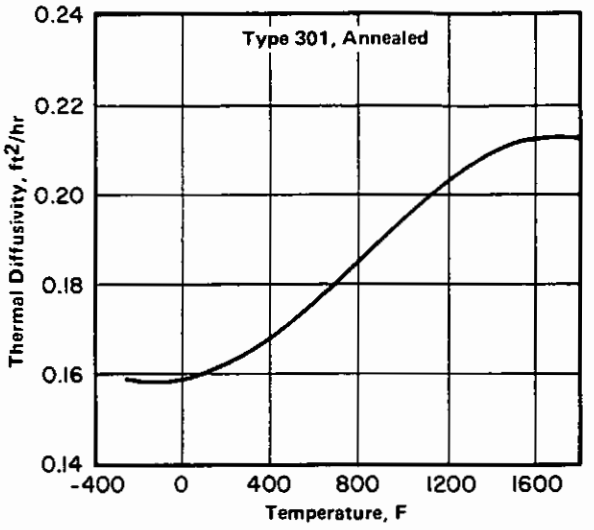


FIGURE 2.015. SPECIFIC HEAT (14)



Fe
18 Cr
8 Ni

Type 301
Type 302

FIGURE 2.016. THERMAL DIFFUSIVITY (14)

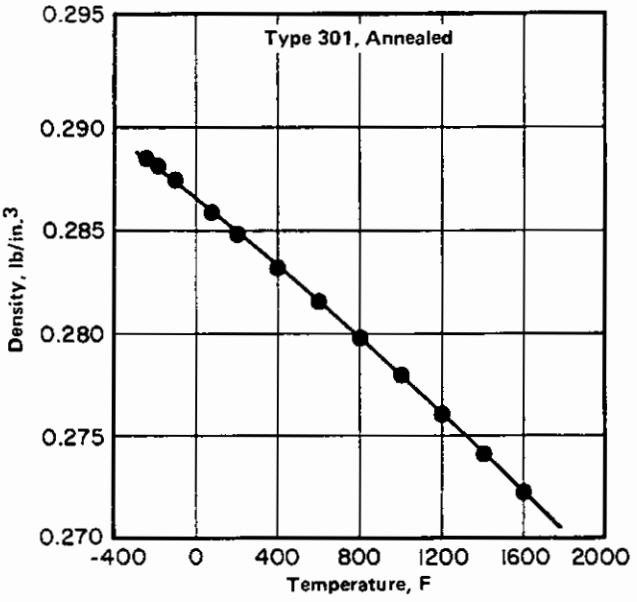


FIGURE 2.021. DENSITY (62)

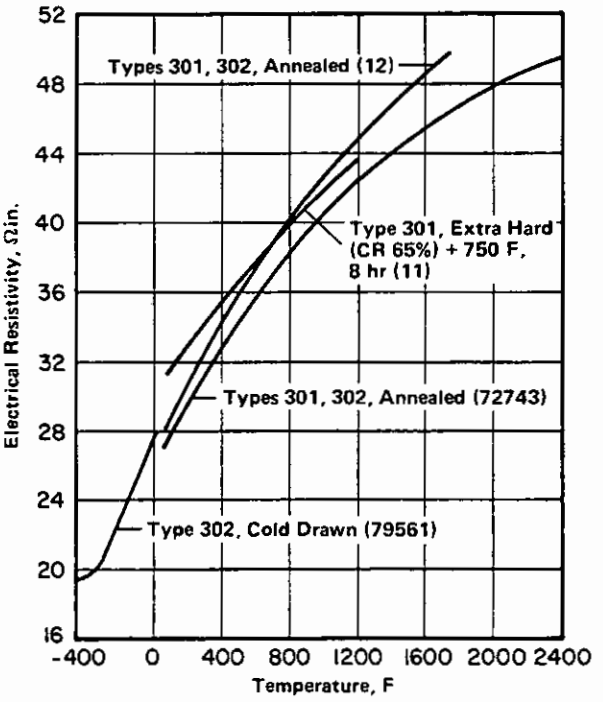


FIGURE 2.0221. ELECTRICAL RESISTIVITY (63)

Fe
18 Cr
8 Ni

Type 301
Type 302

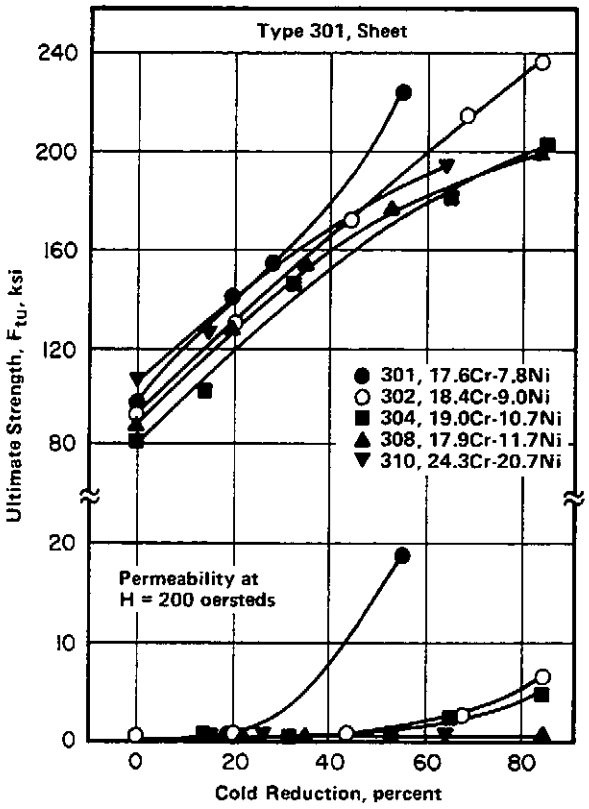


FIGURE 2.0232. EFFECT OF COMPOSITION AND REDUCTION ON MAGNETIC PERMEABILITY AND TENSILE STRENGTH OF 300 SERIES SHEET (22)

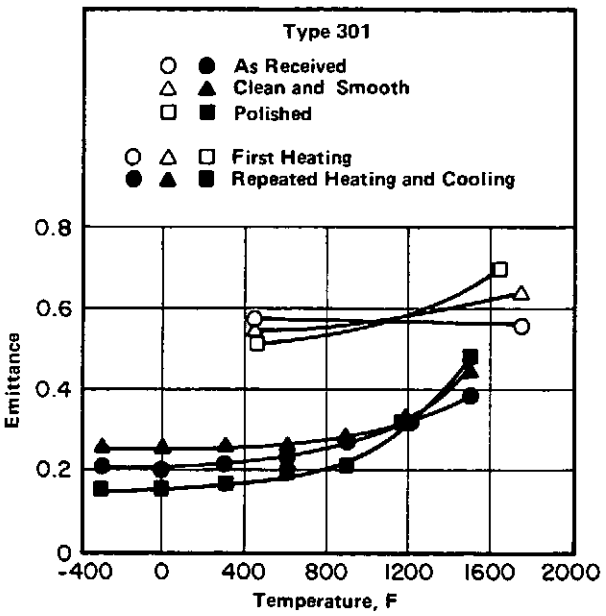


FIGURE 2.024. EMITTANCE (40)

Alloy Type	Exposure[a]	General Corrosion: Weight Loss, g/dm² 1 Yr	8 Yr	16 Yr	General Corrosion: Average Penetration, mils 1 Yr	8 Yr	16 Yr	Steady State Rate, mpy	Pitting Penetration, mils[c] 1 Yr	8 Yr	16 Yr
302	S	2.9	11.0	18.7	1.51	5.51	9.51	(b)	70 (P)	140	151 (P)
	M	0.4	1.8	3.3	0.2	0.9	1.6	(b)	6	58	50 (110)
	L	0.0	0.0	0.0	0.0	0.0	0.0	0.0	<5	<5	<5 (<5)
301	A	0.01	0.01	0.03	0.01	0.01	0.02	0.01	<5	<5	<5 (<5)
	B	0.00	0.01	0.00	0.00	0.00	0.00	0.00	<5	<5	<5 (<5)

(a) S – seawater immersion
M – seawater at mean tide level for intermittent immersion
L – freshwater immersion
A – tropical marine atmospheric exposure
B – tropical inland atmospheric exposure
Panels for aqueous exposures measured 9 x 9 x 0.25 inch; those for atmospheric exposures measured 4 x 8 x 0.063 inch.

(b) Deep local pitting; average penetration not appropriate.

(c) Twenty pit average as determined from the five deepest pits on each surface of duplicate panels. The deepest pit during the 16-year exposure is shown in parentheses. Perforation is shown by a "P".

TABLE 2.0313. CORROSION IN TROPICAL ENVIRONMENTS FOR TIMES UP TO 16 YEARS (65)

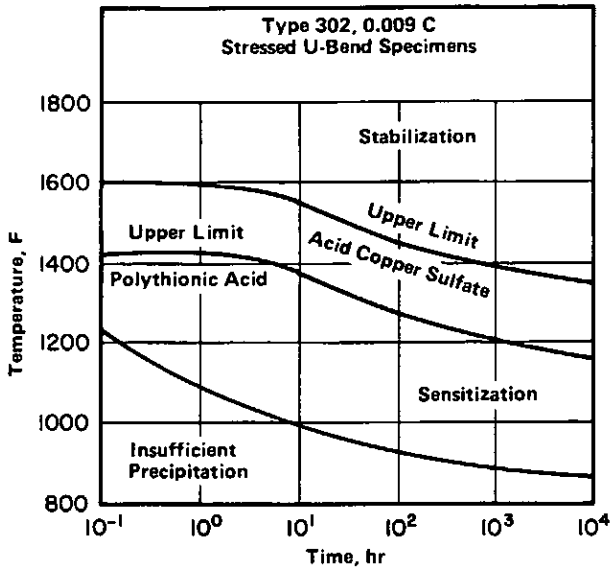
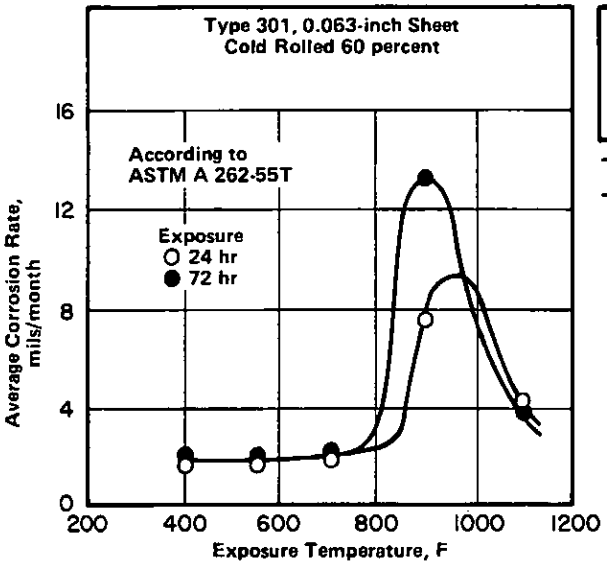


FIGURE 2.0322. EFFECTS OF HEAT TREATMENT ON SUSCEPTIBILITY TO INTERGRANULAR STRESS CORROSION CRACKING IN POLYTHIONIC ACID AND IN ACID COPPER SULFATE (68)



Fe
18 Cr
8 Ni

Type 301
Type 302

FIGURE 2.0323. EFFECT OF PRIOR EXPOSURE TEMPERATURE AND TIME ON AVERAGE CORROSION RATE IN BOILING NITRIC ACID OF COLD-ROLLED SHEET (18)

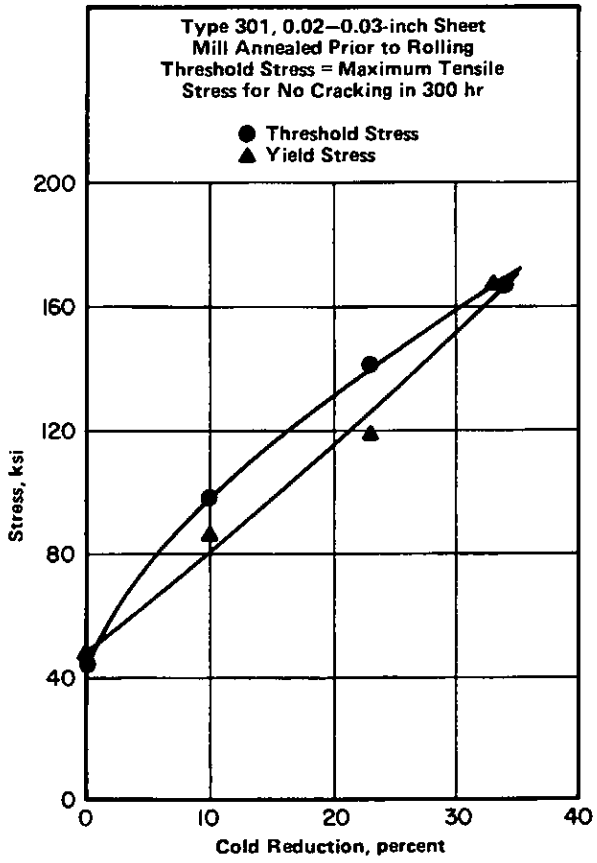


FIGURE 2.0333. EFFECTS OF COLD REDUCTION ON YIELD STRESS IN AIR AND ON THRESHOLD CORROSION STRESS IN BOILING 0.5N NaCl + 0.1N $NaNO_2$ AQUEOUS SOLUTION (72)

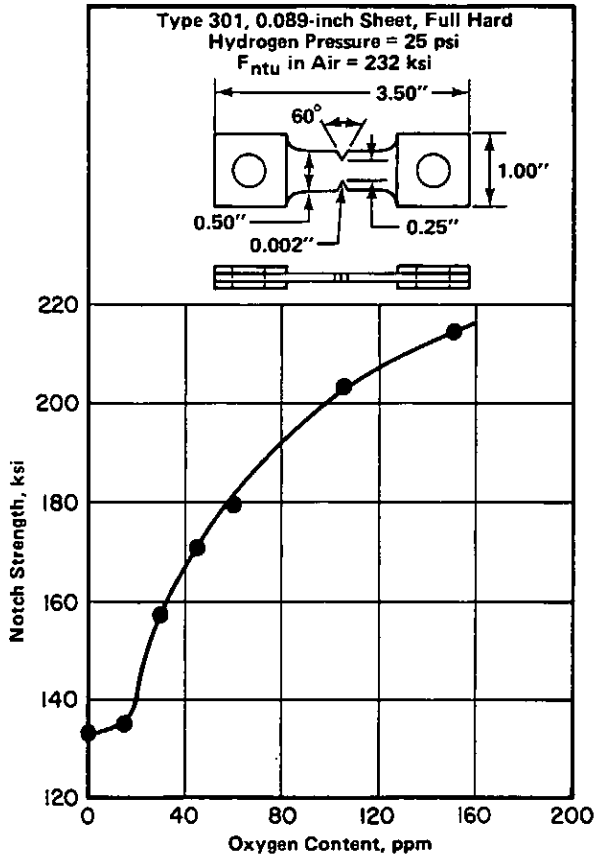


FIGURE 2.0342. EFFECTS OF OXYGEN IMPURITY IN HYDROGEN ON NOTCH STRENGTH OF TYPE 301 (74)

Fe
18 Cr
8 Ni

Type 301
Type 302

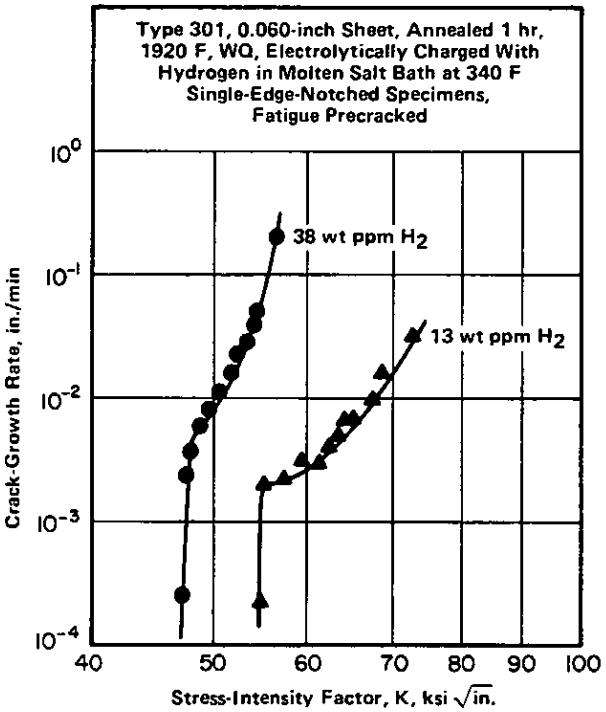


FIGURE 2.0344. SUSTAINED-LOAD CRACK-GROWTH RATE OF HYDROGEN-CHARGED TYPE 301 (73)

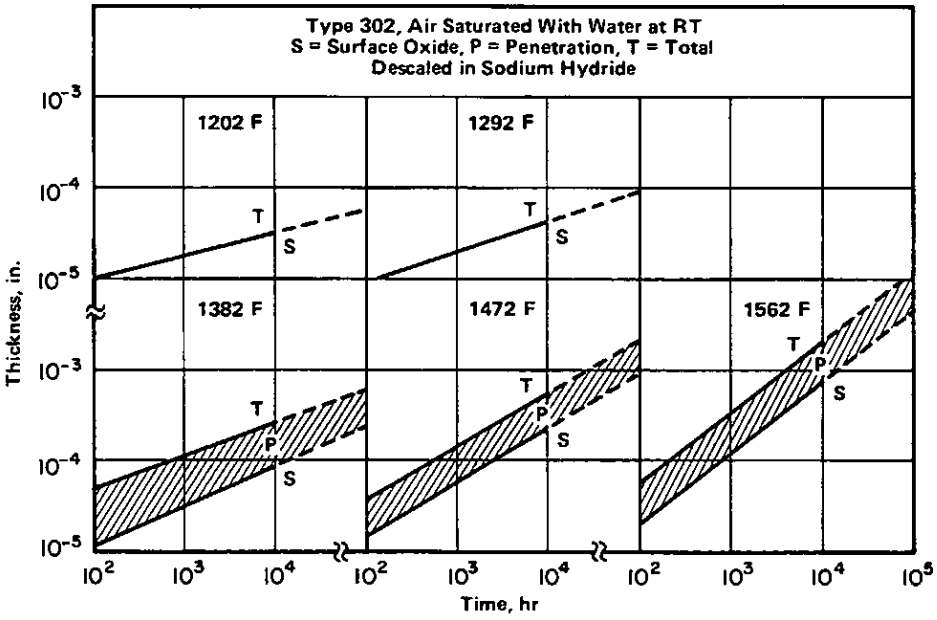


FIGURE 2.0352. TIME DEPENDENCE OF OXIDATION OF TYPE 302 IN AIR AT ELEVATED TEMPERATURES (75)

Fe
18 Cr
8 Ni

Type 301
Type 302

Alloy	Type 301				Type 302	
Condition	Annealed		60% (Cold Worked)		Annealed	
Irradiation Temperature, F	200	–	-416	–	200	–
Irradiation Exposure, $n(m^{-2})$	3.9×10^{9}	Control	2.0×10^{17}	Control	3.9×10^{9}	Control
Test Temperature, F	RT		-423		RT	
F_{tu}, ksi	113.2	98.7	284	391	111.3	95.5
F_{ty}, ksi	87.0	38.4	284	300	84.0	33.8
e, percent	50.0	56.0	8	13	–	–
RA, percent	81.0	83.0	–	–	–	–
Hardness, HRB	94	94	–	–	–	–

TABLE 2.041. EFFECT OF IRRADIATION EXPOSURE ON TENSILE PROPERTIES AND HARDNESS OF ALLOY (35)

Alloy	Types 301 and 302									
AMS Spec	Product Form	Condition[d]	Thickness, in.	F_{tu}, ksi Min	F_{tu}, ksi Max	F_{ty}, ksi Min	F_{ty}, ksi Max	El., percent, Min	RA, percent, Min	Hardness, Max
3517G	Sheet, strip	CR, 125 ksi	–	125	150	75	–	25	–	–
5518F	Sheet, strip	CR, 150 ksi	≤0.015	150	–	110	–	15	–	–
			>0.015	150	–	110	–	18	–	–
5519H	Sheet, strip	CR, 185 ksi	≤0.015	185	–	140	–	8	–	–
			>0.015	185	–	140	–	9	–	–
5358B	Investment cast	SHT	–	–	–	–	–	–	–	174 HB
5515H	Sheet, strip, plate	SHT	<0.025	–	120	–	–	50	–	–
			≥0.025	–	120	–	–	55	–	–
5516J	Sheet, strip, plate	SHT	0.002 ≤ 0.003	75	110	36	60	30	–	–
			>0.003 ≤ 0.004	75	105	36	60	35	–	–
			>0.004 ≤ 0.176	75	100	36	60	40	–	–
			>0.176	75	100	–	–	40	–	–
5636C	Bar	CD, 100 ksi	–	100	–	60	–	32	50	–
5637D	Bar	CD, 125 ksi	–	125	–	100	–	17	45	–
5688G	Wire	Spring temper	0.009–0.394[a]	142	355	–	–	–	–	–
5693	Wire	Cryogenically	0.050–0.148[b]	275	310	–	–	–	–	–
		drawn	0.050–0.148[c]	245	280	–	–	–	–	–
		SR	0.050–0.148[b]	290	340	–	–	–	–	–
			0.050–0.148[c]	260	310	–	–	–	–	–

Note: The original AMS documents should be consulted for complete specification details.
(a) Tensile strengths specified for numerous diameters and thicknesses in range 0.009–0.394 inch.
(b) Round wire.
(c) Square or rectangular wire.
(d) CR = cold rolled; SHT = solution heat treated; CD = cold drawn; SR = stress relieved.

TABLE 3.011. AMS SPECIFIED MECHANICAL PROPERTIES (1–9, 54)

Fe
18 Cr
8 Ni

Type 301
Type 302

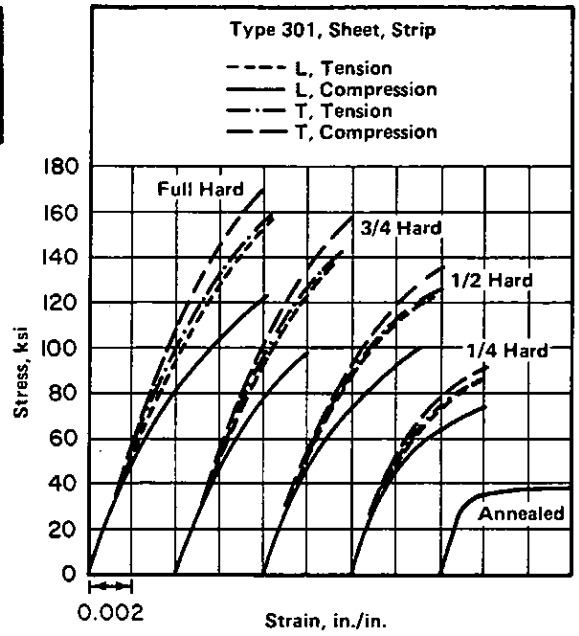


FIGURE 3.0211. STRESS-STRAIN CURVES FOR SHEET AND STRIP COLD ROLLED TO DIFFERENT TEMPER (20)

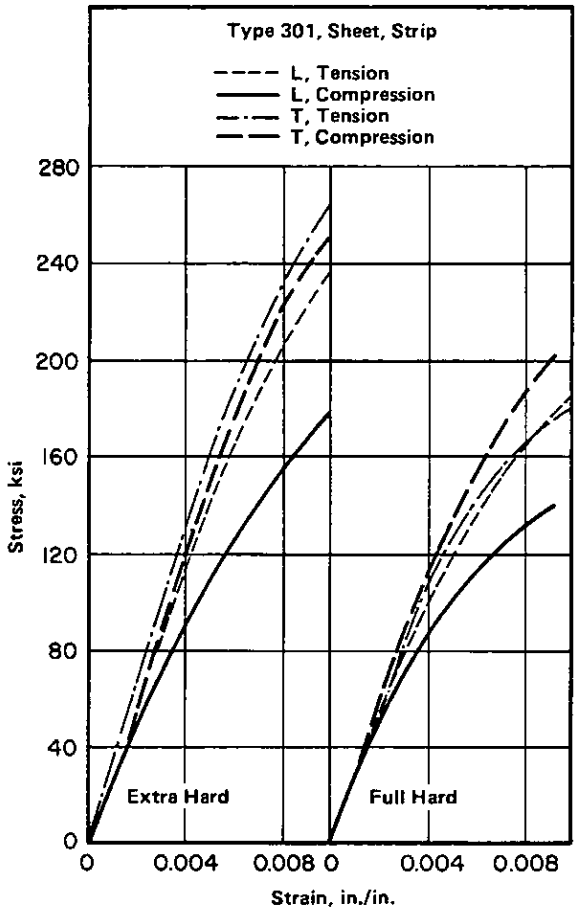


FIGURE 3.0212. STRESS-STRAIN CURVES FOR SHEET AND STRIP COLD ROLLED TO FULL-HARD AND EXTRA-HARD TEMPERS (11)

Alloy	Type 301		Type 302	
Temper	Percent Cold Reduction – Range	F_{tu} – Range, ksi	Percent Cold Reduction – Range	F_{tu} – Range, ksi
1/4 Hard	7–11	125–155	20–22	125–150
1/2 Hard	18–21	150–180	30–33	150–170
3/4 Hard	29–32	175–195	40	170–190
Full Hard	40	190–220	50	185–200
Extra Full Hard	65	240–275	–	–

TABLE 3.0213. PERCENTAGE COLD REDUCTION AND CORRESPONDING TENSILE STRENGTH FOR VARIOUS TEMPERS OF TYPES 301 AND 302 (49)

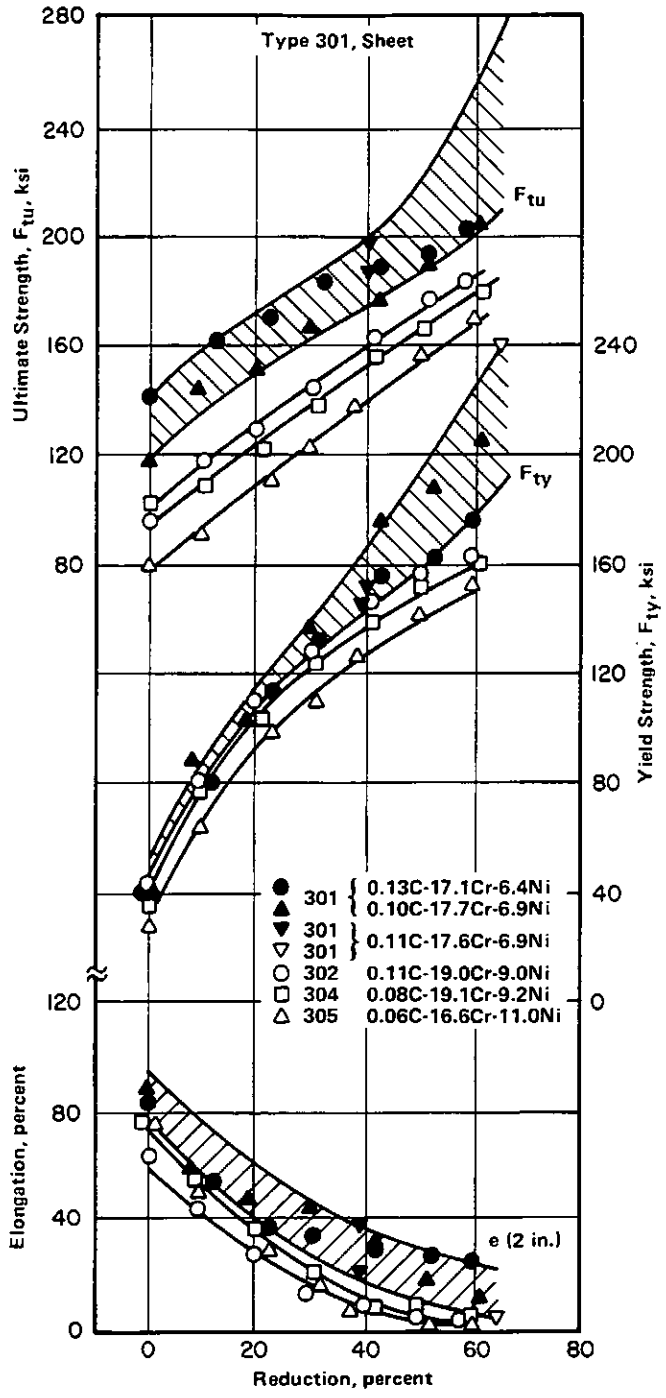
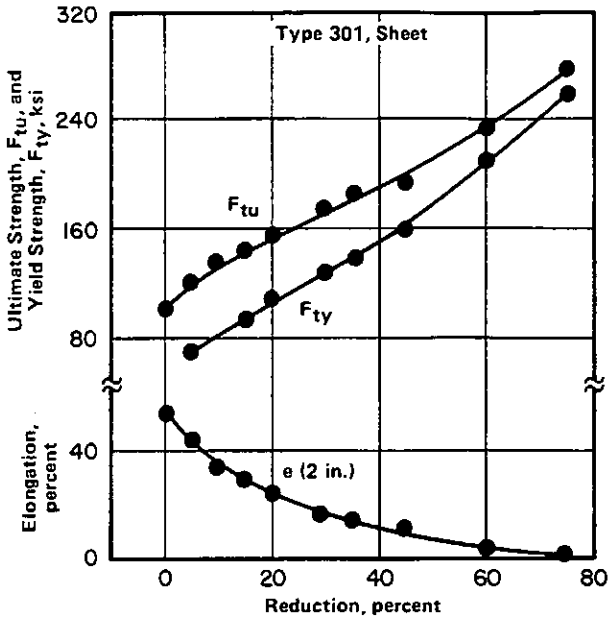


FIGURE 3.0214. EFFECT OF ROLLING REDUCTION AND COMPOSITION ON TENSILE PROPERTIES OF 300 SERIES STEELS (11)



Fe
18 Cr
8 Ni

Type 301
Type 302

FIGURE 3.0215. EFFECT OF COLD REDUCTION ON TENSILE PROPERTIES OF TYPE 301 (28)

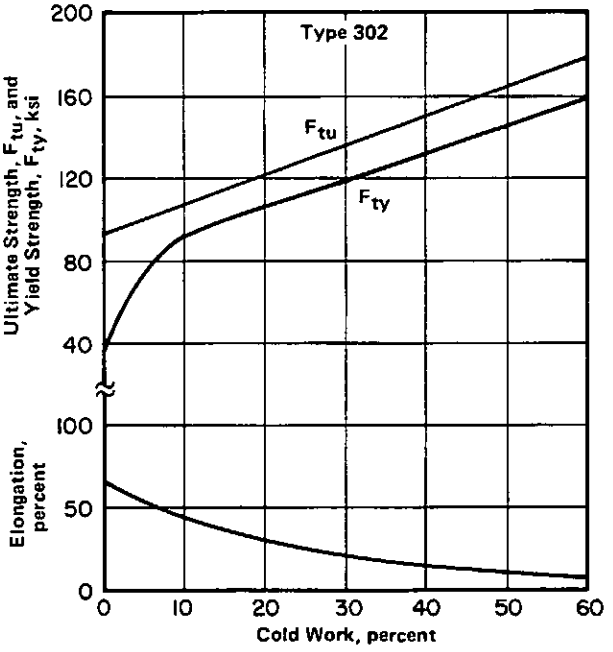


FIGURE 3.0216. EFFECTS OF COLD WORK ON TENSILE PROPERTIES OF TYPE 302 (76)

Fe
18 Cr
8 Ni

Type 301
Type 302

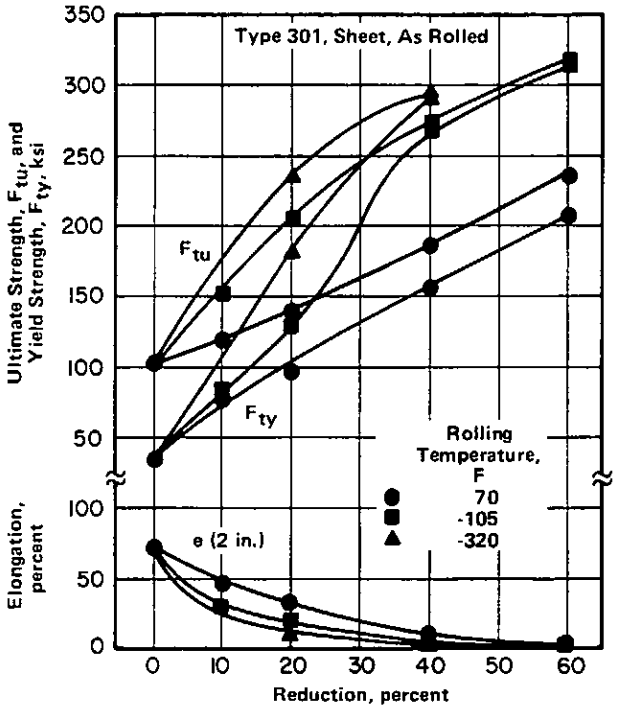


FIGURE 3.0218. EFFECT OF COLD REDUCTION AT ROOM AND CRYOGENIC TEMPERATURES ON TENSILE PROPERTIES OF TYPE 301 (76)

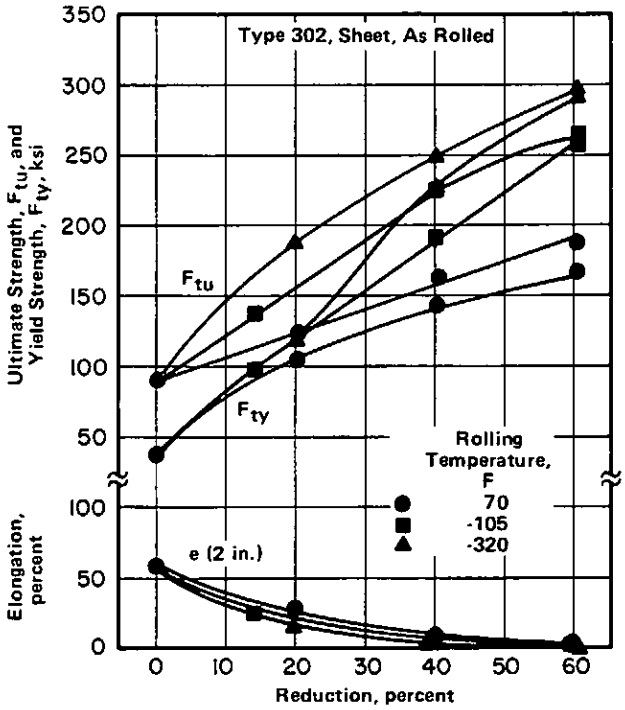


FIGURE 3.0219. EFFECT OF COLD REDUCTION AT ROOM AND CRYOGENIC TEMPERATURES ON TENSILE PROPERTIES OF TYPE 302 (76)

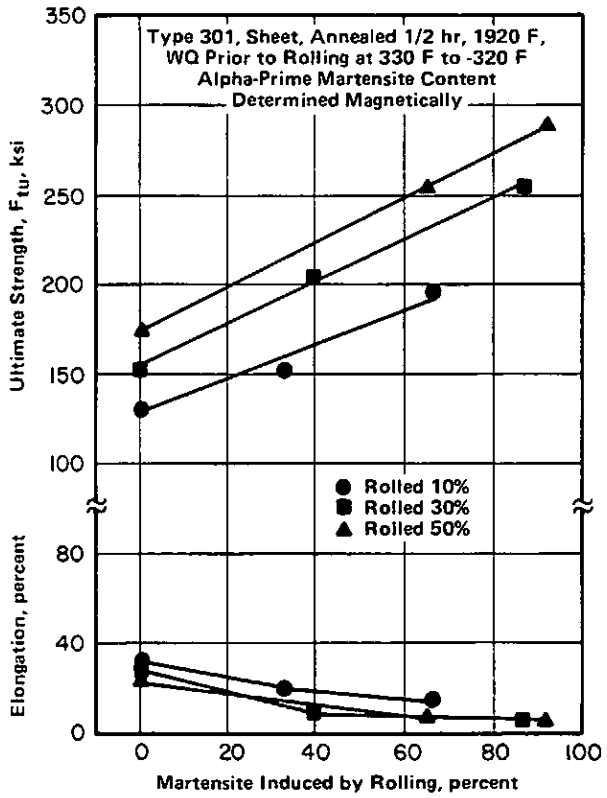


FIGURE 3.02110. RELATIONSHIP BETWEEN TENSILE PROPERTIES AND MARTENSITE CONTENT FOR TYPE 301 (55)

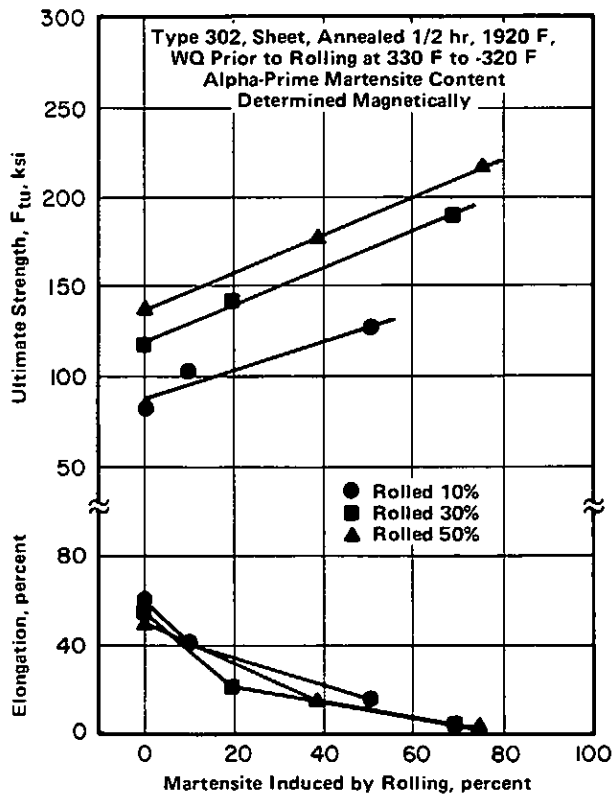


FIGURE 3.02111. RELATIONSHIP BETWEEN TENSILE PROPERTIES AND MARTENSITE CONTENT FOR TYPE 302 (55)

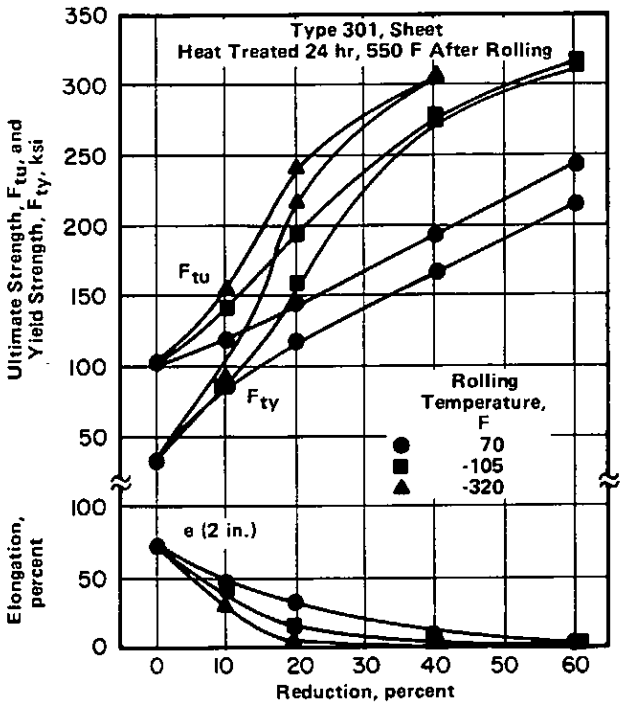


FIGURE 3.02112. EFFECT OF COLD REDUCTION AT ROOM AND CRYOGENIC TEMPERATURES PLUS HEAT TREATMENT ON TENSILE PROPERTIES OF TYPE 301 (76)

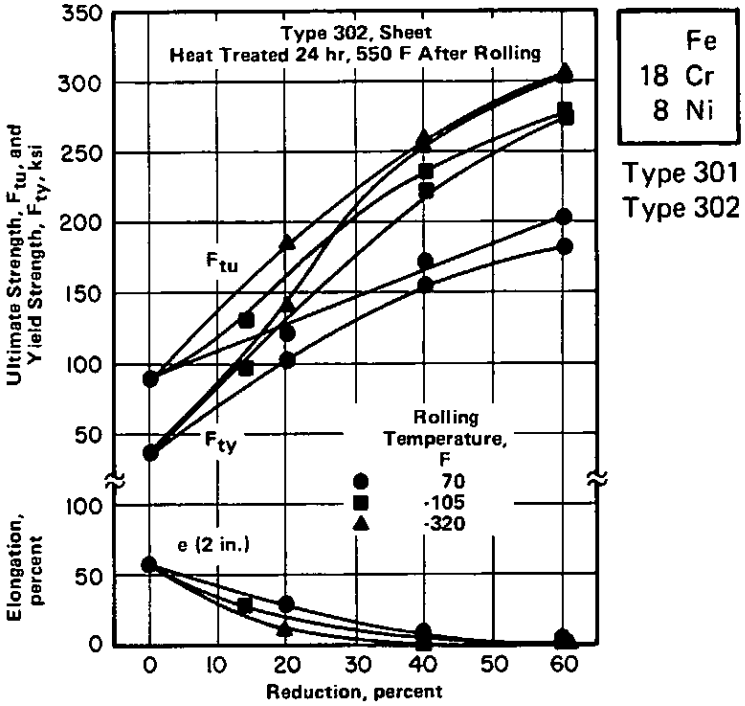


FIGURE 3.02113. EFFECT OF COLD REDUCTION AT ROOM AND CRYOGENIC TEMPERATURES PLUS HEAT TREATMENT ON TENSILE PROPERTIES OF TYPE 302 (76)

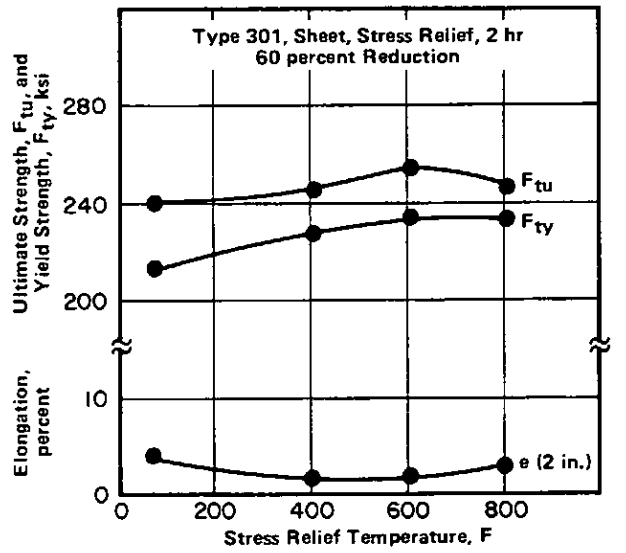


FIGURE 3.02114. EFFECT OF STRESS-RELIEF TEMPERATURE ON TENSILE PROPERTIES OF 60 PERCENT REDUCED SHEET (28)

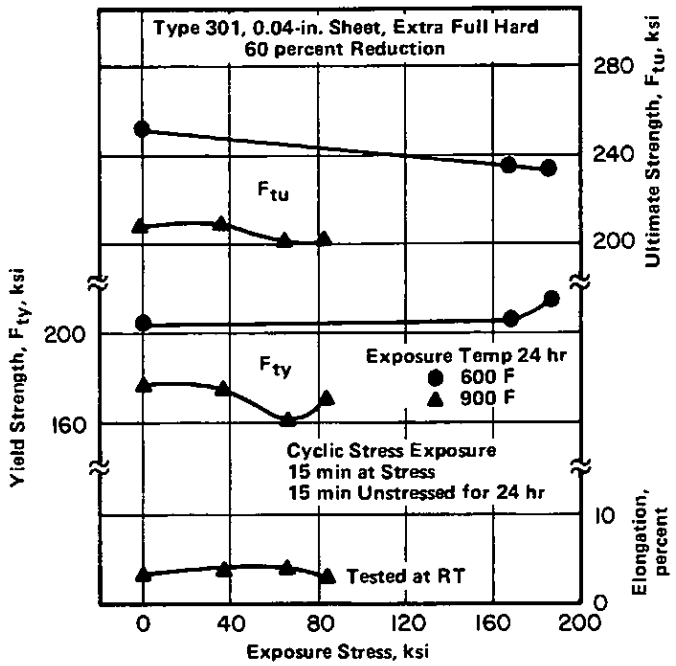


FIGURE 3.02115. EFFECT OF CYCLIC EXPOSURE STRESS ON ROOM-TEMPERATURE TENSILE PROPERTIES OF 60 PERCENT REDUCED SHEET EXPOSED AT 600 AND 900 F (27)

Fe
18 Cr
8 Ni

Type 301
Type 302

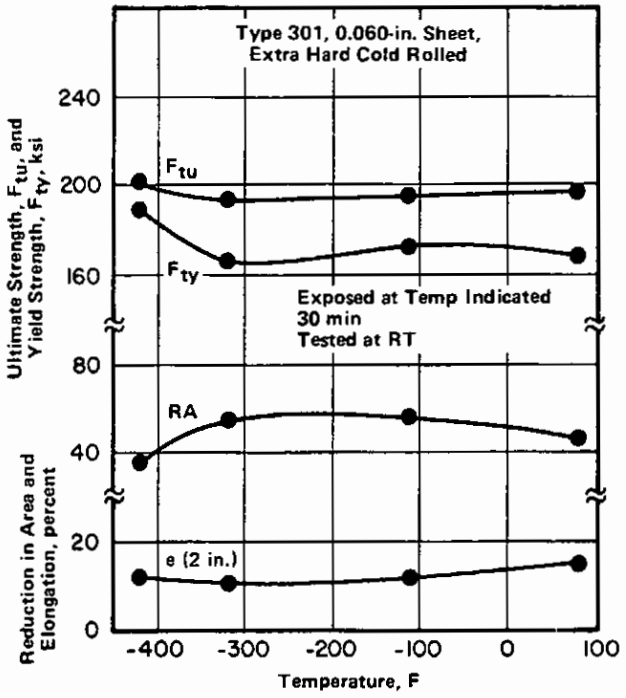


FIGURE 3.02116. EFFECT OF EXPOSURE AT LOW TEMPERATURE ON ROOM-TEMPERATURE TENSILE PROPERTIES OF EXTRA-HARD COLD-ROLLED SHEET (32)

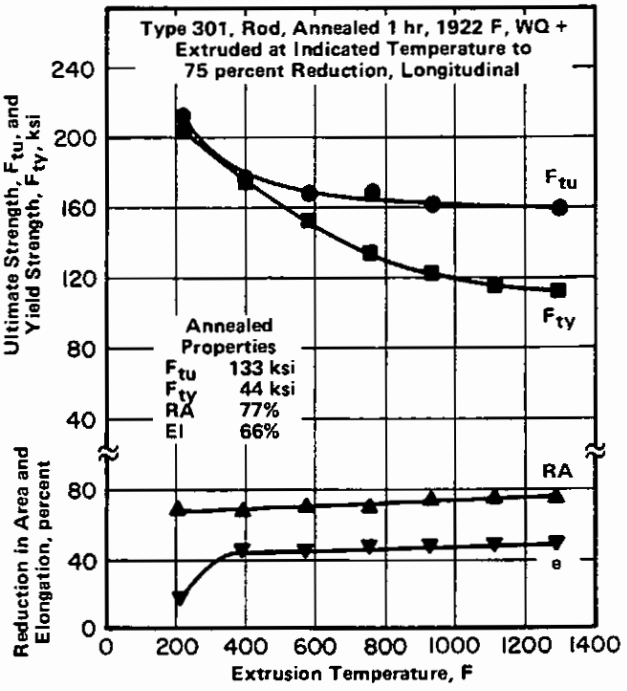


FIGURE 3.02117. EFFECTS OF EXTRUSION TEMPERATURE ON LONGITUDINAL TENSILE PROPERTIES OF TYPE 301 (56)

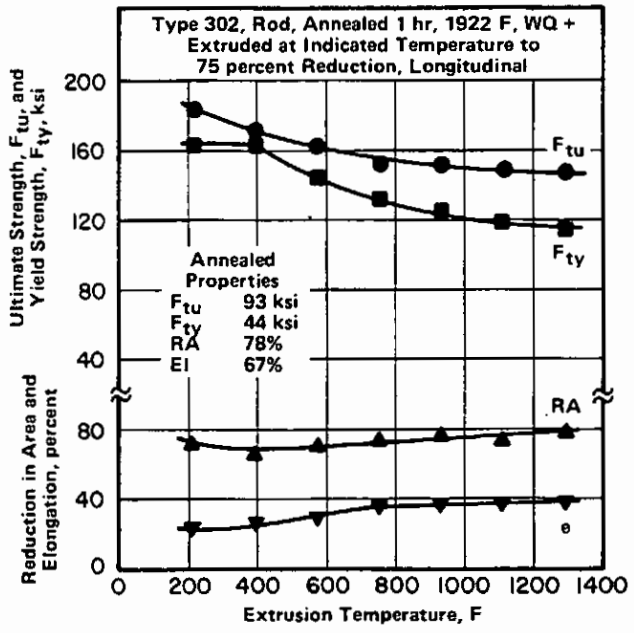


FIGURE 3.02118. EFFECTS OF EXTRUSION TEMPERATURE ON LONGITUDINAL TENSILE PROPERTIES OF TYPE 302 (56)

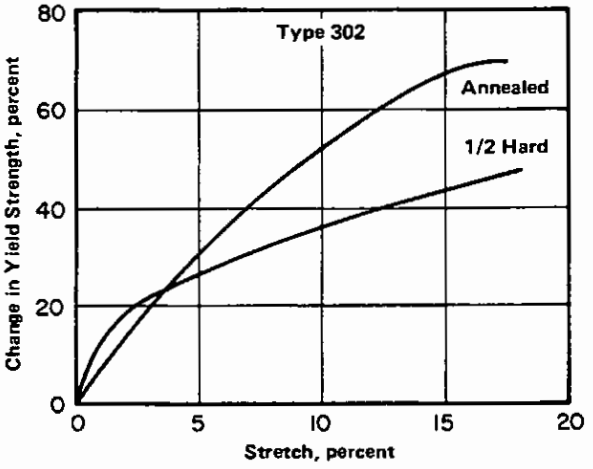


FIGURE 3.02119. EFFECT OF STRETCHING ON TENSILE YIELD STRENGTH OF TYPE 302 (76)

Fe
18 Cr
8 Ni

Type 301
Type 302

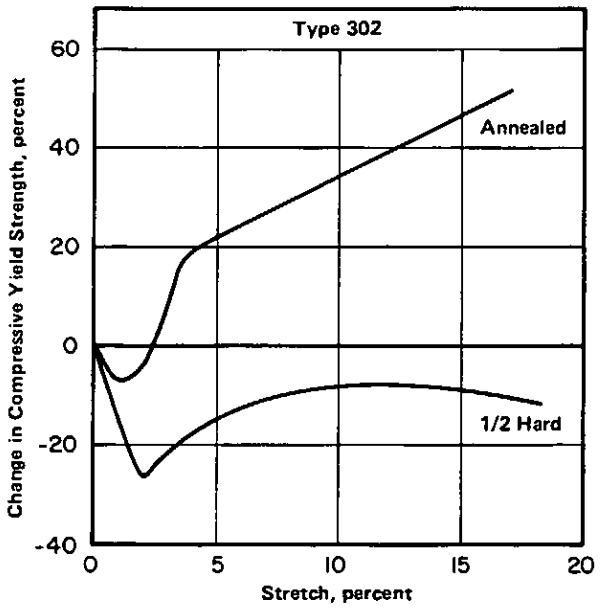


FIGURE 3.0221. EFFECT OF STRETCHING ON COMPRESSIVE YIELD STRENGTH OF TYPE 302 (76)

Type	Impact Energy, ft-lb		
	Izod	Charpy Keyhole Notch	Charpy V Notch
301(a)	70–120	90	110
302(a)	70–120	68–92	–
302B(a)	70–90	–	–
CF-20(b)	–	60	–

(a) Annealed.
(b) Heat treated at 2000 F plus water quench.

TABLE 3.0231. IMPACT PROPERTIES AT ROOM TEMPERATURE (76)

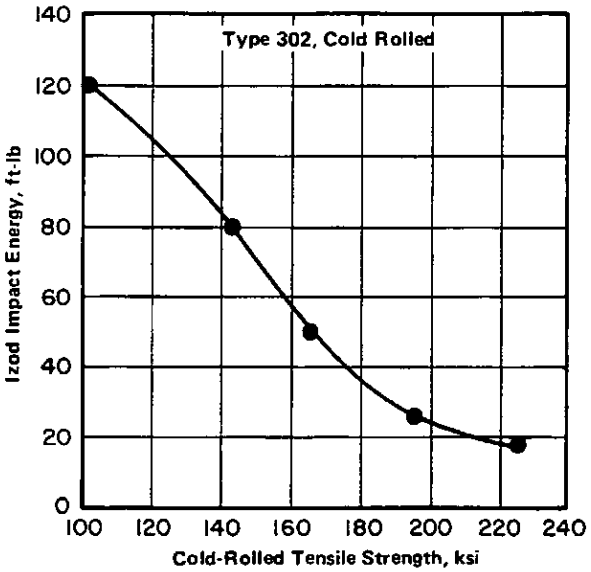


FIGURE 3.0232. RELATION BETWEEN IMPACT ENERGY AND TENSILE STRENGTH FOR COLD-ROLLED TYPE 302 (76)

Fe
18 Cr
8 Ni

Type 301
Type 302

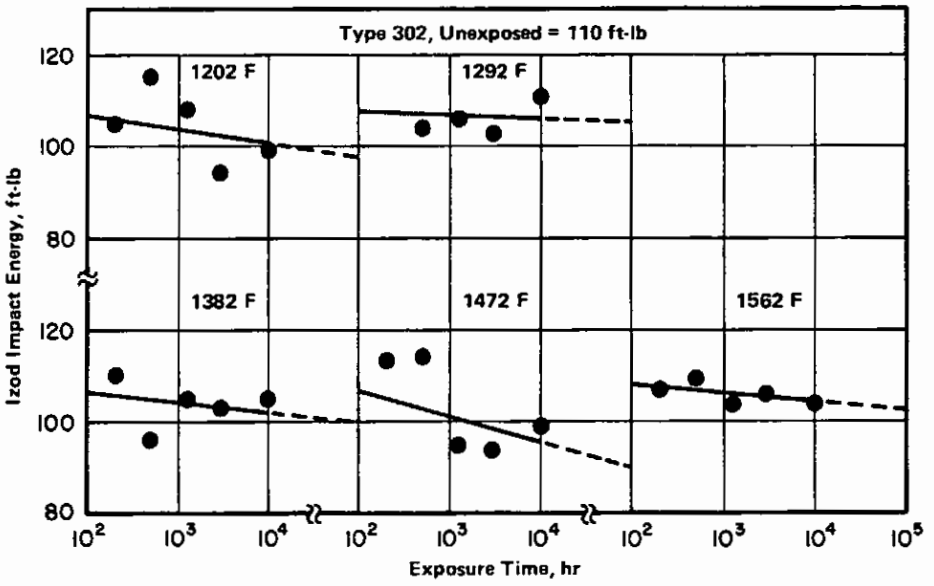


FIGURE 3.0233. EFFECTS OF EXPOSURE TIME IN AIR AT ELEVATED TEMPERATURES ON IMPACT ENERGY (75)

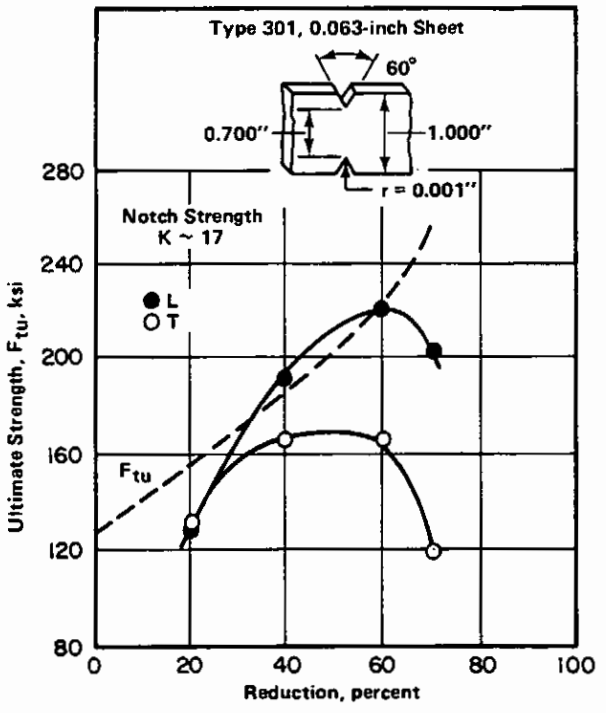


FIGURE 3.02711. EFFECT OF COLD ROLLING AND TEST DIRECTION ON NOTCH STRENGTH OF SHEET

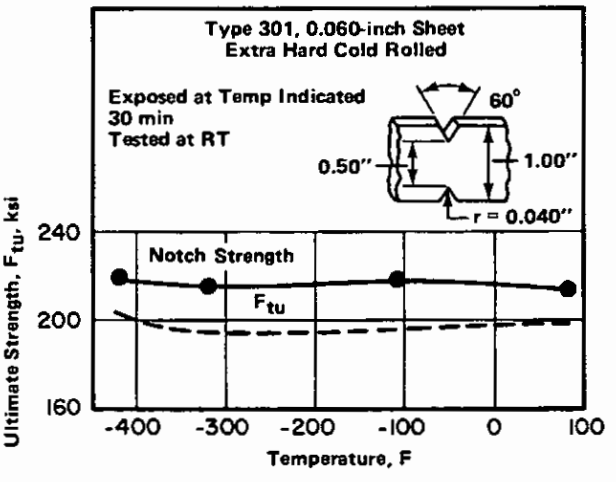


FIGURE 3.02712. EFFECT OF EXPOSURE AT LOW TEMPERATURE ON ROOM-TEMPERATURE NOTCH STRENGTH OF EXTRA-HARD COLD-ROLLED SHEET (32)

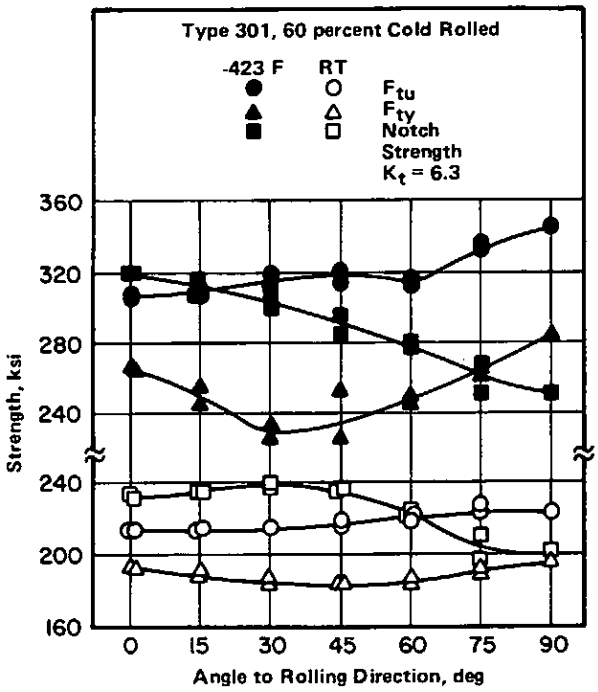
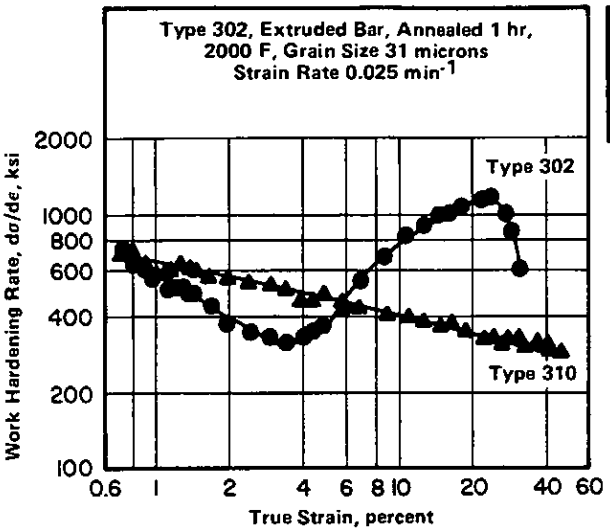


FIGURE 3.02713. EFFECT OF TEST DIRECTION IN RELATION TO ROLLING DIRECTION ON TENSILE PROPERTIES AND NOTCH STRENGTH OF 60 PERCENT COLD-REDUCED SHEET (48)



Fe
18 Cr
8 Ni

Type 301
Type 302

FIGURE 3.03112. TENSILE WORK-HARDENING RATES FOR TYPES 302 AND 310 AT -112 F (78)

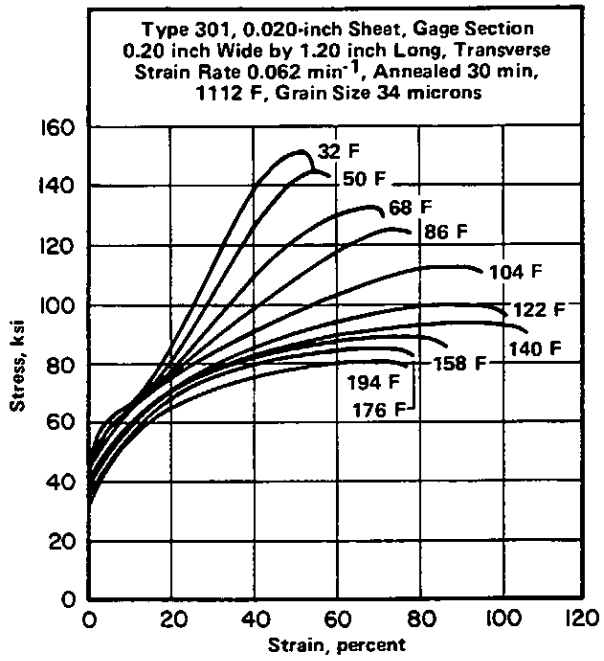


FIGURE 3.03113. STRESS-STRAIN CURVES FOR ANNEALED TYPE 301 (77)

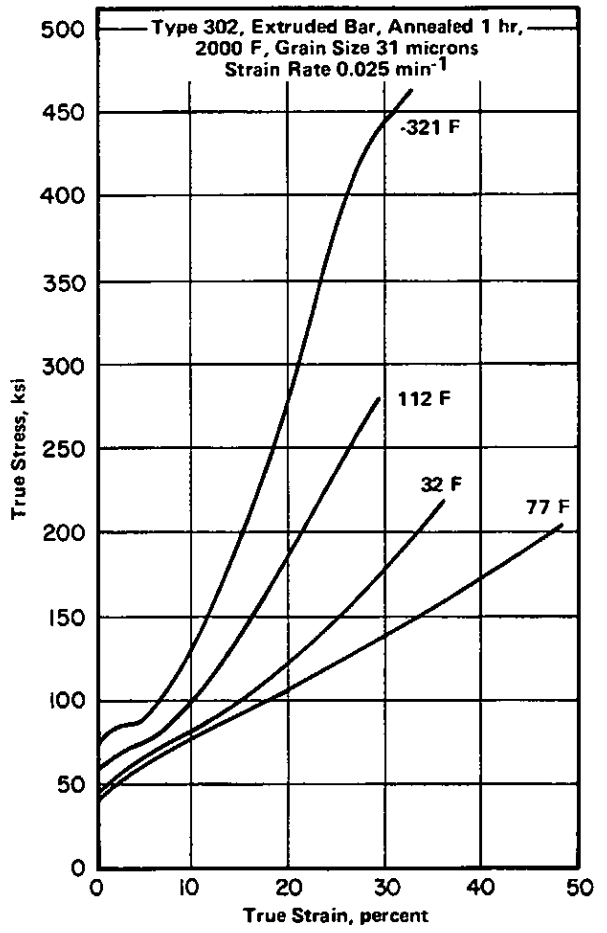


FIGURE 3.03114. TRUE STRESS-STRAIN CURVES FOR ANNEALED TYPE 302 AT ROOM AND CRYOGENIC TEMPERATURES (78)

Fe
18 Cr
8 Ni

Type 301
Type 302

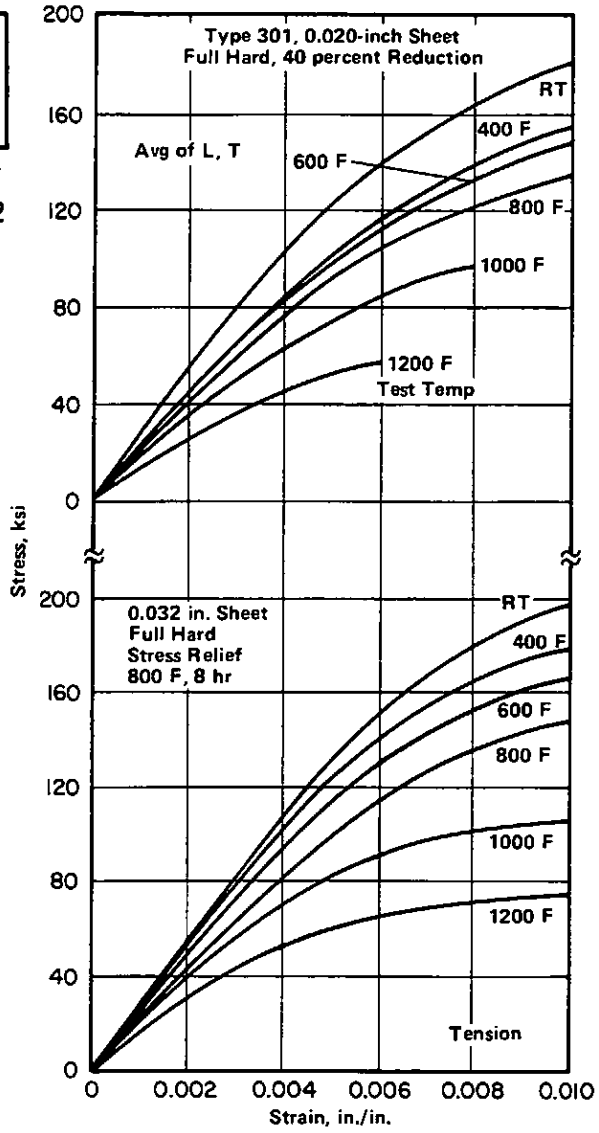


FIGURE 3.03115. STRESS-STRAIN CURVES FOR TYPE 301 FULL-HARD AND FULL-HARD STRESS-RELIEVED SHEET AT ROOM AND ELEVATED TEMPERATURES (11)

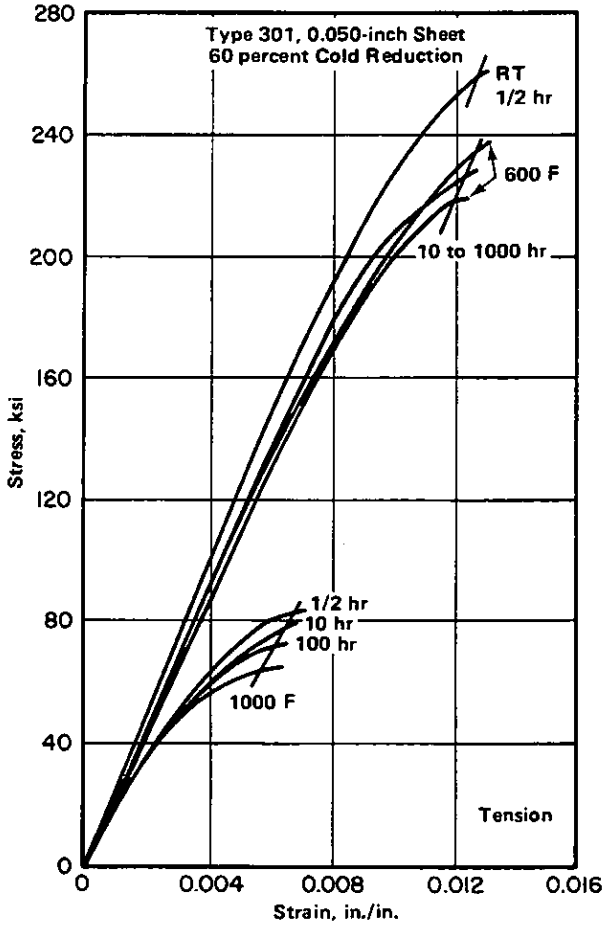


FIGURE 3.03116. STRESS-STRAIN CURVES IN TENSION FOR VARIOUS TEMPERATURES AND EXPOSURE TIMES FOR 60 PERCENT COLD-REDUCED SHEET (38)

Fe
18 Cr
8 Ni

Type 301
Type 302

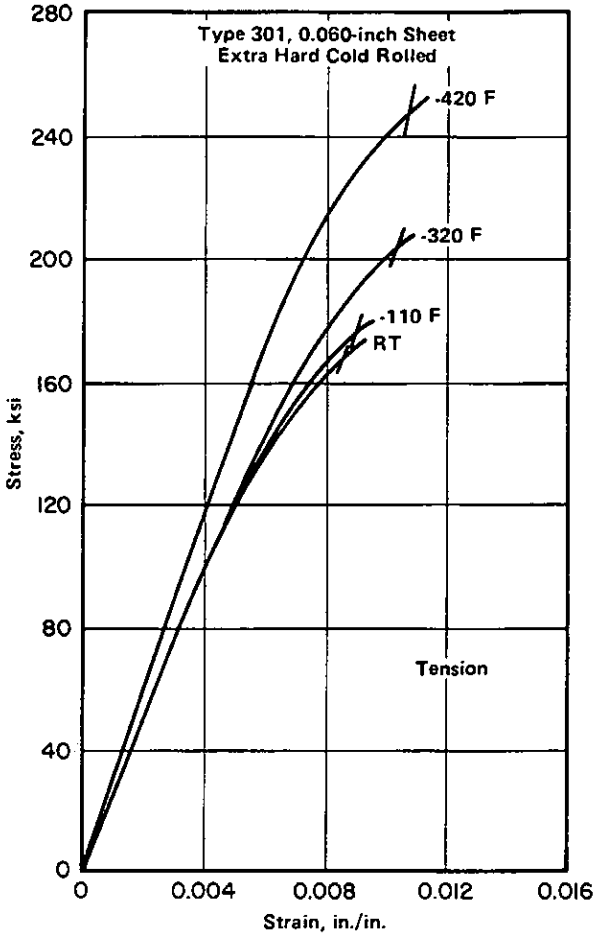


FIGURE 3.03117. STRESS-STRAIN CURVES IN TENSION AT LOW TEMPERATURES OF EXTRA-HARD COLD-ROLLED SHEET (32)

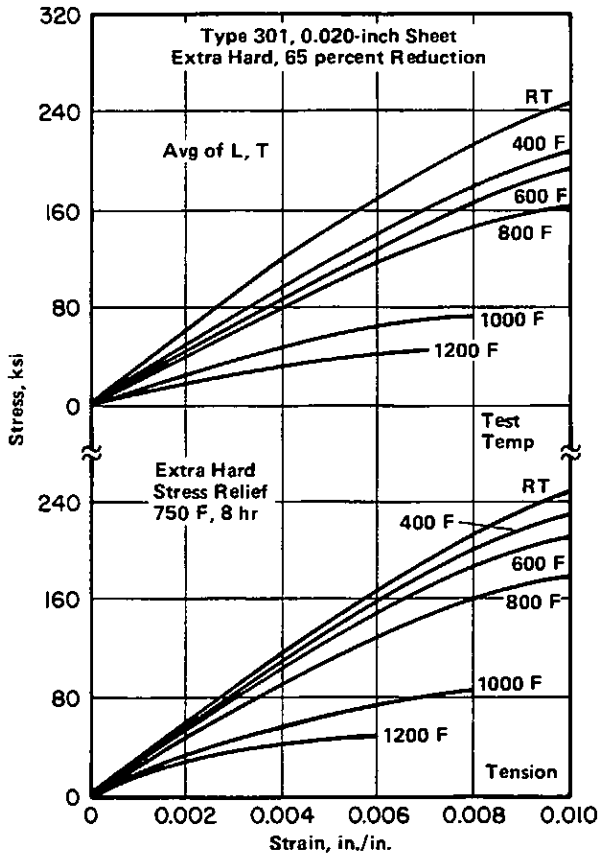


FIGURE 3.03118. STRESS-STRAIN CURVES FOR TYPE 301 EXTRA-HARD AND EXTRA-HARD STRESS-RELIEVED SHEET AT ROOM AND ELEVATED TEMPERATURES (11)

Fe
18 Cr
8 Ni

Type 301
Type 302

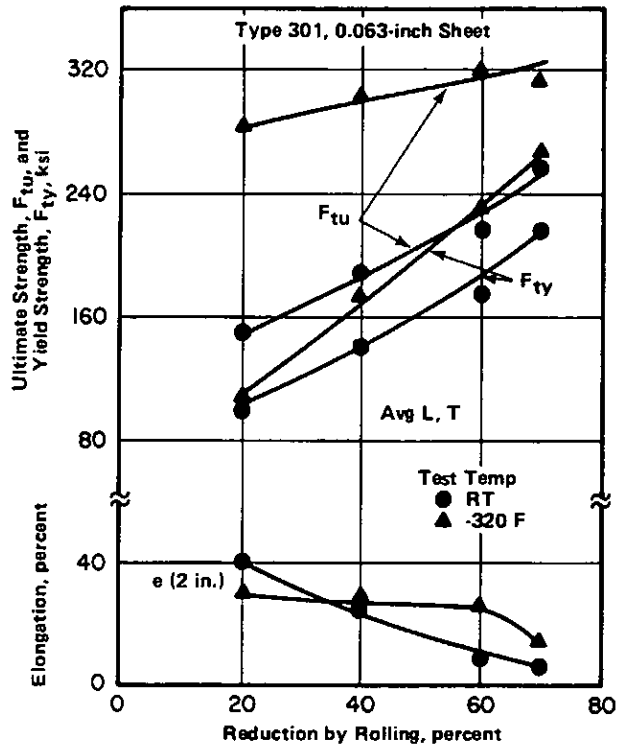


FIGURE 3.03121. EFFECT OF COLD ROLLING ON TENSILE PROPERTIES OF TYPE 301 SHEET AT ROOM TEMPERATURE AND -320 F (18)

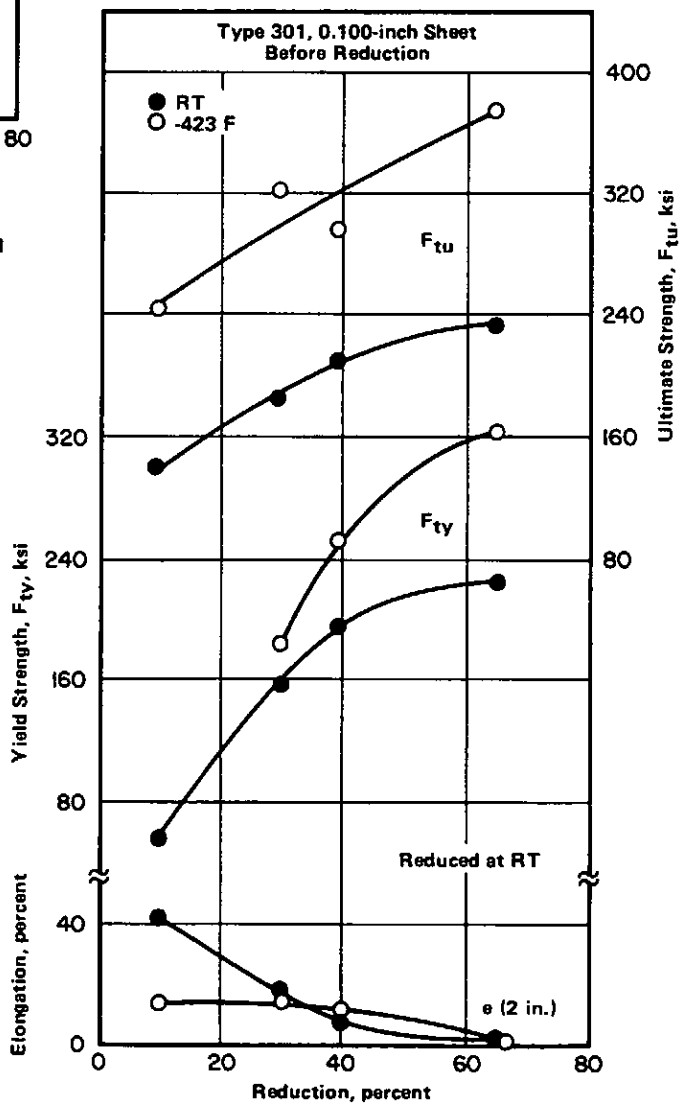


FIGURE 3.03122. EFFECT OF PERCENT REDUCTION ON TENSILE PROPERTIES OF SHEET TESTED AT ROOM TEMPERATURE AND -423 F (24)

Fe
18 Cr
8 Ni

Type 301
Type 302

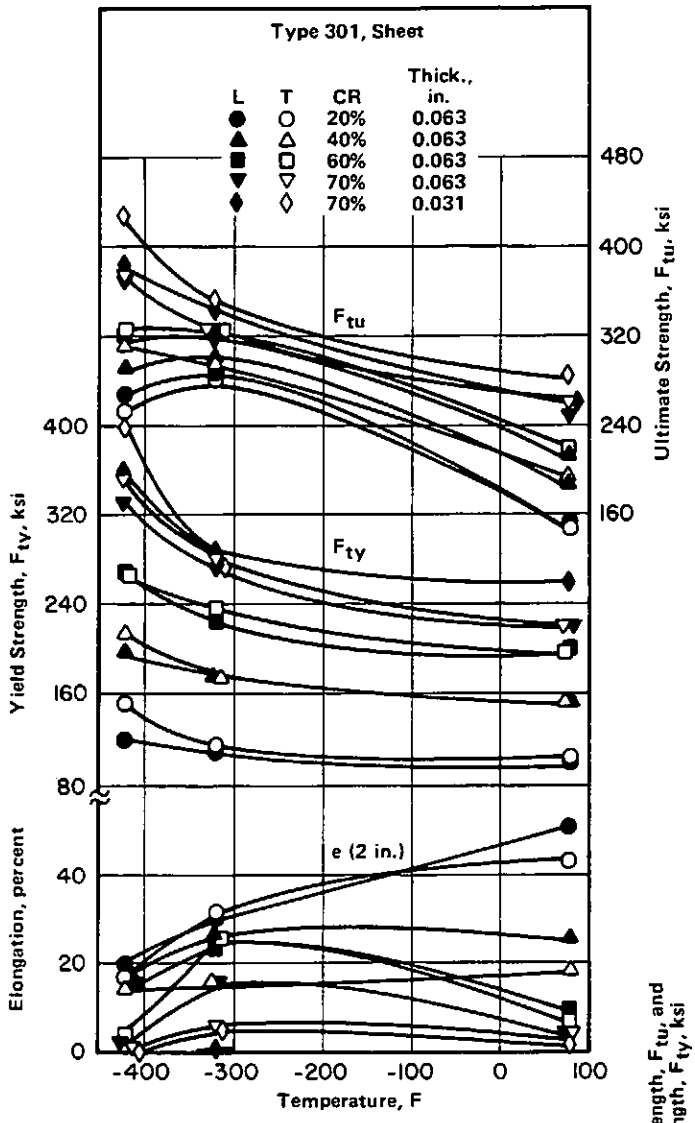


FIGURE 3.03123. EFFECT OF LOW TEMPERATURE AND PERCENT COLD REDUCTION ON TENSILE PROPERTIES OF SHEET (34)

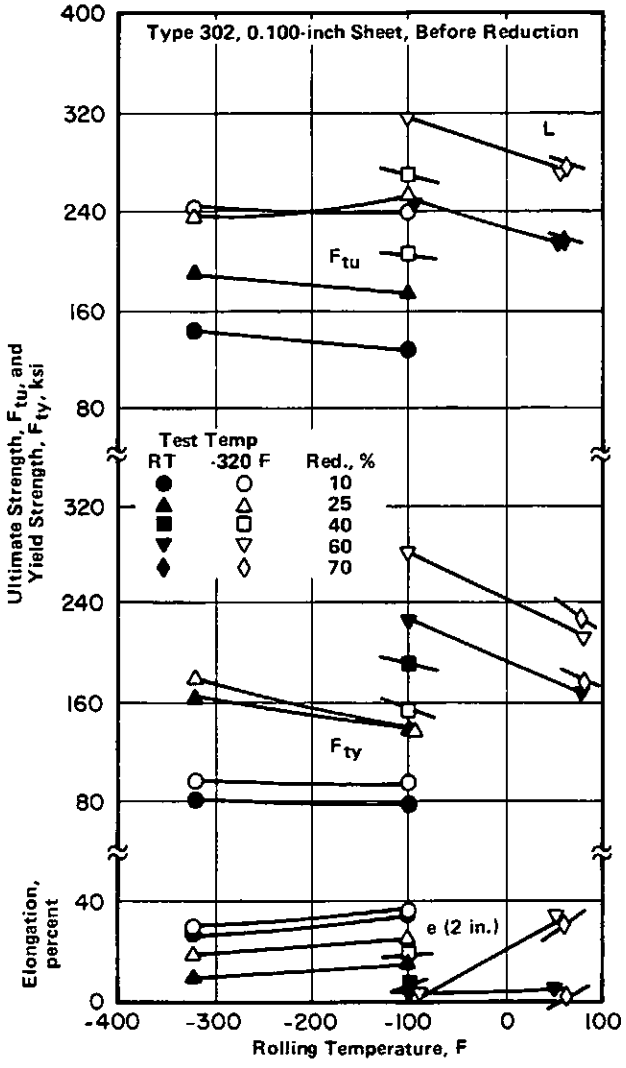


FIGURE 3.03124. EFFECT OF LOW ROLLING TEMPERATURE ON TENSILE PROPERTIES AT ROOM TEMPERATURE AND -320 F OF REDUCED SHEET (24)

Fe
18 Cr
8 Ni

Type 301
Type 302

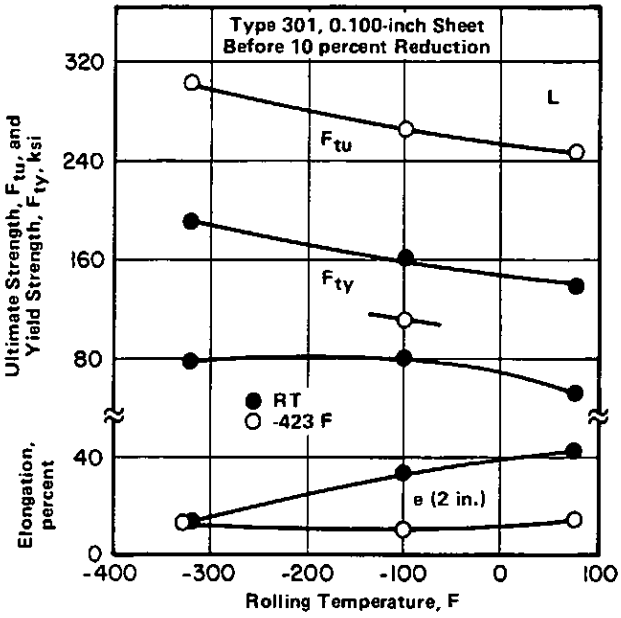


FIGURE 3.03125. EFFECT OF LOW ROLLING TEMPERATURE ON TENSILE PROPERTIES AT ROOM TEMPERATURE AND -423 F OF 10 PERCENT REDUCED SHEET (24)

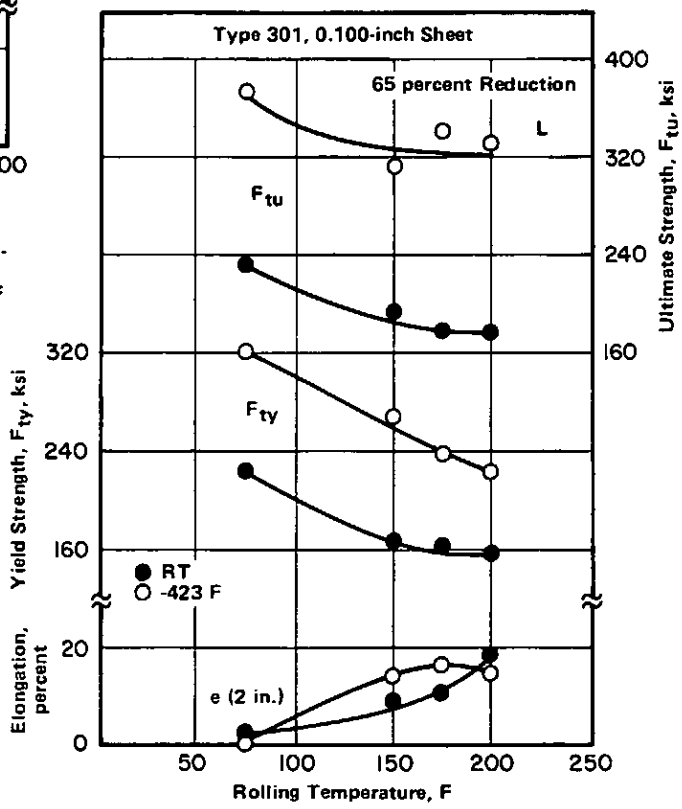


FIGURE 3.03126. EFFECT OF ROLLING TEMPERATURE ON TENSILE PROPERTIES AT ROOM TEMPERATURE AND -423 F OF 65 PERCENT REDUCED SHEET (24)

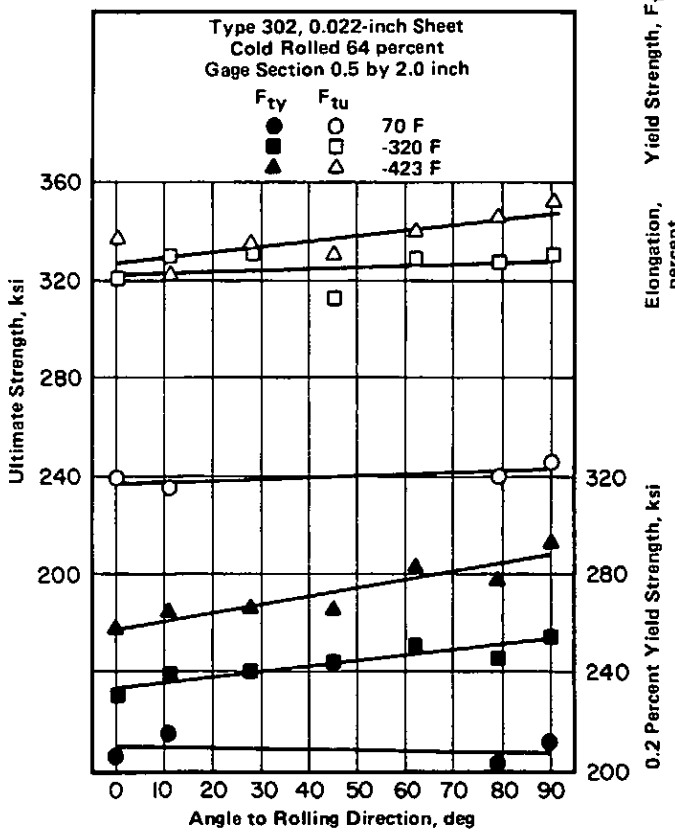


FIGURE 3.03127. EFFECT OF TEST DIRECTION ON TENSILE STRENGTH OF COLD-ROLLED SHEET AT ROOM AND CRYOGENIC TEMPERATURES (79)

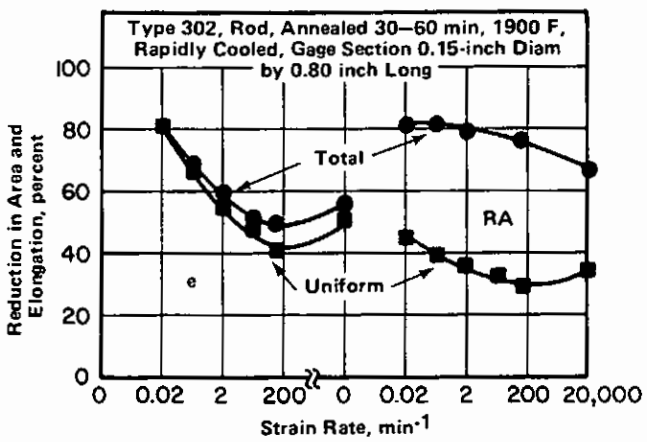


FIGURE 3.03132. EFFECTS OF STRAIN RATE ON TENSILE DUCTILITY OF TYPE 302 AT ROOM TEMPERATURE (80)

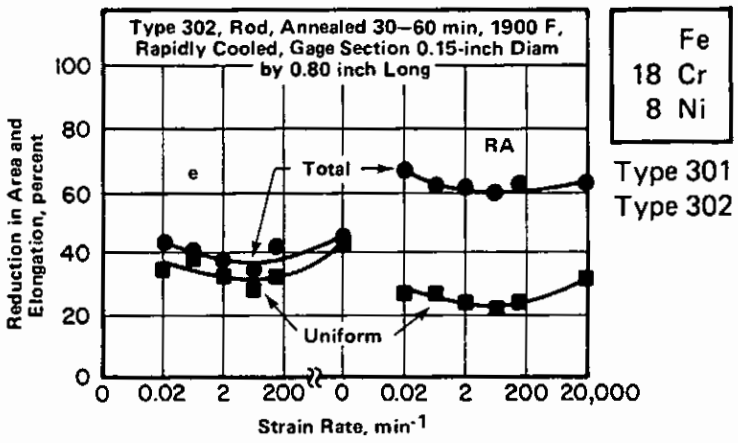


FIGURE 3.03133. EFFECTS OF STRAIN RATE ON TENSILE DUCTILITY OF TYPE 302 AT -321 F (80)

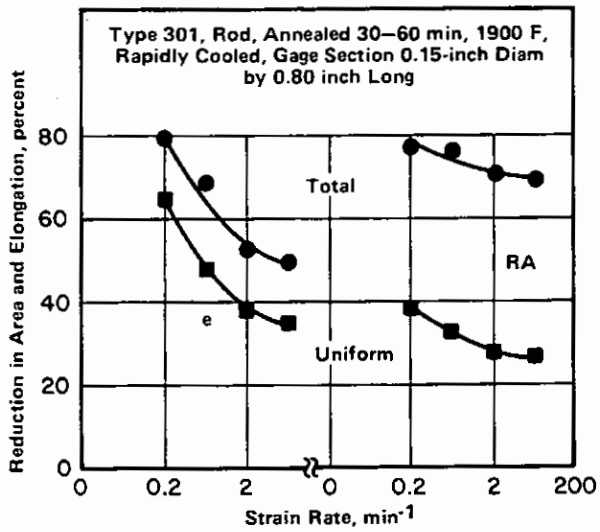


FIGURE 3.03134. EFFECTS OF STRAIN RATE ON TENSILE DUCTILITY OF TYPE 301 AT ROOM TEMPERATURE (80)

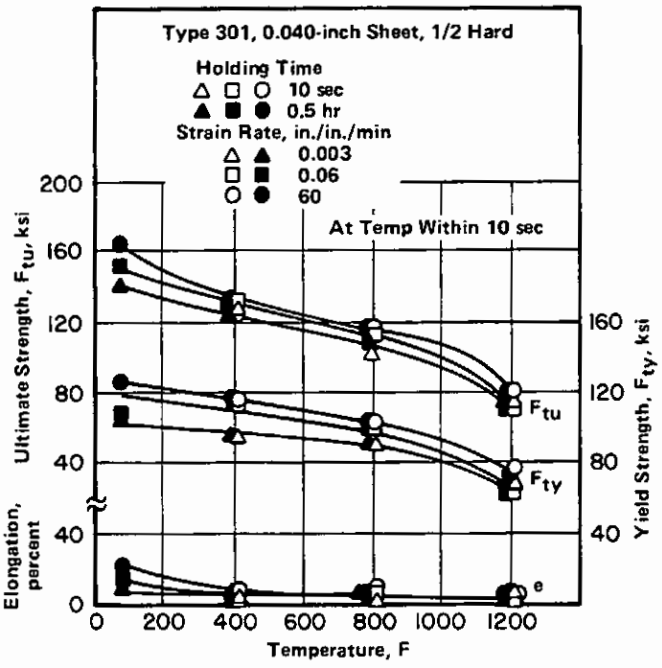


FIGURE 3.03135. EFFECT OF TEST TEMPERATURE, STRAIN RATE, AND HOLDING TIME ON TENSILE PROPERTIES OF TYPE 301 1/2-HARD SHEET (17)

Fe
18 Cr
8 Ni

Type 301
Type 302

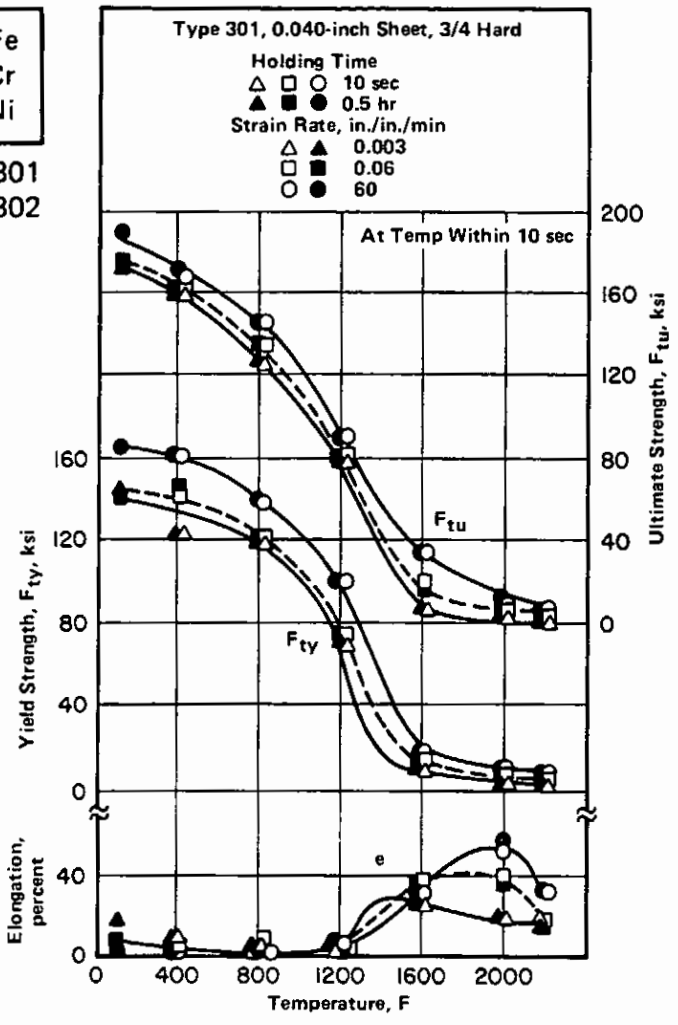


FIGURE 3.03136. EFFECT OF TEST TEMPERATURE, STRAIN RATE, AND HOLDING TIME ON TENSILE PROPERTIES OF TYPE 301 3/4-HARD SHEET (17)

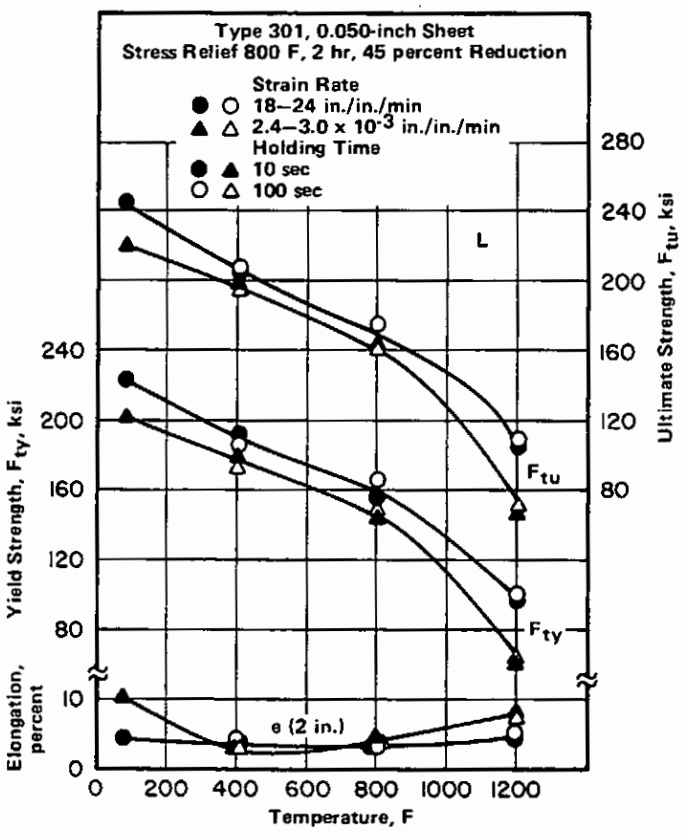


FIGURE 3.03137. EFFECT OF TEST TEMPERATURE, STRAIN RATE, AND HOLDING TIME ON TENSILE PROPERTIES OF 45 PERCENT REDUCED SHEET (28)

Fe
18 Cr
8 Ni

Type 301
Type 302

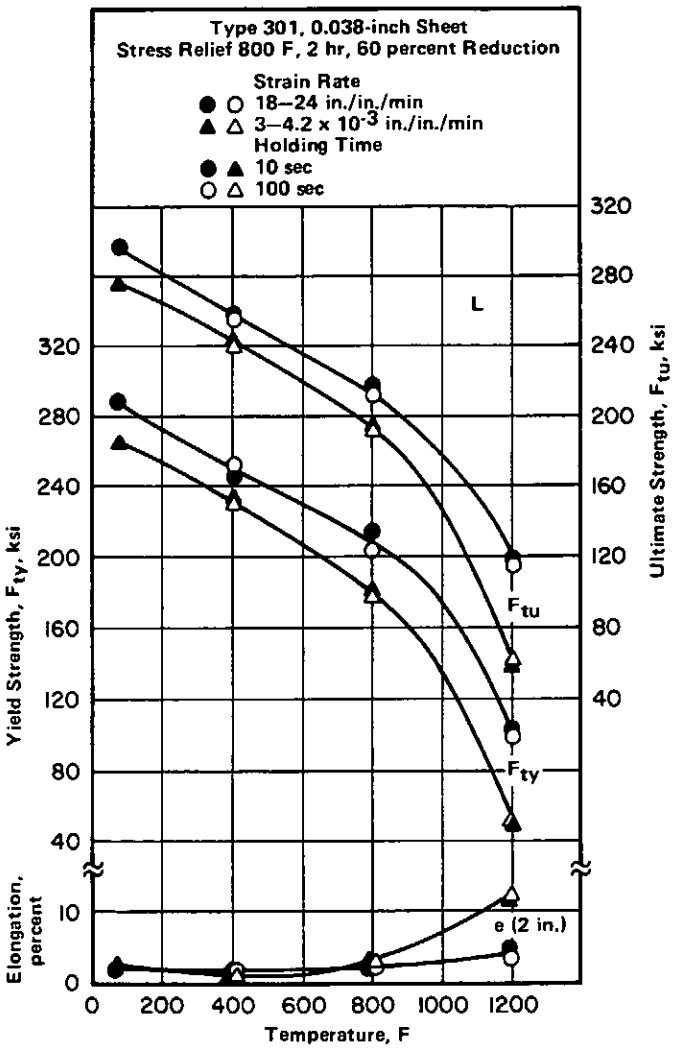


FIGURE 3.03138. EFFECT OF TEST TEMPERATURE, STRAIN RATE, AND HOLDING TIME ON TENSILE PROPERTIES OF 60 PERCENT REDUCED SHEET (28)

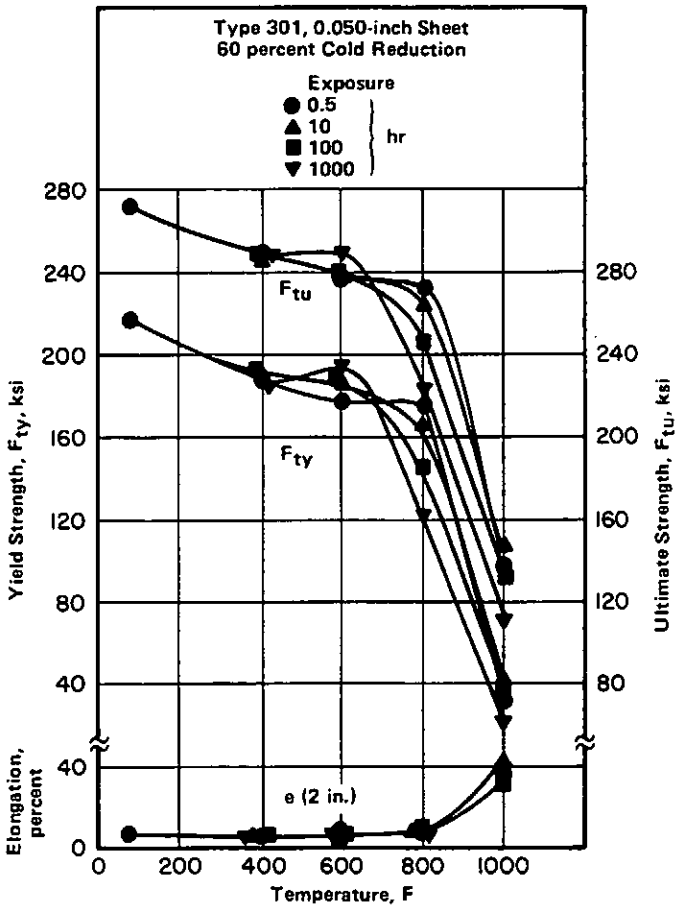


FIGURE 3.03139. EFFECT OF TEST TEMPERATURE AND EXPOSURE TIME ON TENSILE PROPERTIES OF 60 PERCENT COLD-REDUCED SHEET (38)

Fe
18 Cr
8 Ni

Type 301
Type 302

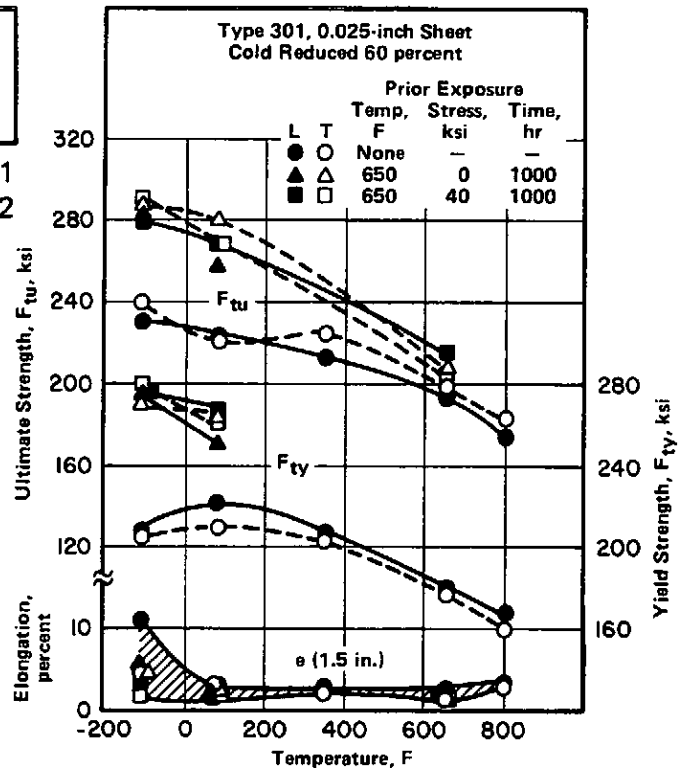


FIGURE 3.031312. EFFECT OF TEST TEMPERATURE AND PRIOR EXPOSURE ON TENSILE PROPERTIES OF 60 PERCENT COLD-REDUCED SHEET (45)

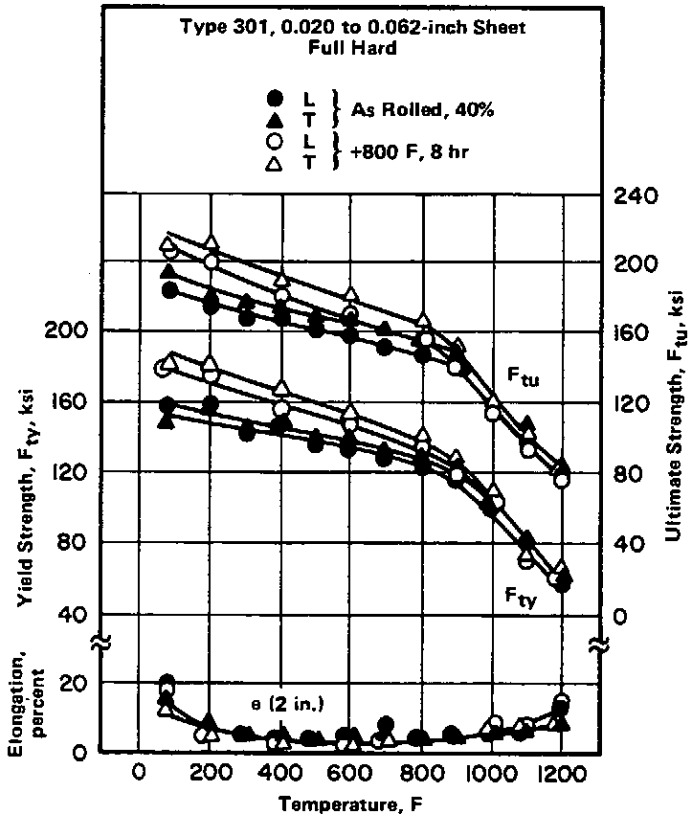


FIGURE 3.03141. EFFECT OF TEST TEMPERATURE, TEST DIRECTION, AND STRESS RELIEF ON TENSILE PROPERTIES OF TYPE 301 FULL-HARD SHEET (11)

Fe
18 Cr
8 Ni

Type 301
Type 302

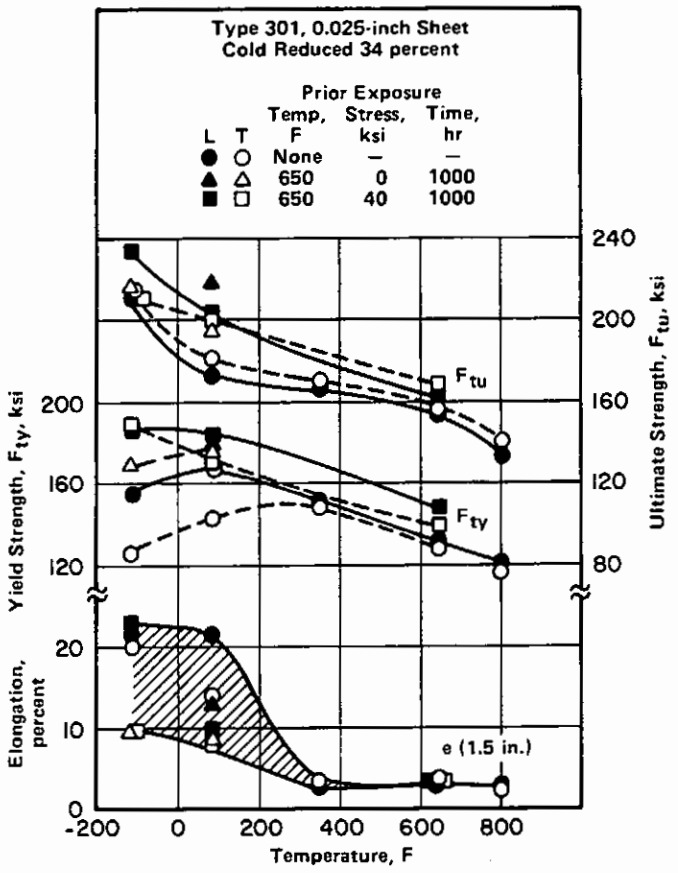


FIGURE 3.031310. EFFECT OF TEST TEMPERATURE AND PRIOR EXPOSURE ON TENSILE PROPERTIES OF 34 PERCENT COLD-REDUCED SHEET (45)

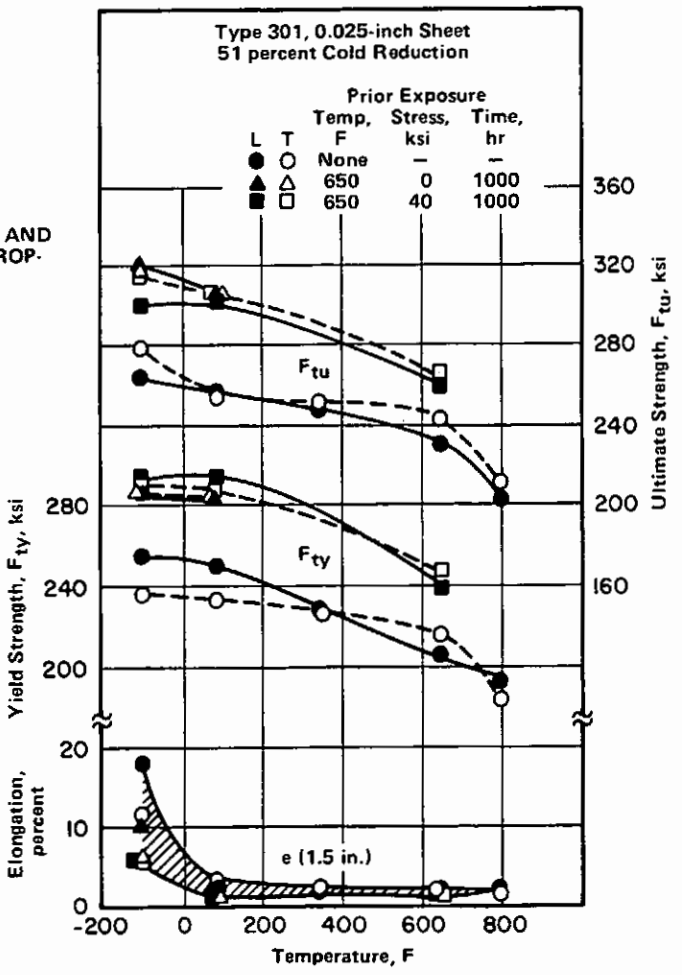


FIGURE 3.031311. EFFECT OF TEST TEMPERATURE AND PRIOR EXPOSURE ON TENSILE PROPERTIES OF 51 PERCENT COLD-REDUCED SHEET (45)

Fe
18 Cr
8 Ni

Type 301
Type 302

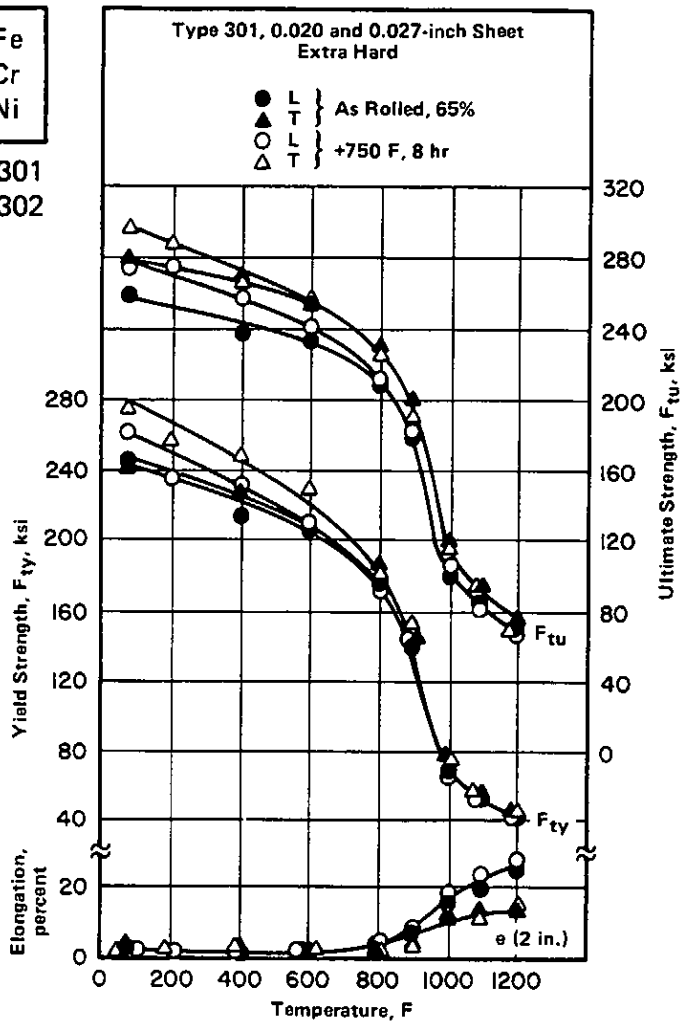


FIGURE 3.03142. EFFECT OF TEST TEMPERATURE, TEST DIRECTION, AND STRESS RELIEF ON TENSILE PROPERTIES OF TYPE 301 EXTRA-HARD SHEET (11)

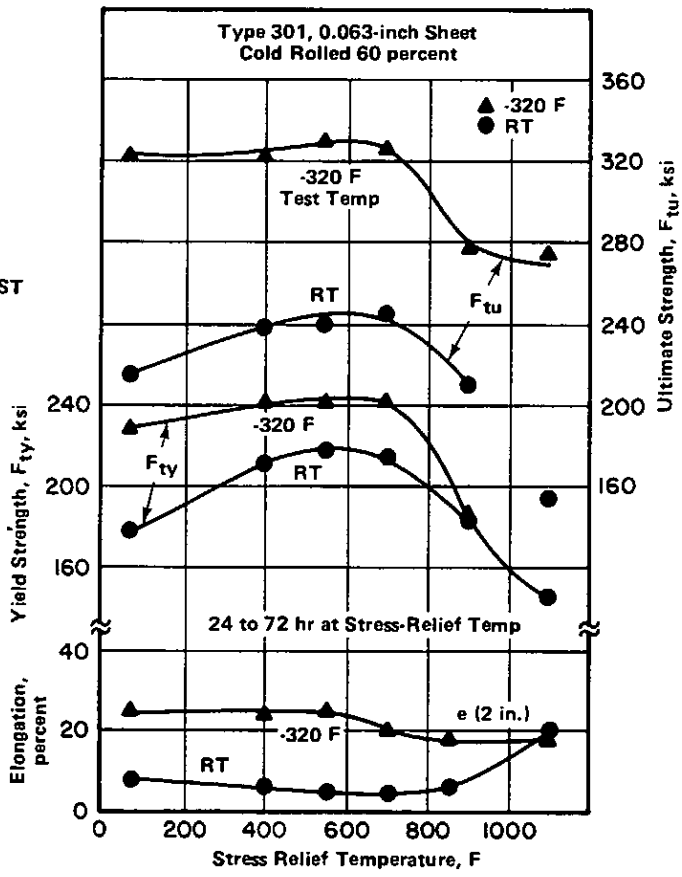


FIGURE 3.03143. EFFECT OF STRESS RELIEF AND TEST TEMPERATURE ON TENSILE PROPERTIES OF COLD-ROLLED SHEET (18)

Fe
18 Cr
8 Ni

Type 301
Type 302

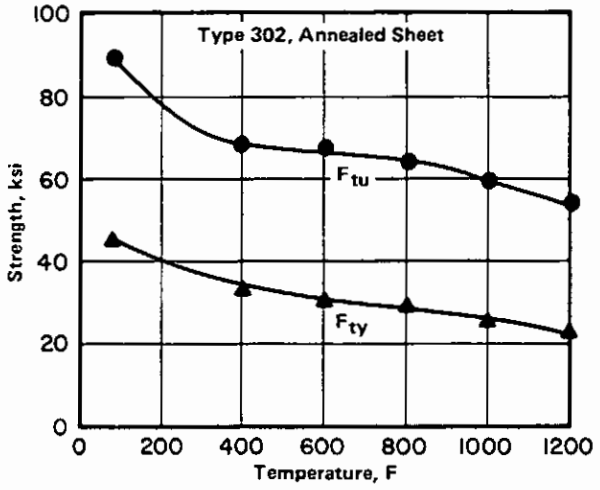


FIGURE 3.03151. EFFECT OF TEST TEMPERATURE ON TENSILE STRENGTH OF ANNEALED TYPE 302 SHEET (62)

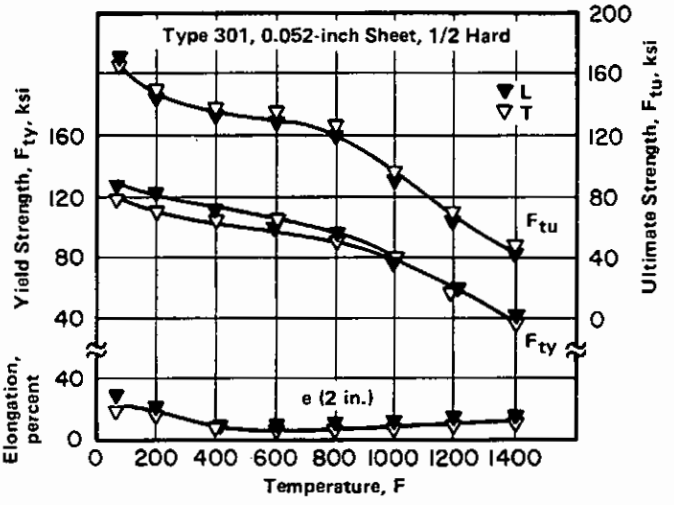


FIGURE 3.03152. EFFECT OF TEST TEMPERATURE ON TENSILE PROPERTIES OF TYPE 301, 1/2 HARD SHEET (11)

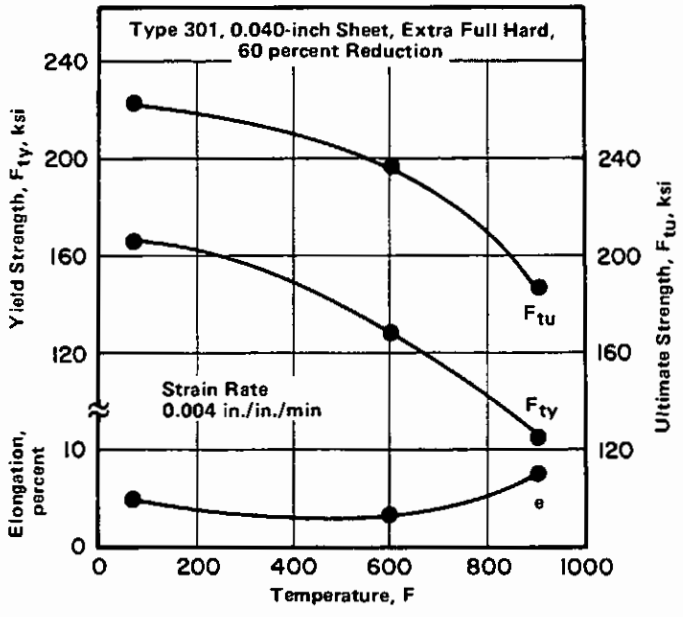


FIGURE 3.03153. EFFECT OF TEST TEMPERATURE ON TENSILE PROPERTIES OF 60 PERCENT REDUCED SHEET (26)

Fe
18 Cr
8 Ni

Type 301
Type 302

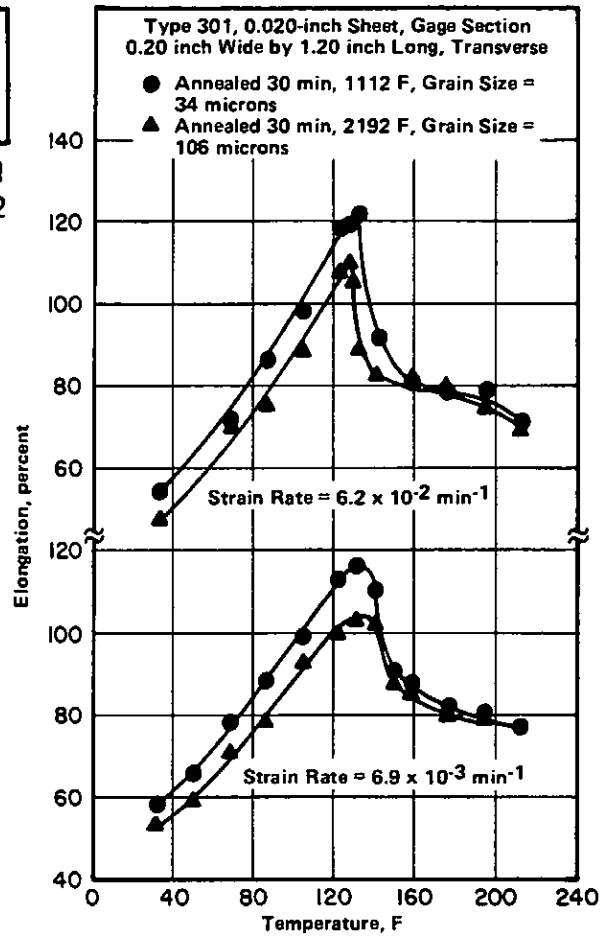


FIGURE 3.03155. EFFECTS OF GRAIN SIZE, STRAIN RATE, AND TEMPERATURE ON TENSILE ELONGATION OF TYPE 301 (77)

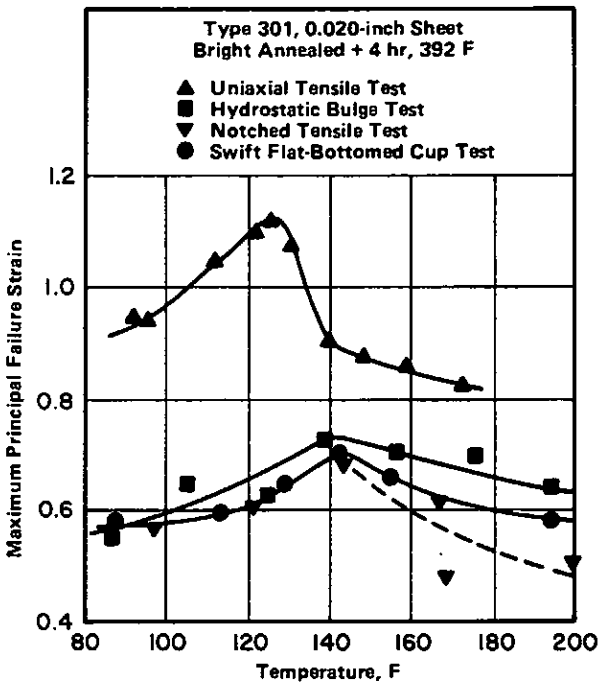


FIGURE 3.03156. EFFECTS OF TEMPERATURE ON FAILURE STRAIN FOR SEVERAL TYPES OF DEFORMATION (81)

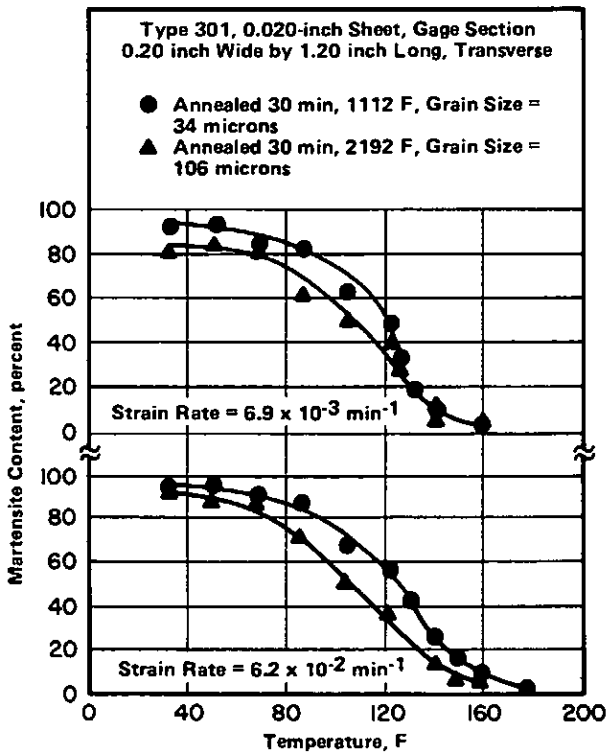


FIGURE 3.03157. EFFECTS OF GRAIN SIZE, STRAIN RATE, AND TEMPERATURE ON MARTENSITE CONTENT OF FRACTURED TENSILE SPECIMENS OF TYPE 301 (77)

Fe
18 Cr
8 Ni

Type 301
Type 302

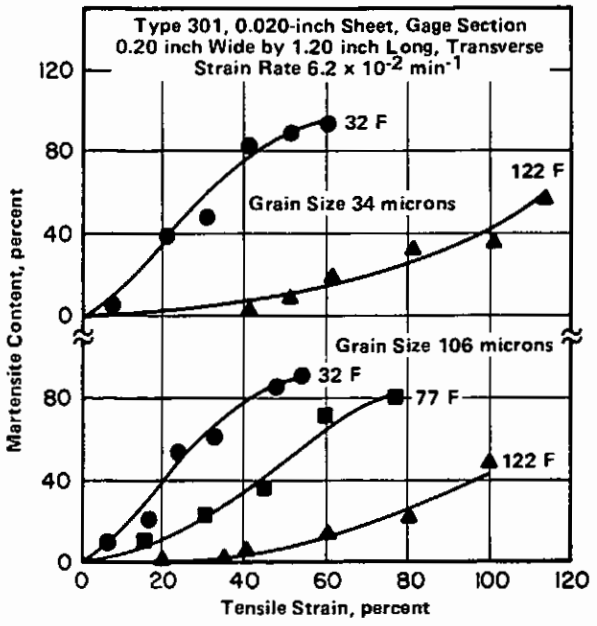


FIGURE 3.03158. EFFECTS OF GRAIN SIZE, TEST TEMPERATURE, AND TENSILE STRAIN ON MARTENSITE CONTENT OF TYPE 301 (77)

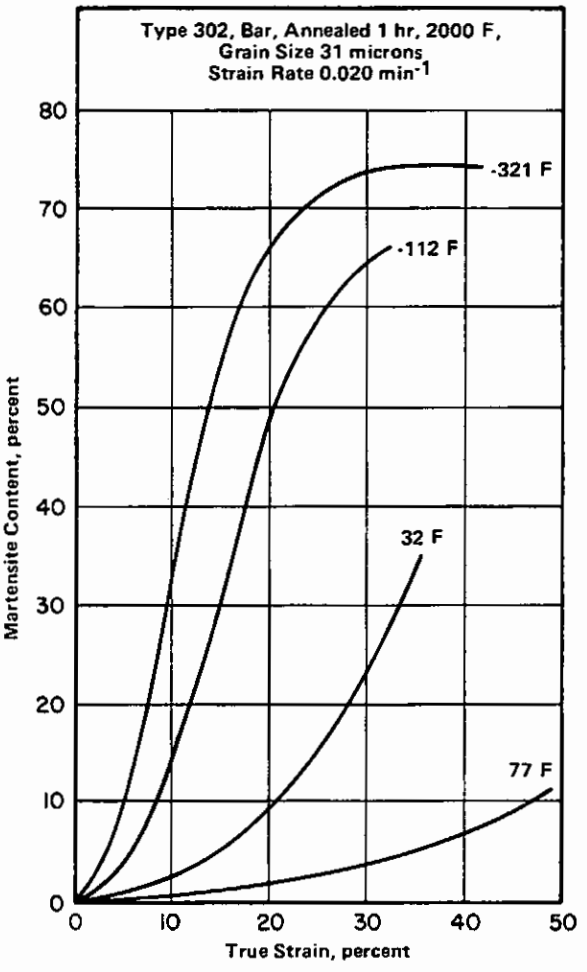


FIGURE 3.03159. EFFECTS OF TEST TEMPERATURE AND TRUE TENSILE STRAIN ON MARTENSITE CONTENT OF TYPE 302 (78)

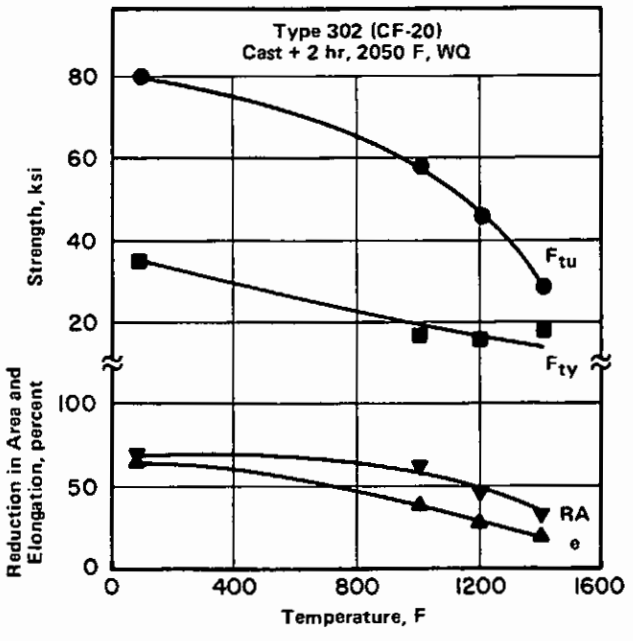


FIGURE 3.031510. EFFECTS OF TEMPERATURE ON TENSILE PROPERTIES OF CAST TYPE 302 (62)

Fe
18 Cr
8 Ni

Type 301
Type 302

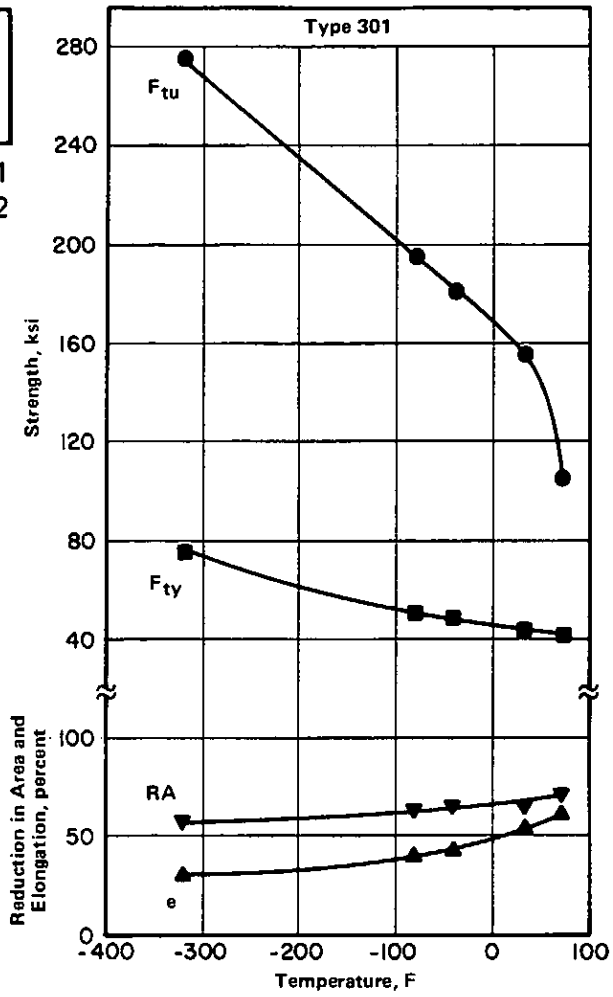


FIGURE 3.03161. EFFECT OF CRYOGENIC TEMPERATURES ON NOMINAL TENSILE PROPERTIES OF ANNEALED TYPE 301 SHEET, STRIP, PLATE, AND BAR (51)

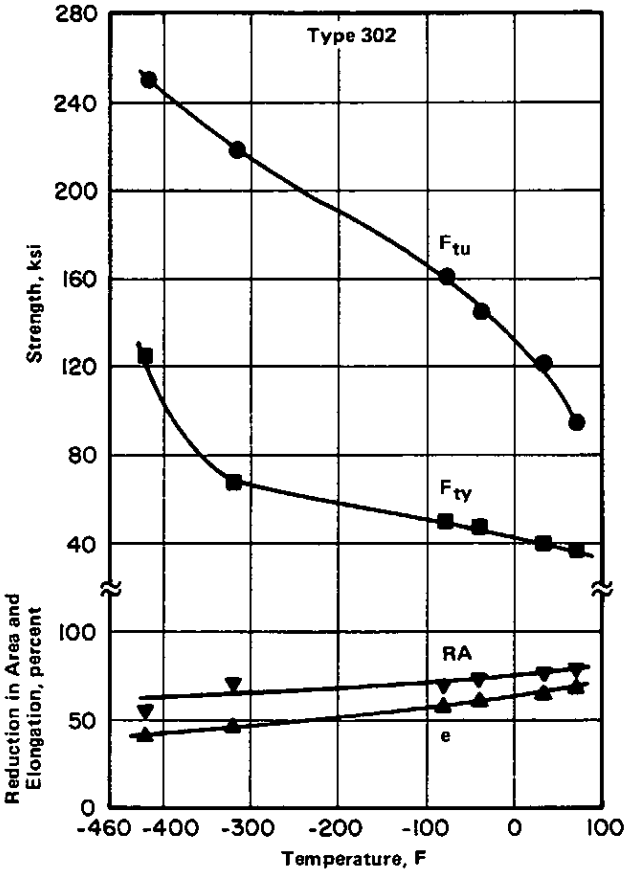


FIGURE 3.03162. EFFECT OF CRYOGENIC TEMPERATURES ON NOMINAL TENSILE PROPERTIES OF ANNEALED TYPE 302 SHEET, STRIP, PLATE, AND BAR (51)

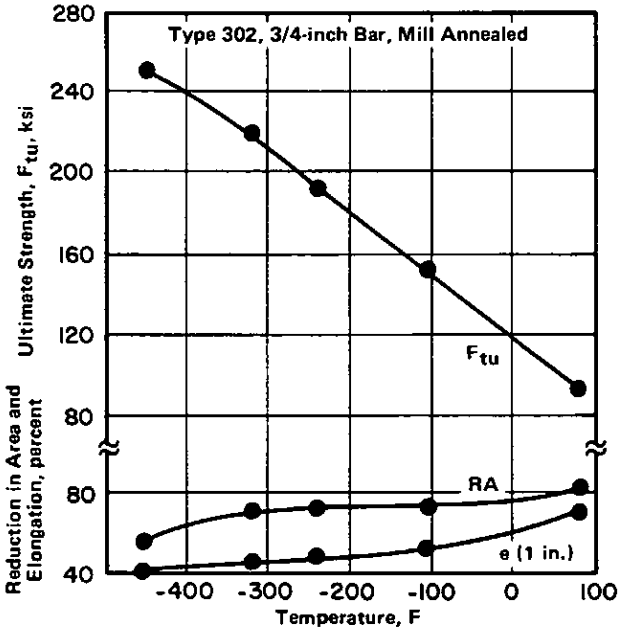


FIGURE 3.03163. EFFECT OF CRYOGENIC TEMPERATURES ON THE TENSILE PROPERTIES OF ANNEALED BAR (33)

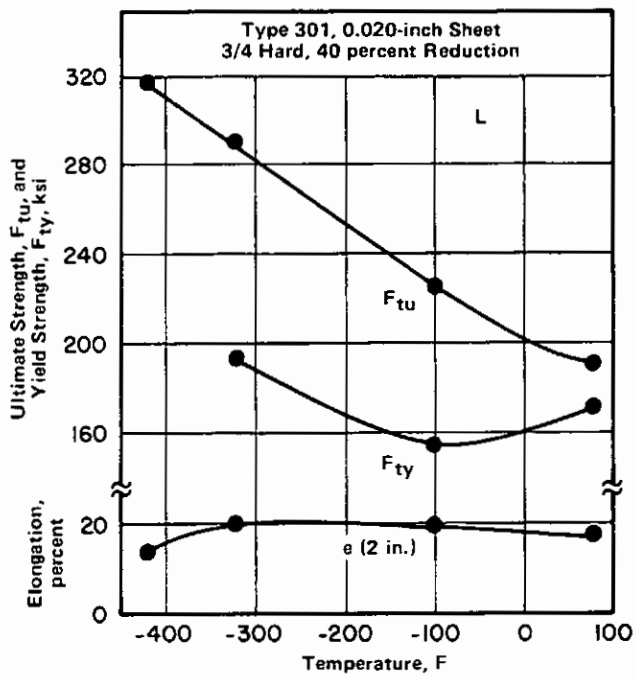
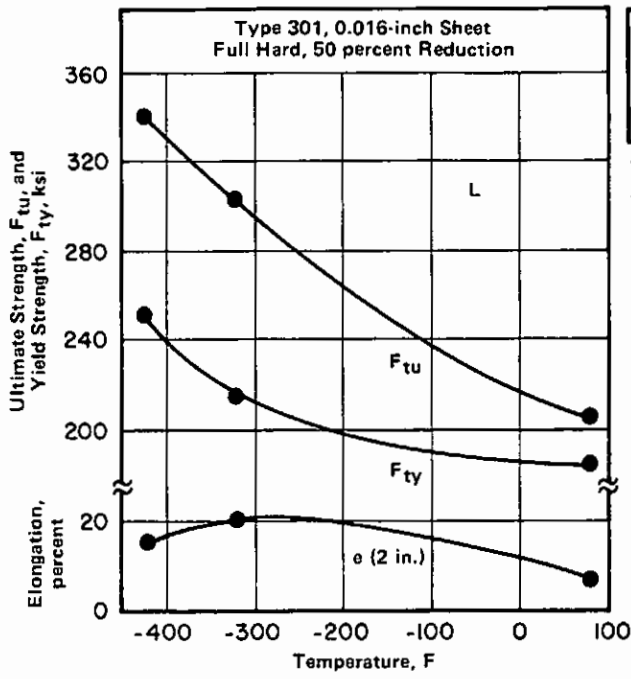


FIGURE 3.03164. EFFECT OF CRYOGENIC TEMPERATURES ON TENSILE PROPERTIES OF 40 PERCENT REDUCED SHEET (31)



Fe
18 Cr
8 Ni

Type 301
Type 302

FIGURE 3.03165. EFFECT OF CRYOGENIC TEMPERATURES ON TENSILE PROPERTIES OF 50 PERCENT REDUCED SHEET (31)

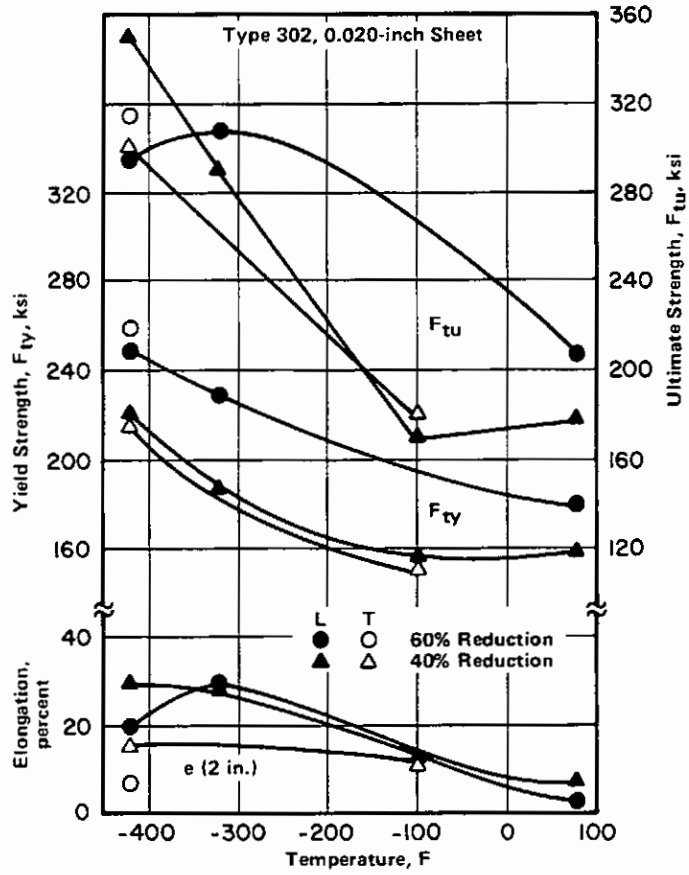


FIGURE 3.03166. EFFECT OF CRYOGENIC TEMPERATURES ON TENSILE PROPERTIES OF 40 AND 60 PERCENT REDUCED SHEET (31)

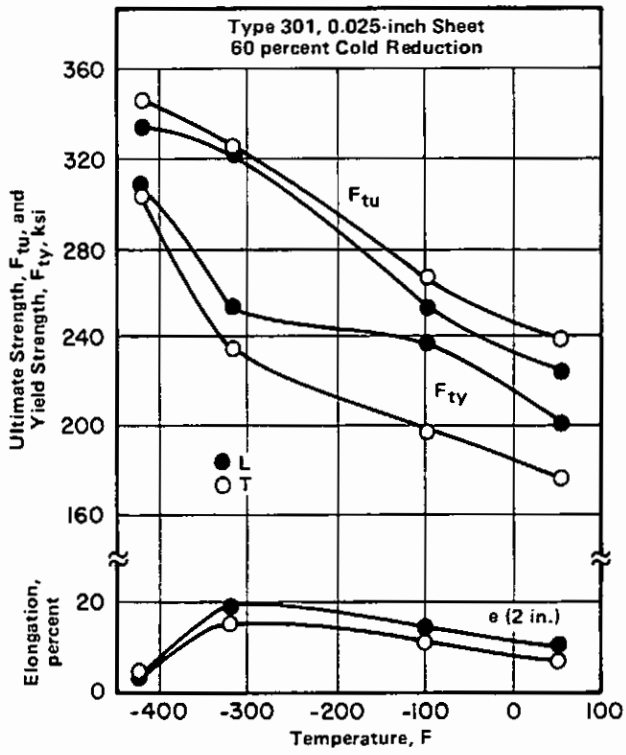


FIGURE 3.03167. EFFECT OF CRYOGENIC TEMPERATURES ON TENSILE PROPERTIES OF 60 PERCENT COLD-REDUCED SHEET (36)

Fe
18 Cr
8 Ni

Type 301
Type 302

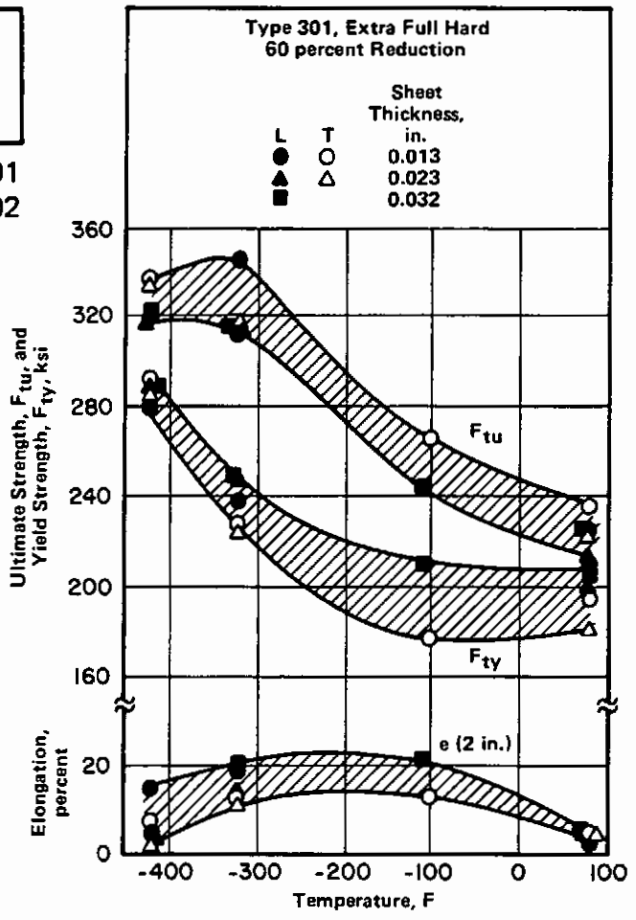


FIGURE 3.03168. EFFECTS OF CRYOGENIC TEMPERATURES AND THICKNESS ON TENSILE PROPERTIES OF 60 PERCENT REDUCED SHEET (31)

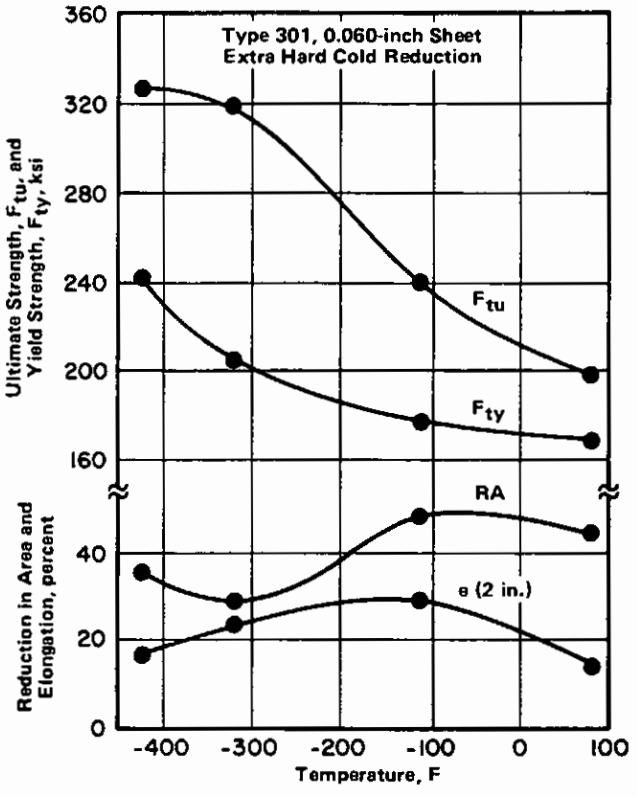


FIGURE 3.03169. EFFECT OF CRYOGENIC TEMPERATURES ON TENSILE PROPERTIES OF EXTRA-HARD COLD-ROLLED SHEET (32)

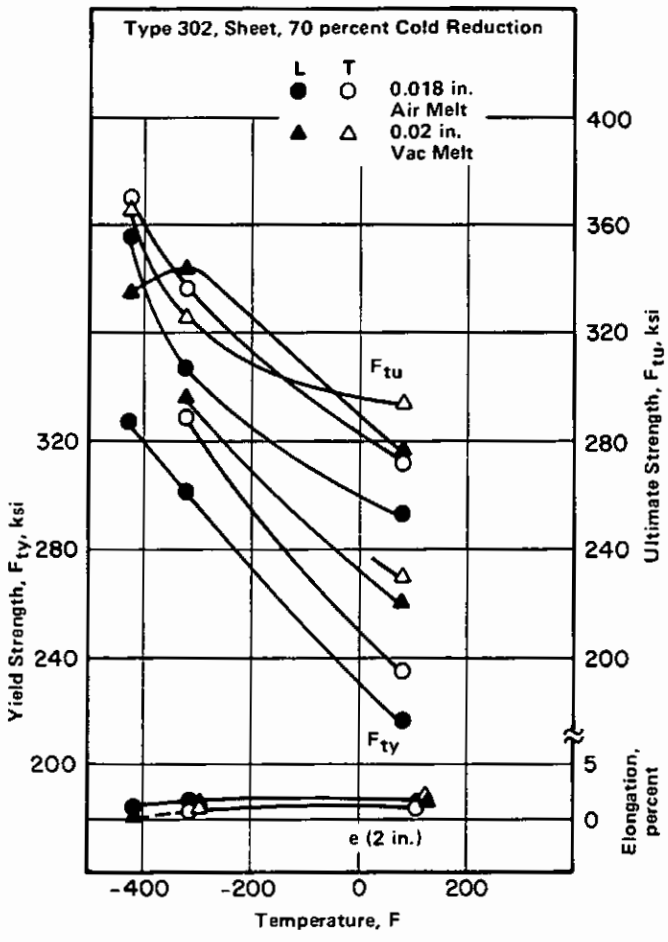
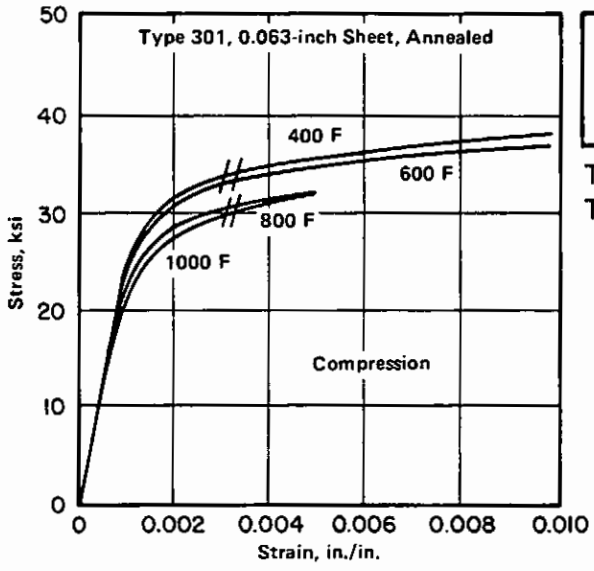


FIGURE 3.031610. EFFECTS OF CRYOGENIC TEMPERATURES AND MELT METHOD ON TENSILE PROPERTIES OF 70 PERCENT REDUCED SHEET (23)



Fe
18 Cr
8 Ni

Type 301
Type 302

FIGURE 3.03211. STRESS-STRAIN CURVES IN COMPRESSION FOR TYPE 301 ANNEALED SHEET AT ELEVATED TEMPERATURES (19)

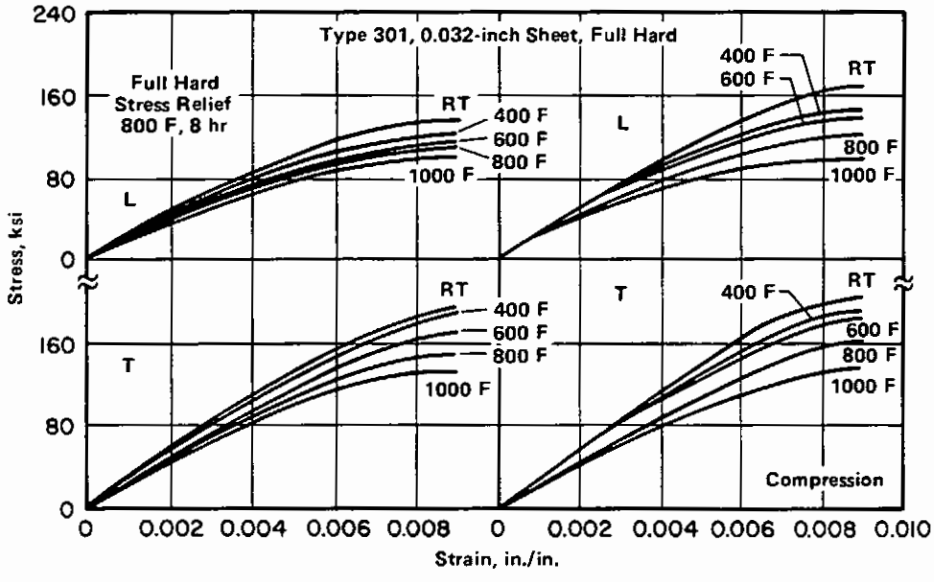


FIGURE 3.03212. STRESS-STRAIN CURVES IN COMPRESSION FOR TYPE 301 FULL-HARD AND FULL-HARD STRESS-RELIEVED SHEET AT ROOM AND ELEVATED TEMPERATURES (11)

Fe
18 Cr
8 Ni

Type 301
Type 302

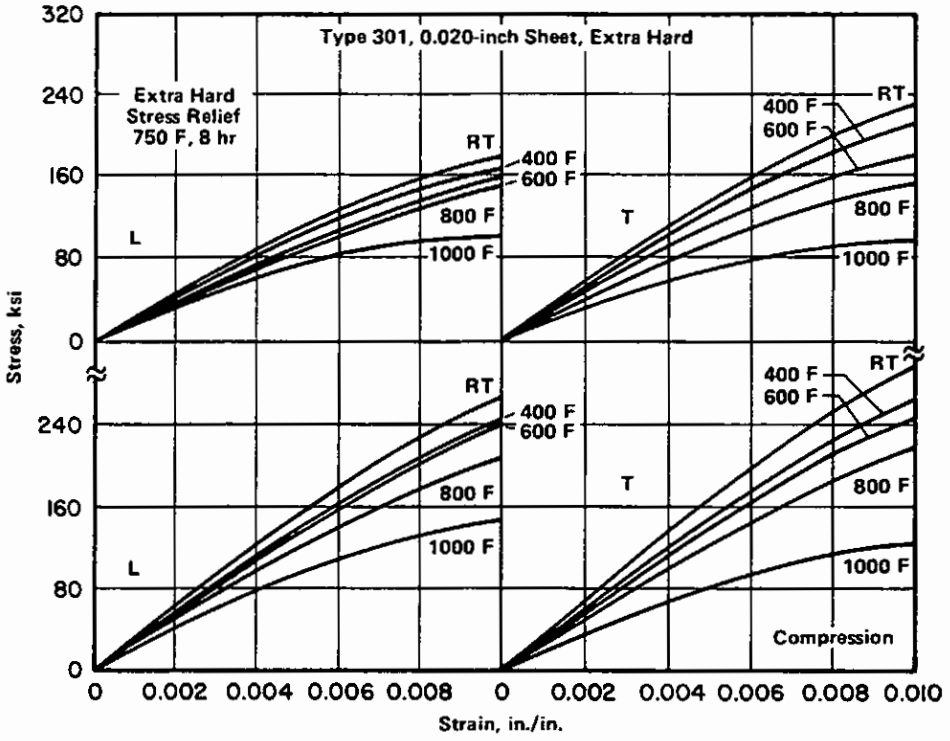


FIGURE 3.03213. STRESS-STRAIN CURVES IN COMPRESSION FOR TYPE 301 EXTRA-HARD AND EXTRA-HARD STRESS-RELIEVED SHEET AT ROOM AND ELEVATED TEMPERATURES (11)

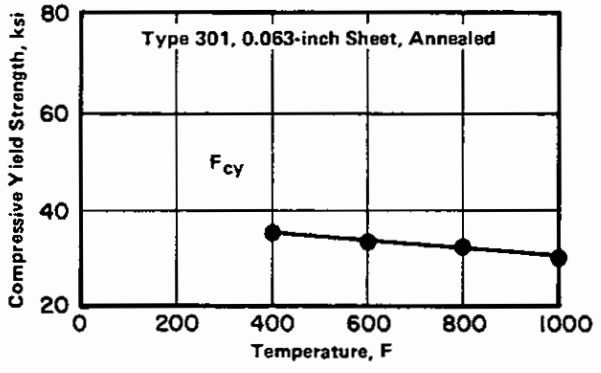


FIGURE 3.0322. EFFECT OF TEST TEMPERATURE ON COMPRESSIVE YIELD STRENGTH OF TYPE 301 ANNEALED SHEET (19)

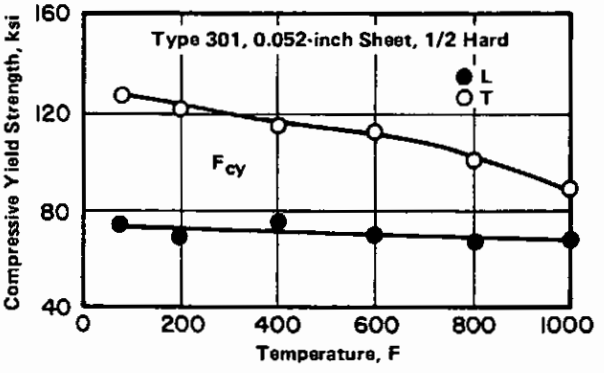


FIGURE 3.0323. EFFECT OF TEST TEMPERATURE AND TEST DIRECTION ON COMPRESSIVE YIELD STRENGTH OF TYPE 301 1/2-HARD SHEET (11)

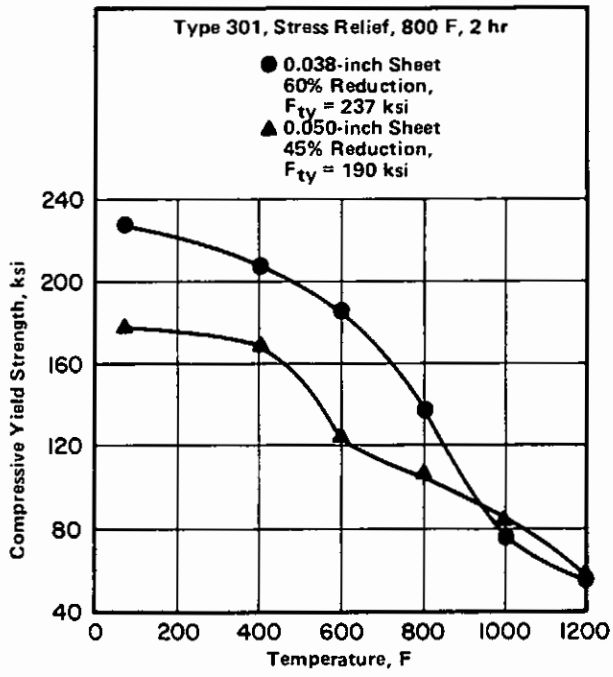
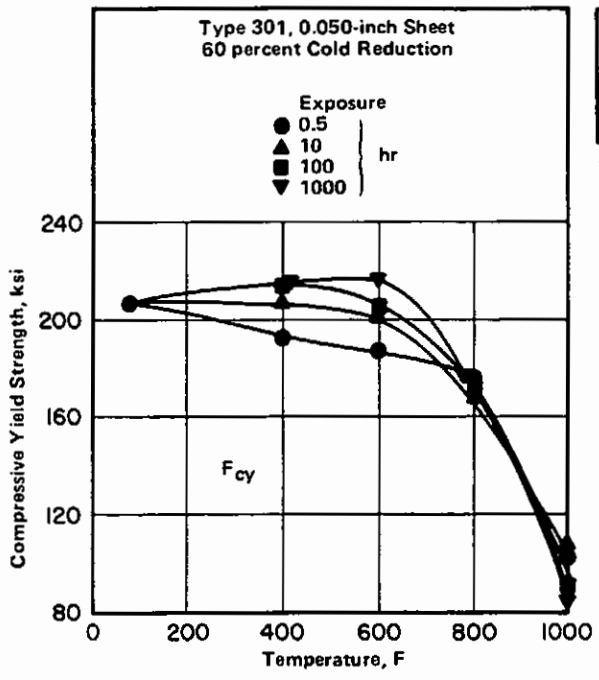


FIGURE 3.0324. EFFECT OF TEST TEMPERATURE ON COMPRESSIVE YIELD STRENGTH OF 45 AND 60 PERCENT REDUCED SHEET (28)



Fe
18 Cr
8 Ni

Type 301
Type 302

FIGURE 3.0325. EFFECT OF TEST TEMPERATURE AND EXPOSURE TIME ON COMPRESSIVE YIELD STRENGTH OF 60 PERCENT COLD-REDUCED SHEET (38)

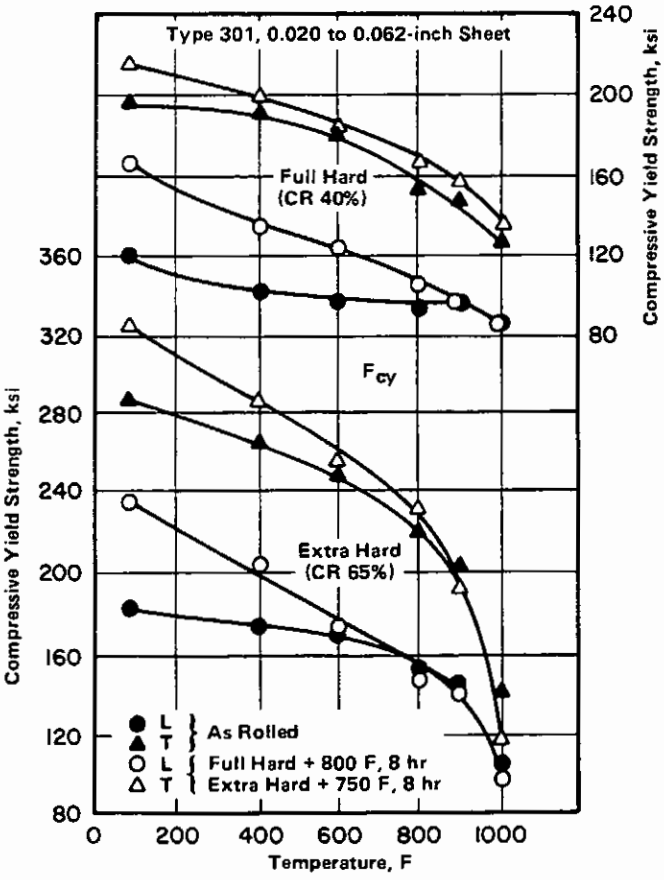


FIGURE 3.0326. EFFECT OF TEST TEMPERATURE, TEST DIRECTION, AND STRESS RELIEF ON COMPRESSIVE YIELD STRENGTH OF TYPE 301 FULL-HARD AND EXTRA-HARD SHEET (11)

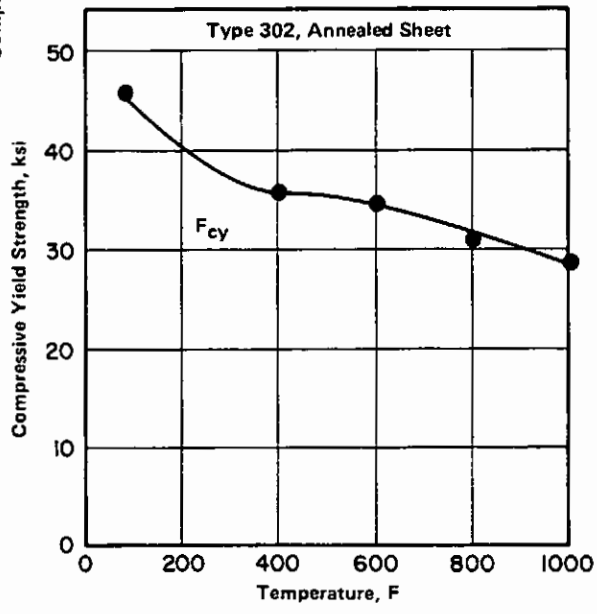


FIGURE 3.0327. EFFECT OF TEST TEMPERATURE ON COMPRESSIVE STRENGTH OF ANNEALED TYPE 302 SHEET (62)

Fe
18 Cr
8 Ni

Type 301
Type 302

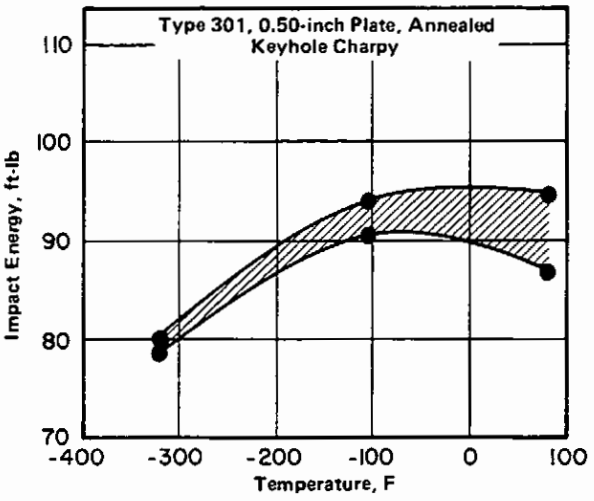


FIGURE 3.0331. IMPACT ENERGY OF TYPE 301 PLATE AT ROOM AND CRYOGENIC TEMPERATURES (82)

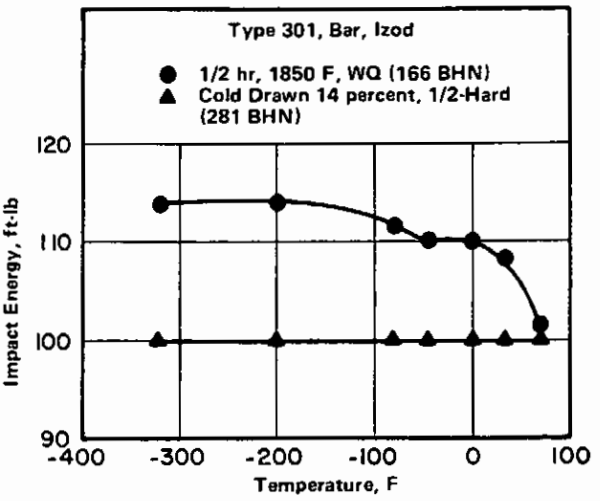


FIGURE 3.0332. IMPACT ENERGY OF TYPE 301 BAR AT ROOM AND CRYOGENIC TEMPERATURES (82)

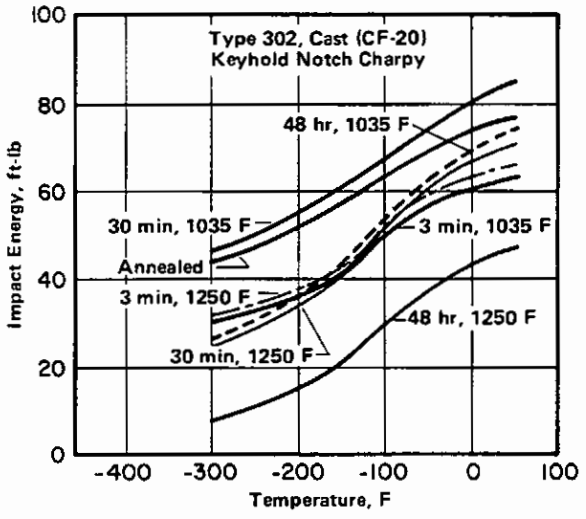


FIGURE 3.0334. EFFECT OF SENSITIZING HEAT TREATMENTS ON THE IMPACT ENERGY OF CAST TYPE 302 AT CRYOGENIC TEMPERATURES (83)

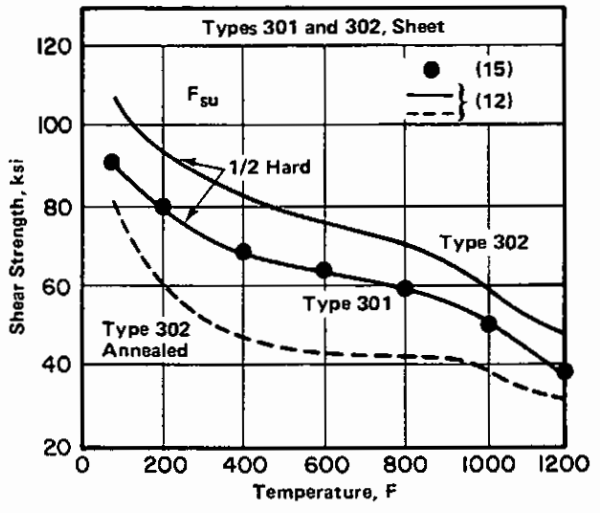


FIGURE 3.0351. EFFECT OF TEST TEMPERATURE ON SHEAR STRENGTH OF TYPES 301 AND 302 (12,15)

Fe
18 Cr
8 Ni

Type 301
Type 302

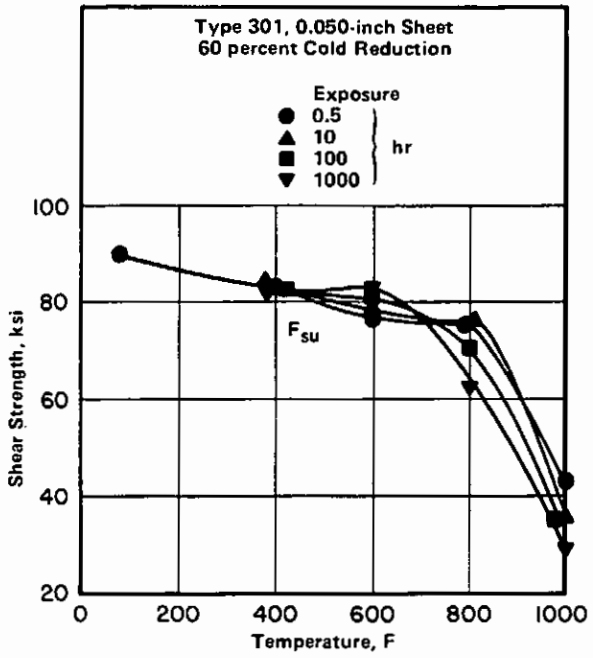


FIGURE 3.0352. EFFECT OF TEST TEMPERATURE AND EXPOSURE TIME ON SHEAR STRENGTH OF 60 PERCENT COLD-REDUCED SHEET (38)

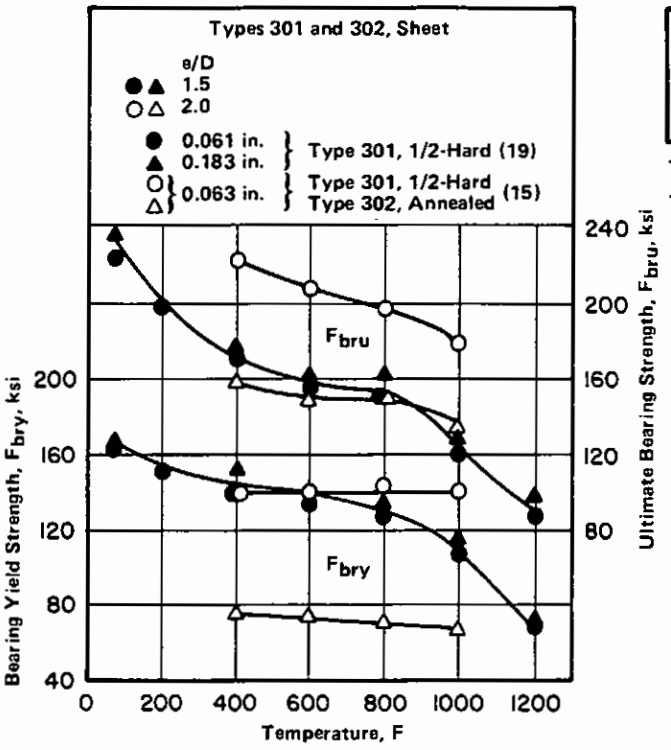


FIGURE 3.0361. EFFECT OF TEST TEMPERATURE ON BEARING PROPERTIES OF TYPES 301 AND 302 SHEET (15,19)

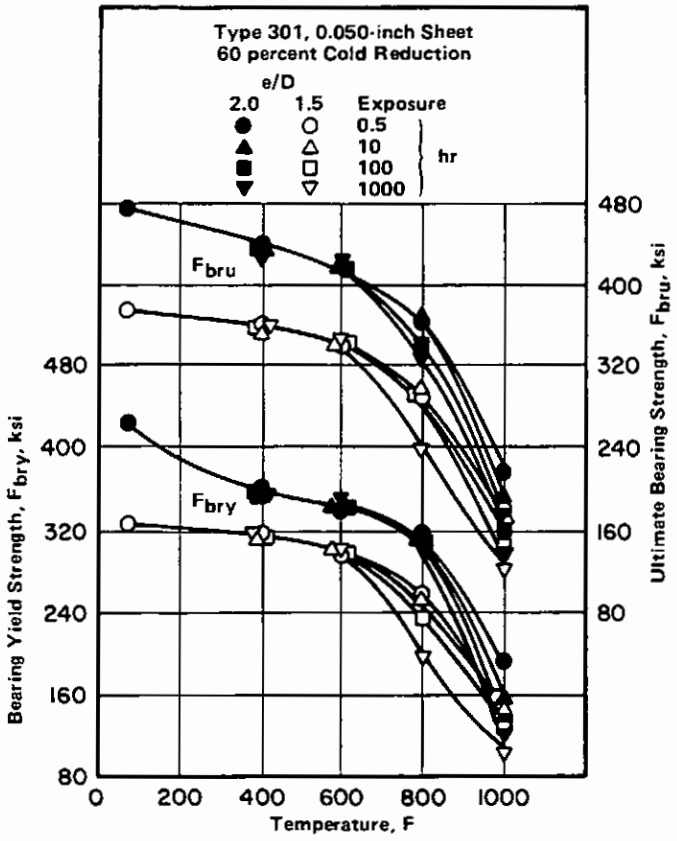


FIGURE 3.0362. EFFECT OF TEST TEMPERATURE AND EXPOSURE TIME ON BEARING PROPERTIES OF 60 PERCENT COLD-REDUCED SHEET (38)

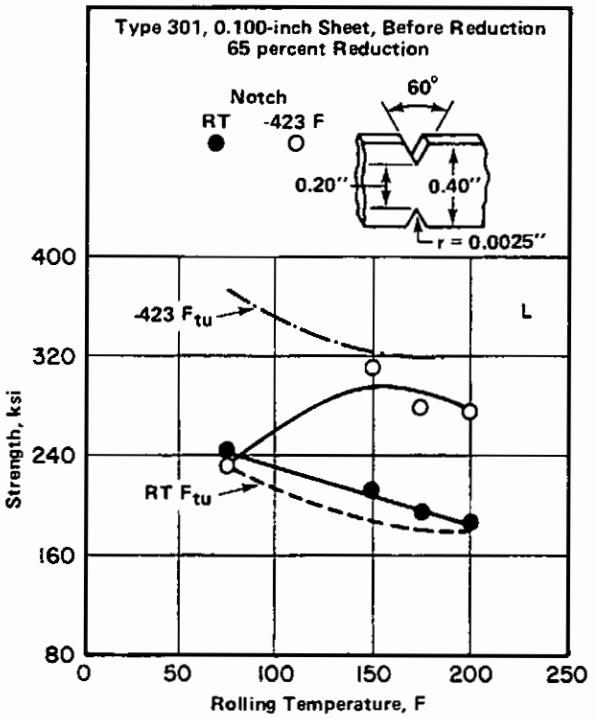


FIGURE 3.03711. EFFECT OF ROLLING TEMPERATURE ON NOTCH STRENGTH AT ROOM TEMPERATURE AND -423 F OF 65 PERCENT REDUCED SHEET (24)

Fe
18 Cr
8 Ni

Type 301
Type 302

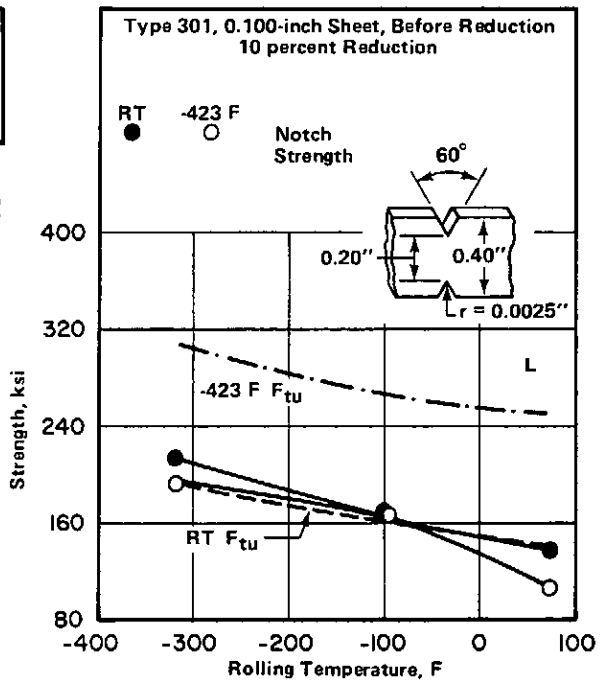


FIGURE 3.037112. EFFECT OF LOW ROLLING TEMPERATURE ON NOTCH STRENGTH AT ROOM TEMPERATURE AND -423 F OF 10 PERCENT REDUCED SHEET (24)

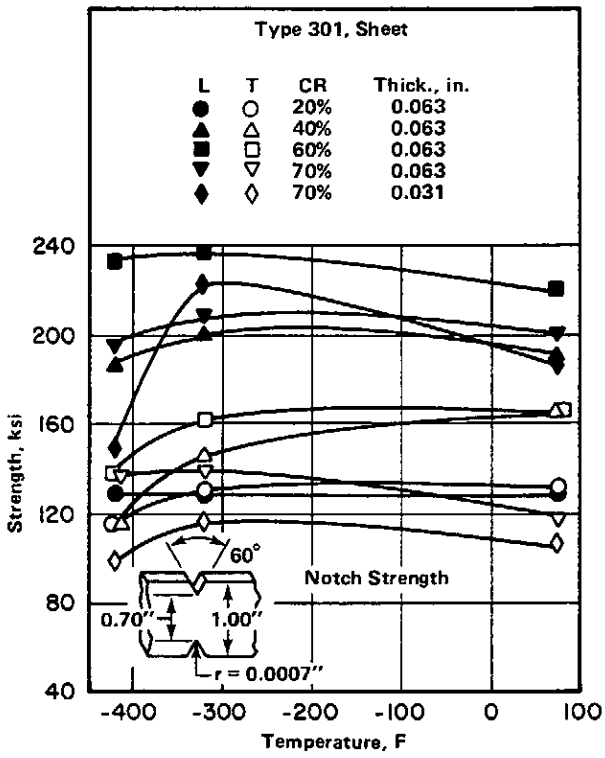


FIGURE 3.037113. EFFECT OF LOW TEMPERATURE AND PERCENT COLD REDUCTION ON NOTCH STRENGTH OF SHEET (34)

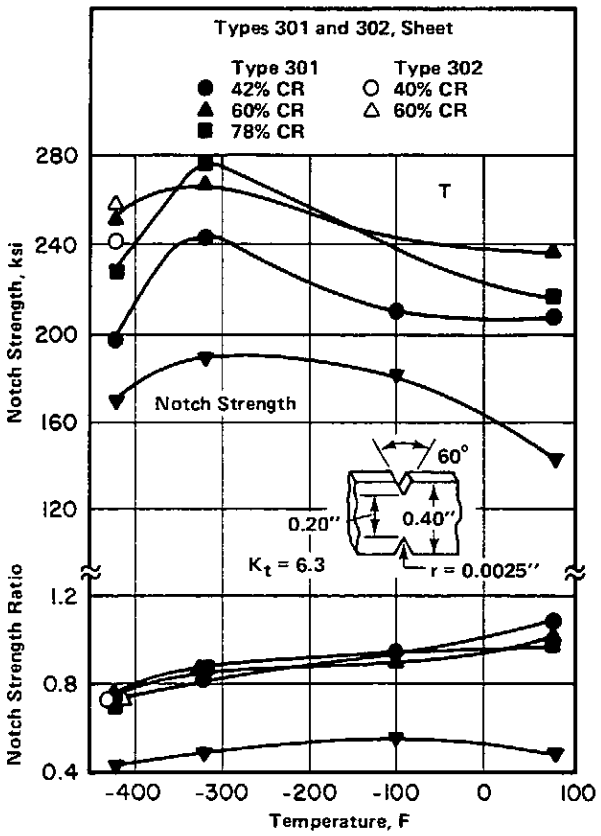


FIGURE 3.037114. EFFECT OF LOW TEMPERATURE AND PERCENT COLD REDUCTION ON NOTCH STRENGTH OF VARIOUS PERCENT REDUCED SHEET (25)

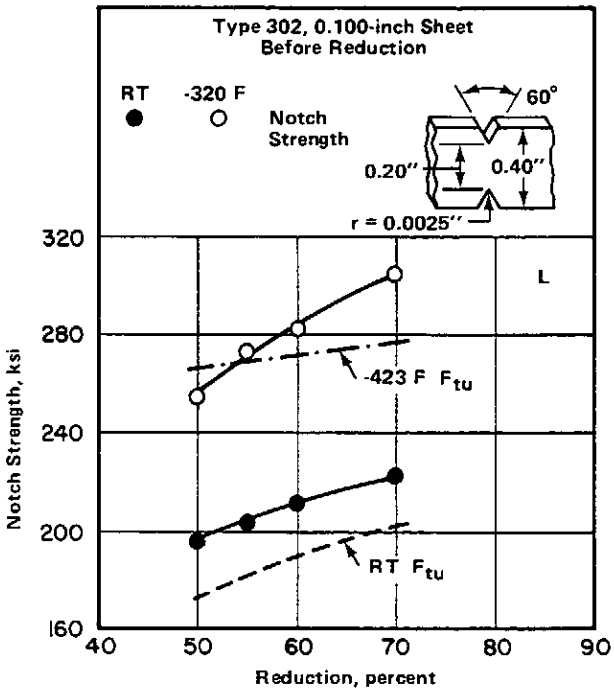


FIGURE 3.037115. EFFECT OF PERCENT COLD REDUCTION ON NOTCH STRENGTH OF SHEET TESTED AT ROOM TEMPERATURE AND -320 F (24)

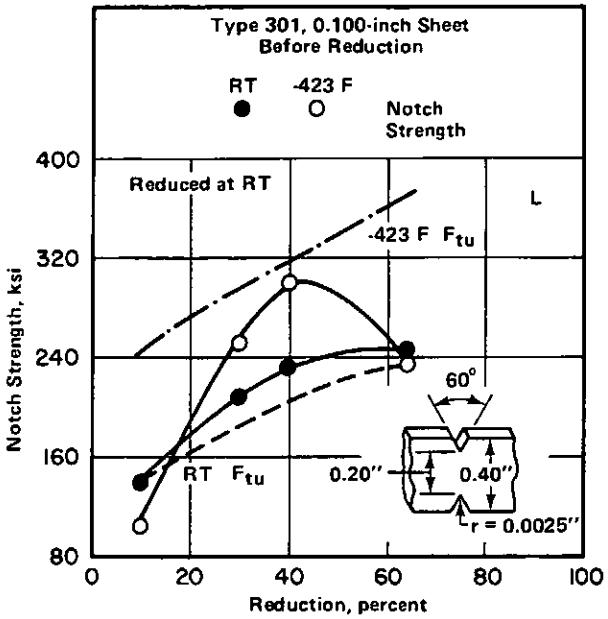


FIGURE 3.037116. EFFECT OF PERCENT COLD REDUCTION ON NOTCH STRENGTH OF SHEET TESTED AT ROOM TEMPERATURE AND -423 F (24)

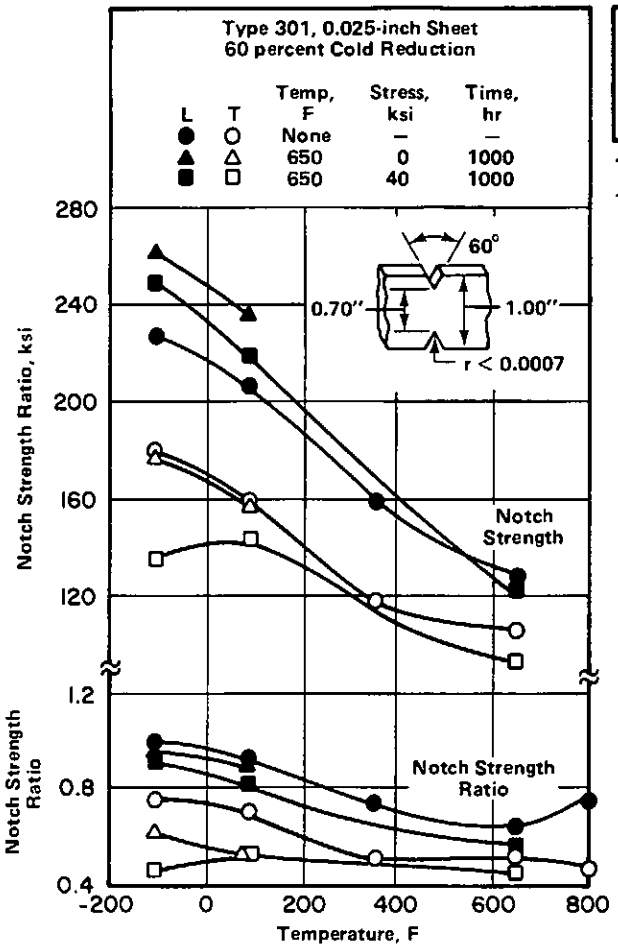


FIGURE 3.037121. EFFECT OF TEST TEMPERATURE AND PRIOR EXPOSURE ON NOTCH PROPERTIES OF 60 PERCENT COLD-REDUCED SHEET (45)

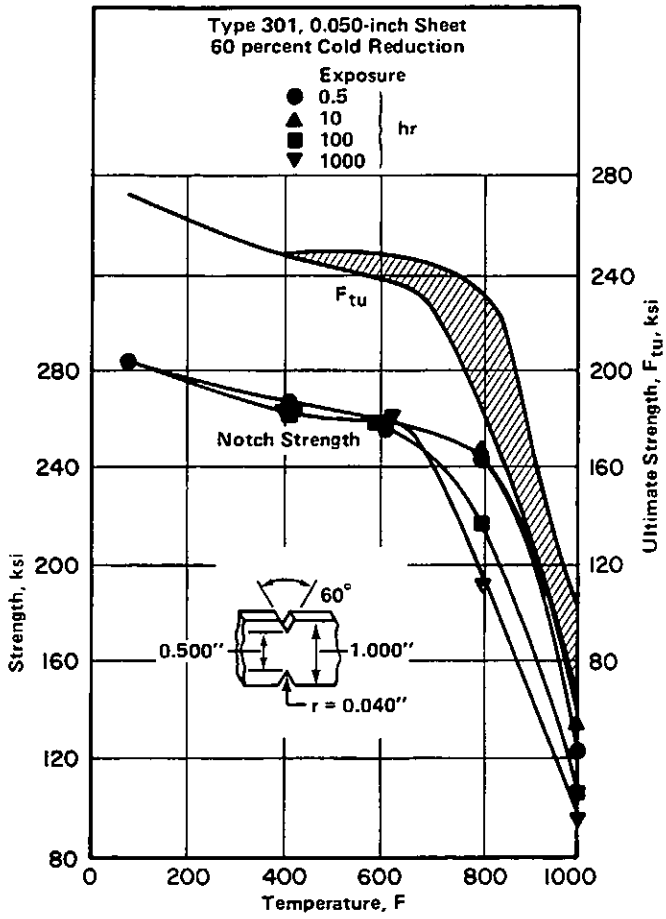


FIGURE 3.037122. EFFECT OF TEST TEMPERATURE AND EXPOSURE TIME ON NOTCH STRENGTH OF 60 PERCENT COLD-REDUCED SHEET (38)

Fe
18 Cr
8 Ni

Type 301
Type 302

Fe
18 Cr
8 Ni

Type 301
Type 302

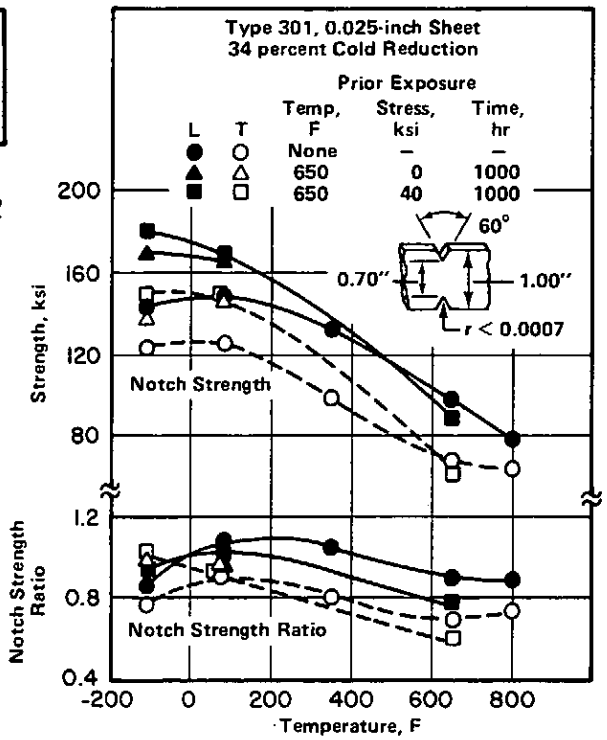


FIGURE 3.037123. EFFECT OF TEST TEMPERATURE AND PRIOR EXPOSURE ON NOTCH PROPERTIES OF 34 PERCENT COLD-REDUCED SHEET (45)

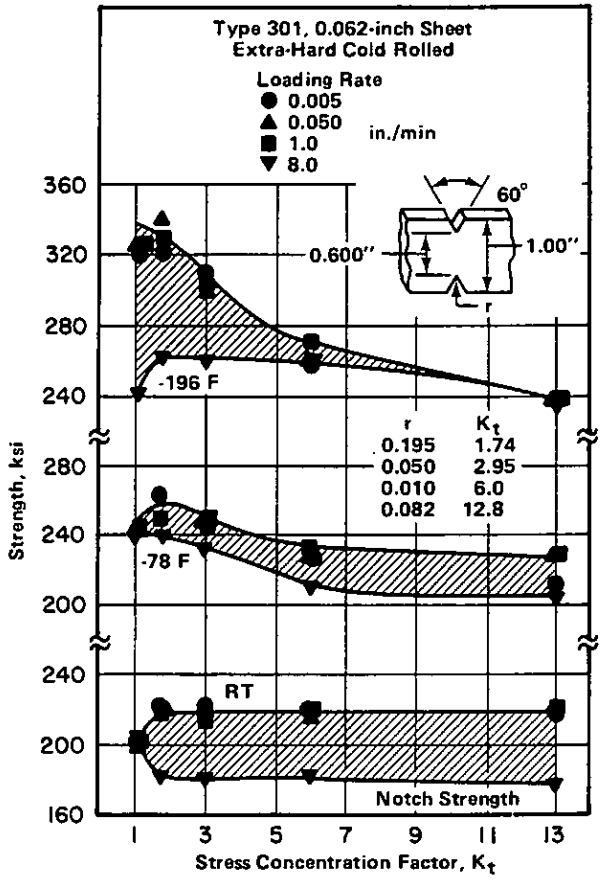


FIGURE 3.037124. EFFECT OF STRESS CONCENTRATION FACTOR, TEMPERATURE, AND LOADING RATE ON NOTCH STRENGTH OF EXTRA-HARD COLD-ROLLED SHEET (44)

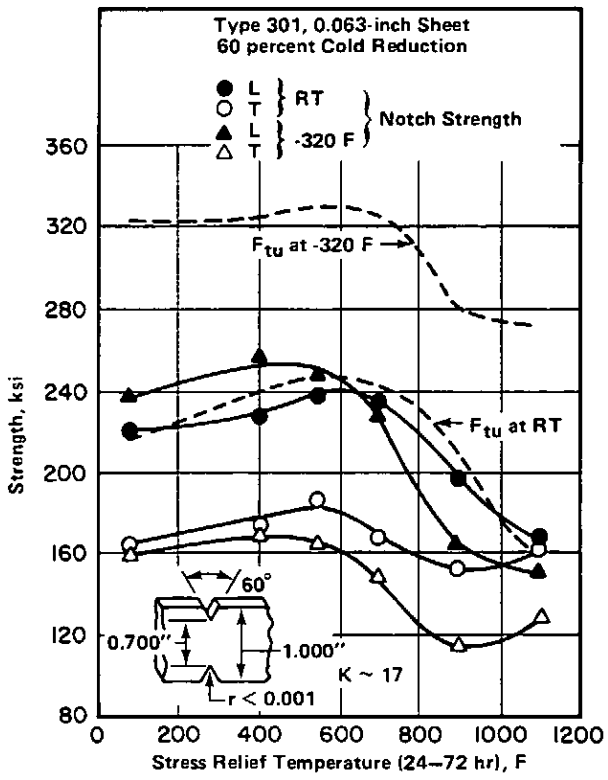


FIGURE 3.037131. EFFECT OF STRESS RELIEF AND LOW TEST TEMPERATURE ON NOTCH STRENGTH OF TYPE 301 SHEET (18)

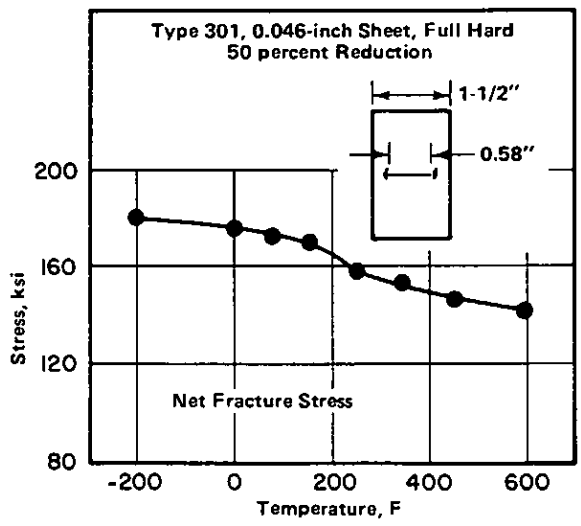


FIGURE 3.037141. EFFECT OF TEST TEMPERATURE ON NET FRACTURE STRESS OF FULL-HARD SHEET (30)

Fe
18 Cr
8 Ni

Type 301
Type 302

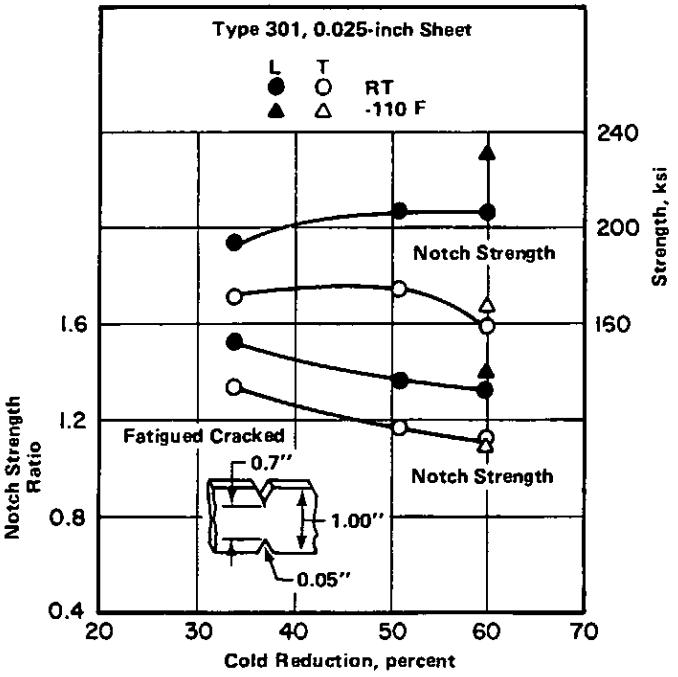


FIGURE 3.037142. EFFECT OF PERCENT COLD REDUCTION ON EDGE-CRACKED PROPERTIES OF SHEET AT ROOM TEMPERATURE AND -110 F (45)

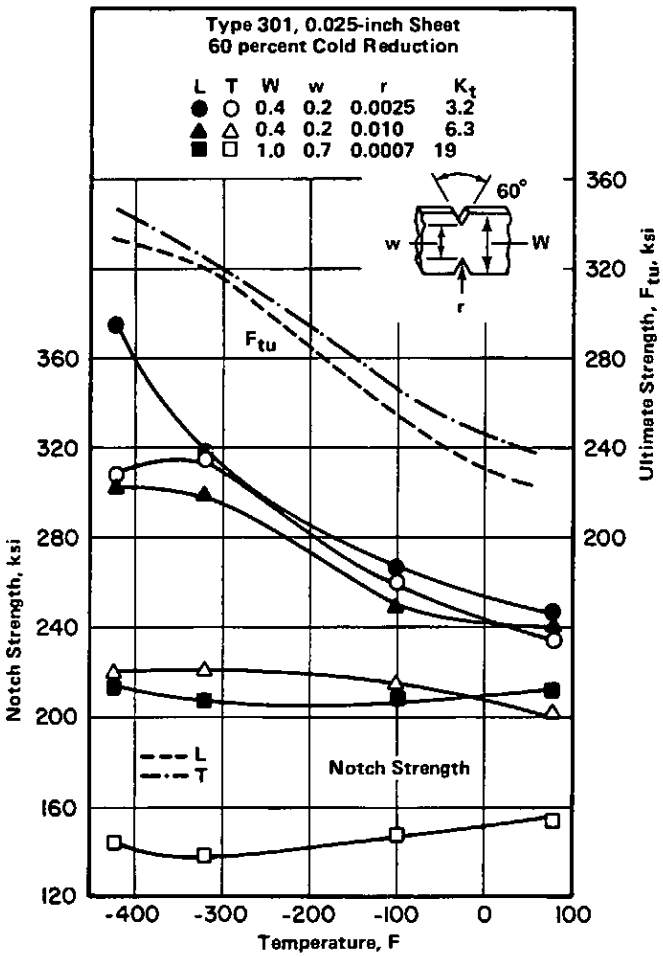


FIGURE 3.037151. EFFECT OF LOW TEST TEMPERATURE ON NOTCH STRENGTH OF 60 PERCENT COLD-REDUCED SHEET (36)

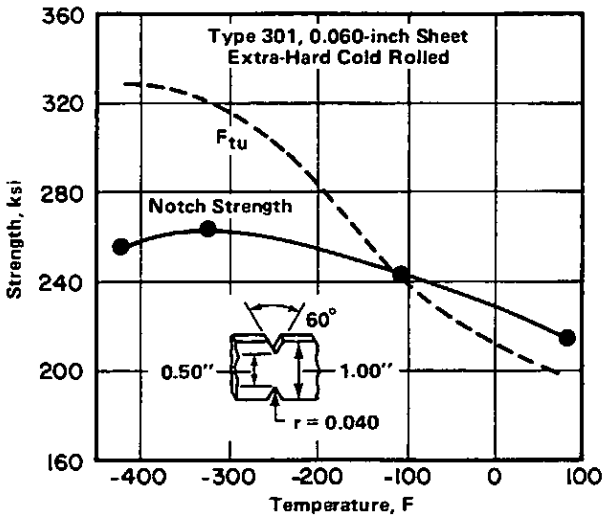


FIGURE 3.037152. EFFECT OF LOW TEMPERATURE ON NOTCH STRENGTH OF EXTRA-HARD COLD-ROLLED SHEET (32)

Fe
18 Cr
8 Ni

Type 301
Type 302

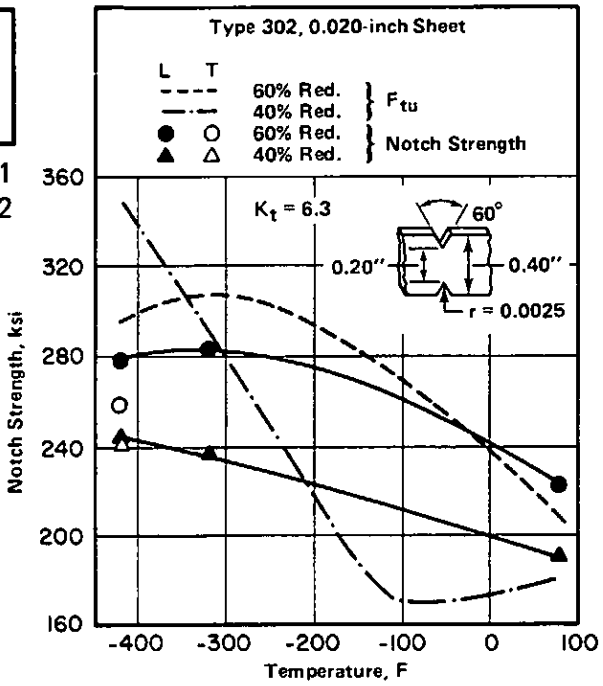


FIGURE 3.037153. EFFECT OF LOW TEST TEMPERATURE ON NOTCH STRENGTH OF 40 AND 60 PERCENT REDUCED TYPE 302 SHEET (31)

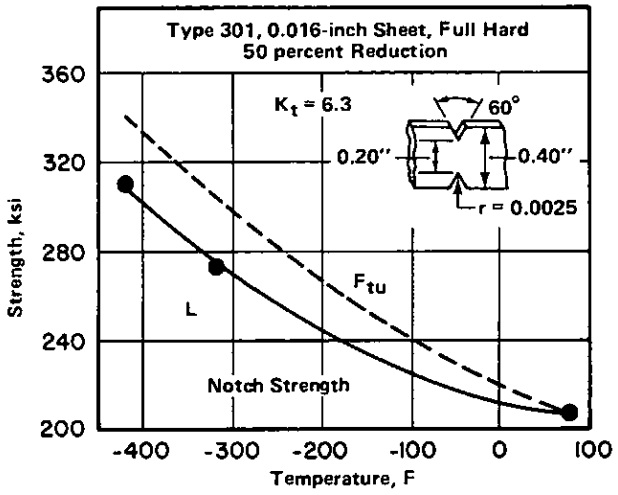


FIGURE 3.037154. EFFECT OF LOW TEST TEMPERATURE ON NOTCH STRENGTH OF 50 PERCENT REDUCED SHEET (31)

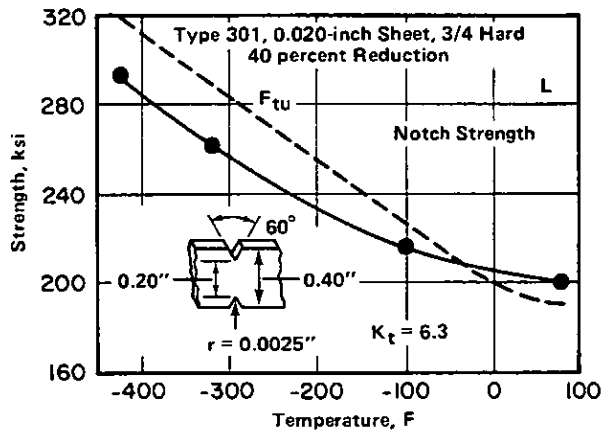


FIGURE 3.037155. EFFECT OF LOW TEST TEMPERATURE ON NOTCH STRENGTH OF 40 PERCENT REDUCED SHEET (31)

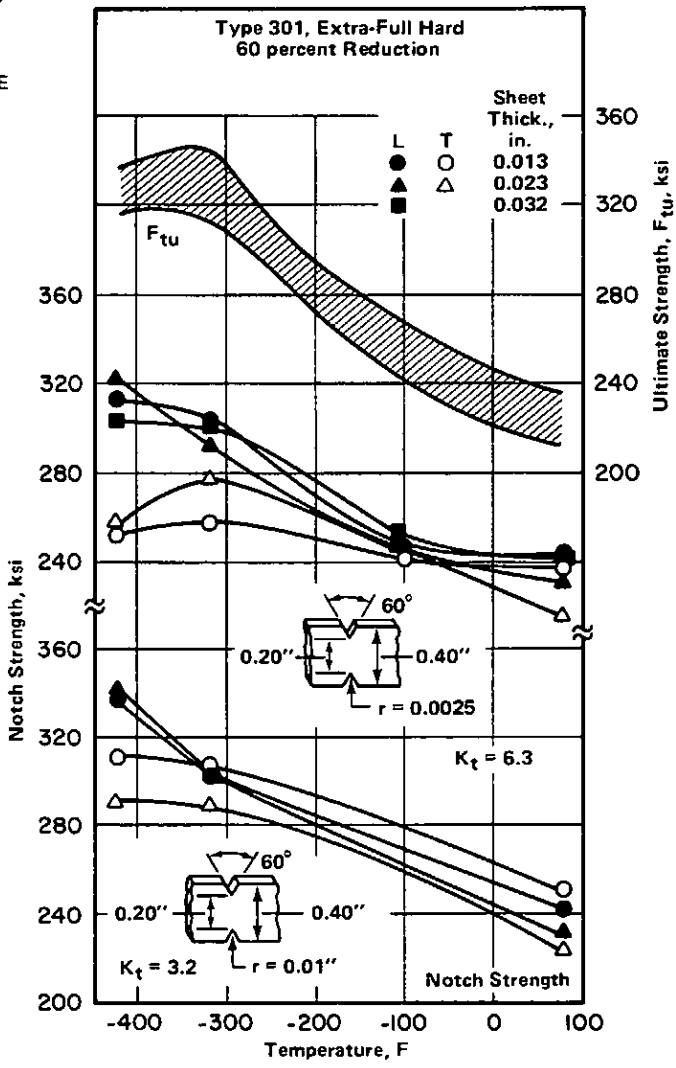


FIGURE 3.037156. EFFECT OF LOW TEST TEMPERATURE AND THICKNESS OF NOTCH STRENGTH OF 60 PERCENT REDUCED SHEET (31)

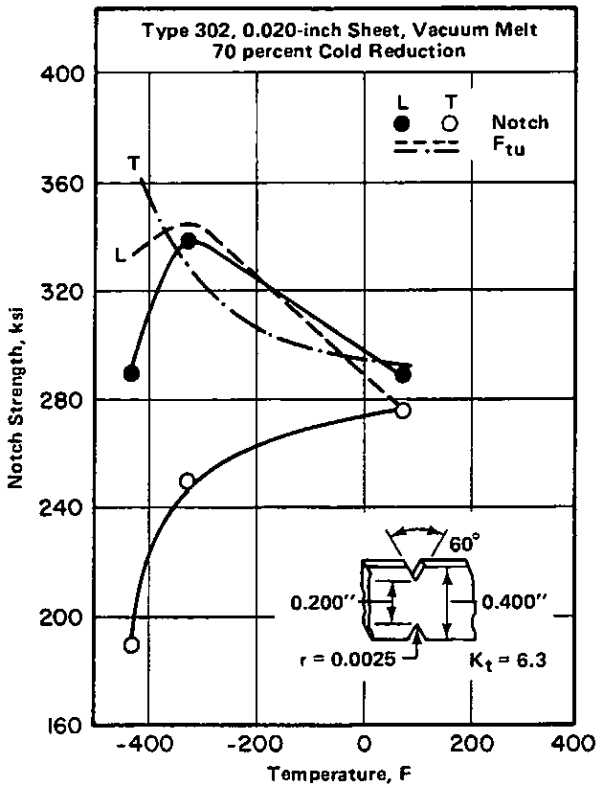
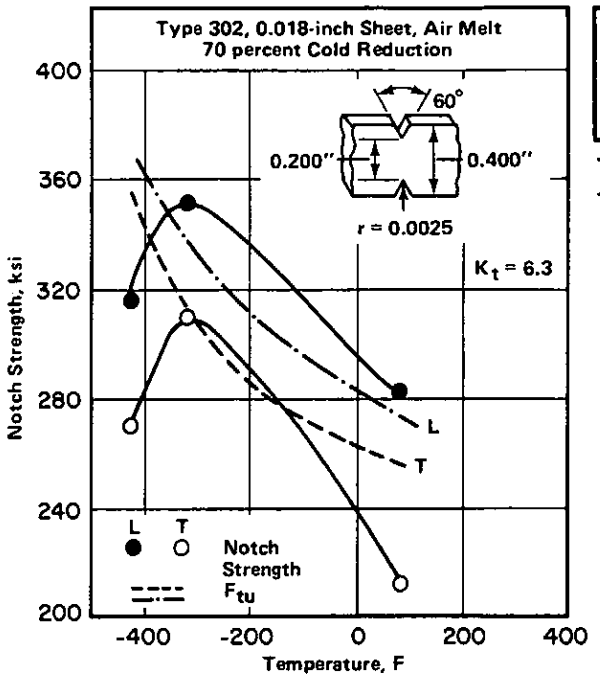


FIGURE 3.037157. EFFECT OF LOW TEST TEMPERATURE ON NOTCH STRENGTH OF 70 PERCENT REDUCED VACUUM-MELT SHEET (23)



Fe
18 Cr
8 Ni

Type 301
Type 302

FIGURE 3.037158. EFFECT OF LOW TEST TEMPERATURE ON NOTCH STRENGTH OF 70 PERCENT REDUCED AIR-MELT SHEET (23)

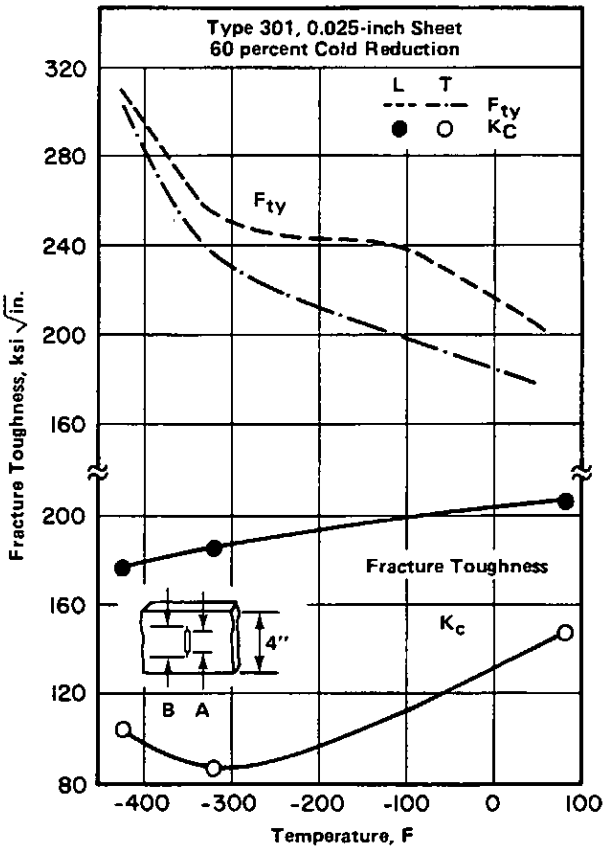


FIGURE 3.03721. EFFECT OF LOW TEST TEMPERATURE ON FRACTURE TOUGHNESS OF 60 PERCENT COLD-REDUCED SHEET (37)

A. Notch length 1.22 ± 0.03.
B. Critical crack length 1.19 to 2.02. Critical crack length telescopically measured.

Fe
18 Cr
8 Ni

Type 301
Type 302

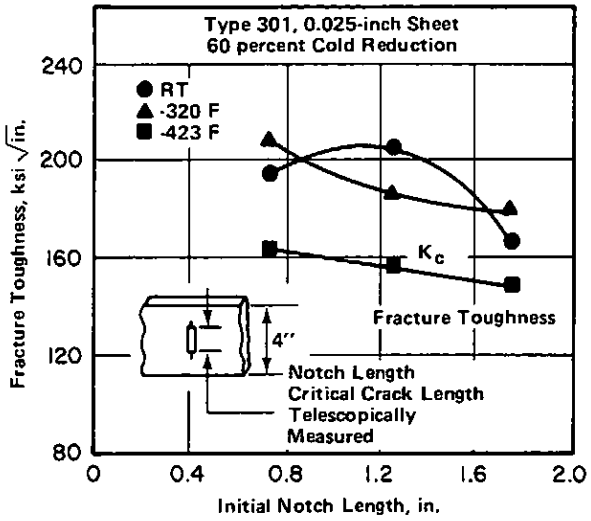


FIGURE 3.03722. EFFECT OF INITIAL NOTCH LENGTH ON FRACTURE TOUGHNESS OF 60 PERCENT COLD-REDUCED SHEET AT ROOM TEMPERATURE, -320, AND -423 F (37)

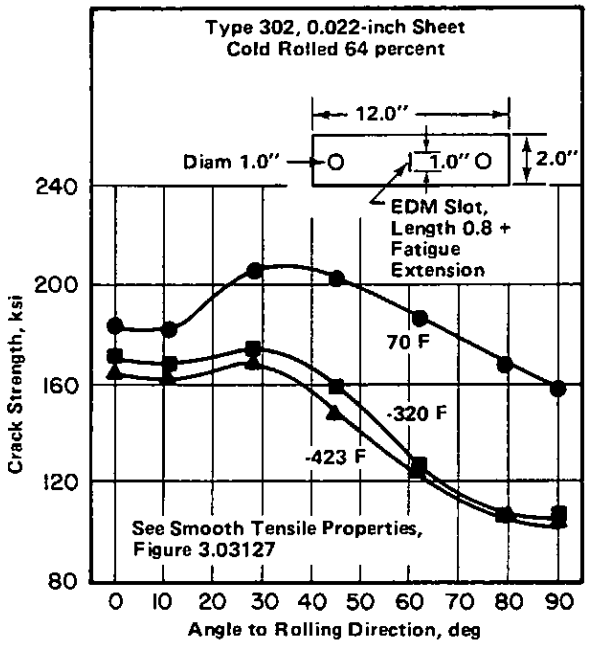


FIGURE 3.03724. EFFECTS OF CENTER CRACK AND TEST DIRECTION ON TENSILE STRENGTH OF COLD-ROLLED SHEET AT ROOM AND CRYOGENIC TEMPERATURES (79)

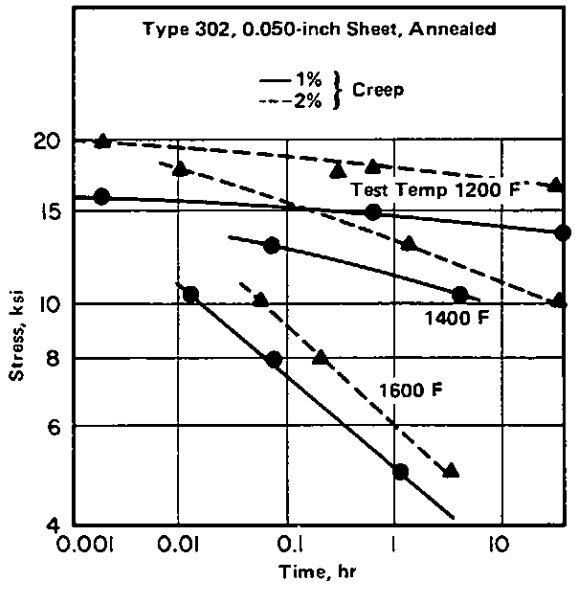


FIGURE 3.041. CREEP CURVES FOR TYPE 302 ANNEALED SHEET AT 1200 TO 1600 F (16)

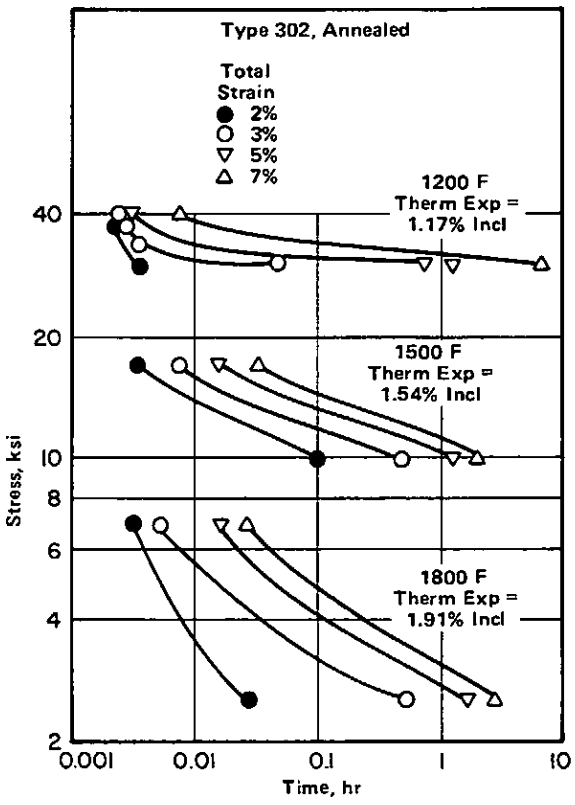


FIGURE 3.042. SHORT-TIME TOTAL STRAIN CURVES FOR ANNEALED TYPE 302 AT 1200 TO 1800 F (12)

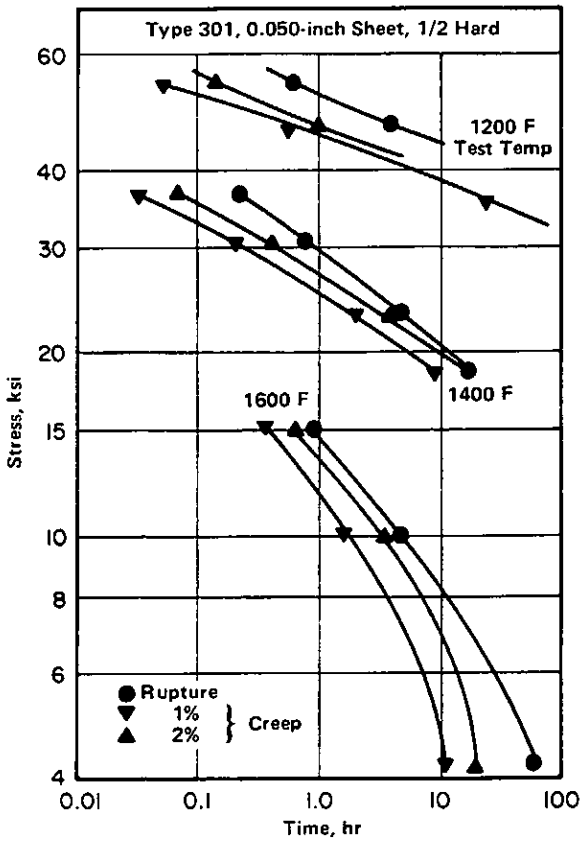
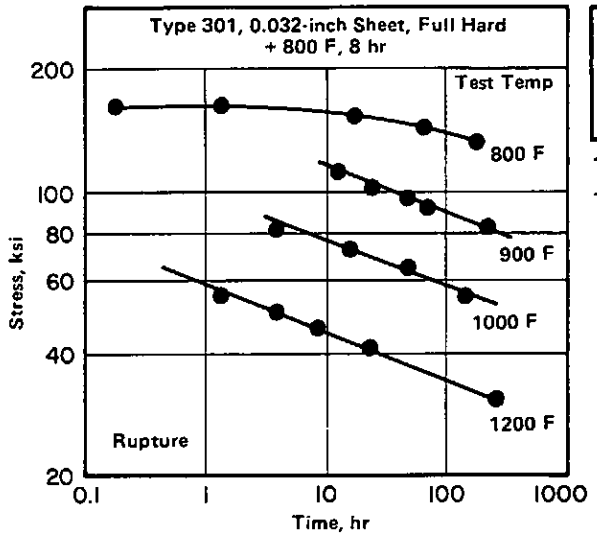


FIGURE 3.043. CREEP AND CREEP-RUPTURE CURVES FOR TYPE 301 1/2-HARD SHEET AT 1200 TO 1500 F (16)



Fe
18 Cr
8 Ni

Type 301
Type 302

FIGURE 3.044. CREEP-RUPTURE CURVES FOR TYPE 301 FULL-HARD AND STRESS-RELIEVED SHEET AT 800 TO 1200 F (11)

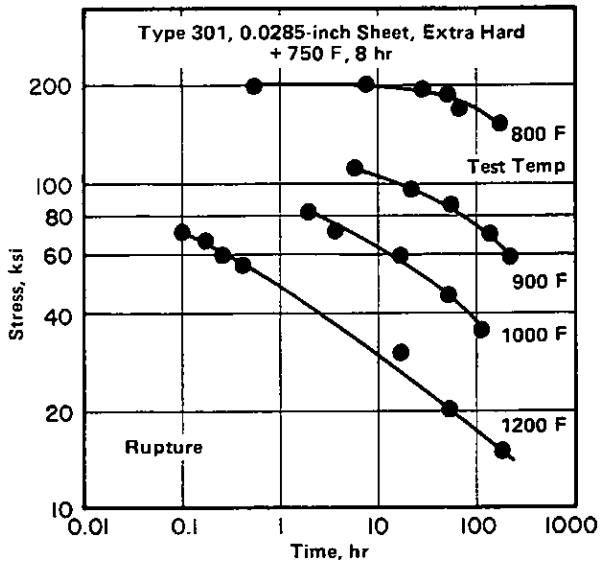


FIGURE 3.045. CREEP-RUPTURE CURVES FOR TYPE 301 EXTRA-HARD AND STRESS-RELIEVED SHEET AT 800 TO 1200 F (11)

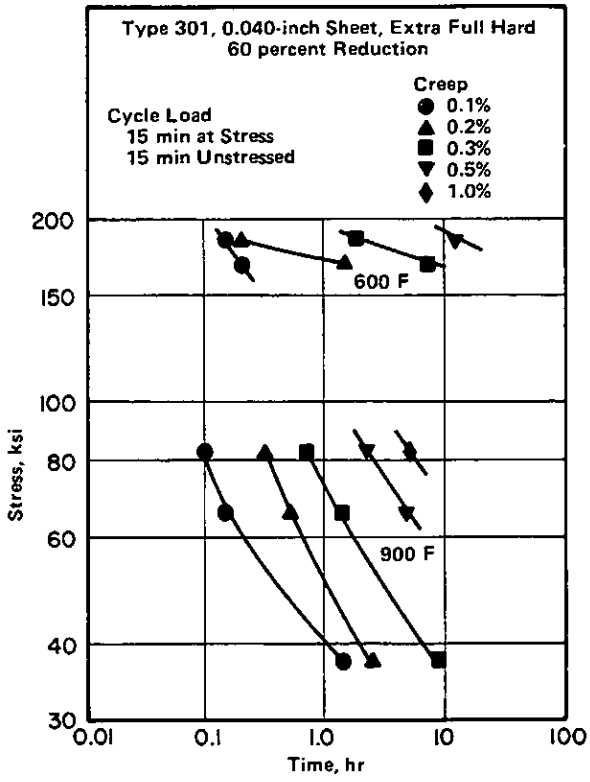


FIGURE 3.046. CREEP CURVES FOR TYPE 301 60 PERCENT REDUCED SHEET UNDER CYCLIC LOAD AT 600 AND 900 F (27)

Fe
18 Cr
8 Ni

Type 301
Type 302

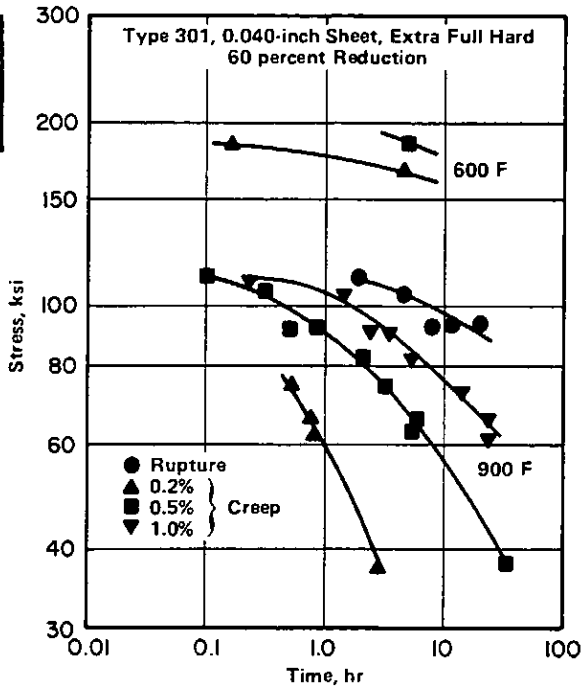


FIGURE 3.047. CREEP AND CREEP-RUPTURE CURVES FOR TYPE 301 60 PERCENT REDUCED SHEET AT 600 AND 900 F (26)

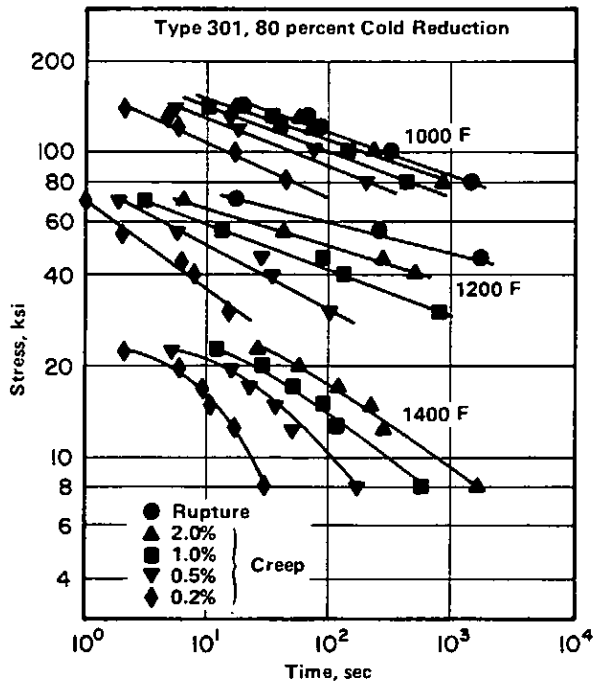


FIGURE 3.048. CREEP AND CREEP-RUPTURE CURVES FOR 80 PERCENT COLD-REDUCED SHEET AT 1000, 1200, AND 1400 F (47)

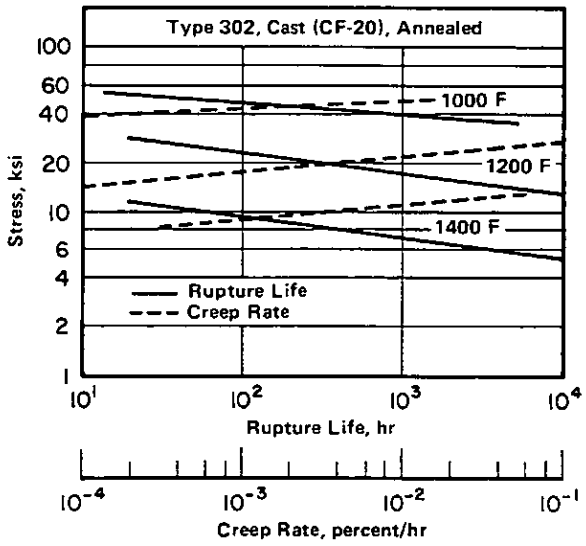


FIGURE 3.049. CREEP-RUPTURE PROPERTIES OF CAST TYPE 302 (62)

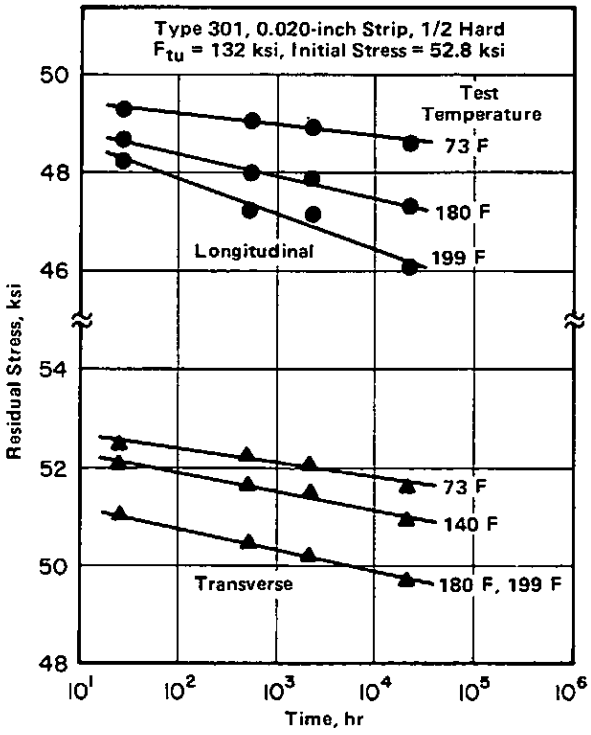


FIGURE 3.0410. STRESS RELAXATION AT ROOM AND SLIGHTLY ELEVATED TEMPERATURES (84)

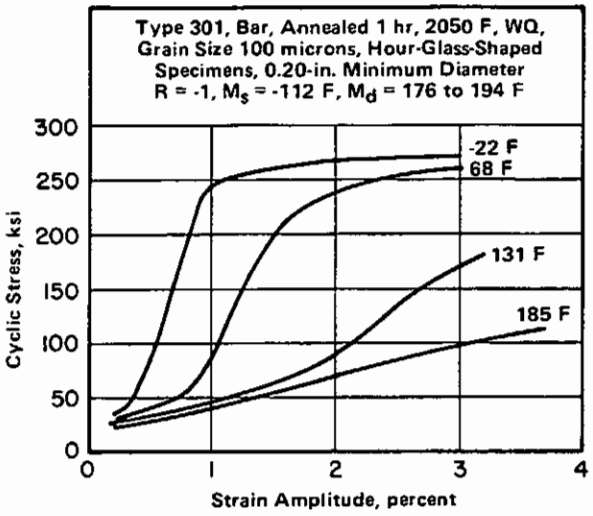
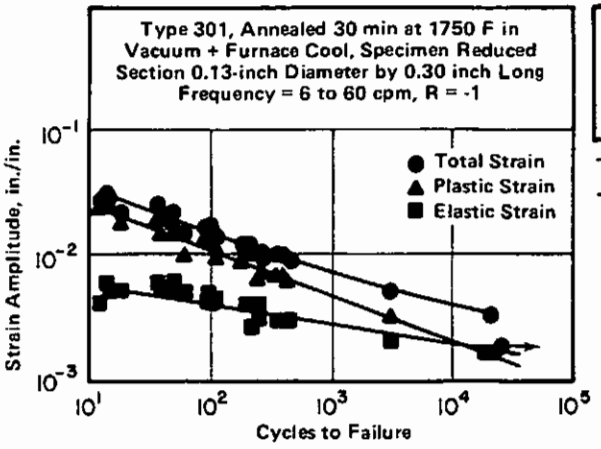


FIGURE 3.051. CYCLIC STRESS-STRAIN CURVES FOR ANNEALED TYPE 301 AT TEMPERATURES BETWEEN M_s AND M_d (58)



Fe
18 Cr
8 Ni

Type 301
Type 302

FIGURE 3.052. STRAIN-CONTROLLED FATIGUE BEHAVIOR OF ANNEALED ROD AT ROOM TEMPERATURE (85)

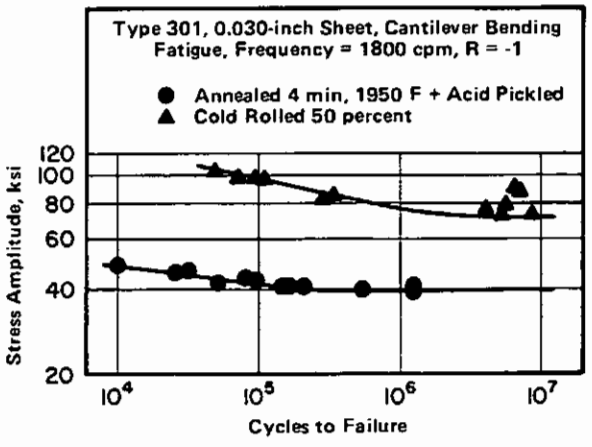


FIGURE 3.053. BENDING FATIGUE BEHAVIOR OF COLD-WORKED AND OF ANNEALED SHEET AT ROOM TEMPERATURE (86)

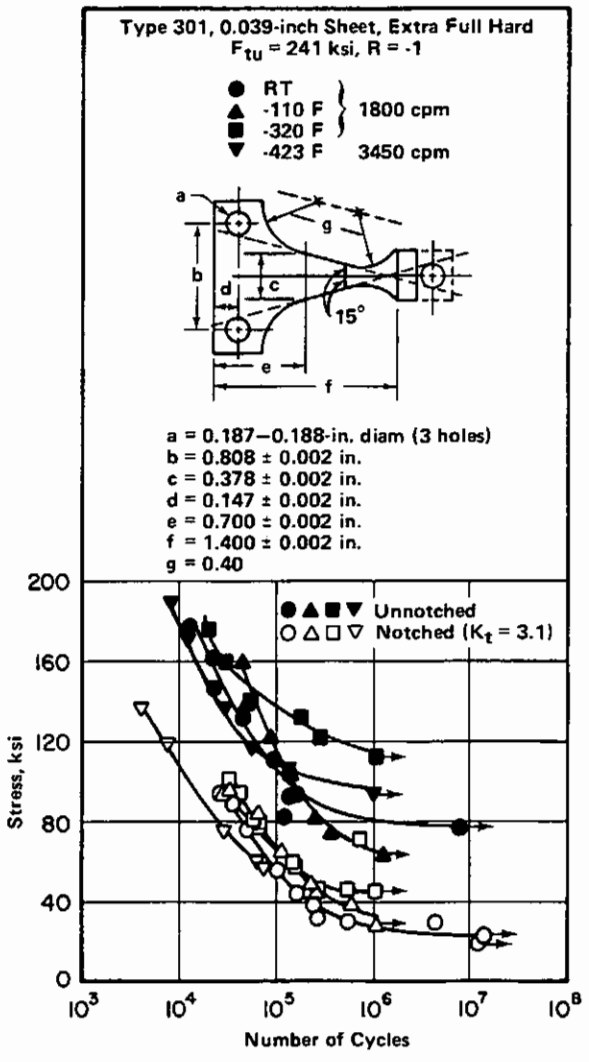


FIGURE 3.054. S-N CURVES IN FLEXURE FOR EXTRA-FULL-HARD SHEET AT LOW TEMPERATURES (39,42)

Fe
18 Cr
8 Ni

Type 301
Type 302

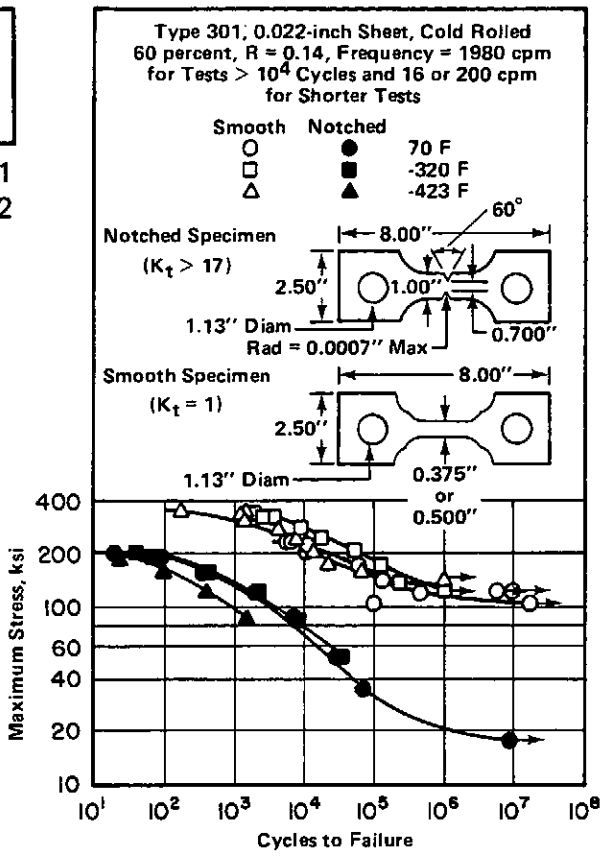


FIGURE 3.055. AXIAL TENSION FATIGUE BEHAVIOR OF SMOOTH AND NOTCHED SHEET AT ROOM AND CRYOGENIC TEMPERATURES (87)

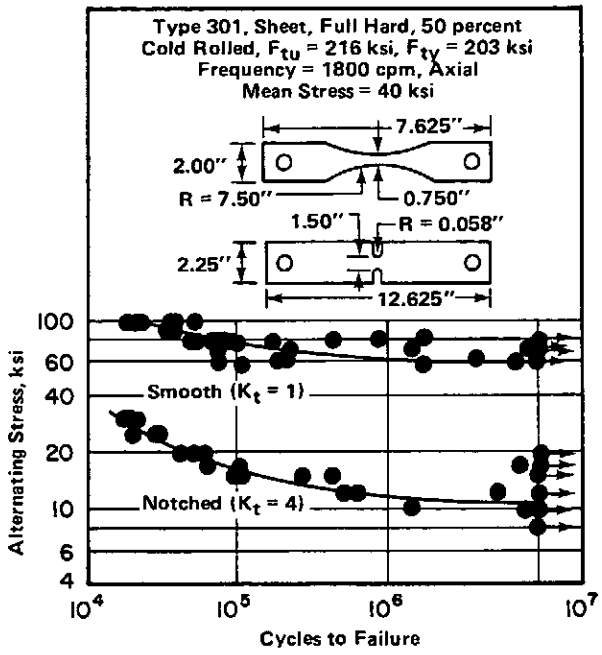


FIGURE 3.057. EFFECTS OF NOTCHES ON FATIGUE BEHAVIOR OF SHEET (89)

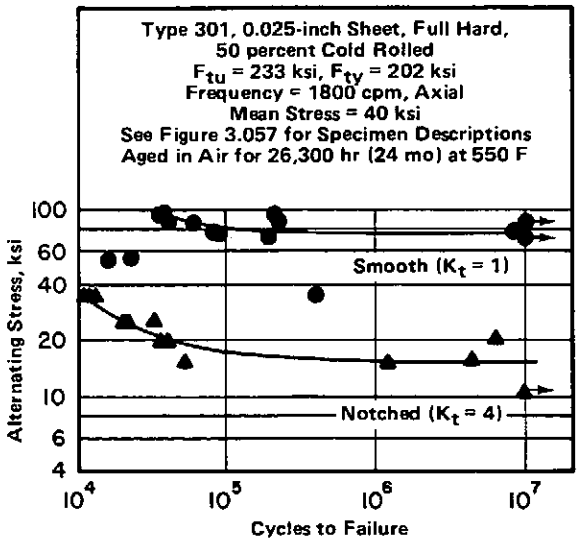


FIGURE 3.058. FATIGUE BEHAVIOR OF SMOOTH AND NOTCHED SHEET AT ROOM TEMPERATURE AFTER AGING FOR 26,300 HOURS AT 550 F (88)

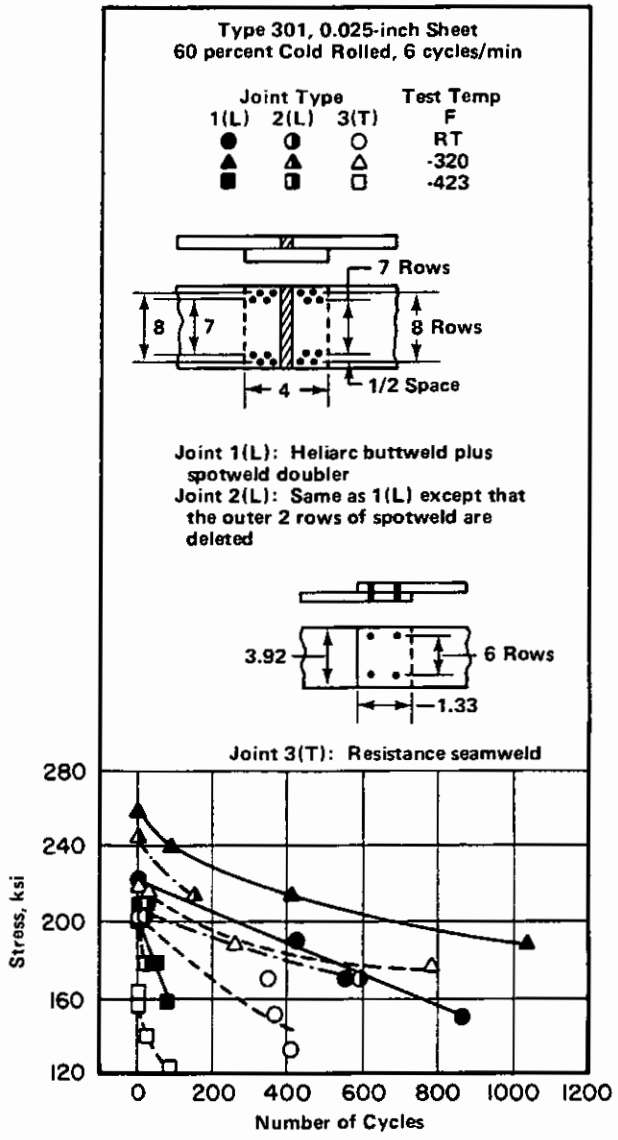
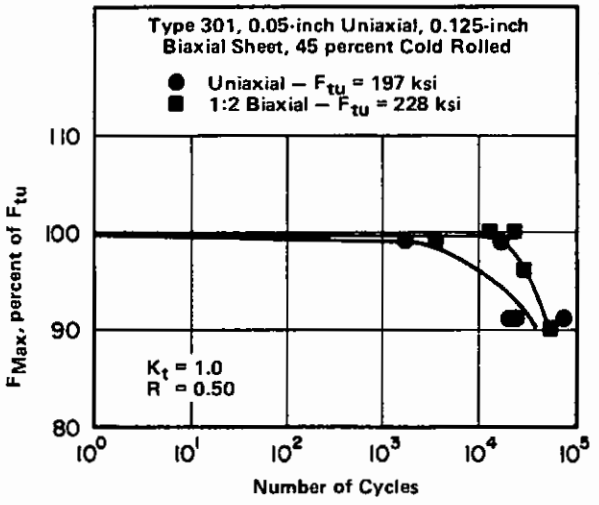


FIGURE 3.059. LOW-CYCLE S-N CURVES FOR COMPLEX WELDED JOINTS OF 60 PERCENT COLD-ROLLED SHEET (36)



Fe
18 Cr
8 Ni

Type 301
Type 302

FIGURE 3.0510. S-N CURVES FOR UNIAXIAL AND BIAXIAL SHEET FOR R = 0.50 (46)

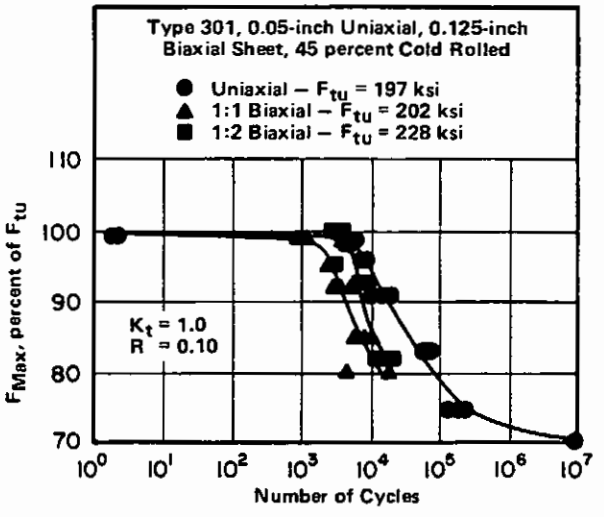


FIGURE 3.0511. S-N CURVES FOR UNIAXIAL AND BIAXIAL SHEET FOR R = 0.10 (46)

Fe
18 Cr
8 Ni

Type 301
Type 302

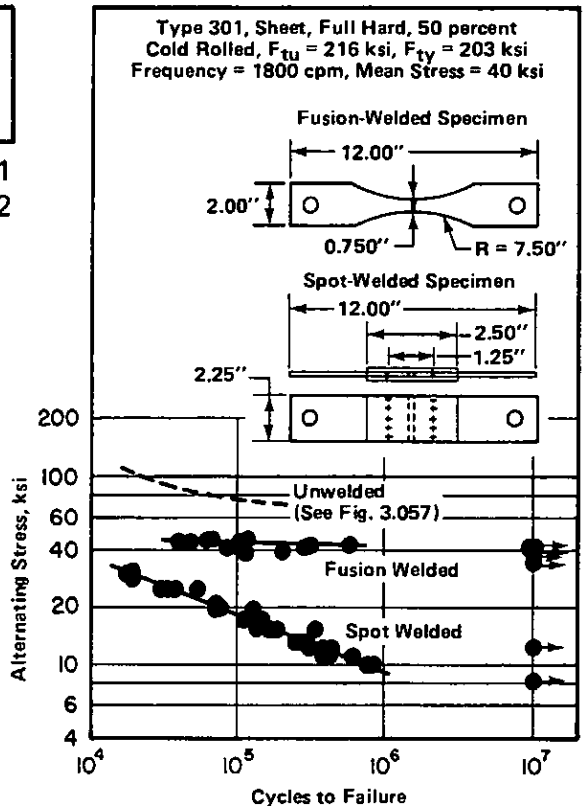


FIGURE 3.0512. EFFECTS OF FUSION AND SPOT WELDING ON FATIGUE BEHAVIOR OF SHEET (89)

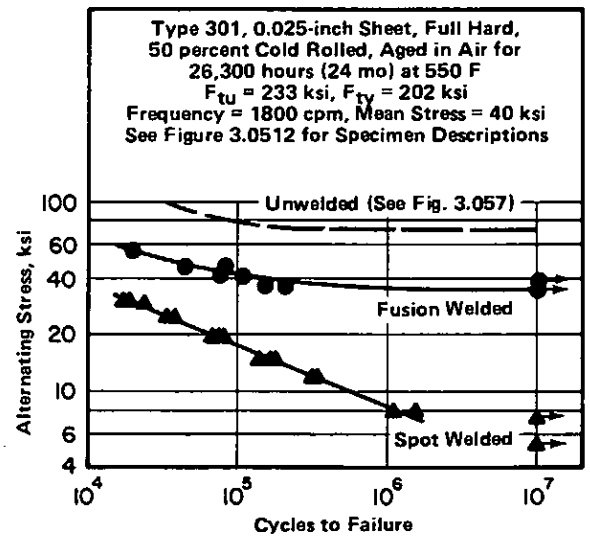


FIGURE 3.0513. FATIGUE BEHAVIOR OF WELDED SHEET AT ROOM TEMPERATURE AFTER AGING FOR 26,300 HOURS AT 550 F (88)

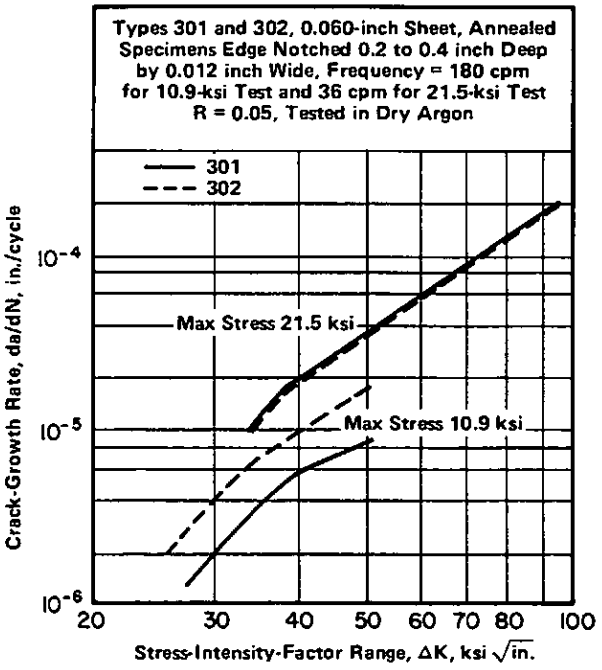


FIGURE 3.0515. FATIGUE CRACK-GROWTH BEHAVIOR AT ROOM TEMPERATURE FOR TYPES 301 AND 302 ANNEALED SHEET TESTED AT TWO DIFFERENT STRESS LEVELS (59)

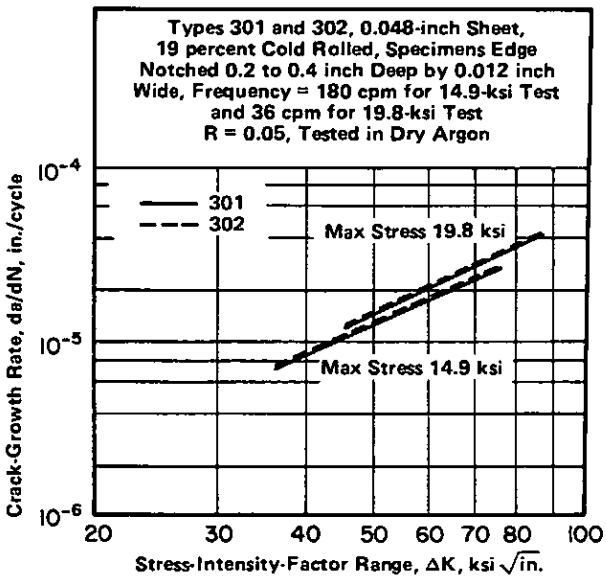


FIGURE 3.0516. FATIGUE CRACK-GROWTH BEHAVIOR AT ROOM TEMPERATURE FOR TYPES 301 AND 302 COLD-ROLLED SHEET TESTED AT TWO DIFFERENT STRESS LEVELS (59)

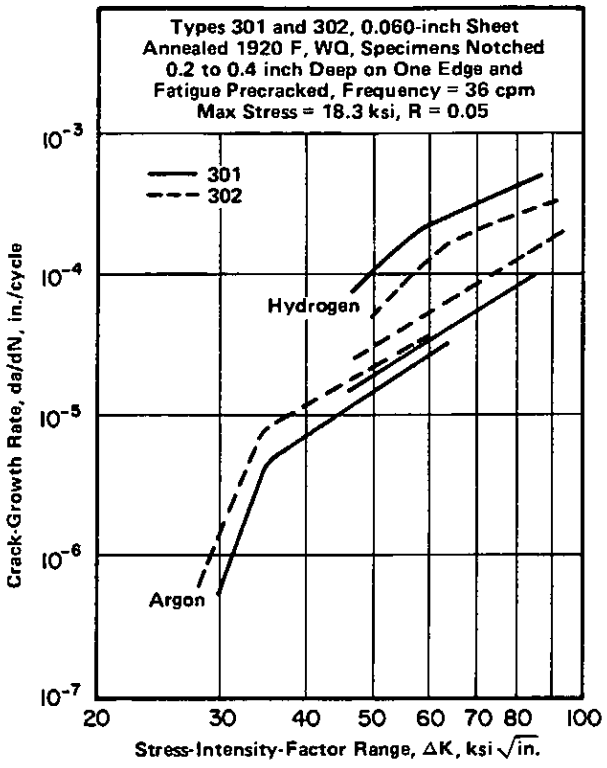
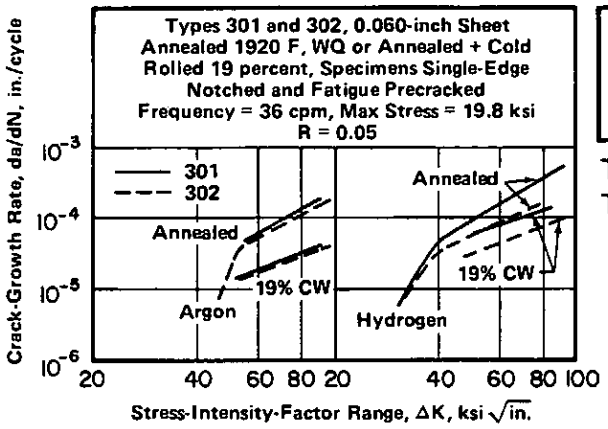


FIGURE 3.0518. FATIGUE CRACK-GROWTH BEHAVIOR AT ROOM TEMPERATURE FOR TYPES 301 AND 302 ANNEALED SHEET TESTED IN DRY HYDROGEN, DRY ARGON, AND AIR (90)



Fe
18 Cr
8 Ni

Type 301
Type 302

FIGURE 3.0519. FATIGUE CRACK-GROWTH BEHAVIOR AT ROOM TEMPERATURE FOR ANNEALED AND COLD-WORKED SHEET TESTED IN ARGON AND HYDROGEN (90)

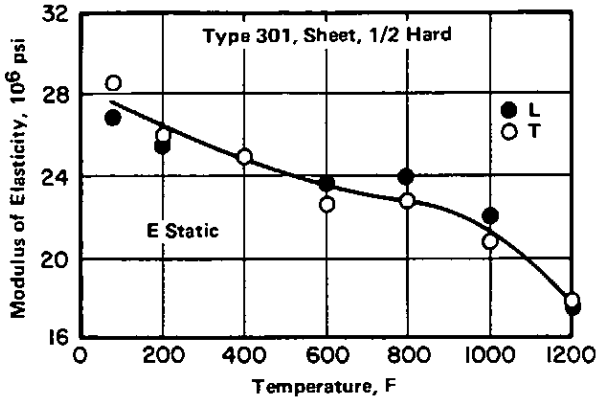


FIGURE 3.0621. MODULUS OF ELASTICITY FOR TYPE 301 1/2-HARD SHEET AT ROOM AND ELEVATED TEMPERATURES (11)

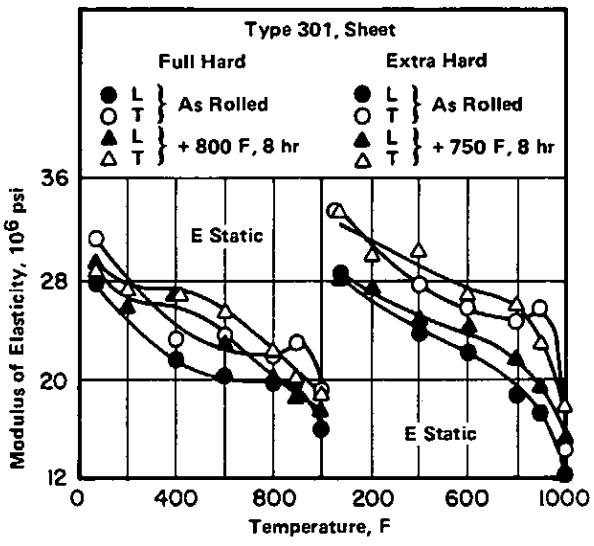


FIGURE 3.0622. MODULUS OF ELASTICITY IN TENSION FOR TYPE 301 FULL-HARD AND EXTRA-HARD SHEET (11)

Fe
18 Cr
8 Ni

Type 301
Type 302

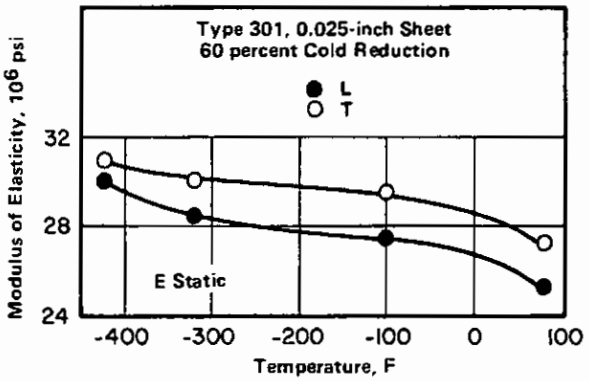


FIGURE 3.0623. EFFECT OF LOW TEST TEMPERATURE ON MODULUS OF ELASTICITY FOR 60 PERCENT REDUCED SHEET (36)

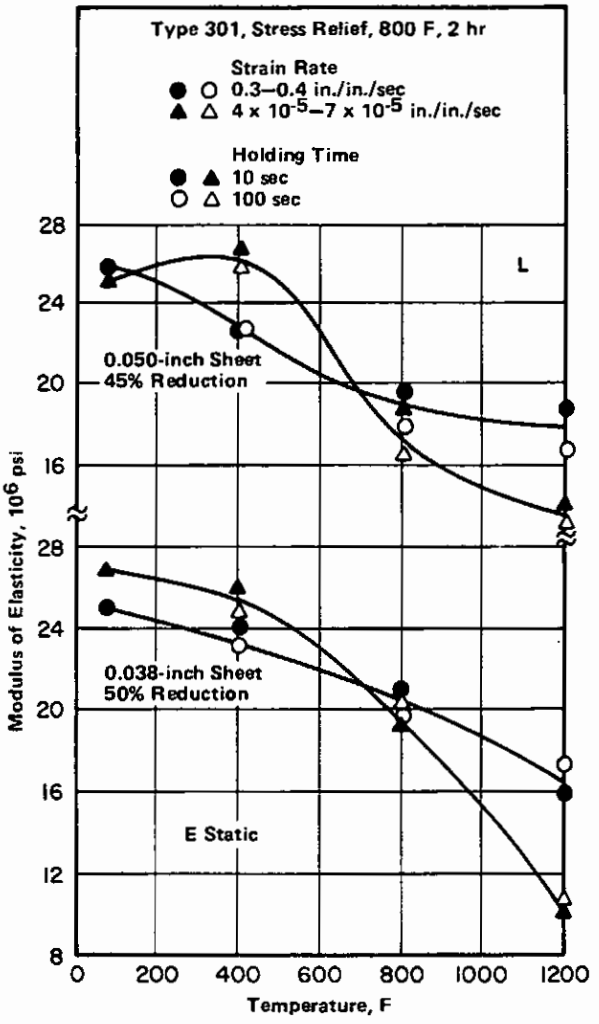


FIGURE 3.0624. EFFECT OF TEST TEMPERATURE, STRAIN RATE, AND HOLDING TIME ON MODULUS OF ELASTICITY IN TENSION OF 45 AND 60 PERCENT REDUCED SHEET (28)

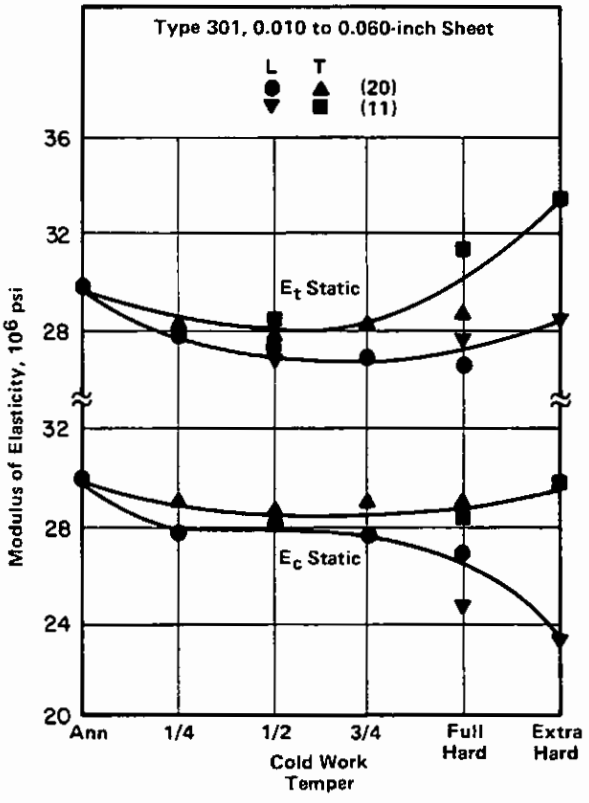


FIGURE 3.0625. EFFECT OF TEMPER ON STATIC MODULUS OF ELASTICITY IN TENSION AND COMPRESSION FOR TYPE 301 SHEET (11,20)

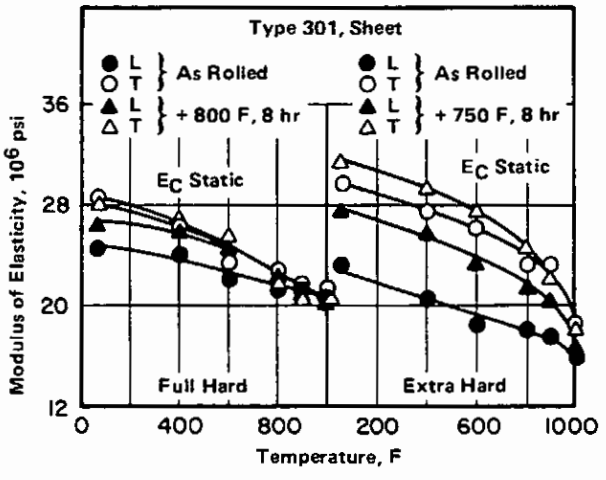


FIGURE 3.0626. MODULUS OF ELASTICITY IN COMPRESSION FOR TYPE 301 FULL-HARD AND EXTRA-HARD SHEET (11)

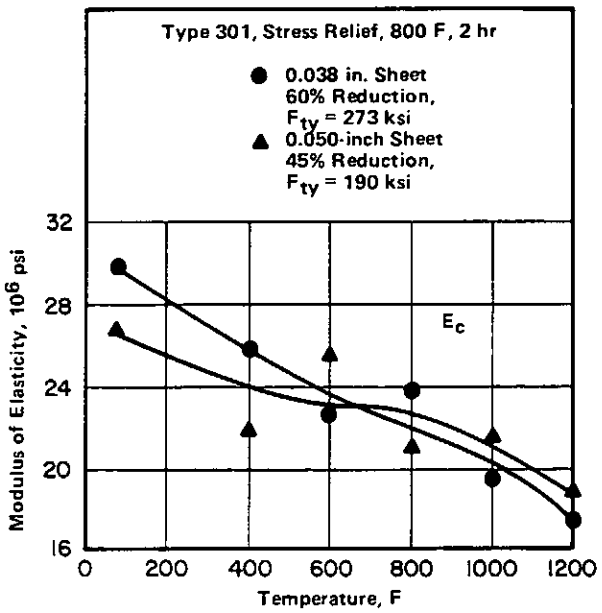
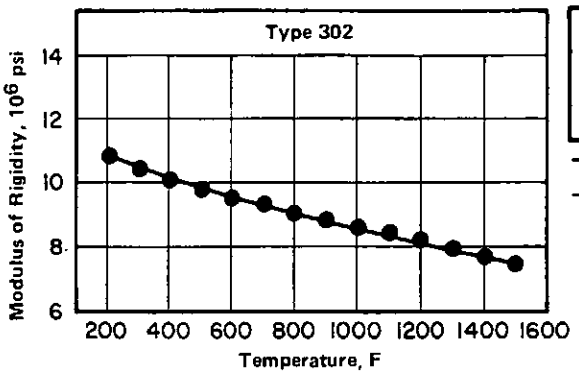


FIGURE 3.0627. EFFECT OF TEST TEMPERATURE ON MODULUS OF ELASTICITY IN COMPRESSION OF 45 AND 60 PERCENT REDUCED SHEET (28)



Fe
18 Cr
8 Ni

Type 301
Type 302

FIGURE 3.0631. MODULUS OF RIGIDITY (62)

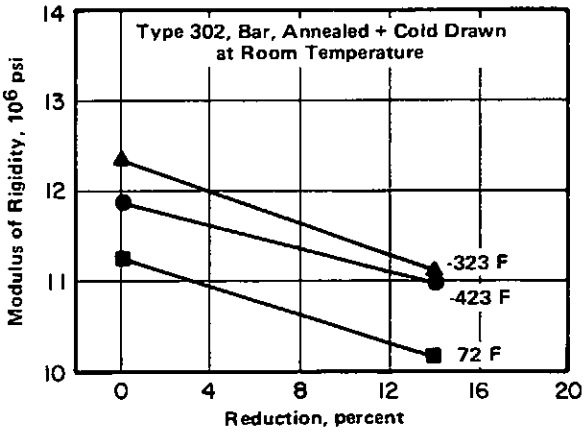


FIGURE 3.0632. EFFECTS OF COLD REDUCTION AND TEMPERATURE ON MODULUS OF RIGIDITY (93)

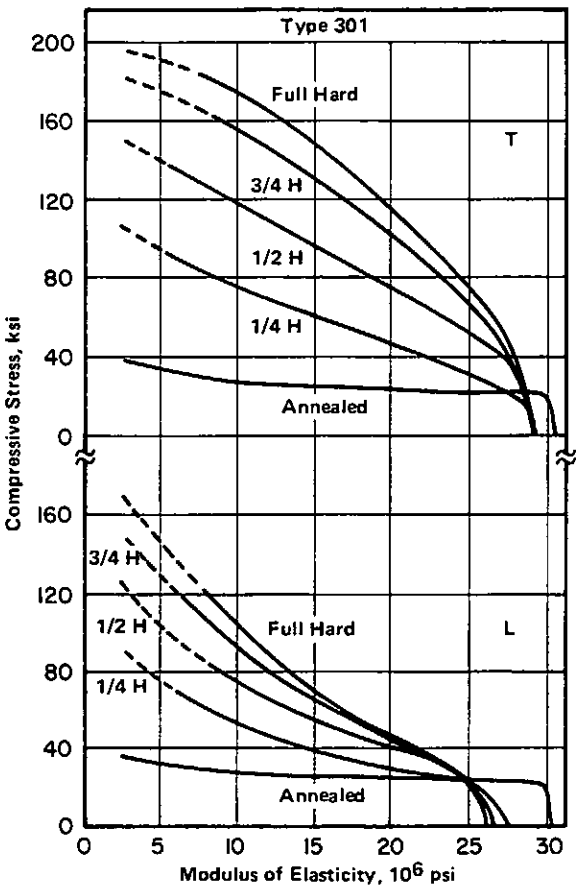


FIGURE 3.0641. COMPRESSIVE TANGENT MODULUS CURVES FOR TYPE 301 SHEET IN VARIOUS CONDITIONS (20)

Fe
18 Cr
8 Ni

Type 301
Type 302

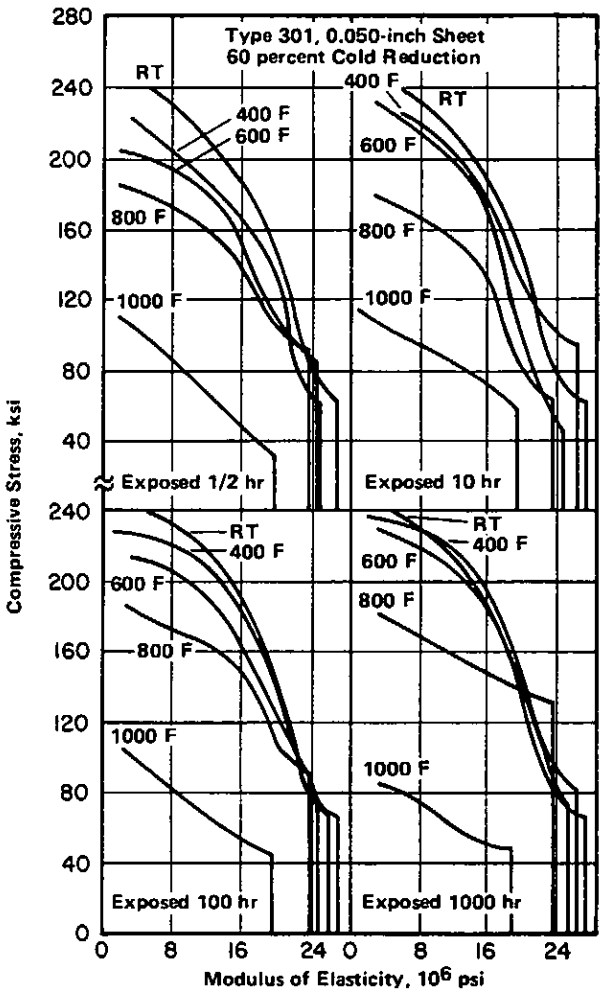


FIGURE 3.0642. COMPRESSIVE TANGENT MODULUS CURVES FOR 60 PERCENT COLD-REDUCED SHEET FOR VARIOUS EXPOSURE TIMES AND TEMPERATURES (38)

Temper	Anneal	1/4 H	1/2 H	3/4 H	Full H
Bend Factor, t	1/2 to 1-1/4	1 to 2-1/4	2-1/2 to 4	3 to 4	4 to 6

TABLE 4.0121. PRACTICAL BEND FACTORS FOR SHEET

REVISED: MARCH 1972
AUTHOR: DR. R. P. WEI

FERROUS ALLOYS

	Fe
18	Cr
9	Ni
+	S
or	Se

TYPES 303, 303 Se

1. GENERAL

These varieties of the 18-8 austenitic stainless steel family contain additions of sulfur or selenium for the purpose of improving machining characteristics, and are limited to service temperatures below 700 F. Because of the presence of these elements they are inferior to the basic Type 302 in formability and corrosion resistance. Type 303Se is superior to Type 303 in these respects, and its formability can be further improved by keeping the nickel content between 10 and 12 percent and reducing the selenium content to 0.07 percent minimum (also called Type 303A). Low carbon, columbium-tantalum stabilized types (AMS 5642C) are made to provide increased service and fabrication temperatures. In addition, types containing increased manganese (Type 303 Mod, AMS 5640J - Type 3) and lead additions (AMS 5635) are produced. Cast forms of these alloys containing suitable combinations of selenium, phosphorous and molybdenum and of sulfur and molybdenum are also known under the designations CF-16Fa and CF-16F respectively. Most properties of these alloys are nearly identical with those of the basic Types 302 and 304, and references should be made to these basic alloys.

1.01 Commercial Designation

Wrought: Type 303, Type 303Se, and Type 303Pb.
Cast: CF-16F and CF-16Fa.

1.02 Alternate Designations

AISI Type 303 and Type 303Se austenitic stainless steels, free machining 18-8 stainless steels, 18-8FM, SAE 30303, SAE 30303Se, SAE 30303 Mod, SAE 30303F, SAE 30303F + Cb.

1.03 Specifications

Table 1.03

1.04 Composition

1.041 AMS specified composition.
1.0411 AMS specified composition for Type 303 alloys, Table 1.0411.
1.0412 AMS specified composition for Type 303Se alloys, Table 1.0412.
1.042 ASTM specified composition.
1.0421 ASTM specified composition for Type 303 alloys, Table 1.0421.
1.0422 ASTM specified composition for Type 303Se alloys, Table 1.0422.

1.05 Heat Treatment

1.051 Annealing or solution treatment. 1900 to 2050 F, air cool or quench, depending on section thickness; cooling to 800 F maximum should be within 3 minutes.
1.0511 Bar and forgings. 1900 to 1950 F, 1/2 hr per in thickness water quench.
1.0512 Sheet and tubing. 1900 to 1950 F, 10 min, air cool up to 0.064 in thickness, water quench 0.065 in and thicker.
1.0513 Castings. 1900 to 2100 F, 30 min minimum, water quench or rapid cool by other means.
1.052 Heat treatment for maximum dimensional stability. 1950 F, 1/2 hr, water quench + 600 F, 1 hr, air cool + 200 F, 20 hr, air cool (13).

1.06 Hardness

These alloys can be hardened only by cold work, which increases both strength and hardness. The extent of possible cold working is less than for the other 18-8 grades because of embrittlement by the sulfur or selenium content (14, p. 116).

1.07 Forms and Conditions Available

The steel is available in the full commercial range of sizes for bar, wire, forgings, sheet and tubing(14, p. 8). All wrought products are available in the annealed condition. Sheet, bar and wire are also available in cold worked condition to various reductions. Castings are available in the annealed condition.

1.08 Melting and Casting Practice

Electric-arc, electric-induction, or other suitable commercial processes.

1.09 Special Considerations

When chromium-nickel steels containing more than about 0.04C are subject to annealing at temperatures of 1850 to 2050 F and are then reheated to or held at temperatures of approximately 800 to 1600 F, chromium carbides will precipitate at the austenite grain boundaries (15, p. 24). This intergranular precipitation or sensitization promotes intergranular corrosion cracking and reduces corrosion resistance of these steels. Heat treatment and welding conditions should be chosen to avoid carbide formation. Additions of columbium and titanium are used to stabilize these alloys and reduce intergranular corrosion sensitivity.

2. PHYSICAL AND CHEMICAL PROPERTIES

2.01 Thermal Properties

2.011 Melting range. 2550 to 2590 F (14, p. 43) (15, p. 38-39), (16, p. 22).
2.012 Phase changes. Severe cold working will transform a small amount of austenite to ferrite (martensite).
2.0121 Time-temperature-transformation diagrams.
2.013 Thermal conductivity, Figure 2.013.
2.014 Thermal expansion, Figure 2.014.
2.015 Specific heat. 0.12 Btu/F/lb from 32-212 F (14, p. 40) (15, p. 38)(16, p. 22).
2.016 Thermal diffusivity.

2.02 Other Physical Properties

2.021 Density. 0.286 lb per cu in, 7.93 gm per cu cm.
2.022 Electrical properties.
2.0221 Electrical resistivity, Figure 2.0221.
2.023 Magnetic properties. This steel is nonmagnetic in the annealed condition (15)(16). Permeability of annealed material is less than 1.01. It becomes slightly magnetic when severely cold worked as a result of transformation of a small amount of austenite to ferrite (martensite).
2.024 Emittance.
2.0241 Total hemispherical emittance, Figure 2.0241.
2.025 Damping capacity.

2.03 Chemical Properties

2.031 Corrosion resistance. General corrosion resistance in mildly corrosive atmospheres is slightly inferior and under severe corrosive conditions greatly inferior to that of Type 302. This steel resists nitric acid well, halogen acids poorly and sulfuric acid moderately (14, p. 116).
2.032 Type 303 is susceptible to stress corrosion cracking if cold worked. Type 303Se, therefore, is preferred for applications involving cold forming.
2.033 Oxidization resistance is similar to that of Type 302, but nonuniform scaling may be encountered in strongly oxidizing atmospheres above 1400 F.

2.04 Nuclear Properties

Similar to Type 304.

3. MECHANICAL PROPERTIES

3.01 Specified Mechanical Properties

3.011 AMS specified mechanical properties.
3.0111 AMS specified mechanical properties for bar, Type and 303Se, Table 3.0111.
3.0112 AMS specified mechanical properties for bar, Types 303(Cb + Ta), 303Se (Cb + Ta) and 303Pb, Table 3.0112.
3.0113 AMS specified mechanical properties for forgings, Table 3.0113.
3.0114 AMS specified mechanical properties for wire, Table 3.0114.
3.012 ASTM specified mechanical properties.
3.0121 ASTM specified mechanical properties for bar and bolting, Table 3.0121.

Fe
18 Cr
9 Ni
\+ S
or Se

TYPES 303, 303Se

3.0122 ASTM specified mechanical properties for forgings, Table 3.0122.
3.0123 ASTM specified mechanical properties for wire, Table 3.0123.
3.0124 ASTM specified mechanical properties for castings, Table 3.0124.

3.02 Mechanical Properties at Room Temperature
3.021 Tension.
3.0211 Stress-strain diagrams (see 3.0311).
3.0212 Typical room temperature mechanical properties, Table 3.0212.
3.0213 Effect of cold work on tensile properties.
3.02131 Effect of cold drawing on tensile properties of wire, Figure 3.02131.
3.022 Compression (see 3.032).
3.0221 Stress-strain diagrams.
3.023 Impact (see Table 3.0212).
3.024 Bending.
3.025 Torsion and shear.
3.026 Bearing.
3.027 Stress concentration.
3.0271 Notch properties.
3.0272 Fracture toughness.
3.028 Combined properties.

3.03 Mechanical Properties at Various Temperatures
3.031 Tension.
3.0311 Stress-strain diagrams.
3.03111 Stress-strain diagrams at room and cryogenic temperatures, Figure 3.03111.
3.0312 Tensile properties of Type 303 +S annealed bar at room and cryogenic temperatures, Figure 3.0312.
3.0313 Tensile properties of annealed bar at room and elevated temperatures, Figure 3.0313.
3.0314 Tensile properties of annealed Type 303+Se bar at room and cryogenic temperatures, Figure 3.0314.
3.032 Compression.
3.0321 Stress-strain diagrams.
3.0322 Compressive yield strength and elastic limit at room and cryogenic temperatures, Figure 3.0322.
3.033 Impact.
3.0331 Range and average values of impact energy for annealed bar of Type 303+Se, Figure 3.0331.
3.0332 Range and average values of impact energy for annealed bar of Type 303+S, Figure 3.0332.
3.034 Bending.
3.035 Torsion and shear.
3.036 Bearing.
3.037 Stress concentration.
3.0371 Notch properties.
3.0372 Fracture toughness.
3.038 Combined properties.

3.04 Creep and Creep Rupture Properties
3.041 Creep strength for 1 percent elongation at 10,000 hours, Figure 3.041.

3.05 Fatigue Properties
3.051 Endurance limit of 1/4 hard 303 is about 48 ksi (27).

3.06 Elastic Properties
3.061 Poisson's ratio.
3.062 Modulus of elasticity. 28.0 x 10^3 ksi (14, p. 40)(15, p. 38)(16, p. 22).
3.063 Modulus of rigidity.

4. FABRICATION

4.01 Formability
4.011 Forging. Starting temperature 2200F maximum, finishing temperature 1700F minimum. These steels will take only light reductions below 1800F.
4.0111 Scaling. Starting temperature 1600F maximum, finishing temperature 1900F maximum for continuous service (14, p. 116).
4.012 Cold forming of these types is possible to a limited extent with Type 303Se being superior to Type 303 in this respect. Type 303 should be annealed after severe forming to prevent stress cracking. A special high nickel, low selenium composition is recommended for more severe cold forming.

4.02 Machining and Grinding
These steels are the most readily machinable of all the austenitic stainless steels. Type 303 permits heavy feeds and deep cuts, while the use of Type 303Se is indicated where a high finish is desired. As with other austenitic steels very sharp tools, low speeds and feeds, and heavy equipment are required. Machining speeds between 60 to 75 percent of those used for mild carbon steels are suitable.

4.03 Welding
Welding of these steels is generally not recommended. Fusion welding with Type 310 electrodes is possible to a very limited extent and post weld annealing is necessary. The columbium bearing types need no post weld annealing.

4.04 Surface Treatment

TABLE 1.03

Form	AMS	ASTM
Bar, forgings, wire (solution treated), forging stock	5640J	A-582, A-473, A-314, A-581
Bar, forgings, (solution treated) (swaging and hot upsetting), forging stock	5641A	
Bar (cold drawn)	5738	
Bolting		A-194, A-320
Casting		A-296
Bar, forgings (solution treated), forging stock (Cb + Ta stabilized)	5642C	
Bar, forgings (solution treated), forging stock (Pb added)	5635	

TABLE 1.0411

Source	AMS (1)				AMS(4)		AMS(5)	
Alloy	Fe-18Cr-9Ni + S							
	Type 303		Type 303 Mod		Type 303 (Cb + Ta)		Type 303Pb	
	Percent		Percent		Percent		Percent	
	min	max	min	max	min	max	min	max
Carbon	-	0.15	-	0.15	-	0.08	-	0.15
Manganese	-	2.00	2.50	4.50	-	2.00	-	2.00
Phosphorus	-	0.15	-	0.20	-	0.040	-	0.040
Sulfur	0.18	0.40	0.15	0.40	0.18	0.35	0.12	0.30
Silicon	-	1.00	-	1.00	-	1.00	-	1.00
Chromium	17.00	19.00	17.00	19.00	17.00	19.00	17.00	19.00
Nickel	8.00	10.00	7.00	10.00	9.00	12.00	8.00	10.00
Molybdenum	-	0.75	-	0.60	-	0.75	-	0.60
Columbium + Tantalum	-	-	-	-	10xC	1.10	-	-
Copper	-	0.50	-	0.50	-	0.50	-	0.50
Lead	-	-	-	-	-	-	0.12	0.30
Iron	Balance		Balance		Balance		Balance	

TABLE 1.0412

Source	AMS (1)		AMS(2)		AMS(3)		AMS(4)	
Alloy	Fe-18Cr-9Ni + Se							
Designation	Type 303Se						Type 303Se (Cb + Ta)	
	Percent		Percent		Percent		Percent	
	min	max	min	max	min	max	min	max
Carbon	-	0.15	-	0.12	-	0.12	-	0.08
Manganese	-	2.00	-	2.00	0.20	2.00	-	2.00
Phosphorus	0.12	0.17	0.11	0.17	-	0.17	0.11	0.17
Sulfur	-	0.04	-	0.040	-	0.10	-	0.030
Silicon	-	1.00	-	0.70	-	1.00	-	1.00
Chromium	17.00	19.00	17.00	20.00	17.00	19.00	17.00	19.00
Nickel	8.00	10.00	8.00	12.00	8.00	10.00	9.00	12.00
Molybdenum	-	0.50	-	0.50	-	0.75	-	0.50
Selenium	0.15	0.40	0.15	0.30	0.15	0.35	0.15	0.35
Columbium + Tantalum	-	-	-	-	-	-	10xC	1.10
Copper	-	0.50	-	-	-	0.50	-	0.50
Iron	Balance		Balance		Balance		Balance	

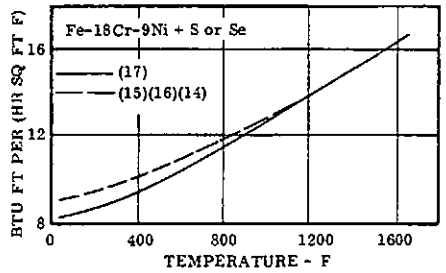


FIG. 2.013 THERMAL CONDUCTIVITY. (17)(15, p.38) (16, p. 22)(14, p. 40)

Fe
18 Cr
9 Ni
+ S
or Se

TYPES 303, 303Se

TABLE 1.0421

Source	ASTM(6)(8)		ASTM(7)(9)		ASTM(10)(11)		ASTM(12)	
Alloy	Fe-18Cr-9Ni + S							
Designation	Type 303						Type 303 (CF-16Fa)	
	Percent		Percent		Percent		Percent	
	min	max	min	max	min	max	min	max
Carbon	-	0.15	-	0.15	-	0.15	-	0.16
Manganese	-	2.00	-	2.00	-	2.00	-	1.50
Phosphorus	-	0.20	-	0.20	-	0.20	-	0.04
Sulfur	0.15	-	0.15	-	0.15	0.35	0.20	0.40
Silicon	-	1.00	-	1.00	-	1.00	-	2.00
Chromium	17.00	19.00	17.00	19.00	17.00	19.00	18.00	21.0
Nickel	8.00	10.00	8.00	10.00	8.00	10.00	9.0	12.0
Molybdenum	-	0.60(b)	-	0.60	-	0.60(b)	0.40	0.80
Zirconium	-	-	-	-	-	0.60(a)	-	-
Iron	Balance		Balance		Balance		Balance	

(a) Optional additions
(b) Optional addition for A320-68 (11)

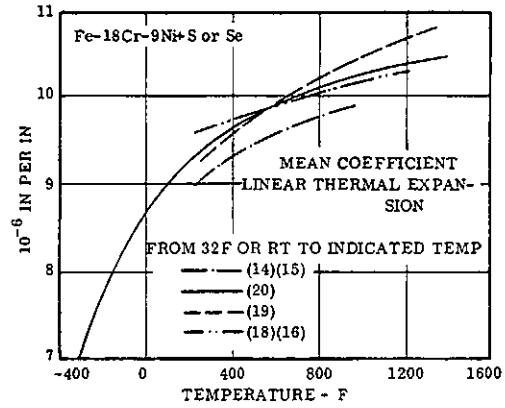


FIG. 2.014 THERMAL EXPANSION. (14, p. 40)(15, p.38) (16, p. 22)(18)(19)(20)

TABLE 1.0422

Source	ASTM(6)(7)(8)(10)		ASTM (11)		ASTM (12)	
Alloy	Fe-18Cr-9Ni + Se					
Designation	Type 303Se				Type 303Se (CF-16F)	
	Percent		Percent		Percent	
	min	max	min	max	min	max
Carbon	-	0.15	-	0.15	-	0.16
Manganese	-	2.00	-	2.00	-	1.50
Phosphorus	-	0.20	-	0.20	-	0.17
Sulfur	-	0.06	-	0.06	-	0.04
Silicon	-	1.00	-	1.00	-	2.00
Chromium	17.00	19.00	17.00	19.00	18.0	21.0
Nickel	8.00	10.00	8.00	10.00	9.0	12.0
Molybdenum	-	-	-	-	-	1.50
Selenium	0.15	-	0.15	0.35	0.20	0.35
Iron	Balance		Balance		Balance	

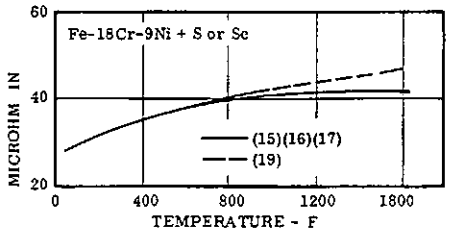


FIG. 2.0221 ELECTRICAL RESISTIVITY. (15, p.38) (16, p. 22)(17)(19)

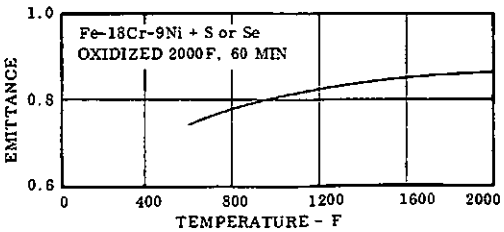


FIG. 2.0241 TOTAL HEMISPHERICAL EMITTANCE. (21)

	Fe
18	Cr
9	Ni
+	S
or	Se

TYPES 303, 303Se

TABLE 3.0111

Source	(1)	(2)	(3)			
Alloy	Fe-18Cr-9Ni+S or Se (Types 303 and 303Se)					
Form	Bar					
Condition	ST(a)	ST(a)	ST + Cold Finish			
Diameter or least distance between parallel sides - in	(a)	(a)	≤0.750	0.751 to 1.000	1.001 to 1.250	1.251 to 1.750
F_{tu} - min - ksi	-	75	125	115	105	95
- max - ksi	-	115	-	-	-	-
F_{ty} - min - ksi	-	-	100	80	65	45
e(2 in or 4D) - min - percent	-	35	12	15	20	28
RA - min - percent	-	-	35	35	35	45
Hardness, BHN(b) min	140	-	-	-	-	-
max	255	-	-	-	-	-

(a) Bars ≤2.75 inch shall be cold finished, unless specified otherwise.
(b) Hardness taken approximately midway between surface and center.

TABLE 3.0112

Source	AMS (4)(c)			AMS (5)		
Alloy	Fe-18Cr-9Ni+S or Se (Cb+Ta), Types 303 (Cb+Ta) and 303Se (Cb+Ta)			Fe-18Cr-9Ni + Pb Type 303Pb		
Form	Bar					
Condition	ST(a)			ST Hot finished	ST Cold finished	
Diameter or least distance between parallel sides-in	≤0.75	>0.75 to 1.50	>1.50	-	≤0.500	>0.500
F_{tu} - min - ksi	-	-	-	75	90	75
F_{ty} - min - ksi	-	-	-	30	45	30
e(2 in or 4D) - min - percent	-	-	-	40	35	40
RA - min - percent	-	-	-	50	45	50
Hardness, BHN(b)						
- minimum	175	163	140	170(d)	140(e)	
- maximum	255	255	241	255(d)	241(e)	

(a) Bars ≤2.75 inch shall be cold finished, unless specified otherwise.
(b) Hardness taken approximately midway between surface and center.
(c) Embrittlement: material shall be capable of meeting specified test for embrittlement.
(d) For bars ≤0.75 inch
(e) For bars >0.75 inch

TABLE 3.0113

Source	AMS(1)(5)	AMS(2)
Alloy	Fe-18Cr-9Ni+S or Se (Types 303 and 303Se) and Fe-18Cr-9Ni(+Pb) (Type 303Pb)	
Form	Forgings	
Condition	ST	
Hardness, BHN - min	-	149
- max	187	229

TABLE 3.0114

Source	AMS (1)
Alloy	Fe-18Cr-9Ni+S or Se (Types 303 and 303Se)
Form	Wire
Condition	ST
F_{tu} - minimum - ksi	85
- maximum - ksi	125

TABLE 3.0121

Source	(7)	(10)	(11)				
Alloy	Fe-18Cr-9Ni + S or Se (Types 303 and 303Se)						
Form	Bar	Bolting					
Condition	ST	ST	ST	ST + Cold Work			
Diameter or least distance between parallel sides - inches	-	-	-	≤0.75	>0.75 to 1.00	>1.00 to 1.25	>1.25 to 1.50
F_{tu} - min - ksi	-	-	75	125	115	105	100
F_{ty} - min - ksi	-	-	30	100	80	65	50
e(2 in) - min - percent	-	-	35	12	15	20	28
RA - min - percent	-	-	50	35	35	35	45
Hardness - BHN							
- minimum	-	149	-	-	-	-	-
- maximum	262	-	-	-	-	-	-

TABLE 3.0122

Source	ASTM (8)
Alloy	Fe-18Cr-9Ni + S or Se (Types 303 and 303Se)
Form	Forgings
Condition	ST
F_{tu} - minimum - ksi	75
F_{ty} - minimum - ksi	30
e(2 in) - minimum - percent	40
RA - minimum - percent	50

TABLE 3.0123

Source	ASTM (9)	
Alloy	Fe-18Cr-9Ni + S or Se (Types 303 and 303Se)	
Form	Wire	
Condition	Annealed	Annealed + Cold Drawn
F_{tu} - minimum - ksi	85	115
maximum - ksi	125	145

TABLE 3.0124

Source	ASTM (12)
Alloy	Fe-18Cr-9Ni + S or Se (CF16-F and CF-16Fa)
Form	Castings
Condition	Annealed
F_{tu} - minimum - ksi	70
F_{ty} - minimum - ksi	30
e(2 in) - minimum - percent	25

TABLE 3.0212

Source	(22)										(18)	(15)	(14)
Alloy	Fe-18Cr-9Ni- + S or Se												
Form	Bar				Wire						Cast test bars	Bar	
Condition	Ann	CD	High tensile		Annealed		Soft temper		Hard temper			Annealed	
Diameter - inches	-	1	7/8	1 1/2	0.062	0.500	0.062	0.500	0.062	0.500	-	-	1
F_{tu} - typical - ksi	90	100	125	110	105	90	125	100	160	140	77	85	90
F_{ty} - typical - ksi	35	60	95	75	35	35	90	60	125	105	40	35	35
e(2 in) - min - percent	50	40	20	30	50	50	30	40	15	20	52	55	50
RA - percent	55	53	50	50	60	60	55	55	45	50	-	60	55
Hardness - BHN	160	228	277	240	-	-	-	-	-	-	152	150	160
Impact Strength													
Izod - ft lb	80	-	35	-	-	-	-	-	-	-	-	85	80
Charpy Keyhole - ft lb	-	-	-	-	-	-	-	-	-	-	75	-	-

	Fe
18	Cr
9	Ni
+	S
or	Se

TYPES 303, 303 Se

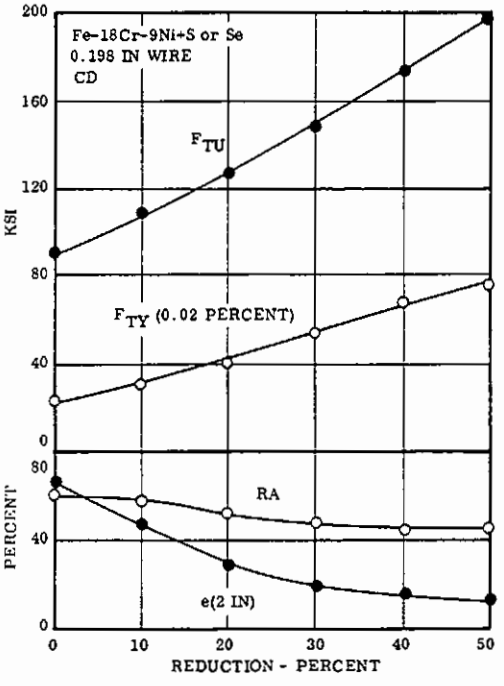


FIG. 3.02131 EFFECT OF COLD DRAWING ON TENSILE PROPERTIES OF WIRE. (19)

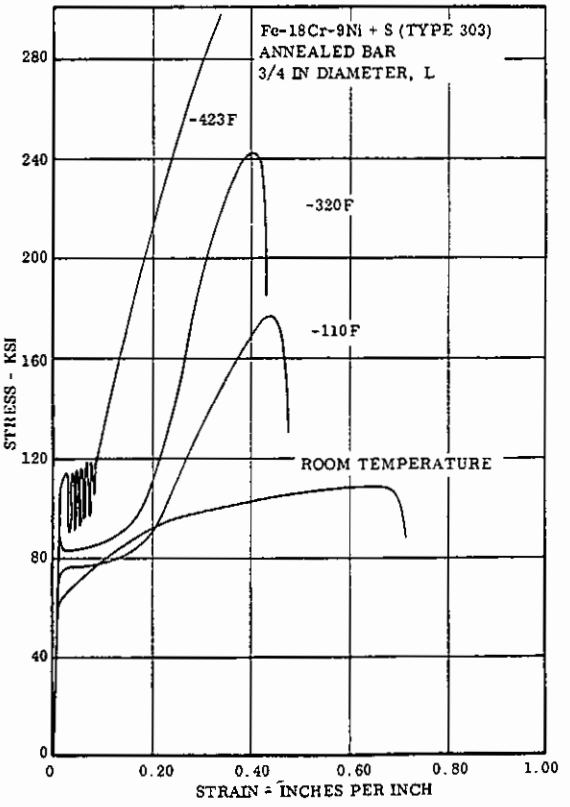


FIG. 3.03111 STRESS-STRAIN DIAGRAMS AT ROOM AND CRYOGENIC TEMPERATURES. (23, p. 40)

	Fe
18	Cr
9	Ni
+	S
or	Se

TYPES 303, 303 Se

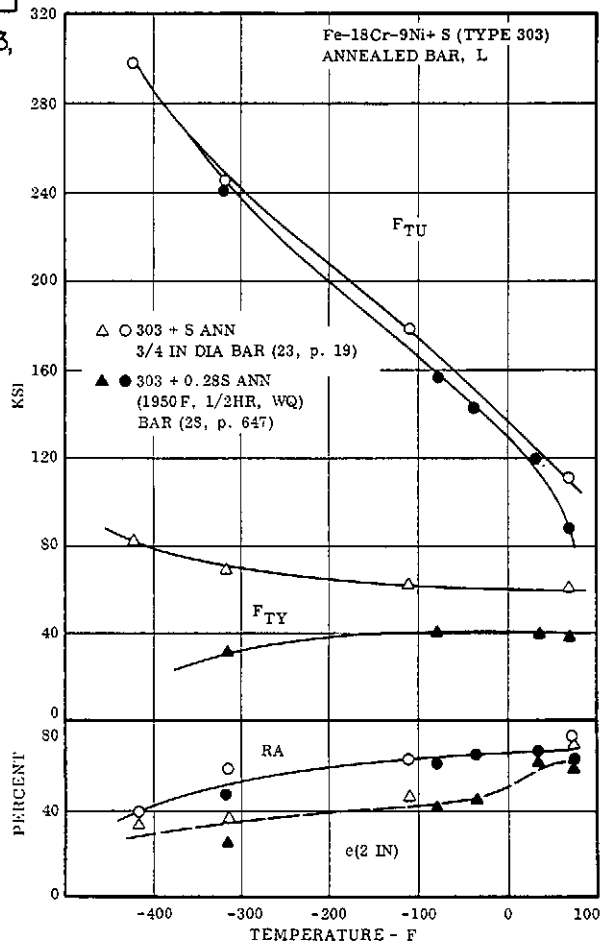


FIG. 3.0312 TENSILE PROPERTIES OF TYPE 303 + S ANNEALED BAR AT ROOM AND CRYOGENIC TEMPERATURES. (23)(28)

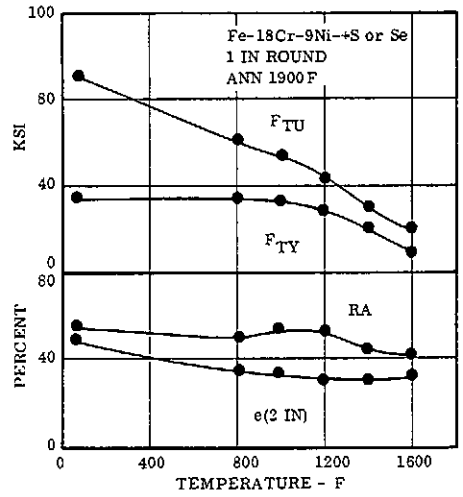


FIG. 3.0313 TENSILE PROPERTIES OF ANNEALED BAR AT ROOM AND ELEVATED TEMPERATURES. (14, p. 117)

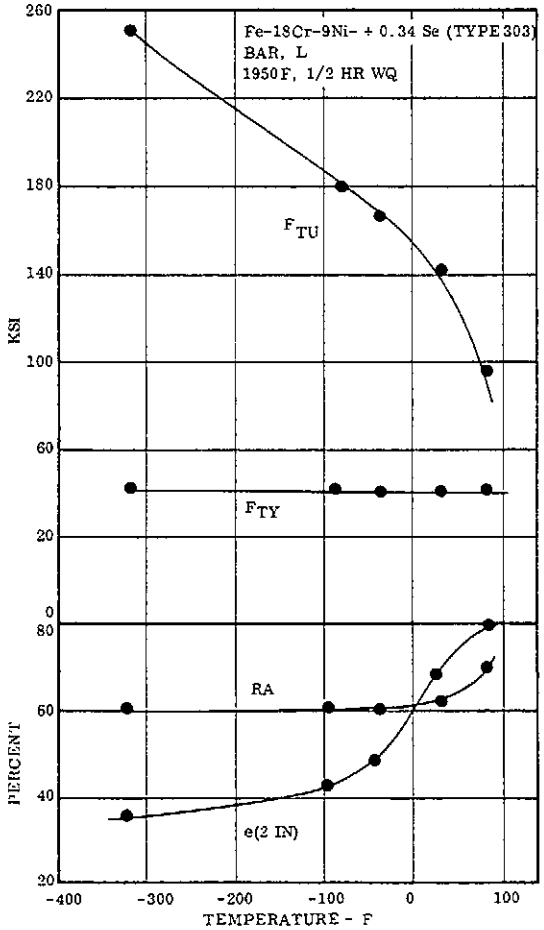


FIG. 3.0314 TENSILE PROPERTIES OF ANNEALED TYPE 303+Se BAR AT ROOM AND CRYOGENIC TEMPERATURES. (28, p. 647)

	Fe
18	Cr
9	Ni
+	S
or	Se

TYPES 303, 303 Se

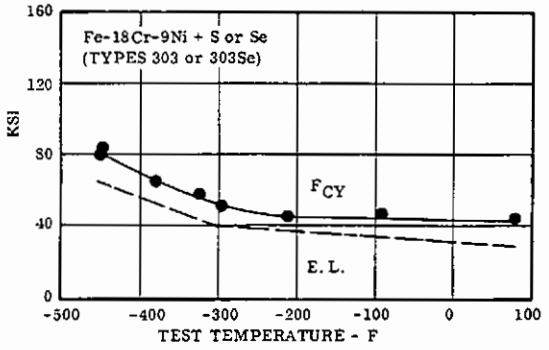


FIG. 3.0322 COMPRESSIVE YIELD STRENGTH AND ELASTIC LIMIT AT ROOM AND CRYOGENIC TEMPERATURES. (24, Fig B5)

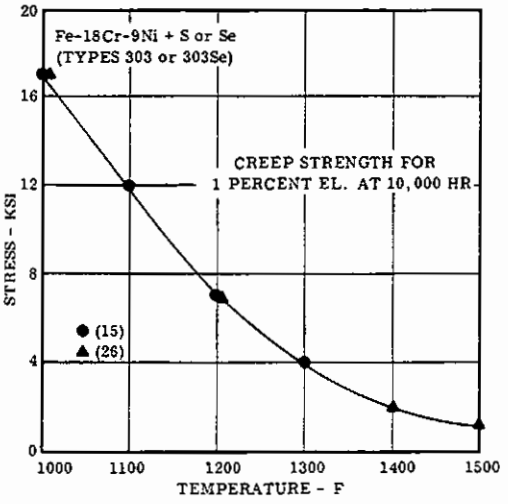


FIG. 3.041 CREEP STRENGTH FOR 1 PERCENT ELONGATION AT 10,000 HOURS. (15, p. 38)(26, p. 112)

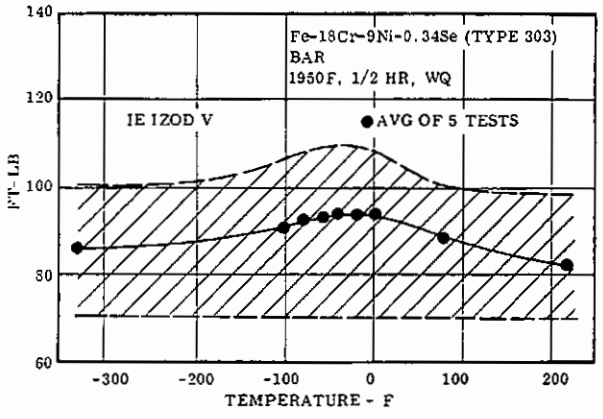


FIG. 3.0331 RANGE AND AVERAGE VALUES OF IMPACT ENERGY FOR ANNEALED BAR OF TYPE 303+Se. (29, p. 647)

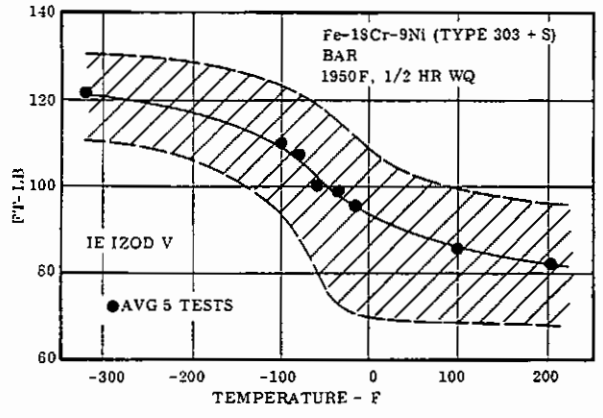


FIG. 3.0332 RANGE AND AVERAGE VALUES OF IMPACT ENERGY FOR ANNEALED BAR OF TYPE 303 + S. (29, p. 647)

REFERENCES

1. AMS 5640J, Bars and Forgings - 18Cr-9Ni, Free Machining (November 1, 1969).

	Fe
18	Cr
9	Ni
+	S
or	Se

TYPES 303, 303 Se

2. AMS 5641A, Bars and Forgings - 18.5Cr-10Ni, Free Machining, Swaging or Hot Upsetting (October 1, 1951).
3. AMS 5738, Bars, Cold Drawn - 18Cr-9Ni, Free Machining, High Yield Strength (February 1, 1956).
4. AMS 5642C, Bars and Forgings - 18.5Cr-11Ni-(Cb+Ta), Free Machining (August 15, 1955).
5. AMS 5635, Bars and Forgings - 18Cr-9Ni (303Pb), Free Machining (January 31, 1964).
6. ASTM A314-63, Standard Specification for Stainless and Heat-Resisting Steel Billets and Bars for Reforging (September 30, 1963).
7. ASTM A582-67, Standard Specification for Free-Machining Stainless and Heat-Resisting Steel Bars, Hot Rolled or Cold Finished (December 12, 1967).
8. ASTM A473-63, Standard Specification for Stainless and Heat-Resisting Steel Forgings (September 30, 1963).
9. ASTM A581-67, Standard Specification for Free-Machining Stainless and Heat-Resisting Steel Wire (December 12, 1967).
10. ASTM A194-68, Standard Specification for Carbon and Alloy Steel Nuts for Bolts for High-Pressure and High-Temperature Service (May 9, 1968).
11. ASTM A320-68, Standard Specification for Alloy Steel Bolting Materials for Low Temperature Service (March 26, 1968).
12. ASTM A296-68, Standard Specification for Corrosion Resistant Iron-Chromium, Iron-Chromium-Nickel, and Nickel Base Alloy Castings for General Application (August 15, 1968).
13. DMIC, "A Review of Dimensional Stability of Metals," DMIC Memo 189 (March 19, 1964).
14. Carpenter Steel Company, "Carpenter Stainless and Heat-Resisting Steels - Selection, Description, Fabrication," Working Data (1962).
15. Republic Steel Corporation, "Republic ENDURO Stainless Steel - Chromium-Nickel Types, 300 Series," ADV 1124 R4-15M-3-66 (1966).
16. Superior Tube Company, "Stainless Steel Tubing," Catalog Section 22 (1957).
17. Hogan, C. L. and Sawyer, R. B., "Thermal Conductivity of Metals at High Temperature," Journal of Applied Physics, American Institute of Physics, Volume 23 (January - December 1952).
18. Schoefer, E. A., "Corrosion Resistant Type CF-16F," Data Sheet, Alloy Casting Institute (June 1954).
19. Allegheny Ludlum Steel Corporation, "Allegheny Free Machining Stainless Steels, Types 303, 416, 430F," Allegheny Ludlum Blue Sheet (1957).
20. North American Aviation, "Stainless Steel Type 303," Data Sheet (1957).
21. Wade, W. R., "Measurements of Total Hemispherical Emissivity of Various Oxidized Metals at High Temperature," NACA TN 4206 (March 1958).
22. American Iron and Steel Institute, "Stainless and Heat Resisting Steels," Steel Products Manual (June 1957).
23. Warren, K. A. and Reed, R. P., "Tensile and Impact Properties of Selected Materials from 20 to 300K," National Bureau of Standards Monograph 63 (June 28, 1963).
24. Hurlich, A., "Properties of Materials at Liquid Oxygen and Liquid Hydrogen Temperatures," GD/Astronautics, San Diego, California, Report No. AA-M-23, (March 15, 1957)(AD676736).
25. ASTM STP52A - Data on Corrosion and Heat Resistant Steels and Alloys (1950).
26. Levy, A.V. and Friedman, "Properties of Metallic Materials Considered in the Design of Ramjet Engine and Associated Accessories for the Advanced Component Development Program," Report 5388, Marquardt Aircraft Company, Contract AF33(616)-38, E.O.R.-448-83, AD-7 (April 1, 1954).
27. Chromium-Nickel Stainless Steel Data, Section 1, Bulletin A, International Nickel Company, New York, New York (1963) p. 1A.
28. Hoke, J.H., Mabus, P.G., and Goller, G.N. "Mechanical Properties of Stainless Steels at Subzero Temperatures," Metal Progress (May 1949) p. 643.

REVISED : MARCH 1973
AUTHOR : C. F. HICKEY, JR.

FERROUS ALLOYS

	Fe
Low	C
19	Cr
10	Ni

TYPES 304, 304L

1. GENERAL

The low carbon members of the straight 18-8 austenitic stainless steel family are produced in two grades. Type 304 with 0.08 percent maximum carbon and Type 304L with 0.03 percent maximum carbon. They have properties similar to those of Type 302 but their corrosion resistance is slightly higher because of the lower carbon and the increased chromium and nickel contents. The susceptibility of these steels to intergranular corrosion decreases considerably with decreasing carbon content, although long exposure to elevated temperatures may even sensitize Type 304L. The normal nitrogen content for Type 304 is 0.04 percent. Increasing the nitrogen to between 0.10 and 0.16 percent is a means of increasing the strength and creep rupture properties of Type 304. This higher nitrogen version is referred to as Type 304N. Types 304 and 304L are available in all common wrought forms and also as castings under the designations of CF-8 and CF-3. respectively. The wrought forms possess very good formability and the steels can be readily welded by all common methods.

1.01 Commercial Designations

Wrought: Type 304, Type 304L and Type 304N.
Cast: CF-8 and CF-3.

1.02 Alternate Designations

Low carbon 18-8S stainless steels. AISI Type 304 and Type 304L austenitic stainless steels.

1.03 Specifications

Table 1.03.

1.04 Composition

1.041 AMS compositions, Table 1.041.
1.042 AISI and ACI compositions, Table 1.042.

1.05 Heat Treatment

1.051 Anneal or solution treat. 1800 to 1950F, 30 minutes to 1 hour per inch thickness, 2 hours minimum for plate, air cool or quench depending on section size. Cooling to 800F maximum should be within 3 minutes.
1.0511 Sheet and tubing. 1900 to 1950F, 10 minutes, air cool up to 0.064 inch thickness, water quench 0.065 and thicker.
1.0512 Castings (AMS 5370, 5371). 1950 to 2050F, 30 minutes minimum, air cool.
1.052 Stress relief (see also 1.09).
1.0521 To improve elastic characteristics of cold rolled sheet or cold drawn bar. 650 to 800F, 4 to 8 hours.
1.05211 Casting (AMS 5370). 400 to 750F, 1/2 to 2 hours, air cool (14).

1.06 Hardness

1.061 Hardness of annealed alloy is RB 75-90 and BHN 135-185 (15).
1.062 Typical hardness for alloy of different forms and conditions (see Table 3.0212).
1.063 Effect of time and temperature of exposure on room temperature hardness of alloy, Figure 1.063.
1.064 Effect of low temperature on hardness of bar, Figure 1.064.
1.065 Effect of test temperature on hot hardness, Figure 1.065.

1.07 Forms and Conditions Available

1.071 The steel is available in the full commercial range of sizes for all wrought forms common for stainless steels.
1.072 These forms are generally available in the annealed, cold worked or cold worked and stress relieved conditions.
1.073 Sand and centrifugal castings are available up to 6000 lb in the annealed condition.

1.08 Melting and Casting Practice

Electric furnace air melts and induction vacuum melts. Castability, fluidity, shrinkage and resistance to hot tearing characteristics are excellent (14).

1.09 Special Considerations

(see also 2.03).
1.091 Intergranular corrosion after welding or heating may occur in Type 304, but usually not in Type 304L.
1.092 Stress corrosion cracking may occur in hot dilute chloride solutions.
1.093 The normal nitrogren content for Type 304 is 0.04 percent. Increasing the nitrogen content to between 0.10 and 0.16 percent results in an increase in strength properties in the temperature range of room temperature to 1200F (Table 3.03138).

The higher nitrogen material is designated as Type 304N. Higher creep and creep rupture properties are also exhibited at temperatures ranging from 1050 to 1500F for Type 304N (Table 3.046). Ductility of Type 304N, as measured by elongation and reduction, is not adversely affected at testing temperatures up to 1100F (43). At cryogenic temperatures the yield strength of Type 304N is superior to that of Type 304, whereas the tensile and toughness properties of Type 304N are similar to those of Type 304, see Table 1.093 for typical values.
1.094 Helium reduces the rupture life of Type 304 (see Figure 3.047).

2. PHYSICAL AND CHEMICAL PROPERTIES

2.01 Thermal Properties

2.011 Melting range. 2550 to 2650F.
2.012 Phase changes.
2.0121 Time-temperature-transformation diagrams.
2.0122 These steels are subject to carbide precipitation at 800 to 1600F.
2.0123 Cold work will transform a small amount of austenite to ferrite (martensite).
2.013 Thermal conductivity, Figure 2.013.
2.014 Thermal expansion, Figure 2.014.
2.015 Specific heat, Figure 2.015.
2.016 Thermal diffusivity.

2.02 Other Physical Properties

2.021 Density. 0.287 to 0.292 lb per cu in. 7.94 to 8.07 gr per cu cm.
2.022 Electrical resistivity, Figure 2.022.
2.023 Magnetic properties. This steel is nonmagnetic in the annealed condition. Permeability of annealed materials is less than 1.02. It becomes slightly magnetic when severely cold worked, but to a lesser extent than Type 302 and particularly, Type 301.
2.0231 Effect of cold reduction on magnetic permeability, Figure 2.0231.
2.0232 The intrinsic saturation magnetization, B_S, is structure insensitive and depends only on the quantity of the ferromagnetic phase, α (28). Stress induced transformation of γ to α occurs as a function of low temperature deformation thus resulting in an increase in magnetization, Figure 2.0232.
2.024 Emittance (Black Body = 1.0) At 80F 0.08
-320F 0.048 (27).
2.025 Damping capacity.

2.03 Chemical Properties

2.031 Corrosion resistance.
2.0311 General corrosion resistance of these steels to various atmospheres, most acids, hot petroleum products and steam and combustion gases is very good.
2.0312 Intergranular corrosion in Types 304 and 304L when subjected to a nitric-dichromate solution is associated with the presence of continuous grain boundary paths of either second phase or solute-segregated regions. The susceptibility of these types to intergranular corrosion may be substantially reduced by suitable heat treatments, Table 2.0312.
2.0313 Intergranular corrosion of Type 304 may occur in certain corrosive media after it is welded or otherwise heated to temperatures between 800 and 1600F. Type 304L will become sensitized only after prolonged heating in this temperature range, but its use over 800F is not recommended because of its relatively low strength. Complete immunity from intergranular corrosion is obtained only in the stabilized types 321 and 347. Effect of carbon content on corrosion rate, Figure 2.0313.

	Fe
Low	C
19	Cr
10	Ni

TYPES 304, 304L

2.0314 Type 304 is susceptible to pitting and crevice attack. In quiet sea water, cathodic protection is essential to control pitting and crevice attack (32). Deep ocean behavior of Types 304 and 304L varies, but local attack often takes place, Table 2.0314.

2.0315 Corrosion rate and attack depth. Results of corrosion rate and maximum depth of attack of sheet in sea water at a depth of 5600 feet in the Tongue of the Ocean (TOTO) waters, Bahama Islands, Table 2.0315.

2.0316 Type 304 is highly resistant to stress corrosion cracking in a moist environment containing chlorides at room temperature. Types 304 and 304L are susceptible to stress corrosion in hot dilute chloride solutions. The presence of oxygen in the solution increases the tendency to stress corrosion. Making the steels anodic accelerates stress cracking, while cathodic currents prevent it.

2.0317 The best corrosion resistance comes from a clean surface free of all organic and metallic contaminants. Such surfaces can be obtained by a thorough degreasing treatment and a nitric acid rinse (37).

2.0318 Nitriding significantly increased the resistance to stress corrosion cracking, Table 2.0318.

2.0319 Threshold stress (maximum stress that will not produce stress-corrosion cracking or failure in 300 hr) determined in 0.5N NaCl + 0.1N $NaNo_2$ boiling solution for Type 304, Table 2.0319.

2.03191 Mechanical properties and threshold stress values, which were determined in a boiling solution of 0.5N NaCl + 0.1N $NaNo_2$, for specimens of annealed sheet which were cold reduced by various amounts, Table 2.03191.

2.032 Oxidation resistance of these steels is good up to 1700F for continuous service and up to 1600F for intermittent service.

2.0321 The presence of high pressure hydrogen during loading to failure leads to a marked reduction in the tensile strength and ductility of Type 304L at room temperature. This reduction in strength is dependent upon the state of stress at the root of the notch, increasing both with increasing notch severity and with increasing hydrogen pressure (36), (see Figures 2.03211 and 2.03212).

2.03211 Ultimate tensile and notch strength versus hydrogen pressure for Type 304L exposed for 24 hr and then pulled to fracture in high pressure hydrogen, Figure 2.03211.

2.03212 Percent elongation versus hydrogen pressure for Type 304L exposed for 24 hr and then tested in high pressure hydrogen, Figure 2.03212.

2.04 Nuclear Properties

Austenitic stainless steels, particularly 304L, 304 and 347 are used extensively in nuclear power reactor construction.

2.041 Irradiation effects on austenitic stainless steels are generally the following:

2.0411 Magnetic susceptibility is increased depending on condition of material, irradiation variables, such as total flux and temperature, and method of measurement. At nvt = 10^{19} and 400 to 500F, the susceptibility of Type 304 shows an increase in the order of 500 percent, if measured by the Guoy method.

2.0412 Changes in mechanical properties consist of increases in tensile strength, yield strength and hardness , decrease in elongation, development of a yield point jog and high strain rate dependence. At room temperature and about 5×10^{19} nvt, the tensile strength of annealed Type 304 is found to increase by approximately 20 percent and the yield strength by 200 percent. At 400 to 500F and 10^{19} nvt, effects of irradiation are small.

2.0413 Austenitic stainless steels retain their high impact strength after irradiation in contrast to ferritic steels which may become extremely brittle because of an increase in the transition temperature.

2.042 Austenitic steels exhibit good resistance to intergranular corrosion in high purity water containing oxygen at 500 to 600F. This also applies to welded parts, including intergranular corrosion between different types of the 300 series. Sensitizing of the steels does not effect this corrosion resistance.

2.043 Type 304L can be used in applications where it is in contact with molten sodium, even though sodium is an excellent medium for transferring carbon (37).

2.044 Type 304 is used with an additional content of up to 2 percent boron for such applications as control rods and thermoshields because of the high nuclear cross-section of boron. However, boron increases the susceptibility of the alloy to radiation damage.

2.045 Nitrogen alloyed Type 304 has the advantage of increasing the strength level by somewhat more than 10 percent without degrading the properties for reactor construction (38).

2.046 Effect of irradiation below 100C (212F) on yield strength, Figure 2.046.

2.047 Strain rate dependence of tensile properties for Type 304 at 1300F after irradiation to 3.4 nvt total, Figure 2.047.

2.048 S-N curve for irradiated and unirradiated smooth specimens of 304 stainless steel, Figure 2.048.

3. MECHANICAL PROPERTIES

3.01 Specified Mechanical Properties

3.011 AMS specified mechanical properties for all products except tubing, Table 3.011.

3.012 AMS specified mechanical properties for tubing, Table 3.012.

3.02 Mechanical Properties at Room Temperature

3.021 Tension.

3.0211 Stress-strain diagrams (see 3.0311).

3.0212 Typical tensile properties for various forms and conditions of alloys, Table 3.0212.

3.0213 Effect of cold rolling on tensile properties of Types 304 and 304L sheet, Figure 3.0213.

3.0214 Effect of cold rolling at -105F on tensile strength of sheet, Figure 3.0214.

3.0215 Effect of exposure to elevated temperatures on tensile properties of cold rolled sheet, Figure 3.0215.

3.0216 Effect of exposure of 10,000 hours to elevated temperatures on tensile properties of annealed alloy, Figure 3.0216.

3.0217 Effect of annealing temperature and exposure to elevated temperatures on tensile properties of bar, Figure 3.0217.

3.0218 Yield strength of Type 304 at room temperature after aging 1-1/2 hours at the temperatures shown following tensile deformation at -319F, Figure 3.0218.

3.0219 Ultimate tensile strength of Type 304 at room temperature after aging 1-1/2 hours at the temperature shown following tensile deformation at -319F, Figure 3.0219.

3.02110 Elongation of Type 304 at room temperature after aging 1-1/2 hours at the temperatures shown following tensile deformation at -319F, Figure 3.02110.

3.02111 AISI tensile strength range for various sizes of spring wire, Figure 3.02111.

3.022 Compression.

3.0221 Stress-strain diagrams.

3.023 Impact.

3.0231 Typical impact properties of annealed plate, and cold drawn bar, Table 3.0231.

3.024 Bending.

3.025 Torsion and shear.

3.026 Bearing.

3.027 Stress concentration.

3.0271 Notch properties.

3.02711 Effect of cold-rolling and test direction on notch strength of sheet, Figure 3.02711.

3.02712 Effect of stress relief temperature on sharp notch strength ratio for cold rolled 304L sheet, Figure 3.02712.

3.0272 Fracture toughness.

3.028 Combined properties.

3.03 Mechanical Properties at Various Temperatures.

3.031 Tension.

3.0311 Stress-strain diagrams.

3.03111 Stress-strain curves to failure at room and elevated temperatures. Figure 3.03111.

3.03112 Stress-strain curves at room and elevated temperatures, Figure 3.03112.

3.03113 Stress-strain curves at room and low temperatures, Figure 3.03113.

	Fe
Low	C
19	Cr
10	Ni

TYPES 304, 304L

3.03114 True stress-strain curves at room and elevated temperatures, Figure 3.03114.
3.03115 True stress-strain curves at room and low temperatures, Figure 3.03115.
3.0312 Effect of cold reduction on tensile properties.
3.03121 Effect of cold rolling on tensile properties of sheet at room and low temperatures, Figure 3.03121.
3.03122 Effect of cold reduction on -320F tensile properties of 304L sheet, Figure 3.03122.
3.0313 Effect of elevated temperatures on tensile properties.
3.03131 Effect of elevated test temperature on tensile properties of rolled tubing, Figure 3.03131.
3.03132 Range of tensile property values at elevated temperatures for annealed alloy, Figure 3.03132.
3.03133 Effect of elevated test temperatures on alloy, Figure 3.03133.
3.03134 Effect of elevated test temperature on annealed alloy, Figure 3.03134.
3.03135 Effect of annealing and test temperature on tensile properties of cold drawn bar, Figure 3.03135.
3.03136 Effect of elevated temperature on Zerolled 304 stainless, Figure 3.03136.
3.03137 Effect of test temperature on tensile properties of castings, Figure 3.03137.
3.03138 Comparison of strength properties of types 304 and 304N at room and elevated temperatures, Table 3.03138.
3.0314 Effect of low temperature on tensile properties.
3.03141 Effect of low test temperature on tensile properties of annealed alloy, Figure 3.03141.
3.03142 Effect of low test temperature and strain rate on tensile properties of cold drawn bar, Figure 3.03142.
3.03143 Effect of low test temperature on tensile properties of cold rolled sheet, Figure 3.03143.
3.03144 Effect of low test temperature and percent cold reduction on tensile properties of sheet, Figure 3.03144.
3.03145 Effect of nitrogen content and test temperature (+80 to -320F) on the tensile properties of Type 304N, Table 3.03145.
3.03146 Effect of low temperatures on tensile properties of 304 cast stainless steel, Figure 3.03146.
3.03147 Effect of low temperature on the yield strength to density ratio, Figure 3.03147.
3.03148 Effect of low test temperature on true tensile properties of alloy, Figure 3.03148.
3.032 Compression.
3.0321 Stress-strain diagrams.
3.0322 Effect of low temperature on compressive yield strength of alloy, Figure 3.0322.
3.033 Impact.
3.0331 Probable range of Charpy impact properties of annealed Types 304 and 304L stainless steels, Figure 3.0331.
3.0332 Effect of low temperature on impact properties of annealed plate and bar, Figure 3.0332.
3.0333 Low temperature impact properties of Type 304 as a function of exposure time, Table 3.0333.
3.0334 Effect of sensitization heat treatment on Charpy keyhole impact properties of Types 304 and 304L, Figure 3.0334.
3.0335 Effect of nitrogen content and test temperature on the Charpy V-notch impact properties of Type 304N, Table 3.0335.
3.034 Bending.
3.035 Torsion and shear.
3.036 Bearing.
3.037 Stress concentration.
3.0371 Notch properties.
3.03711 Effect of low temperature on notch strength of cold rolled sheet, Figure 3.03711.
3.03712 Effect of low temperature on the notch and tensile strength of cold rolled sheet, Table 3.03712.
3.03713 Effect of test temperature on notch strength of annealed plate, Figure 3.03713.
3.03714 Effect of cold reduction on -320F sharp notch strength of 304L sheet, Figure 3.03714.
3.03715 Effect of stress relief temperature on sharp notch strength ratio at -320F for cold rolled 304L sheet, Figure 3.03715.
3.0372 Fracture toughness.
3.038 Combined properties.

3.04 Creep and Creep Rupture Properties
3.041 Creep rupture curves for bar at 1000 to 1800F, Figure 3.041.
3.042 Creep rupture curves for bar at 1200 to 1800F, Figure 3.042.
3.043 Creep rupture curves for bar at 900 to 1500F, Figure 3.043.
3.044 Creep rupture curves for bar at 1050 to 1350F, Figure 3.044.
3.045 Creep rupture curves for Type 304N bar at 1050 to 1500F, Figure 3.045.
3.046 Comparison of rupture stress of Type 304 and Type 304N as a function to temperature and time, Table 3.046
3.047 Effect of helium on creep rupture of sheet tested in vacuum at 1400F, Figure 3.047.
3.048 Short time creep rupture curves for sheet at 1200 to 2000F Figure 3.048.
3.049 Isochronous stress-strain curves for Type 304 at 1000F, Figure 3.049
3.0410 Isochronous stress-strain curves for Type 304 at 1100F, Figure 3.0410
3.0411 Isochronous stress-strain curves for Type 304 at 1200F, Figure 3.0411

3.05 Fatigue Properties
(See also Figure 2.048).
3.051 Fatigue properties of 1 inch diameter annealed bar, Table 3.051.
3.052 Results of vibrating beam tests of notched and unnotched Type 304 bar, Figure 3.052.
3.053 S-N curves for notched and smooth sheet as a function of temperature in the annealed condition, Figure 3.053.
3.054 Fatigue crack propagation rate at R.T. as a function of stress intensity range for plate, Figure 3.054.
3.055 Fatigue crack propagation rate at 1000F as a function of stress intensity range for plate, Figure 3.055.
3.056 Fatigue crack propagation rate at 1200F as a function of stress intensity range for plate, Figure 3.056.
3.057 Fatigue crack growth rate as a function of stress intensity range and temperature for plate in the annealed condition, Figure 3.057.

3.06 Elastic Properties
3.061 Poisson's ratio at room and elevated temperatures, Figure 3.061.
3.062 Modulus of elasticity.
3.0621 Modulus of elasticity at room and elevated temperatures, Figure 3.0621.
3.0622 Modulus of elasticity at room and low temperatures, Figure 3.0622.
3.063 Modulus of rigidity at room and elevated temperatures, Figure 3.063.

4. FABRICATION
(See Type 301 also).

4.01 Formability
4.011 General. This steel has excellent formability in the annealed condition, although other straight 18-8 grades may be preferred for certain operations. It has a low yield strength and high strain hardening capacity and requires considerably more power than carbon steels. Severe forming operations may require intermediate anneals and a final anneal immediately after forming should be applied to prevent stress cracking.
4.012 Forging. Starting forging temperature 2300F maximum, finishing temperature 1500F minimum. Severe reductions below 1700F should be avoided.
4.013 The casting characteristics of this alloy are excellent. Many of the casters use this composition as a base for making comparisons of casting characteristics. (Also see 1.08).

4.02 Machining and Grinding
4.021 General. Because of their high strain hardening, machining of austenitic stainless steels requires positive feeds,

	Fe
Low	C
19	Cr
10	Ni

TYPES 304, 304L

correctly contoured and sharp tools and an ample supply of coolant. While comparison with other material varies with the operation, Type 304 is generally rated as possessing 35 to 45 percent of the machinability of Bessemer steel screw stock.

4.022 Special measures, such as chip curlers, are required to handle the very long chips formed by these steels.

4.03 Welding

4.031 General. This steel can be welded readily by any of the common welding methods.

4.032 Fusion welding of sheet up to 1/8 inch thick is generally done by the inert gas tungsten arc (TIG) method. The shielded metal arc welding process is preferred for sheet over 1/8 inch thick and other products. Type 308 filler rod and electrodes are used.

4.033 Some sensitization on welding may occur in Type 304, particularly if the metal is over 1/8 inch thick. Type 304L will become susceptible to intergranular corrosion only if subjected to heating at about 1200F for a long time.

4.04 Heat Treatment

4.041 Furnace atmosphere should be neutral or slightly oxidizing to produce a readily removable scale and to avoid carburization. Heating with high sulfur fuels should be avoided.

4.042 Bright annealing is done in a dry hydrogen, cracked ammonia or argon atmosphere with a dew point of -80F maximum.

4.043 Prolonged heating at temperatures in the range of 800 - 1600F should be avoided because of possible embrittlement and increase in stress corrosion sensitivity.

4.05 Surface Treatment

4.051 Cleaning prior to heating and welding should include thorough removal of carbonaceous material and of any pickup of zinc or lead from dies. Contamination from these sources may reduce the corrosion resistance, cause embrittlement and susceptibility of intergranular attack during service or processing.

4.052 See 2.0317.

Source	AMS (1)(2)		AMS(3)(4)(5) (6)(7)(8)(9)		AMS (10)(11)	
Type	304L		304		304L	
	Percent		Percent		Percent	
	Min	Max	Min	Max	Min	Max
Carbon	-	0.050	-	0.08	-	0.030
Chromium	18.0	21.0	18.00	20.00	18.00	20.00
Copper	-	0.5	-	0.50	-	-
Manganese	1.00	2.00	-	2.00	-	2.00
Molybdenum	-	0.5	-	0.50	-	-
Nickel	8.0	11.0	8.00	11.00(c)	8.00	11.00
Phosphorus	-	0.04	-	0.040	-	0.040
Silicon	0.75(a)	1.50(a)	-	1.00(d)	0.50(e)	1.00
Sulfur	-	0.03(b)	-	0.030	-	0.030
Iron	Balance		Balance		Balance	

(a) AMS 5371 only, AMS 5370 specified 1.0 percent maximum only.
(b) AMS 5371 gives 0.04.
(c) AMS 5560D and 5566D gives 12.0.
(d) AMS 5566 gives 0.75.
(e) AMS 5647 only.

TABLE 1.041 AMS COMPOSITIONS.

Source	AISI (12)				ACI (13)			
Type	304		304L		CF 8		CF 3	
	Percent		Percent		Percent		Percent	
	Min	Max	Min	Max	Min	Max	Min	Max
Carbon	-	0.08	-	0.03	-	0.08	-	0.03
Chromium	18.00	20.00	18.00	20.00	18.0	21.0	18.0	21.0
Manganese	-	2.00	-	2.00	-	1.50	-	1.50
Nickel	8.00	12.00	8.00	12.00	8.0	11.0	8.0	11.0
Phosphorus	-	0.045	-	0.045	-	0.04	-	0.04
Silicon	-	1.00	-	1.00	-	2.00	-	2.00
Sulfur	-	0.030	-	0.030	-	0.04	-	0.04
Iron	Balance		Balance		Balance		Balance	

TABLE 1.042 AISI AND ACI COMPOSITIONS

AMS	Type	Form	Military
5370	304L	Castings, prec. invest.	—
5371	304L	Castings, sand	—
5513	304	Sheet, strip, plate (ST)	MIL-S-5059
5560D	304	Tubing, seamless (ST)	MIL-T-8506
5565D	304	Tubing, welded (ST)	MIL-T-8506
5566D	304	Tubing, hydraulic (CD)	MIL-T-6845
5567	304	Tubing, seamless or welded, hydraulic (ST)	MIL-T-8504
5639A	304	Bar, forgings, tubing (ST)	QQ-S-763 (a)
5697	304	Wire (ST) (CD)	QQ-S-423 (a)
5511A	304L	Sheet, strip, plate (ST)	MIL-S-4043
5647B	304L	Bar, forging stock, forgings, tubing (ST)	QQ-S-763 (a)

(a) Federal Specifications

TABLE 1.03 SPECIFICATIONS

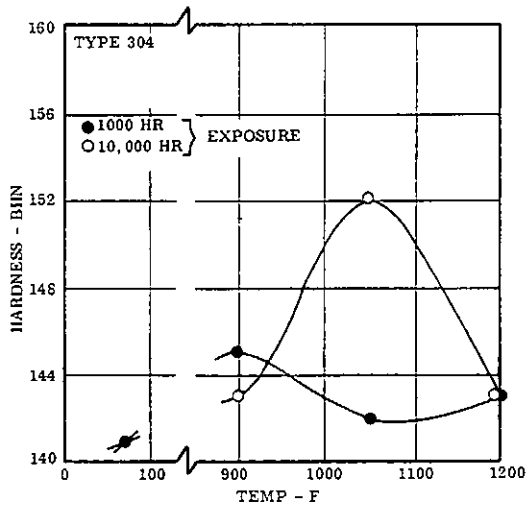


FIG 1.063 EFFECT OF TIME AND TEMPERATURE OF EXPOSURE ON ROOM TEMPERATURE HARDNESS OF ALLOY (17)

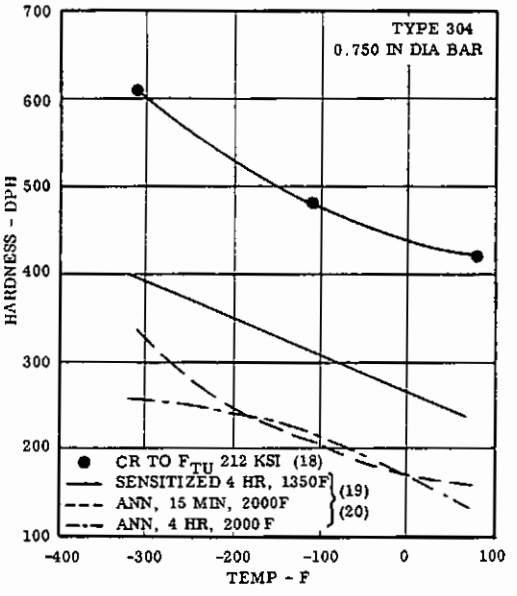


FIG 1.064 EFFECT OF LOW TEMPERATURES ON HARDNESS OF BAR (18)(19)(20)

Source	(27) (43)			
Form	Bar			
Condition	Annealed			
Test temp	-320 F	F_{ty} - ksi	F_{tu} - ksi	Ft-lbs (b)
Type 304		57	220	115(a)
Type 304L		98	220	125

(a) Ref. 27 (b) IE charpy V-notch

TABLE 1.093 TYPICAL VALUES OF TENSILE AND TOUGHNESS PROPERTIES AT CRYOGENIC TEMPERATURES.

	Fe
Low	C
19	Cr
10	Ni

TYPES 304, 304L

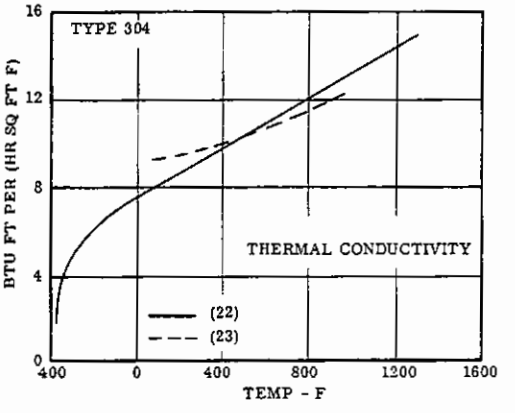


FIG 2.013 THERMAL CONDUCTIVITY (22)(23)

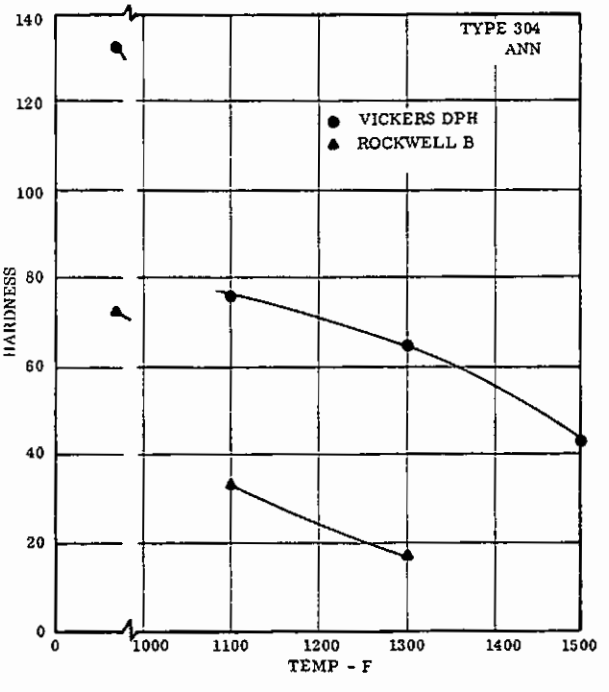


FIG 1.065 EFFECT OF TEST TEMPERATURE ON HOT HARDNESS (21)

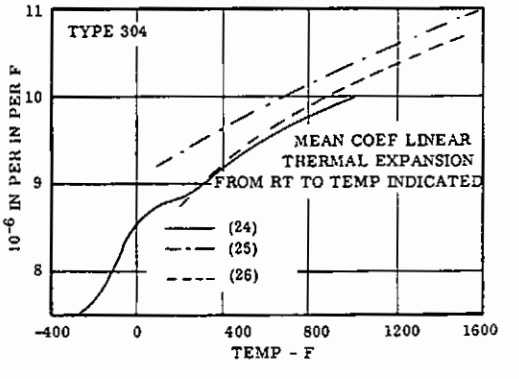


FIG 2.014 THERMAL EXPANSION (21, p. 22)(24)(25, p. 6)(26)

	Fe
Low	C
19	Cr
10	Ni

TYPES 304, 304L

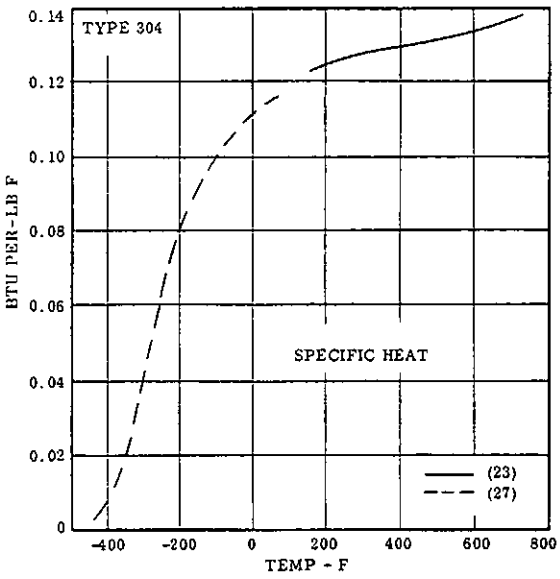


FIG 2.015 SPECIFIC HEAT (23)(27)

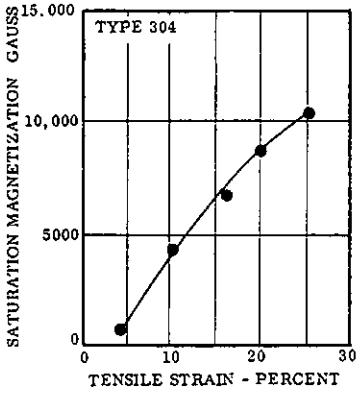


FIG 2.0232 VARIATION IN THE SATURATION MAGNETIZATION AT ROOM TEMPERATURE AFTER TENSILE DEFORMATION IN LIQUID NITROGEN (28)

Source	(31)	
Form	0.015 Inch Sheet	
Corrosion Medium	Nitric-Dichromate (after heat treatment)	
Type	Heat Treatment	Corrosion Rate $mg/cm^2/hr$
304	1920F-2 hrs-WQ	6.2
	1920F-2 hrs-WQ, 1650F-2 hrs-WQ	1.9
	1920F-2 hrs, cooled to 1650F within 20 min, 1650F-2 hrs-WQ	6.2
	2370F-4 hrs, cool to 1110F at approx. 36F per min, 1110F-1 hr-WQ	6.1
	2370F-4 hrs, cool to 1650F at approx. 36F per min, 1650F-1 hr-WQ	6.1
304L	1920F-2 hrs-WQ	8.3
	1920F-2 hrs-WQ, 1650F-2 hrs-WQ	7.7
	1920F-2 hrs-WQ, 1470F-2 hrs-WQ	3.3
	1920F-2 hrs-WQ, 1110F-2 hrs-WQ	8.9

TABLE 2.0312 INTERGRANULAR CORROSION IN TYPES 304 AND 304L WHEN SUBJECTED TO A NITRIC-DICHROMATE SOLUTION.

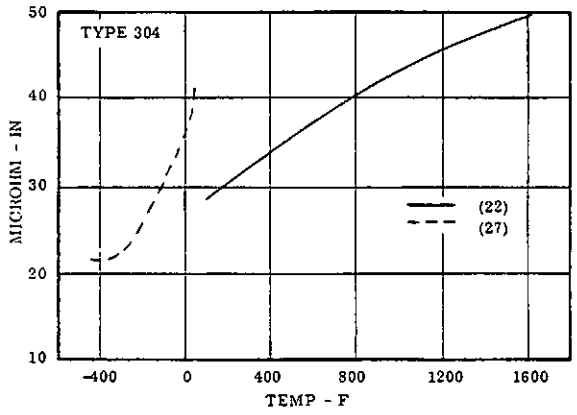


FIG 2.022 ELECTRICAL RESISTIVITY (22)(27)

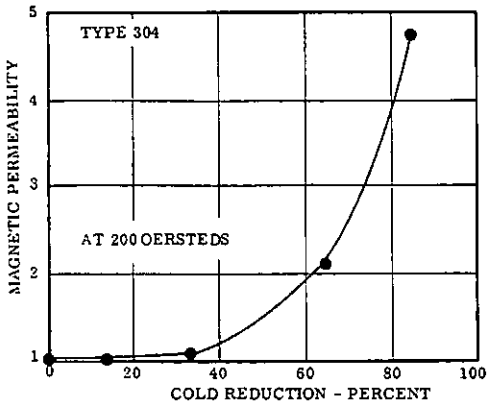


FIG 2.0231 EFFECT OF COLD REDUCTION ON MAGNETIC PERMEABILITY (30)

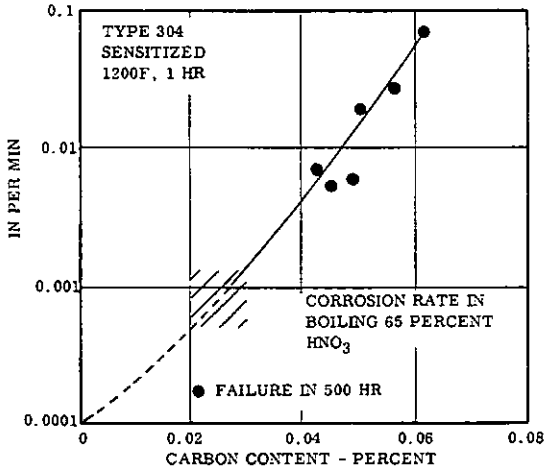


FIG 2.0313 EFFECT OF CARBON CONTENT ON CORROSION RATE (25, p. 273)

Source	(32, p. 26)				
Alloy	Depth(a) ft.	Exposure time, days	Crevice attack, mils		Local Corrosion
			Water	Mud	
304	2,340	197	11	slight	Edge, tunnel
	5,300	1,064	21	29	None in water tunnel in mud
304L	2,340	197	8	18	Tunnel
	5,300	1,064	27, perforated	0	Severe tunnel
(a) Oxygen level at 2,340 feet is 0.60 ppm; that at 5,300 feet is about 1.70 ppm.					

TABLE 2.0314 CREVICE ATTACK IN QUIET SEA WATER

Source	(35, p.141)				
Alloy	Type 304				
Corrosion Environment	0.5N NaCl + 0.1N $NaNo_3$ boiling solution				
Cold reduction percent	Final sheet thickness, in	F_{ty} (ksi)	F_{tu} (ksi)	Threshold stress (a) (ksi)	
0 (b)	0.031	40	91	26	
14.5(c)	0.027	85	113	66(d)	
26 (c)	0.023	114	143	93	
35 (c)	0.020	134	163	74	
(a) See Table 2.0319 for definition.					
(b) Values are average of two specimens.					
(c) Values are average of four specimens.					
(d) Approximate value.					

TABLE 2.03191 MECHANICAL PROPERTIES AND THRESHOLD STRESS VALUES.

	Fe
Low	C
19	Cr
10	Ni

TYPES 304, 304L

Source	(33, p.13)			
Alloy	Type 304			
Form	0.063 inch sheet			
	Avg. corrosion rate Mils per year (MPY)		Maximum Depth of attack (MILS)	
Condition	111 days	1050 days	111 days	1050 days
Annealed	0	0.24	27	63(a)
(a) Localized penetration by corrosion				

TABLE 2.0315 CORROSION RATE AND ATTACK DEPTH

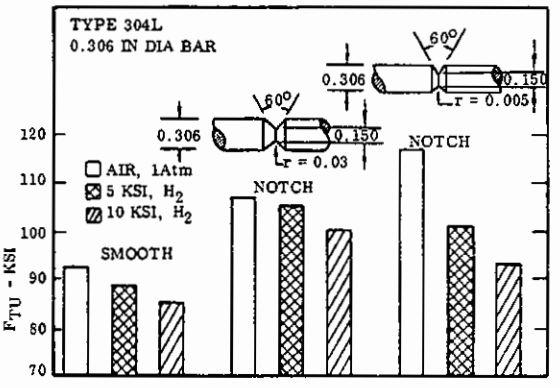


FIG 2.03211 ULTIMATE TENSILE AND NOTCH STRENGTH VERSUS HYDROGEN PRESSURE FOR TYPE 304L EXPOSED FOR 24HR AND THEN PULLED TO FRACTURE IN HIGH PRESSURE HYDROGEN (36, p244)

Source	(34, p.8)		
Alloy	Type 304		
Form	0.047 in dia wire		
Testing Condition	Boiling $MgCl_2$ (42 percent-310F) at 60,000 psi		
Heat Treatment		Specimen No.	Time of Test
A) Annealed in argon 1 hr. at 1832F		1	Failed after 6.5 hours
		2	Failed after 14.0 hours
		3	Failed after 9.3 hours
B) Treated as in (A) then annealed in hydrogen 3 hr at 1380F		4	Failed after 5.0 hours
		5	Failed after 8.7 hours
		6	Failed after 6.5 hours
C) Treated as in (A) then nitrided in 5 percent NH_3-H_2 3 hr at 1380F		7	Unbroken after 85 hours
		8	Unbroken after 95 hours
		9	Unbroken after 93 hours

TABLE 2.0318 NITRIDING SIGNIFICANTLY INCREASED THE RESISTANCE TO STRESS CORROSION CRACKING

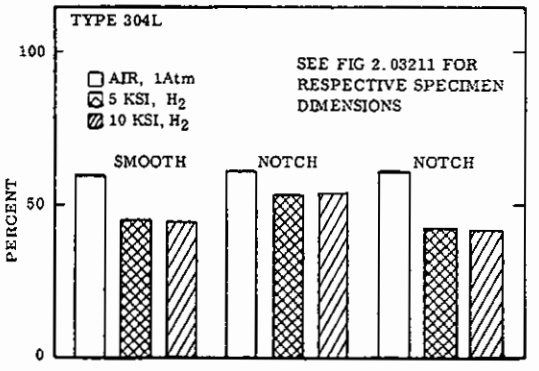


FIG 2.03212 PERCENT ELONGATION VERSUS HYDROGEN PRESSURE FOR TYPE 304L EXPOSED FOR 24HR AND THEN TESTED IN HIGH PRESSURE HYDROGEN (36, p244)

Source	(35, p.141)				
Alloy	Type 304				
Corrosion Environment	0.5N NaCl + 0.1N $NaNo_2$ Boiling Solution				
Condition	Sheet Thickness in.	F_{ty} ksi	F_{tu} ksi	Threshold Stress (a) ksi	Percent of F_{ty}
Cold rolled(b)	0.044	149	166	83	56
Cold rolled(b)	0.030	135	157	149	111
Annealed(b)	0.031	40	91	26	65(c)
(a) Threshold stress is the maximum stress that will not produce stress corrosion cracking or failure in 300 hrs.					
(b) As received condition, values average of two specimens.					
(c) Approximate value.					

TABLE 2.0319 THRESHOLD STRESS DETERMINED IN 0.5N NaCl + 0.1N $NaNo_2$ BOILING SOLUTION FOR TYPE 304.

	Fe
Low	C
19	Cr
10	Ni

TYPES 304, 304L

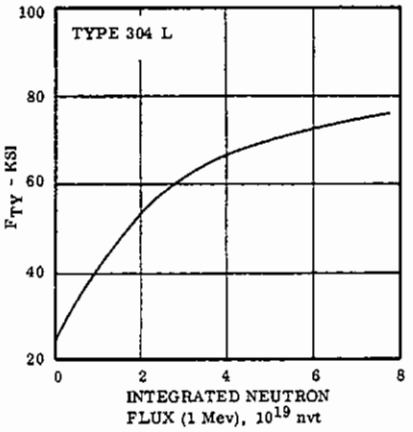


FIG 2.046 EFFECT OF IRRADIATION BELOW 100C (212F) ON YIELD STRENGTH (39)

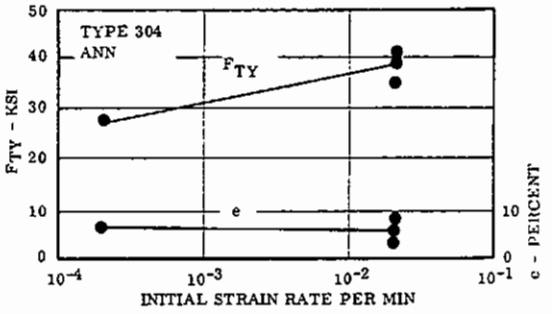


FIG 2.047 STRAIN RATE DEPENDENCE OF TENSILE PROPERTIES FOR TYPE 304 AT 1300F AFTER IRRADIATION TO 3.4 X 10^{22} NVT TOTAL (40, p10)

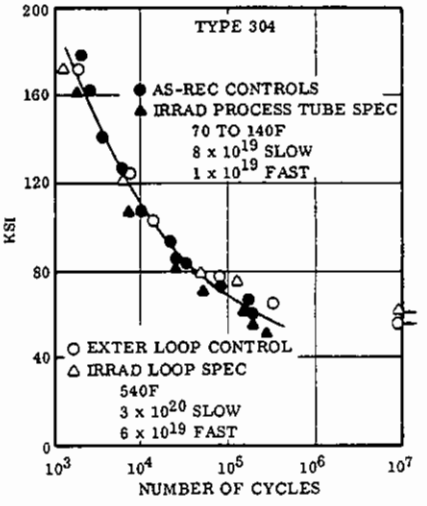


FIG. 2.048 S-N CURVE FOR IRRADIATED AND UNIRRADIATED SMOOTH SPECIMENS OF STAINLESS STEEL. (39)

Source	AMS (3)	AMS (8)			AMS(9)	AMS(1)	AMS(2)	AMS(10)	AMS (11)	
Alloy	Type 304							Type 304L		
Form	Sheet, strip, plate	Bar		Tube	Wire	Castings, invest.	Castings sand	Sheet, strip, plate	Bar	
Condition	ST	ST			ST	ST	ST	ST	ST	
Thickness - in	-	≤ 0.75	> 0.75	-	-	-	-	-	≤ 0.75	> 0.75
F_{tu} - min - ksi	-	-	-	-	90	-	-	-	-	-
max - ksi	100	-	-	-	125	-	-	100	-	-
e(2 in)-min-percent	40	-	-	-	35	-	-	40	-	-
Hardness										
BHN-min	-	170	140	-	-	-	-	-	170	140
max	-	255	241	-	-	-	170	-	255	241
RB - min	-	-	-	-	-	-	-	-	-	-
max	-	-	-	-	-	86	-	-	-	-

TABLE 3.011 AMS SPECIFIED MECHANICAL PROPERTIES

	Fe
Low	C
19	Cr
10	Ni

TYPES 304, 304L

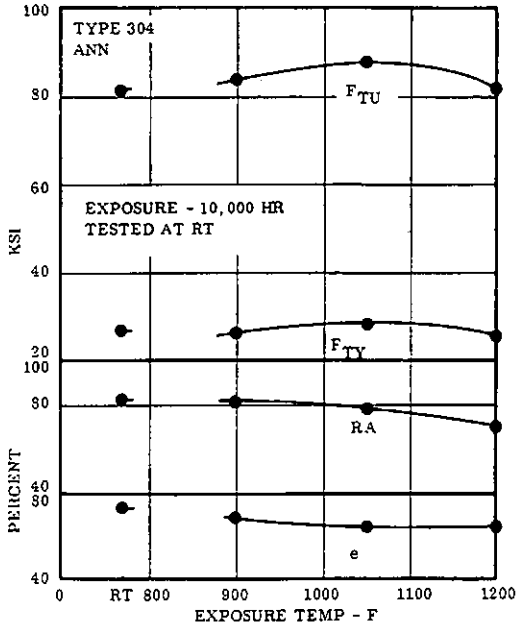


FIG 3.0216 EFFECT OF EXPOSURE OF 10,000 HOURS TO ELEVATED TEMPERATURES ON TENSILE PROPERTIES OF ANNEALED ALLOY (17)

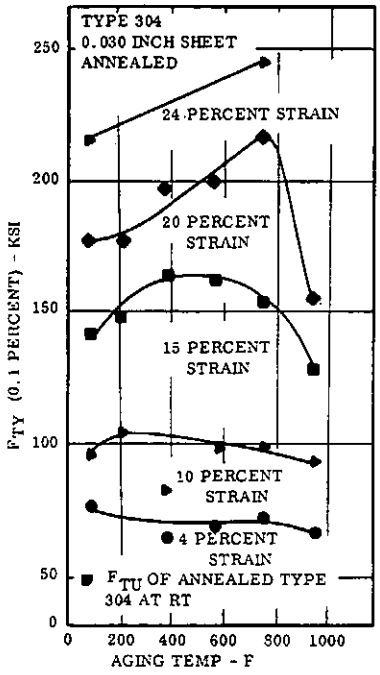


FIG 3.0218 YIELD STRENGTH OF TYPE 304 AT ROOM TEMPERATURE AFTER AGING 1 1/2 HOURS AT THE TEMPERATURES SHOWN FOLLOWING TENSILE DEFORMATION AT -319F. (29, p 1538)

NOTE: ALL SPECIMENS STRAINED 10 AND 20 PERCENT (EXCEPT 932F SPECIMEN FOR 20 PERCENT STRAIN) BROKE OUTSIDE OF 2 INCH GAGE MARKS. THIS APPLIES FOR THE TENSILE DATA IN FIGS. 3.0218 AND 3.0219, AND ACCOUNTS FOR THE ABSENCE OF 10 AND 20 PERCENT ELONG. CURVES IN FIG. 3.02110.

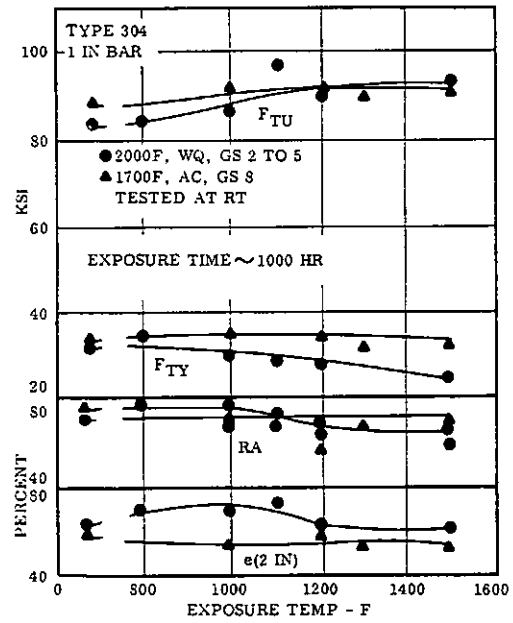


FIG. 3.0217 EFFECT OF ANNEALING TEMPERATURE AND EXPOSURE TO ELEVATED TEMPERATURES ON TENSILE PROPERTIES OF BAR. (26)

	Fe
Low	C
19	Cr
10	Ni

TYPES 304, 304L

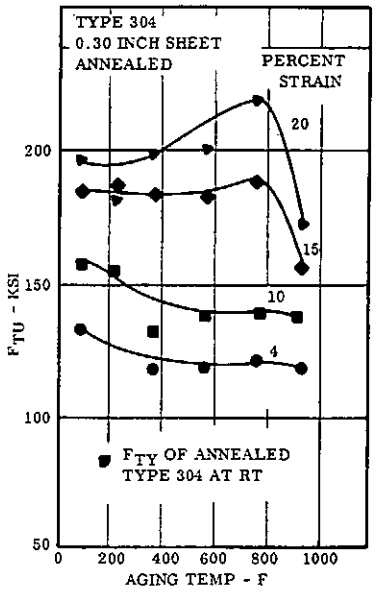


FIG 3.0219 ULTIMATE TENSILE STRENGTH OF TYPE 304 AT ROOM TEMPERATURE AFTER AGING 1 1/2 HOURS AT THE TEMPERATURES SHOWN FOLLOWING TENSILE DEFORMATION AT -319F. (29, p 1588)
SEE NOTE ON FIG 3.0218

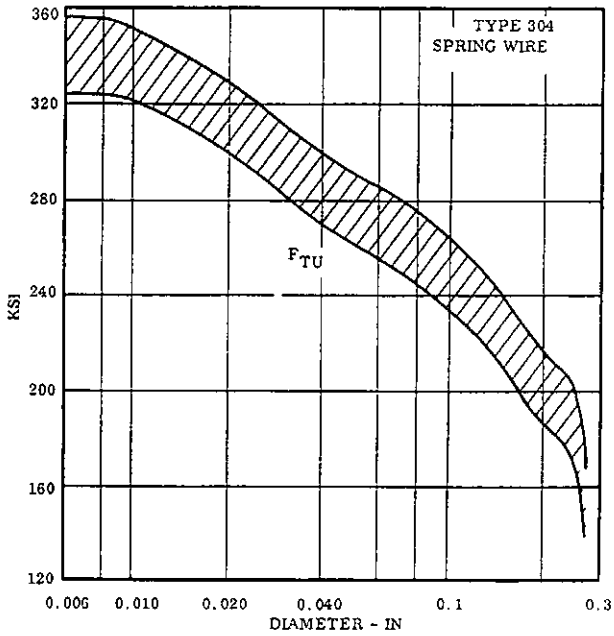


FIG 3.02111 AISI TENSILE STRENGTH RANGE FOR VARIOUS SIZES OF SPRING WIRE (12)

Source	(12)	
Alloy	Type 304	
Form	Plate, bar	Bar
Condition	Ann	CD to high tensile strength
Thickness - in	-	1-1/2
Impact Strength Izod-ft-lb	110	90

TABLE 3.0231 TYPICAL IMPACT PROPERTIES OF ANNEALED PLATE AND COLD DRAWN BAR.

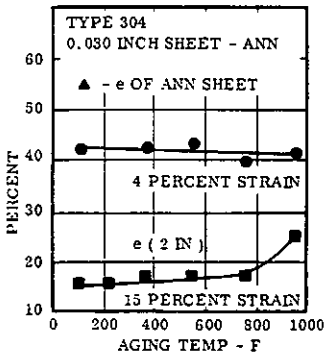


FIG 3.02110 ELONGATION OF TYPE 304 AT ROOM TEMPERATURE AFTER AGING 1 1/2 HOURS AT THE TEMPERATURES SHOWN FOLLOWING TENSILE DEFORMATION AT -319F. (29, p1588)
SEE NOTE ON FIG 3.0218

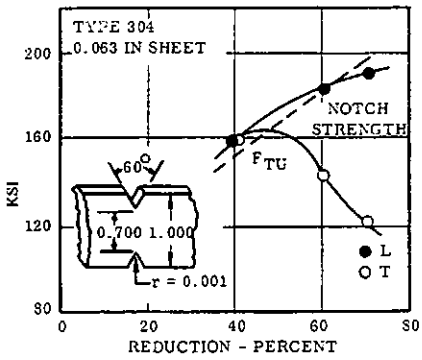


FIG 3.02711 EFFECT OF COLD ROLLING AND TEST DIRECTION ON NOTCH STRENGTH OF SHEET (42)

Fe
Low C
19 Cr
10 Ni

TYPES 304, 304L

Source	AMS (4)(5)(7)						AMS (6)		AMS (8)	AMS (11)
Alloy	Type 304									
Form	Tubing, seamless or welded						Tubing, hydraulic		Tubing, mechanical	
Condition	ST						CD		ST	
Outside dia - in	≤ 0.188		>0.188 to 0.500		>0.500		0.188	≥ 0.250	-	-
Wall thickness-in	≤ 0.016	>0.016	≤ 0.010	>0.010	≤ 0.010(a)	>0.010	≥ 0.016	All	-	-
F_{tu} - min - ksi	-	-	-	-	-	-	95	105	-	-
max - ksi	115	100	110	100	100	100	130	140	-	-
F_{ty} - min - ksi	30(b)(c)	30(b)	-	30(b)	-	30(b)	60	75	-	-
max - ksi	-	-	-	-	-	-	90	110	-	-
e(2in)-min-percent										
Tube	35	40	37	40	32	35(d)	25	20	-	-
Strip	-	-	32(a)	35(a)	27	30(e)	-	-	-	-
Hardness										
RB-min	-	-	-	-	-	-	-	-	-	75
max	-	-	-	-	-	-	-	-	≤ 90	90

(a) AMS 5567 not included.
(b) AMS 5567 only.
(c) Tubes having a wall thickness 0.010 inch and under, the yield strength need not to be determined.
(d) 40 ksi for AMS 5567.
(e) 35 ksi for AMS 5567.

TABLE 3.012 AMS SPECIFIED MECHANICAL PROPERTIES FOR TUBING

Source	(16)		(12)										
Alloy	Type 304												
Form	Sheet(a)		Sheet, strip	Plate, bar	Bar			Wire				Sheet Strip	Ann
Condition	Ann		Ann	Ann	Ann + CD	CD to high tensile		Ann	Soft temper	Hard temper	Spring temper	Ann	Ann
Thickness - in	<0.118	>0.118	-	-	1	7/8	1-1.2	0.062 to 0.500			0.062 to 0.307	-	-
F_{tu} - ksi	78	78	85	85	100	125	110	105 to 90	125 to 100	160 to 140	260 to 170	75	75
F_{ty} - ksi	29	26	35	30	60	95	75	35	90 to 60	125 to 105	-	28	28
e (2 in) - percent	-	-	50	60	45	25	60	55 to 60	40 to 45	20 to 25	-	50	50
RA - percent	55	55	-	70	-	-	-	65	65	55	-	-	-
Hardness													
BHN	-	-	-	150	212	277	240	-	-	-	-	-	140
RB	90	90	80	-	-	-	-	83	95	-	-	70	-
RC	-	-	-	-	-	-	-	-	-	33	-	-	-
Impact strength izod ft-lb	-	90 max	-	110	-	-	90	-	-	-	-	-	-

(a) Minimum values

TABLE 3.0212 TYPICAL TENSILE PROPERTIES FOR VARIOUS FORMS AND CONDITIONS OF ALLOYS.

	Fe
Low	C
19	Cr
10	Ni

TYPES 304, 304L

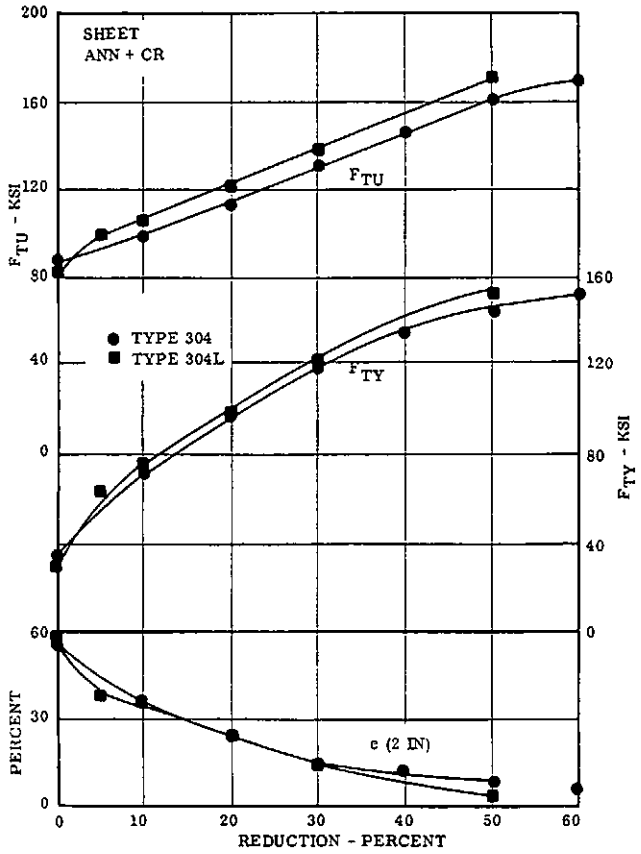


FIG 3.0213 EFFECT OF COLD ROLLING ON TENSILE PROPERTIES OF TYPES 304 AND 304L SHEET (41)

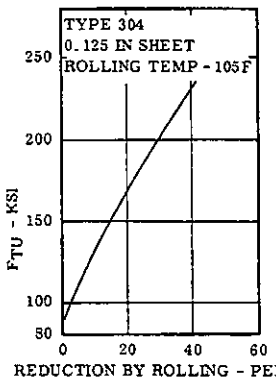


FIG. 3.0214 EFFECT OF COLD ROLLING AT -105F ON TENSILE STRENGTH OF SHEET. (47)

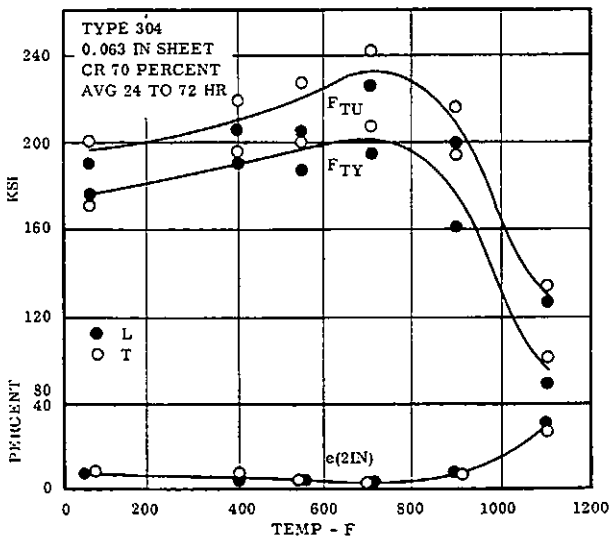


FIG 3.0215 EFFECT OF EXPOSURE TO ELEVATED TEMPERATURES ON TENSILE PROPERTIES OF COLD ROLLED SHEET (42)

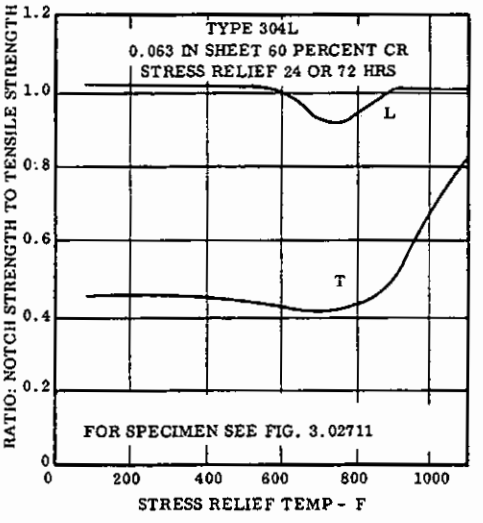
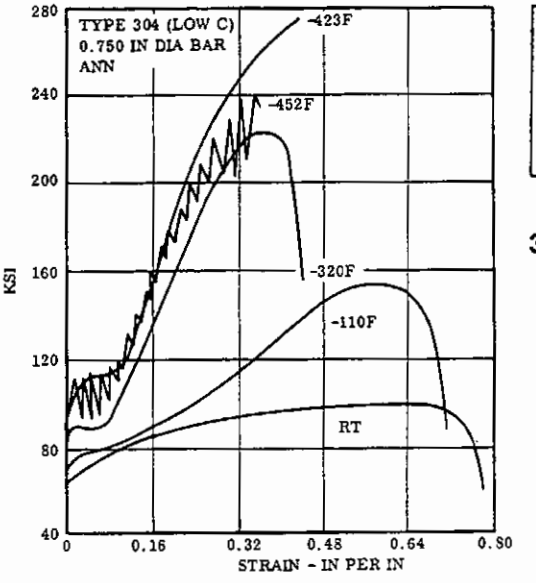


FIG. 3.02712 EFFECT OF STRESS RELIEF TEMPERATURE ON SHARP NOTCH STRENGTH RATIO FOR COLD ROLLED 304L SHEET. (73, fig. 14)



	Fe
Low	C
19	Cr
10	Ni

TYPES 304, 304L

FIG 3.03113 STRESS - STRAIN CURVES AT ROOM AND LOW TEMPERATURES (44)

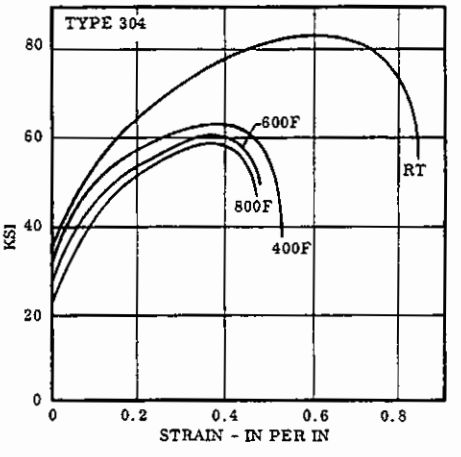


FIG 3.03111 STRESS - STRAIN CURVES TO FAILURE AT ROOM AND ELEVATED TEMPERATURES (23)

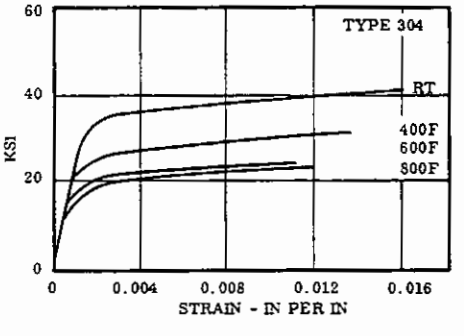


FIG 3.03112 STRESS - STRAIN CURVES AT ROOM AND ELEVATED TEMPERATURES (23)

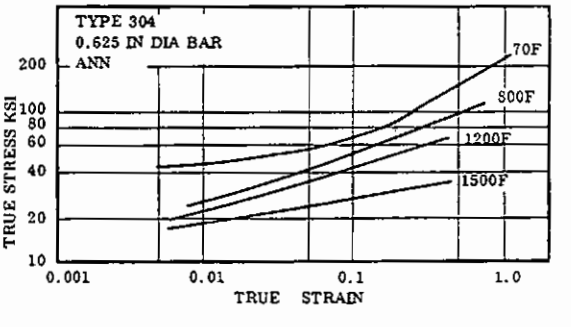


FIG 3.03114 TRUE STRESS - STRAIN CURVES AT ROOM AND ELEVATED TEMPERATURES (45)

	Fe
Low	C
19	Cr
10	Ni

TYPES 304, 304L

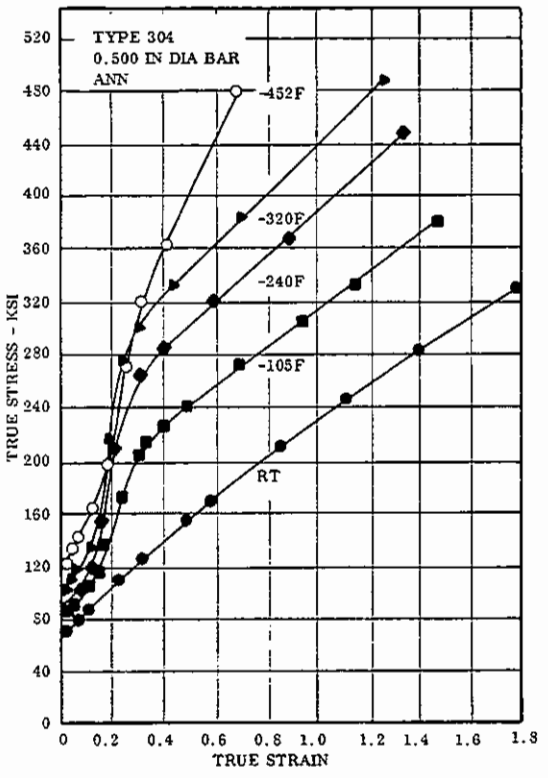


FIG 3.03115 TRUE STRESS - STRAIN CURVES AT ROOM AND LOW TEMPERATURES (46)

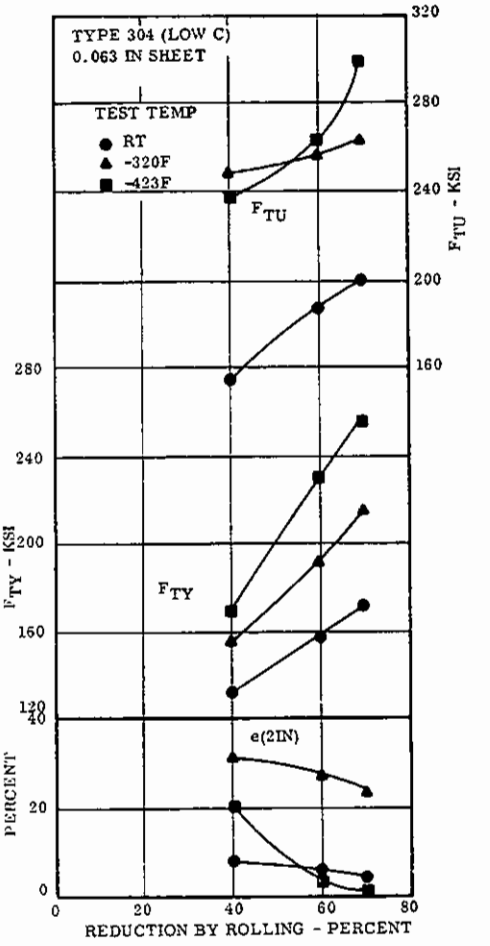


FIG 3.03121 EFFECT OF COLD ROLLING ON TENSILE PROPERTIES OF SHEET AT ROOM AND LOW TEMPERATURES (48)

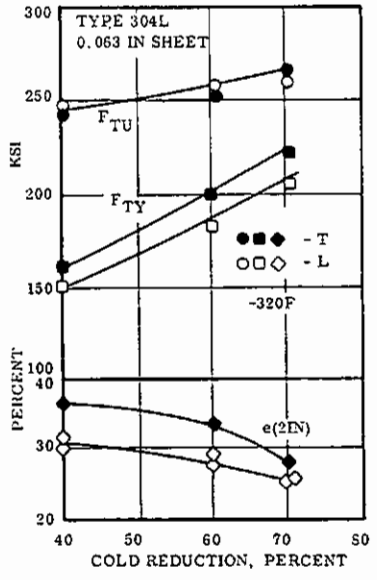


FIG 3.03122 EFFECT OF COLD REDUCTION ON -320F TENSILE PROPERTIES OF 304L SHEET (73)

	Fe
Low	C
19	Cr
10	Ni

TYPES 304, 304L

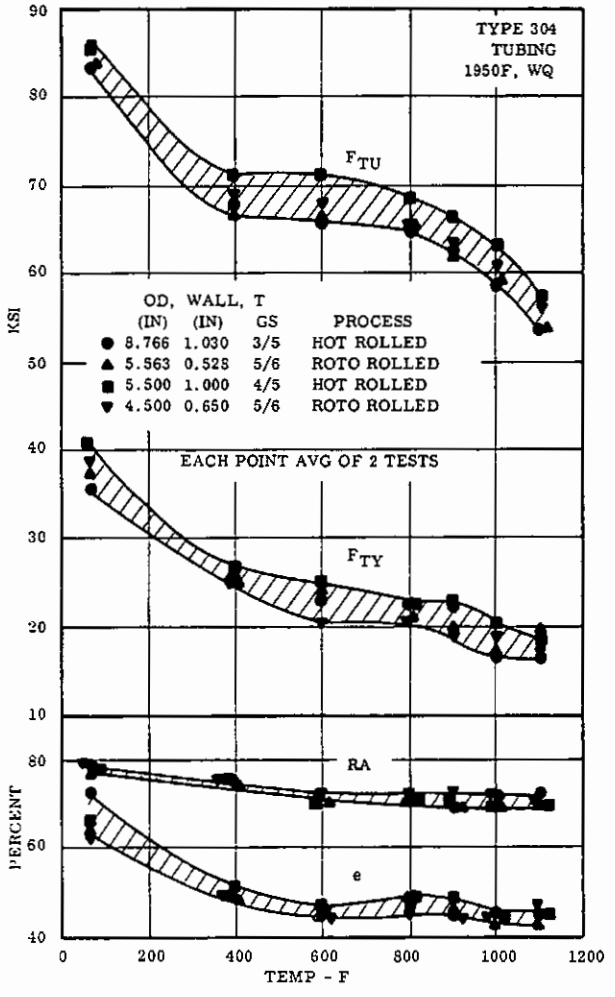


FIG 3.03131 EFFECT OF ELEVATED TEST TEMPERATURE ON TENSILE PROPERTIES OF ROLLED TUBING (49)

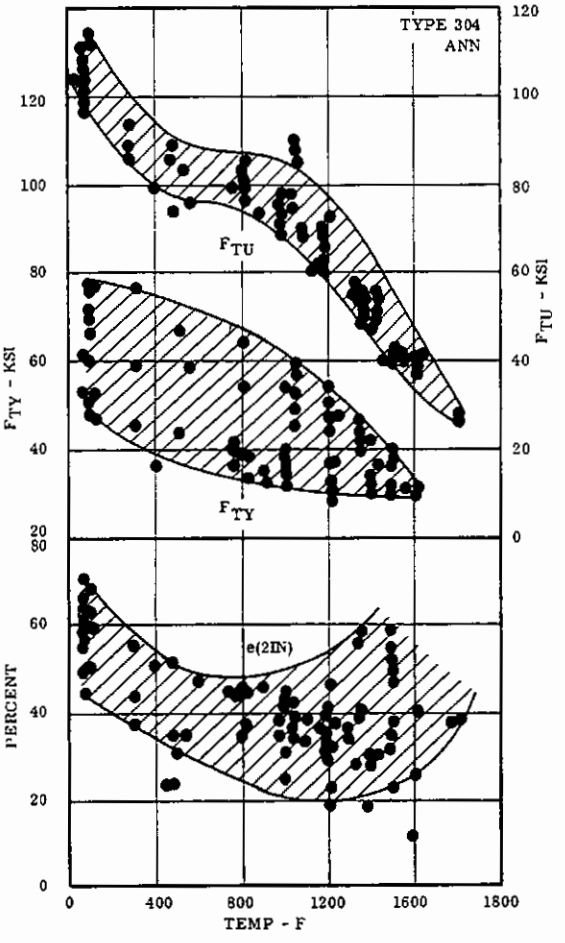


FIG 3.03132 RANGE OF TENSILE PROPERTY VALUES AT ELEVATED TEMPERATURES FOR ANNEALED ALLOY (50)

	Fe
Low	C
19	Cr
10	Ni

TYPES 304, 304L

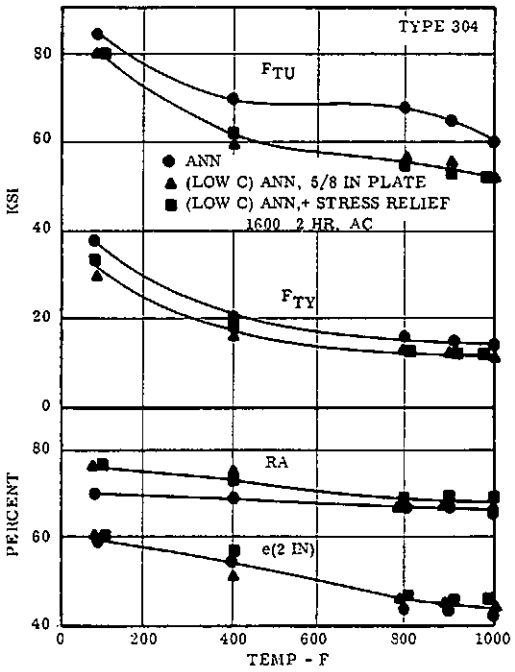


FIG 3.03133 EFFECT OF ELEVATED TEST TEMPERATURE ON ALLOY (51)

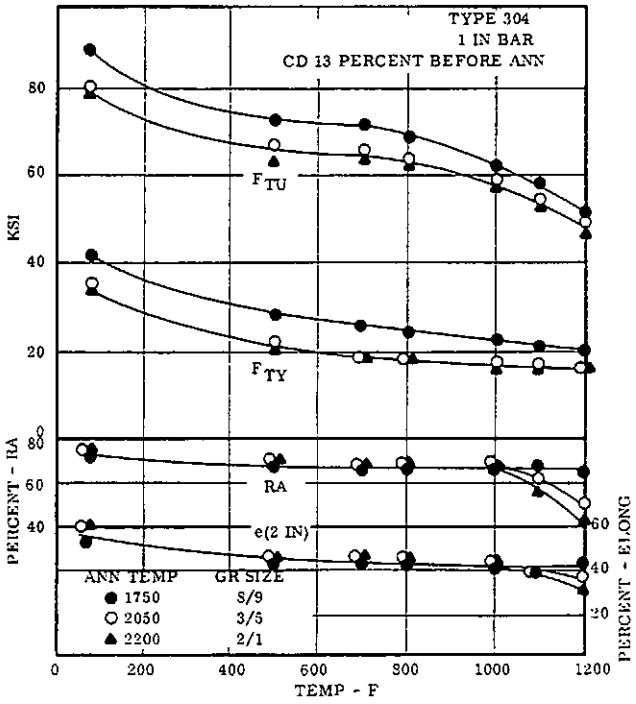


FIG 3.03135 EFFECT OF ANNEALING AND TEST TEMPERATURE ON TENSILE PROPERTIES OF COLD DRAWN BAR (53)

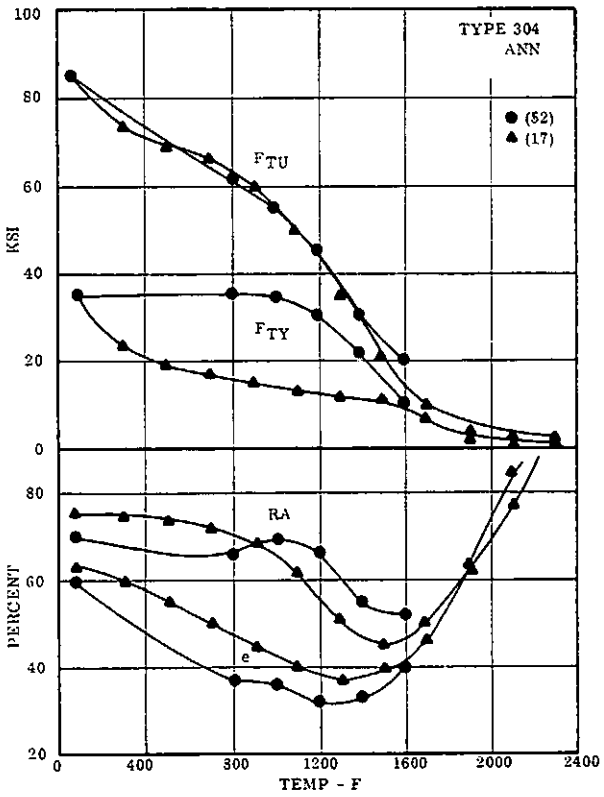


FIG 3.03134 EFFECT OF ELEVATED TEST TEMPERATURE ON ANNEALED ALLOY (17)(52)

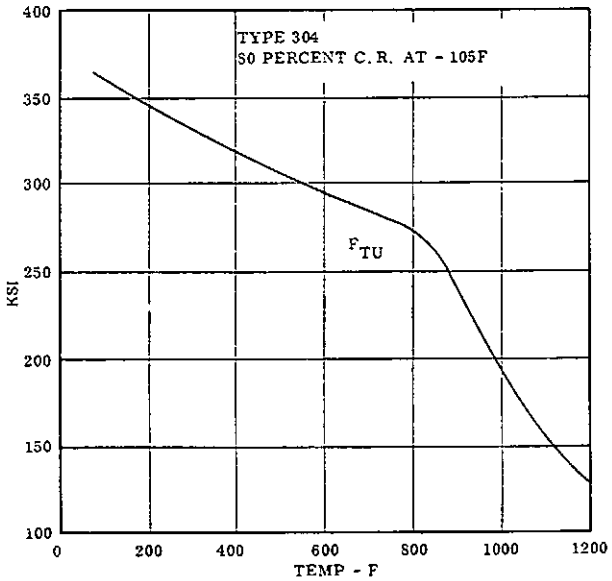


FIG. 3.03136 EFFECT OF ELEVATED TEMPERATURES ON ZEROLLED 304 STAINLESS. (54)

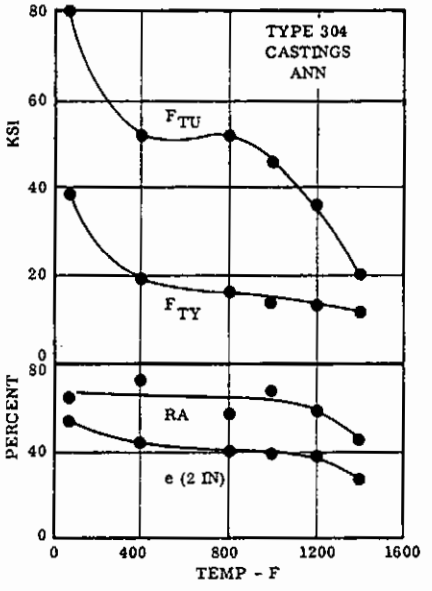


FIG 3.03137 EFFECT OF TEST TEMPERATURE ON TENSILE PROPERTIES OF CASTINGS (55)

Source	(43)			
Form	3 in sq bar (a)			
Condition	Annealed 1975F - 1 hr - WQ(a)			
Type	304(b)		304N(c)	
Test Temp F	F_{ty} - ksi	F_{tu} - ksi	F_{ty} - ksi	F_{tu} - ksi
RT	31.0 - 34.5	80.5 - 86.0	40.1 - 43.3	86.7 - 90.7
200	28.5 - 33.1	69.1 - 72.1	33.2 - 34.4	77.6 - 80.1
400	23.5 - 28.0	61.9 - 65.0	26.2 - 28.4	69.4 - 73.0
600	21.0 - 24.1	61.0 - 64.5	22.4 - 24.5	66.5 - 71.0
800	18.5 - 22.1	59.0 - 64.0	21.0 - 24.6	66.0 - 68.8
1000	18.1 - 19.7	54.2 - 64.1	19.6 - 20.2	60.2 - 63.8
1200	17.5 - 18.1	42.8 - 51.1	17.9 - 18.9	51.6 - 54.5
(a) Specimens annealed in blank form and finish machined to 0.250 in dia tension bars.				
(b) Range of strength values for a nitrogen range of 0.004 - 0.006 percent.				
(c) Range of strength values for a nitrogen range of 0.12 - 0.16 percent.				

TABLE 3.03138 COMPARISON OF STRENGTH PROPERTIES OF TYPES 304 AND 304N AT ROOM AND ELEVATED TEMPERATURES.

	Fe
Low	C
19	Cr
10	Ni

TYPES 304, 304L

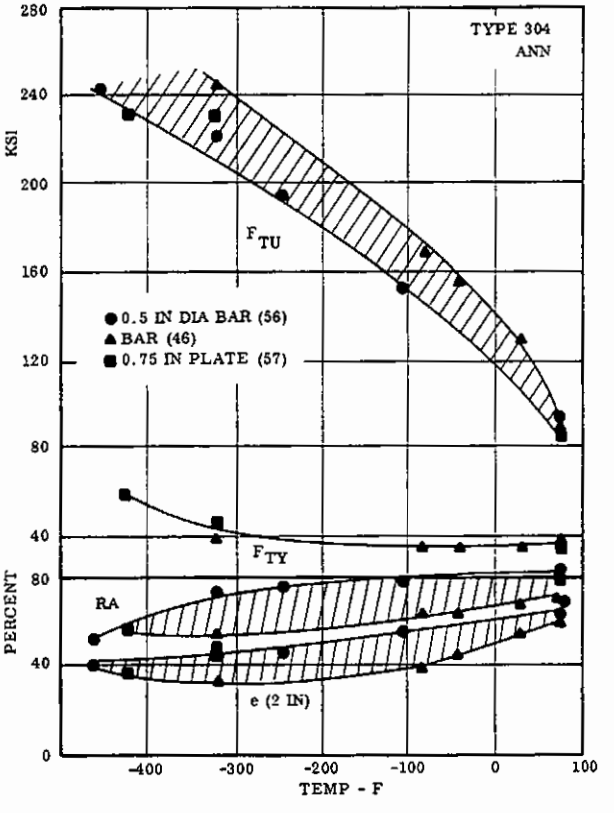


FIG 3.03141 EFFECT OF LOW TEST TEMPERATURE ON TENSILE PROPERTIES OF ANNEALED ALLOY (46)(56)(57)

	Fe
Low	C
19	Cr
10	Ni

TYPES 304, 304L

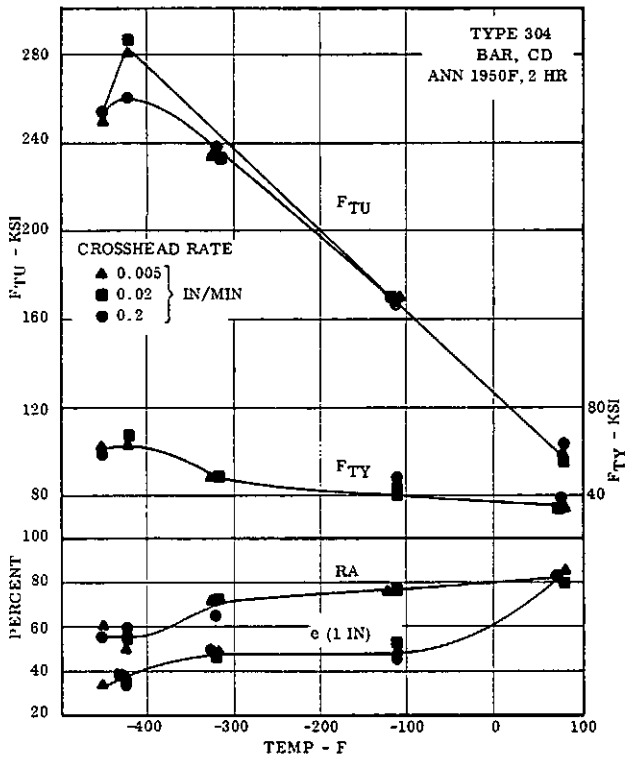


FIG 3.03142 EFFECT OF LOW TEST TEMPERATURE AND STRAIN RATE ON TENSILE PROPERTIES OF COLD DRAWN BAR (58)

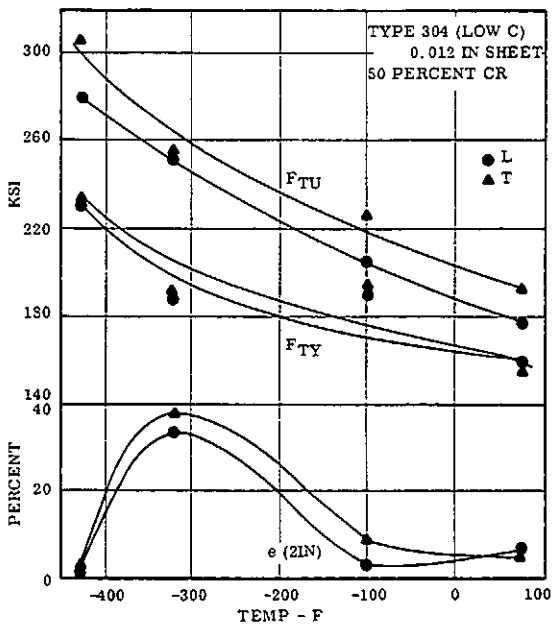


FIG 3.03143 EFFECT OF TEST TEMPERATURE ON TENSILE PROPERTIES OF COLD ROLLED SHEET (59)

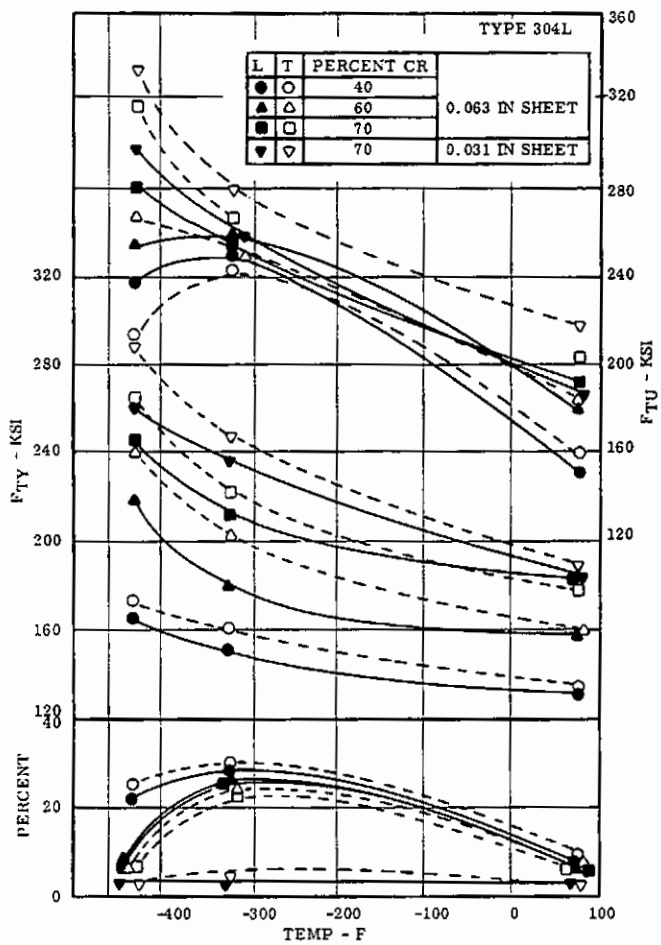


FIG 3.03144 EFFECT OF LOW TEST TEMPERATURE AND PERCENT COLD REDUCTION ON TENSILE PROPERTIES OF SHEET (48)

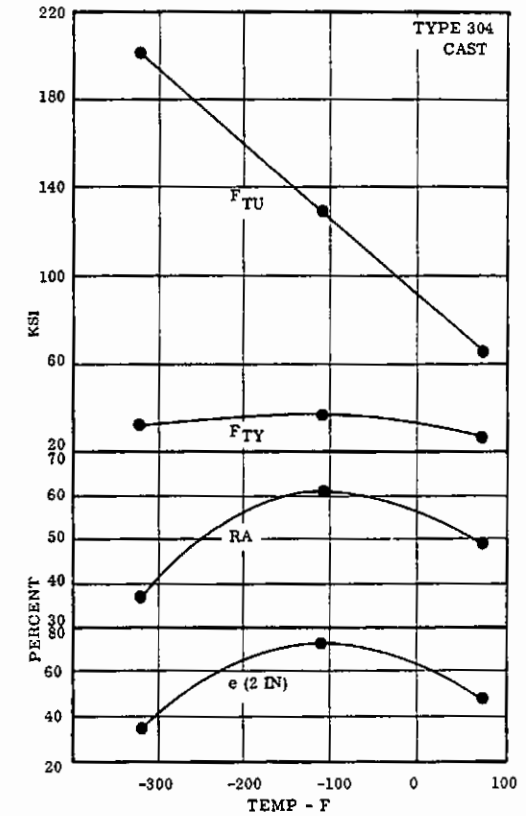


FIG 3.03146 EFFECT OF LOW TEMPERATURES ON TENSILE PROPERTIES OF 304 CAST STAINLESS STEEL (60)

Fe
Low C
19 Cr
10 Ni

TYPES 304, 304L

Source	(43)				
Alloy	304N				
Form	3 in sq. bar (a)				
Condition	Annealed - 1975 F - 1 hr - WQ(a)				
Nitrogen Content wt. percent	Test Temp F	F_{ty} ksi	F_{tu} ksi	e (1 in) percent	RA percent
0.12	80	40.1	86.7	57	76
	-100	63.4	147.1	66	76
	-320	94.2	220.8	49	66
0.13	80	40.8	87.9	55	75
	-100	64.4	150.8	64	75
	-320	95.6	227.8	47	64
0.14	80	43.3	87.6	57	78
	-100	66.2	144.0	71	77
	-320	100.0	223.0	50	66
0.16	80	43.6	90.7	51	75
	-100	66.6	145.4	66	75
	-320	101.5	225.8	47	63

(a) Specimens annealed in blank form and finish machined to 0.250 in dia tension bars.

Data are the average of two tests.

TABLE 3.03145 EFFECT OF NITROGEN CONTENT AND TEST TEMPERATURE (+80 to -320F) ON THE TENSILE PROPERTIES OF TYPE 304N.

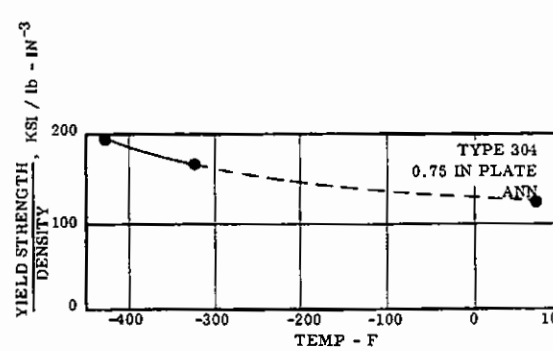


FIG 3.03147 EFFECT OF LOW TEMPERATURE ON THE YIELD STRENGTH - DENSITY RATIO (57)

Low	Fe
19	C
10	Cr
	Ni

TYPES 304, 304L

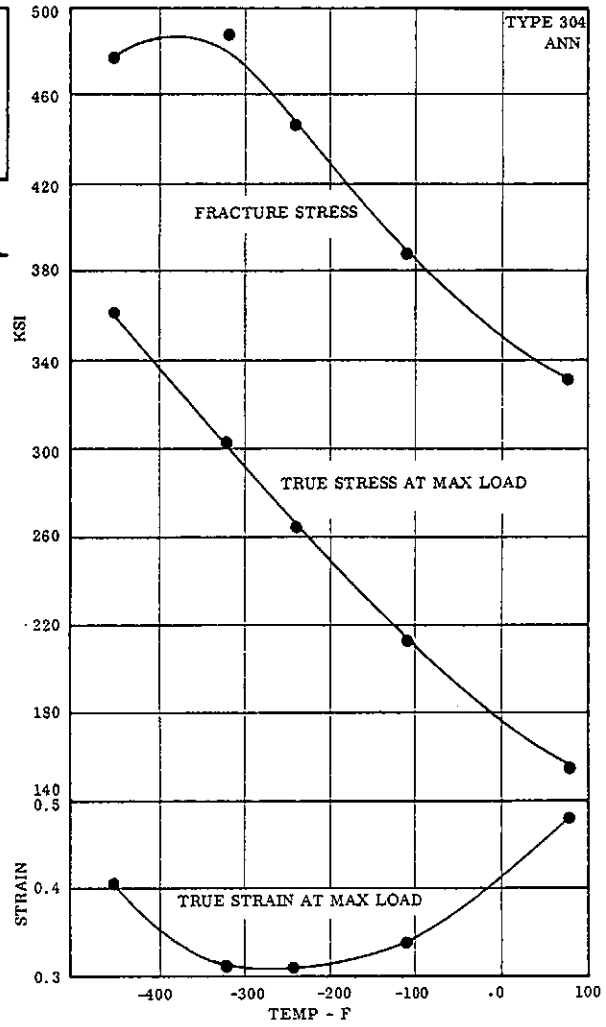


FIG 3.03148 EFFECT OF LOW TEST TEMPERATURE ON TRUE TENSILE PROPERTIES OF ALLOY (46)

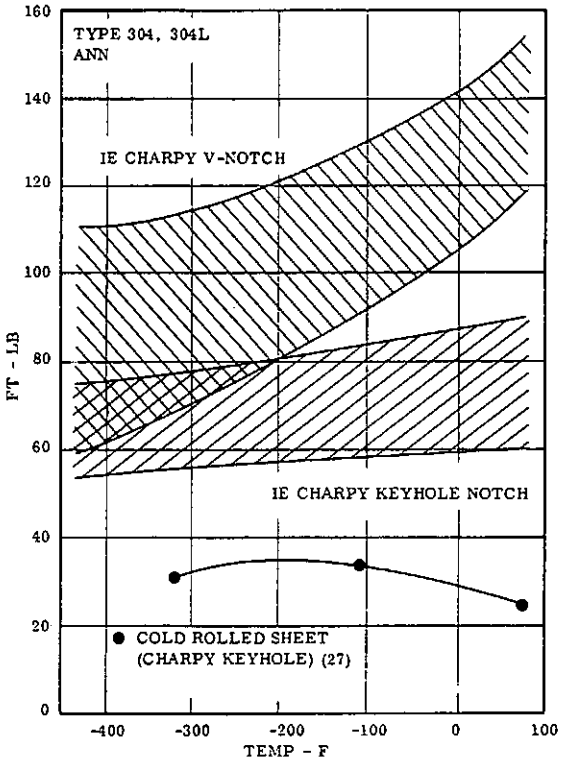


FIG 3.0331 PROBABLE RANGE OF CHARPY IMPACT PROPERTIES OF ANNEALED TYPES 304 AND 304L STAINLESS STEELS (27)(51)

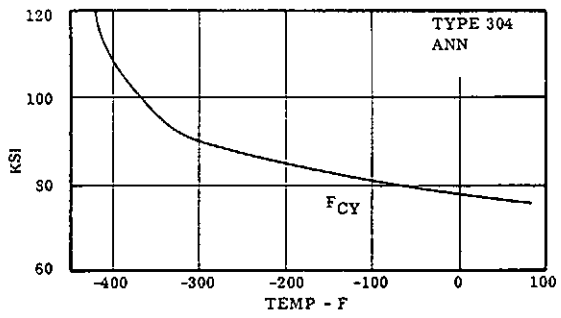


FIG 3.0322 EFFECT OF LOW TEMPERATURE ON COMPRESSIVE YIELD STRENGTH OF ALLOY (44)

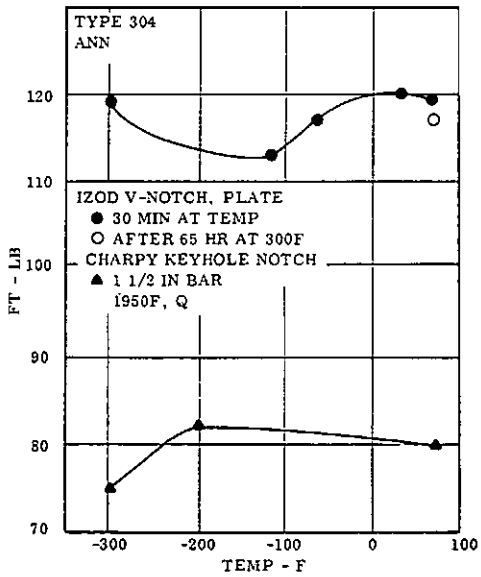


FIG 3.0332 EFFECT OF LOW TEMPERATURE ON IMPACT PROPERTIES OF ANNEALED PLATE AND BAR (61)

Source	(62)	
Alloy	304	
Form	Plate	
Condition	Annealed	
Exposure time to test temp.	Test temp - F	Charpy keyhole notch impact strength - ft-lb
0	-320	85
30 min	-320	72
6 mo	-320	73
12 mo	-320	75

TABLE 3.0333 LOW TEMPERATURE IMPACT PROPERTIES OF TYPE 304 AS A FUNCTION OF EXPOSURE TIME

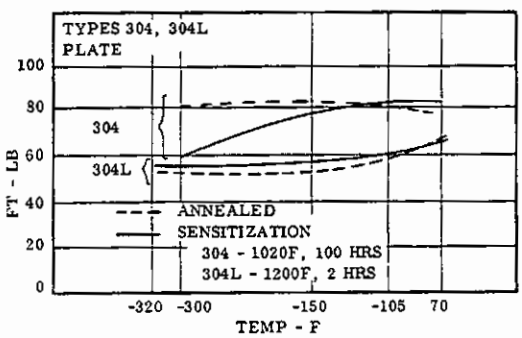
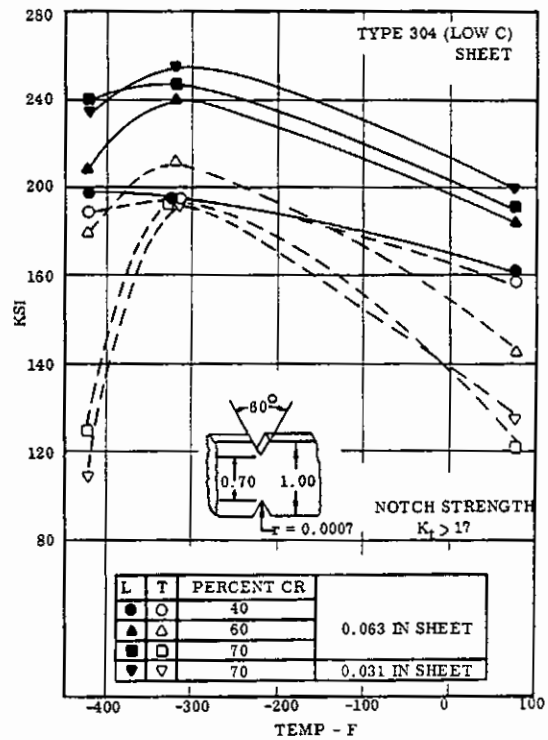


FIG. 3.0334 EFFECT OF SENSITIZATION HEAT TREATMENT ON CHARPY KEYHOLE IMPACT PROPERTIES OF TYPES 304 AND 304L. (62)



Fe	
Low	C
19	Cr
10	Ni

TYPES 304, 304L

FIG 3.03711 EFFECT OF LOW TEMPERATURES ON NOTCH STRENGTH OF COLD ROLLED SHEET (48)

Source	(43)		
Alloy	304N		
Form	3 in sq bar (a)		
Condition	Annealed 1975 F - 1 hr - WQ(a)		
Nitrogen Content wt. percent	Test Temp F	Charpy V-notch Impact Energy ft-lb	
		Longitudinal	Transverse
0.12	80	240(b)	105
	-100	240(b)	82
	-320	141	66
0.13	80	240(b)	90
	-100	240(b)	71
	-320	152	61
0.14	80	240(b)	95
	-100	230	62
	-320	125	52
0.16	80	240(b)	102
	-100	240(b)	80
	-320	158	58
(a) Specimens annealed in blank form and finish machined to standard 0.394 Charpy V-notch impact bars.			
(b) Specimens did not break.			
Data are average of two tests			

TABLE 3.0335 EFFECT OF NITROGEN CONTENT AND TEST TEMPERATURE ON THE CHARPY V-NOTCH IMPACT PROPERTIES OF TYPE 304N.

Source	(62)		
Form	0.012 in sheet		
Condition	50 percent CR		
Type	304L		
Test Temp (F)	F_{ty} (ksi)	F_{tu} (ksi)	Notch F_{tu} (a) (ksi)
78	158	176	192
-100	186	198	217
-320	187	251	262
-423	231	279	304

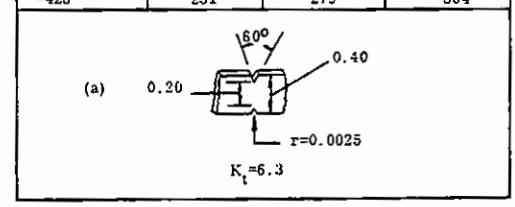


TABLE 3.03712 EFFECT OF LOW TEMPERATURE ON THE NOTCH AND TENSILE STRENGTH OF COLD ROLLED SHEET.

Fe
Low C
19 Cr
10 Ni

TYPES 304, 304L

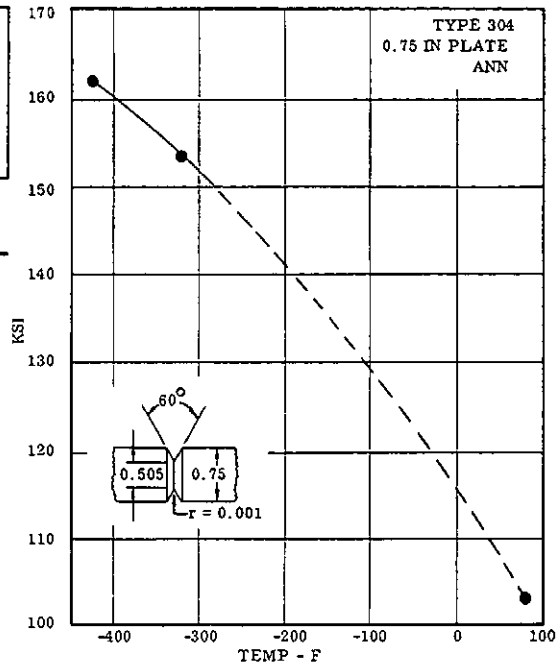


FIG 3.03713 EFFECT OF TEST TEMPERATURE ON NOTCH STRENGTH OF ANNEALED PLATE (57)

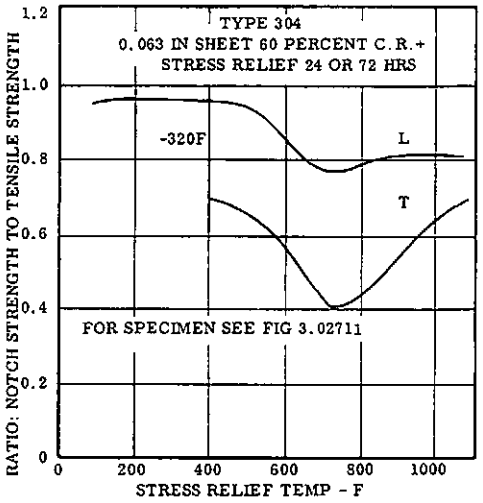


FIG 3.03715 EFFECT OF STRESS RELIEF TEMPERATURE ON SHARP NOTCH STRENGTH RATIO AT -320F FOR COLD ROLLED 304L SHEET (73, fig 14)

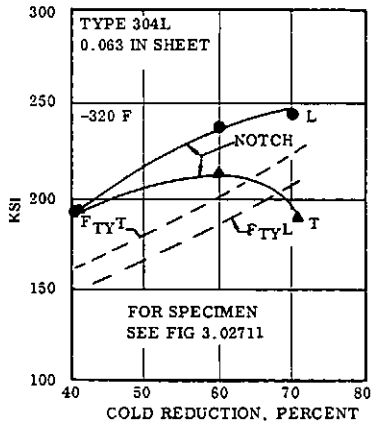


FIG 3.03714 EFFECT OF COLD REDUCTION ON -320F SHARP NOTCH STRENGTH OF 304L SHEET (73) FIG 3

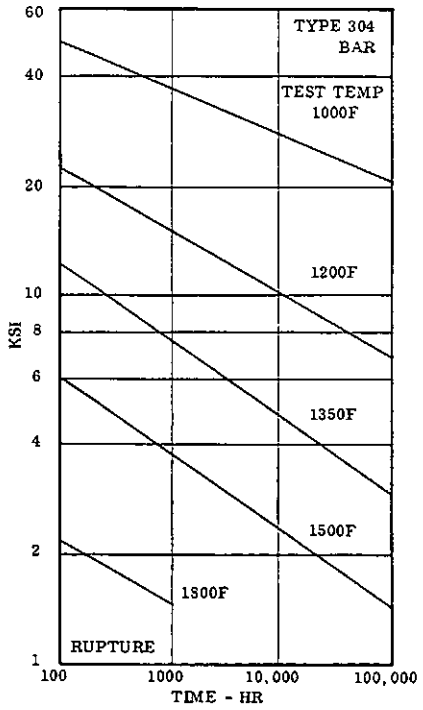


FIG 3.041 CREEP RUPTURE CURVES FOR BAR AT 1000F TO 1800F (64)

Fe
Low C
19 Cr
10 Ni

TYPES 304, 304L

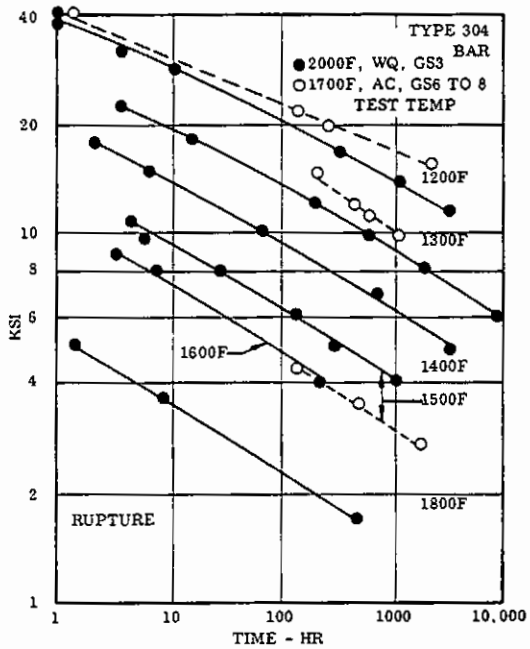


FIG 3.042 CREEP RUPTURE CURVES FOR BAR AT 1200 TO 1800F (26)

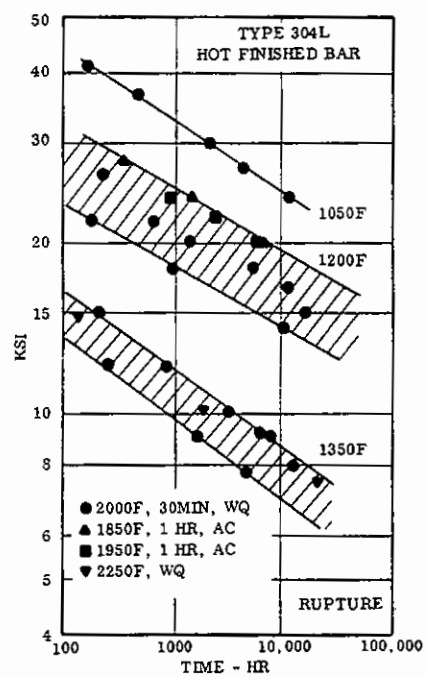


FIG 3.044 CREEP RUPTURE CURVES FOR BAR AT 1050F TO 1350F (65)

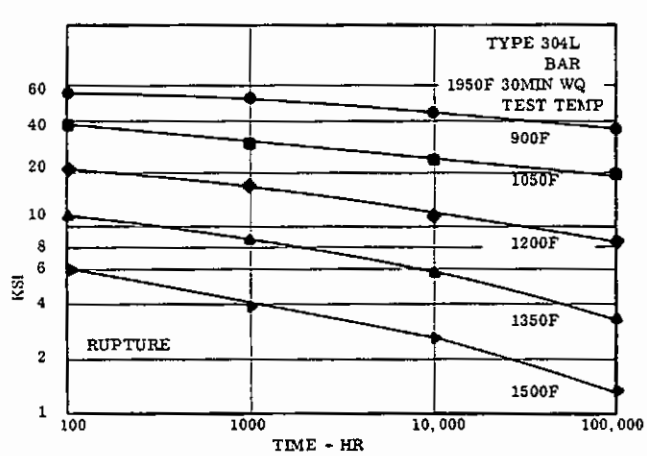


FIG 3.043 CREEP RUPTURE CURVES FOR BAR AT 900 TO 1500F (64)

	Fe
Low	C
19	Cr
10	Ni

TYPES 304, 304L

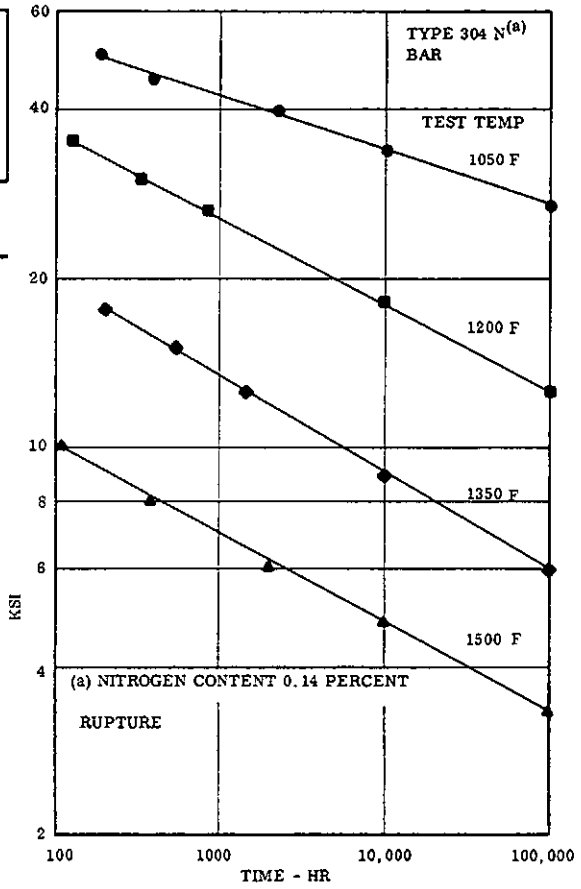


FIG 3.045 CREEP RUPTURE CURVES FOR TYPE 304N BAR AT 1050 TO 1500F (66)

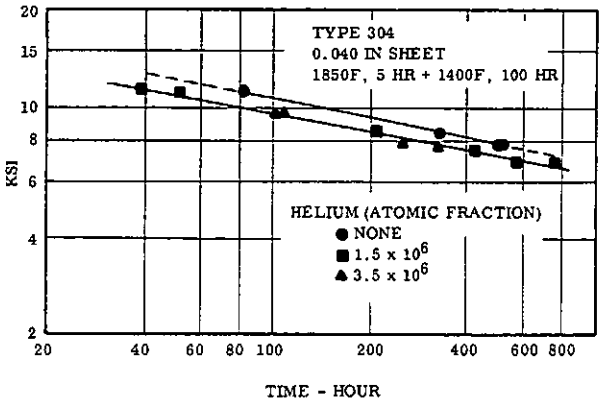


FIG. 3.047 EFFECT OF HELIUM ON CREEP RUPTURE OF SHEET TESTED IN VACUUM AT 1400F. (67)

Source	(66)			
Form	Bar			
Type	304		304N(a)	
Test Temp (F).	Rupture stress - ksi			
	10,000 Hr.	100,000 Hr.	10,000 Hr.	100,000 Hr.
1050	28.0	20.0	34.0	27.0
1200	13.8	9.8	18.0	12.5
1350	6.7	4.7	8.8	6.0
1500	3.25	2.3	3.3	4.0

(a) Nitrogen content 0.14 percent.

TABLE 3.046 COMPARISON OF RUPTURE STRESS OF TYPE 304 AND TYPE 304N AS A FUNCTION TO TEMPERATURE AND TIME.

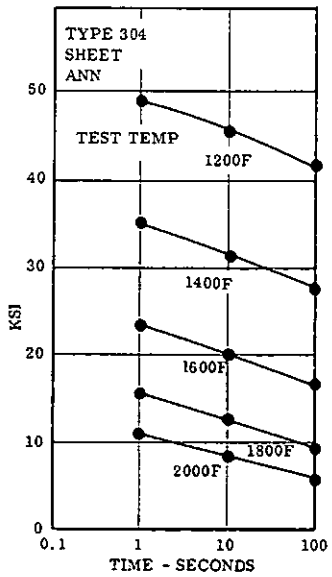


FIG. 3.048 SHORT TIME CREEP RUPTURE CURVES FOR SHEET AT 1200 TO 2000F. (68)

	Fe
Low	C
19	Cr
10	Ni

TYPES 304, 304L

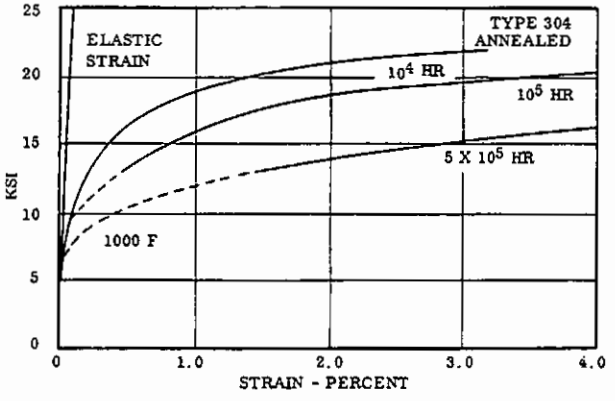


FIG 3.049 ISOCHRONOUS STRESS - STRAIN CURVES FOR TYPE 304 AT 1000 F (69)

Source	(70)						
Alloy	Type 304						
Form	1 in bar						
Condition	Ann						
Temp - F	Method	Stress Ratio		Stress Concentration	Fatigue strength-ksi at cycles		
		A	R		10^5	10^6	10^7
RT	Rot Beam	∞	-1	Smooth K = 1	45	41	40
800					32	31	31
1000					34	32	31
1200					31	29	29

TABLE 3.051 FATIGUE PROPERTIES OF 1 INCH DIAMETER ANNEALED BAR.

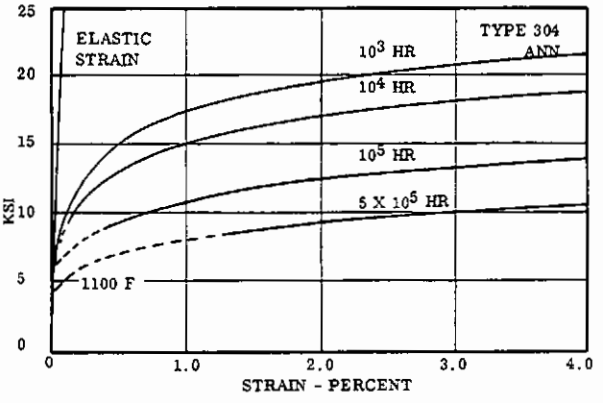


FIG. 3.0410 ISOCHRONOUS STRESS - STRAIN CURVES FOR TYPE 304 AT 1100 F (69)

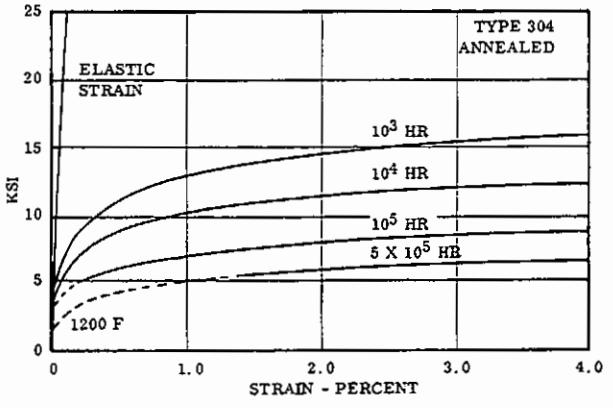


FIG 3.0411 ISOCHRONOUS STRESS - STRAIN CURVES FOR TYPE 304 AT 1200 F (69)

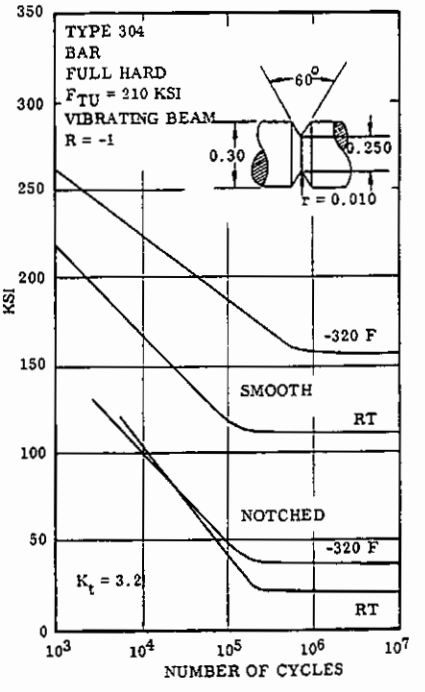


FIG 3.052 RESULTS OF VIBRATING BEAM TESTS OF NOTCHED AND SMOOTH TYPE 304 BAR (18)

	Fe
Low	C
19	Cr
10	Ni

TYPES 304, 304L

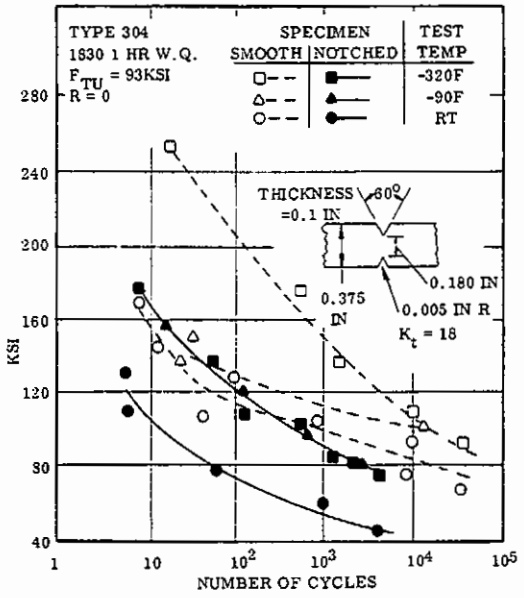


FIG 3.053 S-N CURVES FOR NOTCHED AND SMOOTH SHEET AS A FUNCTION OF TEMPERATURE IN THE ANNEALED CONDITION (75)

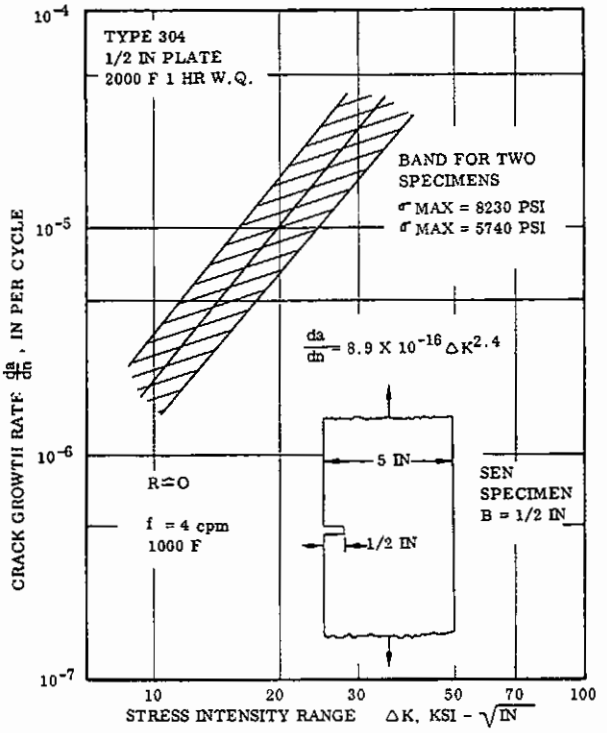


FIG 3.055 FATIGUE CRACK PROPAGATION RATE AT 1000 F AS A FUNCTION OF STRESS INTENSITY RANGE FOR PLATE (73, fig 5)

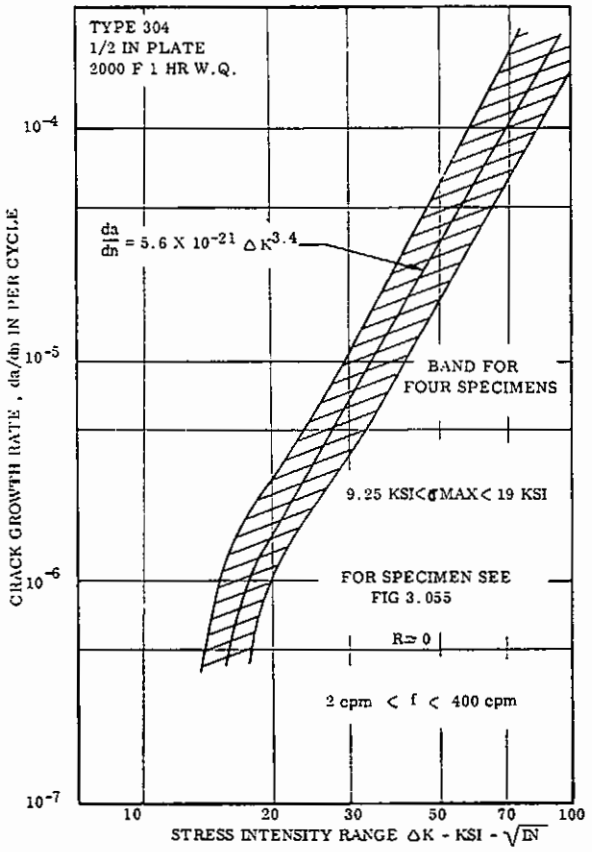


FIG 3.054 FATIGUE CRACK PROPAGATION RATE AT R.T. AS A FUNCTION OF STRESS INTENSITY RANGE FOR PLATE (73, fig 8)

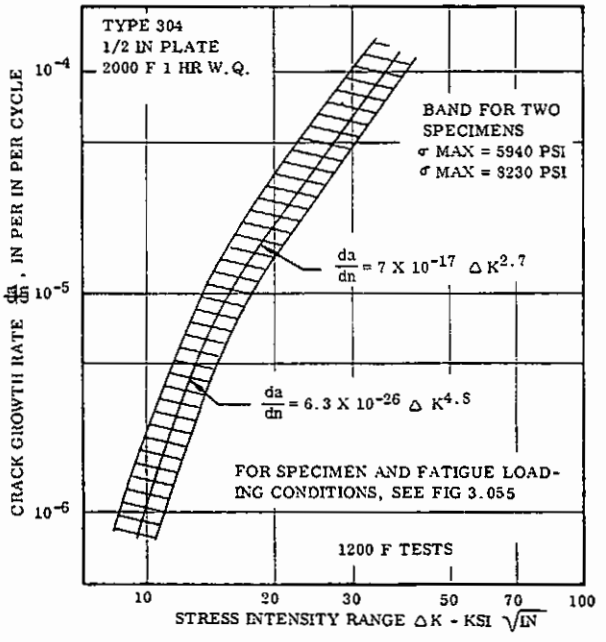


FIG 3.056 FATIGUE CRACK PROPAGATION RATE AT 1200F AS A FUNCTION OF STRESS INTENSITY RANGE FOR PLATE (73, fig 6)

Fe	
Low	C
19	Cr
10	Ni

TYPES 304, 304L

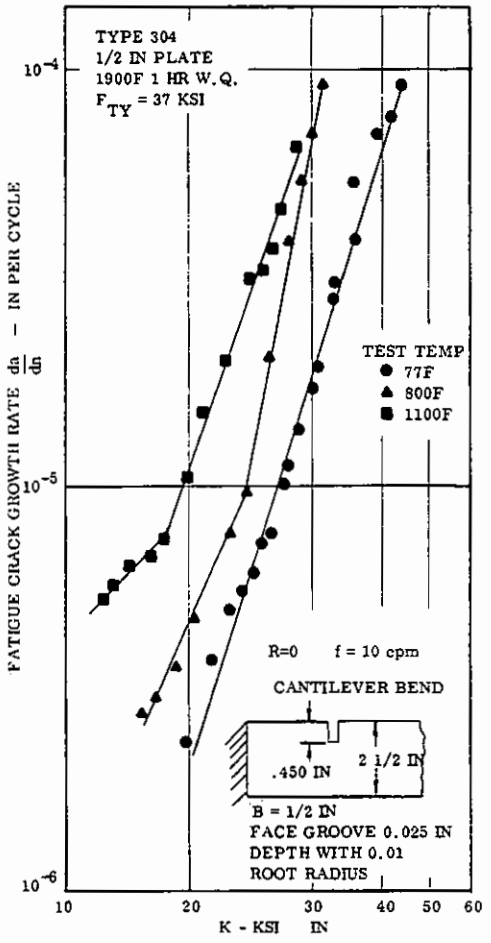


FIG 3.057 FATIGUE CRACK GROWTH RATE AS A FUNCTION OF STRESS INTENSITY RANGE AND TEMPERATURE FOR PLATE IN THE ANNEALED CONDITION (76)

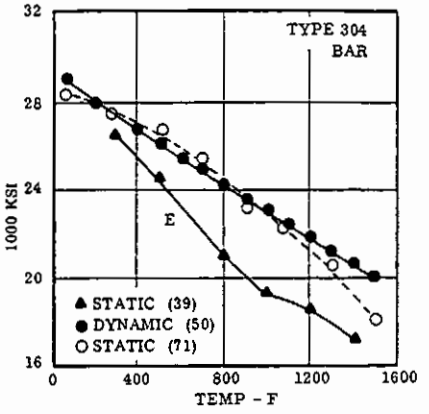


FIG 3.0621 MODULUS OF ELASTICITY AT ROOM AND ELEVATED TEMPERATURES (39)(50, p. 82)(71)

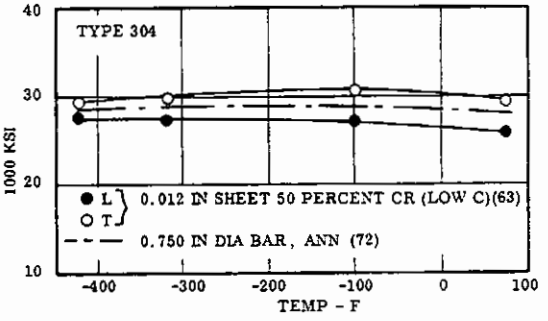


FIG 3.0622 MODULUS OF ELASTICITY AT ROOM AND LOW TEMPERATURES (63) (72)

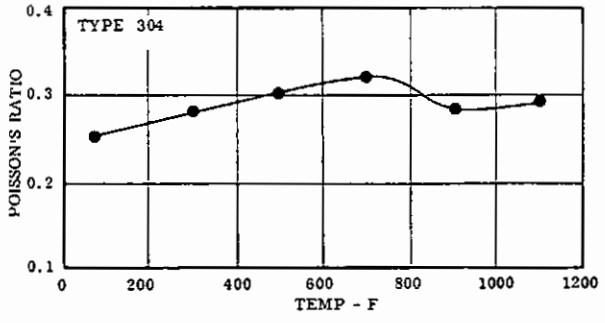


FIG 3.061 POISSON'S RATIO AT ROOM AND ELEVATED TEMPERATURES (21)

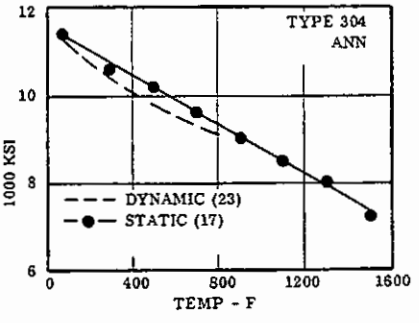


FIG 3.063 MODULUS OF RIGIDITY AT ROOM AND ELEVATED TEMPERATURES (17)(23)

	Fe
Low	C
19	Cr
10	Ni

TYPES 304, 304L

REFERENCES

1. AMS 5370, Castings - Precision Investment 19.5 Cr - 10 Ni (Low Carbon)(March 1, 1955).
2. AMS 5371, Castings - Sand 19.5 Cr - 10 Ni (Low Carbon) (March 1, 1955).
3. AMS 5513, Plate, Sheet and Strip 19 Cr - 9 Ni (June 15, 1958).
4. AMS 5560D, Tubing, Seamless 19 Cr - 10 Ni (January 15, 1958).
5. AMS 5565D, Tubing, Welded 19 Cr - 9 Ni (January 15, 1958).
6. AMS 5566D, Tubing, Seamless or Welded-Hydraulic 19 Cr-10 Ni High Pressure (July 15, 1963).
7. ASM 5567, Tubing, Hydraulic - Seamless or Welded 19 Cr-10 Ni Solution Treated (January 31, 1964).
8. AMS 5639A, Bars, Forgings, Mech. Tubing and Rings 19 Cr - 9 Ni (June 15, 1959).
9. AMS 5697, Wire 19 Cr - 9 Ni Solution Treated (November 1, 1954).
10. AMS 5511A, Plate, Sheet and Strip 18 Cr - 8 Ni Extra Low Carbon (June 15, 1952).
11. AMS 5647B, Bars, Forgings, Mech. Tubing and Rings 18 Cr - 8 Ni (March 15, 1966).
12. American Iron and Steel Institute, "Type 304 and 304L Stainless and Heat Resisting Steels" (June 1957).
13. American Casting Institute, "Corrosion Resistant Type CF-8", Data Sheet (June 1954).
14. Morykwas, S., "304 and 304L Alloy Data", Cannon-Muskegon Corporation (August 1967).
15. United States Steel, "Data on USS-18-8S, Type 304 and USS 18-8L Stainless Steel" (April 1962).
16. Alloy Digest, "Fagersta - R350 (Stainless Steel - Type 304)" (October 1968).
17. National Tube Division, United States Steel Corp., "Pipe and Tubes for Elevated Temperature Service", Bulletin No. 26 (1956).
18. Spretnak, J.W., et. al., "Notched and Unnotched Tensile and Fatigue Properties of Ten Engineering Alloys at 25°C and 196°K", Trans. American Society for Metals, Vol. 43 (1951).
19. Fontana, M.G., "Investigation of Mechanical Properties and Physical Metallurgy of Aircraft Alloys at Very Low Temperatures", WADC-TR-5662, Part II, Ohio State Foundation (October 1958).
20. Zambrow, J.L. and Fontana, M.G., "Impact Strength and Hardness of Aircraft Alloys Down to -423°F", Metals Progress, Vol. 53 (1948).
21. Universal Cyclops Steel Corporation, "High Temperature Metals Uniloy 18-8S (AISI Type 304)", p. 22 (1959).
22. North American Aviation, Inc., "Stainless Steel - Type 304", Data Sheet (1957).
23. Westinghouse Electric Corporation, Standards Engineering Section, "Bettis Plant Materials Manual" (May 1957).
24. Furman, T., AIME (1950).
25. Allegheny Ludlum Steel Corporation, "Stainless Steel Fabrication", p. 273 (1958).
26. The Timken Roller Bearing Company, Steel and Tube Division, "Digest of Steels", p. 56-57 (1957).
27. The International Nickel Co. Inc., "Low Temperature Data Sheet Type 304 and 304L Stainless Steel" (February 1963).
28. Hoselitz, K., "Ferromagnetic Properties of Metals and Alloys", Oxford Clarendon Press, Oxford (1952).
29. Mangonon, P.L. Jr.and Thomas, G., "Structure and Properties of Thermal-Mechanically Treated 304 Stainless Steel", Metallurgical Trans., Vol. 1 (June 1970).
30. The International Nickel Co., Inc., "Heat Treatment and Physical Properties of the Austenitic Chromium - Nickel Stainless Steels", Nickel Alloy Steels, Section 7, Data Sheet A (1947).
31. Aust, K.T. et. al., "Intergranular Corrosion and Electron Microscopic Studies of Austenitic Stainless Steels", Trans. American Society for Metals, Vol. 60 (1967).
32. Fink, F.W. and Boyd, W.K., "The Corrosion of Metals in Marine Environments", DMIC Report 245 (May 1970).
33. Lennox, T.J. Jr., Peterson, M.H.and Groover, R.E., "Marine Corrosion Studies", NRL Report 1948 (November 1968).
34. Mannheimer, W.A. and Paxton, H.W., "Some Effects of Nitrogen on the Resistance to Stress Corrosion Cracking of Type 304 Stainless Steel Wires", Carnegie Institute of Technology, Contract Nonr 760 (14) NR 036-029 (June 15, 1966).
35. Logan, H.L. and McBee, M.J., "Stress-Corrosion Cracking of Cold Reduced Austenitic Stainless Steel", MR&S, ASTM, Vol. 7, No. 4 (April 1967).
36. Vennett, R.M. and Ansell, G.S., "The Effect of High-Pressure Hydrogen Upon the Tensile Properties and Fracture Behavior of 304L Stainless Steel", Trans. ASM, Vol. 60 (1967).
37. Personal Communication, Lovejoy, P.T., Allegheny Ludlum Industries, Inc. to C.F. Hickey, Jr. (September 22, 1970).
38. Guinia, R.B. and Woodrow, G.R., "Nitrogen Improves Engineering Properties of Chromium-Nickel Stainless Steels", Journal of Mats., ASTM, Vol. 5, No. 2 (1970).
39. Tipton, C.R., Jr., Editor, "Reactor Handbook", 2nd Edition Interscience Publishers, New York (1960).
40. Comprelli, F.A., Busboom, H.J. and Gebhardt, M.F., "Mechanical Properties of Irradiated Type 304 and Type 316 Stainless Steel in Fast Reactors", GEAP-10062, AEC Research and Development Report (June 1969).
41. Allegheny Ludlum Steel Corp., "Types 302, 304, 304L and 305", Allegheny Ludlum Blue Sheet (October 1963).
42. NASA (E-502) (1959).
43. Spaeder, C.E. and Domis, W.F., "Cryogenic and Elevated Temperature Mechanical Properties of a High-Nitrogen Type 304 Stainless Steel", Applied Research Laboratory, United States Steel, Proj. No. 44.012-062(2) (April 30, 1969).
44. "Cryogenic Materials Data Handbook", ML-TRD-64-280, Martin Co., Denver (August 1964).
45. Conway, J.B., "Evaluation of Plastic Fatigue Properties of Heat-Resistant Alloys", GEMP-740, General Electric Co., - NSP (December 1969).
46. DeSisto, T.S. and Carr, F.L., "Low Temperature Mechanical Properties of 300 Series Stainless Steels and Titanium" WAL TR 323.4/1 (December 1961).
47. Krivobok, V.N. and Tolbot, A.M., "Effect of Temperature on the Mechanical Properties, Characteristics and Processing of Austenitic Stainless Steels", ASTM, Vol. 50 (1950).
48. Hanson, M.P., "Smooth and Sharp-Notch Tensile Properties of Cold-Reduced AISI 301 and 304L Stainless Steel Sheet at 75F and -423F", NASA TN D-592 (February 1961).
49. The Timken Roller Bearing Company, Steel and Tube Division, "Resume of High Temperature Investigations Conducted During 1948 to 1950", p. 32 (1950).
50. American Society for Metals, "Metals Handbook", Vol. 1, 8th Edition (1961).
51. Engineering Alloys Digest, Inc., "Alloy Digest Filing Code: SS-5S Stainless Steel" (May 1957).
52. The Carpenter Steel Corporation, "Working Data - Carpenter Stainless and Heat Resisting Steels" (1962).
53. Timken Roller Bearing Co., Data Sheet (1959).
54. McDowell, D.W., Jr and Mihalisin, J.L., "Zerolling Boosts Strength of Stainless Sheet", Materials in Design Engineering, Vol. 53, No. 5 (May 1961).
55. Allegheny Ludlum Steel Corporation, "Allegheny Metal 18-8", Allegheny Ludlum Blue Sheet (1958).
56. Allegheny Ludlum Steel Corporation, "Stainless Steel Handbook", p. 66 (1956).
57. Rice, L.P., Campbell, J.E. and Simmons, W.F., "Tensile Behavior of Parent Metals and Welded 5000 Series Aluminum Alloy Plate at Room and Cryogenic Temperatures", Cryogenic Engineering Conference, Ann Arbor, Michigan (August 1961).
58. Gunter, C.F. and Reed, R.P., "The Effect of Experimental Variables Including the Martensitic Transformation on the Low Temperature Properties of Austenitic Stainless Steel", Trans. ASM, Vol. 55 (1962).
59. ASTM STP 287,"Symposium on Low Temperature Properties of High Strength Aircraft Missile Materials"(1960).
60. ASTM STP 302,"Symposium on Evaluation of Metallic Materials in Design for Low Temperature Service"(1961).
61. Republic Steel Corporation, "Republic Enduro Stainless Steel, Chromium Nickel Type 300 Series" (1964).

62. United States Steel, "Low Temperature and Cryogenic Steels Materials Manual" (1966).
63. Christian, J.L., "Physical and Mechanical Properties of Pressure Vessel Materials for Applications in a Cryogenic Environment", ASD TDR 62-258, General Dynamics/Astronautics (March 1962).
64. ASTM Data Series DS5 Report on the Elevated Temperature Properties of Stainless Steels; DS5-S1 Supplement; and DS 5-S2 Strength of Wrought 304, 316, 321 and 347 of Elevated Temperatures(1969).
65. The Babcock and Wilcox Company, "The Long Time Creep Rupture Strength of Croyloy 304".
66. Domis, W.F., "Creep and Creep Rupture Properties of Types 304N and 316N Stainless Steels", ASME, Pet-34(1971)
67. Garr, K.R., Kramer, D. and Rhodes, C.G., "Effect of Hellum on Stress-Rupture Behavior of Types 304 and 316 Stainless Steels", AI-AEC-12932 (April 15, 1970).
68. Moon, D.P. and Simmons, W.F., "Selected Short-Time Tensile and Creep Data Obtained Under Conditions of Rapid Heating", DMIC Report 130 (June 17, 1960).
69. "Isochronous Stress-Strain Curves for 2-1/4 Cr-1Mo, Type 304-304H, and Type 316-316H Steels", TR 2012-Part 1, Prepared for U.S. Atomic Energy Commission, Contract No. AT(04-3)-781, Braun Project 4122-W, United Nuclear Project 2351 (October 16, 1970).
70. Cross, T., ASME (1934).
71. ASTM STP 129, Symposium on Determination of Elastic Constants (1952).
72. Warren, K.A. and Reed, R.P., "Tensile and Impact Properties of Selected Materials from 70 too 300°K", Monograph 63, National Bureau of Standards (June 1963).
73. Espey, G.B., Repko, A.J. and Brown, W.F., Jr., "Effect of Cold Rolling and Stress Relief on Sharp Edge Notch Tensile Characteristics of Austenitic Stainless Sheet Alloys", Proc. ASTM Vol. 59, 159, p. 816.
74. James, L.A., "Fatigue Crack Propagation Behavior of Type 304 Stainless Steel at Elevated Temperatures", 4th National Symposium on Fracture Mechanics, Carnegie Mellon Univ. (August 1970).
75. Reed, R.P., Durcholz, R.L., Schramm, R.E. and Patrician, T.J., "Study of Cryogenic Tank Fatigue Life", Technical Note 609, National Bureau of Standards (August 1971).
76. Steele, L.E. et. al., "Irradiation Effects on Structural Materials", Memorandum Report 2398, Naval Research Laboratory (February 1972).

	Fe
Low	C
19	Cr
10	Ni

TYPES 304, 304L

REVISED: MARCH 1972
AUTHOR: DR. R. P. WEI

FERROUS ALLOYS

	Fe
18	Cr
12	Ni

TYPE 305

1. GENERAL

Type 305 austenitic stainless steel is the member of the 18Cr-8Ni steel family having the highest nickel content considered to be within this classification. It is, therefore, the austenitic stainless steel with the lowest rate of strain hardening. It is used in sheet, strip and plate form for difficult drawing, spinning and other forming operations and in wire form for severe upsetting. It also becomes less magnetic on cold work than other 18-8 steels, particularly Type 301. This steel has a higher carbon content than Type 304 and, therefore, a greater susceptibility to intergranular corrosion after exposure at 800 to 1500F. The properties of this alloy are otherwise nearly identical to those of Type 304.

1.01 Commercial Designation

Type 305

1.02 Alternate Designations

AISI Type 305 austenitic stainless steel, 18-8 FS stainless steel, 18-12 steel, 30305.

1.03 Specifications

Table 1.03.

1.04 Composition

1.041 AMS specified chemical composition, Table 1.041.
1.042 ASTM specified chemical compositions, Table 1.042.

1.05 Heat Treatment

1.051 Anneal or solution heat treat. 1850 to 2000F, 1/2 to 1 hr per in thickness, 2 hr minimum for plate, air cool or quench, depending on section size. Cooling to 800F maximum should be within 3 minutes.

1.06 Hardness

This steel can be hardened only by cold working, and this to a lesser degree than the other steels of the 18-8 family.

1.061 Typical hardness for annealed and soft temper conditions. 78 to 82 Rockwell B, (94 maximum) (14).
1.062 Effect of cold rolling on hardness of various 18-8 stainless steel sheets, Figure 1.062.

1.07 Forms and Conditions Available

This steel is available in plate, sheet, strip, bar, shapes billet, forging and wires. Plate, sheet, strip, bar, shapes and wires may be obtained in hot finished and annealed, cold finished and annealed and cold worked conditions.

1.08 Melting and Casting Practice

Electric arc, electric induction, or other suitable commercial processes.

1.09 Special Considerations

When chromium-nickel steels containing more than about 0.04C are subjected to annealing at temperatures of 1850 to 2050F and are then reheated to or held at temperatures of approximately 800 to 1600F, chromium carbides will precipitate at the austenite boundaries (16, p. 24). This intergranular precipitation or sensitization promotes intergranular corrosion cracking and reduces corrosion resistance of these steels. Heat treatment and welding conditions should be chosen to avoid carbide formation. Additions of columbium and titanium are used to stabilize these alloys and reduce intergranular corrosion sensitivity.

2. PHYSICAL AND CHEMICAL PROPERTIES

2.01 Thermal Properties

2.011 Melting range. 2550 to 2650F.
2.012 Phase changes. Some transformation from austenite to ferrite (martensite) occurs when alloy is severely cold worked.
2.0121 Time-temperature-transformation diagrams.
2.013 Thermal conductivity. Typical values (16):
At 212F 9.4 Btu per (hr sq ft)(F per ft)
At 932F 12.4 Btu per (hr sq ft)(F per ft).
2.014 Thermal expansion, Table 2.014.
2.015 Specific heat. 0.12 Btu (lb ft) for 32-212F (16).
2.016 Thermal diffusivity.

2.02 Other Physical Properties

2.021 Density. 0.29 lb per cu in (16).
2.022 Electrical properties.
2.0221 Electrical resistivity. 72.0 microhm - cm at 70F (16).
2.023 Magnetic properties. This steel is non-magnetic in the annealed condition. It becomes slightly magnetic when severely cold worked as a result of transformation of austenite to ferrite (martensite)(this effect is less pronounced than for the other 18-8 grades).
2.0231 Effect of cold reduction on permeability at various temperatures at H=200 oersteds, Table 2.0231.
2.0232 Effect of cold reduction on permeability of cold rolled strip, Figure 2.0232.
2.024 Emittance.
2.025 Damping capacity.

2.03 Chemical Properties

2.031 General corrosion resistance of this steel is similar to that of Type 304.
2.032 This steel is only slightly embrittled by high pressure (10,000 psi) gaseous hydrogen environment, Table 2.032.

2.04 Nuclear Properties

2.041 Effect of neutron irradiation on room temperature tensile properties of annealed bar, Table 2.041.

3. MECHANICAL PROPERTIES

3.01 Specified Mechanical Properties

3.011 AMS specified mechanical properties.
3.0111 AMS specified mechanical properties for plate, sheet, and strip, Table 3.0111.
3.0112 AMS specified mechanical properties for wire, Table 3.0112.
3.012 ASTM specified mechanical properties.
3.0121 ASTM specified mechanical properties for plate, sheet, and strip, Table 3.0121.
3.0122 ASTM specified mechanical properties for bar and shapes, Table 3.0122.
3.0123 ASTM specified mechanical properties of bar for cold heading and cold forging, Table 3.0123.
3.0124 ASTM specified mechanical properties for tube, Table 3.0124.
3.0125 ASTM specified mechanical properties for forging, Table 3.0125.
3.0126 ASTM specified mechanical properties of wire for cold heading and cold forging, Table 3.0126.
3.0127 ASTM specified mechanical properties of rope wire, Table 3.0127.

3.02 Mechanical Properties at Room Temperature

3.021 Tension.
3.0211 Stress-strain diagrams.
3.0212 Typical tensile properties, Table 3.0212.
3.0213 Effect of cold work on tensile properties.
3.02131 Range of tensile properties and hardness for various tempers and diameters of cold draw wire, Table 3.02131.
3.02132 Effect of cold rolling on tensile properties of strip, Figure 3.02132
3.02133 Effect of cold drawing on tensile properties of bar, Figure 3.02133.
3.02134 Effect of cold drawing on tensile properties of coiled bar, Figure 3.02134.
3.022 Compression.
3.0221 Stress-strain diagrams.
3.023 Impact.
3.024 Bending.
3.025 Torsion and shear.
3.026 Bearing.
3.027 Stress concentration.

Fe
18 Cr
12 Ni

TYPE 305

3.0271 Notch properties.
3.0272 Fracture toughness.
3.028 Combined properties.

3.03 Mechanical Properties at Various Temperatures
3.031 Tension.
3.0311 Stress-strain diagrams.
3.032 Compression.
3.0321 Stress-strain diagrams.
3.033 Impact.
3.034 Bending.
3.035 Torsion and shear.
3.036 Bearing.
3.037 Stress concentration.
3.0371 Notch properties.
3.0372 Fracture toughness.
3.038 Combined properties.

3.04 Creep and Creep Rupture Properties

3.05 Fatigue Properties
3.051 Fatigue crack growth in annealed sheet, (longitudinal or RW orientation), Figure 3.051.
3.052 Fatigue crack growth in annealed sheet (transverse or WR orientation), Figure 3.052.
3.053 Fatigue crack growth in cold rolled sheet (longitudinal or RW orientation), Figure 3.053.
3.054 Fatigue crack growth in cold rolled sheet (transverse or WR orientation), Figure 3.054.

3.06 Elastic Properties
3.061 Poisson's ratio.
3.062 Modulus of elasticity. 28×10^6 psi, typical.
3.063 Modulus of rigidity.

4. FABRICATION

4.01 Formability
4.011 General. Forming of this steel differs in various respects from that of Types 301 and 302, but it is similar to that of Type 304. Because of its lower strain hardening, Type 305 requires less power and requires fewer intermediate anneals in multi-stage forming. Its stretch forming ability, however, is lower than that of Types 301 and 302, because of its lower elongation.
4.012 Deep drawing of this steel is usually performed with the same or less reduction in the first draw than that of Types 301 and 302, but without intermediate anneals before the second, and possibly further draws. The reductions in these draws should be considerably lower than those possible for Type 301 which needs annealing after each draw. Type 305 also has a greater tendency to become thin at sharp radii than Types 301 and 302. Annealing is necessary if the hardness exceeds 35 to 40 R_C.
4.013 Type 305 is preferred for spinning applications because of its lower strain hardening. The surface should be kept clean and free from foreign particles during spinning.

4.02 Machining and Grinding
All 300 series austenitic stainless steels can be machined. Use of high speed or carbide tools, positive feed, and abundant flow of coolant or lubricant is recommended.

4.03 Welding
Thermal properties of this steel should be considered in the design of welded equipment and welding fixtures to minimize warpage or distortion at the weld. Welding rods of similar chemical analysis, or with slightly higher chromium-nickel content, as the base metal should be used. The use of fluxes, coated rods and inert gas shields is recommended.

4.04 Surface Treatment
See ASTM A380-57 "Recommended Practice for Descaling and Cleaning Stainless Steel Surfaces."

TABLE 1.03

Form	AMS	ASTM
Sheet, strip and plate	5514A	A-167, A-240
Bar and billet		A-276, A-314
Tube		A-249
Forging		A-473
Wire; rope and safety	5685D	A-492
Wire, riveting and cold heading	5686A	A-493
Wire, cold finished or cold drawn rounds and shapes		A-580
Wire, weaving		A-478

TABLE 1.041

Source	AMS (1)		AMS (2)		AMS (3)	
Alloy	Fe-18Cr-12Ni (Type 305)					
Form	Plate, sheet, strip		Wire, safety		Wire, riveting	
	Percent		Percent		Percent	
	min	max	min	max	min	max
Carbon	-	0.12	-	0.08	-	0.08
Manganese	-	2.00	-	2.00	-	2.00
Phosphorous	-	0.040	-	0.040	-	0.040
Sulfur	-	0.030	-	0.030	-	0.030
Silicon	-	1.00	-	1.00	-	1.00
Chromium	17.00	19.00	17.00	19.00	17.00	19.00
Nickel	10.00	13.00	10.00	13.00	10.00	13.00
Copper	-	0.50	-	0.50	-	0.50
Molybdenum	-	0.50	-	0.50	-	-
Iron	Balance		Balance		Balance	

TABLE 1.042

Source	ASTM (4)(5)(6)(7)(8)(9))10)(11)(12)(13)			
Alloy	Fe-18Cr-12Ni (Type 305)			
Form	Sheet, strip and plate; bar and billet; tube; forging; and wire		Bar and wire for cold heading and cold forging	
	Percent		Percent	
	minimum	maximum	minimum	maximum
Carbon	-	0.12	-	0.12
Manganese	-	2.00	-	2.00
Phosphorous	-	0.045	-	0.045
Sulfur	-	0.030	-	0.030
Silicon	-	1.00	-	1.00
Chromium	17.00	19.00	17.00	19.00
Nickel	10.00	13.00	11.00	13.00
Iron	Balance		Balance	

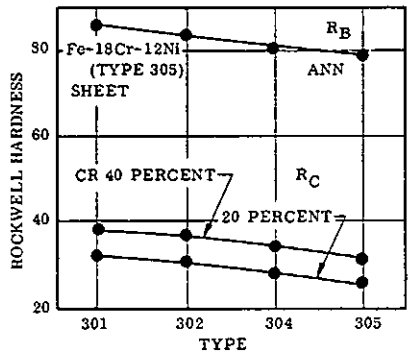


FIG. 1.062 EFFECT OF COLD ROLLING ON HARDNESS OF VARIOUS 18-8 STAINLESS STEEL SHEETS. (19)

TABLE 2.014

Source	(16)
Alloy	Fe-18Cr-12Ni (Type 305)
Temperature Range F	Mean Coefficient of Thermal Expansion 10^{-6} in/in/F
32-212	9.6
32-600	9.9
32-1000	10.2
32-1200	10.4

TABLE 2.032

Source	(17)	
Alloy	Fe-18Cr-12Ni (Type 305)	
Condition	Anneal + Cold Drawn	
Environment	10,000 psi He*	10,000 psi H_2
F_{tu} - ksi	90*	87
F_{ty} - ksi	51	-
e(1.25 in) - percent	63	65
RA - percent	78	75
Notch Strength - ksi (K_t 8.6)	165*	147
RA (Notched Bar) - percent	19	17

* He was contaminated with H_2. Strength reported are those for tests in ambient air minus 10 ksi to compensate for effect of 10,000 psi pressure.

	Fe
18	Cr
12	Ni

TYPE 305

TABLE 2.0231

Source	(15)	
Alloy	Fe-18Cr-12Ni (Type 305)*	
Condition	Anneal + Cold Reduced	
Percent Cold Reduction	Temperature Range - F	Permeability at H = 200 oersteds
0	20-100	1.003
25	20-300	1.005
50	20-871	1.025
C 1.069, Mn 0.94, P 0.021, S 0.013, Si 0.52, Cr 17.19, Ni 11.65		

TABLE 2.041

Source	(18)	
Alloy	Fe-18Cr-12Ni (Type 305)	
Form	Bar	
Condition	Annealed	
	Unirradiated	Irradiated*
F_{tu} - ksi	98.0	103.6
F_{ty} - ksi	32.1	71.4

* Irradiation - 3.9×10^{19} n/cm^2 at 80C

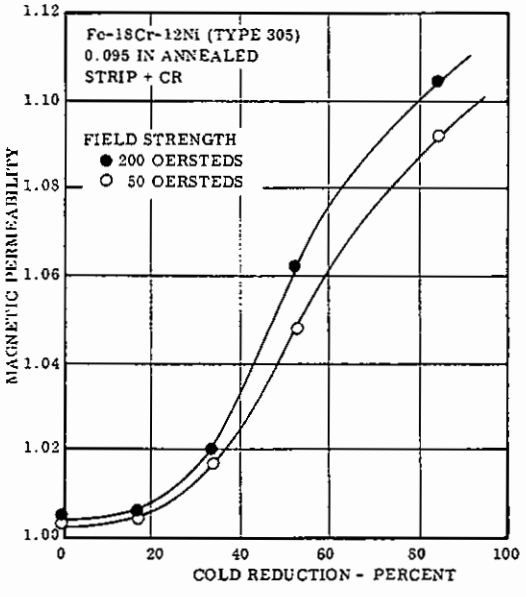


FIG. 2.0232 EFFECT OF COLD REDUCTION ON PERMEABILITY OF COLD ROLLED STRIP. (24)

TABLE 3.0111

Source	AMS (1)	
Alloy	Fe-18Cr-12Ni (Type 305)	
Form	Plate, sheet, strip	
Condition	CR + Sol Treat (sheet, strip) HR + Sol Treat (Plate)	
Thickness - inch	<0.025	≥ 0.025
F_{tu} - maximum* - ksi	100	100
e(2 in) - minimum* percent	45	50

* L specimens for width <9 in, T specimens for width ≥ 9 in.

TABLE 3.0112

Source	AMS (2)		AMS (3)
Alloy	Fe-18Cr-12Ni (Type 305)		
Form	Wire, safety coiled	Wire, safety straight	Wire, riveting
Condition	Solution treat + cold finish		Solution treat
F_{tu} - max - ksi	110	120	110

	Fe
18	Cr
12	Ni

TYPE 305

TABLE 3.0121

Source	ASTM (4)(5)
Alloy	Fe-18Cr-12Ni (Type 305)
Form	Plate, sheet, strip
Condition	Soft
F_{tu} - minimum - ksi	70
F_{ty} - minimum - ksi	25
e(2 in) - minimum - percent	40.0
Hardness	
Rockwell B - maximum	94
Brinell - maximum	202

TABLE 3.0122

Source	ASTM (6)		
Alloy	Fe-18Cr-12Ni (Type 305)		
Form	Bar and Shapes		
Condition	Hot Finish and Annealed	Cold Finish and Annealed	
Size (Dia or Thickness)	all	≤1/2 in	>1/2 in
F_{tu} - minimum - ksi	75(70)*	90	75(70)*
F_{ty} - minimum - ksi	30(25)*	45	30(25)*
e(2 in) - min - percent	40	35	35
RA - minimum - percent	50	45	50

* extrusions

TABLE 3.0123

Source	(12)	
Alloy	Fe-18Cr-12Ni (Type 305)	
Form and Size	Bar >1/2 in diameter	
Condition	Lightly Drafted	Annealed
F_{tu} - ksi	75-95	70-90

TABLE 3.0124

Source	ASTM (9)
Alloy	Fe-18Cr-12Ni (Type 305)
Form and Size	Tube 1/2 to 5 in O D ; 0.035 to 0.32 in wall thickness
Condition	1900 F min + WQ or rapid cool
F_{tu} - min - ksi	75
F_{ty} - min - ksi	30
e(2 in) - min - percent	35*

* For longitudinal strip tests the width of the gage section shall be 1 inch and the basic minimum elongation shall be reduced by 1.75 percent** for each 1/32 inch decrease in wall thickness below 5/16 inch.

** Not applicable to tubes less than 1/8 inch O D or having wall thickness below 0.015 inch or both.

TABLE 3.0125

Source	ASTM (8)
Alloy	Fe-18Cr-12Ni (Type 305)
Form	Forging
Condition	1900 F min + WQ or Rapid AC
F_{tu} - minimum - ksi	75
F_{ty} - minimum - ksi	30
e(2 in) - minimum - percent	40
RA - minimum - percent	50

TABLE 3.0126

Source	(12)			
Alloy	Fe-18Cr-12Ni (Type 305)			
Form	Wire, Cold Heading and Forging			
Diameter	< 0.156 inch		> 0.156 inch	
Condition	Lightly Drafted	Annealed	Lightly Drafted	Annealed
F_{tu} - ksi	80-110	75-105	80-100	75-95

TABLE 3.0127

Source	(11)							
Alloy	Fe-18Cr-12Ni (Type 305)							
Form	Rope Wire							
Condition	Cold Drawn							
Diameter - inch	less than 0.010	0.011 to 0.019	0.020 to 0.040	0.041 to 0.050	0.051 to 0.060	0.061 to 0.070	0.071 to 0.090	0.091 to 0.100
F_{tu} - ksi	245	240	235	230	225	220	210	205

TABLE 3.0212

Source	AISI (20)			
Alloy	Fe-18Cr-12Ni (Type 305)			
Form	Plate	Sheet, Strip	Wire	
Condition	Annealed			Soft Temper
F_{tu}-typical-ksi	85	85	85	100
F_{ty}-typical-ksi	35	38	47	54
e(2 in)-typ-percent	55	50	60	58
RA-typical-percent	-	-	77	74
Hardness - R_B -typical	-	80	78	82

TABLE 3.02131

Source	(25, p. 6)											
Alloy	Fe-18Cr-12Ni (Type 305)											
Form	Wire											
Condition	Cold Drawn											
Temper	1/4 Hard			1/2 Hard			3/4 Hard			Full Hard		
Diameter - in(a)	A	B	C	A	B	C	A	B	C	A	B	C
F_{tu} - ksi	130 to 165	130 to 160	110 to 130	165 to 200	150 to 190	140 to 160	200 to 250	180 to 230	160 to 190	230 to 300	210 to 260	190 to 220
F_{ty} - ksi	100 to 140	95 to 125	90 to 110	150 to 180	120 to 165	110 to 130	180 to 210	150 to 200	130 to 160	210 to 260	180 to 240	160 to 190
e(2 in)-percent	20 to 30	15 to 25	20 to 30	12 to 19	11 to 18	12 to 20	7 to 12	6 to 12	8 to 12	1 to 2	2 to 5	3 to 6
Hardness R_C	-	-	23 to 28	-	-	29 to 32	-	-	33 to 37	-	-	38 to 43

(a) A - 0.002 to 0.020 inch
B - 0.021 to 0.125 inch
C - 0.125 to 0.375 inch

	Fe
18	Cr
12	Ni

TYPE 305

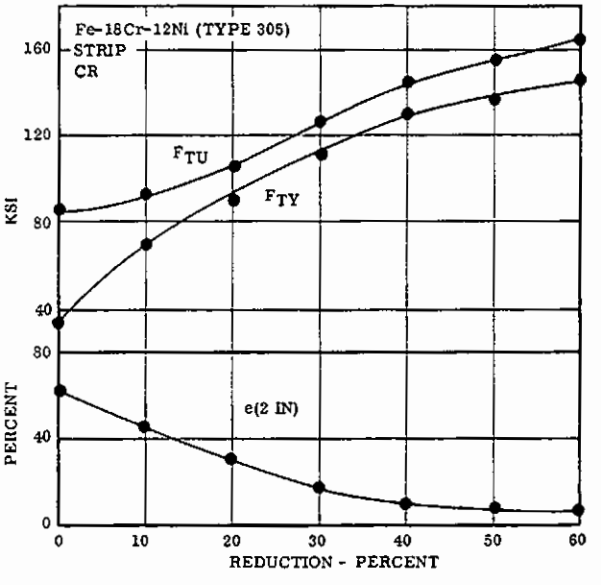


FIG. 3.02132 EFFECT OF COLD ROLLING ON TENSILE PROPERTIES OF STRIP. (21, p. 7)

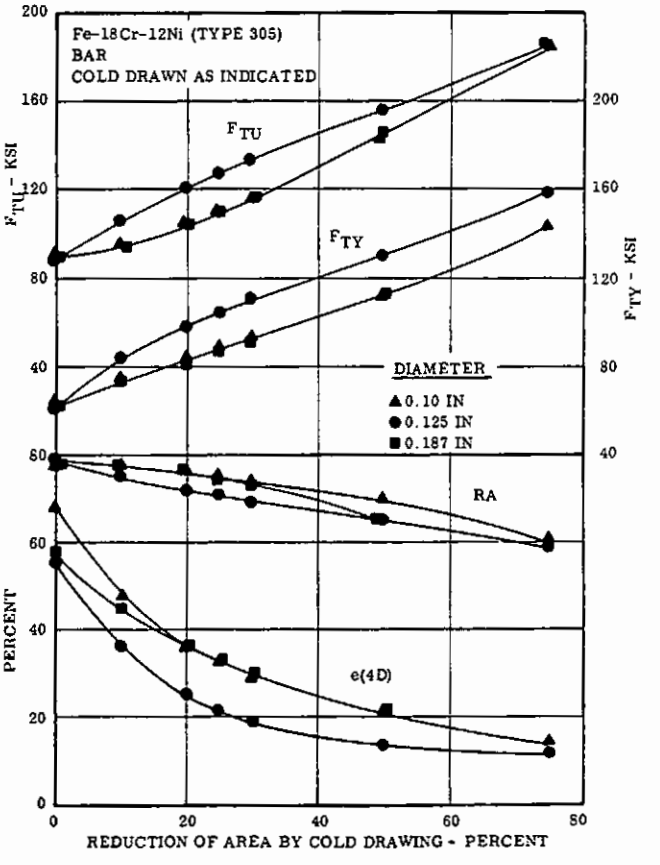


FIG. 3.02133 EFFECT OF COLD DRAWING ON TENSILE PROPERTIES OF BAR. (22)

	Fe
18	Cr
12	Ni

TYPE 305

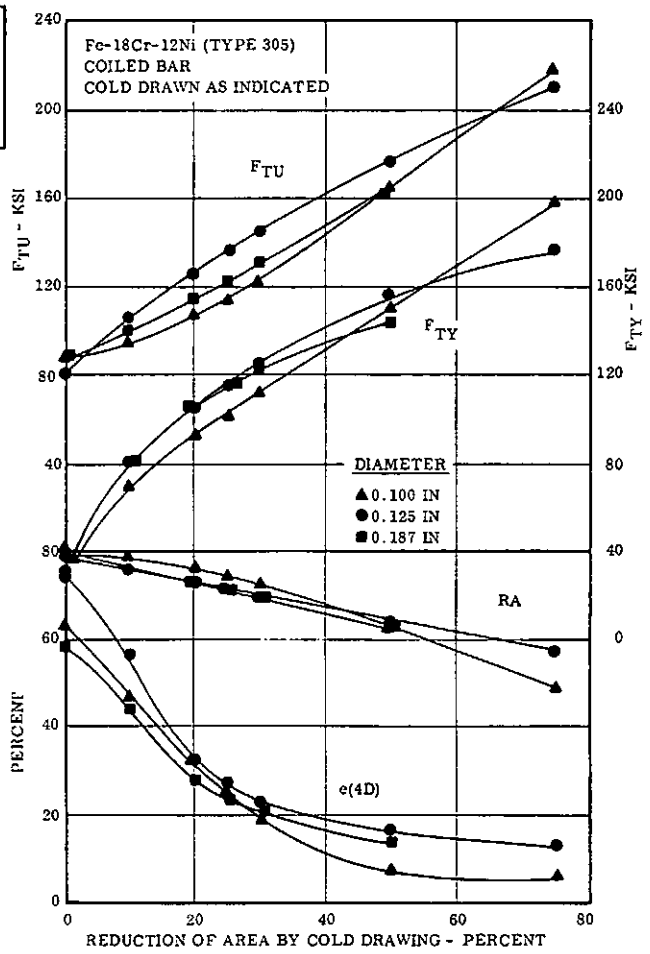


FIG. 3.02134 EFFECT OF COLD DRAWING ON TENSILE PROPERTIES OF COILED BAR. (22)

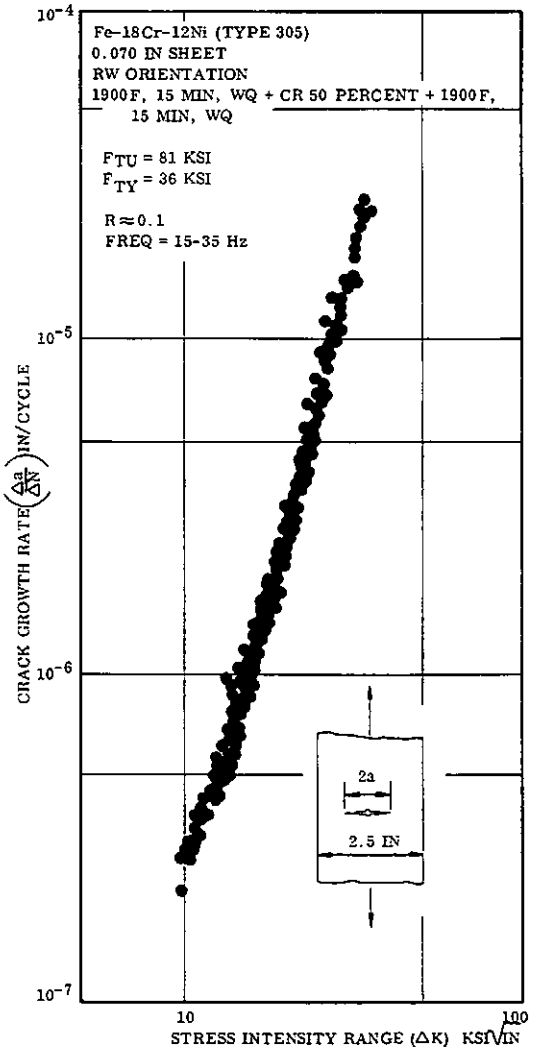


FIG. 3.051 FATIGUE CRACK GROWTH IN ANNEALED SHEET (LONGITUDINAL OR RW ORIENTATION). (23)

	Fe
18	Cr
12	Ni

TYPE 305

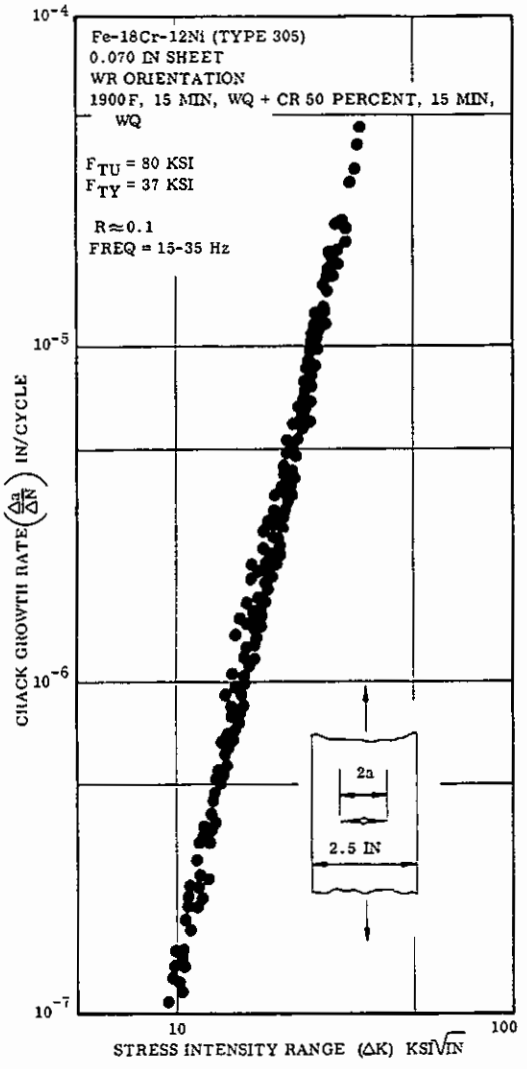


FIG. 3.052 FATIGUE CRACK GROWTH IN ANNEALED SHEET (TRANSVERSE OF WR ORIENTATION). (23)

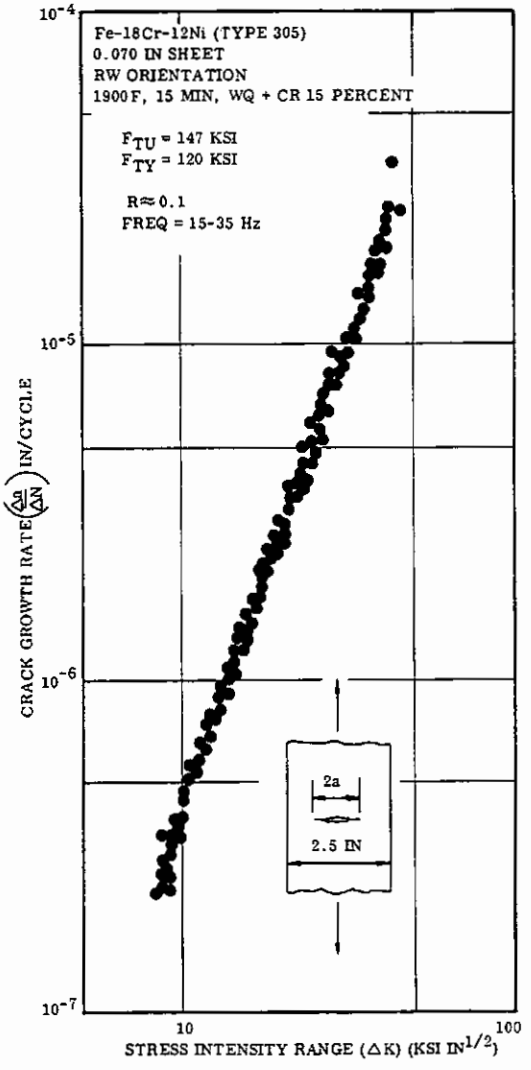


FIG. 3.053 FATIGUE CRACK GROWTH IN COLD ROLLED SHEET (LONGITUDINAL OR RW ORIENTATION). (23)

	Fe
18	Cr
12	Ni

TYPE 305

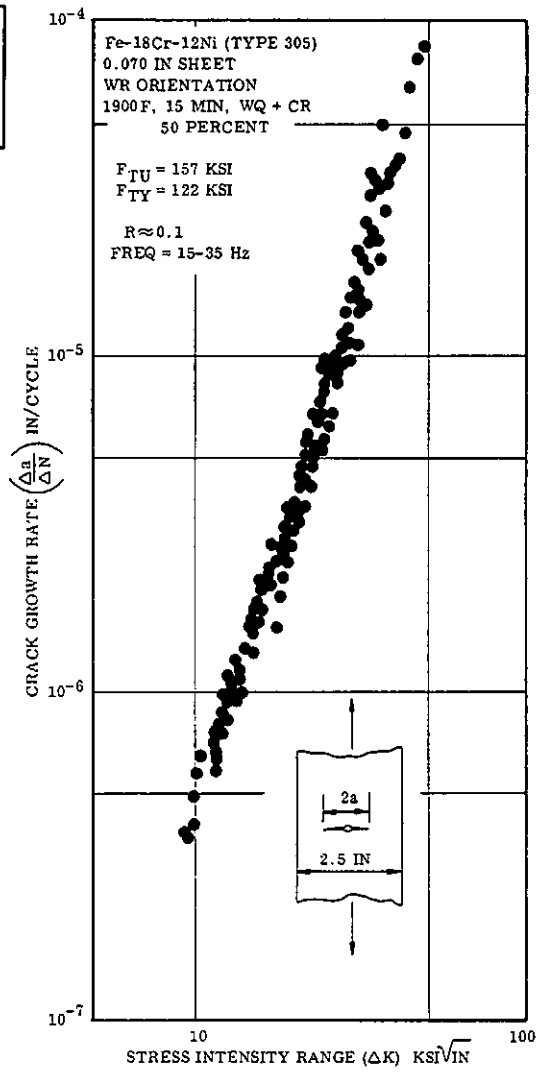


FIG. 3.054 FATIGUE CRACK GROWTH IN COLD ROLLED SHEET (TRANSVERSE OR WR ORIENTATION). (23)

REFERENCES

1. AMS 5514A, Plate, Sheet and Strip - 18Cr-11Ni, Deep Drawing and Spinning (February 15, 1952).
2. AMS 5685D, Wire, Safety - 18Cr-11.5Ni, Solution Heat Treated (May 1, 1968).
3. AMS 5686A, Wire, Riveting - 18Cr-11Ni, Solution Heat Treated (February 15, 1952).
4. ASTM A167-63, Standard Specification for Corrosion-Resisting Chromium-Nickel Steel Plate, Sheet, and Strip (September 30, 1963).
5. ASTM A240-67, Standard Specification for Chromium and Chromium-Nickel Stainless Steel Plate, Sheet, and Strip for Fusion-Welded Unfired Pressure Vessels (December 12, 1967).
6. ASTM A276-67, Standard Specification for Stainless and Heat-Resisting Steel Bars and Shapes (December 12, 1967).
7. ASTM A314-63, Standard Specification for Stainless and Heat-Resisting Steel Billets and Bars for Forging (September 30, 1963).
8. ASTM A473-63, Standard Specification for Stainless and Heat-Resisting Steel Forgings (September 30, 1963).
9. ASTM A249-65, Standard Specification for Welded Austenitic Stainless Steel Boiler, Superheater, Heat-Exchanger, and Condenser Tubes (August 31, 1965).
10. ASTM A478-67, Standard Specification for Chromium-Nickel Stainless and Heat-Resisting Steel Weaving Wires (March 6, 1967).
11. ASTM A492-67, Standard Specification for Stainless and Heat-Resisting Steel Rope Wire (March 6, 1967).
12. ASTM A493-68, Standard Specification for Stainless and Heat-Resisting Steel for Cold Heading and Cold Forging - Bar and Wire (February 14, 1968).
13. ASTM A580-67, Standard Specification for Stainless and Heat-Resisting Steel Wire (December 12, 1967).
14. American Iron and Steel Institute, "Stainless and Heat Resisting Steels - Type 305," Steel Products Manual (June 1957).
15. Kiss, L., Allegheny Ludlum Industries, "Personal Communication to W. F. Brown, Jr." (September 18, 1970).
16. Republic Steel Corporation, "Republic ENDURO Stainless Steel - Chromium-Nickel Types, 300 Series," Adv 1124R4-15M-3-66 (1966).
17. Walter, R. J., Jewett, R. P. and Chandler, W. T., "On the Mechanism of Hydrogen-environment Embrittlement of Iron- and Nickel-base Alloys," Materials Science and Engineering, 5 (1969/70) pp. 98-110.
18. Wilson, J. C. and Berggren, R. G., "Effects of Neutron Irradiation in Steel," Proc. ASTM, 55 (1955) p. 689.
19. Allegheny Ludlum (1959).
20. American Iron and Steel Institute, "Stainless and Heat Resisting Steels - Type 305," Steel Products Manual (June 1957).
21. Allegheny Ludlum Steel Corporation, "Allegheny Metal 18-8," Allegheny Ludlum Blue Sheets (1948).
22. Kiss, L., Allegheny Ludlum Industries, "Private Communication to W. F. Brown, Jr.," (September 11, 1970).
23. Weber, J. H., Jr., "Effects of Crystallography and Thermo-Mechanical Treatment on Fatigue Crack Propagation," Ph.D. Dissertation, Lehigh University (1969).
24. Post, C. B. and Eberly, W. S., "Stability of Austenite in Stainless Steels," Trans. ASM, Volume 39 (1947) p. 868.
25. Chromium-Nickel Stainless Steel Data, Section 1, Bulletin A, International Nickel Company, New York, New York (1963).

Fe
25 Cr
20 Ni

Types 310, 310 S, CK-20, & HK

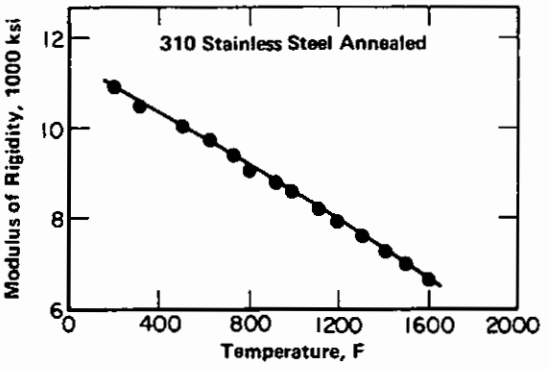


FIGURE 3.063. MODULUS OF RIGIDITY AT ELEVATED TEMPERATURES (34)

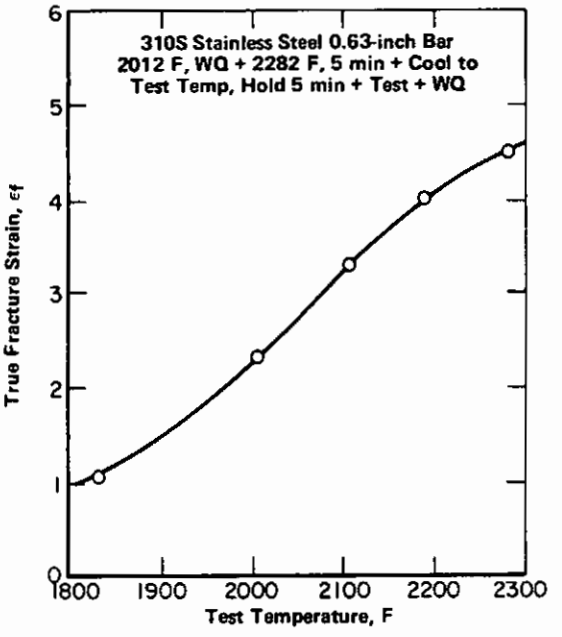


FIGURE 4.013. EFFECT OF TEST TEMPERATURE ON TRUE FRACTURE STRAIN OF 310S BAR COOLED FROM 2282 F TO TEST TEMPERATURE (59)

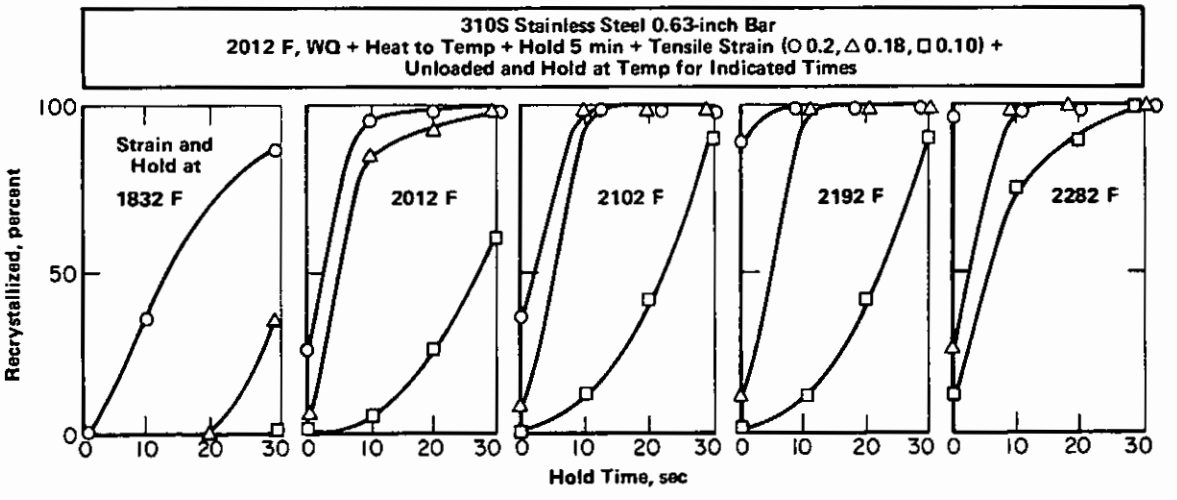


FIGURE 4.014. STATIC RECRYSTALLIZATION OF 310S BAR FOLLOWING TENSILE STRAIN AT VARIOUS TEMPERATURES (59)

	Fe
25	Cr
20	Ni
2	Si

Type 314

1 **GENERAL**

This non-heat treatable stainless steel is generally used in the annealed condition. In this condition it possesses excellent general corrosion resistance and has the highest resistance to scaling and carburization of any of the austenitic Cr-Ni alloys. It is used primarily for parts and welded assemblies requiring both corrosion and oxidation resistance up to 2000 F. Its high silicon content improves corrosion resistance over other austenitic Cr-Ni steels, but with some sacrifice in ductility and weldability. This alloy is subject to embrittlement after long-time exposure at 1200 to 1600 F (2, 5, 7).

1.01 **Commercial Designation**

Type 314.

1.02 **Alternate Designations**

SAE 30314 and UNS S31400.

1.03 **Specifications**

1.031 Specifications, Table 1.031.

1.04 **Composition**

1.041 Composition, Table 1.041.

1.05 **Heat Treatment**

1.051 Anneal (solution treat) 1900 to 2100 F, rapid air cooling (sheet and light plates) or water quench (heavier sections) (5, 7).

1.052 Final anneal at 1900 F, minimum, is recommended to relieve strain and achieve best corrosion resistance and high temperature properties (5).

1.06 **Hardness**

1.061 Alloy is normally strengthened by cold work. (See Figure 3.0212 and Section 3.043.)

1.062 Aging at 1650 F with or without prior cold work causes a hardness peak after about 300 hours. A milder peak occurs after aging at 1740 F for 1 to 10 hours, shown in Figure 1.063. These hardness increases are attributed to precipitation of fine acicular particles within the matrix and coarser particles at the grain boundaries. The precipitate is an intermetallic compound containing approximately 35Cr, 47Fe, and 18Ni, presumably sigma phase. The amount of $M_{23}C_6$ carbide precipitate also increases during aging (8).

1.063 Room temperature hardness of cold worked and annealed alloy, Figure 1.063 [(a) 1650 F and (b) 1740 F].

1.07 **Forms and Conditions Available**

1.071 The alloy is available in bar, sheet, strip, plate, tubing and wire (7).

1.08 **Melting and Casting Practice**

Electric furnace melt.

1.09 **Special Considerations**

Prolonged exposure at 1200 to 1600 F may cause embrittlement through carbide precipitation and sigma phase formation. Ductility may be restored by annealing at 1900 to 1950 F for 10 to 60 minutes. This treatment is recommended after 1000-hr exposure at 1400 to 1600 F (5, 7).

2 **PHYSICAL PROPERTIES AND CHEMICAL PROPERTIES**

2.01 **Thermal Properties**

2.011 Melting range, 2500 to 2600 F (5).

2.012 Phase changes, none.

2.0121 Time-temperature-transformation diagrams.

2.013 Thermal conductivity, Table 2.013.

2.014 Thermal expansion, Figure 2.014.

2.015 Specific heat, 0.12 Btu/lb F, 32 to 212 F (5, 7).

2.016 Thermal diffusivity.

2.02 **Other Physical Properties**

2.021 Density, 0.279 lb/in.^{3}, 7.72 g/cm^3 (5, 7).

2.022 Electrical resistivity, 30.31 microhm-in. at 68 F (7).

2.023 Magnetic properties. Alloy is nonmagnetic.

2.024 Emittance.

2.025 Damping capacity.

2.03 **Chemical Properties**

2.031 Corrosion.

2.0311 This alloy has excellent general corrosion resistance, comparable to 18 Cr-8 Ni austenitic stainless steels. It is slightly inferior to Type 310 under wet corrosion conditions (7).

2.0312 Type 314 exhibits good resistance to fuming nitric acid at room temperature and to fused nitrates up to 800 F (7).

2.0313 This alloy is particularly recommended for handling SO_2 gas, but is inferior to Type 311 where a high percentage of SO_3 is present (5).

2.032 Oxidation.

2.0321 Type 314 has the highest scale resistance of any of the austenitic Cr-Ni stainless steels, because of its high silicon content and lower coefficient of expansion, tending to form a more tightly adherent film, particularly in the range 1200 to 1600 F (5, 7).

2.0322 Recommended maximum operating temperatures are 1900 F for intermittent service and 2100 F for continuous service (7).

2.033 Carburization.

2.0331 Type 314 has good resistance to carburization in high temperature carbonaceous atmospheres relative to other austenitic stainless steels. This behavior is attributed to its high silicon content, which causes a dramatic decrease in the amount of carbon absorbed. The weight gain behavior of electropolished Type 314 in hydrogen-methane gas mixtures, shown in Figure 2.0332, is approximately parabolic, indicating a diffusion-controlled reaction. The uptake of carbon after 100 hours at 1830 F under these conditions is large, as seen from the concentration profile in Figure 2.0333. Oxidation of the alloy to form a continuous Cr_2O_3 surface scale can be induced by the presence of water vapor in the gas stream; this minimizes carburization and accompanying deleterious effects on mechanical properties up to exposure temperatures of about 1700 F (9).

2.0332 Carburization weight gain of Type 314 in hydrogen-methane gas at elevated temperatures, Figure 2.0332.

2.0333 Carbon concentration profile through thickness of specimen after exposure to hydrogen-methane gas mixture for 100 hours at 1830 F, Figure 2.0333.

2.04 **Nuclear Properties**

Fe
25 Cr
20 Ni
2 Si

Type 314

3 MECHANICAL PROPERTIES

3.01 Specified Mechanical Properties

3.011 AMS specified mechanical properties at room temperature, Table 3.011.

3.02 Mechanical Properties at Room Temperature

3.021 Tension—stress-strain diagrams—tension properties.

3.0211 Typical mechanical properties for bar, plate, sheet, and wire, Table 3.0211.

3.0212 Effect of cold work on room temperature properties of bar, Figure 3.0212.

3.0213 Effect of long-time exposure at elevated temperatures on room temperature elongation of annealed alloy, Figure 3.0213.

3.022 Compression—stress-strain diagrams—compression properties.

3.023 Impact.

3.024 Bending.

3.025 Torsion and shear.

3.026 Bearing.

3.027 Stress concentration.

3.0271 Notch properties.

3.0272 Fracture toughness.

3.028 Combined properties.

3.03 Mechanical Properties at Various Temperatures

3.031 Tension—stress-strain properties—tension properties.

3.0311 Short time tension properties of annealed bar and sheet at elevated temperatures, Figure 3.0311.

3.032 Compression—stress-strain diagrams—compression properties.

3.033 Impact.

3.034 Bending.

3.035 Torsion and shear.

3.036 Bearing.

3.037 Stress concentration.

3.0371 Notch properties.

3.0372 Fracture toughness.

3.038 Combined properties.

3.04 Creep and Creep-Rupture Properties

3.041 Creep rupture strength at 1200 to 1800 F, Figure 3.041.

3.042 Creep curves for annealed sheet at 1200 to 1800 F, Figure 3.042.

3.043 Prior cold work usually lowers the minimum creep rate of steel provided that substantial recovery does not take place and the creep temperature does not exceed the recrystallization temperature for the particular degree of cold work. As shown in Figure 3.044, the introduction of 14 percent cold work improves the creep strength of Type 314 at 1650 F at creep rates faster than 10^{-3} percent per hour and at 1740 F at creep rates faster than 10^{-2} percent per hour. These improvements are attributed to an increase in the density of "free" dislocations, i.e., those not comprising subgrain boundaries. The increase in free dislocation density is temporary since dislocations are annealed out at long times and high temperatures. The creep rates then approximate those of the unpredeformed alloy. Sigma phase also precipitates during creep but does not affect the creep rate (8).

3.044 Effect of prior cold work on creep properties of Type 314 at elevated temperatures, Figure 3.044 [(a) 1650 F and (b) 1740 F].

3.05 Fatigue Properties

3.06 Elastic Properties

3.061 Poisson's ratio.

3.062 Modulus of elasticity, 29,000 ksi at room temperature (4, 5).

3.063 Modulus of rigidity.

3.064 Tangent modulus.

3.065 Secant modulus.

4 FABRICATION

4.01 Forming

4.011 An anneal prior to forming operations is recommended since the alloy is susceptible to work hardening.

4.012 Forging. Starting temperature at 1900 to 2050 F, maximum, finishing temperature at 1700 F, minimum. For upset forgings, work should be finished between 1700 and 1850 F (5, 6).

4.02 Machining and Grinding

4.021 General. Because of work hardening the feed should be as heavy as possible in order to obtain a high metal removal at a relatively low surface speed. Sharp tools at all times are necessary. Sulfurized cutting oils diluted with paraffin oil are recommended (5, 7).

4.03 Joining

4.031 General. The alloy can be welded by gas or arc methods without the use of pre- or postheat. However, annealing is recommended after welding for maximum corrosion resistance (7).

4.032 Type 310 electrodes are recommended (5).

4.04 Surface Treating

REFERENCES

1 AMS 5522D (January 15, 1978).

2 AMS 5652D (October 15, 1980).

3 "Elevated Temperature Properties of Stainless Steels", ASTM S. T. P. No. 124 (January 1952).

4 "Physical and Mechanical Properties of Some High-Strength Fine Wires", DMIC Memo 80 (January 20, 1961).

5 Crucible Steel Co. of America, "Crucible 314 Stainless Steel", Data Sheet, 4th Revision (February 1959).

6 Wyman-Gordon Co., "Forging Temperature for Stainless Steels and High Temperature Alloys", Data Sheets (January 19, 1959).

7 Alloy Digest, "AISI Type 314", Filing Code: SS-100, Stainless Steel (February 1960).

8 Adelus, J. L., and Guttmann, V., "Effect of Prior Cold Working on the Creep of 314 Alloy Steel", *Materials Science and Engineering*, Vol. 44, No. 2 (July 1980), pp 195-204.

9 Harrison, J. M., Norton, J. F., Derricott, R., and Marriott, J. B., "The Gaseous Carburisation of Austenitic Stainless Steels", *Materials and Corrosion*, Vol. 30, No. 11 (November 1979), pp 785-794.

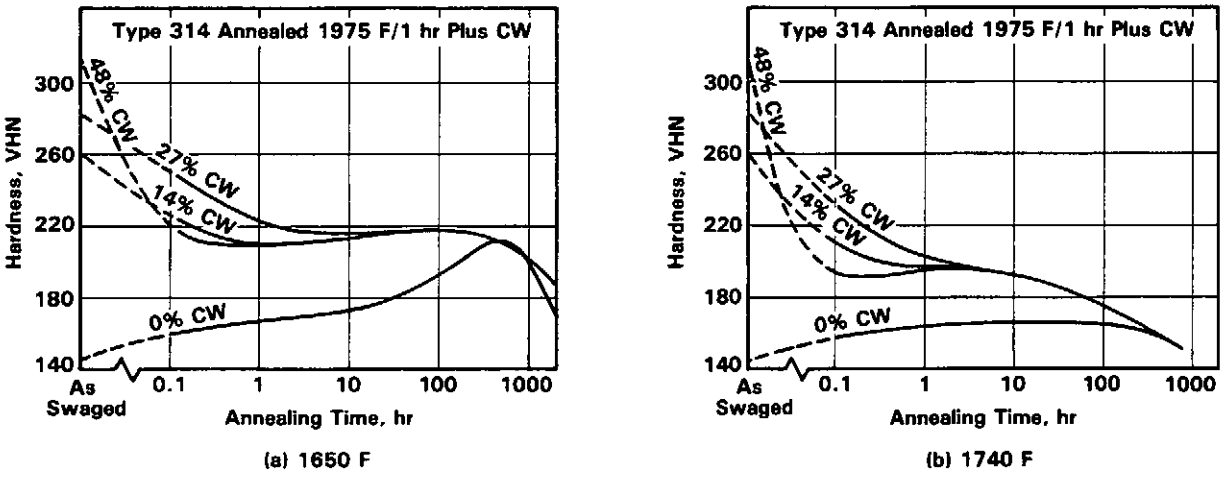
AMS	Form	Military
5652D	Bar, forgings, flash welded rings, mechanical tubing	—
5522D	Plate, sheet, strip	—

TABLE 1.031. SPECIFICATIONS

Type 314				
Specification	AMS 5522D		AMS 5652D	
	Percent		Percent	
Element	Min	Max	Min	Max
Chromium	23.00	25.00	23.00	25.00
Nickel	19.00	22.00	19.00	22.00
Silicon	1.70	2.30	1.50	2.30
Manganese	1.00	2.00	1.00	2.00
Molybdenum	—	0.75	—	0.75
Copper	—	0.50	—	0.50
Carbon	—	0.12	—	0.18
Phosphorus	—	0.040	—	0.040
Sulfur	—	0.030	—	0.030

TABLE 1.041. COMPOSITION (1, 2)

Fe
25 Cr
20 Ni
2 Si
Type 314



(a) 1650 F

(b) 1740 F

FIGURE 1.063. ROOM TEMPERATURE HARDNESS OF COLD WORKED AND ANNEALED ALLOY (8)

Alloy	Type 314
Temp, F	Btu/ft/hr ft² F
212	10.1
932	12.1

TABLE 2.013. THERMAL CONDUCTIVITY (7)

Fe
25 Cr
20 Ni
2 Si

Type 314

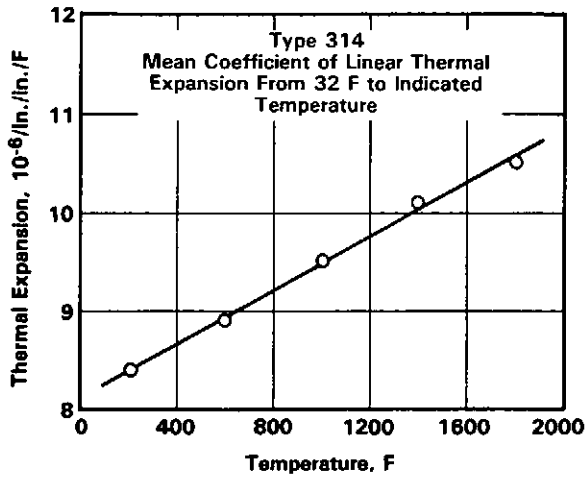


FIGURE 2.014. THERMAL EXPANSION (3)

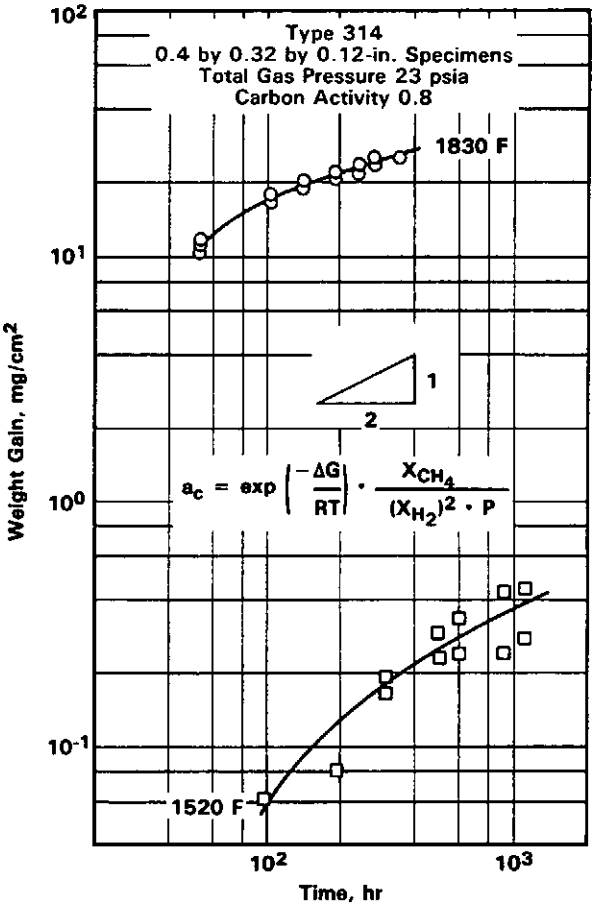


FIGURE 2.0332. CARBURIZATION WEIGHT GAIN OF TYPE 314 IN HYDROGEN-METHANE GAS AT ELEVATED TEMPERATURES (9)

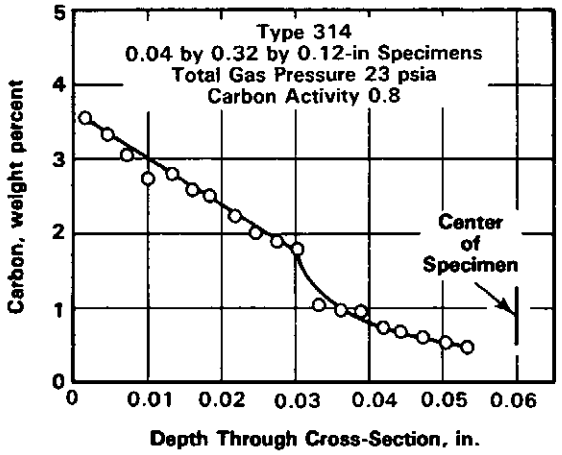


FIGURE 2.0333. CARBON CONCENTRATION PROFILE THROUGH THICKNESS OF SPECIMEN AFTER EXPOSURE TO HYDROGEN-METHANE GAS MIXTURE FOR 100 HOURS AT 1830 F (9)

Fe
25 Cr
20 Ni
2 Si

Type 314

Type 314									
AMS Spec	Product Form	Metallurgical Condition[a]	Thickness, in.	F_{tu}, ksi, Max	Hardness		Bending		
					Min	Max	Type of Bend	Angle, deg, Min	Bend Factor
5522D	Sheet, Strip	CR, SHT	All	—	70 HRB	90 HRB	—	—	—
	Plate	HR, SHT	≤0.249	—	—	—	Free bend	180	1
			≤0.249	—	—	—	V-block	135	1
			>0.249, ≤0.749	—	—	—	Free bend	90	1
			>0.249, ≤0.749	—	—	—	V-block	135	2
5652D	Bars	SHT, CF	≤2.75 dia	—	—	229 BHN	—	—	—
	Bars	SHT, HF	>2.75 dia	—	—	187 BHN	—	—	—
	Forgings	Not Spec.	—	—	—	187 BHN	—	—	—
	Mechanical Tubing	SHT, CF	—	—	—	90 HRB	—	—	—
	Wire	SHT, CF	—	125[b]	—	—	—	—	—

Note: The original AMS documents should be consulted for complete specification details.

(a) SHT = solution heat treated; CR = cold rolled; HR = hot rolled; CF = cold finished; HF = hot finished.
(b) Specified tensile strength or equivalent hardness.

TABLE 3.011. AMS SPECIFIED MECHANICAL PROPERTIES AT ROOM TEMPERATURE (1, 2)

Alloy	Type 314				
Form	Bar	Plate	Sheet	Wire	
Condition	Ann				Hard Drawn
Thickness, in.	1 Dia			0.002 to 0.010	0.002 to 0.010
F_{tu}, ksi	100	100	100	95 to 130	245 to 275
F_{ty}, ksi	50	50	50	35 to 70	230 to 260
e (2 in.), percent	45	45	40	60 Max	1 to 2
RA, percent	60	60	—	—	—
Hardness, HRB	89	89	85	—	—

TABLE 3.0211. TYPICAL MECHANICAL PROPERTIES FOR BAR, PLATE, SHEET, AND WIRE (4, 5)

Fe
25 Cr
20 Ni
2 Si

Type 314

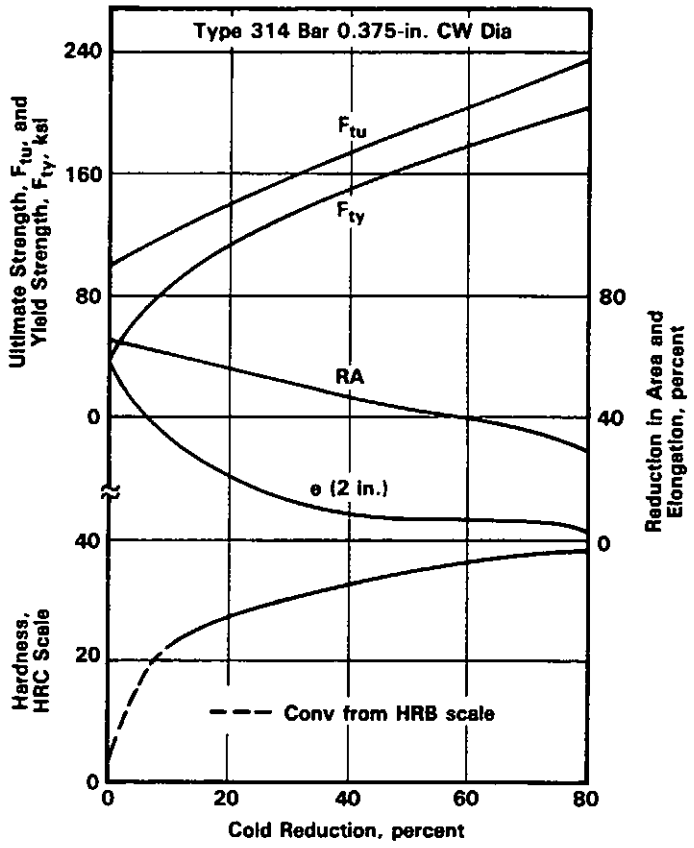


FIGURE 3.0212. EFFECT OF COLD WORK ON ROOM TEMPERATURE PROPERTIES OF BAR (5)

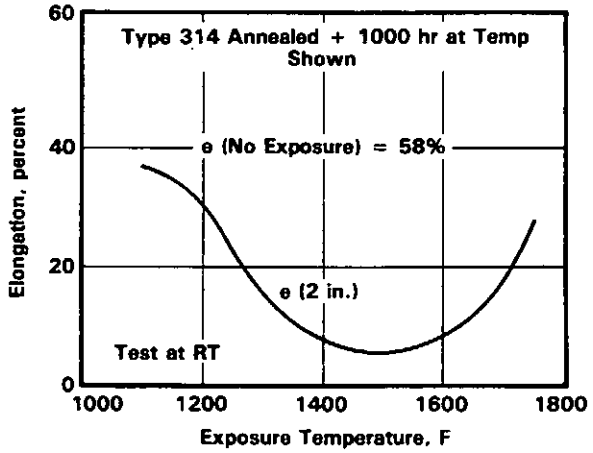


FIGURE 3.0213. EFFECT OF LONG-TIME EXPOSURE AT ELEVATED TEMPERATURES ON ROOM TEMPERATURE ELONGATION OF ANNEALED ALLOY (5)

Fe
25 Cr
20 Ni
2 Si

Type 314

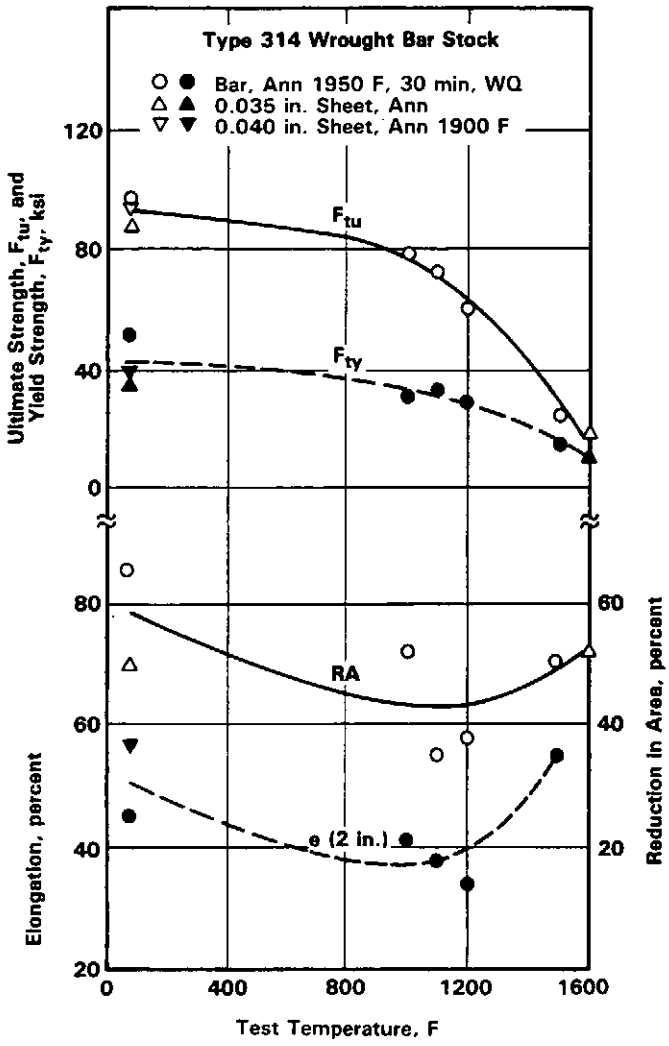


FIGURE 3.0311. SHORT-TIME TENSION PROPERTIES OF ANNEALED BAR AND SHEET AT ELEVATED TEMPERATURES (3)

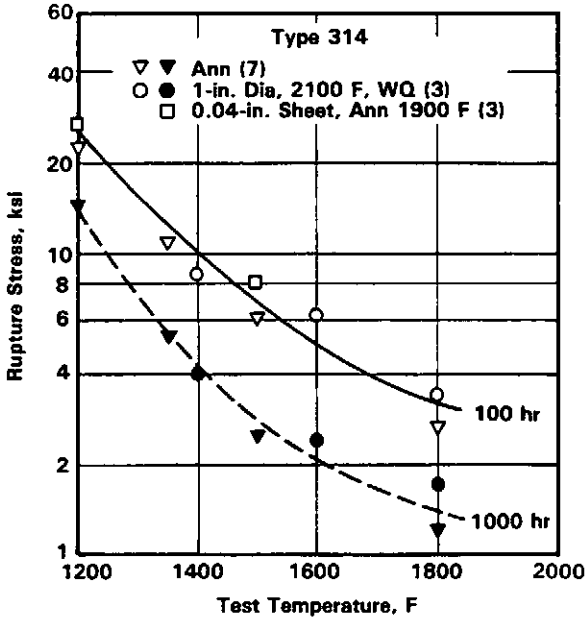


FIGURE 3.041. CREEP RUPTURE STRENGTH AT 1200 TO 1800 F (3, 7)

Fe
25 Cr
20 Ni
2 Si

Type 314

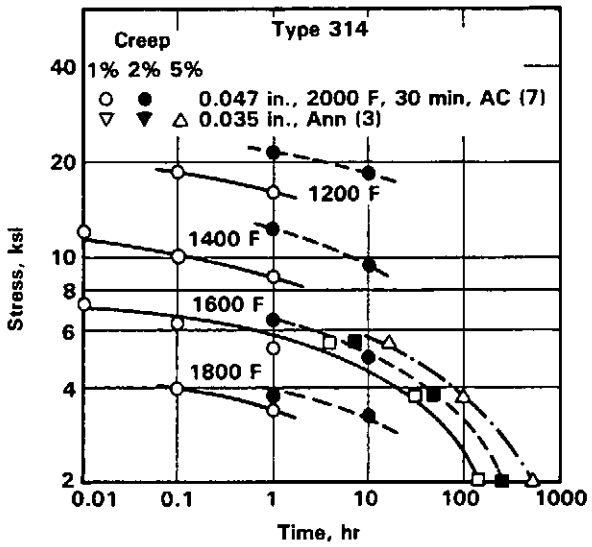
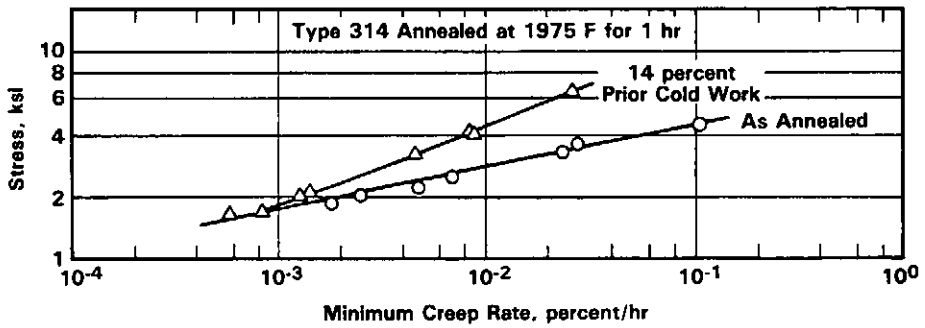
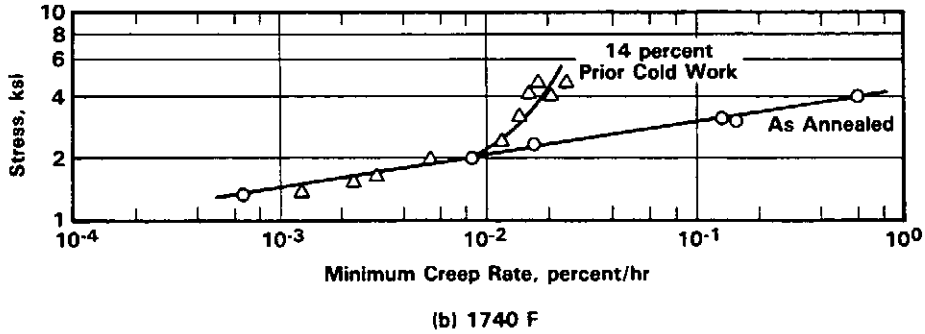


FIGURE 3.042. CREEP CURVES FOR ANNEALED SHEET AT 1200 TO 1800 F (3, 7)



(a) 1650 F



(b) 1740 F

FIGURE 3.044. EFFECT OF PRIOR COLD WORK ON CREEP PROPERTIES OF TYPE 314 AT ELEVATED TEMPERATURES (8)

Fe
18 Cr
13 Ni
+ Mo

Type 316
Type 317

1 GENERAL

Types 316 and 317 are austenitic stainless steels which contain molybdenum for improved corrosion resistance and increased high-temperature strength. Type 316 contains 2 to 3 percent molybdenum and is widely used because of its good resistance to pitting corrosion. Type 317 contains 3 to 4 percent molybdenum and is superior to Type 316 in corrosion resistance and high-temperature strength but is less widely used. Both alloys retain usable strength and oxidation resistance at temperatures up to 1500 F. They are, however, susceptible to carbide precipitation and accompanying sensitization to intergranular corrosion if heated in or slowly through the temperature range 1000 to 1500 F. The low-carbon modifications 316L and 317L are recommended when exposure in this temperature range is required, although the lower carbon content results in lower strength. These alloys are strengthened only by cold work; they are not amenable to strengthening by heat treatment.

In cast form, Type 316 is generally designated CF3M and CF8M, corresponding to carbon contents of 0.03 and 0.08 percent, respectively. The wrought and cast forms are readily weldable, and the wrought forms have good formability in the annealed condition. These alloys are used in various jet-engine parts, exhaust manifolds, heat exchangers, chemical processing equipment, furnace parts, and orthopedic implants (20,30,39).

1.01 Commercial Designations

1.011 Wrought form: Types 316, 316L, 317, 317L.

1.012 Cast form: CF3M, CF8M.

1.02 Alternate Designations

UNS J92810, UNS J92900, UNS J92910, UNS S31600, UNS S31609, UNS J92800, UNS S31603, UNS J93000, UNS S31700, UNS S31703.

1.03 Specifications

1.031 AMS specifications, Table 1.031.

1.04 Composition

1.041 Composition specifications for wrought types 316, 316L, 317, and 317L, Table 1.041.

1.042 Composition specifications for cast Type 316, Table 1.042.

1.043 For effects of specific elements and compositional modifications on properties, see paragraphs 2.01215, 3.03121, 3.03122, 3.0424, 3.0519, 4.014, and 4.0314.

1.05 Heat Treatment

1.051 Annealing is the only heat treatment generally applied to these alloys. The annealing treatment produces maximum formability and corrosion resistance; it can also be used to redissolve intergranular carbides (39,42).

1.052 Wrought products are annealed by heating to the range 1900 to 2150 F and cooling rapidly. Thin sections such as strip may be air cooled, whereas heavier sections, such as forgings, should be water quenched in order to avoid excessive carbide precipitation in the range of about 900 to 1600 F. The rate of cooling is not critical for Types 316L and 317L (38,39,41,42).

1.053 Castings of the CF8M composition should be annealed in the temperature range 1950 to 2150 F followed by water quenching; the CF3M composition may be air cooled rather than water quenched (33).

1.06 Hardness

1.061 Effect of exposures to elevated temperatures on room-temperature hardness, Figure 1.061.

1.062 Hardness of annealed castings, BHN 156 to 170 (33).

1.063 Effect of cold straining on hardness, Figure 1.063.

1.064 Effect of grain size on hardness, Figure 1.064.

1.07 Forms and Conditions Available

1.071 Wrought products are available in the full range of sizes and forms including plate, sheet, strip, bar, forgings, tubing, and wire. Most products are available in both the annealed and cold-worked conditions (20,38,39).

1.072 Sand, centrifugal, and investment castings are available in the as-cast and annealed conditions (33).

1.08 Melting and Casting Practice

1.081 The alloys are generally air melted in electric-arc furnaces with subsequent vacuum refining/degassing and/or argon-oxygen decarburization. Close chemistry control for special applications is provided by vacuum-induction melting. Remelting by vacuum-arc or electroslag processes is also utilized to improve cleanliness and chemical and microstructural homogeneity where required (53).

1.09 Special Considerations

1.091 Intergranular carbide precipitates, which occur when the Types 316, 317, and CF8M grades are exposed to temperatures from 1000 to 1500 F, are detrimental to corrosion resistance; therefore, it is important that the low-carbon grades, Types 316L, 317L, and CF3M be used when such exposures are unavoidable. See Figures 3.0231 and 3.0232 and paragraph 2.0321.

1.092 In addition to carbide precipitation and accompanying corrosion sensitization, Types 316 and 317 are subject to precipitation of embrittling intermetallics during long-time aging in the 1000 to 1500 F temperature range. These phases include primarily sigma, chi, and eta intermetallics. The brittleness of the precipitated phases reduces the toughness of the alloy. Additionally, loss of molybdenum from the alloy matrix reduces creep strength. See paragraphs 2.01211, 3.0231, 3.0232, and 3.0420.

1.093 The delta ferrite phase, which is incorporated into welds to reduce hot cracking, is metastable and transforms into brittle intermetallics on aging at intermediate temperatures. Precautions should be taken if welded components are to be exposed for long times in the temperature range 1100 to 1700 F. See paragraph 4.038.

1.094 Trace amounts of lead, tellurium, and bismuth reduce hot fabricability. Contents of these elements

Fe
18 Cr
13 Ni
+ Mo

Type 316
Type 317

must be kept at very low levels to allow high fabrication yields. See paragraph 4.014.

1.095 Prolonged heating above 2000 F causes excessive grain growth.

1.0951 Effect of time and temperature on grain growth, Figure 1.0951.

2 PHYSICAL PROPERTIES AND ENVIRONMENTAL EFFECTS

2.01 Thermal Properties

2.011 Melting range, 2500 to 2550 F (38).

2.012 Phase changes.

2.0121 Time-temperature-transformation diagrams.

2.01211 The major precipitates occurring in Type 316 steel are $M_{23}C_6$, chi, eta, and sigma phases. The precipitation reactions at elevated temperatures in this metastable alloy are extremely complex and are influenced by such factors as composition, temperature, and thermomechanical pretreatment: Figure 2.01212 shows the time-temperature-precipitation (TTP) diagram for a medium-carbon heat of Type 316.

$M_{23}C_6$ is usually the first precipitate phase to form. The chemical formula, based on analyses of extracted precipitate, is approximately $(Cr_{16}Fe_5Mo_2)C_6$. Other metallic elements such as tungsten, vanadium, and manganese, are substitutionally soluble in $M_{23}C_6$. Boron and nitrogen can also partially substitute for carbon. Precipitation of $M_{23}C_6$ occurs first at grain bounaries, then on incoherent twin boundaries and coherent twin boundaries and, finally, on dislocations. The rate-controlling reaction for coarsening of $M_{23}C_6$ precipitate is thought to be substitutional diffusion of either chromium or iron. The precipitation kinetics of $M_{23}C_6$ follow the Johnson-Mehl reaction:

$$(w/w_{tot}) = 1 - e^{-(t/t_o)^n}$$

where w = weight percent of precipitate, w_{tot} = weight percent of precipitate at saturation, t_o = characteristic time, and n = a constant approximately equal to unity for the data shown in Figure 2.01213. With n = 1, this relation reduces to a simple exponential-decay law similar to that encountered in radioactive decay. It suggests that the rate of formation of carbide in Type 316 steel is directly proportional to the amount of carbon in solution at a given time.

The chi phase, which precipitates later, has a typical composition of $Fe_{36}Cr_{12}Mo_{10}$, but possesses an appreciable composition range with a high tolerance for metal interchange. The nucleation sites for chi phase are grain boundaries, incoherent twin boundaries, and intragranular dislocations. The precipitation kinetics are shown in Figure 2.01214.

Eta or Laves phase in Type 316 has the composition Fe_2Mo. This phase has a small homogeneity range and usually appears as intragranular particles. Sigma phase has a broad homogeneity range and the composition and temperature range of stability vary in different alloy systems. The nucleation of sigma phase requires high-energy interfaces, such as large-angle grain boundaries, incoherent twin boundaries, or high-energy interfaces with second phases such as oxide inclusions. At long aging times, sigma can form at previous $M_{23}C_6$ sites or can grow on $M_{23}C_6$ particles which apparently are dissolving. The composition of sigma phase precipitating in Type 316 can be expressed by the formula $(CrMo)_{35}(FeNi)_{65}$. The exact composition is temperature dependent, with molybdenum and iron contents increasing and chromium and nickel contents decreasing with increasing temperature.

The effect of cold work on aging is to shift the TTP diagram to shorter times and lower temperatures. The formation of $M_{23}C_6$ and sigma is markedly accelerated, while the formation of eta phase is accelerated to a smaller extent. The precipitation of sigma is also enhanced during recrystallization (54–56).

2.01212 Time-temperature-precipitation diagram, Figure 2.01212.

2.01213 Effect of aging time on amount of $M_{23}C_6$ precipitate at 1160 F, Figure 2.01213.

2.01214 Effects of aging conditions on amount of chi-phase precipitate, Figure 2.01214.

2.01215 Modification of Type 316 by the addition of titanium, which is of interest for improvement of post-irradiation ductility, promotes formation of additional precipitates of TiC, TiN, and $Ti_4C_2S_2$. The time-temperature-precipitation diagrams for annealed and cold-worked alloy are shown in Figures 2.01216 (a) and (b), respectively. As seen by comparison with the diagram for Standard Type 316 in Figure 2.01212, formation of $M_{23}C_6$ is substantially delayed in the annealed modified alloy. Cold work accelerates the precipitation of both $M_{23}C_6$ and sigma phases by about one hundredfold. The amount of precipitate, equated to the amount of electrolytically extracted residue, increases greatly with cold work, particularly at 1400 F, as shown in Figure 2.01217 (57).

2.01216 Effects of titanium addition and cold work on time-temperature-precipitation diagram, Figure 2.01216, (a) annealed, and (b) cold worked 40 percent.

2.01217 Effects of cold work and aging temperature on amount of precipitate, Figure 2.01217.

2.0122 The solubility of carbon in Type 316 steel from 1280 to 2040 F is given by:

$$\log (C) = 7.771 - [11290/(T + 460)]$$

where C is carbon solubility in weight parts per million and T is temperature in degrees F (54).

2.013 Thermal conductivity, Figure 2.013.

2.014 Thermal expansion, Figure 2.014.

2.015 Specific heat, Figure 2.015.

2.016 Thermal diffusivity, Figure 2.016.

2.02 Other Physical Properties

Fe
18 Cr
13 Ni
+ Mo

Type 316
Type 317

2.021 Density, 0.29 lb/in.^{3} (38,39,41); 8.03 gr/cm^3 (41).

2.0211 Effect of temperature on density, Figure 2.0211.

2.022 Electrical properties.

2.0221 Electrical properties of annealed alloy, Table 2.0221.

2.0222 Electrical resistivity, Figure 2.0222.

2.0223 Electrical resistivity at cryogenic temperatures, Figure 2.0223.

2.023 Magnetic properties.

2.0231 The wrought alloys are practically nonmagnetic in the annealed condition; the maximum permeability is 1.02. Cold work induces a slight amount of magnetic permeability, which varies with the amount of cold work and the composition (20).

2.0232 Castings are usually slightly magnetic, with permeability between 1.5 and 2.5, but nonmagnetic castings can be produced by careful balancing of the composition.

2.024 Emittance.

2.0241 Normal spectral emittance at various wavelengths at room and elevated temperature, Figure 2.0241.

2.0242 Effects of temperature and preoxidation on emittance, Figure 2.0242.

2.025 Damping capacity.

2.03 **Chemical Environments**

2.031 General corrosion.

2.0311 These molybdenum-bearing stainless steels are more corrosion resistant than unmodified chromium-nickel grades in the atmosphere and in sulfuric acid, especially dilute solutions at temperatures up to 150 F. They are also more resistant to pitting and pinhole corrosion in acetic, phosphoric, formic, and tartaric acids and in solutions of chlorides, bromides, and iodides (20,39).

2.0312 In certain oxidizing acids, for example nitric acid, these grades are less resistant than the regular chromium-nickel grades (20.39).

2.0313 In seawater these alloys are highly resistant to stress corrosion, but are somewhat susceptible to pitting, crevice, and tunneling corrosion although less susceptible than the non-molybdenum-bearing grades (16,17).

2.0314 They can be completely protected against seawater corrosion by galvanically coupling to zinc, aluminum, or carbon steel anodes (18).

2.032 Intergranular corrosion.

2.0321 Types 316 and 317 become sensitized to intergranular corrosion on heating in the temperature range 1000 to 1500 F. This exposure causes grain-boundary precipitation of chromium-rich $M_{23}C_6$, with accompanying loss of both chromium and molybdenum from the regions adjacent to the grain boundaries and resultant decrease in the local corrosion resistance. The time-temperature conditions for sensitization, based on subsequent corrosion tests in acidic copper sulfate, are shown in Figure 2.0322. This curve is similar to that for $M_{23}C_6$ precipitation, shown earlier in Figure 2.01212. Sensitization resulting from welding or exposure in the sensitization temperature range can be eliminated by full annealing followed by rapid cooling. This treatment redissolves the carbide precipitate and restores the alloy matrix to its original chromium and molybdenum levels. Alternatively, sensitization can be minimized through the use of Types 316L or 317L. However, even these low-carbon grades become sensitized after very long exposures in the 1000 to 1500 F temperature range (20.61,62).

2.0322 Time-temperature curve for sensitization of Type 316, Figure 2.0322.

2.033 Stress corrosion.

2.0331 Stress-corrosion cracking occurs in Type 316. As shown in Figure 2.0332, cracking occurs in a hot $MgCl_2$ solution at stress-intensity (K_I) factors above a threshold value of about 12 ksi $\sqrt{in.}$ Three successive regions of crack growth are apparent with increasing K_I. Region I shows sharply increasing crack-growth rate with increasing K_I, region II shows constant crack-growth rate with increasing K_I, and region III again shows crack-growth rate dependent on K_I. Increasing cold work and increasing exposure temperature both tend to increase the crack-growth rate. The relative proportions of intergranular and transgranular cracking are dependent on the level of K_I, with intergranular cracking increasing with increasing K_I (63,64).

2.0332 Effects of cold work and exposure temperature on stress-corrosion crack-growth rate in hot $MgCl_2$ solution, Figure 2.0332.

2.0333 In stress corrosion in boiling $MgCl_2$, the time to failure at a constant initial stress of 16.2 ksi first decreases and then increases with increasing cold work, as shown in Figure 2.0334. At initial stresses corresponding to 40 percent of the yield strength for each cold-work condition, the time to failure initially decreases with increasing cold work and then remains approximately flat. Stress-corrosion cracking initiates in the transgranular mode, but subsequent propagation is intergranular (65).

2.0334 Effects of cold work on stress-corrosion time to failure in boiling $MgCl_2$ solution, Figure 2.0334.

2.034 Oxidation.

2.0341 Types 316 and 317 have good resistance to oxidation in air at temperatures up to at least 1500 F (30.39).

2.0342 Type 316 oxidizes more rapidly in air at 1740 F than Type 310, but less rapidly than Types 304 and 321, as shown in Figure 2.0343. The scale formed on Type 316 is adherent if the alloy is slow cooled after oxidation, but tends to spall if air cooled or water quenched (not shown). Internal oxidation is noted at grain boundaries, particularly after several cycles of oxidation exposure (66).

2.0343 Oxidation-weight-change behavior of Type 316 in air at 1740 F as compared with Types 304, 310, and 321, Figure 2.0343.

2.0344 Oxidation behavior at 1000 F in 3500-psi supercritical steam, Figure 2.0344.

2.035 Reaction with hydrogen.

2.0351 The hydrogen permeability of Type 316 is 3×10^{-7} cm^2 sec^{-1} atm$^{-1/2}$ at 1400 F. The hydrogen permeability, which is of interest for hot hydrogen-containment applications such as the Stirling engine, can be reduced by a factor of two by doping the hydrogen with 5 volume percent CO. This causes formation of a surface oxide layer which has low permeability for hydrogen (68).

2.036 Liquid-metal corrosion.

2.0361 Corrosion of Types 316 and 316L by static molten lithium at 1000 F in 2500 hours is relatively small

Fe
18 Cr
13 Ni
+ Mo

Type 316
Type 317

(less than 0.4-mil penetration). There is no evidence of cracking on either a macro- or microscopic scale. These steels are adequate long-term containment materials for static molten lithium (69).

2.0362 Type 316 is resistant to corrosion by Pb-17 atomic percent Li at 750 F but not at 930 F (70).

2.04 **Nuclear Environments**

2.041 The effects of neutron-irradiation fluence on tensile yield strength and elongation are shown in Figure 2.042. The yield strength of material irradiated near 700 F exhibits pronounced defect hardening at temperatures up to 1000 F, but this hardening is annealed out at 1400 F. The elongation of the 700 F-irradiated material at temperatures above 700 F is relatively independent of test temperature and decreases with increasing fluence. The yield strength of material irradiated near 1100 F decreases with increasing fluence due to thermal annealing during irradiation. Helium embrittlement causes decreased ductility in 1100 F-irradiated material tested at 1100 F or higher at high fluence levels (71).

2.042 Effect of fluence on tensile yield strength and elongation of cold-worked Type 316 at elevated temperatures, (a) irradiated near 700 F, and (b) irradiated near 1100 F, Figure 2.042.

2.043 Effects of fast-neutron irradiation on yield strength at elevated temperatures, Figure 2.043.

2.044 Neutron irradiation at 1200 F has no significant effect on the fatigue-crack-growth rate of annealed Type 316 in continuous cyclic loading at 1100 or 1200 F, as shown in Figure 2.045. However, in the cold-worked condition, the crack-growth rate is substantially increased by neutron irradiation, as shown in Figure 2.046. The inclusion of a 1- or 2-minute hold time also substantially increases the crack-growth rate of irradiated alloy in both the annealed and cold-worked conditions, as shown in Figures 2.047 and 2.048. The crack-propagation mode of unirradiated materials is primarily transgranular, while an intergranular mode is observed for irradiated materials with increased crack-growth rates (73).

2.045 Effects of fast-neutron irradiation on low-cycle fatigue-crack-growth rate of annealed alloy in air at elevated temperatures, Figure 2.045.

2.046 Effects of fast-neutron irradiation on low-cycle fatigue-crack-growth rate of cold-worked alloy in air at elevated temperatures, Figure 2.046.

2.047 Effects of hold time and fast-neutron irradiation on low-cycle fatigue-crack-growth rate of annealed alloy in air at elevated temperatures, Figure 2.047.

2.048 Effects of hold time and fast-neutron irradiation on low-cycle fatigue-crack-growth rate of cold-worked alloy in air at elevated temperatures, Figure 2.048.

3 MECHANICAL PROPERTIES

3.01 Specified Mechanical Properties

3.011 AMS-specified mechanical properties, Table 3.011.

3.02 Mechanical Properties at Room Temperature

3.021 Tension – stress-strain diagrams – tension properties.

3.0211 Effects of grain size on true stress-true strain curves at room temperature, Figure 3.0211.

3.0212 Effect of cold work on tensile properties of Types 316 and 317 sheet, Figure 3.0212.

3.0213 Effect of grain size on tensile strength at room temperature, Figure 3.0213.

3.0214 Effect of 100,000-hour exposures to elevated temperatures on room-temperature tensile properties of bar, Figure 3.0214.

3.0215 Effects of prior creep and soaking on tensile properties at room temperature, Figure 3.0215.

3.0216 Effect of carburizing on room-temperature tensile properties of tube, Figure 3.0216.

3.0217 Tensile properties of wire, Table 3.0217.

3.022 Compression – stress-strain diagrams – compression properties.

3.023 Impact.

3.0231 Effect of exposures to elevated temperatures on room-temperature Charpy V-notch impact properties, Figure 3.0231.

3.0232 Effect of exposures to elevated temperatures on room-temperature Charpy-keyhole impact properties, Figure 3.0232.

3.0233 Effects of prior creep and soaking on impact energy at room temperature, Figure 3.0233.

3.024 Bending.

3.025 Torsion and shear.

3.026 Bearing.

3.027 Stress concentration.

3.0271 Notch properties.

3.0272 Fracture toughness.

3.028 Combined properties.

3.03 Mechanical Properties at Various Temperatures

3.031 Tension – stress-strain diagrams – tension properties.

3.0311 Stress-strain curves for annealed and cold-worked sheet from 75 to 1800 F, Figure 3.0311.

3.0312 Stress-strain curves for bar from 75 to 2300 F, Figure 3.0312.

3.0313 Complete true stress-true strain curves for Type 316 bar from room temperature to -452 F, Figure 3.0313.

3.0314 Complete true stress-true strain curves for Type 316 bar from room temperature to 1500 F at two strain rates, Figure 3.0314.

3.0315 Complete engineering stress-strain curves for Type 316 bar from 75 to 1500 F at two strain rates, Figure 3.0315.

3.0316 The shape of the true stress-true strain flow curve is strongly influenced by test temperature, as shown in Figure 3.0317. The work-hardening rate (slope of the stress-strain curve) decreases monotonically with increasing strain at room temperature, but increases with strains greater than 30 percent at -94 F and 15 percent at -320 F. The increases in work hardening at cryogenic temperatures are related to the production of deformation-induced martensite. At room temperature and -94 F, only small amounts of martensite are detected. However, at -320 F, significant amounts of both epsilon- and alpha-martensite are formed, as shown in Figure 3.0318. The strain at which the

work-hardening rate begins to increase at -320 F corresponds to the onset of the transformation to alpha-martensite. The volume fraction of epsilon-martensite peaks at between 10 and 15 percent plastic strain and thereafter decreases with increasing strain. The sequence of transformations during deformation thus appears to be gamma- to epsilon-martensite to alpha-martensite (76).

3.0317 True stress-true strain curves at room and cryogenic temperatures, Figure 3.0317.

3.0318 Volume fractions of martensite formed during tensile deformation at -320 F, Figure 3.0318.

3.0319 Type 316L (and probably also Types 316, 317, and 317L) does not form martensite on cooling to -452 F. However, up to 50 percent martensite does form (again, probably for all types) during tensile straining at this temperature (77).

3.03110 Elevated-temperature tensile properties of Types 316 and 316L, Figure 3.03110.

3.03111 Elevated-temperature tensile properties of Type 316 heavy-wall tube, Figure 3.03111.

3.03112 Elevated-temperature tensile properties of Type 317, Figure 3.03112.

3.03113 Effect of temperatures up to 2300 F on tensile properties of bar, Figure 3.03113.

3.03114 Effect of temperatures up to 1800 F on tensile properties of annealed and cold-worked Type 316 sheet, Figure 3.03114.

3.03115 Effects of strain rate on tensile properties of plate at room and elevated temperatures, (a) yield strength, (b) ultimate tensile strength, and (c) reduction in area, Figure 3.03115.

3.03116 Low-temperature tensile properties of Type 316 bar, Figure 3.03116.

3.03117 A minimum in tensile ductility occurs in the temperature range 800 to 1400 F, as measured by reduction in area and total elongation. The temperature at which minimum ductility is observed increases with increasing grain size, as shown in Figure 3.03118. At high temperatures, where fracture is largely intergranular, ductility increases sharply with decreasing grain size. However, at low temperatures, fracture is primarily transgranular and ductility decreases slightly with decreasing grain size. The ductility minimum is attributed to a maximum in the amount of grain-boundary sliding. At intermediate temperatures, ductility is also dependent on strain rate. As shown in Figure 3.03119, total elongation decreases with decreasing strain rate. This behavior is consistent with the increased importance of grain-boundary sliding at high temperatures and low strain rates (79).

3.03118 Effects of temperature and grain size on tensile ductility parameters, Figure 3.03118.

3.03119 Effects of strain rate and grain size on total elongation at 1110 F, Figure 3.03119.

3.03120 Effect of temperature on tensile properties of castings, Figure 3.03120.

3.03121 Effects of grain size and nitrogen content on yield strength at room and elevated temperatures, Figure 3.03121.

3.03122 Effects of nitrogen content on yield strength at room and elevated temperatures, Figure 3.03122.

3.032 Compression – stress-strain diagrams – compression properties.

3.033 Impact.

3.0331 Subzero temperatures have very little effect on the impact resistance of wrought Type 316, Izod V-notch values remaining constant at about 110 ft-lb from room temperature to -320 F (30,39).

3.0332 Effect of low temperatures on impact resistance of castings, Figure 3.0332.

3.034 Bending.

3.035 Torsion and shear.

3.036 Bearing.

3.037 Stress concentration.

3.0371 Notch properties.

3.03711 Low-temperature notched tensile characteristics of Type 316 plate, Figure 3.03711.

3.0372 Fracture toughness.

3.038 Combined properties.

Fe
18 Cr
13 Ni
+ Mo

Type 316
Type 317

3.04 Creep and Creep-Rupture Properties

3.041 Creep-rupture properties of tube and pipe, Figure 3.041.

3.042 Stress-rupture behavior of sheet at elevated temperatures, Figure 3.042.

3.043 Creep behavior of sheet at elevated temperatures, Figure 3.043.

3.044 Creep-rupture curves for bar at 1200 to 2000 F, Figure 3.044.

3.045 Creep behavior of bar at elevated temperatures, Figure 3.045.

3.056 The creep-rupture strength of cast Type 316 is about 20 percent less than that of wrought Type 316 when tested in air at 1000 to 1200 F. The cast material shows strain bursts as large as 1.7 percent, probably as a result of nonuniform distribution of molybdenum. The rupture time is a strong function of grain size, being greater for fine grain-size and lesser for coarse grain-size material (83).

3.047 Creep-rupture curves for castings at 1200 to 1650 F, Figure 3.047.

3.048 Long-time stress-rupture behavior at elevated temperatures, Figure 3.048.

3.049 Creep behavior in vacuum at very high temperatures, Figure 3.049.

3.0410 Summary of European creep-rupture data, Figure 3.0410.

3.0411 Stresses for creep-rupture in 1000 and 10,000 hours for Types 316 and 316L at temperatures from 1000 to 1500 F, Figure 3.0411.

3.0412 Stresses for minimum creep rates of 0.0001 and 0.00001 percent per hour for Type 316 at temperatures from 1000 to 1500 F, Figure 3.0412.

3.0413 Stresses for creep rupture in 100, 1000, and 10,000 hours for Type 316 castings at temperatures from 1100 to 1300 F, Figure 3.0413.

3.0414 Under cyclic creep-rupture conditions in which Type 316 is alternately loaded in tension and compression, pure tensile time to rupture is considerably longer than rupture time under equal constant tensile load, as shown in Figure 3.0415.

3.0415 Creep-rupture curves for monotonic and cyclic loading at 1300 F, Figure 3.0415.

3.0416 Isochronous stress-strain curves for Type 316 at 1000, 1100, and 1200 F, Figure 3.0416.

3.0417 Plastic strain resulting from constant stress for 2-minute period at elevated temperatures for Type 316 sheet in the annealed and cold-worked conditions, Figure 3.0417.

Fe
18 Cr
13 Ni
+ Mo

Type 316
Type 317

3.0418 The variation of creep rate with grain size depends on applied stress and creep temperature. Decreasing grain size causes decreased creep rate at 1110 F for stresses of 26.1 ksi and greater, as shown in Figure 3.0419(a). However, at 1290 F, the creep rate is not significantly influenced by grain size for stresses in the range 13.1 to 20.3 ksi. At 10.2 ksi, a minimum exists in the creep rate-grain size curve, as shown in Figure 3.0419(b) (87).

3.0419 Effects of grain size on creep rate of plate at various stresses at elevated temperatures, (a) 1110 F, and (b) 1290 F, Figure 3.0419.

3.0420 Prior aging increases the creep rate at 1175 F by up to twentyfold, as shown in Figure 3.0421. The strain to fracture also increases slightly with increased prior aging time at 1520 F. These effects are attributed to reduction of solute elements in the matrix by precipitation of carbide and intermetallic second phases and to overaging of strengthening precipitates (88,89).

3.0421 Effects of prior aging on creep properties of plate, Figure 3.0421.

3.0422 The creep crack-growth behavior of Type 316 can be better correlated with the energy parameter J than with the stress-intensity parameter K, which is useful for correlating fatigue crack-growth behavior. The creep crack-growth curve, shown in Figure 3.0423, can be separated into three regions. In Region I, there is a linear relationship between the crack-growth rate and J, while in Region II, the rate appears to be independent of J. The onset of Region III coincides with J_{IC}, above which rates again increase with increasing J (90).

3.0423 Creep crack-growth behavior in air at 1100 F, Figure 3.0423.

3.0424 Alloying of Type 316 with elements forming stable carbide and nitride precipitates improves the high-temperature creep strength. Thus, the addition of 40 ppm boron, 0.4 percent vanadium, and 0.12 percent nitrogen to Type 316L reduces the mean creep rate by more than one order of magnitude compared to commercial Type 316L, as shown in Figure 3.0425. This modified alloy contains equiatomic proportions of vanadium and nitrogen and is stronger than a similar alloy containing excess nitrogen (also shown in Figure 3.0425). The improved creep properties are attributed to dislocation pinning by a fine vanadium nitride precipitate and to increased stability of boron-containing $M_{23}C_6$ at the grain boundaries (91).

3.0425 Effects of vanadium-nitrogen-boron additions on creep behavior at 1200 F, Figure 3.0425.

3.0426 The optimum carbon content for maximum creep-rupture strength at 1100 to 1200 F is about 0.05 percent. Silicon appears to be detrimental; a heat containing 0.32 percent silicon was consistently weaker in creep-rupture than one containing 0.18 percent silicon. Boron improves creep life by forming complex grain-boundary carbides and delaying the onset of tertiary creep. Sulfur and phosphorus appear innocuous to creep strength. Substitution of nitrogen for part of the carbon in Type 316 improves the rupture strength below about 1470 F, but above this temperature, the standard Type 316 is stronger (92,93,94).

3.0427 Fracture-mechanism maps based on homologous temperature and on failure time are shown in Figures 3.0428(a) and (b), respectively. These maps define the regimes of stress, temperature, and time to fracture over which each type of fracture mechanism is dominant. The heavy lines indicate the estimated midpoint of the transition from one mechanism to another. The shaded areas represent mixed or transitional modes of fracture. At low temperatures, the material work hardens strongly and can be considered as a rate-independent plastic solid; at higher temperatures, it work hardens less strongly but is rate dependent and is properly considered as a creeping solid. The dotted line at the top of the homologous-temperature map indicates the stress which would lead to a strain rate of about 10^6/sec. Above this stress level, fracture becomes a dynamic problem, limited by the velocity of elastic or plastic waves within the material. Although the fracture mechanisms in the dynamic fracture region may resemble those in slower tests, extrapolation of field boundaries into this region is not justified.

In tensile tests up to about 0.65 T_m, the steel fails predominantly by ductile transgranular failure. This fracture mode is characterized by considerable necking, internal holes, and a cup-and-cone fracture. In the temperature range of 0.4 to 0.65 T_m, fast creep tests result in a transgranular creep fracture which resembles that observed in tensile tests but has reduced extension to fracture. At lower stresses in the temperature range of 0.4 to 0.65 T_m, failure occurs by intergranular creep fracture. The material shows little elongation or necking and cracks originating at the surface or at grain boundaries propagate intergranularly to the final failure. Above 0.65 T_m, Type 316 fails by rupture, necking to zero cross-section. This may result from re-solution of carbides (the shaded band indicates the carbide solutioning range) and other inclusions, thereby removing the nuclei for cavity formation. Several lines of constant fracture time are also shown in this figure. The second map, based on failure time, shows these same fracture-mechanism regions translated to axes of the conventional stress-rupture plot, log stress and log failure time. The constant-temperature lines in this figure emphasize that a change in slope of the creep-rupture plot often reflects a change in fracture mechanism. However, the apparent change in slope around 10^8 seconds may result from a microstructural change (such as carbide re-solution) rather than a change in fracture mechanism. It may be noted that within a field of the fracture map a single mechanism is dominant and simple empirical extrapolation should be satisfactory for strength calculations. However, on crossing a field boundary, the mechanism – and its underlying kinetics and stress dependence – changes and there is no justification for further extrapolation (95).

3.0428 Fracture map, (a) based on homologous temperature, and (b) based on failure time, Figure 3.0428.

3.05 **Fatigue Properties**

Fe
18 Cr
13 Ni
+ Mo

Type 316
Type 317

3.051 Cyclic and monotonic stress-strain curves in air at 1160 F, Figure 3.051.

3.052 Low-cycle axial fatigue behavior in air at room and elevated temperatures (a) room temperature, (b) 840 F, (c) 1110 F, (d) 1290 F, and (e) 1470 F, Figure 3.052.

3.053 Effects of heat-to-heat variations on low-cycle axial fatigue behavior in air at 1160 F, Figure 3.053.

3.054 Jaske and Frey (99) summarized the results of their studies and those of others to arrive at the long-time fatigue curves shown in Figure 3.055. These are best-fit curves to the relation:

$$\epsilon = AN_f^{-b} + C \quad ,$$

where ϵ is total strain range, N_f is cycles to failure, and A, b, and C are empirical constants which are functions of temperature. At short times, the fatigue life decreases with increasing temperature, but at longer times (above about 10^4 cycles), this order disappears. The apparent low-cycle fatigue limit implied by this relationship may or may not be real.

3.055 Long-time low-cycle axial fatigue behavior in air at room and elevated temperatures, Figure 3.055.

3.056 Low-cycle axial fatigue life as a function of plastic, elastic, and total strain ranges in air at 1100 F, Figure 3.056.

3.057 Surface finish has a significant effect on fatigue life. As shown in Figure 3.058, the fatigue life of electropolished specimens is about fourfold greater than that of finely machined or ground specimens. This difference in fatigue life is attributed to the difference in crack-growth rate. In electropolished material, cracks grow from localized semicircular fronts. However, in machined or ground material, crack nucleation occurs at roots of machining marks and leads to a continuous crack front all around the specimen circumference. The growth rate of the semicircular cracks is about fourfold less than that of the continuous cracks (101).

3.058 Effects of surface finish on low-cycle axial fatigue behavior in air at 750 F, Figure 3.058.

3.059 There is little difference in fatigue life between the annealed and cold-worked conditions in terms of total strain amplitude, as shown in Figure 3.0510 (102).

3.0510 Effects of cold work on low-cycle axial fatigue behavior, Figure 3.0510.

3.0511 The fatigue life at 1110 F is reduced by the presence of notches, as shown in Figure 3.0512. An empirical relationship relating fatigue life (N_f), frequency (ν), and stress-concentration factor (K_t) has been proposed as:

$$N_f = N_{fo} K_t^m \nu^l$$

where N_{fo} is cycles to failure under unit conditions, and m and l are empirical constants equal to -1.43 and 0.15, respectively. The lines in the figure are calculated from this relation (103).

3.0512 Effects of stress-concentration factor on low-cycle fatigue life in air at 1110 F, Figure 3.0512.

3.0513 The effect of cyclic frequency on low-cycle fatigue behavior increases with increasing temperature. As shown in Figure 3.0514, little effect of frequency is apparent at room temperature. However, at 840 and 1470 F, the fatigue life is notably shorter at cyclic strain rates of 0.4 and 4 percent/min (about 0.1 to 0.3 cpm and 1 to 3 cpm, respectively) than at 40 percent/min (about 10 to 30 cpm). The decreased fatigue life is due to a greater creep component of fatigue at the lower frequency (97).

3.0514 Low-cycle fatigue life at room and elevated temperatures, Figure 3.0514.

3.0515 The low-cycle fatigue life in vacuum is little affected by temperature up to 1470 F, as shown in Figure 3.0516. In contrast, the fatigue life in air decreases with increasing temperature. This behavior is attributed to the deleterious effect of air on crack-initiation and -propagation behavior (104,105).

3.0516 Low-cycle axial fatigue behavior in vacuum at room and elevated temperatures, Figure 3.0516.

3.0517 Effects of hold time on low-cycle axial fatigue behavior in air at 1160 F, Figure 3.0517.

3.0518 Variation of low-cycle axial fatigue life in air at 1110 F with hold time, Figure 3.0518.

3.0519 The low-cycle fatigue behavior of Type 316L is improved by the addition of nitrogen. As shown in Figure 3.0520, the fatigue life is increased by alloying with up to 0.12 percent nitrogen, especially at higher total-strain-range levels. Increasing the nitrogen content from 0.12 to 0.25 percent appears not to effect further improvement. Nitrogen alloying causes deformation to be more planar and inhibits dislocation cell formation (106).

3.0520 Effects of nitrogen content on low-cycle fatigue behavior at room temperature, Figure 3.0520.

3.0521 The fatigue life of Type 316 in flowing lithium at 900 F is approximately sixfold greater than in air (107).

3.0522 High-frequency rotating bending fatigue behavior at room and elevated temperatures, Figure 3.0522.

3.0523 Temperature dependence of rotating bending fatigue strength at 10^8 cycles, Figure 3.0523.

3.0524 Fatigue life of sheet at 1500 F as a function of plastic cyclic strain range in air and vacuum, Figure 3.0524.

3.0525 Fatigue life at 1500 F as a function of total cyclic strain range, Figure 3.0525.

3.0526 Fatigue limit for Type 316 in various forms in reversed bending (R = -1), Table 3.0526.

3.0527 The effect of cyclic frequency on crack-growth behavior in air at 800, 1000, and 1200 F is shown in Figure 3.0528. Although different slopes are observed at different frequencies, the general trend is for increasing crack-growth rate with decreasing frequency, consistent with observations on other materials (109).

3.0528 Effects of cyclic frequency on low-cycle fatigue crack-growth behavior in air at elevated temperatures, (a) 800 F, (b) 1000 F, and (c) 1200 F, Figure 3.0528.

3.0529 The low-cycle fatigue crack-growth rate increases with increasing temperature, as shown in Figure 3.0530 for annealed alloy and in Figure 3.0531 for 20 percent cold-worked alloy. The rates at 1200 F are fourfold to tenfold greater than those at room temperature. The crack-growth rates for the

Fe
18 Cr
13 Ni
+ Mo

Type 316
Type 317

annealed alloy are also about twofold greater than those for the cold-worked alloy at room temperature to 1200 F. Crack propagation is transgranular for both materials (110).

3.0530 Effects of temperature on low-cycle fatigue crack-growth behavior of annealed alloy, (a) room temperature and 1000 F, and (b) 600 and 1200 F, Figure 3.0530.

3.0531 Effects of temperature on low-cycle fatigue crack-growth behavior of cold-worked alloy, (a) room temperature and 1000 F, and (b) 600 and 1200 F, Figure 3.0531.

3.0532 Fatigue crack-growth rate of annealed alloy at -452 F, Figure 3.0532.

3.0533 Low-cycle fatigue crack-growth behavior in vacuum at room and elevated temperatures, Figure 3.0533.

3.0534 In the unaged solution-annealed condition for stress-intensity-factor ranges between 25 and 40 ksi $\sqrt{in.}$, tension hold times at 1100 F of 0.1 and 1.0 minute produce a small increase in crack-growth rates. However, at stress-intensity factor ranges greater than 40 ksi $\sqrt{in.}$, relatively large increases in crack-growth rates are produced by 1.0-minute hold times, as shown in Figure 3.0535. A hold time of 1.0 minute does not increase the crack-growth rate in the annealed-and-aged condition; but aging per se reduces the crack-growth rate by about twofold as compared to the unaged condition. In the cold-worked condition, the 1100 F crack-growth rate is increased both by aging and by a 1.0-minute hold time, as shown in Figure 3.0536. At 800 F, hold times of 0.1 and 1.0 minute have little effect on crack-growth rate in either the solution-annealed or solution annealed-and-aged condition, as shown in Figures 3.0537 and 3.0538. As at 1100 F, the crack-growth rate at 800 F is reduced by aging of solution-annealed material (113).

3.0535 Effects of aging and hold time on low-cycle bending fatigue crack-growth rate of annealed alloy in air at 1100 F, Figure 3.0535.

3.0536 Effects of aging and hold time on low-cycle bending fatigue crack-growth rate of cold-worked alloy in air at 1100 F, Figure 3.0536.

3.0537 Effects of hold time on low-cycle bending fatigue crack-growth rate of annealed alloy in air at 800 F, Figure 3.0537.

3.0538 Effects of hold time on low-cycle bending fatigue crack-growth rate of annealed-and-aged alloy in air at 800 F, Figure 3.0538.

3.0539 The stress ratio ($R = K_{min}/K_{max}$) significantly affects the fatigue crack-growth rate. As shown in Figure 3.0540, the crack-growth rates at 800 and 1000 F increase with increasing stress ratio. The effect of stress ratio can be accounted for by expressing the crack-growth rate as a function of an "effective stress intensity factor", as

$$da/dN = C(K_{eff})^n$$

where

$$K_{eff} = K_{max}(1 - R)^m$$

The exponent m is an empirically determined constant between zero and unity which depends on material and test condition. Values of m determined for Type 316 range between 0.35 and 0.65 (114).

3.0540 Effects of stress ratio on low-cycle fatigue crack-growth behavior in air at elevated temperatures, (a) 800 F, and (b) 1000 F, Figure 3.0540.

3.06 **Elastic Properties**

3.061 Poisson's ratio.

3.0611 Effect of temperatures up to 1500 F on Poisson's ratio, Figure 3.0611.

3.0612 Poisson's ratio at room and cryogenic temperatures, Figure 3.0612.

3.062 Modulus of elasticity.

3.0621 Effect of temperatures up to 1500 F on modulus of elasticity, Figure 3.0621.

3.0622 Modulus of elasticity of annealed and cold-worked sheet at room temperature and from 1400 to 1800 F, Figure 3.0622.

3.0623 Modulus of elasticity at room and cryogenic temperatures, Figure 3.0623.

3.063 Modulus of rigidity.

3.0631 Effect of temperatures up to 1500 F on modulus of rigidity, Figure 3.0631.

3.0632 Modulus of rigidity at room and cryogenic temperatures, Figure 3.0632.

3.064 Tangent modulus.

3.065 Secant modulus.

4 **FABRICATION**

4.01 **Forming**

4.011 In the annealed condition, these alloys have excellent ductility and may be readily formed by such methods as roll forming, deep drawing, bending, upsetting, etc. When severe cold working is required, intermediate anneals may be necessary to restore ductility and lower hardness for subsequent forming. Severely cold-formed parts should be annealed to relieve stresses (39).

4.012 These alloys are amenable to practically all hot-forming operations, although their good high-temperature strength requires the application of more power than for non-molybdenum-bearing stainless steels. Heating should be done slowly and uniformly; preheating at 1500 to 1600 F is recommended. Forming should be started at 2100 to 2300 F and finished at 1700 F or higher. Annealing is recommended after hot forming. If annealing is not practical, parts should be rapidly cooled from the final hot-forming temperature (11).

4.013 Type 317 has a higher flow stress than Type 316 at elevated temperatures. It consequently requires a mill loading approximately 20 percent greater during hot rolling (116).

4.014 The effects of trace elements on the hot ductility of cast and wrought Type 316L at strain rates similar to those encountered during hot working are shown in Figures 4.015 and 4.016, respectively. Lead, tellurium, and bismuth are quite detrimental to the ductility of the cast alloy. Tin is less detrimental than these three elements, particularly at

2190 F. Wrought alloy is less sensitive than cast alloy to all four trace elements. The tolerances for lead and tin, in particular, are greater in the wrought condition although bismuth and tellurium remain rather embrittling. Levels of lead, bismuth, and tellurium must be kept low in order to achieve high yields during hot working. The negative effects of lead may be alleviated by increasing the initial hot-working temperature (117).

4.015 Effects of lead, tin, bismuth, and tellurium on hot ductility of cast Type 316L, Figure 4.015.

4.016 Effects of lead, tin, bismuth, and tellurium on hot ductility of wrought Type 316L, Figure 4.016.

4.02 **Machining and Grinding**

4.021 Because of their toughness and work-hardening characteristics, these grades of stainless require rigid machine setups and sharp tools. In general, they are machined at speeds about 40 percent of those used for AISI B1112, except the free-machining grade, which approaches 60 percent. Better finishes are obtained with moderately cold-worked material rather than annealed. Heavy feeds and an adequate supply of coolant are recommended (39).

4.03 **Joining**

4.031 The alloys are readily weldable by the conventional automatic and manual electric-arc techniques. The filler material should be the same alloy as the parent material. Types 316 and 317 are subject to carbide precipitation in the heat-affected zones; therefore, susceptibility to intergranular corrosion should be eliminated by a post-weld annealing treatment. Types 316L and 317L do not require remedial annealing after welding and are, therefore, widely used in welded structures.

4.032 Low-temperature tensile and notched tensile properties of plate, butt welded with Type 316 coated stick electrodes, Figure 4.032.

4.033 Comparison of complete true stress-true strain curves of plate and of weld metal after plate had been butt welded with Type 316 coated stick electrodes, Figure 4.033.

4.034 Low-temperature impact properties of plate and of weld metal after plate had been butt welded with Type 316 coated stick electrodes, Figure 4.034.

4.035 Creep-rupture curves for annealed parent metal and for tungsten-inert-gas-welded specimens in various heat-treated conditions, Figure 4.035.

4.036 Minimum creep rates for annealed parent metal and for tungsten-inert-gas-welded specimens in various heat-treated conditions, Figure 4.036.

4.037 Effect of temperature on tensile properties of annealed sheet butt welded by the inert-gas-shielded-arc process, Figure 4.037.

4.038 The microstructure of shielded metal-arc weldments is duplex in nature, consisting of an austenite and a delta ferrite phase. A minimum of about 3 percent ferrite is desirable to minimize hot cracking in the weld. An upper limit for delta ferrite content is also frequently specified when welds are intended for high-temperature service since ferrite is metastable and decomposes into more stable intermetallic phases which are detrimental to mechanical properties. Toughness of weld metal at cryogenic temperatures decreases with increasing (undecomposed) ferrite content, as shown for Charpy impact energy in Figure 4.039 and for fracture toughness in Figure 4.0310. The decreased toughness may be related to cold brittleness of the bcc ferrite phase. Tensile properties at cryogenic temperatures and toughness at room temperature and above are not adversely affected by the presence of the ferrite phase.

Fe
18 Cr
13 Ni
+ Mo

Type 316
Type 317

At elevated temperatures, ferrite transforms into several different phases, predominantly into austenite and $M_{23}C_6$ carbide at 1000 to 1200 F and into chi-phase at 1470 F. The transformation curve is sigmoidal in shape and exhibits a close fit to the Johnson-Mehl relation, as shown in Figure 4.0311. The time-temperature-transformation diagram in Figure 4.0312 was constructed from a series of experimentally determined isothermal transformation curves. The diagram resembles that shown in Figure 2.01212 for intermetallic formation in wrought Type 316, but transformation times are much shorter in the ferrite-containing weld metal. In addition to austenite, $M_{23}C_6$, and chi-phase, the ferrite transformation products include sigma-phase and R-phase (a complex hcp intermetallic phase similar to chi and sigma). These transformation products are brittle and cause a decrease in subsequent impact energy after aging at 1290 or 1470 F, as shown in Figure 4.0313. This embrittlement reaction is related to the original presence of ferrite in the weld metal. Embrittlement does not occur in weld metal free of delta ferrite phase on aging for up to 1000 hours at 1000 to 1470 F. Precautions should be taken in the use of welded components in high-temperature applications, such as specifying a maximum in the ferrite content of the weld, solution annealing the component to dissolve both the ferrite and the deleterious transformation products, or limiting service conditions to those which will not seriously degrade properties (118–122).

4.039 Effect of delta ferrite content on Charpy impact energy of weld metal at -320 F, Figure 4.039.

4.0310 Effect of delta ferrite content on fracture toughness of weld metal at cryogenic temperatures, Figure 4.0310.

4.0311 Effect of aging time at 1380 F on transformation of delta ferrite in Type 316 weld metal, Figure 4.0311.

4.0312 Time-temperature-transformation diagram for transformation of delta ferrite in weld metal, Figure 4.0312.

4.0313 Effects of aging time and temperature on impact energy of weld metal at room temperature, Figure 4.0313.

4.0314 Improved mechanical properties in Type 316 weld metal can be achieved by alloying of the weld metal with small amounts of boron, phosphorus, and titanium. This is accomplished by using coated Type 316 electrodes with the coating composition modified to produce controlled amounts of residual elements (CRE) in the finished welds. The Type 316 CRE weld has good tensile properties at room temperature to 1200 F, as shown in Figure 4.0315. The creep-rupture strength at

Fe
18 Cr
13 Ni
+ Mo

Type 316
Type 317

1200 F is higher than that generally observed for the base metal, as shown in Figure 4.0316. The CRE contents for these welds were 0.007 percent boron, 0.045 percent phosphorus, and 0.06 percent titanium (123).

4.0315 Tensile properties of CRE shielded-metal-arc weld metal at room and elevated temperatures, Figure 4.0315.

4.0316 Stress-rupture behavior of CRE shielded-metal-arc weld metal at 1200 F, Figure 4.0316.

4.04 **Surface Treating**

4.041 Because of their good resistance to corrosion and oxidation, protective surface treatments and coatings are not normally needed for these alloys.

4.042 For optimum corrosion resistance the surfaces must be free of scale and foreign metallic contaminants. Preferred cleaning treatments are either mechanical methods such as sand or vapor blasting, or scale conditioning in a molten caustic bath followed by light acid pickling.

REFERENCES

1 AMS 5524F (October 1, 1984).
2 AMS 5507D (October 1, 1984).
3 AMS 5573G (January 1, 1983).
4 AMS 5648F (July 1, 1982).
5 AMS 5649C (July 1, 1982).
6 AMS 5653B (October 1, 1982).
7 AMS 5690H (July 1, 1982).
8 "Resumé of Investigations on Steels for High Temperature High Pressure Applications 1960–1962", The Timken Roller Bearing Company (1962).
9 DeSisto, T. S., and Carr, F. L., "Low Temperature Mechanical Properties of 300 Series Stainless Steels and Titanium", WAL TR 323.4/1, Watertown Arsenal Laboratories (December 1961).
10 DeSisto, T. S., "Low Temperature Mechanical Properties of Base and Weld Deposits of Selected Austenitic Stainless Steels", AMRA TR 63-08, U.S. Army Materials Research Agency (July 1963).
11 "Steels for Elevated Temperature Service", United States Steel Corporation (June 1972).
12 Halford, G. R., "Cyclic Creep-Rupture Behavior of Three High Temperature Alloys", NASA TN D-6309, Lewis Research Center (May 1971).
13 "Isochronous Stress-Strain Curves for 2-1/4 Cr-1Mo, Type 304-304H, and Type 316-316H Steels", Technical Report 2012 – Part I, United Nuclear Corporation (September 1970).
14 Stanley, J. K., "Mechanical Properties of Carburized Austenitic Stainless Steels as Related to Microstructure", The Aerospace Corporation, Reprint No. TR-0066 (5250-10)-1 (July 31, 1969).
15 Stanley, J. K., and Perrotta, A. J., "Grain Growth in Austenitic Stainless Steels", *Metallography*, Vol 2 (December 1969), pp 349–362.
16 Reinhart, F. M., "Corrosion of Materials in Hydrospace", U.S. Naval Civil Engineering Laboratory, Technical Report R-504 (December 1966).
17 Reinhart, F. M., "Corrosion of Materials in Hydrospace – Part VI – Stainless Steels", Naval Civil Engineering Laboratory, Technical Note N-1172 (September 1971).
18 Waldron, L. J., Forgeson, B. W., Peterson, M. H., and Brown, B. F., "Performance of Stainless Steel Galvanically Coupled to Other Metals", U.S. Naval Research Laboratory Memorandum Report 1388 (January 1963).
19 "Effect of Elevated Temperature Exposure on Types 216 and 316 Impact Properties", Allegheny-Ludlum Data Sheet 272-12370-216-316 (January 23, 1970).
20 "Stainless Steels Chromium-Nickel-Molybdenum Types 316, 316L, 317, 317L", Allegheny-Ludlum Blue Sheet.
21 Furman, D. E., "Thermal Expansion Characteristics of Stainless Steels Between -300 and 1000 F", *Journal of Metals*, Vol 188 (April 1950).
22 Rowe, G. H., and Stewart, J. R., "Creep-Rupture Behavior of Type 316 Stainless Steel Weldments Prepared With and Without Restraint", *Welding Journal*, Vol 41 (December 1962), pp 534S-541S.
23 "Fundamental Behavior of Structural Materials in Fast Reactor Environments", Oak Ridge National Laboratory, paper for the Fourth U.N. International Conference on Peaceful Uses of Atomic Energy (September 1971).
24 Gibbs, T. W., and Wyatt, H. W., "Short-Time Tensile Properties of Type 316 Stainless Steel at Very High Temperatures", ASME Paper No. 60-WA-11.
25 Swindeman, R. W., "Fatigue of Austenitic Stainless Steels in the Low and Intermediate Cycle Range", Oak Ridge National Laboratory, ORNL-TM-1363.
26 Conway, J. B., et al., "Stress-Strain Behavior of Several Stainless Steels to Elevated Temperatures", Nuclear Systems Program, General Electric Company, GEMP-686 (May 1969).
27 Conway, J. B., and Flagella, P. N., "Physical and Mechanical Properties of Reactor Materials", General Electric Co., Nuclear Systems Programs, GEMP-727 (December 1969).
28 Simmons, W. F., and Van Echo, J., "Elevated Temperature Properties of Stainless Steels", ASTM Data Series Publication DS5-S1 (1965).
29 Garofalo, F., "Temperature Dependence of the Elastic Moduli of Several Stainless Steels", *Proceedings ASTM*, Vol 60 (1960), pp 738–749.
30 "Working Data Carpenter Stainless Steels", Carpenter Technology Corporation (1971).
31 "Armco Stainless Steels", Armco Steel Corporation (1972).
32 "Cross-Index of Chemically Similar Specifications and Identification Codes", MIL-HDBK-H1D (June 22, 1970).
33 "A Selection Guide to Heat-Resistant Cast High Alloys Corrosion-Resistant Cast High Alloys", Steel Founders' Society of America (1970).
34 "Steel Casting Design – Specifications", Steel Founders' Society of America (January 1, 1971).
35 Lucks, C. F., and Deem, H. W., "Thermal Properties of 13 Metals", ASTM STP No. 227 (1958).
36 Danek, G. J., Smith, H. H., and Archer, M. R., "High Temperature Fatigue and Bending Strain Measurements in Controlled Environment", *Proceedings ASTM*, Vol 61 (1961), p 775.
37 Schoefer, E. G., "Cast High Alloys", *Chemical Engineering*, Vol 60 (October 1953), p 298.

38 "Type 316", Data Sheet from AISI.

39 "Uniloy 316/317/318 Stainless Steels", Universal-Cyclops Specialty Steel Division (1966).

40 Bates, J. M., "Why So Many Stainless Steels", *Chemical Engineering Progress*, Vol 59 (June 1963), pp 92–96.

41 "Carpenter Stainless Type 316", Carpenter Technology Corporation (May 1972).

42 "Haynes Investment-Cast Steels", Haynes-Stellite Company Data Booklet (April 1958).

43 "Digest of Steels for High Temperature Service", Timken Roller Bearing Company, Sixth Edition (1958).

44 Sessler, J. G., "The Creep-Rupture and Low-Strain Creep Properties of Several Heat-Resistant Alloys Tested in Air at Elevated Temperatures", SURI Chemical and Metallurgical Engineering Department, Report No. MET 383-581 F1 (June 1957).

45 Parr, J. G., and Hanson, A., "An Introduction to Stainless Steel", ASM (1965).

46 AMS 5360D (October 1, 1982).

47 AMS 5361D (July 1, 1985).

48 AMS 5691E (October 1, 1982).

49 AMS 5692 (October 1, 1982).

50 AMS 5696 (July 1, 1984).

51 Renken, C. J., Reimann, K. J., and Berger, H., "Nondestructive Measurements of Cold Work in Type 316 Stainless Steel", *Materials Evaluation*, Vol 32, No. 6 (June 1974), pp 109–116.

52 Scott, J. A., and Spruiell, J. E., "Grain Refinement of Wrought Austenitic Stainless Steels by Rapid Heating", *Metallurgical Transactions*, Vol 5, No. 1 (January 1974), pp 255–259.

53 Bishop, J. L., Jr., "Melting and Refining Specialty Steels at Allegheny Ludlum Industries", *Metal Progress*, Vol 106, No. 3 (August 1974), pp 53–59.

54 Lai, J.K.L., "A Review of Precipitation Behavior in AISI Type 316 Stainless Steel", *Materials Science and Engineering*, Vol 61, No. 2 (November 1983), pp 101–109.

55 Barcik, J., and Brzycha, B., "Chemical Composition of Sigma Phase Precipitated in Chromium-Nickel Austenitic Steels", *Metal Science*, Vol 17, No. 5 (May 1983), pp 256–260.

56 Lai, J.K.L., and Meshkat, M., "Kinetics of Precipitation of Chi-Phase and $M_{23}C_6$ Carbide in a Cast of Type 316 Stainless Steel", *Metal Science*, Vol 12, No. 9 (September 1978), pp 415–420.

57 Grot, A. S., and Spruiell, J. E., "Microstructural Stability of Titanium-Modified Type 316 and Type 321 Stainless Steel", *Metallurgical Transactions*, Vol 6A, No. 11 (November 1975), pp 2023–2030.

58 Makino, T., Kunitomo, T., and Mori, T., "Study on Radiative Properties of Heat Resisting Metals and Alloys (2nd Report, Optical Properties and Emissivities of Stainless Steels and Superalloys)", *Bulletin of the JSME*, Vol 27, No. 223 (January 1984), pp 57–63.

59 Clark, A. F., and Tryon, P. V., "Material Variability as Measured by Low Temperature Electrical Resistivity", *Cryogenics*, Vol 12, No. 6 (December 1972), pp 451–461.

60 Iselli, C., and Nannei, E., "Total Normal Emittance of Stainless Steel at High Temperatures: Influence of Oxide Layer Growth", *High Temperatures-High Pressures*, Vol 12, No. 3 (1980), pp 307–310.

61 Hall, E. L., and Briant, C. L., "Chromium Depletion in the Vicinity of Carbides in Sensitized Austenitic Stainless Steels", *Metallurgical Transactions*, Vol 15A, No. 5 (May 1984), pp 793–811.

62 Srinivasan, S. R., "A Method for Predicting the Critical Cooling Rate to Prevent Sensitization, *Journal of Heat Treating*, Vol 1, No. 1 (June 1979), pp 87–92.

63 Russell, A. J., and Tromans, D., "A Fracture Mechanics Study of Stress Corrosion Cracking of Type-316 Austenitic Steel", *Metallurgical Transactions*, Vol 10A, No. 9 (September 1979), pp 1229–1238.

64 Dickson, J. I., Russell, A. J., and Tromans, D., "Stress Corrosion Crack Propagation in Annealed and Cold Worked 310 and 316 Austenitic Stainless Steels in Boiling (154 C) Aqueous $MgCl_2$ Solution", *Canadian Metallurgical Quarterly*, Vol 19, No. 1 (January–March 1980), pp 161–167.

65 Muraleedharan, P., Khatak, H. S., Gnanamoorthy, J. B., and Rodriguez, P., "Effect of Cold Work on Stress Corrosion Cracking Behavior of Types 304 and 316 Stainless Steels", *Metallurgical Transactions*, Vol 16A, No. 2 (February 1985), pp 285–289.

66 Moccari, A., and Ali, S. I., "Studies on the Oxidation and Spalling Resistance of Austenitic Stainless Steels", *British Corrosion Journal*, Vol 14, No. 2 (1979), pp 91–96.

67 McCoy, H. E., and McNabb, B., "Corrosion of Several Iron- and Nickel-Base Alloys in Supercritical Steam at 1000 F", Oak Ridge National Laboratory, ORNL-TM-4552 (August 1974).

68 Misencik, J. A., "Evaluation of Dopants in Hydrogen to Reduce Hydrogen Permeation in Candidate Stirling Engine Heater Head Tube Alloys at 760 and 820 C", National Aeronautics and Space Administration, Lewis Research Center, Cleveland, Ohio, NASA-TM-82920 (October 1982).

69 Kelsey, P. V., Jr., Reimann, G. A., and Malik, R. K., "Corrosion of 316, 316L and 321 Stainless Steels in Static Molten Lithium", EG and G, Idaho Falls, Idaho, EGG-RE-M-78-024 (September 1978)

70 Tortorelli, P. F., and Devan, J. H., "Compatibility of Stainless Steel with Pb-17 At. Pct Li", *Journal of Materials for Energy Systems*, Vol 4, No. 2 (September 1982), pp 78–83.

71 Fish, R. L., and Watrous, J. D. "Effect of Fast Reactor Irradiation on the Tensile Properties of 20 Percent Cold-Worked Type 316 Stainless Steel", Irradiation Effects on the Microstructure and Properties of Metal, ASTM STP 611, American Society for Testing and Materials (1976), pp 91–100.

72 Blackburn, L. D., Greenslade, D. L., and Ward, A. L., "Mechanical Properties of Type 316 Stainless Steel Materials After Irradiation at 515 C and 585 C", Hanford Engineering Development Laboratory, Richland, Washington, HEDL-TME-81-4 (April 1981).

73 Michel, D. J., and Smith, H. H., "Neutron Irradiation Effects on Fatigue Crack Propagation in Type 316 Stainless Steels at 649 C", Naval Research Laboratory, Washington, D.C., Memorandum Report, NRL-MR-4282 (August 1, 1980).

Fe
18 Cr
13 Ni
+ Mo

Type 316
Type 317

Fe
18 Cr
13 Ni
+ Mo

Type 316
Type 317

74 Norstrom, L.-A., "Influence of Grain Size on Flow Stress in an Austenitic Stainless Steel", *Scandinavian Journal of Metallurgy*, Vol 6, No. 4 (1977), pp 145–150.

75 Gan, D., "Tensile and Fracture Properties of Type 316 Stainless Steel After Creep", *Metallurgical Transactions*, Vol 13A, No. 12 (December 1982), pp 2155–2163.

76 Seetharaman, V., and Krishnan, R., "Influence of the Martensitic Transformation on the Deformation Behavior of an AISI 316 Stainless Steel at Low Temperatures", *Journal of Materials Science*, Vol 16, No. 2 (February 1981), pp 523–530.

77 Larbalestier, D. C., and King, H. W., "Austenitic Stainless Steels at Cryogenic Temperatures. I-Structural Stability and Magnetic Properties", *Cryogenics*, Vol 13, No. 3 (March 1973), pp 160–168.

78 Sikka, V. K., "Tensile and Creep Properties of Type 316 Stainless Steel", presented at the UK/UKAEA Specialists Meeting on Mechanical Properties, Oak Ridge, Tennessee (December 4, 1978).

79 Mannan, S. L., Samuel, K. G., and Rodriguez, P., "Influence of Temperature and Grain Size on the Tensile Ductility of AISI 316 Stainless Steel", *Materials Science and Engineering*, Vol 68, No. 2 (January 1985), pp 143–149.

80 Norstrom, L.-A., "Influence of Nitrogen and Grain Size on Yield Strength in Type AISI 316L Austenitic Stainless Steel", *Metal Science Journal*, Vol 11, No. 6 (June 1977), pp 208–212.

81 Witzke, W. R., and Stephens, J. R., "Creep-Rupture Behavior of Seven Iron-Base Alloys After Long Term Aging at 760 Deg in Low Pressure Hydrogen", National Aeronautics and Space Administration, Lewis Research Center, Cleveland, Ohio, Technical Memorandum, NASA TM-81534 (August 1980).

82 da Silveira, T. L. and Monteiro, S. N. "Strengthened Creep Substructures in 316 Stainless Steel", Proceedings, Second International Conference on Mechanical Behavior of Materials, Boston, Massachusetts (August 16–20, 1976).

83 Sikka, V. K., and David, S. A., "Discontinuous Creep Deformation in a Type 316 Stainless Steel Casting", *Metallurgical Transactions*, Vol 12A, No. 5 (May 1981), pp 883–892.

84 Lai, J. K., and Wickens, A., "Microstructural Changes and Variations in Creep Ductility of 3 Casts of Type 316 Stainless Steel", *Acta Metallurgica*, Vol 27, No. 2 (February 1979) pp 217–230.

85 Boerman, D. J., and Zhu, J. H., "Study of the Accelerated Creep Fracture Process in AISI 316H Stainless Steel Above 800 C", *Materials Science and Engineering*, Vol 67, No. 2 (November 1984), pp 221–227.

86 Brunori, G., Cappellato, S., Vacchiano, S., and Guglielmi, F., "Comparison Among Creep Rupture Strength Extrapolation Methods With Application to Data for AISI 316 SS From Italy, France, U.K., and F.R.G.", European Atomic Energy Community, Brussels, Belgium, Technical Report, EUR-7796-EN (1982).

87 Mannan, S. L., and Rodriguez, P., "Effect of Grain Size on Creep Rate in Type 316 Stainless Steel at 873 and 973 K", *Metal Science*, Vol 17, No. 2 (February 1983), pp 63–69.

88 Singh, G., Boyd, G.A.C., and Henshall, J. L., "Effect of Prior Aging on the Creep Properties of Type 316L Stainless Steel", *Metallurgical Transactions*, Vol 11A, No. 3 (March 1980), pp 539–542.

89 Lai, J.K.L., and Horton, C.A.P., "Some Effects of Thermal Aging and Grain Size on the Creep Behavior of a Cast of AISI Type 316 Stainless Steel", *Materials Science and Engineering*, Vol 54, No. 2 (July 1982), pp 285–289.

90 Saxena, A., Ernst, H. A., and Landes, J. D., "Creep Crack Growth Behavior in 316 Stainless Steel at 594 C (1100 F)", *International Journal of Fracture*, Vol 23, No. 4 (December 1983), pp 245–257.

91 Liljestrand, L. G., and Omsen, A., "The Mechanisms of Improved Creep Strength in a New Austenitic Stainless Steel", *Metallurgical Transactions*, Vol 6A, No. 2 (February 1975), pp 279–286.

92 Grover, H. K., and Wickens, A., "Effects of Minor Elements on the Long Term Creep-Rupture Properties of Type 316 Austenitic Stainless Steel in the Range 550–700 C", presented at Conference on Mechanical Behavior and Nuclear Applications of Stainless Steel at Elevated Temperatures, Varese, Italy (May 20–22, 1981).

93 Swindeman, R. W., Sikka, V. K., and Klueh, R. L., "Residual and Trace Element Effects on the High-Temperature Creep Strength of Austenitic Stainless Steels", paper based on presentation at TMS-AIME Annual Meeting, Dallas, Texas (February 14–18, 1982).

94 Solberg, J. K., "The Influence of Carbon and Nitrogen on the High Temperature Creep Properties of AISI Type 316 Austenitic Stainless Steel", *Materials Science and Engineering*, Vol 55, No. 1 (August 1982), pp 39–44.

95 Fields, R. J., Weerasooriya, T., and Ashby, M. F., "Fracture-Mechanisms in Pure Iron. Two Austenitic Steels, and One Ferritic Steel", *Metallurgical Transactions*, Vol 11A, No. 2 (February 1980), pp 333–347.

96 Wood, D. S., Wynn, J., Baldwin, A. B., and O'Riordan, P., "Some Creep/Fatigue Properties of Type 316 Steel at 625 C", *Fatigue of Engineering Materials and Structures*, Vol 3, No. 1 (1980), pp 39–57.

97 Yoshida, S., Kanazawa, K., Yamaguchi, K. Sasaki, M., and Kobayashi, K., "Elevated-Temperature Fatigue Properties of Engineering Materials, Part I – Section 3: Elevated-Temperature Fatigue Properties of 18Cr-10Ni-Mo Stainless Steel Bars for General Application (SUS316-B)", *Transactions of National Research Institute for Metals*, Vol 19, No. 5 (September 1977), pp 262–272.

98 Yamaguchi, K., and Kanazawa, K., "Effect of Strain Wave Shape on High Temperature Fatigue Life of a Type 316 Steel and Application of the Strain Range Partitioning Method", *Metallurgical Transactions*, Vol 11A, No. 12 (December 1980), pp 2019–2027.

99 Jaske, C. E., and Frey, N. D., "Long-Life Fatigue of Type 316 Stainless Steel at Temperatures up to

593 C", *Transactions of the ASME, Journal of Engineering Materials and Technology*, Vol 104, No. 2 (April 1982), pp 137–144.

100 Levaillant, C., and Pineau, A., "Assessment of High-Temperature Low-Cycle Fatigue Life of Austenitic Stainless Steels by Using Intergranular Damage as a Correlating Parameter", Low-Cycle Fatigue and Life Prediction, ASTM STP 770, C. Amzallag, B. N. Leis, and P. Rabbe, Eds., American Society for Testing and Materials (1982), pp 169–193.

101 Wareing, J., and Vaughan, H. G., "Influence of Surface Finish on Low-Cycle Fatigue Characteristics of Type 316 Stainless Steel at 400 C", *Metal Science*, Vol 13, No. 1 (January 1979), pp 1–8.

102 Plumbridge, W. J., Dalski, M. E., and Castle, P. J., "High Strain Fatigue of a Type 316 Stainless Steel", *Fatigue of Engineering Materials and Structures*, Vol 3, No. 2 (1980), pp 177–188.

103 Sakane, M., and Ohnani, M., "A Study on the Notch Effect on the Low Cycle Fatigue of Metals in Creep-Fatigue Interacting Conditions at Elevated Temperature", *Transactions of the ASME, Journal of Engineering Materials and Technology*, Vol 105, No. 2 (April 1983), pp 75–80.

104 Furuya, K., Nagata, N., and Watanabe, R., "Low Cycle Fatigue Properties of Type 316 Stainless Steel in Vacuum", *Journal of Nuclear Materials*, Vol 89, No. 2/3 (April 1980), pp 372–382.

105 Levailland, C., Rezgui, B., and Pineau, A., "Effects of Environment and Hold Times on High Temperature Low Cycle Fatigue Behavior of 316L Stainless Steel", Proceedings of the Third International Conference on Mechanical Behavior of Materials, Cambridge, England (August 20–24, 1979), pp 163–172.

106 Vogt, J. B., Degallaix, S., and Foct, J., "Low Cycle Fatigue Life Enhancement of 316L Stainless Steel by Nitrogen Alloying", *International Journal of Fatigue*, Vol 6, No. 4 (October 1984), pp 211–215.

107 Chopra, O. K., and Smith, D. L., "Influence of a Flowing-Lithium Environment on the Fatigue and Tensile Properties of Type 316 Stainless Steel", paper presented at the 3rd Topical Meeting on Fusion Reactor Materials, Albuquerque, New Mexico (September 19–22, 1983).

108 Kanazawa, K., and Yoshida, S., "High Temperature Rotating Bending Fatigue Behavior of the Austenitic Stainless Steels, SUS 304-B and 316-B", *Transactions of National Research Institute for Metals*, Vol 16, No. 3 (June 1974), pp 90–98.

109 James, L. A., "Frequency Effects in the Elevated Temperature Crack Growth Behavior of Austenitic Stainless Steels – A Design Approach", *Transactions of the ASME, Journal of Pressure Vessel Technology*, Vol 101, No. 2 (May 1979), pp 171–176.

110 James, L. A., "The Effect of Elevated Temperature Upon the Fatigue-Crack Propagation Behavior of Two Austenitic Stainless Steels", Proceedings of the International Conference on Mechanical Behavior of Materials, Volume III, Temperature Effects of Metals; Environmental Effects; Polymers, Kyoto, Japan (August 15–20, 1971).

111 Tobler, R. L., and Reed, R. P., "Fatigue Crack Growth Rates of Structural Alloys at 4 K", *Advances in Cryogenic Engineering*, Vol 22 (1977), pp 35–46.

112 Sadananda, K., and Shahinian, P., "Effect of Environment on Crack Growth Behavior in Austenitic Stainless Steels Under Creep and Fatigue Conditions", *Metallurgical Transactions*, Vol 11A, No. 2 (February 1980), pp 267–276.

113 Michel, D. J., and Smith, H. H., "Effect of Hold Time on Elevated Temperature Fatigue Crack Propagation in Types 304 and 316 Stainless Steels", Proceedings of 1976 ASME-MPC Symposium on Creep-Fatigue Interaction, held at ASME Winter Annual Meeting, New York, New York (December 1976).

114 James, L. A., "The Effect of Stress Ratio Upon the Elevated Temperature Fatigue-Crack Growth Behavior of Several Reactor Structural Materials", Hanford Engineering Laboratory, Richland, Washington, Summary Report, HEDL-TME-75-20 (February 1975).

115 Ledbetter, H. M., "Stainless-Steel Elastic Constants at Low Temperatures", *Journal of Applied Physics*, Vol 52, No. 3, Pt 1 (March 1981), pp 1587–1589.

116 Ryan, N. D., McQueen, H. J., and Jonas, J. J., "The Deformation Behavior of Types 304, 316, and 317 Austenitic Stainless Steels During Hot Torsion", *Canadian Metallurgical Quarterly*, Vol 22, No. 3 (July–September 1983), pp 369–378.

117 Ljungstrom, L. G., "The Influence of Trace Elements on the Hot Ductility of Austenitic 17Cr-13Ni-Mo Steel", *Scandinavian Journal of Metallurgy*, Vol 6, No. 4 (1977), pp 176–184.

118 Raghunathan, V. S., Seetharaman, V., Venkadesan, S., and Rodriguez, P., "The Influence of Post Weld Heat Treatments on the Structure, Composition and the Amount of Ferrite in Type 316 Stainless Steel Welds", *Metallurgical Transactions*, Vol 10A, No. 11 (November 1979), pp 1683–1689.

119 Thomas, R. G., and Yapp, D., "The Effect of Heat Treatment on Type 316 Stainless Steel Weld Metal", *Welding Journal*, Vol 57, No. 12 (December 1978), pp 361-s–366-s.

120 Lai, J. K., and Haigh, J. R., "Delta-Ferrite Transformations in a Type 316 Weld Metal", *Welding Journal*, Vol 58, No. 1 (January 1979), pp 1-s–6-s.

121 Read, D. T., McHenry, H. I., Steinmeyer, P. A., and Thomas, R. D., Jr., "Metallurgical Factors Affecting the Toughness of 316L SMA Weldments at Cryogenic Temperatures", *Welding Journal*, Vol 59, No. 4 (April 1980), pp 104-s–113-s.

122 Keown, S. R., and Thomas, R. G., "Role of Delta Ferrite in Thermal Aging of Type 316 Weld Metals", *Metal Science*, Vol 15, No. 9 (September 1981), pp 386–392.

123 King, R. T., Cole, N. C., and Goodwin, G. M., "Creep Behavior of SMA Type 316 Weld Metal With Controlled Residual Elements", *Transactions of the ASME, Series J, Journal of Pressure Vessel Technology*, Vol 98, No. 3 (August 1976), pp 194–198.

124 ASTM A743/A743M-85(1985).

Fe
18 Cr
13 Ni
+ Mo

Type 316
Type 317

Fe
18 Cr
13 Ni
+ Mo

Type 316
Type 317

Alloy	Types 316 and 316L	
Alloy Type	Product Form	AMS Specification
316	Sand and centrifugal castings	5361D
	Investment castings	5360D
	Bars, forgings, tubing, and rings	5648F
	Bars and forgings, free machining	5649C
	Sheet, strip, plate	5524F
	Tubing, seamless	5573G
	Wire	5690H
	Welding electrodes, covered	5691E
	Welding wire	5692
	Welding wire, high ferrite	5696
316L	Bars, forgings, tubing, and rings	5653B
	Sheet, strip, and plate	5507D

Note: There are no AMS specifications covering Types 317 and 317L.

TABLE 1.031. AMS SPECIFICATIONS (1–7,46–50)

Alloy	316		316 – Free Machining		316L		317		317L	
Source	AMS 5524F AMS 5573G[a] AMS 5648F[a] AMS 5690H		AMS 5649C		AMS 5507D AMS 5653B[b]		(30)		(30)	
	Percent		Percent		Percent		Percent		Percent	
Element	Min	Max	Min	Max	Min	Max	Min	Max	Min	Max
Chromium	16.00	18.00	17.00	19.00	16.00	18.00	18.00	20.00	18.00	20.00
Nickel	10.00	14.00	12.00	14.00	10.00	14.00	11.00	15.00	11.00	15.00
Molybdenum	2.00	3.00	1.75	2.50	2.00	3.00	3.00	4.00	3.00	4.00
Carbon	–	0.08	–	0.08	–	0.03	–	0.08	–	0.03
Manganese	–	2.00	1.00	2.00	–	2.00	–	2.00	–	2.00
Silicon	–	1.00	–	1.00	–	1.00	–	1.00	–	1.00
Copper	–	0.75	–	0.75	–	0.75	–	–	–	–
Phosphorus	–	0.040	–	0.20	–	0.040	–	0.045	–	0.045
Sulfur	–	0.030	0.10	0.20	–	0.030	–	0.030	–	0.030

(a) AMS 5573G and AMS 5648F specify 1.25 percent minimum manganese.
(b) AMS 5653B specifies 1.25 percent minimum manganese.

TABLE 1.041. COMPOSITION SPECIFICATIONS FOR WROUGHT TYPES 316, 316L, 317, AND 317L (1–7,30)

Alloy	316		316		CF3M		CF8M	
Form	Investment Castings		Sand, Centrifugal Castings		Cast		Cast	
Source	AMS 5360D		AMS 5361D		ASTM A743		ASTM A743	
	Percent		Percent		Percent		Percent	
Element	Min	Max	Min	Max	Min	Max	Min	Max
Chromium	16.00	18.00	17.00	20.00	17.00	21.00	18.00	21.00
Nickel	12.00	14.00	12.00	15.00	9.00	13.00	9.00	12.00
Molybdenum	1.50	2.25	1.75	2.50	2.00	3.00	2.00	3.00
Carbon	–	0.15	0.15	0.25	–	0.03	–	0.08
Manganese	–	2.00	–	2.00	–	1.50	–	1.50
Silicon	–	0.75	–	1.00	–	1.50	–	2.00
Copper	–	0.75	–	0.75	–	–	–	–
Phosphorus	–	0.04	–	0.04	–	0.04	–	0.04
Sulfur	–	0.03	–	0.04	–	0.04	–	0.04

TABLE 1.042. COMPOSITION SPECIFICATIONS FOR CAST TYPE 316 (46,47,124)

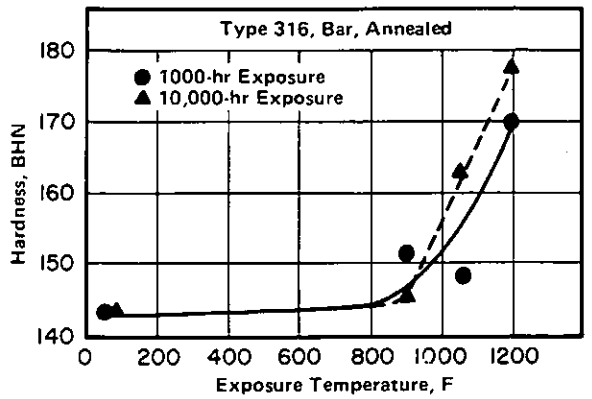


FIGURE 1.061. EFFECT OF EXPOSURES TO ELEVATED TEMPERATURES ON ROOM-TEMPERATURE HARDNESS (11)

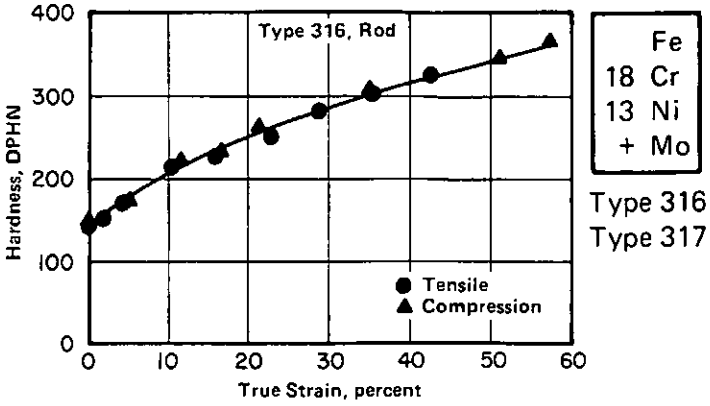


FIGURE 1.063. EFFECT OF COLD STRAINING ON HARDNESS (51)

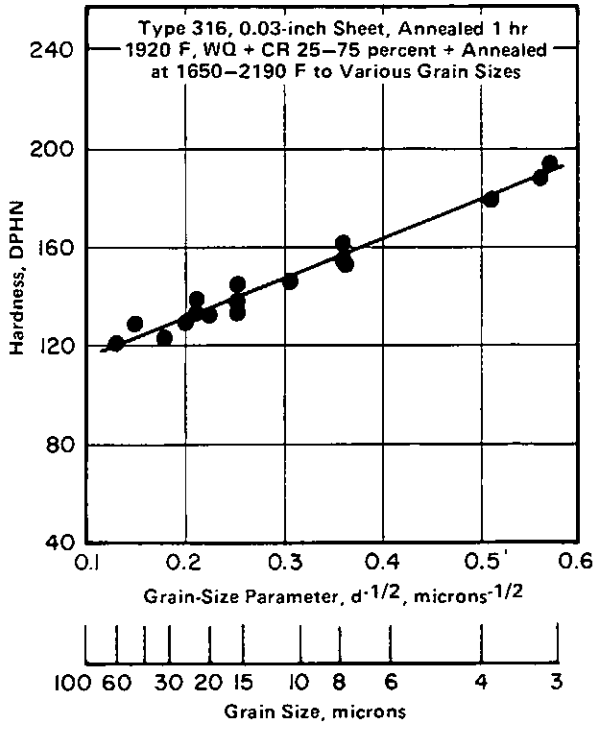


FIGURE 1.064. EFFECT OF GRAIN SIZE ON HARDNESS (52)

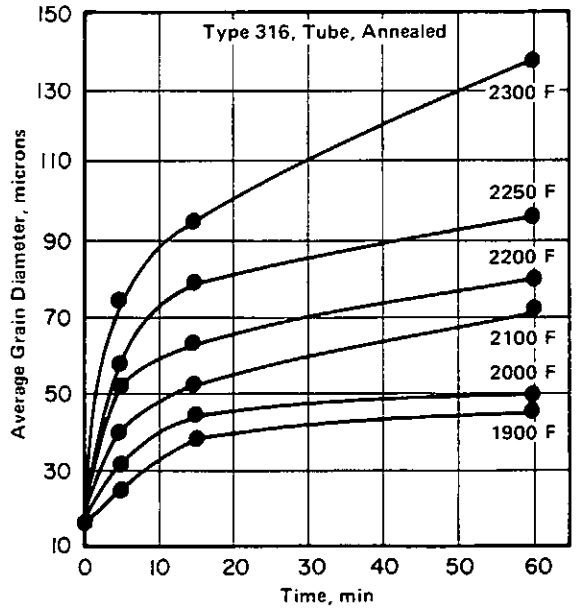


FIGURE 1.0951. EFFECT OF TIME AND TEMPERATURE ON GRAIN GROWTH (15)

Fe
18 Cr
13 Ni
+ Mo

Type 316
Type 317

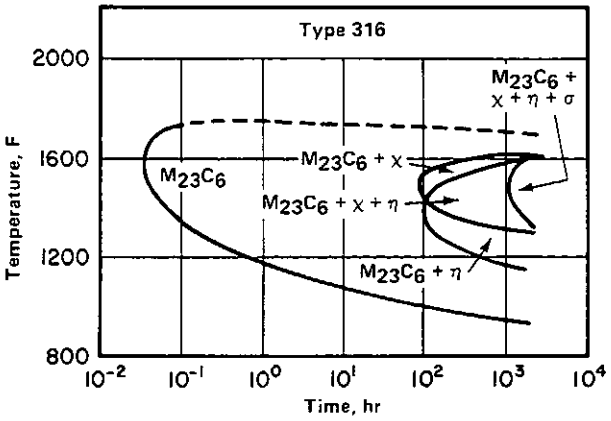


FIGURE 2.01212. TIME-TEMPERATURE-PRECIPITATION DIAGRAM (54)

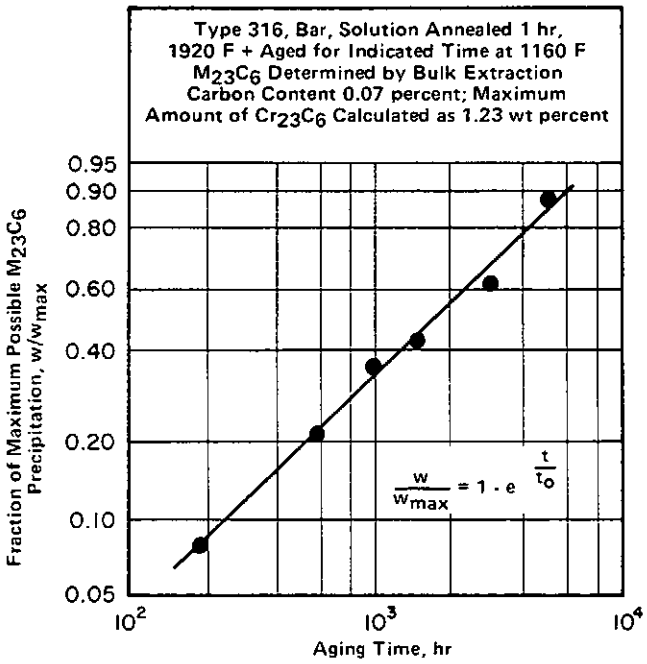


FIGURE 2.01213. EFFECT OF AGING TIME ON AMOUNT OF $M_{23}C_6$ PRECIPITATE AT 1160 F (56)

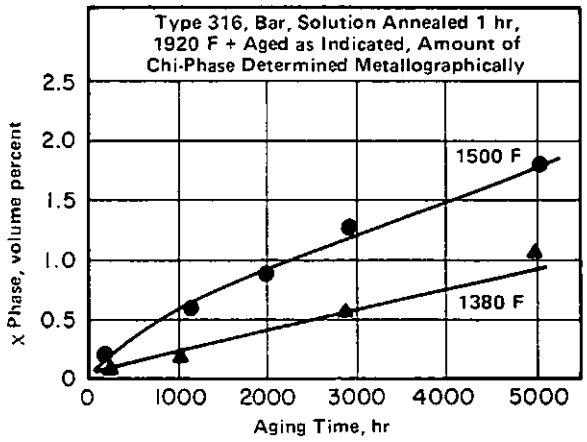


FIGURE 2.01214. EFFECTS OF AGING CONDITIONS ON AMOUNT OF CHI-PHASE PRECIPITATE (56)

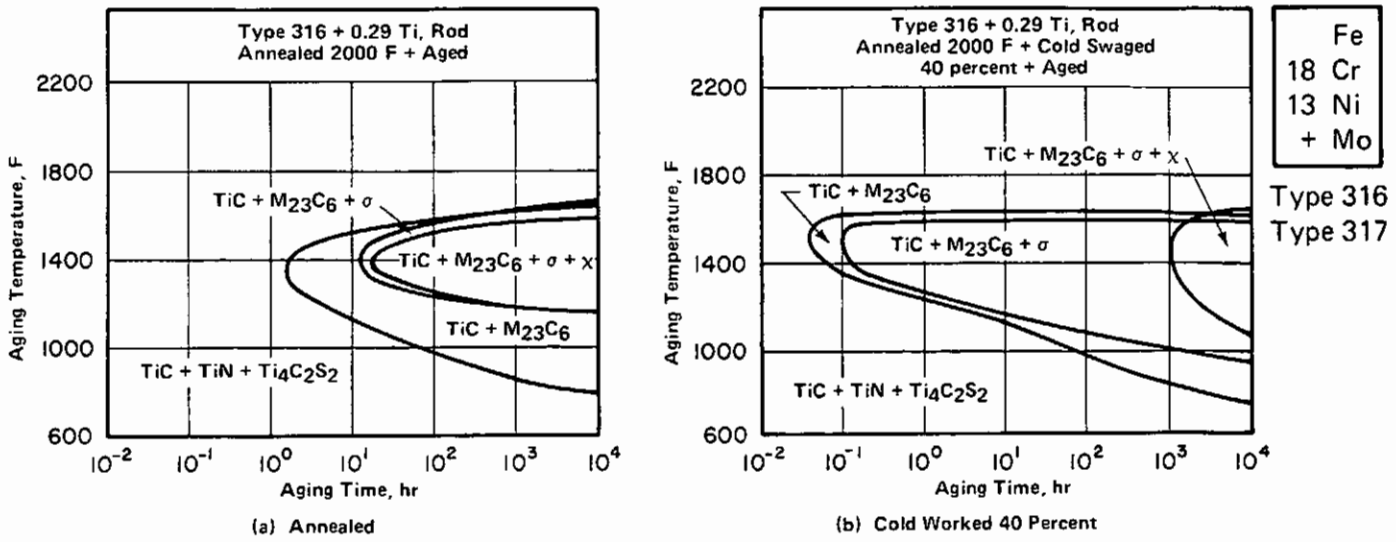


FIGURE 2.01216. EFFECTS OF TITANIUM ADDITION AND COLD WORK ON TIME-TEMPERATURE-PRECIPITATION DIAGRAM (57)

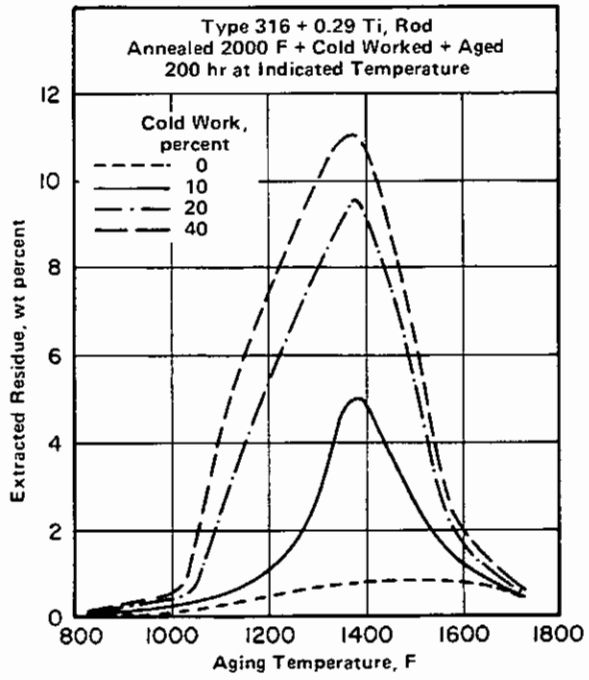


FIGURE 2.01217. EFFECTS OF COLD WORK AND AGING TEMPERATURE ON AMOUNT OF PRECIPITATE (57)

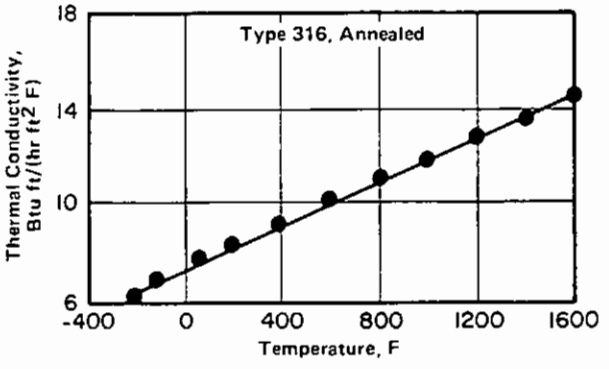


FIGURE 2.013. THERMAL CONDUCTIVITY (35)

Fe
18 Cr
13 Ni
+ Mo

Type 316
Type 317

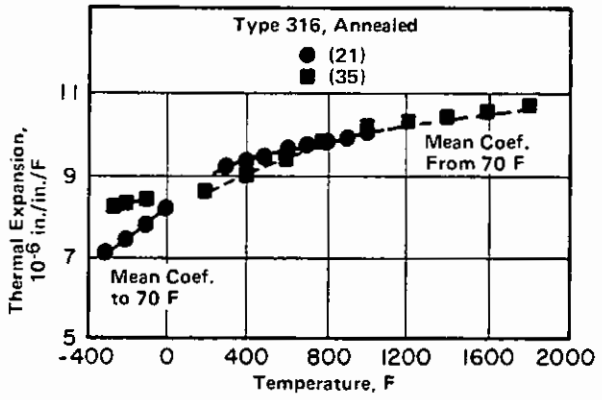


FIGURE 2.014. THERMAL EXPANSION (21,35)

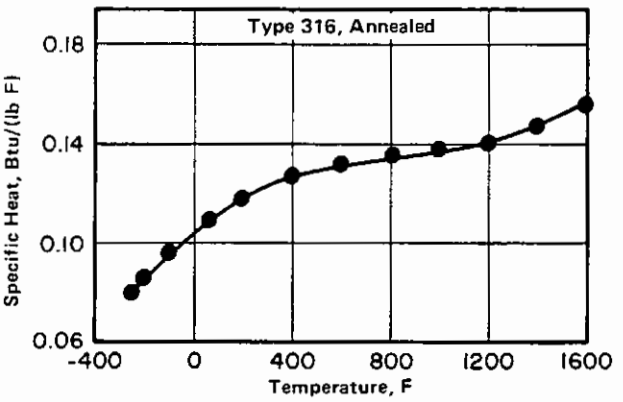


FIGURE 2.015. SPECIFIC HEAT (35)

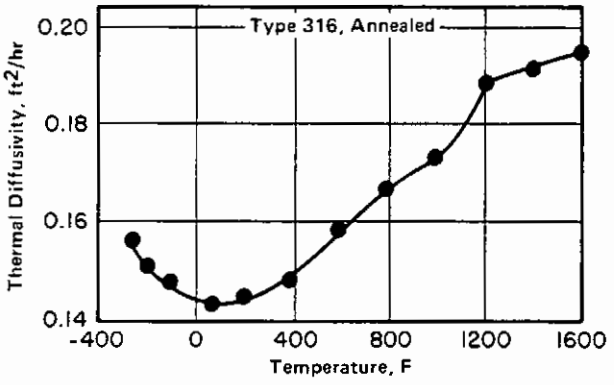


FIGURE 2.016. THERMAL DIFFUSIVITY (35)

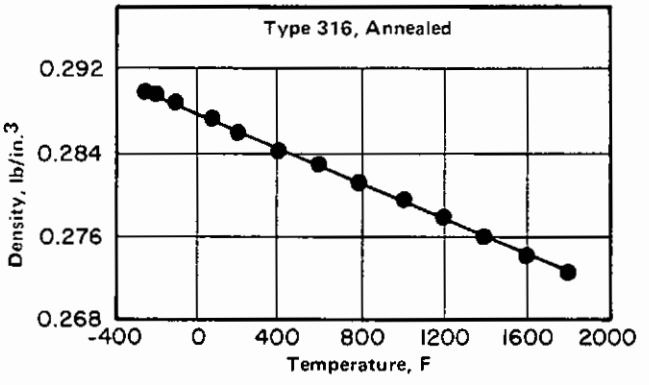


FIGURE 2.0211. EFFECT OF TEMPERATURE ON DENSITY (35)

Alloy	Condition	Temp., F	Electrical Conductivity		Electrical Resistivity, microhm-in.
			Percent IACS	Mmho/in.^{3}	
316	Annealed	68	2.44	0.0344	29.1
317	Annealed	68	2.24	0.0330	31.1
316	Annealed	1200	1.93	0.0285	45.7

TABLE 2.0221. ELECTRICAL PROPERTIES OF ANNEALED ALLOY (20)

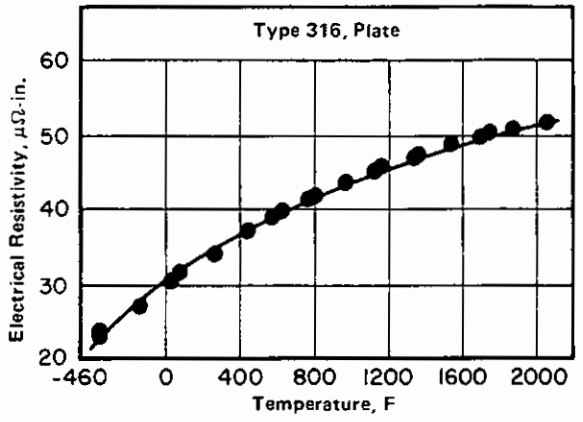


FIGURE 2.0222. ELECTRICAL RESISTIVITY (58)

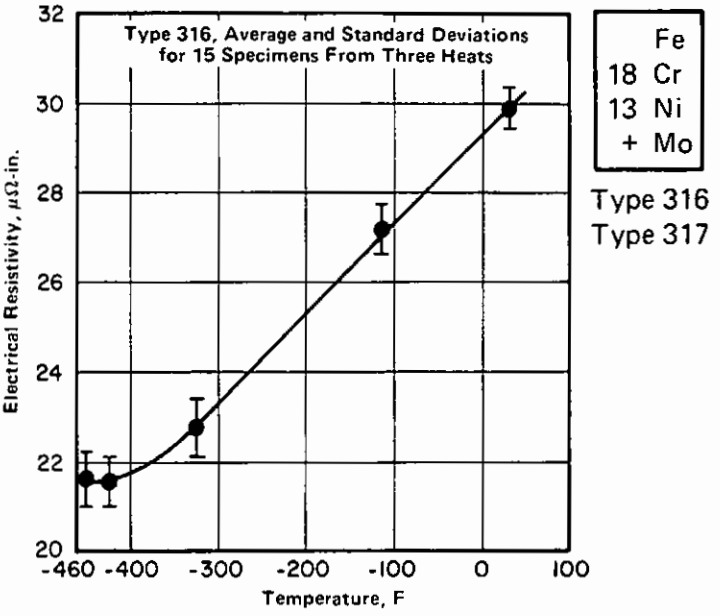


FIGURE 2.0223. ELECTRICAL RESISTIVITY AT CRYOGENIC TEMPERATURES (59)

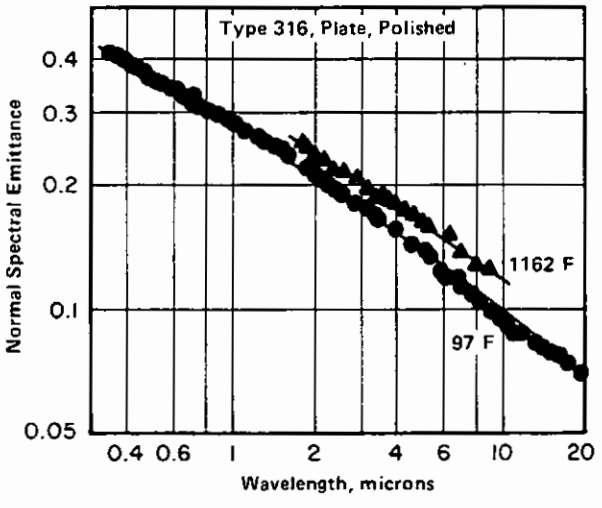


FIGURE 2.0241. NORMAL SPECTRAL EMITTANCE AT VARIOUS WAVELENGTHS AT ROOM AND ELEVATED TEMPERATURE (58)

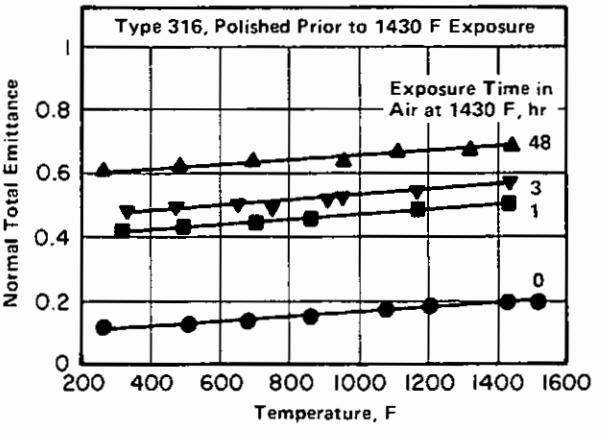


FIGURE 2.0242. EFFECTS OF TEMPERATURE AND PRE-OXIDATION ON EMITTANCE (60)

Fe
18 Cr
13 Ni
+ Mo

Type 316
Type 317

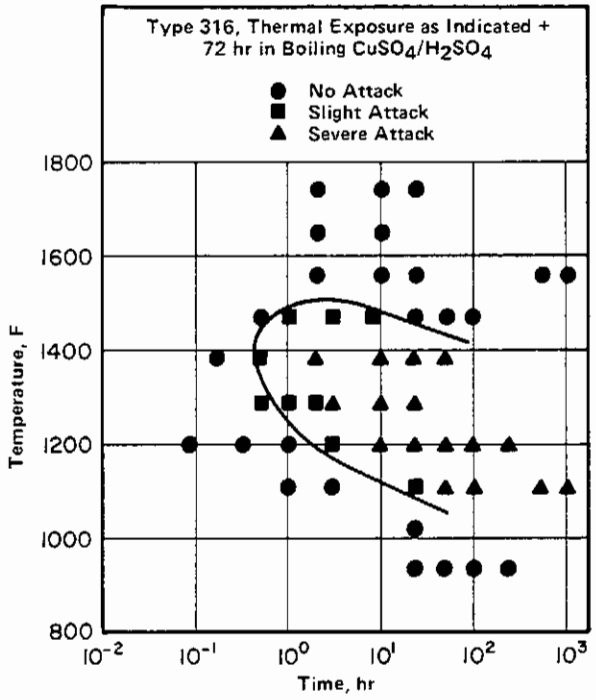


FIGURE 2.0322. TIME-TEMPERATURE CURVE FOR SENSITIZATION OF TYPE 316 (62)

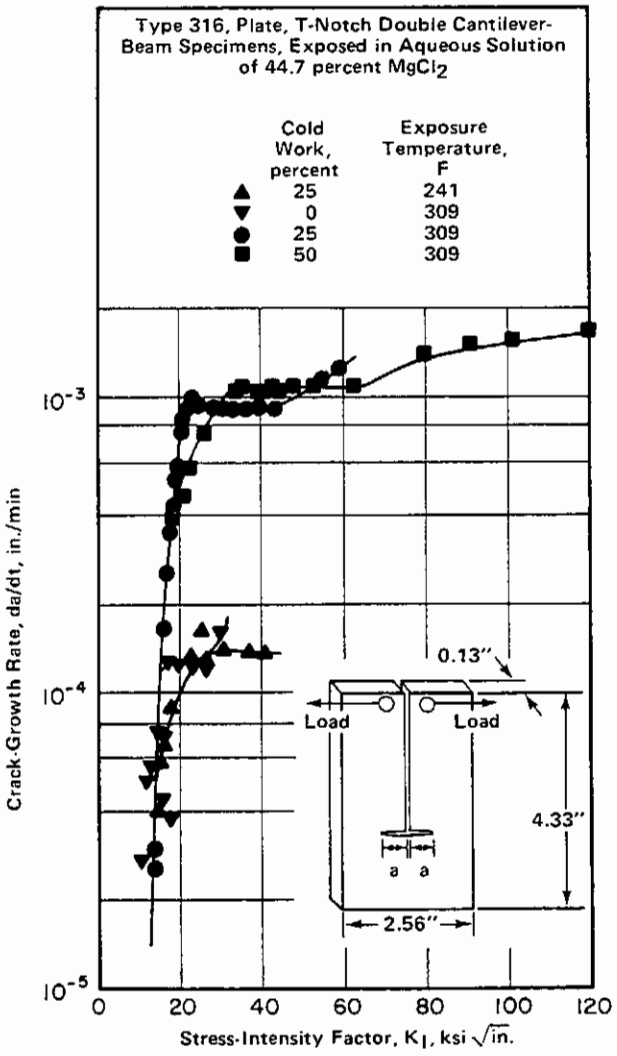


FIGURE 2.0332. EFFECTS OF COLD WORK AND EXPOSURE TEMPERATURE ON STRESS-CORROSION CRACK-GROWTH RATE IN HOT $MgCl_2$ SOLUTION (63,64)

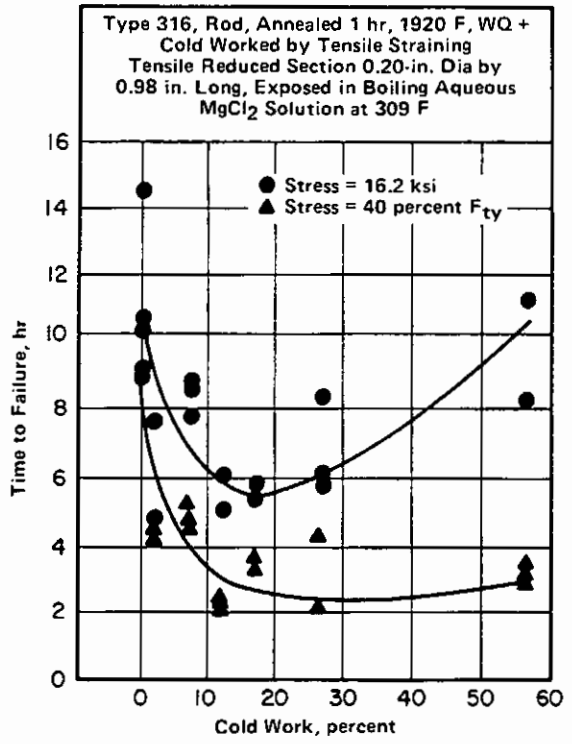


FIGURE 2.0334. EFFECTS OF COLD WORK ON STRESS-CORROSION TIME TO FAILURE IN BOILING $MgCl_2$ SOLUTION (65)

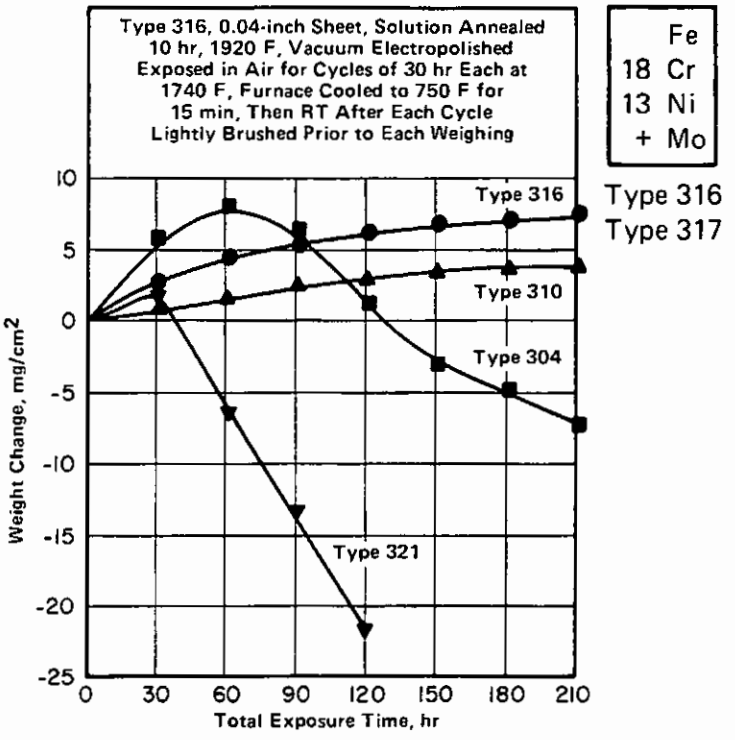


FIGURE 2.0343. OXIDATION-WEIGHT-CHANGE BEHAVIOR OF TYPE 316 IN AIR AT 1740 F AS COMPARED WITH TYPES 304, 310, AND 321 (66)

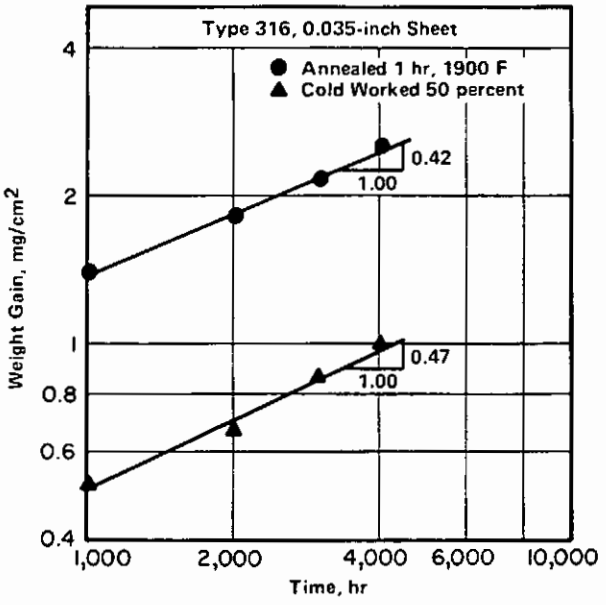


FIGURE 2.0344. OXIDATION BEHAVIOR AT 1000 F IN 3500-PSI SUPERCRITICAL STEAM (67)

Fe
18 Cr
13 Ni
+ Mo

Type 316
Type 317

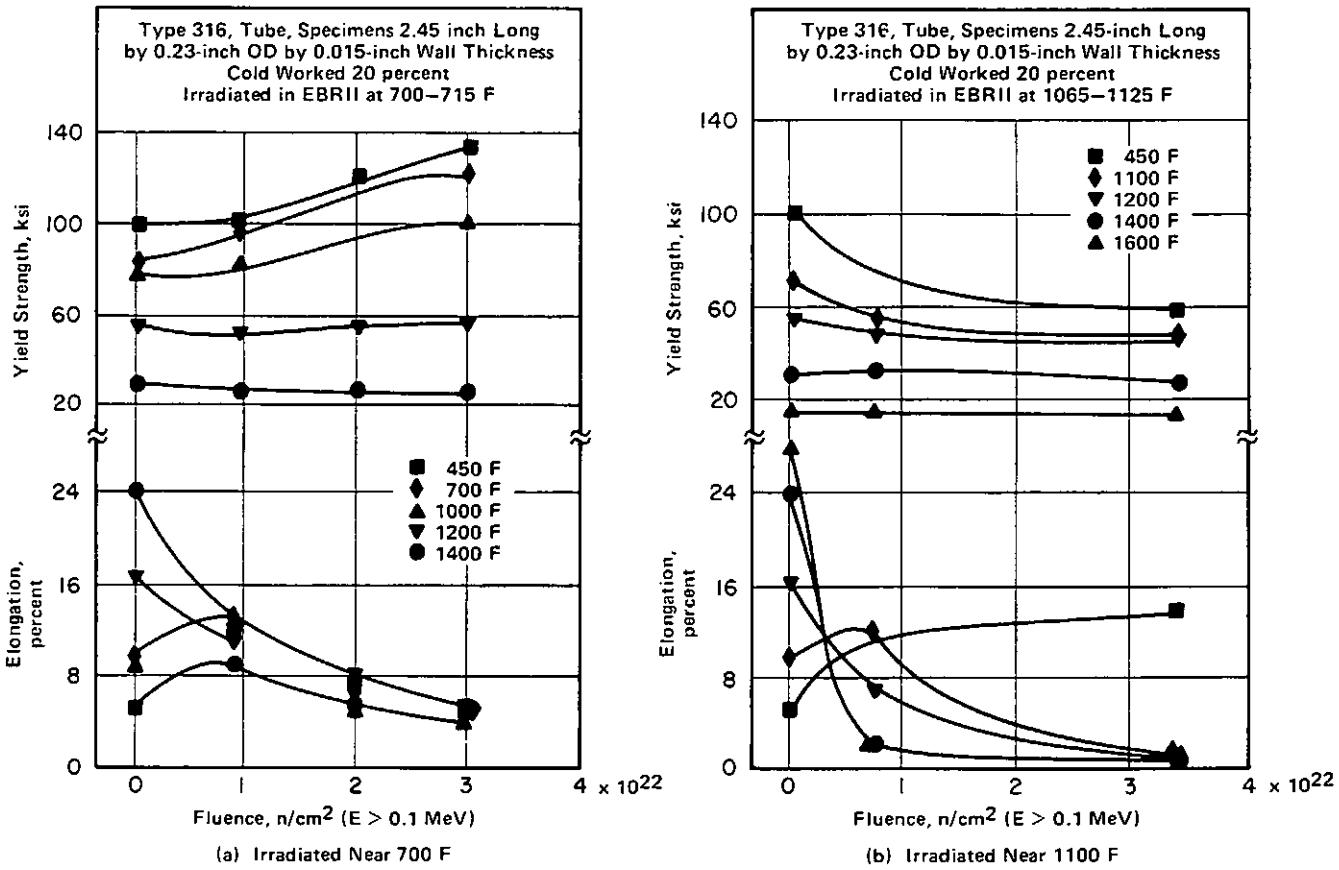


FIGURE 2.042. EFFECT OF FLUENCE ON TENSILE YIELD STRENGTH AND ELONGATION OF COLD-WORKED TYPE 316 AT ELEVATED TEMPERATURES (71)

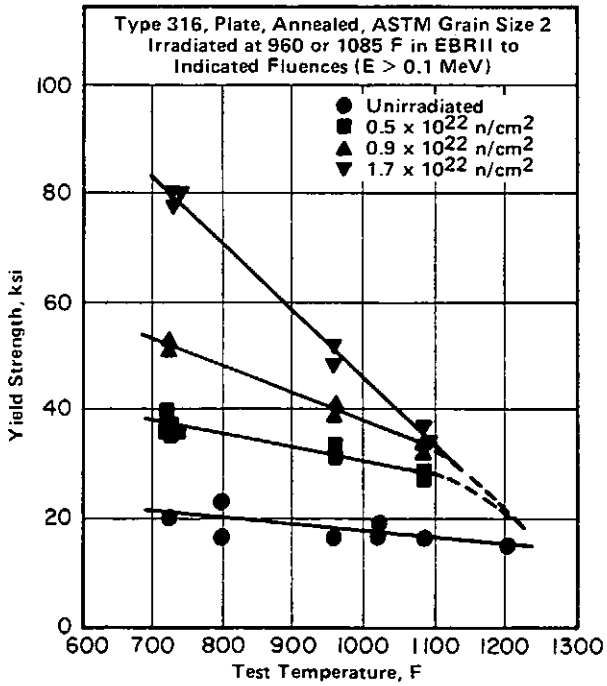


FIGURE 2.043. EFFECTS OF FAST-NEUTRON IRRADIATION ON YIELD STRENGTH AT ELEVATED TEMPERATURES (72)

Fe
18 Cr
13 Ni
+ Mo

Type 316
Type 317

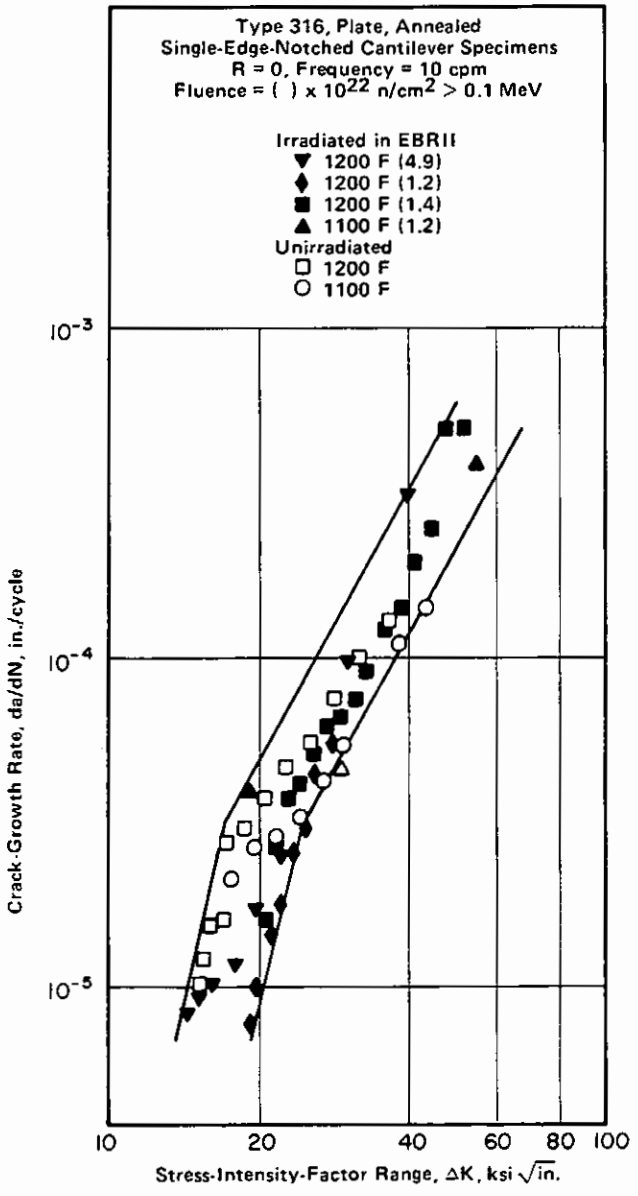


FIGURE 2.045. EFFECTS OF FAST-NEUTRON IRRADIATION ON LOW-CYCLE FATIGUE-CRACK-GROWTH RATE OF ANNEALED ALLOY IN AIR AT ELEVATED TEMPERATURES (73)

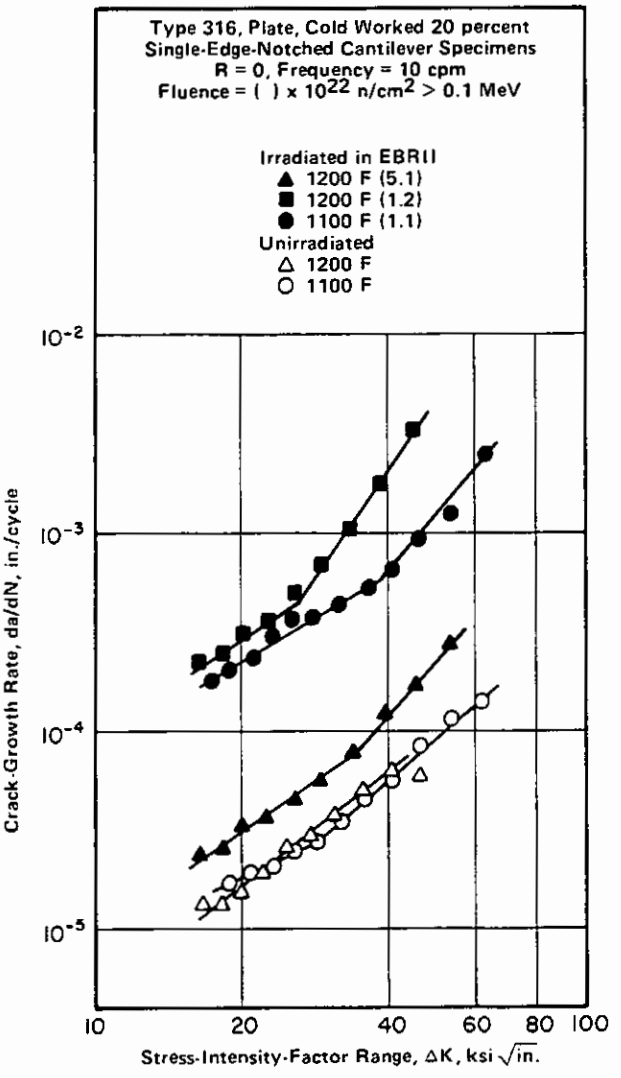


FIGURE 2.046. EFFECTS OF FAST-NEUTRON IRRADIATION ON LOW-CYCLE FATIGUE-CRACK-GROWTH RATE OF COLD-WORKED ALLOY IN AIR AT ELEVATED TEMPERATURES (73)

Fe
18 Cr
13 Ni
+ Mo

Type 316
Type 317

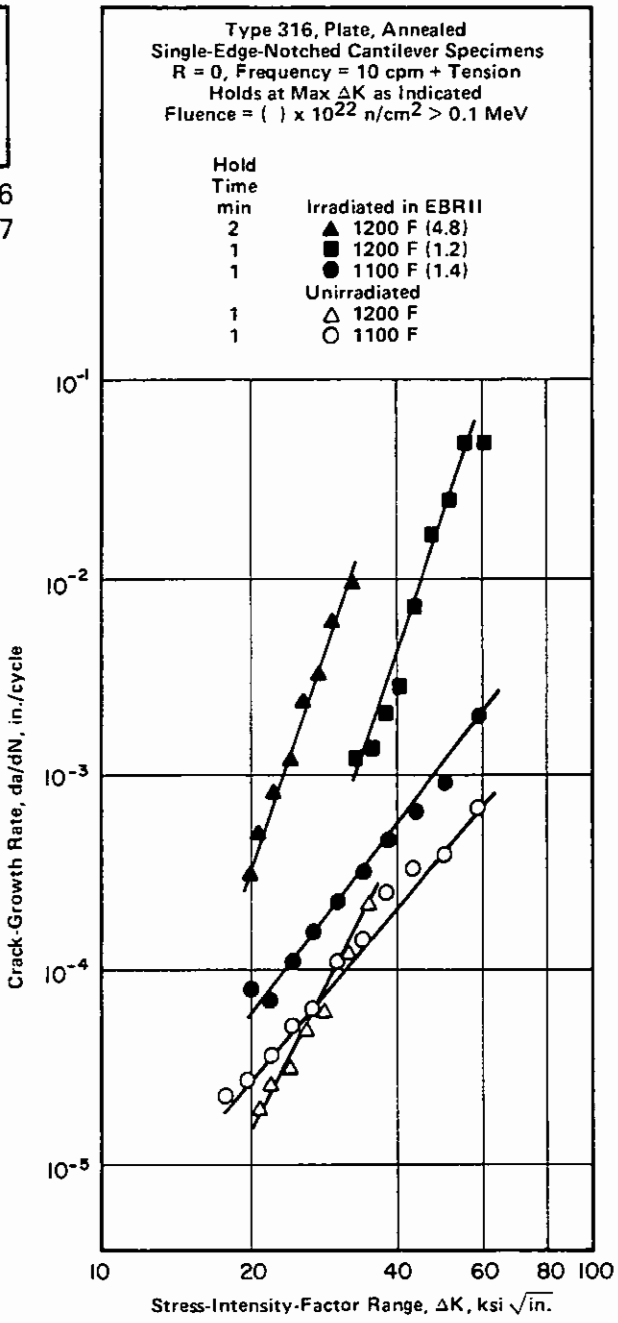


FIGURE 2.047. EFFECTS OF HOLD TIME AND FAST-NEUTRON IRRADIATION ON LOW-CYCLE FATIGUE-CRACK-GROWTH RATE OF ANNEALED ALLOY IN AIR AT ELEVATED TEMPERATURES (73)

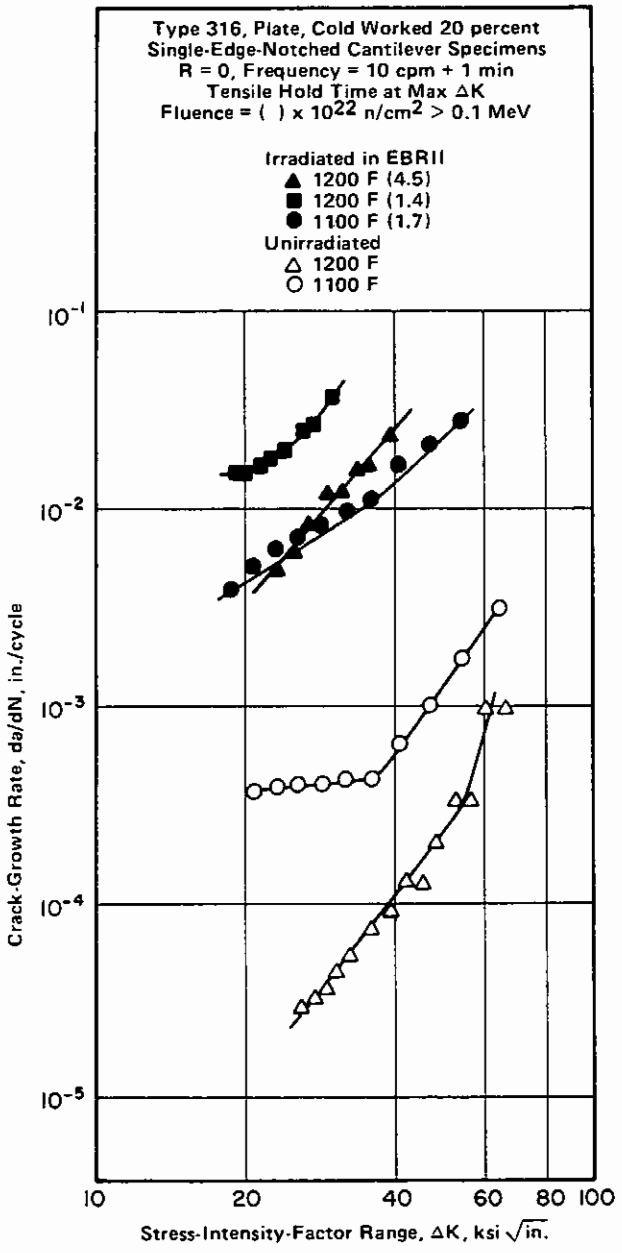


FIGURE 2.048. EFFECTS OF HOLD TIME AND FAST-NEUTRON IRRADIATION ON LOW-CYCLE FATIGUE-CRACK-GROWTH RATE OF COLD-WORKED ALLOY IN AIR AT ELEVATED TEMPERATURES (73)

Fe
18 Cr
13 Ni
+ Mo

Type 316
Type 317

Alloy Type	AMS Spec.	Product Form	Thickness, in.	F_{tu}, ksi (Max)	e, percent (Min)	Hardness Min	Hardness Max
316	5360D	Casting					187 BHN
	5361D	Casting					212 BHN
	5648F	Wire		125			
		Bars	≤2.000			140 BHN	255 BHN
			>2.000				255 BHN
		Forgings, rings					187 BHN
		Tubing					90 HRB
	5524F	Sheet, strip, and plate	<0.025	100	40		
			≥0.025	100	45		
	5649C	Wire		125			
		Bars				20 HRC	28 HRC
		Forgings					187 BHN
	5573G	Tubing	≤0.188 OD; ≤0.016 wall	115			
			≤0.188 OD; >0.016 wall	100			
			0.188–0.500 OD; ≤0.010 wall	110	32		
			0.188–0.500 OD; >0.010 wall	100	35		
			>0.500 OD; ≤0.010 wall	100	27		
			>0.500 OD; >0.010 wall	100	30		
316L	5653B	Bar	≤2.000			140 BHN	255 BHN
			>2.000				255 BHN
		Tubing					90 HRB
		Forgings, rings					187 BHN
		Wire		125			
	5507D	Sheet, strip, and plate	≤0.025	100	40		
			>0.025	100	45		

Note: The original AMS documents should be consulted for complete specification details.

TABLE 3.011. AMS-SPECIFIED MECHANICAL PROPERTIES (1–6,46,47)

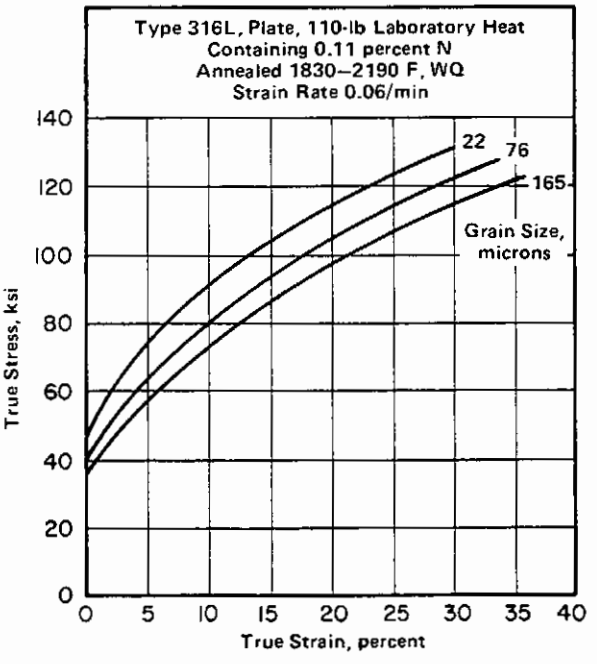


FIGURE 3.0211. EFFECTS OF GRAIN SIZE ON TRUE STRESS-TRUE STRAIN CURVES AT ROOM TEMPERATURE (74)

Fe
18 Cr
13 Ni
+ Mo

Type 316
Type 317

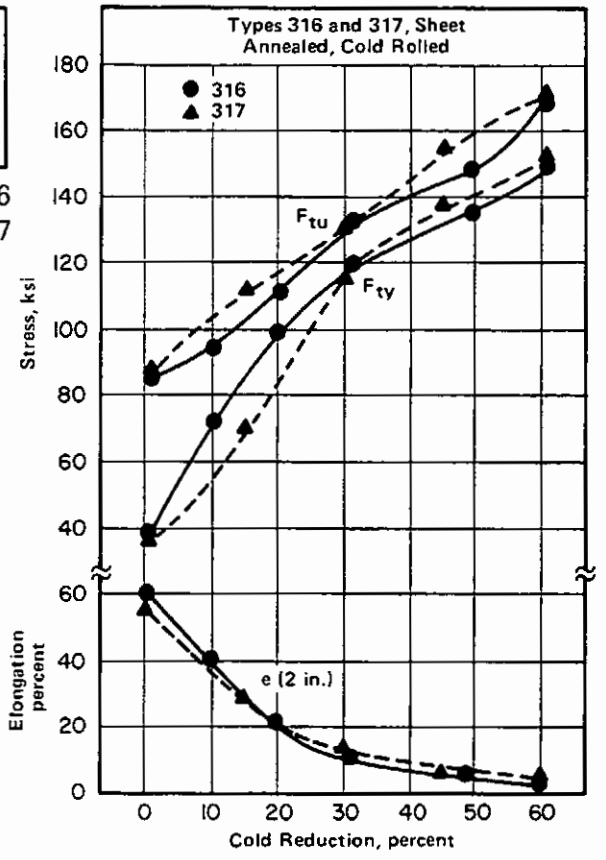


FIGURE 3.0212. EFFECT OF COLD WORK ON TENSILE PROPERTIES OF TYPES 316 AND 317 SHEET (20)

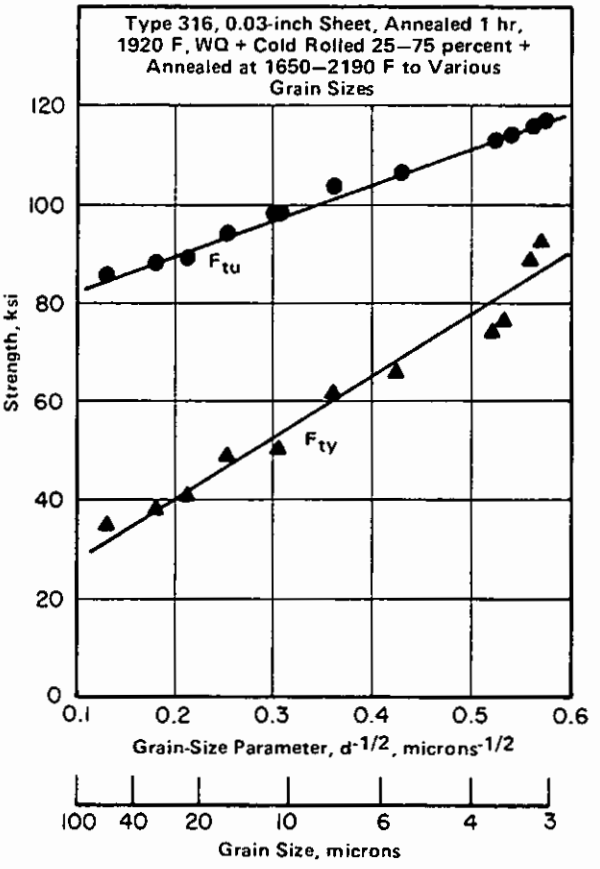


FIGURE 3.0213. EFFECT OF GRAIN SIZE ON TENSILE STRENGTH AT ROOM TEMPERATURE (52)

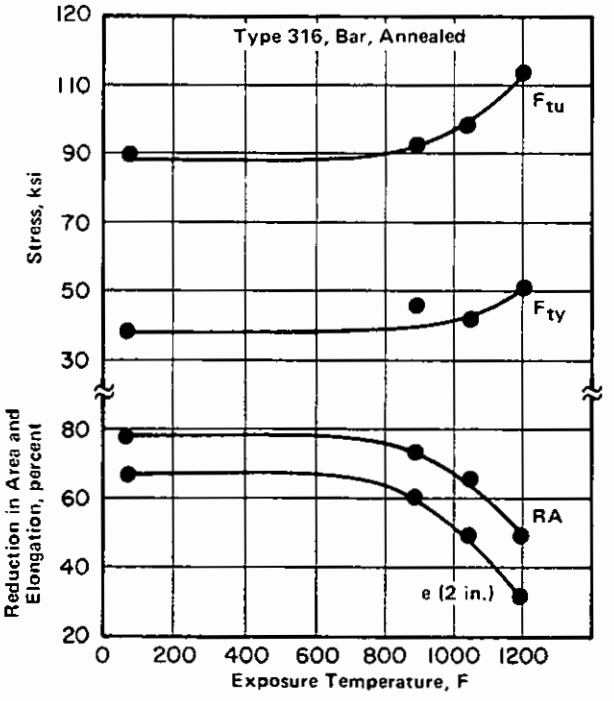


FIGURE 3.0214. EFFECT OF 100,000-HOUR EXPOSURES TO ELEVATED TEMPERATURES ON ROOM-TEMPERATURE TENSILE PROPERTIES OF BAR (11)

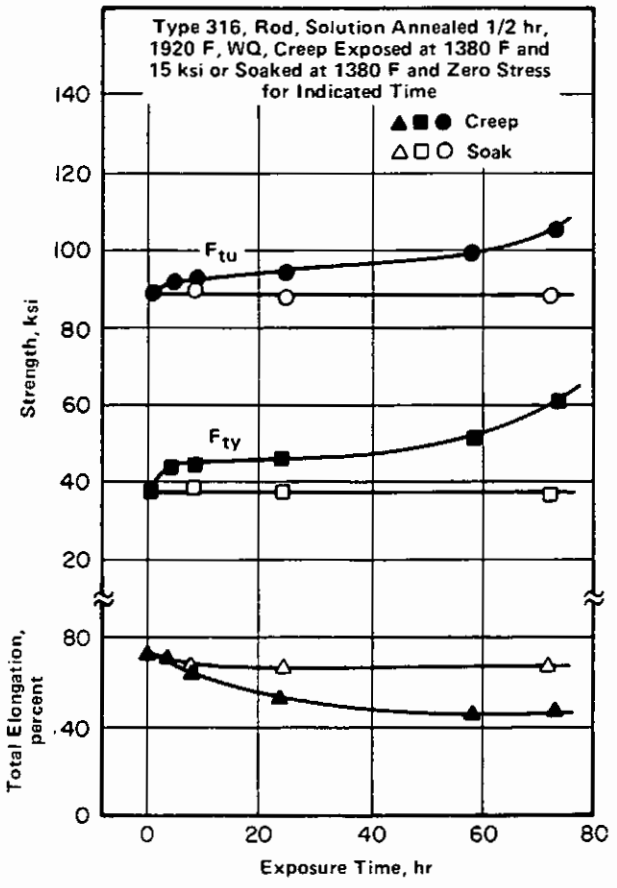
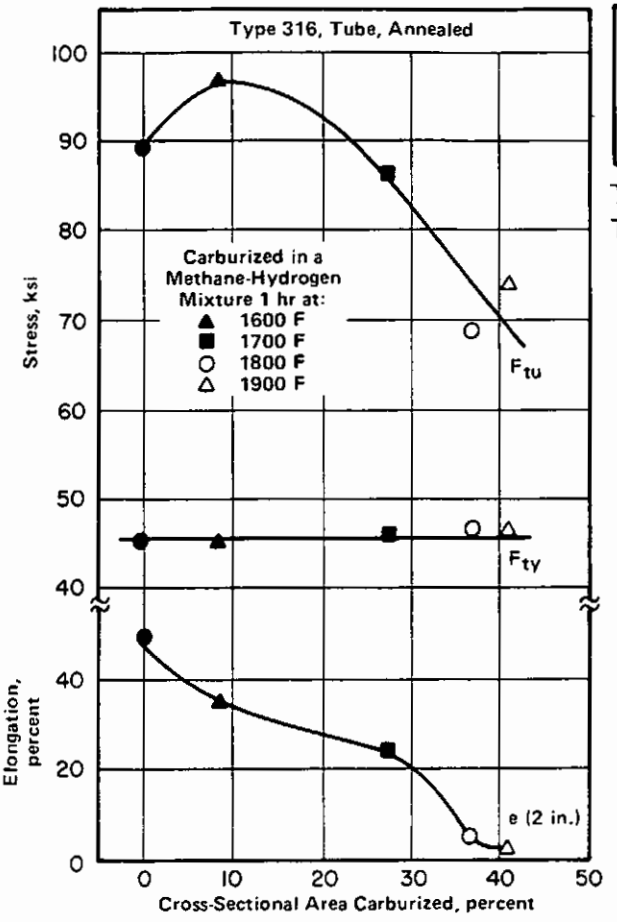


FIGURE 3.0215. EFFECTS OF PRIOR CREEP AND SOAKING ON TENSILE PROPERTIES AT ROOM TEMPERATURE (75)



Fe
18 Cr
13 Ni
+ Mo

Type 316
Type 317

FIGURE 3.0216. EFFECT OF CARBURIZING ON ROOM-TEMPERATURE TENSILE PROPERTIES OF TUBE (14)

Alloy	Type 316				
Form	Wire				
Wire Dia., in.	Condition	F_{ty}, ksi	F_{tu}, ksi	e (4x Dia.), percent	RA percent
0.062	Annealed	30	90	55	65
0.062	Soft temper	75	100	40	65
0.062	Spring temper	–	230	–	–
0.250	Spring temper	–	160	–	–
0.307	Spring temper	–	150	–	–
0.500	Soft temper	60	90	50	65

TABLE 3.0217. TENSILE PROPERTIES OF WIRE (38)

Fe
18 Cr
13 Ni
+ Mo

Type 316
Type 317

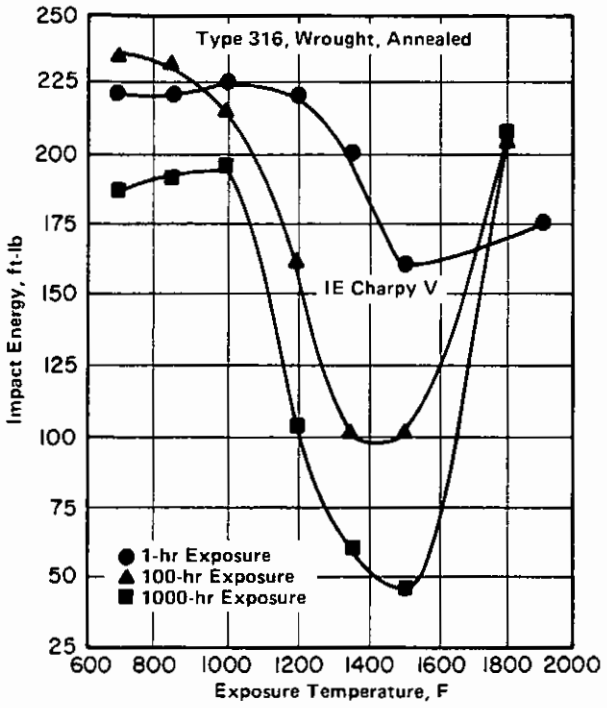


FIGURE 3.0231. EFFECT OF EXPOSURES TO ELEVATED TEMPERATURES ON ROOM-TEMPERATURE CHARPY V-NOTCH IMPACT PROPERTIES (19)

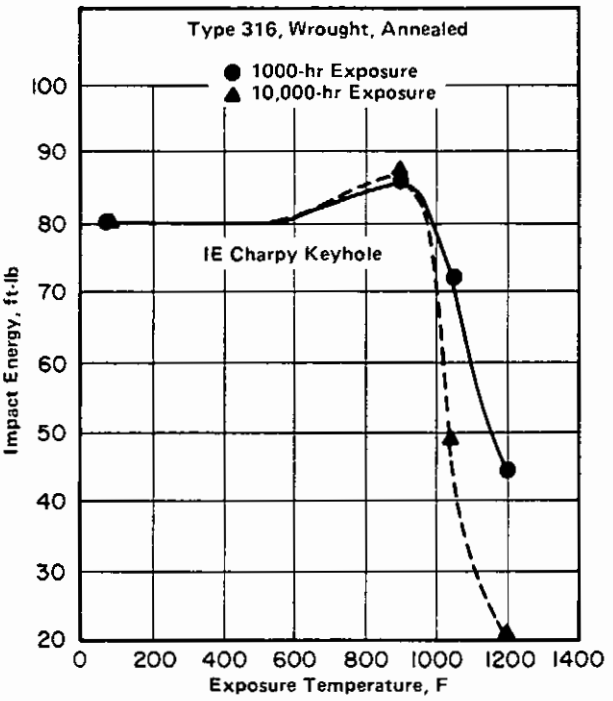


FIGURE 3.0232. EFFECT OF EXPOSURES TO ELEVATED TEMPERATURES ON ROOM-TEMPERATURE CHARPY-KEYHOLE IMPACT PROPERTIES (11)

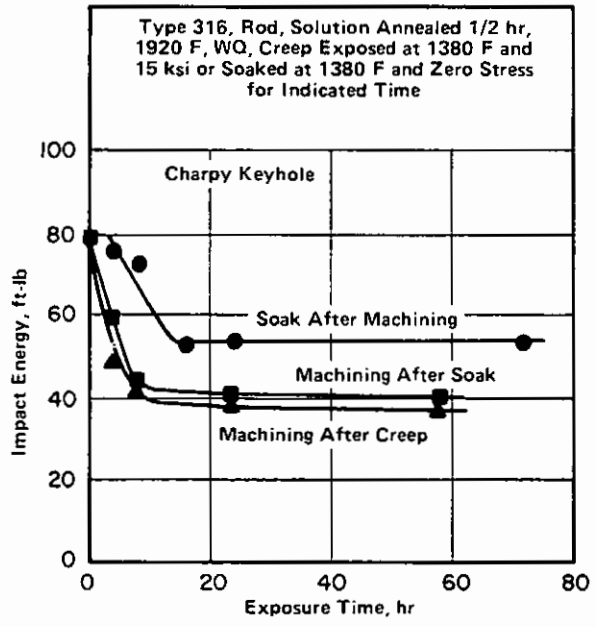


FIGURE 3.0233. EFFECTS OF PRIOR CREEP AND SOAKING ON IMPACT ENERGY AT ROOM TEMPERATURE (75)

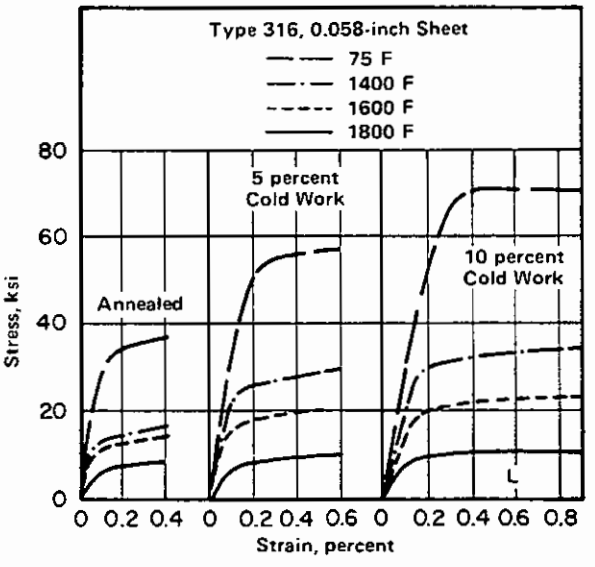


FIGURE 3.0311. STRESS-STRAIN CURVES FOR ANNEALED AND COLD-WORKED SHEET FROM 75 TO 1800 F (24)

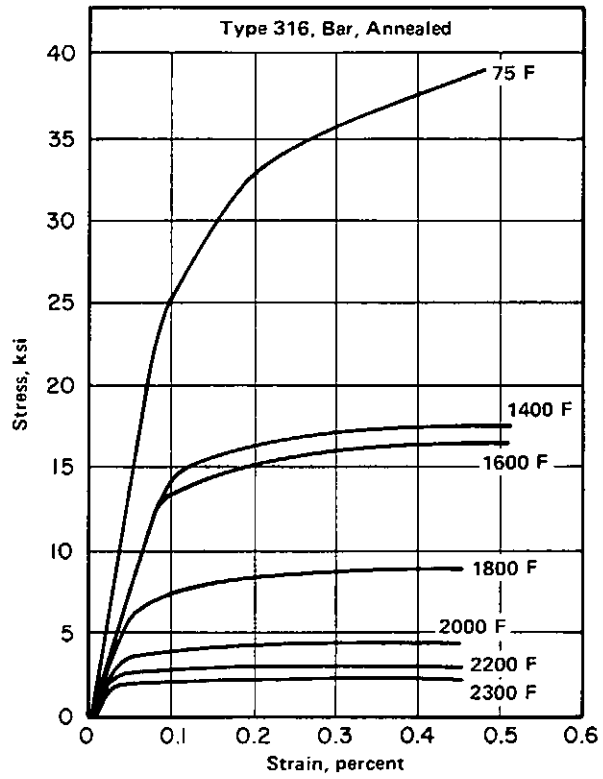


FIGURE 3.0312. STRESS-STRAIN CURVES FOR BAR FROM 75 TO 2300 F (24)

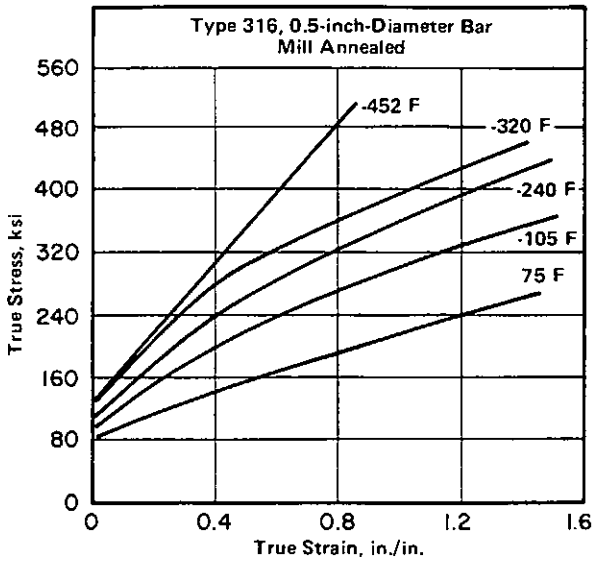


FIGURE 3.0313. COMPLETE TRUE STRESS-TRUE STRAIN CURVES FOR TYPE 316 BAR FROM ROOM TEMPERATURE TO -452 F (9)

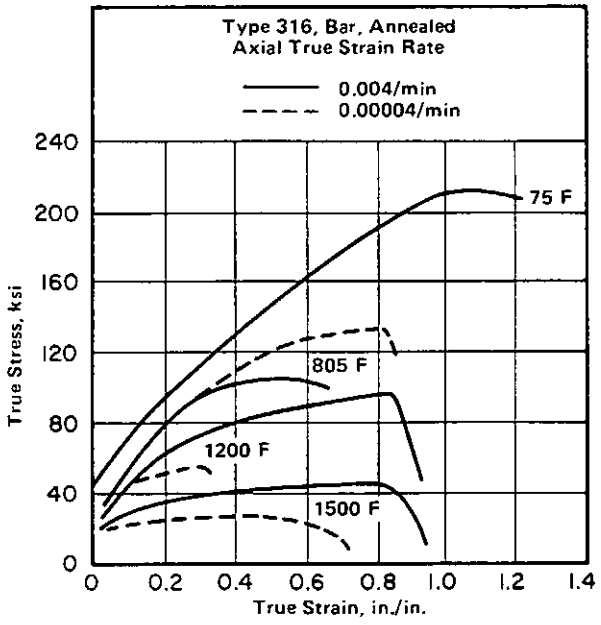


FIGURE 3.0314. COMPLETE TRUE STRESS-TRUE STRAIN CURVES FOR TYPE 316 BAR FROM ROOM TEMPERATURE TO 1500 F AT TWO STRAIN RATES (26)

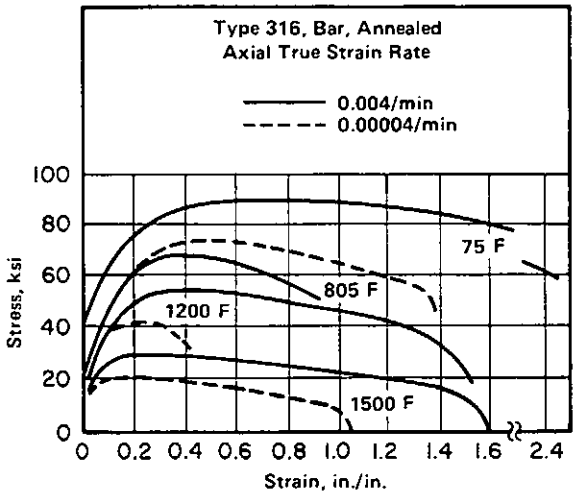


FIGURE 3.0315. COMPLETE ENGINEERING STRESS-STRAIN CURVES FOR TYPE 316 BAR FROM 75 TO 1500 F AT TWO STRAIN RATES (26)

Strain values calculated from true strain values in Figure 3.0314 by the formula: $\epsilon_E = e^{\epsilon}-1$ where ϵ_E = engineering strain, ϵ is true axial strain, and e is natural log base.

Fe
18 Cr
13 Ni
+ Mo

Type 316
Type 317

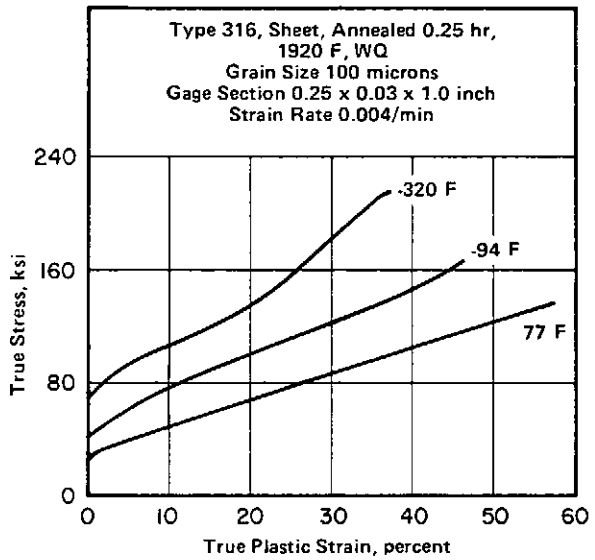


FIGURE 3.0317. TRUE STRESS-TRUE STRAIN CURVES AT ROOM AND CRYOGENIC TEMPERATURES (76)

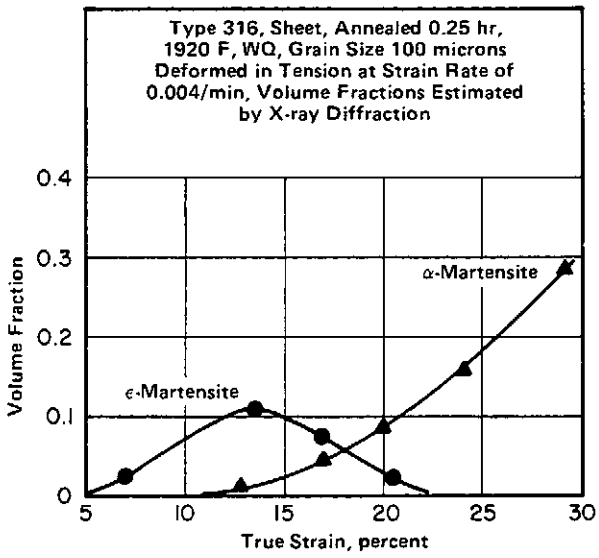


FIGURE 3.0318. VOLUME FRACTIONS OF MARTENSITE FORMED DURING TENSILE DEFORMATION AT -320 F (76)

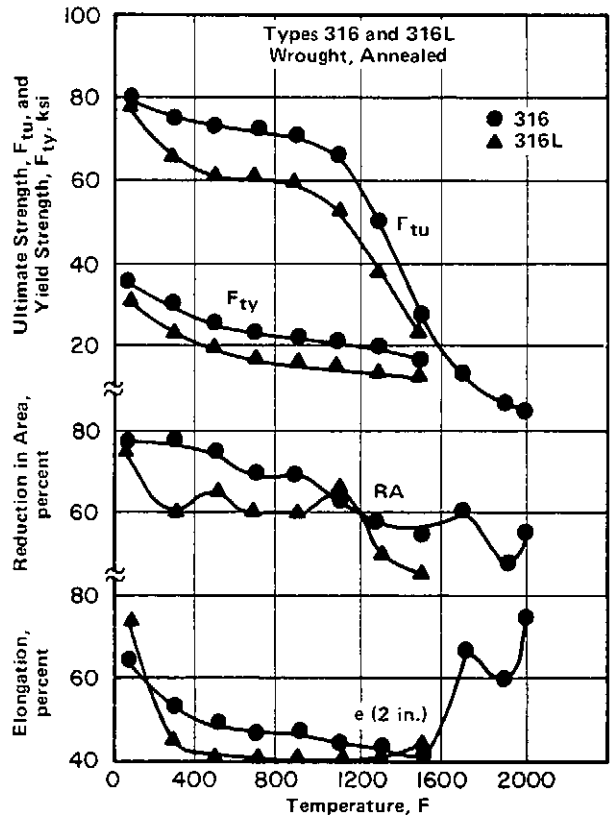


FIGURE 3.03110. ELEVATED-TEMPERATURE TENSILE PROPERTIES OF TYPES 316 AND 316L (11)

Fe
18 Cr
13 Ni
+ Mo

Type 316
Type 317

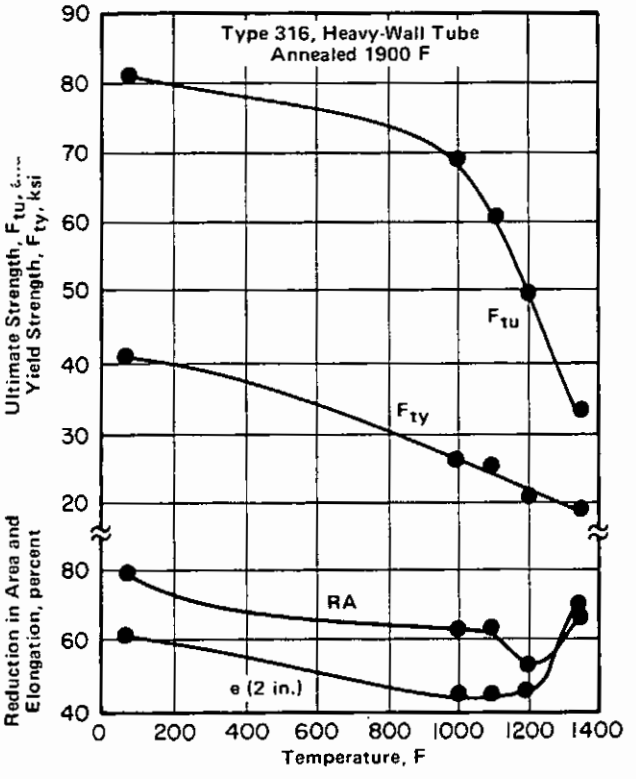


FIGURE 3.03111. ELEVATED-TEMPERATURE TENSILE PROPERTIES OF TYPE 316 HEAVY-WALL TUBE (8)

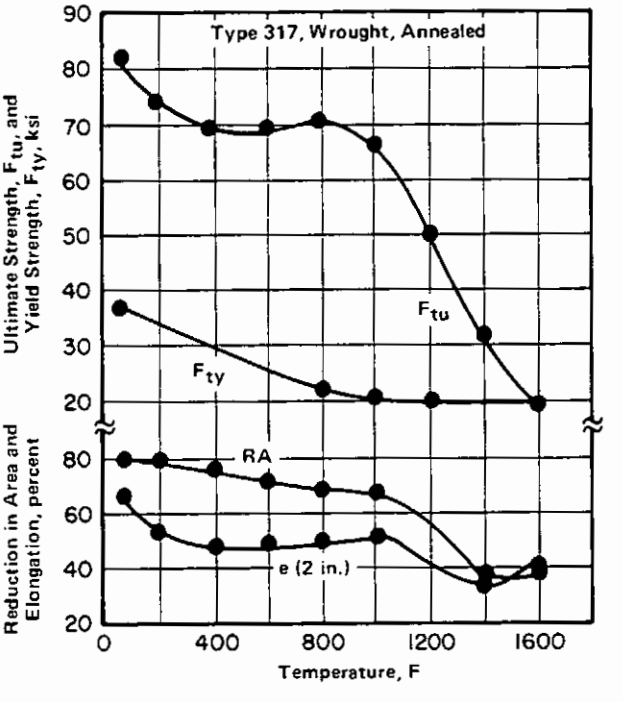


FIGURE 3.03112. ELEVATED-TEMPERATURE TENSILE PROPERTIES OF TYPE 317 (20)

Fe
18 Cr
13 Ni
+ Mo

Type 316
Type 317

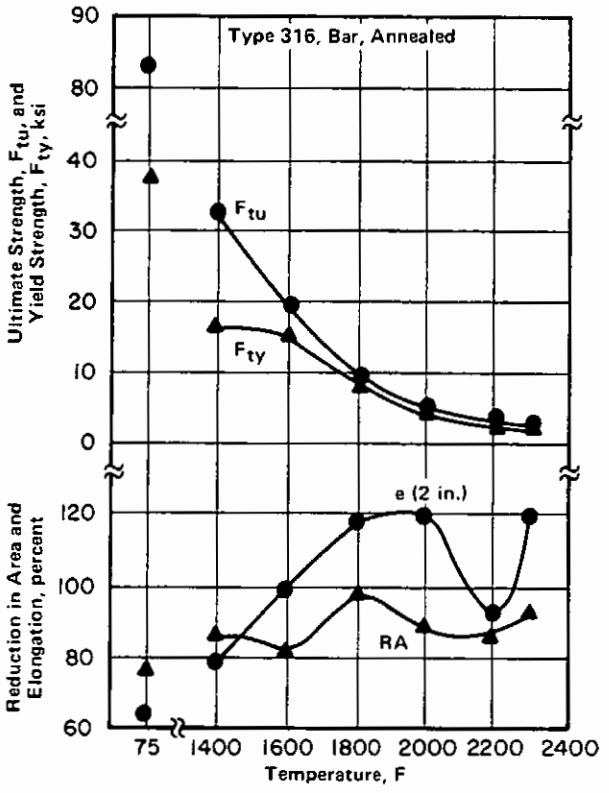


FIGURE 3.03113. EFFECT OF TEMPERATURES UP TO 2300 F ON TENSILE PROPERTIES OF BAR (24)

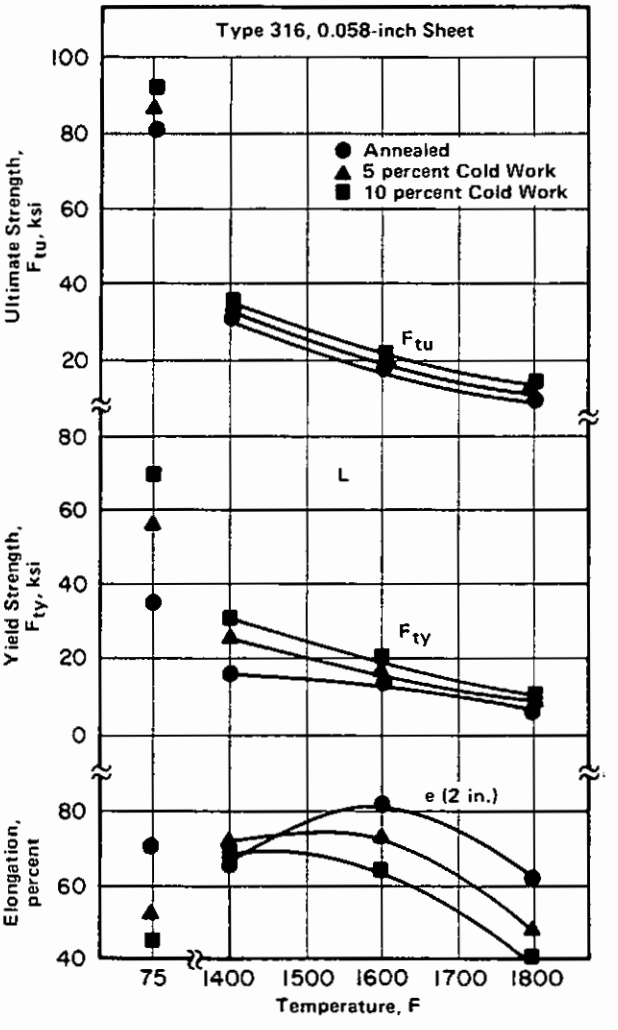
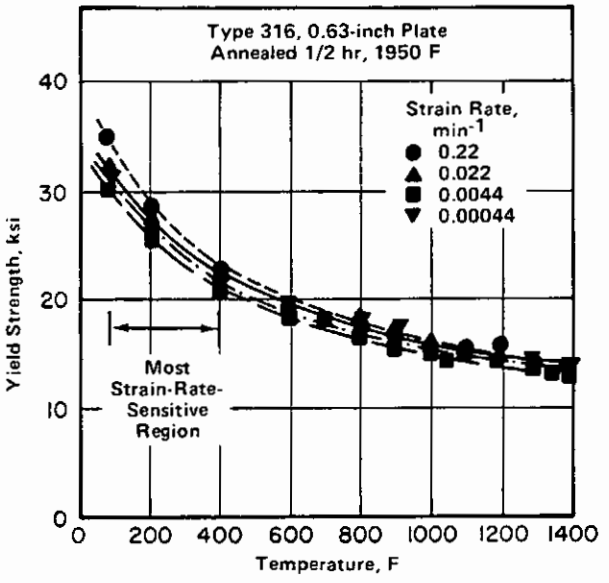
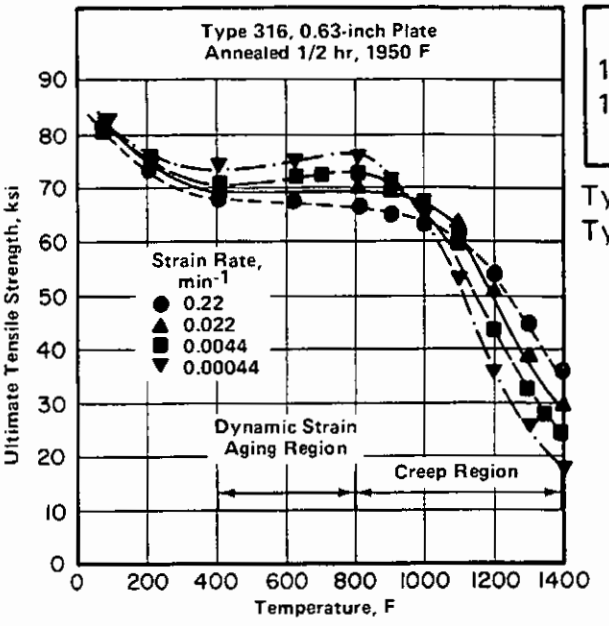


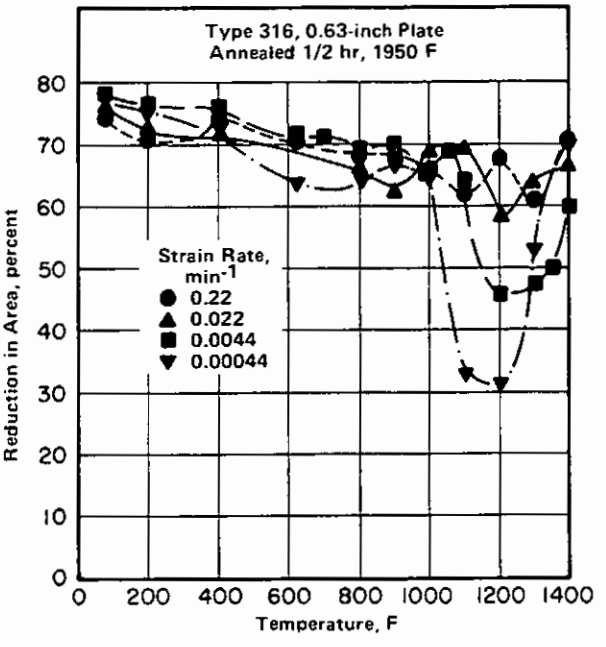
FIGURE 3.03114. EFFECT OF TEMPERATURES UP TO 1800 F ON TENSILE PROPERTIES OF ANNEALED AND COLD-WORKED TYPE 316 SHEET (24)



(a) Yield Strength



(b) Ultimate Tensile Strength



(c) Reduction in Area

FIGURE 3.03115. EFFECTS OF STRAIN RATE ON TENSILE PROPERTIES OF PLATE AT ROOM AND ELEVATED TEMPERATURES (78)

Fe
18 Cr
13 Ni
+ Mo

Type 316
Type 317

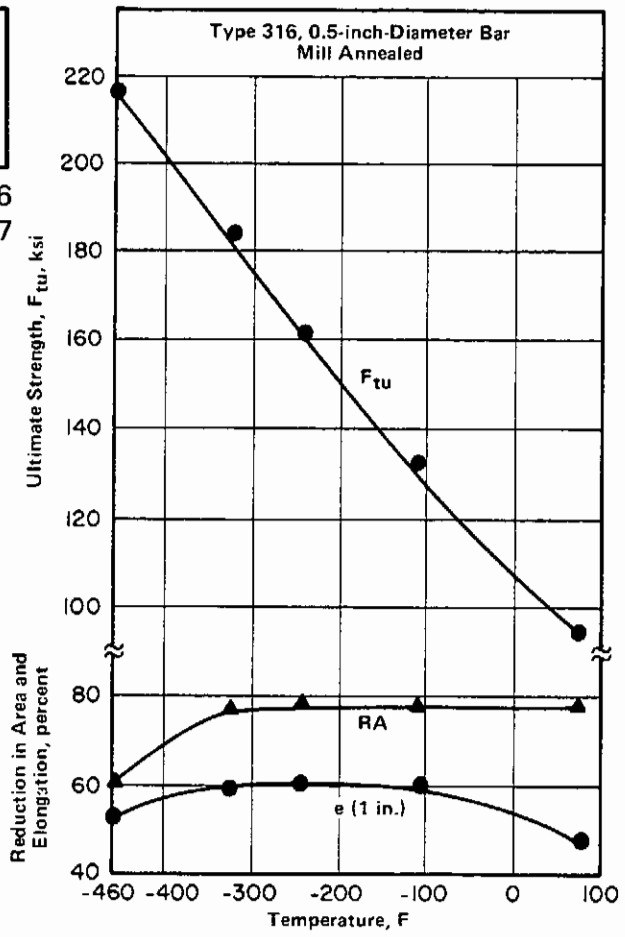


FIGURE 3.03116. LOW-TEMPERATURE TENSILE PROPERTIES OF TYPE 316 BAR (9)

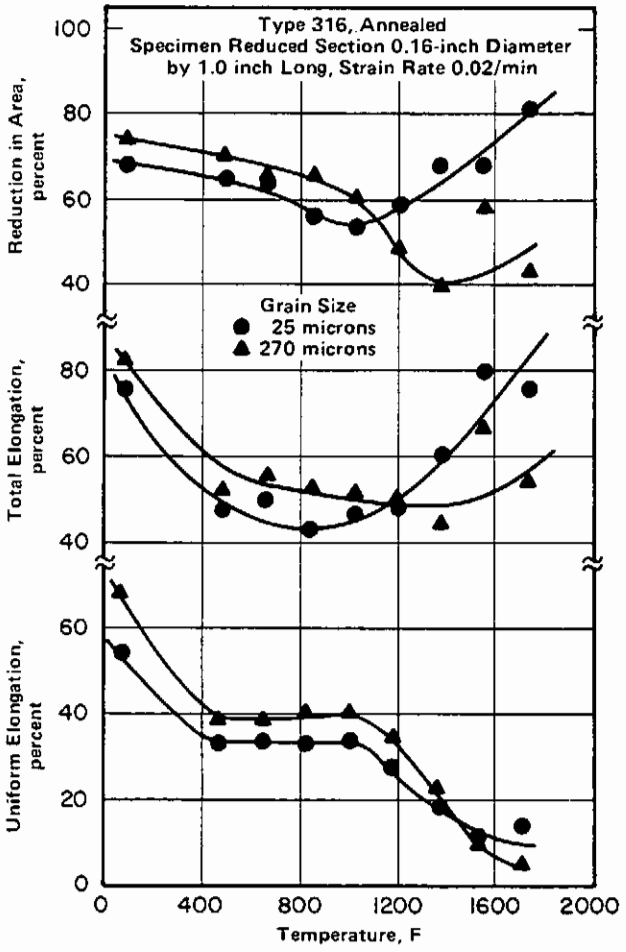


FIGURE 3.03118. EFFECTS OF TEMPERATURE AND GRAIN SIZE ON TENSILE DUCTILITY PARAMETERS (79)

Fe
18 Cr
13 Ni
+ Mo

Type 316
Type 317

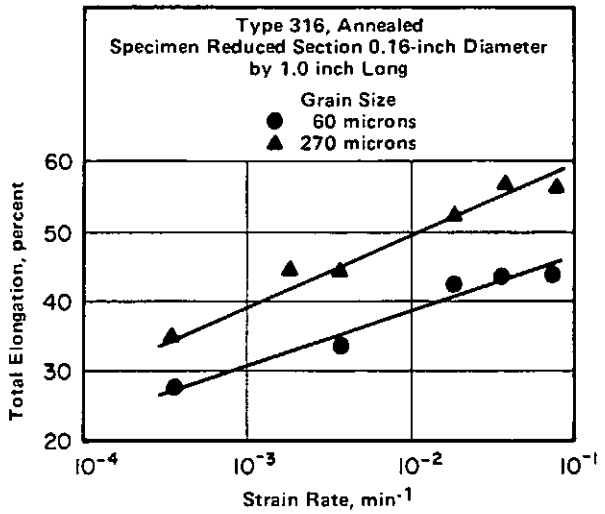


FIGURE 3.03119. EFFECTS OF STRAIN RATE AND GRAIN SIZE ON TOTAL ELONGATION AT 1110 F (79)

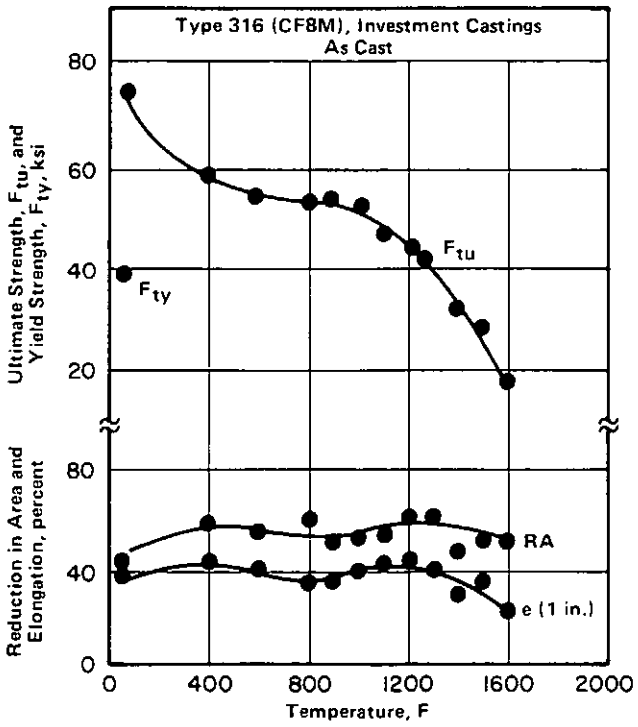


FIGURE 3.03120. EFFECT OF TEMPERATURE ON TENSILE PROPERTIES OF CASTINGS (42)

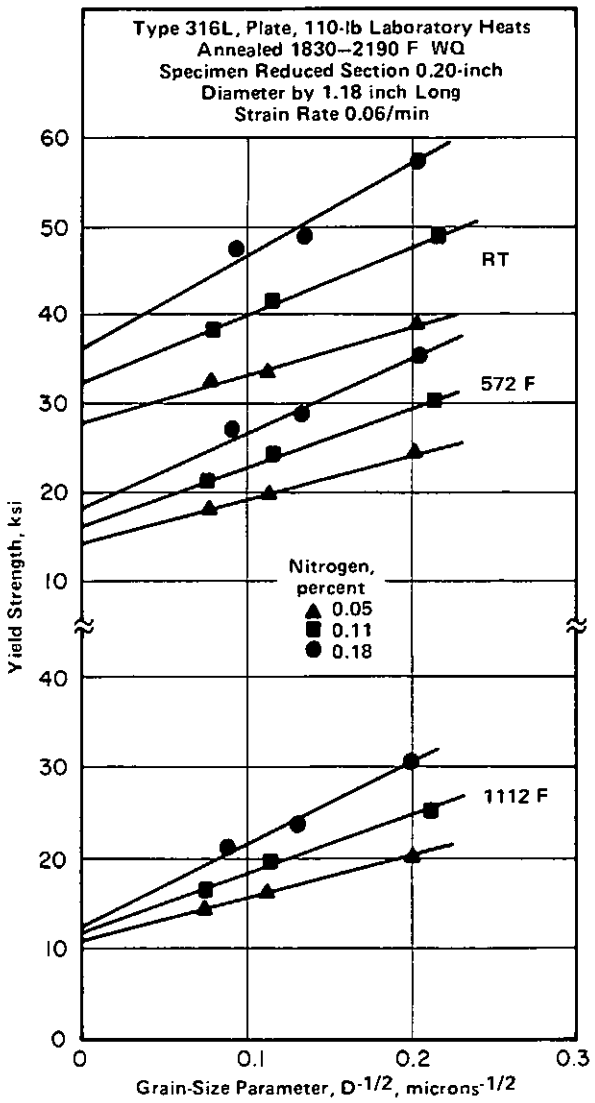


FIGURE 3.03121. EFFECTS OF GRAIN SIZE AND NITROGEN CONTENT ON YIELD STRENGTH AT ROOM AND ELEVATED TEMPERATURES (80)

Fe
18 Cr
13 Ni
+ Mo

Type 316
Type 317

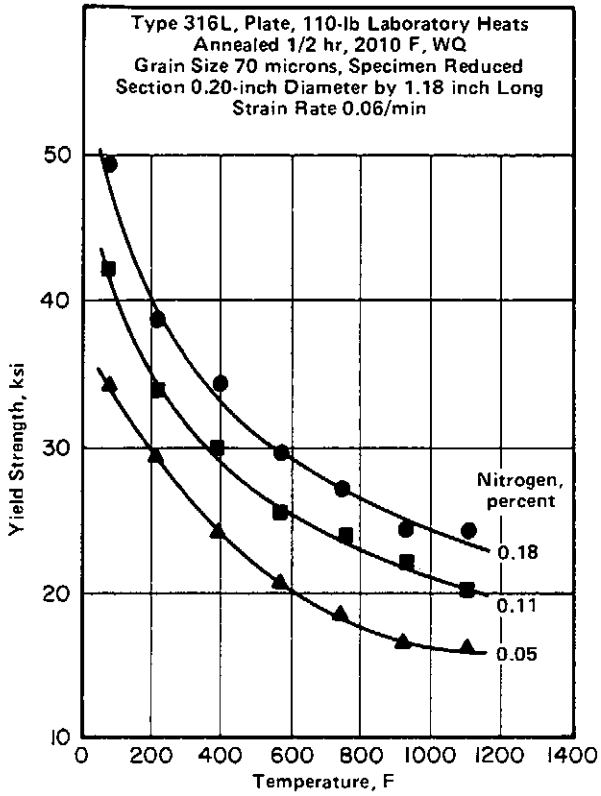


FIGURE 3.03122. EFFECTS OF NITROGEN CONTENT ON YIELD STRENGTH AT ROOM AND ELEVATED TEMPERATURE (80)

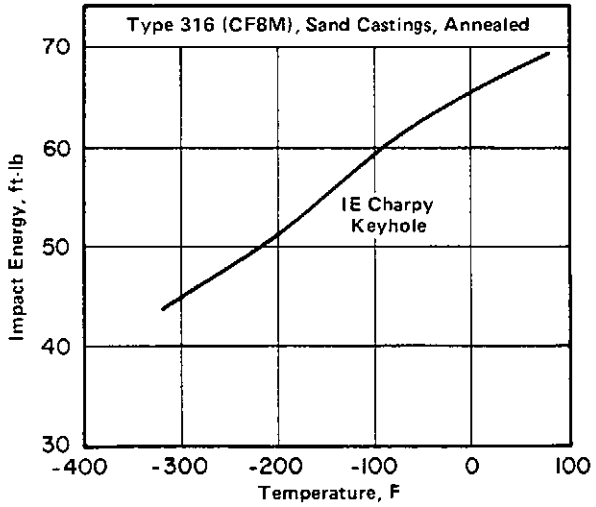


FIGURE 3.0332. EFFECT OF LOW TEMPERATURES ON IMPACT RESISTANCE OF CASTINGS (37)

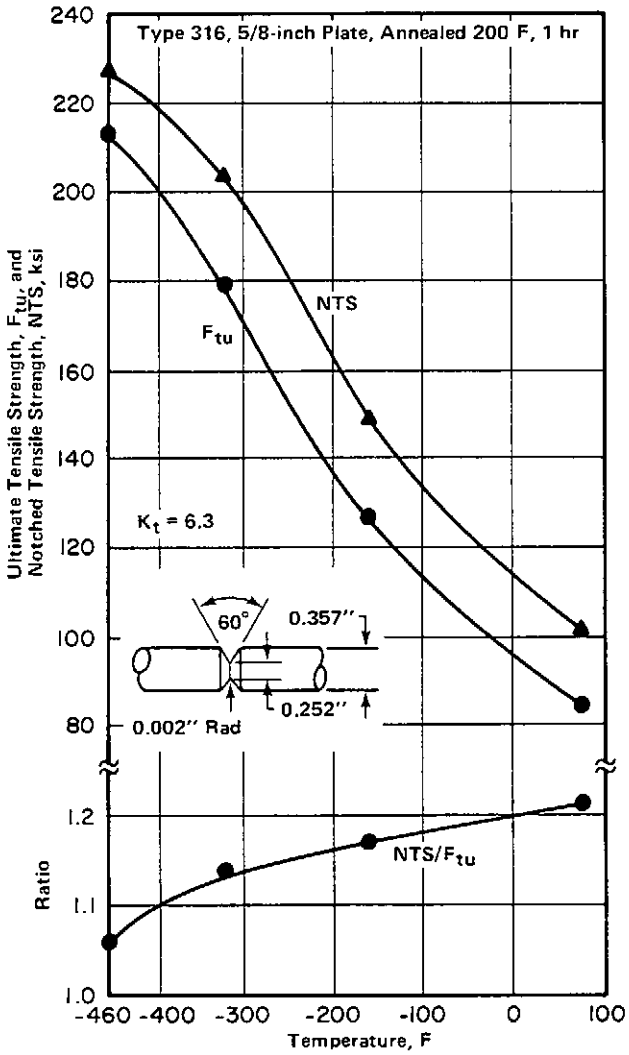


FIGURE 3.03711. LOW-TEMPERATURE NOTCHED TENSILE CHARACTERISTICS OF TYPE 316 PLATE (10)

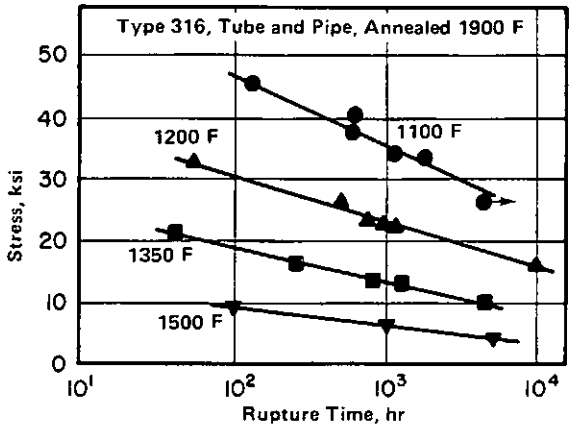


FIGURE 3.041. CREEP-RUPTURE PROPERTIES OF TUBE AND PIPE (8,28)

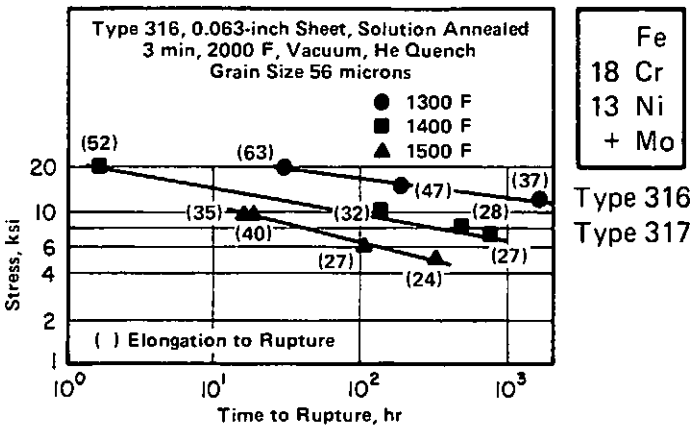


FIGURE 3.042. STRESS-RUPTURE BEHAVIOR OF SHEET AT ELEVATED TEMPERATURES (81)

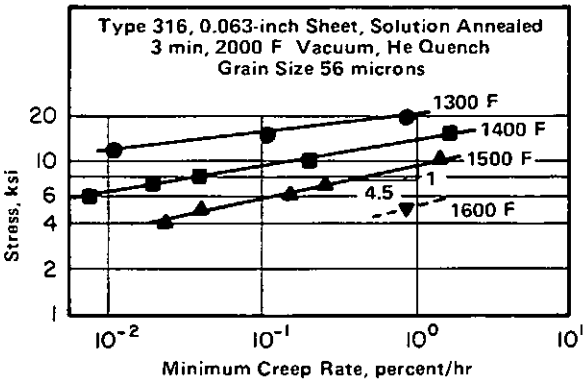


FIGURE 3.043. CREEP BEHAVIOR OF SHEET AT ELEVATED TEMPERATURES (81)

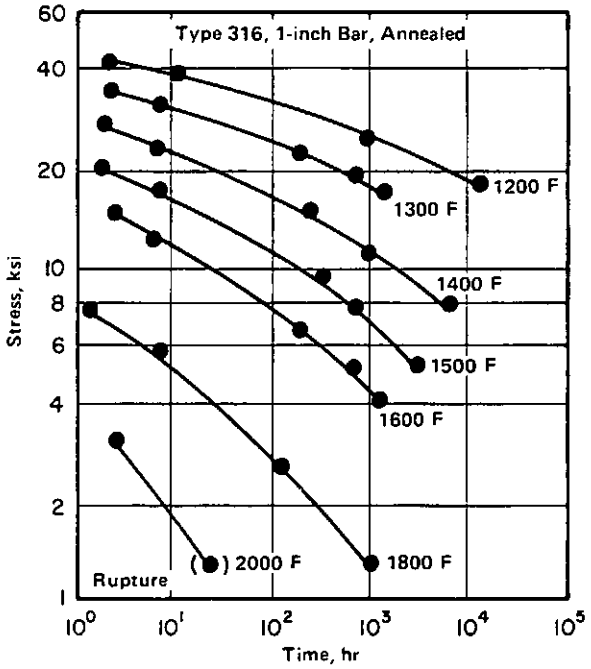


FIGURE 3.0444. CREEP-RUPTURE CURVES FOR BAR AT 1200 TO 2000 F (43)

Fe
18 Cr
13 Ni
+ Mo

Type 316
Type 317

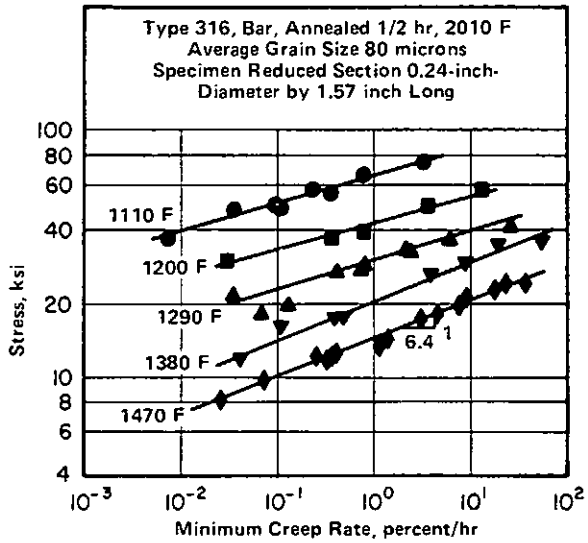


FIGURE 3.045. CREEP BEHAVIOR OF BAR AT ELEVATED TEMPERATURES (82)

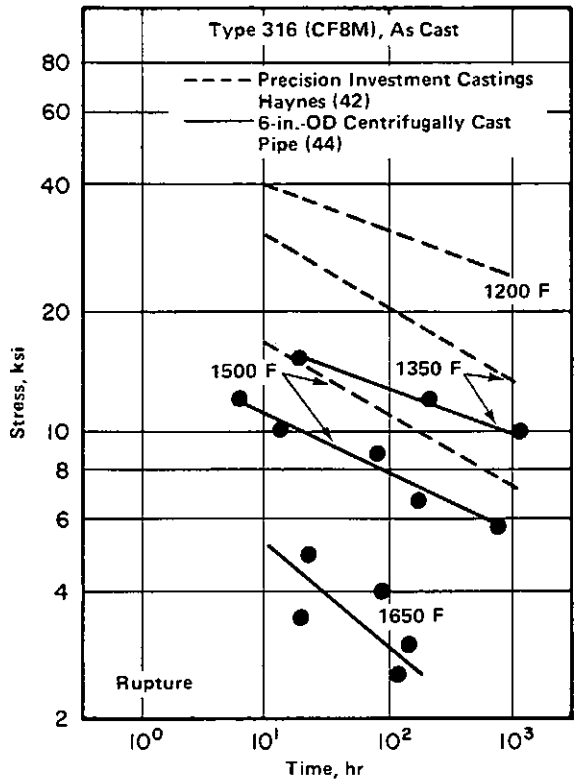


FIGURE 3.047. CREEP-RUPTURE CURVES FOR CASTINGS AT 1200 TO 1650 F (42,44)

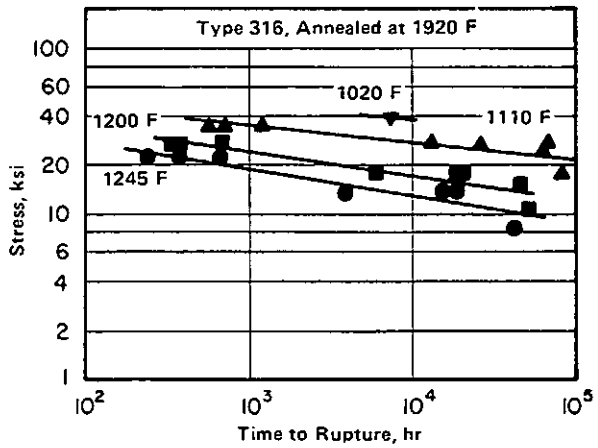


FIGURE 3.048. LONG-TIME STRESS-RUPTURE BEHAVIOR AT ELEVATED TEMPERATURES (84)

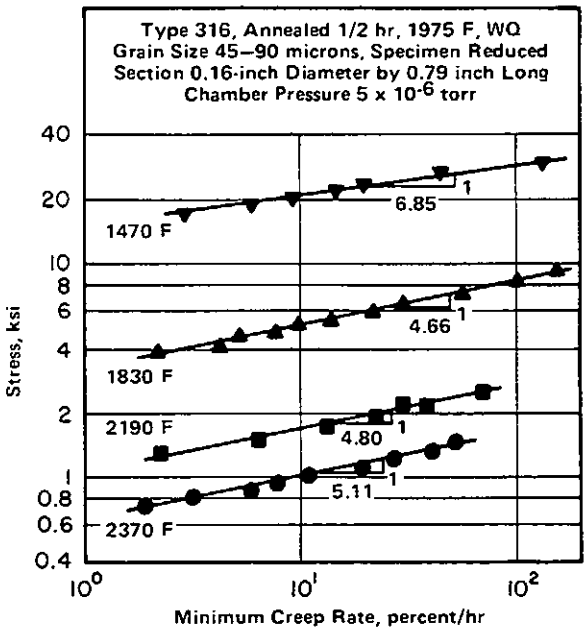


FIGURE 3.049. CREEP BEHAVIOR IN VACUUM AT VERY HIGH TEMPERATURES (85)

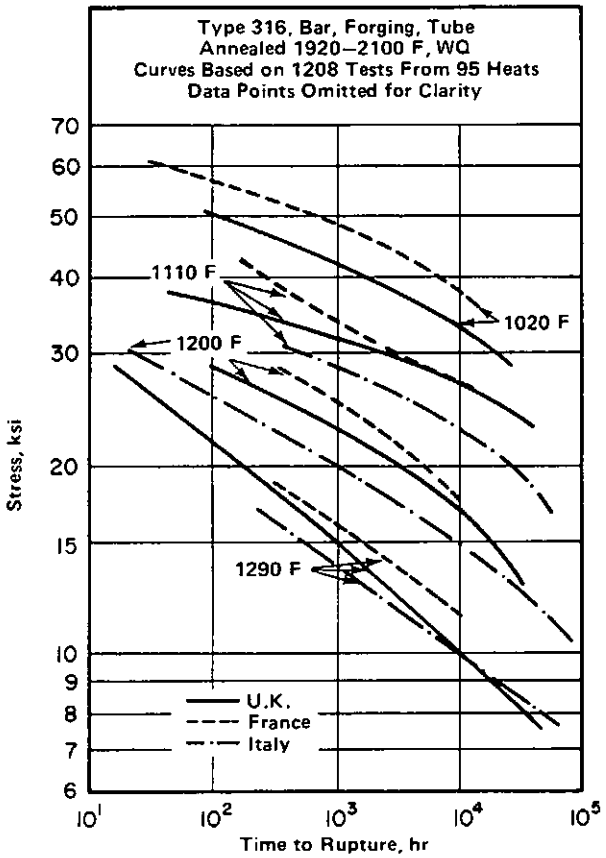
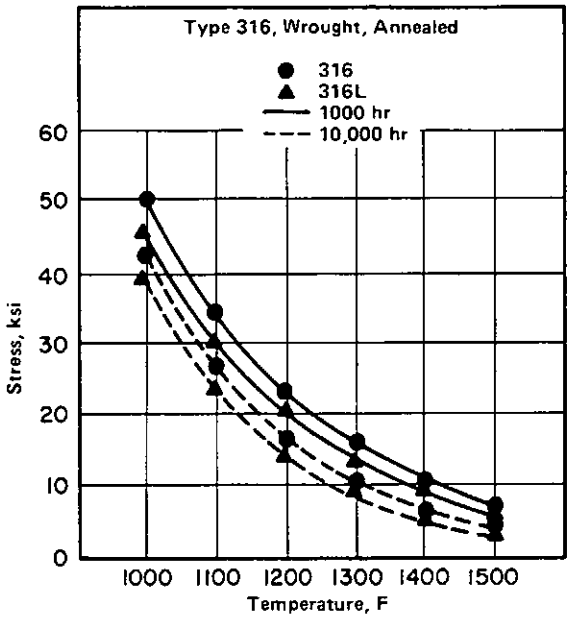


FIGURE 3.0410. SUMMARY OF EUROPEAN CREEP-RUPTURE DATA (86)



Fe
18 Cr
13 Ni
+ Mo

Type 316
Type 317

FIGURE 3.0411. STRESSES FOR CREEP RUPTURE IN 1000 AND 10,000 HOURS FOR TYPES 316 AND 316L AT TEMPERATURES FROM 1000 TO 1500 F (11)

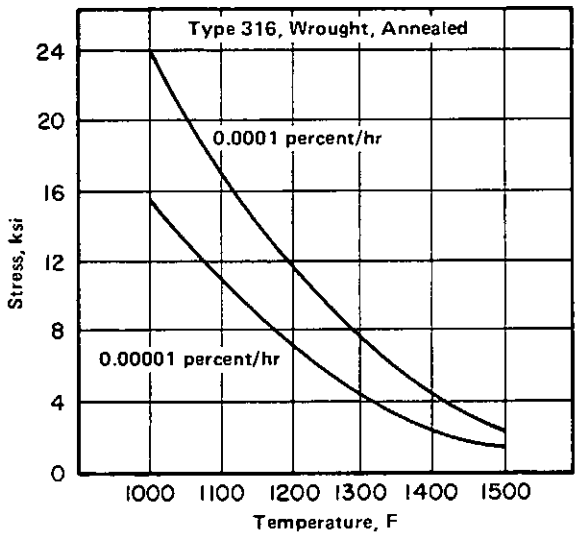


FIGURE 3.0412. STRESSES FOR MINIMUM CREEP RATES OF 0.0001 AND 0.00001 PERCENT PER HOUR FOR TYPE 316 AT TEMPERATURES FROM 1000 TO 1500 F (20)

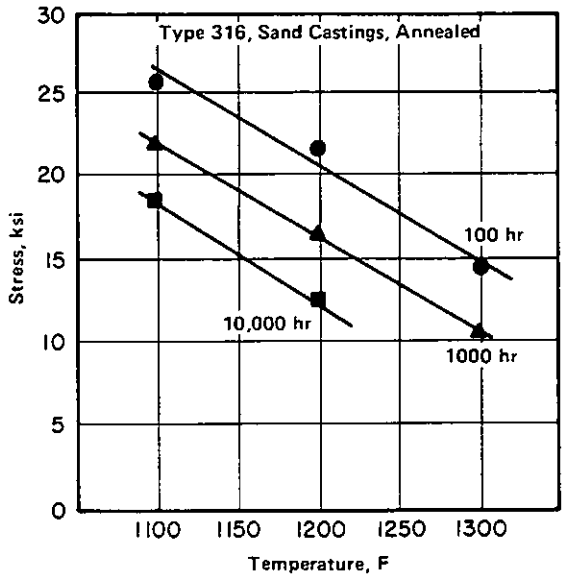


FIGURE 3.0413. STRESSES FOR CREEP RUPTURE IN 100, 1000, AND 10,000 HOURS FOR TYPE 316 CASTINGS AT TEMPERATURES FROM 1100 TO 1300 F (28)

Fe
18 Cr
13 Ni
+ Mo

Type 316
Type 317

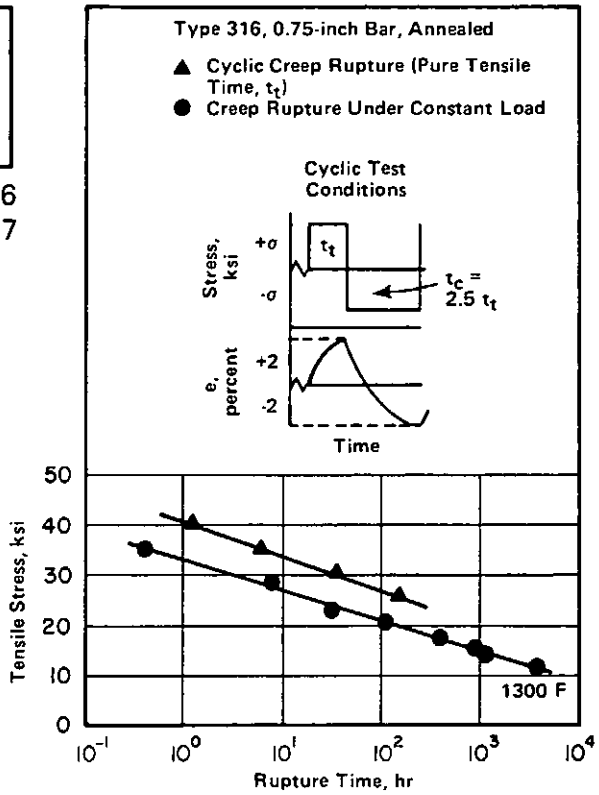


FIGURE 3.0415. CREEP-RUPTURE CURVES FOR MONOTONIC AND CYCLIC LOADING AT 1300 F (12)

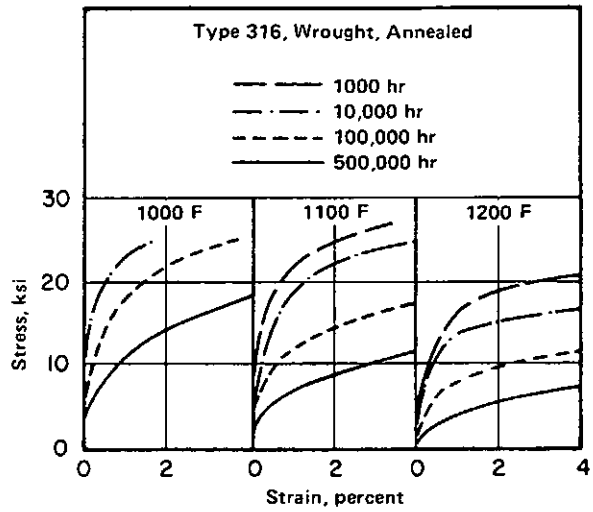


FIGURE 3.0416. ISOCHRONOUS STRESS-STRAIN CURVES FOR TYPE 316 AT 1000, 1100, AND 1200 F (13)

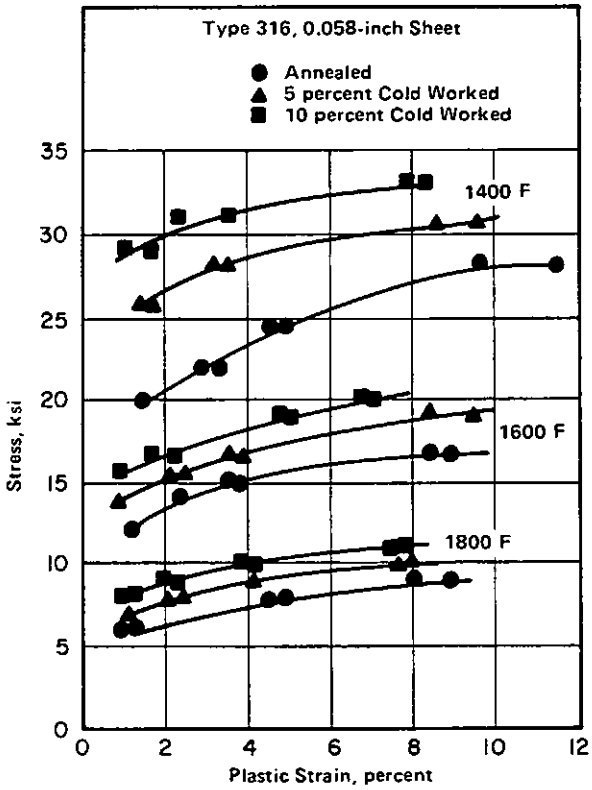
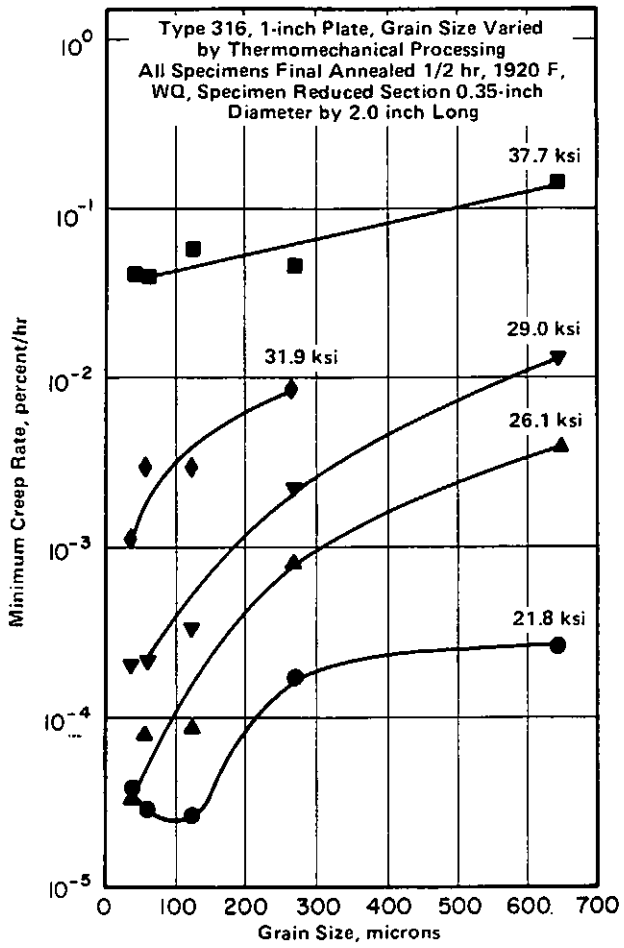


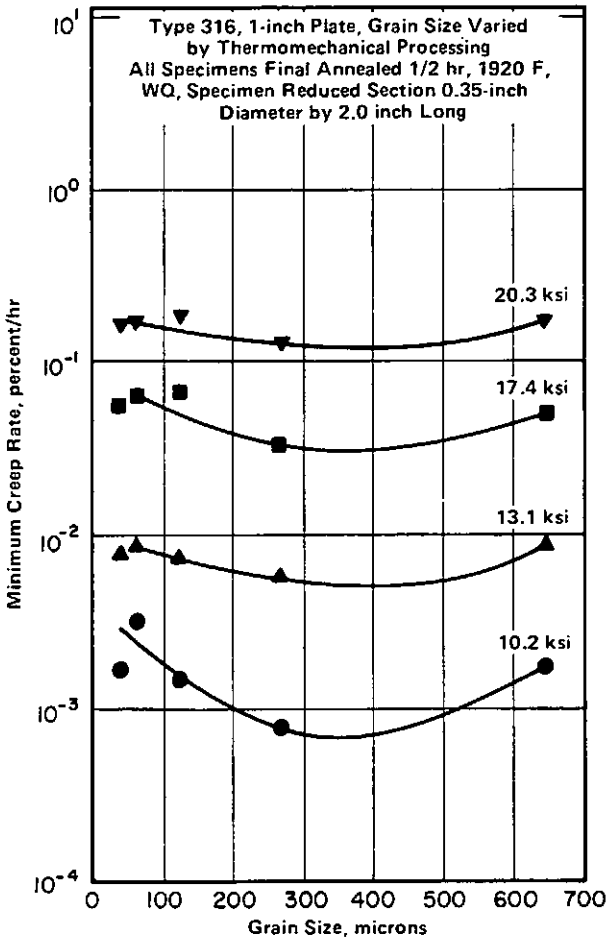
FIGURE 3.0417. PLASTIC STRAIN RESULTING FROM CONSTANT STRESS FOR 2-MINUTE PERIOD AT ELEVATED TEMPERATURES FOR TYPE 316 SHEET IN THE ANNEALED AND COLD-WORKED CONDITIONS (24)

Fe
18 Cr
13 Ni
+ Mo

Type 316
Type 317



(a) 1110 F



(b) 1290 F

FIGURE 3.0419. EFFECTS OF GRAIN SIZE ON CREEP RATE OF PLATE AT VARIOUS STRESSES AT ELEVATED TEMPERATURES (87)

Fe
18 Cr
13 Ni
+ Mo

Type 316
Type 317

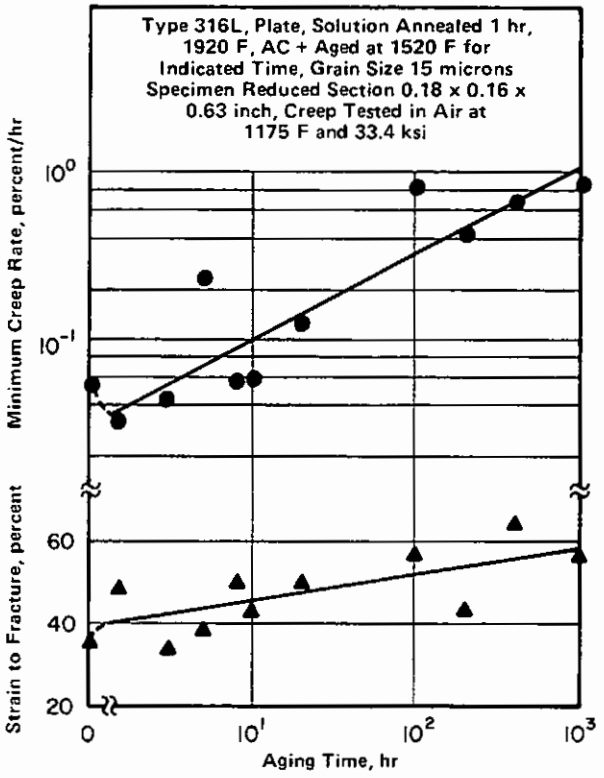


FIGURE 3.0421. EFFECTS OF PRIOR AGING ON CREEP PROPERTIES OF PLATE (88)

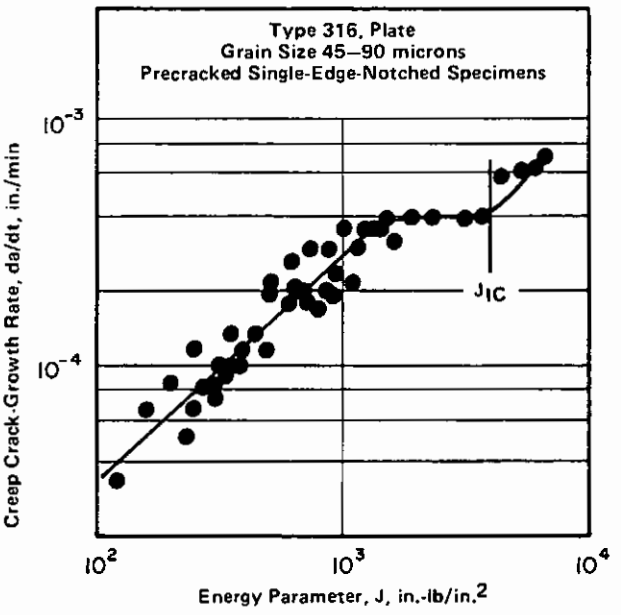


FIGURE 3.0423. CREEP CRACK-GROWTH BEHAVIOR IN AIR AT 1100 F (90)

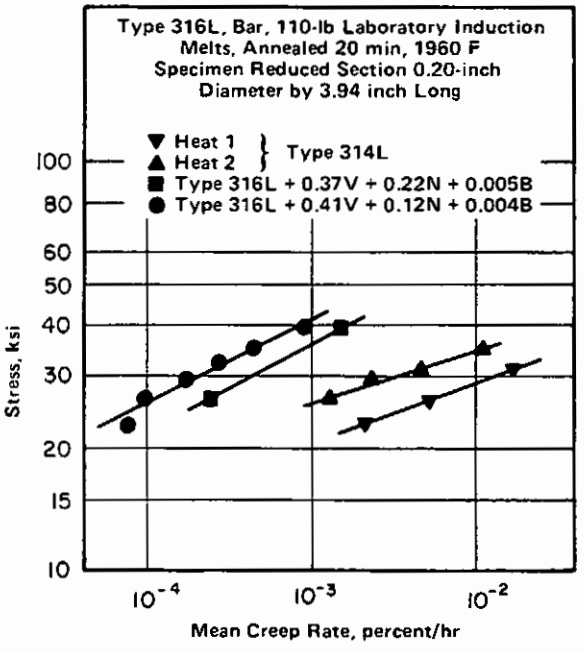


FIGURE 3.0425. EFFECTS OF VANADIUM-NITROGEN-BORON ADDITIONS ON CREEP BEHAVIOR AT 1200 F (91)

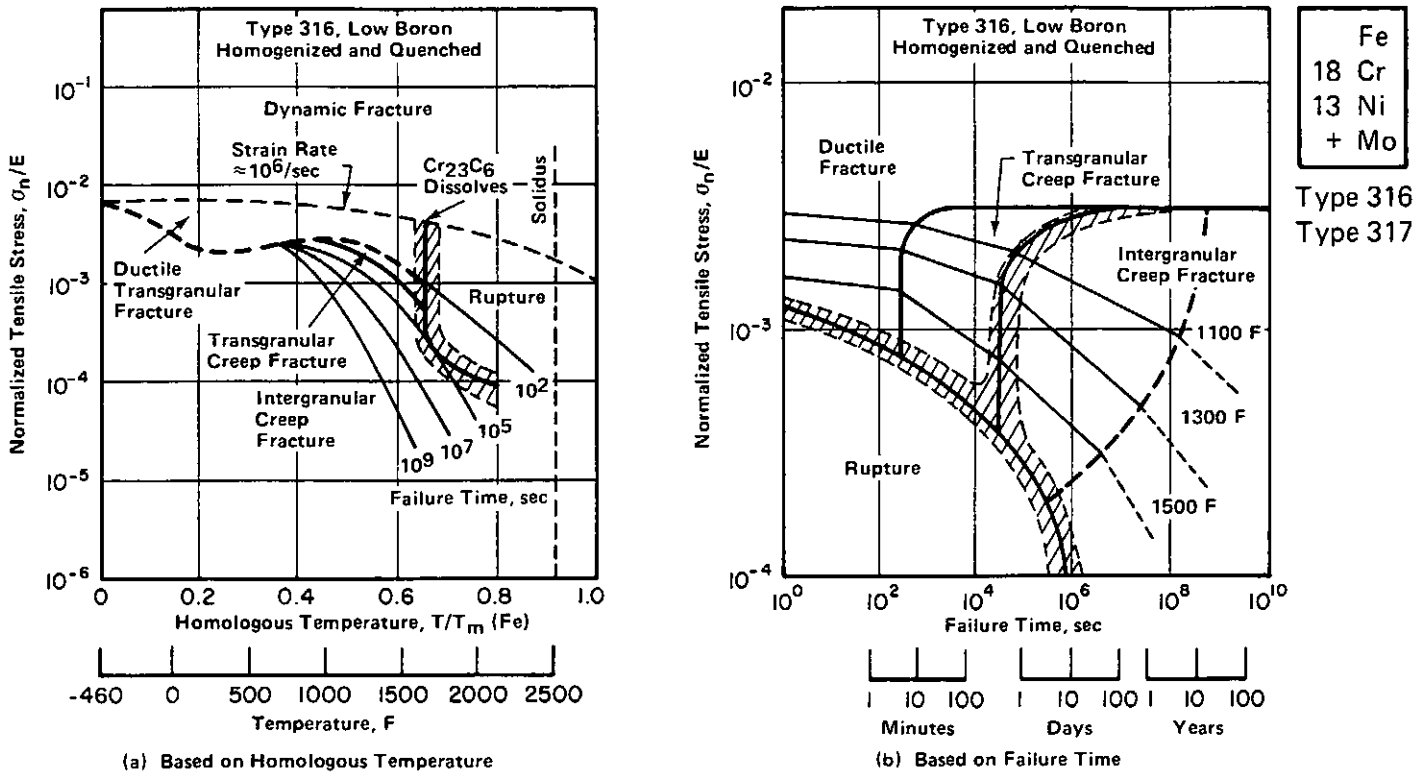


FIGURE 3.0428. FRACTURE MAP (95)

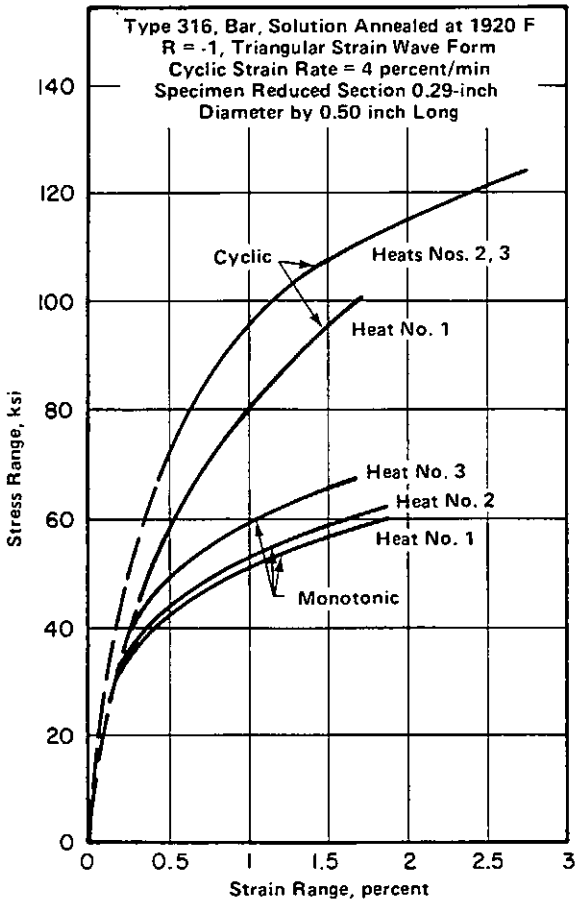
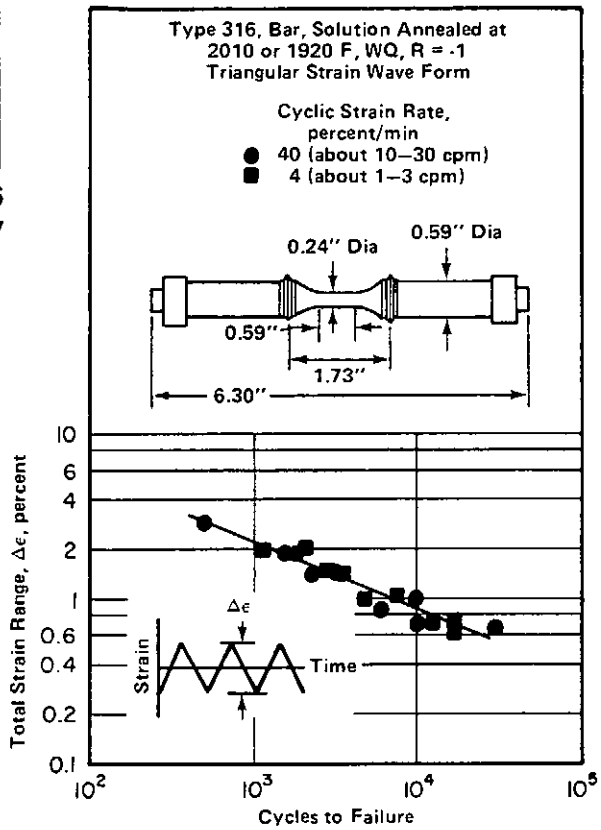


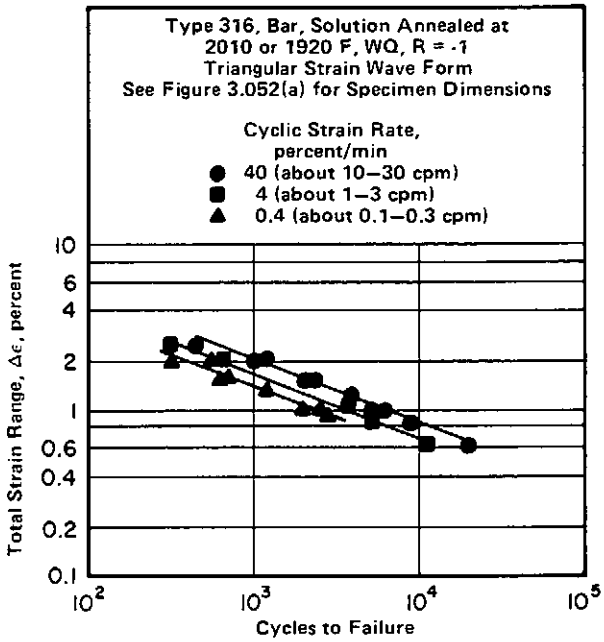
FIGURE 3.051. CYCLIC AND MONOTONIC STRESS-STRAIN CURVES IN AIR AT 1160 F (96)

Fe
18 Cr
13 Ni
+ Mo

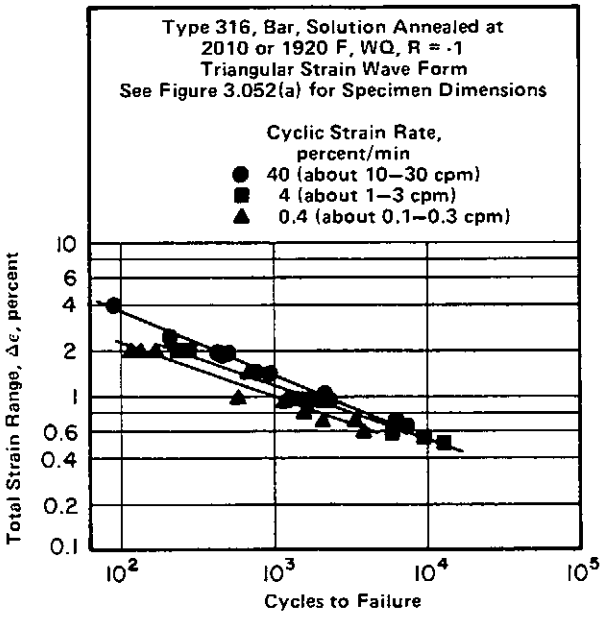
Type 316
Type 317



(a) Room Temperature

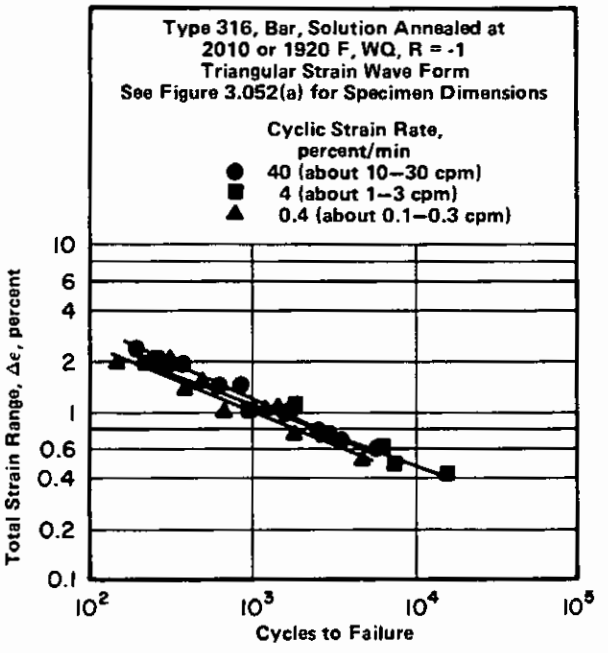


(b) 840 F

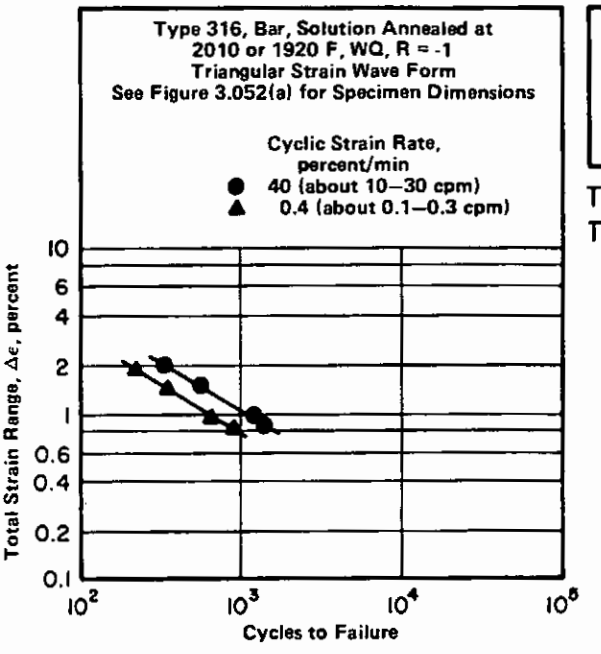


(c) 1110 F

FIGURE 3.052. LOW-CYCLE AXIAL FATIGUE BEHAVIOR IN AIR AT ROOM AND ELEVATED TEMPERATURES (97,98)



(d) 1290 F



(e) 1470 F

Fe
18 Cr
13 Ni
+ Mo

Type 316
Type 317

FIGURE 3.052. LOW-CYCLE AXIAL FATIGUE BEHAVIOR IN AIR AT ROOM AND ELEVATED TEMPERATURES (97,98)

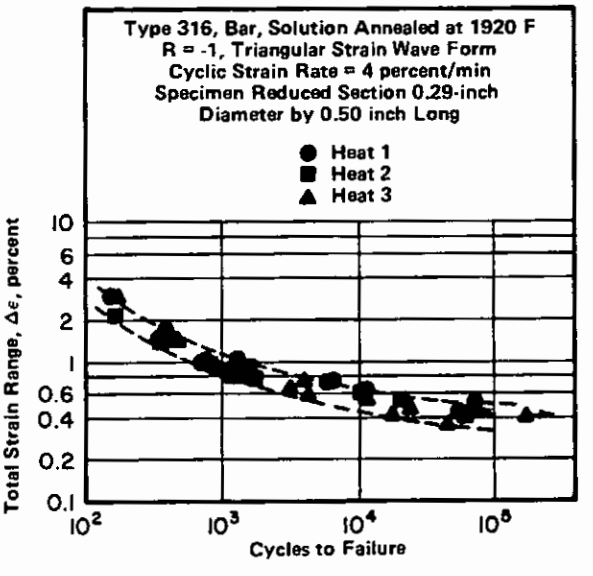


FIGURE 3.053. EFFECTS OF HEAT-TO-HEAT VARIATIONS ON LOW-CYCLE AXIAL FATIGUE BEHAVIOR IN AIR AT 1160 F (96)

Fe
18 Cr
13 Ni
+ Mo

Type 316
Type 317

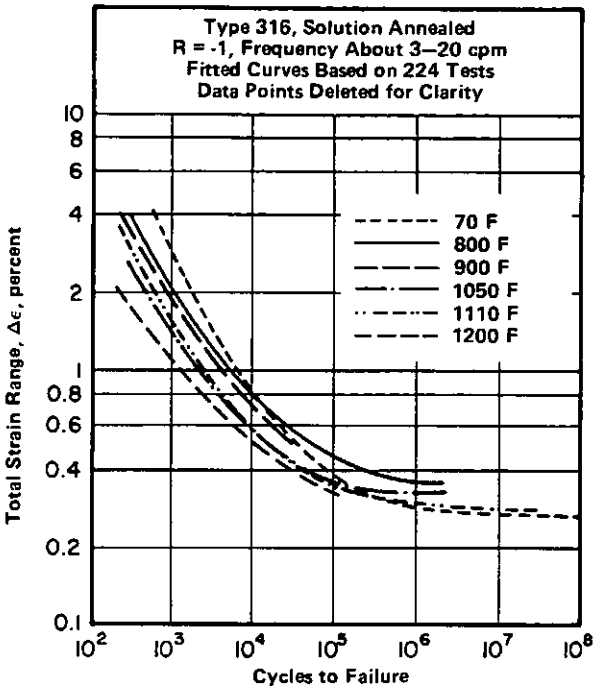


FIGURE 3.055. LONG-TIME LOW-CYCLE AXIAL FATIGUE BEHAVIOR IN AIR AT ROOM AND ELEVATED TEMPERATURES (99)

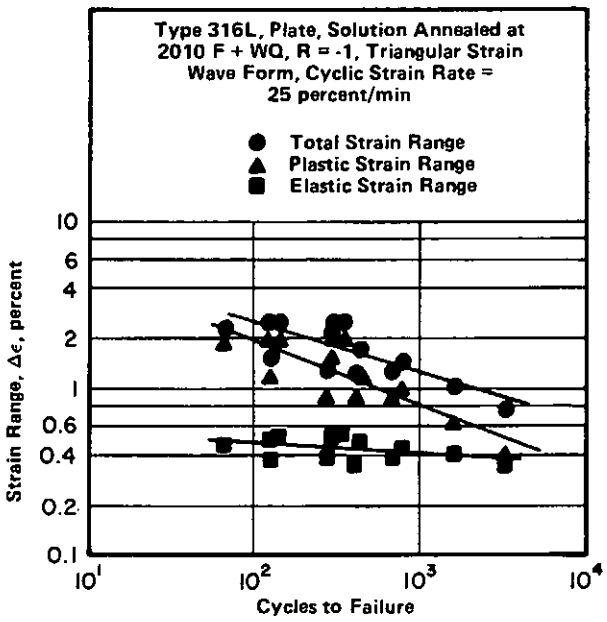


FIGURE 3.056. LOW-CYCLE AXIAL FATIGUE LIFE AS A FUNCTION OF PLASTIC, ELASTIC, AND TOTAL STRAIN RANGES IN AIR AT 1110 F (100)

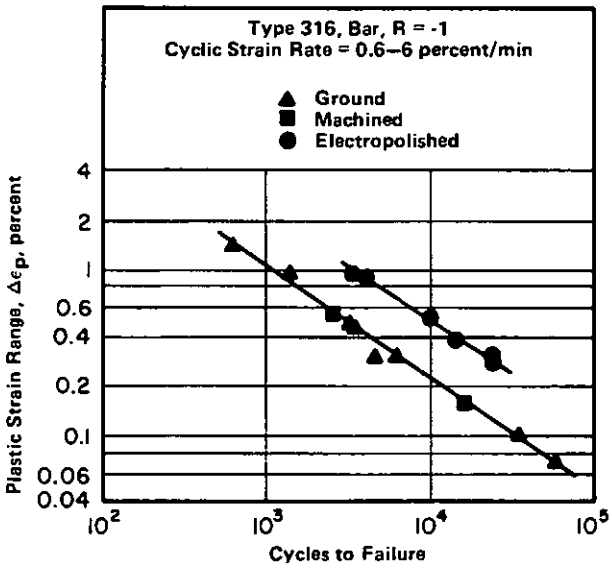


FIGURE 3.058. EFFECTS OF SURFACE FINISH ON LOW-CYCLE AXIAL FATIGUE BEHAVIOR IN AIR AT 750 F (101)

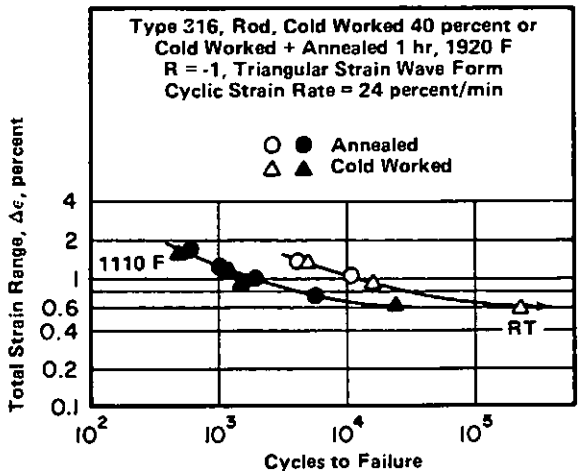


FIGURE 3.0510. EFFECTS OF COLD WORK ON LOW-CYCLE AXIAL FATIGUE BEHAVIOR (102)

Fe
18 Cr
13 Ni
+ Mo

Type 316
Type 317

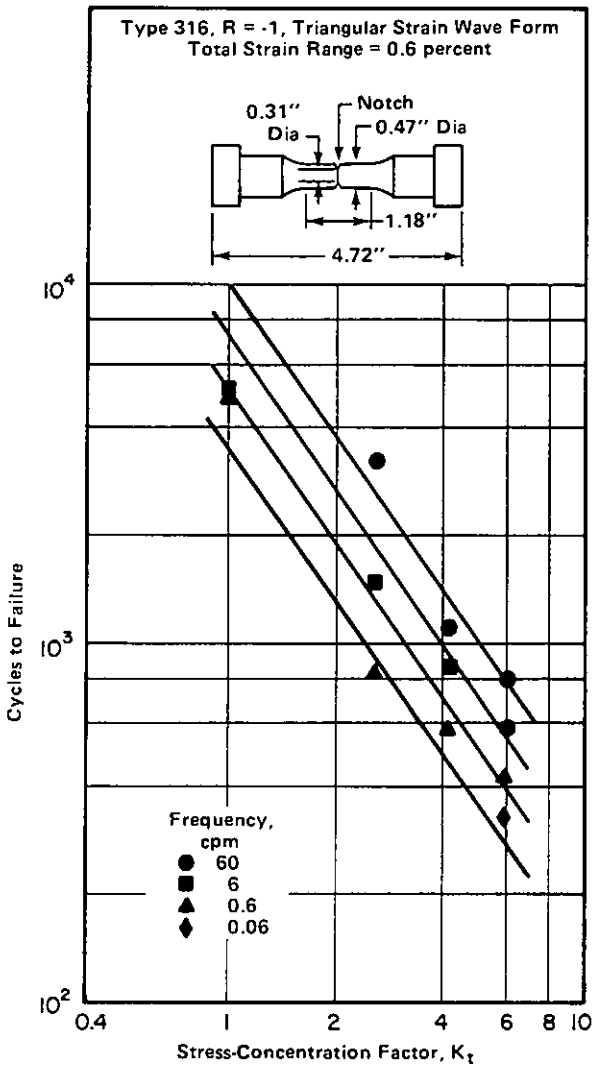


FIGURE 3.0512. EFFECTS OF STRESS-CONCENTRATION FACTOR ON LOW-CYCLE AXIAL FATIGUE LIFE IN AIR AT 1110 F (103)

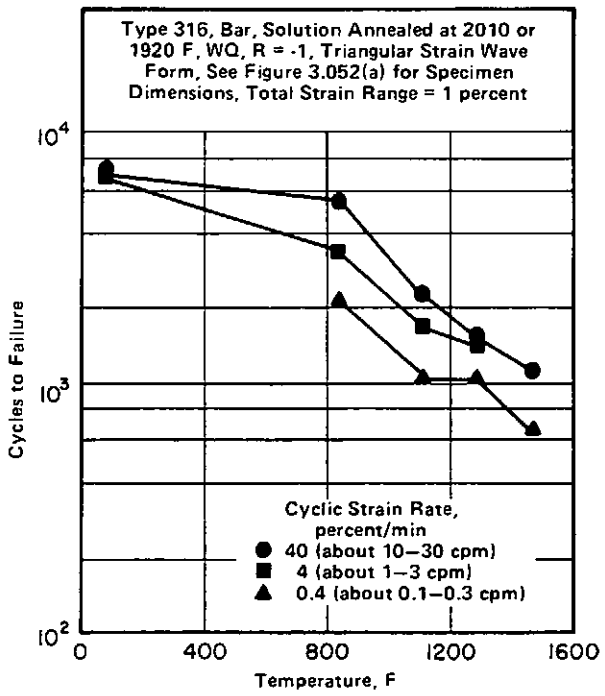


FIGURE 3.0514. LOW-CYCLE FATIGUE LIFE AT ROOM AND ELEVATED TEMPERATURES (97)

Fe
18 Cr
13 Ni
+ Mo

Type 316
Type 317

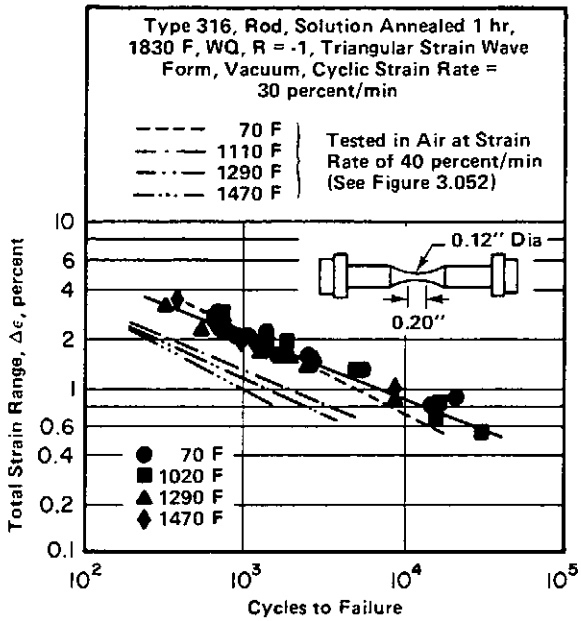


FIGURE 3.0516. LOW-CYCLE AXIAL FATIGUE BEHAVIOR IN VACUUM AT ROOM AND ELEVATED TEMPERATURES (104)

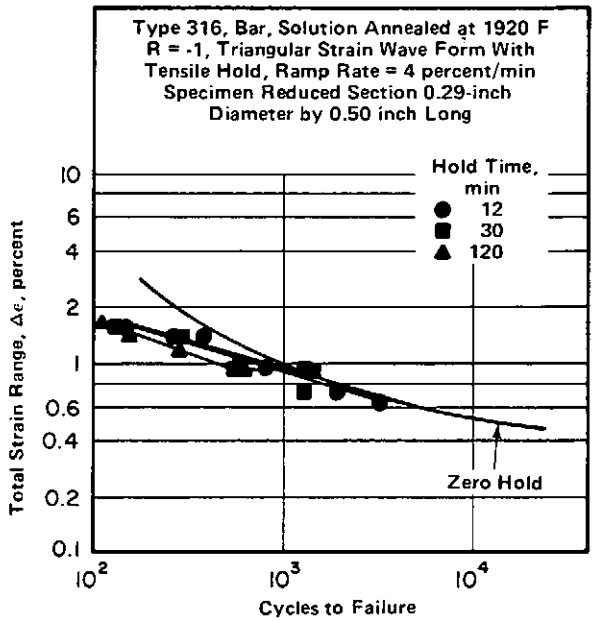


FIGURE 3.0517. EFFECTS OF HOLD TIME ON LOW-CYCLE AXIAL FATIGUE BEHAVIOR IN AIR AT 1160 F (96)

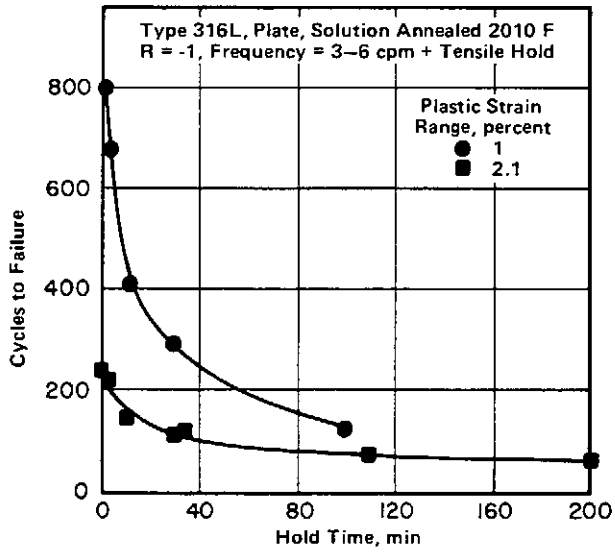


FIGURE 3.0518. VARIATION OF LOW-CYCLE AXIAL FATIGUE LIFE IN AIR AT 1110 F WITH HOLD TIME (105)

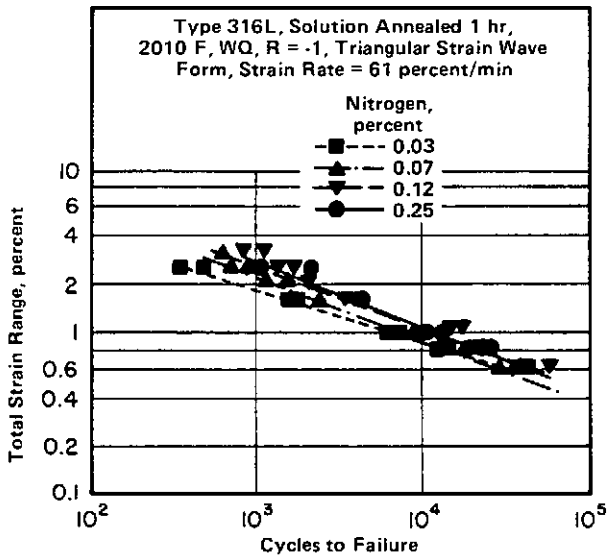


FIGURE 3.0520. EFFECTS OF NITROGEN CONTENT ON LOW-CYCLE FATIGUE BEHAVIOR AT ROOM TEMPERATURE (106)

Fe
18 Cr
13 Ni
+ Mo

Type 316
Type 317

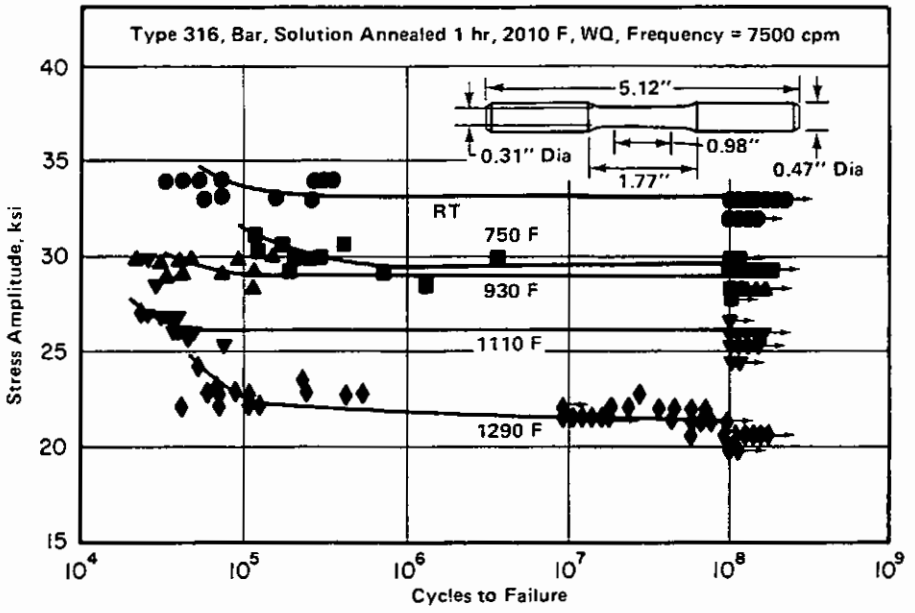


FIGURE 3.0522. HIGH-FREQUENCY ROTATING BENDING FATIGUE BEHAVIOR AT ROOM AND ELEVATED TEMPERATURES (108)

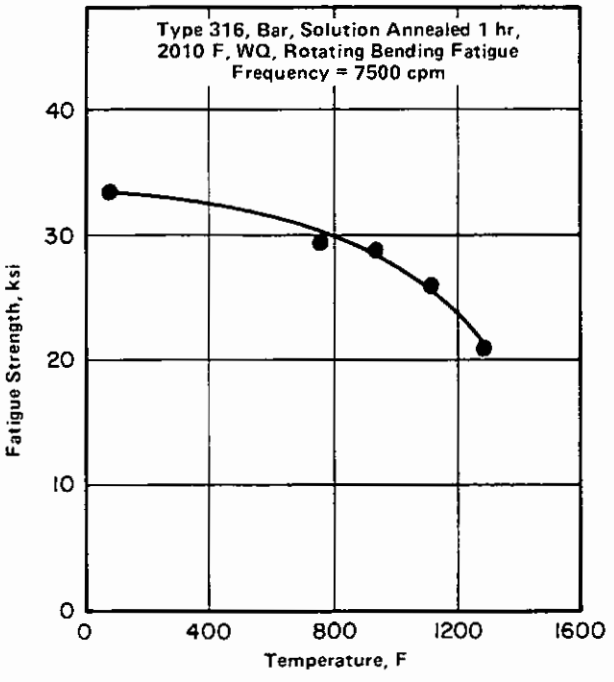


FIGURE 3.0523. TEMPERATURE DEPENDENCE OF ROTATING BENDING FATIGUE STRENGTH AT 10^8 CYCLES (108)

Fe
18 Cr
13 Ni
+ Mo

Type 316
Type 317

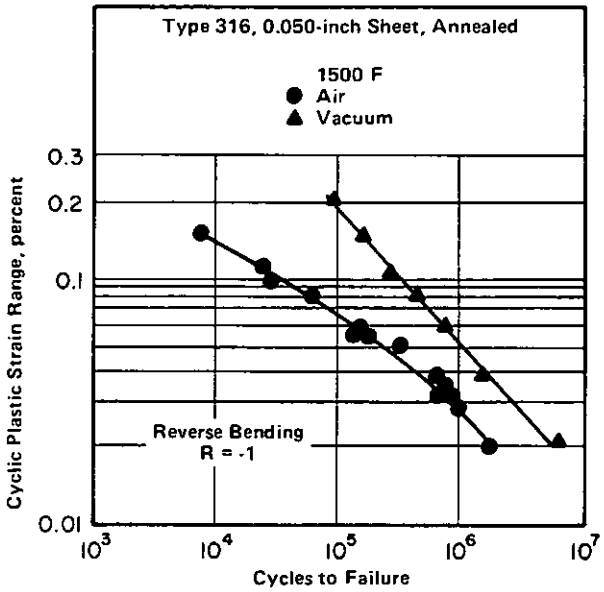


FIGURE 3.0524. FATIGUE LIFE OF SHEET AT 1500 F AS A FUNCTION OF PLASTIC CYCLIC STRAIN RANGE IN AIR AND VACUUM (36)

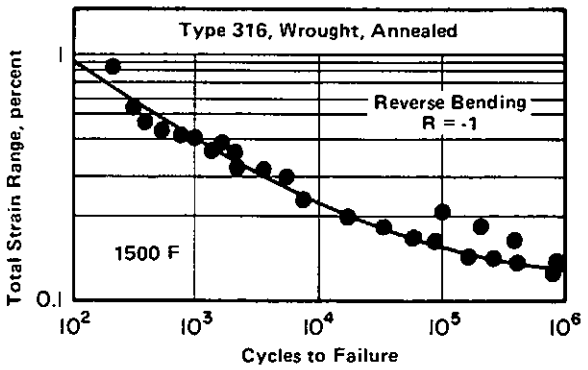


FIGURE 3.0525. FATIGUE LIFE AT 1500 F AS A FUNCTION OF TOTAL CYCLIC STRAIN RANGE (25)

Alloy	Type 316	
Form	Condition	Fatigue Limit, ksi
Sheet	Annealed	39
Strip	Annealed	39
Plate	Annealed	39
Bar	Annealed	38
Bar	Annealed and cold drawn	40

TABLE 3.0526. FATIGUE LIMIT FOR TYPE 316 IN VARIOUS FORMS IN REVERSED BENDING (R = -1) (38)

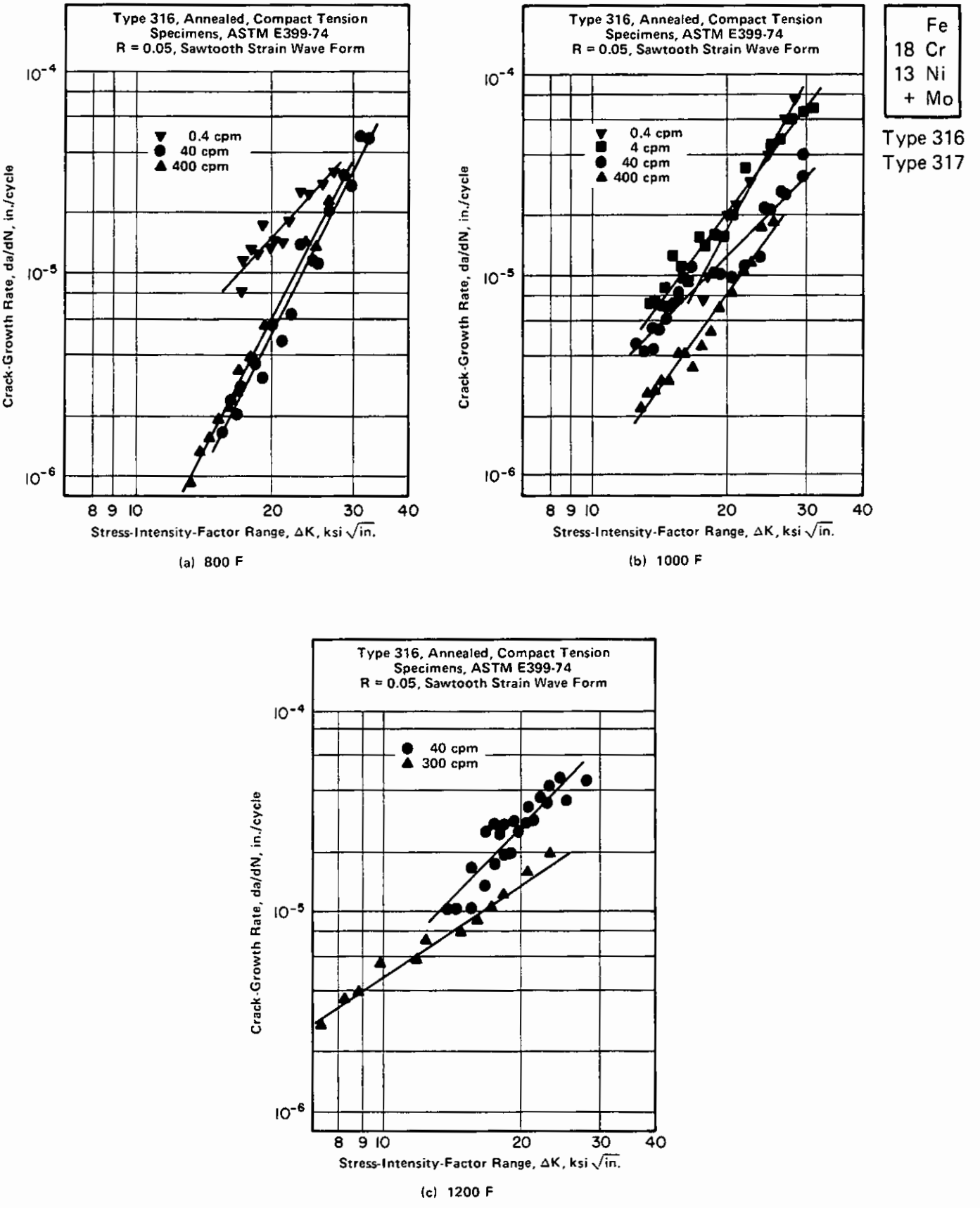
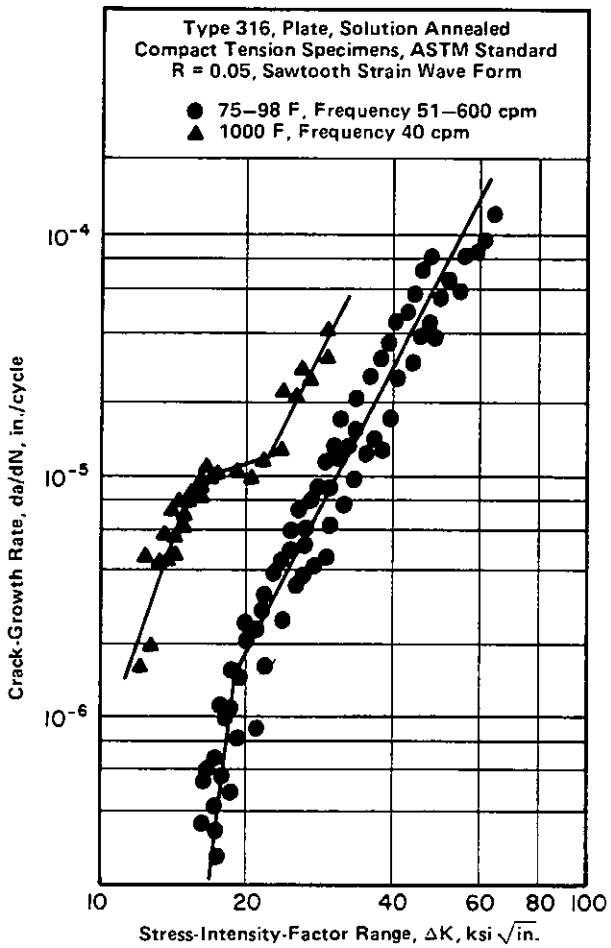


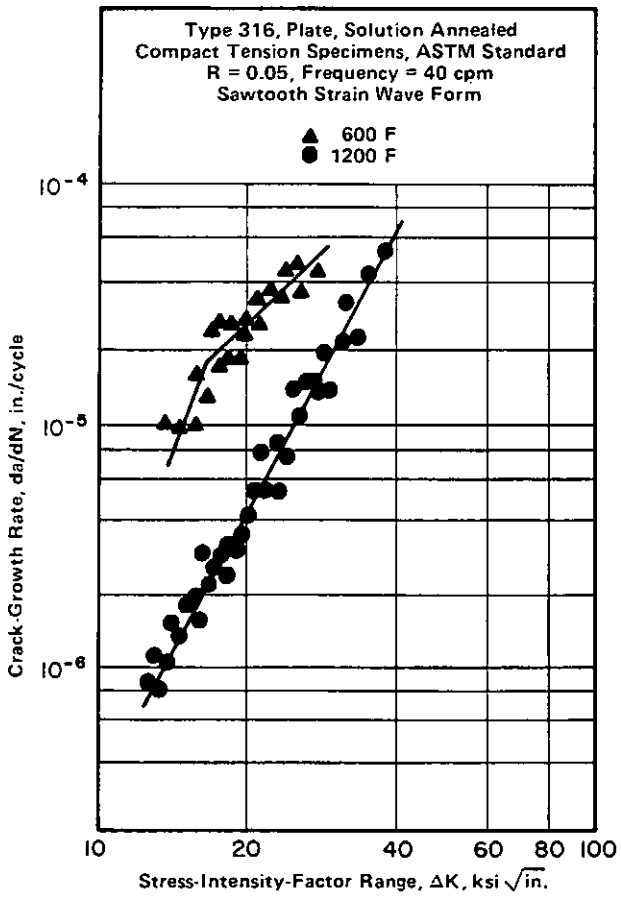
FIGURE 3.0528. EFFECTS OF CYCLIC FREQUENCY ON LOW-CYCLE FATIGUE CRACK-GROWTH BEHAVIOR IN AIR AT ELEVATED TEMPERATURES (109)

Fe
18 Cr
13 Ni
+ Mo

Type 316
Type 317



(a) Room Temperature and 1000 F

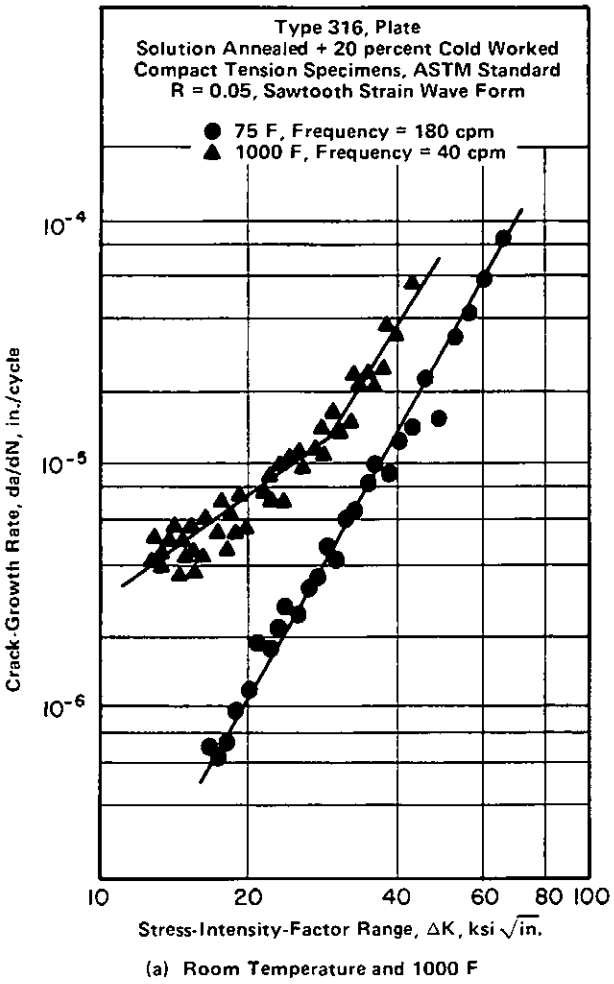


(b) 600 and 1200 F

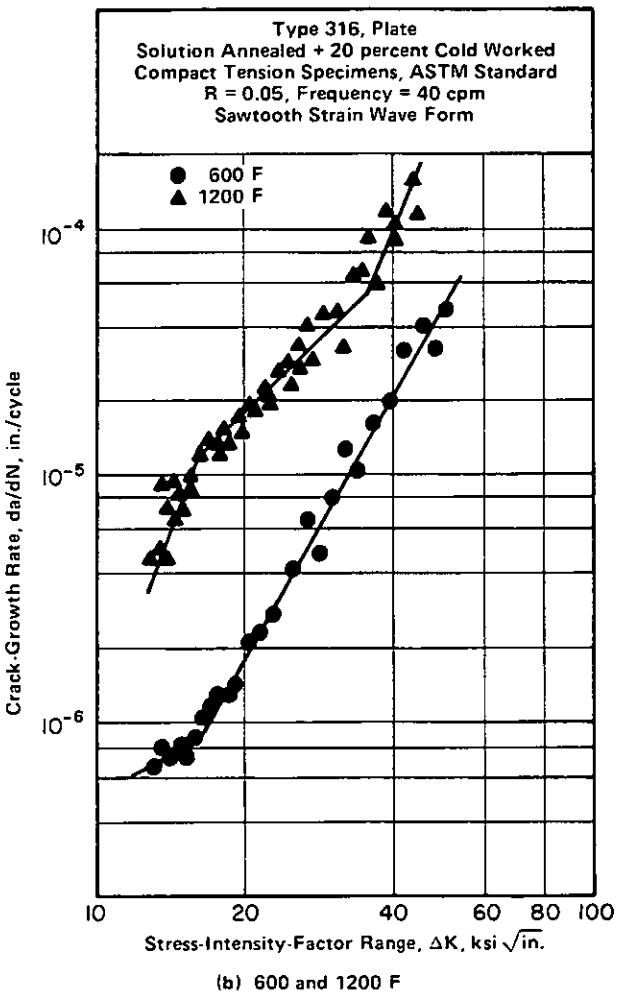
FIGURE 3.0530. EFFECTS OF TEMPERATURE ON LOW-CYCLE FATIGUE CRACK-GROWTH BEHAVIOR OF ANNEALED ALLOY (110)

Fe
18 Cr
13 Ni
+ Mo

Type 316
Type 317



(a) Room Temperature and 1000 F



(b) 600 and 1200 F

FIGURE 3.0531. EFFECTS OF TEMPERATURE ON LOW-CYCLE FATIGUE CRACK-GROWTH BEHAVIOR OF COLD-WORKED ALLOY (110)

Fe
18 Cr
13 Ni
+ Mo

Type 316
Type 317

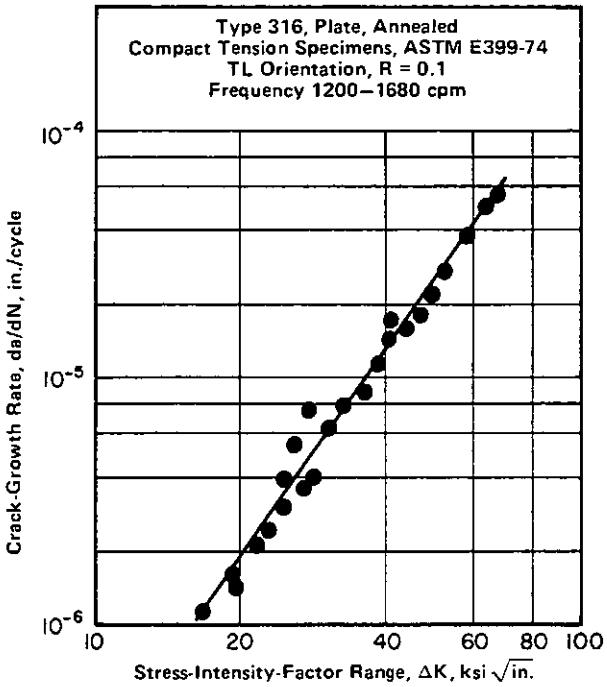


FIGURE 3.0532. FATIGUE CRACK-GROWTH RATE OF ANNEALED ALLOY AT -452 F (111)

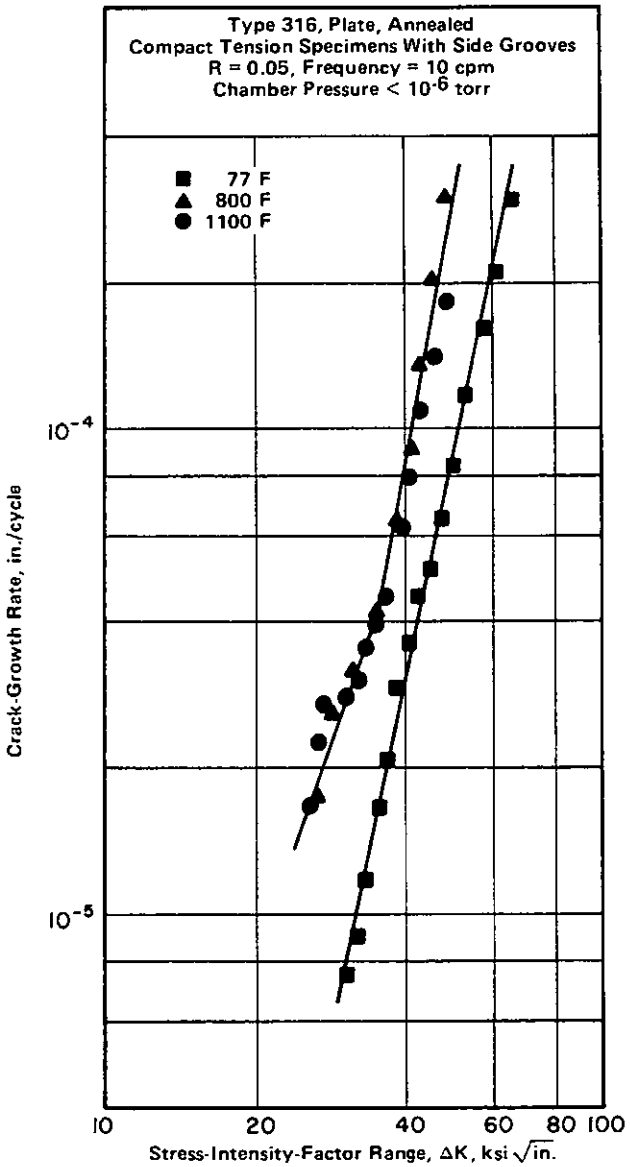


FIGURE 3.0533. LOW-CYCLE FATIGUE CRACK-GROWTH BEHAVIOR IN VACUUM AT ROOM AND ELEVATED TEMPERATURES (112)

Fe
18 Cr
13 Ni
+ Mo

Type 316
Type 317

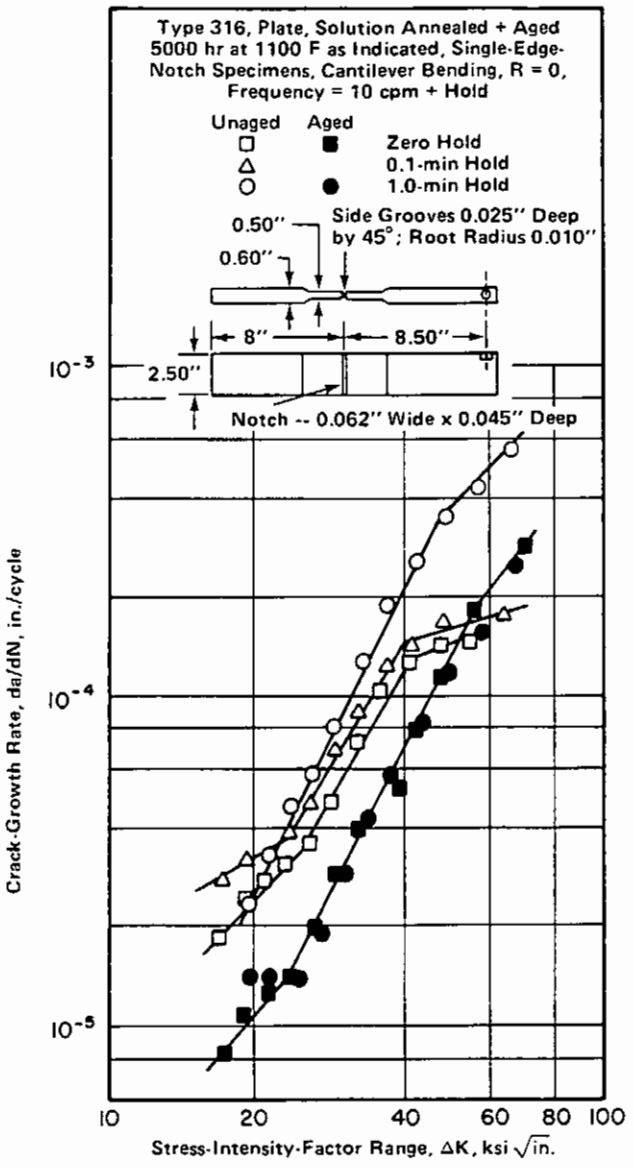


FIGURE 3.0535. EFFECTS OF AGING AND HOLD TIME ON LOW-CYCLE BENDING FATIGUE CRACK-GROWTH RATE OF ANNEALED ALLOY IN AIR AT 1100 F (113)

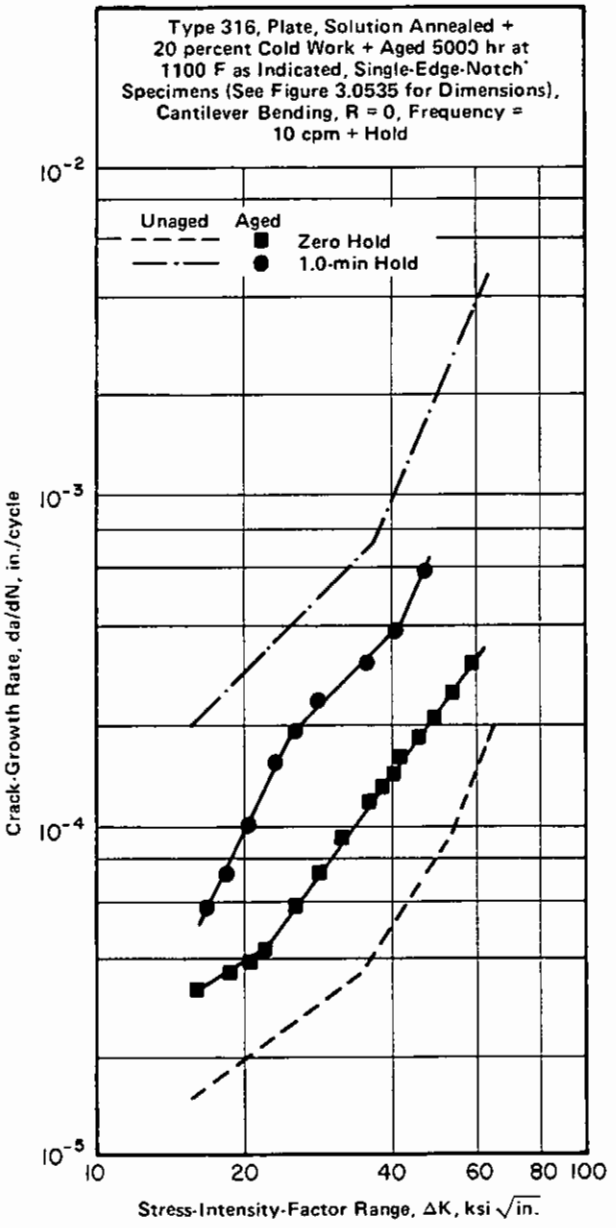


FIGURE 3.0536. EFFECTS OF AGING AND HOLD TIME ON LOW-CYCLE BENDING FATIGUE CRACK-GROWTH RATE OF COLD-WORKED ALLOY IN AIR AT 1100 F (113)

Fe
18 Cr
13 Ni
+ Mo

Type 316
Type 317

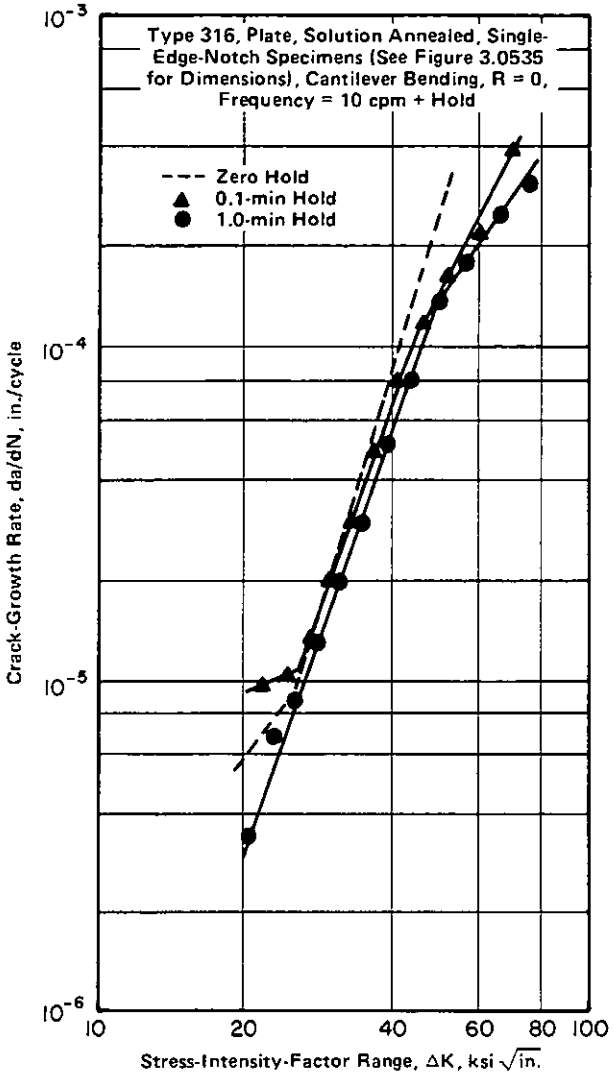


FIGURE 3.0537. EFFECTS OF HOLD TIME ON LOW-CYCLE BENDING FATIGUE CRACK-GROWTH RATE OF ANNEALED ALLOY IN AIR AT 800 F (113)

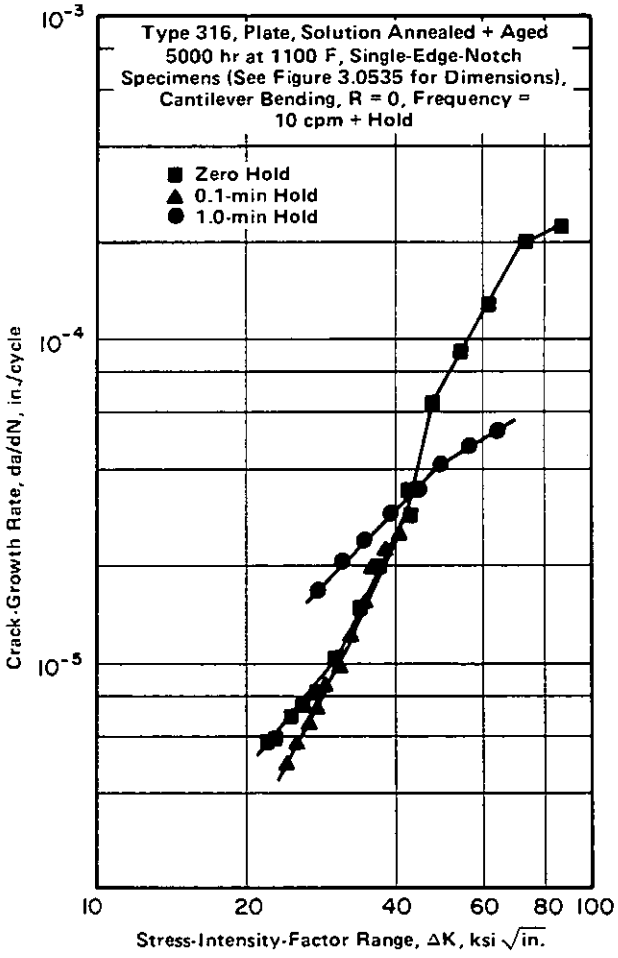


FIGURE 3.0538. EFFECTS OF HOLD TIME ON LOW-CYCLE BENDING FATIGUE CRACK-GROWTH RATE OF ANNEALED-AND-AGED ALLOY IN AIR AT 800 F (113)

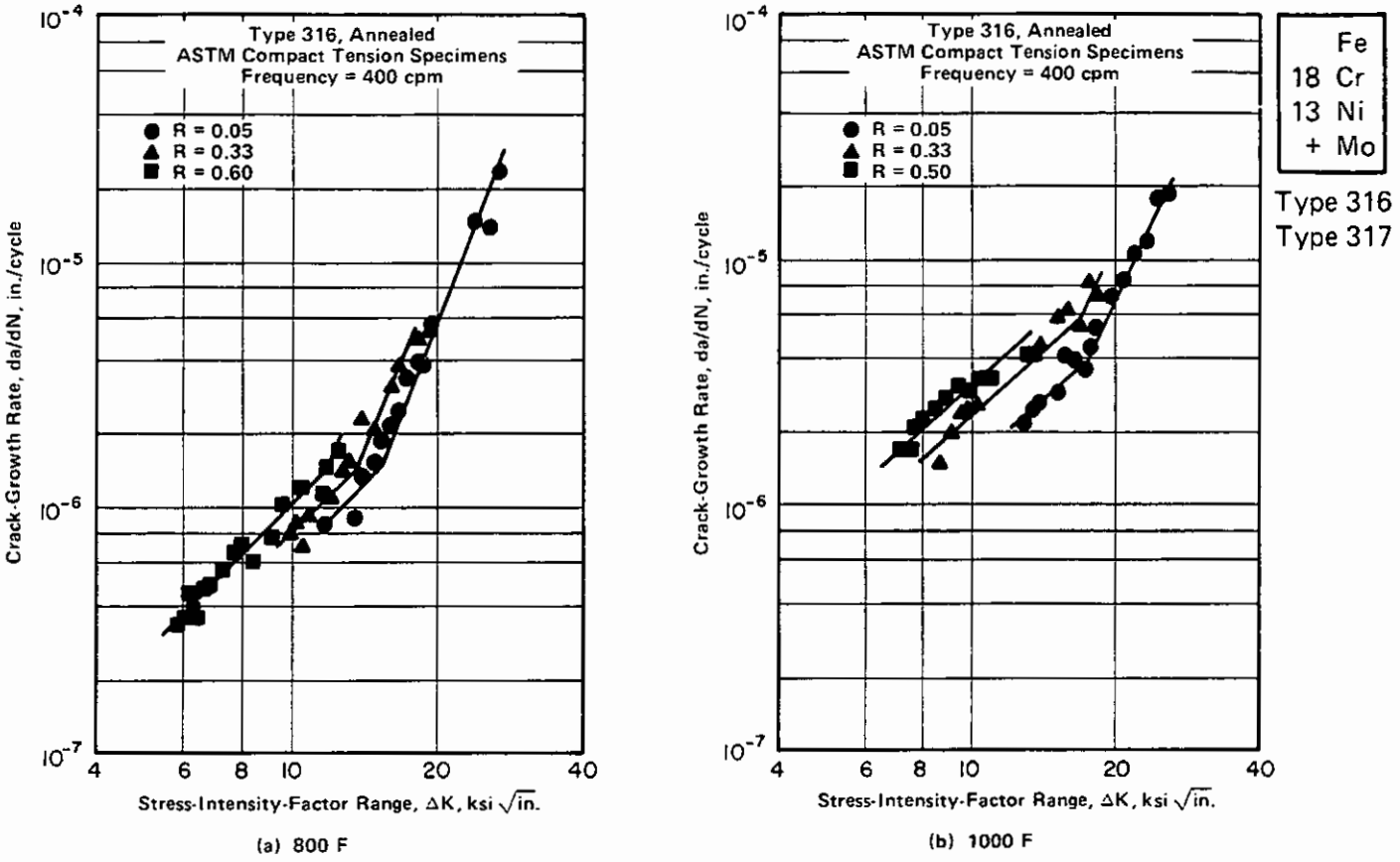


FIGURE 3.0540. EFFECTS OF STRESS RATIO ON LOW-CYCLE FATIGUE CRACK-GROWTH BEHAVIOR IN AIR AT ELEVATED TEMPERATURES (114)

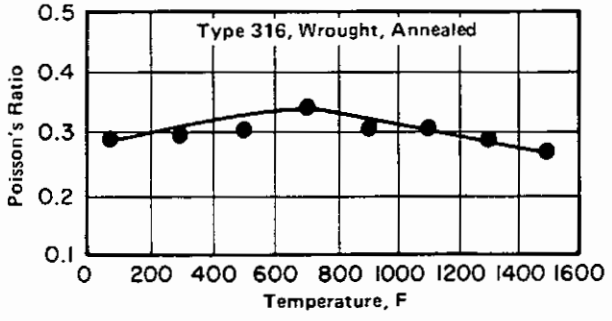


FIGURE 3.0611. EFFECT OF TEMPERATURES UP TO 1500 F ON POISSON'S RATIO (29)

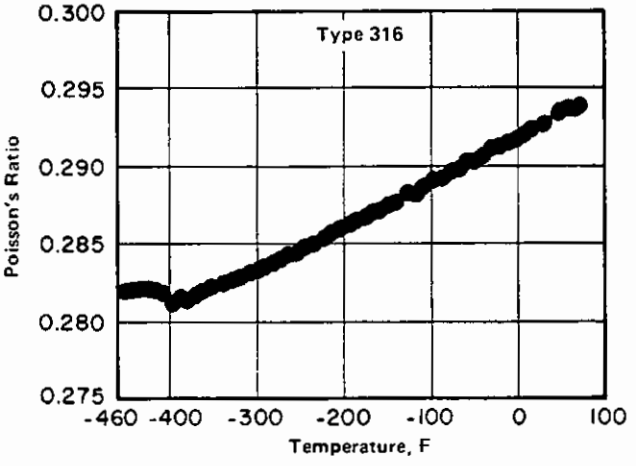


FIGURE 3.0612. POISSON'S RATIO AT ROOM AND CRYOGENIC TEMPERATURES (115)

Fe
18 Cr
13 Ni
+ Mo

Type 316
Type 317

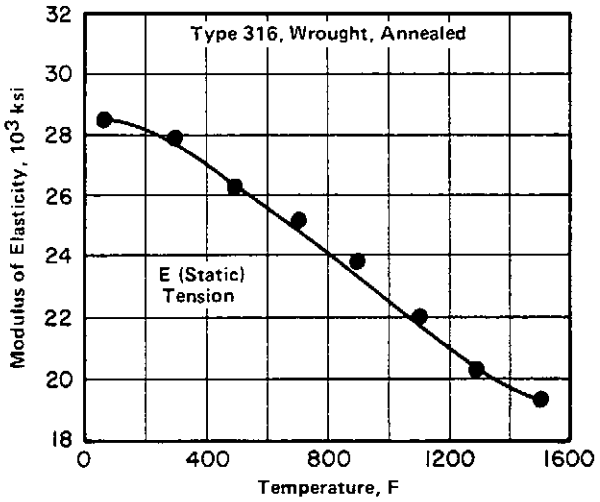


FIGURE 3.0621. EFFECT OF TEMPERATURES UP TO 1500 F ON MODULUS OF ELASTICITY (29)

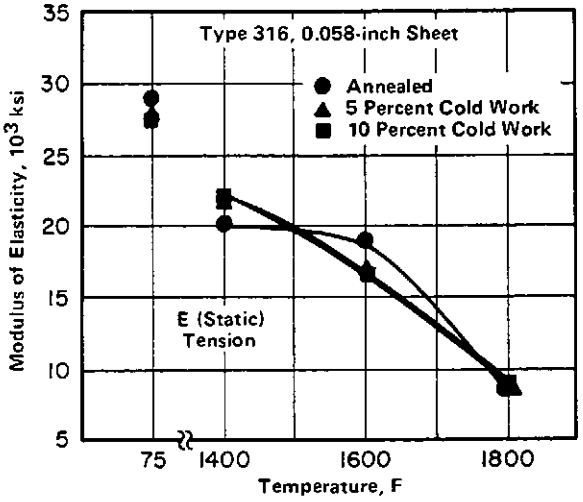


FIGURE 3.0622. MODULUS OF ELASTICITY OF ANNEALED AND COLD-WORKED SHEET AT ROOM TEMPERATURE AND FROM 1400 TO 1800 F (24)

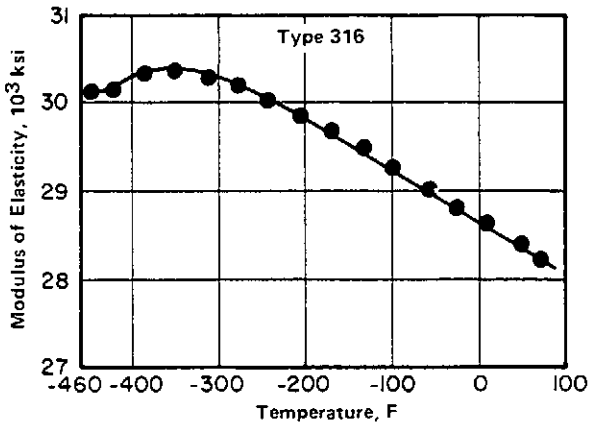


FIGURE 3.0623. MODULUS OF ELASTICITY AT ROOM AND CRYOGENIC TEMPERATURES (115)

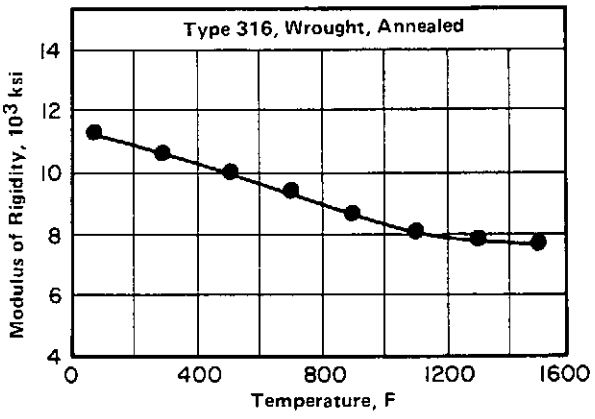


FIGURE 3.0631. EFFECT OF TEMPERATURES UP TO 1500 F ON MODULUS OF RIGIDITY (29)

Fe
18 Cr
13 Ni
+ Mo

Type 316
Type 317

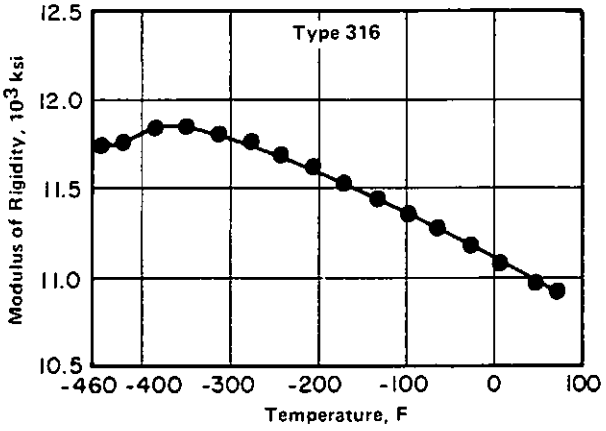


FIGURE 3.0632. MODULUS OF RIGIDITY AT ROOM AND CRYOGENIC TEMPERATURES (115)

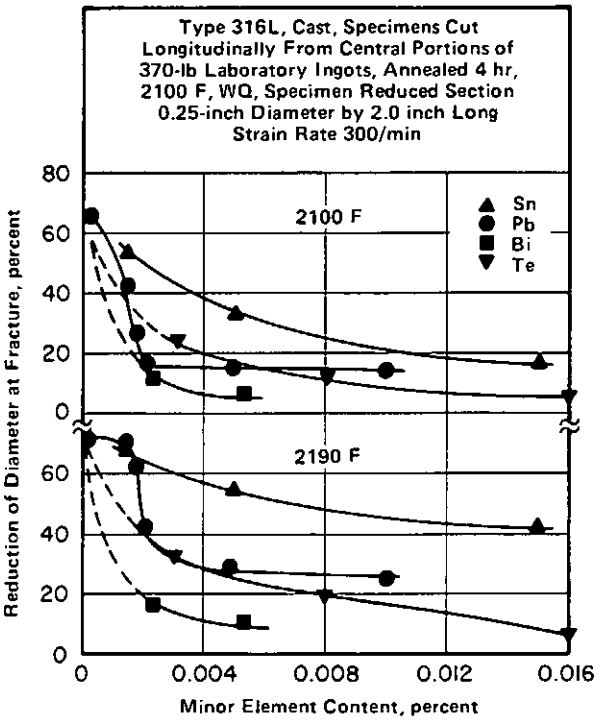


FIGURE 4.015. EFFECTS OF LEAD, TIN, BISMUTH, AND TELLURIUM ON HOT DUCTILITY OF CAST TYPE 316L (117)

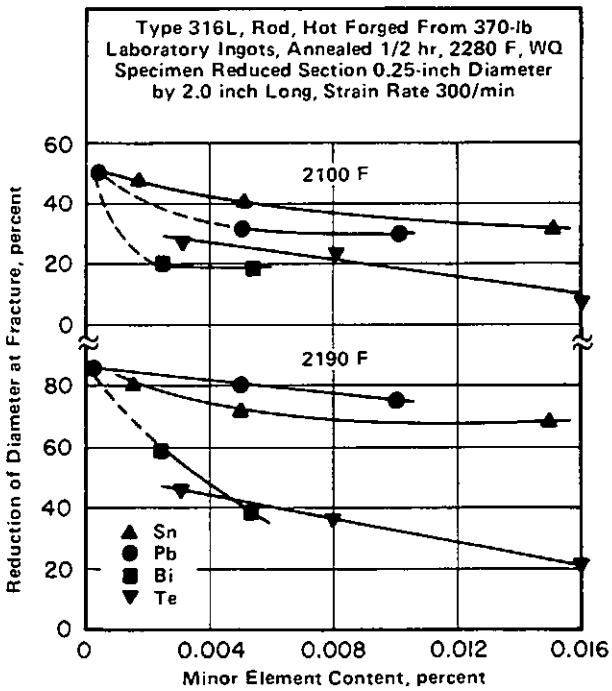


FIGURE 4.016. EFFECTS OF LEAD, TIN, BISMUTH, AND TELLURIUM ON HOT DUCTILITY OF WROUGHT TYPE 316L (117)

Fe
18 Cr
13 Ni
+ Mo

Type 316
Type 317

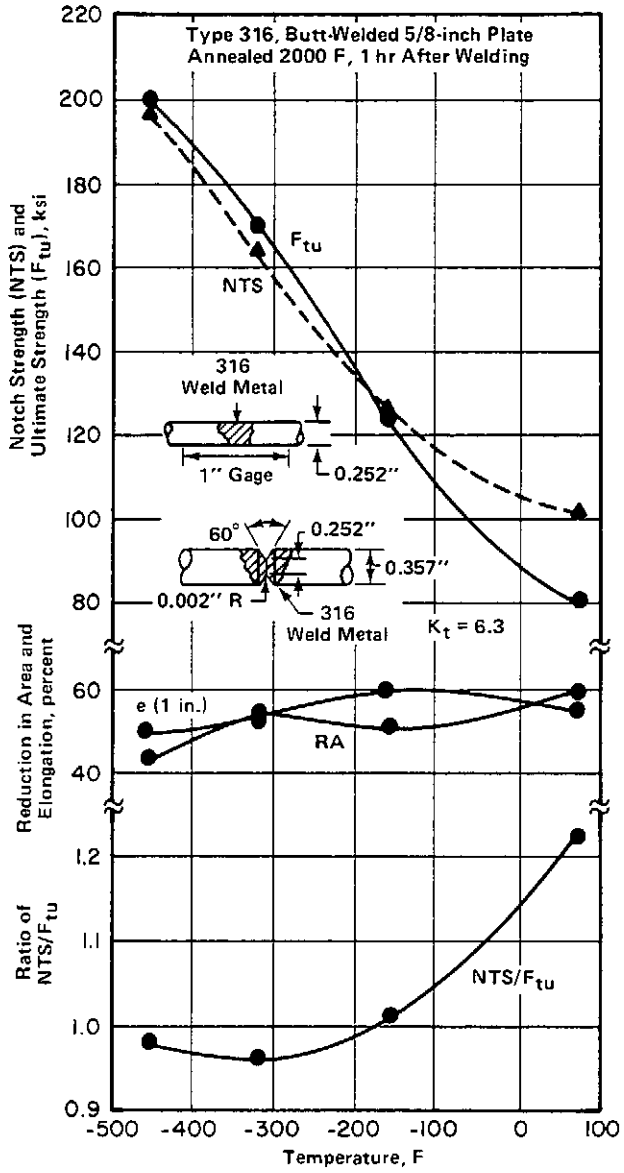


FIGURE 4.032. LOW-TEMPERATURE TENSILE AND NOTCHED TENSILE PROPERTIES OF PLATE, BUTT WELDED WITH TYPE 316 COATED STICK ELECTRODES (10)

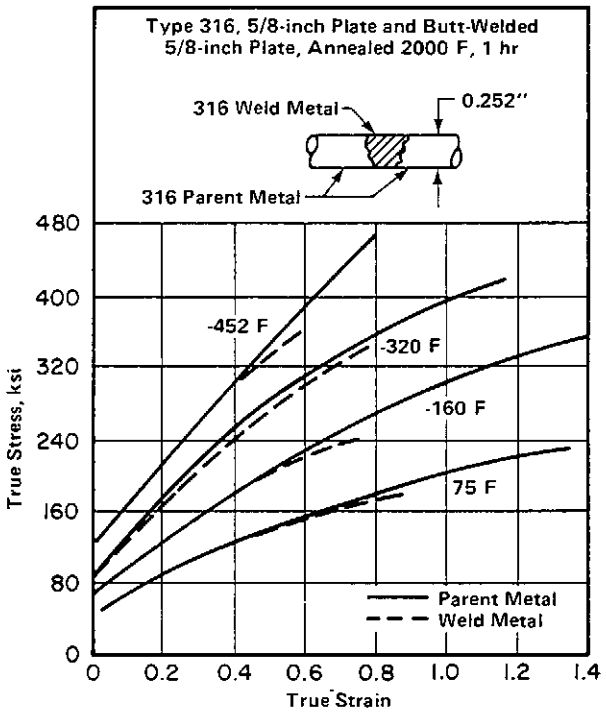


FIGURE 4.033. COMPARISON OF COMPLETE TRUE STRESS-TRUE STRAIN CURVES OF PLATE AND OF WELD METAL AFTER PLATE HAD BEEN BUTT WELDED WITH TYPE 316 COATED STICK ELECTRODES (10)

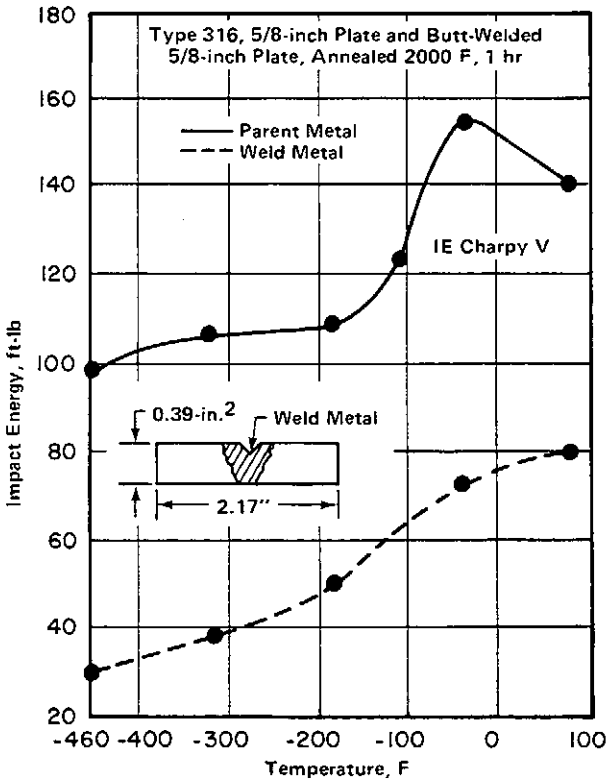


FIGURE 4.034. LOW-TEMPERATURE IMPACT PROPERTIES OF PLATE AND OF WELD METAL AFTER PLATE HAD BEEN BUTT WELDED WITH TYPE 316 COATED STICK ELECTRODES (10)

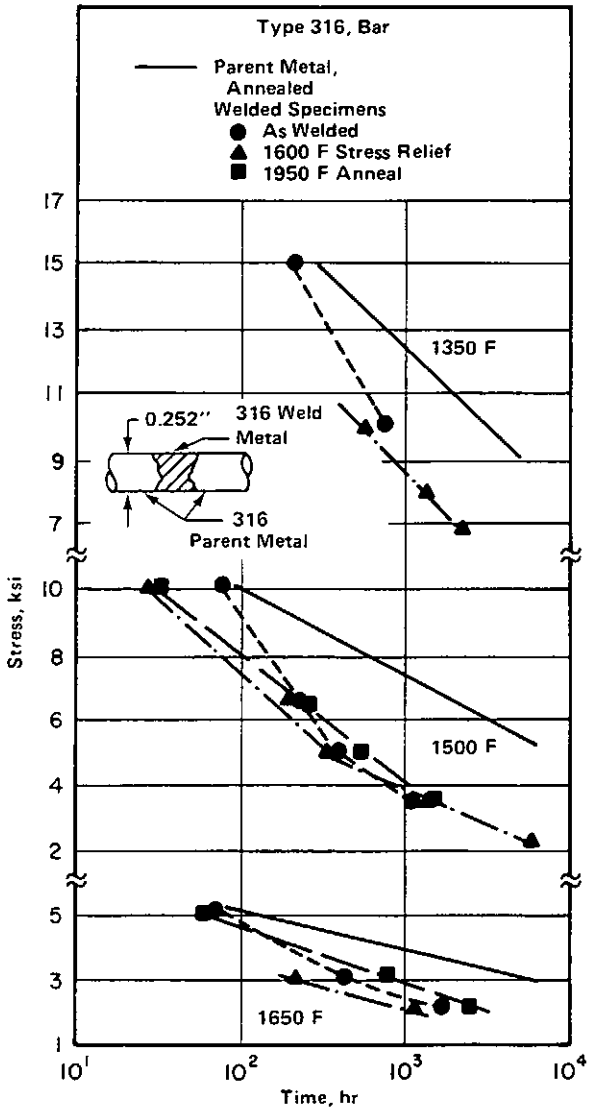


FIGURE 4.035. CREEP-RUPTURE CURVES FOR ANNEALED PARENT METAL AND FOR TUNGSTEN-INERT-GAS-WELDED SPECIMENS IN VARIOUS HEAT-TREATED CONDITIONS (22)

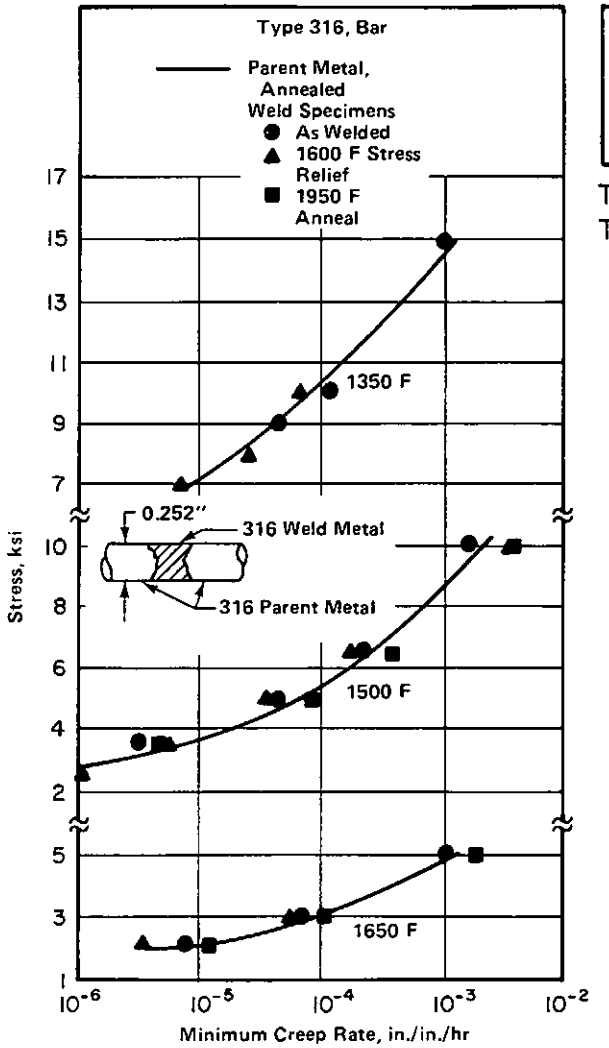


FIGURE 4.036. MINIMUM CREEP RATES FOR ANNEALED PARENT METAL AND FOR TUNGSTEN-INERT-GAS-WELDED SPECIMENS IN VARIOUS HEAT-TREATED CONDITIONS (22)

Fe
18 Cr
13 Ni
+ Mo

Type 316
Type 317

Fe
18 Cr
13 Ni
+ Mo

Type 316
Type 317

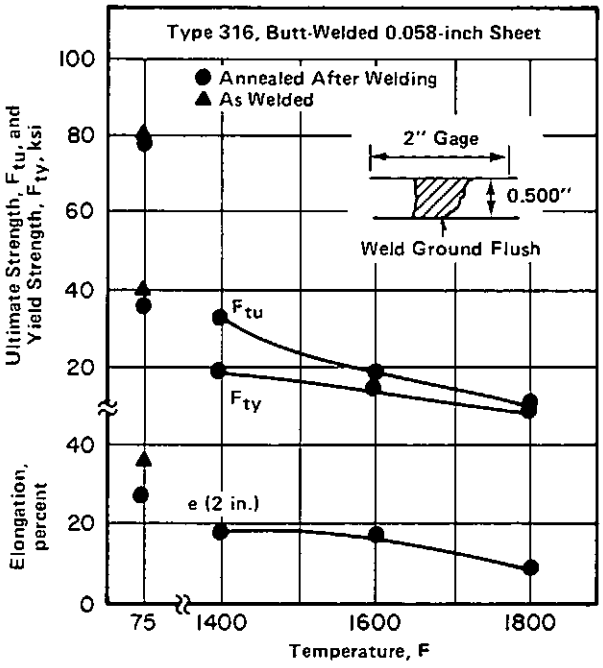


FIGURE 4.037. EFFECT OF TEMPERATURE ON TENSILE PROPERTIES OF ANNEALED SHEET BUTT WELDED BY THE INERT-GAS-SHIELDED-ARC PROCESS (24)

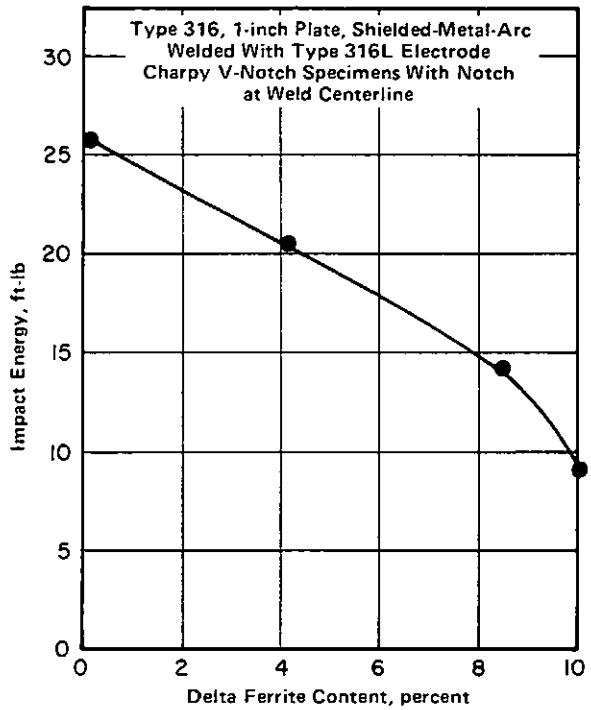


FIGURE 4.039. EFFECT OF DELTA FERRITE CONTENT ON CHARPY IMPACT ENERGY OF WELD METAL AT -320 F (121)

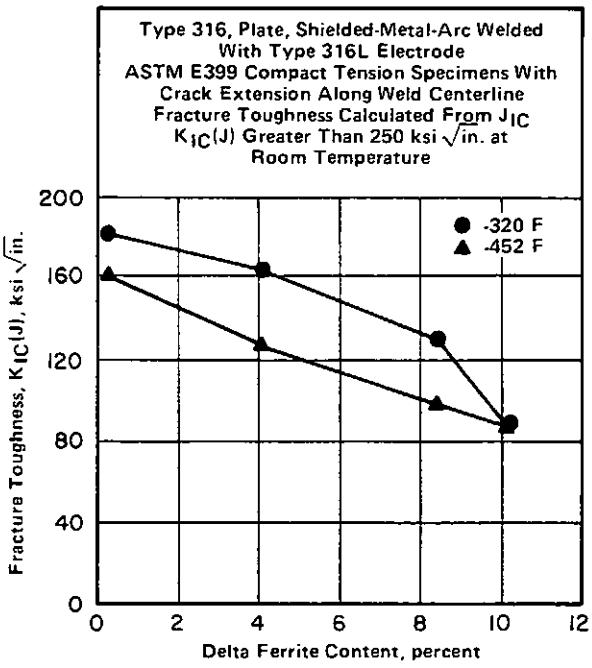


FIGURE 4.0310. EFFECTS OF DELTA FERRITE CONTENT ON FRACTURE TOUGHNESS OF WELD METAL AT CRYOGENIC TEMPERATURES (121)

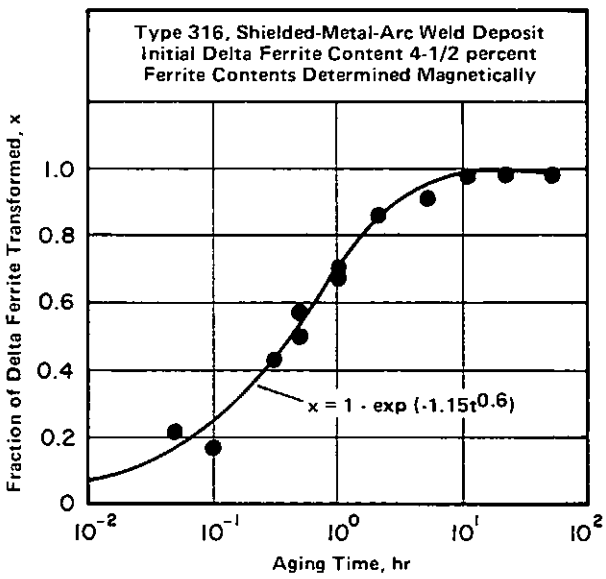


FIGURE 4.0311. EFFECT OF AGING TIME AT 1380 F ON TRANSFORMATION OF DELTA FERRITE IN TYPE 316 WELD METAL (119)

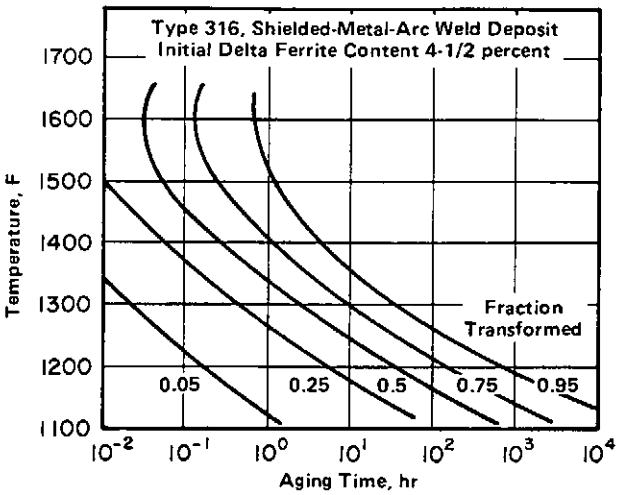


FIGURE 4.0312. TIME-TEMPERATURE-TRANSFORMATION DIAGRAM FOR TRANSFORMATION OF DELTA FERRITE IN WELD METAL (119)

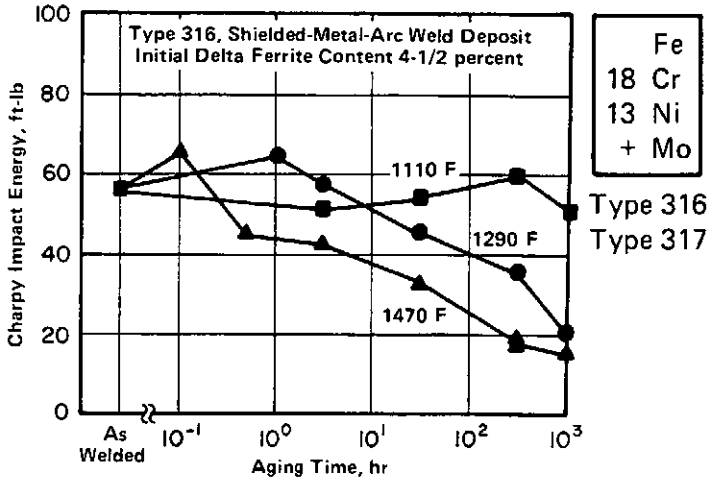


FIGURE 4.0313. EFFECTS OF AGING TIME AND TEMPERATURE ON IMPACT ENERGY OF WELD METAL AT ROOM TEMPERATURE (119)

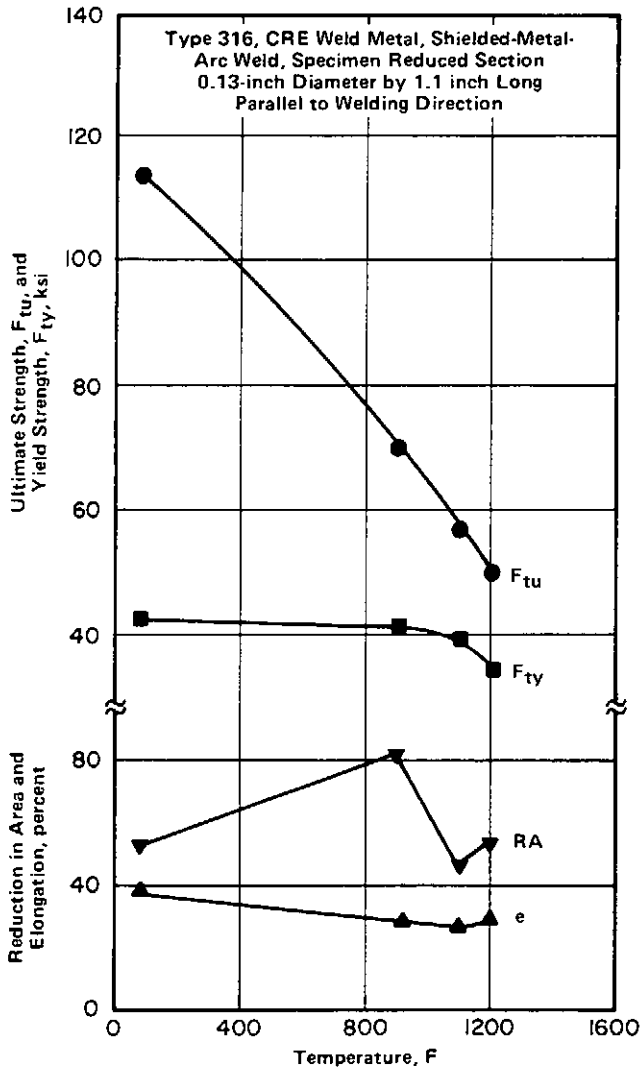


FIGURE 4.0315. TENSILE PROPERTIES OF CRE SHIELDED-METAL-ARC WELD METAL AT ROOM AND ELEVATED TEMPERATURES (123)

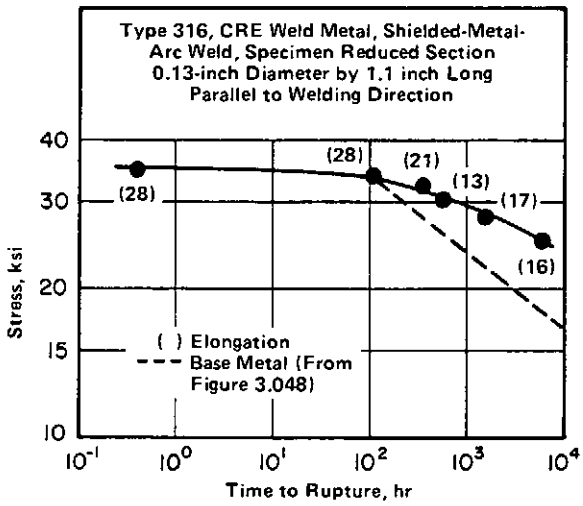


FIGURE 4.0316. STRESS-RUPTURE BEHAVIOR OF CRE SHIELDED-METAL-ARC WELD METAL AT 1200 F (123)

	Fe
18	Cr
10	Ni
+	Ti

Type 321

1 GENERAL

Type 321 is an austenitic stainless steel, which can be hardened by cold work but not by heat treatment. Its composition is similar to that of Type 304, except that titanium is added to form stable precipitates of titanium carbide randomly distributed within the grains. In the stabilization heat-treated condition, harmful precipitation of chromium carbides at the grain boundaries in the sensitization range of 800 to 1600 F is prevented and the alloy has good resistance to intergranular corrosion. Type 321 and other stabilized grades of stainless steels such as Types 347 and 348 are preferred for long-time service in the 800 to 1600 F range, while Type 304L is frequently employed for applications involving welding or short-time heating in this temperature range. Although they are both equally insensitive to grain-boundary carbide precipitation and intergranular corrosion, Type 321 is somewhat inferior to Type 347 in general corrosion resistance. Since the titanium in Type 321 is readily oxidized during melting, it is rarely employed for welding rods or for castings. Some of the more important applications for this alloy are in aircraft collector rings and exhaust manifolds, expansion joints, high-temperature chemical processing equipment, and pressure vessels (8,9,11,33).

1.01 Commercial Designation

Type 321.

1.02 Alternate Designations

Type 321H (11), UNS S32100, UNS S32109-(321H), UNS J92630.

1.03 Specifications

1.031 Table 1.031.

1.04 Composition

1.041 Table 1.041.

1.05 Heat Treatment

1.051 Anneal: 1750 F to 2050 F, air cool or water quench. This treatment results in maximum ductility and workability and minimum hardness (8,9,33). Highly reducing annealing atmospheres should be avoided (11).

1.052 Stabilization: 1550 to 1650 F 2 hours, air cool or water quench. This treatment, following the annealing treatment, is recommended for the most severe conditions of service, particularly those above 800 F. (See also 1.091.) The purpose is to reprecipitate, as titanium carbide, carbon dissolved during the anneal, and thereby to reduce the tendency to form chromium carbides during service. Generally, the higher the annealing temperature, the greater the need for a stabilizing heat treatment (8,33).

1.053 Process anneal or stress relief: 1300 F, air cool. This treatment or, alternatively, a full anneal is used between stages and after severe cold work (8,9).

1.054 Grain growth in Type 321 can be expressed by $D^n - D_o^n = At \exp(-Q/RT)$, where D_o is the initial grain size, D is the grain size after an isothermal exposure at temperature T for a period t, Q is the activation energy, R is the gas constant, and n and A are constants. The exponent n for Type 321 has a best-fit value of 4. The activation energy is estimated as 100 ± 25 kcal/g mol. This large value of activation energy reflects grain-boundary pinning by carbides (45).

1.06 Hardness

1.061 Hardness of various forms, Table 1.061.

1.062 Effects of exposures to elevated temperatures on hardness at room temperature, Table 1.062.

1.063 Effect of cold rolling on hardness of strip, Table 1.063.

1.07 Forms and Conditions Available

Table 1.07.

1.08 Melting and Casting Practice

1.081 The alloy is normally air melted in electric-arc furnaces. For applications requiring exceptional quality, it can be induction or consumable-electrode remelted in vacuum.

1.082 The alloy can be cast as single ingots or continuous strands (46).

1.083 Grain refinement and more homogeneous carbide distribution can be effected by electromagnetic stirring during solidification (47).

1.09 Special Considerations

1.091 Solution annealing at temperatures above 1900 F results in partial dissolution of TiC, the extent of dissolution increasing with increasing annealing temperature. In the solution-annealed condition, the alloy can be subsequently sensitized by welding or by heating in the sensitization temperature range of about 800 to 1500 F. A stabilization anneal of 2 hours or longer at 1650 F after solution annealing is required to promote TiC precipitation and prevent subsequent sensitization (48).

1.092 Prolonged heating at 2000 F and above causes excessive grain growth.

1.0921 Effects of time and temperature on grain growth, Figure 1.0921.

1.093 Prolonged exposure in the temperature range 900 to 1500 F can significantly reduce room-temperature ductility and notched impact strength. See Tables 3.0213, 3.0214, 3.0231, and 3.0232.

1.094 In both the annealed and cold-worked conditions, a minimum in tensile ductility occurs in the temperature range 1100 to 1400 F. See Figures 3.0315, 3.0316, and 3.0319.

2 PHYSICAL AND CHEMICAL PROPERTIES

2.01 Thermal Properties

2.011 Melting range: 2500 to 2550 F (8), 2550 to 2600 F (9).

2.012 Phase changes.

2.0121 Time-temperature-transformation diagrams.

2.0122 The second phases in Type 321 vary with exposure time and temperature, prior thermomechanical history, and composition. In particular, the chemistries of the carbide phase(s) and hence the sensitization of the alloy to intergranular corrosion vary with aging conditions. After furnace aging of

Fe
18 Cr
10 Ni
+ Ti

Type 321

2000 F solution-annealed material for times up to 3000 hours at temperatures between 840 and 1740 F, $M_{23}C_6$ was determined as the major precipitating phase. However, after a service exposure of 17 years at 1050 to 1124 F, the major second phases were TiC and sigma. No $M_{23}C_6$ was observed in the service-exposed material, even though its chemistry was very similar to that of the furnace-aged material. It is suggested that TiC precipitate aligns into stringers during fabrication. On solution annealing, the precipitate dissolves and the carbon is well dispersed. However, the titanium, because of its lower diffusivity, remains in the vicinity of the original precipitate. During subsequent aging in the sensitization temperature range, the carbon near the titanium precipitates as TiC, while the remaining carbon reacts with the more abundant chromium to form $M_{23}C_6$ at the grain boundaries. Over a long time period, the $M_{23}C_6$ converts gradually to the more stable MC precipitate. Thus, while under equilibrium conditions enough titanium may be present to completely react with the carbon present, kinetic factors can permit the formation of metastable $M_{23}C_6$. The inclusion of a stabilization anneal at 1650 F after solution annealing will promote the formation of MC precipitate and prevent possible subsequent sensitization (49).

2.0123 Small amounts of sigma phase can form in Type 321 after long exposures at intermediate temperatures, depending on the chromium content. The critical chromium content for sigma formation in Type 321 has been established as 17.8 weight percent. At chromium contents above this value, sigma phase can form, while at lower levels it cannot. Sigma phase is detrimental to toughness and corrosion resistance. It can be removed by annealing (49).

2.0124 Sulfur in Type 321 precipitates as $Ti_4C_2S_2$ (49).

2.0125 Cold work transforms a small amount of austenite to ferrite.

2.013 Thermal conductivity, Figure 2.013.

2.014 Thermal expansion, Figure 2.014.

2.015 Specific heat. 0.12 Btu/(lb F) (8,33).

2.016 Thermal diffusivity.

2.02 **Other Physical Properties**

2.021 Density. 0.29 lb/in.^{3}, 8.0 g/cm^3 (8,33).

2.022 Electrical properties.

2.0221 Electrical properties at various temperatures, Table 2.0221.

2.023 Magnetic properties.

2.0231 In the annealed condition, Type 321 is practically nonmagnetic; the maximum permeability is 1.02 at 200H. Cold work induces a slight amount of magnetic permeability, which varies with the amount of cold work and the chemical composition (9).

2.0232 The Néel temperature for Type 321 is predicted as -420 to -360 F (50).

2.024 Emittance.

2.0241 Total normal emittance at elevated temperatures, Figure 2.0241.

2.025 Damping capacity.

2.03 **Chemical Environments**

2.031 General corrosion.

2.0311 Type 321 withstands ordinary rusting and is immune to all foodstuffs, sterilizing solutions, most organic chemicals and dyestuffs, and a wide variety of inorganic chemicals. It resists nitric acid well, halogen acids poorly, and sulfuric acids moderately. Although long-time exposure in the range 800 to 1600 F may lower its general corrosion resistance, it nevertheless maintains immunity to intergranular corrosion, which does occur in similarly exposed unstabilized grades of stainless steel (8,9,33).

2.0312 Type 321 is highly resistant to general corrosion and stress corrosion in contact with the dense hydrocarbon fuel RJ-5 (Shelldyne H) (25).

2.0313 It is susceptible to pitting, tunneling, and crevice types of corrosion in seawater, the susceptibility being greater near the surface of the ocean than at the bottom or at intermediate depths. The susceptibility of Type 321 to corrosion in seawater is less than that of Types 301 or 304, but greater than that of the higher chromium-nickel grades such as 309 and 310. Type 321, as well as most other stainless steels, is not recommended for long-time service in seawater unless protective measures are taken such as the application of an inert coating (26).

2.0314 Hydrochloric acid is highly aggressive to Type 321 and other stainless steels, since the protective surface oxide film normally present reacts with this chemical. Various organic additives inhibit the corrosion of Type 321 in hydrochloric acid, including hexamine [also known as hexamethylene-tetramine $(CH_2)_6N_4$]. As shown in Figure 2.0315, the corrosion rate of Type 321 in 1N HCl decreases with increasing hexamine concentration, with a maximum improvement of about 15-fold at 4 percent hexamine. Hexamine is effective over a range of acid concentrations from at least 1N to 10N, as shown in Figure 2.0316, and at temperatures up to 176 F, as shown in Figure 2.0317. The protection against corrosion is attributed to a chemisorbed passive film which prevents reaction of the alloy with the acid (51).

2.0315 Effects of hexamine on corrosion of Type 321 in 1N HCl, Figure 2.0315.

2.0316 Effects of hydrochloric acid concentration and hexamine on corrosion of Type 321, Figure 2.0316.

2.0317 Effects of temperature and hexamine on corrosion of Type 321 in hydrochloric acid, Figure 2.0317.

2.0318 The corrosion rate of Type 321 in sulfuric acid is reduced by the presence of small amounts of potassium iodide. The addition of 10^{-3} to 10^{-1}N KI is effective in inhibiting corrosion at sulfuric acid concentrations up to 15N, as shown in Figure 2.0319. However, at higher potassium iodide concentrations, localized pitting and perforation occur after 14 to 28 days' exposure, as indicated in Figure 2.03110. Increasing temperature increases the rate of corrosion. However, as shown in Figure 2.03111, inhibition by 10^{-3} to 10^{-1}N KI

Fe
18 Cr
10 Ni
+ Ti

Type 321

is effective up to at least 176 F. The reduced corrosion rates are attributed to chemisorption of a monolayer of the inhibitor, preventing corrosion on that fraction of the surface covered by the inhibitor (52).

2.0319 Effects of potassium iodide on sulfuric acid corrosion of Type 321, Figure 2.0319.

2.03110 Effects of potassium iodide and exposure time on corrosion weight loss in 1N sulfuric acid, Figure 2.03110.

2.03111 Effect of temperature and potassium iodide on corrosion of Type 321 in sulfuric acid, Figure 2.03111.

2.032 Intergranular corrosion.

2.0321 The intergranular corrosion behavior of Type 321 is greatly influenced by prior thermal history and its effect on distribution of carbon. In common with the unstabilized austenitic 18-8 stainless steels, solution-annealed Type 321 is sensitized by welding or by exposure in a critical temperature range, which causes precipitation of chromium-rich carbides at the grain boundaries. This precipitation depletes the chromium content of the matrix adjacent to the grain boundaries and, in turn, significantly decreases the local corrosion resistance. However, Type 321 contains titanium to preferentially react with free carbon and precipitate TiC rather than $Cr_{23}C_6$. The alloy can be stabilized so that it is not subject to sensitization. The corrosion rate of sensitized Type 321 increases with increasing solution-heat-treatment temperature as shown in Figure 2.0322. This change in corrosion rate is related to the change in amount of free carbon in solution after heat treatment. Solution annealing at 2192 F causes dissolution of most of the TiC so that the carbon is free to reprecipitate as $Cr_{23}C_6$ during subsequent sensitization. Initial heat treatments at lower temperatures, such as 1832 to 2066 F, leave a greater fraction of the carbon content tied up as TiC so that less chromium is removed by $Cr_{23}C_6$ precipitation. The nature of the TiC precipitate is also affected by solution-heat-treatment temperature. Above 1900 to 2000 F, the initial TiC is probably incoherent with the matrix and large enough to be stable. Below 1900 to 2000 F, the initial TiC forms on dislocations, is probably coherent, and is not large enough to be stable without further growth.

The corrosion behavior of solution-annealed alloy is also influenced by the temperature and time of the sensitization exposure, as shown in Figure 2.0323. At exposure times of less than 100 hours, sensitization occurs at 1022 and 1112 F because precipitation of $Cr_{23}C_6$ occurs more rapidly than precipitation of TiC However, at longer times, rehealing takes place through conversion of $Cr_{23}C_6$ to TiC with accompanying restoration of chromium to the depleted regions. At 1202 F, both $Cr_{23}C_6$ and TiC precipitate from the matrix, with subsequent gradual conversion of $Cr_{23}C_6$ to TiC. The corrosion rates in Figure 2.0323 reflect these changes in chromium content of the matrix, increasing as chromium is lost through precipitation of $Cr_{23}C_6$ and decreasing as chromium is restored by conversion of the precipitate to TiC.

The relationship between carbon content of the matrix and sensitization time and temperature for 18-8 type stainless steels is summarized by the C-curve in Figure 2.0324. At time-temperature combinations below the $M_{23}C_6$ nucleation line, the rate of $Cr_{23}C_6$ precipitation is too sluggish for sensitization to occur. However, at longer times and at temperatures up to about 1130 F, precipitation of $Cr_{23}C_6$ occurs in Type 321, depending on the free carbon content of the matrix. At temperatures above about 1130 F, as indicated by the dotted line, TiC precipitates concurrently with $Cr_{23}C_6$. After long times above 1200 F and short times above about 1600 F, only TiC is present and sensitization is avoided (53,54).

2.0322 Effects of high-temperature heat treatment on corrosion rate of Type 321, Figure 2.0322.

2.0323 Effects of sensitization reheating on corrosion rates of solution-annealed Type 321, Figure 2.0323.

2.0324 Time-temperature-dissolved carbon relationships for $Cr_{23}C_6$ precipitation and for stabilization in 18Cr-8Ni type stainless steels, Figure 2.0324.

2.0325 Cold work affects sensitization by enhancing diffusion and carbide precipitation rates. It also promotes finer and more uniformly distributed precipitate. Heavy cold work can improve the corrosion resistance of sensitized material, while lesser amounts of cold work can enhance sensitization and lead to transgranular corrosion. Hot fatigue cycling is seen to increase the corrosion rate as compared to material which was heat treated only (for similar time at the same temperature), as shown in Figure 2.0326 for Types 321 and 304. Type 321 is seen to have far superior corrosion resistance in all conditions as compared to Type 304. Although sensitization heat treatment increases the corrosion rates for both steels, the increase for Type 321 is less than that for Type 304. Deformation by fatigue at the sensitization temperature further reduces the corrosion resistance by increasing the amount of carbide precipitation (55).

2.0326 Effects of sensitizing heat treatment and fatigue cycling on corrosion behavior in boiling copper sulfate, Figure 2.0326.

2.0327 The heat-affected zone of fusion-welded material is subject to accelerated corrosion if the assembly is sensitized by aging or during exposure after welding. The susceptibility to localized corrosion is caused by a sensitization reaction similar to that which affects improperly solution-annealed and aged material, as described above in Paragraph 2.0321. During welding, material adjacent to the molten weld is heated sufficiently to dissolve most of the MC and $M_{23}C_6$ precipitates. Delta ferrite also forms in the matrix at this time. Rapid cooling after welding retards carbide reprecipitation. During subsequent aging at about 1020 to 1560 F, chromium-rich $M_{23}C_6$ precipitates at the gamma grain boundaries and in the delta ferrite, decreasing the chromium content of these regions and causing sensitization. Some MC-type carbides also

Fe
18 Cr
10 Ni
+ Ti

Type 321

precipitate during aging, but insufficient carbon is tied up as MC to prevent precipitation of $M_{23}C_6$. The localized increased corrosion in the weld heat-affected zone is termed knife-line attack because of the sharp boundary line between corrosion-resistant and non-corrosion-resistant material. As seen in Figure 2.0328, the localized corrosion rate is maximized after an exposure of about 50 hours at 1202 F. At longer exposure times, the corrosion resistance improves, probably due to desensitization (rehealing) by conversion of the precipitate from $M_{23}C_6$ to MC. The corrosion resistance also improves with increasing welding heat input. Accelerated knife-line attack can be considerably reduced by a stabilization heat treatment of 2 hours at 1650 F after welding. This stabilization heat treatment ties up the carbon by precipitation as MC, reducing the loss of chromium as $M_{23}C_6$ during subsequent lower temperature aging. Knife-line-attack sensitivity in Type 321 can also be reduced by alloying with about 0.11 weight percent mischmetal, which accelerates precipitation of MC-type carbides. This level of mischmetal addition has no significant adverse effect on tensile properties (56–60).

2.0328 Effects of aging time on knife-line corrosion rate of arc-welded alloy, Figure 2.0328.

2.033 Stress corrosion.

2.0331 Austenitic stainless steels are particularly susceptible to stress-corrosion cracking as compared to the martensitic (400 series) and ferritic (430 series) stainless steels. Chloride-containing media are most corrosive and austenitic stainless steel components must be entirely stress-free for use in chloride-containing environments (61).

2.0332 Stress-corrosion crack-growth rates as a function of stress-intensity factor for Types 321, 304, 304L, and 316L in hot NaCl solutions are compared in Figure 2.0333. All four alloys exhibit a threshold stress-intensity factor below which no cracking occurs. As the stress-intensity factor increases above the threshold, the crack-growth rate increases sharply to a plateau rate of between 10^{-5} and 10^{-6} in./min. The threshold stress-intensity factor for Type 321 is higher than those for Types 304L and 316L but lower than that for solution-annealed Type 304. The stress-corrosion cracking of iron-nickel-chromium alloys is largely determined by nickel content, as shown in Figure 2.0334. Minimum corrosion resistance is exhibited by alloys containing 10 to 25 percent nickel. Alloys containing more than 25 percent nickel are resistant to chloride stress corrosion, while those containing less than 10 percent tend to be more corrosion resistant but are affected by heat treatment. For example, sensitized Type 304 has a substantially lower threshold stress-intensity factor than that for annealed Type 304. Type 321, being stabilized by titanium, does not exhibit the intergranular stress-corrosion cracking which occurs with sensitized Type 304, but rather shows transgranular cracking which is typical of unsensitized alloys (62).

2.0333 Effect of stress-intensity factor on stress-corrosion crack-growth rate in hot NaCl solution for Type 321 and three other austenitic stainless steels, Figure 2.0333.

2.0334 Effect of nickel content on threshold stress intensity for corrosion cracking in hot NaCl solution for iron-nickel alloys containing about 18 percent chromium, Figure 2.0334.

2.0335 The corrosion resistance of Type 321 weldments can be improved by shot peening. An unpeened welded assembly cracked severely after 22-hour immersion in boiling $MgCl_2$, while a similar peened assembly showed no stress-corrosion cracking after 264 hours (80).

2.0336 Type 321 is resistant to stress-corrosion cracking in seawater, but it is susceptible to both stress corrosion and pitting corrosion in marine atmospheric environment such as seashores and aboard ship. Zinc-rich and aluminum-rich coatings are effective in preventing or retarding the corrosion; surface treatments, such as electropolishing and chemical passivation, are less effective (27).

2.034 Hydrogen embrittlement.

2.0341 A modest degree of low-temperature hydrogen embrittlement is exhibited by Type 321 during tensile testing. This embrittlement occurs in material which has been sensitized by heat treatment prior to cathodic hydrogen charging. The degree of embrittlement at -321 F increases with increasing sensitization time at 1472 F, as shown in Figure 2.0342. The degree of embrittlement by hydrogen also increases with increasing solution-annealing temperature, as shown in Figure 2.0343. Type 321 is more resistant to low-temperature hydrogen embrittlement than the standard grades of Types 304 and 316 but less resistant than the low-carbon modifications of these two alloys and Types 310 and 347 (63).

2.0342 Effects of hydrogen charging and sensitization on tensile ductility at -321 F, Figure 2.0342.

2.0343 Effects of solution-annealing temperature on elongation ratio at -321 F for Type 321 and six other austenitic stainless steels, Figure 2.0343.

2.0344 Type 321 suffers hydrogen embrittlement at room temperature when cathodically charged with hydrogen during tensile testing. As shown in Figure 2.0345, embrittlement under these conditions is observed both in the solution-annealed condition and after sensitization heat treating. Large-grained material is slightly more susceptible to embrittlement than finer grained material (64).

2.0345 Effects of grain size and heat treatment on hydrogen embrittlement during tensile testing at room temperature, Figure 2.0345.

2.0346 Type 321 is subject to hydrogen-induced slow crack growth when charged under load, as shown in Figure 2.0347. Slow crack growth also occurs when precharged specimens are tested in air at stress intensities near the plane-strain fracture toughness. However, hydrogen outgasses at room temperature in about 10 hours, so that material which does not fail in shorter times then does not fail by hydrogen embrittlement. Slow crack growth does not occur at any stress if precharged specimens are outgassed before testing. The fracture mode changes from ductile tearing to brittle quasi-cleavage as the stress intensity is decreased under hydrogen-embrittlement conditions (65,66).

2.0347 Effects of hydrogen charging on delayed failure behavior of Type 321, Figure 2.0347.

2.0348 Exposure to hydrogen at a pressure of 2900 psi and 1112 F for 20 days causes hydrogen attack in Type 321. This attack is in the form of internal bubbles containing methane, ethane, and hydrogen, which form at $M_{23}C_6$, and MC carbide particles. The effects of these bubbles on mechanical properties have not been reported (67).

2.0349 At room and cryogenic temperatures, hydrogen at a pressure of 5000 psi has no significant effect on smooth or notched tensile properties, as shown later in Table 3.03711.

2.035 Oxidation.

2.0351 Type 321 oxidizes more rapidly in air at 1742 F than Types 304, 310, and 316, as shown in Figure 2.0352. The scale formed on Type 321 spalls on cooling, while scales on Types 310 and 316 remain adherent if the alloys are slow cooled after oxidation exposure. Internal oxidation is also noted in Type 321, particularly after several cycles of oxidation exposure (68).

Type 321 can be used in air at temperatures up to 1600 F without excessive scaling (8,11,33).

2.0352 Oxidation weight-change behavior of Type 321 in air at 1742 F as compared to Types 304, 310, and 316, Figure 2.0352.

2.036 Liquid-metal corrosion.

2.0361 Type 321 is suitable for the containment of liquid cesium and rubidium for possible application in liquid-metal-cooled nuclear reactors. It is less suitable for potassium and lithium (28).

2.04 **Nuclear Environments**

2.041 Neutron irradiation increases the strength and reduces the ductility of Type 321. The effect on strength is pronounced at test temperatures up to 1100 F, but decreases with further increases in temperature with full recovery occurring at about 1500 F. The marked deterioration in ductility, however, persists to at least 1500 F (23).

2.042 Effects of fast-neutron irradiation on tensile properties at elevated temperatures, Table 2.042.

2.043 Ion-bombardment results indicate that austenitic stainless steels such as Type 321 tend to swell large amounts under conditions such as would be encountered in a liquid-metal fast-breeder reactor (69).

3 MECHANICAL PROPERTIES

3.01 **Specified Mechanical Properties**

3.011 AMS specified mechanical properties, Table 3.011.

3.02 **Mechanical Properties at Room Temperature**

3.021 Tension – stress-strain diagrams – tension properties.

3.0211 Stress-strain curves (see Figures 3.0311 through 3.0314).

3.0212 Tensile properties of various forms, Table 3.0212.

3.0213 Effects of 100,000-hour exposures to elevated temperatures on room-temperature tensile properties, Table 3.0213.

3.0214 Effects on room-temperature tensile properties of elevated-temperature exposures under load, Table 3.0214.

3.0215 Tensile properties of extrusions, Table 3.0215.

3.0216 Effect of carburizing on room-temperature tensile properties, Figure 3.0216.

3.022 Compression – stress-strain diagrams – compression properties.

3.0221 Stress-strain curves (see Figure 3.0321).

3.0222 Compressive yield strength (see Figure 3.0322).

3.023 Impact.

3.0231 Effects of exposures to elevated temperatures on room-temperature impact properties, Table 3.0231.

3.0232 Effects on room-temperature impact properties of elevated-temperature exposures under load, Table 3.0232.

3.024 Bending.

3.025 Torsion and shear (see Figure 3.0351).

3.026 Bearing (see Figure 3.0361).

3.027 Stress concentration.

3.0271 Notch properties (see Table 3.03711).

3.0272 Fracture toughness.

3.028 Combined properties.

3.03 **Mechanical Properties at Various Temperatures**

3.031 Tension – stress-strain diagrams – tension properties.

3.0311 Stress-strain curves for sheet at room and elevated temperatures, Figure 3.0311.

3.0312 Complete stress-strain curves for sheet at room and elevated temperatures, Figure 3.0312.

3.0313 Stress-strain curves for sheet at room and low temperatures, Figure 3.0313.

3.0314 Complete stress-strain curves for bar at room and low temperatures, Figure 3.0314.

3.0315 Scatter bands for tensile properties of bar at room and elevated temperatures, Figure 3.0315.

3.0316 Effect of elevated temperatures on tensile properties of sheet, Figure 3.0316.

3.0317 Effects of low temperatures on tensile properties of bar and sheet, Figure 3.0317.

3.0318 Effects of cold work induced by hydraulic expansion on tensile properties of tubing at 70 F and -320 F, Figure 3.0318.

3.0319 Effects of temperature on tensile properties of annealed and cold-rolled bar, Figure 3.0319.

3.03110 Effects of temperature, after two different exposure times at temperature, on tensile properties of sheet, Figure 3.03110.

3.03111 Effects of temperature, rapid strain rates, and short holding times at temperature on tensile properties of sheet heated to test temperatures within 10 seconds, Figure 3.03111.

3.03112 Effects of temperature on tensile properties of bar annealed at various temperatures, Figure 3.03112.

3.032 Compression – stress-strain diagrams – compression properties.

3.0321 Compressive stress-strain curves for sheet at room and elevated temperatures, Figure 3.0321.

3.0322 Effects of temperature, after two different exposure times at temperature, on compressive yield strength of sheet, Figure 3.0322.

3.033 Impact.

3.034 Bending.

3.035 Torsion and shear.

3.0351 Effects of temperature, after two different exposure times at temperature, on shear strength of sheet, Figure 3.0351.

3.036 Bearing.

Fe
18 Cr
10 Ni
+ Ti

Type 321

Fe
18 Cr
10 Ni
+ Ti

Type 321

3.0361 Effects of temperature, after two different exposure times at temperature, on bearing properties of sheet, Figure 3.0361.

3.037 Stress concentration.

3.0371 Notch properties.

3.03711 Smooth and notched tensile properties in high-pressure helium and hydrogen at 70 F and -200 F, Table 3.03711.

3.0372 Fracture toughness.

3.038 Combined properties.

3.04 **Creep and Creep Rupture Properties**

3.041 Effect of temperature on creep-rupture strength, Figure 3.041.

3.042 Creep and creep-rupture curves for sheet at 1200 and 1500 F, Figure 3.042.

3.043 Creep curves for sheet at 1000 to 1350 F, Figure 3.043.

3.044 Creep rates for sheet at 1000 to 1350 F, Figure 3.044.

3.045 Short-time total-strain curves for sheet at 1500 and 1800 F, Figure 3.045.

3.046 Creep-rupture curves for bar at 1100 to 1500 F, Figure 3.046.

3.047 Effects of annealing temperature and cold work on creep-rupture properties at 1200 F, Figure 3.047.

3.05 **Fatigue Properties**

3.051 Type 321 exhibits cyclic strain hardening at room temperature to 1292 F, as shown by comparison of the cyclic and monotonic stress-strain curves in Figure 3.052 (70).

3.052 Monotonic and cyclic stress-strain curves for bar at room and elevated temperatures, (a) room temperature, (b) 842 F, (c) 1112 F, (d) 1292 F, Figure 3.052.

3.053 Low-cycle fatigue life at room and elevated temperatures, Figure 3.053.

3.054 High-cycle fatigue strength at room and elevated temperatures, Figure 3.054.

3.055 Fatigue properties of air-melted and vacuum-melted sheet, Figure 3.055.

3.056 The effects of thermal aging on fatigue behavior at 1112 and 1292 F are shown in Figure 3.057. At a cyclic strain rate of 40 percent/min, there is minimal effect of thermal aging on fatigue life. The fracture surface is transgranular and well-defined striations are observed. At a cyclic strain rate of 0.4 percent/min, thermal aging increases the fatigue life, with the effect being greater at 1292 F than at 1112 F. The fracture mode at the lower cyclic strain rate is intergranular. The improvement in fatigue life by aging is attributed to large chromium carbide precipitate particles at the grain boundaries which inhibit grain-boundary sliding (74).

3.057 Effects of aging and cyclic strain rate on fatigue behavior at elevated temperatures, (a) 1112 F, (b) 1292 F, Figure 3.057.

3.058 The effect of cyclic frequency on low-cycle fatigue behavior increases with increasing temperature. As shown in Figure 3.059, little effect of frequency is apparent at room temperature and at 842 F. However, at 1112 to 1472 F, the fatigue life is notably shorter at a cyclic strain rate of 0.4 percent/min than at 40 percent/min. This decreased fatigue life is attributed to a greater creep component of fatigue at the lower frequency (70,73). Surface cracks show a greater tendency to propagate intergranularly with increasing temperature, decreasing cyclic strain rate, and increasing strain range (75).

3.059 Low-cycle axial fatigue behavior in air at room and elevated temperatures, Figure 3.059, (a) room temperature, (b) 842 F, (c) 1112 F, (d) 1292 F, (e) 1472 F.

3.0510 Fatigue life at 1112 F is affected by grain size at a cyclic strain rate of 0.4 percent/min but not at a cyclic strain rate of 40 percent/min, as shown in Figure 3.0511. The fracture mode is also affected by strain rate and grain size. At the higher cyclic strain rate, fracture is transgranular with a striated fracture surface. However, at the lower cyclic strain rate, the fracture mode changes from primarily transgranular at a grain size of 9 (small grain size) to completely intergranular at a grain size of 1 (large grain size). The fatigue lives of Type 321 and seven other austenitic stainless steels at 1112 F are compared in Figure 3.0512. The effect of composition is minor as compared to the effects of grain size and cyclic strain rate. At a cyclic strain rate of 40 percent/min, grain size has no effect on any of these alloys. At a cyclic strain rate of 0.4 percent/min, the fatigue life is decreased at smaller grain size numbers. When a tensile hold time of 30 minutes is incorporated into the fatigue cycle, the fatigue life is further reduced. Fracture under these conditions is completely intergranular at all grain sizes and the intergranular mode becomes more distinct with decreasing grain-size number. Similar behavior is also observed at 1292 F (76).

3.0511 Effects of grain size and cyclic frequency on axial fatigue behavior at 1112 F, Figure 3.0511.

3.0512 Effects of grain size, cyclic frequency, and hold time on axial fatigue life of austenitic stainless steels at 1112 F, Figure 3.0512.

3.0513 At room temperature and 842 F, the fatigue life of electropolished material is about twice that of as-machined material, as shown in Figure 3.0514. At 1292 F, no effect of surface finish is observed. The shorter life of the as-machined material at room temperature and 842 F is attributed to the presence of a work-hardened surface layer which allows earlier crack initiation than does a stress-free (electropolished) surface. At room temperature and 842 F, surface cracks are initiated at twin boundaries, while at 1292 F, they initiate at grain boundaries (75).

3.0514 Effect of surface finish on axial fatigue behavior at room and elevated temperatures, Figure 3.0514.

3.0515 Effects of low temperatures and surface finish on fatigue properties, Figure 3.0515.

3.0516 Fatigue crack-growth rate as a function of stress-intensity-factor range at various temperatures, Figure 3.0516.

3.0517 Thermal aging decreases the fatigue crack-propagation rate at 1100 F, as shown in Figure 3.0518. The incorporation of 0.1- and 1-minute hold times increases the crack-propagation rate in the aged condition (77).

3.0518 Effects of aging and cyclic hold time on bending-fatigue crack-growth rate at 1100 F, Figure 3.0518.

3.0519 Under conditions where the fatigue stress is above the yield stress and a linear elastic fracture mechanics treatment is not applicable, the fatigue crack-growth rate can be represented as a function of crack length. As shown in Figure 3.0520, the crack-growth rate increases with increasing total strain range at 1112 F. The crack-growth rate also increases with decreasing cyclic strain rate (frequency) and is decreased by aging. Increasing temperature slightly increases the crack-growth rate. The fatigue life is inversely dependent on the crack-growth rate, as shown in Figure 3.0521. This relationship also indicates that fatigue life is related inversely to those variables which affect the fatigue crack-growth rate (78).

3.0520 Relation between crack-growth rate and crack length at room and elevated temperatures, (a) room temperature and 842 F, (b) 1112 F, (c) 1292 F, Figure 3.0520.

3.0521 Relation between fatigue life and crack-propagation rate, Figure 3.0521.

3.0522 The room-temperature yield strength after high-cycle fatigue is initially increased by flow stress hardening, but eventually decreases to a value approximately equal to that of the cyclic stress level applied. This behavior is shown in Figure 3.0523 (71).

3.0523 Effect of axial fatigue on subsequent yield strength at room temperature, Figure 3.0523.

3.06 **Elastic Properties**

3.061 Poisson's ratio.

3.0611 Effect of temperature on Poisson's ratio, Figure 3.0611.

3.062 Modulus of elasticity.

3.0621 Modulus of elasticity at room and elevated temperatures, Figure 3.0621.

3.0622 Modulus of elasticity at low temperatures, Figure 3.0622.

3.0623 Tangent modulus curves in compression, Figure 3.0623.

3.063 Modulus of rigidity.

3.0631 Modulus of rigidity at room and elevated temperatures, Figure 3.0631.

4 FABRICATION

4.01 **Forming**

4.011 In the annealed condition, Type 321 is sufficiently tough and ductile to be cold formed by most commercial methods, such as deep drawing, bending, and upsetting. Since it work hardens rapidly, intermediate process anneals or full anneals may be necessary for severely cold-worked parts (8,33).

4.012 It has good hot-forming characteristics by any of the conventional methods, such as forging, rolling, extrusion, and upsetting. Because of its higher hot hardness, more power for a given reduction is required than with mild steel. High-sulfur fuels and strongly reducing atmospheres should be avoided. The material to be hot formed should be preheated to 1500 to 1600 F and then hot formed in the range 2300 to 1700 F. Air cooling after hot forming is usually adequate to retain good corrosion resistance (8,11,33).

4.013 Austenitic stainless steels, such as Type 321, are usually extruded in the range 2100 to 2250 F It is essential that the extrusion billet is lubricated both at the billet/liner interface and at the billet/die interface in order to achieve acceptable low extrusion pressures and good extrusion surface quality. Soda lime and borosilicate glasses are used for this purpose. Inadequate or uneven lubrication can result in transverse cracking, tearing, or surface roughness. The surface quality of properly extruded products can be better than that obtained by hot rolling, especially in the case of shapes. Extrusion pressures for Type 321 as a function of temperature, ram speed, and extrusion ratio are shown in Figure 4.014 (79).

Fe
18 Cr
10 Ni
+ Ti
Type 321

4.014 Effects of extrusion ratio, reheat temperature, and ram speed on peak extrusion pressure, Figure 4.014.

4.02 **Machining and Grinding**

4.021 Because of its toughness and work-hardening characteristics, Type 321 requires rigid machine setups and sharp tools. Better chip action on chip-breaker tools and a better finish are obtained with moderately cold-worked material than with annealed. Heavy feeds and an adequate supply of coolant are recommended. In general, it is machined at speeds about 45 percent of those used for free-machining AISI B1112 steel. In turning operations, speeds of 50 to 90 sfm can be used. (8,33).

4.03 **Joining**

4.031 Type 321 is readily welded by the various electric-arc, oxyacetylene, resistance, and electron-beam methods. Since titanium tends to be lost during welding, another stabilized grade of stainless steel, Type 347, is recommended for electrodes and filler wire. Weldments should be stabilization heat treated to prevent possible subsequent sensitization and intergranular corrosion. Type 321 has low susceptibility to weld-metal hot cracking (8,33,55–60,81).

4.0311 Tensile properties of specimens butt welded in vacuum by low-voltage and high-voltage electron-beam processes; no preheat or postheat treatments, Table 4.0311.

4.032 Type 321 can be brazed with various nickel-base, copper-base, and exotic brazing alloys, such as 82 percent gold-18 percent nickel. Vacuum or hydrogen brazing atmospheres are desirable (18).

4.0321 Shear strength of brazed joints, Table 4.0321.

4.04 **Surface Treatment**

4.041 Because of its inherent good corrosion resistance, protective coatings and surface treatments are not normally needed for Type 321. Nevertheless, improved corrosion resistance when needed can be obtained by coating, preferably with zinc- or aluminum-rich paints or by passivating for 20 to 30 minutes in a warm solution of 20 percent (volume) nitric acid to which 3 ounces per gallon of sodium dichromate has been added (27,33).

Fe
18 Cr
10 Ni
+ Ti

Type 321

4.042 For optimum corrosion resistance the surface must be free of scale and foreign metallic contaminants. Preferred cleaning treatments are either mechanical methods such as buffing, sandblasting, or vapor blasting, or scale conditioning in a molten caustic salt bath followed by light acid pickling.

4.043 Type 321 can be satisfactorily cleaned of oxide by pickling in a mixed solution of nitric acid and hydrofluoric acid at 120 to 140 F. The bath composition varies, depending on the thickness of the scale, ranging from 10 to 25 percent nitric acid and 1 to 4 percent hydrofluoric acid. The ratio of nitric acid to hydrofluoric acid is decreased for thicker scales (85).

4.044 Type 321 can be surface hardened by nitriding or boronizing for improved wear resistance. Figure 4.045 shows the extent of hardening by nitriding for 24 hours at 1020 to 1560 F in a $90NH_3$-$10N_2$ mixture at atmospheric pressure and also by pack boronizing. A layer of M_4N is formed at the surface by nitriding at 1020 to 1380 F, while a mixture of M_4N and M_2N is formed at 1560 F. Very good wear characteristics are exhibited by Type 321 nitrided at 1220 F. Pack-boronizing with a commercial compound containing boron carbide produced a hard but thinner surface layer than that obtained by nitriding. The outer portion of the surface was an alloy boride with stoichiometry corresponding to MB, while the inner portion of the layer corresponded to M_2B. The wear resistance of boronized Type 321 was not evaluated but would be expected to be good based on results obtained with pack-boronized Type 316 (82,83).

4.045 Hardness-depth profiles for Type 321 after nitriding at 1020 to 1560 F or boronizing at 1740 F, Figure 4.045.

4.046 Type 321 can also be hard-coated by liquid-phase-sintering of Ni-Cr-B-Si powder mixtures onto the substrate. The smoothness of the coating surface is better than that obtained with thermospraying and subsequent melting techniques (84).

REFERENCES

1 Aerospace Material Specification, AMS 5510M (April 1, 1983).

2 Aerospace Material Specification, AMS 5557F (January 1, 1983).

3 Aerospace Material Specification, AMS 5559E (January 1, 1983).

4 Aerospace Material Specification, AMS 5570L (January 1, 1983).

5 Aerospace Material Specification, AMS 5576G (April 1, 1983).

6 Aerospace Material Specification, AMS 5645L (April 1, 1983).

7 Aerospace Material Specification, AMS 5689C (April 1, 1983).

8 "Uniloy 321/347/348 Stainless Steels", Universal-Cyclops, Specialty Steel Division (1966).

9 "Stainless Steel Types 347, 348, and 321", Allegheny-Ludlum Steel Corp. Blue Sheet (1970).

10 "Armco Stainless Steels", Armco Steel Corp., Bulletin LA-172 (1972).

11 "Steels for Elevated Temperature Service", U.S. Steel Corporation (June 1972).

12 "Fatigue Properties of Air-Melted and Consutrode-Melted Type 321", Allegheny-Ludlum, Data Sheet 135-121859-321.

13 Schmidt, E. H., and Green, E. F., "Fatigue Properties of Sheet, Bar and Cast Metallic Materials for Cryogenic Applications", Rocketdyne R-7564 (August 1968).

14 "Mechanical Test Results on Various Extruded Materials", Allegheny-Ludlum (January 1, 1956).

15 Stanley, J. K., and Perrotta, A. J., "Grain Growth in Austenitic Stainless Steels", *Metallography*, Vol 2 (December 1969).

16 Stanley, J. K., "Mechanical Properties of Carburized Austenitic Stainless Steels as Related to Microstructure", Aerospace Corporation, Report No. TR-0066(5250-10)-1 (July 1969).

17 "Resumé of Investigations for High-Temperature, High Pressure Applications 1960–1962", Timken Roller Bearing Company (1962).

18 Fazio, F., "Gold-Nickel Eutectic Filler Metal for Brazing Iron, Nickel and Cobalt Base Alloys", Boeing Report No. MDR 2-33008 (March 1971).

19 Mischel, H. T., "Optimum Materials for Ducting Flexible Components", Solar Div. ER 1925 (December 1967).

20 Burrows, C. F., "Manufacturing Methods and Technology Study Covering Parameters for the Application of Electron-Beam Welding", Martin Marietta Corporation Report No. IE-TR-69-5 (August 1969).

21 Stanley, J. K., "Effect of Silicon Additions on the Carburization Resistance, Mechanical Properties, and Joining Characteristics of Stabilized Austenitic Stainless Steels", Aerospace Corporation, Report No. TR-0172 (2250-10)-4 (November 15, 1971).

22 Steels, L. E., et al., "Irradiation Effects on Reactor Structural Materials", Naval Research Lab Memorandum Report 2398 (February 15, 1972).

23 Lauritzen, T., Withop, A., and Ferguson, G. P., "Mechanical Properties Evaluation of Austenitic Stainless Steels Irradiated in EBR-II", General Electric, Report GEAP 10066 (July 1969).

24 "Emissivity of Metals at Elevated Temperatures", McDonnell Aircraft Corporation, Report 9069, Serial No. 28 (October 1962).

25 Sargent, D. H., and Bielawski, C., "Advanced Fuel Systems for Ramjet-Powered Vehicles", Atlantic Research Corporation, TR-PL-9870-03 (March 1970).

26 Reinhard, F. M., "Corrosion of Materials in Hydrospace, Part VI, Stainless Steels", Naval Civil Engineering Lab TN N-1172 (September 1971).

27 Morrison, J. D., "Corrosion Study of Bare and Coated Stainless Steel", Kennedy Space Flight Center, NASA TN D-6519 (July 1972).

28 Phillips, W., "Effects of Alkali Metal Gettering Agents on Stainless Steel Corrosion", Jet Propulsion Lab, TR32-1239 (April 1, 1968).

29 Walker, R. J., "Influence of Gaseous Hydrogen on Metals", Rocketdyne Report N71-32489 (May 24, 1971).

30 Military Standardization Handbook, Cross Index of Chemically Similar Specifications, MIL-HDBK-H1D (June 22, 1970).

31 Metal Progress, 1974 Databook, Vol 106 (June 1974).

32 Carden, A. E., McEvily, A. J., and Wells, C. H., "Fatigue at Elevated Temperatures", ASTM STP 520 (June 1972).

33 "Carpenter Stainless Type 321", Carpenter Technology Corporation (1970).

34 "Stainless Steel Type 321", North American Aviation Summary Report AL-2604 (October 30, 1957).

35 "Digest of Steels for High-Temperature Service", Timken Roller Bearing Co., Sixth Edition (1957).

36 Miller, D. E., "Determination of the Physical Properties of Ferrous and Non-Ferrous Structural Sheet Materials at Elevated Temperatures", AFTR 6517, Pt. 4 (December 1954).

37 Dedman, H. E., Wheelahan, E. J., and Kattus, J. R., "Tensile Properties of Aircraft-Structural Metals at Various Rates of Loading After Rapid Heating", WADC TR58-440, Part 1 (November 1958).

38 Durham, T. F., McClintock, R. M., and Reed, R. P., "Cryogenic Materials Data Handbook", U.S. Dept. of Commerce (1960).

39 Simmons, W. F., and Cross, H. C., "Report on the Elevated-Temperature Properties of Stainless Steels", ASTM STP 124 (January 1952).

40 Dotson, C. L., and Kattus, J. R., "Tensile Properties of Aircraft-Structural Materials at Various Rates of Loading After Rapid Heating", WADC TR55-199, Pt. 1 (August 1955).

41 Perlmutter, I., "Stress-Rupture Tests on Sheet Alloys for High-Temperature Applications", AFTR No. 6188 (July 1950).

42 Perlmutter, I., and Rector, W. H., "Investigation of Sheet Materials for Application at High Temperatures", AFTR No. 5712 (July 13, 1948).

43 Van Echo, J. A., Worth, W. F., and Simmons, W. F., "Short-Time Creep Properties of Structural Sheet Materials for Aircraft and Missiles", AFTR No. 6731, Pt. III (May 1955).

44 Garofalo, F., Malenock, P. R., and Smith, G. V., "The Influence of Temperature on Elastic Constants of Some Commercial Steels", Symposium on Determination of Elastic Constants, ASTM STP 129 (June 25, 1952).

45 German, R. M., "Grain Growth in Austenitic Stainless Steels", *Metallography*, Vol 11, No. 2 (April 1978), pp 235–239.

46 Nakano, Y., Noguchi, Y., Hoshi, F., and Muranaka, Y., "Continuous Casting of Stainless Steel Slabs", *Ironmaking and Steelmaking*, Vol 4, No. 6 (1977), pp 361–367.

47 Takeuchi, H., Ikehara, Y., Yanai, T., and Matsumura, S., "Quality Improvement of Continuously Cast Stainless Steel Blooms Through Electromagnetic Stirring", *Journal of the Iron and Steel Institute of Japan*, Vol 63, No. 8 (July 1977), pp 1287–1296.

48 Hotaling, A. C., and Scharfstein, L. R., "The Effect of Heat Treatments in the Prevention of Intergranular Corrosion Failures of AISI 321 Stainless Steel", *Materials Performance*, Vol 22, No. 9 (September 1983), pp 22–24.

49 Leitnaker, J. M., and Bentley, J., "Precipitate Phases in Type 321 Stainless Steel After Aging 17 Years at Approximately 600 C", *Metallurgical Transactions*, Vol 8A, No. 10 (October 1977), pp 1605–1613.

50 Warnes, L.A.A., and King, H. W., "The Low Temperature Magnetic Properties of Austenitic Fe-Cr-Ni Alloys – 2. The Prediction of Neel Temperatures and Maximum Susceptibilities", *Cryogenics*, Vol 16, No. 11 (November 1976), pp 659–667.

51 Pandey, G. N., and Sanyal, B., "Inhibition of the Corrosion of Stainless Steel (AISI 321) in Hydrochloric Acid", *Corrosion Prevention and Control*, Vol 27, No. 3 (June 1980), pp 13–17.

52 Gupta, S., Pandey, G. N., and Sanyal, B., "Effect of Potassium Iodide on the Attack of Stainless Steel by Sulfuric Acid", *Metal Finishing*, Vol 80, No. 8 (August 1982), pp 51–54.

53 Samans, C. H., Kinoshita, K., and Matsushima, I., "Further Observations on Sensitization of Chemically Stabilized Stainless Steels", Vol 33, No. 8 (August 1977), pp 271-279.

54 Samans, C. H., Kinoshita, K., and Matsushima, I., "Sensitization and Stabilization of Type 321 Stainless Steels", presented at Corrosion/75, Toronto, Canada (April 14–18, 1975), pp 4/1–4/11.

55 Hoffman, C., and McEvily, A. J., "The Effect of High Temperature Low Cycle Fatigue on the Corrosion Resistance of Austenitic Stainless Steels", *Metallurgical Transactions*, Vol 13A, No. 5 (May 1982), pp 923–927.

56 Ikawa, H., Shin, S., Nakao, Y., and Nishimoto, K., "Knife Line Attack Phenomenon in Stabilized Stainless Steels – Effect of Heat Treatment on Knife Line Attack Phenomenon", *Technical Reports of the Osaka University*, Vol 25 (October 1975), pp 337–345.

57 Ikawa, H., Shin, S., Nakao, Y., and Nishimoto, K., "Knife Line Attack Phenomenon in Stabilized Stainless Steels – Mechanism of Knife Line Attack Phenomenon II", *Technical Reports of the Osaka University*, Vol 26 (October 1976), pp 427–435.

58 Ikawa, H., Shin, S., Nakao, Y., and Nishimoto, K., "Knife Line Attack Phenomenon in Stabilized Stainless Steels – Dissolution Phenomenon of Carbides in Thermal Cycles", *Technical Reports of the Osaka University*, Vol 27 (October 1977), pp 381–388.

59 Ikawa, H., Nakao, Y., and Nishimoto, K., "Knife Line Attack Phenomenon in Stabilized Stainless Steels – Precipitation Phenomenon of Carbides During Post-Heat Treatment", *Technical Reports of the Osaka University*, Vol 28 (March 1978), pp 67–74.

60 Ikawa, H., Nakao, Y., and Nishimoto, K., "Improvement of Knife Line Attack Phenomenon in Stabilized Stainless Steels by Addition of REM", *Technical Reports of the Osaka University*, Vol 28 (March 1978), pp 75–83.

61 Keys, L. H., "The Corrosion of Stainless Steels", *Australasian Corrosion Engineering*, Vol 20, No. 3 (March 1976), pp 9–16.

62 Speidel, M. O., "Stress Corrosion Cracking of Stainless Steels in NaCl Solutions", *Metallurgical Transactions*, Vol 12A, No. 5 (May 1981), pp 779–789.

Fe
18 Cr
10 Ni
+ Ti

Type 321

Fe
18 Cr
10 Ni
+ Ti

Type 321

63 Kuribayashi, M., Okabayashi, H., "The Influence of Heat-Treatment and Cold-Work on the Low Temperature Hydrogen Embrittlement of Austenitic Stainless Steels", *Journal of the Japan Institute of Metals*, Vol 47, No. 4 (April 1983), pp 365–372.

64 Rozenak, P., and Eliezer, D., "Effects of Metallurgical Variables on Hydrogen Embrittlement in AISI Type 316, 321 and 347 Stainless Steels", *Materials Science and Engineering*, Vol 61, No. 1 (October 1983), pp 31–41.

65 Eliezer, D., Arbel, A., and Rozenak, P., "Hydrogen Induced Delay Failure of AISI 316L and 321 Types Stainless Steels", *Journal of Materials Science Letters*, Vol 2, No. 10 (October 1983), pp 602–604.

66 Chu, W-Y., Yao, J., and Hsiao, C-M., "Hydrogen Induced Slow Crack Growth in Stable Austenitic Stainless Steels", *Metallurgical Transactions*, Vol 15A, No. 4 (April 1984), pp 729–733.

67 Yacaman, M. J., Parthasarathy, T. A., and Hirth, J. P., "Hydrogen Attack in an Austenitic Stainless Steel", *Metallurgical Transactions*, Vol 15A (September 1984), pp 1485–1490.

68 Moccari, A., and Ali, S. I., "Studies on the Oxidation and Spalling Resistance of Austenitic Stainless Steels", *British Corrosion Journal*, Vol 14, No. 2 (1979), pp 91–96.

69 Johnston, W. G., Lauritzen, T., Rosolowski, J. H., and Turkalo, A. M., "Void Swelling in Fast Reactor Materials – A Metallurgical Problem", *Journal of Metals*, Vol 28, No. 6 (June 1976), pp 19–24.

70 Yamaguchi, K., Kanazawa, K., and Yoshida, S., "Dependence of Temperature and Strain Rate on the Low-Cycle Fatigue Life of Type 321 Stainless Steel", *Journal of the Iron and Steel Institute of Japan*, Vol 64, No. 8 (July 1978), pp 1199–1208.

71 Luther, R. G., and Williams, T.R.G., "Fatigue Cycling of an Austenitic Stainless Steel in R = -1 Loadings", *Metal Science*, Vol 14, No. 1 (January 1980), pp 29–33.

72 Koster, W. P., Field, M., and Fritz, L. J., "Low Stress Creep Testing of 321 Stainless Steel", Research Report, Contract AF 33(600)-36430 (April 22, 1959).

73 Yoshida, S., Kanazawa, K., Yamaguchi, K., Sato, M., and Kobayashi, K., "Elevated-Temperature Fatigue Properties of Engineering Materials, Part II – Section 4: Elevated-Temperature Fatigue Properties of 18Cr-10Ni-Ti Stainless Steel Bars for General Application (SUS 321-B)", *Transactions of the National Research Institute for Metals*, Vol 20, No. 1 (January 1978), pp 60–73.

74 Yamaguchi, K., and Kanazawa, K., "Influence of Thermal Aging on High Temperature, Low-Cycle Fatigue Life of SUS 321 Stainless Steel", *Transactions of the National Research Institute for Metals*, Vol 25, No. 3 (September 1983), pp 143–147.

75 Yamaguchi, K., Kanazawa, K., and Yoshida, S., "Some Aspects of Cracks in Austenitic Stainless Steels Low-Cycle Fatigued at High Temperatures", *Transactions of the National Research Institute for Metals*, Vol 18, No. 4 (July 1976), pp 128–132.

76 Yamaguchi, K., and Kanazawa, K., "Influence of Grain Size on the Low-Cycle Fatigue Lives of Austenitic Stainless Steels at High Temperatures", *Metallurgical Transactions*, Vol 11A, No. 10 (October 1980), pp 1691–1699.

77 Michel, D. J., and Smith, H. H., "Effect of Hold Time and Thermal Aging on Elevated Temperature Fatigue Crack Propagation in Austenitic Stainless Steels", Naval Research Laboratory Report NRL-MR-3627 (October 1977).

78 Yamaguchi, K., and Kanazawa, K., "Crack Propagation Rates of Austenitic Stainless Steels Under High-Temperature Low-Cycle Fatigue Conditions", *Metallurgical Transactions*, Vol 10A, No. 10 (October 1979), pp 1445–1451.

79 Gupta, A. K., Hughes, K. E., and Sellars, C. M., "Glass-Lubricated Hot Extrusion of Stainless Steel", *Metals Technology*, Vol 7, No. 8 (August 1980), pp 323–331.

80 Daly, J. J., "Weldments Live Longer With Shot-Peening", *Welding Design and Fabrication*, Vol 50, No. 7 (July 1977), pp 74–76.

81 Iwami, J-I., Kishimoto, K., and Yamaguchi, A., "Solidification Crack Susceptibility in the Weld Metals of Austenitic Stainless Steels and Ni-Base Super Alloys", *Transactions of the Iron and Steel Institute of Japan*, Vol 23, No. 6 (June 1983), p B-217.

82 Whittle, R.D.T., and Scott, V. D., "Sliding-Wear Evaluation of Nitrided Austenitic Alloys", *Metals Technolgoy*, Vol 11, No. 6 (June 1984), pp 231–241.

83 Whittle, R.D.T., and Scott, V. D., "Sliding-Wear Evaluation of Boronized Austenitic Alloys", *Metals Technology*, Vol 11, No. 12 (December 1984), pp 522–529.

84 Knotek, O., Lugschieder, E., and Reimann, H., "Wear-Resistant and Corrosion-Resistant Nickel-Base Alloys for Coating by Furnace Melting", *Thin Solid Films*, Vol 64, No. 3 (December 17, 1979), pp 365–369.

85 "AISI Type 321", Alloy Digest, Filing Code: SS-124 (November 1961).

Alloy	Type 321
AMS Specification	Product Form
5645L	Bars, Forgings
5510M	Sheet, Strip, Plate
5689C	Wire
5576G	Tubing, Welded
5559E	Tubing, Welded, Thin Wall
5570L	Tubing, Seamless
5557F	Tubing, Seamless and Welded, Hydraulic

Fe
18 Cr
10 Ni
+ Ti

Type 321

TABLE 1.031. SPECIFICATIONS (1–7)

Alloy	Type 321											
AMS Specification	5645L		5689C		5510M, 5559E		5576G		5570L		5557F	
	Percent											
Element	Min	Max	Min	Max	Min	Max	Min	Max	Min	Max	Min	Max
Chromium	17.00	19.00	17.00	19.00	17.00	19.00	17.00	19.00	17.00	19.00	17.00	20.00
Nickel	8.00	12.00	8.00	11.00	9.00	12.00	9.00	12.00	9.00	13.00	8.00	13.00
Titanium	5x(C+N)	0.70	5x(C+N)	0.70	5x(C+N)	0.70	5x(C+N)	0.70	5x(C+N)	0.70	5x(C+N)	0.70
Carbon	–	0.08	–	0.08	–	0.08	–	0.08	–	0.08	–	0.08
Manganese	–	2.00	–	2.00	–	2.00	–	2.00	–	2.00	–	2.00
Silicon	–	1.00	–	1.00	0.40	1.00	–	1.00	0.40	1.00	0.40	1.00
Copper	–	0.75	–	0.75	–	0.75	–	0.75	–	0.75	–	0.75
Molybdenum	–	0.75	–	0.75	–	0.75	–	0.75	–	0.75	–	0.75
Nitrogen	–	0.10	–	0.10	–	0.10	–	0.10	–	0.10	–	0.10
Phosphorus	–	0.040	–	0.040	–	0.040	–	0.040	–	0.040	–	0.040
Sulfur	–	0.030	–	0.030	–	0.030	–	0.030	–	0.030	–	0.030

TABLE 1.041. COMPOSITION (1–7)

Alloy	Type 321
Condition	Annealed
Form	Hardness
Bars, Plates	150–228 BHN
Tube, Sheet, Strip	80–95 HRB
Wire	95 HRB

TABLE 1.061. HARDNESS OF VARIOUS FORMS (8,9,10,31)

Alloy	Type 321	
Condition	Annealed	
Exposure Time, hr	1000	10,000
Exposure Temperature, F	BHN	
Unexposed	168	168
900	143	156
1050	149	151
1200	166	148

TABLE 1.062. EFFECTS OF EXPOSURES TO ELEVATED TEMPERATURES ON HARDNESS AT ROOM TEMPERATURE (11)

Fe
18 Cr
10 Ni
+ Ti

Type 321

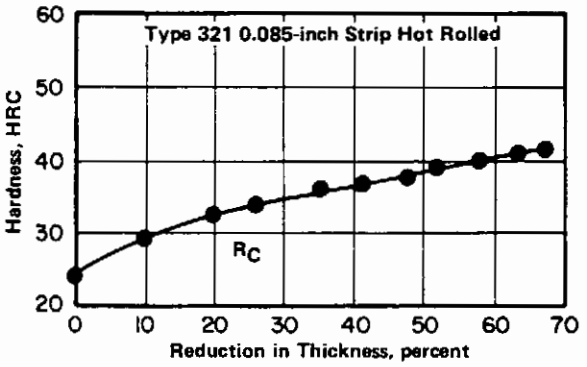


FIGURE 1.063. EFFECT OF COLD ROLLING ON HARDNESS OF STRIP (21)

Alloy	Type 321
Forms	Conditions
Forgings	Annealed
Billets	Annealed
Bars	Hot Rolled or Cold Drawn
Sheet and Strip	Annealed or Temper Rolled up to 1/2 Hard
Wire	Annealed or Cold Drawn to Specified Temper
Wire Rod	Annealed
Plates	Annealed

TABLE 1.07. FORMS AND CONDITIONS AVAILABLE (9,10,33)

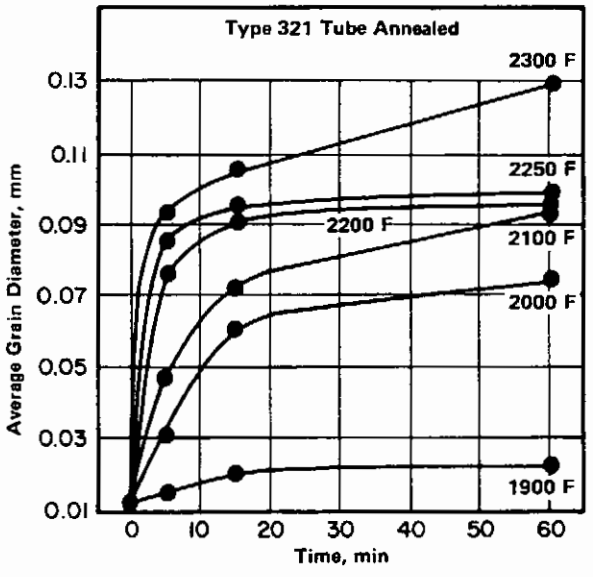


FIGURE 1.0921. EFFECTS OF TIME AND TEMPERATURE ON GRAIN GROWTH (15)

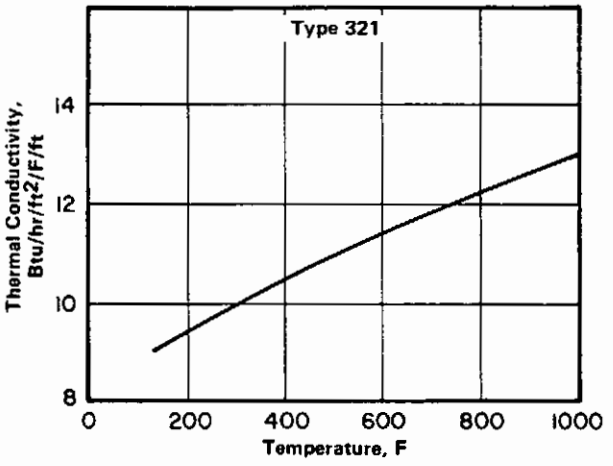


FIGURE 2.013. THERMAL CONDUCTIVITY (34)

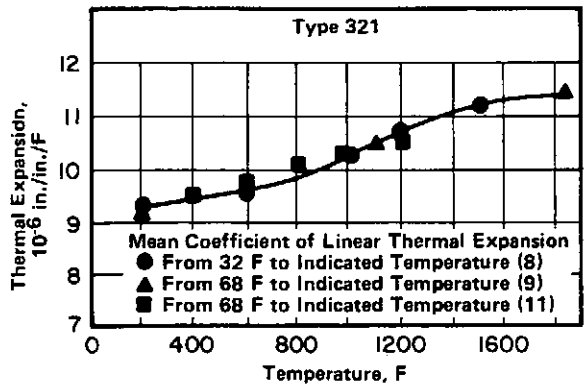


FIGURE 2.014. THERMAL EXPANSION (8,9,11)

Alloy	Type 321		
Condition	Annealed		
	Electrical Conductivity		Electrical Resistivity, μΩ-in.
Temperature, F	Percent IACS	Mmhos/in.^{3}	
68	2.41	0.0354	28.3
212	2.22	0.0326	30.7
392	2.01	0.0296	33.8
752	1.73	0.0254	39.4
1112	1.56	0.0229	43.7
1472	1.43	0.0210	47.6
1652	1.37	0.0202	49.6

TABLE 2.0221. ELECTRICAL PROPERTIES AT VARIOUS TEMPERATURES (9)

Fe
18 Cr
10 Ni
+ Ti

Type 321

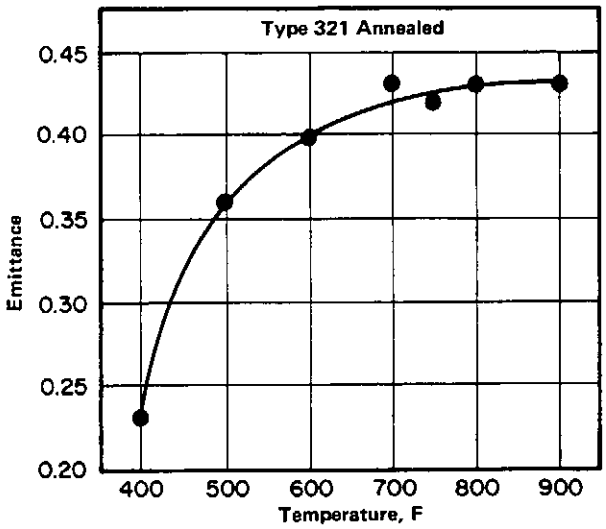


FIGURE 2.0241. TOTAL NORMAL EMITTANCE AT ELEVATED TEMPERATURES (24)

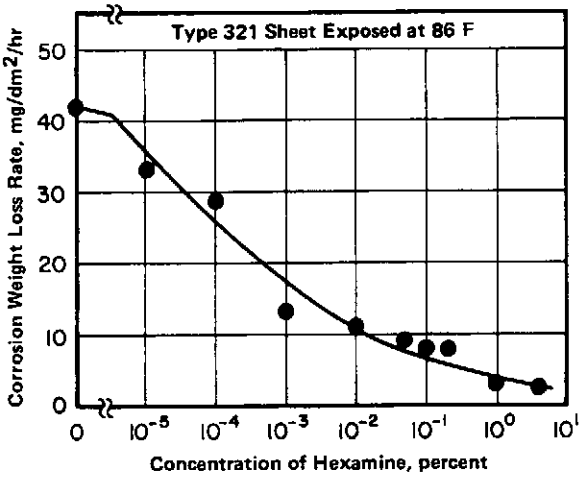


FIGURE 2.0315. EFFECTS OF HEXAMINE ON CORROSION OF TYPE 321 IN 1N HCl (51)

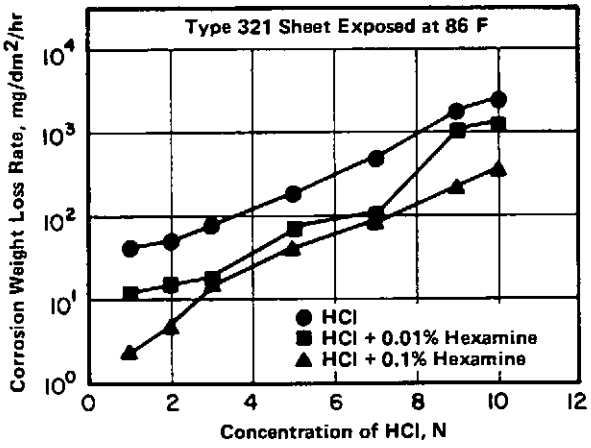


FIGURE 2.0316. EFFECTS OF HYDROCHLORIC ACID CONCENTRATION AND HEXAMINE ON CORROSION OF TYPE 321 (51)

Fe
18 Cr
10 Ni
+ Ti

Type 321

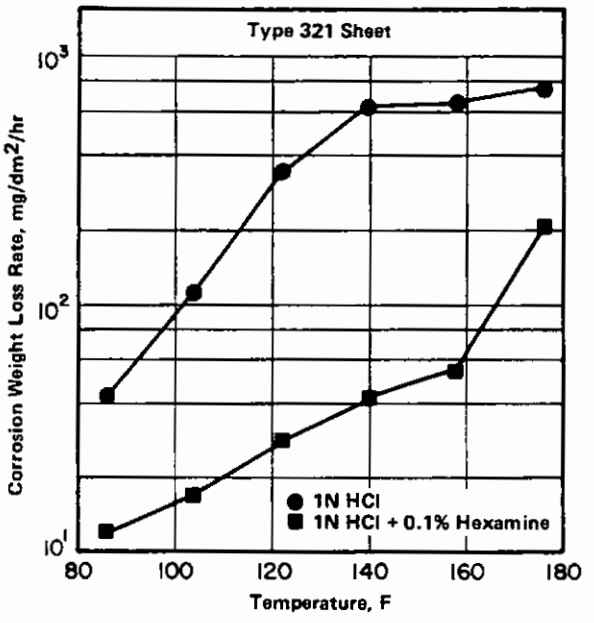


FIGURE 2.0317. EFFECTS OF TEMPERATURE AND HEXAMINE ON CORROSION OF TYPE 321 IN HYDROCHLORIC ACID (51)

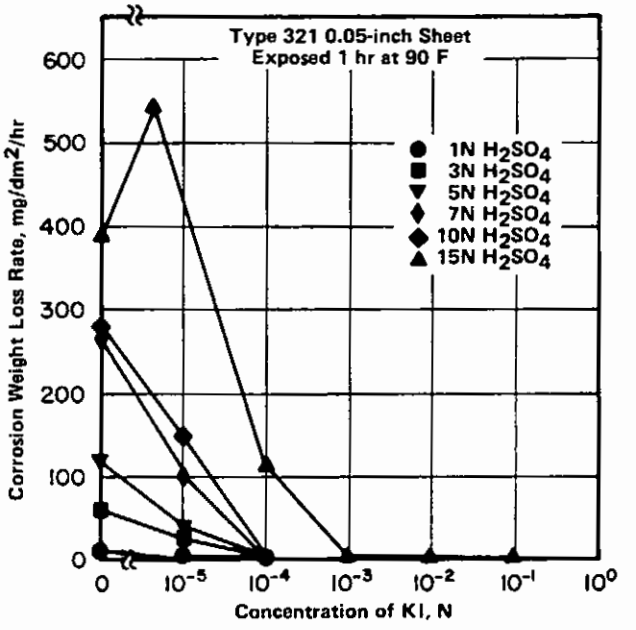


FIGURE 2.0319. EFFECTS OF POTASSIUM IODIDE ON SULFURIC ACID CORROSION OF TYPE 321 (52)

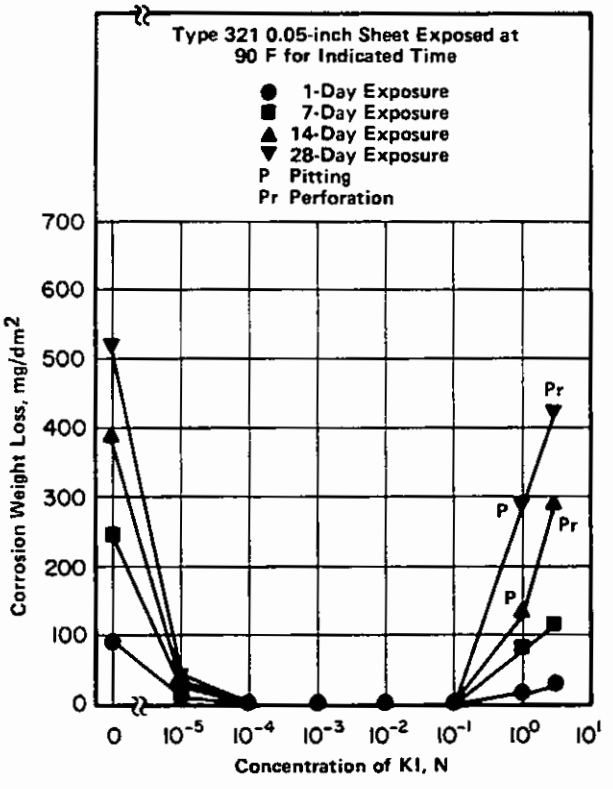


FIGURE 2.03110. EFFECTS OF POTASSIUM IODIDE AND EXPOSURE TIME ON CORROSION WEIGHT LOSS IN 1N SULFURIC ACID (52)

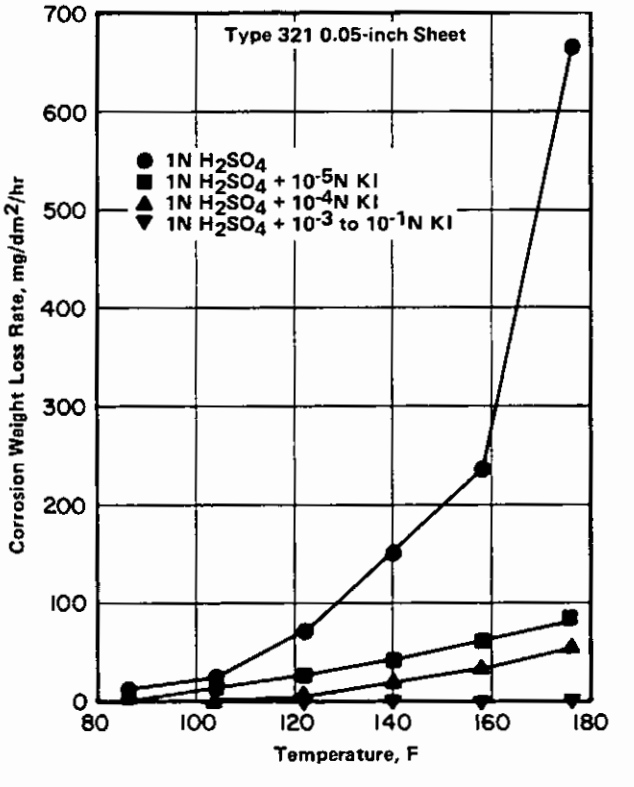


FIGURE 2.03111. EFFECT OF TEMPERATURE AND POTASSIUM IODIDE ON CORROSION OF TYPE 321 IN SULFURIC ACID (52)

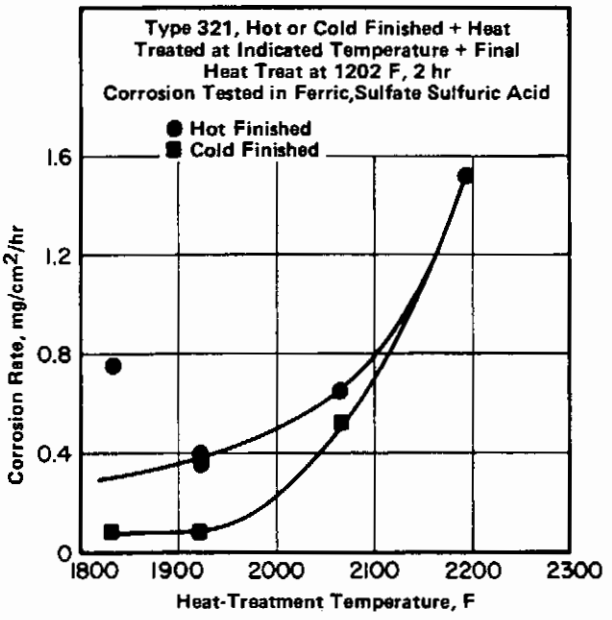


FIGURE 2.0322. EFFECTS OF HIGH-TEMPERATURE HEAT TREATMENT ON CORROSION RATE OF TYPE 321 (53)

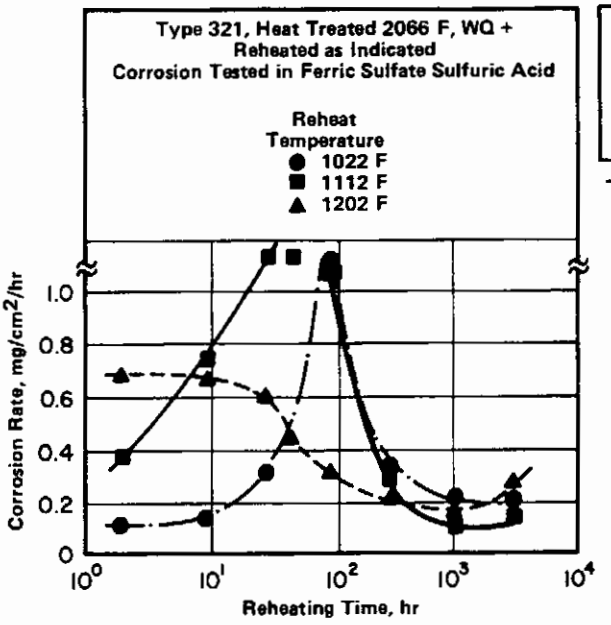


FIGURE 2.0323. EFFECTS OF SENSITIZATION REHEATING ON CORROSION RATES OF SOLUTION-ANNEALED TYPE 321 (53)

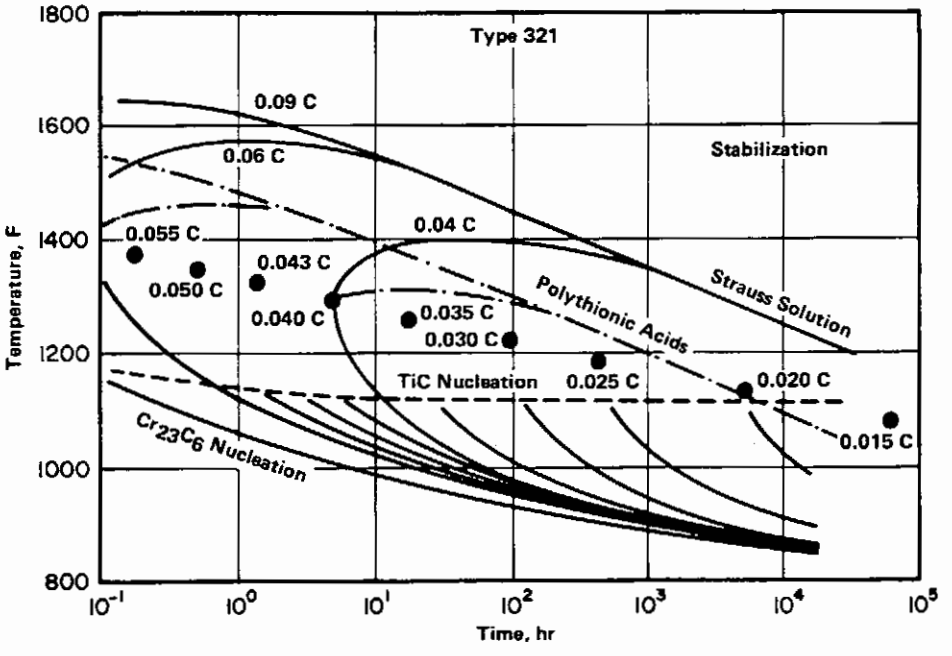


FIGURE 2.0324. TIME-TEMPERATURE-DISSOLVED CARBON RELATIONSHIPS FOR $Cr_{23}C_6$ PRECIPITATION AND FOR STABILIZATION IN 18Cr-8Ni TYPE STAINLESS STEELS (53)

Fe
18 Cr
10 Ni
+ Ti

Type 321

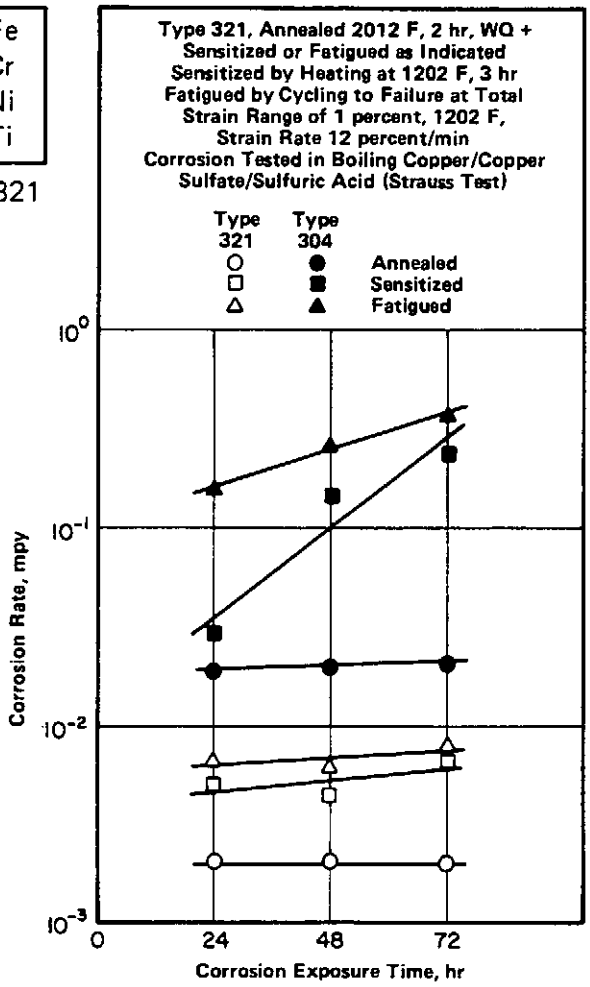


FIGURE 2.0326. EFFECTS OF SENSITIZING HEAT TREATMENT AND FATIGUE CYCLING ON CORROSION BEHAVIOR IN BOILING COPPER SULFATE (55)

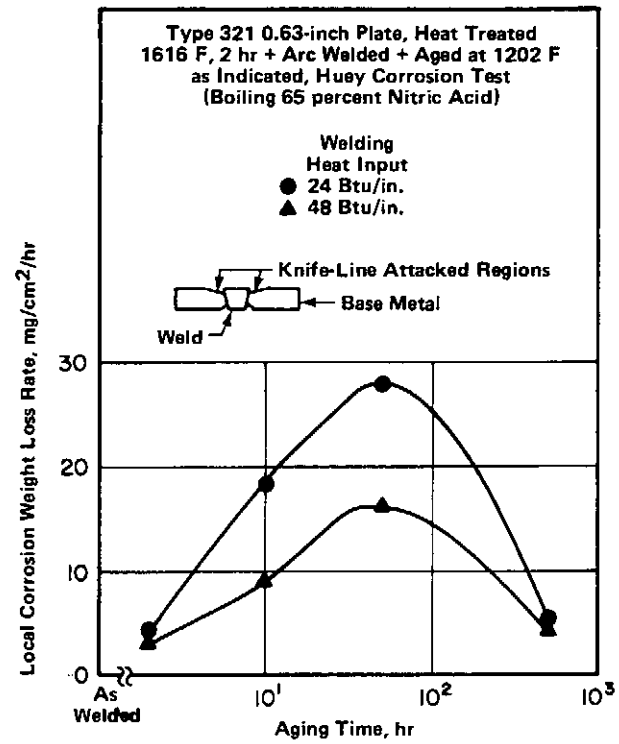


FIGURE 2.0328. EFFECTS OF AGING TIME ON KNIFE-LINE CORROSION RATE OF ARC-WELDED ALLOY (56)

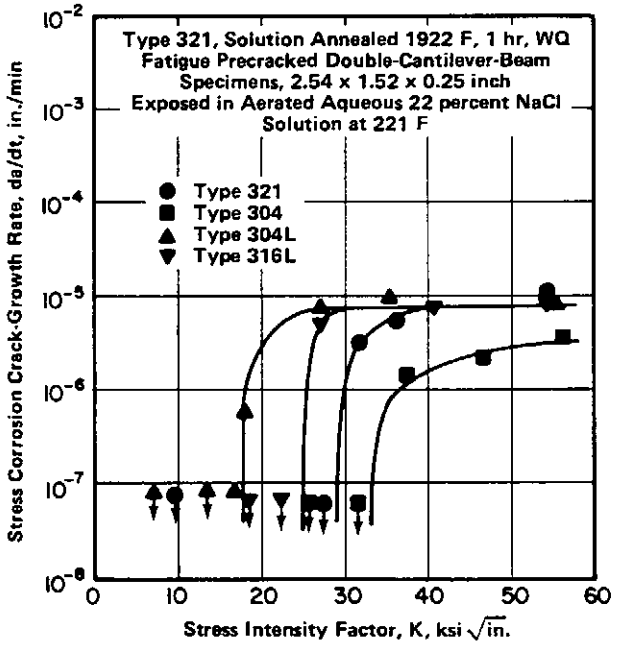


FIGURE 2.0333. EFFECT OF STRESS-INTENSITY FACTOR ON STRESS-CORROSION CRACK-GROWTH RATE IN HOT NaCl SOLUTION FOR TYPE 321 AND THREE OTHER AUSTENITIC STAINLESS STEELS (62)

Fe
18 Cr
10 Ni
+ Ti

Type 321

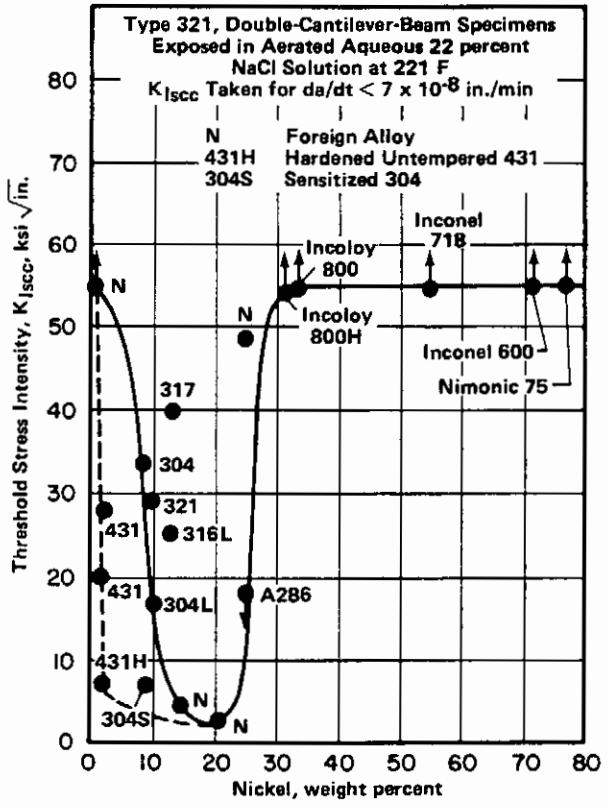


FIGURE 2.0334. EFFECT OF NICKEL CONTENT ON THRESHOLD STRESS INTENSITY FOR CORROSION CRACKING IN HOT NaCl SOLUTION FOR IRON-NICKEL ALLOYS CONTAINING ABOUT 18 PERCENT CHROMIUM (62)

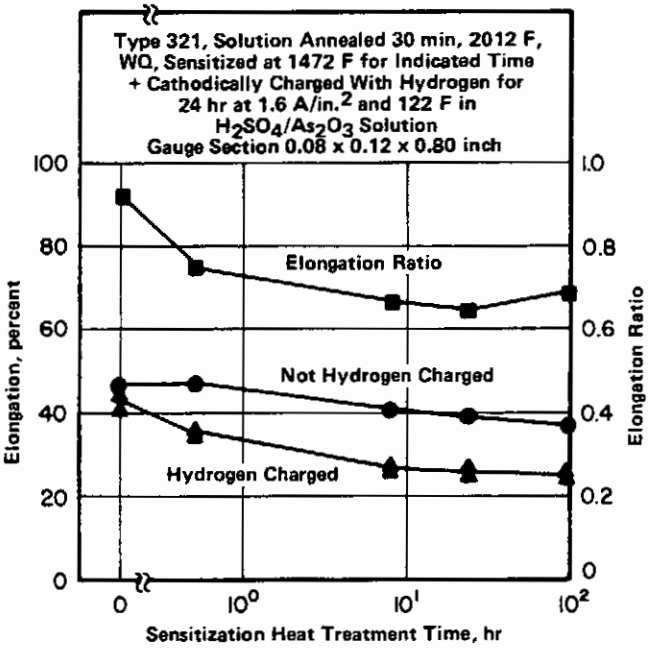


FIGURE 2.0342. EFFECTS OF HYDROGEN CHARGING AND SENSITIZATION ON TENSILE DUCTILITY AT -321 F (63)

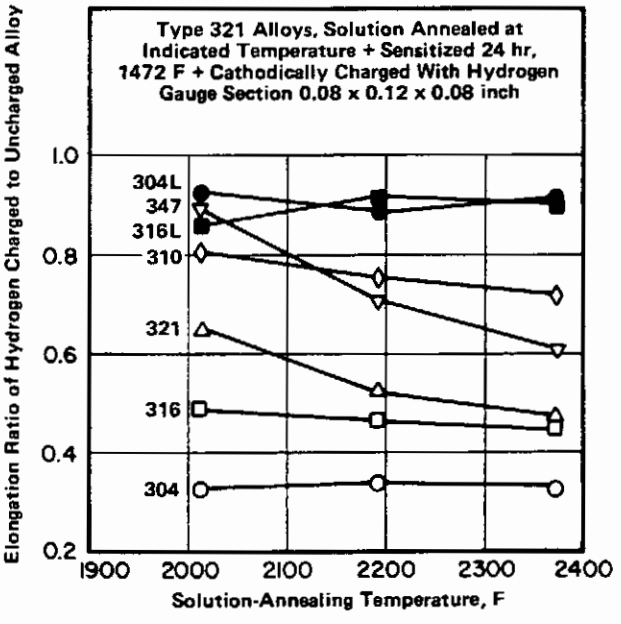


FIGURE 2.0343. EFFECTS OF SOLUTION-ANNEALING TEMPERATURE ON ELONGATION RATIO AT -321 F FOR TYPE 321 AND SIX OTHER AUSTENITIC STAINLESS STEELS (63)

Fe
18 Cr
10 Ni
+ Ti

Type 321

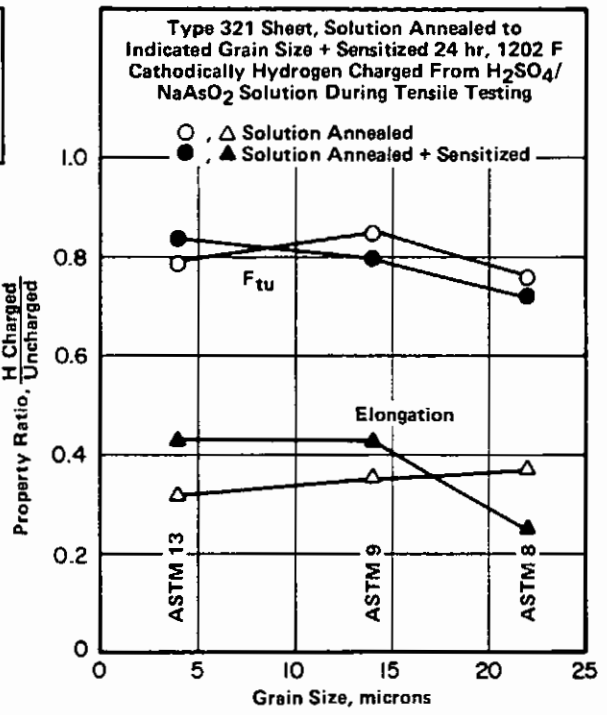


FIGURE 2.0345. EFFECTS OF GRAIN SIZE AND HEAT TREATMENT ON HYDROGEN EMBRITTLEMENT DURING TENSILE TESTING AT ROOM TEMPERATURE (64)

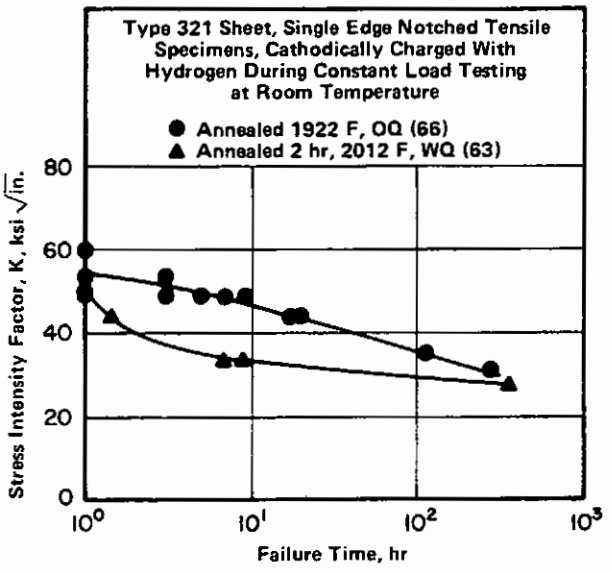


FIGURE 2.0347. EFFECTS OF HYDROGEN CHARGING ON DELAYED FAILURE BEHAVIOR OF TYPE 321 (65,66)

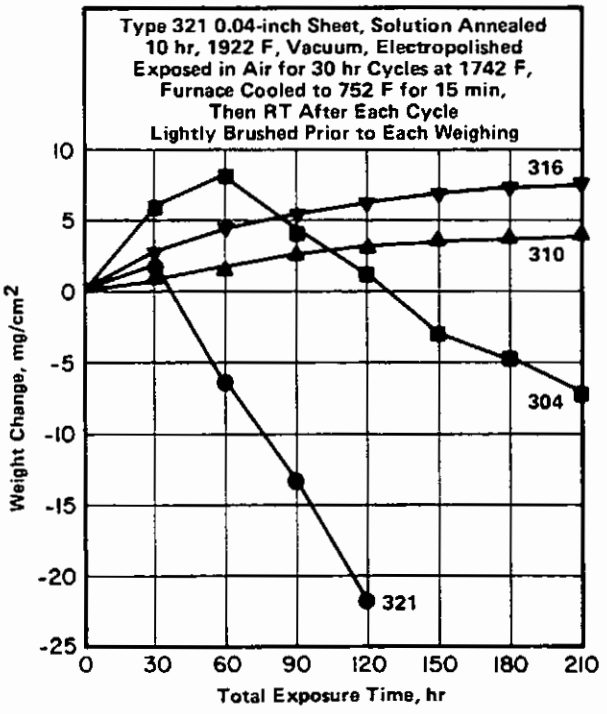


FIGURE 2.0352. OXIDATION WEIGHT-CHANGE BEHAVIOR OF TYPE 321 IN AIR AT 1742 F AS COMPARED TO TYPES 304 310, AND 316 (68)

Fe
18 Cr
10 Ni
+ Ti

Type 321

Alloy	Type 321				
Form	Tubing				
Condition Prior to Neutron Exposure	Test Temp., F	Neutron Fluence at 1000 to 1300 F, nvt (E > 1 MeV)	F_{ty}, ksi	F_{tu}, ksi	e (1 in.), percent
Annealed	75	Unexposed	34.4	79.0	59
	1100	Unexposed	35.6	51.5	28
	1300	Unexposed	26.5	32.2	31
	1500	Unexposed	13.2	16.2	32
Annealed	1100	6.7×10^{21}	60.9	65.5	3.8
	1300	1.3×10^{21}	34.1	36.0	7.8
	1300	6.7×10^{21}	35.9	37.3	2.0
Ann. + Exposed 24 hr at 1650 F	1100	2.5×10^{21}	57.6	60.0	2.8
	1300	0.76×10^{21}	24.5	29.6	15.0
	1300	3.0×10^{21}	29.6	32.0	5.6
	1500	2.4×10^{21}	14.2	15.4	10.0

TABLE 2.042. EFFECTS OF FAST-NEUTRON IRRADIATION ON TENSILE PROPERTIES AT ELEVATED TEMPERATURES (23)

Alloy	Type 321							
AMS Spec.	Product Form[a]	Thickness, in.	F_{ty}, ksi, Min	F_{tu}, ksi		El., percent, Min	Hardness, BHN	
				Min	Max		Min	Max
5559E	Tubing	–	35	75	105	40[b]	–	–
5576G, 5570L	Tubing	Up to 0.188 in. OD						
		Up to 0.016 in. Wall	–	–	120	33	–	–
		Over 0.016 in. Wall	–	–	105	35	–	–
		Over 0.188 to 0.500 in. OD						
		Up to 0.010 in. Wall	–	–	115	35[b]	–	–
		Over 0.010 in. Wall	–	–	105	35[b]	–	–
		Over 0.500 in. OD						
		Up to 0.010 in. Wall	–	–	120	30[b]	–	–
		Over 0.010 in. Wall	–	–	105	35[b]	–	–
5557F	Tubing	Up to 0.188 in. OD						
		Up to 0.016 in. Wall	30	75	120	33	–	–
		Over 0.016 in. Wall	30	75	105	35	–	–
		Over 0.188 to 0.500 in. OD						
		Up to 0.010 in. Wall	30	75	115	35[b]	–	–
		Over 0.010 in. Wall	30	75	105	35[b]	–	–
		Over 0.500 in. OD						
		Over 0.010 in. Wall	30	75	105	35[b]	–	–
5510M	Sheet, Strip, Plate	>0.002–0.003	–	–	110	20	–	–
		>0.003–0.004	–	–	105	30	–	–
		>0.004	–	–	100	40	–	–
5645L	Wire[c]	–	–	85	125	–	–	–
	Bars	Up to 2.00	–	–	–	–	140	255
		Over 2.00	–	–	–	–	–	255
	Forgings, Rings	–	–	–	–	–	–	187
5689C	Wire[c]	0.010–0.020	–	–	135	–	–	–
		>0.020–0.125	–	–	125	–	–	–
		>0.125–0.250	–	–	115	–	–	–

Note: The original AMS documents should be consulted for complete specification details.
(a) All materials in solution-heat-treated condition.
(b) Tube elongation values pertain to full tube; strip specimens 5 percent lower.
(c) Wire F_{tu} values pertain to straight lengths; coil specimens 10 ksi lower.

TABLE 3.011. AMS SPECIFIED MECHANICAL PROPERTIES

Fe
18 Cr
10 Ni
+ Ti

Type 321

Alloy	Type 321		
Condition	Annealed		
Form	F_{ty}, ksi	F_{tu}, ksi	e (2 in.), percent
Bar	35	85	55
Plate	30	85	55
Sheet	35	90	45
Strip	35	90	45
Tubing	35	85	50
Wire	65	95	40

TABLE 3.0212. TENSILE PROPERTIES OF VARIOUS FORMS (31)

Alloy	Type 321			
Condition	Annealed			
100,000-hr Exposure Temp, F	F_{ty}, ksi	F_{tu}, ksi	e (2 in.), percent	RA, percent
Unexposed	30.0	77.3	61	81
900	45.6	84.7	51	81
1050	32.2	86.6	48	70
1200	25.8	82.1	48	62

TABLE 3.0213. EFFECTS OF 100,000-HOUR EXPOSURE TO ELEVATED TEMPERATURES ON ROOM-TEMPERATURE TENSILE PROPERTIES (11)

Alloy	Type 321					
Condition	Annealed at 1900 F					
Form	1-inch-Dia Bar					
Exposure Temp, F	Exposure Load, ksi	Exposure Time, hr	F_{ty}, ksi	F_{tu}, ksi	e (2 in.), percent	RA, percent
70	–	–	67.0	93.0	49	75
1100	12.5	1679	61.0	96.5	48	70
1200	7.0	1367	59.7	96.3	42	56
1300	5.0	1656	54.5	96.5	39	52

TABLE 3.0214. EFFECTS ON ROOM-TEMPERATURE TENSILE PROPERTIES OF ELEVATED-TEMPERATURE EXPOSURES UNDER LOAD (35)

Alloy	Type 321				
Form	0.75 inch x 3-1/8 inch Extruded Flat				
Condition	Orientation	F_{ty}, ksi	F_{tu}, ksi	e (4D), percent	RA, percent
As Hot Extruded	L	20.8	67.2	62.5	75
	T	27.0	65.0	69	75
Ann. 1950 F, 1 hr, WQ	L	24.2	67.0	58	79
	T	22.5	64.4	67	75

TABLE 3.0215. TENSILE PROPERTIES OF EXTRUSIONS (14)

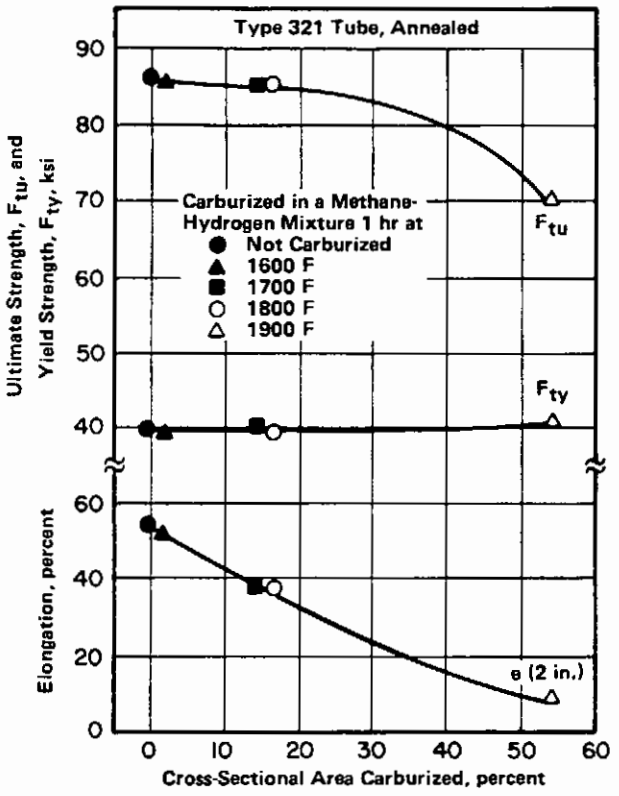


FIGURE 3.0216. EFFECT OF CARBURIZING ON ROOM-TEMPERATURE TENSILE PROPERTIES (16)

Alloy	Type 321	
Condition	Annealed	
Exposure Time, hr	1000	10,000
Exposure Temp, F	Charpy Keyhole, ft-lb	
Unexposed	107	107
900	101	88
1050	90	72
1200	69	62

Fe
18 Cr
10 Ni
+ Ti
Type 321

TABLE 3.0231. EFFECTS OF EXPOSURES TO ELEVATED TEMPERATURES ON ROOM-TEMPERATURE IMPACT PROPERTIES (11)

Alloy	Type 321		
Condition	Annealed at 1900 F		
Form	1-inch Dia Bar		
Exposure Temp, F	Exposure Load, ksi	Exposure Time, hr	Izod IE, ft-lb
70	–	–	92
1100	7.0	2750	54
1200	4.0	2753	49
1300	2.0	2612	46
1500	1.0	1601	41

TABLE 3.0232. EFFECTS ON ROOM-TEMPERATURE IMPACT PROPERTIES OF ELEVATED-TEMPERATURE EXPOSURES UNDER LOAD (35)

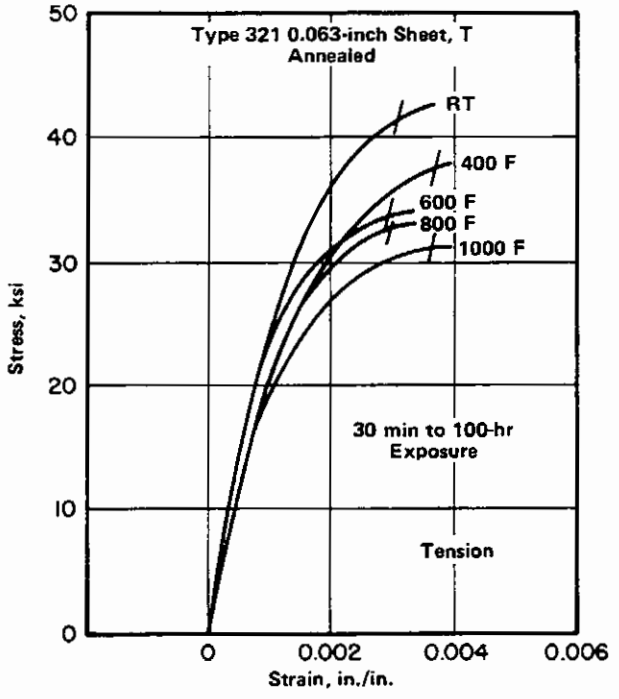


FIGURE 3.0311. STRESS-STRAIN CURVES FOR SHEET AT ROOM AND ELEVATED TEMPERATURES (36)

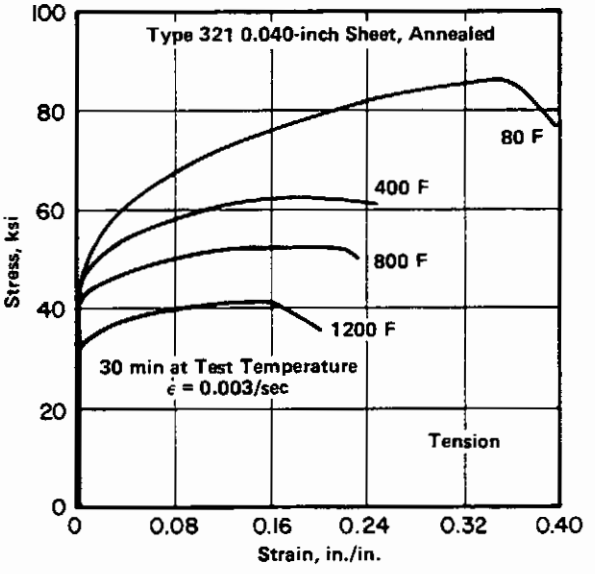


FIGURE 3.0312. COMPLETE STRESS-STRAIN CURVES FOR SHEET AT ROOM AND ELEVATED TEMPERATURES (37)

Fe
18 Cr
10 Ni
+ Ti

Type 321

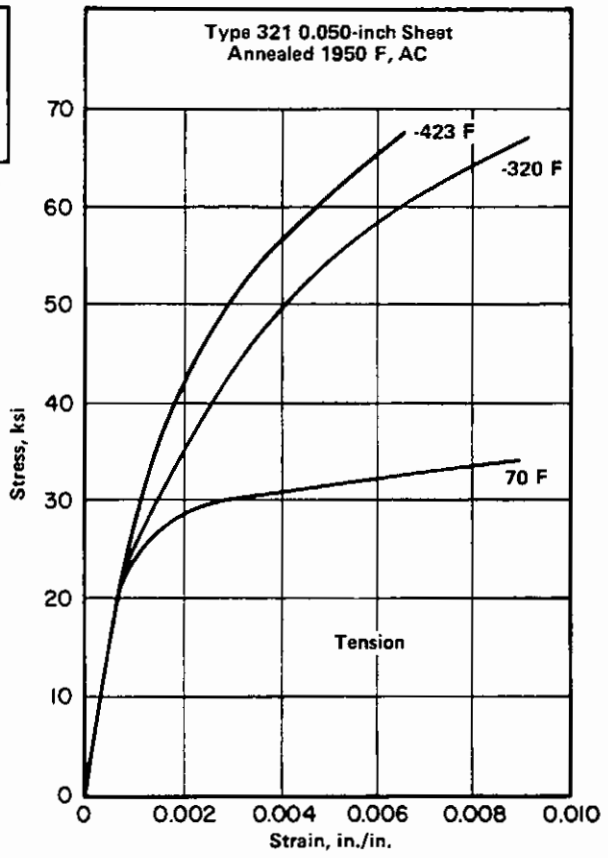


FIGURE 3.0313. STRESS-STRAIN CURVES FOR SHEET AT ROOM AND LOW TEMPERATURES (13)

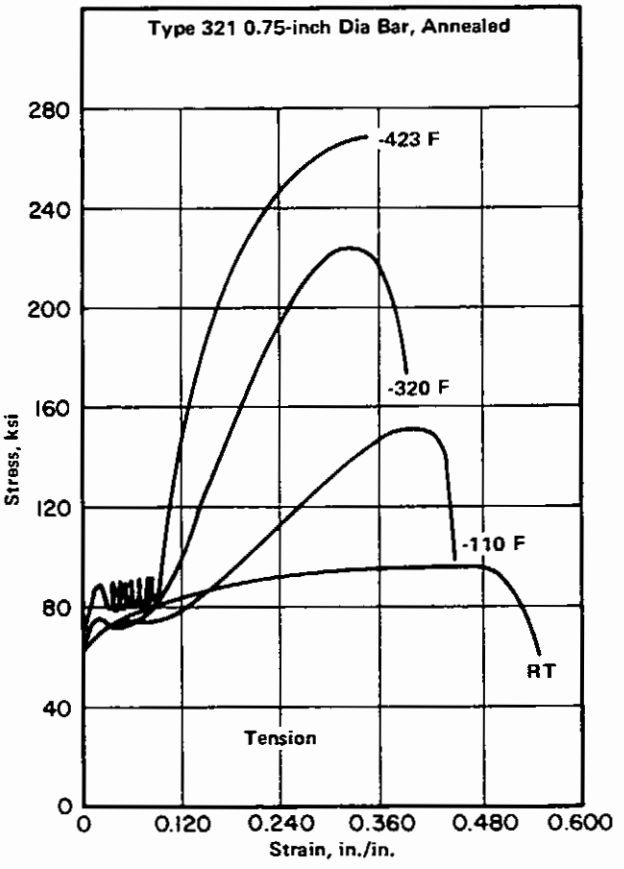


FIGURE 3.0314. COMPLETE STRESS-STRAIN CURVES FOR BAR AT ROOM AND LOW TEMPERATURES (38)

Fe
18 Cr
10 Ni
+ Ti

Type 321

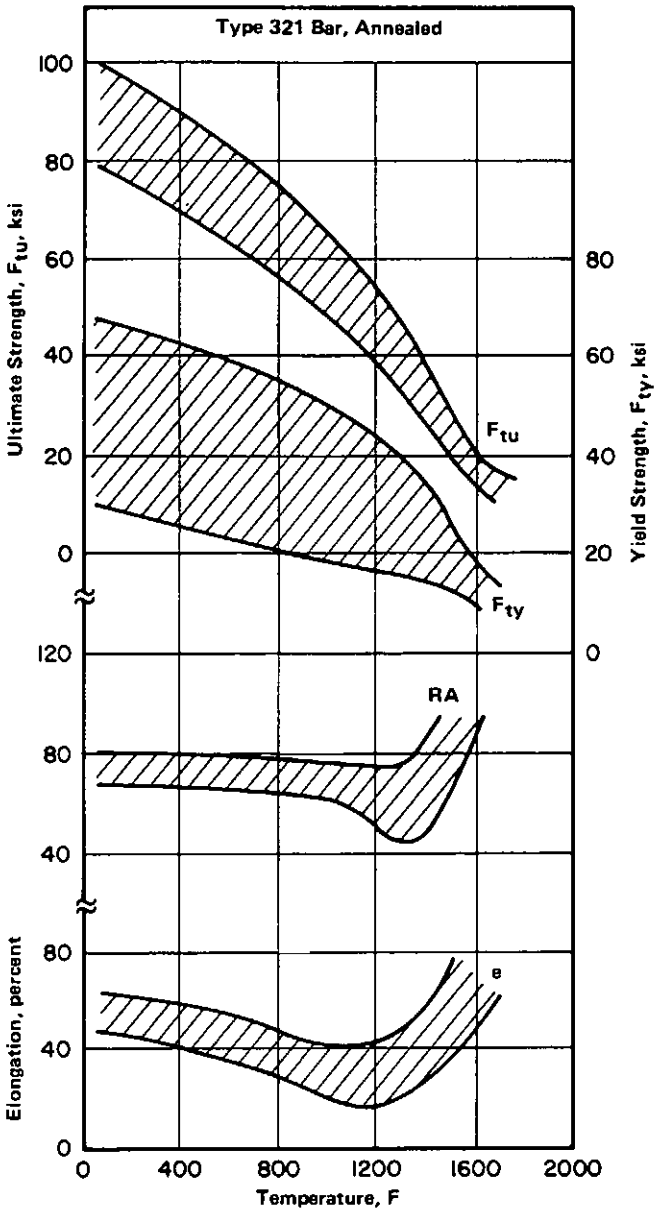


FIGURE 3.0315. SCATTER BANDS FOR TENSILE PROPERTIES OF BAR AT ROOM AND ELEVATED TEMPERATURES (39)

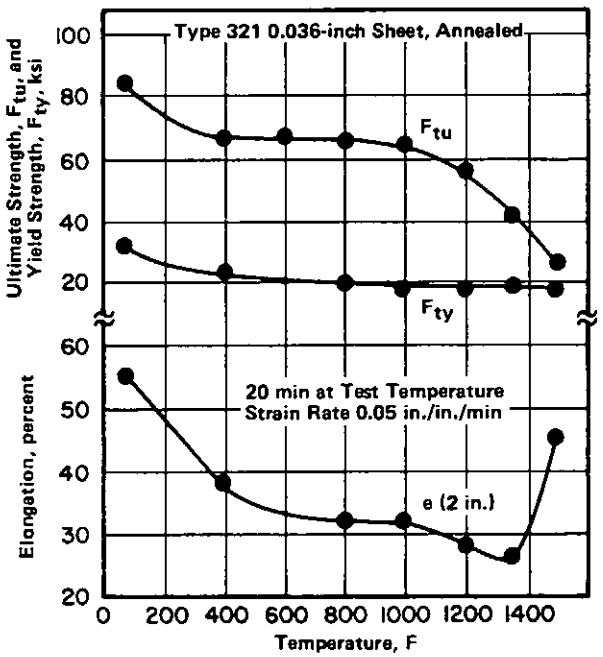


FIGURE 3.0316. EFFECT OF ELEVATED TEMPERATURES ON TENSILE PROPERTIES OF SHEET (9)

Fe
18 Cr
10 Ni
+ Ti

Type 321

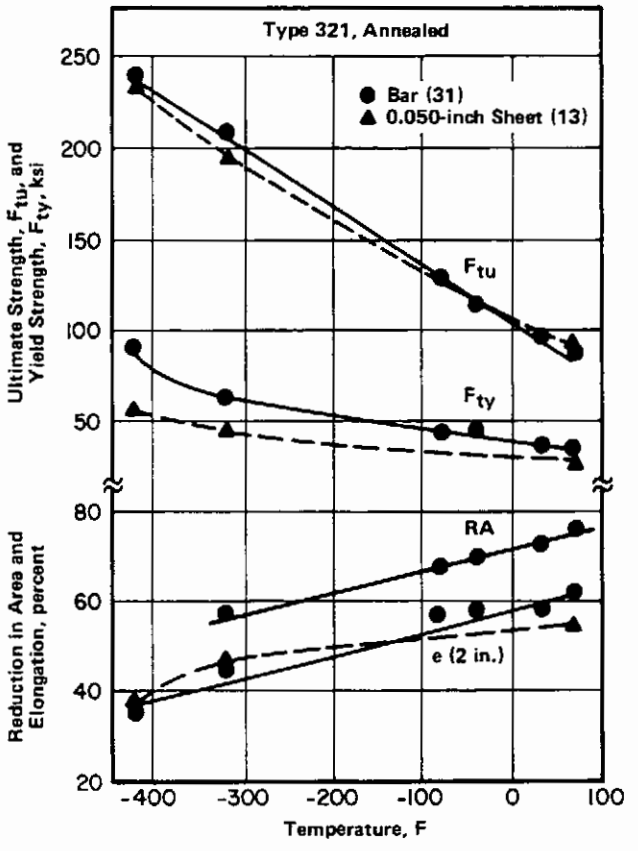


FIGURE 3.0317. EFFECTS OF LOW TEMPERATURES ON TENSILE PROPERTIES OF BAR AND SHEET (13,31)

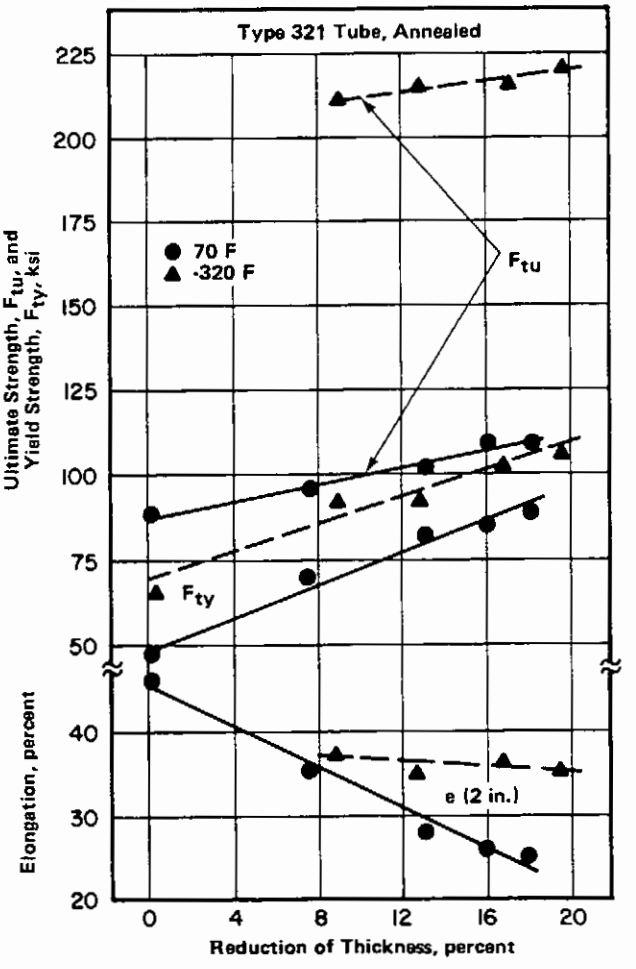


FIGURE 3.0318. EFFECTS OF COLD WORK INDUCED BY HYDRAULIC EXPANSION ON TENSILE PROPERTIES OF TUBING AT 70 F AND -320 F (19)

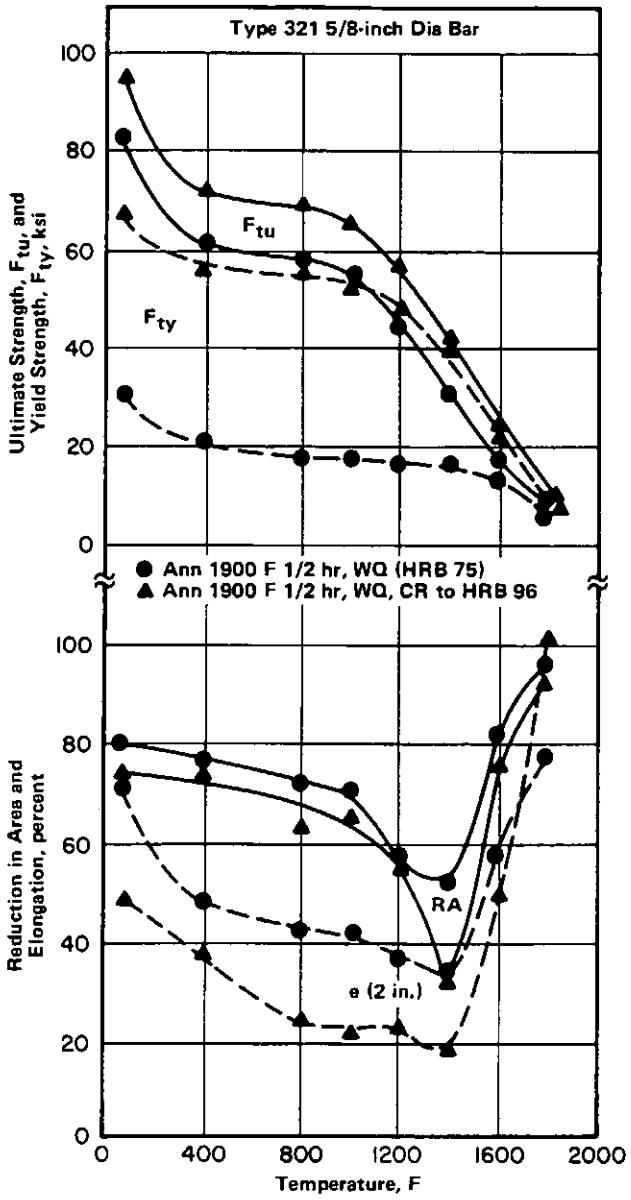


FIGURE 3.0319. EFFECTS OF TEMPERATURE ON TENSILE PROPERTIES OF ANNEALED AND COLD-ROLLED BAR (8)

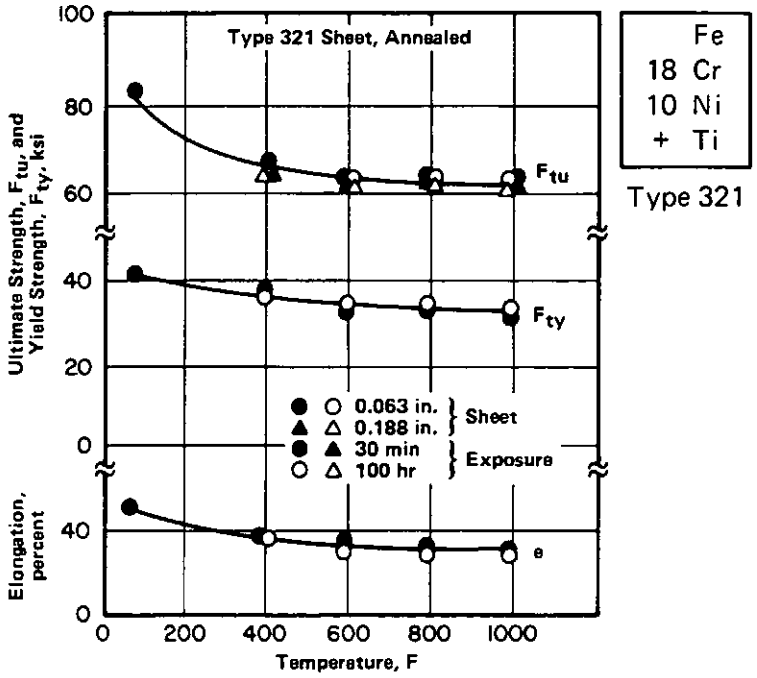


FIGURE 3.03110. EFFECTS OF TEST TEMPERATURE, AFTER TWO DIFFERENT EXPOSURE TIMES AT TEMPERATURE, ON TENSILE PROPERTIES OF SHEET (36)

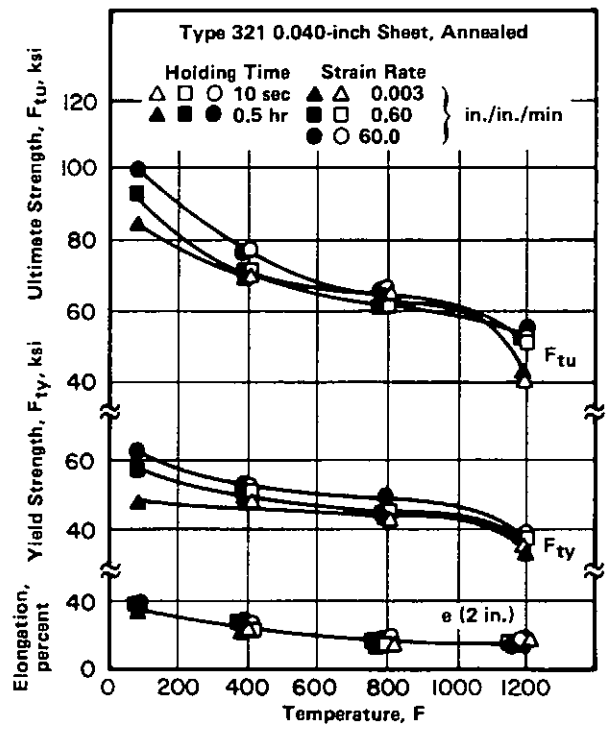


FIGURE 3.03111. EFFECTS OF TEMPERATURE, RAPID STRAIN RATES, AND SHORT HOLDING TIMES AT TEMPERATURE ON TENSILE PROPERTIES OF SHEET HEATED TO TEST TEMPERATURES WITHIN 10 SECONDS (40)

Fe
18 Cr
10 Ni
+ Ti

Type 321

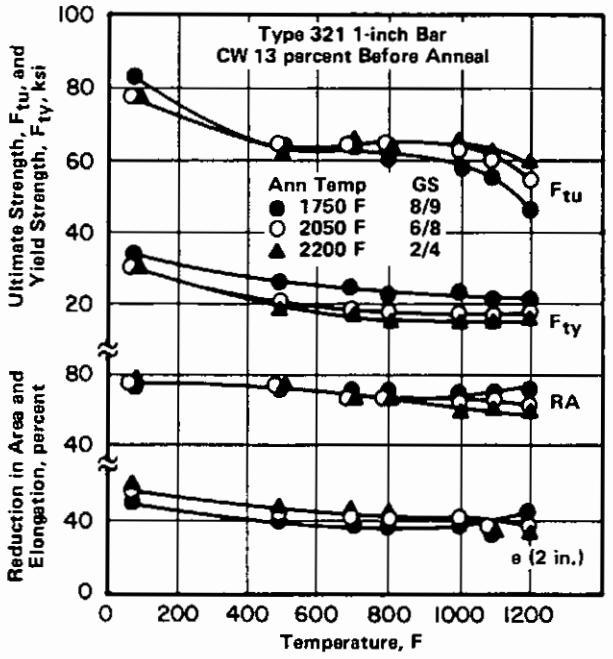


FIGURE 3.03112. EFFECTS OF TEMPERATURE ON TENSILE PROPERTIES OF BAR ANNEALED AT VARIOUS TEMPERATURES (35)

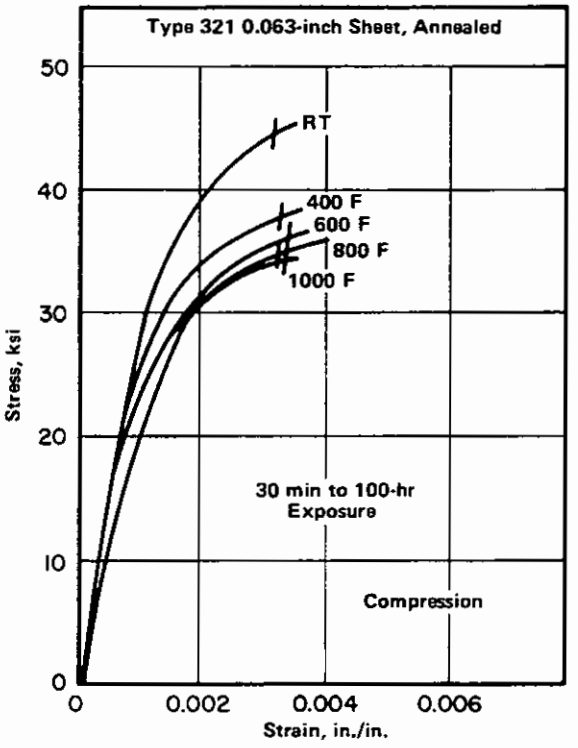


FIGURE 3.0321. COMPRESSIVE STRESS-STRAIN CURVES FOR SHEET AT ROOM AND ELEVATED TEMPERATURES (36)

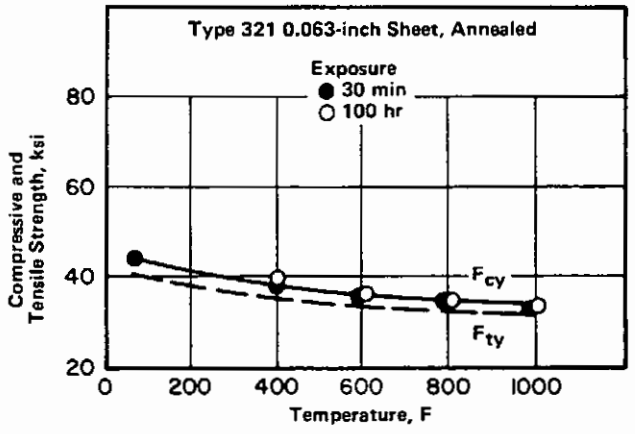


FIGURE 3.0322. EFFECTS OF TEMPERATURE, AFTER TWO DIFFERENT EXPOSURE TIMES AT TEMPERATURE, ON COMPRESSIVE YIELD STRENGTH OF SHEET (36)

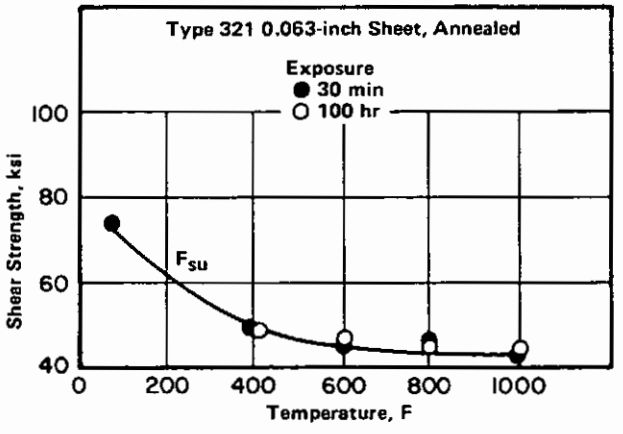


FIGURE 3.0351. EFFECTS OF TEMPERATURE, AFTER TWO DIFFERENT EXPOSURE TIMES AT TEMPERATURE, ON SHEAR STRENGTH OF SHEET (36)

Fe
18 Cr
10 Ni
+ Ti

Type 321

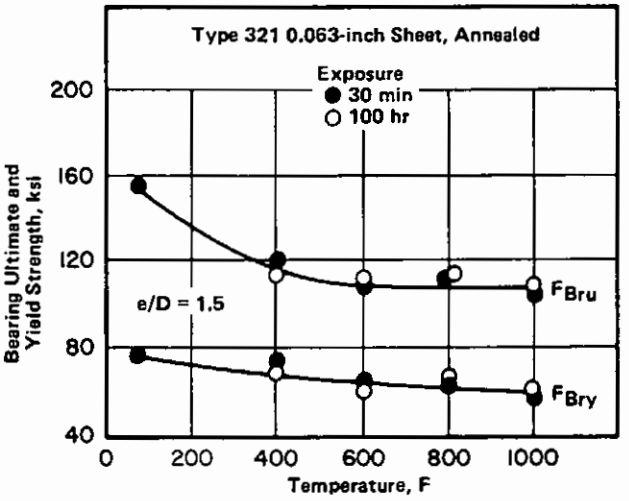


FIGURE 3.0361. EFFECTS OF TEMPERATURE, AFTER TWO DIFFERENT EXPOSURE TIMES AT TEMPERATURE, ON BEARING PROPERTIES OF SHEET (36)

Alloy	Type 321						
Condition	Annealed						
Form	Plate						
Temp, F	Specimen Type	Environment	Pressure, psig	F_{ty}, ksi	F_{tu}, ksi	e (4D), percent	RA, percent
70	Smooth	Air	0	32	87	77	71
70	Smooth	Helium	5000	29	84	63	66
70	Smooth	Hydrogen	5000	37	86	64	60
70	Notched	Helium	5000	–	113	–	6.4
70	Notched	Hydrogen	5000	–	99	–	2.3
-200	Smooth	Helium	5000	–	124	48	67
-200	Smooth	Hydrogen	5000	–	122	43	56
-200	Notched	Helium	5000	–	143	–	12
-200	Notched	Hydrogen	5000	–	141	–	12

Notched specimen

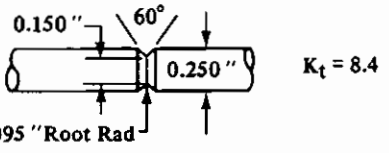


TABLE 3.03711. SMOOTH AND NOTCHED TENSILE PROPERTIES IN HIGH-PRESSURE HELIUM AND HYDROGEN AT 70 F AND -200 F

Fe
18 Cr
10 Ni
+ Ti

Type 321

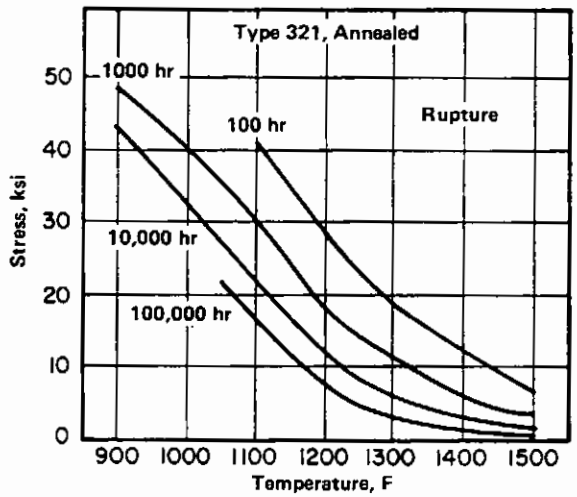


FIGURE 3.041. EFFECT OF TEMPERATURE ON CREEP-RUPTURE STRENGTH (9,10)

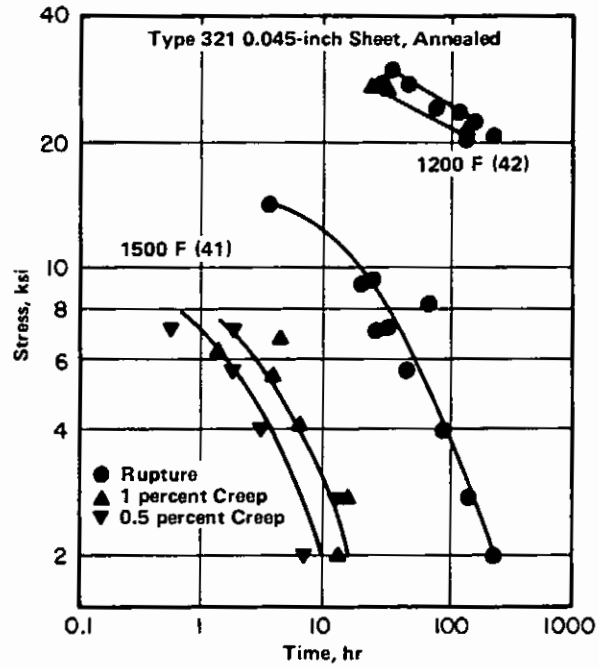


FIGURE 3.042. CREEP AND CREEP-RUPTURE CURVES FOR SHEET AT 1200 AND 1500 F (41,42)

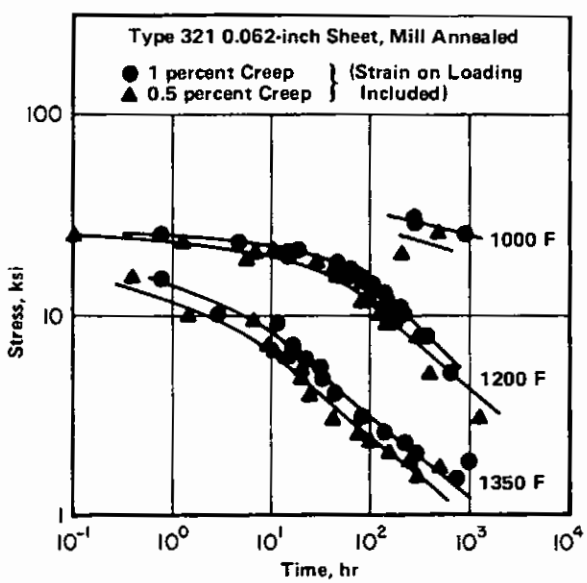


FIGURE 3.043. CREEP CURVES FOR SHEET AT 1000 TO 1350 F (72)

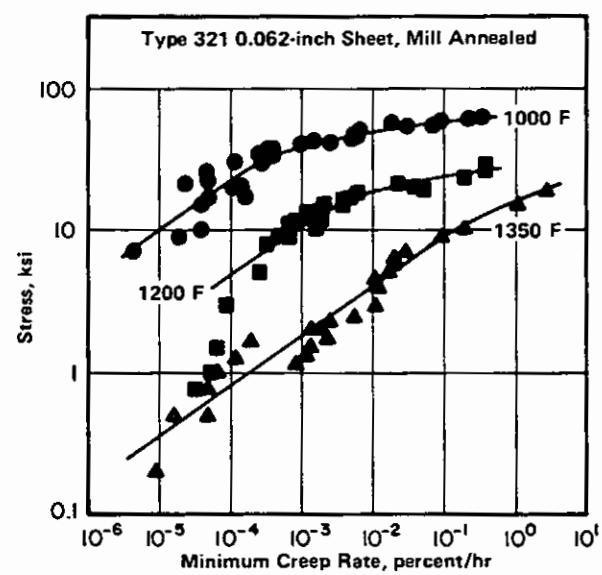


FIGURE 3.044. CREEP RATES FOR SHEET AT 1000 TO 1350 F (72)

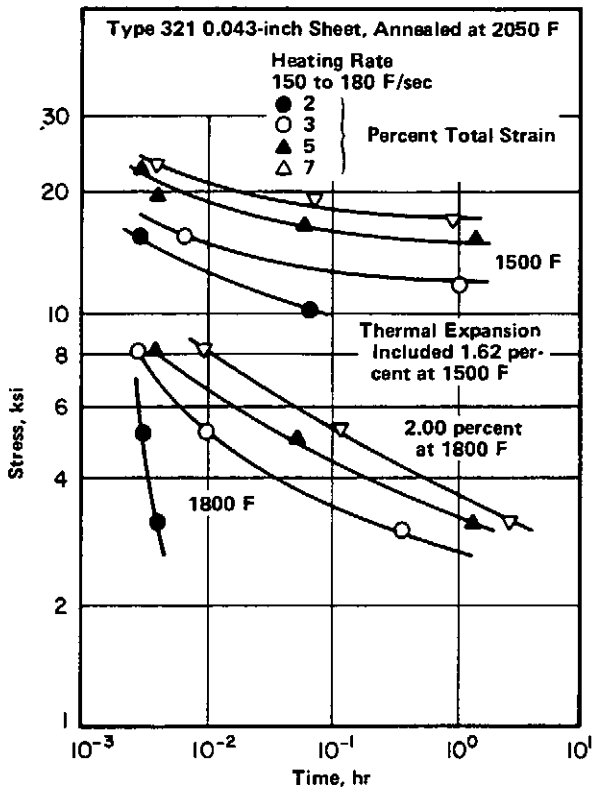
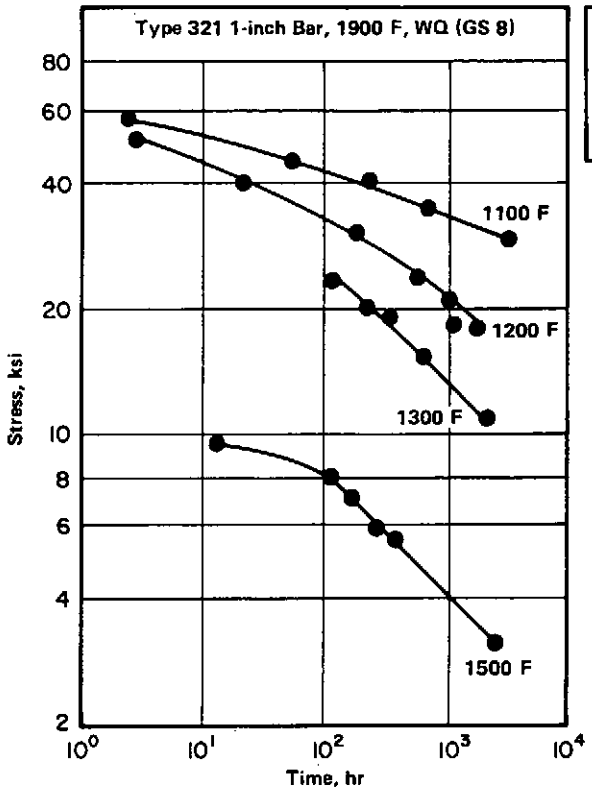


FIGURE 3.045. SHORT-TIME TOTAL-STRAIN CURVES FOR SHEET AT 1500 AND 1800 F (43)



Fe
18 Cr
10 Ni
+ Ti

Type 321

FIGURE 3.046. CREEP-RUPTURE CURVES FOR BAR AT 1100 TO 1500 F (35)

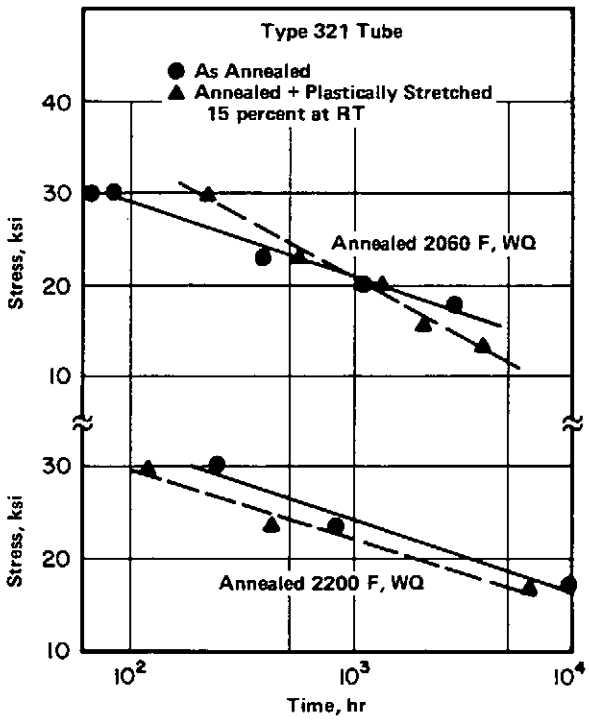
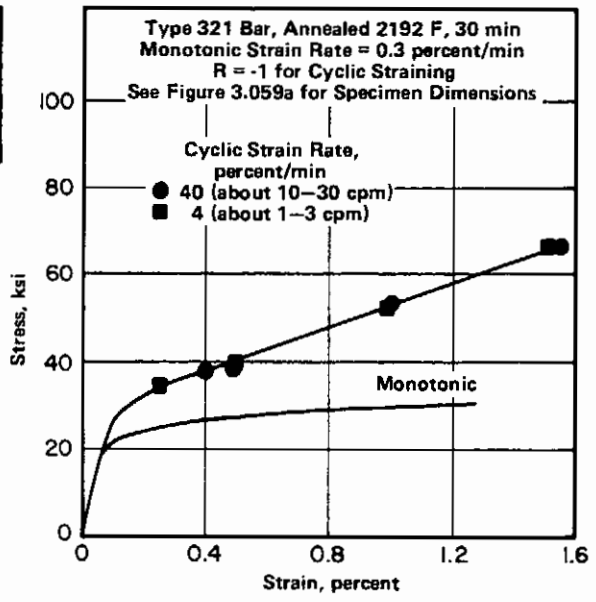


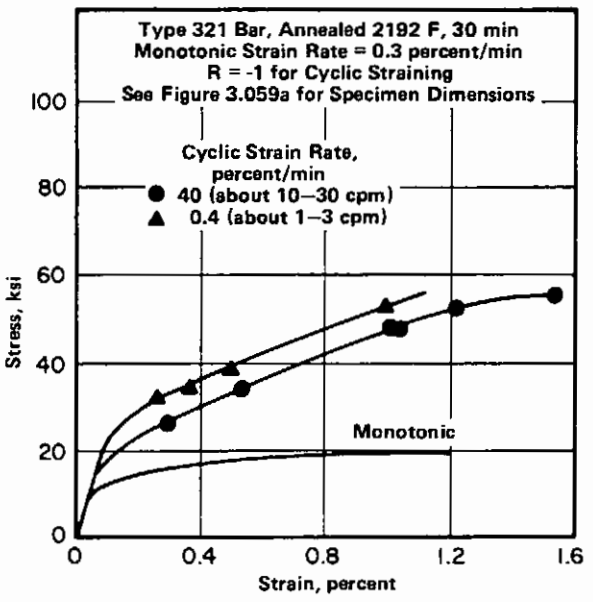
FIGURE 3.047. EFFECTS OF ANNEALING TEMPERATURE AND COLD WORK ON CREEP-RUPTURE PROPERTIES AT 1200 F (17)

Fe
18 Cr
10 Ni
+ Ti

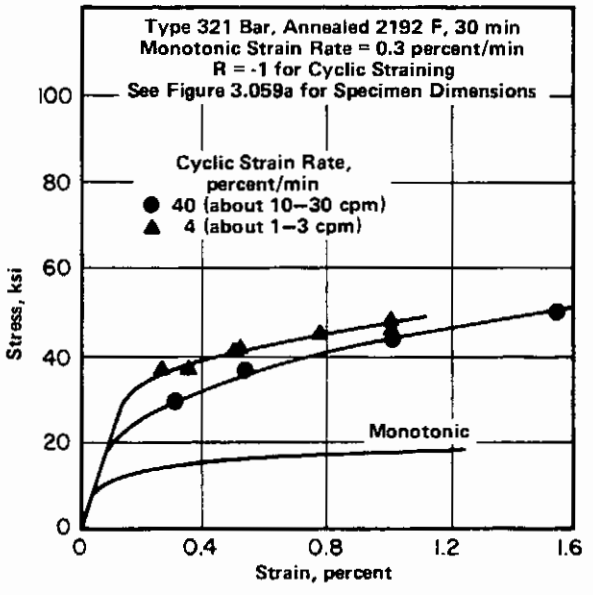
Type 321



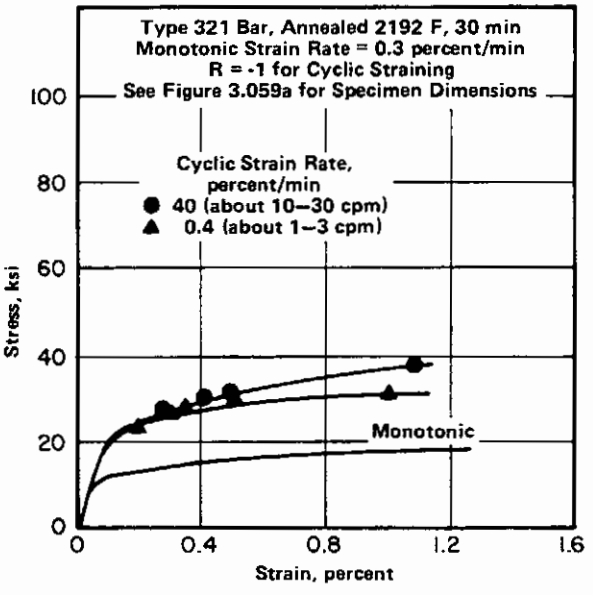
a. Room Temperature



b. 842 F



c. 1112 F



d. 1292 F

FIGURE 3.052. MONOTONIC AND CYCLIC STRESS-STRAIN CURVES FOR BAR AT ROOM AND ELEVATED TEMPERATURES (70)

Fe
18 Cr
10 Ni
+ Ti

Type 321

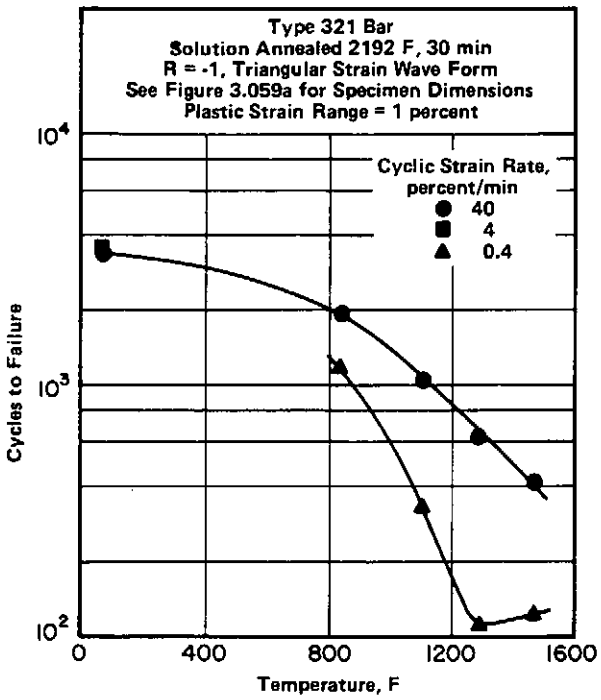


FIGURE 3.053. LOW-CYCLE FATIGUE LIFE AT ROOM AND ELEVATED TEMPERATURES (70,73)

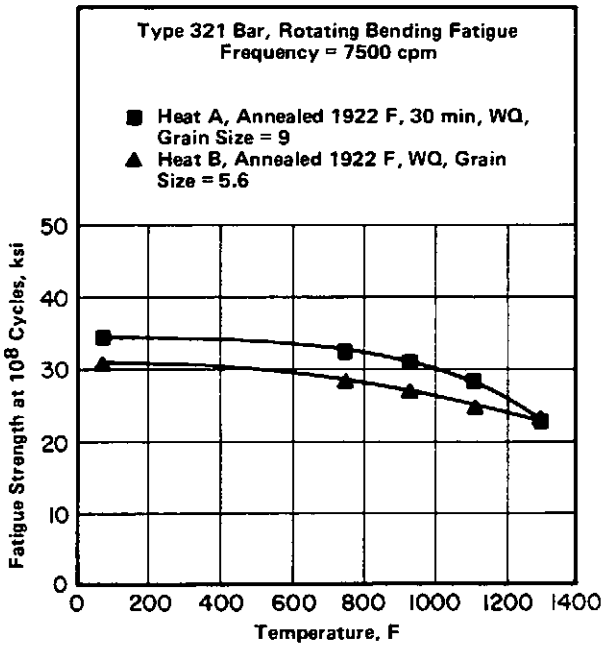


FIGURE 3.054. HIGH-CYCLE FATIGUE STRENGTH AT ROOM AND ELEVATED TEMPERATURES (73)

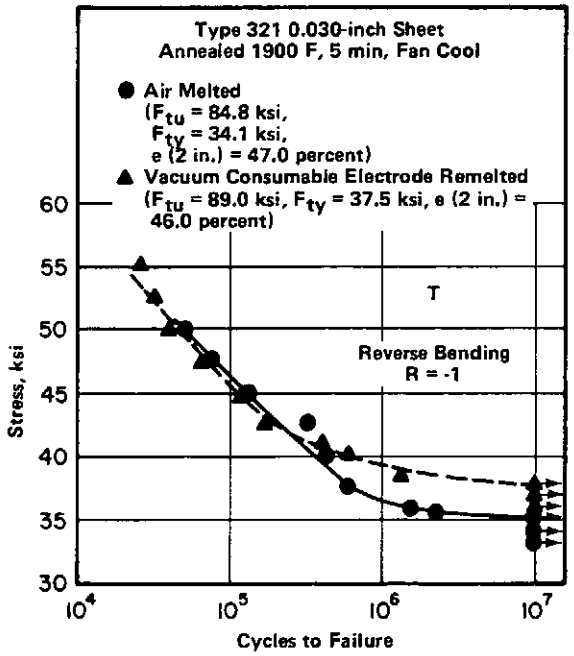


FIGURE 3.055. FATIGUE PROPERTIES OF AIR-MELTED AND VACUUM-MELTED SHEET (12)

Fe
18 Cr
10 Ni
+ Ti

Type 321

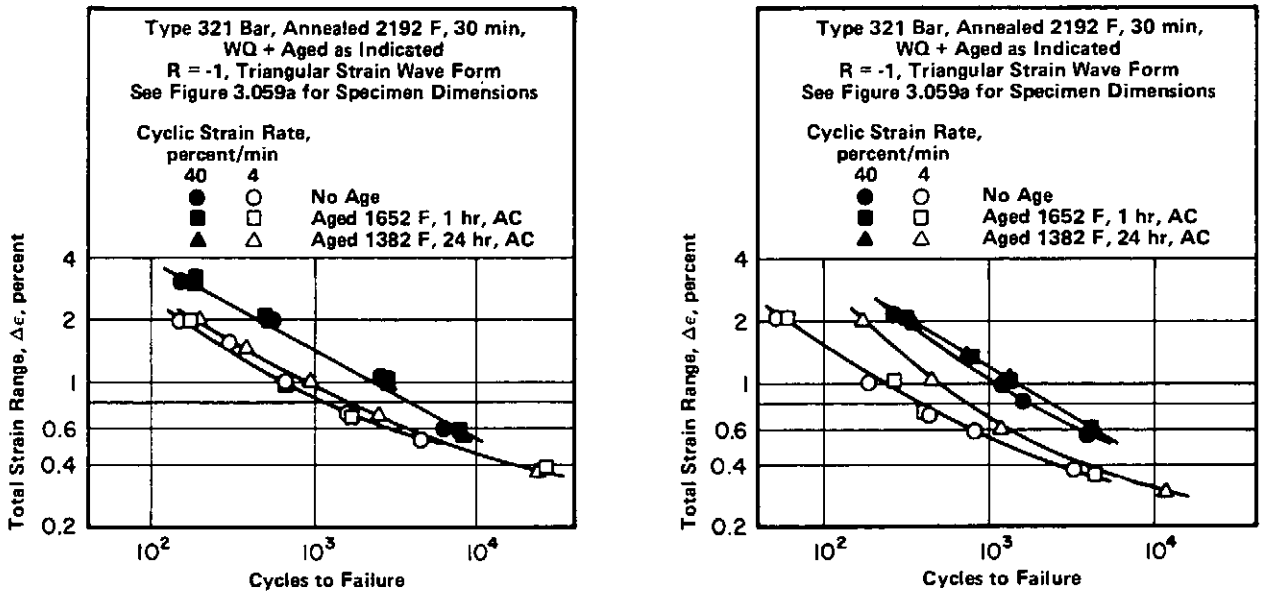


FIGURE 3.057. EFFECTS OF AGING AND CYCLIC STRAIN RATE ON FATIGUE BEHAVIOR AT ELEVATED TEMPERATURES (74)

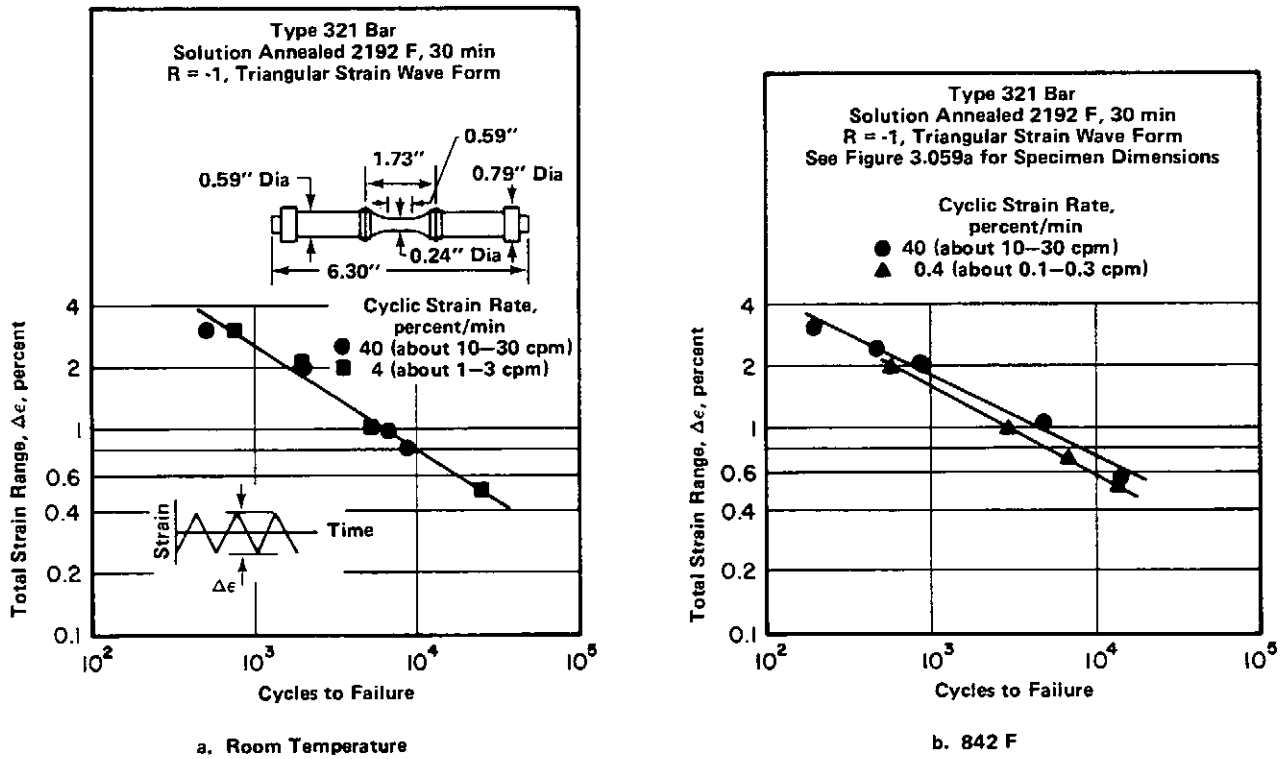
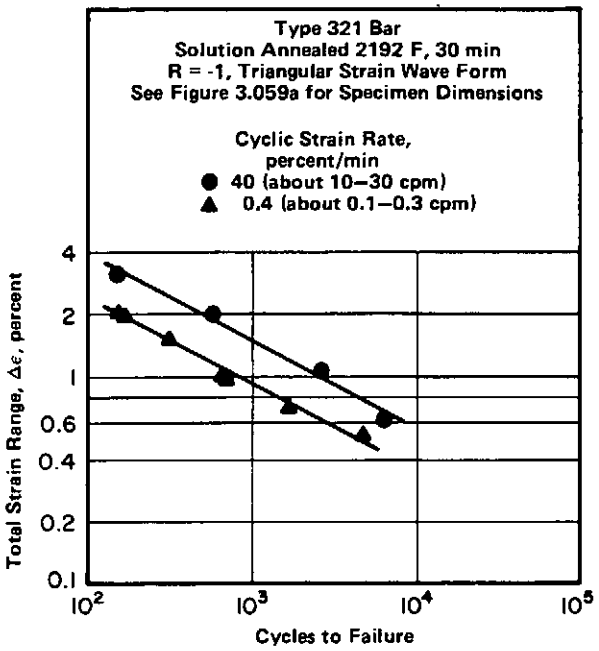
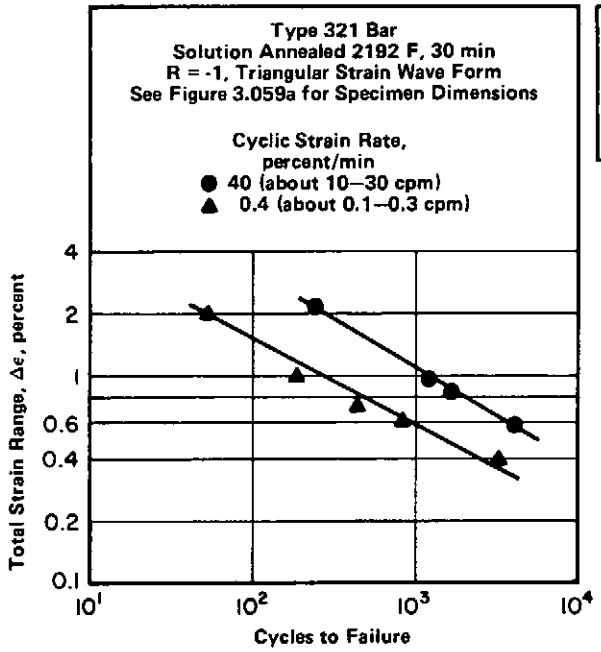


FIGURE 3.059. LOW-CYCLE AXIAL FATIGUE BEHAVIOR IN AIR AT ROOM AND ELEVATED TEMPERATURES (70, 73)



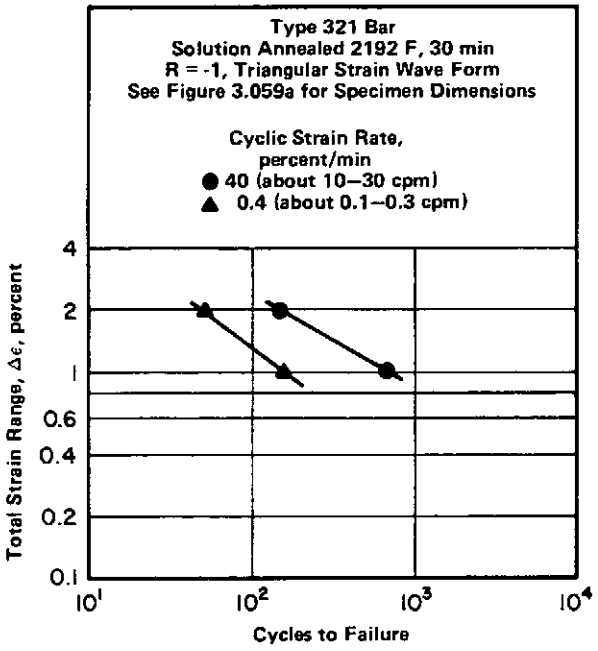
c. 1112 F



d. 1292 F

Fe
18 Cr
10 Ni
+ Ti

Type 321



e. 1472 F

FIGURE 3.059. (CONTINUED)

Fe
18 Cr
10 Ni
+ Ti

Type 321

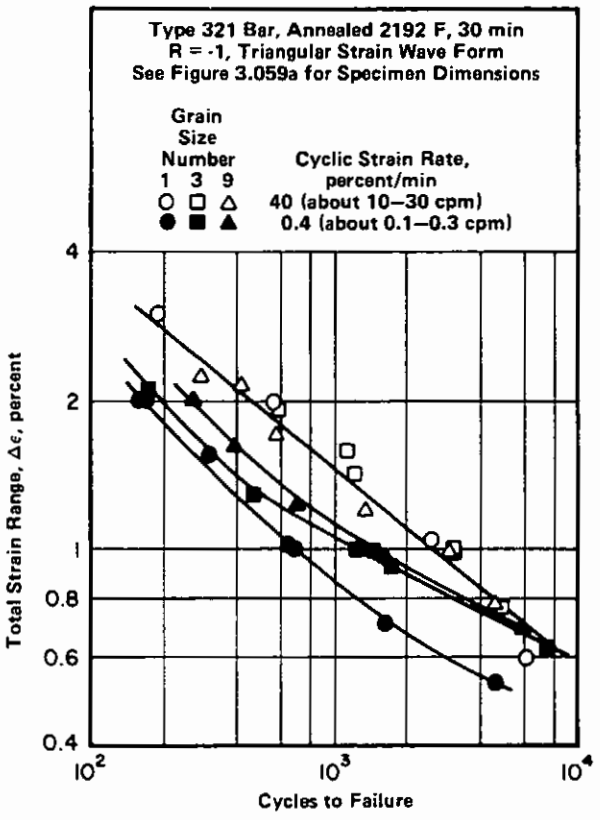


FIGURE 3.0511. EFFECTS OF GRAIN SIZE AND CYCLIC FREQUENCY ON AXIAL FATIGUE BEHAVIOR AT 1112 F (76)

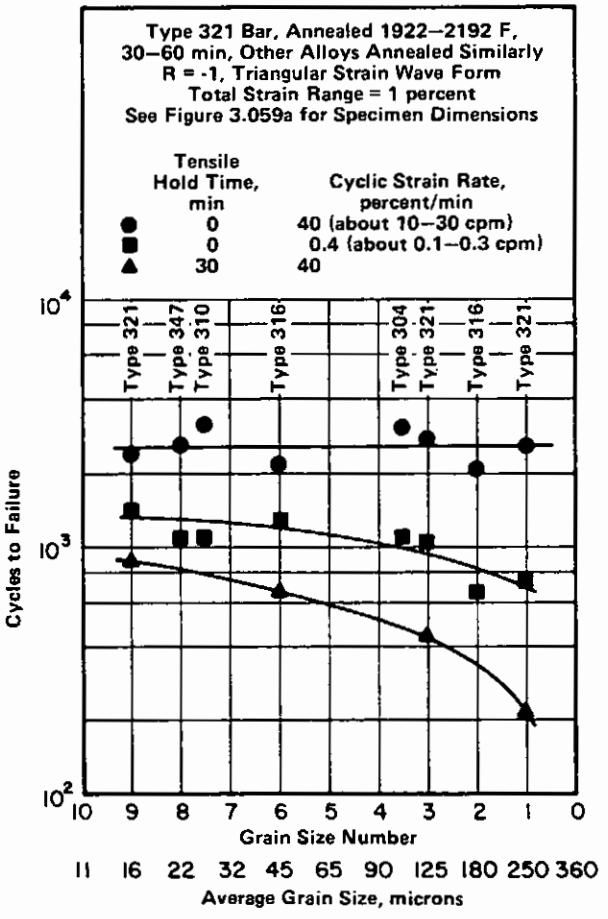


FIGURE 3.0512. EFFECTS OF GRAIN SIZE, CYCLIC FREQUENCY, AND HOLD TIME ON AXIAL FATIGUE LIFE OF AUSTENITIC STAINLESS STEELS AT 1112 F (76)

Fe
18 Cr
10 Ni
+ Ti

Type 321

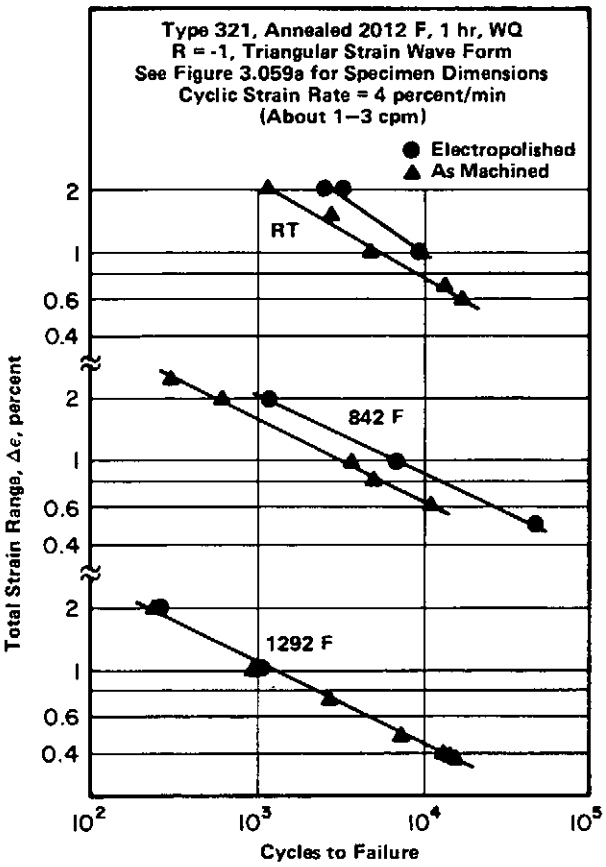


FIGURE 3.0514. EFFECT OF SURFACE FINISH ON AXIAL FATIGUE BEHAVIOR AT ROOM AND ELEVATED TEMPERATURES (75)

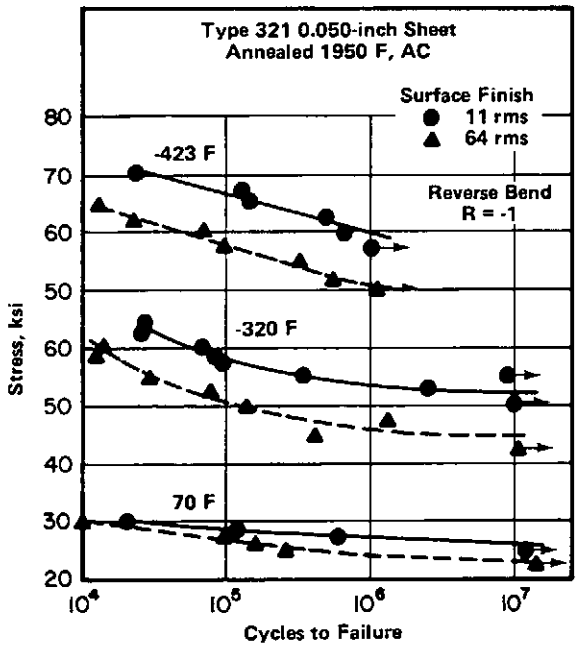


FIGURE 3.0515. EFFECTS OF LOW TEMPERATURES AND SURFACE FINISH ON FATIGUE PROPERTIES (13)

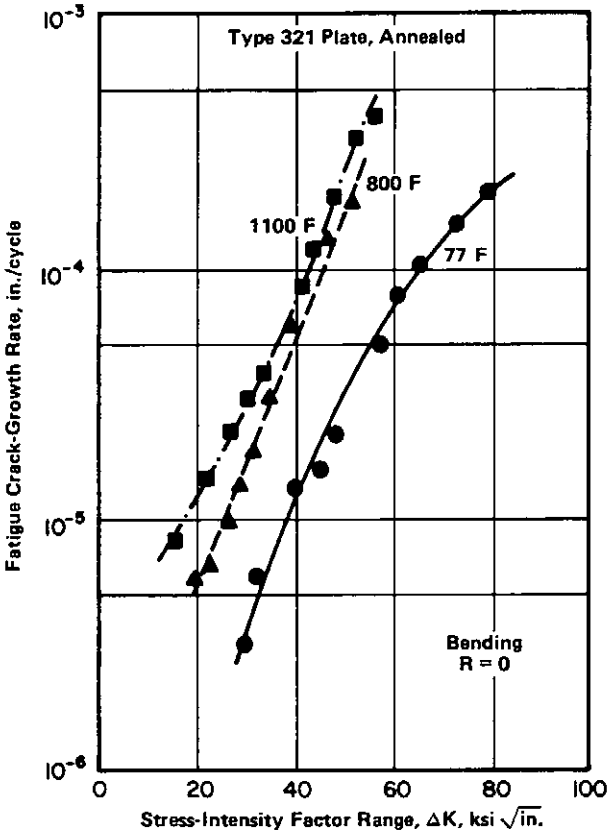


FIGURE 3.0516. FATIGUE CRACK-GROWTH RATE AS A FUNCTION OF THE STRESS-INTENSITY-FACTOR RANGE AT VARIOUS TEMPERATURES (22,32)

Fe
18 Cr
10 Ni
+ Ti

Type 321

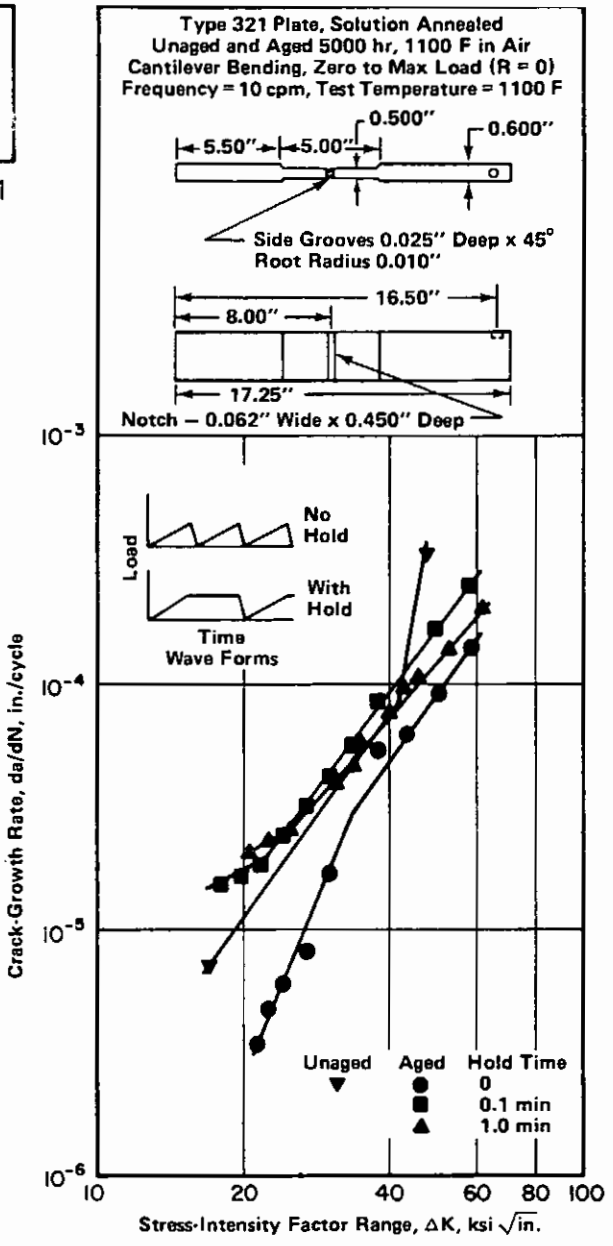
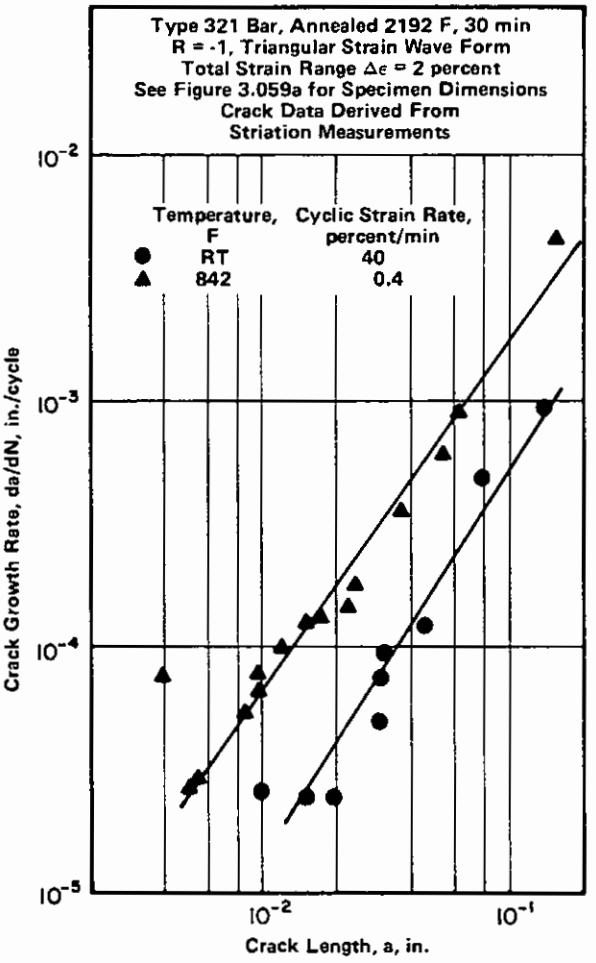


FIGURE 3.0518. EFFECTS OF AGING AND CYCLIC HOLD TIME ON BENDING-FATIGUE CRACK-GROWTH RATE AT 1100 F (77)

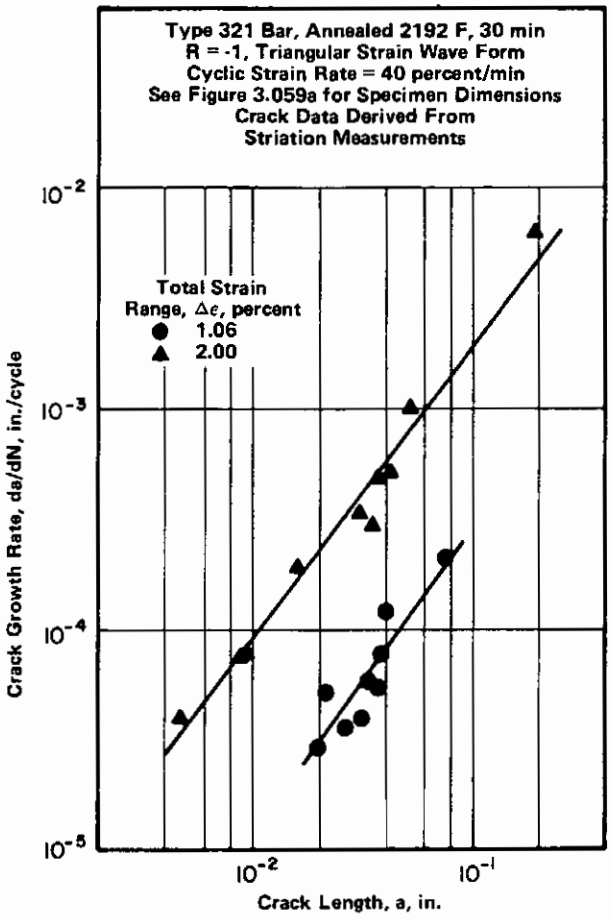


a. Room Temperature and 842 F

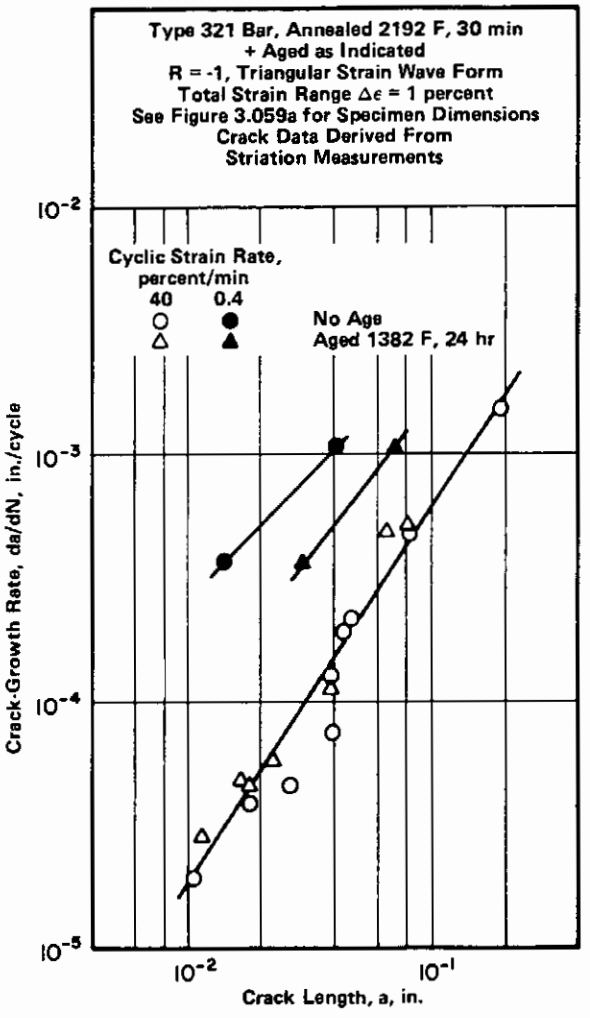
FIGURE 3.0520. RELATION BETWEEN CRACK-GROWTH RATE AND CRACK LENGTH AT ROOM AND ELEVATED TEMPERATURES (78)

Fe
18 Cr
10 Ni
+ Ti

Type 321



b. 1112 F



c. 1292 F

FIGURE 3.0520. (CONTINUED)

Fe
18 Cr
10 Ni
+ Ti

Type 321

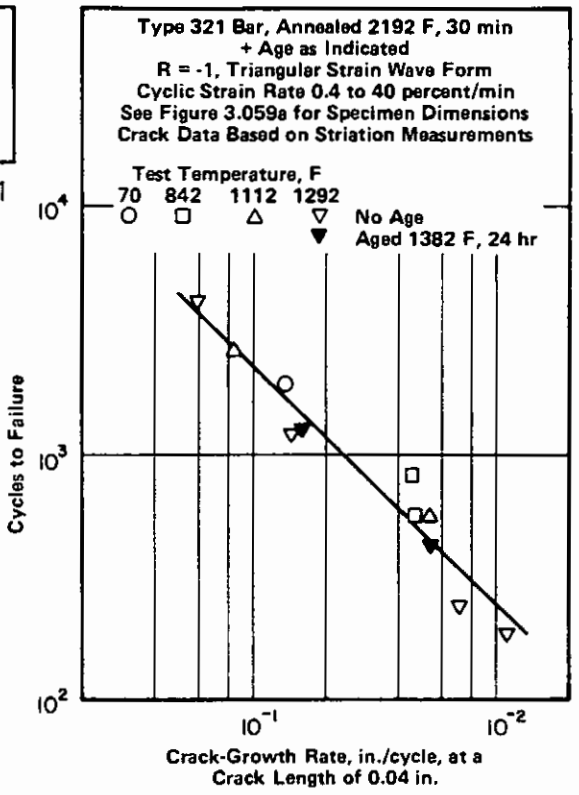


FIGURE 3.0521. RELATION BETWEEN FATIGUE LIFE AND CRACK-PROPAGATION RATE (78)

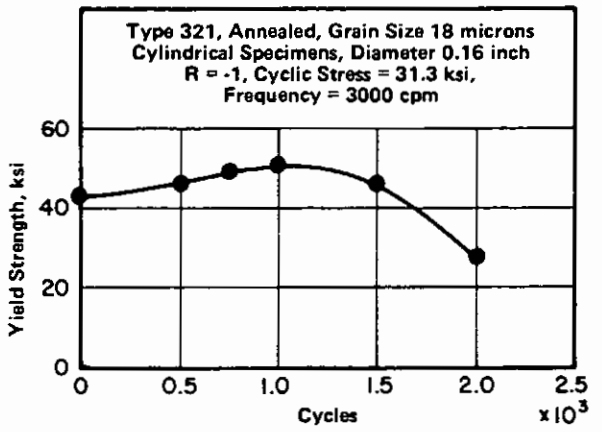


FIGURE 3.0523. EFFECT OF AXIAL FATIGUE ON SUBSEQUENT YIELD STRENGTH AT ROOM TEMPERATURE (71)

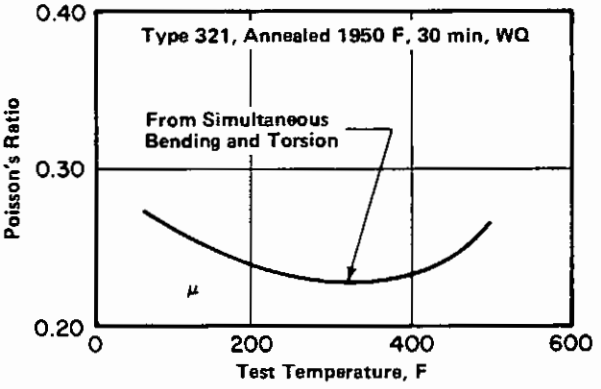


FIGURE 3.0611. EFFECT OF TEMPERATURE ON POISSON'S RATIO (38)

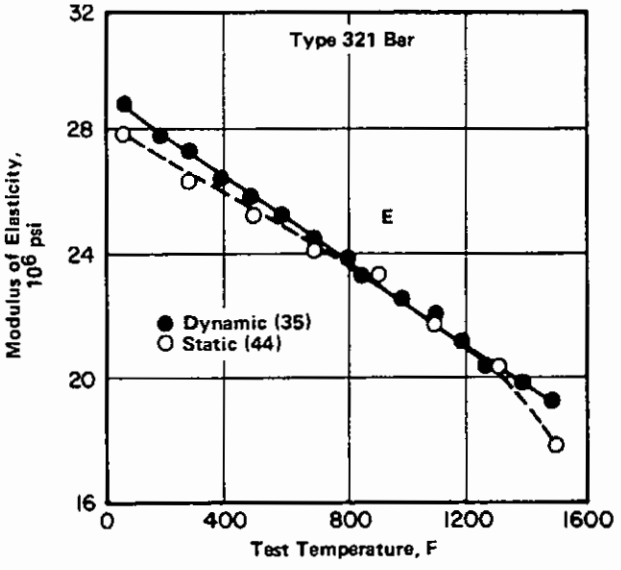


FIGURE 3.0621. MODULUS OF ELASTICITY AT ROOM AND ELEVATED TEMPERATURES (35,44)

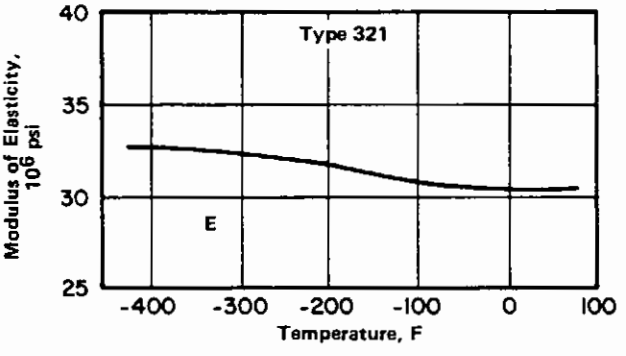


FIGURE 3.0622. MODULUS OF ELASTICITY AT LOW TEMPERATURES (38)

Fe
18 Cr
10 Ni
+ Ti

Type 321

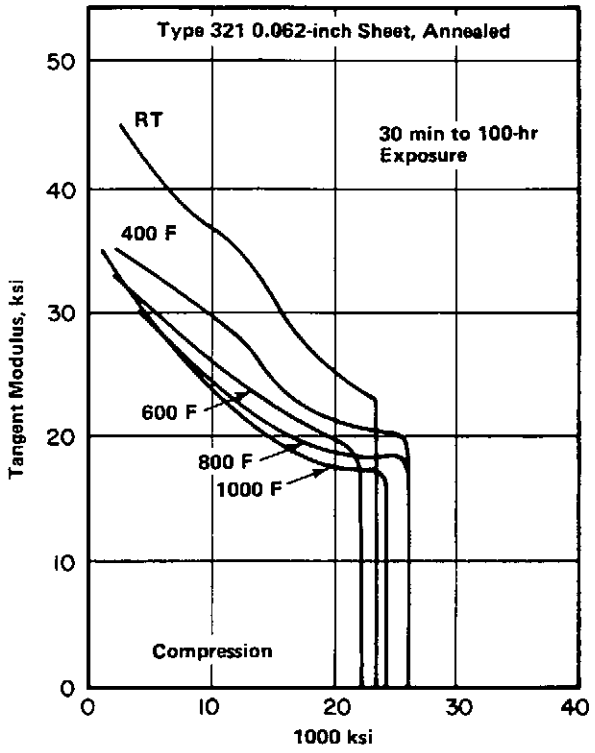


FIGURE 3.0623. TANGENT MODULUS CURVES IN COMPRESSION (36)

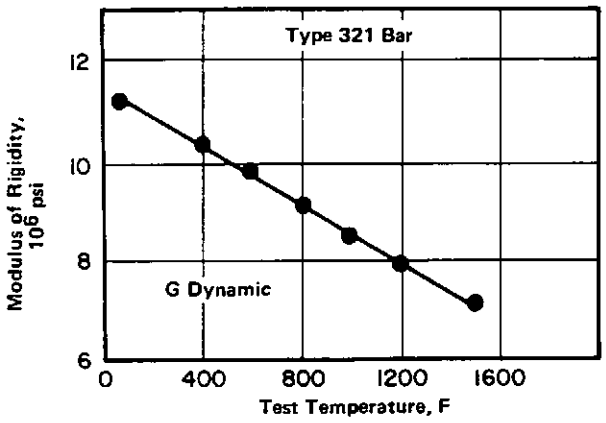


FIGURE 3.0631. MODULUS OF RIGIDITY AT ROOM AND ELEVATED TEMPERATURES (35)

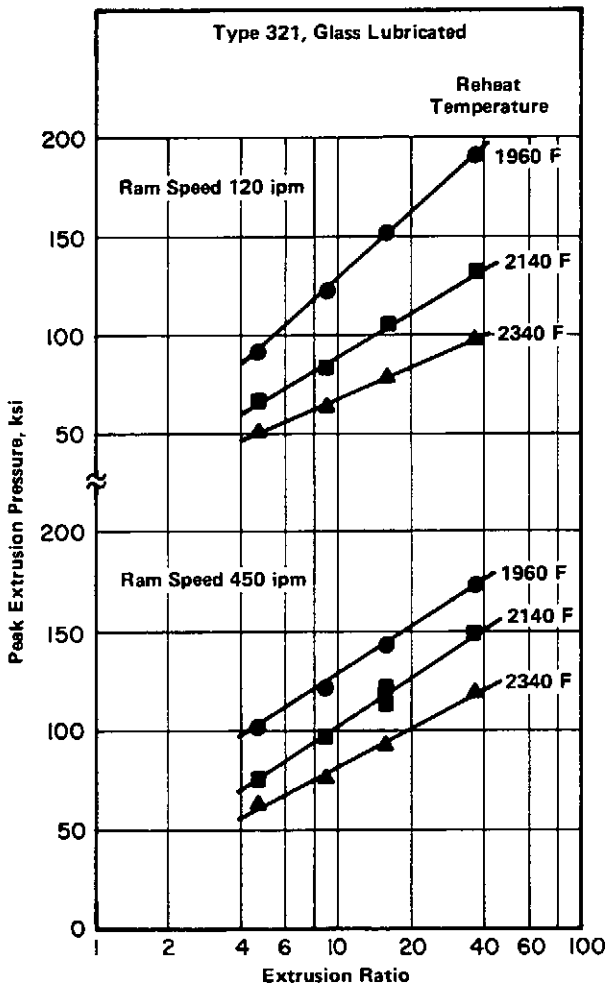


FIGURE 4.014. EFFECTS OF EXTRUSION RATIO, RE-HEAT TEMPERATURE, AND RAM SPEED ON PEAK EXTRUSION PRESSURE (79)

Fe
18 Cr
10 Ni
+ Ti

Type 321

Alloy	Type 321			
Form	Sheet and Plate			
Condition	Annealed			
Material Thickness, in.	Type Weld	F_{ty}, ksi	F_{tu}, ksi	e (2 in.), percent
0.060	Parent Metal	40.1	92.1	48.8
	Low Voltage	39.6	92.7	55.6
	High Voltage	39.4	91.7	44.0
0.125	Parent Metal	42.7	89.3	48.6
	Low Voltage	43.7	89.0	39.0
	High Voltage	43.6	88.0	33.3
0.800	Parent Metal	28.9	79.3	66.3
	Low Voltage	31.8	80.0	60.3
	High Voltage	30.7	82.3	62.0

TABLE 4.0311. TENSILE PROPERTIES OF SPECIMENS BUTT-WELDED IN VACUUM BY LOW-VOLTAGE ELECTRON-BEAM PROCESSES; NO PREHEAT OR POSTHEAT TREATMENTS (20)

Alloy	Type 321	
Condition	Annealed	
Form	Brazed Joints	
Braze Temp, F	1800	1850
F_{su}, ksi	68.0	77.3

Note: Brazed in vacuum with 82 percent gold – 18 percent nickel brazing alloy.

TABLE 4.0321. SHEAR STRENGTH OF BRAZED JOINTS (18)

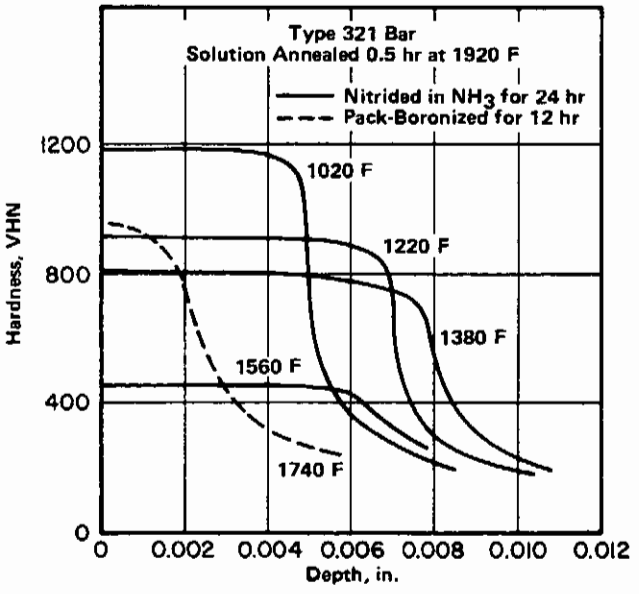


FIGURE 4.045. HARDNESS-DEPTH PROFILES FOR TYPE 321 AFTER NITRIDING AT 1020 TO 1560 F OR BORONIZING AT 1740 F (82,83)

REVISED: DECEMBER 1977
AUTHOR: J.R. KATTUS

FERROUS ALLOYS

	Fe
18	Cr
12	Ni
+	Cb

TYPES 347,348

1.0 GENERAL

Type 347 stainless steel, like Type 321, is a stabilized austenitic stainless steel, which can be hardened by cold work but not by heat treatment. Stabilization is provided by a small addition of columbium plus tantalum, which forms stable carbides scattered throughout the microstructure. Consequently, Type 347 is resistant to sensitization, which is a drastic reduction in intergranular-corrosion resistance associated with the precipitation of chromium carbides at grain boundaries when unstabilized grades of austenitic stainless steels are heated into the range of 800 to 1600F. Type 347 has slightly better general corrosion resistance than Type 321. Unlike Type 321, it is widely used for castings and welding rods since columbium and tantalum do not oxidize out during melting or welding. Type 347 is used primarily for applications requiring long-time exposures to temperatures from 800 to 1500F, such as aircraft collector rings, exhaust manifolds, after burners, pressure vessels, expansion joints and high-temperature chemical processing equipment. When the tantalum addition is restricted to a maximum of 0.10 percent, the alloy designation becomes Type 348. This grade was designed for nuclear applications in order to avoid the active long-life isotopes produced by irradiation of tantalum. Otherwise, its properties are the same as Type 347 (12)(13)(14)(15).

1.01 Commercial Designation

Wrought: Type 347 and Type 348 stainless steel.
Cast: CF-8C.

1.02 Alternate Designations

Type 347H and Type 348H (15), UNS S34700 and S34800.

1.03 Specifications

Table 1.03.

1.04 Composition

Table 1.04.

1.05 Heat Treatment

1.051 Anneal or solution treatment: 1800 to 2050F, one-half hour minimum, air cool or water quench. This treatment results in maximum ductility and workability and minimum hardness (1)(2)(12)(13)(14). Highly reducing annealing atmospheres should be avoided (15).

1.052 Stabilization: 1550F to 1650F, two hours, air cool or water quench. When service temperatures are to be between 800 and 1600F, this treatment is often used after annealing to assure the maximum random precipitation of columbium carbides and to minimize the possibility of chromium carbides precipitating during service (12)(13).

1.053 Stress relief or process anneal: 1300F, air cool. This treatment, or alternatively a full anneal, is used between stages or after severe cold work (12)(14).

1.06 Hardness

1.061 Hardness of various forms, Table 1.061.

1.062 Effects of exposures of 1000 and 10,000 hours to elevated temperatures on room-temperature hardness, Figure 1.062.

1.063 Effect of cold rolling on hardness of strip, Figure 1.063.

1.064 Effects of elevated temperatures on hardness, Figure 1.064.

1.07 Forms and Conditions Available

Table 1.07.

1.08 Melting and Casting Practice

1.081 Normally air melted in electric-arc furnaces or induction furnaces. For applications requiring exceptional quality, it can be vacuum remelted in consumable-electrode or induction furnaces.

1.09 Special Considerations

1.091 Although the alloy is resistant to sensitization and associated intergranular-corrosion, its general corrosion resistance is lowered slightly by prolonged exposures in the sensitization range of 800 to 1600F (14)(15).

1.092 Heating to temperatures of 2100F and above causes excessive grain growth.

1.0921 Effects of time and temperature on grain growth, Figure 1.0921.

1.093 Prolonged exposures at temperatures between 900 and 1500F can significantly reduce room-temperature ductility and notched impact strength, See Figures 3.0214, 3.0215 and 3.0231.

1.094 A selenium-bearing modification of Type 347 is offered by some producers because it provides markedly improved machinability. However, the selenium addition causes some loss in transverse ductility, weldability and corrosion resistance. Careful consideration is necessary, therefore, before attempting to substitute the selenium grade for Type 347 (12).

1.095 The ductility of Type 347 tends to decrease drastically while strength increases when it is exposed to neutron irradiation (See Tables 2.0411, 2.0412 and 2.0413).

1.096 The fatigue life of Type 347 decreases markedly with increasing surface roughness, particularly at cryogenic temperatures (See Figure 3.052).

2. PHYSICAL AND CHEMICAL PROPERTIES

2.01 Thermal Properties

2.011 Melting range, 2550 - 2600F (12)(14)(21).

2.012 Phase changes.

2.0121 Time-temperature-transformation diagrams. In the annealed condition Type 347 and 348 consist primarily of austenitic with randomly distributed carbides of columbium and tantalum. Small amounts of ferrite may or may not be present. Small amounts of sigma phase will form during long exposure in the 1100 to 1500F temperature range. Additional ferrite tends to form during cold work. These phases are stable up to the annealing temperature range at which temperatures all of the phases tend to dissolve into the austenite (14).

2.013 Thermal conductivity, Figure 2.013.

2.014 Thermal expansion, Figure 2.014.

2.015 Specific heat, Figure 2.015.

2.016 Thermal diffusivity, Figure 2.016.

2.02 Other Physical Properties

2.021 Density, Figure 2.021.

2.022 Electrical properties, Table 2.022.

2.023 Magnetic properties.

2.0231 Magnetic permeability in the annealed and cold-worked conditions, Table 2.0231.

2.024 Emittance.

2.0241 Emittance of oxidized sheet, Figure 2.0241.

2.025 Damping capacity.

2.03 Chemical Environment

2.031 Types 347 and 348 have good scaling resistance in air at temperatures up to 1600F, but scaling can be appreciable at higher temperatures (12)(13).

2.0311 Loss of weight caused by oxidation of 0.031 inch thick sheet exposed to cycles of 15 minutes at 1800F and 5 minutes in room temperature air, Figure 2.0311.

2.032 These steels are resistant to ordinary rusting and are immune to all foodstuffs, sterilizing solutions, most organic chemicals and dyes and a wide variety of inorganic chemicals. They are highly resistant to nitric acid, but are readily attacked by halogen acids and moderately attacked by sulfuric acid (13).

2.033 Types 347 and 348 are susceptible to pitting and crevice corrosion in sea water, expecially near the ocean surface. At increasing depths, susceptibility decreases, but varying amounts of corrosion, particularly the crevice type, can occur at all depths. For these reasons, these alloys as well as most other stainless grades, are not recommended for long-time applications in sea water. If they must be used in sea water for any reason, an inert coating or anodic protection should be used (30).

2.034 Type 347 is susceptible to pitting corrosion and to stress

	Fe
18	Cr
12	Ni
+	Cb

TYPES 347,348

corrosion in marine atmospheric environments such as sea shores and aboard ship. Zinc-rich and aluminum-rich coatings are effective in preventing or retarding corrosion; surface treatments, such as electro-polishing and chemical passivation are less effective (32).

2.035 Type 347, both in the annealed and as-welded conditions, is compatible with rocket propellants, such as nitrogen tetroxide, monomethyl-hydrazine, chlorine trifluoride and perchloryl fluoride, at temperatures up to at least 125 to 150F; but the presence of 100 ppm moisture significantly increases corrosion (44).

2.036 Type 347 resists hot corrosion in contact with the products of combustion of gas turbine engines at temperatures up to 1300F, but hot corrosion damage increases rapidly as temperature is increased above 1300F (46).

2.037 Type 347 is not susceptible to stress-corrosion cracking in oxygenated high-temperature water at temperatures up to 550F (52).

2.038 It is not attacked by liquid sodium (53).

2.039 In a hydrogen environment at 5000 psig at temperatures from -260F to 1250F, its mechanical properties are the same as in air (55).

2.0310 Type 347 is highly resistant to attack by liquid fluorine (56).

2.04 Nuclear Environment

2.041 Neutron irradiation increases the tensile strength and reduces the ductility of Types 347 and 348, but the effects, particularly on strength properties, tend to decrease with increasing irradiation temperature and with increasing test temperature. The irradiation-induced property changes can normally be eliminated with a full anneal except for an embrittling type of damage that is sometimes exhibited at high test temperatures after large neutron irradiation doses (See Table 2.0412). The mechanism of this type of radiation embrittlement is not known, although some investigators attribute it to the formation of helium bubbles at grain boundaries when the irradiated metal is deformed at high temperatures (48)(49)(50).

2.0411 Effects of small doses of fast neutron irradiation on tensile properties at elevated temperatures, Table 2.0411.

2.0412 Effects of large doses of fast neutron irradiation on tensile properties at room and elevated temperatures, Table 2.0412.

2.0413 Effects of neutron irradiation, irradiation temperature and test temperature on tensile properties, Table 2.0413.

2.0414 Effects of fast neutron irradiation and annealing on stress-strain curves, Figure 2.0414.

2.042 Effects of temperature and fast neutron irradiation on impact properties, Figure 2.042.

2.043 Effects of fast neutron irradiation on fatigue life as a function of cyclic total strain and plastic strain, Figure 2.043.

2.044 Effects of nuclear irradiation on fatigue life at 550F in dry air, water vapor and vacuum, Figure 2.044.

3. MECHANICAL PROPERTIES

3.01 Specified Mechanical Properties
Table 3.01.

3.02 Mechanical Properties at Room Temperature

3.021 Tension-stress-strain diagrams-tension properties.

3.0211 Stress-strain curves: See Figures 3.0311, 3.0312, 3.0313, 3.0314 and 3.0316.

3.0212 Tensile properties of various forms at room temperature, Table 3.0212.

3.0213 Room-temperature properties of extrusions, Table 3.0213.

3.0214 Effects of exposures of 100,000 hours to elevated temperatures on room-temperature tensile properties of bar, Figure 3.0214.

3.0215 Effects of exposures of 10,000 hours to elevated temperatures on room-temperature tensile properties of sheet, forgings and plate, Figure 3.0215.

3.0216 Effects of cold work on tensile properties of sheet, Figure 3.0216.

3.0217 Effects of carburizing on room-temperature tensile properties, Figure 3.0217.

3.022 Compression-stress-strain diagrams-compression properties.

3.0221 Stress-strain curve: See Figure 3.0321.

3.023 Impact.

3.0231 Effects of exposures of 1000 and 10,000 hours to elevated temperatures on room-temperature impact properties, Figure 3.0231.

3.024 Bending.

3.025 Torsion and shear.

3.0251 Fsu = 53.3 ksi (57).

3.026 Bearing.

3.027 Stress concentration.

3.0271 Notch properties (See Figure 3.03711).

3.0272 Fracture toughness.

3.028 Combined properties.

3.03 Mechanical Properties at Various Temperatures

3.031 Tension-stress-strain diagrams-tension properties.

3.0311 Stress-strain curves for sheet at room-temperature and at low temperatures, Figure 3.0311.

3.0312 Stress-strain curves for sheet at room-temperature and elevated temperatures, Figure 3.0312.

3.0313 Complete engineering stress-strain curves at room temperature and low temperatures, Figure 3.0313.

3.0314 Complete engineering stress-strain curves at room temperature and elevated temperatures, Figure 3.0314.

3.0315 Complete engineering stress-strain curves for Type 348 bar at elevated temperatures at two strain rates, Figure 3.0315.

3.0316 Complete true stress-true strain curves for bar from room temperature to -452F, Figure 3.0316.

3.0317 Complete true stress-true strain curves for Type 348 bar at elevated temperatures at two strain rates, Figure 3.0317.

3.0318 Effects of elevated temperatures on tensile properties of bar, sheet and tube, Figure 3.0318.

3.0319 Low-temperature tensile properties of annealed and cold-worked bar, Figure 3.0319.

3.03110 Low-temperature tensile properties of sheet, Figure 3.03110.

3.03111 Effects of low temperatures on tensile properties of sand castings, Figure 3.03111.

3.03112 Effects of low temperatures on tensile properties of investment castings, Figure 3.03112.

3.03113 Effects of elevated temperatures on tensile properties of investment castings, Figure 3.03113.

3.03114 Effects of annealing temperatures and test temperatures on tensile properties of cold-worked bar, Figure 3.03114.

3.032 Compression-stress-strain diagrams-compression properties.

3.0321 Stress-strain curves in compression for sheet at room temperature and 1000F, Figure 3.0321.

3.033 Impact.

3.0331 Effects of low temperatures on impact properties, Figure 3.0331.

3.034 Bending.

3.035 Torsion and shear.

3.036 Bearing.

3.037 Stress concentration.

3.0371 Notch properties.

3.03711 Low-temperature notched tensile properties, Figure 3.03711.

3.0372 Fracture toughness.

3.038 Combined properties.

3.04 Creep and Creep Rupture Properties

3.041 Creep-rupture curves for tube, Figure 3.041.

3.042 Creep-rupture curves for bar, Figure 3.042.

3.043 Effects of temperature on 1000 hour and 10,000 hour creep-rupture strength of bar, Figure 3.043.

3.044 Effects on creep-rupture strength of exposures of 100,000 hours at test temperature prior to testing, Figure 3.044.

3.045 Effects of temperature on creep-rupture strength of castings, Figure 3.045.

3.046 Total creep-strain curves for sheet at 1200 to 1600F, Figure 3.046.

3.047 Short-time total creep-strain curves at 1200 to 1800F, Figure 3.047.

3.05 Fatigue Properties

3.051 Fatigue life of notched and unnotched sheet, Figure 3.051.

3.052 Effects of surface finish and low temperatures on fatigue life of sheet, Figure 3.052.

3.053 Effects of low temperatures on fatigue life of sheet, Figure 3.053.

3.054 Fatigue crack growth rate as a function of stress-intensity factor range at various temperatures, Figure 3.054.

3.06 Elastic Properties

3.061 Poisson's ratio.

3.0611 Effects of elevated temperatures on Poisson's ratio, Figure 3.0611.

3.062 Modulus of elasticity.

3.0621 Effects of elevated temperatures on modulus of elasticity, Figure 3.0621.

3.063 Modulus of rigidity.

3.0631 Effects of elevated temperatures on modulus of rigidity, Figure 3.0631.

3.064 Tangent modulus.

3.0641 Tangent modulus curves in compression for sheet at room temperature and 1000F, Figure 3.0641.

3.065 Secant modulus.

4. FABRICATION

4.01 Forming

4.011 Because of their excellent ductility and toughness, annealed Types 347 and 348 can be cold worked by most of the common forming methods including deep drawing, bending and upsetting. Since they work harden rather rapidly, intermediate full or process anneals may be necessary. Cold forming, in addition to increasing strength and reducing ductility, tends to transform some of the austenite structure from austenite to ferrite resulting in increased magentic permeability. All of these effects can best be removed by a full anneal (12)(13).

4.012 The alloys can be readily hot worked by any of the conventional methods such as forging, rolling, extrusion, hot heading, upsetting, etc., but more power for a given reduction is required than for mild steel. Hot working should be started in the temperature range of 2100 to 2300F and finished above 1700F. High-sulfur fuels and strongly reducing atmospheres should be avoided (12)(13)(15).

4.02 Machining and Grinding

4.021 The machinability is the same as for Type 321, Code 1308, Section 4.021.

4.03 Joining.

4.031 Types 347 and 348 are weldable by most commercial methods including electric-arc, oxyacetylene, resistance and electron beam, but there is danger of cracking in heavy-section weldments. For the electric-arc techniques, Type 347 electrodes are recommended. Since the alloys are stabilized, no post anneal is necessary, but for complicated weldments stress relief is sometimes desirable (12)(13).

4.0311 Comparison of complete true stress-true strain curves of plate and of weld metal after plate had been butt welded with Type 347 coated stick electrodes, Figure 4.0311.

4.0312 Low-temperature tensile and notched tensile properties of plate butt welded with Type 347 coated stick electrodes, Figure 4.0312.

4.0313 Low-temperature impact properties of plate butt welded with Type 347 stick electrodes, Figure 4.0313.

4.0314 Effects of low temperatures and post-weld heat treatment on impact properties of weld metal deposited from coated stick electrodes, Figure 4.0314.

4.032 Brazing: See Type 321, Code 1308, Section 4.032.

4.04 Surface Treatment

4.041 Same as for Type 321, Code 1308, Section 4.041 and 4.042.

Alloy	347 - 348					
Source	(15)(51)					
AMS	ASTM	Military	Federal	AISI	SAE	ACI
5362	A167	MIL-E-16715	QQ-S-763	347	30347	CF-8C
5363	A182	MIL-E-19933	QQ-S-766	348	30348	
5512	A193	MIL-R-5031				
5556	A194	MIL-S-862				
5558	A213	MIL-S-6721				
5571	A240	MIL-S-17509				
5575	A249	MIL-S-18170				
5646	A264	MIL-S-23195				
5654	A269	MIL-S-23196				
5674	A271	MIL-T-6737				
5680	A276	MIL-T-8606				
5681	A296	MIL-T-8808				
7229	A312	MIL-P-1144				
	A314	MIL-S-81591				
	A320	MIL-S-867				
	A358	MIL-S-18171				
	A376					
	A409					
	A430					
	A473					
	A479					
	A493					
	A511					
	A580					
	A632					

TABLE 1.03 SPECIFICATIONS

	Fe
18	Cr
12	Ni
+	Cb

TYPES 347,348

Alloy	347 - 348			
Form	Bars, Tube, Forgings, Wire, Sheet, Strip, Plate		Castings	
Source	AMS 5512E, 5558B, 5575H, 5646F, 5674A		AMS 5363B	
	min.	max.	min	max.
Carbon	--	0.08	--	0.10
Manganese	--	2.00	--	2.0
Silicon	--(a)	1.00	--	1.5
Phosphorus	--	0.040(b)	--	0.04
Sulfur	--	0.030(b)	--	0.04
Chromium	17.00	19.00	17.0	20.0
Nickel	9.00	12.00	9.0	12.0
Columbium plus Tantalum	10 x C	1.10(c)	10 x C	1.35
Molybdenum	--	0.75	--	0.50
Copper	--	0.50	--	0.50

(a) AMS 5512E and 5558B require 0.50 min. Si.
(b) AMS 5654A, covering consumable-electrode-melted material, requires 0.020 max. S and P.
(c) Type 348 specifies a maximum Tantalum content of 0.10 percent; otherwise it is the same as Type 347.
In the many specifications covering this alloy there are minor variations in composition.

TABLE 1.04 COMPOSITION.

	Fe
18	Cr
12	Ni
+	Cb

TYPES 347,348

Alloy	347		
Condition	Annealed		
Form	Source	Hardness BHN	Hardness Rb
Bar	(12)	160	--
Bar	(13)	150	--
Bar - plate	(14)	228	--
Bar - plate	(20)	160	--
Sheet - strip	(14)	--	90
Sheet - strip	(12)(20)	--	85
Cast	(21)	149	--

TABLE 1.061 HARDNESS OF VARIOUS FORMS.

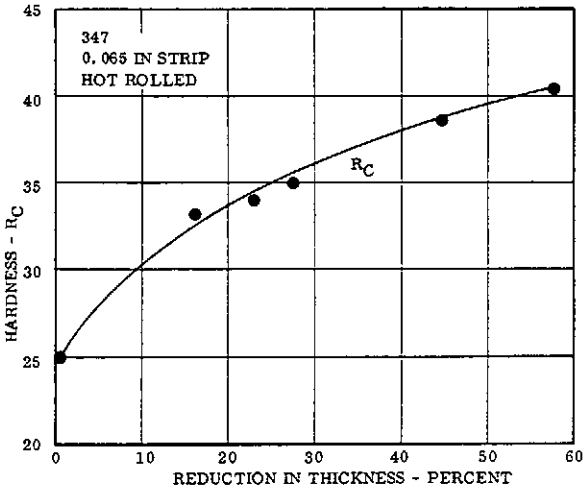


FIG. 1.063 EFFECT OF COLD ROLLING ON HARDNESS OF STRIP. (40)

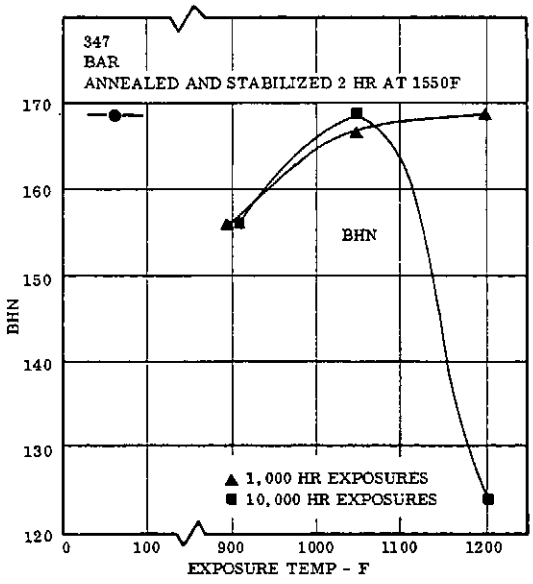


FIG. 1.062 EFFECTS OF EXPOSURES OF 1,000 AND 10,000 HOURS TO ELEVATED TEMPERATURES ON ROOM-TEMPERATURE HARDNESS. (27)

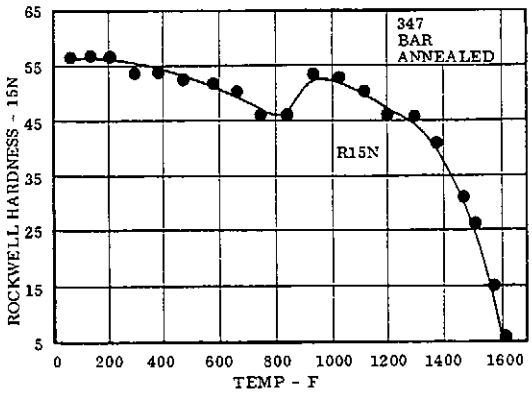


FIG. 1.064 EFFECTS OF ELEVATED TEMPERATURES ON HARDNESS. (15)

Alloy	347
Source	(13)(14)
Forms	Conditions
Forgings	Annealed
Castings	Annealed
Tube and pipe	Annealed
Bars	Annealed or cold drawn
Sheet and strip	Annealed or temper rolled up to 1/2 hard
Wire	Annealed or cold drawn to specified temper
Wire rod	Annealed
Plate	Annealed

TABLE 1.07 FORMS AND CONDITIONS AVAILABLE.

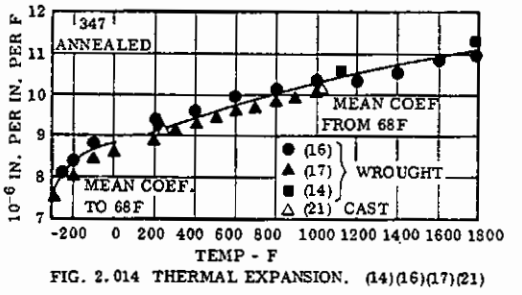


FIG. 2.014 THERMAL EXPANSION. (14)(16)(17)(21)

Fe
18 Cr
12 Ni
+ Cb

TYPES 347,348

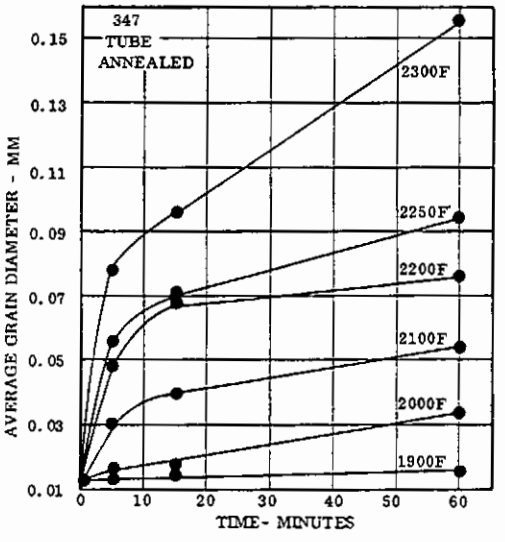


FIG. 1.0921 EFFECT OF TIME AND TEMPERATURE ON GRAIN GROWTH. (29)

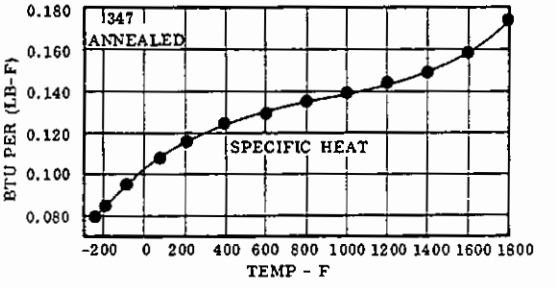


FIG. 2.015 SPECIFIC HEAT. (16)

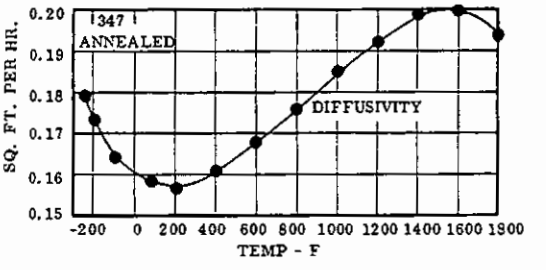


FIG. 2.016 THERMAL DIFFUSIVITY. (16)

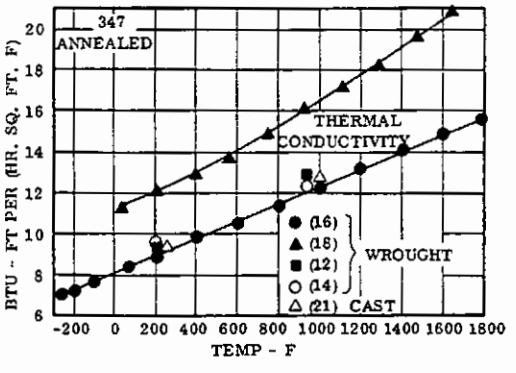


FIG. 2.013 THERMAL CONDUCTIVITY. (12)(14)(16)(18)(21)

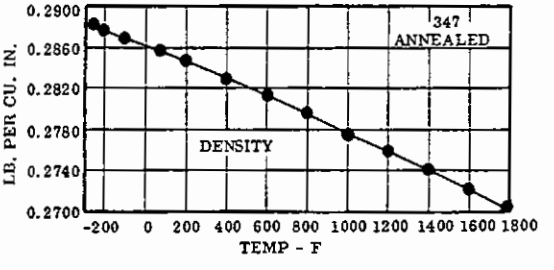


FIG. 2.021 DENSITY. (16)

Fe
18 Cr
12 Ni
+ Cb

TYPES 347,348

Alloy	347		
Condition	Annealed		
Source	(14)		
Temp. F	Electrical Conductivity percent IACS	Electrical Conductivity megmhos per in^3	Electrical Resistivity microhm-in
68	2.40	0.0353	28.3
212	2.22	0.0326	30.7
392	2.01	0.0296	33.8
752	1.73	0.0254	39.4
1112	1.56	0.0229	43.7
1472	1.43	0.0210	47.6
1652	1.37	0.0202	49.6

TABLE 2.022 ELECTRICAL PROPERTIES.

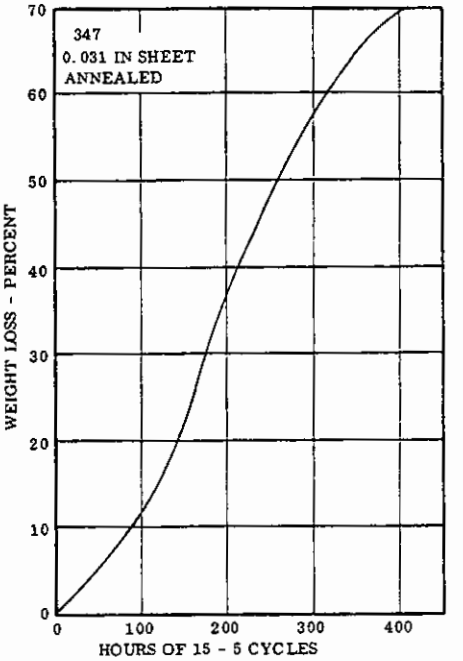


FIG. 2.0311 LOSS OF WEIGHT CAUSED BY OXIDATION OF 0.031 IN THICK SHEET EXPOSED TO CYCLES OF 15 MIN AT 1800F AND 5 MIN IN ROOM-TEMPERATURE AIR. (26)

Alloy	347	
Form	Sheet	
Source	(20)(21)	
Cold reduction precent	Magnetic Permeability at H = 50	at H = 200
0 (wrought, annealed)	1.0037	1.0044
13.5	1.0074	1.0088
40	1.062	1.088
60	1.245	1.445
90	1.97	4.12
0 (cast, annealed)	1.2	1.8

TABLE 2.0231 MAGENTIC PERMEABILITY IN THE ANNEALED AND COLD-WORKED CONDITIONS.

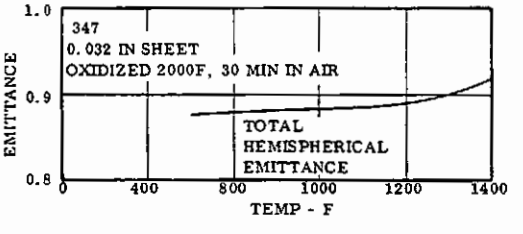


FIG. 2.0241 EMITTANCE OF OXIDIZED SHEET. (54)

	Fe
18	Cr
12	Ni
+	Cb

TYPES 347,348

Alloy	347				
Form	Tube				
Source	(38)				
Condition prior to neutron exposure	Test Temp. F	Neutron Fluence at 1000 to 1300F, 10^{21} n/cm^2 (E>1 Mev)	F_{TY} ksi	F_{TU} ksi	e (1 in) percent
Annealed	75	unexposed	30.3	80.2	40
	1100	unexposed	23.5	46.2	26
	1300	unexposed	--	36.4	38
Annealed	1100	6.2	61.1	62.4	2.4
	1300	1.3	33.4	40.0	7.1
	1300	6.2	43.8	44.2	1.4
	1500	6.2	18.2	18.8	4.3
Annealed and exposed 24 hour at 1650F	1100	2.5	40.5	47.9	10.0
	1300	0.22	22.9	31.8	29.4
	1300	0.76	25.5	31.1	7.5
	1300	3.0	21.7	29.6	11.1
	1500	2.4	13.1	15.6	9.6

TABLE 2.0411 EFFECTS OF SMALL DOSES OF FAST NEUTRON IRRADIATION ON TENSILE PROPERTIES AT ELEVATED TEMPERATURES.

Alloy	347					
Form	Bar					
Condition	Annealed before irradiation					
Source	(48)					
Test Temp. F	Neutron Fluence 10^{21} n/cm^2 (>1 Mev)		F_{TY} ksi	F_{TU} ksi	e (4D) percent	RA percent
70	0		36.9	90.2	64.0	74.0
	5.5		109	112	32.7	70.0
	16		113	113	33.5	74.5
	21		113	113	34.5	67.2
	16	(a)	32.3	84.8	56.6	66.3
600	0		26.8	64.2	36.0	--
	5.5		82.5	84.0	16.3	60.0
	16		84.9	85.2	13.8	59.4
	21		86.0	86.0	10.2	56.8
	16	(a)	20.2	58.2	32.6	55.5
	21	(a)	33.0	61.0	32.6	--
1380	0		22.0	25.5	26.0	--
	21		35.0	35.0	0.5	0
	21	(a)	32.0	32.2	0.6	0
	21	(b)	19.0	20.2	0.5	0

(a) Annealed 1 hour, 1800F after irradiation.
(b) Annealed 1 hour, 2450F after irradiation.

TABLE 2.0412 EFFECTS OF LARGE DOSES OF FAST NEUTRON IRRADIATION ON TENSILE PROPERTIES AT ROOM AND ELEVATED TEMPERATURES.

Fe
18 Cr
12 Ni
+ Cb

TYPES 347,348

Alloy	347
Form	Rod
Condition	Annealed and Cold Worked 10 percent
Source	(50)

	Irradiated 7×10^{20} nvt (fast) and 9×10^{20} (thermal)				Unirradiated			
Test Temp. F	Irrad. Temp. F(a)	F_{TY} ksi	F_{TU} ksi	e (4D) percent	Exposure Temp. F(a)	F_{TY} ksi	F_{TU} ksi	e (4D) percent
68	320	112.6	117.4	28.0	320	60.2	96.0	45.6
	750	83.2	109.5	30.7	750	53.4	98.3	43.8
	1400	43.1	93.5	45.4	1300	52.0	97.5	48.6
750	320	73.5	76.0	9.8	320	48.8	66.8	23.5
	--	--	--	--	500	46.8	66.3	23.4
	770	31.0	71.5	24.8	750	48.8	67.1	21.0
	1100	27.4	66.7	19.0	1300	39.0	63.0	22.3
1100	320	43.2	59.2	22.0	320	43.1	60.0	23.0
	--	--	--	--	500	43.8	60.1	23.7
	750	45.2	60.4	20.4	750	42.7	60.1	25.1
	1100	44.7	57.8	14.6	1100	43.1	59.4	20.5
1300	415	35.2	38.4	14.9	320	39.0	45.3	25.2
	630	36.4	41.6	12.3	750	36.6	44.3	25.0
	1100	27.4	33.9	15.6	1300	32.5	39.4	34.9

(a) Irradiation required about 2000 hours. The unirradiated specimens were exposed to similar temperatures for the same period of time.

FIG. 2.0413 EFFECTS OF NEUTRON IRRADIATION, IRRADIATION TEMPERATURE AND TEST TEMPERATURE ON TENSILE PROPERTIES.

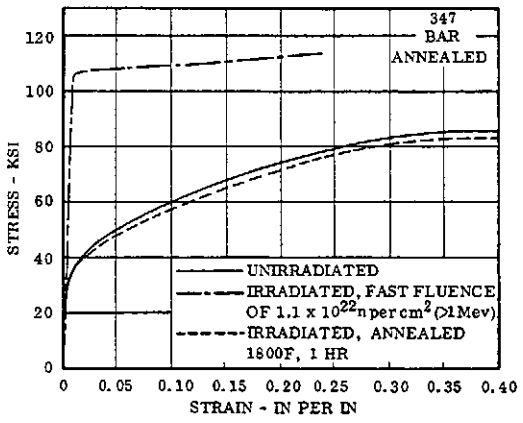


FIG. 2.0414 EFFECTS OF FAST NEUTRON IRRADIATION AND ANNEALING ON STRESS-STRAIN CURVES. (49)

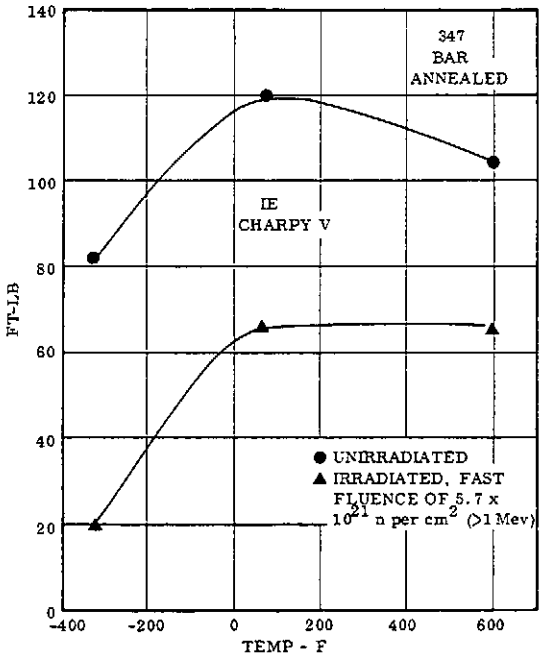


FIG. 2.042 EFFECTS OF TEMPERATURE AND FAST NEUTRON IRRADIATION ON IMPACT PROPERTIES. (48)

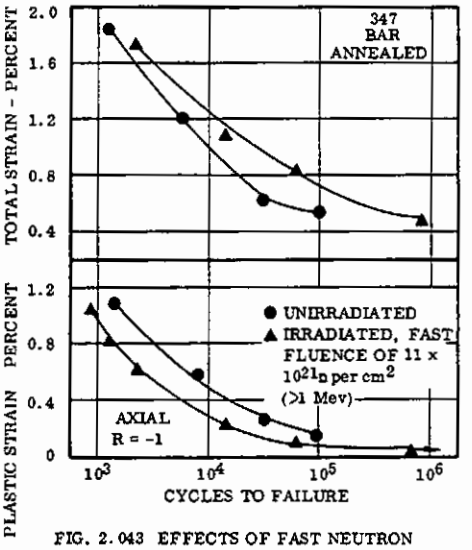


FIG. 2.043 EFFECTS OF FAST NEUTRON IRRADIATION ON FATIGUE LIFE AS A FUNCTION OF CYCLIC TOTAL STRAIN AND PLASTIC STRAIN. (48)

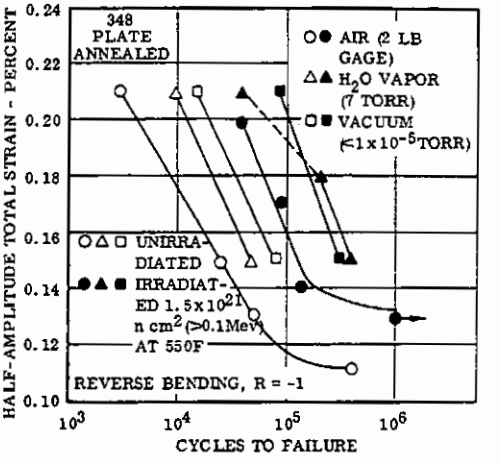


FIG. 2.044 EFFECTS OF NUCLEAR IRRADIATION ON FATIGUE LIFE AT 550F IN DRY AIR, WATER VAPOR AND VACUUM. (35)

	Fe
18	Cr
12	Ni
+	Cb

TYPES 347,348

Alloy	347							
Source	Form	Condition	F_{TY}, ksi min.	F_{TU}, ksi min.	F_{TU}, ksi max.	e (2 in.) min.	BHN min.	BHN max.
AMS 5556C	Tube (hydraulic) up to 0.188 in. OD	Annealed						
	≤0.0161 in. wall		30	75	120	33(a)	--	--
	≥0.016 in. wall		30	75	105	35	--	--
	0.188 to 0.500 in. OD							
	≤0.0101 in. wall		30	75	115	35	--	--
	≥0.010 in. wall		30	75	105	35	--	--
	Over 0.500 in. OD							
	≥0.010 in. wall		30	75	105	35	--	--
AMS 5512E	Sheet, strip, plate 0.002 to 0.003 in. thick	Annealed	--	--	115	20	--	--
	≥0.003 to 0.004 in. thick		--	--	110	30	--	--
	Over 0.004 in. thick		--	--	105	40	--	--
AMS 5646F	Bar	Annealed						
	up to 0.75 in. dia.		--	--	--	--	170	255
	Over 0.75 in. dia.		--	--	--	--	140	241
	Forgings		--	--	--	--	--	187
	Wire		--	85	125	--	--	--
AMS 5363B	Castings	Annealed	--	--	--	--	--	180
AMS 5362E	Investment Castings	Annealed	30	70	--	30	--	175

(a) Tube elongation values pertain to full tube; strip specimens 5 percent lower.

TABLE 3.01 SPECIFIED MECHANICAL PROPERTIES.

	Fe
18	Cr
12	Ni
+	Cb

TYPES 347,348

Alloy	347				
Condition	Annealed				
Form	Source	F_{TY} ksi	F_{TU} ksi	e (2 in) percent	RA percent
Sheet	(12)(20)	40	95	45	--
Plate	(20)	35	90	50	--
Bar	(12)(20)	35	90	50	65
Cast	(21)	38	77	39	--
Forgings	(20)	37	87	66	76

TABLE 3.0212 TENSILE PROPERTIES OF VARIOUS FORMS AT ROOM TEMPERATURE.

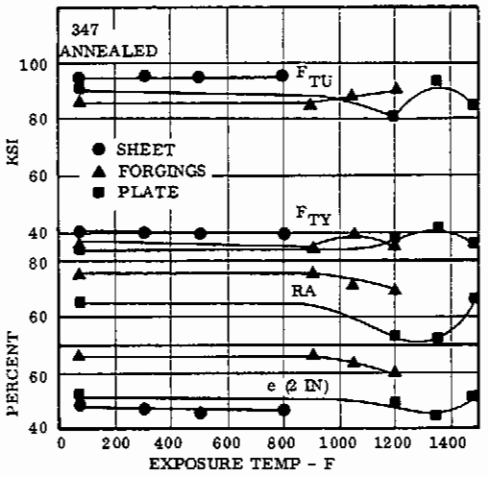


FIG. 3.0215 EFFECTS OF EXPOSURES OF 10,000 HOURS TO ELEVATED TEMPERATURES ON ROOM TEMPERATURE TENSILE PROPERTIES OF SHEET, FORGINGS AND PLATE. (20)

Alloy	347	
Source	(37)	
Form	0.75 in. x 3 1/8 in. extruded flat	
Condition	As hot extruded	
Orientation	L	T
F_{TY}, ksi	28.4	29.4
F_{TU}, ksi	73.1	77.6
e (4D), percent	64	67
RA, percent	78	69

TABLE 3.0213 ROOM TEMPERATURE TENSILE PROPERTIES OF EXTRUSIONS.

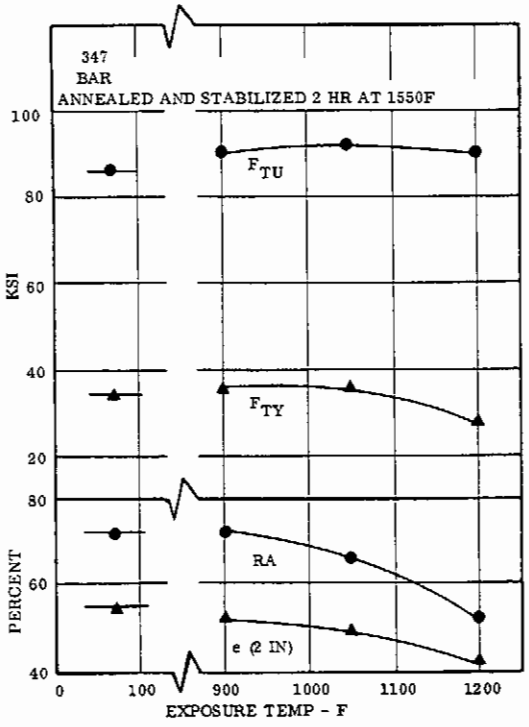


FIG. 3.0214 EFFECTS OF EXPOSURES OF 100,000 HOURS TO ELEVATED TEMPERATURES ON ROOM-TEMPERATURE TENSILE PROPERTIES OF BAR. (15)

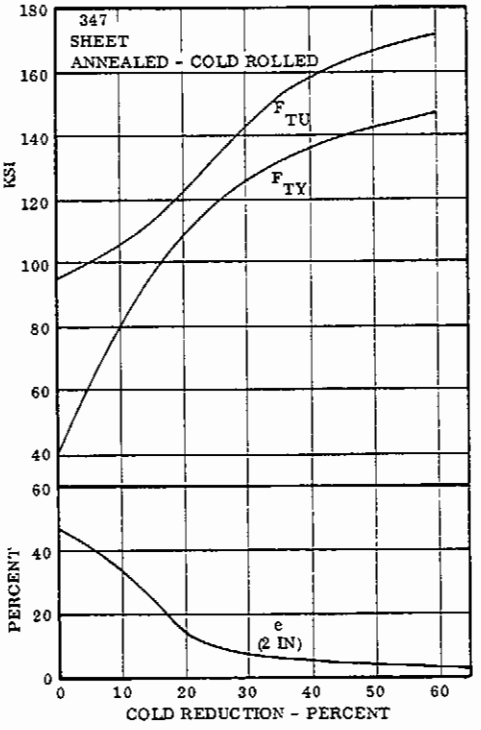


FIG. 3.0216 EFFECTS OF COLD WORK ON TENSILE PROPERTIES OF SHEET. (20)

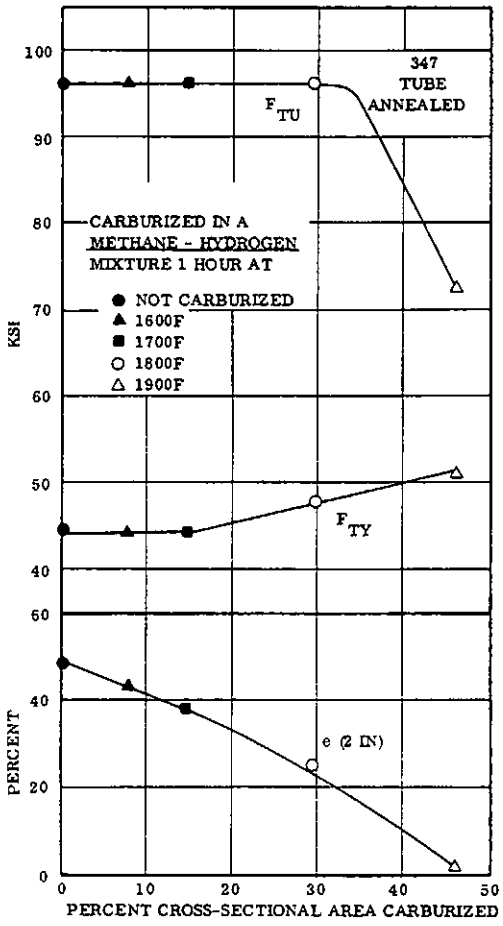
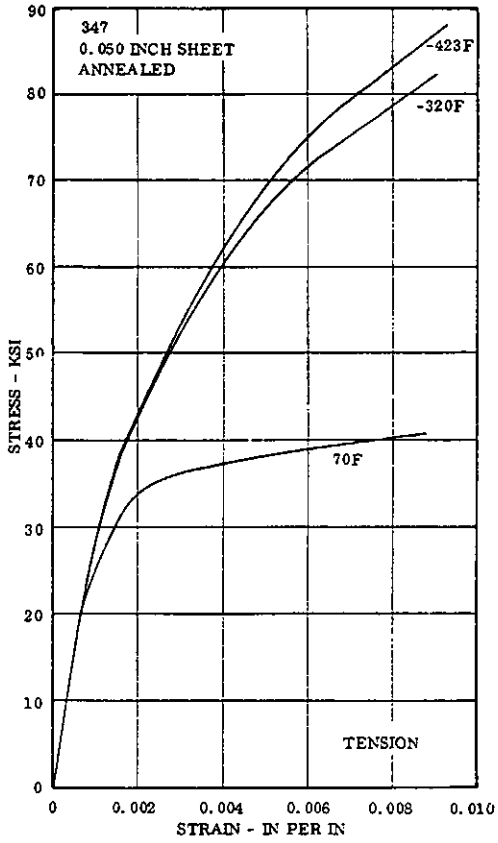


FIG. 3.0217 EFFECTS OF CARBURIZING ON ROOM-TEMPERATURE TENSILE PROPERTIES. (36)



	Fe
18	Cr
12	Ni
+	Cb

TYPES 347,348

FIG. 3.0311 STRESS-STRAIN CURVES FOR SHEET AT ROOM TEMPERATURE AND AT LOW TEMPERATURES. (45)

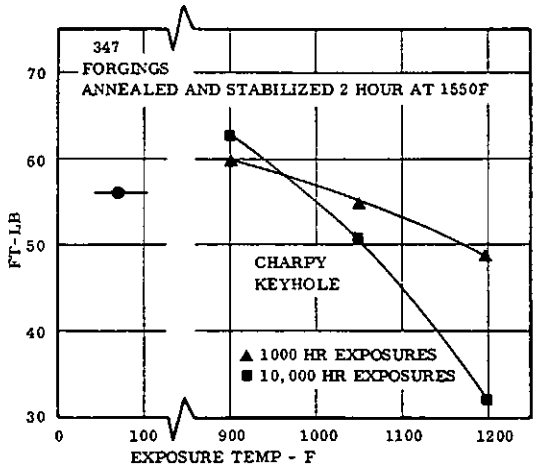


FIG. 3.0231 EFFECTS OF EXPOSURES OF 1000 AND 10,000 HOURS TO ELEVATED TEMPERATURES ON ROOM-TEMPERATURE IMPACT PROPERTIES. (15)(20)

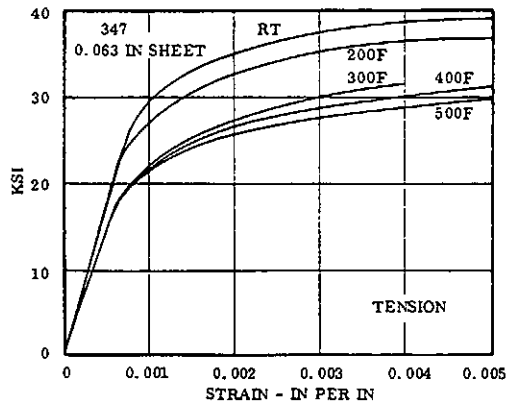


FIG. 3.0312 STRESS-STRAIN CURVES FOR SHEET AT ROOM TEMPERATURE AND ELEVATED TEMPERATURES. (58)

	Fe
18	Cr
12	Ni
+	Cb

TYPES 347,348

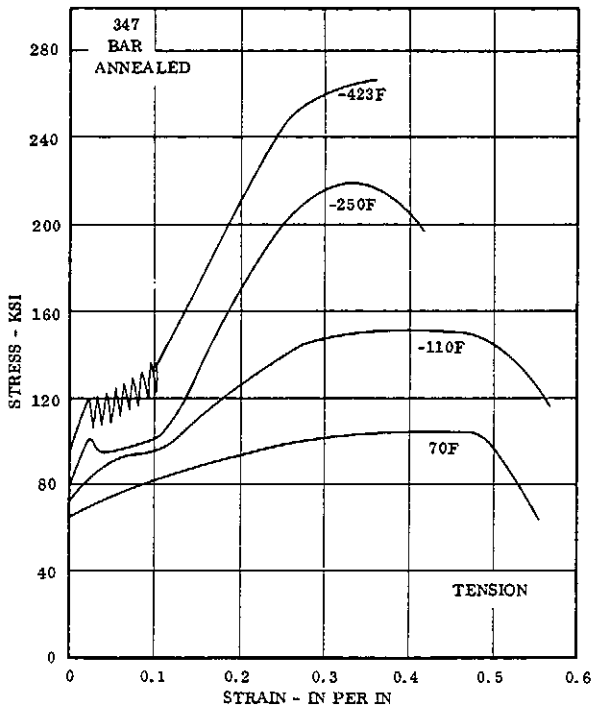


FIG. 3.0313 COMPLETE ENGINEERING STRESS-STRAIN CURVES AT ROOM TEMPERATURE AND LOW TEMPERATURES. (47)

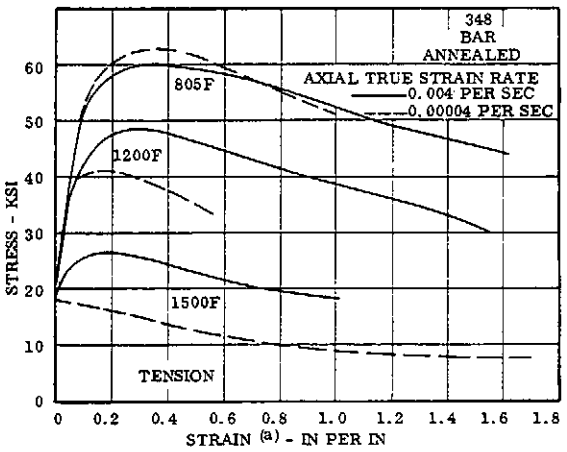


FIG. 3.0315 COMPLETE ENGINEERING STRESS-STRAIN CURVES FOR TYPE 348 BAR AT ELEVATED TEMPERATURES AT TWO STRAIN RATES. (41)

(a) STRAIN VALUES CALCULATED FROM TRUE STRAIN VALUES IN FIG. 3.0317 BY THE FORMULA: E (engineering) = $e^{\epsilon} - 1$ WHERE ϵ IS TRUE ACTUAL STRAIN AND e IS NATURAL LOG BASE.

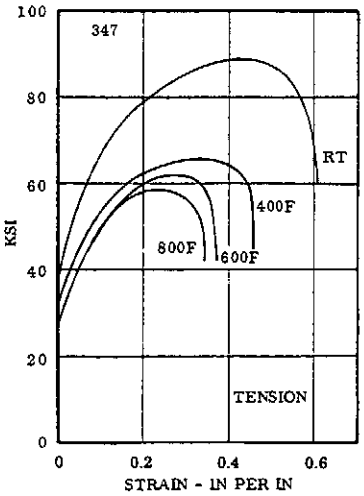


FIG. 3.0314 COMPLETE ENGINEERING STRESS-STRAIN CURVES AT ROOM TEMPERATURE AND ELEVATED TEMPERATURES. (59)

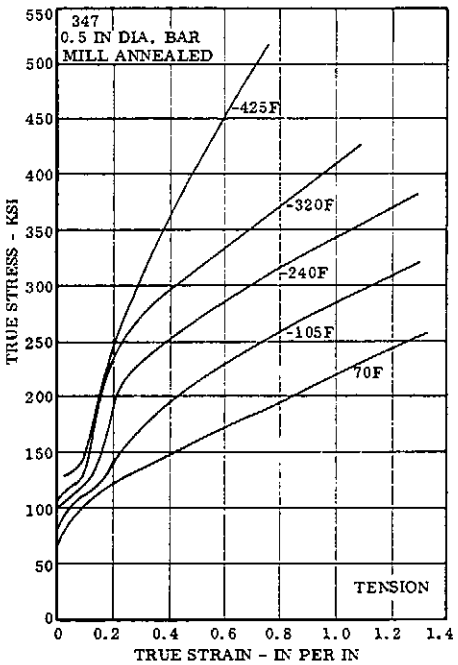


FIG. 3.0316 COMPLETE TRUE STRESS-TRUE STRAIN CURVES FOR BAR FROM ROOM TEMPERATURE TO -425F. (39)

	Fe
18	Cr
12	Ni
+	Cb

TYPES 347,348

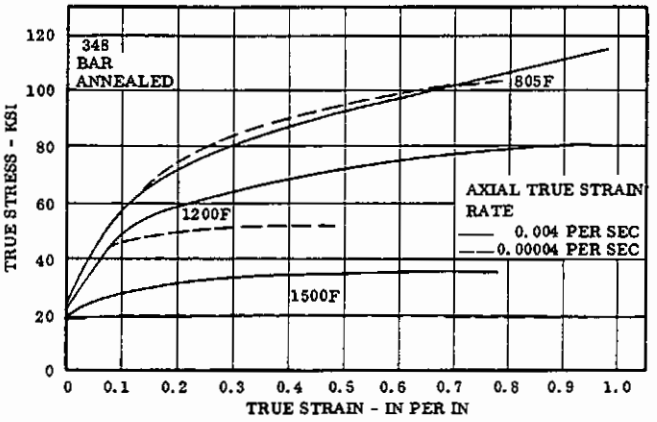


FIG. 3.0317 COMPLETE TRUE STRESS-TRUE STRAIN CURVES FOR TYPE 348 BAR AT ELEVATED TEMPERATURES AT TWO STRAIN RATES. (41)

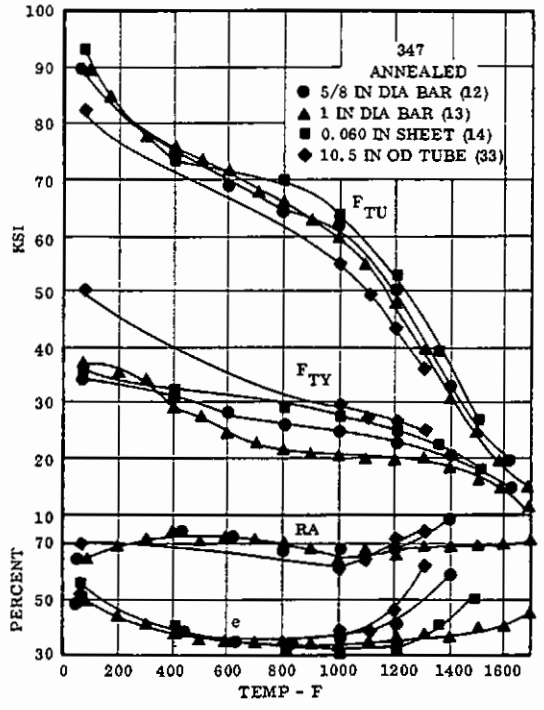


FIG. 3.0318 EFFECTS OF ELEVATED TEMPERATURES ON TENSILE PROPERTIES OF BAR, SHEET AND TUBE. (12)(13)(14)(33)

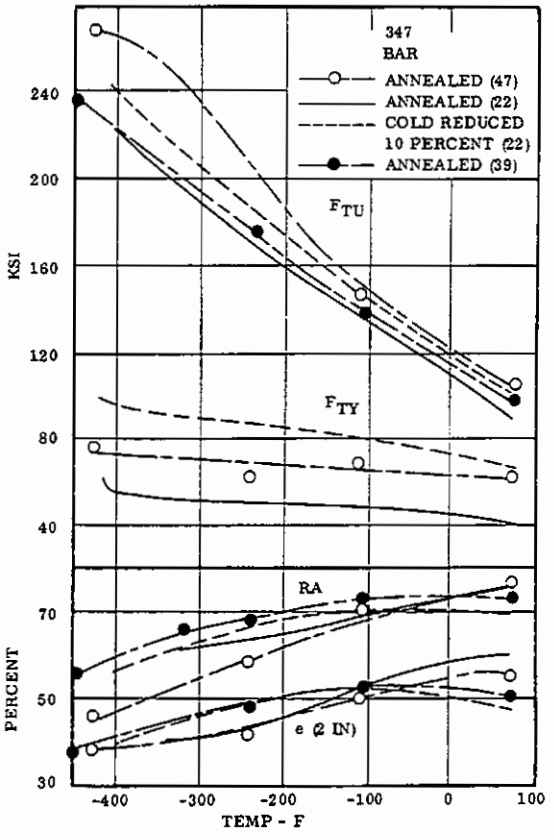


FIG. 3.0319 LOW-TEMPERATURE TENSILE PROPERTIES OF ANNEALED AND COLD-WORKED BAR. (22)(39)(47)

	Fe
18	Cr
12	Ni
+	Cb

TYPES 347,348

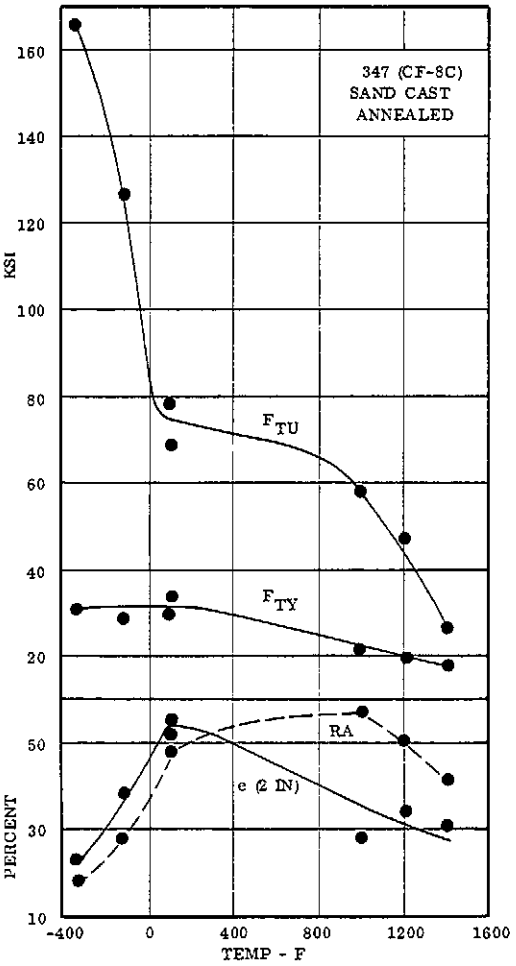


FIG. 3.03111 EFFECTS OF LOW AND ELEVATED TEMPERATURES ON TENSILE PROPERTIES OF SAND CASTINGS. (23)

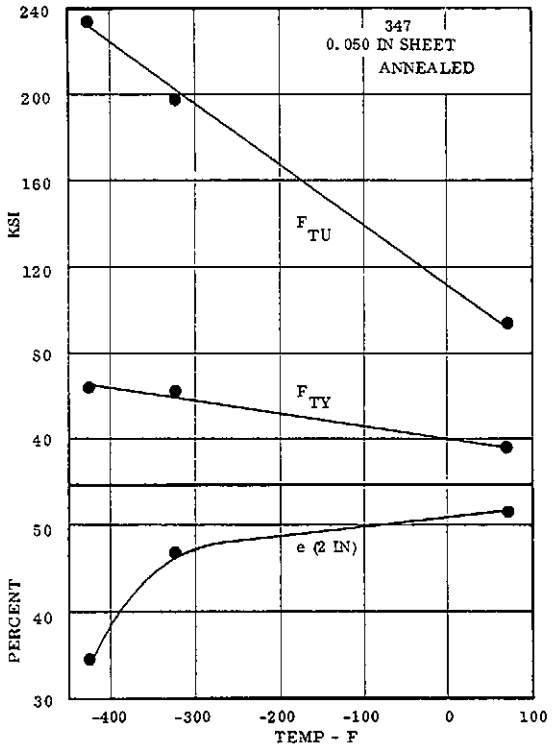


FIG. 3.03110 LOW-TEMPERATURE TENSILE PROPERTIES OF SHEET. (45)

	Fe
18	Cr
12	Ni
+	Cb

TYPES 347,348

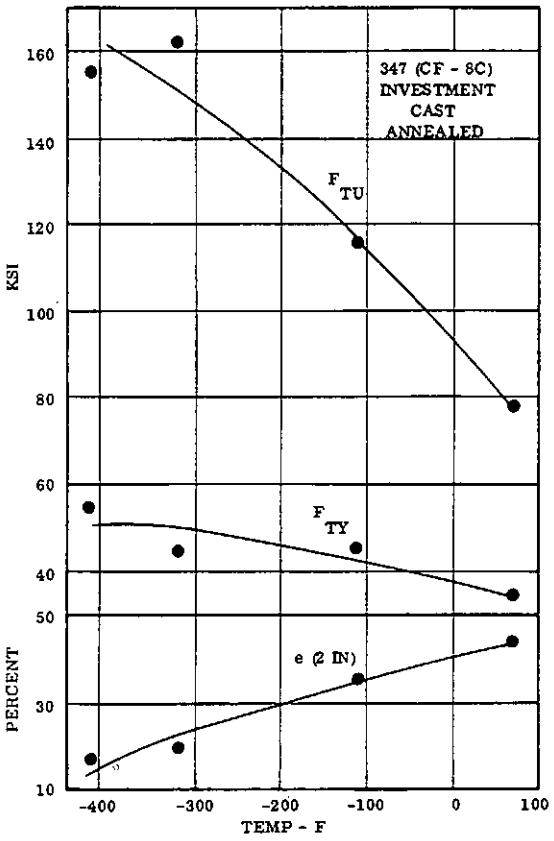


FIG. 3.03112 EFFECTS OF LOW TEMPERATURES ON TENSILE PROPERTIES OF INVESTMENT CASTINGS. (34)

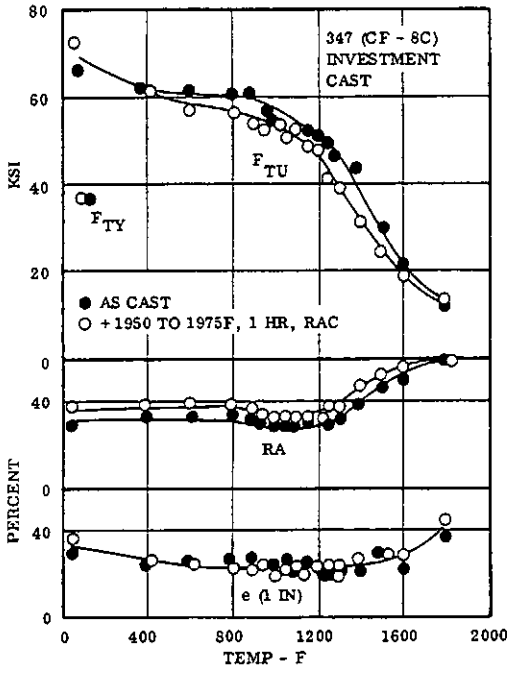


FIG. 3.03113 EFFECTS OF ELEVATED TEMPERATURES ON TENSILE PROPERTIES OF INVESTMENT CASTINGS. (60)

	Fe
18	Cr
12	Ni
+	Cb

TYPES 347,348

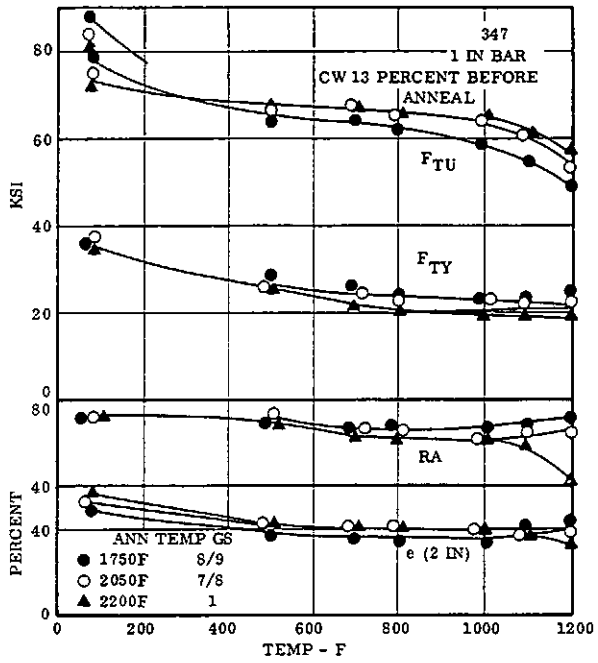


FIG. 3.03114 EFFECTS OF ANNEALING TEMPERATURE AND TEST TEMPERATURE ON TENSILE PROPERTIES OF COLD-WORKED BAR. (61)

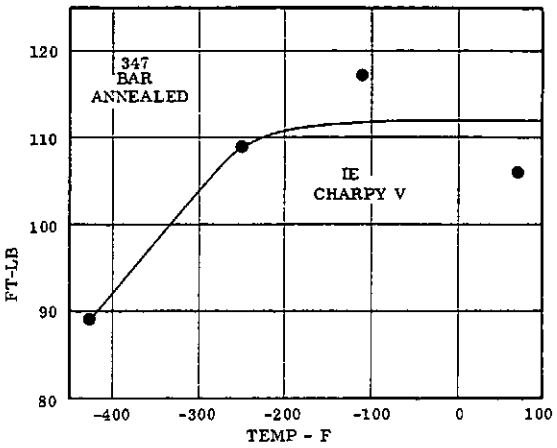


FIG. 3.0331 EFFECTS OF LOW TEMPERATURES ON IMPACT PROPERTIES. (47)

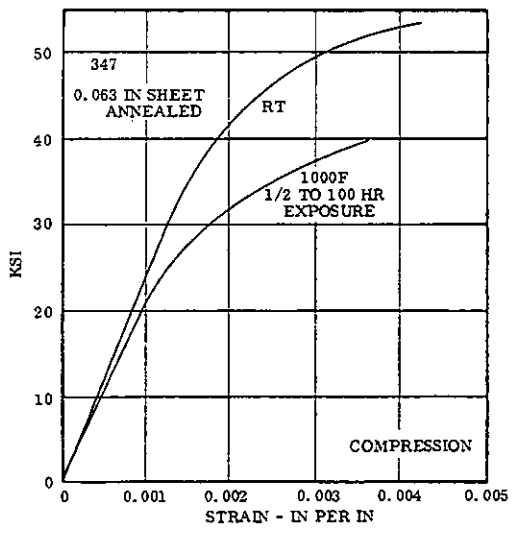


FIG. 3.0321 STRESS-STRAIN CURVES IN COMPRESSION FOR SHEET AT ROOM TEMPERATURE AND 1000F. (62)

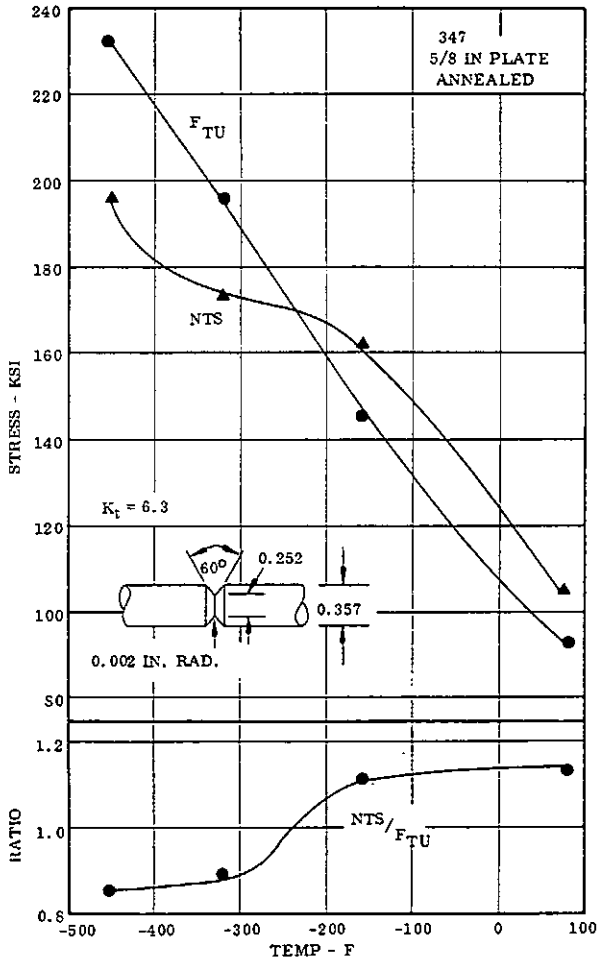


FIG. 3.03711 LOW-TEMPERATURE NOTCHED TENSILE CHARACTERISTICS. (25)

	Fe
18	Cr
12	Ni
+	Cb

TYPES 347,348

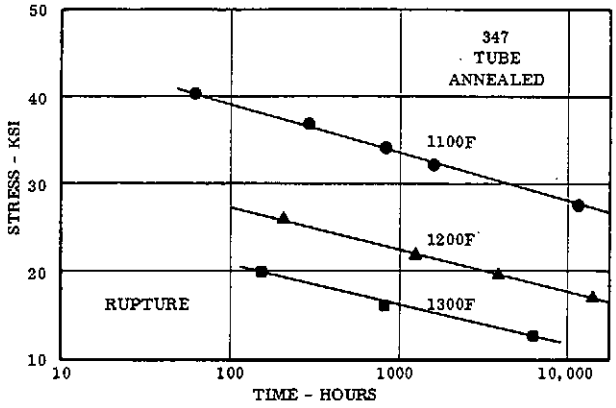


FIG. 3.041 CREEP-RUPTURE CURVES FOR TUBE. (33)

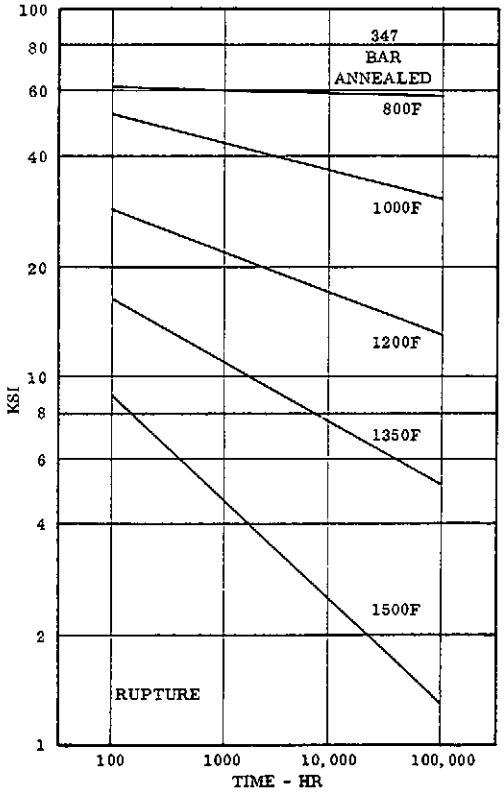


FIG. 3.042 CREEP-RUPTURE CURVES FOR BAR. (63)

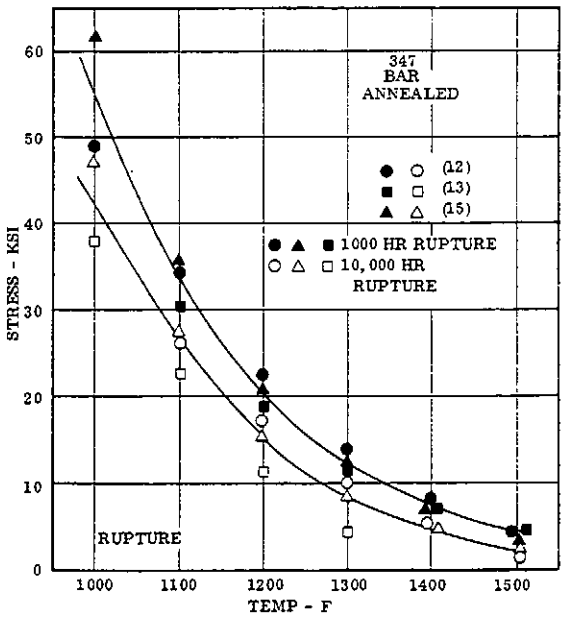


FIG. 3.043 EFFECTS OF TEMPERATURE ON 1000 HOUR AND 10,000 HOUR CREEP-RUPTURE STRENGTH OF BAR. (12)(13)(15)

	Fe
18	Cr
12	Ni
+	Cb

TYPES 347,348

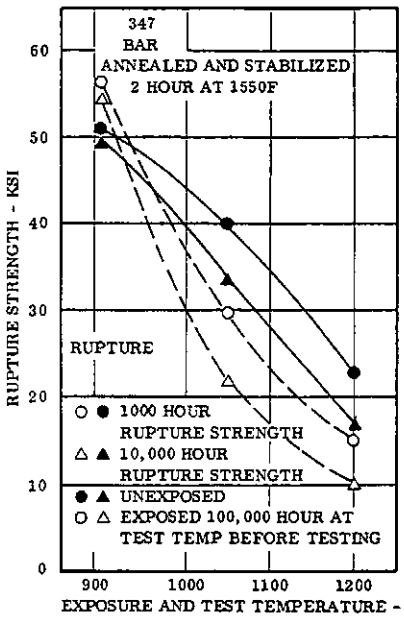


FIG. 3.044 EFFECTS ON CREEP-RUPTURE STRENGTH OF EXPOSURES OF 100,000 HOURS AT TEST TEMPERATURE PRIOR TO TESTING. (15)

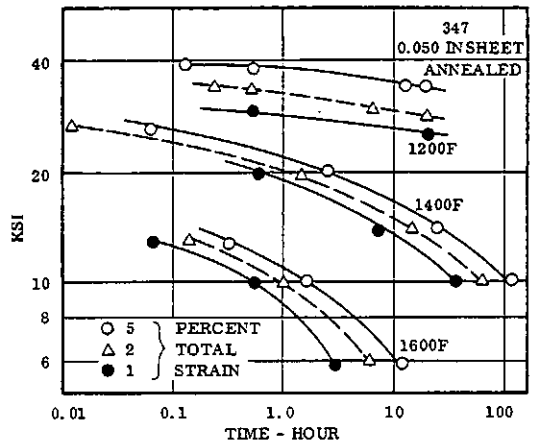


FIG. 3.046 TOTAL CREEP STRAIN CURVES FOR SHEET AT 1200 TO 1600F. (64)

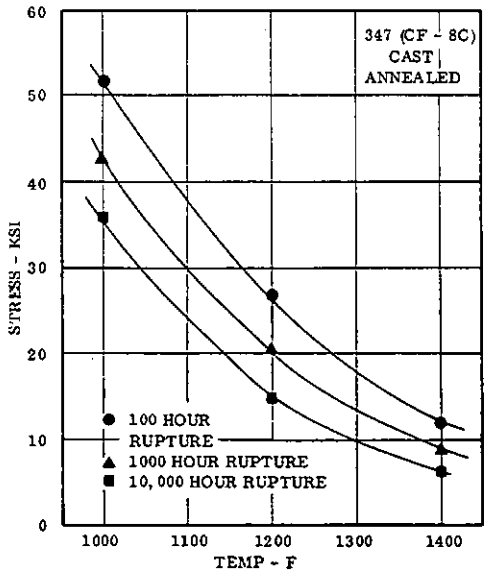


FIG. 3.045 EFFECTS OF TEMPERATURE ON CREEP-RUPTURE STRENGTH OF CASTINGS. (23)

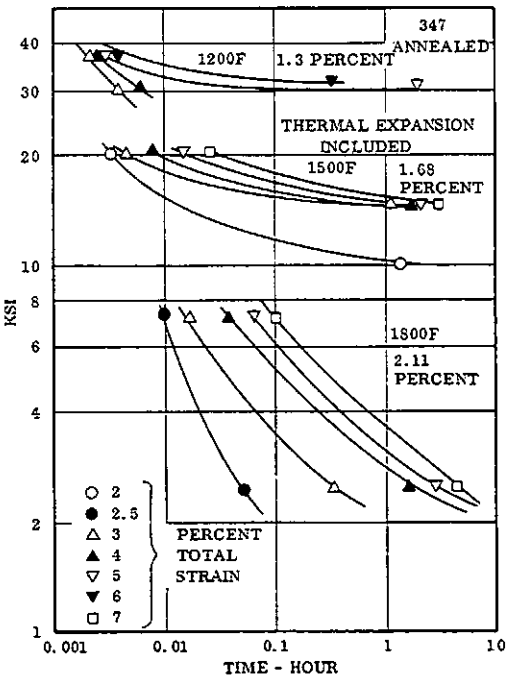


FIG. 3.047 SHORT-TIME TOTAL CREEP STRAIN CURVES AT 1200 TO 1800F. (65)

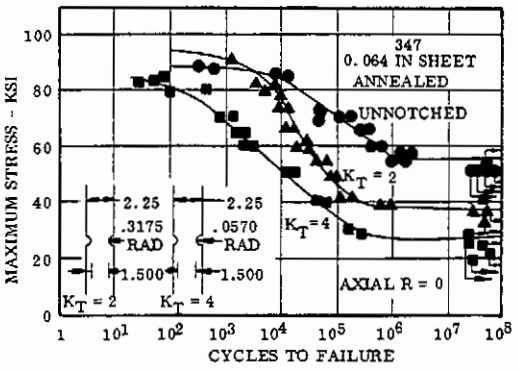


FIG. 3.051 FATIGUE LIFE OF NOTCHED AND UNNOTCHED SHEET. (42)

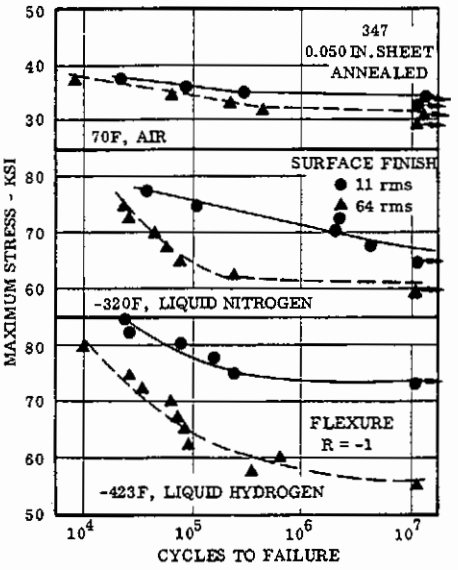


FIG. 3.052 EFFECTS OF SURFACE FINISH AND TEMPERATURES ON FATIGUE LIFE OF SHEET. (45)

	Fe
18	Cr
12	Ni
+	Cb

TYPES 347,348

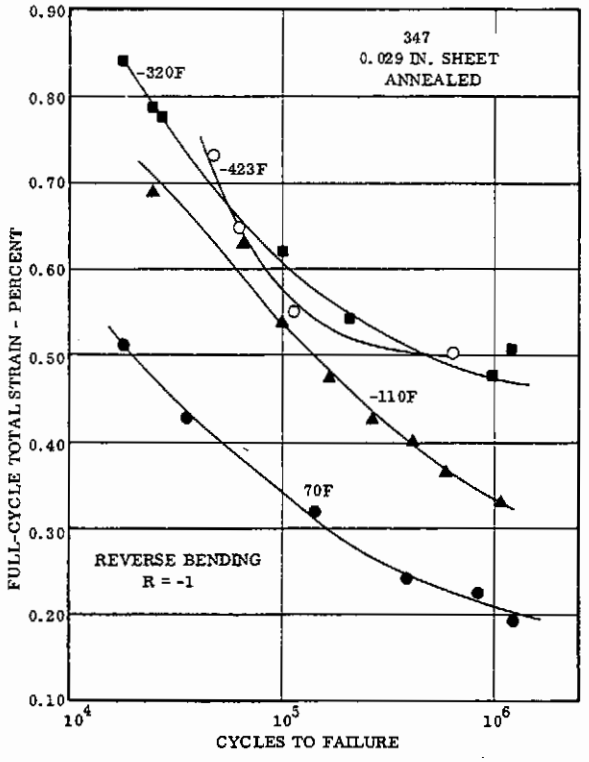


FIG. 3.053 EFFECTS OF LOW TEMPERATURES ON FATIGUE LIFE OF SHEET. (43)

	Fe
18	Cr
12	Ni
+	Cb

TYPES 347,348

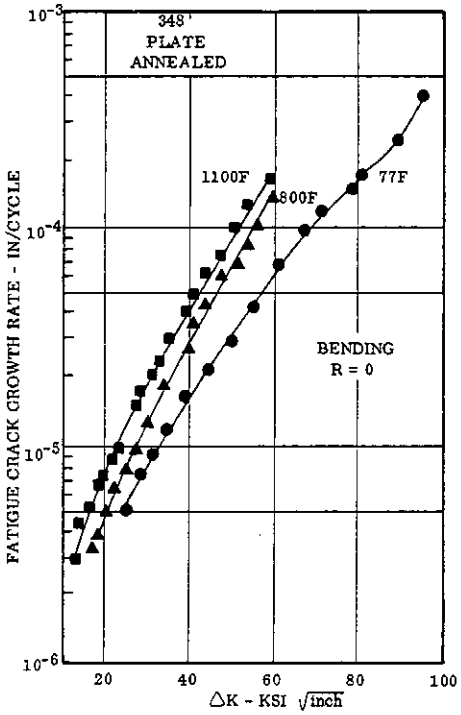


FIG. 3.054 FATIGUE CRACK GROWTH RATE AS A FUNCTION OF THE STRESS-INTENSITY-FACTOR RANGE AT VARIOUS TEMPERATURES. (28)

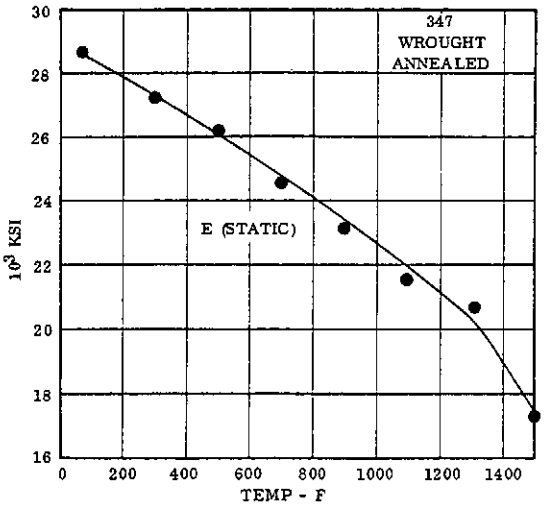


FIG. 3.0621 EFFECTS OF ELEVATED TEMPERATURES ON MODULUS OF ELASTICITY. (19)

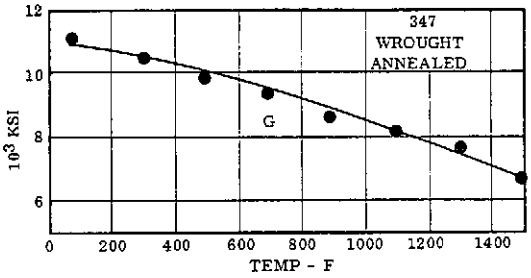


FIG. 3.0631 EFFECTS OF ELEVATED TEMPERATURES ON MODULUS OF RIGIDITY. (19)

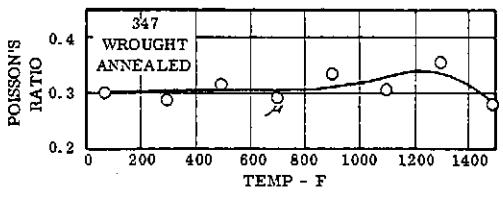


FIG. 3.0611 EFFECTS OF ELEVATED TEMPERATURES ON POISSON'S RATIO. (19)

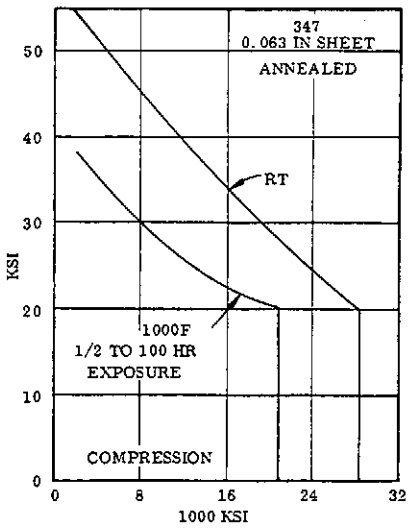


FIG. 3.0641 TANGENT MODULUS CURVES IN COMPRESSION FOR SHEET AT ROOM TEMPERATURE AND 1000F. (62)

	Fe
18	Cr
12	Ni
+	Cb

TYPES 347,348

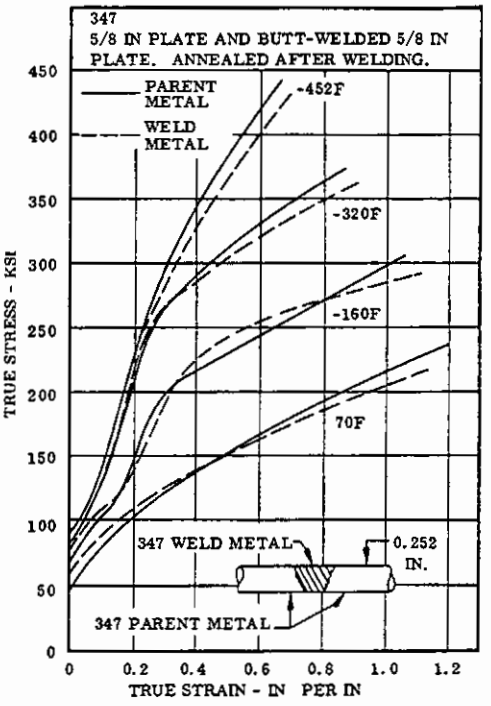


FIG. 4.0311 COMPARISON OF COMPLETE TRUE STRESS-TRUE STRAIN CURVES OF PLATE AND OF WELD METAL AFTER PLATE HAD BEEN BUTT-WELDED WITH TYPE 347 COATED STICK ELECTRODES. (25)

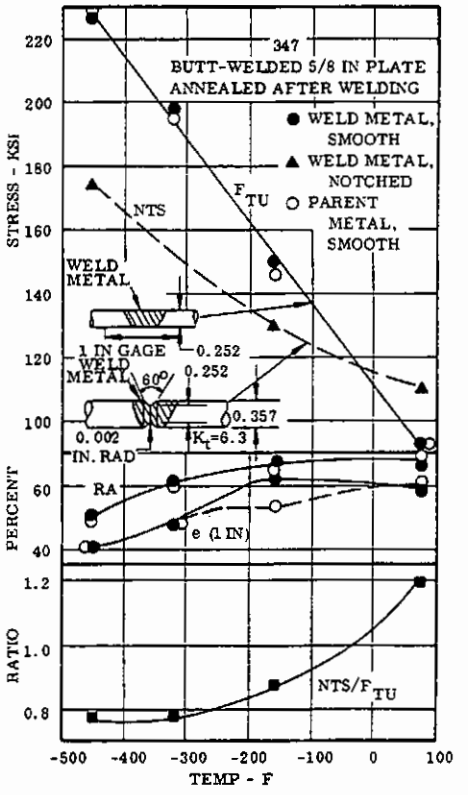


FIG. 4.0312 LOW-TEMPERATURE TENSILE AND NOTCHED-TENSILE PROPERTIES OF PLATES BUTT WELDED WITH TYPE 347 COATED STICK ELECTRODES. (25)

	Fe
18	Cr
12	Ni
+	Cb

TYPES 347,348

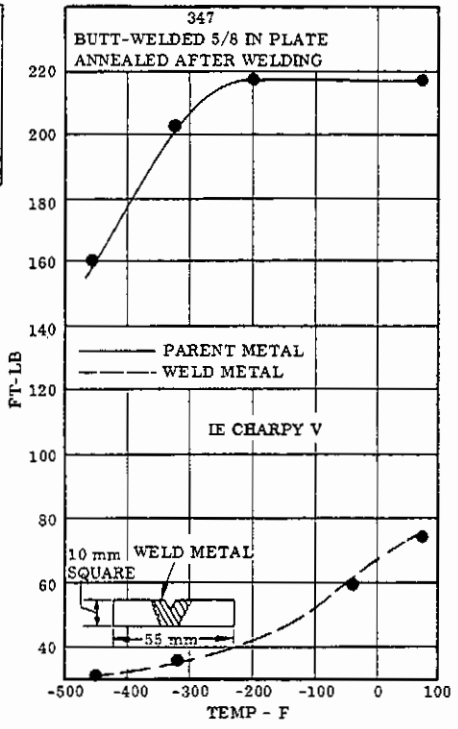


FIG. 4.0313 LOW-TEMPERATURE IMPACT PROPERTIES OF PLATE BUTT-WELDED WITH TYPE 347 STICK ELECTRODES. (25)

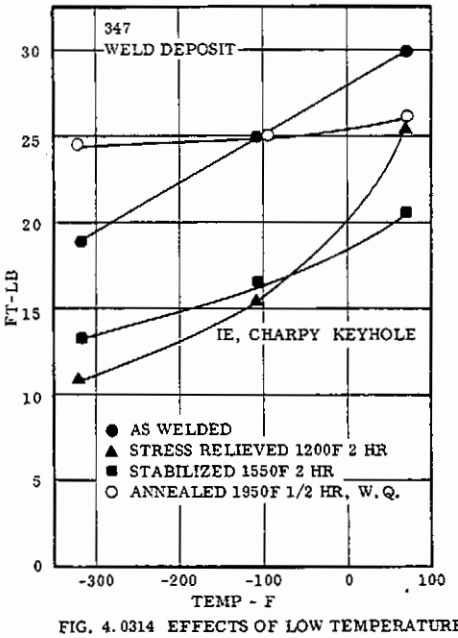


FIG. 4.0314 EFFECTS OF LOW TEMPERATURES AND POST-WELD HEAT TREATMENT ON IMPACT PROPERTIES OF WELD METAL DEPOSITED FROM COATED STICK ELECTRODES. (24)

REFERENCES

1. AMS 5362 E (January 15, 1976).
2. AMS 5363 B (April 15, 1958).
3. AMS 5512 E (January 15, 1976).
4. AMS 5556 C (November 15, 1972).
5. AMS 5558 B (January 15, 1976).
6. AMS 5575 H (January 15, 1976).
7. AMS 5646 F (November 15, 1971).
8. AMS 5654 A (May 15, 1971).
9. AMS 5674 A (May 15, 1971).
10. AMS 5680 D (May 15, 1973).
11. AMS 5681 B (May 15, 1971).
12. "Uniloy 321/347/348 Stainless Steels", Universal-Cyclops Specialty Steel Division (1966).
13. "Carpenter Stainless Type 347, 348", Carpenter Technology Corporation (1975).
14. "Stainless Steel Types 347, 348, 321", Allegheny-Ludlum Steel Corporation Blue Sheet (1970).
15. "Steels for Elevated Temperature Service", United States Steel Corporation (1972).
16. Lucks, C. F., Deem, H. W., "Thermal Properties of Thirteen Metals", ASTM STP No. 227 (1958).
17. Furman, D. E., "Thermal Expansion Characteristics of Stainless Steels Between -300 and 1000F", Trans. AIME Vol. 188 (1950) p. 688.
18. Hogan, C. L., Sawyer, R. B., "The Thermal Conductivity of Metals at High Temperatures", Journal of Applied Physics, Vol. 23 (February 1952) p. 177.
19. Garofalo, F., Malenock, P. R., Smith, G. V., "The Influence of Temperature on the Elastic Constants of Some Commercial Steels", ASTM STP No. 129 (1952) p. 10.
20. "Mechanical and Physical Properties of Austenitic Chromium-Nickel Stainless Steels at Ambient Temperatures", The International Nickel Company (1963).
21. "High-Alloy Data Sheets, Corrosion Series", Alloy Casting Institute (January 1973).
22. "Mechanical and Physical Properties of Austenitic Chromium-Nickel Stainless Steels at Subzero Temperatures", The International Nickel Company (1970).
23. "Cast Stainless Steels", The International Nickel Company (1973).
24. Krivobok, V. N., Thomas, R. D., Jr., "Impact Tests of Welded Austenitic Stainless Steels", Welding Journal, Vol. 19 (1950) p. 493S.
25. DeSisto, T. S., "Low Temperature Mechanical Properties of Base and Weld Deposits of Selected Austenitic Stainless Steels", AMRA TR 63-08, United States Army Materials Research Agency (July 1963).
26. Eiselstein, H. L. and Skinner, E. N., "The Effect of Composition on the Scaling of Iron-Chromium-Nickel Alloys Subjected to Cyclic Temperature Conditions", ASTM STP No. 165 (1954).
27. Hallerman, G., Gray, R. J., "Equipment for Hardness Testing at Elevated Temperatures", Oak Ridge National Laboratory, ORNL-3448 (July 31, 1963).
28. Shahinian, P., Smith, H. H., Watson, H. E., "Fatigue Crack Growth Characteristics of Several Austenitic Stainless Steels at High Temperatures", ASTM STP No. 520 (1973) p. 387-400.
29. Stanley, J. K., Perretta, A. J., "Grain Growth in Austenitic Stainless Steels", Metallography, Vol. 2 (1969) p. 349-362.
30. Reinhart, F. M., "Corrosion of Materials in Hydrospace Part VI - Stainless Steels", Technical Note N-1172, Naval Civil Engineering Laboratory (September 1971).
31. "Stress Corrosion One Year Coupon Test Report", Bell Aerosystems, Company, Report 8477-927288 (April 1970).
32. Morrison, J. D., "Corrosion Study of Base and Coated Stainless Steel", NASA TN D-6519, John F. Kennedy Space Center (July 1972).
33. "Resume' of Investigations on Steels for High-Temperature, High-Pressure Applications 1960-1962", Timken Roller Bearing Company (1962).
34. Malin, C. O., "Low-Temperature Properties of Cast 310 and 347 CRES", Rocketdyne, NAR 80001, NASW 16 (June 1968).
35. Smith, H. H., Shahinian, P., "Fatigue Resistance of Type

348 Stainless Steel Under Simulated Water Reactor Conditions", NRL Report 7770, Naval Research Laboratory (June 26, 1974).

36. Stanley, J. K., "Mechanical Properties of Carburized Austenitic Stainless Steels as Related to Microstructure", Aerospace Corporation Report No. TR-0066 (5250-10)-1 (July 31, 1969).

37. "Mechanical Test Results on Various Extruded Materials", Allegheny-Ludlum Steel Corporation (January 1, 1956).

38. Lauritzen, T., Withop, A., Ferguson, G. P., "Mechanical Properties Evaluation of Austenitic Stainless Steels Irradiated in ERB-11", AEC R & D Report, General Electric Company (July 1969).

39. DeSisto, T. S., Carr, F. L., "Low Temperature Mechanical Properties of 300 Series Stainless Steels and Titanium", WAL TR 323.4/1, Watertown Arsenal (December 1961).

40. Stanely, J. K., "Effect of Silicon Additions on the Carburization Resistance, Mechanical Properties and Joining Characteristics of Stabilized Austenitic Stainless Steels", Aerospace Corporation Report No. TR-0172 (2250-10)-4 (November 15, 1971).

41. Conway, J. B., Berling, J. T., Stentz, R. H., Salyards, D. G., "Stress-Strain Behavior of Several Stainless Steels to Elevated Temperatures", GEMP 686, General Electric Company, Nuclear Systems Programs (May 1969).

42. Hardrath, H. F., Landers, C. B., Utley, E. C., Jr., "Axial-Load Fatigue Tests on Notched and Unnotched Sheet Specimen of 61S-T6 Aluminum, Annealed Type 347 Stainless and Heat-Treated 403 Stainless", NASA Technical Note 3017 (October 1953).

43. Gidean, D. N., Favor, R. J., MacClure, G. M., Grover, H. J. and Koppenhafer, A., "Investigation of Notched Fatigue Behavior of Certain Alloys in the Temperature Range of Room Temperature to -423F", ASD-TDR-62-351, Battelle (August 1962).

44. Grigger, J. C., Miller, H. C., "The Compatibility of Welded Structural Materials With Chlorine Trifluoride and Perchloryl Fluoride", ML-TRD-64-22, Pensalt Chemical Corporation (February 1964).

45. Green, E. F., Schmidt, E. H., "Fatigue Properties of Metallic Materials for Cryogenic Applications", R-7564, Rocketdyne (August 1968).

46. Curbishley, G., Larson, W., McGrath, D. W., Gellessen, E. W., "Hot Corrosion Resistance of Materials for Small Gas Turbine Recuperators", TR 69-92, Airesearch Manufacturing Company (December 1969).

47. Warren, K. A., Reed, R. P., "Tensile and Impact Properties of Selected Materials from 20 to 300 K", National Bureau of Standards Monograph 63 (June 28, 1963).

48. Kangilaski, M., Shober, F. R., DeMastry, J. A., Gates, J. E., "Effects of Large Fast Fluences on Mechanical Properties of Type 347 Stainless Steel and Aluminum", Report BMI-1834, Battelle (March 27, 1968).

49. Murr, W. E., Shober, F. R., Lieberman, R., Dickerson, R. F., "Effects of Large Neutron Doses and Elevated Temperatures on Type 347 Stainless", Report BMI-1609, Battelle (January 21, 1963).

50. Martin, W. R., Weir, J. R., "Effect of Irradiation Temperature on the Postirradiation Stress-Strain Behavior of Stainless Steel", ORNL-TM-906, ORNL (October 1964).

51. "Specifications and Foreign Equivalents for Stainless Steels", The International Nickel Company (1975).

52. Berry, W. E., White, E. L., Boyd, W. K., "Stress-Corrosion Cracking of Stainless Steel in Oxygenated High-Temperature Water", Corrosion, Vol. 29 (December 1973) p. 451-469.

53. Greenberg, S., "How Structural Alloys Perform in ERB-11", Metal Progress, Vol. 107 (March 1975) p. 89-94.

54. Wade, W. R., "Measurement of Total Hemispherical Emissivity of Several Stably Oxidized Metals", NASA Memorandum 1-20-59L (January 1959).

55. Harris, J. A., Jr., Van Wanderham, M.C., "Properties of Materials in High Pressure Hydrogen", Pratt and Whitney Aircraft, Florida R & D Center, FR-5768 (July 31, 1973).

56. Slerner, C. J., Singleton, A. H., "The Compatibility of Various Metals and Carbon with Liquid Fluorine", WADD TR-60-436, Air Products Incorporated (August 1960).

57. Muhlenbruch, C. W., Wayne, C. R., Krivobok, V. N., "Mechanical Properties in Torsion and Poisson's Ratio for Certain Stainless Steels", ASTM Proceedings, Vol. 51 (1951) p. 382-856.

58. "Short-Time High Temperature Data", No. BLR 53-195, Bell Aircraft Corporation (July 16, 1954).

59. "Properties of AISI Type 347 and 348 Stainless Steel", Bettis Plant Materials Manual, Westinghouse (May 1957).

60. "Haynes Investment Cast Steels", Haynes-Stellite Company (April 1958).

61. "Resume' of High-Temperature Investigations Conducted During 1957-59", Timken (1959).

62. Miller, D. E., "Determination of the Physical Properties of Structural Sheet Materials at Elevated Temperatures", WADC AFTR 6517, Pt. 4 (December 1954).

63. Simmons, W. F., Cross, H. C., "The Elevated Temperature Properties of Stainless Steels", ASTM STP No. 124 (1952).

64. Miller, J., Smith, L. M., Porter, P. K., "Utilization of Low-Alloy Materials for High-Temperature Service Applications", AFTR 5929 (June 1949).

65. "Materials Property Manual and Summary Report", North American Aviation Incorporated (October 30, 1957).

	Fe
18	Cr
12	Ni
+	Cb

TYPES 347,348

Fe
12 Cr
Low C

Types 403, 410, 416

1 **GENERAL**

The low-carbon versions of the martensitic 12 percent chromium stainless steels have long been used in various forms as relatively low-cost, air-hardening stainless steels. These steels are hardenable by quenching and tempering. They are magnetic in all conditions, being ferritic as annealed and martensitic as hardened. They have sufficient corrosion resistance for many applications but are inferior to both austenitic and ferritic grades in this respect. The highest strength conditions, obtained by tempering at 550 to 1050 F, are quite susceptible to stress corrosion and possess poor toughness at room and low temperatures. Delta ferrite phase can form in 12 percent chromium steels containing excess chromium and low carbon. This phase adversely affects mechanical properties and formability. These alloys are more difficult to weld than austenitic grades because they tend to crack in the weld bead during cooling after welding. The low-silicon Type 403 is used primarily in the form of forgings for compressor blading and other turbine parts, while the higher silicon Type 410 finds wide applications in wrought form and as sand and investment castings. Specialty grades such as free-machining Types 416 and 416Se are used in both cast and wrought form where their slightly reduced corrosion resistance and formability are acceptable.

See also Code 1410 on columbium-modified Type 410.

1.01 **Commercial Designations**

Wrought: AISI Type 403, 410, 416, and 416Se.
Cast: CA-15 and CA-40.

1.02 **Alternate Designations**

Type 403: UNS S40300
Type 410: UNS J91150, UNS J91152, UNS K91151, UNS K91161, UNS S41000, UNS S41040, UNS S41025
Type 416: UNS J91161, UNS S41600
Type 416Se: UNS S41623.

1.03 **Specifications**

1.031 AMS specifications Types 403, 410, and 416, Table 1.031.

1.04 **Composition**

1.041 Compositions specifications for Types 403 and 416, Table 1.041.

1.042 Composition specifications for Type 410, Table 1.042.

1.05 **Heat Treatment**

1.051 Normalize sand castings. 1825 to 1875 F, 1 hour per inch of thickness, 30-minute minimum, air cool (2).

1.052 All grades. Fully anneal for maximum formability. 1450 to 1650 F, usually 1550 to 1650 F, furnace cool at 50 F per hour maximum to 1100 F. Hardness should be about 155 BHN.

1.053 Subcritical anneal for machining. 1200 to 1400 F. Hardness should be about 185 BHN.

1.054 Austenitize. 1750 to 1850 F, air cool or oil quench depending on section size and shape. Users generally prefer oil quenching.

1.055 Temper. 400 to 1400 F, 1 to 4 hours. Tempering at temperatures between 550 and 1050 F should be avoided because of reduced resistance to stress corrosion and increased notch sensitivity (10,25). Recommended heat treatment for obtaining high dimensional stability in Type 410: 1800 F, 1/2 hour, oil quench; 450 F, 1 hour, air cool or 600 F, 1 hour, air cool (41).

1.056 Tempering temperature affects both mechanical properties and microstructure (as well as corrosion behavior) of Type 410 and other 12 percent chromium steels. After quenching from the austenitizing temperature of about 1800 F, Type 410 is fully martensitic and is characterized by high values of hardness and tensile strength (see Figures 1.062 and 3.0212). The tensile strength and hardness decrease with increasing tempering temperature up to about 570 F. This behavior is related to decomposition of the martensite phase, which loses its tetragonality as carbon precipitates from solid solution. Simultaneously, M_3C carbide appears in the martensite laths. This carbide is stable to about 660 F. At tempering temperatures between 570 and 930 F, hardness values are constant while tensile strength increases slightly with increasing tempering temperature. The tensile strength peak at about 930 F is caused by secondary hardening due to precipitation of M_7C_3 carbide. Above 930 F, the yield and ultimate tensile strengths and hardness decrease rapidly because of dissolution of M_7C_3 carbide. The $M_{23}C_6$ carbide is predominant at temperatures above 930 F (54).

1.057 AMS-specified heat-treatment conditions for Types 403, 410, and 416, Table 1.057.

1.058 A neutral or slightly reducing atmosphere must be maintained when austenitizing or annealing to minimize decarburization and scaling.

1.06 **Hardness**

1.061 These steels harden by transformation to martensite on air cooling after austenitizing. AMS 5349B, 5350F, and 5613M require that material be capable of developing a hardness of at least 35 HRC after being austenitized at 1750 F. AMS 5610K requires similar hardening capability after being austenitized at 1825 F. AMS 5351D and 5504H require that material be capable of developing a hardness of between 35 and 45 HRC after being austenitized at 1750 F. AMS 5591F requires that a specimen cut from tubing, when austenitized, shall have a minimum F_{tu} of 150 ksi. Similarly, AMS 5776B and 5777B require that deposited weld metal about 0.25 inch thick, when austenitized, have a hardness of 35 to 45 HRC.

1.062 Effect of tempering temperature on hardness of Type 410, Figure 1.062.

1.07 **Forms and Conditions Available**

1.071 Type 403 is available in the form of bar and forgings in all commercial sizes.

1.072 Type 410 is available in a full range of forms and sizes regularly produced in stainless steels.

Fe
12 Cr
Low C

Types 403, 410, 416

1.073 Type 410 sand and precision investment castings are available in various conditions as desired.

1.074 Type 410 sheet, strip, bar, and wire are available in the annealed condition. Bar and wire are also available in the cold-drawn condition and wire and forgings in various heat-treated conditions.

1.075 Types 416 and 416Se are available in the form of bar and forgings in all commercial sizes.

1.076 Type 416 precision investment castings are available in various conditions as desired.

1.077 Type 416 is also commercially available in compositional modifications for maximum hardenability and for maximum machinability but nonhardenable (55).

1.078 The 12.5Cr grade (AMS 5821B) is used as a filler material for welding corrosion-resistant alloys of similar compositions which have requirements for control of ferrite.

1.08 **Melting and Casting Practice**

Electric-furnace air melt. Induction and consumable-electrode melts and remelts are also available, as well as vacuum-degassed materials.

1.09 **Special Considerations**

1.091 Tempering in the temperature range of about 550 to 1050 F should be avoided. This temper causes impact embrittlement and increased notch sensitivity as well as a tendency toward reduced resistance to general corrosion and to stress corrosion. See Figure 2.0316, Section 2.0321, Figure 3.0231, Figure 3.0271, Section 3.0331, and Figure 3.0333.

1.092 The high manganese and sulfur contents which are added to Type 416 in order to improve machinability cause decreased corrosion resistance. Manganese contents of 1 percent or more with a manganese-to-sulfur ratio of 7:1 or greater promote formation of soft alpha-MnS inclusions and improved machinability. However, this same alpha-MnS promotes decreased corrosion resistance in the alloy. Type 416 should be used only in applications where its decreased corrosion resistance is acceptable. (See Sections 2.0313 and 4.023.)

1.093 The proper chemical balance is necessary in Types 403 and 410 to insure against the formation of delta ferrite which can affect the mechanical properties, especially hardness and toughness. The hardness decreases with an increase in the ferrite content, while the toughness as measured by impact strength increases for longitudinal tests but decreases for transverse tests. These effects on impact strength are due to the mechanical fibering associated with the presence of ferrite and their magnitude will depend on both the amount of ferrite present and the degree of work in the structure. The effect of carbon, an austenite former, and chromium, a ferrite former, on the amount of ferrite is shown in Figure 2.01204,

1.094 Welding of 12 percent chromium steels requires special precautions to prevent weld cracking. Welds require preheating and post-weld stress relief. Cracking can be eliminated through the use of special electrode compositions. (See Sections 4.031 and 4.032.)

1.095 Type 410 is subject to stress-corrosion cracking in hydrazine and related rocket fuels. This cracking is related to impurities in the hydrazine, particularly carbon dioxide. Susceptibility to stress corrosion can be reduced or eliminated through the use of high-purity or BaO-treated (purified) fuel. (See Section 2.0326.)

2 PHYSICAL PROPERTIES AND ENVIRONMENTAL EFFECTS

2.01 **Thermal Properties**

2.011 Melting range. 2700 to 2790 F.

2.012 Phase changes.

2.01201 Transformation temperature from austenite to ferrite are above 1450 F, but depend on chemistry. Heating to about 1750 F is necessary to insure completely martensitic structure on quenching.

2.01202 Transformation temperatures for Type 410 are (54,56):

Ac_1	1510 F
Ac_3	1670 F
Ac_4	2240 F
M_s	680 F
M_f	260 F

2.01203 Equilibrium phase diagram for Types 403, 410, and 416 with respect to carbon content, Figure 2.01203.

2.01204 Effect of carbon and chromium content on delta ferrite content of Type 410, Figure 2.01204.

2.0121 Time-temperature-transformation diagrams.

2.01211 Time-temperature-transformation diagram for Type 403, Figure 2.01211.

2.013 Thermal conductivity of Types 410 and 416, Figure 2.013.

2.014 Thermal expansion of Types 403, 410, and 416, Figure 2.014.

2.015 Specific heat of Type 410, Figure 2.015.

2.016 Thermal diffusivity.

2.02 **Other Physical Properties**

2.021 Density. 0.280 lb/in.^{3} (7.75 gr/cm^3).

2.022 Electrical resistivity of Types 410 and 416, Figure 2.022.

2.023 Magnetic properties.

2.0231 The 400 series of corrosion-resistant steels are magnetic.

2.0232 Magnetization curves for Type 410, Figure 2.0232.

2.0233 Residual induction and coercive force of Type 410 after magnetizing at 1200 oersteds, and maximum permeability, Table 2.0233.

2.024 Emittance.

2.025 Damping capacity.

2.03 **Chemical Environments**

2.031 General corrosion.

2.0311 These steels are resistant to atmospheric and fresh-water corrosion and to a variety of mild acids and alkalines, but they are inferior to the 300 series of stainless steels and in some cases may require corrosion protection. Maximum corrosion resistance is obtained in the hardened condition but is usually reduced after tempering between 550 and 1050 F. The requirements for clean surfaces are similar to those for the 300 series.

Fe
12 Cr
Low C

Types 403, 410, 416

Type 416 is slightly less corrosion resistant than Types 403 and 410.

2.0312 Types 403 and 410 exhibit poor and erratic corrosion resistance at 500 to 600 F in high-purity water containing oxygen. They are considerably inferior to austenitic stainless steels in this respect.

2.0313 High manganese content in the presence of sulfur promotes rusting and corrosion of 12 percent chromium steels such as Type 416. As shown in Figure 2.0314, manganese contents over 0.4 percent considerably reduce the time for appearance of rust spots on steel containing 0.35 percent sulfur. Similarly, manganese contents of 0.8 percent or higher greatly increase the corrosion rate in a nitric acid solution at sulfur contents of 0.25 and 0.35 percent, as shown in Figure 2.0315. The corrosion behavior in several acids is shown in Figure 2.0316 for two sulfur levels, two manganese levels, and three heat treatments. At a sulfur level of 0.007 percent (not characteristic of commercially available materials), corrosion resistance is good and does not vary with manganese content. However, at a normal sulfur level of 0.35 percent, corrosion rates are considerably increased at the higher manganese level. The effect of limited variations in heat treatment here is minor, with the austenitized-and-tempered materials having improved corrosion resistance as compared to 1300 F-annealed material. The poor corrosion resistance of 12 percent chromium steels containing both manganese and sulfur is attributed to the presence of manganese sulfide (MnS). In low-manganese materials, a chromium-rich sulfide forms which has good corrosion resistance. However, in high-manganese materials, the corrosion-prone manganese sulfide forms. Sulfide composition also affects the behavior of these steels during nitric acid passivation treatments. Highly oxidizing solutions such as nitric acid with a 2 percent addition of sodium dichromate must be used to avoid corrosion attack during these treatments, particularly for steels with high manganese-to-sulfur ratios (59).

2.0314 Effect of manganese on time for first appearance of rust spots on Type 416 in humid air at room temperature, Figure 2.0314.

2.0315 Effect of manganese content on corrosion of Type 416 in aqueous solution of 10 percent nitric acid at room temperature, Figure 2.0315.

2.0316 Effects of sulfur and manganese contents and heat treatment on corrosion rate of Type 416 in several acids, Table 2.0316.

2.0317 Type 410 has superior corrosion resistance in atmospheric and saltwater environments as compared to other non-stainless steels. It is inferior, however, to Types 302, 316, and 321 stainless steels based on 16-year exposure data. Data for Type 410 are shown in Table 2.0318 (60).

2.0318 Corrosion of Type 410 in tropical environments for times up to 16 years, Table 2.0318.

2.032 Stress corrosion.

2.0321 Martensitic stainless steels such as Type 410 are resistant to stress-corrosion cracking in the annealed condition but can be susceptible to cracking in certain environments in the heat-treated condition. Table 2.0322 shows the effects of heat-treatment conditions on stress-corrosion behavior in a marine atmosphere. In this environment, low austenitizing temperatures (1600 and 1750 F) result in resistance to cracking regardless of the tempering temperature. At an intermediate austenitizing temperature (1900 F), cracking occurs after tempering at 950 F but not at 450, 700, or 1200 F. With steel austenitized at 2050 F, tempering temperatures of 950 F and lower result in cracking. Stress-corrosion cracking in Type 410 has been attributed to chromium depletion at the grain boundaries during tempering. Tempering between 900 and 1100 F causes precipitation of chromium carbide at grain boundaries and within the matrix, causing chromium depletion in the surrounding matrix. Chromium depletion at the grain boundaries creates preferential paths for stress-corrosion cracking. Tempering at 1200 F and above permits diffusion of chromium into the depleted zones, consequently producing a more uniform chromium distribution and improving the resistance to stress-corrosion cracking. The effect of austenitizing temperature is believed to be related to grain size, with coarser grain size promoting cracking. Stress-corrosion cracking can be avoided by control of the environment, control of heat treatment, reduction of tensile stresses, and use of selected coatings. Zinc-rich coatings and metallized aluminum are especially effective in preventing cracking in marine and industrial atmospheres (61).

2.0322 Effect of heat treatment on stress-corrosion behavior of Type 410 in marine atmosphere, Figure 2.0322.

2.0323 The resistance of Type 410 to both general corrosion and to stress-corrosion cracking in an aqueous 3.5 percent sodium chloride solution is dependent on prior heat treatment. Material austenitized at 1775 F and tempered 3 hours at 1100 F exhibits severe general corrosion with numerous deep pits but is resistant to stress corrosion. Tensile strength is degraded by general corrosion. After austenitizing at 1775 to 1900 F followed by tempering for 3 hours at lower temperatures (400 or 500 F), Type 410 shows only slight general corrosion. However, it is quite susceptible to stress corrosion in this condition when stressed at 75 to 100 percent of the yield strength (62).

2.0324 The fatigue crack-growth rate of Type 403 is greater in boiling water than in air, as shown in Figure 2.0323. Crack-growth rates in aqueous solutions of sodium chloride and sodium sulfate (not shown) are almost identical to those in water for pH values from 2 to 10, while rates in aqueous solutions of sodium phosphate and sodium silicate (not shown) are almost identical to those in air (63).

2.0325 Effects of frequency and environment on fatigue crack-growth behavior of Type 403 at 212 F, Figure 2.0325.

2.0326 Type 410, along with Inconel 718, Ti-6Al-4V, and 6061T6 Al, finds major application for service with hydrazine and related rocket fuels. These alloys are classified in order of decreasing susceptibility to stress-corrosion cracking in hydrazine as follows: Type 410 stainless steel, Inconel 718, Ti-6Al-4V,

Fe
12 Cr
Low C

Types 403, 410, 416

and 6061T6 Al. Type 410 and Inconel 718 are subject to serious deterioration in crack-propagation resistance in hydrazine while 6061T6 Al is essentially unaffected. Data for Type 410 in hydrazine and three other related fuels are shown in Table 2.0327. Increases in load and in fuel-impurity content tend to decrease the incubation period before crack-growth initiation. Cracking is observed in impure hydrazine and in Aerozine 50 but not in monomethyl hydrazine or unsymmetrical dimethylhydrazine (UMDH). Carbon dioxide impurity is particularly harmful, as shown by short incubation periods in hydrazine containing additions of 0.2 and 1.0 percent CO_2. Carbon dioxide can be absorbed into hydrazine from the atmosphere during handling and forms carbazic acid, which promotes susceptibility to cracking. Data for Type 4130 steel (not shown), which is more susceptible to cracking than Type 410, indicates that treatment of hydrazine with BaO eliminates CO_2-induced cracking. Similar behavior is observed for Type 410 (64).

2.0327 Stress-corrosion behavior of Type 410 in hydrazine rocket fuels, Figure 2.0327.

2.033 Hydrogen-environment embrittlement.

2.0331 Type 410 tempered at 700 F has very poor stress-corrosion resistance in the presence of NaCl and H_2S, as shown in Table 2.0332. This type of cracking is attributed to hydrogen absorption and consequent embrittlement. Cracking under these conditions is generally a function of hardness and can be minimized by tempering to a hardness below Rockwell C22. Thus, tempering at 900 F and below results in maximum hardness and consequent susceptibility to hydrogen embrittlement.

2.0332 Stress-corrosion behavior of Type 410 in several environments, Table 2.0332.

2.0333 Type 410 (of unspecified heat treatment) is greatly embrittled by exposure to high-pressure hydrogen at room temperature, as shown by the tensile ductility data in Table 2.0334 (65).

2.0334 Effects of hydrogen environment on tensile properties of Type 410 at room temperature, Table 2.0334.

2.0335 Effect of tempering temperature on hydrogen diffusivity and solubility in Type 403 at room temperature, Figure 2.0335.

2.034 Oxidation.

2.0341 Oxidation resistance of these alloys is good up to 1200 F for continuous service and 1400 F for intermittent service.

2.0342 The dominant constituent of oxide films formed on electropolished Type 410 at 750 to 930 F in oxygen is Fe_2O_3, based on studies of infrared reflectance spectra. At 1560 F, the dominant constituent is Cr_2O_3, with SiO_2 or a metal silicate probably present as a minor constituent (67).

2.0343 Long-time oxidation weight-gain behavior of Type 410 in high-pressure steam at 1000 F, Figure 2.0343.

2.0344 Effects of pressure and temperature on burning of freshly exposed Type 410 in high-velocity flowing oxygen, Figure 2.0344.

2.04 **Nuclear Environments**

2.041 Type 410 is used for high-strength parts in reactors.

2.042 Irradiation effects on these and other martensitic stainless steels are as follows:

The hardness increases, as the total flux and the temperature of irradiation is increased. This effect also appears to be greater for a higher initial hardness, but independent of the carbon content.

Tensile strength and yield strength increase and the ductility decreases if the saturation point appears to be reached below the point of complete embrittlement.

The impact strength in the ductile range is only slightly reduced. The transition temperature from ductile-to-brittle behavior, however, may be raised by 50 to 75 F.

Density is not changed beyond the limits of experimental error.

2.043 The fracture toughness of Type 403 is decreased by fast-neutron irradiation. Compact tension fracture-toughness specimens (ASTM E399-74) were irradiated to a fluence of 6×10^{19} n/cm^2 (greater than 1 Mev) at 570 F in pressurized water. The room-temperature fracture toughness was reduced from 72.6 ksi$\sqrt{\text{in.}}$ (average of five specimens) in the unirradiated condition to 55.2 ksi$\sqrt{\text{in.}}$ (average of four specimens) after irradiation (70).

3 MECHANICAL PROPERTIES

3.01 **Specified Mechanical Properties**

3.011 AMS-specified mechanical properties for Type 410, Table 3.011.

3.012 AMS-specified mechanical properties for Types 403 and 416, Table 3.012.

3.02 **Mechanical Properties at Room Temperature**

3.021 Tension – stress-strain diagrams – tension properties.

3.0211 Typical mechanical properties of Types 403, 410, and 416, Table 3.0211.

3.0212 Effect of tempering temperature on tensile properties of Type 410 sheet and bar, Figure 3.0212.

3.0213 Effect of tempering temperature on mechanical properties of Type 410 sand castings, Figure 3.0213.

3.0214 Effect of tempering temperature on tensile and yield strengths of Type 410 deformed in the metastable austenitic condition, Figure 3.0214.

3.0215 Effect of tempering temperature on reduction of area and elongation of Type 410 deformed in the metastable austenitic condition, Figure 3.0215.

3.0216 Effect of tempering temperature and deformation on tensile properties of Type 410, Figure 3.0216.

3.0217 Effect of deformation on tensile properties and hardness of Type 410 deformed in the metastable austenitic condition, Figure 3.0217.

3.0218 Effect of rolling reduction on tensile properties of Type 410 annealed sheet, Figure 3.0218.

3.0219 Effect of rolling reduction and annealing on as-received tensile properties of Type 410 sheet, Table 3.0219.

3.022 Compression – stress-strain diagrams – compression properties.

Fe
12 Cr
Low C

Types 403, 410, 416

3.023 Impact.

3.0231 Effect of tempering temperature on impact properties of Type 410, Figure 3.0231.

3.0232 Effect of tempering temperature on mechanical properties of sand castings (see Figure 3.0213).

3.0233 The Charpy impact energy of Type 403 is increased by double austenitizing. Charpy V-notch specimens were austenitized by (1) heat treating for 1 hour at 1650 to 1750 F, oil quenching, plus tempering for 8 hours at 1160 F or by (2) heat treating for 1 hour at 1880 F, oil quenching, plus 1 hour at 1620 F, oil quenching, plus tempering for 8 hours at 1160 F. The average room-temperature impact energies and standard deviations from nine tests were 16.1 ± 11.3 ft-lb for single-austenitized specimens and 41.8 ± 16.5 ft-lb for double-austenitized specimens. The increased impact energy is attributed to removal of coarse grain-boundary carbides in the double-austenitized material, which changes the fracture morphology (71).

3.024 Bending.

3.025 Torsion and shear.

3.026 Bearing.

3.027 Stress concentration.

3.0271 Notch properties. Effect of tempering temperature on sharp notch strength of Type 410 sheet, Figure 3.0271.

3.0272 Fracture toughness.

3.028 Combined properties.

3.03 **Mechanical Properties at Various Temperatures**

3.031 Tension – stress-strain diagrams – tension properties.

3.0311 Stress-strain curves in tension at elevated temperatures for Type 410, Figure 3.0311.

3.0312 True stress-strain curves at cryogenic to intermediate temperatures for Type 410, Figure 3.0312.

3.0313 Effect of test temperature on tensile properties of Type 403 bar, Figure 3.0313.

3.0314 Effect of test temperature on tensile properties of Types 403 and 410, Figure 3.0314.

3.0315 Effect of test temperature on tensile properties of Type 410, Figure 3.0315.

3.0316 Effect of test temperature on tensile properties of annealed Type 416, Figure 3.0316.

3.0317 Effect of test temperature on tensile properties of precision investment castings of Type 403 in different conditions, Figure 3.0317.

3.032 Compression – stress-strain diagrams – compression properties.

3.033 Impact.

3.0331 Type 410 exhibits reversible temper embrittlement which is best shown by the variations in impact energy. As shown earlier in Figure 3.0231, the room-temperature impact energy shows a minimum after tempering at 800 to 900 F and increases sharply after tempering at slightly higher temperatures. The data in Figure 3.0332 further show that tempering at 1200 F results in much higher impact energies over a range of temperatures as compared to tempering at 930 F. Retempering at 930 F after tempering at 1200 F decreases the impact-energy values in the test temperature range 0 to 100 F as compared to the 1200 F-tempered material, indicating a modest amount of embrittlement. However, retempering at 1200 F after an initial temper at 930 F removes the embrittlement, as shown by comparison with the curve for the 930 F-tempered material. This behavior illustrates the reversible nature of temper embrittlement in 12 percent chromium steels. The reversible embrittlement is associated with phosphorus and chromium segregation to prior austenite grain boundaries, along which fracture occurs (54).

3.0332 Effects of test and tempering temperatures on Charpy impact energy of Type 410, Figure 3.0332.

3.0333 Effects of test and tempering temperatures on Charpy impact energy of Type 416, Figure 3.0333.

3.0334 Effect of elevated test temperatures on impact properties of Type 403, Figure 3.0334.

3.0335 Effects of elevated test temperatures on impact properties of Types 403 and 410, Table 3.0335.

3.0336 Effect of low test temperatures on impact properties of Types 410 and 416, Figure 3.0336.

3.034 Bending.

3.035 Torsion and shear.

3.036 Bearing.

3.037 Stress concentration.

3.0371 Notch properties.

3.0372 Fracture toughness.

3.03721 Effects of temperature and impurity content on fracture toughness of Type 403, Figure 3.03721.

3.038 Combined properties.

3.04 **Creep and Creep-Rupture Properties**

3.041 Creep-rupture behavior of Type 403 at 840 to 1110 F, Figure 3.041.

3.042 Creep-rupture curves for Type 403 bar at 1000 to 1500 F, Figure 3.042.

3.043 Short-time total-strain curves for as-quenched Type 410 sheet at 1200 to 2000 F, Figure 3.043.

3.044 Creep-rupture curves for smooth and notched Type 410 bars at 600 to 800 F, Figure 3.044.

3.05 **Fatigue Properties**

3.051 Stress-range diagrams at room temperature to 900 F for Type 403 heat treated to 20 to 26 HRC, Figure 3.051.

3.052 Stress-range diagrams at room temperature to 900 F for Type 403 heat treated to 26 to 32 HRC, Figure 3.052.

3.053 Stress-range diagrams at 700 and 900 F for rupture, 1 and 0.5 percent total strain for heat-treated Type 403 bar, Figure 3.053.

3.054 Low-cycle axial fatigue behavior of Type 403 in air at room and elevated temperatures, (a) room temperature, (b) 750 F, (c) 930 F, and (d) 1110 F, Figure 3.054.

3.055 Effects of temperature and cyclic strain rate on low-cycle axial fatigue life of Type 403, Figure 3.055.

3.056 High-frequency axial and torsional fatigue behavior of Type 403 in air at room temperature, Figure 3.056.

3.057 High-frequency bending fatigue behavior of Type 410 in air at room temperature, Figure 3.057.

3.058 High-frequency bending fatigue behavior of smooth and notched Type 403 bar in air at room temperature, Figure 3.058.

Fe
12 Cr
Low C

Types 403, 410, 416

3.059 High-frequency bending fatigue behavior of Type 403 at room and elevated temperatures, Figure 3.059.

3.0510 Fatigue strength at 10^8 cycles for Type 403 at room and elevated temperatures, Figure 3.0510.

3.0511 Fatigue-crack-growth rate of Type 403 in air at room temperature, Figure 3.0511.

3.06 **Elastic Properties**

3.061 Poisson's ratio, 0.27 to 0.29.

3.062 Modulus of elasticity of Type 410 at room and elevated temperatures, Figure 3.062.

3.0621 Effect of heat treatment of Type 410 on modulus of elasticity at room temperature, Table 3.0621.

3.063 Modulus of rigidity at room and elevated temperatures, Figure 3.063.

3.064 Tangent modulus.

3.065 Secant modulus.

4 FABRICATION

4.01 **Forming**

4.011 General. Type 410 is generally formed in the fully annealed condition. Its formability is inferior to that of annealed 18-8 steels but comparable to that of 1/4-hard 18-8 steels.

4.012 Forging. Starting temperature 2200 F maximum, finishing temperature 1700 F minimum. Hot upsetting operations on Type 403 and Type 410 can be performed at temperatures down to 1300 F. Heavy sections must be preheated at 1200 to 1500 F and both heavy sections and complicated shapes should be equalized after forging at about 1300 F and furnace cooled or cooled slowly in an insulating material. Type 416 can be forged to a limited extent but should be annealed after forging.

4.013 The presence of delta ferrite may cause difficulties in hot-working processes, especially during the piercing of seamless tubes and in forgings if upsetting is involved. Reheating one or more times is advisable when the upsetting operation is severe. The amount of delta ferrite that may be present in Type 410, if the chemistry is not properly balanced, is a function of the ingot size as well as of the composition. As the ingot size is reduced by hot working, the amount of delta ferrite present may decrease; also it may vary from the top to the bottom and from the surface to the center of the ingot (48).

4.014 Type 410 can be consolidated from atomized prealloyed powder by pressing followed by sintering in dissociated ammonia at 2190 to 2280 F. Tensile strengths of as-sintered alloy range from 76 to 98 ksi at densities of 85 to 93 percent. Elongation, however, ranges only from 1 to 9 percent as a result of nitriding during sintering. Embrittlement can be avoided by sintering in low-pressure nitrogen, 50 microns for example (82,86).

4.02 **Machining and Grinding**

4.021 Best machinability in Types 403 and 410 is obtained if they are heat treated or annealed and cold worked to 200 to 260 BHN for light fast cuts, or to 180 to 220 BHN for heavy cuts, drilling, or sawing. Machinability rating in this condition is 50 to 55 percent of that of mild steels. In the annealed condition these steels have a tendency to tear and to seize.

4.022 Types 416 and 416Se possess the highest machinability of all stainless steels. The best performance is obtained if heat treated or cold worked to 180 to 240 BHN. A satisfactory lubricant for most operations is a low-concentration sulfur-base oil. The machinability rating of this steel is about 85 percent of that of mild steel.

4.023 The machinability of Type 416 sulfurized stainless steel is greatly affected by both sulfur and manganese contents. High sulfur content and a high manganese-to-sulfur ratio provide significantly improved machinability, as shown in Figure 4.024. (Drill machinability is defined as the ratio of the average time required to drill a standard bar to that required to drill the test bar.) Optimum machinability at any given sulfur level requires a manganese-to-sulfur ratio of at least 7:1. The machinability relates directly to the properties of the sulfide inclusions that are formed. At very low manganese-to-sulfur ratios, chromium sulfide is the equilibrium phase. Higher ratios produce a spinel-type sulfide, then an alpha-MnS which is saturated with chromium and iron, and finally nearly pure alpha-MnS when the ratio exceeds about 7:1. The average hardness of sulfide inclusions decreases as the manganese-to-sulfur ratio increases, being lowest for pure alpha-MnS. The soft sulfides reduce the shear stress required for fracture in the secondary shear zone by providing regions of easy shear. This lowers the required cutting forces and accounts for the higher machinability ratings and improved tool life obtained with high manganese-to-sulfur ratio materials (83).

4.024 Effects of manganese and sulfur contents on machinability of Type 410, Figure 4.024.

4.03 **Joining**

4.031 Martensitic stainless steels, in particular those with carbon contents above 0.25 percent, are difficult to weld. However, the lower carbon martensitic stainless steels can be successfully welded with careful control of preheat temperature and post-weld heat treatment. Types 403 and 410 are commonly joined by a wide variety of welding processes including resistance welding, arc welding, and electroslag welding. When these steels are used in machinery components, fabrication is usually accomplished by one of the arc-welding processes, such as shielded metal arc, gas tungsten arc, or submerged arc. Welding of annealed base material followed by heat treatment of the entire weldment will produce the most homogeneous structure and optimum mechanical properties. However, because of the difficulties of quenching and tempering complex structures, it is common practice to weld fully heat-treated component parts. Despite the use of careful controls, as well as recommended procedures and proper preheat and post-weld heat treatment, center bead cracking can occur in welds during fabrication of 12 percent chromium stainless steels. Concave, single-pass fillet welds with Type 410 filler metal on Types 403

and 410 steels seem particularly vulnerable. Cracking can be eliminated through the use of a 12Cr-4Ni-Mo (Type E-410-Ni or E-410-Ni-Mo) or 12Cr-4Ni-Mo-Ti (AM-363) electrode. Cracking in Type 410 welds is believed to occur between about 1600 and 2500 F. Shrinkage strains produced by weld-bead cooling cause fracture of ferrite grains or fracture at austenite-ferrite grain boundaries. These microcracks produce stress concentrations and propagate into larger cracks as the weld continues to cool and shrinkage stresses continue to increase (84).

4.032 For fusion welding of Type 403 and Type 410, electrodes of the same composition can be used when material is to be subsequently heat treated, and Type 309 or 310 electrodes can be used if the material is to be used in the as-welded condition. Preheating to 300 F minimum and post-heating at 1300 F, followed by cooling at a rate of 100 F per hour maximum to 1100 F, is necessary to prevent cracking. Type 416 is weldable to a very limited extent. This alloy should be annealed at 1450 F after welding to improve both ductility and corrosion resistance.

4.04 **Surface Treating**

4.041 Stainless steels such as Types 410 and 416 (and probably 403 also) can be plated with any of the common metals after preplating using Wood's nickel strike. This strike is a simultaneous activation/plating treatment resulting in a thin adherent deposit of nickel. Specimens plated after a Wood's strike fail in the electroplated deposit rather than at the coating/substrate interface (85).

REFERENCES

1 AMS 5350F (April 1, 1981).
2 AMS 5351D (April 1, 1981).
3 AMS 5504H (July 1, 1985).
4 AMS 5591F (January 15, 1981).
5 AMS 5610K (July 1, 1982).
6 AMS 5613M (July 1, 1984).
7 AMS 5776B (October 1, 1981).
8 AMS 5777B (July 1, 1981).
9 ASTM A 193-69 Alloy – Steel Bolting Materials for High Temperature Service, Book of Standards American Society for Testing Materials, Part 1 (1970), pp 109–117.
10 ASTM A 194-69 Carbon and Alloy Steel Nuts for Bolts for High Pressure and High Temperature Service (ibid.), pp 118–125.
11 ASTM A 276-67 Stainless and Heat Resisting Bars and Shapes, Book of Standards American Society for Testing Materials, Part 3 (1970), pp 235–241.
12 ASTM A 296-68 Corrosion Resistant Iron-Chromium, Iron-Chromium-Nickel and Nickel Base Castings, Book of Standards American Society for Testing Materials, Part 2 (1970), pp 157–163.
13 ASTM A 314-63 Stainless and Heat-Resistant Steel Billets and Bars for Reforging, Book of Standards American Society for Testing Materials, Part 3 (1970), pp 310–313.
14 ASTM A 351-69 Ferrite and Austenitic Steel Castings for High Temperature Service, Book of Standards American Society for Testing Materials, Part 2 (1970), pp 181–187.
15 AMS 5349B (July 1, 1984).
16 American Iron and Steel Institute, "Stainless and Heat Resisting Steels", Steel Products Manual (June 1957), p 38.
17 AMS 5505B (July 16, 1979).
18 AMS 5609A (July 16, 1979).
19 AMS 5611A (July 15, 1980).
20 AMS 5612D (April 1, 1984).
21 AMS 5614A (October 15, 1978).
22 AMS 5655B (July 1, 1983).
23 AMS 5821B (October 15, 1980).
24 Allegheny Ludlum (1958).
25 Epsey, G. B., Jones, M. H., and Brown, W. F., Jr., *Proc. ASTM*, Vol 59 (1959), p 837.
26 Schoefer, E. A., "Corrosion Resistance Type CA-15", Alloy Casting Institute Data Sheet (June 1954).
27 Hosi, Y., and Pinnow, K. E., "The Tensile Properties of Type 410 Stainless Steel Deformed Before and After Martensite Transformation", *Trans. ASM*, Vol 53 (1961), p 591.
28 North American Aviation, Inc., "Materials Property Manual and Summary Report", Materials Research Report No. AL-2604, Appendix 6 (October 30, 1957).
29 Westinghouse Electric Corporation, "Properties of AISI Type 410 Stainless Steel", Bettis Plant.
30 Materials Manual (May 1957) Universal Cyclops Steel Corporation, "High Temperature Metals" (October 1958).
31 Morykawas, S., "Cannon-Muskegon Corporation, 416 Alloy Data" (September 1967).
32 Lennox, T. J., Jr., Peterson, M. H., and Groover, R. E., "Marine Corrosion Studies", NRL Report 1948 (November 1968).
33 Jones and Laughlin Steel Corporation, Jones and Laughlin Stainless Steel Data Sheet (July 25, 1958).
34 Gerberich, W. W., Martens, H. E., and Boundy, R. A., "Tensile Properties of Five Low-Alloy and Stainless Steels Under High-Heating-Rate and Constant-Temperature Conditions", Technical Report No. 32-222, Jet Propulsion Laboratory (June 1962).
35 Chait, R., and Weiss, V., "Isothermal True Stress-Strain Curves of Body Centered Metals", Syracuse University Research Institute Report No. MET. E. 1081-0666 (June 1966); see also Chait, R., "Deformation and Fracture of High Strength BCC Polycrystalline Alloys", Ph.D. Thesis, Syracuse University (1967) (available from University of Michigan, Order No. 68-5451).
36 Report on Strengths of Wrought Steels at Elevated Temperatures, ASTM Data Series D53.
37 Best, G. E., "403 Stainless Steel", General Electric Data Sheets (June 2, 1958).
38 "Development of a Point Deformation Rolling Mill", Ninth Interim Engineering Progress Report, MMP Project Nr 8-252 (July 1966–September 1966).

Fe
12 Cr
Low C

Types 403, 410, 416

39 DeSisto, T. S., unpublished data, Army Materials and Mechanics Research Center, Watertown, Massachusetts.

40 Haynes Stellite Company, "Haynes Investment-Cast Steels", Haynes Type 410 Stainless Steel (April 1958).

41 Holden, F. C., "A Review of Dimensional Instability in Metals", DMIC Memorandum 189 (March 1964).

42 Van Echo, J. A., Gullotti, D. V., Bibler, J. R., and Simmons, W. F., "Short-Time Creep Properties of Structural Sheet Materials for Aircraft and Missiles", AFTR 6731, Part 4 (January 1956).

43 General Electric (1957).

44 Sessler, J., and Brown, W. F., Jr., *Proc. ASTM*, Vol 56 (1956), p 738.

45 Vitovec, F. H., and Lazan, B. J., "Fatigue, Creep and Rupture Properties of Heat Resistant Materials", WADC TR56-181 (August 1956).

46 ASTM STP 129 Symposium on Determination of Elastic Constants.

47 Timken, "Resume of High Temperature Investigations During 1948–50" (1950).

48 Clark, C. C., "High Temperature Alloys", Pitman Publishing Corporation (1953), pp 206–213.

49 Banerjee, B. R., and Hauser, J. J., "Effect of Processing Variables on Crack Propagation of High Strength Steels and Titanium", Crucible Steel Company of America (August 29, 1963).

50 DMIC Data Sheet, 6909-001 (September 1969).

51 Nachman, J. F., and Buehler, W. J., "Applications, Properties, and Fabrication of Thermenol Type Alloys", U.S. Naval Ordnance Report 4237 (May 5, 1956).

52 Favor, R. J., and Popp. H. G., "Materials Property Data Compilation, Part III AISI 410", General Electric Company, Cincinnati, Ohio (January 31, 1964).

53 Warren, K. A., and Reed, R. P., "Tensile and Impact Properties of Selected Materials from 20 to 300 K", National Bureau of Standards Monograph 63 (June 28, 1963).

54 Prabhu, G. V., Huntz, A. M., and Lacombe, P., "Role of Carbon in Embrittlement Phenomena of Tempered Martensite 12Cr-0.15%C Steel", *Metal Science*, Vol 14, No. 7 (July 1980), pp 241–252.

55 Draznik, R. A., "The Versatile 416 Stainless Steels", *Modern Machine Shop*, Vol 56, No. 9 (February 1984), pp 70–74.

56 Breinan, E. M., and Ansell, G. S., "The Influence of Austenite Strength upon the Austenite-Martensite Transformation in Alloy Steels", *Metallurgical Transactions*, Vol 1, No. 6 (June 1970), pp 1513–1520.

57 "AISI Type 403", Alloy Digest, Filing Code: SS-94 (October 1959).

58 Clark, A. F., Childs, G. E., and Wallace, G. H., "Electrical Resistivity of Some Engineering Alloys at Low Temperatures", *Cryogenics*, Vol 10, No. 4 (August 1970), pp 295–305.

59 Henthorne, M., "Corrosion of Resulfurized Free-Machining Stainless Steels", *Corrosion*, Vol 26, No. 12 (December 1970), pp 511-528.

60 Southwell, C. R., and Bultman, J. D., "Corrosion of Metals in Tropical Environments: Part 10 – Final Report of Sixteen-Year Exposures", NRL-7834 (January 2, 1975).

61 Phelps, E. H., "Stress Corrosion of Ferritic-Martensitic Stainless Steels", *Metals Engineering Quarterly*, Vol 13, No. 2 (May 1973), pp 44–49.

62 Nelson, E. E., "Stress Corrosion Cracking of Several High Strength Ferrous and Nickel Alloys", NASA-TM-X-64626 (November 11, 1971).

63 Abrego, L., and Begley, J. A., "Fatigue Crack Propagation of 403 Stainless Steel in Aqueous Solutions at 100 C", paper presented at Corrosion/80, sponsored by the National Association of Corrosion Engineers, Chicago, Illinois (March 3–7, 1980).

64 Gilbreath, W. P., and Adamson, M. J., "The Stress Corrosion Susceptibility of Several Alloys in Hydrazine Fuels", NASA TN-D-7604 (February 1974).

65 Chandler, W. T., and Walter, R. J., "Testing to Determine the Effect of High Pressure Hydrogen Environments on the Mechanical Properties of Metals", paper presented at the Seventy-Fifth Annual Meeting of the American Society for Testing and Materials, Los Angeles, California (June 25–30, 1972).

66 Sakamoto, Y., and Hanada, U., "Effect of Heat Treated Structure on Diffusion of Hydrogen in Martensitic Type 403 Stainless Steel", *Transactions of the Japan Institute of Metals*, Vol 18, No. 6 (June 1977), pp 466–470.

67 Mertens, F. P., "Reflectance Infrared Study of the Oxidation of Stainless Steels and Component Metals", *Corrosion*, Vol 34, No. 10 (October 1978), pp 359–364.

68 McCoy, H. E., and McNabb, B., "Corrosion of Several Iron- and Nickel-Base Alloys in Supercritical Steam at 1000 F", ORNL-TM-4552 (August 1974).

69 Bates, C. E., Wren, J. E., Monroe, R., and Pears, C. D., "Ignition and Combustion of Ferrous Metals in High Pressure, High Velocity, Gaseous Oxygen", *Journal of Materials for Energy Systems*, Vol 1, No. 1 (June 1979), pp 61–76.

70 Hosbons, R. R., Pacey, A. J., and Wotton, B. L., "Effect of Impurity Concentration on the Change in Fracture Toughness of AISI Type 403 Stainless Steel with Fast Neutron Radiation", ASTM STP-570 (1975), pp 103–116.

71 Hosbons, R. R., and Wotton, B. L., "Heat Treatment to Improve the Toughness of 12% Chromium Steels", AECL-6776 (October 1980).

72 Kanazawa, K., Yamaguchi, K., and Yoshida, S., "High-Temperature Rotating Bending Fatigue Behavior of a Martensitic Stainless Steel SUS 403-B", *Transactions of National Research Institute for Metals*, Vol 20, No. 2 (March 1978), pp 98–103.

73 Scott, J. K., and Cox, E. P., "Fracture Characteristics of Two High-Strength, Low-Alloy and Two Stainless Steels", CERL-IR-M-200 (January 1977).

74 Kawada, T., "Data Sheets on the Elevated-Temperature Properties of 12Cr Stainless Steel Bars for Turbine Blades (SUS 403-B), National Research Institute for Metals Data Sheet (1974).

75 Kanazawa, K., Yamaguchi, K., Sato, M., Kobayashi, K., and Suzuki, N., "Elevated-Temperature Fatigue Properties of Engineering Materials, Part IV – Section 10: Elevated-Temperature Fatigue Properties of a 12Cr Stainless Steel Bar for General Application (SUS 403-B)", *Transactions of National Research Institute for Metals*, Vol 20, No. 5 (September 1978), pp 321–329.

76 Kanazawa, K., Yamaguchi, K., and Kobayashi, K., "The Temperature Dependence of Low Cycle Fatigue Behavior of Martensitic Stainless Steels", *Materials Science and Engineering*, Vol 40, No. 1 (September 1979), pp 89–96.

77 Willertz, L. E., and Moon, D. M., "Correlation of Damping and Fatigue Properties of an AISI 403 Stainless Steel", *Journal of Testing and Evaluation*, Vol 3, No. 3 (May 1975), pp 191–198.

78 Wright, R. N., "The High Cycle Fatigue Strength of Commercial Stainless Steel Strip", *Materials Science and Engineering*, Vol 22, No. 3 (March 1976), pp 223–230.

79 Nishijima, S., Matsuda, C., Abe, T., Takeuchi, E., and Komatsu, A., "Statistical Fatigue Properties of Heat Treated JIS Steels, S45C, SCM3, SNCM8, SK5, and SUS403, for Machine Structural Use", *Transactions of National Research Institute for Metals*, Vol 19, No. 6 (November 1977), pp 327–343.

80 Logsdon, W. A., "An Evaluation of the Crack Growth and Fracture Properties of AISI 403 Modified 12Cr Stainless Steel", *Engineering Fracture Mechanics*, Vol 7, No. 1 (March 1975), pp 23–40.

81 Wolfenden, A., "Internal Friction Study of AISI 410 Stainless Steel", *Scripta Metallurgica*, Vol 17, No. 3 (March 1983), pp 321–325.

82 Otto, G., "Vacuum Sintering of Stainless Steel", *Journal of Vacuum Science and Technology*, Vol 11, No. 6 (November/December 1974), pp 1110–1113.

83 Kovach, C. W., and Moskowitz, A., "Effects of Manganese Additions and Sulfur Additions on the Machinability of Martensitic Stainless Steels", *Transactions of the Metallurgical Society of AIME*, Vol 245, No. 8 (October 1969), pp 2157–2164.

84 Castner, H. R., "Cause and Prevention of 12% Chromium Steel Fillet Weld Cracks", *Welding Journal*, Vol 56, No. 7 (July 1977), pp 193-s–200-s.

85 Dini, J. W., and Johnson, H. R., "Plating on Stainless-Steel Alloys", *Plating and Surface Finishing*, Vol 69, No. 11 (November 1982), pp 63–65.

86 Dovydenkov, V. A., Radomysel'skii, I. E., and Napara-Volgina, S. G., "Methods of Production and Properties of Sintered Stainless Steels for Machine Components – A Review", *Soviet Powder Metallurgy and Metal Ceramics*, Vol 17, No. 5 (May 1978), pp 371–379.

Fe
12 Cr
Low C

Types 403, 410, 416

Alloy	Types 403, 410, and 416	
Alloy Type	AMS Specification	Product Form
403	5611A	Bars, forgings, and tubing
410	5350F	Investment castings
	5351D	Sand castings
	5504H	Sheet, strip, plate, annealed
	5505B	Sheet, strip, plate, ferrite controlled
	5591F	Tubing, seamless
	5609A	Bars, forgings, tubing, rings, ferrite controlled
	5612D	Bars, forgings, tubing, rings, ferrite controlled, annealed
	5613M	Bars, forgings, tubing, rings, annealed
	5614A	Bars and forgings
	5776B	Welding wire
	5777B	Electrode, covered welding
	5821B	Welding wire, ferrite control
416	5349B	Investment castings
	5610K	Bars and forgings, free-machining

TABLE 1.031. AMS SPECIFICATIONS FOR TYPES 403, 410, AND 416 (1–8,15,17–21,23)

Fe
12 Cr
Low C

Types 403, 410, 416

Alloy	403		416		416		416		416	
Form	Wrought		Cast		Cast		Wrought		Wrought	
Source	AMS 5611A[b]		AMS 5349B[c]		AMS 5349B[a]		AMS 5610K[c]		AMS 5610K[c]	
	Percent		Percent		Percent		Percent		Percent	
Element	Min	Max	Min	Max	Min	Max	Min	Max	Min	Max
Chromium	11.50	12.50	11.50	14.00	11.50	14.00	11.50	13.50	11.50	13.50
Carbon	0.12	0.15	–	0.15	–	0.15	–	0.15	–	0.15
Manganese	–	0.60	–	1.25	–	1.25	–	1.25	–	2.50
Silicon	–	0.50	–	1.50	–	1.50	–	1.00	–	1.00
Nickel	–	0.75	–	0.50	–	0.50	–	0.75	–	0.75
Copper	–	0.50	–	0.50	–	0.50	–	0.50	–	0.50
Molybdenum	–	0.20	–	0.50	–	0.50	–	0.60[a]	–	0.60[a]
Zirconium	–	–	–	0.50	–	0.50	–	0.60[a]	–	0.60[a]
Aluminum	–	0.05	–	0.05	–	0.05	–	–	–	–
Tin	–	0.05	–	0.05	–	0.05	–	–	–	–
Phosphorus	–	0.025	–	0.04	–	0.04	–	0.06	–	0.06
Sulfur	–	0.025	0.15	0.35	–	0.03	–	0.03	0.15	0.40
Nitrogen	–	0.18	–	–	–	–	–	–	–	–
Selenium	–	–	–	–	0.10	0.30	0.18	0.35	–	–

(a) 0.60 max molybdenum or zirconium.
(b) Ferrite controlled.
(c) AMS 5349B and 5610K each specify a high-sulfur and a selenium-containing modification for Type 416.

TABLE 1.041. COMPOSITION SPECIFICATIONS FOR TYPES 403 AND 416 (5,15,19)

Alloy	410									
Form	Cast				Wrought					
Source	AMS 5350F		AMS 5351F CA-40[a]		AMS 5504H AMS 5591F[b] AMS 5613M[c] AMS 5776B[d] AMS 5777B[d]		AMS 5505B[e] AMS 5609A[e,f] AMS 5612D[e,g] AMS 5821B[h]		AMS 5614A	
	Percent		Percent		Percent		Percent		Percent	
Element	Min	Max	Min	Max	Min	Max	Min	Max	Min	Max
Chromium	11.50	13.50	11.50	14.00	11.50	13.50	11.50	12.50	11.50	12.50
Carbon	0.05	0.15	–	0.15	–	0.15	0.12	0.15	0.07	0.12
Manganese	–	1.00	–	1.00	–	1.00	–	0.60	0.30	0.60
Silicon	–	1.00	–	1.50	–	1.00	–	0.50	–	0.35
Nickel	–	0.50	–	1.00	–	0.75	–	0.75	–	0.60
Copper	–	0.50	–	0.50	–	0.50	–	0.50	–	0.50
Molybdenum	–	0.50	–	0.50	–	0.50	–	0.20	0.40	0.60
Aluminum	–	0.05	–	0.05	–	0.05	–	0.05	–	0.05
Tin	–	0.05	–	0.05	–	0.05	–	0.05	–	0.05
Phosphorus	–	0.04	–	0.04	–	0.04	–	0.025	–	0.04
Sulfur	–	0.03	–	0.03	–	0.03	–	0.025	–	0.03
Nitrogen	–	–	–	–	–	0.08	–	0.08	–	0.08

(a) Carbon 0.20–0.40.
(b) Molybdenum max 0.60.
(c) Carbon min 0.10.
(d) Phosphorus max 0.023; sulfur max 0.015; phosphorus + sulfur max 0.030.
(e) Ferrite controlled.
(f) Plus 0.05 to 0.20 columbium.
(g) Molybdenum max 0.50.
(h) Carbon min 0.11.

TABLE 1.042. COMPOSITION SPECIFICATIONS FOR TYPE 410 (1–4,6–8,12,17,18,20,21,23)

Fe
12 Cr
Low C

Types 403, 410, 416

Alloy	Types 403, 410, and 416		
Alloy Type	AMS Specification	Austenitizing Conditions	Tempering Conditions
403	5611A[a]	1735 F, 1 hr, AC	600 F, 2 hr, AC
410	5350F	1750 F, 1 hr, AC	1350 F, 1 hr
	5351D	1850 F, 30 min, AC	1100 F min, AC
	5504H, 5591F, 5613M, 5776B, 5777B	1750 F, 30 min, AC	–
	5505B[b], 5609A, 5612D[a], 5821B[b]	1700 F, 1 hr, AC	600 F, 2 hr, AC
	5614A	1750 F, 30 min, AC	1100 F min, 1 hr, AC
416	5349B	1750 F, 30 min, AC	1100 F, 1 hr, AC
	5610K	1825 F, 30 min, AC	–

Note: The original AMS documents should be consulted for complete specification details.

(a) Austenitized in a neutral atmosphere.
(b) Tempered twice.

TABLE 1.057. AMS-SPECIFIED HEAT-TREATMENT CONDITIONS FOR TYPES 403, 410, AND 416 (1–8,15,17–21,23)

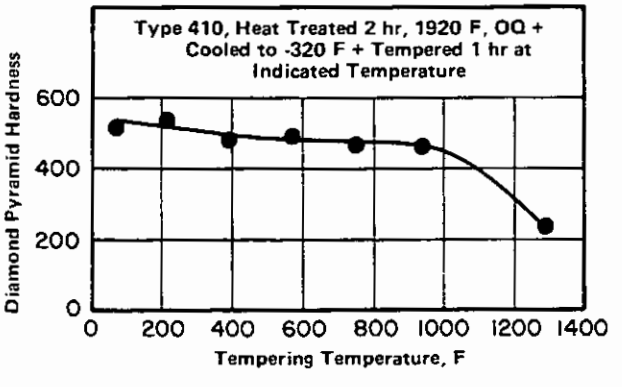


FIGURE 1.062. EFFECT OF TEMPERING TEMPERATURE ON HARDNESS OF TYPE 410 (54)

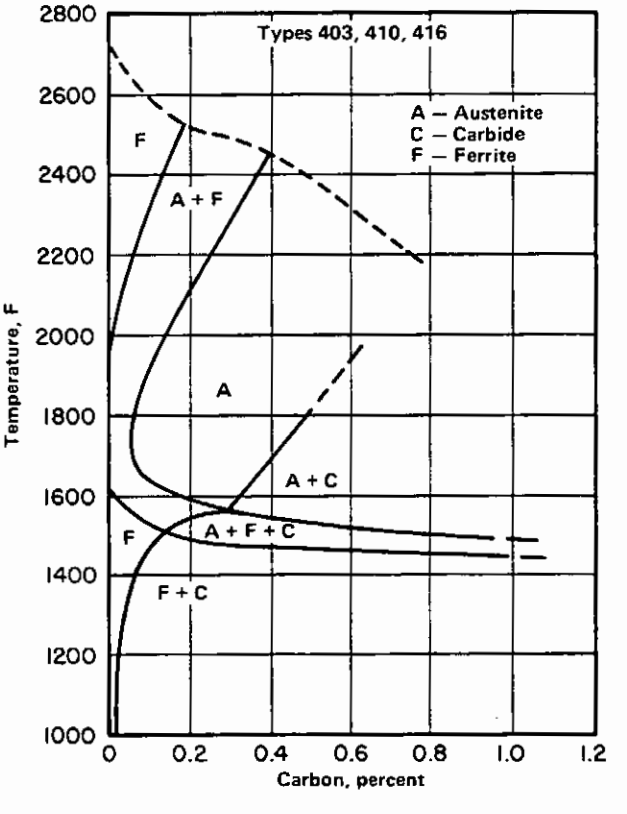


FIGURE 2.01203. EQUILIBRIUM PHASE DIAGRAM FOR TYPES 403, 410, AND 416 WITH RESPECT TO CARBON CONTENT (54)

Fe
12 Cr
Low C

Types 403, 410, 416

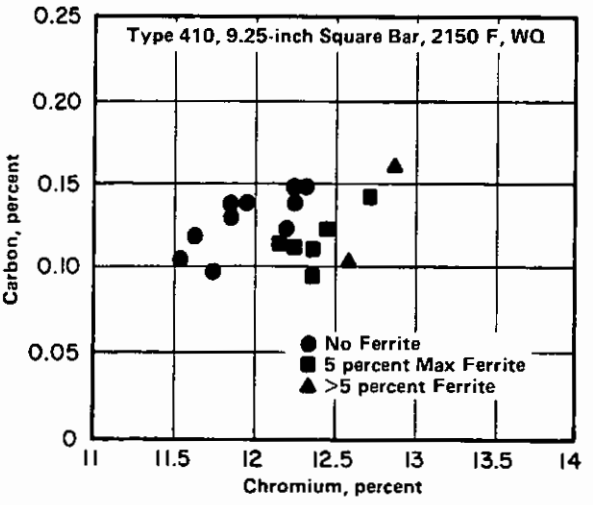


FIGURE 2.01204. EFFECT OF CARBON AND CHROMIUM CONTENT ON DELTA FERRITE CONTENT OF TYPE 410 (48)

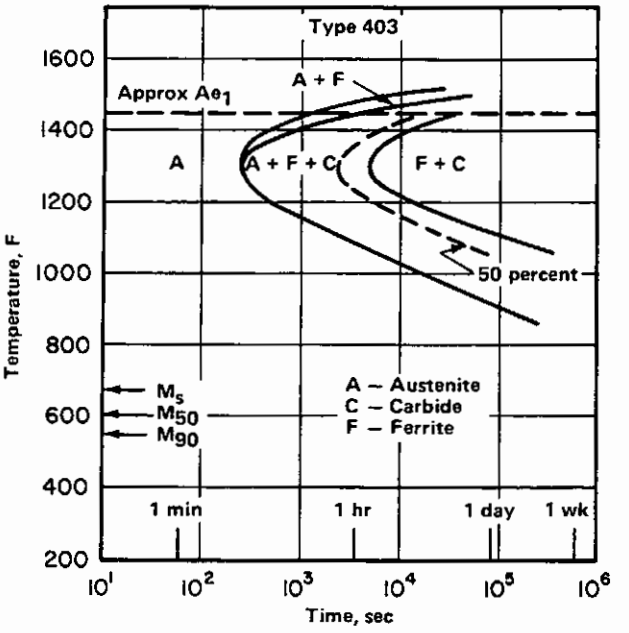


FIGURE 2.01211. TIME-TEMPERATURE-TRANSFORMATION DIAGRAM FOR TYPE 403 (57)

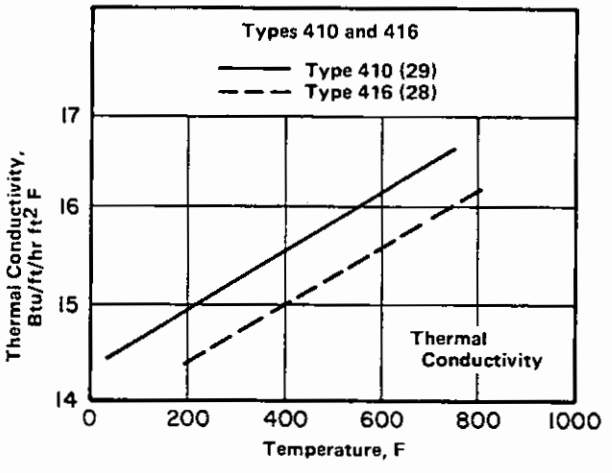


FIGURE 2.013. THERMAL CONDUCTIVITY OF TYPES 410 AND 416 (28,29)

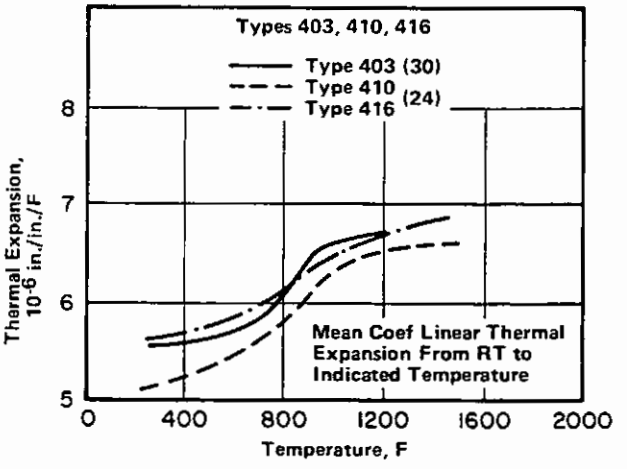


FIGURE 2.014. THERMAL EXPANSION OF TYPES 403, 410, AND 416 (24,30)

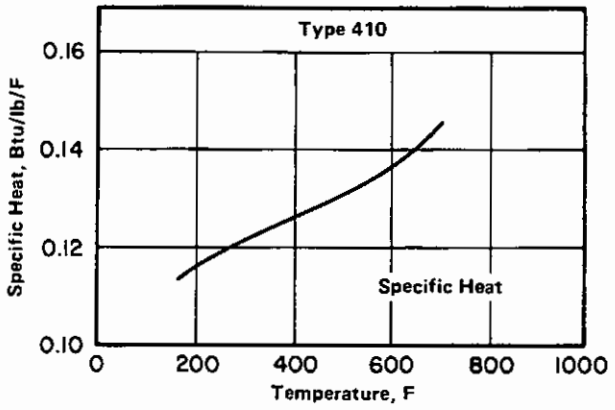


FIGURE 2.015. SPECIFIC HEAT OF TYPE 410 (29)

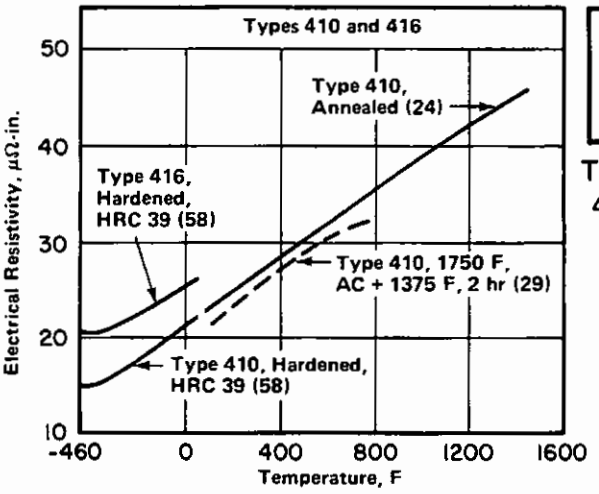


FIGURE 2.022. ELECTRICAL RESISTIVITY OF TYPES 410 AND 416 (24,29,38)

Fe
12 Cr
Low C

Types 403, 410, 416

Alloy	Type 410	
Condition	1350 F, 4 hr, FC	1850 F, AC + 500 F, 2 hr
Max Permeability	850	82
Residual Induction, G	12,000	6,000
Coercive Force, Oe	33	48

TABLE 2.0233. RESIDUAL INDUCTION AND COERCIVE FORCE OF TYPE 410 AFTER MAGNETIZING AT 1200 OERSTEDS, AND MAXIMUM PERMEABILITY (29)

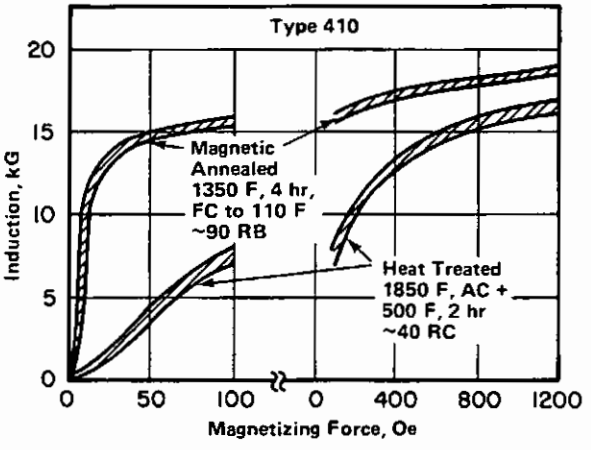


FIGURE 2.0232. MAGNETIZATION CURVES (29)

Fe
12 Cr
Low C

Types 403, 410, 416

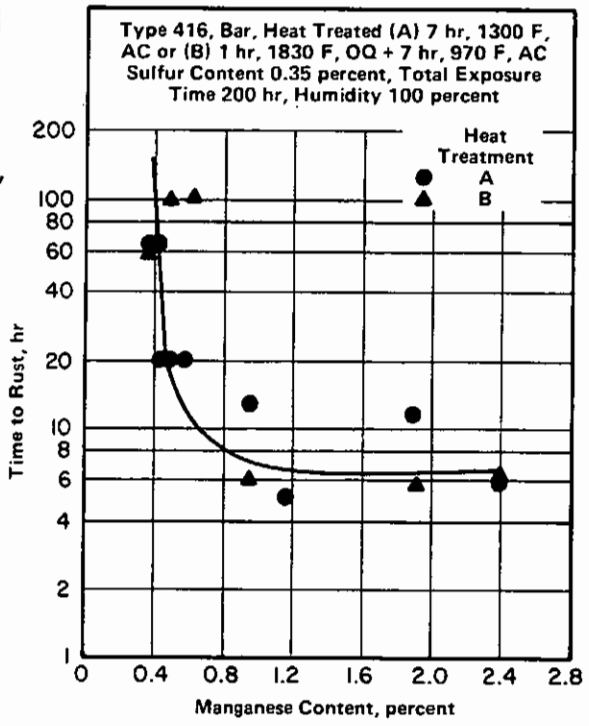


FIGURE 2.0314. EFFECT OF MANGANESE ON TIME FOR FIRST APPEARANCE OF RUST SPOTS ON TYPE 416 IN HUMID AIR AT ROOM TEMPERATURE (59)

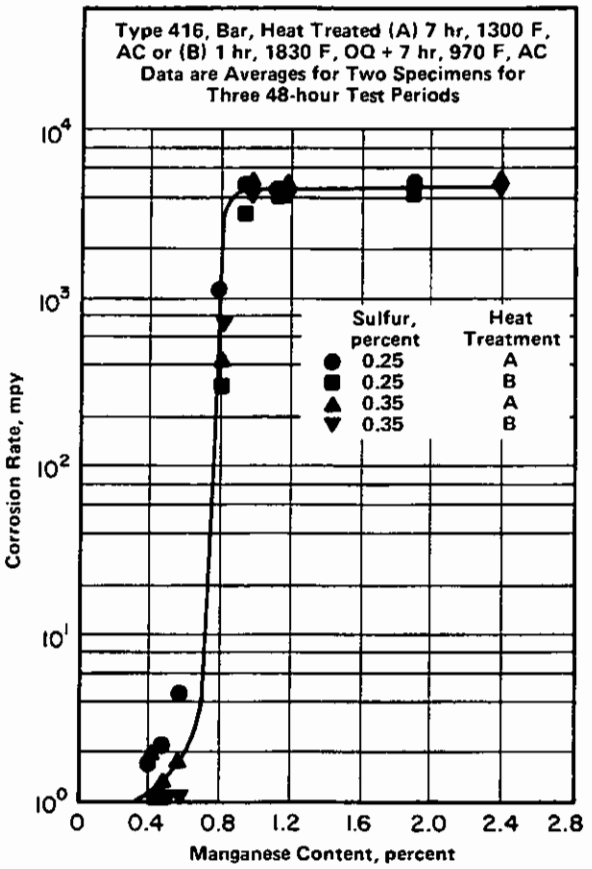


FIGURE 2.0315. EFFECT OF MANGANESE CONTENT ON CORROSION OF TYPE 416 IN AQUEOUS SOLUTION OF 10 PERCENT NITRIC ACID AT ROOM TEMPERATURE (59)

Alloy	Type 416				
Sulfur Content, percent	Corrosion Conditions		Material Heat Treatment[a]	Corrosion Rate, mpy[b], for Indicated Percent Manganese Content	
	Acid	Temperature, F		0.4 Mn	2.0 Mn
0.007	Nitric, 10 percent	75	A	50	42
			B	35	60
	Citric acid buffer	122	A	<1	<1
			B	<1	<1
	Acetic, 3 percent	Boiling	A	<1	<1
			B	<1	<1
0.35	Nitric, 10 percent	75	A	6	3700
	Citric acid buffer	122	A	3	710
			B	1	650
			C	1	450
	Acetic, 3 percent	Boiling	A	201	580
			B	135	260
			C	50	180
	Sulfuric, 0.5 percent	75	A	730	725

(a) A – 7 hr, 1300 F, AC
B – 1 hr, 1830 F, OQ plus 7 hr, 970 F, AC
C – 1 hr, 1830 F, OQ plus 2 hr, 600 F, AC.
(b) Based on 48-hr exposure.

TABLE 2.0316. EFFECTS OF SULFUR AND MANGANESE CONTENTS AND HEAT TREATMENT ON CORROSION RATE OF TYPE 416 IN SEVERAL ACIDS (59)

Fe
12 Cr
Low C

Types 403, 410, 416

Alloy	Type 410									
	General Corrosion						Steady State Rate, mpy	Pitting Penetration, mils(b)		
	Weight Loss, g/dm^2			Average Penetration, mils						
Exposure(a)	1 Yr	8 Yr	16 Yr	1 Yr	8 Yr	16 Yr		1 Yr	8 Yr	16 Yr
S	6.0	28.1	46.8	3.1(c)	14.3(c)	23.9(c)	(c)	61 (P)	161 (P)	212 (P)
M	1.0	6.7	12.6	0.5	3.4(c)	6.4(c)	(c)	46	67	107 (P)
L	0.0	1.1	1.8	0.0	0.5	0.9(c)	(c)	<5	<5	94 (P)
A	0.08	0.05	0.35	0.04	0.04	0.18	<0.01	<5	<5	<5
B	0.01	0.00	0.02	0.00	0.00	0.01	0.00	<5	<5	<5

(a) S – seawater immersion
M – seawater at mean-tide level for intermittent immersion
L – freshwater immersion
A – tropical marine atmospheric exposure
B – tropical inland atmospheric exposure
Panels for aqueous exposures measured 9 x 9 x 0.25 in.; those for atmospheric exposures measured 4 x 8 x 0.063 in.

(b) Twenty-pit average as determined from the five deepest pits on each surface of duplicate panels; "P" denotes perforation.

(c) Deep local pitting; average penetration not appropriate.

TABLE 2.0318. CORROSION OF TYPE 410 IN TROPICAL ENVIRONMENTS FOR TIMES UP TO 16 YEARS (60)

Alloy	Type 410		
Austenitizing Temperature, F	Tempering Temperature, F	Yield Strength, ksi	Time to Failure, days(a)
1600	450	140	NF
	700	138	NF
	950	130	NF
	1200	80	NF
1750	450	150	NF
	700	144	NF
	950	140	NF
	1200	90	NF
1900	450	141	NF
	700	139	NF
	950	138	404
	1200	90	NF
2050	450	136	1500
	700	134	1000
	800	135	280
	950	132	140
	1200	88	NF

(a) NF – No failure in 10-year exposure. Bent beam specimens stressed at 75 percent of the yield strength and exposed at Kure Beach, North Carolina.

TABLE 2.0322. EFFECT OF HEAT TREATMENT ON STRESS-CORROSION BEHAVIOR OF TYPE 410 IN MARINE ATMOSPHERE (61)

Fe
12 Cr
Low C

Types 403, 410, 416

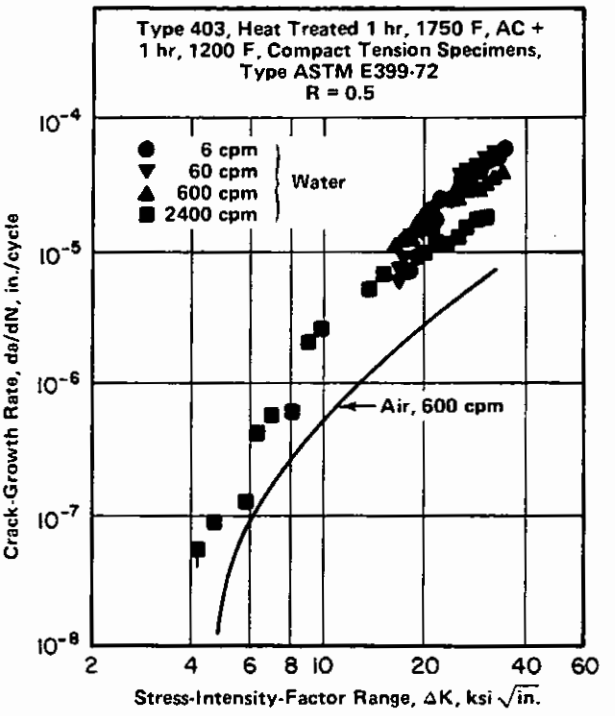


FIGURE 2.0323. EFFECTS OF FREQUENCY AND ENVIRONMENT ON FATIGUE CRACK-GROWTH BEHAVIOR OF TYPE 403 AT 212 F (63)

Alloy	Type 410[a]			
Fuel[b]	Initial Stress Intensity, ksi √in.	Incubation Period, hr[c]	Total Immersion Time, hr	Final Stress Intensity, ksi √in.
H-1	28.7	>200	200	28.7
	64.8	380	3140	36.2
H-2	45.5	>245	245	45.5
	55.6	>510	510	55.6
	56.0	>420	420	56.0
	56.1	>640	640	56.1
H-2/0.2 CO_2	56.1	20	168	28.3
H-2/1.0 CO_2	44.5	24	220	27.5
H-2/BaO	62.3	>1400	1400	62.3
H-3	18.4	>460	460	18.4
A-50	48.5	>4600	4600	48.5
	57.5	290	1040	30.5
MMH	42.9	>3320	3320	42.9
UDMH	61.3	>3060	3060	61.3

(a) 0.13-in. thick; heat treated 1880 F, AC plus tempered at 620 F to HRC 43. Specimens were wedge-opening, loaded, precracked compact tension.

(b) H-1 – 97 percent hydrazine
H-2 – propellant-grade hydrazine
H-3 – refined-grade hydrazine
A-50 – Aerozine 50 (1:1 mixture of hydrazine and unsymmetrical dimethylhydrazine)
MMH – 98 percent grade monomethyl hydrazine
UDMH – unsymmetrical dimethylhydrazine.

(c) Stable period before crack growth commences.

TABLE 2.0327. STRESS-CORROSION BEHAVIOR OF TYPE 410 IN HYDRAZINE ROCKET FUELS (64)

Fe
12 Cr
Low C

Types 403, 410, 416

Alloy	Type 410[a]
Environment	Time to Failure[b], hr
3 percent NaCl, aerated with O_2	NF 650
10 percent NaCl + H_2O_2	NF 350
10 percent $FeCl_3$	NF 200[c]
42 percent $MgCl_2$, boiling	NF 500
3 percent NaCl + 0.5 percent acetic acid	NF 700
3 percent NaCl + H_2S	2
3 percent NaCl + 0.5 percent acetic acid + H_2S	2

(a) Austenitized 0.25 hr, 1800 F, AC plus tempered 700 F, AC.
(b) NF – No failure in time indicated. Tests were conducted with U-bend specimens exposed in triplicate.
(c) Failure occurred by pitting but no cracking.

TABLE 2.0332. STRESS-CORROSION BEHAVIOR OF TYPE 410 IN SEVERAL ENVIRONMENTS (61)

Alloy		Type 410			
Strength Ratio, Hydrogen/Helium[a]		Unnotched Ductility			
		Elongation, percent		Reduction in Area, percent	
Notched[b]	Unnotched	Helium	Hydrogen	Helium	Hydrogen
0.22	0.79	15	1.3	60	12

(a) Hydrogen and helium gas pressures 10,000 psi.
(b) K_t = 8.4.

TABLE 2.0334. EFFECTS OF HYDROGEN ENVIRONMENT ON TENSILE PROPERTIES OF TYPE 410 AT ROOM TEMPERATURE (65)

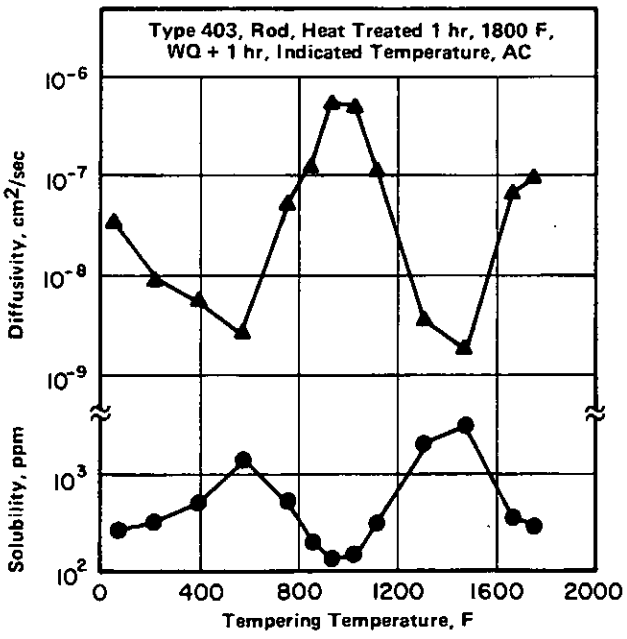


FIGURE 2.0335. EFFECT OF TEMPERING TEMPERATURE ON HYDROGEN DIFFUSIVITY AND SOLUBILITY IN TYPE 403 AT ROOM TEMPERATURE (66)

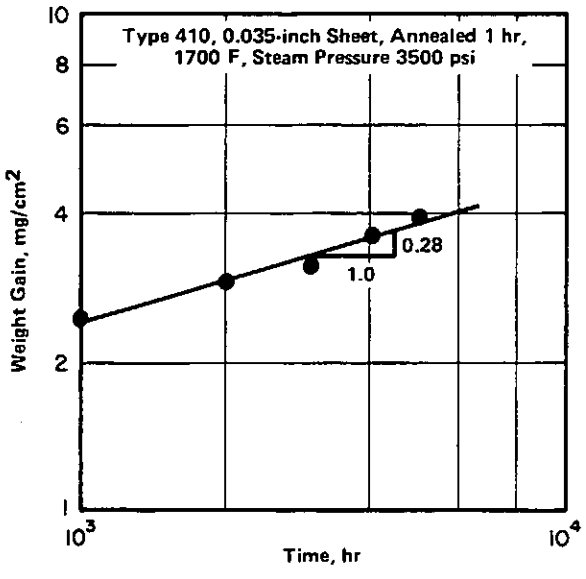


FIGURE 2.0343. LONG-TIME OXIDATION WEIGHT-GAIN BEHAVIOR OF TYPE 410 IN HIGH-PRESSURE STEAM AT 1000 F (68)

Fe
12 Cr
Low C

Types 403, 410, 416

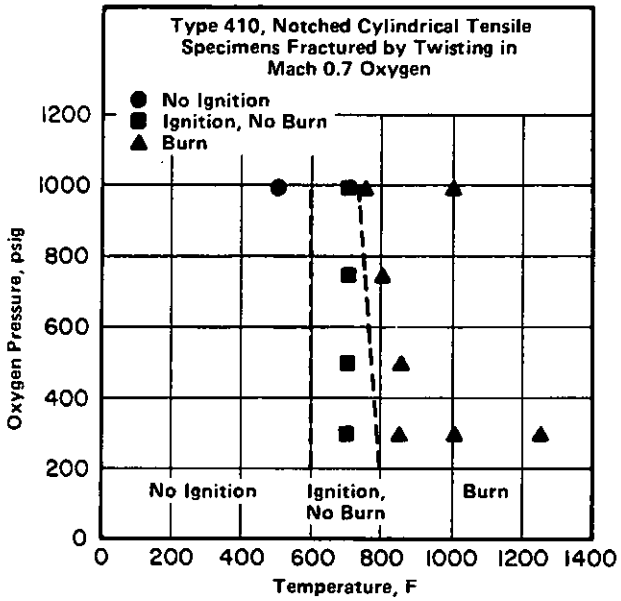


FIGURE 2.0344. EFFECTS OF PRESSURE AND TEMPERATURE ON BURNING OF FRESHLY EXPOSED TYPE 410 IN HIGH-VELOCITY FLOWING OXYGEN (69)

Alloy	Type 410										
AMS Specification	Condition[a]	Thickness, in.	F_{tu}, ksi Min	F_{tu}, ksi Max	F_{ty}, ksi (Min)	e, percent (Min)	RA, percent (Min)	Hardness Min	Hardness Max	Bend Radius, t V-Block[b]	Bend Radius, t Free[c]
5350F	C: 1750 F, 1 hr	–	–	–	–	–	–	35 HRC	–	–	–
	C: 1750 F, 1 hr + 1350 F, 1 hr	–	95	–	75	8	20	94 HB	100 HB	–	–
5351D	C: 1850 F, 1 hr + 1100 F[d]	–	–	–	–	–	–	217 HB	248 HB	–	–
	C: 1750 F, 15–45 min	<0.375	–	–	–	–	–	35 HRC	45 HRC	–	–
5504H	W: annealed	<0.030	–	95	–	12	–	–	–	–	–
		>0.030	–	95	–	15	–	–	–	–	–
		<0.375	–	–	–	–	–	–	–	2	1
		>0.375–0.500	–	–	–	–	–	–	–	4	2
	W: 1750 F, 15–30 min	<0.500	–	–	–	–	–	35 HRC	45 HRC	–	–
5505B	W: annealed	<0.030	–	95	–	15	–	–	–	–	–
		>0.030	–	95	–	20	–	–	–	–	–
		<0.375	–	–	–	–	–	–	–	2	1
		>0.375–0.500	–	–	–	–	–	–	–	4	2
	W: 1700 F, 1 hr + 2X 600 F, 2 hr	<0.035	180	–	147	4	–	39 HRC	44 HRC	–	–
		>0.035 < 0.070	180	–	147	5	–	39 HRC	44 HRC	–	–
		>0.070 < 0.110	180	–	147	7	–	39 HRC	44 HRC	–	–
		>0.110 < 0.150	180	–	147	9	–	39 HRC	44 HRC	–	–
		>0.150	180	–	147	11	–	39 HRC	44 HRC	–	–
5591F	W: annealed	–	–	100	–	20[d]	–	–	–	–	–
	W: 1750 F, 30 min	–	150	–	–	–	–	–	–	–	–
5609A	W: annealed	–	–	115[e]	–	–	–	–	241 HB[f]	–	–
	W: 1700 F, 1 hr + 600 F, 2 hr	<0.500	185	–	152	10	30	40 HRC	45 HRC	–	–
5612D	W: annealed	–	–	115[e]	–	–	–	–	241 HB[f]	–	–
	W: 1700 F, 1 hr + 600 F, 2 hr	<0.500	180	–	147	10	30	39 HRC	44 HRC	–	–
5613M	W: annealed	–	–	115[e]	–	–	–	–	241 HB[f]	–	–
	W: 1750 F, 30–35 min	<0.375	–	–	–	–	–	35 HRC	–	–	–
5614A	W: annealed	–	–	115[e]	–	–	–	–	223 HB[g]	–	–
	W: 1750 F, 30 min + 1100 F[d], 1 hr	<0.375[h]	100	–	80	21	60	217 HB	248 HB	–	–
5776B	WD: 1750 F, 30 min	~0.25	–	–	–	–	–	35 HRC	45 HRC	–	–
5777B	WD: 1750 F, 30 min	~0.25	–	–	–	–	–	35 HRC	45 HRC	–	–
5821B	WD: 1700 F, 1 hr + 2X 600 F, 2 hr	~0.25	–	–	–	–	–	39 HRC	44 HRC	–	–

Note: The original AMS documents should be consulted for complete specification details.

(a) C – cast; W – wrought; WD – weld deposit.
(b) 135-degree bend.
(c) 180-degree bend.
(d) Minimum tempering temperature.
(e) Applicable to wire only.
(f) Applicable to bars, forgings, and tubing.
(g) Applicable to bars only.
(h) Specification also requires Izod impact energy of not less than 50 ft-lb.

TABLE 3.011. AMS-SPECIFIED MECHANICAL PROPERTIES FOR TYPE 410 (1–4,6–8,17,18,20,21,23)

Alloy	Types 403 and 410								Type 416					
Form	Sheet, Strip	Plate	Bar			Wire			Bar			Wire		
Condition	Ann.	Ann.	Ann.	Tempered	Cold Drawn	Ann.	Cold Drawn	Heat Treated	Ann.	Tempered	Cold Drawn	Ann.	Cold Drawn	Heat Treated
Thickness, in.	–	–	All	All	1		0.250		All	All	1		0.250	
F_{tu}, typical, ksi	65	70	75	110	100	75	95	135	75	110	100	75	95	135
F_{ty}, typical, ksi	35	35	40	85	85	40	80	105	40	85	85	40	80	105
e (2 in.), typical, percent	25	30	35	23	17	–	–	–	30	18	13	–	–	–
e (4D), typical, percent	–	–	–	–	–	30	15	10	–	–	–	20	10	5
RA, typical, percent	–	–	70	65	60	70	60	50	60	55	50	60	50	40
Hardness														
HRB, typical	80	80	82	97	94	82	92	–	–	–	–	82	92	–
HRC, typical	–	–	–	–	–	–	–	29	–	–	–	–	–	29
BHN, typical	–	–	155	225	205	155	–	–	155	230	205	–	–	–

Fe
12 Cr
Low C

Types 403, 410, 416

TABLE 3.0211. TYPICAL MECHANICAL PROPERTIES OF TYPES 403, 410, AND 416 (33)

Alloy	Types 403 and 416								
Alloy Type	AMS Specification	Condition[a]	Thickness, in.	F_{tu}, ksi		F_{ty}, ksi	e, percent	RA, percent	Hardness	
				Min	Max	(Min)	(Min)	(Min)	Min	Max
403	5611A	W; annealed	–	–	115[b]	–	–	–	–	241 HB[c]
		W; 1735 F, 1 hr + 600 F, 2 hr	≤0.500	180	–	145	10	30	39 HRC	44 HRC
416	5349B	C; 1750 F, 1 hr	–	–	–	–	–	–	35 HRC	–
		C; 1750 F, 30 min + 1100 F, 1 hr	–	90	–	65	8	15	90 HRB	100 HRB
	5610K	W; annealed	–	–	125[b]	–	–	–	–	241 HB[d]
		W; 1825 F, 30 min	≤0.375	–	–	–	–	–	35 HRC	–

Note: The original AMS documents should be consulted for complete specification details.

(a) W – wrought; C – cast.
(b) Wire.
(c) Bars, forgings, and tubing.
(d) Bars.

TABLE 3.012. AMS-SPECIFIED MECHANICAL PROPERTIES FOR TYPES 403 AND 416 (5,15,19)

Fe
12 Cr
Low C

Types 403, 410, 416

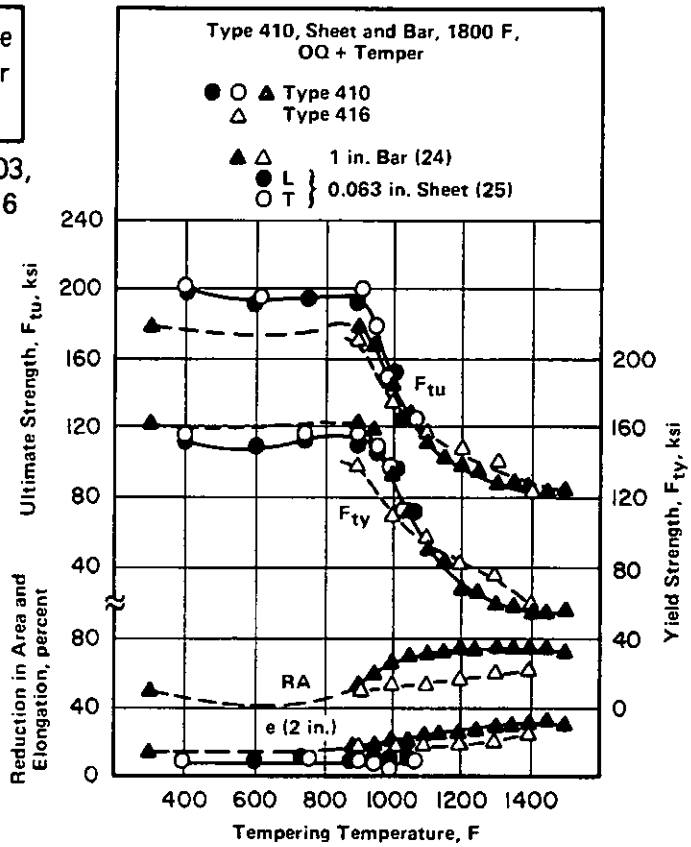


FIGURE 3.0212. EFFECT OF TEMPERING TEMPERATURE ON TENSILE PROPERTIES OF TYPE 410 SHEET AND BAR (24,25)

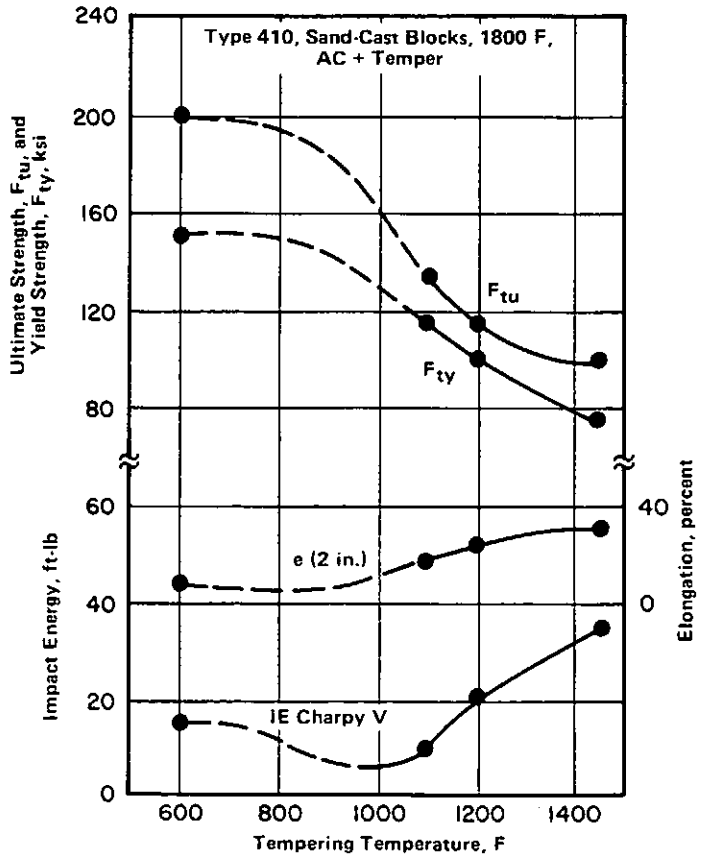


FIGURE 3.0213. EFFECT OF TEMPERING TEMPERATURE ON MECHANICAL PROPERTIES OF TYPE 410 SAND CASTINGS (26)

Fe
12 Cr
Low C

Types 403, 410, 416

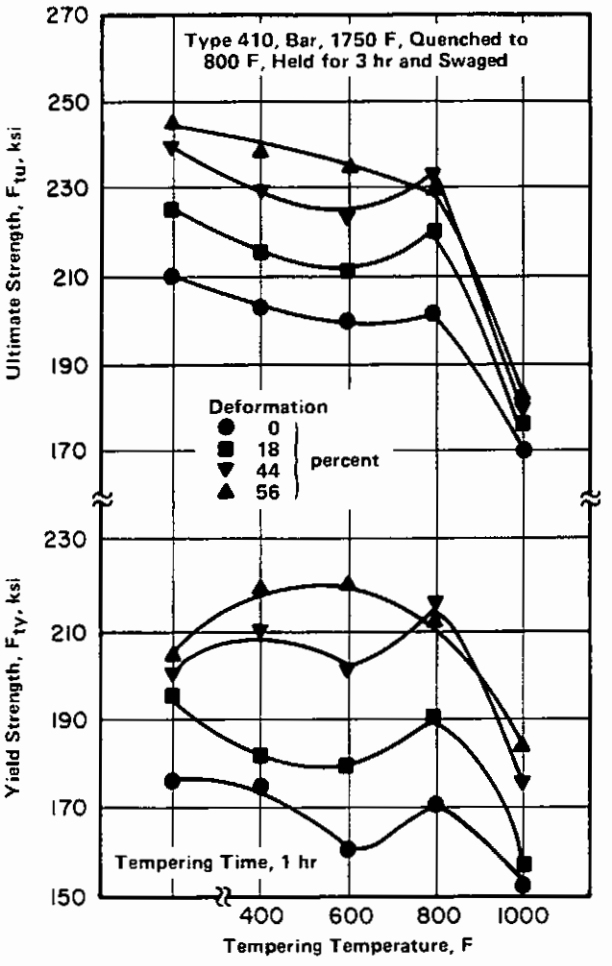


FIGURE 3.0214. EFFECT OF TEMPERING TEMPERATURE ON TENSILE AND YIELD STRENGTHS OF TYPE 410 DEFORMED IN THE METASTABLE AUSTENITIC CONDITIONS (27)

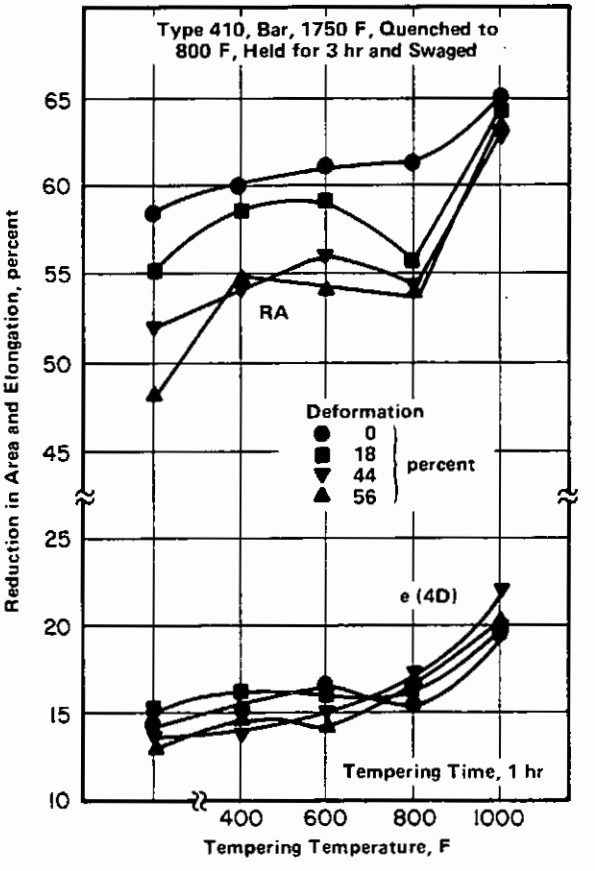


FIGURE 3.0215. EFFECT OF TEMPERING TEMPERATURE ON REDUCTION OF AREA AND ELONGATION OF TYPE 410 DEFORMED IN THE METASTABLE AUSTENITIC CONDITION (27)

Fe
12 Cr
Low C

Types 403, 410, 416

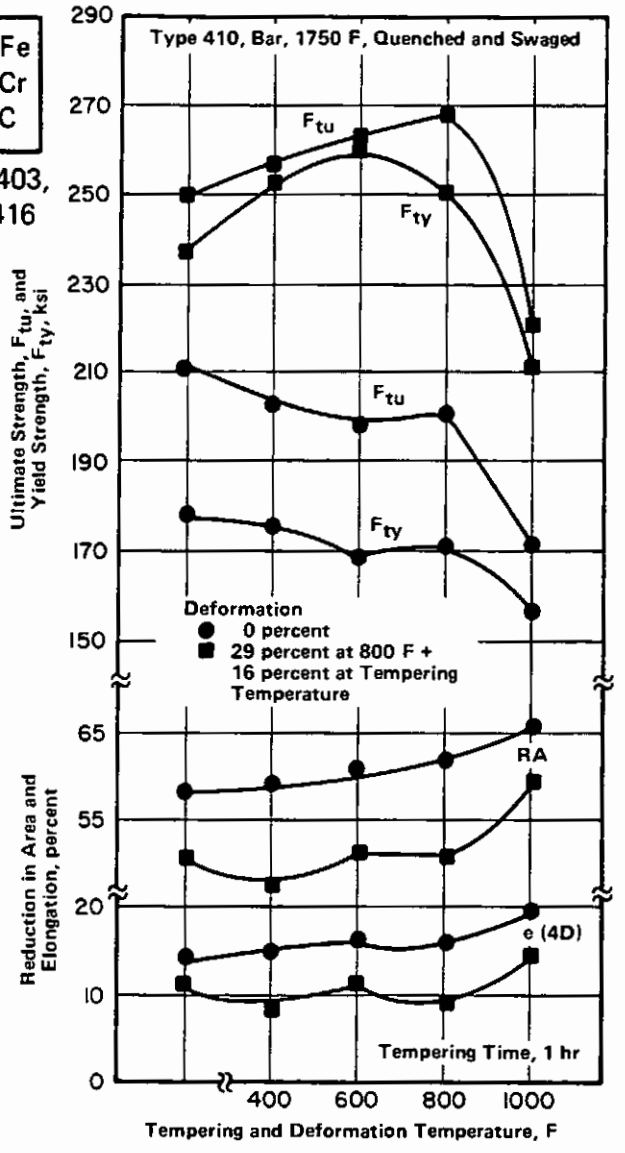


FIGURE 3.0216. EFFECT OF TEMPERING TEMPERATURE AND DEFORMATION ON TENSILE PROPERTIES OF TYPE 410 (27)

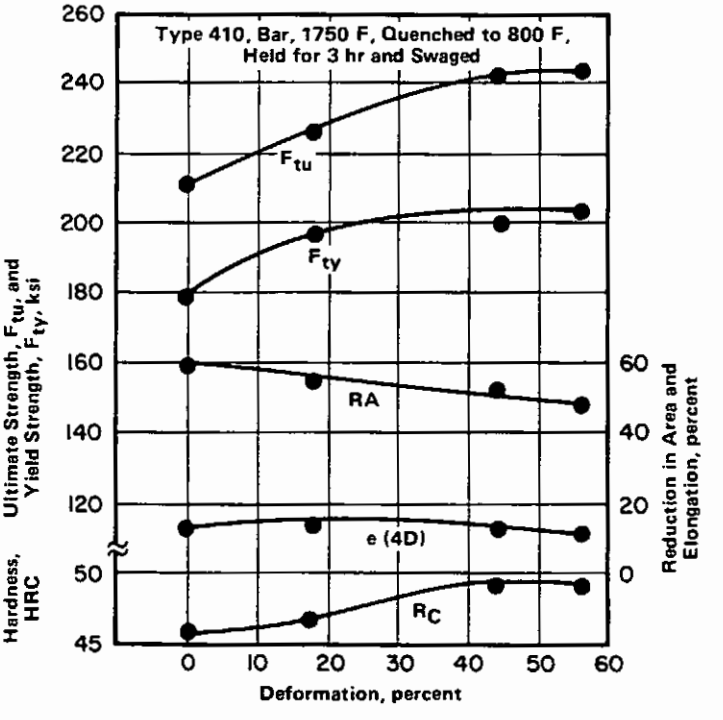


FIGURE 3.0217. EFFECT OF DEFORMATION ON TENSILE PROPERTIES AND HARDNESS OF TYPE 410 DEFORMED IN THE METASTABLE AUSTENITIC CONDITION (27)

Fe
12 Cr
Low C

Types 403, 410, 416

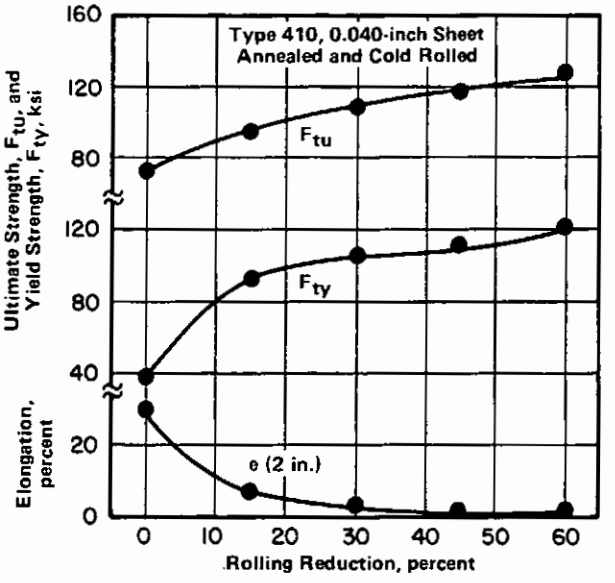


FIGURE 3.0218. EFFECT OF ROLLING REDUCTION ON TENSILE PROPERTIES OF TYPE 410 ANNEALED SHEET (24)

Alloy	Type 410			
Form	0.062-inch Sheet (Initial Thickness)			
Condition	As Rolled or Rolled and Annealed			
Reduction in Thickness (by rolling), percent	Direction	F_{ty}, ksi, 0.2 percent	F_{tu}, ksi	e (2 in.), percent
0	L	49.4	83.5	24.5
	T	47.9	83.6	27.5
15	L	102	108	5.3
	L	34.8	74.8	27.0
18(a)	L	99	109.2	5.0
	L	37.6	75.3	27.8

(a) Rolled + 1550 F, 10 min, AC.

TABLE 3.0219. EFFECT OF ROLLING REDUCTION AND ANNEALING ON AS-RECEIVED TENSILE PROPERTIES OF TYPE 410 SHEET (38)

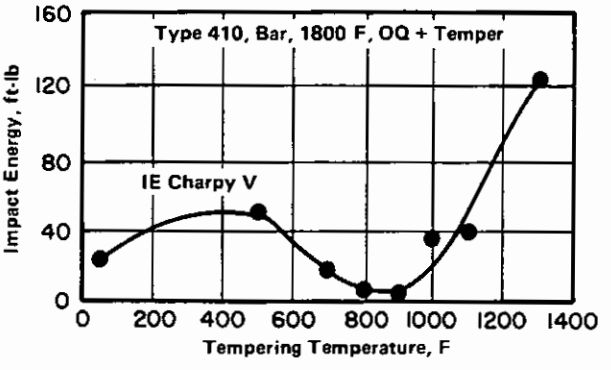


FIGURE 3.0231. EFFECT OF TEMPERING TEMPERATURE ON IMPACT PROPERTIES OF TYPE 410 (49)

Fe
12 Cr
Low C

Types 403, 410, 416

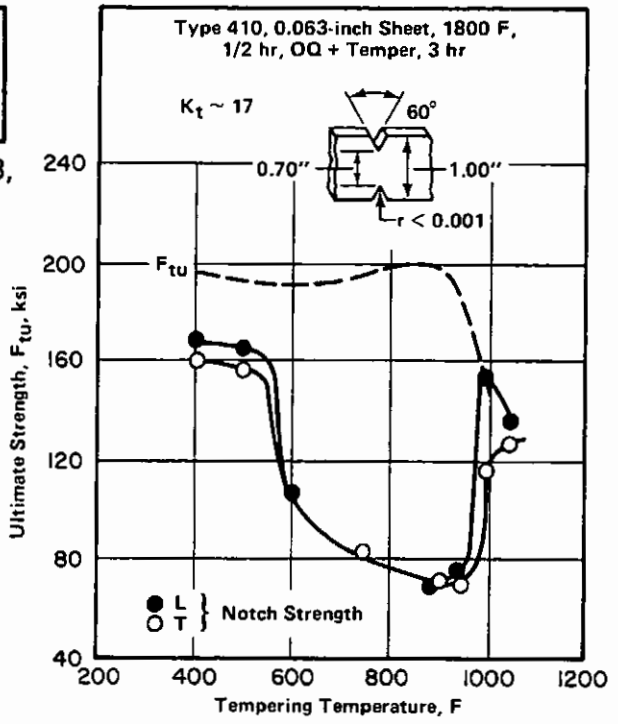


FIGURE 3.0271. EFFECT OF TEMPERING TEMPERATURE ON SHARP NOTCH STRENGTH OF TYPE 410 SHEET (25)

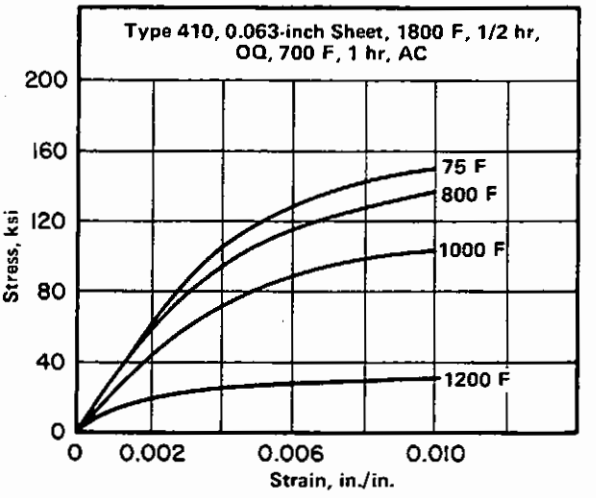


FIGURE 3.0311. STRESS-STRAIN CURVES IN TENSION AT ELEVATED TEMPERATURES FOR TYPE 410 (34)

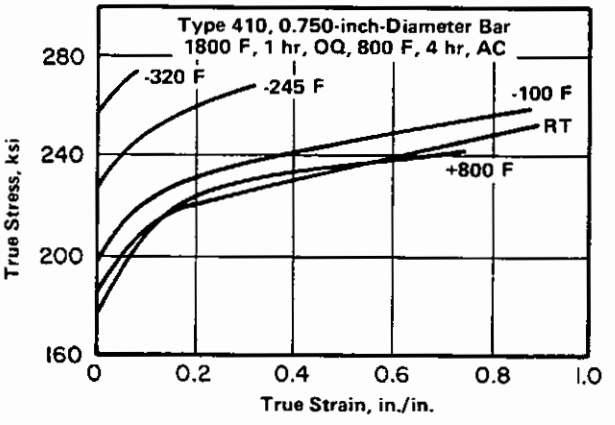


FIGURE 3.0312. TRUE STRESS-STRAIN CURVES AT CRYOGENIC TO INTERMEDIATE TEMPERATURES FOR TYPE 410 (35)

Fe
12 Cr
Low C

Types 403, 410, 416

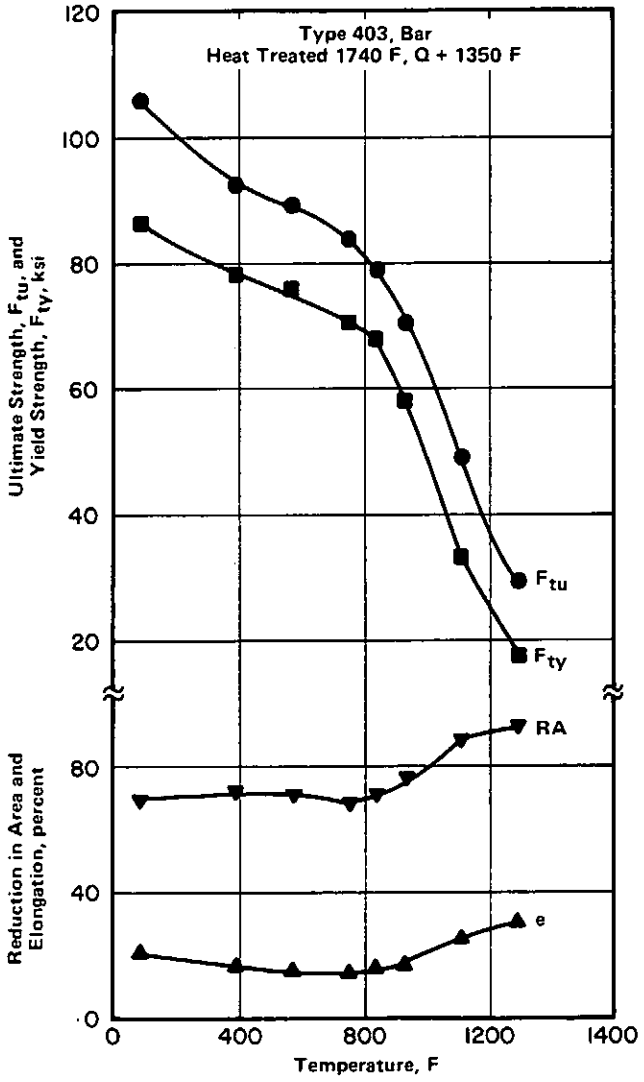


FIGURE 3.0313. EFFECT OF TEST TEMPERATURE ON TENSILE PROPERTIES OF TYPE 403 BAR (72)

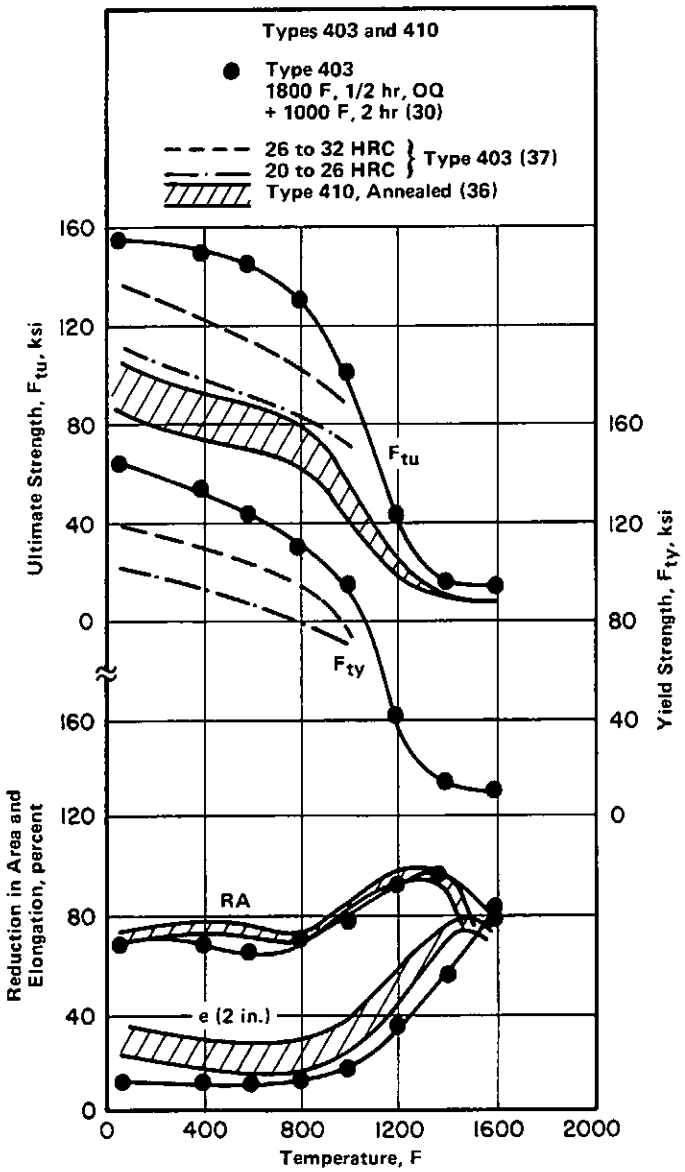


FIGURE 3.0314. EFFECT OF TEST TEMPERATURE ON TENSILE PROPERTIES OF TYPES 403 AND 410 (30,36,37)

Fe
12 Cr
Low C

Types 403, 410, 416

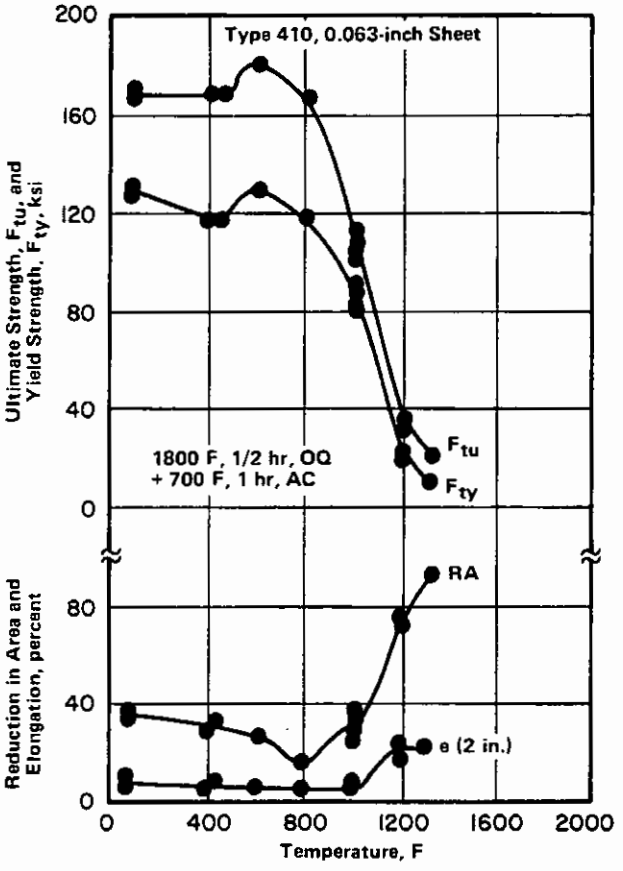


FIGURE 3.0315. EFFECT OF TEST TEMPERATURE ON TENSILE PROPERTIES OF TYPE 410 (34)

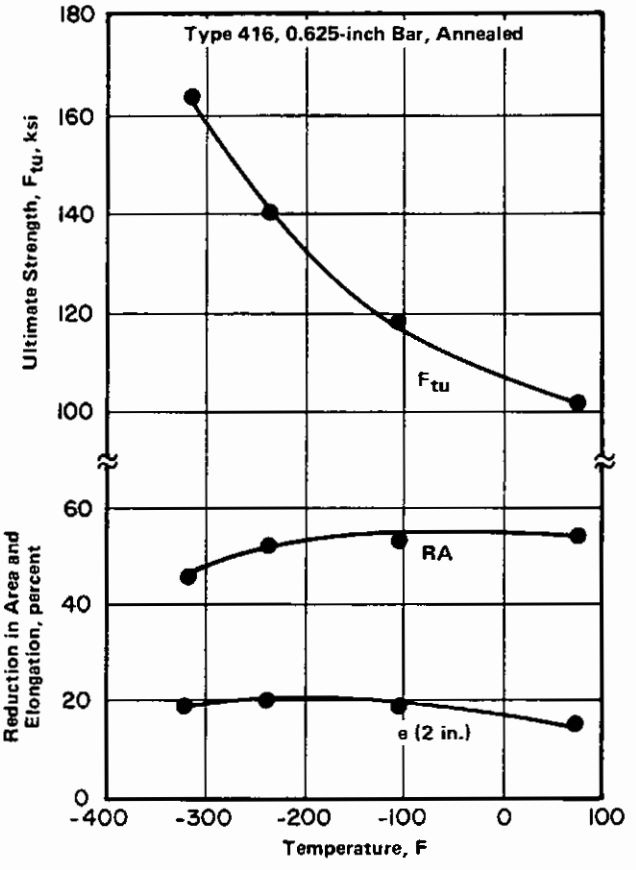


FIGURE 3.0316. EFFECT OF TEST TEMPERATURE ON TENSILE PROPERTIES OF ANNEALED TYPE 416 (39)

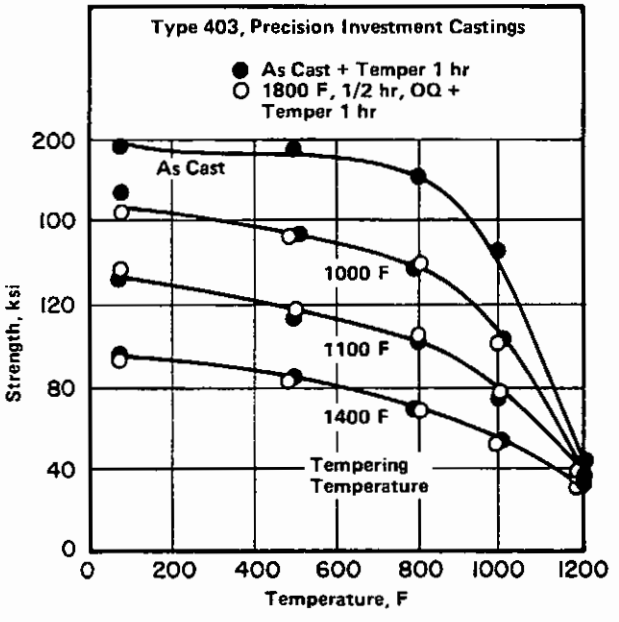


FIGURE 3.0317. EFFECT OF TEST TEMPERATURE ON TENSILE PROPERTIES OF PRECISION INVESTMENT CASTINGS OF TYPE 403 IN DIFFERENT CONDITIONS (40)

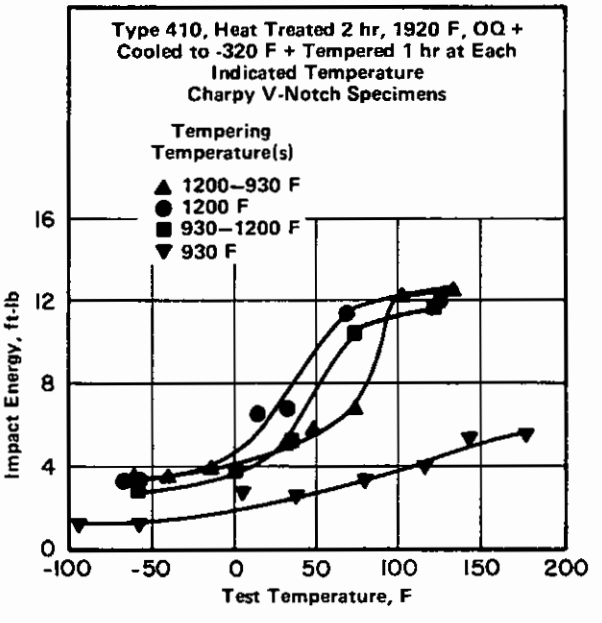


FIGURE 3.0332. EFFECTS OF TEST AND TEMPERING TEMPERATURES ON CHARPY IMPACT ENERGY OF TYPE 410 (54)

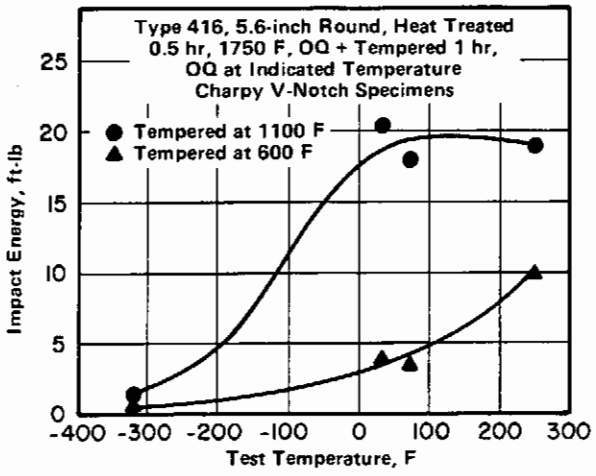


FIGURE 3.0333. EFFECTS OF TEST AND TEMPERING TEMPERATURES ON CHARPY IMPACT ENERGY OF TYPE 416 (73)

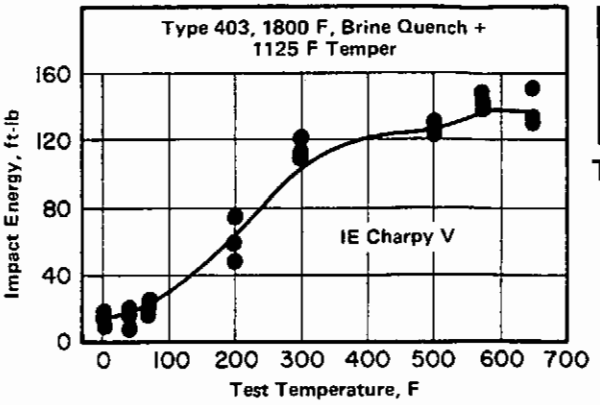


FIGURE 3.0334. EFFECT OF ELEVATED TEST TEMPERATURES ON IMPACT PROPERTIES OF TYPE 403 (50)

Fe
12 Cr
Low C

Types 403, 410, 416

Alloy	Type 403	Type 410[a]	
Form	Bar		
Condition	1750 F, 1 hr, AC; 1050 F, 1 hr, AC	1800 F, 1 hr, OQ; 1075 F, 3 hr, AC 1100 F, 2 hr, AC	1800 F, 1 hr, OQ 950 F, 3 hr, AC 975 F, 2 hr, AC
Test Temperature, F	IE Charpy V, ft-lb		
RT	–	16.0	8.5
500	105	–	–
600	98	34.3	19.3
700	–	35.5	20.3
800	81	41.3	17.5

(a) Average of two tests.

TABLE 3.0335. EFFECT OF ELEVATED TEST TEMPERATURES ON IMPACT PROPERTIES OF TYPES 403 AND 410 (51,52)

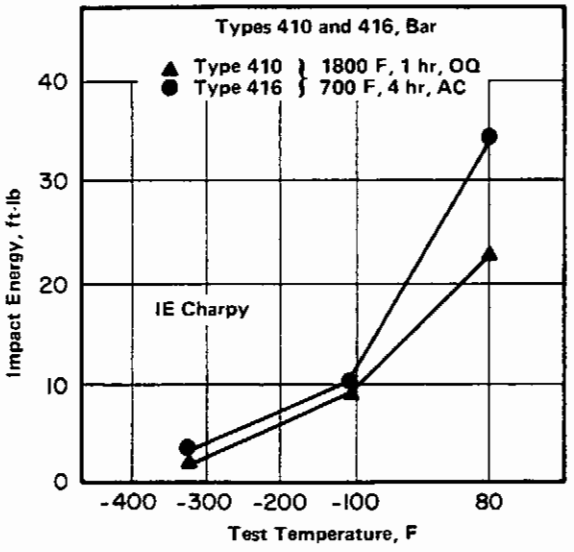


FIGURE 3.0336. EFFECT OF LOW TEST TEMPERATURES ON IMPACT PROPERTIES OF TYPES 410 AND 416 (53)

Fe
12 Cr
Low C

Types 403, 410, 416

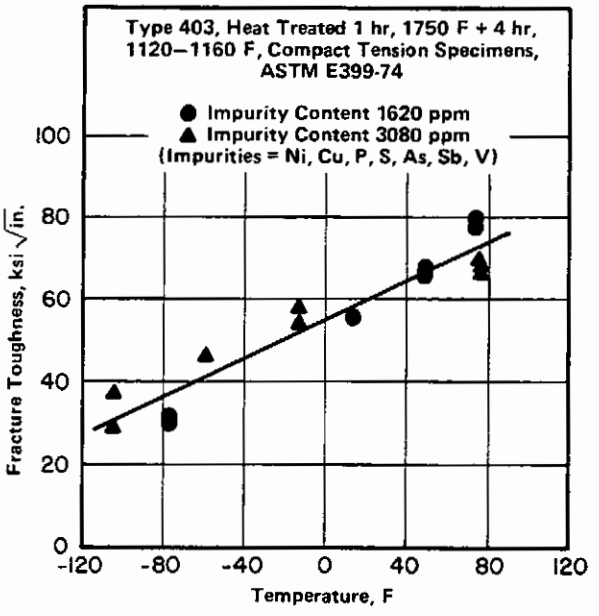


FIGURE 3.03721. EFFECTS OF TEMPERATURE AND IMPURITY CONTENT ON FRACTURE TOUGHNESS OF TYPE 403 (70)

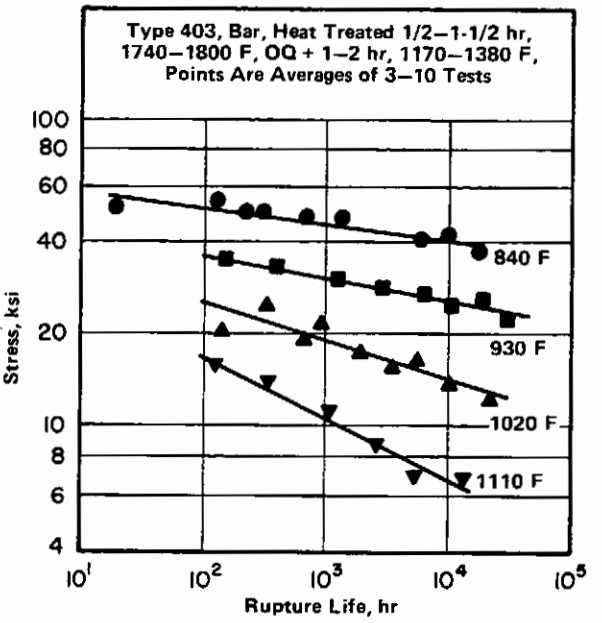


FIGURE 3.041. CREEP-RUPTURE BEHAVIOR OF TYPE 403 AT 840 TO 1110 F (74)

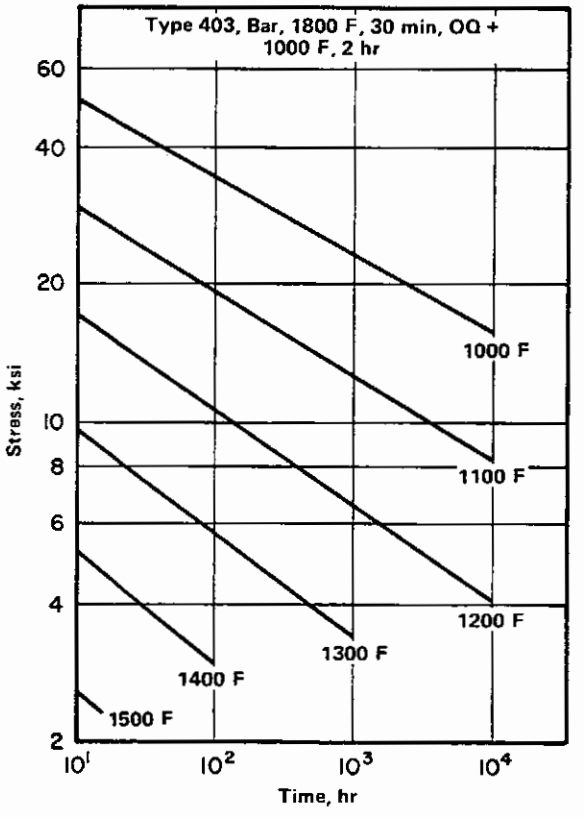


FIGURE 3.042. CREEP-RUPTURE CURVES FOR TYPE 403 BAR AT 1000 TO 1500 F (30)

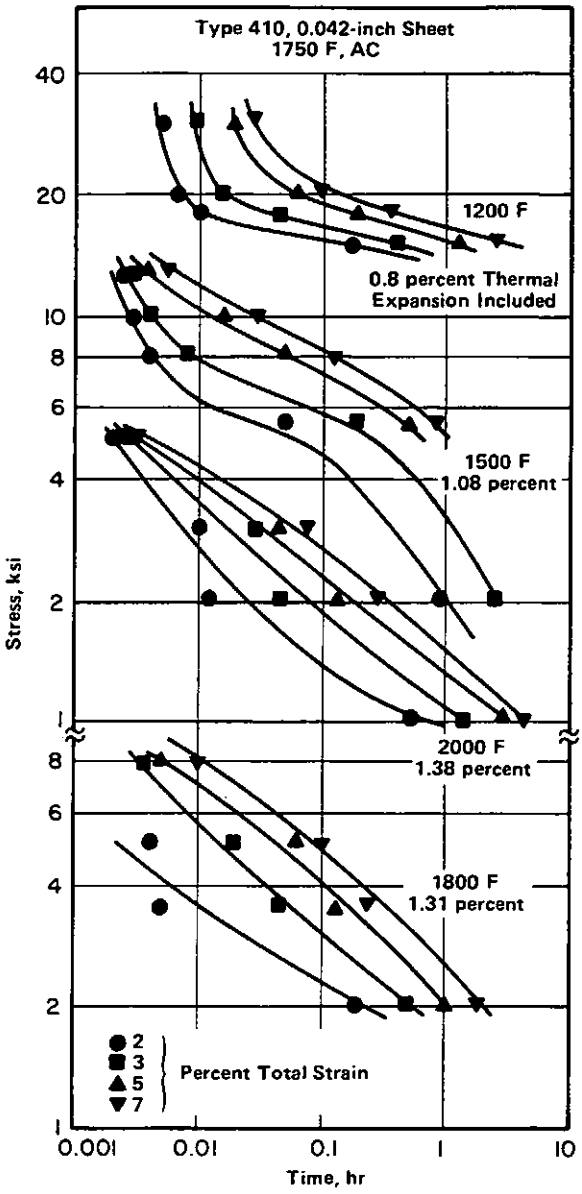
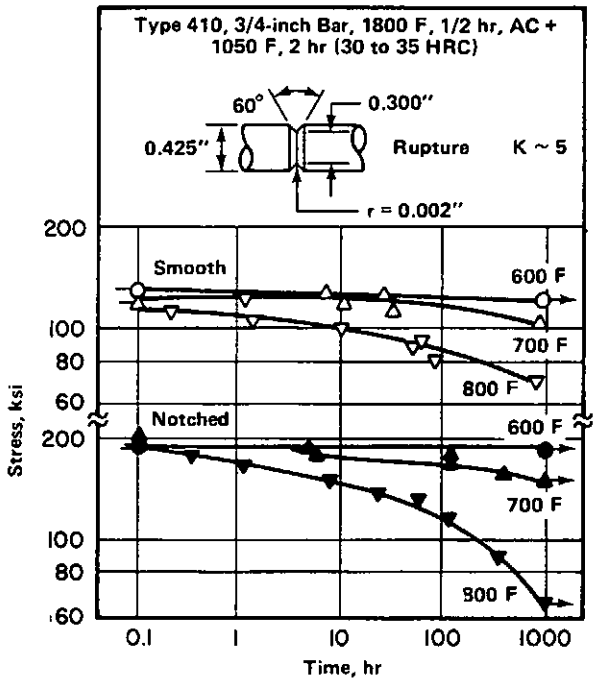


FIGURE 3.043. SHORT-TIME TOTAL-STRAIN CURVES FOR NORMALIZED TYPE 410 SHEET AT 1200 TO 2000 F (42)



Fe
12 Cr
Low C

Types 403, 410, 416

FIGURE 3.044. CREEP-RUPTURE CURVES FOR SMOOTH AND NOTCHED TYPE 410 BAR AT 600 TO 800 F (44)

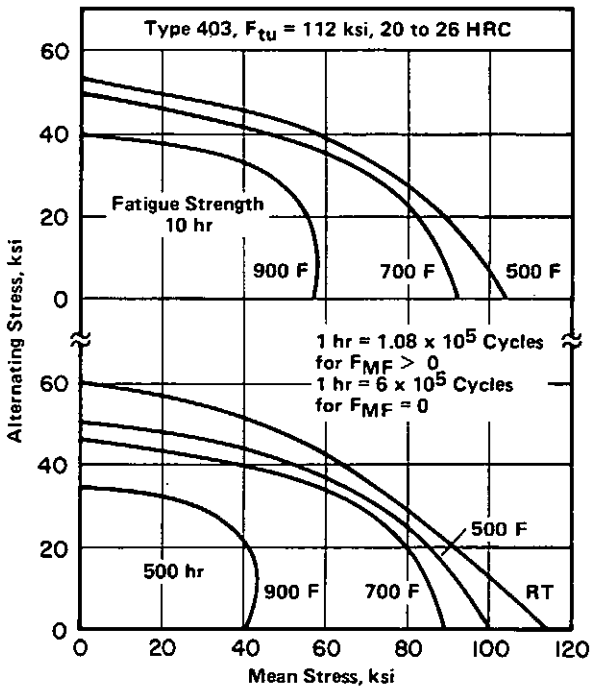


FIGURE 3.051. STRESS-RANGE DIAGRAMS AT ROOM TEMPERATURE TO 900 F FOR TYPE 403 HEAT TREATED TO 20 TO 26 HRC (43)

(Caption revised September, 1989)

Fe
12 Cr
Low C

Types 403, 410, 416

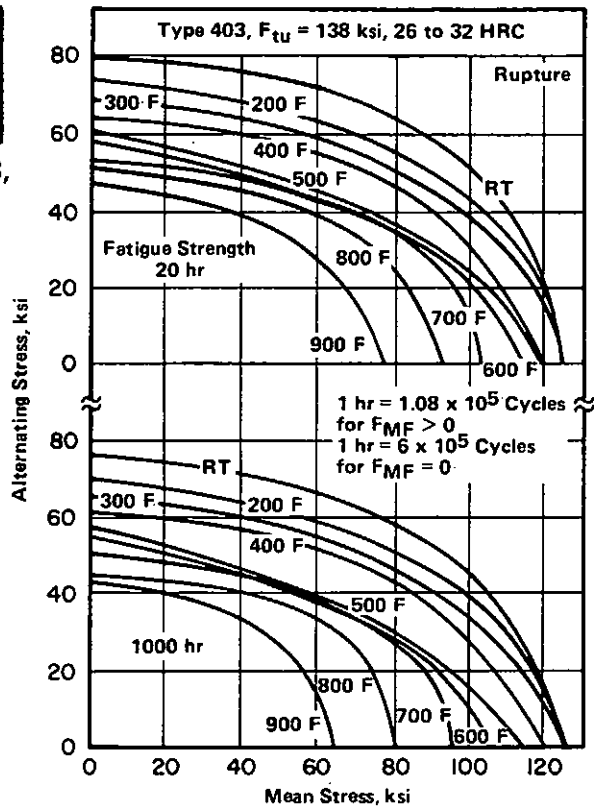


FIGURE 3.052. STRESS-RANGE DIAGRAMS AT ROOM TEMPERATURE TO 900 F FOR TYPE 403 HEAT TREATED TO 26 TO 32 HRC (43)

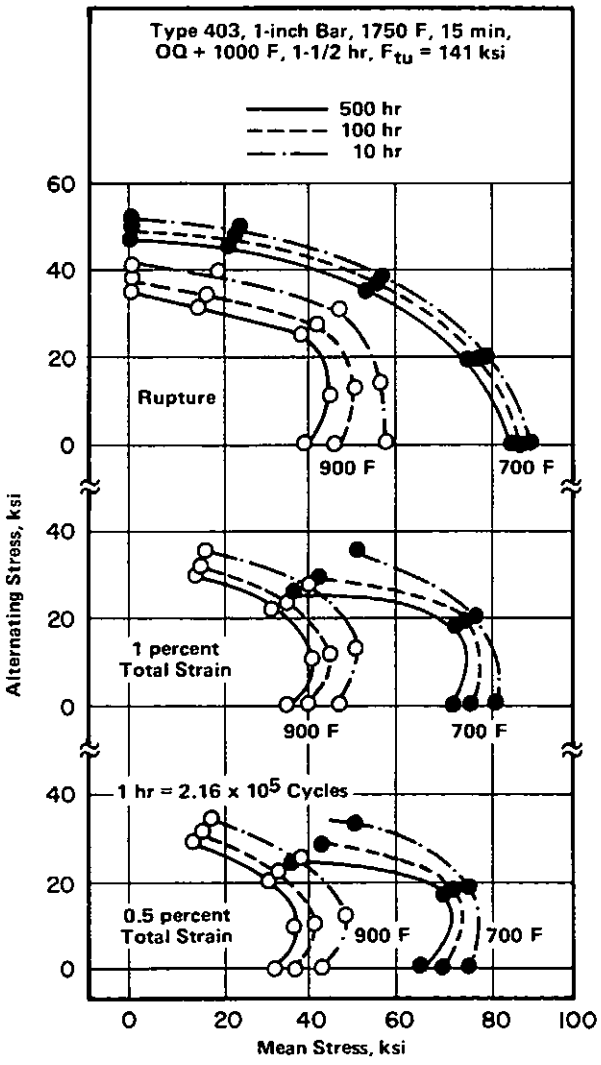
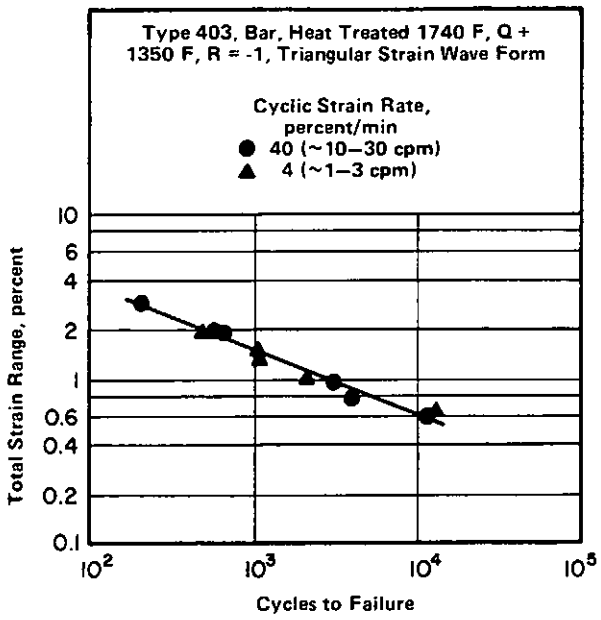
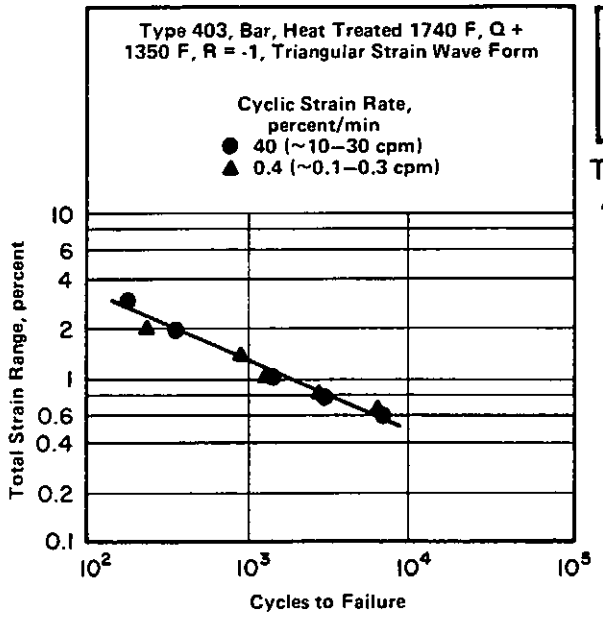


FIGURE 3.053. STRESS-RANGE DIAGRAMS AT 700 AND 900 F FOR RUPTURE, 1.0 AND 0.5 PERCENT TOTAL STRAIN FOR HEAT-TREATED TYPE 403 BAR (48)



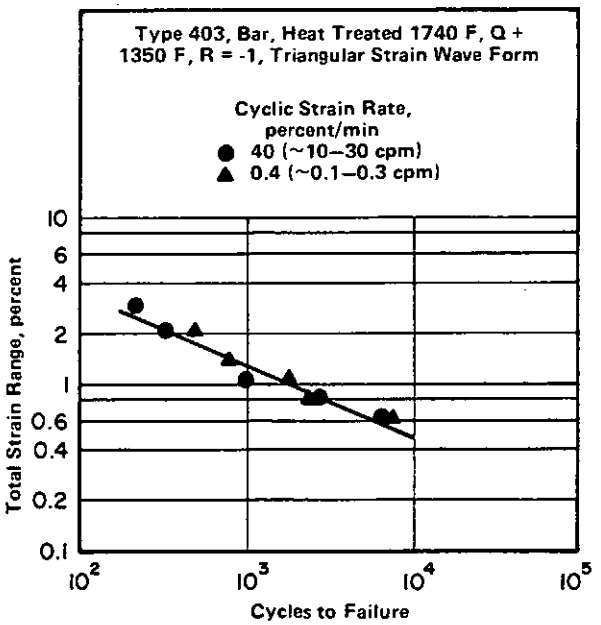
(a) Room Temperature



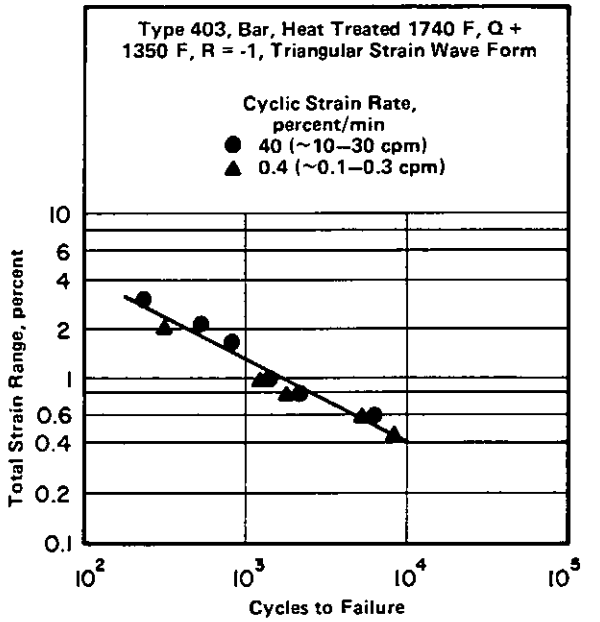
(b) 750 F

Fe
12 Cr
Low C

Types 403, 410, 416



(c) 930 F



(d) 1110 F

FIGURE 3.054. LOW-CYCLE AXIAL FATIGUE BEHAVIOR OF TYPE 403 IN AIR AT ROOM AND ELEVATED TEMPERATURES (75,76)

Fe
12 Cr
Low C

Types 403, 410, 416

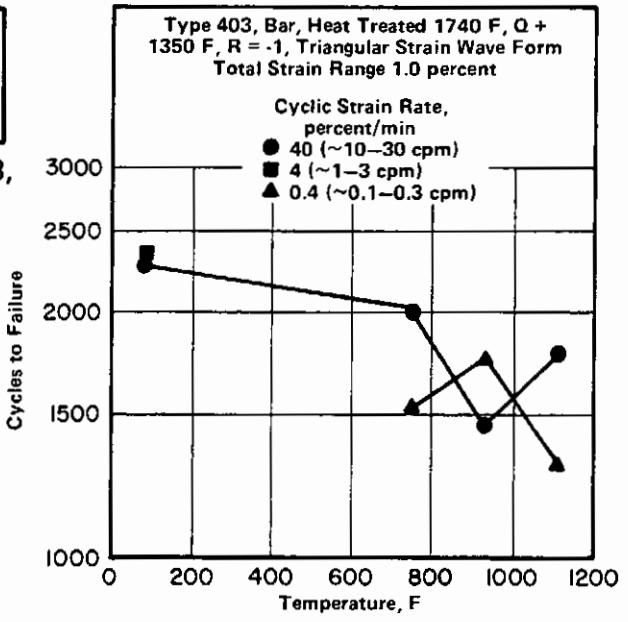


FIGURE 3.055. EFFECTS OF TEMPERATURE AND CYCLIC STRAIN RATE ON LOW-CYCLE AXIAL FATIGUE LIFE OF TYPE 403 (75)

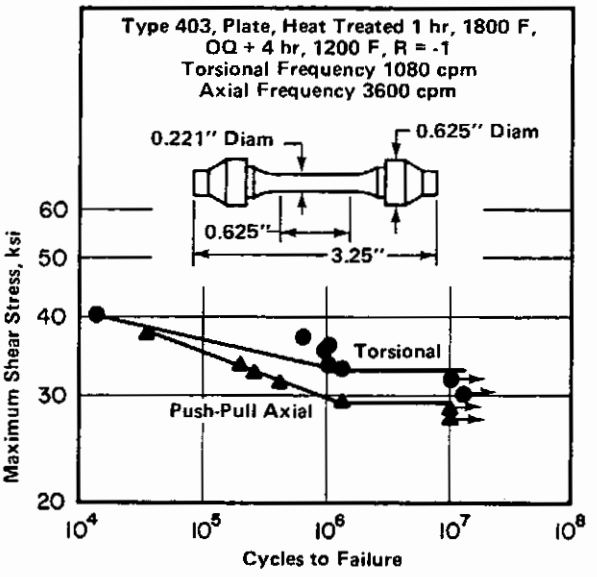


FIGURE 3.056. HIGH-FREQUENCY AXIAL AND TORSIONAL FATIGUE BEHAVIOR OF TYPE 403 IN AIR AT ROOM TEMPERATURE (77)

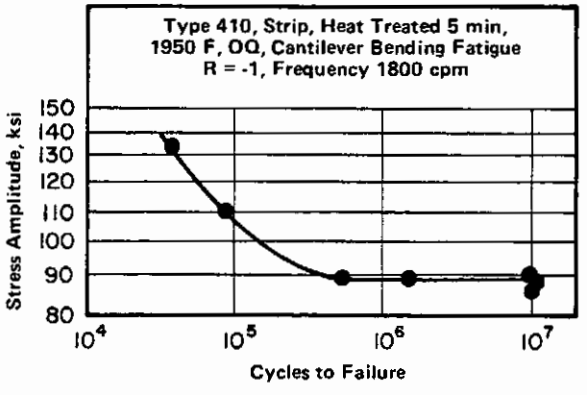


FIGURE 3.057. HIGH-FREQUENCY BENDING FATIGUE BEHAVIOR OF TYPE 410 IN AIR AT ROOM TEMPERATURE (78)

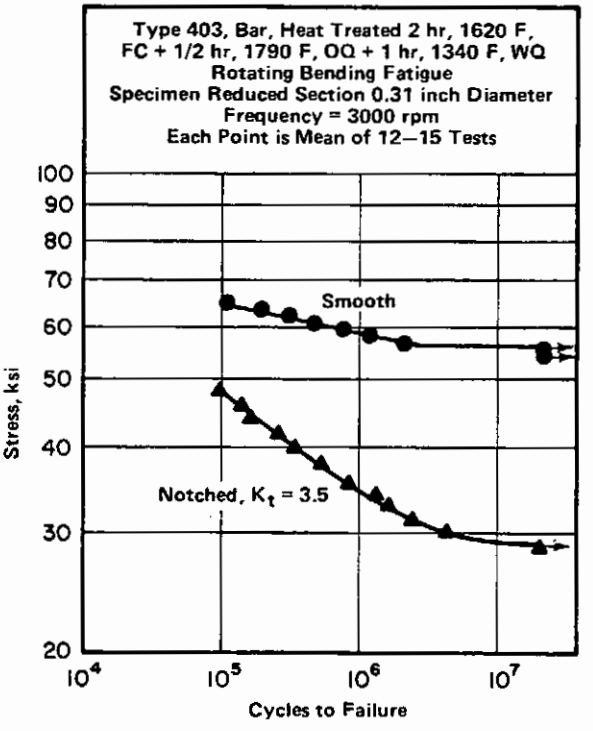


FIGURE 3.058. HIGH-FREQUENCY BENDING FATIGUE BEHAVIOR OF SMOOTH AND NOTCHED TYPE 403 BAR IN AIR AT ROOM TEMPERATURE (79)

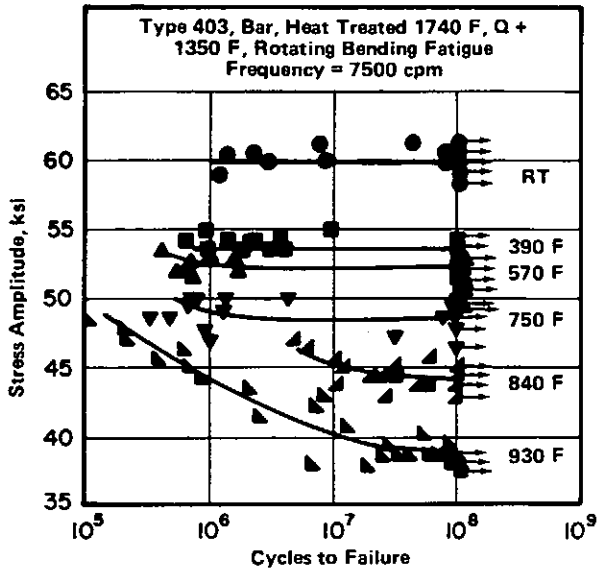


FIGURE 3.059. HIGH-FREQUENCY BENDING FATIGUE BEHAVIOR OF TYPE 403 AT ROOM AND ELEVATED TEMPERATURES (72)

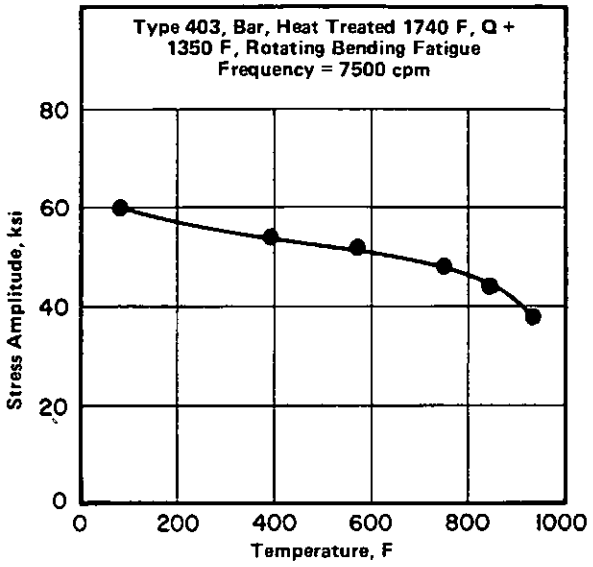


FIGURE 3.0510. FATIGUE STRENGTH AT 10^8 CYCLES FOR TYPE 403 AT ROOM AND ELEVATED TEMPERATURES (72)

(Caption revised September, 1989)

Fe
12 Cr
Low C

Types 403, 410, 416

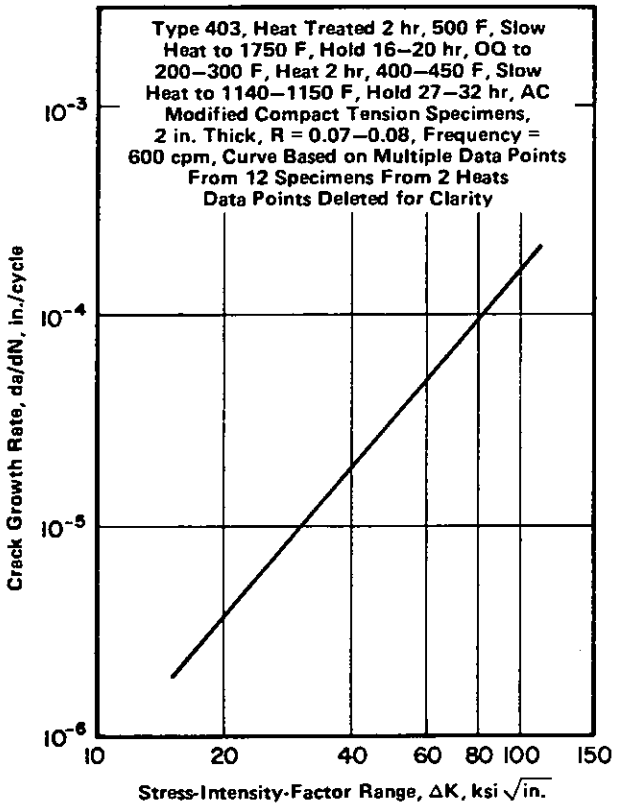


FIGURE 3.0511. FATIGUE-CRACK-GROWTH RATE OF TYPE 403 IN AIR AT ROOM TEMPERATURE (80)

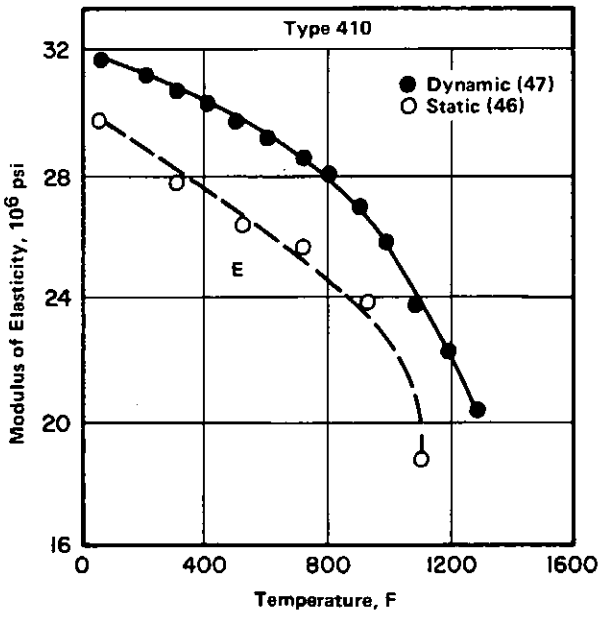


FIGURE 3.062. MODULUS OF ELASTICITY OF TYPE 410 AT ROOM AND ELEVATED TEMPERATURES (47,47)

Fe
12 Cr
Low C

Types 403, 410, 416

Alloy	Type 410
Tempering Conditions(a)	Dynamic Modulus, 1000 ksi
1 hr, 480 F	30.6
1-1/2 hr, 1200 F	31.2
3 hr, 1200 F, FC	31.6
1 hr, 1440 F	31.2

(a) Austenitized 1760 F, OQ prior to tempering.

TABLE 3.0621. EFFECT OF HEAT TREATMENT OF TYPE 410 ON MODULUS OF ELASTICITY AT ROOM TEMPERATURE (81)

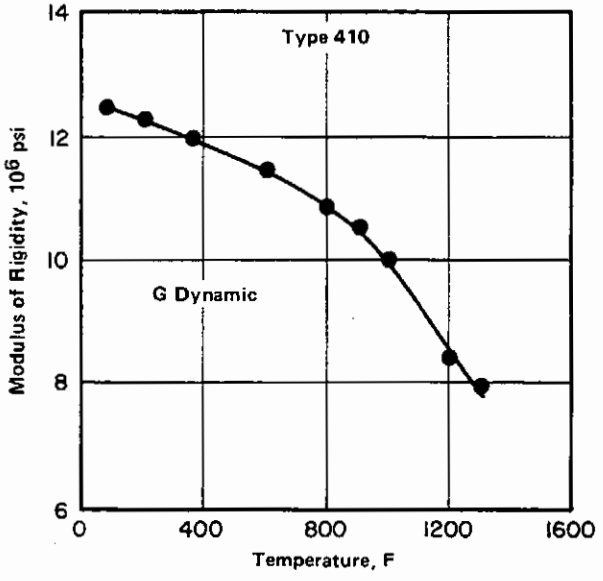


FIGURE 3.063. MODULUS OF RIGIDITY OF TYPE 410 AT ROOM AND ELEVATED TEMPERATURES (47)

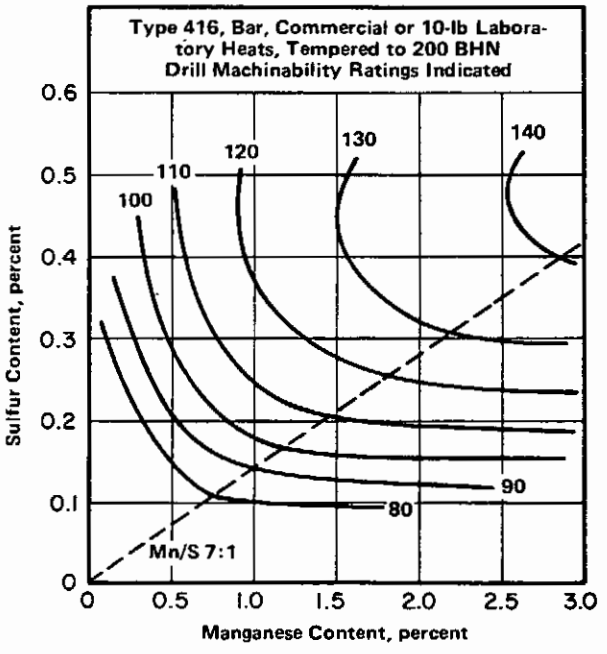


FIGURE 4.024. EFFECTS OF MANGANESE AND SULFUR CONTENTS OF MACHINABILITY OF TYPE 416 (83)

RELEASED: JUNE 1972
AUTHOR: W. W. DYRKACZ

FERROUS ALLOYS

	Fe
Low	C
12	Cr
+	Cb

410 Cb

1. GENERAL

410Cb is an improved version of the standard Type 410 stainless steel. By the addition of about 0.15 percent Cb, certain properties are improved without altering any of the desirable characteristics of Type 410. The 410Cb stainless grade offers these major advantages over Type 410:

a. higher strength, ductility, and toughness at room, elevated and sub-zero temperatures
b. refinement in grain size
c. easier control of tempered hardness thru decreased sensitivity to time and temperature variations

It is used as an alternate to Type 410 in applications requiring uniformly high properties, uniform response to tempering and where the control of ferrite content is necessary (1)(2).

1.01 Commercial Designation

410Cb

1.02 Alternate Designations

AMS 5609; SAE 51410 Cb modified.

1.03 Specifications

Table 1.03.

1.04 Composition

Table 1.04.

1.05 Heat Treatment

(see also 1.09).

1.051 Fully anneal for maximum formability at 1450 to 1650F, usually 1550-1650F, followed by furnace cooling at 50F per hour maximum to 1100F. Hardness should be about Rockwell C 20.

1.052 Austenitize at 1700 to 1850F followed by an air cool or oil quench depending on section size and shape. As-quenched hardness should be about 42 to 44 Rockwell C (3).

1.0521 Effect of austenitizing temperature on grain size. The small addition of .10 to .15 columbium to Type 410 produces a marked refinement in its grain structure as shown by grain size measurements conducted on 1 1/2 inch diameter bars held one hour at various heating temperatures (3). Effect of columbium on grain size of Type 410 when austenitized at various temperatures, Table 1.0521.

1.053 Temper at 400 to 1400F for 1 to 12 hours, generally 4 hours. Tempering at temperatures between 700 and 1050F is not generally recommended, because of reduced resistance to corrosion and stress corrosion, and reduction of impact strength. However, 410Cb displays reduced susceptibility to temper embrittlement compared to regular Type 410 stainless steel (3).

1.0531 Effect of tempering temperature on hardness, Master tempering curves for 410Cb and regular Type 410, Figure 1.0531.

1.06 Hardness

This steel is air hardening. Also, sections up to 10 inches x 10 inches can be hardened to Rockwell C 42 to 44 by oil quenching from 1800F (3)(5).

1.061 Since 410Cb is more resistant to tempering than regular Type 410, a higher hardness is obtained with the 410Cb steel at any specified temperature when tempered between 950 and 1400F, Figure 1.061.

1.062 Hardness versus tempering temperature with constant tempering time for 410Cb versus regular Type 410, Table 1.062.

1.07 Forms and Conditions Available

410Cb is available as forging billets, bars, wire, forgings, and mechanical tubing in a wide range of commercial sizes in the annealed condition or heat treated to a broad range of mechanical properties (1)(2).

1.08 Melting and Casting Practice

Electric furnace air melt.

1.09 Special Considerations

1.091 Avoid tempering at 700 to 1050F because of reduced corrosion resistance, stress corrosion resistance, and impact strength. However, 410Cb exhibits a significantly higher level of notch impact strength than Type 410 when tempered between 700 and 1050F, and 410Cb shows a faster recovery of toughness in the trough region with tempering temperatures above 950F, as well (see Figure 3.0234).

1.092 Variation in tempering time and temperature are considerably less critical for 410Cb than for regular Type 410 stainless steel in the range of 950 to 1150F as shown by the early development of hardness plateaus (see Figure 1.061). These tempering characteristics of 410Cb can be used to advantage to enable close control of hardness and to produce uniformity of hardness within a furnace load when working to narrow specified hardness levels particularly within the broad range of Rockwell C 25 to 35. Substitution of 410Cb for Type 410 in such situations results in virtual elimination of re-heat treatments, permits larger furnace loads, and allows the mixing of parts with dissimilar and varying cross sections within the same furnace load (1)(3)(7).

1.093 The applicability of a comparatively high tempering temperature for hardness levels within the range of Rockwell C 20 to 32 is beneficial from the standpoint of additional relief of internal mechanical stresses and for dimensional stability in parts made from 410Cb (3).

2. PHYSICAL AND CHEMICAL PROPERTIES

2.01 Thermal Properties

2.011 Melting range. Same as for Type 410 stainless steel(4). (see also Code 1401)

2.012 Phase changes. Same as for Type 410 (4).

2.013 Thermal conductivity. Same as for Type 410 (4).

2.014 Thermal expansion. Same as for Type 410 (4).

2.015 Specific heat. Same as for Type 410 (4).

2.016 Thermal diffusivity.

2.02 Other Physical Properties

2.021 Density. Same as for Type 410 stainless steel (4) (see also Code 1401).

2.022 Electrical properties. Same as for Type 410 (4).

2.023 Magnetic properties. Same as for Type 410 (4).

2.024 Emittance.

2.025 Damping capacity.

2.03 Chemical Properties

2.031 Corrosion resistance.

2.0311 410Cb is resistant to atmospheric and fresh water corrosion and to a variety of mild acids and alkalines. It is inferior to the Type 300 stainless steels and may require corrosion protection. Maximum corrosion resistance is developed in the hardened condition, but the corrosion resistance is reduced by tempering between 700 and 1050F. The surface must be free from scale and foreign particles to prevent galvanic corrosion. The results of laboratory and actual service tests indicate that the minor addition of columbium is neutral insofar as affecting the general corrosion resistance of Type 410 stainless steel (3).

2.0312 410Cb is susceptible to both stress corrosion and to hydrogen embrittlement, if heat treated to high strength levels. In certain accelerated stress corrosion cracking tests conducted in the laboratory, the small addition of columbium to Type 410 indicates a slight trend toward improved resistance to stress corrosion cracking (3). The higher tempering temperature required for 410Cb to develop tensile strengths equivalent to those of regular Type 410 results in more effective relief of residual internal stresses that, in some environments, promote stress corrosion cracking (1).

2.032 Oxidation resistance of 410Cb is good up to 1200F for continuous service and up to 1400F for intermittent service (4).

2.04 Nuclear Properties

	Fe
Low	C
12	Cr
+	Cb

410 Cb

3. MECHANICAL PROPERTIES

3.01 Specified Mechanical Properties

3.011 AMS specified mechanical properties, Table 3.011.

3.02 Mechanical Properties at Room Temperature

3.021 Typical mechanical properties, Table 3.021.

3.0212 Typical tensile properties of 410Cb compared with regular Type 410 at various tempering temperatures, Figure 3.0212.

3.0213 Effect of size of cross section,. Table 3.0213.

3.0214 Effect of austenitizing and tempering temperatures, Table 3.0214.

3.0215 Tensile strength versus elongation of 410Cb compared with regular Type 410, Figure 3.0215.

3.0216 Effect of exposure at elevated temperature on room temperature properties, Table 3.0216.

3.022 Compression.

3.023 Impact.

3.0231 Effect of tempering temperature on impact strength (see Table 3.021).

3.0232 Effect of austenitizing temperature on impact strength (see Table 3.0214).

3.0233 Effect of size of cross section on impact strength (see Table 3.0213).

3.0234 Charpy V-notch impact strength of 410Cb compared with regular Type 410 after various tempering treatments, Figure 3.0234.

3.024 Bending.

3.025 Torsion and shear.

3.026 Bearing.

3.027 Stress concentration.

3.0271 Notch properties (see Table 3.0216).

3.0272 Fracture toughness.

3.028 Combined properties.

3.03 Mechanical Properties at Various Temperatures

3.031 Typical short time, elevated temperature tensile properties using two different tempering temperatures, Table 3.031.

3.0312 Elevated temperature tensile properties of 410Cb compared with regular type 410 stainless steel (typical), Figure 3.0312.

3.032 Compression.

3.033 Impact.

3.0331 Charpy V-notch impact strength of 410Cb at room and sub-zero temperatures versus Type 410, Figure 3.0331.

3.0332 Effect of tempering temperature on impact strength of 410Cb and Type 410 bar at room and sub-zero temperatures, Figure 3.0332.

3.034 Bending.

3.035 Torsion and shear.

3.036 Bearing.

3.037 Stress concentration.

3.038 Combined properties.

3.04 Creep and Creep Rupture Properties

3.041 Creep rupture curves at 900 to 1100F for bar tempered at 1200F for 410Cb versus Type 410, Figure 3.041.

3.042 Creep rupture curves at 900 to 1100F for 410Cb tempered bar using 1850F and 2000F austenitizing temperatures, Figure 3.042.

3.05 Fatigue Properties

3.051 S-N curves for heat treated bar, Figure 3.051.

3.06 Elastic Properties

3.061 Poisson's ratio. Same as Type 410 (4).

3.062 Modulus of elasticity. Same as Type 410 (4).

3.063 Modulus of rigidity. Same as Type 410 (4).

4. FABRICATION

4.01 Formability

4.011 410Cb is generally formed in the fully annealed condition utilizing the same practice used for Type 410.

4.012 Forgeability and forging procedures. Same as Type 410.

4.02 Machining and Grinding

4.021 Machinability and machining practice. Same as for Type 410.

4.03 Welding

4.031 Weldability and welding procedures. Same as for Type 410.

4.04 Surface Treatment

AMS	Form	Military
5609	Bars, Forgings, Forging Stock and Mechanical Tubing	-

TABLE 1.03 SPECIFICATIONS.

Source	AMS 5609 (2)		(3)
	Percent		
	Minimum	Maximum	Typical
Carbon	.12	.15	.13
Manganese	-	.60	.50
Silicon	-	.50	.25
Phosphorus	-	.025	.012
Sulfur	-	.025	.018
Chromium	11.50	12.50	11.95
Nickel	-	.75	.20
Molybdenum	-	.20	-
Aluminum	-	.05	-
Copper	-	.50	-
Columbium	.05	.25	.12
Tin	-	.05	-
Nitrogen	-	.08	-
Iron	Balance		Balance

TABLE 1.04 COMPOSITION.

Heating Temperature F - 1 hr	ASTM Grain Size (avg at 100x)	
	Type 410	410Cb
1700	6	8 to 9
1800	5	8
1900	4 to 5	8
2000	4	7 to 8

TABLE 1.0521 EFFECT OF COLUMBIUM ON GRAIN SIZE OF TYPE 410 WHEN AUSTENITIZED AT VARIOUS TEMPERATURES.

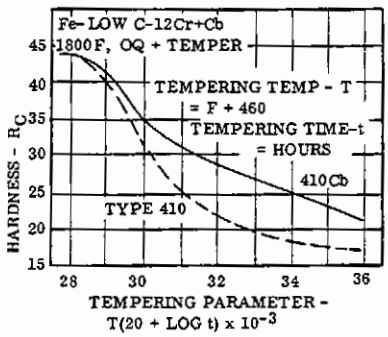


FIG. 1.0531 MASTER TEMPERING CURVES FOR 410Cb AND TYPE 410. (3, p. 81)

Fe
Low C
12 Cr
+ Cb

410 Cb

Source	AMS 5609 (2)
Alloy	Fe-low C-12Cr + Cb
Form	Bar, Forgings, Mechanical Tubing, and Forging Stock
Condition	1700F, 1 hr, AC + 600F, 2 hr (double temper)
F_{tu} - min - ksi	185*
F_{ty} - min - ksi	152
e(2 in or 4D) min - percent	10
RA - min - percent	30
Hardness - R_C	40-45

* Capability requirement of material 0.500 in or less in diameter, wall thickness, or distance between parallel sides or 0.500 in diameter specimens cut from larger bars, forgings, or tubing and given heat treatment specified above.

TABLE 3.011 AMS SPECIFIED MECHANICAL PROPERTIES.

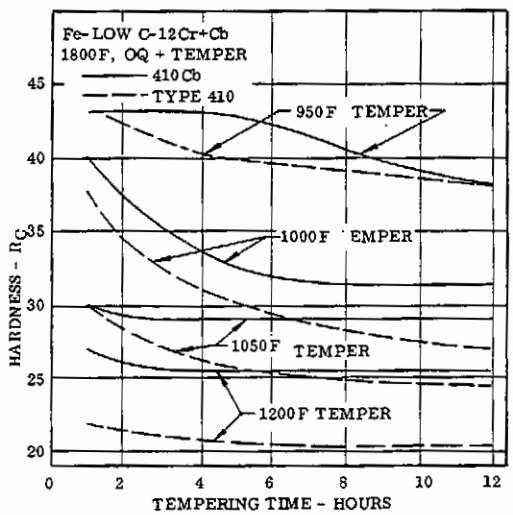


FIG. 1.061 TEMPERING CHARACTERISTICS OF 410Cb AND TYPE 410. (3, p. 81)

Source	(3)(4)								
Alloy	Fe-Low C-12Cr + Cb								
Form	Bar - 1 inch diameter								
Condition	1850F, oil quench +(F) Temper, 4 hr, AC								Ann
Temper - F	500	700	900	1000	1100	1200	1300	1400	-
F_{tu} - ksi	195	194	199	157	137	125	114	101	100
F_{ty} - ksi	161	162	156	138	121	109	94	79	75
e(2 in)-percent	16	16	18	18	19	20	22	26	25
RA - percent	61	61	60	64	64	65	69	72	70
Hardness-R_C	43	43	43	34	28	25	22	-	-
-R_B	-	-	-	-	-	-	-	99	99
Charpy V-Notch Impact - ft lb	50	55	30	37	68	95	110	110	-

TABLE 3.021 TYPICAL MECHANICAL PROPERTIES.

Source	(3)	
Form	Bar - 1 in diameter	
Condition	1850F, oil quench +(F) temper, 4 hr, AC	
Tempering Temperature - F	Rockwell Hardness	
	410Cb	Type 410
500	C43	C43
700	C43	C41
900	C43	C42
1000	C34	C28
1100	C28	C24
1200	C25	C20
1300	C22	B97
1400	B99	B92

TABLE 1.062 HARDNESS VERSUS TEMPERING TEMPERATURE WITH CONSTANT TEMPERING TIME FOR 410Cb VERSUS REGULAR TYPE 410.

	Fe
Low	C
12	Cr
+	Cb

410 Cb

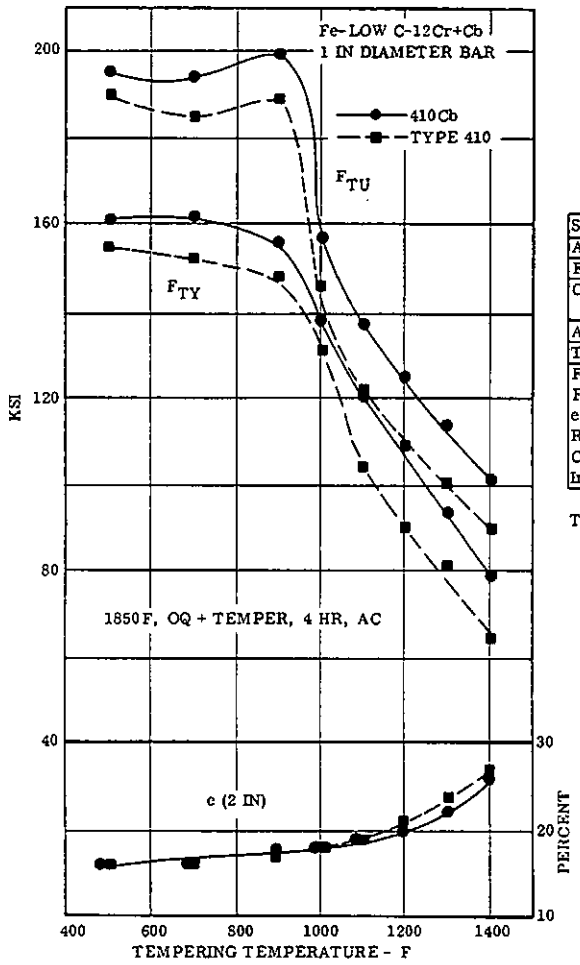


FIG. 3.0212 EFFECT OF TEMPERING TEMPERATURE ON ROOM TEMPERATURE TENSILE PROPERTIES OF 410Cb AND TYPE 410 BAR. (3, p. 82)

Source	(6)									
Alloy	Fe-Low C-12Cr + Cb									
Form	Bar - 1 inch diameter									
Condition	Austenitize (F), 0.5 hr, oil quench + Temper (F), 4 hr, AC									
Austenitize - F	1700	1850	1700	1850	1700	1850	1700	1850	1700	1850
Temper - F	700		1000		1100		1200		1300	
F_{tu} - ksi	193	194	146	157	129	137	120	125	111	114
F_{ty} - ksi	166	162	130	138	115	121	103	109	95	99
e(2 in)-percent	16	16	20	18	20	19	21	20	22	22
RA - percent	50	51	67	64	67	64	67	65	70	69
Charpy V-Notch Impact - ft lb	54	56	64	37	64	68	110	96	117	110

TABLE 3.0214 EFFECT OF AUSTENITIZING AND TEMPERING TEMPERATURES.

Source	(5)		
Alloy	Fe-Low C-12Cr + Cb		
Condition	1850 F, oil quench + 1200 F, 4 hr, AC		
Form - Bar	2 5/8 inch diameter	4 5/8 inch diameter	5 1/4 inch diameter
F_{tu} - ksi	125	124	126
F_{ty} - ksi	112	112	110
e(2 in) - percent	20	21	20
RA - percent	65	64	61
Hardness - R_C	26	26	26
Charpy V-Notch Impact - ft lb	90 to 96	40 to 46	55 to 65
Longitudinal tests at mid-radius location.			

TABLE 3.0213 EFFECT OF SIZE OF CROSS SECTION.

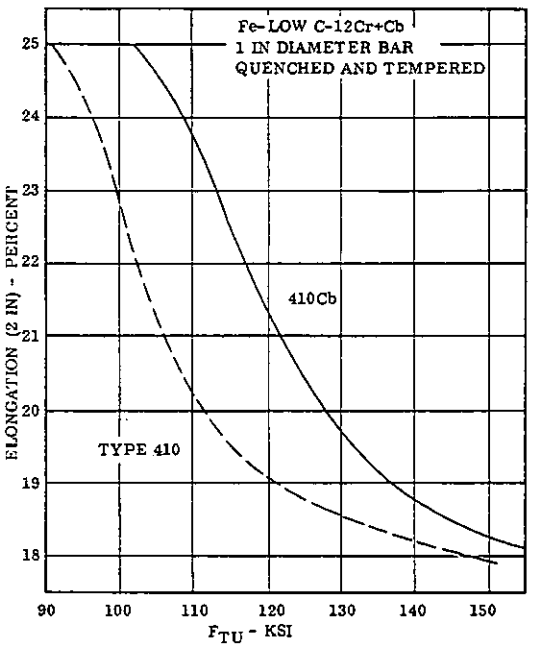


FIG. 3.0215 TENSILE STRENGTH VERSUS ELONGATION OF 410Cb AND TYPE 410. (1, p. 4)

Source	(5)			
Alloy	Fe-Low C-12Cr + Cb			
Form	1 inch diameter bar			
Condition	1850F, 0.5 hr, oil quench + 1200F temper + exposure			
Exposure Temp and Stress	None	900F-50 ksi	None	900F-55 ksi
Exposure Time - hours	None	17,229	None	16,818
F_{tu} - smooth - ksi	127	128	-	-
notched - ksi	-	-	208	223
e(4D) - percent	20	18	-	-
Hardness - R_C	26	27	26	27
Notch specimen: K_t = 3.0, 60° notch with .005 R, .375 inch diameter smooth section.				

TABLE 3.0216 EFFECT OF EXPOSURE AT ELEVATED TEMPERATURE ON ROOM TEMPERATURE PROPERTIES.

	Fe
Low	C
12	Cr
+	Cb

410 Cb

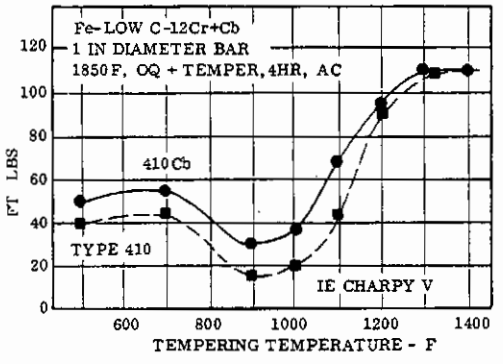


FIG. 3.0234 EFFECT OF TEMPERING TEMPERATURE ON ROOM TEMPERATURE IMPACT STRENGTH OF 410Cb AND TYPE 410 BAR. (3, pp. 82, 83)

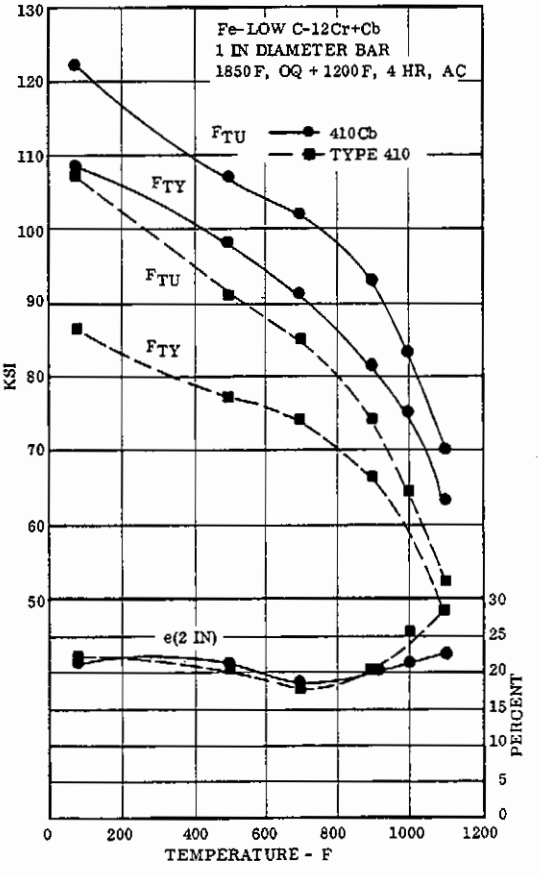


FIG. 3.0312 EFFECT OF TEST TEMPERATURE ON TENSILE PROPERTIES OF 410Cb AND TYPE 410 BAR. (3, p. 86)

Source	(1)(3)(6)									
Alloy	Fe-low C-12Cr + Cb									
Form	Bar - 1 inch diameter									
Condition	1850F, oil quench + (F) Temper, 4 hr, AC									
Tempering Temp - F	1200					1100				
Test Temp F	500	700	900	1000	1100	500	700	900	1000	1100
F_{tu} - ksi	107	102	93	83	70	117	110	97	-	74
F_{ty} - ksi	98	91	81	75	63	107	101	92	-	71
e(2 in)-percent	21	18	20	21	22	17	15	18	-	21
RA - percent	67	65	67	-	80	70	68	72	-	81

TABLE 3.031 TYPICAL SHORT TIME, ELEVATED TEMPERATURE TENSILE PROPERTIES USING TWO DIFFERENT TEMPERING TEMPERATURES.

	Fe
Low	C
12	Cr
+	Cb

410 Cb

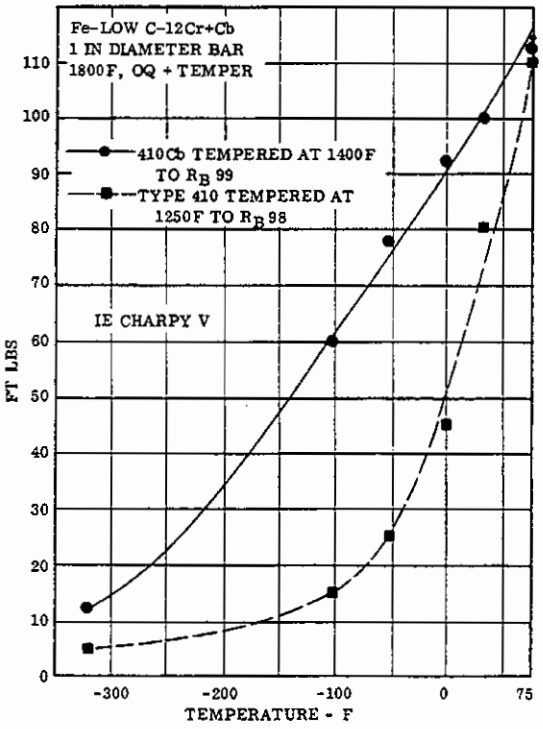


FIG. 3.0331 EFFECT OF TEST TEMPERATURE ON IMPACT STRENGTH OF 410Cb AND TYPE 410 TEMPERED BAR. (5)

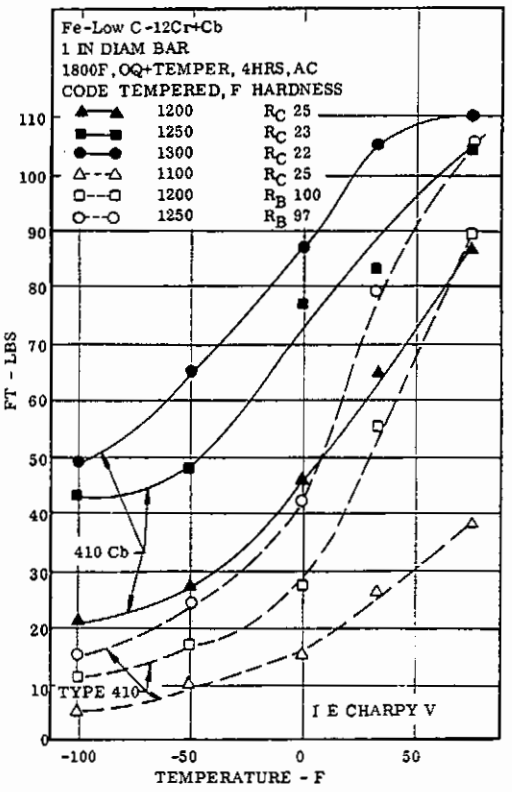


FIG. 3.0332 EFFECT OF TEMPERING TEMPERATURE ON IMPACT STRENGTH OF 410 Cb AND TYPE 410 BAR AT ROOM AND SUB-ZERO TEMPERATURES.

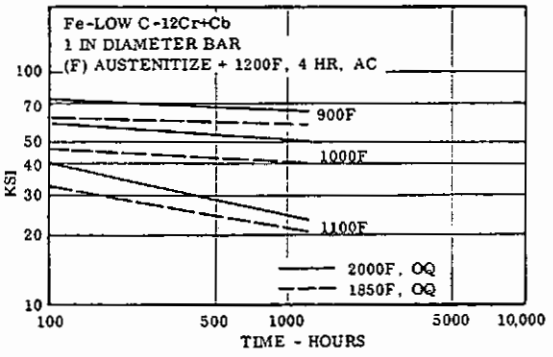


FIG. 3.042 CREEP RUPTURE CURVES AT 900 TO 1100F FOR 410 Cb TEMPERED BAR USING TWO AUSTENITIZING TEMPERATURES. (1, p. 6)

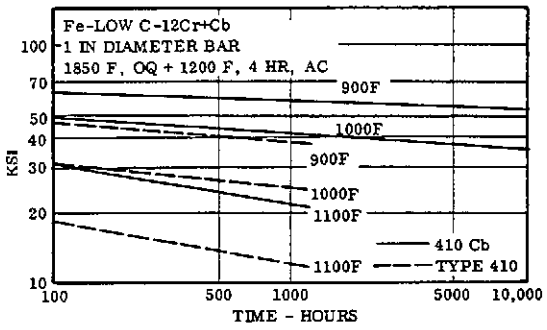


FIG. 3.041 CREEP RUPTURE CURVES AT 900 TO 1100F FOR 410Cb AND TYPE 410 TEMPERED BAR. (1,p.6)(5)

	Fe
Low	C
12	Cr
+	Cb

410 Cb

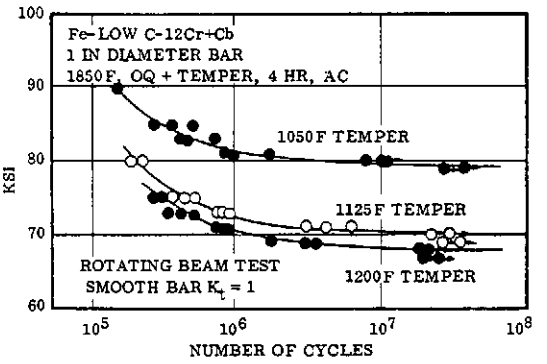


FIG. 3.051 S-N CURVES AT ROOM TEMPERATURE FOR 410Cb BAR. (8)

REFERENCES

1. Armco Steel Corporation, Product Data Bulletin S-32, "Armco 410Cb Stainless Steel" (September 1966).
2. AMS 5609 (January 31, 1964).
3. Tanczyn, H., "Properties of 12 Percent Chromium Alloys Modified with Small Columbium Additions," ASTM Special Technical Publication No. 369 (1965).
4. Private communication with A. C. Burton, Research Engineer, Armco Steel Corporation, Baltimore, Maryland (February 1971).
5. Tanczyn, H., "What Columbium Does to Type 410 Stainless Steel," Metal Progress (November 1966).
6. "Stainless Steel Properties Bettered with Columbium," STEEL (September 3, 1962).
7. "Columbium Addition Toughens Type 410 Stainless Steel" IRON AGE (August 30, 1962).
8. Private communication with H. Tanczyn, Senior Research Engineer, Armco Steel Corporation, Baltimore, Maryland (July 1971).

REVISED: SEPTEMBER 1973
AUTHOR: J. R. KATTUS

FERROUS ALLOYS

Fe
0.35 C
13 Cr

TYPE 420

1. GENERAL

Type 420 is a medium-carbon version of the hardenable (martensitic) family of stainless steels containing about 13 percent chromium. Its carbon content of about 0.35 percent provides heat-treated hardness and strength higher thanType 410 stainless steel. In the hardened condition (quenched and tempered), Type 420 has high strength and wear resistance. It develops its maximum corrosion resistance when hardened and polished. Type 420 has long been used for cutlery, gears, valve and pump parts, surgical instruments, dies, hand tools, and many parts requiring high spring tempers. It can be used up to about 900F in aerospace applications, but its use at elevated temperatures has, to a great extent, been superseded by the modified, more-highly-alloyed Type 422 (Code 1403). Type 420 should not be used for heavily stressed parts that operate at subzero temperatures. It is sometimes welded, but both pre-heat and post-heat are needed for optimum results. Free-machining sulfur-bearing (420F) and selenium-bearing (420F-Se) modifications are produced. They have about 10 percent better machinability than standard Type 420. Aside from somewhat reduced formability and corrosion resistance, the free-machining grades exhibit properties similar to the standard grade. The alloy is also produced in the form of castings for corrosion-resisting applications.

1.01 Commercial Designations

Type 420 stainless steel
CA-40 cast stainless steel
Type 420F stainless steel (sulfur-bearing)
Type 420F-Se stainless steel (selenium-bearing)

1.02 Alternate Designations

1.03 Specifications

Table 1.03.

1.04 Composition

Table 1.04.

1.05 Heat Treatment

1.051 Full anneal: Heat to 1550 - 1650F, soak 1 hour per inch of thickness, furnace cool to 1100F or lower. This treatment results in a hardness of about 185 Brinell, which provides optimum formability and machinability. Extreme care must be taken to maintain a very slow cooling rate of no more than 50F per hour through the critical range in order to avoid rehardening (3)(7)(23)(24).

1.052 Process anneal: Heat to 1350 to 1450F, soak 4 hours, air cool. This treatment results in a hardness of about 215 Brinell, which provides limited formability and fair machinability (7)(23)(24).

1.053 Hardening: Austenitize at 1800 - 1900F for at least 15 minutes, oil- or air-quench to room temperature. For large parts, complex shapes, or parts already hardened or otherwise stressed, preheating at a temperature in the range 1000 to 1450F is recommended. The austenitizing should be done in inert or endothermic atmosphere if possible to avoid decarburization; if controlled atmosphere is not available, time at temperature should not be unnecessarily prolonged. The alloy is air hardening in sections up to at least 4 inches; larger sections should generally be oil quenched (7)(23)(24).

1.054 Tempering: Hold at temperature in the range 300 to 700F or 1050 to 1300F for 1 to 4 hours. The secondary hardening range from about 700 to 1000F should generally be avoided because tempering in that range induces reduced resistance to corrosion and stress corrosion and reduced toughness (7)(23)(24).

1.055 Stress relief: Hold at 1300 to 1400F, 6 to 8 hours, and air cool. This treatment, which is quite similar to a process anneal, is recommended after welding and after severe cold forming (7)(19).

1.06 Hardness

1.061 Effect of tempering temperature on hardness, Figure 1.061.

1.062 Effect of temperature on hardness, Figure 1.062.

1.063 Effect of exposures at elevated temperatures on room-temperature hardness, Figure 1.063.

1.07 Forms and Conditions Available

Table 1.07.

1.08 Melting and Casting Practice

1.081 For wrought products, Type 420 is generally air melted in electric-arc furnaces. For some applications requiring exceptional quality, it is vacuum remelted by consumable-electrode or induction methods.

1.082 For castings, the alloy is usually air melted. Its castability - fluidity, shrinkage, resistance to hot tearing - is rated as good. During melting and casting, clean crucibles, ladles, molds, and other refractories should be used. The metal should be melted rapidly with care to avoid superheat in the molten portion of the charge while solid or cold melting stock is still present. Calcium - manganese - silicon is used for deoxidation. The amount added must be calculated on the basis of silicon and manganese content of the charge, so that the final silicon content is within 10 percent of the maximum limit of the specification. The addition should be mixed into the melt about 30 to 60 seconds before pouring; the deoxidation products should then be skimmed off, the temperature adjusted, and the metal poured. Carbon content must be maintained within the specified limits to obtain proper response to heat treatment. Carbon losses should be established on standard melt cycles and additions made in the form of an iron-carbon alloy. The following precautions are helpful in minimizing pitting and other surface defects:

1. Maintain carbon level near the upper limit.
2. Maintain chromium level at the mid or lower end of the range.
3. Use clean furnaces and ladles.
4. Cool castings through the solidification range as rapidly as possible.
5. When feasible, introduce an inert atmosphere into the mold before pouring.

The pouring temperature should normally be 2900 to 2950F; however, it can vary from this level dependent upon complexity of the casting and section size. Pouring of the molds should be done from a minimum height with gates and risers designed to minimize turbulence. For investment castings all traces of wax or plastic pattern material and moisture must be removed from the molds to prevent carbon pickup from the pattern material and gas holes or pin-hole porosity from the moisture (31).

1.09 Special Considerations

1.091 See Type 422, Code 1403, Sections 1.091 and 1.092.

1.092 The strength and toughness of Type 420 can be significantly improved by ausforming at about 1000F (29).

1.093 Quenching and tempering induce small dimensional changes which vary with the heat-treating conditions.

1.0931 Dimensional changes as a result of hardening and tempering, Figure 1.0931.

2. PHYSICAL AND CHEMICAL PROPERTIES

2.01 Thermal Properties

2.011 Melting range - 2650 to 2750F (2).

2.012 Phase changes.

2.0121 Time-temperature-transformation diagrams.

2.0122 The exact temperatures for the various phase changes have not been studied as thoroughly as those in Type 422, but the changes and their temperatures closely parallel those of Type 422 (See Code 1403, Sections 2.0122 through 2.0125).

2.013 Thermal conductivity, Figure 2.013.

2.014 Thermal expansion, Figure 2.014.

2.015 Specific heat, Figure 2.015.

Fe
0.35 C
13 Cr

TYPE 420

2.016 Thermal diffusivity, Figure 2.016.

2.02 Other Physical Properties

2.021 Density. 0.28 lb per in^3; 7.75 gr per cm^3 (10)(12)(23)(24).

2.022 Electrical properties, Table 2.022.

2.023 Magnetic properties. Ferromagnetic in all conditions (24).

2.024 Emittance.

2.025 Damping capacity.

2.03 Chemical Properties

2.031 Type 420 attains its optimum resistance to both general and stress corrosion when quenched and tempered except that tempering in the secondary-hardening range - about 700 to 1000F - results in a marked deterioration in corrosion resistance. See Table 2.0311 and Figures 2.0312 and 2.0313. Inferior corrosion resistance is also exhibited by annealed material and by material with scale and other surface contaminants (7)(10).

2.0311 Effect of tempering temperature on susceptibility to stress corrosion in salt spray, Table 2.0311.

2.0312 Effect of tempering temperature on susceptibility to stress corrosion of bar totally immersed in 3 percent sodium-chloride solution, Figure 2.0312.

2.0313 Effect of tempering temperature on general corrosion resistance of bar totally submerged in 3 percent sodium-chloride solution, Figure 2.0313.

2.032 Hardened and cleaned Type 420 resists corrosion from the atmosphere, water, steam, carbonic acid, crude oil, gasoline, blood, perspiration, alcohol, ammonia, mercury, sterilizing solutions, soaps and oxidizing solutions such as nitric acid and nitrates. Deairated or reducing solutions tend to attack the alloy (10)(30).

2.033 Resists excessive oxidation in continuous service at temperatures up to 1200F.

2.04 Nuclear Properties

3. MECHANICAL PROPERTIES

3.01 Specified Mechanical Properties
Table 3.01.

3.02 Mechanical Properties at Room Temperature

3.021 Tension.

3.0211 Stress-strain diagrams (see Figure 3.03111).

3.0212 Effect of tempering temperature on tensile properties of bar, Figure 3.0212.

3.0213 Effect of tempering temperature in tensile properties of castings, Figure 3.0213.

3.0214 Effect of ausforming on tensile properties of sheet, Table 3.0214.

3.0215 Tensile properties of non-hardened material, Table 3.0215.

3.022 Compression.

3.0221 Stress-strain diagrams (see Figure 3.03211).

3.0222 Compressive yield strength (see Figure 3.0322).

3.023 Impact.

3.0231 Effect of tempering temperature on impact properties of bar at room temperature, Figure 3.0231.

3.0232 Effect of tempering temperature on impact properties of castings at room temperature, Figure 3.0232.

3.024 Bending.

3.025 Torsion and shear.

3.0251 Shear strength (see Figure 3.0351).

3.026 Bearing.

3.0261 Bearing ultimate and yield strengths (see Figure 3.0361).

3.027 Stress concentration.

3.0271 Notch properties.

3.0272 Fracture toughness.

3.028 Combined properties.

3.03 Mechanical Properties at Various Temperatures.

3.031 Tension.

3.0311 Stress-strain diagrams.

3.03111 Tensile stress-strain curves for sheet at room and elevated temperatures, Figure 3.03111.

3.0312 Effect of temperature on tensile properties of bar, Figure 3.0312.

3.0313 Effect of temperature on tensile properties of sheet of different thicknesses, Figure 3.0313.

3.0314 Effect of exposure time at test temperature on the tensile properties of sheet, Figure 3.0314.

3.032 Compression.

3.0321 Stress-strain diagrams.

3.03211 Compressive stress-strain curves for sheet at room and elevated temperatures, Figure 3.03211.

3.0322 Effect of temperature on compressive yield strength after two different exposure times at test temperature, Figure 3.0322.

3.033 Impact.

3.0331 Effect of temperature on impact properties, Figure 3.0331.

3.034 Bending.

3.035 Torsion and shear.

3.0351 Effect of temperature on shear strength after two different exposure times at test temperature, Figure 3.0351.

3.036 Bearing.

3.0361 Effect of temperature on bearing properties after two different exposure times at test temperature, Figure 3.0361.

3.037 Stress concentration.

3.0371 Notch properties.

3.0372 Fracture toughness.

3.038 Combined properties.

3.04 Creep and Creep-Rupture Properties

3.041 Creep-rupture curves at 800 to 1100F, Figure 3.041.

3.042 Stresses to cause various amounts of creep deformation in 1000 hours at 700, 800, and 900F, Figure 3.042.

3.043 Stress to cause 1 percent creep deformation in 10,000 hours at 1000 to 1300F, Figure 3.043.

3.05 Fatigue Properties

3.06 Elastic Properties

3.061 Poisson's ratio.

3.062 Modulus of elasticity.

3.0621 Effect of temperature on modulus of elasticity in tension and compression, Figure 3.0621.

3.0622 Tangent modulus curves in compression for sheet at room and elevated temperatures, Figure 3.0622.

3.063 Modulus of rigidity - 11.7×10^3 ksi (2)(24).

4. FABRICATION

4.01 Formability

4.011 Hot working. The alloy can be readily hot worked by starting at 2000 to 2200F and finishing above 1650F. If necessary, it should be reheated to maintain the hot working temperature above 1650F. Material to be hot worked should be preheated at 1400 to 1500F and then heated to the working temperature. Cooling cracks should be prevented by slow cooling after hot work. This can be accomplished by charging the hot worked material into a furnace at 1550F and furnace cooling or by burying the material in an insulating material such as dry lime or ashes (7)(10).

4.012 Cold working. Type 420 can be cold formed moderately in the fully annealed condition and only to a very limited extent in the process-annealed condition. A full anneal or stress-relief anneal is recommended after severe cold forming (7)(10).

4.02 Machining and Grinding

4.021 Type 420 is usually machined in the fully annealed condition at speeds about 50 percent of those used for free-machining AISI B1112 steel. For the free-machining grades machining speeds are about 10 percent higher. Machinability in the process-annealed condition is somewhat less. Machining of the quenched-and-tempered

material is difficult but possible with carbide cutting tools (7)(10).

4.03 Welding

4.031 The alloy can be arc welded by any of the common manual and automatic techniques. Because of its air-hardening characteristic and resulting tendency toward weld embrittlement, it should be preheated to 450F and immediately after welding should be stress relieved (see Section 1.055). Type 420 may be used as filler metal. Higher weld ductility but lower strength is provided by an austenitic stainless filler, such as Type 309 or 310 (7)(10).

4.04 Surface Treatment

See Type 422, Code 1403, Sections 4.041 and 4.042.

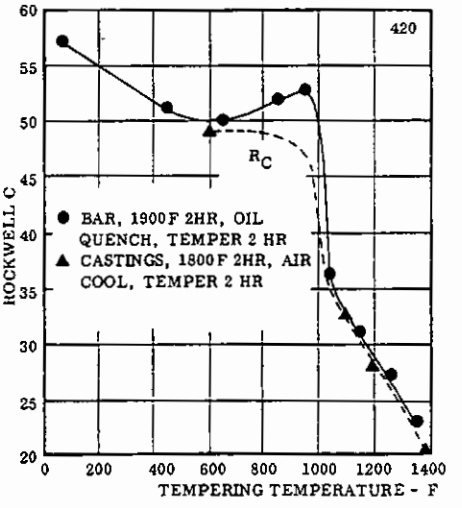


FIG. 1.061 EFFECT OF TEMPERING TEMPERATURE ON HARDNESS (7)(19)

Fe
0.35 C
13 Cr

TYPE 420

Alloy	420
Source	(4)(5)(6)(8)(9)(18)
Specification	Forms
AMS 5621	Bars, forgings, forging stock
AMS 5620B	Free-machining bars, forgings, forging stock
AMS 5506A	Sheet, strip, plate
QQ-S-763C (1) Cl.420	Bars, forgings
QQ-S-766C (5) Cl.420	Plates, sheet, strip
QQ-W-423A	
ASTM A276	Bars
ASTM A314	Billets and bars for reforging
ASTM A473	Forgings
ASTM A296	Castings
MIL-S-862B, Cl.420	Bars
MIL-S-22216	Castings
MIL-S-8142	
MIL-W-17481A	
SAE 51420	Martensitic stainless steel
SAE 60420	Corrosion-resistant castings
AISI 420	Stainless steel
AWS A5.9-69 ER420	Electrode and rod
ACI CA40	Castings

TABLE 1.03 SPECIFICATIONS

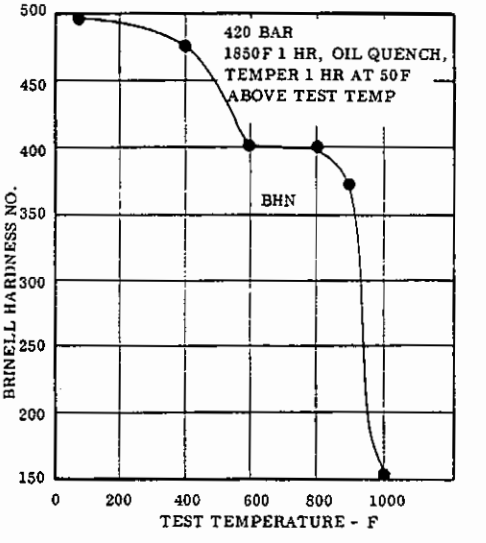


FIG. 1.062 EFFECT OF TEMPERATURE ON HARDNESS (10)

Alloy	420		420F		420F-Se		420		420 (CA-40)	
Source	AMS 5621 (4) AMS 5506 (5)		AMS 5620B (6)		AMS 5620B (6)		ASTM A276(15) ASTM A314(16) ASTM A473(17)		ASTM A296 (18) SAE 60420	
Form	Wrought		Wrought		Wrought		Wrought		Cast	
	min	max	min	max	min	max	min	max	min	max
Carbon	0.30	0.40	0.30	0.40	0.30	0.40	0.15	-	0.20	0.40
Manganese	-	1.00	-	1.25	-	1.25	-	1.00	-	1.00
Silicon	-	1.00	-	1.00	-	1.00	-	1.00	-	1.50
Phosphorus	-	0.040	-	0.040	-	0.040	-	0.040	-	0.04
Sulfur	-	0.030	0.15	0.35	-	0.030	-	0.030	-	0.04
Chromium	12.00	14.00	12.00	14.00	12.00	14.00	12.00	14.00	11.5	14.0
Nickel	-	0.50	-	0.50	-	0.50	-	-	-	1.00
Mo or Zr	-	0.50	-	0.60	-	0.60*	-	-	-	0.50
Selenium	-	-	-	-	0.18	0.35	-	-	-	-
Iron	Balance		Balance		Balance		Balance		Balance	

TABLE 1.04 COMPOSITION

Fe
0.35 C
13 Cr

TYPE 420

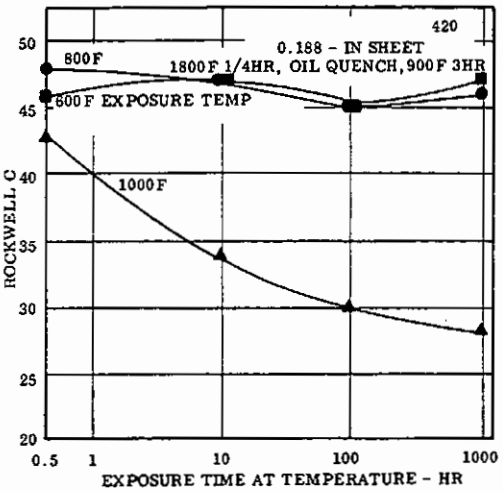


FIG. 1.063 EFFECT OF EXPOSURES AT ELEVATED TEMPERATURES ON ROOM - TEMPERATURE HARDNESS (11)

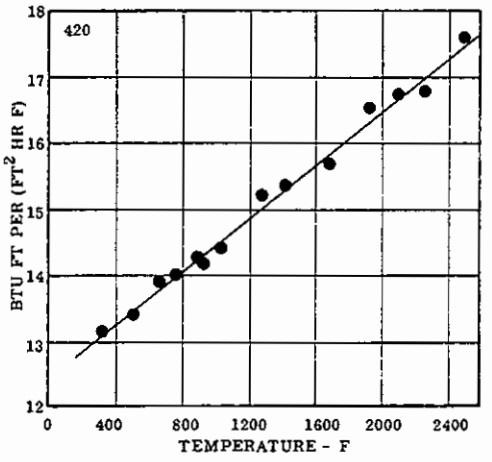


FIG. 2.012 THERMAL CONDUCTIVITY (1)

Alloy	420
Source	(9)(10)(12)(19)(26)(27)(28)
Form	Condition
Forging billets and bars	Annealed
Bars	Hot rolled or cold finished
Tubular products	Annealed
Wire	Annealed or cold finished
Wire rods	Annealed or cold finished
Sheet and strip	Annealed or cold rolled
Plate	Annealed or hot rolled
Forgings	Annealed or hardened
Castings	Annealed or hardened

TABLE 1.07 FORMS AND CONDITIONS AVAILABLE

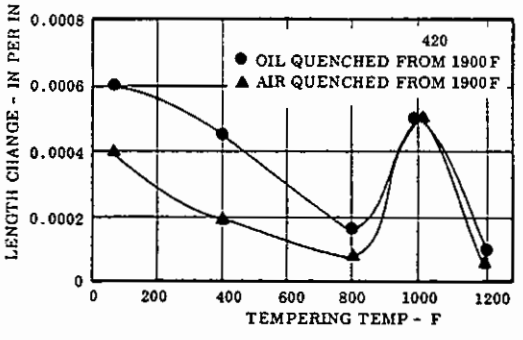


FIG. 1.0931 DIMENSIONAL CHANGES AS A RESULT OF HARDENING AND TEMPERING (10)

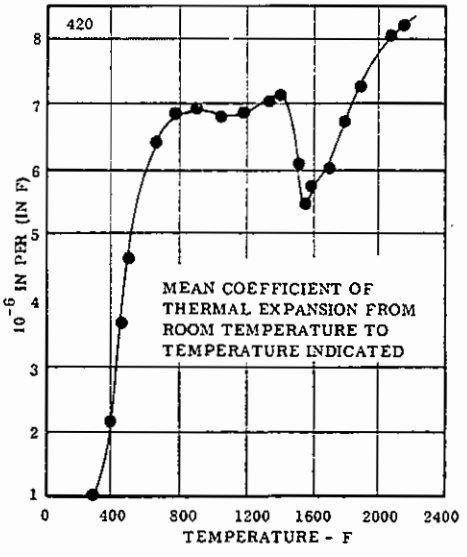


FIG. 2.014 THERMAL EXPANSION (1)

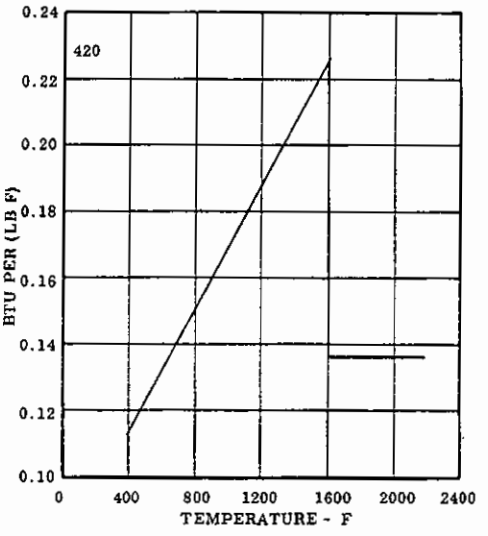


FIG. 2.015 SPECIFIC HEAT (1)

Alloy	420
Form	Forgings
Condition	1850F oil quench, tempered 2 hr.
Source	(20)
Tempering Temp. (F)	Stress corrosion,* days to failure
300	no failure
400	no failure
500	no failure
600	no failure
700	no failure
800	4
900	1/2
1000	6
1100	no failure

*Exposed 75 days to 5 percent salt spray under 100 ksi stress.

TABLE 2.0311 EFFECT OF TEMPERING TEMPERATURE ON SUSCEPTIBILITY TO STRESS CORROSION IN SALT SPRAY

Fe
0.35 C
13 Cr

TYPE 420

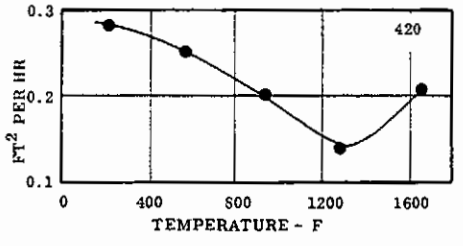


FIG. 2.016 THERMAL DIFFUSIVITY (2)

Alloy	420		
Condition	Annealed		
Source	(2)(3)		
	Electrical Conductivity		Electrical Resistivity, microhm in.
Temperature - F	Percent IACS	megmhos per in^3	
32 - 70	3.15	0.0463	21.6

TABLE 2.022 ELECTRICAL PROPERTIES

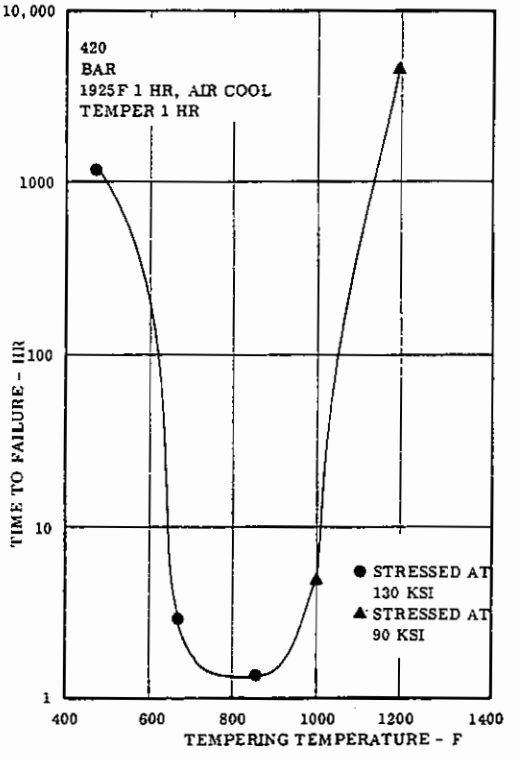


FIG. 2.0312 EFFECT OF TEMPERING TEMPERATURE ON SUSCEPTIBILITY TO STRESS CORROSION OF BAR TOTALLY IMMERSED IN 3 - PERCENT SODIUM - CHLORIDE SOLUTION (22)

Fe
0.35 C
13 Cr

TYPE 420

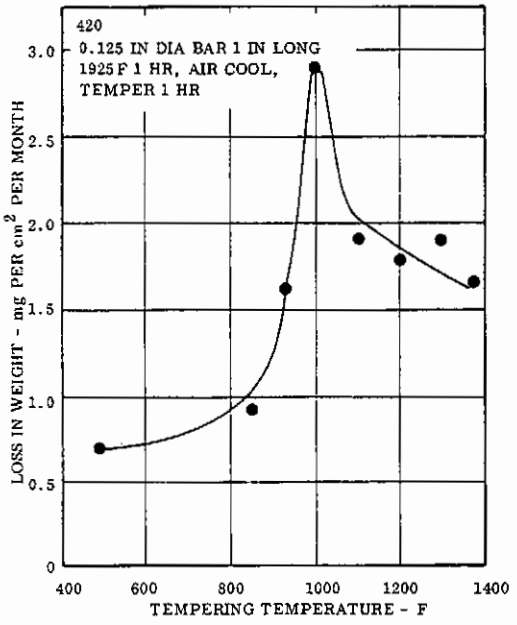


FIG. 2.0313 EFFECT OF TEMPERING TEMPERATURE ON GENERAL CORROSION RESISTANCE OF BAR TOTALLY SUBMERGED IN 3 - PERCENT SODIUM - CHLORIDE SOLUTION (22)

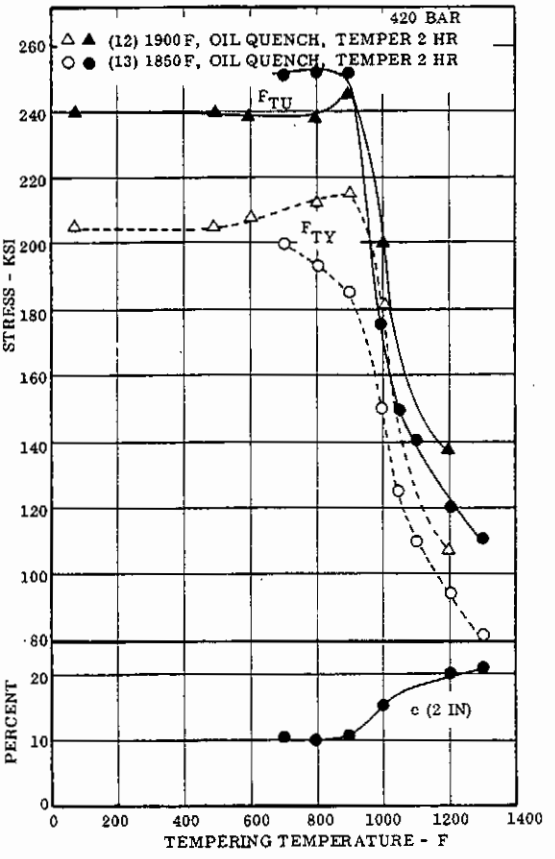


FIG. 3.0212 EFFECT OF TEMPERING TEMPERATURE ON TENSILE PROPERTIES OF BAR (12)(13)

Alloy	420						
Source	AMS 5506A (5)	AMS 5621 (4) AMS 5620B (6)	ASTM A276 (15)	ASTM A276 (15)	ASTM A473 (17)		ASTM A296 (18)
Form	Sheet, strip	Bars, forging	Bars	Bars	Forgings		Castings
Condition	Annealed	Annealed	Hot finished	Cold finished	Anneal.	1900F OQ	Annealed
F_{tu}, ksi, max.	100	-	-	-	-	-	-
F_{tu}, ksi, min.	-	-	-	-	-	-	100
F_{ty}, ksi, min.	-	-	-	-	-	-	70
e (2 in.), percent, min.	-	-	-	-	-	-	15
under 0.030 in. thick	12	-	-	-	-	-	-
0.030 in. and over	15	-	-	-	-	-	-
RA, percent, min.	-	-	-	-	-	-	25
BHN, max.	-	241	241	255	223	-	-
RC, min.	-	-	-	-	-	50	-

TABLE 3.01 SPECIFIED MECHANICAL PROPERTIES

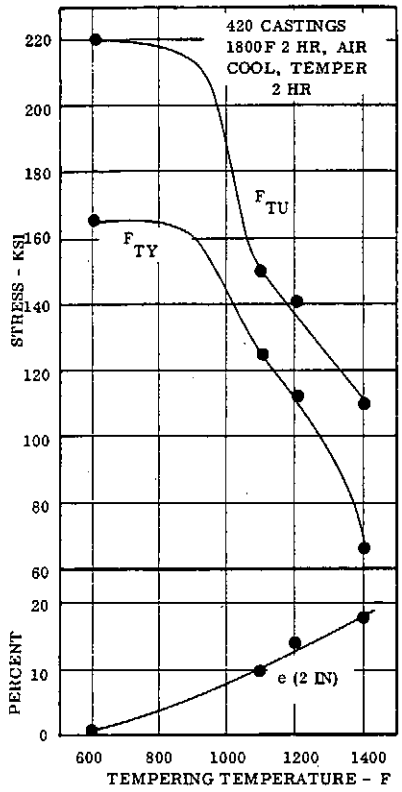


FIG. 3.0213 EFFECT OF TEMPERING TEMPERATURE ON TENSILE PROPERTIES OF CASTINGS (19)

Alloy	420				
Source	(24)				
Form	Condition	F_{ty} ksi	F_{tu} ksi	e (2 in.) percent	RA percent
Strip	Fully annealed	50	95	20	-
Bar	Fully annealed	50	95	25	55
Bar	Annealed & cold drawn	85	105	17	50
Wire	Fully annealed	50	95	20*	65

* Gage length equal to 4 times diameter.

Fe
0.35 C
13 Cr

TYPE 420

TABLE 3.0215 TENSILE PROPERTIES OF NON-HARDENED MATERIAL

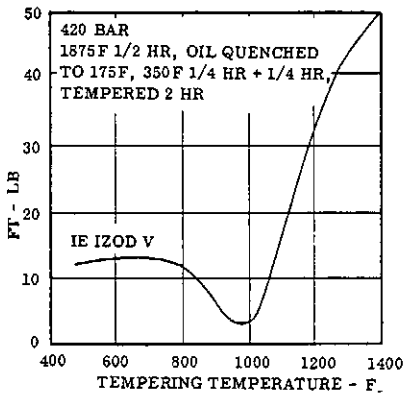


FIG. 3.0231 EFFECT OF TEMPERING TEMPERATURE ON IMPACT PROPERTIES OF BAR AT ROOM TEMPERATURE (14)

Alloy	420	
Form	Sheet	
Source	(29)	
Condition	1900F, OQ, 900F, 2 hr.	1900F, AC to 1000F, Ausformed 85 percent by rolling, OQ, 1000F, 2 hr.
F_{ty}, ksi	195	220
F_{tu}, ksi	236	245
RA, percent	60	40

TABLE 3.0214 EFFECT OF AUSFORMING ON TENSILE PROPERTIES OF SHEET

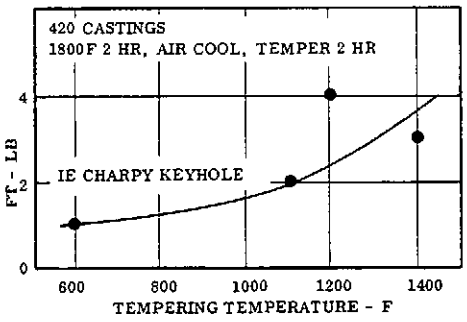


FIG. 3.0232 EFFECT OF TEMPERING TEMPERATURE ON IMPACT PROPERTIES OF CASTINGS AT ROOM TEMPERATURE (19)

Fe
0.35 C
13 Cr

TYPE 420

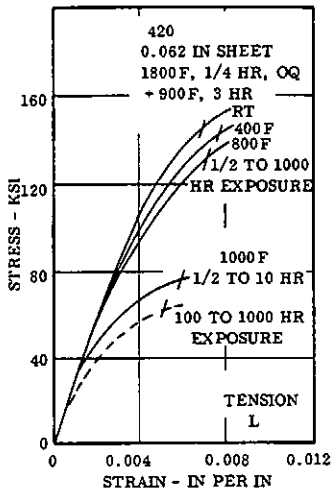


FIG. 3.03111 TENSILE STRESS - STRAIN CURVES FOR SHEET AT ROOM AND ELEVATED TEMPERATURES (11)

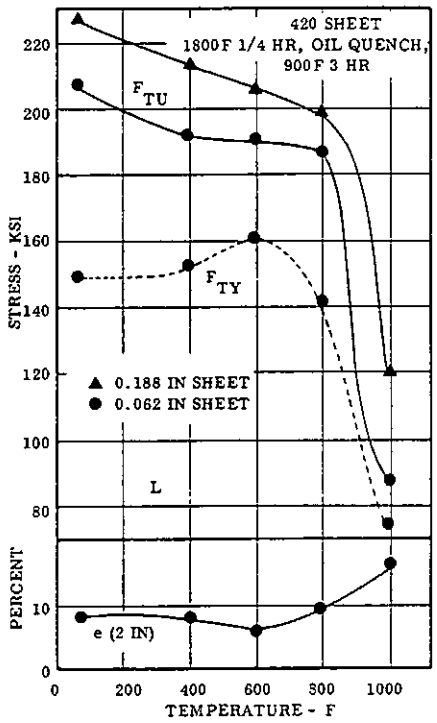


FIG. 3.0313 EFFECT OF TEMPERATURE ON TENSILE PROPERTIES OF SHEET OF DIFFERENT THICKNESSES (11)

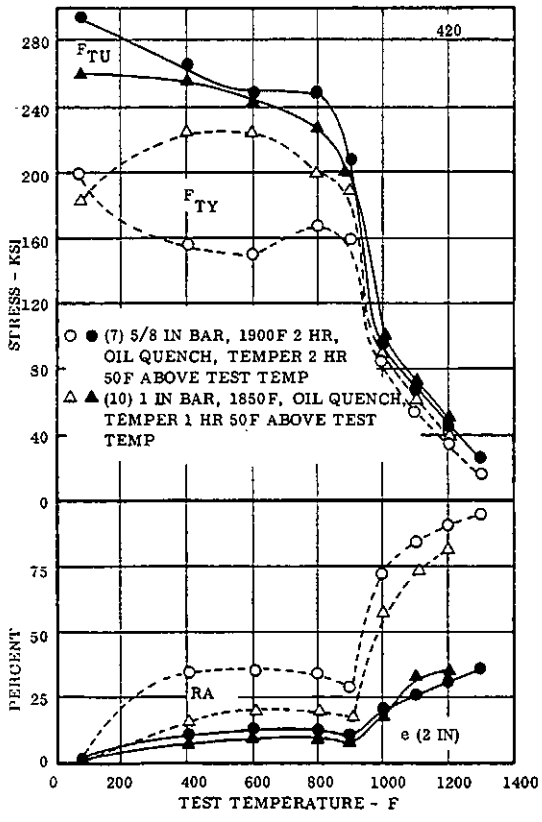


FIG. 3.0312 EFFECT OF TEMPERATURE ON TENSILE PROPERTIES OF BAR (7)(10)

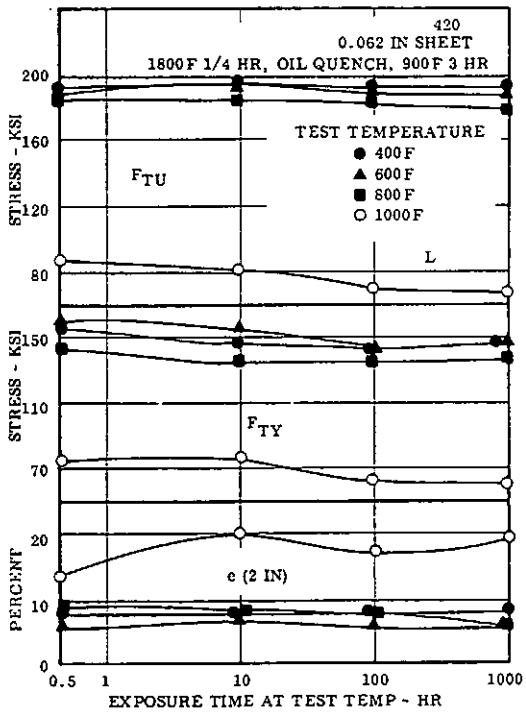


FIG. 3.0314 EFFECT OF EXPOSURE TIME AT TEST TEMPERATURE ON THE TENSILE PROPERTIES OF SHEET (11)

Fe
0.35 C
13 Cr

TYPE 420

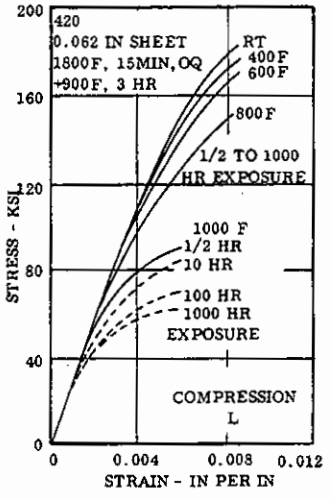


FIG. 3.03211 COMPRESSIVE STRESS - STRAIN CURVES FOR SHEET AT ROOM AND ELEVATED TEMPERATURES (11)

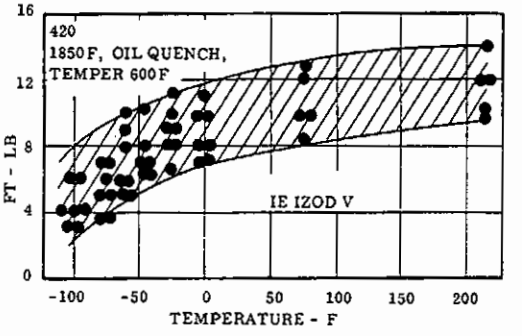


FIG. 3.0331 EFFECT OF TEMPERATURE ON IMPACT PROPERTIES (13)

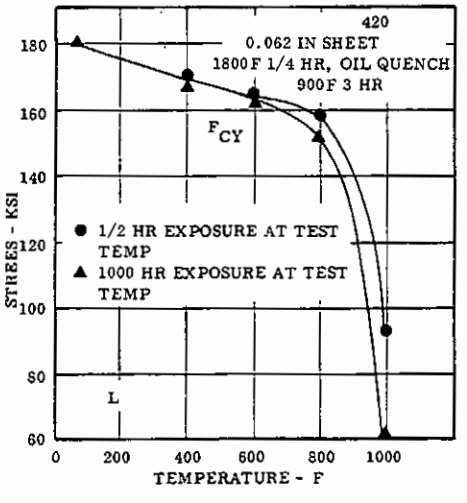


FIG. 3.0322 EFFECT OF TEMPERATURE ON COMPRESSIVE YIELD STRENGTH AFTER TWO DIFFERENT EXPOSURE TIMES AT TEST TEMPERATURE (11)

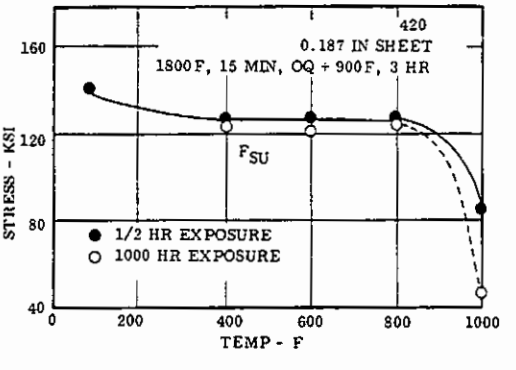


FIG. 3.0351 EFFECT OF TEMPERATURE ON SHEAR STRENGTH AFTER TWO DIFFERENT EXPOSURE TIMES AT TEST TEMPERATURE (11)

Fe
0.35 C
13 Cr

TYPE 420

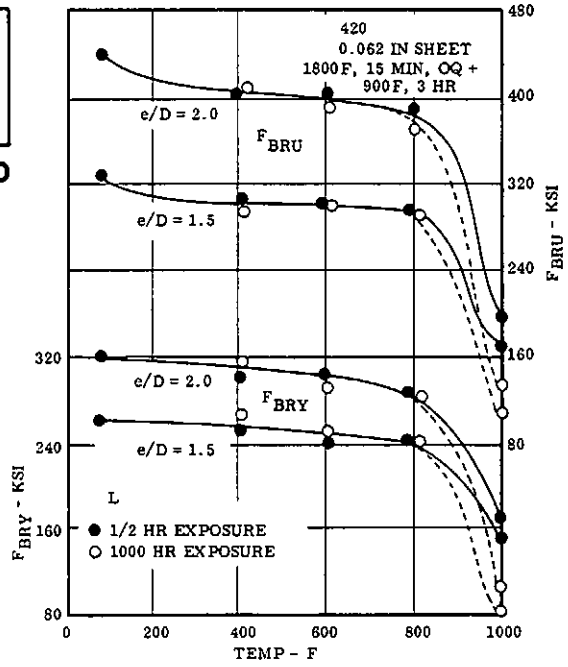


FIG. 3.0361 EFFECT OF TEMPERATURE ON BEARING PROPERTIES AFTER TWO DIFFERENT EXPOSURE TIMES AT TEST TEMPERATURE (11)

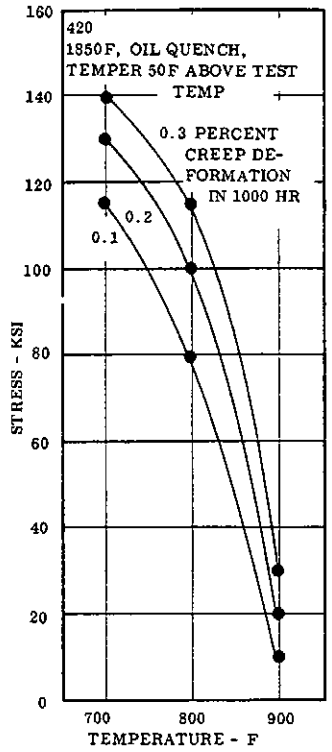


FIG. 3.042 STRESSES TO CAUSE VARIOUS AMOUNTS OF CREEP DEFORMATION IN 1000 HOURS AT 700, 800, AND 900F (25)

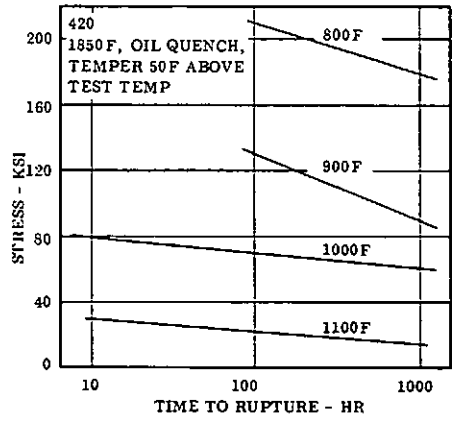


FIG. 3.041 CREEP - RUPTURE CURVES AT 800 TO 1100F (25)

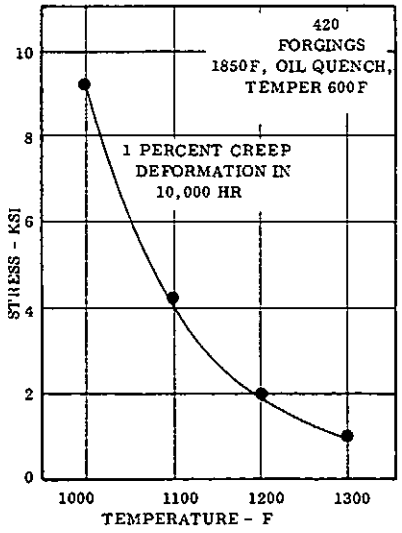


FIG. 3.043 STRESS TO CAUSE 1 PERCENT CREEP DEFORMATION IN 10,000 HOURS AT 1000 TO 1300F (21)

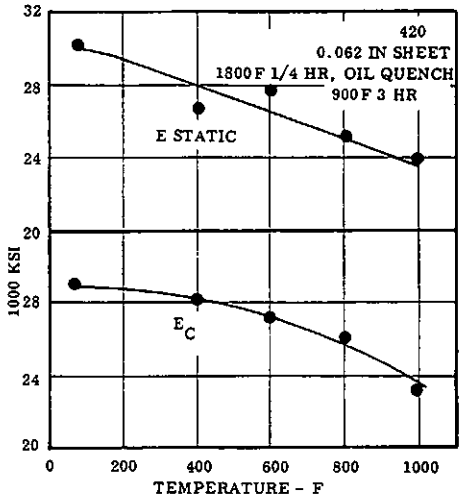


FIG. 3.0621 EFFECT OF TEMPERATURE ON MODULUS OF ELASTICITY IN TENSION AND COMPRESSION (11)

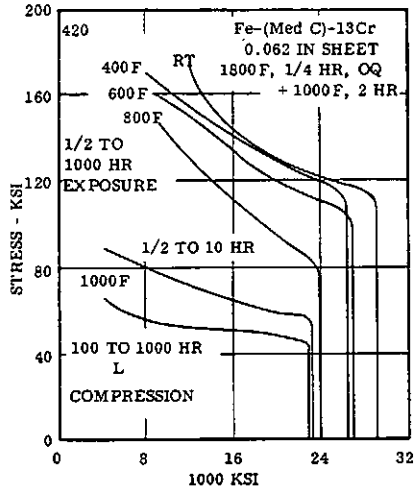


FIG. 3.0622 TANGENT MODULUS CURVES IN COMPRESSION FOR SHEET AT ROOM AND ELEVATED TEMPERATURES (11)

REFERENCES

1. Fieldhouse, I.B. and Lang, J.I., "Measurement of Thermal Properties", WADD Technical Report 60-904, Armour Research Foundation (January 1961).
2. "Some Physical Properties of Martensitic Stainless Steels", DMIC Memorandum 68, Battelle Memorial Institute (September 28, 1960).
3. "Properties of 200, 300, 400 Series", Republic Steel Corporation (1972).
4. AMS 5621 (November 1, 1952).
5. AMS 5506A (August 15, 1958).
6. AMS 5620B (June 15, 1952).
7. "Uniloy Hardenable 400 Series Stainless Steels", Universal-Cyclops Specialty Steel Division, Bulletin S-2029 (1966).
8. "Military Standardization Handbook", MIL-HDBK-H1D (22 June 1970).
9. "Armco Stainless Steels", Armco Steel Corporation, Bulletin LA172 16M (June 1972).
10. "Carpenter Stainless Type 420", Carpenter Technology Corporation, Technical Data Sheet (August 1970).
11. Kattus, J.R., Preston J.B. and Lessley, H.L., "Determination of Tensile, Compressive, Bearing, and Shear Properties of Sheet Steels at Elevated Temperatures", WADC TR 58-365, ASTIA Document No. 206075 Southern Research Institute (November 1958).
12. "Types 440A, B and C and 420", Allegheny-Ludlum Steel Corporation, Bulletin B102-Ed17-10M-470G.
13. "Properties of Corrosion-Resistant Steel Castings", Metals Handbook, Vol. 1, American Society for Metals (1961), p. 439.
14. Parr, J.G. and Hanson, A., "An Introduction to Stainless Steel", American Society for Metals (1966).
15. ASTM A276.
16. ASTM A314.
17. ASTM A473.
18. ASTM A296.
19. Schoeffer, E.A., "A Selection Guide to Corrosion-Resistant Cast Alloys", Steel Founders Society, Bulletin 25M (January 1970).
20. Lillys, P., and Nehrenberg, A.E., "Effect of Tempering Temperature on Stress Corrosion and Hydrogen Embrittlement of Martensitic Stainless Steel", Transactions ASM, Vol. 48 (1956), p. 327-346.
21. "Typical Properties of Wrought Stainless Steel", Metal Progress, Vol. 92 (August 1967), p. 106.
22. Truman, J.E., and Chapman, G.N., "Stress-Corrosion Cracking of Martensitic Stainless Steel", Journal of the Iron and Steel Institute, Vol. 202 (September 1964), p. 745-746.
23. "Selection of Stainless Steel", Universal-Cyclops Specialty Steel Div., Bulletin S-2024.1 (1966).
24. "Type 420" Data Bulletin Supplied by American Iron and Steel Institute.
25. Hall, A.M., "High-Strength Steels", Machine Design, Vol. 32 (July 21, 1960), p. 174-176.
26. "B&W Stainless Croloy Steels", Babcock & Wilcox Co., Bulletin T411 (August 1972).
27. "The 400 Series", Republic Steel Corporation, Bulletin 2197 10M (November 1971).
28. "Working Data Carpenter Stainless Steels", Carpenter Technology Corporation (August 1971).
29. Justusson, W.M., Faunce, R.L., and Telang, Y.P., "Half-Million Psi Steels by Ausforming", Materials in Design Engineering, Vol. 598 (May 1964), p. 92-95.
30. Schoeffer, E.A., "Cast High Alloys", Chemical Engineering, Vol. 60 (October 1953), p. 298.
31. Morykwas, S., "Alloy Data, re: 420", Cannon-Muskegon Corporation (1967).

Fe
0.35 C
13 Cr

TYPE 420

REVISED: SEPTEMBER 1973
AUTHOR: J.R. KATTUS

FERROUS ALLOYS

	Fe
0.23	C
12	Cr
1	Mo
1	W
0.8	Ni
0.25	V

TYPE 422

1. GENERAL

Type 422 is a hardenable (martensitic) 13 percent chromium stainless steel which is a modification of Type 420. The modification consists of additions of nickel, molybdenum, tungsten, and vanadium which improve elevated-temperature strength and resistance to stress corrosion and minimize anisotropic behavior. A wide range of mechanical properties, up to about 260 KSI F_{tu} can be obtained by quench-and-temper heat treatments, however, the highest strength condition possesses relatively poor toughness and corrosion resistance. Good creep-rupture properties up to about 900F and resistance to stress-corrosion cracking in the heat-treated condition make this grade suitable for applications in jet engines. Other uses include buckets for steam and gas turbines, discs, bolts, wheels, and blades, as well as structural components of aircraft and missiles. This alloy is also used for a number of valve applications. Because of its chromium content, it does not need to be protected against corrosion throughout its application temperature range. If welding is required, both pre-heat and post-heat are recommended.

1.01 Commercial Designation

Type 422 stainless steel

1.02 Alternate Designations

AISI 616
Carpenter 636 alloy
Unitemp 1420 WM (Universal Cyclop Specialty Steel)
Crucible 422

1.03 Specifications

Table 1.03.

1.04 Composition

Table 1.04.

1.05 Heat Treatment

1.051 Sub-critical anneal: Heat to 1350 to 1450F, 4 hours at temperature, furnace or air cool. This treatment softens the material to about 240 Brinell which is suitable for machining and light forming (3)(4).

1.052 Full anneal: Heat to 1600F, hold 1-1/2 hours per inch of cross section, cool to 1300F no faster than 25F per hour, hold 6 hours, cool 50F per hour in the furnace to 1000F. Heavy sections of 12 inches and more should be cooled at 50F per hour to 150F to prevent cracking. This treatment results in a hardness of about 210 Brinell, which provides optimum formability for this alloy. Full annealing is infrequently used because extremely slow cooling rates are required to prevent a martensitic transformation during cooling (3)(5).

1.053 Hardening: Austenitize above 1750F for 15 minutes minimum; 1900 to 1925 is preferred; oil- or air-quench to room temperature. Austenitizing should be done in inert or endothermic atmospheres. If controlled atmosphere is not available, time at temperature should not be unnecessarily prolonged since decarburization tends to occur. The alloy is air hardening in sections up to at least 4 inches. Large sections should generally be oil quenched. Limited experimental evidence indicates that air quenching results in better toughness for a given hardness. Some heat treaters have followed the quench with a cryogenic treatment (-320F) but direct experimental evidence shows no beneficial effect (2)(4)(5)(9)(13).

1.054 Tempering: 500 to 600F or 1050 to 1300F, 1 hour minimum. The secondary hardening range of about 700 to 1050F should generally not be used because it results in a marked deterioration in fracture toughness. Tempering in the range 500 to 600F provides the best combination of strength and toughness. The higher tempering-temperature range provides appreciably lower strength but is required for applications above 600F to avoid embrittlement during service. A double temper is desirable for heavy sections and whenever extreme dimensional stability is required (3)(4)(5)(9).

1.055 Martempering: Austenitize at 1900 to 1925F, quench in salt bath to 500F, hold until the parts are heated uniformly to this temperature, air cool to room temperature. Temper in accordance with Section 1.04. This treatment can be used in exceptional cases, such as heavy forgings, where the differential in stress levels developed upon rapid cooling through the martensitic-transformation range can cause cracking. In addition, there is evidence that marquenching results in some improvement in toughness as compared with oil quenching (3)(9). (See Figure 3.02712).

1.056 Stress relief: Hold at 1200 to 1300F, 8 hours, or at 1300 to 1400F, 4 hours, air cool. This treatment, which is quite similar to a sub-critical anneal is recommended after welding and after severe cold forming (3)(4).

1.06 Hardness

1.061 Effect of tempering temperature on hardness of sheet, Figure 1.061.

1.062 Effect of tempering temperature and time on hardness of bar, Figure 1.062.

1.063 Effect of tempering temperature and ausforming in the range 1150 to 900F on hardness of vacuum-melted sheet, Figure 1.063.

1.064 Effect of temperature on hardness of bar after two different tempering treatments, Figure 1.064.

1.07 Forms and Conditions Available

Table 1.07.

1.08 Melting and Casting Practice

1.081 The alloy is generally air melted in electric arc furnaces. For some applications requiring exceptional quality, it is vacuum remelted by consumable electrode or induction techniques (1)(5).

1.082 Ingots are normally cast in air, but vacuum pouring is sometimes employed after vacuum melting (1)(5).

1.083 Since Type 422 is sensitive to cracking in ingot form, ingots are generally stripped hot and slowly cooled in an insulating material or moved hot to a reheating furnace for further processing (1).

1.09 Special Considerations

1.091 Segregation can be a serious problem with large ingots in which segregates of non-metallics, massive carbides, and delta ferrite-carbide aggregates tend to form. Such segregates cause difficulties in hot working and also decrease mechanical properties, particularly ductility and toughness. A method of prevention is to balance the composition to prevent delta ferrite, which is residual ferrite retained in the microstructure when the metal is cooled from the austenitic range, as distinguished from ferrite formed at lower temperatures. It has been suggested that a balanced composition is one in which the "chromium equivalent" does not exceed 10 as calculated by the following formula: percent Cr + 6 (percent Si) + 4 (percent Mo) + 11 (percent V) - 40 (percent C) -2 (percent Mn) -4 (percent Ni) - 30 (percent N) (1)(23).

1.092 Vacuum melting provides better toughness and, in some instances, better creep strength than air melting, probably because of lower hydrogen and oxygen contents and fewer inclusions. The superior quality of vacuum melting is particularly desirable in producing large sections and parts for highly critical service, especially where transverse ductility is important.

1.093 The ultimate and yield strengths, notched strength (see Table 3.02714) and resistance to stress-corrosion cracking (see Table 2.0312) of Type 422 can be significantly improved by ausforming in the temperature range 1150 to 900F. (See Appendix B for definition.)

2. PHYSICAL AND CHEMICAL PROPERTIES

2.01 Thermal Properties

2.011 Melting range. 2675 - 2700F (2)(3).

2.012 Phase changes.

2.0121 Time-temperature-transformation diagram, Figure 2.0121.

	Fe
0.23	C
12	Cr
1	Mo
1	W
0.8	Ni
0.25	V

TYPE 422

2.0122 Upon heating under equilibrium conditions, the transformation from ferrite or martensite to austenite starts at about 1500F (AC1) and is complete at about 1625F (AC3) (4)(14).

2.0123 Upon oil quenching or air cooling the transformation from austenite to martensite starts at about 475F (MS) and is complete at about 275F (Mf) (4)(9)(14).

2.0124 After oil quenching or air cooling from the austenitic condition, about 1 to 3 percent austenite tends to remain in the martensitic matrix. This austenite is not appreciably reduced by refrigeration down to -320F; it can be decomposed by tempering above 1000F. Generally, the retained austenite has little effect upon properties (9).

2.0125 During tempering in the range 400 to 800, carbides of the form M_3C precipitate in a highly dispersed form from the martensite. At higher tempering temperatures, resolution of the M_3C and simultaneous precipitation of $M_{23}C_6$ alloy carbides occur (9).

2.013 Thermal conductivity, Figure 2.013.

2.014 Thermal expansion, Figure 2.014.

2.015 Specific heat. 0.11 Btu per (lb F) (2).

2.016 Thermal diffusivity. 0.27 ft^2 per hour (2).

2.02 Other Physical Properties

2.021 Density. 0.281 lb per in^3; 7.78 gr per cm^3 (2)(3)(4)(5).

2.022 Electrical properties.

2.0221 Electrical properties at 70F and 1470F with variations in tempering temperature, Table 2.0221.

2.023 Magnetic properties. Alloy is ferromagnetic.

2.0231 Magnetic permeability at room temperature, Table 2.0231.

2.024 Emittance.

2.025 Damping capacity.

2.0251 Damping capacity determined in torsional vibration damping tests, Table 2.0251.

2.03 Chemical Properties

2.031 Type 422 has good resistance to both general and stress corrosion when hardened and tempered in the ranges 500 to 600F and above 1050F. Tempering in the secondary-hardening range - 700 to 1050F - and annealing markedly reduce resistance to both general corrosion and stress corrosion. Ausforming appreciably improves stress-corrosion resistance of material tempered in the secondary hardening range (5)(9)(14).

2.0311 Effect of tempering temperature on susceptibility to stress corrosion and general corrosion, Table 2.0311.

2.0312 Effect of ausforming on resistance of vacuum melted sheet to stress corrosion in sodium chloride and to cathodic hydrogen cracking, Table 2.0312.

2.032 Scaling resistance in air is good up to 1300F. At room temperature, Type 422 is resistant to atmospheric corrosion although surface discoloration may occur. It also resists steam and humidity above room temperature when the surface is clean, but shallow rust spots can occur under these conditions if the surface has not been adequately descaled and cleaned after high temperature processing (3)(4)(5).

2.033 It resists weak organic acids and oxidizing acids such as nitric acid, but it does not have the superior resistance to pitting by dilute reducing acids characteristic of austenitic stainless steels (3)(4)(5).

2.04 Nuclear Properties

3. MECHANICAL PROPERTIES

3.01 Specified Mechanical Properties
Table 3.01.

3.02 Mechanical Properties at Room Temperature

3.021 Tension.

3.0211 Stress-strain diagrams (see Figure 3.03111).

3.0212 Effect of tempering temperature on tensile properties of 0.120 inch sheet at room temperature, Figure 3.0212.

3.0213 Effect of tempering temperature on tensile properties of 0.025 inch sheet at room temperature, Figure 3.0213.

3.0214 Effect of tempering temperature on tensile properties of bar at room temperature, Figure 3.0214.

3.0215 Tensile properties of specimens machined from forged jet engine parts, Table 30215.

3.0216 Effect of ausforming in the temperature range 1150 to 900F on tensile properties, Figure 3.0216.

3.0217 Tensile properties of fully annealed sheet, Table 3.0217.

3.022 Compression.

3.0221 Stress-strain diagrams (see Figure 3.03211).

3.0222 Compressive yield strength (see Figure 3.0322).

3.023 Impact.

3.0231 Effect of tempering temperature and time on impact properties at room temperature, Figure 3.0231.

3.024 Bending.

3.025 Torsion and shear.

3.0251 Shear strength (see Figure 3.0351).

3.026 Bearing.

3.0261 Bearing ultimate and yield strengths (see Figure 3.0361).

3.027 Stress concentration.

3.0271 Notch properties.

3.02711 Crack strength (net fracture stress at cracked section) compared with ultimate and yield strengths after tempering at various temperatures, Figure 3.02711.

3.02712 Effect of tempering temperature on crack strength (net fracture stress at cracked section) after various cooling methods from austenitizing temperature, Figure 3.02712.

3.02713 Effect of ausforming in the temperature range 1150 to 900F on notched tensile strength, Figure 3.02713.

3.02714 Effect of ausforming in the temperature range 1150 to 900F on the crack strength (net fracture stress at cracked section) of vacuum-melted sheet, Table 3.02714.

3.0272 Fracture toughness.

3.028 Combined properties.

3.03 Mechanical Properties at Various Temperatures

3.031 Tension.

3.0311 Stress-strain diagrams.

3.03111 Tensile stress-strain curves for sheet at room and elevated temperatures, Figure 3.03111.

3.0312 Effect of temperature on tensile properties of bar and forgings with various tempering temperatures, Figure 3.0312.

3.0313 Effect of temperature on tensile properties of sheet of different thicknesses and with various tempering treatments, Figure 3.0313.

3.0314 Effect of exposure time at test temperature on the tensile properties of sheet, Figure 3.0314.

3.0315 Effect of ausforming on tensile properties of vacuum-melted sheet at room temperature and at 1000F, Table 3.0315.

3.032 Compression.

3.0321 Stress strain diagrams.

3.03211 Compressive stress-strain curves for sheet at room and elevated temperatures, Figure 3.03211.

3.0322 Effect of temperature on compressive yield strength after two different exposure times at test temperature, Figure 3.0322.

3.033 Impact.

3.0331 Effect of temperature on impact properties, Figure 3.0331.

3.0332 Effect of exposures at 1000F on impact properties at various temperatures after two different tempering treatments, Figure 3.0332.

3.034 Bending.

3.035 Torsion and shear.

3.0351 Effect of temperature on shear strength after two different exposure times at test temperature, Figure 3.0351.

3.036 Bearing.

3.0361 Effect of temperature on bearing properties after two different exposure times at test temperature, Figure 3.0361.

3.037 Stress concentration.

3.0371 Notch properties.
3.03711 Crack strength (net fracture stress at cracked section) compared with tensile ultimate and yield strengths at various temperatures, Figure 3.03711.
3.0372 Fracture toughness.
3.038 Combined properties.

3.04 Creep and Creep Rupture Properties
3.041 Creep and rupture curves for sheet at 600, 800, and 900F, Figure 3.041.
3.042 Creep rupture curves for sheet at 800 to 1200F, Figure 3.042.
3.043 Creep and rupture curves for forgings at 1000, 1100, and 1200F, Figure 3.043.
3.044 Creep and rupture curves for bar at 1000, 1100, and 1200F, Figure 3.044.
3.045 Minimum creep rate for bar at various stresses at 1000 and 1100F, Figure 3.045.
3.046 Creep-rupture curves for smooth and notched specimens at 1000, 1100, and 1200F, Figure 3.046.
3.047 Isochronous stress-strain curves at 800, 1000, and 1200F for various tempers, Figure 3.047.

3.05 Fatigue Properties
3.051 Reverse-bend fatigue properties at room and elevated temperatures for bar tempered at 980, 1150, and 1200F, Figure 3.051.
3.052 Stress-range diagram for bar at 900 and 1100F, Figure 3.052.

3.06 Elastic Properties
3.061 Poisson's ratio.
3.0611 Effect of temperature on Poisson's ratio, Figure 3.0611.
3.062 Modulus of elasticity.
3.0621 Effect of temperature on modulus of elasticity in tension and compression, Figure 3.0621.
3.0622 Tangent modulus curves in compression for sheet at room and elevated temperatures, Figure 3.0622.
3.063 Modulus of rigidity.
3.0631 Effect of temperature on modulus of rigidity, Figure 3.0631.

4. FABRICATION

4.01 Formability
4.011 Hot working. The hot working range is from a maximum of 2150F to a minimum of 1600F. For large and nonuniform parts, a preheat in the range 1200 to 1400F reduces thermal stress and facilitates temperature uniformity in heating to the hot-working temperature. The susceptibility of large sections (over 4 inch diameter) or intricately designed sections to crack due to thermal stresses is avoided by annealing immediately after hot working and before cooling to room temperature or by retarding the cooling rate, which may be accomplished by charging the hot-worked material directly into a furnace at about 1300F, holding the work until equalized, and then air cooling. Slow cooling also may be accomplished by burying the material in Sil-O-Cel or some other insulating material. In order to avoid cracking, surface imperfections should be removed before hardening and tempering. Small components, such as compressor blading, usually can be directly air cooled after hot work (3).
4.012 Cold working. Fully annealed Type 422 can be moderately cold formed, in which condition free bends of two to three times the sheet thickness can be made. In the sub-critical-annealed condition it can be lightly cold formed. Although its annealed hardness is higher its general forming behavior is similar to Types 403 and 410. It is not as ductile nor does it work harden as much as the 18-8 austenitic stainless steels. Depending on the degree and nature of deformation, in-process annealing may or may not be required. Annealing or stress relieving is recommended after severe cold forming operations (3).

4.02 Machining and Grinding
4.021 Type 422 has good machinability in the fully annealed and sub-critical annealed conditions, its machinability rating being 55 percent in comparison with 100 percent for B1112 resulfurized steel. Generally its machinability is somewhat better than the austenitic stainless steels. It can be machined with more difficulty in the hardened and tempered condition (3).

4.03 Welding
4.031 Type 422 can be arc welded manually with coated low-hydrogen electrodes or automatically by metal-inert-gas or tungsten-inert-gas methods. Filler metal of the same composition can be used, or for greater weld ductility austenitic stainless steel filler metal, such as Type 310 or 304, can be used. To avoid the danger of weld cracking caused by the high hardenability of Type 422, preheating to 400F and post-weld stress relief (see Section 1.056) are recommended (2)(3)(4).
4.032 Type 422 sheet can be successfully spot welded provided post-weld tempering or stress relief is carried out to avoid brittleness (21).

4.04 Surface Treatment
4.041 Because of its good resistance to oxidation and corrosion, protective surface treatments and coatings are not normally needed. There is some evidence that anodic coatings, such as zinc dust dibutyl titanate, sprayed aluminum, and nickel-cadmium electroplate, are effective in appreciably inhibiting stress-corrosion cracking (3)(20).
4.042 Preferred methods for removal of hot-work and heat-treat scales are either mechanical methods such as sand or vapor blasting, or scale conditioning in a molten caustic bath followed by light acid pickling. After acid pickling of hardened and tempered parts, it is advisable to bake the parts at about 400F as a precaution against hydrogen embrittlement (3).

Fe
0.23 C
12 Cr
1 Mo
1 W
0.8 Ni
0.25 V

TYPE 422

Alloy	422
Source	(4)(13)(14)
Specification	Forms
AMS 5655	Bars, forgings, forging stock
MIL-S-861A	Bars, billets
ASTM A565 (Grade 616)	Bars, forgings, forging stock

TABLE 1.03 SPECIFICATIONS

Alloy	422					
Source	AMS 5655 (13)		Carpenter (4)		ASTM A565 (15)	
	Percent		Percent		Percent	
	min.	max.	min.	max.	min.	max.
Carbon	0.20	0.25	0.20	0.25	0.20	0.25
Manganese	-	1.00	-	1.00	0.50	1.00
Silicon	0.20	0.60	-	1.00	-	0.50
Phosphorus	-	0.040	-	0.04	-	0.025
Sulfur	-	0.030	-	0.03	-	0.025
Chromium	11.50	13.50	12.00	14.00	11.00	12.50
Nickel	0.50	1.00	0.50	1.00	0.50	1.00
Molybdenum	0.75	1.25	0.75	1.25	0.90	1.25
Tungsten	0.75	1.25	0.75	1.25	0.90	1.25
Vanadium	0.17	0.27	0.20	0.50	0.20	0.30
Iron	Balance		Balance		Balance	

TABLE 1.04 COMPOSITION

	Fe
0.23	C
12	Cr
1	Mo
1	W
0.8	Ni
0.25	V

TYPE 422

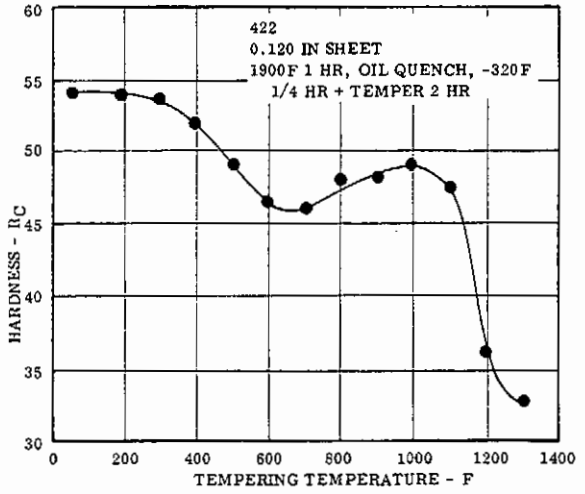


FIG. 1.061 EFFECT OF TEMPERING TEMPERATURE ON HARDNESS OF SHEET. (8)

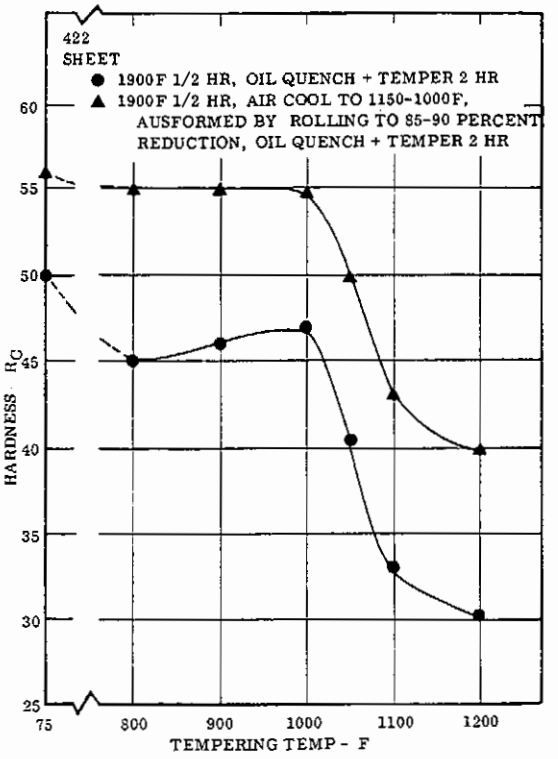


FIG. 1.063 EFFECT OF TEMPERING TEMPERATURE AND AUSFORMING IN THE RANGE 1150 TO 900F ON HARDNESS OF VACUUM-MELTED SHEET. (14)

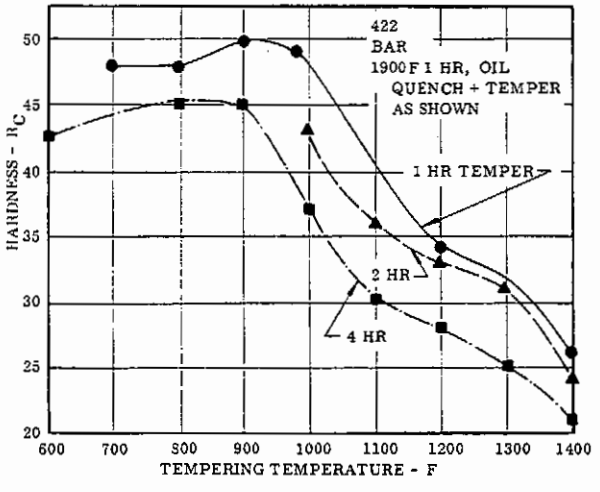


FIG. 1.062 EFFECT OF TEMPERING TEMPERATURE AND TIME ON HARDNESS OF BAR. (3)(4)(5)

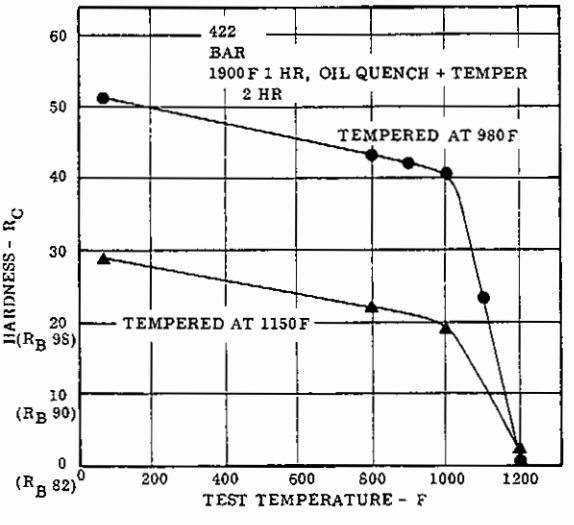


FIG. 1.064 EFFECT OF TEMPERATURE ON HARDNESS OF BAR AFTER TWO DIFFERENT TEMPERING TREATMENTS. (1)

Alloy	422
Source	(4)(5)
Form	Condition
Forging-quality bars and billets	Annealed
Bars	Hot rolled and cold finished
Extruded shapes	Annealed
Tubular products	Annealed
Wire	-
Strip	Cold rolled
Forgings	Annealed or hardened
Castings	Annealed or hardened

TABLE 1.07 FORMS AND CONDITIONS AVAILABLE

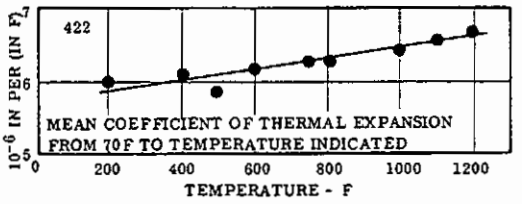


FIG. 2.014 THERMAL EXPANSION. (2)(4)

	Fe
0.23	C
12	Cr
1	Mo
1	W
0.8	Ni
0.25	V

TYPE 422

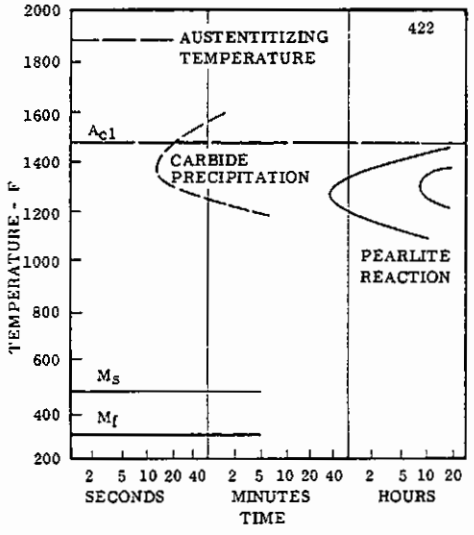


FIG. 2.0121 TIME-TEMPERATURE-TRANSFORMATION DIAGRAM. (14)

Alloy	422		
Condition	Quenched and tempered		
Source	(1)(2)		
Temperature F	Tempering Temperature F	Electrical Conductivity percent IACS	Electrical Conductivity megmhos per in^3	Electrical Resistivity microhm in.
70	700	2.79	0.0410	24.4
	800	2.83	0.0416	24.0
	900	2.86	0.0420	23.8
1470	700-900	1.57-1.43	0.0231-0.0211	43.4-47.4

TABLE 2.0221 ELECTRICAL PROPERTIES AT 70F AND 1470F WITH VARIATIONS IN TEMPERING TEMPERATURE

Alloy	422	
Condition	Quenched and tempered	
Source	(2)	
Tempering Temp. F	At 100 Oersteds	Maximum
700	85	85
800	75	92
900	93	100

TABLE 2.0231 MAGNETIC PERMEABILITY

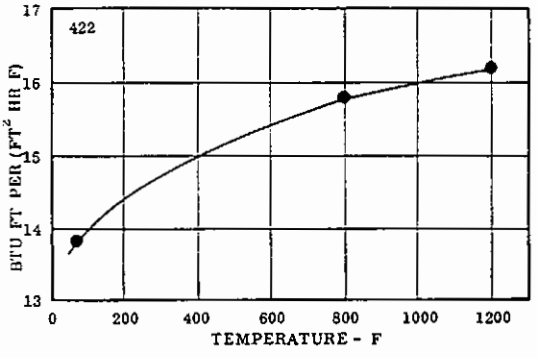


FIG. 2.013 THERMAL CONDUCTIVITY. (2)

Alloy	422	
Condition	1900F 1 hour, oil quench, 1200F 2 hour	
Source	(11)	
Specific damping, percent per cycle at		
10 ksi	20 ksi	30 ksi
1.4	1.4	1.2

TABLE 2.0251 DAMPING CAPACITY DETERMINED IN TORSIONAL VIBRATION DAMPING TESTS

Fe	
0.23	C
12	Cr
1	Mo
1	W
0.8	Ni
0.25	V

TYPE 422

Alloy	422	
Condition	1900F 1 hr., oil quench, -320F 1/4 hr. + tempered 2 hr.	
Form	0.120 inch sheet	
Source	(9)	
Tempering Temperature F	Stress Corrosion, (a) days to failure	General Corrosion (b) in 2 days
550	No failure	None
700	No failure	None
900	-	Slight
950	2.2	-
1000	2.2 - 4.4	Heavy
1050	2.7 - 4.3	-
1100	21 - 32	Slight
1200	No failure	Slight

(a) Exposed 60 days to 4-5 percent salt spray under 100 ksi stress.
(b) Exposed to 10 percent nitric acid at 125F.

TABLE 2.0311 EFFECT OF TEMPERING TEMPERATURE ON SUSCEPTIBILITY TO STRESS CORROSION AND GENERAL CORROSION

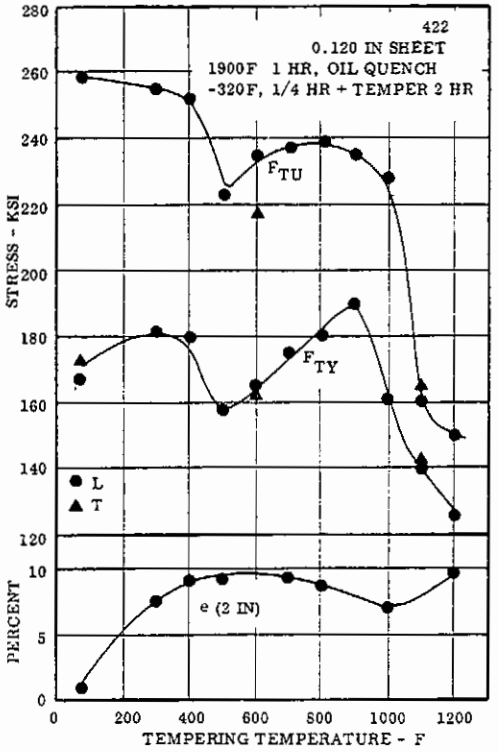


FIG. 3.0212 EFFECT OF TEMPERING TEMPERATURE ON TENSILE PROPERTIES OF 0.120 - IN SHEET AT ROOM TEMPERATURE (8)

Alloy	422		
Form	Sheet		
Condition	1900F 1 hour (a), Temper 980F		
Source	(14)		
Ausforming	Stress, ksi	Failing Time NaCl solution (b)	Cathodic H_2 (c)
None	150	2 days	6 min.
		14 days	6 min.
85 percent	150	>36 days	16 min.
		>36 days	16 min.
90 percent	150	>36 days	16 min.
		>36 days	18 min.

(a) Material that was not ausformed was oil quenched. Ausformed material was air cooled to 1150-1000F, ausformed by rolling to 85 or 90 percent reduction, and then oil quenched.
(b) Specimens held at 100F at relative humidity of 98 percent. 5 percent sodium chloride solution was applied twice a day. Failure criterion was cracks visible at 40X.
(c) Cathodic hydrogen cracking tests at a current density of of 0.6 amp/in^2in 0.1 N sulfuric acid containing 3 mg arsenic per liter. Failure criterion was cracks visible at 10X.

TABLE 2.0312 EFFECT OF AUSFORMING ON RESISTANCE OF VACUUM-MELTED SHEET TO STRESS CORROSION IN SODIUM CHLORIDE AND TO CATHODIC HYDROGEN CRACKING

Alloy	422			
Form	Bars and Forgings			
Source	AMS 5655 (13)	ASTM A565 (15)		
Condition	Hardened (a)	Hardened (b)	Full Anneal	Sub-crit Anneal
F_{tu}, ksi, (min.)	140	140	-	-
F_{ty}, ksi, (min.)	115	110	-	-
e (2 in.), percent, (min.)	13	13	-	-
RA, percent, (min.)	25	30	-	-
BHN	293-341	302-352	247 max.	285 max.
IE, Izod V, ft. lb., (min.)	8	-	-	-
IE, Charpy V, ft. lb., (min.)	-	8	-	-

(a) 1925F 1 hour, oil or air quench + 1100F 4 hours + 1000F 4 hours.
(b) 1900F, oil or air quench + 1150F min. 2 hours min.

TABLE 3.01 SPECIFIED MECHANICAL PROPERTIES

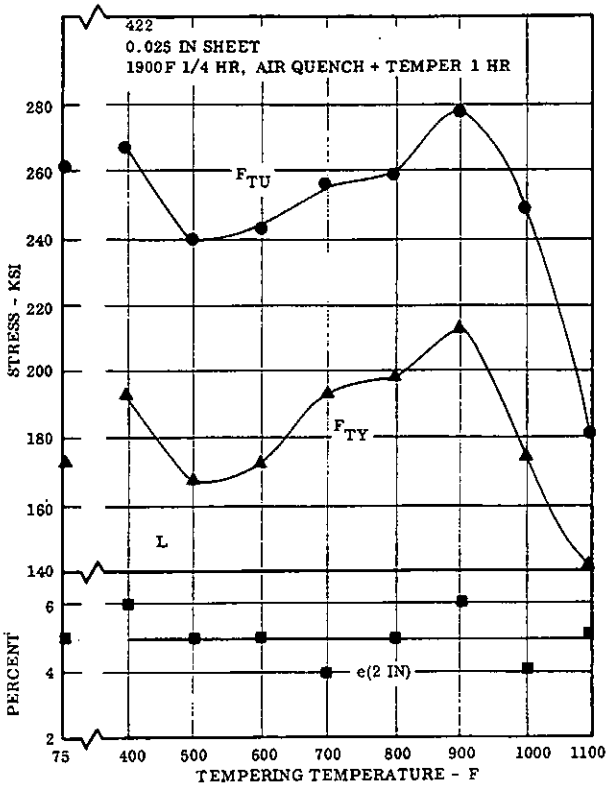


FIG. 3.0213 EFFECT OF TEMPERING TEMPERATURE ON TENSILE PROPERTIES OF 0.025 IN SHEET AT ROOM TEMPERATURE. (7)

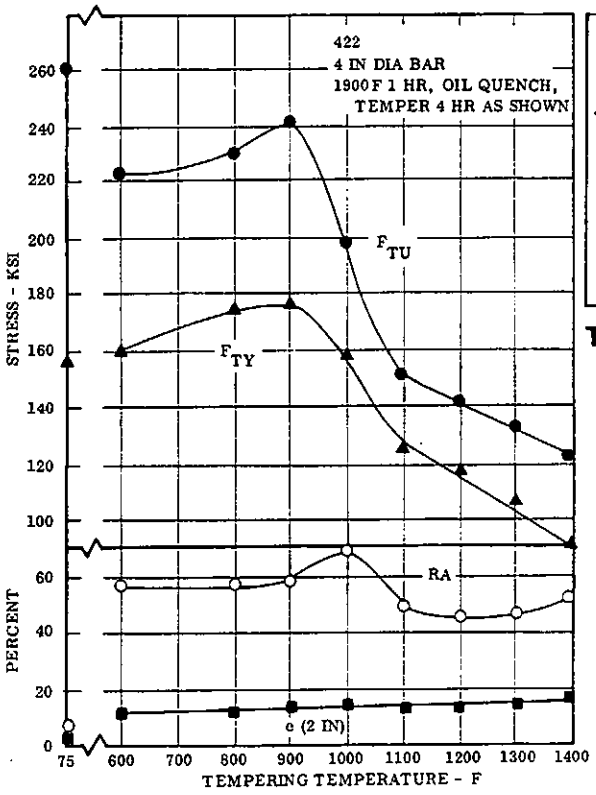


FIG. 3.0214 EFFECT OF TEMPERING TEMPERATURE ON TENSILE PROPERTIES OF BAR AT ROOM TEMPERATURE. (5)

Fe
0.23 C
12 Cr
1 Mo
1 W
0.8 Ni
0.25 V

TYPE 422

Alloy	422			
Condition	1900F 1/2 hour, air quench + 1150F 2 hours			
Source	(12)			
Part	F_{tu} ksi	F_{ty} ksi	e(2 in.) percent	RA percent
First stage fan vane	153.8	134.8	23.8	46.8
Third stage compressor vane	155.9	129.0	26.2	51.4
Fifth stage compressor vane	153.3	125.7	23.8	48.6
Sixth stage compressor vane	154.5	128.2	22.6	46.4

TABLE 3.0215 TENSILE PROPERTIES OF SPECIMENS MACHINED FROM FORGED JET ENGINE PARTS

	Fe
0.23	C
12	Cr
1	Mo
1	W
0.8	Ni
0.25	V

TYPE 422

Alloy	422			
Form	Sheet			
Condition	Fully annealed			
Source	(7)			
Thickness, in.	Orientation	F_{ty} ksi	F_{tu} ksi	e (2 in.) percent
0.165	L	73.7	96.8	26.0
	T	74.5	98.5	23.0
0.031	L	64.5	95.0	25.5
	T	66.3	96.5	24.0
0.025	L	69.5	100.5	23.5
	T	69.2	101.0	23.0

TABLE 3.0217 TENSILE PROPERTIES OF FULLY ANNEALED SHEET

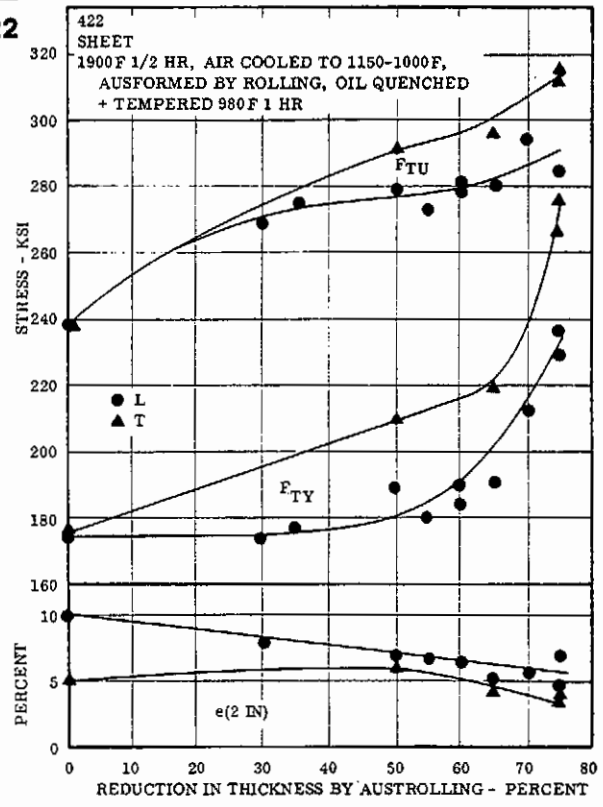


FIG. 3.0216 EFFECT OF AUSFORMING IN THE TEMPERATURE RANGE 1150 TO 900F ON TENSILE PROPERTIES. (14)

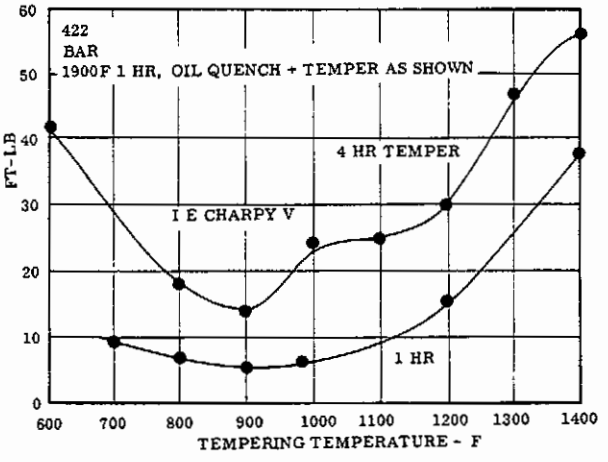


FIG. 3.0231 EFFECT OF TEMPERING TEMPERATURE AND TIME ON IMPACT PROPERTIES AT ROOM TEMPERATURE. (3)(5)

	Fe
0.23	C
12	Cr
1	Mo
1	W
0.8	Ni
0.25	V

TYPE 422

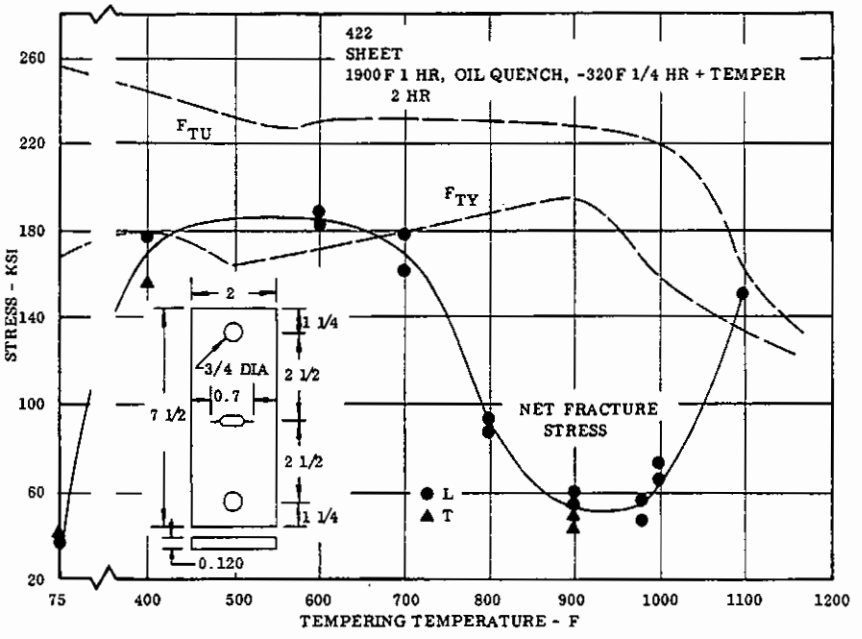


FIG. 3.02711 CRACK STRENGTH (NET FRACTURE STRESS AT CRACKED SECTION) COMPARED WITH ULTIMATE AND YIELD STRENGTHS AFTER TEMPERING AT VARIOUS TEMPERATURES. (9)

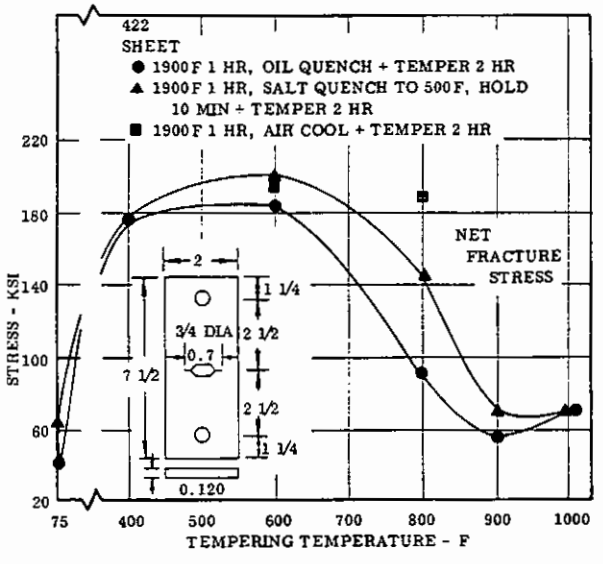


FIG. 3.02712 EFFECT OF TEMPERING TEMPERATURE ON CRACK STRENGTH (NET FRACTURE STRESS AT CRACKED SECTION) AFTER VARIOUS COOLING METHODS FROM AUSTENITIZING TEMPERATURE. (9)

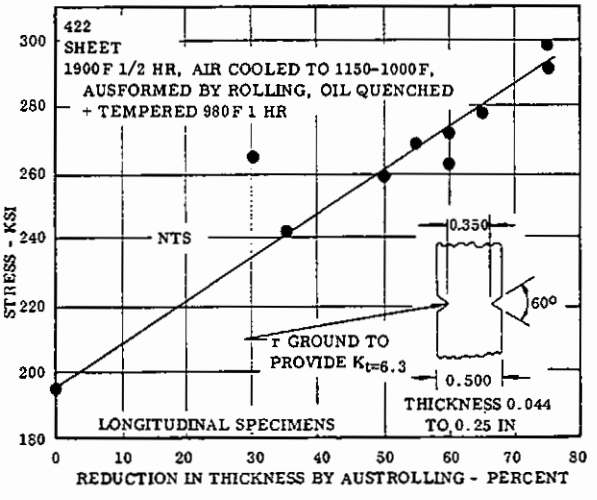


FIG. 3.02713 EFFECT OF AUSFORMING IN THE TEMPERATURE RANGE 1150 TO 900 F ON NOTCHED TENSILE STRENGTH. (14)

Fe	
0.23	C
12	Cr
1	Mo
1	W
0.8	Ni
0.25	V

TYPE 422

Alloy	422		
Form	Sheet		
Condition	1900F 1 hour (a), Temper 980F 1 hour		
Source	(14)		
Ausforming	Net Fracture Strength (b) ksi	F_{ty} ksi	Ratio, NFS to F_{ty}
None	122	168	0.73
85 percent	212	246	0.86
90 percent	164	238	0.68

(a) Material that was not ausformed was oil quenched. Ausformed material was air cooled to 1150-1000F, ausformed by rolling to 85 or 90 percent reduction, and then oil quenched.
(b) See Figure 3.02711 for specimen configuration.

TABLE 3.02714 EFFECT OF AUSFORMING IN THE TEMPERATURE RANGE 1150 TO 900 ON THE CRACK STRENGTH (NET FRACTURE STRESS AT CRACKED SECTION) OF VACUUM-MELTED SHEET.

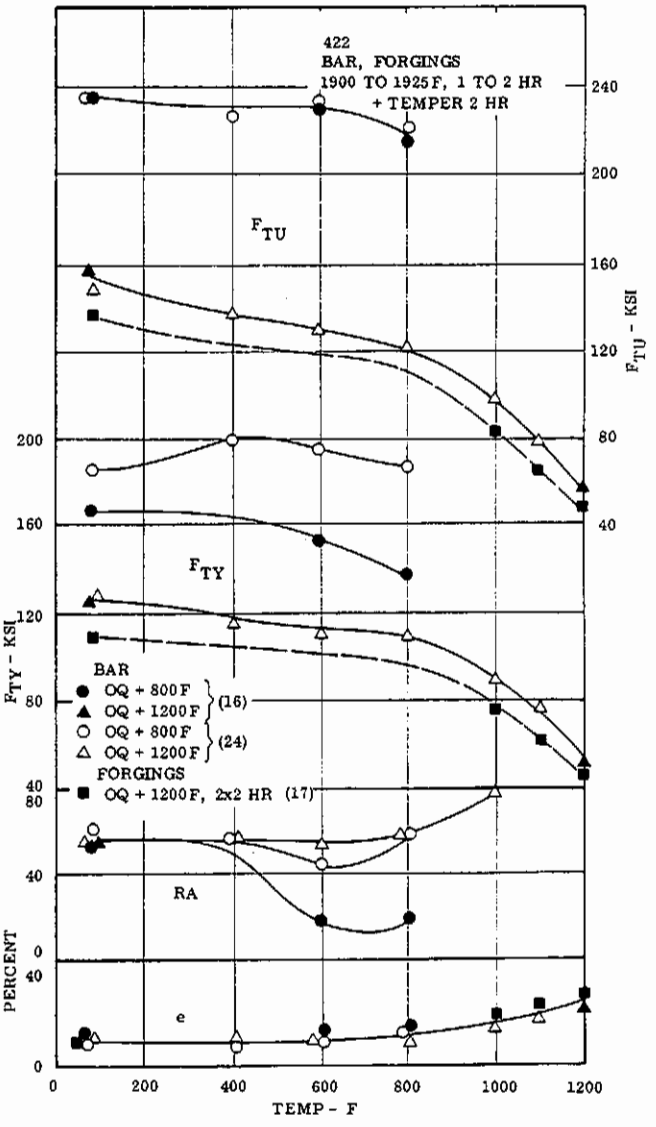


FIG. 3.0312 EFFECT OF TEMPERATURE ON TENSILE PROPERTIES OF BAR AND FORGINGS WITH VARIOUS TEMPERING TEMPERATURES. (16)(17)(24)

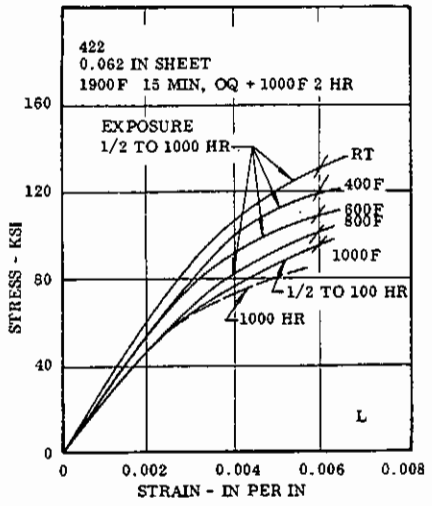


FIG. 3.03111 TENSILE STRESS-STRAIN CURVES FOR SHEET AT ROOM AND ELEVATED TEMPERATURES. (10)

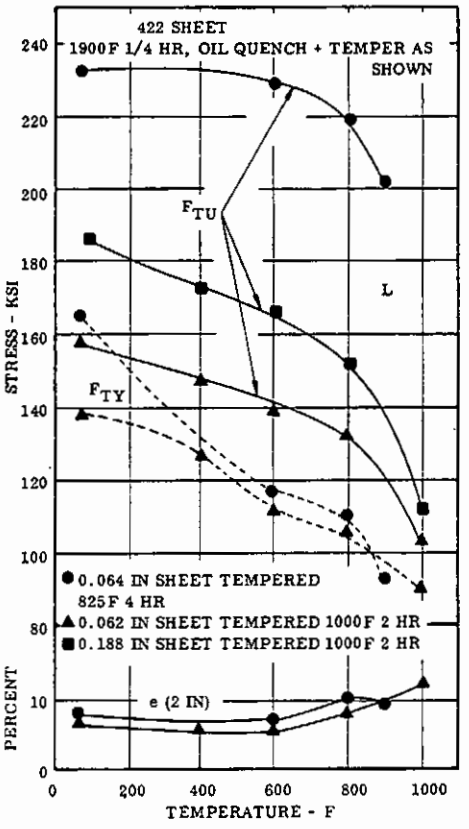


FIG. 3.0313 EFFECT OF TEMPERATURE ON TENSILE PROPERTIES OF SHEET OF DIFFERENT THICKNESSES AND WITH DIFFERENT TEMPERING TREATMENTS (6)(10)

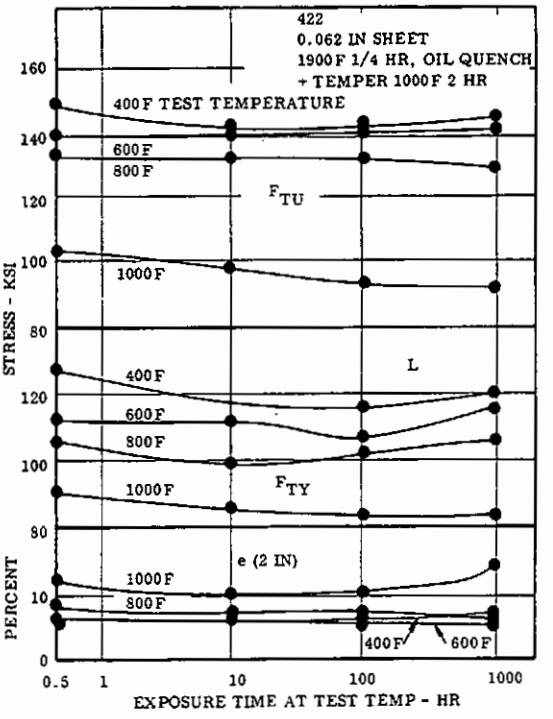


FIG. 3.0314 EFFECT OF EXPOSURE TIME AT TEST TEMPERATURE ON THE TENSILE PROPERTIES OF SHEET (10)

Fe
0.23 C
12 Cr
1 Mo
1 W
0.8 Ni
0.25 V

TYPE 422

Alloy	422				
Form	Sheet				
Condition	1900F 1 hour*, Temper 980F 1 hour				
Source	(14)				
Ausforming	Test Temp. F	Specimen Orientation	F_{ty} ksi	F_{tu} ksi	e (2 in.) percent
None	75	L	168	222	12.0
		T	168	216	11.0
85 percent	75	L	246	288	9.0
		T	276	310	7.0
90 percent	75	L	238	279	6.5
		T	280	308	6.0
None	1000	L	122	168	8.0
85 percent	1000	L	145	192	6.0
90 percent	1000	L	130	176	9.0

* Material that was not ausformed was oil quenched. Ausformed material was air cooled to 1150-1000F, ausformed by rolling to 85 or 90 percent reduction, and then oil quenched.

TABLE 3.0315 EFFECT OF AUSFORMING ON TENSILE PROPERTIES OF VACUUM-MELTED SHEET AT ROOM TEMPERATURE AND AT 1000F

	Fe
0.23	C
12	Cr
1	Mo
1	W
0.8	Ni
0.25	V

TYPE 422

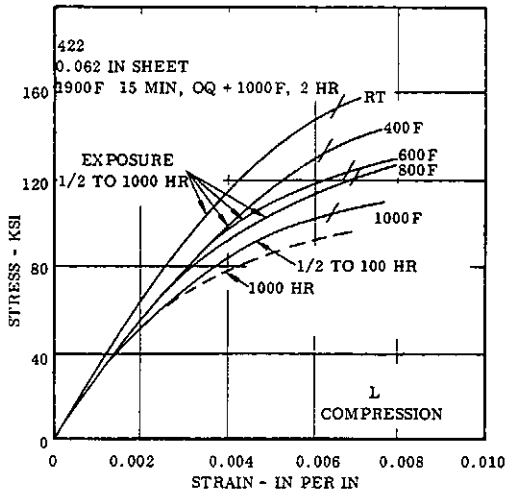


FIG. 3.03211 COMPRESSIVE STRESS-STRAIN CURVES FOR SHEET AT ROOM AND ELEVATED TEMPERATURES. (10)

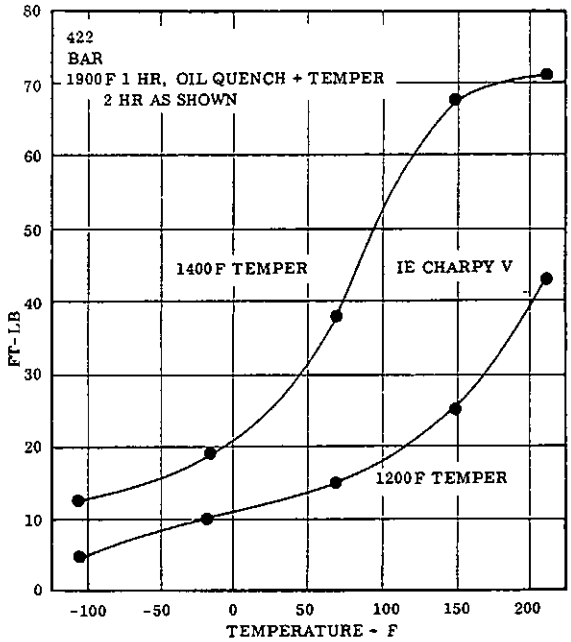


FIG. 3.0331 EFFECT OF TEMPERATURE ON IMPACT PROPERTIES. (3)

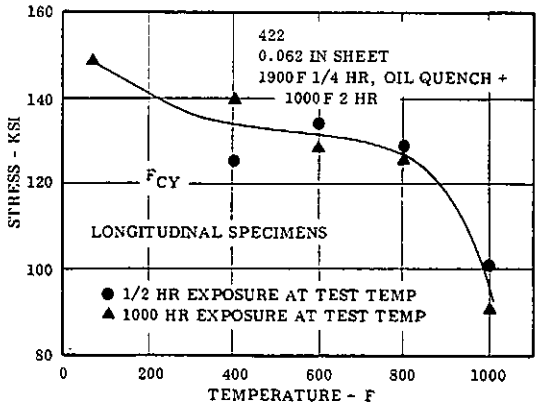


FIG. 3.0322 EFFECT OF TEMPERATURE ON COMPRESSIVE YIELD STRENGTH AFTER TWO DIFFERENT EXPOSURE TIMES AT TEST TEMPERATURE. (10)

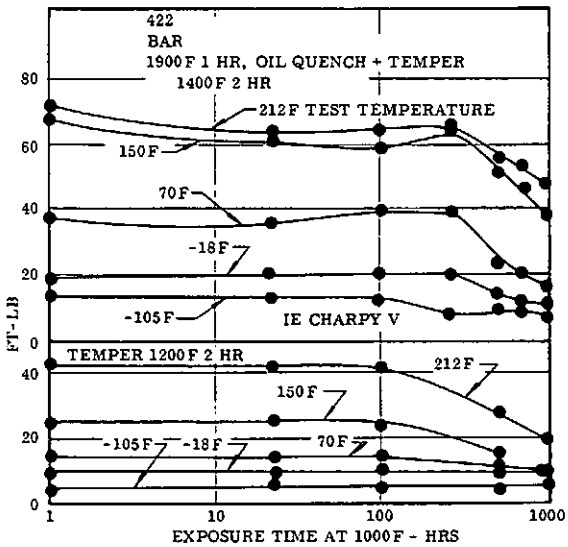


FIG. 3.0332 EFFECT OF EXPOSURES AT 1000F ON IMPACT PROPERTIES AT VARIOUS TEMPERATURES AFTER TWO DIFFERENT TEMPERING TREATMENTS. (3)

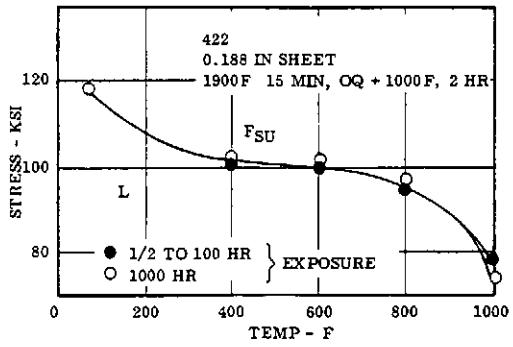
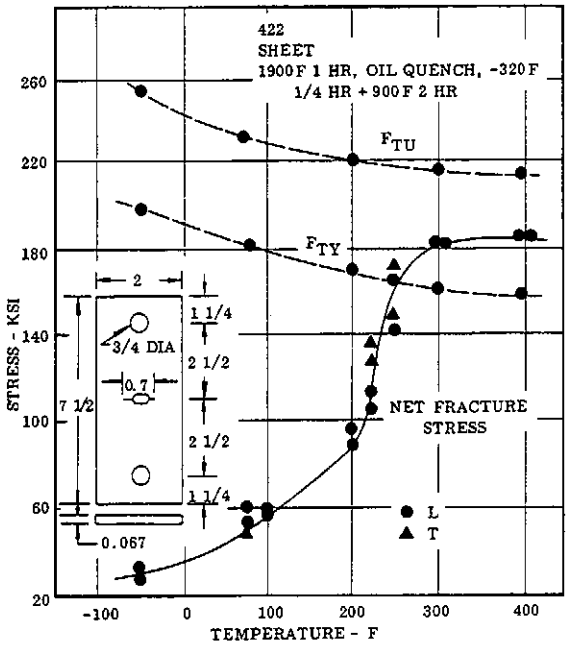


FIG. 3.0351 EFFECT OF TEMPERATURE ON SHEAR STRENGTH AFTER TWO DIFFERENT EXPOSURE TIMES AT TEST TEMPERATURE. (10)



	Fe
0.23	C
12	Cr
1	Mo
1	W
0.8	Ni
0.25	V

TYPE 422

FIG. 3.03711 CRACK STRENGTH (NET FRACTURE STRESS AT CRACKED SECTION) COMPARED WITH TENSILE ULTIMATE AND YIELD STRENGTH AT VARIOUS TEMPERATURES. (8)

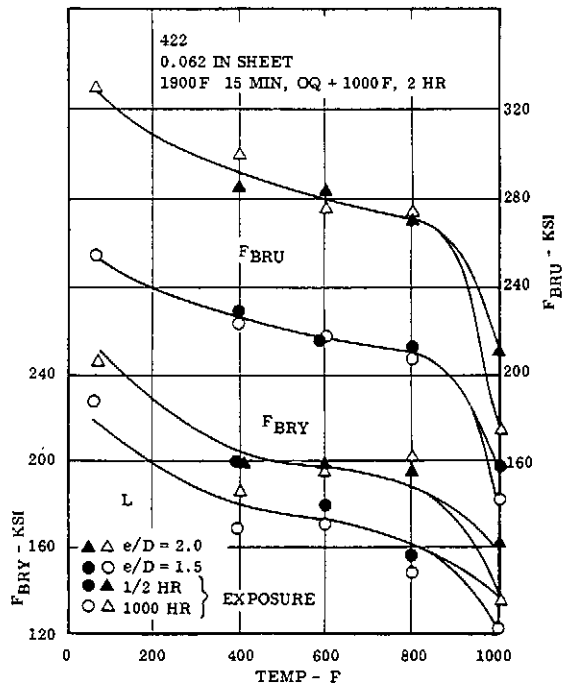


FIG. 3.0361 EFFECT OF TEMPERATURE ON BEARING PROPERTIES AFTER TWO DIFFERENT EXPOSURE TIMES AT TEST TEMPERATURE. (10)

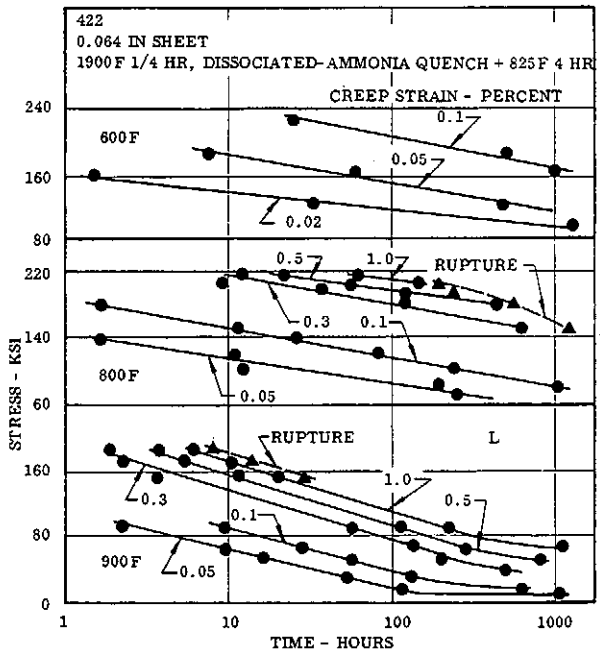


FIG. 3.041 CREEP AND RUPTURE CURVES FOR SHEET AT 600, 800, AND 900F. (6)

Fe	
0.23	C
12	Cr
1	Mo
1	W
0.8	Ni
0.25	V

TYPE 422

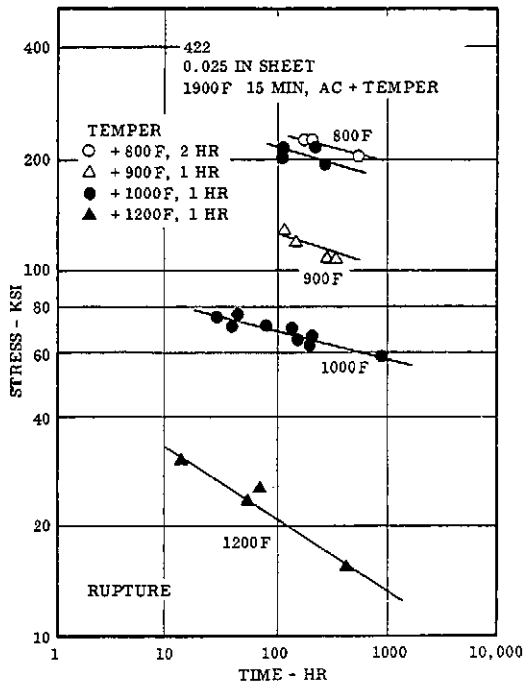


FIG. 3.042 CREEP RUPTURE CURVES FOR SHEET AT 800 TO 1200F. (16)

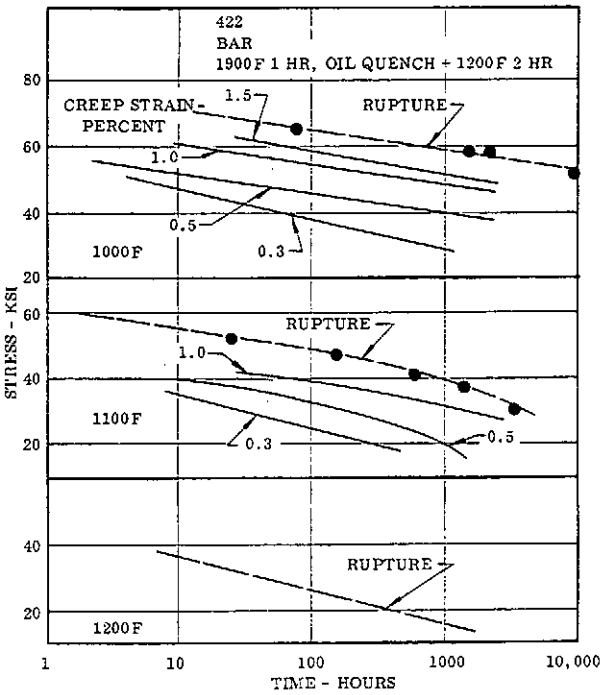


FIG. 3.044 CREEP AND RUPTURE CURVES FOR BAR AT 1000, 1100, AND 1200F. (1)(11)

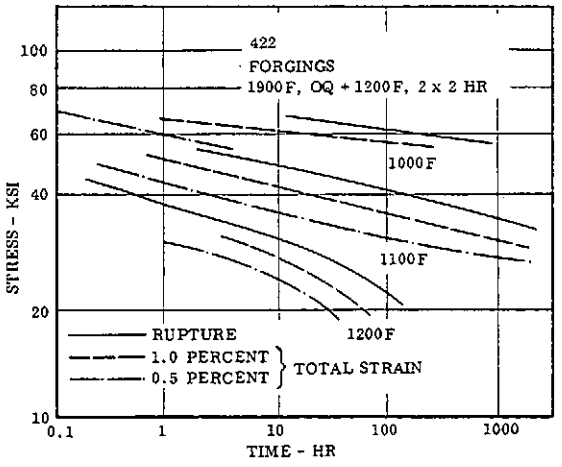


FIG. 3.043 CREEP AND RUPTURE CURVES FOR FORGINGS AT 1000, 1100, AND 1200 F. (17)

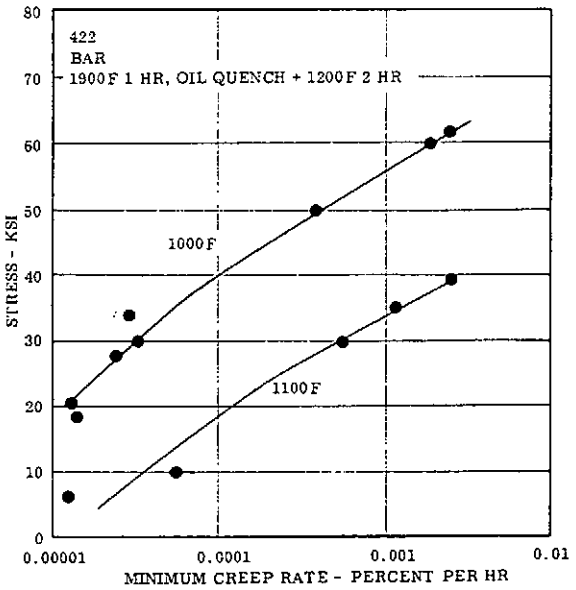


FIG. 3.045 MINIMUM CREEP RATE FOR BAR AT VARIOUS STRESSES AT 1000 AND 1100F. (11)

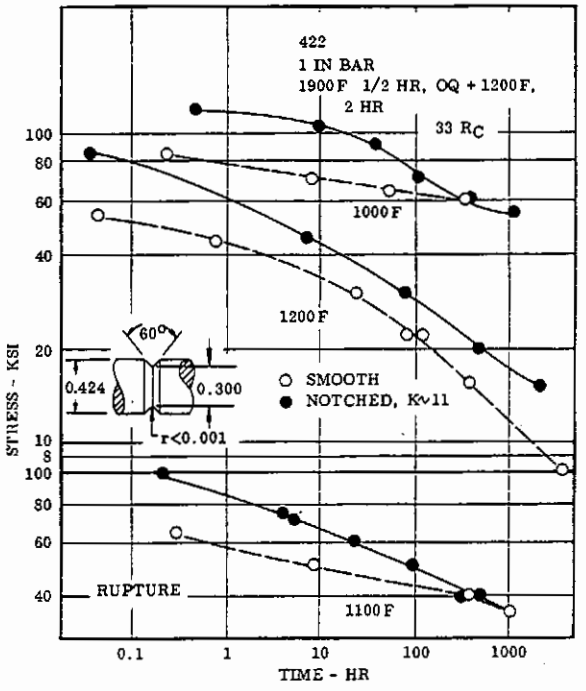


FIG. 3.046 CREEP RUPTURE CURVES FOR SMOOTH AND NOTCHED SPECIMENS AT 1000, 1100, AND 1200F. (18)

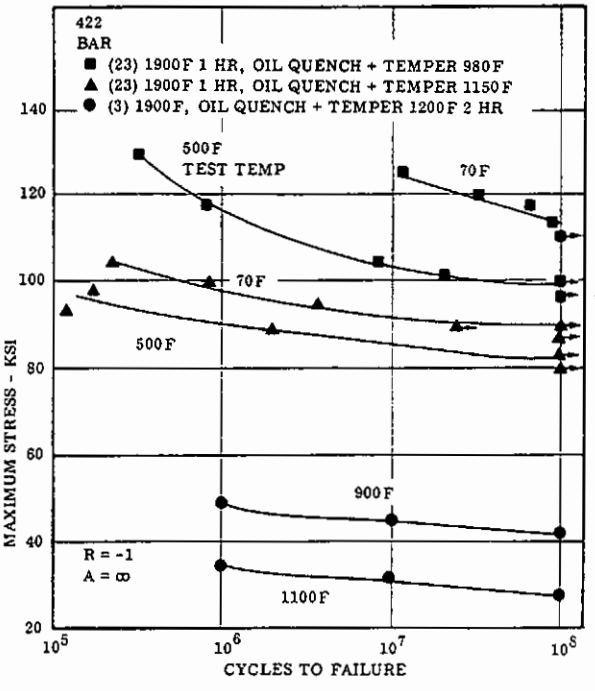


FIG. 3.051 REVERSE-BEND FATIGUE PROPERTIES AT ROOM AND ELEVATED TEMPERATURES FOR BAR TEMPERED AT 980, 1150, AND 1200F. (3)(23)

Fe	
0.23	C
12	Cr
1	Mo
1	W
0.8	Ni
0.25	V

TYPE 422

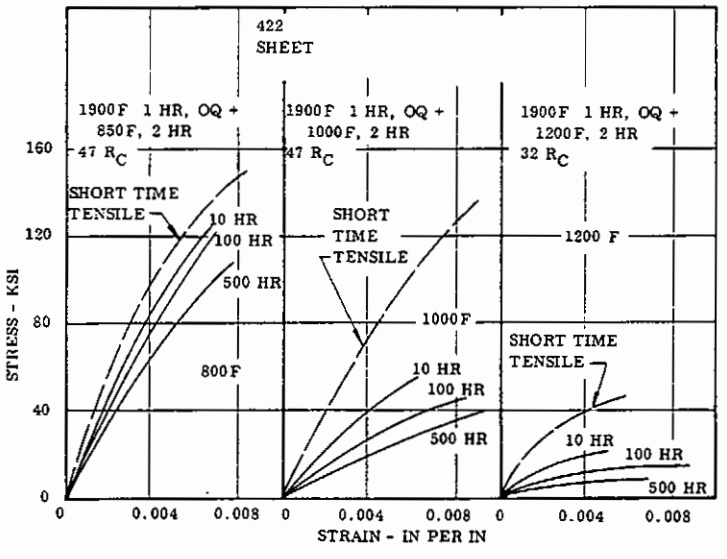


FIG. 3.047 ISOCHRONOUS STRESS STRAIN CURVES AT 800, 1000, AND 1200F FOR VARIOUS TEMPERS. (16)

	Fe
0.23	C
12	Cr
1	Mo
1	W
0.8	Ni
0.25	V

TYPE 422

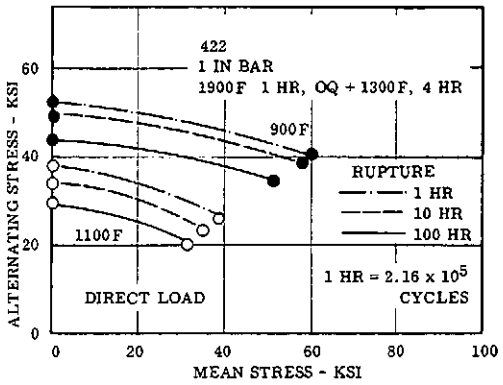


FIG. 3.052 STRESS RANGE DIAGRAM FOR BAR AT 900 AND 1100F. (19)

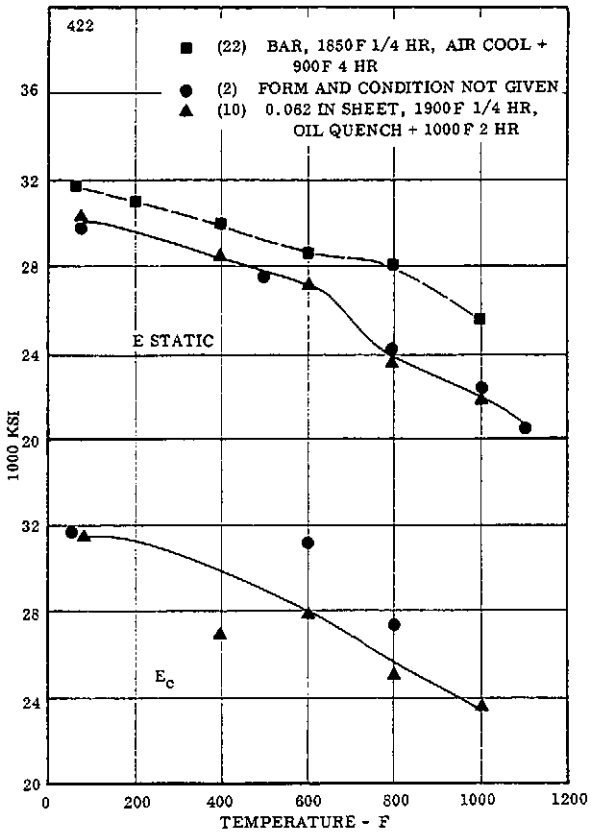


FIG. 3.0621 EFFECT OF TEMPERATURE ON MODULUS OF ELASTICITY IN TENSION AND COMPRESSION. (2)(10)(22)

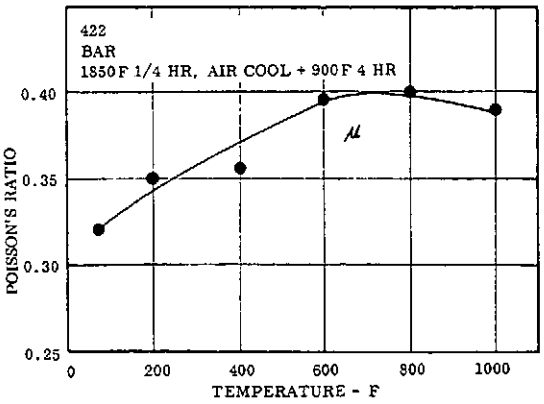


FIG. 3.0611 EFFECT OF TEMPERATURE ON POISSON'S RATIO. (22)

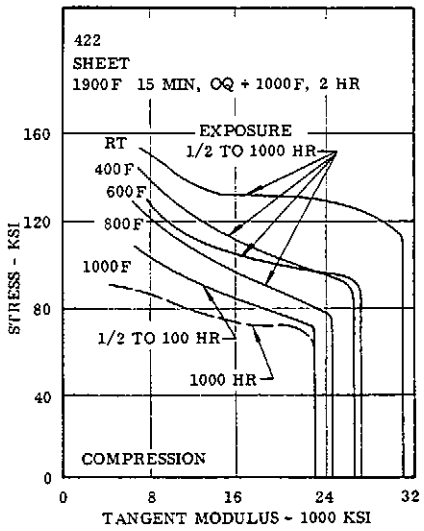


FIG. 3.0622 TANGENT MODULUS CURVES IN COMPRESSION FOR SHEET AT ROOM AND ELEVATED TEMPERATURES. (10)

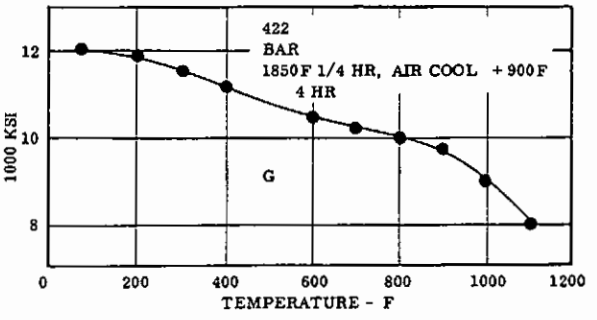


FIG. 3.0631 EFFECT OF TEMPERATURE ON MODULUS OF RIGIDITY. (22)

	Fe
0.23	C
12	Cr
1	Mo
1	W
0.8	Ni
0.25	V

TYPE 422

REFERENCES

1. Briggs, J.Z., and Parker, T.D., "The Super 12 Percent Cr Steels", Climax Molybdenum Co. (1965).
2. Battelle Memorial Institute, "Some Physical Properties of Martensitic Stainless Steels", DMIC Memorandum 68 (September 28, 1960).
3. Universal-Cyclops, "Unitemp 1420WM", Bulletin HT-3026 (1971).
4. Cartech Carpenter Technology Corporation, "Carpenter 636 Alloy (Type 422)", Technical Data Sheet (October 1969).
5. Allegheny Ludlum Steel Corp., "Properties of Type 422", 300-62272-422 Data Sheet (January 23, 1972).
6. Fritz, L.J. and Koster, W.P., "Low-Stress Creep Testing of 422 Stainless Steel", Report No. 363-1535 for Air Material Command by Metcut Research Associates (April 5, 1960).
7. Battelle Memorial Institute, "Mechanical and Physical Property Data on Modified 12 Percent Chromium Martensitic Stainless Steels for Airframe Applications", DMIC Memorandum 15 (April 18, 1959).
8. Banerjee, B.R. and Hauser, J.J., "Research and Application Engineering to Determine the Effect of Processing Variables on Crack Propagation of High-Strength Steels and Titanium", ASD-TDR-62-1034, Part 1, Crucible Steel Company of America (April 1963).
9. Banerjee, B.R. and Hauser, J.J., "Fracture Micro-Mechanics in High-Strength Steels and Titanium", AFML TDR-64-182, Crucible Steel Company of America (July 31, 1964).
10. Kattus, J.R., Preston, J.B. and Lessley, H.L., "Determination of Tensile, Compressive, Bearing and Shear Properties of Sheet Steels at Elevated Temperatures", WADC TR 58-365, ASTIA Document No. 206075, Southern Research Institute (November 1958).
11. Williams, W.L., "Properties of Type 422 Modified 12 Percent Chromium Steel", E.E.S. Report 040038B, U.S. Naval Engineering Experiment Station (November 9, 1953).
12. Cvercko, E., "Mechanical Properties Evaluation of Twenty-Nine Prototype Parts", by Wright Aeronautical Division for ASD under Contract AF33(657)-15787 (February 28, 1967).
13. AMS 5655 (January 15, 1959).
14. Westgren, R.C. and Dulis, E.J., "Advances in the Technology of Stainless Steels and Related Alloys", ASTM STP369 (March 1963).
15. ASTM A565 (1972).
16. Crucible Steel Company of America, "Crucible 422 Stainless Steel", Data Sheet, Rev. No. 3 (August 1958)
17. Zonder, A., Rush, I.A. and Freeman, J.W., "High Temperature Properties of Four Low-Alloy Steels for Jet Engine Turbine Wheels", WADC TR 53-277, Part 1 (November 1953).
18. Brown, W.F. Jr., Jones, M.H. and Newman, D.P., "Influence of Sharp Notches on the Stress-Rupture Characteristics of Heat-Resisting Alloys: Part II", ASTM Proc., Vol. 53, p. 665 (1953).
19. Vitovec, F.H. and Lazan, B.J., "Fatigue, Creep and Rupture Properties of Heat-Resistant Materials", WADC TR 56-181 (August 1956).
20. Phelps, E.H. and Loginow, A.W., "Stress Corrosion of Steels for Aircraft and Missiles", Corrosion, Vol. 16 (1960), p. 325t - 335t.
21. Nippes, E.F., Savage, W.F., Ianniello, L.C. and Owczareski, W.A., "Spot Welding of 12 Percent Cr Martensitic Stainless Steel, Welding Journal, Vol. 38 (September 1959), p. 360-s - 366-s.
22. Garafalo, F., "Temperature Dependence of the Elastic Moduli of Several Stainless Steels", Proceedings ASTM, Vol. 60 (1960), p. 738 - 749.
23. Loria, E.A., "Influence of Delta Ferrite-Carbide Segregates on the Properties of 12 Percent Chromium Steel", Transactions ASM, Vol. 54 (1961), p. 31-49.

REVISED : MARCH 1973
AUTHOR : DR. R. P. WEI

FERROUS ALLOYS

	Fe
0.2	C
16	Cr
2	Ni

TYPE 431 Stainless Steel

1. GENERAL
This alloy is a modification of Type 410 stainless steel with increased chromium and carbon contents and an addition of about 2 percent nickel. It is on the borderline of a heat treatable stainless steel. Because of the rather broad composition limits, it may require special considerations regarding heat treatment, (see 1.09). It is normally used at temperatures up to 800F where moderate strength is required and provides corrosion resistance superior to other hardenable chromium stainless grades. It is frequently used in highly stressed parts where good corrosion resistance is important in design, such as aircraft fittings, pump shafts and valve parts (1, p.20)(2, pp. 3-4)(3)(4, p.1)(5)(6)(7)(8).

1.01 Commercial Designation
Type 431.

1.02 Alternate Designations
AISI 431; SAE 51431 (wrought); ASTM A-314, Type 431; ASTM A-276, Type 431; 431 Mod (cast); ASTM A-296, Grade CB-30 (cast).

1.03 Specifications
1.031 AMS specifications, Table 1.031.
1.032 ASTM specifications. ASTM A-296, Grade CB-30 (castings), ASTM A-314, Type 431 (billets and bars), ASTM A-276, Type 431 (bars).

1.04 Composition
1.041 Specified composition.
1.0411 AMS specified composition, Table 1.0411.
1.0412 ASTM specified composition, Table 1.0412.

1.05 Heat Treatment
1.051 Anneal. Full anneal is impractical because of the long cooling time required. Semi-anneal for bars and forgings, 1500 to 1600F, 30 min, air cool. Reheat to 1250F, 4 hr minimum, air cool (12).
Semi-anneal for castings, 1450F minimum, furnace cool to 1000F, air cool (10).
1.052 Normalize for castings.
1.0521 Sand castings. 1800 to 1850F, 1 hr per inch of section, 30 min minimum, air cool (8).
1.0522 Investment castings. 1850 to 1900F, 1 hr per inch of section, 30 min minimum, air cool to room temperature, and cool to -90F, maximum, 1 hr minimum (7).
1.053 Stress relieve. 1200F, air cool (13, p. 40).
1.054 Austenitize. 1800 to 1950F, 1 hr per inch of section, 30 min minimum, oil quench or air cool depending on size. Depending on composition, it may be necessary to follow quenching by slow cooling to -90F, maximum, and holding for 1 hr minimum, to minimize retained austenite (4, p.1)(7)(8)(12, p. 53).
1.0541 Preheat. For large parts or those already hardened, preheat before austenitizing. Heat slowly from 1000 to 1450F, soak at 1450F, 1 hr, and raise to austenitizing temperature (12, p. 54).
1.0542 Effect of austenitizing temperature on room temperature tensile properties of as-quenched bar, Figure 1.0542.
1.0543 Effect of austenitizing atmosphere on room temperature mechanical properties, Table 1.0543.
1.055 Temper. To avoid embrittlement, do not temper in the range between 700 and 1100F.
Double temper. 1175F, 1 hr per inch, 2 hr minimum (12, p. 53). Sand castings, 1100F, 2 hr minimum, air cool following normalizing (8). Investment casting, 1100F, 2 to 4 hr, air cool; plus following optional heat treatment: austenitize, and temper at 600 to 700F, 2 hr, cool to -90F maximum, hold for 1 hr, retemper at 600 to 700F, 2 hr, air cool (7).

1.06 Hardness
1.061 General. This steel is air hardening in thin sections. Oil quenching is required in large sections.
1.062 Specified hardness.
1.0621 AMS specified hardness.
1.06211 Bars and forgings. Rockwell C 40 minimum in 1 inch sections after 1850 to 1900F, 25 min, oil quench (6).
1.06212 Sand castings. BHN 255 to 311 after normalizing and tempering (see 1.0522 and 1.055). Rockwell C 38 minimum after austenitizing 1875 to 1925F, 30 min, oil quench and tempering 650 to 700F, 3 hr, air cool (8).
1.06213 Investment castings. Rockwell C 24 to 34 after normalizing and tempering, (see 1.0522 and 1.055). Rockwell C 38 to 49 after austenitizing and tempering, (see 1.054 and 1.055)(7).
1.0622 ASTM specified hardness. BHN 241 maximum for ASTM A296-Grade CB-30 (castings) (9).
1.063 Effect of tempering temperature on hardness of investment castings, Figure 1.063.

1.07 Forms and Conditions Available
This alloy is available in bars, wire, rods, tubings, forgings and castings. Bars (over 2.75 in) are hot finished and annealed. Bars (less than 2.75 in), wire and mechanical tubing are annealed and cold finished (6)(7)(8)(17).

1.08 Melting and Casting Practices
Electric furnace air melt, induction vacuum melt and consumable electrode vacuum melt (21, p.5).

1.09 Special Considerations
The composition of this steel is such that difficulties are sometimes encountered in obtaining the expected mechanical properties. The high chromium content tends to keep the structure ferritic during austenitization. This tendency is overcome by the addition of nickel which tends to promote austenite formation. The composition limits, however, are rather broad and significant variations in response to heat treatment and in mechanical properties can be expected within the normal ranges of chemistry. If the chromium is high and nickel is low, the quenched steel may contain ferrite and not develop full strength. Conversely, if the chromium is low and nickel is high, retention of austenite may be a problem and sub-cooling after quenching will be required. In such cases it is not recommended to substitute water quenching for refrigeration as cracking may be encountered. Close temperature control and inert atmosphere for heat treatment at high temperature are recommended. Higher carbon contents tend to increase tensile strength but lower the corrosion resistance. Castings are available in more than one range of carbon contents. Stress relieving or tempering in the range between 700 and 1100F is not recommended because embrittlement may be encountered in this temperature range (1)(5).
1.091 Hydrogen embrittlement may be a problem with this steel at high strength and hardness levels. Embrittlement may be caused by cleaning processes such as pickling.
1.0911 Susceptibility of 0.06 inch diameter wire to embrittlement as a function of pickling time in 7 percent HCl, Figure 1.0911.

2. PHYSICAL AND CHEMICAL PROPERTIES

2.01 Thermal Properties
2.011 Melting range. 2600 to 2750F (1, p.39)(19, p.18).
2.012 Phase changes (14).
A_{c1} = 1500F A_{r1} = 80F
A_{c3} = 1380F A_{r3} = 500F
2.0121 Time-temperature-transformation diagrams.
2.013 Thermal conductivity. 11.7 Btu ft per (hr sq ft F) at 200F (4, p.3).
2.014 Thermal expansion, Figure 2.014.
2.015 Specific heat. 0.11 Btu per (lb F), 32 to 212F (1, p. 39)(19, p.18).
2.016 Thermal diffusivity.

2.02 Other Physical Properties
2.021 Density. 0.28 lb per cu in, 7.74 gm per cu cm, (19, p. 18).
2.022 Electrical properties.
2.0221 Electrical resistivity. 28.35 microhm - in or 72.0 microhm - cm at room temperature (1, p.39)(4, p.3).
2.023 Magnetic properties. The alloy is ferromagnetic (19, p.18).

	Fe
0.2	C
16	Cr
2	Ni

TYPE 431 Stainless Steel

2.024 Emittance.
2.025 Damping capacity.

2.03 Chemical Properties
2.031 Corrosion resistance. The corrosion resistance of Type 431 is superior to other hardenable chromium stainless steels, but is generally inferior to the 18-8 types. For certain applications involving steam, food products and salt sprays, however, this alloy compares very favorably with Type 18-8 stainless steels (4, p.2).
2.032 Oxidation resistance. Scales at about 1600F (3, p.3).

2.04 Nuclear Properties

3. MECHANICAL PROPERTIES

3.01 Specified Mechanical Properties
3.011 AMS specified mechanical properties, Table 3.011.
3.012 ASTM specified mechanical properties, Table 3.012.

3.02 Mechanical Properties at Room Temperature
3.021 Tension.
3.0211 Stress-strain diagrams.
3.0212 Typical mechanical properties of wrought and cast products.
3.02121 Typical mechanical properties for bar, wire, sand castings and precision castings, Table 3.02121.
3.02122 Typical tensile properties of bar, billet and forging, Table 3.02122.
3.0213 Effect of size and elevated temperature exposure on tensile properties.
3.02131 Effect of size and 700F exposure on tensile properties of bar, Figure 3.02131.
3.0214 Effect of tempering temperature on tensile properties.
3.02141 Effect of tempering temperature on tensile properties of bar, Figure 3.02141.
3.02142 Effect of tempering temperature on tensile properties of investment castings, Figure 3.02142.
3.02143 Effect of tempering treatment on tensile properties of extruded bar, Table 3.02143.
3.022 Compression.
3.0221 Stress-strain diagrams.
3.023 Impact.
3.0231 Effect of tempering temperature on impact strength of bar, Figure 3.0231.
3.0232 Impact strength of bar, billet and forging at room temperature and -40F, Table 3.0232. (See 3.02122).
3.0233 Effect of refrigeration and strain on impact strength at room temperature and -40F, Table 3.0233.
3.024 Bending.
3.025 Torsion and shear. (See 3.0351).
3.026 Bearing.
3.027 Stress concentration.
3.0271 Notch properties.
3.0272 Fracture toughness.
3.028 Combined properties.

3.03 Mechanical Properties at Various Temperatures
3.031 Tension.
3.0311 Stress-strain diagrams.
3.0312 Effect of test temperature on tensile properties of bar, Figure 3.0312.
3.0313 Effect of size on tensile properties of bar at 700F, Figure 3.0313. (See Figure 3.02131).
3.032 Compression.
3.0321 Stress-strain diagrams.
3.033 Impact. (See 3.0232 and 3.0233).
3.034 Bending.
3.035 Torsion and shear.
3.0351 Effect of size and exposure at 700F on shear strength of bar at room temperature and 700F, Figure 3.0351.
3.036 Bearing.
3.037 Stress concentration.
3.0371 Notch properties.
3.0372 Fracture toughness.
3.038 Combined properties.

3.04 Creep and Creep Rupture
3.041 Creep and creep rupture curves at 900 to 1200F, Figure 3.041.

3.05 Fatigue Properties

3.06 Elastic Properties
3.061 Poisson's ratio.
3.062 Modulus of elasticity in tension at room temperature. 29.0×10^3 ksi (1, p.39)(4, p.3).
3.063 Modulus of rigidity at room temperature. 10.5×10^3 ksi (18, p.18).

4. FABRICATION

4.01 Formability
4.011 General. Forming in the semi-annealed condition is recommended. In this condition forming is similar to the 18-8 grades except that work hardening is less and that the ductility is lower (3, p.2).
4.012 Forging. Starting temperature 2100 to 2250F maximum; finishing temperature 1500F minimum (21, p.2). Slow cooling or stress relief at 1200F is recommended (3, p.2). To prevent loss of toughness and ductility, this alloy should not be overheated.

4.02 Machining and Grinding
4.021 General. Because of the relative high hardness of this steel in the semi-annealed condition, machinability is poorer than the other 400 grades. Machinability is superior to the 18-8 stainless steels, however. Best machinability is obtained for cold drawn stock. Slow feeds, deep cuts and rigid equipment are recommended. Both carbide and high speed tools may be used with sulphurized cutting oils (17).

4.03 Welding
4.031 General. Welding is recommended only for parts used at elevated temperatures. Welds show grain growth that causes embrittlement at room temperature. Carbon arc or oxyacetylene methods should not be used since they cause carbon pick-up and consequently reduce corrosion resistance and ductility. For metal arc or inert gas arc welding, lime coated type electrodes may be used. In cases where high weld stresses are expected, 18-8 electrodes are recommended. Resistance welding is readily accomplished (4, p.2)(10, p.2).
4.032 Preheating before fusion welding is necessary. 300 to 400F for wrought product and 600 to 800F for castings. Stress relief after welding at 1200F is essential. For improved weld ductility, a semi-anneal may be used (10, p.2)(17, p.2).

4.04 Surface Treatment
4.041 For scale removal, pickle in a bath of 20 percent (by weight) hydrochloric acid at 120 to 140F or in a hot solution of 10 percent sulfuric acid and 6 to 12 percent rock salt by weight. Rinsing in a warm solution of 15 to 30 percent nitric acid (by weight) and wash in water (17, p.2) (See 1.091).

AMS	Form
5628C	Bars, wire, forgings, mechanical tubing, and forging stock
5353	Investment castings
5372	Sand castings

TABLE 1.031 AMS SPECIFICATIONS

Source	AMS(6)		AMS(7)		AMS(8)	
Alloy	Fe-(0.2C)-16Cr-2Ni					
Form	Wrought		Investment Casting		Sand Casting	
	Percent		Percent		Percent	
	Min	Max	Min	Max	Min	Max
Carbon	0.12	0.17	0.08	0.15	0.12	0.20
Chromium	15.50	17.00	15.0	17.0	14.5	17.0
Copper	-	0.50	-	-	-	0.50
Manganese	0.30	0.80	-	1.0	-	1.0
Molybdenum	-	0.25	-	-	-	0.50
Nickel	2.00	3.00	1.5	2.2	1.5	2.25
Silicon	0.20	0.60	-	1.0	-	1.0
Phosphorus	-	0.040	-	0.04	-	0.04
Sulfur	-	0.030	-	0.04	-	0.04
Nitrogen	-	0.10	0.03	0.12	-	-
Carbon + Nitrogen	-	-	-	0.22	-	-
Iron	Balance		Balance		Balance	

TABLE 1.0411 AMS SPECIFIED COMPOSITION

Source	(15, Table 2)		
Alloy	Fe-(0.2C)-16Cr-2Ni		
Form	4 in by 4 in billet (L)		
Condition	1800F, 1/2 hr, OQ + 1150F, 2 hr, AC. Specimens machined after H.T.		
Austenitizing Atmosphere	Argon	Reducing	Air
F_{tu} - ksi	222	223	220
F_{ty} - ksi	151	158	152
e(1 in) - percent	16.4	16.5	16.3
RA - percent	62	59	62
Hardness(a) - R_c	46	46	46
IE Charpy V(b) - ft lb	34.4	25.6	37.9
(a) Avg. of 16 readings; 4 on each impact specimen.			
(b) Avg. of 4 tests.			

TABLE 1.0543 EFFECT OF AUSTENITIZING ATMOSPHERE ON ROOM TEMPERATURE MECHANICAL PROPERTIES

Fe
0.2 C
16 Cr
2 Ni

TYPE 431 Stainless Steel

Source	ASTM (9)		ASTM (23)(24)	
Alloy	Fe-(0.2C)-16Cr-2Ni			
Form	Castings		Bars and Billets	
	Percent		Percent	
	Min	Max	Min	Max
Carbon	-	0.30	-	0.20
Chromium	18.0	21.0	15.0	17.0
Copper	0.90*	1.20*	-	-
Manganese	-	1.0	-	1.0
Nickel	-	2.00	1.25	2.50
Silicon	-	1.50	-	1.00
Phosphorus	-	0.04	-	0.040
Sulfur	-	0.04	-	0.030
Iron	Balance		Balance	
* Optional				

TABLE 1.0412 ASTM SPECIFIED COMPOSITION

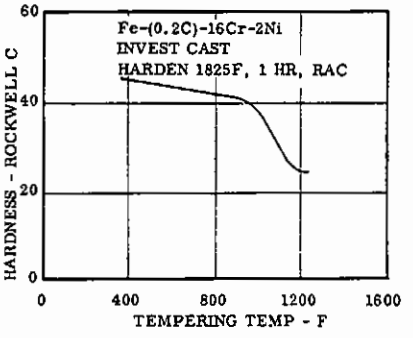


FIG. 1.063 EFFECT OF TEMPERING TEMPERATURE ON HARDNESS OF INVESTMENT CASTINGS. (11, p.21)

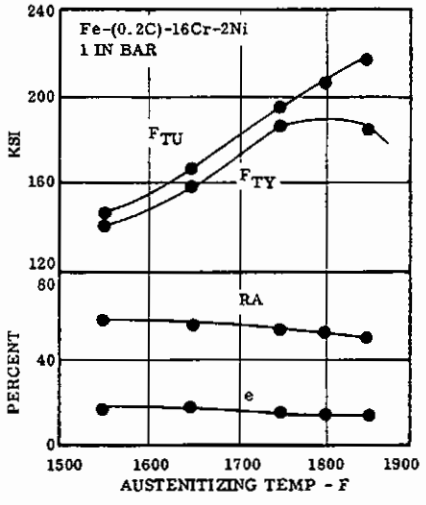


FIG. 1.0542 EFFECT OF AUSTENITIZING TEMPERATURE ON ROOM TEMPERATURE TENSILE PROPERTIES OF AS-QUENCHED BAR. (14)

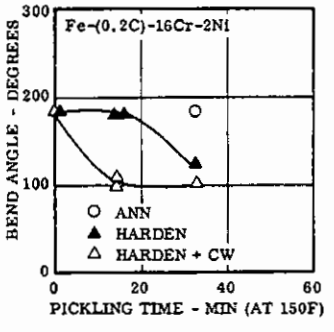


FIG. 1.0911 SUSCEPTIBILITY OF 0.06 IN DIAMETER WIRE TO EMBRITTLEMENT AS A FUNCTION OF PICKLING TIME IN 7 PERCENT HCl. (18, p. 429)

	Fe
0.2	C
16	Cr
2	Ni

TYPE 431 Stainless Steel

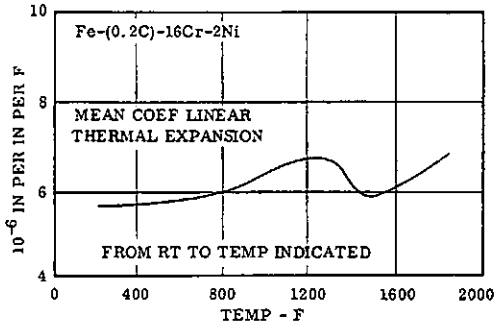


FIG. 2.014 THERMAL EXPANSION. (19, p.18)

Source	(21, p.46)			(17)				(11, p.20, 21)
Alloy	Fe-(0.2C)-16Cr-2Ni							
Form	Bar		Wire	Sand Cast	Prec Cast			Cast
Condition	Ann	Ann +CD	Soft Temper	Ann	Ann	Hardened LD	Hardened HD	As cast
Thickness - in	All	1	0.250	–	–	–	–	–
F_{tu} - ksi	125	130	135	75	120	180	140	109
F_{ty} - ksi	95	110	115	50	90	130	100	85
e (2 in) - percent	20	15	10	5	15	10	15	3
RA - percent	55	35	50	-	20	15	30	1
Hardness								
BHN	260	270	-	170	-	-	-	-
RC	24	26	29	-	26	42	30	46.5

TABLE 3.02121 TYPICAL MECHANICAL PROPERTIES FOR BAR, WIRE, SAND CASTINGS AND PRECISION CASTINGS

Source	(6)(7)(8)						
Alloy	Fe-(0.2C)-16Cr-2Ni						
Form	Bar	Wire	Mech. Tubing	Sand Castings		Investment Castings	
Condition	Ann. + HF or CF	Ann. + CF	Ann. + CF	Norm. + Temper	Aust. + Temper	Norm + Temper	Aust. + Temper
F_{tu} - ksi - min	-	-	-	-	180 (b)	-	170 (d)
max	-	140	-	-	-	-	-
F_{ty} - ksi - min	-	-	-	-	140 (b)	-	130 (d)
e (4D) - min-percent	-	-	-	-	8(b)	-	2 (d)
Hardness							
RC - min	-	-	-	-	38 (b)	24 (c)	38 (c)
max	-	-	-	-	-	34 (c)	49 (c)
BHN - min	-	-	-	255 (a)	-	-	-
max	302	-	285	311 (a)	-	-	-

(a) Castings and test specimens.
(b) Test specimens produced with castings; normalized and tempered with castings + austenitize 1875 to 1925F, 30 min, oil quench, temper 650 to 700F, 3 hr, air cool.
(c) Castings.
(d) Specimens representing master heat or master heat lot.

TABLE 3.011 AMS SPECIFIED MECHANICAL PROPERTIES

Source	(9)
Alloy	Fe-(0.2C)-16Cr-2Ni
Form	Castings
Condition	1450F, minimum, AC or FC
F_{tu} - ksi - min	65
F_{ty} - ksi - min	30

TABLE 3.012 ASTM SPECIFIED MECHANICAL PROPERTIES

Source	(15, Table 3)							
Alloy	Fe-(0.2C)-16Cr-2Ni							
Condition	1850F, 1/2 hr, OQ + 1150F, 2 hr, AC							
Form	6-1/2 in Dia x 3/4 in Pancakes		4 in x 4 in Billet		4-5/8 in Dia. Bar		3-7/8 in Dia. Bar	
Direction	L	T	L	T	L	T	L	T
F_{tu} - ksi	216	219	218	219	226	223	222	222
F_{ty} - ksi	157	153	154	153	156	153	151	152
e (1 in) - percent	15.3	15.1	18.2	12.8	17.5	10.8	18.0	10.7
RA - percent	47.4	48.7	62.8	37.2	62.5	26.8	61.0	24.8

TABLE 3.02122 TYPICAL TENSILE PROPERTIES OF BAR, BILLET AND FORGING

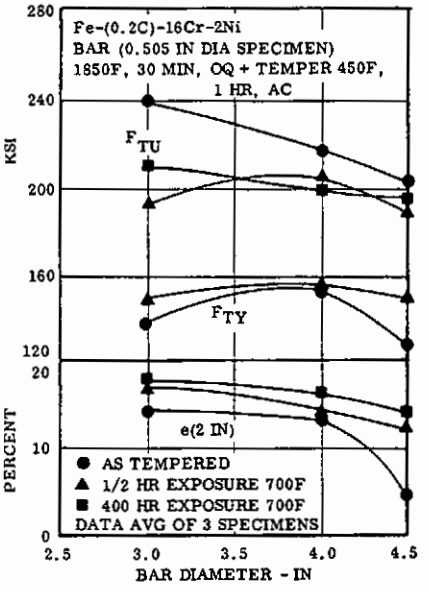


FIG. 3.02131 EFFECT OF SIZE AND 700F EXPOSURE ON ROOM TEMPERATURE TENSILE PROPERTIES OF BAR. (16)

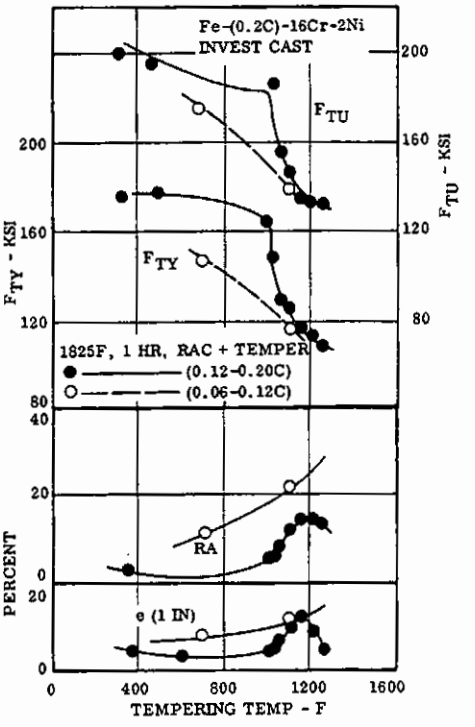


FIG. 3.02142 EFFECT OF TEMPERING TEMPERATURE ON TENSILE PROPERTIES OF INVESTMENT CASTINGS. (11, pp.19,21)

	Fe
0.2	C
16	Cr
2	Ni

TYPE 431 Stainless Steel

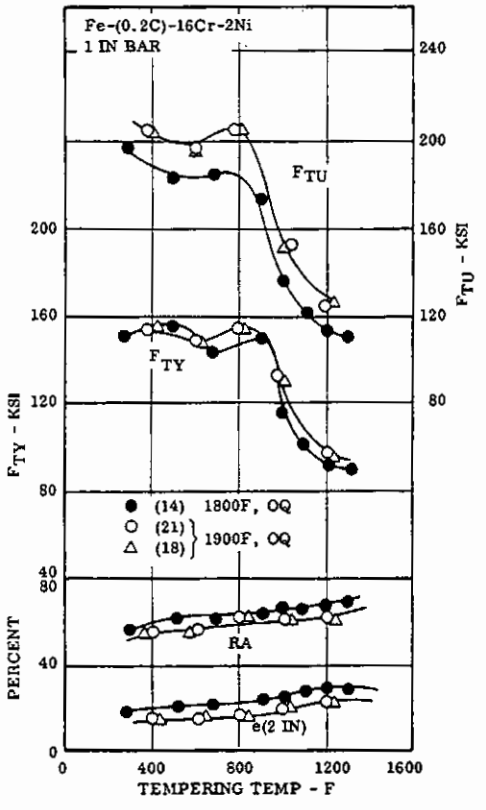


FIG. 3.02141 EFFECT OF TEMPERING TEMPERATURE ON TENSILE PROPERTIES OF BAR. (14)(18, p.414)(21, p.27)

Source	(22)	
Alloy	Fe-(0.2C)-16Cr-2Ni	
Form	Extruded Bar (L)	
Condition	1750F, 1/2 hr, AC +1250F, 2 hr, AC	1800F, 1/2 hr, OQ + 550F, 2 hr, AC
F_{tu} - ksi	126	207
F_{ty} - ksi	104	159
e (2 in) - percent	21	15
RA - percent	59	27

TABLE 3.02143 EFFECT OF TEMPERING TREATMENT ON TENSILE PROPERTIES OF EXTRUDED BAR

	Fe
0.2	C
16	Cr
2	Ni

TYPE 431 Stainless Steel

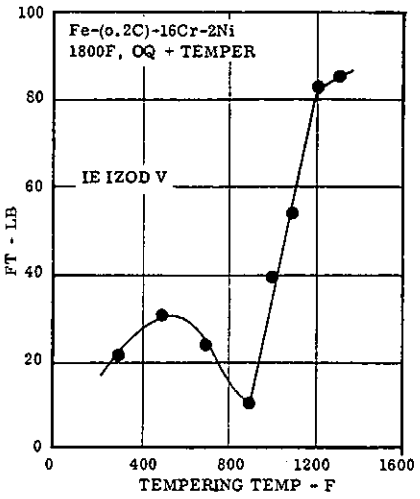


FIG. 3.0231 EFFECT OF TEMPERING TEMPERATURE ON IMPACT STRENGTH OF BAR. (14)

Source	(15, Tables 4-8)								
Alloy	Fe-(0.2C)-16Cr-2Ni								
Condition	1850F, 1/2 hr, OQ + 1150F, 2 hr, AC								
Form	6-1/2 in dia x 3/4 in Pancakes			4 in x 4 in Billet		4-5/8 in Dia. Bar		3-7/8 in Dia. Bar	
Direction		L	T	L	T	L	T	L	T
IE Charpy V-ft lb (Avg. and range of 6 tests)	Temp RT	21.7 (12.9-32.9)	20.9 (13.5-26.3)	37.3 (31.3-40.0)	16.5 (10.7-21.4)	26.8 (21.4-33.6)	11.2 (6.6-19.5)	33.3 (30.5-35.1)	9.0 (7.1-9.6)
	-40F	8.0 (6.2-11.3)	8.6 (6.6-13.5)	14.6 (12.4-17.6)	12.6 (9.1-14.0)	8.6 (7.1-9.6)	7.3 (4.8-11.8)	10.7 (8.5-12.9)	7.9 (7.1-9.6)
IE Izod V- ft lb (Avg. and range of 4 tests)	RT	24.5 (21.0-30.0)	24.2 (24.0-25.0)	31.0 (30.0-32.0)	14.8 (13.0-17.0)	21.0 (18.0-23.0)	6.0 (4.0-9.0)	25.5 (25.0-26.0)	7.2 (5.0-9.0)

TABLE 3.0232 IMPACT STRENGTH OF BAR, BILLET AND FORGING AT ROOM TEMPERATURE AND -40F.

Source		(20)			
Alloy		Fe-(0.2C)-16Cr-2Ni			
Form		1 in Dia Bar			
Condition		1200F, 1/2 hr, AC+1900F 1/2 hr, OQ+double temper 550F, 2 hr, AC		1200F, 1/2 hr, AC+1900F 1/2 hr, OQ+ -140F, 2 hr +double temper 550F, 2 hr, AC	
		As Tempered(b)	Strained(a)	As Tempered(c)	Strained(a)
IE Charpy V ft lb (Avg. of 4)	Temp. RT	53.5	27.3	24.0	17.7
	-40F	28.8	12.8	7.0	4.7

(a) Strained to 138 percent of F_{ty}.
(b) F_{tu} = 216 ksi, F_{ty} = 145 ksi, e(1 in) = 20.6 percent, RA = 59.5 percent.
(c) F_{tu} = 224 ksi, F_{ty} = 158 ksi, e(1 in) = 17.2 percent, RA = 58.7 percent.

TABLE 3.0233 EFFECT OF REFRIGERATION AND STRAIN ON IMPACT STRENGTH AT ROOM TEMPERATURE AND -40F.

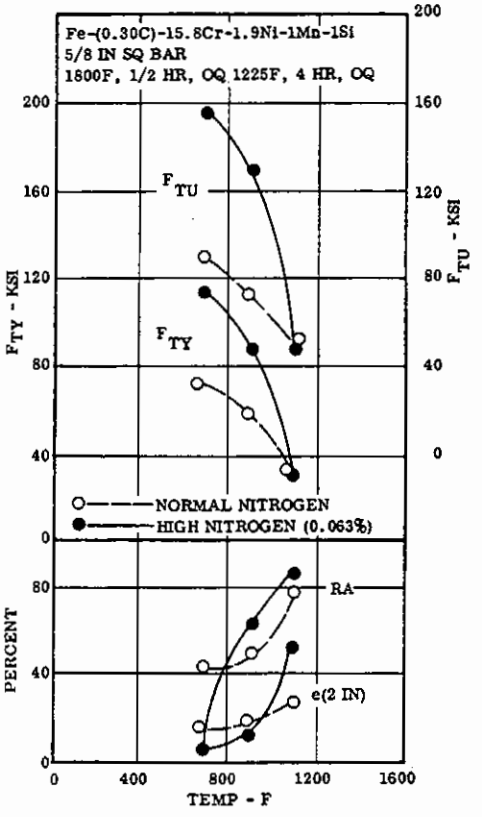


FIG. 3.0312 EFFECT OF TEST TEMPERATURE ON TENSILE PROPERTIES OF BAR. (17)

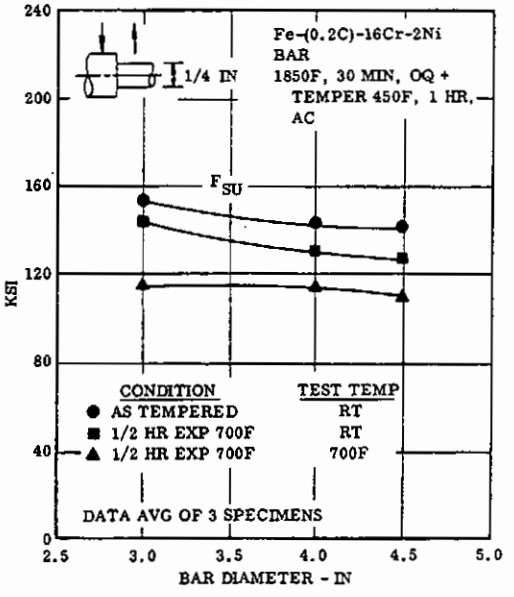


FIG. 3.0351 EFFECT OF SIZE AND EXPOSURE AT 700F ON SHEAR STRENGTH OF BAR AT ROOM TEMPERATURE AND 700F. (16)

	Fe
0.2	C
16	Cr
2	Ni

TYPE 431 Stainless Steel

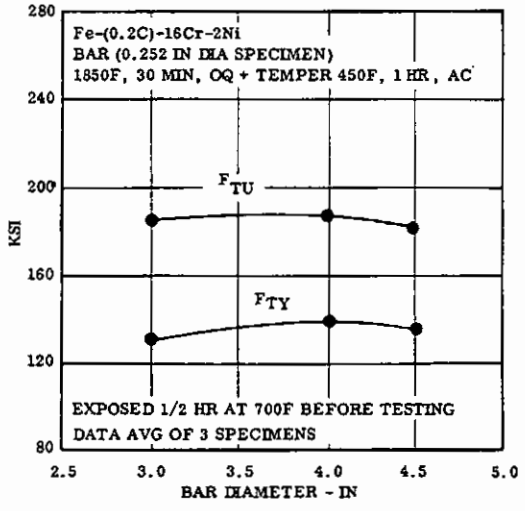


FIG. 3.0313 EFFECT OF SIZE ON TENSILE PROPERTIES OF BAR AT 700F. (16)

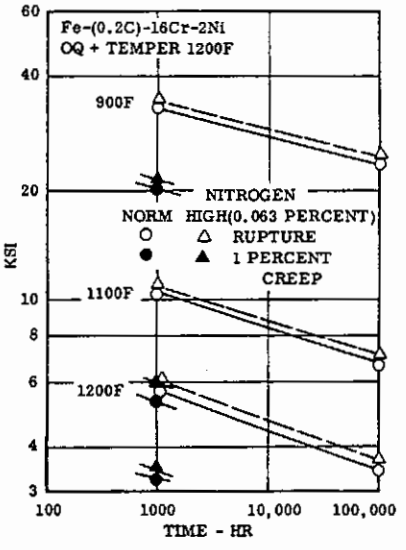


FIG. 3.041 CREEP AND CREEP RUPTURE CURVES AT 900 TO 1200 F. (17)

	Fe
0.2	C
16	Cr
2	Ni

TYPE 431 Stainless Steel

REFERENCES

1. Republic Steel Corp., "Republic Enduro Stainless Steel, Chromium Types - 400 Series", Adv. 1125 R4a-10M-1-66 (1964).
2. Dieter, G.E., "Effect of Microstructure and Heat Treatment on the Mechanical Properties of AISI Type 431 Stainless Steel", ASM Trans., Vol. 50 (1957).
3. Jones & Laughlin Steel Corp., "J & L Type 431, Stainless Steel", Data Sheet DS-458-8 (July 1958).
4. Crucible Steel Co., "Crucible 431 Stainless Steel", Data Sheet DS 163-5M-11/60, Issue #4, and "Resistal 431 Stainless Steel", Data Sheet DS 163-10M-2/57 (issued August 1947), Revision #3 (September 1954).
5. Brown, W.F., Jr., Personal Communication (October 2, 1961).
6. AMS 5628C (Rev. May 1, 1970).
7. AMS 5353 (September 15, 1957).
8. AMS 5372 (March 1, 1955).
9. ASTM A296-68, Grade CB-30 (1968).
10. Alloy Casting Institute, "Corrosion Resistant Type CB-30", Data Sheet 4-54-75 CI (June 1954).
11. Haynes Stellite Co., "Haynes Investment-Cast Steels", (April 1958).
12. Fiorentino, R.J., Roach, D.B., and Hall, A.M., "Heat Treatment of High-Strength Steels for Airframe Applications", DMIC Rept. 119 (November 27, 1959).
13. Mishler, H.W., Monroe, R.E., and Rieppel, P.J., "Welding of High-Strength Steels for Aircraft and Missile Applications", DMIC Rept. 118 (October 12, 1959).
14. Allegheny Ludlum Steel Corp., "Blue Sheet for Allegheny Metal 12-2, 16-1, Stainless Steel".
15. Irish, C.R., and Rosenberg, S.J., "Heat Treatment of Type 431 Stainless Steel", National Bureau of Standards (September 1959).
16. Republic Aviation Corp., "Compilation of Unpublished Materials Information", First Quarterly Rept. No. RAC 767-251(357), (July 14, 1961), and AD 269710 (June 1961).
17. Alloy Digest, "AISI Type 431", Filing Code SS-88 (May 1959).
18. ASM Metals Handbook, Vol. 1, 8th Edition, "Properties and Selection of Metals" (1961).
19. "Some Physical Properties of Martensitic Stainless Steels", DMIC Memo 68 (September 28, 1960).
20. Feinberg, I.J., "Effect of Refrigeration and Strain on the Charpy V-Notch Properties of Type 431 Stainless Steel", National Bureau of Standards Rept. 10-015 (April 1969).
21. American Iron and Steel Institute, "Stainless and Heat Resisting Steels", Steel Products Manual (April 1963).
22. Fiorentino, R.J., and Sabroff, A.M., "Availability and Mechanical Properties of High-Strength Steel Extrusions", DMIC Rept. 138 (October 1960).
23. ASTM A-276-67, Type 431 (1967).
24. ASTM A-314-63, Type 431 (1963).

REVISED: SEPTEMBER 1973
AUTHOR : DR. R. P. WEI

FERROUS ALLOYS

	Fe
High	C
17	Cr
0.5	Mo

TYPE 440 A, B, C, AND F

1. GENERAL

These 17 percent chromium martensitic stainless steels are produced with various carbon contents. Type 440 A contains about 0.70 percent carbon, Type 440 B about 0.85 percent carbon, and Type 440 C about 1.10 percent carbon. Type 440 F is a free machining grade of Type 440 C and contains additions of either sulfur or selenium. All of these types are used in the hardened condition where a combination of high wear and corrosion resistance is required. Their hardness and wear resistance increase with increasing carbon content, while their shock resistance and ductility decrease (1)(2)(3)(4)(5)(6).

1.01 Commercial Designation

Type 440 A, B, C and F stainless steel.

1.02 Alternate Designations

SAE 51440 A, C and F; Type 440 C modified.

1.03 Specifications

1.031 AMS specifications, Table 1.031.

1.04 Composition

1.041 Specified composition.
1.0411 AMS specified composition, Table 1.0411.
1.0412 AISI specified composition, Table 1.0412.

1.05 Heat Treatment

(1, p. 39)(6, p. 47).
1.051 Full anneal.
1.0511 Bar, wire and forgings. 1550 to 1650F, furnace cool.
1.0512 Precision investment castings. 1625 to 1675F, 1 hour minimum, furnace cool at 25F per hour maximum to 1200F maximum.
1.052 Subcritical anneal. 1250 to 1450F.
1.053 Spheroidizing anneal for best machinability of precision investment castings. 1875F, 1 hour, air cool + 1350F, 32 hours.
1.054 Stress relief after forging Type 440 C. 1200F.
1.055 Austenitize. 1850 to 1950F, rapid air cool or oil quench. Heavy sections of Type 440 A should be preheated at 1200F. Types 440 B and 440 C should be preheated at 1450 to 1500F.
1.056 Temper. 300 to 800F, preferably 400 to 500F.

1.06 Hardness

1.061 General. These steels are air hardening.
1.062 Specified hardness.
1.0621 AMS specified hardness.
1.06211 Bar and forgings. Annealed and in a machinable condition. Type 440 A, BHN= 241 maximum (2); Type 440 C, BHN= 255 maximum (3); Type 440 F, BHN= 286 maximum (5). Material up to 0.375 inch thickness, and 0.375 inch thick specimens from thicker material, austenitized at 1865 to 1885F, 25 minutes, air cooled, shall have a minimum hardness as follows: Type 440 A, Rockwell C 55; Types 440 C and 440 F, Rockwell C 58 (2)(3)(5).
1.06212 Investment castings. Annealed condition. Rockwell C 30 maximum. Austenitized 1865 to 1885F, 30 minutes, air cooled. Rockwell C 58 minimum (4).
1.063 Effect of tempering temperature on hardness.
1.0631 Effect of tempering temperature on hardness, Figure 1.0631.
1.0632 Effect of tempering temperature on hardness of bar, Figure 1.0632.

1.07 Forms and Conditions Available

1.071 The various types are available in the full commercial range of sizes for bar, wire and forgings.
1.072 Bar and wire are available on the annealed or cold finished condition, and forgings in the annealed or heat treated condition.
1.073 Precision investment castings are supplied in the as cast, heat treated or spheroidize annealed condition.

1.08 Melting and Casting Practice

Electric furnace air melt. Induction and consumable electrode vacuum melts and remelts are available. Vacuum degassed material is also available.

1.09 Special Considerations

1.091 Cracking may occur on heating, cooling, pickling or after welding.
1.092 These steels are particularly subject to decarburization because of their high carbon content. Use of protective, non-decarburizing atmospheres in heat treatments is recommended.
1.093 Addition of 0.4 to 0.5 weight percent of sulfur to Type 440 C reduces friction, wear and welding normally encountered with these alloys in high vacuum (to 10^{-9} torr) applications (9).
1.094 These steels are subject to severe embrittlement by gaseous hydrogen (10).

2. PHYSICAL AND CHEMICAL PROPERTIES

2.01 Thermal Properties

2.011 Melting range. Types 440 A and B, 2500 to 2750F. Type 440 C, 2500 to 2700F (6, p. 47).
2.012 Phase changes. Alloy transforms from austenite to martensite.
2.0121 Time-temperature-transformation diagrams.
2.013 Thermal conductivity. 14.0 Btu ft per (hr sq. ft. F) at 212F (1, p.39)(6, p. 47).
2.014 Thermal expansion.
2.0141 Mean coefficient of thermal expansion from 32F, Table 2.0141.
2.0142 Mean coefficient of thermal expansion from 68F, Table 2.0142.
2.015 Specific heat. 0.11 Btu per lb F, 32 to 212F, (1, p.39) (8, p. 90).
2.016 Thermal diffusity.

2.02 Other Physical Properties

2.021 Density. 0.28 lb per cu. in. 7.75 gm per cu. cm. (6, p. 47)(8, p. 90).
2.022 Electrical resistivity. 23.6 microhm-in. 60.0 microhm-cm (1, p. 39)(6, p. 47)(8, p. 90).
2.023 Magnetic properties. The alloys are ferromagnetic (6, p. 47)(8, p. 90).
2.024 Emittance.
2.025 Damping capacity.

2.03 Chemical Properties

2.031 Corrosion resistance of these steels is similar to that of Type 410 stainless steels. It is best in the fully hardened condition with a polished surface.
2.032 Oxidation resistance is good up to 1400F for continuous service, and up to 1500F for intermittent service (1, p. 39).

2.04 Nuclear Properties

See Type 410 stainless steel.
2.041 Effect of combined nuclear-cryogenic environments on tensile properties, Table 2.041.

3. MECHANICAL PROPERTIES

3.01 Specified Mechanical Properties

3.011 AMS specified mechanical properties, Table 3.011. (See also 1.0621).

3.02 Mechanical Properties at Room Temperature

3.021 Tension.
3.0211 Stress-strain diagrams.
3.0212 Typical mechanical properties of bar and wire, Table 3.0212.
3.0213 Effect of austenitizing and tempering treatment on mechanical properties.
3.02131 Effect of tempering temperature on mechanical properties of bar austenitized at 1700F, Figure 3.02131.
3.02132 Effect of tempering temperature on mechanical properties of bar austenitized at 1900F, Figure 3.02132.
3.022 Compression.
3.0221 Stress-strain diagrams.
3.023 Impact. (See 3.0213).
3.024 Bending.

Fe
High C
17 Cr
0.5 Mo

TYPE 440 A, B, C, AND F

3.025 Torsion and shear.
3.026 Bearing.
3.027 Stress concentration.
3.0271 Notch properties. (See 2.041).
3.0272 Fracture toughness.
3.028 Combined properties.

3.03 Mechanical Properties at Various Temperatures
3.031 Tension.
3.0311 Stress-strain diagrams.
3.0312 Effect of elevated temperature on tensile properties, Figure 3.0312.
3.032 Compression.
3.0321 Stress-strain diagrams.
3.033 Impact.
3.034 Bending.
3.035 Torsion and shear.
3.036 Bearing
3.037 Stress concentration.
3.0371 Notch properties. (See 2.041).
3.0372 Fracture toughness.
3.039 Combined properties.

3.04 Creep and Creep Rupture Properties

3.05 Fatigue Properties

3.06 Elastic Properties
3.061 Poisson's ratio. Types 440 A and C, 0.284 (11, p. 21).
3.062 Modulus of elasticity. 29.0×10^3 ksi (1, p. 39)(6, p.47). 29.0×10^3 to 31.8×10^3 ksi (11, p. 21).
3.063 Modulus of rigidity. Types 440 A and C, 13.5×10^3 ksi, (11, p. 21).

4. FABRICATION

4.01 Formability
4.011 Forging. Starting temperature 2100F maximum for Types 440 A and B, and 2050F maximum for Type 440 C. Finishing temperature 1700F minimum. Heating time is about twice that for carbon steels. Preheating at 1400 to 1500F is recommended. Furnace cool after forging to 1200F or cool under insulating cover. Alternatively, stress relieve Type 440 C by placing work, after forging, in furnace held at 1200F.
4.012 Drawing or stamping is not recommended (1, p. 39).

4.02 Machining and Grinding
These alloys are difficult to machine. Machining is generally performed in the fully annealed condition for bar and forgings, and in the spheroidized condition for castings. The use of carbide or ceramic tools is recommended. Machinability rating of these alloys is about 40 percent of that of mild steel.

4.03 Welding
Welding is generally not recommended (1, p. 39). However, for fusion welding of these alloys, electrodes of similar composition can be used. If a softer weld can be tolerated, austenitic stainless steel electrodes, Types 309 or 310, can be used. Preheat at 450F and postheat at 1300F, air cool.

4.04 Surface Treatment
4.041 Pickling. The material should be annealed or stress relieved to prevent cracking on pickling. Cleaning by sand blasting or mechanical scale braking of heavy scale is recommended prior to pickling to avoid localized overpickling.

AMS	Type	Form
5631	440 A	Bar, forgings, forging stock
5630 C	440 C	Bar, forgings, forging stock
5352 A	440 C Mod.	Castings, (precision invest.)
5632 C	440 F	Bar, wire, forgings, forging stock

TABLE 1.031 AMS SPECIFICATIONS

Source	AMS (2)		AMS (3)		AMS (4)		AMS (5)	
Type	440 A		440 C		440 C Mod.		440 F	
Form	Wrought		Wrought		Investment Castings		Wrought	
	Percent		Percent		Percent		Percent	
	Min.	Max.	Min.	Max.	Min.	Max.	Min.	Max.
Carbon	0.60	0.75	0.95	1.20	0.95	1.20	0.95	1.20
Manganese	-	1.00	-	1.00	-	1.00	-	1.25
Silicon	-	1.00	-	1.00	-	1.00	-	1.00
Phosphorus	-	0.04	-	0.04	-	0.04	-	0.04
Sulfur	-	0.03	-	0.03	-	0.03	0.10(a)	0.35(a)
Chromium	16.00	18.00	16.00	18.00	16.0	18.0	16.00	18.00
Nickel	-	0.75	-	0.75	-	0.75	-	0.75
Molybdenum	-	0.75	0.40	0.60	0.35	0.75	0.40	0.60
Copper	-	-	-	-	-	-	-	0.50
Nitrogen	-	-	-	-	-	-	-	0.08(b)
Tin	-	-	-	-	-	-	-	0.05
Iron	Balance		Balance		Balance		Balance	

(a) Alternate composition: sulfur 0.030 max. + selinium 0.10 to 0.20.
(b) Determination not required for routine acceptance.

TABLE 1.0411 AMS SPECIFIED COMPOSITION.

Source	AISI (6, p. 47)	
Type	440 B	
Form	Wrought	
	Percent	
	Minimum	Maximum
Carbon	0.75	0.95
Manganese	-	1.00
Silicon	-	1.00
Phosphorus	-	0.040
Sulfur	-	0.030
Chromium	16.00	18.00
Nickel	-	-
Molybdenum	-	0.75
Iron	Balance	

TABLE 1.0412 AISI SPECIFIED COMPOSITION

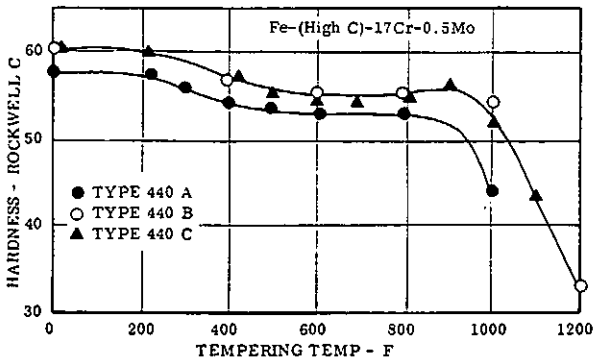


FIG. 1.0631 EFFECT OF TEMPERING TEMPERATURE ON HARDNESS. (7)

FERROUS ALLOYS

	Fe
High	C
17	Cr
0.5	Mo

TYPE 440 A, B, C, AND F

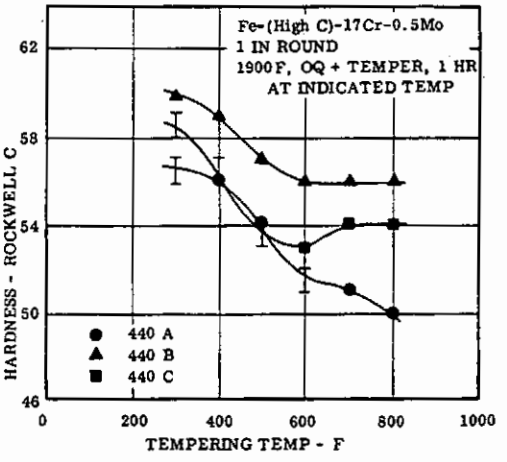


FIG. 1.0632 EFFECT OF TEMPERING TEMPERATURE ON HARDNESS OF BAR. (8, p. 86-91)

Source	(12, p. 67)		
Alloy	Fe- (High C) - 17 Cr - 0.5 Mo (Type 440 C)		
Condition	Austenitized and Tempered		
Test Temperature and Condition	R.T. Not Irradiated	-430F Not Irradiated	-430F Irradiated (1×10^{17} nvt)
F_{tu} (a) - ksi	316	261	218
F_{ty} (a) - ksi	270	(c)	(c)
e (0.5 in) - percent	nil	nil	nil
RA - percent	nil	nil	nil
Sharp Notch (b) - ksi Strength (K_t=6.4)	217	108	119

(a) 0.125 in. diam. specimens
(b) 0.125 in O.D., 0.105 in. I.D., Root Radii 0.007 in, $K_t \simeq 6.4$.
(c) Failed at less than 0.2 percent plastic strain.

TABLE 2.041 EFFECT OF COMBINED NUCLEAR-CRYOGENIC ENVIRONMENTS ON TENSILE PROPERTIES.

Source	(11, p. 19)		
Alloy	Fe - (High C) - 17 Cr - 0.5 Mo		
Type	440 A	440 B	440 C
Temperature - F	Mean Coef. from 32F - 10^{-6} in/in/F		
212	5.7	5.7	5.7
600	6.0	6.1	6.0
1000	6.5	6.6	6.5
1200	6.8	6.8	6.8

TABLE 2.0141 MEAN COEFFICIENT OF THERMAL EXPANSION FROM 32F.

Source	(11, p. 19)	
Alloy	Fe - (High C) - 17 Cr - 0.5 Mo	
Type	440 A	440 C
Temperature - F	Mean Coef. from 68F 10^{-6} in/in/F	
212	5.8	5.6
392	-	5.8
1112	-	6.2
1600	6.2	-

TABLE 2.0142 MEAN COEFFICIENT OF THERMAL EXPANSION FROM 68F.

Source	AMS(2)	AMS(3)	AMS(5)		AMS (4)
Alloy	Fe - (High C) - 17 Cr - 0.5 Mo				
Type	440 A	440 C	440 F		440 C Mod.
Form	Bar		Bar	Wire	Invest. Castings
Condition	Machinable		Ann. Machinable	Ann. +CF	Ann.
F_{tu}, max. - ksi	-	-	-	140	-
Hardness					
BHN, max.	241	255	286	-	-
Rockwell C, max.	-	-	-	-	30

TABLE 3.011 AMS SPECIFIED MECHANICAL PROPERTIES

Source	(6, p. 19, 47-49)(8, p. 86, 88, 90)*														
Alloy	Type 440 A					Type 440 B					Type 440 C				
Form	Bar			Wire		Bar			Wire		Bar			Wire	
Condition	Ann	Ann + CD	Temp*	Ann	Soft Temper	Ann	Ann + CD	Temp*	Ann	Soft Temper	Ann	Ann + CD	Temp*	Ann	Soft Temper
Thickness-in	All	1		0.250		All	1		0.250		All	1		0.250	
F_{tu} - ksi	105	115	260	105	115	107	120	280	107	115	110	125	285	110	125
F_{ty} - ksi	60	90	240	60	85	62	95	270	62	90	65	100	275	65	100
e (2 in) - percent	20	12	5	18	10	18	9	3	16	8	14	7	2	13	6
RA - percent	45	20	20	55	35	35	20	15	40	25	25	20	10	30	20
Hardness															
BHN	215	240	510	-	-	220	250	555	-	-	230	260	580	-	-
R_C	-	-	51	-	-	-	23	55	-	-	-	24	57	-	24
R_B	95	99	-	95	99	96	-	-	96	99	97	-	-	97	-

* 1900F, OQ + 600F

TABLE 3.0212 TYPICAL MECHANICAL PROPERTIES OF BAR AND WIRE.

	Fe
High	C
17	Cr
0.5	Mo

TYPE 440 A, B, C, AND F

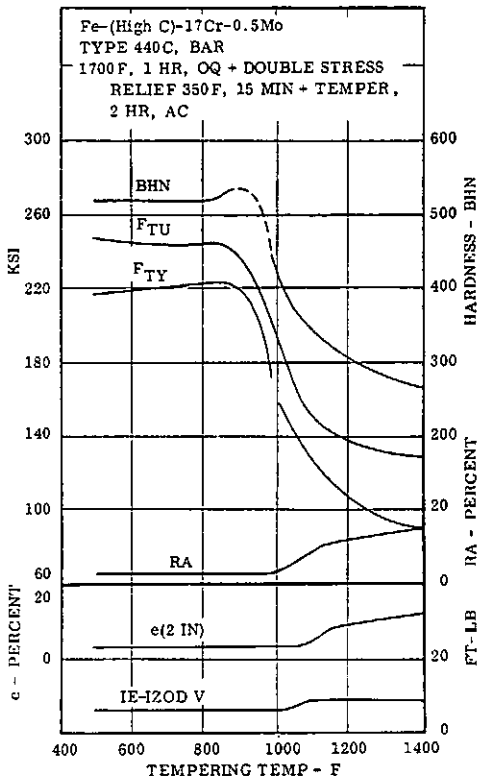


FIG. 3.02131 EFFECT OF TEMPERING TEMPERATURE ON MECHANICAL PROPERTIES OF BAR AUSTENITIZED AT 1700F. (1, p. 23)

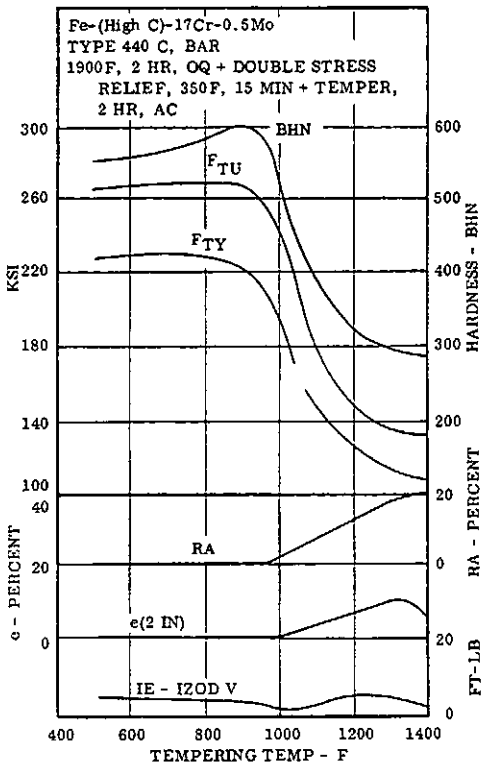


FIG. 3.02132 EFFECT OF TEMPERING TEMPERATURE ON MECHANICAL PROPERTIES OF BAR AUSTENITIZED AT 1900F. (1, p. 23)

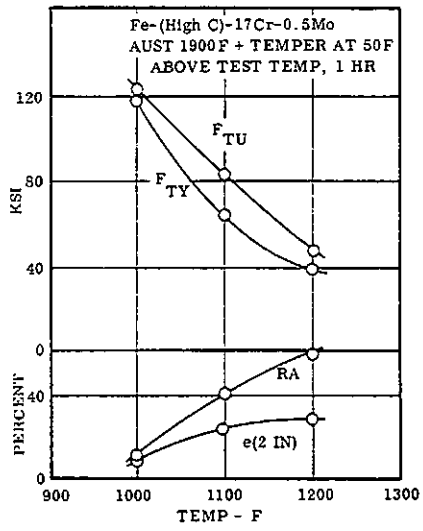


FIG. 3.0312 EFFECT OF ELEVATED TEMPERATURE ON TENSILE PROPERTIES. (8, p. 90)

	Fe
High	C
17	Cr
0.5	Mo

TYPE 440 A, B, C, AND F

REFERENCES

1. Republic Steel Corp., "Republic Enduro Stainless Steel, Chromium Types - 400 Series", Adv. 1125 R4a-10M-1-66 (1964).
2. AMS 5631 (November 1, 1952).
3. AMS 5630C (December 4, 1939, Revised December 1, 1953).
4. AMS 5352A (December 1, 1953, Revised November 15, 1960).
5. AMS 5632C (June 1, 1942, Revised November 1, 1969).
6. American Iron and Steel Institute, "Stainless and Heat Resisting Steels", Steel Products Manual (June 1957).
7. Universal-Cyclops Steel Corp., "Stainless Steels, Tool Steels, Specialty Steels", Data Sheet 2M-7'51 (December 1951).
8. The Carpenter Steel Co., "Carpenter Stainless and Heat Resisting Steels - Selection, Description, Fabrication", Working Data (1962).
9. Buckley, D.H., and Johnson, R.L., "Friction and Wear of Nickel-Aluminum Alloys and Some Sulfur-Modified Steels in Vacuum to 10^{-9} Millimeter of Mercury", Lewis Research Center, NASA TN D-2307 (May 1964).
10. Walter, R.J., and Chandler, W.T., "Effects of High Pressure Hydrogen on Metals at Ambient Temperature", Final Report, Contract NAS8-19, NASA, MSFC, North American Rockwell Corp. - Rocketdyne Report R-7780-1,2,3 (1969).
11. Battelle Memorial Institute, "Some Physical Properties of Martensitic Stainless Steels", DMIC Memo 68 (September 1960).
12. Schwanbeck, C.A., "Effect of Nuclear Radiation on Materials at Cryogenic Temperatures", Lockheed Nuclear Products, NASA CR 54881, NAS3-7987 (January 1965).

ADDITIONAL BIBLIOGRAPHY

1. Sevakis, P. and Tafel, R., "Vanadium Decreases Hardness of Cast Type 440C Stainless", Casting Engineering, p. 14 (September/October 1972).
2. North American Aviation Inc., "Tensile and Fatigue Properties of 440C Stainless Steel Bar at -65F", NAA Report No. TFD-61-756, File No. LP-61-203 (August 11. 1961)(AD 820943).
3. Hutchinson, E. F., "Effect of Fluid Environment on Torsional Fatigue Failure", Nuclide Corp. Technical Report 64-GRX-10 (March 1966)(AD488170).
4. Warren, K.A. and Reed, R.P., "Tensile and Impact Properties of Selected Materials From 20 to 300K", National Bureau of Standards Monograph 63 (June 28, 1963).
5. Zlatin, N., Field, M., Koster, W.P., et al., "Machining of New Materials", AFML-TR-67-339 (October 1967)(AD 824483).

Fe	
0.3	C
0.95	Cr
0.2	Mo

4130

1 GENERAL

This heat-treatable low-alloy steel has relatively low hardenability; nevertheless, it is one of the most popular alloy steels because of its good formability and weldability along with an excellent combination of mechanical properties. Its optimum combination of properties is developed in limited section thicknesses by quench-and-temper heat treatment, but sufficient strength and toughness for many applications can be obtained by normalizing. It is recommended for use at temperatures up to a maximum of 700 F because its strength decreases markedly with increasing temperatures above that level. At sub-zero temperatures it undergoes a transition from ductile to brittle behavior in a Charpy V impact test, when it has poor impact properties. The transition temperature varies with the heat treatment.

This steel is not subject to temper embrittlement, and can be nitrided. It is usually forged at 2000 F to 2200 F and the finishing temperature should never fall below 1800 F. For applications in moist, marine, and other corrosive environments, paint, electroplate, or other protective coatings should be applied to inhibit rusting and other corrosion. It is used in both cast and wrought form for many applications requiring high strength and toughness.

4130 steel is available as billet, bar, rod, forgings, sheet, plate, tubing, and castings. It is used to make automotive connecting rods, engine mounting lugs, shafts, fittings, bushings, gears, bolts, axles, gas cylinders, airframe components, hydraulic lines, and nitrided machinery parts. (30,74)

1.01 **Commercial Designation**

4130.

1.02 **Alternate Designations**

AISI 4130, SAE 4130, 4130H, UNS G41300, UNS H41300.

1.03 **Specifications**

Table 1.03.

1.04 **Composition**

Table 1.04.

1.05 **Heat Treatment**

1.051 Normalize: Heat to 1600 to 1700 F, air cool (tempering at 900 F or above is often carried out after normalizing to raise the relatively low as-normalized yield strength) (30).

1.052 Anneal: Heat to 1525 to 1575 F, furnace cool (30).

1.053 Harden: Heat to 1500 to 1600 F, water quench, or heat to 1575 to 1625 F, oil quench. Inert or endothermic atmosphere is desirable to prevent decarburization (30).

1.054 Temper: Heat to 400 to 1300 F, hold 1/2 hour minimum, air cool or water quench (the alloy is not susceptible to temper embrittlement) (30).

1.055 Spheroidize: Heat to 1400 to 1425 F, hold at temperature for 6 to 12 hours, cool slowly (30).

1.06 **Hardness**

1.061 Effect of tempering temperature on hardness of bar, Figure 1.061.

1.062 Effect of tempering temperature on hardness of oil-quenched and water-quenched bar, Figure 1.062.

1.063 Effect of exposures at elevated temperatures on room-temperature hardness of sheet after three different tempering treatments, Figure 1.063.

1.064 Hardness of bar, plate, sheet, and extrusion in various heat-treated conditions, Table 1.064.

1.065 Effect of diameter on surface hardness of quenched-and-tempered bars, Figure 1.065.

1.066 End-quench hardenability, Figure 1.066.

1.067 Hardness profile through nitrided case, Figure 1.067.

1.068 Effect of repress (forging) pressure and temperature on hardness of powder metallurgy forging, Figure 1.068.

1.069 Effect of fabrication process on hardness properties of powder metallurgy forging, Table 1.069.

1.07 **Forms and Conditions Available**

1.071 Wrought products are available in the full range of sizes and forms including billets, bars, rods, forgings, sheets, plates, strip, and tubing. The products are furnished in the annealed, normalized and tempered, or hardened and tempered conditions (30).

1.072 Sand, centrifugal, and investment castings are available in any desired heat-treated condition (30).

1.08 **Melting and Casting Practice**

1.081 The alloy is generally air melted in basic-electric, basic-open-hearth, or basic-oxygen furnaces. For some applications requiring exceptional quality, it is induction or consumable-electrode remelted in vacuum.

1.09 **Special Considerations**

1.091 Because of the limited hardenability of Type 4130, optimum and uniform mechanical properties can be obtained only in section thicknesses that are small enough to through-harden when quenched from the austenitizing temperature. For critical applications requiring high strength and toughness, therefore, use should be made of precise hardenability calculations to determine the suitability of specific heat compositions.

1.092 Type 4130 is susceptible to hydrogen embrittlement in chrome-, nickel-, and cadmium-plating solutions and in hydrochloric-acid pickling. It is generally not susceptible in alkaline cleaners or anodic acid cleaners. Baking at 375 F for times up to 24 hours, depending upon the severity of the embrittlement, is effective in relieving the embrittlement (19,20).

1.093 Effect of hydrogen gas pressure on embrittlement (see Figure 3.02726).

2 PHYSICAL AND CHEMICAL PROPERTIES

2.01 **Thermal Properties**

2.011 Melting range – about 2795 F.

2.012 Phase changes.

2.0121 Time-temperature-transformation diagram, Figure 2.0121.

Fe
0.3 C
0.95 Cr
0.2 Mo

4130

2.0122 Upon heating under equilibrium conditions, the transformation from pearlite or martensite to austenite starts at 1395 F (AC_1) and is complete at 1490 F (AC_3) (35).

2.0123 Upon slow cooling under equilibrium conditions, the transformation from austenite to pearlite starts at 1390 F (Ar_3) and is complete at 1380 F (Ar_1) (35).

2.0124 Upon rapid quenching from the austenitic condition the transformation to martensite starts at 700 F (M_s) and is complete at 550 F (M_f) (30).

2.013 Thermal conductivity, Figure 2.013.

2.014 Thermal expansion, Figure 2.014.

2.015 Specific heat, Figure 2.015.

2.016 Thermal diffusivity.

2.02 **Other Physical Properties**

2.021 Density, 0.2834 lb/in.^{3}, 7.845 gr/cm^3 (30).

2.0211 Effect of initial compacting pressure on density of powder metallurgy forging, Figure 2.0211.

2.0212 Effect of repress (forging) pressure and temperature on density of powder metallurgy forging, Figure 2.0212.

2.022 Electrical properties.

2.0221 Electrical resistivity as a function ot temperature, Figure 2.0221.

2.023 Magnetic properties, ferromagnetic.

2.024 Emittance.

2.025 Damping capacity.

2.0251 Effect of number of cycles in reversed bending and maximum cyclic tensile strain (Em) on damping capacity, Figure 2.0251.

2.03 **Chemical Properties**

2.031 Type 4130 is susceptible to general corrosion – rusting and pitting – and to stress corrosion, particularly in industrial and marine environments. For most applications it should be protected by suitable electroplating, paint, or a combination of both (21). Corrosion rate in seawater decreases at least by 50 percent with exposure from 1 year to 3-1/2 years, and the rate at a depth of 5500 feet is less than half that in surface waters (67).

2.032 Stress corrosion of cadmium-plated bar and sheet subjected to alternate immersions (10 minutes in and 50 minutes out) in 3-1/2 percent solution of sodium chloride having pH of 6.8 to 7.2, Table 2.032.

2.033 Type 4130 is resistant to corrosion by pure fluorinated hydrocarbons, such as Propellants 113 and 114B2 (Freon-113 and Freon-114B2), which are used as solvents and refrigerants as well as propellants. In the presence of small amounts of moisture, however, these types of hydrocarbons significantly attack the alloy (37).

2.034 Effect of temperature and chloride concentration on "break point" of sheet in two-point bend test, Table 2.034.

2.035 Effect of sulfur hexafluoride (SF_6) on tensile properties (see Section 3.02121).

2.036 Effect of yield strength and flaw depth on threshold stress intensity (K_{Iscc}) (see Figure 3.02725).

3 **MECHANICAL PROPERTIES**

3.01 **Specified Mechanical Properties**
Table 3.01.

3.02 **Mechanical Properties at Room Temperature**

3.021 Tension – stress-strain diagrams – tension properties.

3.0211 Stress-strain curves (see Figure 3.0311).

3.0212 Tensile properties of round bar in various heat-treated conditions, Table 3.0212.

3.0213 Tensile properties of plate in various heat-treated conditions, Table 3.0213.

3.0214 Tensile properties of 3/8 inch plate heat treated to various hardnesses, Table 3.0214.

3.0215 Tensile properties of extruded round bar in various heat-treated conditions, Table 3.0215.

3.0216 Tensile properties of extruded flat bar in various heat-treated conditions, Table 3.0216.

3.0217 Tensile properties of castings in various heat-treated conditions, Table 3.0217.

3.0218 Effect of tempering temperature on room-temperature tensile properties of 0.530 inch bar, Figure 3.0218.

3.0219 Effect of tempering temperature on tensile properties of oil-quenched and water-quenched 1 inch bar, Figure 3.0219.

3.02110 Effect of sheet thickness and tempering temperature on tensile properties, Table 3.02110.

3.02111 Effect of austenitizing temperature and quench medium on tensile properties of as-quenched material, Table 3.02111.

3.02112 Effect of quench medium and tempering temperature on tensile properties of rolled bar, Table 3.02112.

3.02113 Effect of quench medium on tensile properties of sheet, Table 3.02113.

3.02114 Effect of bar diameter on tensile properties in various heat-treated conditions, Figure 3.02114.

3.02115 Tensile properties of quenched and tempered round bar, Figure 3.02115.

3.02116 Effect of explosive forming on tensile properties of plate, Table 3.02116.

3.02117 Effect of fabrication process on tensile properties of powder metallurgy forging, Table 3.02117.

3.02118 Effect of repress (forging) pressure and temperature on ultimate tensile strength of powder metallurgy forging, Figure 3.02118.

3.02119 Effect of Mn plating and elevated temperature exposure on tensile properties of sheet, Table 3.02119.

3.02120 Temperature limits for prolonged unstressed exposure which prevent degradation of tensile strength, Table 3.02120.

3.02121 Exposure to sulfur hexafluoride (SF_6) at a temperature of 440 F and a pressure of 525 psi for up to 24 hours does not degrade the tensile ultimate (F_{tu}) and yield (F_{ty}) strengths of 0.094-inch-thick sheet (64).

3.022 Compression – stress-strain diagrams – compression properties.

3.0221 Stress-strain curves (see Figure 3.0321).

3.0222 Compressive yield strength (see Figure 3.0322).

3.023 Impact.

3.0231 Impact properties of extruded bar, Table 3.0231.

3.0232 Effect of tempering temperature on room-temperature impact strength, Figure 3.0232.

3.0233	Impact resistance of normalized and annealed material, Table 3.0233.
3.0234	Effect of quench medium and tempering temperature on impact properties of rolled bar, Figure 3.0234.
3.0235	Effect of fabrication process and temperature on impact properties of powder metallurgy forging, Table 3.0235.
3.0236	Effect of repress (forging) pressure and temperature on impact properties of powder metallurgy forging, Figure 3.0236.
3.0237	Effect of carburization on impact properties, Figure 3.0237.
3.024	Bending.
3.025	Torsion and shear.
3.0251	Shear strength (see Figures 3.0351 and 3.0352).
3.026	Bearing.
3.0261	Bearing strength (see Figures 3.0361 and 3.0362).
3.027	Stress concentration.
3.0271	Notch properties.
3.02711	Effect of initial crack length ($2\ a_0$) on residual strength (maximum load divided by gross cross-sectional area) of sheet after two different tempering treatments, Figure 3.02711.
3.02712	Effect of temperature on slow-crack-growth rate in gaseous hydrogen, Figure 3.02712.
3.02713	Effect of hydrogen pressure on slow-crack-growth rate, Figure 3.02713.
3.0272	Fracture toughness.
3.02721	Plane-strain fracture toughness of material heat treated to 158 ksi yield (F_{ty}) strength is 100 ksi $\sqrt{in.}$ when tested in three-point loading (73).
3.02722	Effect of sheet thickness on fracture-toughness parameter K_c, Table 3.02722.
3.02723	Effect of yield strength on fracture resistance of sheet, Figure 3.02723.
3.02724	Effect of tempering temperature, carbon content, and quenching medium on plane-strain fracture toughness of flat rolled bar, Figure 3.02724.
3.02725	Effect of yield strength and flaw depth on threshold stress intensity in static loading, Figure 3.02725 (58).
3.02726	Effect of hydrogen pressure and displacement rate on initiation of slow crack growth, K_{Iscg} (embrittlement), Figure 3.02726.
3.02727	Effect of hydrogen pressure on the arrest of crack propagation, Table 3.02727.
3.028	Combined properties.
3.03	**Mechanical Properties at Various Temperatures**
3.031	Tension – stress-strain diagrams – tension properties.
3.0311	Tensile stress-strain curves for sheet at temperatures up to 1000 F after three different tempering treatments; curves apply to specimens held for 0.5 hour up to 100 hours at test temperature, Figure 3.0311.
3.0312	Effect of temperature on tensile properties of sheet after three different tempering treatments and two different exposure times, Figure 3.0312.
3.0313	Effect of temperature and strain rate on tensile properties of normalized sheet after rapid heating; data pertain to specimens held for 10 seconds up to 1/2 hour at test temperature, Figure 3.0313.
3.0314	Effect of temperature and strain rate on tensile properties of heat-treated sheet after rapid heating; data pertain to specimens held for 10 seconds up to 1/2 hour at test temperature, Figure 3.0314.
3.0315	Effect of temperature on tensile properties of sheet after 5-minute soak at temperature, Figure 3.0315.
3.0316	Effect of short-time exposure to elevated temperature on tensile properties of sheet, Figure 3.0316.
3.0317	Effect of prior exposure to test temperature up to 10 hours on tensile properties, Figure 3.0317.
3.032	Compression – stress-strain diagrams – compression properties.
3.0321	Compressive stress-strain curves for sheet at temperatures up to 1000 F after three different tempering treatments; curves apply to specimens held for 1/2 up to 100 hours at test temperatures, Figure 3.0321.
3.0322	Effect of temperature on compressive yield strength of sheet after three different tempering treatments and two different holding times, Figure 3.0322.
3.033	Impact.
3.0331	Effect of grain size and temperature on impact properties, Figure 3.0331.
3.0332	Effect of low temperatures on impact properties in several heat-treated conditions, Figure 3.0332.
3.0333	Effect of low temperatures on impact properties of pipe, Figure 3.0333.
3.0334	Effect of temperature on impact properties of explosively formed and rolled and annealed plate, Figure 3.0334.
3.0335	Effect of temperature on impact properties of explosively formed and cold-rolled heat-treated plate, Figure 3.0335.
3.034	Bending.
3.035	Torsion and shear.
3.0351	Effect of temperature on shear strength of sheet after three different tempering treatments and two different exposure times, Figure 3.0351.
3.0352	Effect of temperature on shear strength of normalized and of cold-worked-and-stress-relieved Type 4130, Figure 3.0352.
3.0353	Effect of prior test temperature exposure up to 10 hours on shear properties, Figure 3.0353.
3.036	Bearing.
3.0361	Effect of temperature on bearing strength (e/D = 2) of sheet after three different tempering treatments and two different exposure times, Figure 3.0361.
3.0362	Effect of temperature on bearing strength (e/D = 1.5) of sheet after three different tempering treatments, Figure 3.0362.
3.0363	Effect of prior test temperature exposure up to 10 hours on bearing properties, Figure 3.0363.
3.037	Stress concentration.
3.0371	Notch properties.
3.03711	Comparison of tensile ultimate (F_{tu}) and yield (F_{ty}) strengths with crack strength (net fracture stress) and fracture appearance of shear-cracked sheet specimens quenched and tempered at 825 F, Figure 3.03711.
3.03712	Comparison of tensile ultimate (F_{tu}) and yield (F_{ty}) strengths with crack strength (net fracture stress) and fracture appearance of shear-cracked sheet specimens quenched and tempered at 400 F, Figure 3.03712.

Fe
0.3 C
0.95 Cr
0.2 Mo

4130

Fe
0.3 C
0.95 Cr
0.2 Mo

4130

3.03713 Effect of temperature and loading rate on crack strength (net fracture stress) and fracture appearance of fatigue cracked sheet specimens quenched and tempered at 400 F, Figure 3.03713.

3.03714 Effect of temperature on crack strength (net fracture stress) and fracture appearance of both fatigue-cracked and shear-cracked sheet specimens quenched and tempered at 825 F, Figure 3.03714.

3.0372 Fracture toughness.

3.038 Combined properties.

3.04 **Creep and Creep Rupture Properties**

3.041 Creep-rupture curves from 700 to 1100 F, Figure 3.041.

3.042 Creep-rupture and minimum-creep-rate characteristics of normalized sheet at 1000 and 1200 F, Figure 3.042.

3.05 **Fatigue Properties**

3.051 Fatigue life as a function of cyclic strain for Type 4130 tempered at 1200 F, Figure 3.051.

3.052 Fatigue life as a function of cyclic strain for Type 4130 tempered at 750 F, Figure 3.052.

3.053 Effect of maximum cyclic tensile strain on fatigue life in reversed bending, Figure 3.053.

3.054 Fatigue-crack growth rate as a function of maximum cyclic stress intensity factor (K) for center cracked specimens, Figure 3.054.

3.055 Fatigue-crack-growth rate in air and vacuum as a function of stress intensity amplitude (ΔK) for compact tension specimen, Figure 3.055.

3.056 Effect of prestressing and removal of surface-layer stress by thermal relaxation on fatigue crack growth rate of plate, Figure 3.056.

3.057 Effect of prestressing and chem-milling on fatigue crack growth rate of sheet, Figure 3.057.

3.058 S-N curve at room temperature in rotating bending, Figure 3.058.

3.059 Comparison of axial-loading and rotating-beam-bending fatigue data, Figure 3.059.

3.0510 Axial-stress S-N curves for edge-notched specimens, Figure 3.0510.

3.0511 Effect of temper treatment (measured by Rockwell hardness) on repeated-bending fatigue properties, Figure 3.0511.

3.0512 Effect of temper treatment (measured by Rockwell hardness) on rotating-beam fatigue properties, Figure 3.0512.

3.0513 Effect of chromium coating on axial-stress fatigue properties of sheet, Figure 3.0513.

3.06 **Elastic Properties**

3.061 Poisson's ratio, 0.25 to 0.29 (22,36).

3.062 Modulus of elasticity.

3.0621 Effect of temperature on modulus of elasticity in tension and compression of sheet after three different tempering treatments, Figure 3.0621.

3.0622 Compressive tangent modulus curves for sheet after three different tempering treatments, Figure 3.0622.

3.063 Modulus of rigidity.

4 FABRICATION

4.01 **Formability**

4.011 In the annealed condition, Type 4130 has good cold formability for a heat-treatable alloy steel; but its cold formability, of course, does not approach that of a low-carbon steel.

4.012 Its hot formability is excellent. All forging should be done within the temperature range 2250 to 1800 F; the optimum forging range is 2200 to 2000 F. Parts should be slow cooled in air or other appropriate environment after hot forming (30,35).

4.013 Effect of temperature on formability of sheet, Figure 4.013.

4.02 **Machining and Grinding**

4.021 Type 4130 can be readily machined in the annealed, normalized, and cold-drawn conditions. In the cold-drawn condition, which provides optimum machinability for this alloy, machinability is 60 to 70 percent of that of AISI B1112 screw stock.

4.03 **Welding**

4.031 Type 4130 has good weldability by oxyacetylene techniques and by any of the automatic or manual electric-arc processes. In oxyacetylene welding, the filler metal should be the same alloy as the base metal. In arc-welding, low-hydrogen low-alloy electrodes should be used. Although good welded properties can be obtained without thermal treatment, preheating to about 400 F and post-weld tempering are recommended when possible for improved weld properties. If complete quench and temper heat treatment can be carried out after welding, joint efficiencies approaching 100 percent can be obtained.

4.032 Tensile properties of parent metal and of 0.5 inch thick plate with butt weld as the center of the specimen gage length, Table 4.032.

4.033 Charpy V-notch impact properties at -65 F of butt-welded 0.50-inch-thick plate, Table 4.033.

4.034 Tensile properties of sheet butt welded by various arc processes, Table 4.034.

4.035 Tensile properties of butt-welded sheet, Table 4.035.

4.036 Effect of electrode alloy and sheet or plate thickness on tensile ultimate strength of bead-off butt welds, Table 4.036.

4.037 Effect of electrode alloy and sheet or plate thickness on shear ultimate strength of longitudinal-weld lap joints, Table 4.037.

4.038 Tensile and shear ultimate-strength design curves for sheet and plate welds heat treated to either 150 or 175 ksi, Figure 4.038.

4.039 Constant-life diagram for an axial-loaded tube splice – stresses calculated in the large tube, Figure 4.039.

4.0310 Constant-life diagram for an axial-loaded tube splice – stresses calculated in the small tube, Figure 4.0310.

4.04 **Surface Treatments**

4.041 With proper surface preparation, protective coatings of paint and electroplating can be applied with excellent results.

REFERENCES

1 AMS 5336D (July 1, 1984).
2 AMS 6348 (October 15, 1979).
3 AMS 6350F (October 16, 1978).
4 AMS 6351C (July 16, 1979).
5 AMS 6356C (April 1, 1983).
6 AMS 6360G (January 15, 1977).
7 AMS 6361B (October 1, 1984).
8 AMS 6362C (January 1, 1985).
9 AMS 6370J (October 1, 1983).
10 AMS 6371F (October 15, 1979).
11 AMS 6373B (July 15, 1978).
12 AMS 6374 (July 1, 1985).
13 AMS 6457 (October 15, 1979).
14 Melonas, J. V., and Kattus, J. R., "Determination of Tensile, Compressive, Bearing, and Shear Properties of Ferrous and Non-Ferrous Structural Sheet Metals at Elevated Temperatures", Southern Research Institute, WADC TR56-340, ASTIA Document No. AD 131 069 (September 1957).
15 Morrison, J. D., and Kattus, J. R., "Tensile Properties of Aircraft-Structural Metals at Various Rates of Loading After Rapid Heating", Southern Research Institute, WADC TR 55-199, Part 2, ASTIA Document No. AD 110 540 (November 1956).
16 "Modern Steels and Their Properties", Seventh Edition, Handbook 2757, Bethlehem Steel Corp. (1972).
17 Sullivan, A. M., and Freed, C. N., "Plane Stress Fracture Resistance of One Sheet Steel and Two Titanium Sheet Alloys", Naval Research Laboratory Report 7332 (October 27, 1971).
18 Simmons, W. F., and Cross, H. C., "Elevated Temperature Properties of Wrought Medium-Carbon Alloy Steels", ASTM STP No. 199 (1957).
19 Cataldo, C. E., "Compatibility of Metals With Hydrogen", NASA TM X-53807, George C. Marshall Space Flight Center (December 26, 1968).
20 Groeneveld, T. P., Fletcher, E. E., Elsea, A. R., "A Review of the Literature on Cleaning, Pickling, and Electroplating Processes and Relief Treatments to Minimize Hydrogen Embrittlement of Ultrahigh-Strength Steels", Battelle Memorial Institute (October 15, 1966).
21 Nelson, E. E., "Stress Corrosion Cracking of Several High Strength Ferrous and Nickel Alloys", NASA TMX-64626, George C. Marshall Space Flight Center (November 11, 1971).
22 Smith, R. W., Hirschberg, M. H., and Manson, S. S., "Fatigue Behavior of Materials Under Strain Cycling in Low and Intermediate Life Range", NASA TN D-1574, Lewis Research Center (October 10, 1962).
23 Horsley, J. J., "Stress Intensity Factors for Selected Alloys", the Boeing Company, No. D3-7326 (April 26, 1968).
24 Blatherwick, A. A., and Mowbray, D. F., "Cyclic Plasticity Effects in Intermediate and Low Cycle Fatigue", AFML ML-TDR-64-120, University of Minnesota (May 1964).
25 Kramer, I. R., and Kumar, A., "Effect of Vacuum Environment on Mechanical Behavior", AFOSR-TR-72-0734, Martin Marietta Corporation (February 1972).
26 Goldman, M., "An Evaluation of Four Heat Treated Conditions of 4130 Steel for Low Temperature Application", Goodyear Aircraft Corp., Serial No. 8753 (June 16, 1958).
27 Haugen, E. B., "Statistical Strength Properties of Common Metal Alloys", North American Aviation, Inc., SID 65-1274 (October 30, 1965).
28 "Cross-Index of Chemically Similar Specifications and Identification Code", MIL-HDBK-H1D (June 22, 1970).
29 "Summary of Steel Castings Specifications", Steel Founders' Society of America (January 1, 1971).
30 "AISI 4130", Alloy Digest, Filing Code: SA-23 (November 1954).
31 Data supplied by C. J. Cooley, American Iron and Steel Institute (June 18, 1973).
32 Rolfe, S. T., and Novak, S. R., "Slow-Bend K_{Ic} Testing of Medium-Strength High-Toughness Steels", ASTM STP 463 (1970).
33 Metals Handbook, Vol 1, 8th Edition, ASM (1961).
34 "Atlas of Isothermal Transformation Diagrams", U.S. Steel Corporation (1951).
35 "Mechanical Properties of Alloy Steel", Republic Steel Corporation (1961).
36 North American Aviation Data Sheet on Alloy Steel – AISI 4130, Al-2604.
37 Jackson, J. D., and Boyd, W. R., "Compatibility of Propellants 113 and 114B2 With Aerospace Structural Materials", DMIC Memorandum 151 (April 27, 1962).
38 Morrison, J. D., and Kattus, J. R., "An Investigation of Methods for Determining the Crack-Propagation Resistance of High-Strength Alloys", Southern Research Institute, Bureau Naval Weapons Contract NOas61-0392-d (February 1962).
39 Morrison, J. D., Jenkins, P. C., and Kattus, J. R., "An Investigation of the Crack-Propagation Resistance of High-Strength Alloys and Heat-Resistant Alloys", Southern Research Institute, Bureau Naval Weapons Contract NOw 61-0392-d (October 23, 1962).
40 Babcock & Wilcox Company, Data Sheet on 4140, 4130, and 410 Steels (1962).
41 Manson, S. S., Nachtigall, A. J., and Freche, J. C., "A Proposed New Relation for Cumulative Fatigue Damage in Bending", Proc. ASTM, Vol 61 (1961).
42 Lange, E. A., and Cooley, L. A., "Fracture Control Plans for Critical Structural Materials Used in Deep-Hole Experiments", Naval Research Laboratory Memorandum Report 2497 (September 1972).
43 Ashauer, R. C., Goodman, S., Rienks, F., and McMaster, J. A., "A Study of Pulsed Arc Welding Applied to Aerospace Alloys", AFML TR-69-332 (December 1960).
44 Sinnott, M. T., "Fatigue Properties of Chromium-Plated Heat-Treated SAE 4130 Steel", Engineering Research Institute, University of Michigan, Ann Arbor (September 1, 1951).
45 "Mechanical Test Results on Various Extruded Materials", Allegheny Ludlum Steel Corporation (January 1, 1956).
46 Westerman, R. E., and Sump, K. R., "Properties of Prealloyed Steel Powder Metallurgy Products – Final Report", Battelle Pacific Northwest

Fe
0.3 C
0.95 Cr
0.2 Mo

4130

Fe
0.3 C
0.95 Cr
0.2 Mo

4130

Laboratories for U.S. Army Weapons Command Contract MIPR A1-1-50248-M1-Ws (December 1972).

47 Troiano, A. R., and Hehemann, R. F., "Hydrogen Sulfide Stress Corrosion Cracking in Materials for Geothermal Power", Materials Performance (January 1979).

48 Paine, R. M., and Stonehouse, A. J., "A Corrosion Protection System for Beryllium in Aircraft Brake Applications", Materials Performance (August 1977).

49 Oberg, T. T., and Rooney, R. J., "Reversed Bending Fatigue Characteristics of Steel and High Strength Aluminum Alloys as Affected by Type of Specimen", U.S. Air Force Air Materiel Command Technical Report No. 5775 (July 1949).

50 Parker, E. R., and Zackay, V. F., "Microstructural Features Affecting Fracture Toughness of High Strength Steels", Engineering Fracture Mechanics, Vol 7 (1975).

51 Wood, W. E., Parker, E. R., and Zackay, V. F., "An Investigation of Metallurgical Factors Which Affect Fracture Toughness of Ultra-High Strength Steels", Army Materials and Mechanics Research Center Report No. CTR 73-24, Lawrence Berkeley Laboratory, University of California (May 1973).

52 McCall, J. L., "Metallography of Vacuum Brazed and Vacuum Heat Treated and Gas Quenched Materials", Welding Journal, Welding Research Supplement (February 1972).

53 "Mechanical Properties at Elevated Temperatures of As-Received Materials", Boeing Airplane Company, Manufacturing Report No. MDR 2-28014 (April 4, 1964).

54 Otto, H. E., and Mikesell, R., "Thermal Properties of Explosively Formed High Strength Low Alloy Steels", presented at the Third International Conference of the Center for High Energy Forming, Vail, Colorado (July 12–16, 1971).

55 Cambell, C. M., "Short Time Tensile Properties of Low Alloy Steels at Elevated Temperatures", North American Aviation Inc., Report No. NA-47-825 (October 15, 1947).

56 Bertke, R. S., "Impact Damage on Various Metal Leading Edges From Small Hard Objects", University of Dayton for Air Force Wright Aeronautical Laboratories, Report No. AFWAL-TR-81-44066 (August 1981).

57 Smith, C. R., "Tests Suggest Coating May Extend Fatigue Life of Mechanical Joints", Assembly Engineering (February 1976).

58 Brown, B. F., "AFPA Coupling Program on Stress-Corrosion Cracking", Naval Research Laboratory, Report No. 7329 (October 27, 1971).

59 Kramer, I. R., and Kumar, A., "The Effects of Surface Layer on Plastic Deformation and Crack Propagation", Martin Marietta Corporation for Army Materials and Mechanics Research Center, Report No. AMMRC CR 71-2/2 (August 1971).

60 Soderberg, E. W., and Roth, R. E., "Low Current Plasma Welding", General Motors Allison Division for Air Force Materials Laboratory, Report No. AFML-TR-66-177 (July 1967).

61 Harris, F. G., and Rowan, R. W., "Axial Load Fatigue Tests on Chromium Molybdenum Steel Tubing With Welded Fish-Mouth Type Splices", Australian Defence Scientific Service Aeronautical Research Laboratories, Report No. ARL/SM 323 (March 1969).

62 Degnan, W. G., Dripchak, P. D., and Matusovich, "Fatigue Crack Propagation in Aircraft Materials", Sikorsky Aircraft for U.S. Army Aviation Materiel Laboratories, USAAVLABS Technical Report No. 66-9 (March 1966).

63 Moon, D. P., "Effect of Temperature on the Short-Time Strength Properties of AISI 4130 and AISI 4340 Steels", Battelle Memorial Institute, Defense Metals Information Center, Technical Note (February 4, 1970).

64 Kirby, C. E., and Ransone, P. O., "Preliminary Investigation of Effects of Exposure to Sulfur Hexafluoride on Tensile and Yield Strengths of Aluminum and Steel", Langley Research Center, NASA Technical Memorandum X-2333 (September 1971).

65 Manson, S. S., and Muralidharan, V., "Fatigue Life Prediction in Bending From Axial Fatigue Information", Case Western Reserve University, NASA CR-165563 (February 1982).

66 Williams, D. P., and Nelson, H. G., "Embrittlement of 4130 Steel by Low-Pressure Gaseous Hydrogen", Metallurgical Transactions, Vol 1 (January 1970).

67 Rynewicz, J., "Corrosion in the Deep Oceans", Ocean Engineering Petroleum Engineer Special Edition (November 15, 1974).

68 Sullivan, A. M., and Stoop, J., "Effect of Sheet Thickness on the Fracture-Resistance Parameter K_c of Steels", Naval Research Laboratory, Report 7601 (August 8, 1973).

69 Loginow, A. W., and Phelps, E. H., "Steel for Seamless Hydrogen Pressure Vessels", Corrosion-NACE (November 1975).

70 Convair Division, General Dynamics Corp., "Heat Treatable Welds in Steel Plate", Report No. ZS-194 (September 30, 1953).

71 Freed, C. N., Sullivan, A. M., and Stoop, J., "Influence of Dimensions of the Center-Cracked Tension Specimen on K_c", ASTM STP 514 (1972).

72 Nguyen-Duy, P., "Effects of Loading Rate and Temperature on Fracture Toughness of 4130 Quenched and Tempered Steel Using Precracked Charpy V-Notch Specimens", Fracture Mechanics: Fourteenth Symposium, Volume II: Testing and Applications, ASTM STP 791, J. C. Lewis and G. Sines, Eds., American Society for Testing and Materials (1983).

73 Campbell, J. E., "Plane-Strain Fracture-Toughness Data for Selected Metals and Alloys", Defense Metals Information Center, Report S-28, Battelle Memorial Institute (June 1969).

74 "Metals Handbook", 9th Edition, Vol 1, American Society for Metals (1978).

Fe
0.3 C
0.95 Cr
0.2 Mo

4130

Alloy	4130				
	Forms				
Sheet, Strip, Plate	Bars, Billets, Forgings	Pipe, Tube	Castings	Welding Wire	General
AMS 6350F	AMS 6348	AMS 6360G	AMS 5336D	AMS 6457	QQ-M-105b
AMS 6351C	AMS 6370J	AMS 6361B	MIL-S-22141		SAE 4130
AMS 6350C	QQ-S-621b	AMS 6362C	ASTM A487		SAE 4130H
QQ-S-626a	MIL-S-6758A	AMS 6371F			AISI 4130
QQ-S-627b	MIL-S-16974B	AMS 6373B			AISI 4130H
MIL-S-18729C	MIL-S-81242	AMS 6374			AISI TS4130
ASTM A505	ASTM A274	QQ-T-00825			AISI TS4130H
ASTM A507	ASTM A304	MIL-T-6736B			
ASTM A410	ASTM A322	ASTM A519			
	ASTM A372	ASTM A513			
	ASTM A322				
	ASTM A331				
	ASTM A274				
	ASTM A372				

TABLE 1.03. SPECIFICATIONS (1–13,28,29)

Alloy	4130							
Form	Wrought		Investment Castings (1)		Castings (29)		Welding Wire	
	Min	Max	Min	Max	Min	Max	Min	Max
Carbon	0.28[a]	0.33[a]	0.05	0.35	–	0.33	0.28	0.33
Manganese	0.40	0.60	0.40	0.80	0.60	1.00	0.40	0.60
Silicon	0.15[b]	0.35	–	1.00	–	0.80	0.15	0.35
Phosphorus	–	0.025	–	0.04	–	0.04	–	0.008[c]
Sulphur	–	0.025	–	0.04	–	0.045	–	0.008[c]
Chromium	0.80	1.10	0.80	1.10	0.75	1.10	0.80	1.10
Molybdenum	0.15	0.25	0.15	0.25	0.15	0.30	0.15	0.25
Nickel	–	0.25	–	0.25	–	0.50	–	0.25
Copper	–	0.35	–	0.25	–	–	–	0.10
Vanadium	–	–	–	–	–	–	–	0.06
Oxygen	–	–	–	–	–	–	–	0.0025
Nitrogen	–	–	–	–	–	–	–	0.005
Hydrogen	–	–	–	–	–	–	–	0.0010
Iron	Balance	Balance	Balance	Balance	Balance	Balance	Balance	Balance

(a) AMS 6336C gives 0.30 min and 0.35 max.
(b) AMS 6360G gives 0.20.
(c) Phosphorus + sulphur 0.012.

TABLE 1.04. COMPOSITION (1–13,29)

Fe
0.3 C
0.95 Cr
0.2 Mo

4130

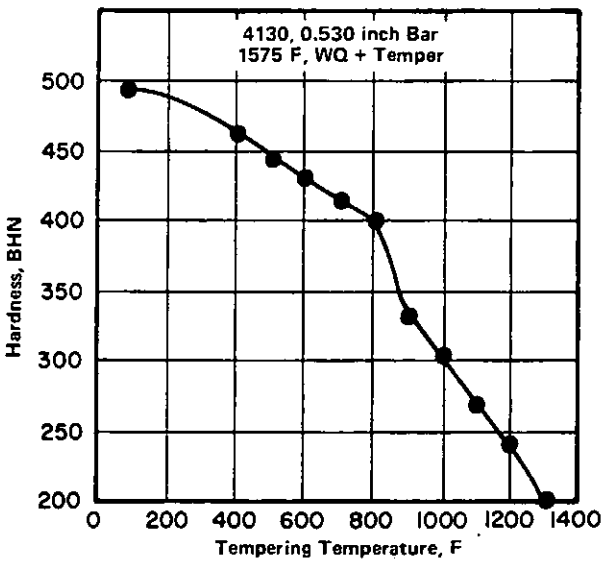


FIGURE 1.061. EFFECT OF TEMPERING TEMPERATURE ON HARDNESS OF BAR (16)

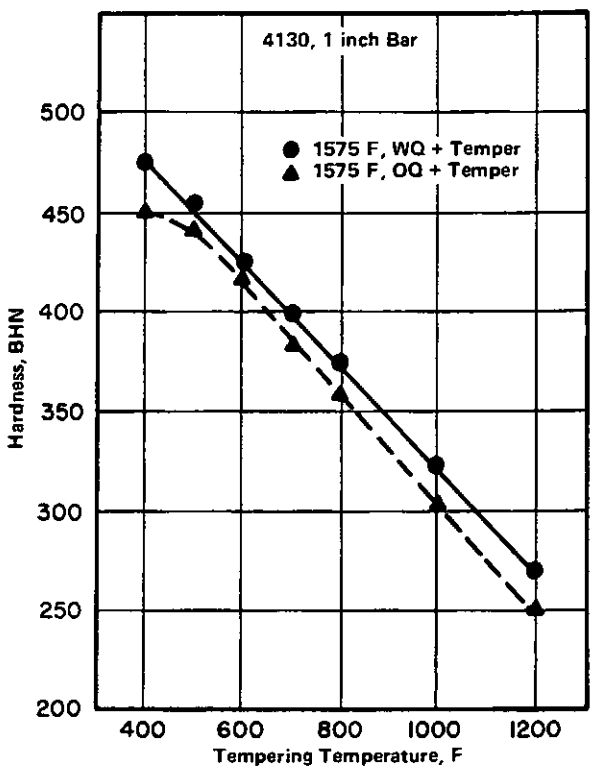


FIGURE 1.062. EFFECT OF TEMPERING TEMPERATURE ON HARDNESS OF OIL-QUENCHED AND WATER-QUENCHED BAR (30)

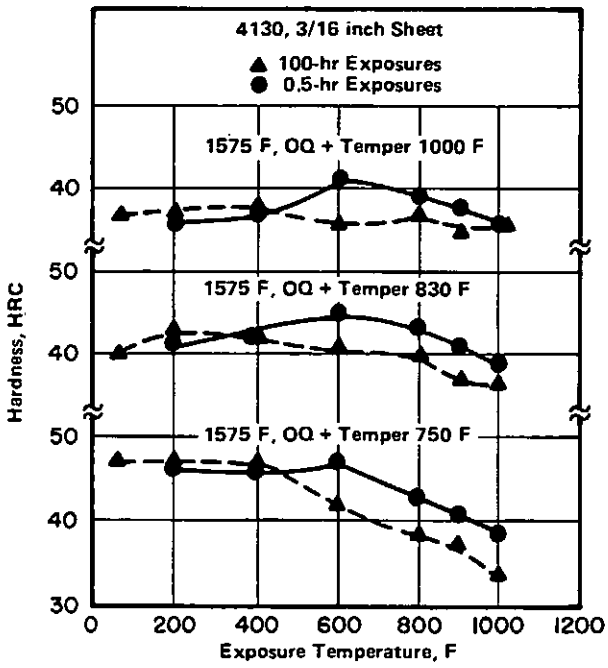


FIGURE 1.063. EFFECT OF EXPOSURES AT ELEVATED TEMPERATURES ON ROOM-TEMPERATURE HARDNESS OF SHEET AFTER THREE DIFFERENT TEMPERING TREATMENTS (14)

Fe
0.3 C
0.95 Cr
0.2 Mo

4130

Alloy	4130			
Form	Condition	Hardness		
		BHN	HRB	HRC
5/8 in. Diam Bar	Normalized 1550 F, WQ, tempered 800 F, 1 hr	–	–	40
1 in. Bar	Hot rolled:			
	As hot rolled	229	–	–
	Normalized 1600 F	207	–	–
	Annealed 1550 F	179	–	–
	Cold drawn:			
	As cold drawn	248	–	–
	Annealed 1550 F	201	–	–
0.50 in. Plate	Normalized 1600 F	–	–	14
	Normalized + tempered 1100 F	–	–	12
	Oil quenched + tempered 1000 F	–	–	34
	Oil quenched + tempered 1200 F	–	–	22
1 in. Diam Extruded Bar, Allegheny Ludlum Steel	Annealed 1550 F, 1 hr + slow cool	–	80	–
	Normalized 1575 F, 1 hr, OQ and			
	Temper 850 F, 2 hr	–	–	32
	Temper 1200 F, 2 hr	–	88	–
3/4 x 3-1/8 in. Extruded Flat Allegheny Ludlum Steel	Normalized 1650 F, 1 hr	–	92	–
	Annealed 1550 F, 1 hr	–	76	–
	Normalized 1575 F, 1 hr, OQ +			
	Tempered 850 F, 2 hr	–	–	29
	Tempered 1200 F, 2 hr	–	93	–
0.063 in. Sheet	Austenitized 1575 F, 1 hr, WQ + temper 700 F, 1/2 hr, air cool	–	–	41
	Austenitized 1575 F, 1/2 hr, WQ + temper 500 F, 1/2 hr, air cool	–	–	46

TABLE 1.064. HARDNESS OF BAR, PLATE, SHEET AND EXTRUSION IN VARIOUS HEAT-TREATED CONDITIONS (11,26,30,44,45)

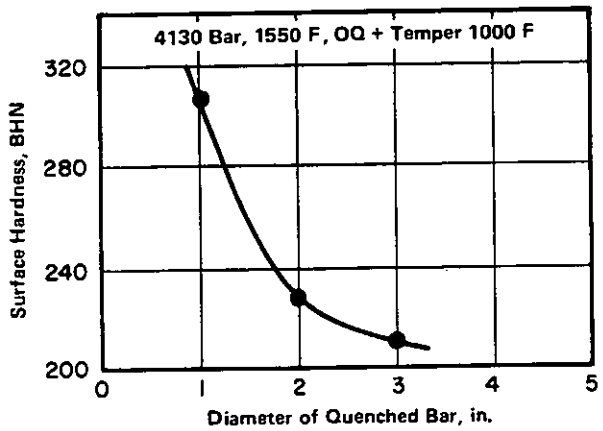


FIGURE 1.065. EFFECT OF DIAMETER ON SURFACE HARDNESS OF QUENCHED-AND-TEMPERED BARS (30)

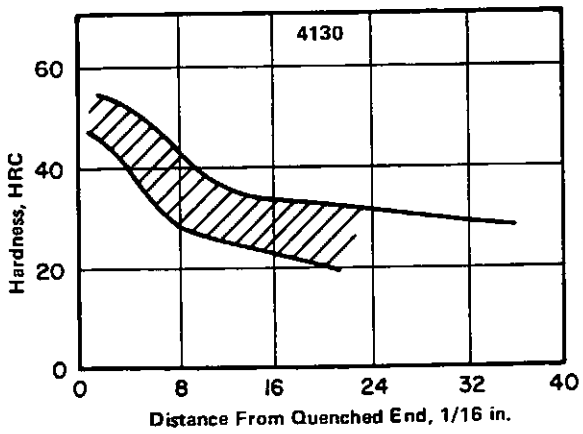


FIGURE 1.066. END-QUENCH HARDENABILITY (33)

	Fe
0.3	C
0.95	Cr
0.2	Mo

4130

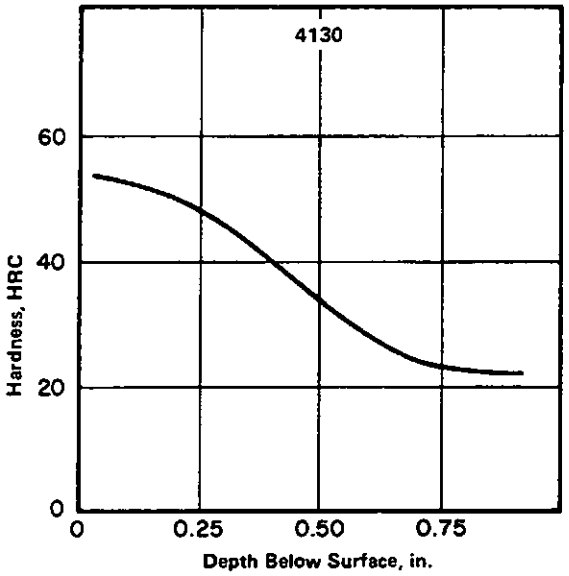


FIGURE 1.067. HARDNESS PROFILE THROUGH NITRIDED CASE (74)

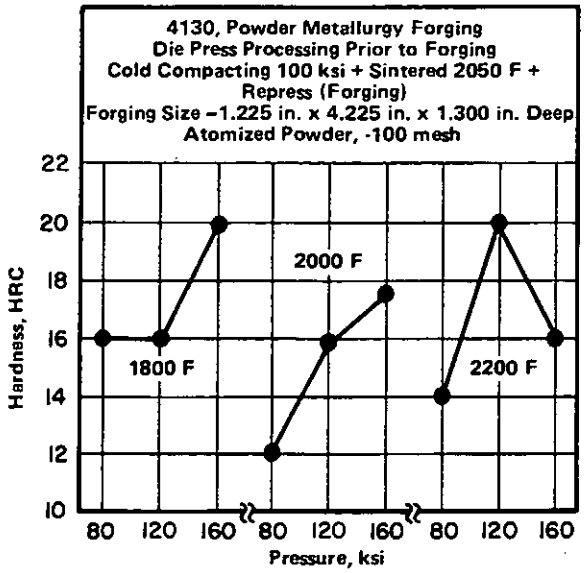


FIGURE 1.068. EFFECT OF REPRESS (FORGING) PRESSURE AND TEMPERATURE ON HARDNESS OF POWDER METALLURGY FORGING (46)

Alloy	4130					
Form	Powder Metallurgy Forgings, Die Press Process – 1.125 x 4.225 x 3.000 inch Deep, Isostatic Press Process – 0.565 x 4.000 x 1.300 inch Deep, High Energy Rate Forming (HERF), 2.5 inch Diameter x 5.5 inch Long Water Atomized Powder, -100 Mesh					
Condition	Austenitized 1575 F, RT Water Quench, Tempered 800 F, 1 hr					
	Compacting		Sinter	Repress (Forging)		
Process	Temperature, F	Pressure, ksi	Temperature, F(a)	Temperature, F	Pressure, ksi	Hardness, HRC
Die Press	RT	100	2050	2200	150	31
Isostatic	RT	50	1650	2200	150	39
HERF	–	–	–	2200	275	35

(a) For 1 hour.

TABLE 1.069. EFFECT OF FABRICATION PROCESS ON HARDNESS PROPERTIES OF POWDER METALLURGY FORGING (46)

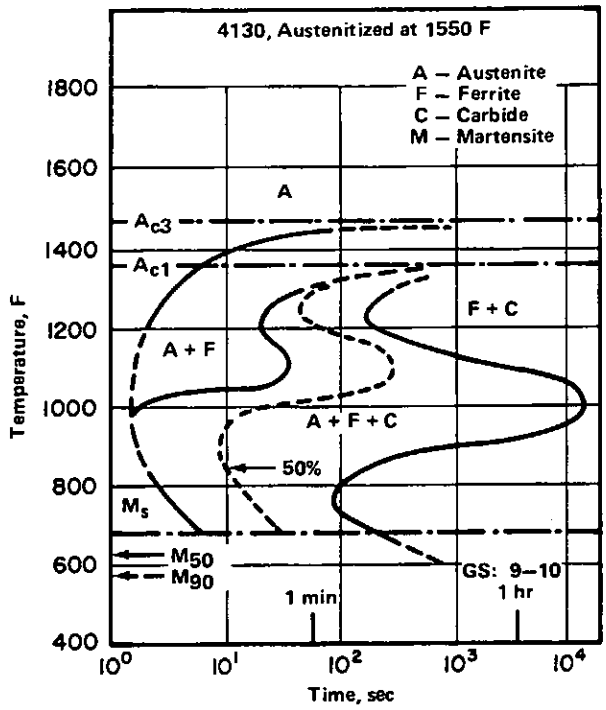


FIGURE 2.0121. TIME-TEMPERATURE-TRANSFORMATION DIAGRAM (34)

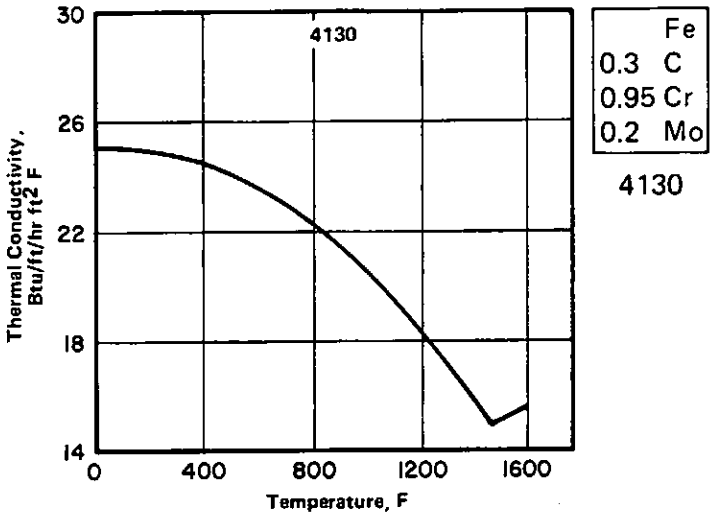


FIGURE 2.013. THERMAL CONDUCTIVITY (36)

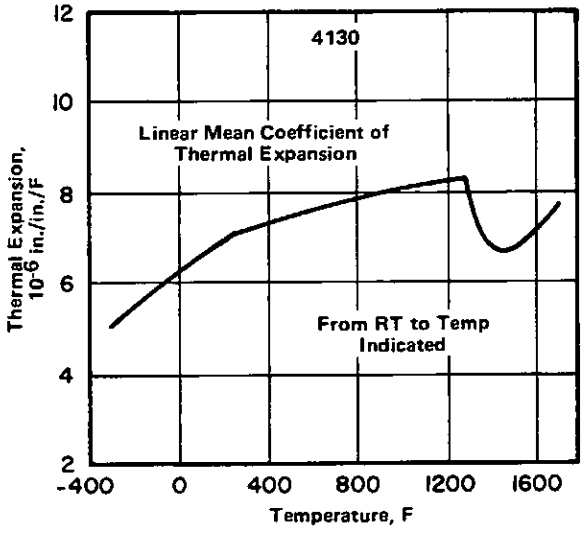


FIGURE 2.014. THERMAL EXPANSION (36)

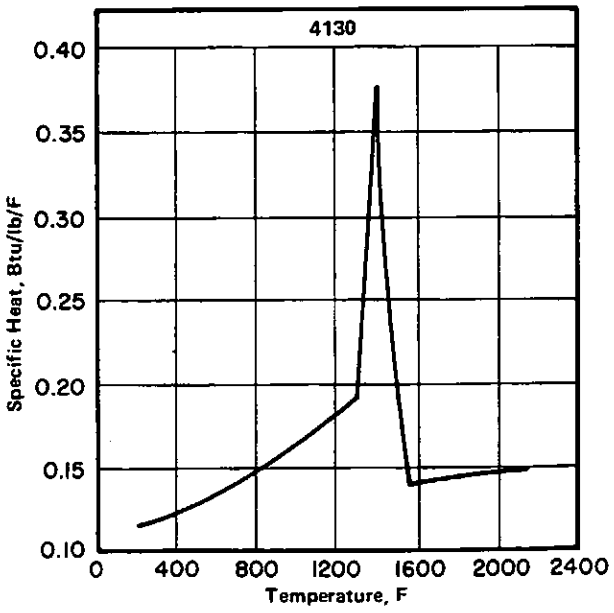


FIGURE 2.015. SPECIFIC HEAT (36)

Fe
0.3 C
0.95 Cr
0.2 Mo

4130

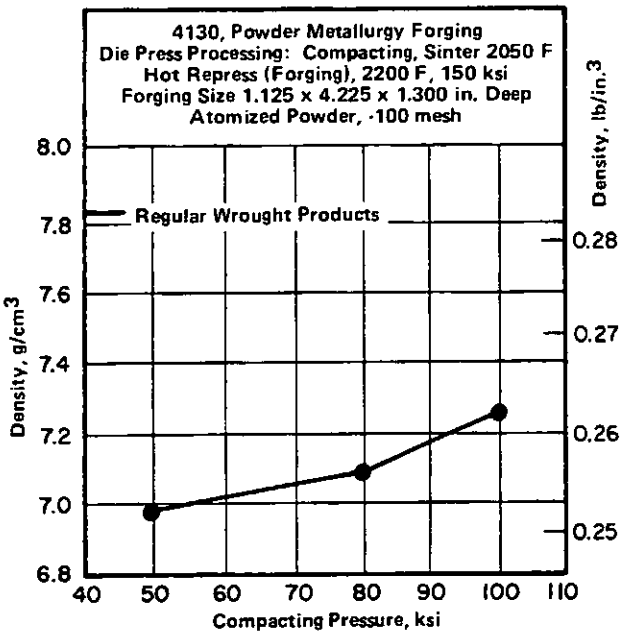


FIGURE 2.0211. EFFECT OF INITIAL COMPACTING PRESSURE ON DENSITY OF POWDER METALLURGY FORGING (46)

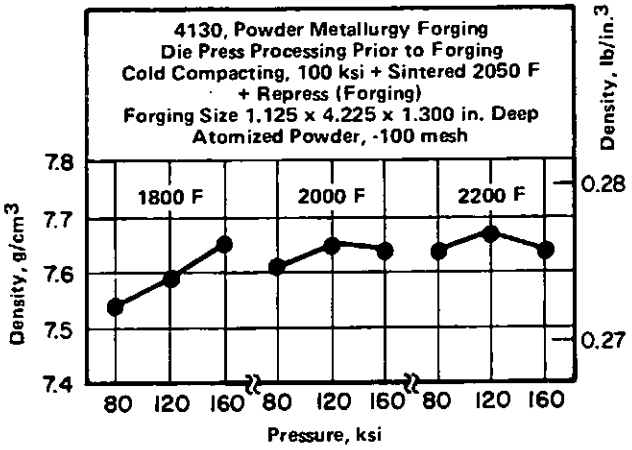


FIGURE 2.0212. EFFECT OF REPRESS (FORGING) PRESSURE AND TEMPERATURE ON DENSITY OF POWDER METALLURGY FORGING (46)

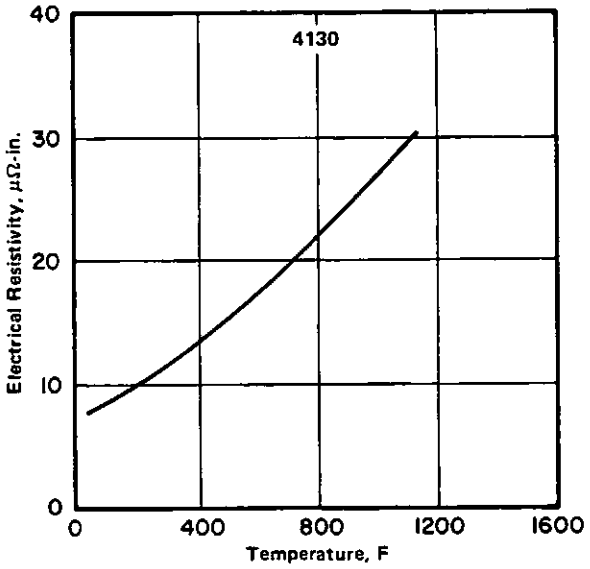


FIGURE 2.0221. ELECTRICAL RESISTIVITY AS A FUNCTION OF TEMPERATURE (36)

Fe
0.3 C
0.95 Cr
0.2 Mo

4130

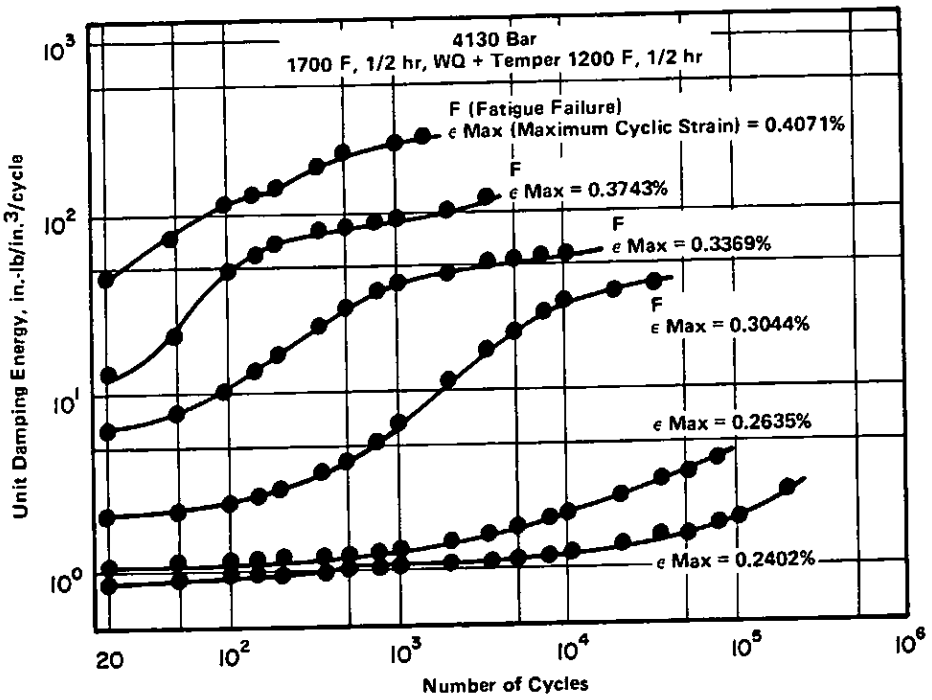


FIGURE 2.0251. EFFECT OF NUMBER OF CYCLES IN REVERSED BENDING AND MAXIMUM CYCLIC TENSILE STRAIN (ϵ MAX) ON DAMPING CAPACITY (24)

Alloy	4130					
Form	Condition	Orientation	F_{ty}, ksi	Applied Stress, ksi	No. Specimens	Days to Failure
2-1/2 inch Diam Bar	A(a)	T	155	116	3	–(c)
			155	155	3	–
		L	154	116	3	–
			154	154	3	–
	B(b)	T	161	121	3	–
			161	161	3	–
		L	148	111	3	–
			148	148	3	–
0.060 inch Sheet	A	T	142	107	3	–
			142	142	3	–
		L	147	110	3	–
			147	147	3	–
	B	T	171	124	3	–
			171	171	3	109,134, 144
		L	171	128	3	–
			171	171	3	28,56

(a) 1575 F, WQ + temper 900 F.
(b) 1575 F, WQ + temper 800 F.
(c) No cracking in maximum exposure time of 180 days.

TABLE 2.032. STRESS CORROSION OF CADMIUM-PLATED BAR AND SHEET SUBJECTED TO ALTERNATE IMMERSIONS (10 MINUTES IN AND 50 MINUTES OUT) IN 3.5 PERCENT SOLUTION OF SODIUM CHLORIDE HAVING pH OF 6.8 TO 7.2 (21)

Fe
0.3 C
0.95 Cr
0.2 Mo

4130

Alloy	4130	
Form	0.035 inch Sheet	
Condition	Normalized and Tempered to Various Yield Strengths	
Specimen Orientation	L	
Temperature, F	Chloride Concentration[a], percent	Yield Strength Break Point[b], ksi
78	0	113
	1	110
	5	110
	20	118
215	5	140
	20	142
425	5	140
	20	138

(a) Modified NACE Solution, which is deaerated aqueous solution of 5% NaCl, 0.5% acetic acid, saturated with a continuous flow of H_2S.

(b) "Break Point" is the highest value of RT yield strength which survived the environment when loaded to approximately its yield strength in a two-point bend test (ASTM G39-73). The yield strengths were varied in the range 100 to 150 ksi by using different tempering times and temperatures.

TABLE 2.034. EFFECT OF TEMPERATURE AND CHLORIDE CONCENTRATION ON "BREAK POINT" OF SHEET IN TWO-POINT BEND TEST (47)

Fe
0.3 C
0.95 Cr
0.2 Mo

4130

Alloy	4130							
			F_{ty}, ksi	F_{tu}, ksi	e (2 in.), percent	RA, percent	Hardness	
Source	Form	Condition	(Min)	(Min)	(Min)	(Min)	Min	Max
AMS 5336D (1)	Casting, investment	Normalized or normalized and tempered Plus: 1600 F ≥ 30 min, OQ, temper at 825 F ≥ 1 hr, air cool, 2nd temper 825 F ≥ 1 hr, air cool	125(a)	150(a)	5(a)	10(a)	30 HRC 32 HRC(b)	– 38 HRC(b)
AMS 6350F (3)	Sheet, strip Plate <0.250 in. sheet, strip, plate	Annealed Hot rolled or annealed 1600 F, OQ + 900 F, 30 min	– – –	– – 125	– – –	– – –	– – 26 HRC	98 HRB 25 HRC –
AMS 6351C (4)	Sheet, strip, plate <0.250 in. sheet, strip, plate	Spheroidized 1600 F, OQ + 900 F, 30 min	– –	– 125	– –	– –	– 26 HRC	85 HRB –
AMS 6356C (5)	Sheet and strip Plate	Cold finished and annealed or hot rolled and annealed Hot rolled, annealed if necessary	– –	– –	– –	– –	– –	95 HRB 95 HRB
AMS 6360G (6)	Tube: Up to 0.500 in. OD <0.1881 in. wall >0.188 in. wall 0.500 in. and over OD <0.1881 in. wall >0.188 in. wall	Cold drawn and stress relieved or normalized	 75 70 75 70	 95 90 95 90	 10 10 12(c) 15(c)	 – – – –	 – – – –	 – – – –
AMS 6361B (7)	Tube	1550 F, Q + temper	100	125	12(c)	–	–	–
AMS 6362C (8)	Tube	1550 F, Q + temper	135	150	10(c)	–	–	–
AMS 6770J (9)	Bars 0.500 in. diam and under Over 0.500 in. diam Over 0.500 in. diam	Cold finished Hot finished Cold finished	130 (Max) – –	– – –	– – –	– – –	– – –	– 229 BHN 241 BHN
AMS 6371F (10)	Tube	Cold finished Hot finished	– –	– –	– –	– –	– –	25 HRC 99 HRB
ASTM A487 (29)	Castings	Normalized + tempered Quenched + tempered	60 85	90 105	20 16	35 35	– –	– –

(a) From separately cast specimens. For properties from casting, see AMS 2360.
(b) From casting or (a).
(c) Elongation values pertain to full tube; strip samples 5 percent lower.

TABLE 3.01. SPECIFIED MECHANICAL PROPERTIES

Alloy	4130				
Form	Bar				
Bar Diameter	Condition	F_{ty}, ksi	F_{tu}, ksi	e (2 in.), percent	RA, percent
1 inch	Hot Rolled:				
	As hot rolled	70	116	22	53
	Normalized 1600 F	65	108	27	57
	Annealed 1550 F	60	88	30	65
	Cold Drawn:				
	As cold drawn	105	122	16	45
	Annealed 1550 F	82	98	20	53
5/8 inch	Cold Drawn: Normalized 1550 F, water quenched, tempered 800 F, 1 hr	164.8(a)	186.1	11.8	59.3

(a) Proportional limit.

TABLE 3.0212. TENSILE PROPERTIES OF ROUND BAR IN VARIOUS HEAT-TREATED CONDITIONS (30,44)

Fe
0.3 C
0.95 Cr
0.2 Mo

4130

Alloy	4130				
Form	Plate				
Thickness, in.	Condition	Specimen Orientation	F_{ty}, ksi	F_{tu}, ksi	Elongation (in 2 In.), percent
0.50	Normalized 1600 F	L	65.2	94.8	30.8
		T	64.4	94.4	26.2
	Normalized + temper	L	64.4	94.0	31.8
	1100 F	T	63.2	93.8	26.2
	Oil quench + temper	L	113.8	130.8	18.8
	1000 F	T	128.4	143.2	13.8
	Oil quench + temper	L	97.4	113.2	24.8
	1200 F	T	94.4	110.0	20.2
>1.00	Normalized 1600 F, 2 hr, oil quench, temper 1175 F, 2 hr, air cool	T	92	119	21

TABLE 3.0213. TENSILE PROPERTIES OF PLATE IN VARIOUS HEAT-TREATED CONDITIONS (26,69)

Alloy	4130		
Form	3/8 inch Plate		
Specimen Orientation	Longitudinal		
Condition	F_{ty}, ksi	F_{tu}, ksi	Elongation (in 0.5 In.), percent
Normalized 1625 F, then			
Tempered to Rc 26	118	129	17.0
Tempered to Rc 34	143	150	14.5
Tempered to Rc 44	194	206	10.0

TABLE 3.0214. TENSILE PROPERTIES OF 3/8 INCH PLATE HEAT TREATED TO VARIOUS HARDNESSES (49)

Alloy	4130			
Form	1-inch Diameter Extruded Bar			
Composition	C-0.31, Mn-0.58, Si-0.23, P-0.009, S-0.014, Cr-0.99, Ni-0.95, Mo-0.21			
Condition	F_{ty}, ksi	F_{tu}, ksi	e (2 in.), percent	RA, percent
1550 F, 1 hr + Slow Cool	46.5	85.2	27.0	56.3
1575 F, 1 hr + OQ +				
Tempered 850 F, 2 hr	145.5	167.0	14.0	55.0
Tempered 1200 F, 2 hr	64.5	82.5	31.0	72.6
Composition	C-0.30, Mn-0.55, Si-0.35, P-0.005, S-0.005, Cr-0.98, Ni-0.11, Mo-0.20			
1550 F, 1 hr + Slow Cool	48.0	83.5	27.5	52.6
1575 F, 1 hr + OQ +				
Tempered 850 F, 2 hr	160.5	174.0	14.0	51.1
Tempered 1200 F, 2 hr	90.0	110.8	23.5	70.2

TABLE 3.0215. TENSILE PROPERTIES OF EXTRUDED ROUND BAR IN VARIOUS HEAT-TREATED CONDITIONS (45)

Fe
0.3 C
0.95 Cr
0.2 Mo

4130

Alloy	4130				
Form	3/4 inch x 3-1/8 inch Extruded Flat				
Composition	C-0.30, Mn-0.50, Si-0.27, P-0.016, S-0.016, Ni-0.11, Cr-0.99, Mo-0.18				
Condition	Specimen Orient.	F_{ty}, ksi	F_{tu}, ksi	e (1 in.), percent	RA, percent
1650 F, 1 hr + Air Cool	L	84.2	115.8	23.5	56.4
	T	81.8	111.0	21.2	54.2
1575 F, 1 hr + OQ + Tempered 850 F, 2 hr	L	157.6	164.9	16.5	57.8
	T	154.0	159.2	11.5	49.6
Tempered 1200 F, 2 hr	L	86.1	103.2	23.5	73.0
	T	84.3	100.2	23.5	56.4
Composition	C-0.31, Mn-0.58, Si-0.23, P-0.009, S-0.014, Cr-0.99, Ni-0.95, Mo-0.21				
1550 F, 1 hr + Slow Cool	L	41.3	76.0	30.0	55.9
	T	40.6	73.6	25.5	52.4
1575 F, 1 hr + OQ + Tempered 850 F, 2 hr	L	155.5	165.5	15.5	58.8
	T	153.0	162.0	12.0	42.8
Tempered 1200 F, 2 hr	L	53.6	77.3	36.5	73.2
	T	58.7	74.8	29.5	61.4
Composition	C-0.30, Mn-0.55, Si-0.35, P-0.005, S-0.005, Cr-0.98, Ni-0.11, Mo-0.20				
1550 F, 1 hr + Slow Cool	L	42.6	77.3	30.0	55.1
	T	41.0	75.4	28.0	43.8
1575 F, 1 hr + OQ + Tempered 850 F, 2 hr	L	160.0	167.5	16.0	59.4
	T	153.6	163.0	14.5	41.0
Tempered 1200 F, 2 hr	L	86.6	104.0	25.0	71.6
	T	84.4	101.8	20.0	59.0

TABLE 3.0216. TENSILE PROPERTIES OF EXTRUDED FLAT BAR IN VARIOUS HEAT-TREATED CONDITIONS (45)

Alloy	4130			
Form	Castings			
Condition	F_{ty}, ksi	F_{tu}, ksi	e (2 in.), percent	RA, percent
Normalized 1650 F and				
Tempered 1100 F	95.0	115.0	16.0	35.0
Tempered 1200 F	61.5	93.5	23.0	37.3
Tempered 1250 F	56.5	88.0	22.0	38.0
1575 F, WQ and				
Tempered 950 F	148.0	176.5	10.0	24.6
Tempered 1100 F	120.0	140.0	17.0	38.5
Tempered 1175 F	95.0	115.0	19.5	42.0

TABLE 3.0217. TENSILE PROPERTIES OF CASTINGS IN VARIOUS HEAT-TREATED CONDITIONS (30)

Fe
0.3 C
0.95 Cr
0.2 Mo

4130

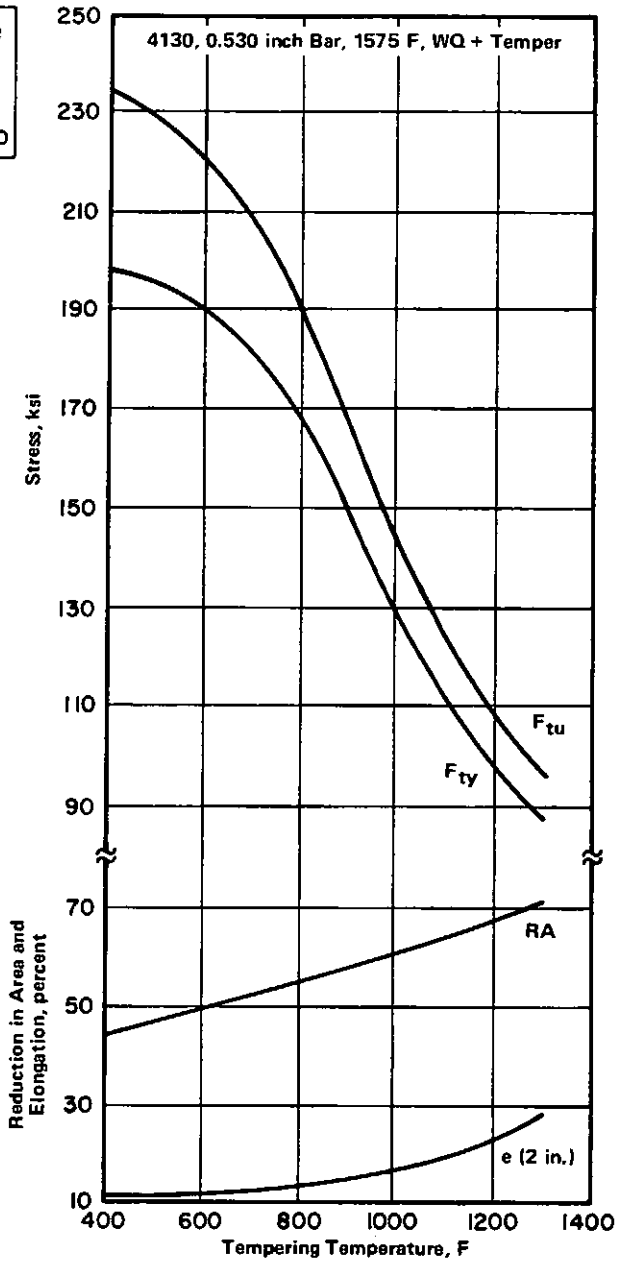


FIGURE 3.0218. EFFECT OF TEMPERING TEMPERATURE ON ROOM TEMPERATURE TENSILE PROPERTIES OF 0.530 INCH BAR (16)

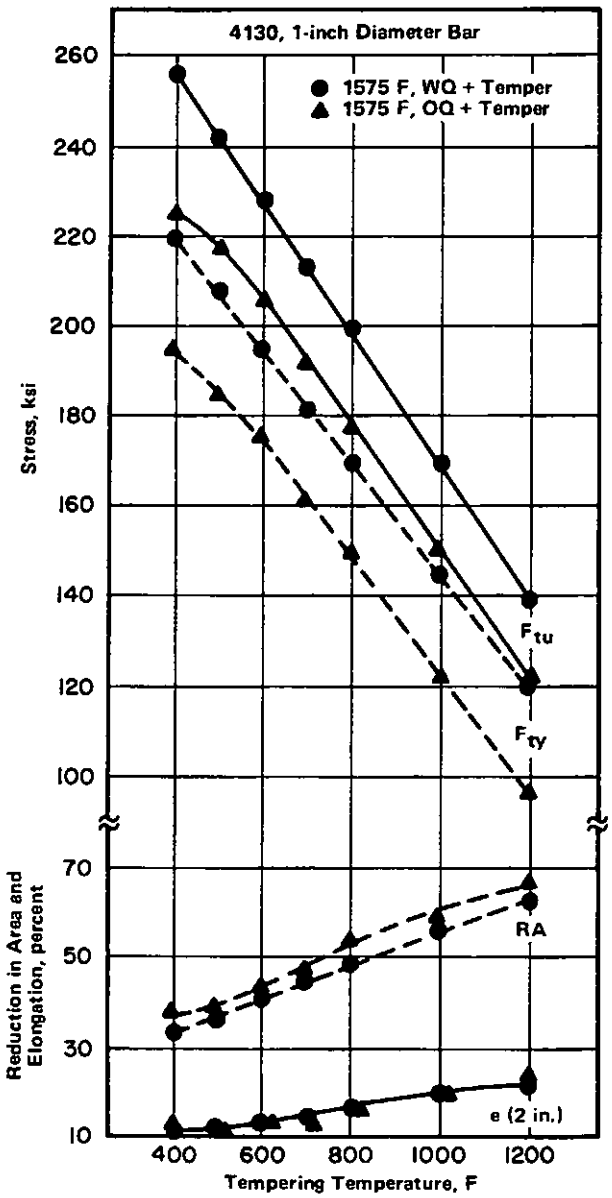


FIGURE 3.0219. EFFECT OF TEMPERING TEMPERATURE ON TENSILE PROPERTIES OF OIL-QUENCHED AND WATER-QUENCHED 1 INCH BAR (30)

Fe
0.3 C
0.95 Cr
0.2 Mo

4130

Alloy	4130					
Form	Sheet					
Condition	Specimen Orient.	Thickness, in.	F_{ty}, ksi	F_{tu}, ksi	e (1 in.), percent	RA, percent
Austenitized 1575 F, 1 hr, WQ, Tempered 700 F, 30 min, Air Cool	T	0.030	167.8	183.4	–	7.1
		0.050	171.6	197.6	3.5	7.5
		0.063	169.5	193.0	3.8	11.2
		0.087	183.4	205.2	3.0	6.5
		0.125	176.4	197.9	4.5	16.5
		0.250	173.7	195.3	7.5	36.8
Austenitized 1575 F, 1/2 hr, WQ, Tempered 500 F, 30 min, Air Cool	T	0.030	185.2	221.4	2.5	7.1
		0.050	184.6	219.8	3.0	10.7
		0.063	178.4	226.0	5.2	27.8
		0.087	200.3	233.2	3.5	20.1
		0.125	191.2	228.1	6.0	23.2
		0.250	185.4	221.5	–	36.9
Austenitized 1650 F, 1 hr, OQ, Tempered 800 F, 1 hr	L	0.125	175(a)	–	–	–

(a) Proportional limit = 163 ksi.

TABLE 3.02110. EFFECT OF SHEET THICKNESS AND TEMPERING TEMPERATURE ON TENSILE PROPERTIES (59,68)

Alloy	4130			
Form	5/8 inch Thick Flat Bar			
Austenitizing Temperature, F, and Quench Medium	F_{ty}, ksi	F_{tu}, ksi	e (4D), percent	RA, percent
1600, Oil	201	284	11.4	32.9
2200, Oil	205	276	5.6	9.9
2200, Ice-Brine	215	249	1.6	6.6

TABLE 3.02111. EFFECT OF AUSTENITIZING TEMPERATURE AND QUENCH MEDIUM ON TENSILE PROPERTIES OF AS-QUENCHED MATERIAL (50)

Alloy	4130						
Form	3/8-inch Thick Rolled Flat Bar						
Specimen Orient.	Longitudinal						
Austenitizing Temperature, Time	Quench Medium	Temper Temperature, F	F_{ty}, ksi	F_{tu}, ksi	e (1.4 in.), percent	RA, percent
2200 F, 1 hr	IBLN(a)	As quenched	167	245	–(b)	–
		392	186	257	–(b)	–
		536	184	225	7.6	21.0
		662	180	209	9.8	37.0
2200 F, 1 hr	Water	As quenched	167	278	5.2	14.0
		392	210	258	9.7	–
		536	182	228	10.3	38.7
		662	180	210	9.8	25.2
2200 F, 1 hr	Oil	As quenched	161	276	5.6	9.8
		392	176	262	7.5	18.1
		536	194	246	8.0	25.5
		662	182	222	7.7	30.6
2200 F, 1 hr, Cooled to 1600 F, 1/2 hr	IBLN	As quenched	170	279	6.6	12.0
		392	195	261	–(b)	–
		536	184	230	7.8	25.9
		662	200	210	9.3	32.4

(a) Ice-brine followed by liquid nitrogen storage.
(b) Quench cracks visible.

TABLE 3.02112. EFFECT OF QUENCH MEDIUM AND TEMPERING TEMPERATURE ON TENSILE PROPERTIES OF ROLLED BAR (51)

Fe
0.3 C
0.95 Cr
0.2 Mo

4130

Alloy	4130		
Form	0.125 inch Sheet		
Condition	Austenitized 1575 F, 15 min, Quenched, Tempered 1050 F, 1 hr		
Quench Medium	F_{ty}, ksi	F_{tu}, ksi	Elongation, percent
Oil	146.0	156.4	14.0
Nitrogen Gas	147.0	162.0	13.0

TABLE 3.02113. EFFECT OF QUENCH MEDIUM ON TENSILE PROPERTIES OF SHEET (52)

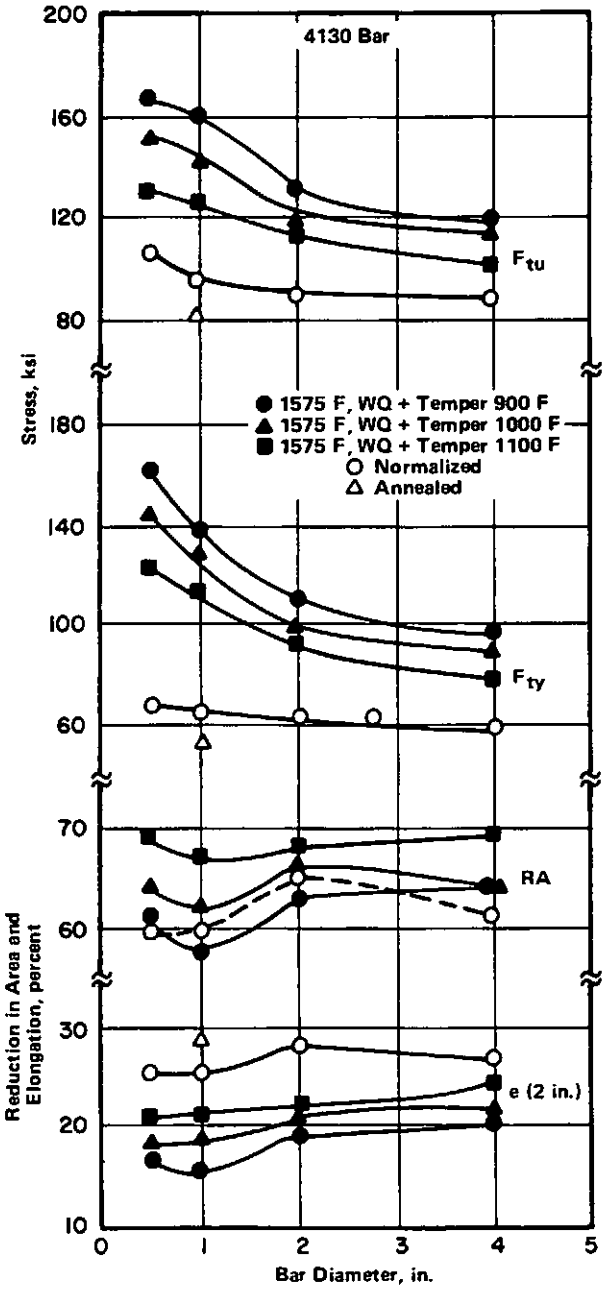


FIGURE 3.02114. EFFECT OF BAR DIAMETER ON TENSILE PROPERTIES IN VARIOUS HEAT-TREATED CONDITIONS (16)

Fe
0.3 C
0.95 Cr
0.2 Mo

4130

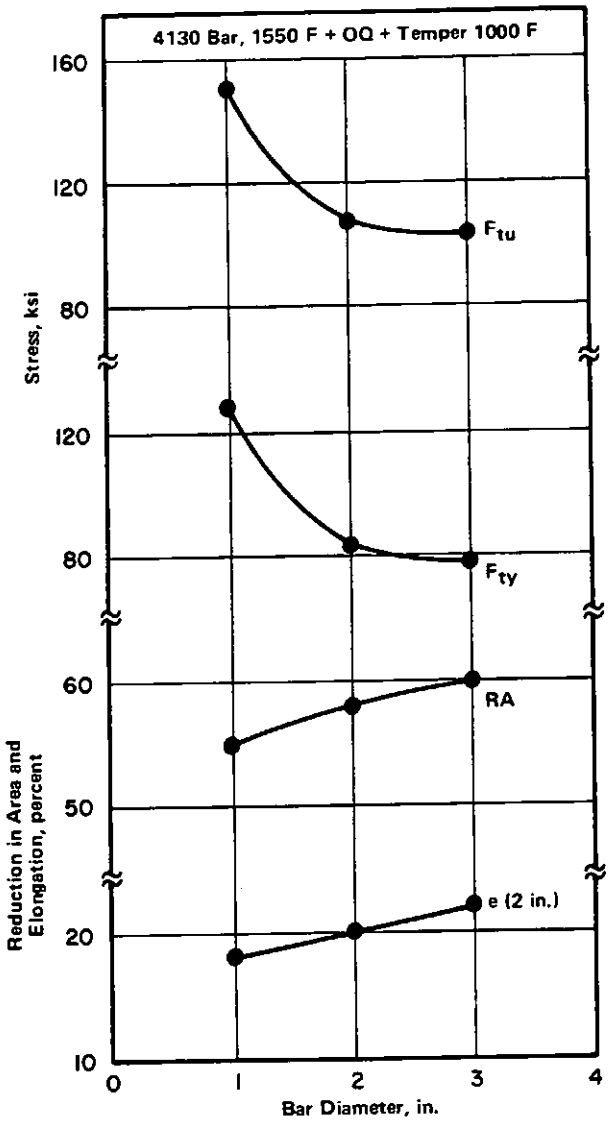


FIGURE 3.02115. TENSILE PROPERTIES OF QUENCHED AND TEMPERED ROUND BAR (74)

Alloy	4130					
Form	1/4 inch Plate					
Orientation	Longitudinal					
Condition	Treatment	Effective Strain	F_{ty}, ksi	F_{tu}, ksi	e (1 in.), percent	RA, percent
Annealed	None	0	66.5	97.1	29.5	60.2
	Explosively formed	0.068	90.7	98	26.5	43.2
	Cold rolled	0.066	68.1	96.7	26.0	43.3
Heat Treated(a)	None	0	149	155	10.5	39.1
	Explosively formed	0.068	148	155	12.3	41.3
	Cold rolled	0.066	140	149	12.5	35.7

(a) Austenitized 1600 F, 40 min, oil quenched, tempered 1000 F, 55 min.

TABLE 3.02116. EFFECT OF EXPLOSIVE FORMING ON TENSILE PROPERTIES OF PLATE (54)

Fe
0.3 C
0.95 Cr
0.2 Mo

4130

Alloy	4130							
Form	Powder Metallurgy Forgings Die Press Process — 1.125 x 4.225 x 3.000 inch Isostatic Press Process — 0.565 x 4.000 x 1.300 inch High Energy Rate Forming (HERF) — 2.5 inch Diam x 5.5 inch Long Water Atomized Powder, -100 mesh							
Condition	Austenitized 1575 F, RT, Water Quench, Tempered 800 F, 1 hr							
	Compacting		Sinter	Repress (Forging)				
Process	Temperature, F	Pressure, ksi	Temperature, F(a)	Temperature, F	Pressure, ksi	F_{ty}, ksi	F_{tu}, ksi	e (1 in.), percent
Die Press	RT	100	2050	2200	150	132	136	1.4
Isostatic Press	RT	50	1650	2200	150	(b)	153	0.5
HERF	–	–	–	2200	275	136	160	1.4

(a) For 1 hour.
(b) Did not have sufficient ductility.

TABLE 3.02117. EFFECT OF FABRICATION PROCESS ON TENSILE PROPERTIES OF POWDER METALLURGY FORGING (46)

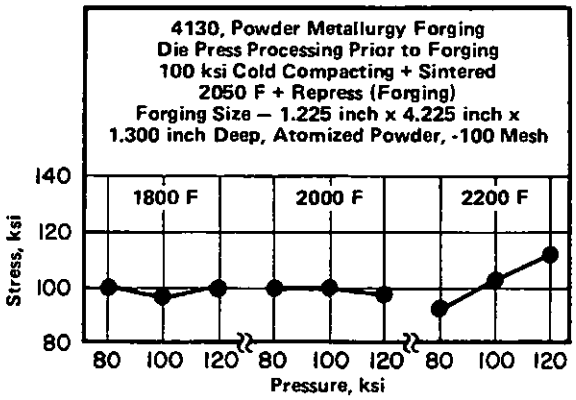


FIGURE 3.02118. EFFECT OF REPRESS (FORGING) PRESSURE AND TEMPERATURE ON ULTIMATE TENSILE STRENGTH OF POWDER METALLURGY FORGING (46)

Alloy	4130				
Form	0.030 inch Sheet				
Condition	F_{ty}, ksi	F_{tu}, ksi	e (1 in.), percent	RA, percent	Prop. Limit, ksi
As received	80.5	106.2	13.2	47	69.9
HT 1800 F, 1 hr	34.8	66.2	23.8	57	29.0
Mn plated	81.5	106.3	12.8	39	77.6
HT 1800 F, 1 hr	37.2	75.3	20.2	34	33.4

TABLE 3.02119. EFFECT OF Mn PLATING AND ELEVATED TEMPERATURE EXPOSURE ON TENSILE PROPERTIES OF SHEET (48)

Fe
0.3 C
0.95 Cr
0.2 Mo

4130

Alloy	4130	
Condition	Quenched and Tempered	
F_{tu}, ksi[a]		
125	150	180
925 F	775 F	575 F

(a) If the material is exposed for more than 10 hours to temperatures exceeding those listed (unstressed), a permanent reduction in strength is likely to occur. The temperatures are approximately 125 F below the tempering temperature used to achieve the various strength levels.

TABLE 3.02120. TEMPERATURE LIMITS FOR PROLONGED UNSTRESSED EXPOSURE WHICH PREVENT DEGRADATION OF TENSILE STRENGTH (63)

Alloy	4130
Form	3/4 x 3-1/2 inch Extruded Bar
Condition	As Extruded
Specimen Orientation	Keyhole Charpy Impact, ft-lb
L	68
T	36

TABLE 3.0231. IMPACT PROPERTIES OF EXTRUDED BAR (45)

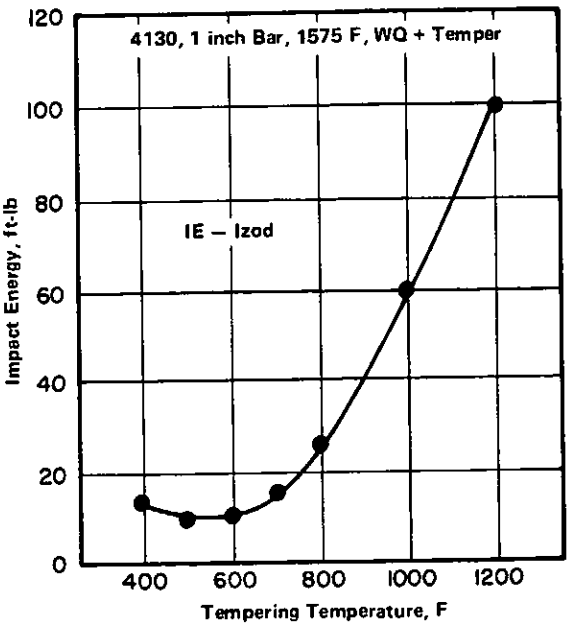


FIGURE 3.0232. EFFECT OF TEMPERING TEMPERATURE ON ROOM TEMPERATURE IMPACT STRENGTH (30)

Fe
0.3 C
0.95 Cr
0.2 Mo

4130

Alloy	4130	
Form	Wrought	
Condition	Izod Impact, ft-lb	F_{tu}, ksi
Normalized	63.7	97.0
Annealed	45.5	81.2

TABLE 3.0233. IMPACT RESISTANCE OF NORMALIZED AND ANNEALED MATERIAL (31)

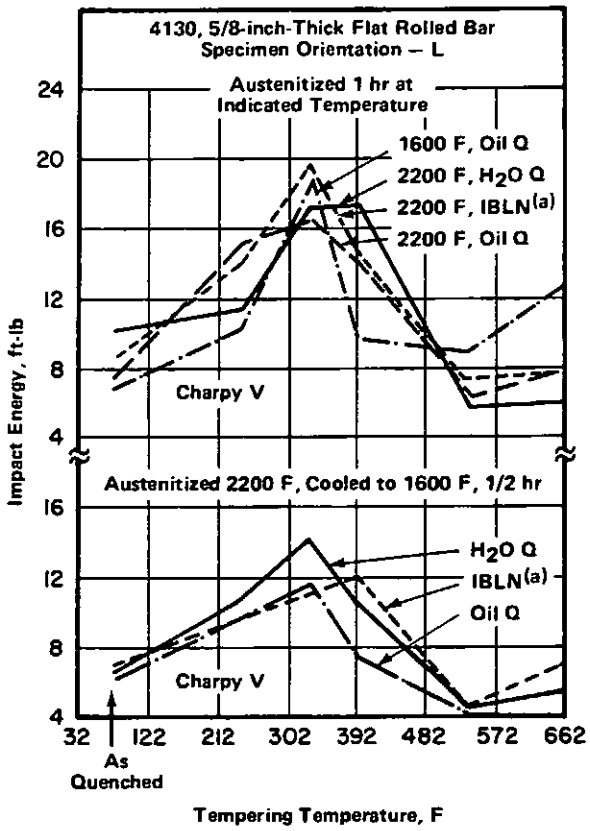


FIGURE 3.0234. EFFECT OF QUENCH MEDIUM AND TEMPERING TEMPERATURE ON IMPACT PROPERTIES OF ROLLED BAR (51)

(a) Ice-brine followed by liquid N_2 storage.

Alloy	4130								
Form	Powder Metallurgy Forgings Die Press Process – 1.125 inch x 4.225 inch x 1.300 inch Deep Isostatic Press Process – 0.565 inch x 4.000 inch x 1.300 inch Deep High Energy Rate Forming (HERF) – 2.5 inch Diameter x 5.5 inch Long Water Atomized Powder – 100 mesh								
Condition	Austenitized 1575 F, RT, H_2O Quench, Tempered 800 F, 1 hr								
	Compacting		Sinter	Repress (Forging)		Charpy-V Notched Impact Energy, ft-lb			
Process	Temperature, F	Pressure, ksi	Temperature, F[a]	Temperature, F	Pressure, ksi	-40 F	77 F	210 F	450 F
Die Press	RT	100	2050	2200	150	4.5	3.2	7.3	5.9
Isostatic Press	RT	50	1650	2200	150	1.0	2.3	2.1	6.2
HERF	–	–	–	2200	275	1.7	1.3	1.2	1.3

(a) For 1 hour.

TABLE 3.0235. EFFECT OF FABRICATION PROCESS AND TEMPERATURE ON IMPACT PROPERTIES OF POWDER METALLURGY FORGING (46)

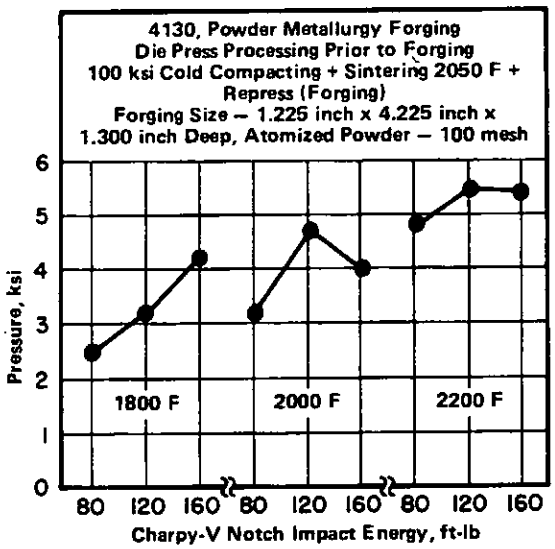


FIGURE 3.0236. EFFECT OF REPRESS (FORGING) PRESSURE AND TEMPERATURE ON IMPACT PROPERTIES OF POWDER METALLURGY FORGING (46)

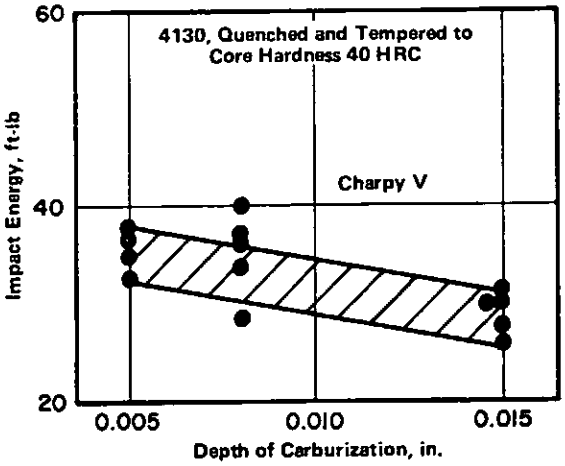


FIGURE 3.0237. EFFECT OF CARBURIZATION ON IMPACT PROPERTIES (74)

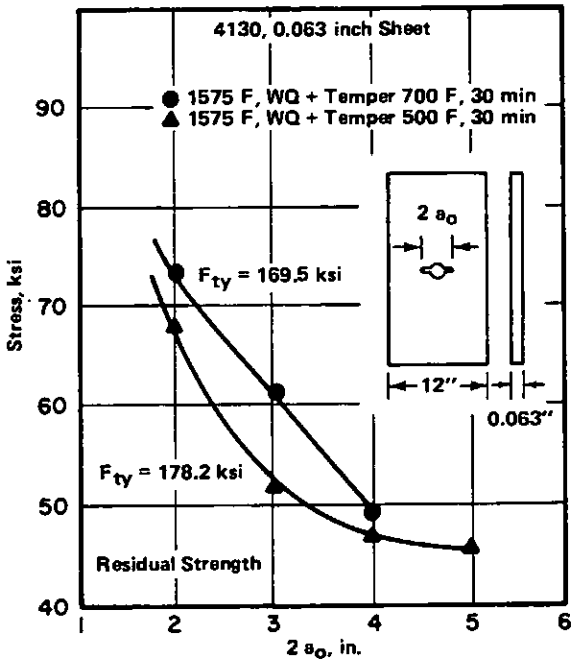


FIGURE 3.02711. EFFECT OF INITIAL CRACK LENGTH (2 a_o) ON RESIDUAL STRENGTH (MAXIMUM LOAD DIVIDED BY GROSS CROSS-SECTIONAL AREA) OF SHEET AFTER TWO DIFFERENT TEMPERING TREATMENTS (17)

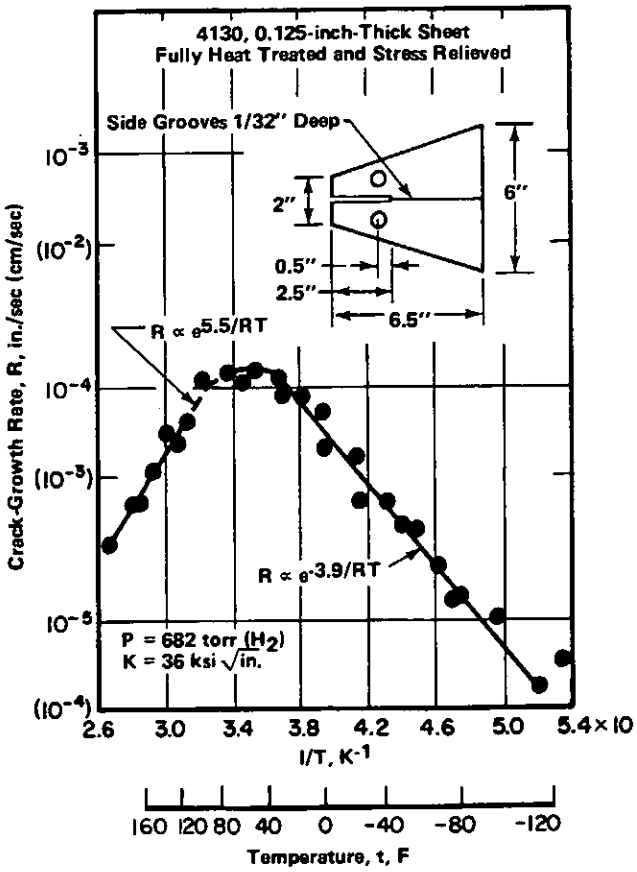


FIGURE 3.02712. EFFECT OF TEMPERATURE ON SLOW-CRACK-GROWTH RATE IN GASEOUS HYDROGEN (66)

Fe
0.3 C
0.95 Cr
0.2 Mo

4130

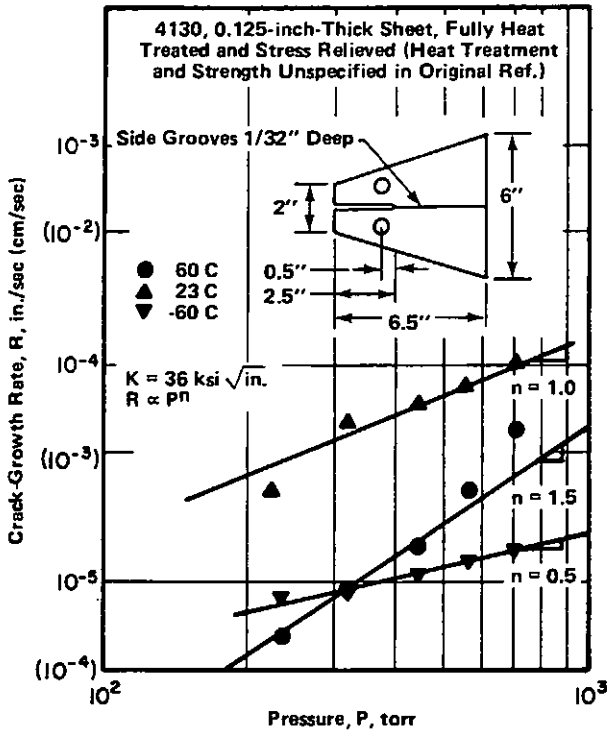


FIGURE 3.02713. EFFECT OF HYDROGEN PRESSURE ON SLOW-CRACK-GROWTH RATE (66)

Alloy	4130		
Form	Sheet		
Condition	Sheet Thickness, in.	K_c, ksi $\sqrt{in.}$ Blunt	K_c, ksi $\sqrt{in.}$ Sharp
Austenitized 1575 F, 1 hr, WQ, Temper 700 F, 30 min, Air Cool	0.030	136	148
	0.050	140	173
	0.063	158	182
	0.087	126	134
	0.125	148	153
Austenitized 1575 F, 1/2 hr, WQ, Temper 500 F, 30 min, Air Cool	0.030	–	158
	0.050	149	152
	0.063	141	129
	0.087	122	125
	0.125	165	146
	0.250	124	142

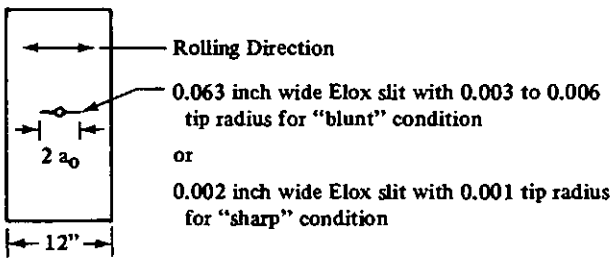


TABLE 3.02722. EFFECT OF SHEET THICKNESS ON FRACTURE-TOUGHNESS PARAMETER K_c (68)

Fe
0.3 C
0.95 Cr
0.2 Mo

4130

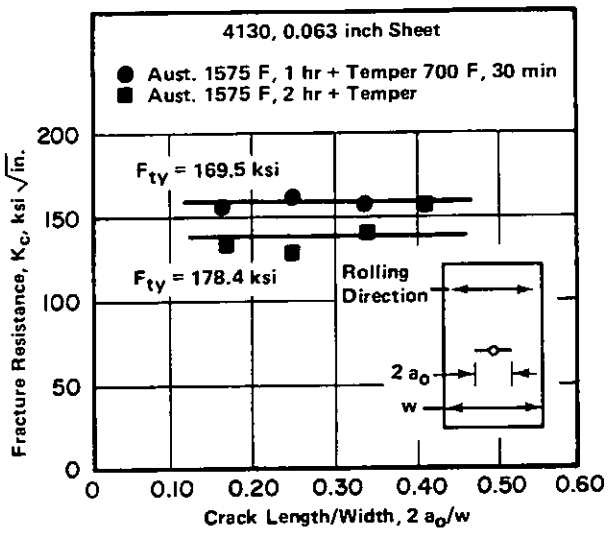


FIGURE 3.02723. EFFECT OF YIELD STRENGTH ON FRACTURE RESISTANCE OF SHEET (71)

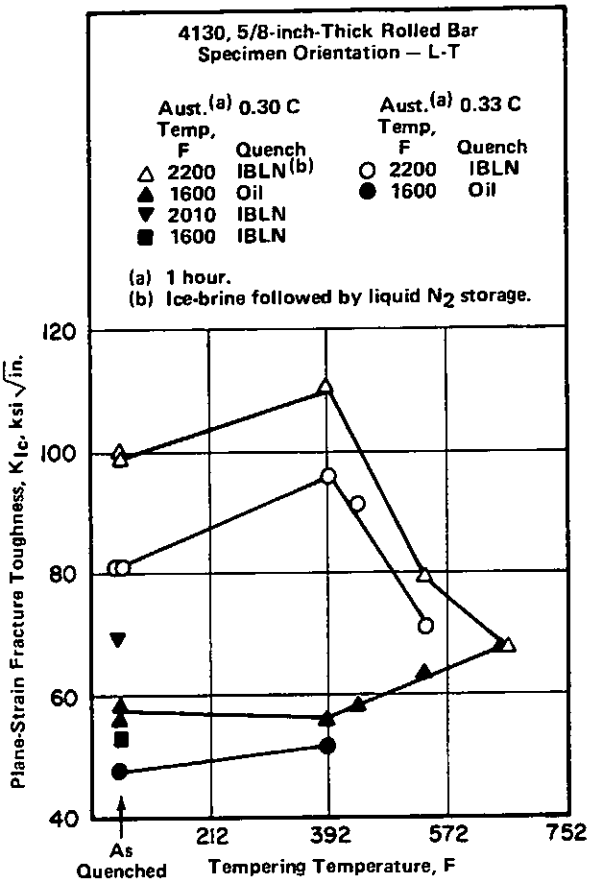


FIGURE 3.02724. EFFECT OF TEMPERING TEMPERATURE, CARBON CONTENT, AND QUENCHING MEDIUM ON PLANE-STRAIN FRACTURE TOUGHNESS OF FLAT ROLLED BAR (51)

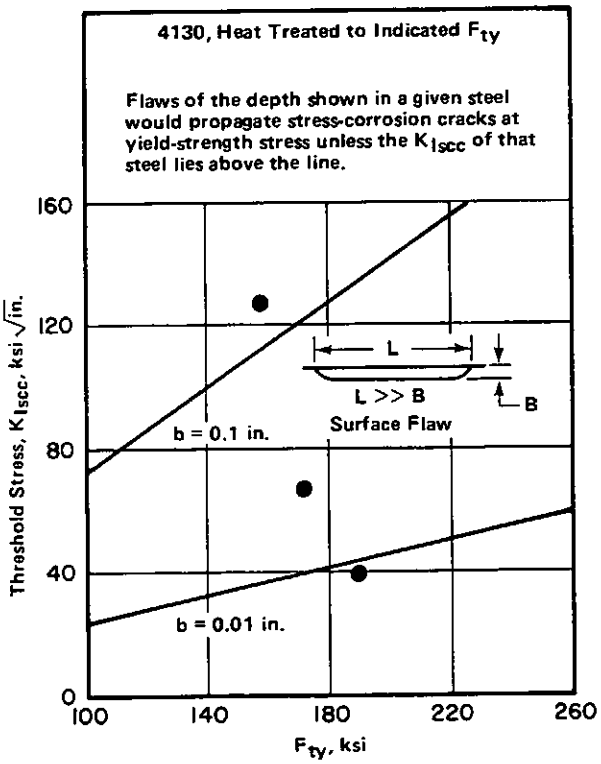


FIGURE 3.02725. EFFECT OF YIELD STRENGTH AND FLAW DEPTH ON THRESHOLD STRESS INTENSITY IN STATIC LOADING (58)

Fe
0.3 C
0.95 Cr
0.2 Mo

4130

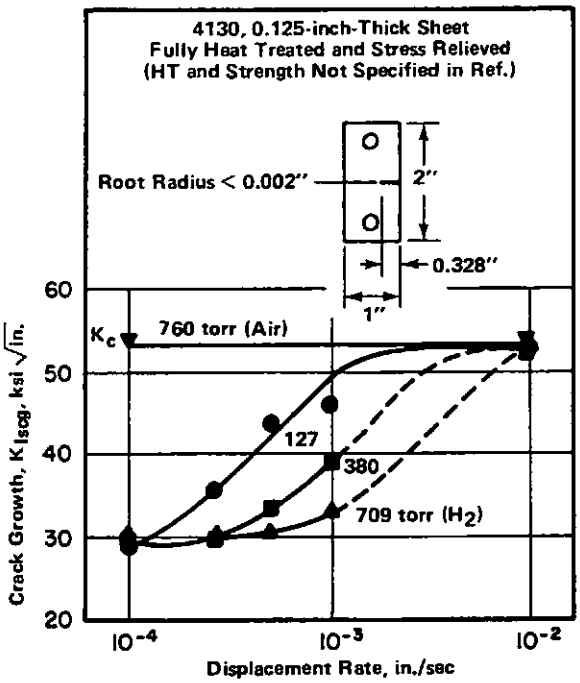


FIGURE 3.02726. EFFECT OF HYDROGEN PRESSURE AND DISPLACEMENT RATE ON INITIATION OF SLOW CRACK GROWTH, K_{Iscg} (EMBRITTLEMENT) (66)

Alloy	4130	
Form	>1 inch Plate	
Condition	1600 F, 2 hr, OQ + 1175 F, 2 hr + AC	
Air, K_Q[(a)], ksi $\sqrt{in.}$	Hydrogen Pressure[(b)], psi	Arrest Stress Intensity, ksi $\sqrt{in.}$
114	3,000	80
	6,000	62
	9,000	41
	10,000	29
	14,000	47

(a) 10 percent secent.
(b) Temperature = 55 F.

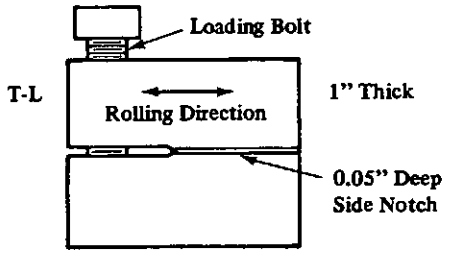


TABLE 3.02727. EFFECT OF HYDROGEN PRESSURE ON THE ARREST OF CRACK PROPAGATION (69)

Fe
0.3 C
0.95 Cr
0.2 Mo

4130

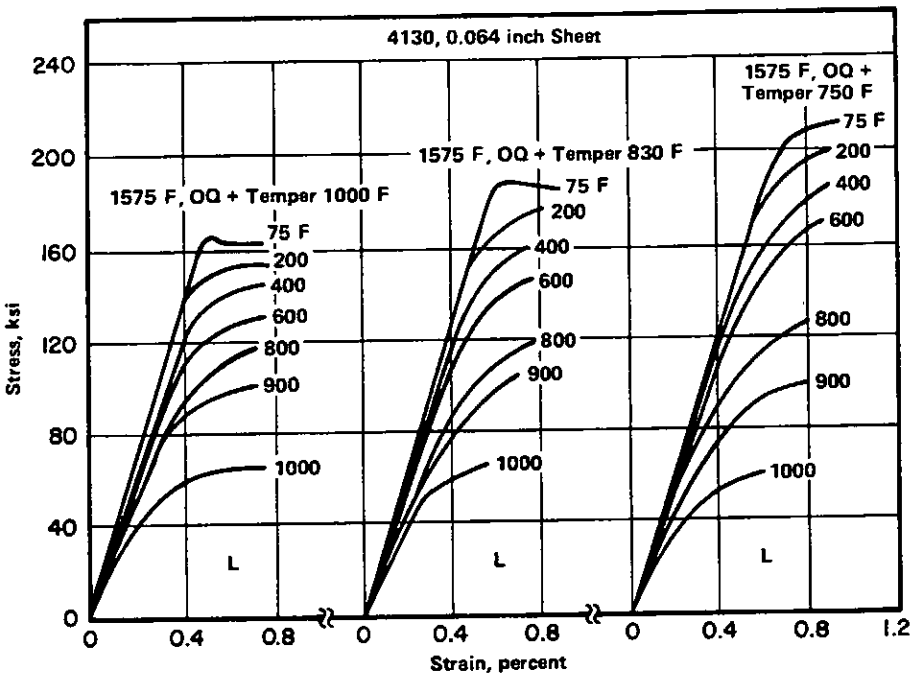


FIGURE 3.0311. TENSILE STRESS-STRAIN CURVES FOR SHEET AT TEMPERATURES UP TO 1000 F AFTER THREE DIFFERENT TEMPERING TREATMENTS: CURVES APPLY TO SPECIMENS HELD FOR 0.5 UP TO 100 HOURS AT TEST TEMPERATURE (14)

Fe
0.3 C
0.95 Cr
0.2 Mo

4130

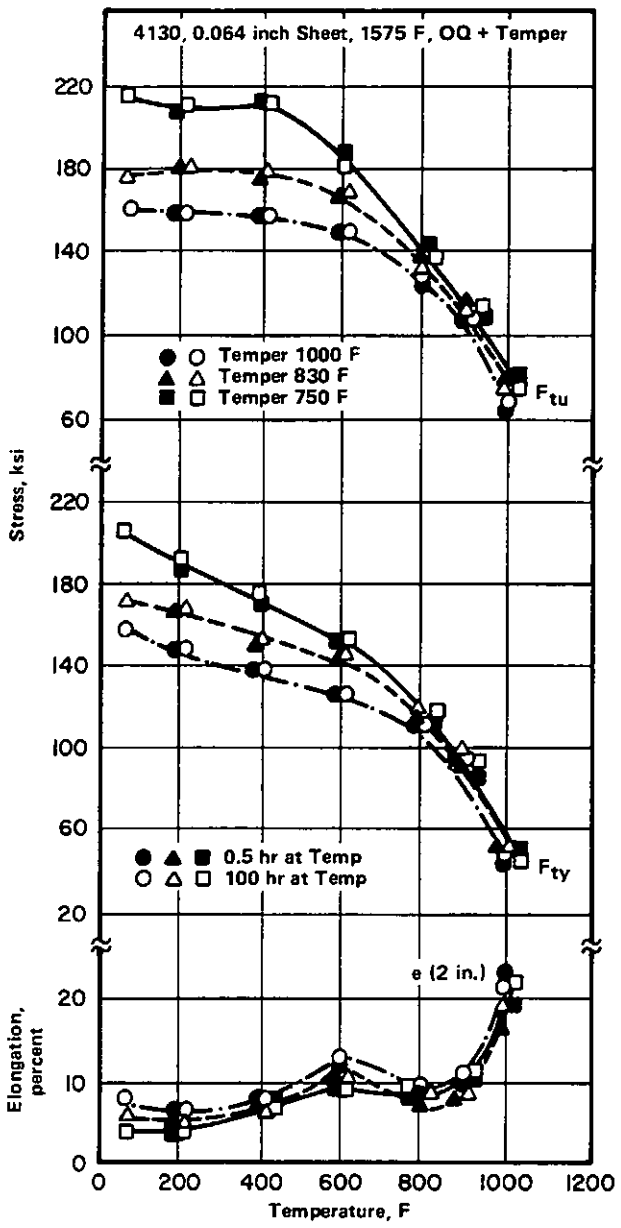


FIGURE 3.0312. EFFECT OF TEMPERATURE ON TENSILE PROPERTIES OF SHEET AFTER THREE DIFFERENT TEMPERING TREATMENTS AND TWO DIFFERENT EXPOSURE TIMES (14)

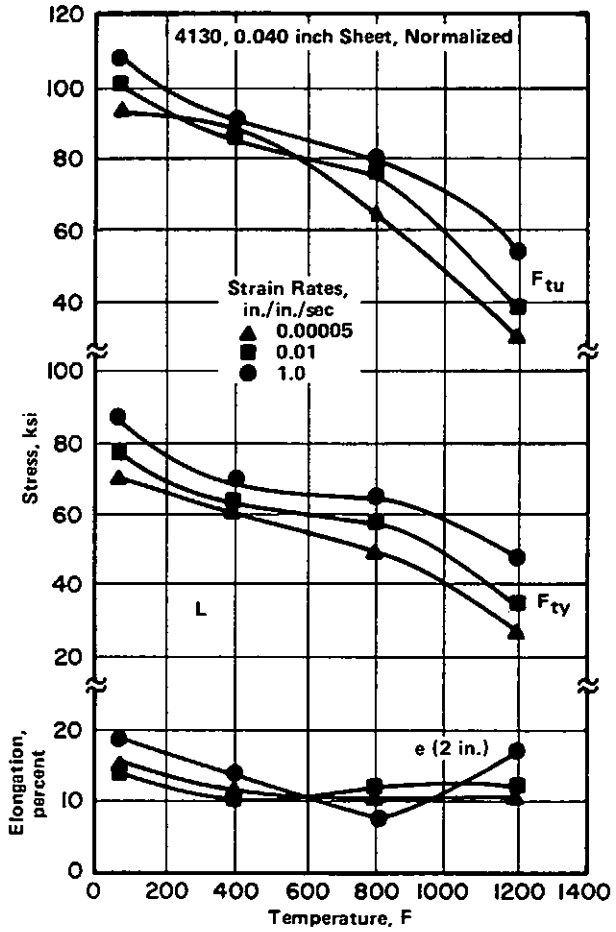


FIGURE 3.0313. EFFECT OF TEMPERATURE AND STRAIN RATE ON TENSILE PROPERTIES OF NORMALIZED SHEET AFTER RAPID HEATING; DATA PERTAIN TO SPECIMENS HELD FOR 10 SECONDS UP TO 1/2 HOUR AT TEST TEMPERATURES (15)

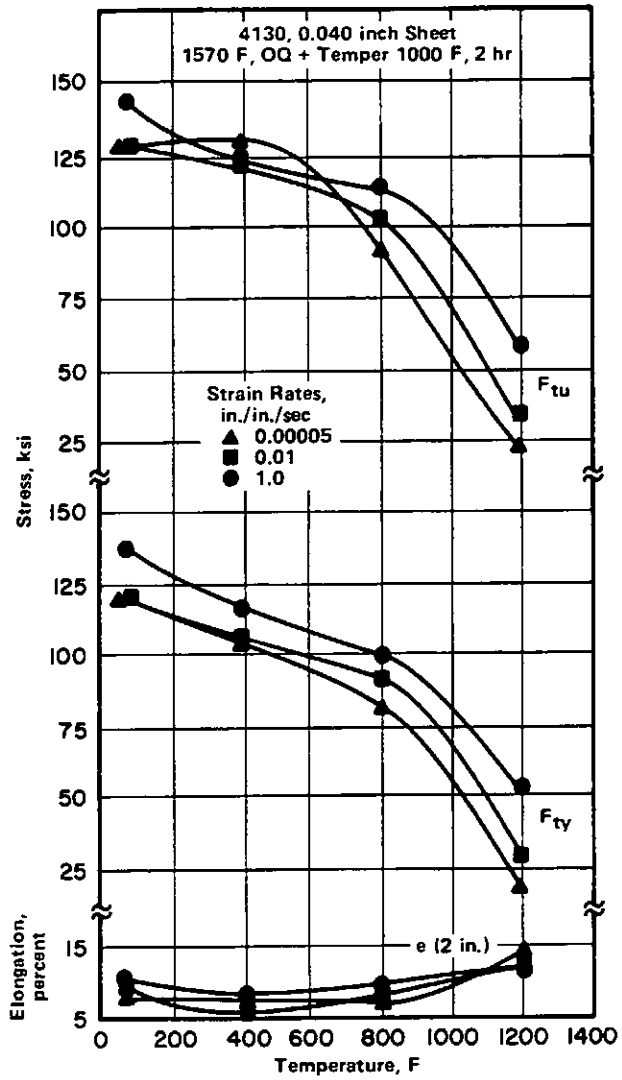


FIGURE 3.0314. EFFECT OF TEMPERATURE AND STRAIN RATE ON TENSILE PROPERTIES OF HEAT TREATED SHEET AFTER RAPID HEATING; DATA PERTAIN TO SPECIMENS HELD FOR 10 SECONDS UP TO 1/2 HOUR AT TEST TEMPERATURE (15)

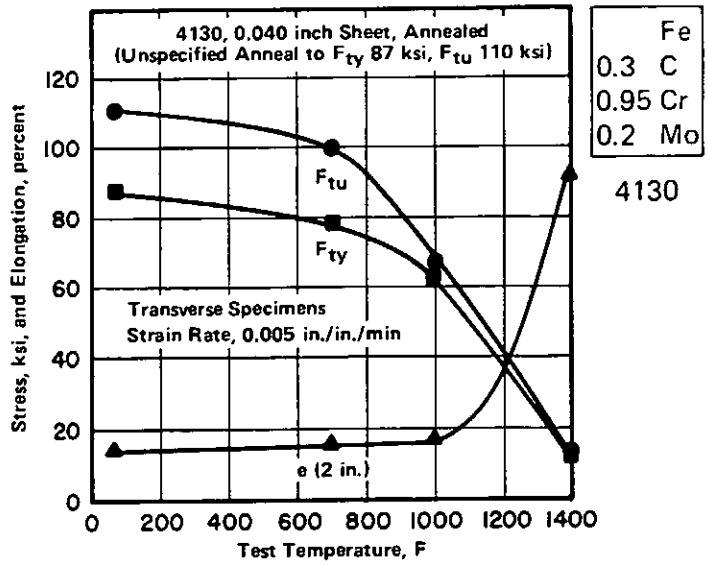


FIGURE 3.0315. EFFECT OF TEMPERATURE ON TENSILE PROPERTIES OF SHEET AFTER 5-MINUTE SOAK AT TEMPERATURE (53)

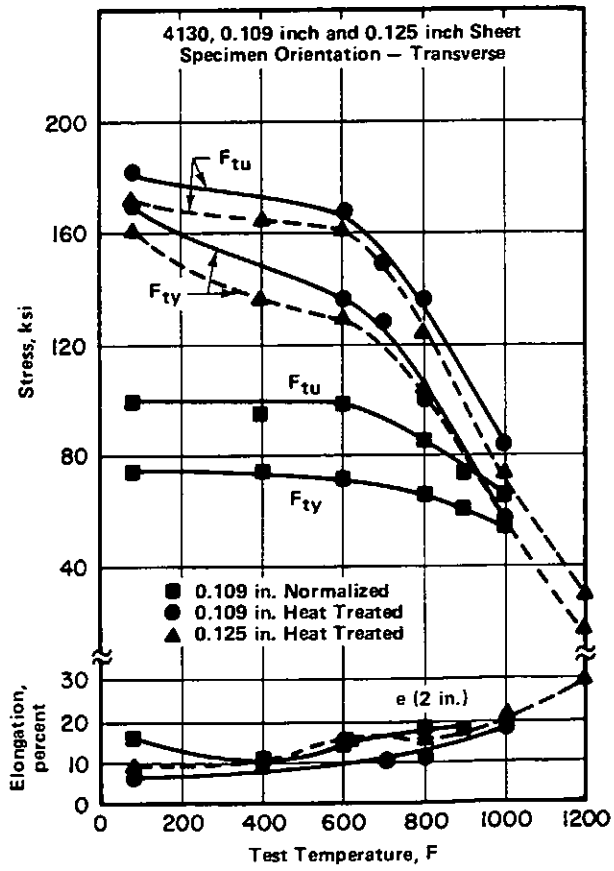


FIGURE 3.0316. EFFECT OF SHORT-TIME EXPOSURE TO ELEVATED TEMPERATURE ON TENSILE PROPERTIES OF SHEET (55)

Fe
0.3 C
0.95 Cr
0.2 Mo

4130

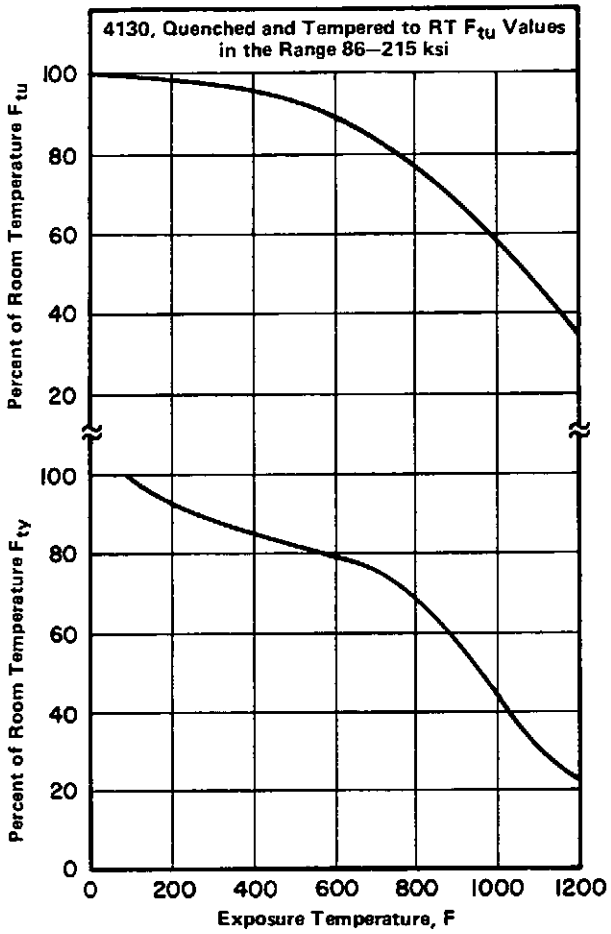


FIGURE 3.0317. EFFECT OF PRIOR EXPOSURE TO TEST TEMPERATURE UP TO 10 HOURS ON TENSILE PROPERTIES (63)

Fe
0.3 C
0.95 Cr
0.2 Mo

4130

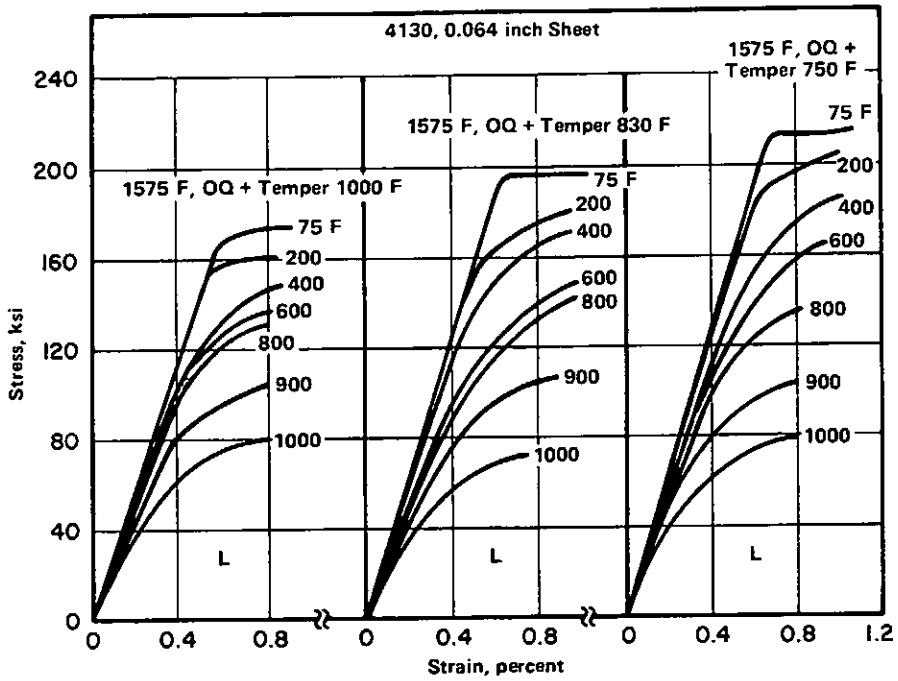


FIGURE 3.0321. COMPRESSIVE STRESS-STRAIN CURVES FOR SHEET AT TEMPERATURES UP TO 1000 F AFTER THREE DIFFERENT TEMPERING TREATMENTS; CURVES APPLY TO SPECIMENS HELD FOR 0.5 UP TO 100 HOURS AT TEST TEMPERATURES (14)

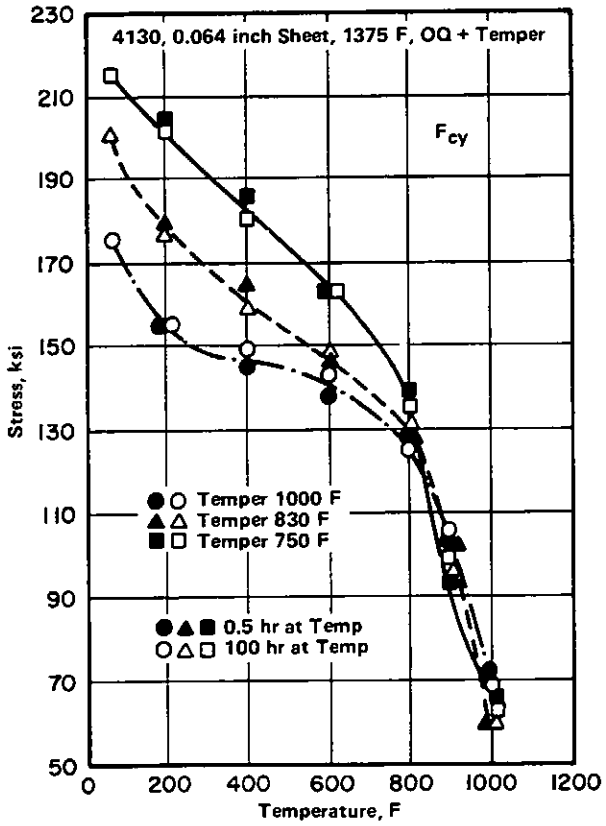


FIGURE 3.0322. EFFECT OF TEMPERATURE ON COMPRESSIVE YIELD STRENGTH OF SHEET AFTER THREE DIFFERENT TEMPERING TREATMENTS AND TWO DIFFERENT EXPOSURE TIMES (14)

Fe
0.3 C
0.95 Cr
0.2 Mo

4130

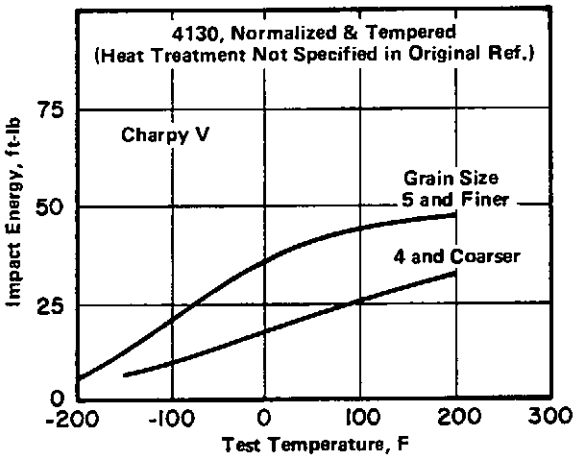


FIGURE 3.0331. EFFECT OF GRAIN SIZE AND TEMPERATURE ON IMPACT PROPERTIES (33)

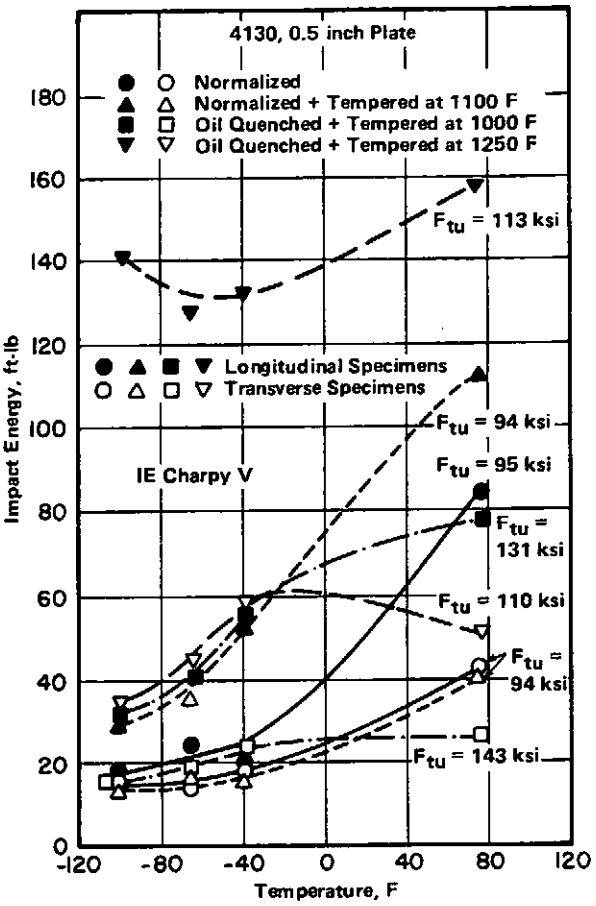


FIGURE 3.0332. EFFECT OF LOW TEMPERATURES ON IMPACT PROPERTIES IN SEVERAL HEAT-TREATED CONDITIONS (26)

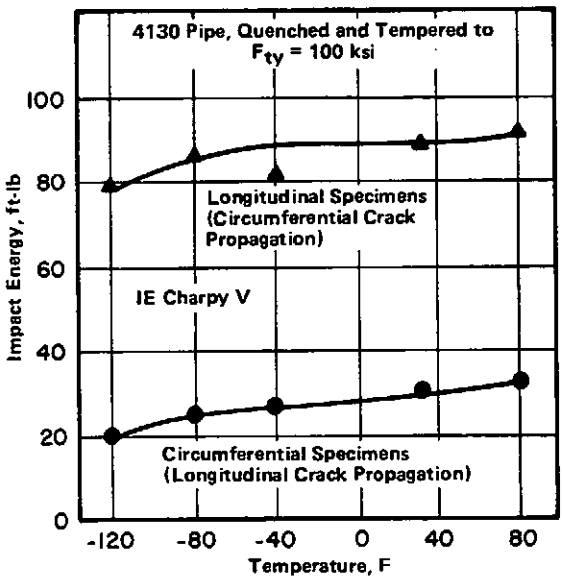


FIGURE 3.0333. EFFECT OF LOW TEMPERATURES ON IMPACT PROPERTIES OF PIPE (42)

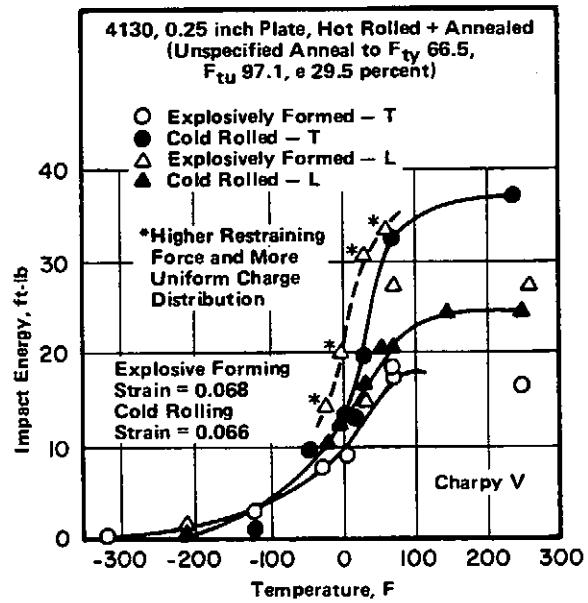


FIGURE 3.0334. EFFECT OF TEMPERATURE ON IMPACT PROPERTIES OF EXPLOSIVELY FORMED AND ROLLED AND ANNEALED PLATE (54)

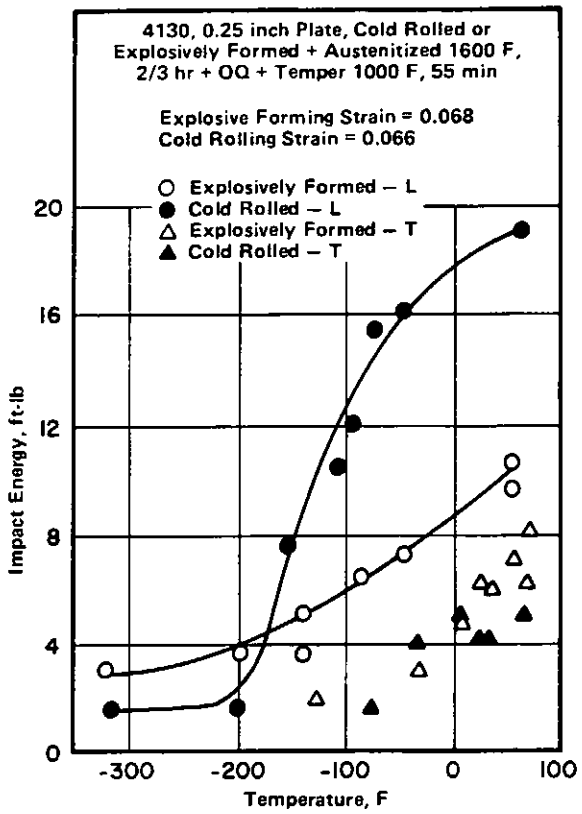


FIGURE 3.0335. EFFECT OF TEMPERATURE ON IMPACT PROPERTIES OF EXPLOSIVELY FORMED AND COLD-ROLLED HEAT-TREATED PLATE (54)

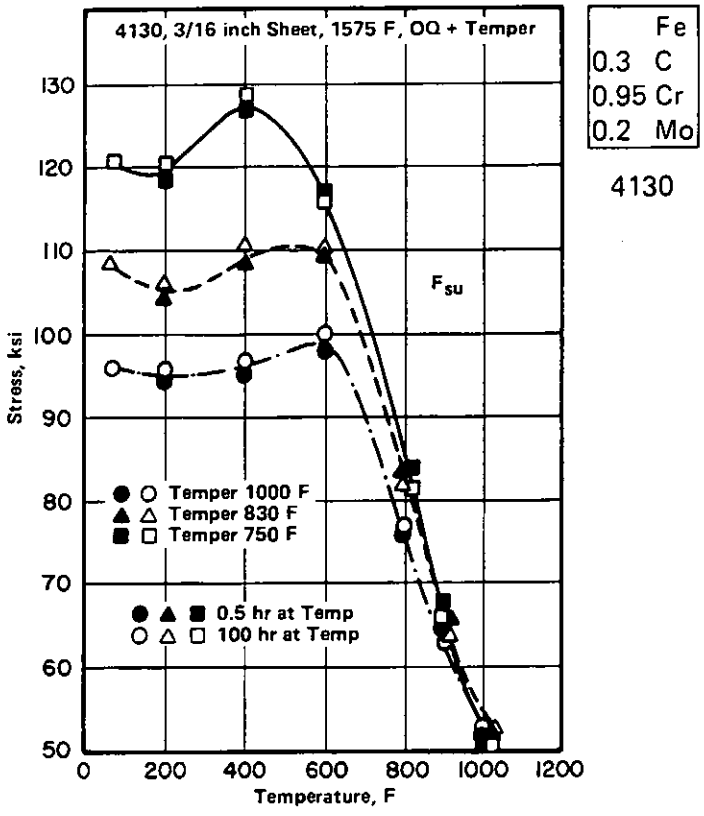


FIGURE 3.0351. EFFECT OF TEMPERATURE ON SHEAR STRENGTH OF SHEET AFTER THREE DIFFERENT TEMPERING TREATMENTS AND TWO DIFFERENT EXPOSURE TIMES (14)

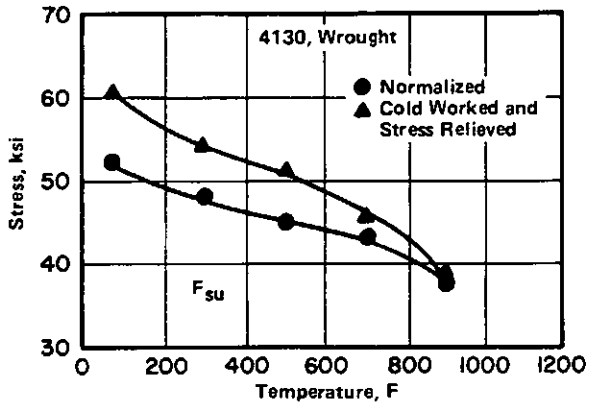


FIGURE 3.0352. EFFECT OF TEMPERATURE ON SHEAR STRENGTH OF NORMALIZED AND OF COLD-WORKED-AND-STRESS-RELIEVED TYPE 4130 (27)

Fe
0.3 C
0.95 Cr
0.2 Mo

4130

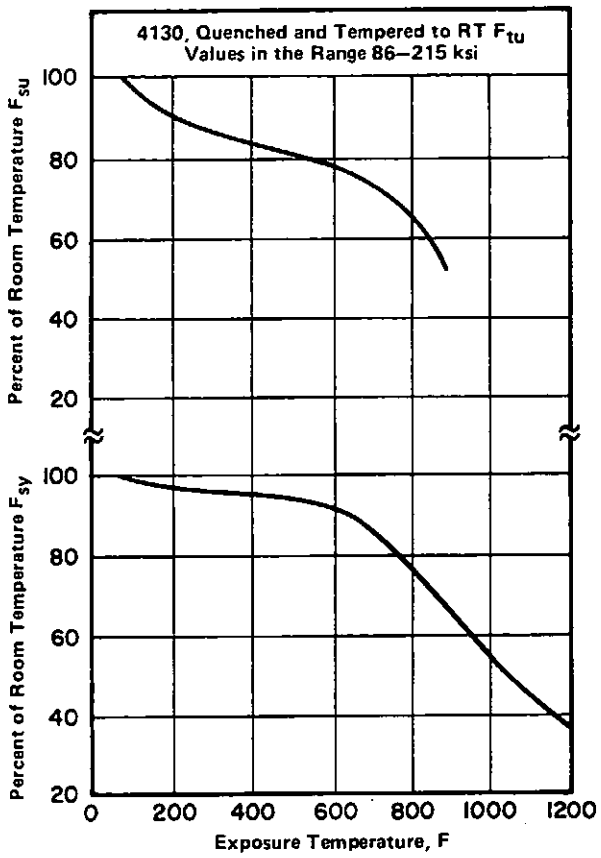


FIGURE 3.0353. EFFECT OF PRIOR TEST TEMPERATURE EXPOSURE UP TO 10 HOURS ON SHEAR PROPERTIES (63)

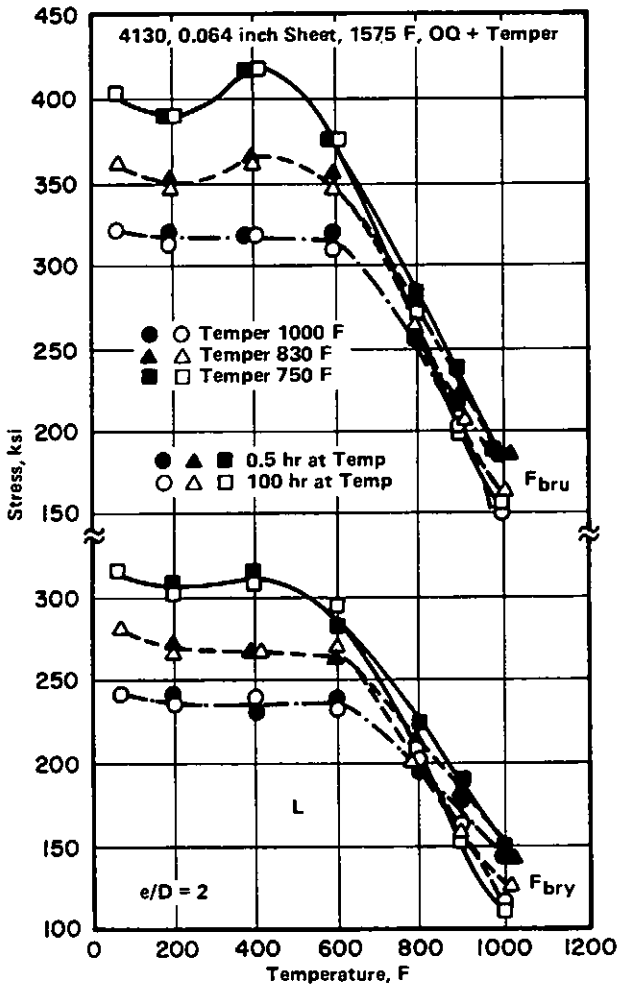


FIGURE 3.0361. EFFECT OF TEMPERATURE ON BEARING STRENGTH (e/D = 2) OF SHEET AFTER THREE DIFFERENT TEMPERING TREATMENTS AND TWO DIFFERENT EXPOSURE TIMES (14)

Fe
0.3 C
0.95 Cr
0.2 Mo

4130

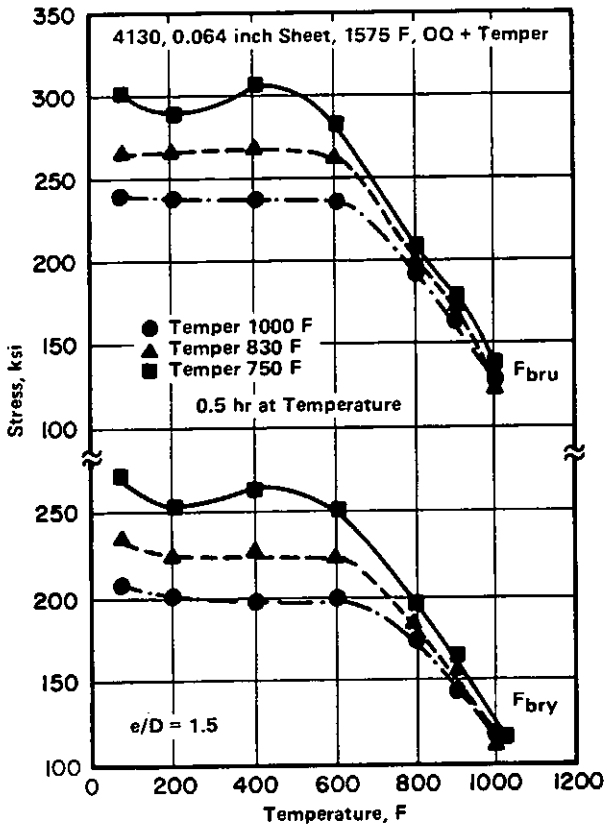


FIGURE 3.0362. EFFECT OF TEMPERATURE ON BEARING STRENGTH (e/D = 1.5) OF SHEET AFTER THREE DIFFERENT TEMPERING TREATMENTS (14)

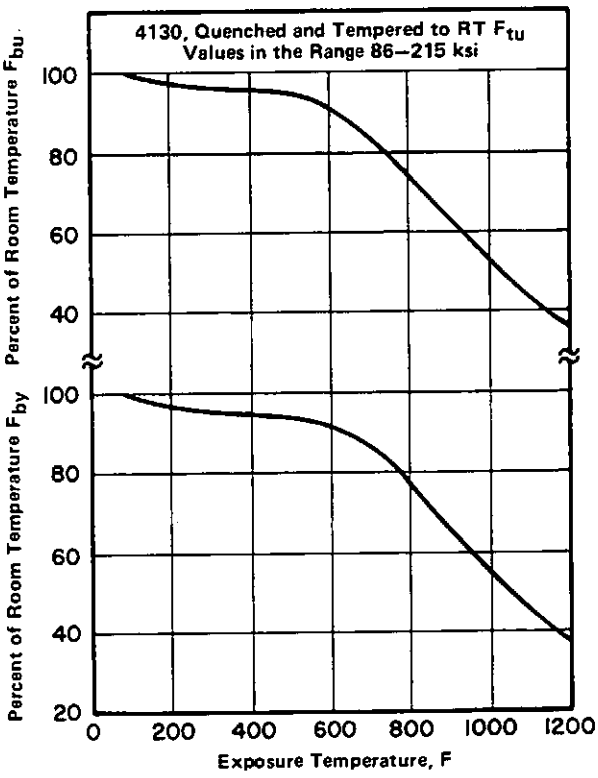


FIGURE 3.0363. EFFECT OF PRIOR TEST TEMPERATURE EXPOSURE UP TO 10 HOURS ON BEARING PROPERTIES (63)

Fe
0.3 C
0.95 Cr
0.2 Mo

4130

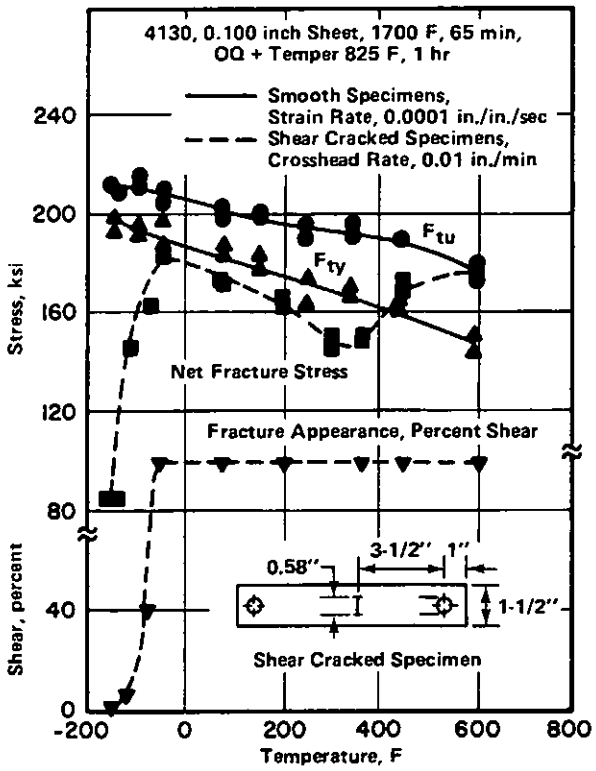


FIGURE 3.03711. COMPARISON OF TENSILE ULTIMATE (F_{tu}) AND YIELD (F_{ty}) STRENGTHS WITH CRACK STRENGTH (NET FRACTURE STRESS) AND FRACTURE APPEARANCE OF SHEAR-CRACKED SHEET SPECIMENS QUENCHED AND TEMPERED AT 825 F (38)

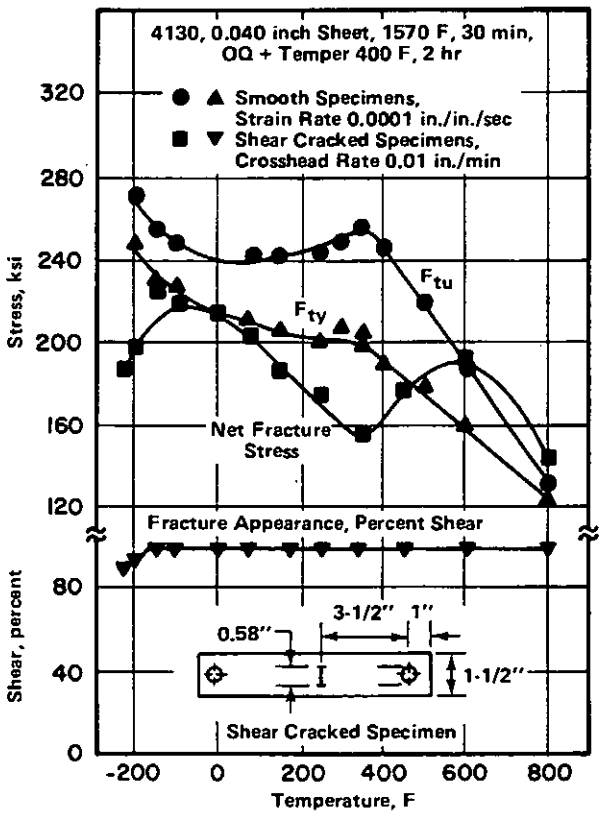


FIGURE 3.03712. COMPARISON OF TENSILE ULTIMATE (F_{tu}) AND YIELD (F_{ty}) STRENGTHS WITH CRACK STRENGTH (NET FRACTURE STRESS) AND FRACTURE APPEARANCE OF SHEAR-CRACKED SHEET SPECIMENS QUENCHED AND TEMPERED AT 400 F (38)

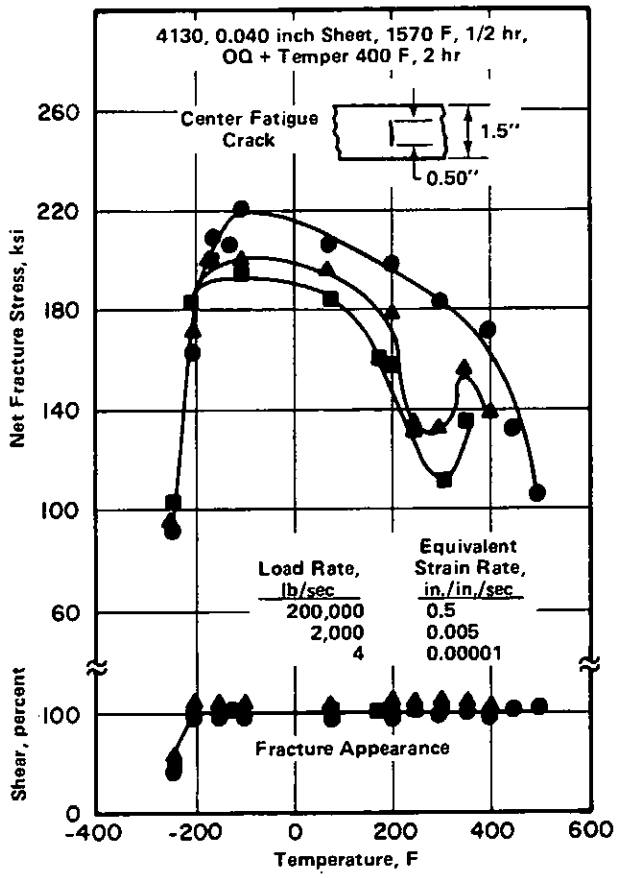


FIGURE 3.03713. EFFECT OF TEMPERATURE AND LOADING RATE ON CRACK STRENGTH (NET FRACTURE STRESS) AND FRACTURE APPEARANCE OF FATIGUE-CRACKED SHEET SPECIMENS QUENCHED AND TEMPERED AT 400 F (39)

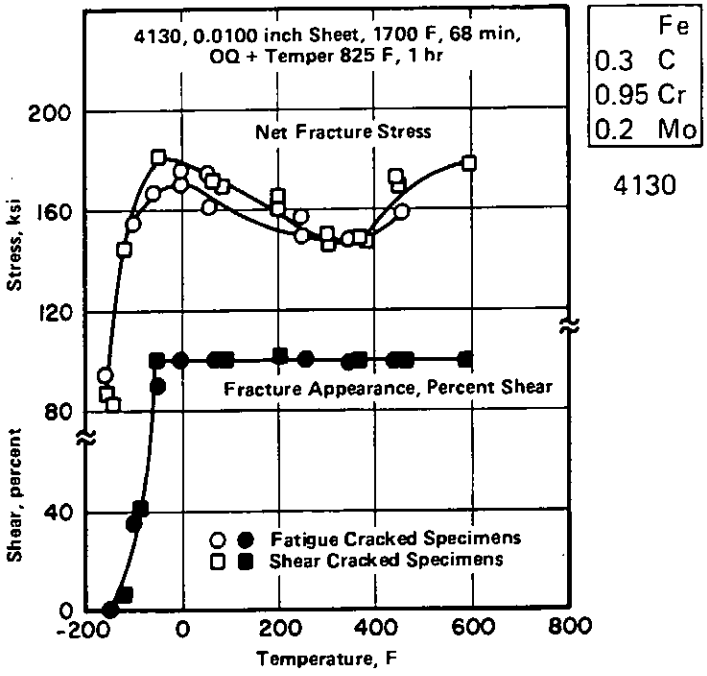


FIGURE 3.03714. EFFECT OF TEMPERATURE ON CRACK STRENGTH (NET FRACTURE STRESS) AND FRACTURE APPEARANCE OF BOTH FATIGUE-CRACKED AND SHEAR-CRACKED SHEET SPECIMENS QUENCHED AND TEMPERED AT 825 F (38)

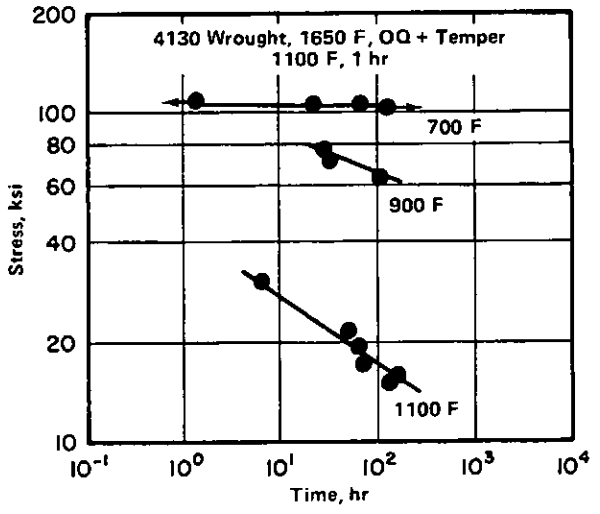


FIGURE 3.041. CREEP-RUPTURE CURVES FROM 700 TO 1100 F (40)

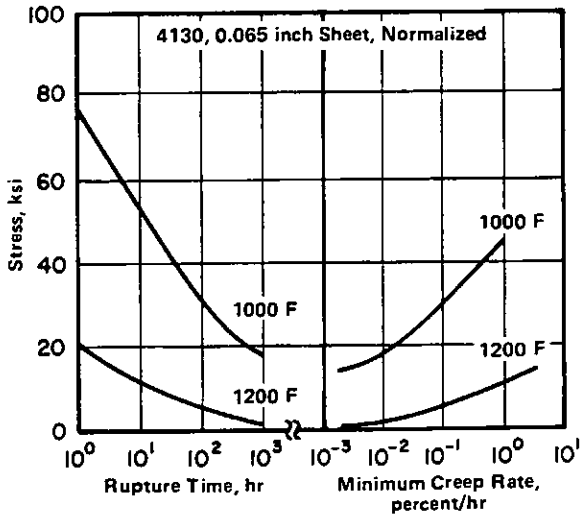


FIGURE 3.042. CREEP-RUPTURE AND MINIMUM-CREEP-RATE CHARACTERISTICS OF NORMALIZED SHEET AT 1000 AND 1200 F (18)

Fe
0.3 C
0.95 Cr
0.2 Mo

4130

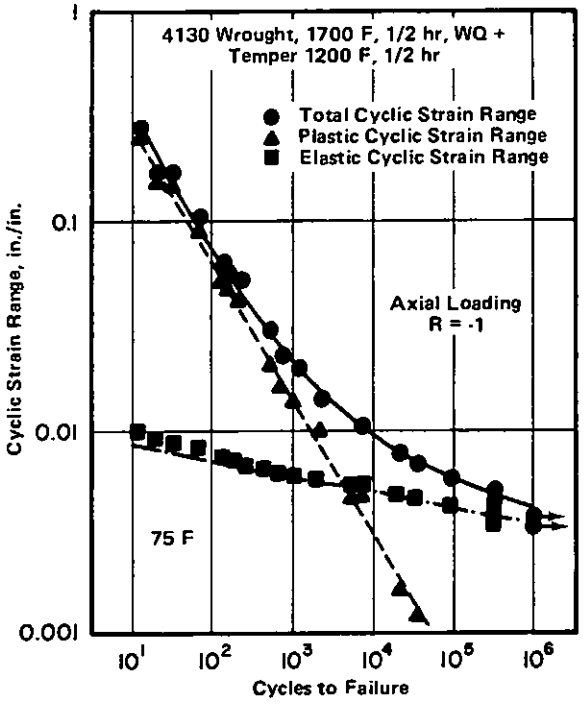


FIGURE 3.051. FATIGUE LIFE AS A FUNCTION OF CYCLIC STRAIN FOR TYPE 4130 TEMPERED AT 1200 F (22)

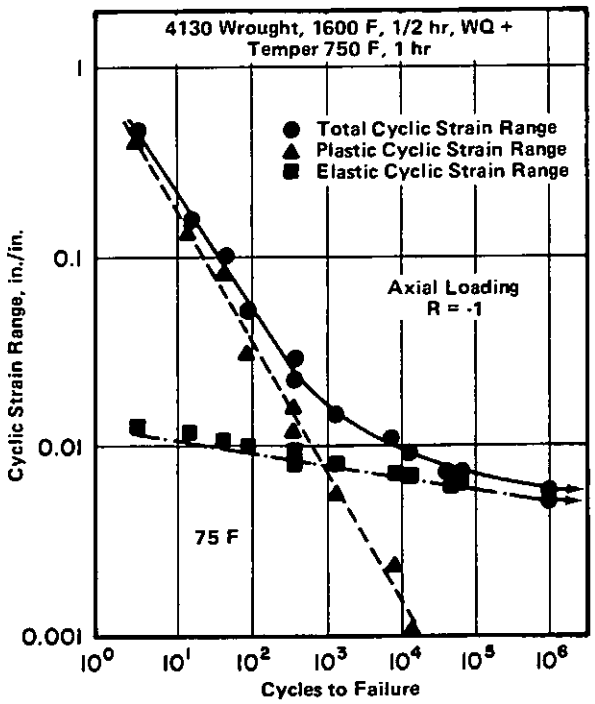


FIGURE 3.052. FATIGUE LIFE AS A FUNCTION OF CYCLIC STRAIN FOR TYPE 4130 TEMPERED AT 750 F (22)

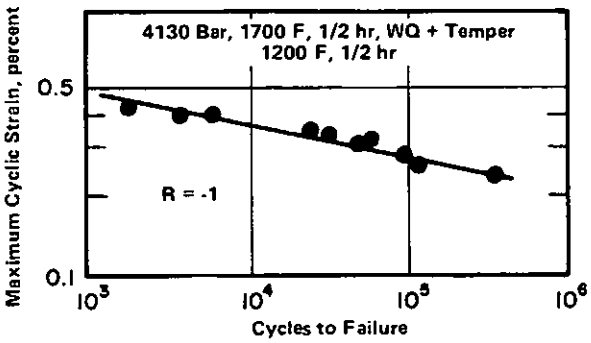


FIGURE 3.053. EFFECT OF MAXIMUM CYCLIC TENSILE STRAIN ON FATIGUE LIFE IN REVERSED BENDING (24)

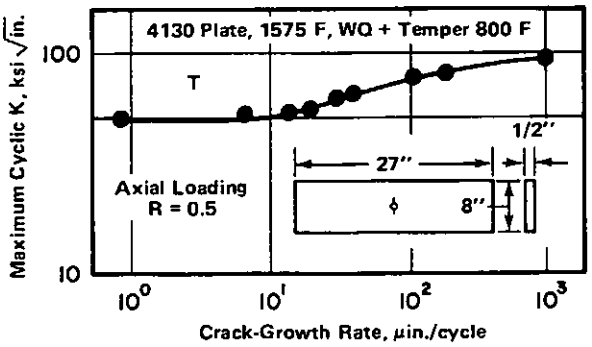


FIGURE 3.054. FATIGUE-CRACK-GROWTH RATE AS A FUNCTION OF MAXIMUM CYCLIC STRESS INTENSITY FACTOR (K) FOR CENTER-CRACKED SPECIMENS (23)

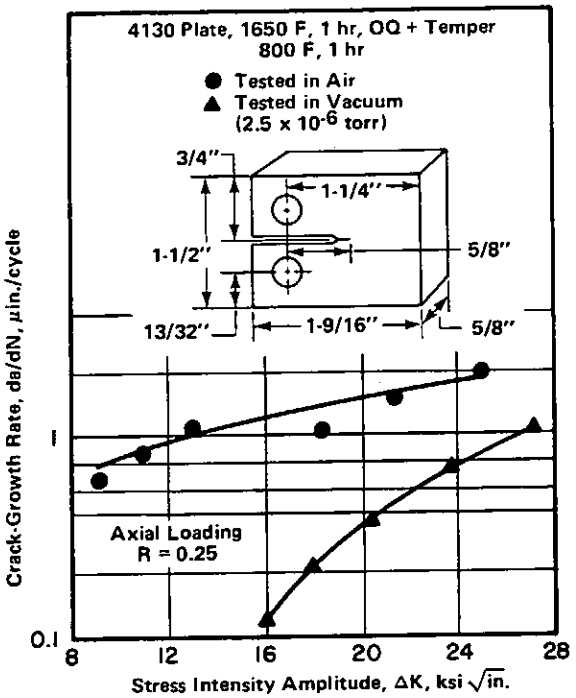


FIGURE 3.055. FATIGUE-CRACK-GROWTH RATE IN AIR AND VACUUM AS A FUNCTION OF STRESS INTENSITY AMPLITUDE (ΔK) FOR COMPACT TENSION SPECIMEN (25)

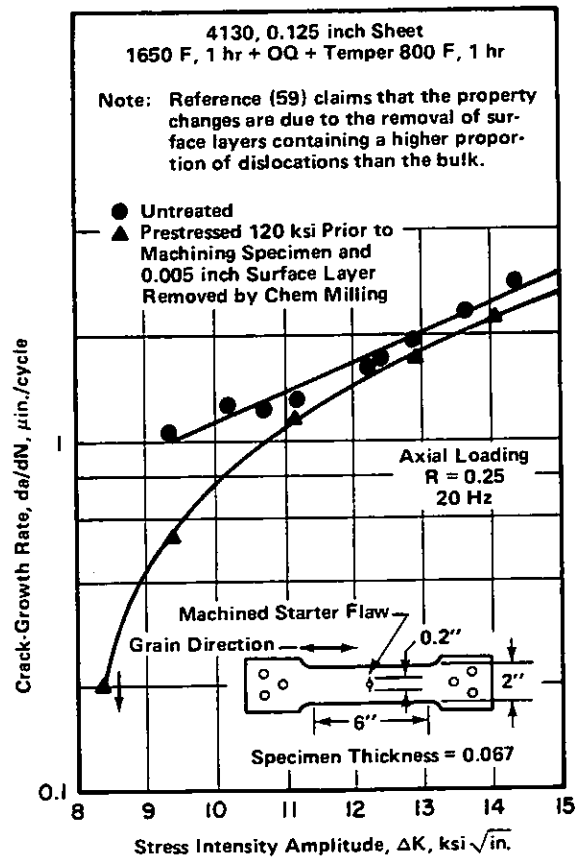
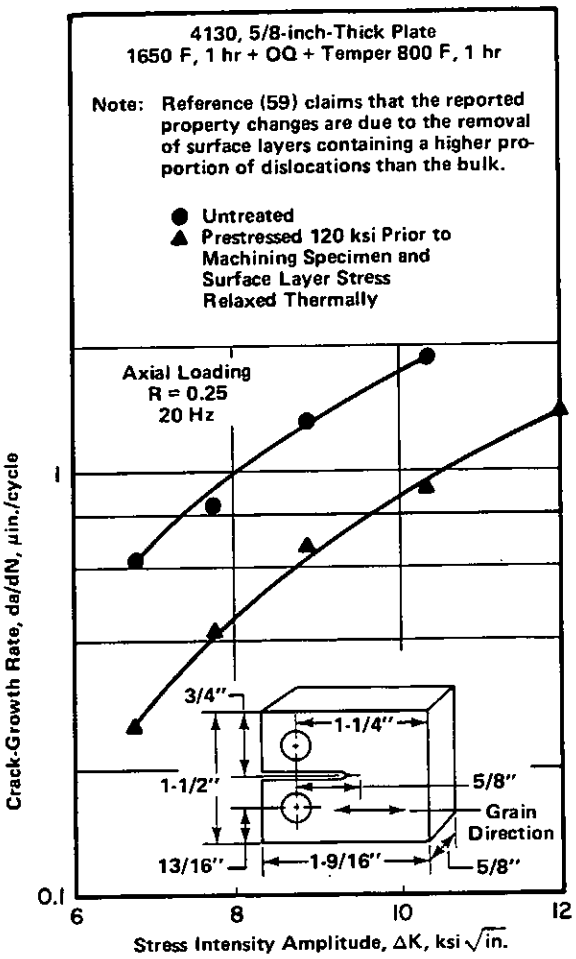


FIGURE 3.057. EFFECT OF PRESTRESSING AND CHEMMILLING ON FATIGUE CRACK GROWTH RATE OF SHEET (59)



Fe
0.3 C
0.95 Cr
0.2 Mo

4130

FIGURE 3.056. EFFECT OF PRESTRESSING AND REMOVAL OF SURFACE-LAYER STRESS BY THERMAL RELAXATION ON FATIGUE CRACK GROWTH RATE OF PLATE (59)

Fe
0.3 C
0.95 Cr
0.2 Mo

4130

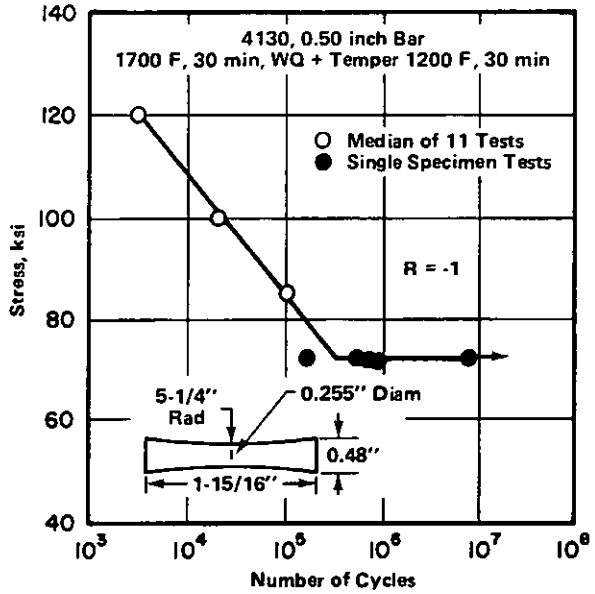


FIGURE 3.058. S-N CURVE AT ROOM TEMPERATURE IN ROTATING BENDING (41)

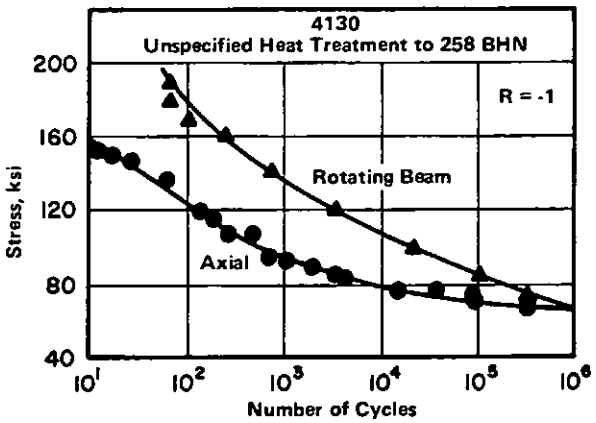


FIGURE 3.059. COMPARISON OF AXIAL-LOADING AND ROTATING-BEAM-BENDING FATIGUE DATA (65)

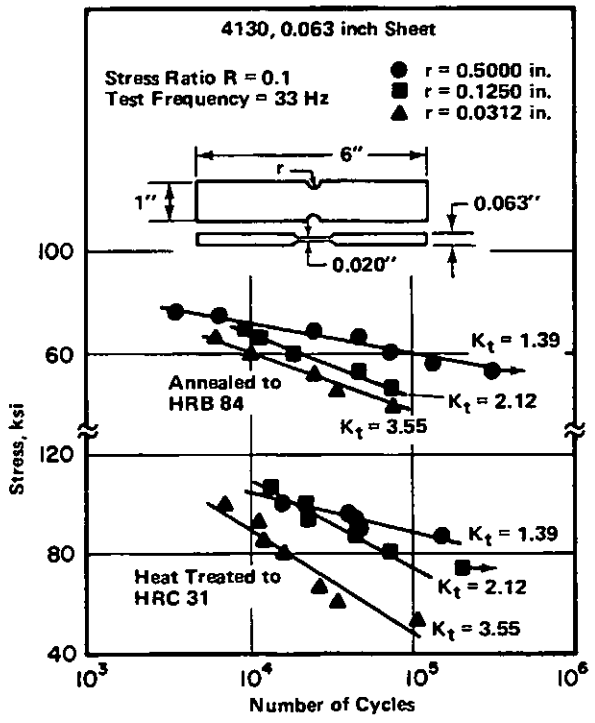


FIGURE 3.0510. AXIAL-STRESS S-N CURVES FOR EDGE-NOTCHED SPECIMENS (65)

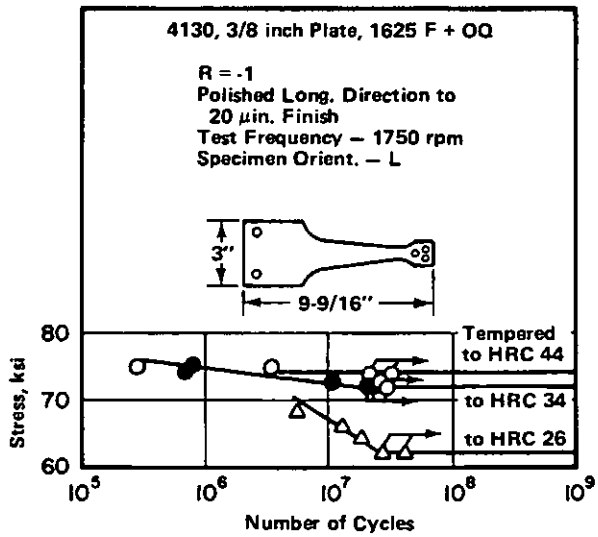


FIGURE 3.0511. EFFECT OF TEMPER TREATMENT (MEASURED BY ROCKWELL HARDNESS) ON REPEATED-BENDING FATIGUE PROPERTIES (49)

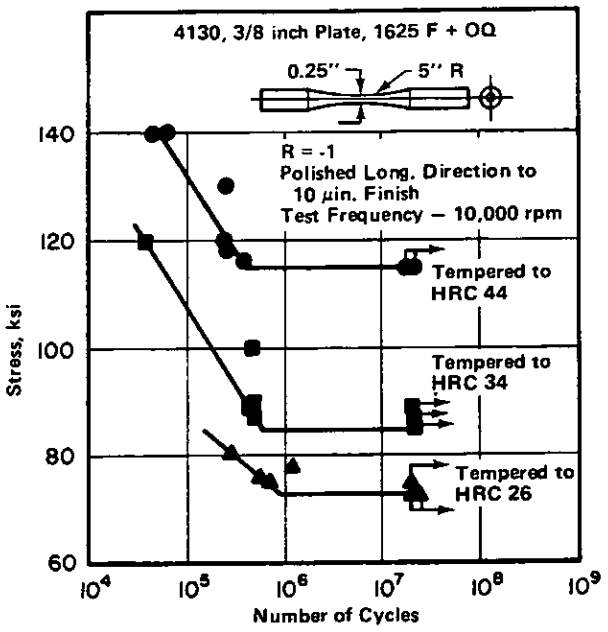


FIGURE 3.0512. EFFECT OF TEMPER TREATMENT (MEASURED BY ROCKWELL HARDNESS) ON ROTATING-BEAM FATIGUE PROPERTIES (49)

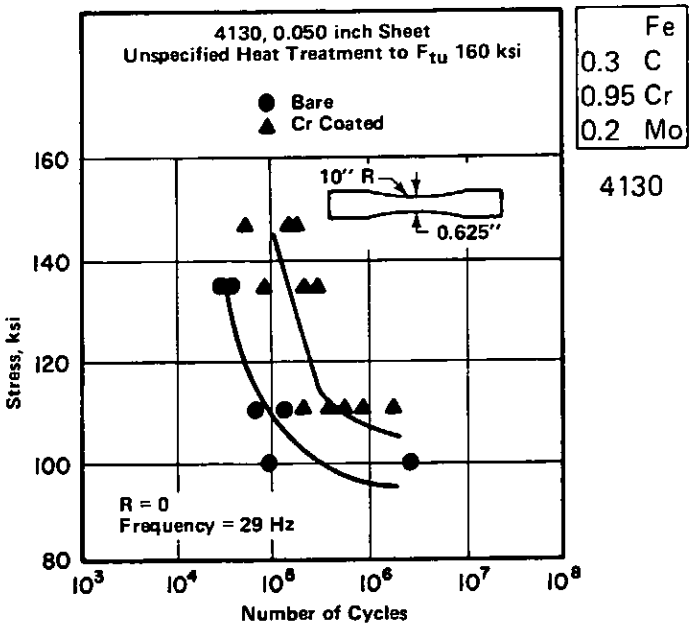


FIGURE 3.0513. EFFECT OF CHROMIUM COATING ON AXIAL-STRESS FATIGUE PROPERTIES OF SHEET (57)

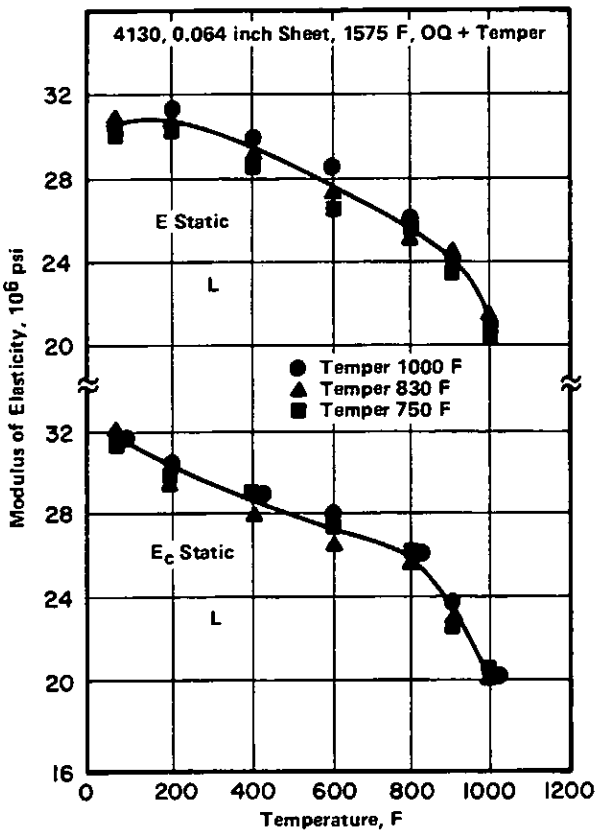


FIGURE 3.0621. EFFECT OF TEMPERATURE ON MODULUS OF ELASTICITY IN TENSION AND COMPRESSION OF SHEET AFTER THREE DIFFERENT TEMPERING TREATMENTS (14)

Fe
0.3 C
0.95 Cr
0.2 Mo

4130

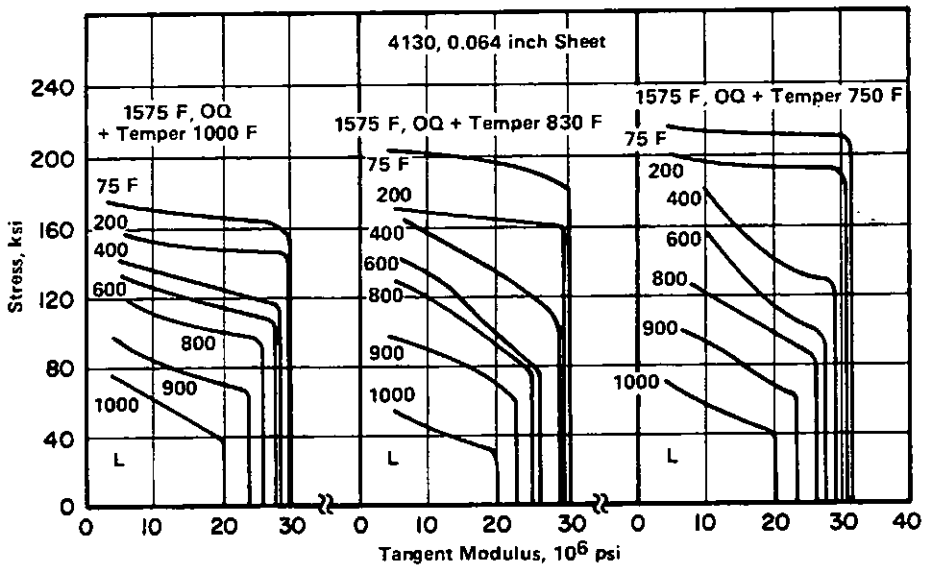


FIGURE 3.0622. COMPRESSIVE TANGENT MODULUS CURVES FOR SHEET AFTER THREE DIFFERENT TEMPERING TREATMENTS (14)

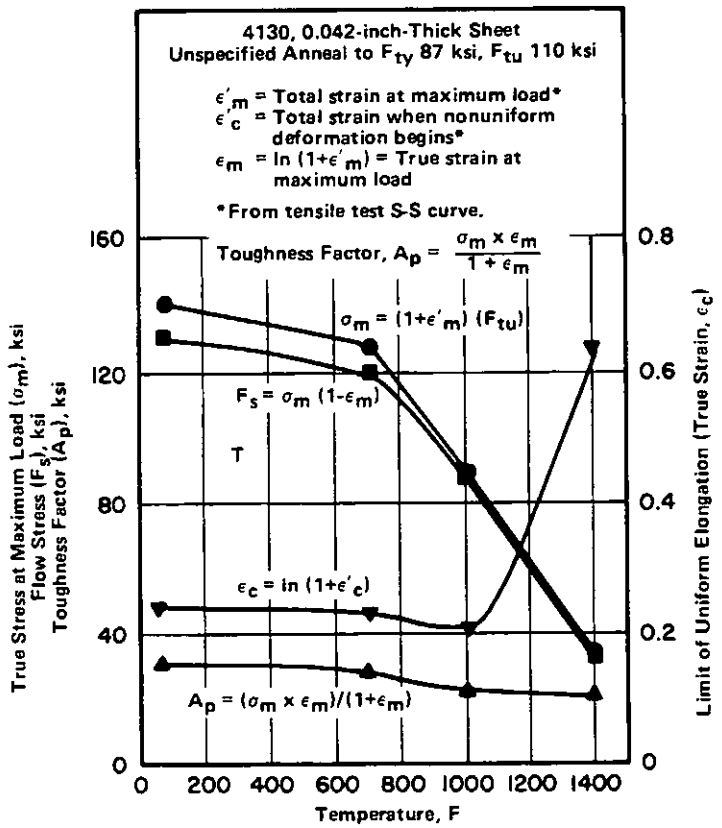


FIGURE 4.013. EFFECT OF TEMPERATURE ON FORMABILITY OF SHEET (53)

Fe
0.3 C
0.95 Cr
0.2 Mo

4130

Alloy	4130			
Form	0.50-inch-Thick Plate			
Condition	OQ + 1250 F + Weld With 8016N Coated Stick Electrodes (2.5 percent Ni)			
Specimens	Orientation	F_{ty}, ksi	F_{tu}, ksi	e (2 in.), percent
Parent metal	L	97.5	113	24.8
	T	94.5	110	20.2
As welded	L	79.0	105	20.2
	T	81.0	106	21.2

TABLE 4.032. TENSILE PROPERTIES OF PARENT METAL AND OF 0.5 INCH THICK PLATE WITH BUTT WELD AT THE CENTER OF THE SPECIMEN GAGE LENGTH (26)

Alloy	4130
Form	0.50-inch-Thick Plate
Condition	OQ + 1250 F + Weld With 8016Q Coated Stick Electrodes (2.5 percent Ni)
Test Temp, F	-65
Notch Position	Charpy V, ft-lb
In weld metal	22
In heat-affected zone	34
In outer edge of heat-affected zone	31
In parent metal (longitudinal)	130
In parent metal (transverse)	44

TABLE 4.033. CHARPY-V NOTCH IMPACT PROPERTIES AT -65 F OF BUTT-WELDED 0.50-INCH-THICK PLATE (26)

Alloy	4130					
Form	0.090 inch Sheet					
Condition	Annealed or As Welded			1575 F, 1 hr, OQ + 900 F, 1 hr		
	F_{ty}, ksi	F_{tu}, ksi	e (2 in.), percent	F_{ty}, ksi	F_{tu}, ksi	e (2 in.), percent
Base Metal	43.6	68.6	30.4	151.6	167.5	8.9
GTA[a]	46.3	67.1	21.8	150.4	163.5	8.6
PGTA[b]	17.3	66.5	19.6	153.8	165.7	8.6
GMA[c]	45.4	66.4	18.2	151.9	165.5	7.8
PGMA[d]	48.1	69.2	16.5	153.9	164.1	7.2

(a) Gas tungsten arc welded.
(b) Pulsed gas tungsten arc welded.
(c) Gas metal arc welded.
(d) Pulsed gas metal arc welded.

TABLE 4.034. TENSILE PROPERTIES OF SHEET BUTT WELDED BY VARIOUS ARC PROCESSES (43)

Fe
0.3 C
0.95 Cr
0.2 Mo

4130

Alloy	4130		
Form	0.125 inch Sheet		
	F_{ty}, ksi	F_{tu}, ksi	e (2 in.), percent
Annealed	48.9	68.4	30.7
GTA Welded	47.8	67.0	22.9

TABLE 4.035. TENSILE PROPERTIES OF BUTT-WELDED SHEET (60)

Alloy	4130			
Form	Sheet and Plate Butt Welds – Beads Off			
			Duplicate Tests	
Type Electrode	Weld Heat Treatment (to F_{tu} Listed)	Thickness, in.	F_{tu}, ksi	Failure Location[a]
Arcaloy 502	150 ksi	0.185	158	H B
		0.236	150	– –
		0.375	161	H W
		0.500	152	H H
	175 ksi	0.078	165	– –
		0.100	177	– –
		0.236	176	W B
		0.245	159	– –
		0.375	178	H H
		0.500	162	W W
P & H21	150 ksi	0.235	156	B B
		0.350	155	B B
		0.492	154	W H
	175 ksi	0.077	176	– –
		0.162	180	– –
		0.235	166	W W
		0.255	164	– –
		0.235	173	W W
		0.492	166	W W
AW-4	175 ksi	0.095	175	– –

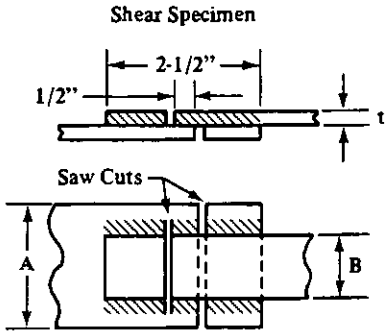
(a) H = heat-affected zone, W = weld metal, B = base metal.

TABLE 4.036. EFFECT OF ELECTRODE ALLOY AND SHEET OR PLATE THICKNESS ON TENSILE ULTIMATE STRENGTH OF BEAD-OFF BUTT WELDS (70)

Fe
0.3 C
0.95 Cr
0.2 Mo

4130

Alloy	4130		
Form	Sheet and Plate Fillet Welds		
Type Electrode	Weld Heat Treatment (to F_{tu} Listed)	Thickness, in.	F_{su}, ksi
Arcaloy	150 ksi	0.076	93.3
		0.190	68.6
		0.248	64.5
		0.258	60.5
		0.385	62.5
		0.496	44.3
	175 ksi	0.076	98.7
		0.190	74.3
		0.250	66.5
		0.260	62.9
		0.388	62.1
		0.496	44.3
P & H21	150 ksi	0.076	98.1
		0.156	78.8
		0.246	77.5
		0.250	65.8
		0.380	55.5
		0.512	50.3
	175 ksi	0.076	93.4
		0.156	83.4
		0.245	74.8
		0.250	57.1
		0.380	54.6
		0.512	52.0
AW-4	150 ksi	0.076	100.8
		0.093	93.8
		0.123	87.0
		0.255	58.8
		0.258	60.8
		0.388	58.8
		0.500	49.2
	175 ksi	0.078	99.1
		0.093	94.3
		0.123	90.1
		0.255	58.6
		0.260	61.6
		0.386	53.5
		0.496	40.8



t	A	B
1/4	2	1
3/8	2	1
1/2	3	1-1/2

TABLE 4.037. EFFECT OF ELECTRODE ALLOY AND SHEET OR PLATE THICKNESS ON SHEAR ULTIMATE STRENGTH OF LONGITUDINAL-WELD LAP JOINTS (70)

Fe
0.3 C
0.95 Cr
0.2 Mo

4130

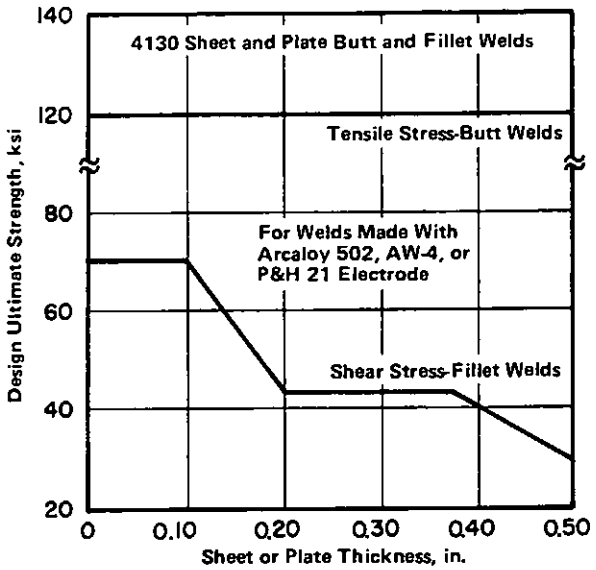


FIGURE 4.038. TENSILE AND SHEAR ULTIMATE-STRENGTH DESIGN CURVES FOR SHEET AND PLATE WELDS HEAT TREATED TO EITHER 150 OR 175 KSI (70)

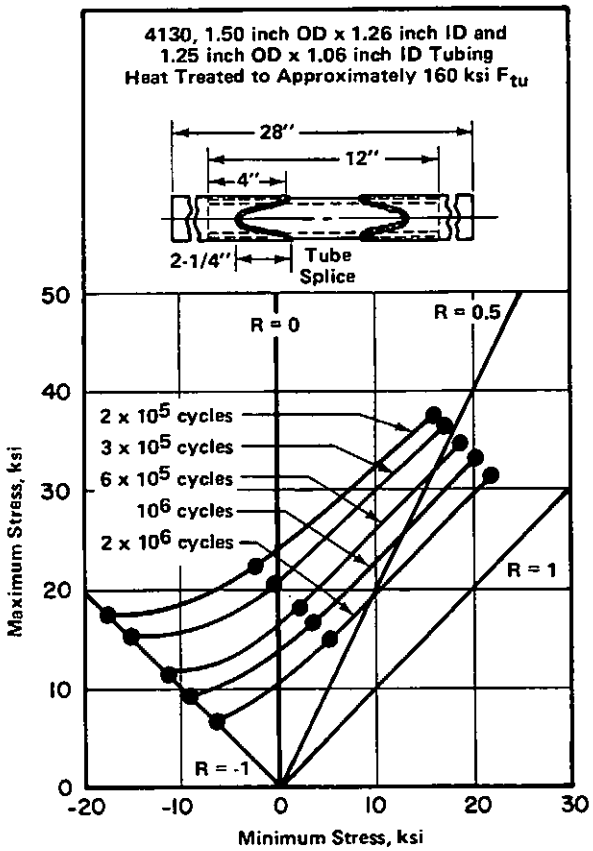


FIGURE 4.039. CONSTANT-LIFE DIAGRAM FOR AN AXIAL-LOADED TUBE SPLICE – STRESSES CALCULATED IN THE LARGE TUBE (61)

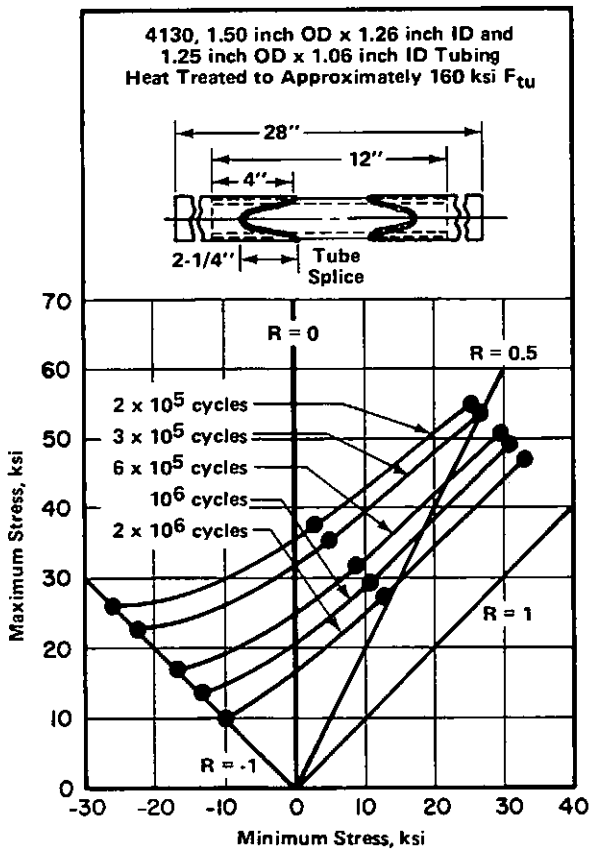


FIGURE 4.0310. CONSTANT-LIFE DIAGRAM FOR AXIAL-LOADED TUBE SPLICES – STRESSES CALCULATED IN SMALL TUBE (61)

Fe
0.4 C
1 Cr
0.2 Mo

4140

1 **GENERAL**

This heat treatable low-alloy steel is similar in chemical composition to Type 4130, except that 4140 has higher carbon content. The increased carbon content provides greater hardenability and strength with some sacrifice in formability and weldability. It is generally used in the oil-quenched and tempered condition, which provides optimum properties; nevertheless, the somewhat lower mechanical properties of the normalized and normalized-and-tempered conditions are adequate for some applications. It can be used to a maximum temperature of about 900 F, above which its strength decreases rapidly with increasing temperature. Like other martensitic and ferritic steels, Type 4140 undergoes a transition from ductile to brittle behavior at low temperatures, the temperature level varying with heat treatment and degree of stress concentration. Since it is susceptible to rusting, it should be protected by paint, electroplate, or other protective coatings for applications in moist, marine, or other corrosive environments. It is widely used in applications requiring a good combination of moderate hardenability, strength, and toughness.

1.01 **Commercial Designation**

4140.

1.02 **Alternate Designations**

AISI 4140, SAE 4140, 4140H, UNS G41400, and UNS J14046.

1.021 The 4140H designation indicates that the steel is made within strict hardenability limits.

1.03 **Specifications**

1.031 Specifications, Table 1.031.

1.04 **Composition**

1.041 Composition, Table 1.041.

1.05 **Heat Treatment**

1.051 Normalize: 1550 to 1650 F, air cool (2, 32).

1.052 Anneal: 1450 to 1600 F, furnace cool (2, 16, 32).

1.053 Harden: 1525 to 1600 F, oil quench. (For water quench, which is rarely used for 4140, 1500 to 1550 F) (2, 32).

1.054 Temper: 350 to 450 F or 700 to 1250 F, 1/2 hour minimum, air cool or water quench. Tempering in the range 450 to 700 F is usually not recommended because the blue-brittleness phenomenon occurs in that range. The alloy is not susceptible to temper embrittlement which occurs in some low-alloy steels in the range 800 to 1100 F (2).

1.055 Spheroidize: 1400 to 1425 F, 6 to 12 hours, furnace cool (2), or 1550 F, furnace cool to 1300 to 1350 F, 6 hours, air cool (16).

1.056 Stress relieve: 1100 to 1250 F, air cool.

1.06 **Hardness**

1.061 Effect of tempering temperature on hardness, Figure 1.061.

1.062 Effect of diameter on surface hardness of quenched and tempered bar, Figure 1.062.

1.063 Effect of diameter on as-quenched hardness at various locations on cross section of bar, Figure 1.063.

1.064 Effects on room temperature hardness of exposures up to 30 hours at various elevated temperatures, Figure 1.064.

1.065 Hardness in unhardened conditions, Table 1.065.

1.066 Effects of 1-hour exposures to elevated temperatures on the room temperature hardness of bars cold rolled various amounts after heat treatment, Figure 1.066.

1.067 Effects of 1-hour exposures to elevated temperatures on the room temperature hardness of bars that had been annealed and then cold rolled various amounts, Figure 1.067.

1.068 End-quench hardenability, Figure 1.068.

1.069 Increased phosphorus (within the specified composition limit) increases the hardenability of Type 4140, as shown in Figure 1.0610. This behavior is attributed to segregation and interaction of phosphorus and carbon at austenite grain boundaries (43).

1.0610 End-quench hardenability curves for 4140 containing high and low phosphorus, Figure 1.0610.

1.07 **Forms and Conditions Available**

1.071 Wrought products are available in the full range of sizes and forms including plate, sheet, strip, bars, rods, billets, forgings, and tubing. The products can be furnished in the annealed, normalized, spheroidized hot-finished, cold-finished, die-drawn-and-tempered, and hardened-and-tempered conditions (1, 2, 16)

1.072 Sand, centrifugal, and investment castings are available in all heat treated conditions.

1.08 **Melting and Casting Practice**

1.081 The alloy is generally air melted in basic-electric, basic-open-hearth, or basic-oxygen furnaces. For some applications requiring exceptional quality, it is induction or consumable-electrode remelted in vacuum.

1.09 **Special Considerations**

1.091 Most of the common acid-pickling processes can cause hydrogen embrittlement of Type 4140 that has been heat treated to high strength levels. However, nitric acid has been reported to be hydrogen embrittling only when used in the range 0.3 to 0.8N. Higher concentrations are recommended for pickling purposes. Anodic cleaning processes are nonhydrogen embrittling because the workpiece is made the anode during electrolysis; consequently, no hydrogen is deposited on it. Alkaline descaling has also been reported to provide complete freedom from hydrogen embrittlement. Hydrogen embrittlement resulting from acid pickling can generally be relieved by baking about 2 to 4 hours at 375 F (15).

1.092 Cadmium plating and chromium plating can induce hydrogen embrittlement in Type 4140 that has been heat treated to tensile strength levels above 180 ksi. Ductility can be restored by baking at 375 F for 4 hours after cadmium plating and for 2 hours after chromium plating (9).

1.093 Hydrogen embrittlement can also occur in Type 4140, heat treated to F_{tu} above 180 ksi, when it is exposed to an environment of high-pressure hydrogen. The embrittlement can be relieved by

Fe
0.4 Cr
1 Cr
0.2 Mo
4140

exposure to air at room temperature for one or more days (8, 14).

1.0931 Effects of exposures to high pressure hydrogen on notched tensile strength, Table 1.0931.

1.094 In commercial wrought grades, transverse mechanical properties are inferior to longitudinal due to inclusions which act as stress raisers with their major effects in the transverse direction. (See Tables 3.0216, 3.0217, and 3.0233 and Figure 3.051.) Available data indicate that this directionality is more pronounced the larger the section size and the higher the strength. It can be minimized by vacuum melting or any other means of reducing nonmetallic inclusions (29).

1.095 Studies of Type 4140 castings have shown that gas holes and shrinkage defects cause percentage decreases in tensile strength appreciably greater than the percentage of cross section that they occupy (3).

1.0951 Effect of gas holes and shrinkage defects on tensile strength of castings, Figure 1.0951.

1.096 Type 4140 is subject to stress corrosion and to corrosion fatigue, especially when heat treated to high hardness levels. Crack propagation rates are increased and fatigue strength is considerably reduced in aqueous or seawater environments. (See Section 2.031.)

1.097 Type 4140 is embrittled at intermediate temperatures when in contact with lead, cadmium, or other low melting point metals. Type 4140 to which lead has been added for improved machinability and Type 4140 which has been cadmium plated for improved corrosion resistance are not suitable for use above 450 F. (See Sections 2.033 and 3.0315.)

2 PHYSICAL PROPERTIES AND ENVIRONMENTAL EFFECTS

2.01 Thermal Properties

2.011 Melting range, about 2790 F.

2.012 Phase changes.

2.0121 Time-temperature-transformation diagram, Figure 2.0121.

2.0122 Upon heating under equilibrium conditions, transformation from pearlite or martensite to austenite starts at 1380 F (Ac1) and is complete at 1460 F (Ac3) (2).

2.0123 Upon slow cooling under equilibrium conditions, the transformation from austenite to pearlite starts at 1370 F (Ar3) and is complete at 1280 F (Ar1) (2).

2.0124 Upon rapid quenching from the austenitic condition the transformation to martensite starts at 650 F (Ms) and is complete at 500 F (Mf) (2).

2.013 Thermal conductivity, 22 Btu ft/hr ft^2 F (34).

2.014 Thermal expansion, 6.3 x 10^{-6} in./in./F from 0 to 200 F (34).

2.015 Specific heat, 0.107 Btu/lb F (34).

2.016 Thermal diffusivity.

2.02 Other Physical Properties

2.021 Density, 0.283 lb/$in.^3$, 7.83 gr/cm^3 (34).

2.022 Electrical properties.

2.023 Magnetic properties, ferromagnetic.

2.024 Emittance.

2.025 Damping capacity.

2.03 Chemical Environments

2.031 Stress corrosion.

2.0311 Type 4140 heat treated to high strength levels is subject to stress corrosion cracking in aqueous environments, including distilled water. Hardness or strength level is the primary criterion for assessing susceptibility to stress corrosion. As shown in Figure 2.0312, the critical hardness level for stress corrosion cracking in boiling distilled water is 40 to 42 HRC, corresponding to a yield strength of 170 to 185 ksi. Harder material failed in a matter of hours under the conditions shown, while softer material did not fail after 200 hours' exposure. Similar behavior may be expected at room temperature at longer times. This critical hardness level is confirmed by laboratory tests, atmospheric service tests, and practical experience.

Type 4140 steel at all hardness levels fails more readily by stress corrosion cracking in nitrate solutions than in distilled water or in aqueous sodium chloride solutions. Stress corrosion cracking in nitrate solutions is attributed to reduction in metal bond strength by NO_3^- ions adsorbed on appropriate imperfection sites associated with carbon atoms. At higher hardness levels, adsorbed water alone reduces metal bond strength sufficiently to initiate cracks (44, 45). (See also Table 3.0281.)

2.0312 Effect of heat treated hardness on stress corrosion cracking in aqueous solutions, Figure 2.0312.

2.0313 The resistance to stress corrosion cracking is improved by cold work, as shown in Figure 2.0314.

2.0314 Effect of cold rolling on stress corrosion cracking in boiling aqueous solutions, Figure 2.0314.

2.0315 A thin decarburized soft surface layer over a core of hardness greater than HRC 40 effectively prevents initiation of stress corrosion cracking (45).

2.0316 The stress corrosion crack-growth rate is faster in distilled water than in air, as shown in Figure 2.0317.

2.0317 Stress corrosion crack-growth rate as a function of stress intensity in water and in air at room temperature, Figure 2.0317.

2.0318 The fatigue strength is considerably reduced in seawater as compared to air because of corrosion fatigue, as shown in Figure 2.0319.

2.0319 Corrosion fatigue in natural seawater as compared to air at room temperature, Figure 2.0319.

2.032 Oxidation.

2.0321 Type 4140 will ignite and burn when fractured in 1000 psig oxygen flowing at 1400 fps at a nominal temperature of about 600 F. The ignition temperature increases as the oxygen pressure is reduced (46).

2.033 Metal-induced embrittlement.

2.0331 Although wrought 4140 steel is normally ductile, embrittlement and delayed fracture can result when the alloy is placed under tensile stress and simultaneously into intimate contact with certain lower-melting metals. This phenomenon, termed metal-induced embrittlement, has been observed with solid cadmium, lead, tin, zinc, and solid and liquid indium (47); it is very similar to the tensile embrittlement discussed later in Section 3.0315.

The lowered fracture stress can be lower than the normal yield stress. Delayed fracture can be separated into two component processes, crack initiation and crack propagation. The temperature dependence of the time required for each of these two processes is shown in Figure 2.0332 for 4140 steel coated with indium in the center of the reduced section of tensile specimens. Crack initiation occurs after an incubation period of minutes to hours below the melting point of indium and after minutes or fractions of a minute above the melting point. This process is stress dependent and occurs more rapidly with increasing stress above a threshold stress of 150 ksi at temperatures near the melting point of indium. Crack propagation time, however, is independent of stress. It is temperature dependent below the melting point of indium, but occurs almost instantaneously above the melting point. The time for crack initiation is believed dependent on diffusion of indium along grain boundaries of the 4140 steel. Crack propagation depends on the presence of indium at the advancing crack tip, which is governed by indium self-diffusion in the solid state or liquid metal flow in the liquid state (47, 48).

2.0332 Delayed fracture of 4140 steel caused by metal-induced embrittlement with indium [(a) crack initiation and (b) crack propagation], Figure 2.0332.

2.04 **Nuclear Environments**

3 MECHANICAL PROPERTIES

3.01 **Specified Mechanical Properties**

3.011 AMS specified mechanical properties at room temperature, Table 3.011.

3.02 **Mechanical Properties at Room Temperature**

3.021 Tension – stress-strain diagrams – tension properties.

3.0211 Effect of tempering temperature on tensile properties of bar, Figure 3.0211.

3.0212 Effect of tempering temperature on tensile properties of castings, Figure 3.0212.

3.0213 Effect of diameter on tensile properties of quenched and tempered bar, Figure 3.0213.

3.0214 Tensile properties of normalized bars from 1/2 to 4 inch in diameter and of annealed bar 1.0 inch in diameter, Figure 3.0214.

3.0215 Effect of cold rolling on tensile properties of bar, Figure 3.0215.

3.0216 Tensile properties of extrusions, Figure 3.0216.

3.0217 Effect of specimen orientation on tensile properties of 6-inch-diameter bar heat treated to two hardness levels, Figure 3.0217.

3.0218 Tensile properties of bar in unhardened conditions, Table 3.0218.

3.0219 Tensile properties of castings, Table 3.0219.

3.02110 Relation between yield strength and hardness for 4140 steel, Figure 3.02110.

3.02111 The ultimate tensile strength of 4140 steel varies with carbide particle size and shape as shown in Figure 3.02112. Carbides in as-quenched material or in material tempered at 390 F or 570 F are needle-shaped, while those produced by tempering at 1020 F or higher are spheroidal. The latter carbides are larger and less strengthening than the former. The spheroidal carbides reflect diffusional coarsening and the reduction of total surface energy as compared to newly precipitated needle-shaped carbides (49). The ultimate tensile strength of as-quenched 4140 steel is approximately equal to the stress for microvoid formation. The initiation of microvoids, either by decohesion at the carbide/matrix interface or by cracking of the carbides themselves, may be the critical stage in the ductile fracture process (50).

Fe
0.4 C
1 Cr
0.2 Mo

4140

3.02112 Variation of ultimate tensile strength with carbide size and shape, Figure 3.02112.

3.02113 The monotonic and cyclic stress-strain curves for as-quenched material and for material tempered at 390, 750, and 1200 F (determined by the incremental step test) are shown in Figure 3.02114. Cyclic hardening is exhibited in the as-quenched condition, while the tempered materials all show cyclic softening. Cyclic softening is at a maximum for material tempered at 750 F. This softening is attributed to (a) mechanical "unpinning" of dislocations and (b) reduction in internal stress through generation of a fatigue substructure. Both the monotonic and cyclic stress-strain curves show a stress-differential effect, with compressive flow stresses being higher than the tensile flow stresses (51).

3.02114 Monotonic and cyclic true stress-true strain curves for 4140 steel [(a) austenitized and quenched, (b) tempered at 390 F, (c) tempered at 750 F, and (d) tempered at 1200 F], Figure 3.02114.

3.022 Compression – stress-strain diagrams – compression properties. (See also Section 3.02113.)

3.0221 Compressive yield strength. (See Figure 3.0321.)

3.023 Impact.

3.0231 Effect of tempering temperature on impact properties at room temperature, Figure 3.0231.

3.0232 Transverse impact properties of leaded and non-leaded 6-inch-diameter bar at room temperature, Figure 3.0232.

3.0233 Impact properties of extruded bar at room temperature in various heat treated conditions, Table 3.0233.

3.024 Bending.

3.025 Torsion and shear (see Figure 3.0351).

3.0251 Effect of tempering temperature on torsional properties, Figure 3.0251.

3.026 Bearing (see Figure 3.0361).

3.027 Stress concentration.

3.0271 Notch properties (see Table 1.0931).

3.0272 Fracture toughness.

3.02721 Effect of quenching and tempering temperature on plane strain fracture toughness, Figure 3.02721.

3.028 Combined properties.

3.0281 Burst properties of small pressure vessels, Table 3.0281.

3.03 **Mechanical Properties at Various Temperatures**

3.031 Tension – stress-strain diagrams – tension properties.

3.0311 Effect of elevated temperatures on tensile properties of quenched and tempered bar, Figure 3.0311.

Fe
0.4 Cr
1 Cr
0.2 Mo

4140

3.0312 Effect of exposure time at test temperature on elevated temperature tensile properties, Figure 3.0312.

3.0313 Effects of temperatures from -100 F to 200 F on tensile properties, Figure 3.0313.

3.0314 Effects of temperatures from -200 F to 80 F on tensile properties of 4140 tempered at 1050 F and at 725 F [(a) tempered at 1050 F, and (b) tempered at 725 F], Figure 3.0314.

3.0315 Type 4140 is embrittled during tensile testing at intermediate temperatures (roughly 400 F to 900 F) when in intimate contact with lead, cadmium, zinc, tin, or indium. The embrittling agent can be present internally, such as leaded 4140 for improved machinability, or on the surface, such as cadmium electroplated 4140 for improved corrosion resistance. Embrittlement becomes apparent above about 0.75 of the melting point of the low melting metal and is recovered at some temperature above this melting point. Tensile data for Type 4140 externally wetted with high purity lead are compared in Figure 3.0316 with similar data for clean Type 4140. Above about 350 F, or 0.75 of the absolute melting point of lead (621 F), the reduction in area and true fracture strength are significantly reduced. The effects of solid cadmium, zinc, tin, and indium are similar, with losses of RA noted at temperatures which are relative to the melting points of the respective embrittling metals (52).

External wetting with lead alloys containing small amounts of tin, antimony, zinc, or bismuth intensify the severity of embrittlement and/or extend the temperature range of embrittlement as compared to wetting with pure lead. The temperature for ductility recovery ranges from just above the melting point of lead for material wet with high purity lead to above 900 F for material wet with Pb-25Bi or Pb-0.1Zn (53).

Embrittlement is associated with the presence of the low melting metal at the crack tip during deformation of 4140. At temperatures above the melting point, the embrittling metal is believed to proceed down the crack as a liquid, aided by surface tension effects, and to complete its path to the crack tip as a vapor. At temperatures below the melting point, it has been proposed that the transit is by vapor transport alone (54), in contrast to the diffusional mechanism proposed for metal-induced embrittlement (47). (See Section 2.033.)

3.0316 Effects of surface wetting with lead on tensile properties [(a) unwetted and (b) wetted with pure lead], Figure 3.0316.

3.0317 The susceptibility to lead embrittlement can be reduced by prior cold work, as shown in Figure 3.0318. The entire embrittlement trough, which extends from 400 F to 850 F, can virtually be eliminated by combining cold work with heat treatment to produce material with the desired tensile strength, in this case 200 ksi. The room temperature ductility, however, is reduced by cold work. A second technique for elimination of lead embrittlement involves rare earth alloying through the addition of mischmetal during melting. In this case, cerium associates with the lead and eliminates embrittlement, as shown in Figure 3.0319 (54).

3.0318 Elimination of lead embrittlement by prior cold deformation, Figure 3.0318.

3.0319 Elimination of lead embrittlement by the addition of rare earth elements, Figure 3.0319.

3.032 Compression -- stress-strain diagrams -- compression properties.

3.0321 Effect of temperature on compressive yield strength of bar and forgings heat treated to various strength levels, Figure 3.0321.

3.033 Impact.

3.0331 Effects of test temperature, tempering temperature, and percentage of martensite in microstructure on impact properties, Figure 3.0331.

3.0332 Effects of exposures up to 30 hours at various elevated temperatures on impact resistance at -40 F, Figure 3.0332.

3.0333 Effects of temperature and prestrain on impact resistance of annealed bar, Figure 3.0333.

3.0334 Impact properties of castings at 70 F and -50 F, Table 3.0334.

3.0335 Effects of temperature from -200 F to 80 F on impact energy of 4140 tempered at 1050 F and at 725 F, Figure 3.0335.

3.0336 Effect of tempering temperature on impact resistance at -40 F, Figure 3.0336.

3.0337 Effect of tempering temperature on impact ductile-brittle transition temperature, Figure 3.0337.

3.034 Bending.

3.035 Torsion and shear.

3.0351 Effect of temperature on shear strength of bar and forgings heat treated to various strength levels, Figure 3.0351.

3.0352 Effects of temperature from -200 F to 80 F on shear strength of 4140 tempered at 1050 F and at 725 F, Figure 3.0352.

3.036 Bearing.

3.0361 Effect of temperature on bearing strength of bar and forgings heat treated to various strength levels, Figure 3.0361.

3.037 Stress concentration.

3.0371 Notch properties.

3.03711 Effects of temperature from -200 F to 80 F on notched/unnotched tensile strength ratio of 4140 tempered at 1050 F and at 725 F, Figure 3.03711.

3.0372 Fracture toughness.

3.03721 A transition in crack arrest fracture toughness at 0 F is observed for 4140 tempered to 160 ksi or 180 ksi, as shown in Figure 3.03722. This transition appears to be associated with a change in fracture mechanism from cleavage at subtransition temperatures to dimpled rupture at supertransition temperatures (55).

3.03722 Crack arrest fracture toughness of 4140 steel as a function of test temperature, Figure 3.03722.

3.038 Combined properties.

3.04 **Creep and Creep-Rupture Properties**

3.041 Creep properties at 1000 F and 1200 F of sheet in various heat treated conditions, Figure 3.041.

3.042 Effect of cold rolling on creep-rupture time of quenched and tempered rod at various combinations of temperature and stress, Figure 3.042.

3.043 Effect of cold rolling on minimum creep rate of quenched and tempered rod at various combinations of temperature and stress, Figure 3.043.

3.05 **Fatigue Properties**

3.051 Longitudinal and transverse fatigue properties of smooth and notched specimens, Figure 3.051.

3.052 Fatigue properties of smooth bars heat treated to various strength levels, Figure 3.052.

3.053 Fatigue properties of notched bars heat treated to various strength levels, Figure 3.053.

3.054 Effects of decarburization on fatigue properties of smooth and notched specimens, Figure 3.054.

3.055 Fatigue properties of leaded and nonleaded bar at two hardness levels, Figure 3.055.

3.056 Fatigue properties of annealed bar, Figure 3.056.

3.057 Effects of various environments on fatigue properties in different heat treated conditions, Figure 3.057.

3.058 Fatigue data for investment-castings showing improvement in fatigue life and consistency of results produced by machining and sand blasting, Figure 3.058.

3.059 Room temperature fatigue behavior of quenched and tempered 4140 [(a) tempered at 390 F and (b) tempered at 1200 F], Figure 3.059.

3.0510 Effects of notches on cyclic fatigue life at room temperature, Figure 3.0510.

3.0511 Tempering after quenching from 1830 F reduces the room temperature fatigue crack-growth rate, as shown in Figure 3.0512. Lowest crack-growth rates are observed for material tempered at 750 F to 1200 F. Crack-growth rates after tempering are higher in compression-tension fatigue (R = -1) than in zero-tension fatigue (R = 0) for the 970 F and 1230 F tempers, as shown in Figure 3.0513. The threshold stress for fatigue crack propagation in quenched and tempered alloy is approximately 3.6 ksi$\sqrt{\text{inch}}$, as shown in Figure 3.0514.

3.0512 Room temperature fatigue crack-growth behavior of 4140 steel austenitized at 1830 F and tempered at 390 F to 1200 F, Figure 3.0512.

3.0513 Room temperature fatigue crack-growth behavior of 4140 steel austenitized at 1550 F and tempered at 720 F to 1550 F [(a) R = 0, and (b) R = -1], Figure 3.0513.

3.0514 Room temperature fatigue crack-growth behavior of quenched and tempered 4140 steel at low stresses, Figure 3.0514.

3.06 **Elastic Properties**

Elastic properties are generally assumed to be equivalent to those of Type 4130, Code 1201.

3.061 Poisson's ratio.

3.062 Modulus of elasticity.

3.063 Modulus of rigidity.

3.064 Tangent modulus.

3.065 Secant modulus.

4 FABRICATION

4.01 **Forming**

4.011 Type 4140 can be cold formed to a reasonable extent in the annealed condition, but its cold formability is somewhat inferior to that of Type 4130, Code 1201.

4.012 4140 has good hot workability. Forging should be carried out within the range 2200 F to 1700 F, the optimum range being 2200 F to 2000 F. Hot rolling should be started in the range 2250 F to 2350 F. Parts should be cooled slowly after hot forming (2, 16).

	Fe
0.4	C
1	Cr
0.2	Mo

4140

4.02 **Machining and Grinding**

4.021 Type 4140 has good machinability in the annealed and cold drawn conditions. Cold drawn material has a machinability rating of 62 percent of AISI B1112 Bessemer screw stock. When annealed prior to cold drawing, the machinability rating advances about 10 percent for most machining operations. The leaded grade has appreciably better machinability than the standard grade (2).

4.03 **Joining**

4.031 This alloy can be readily welded by any of the manual or automatic electric-arc techniques. Low-hydrogen electrodes of the appropriate strength level are recommended. Since there is danger of embrittlement in the heat-affected zone, preheating is required and postweld heat treating may be necessary depending on the application. If postweld heat treating is not done, preheat and interpass temperature of 600 F minimum, followed by slow cooling, is recommended. If postweld heat treating is done, preheat and interpass temperature of 400 F minimum is suggested, followed by transfer of weldment into furnace immediately after welding for postweld heat treatment at 1100 F to 1250 F, followed by slow cooling. If the postweld treatment cannot be done immediately after welding, the weldment should be heated to 600 F immediately following welding, held at temperature 1 hour per inch of thickness, slow cooled to ambient temperature and then subsequently postweld heat treated (2, 16).

4.04 **Surface Treating**

4.041 With proper surface preparation, protective coatings of paint and electroplate can be applied with excellent results.

4.042 Type 4140 can be nitrided by gas, salt-bath, or ion-bombardment techniques for improved surface hardness, wear resistance, and fatigue strength. Hardness curves for gas-nitrided and ion-nitrided materials are shown in Figures 4.0421 and 4.0422, respectively. The surface layer generally consists of internal nitrides of alloying elements plus a thin surface layer (termed "white layer") and intergranular network of iron nitride. The presence of iron nitride promotes greater surface hardness and wear resistance but is detrimental to ductility. Fatigue resistance is enhanced by the internal diffusion layer of nitrides of the alloying elements. Anhydrous ammonia is employed as the nitrogen source, with excess hydrogen added to control the nitrogen activity and amount of iron nitride formed. Nitriding times are reduced for ion-nitriding as compared to gas-nitriding (26, 27, 56, 57, 58)

4.0421 Case hardness of alloy nitrided after it had been quenched and tempered at various temperatures, Figure 4.0421.

Fe
0.4 Cr
1 Cr
0.2 Mo

4140

4.0422 Hardness gradient near surface of ion-nitrided 4140 steel, Figure 4.0422.

4.043 Type 4140 can also be surface hardened by laser heat treatment. Surface hardness can be increased from 20 HRC, corresponding to the normalized or annealed condition, to as high as 59 HRC, corresponding to a martensite content of 95 to 100 percent by laser heating a thin surface layer and air quenching (59).

REFERENCES

1 "Modern Steels and Their Properties", Seventh Edition, Handbook 2757, Bethlehem Steel Corp. (1972).

2 "AISI 4140", Alloy Digest, Filing Code: SA-18 (May 1954).

3 Bramfitt, B. L., and Luizzi, L., "A Study of the Effect of Solidification Imperfections on the Tensile Properties of Cast Steel", Benet R & E Labs, Watervliet Arsenal, WVT-6420 (September 1964).

4 DeFries, R. S., "The Elevated Temperature Properties of Two 81MM Mortar Tube Alloys 4337M and 4140", Benet R & E Labs, Watervliet Arsenal, WVT-7106 (June 1971).

5 Thorkildsen, R. L., "High-Temperature Materials Program", Materials Technology Inc., MTI 65TR45 (September 2, 1965).

6 Larson, F. R., "The Effect of Microstructure on the Impact Properties of Some Commercial Alloy Steels With and Without Boron", Watertown Arsenal, WAL TR 310/215 (April 1958).

7 "Fatigue Properties of Investment Castings", U.S. Army Weapons Command, Technical Report RE-71-2 (April 1971).

8 Owens, W. H., "The Effect of High-Pressure Hydrogen on SAE 4140 and 1018 Steels at Ambient Temperatures", Aro, Inc., AEDC-TR-66-269 (December 1977).

9 "Methods for Minimizing the Embrittling Effect of Hydrogen in Electroplated High Strength Alloy Steel Items", Frankfort Arsenal, IEP 60-6110-2 (March 1963).

10 "Mechanical Tests on Various Extruded Materials", Allegheny-Ludlum Steel Corp. (January 1, 1956).

11 Romine, H. E., "Correlation of Laboratory Fracture Toughness Tests With Burst Tests of Thin-Wall Steel Pressure Vessels Containing a 2t Through-Crack Flaw", Naval Weapons Lab, NWL Technical Report TR-2270 (March 1969).

12 "Atlas of Isothermal Transformation Diagrams", U.S. Steel Corp. (1951).

13 SAE Handbook, 1972 Edition.

14 Cataldo, C. E., "Compatibility of Metals With Hydrogen", Geo. C. Marshall Space Flight Center, NASA TM X-53807 (December 26, 1968).

15 Groeneveld, T. P., Fletcher, E. E., and Elsea, A. R., "A Review of the Literature on Cleaning, Pickling, and Electroplating Processes and Relief Treatments to Minimize Hydrogen Embrittlement of Ultrahigh-Strength Steels", Battelle Memorial Institute, Contract NAS8-20029 (October 15, 1966).

16 "Steels for Elevated Temperature Service", U.S. Steel Corp. (June 1972).

17 AMS 5338C (October 1, 1982).

18 AMS 6378C (April 1, 1983).

19 AMS 6381C (May 15, 1972).

20 AMS 6382J (July 1, 1981).

21 AMS 6390B (July 1, 1976).

22 AMS 6395B (October 15, 1979).

23 "Cross-Index of Chemically Similar Specifications and Identification Code", MIL-HDBK-H1D (June 22, 1970).

24 Metals Handbook, 8th Edition, ASM (1961).

25 Lee, R. H., and Uhlig, H. H., "Corrosion Fatigue of Type 4140 High-Strength Steel", *Metallurgical Transactions*, Vol. 3 (November 1972), pp 2949–2957.

26 Schwartzkopf, A. J., "New Facts on the Nitriding of 4140 and 4340", *Iron Age*, Vol. 181 (May 29, 1958), pp 90–93.

27 Boempler, D., "The Load Carrying Capacity of Bath Nitrided Gears", American Gear Manufacturers Institute, AGMA 109.18 (October 1966).

28 Simmons, W. F., and Cross, H. C., "Elevated-Temperature Properties of Wrought Medium-Carbon Alloy Steels", *ASTM STP*, No. 199 (1957).

29 Simon, W., "Fatigue, Impact, and Tensile Properties of High-Strength Leaded and Non-Leaded SAE 4140 Steel", SAE Transactions, Vol. 69 (1961), pp 69–76.

30 Evans, E. B., Ebert, L. J., and Briggs, C. W., "Fatigue Properties of Comparable Cast and Wrought Steels", *Proceedings ASTM*, Vol. 56 (1956), pp 979–1009.

31 Jackson, L. R., and Pochapsky, T. E., "The Effect of Composition on the Fatigue Strength of Decarburized Steel", *Transactions ASM*, Vol. 39 (1947), pp 45–57.

32 "Mechanical Properties of Alloy Steel", Republic Steel Corp. (1961).

33 Shahinian, P., Achter, M. R., and Pennington, W. A., "The Effect of Cold Work and Temperature on Strength and Structure of Steel", *Trans. ASM*, Vol. 53 (1961).

34 "Strength of Aircraft Elements", MIL-HDBK-5B (September 1971).

35 "Guide to Steel Selection", Joseph T. Ryerson & Son, Inc., Bulletin No. R-8-6-2.

36 "Haynes Low Alloy Steels", Haynes-Stellite Co. (1959).

37 Fiorentino, R. J., and Sabroff, A. M., "Availability and Mechanical Properties of High-Strength Steel Extrusions", DMIC Report 138 (October 26, 1960).

38 Grobecker, D. W., "Metals for Supersonic Aircraft and Missiles", Proceedings of the Conference on Heat Tolerant Metals for Aerodynamic Applications (January 1957).

39 Steigerwald, E. A., "Plane Strain Fracture Toughness for Handbook Presentation", TRW Inc., AFML TR-67-187 (July 1967). (This publication is subject to export control. Export permitted only with the approval of AFML.)

40 Miller, J., Smith, L. W., and Porter, P. K., "Utilization of Low-Alloy Materials for High-Temperature Service Applications", U.S. Air Force, AF TR-5929 (June 1949).

41 "Nitralloy and Nitriding", The Nitralloy Corp. (1954).

42 Wood, W. E., Parker, E. R., and Zackay, V. F., "An Investigation of Metallurgical Factors Which Affect Fracture Toughness of Ultra High Strength Steels", Army Materials and Mechanics Research Center Report No. AMMRC CTR 73-24 (May 1973).

43 Jacobs, F. A., and Krauss, G., "The Effects of Phosphorus and Carbon on the Hardenability of 41XX Type Steels", *Journal of Heat Treating*, Vol. 2, No. 2 (December 1981), pp 139–146.

44 Uhlig, H. H., "Critical Potentials for Stress Corrosion Cracking (Mechanism of Stress Corrosion Cracking)", Massachusetts Institute of Technology, Final Report ARO 11266.4-MC (April 1975).

45 Asphahani, A., and Uhlig, H. H., "Stress Corrosion Cracking of 4140 High Strength Steel in Aqueous Solutions", *Journal of the Electrochemical Society*, Vol. 122, No. 2 (February 1975), pp 174–179.

46 Bates, C. E., Wren, J. E., Monroe, R., and Pears, C. D., "Ignition and Combustion of Ferrous Metals in High Pressure, High Velocity, Gaseous Oxygen", *Journal of Materials for Energy Systems*, Vol. 1, No. 1 (June 1979), pp 61–76.

47 Gordon, P., "The Mechanisms of Crack Initiation and Crack Propagation in Metal-Induced Embrittlement of Metals. Part II. Theoretical Aspects of Crack Initiation", Illinois Institute of Technology, Final Report N00014-79-C-0580, NSF-DMR 79-08674 (February 1981).

48 Gordon, P., "The Mechanisms of Crack Initiation and Crack Propagation in Metal-Induced Embrittlement of Metals. Part I. Delayed Failure in the Embrittlement of 4140 Steel", Technical Report N00014-79-C-0580, NSF-DMR 79-08674 (December 1980).

49 Lui, M. W., and Le May, I., "Relations Between Tensile Strength and Carbide Size in AISI 4140 Steel", *Metallurgical Transactions*, Vol. 6A, No. 3 (March 1975), pp 583–584.

50 Lui, M. W., and Le May, I., "The Relation Between Ultimate Tensile Strength and Carbide Size in Steel", *Transactions of the ASME, Series H, Journal of Engineering Materials and Technology*, Vol. 98, No. 2 (April 1976), pp 173–179.

51 Thielen, P. N., Fine, M. E., and Fournelle, R. A., "Cyclic Stress Strain Relations and Strain-Controlled Fatigue of 4140 Steel", *Acta Metallurgica*, Vol. 24, No. 1 (January 1976), pp 1–10.

52 Lynn, J. C., Warke, W. R., and Gordon, P., "Solid Metal-Induced Embrittlement of Steel", *Materials Science and Engineering*, Vol. 18, No. 1 (March 1975), pp 51–62.

53 Landow, M., Harsolia, A., and Breyer, N. N., "Liquid Metal Embrittlement of 4145 Steel by Lead Alloys", *Journal of Materials for Energy Systems*, Vol. 2, No. 4 (March 1981), pp 50–59.

54 Breyer, N. N., and Gordon, P., "Lead Induced Brittle Failures of High Strength Steels", Proceedings of the Third International Conference on the Strength of Metals and Alloys, Vol. I, The Microstructure and Design of Alloys, held in Cambridge, England (August 20–25, 1973), Paper 101.

55 Ripling, E. J., Mulherin, J. H., and Crosley, P. B., "Crack Arrest Toughness of Two High Strength Steels (AISI 4140 and AISI 4340)", *Metallurgical Transactions*, Vol. 13A (April 1982), pp 657–664

56 Jindal, P. C., "Ion Nitriding of Steels", *Journal of Vacuum Science and Technology*, Vol. 15, No. 2 (March/April 1978), pp 313–317.

57 Knechtel, H. E., and Podgurski, H. H., "Bright Nitriding in Bell-Type Furnace With Continuous Recirculation of Atmosphere", *Industrial Heating*, Vol. 46, No. 6 (June 1979), pp 12–14, 16.

58 Anonymous, "Ion Nitriding: A Particularly Versatile Case Hardening Process – Part 1: Function of the Method", *Industrial Heating*, Vol. 48, No. 9 (September 1981), pp 24–25, 27, 29.

59 Grotke, G. E., Bruck, G. J., Smith, J. E., and Nurminen, J. I., "A Parametric Study of Surface Transformation Hardening With High-Power Lasers", Westinghouse Research and Development Center, Pittsburgh, Pennsylvania, Report 84-9D4-SURFC-R1 (February 2, 1984).

60 Briggs, A., Airey, R., and Edwards, B. C., "A Double Torsion Fracture Mechanics and Auger Electron Spectroscopy Approach to the Study of Stress Corrosion Cracking in Low Alloy Steels", *Journal of Materials Science*, Vol. 16, No. 1 (January 1981), pp 125–140.

61 Tipton, D. G., "Corrosion Fatigue of High Strength Fastener Materials in Seawater", Laque Center for Corrosion Technology, Incorporated, Wrightsville Beach, North Carolina, NASA CR-174677 (December 1983).

62 DeFries, R. S., "The Estimation of Yield Strength From Hardness Measurements", Watervliet Arsenal, New York, WVT-TN-75051 (August 1975).

63 Montano, J. W., "Low Temperature Mechanical Properties, Fractographic and Metallographic Evaluation of Several Alloy Steels", National Aeronautics and Space Administration, Marshall Space Flight Center, Huntsville, Alabama, NASA TM X-64791 (November 1973).

64 Tauscher, S., and Thornton, P., "Temper Embrittlement in 4140 Seamless Tubing", Army Armament Research and Development Command, Dover, New Jersey, ARLCB-TR-77043 (November 1977).

65 Ripling, E. J., and Crosley, P. B., "Crack Arrest Toughness of 4140, 1340, and 4340 Steel", Materials Research Laboratory, Incorporated, Glenwood, Illinois, MRL-792 (November 1981).

66 Haibach, E., and Matschke, C., "The Concept of Uniform Scatter Bands for Analyzing S-N Curves of Unnotched and Notched Specimens in Structural Steel", Proceedings of a Symposium, Low-Cycle Fatigue and Life Prediction, ASTM-STP-770, Firminy, France (September 23–25, 1980), pp 549–571.

67 Thielen, P. N., and Fine, M. E., "Fatigue Crack Propagation in 4140 Steel", *Metallurgical Transactions*, Vol. 6A, No. 11 (November 1975), pp 2133–2141.

68 Stephens, R. I., Benner, P. H., Mauritzson, G., and Tindall, G. W., "Constant and Variable Amplitude Fatigue Behavior of Eight Steels", *Journal of Testing and Evaluation*, Vol. 7, No. 2 (March 1979), pp 68–81.

69 Kwun, S. I., and Fine, M. E., "Fatigue Microcrack Growth in Tempered HY80, HY130, and 4140 Steels: Threshold and Mid-Delta K Range", *Fatigue of Engineering Materials and Structures*, Vol. 3, No. 4 (1980), pp 367–382.

	Fe
0.4	C
1	Cr
0.2	Mo

4140

Fe
0.4 Cr
1 Cr
0.2 Mo

4140

Alloy	4140
AMS Specification	Product Form
5338C	Castings
6378C	Bars
6381C	Tubing
6382J	Bars, Forgings, Rings
6390B	Tubing
6395B	Sheet, Strip, Plate

TABLE 1.031. SPECIFICATIONS (17–22)

Alloy	4140					
AMS Specifications	5338C		6378C		6381C, 6382J, 6390B, 6395B	
	Percent		Percent		Percent	
Element	Min	Max	Min	Max	Min	Max
Carbon	0.35	0.45	0.39	0.48	0.38	0.43
Chromium	0.80	1.10	0.75	1.20	0.80	1.10
Molybdenum	0.15	0.25	0.15	0.25	0.15	0.25
Manganese	0.75	1.00	0.70	1.10	0.75	1.00
Silicon	–	1.00	0.15	0.35	0.20[a]	0.35
Copper	–	0.35	–	0.35	–	0.35
Nickel	–	0.25	–	0.25	–	0.25
Phosphorus	–	0.04	–	0.040	–	0.025
Sulfur	–	0.04	0.04	0.060	–	0.025
Tellurium	–	–	0.01	0.02	–	–

(a) 0.15 percent silicon minimum for AMS 6382J and 6395B.

TABLE 1.041. COMPOSITION (17–22)

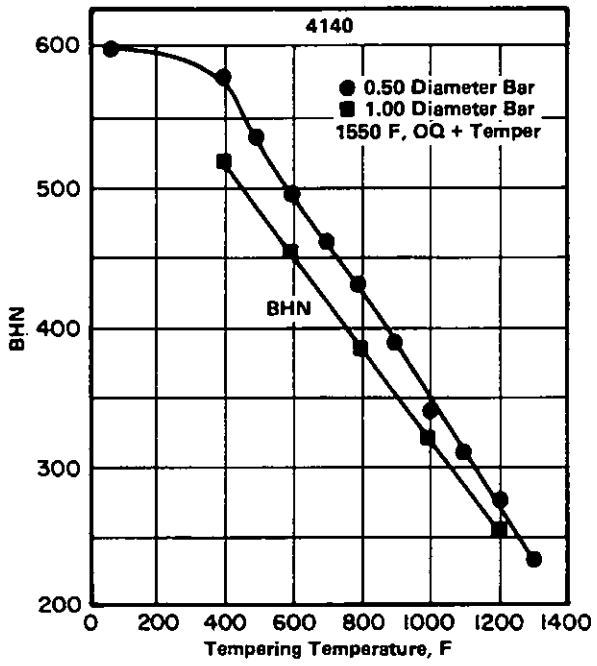


FIGURE 1.061. EFFECT OF TEMPERING TEMPERATURES ON HARDNESS (1, 2)

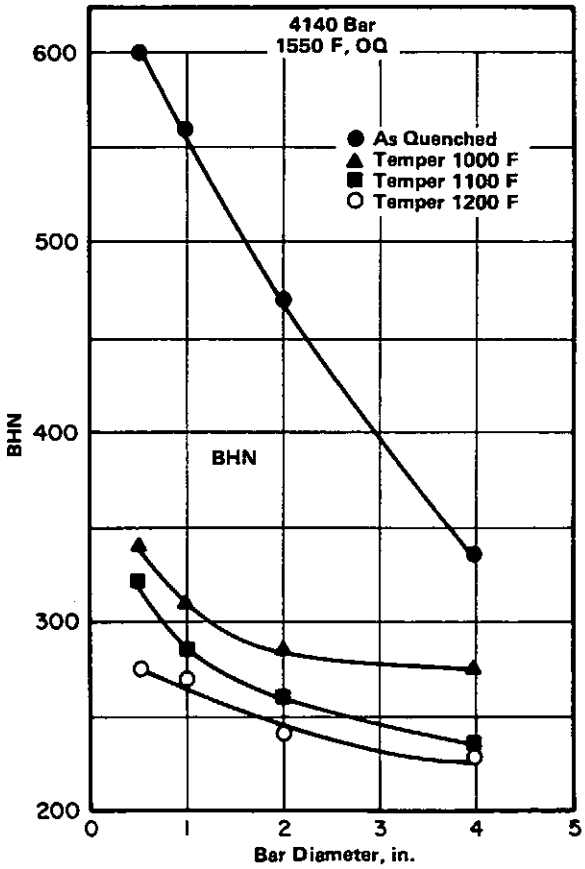


FIGURE 1.062. EFFECT OF DIAMETER ON SURFACE HARDNESS OF QUENCHED AND TEMPERED BAR (1)

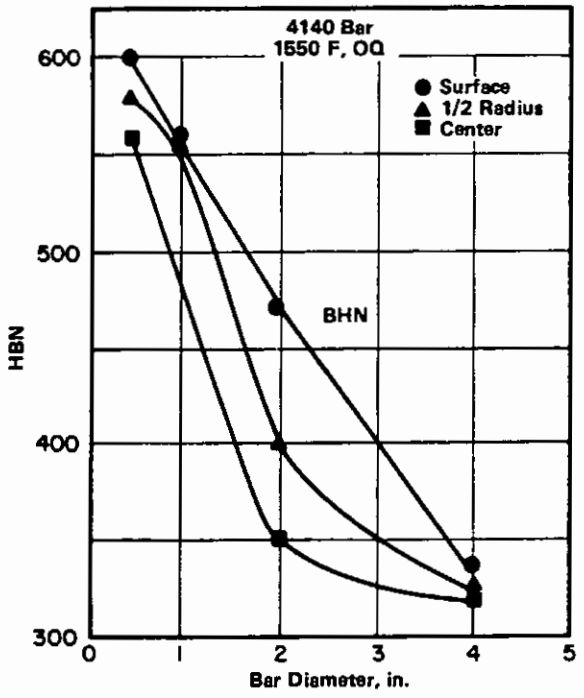


FIGURE 1.063. EFFECT OF DIAMETER ON AS-QUENCHED HARDNESS AT VARIOUS LOCATIONS ON CROSS SECTION OF BAR (1)

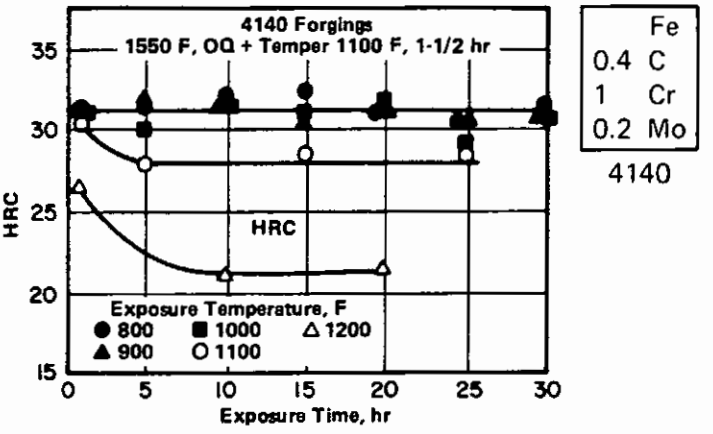


FIGURE 1.064. EFFECTS ON ROOM TEMPERATURE HARDNESS OF EXPOSURES UP TO 30 HOURS AT VARIOUS ELEVATED TEMPERATURES (4)

Alloy	4140	
Condition	Form	BHN
Annealed	1-inch-Diameter Bar	197
	Castings	220
Normalized	1/2-inch-Diameter Bar	302
	1-inch-Diameter Bar	302
	2-inch-Diameter Bar	285
	4-inch-Diameter Bar	241
	Castings	275
Hot Rolled	1-inch-Diameter Bar	229 – 270

TABLE 1.065. HARDNESS IN UNHARDENED CONDITIONS (1, 2)

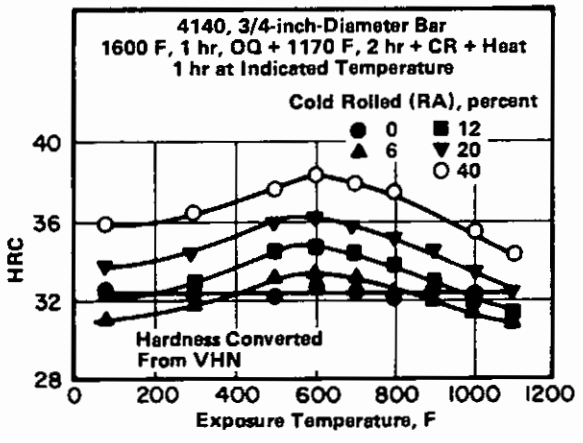


FIGURE 1.066. EFFECTS OF ONE-HOUR EXPOSURES TO ELEVATED TEMPERATURES ON THE ROOM TEMPERATURE HARDNESS OF BARS COLD ROLLED VARIOUS AMOUNTS AFTER HEAT TREATMENT (33)

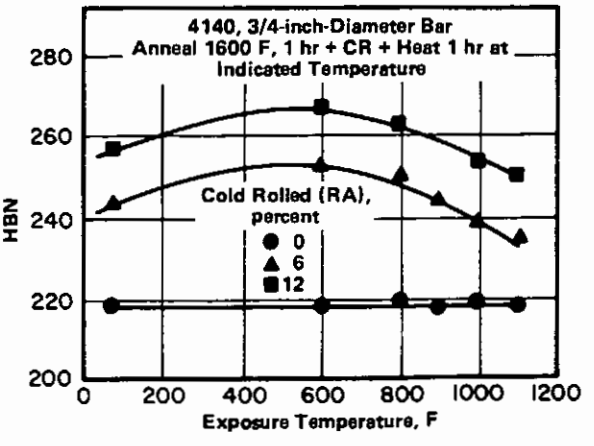


FIGURE 1.067. EFFECTS OF ONE-HOUR EXPOSURES TO ELEVATED TEMPERATURES ON THE ROOM TEMPERATURE HARDNESS OF BARS THAT HAD BEEN ANNEALED AND THEN COLD ROLLED VARIOUS AMOUNTS (33)

Fe
0.4 Cr
1 Cr
0.2 Mo
4140

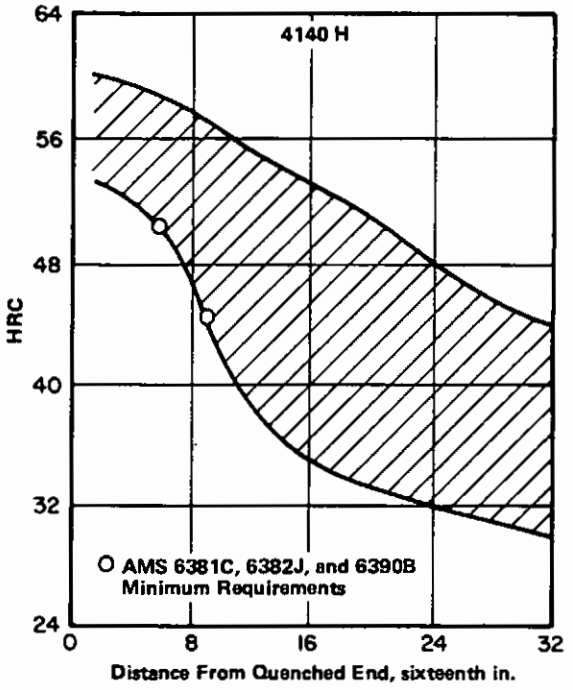


FIGURE 1.068. END-QUENCH HARDENABILITY (13)

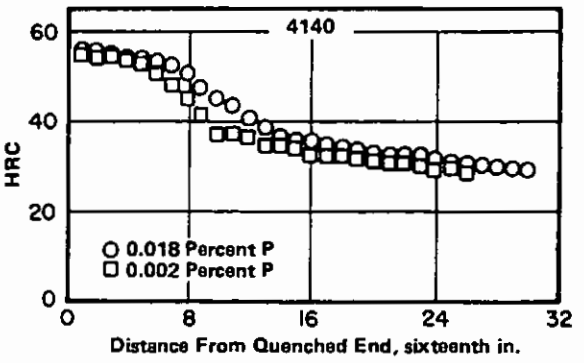
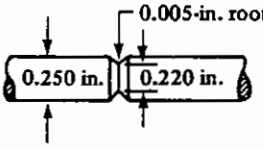


FIGURE 1.0610. END-QUENCH HARDENABILITY CURVES FOR 4140 CONTAINING HIGH AND LOW PHOSPHORUS (43)

Alloy	4140		
Form	Bar		
Condition	Quenched and Tempered to Two Hardness Levels		
Exposure to 6000 psi H_2 at 75 F[b]	NTS, ksi[a]	HRC	F_{tu}, ksi
None	257	48	230
25 Days[c]	170	47	–
50 Days[c]	165	46	–
55 Days[c]	169	47	–
10 Days in Air After 55-Day Exposure	260	47	–
1 Day in Air After 25-Day Exposure	251	47	–
None	169	30	130
25 Days[c]	167	31	–
50 Days[c]	169	30	–
55 Days[c]	170	30	–

(a) Notched specimen.



(b) Specimens under nominal tensile stress of 33,000 psi during exposures to hydrogen.

(c) Tested in air within 23 minutes after removal from hydrogen pressure chamber.

TABLE 1.0931. EFFECTS OF EXPOSURE TO HIGH-PRESSURE HYDROGEN ON NOTCHED TENSILE STRENGTH (8)

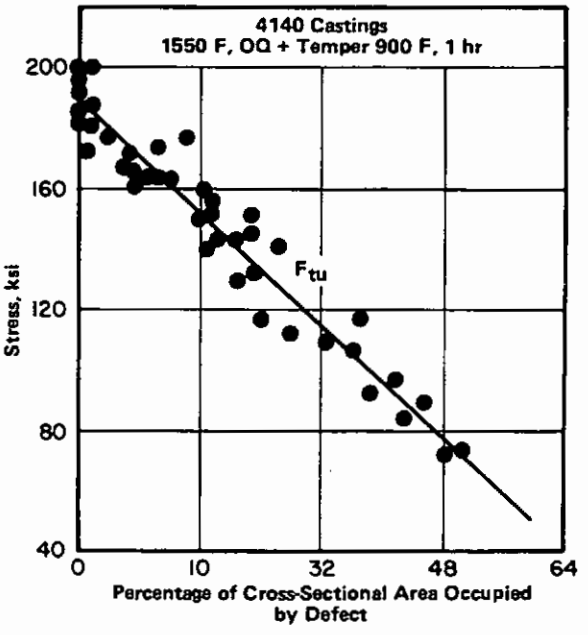


FIGURE 1.0951. EFFECT OF GAS HOLES AND SHRINKAGE DEFECTS ON TENSILE STRENGTH OF CASTINGS (3)

	Fe
0.4	C
1	Cr
0.2	Mo

4140

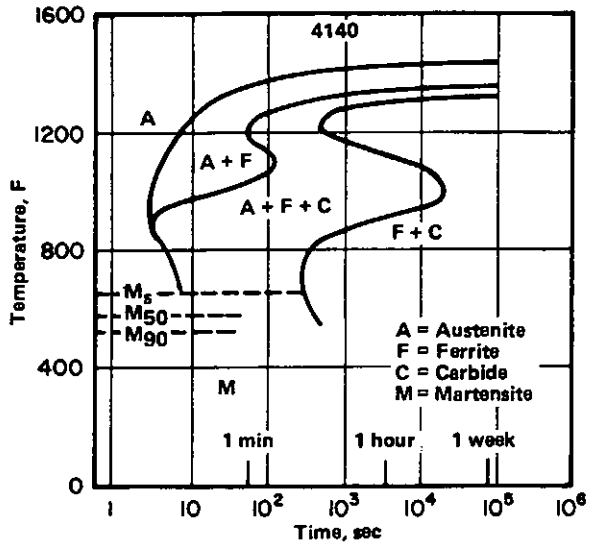


FIGURE 2.0121. TIME-TEMPERATURE-TRANSFORMATION DIAGRAM (12)

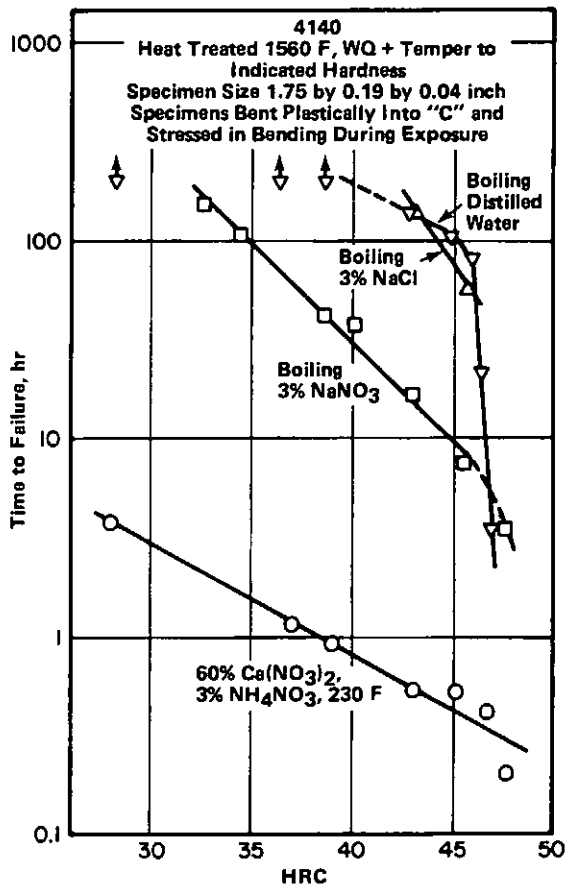


FIGURE 2.0312. EFFECT OF HEAT TREATED HARDNESS ON STRESS CORROSION CRACKING IN AQUEOUS SOLUTIONS (44, 45)

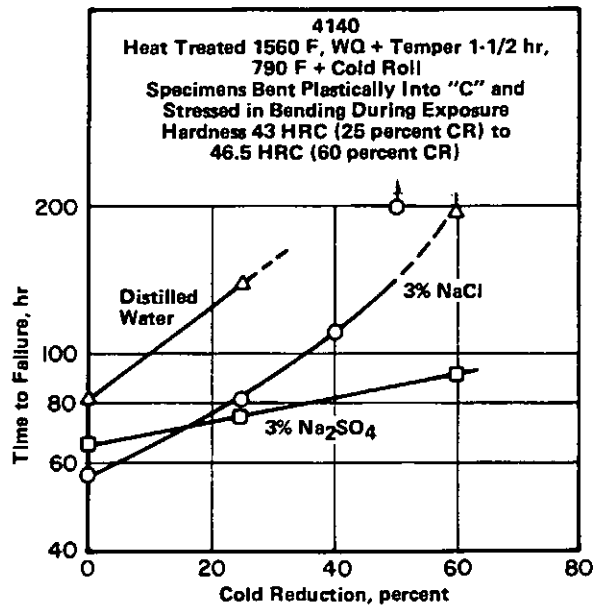


FIGURE 2.0314. EFFECT OF COLD ROLLING ON STRESS CORROSION CRACKING IN BOILING AQUEOUS SOLUTIONS (45)

Fe
0.4 Cr
1 Cr
0.2 Mo

4140

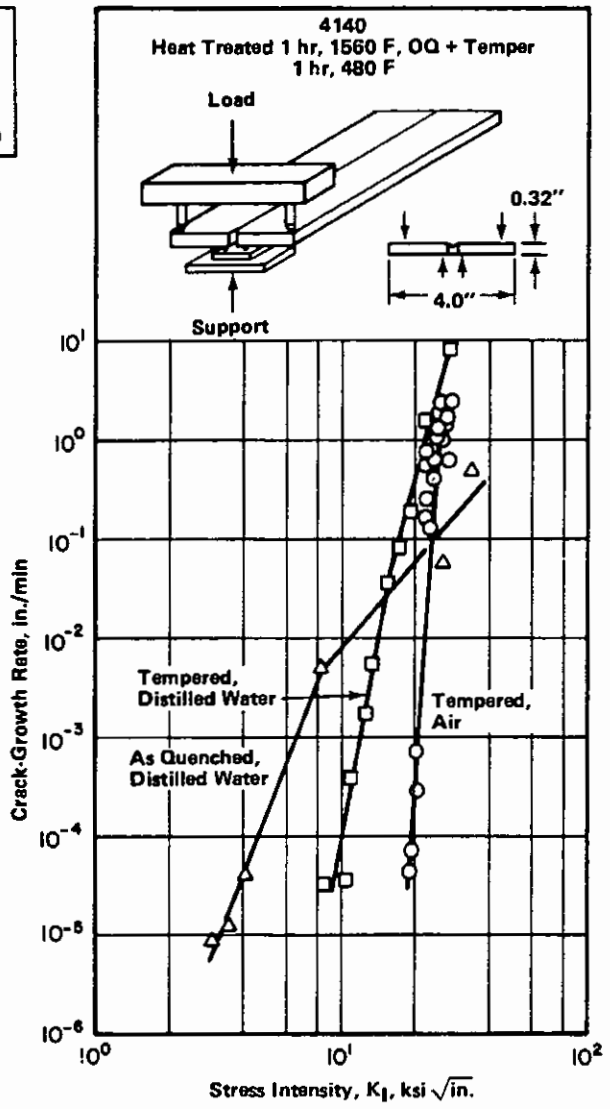


FIGURE 2.0317. STRESS CORROSION CRACK-GROWTH RATE AS A FUNCTION OF STRESS INTENSITY IN WATER AND IN AIR AT ROOM TEMPERATURE (60)

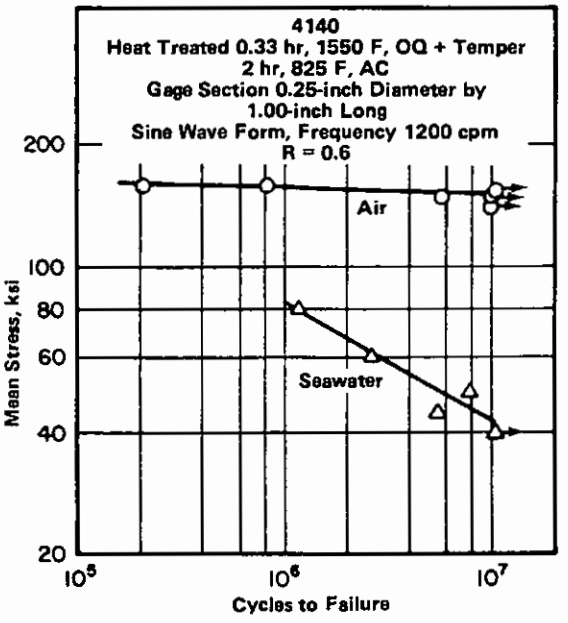


FIGURE 2.0319. CORROSION FATIGUE IN NATURAL SEAWATER AS COMPARED TO AIR AT ROOM TEMPERATURE (61)

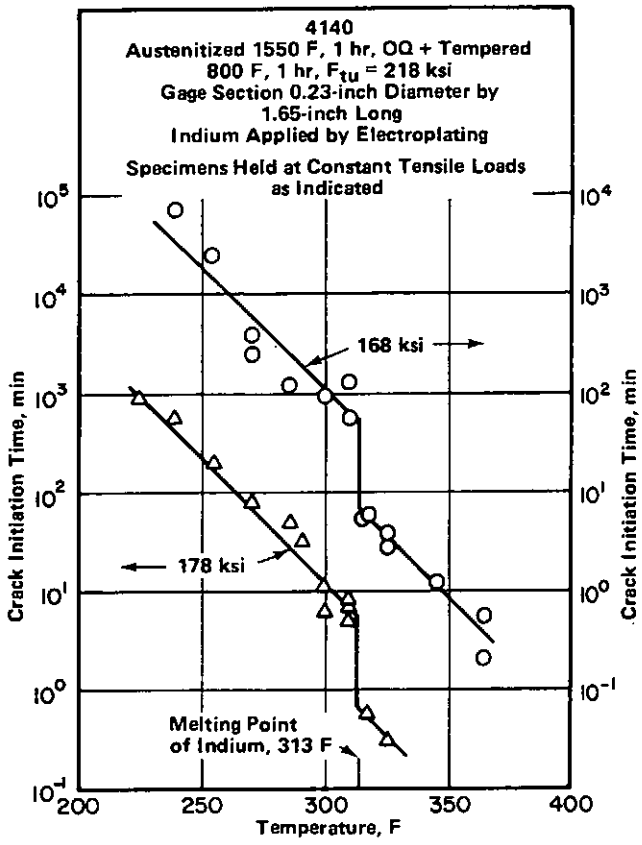


FIGURE 2.0332. DELAYED FRACTURE OF 4140 STEEL CAUSED BY METAL-INDUCED EMBRITTLEMENT WITH INDIUM (48)

FIGURE 2.0332. DELAYED FRACTURE OF 4140 STEEL CAUSED BY METAL-INDUCED EMBRITTLEMENT WITH INDIUM (48)

Alloy	4140										
AMS Specification	Product Form	Metallurgical Condition	Thickness, in.	F_{tu}, ksi Min	F_{tu}, ksi Max	F_{ty}, ksi, Min	Elongation, %, Min	RA, %, Min	Hardness[a] Min	Hardness[a] Max	Bend Angle, degrees[b]
5338C	Castings	Tempered	–	175	–	160	3	6	38 HRC	43 HRC	–
6378C	Bars	Hot Die-Drawn	–	150	–	130	5	20	(302 HBN)	(341 HBN)	–
6381C, 6390B	Tubing	Cold Finished	–	–	–	–	–	–	–	25 HRC	–
		Hot Finished	–	–	–	–	–	–	–	99 HRB	–
6382J	Bars, Forgings, and Rings	Cold Finished	≤0.50	–	125	–	–	–	–	–	–
		Cold Finished	>0.50	–	–	–	–	–	–	241 HBN	–
		Hot Finished	>0.50	–	–	–	–	–	–	229 HBN	–
6395B	Sheet, Strip, and Plate	–	"Sheet, Strip"	–	–	–	–	–	–	98 HRB	–
		–	"Plate"	–	–	–	–	–	–	25 HRC	–
		Tempered	≤0.875	180	–	–	–	–	(40 HRC)	–	–
		–	≤0.249	–	–	–	–	–	–	–	180
		–	0.249 – 0.749	–	–	–	–	–	–	–	90

Note: The original AMS documents should be consulted for complete specification details.

(a) Hardness specifications in parentheses need not be met if tensile specifications are met.
(b) Free bend around a diameter equal to the nominal thickness of the product.

TABLE 3.011. AMS SPECIFIED MECHANICAL PROPERTIES AT ROOM TEMPERATURE (17–22)

Fe
0.4 Cr
1 Cr
0.2 Mo

4140

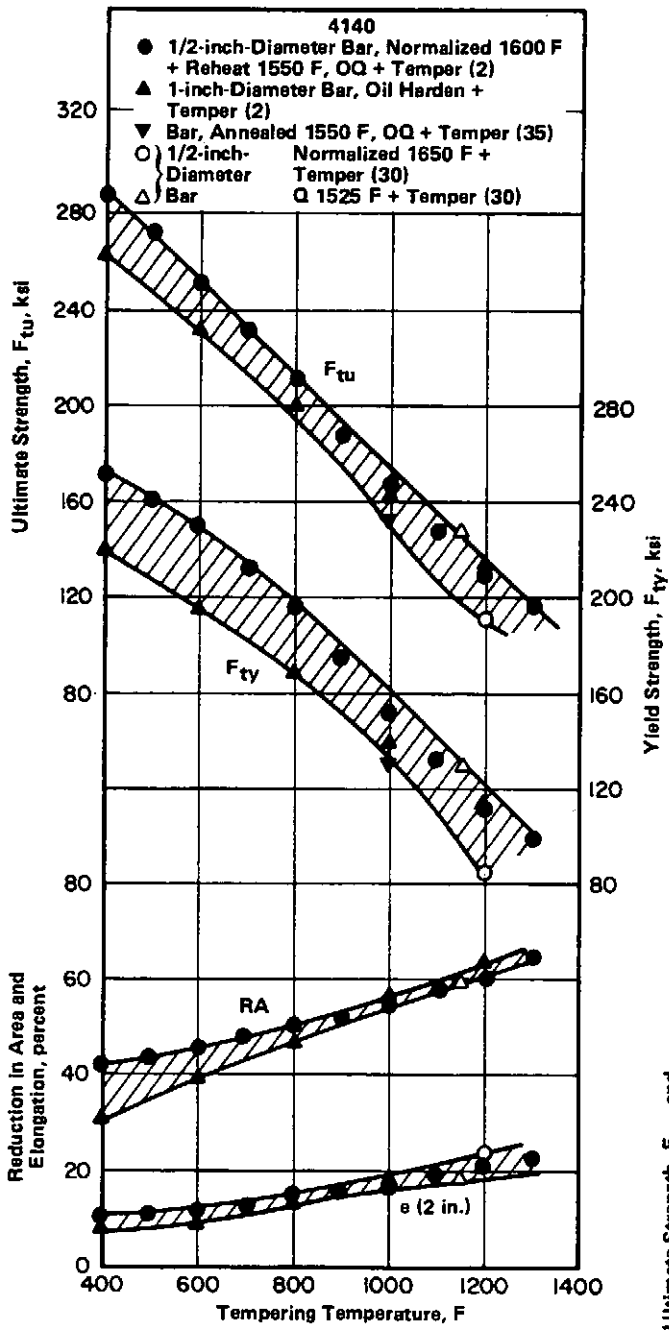


FIGURE 3.0211. EFFECT OF TEMPERING TEMPERATURE ON TENSILE PROPERTIES OF BAR (2, 30, 35)

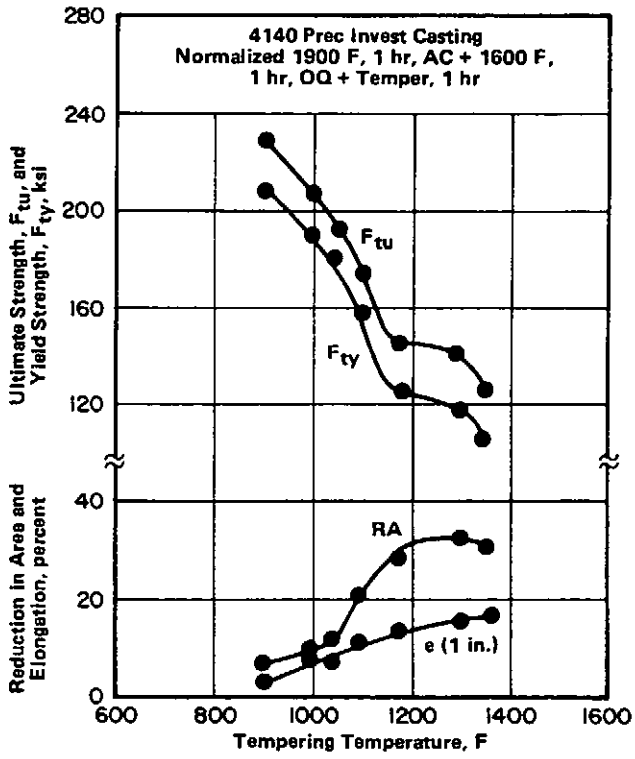


FIGURE 3.0212. EFFECT OF TEMPERING TEMPERATURE ON TENSILE PROPERTIES OF CASTINGS (36)

	Fe
0.4	C
1	Cr
0.2	Mo

4140

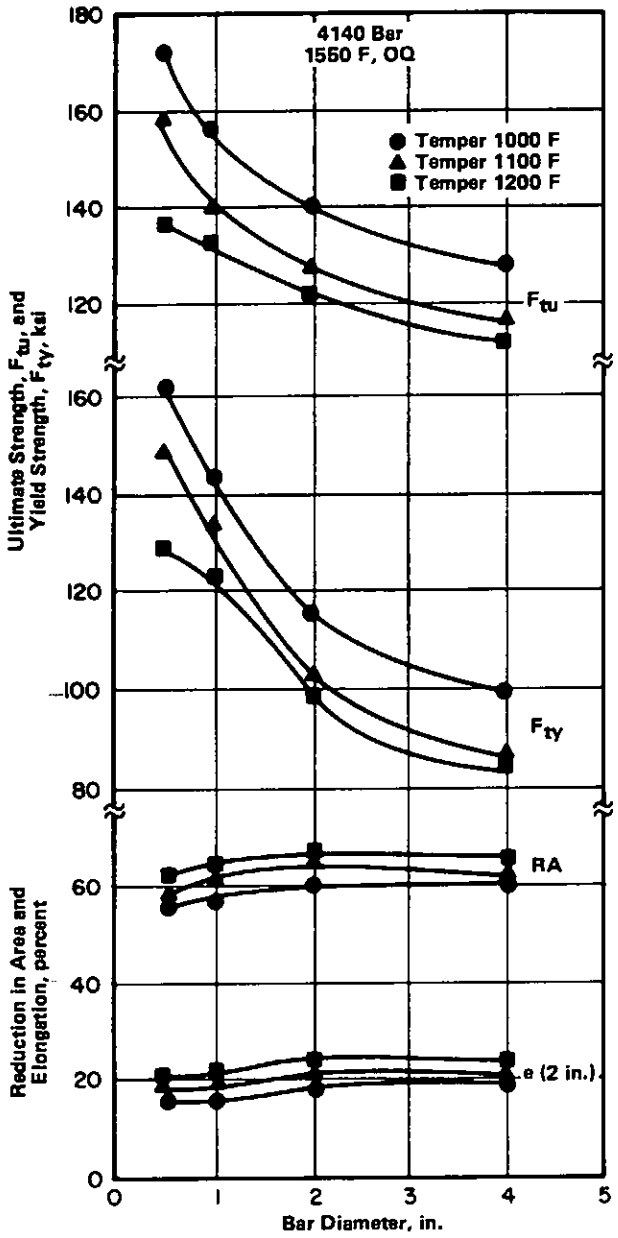


FIGURE 3.0213. EFFECT OF DIAMETER ON TENSILE PROPERTIES OF QUENCHED AND TEMPERED BAR (1)

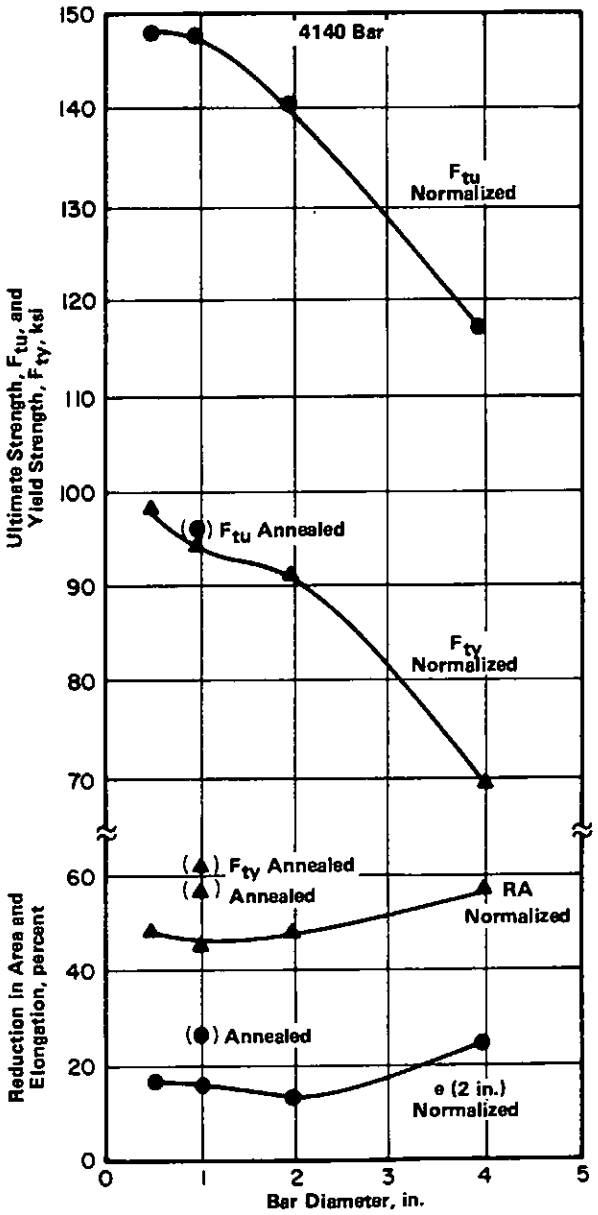


FIGURE 3.0214. TENSILE PROPERTIES OF NORMALIZED BARS FROM 1/2 TO 4 INCHES IN DIAMETER AND OF ANNEALED BAR 1.0 INCH IN DIAMETER (1)

Fe
0.4 Cr
1 Cr
0.2 Mo
4140

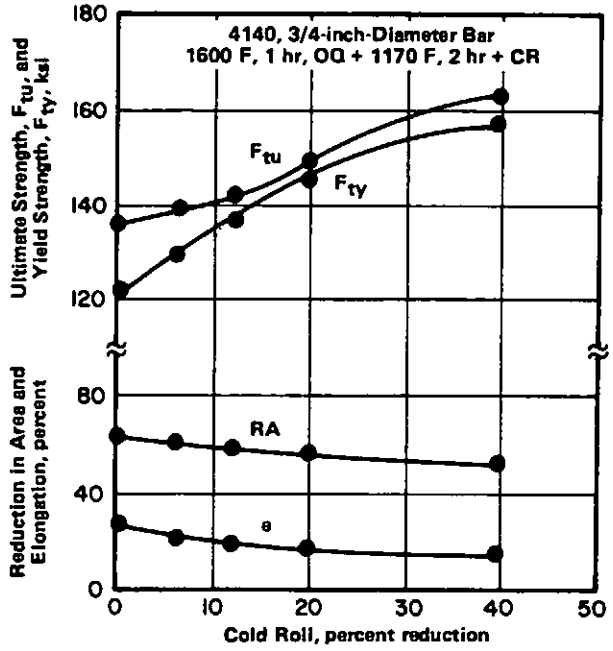


FIGURE 3.0215. EFFECT OF COLD ROLLING ON TENSILE PROPERTIES OF BAR (33)

Alloy	4140			
Form	Extrusions			
Condition	1550 F, OQ + Temper 600 F			
Specimen Orientation	F_{tu}, ksi	F_{ty}, ksi	e (2 in.), percent	RA, percent
Longitudinal	239	221	11.9	46.7
Transverse	230	210	4.7	17.0

TABLE 3.0216. TENSILE PROPERTIES OF EXTRUSIONS (10)

Alloy	4140							
Form	6-inch Diameter Bar							
Condition	OQ + Tempered to Two Hardness Levels							
		Nonleaded				Leaded			
HRC	Specimen Orientation	F_{tu}, ksi	F_{ty}, ksi	e (2 in.), percent	RA, percent	F_{tu}, ksi	F_{ty}, ksi	e (2 in.), percent	RA, percent
47	L	220	206	6.8	47.7	222	210	7.6	46.4
	T	166	126	3.5	3.3	169	126	2.8	6.5
55	L	269	228	7.9	45.2	272	246	5.8	36.6
	T	169	115	3.5	6.5	180	117	2.8	8.9

TABLE 3.0217. EFFECT OF SPECIMEN ORIENTATION ON TENSILE PROPERTIES OF 6-INCH-DIAMETER BAR HEAT TREATED TO TWO HARDNESS LEVELS (29)

Alloy	4140			
Form	Bar			
Condition	F_{tu}, ksi	F_{ty}, ksi	e (2 in.), percent	RA, percent
Hot Rolled	130 – 110	95 – 65	20 – 15	45 – 40
Annealed	100 – 90	70 – 65	27 – 25	55 – 50
Normalized	138 – 120	100 – 95	22 – 18	55 – 44

TABLE 3.0218. TENSILE PROPERTIES OF BAR IN UNHARDENED CONDITION (2)

Alloy	4140			
Form	Castings			
Condition	F_{tu}, ksi	F_{ty}, ksi	e (2 in.), percent	RA, percent
Annealed	90	60	25	45
Normalized	135	100	16	28
1600 F, WQ + Temper 1250 F, 5 hr	130	108	20	38

TABLE 3.0219. TENSILE PROPERTIES OF CASTINGS (2)

	Fe
0.4	C
1	Cr
0.2	Mo

4140

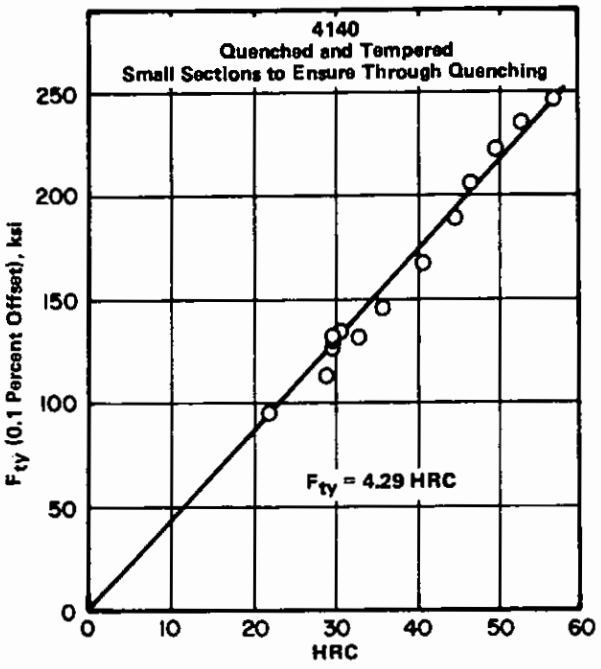


FIGURE 3.02110. RELATION BETWEEN YIELD STRENGTH AND HARDNESS FOR 4140 STEEL (62)

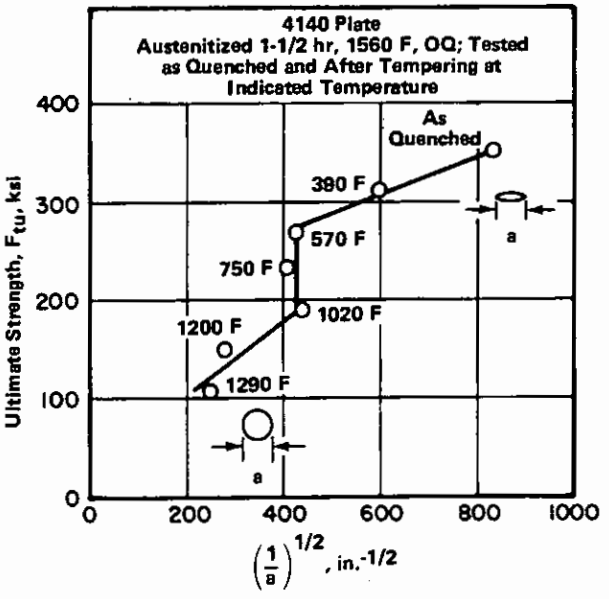
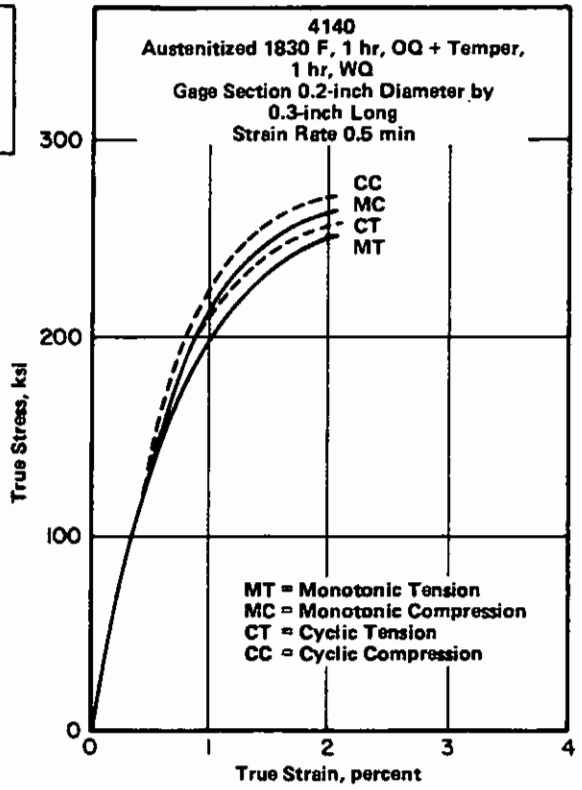


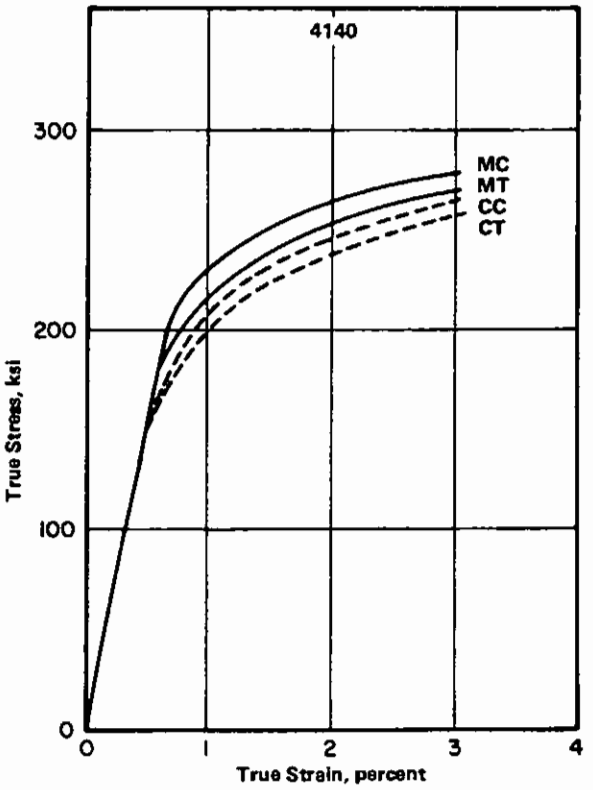
FIGURE 3.02112. VARIATION OF ULTIMATE TENSILE STRENGTH WITH CARBIDE SIZE AND SHAPE (50)

Fe
0.4 Cr
1 Cr
0.2 Mo
4140



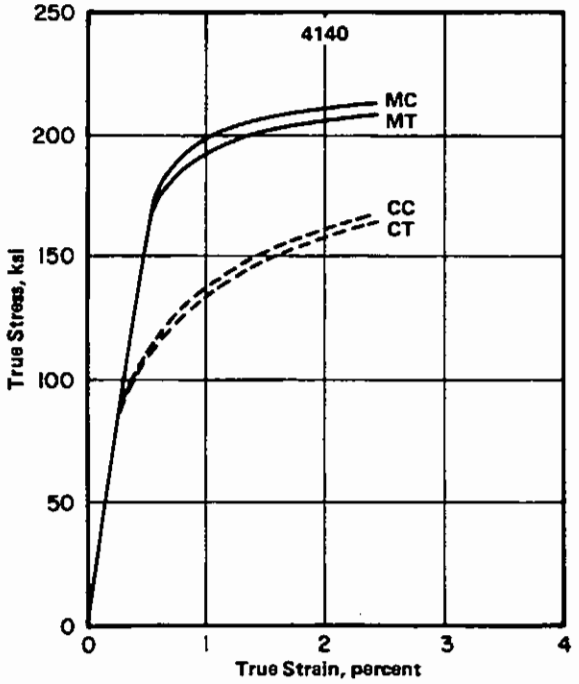
(a) Austenitized and Quenched

FIGURE 3.02114. MONOTONIC AND CYCLIC TRUE STRESS-TRUE STRAIN CURVES FOR 4140 STEEL (51)



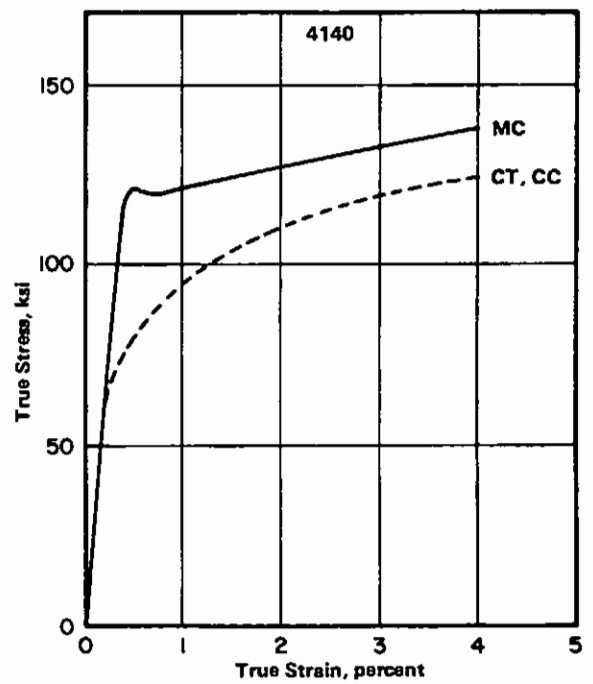
(b) Tempered at 390 F

FIGURE 3.02114. MONOTONIC AND CYCLIC TRUE STRESS-TRUE STRAIN CURVES FOR 4140 STEEL (51)



(c) Tempered at 750 F

FIGURE 3.02114. MONOTONIC AND CYCLIC TRUE STRESS-TRUE STRAIN CURVES FOR 4140 STEEL (51)



(d) Tempered at 1200 F

FIGURE 3.02114. MONOTONIC AND CYCLIC TRUE STRESS-TRUE STRAIN CURVES FOR 4140 STEEL (51)

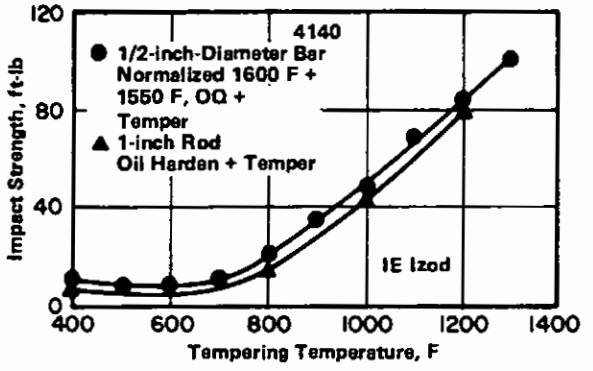


FIGURE 3.0231. EFFECT OF TEMPERING TEMPERATURE ON IMPACT PROPERTIES AT ROOM TEMPERATURE (2)

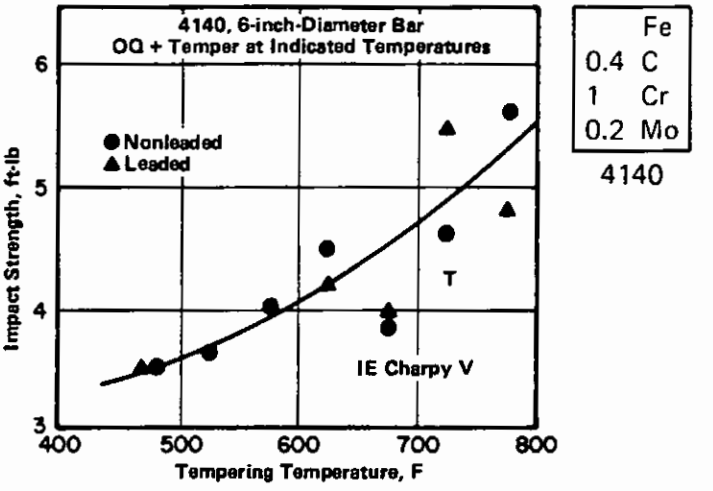


FIGURE 3.0232. TRANSVERSE IMPACT PROPERTIES OF LEADED AND NONLEADED 6-INCH-DIAMETER BAR AT ROOM TEMPERATURE (29)

Alloy	4140		
Form	Extruded Bar, 3/4 inch x 3-1/8 inch		
Condition	Specimen Orientation	Hardness	Impact, Charpy Keyhole, ft-lb
As Hot Extruded	L	89 HRB	25
	T	89 HRB	16
1550 F, OQ + Temper 600 F, 2 hr	L	49 HRC	14
	T	49 HRC	9
1550 F, OQ + Temper 900 F, 2 hr	L	40 HRC	23
	T	40 HRC	11

TABLE 3.0233. IMPACT PROPERTIES OF EXTRUDED BAR AT ROOM TEMPERATURE IN VARIOUS HEAT TREATED CONDITIONS (10)

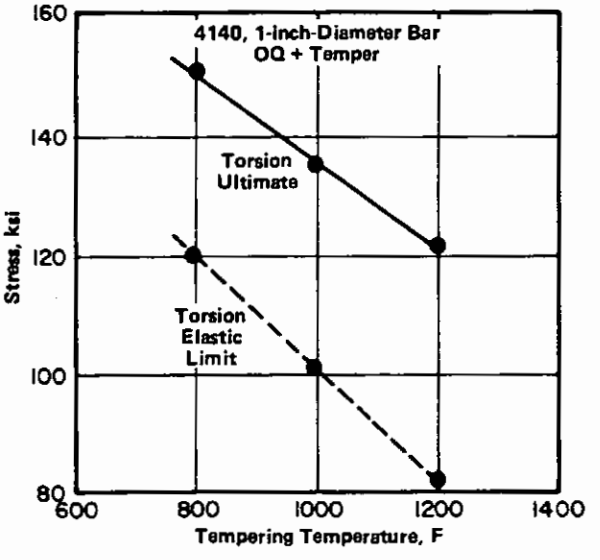


FIGURE 3.0251. EFFECT OF TEMPERING TEMPERATURE ON TORSIONAL PROPERTIES (2)

Fe
0.4 Cr
1 Cr
0.2 Mo

4140

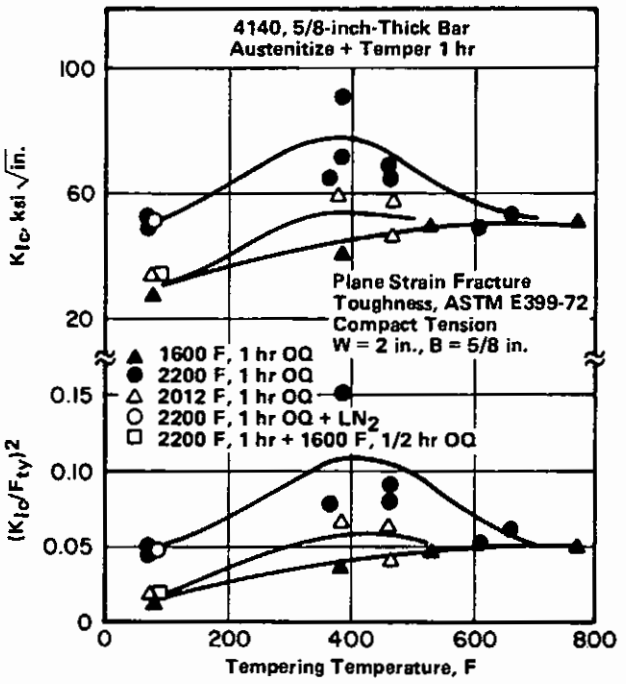


FIGURE 3.02721. EFFECT OF QUENCHING AND TEMPERING TEMPERATURE ON PLANE STRAIN FRACTURE TOUGHNESS (42)

Alloy	4140	
Condition	1550 F, 2 hr, Salt Quench to 325 F, AC + Double Temper 425 F, 2 hr	
Property	Type Test Uniaxial Tension	
F_{ty}, ksi	196	
F_{tu}, ksi	240	
e (2 in.), percent	5.5	
	Burst[a] With No Notch	
Biaxial Yield Strength (0.2 percent Offset), ksi	232	
Biaxial Ultimate Strength, ksi	265	
	Burst[a] With Fatigue-Cracked Through-Thickness Notch About 0.230-inch Long	
	Notch Environment	
	Air	Water
Hoop Stress at Fracture Start, ksi (σ i)	110	53
Hoop Stress at Burst, ksi (σ c)	115	73
	Burst With Machined Through-Thickness Notch (0.001-inch Root Rad), About 0.205-inch Long	
	Notch Environment	
	Air	Water
Hoop Stress at Fracture Start, ksi	69	51
Hoop Stress at Burst, ksi	124	67

(a) Burst tests by hydraulic pressurization of deep-drawn vessels 55-inches long, 11.45-inches ID, and 0.105 wall, open at one end. Notch located longitudinally 8 inches from open end.

TABLE 3.0281. BURST PROPERTIES OF SMALL PRESSURE VESSELS (11)

	Fe
0.4	C
1	Cr
0.2	Mo

4140

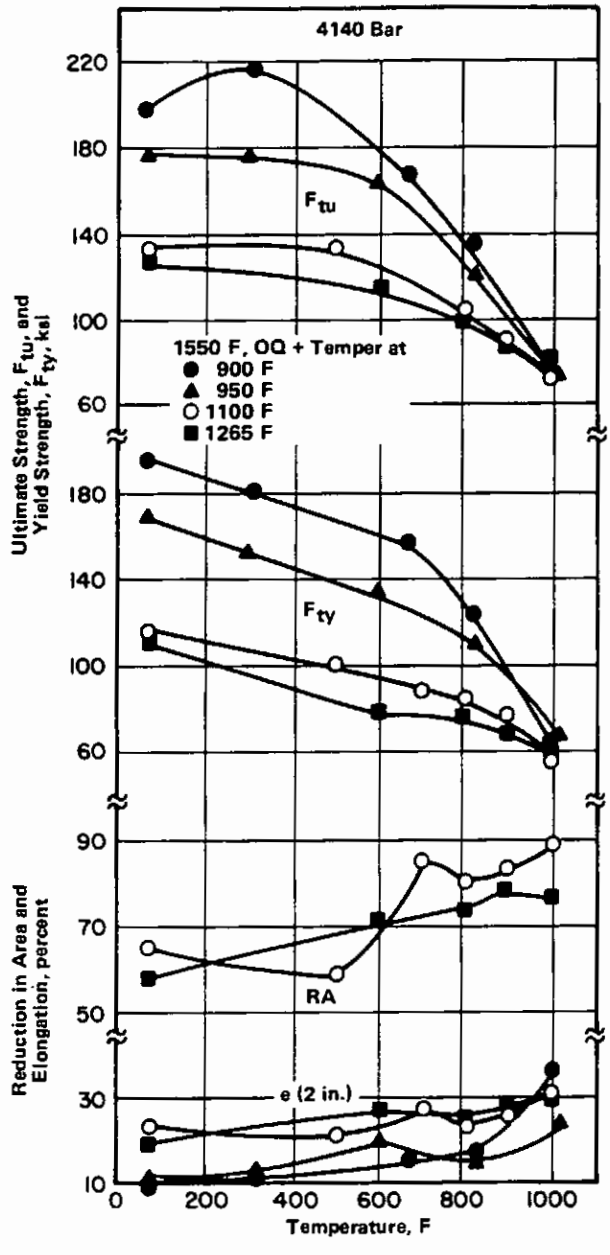


FIGURE 3.0311. EFFECT OF ELEVATED TEMPERATURES ON TENSILE PROPERTIES OF QUENCHED AND TEMPERED BAR (28)

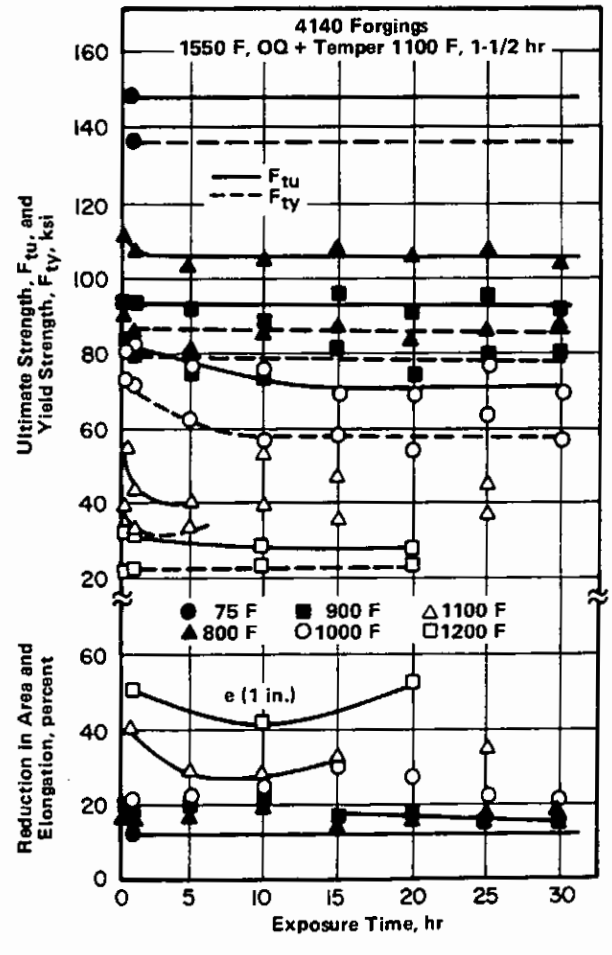


FIGURE 3.0312. EFFECT OF EXPOSURE TIME AND TEST TEMPERATURE ON ELEVATED TEMPERATURE TENSILE PROPERTIES (4)

Fe
0.4 Cr
1 Cr
0.2 Mo

4140

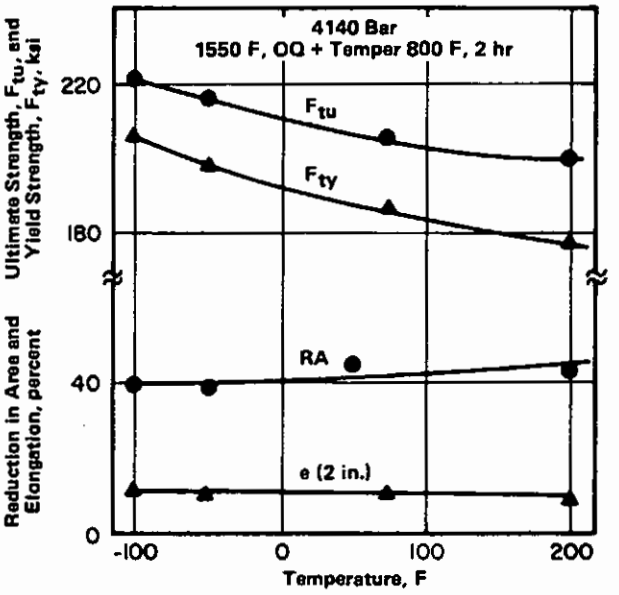
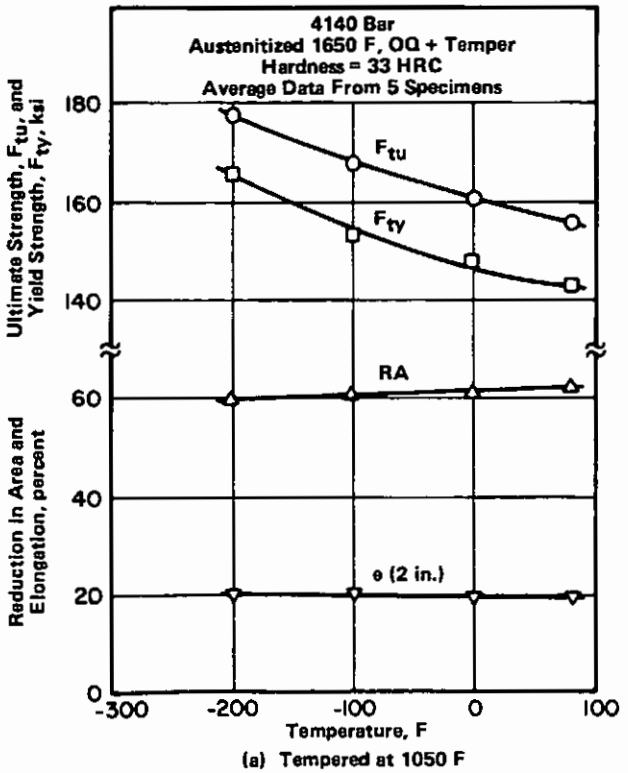
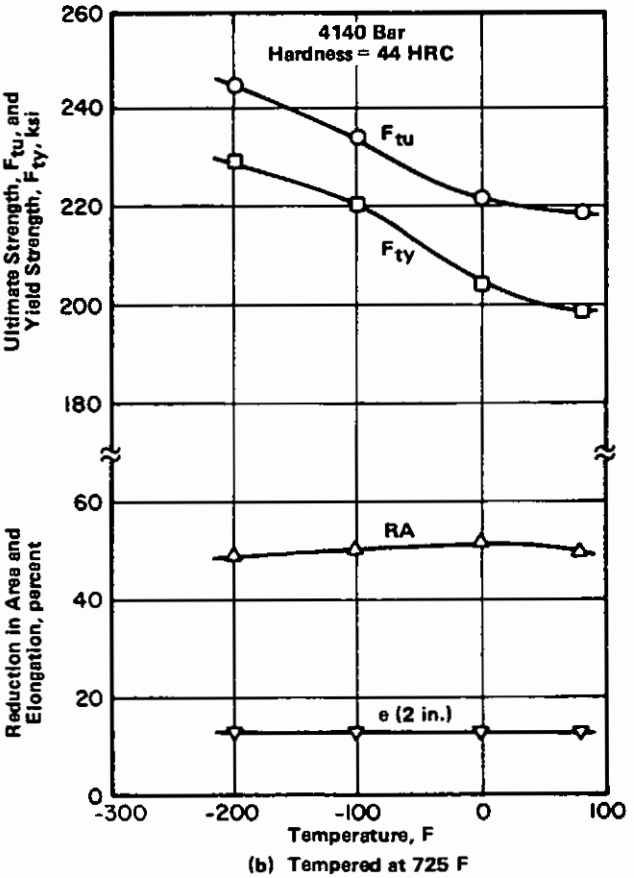


FIGURE 3.0313. EFFECTS OF TEMPERATURES FROM -100 F TO 200 F ON TENSILE PROPERTIES (39)



(a) Tempered at 1050 F

FIGURE 3.0314. EFFECTS OF TEMPERATURES FROM -200 F TO 80 F ON TENSILE PROPERTIES OF 4140 TEMPERED AT 1050 F AND AT 725 F (63)



(b) Tempered at 725 F

FIGURE 3.0314. EFFECT OF TEMPERATURES FROM -200 F TO 80 F ON TENSILE PROPERTIES OF 4140 TEMPERED AT 1050 F AND AT 725 F (63)

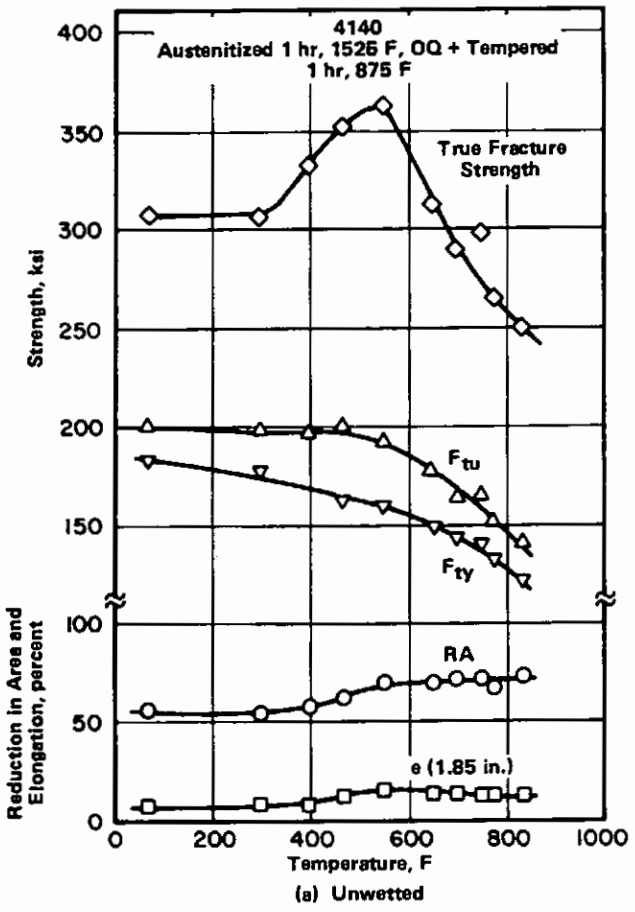


FIGURE 3.0316. EFFECTS OF SURFACE WETTING WITH LEAD ON TENSILE PROPERTIES (53)

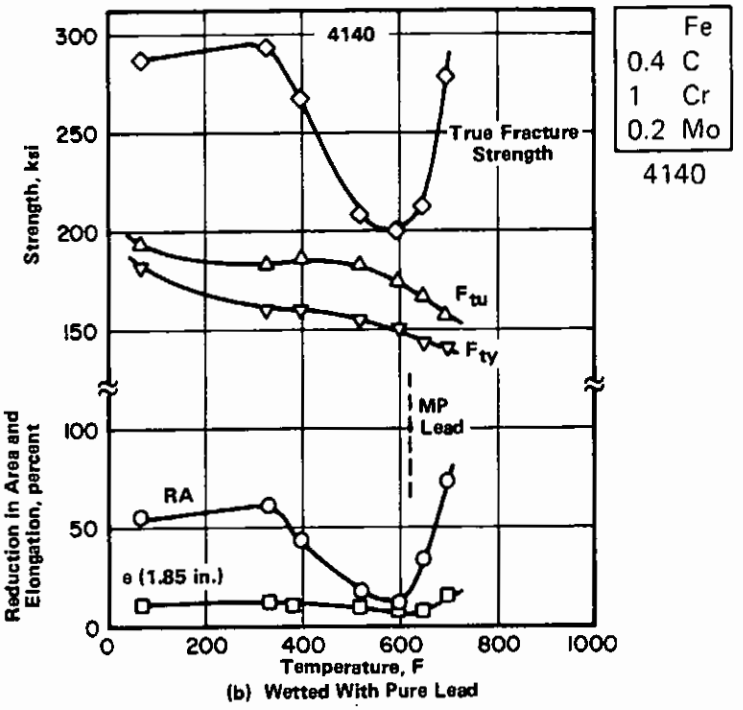


FIGURE 3.0316. EFFECTS OF SURFACE WETTING WITH LEAD ON TENSILE PROPERTIES (53)

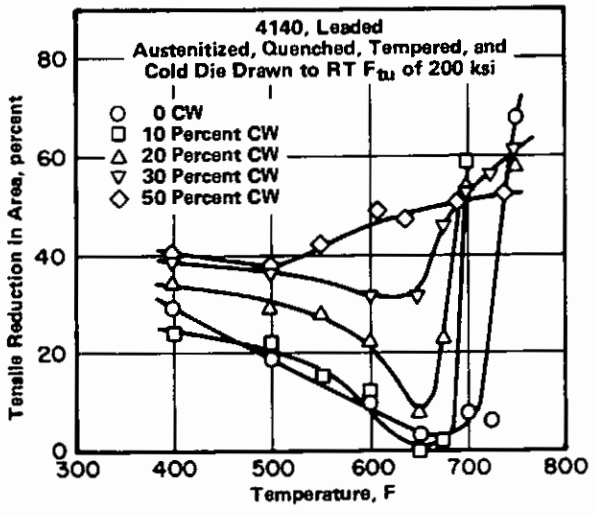


FIGURE 3.0318. ELIMINATION OF LEAD EMBRITTLEMENT BY PRIOR COLD DEFORMATION (54)

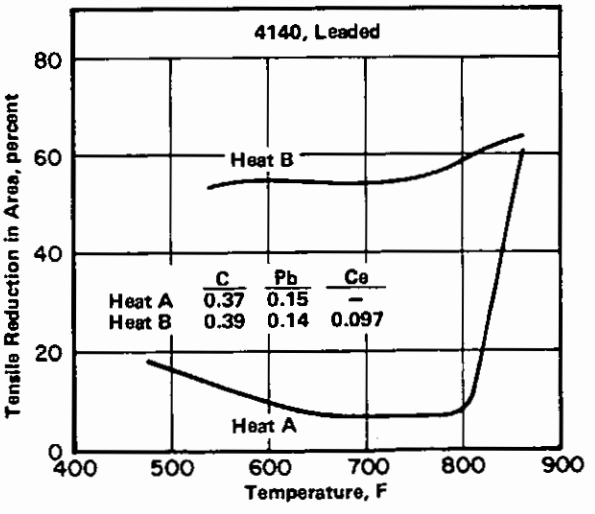


FIGURE 3.0319. ELIMINATION OF LEAD EMBRITTLEMENT BY THE ADDITION OF RARE EARTH ELEMENTS (54)

Fe
0.4 Cr
1 Cr
0.2 Mo

4140

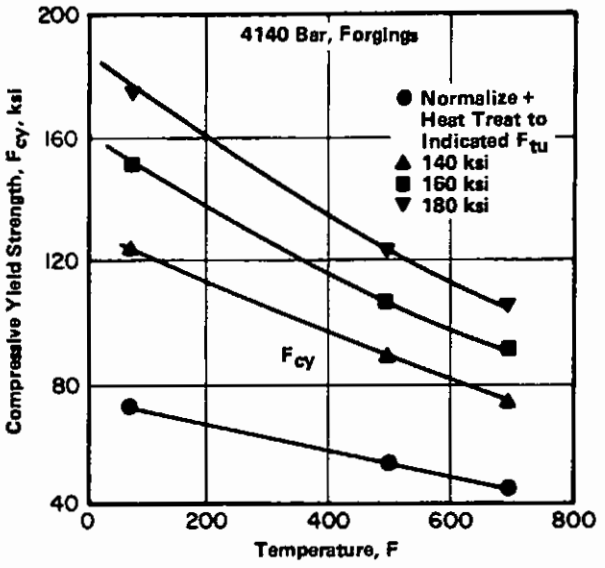


FIGURE 3.0321. EFFECT OF TEMPERATURE ON COMPRESSIVE YIELD STRENGTH OF BAR AND FORGINGS HEAT TREATED TO VARIOUS STRENGTH LEVELS (38)

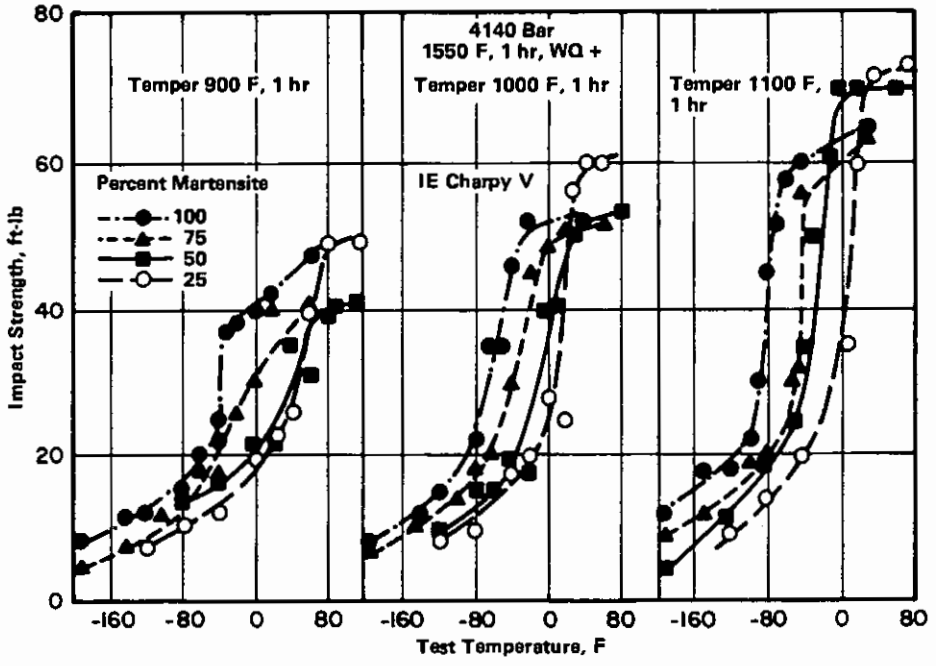


FIGURE 3.0331. EFFECTS OF TEST TEMPERATURE, TEMPERING TEMPERATURE, AND PERCENTAGE OF MARTENSITE IN MICROSTRUCTURE ON IMPACT PROPERTIES (6)

Note: Percent martensite controlled by use of specially designed end-quench specimens.

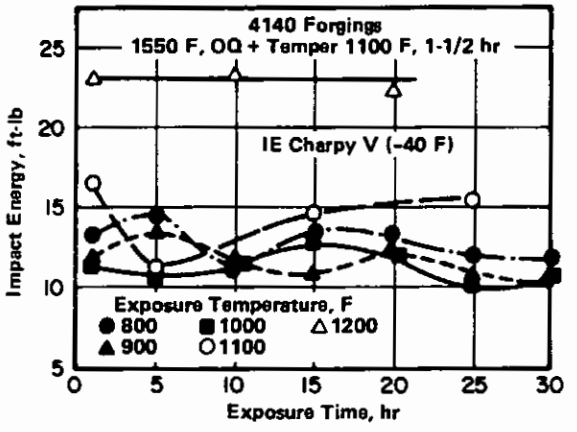


FIGURE 3.0332. EFFECTS OF EXPOSURES UP TO 30 HOURS AT VARIOUS ELEVATED TEMPERATURES ON IMPACT ENERGY AT -40 F (4)

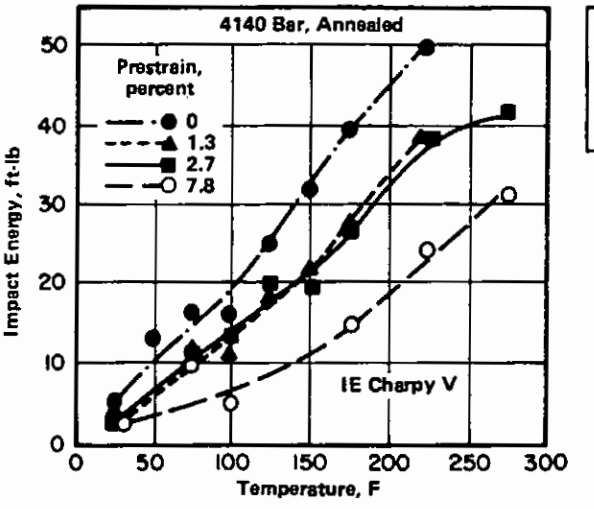


FIGURE 3.0333. EFFECTS OF TEMPERATURE AND PRE-STRAIN ON IMPACT ENERGY OF ANNEALED BAR (5)

Alloy	4140
Form	Castings
Condition	1600 F, WQ + Temper 1250 F, 5 hr
Temperature, F	Charpy V-Notch, ft-lb
70	22
-50	16

TABLE 3.0334. IMPACT PROPERTIES OF CASTINGS AT 70 AND -50 F (2)

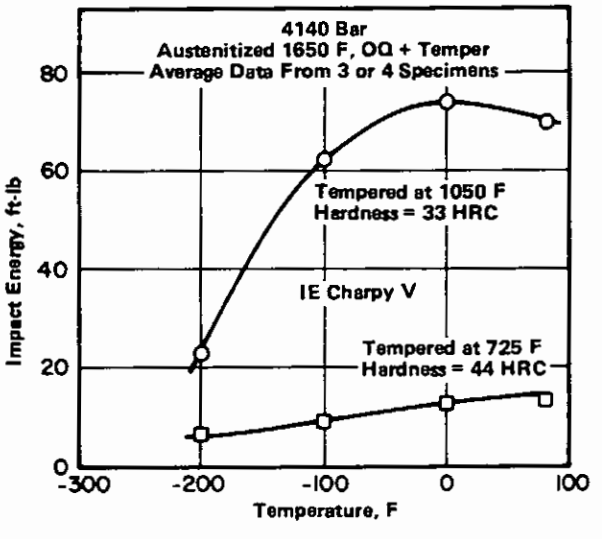


FIGURE 3.0335. EFFECTS OF TEMPERATURE FROM -200 F TO 80 F ON IMPACT ENERGY OF 4140 TEMPERED AT 1050 F AND AT 725 F (63)

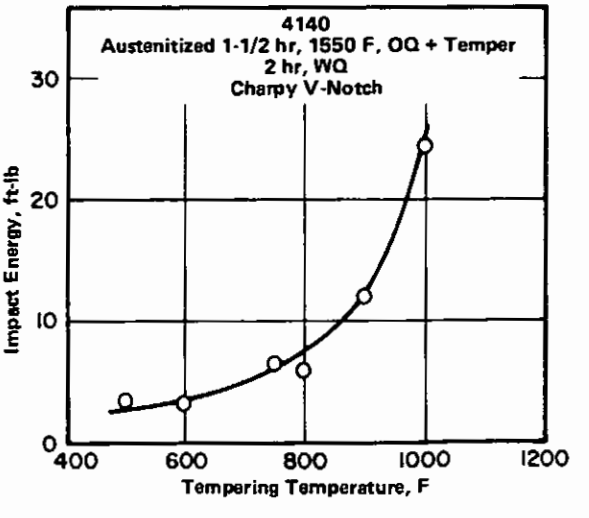


FIGURE 3.0336. EFFECT OF TEMPERING TEMPERATURE ON IMPACT ENERGY AT -40 F (64)

Fe
0.4 Cr
1 Cr
0.2 Mo

4140

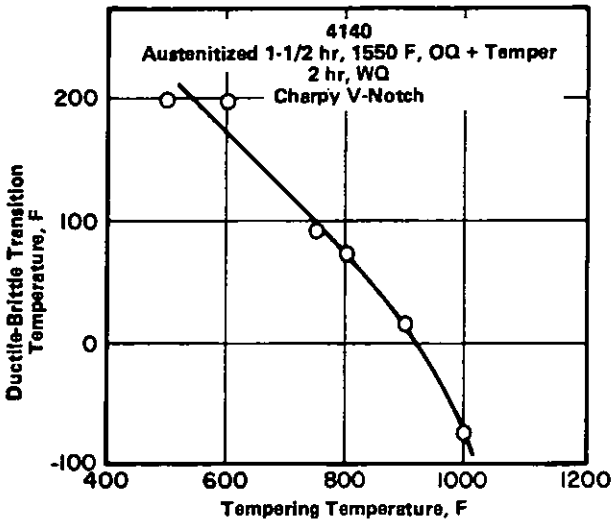


FIGURE 3.0337. EFFECT OF TEMPERING TEMPERATURE ON IMPACT DUCTILE-BRITTLE TRANSITION TEMPERATURE (64)

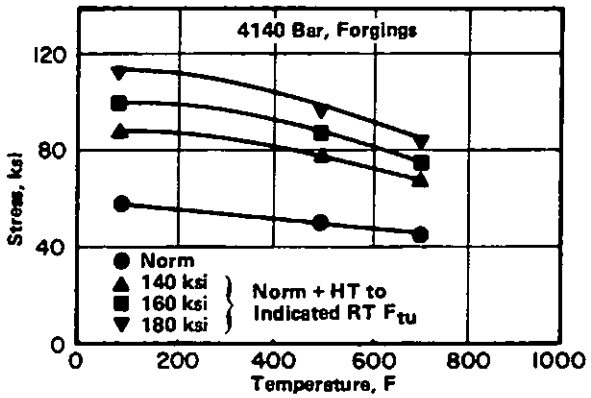


FIGURE 3.0351. EFFECT OF TEMPERATURE ON SHEAR STRENGTH OF BAR AND FORGINGS HEAT TREATED TO VARIOUS STRENGTH LEVELS (38)

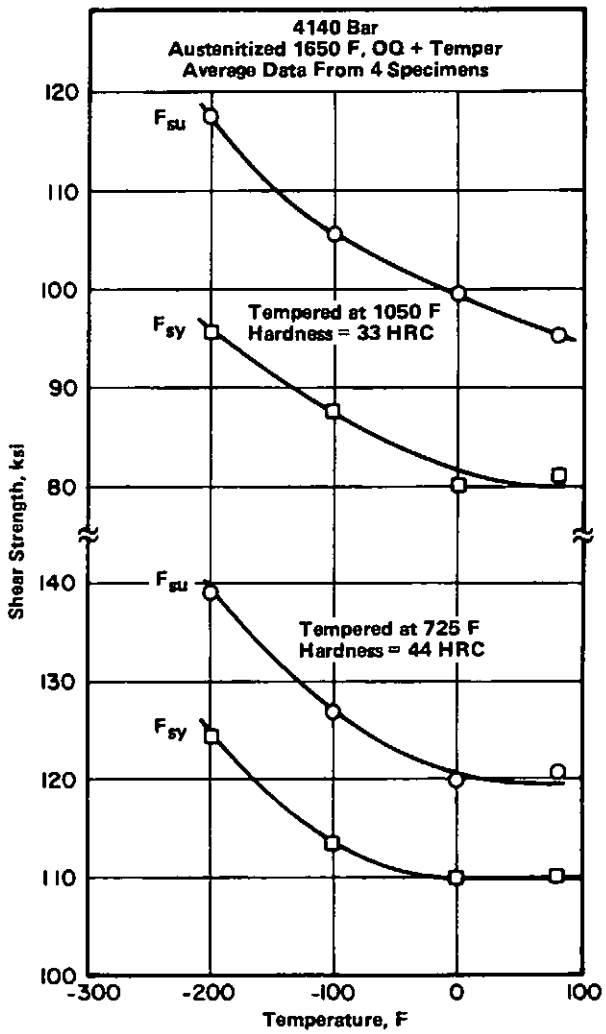


FIGURE 3.0352. EFFECTS OF TEMPERATURE FROM -200 F TO 80 F ON SHEAR STRENGTH OF 4140 TEMPERED AT 1050 F AND AT 725 F (63)

Fe
0.4 C
1 Cr
0.2 Mo

4140

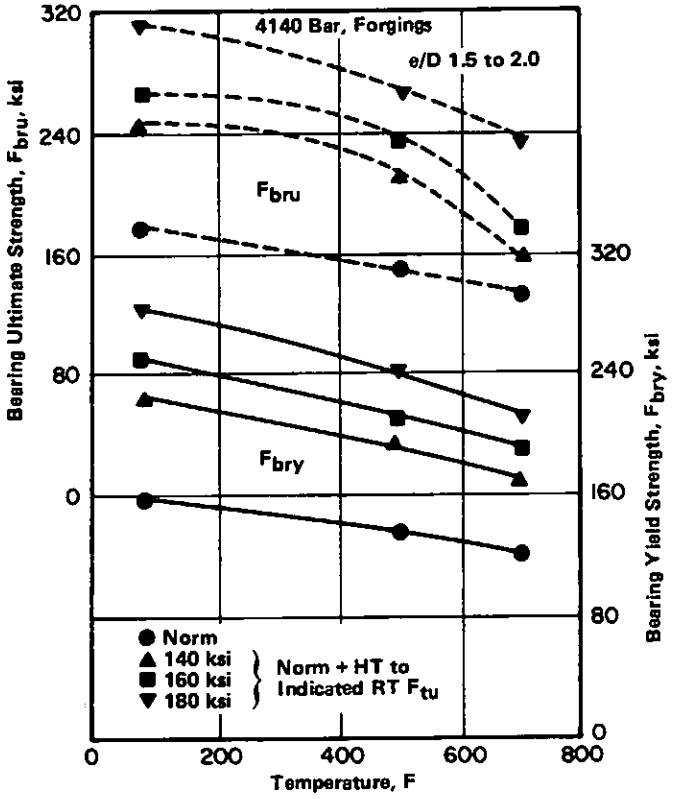


FIGURE 3.0361. EFFECT OF TEMPERATURE ON BEARING STRENGTH OF BAR AND FORGINGS HEAT TREATED TO VARIOUS STRENGTH LEVELS (38)

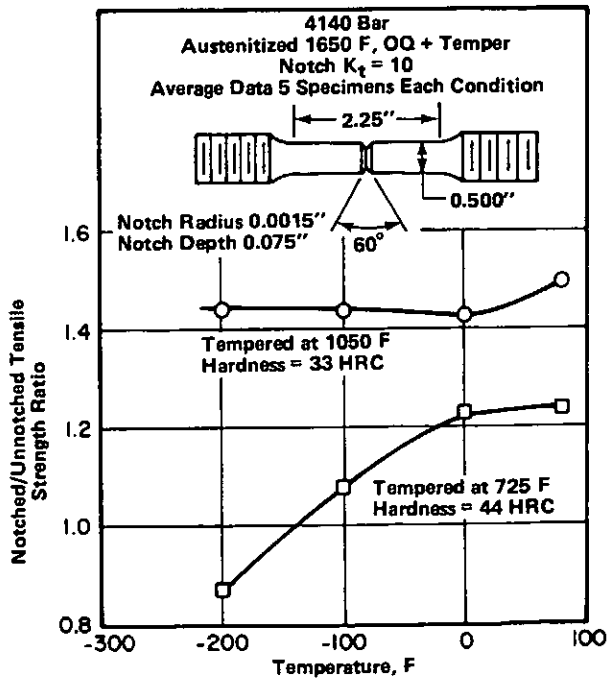


FIGURE 3.03711. EFFECTS OF TEMPERATURE FROM -200 F TO 80 F ON NOTCHED/UNNOTCHED TENSILE STRENGTH RATIO OF 4140 TEMPERED AT 1050 F AND AT 725 F (63)

Fe
0.4 Cr
1 Cr
0.2 Mo

4140

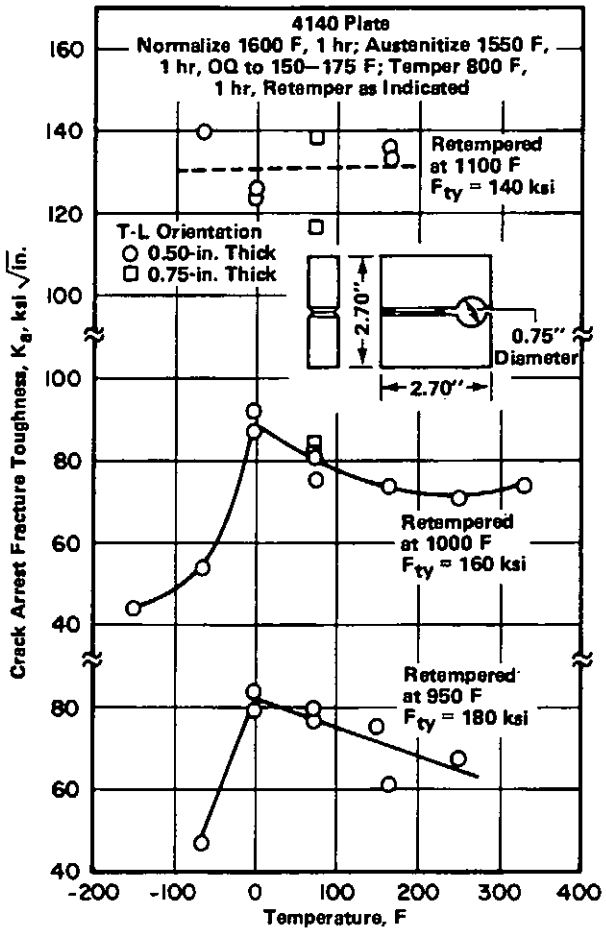


FIGURE 3.03722. CRACK ARREST FRACTURE TOUGHNESS OF 4140 STEEL AS A FUNCTION OF TEST TEMPERATURE (65)

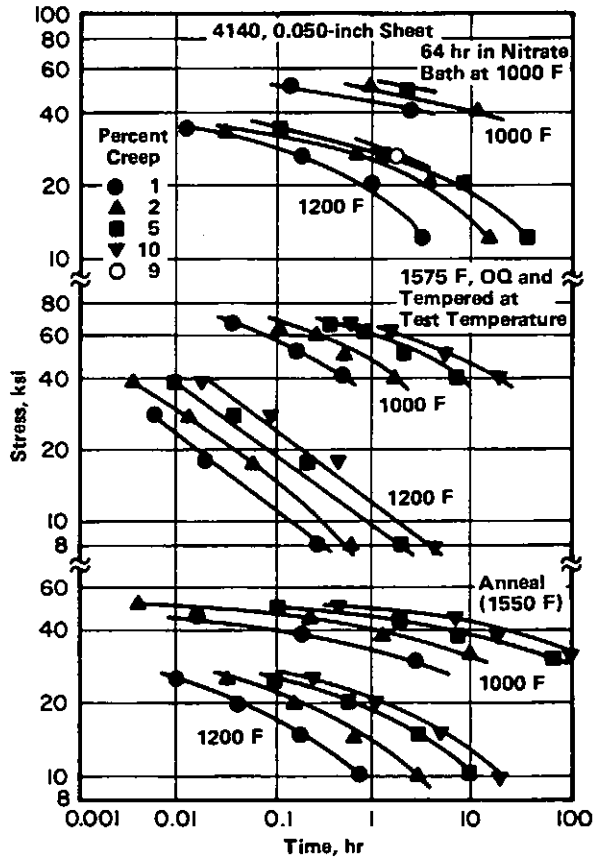


FIGURE 3.041. CREEP PROPERTIES AT 1000 F AND 1200 F OF SHEET IN VARIOUS HEAT TREATED CONDITIONS (40)

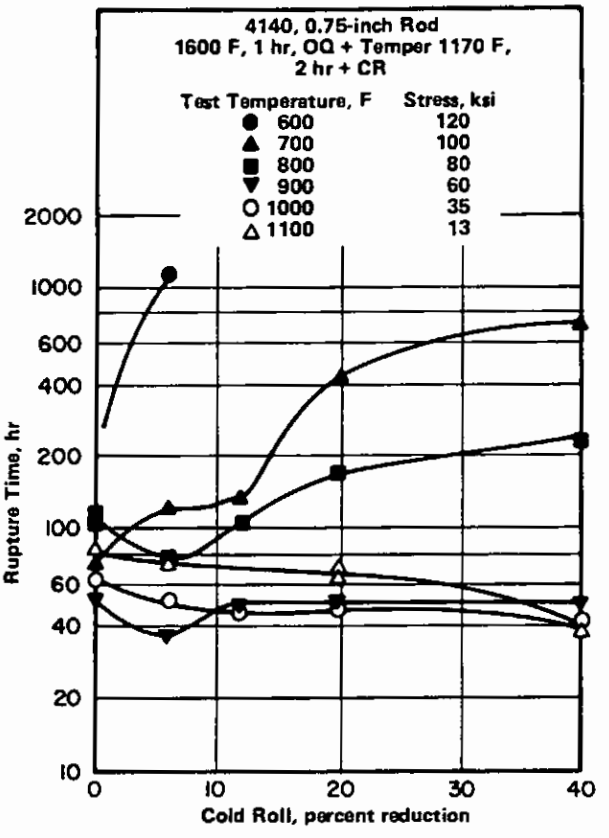


FIGURE 3.042. EFFECT OF COLD ROLLING ON CREEP-RUPTURE TIME OF QUENCHED AND TEMPERED ROD AT VARIOUS COMBINATIONS OF TEMPERATURE AND STRESS (33)

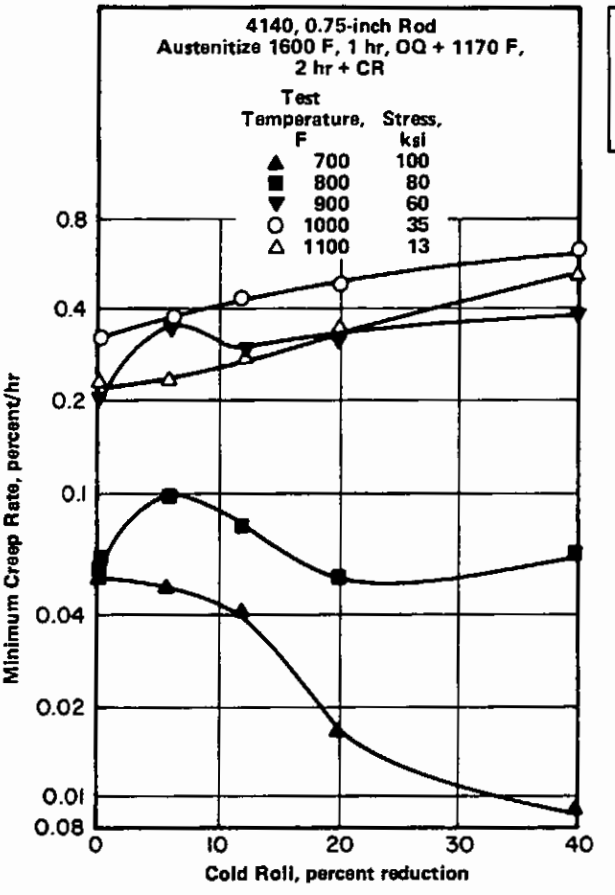


FIGURE 3.043. EFFECT OF COLD ROLLING ON MINIMUM CREEP RATE OF QUENCHED AND TEMPERED ROD AT VARIOUS COMBINATIONS OF TEMPERATURE AND STRESS (33)

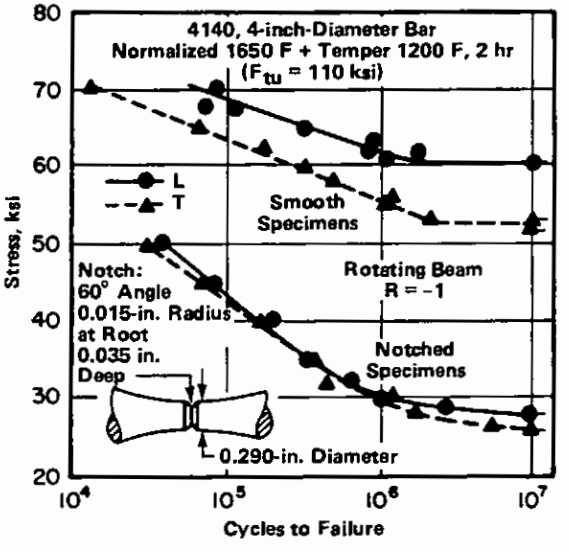


FIGURE 3.051. LONGITUDINAL AND TRANSVERSE FATIGUE PROPERTIES OF SMOOTH AND NOTCHED SPECIMENS (30)

Fe
0.4 Cr
1 Cr
0.2 Mo
4140

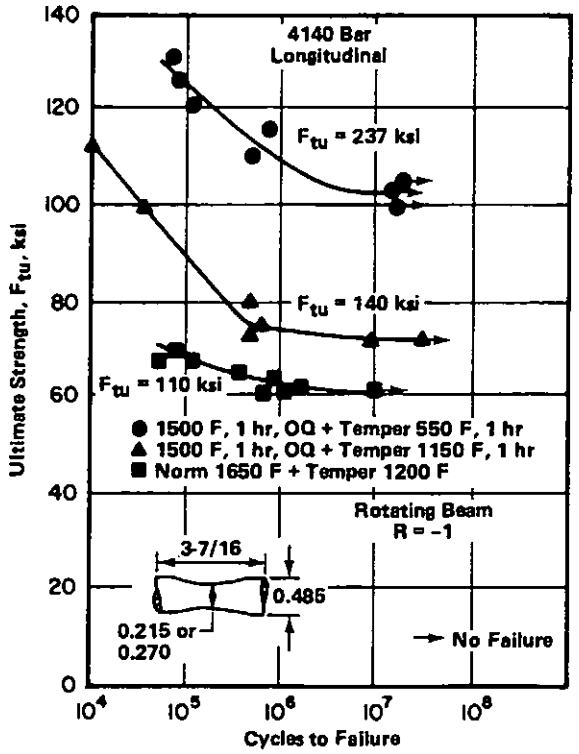


FIGURE 3.052. FATIGUE PROPERTIES OF SMOOTH BARS HEAT TREATED TO VARIOUS STRENGTH LEVELS (30, 31)

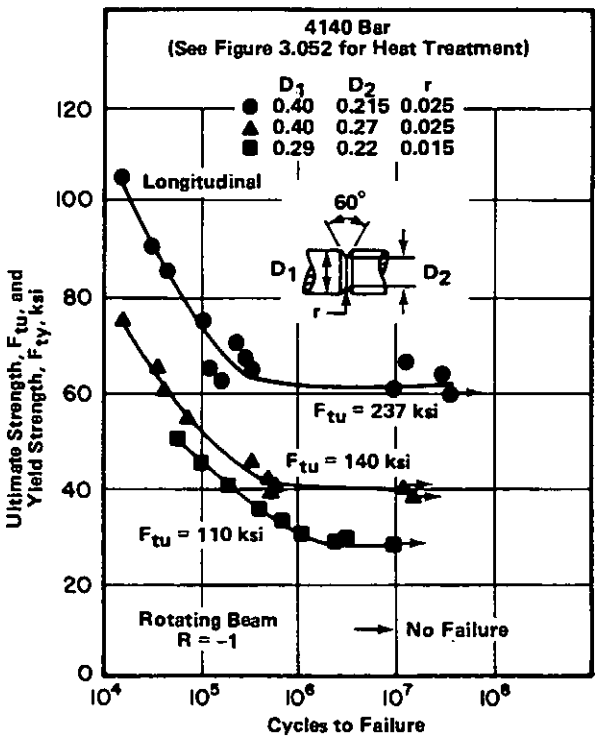


FIGURE 3.053. FATIGUE PROPERTIES OF NOTCHED BARS HEAT TREATED TO VARIOUS STRENGTH LEVELS (30, 31)

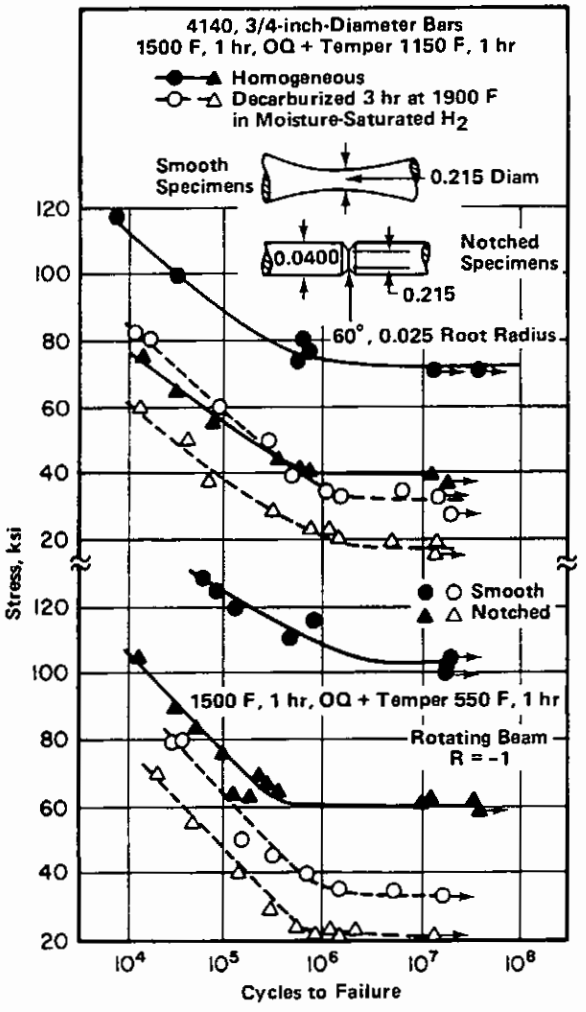


FIGURE 3.054. EFFECTS OF DECARBURIZATION ON FATIGUE PROPERTIES OF SMOOTH AND NOTCHED SPECIMENS (31)

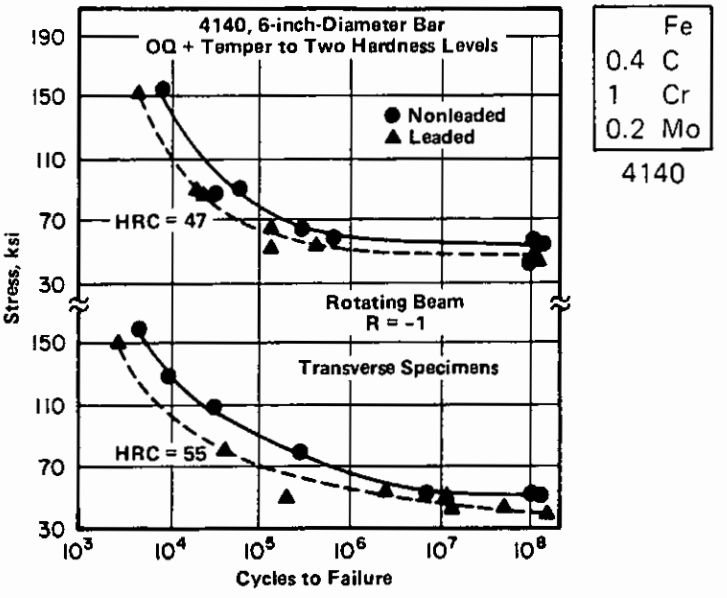


FIGURE 3.055. FATIGUE PROPERTIES OF LEADED AND NONLEADED BAR AT TWO HARDNESS LEVELS (29)

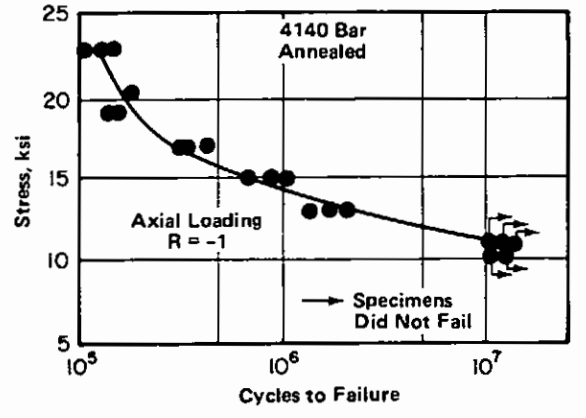


FIGURE 3.056. FATIGUE PROPERTIES OF ANNEALED BAR (5)

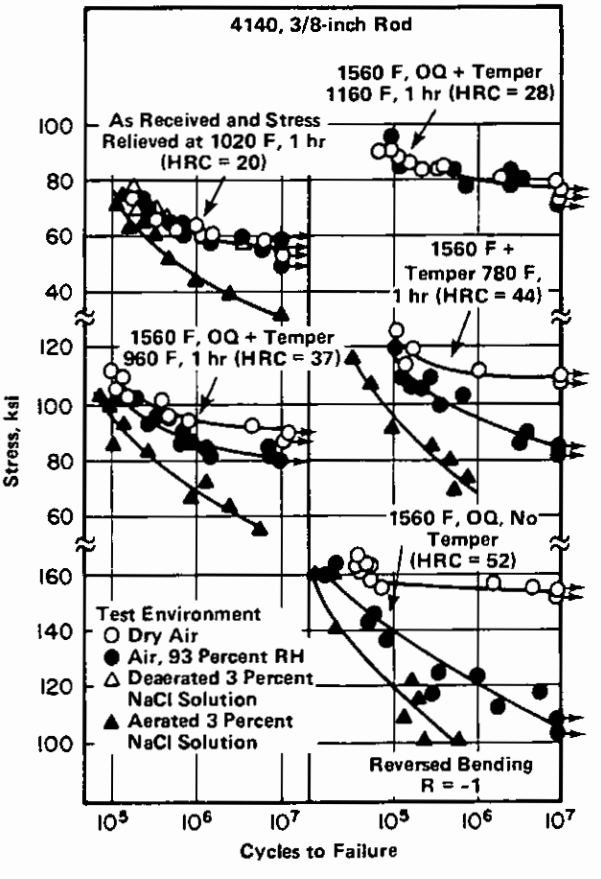


FIGURE 3.057. EFFECTS OF VARIOUS ENVIRONMENTS ON FATIGUE PROPERTIES IN DIFFERENT HEAT TREATED CONDITIONS (25)

Fe
0.4 Cr
1 Cr
0.2 Mo
4140

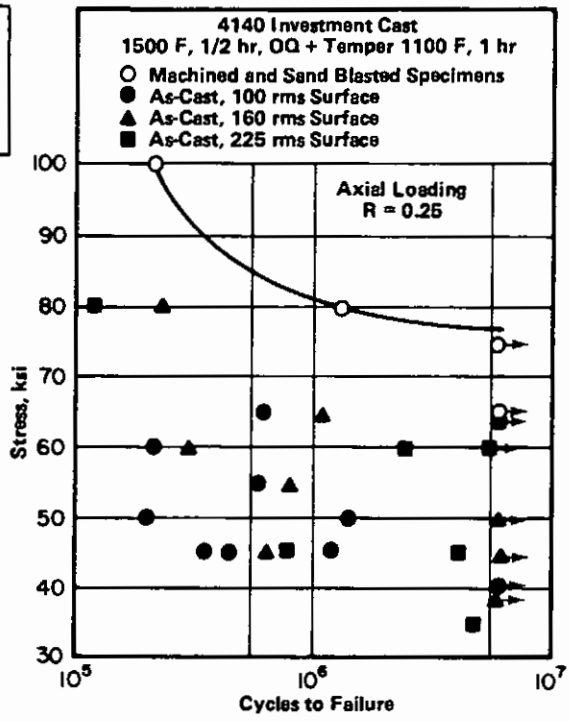
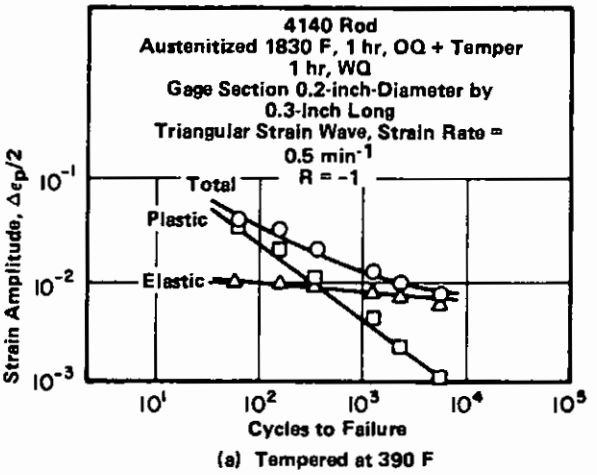
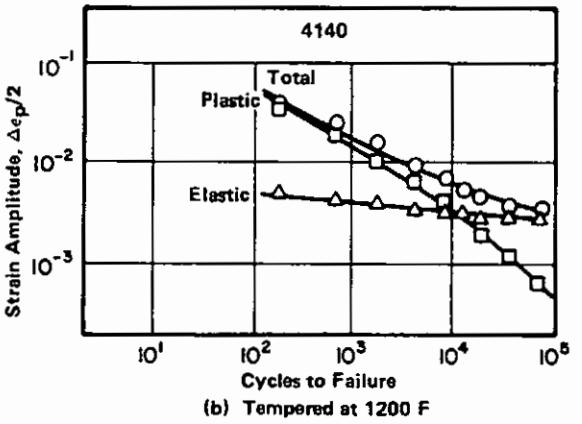


FIGURE 3.058. FATIGUE DATA FOR INVESTMENT CASTINGS SHOWING IMPROVEMENT IN FATIGUE LIFE AND CONSISTENCY OF RESULTS PRODUCED BY MACHINING AND SAND BLASTING (7)



(a) Tempered at 390 F

FIGURE 3.059. ROOM TEMPERATURE FATIGUE BEHAVIOR OF QUENCHED AND TEMPERED 4140 (51)



(b) Tempered at 1200 F

FIGURE 3.059. ROOM TEMPERATURE FATIGUE BEHAVIOR OF QUENCHED AND TEMPERED 4140 (51)

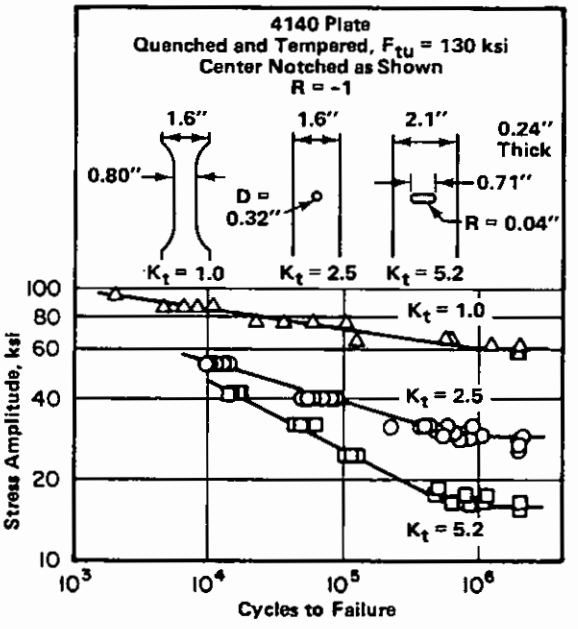


FIGURE 3.0510. EFFECTS OF NOTCHES ON CYCLIC FATIGUE LIFE AT ROOM TEMPERATURE (66)

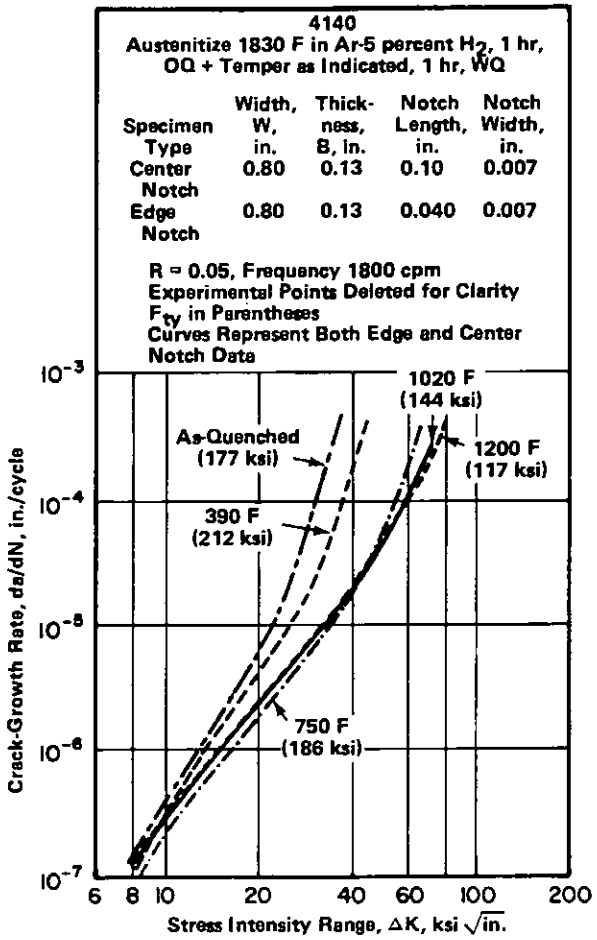
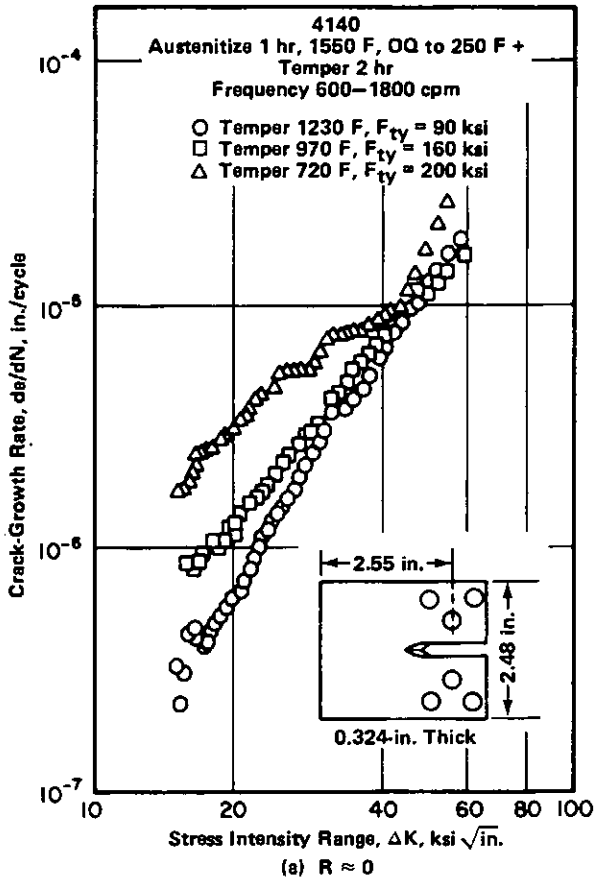


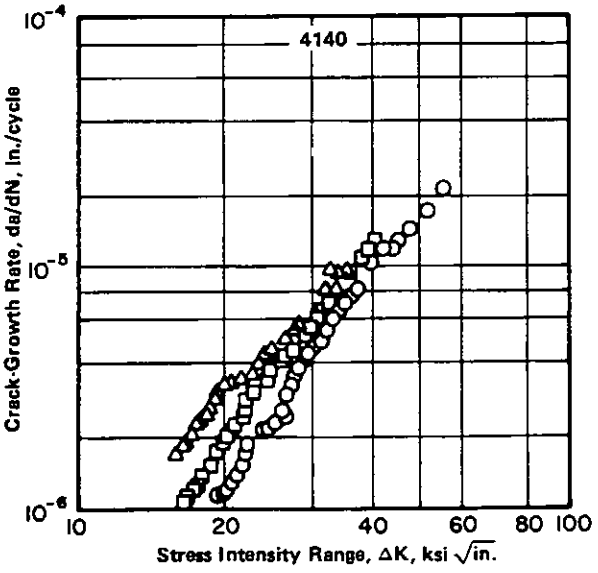
FIGURE 3.0512. ROOM TEMPERATURE FATIGUE CRACK GROWTH BEHAVIOR OF 4140 STEEL AUSTENITIZED AT 1830 F AND TEMPERED AT 390 F TO 1200 F (67)



(a) R ≈ 0

Fe
0.4 C
1 Cr
0.2 Mo
4140

FIGURE 3.0513. ROOM TEMPERATURE FATIGUE CRACK-GROWTH BEHAVIOR OF 4140 STEEL AUSTENITIZED AT 1550 F AND TEMPERED AT 720 F TO 1230 F (68)



(b) R = -1

FIGURE 3.0513. ROOM TEMPERATURE FATIGUE CRACK-GROWTH RATE OF 4140 STEEL AUSTENITIZED AT 1550 F AND TEMPERED AT 720 F TO 1230 F (68)

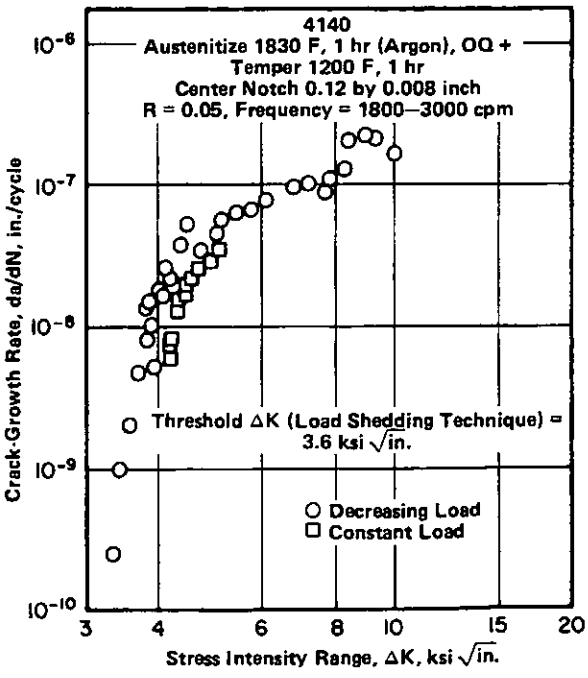


FIGURE 3.0514. ROOM TEMPERATURE FATIGUE CRACK-GROWTH BEHAVIOR OF QUENCHED AND TEMPERED 4140 STEEL AT LOW STRESSES (69)

	Fe
0.4	Cr
1	Cr
0.2	Mo

4140

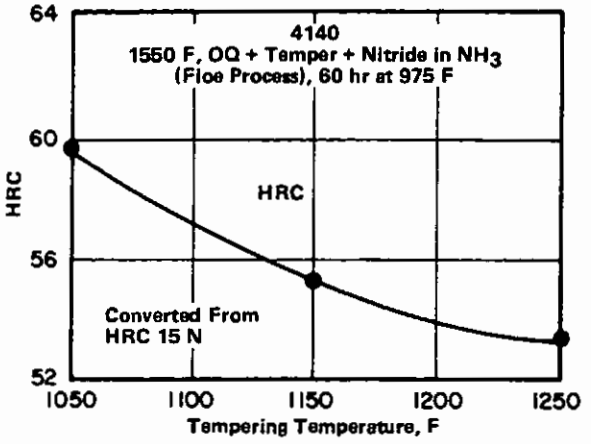


FIGURE 4.0421. CASE HARDNESS OF ALLOY NITRIDED AFTER IT HAD BEEN QUENCHED AND TEMPERED AT VARIOUS TEMPERATURES (41)

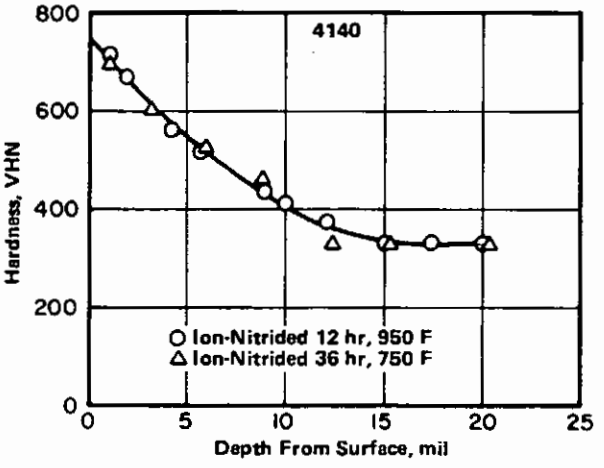


FIGURE 4.0422. HARDNESS GRADIENT NEAR SURFACE OF ION-NITRIDED 4140 STEEL (56)

1 General

Type 4330V is one of a group of low-alloy steels of similar composition based on the Type 4340 composition. These steels derive their high strengths from hardening and tempering treatments which produce a martensitic microstructure. The lower-carbon content of Type 4330V improves its performance in the areas of fracture toughness, weldability, and general fabricability with minimal reduction in strength relative to Type 4340. The presence of vanadium in Type 4330V provides improved hardenability and imparts some secondary strengthening. A further addition of 1.5 percent silicon has been shown to give additional strength improvement. This modification, termed Type 4330V (Mod + Si), has been studied in the laboratory but is not yet covered by AMS specifications. The mechanical properties of Type 4330V can be varied by varying the tempering conditions. It is most frequently heat treated to a tensile strength of 220-240 ksi. Type 4330V is employed in a variety of critical military, aerospace, and commercial applications. High quality alloy produced by arc-melting and vacuum degassing is the prime material for gun tubes of 3-inch-diameter or larger because of its high ductility and good resistance to cold impact. Type 4330V is also widely used for both civil and military landing gear applications (Refs. 24, 25, and 26).

1.1 Commercial Designation

4330V.

1.2 Alternate Designations

4330, 4330 Mod, 4330V Mod, 4330V (Mod + Si), UNS J23260 (Castings), UNS K23080 (Bars, Forgings, Tubing).

1.3 Specifications

1.3.1 *[Table]* AMS Specifications.

1.4 Composition

1.4.1 *[Table]* Specified Compositions.

1.5 Heat Treatment

1.5.1 General. The effects of microalloying with vanadium on hardenability in high-strength, low-alloy steels such as Type 4330V are complex but have received attention in recent years. Vanadium is the most effective hardener of all the usual alloying elements in steel, with a multiplying factor of about 1.4 at the 0.1 percent vanadium level based on the Jominy hardenability test. At the same alloying level, molybdenum has a hardenability multiplying factor of slightly less, about 1.35. A synergistic effect is obtained when both vanadium and molybdenum are present so that their combined hardenability is greater than the sum of their individual hardenabilities. However, only that portion of the vanadium which is dissolved in the austenite during the austenitizing heat treatment is effective in improving hardenability. Vanadium that is removed from solution by precipitation as carbide and/or nitride does not contribute directly to hardenability.

Fe
0.03 C
1.80 Ni
0.80 Cr
0.40 Mo
0.07 V

Hardenability studies have shown that the effectiveness of hardeners such as vandium is decreased at very high austenitizing temperatures, particularly above 2200F. It has been suggested that at low austenitizing temperatures, dissolved vanadium preferentially segregates to austentite grain boundaries, possibly as clusters with carbon or nitrogen, and inhibits grain-boundary nucleation of non-martensitic transformation products, thereby increasing hardenability. Conversely, high austenitizing temperatures cause the grain boundary segregation to be thermally dispersed with a consequent loss in hardenability. The austenitizing temperature must be higher than the ferrite-to-austenite transformation temperature (A_{c3}), but it should be below the temperature at which vanadium and molybdenum alloying additions lose their hardening effectiveness (i.e., in the range 1440 to 2200F).

Vanadium also affects the response to tempering of austenitized and quenched Type 4330V. Specifically, vanadium retards softening during tempering at 600 to 1100F by reducing precipitation of Fe_3C, possibly by slowing diffusion rates. Vanadium also promotes secondary hardening by precipitation of VC at temperatures above about 950F. Secondary hardening is at a maximum in the tempering temperature range 1100 to 1200F. Overageing and softening occur on tempering above 1200F (Refs. 27, 28).

1.5.2 Normalizing: Heat to 1675 - 1775F, air cool. After normalizing, tempering at 1250F gives a partially spheroidized structure which may be preferable to an annealed structure for easy machining (Ref. 29).

1.5.3 Annealing: Heat to 1550 - 1650F, furnace cool. Brinell hardness should be 200 to 240 for easy machining.

1.5.4 Austenitizing: Heat to 1525 - 1625F, hold 15 minutes per inch of thickness, oil quench (Ref. 29). (See Sections 3.2 - 3.3 for effects of austenitizing temperature and quenching on mechanical properties.)

1.5.5 Tempering: Heat to 400 - 1200F, air cool. Following are approximate tempering temperatures for indicated strength ranges:

F_{tu} 180 to 200 ksi, 950 to 1100F, 4 hr
F_{tu} 200 to 220 ksi, 750 to 950F, 4 hr
F_{tu} 220 to 240 ksi, 625 to 750F, 2 + 2 hr

© 1992 by Purdue Research Foundation, West Lafayette, Indiana 47907.
All Rights Reserved.

The maximum safe tempering temperature is about 1200F to avoid overageing and softening (Ref. 29). (See Sections 3.2 - 3.3 for effects of tempering temperature on mechanical properties.)

1.5.6 Stress Relieving: Heat to 400 - 450F, air cool. This treatment is beneficial after machining of material heat treated to high strength levels (Ref. 29).

1.5.7 Heat treatments should be conducted in a protective atmosphere to prevent excessive surface decarburization. Pure nitrogen, nitrogen-methanol blends, and endothermic gas are adequate. Depths of decarburization typically range from 0.002 to 0.0025 inch after heat treatment in a nitrogen-based atmosphere (Ref. 30).

1.6 Hardness

1.6.1 *[Figure]* End quench hardenability.

1.6.2 *[Figure]* Hardness distribution in oil quenched bars of different diameters.

1.6.3 *[Figure]* Effect of tempering temperature on hardness.

1.7 Forms and Conditions Available

1.7.1 Alloy is available in the full commercial range of sizes for low-alloy steels in the form of bar, forging, plate, and tubing.

1.7.2 All products are available in the annealed or normalized condition, forgings also in heat-treated condition.

1.8 Melting and Casting Practice

Electric furnace air melt. Induction and consumable electrode vacuum melts. (See Table 3.2.1.1.1 for effects of melting practice on mechanical properties.)

1.9 Special Considerations

1.9.1 Decarburization, although less pronounced than in the higher carbon steels, should not exceed a very small amount, particularly for applications involving repeated stresses. Decarburization or carburization during normal heat treatment (normalization and austenitization) should be avoided by using suitable, neutral protective atmospheres, unless the surface layer can be removed following heat treatment.

1.9.2 Material heat treated to F_{tu} = 220 to 260 ksi requires careful designing to keep stress concentrations at a minimum, and special measures during fabrication for 4337 and 4340 are given as guides:

(a) Decarburization must be completely removed.

(b) Straightening of heat-treated parts should be limited to 1/4 degree and performed at temperatures between 70 to 200F, followed by retempering at 390 to 410F, 4 hours. Straightened sections must be shot peened.

(c) Grinding of heat-treated parts must be performed with extreme caution and must be followed by baking at 365 to 385F and shot peening.

(d) Scale and rust removal should be by machining, sand blasting, or wet blasting.

(e) Vapor or solvent degreasing must be used. Pickling and cathodic cleaning are prohibited because of the susceptibility of inducing hydrogen embrittlement.

(f) Plating must be followed by baking at 365 to 385F, 8 hours, minimum. If parts are plated for oxidation protection before austenitizing, this must be followed by baking at 350 to 400F, 3 hours.

(g) A final baking at 250F, 24 hours is required to stabilize austenite. Alternatively, refrigeration can be used. (Cleveland Pneumatic Tool 1958). Honing to a depth not exceeding 0.010 inch may follow shot peening, but grinding after peening is not permissible.

1.9.3 Hydrogen embrittlement is a problem if the steel is heat treated to F_{tu} above 200 ksi.

2 Physical Properties and Environmental Effects

2.1 Thermal Properties

2.1.1 Melting Range, 2645 - 2845F.

2.1.2 Phase Changes.

2.1.2.1 Time-temperature-transformation diagrams.

2.1.2.2 Transformation temperatures. This steel transforms from austenite to ferrite and carbides on slow cooling and to martensite on fast cooling. Critical temperatures (approximate):

A_{e1} = 1290F

A_{e3} = 1340F (est)

A_{c1} = 1345-1364F (est)

A_{c3} = 1430-1436F (est)

A_{r1} = 610F

A_{r3} = 915F

M_9 = 576-640F (est)

M_{90} = 455F (est)

M_f = 360F (est)

(Refs. 5, 31, 32, 33.)

2.1.3 Thermal Conductivity, 22 Btu/ft/hr-ft^2-F (Ref. 29); 29 Btu/ft/hr-ft^2-F (Ref. 33).

2.1.4 Thermal Expansion.

2.1.4.1 *[Figure]* Mean coefficient of linear thermal expansion.

2.1.5 Specific heat, 0.12 Btu/1b-F (70-212F) (Ref. 29); 0.16 Btu/1b-F (Ref. 33).

2.1.6 Thermal Diffusivity, 0.37 ft^2/hr (Ref. 33).

2.2 Other Physical Properties

2.2.1 Density.

2.2.1.1 *[Figure]* Effect of temperature on density.

2.2.2 Electrical Properties.

2.2.3 Magnetic Properties.

2.2.4 Emissivity.

2.2.5 Damping Capacity.

2.3 Chemical Environments

2.3.1 General Corrosion.

2.3.2 Stress Corrosion.

2.3.2.1 Type 4330V steel suffers from accelerated stress corrosion cracking (SCC) in water, as do other similar steels. The threshold stress intensity for SCC in distilled water, shown in Figure 2.3.2.2, is less than half the fracture toughness for similarly quenched-and-tempered materials, shown later in Figure 3.2.7.2.1. Although both the threshold stress intensity and SCC crack-growth rate vary with austenitizing temperature, the controlling factor appears to be grain boundary segregation of phosphorus and sulfur rather than grain size (with which fracture toughness is better correlated). The threshold stress intensity for SCC is least after final austenitizing at 1598F and is similar for both large-grained and small-grained material. The highest threshold stress intensity is observed for material austenitized at 2012F. As shown in Figure 2.3.2.3, large- and small-grained material austenitized at 1598F had similar high SCC crack-growth rates, while material austenitized at 2012F had the lowest. Intergranular fracture and grain boundary segregation of phosphorus and sulfur were observed in specimens austenitized at 1598 or 1832F, while transgranular fracture and lack of detectable segregation of these elements characterized the materials austenitized at 2012 and 2192F. These observations indicate that hydrogen embrittlement, which is generally accepted as the mechanism of SCC of high-strength steels in water, is likely to be enhanced along grain boundaries by low-temperature austenitizing. It is suggested that the enhanced hydrogen embrittlement is related to increased phosphorus and sulfur segregation and consequent increased hydrogen trapping at grain boundaries after austenitizing at lower temperatures, resulting in decreased resistance to SCC. At higher temperatures, grain boundary segregation and hydrogen embrittlement are both decreased, leading to improved stress corrosion resistance (Refs. 34, 35).

2.3.2.2 *[Figure]* Effects of austenitizing temperature on threshold stress intensity for stress corrosion cracking in distilled water at 95F.

2.3.2.3 *[Figure]* Effects of austenitizing temperature on state II constant crack-growth rate during stress corrosion in distilled water at 95F.

2.3.2.4 The threshold stress intensity for SCC in aqueous 3.5 percent NaCl solution is reported as 25 ksi $(in)^{1/2}$ using 0.5-inch thick cantilever-loaded specimens tempered at 500F (Ref. 36). This value is close to those shown in Figure 2.3.2.2, indicating similar behavior in both distilled water and saline solutions.

2.3.2.5 High-strength steels such as Type 4330 are also susceptible to both general corrosion and stress corrosion during long-time exposures to marine atmosphere. Two-point loaded stress corrosion specimens of Type 4330, 0.08 to 0.24 inch thick, were initially exposed in low-velocity seawater for 6 months and then re-exposed to marine atmosphere at Kure Beach, North Carolina, for 4 years. After this time, they were removed from test due to severe corrosion although no cracks were found. Thirty additional two-point loaded welded specimens were exposed to marine atmosphere for 24 years. Five specimens failed during this exposure due to cracking while the other 25 were discontinued from further testing because of severe corrosion. In contrast, a plate specimen of Type 4330 stressed by a circular weld was in satisfactory condition after 22 years exposure to marine atmosphere (Ref. 37).

2.4 Nuclear Environments

3 Mechanical Properties

3.1 Specified Mechanical Properties

3.1.1 *[Table]* AMS Specified Mechanical Properties.

3.2 Mechanical Properties at Room Temperature

3.2.1 Tension Stress-strain Diagrams and Tensile Properties.

3.2.1.1 Effects of melting.

3.2.1.1.1 *[Table]* Effects of melting practice on mechanical properties.

3.2.1.2 Effects of austenitizing.

3.2.1.2.1 Increasing the austenitizing temperature in the range 1598 to 2192F

results in a progressive decrease in yield and ultimate tensile strength and in reduction in area, as shown in Figure 3.2.1.2.2. These effects are probably related to the increase in austenite grain size.

3.2.1.2.2 *[Figure]* Effects of austenitizing temperature on tensile properties.

3.2.1.2.3 The effects of mixed microstructures comprised of martensite and bainite are of interest because of the possibility of their occurrence when Type 4330 and other low-alloy steels are commercially processed in heavy sections. Figure 3.2.1.2.4 shows the effects on tensile properties of holding at 662F to develop a mixed structure of martensite and lower bainite and of holding at 932F to develop a structure of martensite plus upper bainite. Comparison of the 662F-hold data with baseline data for direct oil-quenched materials indicates that intermediate holding at this temperature causes a progressive decrease in tensile strength and an increase in ductility (as measured by RA). In contrast, holding for longer times at 932F does not significantly affect tensile properties. Similar effects are observed on impact energy, shown later in Figure 3.2.3.2 (Ref. 38).

3.2.1.2.4 *[Figure]* Effects of hold time at intermediate temperatures after austenitizing on tensile properties.

3.2.1.2.5 *[Figure]* Effect of as-quenched section size on the tensile properties of bar tempered at 1000F.

3.2.1.2.6 *[Figure]* Effect of as-quenched section size on the tensile properties of bars at 1200F.

3.2.1.2.7 Quenching medium after austenitizing affects the microstructure but has only minor effects on mechanical properties, as shown in Table 3.2.1.2.8. Quenching into water at 75F provided the severest quench and produced a fully martensitic microstructure. A 400F salt bath comprised the least severe quench and resulted in a largely bainitic structure, while the intermediate severity oil quench gave a mixed bainite/martensite structure (Ref. 39).

3.2.1.2.8 *[Table]* Effects of quenching medium on mechanical properties and microstructure.

3.2.1.3 Effects of ausforming.

3.2.1.3.1 The introduction of a forging step between austenitizing and tempering effects a modest increase in tensile strength, as shown in Figure 3.2.1.3.2.

3.2.1.3.2 *[Figure]* Effects of ausforming by forging on tensile properties.

3.2.1.4 Effects of tempering.

3.2.1.4.1 A general trend is evident for decreasing tensile strength and moderately increasing tensile ductility with increasing tempering temperature, seen in Figures 3.2.1.4.2 - 3.2.1.4.7.

3.2.1.4.2 *[Figure]* Effects of tempering temperature on tensile properties of rod.

3.2.1.4.3 *[Figure]* Effect of tempering temperature on tensile properties of bar.

3.2.1.4.4 *[Figure]* Effect of tempering temperature on tensile properties of plate.

3.2.1.4.5 *[Figure]* Effects of specimen location and tempering temperature on tensile properties of a large forging.

3.2.1.4.6 *[Figure]* Effects of as-quenched section size and tempering temperature on tensile properties of bar.

3.2.1.4.7 *[Figure]* Effects of tempering temperature on tensile properties of electro-slag-melted alloy.

3.2.1.5 Effects of alloying.

3.2.1.5.1 *[Figure]* Effects of austenitizing and tempering temperatures on tensile properties of Type 4330V (Mod + Si).

3.2.1.5.2 *[Figure]* Effects of tempering temperature and quenching rate on tensile properties of Type 4330V (Mod + Si).

3.2.1.5.3 The addition of 2 percent silicon to a base Type 4330 composition (no vanadium) significantly improves the mechanical properties after quenching and tempering. As shown in Figure 3.2.1.5.4, the silicon-containing material had notably higher yield and ultimate strengths with no decrease in elongation as compared to the unmodified Type 4330. Fracture toughness was also improved by the silicon addition, as shown later in Figure 3.2.7.2.4 (Ref. 40).

3.2.1.5.4 *[Figure]* Effects of tempering temperature and silicon addition on tensile properties of Type 4330.

3.2.1.5.5 *[Figure]* Tensile properties of plate containing silicon and chromium additions.

3.2.2 Compression Stress-strain Diagrams and Compression Properties.

3.2.3 Impact.

3.2.3.1 *[Figure]* Effects of austenitizing temperature on impact energy.

3.2.3.2 *[Figure]* Effects of hold time at intermediate temperature after austenitizing on impact energy.

3.2.3.3 *[Figure]* Effects of carbon content and tempering temperature on impact energy of bar.

3.2.3.4 *[Figure]* Effects of specimen location and tempering temperature on impact energy of bar and forgings.

3.2.3.5 *[Figure]* Effects of as-quenched section size and tempering temperature on impact energy of bar.

3.2.4 Bending.

3.2.5 Torsion and Shear.

3.2.6 Bearing.

3.2.7 Stress Concentration.

3.2.7.1 Notch properties.

3.2.7.1.1 *[Figure]* Effects of carbon content and tempering temperature on notch strength of bar.

3.2.7.1.2 *[Figure]* Effects of specimen location and tempering temperature on notch strength of a large forging.

3.2.7.1.3 *[Figure]* Effects of specimen size and test direction on notch strength of bar at various strength levels.

3.2.7.1.4 *[Figure]* Effects of stress concentration, tempering temperature, specimen size, and test direction on notch strength ratio of bar.

3.2.7.2 Fracture toughness.

3.2.7.2.1 *[Figure]* Effects of grain size and austenitizing temperature on fracture toughness.

3.2.7.2.2 *[Figure]* Effects of tempering temperature on fracture toughness.

3.2.7.2.3 *[Table]* Fracture toughness of plate, bar, and billet.

3.2.7.2.4 *[Figure]* Plane-strain fracture toughness of plate with additions of silicon and chromium.

3.2.8 Combined Properties.

3.3 Mechanical Properties at Various Temperatures

3.3.1 Tension Stress-strain Diagrams and Tensile Properties.

3.3.1.1 *[Figure]* Effect of cyclic exposure and test temperature on tensile properties of bar.

3.3.1.2 *[Figure]* Effect of test temperature on tensile properties of plate with silicon and chromium additions.

3.3.1.3 *[Figure]* Effects of test temperature on tensile properties of Type 4330V (Mod + Si).

3.3.2 Compression Stress-strain Diagrams and Compression Properties.

3.3.3 Impact.

3.3.3.1 *[Figure]* Effects of test temperature, section size, and test direction of impact energy of bar.

3.3.3.2 *[Figure]* Effects of austenitizing and tempering temperatures on impact energy at -40F.

3.3.3.3 *[Figure]* Effect of tempering temperature on impact energy at -40F.

3.3.3.4 *[Figure]* Effect of ausforming on impact energy ductile-brittle transition temperature.

3.3.3.5 *[Figure]* Effects of austenitizing and tempering temperatures on impact energy of Type 4330V (Mod + Si) at -40F.

3.3.3.6 *[Figure]* Effects of tempering temperature and quenching rate on impact energy of Type 4330V (Mod + Si) at -40F.

3.3.4 Bending.

3.3.5 Torsion and Shear.

3.3.6 Bearing.

3.3.7 Stress Concentration.

3.3.7.1 Notch properties.

3.3.7.1.1 *[Table]* Effect of tempering temperature on the crack strength of forged billet at two test temperatures.

3.3.7.1.2 *[Figure]* Effects of test temperature on notch and ultimate tensile strength of Type 4330V (Mod + Si).

3.3.7.2 Fracture toughness.

3.3.7.2.1 *[Table]* Plane-strain fracture toughness of forgings at two test temperatures.

3.3.7.2.2 *[Figure]* Effect of test temperature on plane-strain fracture toughness of plate with silicon and chromium additions.

3.3.8 Combined Properties.

3.4 Creep and Creep Rupture Properties

3.4.1 *[Figure]* Creep curves for Type 4330 at 842F for times up to 12 years.

3.5 Fatigue Properties.

3.5.1 *[Table]* Fatigue properties of smooth and notched bar at room temperature.

3.5.2 *[Table]* Fatigue properties of notched billet at room temperature.

3.5.3 *[Figure]* Effects of double tempering on fatigue properties of smooth and notched bar.

3.5.4 *[Figure]* Fatigue crack growth rate for forgings (F_{tu} = 240 ksi).

3.5.5 *[Figure]* Fatigue crack growth rate for forgings (F_{tu} = 230 ksi).

3.5.6 *[Figure]* Fatigue crack growth rate for forged bar (F_{tu} = 220 to 240 ksi).

3.5.7 An extensive investigation of fatigue and related mechanical properties was conducted on material austenitized at 1550F, 2 hours, oil quenched, plus tempered at 600 to 1300F, and water quenched. Based on the observed crack propagation rates [for maximum stress intensities of 30 to 80 ksi(in.)$^{1/2}$] and correlations with fracture toughness and tensile properties, it was concluded that optimum fatigue resistance (minimum crack propagation rate) is provided by tempering at about 1100F (Ref. 41).

3.6 Elastic Properties

3.6.1 Poisson's Ratio.

3.6.2 Modulus of Elasticity.

3.6.2.1 *[Figure]* Effect of temperature on dynamic modulus of elasticity.

3.6.3 Modulus of Rigidity.

3.6.4 Tangent Modulus.

3.6.5 Secant Modulus.

4 Fabrication

4.1 Forming

4.1.1 Type 4330V can be hot worked by forging or rolling in the temperature range 2250 to 1950F. Preheating at 1300 to 1500F is recommended. After hot working, parts should be furnace cooled (Ref. 29).

4.2 Machining and Grinding

4.2.1 Type 4330V can be readily machined in the annealed or normalized-and-tempered condition. Material which has been quenched and tempered to high strength levels is also machinable but should be stress-relieved at 400 to 450F after machining (Ref. 29).

4.3 Joining

4.3.1 Type 4330V can be gas welded, arc welded, and resistance welded. A welding rod of the same composition is recommended. Preheating and post-weld heat treating are desirable to prevent cracking (Ref. 29).

Table 1.3.1 AMS specifications (Refs. 1, 42-44)

Alloy: 4330V	
AMS Specification	**Product Form**
5328C	Investment castings
5329D	Sand castings
6411D	Bars, forgings, tubing (Premium quality, consumable electrode remelted)
6427G	Bars, forgings, tubing

Table 1.4.1 Specified compositions

Alloy	4330 Mod		4330V Mod				4330V (Mod + Si)	
AMS Specification	5328C, 5329D		6411D		6427G		(None)	
Reference	42, 43		44		1		3	
Element	Percent		Percent		Percent		Percent	
	Min	Max	Min	Max	Min	Max	Min	Max
Carbon	0.28	0.36	0.28	0.33	0.28	0.33	0.28	0.33
Nickel	1.65	2.00	1.65	2.00	1.65	2.00	1.65	2.00
Chromium	0.65	1.00	0.75	1.00	0.75	1.00	0.70	0.90
Molybdenum	0.30	0.45	0.35	0.50	0.35	0.50	0.20	0.30
Vanadium	-	-	0.05	0.10	0.05	0.10	0.10 Typical	
Manganese	0.60	1.00	0.65	1.00	0.75	1.00	0.65	0.85
Silicon	0.50	1.00 (a)	0.15	0.35	0.15	0.35	1.45 Typical	
Phosphorus	-	0.025	-	0.015	-	0.025	-	-
Sulfur	-	0.025	-	0.015	-	0.025	-	-
Copper	-	0.35	-	0.35	-	0.35	-	-
Iron	Balance		Balance		Balance		Balance	

(a) Max silicon content is 0.90 percent for AMS 5329D.

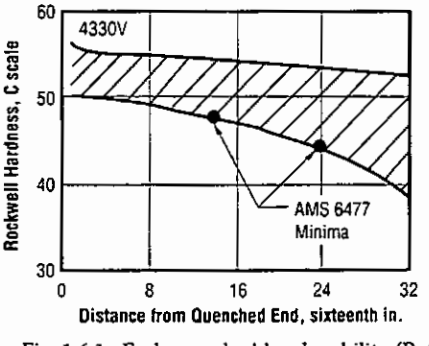


Fig. 1.6.1 End quenched hardenability (Ref. 12)

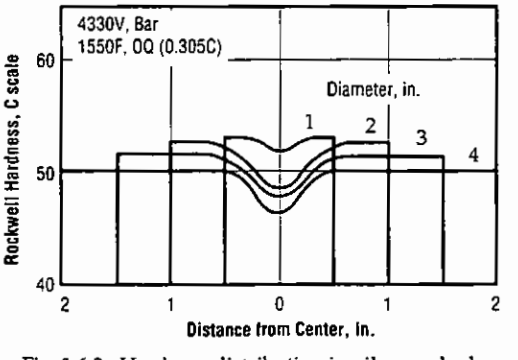


Fig. 1.6.2 Hardness distribution in oil quenched bars of different diameters (Ref. 13)

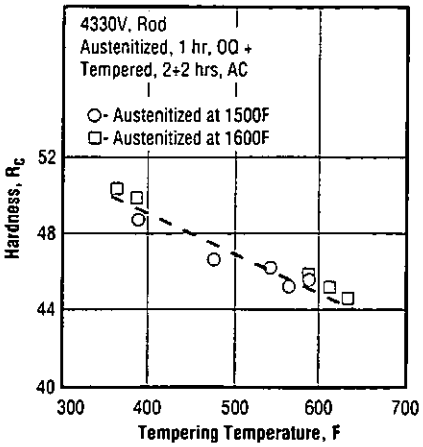


Fig. 1.6.3 Effect of tempering temperature on hardness (Ref. 26)

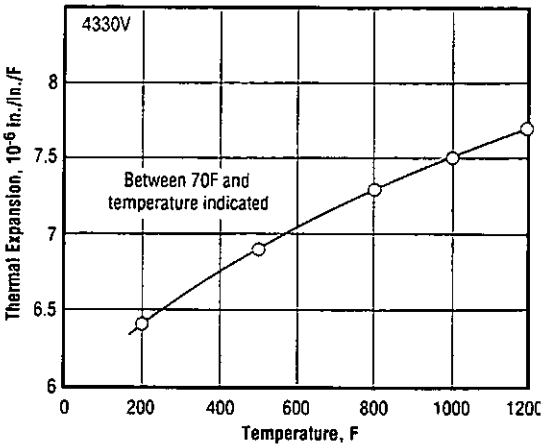


Fig. 2.1.4.1 Mean coefficient of linear thermal expansion (Ref. 29)

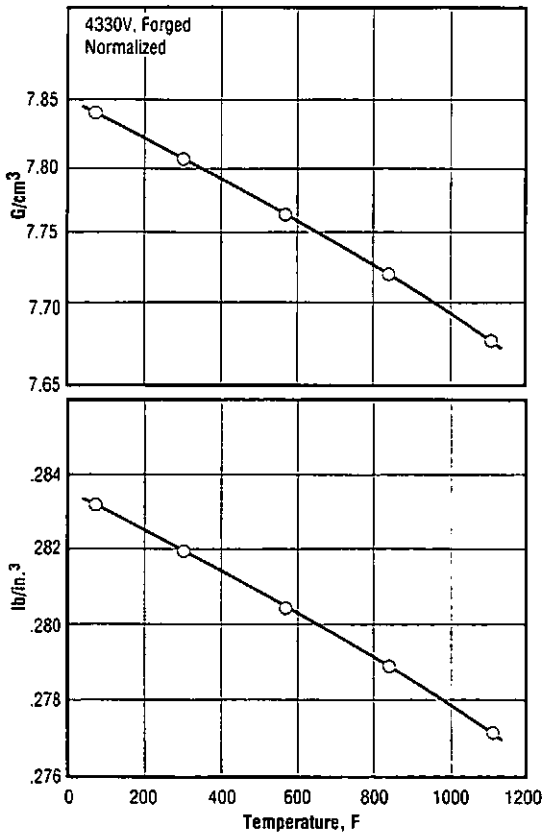


Fig. 2.2.1.1 Effect of temperature on density (Ref. 45)

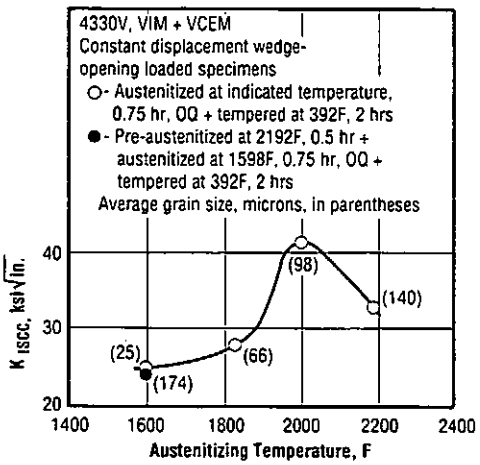


Fig. 2.3.2.2 Effects of austenitizing temperature on threshold stress intensity for stress corrosion cracking in distilled water at 95F (Refs. 34, 35)

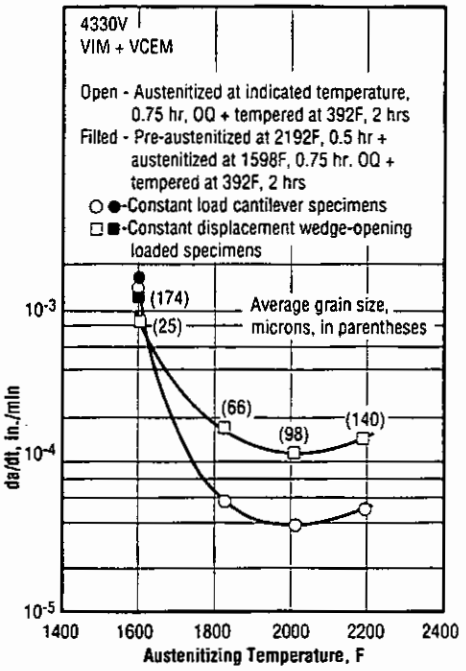


Fig. 2.3.2.3 Effects of austenitizing temperature on stage II constant crack growth rate during stress corrosion in distilled water at 95F (Refs. 34, 35)

Table 3.1.1 AMS specified properties (Refs. 1, 42-44)

Alloy	AMS Specification	Form	Heat Treatment	Orientation	Cross-Sectional Area, (sq, in.)	Tensile Properties				Izod Impact Energy (ft - lb, min)
						F_{ty} (ksi, min)	F_{tu} (ksi, min)	e (pct, min)	RA (pct, min)	
4330 Mod	5328C	Investment casting	1500F, 0.5 hr min, OQ + 750F, 2+2 hr, AC	-	-	160	180	5	-	-
	5329D	Sand casting	1575F, 0.5 hr min, OQ + 750F, 2+2 hr, AC	-	-	160	180	5	-	-
4330V Mod	6411D	Bars, forgings, tubing	1700F, 1 hr min, AC + 1550F, 1 hr, OQ + temper, 1 hr min, AC	Long.	-	185	220	10	35	-
				Trans.	Up to 144	185	220	-	35	-
					144 to 225	185	220	-	30	-
					Over 225	185	220	-	25	-
	6427G	Bars, forgings, tubing	1550F, OQ + 600F	Long.	-	-	-	-	-	15

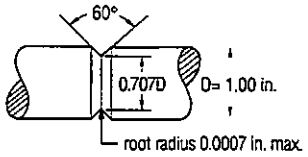
Note: The original AMS documents should be consulted for complete specification details.

Table 3.2.1.1.1 Effects of melting practice on mechanical properties (Ref. 11)

Alloy: 4330V						
Form	**4 inch dia bar**		**3x5 plate**		**4 inch dia bar**	
Melting Practice	**(a)**		**(b)**		**(c)**	
Condition	**(d)**					
Actual Carbon Level	**0.33C**		**0.31C**		**0.30C**	
Direction	**L**	**T**	**L**	**ST**	**L**	**T**
F_{tu} (ksi)	220.4	222.2	213.7	216.2	229.9	230.1
F_{ty} (ksi)	193.5	194.0	185.5	187.5	198.6	201.3
e,1 in. (percent)	11.0	5.0	12.0	5.0	13.0	4.0
RA (percent)	36.5	15.0	56.3	11.7	56.4	10.2
Sharp Notch Strength** (ksi)	233.7	168.2	250.6	198.8	251.9	192.9

(a) Electric furnace air melt
(b) Vacuum stream degas
(c) Cyclic vacuum degas*
(d) 1700F, 1 hr, AC + 1600F, 1 hr, OQ + Temper at 600F, 2 hr, AC

*Dortmund - Horder (cyclic vacuum degassing) process



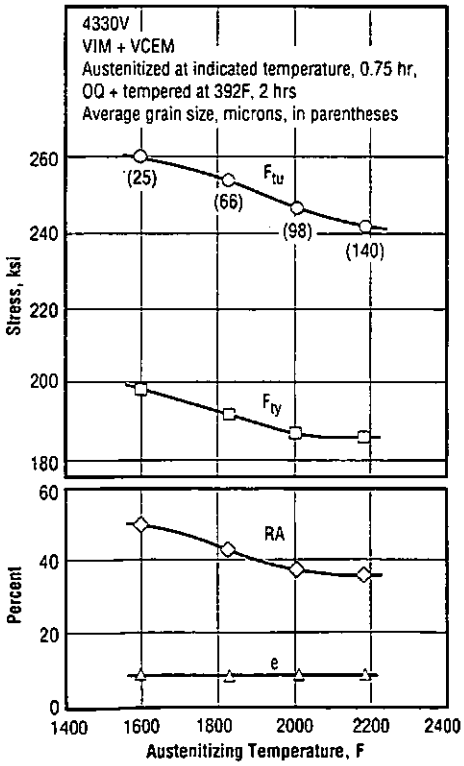


Fig. 3.2.1.2.2 Effects of austenitizing temperature on tensile properties (Ref. 35)

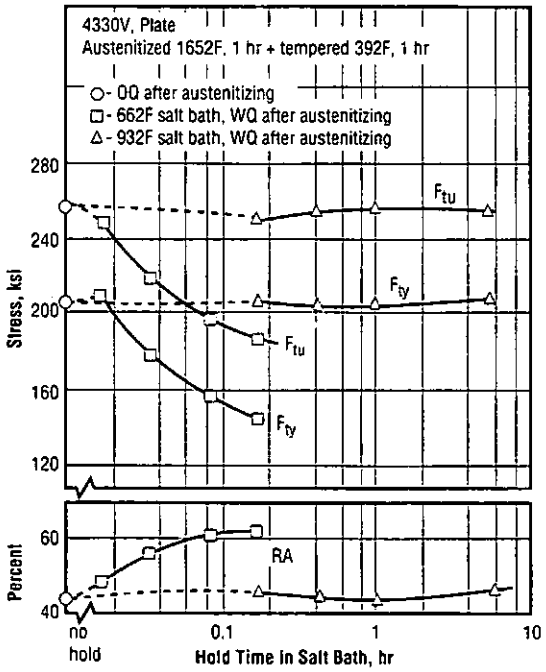


Fig. 3.2.1.2.4 Effects of hold time at intermediate temperature after austenitizing on tensile properties (Ref. 38)

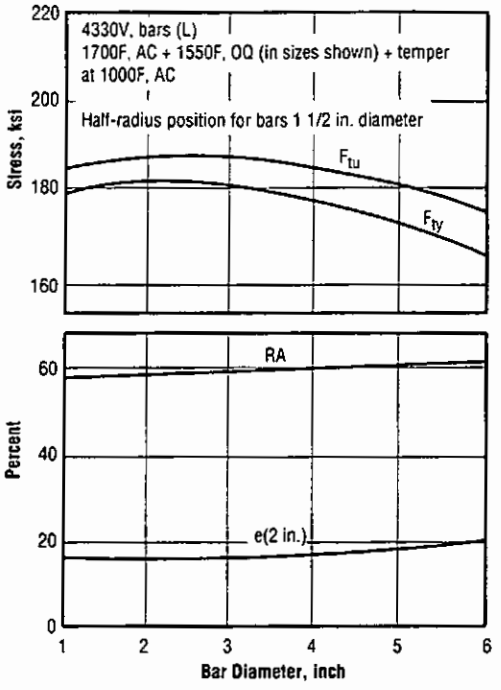


Fig. 3.2.1.2.5 Effect of as quenched section size on the tensile properties of bars tempered at 1000F (Ref. 5)

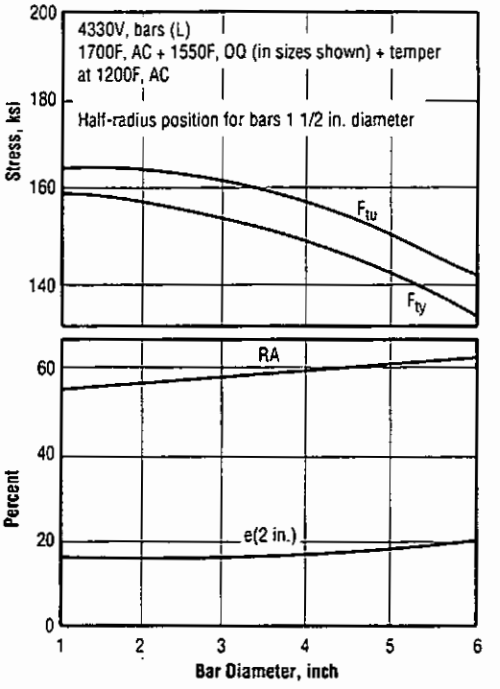


Fig. 3.2.1.2.6 Effect of as quenched section size on the tensile properties of bars tempered at 1200F (Ref. 5)

Table 3.2.1.2.8 Effects of quenching medium on mechanical properties and microstructure (Ref. 39)

Alloy: Type 4330V										
Form	**Block, 2.25 x 5.00 x 5.25 in.**									
Heat Treatment	**Austenitize 1550F, 1 hr, Q + Temper, 1000F, 1 hr, Oil Cool**									
Quench Medium	**Mechanical Properties (a)**								**Microstructure**	
	Tensile Properties at RT				**Charpy-V Impact Energy (ft-lb)**		**Fracture Toughness, K_{Ic} (ksi$\sqrt{in.}$)**	**Hardness (R_c)**	**ASTM Grain Size**	**Major Phases Present**
	F_{ty} (ksi)	**F_{tu} (ksi)**	**El, 2 in. (pct)**	**RA (pct)**	**-40F**	**+80F**				
Salt, 400F	167	184	15	41	12.3	22.0	109	40	9.4	Tempered Bainite
Oil, 200F	180	193	13	40	10.6	22.4	118	43	8.8	Tempered Martensite + Bainite
Water, 75F	174	186	16	49	11.9	25.8	124	42	9.6	Tempered Martensite

(a) All values are averages from 2 or 3 tests on specimens taken from mid-section of heat-treated block.

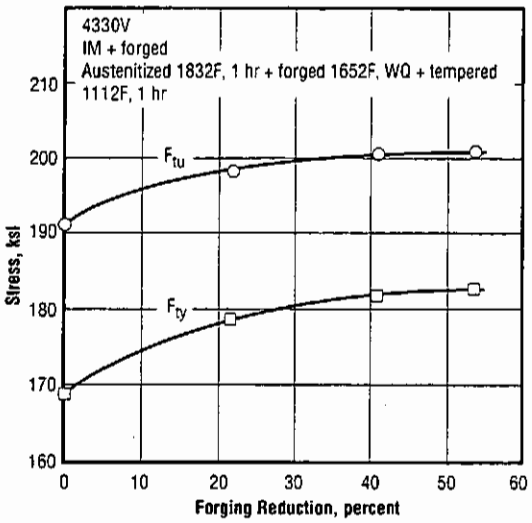


Fig. 3.2.1.3.2 Effects of ausforming by forging on tensile properties (Ref. 32)

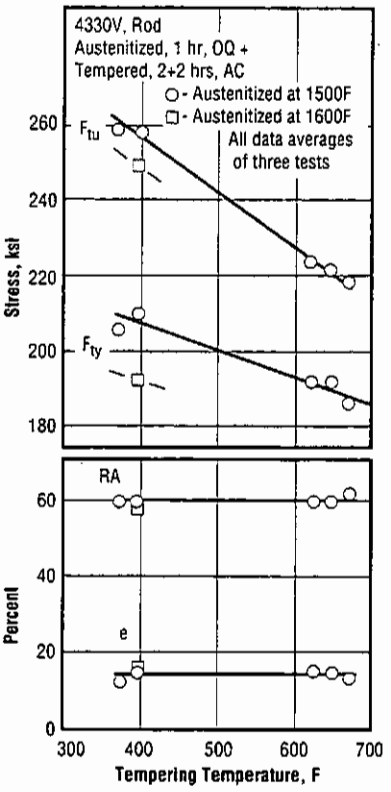


Fig. 3.2.1.4.2 Effects of tempering temperature on tensile properties of rod (Ref. 26)

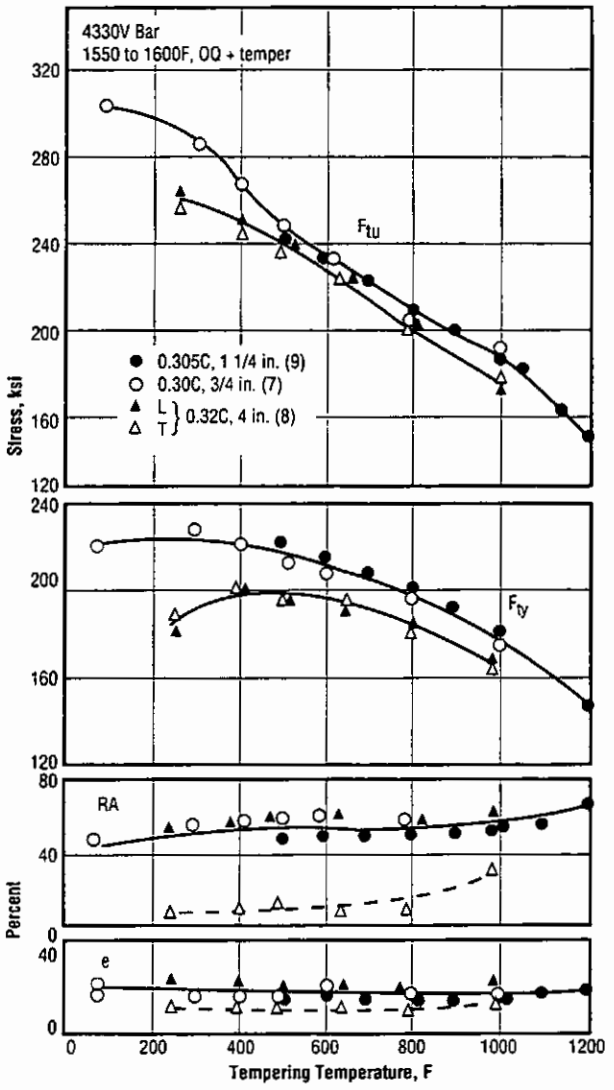


Fig. 3.2.1.4.3 Effect of tempering temperature on tensile properties of bar (Refs. 7, 8, 9)

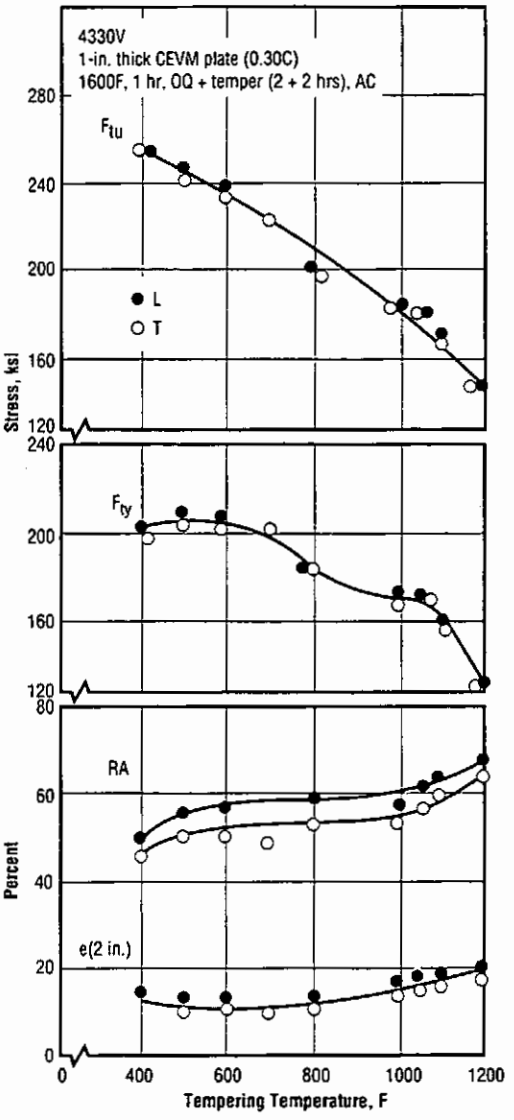


Fig. 3.2.1.4.4 Effect of temperature on the tensile properties of plate (Ref. 10)

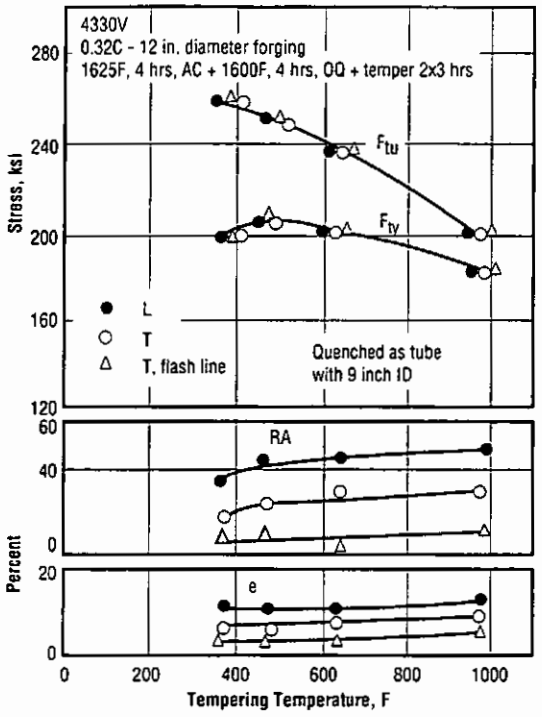


Fig. 3.2.1.4.5 Effects of specimen location and tempering temperature on tensile properties of a large forging (Ref. 14)

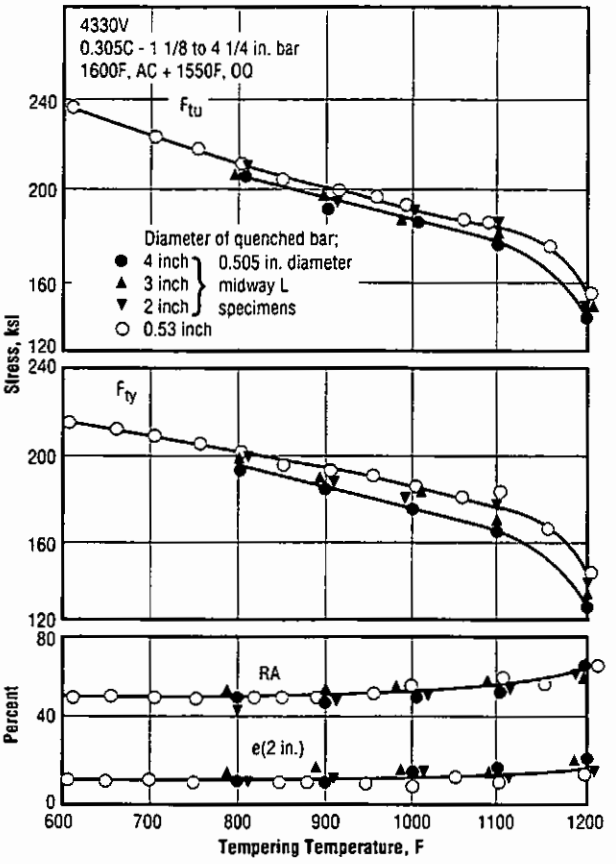


Fig. 3.2.1.4.6 Effects of as quenched section size and tempering temperature on tensile properties of bar (Ref. 13)

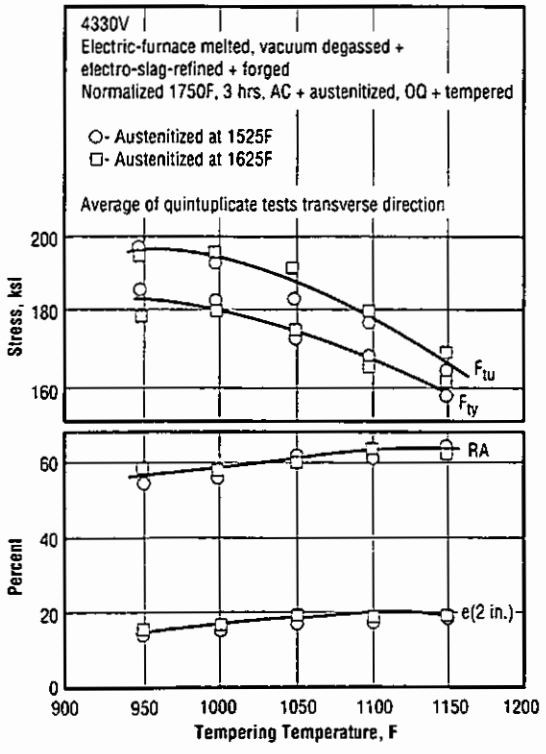


Fig. 3.2.1.4.7 Effects of tempering temperature on tensile properties of electro-slag-refined alloy (Ref. 29)

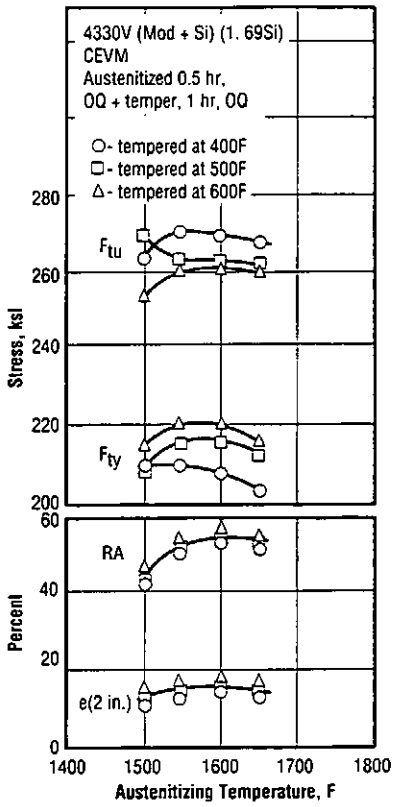


Fig. 3.2.1.5.1 Effects of austenitizing and tempering temperatures on tensile properties of Type 4330V (Mod + Si) (Ref. 46)

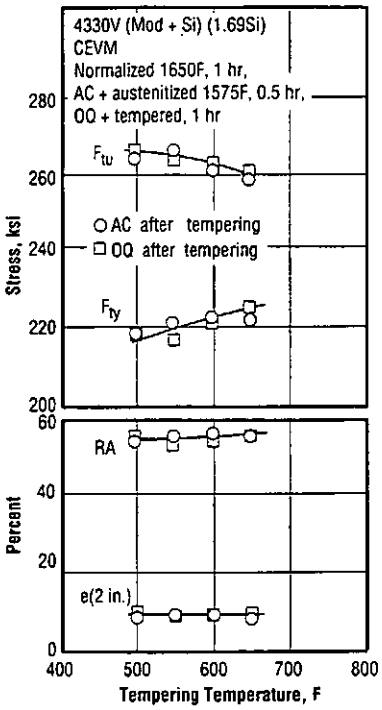


Fig. 3.2.1.5.2 Effects of tempering temperatures and quenching rate on tensile properties of Type 4330V (Mod + Si) (Ref. 46)

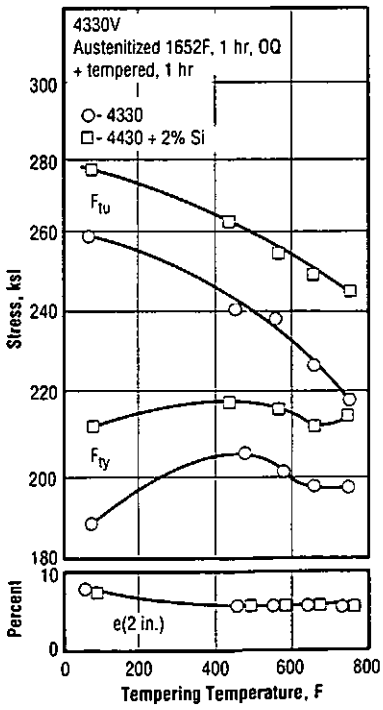


Fig. 3.2.1.5.4 Effects of tempering temperature and silicon addition on tensile properties of Type 4330 (Ref. 40)

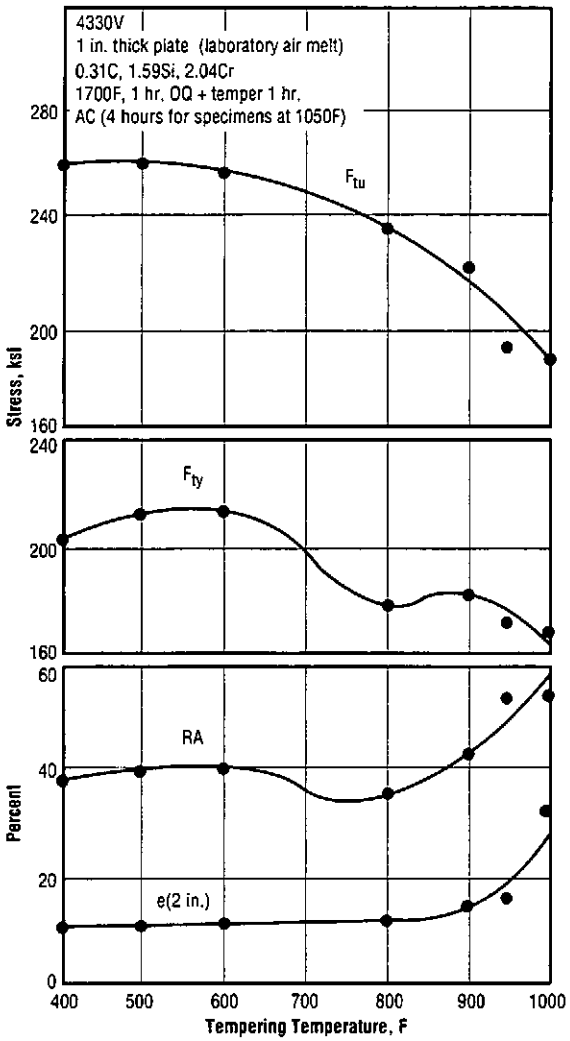


Fig. 3.2.1.5.5 Tensile properties of plate containing silicon and chromium additions (Refs. 16, 17)

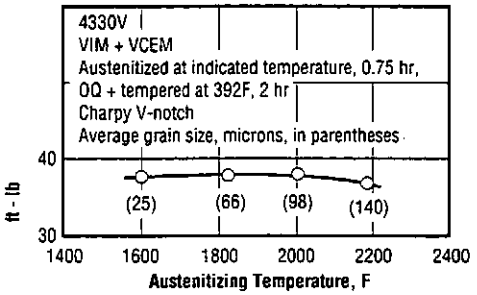


Fig. 3.2.3.1 Effects of austenitizing temperature on impact energy (Ref. 35)

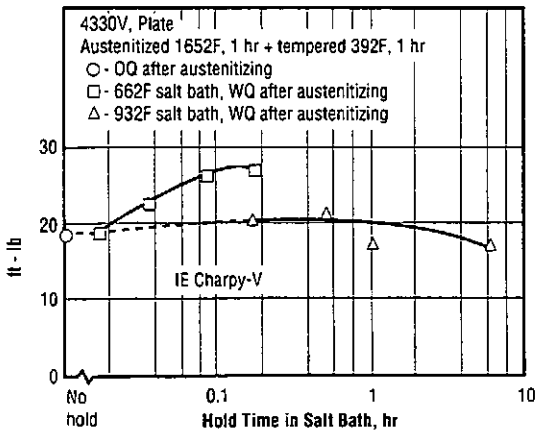


Fig. 3.2.3.2 Effects of hold time at intermediate temperature after austenitizing on impact energy (Ref. 38)

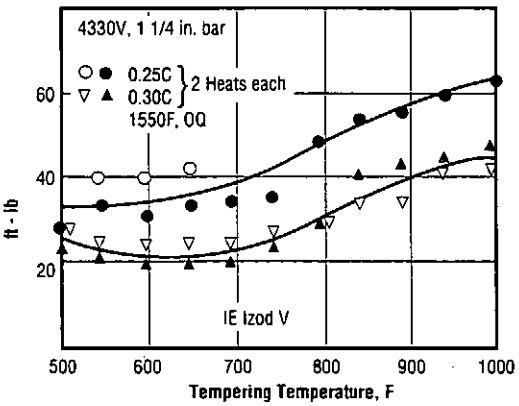


Fig. 3.2.3.3 Effects of carbon content and tempering temperature on impact energy of bar (Ref. 14)

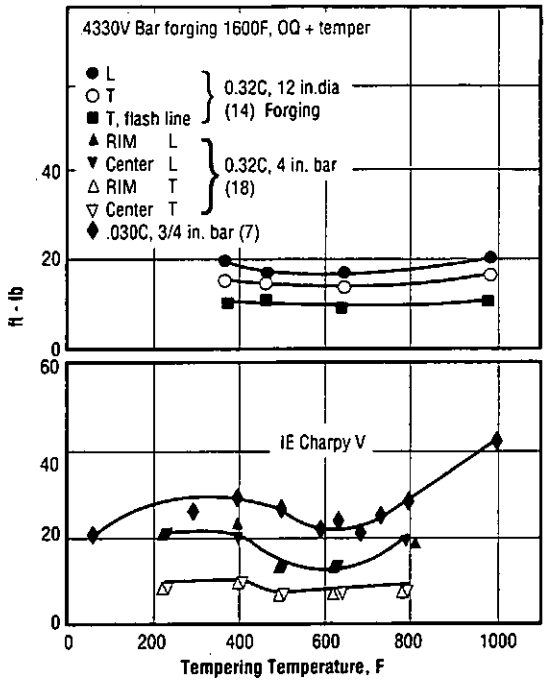


Fig. 3.2.3.4 Effects of specimen location and tempering temperature on impact energy of bar and forgings (Refs. 18, 7, 14)

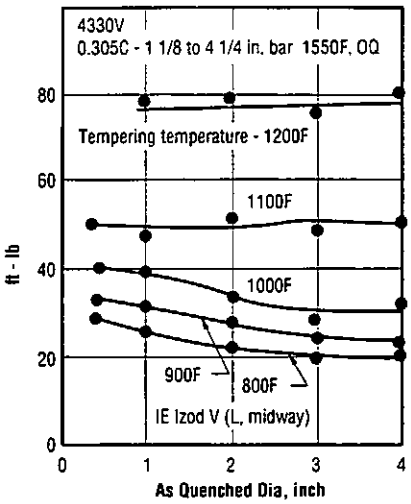


Fig. 3.2.3.5 Effects of as quenched section size and tempering temperature on impact energy of bar (Ref. 13)

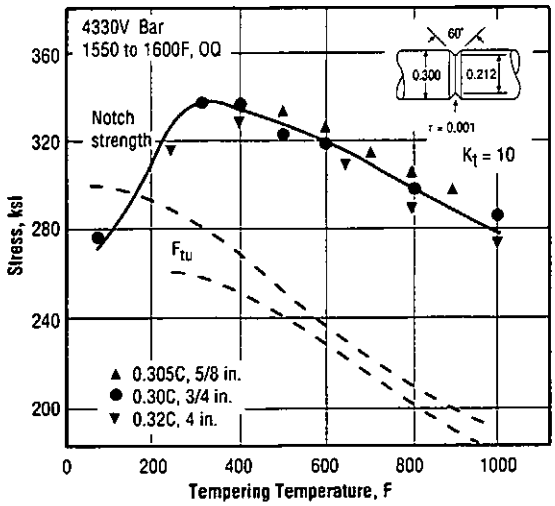


Fig. 3.2.7.1.1 Effects of carbon content and tempering temperature on notch strength of bar (Refs. 7, 8, 19)

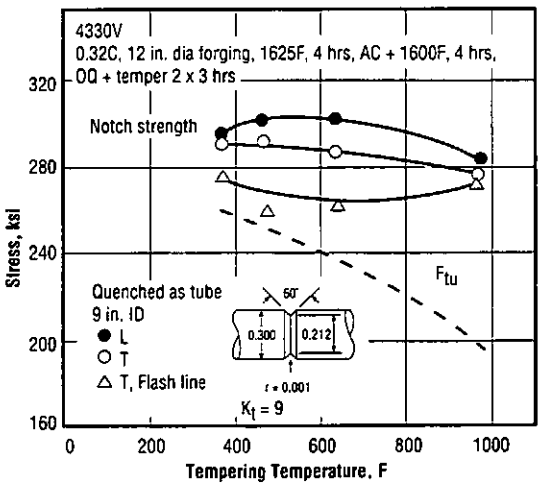


Fig. 3.2.7.1.2 Effects of specimen location and tempering temperature on notch strength of a large forging (Ref. 14)

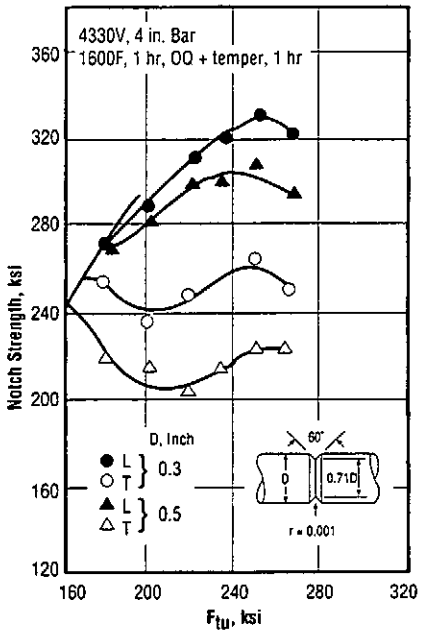


Fig. 3.2.7.1.3 Effects of specimen size and test direction on notch strength of bar at various strength levels (Ref. 8)

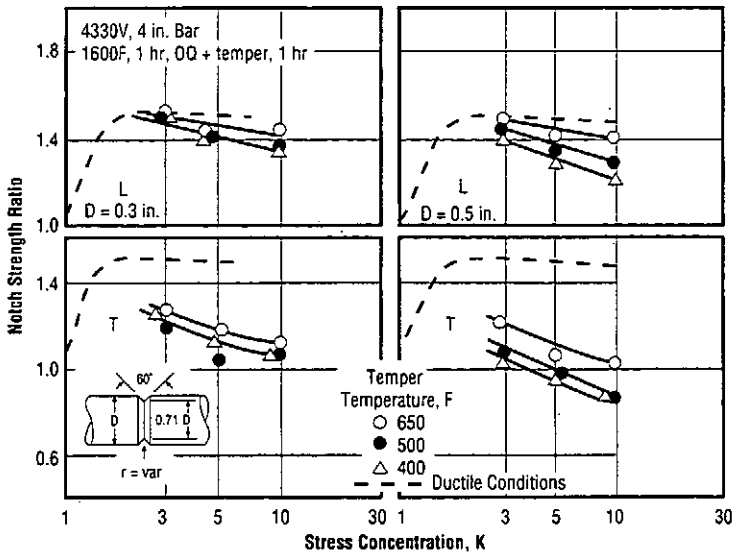


Fig. 3.2.7.1.4 Effects of stress concentration, tempering temperature, specimen size and test direction on notch strength ratio of bar (Ref. 18)

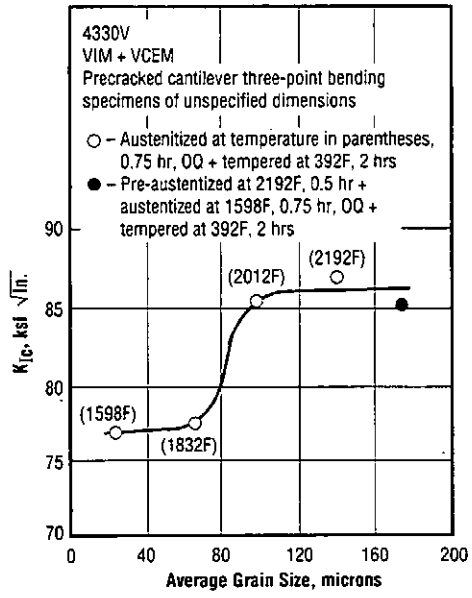


Fig. 3.2.7.2.1 Effects of grain size and austentizing temperature on fracture toughness (Refs. 34, 35)

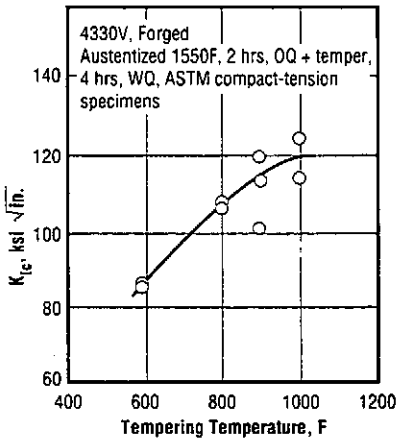


Fig. 3.2.7.2.2 Effects of tempering temperature on fracture toughness (Ref. 41)

Table 3.2.7.2.3 Fracture toughness of plate, bar, and billet (Ref. 51)

Alloy: 4330V Mod				
Form	**Heat Treatment**	**Specimen Orientation**	**Number of Tests**	**Average Fracture Toughness, K_{Ic} (ksi $\sqrt{in.}$)**
Plate	Heat treated to 46 R_c harndess	T-L	2	75
Forged Bar	1600F, 1 hr, OQ + 400F, 1 hr	L-T	1	88
	1600F, 1 hr, OQ + 535F, 1 hr	L-T	2	97
Billet	1650F, 1 hr, AC + 1575F, 1 hr, OQ + 800F, 2+2 hr	L-T	3	96
	1650F, 1 hr, AC + 1575F, 1 hr, OQ + 525F, 2+2 hr	L-T	6	82

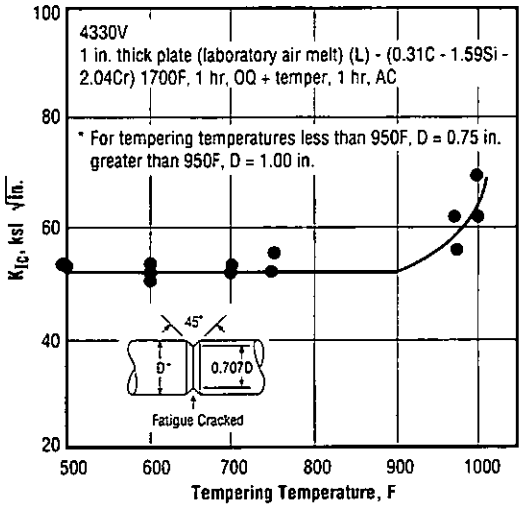


Fig. 3.2.7.2.4 Plane strain fracture toughness of plate with additions of silicon and chromium (Ref. 16)

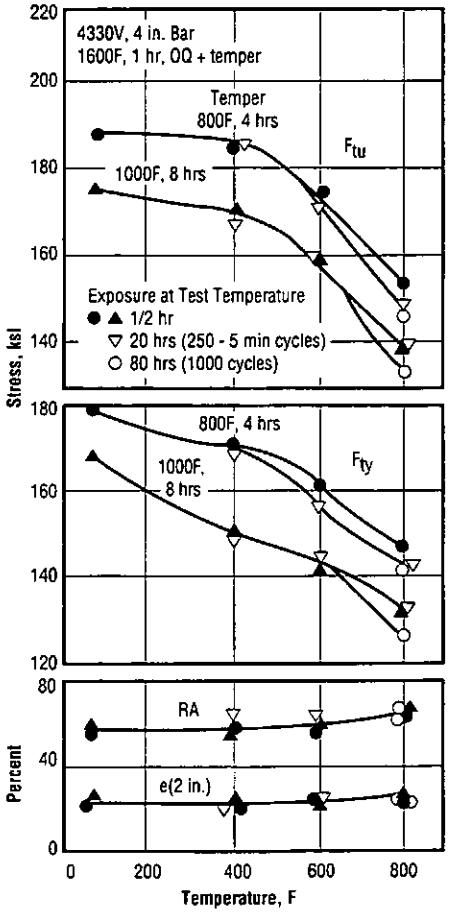


Fig. 3.3.1.1 Effects of cyclic exposure and test temperature on tensile properties of bar (Ref. 21)

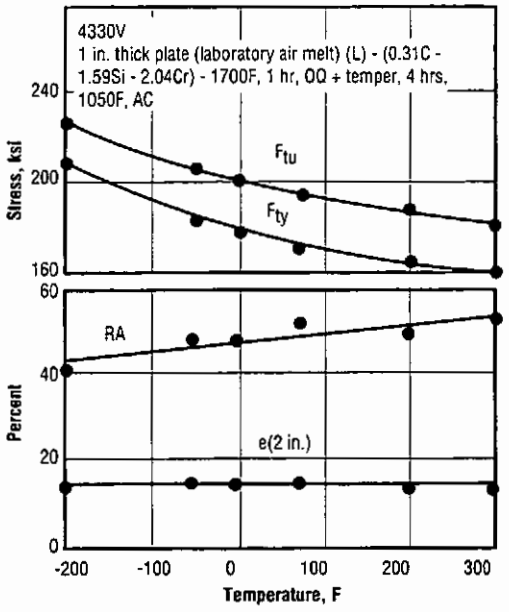


Fig. 3.3.1.2 Effect of test temperature on tensile properties of plate with silicon and chromium (Ref. 17)

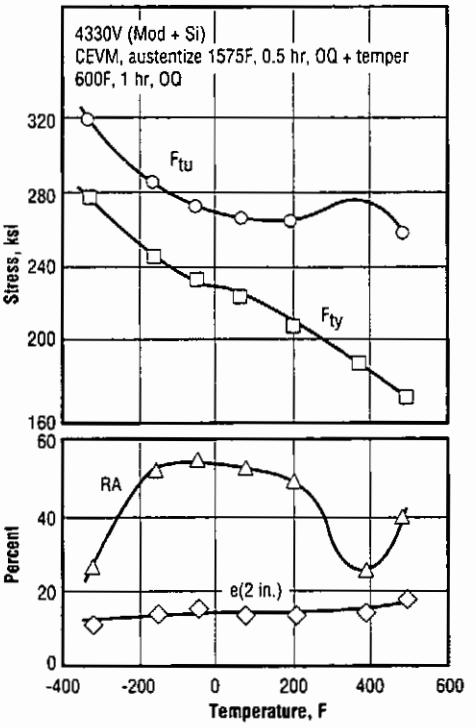


Fig. 3.3.1.3 Effects of test temperature on tensile properties of Type 4330V (Mod + Si) (Ref. 46)

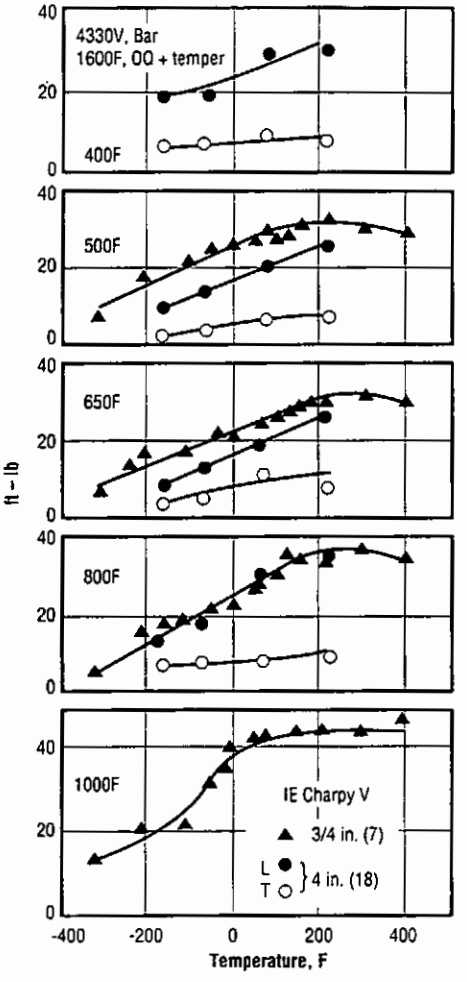


Fig. 3.3.3.1 Effects of test temperature, section size, and test direction on impact energy of bar (Refs. 7, 18)

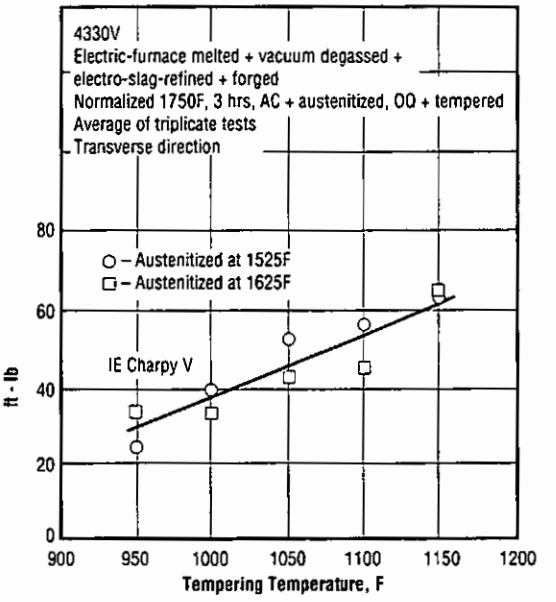


Fig. 3.3.3.2 Effects of austenitizing and tempering temperatures on impact energy at -40F (Ref. 47)

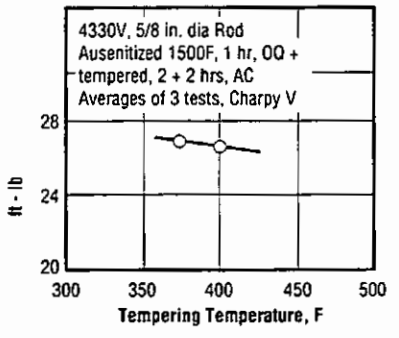


Fig. 3.3.3.3 Effect of tempering temperature on impact energy at -40F (Ref. 26)

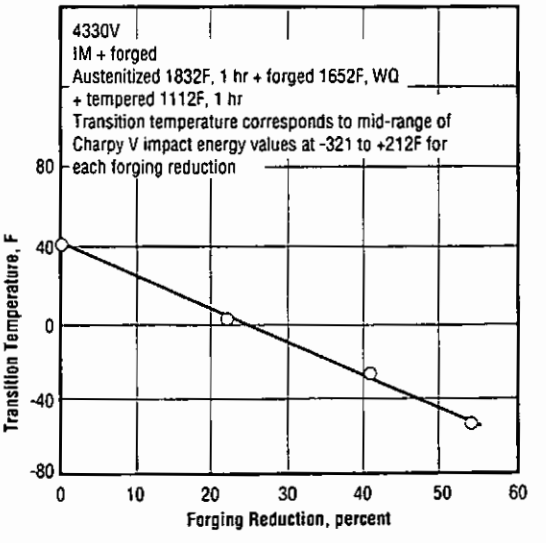


Fig. 3.3.3.4 Effect of ausforming on impact energy ductile-brittle transition temperature (Ref. 32)

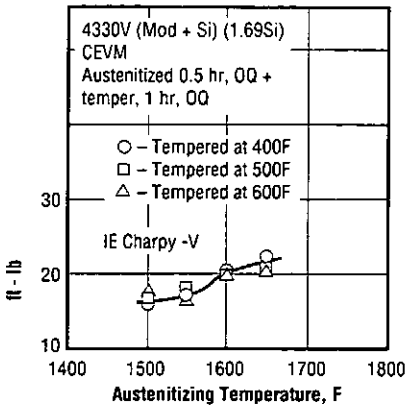


Fig. 3.3.3.5 Effects of austenitizing and tempering temperatures on impact energy of Type 4330V (Mod + Si) at -40F (Ref. 46)

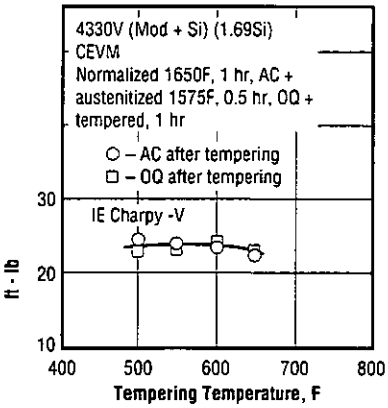
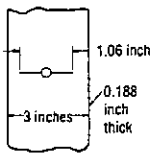


Fig. 3.3.3.6 Effects of tempering temperature and quenching rate on impact energy of Type 4330V (Mod + Si) at -40F (Ref. 46)

Table 3.3.7.1.1 Effect of tempering temperature on the crack strength of forged billet at two test temperatures (Ref. 22)

Alloy: Type 4330V				
Form	**Forged Billet**			
Condition	**Austenitize, OQ + Temper, AC**			
Tempering Temp.	**450F**		**625F**	
Test Temperature	**RT**	**-65F**	**RT**	**-65F**
Crack Strength (ksi) T orientation 	98	54	77	52
	103	56	77	
	109	61	84	
	113		89	
	114		100	
			102	

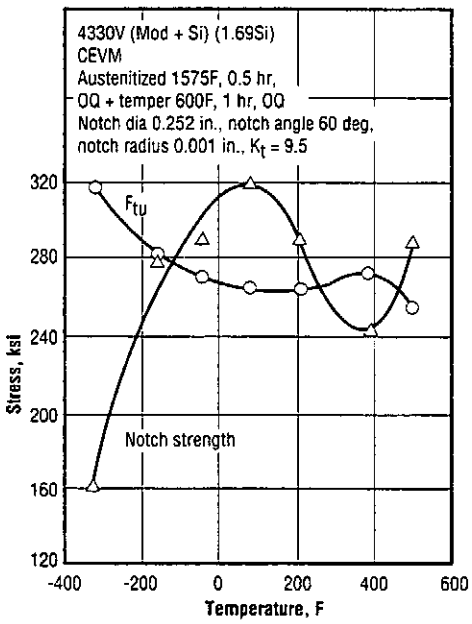
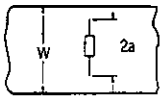


Fig. 3.3.7.1.2 Effects of test temperature on notch and ultimate tensile strength of Type 4330V (Mod + Si) (Ref. 46)

Table 3.3.7.2.1 Plane-strain fracture toughness of plate with silicon and chromium additions (Ref. 23)

Alloy: Type 4330V				
Form	**Forgings**			
Condition	**Heat Treated to F_{tu} = 220 - 240 ksi**			
Test Temp.	**70F**		**-66F**	
Direction	**L**	**T**	**L**	**T**
Fracture toughness K_{Ic} - ksi $\sqrt{in.}$	51		39 **	40
	52		41 **	41
(Center - cracked specimens)			42	
			48	
			49	
			50	

*W = 1.5 inch to 3.4 inch; 2a/W = 0.4 to 0.5; 0.2 inch thick (except ** 0.4 inch thick)

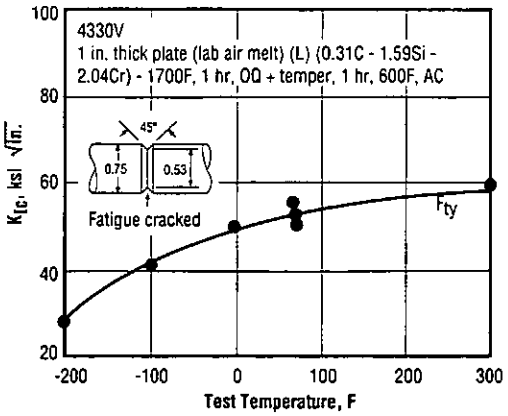


Fig. 3.3.7.2.2 Effect of test temperature on plane-strain fracture toughness of plate with silicon and chromium additions (Ref. 17)

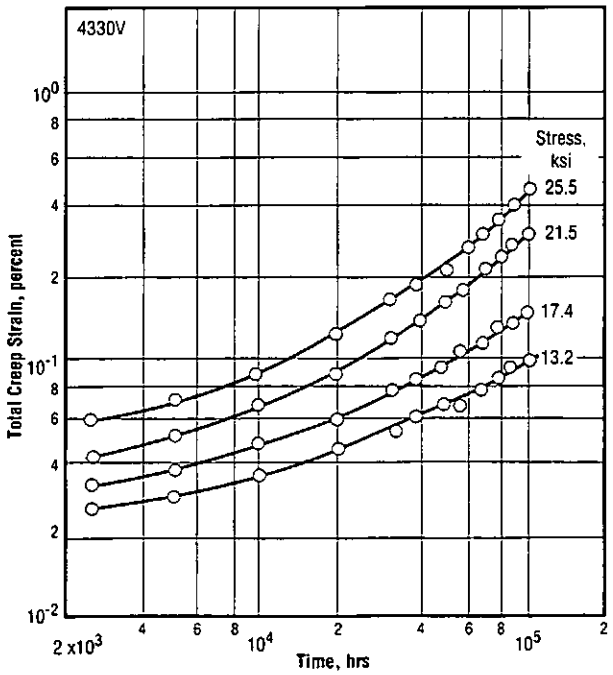
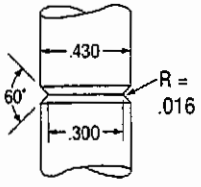


Fig. 3.4.1 Creep curves for Type 4330V at 842F for times up to 12 years (Ref. 50)

Table 3.5.1 Fatigue properties of smooth and notched bar at room temperature (Ref. 18)

Alloy: Type 4330V							
Form	**4 inch bar**						
Condition	**1600F + Temper 1 hour to F_{tu} below**						
F_{tu} (ksi)	**Method**	**Stress Ratio**		**Stress Concentraton**	**Fatigue strength (ksi at cycles)**		
		A	**R**		**10^5**	**10^6**	**10^7**
201	Rotating Beam	∞	-1	Smooth $K_t = 1$	105	85	85
222					105	90	90
236					115	95	90
250					120	95	90
263					130	95	80
201				Notched $K_t = 8$	50	40	40
250					60	50	50
263					65	65	65

Table 3.5.2 Fatigue properties of notched billet at room temperature (Ref. 22)

Alloy: 4330V		
Form	**Forged Billet**	
Condition	**Heat Treated to F_{tu} = 220 - 240 ksi**	
Stress Concentration	**$K_t = 3$**	
Stress Ratio	**R = 0.1, A = 0.82**	
Axial load (L) 	**Maximum Stress (ksi)**	**Fatigue Life (cycles, avg of 4)**
	150	4.4×10^3
	130	7.8×10^3
	118	1.3×10^4
	100	2.0×10^4
	82	6.0×10^4
	70	1.1×10^5
	60	1.0×10^6

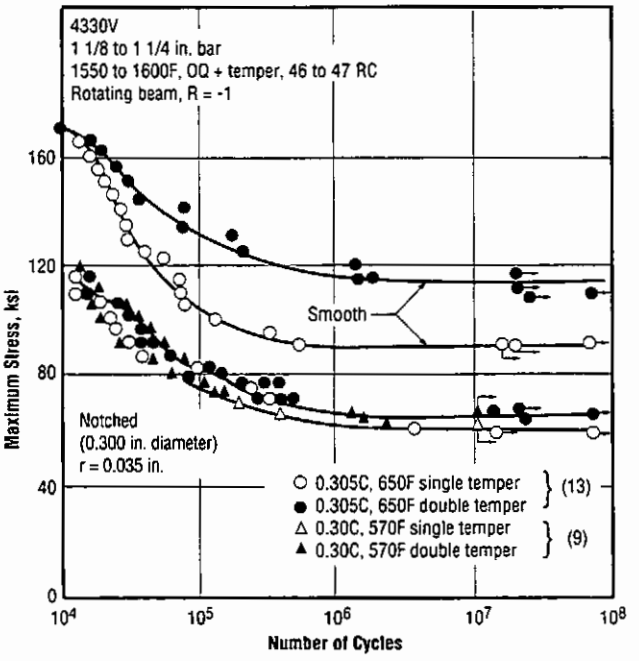


Fig. 3.5.3 Effect of double tempering on fatigue properties of smooth and notched bar (Refs. 9, 13)

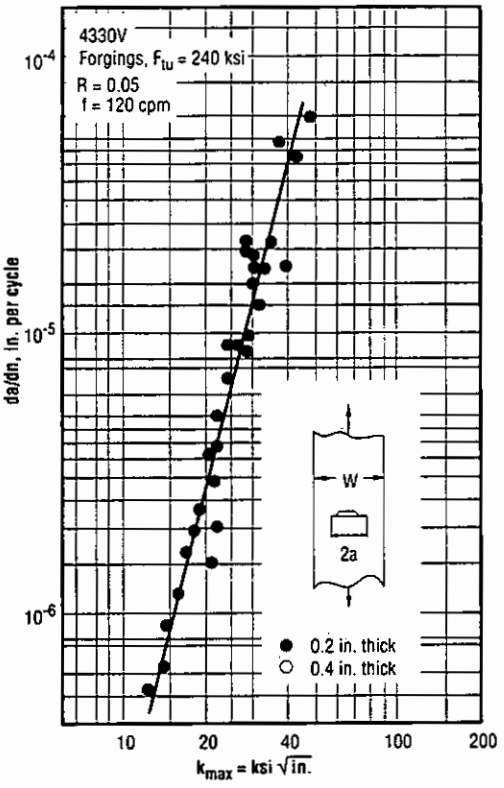


Fig. 3.5.4 Fatigue crack growth rate for forgings (F_{tu} = 240 ksi) (Ref. 23)

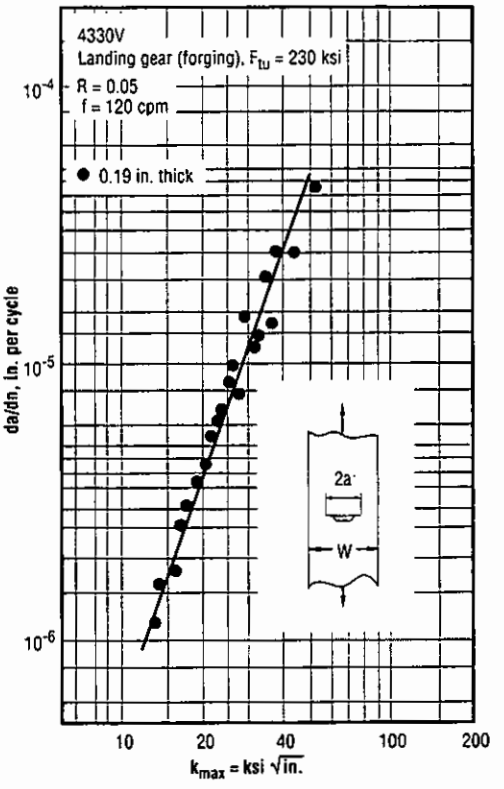


Fig. 3.5.5 Fatigue crack growth rate for forgings (F_{tu} = 230 ksi) (Ref. 23)

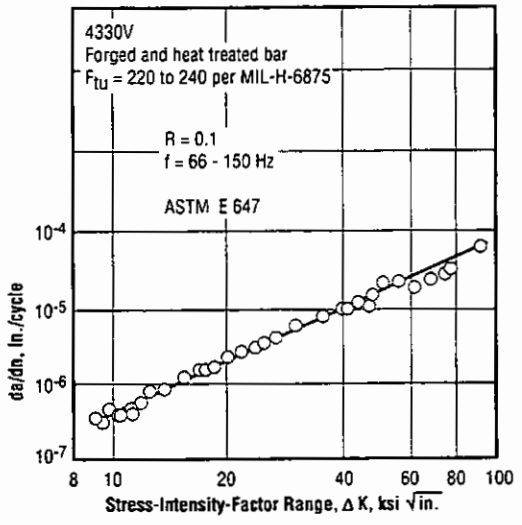


Fig. 3.5.6 Fatigue crack growth rate for forged bar (F_{tu} = 220 to 240 ksi) (Ref. 49)

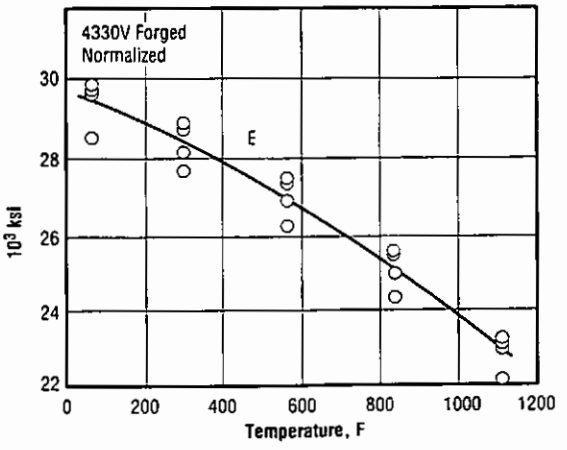


Fig. 3.6.2.1 Effect of temperature on dynamic modulus of elasticity (Ref. 45)

References

1. AMS 6427G, Society of Automotive Engineers (April 1, 1987).
2. Bendix Products Division, "Heat Treatment of Low-Alloy Steels" (Mar. 18, 1958).
3. DMIC Memo 239.
4. DMIC Report 119 (Nov. 27, 1959).
5. Republic Steel Corporation, "Mechanical Properties of Alloy Steels," ADV. 13036-10M-266 (1961).
6. Bendix Aviation, "Personal Communication," Trodrian, J. (Oct. 12, 1959).
7. Kinler, L. J.; Barnett, W. J.; Frohmberg, R. P.; and Troiano, A. R., "The Embrittlement of Alloy Steels at High Strength Levels," WADC TR 53-205 (July 1953).
8. Muvdi, B. B.; Sachs, G.; and Klier, E. P., "Design Properties of High Strength Steels in the Presence of Stress Concentration," WADC TR 56-395, Part I (Dec. 1956).
9. Bendix Aviation Corporation, "A Comparison of Two High Strength Low Alloy Steels" (May 6, 1953).
10. Puzak, P. O. et al, "Metallurgical Characteristics of High Strength Structural Materials" (Third Quarterly Report), NRL Report 6086 (Jan. 1964).
11. "Vacuum Degasssing in the Production of Premium-Quality Steels" (Mar. 11, 1964).
12. MacLaren, A. W., "Personal Communication," U. S. Steel Corporation Data Sheet (June 26, 1959).
13. Republic Steel Corporation, "Experimental Testing of a Heat of High Tensile Alloy Steel" (Sept. 22, 1949).
14. Ragland, F. J., Jr. and Barrett, G. N., Jr., "Evaluation of Forging of 4330 Modified, 4340, and 9840 Steels at High-Strength Levels," WADC TR 54-89 (March 1954).
15. Carman, C. M.; Armiento, D. F.; and Markus, H., "Fracture Toughness and Pressure Vessel Performance," ASME Paper No. 63-WA-138 (1963).
16. Baker, A. J.; Lauta, F. J.; and Wei, R. P., "Relationship between Microstructure and Toughness in Quenched and Tempered Ultrahigh-Strength Steels," ASTM STP 370, p. 3 (1965).
17. U. S. Steel Corporation, Applied Research Laboratory, "Unpublished Data," communication to R. P. Wei (1969).
18. Muvdi, B. B.; Klier, E. P.; and Sachs, G., "Design Properties of High-Strength Steels in the Presence of Stress-Concentration," WADC TR 55-103 (Jan. 1956).
19. Sachs, G., and Klier, E. P., "Survey of Low-Alloy Aircraft Steels Heat Treated to High Strength Levels," WADC TR 53-254, Part 5 (Sept. 1954).
20. Klier, E. P.; Muvdi, B. B.; and Sachs, G., "The Response of High-Strength Steels in the Range of 180 to 300 ksi to Hydrogen Embrittlement from Cadmium Plating," *Proc. ASTM*, Vol. 58, pp. 597-622 (1958).
21. Sachs, G.; Muvdi, B.; and Klier, E. P., WADC TR 55-103, Supplement 2 (1956).
22. General Dynamics Corporation, "Steel Alloy Selection for F-111, Justification Data for D6AC Steel," Report FZM-12-408 (Feb. 1964).
23. Smith, S. H., Personal Communication, The Boeing Company, Commercial Airplane Division (Oct. 29, 1968).
24. Best, K. F., "High Strength Materials for Aircraft Landing Gear," *Aircraft Engineering*, Vol. 58, No. 7, pp. 14-24 (July 1986).
25. Anon., "The Art of the Gun Tube," *Compressed Air*, Vol. 91, No. 2, pp. 8-12 (Feb. 1986).
26. Hickey, C. F., Jr.; Dix, D. W.; and O'Donovan, M. E., "Heat Treatment Investigation of 4330 Vanadium-Modified Steel," MTL TR 89-84, U.S. Army Materials Technology Laboratory, Watertown, Massachusetts (Aug. 1989).
27. Pickering, F. B., "Vanadium as a Hardenability Additive in Quenched and Tempered Steels," presented at HSLA Steels '85, Beijing, China (Nov. 4-8, 1985), published by Chinese Society of Metals, Beijing, China..
28. Mangonon, P. L., "Hardenabilities of Vanadium-Modified 4330 Low Alloy Constructional Steels," *Journal of Heat Treating*, Vol. 1, No. 4, pp. 47-60 (Dec. 1980).
29. "ESR 4330 Mod," *Alloy Digest*, Filing Code SA-388 (April 1983).
30. Ambrus, Z., and Pellman, M. A., "Hardening of Aerospace Alloys in Nitrogen Base Atmospheres," *Metal Progress*, pp. 47-51 (May 1983).
31. "Lescalloy 4330+V Vac Arc," *Alloy Digest*, Filing Code SA-314 (May 1975).
32. Lee, J. S., and Chun, J. S., "Effect of High Temperature Thermomechanical Treatment on the Mechanical Properties of Vanadium-Modified AISI 4330 Steel," *Journal of Materials Science*, Vol. 16, No. 6, pp. 1557-1566 (June 12, 1981).
33. Gourdin, W. H., "Local Microstructural Modification in Dynamically Consolidated Metal Powders," *Metallurgical Transactions A*, Vol. 15A, pp. 1653-1664 (Sept. 1984).
34. Lan, Y., and Lin, T. L., "Research on the Cause of Surface Crack Tip Plastic Zone Growth in Stress

Corrosion Cracking," *Scripta Metallurgica*, Vol. 23, No. 5, pp. 677-683 (May 1989).

35. Lin, T. L.; Lan, Y.; and Wu, J., "Influence of Austenitizing Temperature on Stress Corrosion in 4330M Steel - The Role of Impurity Segregation in Stress Corrosion Cracking of High Strength Steel," *Metallurgical Transactions A*, Vol. 19A, pp. 2225-2231 (Sept. 1988).
36. Carter, C. S., "Stress Corrosion Crack Branching in High-Strength Steels," *Engineering Fracture Mechanics*, Vol. 3, No. 1-A, pp. 1-13 (July 1971).
37. Baker, E. A., "Long-Term Corrosion Behavior of Materials in the Marine Atmosphere," *Degradation of Metals in the Atmosphere*, ASTM STP 965, S. W. Dean and T. S. Lee, Eds., American Society for Testing and Materials, Philadelphia, pp. 125-144 (1988).
38. Rao, T. V. L. N.; Dikshit, S. N.; Malakondaiah, G.; and Rao, P. R., "On Mixed Upper Bainite-Martensite in an AISI 4330 Steel Exhibiting an Uncommonly Improved Strength-Toughness Combination," *Scripta Metallurgica et Materialia*, Vol. 24, No. 7, pp. 1323-1328 (July 1990).
39. Niccolls, E. H., "Effects of Quenching Techniques upon Gun Steel," ARLCB-MR-77026, Benet Weapons Laboratory, Watervliet Arsenal, Watervliet, NY (May 1977).
40. Parker, E. R., "Interrelations of Compositions, Transformation Kinetics, Morphology, and Mechanical Properties of Alloy Steels," *Metallurgical Transactions A*, Vol. 8A, pp. 1025-1042 (July 1977).
41. Throop, J. F., and Miller, G. A., "Optimum Fatigue Crack Resistance," WVT-7006, Bethlehem Steel Corporation, Bethlehem, Pennsylvania (Jan. 1970).
42. AMS 5328C, Society of Automotive Engineers (Oct. 1, 1987).
43. AMS 5329D, Society of Automotive Engineers (Oct. 1, 1987).
44. AMS 6411D, Society of Automotive Engineers (Oct. 1, 1990).
45. Cook, L. S.; Wolfenden, L. S.; and Ludtka, G. M., "Longitudinal and Flexural Resonance Methods for the Determination of the Variation with Temperature of Dynamic Young's Modulus in 4330V Steel," *Dynamic Elastic Modulus Measurements in Materials*, ASTM STP 1045, A. Wolfenden, Ed., American Society for Testing and Materials, Philadelphia (1990).
46. Rizzitano, F. J., "Request for Mechanical Properties Data on 4330V (Modified + Si) Steel," Letter from Army Materials and Mechanics Research Center, Watertown, Massachusetts, to Mechanical Property Data Center, Traverse City, Michigan (Feb. 3, 1978).
47. "Cabot ESR 4330 Mod," *Alloy Digest*, Filing Code SA-364 (Sept. 1979).
48. Man'kovskii, V. A., "Analysis of Long-Time Creep Curves," *Mashinovedenie*, No. 1, pp. 78-86 (Jan.-Feb. 1983).
49. Wanhill, R. J. H., "Fatigue Fracture in Steel Landing Gear Components," presented at International Symposium for Testing and Failure Analysis 1985, Long Beach, California (Oct. 21-23, 1985).
50. Robinson, E. L., "1,000,000-Hour Creep Test," *Mechanical Engineering*, pp. 166-168 (Mar. 1943).
51. Gallagher, J., "Damage Tolerant Design Handbook," CINDAS/Purdue University, West Lafayette, Indiana, pp. 6.28-1 - 6.28-6 (1983).

This page is blank.

	Fe
0.35	C
1.8	Ni
0.8	Cr
0.35	Mo
0.2	V

4335 V Mod

1 GENERAL

This steel is a development of 4330 and 4330 V Mod. The higher carbon content appreciably increases the tensile and yield strengths at low tempering temperatures. The alloy is used primarily in a condition heat treated to F_{ty} = 210 ksi minimum. It is available in the form of sheet, strip, plate, bar, forgings and tubing. It possesses good welding characteristics and the formability of the steel, if spheroidized, is also good.

1.01 Commercial Designation

4335 V Modified.

1.02 Alternate Designations

4335 Modified.
UNS Number: K33517.

1.03 Specifications

1.031 AMS Specifications, Table 1.031.

1.04 Composition

Table 1.04.

1.05 Heat Treatment

1.051 Normalize. 1600 to 1750 F, air cool. Normalizing temperature is frequently kept low (e.g., 1585 to 1615 F, 20 minutes). AMS 6428 gives 1690 to 1710 F.

1.052 Full anneal. 1585 to 1615 F, 1 hour per inch thickness, furnace cool to 1400 F, continue furnace cool at 30 F per hour maximum to 1000 F maximum.

1.053 Spheroidize anneal sheet and plate for maximum formability. 1435 to 1465 F, 10 hours, furnace cool 20 F per hour maximum to 800 F maximum.

1.054 Intermediate anneal to remove strain hardening of cold worked spheroidized sheet. 1200 to 1250 F, 2 to 8 hours.

1.055 Stress relief welded material. 1025 to 1075 F, 30 minutes, furnace cool to 500 F.

1.056 Austenitize. 1600 to 1650 F, 20 minutes per inch thickness, 30 minutes minimum, air cool or oil quench. Below 1600 F, the properties may be irregular. Tensile properties decrease slightly with increasing austenitizing temperatures. Normalizing should precede austenitizing if steel has been previously spheroidized.

1.057 Temper. 400 to 500 F, 2 hours minimum, to obtain F_{ty} = 210 ksi minimum, and 700 F minimum for at least 2 hours to obtain F_{ty} = 190 ksi minimum. AMS specified tensile properties, Table 1.057.

1.058 Alternate heat treatment for sheet. 1635 to 1665 F, 20 minutes, quench in salt bath at 375 to 415 F until metal reaches temperature of 400 to 500 F, hold 2 hours minimum. This treatment produces less distortion than oil quenching.

1.06 Hardness

1.061 End quench hardenability, Figure 1.061.

1.062 Effect of tempering temperature, quenching media and melt method on hardness of sheet, Figure 1.062.

1.063 Rockwell number for extruded bar with typical tempered martensite structure: 50 HRC (35).

1.064 Effect of thickness, melting practice, austenitizing temperature and tempering temperature on hardness of sheet, Table 1.064.

1.065 Effect of below-normal austenitizing temperature on hardness of forging, Figure 1.065.

1.07 Forms and Conditions Available

1.071 Alloy is available in the full commercial range of sizes for sheet, strip, plate, bar, tube and flash-welded rings.

1.072 Bar and forgings are available in the normalized condition. Sheet and plate are available in various annealed conditions.

1.08 Melting and Casting Practice

Electric furnace air melt. Induction and consumable electrode vacuum melts.

1.09 Special Considerations

See 4340.

2 PHYSICAL AND CHEMICAL PROPERTIES

2.01 Thermal Properties

2.011 Melting range. 2645 to 2845 F.

2.012 Phase changes. Transformation temperatures from ferrite to austenite,

A_{c1} = 1310 F
A_{c3} = 1480 F
M_s point = 575 F
M_f point near 360 F.

Determined on specimens with 0.35C (12).

2.0121 Time-temperature-transformation diagram, determined by (12), Figure 2.0121.

2.0122 Time-temperature-transformation diagram, determined by (26), Figure 2.0122.

2.013 Thermal conductivity. 29.2 Btu/ft/hr/ft^2/F.

2.014 Thermal expansion, Figure 2.014.

2.015 Specific heat. 0.16 Btu/lb/F.

2.016 Thermal diffusivity.

2.02 Other Physical Properties

2.021 Density. 0.283 lb/in.^{3}, 7.83 g/cm^3.

2.022 Electrical resistivity.

2.023 Magnetic properties. Alloy is ferromagnetic.

2.024 Emissivity.

2.025 Damping capacity.

2.03 Chemical Properties

Similar to 4340.

2.04 Nuclear Properties

3 MECHANICAL PROPERTIES

3.01 Specified Mechanical Properties

3.011 AMS specifications.

3.0111 AMS specifications for sheet, strip and plate, Table 3.0111.

3.0112 AMS specifications for bars, forgings, stock or billets, Table 3.0112.

3.012 Fabricators' specified mechanical properties, Table 3.012.

3.02 Mechanical Properties at Room Temperature

3.021 Tension.

3.0211 Stress-strain diagrams.

Fe
0.35 C
1.8 Ni
0.8 Cr
0.35 Mo
0.2 V

4335 V Mod

3.02111 Stress-strain curve in tension for bar, Figure 3.02111.
3.0212 Effect of austenitizing temperature and time on tensile properties.
3.02121 Effect of austenitizing time and temperature on tensile properties of bar, Figure 3.02121.
3.02122 Effect of austenitizing temperature on tensile properties of sheet, Figure 3.02122.
3.02123 Effect of austenitizing time on tensile properties of sheet, Figure 3.02123.
3.02124 Effect of quenching time at 400 F in salt on tensile properties of sheet, Figure 3.02124.
3.02125 Effect of normalizing and austenitizing temperature on tensile properties of sheet and plate, Figure 3.02125.
3.02126 Effect of below-normal austenitizing temperature on tensile properties of forging, Figure 3.02126.
3.0213 Effect of tempering temperature and time on tensile properties of sheet and plate.
3.02131 Effect of austenitizing and tempering temperatures on tensile properties of sheet, Figure 3.02131.
3.02132 Effect of melting practice and tempering temperature on tensile properties of sheet, Figure 3.02132.
3.02133 Effect of tempering time and temperature and time of austenitizing on tensile properties of sheet and plate austenitized at 1550 F, Figure 3.02133.
3.02134 Effect of tempering time and temperature and time of austenitizing on tensile properties of sheet and plate austenitized at 1600 F, Figure 3.02134.
3.02135 Effect of tempering time and temperature and time of austenitizing on tensile properties of sheet and plate austenitized at 1650 F, Figure 3.02135.
3.02136 Effect of tempering temperature and quenching media and melt method on tensile properties of sheet, Figure 3.02136.
3.02137 Effect of tempering time and quenching media on tensile properties of sheet, Figure 3.02137.
3.02138 Effect of tempering temperature on uniaxial and biaxial tensile stress properties of sheet, Figure 3.02138.
3.0214 Effect of tempering temperature and time on tensile properties of bar.
3.02141 Effect of quenching and tempering temperature on tensile properties of bar, Figure 3.02141.
3.02142 Effect of tempering time and temperature on tensile properties of bar, Figure 3.02142.
3.0215 Size effects on tensile properties.
3.02151 Effect of thickness on tensile properties of sheet and plate, Figure 3.02151.
3.02152 Effect of thickness of sheet from two melting practices and various heat treatments, Table 3.02152.
3.0216 Tensile properties of gun-tube extrusion, Table 3.0216.
3.0217 Tensile properties of forging, Table 3.0217.
3.022 Compression.
3.0221 Stress-strain diagrams.
3.02211 Stress-strain curve in compression for bar, Figure 3.02211.
3.023 Impact.
3.0231 Effect of quenching and tempering temperature on impact strength of bar, Figure 3.0231.
3.0232 Effect of tempering time and temperature on impact strength of bar, Figure 3.0232.
3.0233 Effect of below-normal austenitizing temperature on impact properties of forging, Figure 3.0233.
3.0234 Impact properties of gun-tube extrusion, Table 3.0234.
3.0235 Correlation of Charpy-V shelf energy with dynamic tear shelf energy in comparison to a range of various high-strength steels (37), Figure 3.0235.
3.024 Bending.
3.025 Torsion and shear.
3.0251 Effect of diameter-to-thickness ratio on ultimate shear strength of hollow cylinders, Figure 3.0251.
3.026 Bearing.
3.027 Stress concentration.
3.0271 Notch properties; see also 3.0272 and 3.0371.
3.02711 Effect of tempering temperature on tensile properties and notch strength of plate, Figure 3.02711.
3.02712 Effect of tempering temperature, melting practice and sheet thickness on notch strength of sheet, Figure 3.02712.
3.02713 Effect of stress concentration on notch strength of sheet, Figure 3.02713.
3.02714 Effect of tempering temperature on notch strength of sheet austenitized at 1650 F, Figure 3.02714.
3.02715 Effect of tempering temperature on notch strength of plate austenitized at 1650 F, Figure 3.02715.
3.02716 Effect of tempering time and temperature on notch strength of bar, Figure 3.02716.
3.02717 Effect of quenching and tempering temperature on notch strength of bar, Figure 3.02717.
3.02718 Notch tensile properties of forging, Table 3.02718.
3.0272 Fracture toughness.
3.02721 Effect of austenitizing temperature on notch strength of sheet, Figure 3.02721.
3.02722 Effect of tempering temperature on notch strength of sheet, Figure 3.02722.
3.02723 Effect of tempering temperature on notch strength of sheet austenitized at 1625 F, Figure 3.02723.
3.02724 Effect of tempering temperature on notch strength of plate austenitized at 1625 F, Figure 3.02724.
3.02725 Effect of tempering temperature on notch strength of sheet austenitized at 1650 F, Figure 3.02725.
3.02726 Effect of tempering temperature on notch strength of plate austenitized at 1650 F, Figure 3.02726.
3.02727 Effect of thickness on notch strength of sheet, Figure 3.02727.
3.02728 Fracture-toughness properties of gun-tube extrusion, Table 3.02728.
3.028 Combined properties.

3.03 **Mechanical Properties at Various Temperatures**
3.031 Tension.
3.0311 Stress-strain diagrams.
3.0312 Effect of test temperature on tensile properties of sheet, Figure 3.0312.
3.032 Compression.
3.0321 Stress-strain diagrams.
3.033 Impact.
3.0331 Effect of test temperature on impact strength of plate, Figure 3.0331.
3.034 Bending.
3.035 Torsion and shear.
3.036 Bearing.
3.037 Stress concentration.
3.0371 Notch properties.
3.03711 Effect of test temperature on net fracture stress and fracture appearance of shear-cracked sheet, Figure 3.03711.

3.03712	Effect of test temperature on tensile properties, fracture appearance, and net section fracture stress of air melted, quenched and tempered 0.015 inch sheet, Figure 3.03712 (38).
3.03713	Effect of test temperature on tensile properties, fracture appearance, and net section fracture stress of air melted, quenched and tempered 0.015 inch sheet, Figure 3.03713 (38).
3.03714	Effect of test temperature on tensile properties, fracture appearance, and net section fracture stress of air melted, quenched and tempered 0.015 inch sheet, Figure 3.03714 (38).
3.03715	Effect of test temperature on tensile properties, fracture appearance, and net section fracture stress of air melted, quenched and tempered 0.030 inch sheet, Figure 3.03715 (38).
3.03716	Effect of test temperature on tensile properties, fracture appearance, and net section fracture stress of air melted, quenched and tempered 0.030 inch sheet, Figure 3.03716 (38).
3.03717	Effect of test temperature on tensile properties, fracture appearance, and net section fracture stress of air melted, quenched and tempered 0.030 inch sheet, Figure 3.03717 (38).
3.03718	Effect of test temperature on tensile properties, fracture appearance, and net section fracture stress of air melted, quenched and tempered 0.063 inch sheet, Figure 3.03718 (38).
3.03719	Effect of test temperature on tensile properties, fracture appearance, and net section fracture stress of air melted, quenched and tempered 0.063 inch sheet, Figure 3.03719 (38).
3.03720	Effect of test temperature on tensile properties, fracture appearance, and net section fracture stress of air melted, quenched and tempered 0.063 inch sheet, Figure 3.03720 (38).
3.03721	Effect of test temperature on tensile properties, fracture appearance, and net section fracture stress of air melted, quenched and tempered 0.125 inch sheet, Figure 3.03721 (38).
3.03722	Effect of test temperature on tensile properties, fracture appearance, and net section fracture stress of air melted, quenched and tempered 0.125 inch sheet, Figure 3.03722 (38).
3.03723	Effect of test temperature on tensile properties, fracture appearance, and net section fracture stress of air melted, quenched and tempered 0.125 inch sheet, Figure 3.03723 (38).
3.03724	Effect of test temperature on tensile properties, fracture appearance, and net section fracture stress of consutrode vacuum melted, quenched and tempered 0.015 inch sheet, Figure 3.03724 (38).
3.03725	Effect of test temperature on tensile properties, fracture appearance, and net section fracture stress of consutrode vacuum melted, quenched and tempered 0.015 inch sheet, Figure 3.03725 (38).
3.03726	Effect of test temperature on tensile properties, fracture appearance, and net section fracture stress of consutrode vacuum melted, quenched and tempered 0.015 inch sheet, Figure 3.03726 (38).
3.03727	Effect of test temperature on tensile properties, fracture appearance, and net section fracture stress of consutrode vacuum melted, quenched and tempered 0.063 inch sheet, Figure 3.03727 (38).
3.03728	Effect of test temperature on tensile properties, fracture appearance, and net section fracture stress of consutrode vacuum melted, quenched and tempered 0.063 inch sheet, Figure 3.03728 (38).
3.03729	Effect of test temperature on tensile properties, fracture appearance, and net section fracture stress of consutrode vacuum melted, quenched and tempered 0.063 inch sheet, Figure 3.03729 (38).
3.03730	Effect of test temperature on tensile properties, fracture appearance, and net section fracture stress of consutrode vacuum melted, quenched and tempered 0.063 inch sheet, Figure 3.03730 (38).
3.0372	Fracture toughness.
3.038	Combined properties.

Fe
0.35 C
1.8 Ni
0.8 Cr
0.35 Mo
0.2 V

4335 V Mod

3.04	**Creep and Creep Rupture Properties**
3.05	**Fatigue Properties**
3.051	S-N curves for bar with various surface treatments, Figure 3.051.
3.052	S-N curves for smooth and notched bar, Figure 3.052.
3.053	Fatigue life at 80 ksi (R = 0) for forging, Figure 3.053.
3.054	Fatigue crack propagation rate of gun-tube extrusion, Table 3.054.
3.06	**Elastic Properties**
3.061	Poisson's ratio. Dynamic bending, 0.303. Static tension, 0.293.
3.062	Modulus of elasticity, 30,000 ksi.
3.063	Modulus of rigidity, 11,000 ksi.
4	**FABRICATION** Similar to 4330 V Mod.
4.01	**Formability** Severe forming of sheet and strip is performed in the spheroidized condition, with the hardness limited to 95 RB maximum.
4.011	Forging range, 2000–2200 F (20).
4.02	**Machining and Grinding** Bar and forgings can be machined in the normalized condition, with additional tempering at 1275 F recommended for best machinability.
4.03	**Welding**
4.031	Flash welding of air melted plate results in reduced joint efficiency when heat treated to maximum strength. Effects of flash welding and tempering temperature on tensile properties and endurance limit of air melted plate, Figure 4.031.
4.032	Flash welding of vacuum melted plate results in better joint efficiency and considerably increased endurance limit. Effect of flash welding and tempering temperature on tensile properties and endurance limit of vacuum melted plate, Figure 4.032.
4.033	Multipass welding technique is required for welding 0.220 inch thick material. A 500 F preheat and a 500 F postheat for 30 minutes results in the optimum as-welded weld ductility (31).
4.034	Tests of welded 0.093 inch sheet, containing weld repairs after heat treatment, show F_{tu} reduced 20 to 30 ksi and F_{ty} reduced 10 to 15 ksi. Fracture toughness of repair weld after heat treatment

Fe
0.35 C
1.8 Ni
0.8 Cr
0.35 Mo
0.2 V

4335 V Mod

generally was better than a normal heat-treated weld (32).

4.04 Heat Treatment

4.05 Surface Treatment

REFERENCES

1. AMS 5029B (October 1, 1984).
2. AMS 6428C (April 15, 1980).
3. AMS 6429C (April 1, 1985).
4. AMS 6430C (January 15, 1980).
5. AMS 6433C (April 15, 1980).
6. AMS 6434C (October 1, 1983).
7. AMS 6435C (October 1, 1984).
8. Aerojet-General Corporation, Material Data Sheet No. P 2101 (January 17, 1959).
9. Aerojet-General Corporation, "Steel Plates, Sheets and Strips; Chromium-Nickel-Molybdenum-Vanadium", Development Material Specification, AMS – M255a (July 14, 1958).
10. Aerojet-General Corporation, "List of Data Sheets and Reports on AMS 6434, Alloy Steel" (1959).
11. Warga, J. J., "Mechanical Properties of AMS 6434 Steel", Aerojet-General Corporation, Report No. SRP 121 (Special) (June 19, 1958).
12. Gable, G. W., "Critical Points and Heat Treatment of 1-3/4 Ni-Cr-Mo-V Steel Heat 654550", Republic Steel Corporation, Y.S. 625 (December 12, 1958).
13. Espey, G. B., Jones, M. H., and Brown, W. F., Jr., "The Sharp Edge Notch Tensile Strength of Several High Strength Steel Sheet Alloys", ASTM Proceedings, Vol 59 (1959).
14. Sachs, G., and Sessler, J. G., "Effect of Stress Concentration on Tensile Strength of Titanium and Steel Alloy Sheet at Various Temperatures", Symposium on Low-Temperature Properties of High-Strength Aircraft and Missile Materials, ASTM STP No. 287, pp 122–135 (June 30, 1960).
15. Kreger, J., and Mayer, H., "Comparative Properties of Air Melt and Vacuum Melt AMS 6434 Steel in the Ultra-High Strength Tensile Range", A. O. Smith Corporation, Aeronautical Division Report No. AD-282 (December 4, 1956).
16. MacLaren, A. W., Personal Communication, United States Steel Corporation (June 26, 1959).
17. Republic Steel Corporation, 4335 V Mod., Data Sheet (May 28, 1959).
18. Aerojet-General Corporation (1958).
19. March, J. L., "AMS 6434 (Modified) Steel Sheet Material Characteristics and Heat Treatment", American Car and Foundry Division, ACF Industries, Major Report 458 (June 18, 1959).
20. Climax Molybdenum Company, "Ultra-Strength Steels" (1957).
21. Aerojet-General Corporation, "Heat Treatment of a 4335 V Type Low Alloy Steel (October 15, 1962).
22. Campbell, J. E., "Steels for Large Solid-Propellant Rocket Motor Cases", DMIC Report 178 (November 20, 1962).
23. Morrison, J. D., and Kattus, J. R., "An Investigation of Methods for Determining the Crack-Propagation Resistance of High Strength Alloys", Summary Technical Report, Southern Research Institute (March 7, 1961).
24. Jones, R. C., "Materials – SAE 4335 (Modified) Steel 260,000 to 280,000 psi Heat Treatment – Development of Process Control and Mechanical Properties for", Convair Division – General Dynamics (October 24, 1962).
25. Whitney, R. C., "Material – SAE 4335 (Modified) Steel Process Control and Mechanical Properties – Development of", General Dynamics, Convair Division, Report 1659 (November 9, 1962).
26. Fiorentino, R. J., Roach, D. B., and Hall, A. M., "Heat Treatment of High-Strength Steels for Airframe Applications", DMIC Report 119 (November 27, 1959).
27. Gilbert, L. L., and Brown, J. A., "Materials and Fabrication Problems Associated With High Strength Lightweight Homogeneous Pressure Vessels", Proceedings of the Golden Gate Metals Conference on High Strength Steels, for the Missile Industry, ASM (1961).
28. Bhat, G. K., and Lindh, D. V., "Evaluation of Ultra-High Strength Steels for Thin Walled Pressure Vessels and Rocket Motor Cases", ASME, Paper No. 62, Met-16 (April 1962).
29. Bernstein, H. K., and Young, G. C., "Progress Report on Fracture Toughness Tests of High Strength Sheet Metals", NAVORD Report 6496 NGF-T-7-59 (May 18, 1959).
30. Bernstein, H., and Young, G. C., "2nd Progress Report on Fracture Toughness of High Strength Sheet Metals", NAVORD Report 6496 (Part 21, NRL 108) (January 28, 1960).
31. "Welding Thick Section of 4335 V Type Low Alloy Steel", Aerojet-General Corporation (October 15, 1962).
32. "Repair Welding 4335 V Type Alloy Steel After Final Heat Treatment", Aerojet-General Corporation (January 15, 1963).
33. Thornton, P. A., "The Austenitizing Behavior of a Low Alloy Steel", U.S. Army Armament Research and Development Command Research Report No. ARLCB-TR-80013 (May 1980).
34. Jones, R. L., "B-58 A. O. Smith Pylon Box Forgings – Mechanical Properties – Determination of –", Convair/General Dynamics Test Data Memorandum No. 2796 (February 11, 1963).
35. Stonesifer, F. R., and Smith, H. L., "Failure Analysis of Shrike Mounting Lugs", Naval Research Laboratory, Section 2 of "Case Studies of Fracture Mechanics", Army Materials and Mechanics Research Center Report No. AMMRC MS 77-5 (June 1977).
36. Farrara, R. A., "Gun Tube Extrusions", U.S. Army Armament Research and Development Command Technical Report ARLCB-TR-83012 (April 1983).
37. Lange, E. A., "Fracture Toughness of Structural Metals", U.S. Naval Research Laboratory Report No. 7046 (May 4, 1970).
38. Beachem, C. D., and Srawley, J. E., "Crack Propagation Tests of High-Strength Sheet Materials – Part V – Air Melted and Consutrode AMS 6434 Steel", U.S. Naval Research Laboratory Report 5507 (August 18, 1960).

Alloy	4335 V Mod	
Source	AMS	Form
1	5029B	Welding wire
2	6428C	Bars, forgings, forging stock and mechanical tubing
3	6429C	Bars, forgings, mechanical tubing, flash-welded rings, and stock for forging or flash-welded rings (vacuum melt)
4	6430C	Bars, forgings, mechanical tubing, flash-welded rings, and stock for forging or flash-welded rings (special grade)
5	6433C	Sheet, strip and plate (special grade)
6	6434C	Sheet, strip and plate
7	6435C	Sheet, strip and plate (vacuum melt)

TABLE 1.031. AMS SPECIFICATIONS

Fe
0.35 C
1.8 Ni
0.8 Cr
0.35 Mo
0.2 V

4335 V Mod

Alloy	4335 V Mod			
Source	AMS (2,6)		AMS (3,4,5,7)	
	Percent		Percent	
Composition	Min	Max	Min	Max
Carbon	0.32[a]	0.38	0.33[b]	0.38
Chromium	0.65	0.90	0.65	0.90
Copper	–	0.35	–	0.35
Manganese	0.60	0.80	0.60	0.90
Molybdenum	0.30	0.40	0.30	0.40
Nickel	1.65	2.00	1.65	2.00
Phosphorus	–	0.025	–	0.010[c]
Silicon	0.15	0.35	0.40	0.60
Sulfur	–	0.025	–	0.010[c]
Vanadium	0.17	0.23	0.17	0.23
Iron	Balance		Balance	

(a) AMS 6434C gives 0.33.
(b) AMS 6430C gives 0.32.
(c) AMS 6430C and AMS 6433C give 0.015.

TABLE 1.04. COMPOSITION

Alloy	4335 V Mod			
Condition	Austenitized 1600–1650 F, 1 hr, OQ			
Source	Form of Product	Temper	F_{tu}, ksi (Min)	F_{ty}, ksi (Min)
AMS 6429C	Bars, forgings, tube (vacuum melted)	400–500 F 2 hr (min)	240	210
AMS 6430C	Bars, forgings, tube (special grade)	700 F 2 hr (min)	205	190
AMS 6433C	Sheet, strip and plate (special grade)	700 F 2 hr (min)	205	190
AMS 6435C	Sheet, strip and plate (vacuum melted)	400–500 F 2 hr (min)	240	210

TABLE 1.057. AMS SPECIFIED TENSILE PROPERTIES

Fe
0.35 C
1.8 Ni
0.8 Cr
0.35 Mo
0.2 V

4335 V Mod

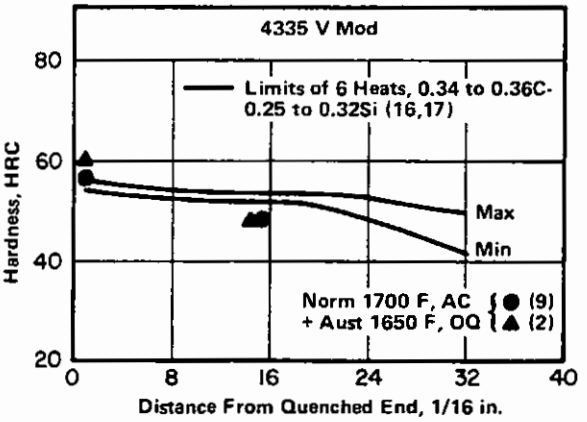


FIGURE 1.061. END QUENCH HARDENABILITY (2,9,16,17)

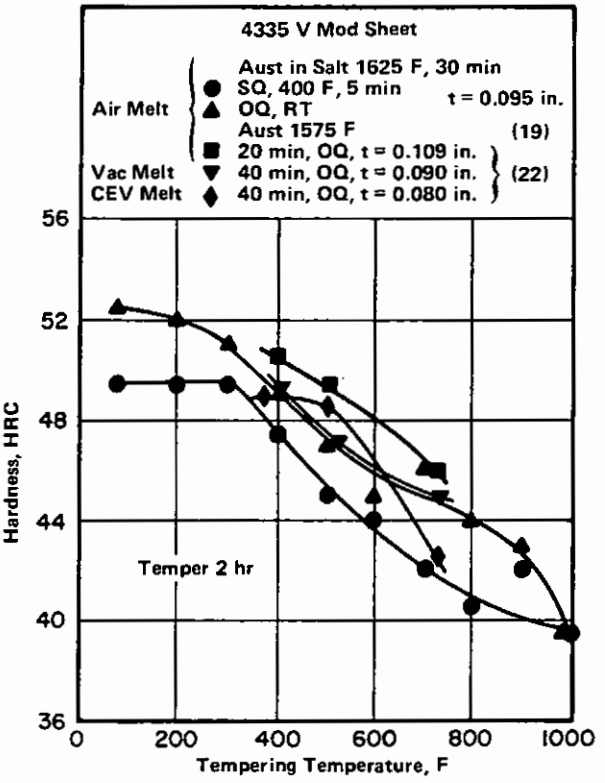


FIGURE 1.062. EFFECT OF TEMPERING TEMPERATURE, QUENCHING MEDIA AND MELT METHOD ON HARDNESS OF SHEET (19,22)

Alloy	4335 V Mod			
Form	Sheet			
		Condition		
Melting Practice	Thickness, in.	Austenitizing Temperature, F(a)	Tempering Temperature, F(b)	Hardness, HRC
Air Melt	0.03	1575	400	49–50
		1575	725	41–43
		1620	400	48–50
	0.063	1575	400	52–54
		1575	725	44–45
		1620	400	48–52
	0.125	1575	400	47–50
		1575	725	42–44
		1620	400	47–51
Consumable Electrode	0.063	1575	400	48–50
		1575	725	43–44
		1620	400	48–50

(a) Austenitized at 1575 F in neutral salt, or in argon at 1620 F, oil quenched.
(b) Tempered for 2 hours and air cooled.

TABLE 1.064. EFFECT OF THICKNESS, MELTING PRACTICE, AUSTENITIZING TEMPERATURE AND TEMPERING TEMPERATURE ON HARDNESS OF SHEET (38)

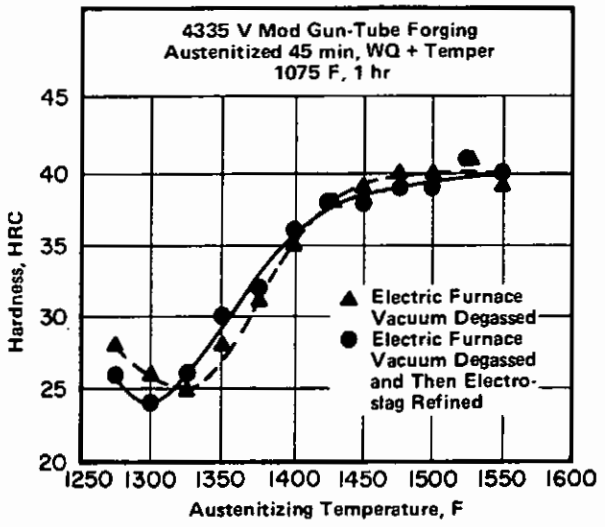


FIGURE 1.065. EFFECT OF BELOW-NORMAL AUSTENITIZING TEMPERATURE ON HARDNESS OF FORGING (33)

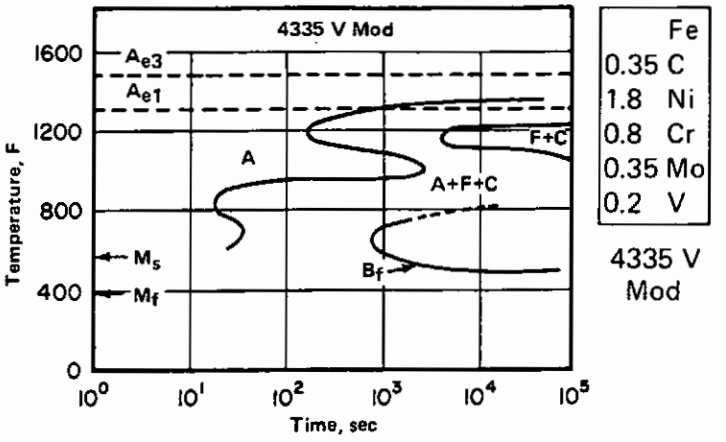


FIGURE 2.0121. TIME-TEMPERATURE-TRANSFORMATION DIAGRAM, DETERMINED BY (12)

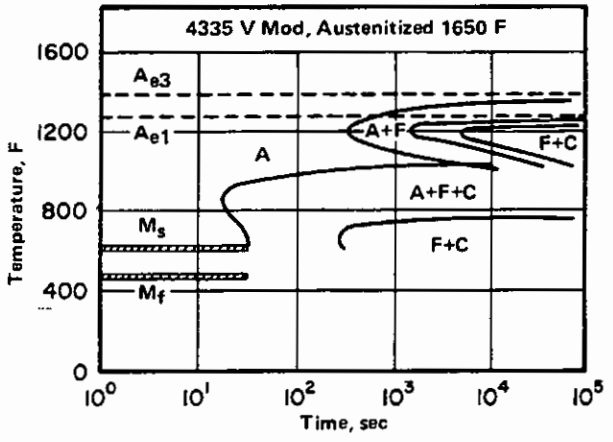


FIGURE 2.0122. TIME-TEMPERATURE-TRANSFORMATION DIAGRAM, DETERMINED BY (26)

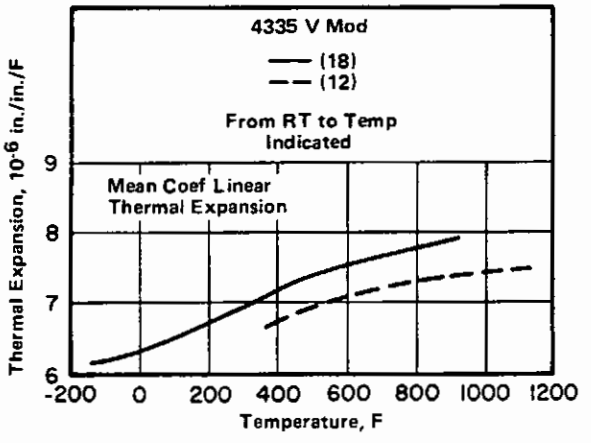


FIGURE 2.014. THERMAL EXPANSION (12,18)

Alloy	4335 V Mod						
Form	Sheet, Strip and Plate						
Condition	1600 to 1650 F, 1 hr, OQ +						
	>700 F, 2 hr				400 to 500 F, 2 hr		
Thickness, in.	≤0.070	>0.070 to 0.249	>0.249 to 0.349	>0.349	≥0.070	≥0.070 to 0.249	>0.349
F_{tu} (Min), ksi	205	205	205	205	240	240	240
F_{ty} (Min), ksi	190	190	190	190	210	210	210
e (2 in.) (Min), percent	5	6	8	10	5	6	8

TABLE 3.0111. AMS SPECIFICATIONS FOR SHEET, STRIP AND PLATE (5,7)

Fe
0.35 C
1.8 Ni
0.8 Cr
0.35 Mo
0.2 V

4335 V Mod

Alloy	4335 V Mod			
Condition	1600 to 1650 F, 1 hr, OQ + >700 F, 2 hr		400 to 500 F, 2 hr	
Form	Bar	Forgings, Stock, Billets	Bar	Forgings, Stock, Billets
Thickness, in.	Not given			
F_{tu} (Min), ksi		240		205
F_{ty} (Min), ksi		210		190
e (4D) (Min), percent	10 (L)	7 (T)	10 (L)	7 (T)

TABLE 3.0112. AMS SPECIFICATIONS FOR BARS, FORGINGS, STOCK OR BILLETS (3,4)

Alloy	4335 V Mod		
Condition	1625 F, OQ + 400 to 500 F, 2 hr Minimum		
Form	Sheet, Strip, Plate	Bar	Billet
F_{ty} (Min), ksi	–	210	210
L	–	–	–
T	210	–	–
e (2 in.) (Min), percent	–	–	–
L	–	10	–
T	6	–	7

TABLE 3.012. FABRICATORS' SPECIFIED MECHANICAL PROPERTIES (9)

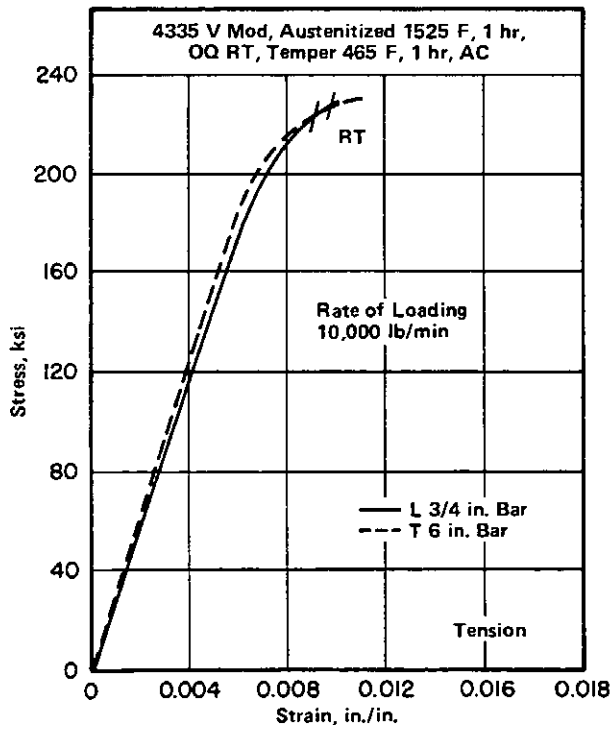


FIGURE 3.02111. STRESS-STRAIN CURVE IN TENSION FOR BAR (24)

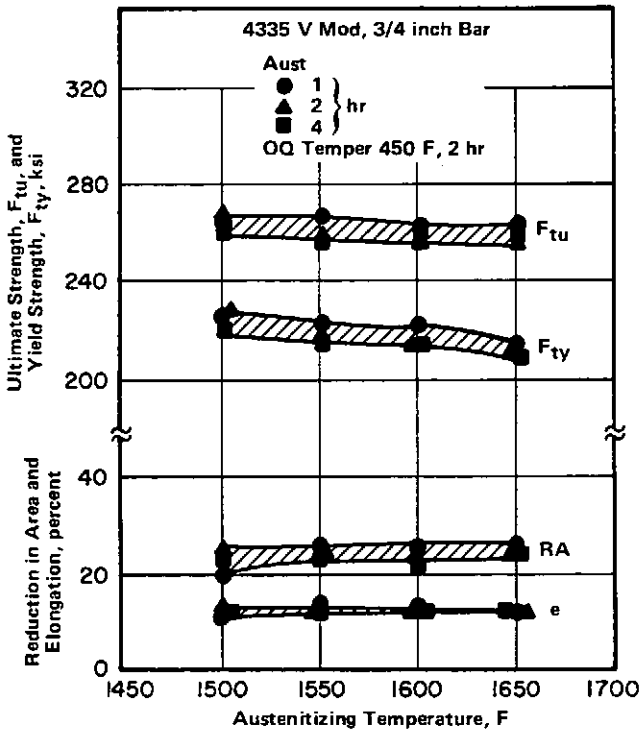


FIGURE 3.02121. EFFECT OF AUSTENITIZING TIME AND TEMPERATURE ON TENSILE PROPERTIES OF BAR (24)

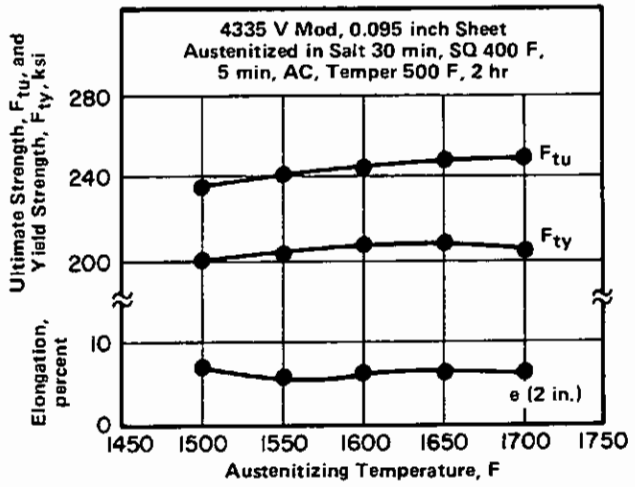


FIGURE 3.02122. EFFECT OF AUSTENITIZING TEMPERATURE ON TENSILE PROPERTIES OF SHEET (19)

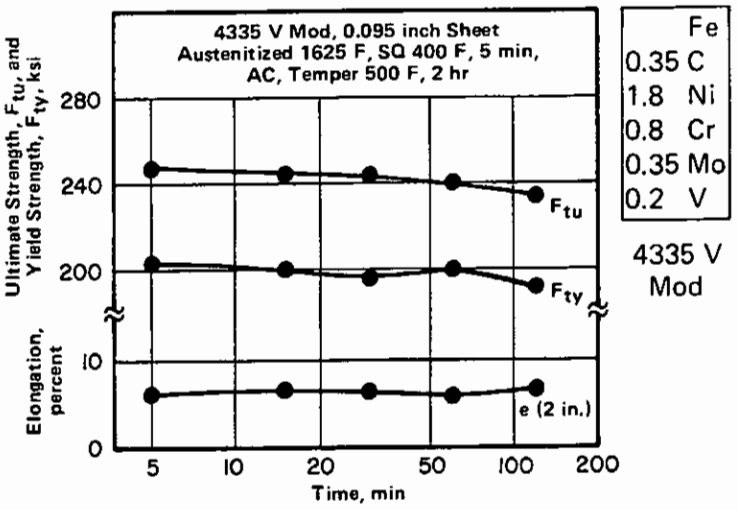


FIGURE 3.02123. EFFECT OF AUSTENITIZING TIME ON TENSILE PROPERTIES OF SHEET (19)

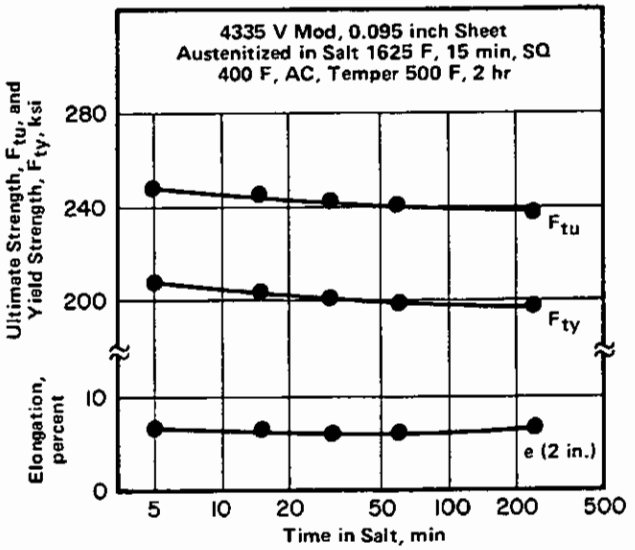


FIGURE 3.02124. EFFECT OF QUENCHING TIME AT 400 F IN SALT ON TENSILE PROPERTIES OF SHEET (19)

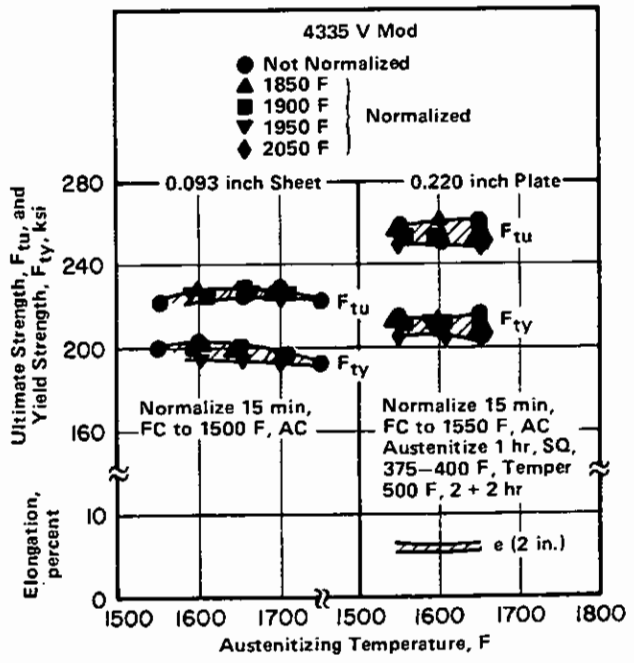


FIGURE 3.02125. EFFECT OF NORMALIZING AND AUSTENITIZING TEMPERATURE ON TENSILE PROPERTIES OF SHEET AND PLATE (21)

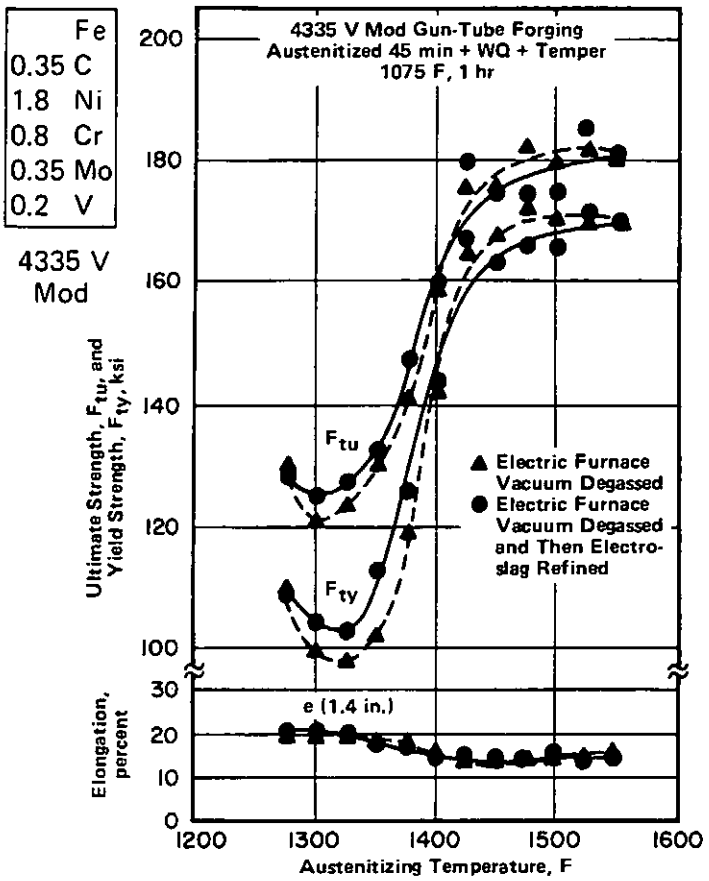


FIGURE 3.02126. EFFECT OF BELOW-NORMAL AUSTENITIZING TEMPERATURE ON TENSILE PROPERTIES OF FORGING (33)

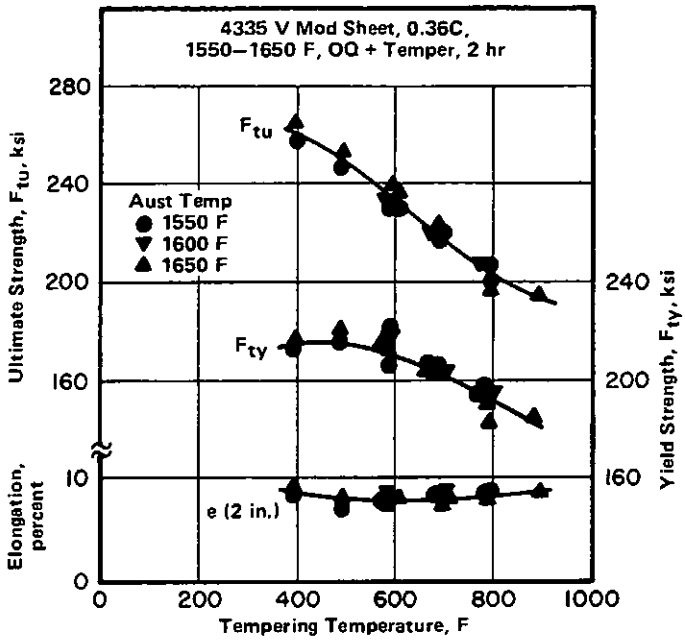


FIGURE 3.02131. EFFECT OF AUSTENITIZING AND TEMPERING TEMPERATURES ON TENSILE PROPERTIES OF SHEET (11)

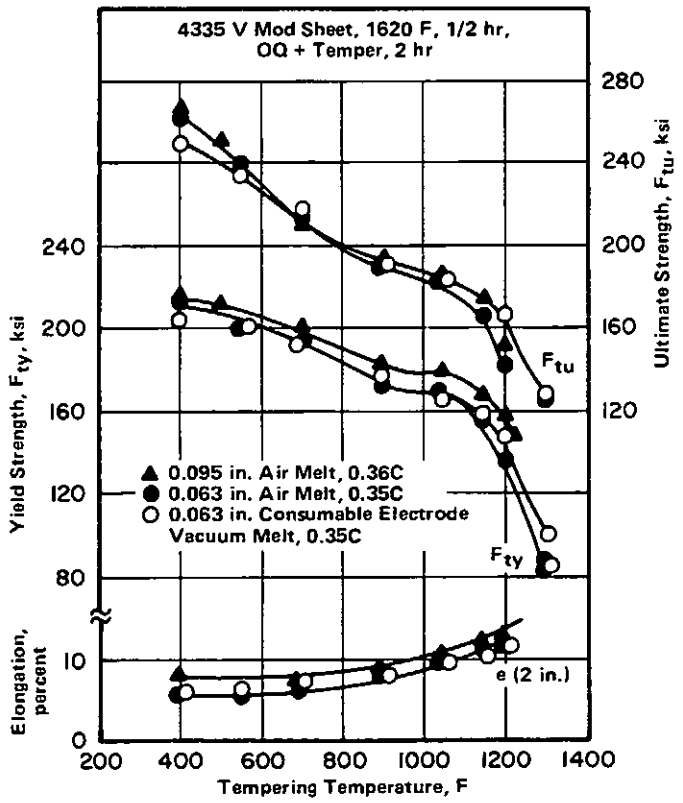


FIGURE 3.02132. EFFECT OF MELTING PRACTICE AND TEMPERING TEMPERATURE ON TENSILE PROPERTIES OF SHEET (13)

Fe
0.35 C
1.8 Ni
0.8 Cr
0.35 Mo
0.2 V

4335 V Mod

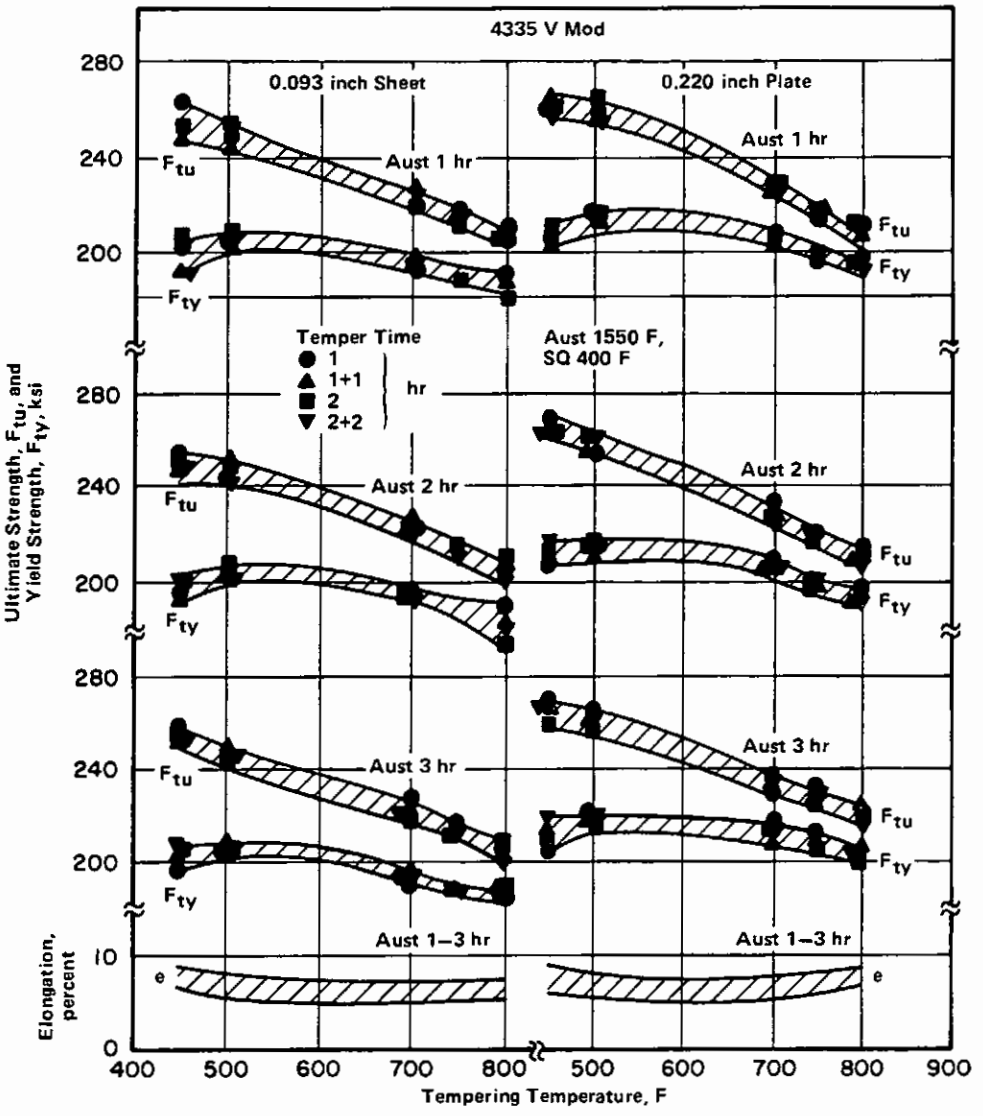


FIGURE 3.02133. EFFECT OF TEMPERING TIME AND TEMPERATURE AND TIME OF AUSTENITIZING ON TENSILE PROPERTIES OF SHEET AND PLATE AUSTENITIZED AT 1550 F (21)

Fe
0.35 C
1.8 Ni
0.8 Cr
0.35 Mo
0.2 V

4335 V Mod

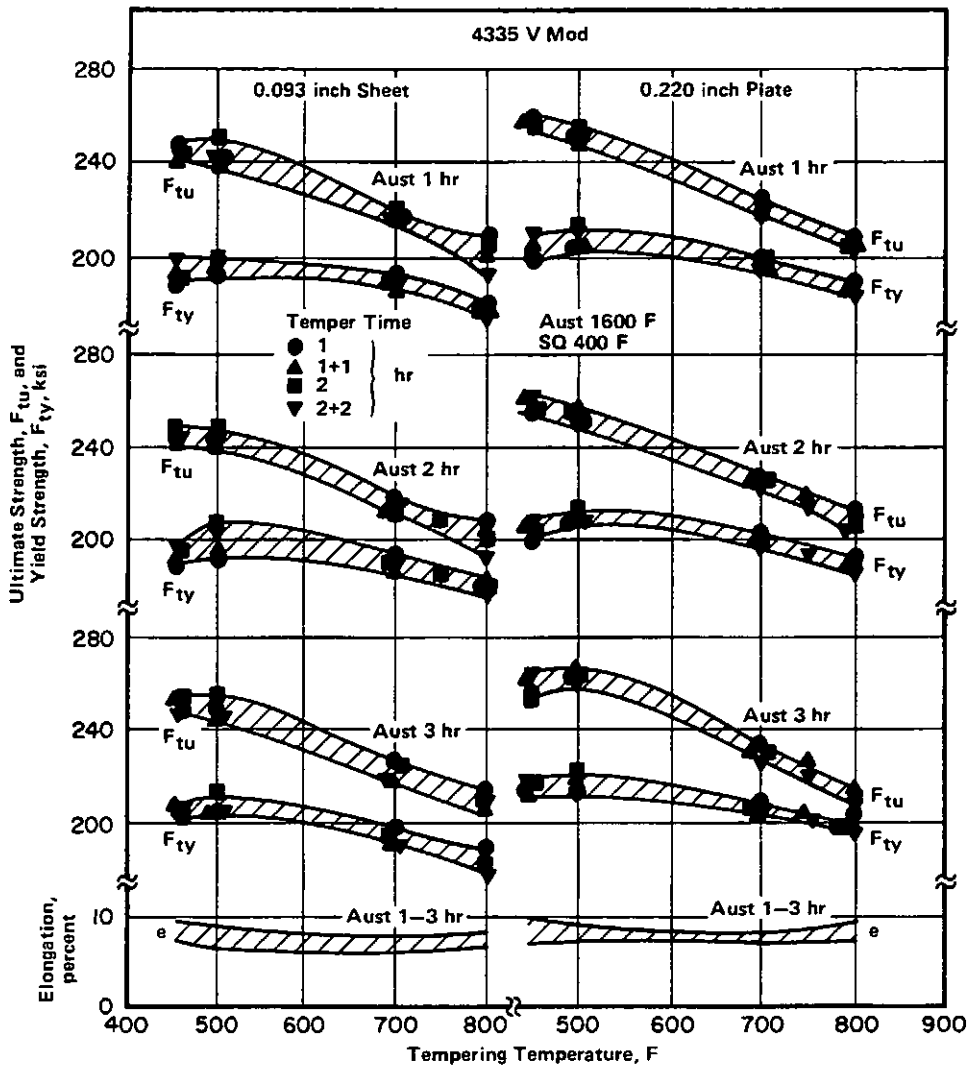


FIGURE 3.02134. EFFECT OF TEMPERING TIME AND TEMPERATURE AND TIME OF AUSTENITIZING ON TENSILE PROPERTIES OF SHEET AND PLATE AUSTENITIZED AT 1600 F (21)

Fe
0.35 C
1.8 Ni
0.8 Cr
0.35 Mo
0.2 V

4335 V Mod

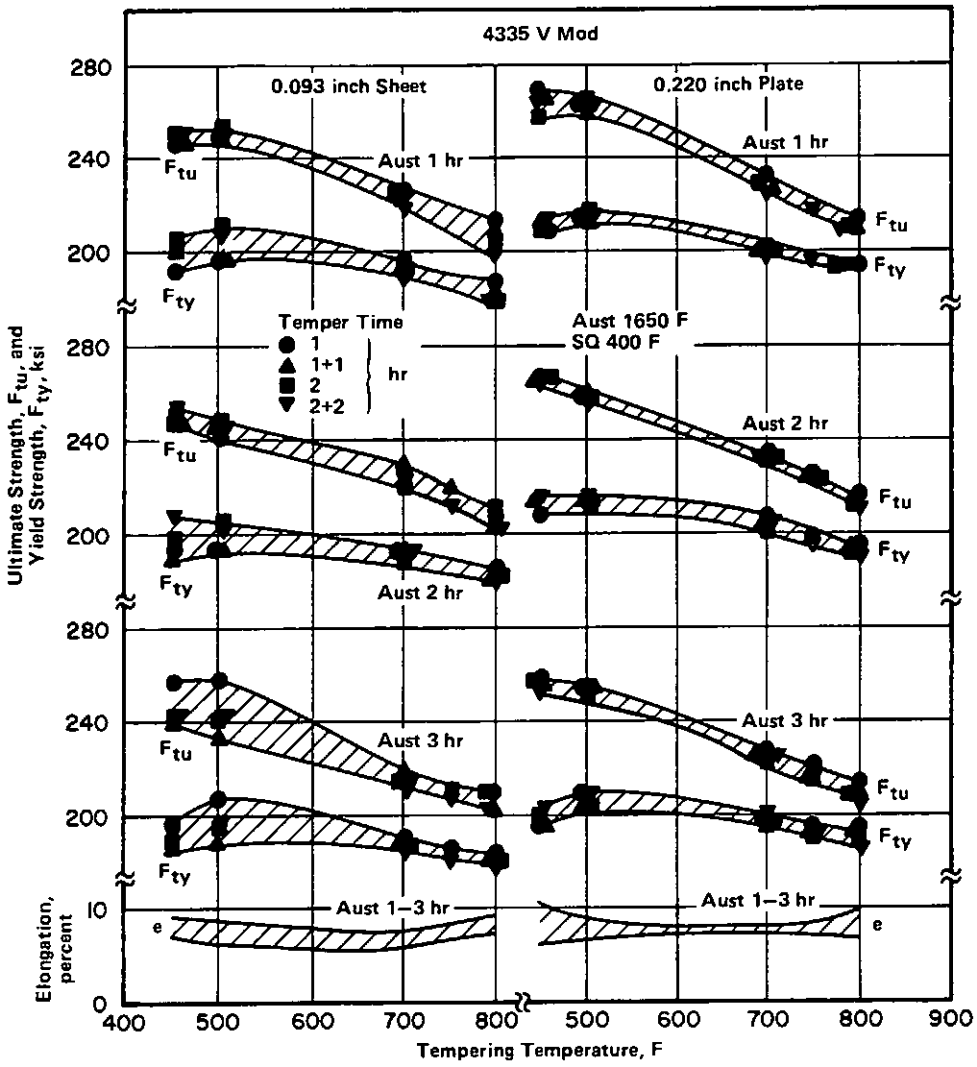


FIGURE 3.02135. EFFECT OF TEMPERING TIME AND TEMPERATURE AND TIME OF AUSTENITIZING ON TENSILE PROPERTIES OF SHEET AND PLATE AUSTENITIZED AT 1650 F (21)

Fe
0.35 C
1.8 Ni
0.8 Cr
0.35 Mo
0.2 V

4335 V Mod

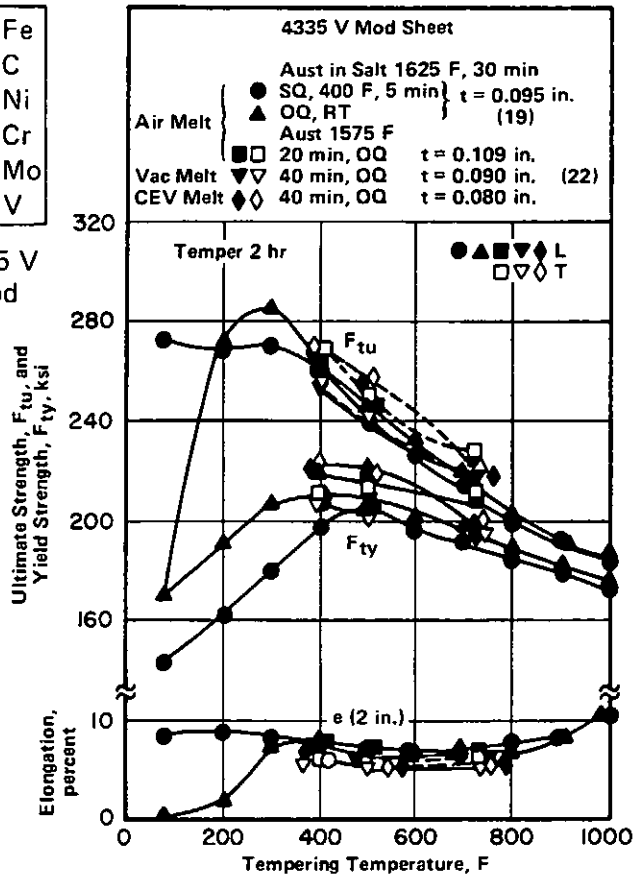


FIGURE 3.02136. EFFECT OF TEMPERING TEMPERATURE AND QUENCHING MEDIA AND MELT METHOD ON TENSILE PROPERTIES OF SHEET (19,22)

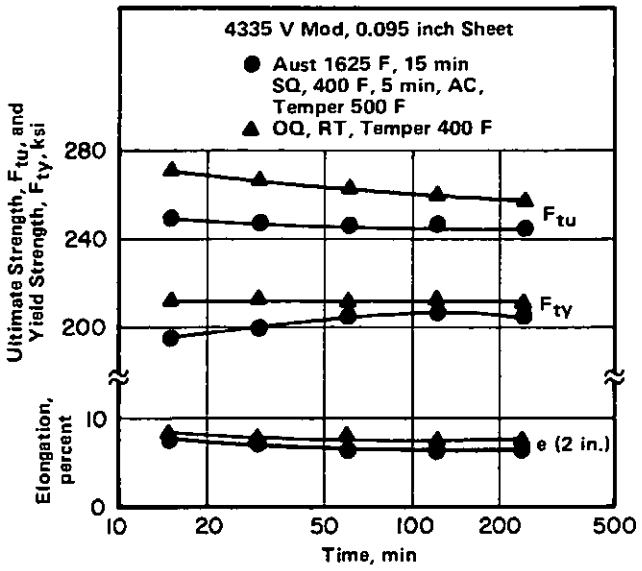


FIGURE 3.02137. EFFECT OF TEMPERING TIME AND QUENCHING MEDIA ON TENSILE PROPERTIES OF SHEET (19)

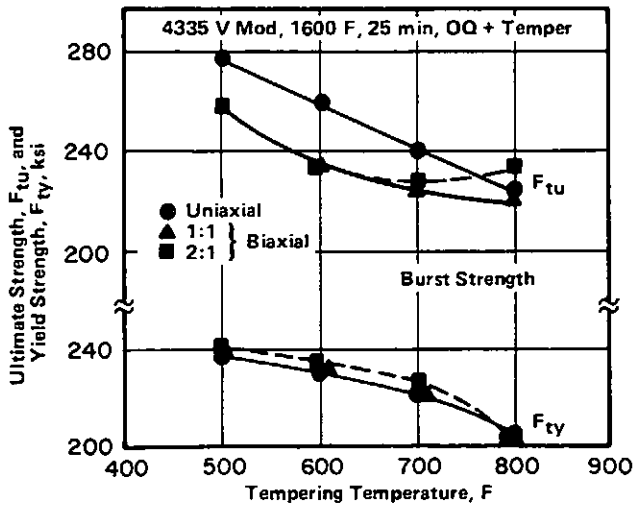


FIGURE 3.02138. EFFECT OF TEMPERING TEMPERATURE ON UNIAXIAL AND BIAXIAL TENSILE STRESS PROPERTIES OF SHEET (28)

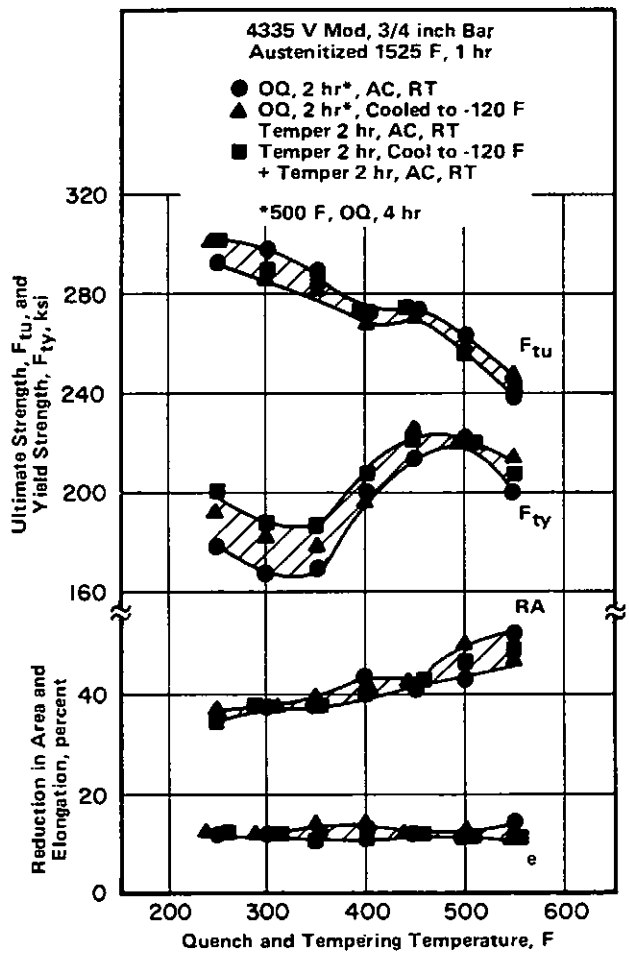


FIGURE 3.02141. EFFECT OF QUENCHING AND TEMPERING TEMPERATURE ON TENSILE PROPERTIES OF BAR (24)

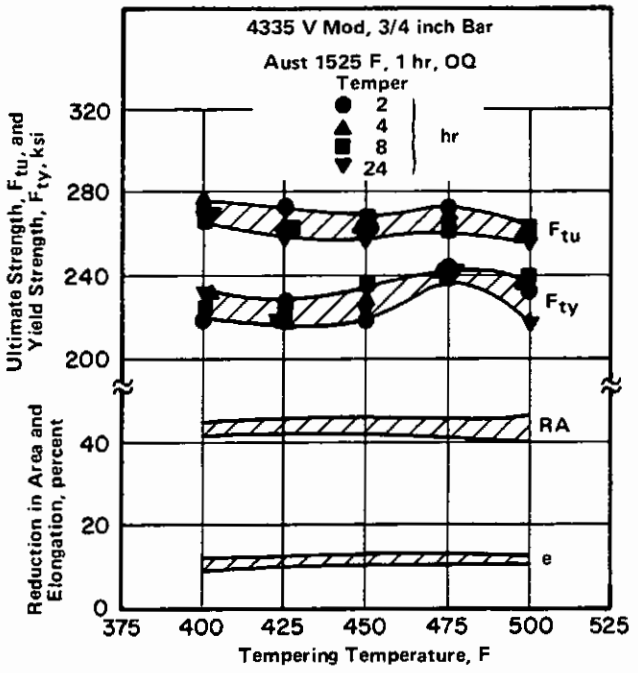
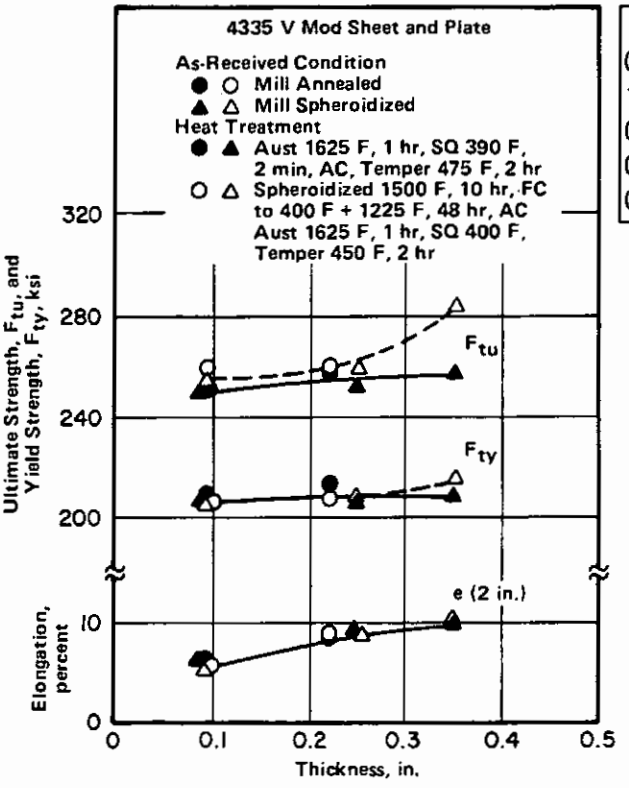


FIGURE 3.02142. EFFECT OF TEMPERING TIME AND TEMPERATURE ON TENSILE PROPERTIES OF BAR (24)



Fe
0.35 C
1.8 Ni
0.8 Cr
0.35 Mo
0.2 V

4335 V Mod

FIGURE 3.02151. EFFECT OF THICKNESS ON TENSILE PROPERTIES OF SHEET AND PLATE (21)

Alloy	4335 V Mod					
Form	Sheet					
Orientation	L					
		Condition				
Melting Practice	Thickness, in.	Austenitizing Temperature, F(a)	Tempering Temperature, F(b)	F_{ty}, ksi	F_{tu}, ksi	Elongation, percent
Air Melt	0.015	1575	400	192	220	2.5
		1575	725	180	193	2
		1620	400	183	217	2.3
	0.03	1575	400	208	251	5
		1575	725	192	211	3.5
		1620	400	189.5	232.5	4
	0.063	1575	400	207	256	7
		1575	725	182	202	5.5
		1620	400	205	254	5.5
		1620(c)	400	204	254	7
	0.125	1575	400	205	254	8
		1575	725	191	209	7.5
		1620	400	196	250	8
Consumable Electrode	0.015	1575	400	185	215	–
		1575	725	173.5	186.5	–
		1620	400	190	229	4
	0.063	1575	400	199	240	6.5
		1575	725	186	205	–
		1620	400	202	248	6.5
		1620(c)	400	201	246	7

(a) Austenitized at 1575 F in neutral salt, or in argon at 1620 F, oil quenched.
(b) Tempered for 2 hours and air cooled.
(c) Transverse specimen.

TABLE 3.02152. EFFECT OF THICKNESS OF SHEET FROM TWO MELTING PRACTICES AND VARIOUS HEAT TREATMENTS (38)

Fe
0.35 C
1.8 Ni
0.8 Cr
0.35 Mo
0.2 V

4335 V Mod

Alloy	4335 V Mod			
Form	Hollow Extrusions With Two External Diameters (Approx. 9.5 in. and 7 in.) for 105 mm Gun Tube			
Condition	Austenitized at 1550 F, OD and ID Quenched With Agitated Water, Tempered 1060 F for 4 hr			
Specimen Orientation	T			
Condition	Tube No.	Location	F_{ty} Range[a], ksi	RA Range, percent
Original Heat Treatment (Above)	1	Breech	165.4–168.1	29–36
		Muzzle	162.1–163.4	34–39
	4	Breech	168.7–170.8	35–43
		Muzzle	169.8–171.0	41–48
	8	Breech	167.1–170.1	26–34
		Muzzle	162.3–164.1	26–37
Reheat Treatment[b]	1	Breech	162.6–162.6	42.8–43.6
		Muzzle	158.1–159.6	36.3–40.7
	4	Breech	165.6–165.6	43.6–46.2
		Muzzle	164.1–165.6	44.9–48.6
	8	Breech	172.7–172.7	35.4–38.5
		Muzzle	169.7–169.7	34.0–37.7

(a) Range of values from four specimens.
(b) Austenitized at 1560–1580 F for 3 hours; ID and OD water spray quenched; Tubes 1 and 4 tempered 1100 F for 5 hours, Tube 8 tempered 1080 F for 5 hours.

TABLE 3.0216. TENSILE PROPERTIES OF GUN-TUBE EXTRUSION (36)

Alloy	4335 V Mod			
Form	B-58 Wing, A. O. Smith Pylon Box Forging			
Condition	Austenitized at 1550 F, 30 min, Quenched Into Agitated Molten Salt at 420–435 F for 10 min, Cooled to RT, Tempered 2 hr at 975 F			
Direction	F_{ty}, ksi	F_{tu}, ksi	Elongation, percent	Reduction in Area, percent
L	183.0	188.4	11.4	47.4
T	182.8	189.1	9.3	33.3

TABLE 3.0217. TENSILE PROPERTIES OF FORGING (34)

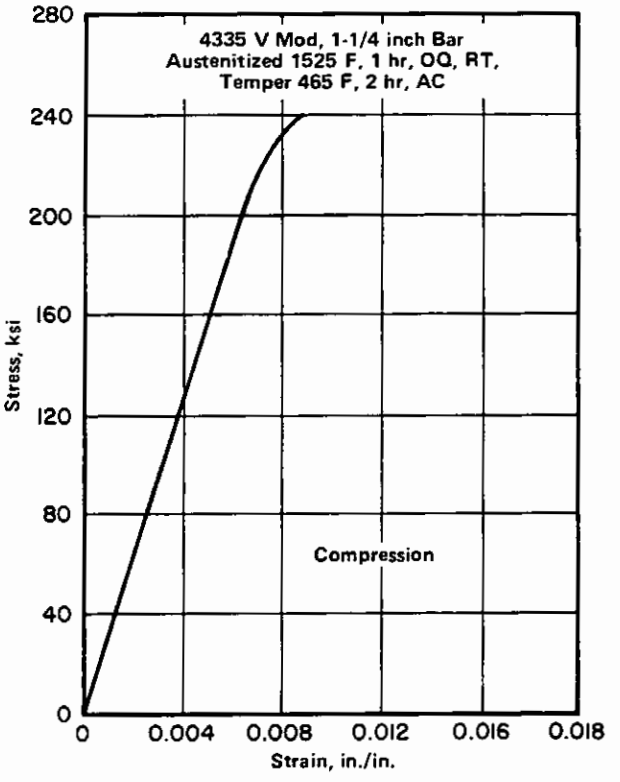


FIGURE 3.02211. STRESS-STRAIN CURVE IN COMPRESSION FOR BAR (24)

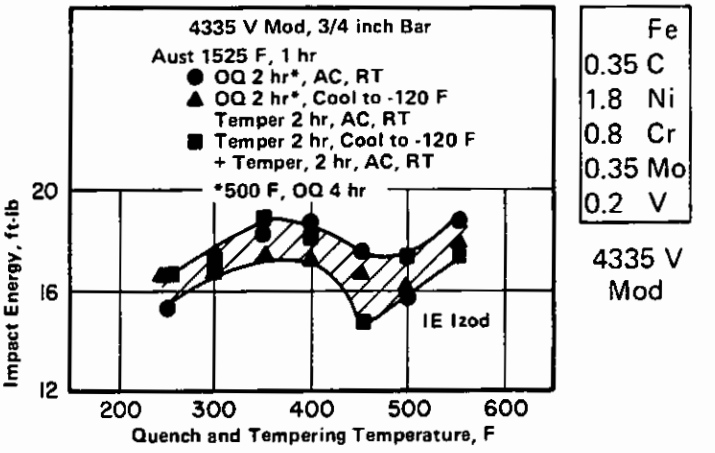


FIGURE 3.0231. EFFECT OF QUENCHING AND TEMPERING TEMPERATURE ON IMPACT STRENGTH OF BAR (24)

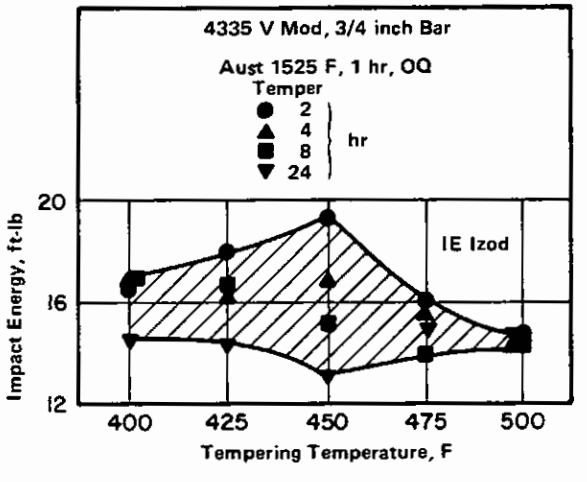


FIGURE 3.0232. EFFECT OF TEMPERING TIME AND TEMPERATURE ON IMPACT STRENGTH OF BAR (24)

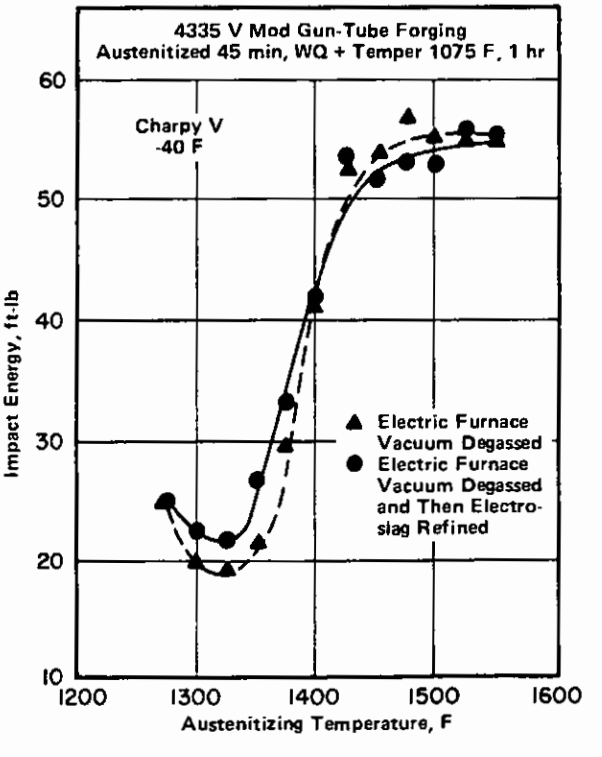


FIGURE 3.0233. EFFECT OF BELOW-NORMAL AUSTENITIZING TEMPERATURE ON IMPACT PROPERTIES OF FORGING (33)

Fe
0.35 C
1.8 Ni
0.8 Cr
0.35 Mo
0.2 V

4335 V Mod

Alloy	4335 V Mod		
Form	Hollow Extrusions With Two External Diameters (Approx. 9.5 in. and 7 in.) for 105 mm Gun Tube		
Condition	Austenitized at 1550 F, OD and ID Quenched With Agitated Water, Tempered 1060 F for 4 hr		
Specimen Orientation	T		
Condition	Tube No.	Location	Charpy V-Notch Range[a] at -40 F, ft-lb
Original Heat Treatment (Above)	1	Breech	15–16
		Muzzle	17–18
	4	Breech	17–20
		Muzzle	19–20
	8	Breech	16–17
		Muzzle	15.5–16
Reheat Treatment[b]	1	Breech	18.3–20.0
		Muzzle	17.5–17.5
	4	Breech	21–22
		Muzzle	23–23
	8	Breech	14.5–14.5
		Muzzle	15.5–15.5

(a) Range of values from four specimens.
(b) Austenitized at 1560–1580 F for 3 hours; ID and OD water spray quenched; Tubes 1 and 4 tempered 1100 F for 5 hours, Tube 8 tempered 1080 F for 5 hours.

TABLE 3.0234. IMPACT PROPERTIES OF GUN-TUBE EXTRUSION (36)

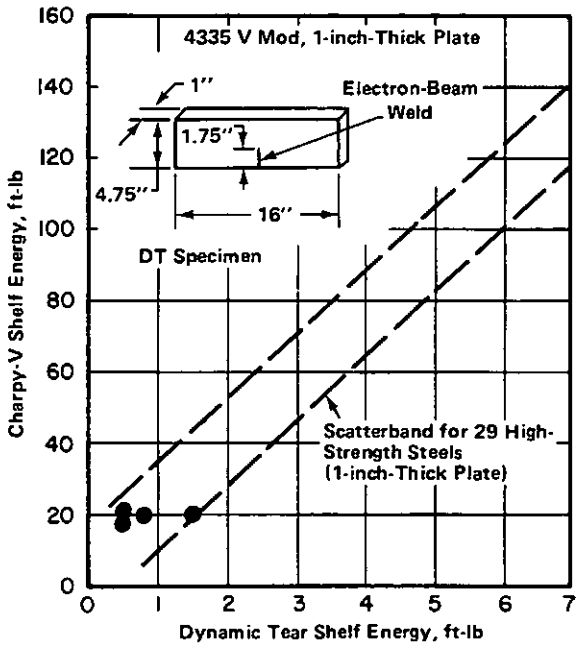


FIGURE 3.0235. CORRELATION OF CHARPY-V SHELF ENERGY WITH DYNAMIC TEAR SHELF ENERGY IN COMPARISON TO A RANGE OF VARIOUS HIGH-STRENGTH STEELS (37)

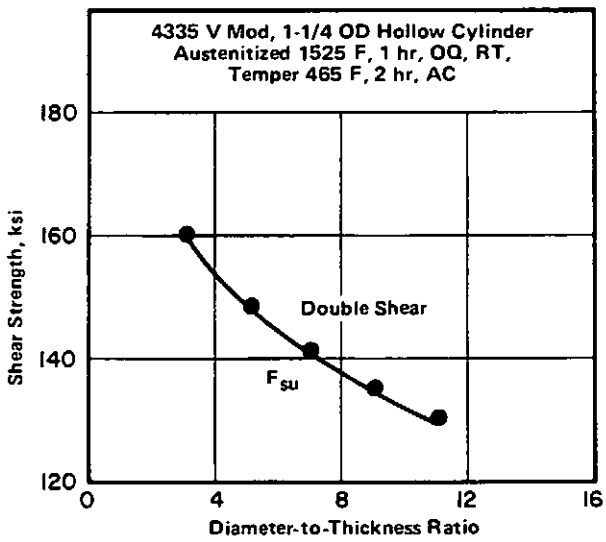


FIGURE 3.0251. EFFECT OF DIAMETER-TO-THICKNESS RATIO ON ULTIMATE SHEAR STRENGTH OF HOLLOW CYLINDERS (24)

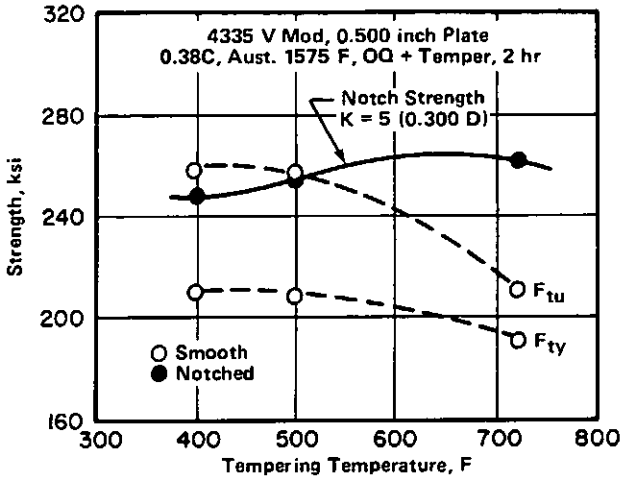


FIGURE 3.02711. EFFECT OF TEMPERING TEMPERATURE ON TENSILE PROPERTIES AND NOTCH STRENGTH OF PLATE (8)

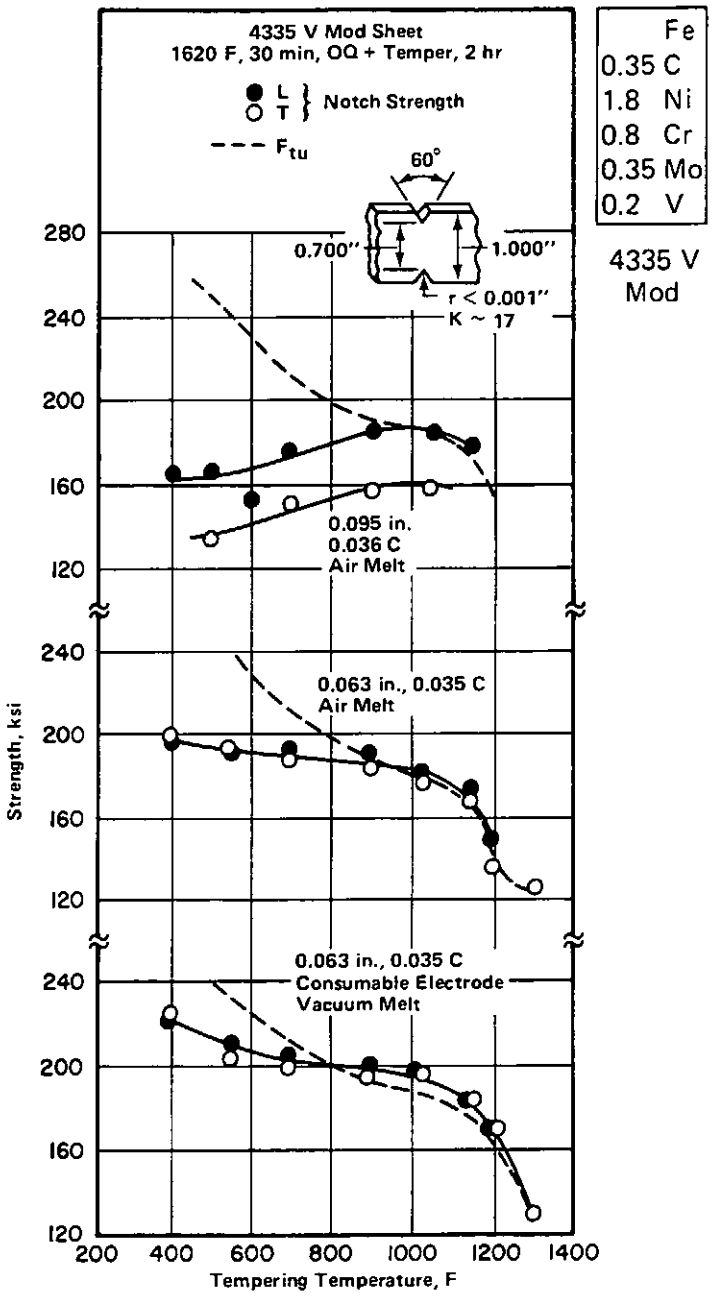


FIGURE 3.02712. EFFECT OF TEMPERING TEMPERATURE, MELTING PRACTICE AND SHEET THICKNESS ON NOTCH STRENGTH OF SHEET (13)

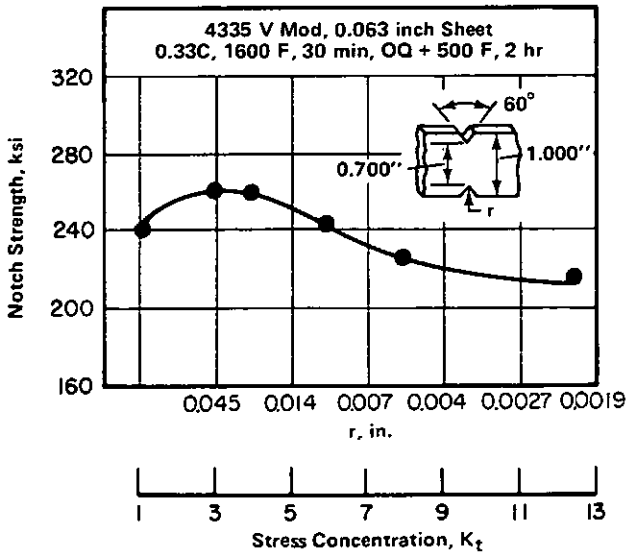


FIGURE 3.02713. EFFECT OF STRESS CONCENTRATION ON NOTCH STRENGTH OF SHEET (14)

Fe
0.35 C
1.8 Ni
0.8 Cr
0.35 Mo
0.2 V

4335 V Mod

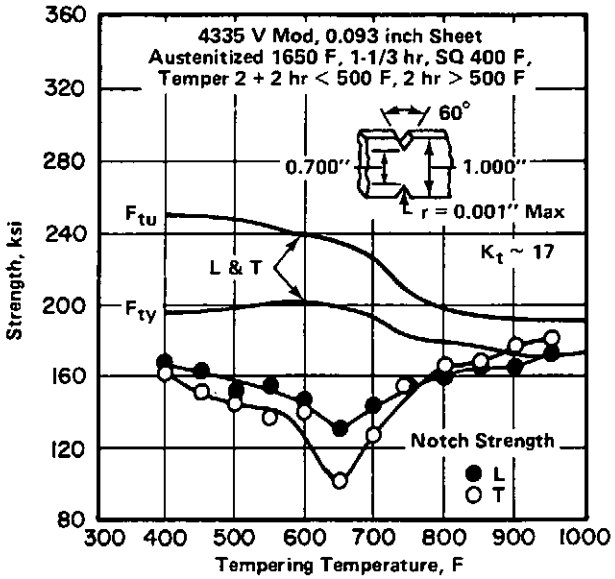


FIGURE 3.02714. EFFECT OF TEMPERING TEMPERATURE ON NOTCH STRENGTH OF SHEET AUSTENITIZED AT 1650 F (21)

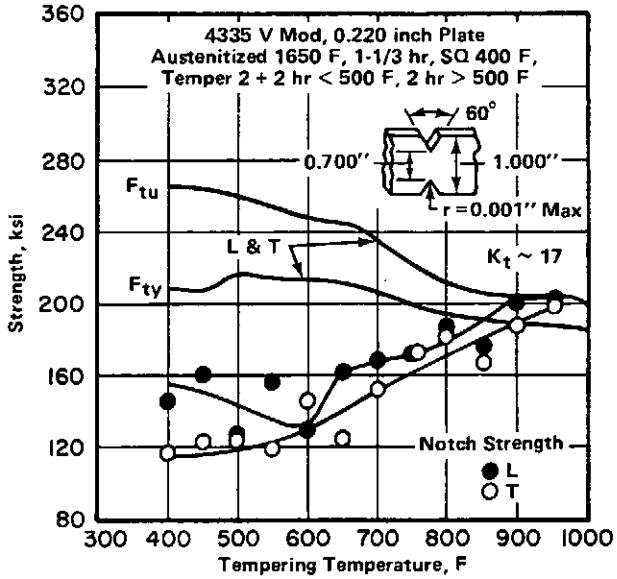


FIGURE 3.02715. EFFECT OF TEMPERING TEMPERATURE ON NOTCH STRENGTH OF PLATE AUSTENITIZED AT 1650 F (21)

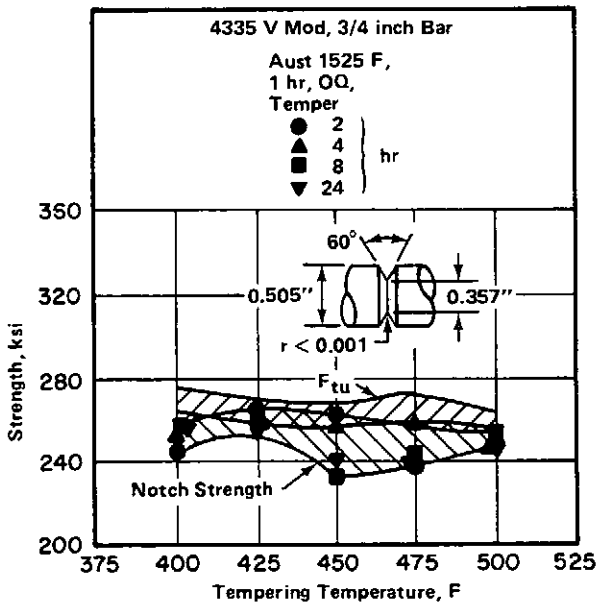


FIGURE 3.02716. EFFECT OF TEMPERING TIME AND TEMPERATURE ON NOTCH STRENGTH OF BAR (24)

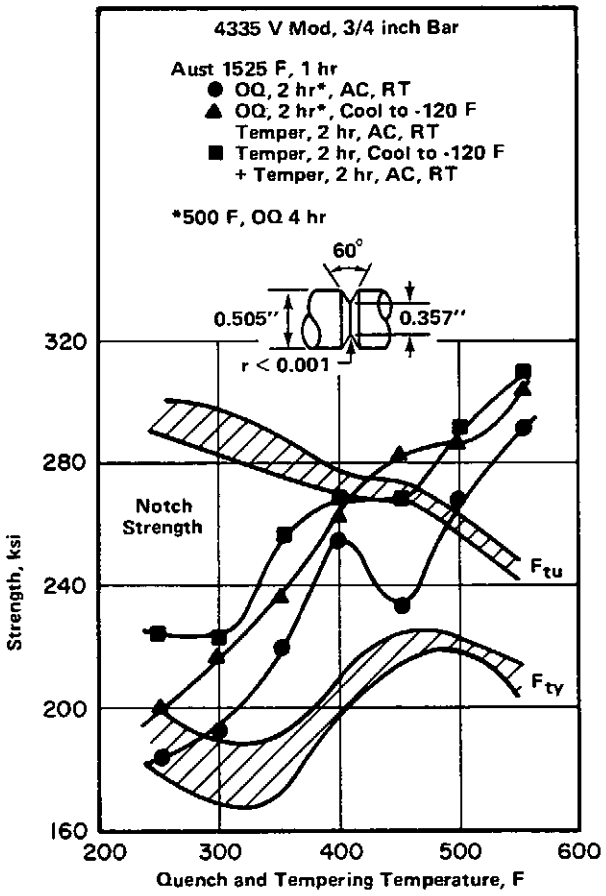


FIGURE 3.02717. EFFECT OF QUENCHING AND TEMPERING TEMPERATURE ON NOTCH STRENGTH OF BAR (24)

Fe
0.35 C
1.8 Ni
0.8 Cr
0.35 Mo
0.2 V

4335 V Mod

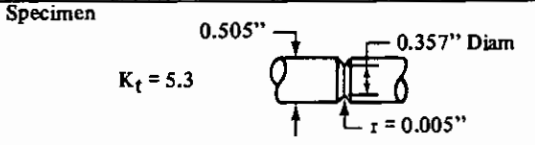
Alloy	4335 V Mod	
Form	B-58 Wing, O. A. Smith Pylon Box Forging	
Condition	Austenitized 1550 F, 30 min, Quench Into Agitated 420–435 F Molten Salt, 10 min, Cooled to RT, Tempered 2 hr at 975 F	
Specimen		
Direction	Notch Strength, ksi	Notch Strength-Ultimate Strength Ratio
Long.	268.4	1.42
L. Trans.	262.2	1.39

TABLE 3.02718. NOTCH TENSILE PROPERTIES OF FORGING (34)

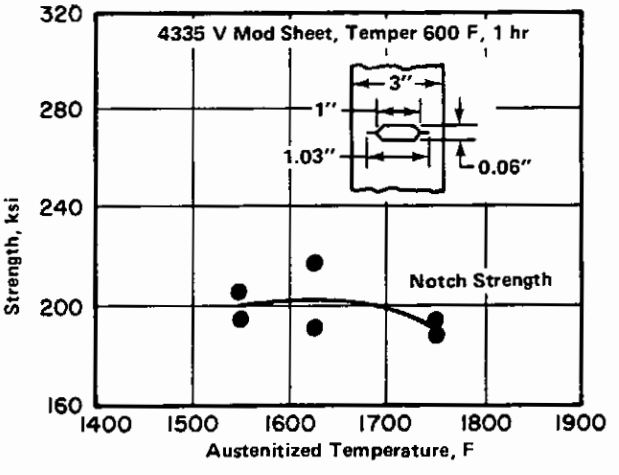


FIGURE 3.02721. EFFECT OF AUSTENITIZING TEMPERATURE ON NOTCH STRENGTH OF SHEET (29)

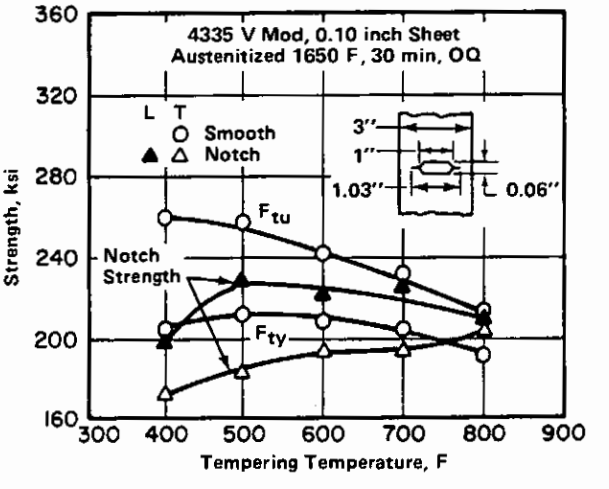


FIGURE 3.02722. EFFECT OF TEMPERING TEMPERATURE ON NOTCH STRENGTH OF SHEET (30)

Fe
0.35 C
1.8 Ni
0.8 Cr
0.35 Mo
0.2 V

4335 V Mod

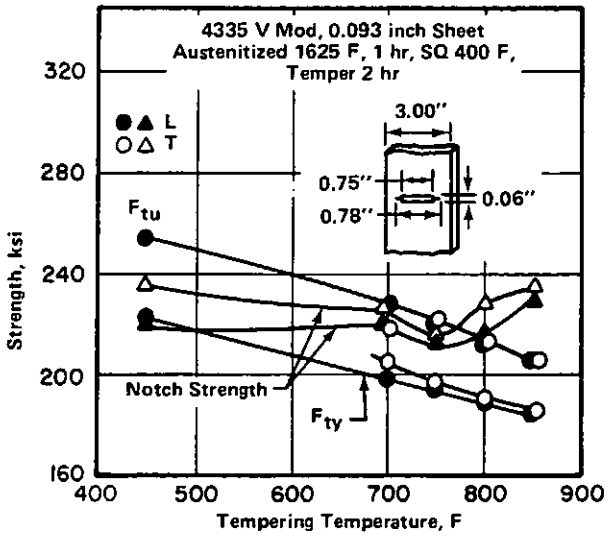


FIGURE 3.02723. EFFECT OF TEMPERING TEMPERATURE ON NOTCH STRENGTH OF SHEET AUSTENITIZED AT 1625 F (21)

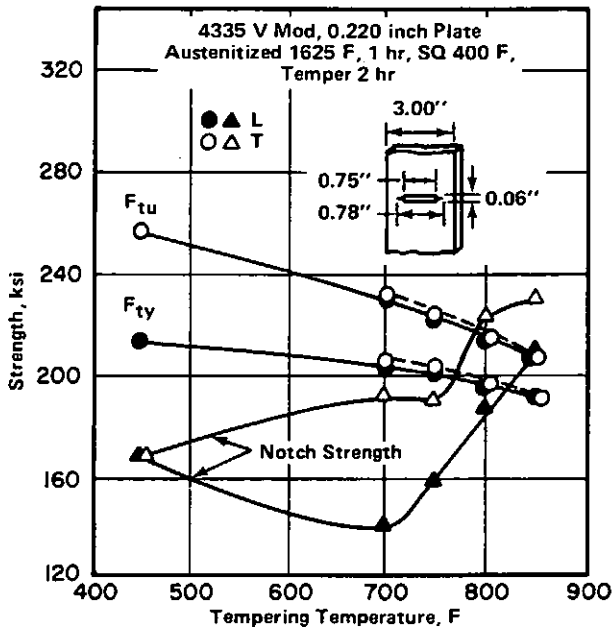


FIGURE 3.02724. EFFECT OF TEMPERING TEMPERATURE ON NOTCH STRENGTH OF PLATE AUSTENITIZED AT 1625 F (21)

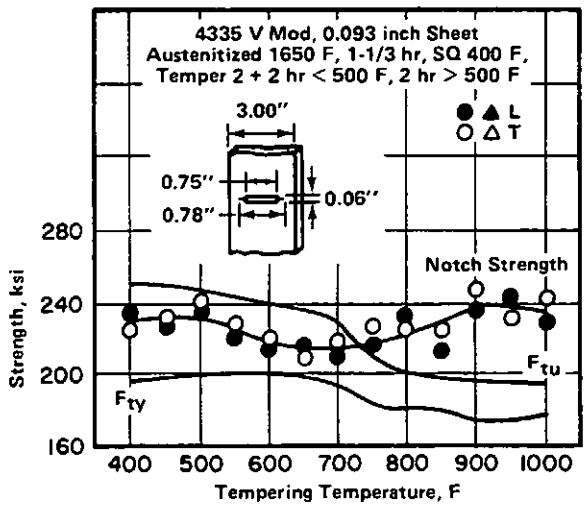


FIGURE 3.02725. EFFECT OF TEMPERING TEMPERATURE ON NOTCH STRENGTH OF SHEET AUSTENITIZED AT 1650 F (21)

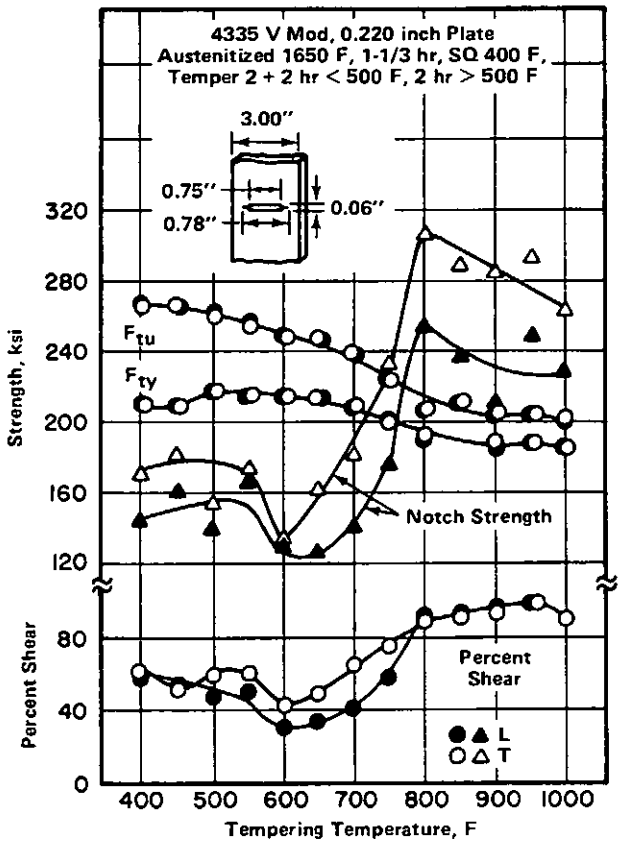


FIGURE 3.02726. EFFECT OF TEMPERING TEMPERATURE ON NOTCH STRENGTH OF PLATE AUSTENITIZED AT 1650 F (21)

Fe
0.35 C
1.8 Ni
0.8 Cr
0.35 Mo
0.2 V

4335 V Mod

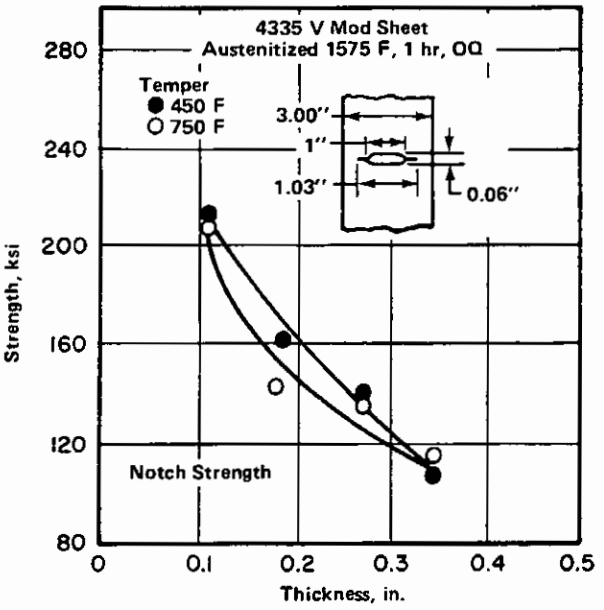


FIGURE 3.02727. EFFECT OF THICKNESS ON NOTCH STRENGTH OF SHEET (30)

Alloy	4335 V Mod	
Form	Hollow Extrusions With Two External Diameters (Approx. 9.5 in. and 7 in.) for 105 mm Gun Tube	
Condition	Austenitized at 1550 F, OD and ID Quenched With Agitated Water, Tempered 1060 F for 4 hr	
Specimen and Orientation	C Shape, T-S	
	K_{Ic}, ksi $\sqrt{in.}$	
Location	Average(a)	Range
Breech End of Extrusion	109.3	106.4–112.1
Muzzle End of Extrusion	97.4	94.1–102.3
Mid-Length of Breech	113.3	109.1–116.4
Mid-Length of Muzzle	95.6	92.4– 97.7

(a) Average of six specimens, two from each of three extrusions.

TABLE 3.02728. FRACTURE-TOUGHNESS PROPERTIES OF GUN-TUBE EXTRUSION (36)

Fe
0.35 C
1.8 Ni
0.8 Cr
0.35 Mo
0.2 V

4335 V Mod

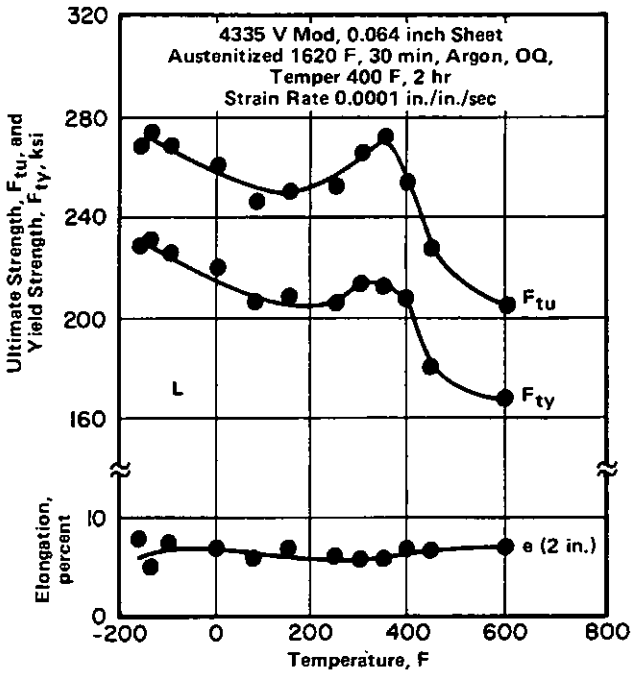


FIGURE 3.0312. EFFECT OF TEST TEMPERATURE ON TENSILE PROPERTIES OF SHEET (23)

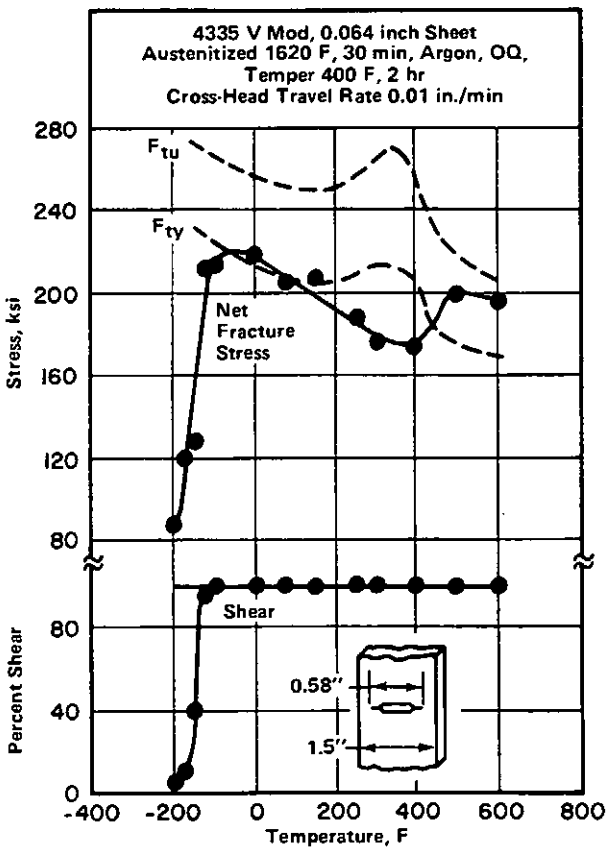


FIGURE 3.03711. EFFECT OF TEST TEMPERATURE ON NET FRACTURE STRESS AND FRACTURE APPEARANCE OF SHEAR CRACKED SHEET (23)

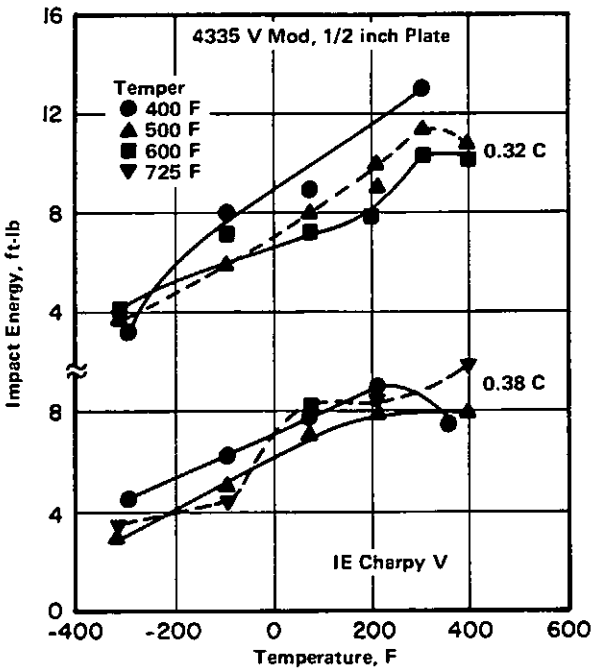


FIGURE 3.0331. EFFECT OF TEST TEMPERATURE ON IMPACT STRENGTH OF PLATE (27)

Fe
0.35 C
1.8 Ni
0.8 Cr
0.35 Mo
0.2 V

4335 V Mod

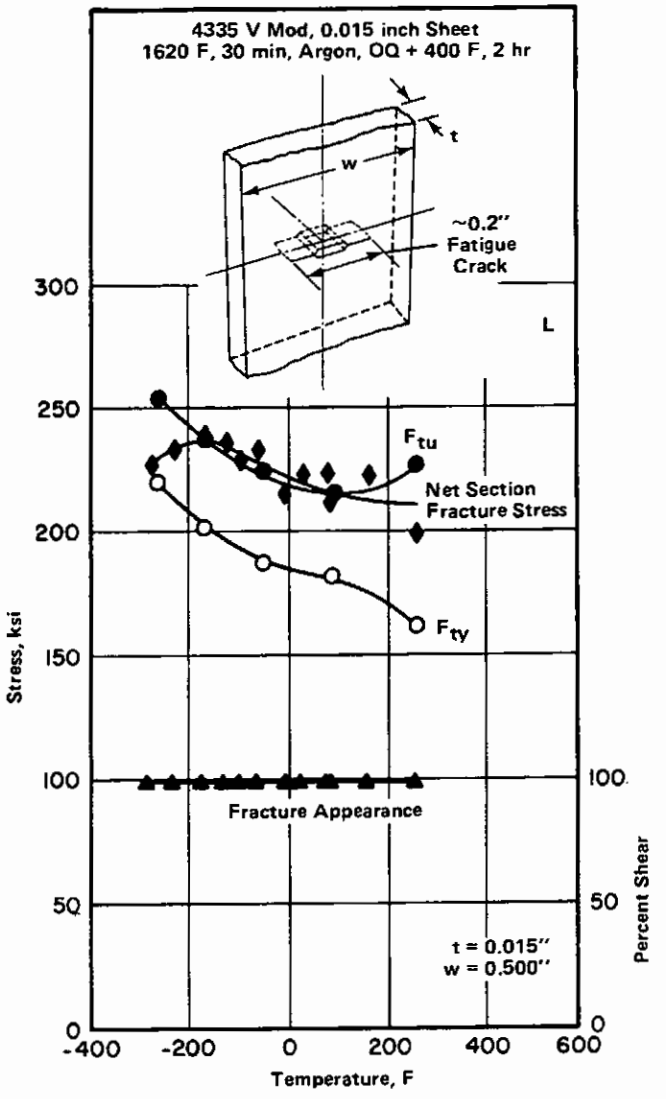


FIGURE 3.03712. EFFECT OF TEST TEMPERATURE ON TENSILE PROPERTIES, FRACTURE APPEARANCE, AND NET SECTION FRACTURE STRESS OF AIR MELTED, QUENCHED AND TEMPERED 0.015 INCH SHEET (38)

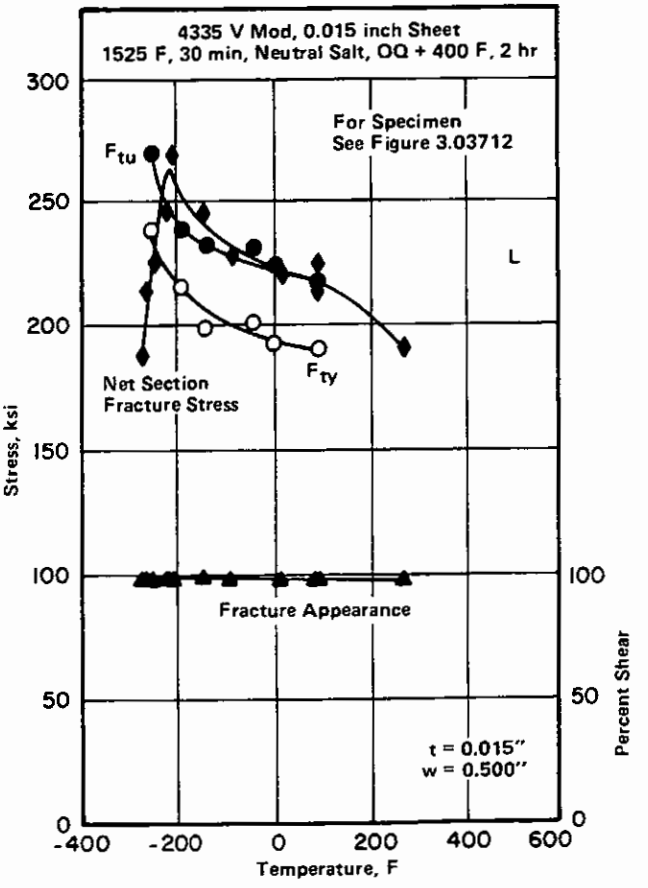


FIGURE 3.03713. EFFECT OF TEST TEMPERATURE ON TENSILE PROPERTIES, FRACTURE APPEARANCE, AND NET SECTION FRACTURE STRESS OF AIR MELTED, QUENCHED AND TEMPERED 0.015 INCH SHEET (38)

Fe
0.35 C
1.8 Ni
0.8 Cr
0.35 Mo
0.2 V

4335 V Mod

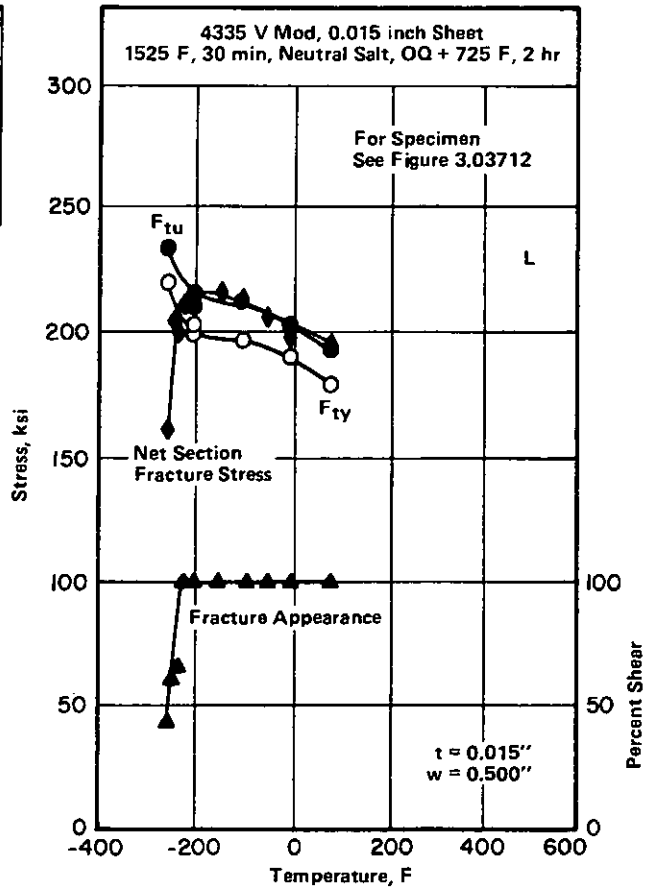


FIGURE 3.03714. EFFECT OF TEST TEMPERATURE ON TENSILE PROPERTIES, FRACTURE APPEARANCE, AND NET SECTION FRACTURE STRESS OF AIR MELTED, QUENCHED AND TEMPERED 0.015 INCH SHEET (38)

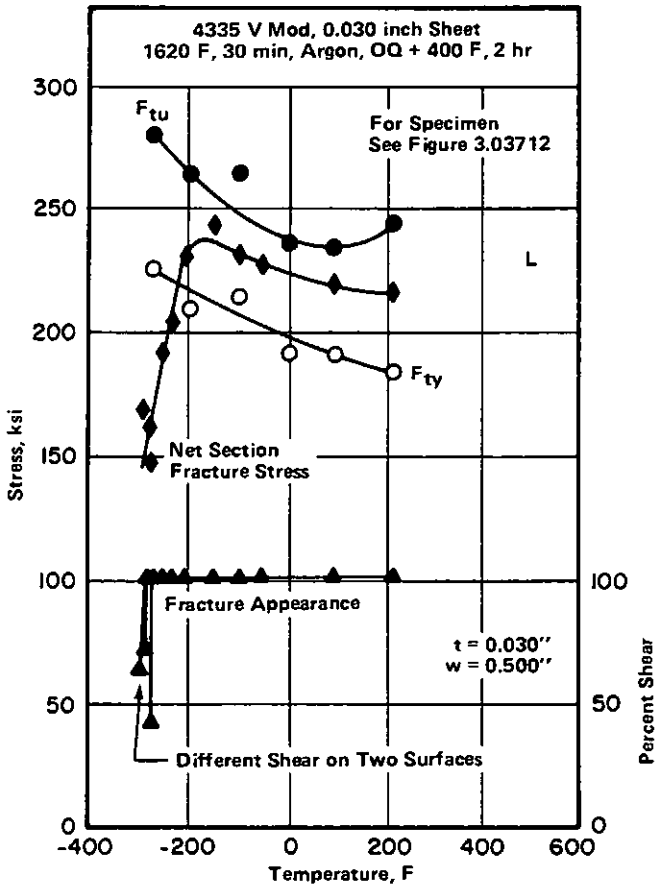


FIGURE 3.03715. EFFECT OF TEST TEMPERATURE ON TENSILE PROPERTIES, FRACTURE APPEARANCE, AND NET SECTION FRACTURE STRESS OF AIR MELTED, QUENCHED AND TEMPERED 0.030 INCH SHEET (38)

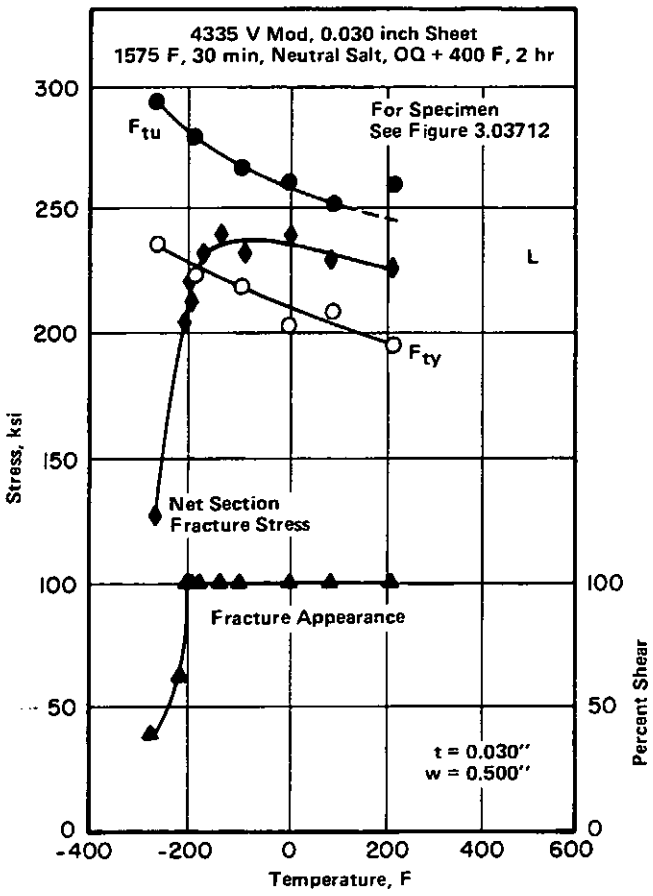


FIGURE 3.03716. EFFECT OF TEST TEMPERATURE ON TENSILE PROPERTIES, FRACTURE APPEARANCE, AND NET SECTION FRACTURE STRESS OF AIR MELTED, QUENCHED AND TEMPERED 0.030 INCH SHEET (38)

Fe
0.35 C
1.8 Ni
0.8 Cr
0.35 Mo
0.2 V

4335 V Mod

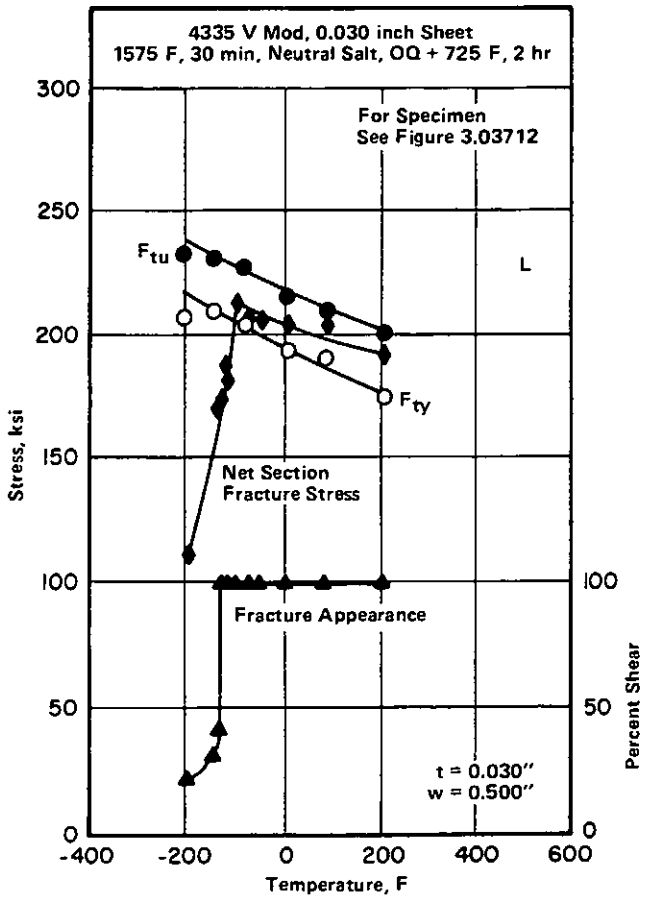


FIGURE 3.03717. EFFECT OF TEST TEMPERATURE ON TENSILE PROPERTIES, FRACTURE APPEARANCE, AND NET SECTION FRACTURE STRESS OF AIR MELTED, QUENCHED AND TEMPERED 0.030 INCH SHEET (38)

Fe
0.35 C
1.8 Ni
0.8 Cr
0.35 Mo
0.2 V

4335 V Mod

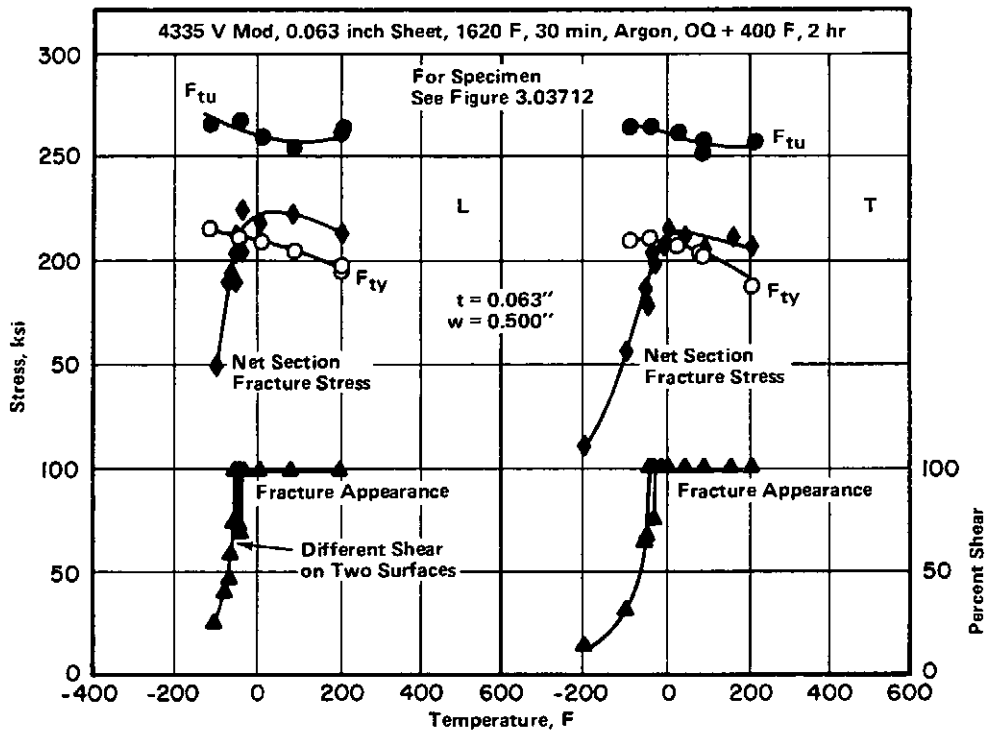


FIGURE 3.03718. EFFECT OF TEST TEMPERATURE ON TENSILE PROPERTIES, FRACTURE APPEARANCE, AND NET SECTION FRACTURE STRESS OF AIR MELTED, QUENCHED AND TEMPERED 0.063 INCH SHEET (38)

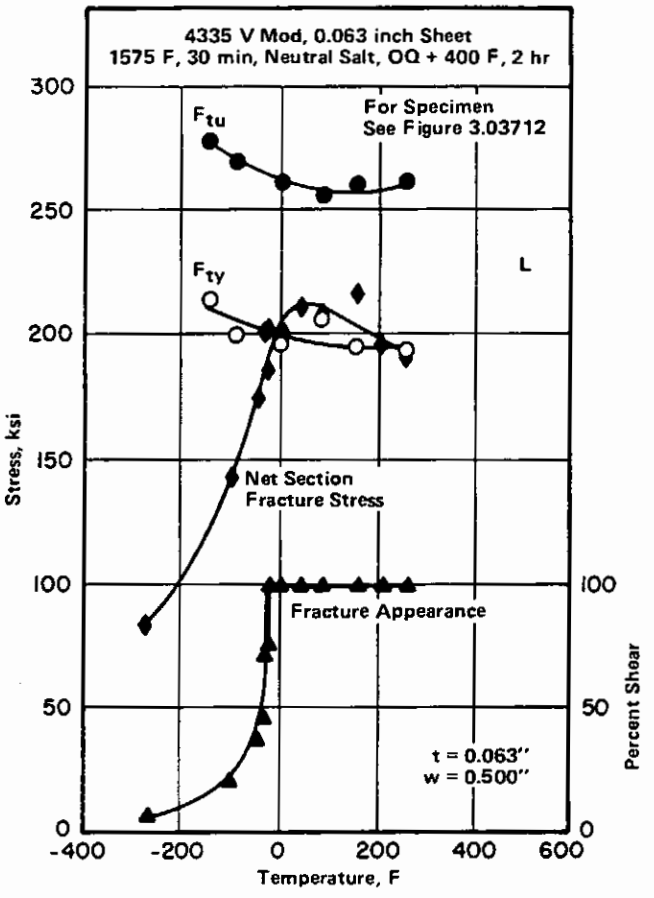


FIGURE 3.03719. EFFECT OF TEST TEMPERATURE ON TENSILE PROPERTIES, FRACTURE APPEARANCE, AND NET SECTION FRACTURE STRESS OF AIR MELTED, QUENCHED AND TEMPERED 0.063 INCH SHEET (38)

Fe
0.35 C
1.8 Ni
0.8 Cr
0.35 Mo
0.2 V

4335 V Mod

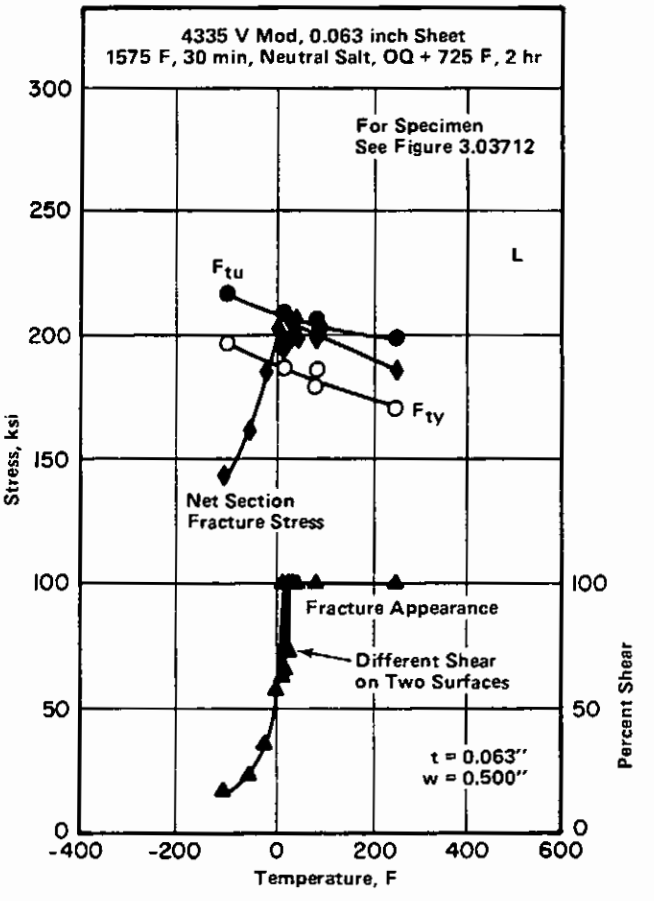


FIGURE 3.03720. EFFECT OF TEST TEMPERATURE ON TENSILE PROPERTIES, FRACTURE APPEARANCE, AND NET SECTION FRACTURE STRESS OF AIR MELTED, QUENCHED AND TEMPERED 0.063 INCH SHEET (38)

Fe
0.35 C
1.8 Ni
0.8 Cr
0.35 Mo
0.2 V

4335 V Mod

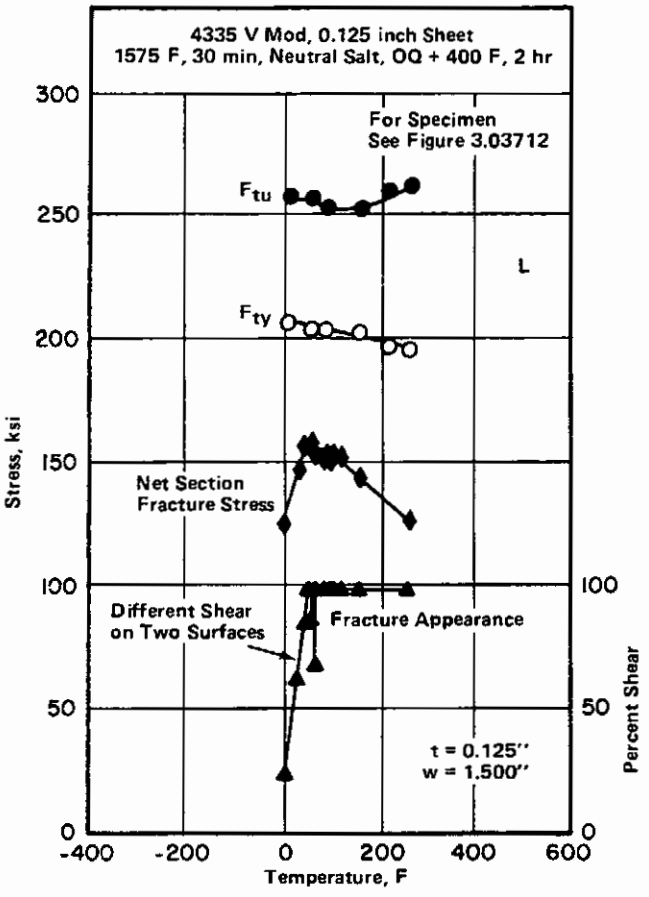


FIGURE 3.03721. EFFECT OF TEST TEMPERATURE ON TENSILE PROPERTIES, FRACTURE APPEARANCE, AND NET SECTION FRACTURE STRESS OF AIR MELTED, QUENCHED AND TEMPERED 0.125 INCH SHEET (38)

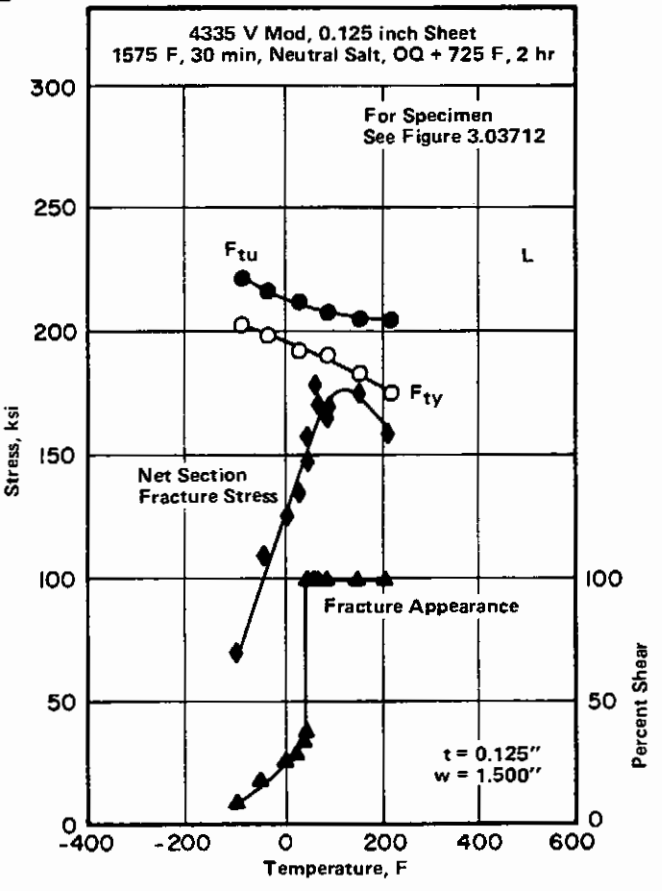


FIGURE 3.03722. EFFECT OF TEST TEMPERATURE ON TENSILE PROPERTIES, FRACTURE APPEARANCE, AND NET SECTION FRACTURE STRESS OF AIR MELTED, QUENCHED AND TEMPERED 0.125 INCH SHEET (38)

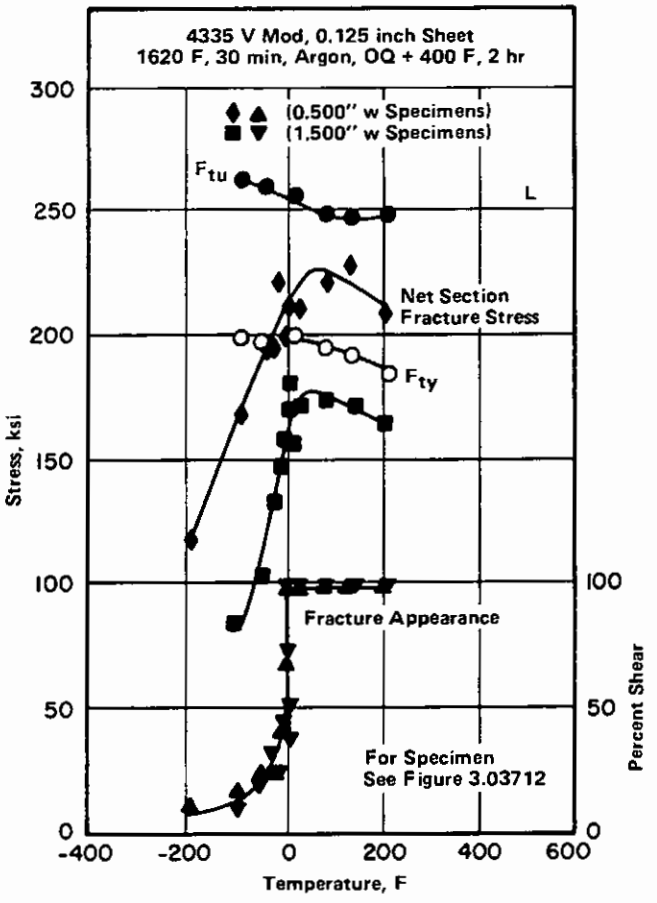


FIGURE 3.03723. EFFECT OF TEST TEMPERATURE ON TENSILE PROPERTIES, FRACTURE APPEARANCE, AND NET SECTION FRACTURE STRESS OF AIR MELTED, QUENCHED AND TEMPERED 0.125 INCH SHEET (38)

Fe
0.35 C
1.8 Ni
0.8 Cr
0.35 Mo
0.2 V

4335 V Mod

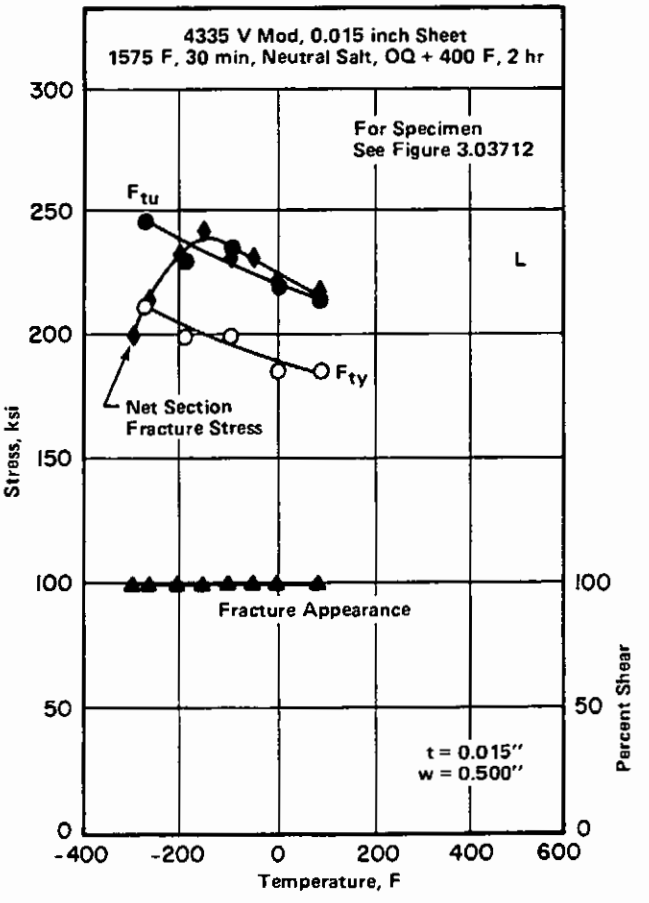


FIGURE 3.03724. EFFECT OF TEST TEMPERATURE ON TENSILE PROPERTIES, FRACTURE APPEARANCE, AND NET SECTION FRACTURE STRESS OF CONSUTRODE VACUUM MELTED, QUENCHED AND TEMPERED 0.015 INCH SHEET (38)

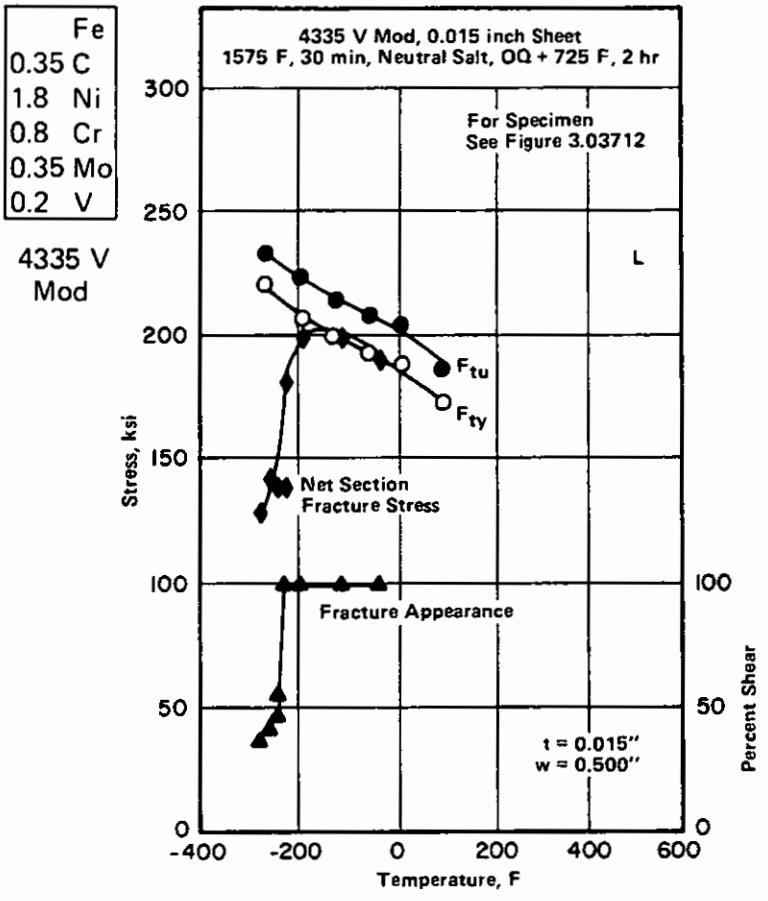


FIGURE 3.03725. EFFECT OF TEST TEMPERATURE ON TENSILE PROPERTIES, FRACTURE APPEARANCE, AND NET SECTION FRACTURE STRESS OF CONSUTRODE VACUUM MELTED, QUENCHED AND TEMPERED 0.015 INCH SHEET (38)

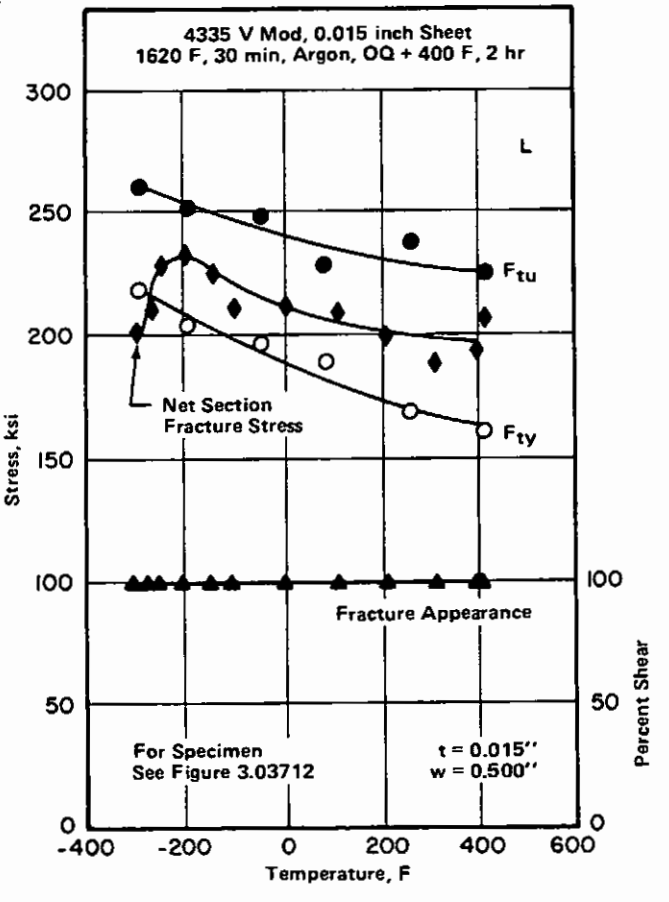


FIGURE 3.03726. EFFECT OF TEST TEMPERATURE ON TENSILE PROPERTIES, FRACTURE APPEARANCE, AND NET SECTION FRACTURE STRESS OF CONSUTRODE VACUUM MELTED, QUENCHED AND TEMPERED 0.015 INCH SHEET (38)

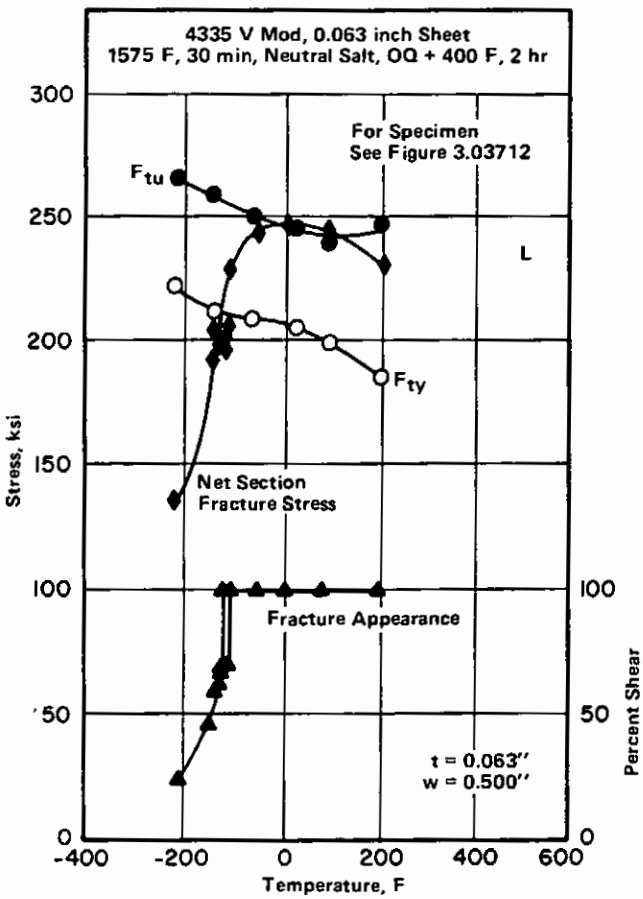


FIGURE 3.03727. EFFECT OF TEST TEMPERATURE ON TENSILE PROPERTIES, FRACTURE APPEARANCE, AND NET SECTION FRACTURE STRESS OF CONSUTRODE VACUUM MELTED, QUENCHED AND TEMPERED 0.063 INCH SHEET (38)

Fe
0.35 C
1.8 Ni
0.8 Cr
0.35 Mo
0.2 V

4335 V Mod

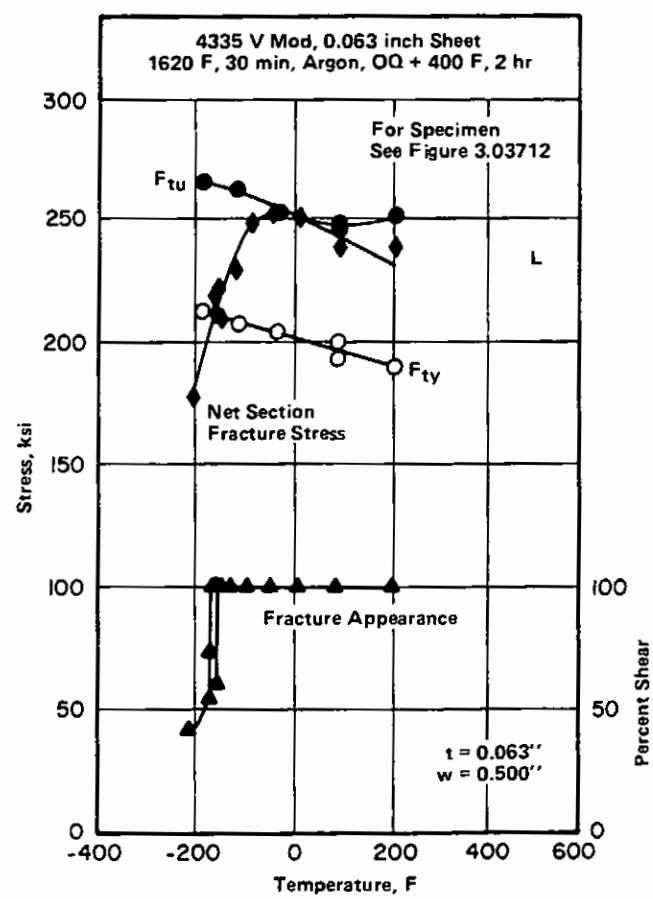


FIGURE 3.03728. EFFECT OF TEST TEMPERATURE ON TENSILE PROPERTIES, FRACTURE APPEARANCE, AND NET SECTION FRACTURE STRESS OF CONSUTRODE VACUUM MELTED, QUENCHED AND TEMPERED 0.063 INCH SHEET (38)

Fe
0.35 C
1.8 Ni
0.8 Cr
0.35 Mo
0.2 V

4335 V Mod

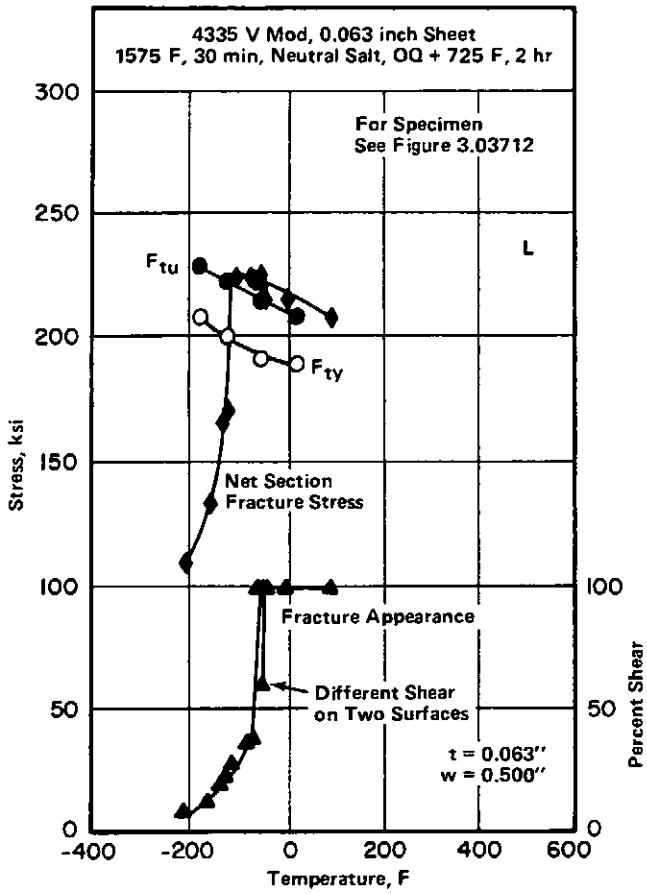


FIGURE 3.03729. EFFECT OF TEST TEMPERATURE ON TENSILE PROPERTIES, FRACTURE APPEARANCE, AND NET SECTION FRACTURE STRESS OF CONSUTRODE VACUUM MELTED, QUENCHED AND TEMPERED 0.063 INCH SHEET (38)

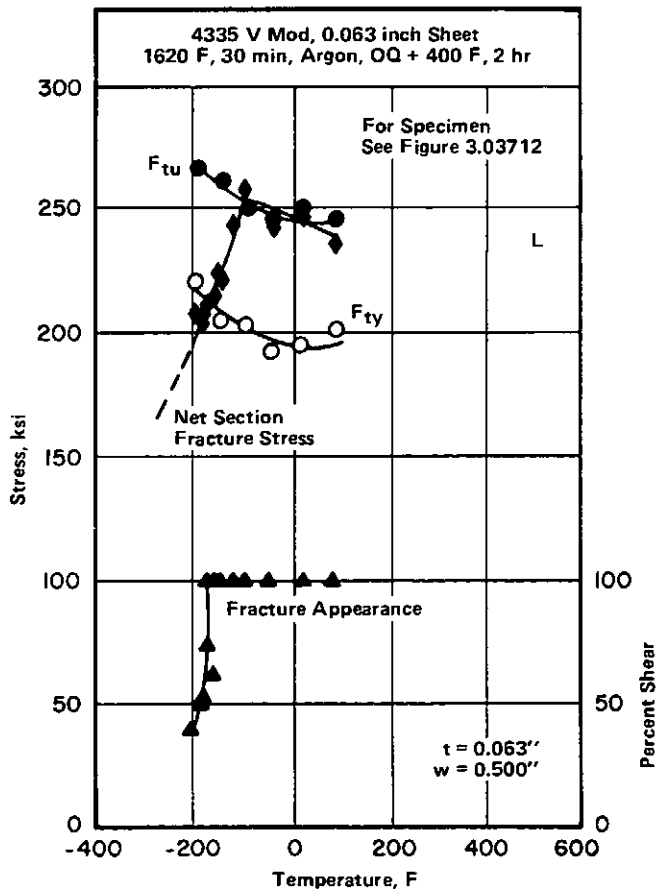


FIGURE 3.03730. EFFECT OF TEST TEMPERATURE ON TENSILE PROPERTIES, FRACTURE APPEARANCE, AND NET SECTION FRACTURE STRESS OF CONSUTRODE VACUUM MELTED, QUENCHED AND TEMPERED 0.063 INCH SHEET (38)

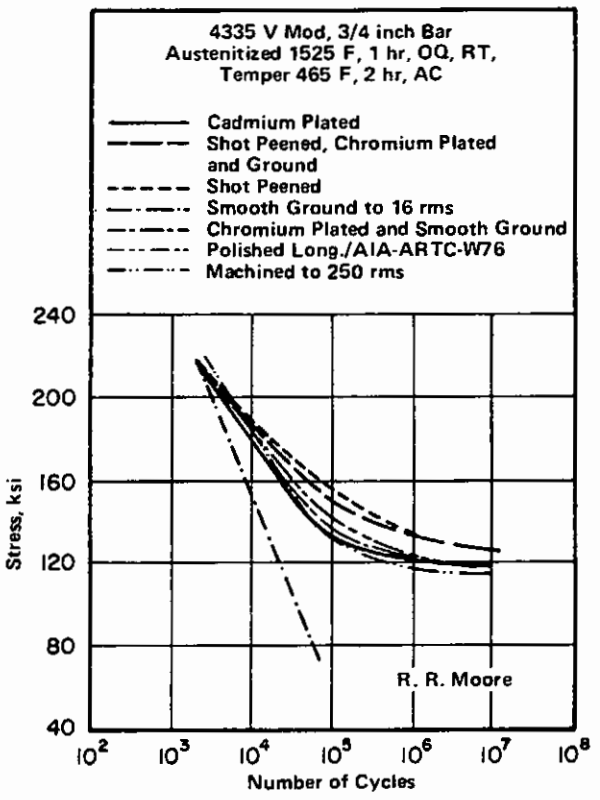
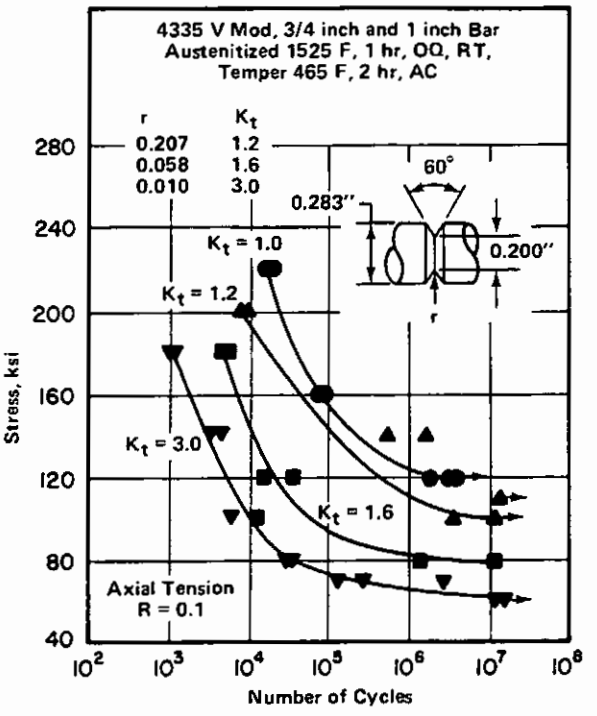


FIGURE 3.051. S-N CURVES FOR BAR WITH VARIOUS SURFACE TREATMENTS (24)



Fe
0.35 C
1.8 Ni
0.8 Cr
0.35 Mo
0.2 V

4335 V Mod

FIGURE 3.052. S-N CURVES FOR SMOOTH AND NOTCHED BAR (25)

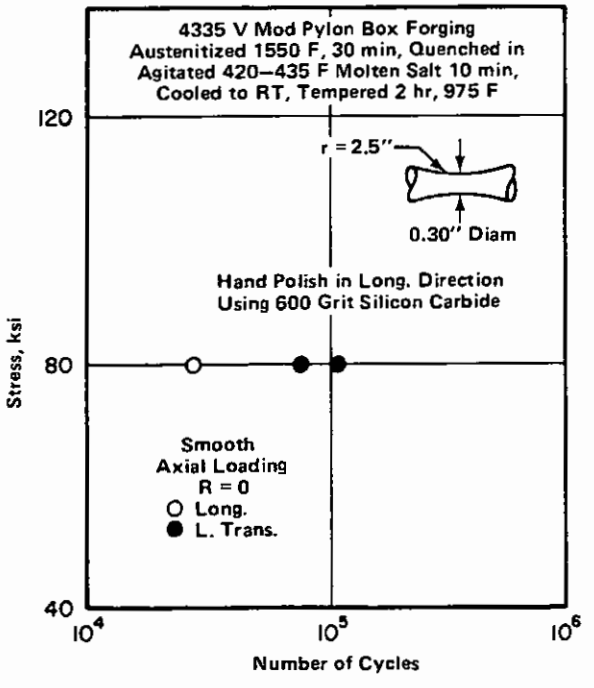


FIGURE 3.053. FATIGUE LIFE AT 80 KSI (R = 0) FOR FORGING (34)

Fe
0.35 C
1.8 Ni
0.8 Cr
0.35 Mo
0.2 V

4335 V Mod

Alloy	4335 V Mod	
Form	Hollow Extrusions With Two External Diameters (Approx. 9.5 in. and 7 in.) for 105 mm Gun Tube	
Condition	Austenitized at 1550 F (Time Unspecified), OD and ID Quenched With Agitated Water, Tempered 1060 F for 4 hr	
Specimen and Orientation	C Shape, T-S	
Location	Applied ΔK, ksi $\sqrt{in.}$	da/dN[(a)], in./cycle
Breech End of Extrusion	27.3	5.05×10^{-6}
Mid-Length of Breech	27.3	5.75×10^{-6}
Muzzle End of Extrusion	35.1	10.8×10^{-6}

(a) Average of two specimens, one from each of two extrusions.

TABLE 3.054. FATIGUE CRACK PROPAGATION RATE OF GUN-TUBE EXTRUSION (36)

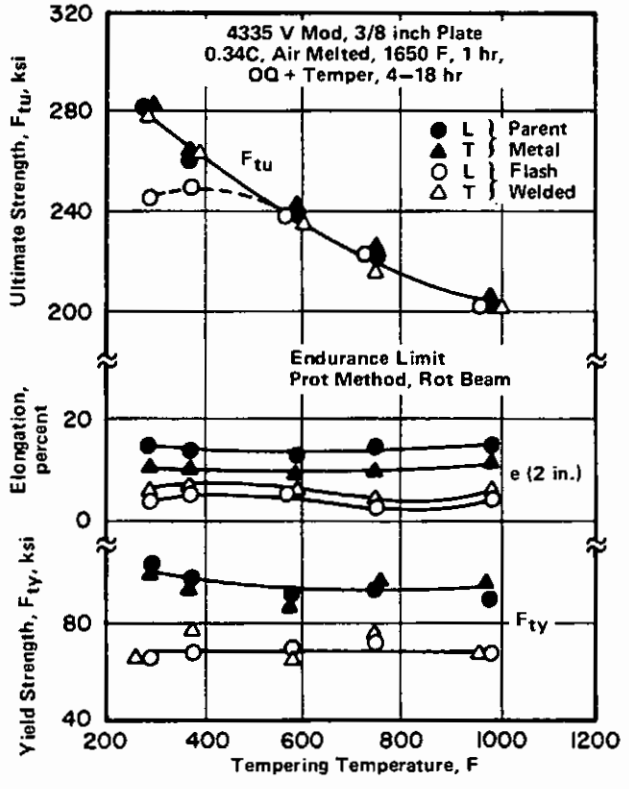


FIGURE 4.031. EFFECT OF FLASH WELDING AND TEMPERING TEMPERATURE ON TENSILE PROPERTIES AND ENDURANCE LIMIT OF AIR MELTED PLATE (15)

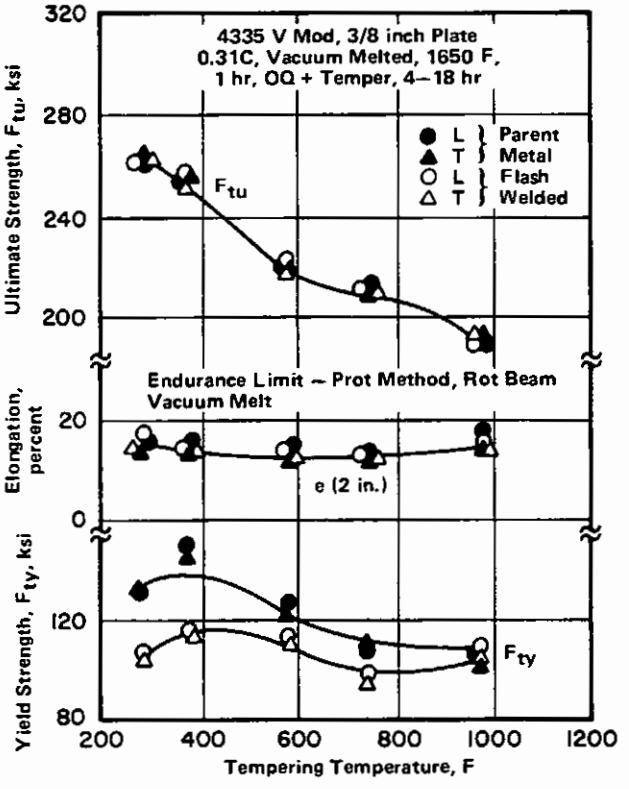


FIGURE 4.032. EFFECT OF FLASH WELDING AND TEMPERATURE ON TENSILE PROPERTIES AND ENDURANCE LIMIT OF VACUUM MELTED PLATE (15)

	Fe
0.4	C
1.8	Ni
0.8	Cr
0.25	Mo

4340

1 **GENERAL**

4340 is a low alloy steel with excellent hardenability because of its appreciable contents of carbon, nickel, chromium, and molybdenum. As a result, quench-and-temper heat treatments develop excellent combinations of strength and toughness uniformly over a wide range of section sizes. These characteristics make the alloy attractive for many critical applications from -200 to 900 F, particularly in heavy sections for which leaner alloy steels are not capable of developing uniformly high properties. Some of the current applications include gears, pinions, crankshafts, piston rods, landing gear, bolts, and other fasteners. Because of its high hardenability, its weldability is inferior to that of steels with lower contents of carbon and other alloying elements. Consequently, it is not normally recommended for applications in which high weld joint efficiently is essential. Nevertheless, with proper precautions it can be welded with arc and gas welding processes and with the electron beam technique.

1.01 **Commercial Designation**

4340.

1.02 **Alternate Designations**

AISI 4340, SAE 4340, E 4340, 4340 H, and UNS G43400.

1.021 The E 4340 designation indicates electric furnace melted.

1.022 The 4340 H designation indicates that the steel is made within strict hardenability limits; consequently, wider composition limits are allowed for individual alloying elements.

1.03 **Specifications**

Specifications, Table 1.03.

1.04 **Composition**

Composition, Table 1.04.

1.05 **Heat Treatment**

1.051 Normalize, 1550 to 1700 F, air cool (30) (33) (69) (70) (76).

1.052 Temper after normalize for improved machinability and toughness, 800 to 1200 F 1/2 hr minimum, air cool.

1.053 Anneal, 1450 to 1575 F, air cool (30) (33) (76).

1.054 Spheroidize anneal, 1275 F hold 2 hr, increase to 1325 F hold 2 hr, cool to 1200 F hold 6 hr, furnace cool to 1100 F, air cool. Alternative schedule, 1375 F several hours, cool to room temperature (33) (76).

1.055 Stress relief, 1100 to 1250 F, air cool (33) (69) (76).

1.056 Harden, 1475 to 1600 F, oil-quench to about 150 F. For sections greater than about 3 inch in diameter, better uniformity is obtained by water-quenching, but the risks of distortion and quench cracks are greatly increased. A modified technique called martempering, which minimizes distortion and cracking, consists of quenching into hot salt at 450 to 525 F, holding until the parts are uniform in temperature which requires about 2 to 6 minutes, and then air cooling. Sections up to about 4 inch in diameter can be fully hardened in this manner (30) (33) (69) (70) (76).

1.057 Temper after hardening, 350 to 450 F or 750 to 1200 F, air cool or water-quench. Tempering in the range 450 to 750 F is not recommended because tempered martensite embrittlement, common to most low alloy steels, occurs in that range. The 4340 alloy is resistant to temper embrittlement which occurs in some low alloy steels in the range 800 to 1100 F. In order to minimize quench cracking, 4340 parts should be placed in the tempering furnace shortly after the quench operation while they are between 150 F and ambient temperature (30) (33) (69) (70) (76).

1.06 **Hardness**

1.061 Effect of tempering temperature on hardness, Figure 1.061.

1.062 Effect of bar diameter on surface hardness for various heat treated conditions, Figure 1.062.

1.063 Effect of bar diameter on as-quenched hardness at various depths in bar, Figure 1.063.

1.064 Effect of temperatures from 80 F to -423 F on hardness of bar heat treated to a hardness level of R_C 51, Figure 1.064.

1.065 End-quench hardenability, Figure 1.065.

1.07 **Forms and Conditions Available**

1.071 Wrought products including bars, rods, plates, sheets, tubes, and billets are available in the annealed, normalized or spheroidized condition. Forgings and castings are available in any heat treated condition.

1.08 **Melting and Casting Practice**

1.081 The 4340 alloy is generally air melted in basic electric, basic open hearth, or basic oxygen furnaces. For some applications requiring exceptional quality, it is induction or consumable electrode remelted in vacuum or electroslag refined.

1.09 **Special Considerations**

1.091 Most of the common electroplating processes including chromium, cadmium, nickel, copper, silver, and zinc tend to induce some degree of hydrogen embrittlement in 4340 steel that has been heat treated to tensile strength (F_{tu}) levels above 180 ksi. Most acid pickling processes can also induce hydrogen embrittlement at high strength levels. One exception is nitric acid pickling at concentrations above 1.0N. Anodic cleaning processes and alkaline descaling are nonhydrogen embrittling. Baking 2 to 6 hr at 375 F normally relieves hydrogen embrittlement resulting from electroplating or acid pickling (4) (5).

1.0911 Adding rare-earths such as cerium and lanthanum to 4340 tends to minimize or prevent hydrogen embrittlement (12).

	Fe
0.4	C
1.8	Ni
0.8	Cr
0.25	Mo

4340

1.09111 Effects of cerium content on delayed fracture in air of 0.5-inch thick precracked specimens that have been cathodically charged with hydrogen, Figure 1.09111.

1.092 Like other martensite and ferrite steels, 4340 undergoes a transition from ductile to brittle behavior at low temperatures; the transition temperature varies with the heat treatment and the degree of stress concentration. (See Figures 3.0331 through 3.0339, 3.03711 through 3.03715, and Figure 3.03721.)

1.093 Increasing contents of sulfur and phosphorus are detrimental to the notch toughness of 4340. (See Figures 3.0237, 3.02724, 3.02727, 3.0337, and 3.0338). Treatment of the molten alloy with rare-earths minimizes the adverse effects of sulfur (see Figure 3.0338).

1.094 Surface decarburization, which can occur during high temperature processing or during heat treatment, is detrimental to fatigue properties, particularly at the higher strength levels. For optimum fatigue properties, decarburization should be prevented, for example, by controlling the atmosphere during heat treatment, or by removing critical decarburized areas by machining.

1.095 Thin sections tend to air harden; that is, they may become hard and brittle (similar to the as-oil-quenched properties rather than the usual normalized properties) when air cooled from temperatures above 1400 F. Tempering restores toughness and ductility and reduces hardness of air hardened materials just as it does for oil-quenched material.

1.096 For quenched-and-tempered 4340, fracture toughness increases with increasing austenitizing temperatures when subsequent tempering temperatures are below 600 F (see Figures 3.02723, 3.02724, and 3.02725 and Table 3.02726). On the other hand, impact properties, as well as other measures of ductility, decrease with increasing austenitizing temperatures (see Figures 3.0234, 3.0235, and 3.0236). Because the reason for this anomaly is not presently understood, the use of unusually high austenitizing temperatures to obtain high fracture toughness is not generally practiced.

2 PHYSICAL AND ENVIRONMENTAL EFFECTS

2.01 Thermal Properties

2.011 Melting range, about 2740 F (31) (32).

2.012 Phase changes.

2.0121 Time-temperature-transformation diagram, Figure 2.0121.

2.0122 Upon heating under equilibrium conditions, transformation from pearlite or martensite to austenite starts at 1335 F (A_c1) and is complete at 1425 F (A_c3) (69).

2.0123 Upon slow cooling under equilibrium conditions, the transformation from austenite to pearlite starts at 1310 F (A_r3) and is complete at 1210 F (A_r1) (69).

2.0124 Upon rapid quenching from the austenitic condition, the transformation to martensite starts at 570 F (Ms) and is complete at 400 F (Mf)(34).

2.013 Thermal conductivity, Figure 2.013.

2.014 Thermal expansion, Figure 2.014.

2.015 Specific heat, 0.107 Btu/lb ft (31) (32).

2.016 Thermal diffusivity.

2.02 Other Physical Properties

2.021 Density, 0.283 lb/in.^{3} (31) (32).

2.022 Electrical properties.

2.0221 Electrical properties from room temperature to 1100 F, Figure 2.0221.

2.023 Magnetic properties. Alloy is ferromagnetic.

2.024 Emittance.

2.025 Damping capacity.

2.03 Chemical Environment

2.031 Since the alloy is susceptible to rusting, it should be protected by means of paint, electroplate, anode, or other suitable corrosion inhibitor for long time exposures in moist, marine, or other corrosive environments.

2.032 An exhaustive study, including laboratory salt spray tests and alternate immersions in salt solutions, as well as outdoor exposures in urban and seacoast environments, showed that 4340 has good resistance to stress-corrosion when heat treated to strength levels below 180 ksi, which requires tempering temperatures above 950 F. The resistance decreases with increasing tensile strength above the 180 ksi level. Also, the susceptibility is greater when stresses are applied in the short transverse and long transverse directions, rather than in the longitudinal direction (13).

2.0321 Threshold stress intensity factor (K_{Iscc}) for stress-corrosion cracking of plate in aerated 3 percent aqueous sodium-chloride solution at various corresponding levels of tensile strength and critical stress intensity factor (K_{Ic}), Table 2.0321.

2.0322 Effect of variations in yield strength on threshold stress intensity factor for stress-corrosion crack growth in 3.5 percent solution of sodium-chloride in water, Figure 2.0322.

2.0323 Effect of yield strength on resistance to stress-corrosion cracking of heat treated 4340 in aqueous salt solutions, Figure 2.0323.

2.0324 Effect of increasing yield strength, induced by decreasing tempering temperature or by increasing amounts of cold rolling up to 50 percent reduction, on resistance to stress-corrosion cracking in an environment of hydrogen-sulfide (H_2S) gas at 50 psig at room temperature, Figure 2.0324.

2.0325 Effect of cold working and stress relief on resistance to stress-corrosion cracking in an environment of hydrogen-sulfide (H_2S) gas at 50 psig at room temperature, Figure 2.0325.

2.0326 Time to stress-corrosion failure of quenched-and-tempered plate in distilled water at various temperatures, Figure 2.0326.

2.0327 Effect of temperature on resistance to stress-corrosion cracking in an environment of dry hydrogen gas at 80 psig, Figure 2.0327.

2.0328 Effect of temperature on resistance to stress-corrosion cracking in an environment of hydrogen-sulfide gas at 50 psig, Figure 2.0328.

2.0329 Effect of gas pressure on resistance to stress-corrosion cracking in environments of hydrogen and hydrogen-sulfide gases at room temperature, Figure 2.0329.

2.03210 Effect of cerium additions on time to stress-corrosion failure in an aqueous 3.5-percent sodium-chloride solution, Figure 2.03210.

2.03211 Effect of a brief prestress of precracked specimens on the threshold stress intensity (K_{Iscc}) for stress-corrosion cracking in 3.5 percent aqueous sodium-chloride solution, Figure 2.03211.

2.04 Nuclear Environment

2.041 In general, nuclear irradiation tends to cause the hardness and strength of low alloy steels to increase and the ductility and toughness to decrease. Quenched and tempered material is affected somewhat less than normalized or annealed material.

3 MECHANICAL PROPERTIES

3.01 Specified Mechanical Properties

Specified mechanical properties, Table 3.01.

3.02 Mechanical Properties at Room Temperature

3.021 Tension – Stress-strain diagrams – Tension properties.

3.0211 Room temperature tensile stress-strain curves for bar heat treated to various strength levels, Figure 3.0211.

3.0212 Complete tensile stress-strain curves at room temperature for tube in two different conditions, Figure 3.0212.

3.0213 Effect of tempering temperature on tensile properties of oil-quenched bar, Figure 3.0213.

3.0214 Effect of tempering temperature on tensile properties of normalized bar, Figure 3.0214.

3.0215 Effect of section size on tensile properties of bar in several heat treated conditions, Figure 3.0215.

3.0216 Effect of strain rate on tensile properties of oil-quenched-and-tempered bar at room temperature, Figure 3.0216.

3.0217 Effect of strain rate on the ultimate tensile strength and elongation of bar in various heat treated conditions, Figure 3.0217.

3.0218 Tensile properties for different orientations in forging, Table 3.0218.

3.0219 Effects of various tempering temperatures on tensile properties of electroslag remelted plate after conventional oil-quenching and after martempering, Table 3.0219.

3.02110 Comparison of tensile properties of air induction melted cross rolled plate of normal purity with those of high purity plate produced by vacuum induction melting followed by vacuum arc remelting, Table 3.02110.

3.02111 Effects of cold working and stress relief on room temperature tensile properties of oil-quenched-and-tempered forgings, Figure 3.02111.

3.02112 Effects of tempering temperature and 10 percent cold reduction and aging at 400 F on tensile properties of oil-quenched bar, Figure 3.02112.

3.02113 Effects of cold working and aging on tensile properties of bar that had previously been oil-quenched-and-tempered at 1000 F, Figure 3.02113.

3.02114 Effects of cold working and aging on tensile properties of bar that had been previously oil-quenched-and-tempered at 1150 F, Figure 3.02114.

3.02115 Effects of cold work by hydrostatic extrusion and of retempering on tensile properties of bar that had been previously oil-quenched-and-tempered, Table 3.02115.

3.02116 Effect of cerium additions on room temperature tensile properties, Figure 3.02116.

3.02117 Tensile properties of annealed bar, Table 3.02117.

3.02118 Comparison of room temperature tensile properties in two heat treated conditions of cast keel block and wrought plate made from the same air induction melted heat, Table 3.02118.

3.022 Compression – Stress-strain diagrams – Compression properties.

3.0221 Room temperature stress-strain curve in compression for bar heat treated to F_{tu} = 260 ksi, Figure 3.0221.

3.0222 Relationship between compressive yield strength and tensile strength, Figure 3.0222.

3.023 Impact.

3.0231 Effect of tempering temperature on impact properties of oil-quenched bar at room temperature, Figure 3.0231.

3.0232 Effect of tempering temperature on impact properties of normalized bar at room temperature, Figure 3.0232.

3.0233 Effects of tempering temperature and melting practice on impact properties at room temperature, Figure 3.0233.

3.0234 Effects of tempering temperature and austenitizing temperature and resulting grain size on impact properties at room temperature of bar that had been air melted and vacuum degassed, Figure 3.0234.

3.0235 Effects of tempering temperature after two different austenitizing treatments on impact properties at room temperature of air melted and electroslag refined forgings, Figure 3.0235.

3.0236 Effect of austenitizing temperature on the room temperature impact properties of oil-quenched-and-tempered vacuum arc remelted plate, Figure 3.0236.

3.0237 Effects of tempering temperature and phosphorus content on impact properties at room temperature of plate that had been vacuum induction melted, Figure 3.0237.

3.0238 Comparison of room temperature Charpy V-notch impact properties in two heat treated conditions of cast keel block and wrought plate made from the same induction melted heat, Table 3.0238.

3.024 Bending.

3.025 Torsion and shear.

	Fe
0.4	C
1.8	Ni
0.8	Cr
0.25	Mo

4340

	Fe
0.4	C
1.8	Ni
0.8	Cr
0.25	Mo

4340

3.0251 Relationship between shear strength in torsion and ultimate tensile strength, Figure 3.0251.

3.0252 Effect of tempering temperature on shear strength in torsion of oil-quenched bar of two different sizes, Figure 3.0252.

3.026 Bearing.

3.0261 Relationship between bearing properties and ultimate tensile strength, Figure 3.0261.

3.027 Stress concentration.

3.0271 Notch properties.

3.02711 Effects of tempering temperature, hydrogen content, stress concentration, and rate of loading on the notched tensile strength of bar, Figure 3.02711.

3.02712 Effect of tempering temperature on sharp-notch strength of sheet, Figure 3.02712.

3.02713 Effect of tempering temperature and specimen orientation on crack strength of bar, Figure 3.02713.

3.02714 Effect of tempering temperature on sharp-notch strength of bar cold reduced 10 percent after tempering, Figure 3.02714.

3.02715 Relationship between ultimate tensile strength (F_{tu}) and notched tensile strength (NTS) for various size test bars, stress concentrations, and orientations, Figure 3.02715.

3.02716 Effect of specimen cross section, notch root radius, and notch depth on notch strength ratio of bar, Figure 3.02716.

3.02717 Effect of cold working on sharp-notch strength of bars previously oil-quenched-and-tempered at 1000 F, Figure 3.02717.

3.0272 Fracture toughness.

3.02721 Effect of tempering temperature on range of fracture toughness resulting from normal variations in melting and processing practices, chemical composition, and impurity content, Figure 3.02721.

3.02722 Effect of tempering temperature on the fracture toughness of aircraft-quality (vacuum arc remelted) bar, Figure 3.02722.

3.02723 Effect of tempering temperature after two different austenitizing treatments on fracture toughness at room temperature of air melted and electroslag refined forgings, Figure 3.02723.

3.02724 Effects of tempering and austenitizing temperatures and phosphorus content on room temperature fracture toughness of plate that has been vacuum induction melted, Figure 3.02724.

3.02725 Effect of austenitizing temperature on the room temperature fracture toughness of oil-quenched-and-tempered vacuum arc remelted plate, Figure 3.02725.

3.02726 Effects of various step-quenching treatments on fracture toughness of aircraft-quality plate initially austenitized at 2190 F and subsequently tempered at 390 F, Table 3.02726.

3.02727 Effect of sulfur plus phosphorus content on fracture toughness, Figure 3.02727.

3.02728 Comparison of room temperature fracture toughness in two heat treated conditions of cast keel block and wrought plate made from the same induction melted heat, Table 3.02728.

3.028 Combined properties.

3.03 Mechanical Properties at Various Temperatures

3.031 Tension – Stress-strain diagrams – Compression properties.

3.0311 Tensile stress-strain curves at room temperature and elevated temperatures for sheet heat treated to F_{tu} = 200 ksi, Figure 3.0311.

3.0312 Tensile stress-strain curves at room temperature and low temperatures for bar heat treated to F_{tu} = 270 ksi, Figure 3.0312.

3.0313 Tensile stress-strain curves at various temperatures for tube in two different conditions, Figure 3.0313.

3.0314 Complete tensile stress-strain curves at 662 F for tube in two different conditions, Figure 3.0314.

3.0315 Effect of elevated temperatures on tensile properties of bar and sheet heat treated to various strength levels, Figure 3.0315.

3.0316 Effect of elevated temperatures up to 850 F on tensile properties of bar in various heat treated conditions, Figure 3.0316.

3.0317 Effect of elevated temperatures on tensile properties of bar normalized and tempered to a hardness level of R_C 32, Figure 3.0317.

3.0318 Effect of elevated temperatures up to 662 F on tensile properties of tube in two different conditions, Figure 3.0318.

3.0319 Effect of temperatures from 1400 to 1900 F on tensile properties of normalized-and-tempered bar, Figure 3.0319.

3.03110 Effect of temperatures from 80 to -200 F on the tensile properties of bar quenched and tempered to two levels of hardness, Figure 3.03110.

3.03111 Effect of temperatures from 80 to -423 F on the tensile properties of plate quenched and tempered to a hardness level of R_C 36, Figure 3.03111.

3.03112 Effect of temperature from 80 to -423 F on the tensile properties of bar quenched and tempered to F_{tu} = 270 ksi, Figure 3.03112.

3.032 Compression – Stress-strain diagrams – Compression properties.

3.0321 Stress-strain curves in compression at room and elevated temperatures for sheeet heat treated to F_{tu} = 200 ksi, Figure 3.0321.

3.0322 Effect of elevated temperatures on compressive yield strength of sheet heat treated to F_{tu} = 200 ksi, Figure 3.0322.

3.033 Impact.

3.0331 Effects of tempering temperature and test temperature on impact properties of oil-quenched bar, Figure 3.0331.

3.0332 Effect of temperatures from 100 F to -300 F on impact properties of oil-quenched bar tempered at 400 to 1200 F, Figure 3.0332.

3.0333 Effect of temperatures from 245 F to -240 F on impact properties of water-quenched bar tempered at 900 to 1100 F, Figure 3.0333.

3.0334 Effect of low temperatures on impact properties of tube in two different conditions, Figure 3.0334.

3.0335 Effect of temperature on impact properties of bar in various heat treated conditions, Figure 3.0335.

3.0336	Effect of low temperatures on the impact properties of bar heat treated to two levels of hardness, Figure 3.0336.
3.0337	Effects of temperature and phosphorus content on impact properties of plate that have been vacuum induction melted, Figure 3.0337.
3.0338	Effects of rare-earth treatment and variations in sulfur content on impact transition curves of vacuum induction melted plate in two heat treated conditions, Figure 3.0338.
3.0339	Comparison of impact properties over a range of temperatures for quenched-and-tempered and normalized-and-tempered 4340, Figure 3.0339.
3.03310	Impact properties at various temperatures for different orientations in forgings, Table 3.03310.
3.03311	Comparison of low temperature impact properties of air induction melted cross rolled plate of normal purity with those of high purity plate produced by vacuum induction melting followed by vacuum arc remelting, Figure 3.03311.
3.034	Bending.
3.035	Torsion and shear.
3.0351	Effect of low temperatures on shear strength of bar quenched and tempered to two levels of hardness, Figure 3.0351.
3.036	Bearing.
3.037	Stress concentration.
3.0371	Notch properties.
3.03711	Effect of temperatures from 80 to -200 F on ratio of notched tensile strength to tensile strength of bar heat treated to two levels of hardness, Figure 3.03711.
3.03712	Effect of temperatures from 80 to -423 F on ratio of notched tensile strength to tensile strength of plate heat treated to a hardness level of R_C 36, Figure 3.03712.
3.03713	Effect of low temperatures on notched strength of bar heat treated to F_{tu} = 270 ksi, Figure 3.03713.
3.03714	Effect of low temperatures on tensile strength and crack strength of sheet in three heat treated conditions, Figure 3.03714.
3.03715	Effect of temperatures from -300 to 300 F on tensile strength and crack strength of vacuum induction melted and vacuum induction remelted bar heat treated to F_{tu} = 265 ksi, Figure 3.03715.
3.0372	Fracture toughness.
3.03721	Effect of temperatures from -100 to 200 F on fracture toughness of plate heat treated to two different strength levels, Figure 3.03721.
3.03722	Fracture toughness at 75 and -200 F of plate heat treated to a room temperature tensile strength level of 275 ksi, Table 3.03722.
3.038	Combined properties.
3.04	Creep and Creep Rutpure Properties
3.041	Stress-rupture properties at 900 - 1100 F of normalized-and-tempered smooth and notched bar, Figure 3.041.
3.05	Fatigue Properties
3.051	Fatigue life of bar at room temperature and at -320 F, Figure 3.051.
3.052	Effect of specimen sizes from 1/8- to 1-inch diameter on fatigue life of bar, Figure 3.052.
3.053	Fatigue life of bare and coated bar in environments of air and 3.5 percent aqueous sodium-chloride solution, Figure 3.053.
3.054	Constant-life fatigue curves at 80 F for smooth and notched bar heat treated to F_{tu} = 260 ksi, Figure 3.054.
3.055	Constant-life fatigue curves at 80 F for smooth and notched bar heat treated to F_{tu} = 150 ksi, Figure 3.055.
3.056	Constant-life fatigue curves at 600 F for smooth and notched bar heat treated to F_{tu} = 150 ksi, Figure 3.056.
3.057	Constant-life fatigue curves at 1000 F for smooth and notched bar heat treated to F_{tu} = 150 ksi, Figure 3.057.
3.058	Fatigue crack-growth rate in air of air melted and electroslag refined forgings that have been oil-quenched and tempered at two different temperatures, Figure 3.058.
3.059	Fatigue crack-growth rate of plate at various strength levels in air and in aerated 3 percent aqueous sodium-chloride solution, Figure 3.059.
3.0510	Effects of various environments and a sodium-borate, sodium-nitrite inhibitor on fatigue crack-growth rate of plate heat treated to two strength levels, Figure 3.0510.
3.0511	Fatigue crack-growth rates for plate tested at room temperature in air at three levels of relative humidity, Figure 3.0511.
3.0512	Fatigue crack-growth rates for plate tested at room temperature in distilled water at three frequencies and in argon at one frequency, Figure 3.0512.
3.0513	Effects of tempering temperature and stress-intensity range on fatigue crack-growth rate in air, Figure 3.0513.
3.06	Elastic Properties
3.061	Poisson's ration, 0.3 (74).
3.062	Modulus of elasticity.
3.0621	Effect of temperatures from -423 to 1200 F on modulus of elasticity, Figure 3.0621.
3.063	Modulus of rigidity, 11.2 x 10^3 ksi (74).
3.064	Tangent modulus.
3.0641	Tangent modulus curves in compression at room and elevated temperatures, Figure 3.0641.
3.065	Secant modulus.
3.0651	Secant modulus curves in compression at room and elevated temperatures, Figure 3.0651.

Fe	
0.4	C
1.8	Ni
0.8	Cr
0.25	Mo

4340

4 FABRICATION

4.01 Forming

4.011 Although the cold formability of 4340 is inferior to that of steels with lower carbon and alloy contents, it can be cold formed to a limited extent. Optimum formability is obtained in the spheroidize annealed condition.

4.012 Forging and other hot working operations can readily be conducted on 4340 in the temperature range of 1950 to 2250 F. Because of its relatively high alloy content, somewhat more

	Fe
0.4	C
1.8	Ni
0.8	Cr
0.25	Mo

4340

force is required than for hot working plain carbon or lower alloy steels. Slow cooling, preferably in a furnace, is recommended after hot work (32) (33) (70).

4.02 Machining and Grinding

4.021 Type 4340 can be machined without difficulty in the annealed and cold drawn conditions. Based on a 100 percent machinability rating for cold rolled B1112 steel, the rating for 4340 is 55 percent in the cold drawn condition and 45 percent in the annealed condition. Machining is more difficult for quenched-and-tempered material; the difficulty increases with increasing hardness. Good machinability is obtained by normalizing and tempering at 1200 F (32) (33).

4.03 Joining

4.031 When fusion welded, 4340 is susceptible to underbead cracking, heat affected zone embrittlement, and thermal stress cracking unless proper precautions and controls are exercised. Proper procedures include the use of low hydrogen electrodes, preheat and interpass temperatures of at least 550 F, and postweld stress relief at 1100 to 1200 F immediately after welding followed by slow cooling. Full quench-and-temper heat treatment after welding is necessary to develop optimum properties in weldments. Type 4340 can be successfully welded by the electron beam method (33) (70) (75).

4.04 Surface Treating

4.041 (See Code 1203, 4140 steel, section 4.04.)

REFERENCES

1 Imhof, E. J., Jr. and Barsom, J. M., "Fatigue and Corrosion Fatigue Crack Growth of 4340 Steel at Various Yield Strengths", Sixth National Symposium on Fracture Mechanics, Philadelphia, PA (August 28-30, 1972).

2 "Fatigue Properties of Sheet, Bar, and Cast Metallic Materials for Cryogenic Applications", Report No. R-7564, Rocketdyne Division, North American Rockwell Corp. (August 30, 1968).

3 Larson, F. R., "Effect of Microstructure on the Impact Properties of Some Commercial Alloy Steels With and Without Boron", WAL TR 310/215, Watertown Arsenal (April 1958).

4 Dougherty, E. E., "Methods for Minimizing the Embrittling Effect of Hydrogen in Electroplated High Strength Steel Items", Frankford Arsenal, IEP 60-6110-2 (March 1963).

5 Groeneveld, T. P., Fletcher, E. E., and Elsea, A. R., "A Review of the Literature on Cleaning, Pickling, and Electroplating Processes and Relief Treatments to Minimize Hydrogen Embrittlement of Ultrahigh-Strength Steels", Battelle Memorial Institute, Contract No. NAS 8-20029 (October 15, 1966).

6 MacKay, K. P., Coldren, A. P., Rush, A. J., and Freeman, J. W., "A Survey of the Effect of Austenitizing Temperature and Rate of Continuous Cooling on the Structure and 700 F to 1200 F Properties of Three Low-Alloy Steels", WADC TR 55-388 (January 1956).

7 "Properties of High-Strength Low-Alloy Steels at Slightly Elevated Temperatures", Timken Co., Resume of Investigations on Steels for High-Temperature High-Pressure Applications (1960-1962).

8 Novak, S. R., et al, "Effect of Purity on Reliability Characteristics of High-Strength Steel", AFML-TR-78-79, U.S. Steel Corp. (July 1978).

9 Speich, G. R. and Spitzig, W. A., "Effect of Volume Fraction and Shape of Sulfide Inclusions on Through-Thickness Ductility and Impact Energy of High Strength 4340 Plate Steels", U.S. Steel Corp., Research Laboratory, Army Research Office Contract No. DAAG29-78-C-0008. (To be published in Metallurgical Transactions.)

10 Levy, M. and Morrossi, J. L., "Corrosion Fatigue Behavior of Coated 4340 Steel for Blade Retention Bolts of the AH-1G Helicopter", AMMRC-TR-34 (October 11, 1976).

11 Wong, A. K., Levy, M., and Czyrklis, W. F., "Fracture Toughness and Stress Corrosion Characteristics of Ultrahigh-Strength 4340 Steel – Summary Review", AMMRC-MS-79-1 (February 11, 1979).

12 Kortovich, C. S., "Inhibition of Hydrogen Embrittlement in High Strength Steel", TRW ER-7814-2 for Office of Naval Research, Contract N00014-74-0365 (February 1977).

13 Sandoz, G., "The Resistance of Some High Strength Steels to Slow Crack Growth in Salt Water", Naval Research Laboratory Memorandum Report 2454 (February 1972).

14 Kortovich, C. S., "Corrosion Fatigue Behavior of 4340 and D6AC Steels Below K_{Iscc}", TRW ET-7717 for Office of Naval Research, Contract N00014-69-0286 (April 1974).

15 Carter, C. S., "Effect of Prestressing on the Stress-Corrosion Resistance of Two High-Strength Steels", Boeing Co. Report D6-25275 (May 1970).

16 Neu, C. E. and Fletcher, A. R., "Fatigue Crack Growth Behavior of Four High Strength Steels in Two Humid Environments", Naval Air Development Center, Report No. NADC-MA-7060 (January 29, 1971).

17 Hickey, C. F., Jr., "Mechanical Property Survey for Electroslag Remelt Processed Steels", AMMRC AD778-169 (March 1974).

18 Mardirosian, M. M., "Strain Rate Effects in Brittle and Tough Materials", AMMRC AD/A 007-141 (December 1974).

19 Throop, J. F. and Miller, G. A., "Optimum Fatigue Crack Resistance", ASTM STP467 (1970).

20 Sheinker, A. A., "Effect of Rare Earth Additions on Stress Corrosion Cracking of 4340 Steel", TRW Inc. ER7814-3 (January 1978).

21 Clark, W. G., Jr., "Effect of Cold Work on K_{Iscc} in a 4340 Steel", Flaw Growth and Fracture, ASTM STP631 (1977).

22 Shah, R. C., "Fracture Under Combined Modes in 4340 Steel", Fracture Analysis, ASTM STP560 (1974).

23 Montano, J. W., "Low Temperature Mechanical Properties, Fractographic, and Metallographic Evaluation of Several Alloy Steels", NASA TM X-64791 (November 1973).

24 Humphries, T. S. and Nelson, E. E., "Evaluation of the Stress Corrosion Cracking Resistance of Several High Strength Low Alloy Steels", NASA TM78276 (May 1980).

25 Gottlieb, T., "Cryogenic Mechanical Testing of AISI 4340", NAR80089 (June 15, 1968).

26 Blankenship, C. P., "Some Effects of Cold Working by Hydrostatic Extrusion on Mechanical Properties of High-Strength Steels", NASA TN D-6186 (February 1971).

27 Anctil, A. A. and Rudy, F. J., "Engineering and True Stress-Strain Tensile Properties of High-Strength ESR 4340 and 4350 Steels", AMMRC SP 75-9 (November 1975).

28 Dolan, T. J. and Hanley, B. C. "The Effect of Size of Specimen on the Fatigue Strength of SAE 4340 Steel", Engineering Experiment Station, University of Illinois (May 1948).

29 Lynch, C. T., Vahldiek, F. W., and Thorton, F., "Comparison of Environmentally Enhanced Crack-Growth Rates of 1410 and Other High-Strength Steels", Proceedings of the 1978 Tri-Service Conference on Corrosion (October 1978).

30 Modern Steels, Bethlehem Steel Corp., Seventh Edition (1972).

31 Peterson, J. V., Timken Co., Private Communication (March 16, 1982).

32 AISI 4340, Alloy Digest (February 1954).

33 Metals Handbook, Ninth Edition, Vol. 1, American Society for Metals (1978).

34 Atlas of Isothermal Transformation and Cooling Transformation Diagrams, American Society for Metals (1977).

35 Hall, A. M., Sr., "Introduction to Today's Ultrahigh-Strength Structural Steels", ASTM STP498 (1971).

36 Agarwala, V. S. and DeLuccia, J. J., "New Inhibitors for Crack Arrestment in Corrosion Fatigue of High-Strength Steels", Corrosion, Vol. 36 (April 1980).

37 MIL-Handbook – 5C, Vol. 1 (December 15, 1978).

38 ASM Metals Reference Book, American Society for Metals (1981).

39 Brown, W. F., Jr., Jones, M. H., and Newman, D. P., "Influence of Sharp Notches on the Stress-Rupture Characteristics of Heat-Resistant Alloys: Part II", ASTM Proceedings, Vol. 53 (1953).

40 Steigerwald, E. A., "Plane Strain Fracture Toughness of High Strength Materials", Engineering Fracture Mechanics, Vol. 1 (1969).

41 Clark, W. G., Jr., "Effect of Temperature and Pressure on Hydrogen Cracking in High Strength Type 4340 Steel", Journal of Materials for Energy Systems, Vol. 1 (June 1979).

42 DiCesare, E., "Mechanical Properties of Cold-Drawn Martensitic SAE 4340 Steel Rod", ASTM Proceedings, Vol. 64 (1964).

43 Klinger, R. F., "Effect of Strain Rate on the Tensile Properties of SAE 4340 Steel", WADC TR 53-507 (February 1955).

44 Sachs, G., "Survey of Low-Alloy Aircraft Steels Heat Treated to High Strength Levels", WADC TR 53-254, Pt. 4 (December 1953).

45 Lodge, J. W. and Manning, G. K., "The Mechanical Properties of Quenched and Tempered Medium-Carbon Alloy Steels", American Iron and Steel Institute (March 1956).

46 Klier, E. P., Muvdi, B. B., and Sachs, G., "Design Properties of High-Strength Steels in the Presence of Stress Concentrations and Hydrogen Embrittlement", WADC TR 55-18, Pt. 1 (November 1954).

47 Espey, G. B., Jones, M. H., and Brown, W. F., Jr., "The Sharp Notch Tensile Strength of Several High Strength Sheet Alloys", Proc. ASTM, Vol. 59, p. 837 (1959).

48 Matas, S. T. and Munger, H. P., "Notch Sensitivity of Candidate Materials for the B-58 Landing Gear Program", Republic Steel Co., Phase Report No. 1, Project 12078 (May 1, 1962).

49 Muvdi, B. B., Sachs, G., and Klier, E. P., "Design Properties of High Strength Steels in the Presence of Stress Concentrations", WADC TR 56-395, Pt. 1 (December 1956).

50 Sachs, G., Sessler, J., and Yeh, T., Syracuse University (1958).

51 Hughes, P. J., Inge, J. E., and Prosser, S. B., "Tensile and Compressive Stress-Strain Properties of Some High Strength Sheet Alloys at Elevated Temperatures", NACA TN 3315 (1954).

52 "Elevated-Temperature Tensile Properties of SAE 4340 Steel Heat Treated to 260,000 – 280,000 psi Ultimated Tensile Strength", ER 9145-4 (May 3, 1957).

53 Sachs, G. and Klier, E. P., "Survey of Low-Alloy Aircraft Steels Heat-Treated to High Strength Levels", WADC TR 53-254, Pt. 5 (September 1954).

54 McGee, R. L., Campbell, J. E., Carlson, L. R., and Manning, G. K., "The Mechanical Properties of Certain Aircraft Structural Metals at Very Low Temperatures", WADC TR 58-386 (November 1958).

55 Banerjee, B. R. and Hauser, J. T., "Research and Application Engineering to Determine the Effect of Processing Variables on Crack Propagation of High-Strength Steels and Titanium", ASD-TDR-62-1034, Pt. 1 (April 1963).

56 Banerji, S. K., McMahon, C. J., and Feng, H. C., "Intergranular Fracture in 4340-Type Steels: Effects of Impurities and Hydrogen", Metallurgical Transactions, Vol. 9A (February 1978).

	Fe
0.4	C
1.8	Ni
0.8	Cr
0.25	Mo

4340

	Fe
0.4	C
1.8	Ni
0.8	Cr
0.25	Mo

4340

57 Hemirl, G. J., and Hughes, P. J., "Structural Efficiencies of Various Aluminum, Titanium and Steel Alloys at Elevated Temperatures", NACA TN 2975 (July 1953).

58 Hesbur, M. G., Abraham, K. P., and Prasad, Y.V.R.K., "Effects of Electroslag Refining on the Fracture Toughness and Fatigue Crack Propagation Rates in Heat Treated AISI 4340 Steel", Engineering Fracture Mechanics, Vol. 13 (1980).

59 AMS 5331 C (November 15, 1972).

60 AMS 6359 D (July 15, 1980).

61 AMS 6414 C (April 15, 1980).

62 AMS 6415 J (October 10, 1979).

63 Alloy Cross Index, Battelle Columbus Laboratories (1982).

64 Unified Numbering System, SAE-ASTM (1977).

65 Unterweiser, P. M. and Penzenik, "Worldwide Guide to Equivalent Irons and Steels", ASM.

66 Arnessen, J. E., Personal Communication, Pratt and Whitney Aircraft Corp. (May 7, 1959).

67 NACA TN 2957 (1953).

68 Ritchie, R. O. and Horn, R. M., "Further Considerations on the Inconsistency in Toughness Evaluation of AISI 4340 Steel Austenitized at Increasing Temperatures", Metallurgical Transactions, Vol. 9A (March 1978).

69 Mechanical Properties of Steel, Republic Steel Corp. (1961).

70 Unterweiser, P. M., Boyer, H. E., and Kubbs, J. J., Heat Treaters Guide, ASM (1982).

71 Khan, K. H. and Wood, W. E., "The Effect of Step Quenching on the Microstructure and Fracture Toughness of AISI 4340 Steel", Metallurgical Transactions, Vol. 9A (July 1978).

72 Horn, R. M. and Ritchie, R. O., "Mechanisms of Tempered Martensite Embrittlement in Low-Alloy Steels", Metallurgical Transactions, Vol. 9A (August 1978).

73 Floreen, S., "The Fracture Toughness of Cast High-Strength Steels", Trans. ASME, Journal of Engineering Materials and Technology, Vol. 99 (January 1977).

74 Metals Handbook, Eighth Edition, Vol. 1, American Society for Metals (1961).

75 Stout, R. D. and Doty, W. D., "Weldability of Steels", Welding Research Council (1971).

76 Metals Handbook, Ninth Edition, Vol. 4, American Society for Metals (1981).

77 Crooker, T. W., "Optimizing Crack-Growth Resistance in Engineering Alloys", Naval Research Laboratory Report 8110 (April 18, 1977).

78 Kula, E. B. and Anctil, A. A., "Tempered Martensite Embrittlement and Fracture Toughness in SAE 4340 Steel", Journal of Materials, Vol. 4 (December 1969).

Alloy	Fe-0.4C-1.8Ni-0.8Cr-0.25Mo				
	Forms				
Bar, Billets, Forgings, and Tubing	Sheet, Strip, and Plate	Castings	Wire	Bolting Material	General
AMS 6414 C AMS 6415 J ASTM A322 ASTM A519 ASTM A304 ASTM A646	AMS 6359 D ASTM A505 Fed. QQ-S-627	AMS 5331 C MIL-S-22141	ASTM A547	ASTM A320	MIL-S-8844B MIL-S-16974 MIL-S-5000 SAE J404j SAE J412h SAE J770c

TABLE 1.03. SPECIFICATIONS (59-65)

Fe	
0.4	C
1.8	Ni
0.8	Cr
0.25	Mo

4340

Alloy	Fe-0.4C-1.8Ni-0.8Cr-0.25Mo					
Form	Wrought 4340 (61)[a]		Wrought 4340H(33)		Castings(59)	
	Percent		Percent		Percent	
Composition	Min	Max	Min	Max	Min	Max
C	0.38	0.43	0.37	0.44	0.38	0.46
Mn	0.60	0.90	0.55	0.90	0.60	1.00
Si	0.15	0.35	0.15	0.30	0.50	0.90
P	–	0.015	–	0.035	–	0.025
S	–	0.015	–	0.040	–	0.025
Cr	0.70	0.90	0.65	0.95	0.65	1.00
Ni	1.65	2.00	1.55	2.00	1.65	2.00
Mo	0.20	0.30	0.20	0.30	0.30	0.45
Cu	–	0.35	–	–	–	0.35

(a) The other AMS specifications for wrought 4340 (references 60 and 62) allow 0.025 percent maximum phosphorus and sulfur; whereas most ASTM and SAE specifications allow 0.035 percent maximum phosphorus and 0.040 percent maximum sulfur for wrought 4340.

TABLE 1.04. COMPOSITION

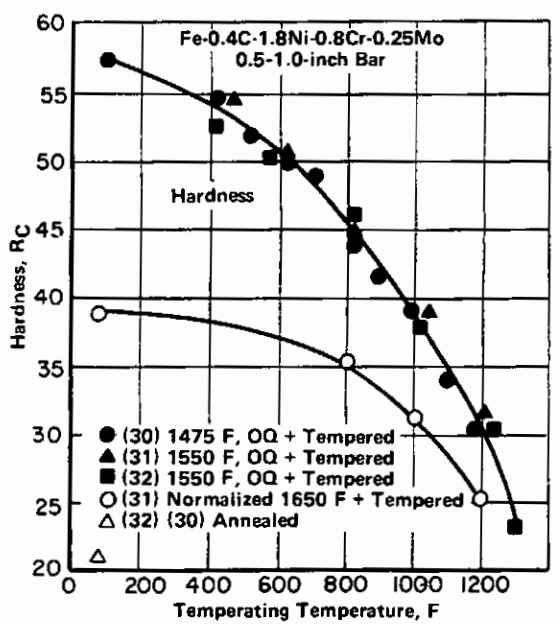


FIGURE 1.061. EFFECT OF TEMPERING TEMPERATURE ON HARDNESS (30, 31, 32)

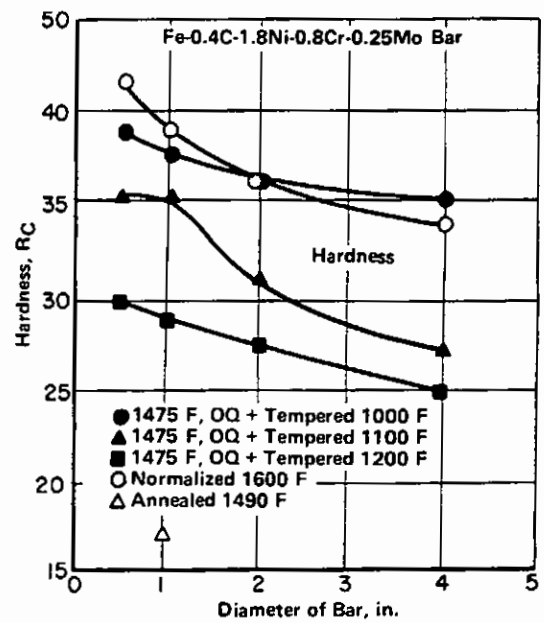


FIGURE 1.062. EFFECT OF BAR DIAMETER ON SURFACE HARDNESS FOR VARIOUS HEAT TREATED CONDITIONS (30)

	Fe
0.4	C
1.8	Ni
0.8	Cr
0.25	Mo

4340

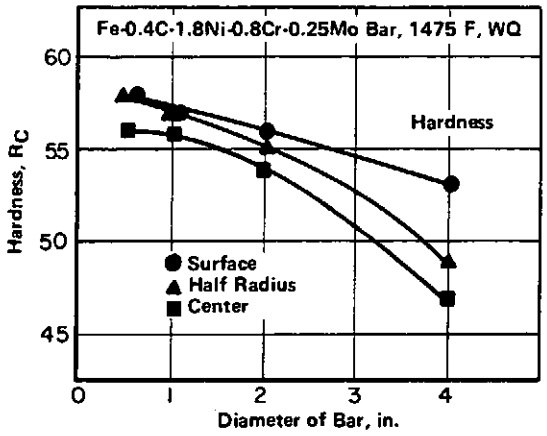


FIGURE 1.063. EFFECT OF BAR DIAMETER ON AS-QUENCHED HARDNESS AT VARIOUS DEPTHS IN BAR (30)

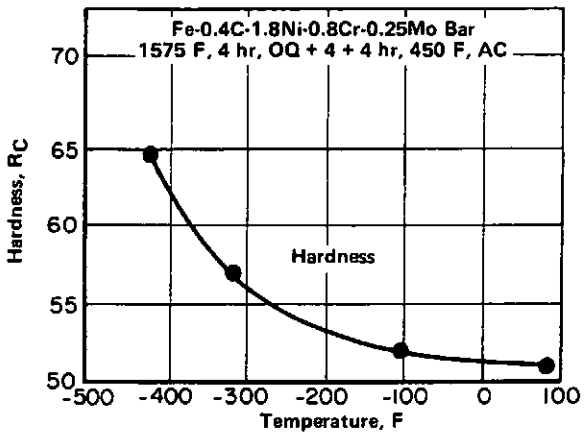


FIGURE 1.064. EFFECT OF TEMPERATURES FROM 80 F TO -423 F ON HARDNESS OF BAR HEAT TREATED TO A HARDNESS LEVEL OF RC 51 (31)

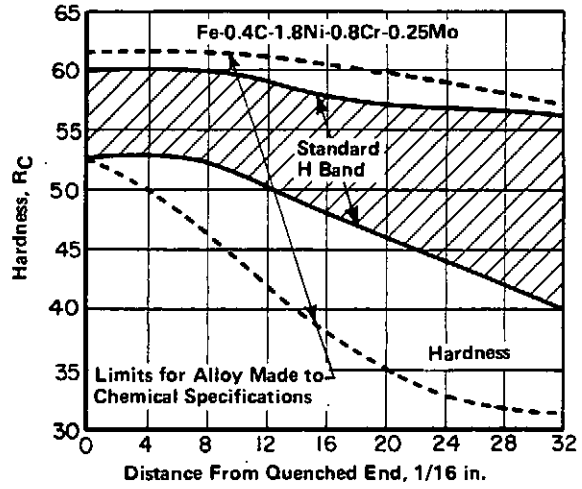


FIGURE 1.065. END-QUENCH HARDENABILITY (33)

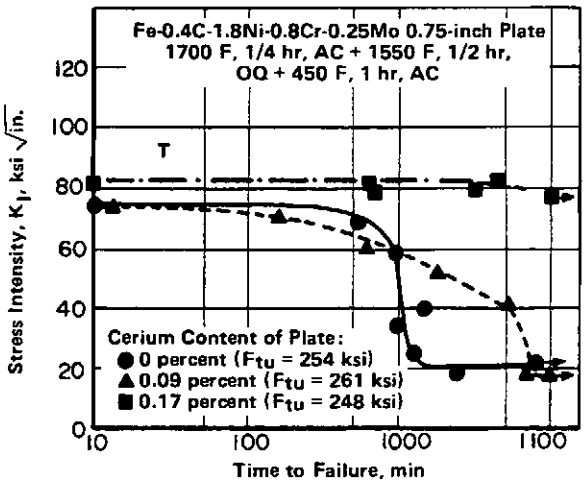
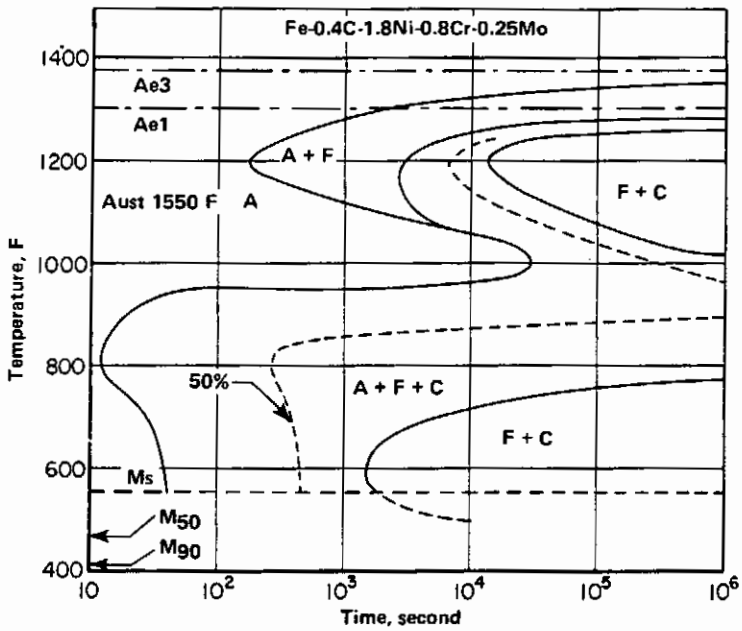


FIGURE 1.09111. EFFECTS OF CERIUM CONTENT ON DELAYED FRACTURE IN AIR OF 0.5-INCH THICK PRECRACKED SPECIMENS THAT HAVE BEEN CATHODICALLY CHARGED WITH HYDROGEN (12)



	Fe
0.4	C
1.8	Ni
0.8	Cr
0.25	Mo

4340

FIGURE 2.0121. TIME-TEMPERATURE-TRANSFORMATION DIAGRAM (34)

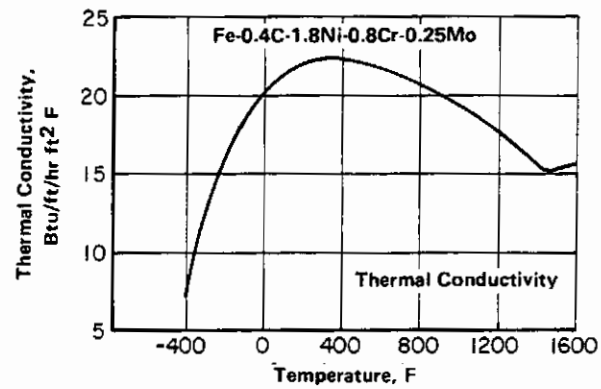


FIGURE 2.013. THERMAL CONDUCTIVITY (37)

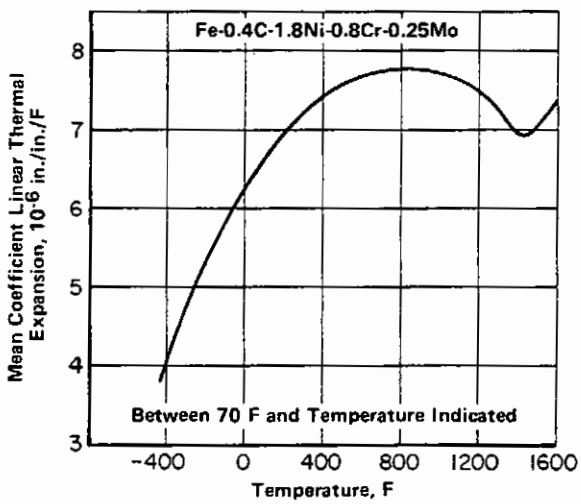


FIGURE 2.014. THERMAL EXPANSION (37)

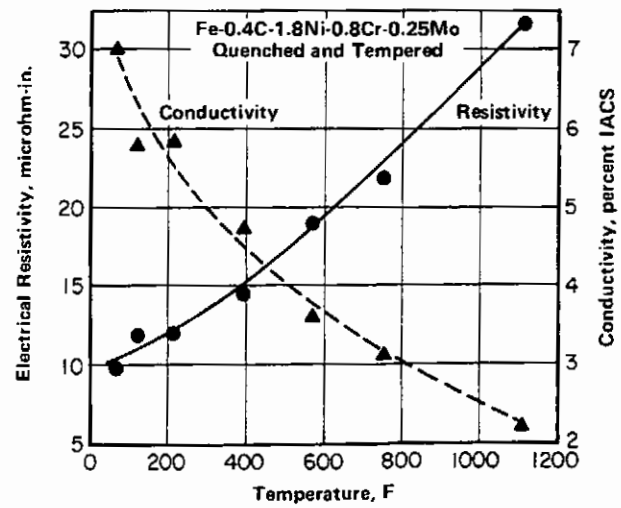


FIGURE 2.0221. ELECTRICAL PROPERTIES FROM ROOM TEMPERATURE TO 1100 F (31, 32, 33)

	Fe
0.4	C
1.8	Ni
0.8	Cr
0.25	Mo

4340

Alloy	Fe-0.4C-1.8Ni-0.8Cr-0.25Mo		
Form	1-inch Plate		
Condition	1600 F 1 hr, AC + 1550 F 1 hr, OQ + Temper 1 hr, AC		
Temper, F	F_{tu}, ksi	K_{Ic}, ksi √in.	K_{Iscc}, ksi √in.
1200	145	>141	111
950	195	104	26
400	285	56	10.5

Note: K_{Ic} and K_{Iscc} specimens, cantilever bending, 1.0 in. thick, T-L direction.

TABLE 2.0321. THRESHOLD STRESS INTENSITY FACTOR (K_{Iscc}) FOR STRESS-CORROSION CRACKING OF PLATE IN AERIATED 3 PERCENT AQUEOUS SODIUM-CHLORIDE SOLUTION AT VARIOUS CORRESPONDING LEVELS OF TENSILE STRENGTH AND CRITICAL STRESS INTENSITY FACTOR (K_{Ic}) [1]

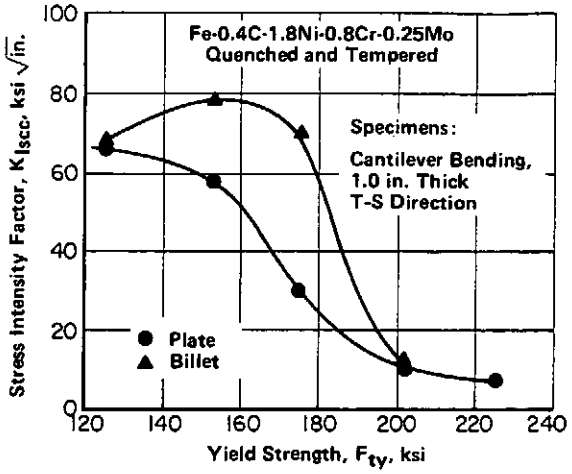


FIGURE 2.0322. EFFECT OF VARIATIONS IN YIELD STRENGTH ON THRESHOLD STRESS INTENSITY FACTOR FOR STRESS-CORROSION CRACK GROWTH IN 3.5 PERCENT SOLUTION OF SODIUM CHLORIDE IN WATER (13)

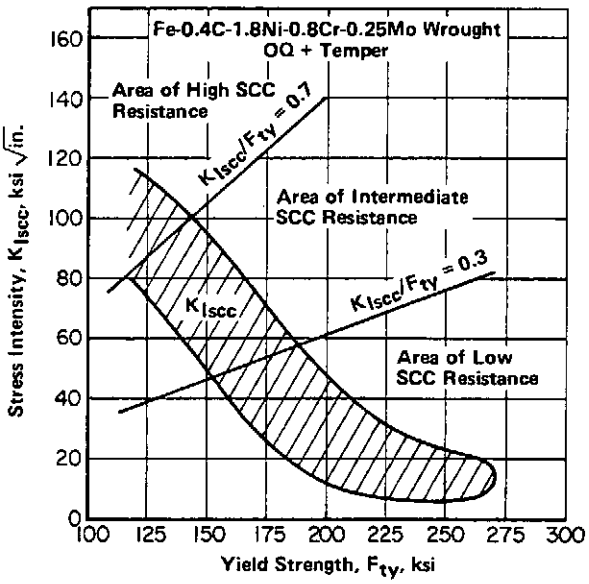


FIGURE 2.0323. EFFECT OF YIELD STRENGTH ON RESISTANCE TO STRESS-CORROSION CRACKING (SCC) OF HEAT TREATED 4340 IN AQUEOUS SALT SOLUTIONS (19)

Note: Shaded range summarizes data from a number of test programs.

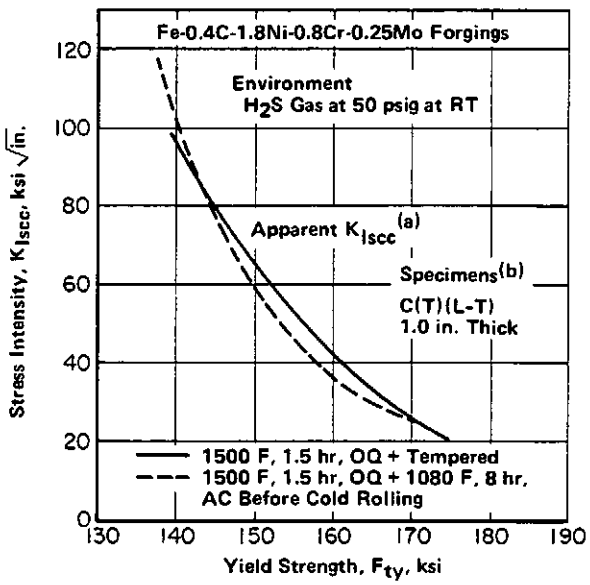


FIGURE 2.0324. EFFECT OF INCREASING YIELD STRENGTH, INDUCED BY DECREASING TEMPERING TEMPERATURE OR BY INCREASING AMOUNTS OF COLD ROLLING UP TO 50 PERCENT REDUCTION ON RESISTANCE TO STRESS-CORROSION CRACKING IN AN ENVIRONMENT OF HYDROGEN-SULFIDE (H_2S) GAS AT 50 PSIG AT ROOM TEMPERATURE (21)

Notes: (a) The term "apparent K_{Iscc}" is used to distinguish between results developed under rising load conditions and results obtained by means of long-time, constant-load or constant-displacement tests.
(b) ASTM Standardization News, May 1982, p 31-32, provides "Standard Designation Code for Fracture Specimens, Loading, and Orientations".

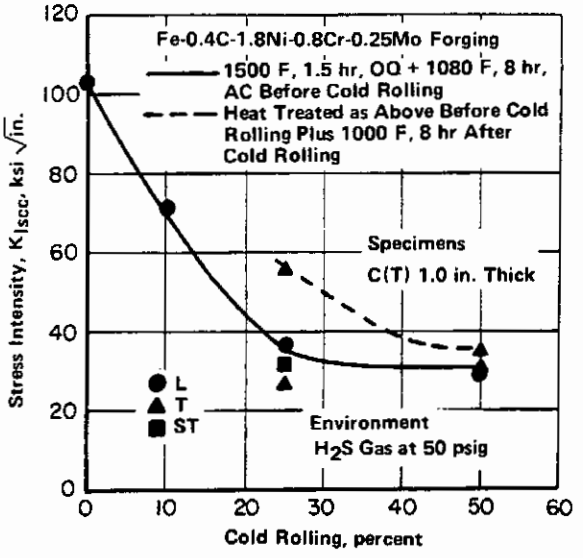


FIGURE 2.0325. EFFECT OF COLD WORKING AND STRESS RELIEF ON RESISTANCE TO STRESS-CORROSION CRACKING IN AN ENVIRONMENT OF HYDROGEN-SULFIDE (H_2S) GAS AT 50 PSIG AT ROOM TEMPERATURE (21)

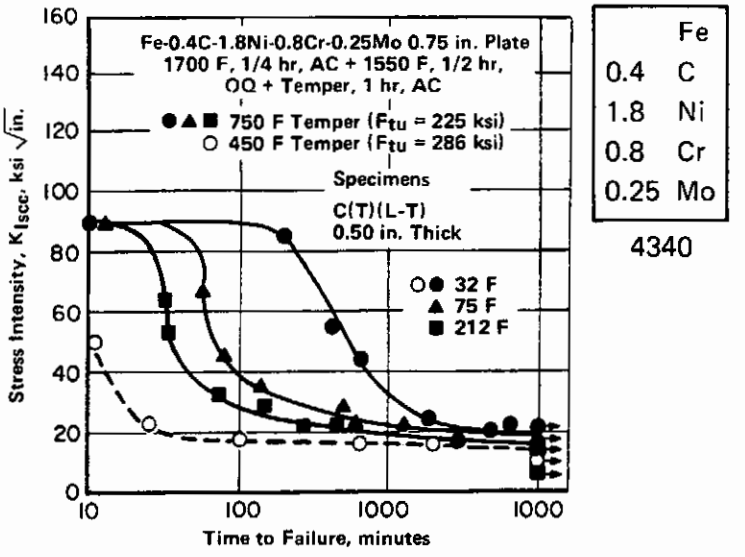


FIGURE 2.0326. TIME TO STRESS-CORROSION FAILURE OF QUENCHED-AND-TEMPERED PLATE IN DISTILLED WATER AT VARIOUS TEMPERATURES (14)

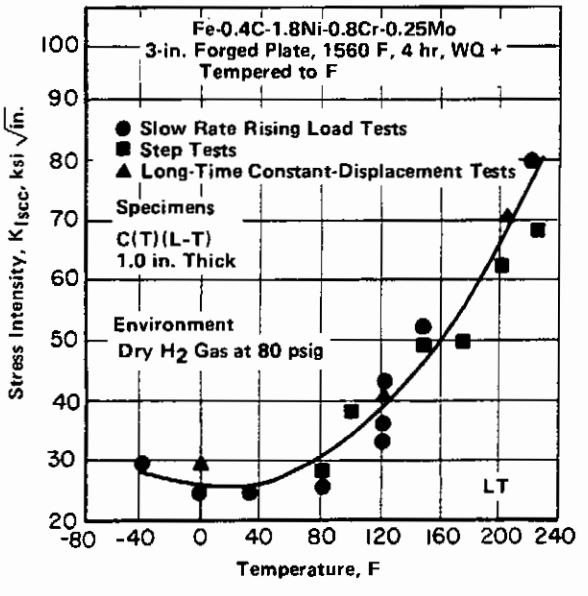


FIGURE 2.0327. EFFECT OF TEMPERATURE ON RESISTANCE TO STRESS-CORROSION CRACKING IN AN ENVIRONMENT OF DRY HYDROGEN GAS AT 80 PSIG (41)

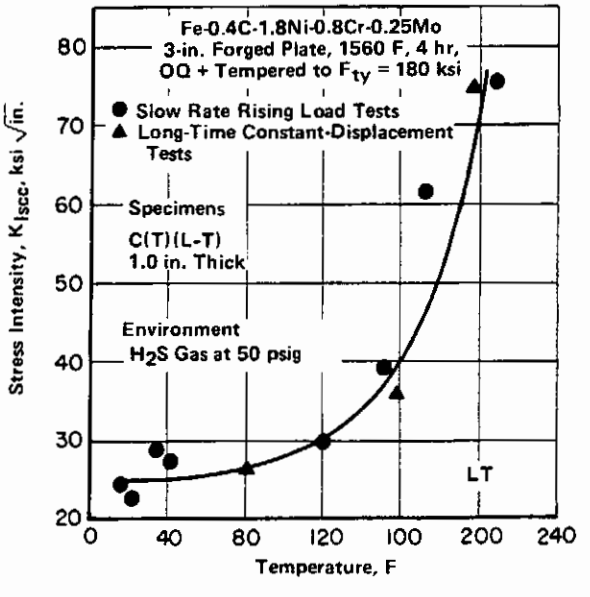


FIGURE 2.0328. EFFECT OF TEMPERATURE ON RESISTANCE TO STRESS-CORROSION CRACKING IN AN ENVIRONMENT OF HYDROGEN-SULFIDE GAS AT 50 PSIG (41)

	Fe
0.4	C
1.8	Ni
0.8	Cr
0.25	Mo

4340

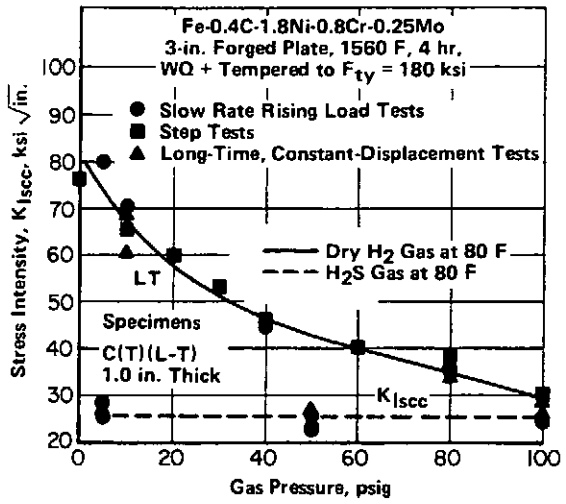


FIGURE 2.0329. EFFECT OF GAS PRESSURE ON RESISTANCE TO STRESS-CORROSION CRACKING IN ENVIRONMENTS OF HYDROGEN AND HYDROGEN-SULFIDE GASES AT ROOM TEMPERATURE (41)

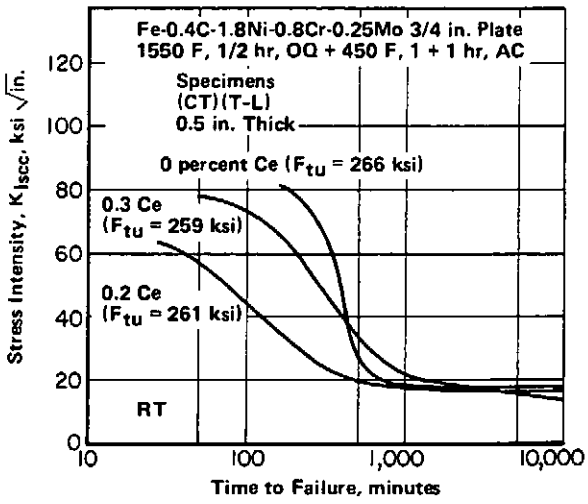


FIGURE 2.03210. EFFECT OF CERIUM ADDITIONS ON TIME TO STRESS-CORROSION FAILURE IN AN AQUEOUS 3.5 PERCENT SODIUM-CHLORIDE SOLUTION (20)

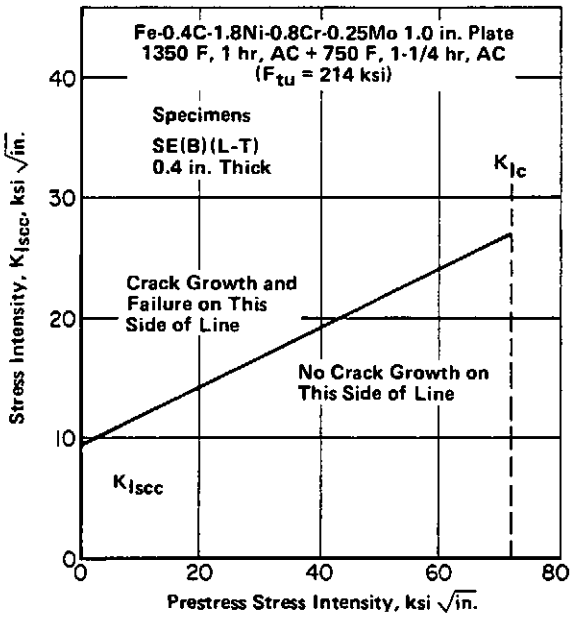


FIGURE 2.03211. EFFECT OF A BRIEF PRESTRESS OF PRECRACKING SPECIMENS ON THE THRESHOLD STRESS INTENSITY (K_{Iscc}) FOR STRESS-CORROSION CRACKING IN 3.5 PERCENT AQUEOUS SODIUM-CHLORIDE SOLUTION (15)

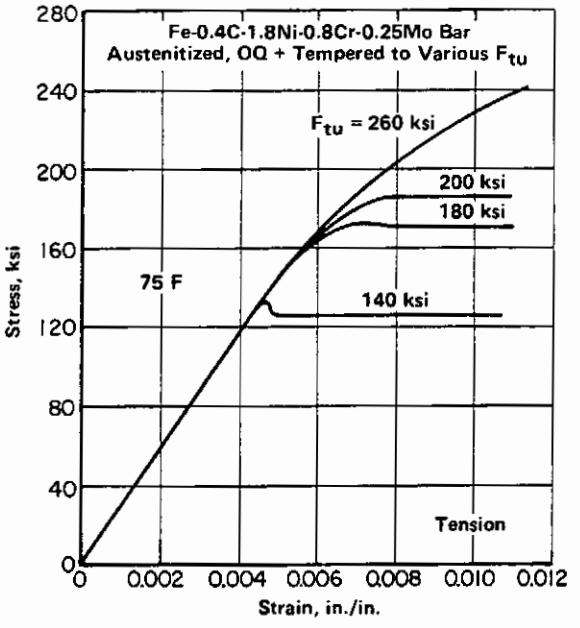
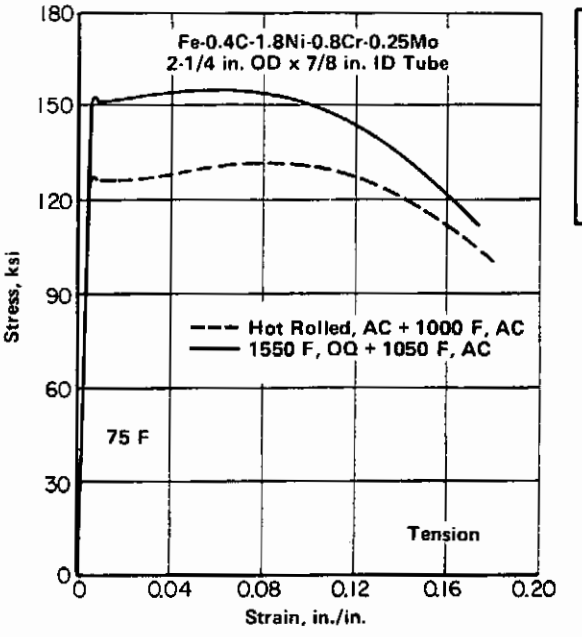


FIGURE 3.0211. ROOM TEMPERATURE TENSILE STRESS-STRAIN CURVES FOR BAR HEAT TREATED TO VARIOUS STRENGTH LEVELS (37)



	Fe
0.4	C
1.8	Ni
0.8	Cr
0.25	Mo

4340

FIGURE 3.0212. COMPLETE TENSILE STRESS-STRAIN CURVES AT ROOM TEMPERATURE FOR TUBE IN TWO DIFFERENT CONDITIONS (7)

Alloy	Fe-0.4C-1.8Ni-0.8Cr-0.25Mo							
Source	Form	Condition	F_{ty}, ksi (Min)	F_{tu}, ksi (Min)	e (2 inch), percent (Min)	RA, percent (Min)	Hardness (Min)	Hardness (Max)
AMS 6415 J (62)	Bars							
	<0.501-inch diam	Cold Finished		125 Max				
	>0.500-inch diam	Hot Finished					–	235 BHN
	>0.500-inch diam	Cold Finished					–	255 BHN
	Tubing	Hot Finished					–	99 R_B
		Cold Finished					–	25 R_C
AMS 6359 D (60)	Sheet and Strip	Annealed or Hot Rolled					–	98 R_B
	Plate	Annealed or Hot Rolled					–	25 R_C
AMS 6414 C (61)	Forgings	Normalized and Tempered					–	269 BHN
	Bars, Tubes, and Forgings	1500 F, OQ + 475 F, AC + 475 F, AC						
	Longitudinal		217	260	10	30		
	Transverse		217	260	–	25(a)		
AMS 5331 C (59)	Castings	Annealed					–	286 BHN
		1500 F, OQ + 800 F, AC + 800 F, AC	180	200	5	–	44 R_C	49 R_C

(a) Lower values of percent elongation allowed for cross-sectional areas greater than 100 $in.^2$

TABLE 3.01. SPECIFIED MECHANICAL PROPERTIES

	Fe
0.4	C
1.8	Ni
0.8	Cr
0.25	Mo

4340

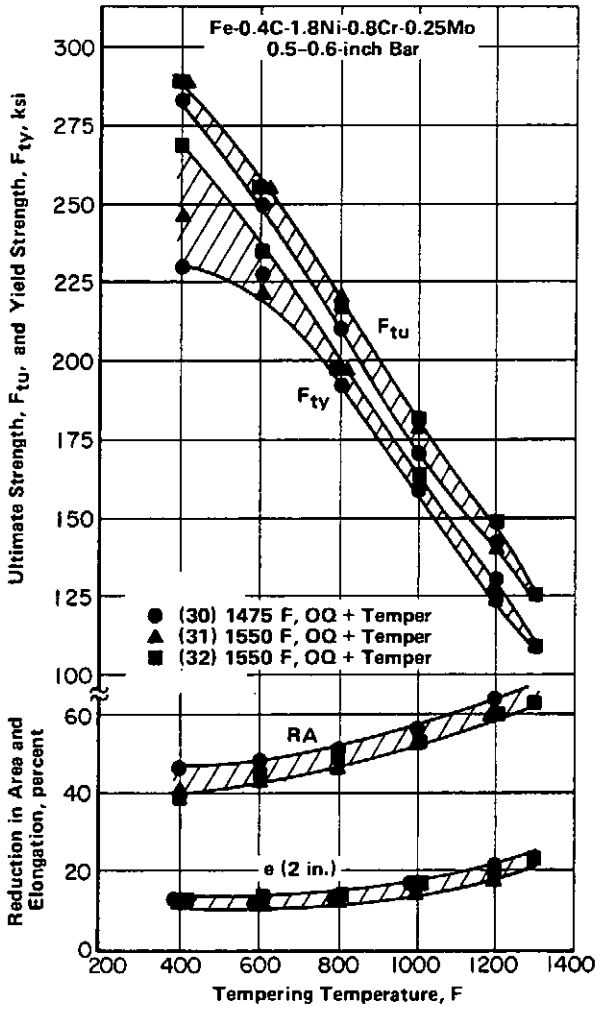


FIGURE 3.0213. EFFECT OF TEMPERING TEMPERATURE ON TENSILE PROPERTIES OF OIL-QUENCHED BAR (30, 31, 32)

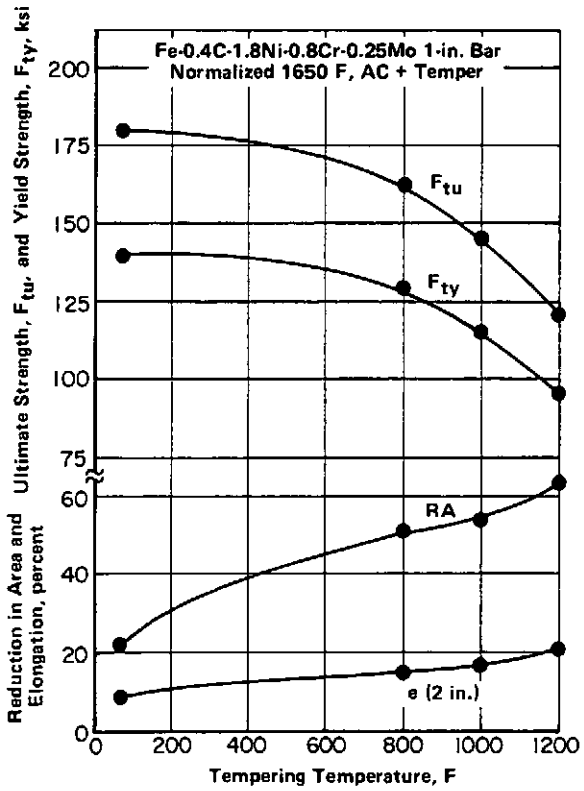


FIGURE 3.0214. EFFECT OF TEMPERING TEMPERATURE ON TENSILE PROPERTIES OF NORMALIZED BAR (31, 32)

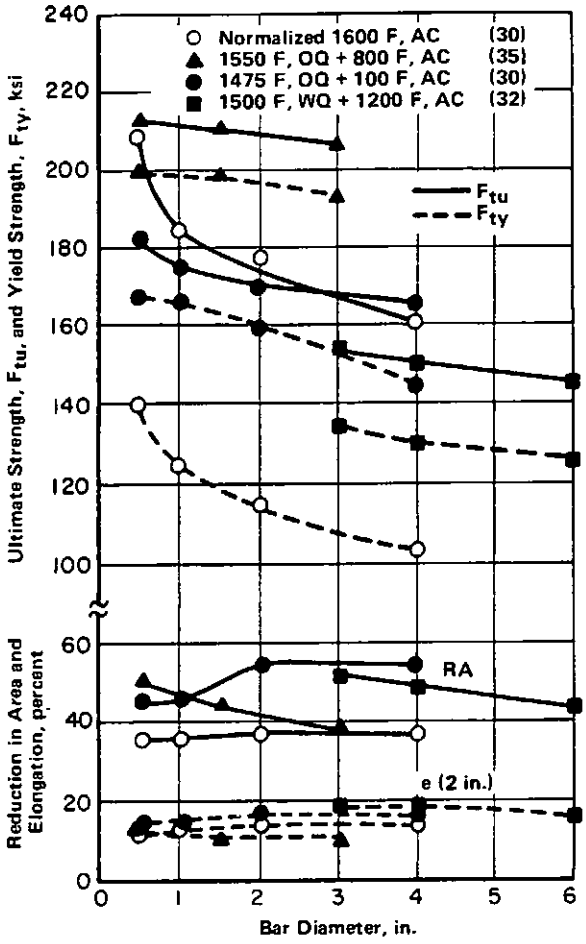


FIGURE 3.0215. EFFECT OF SECTION SIZE ON TENSILE PROPERTIES OF BAR IN SEVERAL HEAT TREATED CONDITIONS (30, 32, 35)

(Tests specimens taken from bars greater than 1 in. in diameter and taken at half radius.)

	Fe
0.4	C
1.8	Ni
0.8	Cr
0.25	Mo

4340

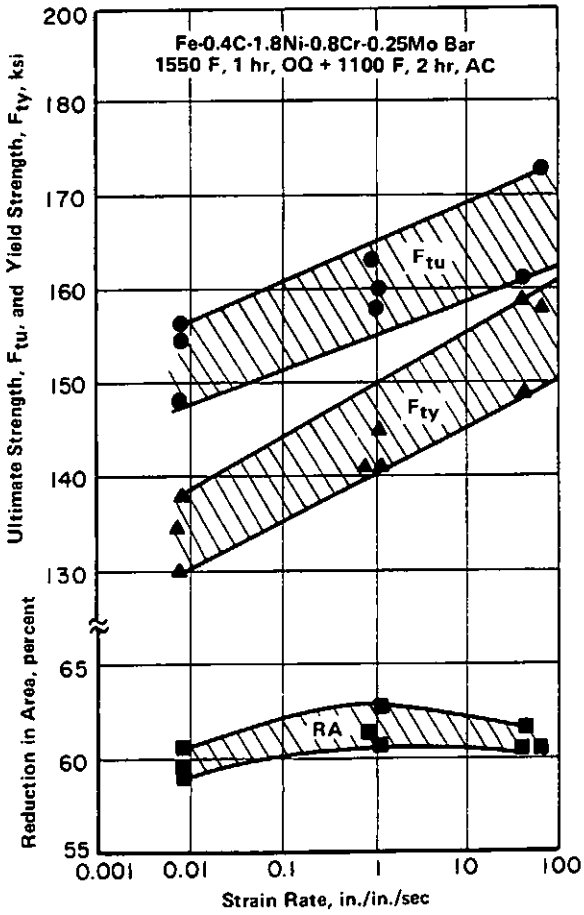


FIGURE 3.0216. EFFECT OF STRAIN RATE ON TENSILE PROPERTIES OF OIL-QUENCHED-AND-TEMPERED BAR AT ROOM TEMPERATURE (18)

	Fe
0.4	C
1.8	Ni
0.8	Cr
0.25	Mo

4340

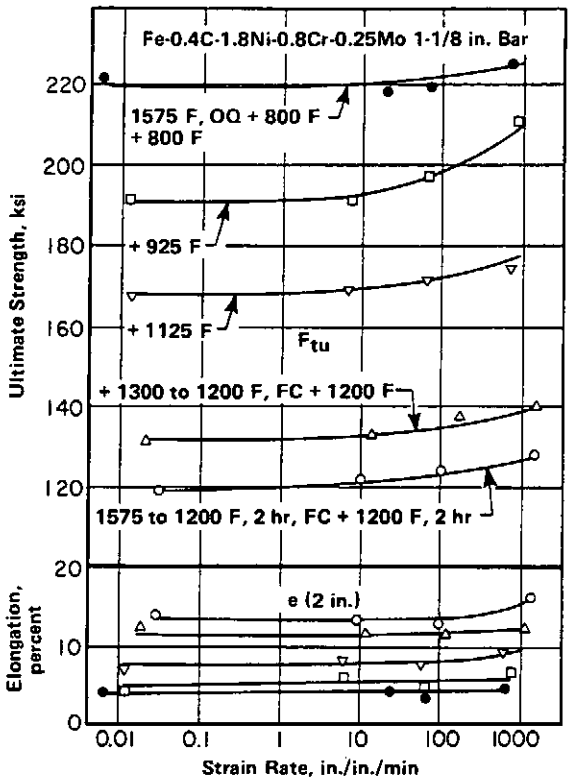
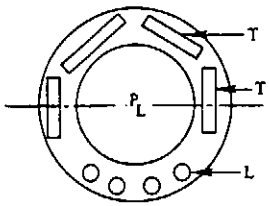


FIGURE 3.0217. EFFECT OF STRAIN RATE ON THE ULTIMATE TENSILE STRENGTH AND ELONGATION OF BAR IN VARIOUS HEAT TREATED CONDITIONS (43)

Alloy	Fe-0.4C-1.8Ni-0.8Cr-0.25Mo			
Form	Forging			
Condition	Oil-Quenched and Tempered to R_C 41			
Orientation	F_{ty}, ksi	F_{tu}, ksi	e (2 inch), percent	RA, percent
Longitudinal	180	191	14.6	48.9
Transverse	181	191	8.2	17.1
Transverse to P_L	176	188	4.6	9.8



Forging section 12-inch OD x 9-inch ID x 48-inch long. Forged to 12-inch diam, bored, and then heat treated.

TABLE 3.0218. TENSILE PROPERTIES FOR DIFFERENT ORIENTATIONS IN FORGING (33)

Alloy	Fe-0.4C-1.8Ni-0.8Cr-0.25Mo				
Form	1-1/2-inch Plate				
Condition	1550 F 1 hr. OQ + Temper 3 hr. AC				
Temper, F	Orientation	F_{ty}, ksi	F_{tu}, ksi	e (4D), percent	RA, percent
300	L	227.3	340.0	10.0	37.4
		228.0	307.6	11.8	41.3
375	L	226.6	318.0	13.7	38.1
	T	216.4	283.1	13.0	45.2
450	L	236.5	295.7	12.7	43.5
	T	228.5	273.5	14.0	44.3
500	L	241.2	286.4	11.2	44.0
Condition	1550 F 1 hr. Salt Q at 450 F 5 Min, AC + Temper 3 hr. AC				
375	L	229.0	325.1	12.3	37.8
450	L	239.9	309.2	10.0	36.1

TABLE 3.0219. EFFECTS OF VARIOUS TEMPERING TEMPERATURES ON TENSILE PROPERTIES OF ELECTROSLAG REMELTED PLATE AFTER CONVENTIONAL OIL-QUENCHING AND AFTER MARTEMPERING (27)

	Fe
0.4	C
1.8	Ni
0.8	Cr
0.25	Mo

4340

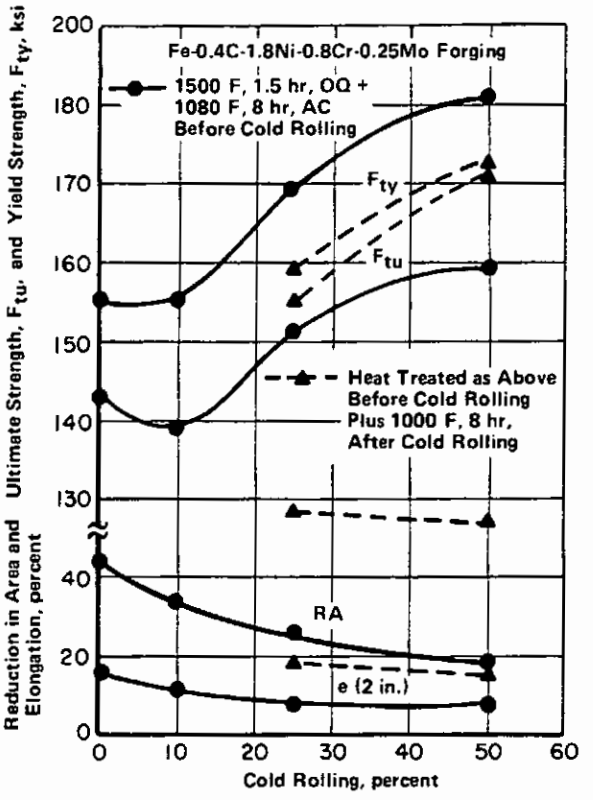


FIGURE 3.02111. EFFECTS OF COLD WORKING AND STRESS RELIEF ON ROOM TEMPERATURE TENSILE PROPERTIES OF OIL-QUENCHED-AND-TEMPERED FORGINGS (21)

Alloy	Fe-0.4C-1.8Ni-0.8Cr-0.25Mo				
Form	1-inch Plate, Cross Rolled				
Condition	1650 F 1 hr, OQ + 1525 F 1 hr, OQ + 475 F 8 hr, AC				
Purity	Orientation	F_{ty}, ksi	F_{tu}, ksi	e (2 inch), percent	RA, percent
Normal	L	219	259	11.6	43.3
	T	221	260	10.0	39.7
High	L	210	247	11.6	45.4
	T	209	248	12.4	51.2

Note. Chemical Analyses

Purity	C	Mn	P	S	Si	Ni	Cr	Mo	Cu
Normal	0.40	0.71	0.010	0.011	0.27	1.80	0.82	0.25	0.006
High	0.40	0.29	<0.0003	0.0008	0.007	1.79	0.75	0.27	0.002

(Cont)	Co	O	Al	N	Ti	As	Sb	Sn
Normal	0.008	0.0016	0.034	0.008	0.005	<0.002	<0.0004	<0.002
High	0.023	0.0010	0.002	0.002	<0.002	<0.002	<0.0004	<0.002

TABLE 3.02110. COMPARISON OF TENSILE PROPERTIES OF AIR INDUCTION MELTED CROSS ROLLED PLATE OF NORMAL PURITY WITH THOSE OF HIGH PURITY PLATE PRODUCED BY VACUUM INDUCTION MELTING FOLLOWED BY VACUUM ARC REMELTING (8)

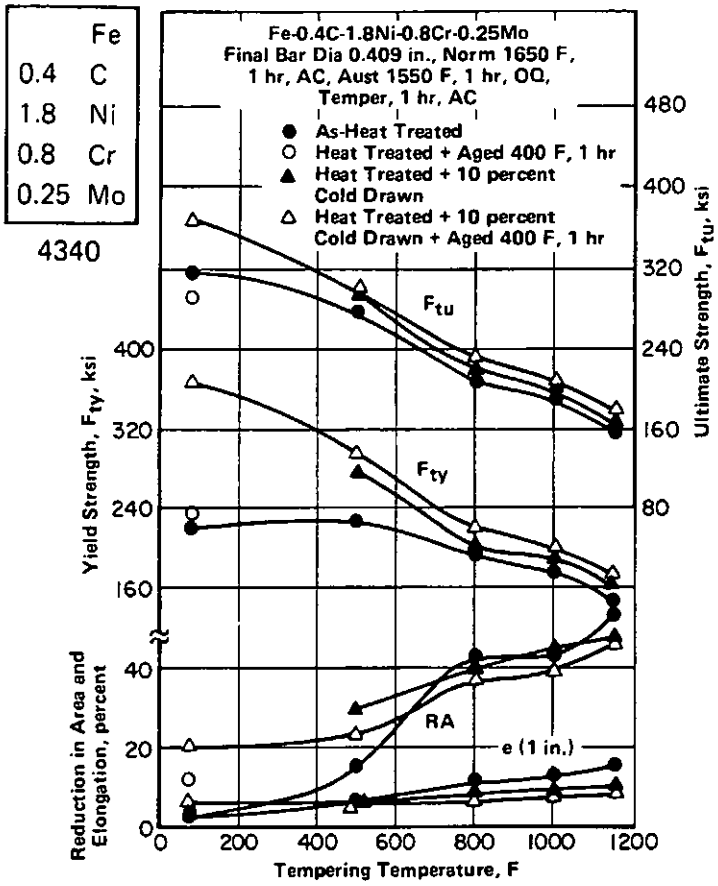


FIGURE 3.02112. EFFECTS OF TEMPERING TEMPERATURE AND 10 PERCENT COLD REDUCTION AND AGING AT 400 F ON TENSILE PROPERTIES OF OIL-QUENCHED BAR (42)

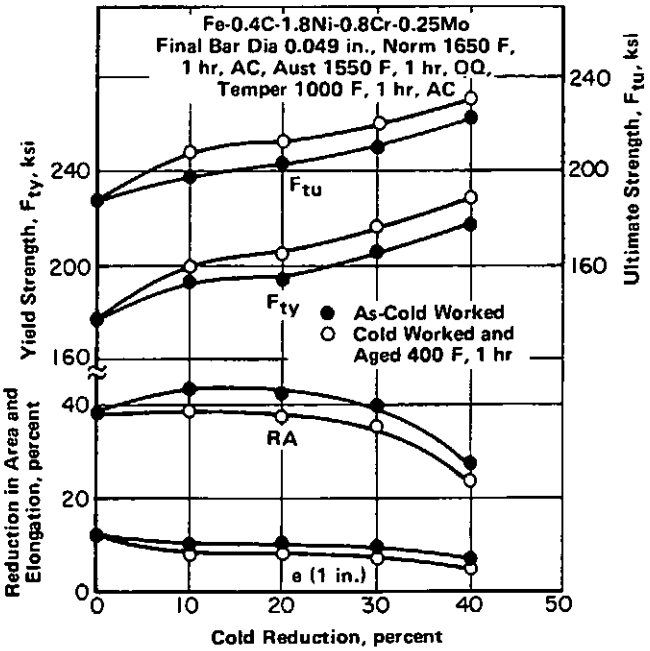


FIGURE 3.02113. EFFECTS OF COLD WORKING AND AGING ON TENSILE PROPERTIES OF BAR THAT HAD PREVIOUSLY BEEN OIL-QUENCHED-AND-TEMPERED AT 1000 F (42)

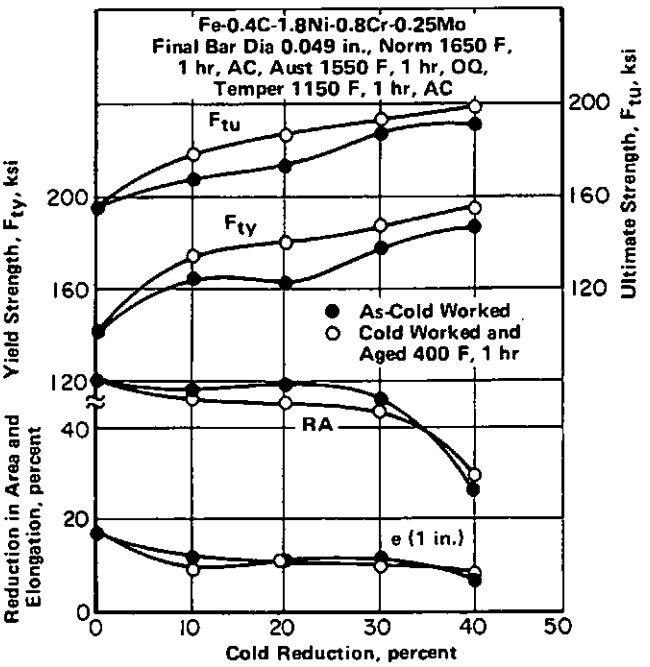


FIGURE 3.02114. EFFECTS OF COLD WORKING AND AGING ON TENSILE PROPERTIES OF BAR THAT HAD BEEN PREVIOUSLY OIL-QUENCHED-AND-TEMPERED AT 1150 F (42)

Alloy	Fe-0.4C-1.8Ni-0.8Cr-0.25Mo					
Form	Bar					
Condition			Tensile Properties			
1550 F 1 hr, OQ + Following			F_{ty}, ksi	F_{tu}, ksi	e (2 inch), percent	RA, percent
Temper	CW, percent	Retemper				
800 F 1 hr (R_C 44)	–	–	197.5	208.5	14.0	54.5
	50 (R_C 47)	–	229.0	239.0	8.6	46.7
	50 (R_C 47)	400 F 1 hr (R_C 49)	258.7	269.2	10.0	48.1
900 F 1 hr (R_C 42)	–	–	182.0	188.6	15.3	56.2
	50 (R_C 43)	–	211.0	229.0	9.3	48.9
	50 (R_C 43)	400 F 1 hr (R_C 46)	227.0	240.0	10.0	48.3
	67	–	225.0	246.5	7.9	43.9
	67	400 F 1 hr	233.8	257.0	8.5	41.2

	Fe
0.4	C
1.8	Ni
0.8	Cr
0.25	Mo

4340

TABLE 3.02115. EFFECT OF COLD WORK BY HYDROSTATIC EXTRUSION AND OF RETEMPERING ON TENSILE PROPERTIES OF BAR THAT HAD BEEN PREVIOUSLY OIL-QUENCHED AND TEMPERED (26)

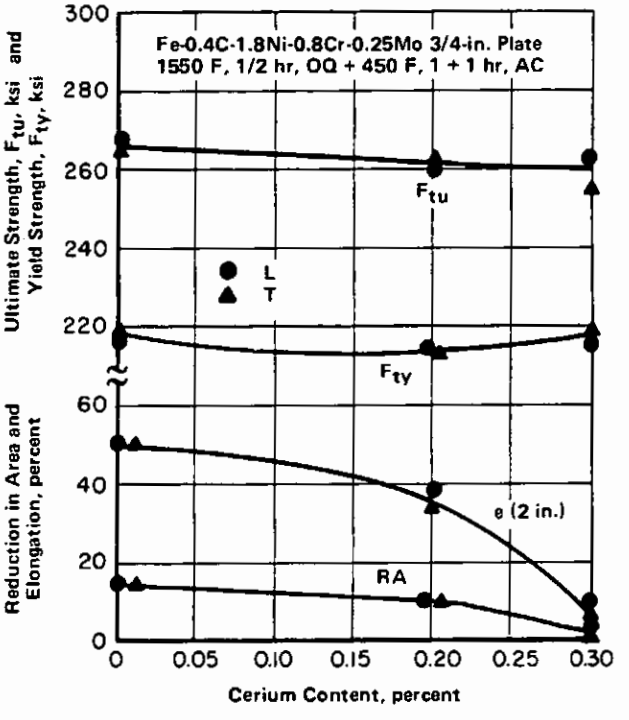


FIGURE 3.02116. EFFECT OF CERIUM ADDITIONS ON ROOM TEMPERATURE TENSILE PROPERTIES (20)

Alloy	Fe-0.4C-1.8Ni-0.8Cr-0.25Mo
Form	Bar
Condition	Annealed: 1490 F, FC 20 F per hr to 670 F, AC
F_{ty}, ksi	68.5
F_{tu}, ksi	108.0
e (2 inch), percent	22.0
RA, percent	49.9

TABLE 3.02117. TENSILE PROPERTIES OF ANNEALED BAR (30)

Alloy	Fe-0.4C-1.8Ni-0.8Cr-0.25Mo			
Condition	1600 F, OQ + Temper 1 hr, AC			
Temper, F	600		905	
Form	Cast	Plate	Cast	Plate
F_{ty}, ksi	211	220	174	181
F_{tu}, ksi	239	236	186	195
e (2 inch), percent	8	9	8	9
RA, percent	21	25	29	39

TABLE 3.02118. COMPARISON OF ROOM TEMPERATURE TENSILE PROPERTIES IN TWO HEAT TREATED CONDITIONS OF CAST KEEL BLOCK AND WROUGHT PLATE MADE FROM THE SAME AIR INDUCTION MELTED HEAT (73)

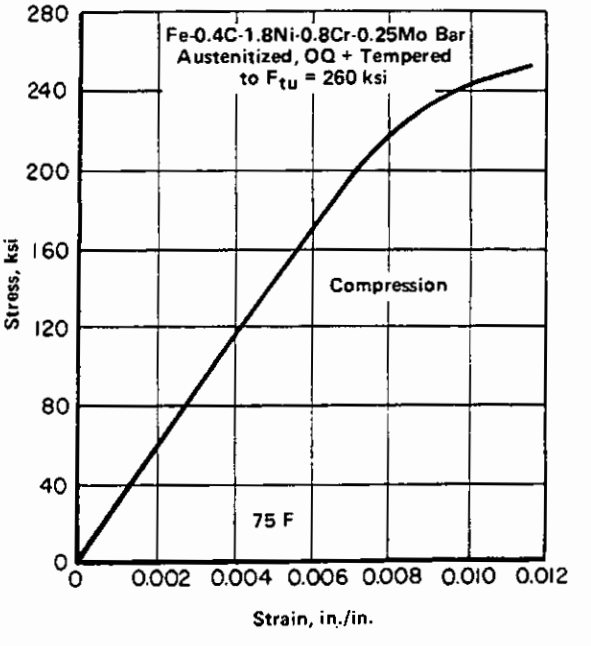


FIGURE 3.0221. ROOM TEMPERATURE STRESS-STRAIN CURVE IN COMPRESSION FOR BAR HEAT TREATED TO F_{tu} = 260 KSI (37)

	Fe
0.4	C
1.8	Ni
0.8	Cr
0.25	Mo

4340

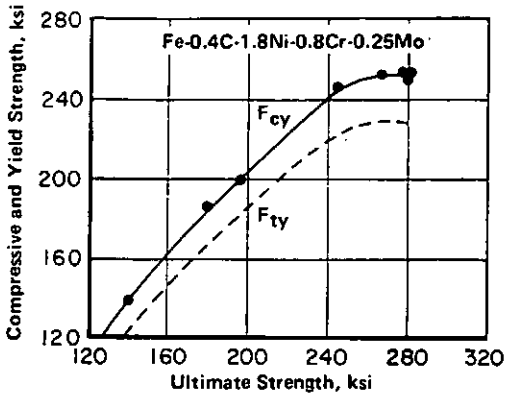


FIGURE 3.0222. RELATIONSHIP BETWEEN COMPRESSIVE YIELD STRENGTH AND TENSILE STRENGTH (44)

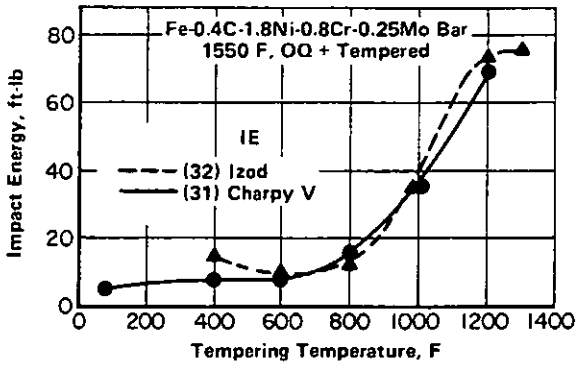


FIGURE 3.0231. EFFECT OF TEMPERING TEMPERATURE ON IMPACT PROPERTIES OF OIL-QUENCHED BAR AT ROOM TEMPERATURE (31, 32)

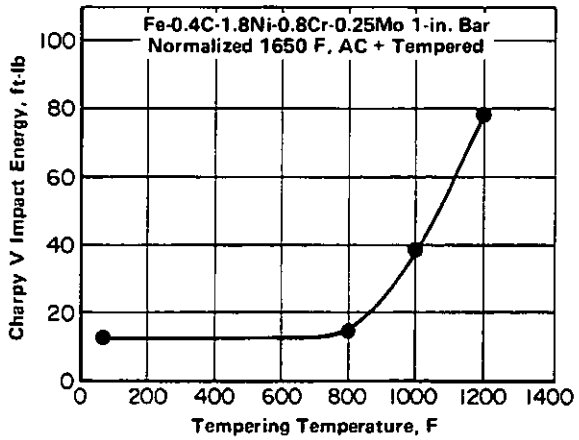


FIGURE 3.0232. EFFECT OF TEMPERING TEMPERATURE ON IMPACT PROPERTIES OF NORMALIZED BAR AT ROOM TEMPERATURE (31, 32)

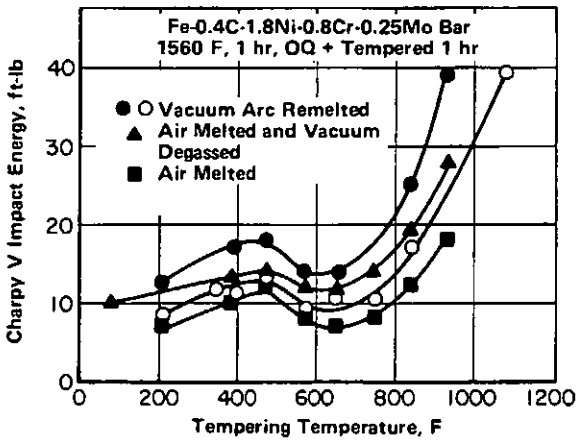


FIGURE 3.0233. EFFECTS OF TEMPERING TEMPERATURE AND MELTING PRACTICE ON IMPACT PROPERTIES AT ROOM TEMPERATURE (56)

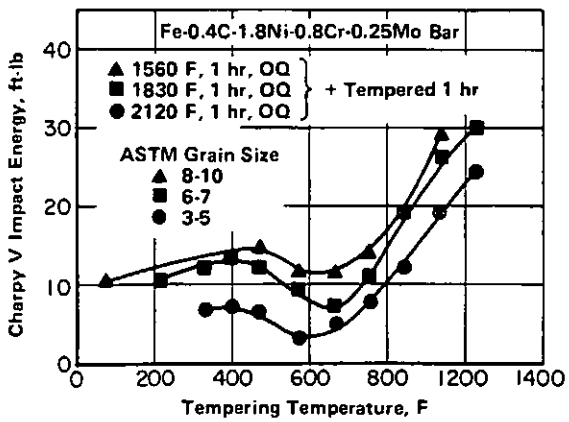


FIGURE 3.0234. EFFECTS OF TEMPERING TEMPERATURE AND AUSTENITIZING TEMPERATURE AND RESULTING GRAIN SIZE ON IMPACT PROPERTIES AT ROOM TEMPERATURE OF BAR THAT HAD BEEN AIR MELTED AND VACUUM DEGASSED (56)

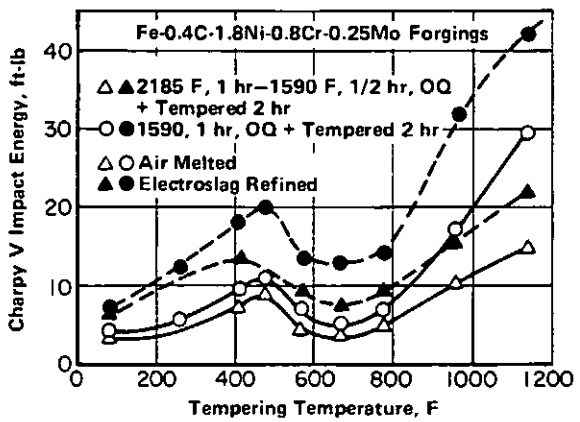


FIGURE 3.0235. EFFECTS OF TEMPERING TEMPERATURE AFTER TWO DIFFERENT AUSTENITIZING TREATMENTS ON IMPACT PROPERTIES AT ROOM TEMPERATURE OF AIR MELTED AND ELECTROSLAG REFINED FORGINGS (58)

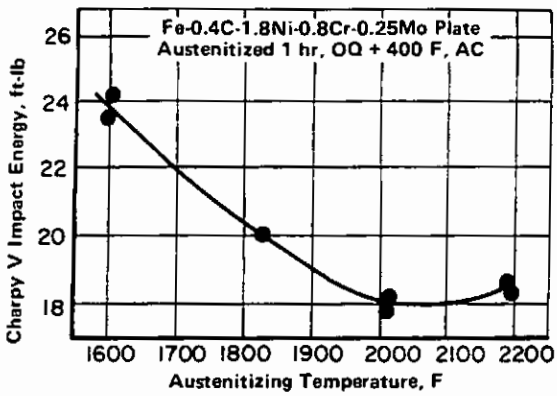


FIGURE 3.0236. EFFECT OF AUSTENITIZING TEMPERATURE ON THE ROOM TEMPERATURE IMPACT PROPERTIES OF OIL-QUENCHED-AND-TEMPERED VACUUM ARC REMELTED PLATE (68)

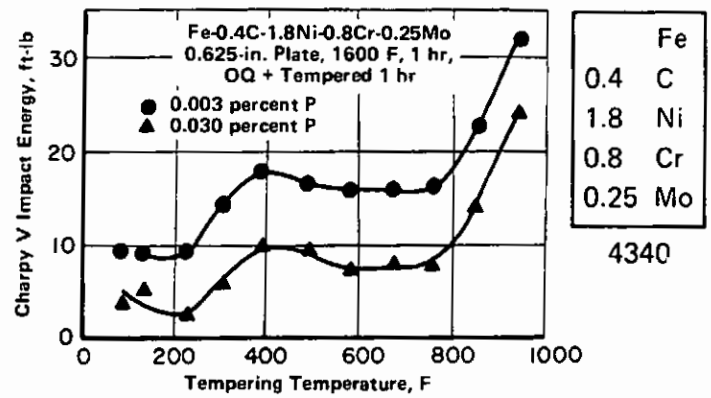


FIGURE 3.0237. EFFECTS OF TEMPERING TEMPERATURE AND PHOSPHORUS CONTENT ON IMPACT PROPERTIES AT ROOM TEMPERATURE OF PLATE THAT HAD BEEN VACUUM INDUCTION MELTED (57)

Alloy	Fe-0.4C-1.8Ni-0.8Cr-0.25Mo			
Condition	1600 F, OQ + Temper 1 hr, AC			
Temper, F	600		905	
Form	Cast	Plate	Cast	Plate
Impact, ft-lb	9.2	10.5	19.9	17.7

TABLE 3.0238. COMPARISON OF ROOM TEMPERATURE CHARPY V-NOTCH IMPACT PROPERTIES IN TWO HEAT TREATED CONDITIONS OF CAST KEEL BLOCK AND WROUGHT PLATE MADE FROM THE SAME INDUCTION MELTED HEAT (73)

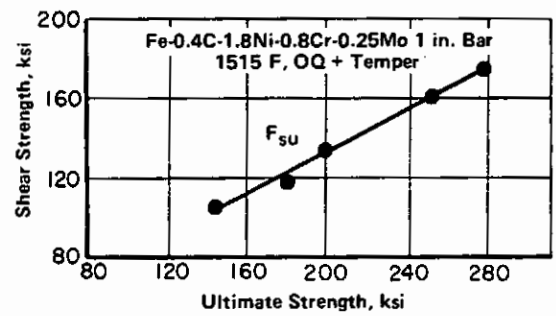


FIGURE 3.0251. RELATIONSHIP BETWEEN SHEAR STRENGTH IN TORSION AND ULTIMATE TENSILE STRENGTH (45)

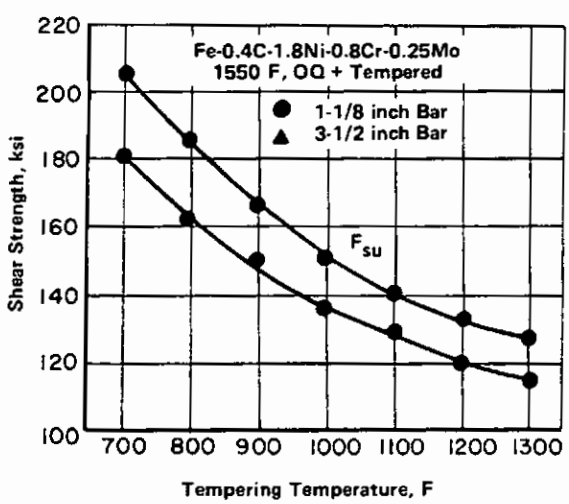


FIGURE 3.0252. EFFECT OF TEMPERING TEMPERATURE ON SHEAR STRENGTH IN TORSION OF OIL-QUENCHED BAR OF TWO DIFFERENT SIZES (32)

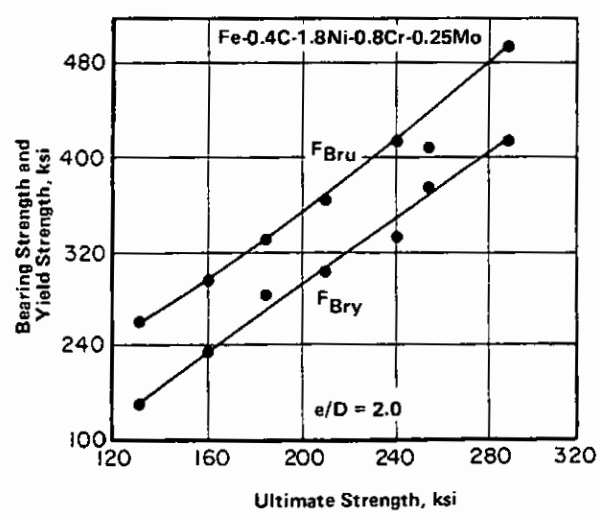


FIGURE 3.0261. RELATIONSHIP BETWEEN BEARING PROPERTIES AND ULTIMATE TENSILE STRENGTH (44)

	Fe
0.4	C
1.8	Ni
0.8	Cr
0.25	Mo

4340

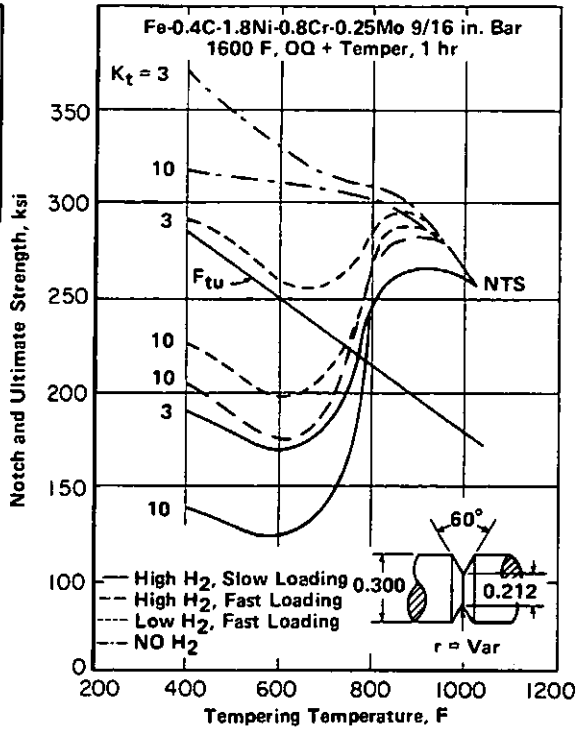


FIGURE 3.02711. EFFECTS OF TEMPERING TEMPERATURE, HYDROGEN CONTENT, STRESS CONCENTRATION, AND RATE OF LOADING ON THE NOTCHED TENSILE STRENGTH OF BAR (46)

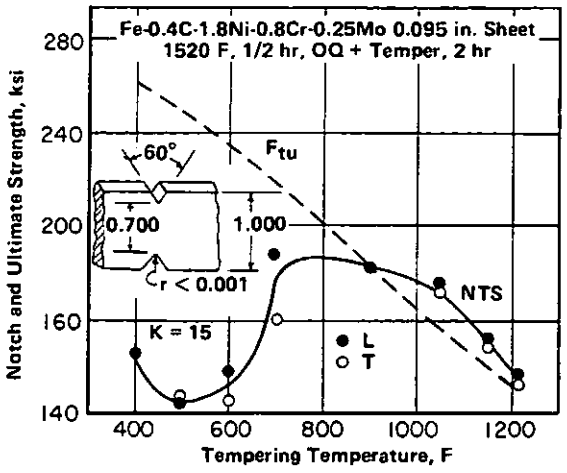


FIGURE 3.02712. EFFECT OF TEMPERING TEMPERATURE ON SHARP-NOTCH STRENGTH OF SHEET (47)

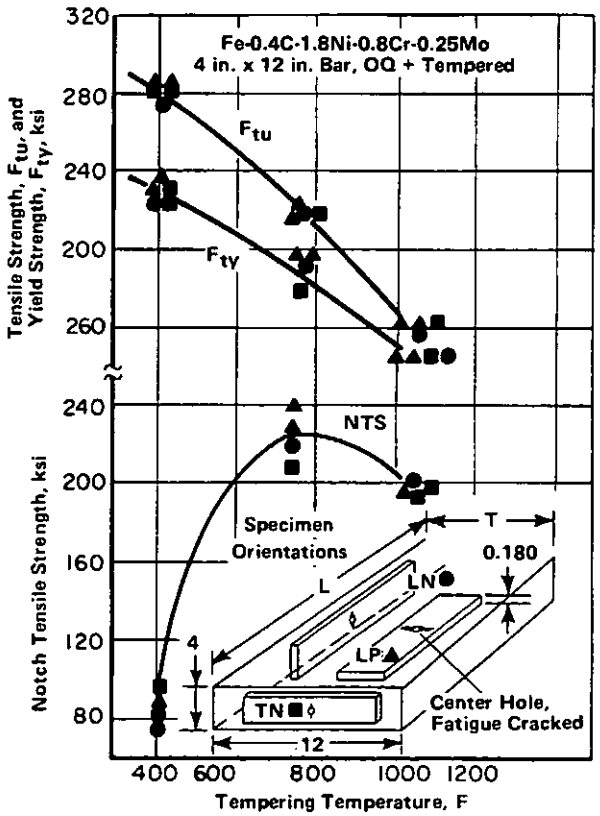


FIGURE 3.02713. EFFECT OF TEMPERING TEMPERATURE AND SPECIMEN ORIENTATION ON CRACK STRENGTH OF BAR (48)

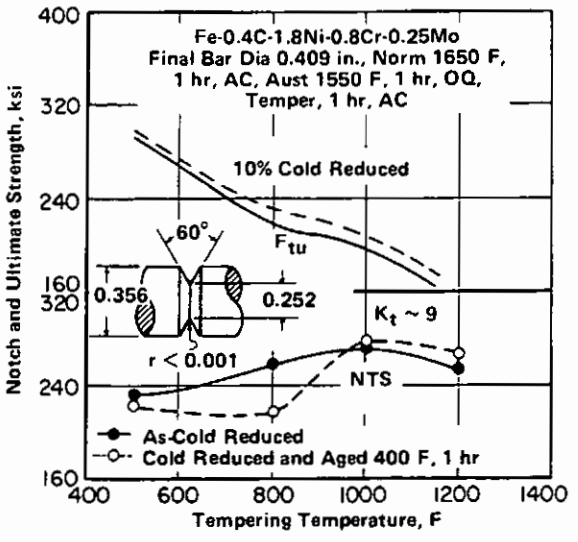


FIGURE 3.02714. EFFECT OF TEMPERING TEMPERATURE ON SHARP-NOTCH STRENGTH OF BAR COLD REDUCED 10 PERCENT AFTER TEMPERING (42)

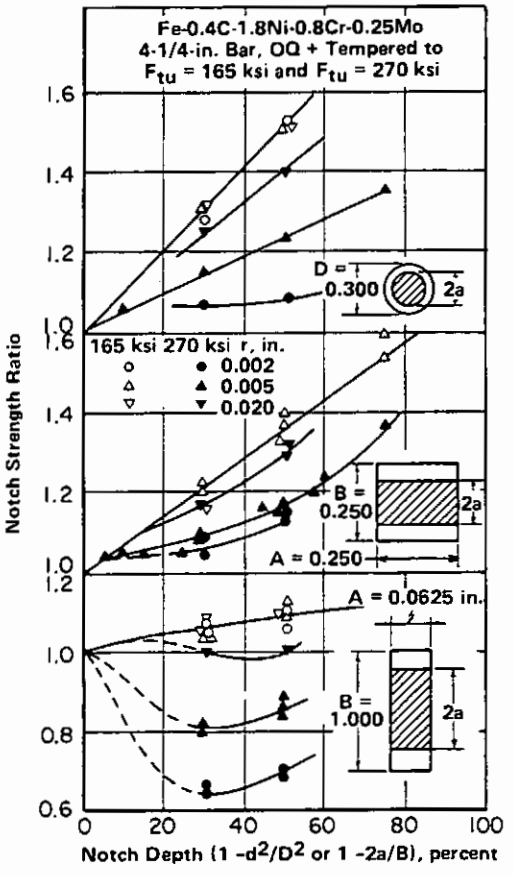


FIGURE 3.02716. EFFECT OF SPECIMEN CROSS SECTION, NOTCH ROOT RADIUS, AND NOTCH DEPTH ON NOTCH STRENGTH RATIO OF BAR (50)

	Fe
0.4	C
1.8	Ni
0.8	Cr
0.25	Mo

4340

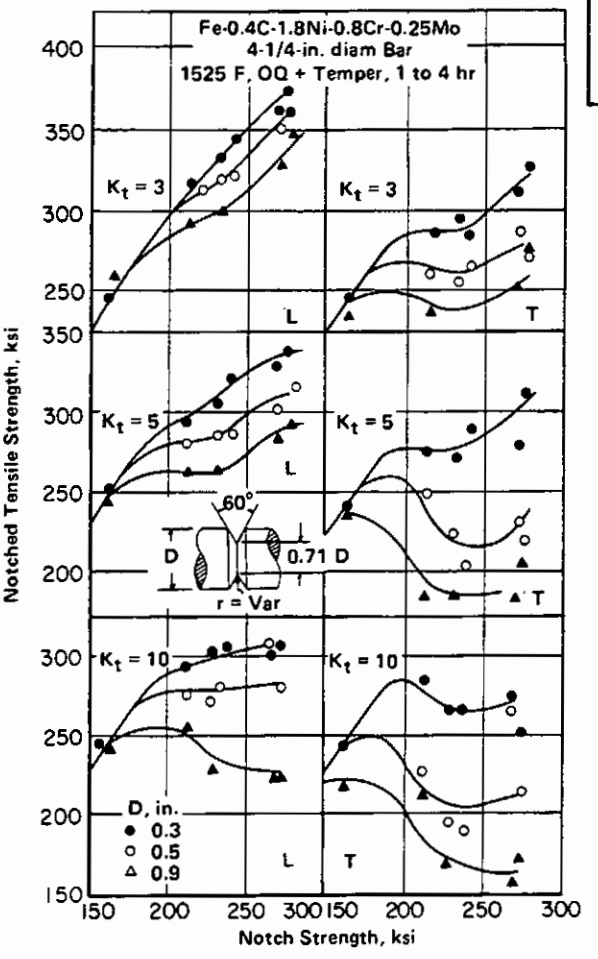


FIGURE 3.02715. RELATIONSHIP BETWEEN ULTIMATE TENSILE STRENGTH (F_{tu}) AND NOTCHED TENSILE STRENGTH (NTS) FOR VARIOUS SIZE TEST BARS, STRESS CONCENTRATIONS, AND ORIENTATIONS (49)

	Fe
0.4	C
1.8	Ni
0.8	Cr
0.25	Mo

4340

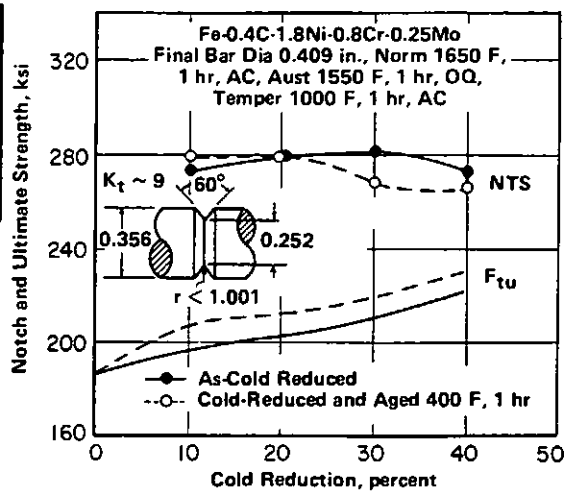


FIGURE 3.02717. EFFECT OF COLD WORKING ON SHARP-NOTCH STRENGTH OF BARS PREVIOUSLY OIL-QUENCHED-AND-TEMPERED AT 1000 F (42)

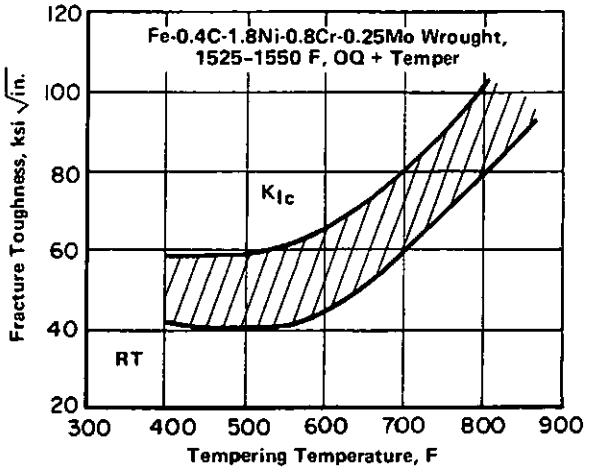


FIGURE 3.02721. EFFECT OF TEMPERING TEMPERATURE ON RANGE OF FRACTURE TOUGHNESS RESULTING FROM NORMAL VARIATIONS IN MELTING AND PROCESSING PRACTICES, CHEMICAL COMPOSITION, AND IMPURITY CONTENT (11)

Note: Shaded range summarizes data gathered from a number of sources.

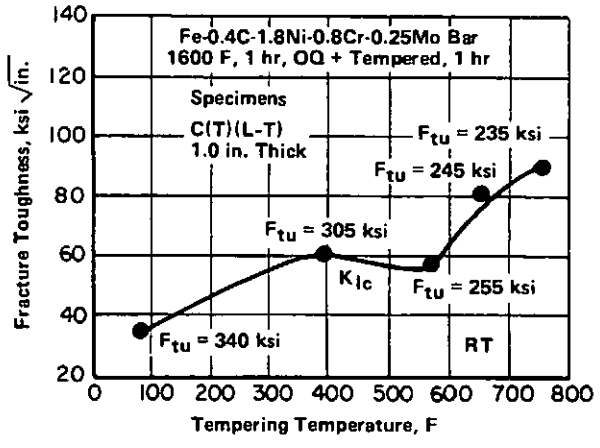


FIGURE 3.02722. EFFECT OF TEMPERING TEMPERATURE ON THE FRACTURE TOUGHNESS OF AIRCRAFT-QUALITY (VACUUM ARC REMELTED) BAR (72)

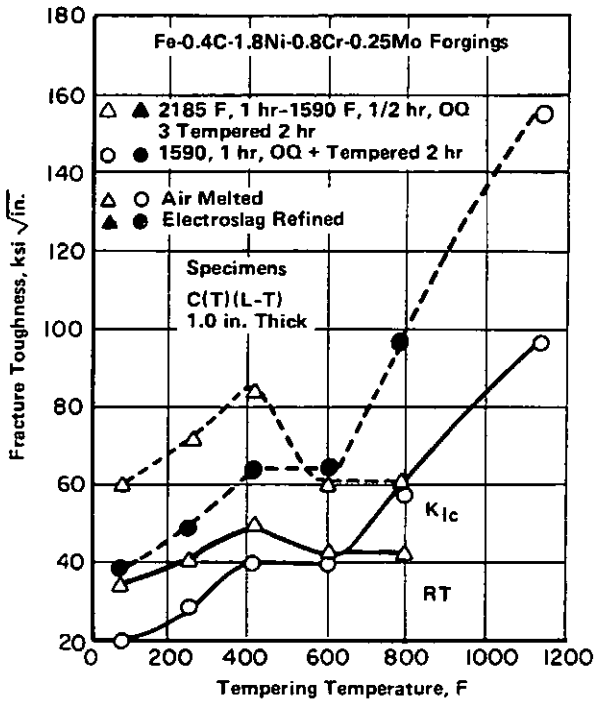


FIGURE 3.02723. EFFECTS OF TEMPERING TEMPERATURE AFTER TWO DIFFERENT AUSTENITIZING TREATMENTS ON FRACTURE TOUGHNESS AT ROOM TEMPERATURE OF AIR MELTED AND ELECTROSLAG REFINED FORGINGS (58)

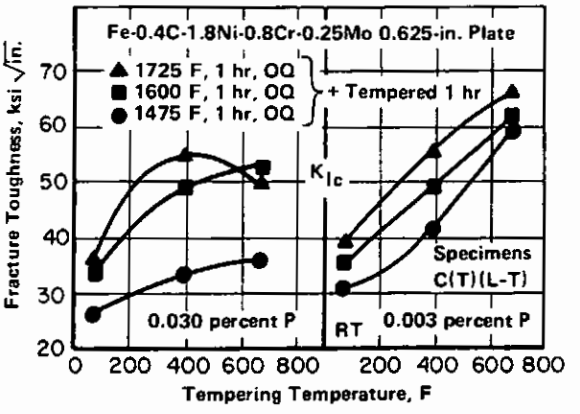


FIGURE 3.02724. EFFECTS OF TEMPERING AND AUSTENITIZING TEMPERATURES AND PHOSPHORUS CONTENT ON ROOM TEMPERATURE FRACTURE TOUGHNESS OF PLATE THAT HAS BEEN VACUUM INDUCTION MELTED (57)

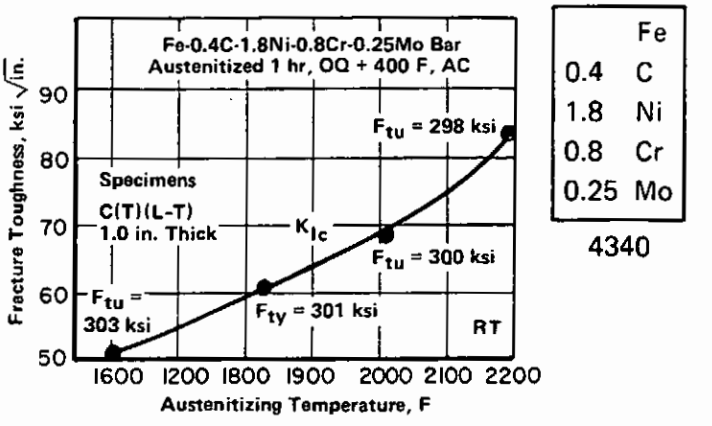


FIGURE 3.02725. EFFECT OF AUSTENITIZING TEMPERATURE ON THE ROOM TEMPERATURE FRACTURE TOUGHNESS OF OIL-QUENCHED-AND-TEMPERED VACUUM-ARC REMELTED PLATE (68)

Alloy	Fe-0.4C-1.8Ni-0.8Cr-0.25Mo
Form	Plate
Condition	K_{Ic}, ksi √in.
2190 F 1 hr, OQ + 390 F 1 hr, AC	89.1
2190 F 1 hr — 2010 F 10 min, OQ + 390 F 1 hr, AC	86.0
2190 F 1 hr — 2010 F 1/2 hr, OQ + 390 F 1 hr, AC	68.0
2190 F 1 hr — 2010 F 1 hr, OQ + 390 F 1 hr, AC	67.0
2190 F 1 hr — 1600 F 1/2 hr, OQ + 390 F 1 hr, AC	60.9

Notes: K_{Ic} specimens, C(T)(L-T), 1.0 in. thick.
F_{ty} approximately 220 ksi for all conditions.

TABLE 3.02726. EFFECTS OF VARIOUS STEP-QUENCHING TREATMENTS ON FRACTURE TOUGHNESS OF AIRCRAFT-QUALITY PLATE INITIALLY AUSTENITIZED AT 2190 F AND SUBSEQUENTLY TEMPERED AT 390 F (71)

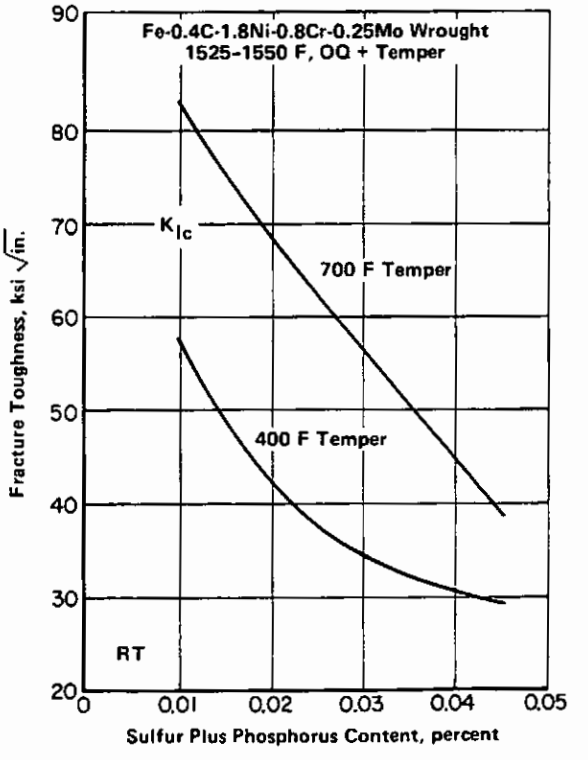


FIGURE 3.02727. EFFECT OF SULFUR PLUS PHOSPHORUS CONTENT ON THE FRACTURE TOUGHNESS (17, 78)

Note: Curves summarize averages of data gathered from a number of sources.

	Fe
0.4	C
1.8	Ni
0.8	Cr
0.25	Mo

4340

Alloy	Fe-0.4C-1.8Ni-0.8Cr-0.25Mo			
Condition	1600 F, OQ + Temper 1 hr, AC			
Temper, F	600		905	
Form	Cast	Plate	Cast	Plate
K_{Ic}, ksi √in.	60	55	104	80

Notes: Specimens, C(T)(T-L) [(T-L) direction applies to plate].
See Table 3.02118 for tensile properties.

TABLE 3.02728. COMPARISON OF ROOM TEMPERATURE FRACTURE TOUGHNESS IN TWO HEAT TREATED CONDITIONS OF CAST KEEL BLOCK AND WROUGHT PLATE MADE FROM THE SAME INDUCTION MELTED HEAT (73)

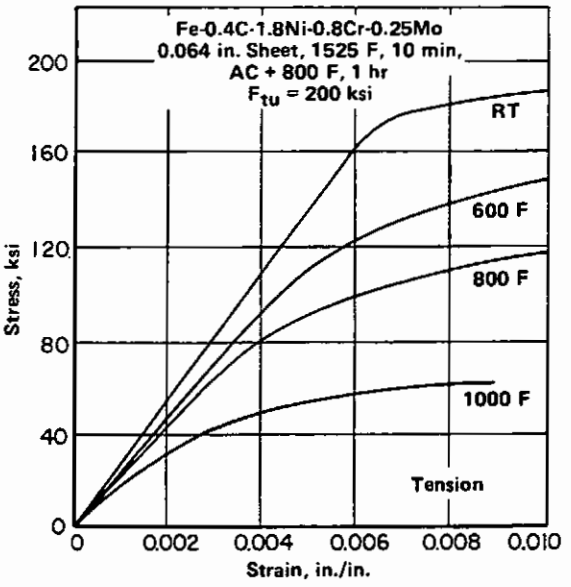


FIGURE 3.0311. TENSILE STRESS-STRAIN CURVES AT ROOM TEMPERATURE AND ELEVATED TEMPERATURES FOR SHEET HEAT TREATED TO F_{tu} = 200 KSI (51)

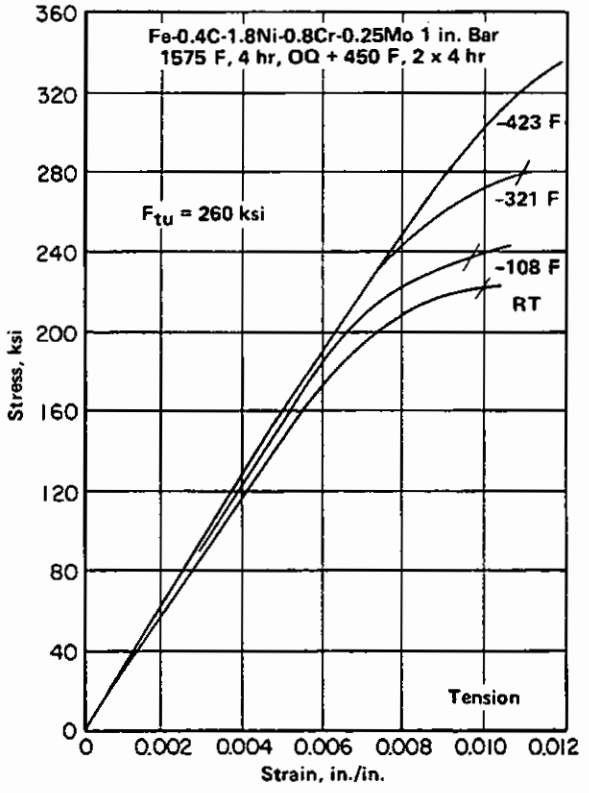


FIGURE 3.0312. TENSILE STRESS-STRAIN CURVES AT ROOM TEMPERATURE AND LOW TEMPERATURES FOR BAR HEAT TREATED TO F_{tu} = 270 KSI (52)

	Fe
0.4	C
1.8	Ni
0.8	Cr
0.25	Mo

4340

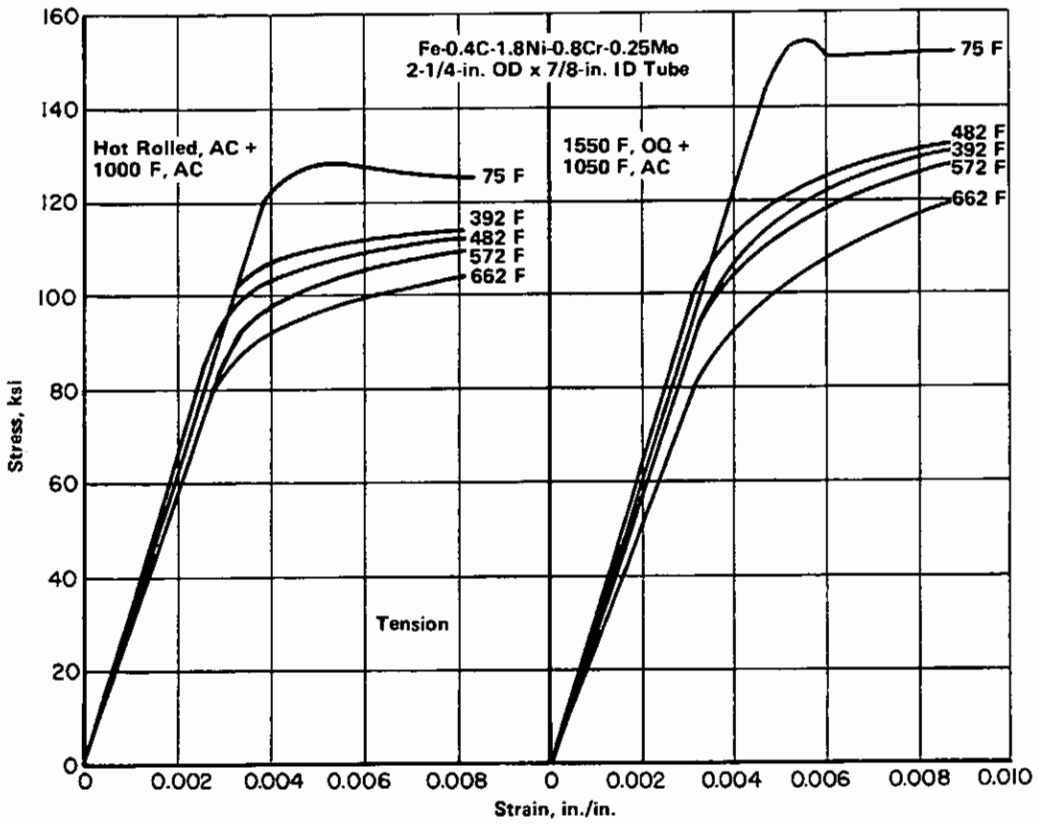


FIGURE 3.0313. TENSILE STRESS-STRAIN CURVES AT VARIOUS TEMPERATURES FOR TUBE IN TWO DIFFERENT CONDITIONS (7)

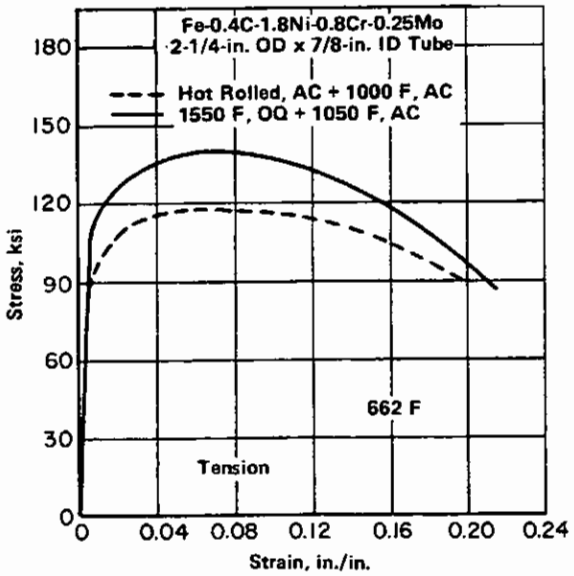


FIGURE 3.0314. COMPLETE TENSILE STRESS-STRAIN CURVES AT 662 F FOR TUBE IN TWO DIFFERENT CONDITIONS (7)

	Fe
0.4	C
1.8	Ni
0.8	Cr
0.25	Mo

4340

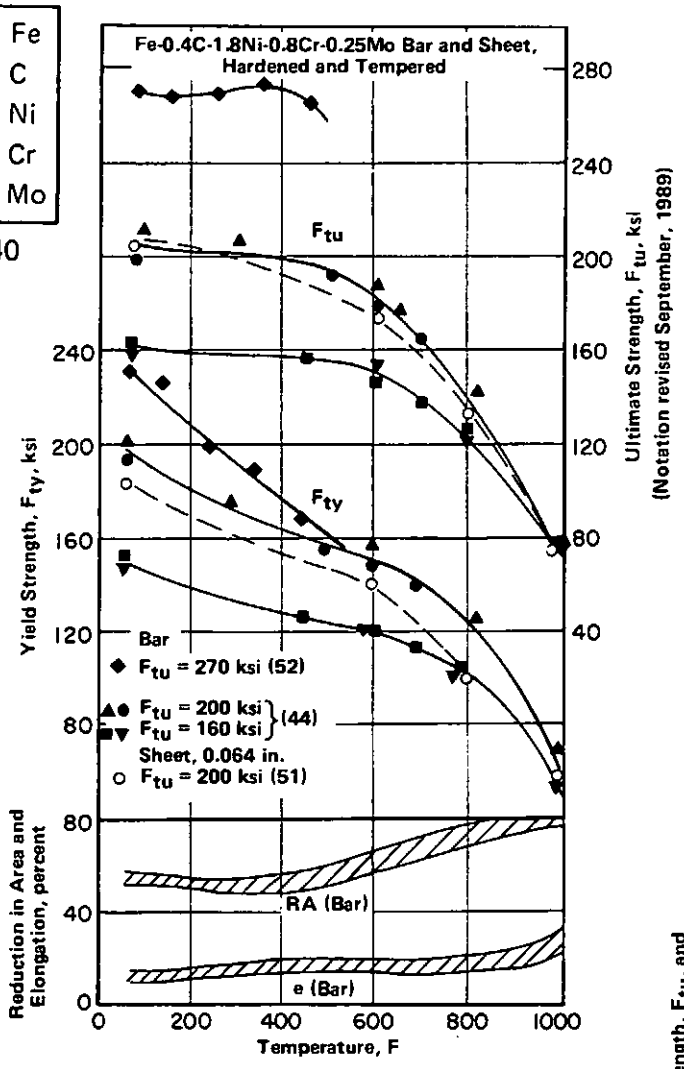


FIGURE 3.0315. EFFECT OF ELEVATED TEMPERATURES ON TENSILE PROPERTIES OF BAR AND SHEET HEAT TREATED TO VARIOUS STRENGTH LEVELS (44, 51, 52)

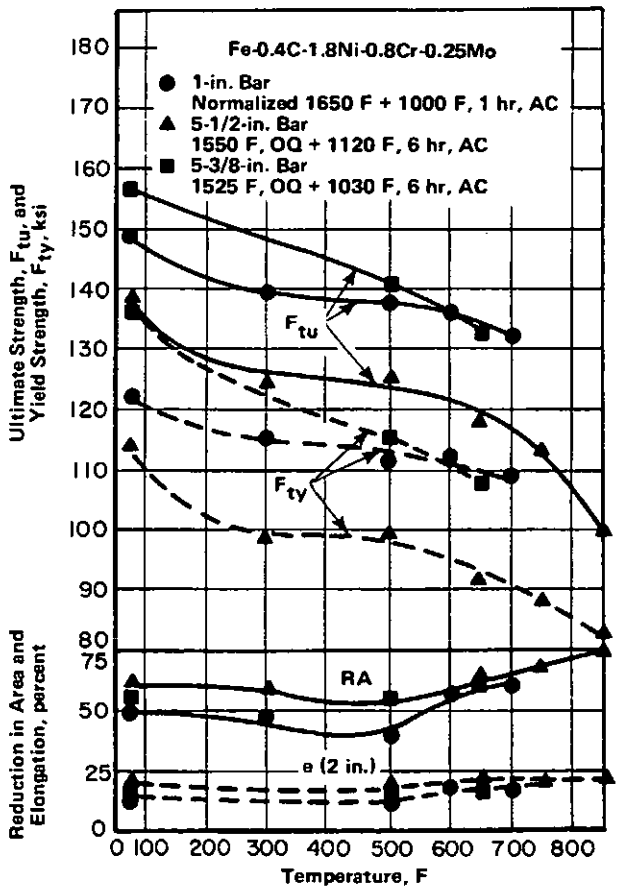


FIGURE 3.0316. EFFECT OF ELEVATED TEMPERATURES UP TO 850 F ON TENSILE PROPERTIES OF BAR IN VARIOUS HEAT TREATED CONDITIONS (7)

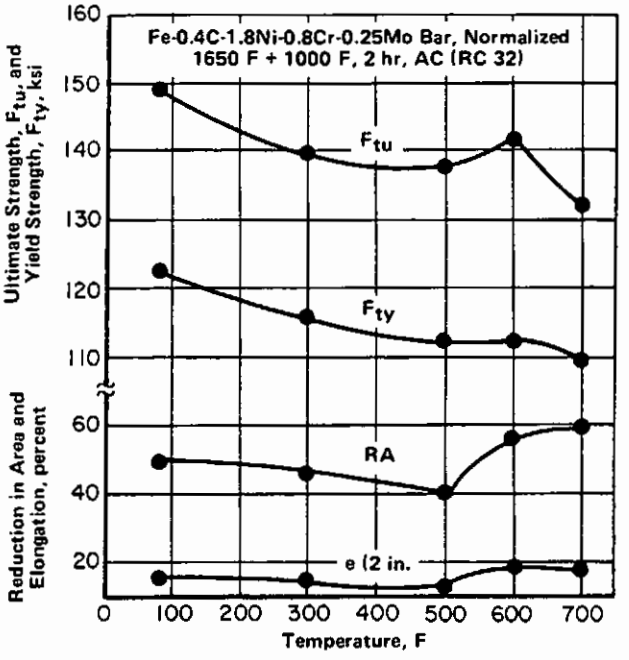


FIGURE 3.0317. EFFECT OF ELEVATED TEMPERATURES ON TENSILE PROPERTIES OF BAR NORMALIZED AND TEMPERED TO A HARDNESS LEVEL OF RC 32 (31)

	Fe
0.4	C
1.8	Ni
0.8	Cr
0.25	Mo

4340

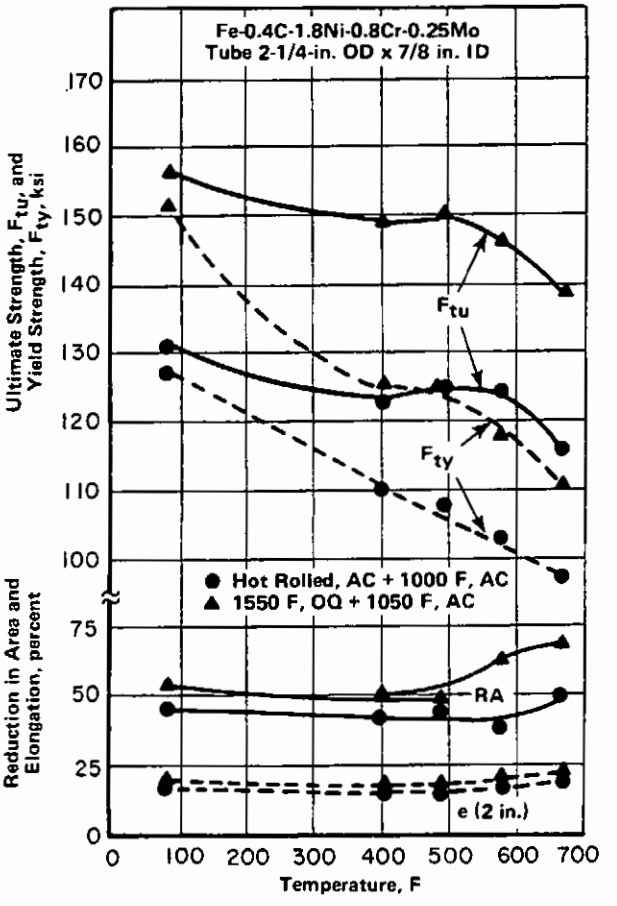


FIGURE 3.0318. EFFECT OF ELEVATED TEMPERATURES UP TO 662 F ON TENSILE PROPERTIES OF TUBE IN TWO DIFFERENT CONDITIONS (7)

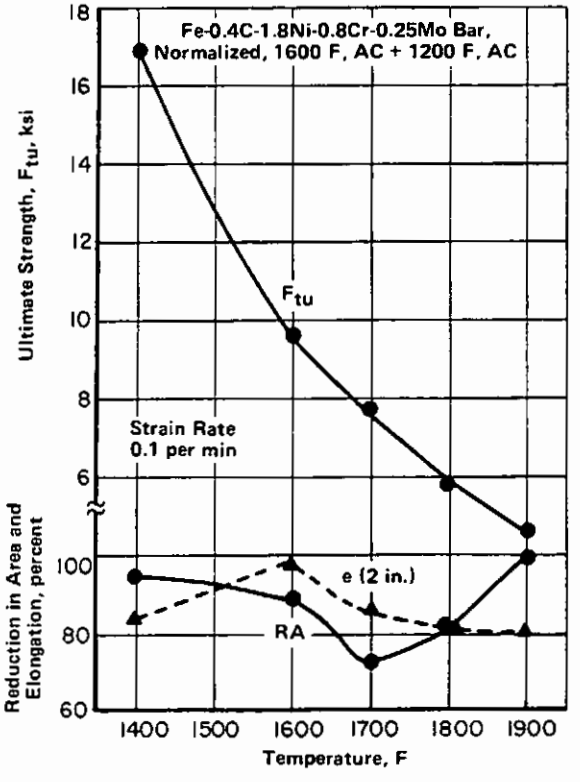


FIGURE 3.0319. EFFECT OF TEMPERATURES FROM 1400 F TO 1900 F ON TENSILE PROPERTIES OF NORMALIZED-AND-TEMPERED BAR (31)

	Fe
0.4	C
1.8	Ni
0.8	Cr
0.25	Mo

4340

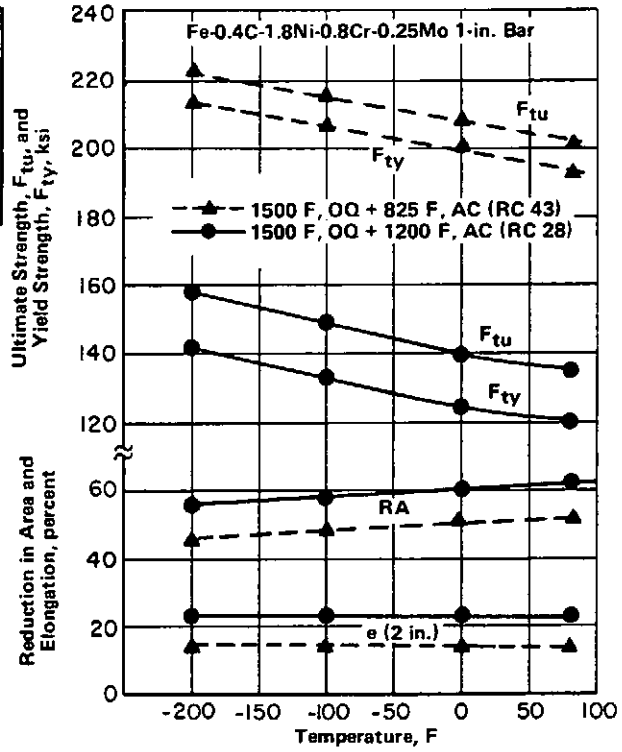


FIGURE 3.03110. EFFECT OF TEMPERATURES FROM 80 TO -200 F ON THE TENSILE PROPERTIES OF BAR QUENCHED AND TEMPERED TO TWO LEVELS OF HARDNESS (23)

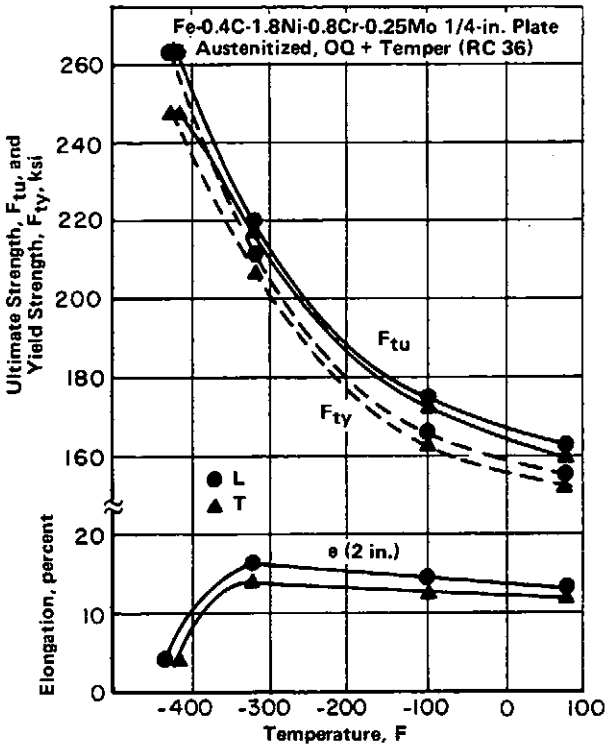


FIGURE 3.03111. EFFECT OF TEMPERATURES FROM 80 TO -423 F ON THE TENSILE PROPERTIES OF PLATE QUENCHED AND TEMPERED TO A HARDNESS LEVEL OF RC 36 (25)

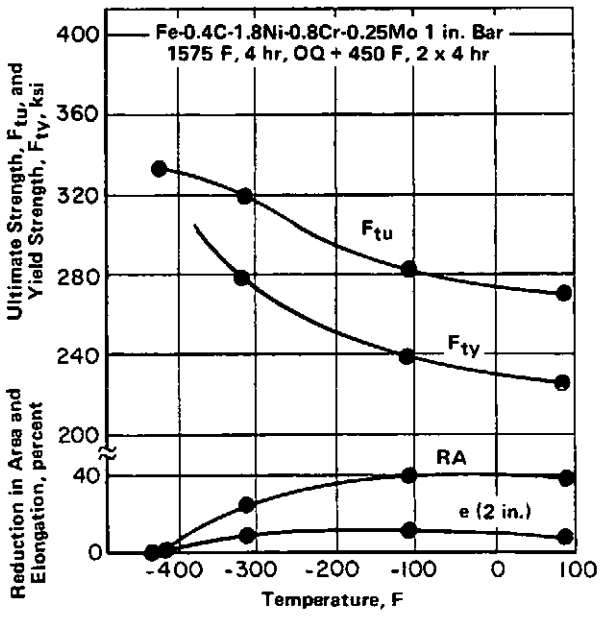


FIGURE 3.03112. EFFECT OF TEMPERATURES FROM 80 TO -423 F ON THE TENSILE PROPERTIES OF BAR QUENCHED AND TEMPERED TO F_{tu} = 270 KSI (31)

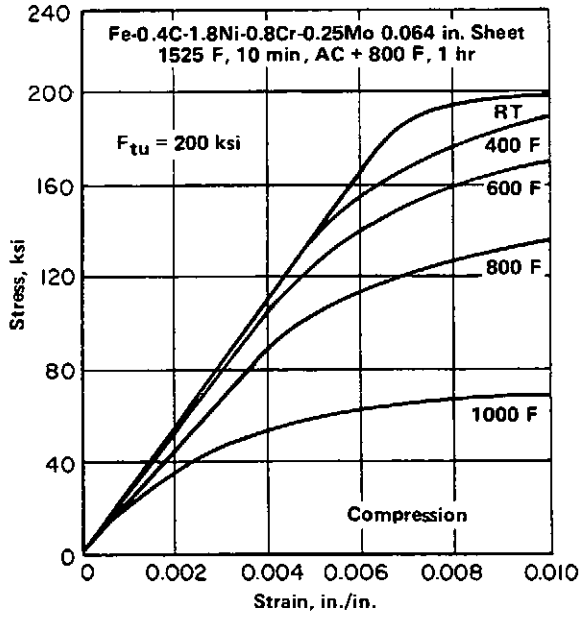


FIGURE 3.0321. STRESS-STRAIN CURVES IN COMPRESSION AT ROOM AND ELEVATED TEMPERATURES FOR SHEET HEAT TREATED TO F_{tu} = 200 KSI (51)

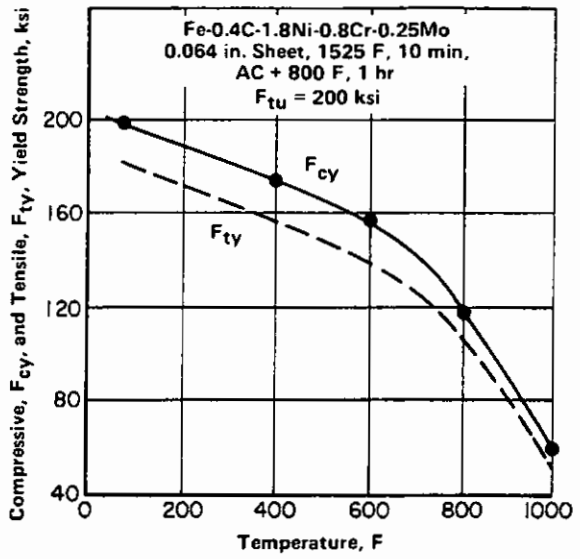


FIGURE 3.0322. EFFECT OF ELEVATED TEMPERATURES ON COMPRESSIVE YIELD STRENGTH OF SHEET HEAT TREATED TO F_{tu} = 200 KSI (51)

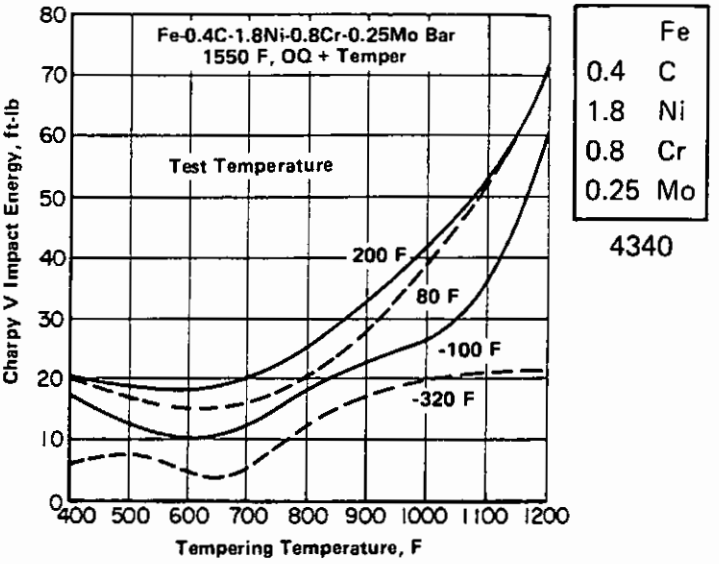


FIGURE 3.0331. EFFECTS OF TEMPERING TEMPERATURE AND TEST TEMPERATURE ON IMPACT PROPERTIES OF OIL-QUENCHED BAR (53)

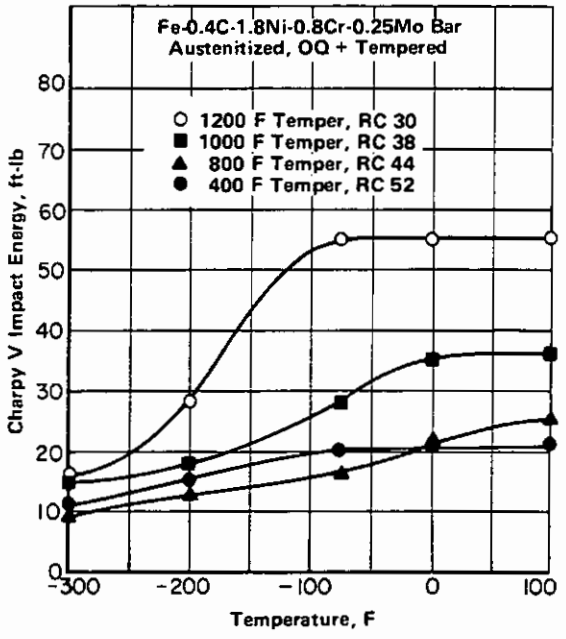


FIGURE 3.0332. EFFECT OF TEMPERATURES FROM 100 F TO -300 F ON IMPACT PROPERTIES OF OIL-QUENCHED BAR TEMPERED AT 400 TO 1200 F (38)

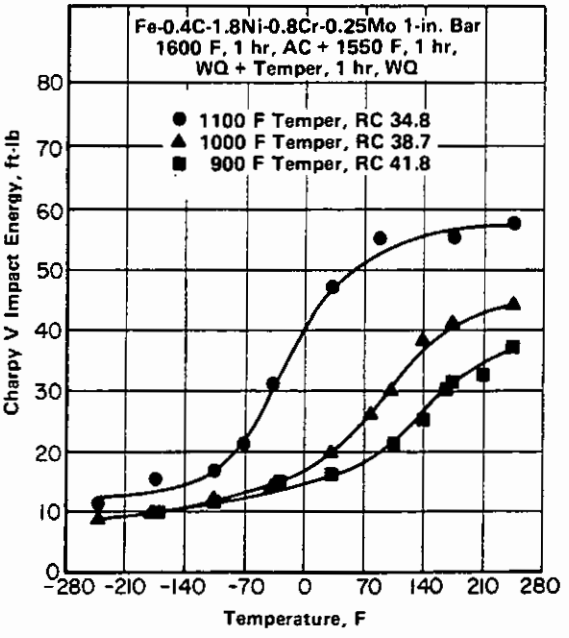


FIGURE 3.0333. EFFECT OF TEMPERATURES FROM 245 F TO -240 F ON IMPACT PROPERTIES OF WATER-QUENCHED BAR TEMPERED AT 900 TO 1100 F (3)

	Fe
0.4	C
1.8	Ni
0.8	Cr
0.25	Mo

4340

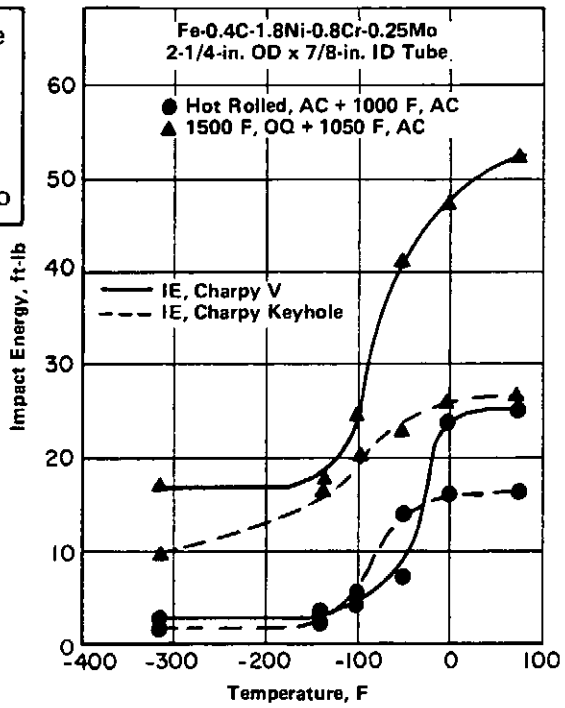


FIGURE 3.0334. EFFECT OF LOW TEMPERATURES ON IMPACT PROPERTIES OF TUBE IN TWO DIFFERENT CONDITIONS (7)

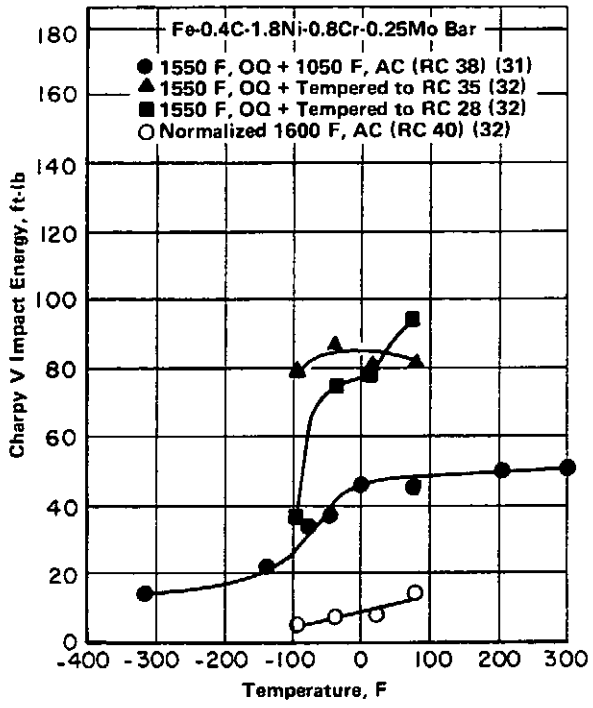


FIGURE 3.0335. EFFECT OF TEMPERATURE ON IMPACT PROPERTIES OF BAR IN VARIOUS HEAT TREATED CONDITIONS (31, 32)

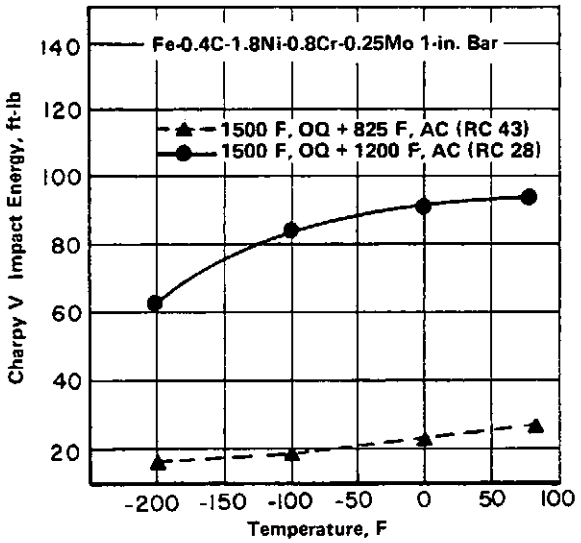


FIGURE 3.0336. EFFECT OF LOW TEMPERATURES ON THE IMPACT PROPERTIES OF BAR HEAT TREATED TO TWO LEVELS OF HARDNESS (23)

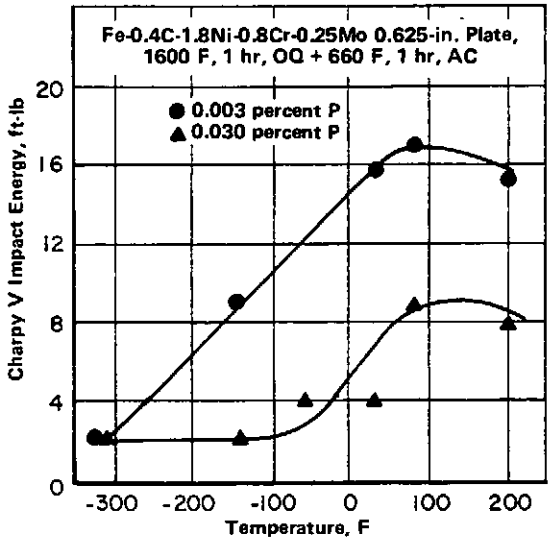
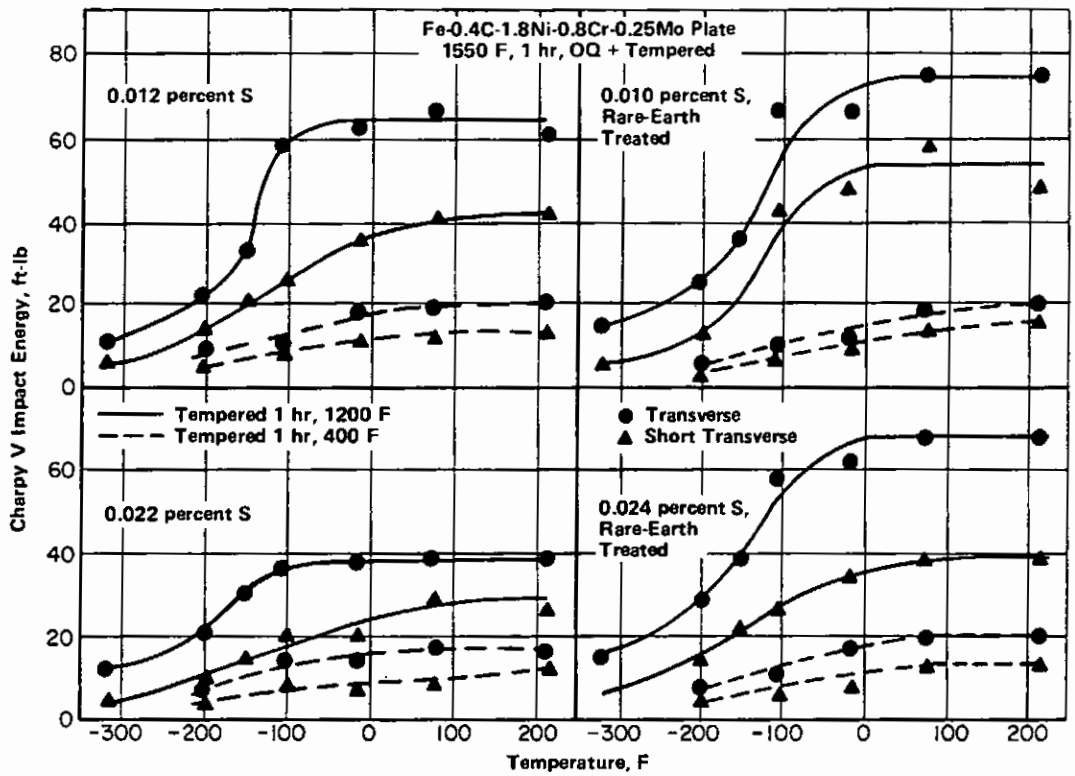


FIGURE 3.0337. EFFECTS OF TEMPERATURE AND PHOSPHORUS CONTENT ON IMPACT PROPERTIES OF PLATE THAT HAVE BEEN VACUUM INDUCTION MELTED (57)



	Fe
0.4	C
1.8	Ni
0.8	Cr
0.25	Mo

4340

FIGURE 3.0338. EFFECTS OF RARE-EARTH TREATMENT AND VARIATIONS IN SULFUR CONTENT ON IMPACT TRANSITION CURVES OF VACUUM INDUCTION MELTED PLATE IN TWO HEAT TREATED CONDITIONS (9)

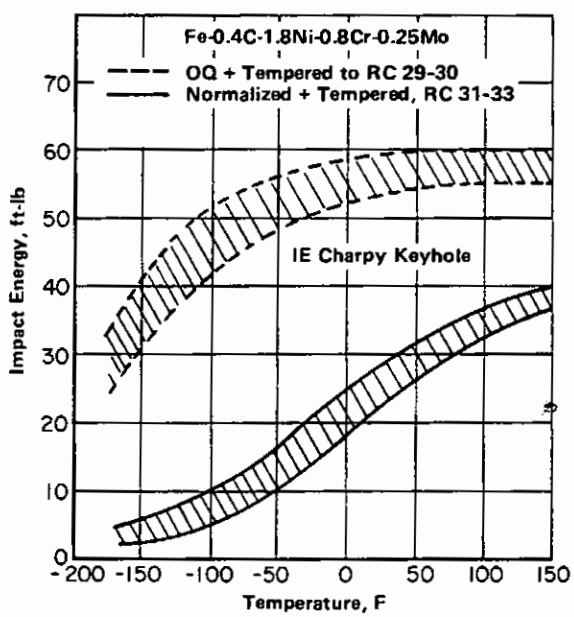
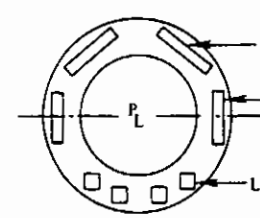


FIGURE 3.0339. COMPARISON OF IMPACT PROPERTIES OVER A RANGE OF TEMPERATURES FOR QUENCHED-AND-TEMPERED AND NORMALIZED-AND-TEMPERED 4340 (33)

Alloy	Fe-0.4C-1.8Ni-0.8Cr-0.25Mo		
Form	Forging		
Condition	Oil-Quenched and Tempered to R_C 41		
	Charpy V-Notch Impact, ft-lb		
Orientation	68 F	32 F	- 65 F
Longitudinal	27.5	20.0	17.3
Transverse	15.5	14.5	11.3
Transverse to P_L	10.9	9.6	8.6



Forging section 12-inch ID x 9-inch OD x 48-inch long. Forged to 12-inch diam, bored, and then heat treated.

TABLE 3.03310. IMPACT PROPERTIES AT VARIOUS TEMPERATURES FOR DIFFERENT ORIENTATIONS IN FORGINGS (33)

	Fe
0.4	C
1.8	Ni
0.8	Cr
0.25	Mo

4340

Alloy	Fe-0.4C-1.8Ni-0.8Cr-0.25Mo			
Form	1-inch Plate, Cross Rolled			
Condition	1650 F 1 hr, OQ + 1525 F 1 hr, OQ + 475 F 8 hr, AC			
		Charpy V-Notch IE, ft-lb		
Purity	Orientation	72 F	0 F	-80 F
Normal	L	12	10	9
	T	11	10	8
High	L	14	11	8
	T	14	11	9

Note: Chemical Analyses

Purity	C	Mn	P	S	Si	Ni	Cr	Mo	Cu
Normal	0.40	0.71	0.010	0.011	0.27	1.80	0.82	0.25	0.006
High	0.40	0.29	<0.0003	0.0008	0.007	1.79	0.75	0.27	0.002

(Cont)	Co	O	Al	N	Ti	As	Sb	Sn
Normal	0.008	0.0016	0.034	0.008	0.005	<0.002	<0.0004	<0.002
High	0.023	0.0010	0.002	0.002	<0.002	<0.002	<0.0004	<0.002

TABLE 3.03311. COMPARISON OF LOW TEMPERATURE IMPACT PROPERTIES OF AIR INDUCTION MELTED CROSS ROLLED PLATE OF NORMAL PURITY WITH THOSE OF HIGH PURITY PLATE PRODUCED BY VACUUM INDUCTION MELTING FOLLOWED BY VACUUM ARC REMELTING (8)

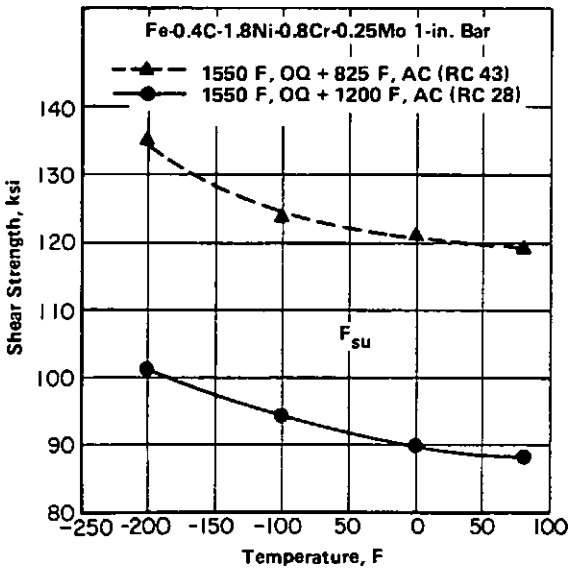


FIGURE 3.0351. EFFECT OF LOW TEMPERATURES ON SHEAR STRENGTH OF BAR QUENCHED AND TEMPERED TO TWO LEVELS OF HARDNESS (23)

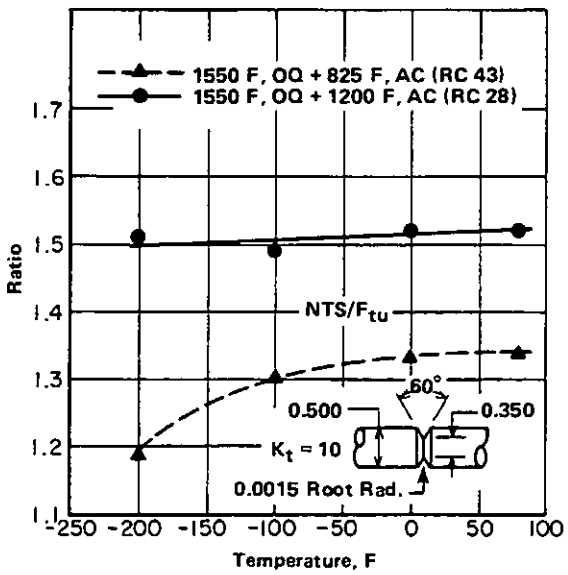


FIGURE 3.03711. EFFECT OF TEMPERATURES FROM 80 TO -200 F ON RATIO OF NOTCHED TENSILE STRENGTH TO TENSILE STRENGTH OF BAR HEAT TREATED TO TWO LEVELS OF HARDNESS (23)

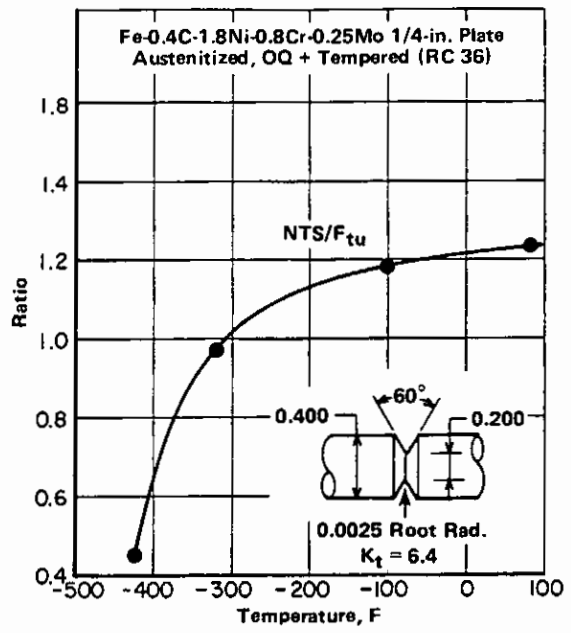


FIGURE 3.03712. EFFECT OF TEMPERATURES FROM 80 TO -423 F ON RATIO OF NOTCHED TENSILE STRENGTH TO TENSILE STRENGTH OF PLATE HEAT TREATED TO A HARDNESS LEVEL OF RC 36 (25)

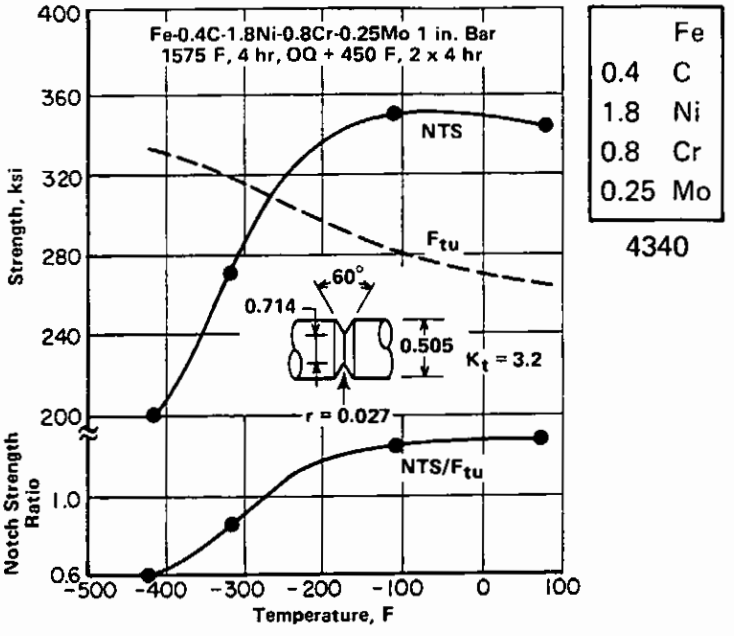


FIGURE 3.03713. EFFECT OF LOW TEMPERATURES ON NOTCHED STRENGTH OF BAR HEAT TREATED TO F_{tu} = 270 KSI (54)

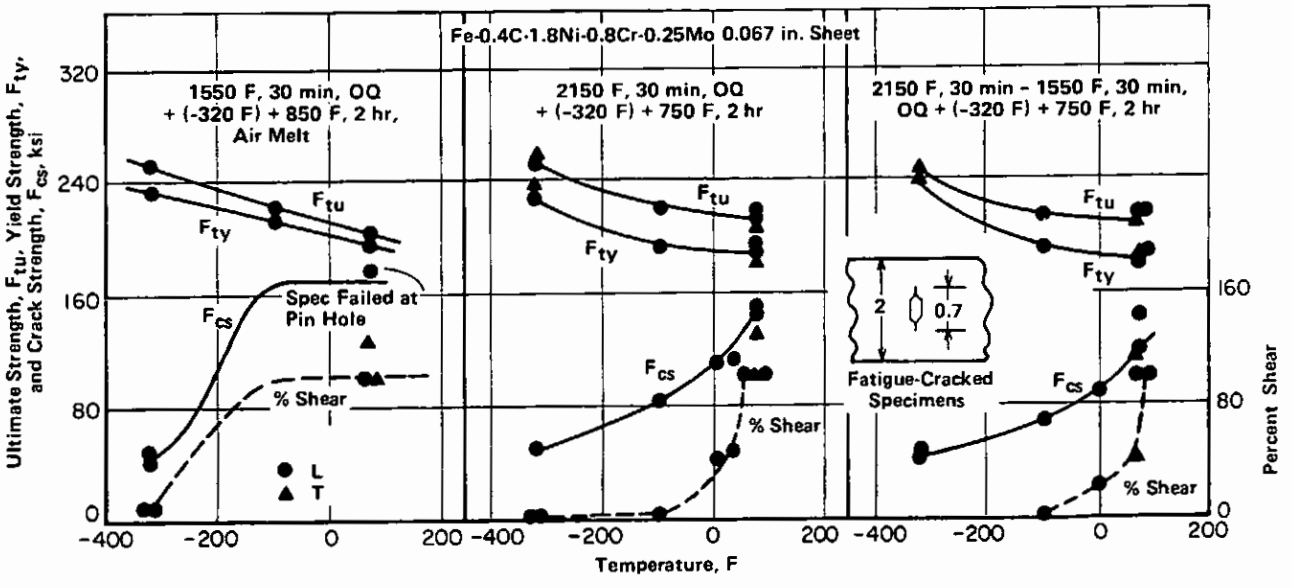


FIGURE 3.03714. EFFECT OF LOW TEMPERATURES ON TENSILE STRENGTH AND CRACK STRENGTH OF SHEET IN THREE HEAT TREATED CONDITIONS (55)

	Fe
0.4	C
1.8	Ni
0.8	Cr
0.25	Mo

4340

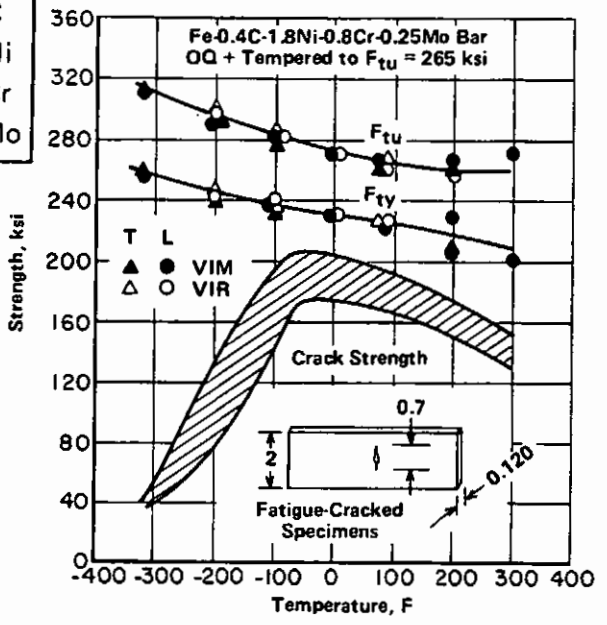


FIGURE 3.03715. EFFECT OF TEMPERATURES FROM -300 TO 300 F ON TENSILE STRENGTH AND CRACK STRENGTH OF VACUUM INDUCTION MELTED AND VACUUM INDUCTION REMELTED BAR HEAT TREATED TO F_{tu} = 265 KSI (55)

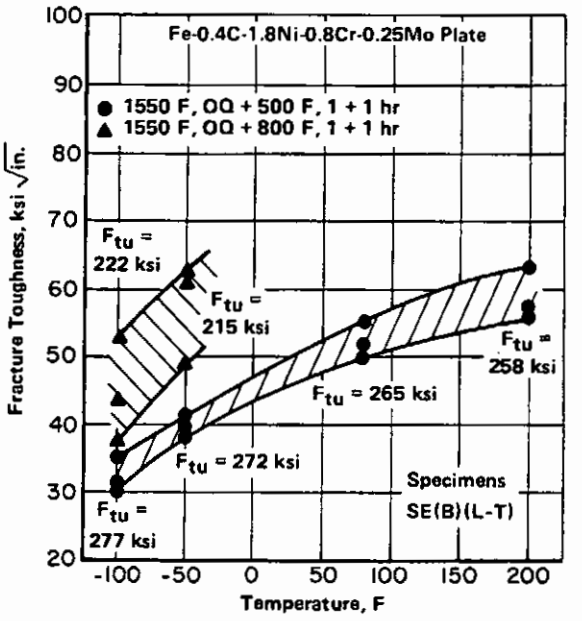


FIGURE 3.03721. EFFECT OF TEMPERATURES FROM -100 TO 200 F ON FRACTURE TOUGHNESS OF PLATE HEAT TREATED TO DIFFERENT STRENGTH LEVELS (40)

Alloy	Fe-0.4C-1.8Ni-0.8Cr-0.25Mo		
Form	1-inch Plate		
Condition	1550 F 1 hr, OQ + 400 F 3 + 3 hr, AC		
		Temp, F	
Property	Orientation(a)	75	-200
F_{ty}, ksi	L	214	225
F_{tu}, ksi	L	275	294
e (2 inch), percent	L	10	3
K_{Ic}, ksi √in.	L-S	72.6	40.1
	L-T	72.1	41.6
	T-S	–	40.6

Note: K_{Ic} specimens, M(T)(LS&LT), 0.25 in. thick.

TABLE 3.03722. FRACTURE TOUGHNESS AT 75 AND -200 F OF PLATE HEAT TREATED TO A ROOM TEMPERATURE TENSILE STRENGTH LEVEL OF 275 KSI (22)

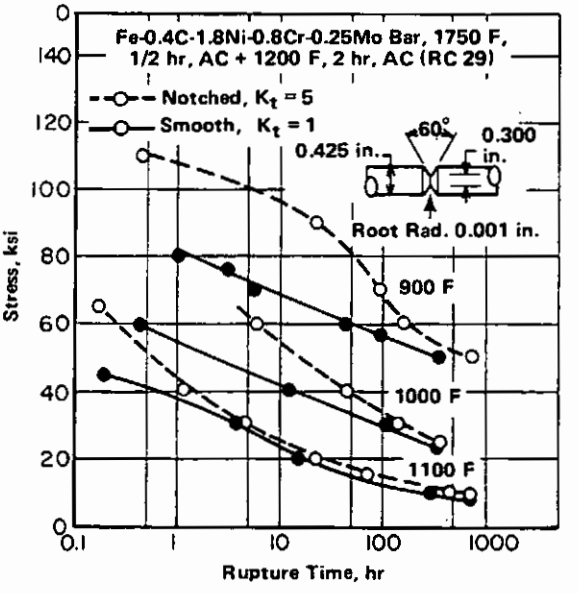


FIGURE 3.041. STRESS-RUPTURE PROPERTIES AT 900-1100 F OF NORMALIZED-AND-TEMPERED SMOOTH AND NOTCHED BAR (39)

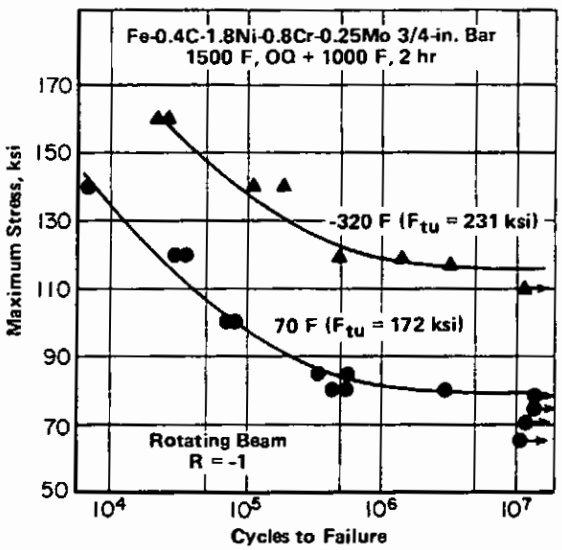


FIGURE 3.051. FATIGUE LIFE OF BAR AT ROOM TEMPERATURE AND AT -320 F (2)

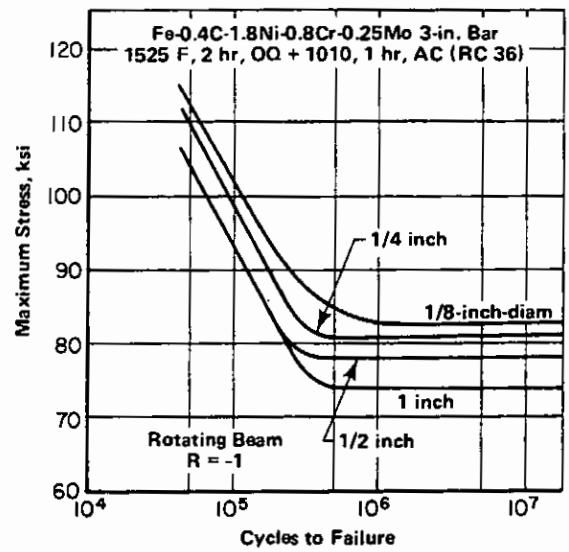


FIGURE 3.052. EFFECT OF SPECIMEN SIZES FROM 1/8 INCH TO 1 INCH DIAMETER ON FATIGUE LIFE OF BAR (28)

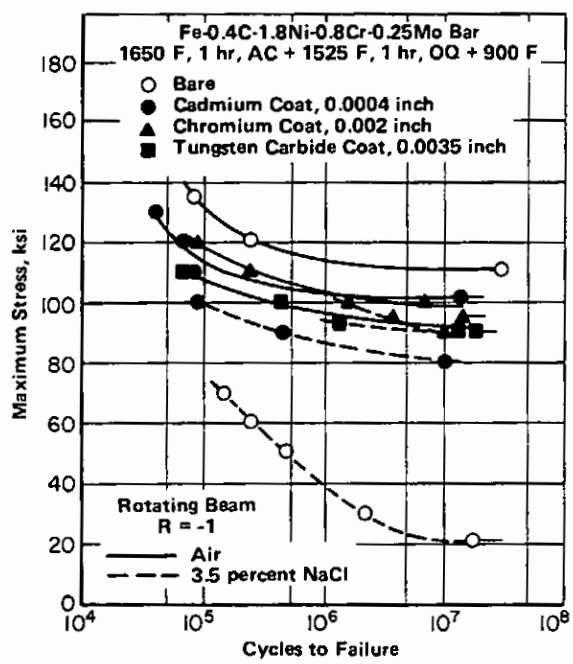


FIGURE 3.053. FATIGUE LIFE OF BARE AND COATED BAR IN ENVIRONMENTS OF AIR AND 3.5 PERCENT AQUEOUS SODIUM-CHLORIDE SOLUTION (10)

	Fe
0.4	C
1.8	Ni
0.8	Cr
0.25	Mo

4340

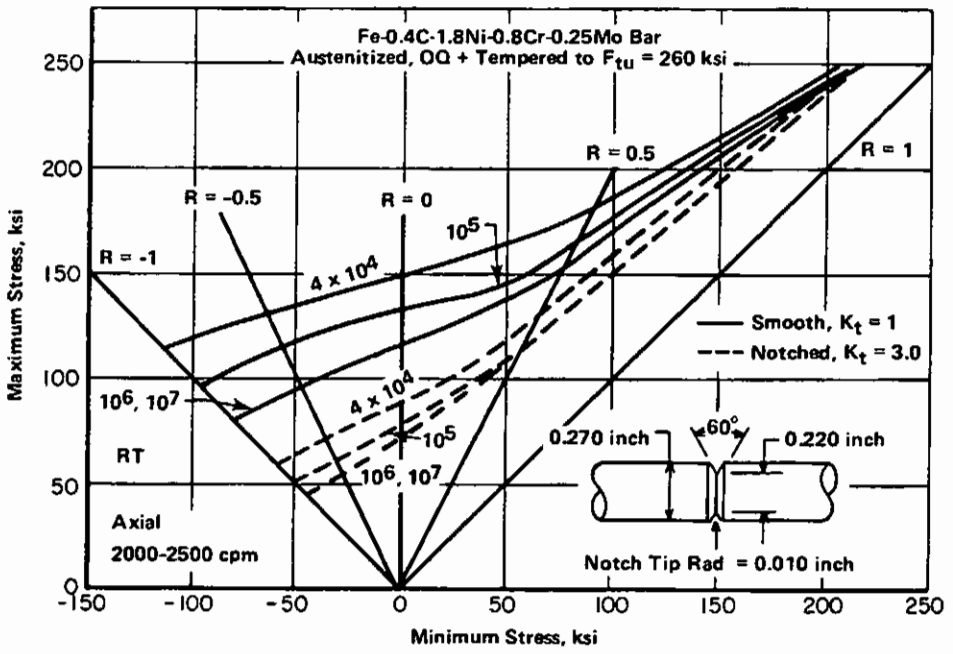


FIGURE 3.054. CONSTANT-LIFE FATIGUE CURVES AT 80 F FOR SMOOTH AND NOTCHED BAR HEAT TREATED TO F_{tu} = 260 KSI (37)

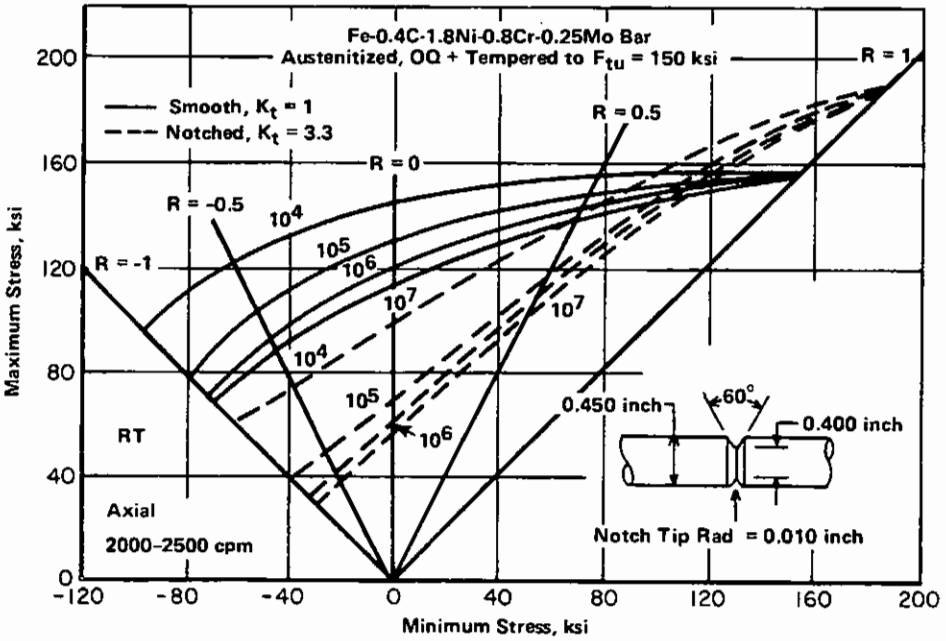


FIGURE 3.055. CONSTANT-LIFE FATIGUE CURVES AT 80 F FOR SMOOTH AND NOTCHED BAR HEAT TREATED TO F_{tu} = 150 KSI (37)

	Fe
0.4	C
1.8	Ni
0.8	Cr
0.25	Mo

4340

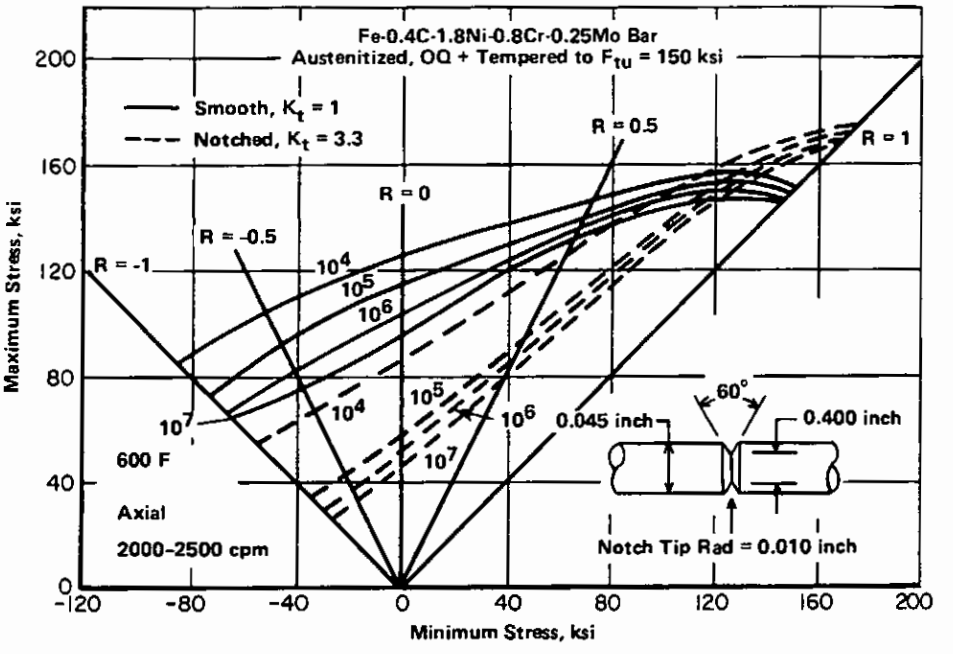


FIGURE 3.056. CONSTANT-LIFE FATIGUE CURVES AT 600 F FOR SMOOTH AND NOTCHED BAR HEAT TREATED TO F_{tu} = 150 KSI (37)

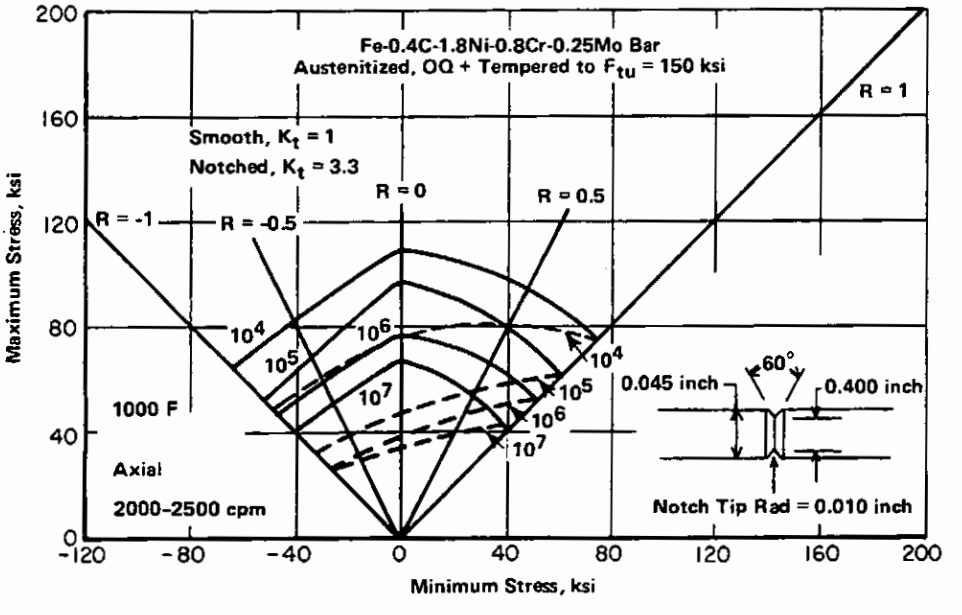


FIGURE 3.057. CONSTANT-LIFE FATIGUE CURVES AT 1000 F FOR SMOOTH AND NOTCHED BAR HEAT TREATED TO F_{tu} = 150 KSI (37)

	Fe
0.4	C
1.8	Ni
0.8	Cr
0.25	Mo

4340

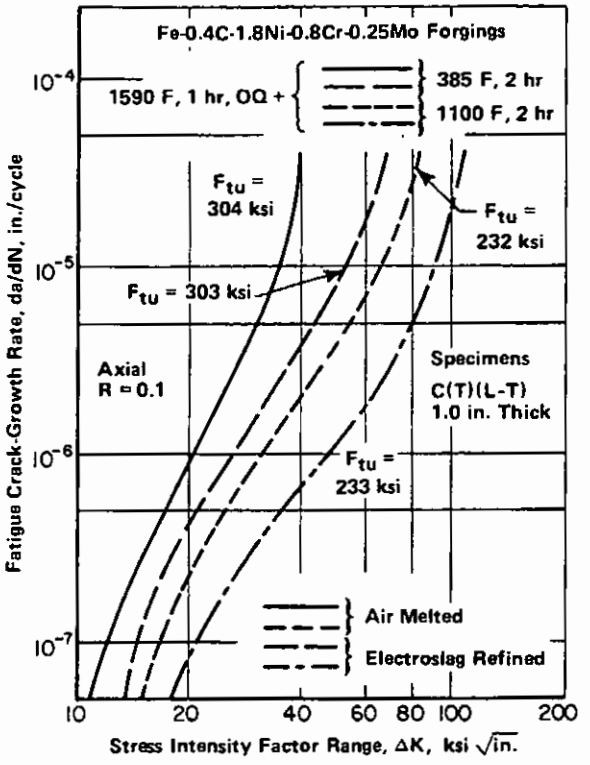


FIGURE 3.058. FATIGUE CRACK-GROWTH RATE IN AIR OF AIR-MELTED AND ELECTRO-SLAG REFINED FORGINGS THAT HAVE BEEN OIL-QUENCHED AND TEMPERED AT TWO DIFFERENT TEMPERATURES (58)

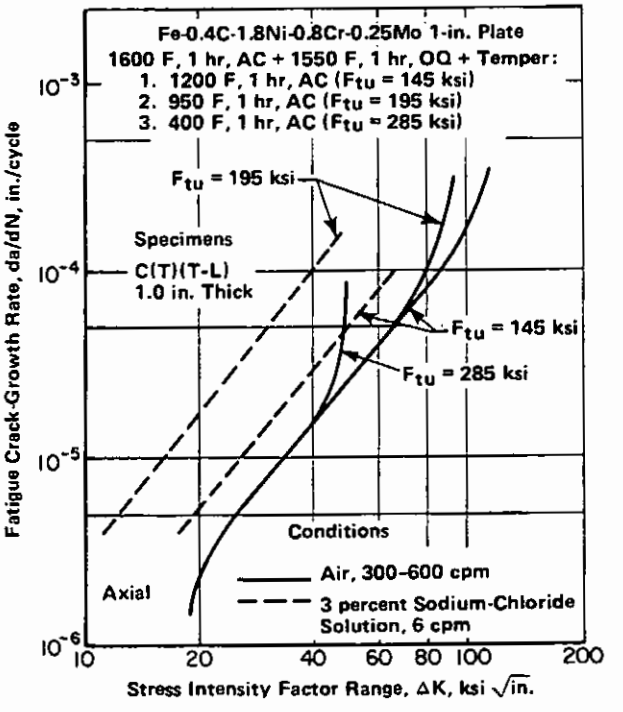


FIGURE 3.059. FATIGUE CRACK-GROWTH RATE OF PLATE AT VARIOUS STRENGTH LEVELS IN AIR AND IN AERATED 3 PERCENT AQUEOUS SODIUM-CHLORIDE SOLUTION (1)

	Fe
0.4	C
1.8	Ni
0.8	Cr
0.25	Mo

4340

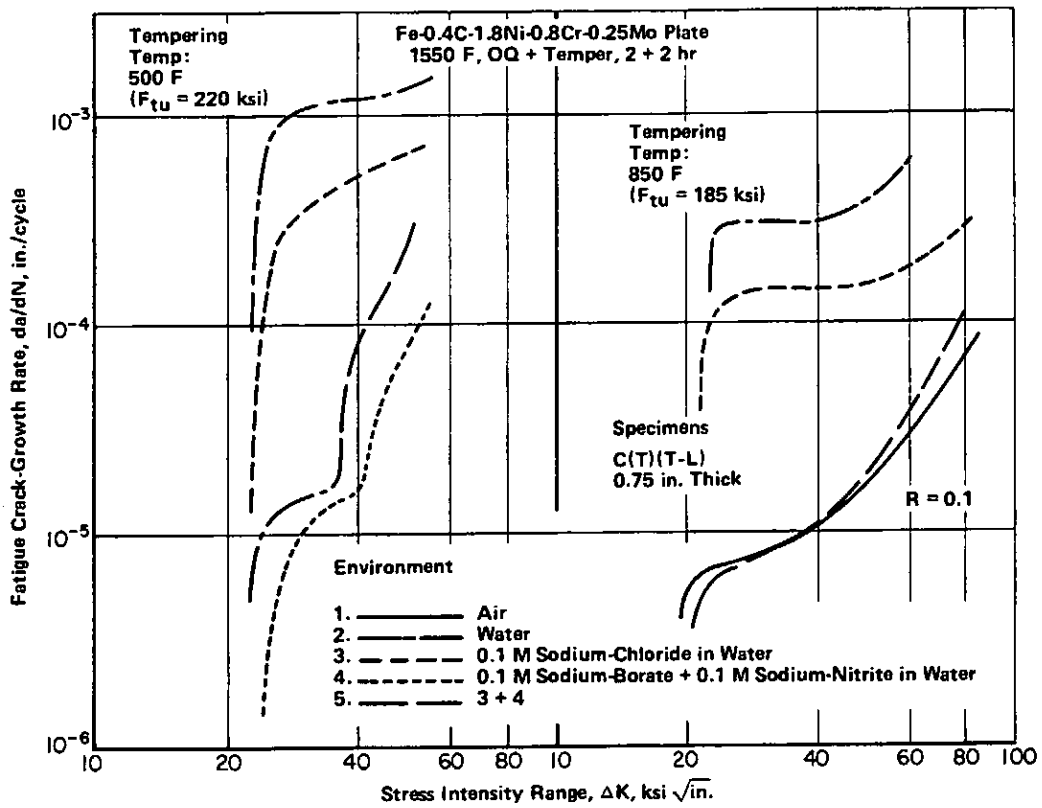


FIGURE 3.0510. EFFECTS OF VARIOUS ENVIRONMENTS AND A SODIUM-BORATE, SODIUM-NITRITE INHIBITOR ON FATIGUE CRACK-GROWTH RATE OF PLATE HEAT TREATED TO TWO STRENGTH LEVELS (29)

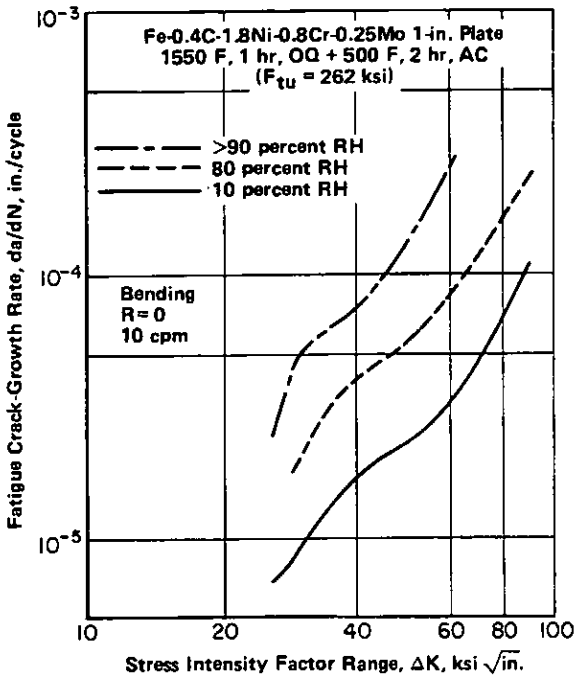


FIGURE 3.0511. FATIGUE CRACK-GROWTH RATES FOR PLATE TESTED AT ROOM TEMPERATURE IN AIR AT THREE LEVELS OF RELATIVE HUMIDITY (16, 36)

	Fe
0.4	C
1.8	Ni
0.8	Cr
0.25	Mo

4340

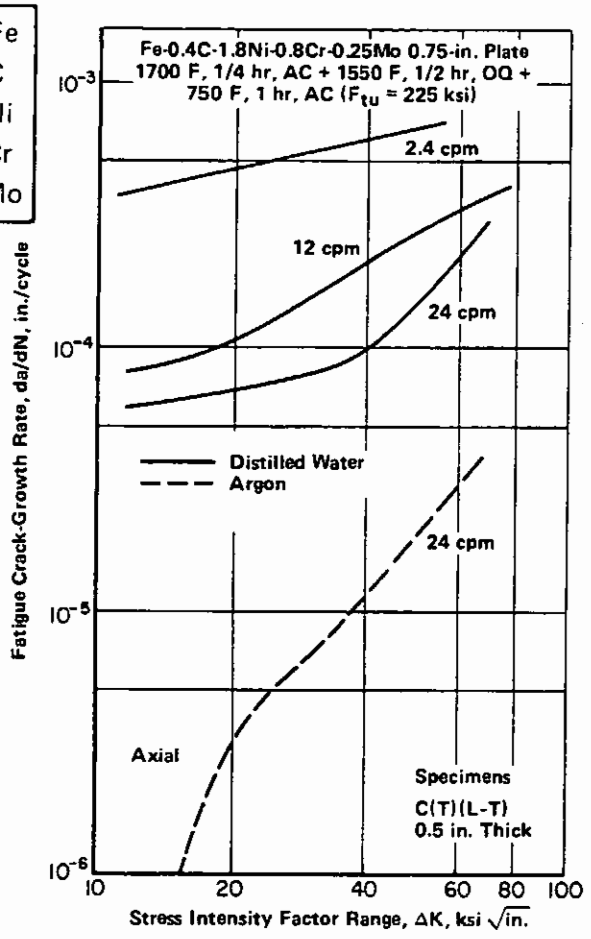


FIGURE 3.0512. FATIGUE CRACK-GROWTH RATES FOR PLATE TESTED AT ROOM TEMPERATURE IN DISTILLED WATER AT THREE FREQUENCIES AND IN ARGON AT ONE FREQUENCY (14)

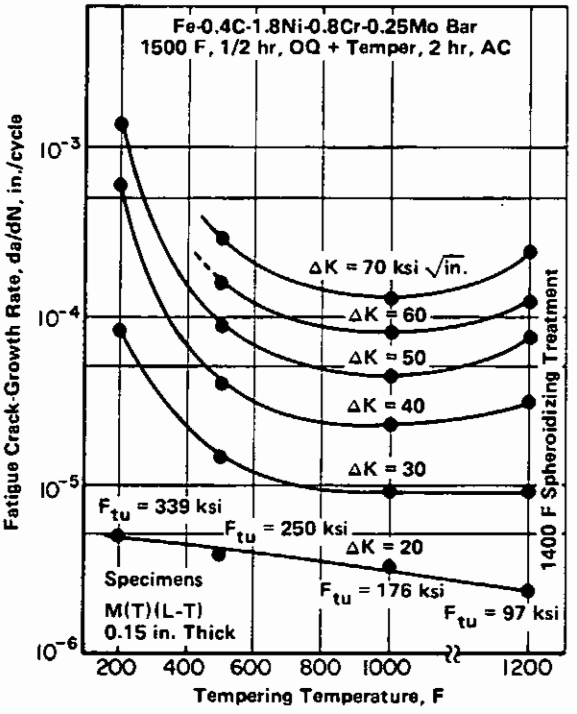


FIGURE 3.0513. EFFECTS OF TEMPERING TEMPERATURE AND STRESS-INTENSITY RANGE ON FATIGUE CRACK-GROWTH RATE IN AIR (19)

	Fe
0.4	C
1.8	Ni
0.8	Cr
0.25	Mo

4340

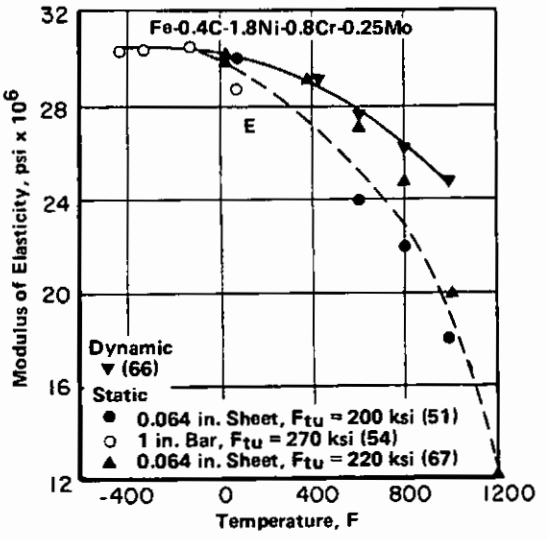


FIGURE 3.0621. EFFECT OF TEMPERATURES FROM -423 TO 1200 F ON MODULUS OF ELASTICITY (51, 54, 66, 67)

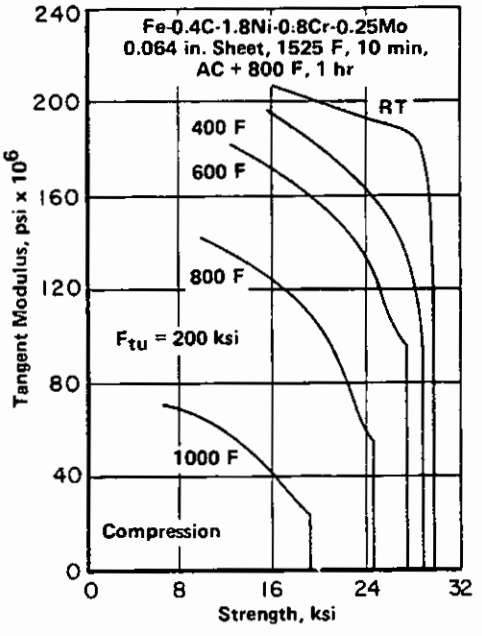


FIGURE 3.0641. TANGENT MODULUS CURVES IN COMPRESSION AT ROOM AND ELEVATED TEMPERATURES (51)

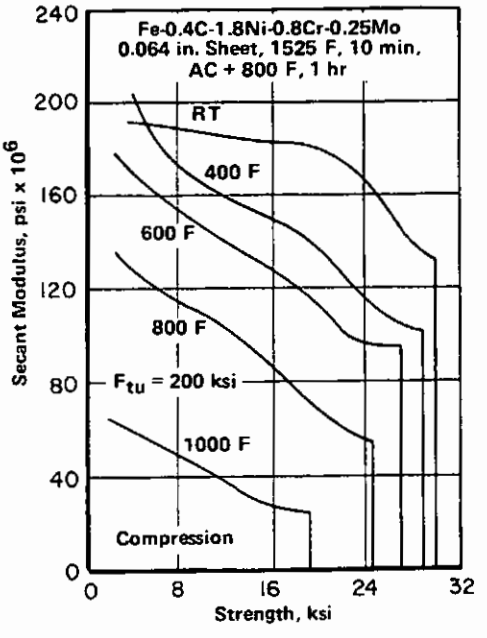


FIGURE 3.0651. SECANT MODULUS CURVES IN COMPRESSION AT ROOM AND ELEVATED TEMPERATURES (51)

1 General

This low-alloy steel, which is quite similar in properties to Type 4130, is hardenable in sections up to about 2 in. in thickness. In the quenched-and-tempered conditions it has an excellent combination of strength, toughness, and fatigue resistance; good formability and machinability are obtained in the annealed and normalized conditions. The alloy has satisfactory weldability if proper preheat and postheat treatments and low-hydrogen electrodes are used. It is useful for long-time applications at temperatures up to about 700F; at higher temperatures its strength decreases markedly. Like other martensitic or ferritic steels, it undergoes a transition from ductile to brittle behavior at low temperatures, which varies with heat treatment, section size, and degree of stress concentration. For long-time applications in moist environments, protective coatings or cathodic protection is desirable to prevent rusting. Typical applications are pinions, gears, shafting, axles, connecting rods, bolts, and air-frame parts.

1.1 Commercial Designation

8630

1.2 Alternate Designations

AISI 8630, SAE 8630, 8630H.

UNS J13042 (Investment Castings).

UNS J13050 (Sand Castings).

UNS G86300 (Wrought Products).

1.3 Specifications

1.3.1 *[Table]* AMS Specifications.

1.4 Composition

1.4.1 *[Table]* AMS Specified Compositions.

1.5 Heat Treatment

1.5.1 Normalize: 1575-1700F, air cool, for wrought products (Refs. 1, 5, 24); 1650-1750F, air cool, for castings (Refs. 15, 16). Tempering at 800-1200F is sometimes carried out after normalizing to improve strength and toughness.

1.5.2 Anneal: 1550F plus either slow cool from 1350 to 1180F at 20F/hr (8.5 hr total) or cool to 1225F and hold for 6 hours. This treatment produces a spheroidized structure, hardness HB 192 (Ref. 37).

1.5.3 Harden: 1525-1600F, oil quench or water quench. Type 8630 is not sensitive to quench cracking or delayed quench cracking. It should be quenched completely to room temperature to ensure transformation of most of the austenite to martensite and to achieve maximum as-quenched hardness (Ref. 37).

1.5.4 Temper: 400-1300F, 1/2 hour minimum, after hardening (Refs. 1, 5, 24).

1.5.5 Martemper: Type 8630 is commonly martempered to full hardness (Ref. 37).

1.5.6 Stress Relief: 675F for 3 hours but no higher than 50F below the tempering temperature. Stress relief of shot-peened parts should be limited to 400F to avoid relaxing compressive surface stresses (Ref. 28).

Fe
0.30 C
0.55 Ni
0.05 Cr
0.25 Mo

1.6 Hardness

1.6.1 *[Figure]* Effect of tempering temperature on hardness of bar.

1.6.2 *[Figure]* Typical hardness of tempered bar.

1.6.3 *[Figure]* Effects of bar diameter on hardness for various heat-treated conditions.

1.6.4 *[Figure]* Effects of bar diameter on as-quenched hardness at various depths in bar.

1.6.5 *[Figure]* Approximate maximum bar diameters hardenable by martempering, oil quenching, and water quenching.

1.6.6 *[Figure]* Effects of cold work on hardness.

1.6.7 *[Figure]* Effects of time at 1000F on room-temperature hardness for various heat treatments.

1.6.8 *[Figure]* End-quench hardenability band.

1.6.9 The end-quench hardenability of Type 8630 can be increased by microalloying with 0.15 percent vanadium (Ref. 29).

1.7 Forms and Conditions Available

1.7.1 The alloy is available in most wrought forms including sheet, strip, plate, bars, rods, tubing, billets, and forgings. Mill products are normally furnished in the hot-rolled, cold-finished, annealed, or normalized condition.

1.7.2 Sand, investment, and centrifugal castings are available in any of the heat-treated conditions.

1.8 Melting and Casting Practice

1.8.1 Type 8630 is generally air melted in basic-electric, basic-open-hearth, or basic-oxygen furnaces. For exceptional quality, it can be induction or consumable-electrode remelted in vacuum.

1.8.2 Ladle desulfurization of acid melted 8630 is recommended as a means of improving tensile elongation and reduction of area and Charpy V-notch properties. Final sulfur levels of 0.010 to 0.014 percent can be consistently achieved by this technique. The reduced sulfur levels also alleviate hot tearing tendencies in complex, thin-walled castings (Ref. 30).

© 1992 by Purdue Research Foundation, West Lafayette, Indiana 47907.
All Rights Reserved.

1.9 Special Considerations

1.9.1 Tempering in the range 500-800F is not recommended for Type 8630 (or other low-alloy steels) because it tends to cause embrittlement and increased ductile-to-brittle transition temperature (Ref. 13, see also Figure 3.3.3.4).

1.9.2 See Type 4130, Code 1201, Section 1.9

2 Physical and Environmental Effects

2.1 Thermal Properties

2.1.1 Melting Range 2740F (approximate) (Ref. 5).

2.1.2 Phase Changes.

2.1.2.1 *[Figure]* Time-temperature-transformation diagram.

2.1.2.2 Upon heating under equilibrium conditions, the transformation from pearlite or martensite to austenite starts at 1365F (A_{c1}) and is complete at 1465F (A_{c3}) (Ref. 1).

2.1.2.3 Upon slow cooling under equilibrium conditions, the transformation from austenite to pearlite starts at 1365F (A_{r3}) and is complete at 1205F (A_{r1}) (Ref. 1).

2.1.2.4 Upon rapid quenching from the austenitic condition the transformation to martensite starts at 700F (M_s) and is complete at 540F (M_f) (Ref. 5).

2.1.3 Thermal Conductivity. 21.7 Btu ft per (hr sq ft F) (Ref. 5).

2.1.4 Thermal Expansion.

2.1.4.1 Mean coefficient, in. per in. per F,

0-200F, 6.3×10^{-6}

0-1200F, 8.1×10^{-6}

2.1.4.2 *[Figure]* Thermal expansion at low temperatures (Ref. 5).

2.1.5 Specific heat 0.107 Btu per (lb F) (Ref. 5).

2.1.6 Thermal Diffusivity.

2.2 Other Physical Properties

2.2.1 Density 0.283 lb per cu. in., 7.83 gr per cu. cm. (Ref. 5).

2.2.2 *[Table]* Electrical Properties.

2.2.3 Magnetic Properties. Ferromagnetic.

2.2.4 Emittance.

2.2.5 Damping Capacity.

2.3 Chemical Environment

2.3.1 General Corrosion.

2.3.1.1 Like other ferritic and martensitic steels, Type 8630 rusts in the presence of moisture and oxygen. The rate of rusting increases as the following environmental variables increase: temperature, acidity of the moisture (low pH), and velocity of the water. Contact with a cathodic metal also increases the rate of rusting.

2.3.1.2 See Type 4130, Code 1201, Section 2.3.

2.3.2 Stress Corrosion.

2.4 Nuclear Environment

3 Mechanical Properties

3.1 Specified Mechanical Properties

3.1.1 *[Table]* AMS Specified Mechanical Properties.

3.2 Mechanical Properties at Room Temperature

3.2.1 Tension Stress-strain Diagrams and Tensile Properties.

3.2.1.1 *[Figure]* Tensile stress-strain curves for sheet in various heat-treated conditions.

3.2.1.2 *[Figure]* Tensile stress-strain curves for bar in various heat-treated conditions.

3.2.1.3 *[Figure]* Effects of tempering temperature after both oil quench and water quench on room-temperature tensile properties of 0.530 in. bar.

3.2.1.4 *[Figure]* Effect of tempering temperature on tensile properties of sheet.

3.2.1.5 *[Figure]* Effects of bar diameter on tensile properties for various heat-treated conditions.

3.2.1.6 *[Figure]* Effects of tempering temperature on tensile properties of bar heat treated to two different metallurgical structures.

3.2.1.7 *[Figure]* Effects of cold drawing on tensile properties of normalized bar.

3.2.1.8 *[Table]* Tensile properties of tube in various heat-treated conditions.

3.2.1.9 *[Table]* Tensile properties of extrusions in two heat-treated conditions.

3.2.1.10 *[Table]* Effect of cold extrusion on tensile properties of annealed bar.

3.2.1.11 *[Table]* Tensile properties of castings in two heat-treated conditions.

3.2.2 Compression Stress-strain Diagrams and Compression Properties.

3.2.2.1 *[Figure]* Compressive stress-strain curves for bar in various heat-treated conditions.

3.2.2.2 *[Figure]* Effects of tempering temperature on compressive yield strength of bar heat treated to two different metallurgical structures.

3.2.3 Impact.

3.2.3.1 *[Figure]* Effects of tempering temperature on room-temperature impact strength.

3.2.4 Bending.

3.2.5 Torsion and Shear.

3.2.5.1 *[Table]* Shear strength of bar determined on pin-type double-shear specimens.

3.2.5.2 *[Figure]* Effects of tempering temperature on torsional properties of bar heat treated to two different metallurgical structures.

3.2.6 Bearing.

3.2.6.1 *[Figure]* Effects of tempering temperature on bearing properties.

3.2.7 Stress Concentration.

3.2.7.1 Notch properties.

3.2.7.1.1 *[Figure]* Effect of tempering temperature on notched tensile strength.

3.2.7.2 Fracture toughness.

3.2.8 Combined Properties.

3.3 Mechanical Properties at Various Temperatures

3.3.1 Tension Stress-strain Diagrams and Tensile Properties.

3.3.1.1 *[Figure]* Stress-strain curves from room temperature to 1200F for sheet quenched and tempered to 125 ksi F_{tu}.

3.3.1.2 *[Figure]* Stress-strain curves from room temperature to 1200F for sheet quenched and tempered to 160 ksi F_{tu}.

3.3.1.3 *[Figure]* Monotonic and cyclic stress-strain curves for cast alloy at room temperature and -50F.

3.3.1.4 *[Figure]* Effects of exposures from one-half to 100 hours at test temperature on elevated-temperature tensile properties of sheet quenched and tempered to two different strength levels.

3.3.1.5 *[Figure]* Effects of low temperatures on tensile properties of both normalized and quenched-and-tempered alloy.

3.3.2 Compression Stress-strain Diagrams and Compression Properties.

3.3.2.1 *[Figure]* Stress-strain curves in compression from room temperature to 1000F for sheet quenched and tempered to 120 ksi F_{tu}.

3.3.2.2 *[Figure]* Stress-strain curves in compression from room temperature to 1000F for sheet quenched and tempered to 160 ksi F_{tu}.

3.3.2.3 *[Figure]* Effects of exposures from one-half hour to 100 hours at test temperature on compressive yield strength of sheet quenched and tempered to two F_{tu} levels.

3.3.3 Impact.

3.3.3.1 *[Figure]* Low-temperature impact properties of bar.

3.3.3.2 *[Figure]* Comparison of low-temperature impact properties of hardened-and-tempered and normalized alloy.

3.3.3.3 *[Figure]* Effects of cold work on impact properties at room temperature and -40F.

3.3.3.4 *[Figure]* Effect of tempering temperature on impact (Charpy V) transition temperature.

3.3.3.5 *[Figure]* Effect of temperature on impact energy of cast alloy.

3.3.3.6 *[Figure]* Effect of tempering temperature on impact energy of cast alloy at low temperatures.

3.3.4 Bending.

3.3.5 Torsion and Shear.

3.3.5.1 *[Figure]* Effects of exposures from one-half hour to 100 hours at test temperature on shear strength of sheet quenched and tempered to two F_{tu} levels.

3.3.6 Bearing.

3.3.6.1 *[Figure]* Effects of exposures from one-half hour to 100 hours at test temperature on bearing properties of sheet quenched and tempered to two F_{tu} levels.

3.3.7 Stress Concentration.

3.3.7.1 Notch properties.

3.3.7.2 Fracture toughness.

3.3.7.2.1 The J_{Ic} fracture toughness was determined using the ASTM E 813 Standard Test for cast, heat-treated (as in Figure 3.5.5) 8630 alloy as 456 in-lb/in^2 at room temperature. Based on this determination, a conservative value for the plane strain fracture toughness, K_{Ic}, was estimated as 123 ksi(in)$^{1/2}$. At -50F, the cleavage fracture toughness, J_{cl}, was measured as 175 in-lb/in^2, from which K_{cl} was estimated as 77 ksi(in)$^{1/2}$ (Ref. 31).

3.4 Creep and Creep Rupture Properties

3.4.1 *[Figure]* Short-time creep properties of sheet heat treated to an F_{tu} level of 125 ksi.

3.4.2 *[Figure]* Short-time creep properties of sheet heat treated to an F_{tu} level of 180 ksi.

3.4.3 *[Figure]* Long-time creep properties of sheet in the annealed and quenched-and-tempered conditions.

3.5 Fatigue Properties

3.5.1 *[Figure]* Fatigue properties of bar at several strength levels and under various loading conditions.

3.5.2 *[Figure]* Low-temperature fatigue properties of notched bar.

3.5.3 *[Figure]* Fatigue properties of castings in the normalized-and-tempered and quenched-and-tempered conditions.

3.5.4 *[Figure]* Effects of cold work on fatigue endurance limit at 10^7 cycles.

3.5.5 *[Figure]* Fatigue behavior of cast alloy at room temperature.

3.5.6 *[Figure]* Fatigue behavior of cast alloy at -50F.

3.5.7 *[Figure]* Fatigue crack-growth rate for cast alloy at R = 0.5.

3.5.8 *[Figure]* Fatigue crack-growth rate for cast alloy at R = 0.

3.5.9 *[Figure]* Threshold and near-threshold fatigue crack-growth rates for cast alloy at room temperature and -50F.

3.6 Elastic Properties

3.6.1 Poisson's Ratio. 0.32 (Ref. 12).

3.6.2 Modulus of Elasticity. 30×10^3 ksi (Ref. 12).

3.6.2.1 *[Figure]* Effects of temperature on modulus of elasticity in tension for sheet quenched and tempered to two F_{tu} levels.

3.6.2.2 *[Figure]* Effects of temperature on modulus of elasticity in compression for sheet quenched and tempered to two F_{tu} levels.

3.6.3 Modulus of Rigidity. 11.3×10^3 ksi (Ref. 12).

3.6.4 Tangent Modulus.

3.6.4.1 *[Figure]* Tangent modulus curves in compression at room and elevated temperatures for sheet quenched and tempered to 120 ksi F_{tu}.

3.6.4.2 *[Figure]* Tangent modulus curves in compression at room and elevated temperatures for sheet quenched and tempered to 160 ksi F_{tu}.

3.6.5 Secant Modulus.4 Fabrication

4 Fabrication

4.1 Forming

4.1.1 The forming characteristics, both cold and hot, of Type 8630 are similar to those of Type 4130. (See Chapter Code 1201, Sections 4.1.1 and 4.1.2.)

4.2 Machining and Grinding

4.2.1 Type 8630 has good machinability in the annealed, normalized, and cold-drawn conditions. Optimum machinability is obtained when the alloy is annealed and then cold drawn, which provides a machinability rating of 63 percent or more of that of AISI B1112 steel (Ref. 5).

4.3 Joining

4.3.1 The weldability of this alloy is similar to that of Type 4130 steel. (See Chapter code 1201, Section 4.3.1.)

4.3.2 Type 8630 steel is subject to underbead cracking after fusion welding. This cracking can be reduced or eliminated by weld pre-heating and by post-weld holding at an elevated temperature. Cast alloy has superior resistance to underbead cracking than wrought alloy because the globular inclusions in the cast material are much less favorable sites for crack initiation than the elongated, almost needle-shaped inclusions in wrought alloy (Ref. 32).

4.4 Surface Treatment

4.4.1 With proper surface preparation, this alloy can be painted or electroplated for both protective and decorative purposes.

4.4.2 Type 8630 heat treated up to 180 ksi can be cleaned by pickling, but higher strength material should be cleaned with alkaline scale conditioner or alkaline electrocleaner or mechanically cleaned by sand blasting (Ref. 28).

Table 1.3.1 AMS specifications (Refs. 15-19)

Alloy: 8630	
AMS Specification	**Product Form**
6280H	Bars, rods, forgings
6355L (a)	Sheet, strip, and plate
6281G	Mechanical tubing
5334D	Investment castings
5335D	Sand castings

(a) Superseded as of December 1990. The requirements of this specification are embodied in the latest issue of AMS 6350H (SAE 4130).

Table 1.4.1 AMS specified compositions

Alloy: 8630						
Form	**All Wrought Forms**		**Sand Cast**		**Investment Cast**	
Reference	**17, 18**		**16**		**15**	
Composition (percent)	**min**	**max**	**min**	**max**	**min**	**max**
Carbon	0.28	0.33	0.25	0.33	0.25	0.35
Manganese	0.70	0.90	0.60	0.95	0.60	0.95
Silicon	0.15	0.35	0.50	0.90	-	1.00
Phosphorus	-	0.025	-	0.025	-	0.04
Sulfur	-	0.025	-	0.025	-	0.04
Chromium	0.40	0.60	0.40	0.90	0.35	0.65
Nickel	0.40	0.70	0.40	1.10	0.35	0.75
Molybdenum	0.15	0.25	0.15	0.25	0.15	0.30
Copper	-	0.35	-	0.35	-	0.35

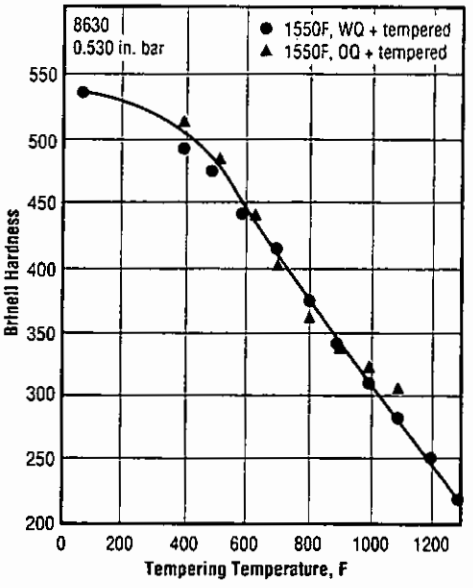


Fig. 1.6.1 Effect of tempering temperature on hardness of bar (Refs. 1, 5)

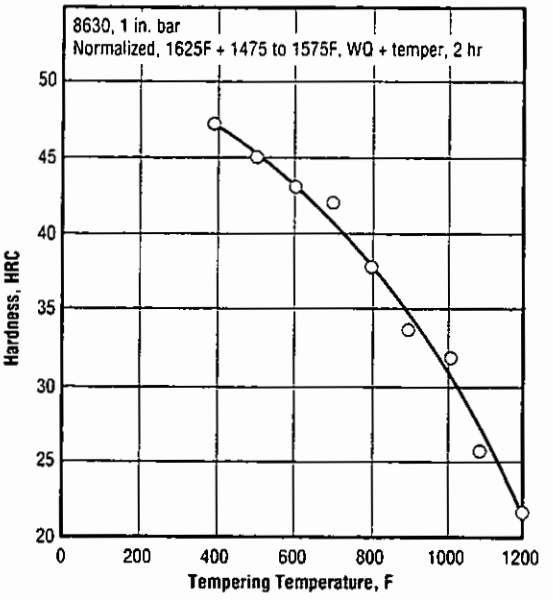


Fig. 1.6.2 Typical hardness of tempered bar (Ref. 37)

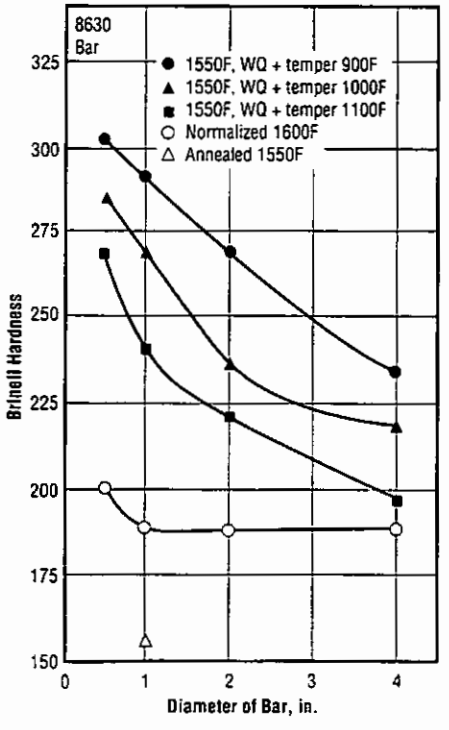


Fig. 1.6.3 Effects of bar diameter on hardness for various heat-treated conditions (Ref. 1)

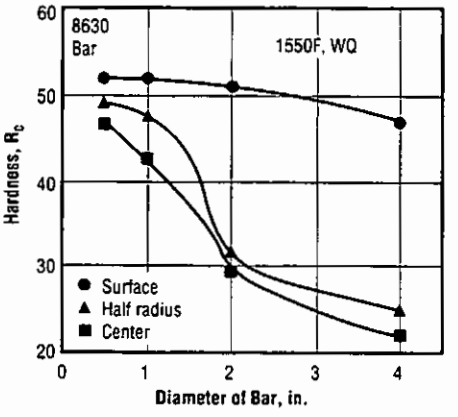


Fig. 1.6.4 Effects of bar diameter on as-quenched hardness at various depths on bar (Ref. 1)

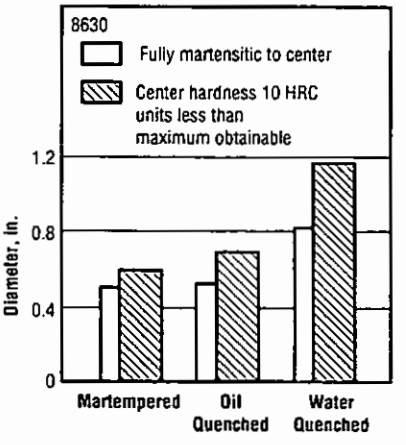


Fig. 1.6.5 Approximate maximum bar diameters hardenable by martempering, oil quenching, and water quenching (Ref. 37)

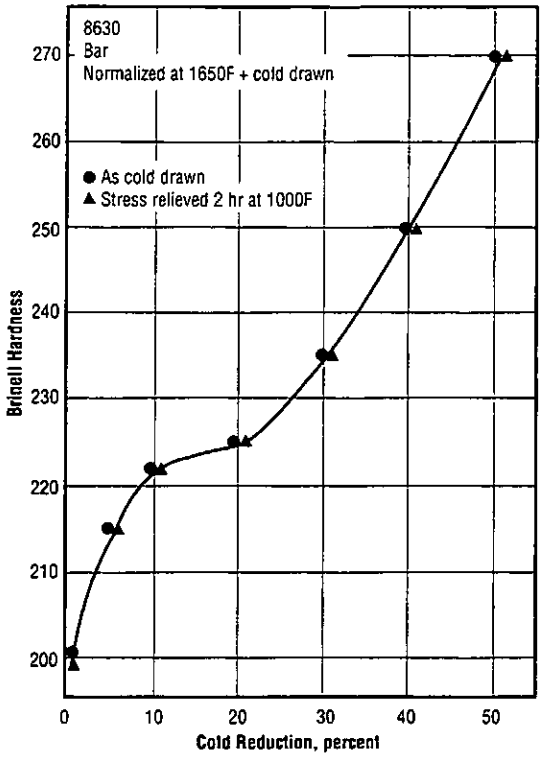


Fig. 1.6.6 Effects of cold work on hardness (Ref. 14)

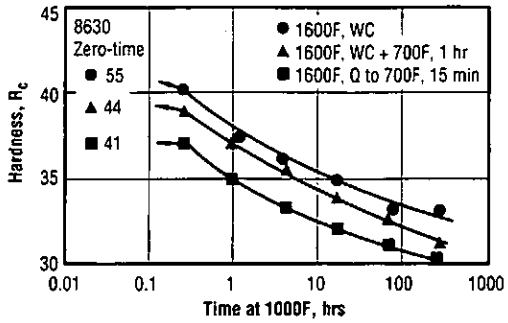


Fig. 1.6.7 Effects of time at 1000F on room-temperature hardness for various heat treatments (Ref. 25)

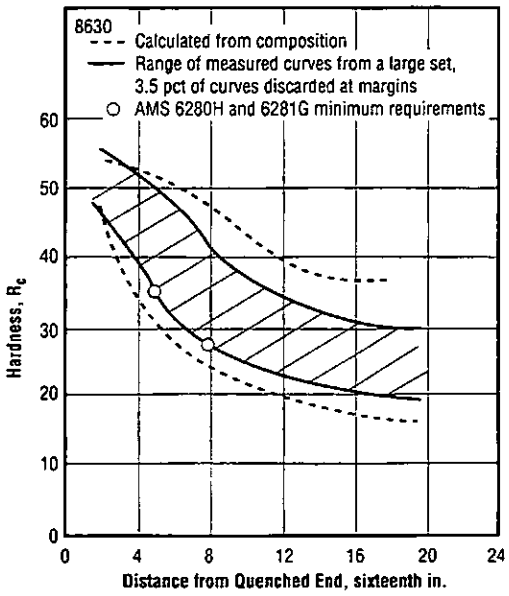


Fig. 1.6.8 End-quench hardenability band (Ref. 33)

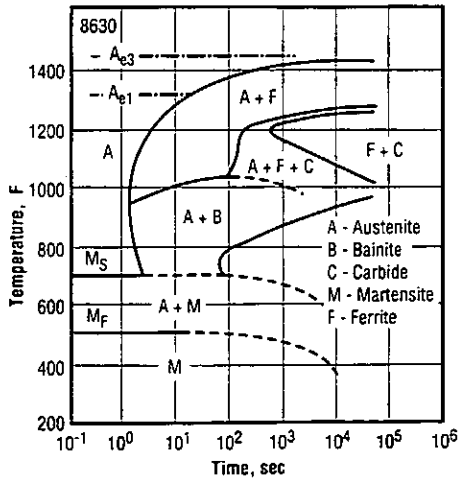


Fig. 2.1.2.1 Time-temperature-transformation diagram (Refs. 2, 37)

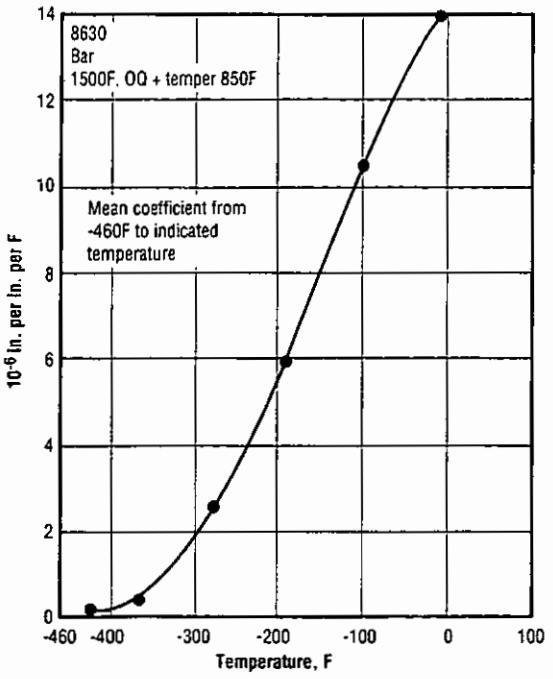


Fig. 2.1.4.2 Thermal expansion at low temperatures (Ref. 9)

Table 2.2.2 Electrical properties (Ref. 5)

Alloy: 8630			
Temperature (F)	Electrical Conductivity		Electrical Resistivity (microhm-in.)
	percent IACS	megohms per in.	
120	5.8	0.085	11.8
570	3.6	0.053	18.9

Table 3.1.1 AMS Specified mechanical properties (Refs. 15-18)

Alloy: 8630								
AMS Specification	Form	Condition	Tensile Properties				Hardness	
			F_{ty} (ksi, min)	F_{tu} (ksi, min)	e (pct, min)	RA (pct, min)	min	max
6281G	Mechanical tubing	Cold finished	-	-	-	-	-	25 R_c
		Hot finished	-	-	-	-	-	99 R_b
6280H	Bars							
	0.500 in. and under	Cold finished	-	125 max	-	-	-	27 R_c
	Over 0.500 in.	Hot finished	-	-	-	-	-	229 BHN
		Cold finished	-	-	-	-	-	248 BHN
5335D	Sand castings	Normalized and tempered	-	-	-	-	183 BHN	229 BHN
		1600F, OQ + temper 800F	150	165	8	-	331 BHN	-
5334D	Investment castings	Normalized and tempered	-	-	-	-	-	99 R_b
		1600F, OQ + temper 825F	125	150	5	10	32 R_c	38 R_c

Note: The original AMS documents should be consulted for complete specification details.

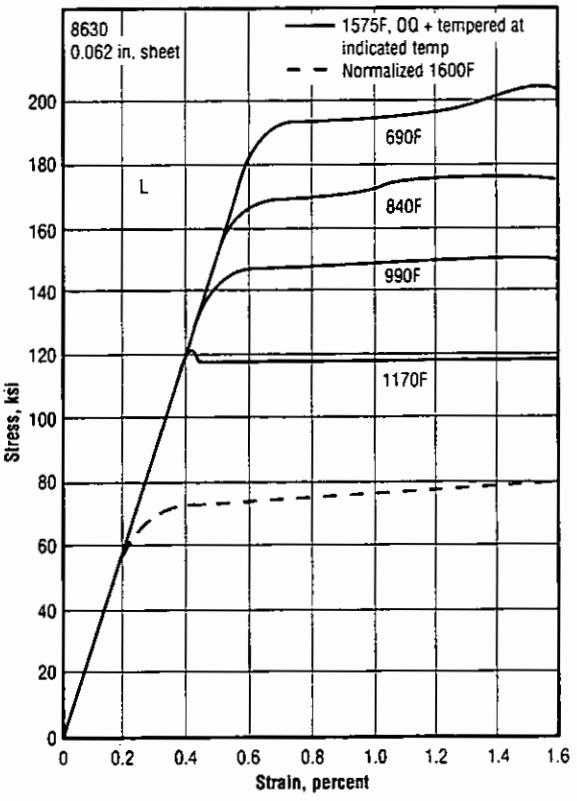


Fig. 3.2.1.1 Tensile stress-strain curves for sheet in various heat treated conditions (Ref. 12)

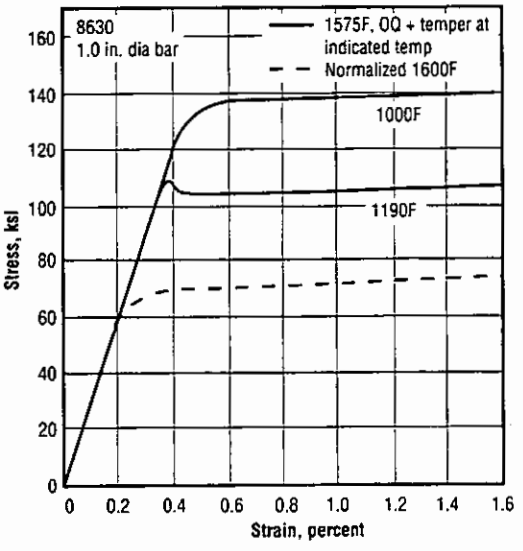


Fig. 3.2.1.2 Tensile stress-strain curves for bar in various heat treated conditions (Ref. 12)

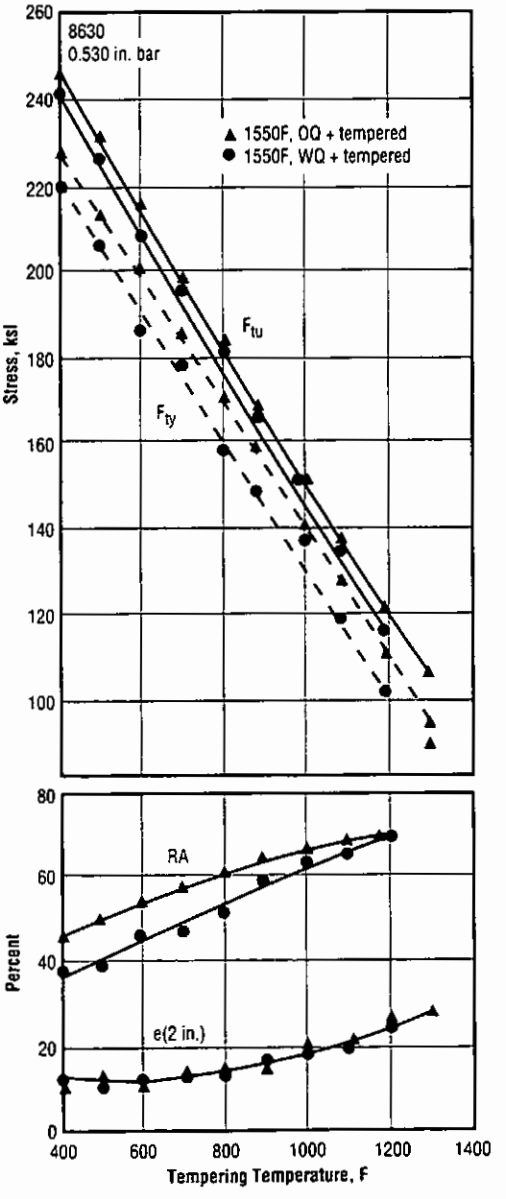


Fig. 3.2.1.3 Effects of tempering temperature after both oil quench and water quench on room temperature tensile properties of 0.530 in bar (Refs. 1, 5)

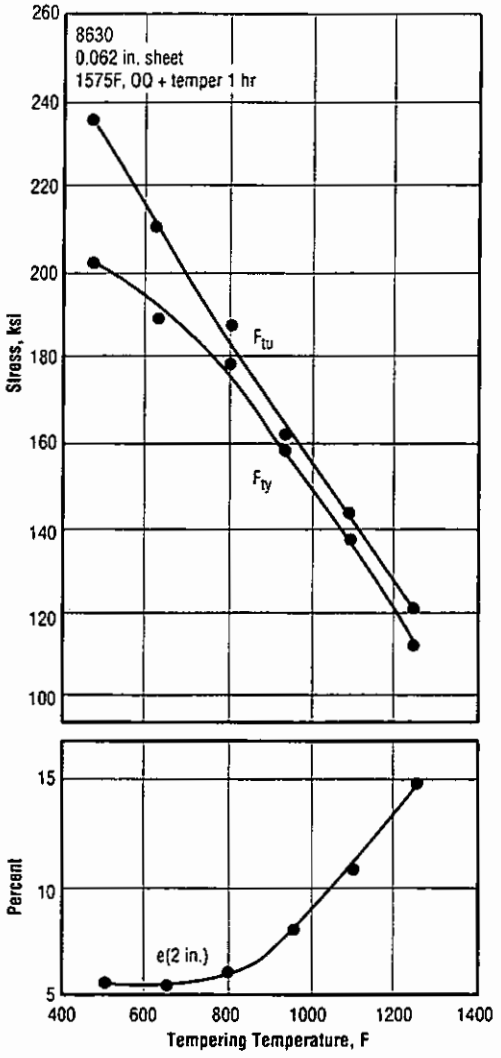


Fig. 3.2.1.4 Effect of tempering temperature on tensile properties of sheet (Ref. 8)

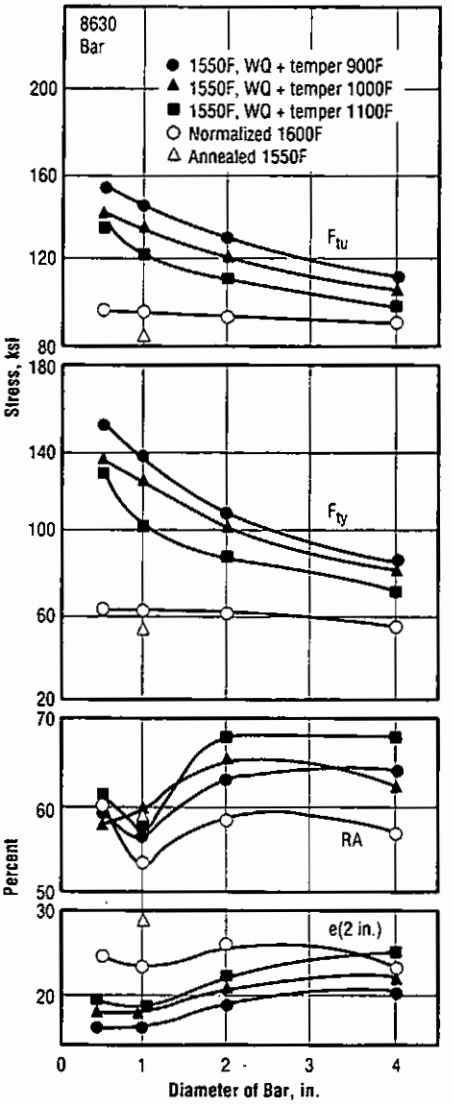


Fig. 3.2.1.5 Effects of bar diameter on tensile properties for various heat treated conditions (Ref. 1)

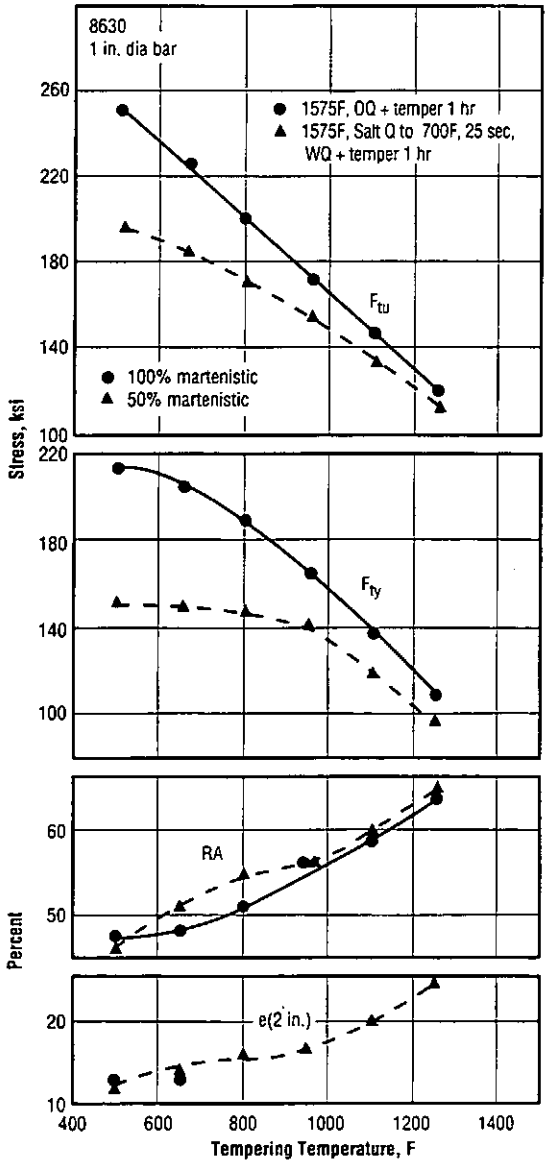


Fig. 3.2.1.6 Effect of tempering temperature on tensile properties of bar heat treated to two different metallurgical structures (Ref. 8)

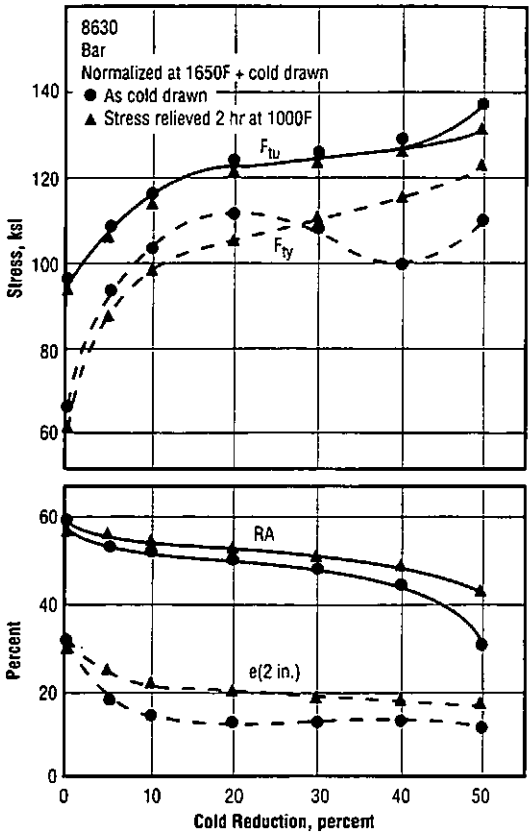


Fig. 3.2.1.7 Effects of cold drawing on tensile properties of normalized bar (Ref. 14)

Table 3.2.1.8 Tensile properties of tube in various heat-treated conditions (Ref. 5)

Alloy: 8630			
Form	**Tube, 1.0 in. OD x 0.062 in. Wall**		
Condition	**F_{ty} (ksi)**	**F_{tu} (ksi)**	**e, 2 in. (percent)**
Normalized 1650F	61.5	114.1	23.8
Normalized 1700F	63.4	118.5	22.2
1550F, OQ + temper 700F	184.2	196.4	8.7
1550F, OQ + temper 900F	160.2	163.4	16.5
1550F, OQ + temper 1100F	126.4	133.2	17.0

Table 3.2.1.9 Tensile properties of extrusions in two heat-treated conditions (Ref. 4)

Alloy: 8630				
Form	Extruded T, 3/4 x 1 3/4 in.			
Condition	F_{ty} (ksi)	F_{tu} (ksi)	e, 2 in. (a) (percent)	RC
1550F, OQ + 800F	193.5	200.0	8.5	43
1550F, OQ + 1100F	127.5	137.9	15.7	31

(a) Flat specimen

Table 3.2.1.10 Effect of cold extrusion on tensile properties of annealed bar (Ref. 6)

Alloy: 8630				
Form	Bar			
Condition	F_{ty} (ksi)	F_{tu} (ksi)	e, 2 in. (percent)	RA (percent)
Annealed	54.0	81.8	29	59
Cold extruded to 60 percent cold reduction	171	166	12	46

Table 3.2.1.11 Tensile properties of castings in two heat-treated conditions (Ref. 7)

Alloy: 8630					
Form	1.0 in. Dia Cast Bars				
Condition	F_{ty} (ksi)	F_{tu} (ksi)	e,4D (percent)	RA (percent)	BHN
Normalized 1650F + tempered 1200F	85.6	110.5	19.0	53.7	223
1550F, WQ + tempered 1200F	125.8	137.5	14.8	34.5	286

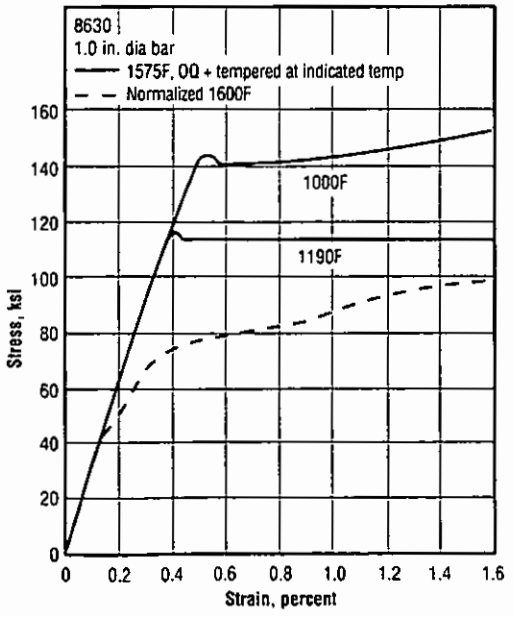


Fig. 3.2.2.1 Compressive stress-strain curves for bar in various heat-treated conditions (Ref. 12)

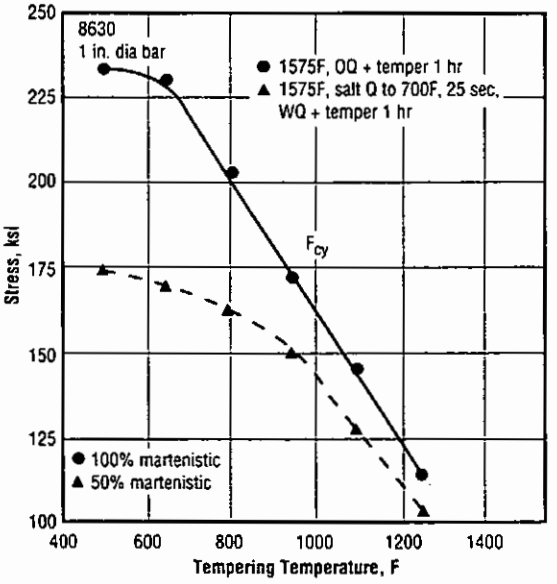


Fig. 3.2.2.2 Effects of tempering temperature on compressive yield strength of bar heat treated to two different metallurgical structures (Ref. 8)

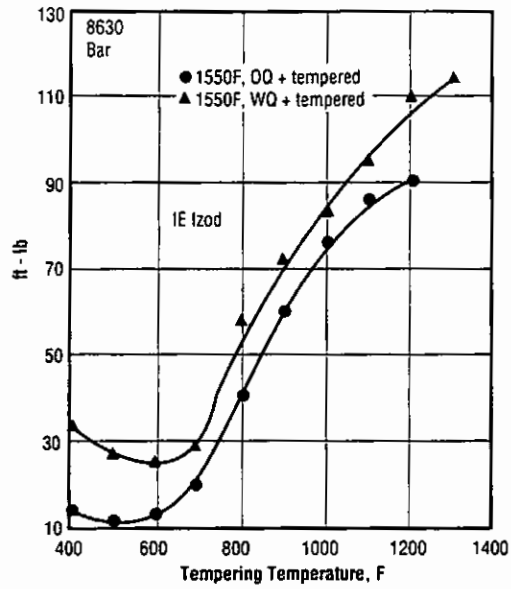


Fig. 3.2.3.1 Effects of tempering temperature on room-temperature impact strength (Ref. 5)

Table 3.2.5.1 Shear strength of bar determined on pin-type double-shear specimens (Ref. 12)

Alloy: 8630		
Form	**1.0 in. dia bar**	
Condition	**F_{tu} (ksi)**	**F_{su} (ksi)**
Normalized 1675F	116.0	81.0
1575F, OQ + temper 1190F	120.5	88.4
1575F, OQ + temper 1000F	147.5	109.0

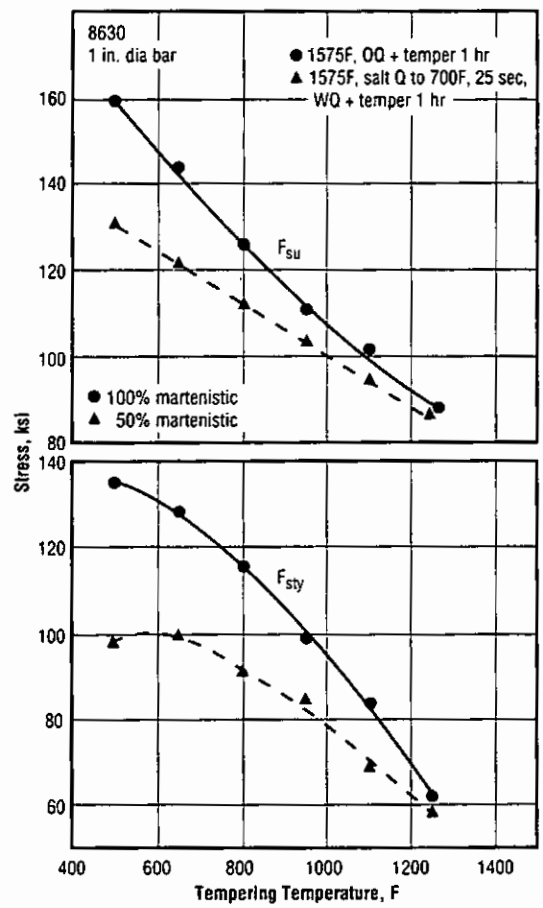


Fig. 3.2.5.2 Effects of tempering temperature on torsional properties of bar heat treated to two different metallurgical structures (Ref. 8)

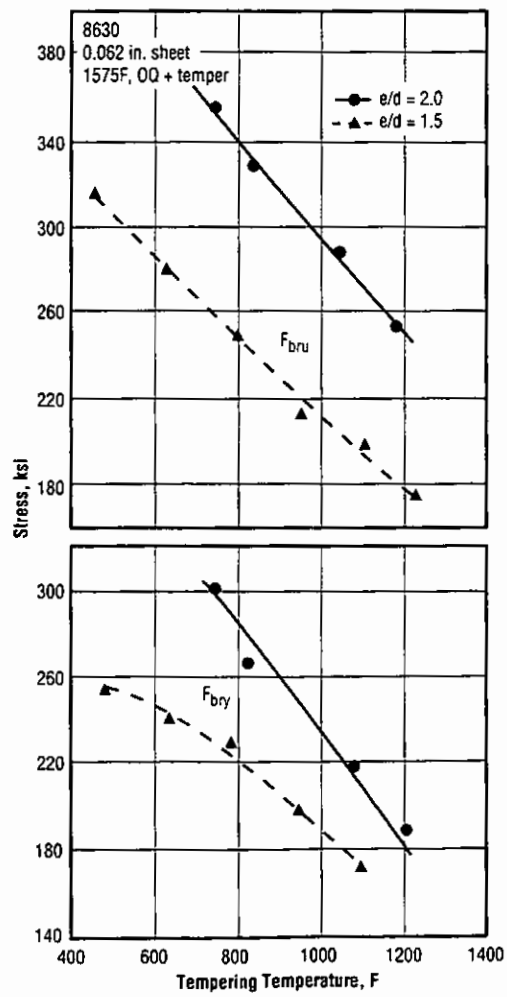


Fig. 3.2.6.1 Effects of tempering temperature on bearing properties (Refs. 8, 12)

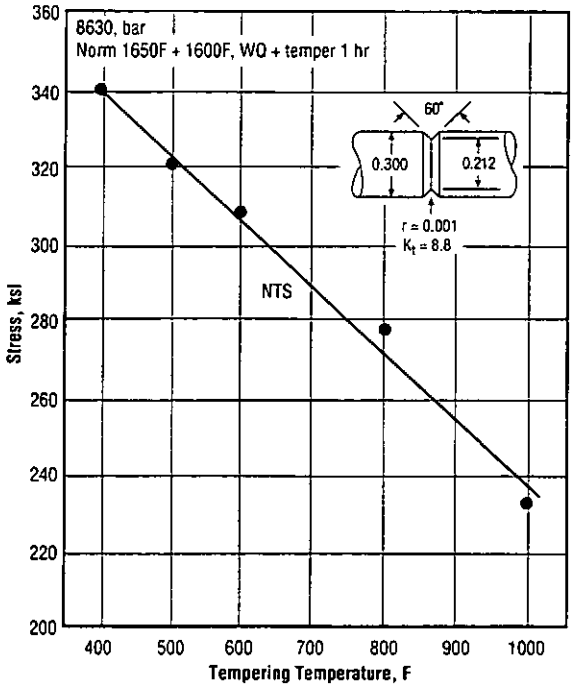


Fig. 3.2.7.1.1 Effect of tempering temperature on notched tensile strength (Ref. 26)

Note: See Fig. 3.2.1.3 for tensile properties of bar in approximately equivalent heat-treated conditions.

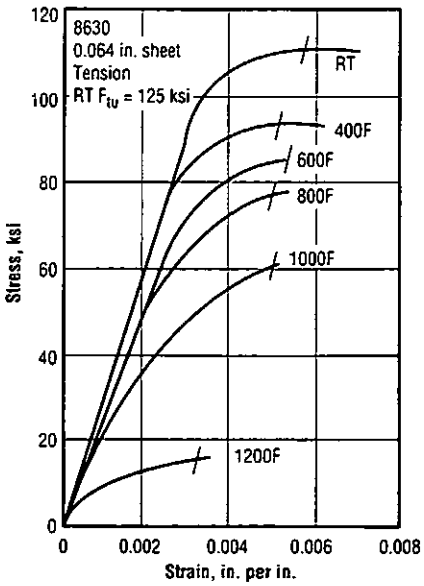


Fig. 3.3.1.1 Stress-strain curves from room temperature to 1200F for sheet quenched and tempered to 125 ksi F_{tu} (Ref. 27)

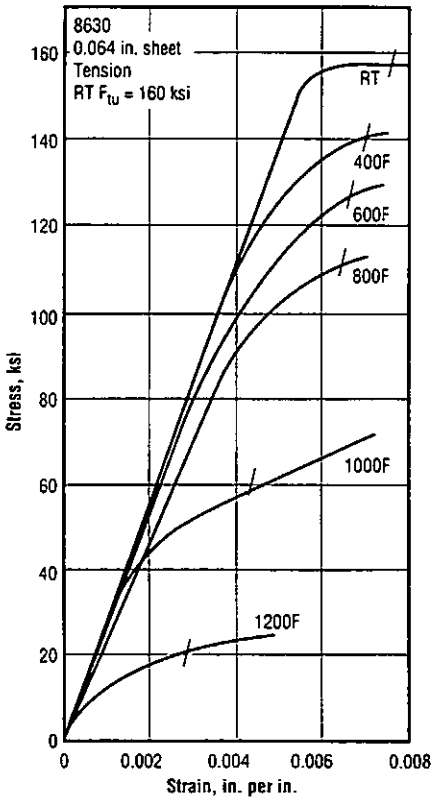


Fig. 3.3.1.2 Stress-strain curves from room temperature to 1200F for sheet quenched and tempered to 160 ksi F_{tu} (Ref. 27)

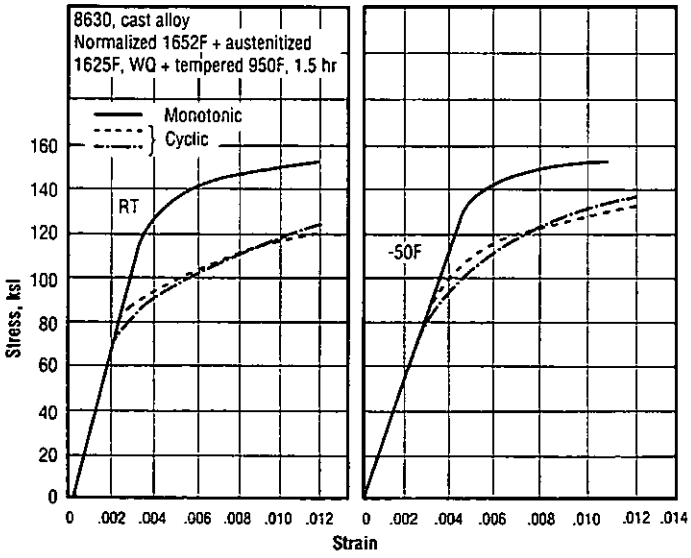


Fig. 3.3.1.3 Monotonic and cyclic stress-strain curves for cast alloy at room temperature and -50F (Ref. 34)

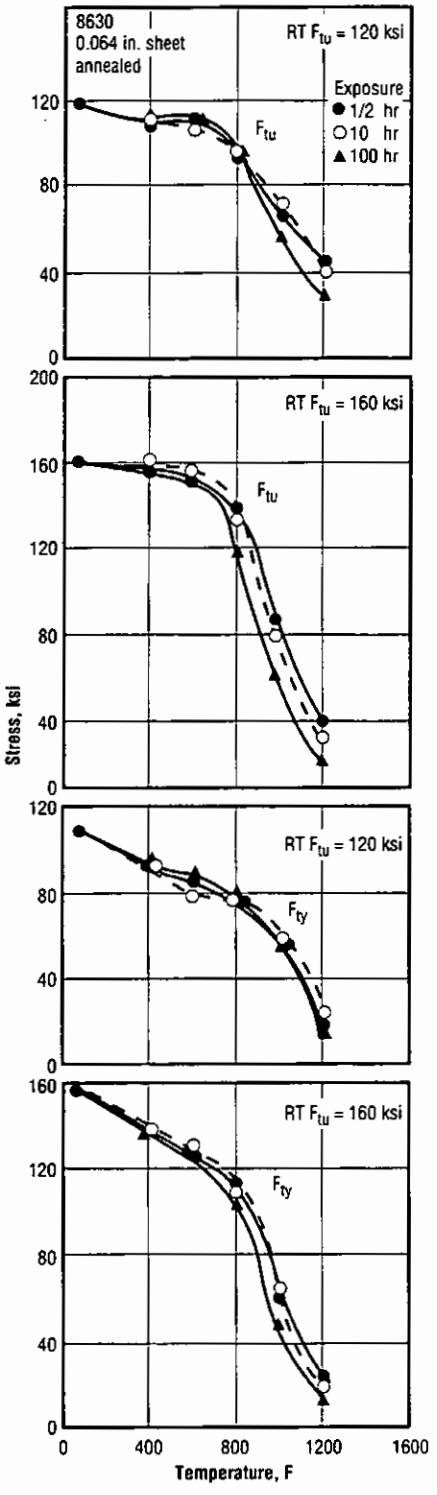


Fig. 3.3.1.4 Effects of exposures from one-half hour to 100 hours at test temperature on elevated-temperature tensile properties of sheet quenched and tempered to two different strength levels (Ref. 27)

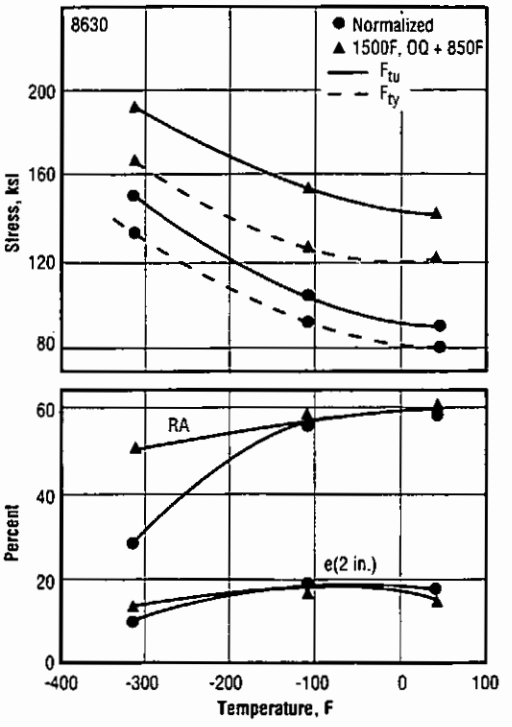


Fig. 3.3.1.5 Effects of low temperature on tensile properties of both normalized and quench-and-tempered alloy (Ref. 27)

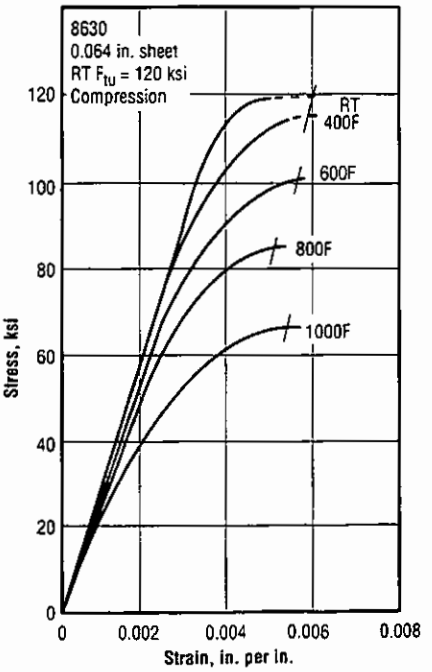


Fig. 3.3.2.1 Stress-strain curves in compression from room temperature to 1000F for sheet quenched and tempered to 120 ksi F_{tu} (Ref. 27)

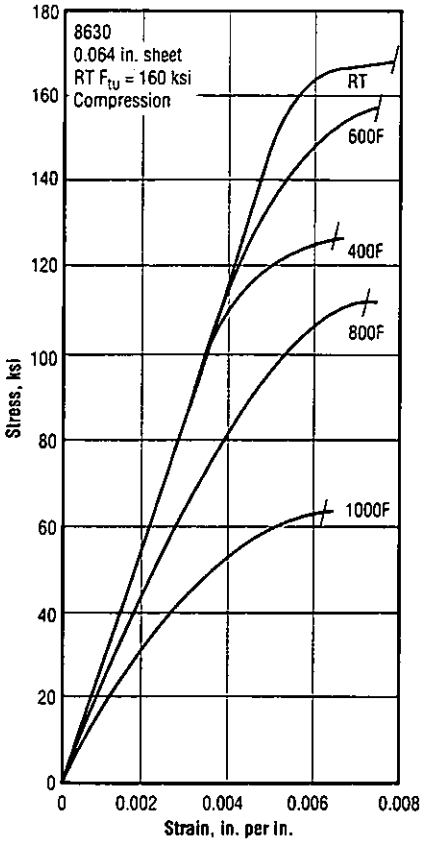


Fig. 3.3.2.2 Stress-strain curves in compression from room temperature to 1000F for sheet quenched and tempered to 160 ksi F_{tu} (Ref. 27)

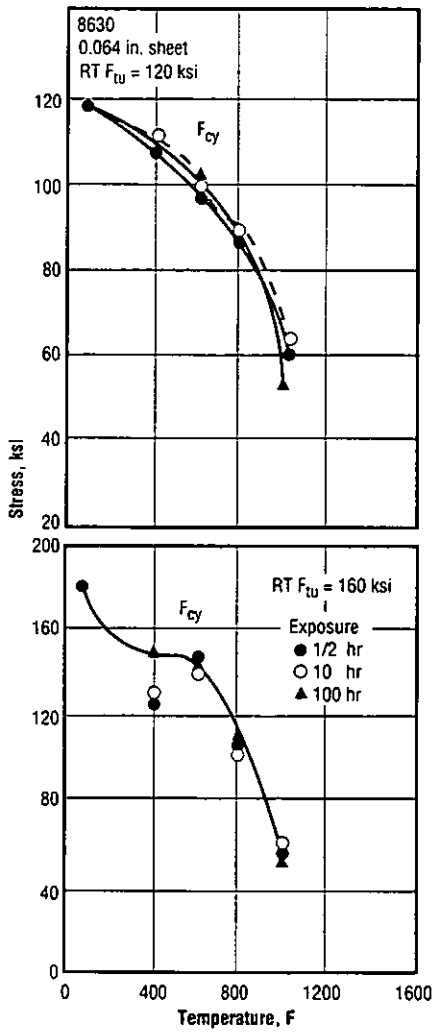


Fig. 3.3.2.3 Effects of exposures from one-half hour to 100 hours at test temperature on compressive yield strength of sheet quenched and tempered to two F_{tu} levels (Ref. 27)

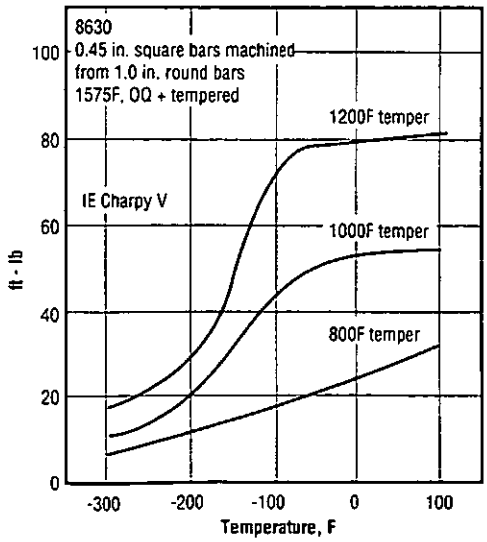


Fig. 3.3.3.1 Low-temperature impact properties of bar (Ref. 3)

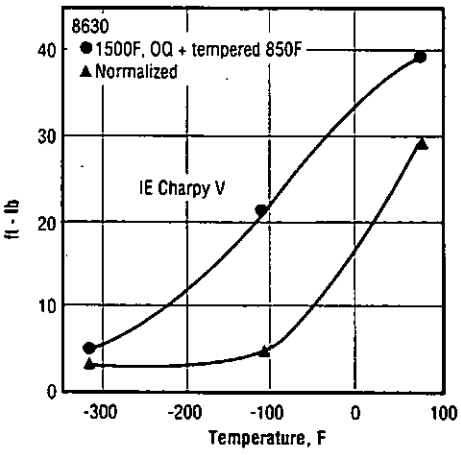


Fig. 3.3.3.2 Comparison of low-temperature impact properties of hardened-and-tempered and normalized alloy (Ref. 5)

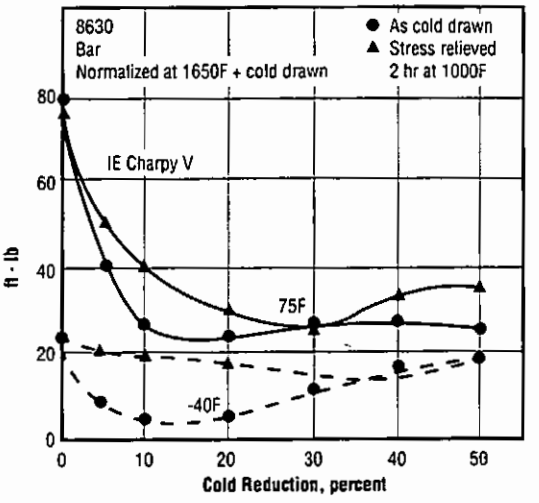


Fig. 3.3.3.3 Effects of cold work on impact properties at room temperature and -40F

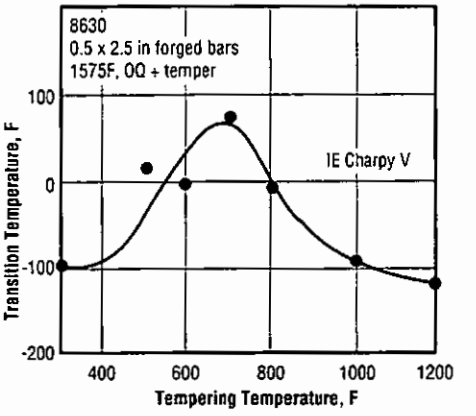


Fig. 3.3.3.4 Effect of tempering temperature on impact (Charpy V) transition temperature. Impact transition temperature in this instance is defined as the temperature at which impact energy absorption is 80 percent of the shelf energy. (Ref. 13)

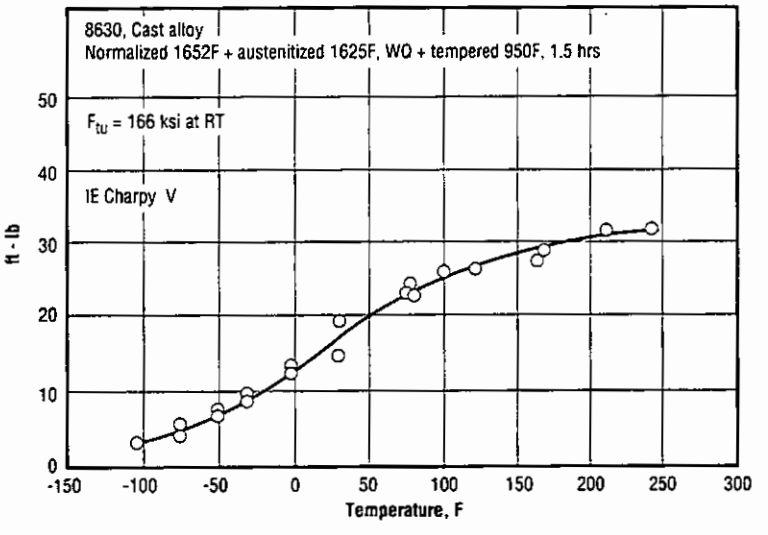


Fig. 3.3.3.5 Effect of temperature on impact energy of cast alloy (Ref. 34)

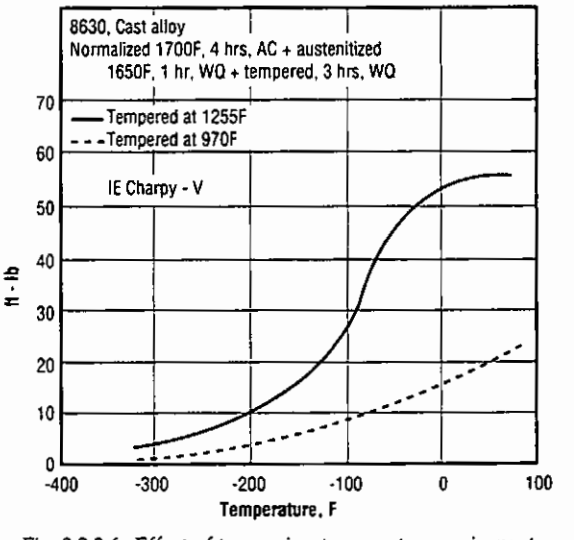


Fig. 3.3.3.6 Effect of tempering temperature on impact energy of cast alloy at low temperatures (Ref. 35)

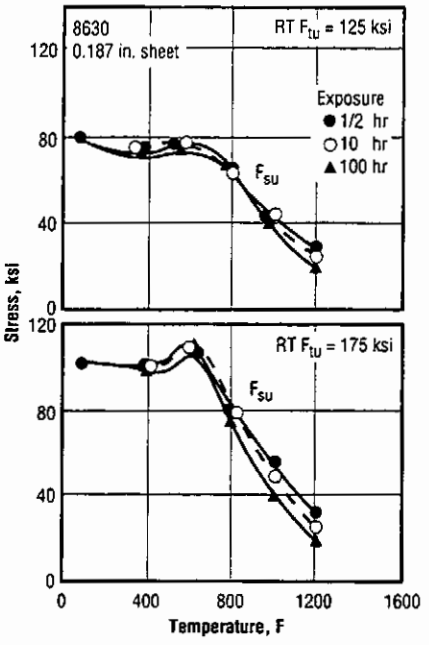


Fig. 3.3.5.1 Effects of exposures from one-half hour to 100 hours at test temperature on shear strength of sheet quenched and tempered to two F_{tu} levels (Ref. 27)

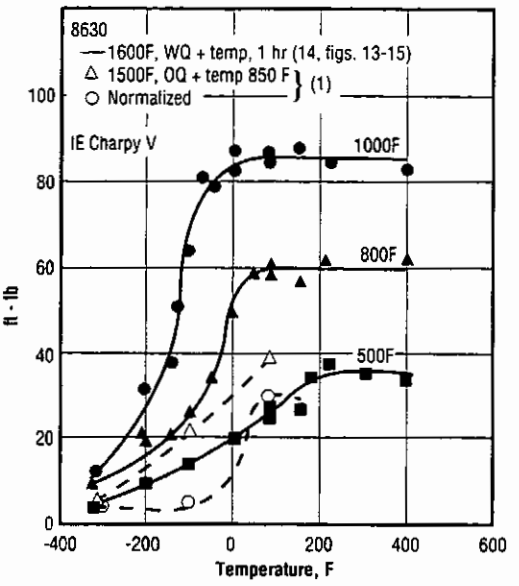


Fig. 3.3.6.1 Effects of exposures from one-half hour to 100 hours at test temperature on bearing properties of sheet quenched and tempered to two F_{tu} levels (Ref. 1, 14)

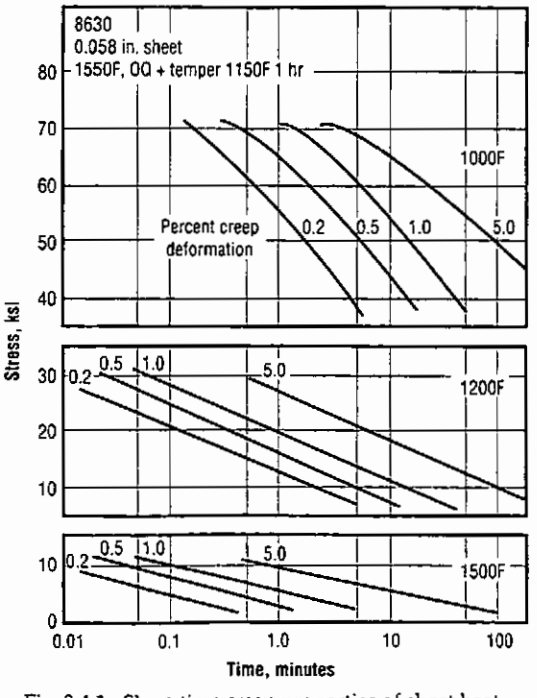


Fig. 3.4.1 Short-time creep properties of sheet heat treated to an F_{tu} level of 125 ksi (Ref. 10)

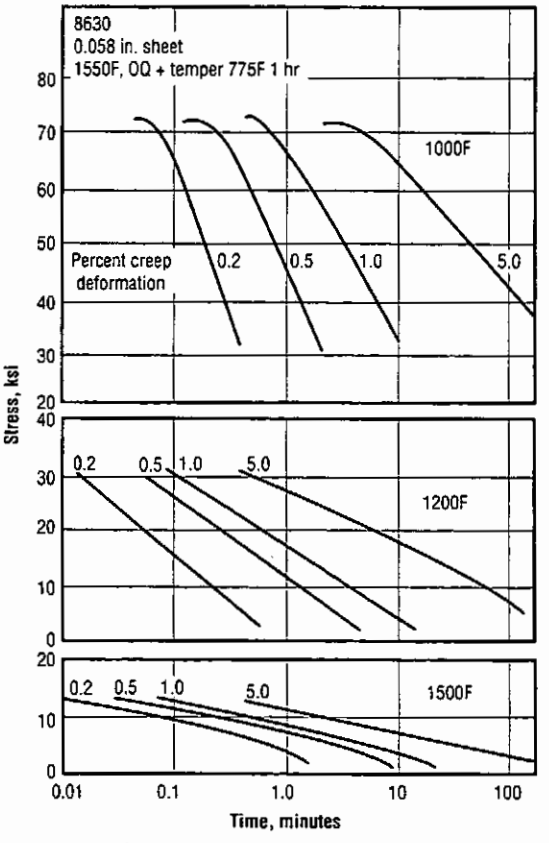


Fig. 3.4.2 Short-time creep properties of sheet heat treated to an F_{tu} level of 180 ksi (Ref. 10)

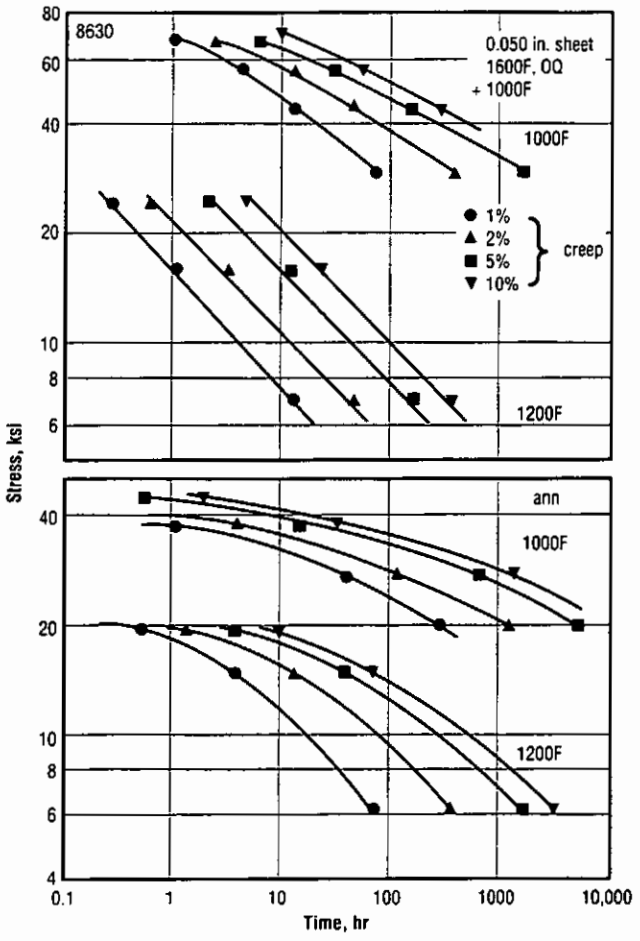


Fig. 3.4.3 Long-time creep properties of sheet in the annealed and quenched-and-tempered conditions (Ref. 25)

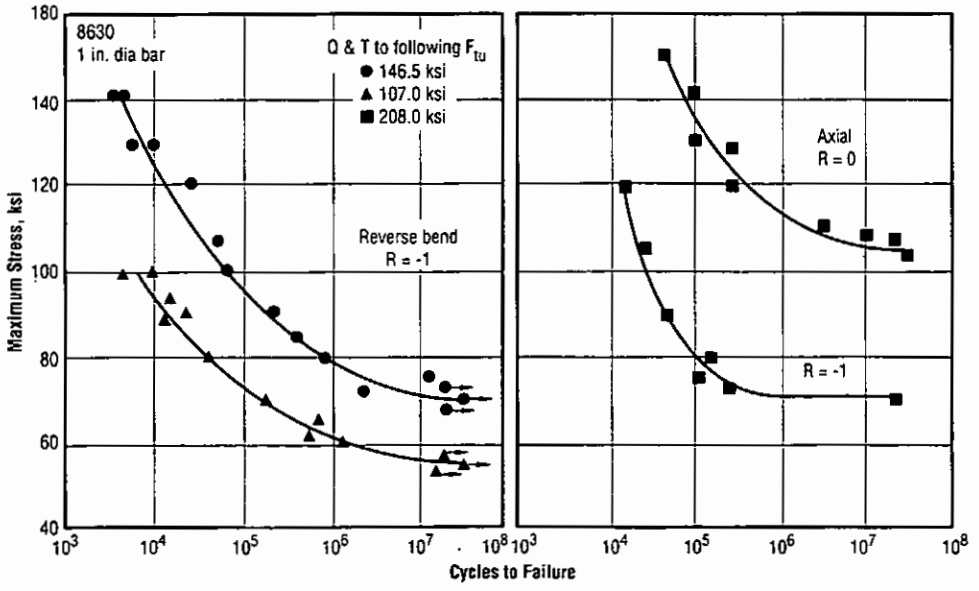


Fig. 3.5.1 Fatigue properties of bar at several strength levels and under various loading conditions (Ref. 11)

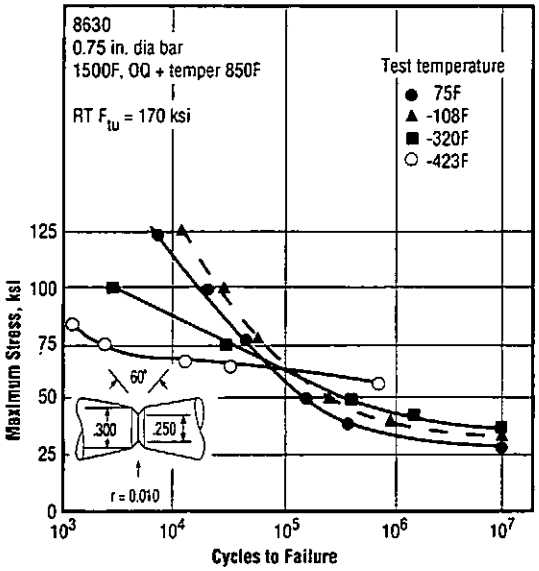


Fig. 3.5.2 Low-temperature fatigue properties of notched bar (Ref. 9)

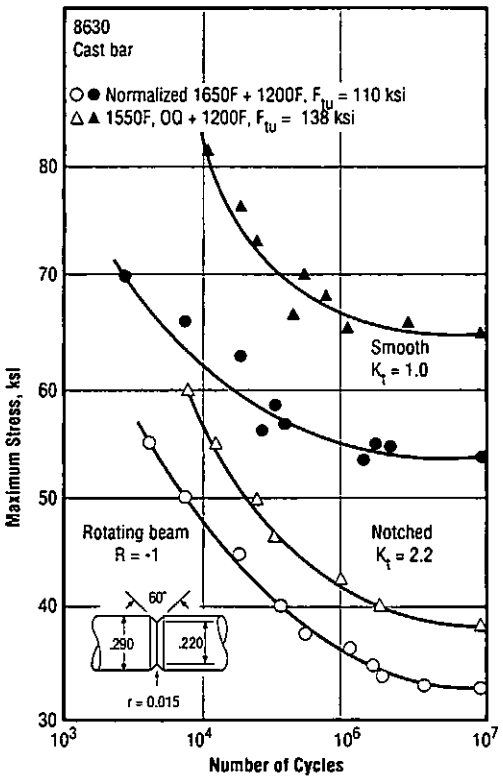


Fig. 3.5.3 Fatigue properties of castings in the normalized-and-tempered and quenched-and-tempered conditions (Ref. 7)

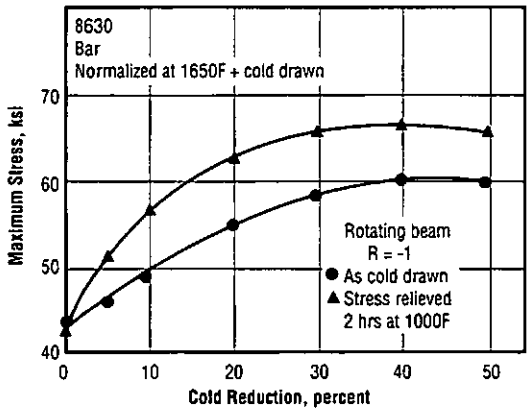


Fig. 3.5.4 Effects of cold work on fatigue endurance limit at 10^7 cycles (Ref. 14)

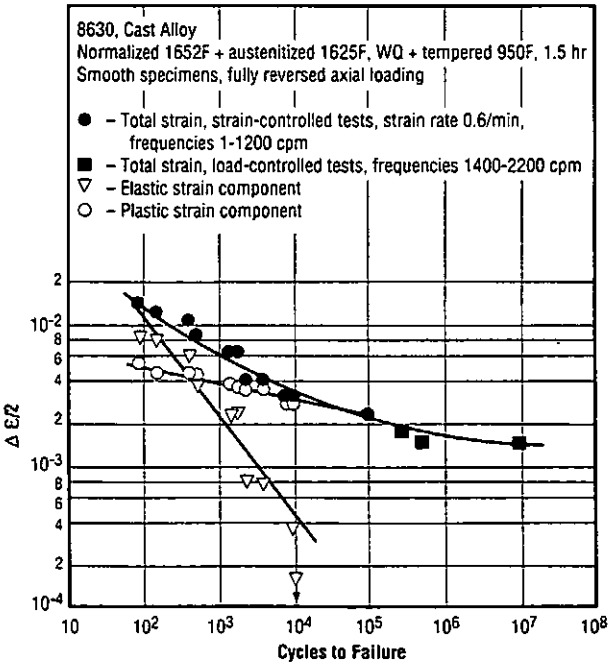


Fig. 3.5.5 Fatigue behavior of cast alloy at room temperature (Ref. 34)

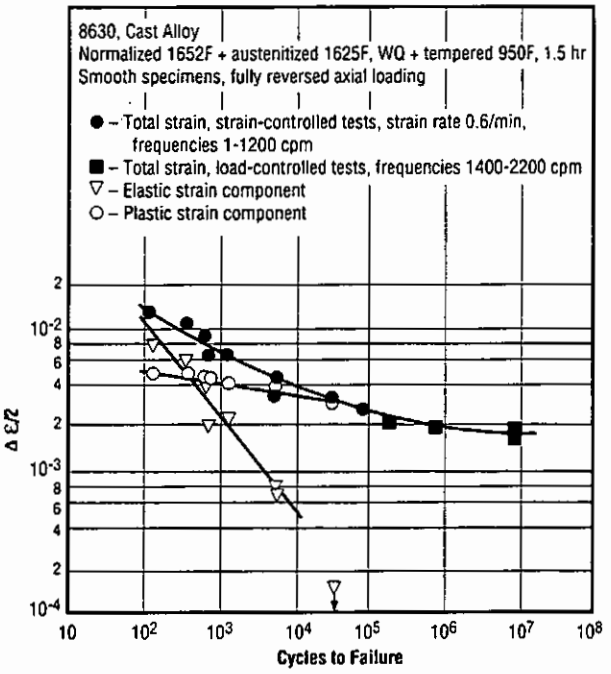


Fig. 3.5.6 Fatigue behavior of cast alloy at -50F (Ref. 34)

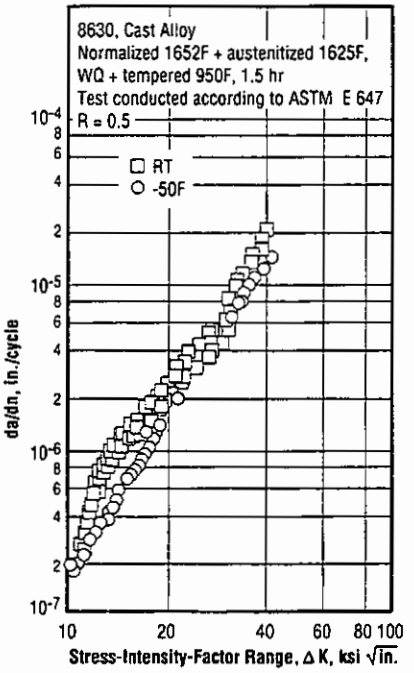


Fig. 3.5.7 Fatigue crack growth rate for cast alloy at R = 0.5 (Ref. 34)

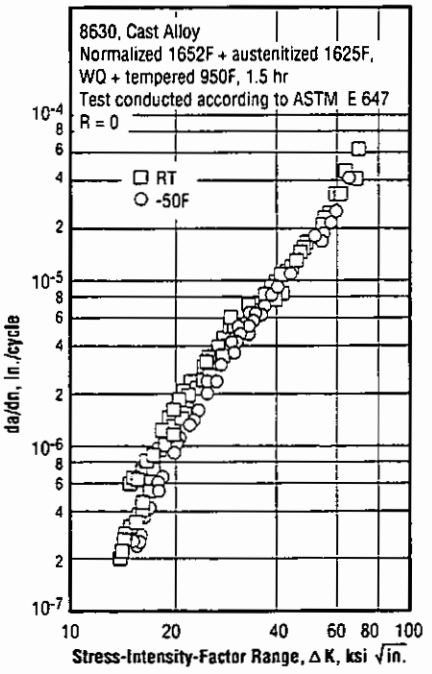


Fig. 3.5.8 Fatigue crack growth rate for cast alloy at R = 0 (Ref. 34)

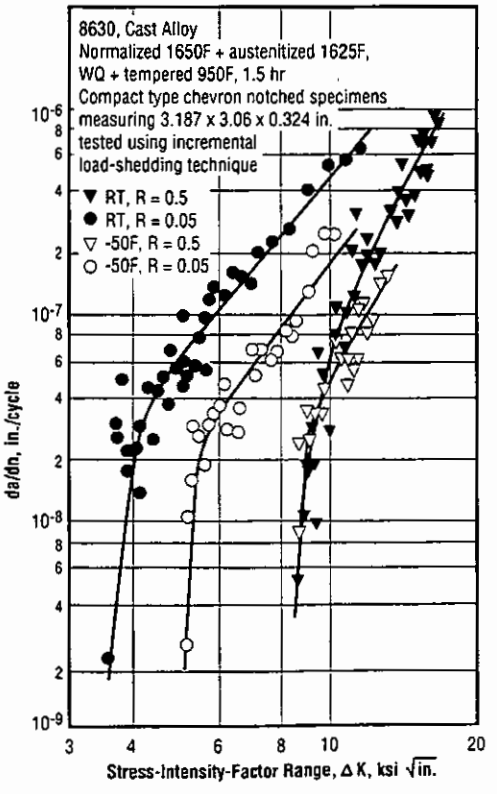


Fig. 3.5.9 Threshold and near-threshold fatigue crack growth rates for cast alloy at room temperature and -50F (Ref. 36)

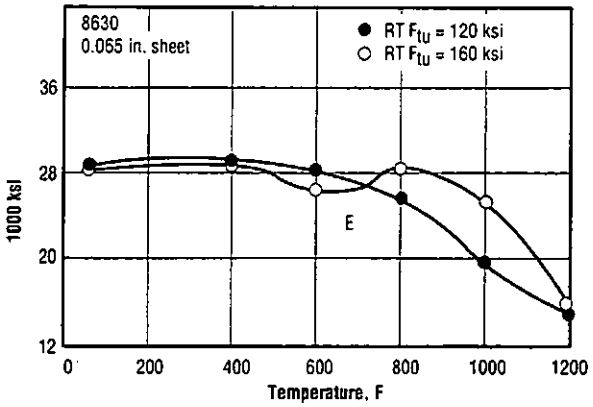


Fig. 3.6.2.1 Effects of temperature on modulus of elasticity in tension for sheet quenched and tempered to two F_{tu} levels (Ref. 27)

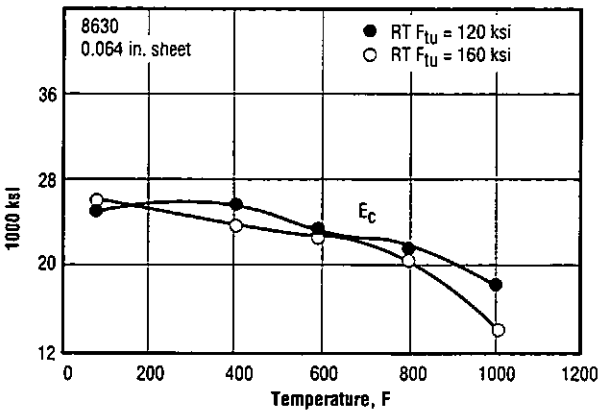


Fig. 3.6.2.2 Effect of temperature on modulus of elasticity in compression for sheet quenched and tempered to two F_{tu} levels (Ref. 27)

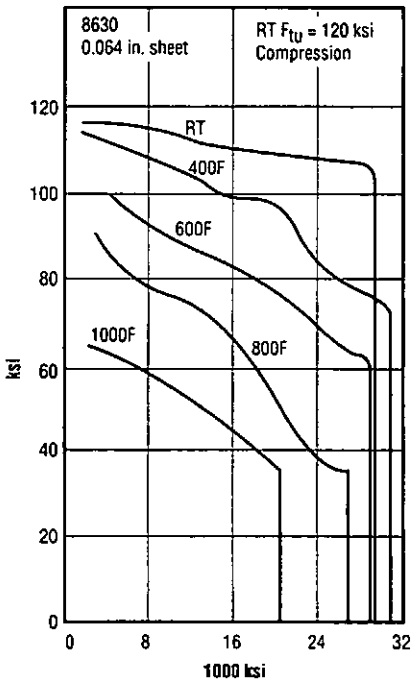


Fig. 3.6.4.1 Tangent modulus curves in compression at room and elevated temperatures for sheet quenched and tempered to 120 ksi F_{tu} (Ref. 27)

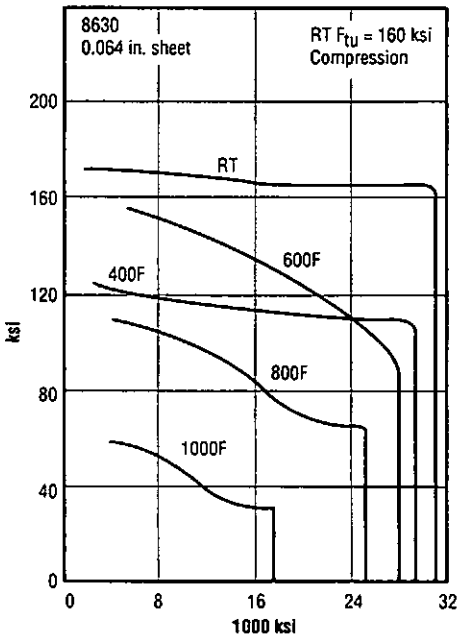


Fig. 3.6.4.2 Tangent modulus curves in compression at room and elevated temperatures for sheet at 160 ksi room temperature F_{tu} (Ref. 15)

References

1. "Modern Steels and Their Properties," Seventh Edition, Handbook 2757, Bethlehem Steel Corp. (1972).
2. "Isothermal Transformation Diagrams of Nickel Alloy Steels," The International Nickel Co. (1965).
3. Metal Progress Data Book (June 1977).
4. Fiorentino, R. J., and Sabroff, A. M., "Availability and Mechanical Properties of High-Strength Steel Extrusions," DMIC Report 138, Battelle Memorial Institute (Oct. 26, 1960).
5. "AISI 8630," *Alloy Digest*, Filing code: SA-49 (Oct. 1956).
6. Parker, Charles, and Chepko, Frank, "Switch to Cold Extrusion Cuts Steel Parts Costs," *Materials Engineering*, Vol. 66 (Oct. 1967).
7. Evans, E. B.; Ebert, L. J.; and Briggs, C. W., "Fatigue Properties of Comparable Cast and Wrought Steels," *ASTM Proceedings*, Vol. 56 (1956).
8. Lodge, J. W., and Manning, G. K., "The Mechanical Properties of Quenched and Tempered Medium-Carbon Alloy Steels," AISI, Contributions to the Metallurgy of Steel (March 1956).
9. Fontana, M. G.; Bishop, S. M.; and Spretnak, J. W., "Investigation of Mechanical Properties and Physical Metallurgy of Aircraft Alloys at Very Low Temperatures," Part 5, AF Technical Report 5662, Wright Air Development Center (Dec. 1953).
10. Van Echo, J. A.; Wirth, W. F.; and Simmons, W. F., "Short-Time Creep Properties of Structural Sheet Materials for Aircraft and Missiles," AF Technical Report 6731, Part III, Wright Air Development Center (May 1955).
11. Oberg, T. T., and Ward, E. J., "Fatigue of Alloy Steels at High Stress Levels," WADC Technical Report 53-256, Wright Air Development Center (Oct. 1953).
12. Jackson, L. R., and Crites, N. A., "Development of Mechanical Properties Information on Carbon and Alloy Steels at Various Strength Levels," Battelle Memorial Institute Report to AISA (Feb. 1, 1951).
13. Schwartzbart, H., and Sheehan, J. P., "Impact Properties of Quenched and Tempered Alloy Steels," Armour Research Foundation, Office of Naval Research Contract N6 onr 274 T.O.I. (Sept. 19, 1955).
14. Elbert, L. J., "Significant Properties and Characteristics of Cold-Worked Steel," Case Institute of Technology for Dept. of the Army, WAL Report No. 310/90-85 (June 1955).
15. AMS 5334D, Society of Automotive Engineers (Jan. 6, 1985).
16. AMS 5335D, Society of Automotive Engineers (July 1984).
17. AMS 6280H, Society of Automotive Engineers (Jan. 1991).
18. AMS 6281G, Society of Automotive Engineers (Oct. 1990).
19. AMS 6355L, Society of Automotive Engineers (July 1991).
20. AMS 6550F, Society of Automotive Engineers (June 1974). (Noncurrent Oct. 1988)
21. AMS 6530F, Society of Automotive Engineers (June 1975). (Noncurrent Oct. 1988)
22. Military Standardization Handbook, Cross-Index of Chemically Similar Specifications and Identification Code (Ferrous and Nonferrous Alloys), MIL-HDBK-HID (22 June 1970).
23. *Metals Handbook*, Vol. 1, 8th Edition, American Society for Metals (1961).
24. "Mechanical Properties of Alloy Steel," Republic Steel Corp. (1961).
25. Miller, J.; Smith, L. W.; and Porter, P. K., "Utilization of Low-Alloy Materials for High Temeprature Service Applications," U.S. Air Force, Air Material Command, AF TR 5929 (June 1949).
26. "The High-Strength Characteristics of Alloy Steels," Metals Research Lab., Case Institute of Technology (June 1952).
27. Doerr, D. D., "Determination of Physical Properties of Ferrous and Non-Ferrous Structural Sheet Materials at Elevated Temperatures," Armour Research Foundation, WADC AF TR 6517, Pt 2 (April 1954).
28. Groshart, E. A., "Design and Finish Requirements of High-Strength Steels," *Metal Finishing*, Vol. 82, No. 3, pp. 49-51 (Mar. 1984).
29. Mangonon, P. L., "The Heat Tretment of Vanadium-Modified Steels," *Journal of Metals*, Vol. 33, No. 6, pp. 18-24 (June 1981).
30. Svoboda, J. M., and Monroe, R. W., "Ladle Desulfurization of Acid Melted Steel," *Transactions of the American Foundrymen's Society*, Vol. 92, American Foundrymen's Society, Inc., Des Plaines, Illinois 60016, pp. 709-728 (1984).
31. Chung, J. H., and Stephens, R. I., "J_{Ic} Determination of Five Cast Steels at Room Temperature and -45C (-50F)," *Journal of Engineering Materials and Technology*, Vol. 106, No. 2, pp. 200-206 (April 1984).
32. Anon., "Weldability Tests Prove Cast Steel Superior to Wrought," *Casting Engineering and Foundry World*, Vol. 14, No. 2, pp. 39, 41-42 (Summer 1982).
33. Kirkaldy, J. S., and Feldman, S. E., "Optimization of Steel Hardenability Control," *Journal of Heat Treating*, Vol. 7, No. 1, pp. 57-64 (1989).

34. Stephens, R. I.; Chung, J. H.; Fatemi, A.; Lee, H. W.; Lee, S. G.; Vaca-Oleas, C.; and Wang, C. M., "Constant and Variable Amplitude Fatigue Behavior of Five Cast Steels at Room Temperature and -45C," *Journal of Engineering Materials and Technology*, Vol. 106, No. 1, pp. 25-37 (Jan. 1984).

35. Voigt, R. C., "Analysis of Intercritical Heat Treatment of Cast Steels," *Journal of Heat Treating*, Vol. 7, No. 2. pp. 95-105 (1989).

36. Stephens, R. I.; Lee, S. G.; and Lee, H. W., "Threshold and Near Threshold Fatigue Crack Growth of Five Cast Steels at Room Temperature and -45C," *Journal of Engineering Materials and Technology*, Vol. 107, No. 2, pp. 166-171 (April 1985).

37. ASM Handbook, *Volume 4, Heat Treating*, ASM International, Metals Park, OH (1991).

	Fe
0.1	C
3.25	Ni
1.2	Cr
0.1	Mo

E 9310

1 GENERAL

E 9310 is a carburizing high hardenability steel. It is normally carburized to a depth of 0.02 to 0.04 inch, followed by austenitizing, quenching, and tempering to produce a high strength core with a hard case. The alloy is widely used as an aircraft alloy because of its ease of processing and excellent core and case properties. It retains good tensile ductility and absence of notch sensitivity down to liquid hydrogen temperature. A major application for this alloy is high performance gears, such as in helicopter power train transmissions. Maximum service temperature in this application is 300 F; above this temperature the alloy softens and gears exhibit scoring, scuffing, and tooth bending fatigue (8–11).

The "H" designated steel (9310 H) is guaranteed by the supplier to meet established AISI-SAE hardenability limits; otherwise its properties and nominal compositions are identical to E 9310 (5).

1.01 Commercial Designation

E 9310.

1.02 Alternate Designations

SAE 9310, AISI E 9310 H, AMS 6260 E, and UNS G93106.

1.03 Specifications

1.031 Specification, Table 1.031.

1.04 Composition

1.041 Composition, Table 1.041.

1.05 Heat Treatment

1.051 Anneal, 1475 to 1575 F, furnace cool (1).

1.052 Normalize, 1600 to 1700 F, air cool (1). AMS specifies 1690 to 1710 F (4, 6, 7).

1.053 Austenitize, 1450 to 1550 F, oil quench (1, 5). AMS specifies 1490 to 1510 F (4, 6, 7).

1.054 Temper, 275 to 450 F for case hardened parts (1).

1.055 Spheroidize, temper, 1175 F maximum, 8 to 10 hr or austenitize at 1400 F and transform isothermally at 1100 F, 12 hr (1).

1.056 Typical case hardening procedures.

1.0561 Direct quench from pot. Carburize at 1700 F, 8 hr, circulating oil quench and temper (1).

1.0562 Single quench and temper. Carburize at 1700 F, 8 hr, pot cool, austenitize, circulating oil quench and temper (1).

1.0563 Double quench and temper. Carburize at 1700 F, 8 hr, pot cool, austenitize, circulating oil quench, repeat previous austenitizing treatment and temper. This treatment yields higher grain refinement in both case and core (1).

1.0564 For maximum core toughness temper at 450 F (see Figure 3.0231).

1.0565 Refrigeration is sometimes employed after austenitizing and quenching but before tempering. This treatment increases hardness and decreases the amount of retained austenite by promoting transformation to martensite (12).

1.06 Hardness

1.061 Effect of carbon content on hardness of bar, Figure 1.061.

1.062 Effect of thickness on as-quenched hardness of bar, Figure 1.062.

1.063 Effect of bar diameter on quenched and tempered hardness of bar, given simulated carburizing cycle, Figure 1.063.

1.064 Short-term hot hardness, Figure 1.064.

1.065 Hardness traverse across thickness of carburized and quenched E 9310, Figure 1.065.

1.066 Hardenability.

1.0661 AMS Specifications 6260J, 6265F, and 6267B all require that the hardenability be J41 = 1 maximum and J32 = 6 minimum for material in the normalized (1700 F) plus austenitized (1500 F) condition. The original AMS documents should be consulted for complete specification details, which also include microstructural requirements (4, 6, 7).

1.0662 End quench hardenability for 9310 H, Figure 1.0662.

1.07 Forms and Conditions Available

1.071 This steel is available as billets, bars, forgings, and annealed hot and cold finished rounds (1, 2), and as centerless ground bars, hot and cold drawn wire, and hot and cold rolled strip (1).

1.08 Melting and Casting Practice

1.081 Open hearth, electric furnace, air, and vacuum melt (3).

1.082 Vacuum melting produces improved impact properties (3) and fatigue properties (see Figure 3.056).

1.09 Special Considerations

1.091 E 9310 is not suitable for use in high load gear applications at temperatures above 300 F. Scuffing, scoring, and tooth fatigue can occur above this temperature (10, 11).

2 PHYSICAL PROPERTIES AND ENVIRONMENTAL EFFECTS

2.01 Thermal Properties

2.011 Melting range.

2.012 Phase changes.

2.0121 Critical temperatures are:

A_{c1} = 1315 F A_{r3} = 1305 F
A_{c3} = 1490 F A_{e1} = 1240 F
A_{r1} = 830 F A_{e3} = 1480 F (1).

2.013 Thermal conductivity.

2.014 Thermal expansion, Figure 2.014.

2.015 Specific heat.

2.016 Thermal diffusivity.

2.02 Other Physical Properties

2.021 Density.

2.022 Electrical properties.

2.023 Magnetic properties.

2.024 Emittance.

2.025 Damping capacity.

2.03 Chemical Environments

2.04 Nuclear Environments

3 MECHANICAL PROPERTIES

3.01 Specified Mechanical Properties

	Fe
0.1	C
3.25	Ni
1.2	Cr
0.1	Mo

E 9310

3.011 AMS specifies no mechanical property requirements for E 9310 but does specify hardenability limits. These are given in Section 1.0661.

3.02 **Mechanical Properties at Room Temperature**

3.021 Tension – stress-strain diagrams – tension properties.

3.0211 Typical properties of bar stock, Table 3.0211.

3.0212 Effect of carbon content on tensile properties of bar, Figure 3.0212.

3.0213 Effect of bar diameter on room temperature tensile properties of bar, given simulated carburizing cycle, Figure 3.0213.

3.0214 Cyclic and monotonic stress-strain curves in tension, Figure 3.0214.

3.022 Compression – stress-strain diagrams – compression properties.

3.023 Impact.

3.0231 Effect of bar diameter and tempering temperature on room temperature impact strength of bar, given simulated carburizing cycle, Figure 3.0231.

3.024 Bending.

3.025 Torsion and shear.

3.026 Bearing.

3.027 Stress concentration.

3.0271 Notch properties.

3.0272 Fracture toughness.

3.02721 Fracture toughness gradient in carburized case, Figure 3.02721.

3.028 Combined properties.

3.03 **Mechanical Properties at Various Temperatures**

3.031 Tension – stress-strain diagrams – tension properties (see Figure 3.03712).

3.032 Compression – stress-strain diagrams – compression properties.

3.033 Impact.

3.034 Bending.

3.035 Torsion and shear.

3.036 Bearing.

3.037 Stress concentration.

3.0371 Notch properties.

3.03711 The alloy exhibits excellent resistance to notch sensitivity at cryogenic temperatures, as indicated by tensile data in Figure 3.03712.

3.03712 Smooth and notched tensile properties at low temperatures, Figure 3.03712.

3.0372 Fracture toughness.

3.038 Combined properties.

3.04 **Creep and Creep Rupture Properties**

3.05 **Fatigue Properties**

3.051 Refrigeration after quenching has little effect on the rotating beam fatigue life in the untempered condition, as shown in Figure 3.052. However, in the quenched and tempered condition, better fatigue life is obtained with nonrefrigerated material containing a larger fraction of retained austenite, as shown in Figures 3.053 and 3.054. Tempering at 300 F effects a significant increase in fatigue strength as seen by comparison of the data for untempered material in Figure 3.052 and for tempered material in Figure 3.053.

3.052 Rotating beam fatigue life at room temperature for carburized and quenched E 9310, Figure 3.052.

3.053 Rotating beam fatigue life at room temperature for carburized and tempered E 9310, Figure 3.053.

3.054 Weibull distribution of rotating beam fatigue life at room temperature for carburized E 9310 with two levels of retained austenite, Figure 3.054.

3.055 Double vacuum processing (vacuum induction melt-vacuum arc remelt) improves the rolling contact fatigue performance over that of single vacuum processed (vacuum arc remelt) material, as shown in Figure 3.056 (10).

3.056 Weibull distribution of rolling contact fatigue life at room temperature for single (VAR) and double (VIM-VAR) vacuum melted material, Figure 3.056.

3.057 The fatigue crack-growth rate in the carburized surface layer is much greater than in the noncarburized core for surface-carburized E 9310. This is illustrated by fatigue data on noncarburized material (representing the core) and through-carburized material (representing the case) shown in Figure 3.058. Other variables such as test frequency and stress ratio have relatively small effects (overlapping data scatter ranges), although wet air promotes rusting and increases the crack-growth rate as compared to dry air (13).

3.058 Fatigue crack-growth behavior at room temperature [(a) noncarburized, f = 204 cpm, R = 0.05, dry air; (b) noncarburized, f = 204 cpm, R = 0.50, dry air; (c) noncarburized, f = 60 cpm, R = 0.05, wet air; (d) noncarburized, f = 6 cpm, R = 0.05, wet air; and (e) carburized, f = 204 cpm, R = 0.05, dry air], Figure 3.058.

3.06 **Elastic Properties**

3.061 Poisson's ratio.

3.062 Modulus of elasticity.

3.063 Modulus of rigidity.

3.064 Tangent modulus.

3.065 Secant modulus.

4 **FABRICATION**

4.01 **Forming**

4.011 Forging.

4.0111 Starting temperature 2200 F maximum, finishing temperature 1950 F minimum (1).

4.012 Powder metallurgy.

4.0121 E 9310 can be consolidated by shock compaction of rapidly solidified powder produced by centrifugal atomization. Hardness of the individual spherical particles is 344 ± 34 DPH, which compares well with the typical value of 340 DPH for wrought 9310 steel. The shock compacted powder is harder than 340 DPH, as shown in Figure 4.0122, reflecting cold work introduced during compaction. Tensile strength of the powder compacts reaches a maximum of 190 ksi at a compaction pressure of 4500 ksi. The maximum pressure is maintained only for 2–3 microseconds due to the dynamic nature of the shock compaction process. The density of the powder compacts is essentially 100 percent for compaction pressures of 1000 ksi and greater (14).

4.0122 Hardness and strength of shock compacted rapidly solidified E 9310 powder, Figure 4.0122.

4.02 Machining and Grinding

4.021 Generally similar to other grades of low carbon low alloy steels. Cold drawn bars have better machinability than annealed stock. General practice for machining gears is to normalize and temper or quench and temper (1200 F, 8 to 10 hr) for best machinability (1). High speed steel tools and sulphurized cutting fluids are recommended (1).

4.022 Cutting rates in E 9310 can be increased by a factor of 2 to 3 by using ultrasonically assisted machining (15).

4.03 Joining

4.031 The steel can be readily welded by oxyacetylene or metallic arc methods. The use of bare type electrodes results in low strength and low ductility welds (1).

4.032 Stress relief after welding, 1150 to 1200 F, is recommended to increase impact properties (1).

4.04 Surface Treating

4.041 Generally, this steel is especially suited for case hardening by carburizing. See Section 1.056. It is recommended that the maximum carbon in the case be limited to 0.90 percent and some specifications limit the carbon to 0.80 percent (1).

4.042 Shot peening is frequently employed in addition to carburizing to provide a desirable residual compressive stress on the surface for gear applications. Shot peening improves the pitting fatigue life of case carburized and hardened spur gears by 50 to 60 percent (11, 16).

	Fe
0.1	C
3.25	Ni
1.2	Cr
0.1	Mo

E 9310

REFERENCES

1 Alloy Digest, "AISI E 9310", Filing Code: SA-43, Steel Alloy (May 1956).

2 Joseph T. Ryerson & Son, Inc., "Ryerson Aircraft Steels", Issue (1958).

3 Ludwigson, D. C., and Morral, F. R., "A Summary of Comparative Properties of Air-Melted and Vacuum-Melted Steels and Superalloys", DMIC Rep. 128 (March 28, 1960).

4 AMS 6260J (October 15, 1979).

5 "Alloy Steel: Semi-Finished Hot Rolled and Cold Finished Bars", Steel Products Manual, AISI (July 1955), Supplement (July 1958).

6 AMS 6265F (July 1, 1982).

7 AMS 6267B (December 1, 1973).

8 Belton, J. H., Godby, L. L., and Taft, B. L., "Materials for Use at Liquid Hydrogen Temperature", paper presented at the 63rd Annual ASTM Meeting, held in Atlantic City, New Jersey (June 26–July 1, 1960).

9 Burroughs, L. R., and FitzGerald, P. C., "Evaluation of Advanced Gear-Forging Techniques", Sikorsky Aircraft Division, United Aircraft Corporation, Stratford, Connecticut, USAAVLABS TR-69-11 (April 1969).

10 Nahm, A. H., "Rolling Element Fatigue Testing of Gear Materials", Aircraft Engine Group, General Electric Company, Cincinnati, Ohio, NASA CR-135450 (June 26, 1978).

11 Anonymous, "Materials for Helicopter Gears", National Materials Advisory Board, Washington, D.C., NMAB-351 (October 1979).

12 Panhans, M. A., and Fournelle, R. A., "High Cycle Fatigue Resistance of AISI E 9310 Carburized Steel With Two Different Levels of Surface Retained Austenite and Surface Residual Stress", *Journal of Heat Treating*, Vol. 2, No. 1 (June 1981), pp 54–61.

13 Au, J. J., and Ke, J. S., "Correlation Between Fatigue Crack Growth Rate and Fatigue Striation Spacing in AISI 9310 (AMS 6265) Steel", Proceedings of Symposium on Fractography and Materials Science, sponsored by ASTM Committee E-24 on Fracture Testing, Williamsburg, Virginia (November 27–28, 1979), ASTM STP-733, pp 202-221.

14 Kasiraj, P., Vreeland, T., Jr., Schwarz, R. B., and Ahrens, T. J., "Shock Consolidation of a Rapidly Solidified Steel Powder", *Acta Metallurgica*, Vol. 32, No. 8 (August 1984), pp 1235-1241.

15 Devine, J., "Ultrasonically Assisted Machining", Sonobond Corporation, West Chester, Pennsylvania, *The Carbide Tool Journal* (September/October 1980).

16 Townsend, D. P., and Zaretsky, E. V., "Effect of Shot Peening on Surface Fatigue Life of Carburized and Hardened AISI 9310 Spur Gears", National Aeronautics and Space Administration, Lewis Research Center, Cleveland, Ohio, NASA TP-2047 (August 1982).

17 Townsend, D. P., and Zaretsky, E. V., "Comparisons of Modified Vasco X-2 and AISI 9310 Gear Steels", National Aeronautics and Space Administration, Lewis Research Center, Cleveland, Ohio, NASA TP-1731 (November 1980).

18 Cavallini, G., Lanciotti, A., Aldinio, G., and Rovellotti, R., "Fatigue Behavior of Helicopter Dynamic Components Under Constant Amplitude and Spectrum Loading", 51st Meeting of the AGARD Structures and Materials Panel, Helicopter Fatigue Life Assessment, Aix-en-Provence, France (September 14–19, 1980), pp 17-1 – 17-14.

19 Diesburg, D. E., "High-Hardenability Carburizing Steels for Rock Bits", Micon 78: Optimization of Processing, Properties, and Service Performance Through Microstructural Control, ASTM STP 672, Edited by Halle Abrams, G. N. Maniar, D. A. Nail, and H. D. Solomon, American Society for Testing and Materials (1979), pp 207–229.

20 Raefsky, M., "Effect of Retained Austenite on the Fatigue Properties of Carburized 9310 Steel", Vertol Division, Boeing Company, Philadelphia, Pennsylvania, Report D8-2123 (June 17, 1968).

	Fe
0.1	C
3.25	Ni
1.2	Cr
0.1	Mo

E 9310

Alloy	E 9310
AMS Specification	Product Form
6260J	Bars, Forgings, Tubing
6265F	Bars, Forgings, Tubing
6267B	Bars, Forgings, Tubing

TABLE 1.031. SPECIFICATIONS (4, 6, 7)

Alloy	E 9310					
AMS Specification	6260J		6265F		6267B	
	Percent		Percent		Percent	
Element	Min	Max	Min	Max	Min	Max
Carbon	0.07	0.13	0.07	0.13	0.07	0.13
Nickel	3.00	3.50	3.00	3.50	3.00	3.50
Chromium	1.00	1.40	1.00	1.40	1.00	1.40
Molybdenum	0.08	0.15	0.08	0.15	0.08	0.15
Manganese	0.40	0.70	0.40	0.70	0.40	0.70
Silicon	0.15	0.35	0.15	0.35	0.20	0.35
Copper	–	0.35	–	0.35	–	0.35
Phosphorus	–	0.025	–	0.015	–	0.015
Sulfur	–	0.025	–	0.015	–	0.015

TABLE 1.041. COMPOSITION (4, 6, 7)

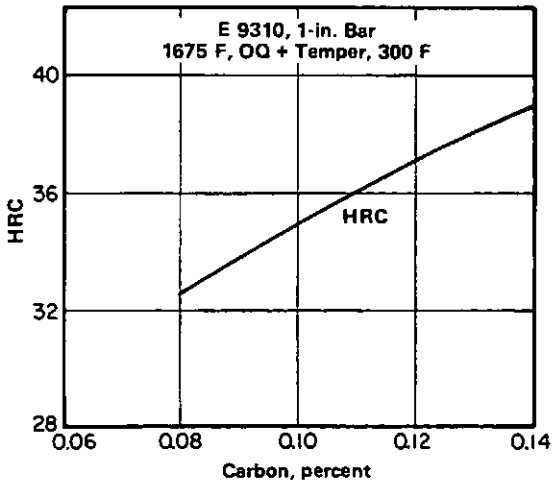


FIGURE 1.061. EFFECT OF CARBON CONTENT ON HARDNESS OF BAR (1)

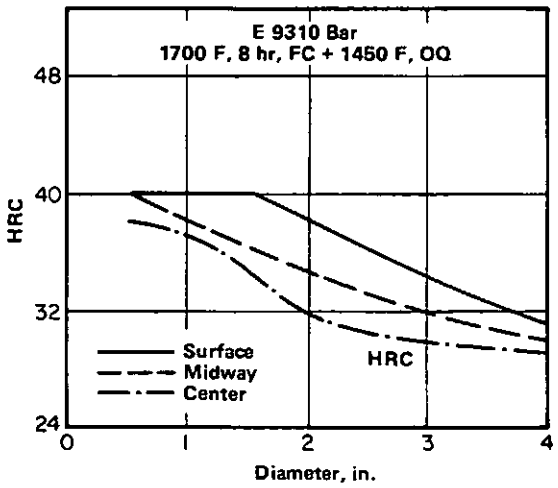


FIGURE 1.062. EFFECT OF THICKNESS ON AS-QUENCHED HARDNESS OF BAR (1)

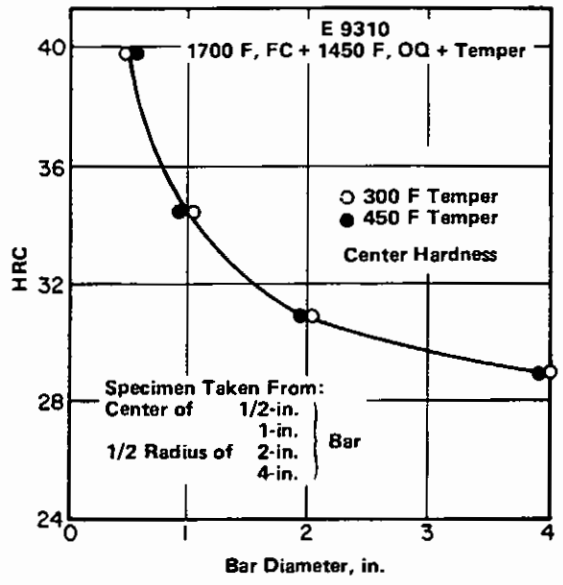


FIGURE 1.063. EFFECT OF BAR DIAMETER ON QUENCHED AND TEMPERED HARDNESS OF BAR, GIVEN SIMULATED CARBURIZING CYCLE (1)

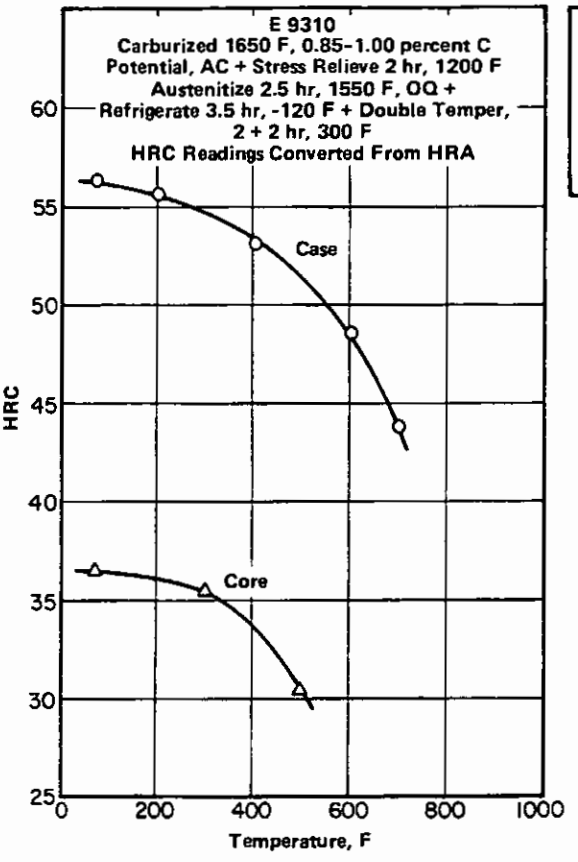


FIGURE 1.064. SHORT-TERM HOT HARDNESS (17)

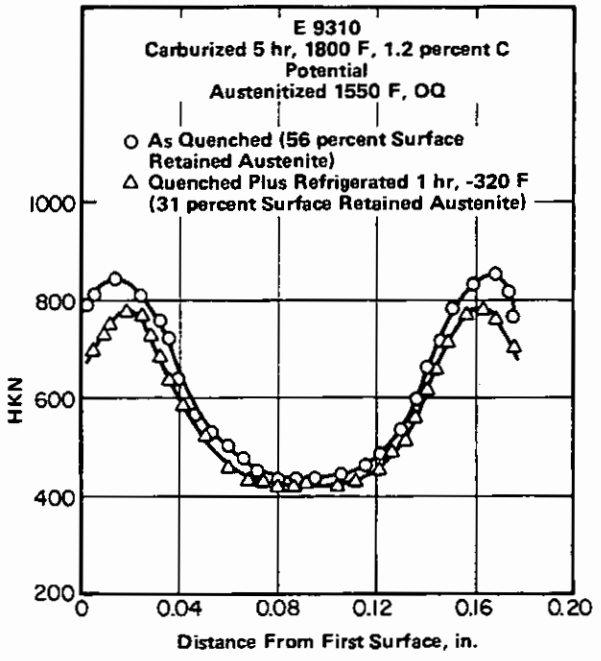


FIGURE 1.065. HARDNESS TRAVERSE ACROSS THICKNESS OF CARBURIZED AND QUENCHED E 9310 (12)

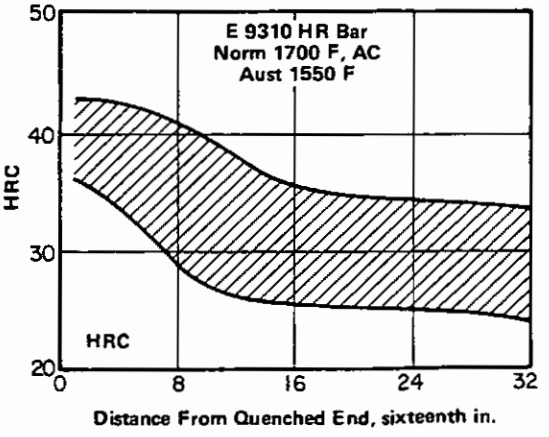


FIGURE 1.0662. END QUENCH HARDENABILITY FOR 9310 H (5)

	Fe
0.1	C
3.25	Ni
1.2	Cr
0.1	Mo

E 9310

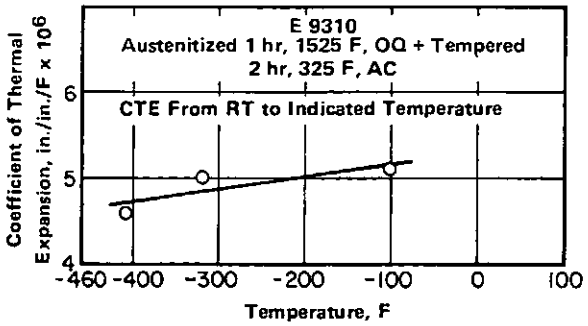


FIGURE 2.014. THERMAL EXPANSION (8)

Alloy	E 9310				
Form	Bar(a)				
Condition	As Rolled		Ann	Norm	
Diameter, in.	1	4	4	1	4
F_{tu}, typ, ksi	131	117.5	100	131.5	125.25
F_{ty}, typ, ksi	88	84	80	82.75	81.75
e (2 in.), percent	19	18.8	25	18.8	19.5
RA, percent	61.5	59.2	60	58.1	61.7
Hardness, BHN	269	241	200	269	255

(a) Tests were taken from center of 1-in. rounds and from 1/2 radius of 4-in. rounds.

TABLE 3.0211. TYPICAL PROPERTIES OF BAR STOCK (1)

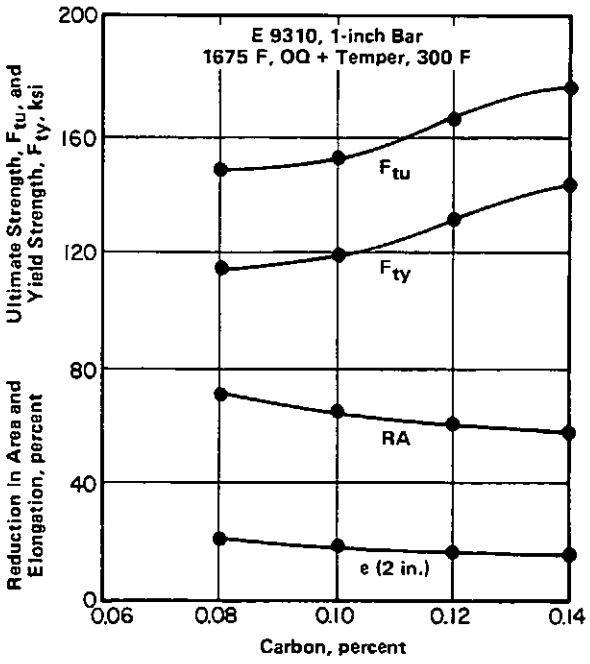


FIGURE 3.0212. EFFECT OF CARBON CONTENT ON TENSILE PROPERTIES OF BAR (1)

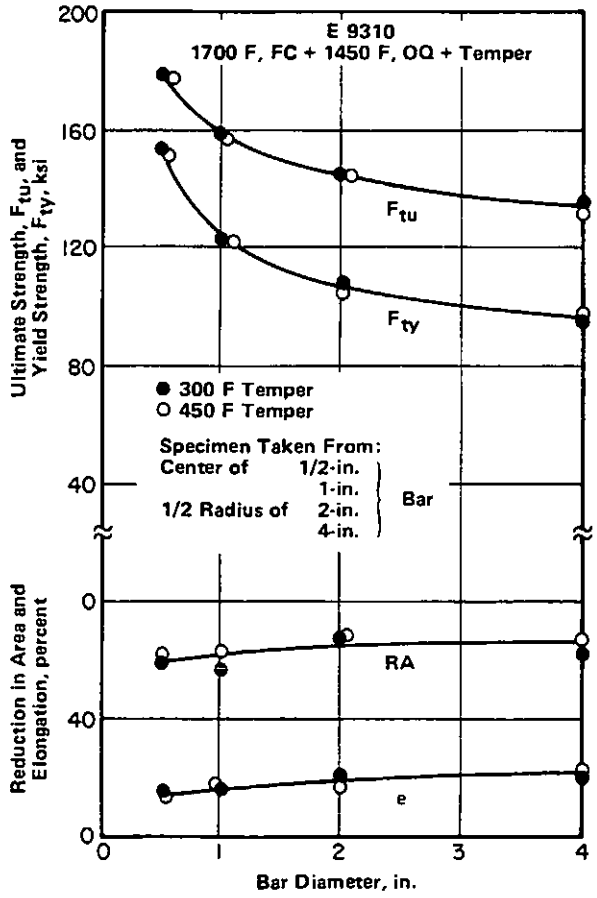


FIGURE 3.0213. EFFECT OF BAR DIAMETER ON ROOM TEMPERATURE TENSILE PROPERTIES OF BAR, GIVEN SIMULATED CARBURIZING CYCLE (1)

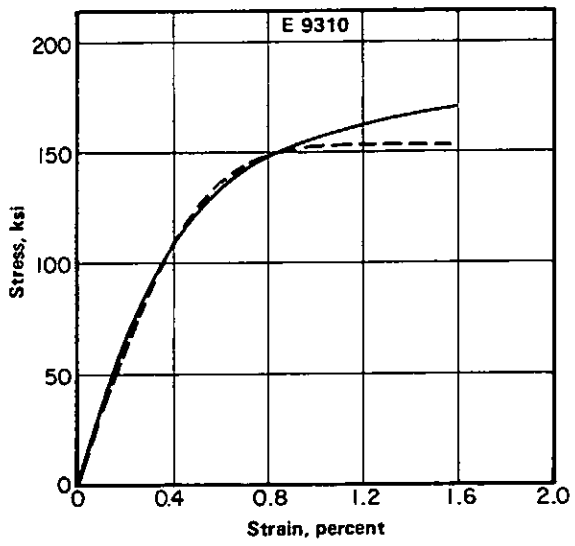


FIGURE 3.0214. CYCLIC AND MONOTONIC STRESS-STRAIN CURVES IN TENSION (18)

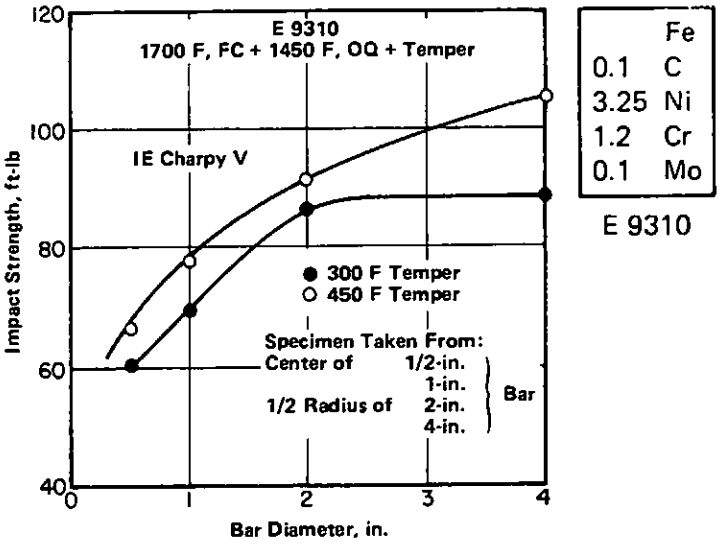


FIGURE 3.0231. EFFECT OF BAR DIAMETER AND TEMPERING TEMPERATURE ON ROOM TEMPERATURE IMPACT STRENGTH OF BAR, GIVEN SIMULATED CARBURIZING CYCLE (1)

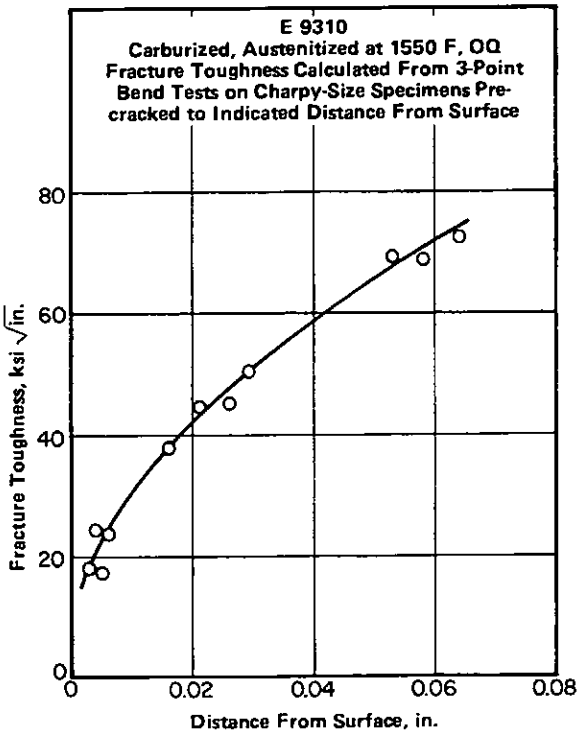


FIGURE 3.02721. FRACTURE TOUGHNESS GRADIENT IN CARBURIZED CASE (19)

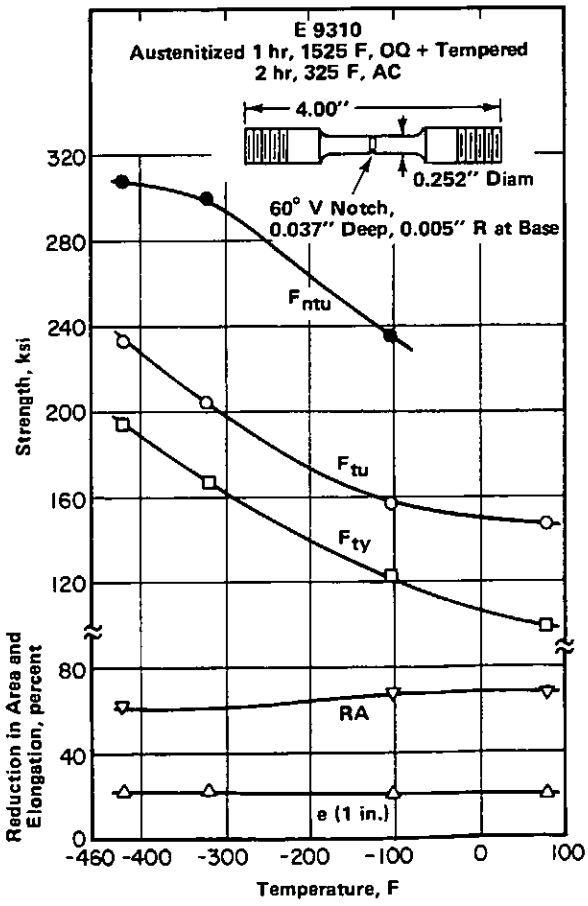


FIGURE 3.03712. SMOOTH AND NOTCHED TENSILE PROPERTIES AT LOW TEMPERATURES (8)

	Fe
0.1	C
3.25	Ni
1.2	Cr
0.1	Mo

E 9310

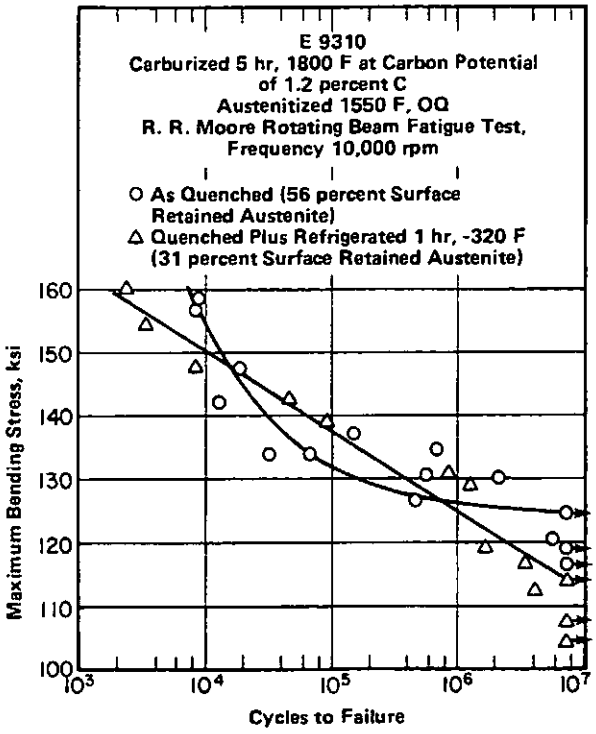


FIGURE 3.052. ROTATING BEAM FATIGUE LIFE AT ROOM TEMPERATURE FOR CARBURIZED AND QUENCHED E 9310 (12)

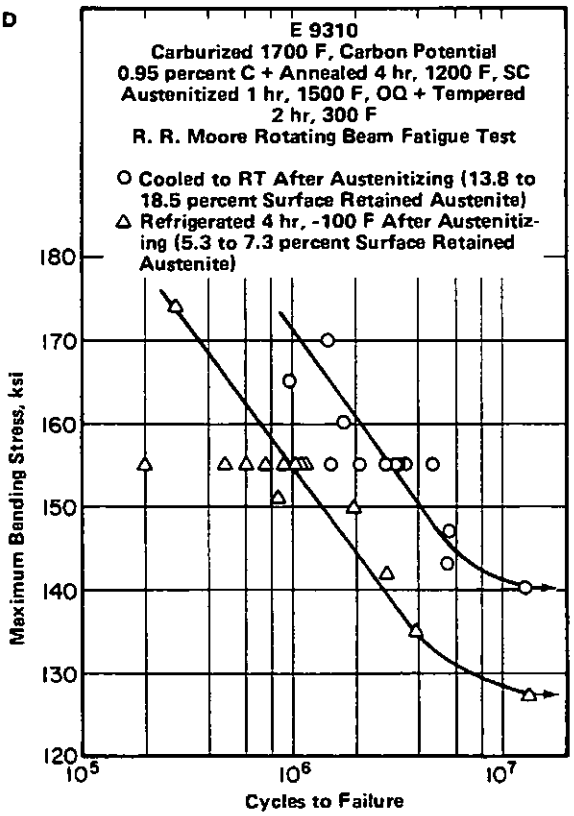


FIGURE 3.053. ROTATING BEAM FATIGUE LIFE AT ROOM TEMPERATURE FOR CARBURIZED AND TEMPERED E 9310 (20)

	Fe
0.1	C
3.25	Ni
1.2	Cr
0.1	Mo

E 9310

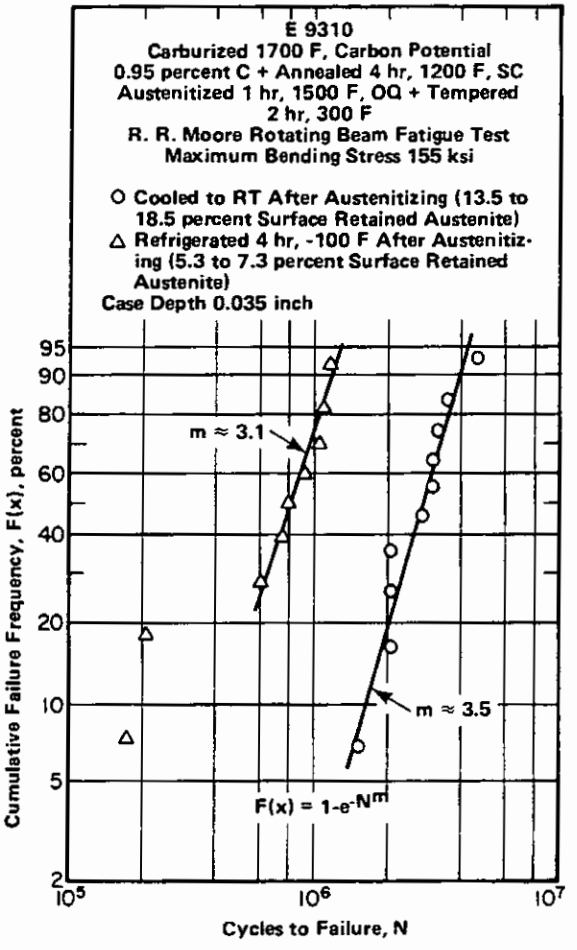


FIGURE 3.054. WEIBULL DISTRIBUTION OF ROTATING BEAM FATIGUE LIFE AT ROOM TEMPERATURE FOR CARBURIZED E 9310 WITH TWO LEVELS OF RETAINED AUSTENITE (20)

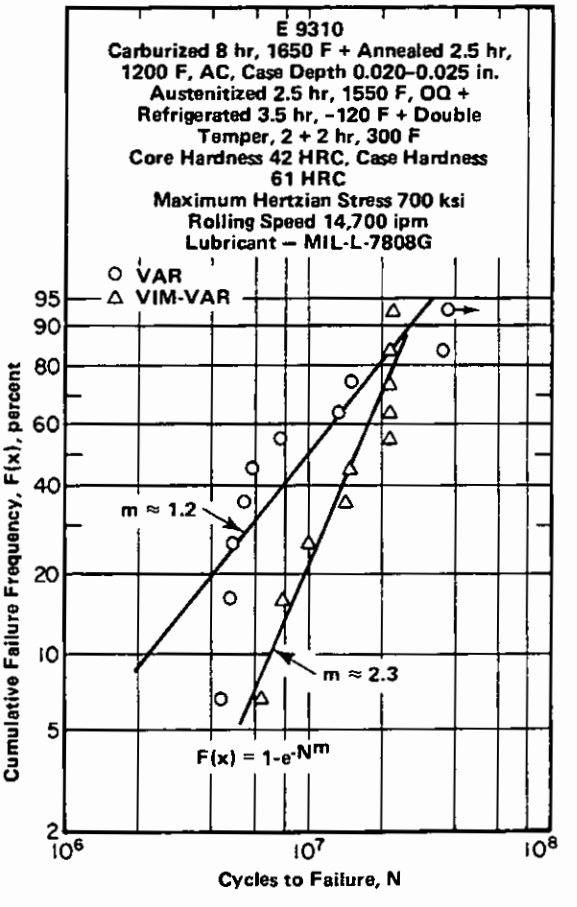
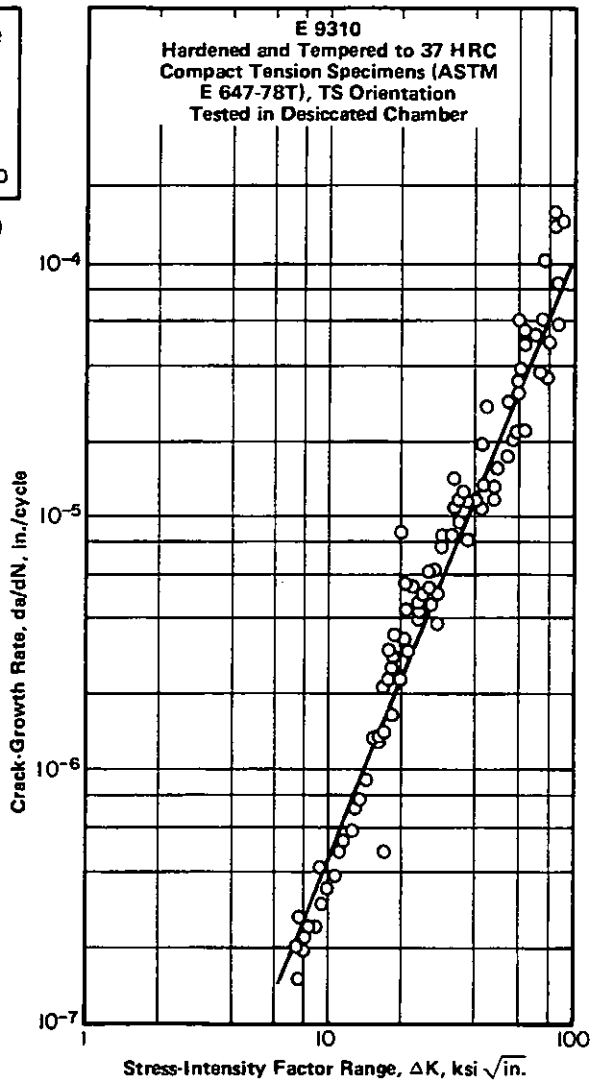


FIGURE 3.056. WEIBULL DISTRIBUTION OF ROLLING CONTACT FATIGUE LIFE AT ROOM TEMPERATURE FOR SINGLE (VAR) AND DOUBLE (VIM-VAR) VACUUM MELTED MATERIAL (10)

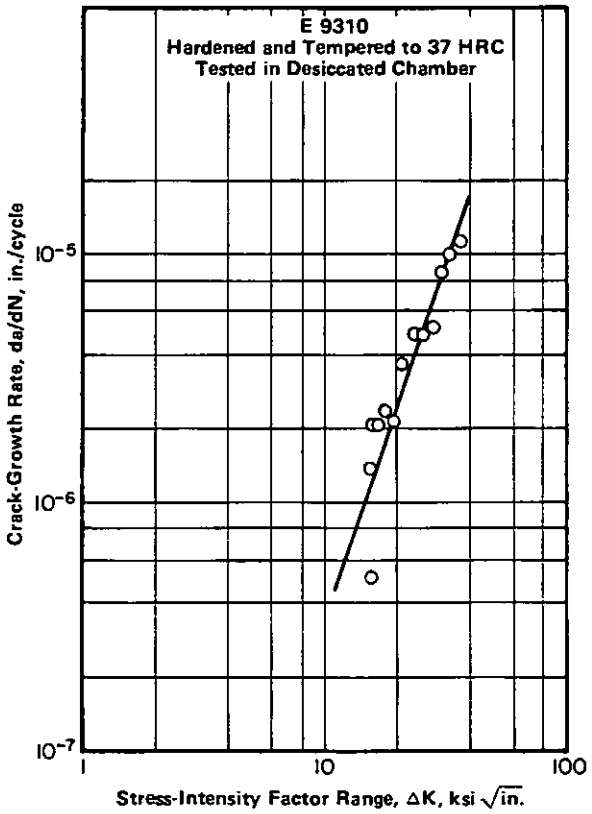
	Fe
0.1	C
3.25	Ni
1.2	Cr
0.1	Mo

E 9310



(a) Noncarburized, f = 204 cpm, R = 0.05, dry air.

FIGURE 0.058. FATIGUE CRACK-GROWTH BEHAVIOR AT ROOM TEMPERATURE (13)

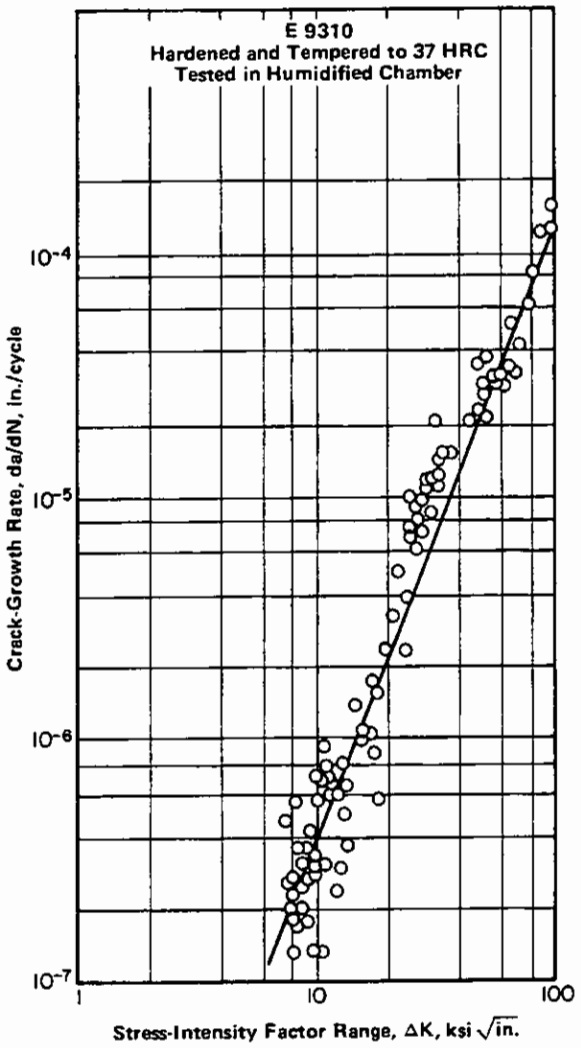


(b) Noncarburized, f = 204 cpm, R = 0.50, dry air.

FIGURE 3.058. FATIGUE CRACK-GROWTH BEHAVIOR AT ROOM TEMPERATURE (13)

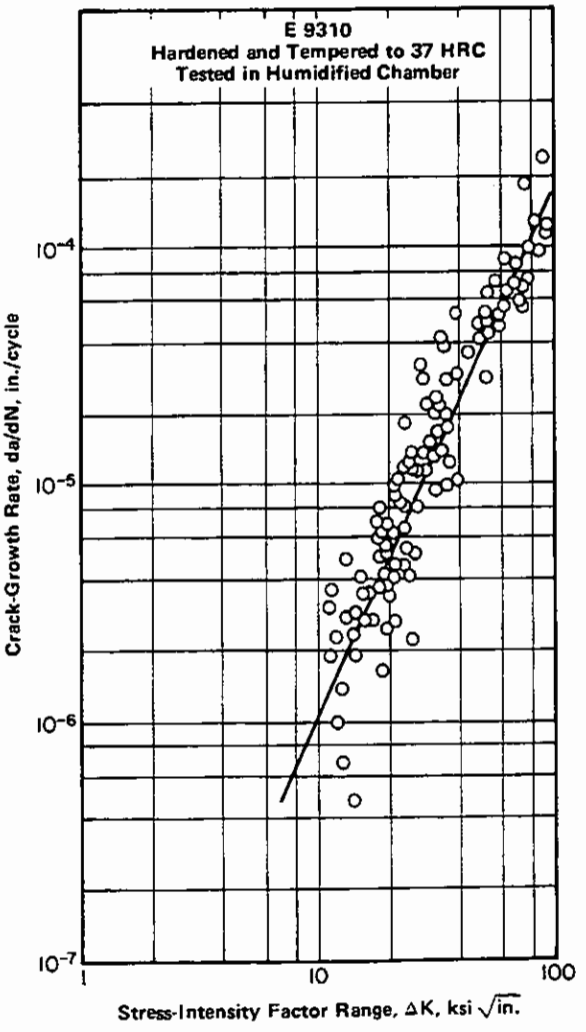
	Fe
0.1	C
3.25	Ni
1.2	Cr
0.1	Mo

E 9310



(c) Noncarburized, f = 60 cpm, R = 0.05, wet air.

FIGURE 3.058. FATIGUE CRACK-GROWTH BEHAVIOR AT ROOM TEMPERATURE (13)

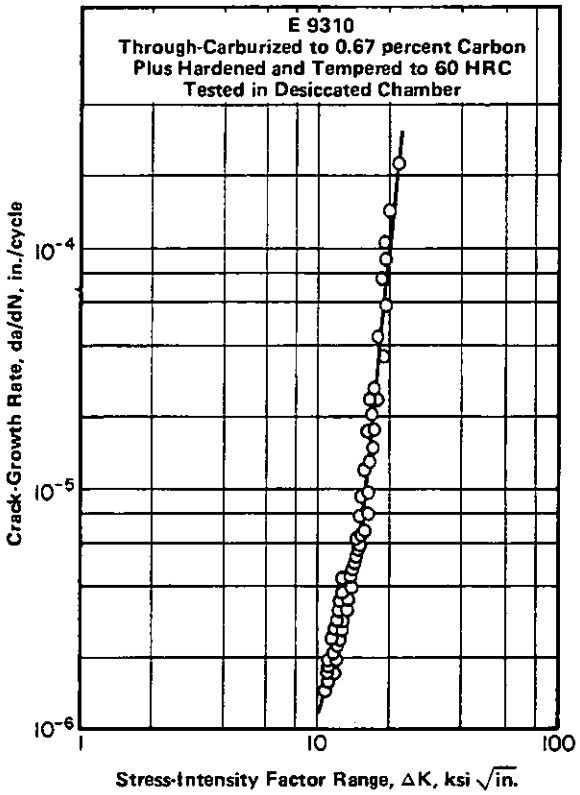


(d) Noncarburized, f = 6 cpm, R = 0.05, wet air.

FIGURE 3.058. FATIGUE CRACK-GROWTH BEHAVIOR AT ROOM TEMPERATURE (13)

	Fe
0.1	C
3.25	Ni
1.2	Cr
0.1	Mo

E 9310



(e) Carburized, f = 204 cpm, R = 0.05, dry air.

FIGURE 3.058. FATIGUE CRACK-GROWTH BEHAVIOR AT ROOM TEMPERATURE (13)

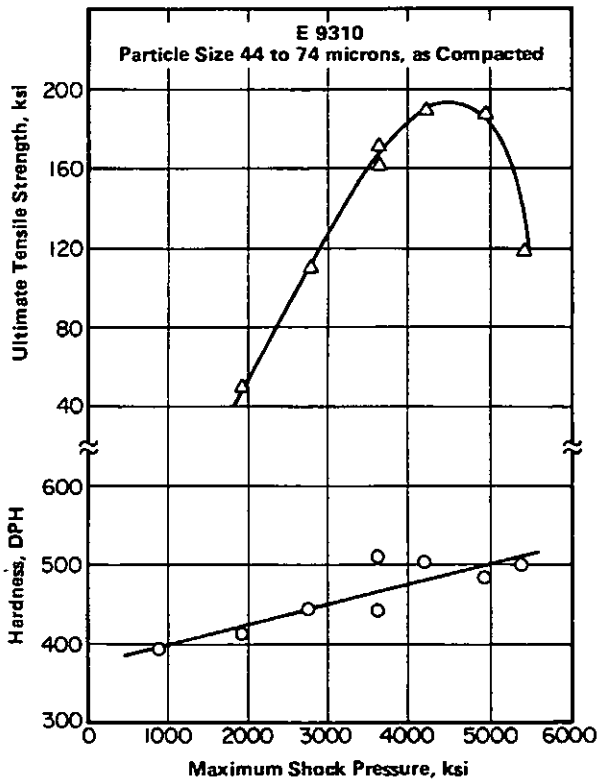


FIGURE 4.0122. HARDNESS AND STRENGTH OF SHOCK COMPACTED RAPIDLY SOLIDIFIED E 9310 POWDER (14)

FERROUS ALLOYS

REVISED: JUNE 1975
AUTHOR: J. R. KATTUS

Fe
1 C
1.45 Cr

52100

GENERAL

This low-alloy steel, which can be hardened by either oil- or water-quenching, has moderate hardenability combined with high compressive strength, abrasion resistance, and fatigue resistance when tempered to high hardness levels. With this combination of properties it is particularly useful in the following applications: ball and roller bearings, bearing races, spindles, gauges, cold working tools, and various hardened machine parts. Since it has poor resistance to softening at elevated temperatures, it is not recommended for use at temperatures above about 400F. Because of its high carbon content, its weldability is relatively poor; consequently, it is not recommended for weldments. It can be machined with moderate ease in the spheroidized, annealed, and hot-worked conditions. Its hot working characteristics are similar to those of carbon steels with equivalent carbon content (6)(7)(8)(13).

1.01 Commercial Designation

52100

1.02 Alternate Designations

E 52100, Teton (Allegheny-Ludlum)

1.03 Specifications

Table 1.03

1.04 Composition

Table 1.04

1.05 Heat Treatment

1.051 Anneal: Heat slowly and uniformly to 1425 to 1475F, hold 4 hours minimum, furnace cool. Resulting hardness 241 BHN max. (6)(7)(13).

1.052 Alternate anneal: Heat slowly and uniformly to 1425 to 1450F, hold 4 hours minimum, furnace cool to 1200 to 1275F, hold 4 to 6 hours, air cool. Resulting hardness 217 BHN max. (7)(8).

1.053 Spheroidize anneal: Heat slowly and uniformly to 1425F, hold 4 hours, furnace cool to 1380F, then cool 10F per hour to 1200F, air cool. Resulting hardness 200 BHN max. (7)

1.054 Normalize: 1650 - 1700F, air cool. Resulting hardness about 363 BHN (13).

1.055 Harden: Heat slowly and uniformly to 1500 to 1600F, oil quench; or 1425 to 1525F, water quench (6)(7)(8)(13).

1.056 Temper: Temperature will vary depending on hardness desired. For most applications tempering consists of 2 hours at 300 to 400F. Tempering should be done promptly after quenching as a precaution against cracking, especially when irregular shaped parts are involved (6)(8).

1.057 Martemper: 1550F, quench in salt at 500F, hold 5 minutes per inch of cross section, air cool, temper 350F. Resulting hardness 60 - 63 R_C (13).

1.06 Hardness

1.061 End-quench hardenability, Figure 1.061.

1.062 Effects of tempering temperature and time on the hardness of water-quenched and oil-quenched 52100, Figure 1.062.

1.063 Effects of mass and tempering temperature on surface hardness, Figure 1.063.

1.064 Effects of temperatures from 400 to 900F on the hardness of rod tempered at various temperatures, Figure 1.064.

1.065 Effect of temperatures up to 450F on the hardness of ball bearings, Figure 1.065.

1.066 Effects of 30 minute exposures at various elevated temperatures on the room-temperature hardness of rod tempered at different temperatures, Figure 1.066.

1.07 Forms and Conditions Available

1.071 Available in the form of bars, forgings, coils, and tubing in the annealed, hot-rolled, cold finished, or oil-quenched conditions (1)(2)(3)(13).

1.08 Melting and Casting Practice

1.081 Type 52100 is generally melted in basic electric furnaces. For applications requiring optimum quality, it is induction or consumable-electrode remelted in vacuum.

1.09 Special Considerations

1.091 The fatigue, impact, and notch-tensile strength of this alloy, at hardnesses between R_C 50 and R_C 65, are improved by vacuum melting as compared with air melting, whereas tensile strength is not significantly affected (16)(18).

1.092 In bearing applications, retained austenite above 4 percent causes increased rolling friction and local yielding at lower contact stresses than those for material containing no retained austenite (19).

1.093 Small amounts of water (0.01 percent) dissolved in hydrocarbon lubricants significantly lower the surface fatigue life of 52100 bearings (20).

1.094 When heat treated to high strength levels, Type 52100 is highly susceptible to hydrogen embrittlement (11).

1.095 Controlled atmosphere or other effective protection is highly recommended during annealing, hardening, or normalizing heat treatments in order to prevent decarburization, which decreases fatigue strength and wear resistance (7).

2. PHYSICAL AND CHEMICAL PROPERTIES

2.01 Thermal Properties

2.011 Melting range.

2.012 Phase changes.

2.0121 Time-temperature-transformation diagram, Figure 2.0121.

2.0122 The critical temperatures for Type 52100 are as follows: A_{c1} = 1400F, A_{c3} = 1440F, A_{r3} = 1310F, A_{r1} = 1300F, M_S = 480F, M_f = 235F (6).

2.013 Thermal conductivity.

2.014 Thermal expansion, Figure 2.014.

2.015 Specific heat.

2.016 Thermal diffusivity.

2.02 Other Physical Properties

2.021 Density. 0.282 lb per cu in., 7.80 grams per cu cm (6)(9).

2.022 Electrical properties.

2.023 Magnetic properties. Ferromagnetic.

2.024 Emittance.

2.025 Damping capacity.

2.03 Chemical Properties

2.031 Type 52100 is susceptible to rusting in moist environments.

2.032 Small amounts of water or oxygen dissolved in hydrocarbon lubricants significantly increase corrosive wear in ball bearings (20).

2.04 Nuclear Properties

3. MECHANICAL PROPERTIES

3.01 Specified Mechanical Properties

Table 3.01

3.02 Mechanical Properties at Room Temperature

3.021 Tension-stress/strain diagrams - tension properties.

3.0211 Tensile stress-strain curve, Figure 3.0211.

3.0212 Tensile properties in various non-hardened conditions, Table 3.0212.

3.0213 Effect of tempering temperature on tensile properties, Figure 3.0213.

3.0214 Relationship between hardness and tensile properties. (See Figure 3.0311).

3.022 Compression-stress/strain diagrams - compression properties.

3.0221 Compressive stress-strain curve, Figure 3.0221.

Fe
1 C
1.45 Cr

52100

3.0222 Effect of tempering temperature on compressive yield strength, Figure 3.0222.
3.0223 Relationship between hardness and compressive yield strength. (See Figure 3.0321).
3.023 Impact.
3.0231 Effect of tempering temperature on unnotched Izod impact properties, Figure 3.0231.
3.024 Bending.
3.025 Torsion and shear.
3.026 Bearing.
3.027 Stress concentration.
3.0271 Notch properties.
3.02711 Notched tensile strength, Table 3.02711.
3.0272 Fracture toughness.
3.028 Combined properties.
3.03 Mechanical Properties at Various Temperatures.
3.031 Tension-stress/strain diagrams - tension properties.
3.0311 Effect of tempering to various hardness levels on tensile properties of air-melted and vacuum-melted 52100 at room temperature and 350F, Figure 3.0311.
3.032 Compression-stress/strain diagrams - compression properties.
3.0321 Effect of tempering to various hardness levels on compressive yield strength of air-melted and vacuum-melted 52100 at room temperature and 350F, Figure 3.0321.
3.033 Impact.
3.034 Bending.
3.035 Torsion and shear.
3.036 Bearing.
3.037 Stress concentration.
3.0371 Notch properties.
3.0372 Fracture toughness.
3.038 Combined properties.

3.04 Creep and Creep Rupture Properties

3.05 Fatigue Properties
3.051 Investigations of the mechanism of fatigue failures in bearings have shown that cracks in Type 52100 nucleate at inclusions containing calcium or aluminum oxides, whereas sulfide inclusions do not appear to play a part in crack initiation. Consequently, melting practices that minimize oxygen and calcium content - vacuum melting or vacuum degassing - are quite beneficial to fatigue properties. Increasing sulfur contents up to at least 0.12 percent improve the fatigue resistance of Type 52100 by modifying the shape and coherence of harmful oxide inclusions (16)(23)(24)(25).
3.052 Fatigue life at various hardness levels for air-electric and vacuum-induction melted material, Figure 3.052.
3.053 Fatigue life of vacuum-melted and air-melted Type 52100 steel, Figure 3.053.
3.054 Effect of hardness and melting practice on fatigue strength at 10^8 cycles, Figure 3.054.
3.055 Fatigue life in torsion as a function of cyclic strain range for specimens in various liquid environments, Figure 3.055.
3.056 Fatigue life in torsion as a function of cyclic strain range for specimens tempered at three different temperatures, Figure 3.056.
3.057 Fatigue life as a function of cyclic strain, Figure 3.057.
3.058 Effect of hardness level on fatigue strength at 10^8 cycles for air-melted and vacuum-melted material at room temperature and 350F, Figure 3.058.
3.059 Weibull plot showing effects of ambient moisture on statistical distribution of fatigue durability at a maximum stress of 125 ksi, Figure 3.059.
3.0510 Weibull plot showing effects of ambient moisture on statistical distribution of fatigue durability at a maximum stress of 170 ksi, Figure 3.0510.

3.06 Elastic Properties
3.061 Poisson's ratio, 0.290 (6).
3.062 Modulus of elasticity.
3.0621 Dynamic modulus, 30,990 ksi (6).
3.0622 Static modulus, 29,000 ksi (9).
3.063 Modulus of rigidity, 12,010 ksi (6)(9).

4. FABRICATION

4.01 Formability
4.011 Type 52100 has moderately good formability in the temperature range 2100 to 1600F. Its cold formability is poor (6)(7)(25).

4.02 Machining
4.021 In the annealed condition, Type 52100 can be readily machined. Fully annealed material has a machinability rating of 45 percent of AISI B 1112 steel, whereas spheroidize annealed material has a rating of 37 percent (13).

4.03 Welding
4.031 Welding is not recommended since the weldability of Type 52100 is relatively poor.

4.04 Surface Treatment
4.041 Since Type 52100 is used primarily in applications requiring its inherent wear resistance, lubricants are normally the only type of coating applied.

Alloy	52100			
Source	(1)(2)(3)(14)			
Form	AMS	ASTM	Military	Federal
Bars	6440F	A322	MIL-S-980B	QQ-S-6246
	6447B	A331	MIL-S-7420B	
Tubing	6441E	A519		
	6447B			
Forgings	6440F		MIL-S-7420B	
	6447B			
Sheet, strip		A505		
		A506		
		A507		
Castings			MIL-S-22141	
Ball & roller bearing steel		A295		

TABLE 1.03 SPECIFICATIONS

Alloy	52100	
Source	ASTM A-295, A-331, A-322 AMS 6440F (1), 6441E (2)	
	percent	
	min.	max.
Carbon (a)	0.98	1.10
Manganese	0.25	0.45
Phosphorus (b)	-	0.025
Sulfur (b)	-	0.025
Silicon	0.20	0.35
Chromium	1.30	1.60
Nickel	-	0.25
Copper	-	0.35
Molybdenum	-	0.08
(a) ASTM A505 and A519: C-0.95 min. 1.10 max.		
(b) AMS 6447B (3): P and S - 0.15 max.		

TABLE 1.04 COMPOSITION

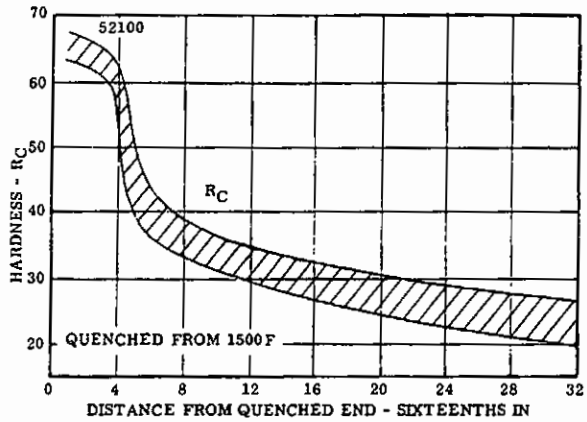


FIG. 1.061 END QUENCH HARDENABILITY. (9)

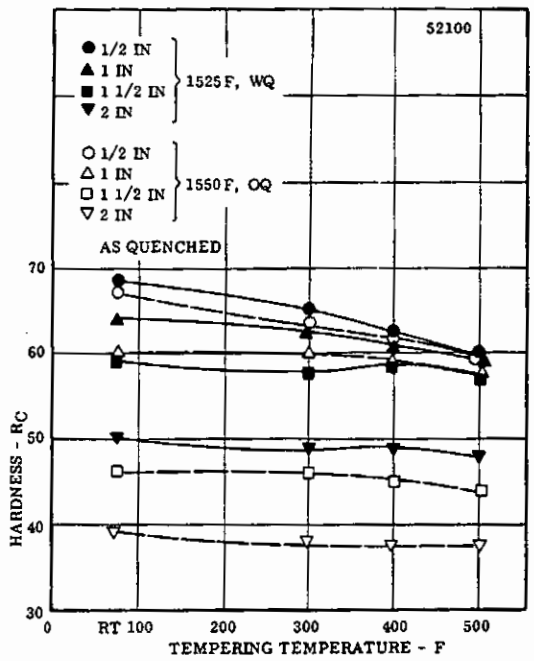


FIG. 1.063 EFFECTS OF MASS AND TEMPERING TEMPERATURE ON SURFACE HARDNESS. (7)

Fe
1 C
1.45 Cr

52100

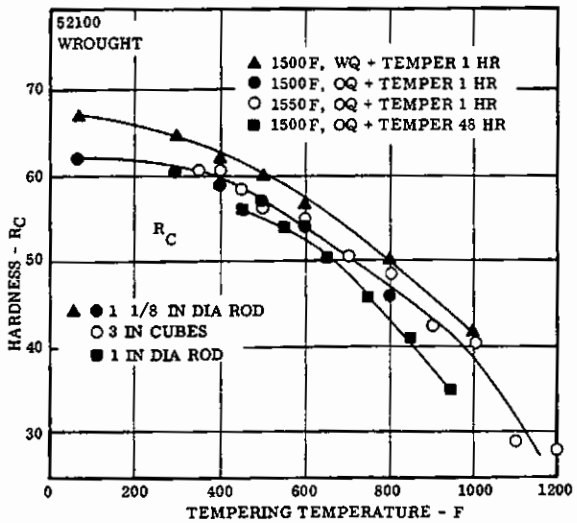


FIG. 1.062 EFFECTS OF TEMPERING TEMPERATURE AND TIME ON THE HARDNESS OF WATER-QUENCHED AND OIL-QUENCHED 52100. (6)(7)

Fe
1 C
1.45 Cr

52100

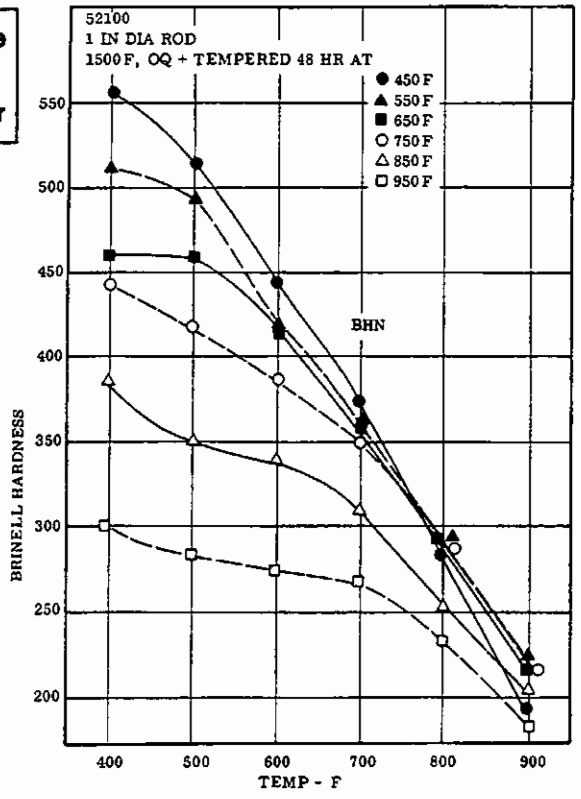


FIG. 1.064 EFFECTS OF TEMPERATURES FROM 400 TO 900 F ON THE HARDNESS OF ROD TEMPERED AT VARIOUS TEMPERATURES. (6)

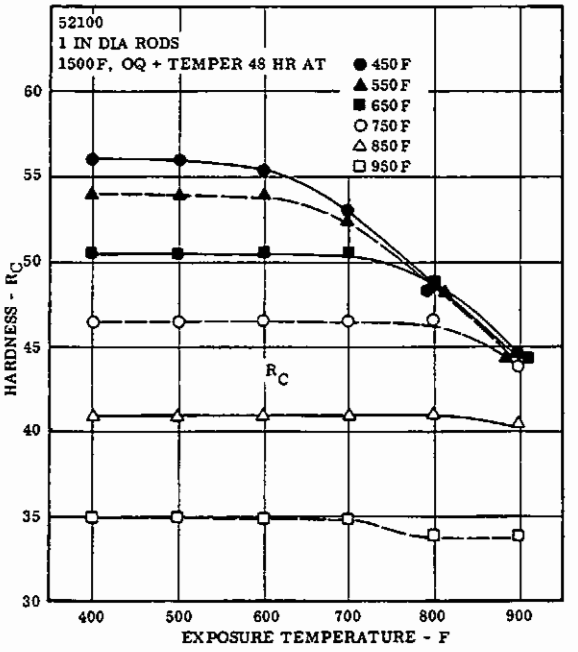


FIG. 1.066 EFFECTS OF 30-MINUTE EXPOSURES AT VARIOUS ELEVATED TEMPERATURES ON THE ROOM TEMPERATURE HARDNESS OF ROD TEMPERED AT DIFFERENT TEMPERATURES. (6)

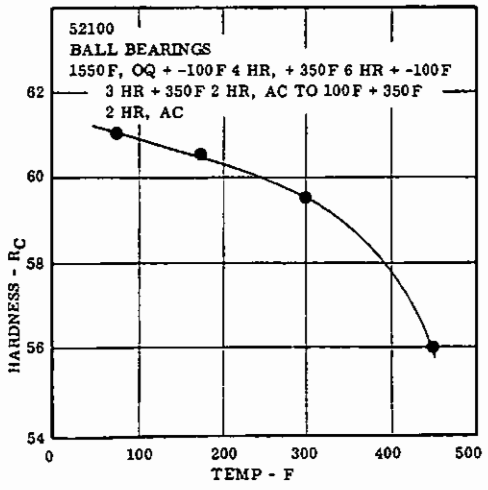


FIG. 1.065 EFFECT OF TEMPERATURES UP TO 450 F ON THE HARDNESS OF BALL BEARINGS. (17)

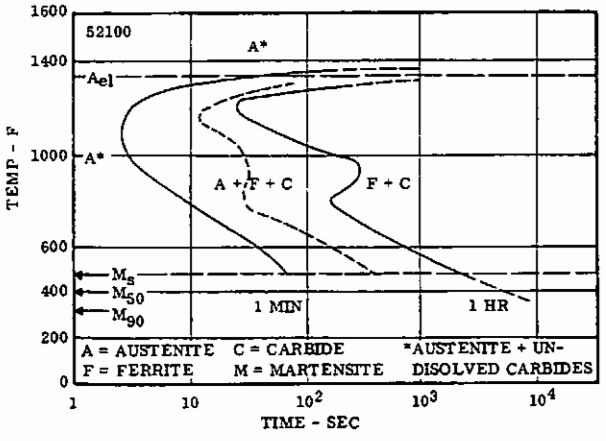


FIG. 2.0121 TIME-TEMPERATURE-TRANSFORMATION DIAGRAM. (21)

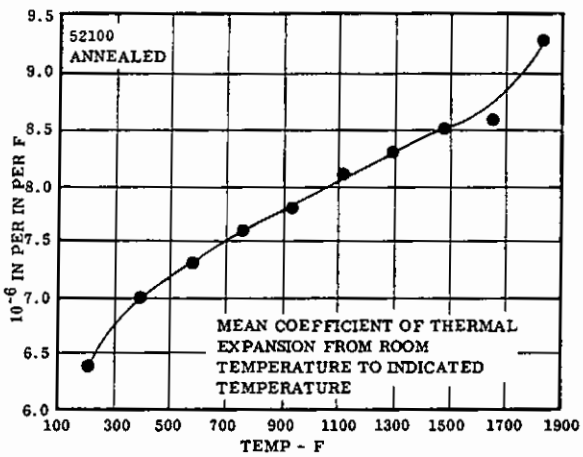


FIG. 2.014 THERMAL EXPANSION. (6)

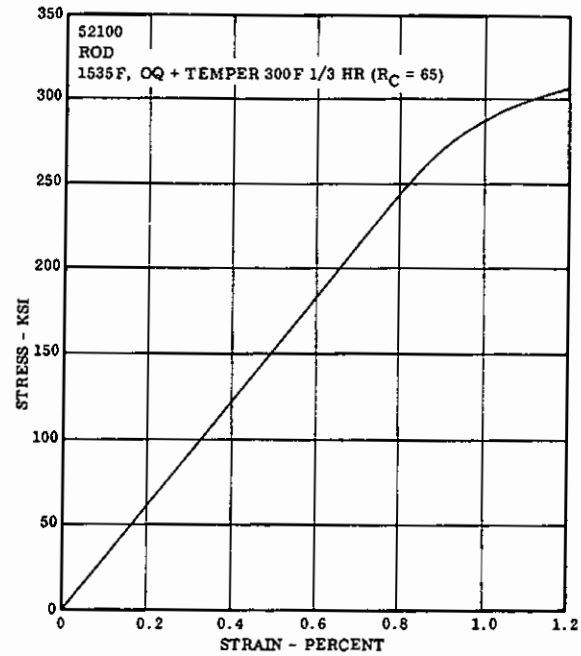


FIG. 3.0211 TENSILE STRESS-STRAIN CURVE. (10)

Fe
1 C
1.45 Cr

52100

Alloy	52100			
Specification	Form	Condition	Hardness	F_{tu} (ksi)
6440F (1)	Bars			
6447B (3)	up to 0.50 in. dia.	cold finished	-	120 max.
	over 0.50 in. dia.	hot finished	207 BHN max.	-
	over 0.50 in. dia.	cold finished	248 BHN max.	-
	bars & forgings	1525F, 20 min., OQ	63 R_c min.	-
6441E (2)	Tubing	hot finished	95 R_b max.	-
6447B (3)		1525F, 20 min., O.Q.	63 R_c min.	-
ASTM A295	Bearing steel			
	coils	annealed	92 R_b max.	-
	bar & tubes	annealed	207 BHN max.	-
	coils	cold drawn-stress rel.	92 R_b max.	-
	coils, bars, tubes	cold drawn	250 BHN max.	-
	coils, bars, tubes	annealed	-	110 max.

TABLE 3.01 SPECIFIED MECHANICAL PROPERTIES

Alloy	52100				
Form	Bar				
Source	(7)(13)				
Condition	F_{ty} (ksi)	F_{tu} (ksi)	e (2 in) (percent)	RA (percent)	BHN
Annealed	81	100	25	57	192
Normalized	139	185	13	20	363
Spheroidized	62	94	27	62	179
Spheroidized and cold drawn 13 percent	98	105	25	57	229
spheroidized and cold drawn 26 percent	106	124	16	50	262

TABLE 3.0212 TENSILE PROPERTIES IN VARIOUS NON-HARDENED CONDITIONS.

Fe
1 C
1.45 Cr

52100

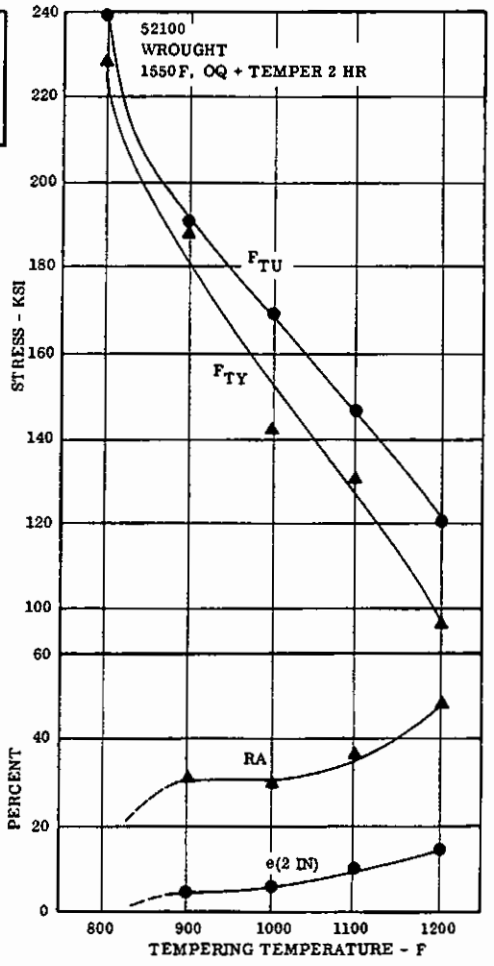


FIG. 3.0213 EFFECT OF TEMPERING TEMPERATURE ON TENSILE PROPERTIES. (9)

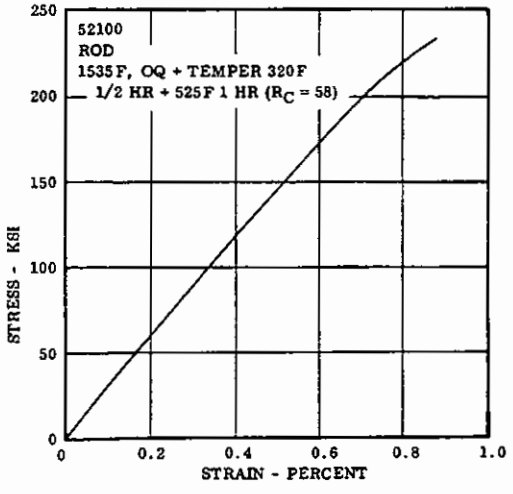


FIG. 3.0221 COMPRESSIVE STRESS-STRAIN CURVE. (10)

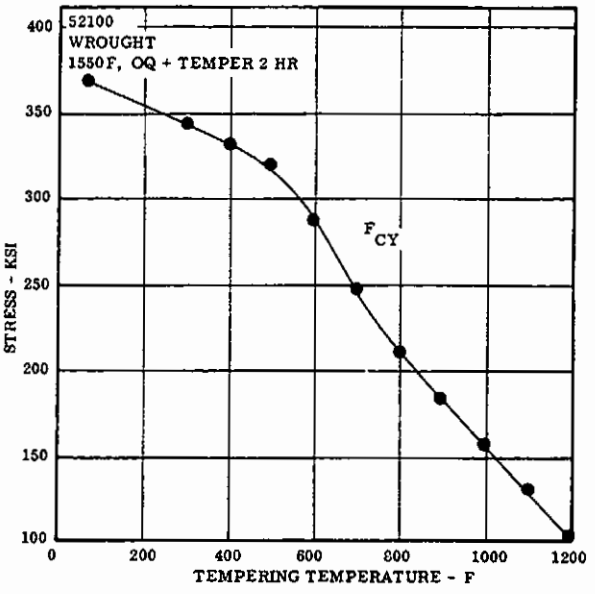


FIG. 3.0222 EFFECT OF TEMPERING TEMPERATURE ON COMPRESSIVE YIELD STRENGTH. (9)

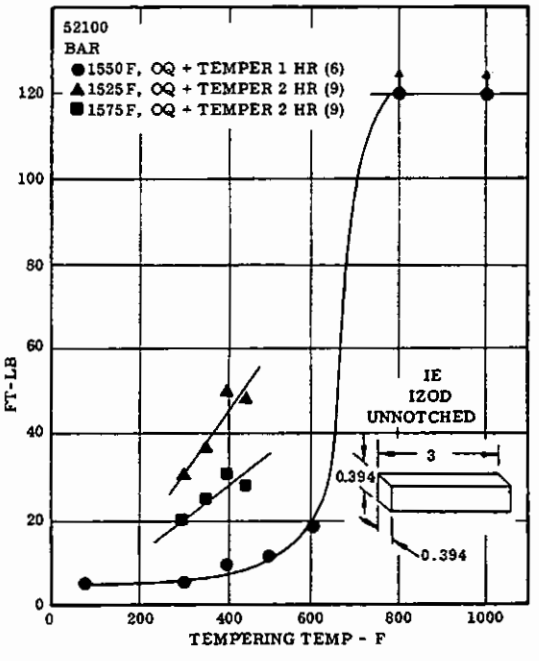


FIG. 3.0231 EFFECT OF TEMPERING TEMPERATURE ON UNNOTCHED IZOD IMPACT PROPERTIES. (6)(9)

Alloy	52100			
Form	Rod			
Source	(11)			
Condition	RC	F_{tu} (ksi)	NTS (ksi)	NTS/F_{ty}
1550F, OQ + temper 300F 1 hr.	64	300	86.8	0.29
1550F, OQ + temper 700F 1 hr.	54	280	176.5	0.63

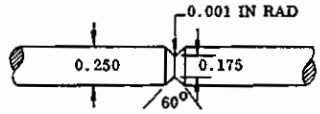
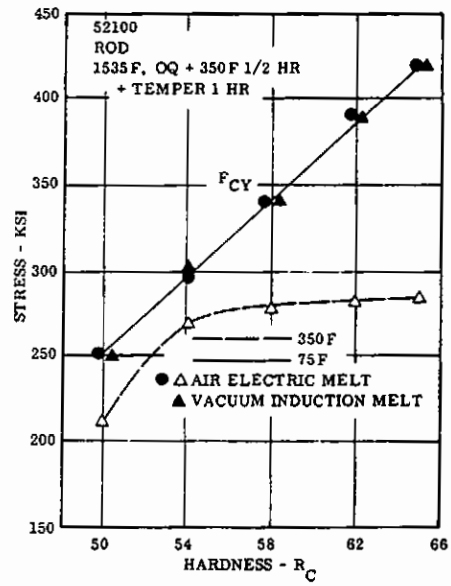


TABLE 3.02711 NOTCHED TENSILE STRENGTH



Fe
1 C
1.45 Cr

52100

FIG. 3.0321 EFFECT OF TEMPERING TO VARIOUS HARDNESS LEVELS ON COMPRESSIVE YIELD STRENGTH OF AIR-MELTED AND VACUUM-MELTED 52100 AT ROOM TEMPERATURE AND 350F. (10)

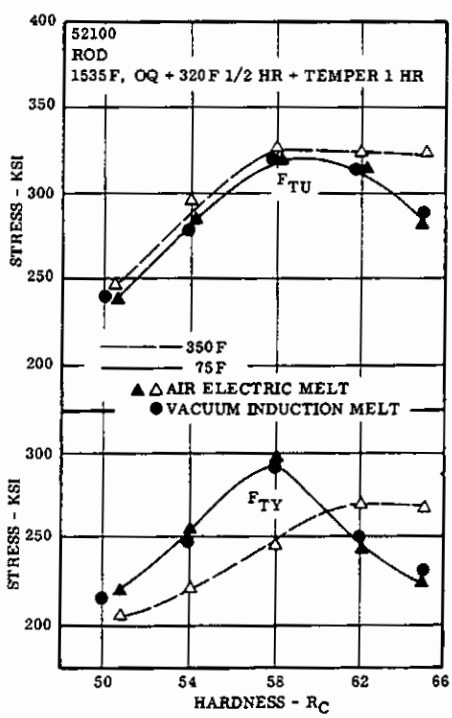


FIG. 3.0311 EFFECT OF TEMPERING TO VARIOUS HARDNESS LEVELS ON TENSILE PROPERTIES OF AIR-MELTED AND VACUUM-MELTED 52100 AT ROOM TEMPERATURE AND 350F. (10)

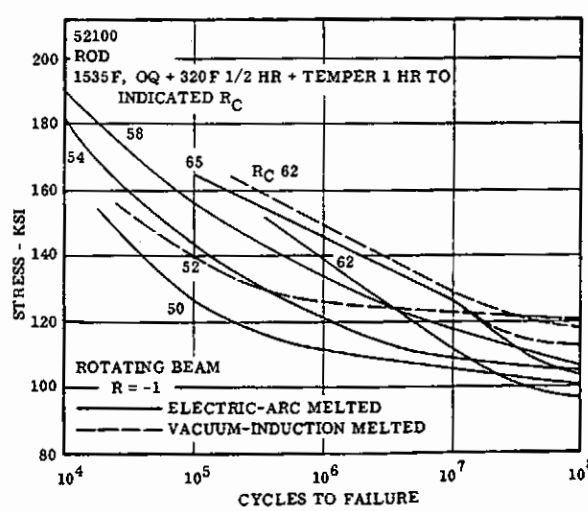


FIG. 3.052 FATIGUE LIFE AT VARIOUS HARDNESS LEVELS FOR AIR-ELECTRIC AND VACUUM-INDUCTION MELTED MATERIAL. (10)

Fe
1 C
1.45 Cr

52100

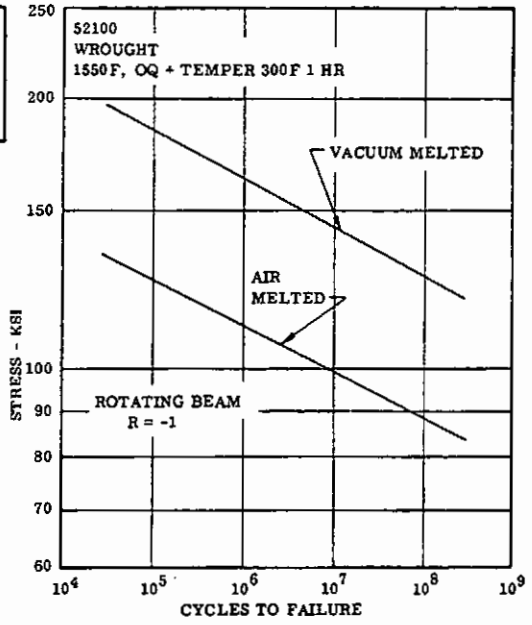


FIG. 3.053 FATIGUE LIFE OF VACUUM-MELTED AND AIR-MELTED TYPE 52100 STEEL. (8)

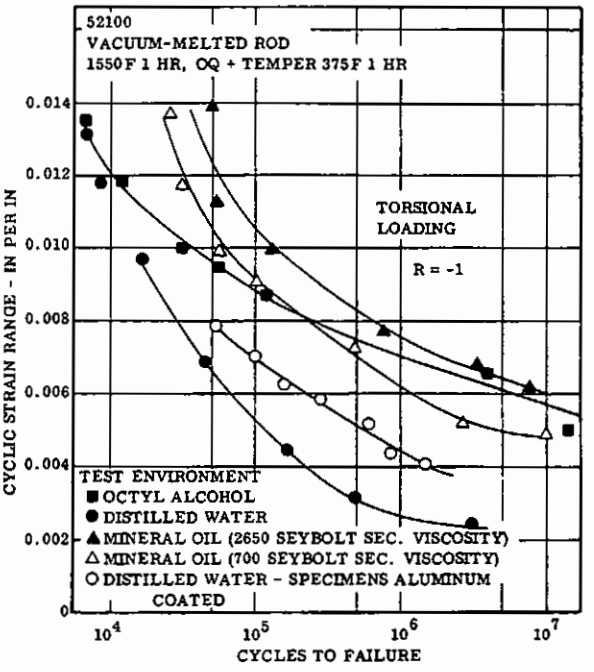


FIG. 3.055 FATIGUE LIFE IN TORSION AS A FUNCTION OF CYCLIC STRAIN RANGE FOR SPECIMENS IN VARIOUS LIQUID ENVIRONMENTS. (4)

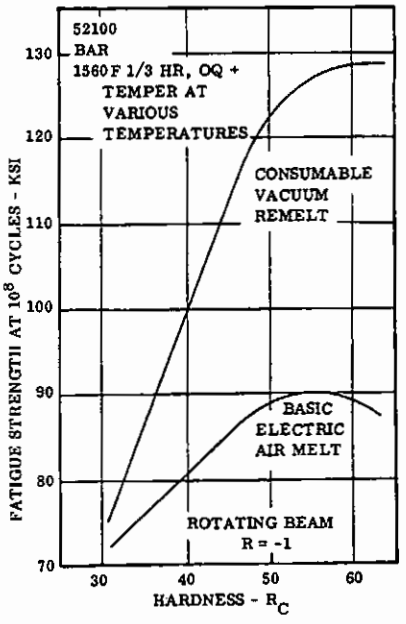


FIG. 3.054 EFFECT OF HARDNESS AND MELTING PRACTICE ON FATIGUE STRENGTH AT 10^8 CYCLES. (16)

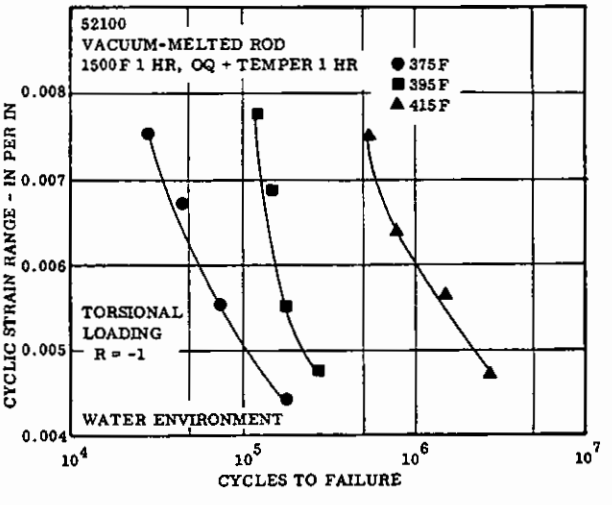


FIG. 3.056 FATIGUE LIFE IN TORSION AS A FUNCTION OF CYCLIC STRAIN RANGE FOR SPECIMENS TEMPERED AT THREE DIFFERENT TEMPERATURES. (4)

Fe
1 C
1.45 Cr

52100

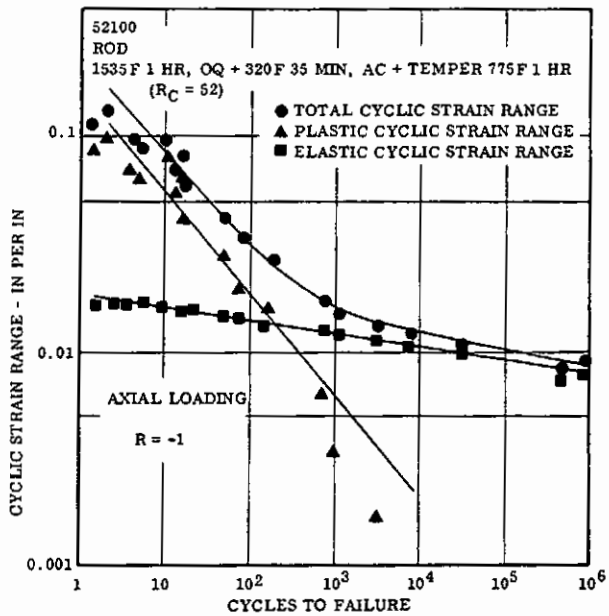


FIG. 3.057 FATIGUE LIFE AS A FUNCTION OF CYCLIC STRAIN. (12)

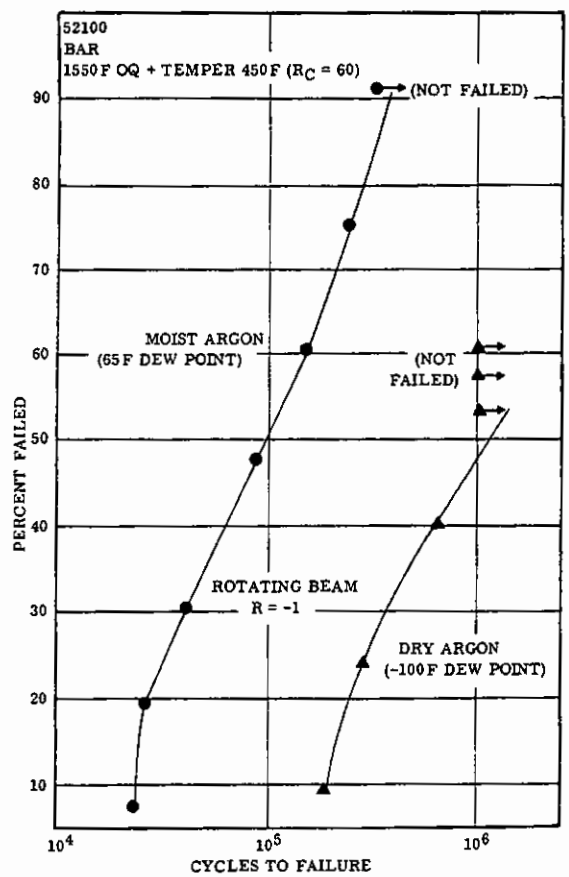


FIG. 3.059 WEIBULL PLOT SHOWING EFFECTS OF AMBIENT MOISTURE ON STATISTICAL DISTRIBUTION OF FATIGUE DURABILITY AT A MAXIMUM STRESS OF 125 KSI. (15)

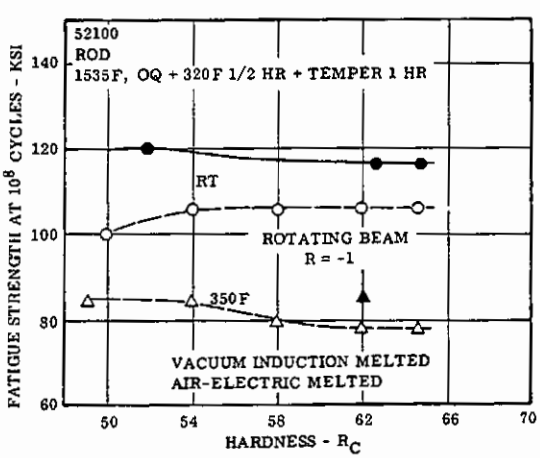


FIG. 3.058 EFFECT OF HARDNESS LEVEL ON FATIGUE STRENGTH AT 10^8 CYCLES FOR AIR-MELTED AND VACUUM-MELTED MATERIAL AT ROOM TEMPERATURE AND 350F. (10)

Fe
1 C
1.45 Cr

52100

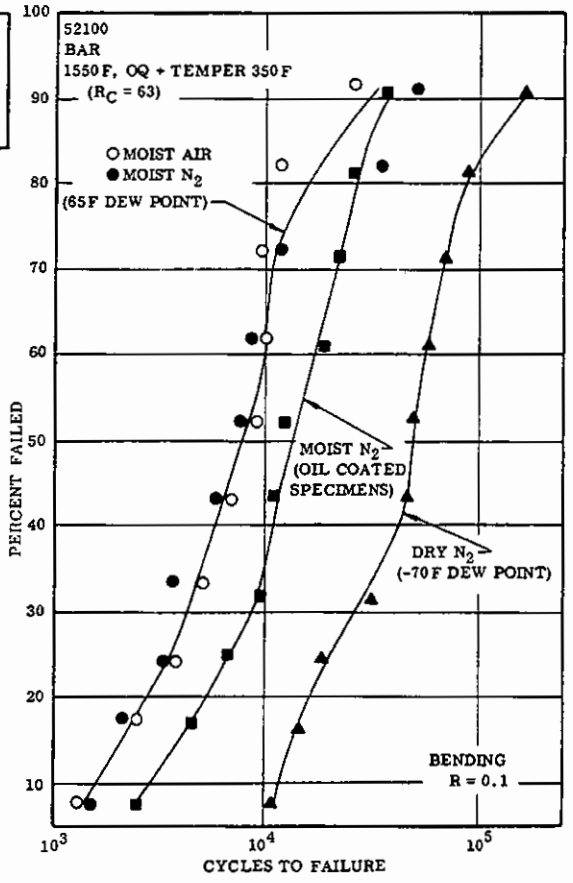


FIG. 3.0510 WEIBULL PLOT SHOWING EFFECTS OF AMBIENT MOISTURE ON STATISTICAL DISTRIBUTION OF FATIGUE DURABILITY AT A MAXIMUM STRESS OF 170 KSI. (15)

REFERENCES

1. AMS 6440F (November 15, 1972).
2. AMS 6441E (November 15, 1972).
3. AMS 6447B (November 15, 1972).
4. Hutchinson, E.F.,"Effect of Fluid Environment on Torsional Fatigue Failure", Nuclide Corp. Technical Report 64-GRX-10 to Bureau of Naval Weapons (March 1966).
5. Borgese, S.F. and Pantalone, W.J., "The tempering Behavior of Deformation Bands in 52100 Steel", SKF Industries Report AL67M051 to Office of Naval Research (May 19, 1967).
6. Private communication and data sheet from P.R. Borneman, Allegheny-Ludlum Steel Corp. (February 6, 1974).
7. "AISI E 52100 Alloy Steel", data sheet from Crucible Steel Co. of America (May 15, 1961).
8. "Ferrovac - 52100", data sheet from Vacuum Metals Corp. (February 1958).
9. "52100", data sheet from Timken Co. (February 18, 1974).
10. Sachs, G., Sell, R. and Brown, W.F. Jr., "Tension, Compression and Fatigue Properties of Several Steels for Aircraft Bearing Applications", Proceedings ASTM, Vol. 59 (1959).
11. Srawley, J.E., "Hydrogen-Embrittlement Susceptibility of Some Steels and Nonferrous Alloys", U.S. Naval Research Laboratory Report 5392 (October 19, 1959).
12. Smith, P.W., Hirschberg, M.H. and Manson, S.S., "Fatigue Behavior of Materials Under Strain Cycling in Low and Intermediate Life Range", NASA, Lewis Research Center, TN D-1574 (October 10, 1962).
13. "AISI E 52100", Alloy Digest, Filing Code: SA-16 (April 1954).
14. "Cross-Index of Chemically Similar Specifications", MIL-HDBK-H1D (June 22, 1970).
15. Mantel, E.R., Robinson, G.H. and Thompson, R.F., "Influence of Atmospheric Moisture on Fatigue of Hardened Steel", Metals Engineering Quarterly, Vol. 1 (August 1961), p. 57-61.
16. Tricot, R., Minnot, J., Lluansi, M., "How Microstructural Alterations Affect Fatigue Properties of 52100 Steel", Metals Engineering Quarterly, Vol. 12 (May 1972), p. 39-47.
17. Parker, R.J., Zeretsky, E.V. and Dietrich, M.W., "Rolling-Element Fatigue Lives of AISI T-1, AISI M-42, AISI 52100, and Halmo at 150F", NASA, Lewis Research Center TN D-6179 (February 1971).
18. Hauser, J.J. and Wells, G.H., "Inclusions in High-Strength Bearing Steels", Crucible Materials Research, AFML-TR-69-339 (February 1970).
19. Drutowski, R.C. and Mikus, E.B., "The Effect of Ball Bearing Steel Structure on Rolling Friction and Contact Plastic Deformation", General Motors Corp. (November 23, 1959).
20. Schatzberg, P., "Influence of Water and Oxygen on Fatigue Life and Wear During Rolling-Contact Lubrication", Naval Ship Research and Development Center, Report 3061 (July 1969).
21. "Atlas of Isothermal Diagrams", United States Steel Corp. (1951).
22. Bhat, G.K. and Nehrenberg, A.E., "A Study of the Metallurgical Properties of Bearing Materials at Temperatures in the Range Room Temperature to 1000 F for Aircraft Service", WADC TR 57-343 (April 1957).
23. Conrad, A.A. and Darby, C.W., "Degassing Improves Quality Extends Fatigue Life of Steel", SAE Journal, Vol. 74 (March 1966), p. 53-56.
24. Lyne, C.M. and Kasak, A., "Effect of Sulfur on the Fatigue Behavior of Bearing Steel", Transactions ASM, Vol. 61 (1968), p. 10-13.
25. Hurley, J.L., Kitchen, A.L. and Crawford, R.R., "Cold Forging of Alloy Steels", Metals Engineering Quarterly, Vol. 11 (August 1971), p. 36-43.

1. General

AerMet 100, a further development of AF 1410 (Chapter 1224), is currently being used in landing gear applications. Because of its high strength, hardness, and fracture toughness, it has potential applications in many critical components in aerospace structures. The AF 1410 alloy has MIL-HDBK 5G (Ref. 1) S-Basis design values of F_{tu} = 235 ksi and F_{ty} = 215 ksi; the corresponding values for AerMet 100 are F_{tu} = 280 ksi and F_{ty} = 235 ksi for the 900F aged condition. Typical K_{Ic} values for AF 1410 vary from 130 to 150 ksi$\sqrt{in}$. with the lower values characteristic of the SL crack orientation in plate; corresponding K_{Ic} values for AerMet 100 forgings (aged at 900F) vary from 105 to 125 ksi$\sqrt{in}$. Aging AerMet 100 at 875F increases the tensile and yield strengths by about 10 ksi with typical K_{Ic} values from 80 to 100 ksi$\sqrt{in}$. These improved strength properties of AerMet 100 coupled with high fracture toughness were obtained by increases in the content of C, Ni, and Cr and reduction in the amount of tramp elements by careful raw material selection and control of the melting practice. From the available information, AerMet 100, on balance, appears to have a superior combination of properties as compared with other high strength steels. Selected comparisons have been published by the alloy producer. (Ref. 16)

1.1 Commercial Designation - AerMet 100

1.2 Alternate Designations - UNS K92580

1.3 Specifications

1.3.1 *[Table]* AMS Specifications

1.4 Composition

1.4.1 *[Table]* Chemical Composition

1.5 Heat Treatment

1.5.1 *[Table]* AMS specified heat treatment for specimens cut from bars and forgings with 100 sq. in. or less in cross-section

1.5.2 Annealing. 1225F to 1275F, 16 hours. Annealing at lower temperatures can result in retained austenite.

1.5.3. Normalize. 1650F, 1 hour, Air Cool

1.5.4 Solution treatment. 1625F, 1 hour, Air Cool or Oil Quench.

Air cooling appears to be sufficient to develop full tensile strength properties in sections up to at least 2 in. in thickness (Fig. 3.2.1.7). This air hardening is associated with a relatively low M_s temperature and a sluggish banite transformation (Fig 2.1.2.1). There appears to be essentially no difference in the tensile strength between air cooling and oil quenching over a wide range of aging temperatures (Fig. 3.2.1.4); however, the tensile yield strength of oil quenched material is lower in the aging temperature range between about 500 and 800F (which is not a normal aging range). At higher aging temperatures this difference diminishes considerably (Fig. 3.2.1.4). Water quenching is not recommended.

	Fe
3.1	Cr
11.5	Ni
13.5	Co
1.2	Mo
0.23	C

1.5.5. Refrigeration. To ensure the transformation of retained austenite, refrigeration at -100F following solution treatment is recommended.

1.5.6. Aging. This alloy possesses strong secondary hardening characteristics (e.g. Figs. 1.6.2 and 3.2.1.3) with peak tensile strength being developed by aging between 800 and 850F. At higher aging temperatures, the strength properties decrease rapidly with a corresponding increase in impact energy and fracture toughness (Figs. 3.2.3.1 and 3.2.7.2.1). Aging temperatures less than 875F are not recommended. From the limited amount of information on aging time (Fig. 3.2.1.6) it appears that aging at 900F in excess of about 6 hours can produces a loss in tensile strength properties.

1.5.7 Stress relief anneal. 800F 1 to 3 hrs, Air Cool

1.5.8 Snap temper. 400F 5 hrs (to permit straightening prior to aging)

1.6 Hardness

Annealed (Overaged) - 37 to 39 R_C (Ref.16)

1.6.1 *[Figure]* Effect of aging temperature on hardness of forging

1.6.2 *[Figure]* Effect of aging temperature on hardness of specimens cut from 10-inch-diameter bar

1.7 Forms and Conditions Available

Bars, Forgings, Plate, Strip, Wire, Castings

1.8 Melting and Casting Practice

Vacuum Induction Melt + Vacuum Arc Remelt

Preliminary development work indicates that the alloy can be vacuum cast and hot isostatically pressed (HIP) to yield mechanical properties equal to the wrought product (Table 1.8.1).

1.8.1 *[Table]* Mechanical properties of vacuum cast and HIP'ed samples

1.9 Special Considerations

1.9.1 The fracture toughness is very sensitive to the aging temperature at temperatures below about 900F and aging below 875F is not recommended (Fig. 3.2.7.2.1).

This section produced with the support of NASA-Lewis Research Center.

© 1995 by Purdue Research Foundation, West Lafayette, Indiana 47907. All Rights Reserved. U.S. Government License. This material may be used, duplicated or disclosed by United States Government agencies without the payment of any royalty.

1.9.2. In common with other ultra high strength steels, the impact energy (Fig. 3.2.3.2) and, probably, the fracture toughness is substantially reduced at very low temperatures.

1.9.3. Inadequate cooling rates from the solution temperature can result in mixed structures containing banite which will increase the strength and reduce the fracture toughness. An indication of such an effect is shown in Fig. 3.2.7.2.3, although these data are insufficient to establish the limiting thickness for air cooling.

1.9.4 Long time elevated temperature exposure at 700F produces small increases in the ultimate tensile and yield strength (compare Figs. 3.3.1.1 and 3.3.1.2) and a substantial reduction in the Charpy V impact energy at 400F (Fig. 3.3.3.1). The fracture toughness (Table 3.2.7.2.4) is also reduced by this 700F exposure. The extent of elevated temperature exposure effects and their mechanisms are unknown at this time.

1.9.5 Decarburization will occur when air exposure exceeds 1000F (Ref. 16)

1.9.6 Water quenching should be avoided because quench cracking may occur in regions having sharp changes in crossection.

1.9.7 Retained austenite increases rapidly with increase in aging temperature above 900F (Fig. 1.9.7.1).

1.9.7.1 *[Figure]* Retained austenite as a function of aging temperature

2. Physical Properties and Environmental Effects

2.1 Thermal Properties

2.1.1 Melting Range. Heating - solidus, 2614F
liquidus, 2729F
Cooling - solidus, 2633F

2.1.2 Phase Changes. A detailed TEM analysis of the hardening phenomena in this alloy (Ref. 14) revealed the phase changes responsible for the variation in mechanical properties with heat treatment. These are briefly summarized as follows. The as-quenched and cryogenically treated alloy was completely martensitic with a mixture of lathes and plates coupled with a high dislocation density. A fine dispersion of spherical complex carbide particles was also present. The amount of retained austenite was extremely small (< 1 percent). Aging at 800F results in the formation of a relatively coarse Fe_3C Widmanstaten structure within the lathes and elongated carbides at lath and twin boundaries. This structure had a low fracture toughness (Fig. 3.2.7.2.1). With further aging at 850F these carbides were largely replaced by extremely fine needle-shaped precipitates coherent with the matrix and corresponding to the peak in secondary hardening. (The composition of the needles could not be identified.) Further aging at 900F produced coarsening of the needle-shaped precipitates, corresponding to the rapid development of overaging and high fracture toughness (Figs. 3.2.1.3 and 3.2.7.2.1). Reverted austenite formation was also present at the lath boundaries for the 900F age. Further aging (950 to 1050F) produced additional precipitate coarsening, loss of matrix precipitate coherency, and increasing amounts of reverted austenite. The precipitates contained in the structures produced by aging at 900 F and above were identified as M_2C carbides containing Cr, Mo, and Fe.

2.1.2.1 *[Figure]* Continuous cooling curves from solution treatment at 1625F

2.1.2.2 Transformation temperatures - A_{c1} = 1065F; A_{c3} = 1525F (Ref. 11)

2.1.3 Thermal Conductivity

2.1.3.1 *[Figure]* Thermal conductivity of annealed bar

2.1.4 Thermal Expansion

2.1.4.1 *[Figure]* Mean coefficient of linear thermal expansion for annealed or solution treated and aged bar

2.1.5 Specific Heat.

2.1.5.1 *[Figure]* Specific heat of rolled bar

2.1.6 Thermal Diffusivity.

2.1.6.1 *[Figure]* Thermal diffusivity of annealed bar

2.2. Other Physical Properties

2.2.1 Density. 0.285 lbs/in.^{3}

2.2.2 Electrical Properties.

2.2.3 Magnetic Properties.

2.2.3.1 *[Figure]* DC normal induction curve for heat treated alloy

2.2.4 Emittance.

2.2.5 Damping Capacity.

2.3 Chemical Environments

2.3.1 General Corrosion.

2.3.2 Stress Corrosion. (see also Figs. 3.5.3.2 to 3.5.3.6) At the time this Chapter was prepared, the only available data were the results from notch tensile specimens subjected to alternate immersion in 3.5 percent NaCl solution and the effects of stress intensity level on failure time in 3.5 percent NaCl solution using precracked, cantilever loaded beam specimens. One purpose of these tests was to establish a stress level or K level (K_{Iscc}) below which no failure would occur in the test environment. The data at hand do not establish these levels. None of the alternate immersion specimens failed (Table 2.3.2.2) and the cantilever bend specimens (Fig. 2.3.2.1) did not establish a K_{Iscc}.

However, the data may be useful for comparative purposes. Thus, AerMet 100 appears to be more resistant to stress corrosion in 3.5 percent NaCl than 300 M (Fig. 2.3.2.1).

2.3.2.1 *[Figure]* Effect of applied stress intensity factor on the failure time of AerMet 100 and 300 M forgings in 3.5 percent NaCl solution

2.3.2.2 *[Table]* Results for notch tensile specimens subjected to steady stress and alternate immersion in 3.5 percent NaCl solution

2.4 Nuclear Environments

3 Mechanical Properties

3.1 Specified Mechanical Properties

3.1.1 *[Table]* AMS minimum properties for bar and forgings aged at 900 F or 875F

3.2 Mechanical Properties at Room Temperature

3.2.1 Tensile Stress-Strain Diagrams and Tensile Properties

3.2.1.1 *[Figure]* Typical tensile stress-strain curve for longitudinal and short-transverse directions

3.2.1.2 *[Figure]* Effect of aging temperature on the tensile properties of forgings for specimens air cooled or oil quenched from the solution temperature

3.2.1.3 *[Figure]* Effect of aging temperature on transverse tensile properties of 10-inch-diameter forging

3.2.1.4 *[Figure]* Effect of aging temperature on the longitudinal tensile properties of forging for specimens air cooled or oil quenched from the solution temperature

3.2.1.5 *[Table]* Effect of aging temperature on the tensile properties and plane strain fracture toughness of specimens cut from two sizes of forgings from a single heat (No. 88287)

3.2.1.6 *[Figure]* Effect of aging time on specimens cut from forgings: one oil quenched from solution temperature, the other gas quenched (< 400F within 20 min.) in vacuum furnace (Data from two suppliers)

3.2.1.7 *[Figure]* Effect of heat-treated section size on the tensile properties of specimens cut from 10-inch-diameter die forged billet

3.2.1.8 *[Table]* Longitudinal and transverse tensile properties of specimens aged at 875F which were cut from various forgings representing seven heats

3.2.1.9 *[Table]* Longitudinal and transverse tensile properties of specimens aged at 900F which were cut from various forgings representing four heats

3.2.1.10 *[Table]* Tensile properties, plane strain fracture toughness, Charpy V energy, and hardness of specimens removed from production landing-gear piston/axle forging

3.2.2 Compression Stress-strain Diagrams and Compression Properties

3.2.2.1 *[Figure]* Typical compression stress-strain curve for longitudinal and short-transverse directions

3.2.2.2 *[Table]* Longitudinal and transverse compression yield strengths of specimens aged at 875F which were cut from various size forgings representing seven heats

3.2.2.3 *[Table]* Longitudinal and transverse compression yield strengths of specimens aged at 900F which were cut from various size forgings representing four heats.

3.2.3 Impact. (see also Table 3.2.1.10)

3.2.3.1 *[Figure]* Effect of aging temperature on Charpy V impact energy of forging for specimens air cooled or oil quenched from the solution temperature

3.2.3.2 *[Figure]* Effect of aging temperature on Charpy V energy of specimens air cooled or oil quenched from the solution temperature

3.2.4 Bending.

3.2.5 Torsion and Shear.

3.2.5.1 *[Table]* Longitudinal and transverse shear strength of specimens aged at 875F which were cut from various size forgings representing seven heats

3.2.5.2 *[Table]* Longitudinal and transverse shear strength of specimens aged at 900F which were cut from various size forgings representing four heats

3.2.6 Bearing.

3.2.6.1 *[Table]* Longitudinal bearing yield and ultimate strengths of specimens aged at 875F which were cut from various size forgings representing seven heats

3.2.6.2 *[Table]* Longitudinal bearing yield and ultimate strengths of specimens aged at 900F which were cut from various size forgings representing four heats

3.2.7 Stress Concentration.

3.2.7.1 Notch Properties

3.2.7.2 Fracture Toughness (see also Tables 3.1.1, 3.2.1.5, and 3.2.1.10 and Section 1.9)

3.2.7.2.1 *[Figure]* Effect of aging temperature on plane strain fracture toughness of forging for specimens air cooled or oil quenched from the solution temperature

3.2.7.2.2 *[Table]* Plane strain fracture toughness of specimens aged at 875F which were cut from various forgings representing seven heats

3.2.7.2.3 *[Figure]* Effect of heat treated section thickness on plane strain fracture toughness of specimens cut from a 10-in.-diameter forged billet

3.2.7.2.4 *[Table]* Effect of 700F, 3000-hour air exposure on the plane strain fracture toughness of specimens cut from forging

3.2.8 Combined Loading

3.3 Mechanical Properties at Various Temperatures

3.3.1. Tension Stress-strain Diagrams and Tensile Properties

3.3.1.1 *[Figure]* Effect of elevated test temperature on tensile properties of a forging aged at 900F

3.3.1.2 *[Figure]* Effect of test temperature on tensile properties following 700F, 3000-hour air exposure for a forging aged at 900F

3.3.2 Compression Stress-strain Diagrams and Compression Properties

3.3.3 Impact.

3.3.3.1 *[Figure]* Effect of test temperature on Charpy V impact energy for specimens cut from forging with and without a prior 700F, 3000-hour air exposure

3.3.3.2 *[Figure]* Effect of cryogenic and elevated temperature on the Charpy V impact energy of specimens from a 10-in.-diameter round forging and aged at several temperatures

3.3.3.3 *[Figure]* Cooling curves for tensile and Charpy V specimens cooled in vermiculite following solution treating to simulate the cooling rate of 1-in.-thick CT K_{Ic} specimens cooled in still air

3.3.4 Bending.

3.3.5 Torsion and Shear.

3.3.6 Bearing.

3.3.7 Stress Concentration.

3.3.7 Notch Properties.

3.3.7.1 Fracture Toughness.

3.3.8 Combined Loading.

3.4 Creep and Creep Rupture Properties

3.5 Fatigue Properties

3.5.1 Conventional High-Cycle Fatigue. The database for high cycle fatigue is small. The majority of the data relates to operational stress spectrum tests obtained for design of a landing gear/axle forging (Ref. 13). These tests involved different frequencies, many surface conditions, different R ratios and several stress concentration factors. By appropriate selection and combination of these data, it was possible to develop fatigue curves over a range of cycles from 10^3 to somewhat beyond 10^6. The results of this analysis are shown in Figs. 3.5.1.1 to 3.5.1.4 which illustrate the following:

(1) There is a negligible effect of frequency between 10 and 20 Hz. The data for 5 Hz are confined to relatively low cyclic lives but do not exhibit a frequency effect within this range .

(2) Grinding after heat treatment appears to result in somewhat higher fatigue lives than heat treating following grinding.

(3) Machining (125 rms surface finish) before heat treatment appears to yield essentially the same fatigue lives as grinding (63 rms surface finish) before heat treatment.

(4) Large improvements in fatigue lives are produced by shot peening when applied to ground or machined surfaces and these improvements are retained when chrome plating followed by grinding is applied to the shot peened surface.

(5) Consistent with an expected trend, fatigue lives at R= - 0.33 appear to be somewhat longer than at R = -1.

Recognizing that the database is small, an attempt was made to estimate the maximum stresses for 10^6 cycles. The results are shown in Table 3.5.1.5. It was not possible to incorporate the data shown in Fig. 3.5.1.6 in these estimates because attempts to discover the details of the test conditions were not successful.

3.5.1.1 *[Figure]* Axial load fatigue data at R = - 1 for smooth specimens cut from a forging and tested with various surface conditions at different frequencies

3.5.1.2 *[Figure]* Axial load fatigue data at R = - 1 and K_t = 3 for specimens cut from a forging and tested with various surface conditions at different frequencies

3.5.1.3 *[Figure]* Axial load fatigue data at R = - 0.33 for smooth specimens cut from a forging and tested with various surface conditions at different frequencies

3.5.1.4 *[Figure]* Axial load fatigue data at R = - 0.33 and K_t = 3 for specimens cut from a forging and tested with various surface conditions and at different frequencies

3.5.1.5 *[Table]* Estimates of the fatigue strength at 10^6 cycles for axial loading of specimens from a landing-gear piston/axle forging

3.5.1.6 *[Figure]* Fatigue data for forgings tested at R = 0 using smooth and notched specimens of unspecified geometry

3.5.1.7 *[Figure]* Torsional fatigue strength at 400F of AerMet 100 and 250 Grade Maraging steel.

3.5.2 Low Cycle Fatigue.

3.5.2.1 *[Figure]* Low cycle fatigue data for crack initiation and failure for specimens cut from a forging.

3.5.3 Fatigue Crack Propagation. As expected, the fatigue crack growth rates are relatively insensitive to the R ratio in the sector where there is a nearly linear relation between log da/dN and log ΔK. In this region, negligible influence of the 3.5 percent NaCl environment is observed. In the region of very low growth rates, K_{th} increases with the R ratio for both the neutral environment and for the 3.5 percent NaCl solution. It is interesting to note that the K_{th} values are higher for the more corrosive NaCl environment. This effect was attributed to corrosion- controlled crack closure (Ref. 7).

3.5.3.1 *[Figure]* Fatigue crack propagation rates in air at several R values for a landing-gear piston/axle forging

3.5.3.2 *[Figure]* Fatigue crack growth rates at R = 0.1 in 3.5 percent NaCl and in dry nitrogen for a forged slab

3.5.3.3 *[Figure]* Fatigue crack growth rates at R = 0.1 for AerMet 100 in dry nitrogen and 300 M in air

3.5.3.4 *[Figure]* Fatigue crack growth rates at R = 0.1 for AerMet 100 and 300 M in 3.5 percent NaCl

3.5.3.5 *[Figure]* Fatigue crack growth rates at R = 0.5 in 3.5 percent NaCl and in dry nitrogen for a forged slab

3.5.3.6 *[Figure]* Fatigue crack growth rates at R = 0.8 in 3.5 percent NaCl and in dry nitrogen for a forged slab

3.6 Elastic Properties

3.6.1 Poisson's Ratio.

3.6.2 Modulus of Elasticity.

3.6.2.1 *[Table]* Tension and compression moduli of elasticity determined for specimens aged at 875F which were cut from various size forgings representing seven heats

3.6.3 Modulus of Rigidity.

3.6.4 Tangent Modulus.

3.6.5 Secant Modulus.

4 Fabrication

4.1 Forming

4.1.1 Forging. Preliminary breakdown - 2150F max.
Finish - 1800F to below 1650F (Ref. 16)

4.2 Machining and Grinding

Normally, machining should be done in the annealed condition which provides a hardness of 37 to 39 R_C. At lower hardnesses, machining is more difficult due to the production of long string-like chips which clog the cutting tools (Ref. 16). In comparative machining tests using various processes, it was reported that AerMet 100 was more difficult to machine at hardnesses of R_C 40 and R_C 53 than was 300 M at the same hardness levels (Ref. 13).

4.3 Joining

4.3.1 Welding. The preliminary results of welding studies that are in progress (August 1995) indicate that the alloy can be welded by the electron beam, cold-wire-feed plasma arc, and GTA processes. Relatively low heat input, multiple pass welds produce the best results. Tensile and impact data are available for GTA welds in plate (Table 4.3.1.1). Of the various pre- and post-heat treatments studied, Condition A (welding annealed material followed by normalizing and reannealing prior to solution treating and aging) produced tensile properties exceeding the minimums specified in AMS 6532 (Table 3.1.1). The remaining conditions did not produce welds meeting the AMS minimum property requirements. The weld impact energies differed little for the various conditions and, in all cases, were well below the values reported for parent material (See Fig. 3.2.3.2) in laboratory tests, but, for Conditon A were close to those reported for specimens removed from production forged parts (see Tale 3.2.1.10). It should be noted that relatively low impact values may not reflect correspondingly low plane strain fracture toughness. For example, Table 3.2.1.10 shows a mean K_{Ic} value of 107.2 ksi$\sqrt{in}$. with a mean impact value of 29.7 ft-lbs.

4.3.1.1 *[Table]* Preliminary results (duplicate tests) for tensile properties and Charpy V impact energies for GTA welds in plate

4.4 Surface Treating

The alloy can be nitrided.

Table 1.3.1 AMS Specifications (Refs. 3, 15)

Alloy	AerMet 100
Form	Bars and Forgings
Specifications	Coverage
AMS 6478	Vacuum Melted, Annealed Heat Treatable to 290 ksi (1999 Mpa) Tensile Strength
AMS 6532	Vacuum Melted, Annealed

Table 1.4.1 Chemical composition (Refs. 3, 15)

Alloy	AerMet 100	
Source	AMS 6478 and 6532	
Composition	Percent	
Element	Minimum	Maximum
C	0.21	0.25
Mn		0.10
Si		0.10
P		0.008
S		0.005
P + S		0.010
Cr	2.9	3.3
Ni	11.0	12.0
Co	13.0	14.0
Mo	1.10	1.30
Ti		0.015
Al		0.015
O_2		20 ppm
N_2		15 ppm

Table 1.5.1 AMS specified heat treatment for specimens cut from bars and forgings with 100 sq. in. or less in cross-section.

Alloy	AerMet 100			
Source	AMS 6532 (Ref. 15)		AMS 6478 (Ref. 3)	
Solution Treat	1600F to 1650F, 60 to 75 minutes			
Quench				
t =< 1.25 in.	Air Cool (AC)			
t > 1.25 in.	Oil Quench (OQ)			
Refrigerate	-85 to -115F, 55 to 65 minutes, Air Warm			
Age	890 to 910F, 5 to 8 hrs, AC		865 to 885F, 5 to 8 hrs, AC	
Form	Bars	Forgings	Bars	Forgings
Anneal	1115 to 1250F, 8 hrs min, AC	1225 to 1275F, 8 hrs min, Fan Cool	1225 to 1275F, 16 hrs min, AC	1225 to 1275F, 8 hrs min, Fan Cool
Normalize	-	1225 to 1275F, 55 to 75 minutes, AC	-	1225 to 1275F, 55 to 75 minutes, AC

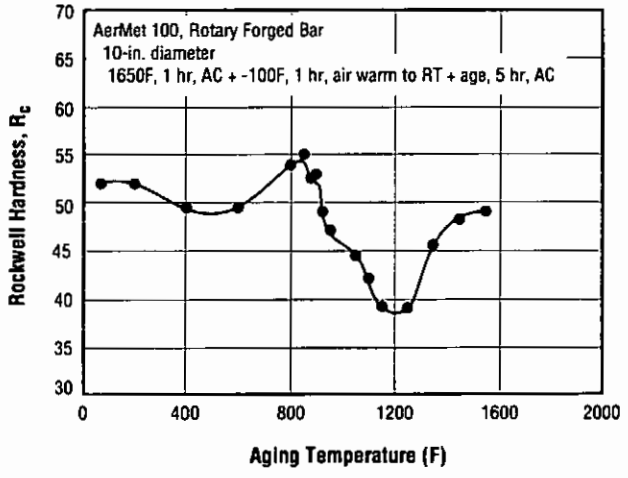


Figure 1.6.1 Effect of aging temperature on hardness of forging (Ref. 5)

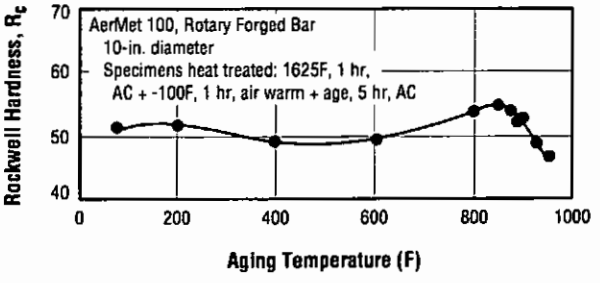


Fig. 1.6.2 Effect of aging temperature on hardness of specimens cut from 10-inch-diameter bar (Ref. 5)

Table 1.8.1 Mechanical properties of vacuum cast and HIP'ed samples (Ref. 18)

Alloy	AerMet 100	
Form	Castings	
HIP Cycle in Argon	1550F, 1 hr., heat to 2250F, 6.5 hr. at 30 ksi pressure, FC	
Heat Treatment	1250F, 16 hr., Cool 600F per hr. to RT + 1650F, 1 hr., AC + -100F, 1 hr., Air Warm to RT + 900F, 5 hr., AC	
Sample	1	2
F_{tu} (ksi)	277	292
F_{ty} (ksi)	242	249
Elongation, E (percent)	12.4	13
Reduction in Area, RA (percent)	57	58
Fracture Toughness, K_{Ic} (ksi $\sqrt{in.}$)	113	118
Charpy V Impact Energy (ft-lb)	26	25

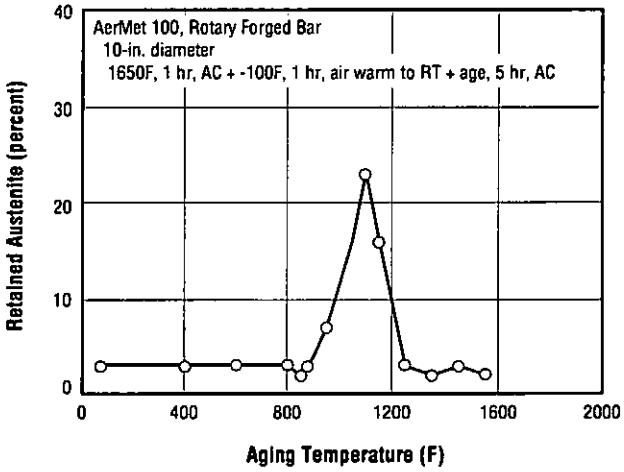


Figure 1.9.7.1 Retained austenite as function of aging temperature (Ref. 5)

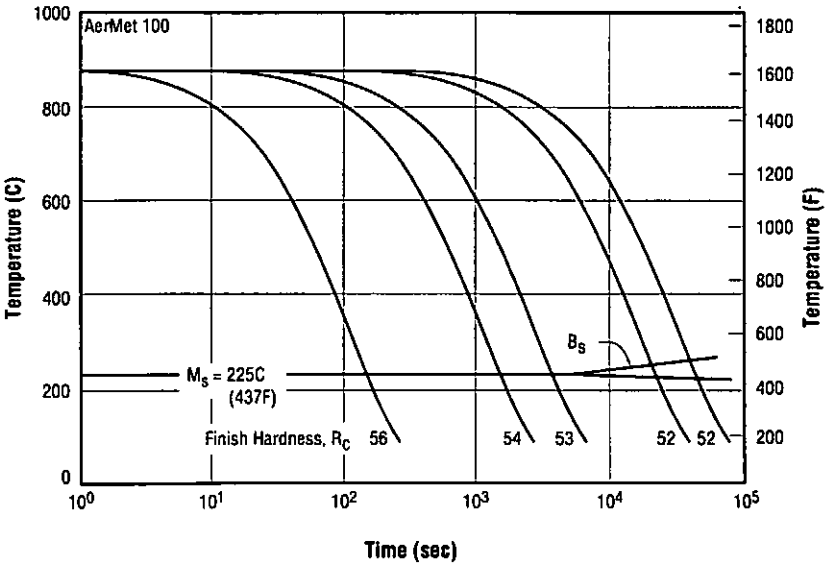


Fig. 2.1.2.1 Continuous cooling curves from solution treatment at 1625F [M_s - Martensite start (1 percent transformation); B_s - Banite start] (Ref. 2)

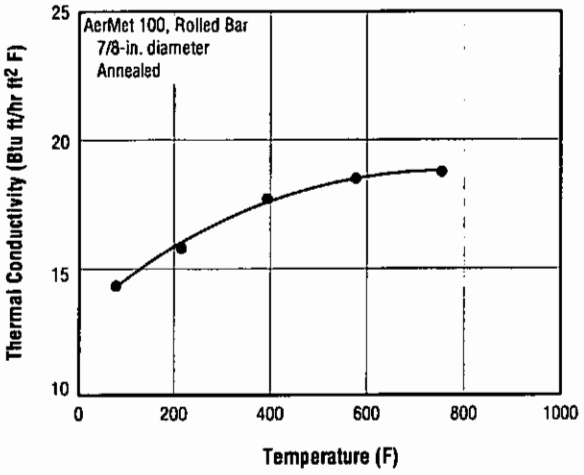


Figure 2.1.3.1 Thermal conductivity of annealed bar (Ref. 10)

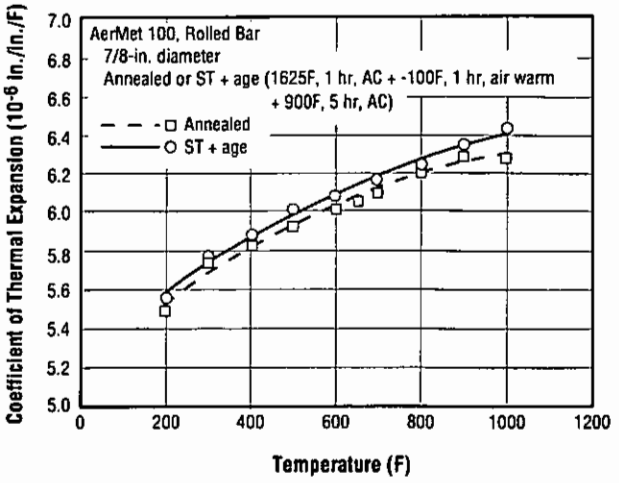


Fig. 2.1.4.1 Mean coefficient of linear thermal expansion for annealed or solution treated and aged bar (Ref. 11)

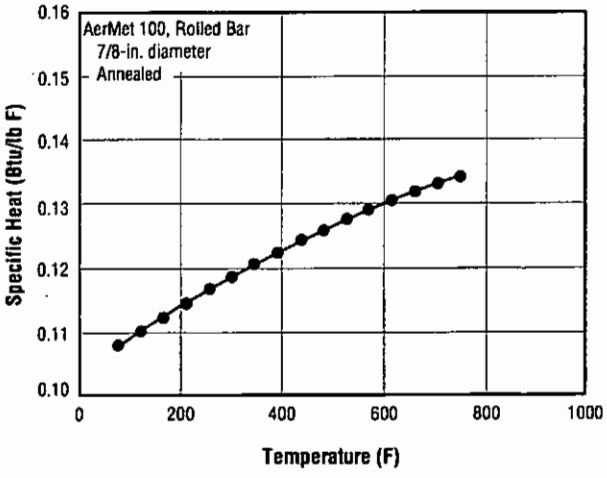


Fig. 2.1.5.1 Specific heat of rolled bar (Ref. 10)

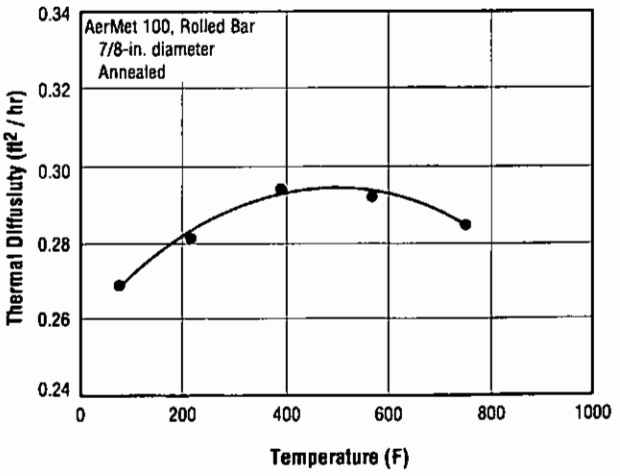


Fig. 2.1.6.1 Thermal diffusivity of annealed bar (Ref. 10)

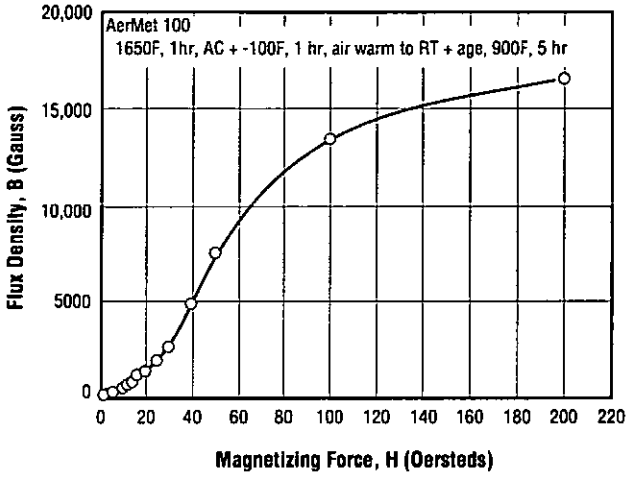


Fig. 2.2.3.1 DC normal induction curve for heat treated alloy (Ref. 2)

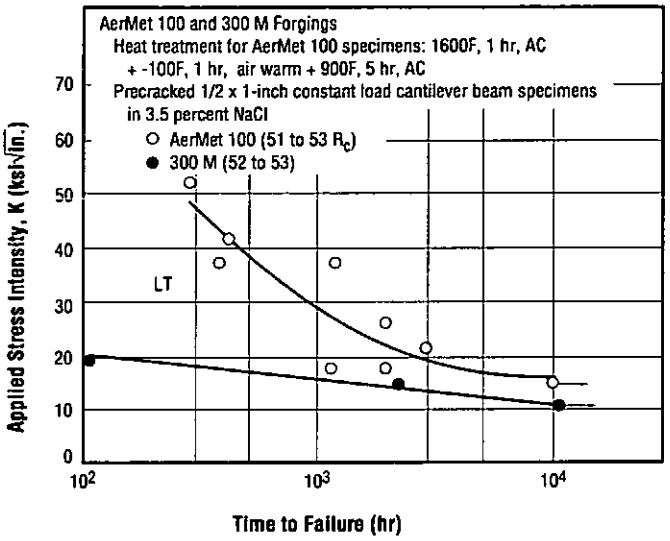
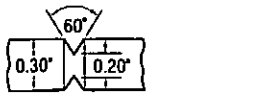


Figure 2.3.2.1 Effect of applied stress intensity factor on the failure time of AerMet 100 and 300 M forgings in 3.5 percent NaCl solution (Ref. 4)

Table 2.3.2.2 Results for notch tensile specimens subjected to steady stress and alternate immersion in 3.5 percent NaCl solution (Ref. 13)

Alloy	AerMet 100		
Form	5 to 6-in.-dia. Landing-Gear Piston/Axle Forging		
Specimen Condition	1625F, 1 hr., OQ + -100F, 1 hr., Air Warm + 900F, 4 hr.		
Environment	Alternate Immersion in 3.5 percent NaCl		
K_t	1	2	3
Stress Range (ksi)	220	240	
Exposure Time (hr)	90		
Failures	None		



Notch radius = 0.031 in. for K_t = 2
= 0.01 in. for K_t = 3

Table 3.1.1 AMS minimum properties for bars and forgings aged at 900F or 875F (Refs. 3, 15)

Alloy	AerMet 100			
Form	Bars and Forgings			
Size[a]	≤ 100 sq in. cross-sectional area			
Source	AMS 6532		AMS 6478	
Condition[b]	ST + 900F Age		ST + 875F Age	
Direction[c]	L	T	L	T
F_{tu}, min (ksi)	280		290	
F_{ty}, min (ksi)	235	233	245	
Elongation, e, min (percent)	10	8	10	8
Reduction in Area, RA, min (percent)	55	45	50	35
Hardness, min (R_C)	53			
Fracture Toughness[d], K_{Ic} (ksi$\sqrt{in.}$) LS or LR Orientations	100		80	

[a] Properties of products > 100 sq in. cross-sectional area to be agreed upon by purchaser and vendor.

[b] For heat treatment details, see Table 1.5.1.

[c] If transverse tensile properties are measured, longitudinal properties are not required.

[d] For products < 3 in., fracture toughness measurement method and minimum values are to be agreed upon by the purchaser and the vendor.

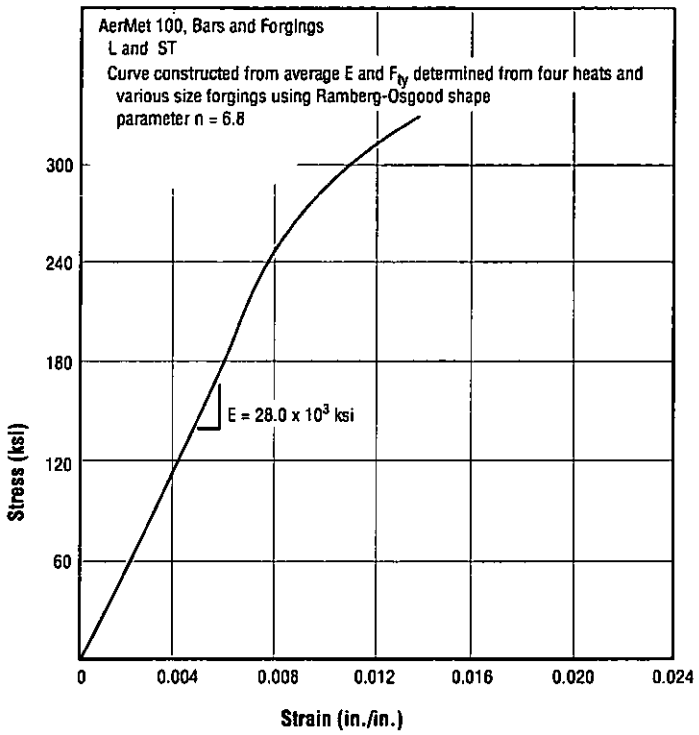


Figure 3.2.1.1 Typical tensile stress-strain curve for longitudinal and short-transverse directions (Refs. 1, 4)

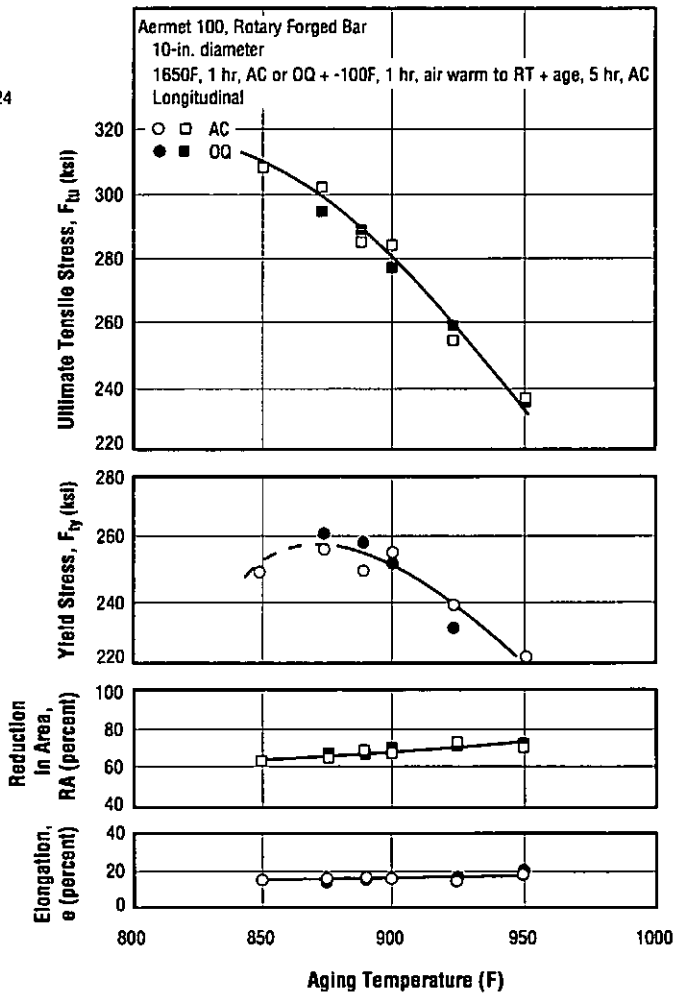


Figure 3.2.1.2 Effect of aging temperature on the tensile properties of forgings for specimens air cooled or oil quenched from the solution temperature (Ref. 5)

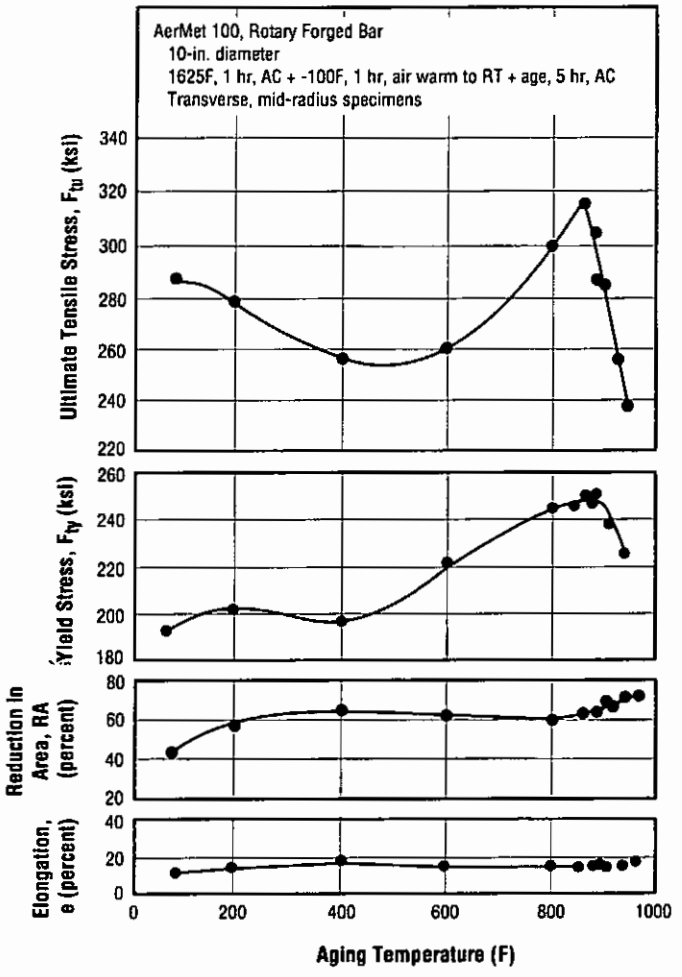


Figure 3.2.1.3 Effect of aging temperature on transverse tensile properties of 10-inch diameter forging (Ref. 8)

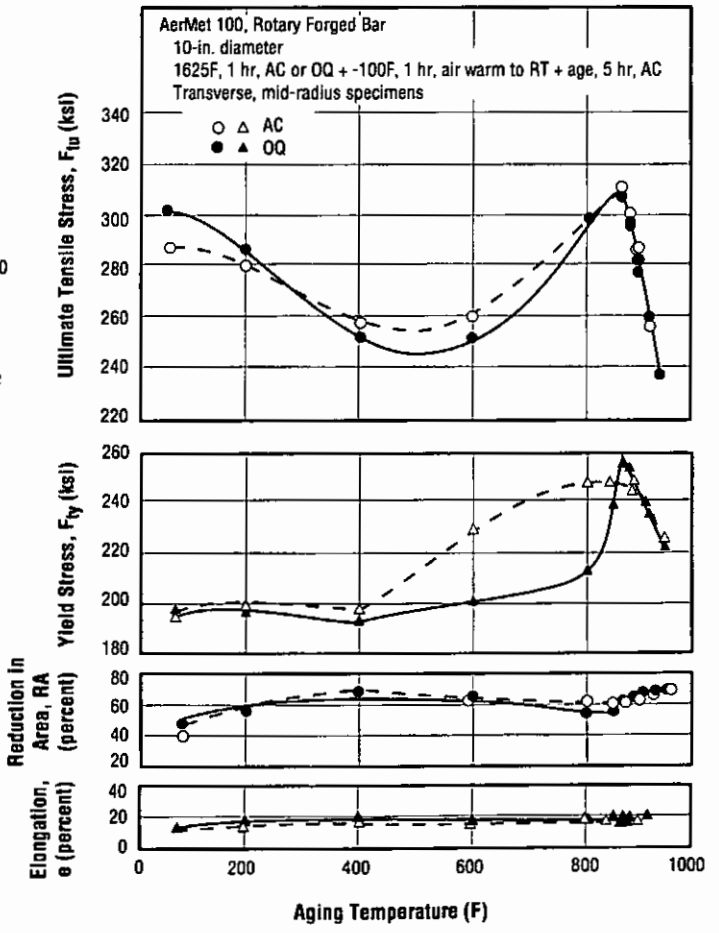


Figure 3.2.1.4 Effect of aging temperature on the longitudinal tensile properties of forging for specimens air cooled or oil quenched from the solution temperature (Ref. 5)

Table 3.2.1.5 Effect of aging temperature on the tensile properties and plane strain fracture toughness of specimens cut from two sizes of forgings from a single heat (No. 88287) (Refs. 2, 6)

Alloy	AerMet 100			
Form	Forgings			
Source	Ref. 2		Ref. 6	
Condition	1625F, 1 hr., OQ + -100F, 1 hr., + Age, 5 hr.			
5 hr. Aging Temperature (F)[c]	875		900	
Size	5 x 8 in.		16-in DOC[a]	
Direction[b]	L	T	L	T
F_{tu}, min (ksi)[c]	302	301	287	289
F_{ty}, min (ksi)	259	258	249	252
Elongation, e (percent)	15	13	16.6	16
Reduction in Area, RA (percent)	66	58	68	59
Fracture Toughness[d], K_{Ic} (ksi$\sqrt{in.}$)	90	78	113	115

[a] Double octagon (16-sided) press forging.

[b] L - Loading axis parallel to grain flow; T - Loading axis normal to grain flow.

[c] Average of duplicate tensile results for the 5 x 8-in. forging; Average of 10 tensile results for the 16-in. DOC.

[d] Average of triplicate toughness results for the 5 x 8-in. forging; Average of five toughness results for the 16-in. DOC.

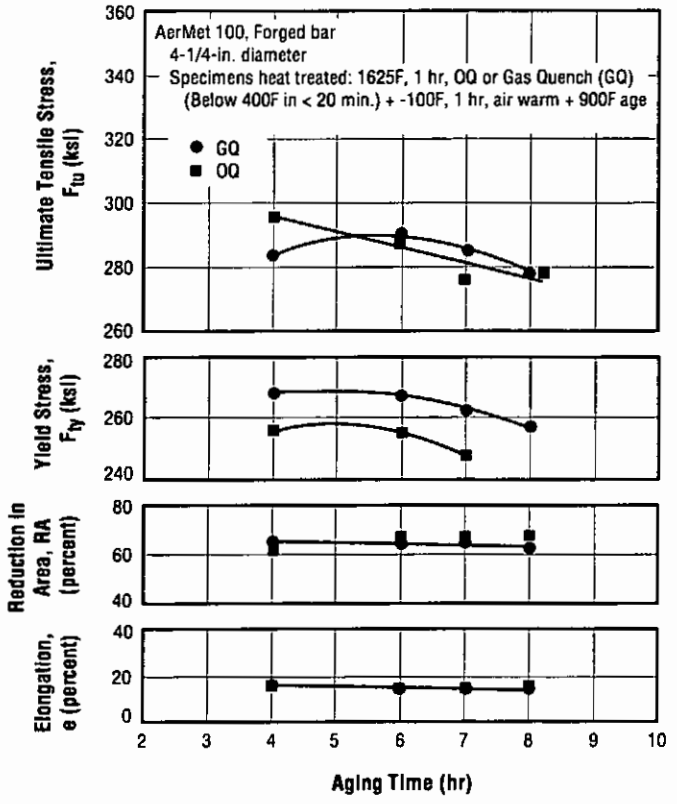


Figure 3.2.1.6 Effect of aging time on specimens cut from forging: one oil quenched from solution temperature, the other gas quenched (< 400F within 20 min.) in vacuum furnace (Data from two suppliers) (Ref. 13)

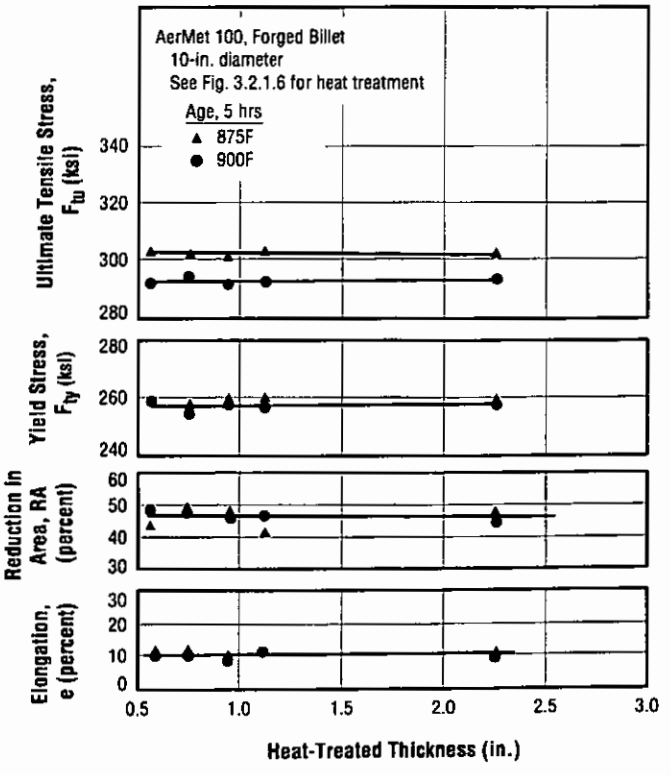


Fig. 3.2.1.7 Effect of heat-treated section size on the tensile properties of specimens cut from 10-inch-diameter die forged billet (Ref. 13)

Table 3.2.1.8 Longitudinal and transverse tensile properties of specimens aged at 875F which were cut from various forgings representing seven heats (Ref. 2)

Alloy	AerMet 100			
Form	Forgings			
Sizes (in.)	Rounds (3, 3.5, 4.25, 5, 6, and 8) Round-cornered square (5 and 7.25) Rectangle (5 x 8)			
Condition	1600 to 1650 in salt, 60 to 75 min, AC + -85 to -115F, 55 to 65 min, Air Warm + 865 to 885F, 5 hr,			
Sampling	D/4 or t/4 locations; 2 specimens from each forging			
	Longitudinal[a]			
	F_{ty} (ksi)	F_{tu} (ksi)	Elongation, e (percent)	Reduction in Area, RA (percent)
Low	251	296	13	58
High	265	307	16	66
Mean	258	302	14.2	64
Standard Deviation	3.9	2.4	0.8	2.3
	Transverse[a, b]			
Low	250	298	10	42
High	268	307	13	61
Mean	259	302	12	50
Standard Deviation	4.7	2.3	1.0	4.9

[a] Results shown for 20 specimens.

[b] For all sizes, loading axis was normal to grain flow.

Table 3.2.1.9 Longitudinal and transverse tensile properties of specimens aged at 900F which were cut from various forgings representing four heats (Ref. 4)

Alloy	AerMet 100			
Form	Forgings			
Sizes (in.)	Rounds (3, 4-5/8, 5, 6, 6-1/2, 8-1/2, and 10) Rectangle (7-1/4 x 7-1/4 and 5 x 8)			
Condition	1600 to 1650 in salt, 60 to 75 min, AC + -85 to -115F, 55 to 65 min, Air Warm + 890 to 910F, 5 to 8 hr, AC			
Sampling	D/4 or t/4 locations; 2 specimens from each forging			
	Longitudinal[a]			
	F_{ty} (ksi)	F_{tu} (ksi)	Elongation, e (percent)	Reduction in Area, RA (percent)
Low	235	280	14	58
High	266	293	18	71
Mean	247	287	16.1	67.3
Standard Deviation	5.9	3.5	0.7	3.3
	Transverse[a, b]			
Low	239	283	11.3	42.1
High	261	293	19.9	58.7
Mean	246	288	14.3	56.6
Standard Deviation	4.8	3.4	1.7	6.0

[a] Results shown for 20 specimens.

[b] For all sizes, loading axis was normal to grain flow.

Table 3.2.1.10 Tensile properties, plane strain fracture toughness, Charpy V energy, and hardness of specimens removed from production landing-gear piston/axle forging (Ref. 13)

Alloy	AerMet 100						
Form	5- to 6-in.-dia. landing-gear piston/axle forging						
Condition	Normalize 1650F + 1250F Overage						
Specimens	1625F, 1 hr., OQ + -100F, 1 hr., air warm + 900F, 5-1/2 hr., AC						
Direction	Transverse				L - R		
	F_{tu} (ksi)	F_{ty} (ksi)	Elongation, e (percent)	Reduction in Area, RA (percent)	K_{Ic} (ksi$\sqrt{in.}$)	Charpy V Energy (ft-lb)	Hardness, R_c
Mean	287.7	263.0	17.4	59.9	107.2	29.7	52.3
Standard Deviation	2.89	4.54	1.67	7.8	4.35	3.83	.516
Number of Tests	8				4	6	

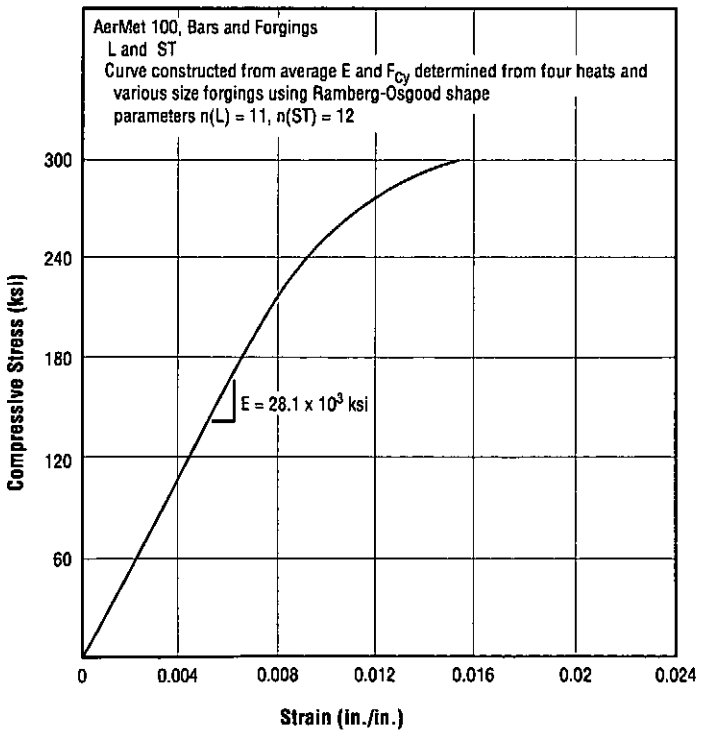


Figure 3.2.2.1 Typical compression stress-strain curve for longitudinal and short-tranverse directions (Refs. 1, 4)

Table 3.2.2.2 Longitudinal and transverse compression yield strengths of specimens aged at 875F which were cut from various size forgiings representing seven heats (Ref. 2)

Alloy	AerMet 100	
Form	Forgings	
Condition	See Table 3.2.1.8	
Sizes		
Sampling		
Direction	Longitudinal	Transverse[a]
	F_{cy} (ksi)	
No. Specimens	20	19
Low	291	291
High	301	303
Mean	297	296
Standard Deviation	3.0	3.7

[a] For all sizes, loading axis normal to grain flow.

Table 3.2.2.3 Longitudinal and transverse compression yield strengths of specimens aged at 900F which were cut from various size forgings representing four heats (Ref. 4)

Alloy	AerMet 100	
Form	Forgings	
Condition	See Table 3.2.1.9	
Sizes (in.)		
Direction	Longitudinal	Transverse[a]
	F_{cy} (ksi)	
Low	267	274
High	283	283
Mean	279	279
Standard Deviation	3.3	2.5

[a] Specimen load axis normal to grain flow.

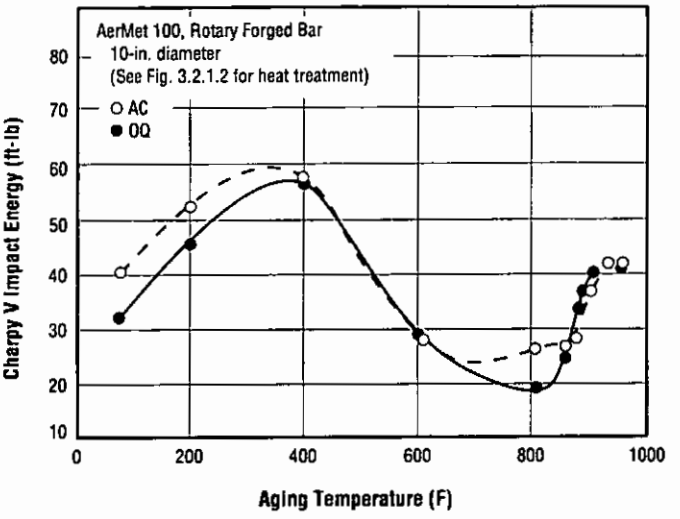


Fig. 3.2.3.1 Effect of aging temperature on the Charpy V impact energy of forging for specimens air cooled or oil quenched from the solution temperature (Ref. 5)

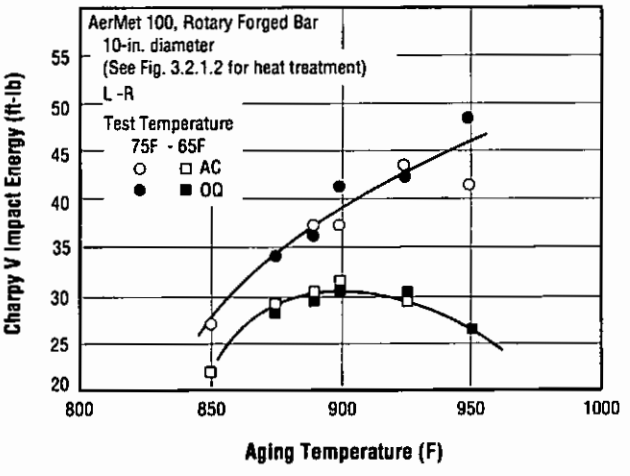


Fig. 3.2.3.2 Effect of aging temperature on Charpy V energy of specimens air cooled or oil quenched from the solution temperature (Ref. 5)

Table 3.2.5.1 Longitudinal and transverse shear strength of specimens aged at 875F which were cut from various size forgings representing seven heats (Ref. 2)

Alloy	AerMet 100	
Form	Forgings	
Condition	See Table 3.2.1.8	
Sampling		
Direction	Longitudinal	Transverse[a]
	F_{su} (ksi)	
Number of Specimens	20	
Low	189	189
High	198	210
Mean	195	198
Standard Deviation	2.3	6.0

[a] Loading axis normal to grain flow.

Table 3.2.5.2 Longitudinal and transverse shear strength of specimens aged at 900F which were cut from various size forgings representing four heats (Ref. 4)

Alloy	AerMet 100	
Form	Forgings	
Condition	See Table 3.2.1.9	
Sizes		
Sampling		
Direction	Longitudinal	Transverse[b]
Number of Specimens[a]	15	14
	F_{su} (ksi)	
Low	174	175
High	184	184
Mean	179	179
Standard Deviation	2.6	3.2

[a] Data for bent specimens excluded.

[b] Load axis normal to grain flow.

Table 3.2.6.2 Longitudinal bearing yield and ultimate strengths for specimens aged at 900F which were cut from various size forgings representing four heats (Ref. 4)

Alloy	AerMet 100			
Form	Forgings			
Condition	See Table 3.2.1.9			
Sizes				
Sampling				
Direction	Longitudinal[a]			
	F_{bry} (ksi)		F_{bru} (ksi)	
	e/D=1.5	e/D=2.0	e/D=1.5	e/D=2.0
Low	375	388	449	506
High	398	474	422	600
Mean	385	439	467	585
Standard Deviation	7.0	17.3	10.9	21.1

[a] Results shown for 20 specimens for each property.

Table 3.2.6.1 Longitudinal bearing yield and ultimate strengths of specimens aged at 875F which were cut from various size forgings representing seven heats (Ref. 2)

Alloy	AerMet 100			
Form	Forgings			
Condition	See Table 3.2.1.8			
Sizes				
Sampling				
Direction	Longitudinal[a]			
	F_{bry} (ksi)		F_{bru} (ksi)	
	e/D=1.5	e/D=2.0	e/D=1.5	e/D=2.0
Low	394	449	451	575
High	414	498	457	633
Mean	403	473	473	614
Standard Deviation	5.9	15.5	10.6	18.5

[a] Results shown for 20 specimens for each property.

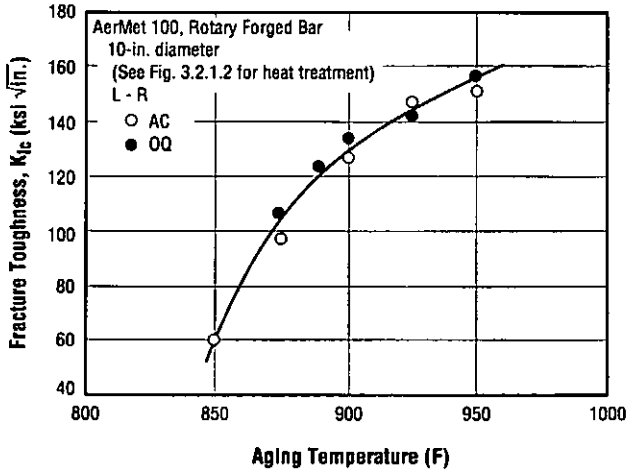


Figure 3.2.7.2.1 Effect of aging temperature on plane strain fracture toughness of forging for specimens air cooled or oil quenched from the solution temperature (Ref. 5)

Table 3.2.7.2.2 Plane strain fracture toughness of specimens aged at 875F which were cut from various forgings representing seven heats (Ref. 2)

Alloy	AerMet 100	
Form	Forgings	
Condition	See Table 3.2.1.8	
Sizes	As inTable 3.2.1.8	As in Table 3.2.1.8, except 3- and 3.5-in. rounds were not tested
Sampling	As in Table 3.2.1.8	
Number of Specimens	30	29
Crack Orientation[a]	LR or LT	CR or ST
	Fracture Toughness[b], K_{Ic} (ksi $\sqrt{in.}$)	
Low	90	73
High	110	101
Mean	99	88
Standard Deviation	6.5	8.6

[a] LR or CR applies to rounds; LT or ST applies to square or rectangular cross sections.

[b] ASTM E 399 1-inch-thick CT specimens.

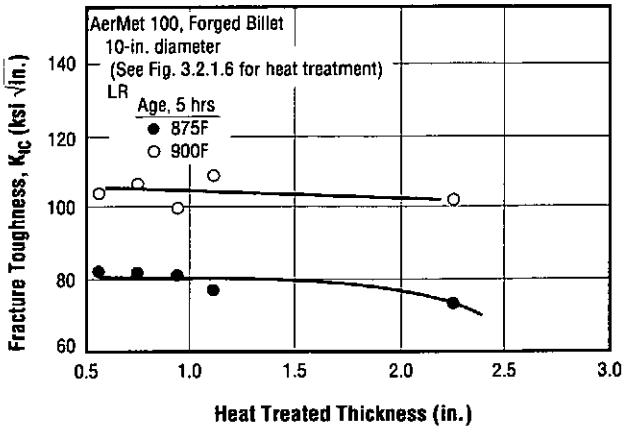


Fig. 3.2.7.2.3 Effect of heat treated section thickness on plane strain fracture toughness of specimens cut from 10-inch-diameter forged billet (Ref. 13)

Table 3.2.7.2.4 Effect of 700F, 3000-hr. air exposure on the plane strain fracture toughness of specimens cut from forging (Ref. 2)

Alloy	AerMet 100	
Form	6-in.-diameter Forging[a]	
Condition	Specimens: 1625F, 1 hr., VC[b] + -100F, 1 hr., air warm + 900F, 5 hr.	
Exposure	None	700F, 3,000 hr.
Fracture Toughness[b], K_{Ic} (ksi $\sqrt{in.}$)	97.1	83
	99.0	86.4
	100.5	

[a] Specimens cut from mid-radius.

[b] VC - Vermiculite Cooling to simulate the cooling rate of 1-in.-thick CT K_{Ic} specimens cooled in still air. See Figure 3.3.3.3.

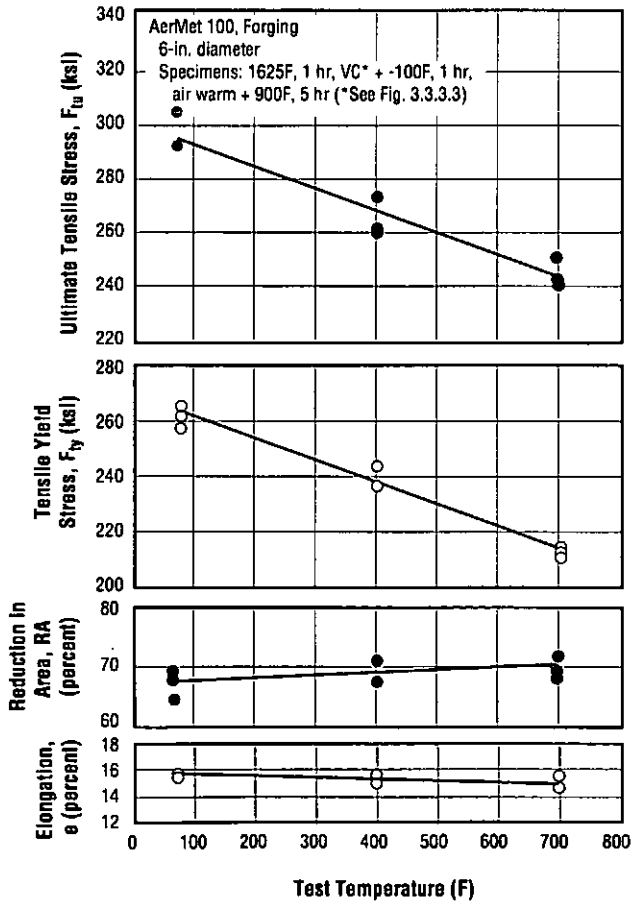


Fig. 3.3.1.1. Effect of elevated test temperature on tensile properties of a forging aged at 900F (Ref. 2)

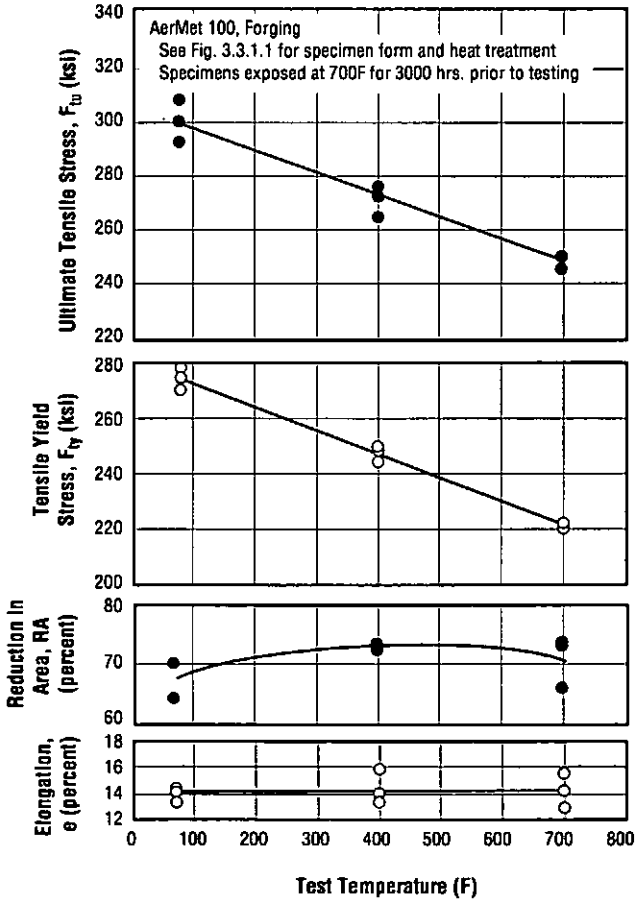


Fig. 3.3.1.2. Effect of test temperature on tensile properties following 700F, 3000 hr. air exposure for a forging aged at 900F (Ref. 2)

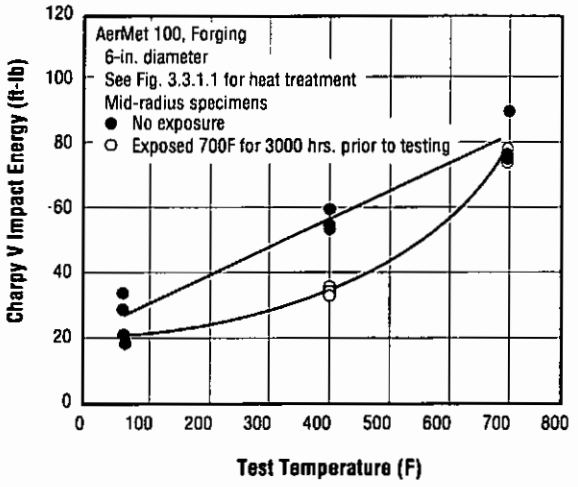


Fig. 3.3.3.1 Effect of test temperature on Charpy V impact energy for specimens cut from forging with and without a prior 700F, 3000 hr. air exposure (Ref. 2)

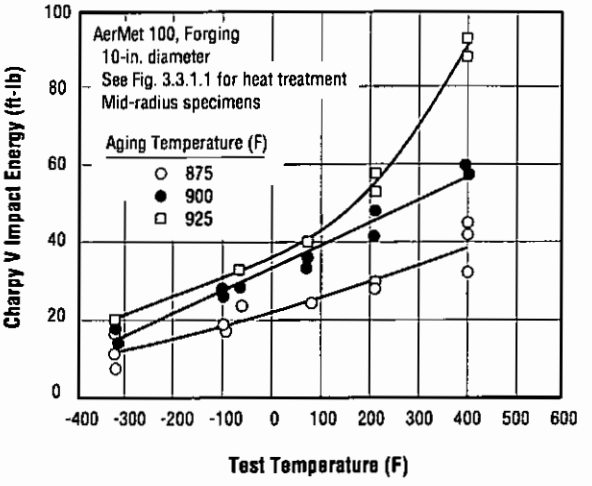


Fig. 3.3.3.2 Effect of cryogenic and elevated test temperature on the Charpy V impact energy of specimens cut from a 10-in.-diameter round forging and aged at several temperatures (Fig. 2)

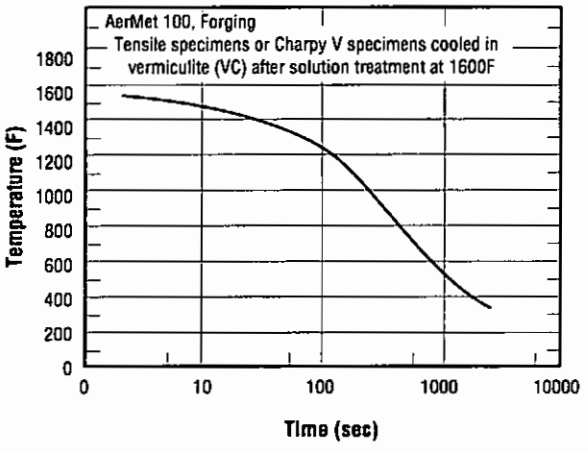


Fig. 3.3.3.3 Cooling curve for tensile and Charpy V specimens cooled in vermiculite following solution treatment to simulate the cooling rate of 1-in.-thick CT K_{Ic} specimens cooled in still air (Ref. 8)

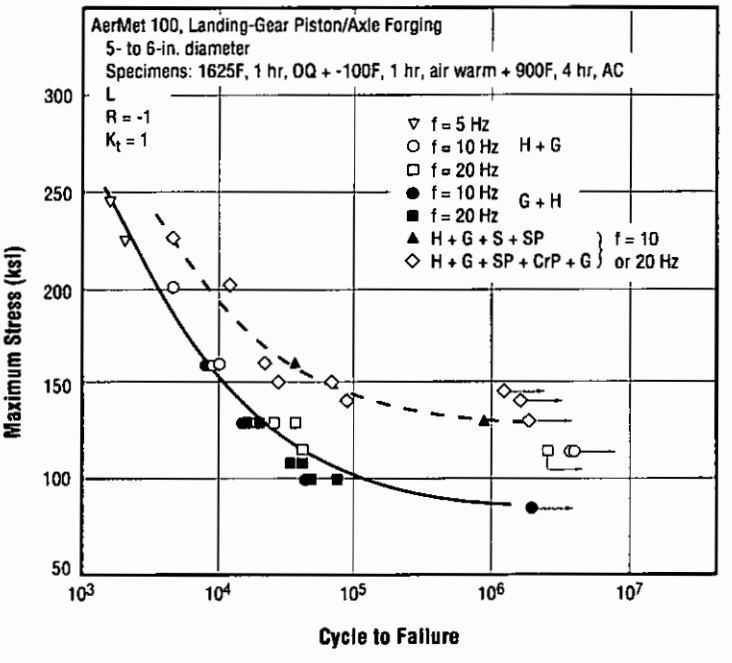


Fig. 3.5.1.1 Axial load fatigue data at R = - 1 for smooth specimens cut from a forging and tested with various surface conditions at different frequencies (Ref. 13)

Surface Condition Code:

H = Heat treated
G = Ground, 63 rms
S = Sand blasted
SP = Shot peened
(0.008 to 0.012 Almen Intensity)
CrP = Chrome plated
M = Machined, 125 rms

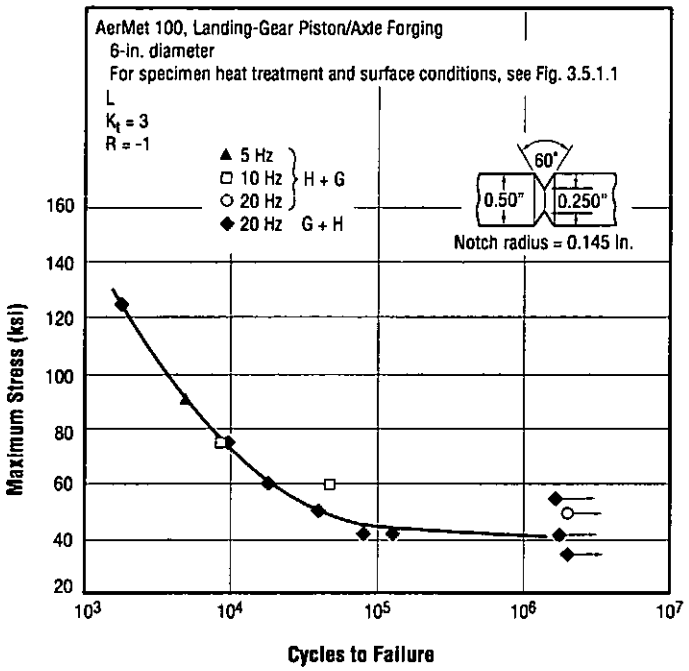


Fig. 3.5.1.2 Axial load fatigue data at R = - 1 and K_t = 3 for specimens cut from a forging and tested with various surface conditions at different frequencies (Ref. 13)

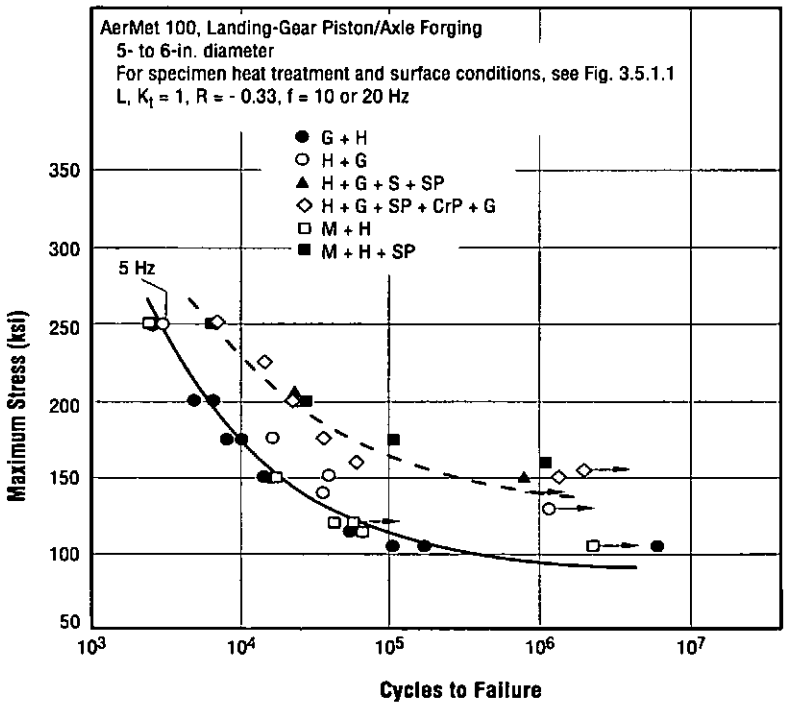


Figure 3.5.1.3 Axial load fatigue data at R = - 0.33 for smooth specimens cut from a forging and tested with various surface conditions at different frequencies (Ref. 13)

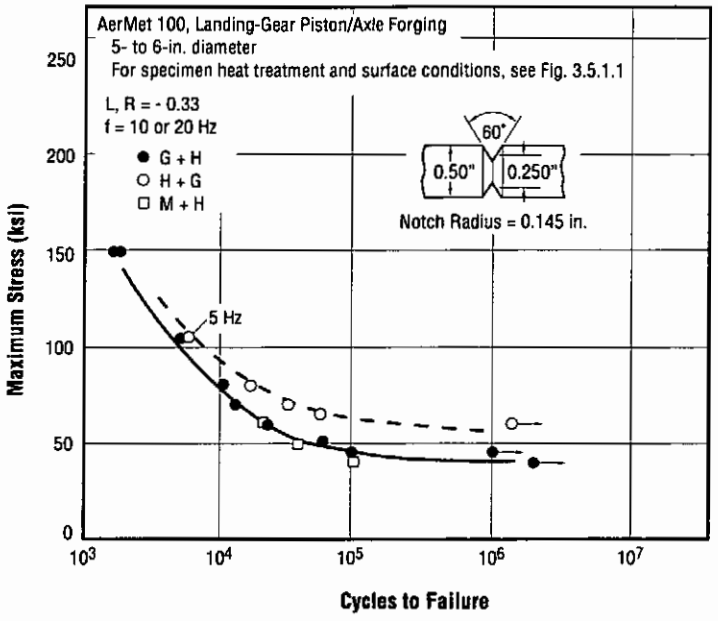


Figure 3.5.1.4 Axial load fatigue data at R = - 0.33 and K_t = 3 for specimens cut from a forging and tested with various surface conditions and at different frequencies (Ref. 13)

Table 3.5.1.5 Estimates of the fatigue strength at 10^6 cycles for axial loading of specimens from a landing-gear piston/axle forging

Alloy	AerMet 100										
Form	Landing-Gear Piston/Axle Forging										
Heat Treatment	See Fig. 3.5.1.1										
Sources	Figures 3.5.1.1 to 3.5.1.4 (Ref. 13)										
R Ratio	-1					- 0.33					
Stress Concentration, K_t	1			3		1				3	
Surface Condition[a]	G+H	H+G	SP	G+H	H+G	G+H	H+G	M+H	SP	G+H	H+G
Maximum Stress at 10^6 cycles (ksi)	75	120	140	50		110	125		170	60	50

[a] See Fig. 3.5.1.1 for surface conditions.

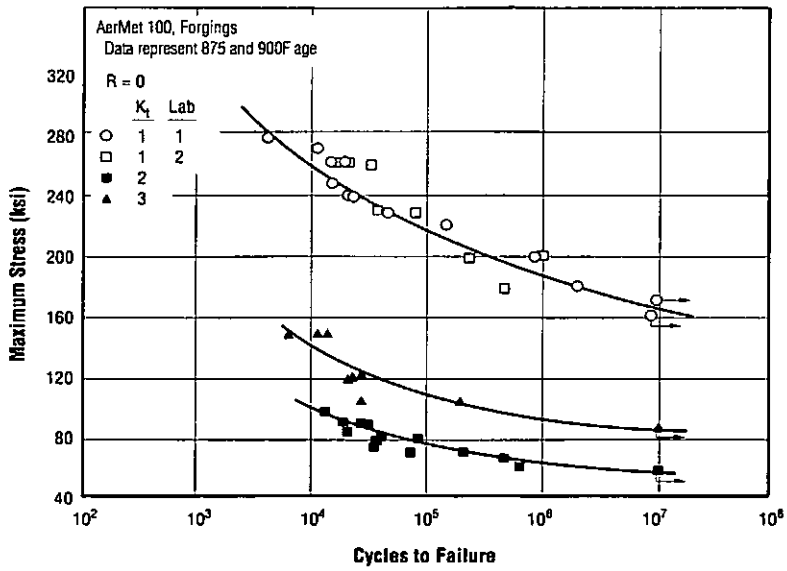


Fig. 3.5.1.6 Fatigue data for forgings tested at R = 0 using smooth and notch specimens of unspecified geometry (Refs. 2, 10)

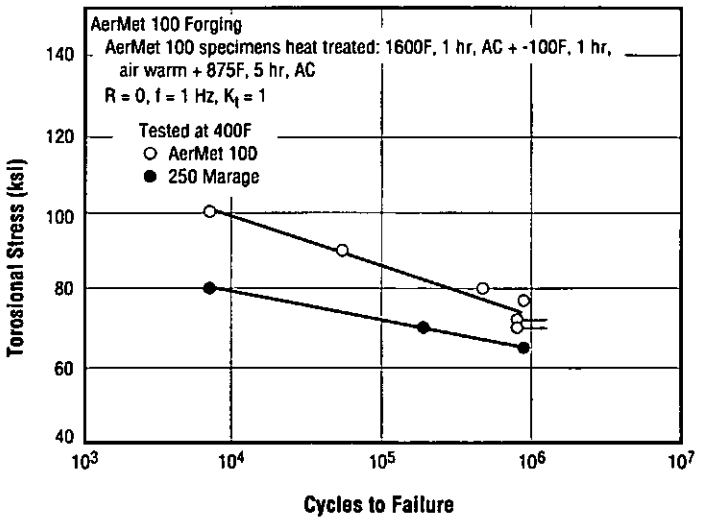


Figure 3.5.1.7 Torsional fatigue strength at 400F of AerMet 100 and 250 Grade Maraging steel (Ref. 9)

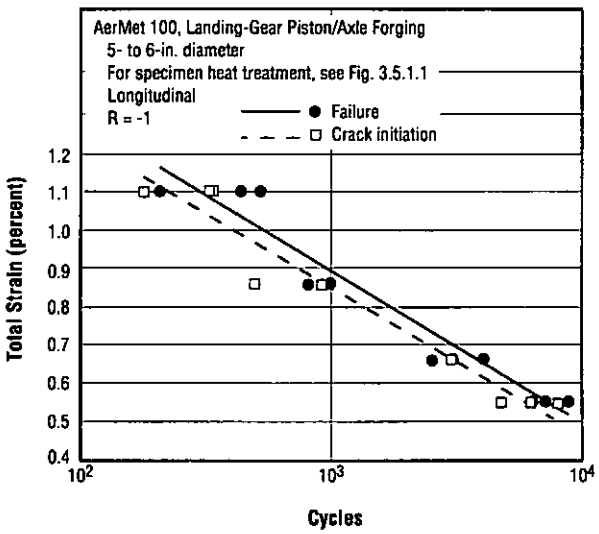


Figure 3.5.2.1 Low cycle fatigue data for crack initiation and failure for specimens cut from a forging (Ref. 13)

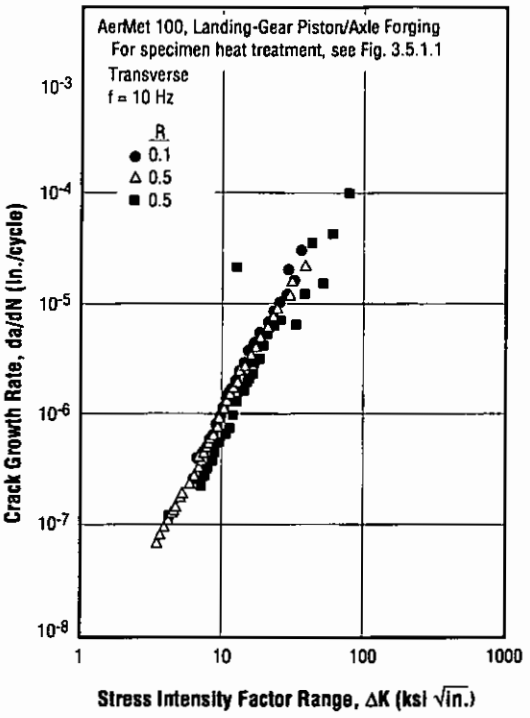


Fig. 3.5.3.1 Fatigue crack propagation rates in air at several R values for landing-gear piston/axle forging (Ref. 13)

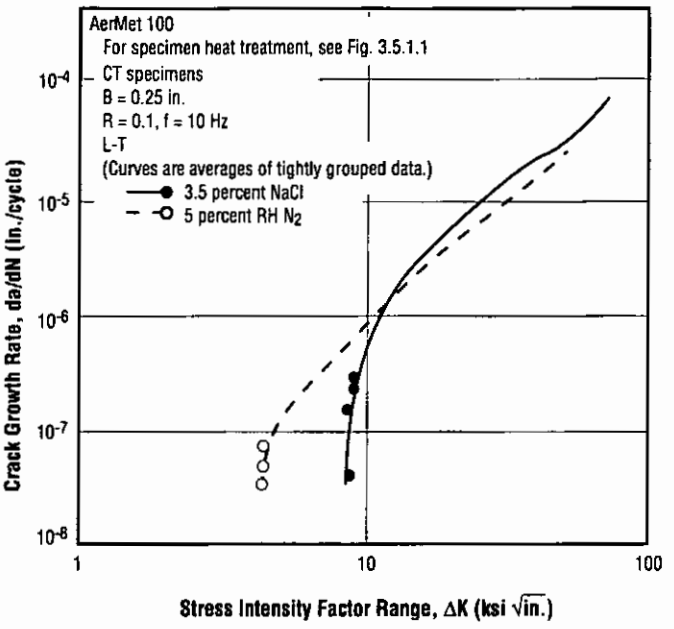


Fig. 3.5.3.2 Fatigue crack growth rates at R = 0.1 in 3.5 percent NaCl and in dry nitrogen for a forged slab (Ref. 7)

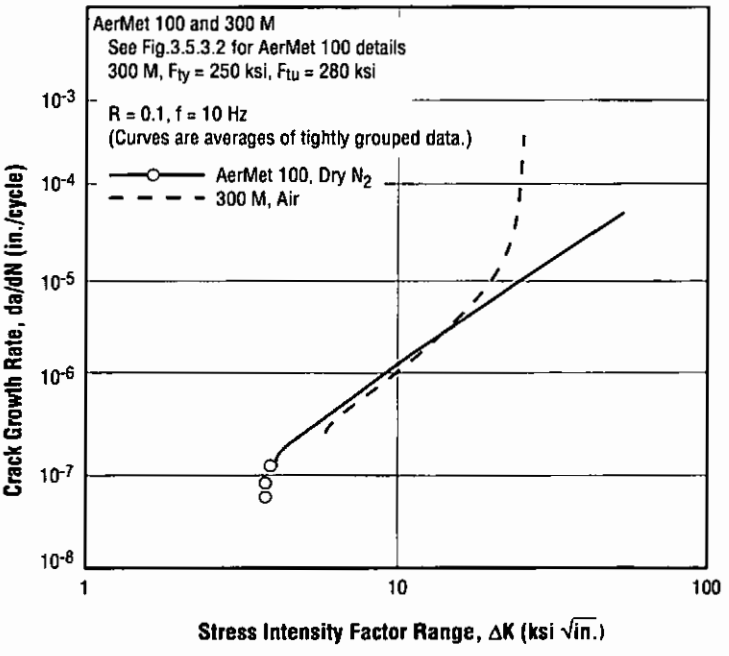


Fig. 3.5.3.3 Fatigue crack growth rates at R = 0.1 for AerMet 100 in dry nitrogen and 300 M in air (Ref. 7)

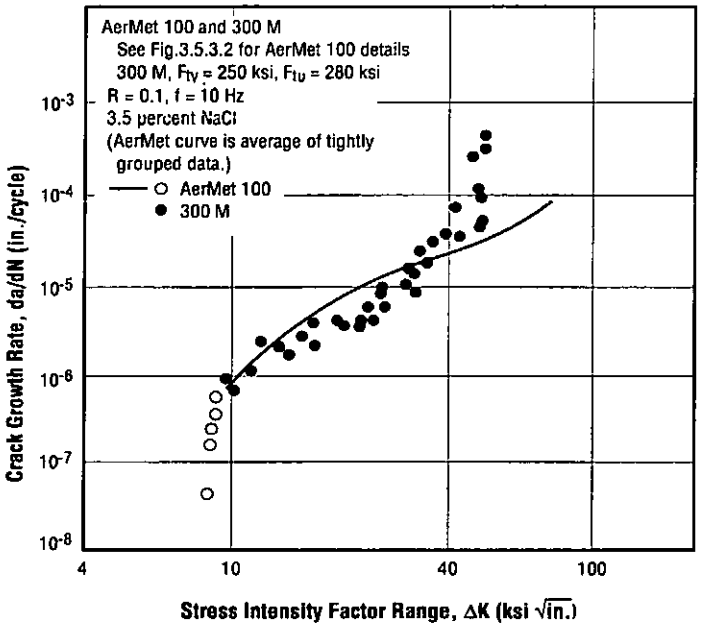


Fig. 3.5.3.4 Fatigue crack growth rates at R = 0.1 for AerMet 100 and 300 M in 3.5 percent NaCl (Ref. 7)

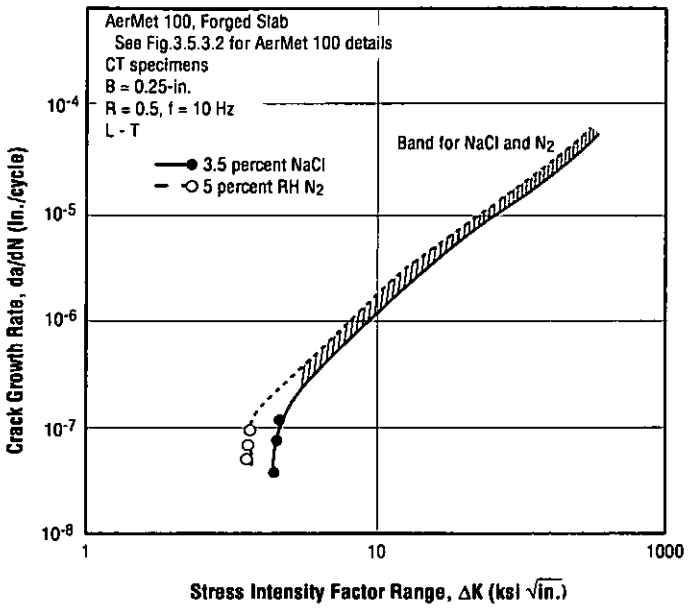


Fig. 3.5.3.5 Fatigue crack growth rates at R = 0.5 in 3.5 percent NaCl and in dry nitrogen for a forged slab (Ref. 7)

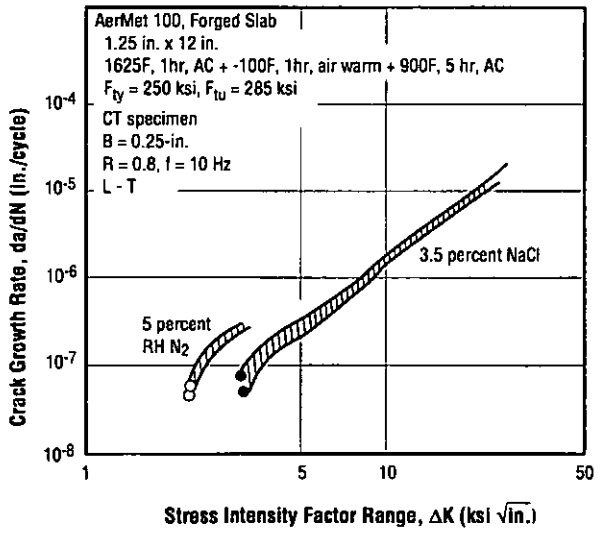


Fig. 3.5.3.6 Fatigue crack growth rates at R = 0.8 in 3.5 percent NaCl and in dry nitrogen for a forged slab (Ref. 6)

Table 3.6.2.1 Tension and compression moduli of elasticity determined for specimens aged at 875F which were cut from various size forgings representing seven heats (Ref. 2)

Alloy	AerMet 100	
Form	Forgings	
Condition	See Fig. 3.5.1.8	
Sizes		
Direction	Longitudinal[a]	
Modulus (10^3 ksi)	Tension	Compression
Mean	27.9	28.2
Standard Deviation	0.3	

[a] Sampling - 30 tests for each property.

Table 4.3.1.1 Preliminary results (duplicate tests) for tensile properties and Charpy V impact energies for GTA welds in plate (Refs. 2, 19)

Alloy	AerMet 100			
Form	60° V-groove GTA multiple-pass welds in 5/8-in. plate			
Condition[a]	A A+W+N+A+STA	B STA+W	C STA+W+SR	D STA+W+Age
F_{tu} (ksi)	281 280	262 260	260 260	268 266
F_{ty} (ksi)	253 252	181 183	176 186	230 233
Elongation, e (percent)	14 13	10 8	15 11	13 8
Reduction in Area, RA (percent)	60 59	16 23	56 25	30 28
Charpy V Impact Energy[b] (ft-lb)	22 27	-	25 24	20 21

[a] A - Anneal 1250F, 16 hr, AC; W - GTA weld; N - Normalize 1650F, 1 hr, AC; SR - Stress relief 200F, 5 hr, AC; STA - 1625F, 1 hr, AC + -100F, 1 hr, Air warm + 900F, AC.

[b] Specimens taken at weld center line.

References

1. Military Handbook 5G, "Metallic Materials and Elements for Aerospace Vehicle Structures", prepared by the U.S. Air Force, November 1994
2. Personal communication from P.M. Novotny, Carpenter Technology, to W. F. Brown Jr. March 29, 1995
3. Aerospace Material Specification, AMS 6478, Society of Automotive Engineers, May 1994.
4. Ruff, P.E.,"Mechanical Properties of AerMet 100 Alloy", *Carpenter Technology Report*, February 14, 1995.
5. Novotny, P. M., "An Aging Study of Carpenter AerMet 100 Alloy", 1992 Gilbert R.Spiech Symposium Proceedings, Fundmentals of Aging and Tempering in Martenistic and Banitic Steel Products, Iron and Steel Institute, Eds. G. Kraus and P.E. Repas, 1992. p.215
6. Wert. D.E., "Statistical Analysis of AerMet 100 Alloy", *Carpenter Steel*, Oct. 11, 1991.
7. Lee E. U., "Fatigue Crack Growth in AerMet 100 Steel", Naval Air Development Center, Report No. NASC-91111-60, Oct. 18, 1991.
8. Novotny, P. M., "Effect of Variations in Hardening and Aging Parameters on the Fracture Toughness and Tensile Properties of Carpenter AerMet 100 Alloy", *Carpenter Research and Technology*, 1991.
9. Novotny, P. M. and Dahl, J. M., "AerMet 100 Alloy for Aerospace Applications", Mechanical Working and Steel Processing Proceedings, 1990, p. 275.
10. Henderson, J. B. , Groot, H. and Ferrier, J.,"Thermal Physical Properties of an Iron Alloy", Report to Carpenter Technology, Purdue University, School of Mechanical Engineering, Report TPRL 1222, Nov. 1992.
11. Alloy Data, "AerMet 100 Alloy", *Carpenter Technology*, 1992
12. Kozol, J. and Neu, C.E., "Stress Corrosion Susceptibility of Ultra High Strength Steels for Naval Aircraft Applications", Report No. NAWCADWAR-92018-60, Naval Air Warfare Center, Jan. 10, 1992.
13. Personal Communication from R. Eybel, Dowty Aerospace, Ontario, Canada, April 1995.
14. Raghavan, A. and Machmeier, P.M., "Analytical Electron Microscopic Examination of Peak Hardening Phenomena in a Secondary Hardening High Strength Steel", Microstructure and Mechanical Properties of Aging Material, The Minerals, Metals and Materials Society, 1993
15. Aerospace Materials Specification, AMS 6532, Society of Automotive Engineers, June 1992
16. Novotny, P. M. and McCaffery, T.J., "An Advanced Alloy for Landing Gear and Aircraft Structural Applications - AerMet 100 Alloy", SAE Technical Paper 922040, 1992.
17. Dahl, J., "AerMet 100 - An Advanced Steel for the Aerospace Industry", *Advanced Materials Technology International*, 1991
18. Novotny, P.M. and Maguire, M. "Navy Fighter Demands Evolve into Tough Castings", *Foundry Management and Technology*, December 1993, p.33
19. Novotny, P.M., Nye, R.D., and Robino, C.V., "Fabricating Characteristics of Ultrahigh-Strength Steel", *Welding Journal*, Feb. 1995

	Fe
0.16	C
14	Co
10	Ni
2	Cr
1	Mo

AF1410

1. GENERAL

AF 1410 is a further development, under Air Force sponsorship, of the Fe-0.11C-10Ni-8Co-2Cr-1Mo advanced submarine hull steel which has a typical room temperature yield strength and plane strain fracture toughness of 200 ksi and 190 ksi-in.$^{1/2}$ respectively. By raising the Co and C content, the F_{ty} has been increased to a typical of 235 ksi. As might be expected this increase in the strength was accompanied by some loss in fracture toughness, the typical value being about 140 ksi-in.$^{1/2}$ However, this combination of strength and toughness exceeds that of other commercially available steels, and the alloy has been considered as a replacement for titanium in certain aircraft parts. Presently available information shows that AF 1410 is air hardening in sections 3 inch thick, and from metallurgical considerations, satisfactory hardening would be expected in even thicker sections. VIM-VAR melting is presently the preferred practice and care must be taken to keep impurity elements at very low levels. Weldability is good using the CW-GTA process providing high purity wire is used and oxygen contamination is avoided. The K_{Ic} value of welds has not been determined. However, from the results of tests on surface cracked specimens, subsized plane strain fracture toughness specimens and Charpy V impact values, it appears that the fracture toughness of the fusion zone and of the heat affected zone is comparable to that of the parent metal. Information on stress corrosion cracking is incomplete and no definite value can be assigned to K_{Iscc} for either parent metal or weldments.

1.01 Commercial Designation

Unimach 1410

1.02 Alternate Designation

AF 1410

1.03 Specifications

1.031 Rockwell International Corporation, B-1 Division Specification LB0160-184

1.04 Composition

Table 1.04

1.05 Heat Treatment (See also 4.0313)

General. The steel is austenitized and aged. Quenching from the austenitizing temperature produces a highly dislocated lath martensite having a relatively low yield strength and a high toughness as measured by the Charpy V impact energy (Fig. 3.0235). Aging produces a complex series of changes in the carbide structure which result in a combination of martensite tempering and secondary hardening due to aging. This secondary hardening produces a maximum in the tensile strength at about 900 F (5 hour age time) and a minimum in the impact energy at about 800 F. In a temperature range between 800 and 1000 F the impact energy exhibits a maximum. At aging temperatures above 1000 F both the tensile strength and the impact energy decrease rather rapidly (Figs. 3.0234 and 3.0235).

This steel is subject to austenite reversion during aging. At normal aging temperatures the retained austenite is generally less than one percent by volume. At aging temperatures of 1000 F and higher, large amounts of austenite will be formed (Fig. 2.0121) and these will weaken the matrix.

1.051 Normalize: 1625 to 1650 F, 1 hour per inch, A. C.

1.052 Both single and double austenitizing treatments have been employed. Double austenitizing appears to produce a higher toughness (Table 1.058 and 3.02724). Both the tensile strength and impact energy appear to exhibit a rather flat maximum between 1500 and 1600 F (Figs. 3.0213 and 3.0232).

1.0521 Single austenitizing. 1475 to 1525 F, 1 hour per inch + 1475 to 1525 F, 1 hour per inch.

1.053 Quenching. Experience to date indicates that air cooling from the austenitizing temperature will produce tensile strength, toughness and fatigue strength essentially equal to oil or water quenching in section sizes up to 3 inches (Tables 1.057, 1.059 and 3.051).

1.054 Refrigeration. A refrigeration treatment of -100 F is sometimes applied in order to reduce the amount of retained austenite. There is no evidence that such a treatment has any substantial effect on the mechanical properties (Table 1.057 and 1.058).

1.055 Aging. 950 F, 4 hours A.C.

1.056 Premachining. As received material may be given a 1250 F, 8 hour treatment to increase machinability. This treatment is normally followed by austenitizing and aging. (Figs. 3.0216 and 3.0233)

1.057 Tensile strength properties and impact energy for VIM-VAR melt plate quenched in air, oil or water following austenitizing. Table 1.057

1.058 Effect of various heat treatments on tensile and impact properties of 5/8 inch and 3 inch VIM-VAR Melt Plate. Table 1.058

1.059 Tensile properties, impact energy and fracture toughness of VIM-VAR Melt 2 inch plate quenched in different media and given a premaching heat treatment. Table 1.059

1.06 Hardness

1.061 End quenched hardenability. Fig. 1.061

1.062 Effect of aging time and temperature on hardness of VIM-VAR Melt Plate. Fig. 1.062

1.07 Forms and Conditions Available

1.071 Sheet, bars, forgings and forging stock. All products as hot finished, overaged (1250 F, 8 hours A. C.) or to specified heat treatment. (14)

1.08 Melting and Casting Practice

1.081 Melting Practice. Vacuum arc remelting of a vacuum induction melted electrode (VIM-VAR melting). Attempts (1 to 5) (10) have been made to produce this steel by other

	Fe
0.16	C
14	Co
10	Ni
2	Cr
1	Mo

AF1410

melting practices with particular emphasis on electroslag remelting of a vacuum induction melted ingot (VIM-ESR). None of these practices were able to produce material with as high a toughness, as measured by impact energy, as VIM-VAR melting (Tables 1.0814 through 1.08110 also compare Figs. 3.0234 and 3.0236). Variations in the ESR slag composition (Table 1.0812) were investigated in an attempt to improve the toughness and reduce directionality but these were unsuccessful (compare Table 1.0814 with VIM-VAR in Table 1.0815 and compare Table 1.0816 with 1.0817). ESR melts contained excessive amounts of oxygen (Table 1.0813) which contributed to the reduced impact energy of the ESR melted material as compared with VIM-VAR melting. This excess oxygen arises from a slag metal reaction which is apparently impossible to prevent. Normally, oxygen produced in this manner is removed by the addition of deoxidizing elements such as Al and Si. However, in this steel such elements are intentionally controlled to low values in order to achieve high fracture toughness. In addition, ESR melted plate material exhibited slits which apparently result from microvoids in the ingot which are not welded during processing. These microvoids arise from a reaction between alloy carbon and oxygen. The total non metallic content of ESR material was considerably higher than VIM or VFM-VAR melts (Fig. 3.0238).

1.0811 Plate and ESR slag compositions for 2000 lb. VIM melt remelted into ESR ingots. Table 1.0811

1.0812 Slag compositions used in making ESR remelts. Table 1.0812

1.0813 Oxygen levels in ingots produced by various melting practices. Table 1.0813

1.0814 Tensile and impact properties of 1-1/4 and 1.4 inch thick plate from VIM-ESR melts. Table 1.0814

1.0815 Tensile and impact properties of 1-1/4 inch thick plate from various melting practices. Table 1.0815

1.0816 Tensile and impact properties of 3 inch thick plate from VIM and VIM-VAR Melts. Table 1.0816

1.0817 Tensile and impact properties of 3 inch thick plate from various melting practices. Table 1.0817

1.0818 Tensile and impact properties of 3 inch thick plate from various ADO melting practices. Table 1.0818

1.0819 Tensile and impact properties of 1-1/2 and 1-3/4 inch thick upset disks from various melting practices. Table 1.0819

1.08110 Tensile and impact properties of 6 inch thick upset disks from various melting practices. Table 1.08110

1.09 Special Considerations (See also 1.05 and 4.03)

1.091 The toughness of this alloy is especially sensitive to the content of impurity elements including those normally used to deoxidize steel. These elements act to reduce the toughness and are closely controlled by good melting practice. (Figs. 1.094 and 3.0238)

1.092 Aging temperature in excess of 1000 F result in a loss in toughness and should be avoided (Figs. 3.0234 and 3.0235). Long time exposure to temperatures above about 500 F results in a loss in impact energy. (Fig. 3.0237)

1.093 The toughness as measured by the impact energy decreases substantially at subzero temperatures and is low at cryogenic temperatures. (Figs. 3.0331 and 3.0332)

1.094 Effect of sulphur and oxygen content on the impact energy of VIM-VAR and VIM-ESR Melt Alloy. Fig. 1.094

2. PHYSICAL PROPERTIES AND ENVIRONMENTAL EFFECTS

2.01 Thermal Properties

2.011 Melting range. Liquidus = 2592 F, Solidus = 2462 F

2.012 Phase Changes. (14)

A_{c1} = 1160 - 1161 F
A_{c3} = 1512 -1523 F
M_s = 635 to 640 F
M_f = 320 to 350 F

2.0121 Time temperature transformation diagrams. (Fig. 2.0121)

2.013 Thermal conductivity

2.014 Thermal expansion

2.0141 Mean coefficient of linear thermal expansion. Figure 2.0141

2.015 Specific heat

2.016 Thermal diffusivity

2.02 Other Physical Properties

2.021 Density 0.283 lbs. per cu. inch.

2.022 Electrical properties

2.023 Magnetic properties

2.024 Emittance

2.025 Damping capacity

2.03 Chemical Environments

2.031 General corrosion resistance. The alloy has a general corrosion resistance similar to the maraging steels. It is more resistant than HY 180 and D6ac steels. (7) Fatigue crack growth rates are essentially the same for parent metal tested in air, 3-1/2 percent salt water or in sump tank water. (Figs. 3.056 to 3.059) The fusion zone of CW-GTA welds appear to exhibit a somewhat lower crack growth rate in air and in 3.5 percent NaCl than that characteristic of parent metal. (Compare Figs. 4.03122 and 4.03123 with Fig. 3.056)

2.032 Attempts to measure K_{Iscc} have been hampered by crack branching. Values as low as 30 ksi-in.$^{1/2}$ have been reported for full heat treated plate in 3.5 percent NaCl. This value is probably quite conservative and considerable additional data will be needed to establish a useful value of K_{Iscc} for this alloy.

2.04 Nuclear Environments

	Fe
0.16	C
14	Co
10	Ni
2	Cr
1	Mo

AF1410

3. MECHANICAL PROPERTIES

3.01 Specified Mechanical Properties

3.011 Fabricators mechanical property specification. Table 3.011

3.02 Mechanical Properties at Room Temperature

3.021 Tension-stress/strain diagrams-tension properties.

3.0211 Effect of aging temperature on the tension stress-strain curves of VIM-VAR plate. Fig. 3.0211

3.0212 Effect of aging time on tension stress-strain curves of VIM-VAR plate. Fig. 3.0212

3.0213 Effect of austenitizing temperature and refrigeration treatment on tensile strength properties of VIM-VAR melt plate WQ from the austenitizing temperature. Fig. 3.0213

3.0214 Effect of austenitizing temperature and refrigeration treatment on tensile strength properties of VIM-VAR melt plate air cooled from the austenitizing temperature. Figure 3.0214

3.0215 Effect of aging time and temperature on tensile properties of VIM-VAR 5/8 inch plate. Fig. 3.0215

3.0216 Effect of aging temperature and time on tensile properties of VIM-VAR melt 1 inch plate given a premachining heat treatment. Fig. 3.0216

3.0217 Effect of exposure to elevated temperature on room temperature tensile properties. Fig. 3.0217

3.0218 Wing sweep actuator VIM-VAR forging showing test locations and mechanical test specimens cut from these areas. Fig. 3.0218

3.0219 Tensile and impact properties for single and double austenitized specimens cut from VIM-VAR melt wing sweep actuator forging. Table 3.0219

3.02110 Tensile and impact properties of single and double austenitized refrigerated specimens cut from VIM-VAR wing sweep actuator forging. Table 3.02110

3.02111 Effect of aging temperature on the tensile properties of three VIM-ESR melts. Fig. 3.02111

3.022 Compression-stress/strain diagrams-compression properties.

3.0221 Compressive yield strength and elastic modulus for single and double austenitized specimens cut from VIM-VAR melt wing sweep actuator forging. Table 3.0221

3.0222 Effect of temperature on compression yield strength of VIM-VAR melt plate. See Fig. 3.0322

3.023 Impact

3.0231 Effect of austenitizing temperatures on impact energy of VIM-VAR melt plate. Fig. 3.0231

3.0232 Effect of austenitizing temperature and refrigeration treatment on impact energy of VIM-VAR melt plate air cooled or water quenched from the austenitizing temperature. Fig. 3.0232

3.0233 Effect of aging temperature and time on impact energy of VIM-VAR melt plate given a premachining heat treatment. Fig. 3.0233

3.0234 Effect of aging temperature on impact energy of VIM-VAR plate. Fig. 3.0234

3.0235 Effect of aging temperature on impact energy and yield strength of VIM-VAR plate. Fig. 3.0235

3.0236 Effect of aging temperature on impact energy of three VIM-ESR melts. Fig. 3.0236

3.0237 Effect of exposure to elevated temperatures on room temperature Charpy V impact energy of VIM-VAR melt plate. Fig. 3.2037

3.0238 Charpy impact energy for plate as function of total non-metallics as determined with quantitative television microscope. Fig. 3.0238

3.024 Bending

3.025 Torsion and shear

3.026 Bearing

3.027 Stress concentration

3.0271 Notch properties

3.0272 Fracture toughness

3.02721 General. This alloy was developed to have high fracture toughness. The developmental program goal specified K_{Ic} = 115 ksi-in.$^{1/2}$. This goal was exceeded and typical values are in excess of 130 ksi-in.$^{1/2}$ at room temperature and greater than 100 ksi-in.$^{1/2}$ at -65 F. Maintaining a high level of fracture toughness requires close attention to alloy purity. (See 1.09)

3.02722 Plane strain fracture toughness of VIM-VAR melt plate tested in two directions at room and low temperature. Table 3.02722

3.02723 Plane strain fracture toughness of 3 inch VIM-VAR melt plate. Table 3.02723

3.02724 Plane strain fracture toughness values for single and double austenitized specimens cut from VIM-VAR melt wing sweep actuator forging. Table 3.02724

3.028 Combined properties

3.03 Mechanical Properties at Various Temperatures

3.031 Tension-stress/strain diagrams-tension properties

3.0311 Effect of test temperature on tensile properties of 3/4 inch and 2 inch VIM-VAR melt plate. Fig. 3.0311

3.0312 Effect of test temperature on tensile properties of VIM-VAR melt plate exposed at the test temperature. Fig. 3.0312

3.0313 Effect of low and elevated temperatures on tensile properties of VIM-VAR melt plate. Fig. 3.0313

3.032 Compression-stress/strain diagrams-compression properties

3.0322 Effect of temperature on the compressive yield strength of VIM-VAR melt plate. Fig. 3.0322

3.033 Impact

3.0331 Effect of test temperature on impact energy of three VIM-ESR melts. Fig. 3.0331

3.0332 Effect of low test temperatures on impact energy of a 300 lb. VIM-VAR melt plate. Fig. 3.0332

3.034 Bending

3.035 Torsion and shear

3.0351 Effect of temperature on shear strength of VIM-VAR melt plate. Fig. 3.0351

3.036 Bearing

3.0361 Effect of temperature on bearing yield strength of VIM-VAR melt plate. Fig. 3.0361

	Fe
0.16	C
14	Co
10	Ni
2	Cr
1	Mo

AF1410

3.0362 Effect of temperature on bearing ultimate strength of VIM-VAR melt plate. Fig. 3.0362

3.037 Stress concentration

3.0371 Notch properties

3.0372 Fracture toughness (See 3.0272

3.038 Combined properties

3.04 Creep and Creep Rupture Properties

3.041 Creep rupture curve at 800 F for VIM-VAR melt plate. Fig. 3.041

3.05 Fatigue

3.051 Axial load S-N data for VIM-VAR melt plate given a premachining heat treatment and then water or air quenched following austenitizing. Fig. 3.051

3.052 S-N curves at room temperature for VIM-VAR melt plate tested in the transverse direction at several stress concentration factors for R = -1. Fig. 3.052

3.053 S-N curve at room temperature for VIM-VAR melt plate tested in the transverse direction at several stress concentration factors for R = 0.5. Fig. 3.053

3.054 S-N curve at room temperature for VIM-VAR melt plate for several stress concentration factors at R = 0.05. Fig. 3.054

3.055 S-N curve for VIM-VAR melt plate for specimens with ground or ground and shot peened surfaces. Fig. 3.055

3.056 Fatigue crack growth rate for VIM-VAR melt 2-inch plate given a premachining heat treatment and then water on air quenched following austenitizing. Fig. 3.056

3.057 Fatigue crack growth rate at two frequencies and two R ratios for VIM-VAR plate at room temperature in low humidity air. Fig. 3.057

3.058 Fatigue crack growth rate at two frequencies and two R ratios for VIM-VAR melt plate at room temperature in 3-1/2 percent salt water. Fig. 3.058

3.059 Fatigue crack growth rate at two frequencies for VIM-VAR melt plate at room temperature in sump tank water. Fig. 3.059

3.0510 Fatigue crack growth rate for VIM-VAR plate at -65 F. Fig. 3.0510

3.0511 Effect of stress ratio on fatigue life of various cracked specimens subjected to constant amplitude loading. Fig. 3.0511

3.06 Elastic Properties

3.061 Poisson's ratio

3.062 Modulus of elasticity

3.0621 Elastic modulus in tension for VIM-VAR 1-1/4 inch plate. Table 3.0621 Elastic modulus in compression (see TAble 3.0221)

3.063 Modulus of rigidity

3.064 Tangent modulus

3.065 Secant modulus

4. FABRICATION

4.01 Forming

General. Only a very limited amount of information is available concerning the forming characteristics of this alloy. One large forging (Fig. 3.0218) has been produced. This closed die forging was forged to final shape after three blocking operations. Semi-finished parts were heated to about 1800 F before final forging. Dies were preheated to 900 F. Forging pressure was 28,000 tons. (6)

4.02 Machining and Grinding

Machinability should be essentially the same as for the maraging steels. A premachining heat treatment of 1250 F, 8 hours A. C. is recommended. (See 1.05)

4.03 Joining

4.031 Welding

4.0311 General. The weldment strength and toughness are dependent on the content of impurity elements and on the welding parameters which directly influence the microstructure of the fusion zone (FZ) and the heat affected zone (HAZ). Impurity elements include S, P, O, N, H, and the deoxidizers Al and Si. These elements can form inclusions and second phase particles in the FZ which may act to nucleate voids at relatively low matrix strain. The improvement in FZ impact energy associated with a reduction in impurity elements is evident when comparing CW-GTA welds made with different fillers as shown in Table 4.03112. Gaseous elements can be introduced during welding and these may be in part responsible for the relatively low impact energies shown in Table 4.03112 for the HW-GTA and CW-PA welds. Microstructural changes in the FZ and HAZ during welding are complex and can have a strong influence on the strength and toughness. An excellent description of these changes is given in (12). The final microstructure is a function of the heat input, number of passes and the post weld aging treatment. High heat inputs tend to produce a relatively coarse FZ structure. The as deposited structure is refined by the thermal reversals associated with subsequent passes. These thermal reversals also produce increasing amounts of austenite and temper the carbide structure in both HAZ and FZ. Multiple pass welds may contain as much as eight percent retained austenite after post weld aging. There is no direct evidence that this austenite has a deleterious effect on the toughness. However, the influence of retained austenite will depend on its composition, form and location. Generally, austenite will reduce the strength of the matrix and efforts should be made to keep the amount below six percent by volume.

	Fe
0.16	C
14	Co
10	Ni
2	Cr
1	Mo

AF1410

The data available indicate that properly made welds will have smooth tensile and yield strengths somewhat lower than the parent plate (e.g. compare Fig. 3.0216 with Table 4.0318 and see also Fig. 4.03110). On the basis of Charpy V impact energy the toughness of the FZ and HAZ are comparable to the parent plat (e.g. compare Table 4.03113 with Fig. 3.0232). Plane strain fracture toughness (K_{Ic}) values for GTA welds are not available. K_Q values ranged from 97 to 139 ksi-in.$^{1/2}$ for specimens having large irregularities in their fatigue crack fronts (12). The rather low K_{Ic} values for electron beam welds (Table 4.03115) may be associated with a lack of stability in the electron beam which produced a heterogeneous solidification structure. The conventional fatigue of some CW-GTA welds appears to be substantially below that of the plate parent material (e. g. compare Figs. 4.03117 and 4.03118 with Figs. 3.052 to 3.054). This difference may be in part due to the fact that the weld data in question was obtained from specimens of rectangular crossection while the parent metal data was obtained from specimens of rectangular crossection while the parent metal data was obtained from specimens with a circular crossection and in part

4.0312 due to subsurface porosity which characterized the fusion zone of the welded specimens. Welding Conditions: To date the most satisfactory welds in terms of strength and toughness have been made using the CW-GTA process. Typical welding parameters are shown in Table 4.0316. No preheat is necessary and the maximum heat input should not exceed 50 Kj/inch. ment work.

4.0313 Post Weld Heat Treatment: The selection of a post weld age is complicated by the thermal reversals experienced in multipass welding. These produce an aging response different than that characteristic of the parent metal, (compare Fig. 3.0216 with Fig. 4.03110) and may require tailoring the post weld aging to the welding parameters. Present recommendations are for a 950 F, four hour age. (12)

4.0314 Filler wire compositions used in certain weld property studies. Table 4.0314

4.0315 Filler wire compositions used in certain weld property studies. Table 4.0315

4.0316 Weld parameters for automatic pulsed arc CW-GTA welding. Table 4.0316

4.0317 Alternate immersion stress corrosion data in 3.5 percent NaCl for CW-GTA welds in VIM-VAR plate. Table 4.0317

4.0318 Tensile properties at room temperature and -65 F for manual CW-GTA plate butt welds and repair welds with and without bead removal. Table 4.0318

4.0319 Hardness and impact energy as a function of distance from the weld centerline for CW-GTA welds in VIM-VAR plate. Fig. 4.0319

4.03110 Fusion zone tensile properties of VIM-VAR melt plate CW-GTA welded with several filler wires and aged for various times at 900 to 950 F. Fig. 4.03110

4.03111 Fusion zone charpy impact energy of VIM-VAR plate CW-GTA welded using several filler wires and aged for various times at 900 and 950 F. Fig. 4.03111

4.03112 Effects of heat input and filler wire impurities on fusion zone impact energy. Table 4.03112

4.03113 Impact energy for GTA weld metal and heat affected zone in VIM-VAR melt 1/2 inch plate. Table 4.03113

4.03114 Effect of temperature on fusion zone impact energy of CW-GTA welds in VIM-VAR plate. Fig. 4.03114

4.03115 Plane strain fracture toughness of electron beam welds made in VIM-VAR melt plate. Table 4.03115

4.03116 Fusion zone fatigue strength of CW-GTA weld in VIM-VAR melt plate. Fig. 4.03116

4.03117 S-N curves for GTA Butt Welds in VIM-VAR Melt 1/2 inch plate with bead ground off. Fig. 4.03117

4.03118 S-N curves for GTA Butt Welds in VIM-VAR 1/2 inch plate with bead on. Fig. 4.03118

4.03119 S-N curves for GTA repaired Butt Welds in VIM-VAR 1/2 inch plate with beads ground off. Fig. 4.03119

4.03120 S-N curve for full penetration fillet welded VIM-VAR melt cruciforms with non-symmetrical joints. Fig. 4.03120

4.03121 S-N curve for full penetration fillet welded VIM-VAR melt cruciforms with symmetrical joints. Fig. 4.03121

4.03122 Fatigue crack growth rate in air and in 3-1/2 percent NaCl for GTA weld in VIM-VAR 1/2 inch plate. Fig. 4.03122

4.03123 Fatigue crack growth of fusion zone of CW-GTA welds in VIM-VAR melt plate Fig. 4.03123

4.04 Surface Treating

4.041 S-N curves for VIM-VAR melt plate for specimens plated by various processes. Fig. 4.041

REFERENCES

1. Buzzanell, J. D., Shiring, R. R., Black, H. L., "Production Melting and Thermomechanical Processing of Af 1410 Steel", Universal-Cyclops Speciality Steel Division, Report IR-160-6 (I), AF Contract F33615-76-C-5026, (April 15, 1976)
2. ibid Report IR-160-6 (II) AF Contract F33615-76-5026 (July 15, 1976)
3. ibid Report IR-160-6 (III) Air Force Contract F33615-76-C-5026 (October 15, 1976)
4. Shiring, R. R., Milavec, J. L., Black, H. L., "Production Melting and Thermomechanical Processing of AF 1410 Steel", Universal-Cyclops Specialty Steel Division, Report IR 160-6 (IV) AF Contract F33615-76-C-5026 (January 1977)
5. ibid Report IR-160-6 (V), Air Force Contract F33615-76-C-5026 (April 15, 1977)

	Fe
0.16	C
14	Co
10	Ni
2	Cr
1	Mo

AF1410

REFERENCES (Cont'd)

6. ibid Report IR 160-6 (VII), AF Contract F33615-76-C-5026 (October, 1977)
7. Little, C. D., Machmeier, M. P., "Development of a Weldable High Strength Steel", General Dynamics Fort Worth, AFML-TR-76-148, AF Contract 33615-73-C-5093 (September, 1975)
8. Routh, W. E., "Lower Cost by Substituting Steel for Titanium", Rockwell International, Los Angeles Div. AFFDL-TR-77-73 (June 1977)
9. Phase II Development Test Results, Rockwell International, communication from Guy Bennett, Rockwell International to W. F. Brown Jr. (1978)
10. Machmeier, M. P., "Development of a Weldable High Strength Steel", General Dynamics Fort Worth, AFML TR-76-217, AF Contract 33615-76-C-5093/P0006, (December 1976)
11. Shiring, R. R., Milavec, J. L., Black, H. L., "Production Melting and Thermomechanical Processing of AF 1410 Steel", Universal-Cyclops Specialty Steel Div., Report IR-160-6 (VIII) AF Contract F33615-76-C-5026 (January 1978)
12. Machmeier, M. P., Collins, J. C., Jones, R. L., "Weldability of 10 Nickel Modified Type Steel", General Dynamics Fort Worth, AFML-TR-77-61, AF Contract F33615-76-C-5091 (May 1977)
13. Bennet, G., International Rockwell, B-1 Division, Specification No. LB160-184 (June 1, 1978)
14. Black, H. L., Universal-Cyclops Specialty Steel Div. communication to W. F. Brown Jr. (1978)

Alloy	Fe-0.16C-14Co-10Ni-2Cr-1Mo	
Form	Plate, Bar, Forgings & Reforging Stock	
	Percent	
	Min	Max
C	0.13	0.17
Mn	-	0.10
Si	-	0.10
P	-	0.008
S	-	0.005
Cu	1.80	2.20
Ni	9.50	10.50
Co	13.50	14.50
Mo	0.90	1.10
Ti	-	0.015
Al	-	0.015
O	-	0.0015
N	-	0.0015
Total P+S		0.010

TABLE 1.04 COMPOSITION (13)

Alloy	Fe-0.16C-14Co-10Ni-2Cr-1Mo					
Source	(8) p 184-186					
Form	VIM - VAR 1 inch Plate					
Condition	1250F, 8 Hr AC + 1650F, AC + 1500F, 1 Hr Q + R + 950F, 5 Hr					
Quench Medium	Air		Oil		Water	
R-Refrigerated at 100F, 1 Hour	Yes	No	Yes	No	Yes	No
F_{tu}-ksi	246	246	252	252	243	241
F_{ty}-ksi	220	220	229	221	228	223
Charpy V ft. lbs.	47	46	44	44	55	49

TABLE 1.057 TENSILE STRENGTH PROPERTIES & IMPACT ENERGY FOR VIM-VAR MELT PLATE QUENCHED IN AIR, OIL OR WATER FOLLOWING AUSTENITIZING

Alloy	Fe-0.16C-14Co-10Ni-2Cr-1Mo								
Source	(11) p 12 & 13								
Form	VIM - VAR Plate								
Condition	1650F, AC[1] + 1250F, 8 Hr AC + A, B, C or D + 950F, 5 Hr AC								
Thickness (in)	5/8				3				Avg. from many heats
Heat Treat[1][2]	A	B	C	D	A	B	C	D	E
F_{tu} - ksi	229	239	235	241	230	244	215	242	243
F_{ty} - ksi	220	225	216	221	223	223	200	223	231
e - percent	16	17	17	17	16	17	18	17	-
R. A. - percent	69	69	70	73	66	70	68	69	-
Charpy V ft. - lbs.	67	61	62	83	48	60	43	70	68

1. Time at 1600 or 1500F - 5/8 inch plate. 1 Hr, 3 inch plate. 3 Hrs
2. A 1500F, WQ
   B 1500F, AC + (-100F)
   C 1500F, Vermiculite cool + (-100F)
   D 1650F, AC + 1500F, AC + (-100F)
   E 1650F, WQ + 1500F, WQ + 950F, 5 Hr AC

TABLE 1.058 EFFECT OF VARIOUS HEAT TREATMENTS ON TENSILE IMPACT PROPERTIES OF 5/8 IN & 3 IN VIM-VAR MELT PLATE

	Fe
0.16	C
14	Co
10	Ni
2	Cr
1	Mo

AF1410

Alloy	Fe-0.16C-14Co-10Ni-2Cr-1Mo		
Source	(9) p 6 & 7		
Form	VIM - VAR 2 inch Thick Plate		
Condition[2]	1250F, 8 Hr AC[1] + 1650F, 1 Hr Q + 1525F, 1 Hr Q + (-100F, 1 Hr) + 950F, 5 Hr AC		
Quench Medium	Air	Oil	Water
F_{tu} - ksi	244	254	249
F_{ty} - ksi	214	224	223
e - percent	16	16	16
R.A. percent	69	69	70
Charpy V ft. - lbs.	51	48	48
K_{IC} - ksi $\sqrt{in}$	158	140	146

1. Premachining heat treatment
2. Heat treated in 2 inch thickness

TABLE 1.059 TENSILE PROPERTIES, IMPACT ENERGY & FRACTURE TOUGHNESS OF VIM-VAR MELT 2 INCH PLATE QUENCHED IN SEVERAL MEDIA & GIVEN A PREMACHINING HEAT TREATMENT

Alloy	Fe-0.16C-14Co-10Ni-2Cr-1Mo		
Source	(10) p 148-9		
Composition Percent	VIM - ESR Melt Plate		
Melt	A	D	E
C	0.15	0.15	0.16
Co	13.40	13.61	13.76
Ni	9.23	9.66	9.64
Cr	1.46	1.79	1.72
Mo	0.91	1.12	1.07
Mn	0.14	0.18	0.17
Si	< 0.01	< 0.01	< 0.01
Al	< 0.01	< 0.01	< 0.01
Ti	< 0.01	< 0.01	< 0.01
V	< 0.01	< 0.01	< 0.01
S	0.003	0.006	0.007
P	0.010	0.010	0.014
N ppm	13	11	5
O ppm	320	220	88
H ppm	2	2	4
		ESR Slag	
CaF_2	30	70	70
Al_2O_3	15	22	20
CaO	3	6	8
MgO	2	2	2

TABLE 1.0811 PLATE & ESR SLAG COMPOSITIONS FOR 2000 lb VIM MELT REMELTED INTO ESR INGOTS

Alloy	Fe-0.16C-14Co-10Ni-2Cr-1Mo				
Source	(1) p 32 (4) p 8				
Melt Practice	VIM-ESR				
Heat	R3	R4	R5	R6	L3616R1
Slag Composition Percent					
CaF_2	30	55	70	30	30
CaO	40	22	20	40	40
Al_2O_3	30	15	10	30	30
SiO_2	-	8	-	-	-
Ca[1]	0.032	0.047	0.045	0.14	0.02
Mg	-	-	-	-	0.08

1. Ca added as 30% Ca-Si alloy at 5 minute intervals during melting

TABLE 1.0812 SLAG COMPOSITIONS USED IN MAKING ESR REMELTS

Alloy	Fe-0.16C-14Co-10Ni-2Cr-1Mo											
Source	(1) p 10 & 36 (3) p 10											
Melt Practice	VIM		VIM-VAR[1]				VIM-ESR[2]				AOD-ESR[3]	AOD-ESR-VAR[3]
Heat	L3550	L3614	K-19	K-20	K13	K18	R3	R4	R5	R6	R2	K2
Oxygen ppm	10	12	6	6.5	3.5	4.5	36	53	46	47	28	5

1. K-19 & K-20 from L3550
   K13 & K18 from L3614
2. From L3550
3. From 3-957 VIM + Argon Oxygen Deoxidized Electric Furnace Heat (AOD)

TABLE 1.0813 OXYGEN LEVELS IN INGOTS PRODUCED BY VARIOUS MELTING PRACTICES

Alloy	Fe-0.16C-14Co-10Ni-2Cr-1Mo									
Source	(2) p 14									
Form	1.25 and 1.4 inch Plate									
Condition	1650F, 1/2 hour WQ + 1500F, 1/2 hour WQ + 950F, 5 hours AC									
Melt Practice	VIM-ESR[1]								VIM-ESR[2]	
Heat	R3		R4		R5		R6		L3616R1	
Direction	L	T	L	T	L	T	L	T	L	T
F_{tu} - ksi	249	245	245	241	246	241	253	245	245	249
F_{ty} - ksi	229	228	230	229	229	225	236	229	233	236
Charpy V[3] ft - lbs @ OF	37	28	26	29	36	27	14	13	38	32

1. 1.4 inch plate
2. 1.25 inch plate
3. L - LT direction T - TL direction

TABLE 1.0814 TENSILE & IMPACT PROPERTIES OF 1.25 & 1.4 INCH THICK PLATE FROM VIM-ESR MELTS

	Fe
0.16	C
14	Co
10	Ni
2	Cr
1	Mo

AF1410

Alloy	Fe-0.16C-14Co-10Ni-2Cr-1Mo							
Source	(2) p. 6 (3) p. 15 (5) p. 3							
Form	1.25 Inch Plate							
Condition	1650F, ½ hour WQ + 1500F, ½ hour WQ + 950F, 5 hour AC							
Melt Practice	VIM-VAR		ADO[1]-VAR		ARC-ADO-ESR		ARC-ADO-ESR-VAR	
Heat	L3550K20		3-957K11		3-957R2[3]		3-957K2[3]	
Direction	L	T	L	T	L	T	L	T
F_{tu} - ksi	252	255	232	235	229	218	231	231
F_{ty} - ksi	232	233	223	222	226	217	220	220
Charpy V[2] ft-lb at 0 F	62	59	40	40	46	45	73	41

1. Argon oxygen deoxidation electric furnace melt.
2. L - LT direction, T - TL direction.
3. See Table 1.0813 for O_2 content.

TABLE 1.0815 TENSILE & IMPACT PROPERTIES OF 1.25 THICK PLATE FROM VARIOUS MELTING PRACTICES

Alloy	Fe-0.16C-14Co-10Ni-2Cr-1Mo								
Source	(2) p 10								
Form	3 Inch Plate								
Condition	1650F, ½ hour WQ + 1500F, ½ hour WQ + 950F, 5 hours AC								
Melt Practice	VIM			VIM-VAR			VIM-VAR		
Heat	L3550			L3550K19[1]			L3550K20[2]		
Direction	L	T	ST	L	T	ST	L	T	ST
F_{tu} - ksi	253	261	259	241	250	247	247	247	249
F_{ty} - ksi	239	251	239	227	229	227	226	227	230
RA - percent	64	59	53	72	68	67	70	69	65
e - percent	14	14	13	16	15	14	16	16	15
Charpy V[3] ft - lbs at 0 F	37	36	17	65	61	56	56	50	44

1. VAR stirred
2. VAR not stirred
3. L - LT direction, T - TL direction, ST - SL direction

TABLE 1.0816 TENSILE & IMPACT PROPERTIES OF 3 INCH THICK PLATE FROM VIM & VIM-VAR MELTS

Alloy	Fe-0.16C-14Co-10Ni-2Cr-1Mo									
Source	(2) p 12 & 13 (4) p 9									
Form	3 Inch Plate									
Condition	1650F, ½ hour WQ + 1500F, ½ hour WQ + 950F, 3 hours AC									
Melt Practice	VIM-ESR[1, 2]								VIM-ESR[2]	
Heat	R3		R4		R5		R6		L3616R1	
Direction	L	ST	L	ST	L	ST	L	ST	L	ST
F_{tu} - ksi	251	245	256	240	246	244	246	244	232	234
F_{ty} - ksi	228	225	239	218	228	229	232	229	223	222
Charpy V[3] ft - lbs @ 0 F	29	22	31	21	29	23	9	7	33	17

1. Parent VIM Heat L3550
2. See Table 1.083 for slag composition & deoxidation
3. L - LT direction, T - TL direction, ST - SL direction

TABLE 1.0817 TENSILE & IMPACT PROPERTIES OF THREE INCH THICK PLATE FROM VARIOUS MELTING PRACTICES

Alloy	Fe-0.16C-14Co-10Ni-2Cr-1Mo					
Source	(3) p 15 (5) p 7					
Form	3 Inch Plate					
Condition	1650F, ½ hour WQ + 1500F, ½ hour WQ + 950F 5 hours AC					
Melt Practice	ADO-VAR[1]		ARC-ADO-ESR		ARC-ADO-ESR-VAR	
Heat	3-957K11		3-957-R2[3]		3-957-K2[3]	
Direction	L	ST	L	ST	L	ST
F_{tu} - ksi	236	239	229	227	231	227
F_{ty} - ksi	224	226	222	219	222	218
Charpy V[2] ft - lbs @ 0 F	38	31	42	24	47	28

1. Argon oxygen deoxidation
2. L-LT direction, T-TL direction, ST-SL direction
3. See Table 1.0813 for O_2 content

TABLE 1.0818 TENSILE & IMPACT PROPERTIES OF THREE INCH THICK PLATE FROM VARIOUS ADO MELTING PRACTICES

	Fe
0.16	C
14	Co
10	Ni
2	Cr
1	Mo

AF1410

Alloy	Fe-0.16C-14Co-10Ni-2Cr-1Mo							
Source	(3) p 30 (5) p 13							
Form	1 1/2 & 1 3/4 Inch Thick Upset Disks							
Condition	1650F, ½ hour WQ + 1500F, ½ hour WQ + 950F, 5 hours AC							
Melt Practice	VIM-VAR(2)		VIM-ESR(3)		ARC-AOD-VAR(2)		ACR-AOD(1)-ESR(3)	
Heat	L3614K18		L3614R1		3-957K11		3-957R2	
Direction	R	T	R	T	R	T	R	T
F_{tu} - ksi	249	246	245	246	236	241	227	229
F_{ty} - ksi	232	232	234	232	223	224	215	219
RA percent	63	67	60	61	65	64	67	68
Charpy V ft-lbs at O F	45	46	34	32	33	37	49	53

1. Argon oxygen deoxidation electric furnace heat
2. 1 3/4 inch thick
3. 1 1/2 inch thick
4. R - RT direction, T - TR direction

TABLE 1.0819 TENSILE & IMPACT PROPERTIES OF 1 1/2 & 1 3/4 INCH THICK UPSET DISKS FROM VARIOUS MELTING PRACTICES

Alloy	Fe-0.16C-14Co-10Ni-2Cr-1Mo											
Source	(3) p 28 (5) p 11											
Form	6 Inch Thick Upset Disks											
Condition	1650F, ½ hour WQ + 1500F, ½ hour WQ + 950, 5 hours AC											
Melt Practice	VIM-VAR			VIM-ESR			ARC-AOD(1)-VAR			ARC-AOD-ESR		
Heat	L3614K18			L3614R1			3-957K11			3-957R2		
Direction	R	T	ST	R	T	ST	R	T	ST	R	T	ST
F_{tu} - ksi	230	229	229	238	239	239	240	230	236	227	224	224
F_{ty} - ksi	215	212	211	222	223	221	219	211	215	214	210	209
RA percent	68	69	68	50	58	61	62	64	63	67	63	65
Charpy V(2) ft-lbs at O F	44	44	43	20	25	28	28	28	29	28	26	28

1. Argon oxygen deoxidation electric furnace heat
2. R - RT direction, T - TR direction, ST - ST direction

TABLE 1.08110 TENSILE & IMPACT PROPERTIES OF 6 INCH THICK UPSET DISKS FROM VARIOUS MELTING PRACTICES

Alloy	Fe-0.16C-14Co-10Ni-2Cr-1Mo				
Form	Plate, Bar, Forgings & Reforging Stock				
Melting	VIM-VAR				
Condition	1600 to 1650F, 1 hr AC + 1500 to 1550F, 1 hr, AC + (-90 to -110F, 1 hr) + 940 to 960F, 5 hr, AC				
Thickness (inches)	F_{tu}(min), ksi	F_{ty}(min), ksi	e(min), 2 in, %	R. A. (min), %	K_{Ic}(1)(min) ksi $\sqrt{in}$
t < 1.00	235	220	12	60	-
1.00 < t < 1.50	235	215	12	60	-
1.50 < t < 2.00	235	210	12	60	130
2.00 < t < 2.50	235	200	12	60	130
2.50 < t(2)					

1. Applies to product 1.5 inch thick or over. For thinner products report K_Q. WL orientation
2. As negotiated with supplier

TABLE 3.011 FABRICATORS MECHANICAL PROPERTY SPECIFICATION (13)

Alloy	Fe-0.16C-14Co-10Ni-2Cr-1Mo															
Source	11(p 17)															
Form	Wing Sweep Actuator Forging VIM-VAR Melt															
Condition	Forging Heat Treat: 1650F, 1 hour AC + 1250F, 8 hours AC															
Specimen Heat Treat	1650F, ½ hour WQ + 1500F, ½ hour WQ + 950F, 5 hours AC								1500F, ½ hour AC + (-100F, ½ hour) + 950F, 5 hours AC							
Location(1)	1	2	3	4	5	6	7	8	1	2	3	4	5	6	7	8
F_{tu} - ksi	252	256	246	234	244	255	237	243	256	229	233	231	252	235	230	253
F_{ty} - ksi	236	239	229	222	223	236	223	232	237	214	218	217	233	218	217	232
e - percent	17	18	18	17	17	17	17	17	17	17	17	16	17	16	16	15
RA percent	73	73	75	75	74	72	77	72	68	67	68	66	66	67	68	63
Charpy V ft-lbs	86	94	82	-	94	-	-	83	50	53	56	-	50	-	-	51

1. For location in forging, see Fig. 3.0218

TABLE 3.0219 TENSILE & IMPACT PROPERTIES FOR SINGLE & DOUBLE AUSTENITIZED SPECIMENS CUT FROM VIM-VAR MELT WING SWEEP ACTUATOR FORGING

	Fe
0.16	C
14	Co
10	Ni
2	Cr
1	Mo

AF1410

Alloy	Fe-0.16C-14Co-10Ni-2Cr-1Mo	
Source	(11) p 20	
Form[1]	Wing Sweep Actuator Forging (Location 1) VIM-VAR Melt	
Condition	Forging Heat Treat: 1650F, 1 hour AC + 1250F, 8 hours AC	
Specimen Heat Treat	1650F ½ hr AC + 1500F, ½ hr AC + (-100F, ½ hr) + 950F, 5 hrs AC	1500F ½ hr AC + (-100F ½ hr) + 950F, 5 hrs AC
F_{tu} - ksi	254	256
F_{ty} - ksi	228	237
e - percent	17	17
RA - percent	72	68
Charpy V ft - lbs	64	59

1. For specimen location see Fig. 3.0218

TABLE 3.02110 TENSILE & IMPACT PROPERTIES OF SINGLE & DOUBLE AUSTENITIZED & REFRIGERATED SPECIMENS CUT FROM VIM-VAR MELT WING SWEEP ACTUATOR FORGING

Alloy	Fe-0.16C-14Co-10Ni-2Cr-1Mo							
Source	(11) p 23							
Form	Wing Sweep Actuator Forging VIM-VAR Melt							
Condition	Forging Heat Treat: 1650F, 1 hour AC + 1250F, 8 hours AC							
Specimen Heat Treat	1650F, ½ hour WQ + 1500F, ½ hour WQ + 950F, 5 hours AC				1500F, ½ hour AC + (-100F, ½ hour) + 950F, 5 hours AC			
Forging Test Location[1]	1	2	3	4	1	2	3	4
F_{cy} - ksi	256	255	260	259	250	234	250	234
E_c - 1000 ksi	30.1	29.8	29.3	28.7	31.1	29.9	30.5	28.3

1. For test locations see Fig. 3.0218

TABLE 3.0221 COMPRESSIVE YIELD STRENGTH & ELASTIC MODULUS FOR SINGLE & DOUBLE AUSTENITIZED SPECIMENS CUT FROM VIM-VAR MELT WING SWEEP ACTUATOR FORGING

Alloy	Fe-0.16C-14Co-10Ni-2Cr-1Mo			
Source	(8) p 79			
Form	VIM-VAR 2 Inch Plate			
Condition	1650F, 1 hour WQ + 1500F, 1 hour WQ + 950F, 5 hours AC			
Direction	LT		TL	
Temp - F	RT	-65	RT	-65
K_{Ic} - ksi $\sqrt{in}$	140	110	137	111
F_{ty} - ksi	228	236	228	249

TABLE 3.02722 PLANE STRAIN FRACTURE TOUGHNESS OF VIM-VAR MELT PLATE TESTED IN TWO DIRECTIONS AT ROOM AND LOW TEMPERATURE

Alloy	Fe-0.16C-14Co-10Ni-2Cr-1Mo		
Source	(11) p 24 (15)		
Form	Wing Sweep Actuator Forging VIM-VAR Melt		
Condition	Forging Heat Treat: 1650F, 1 hour AC + 1250F, 8 hours AC		
Specimen Heat Treat	1650F, ½ hour WQ + 1500F, ½ hour WQ + 950F, 5 hours AC	1500F, ½ hour AC + (-100F, ½ hour) + 950F, 5 hours AC	
Location[1]	5	1	5
F_{ty} - ksi	228	237	233
K_{Ic} - ksi $\sqrt{in}$[2]	196[3]	151	154

1. For location see Figure 3.0218
2. Specimen 1.5 inch thick
3. K_Q

TABLE 3.02724 PLANE STRAIN FRACTURE TOUGHESS VALUES FOR SINGLE & DOUBLE AUSTENITIZED SPECIMENS CUT FROM VIM-VAR MELT WING SWEEP ACTUATOR FORGING

Alloy	Fe-0.16C-14Co-10Ni-2Cr-1Mo		
Source	(3) p 19, p 15		
Form	VIM-VAR 3 Inch Plate		
Condition	1650F, 1 hour WQ + 1500F, 1 hour WQ + 950F, 5 hours AC		
Direction	LT	TL	SL
K_{Ic} - ksi $\sqrt{in}$	154	142	136
F_{ty} - ksi	233	230	230

TABLE 3.02723 PLANE STRAIN FRACTURE TOUGHNESS OF 3 INCH VIM-VAR MELT PLATE

Alloy	Fe-0.16C-14Co-10Ni-2Cr-1Mo	
Source	(5) p 16	
Form	VIM-VAR 1 1/4 Inch Plate	
Condition	1650F, ½ hour WQ + 1500F, ½ hour WQ + 950F, 5 hours AC	
Direction	L	T
E-1000 ksi	29.3	29.4

TABLE 3.0621 ELASTIC MODULUS IN TENSION FOR VIM-VAR 1 1/4 INCH PLATE

	Fe
0.16	C
14	Co
10	Ni
2	Cr
1	Mo

AF1410

Alloy	Fe-0.16C-14Co-10Ni-2Cr-1Mo			
Source	(12) p 24			
Form	Filler Wire 0.062 Inch Diameter			
Heat	VE 798	VE 799	VE 800	VE 717
C	0.18	0.15	0.16	0.16
Co	14.34	13.76	14.06	14.30
Ni	10.36	9.82	9.99	9.94
Cr	1.92	1.90	1.94	2.13
Mo	1.04	1.00	1.06	0.93
Si	0.16	< 0.01	0.16	0.11
Al	0.015	0.025	0.031	0.028
V	0.029	< 0.01	< 0.01	0.015
Mn	< 0.05	< 0.05	< 0.05	< 0.03
Ti	< 0.01	< 0.01	< 0.01	< 0.01
S	0.007	0.005	0.005	0.007
P	< 0.001	< 0.001	< 0.001	0.006
O	37 ppm	52 ppm	74 ppm	28 ppm
N	3 ppm	4 ppm	2 ppm	4 ppm
H	1 ppm	1 ppm	2 ppm	1 ppm

TABLE 4.0314 FILLER WIRE COMPOSITIONS USED IN CERTAIN WELD PROPERTY STUDIES

Alloy	Fe-0.16C-14Co-10Ni-2Cr-1Mo	
Source	(8) p 64	
Form	Filler Wire	
Heat	L3616K13	TLA2606
C	0.17	0.15
Co	13.98	13.76
Ni	10.10	9.82
Cr	1.91	1.90
Mo	0.97	1.00
Si	0.04	< 0.01
Al	0.003	0.025
Mn	0.06	< 0.05
Ti	0.004	< 0.01
S	0.001	0.005
P	0.004	< 0.001
O	300 ppm	520 ppm
N	200 ppm	400 ppm

TABLE 4.0315 FILLER WIRE COMPOSITIONS USED IN CERTAIN WELD PROPERTY STUDIES

Alloy	Fe-0.16C-14Co-10Ni-2Cr-1Mo		
Source	(12) p 12		
Plate thickness, inch	1/2		1 1/8
Weld groove	40° Double J		40° Double U
Electrode diameter, inch	1/8		1/8
Electrode type	W - 2 Th		W - 2 Th
Wire diameter, inch	0.062		0.062
Total passes	11 - 16		29 - 30
Interpass, F	100 - 150		100 - 160
Back up gas, cu ft per hour	A, 10 - 12		A, 10 - 12
Torch gas, percent	75 He - 25 A		75 He - 25 A
Flowrate, cu ft per hour	60		60
Pulsed arc Current, amp - secs	200-5 / 160-15	or { 200-15 / 160-5	200-15 / 160-5
Arc voltage	14	or 13	13
Arc travel, inch per min.	4		4
Heat input, K_j per inch	35.7	or 37.1	37.1 - 38.5
Deposition Rate - lbs per hour	1.1		1.1

TABLE 4.0316 WELD PARAMETERS FOR AUTOMATIC PULSED ARC GW-GTA WELDING

Alloy	Fe-0.16C-14Co-10Ni-2Cr-1Mo	
Source	(12) p 48	
Form	1 1/8 inch Plate	
Condition	1650F, 1 hour WQ + 1500F, 1 hour WQ + GW-GTA Weld(1) + 950F, 4 hours WQ	
Test Condition	Alternate Immersion (10 min. in 3.5% NaCl + 50 min. Air Dry) at 165 ksi. Specimen Axis Normal to Weld	
Specimen No.	Failure Time, Hours	Remarks
4c4	488	Crack initiated in HAZ
4c6	199	Failed at tool mark in head radius

1. Weld wire heat VE799 (Table 4.0314). See Table 4.0316 for welding parameters.

TABLE 4.0317 ALTERNATE IMMERSION STRESS CORROSION DATA IN 3.5% NaCl FOR GW-GTA WELDS IN VIM-VAR PLATE

	Fe
0.16	C
14	Co
10	Ni
2	Cr
1	Mo

AF1410

Alloy	Fe-0.16C-14Co-10Ni-2Cr-1Mo							
Form	VIM VIM-VAR ½ inch Plate (Rectangular Cross-section Specimens)							
Source	(5) p 125 & 126							
Condition	1650F, 1 hour WQ + 1500F, 1 hour WQ + Weld + 950F, 5 hours AC							
Weld	Double U Groove, Manual, Stringer Bead CW-GTA Butt Welds, 0.062 Matching Filler With Argon Shield							
Surface Condition	Weld Bead On		Bead Ground Off		Single Repair Bead Ground off		Multiple Repair Bead Ground off	
Test Temp F	RT	-65[1]	RT	-65	RT	-65	RT	-65
F_{tu} - ksi[2]	248	255	232	256	236	254	239	254
F_{ty} - ksi	230	-	220	-	219	-	204	-
e(2 in.) percent	12.5	21	12	12	9	11	9	10

1. Specimens failed in parent metal
2. Welds normal to applied load

TABLE 4.0318 TENSILE PROPERTIES AT ROOM TEMPERATURE AND -65F FOR MANUAL CW-GTA PLATE BUTT WELDS AND REPAIR WELDS WITH AND WITHOUT BEAD REMOVAL

Alloy	Fe-0.16C-14Co-10Ni-2Cr-1Mo									
Source	(12) p 33									
Form	½ inch Plate VIM-VAR Melt									
Condition	1650F, ½ hour WQ + 1500F, ½ hour WQ + Weld									
Weld[1] Process	Filler[3] Wire	Heat Input Kj per in.	Deposition Rate, lbs per hr	Fusion Zone Impurities Al	Si	S	P	O	N	Fusion Zone C_{vng}-ft-lbs[4] As Deposit	Aged[2]
CW-GTA	VE717	33.2	1.1	0.086	0.21	0.007	0.006	69	5	35.4	24.4
	VE799	37.1	1.1	0.025	<0.01	0.005	0.001	52	4	40.4	47.3
HW-GTA	VE717	33.8	5.6	0.061	0.20	0.003	0.006	195	62	18.3	16.2
CW-PA	VE717	93.6	3.4	0.095	0.22	0.006	0.007	90	102	23	13.3

1. CW-GTA Cold wire gas tungsten arc
   HW-GTA Hot wire GTA
   CW-PA Cold wire plasma arc
2. Age 950F, 5 hours
3. For wire composition see Table 4.0314
   For weld parameters see Table 4.0316
4. LT orientation, L in weld direction

TABLE 4.03112 EFFECTS OF HEAT INPUT AND FILLER WIRE IMPURITIES ON FUSION ZONE IMPACT ENERGY

Alloy	Fe-0.16C-14Co-10Ni-2Cr-1Mo	
Source	8 (p 131)	
Form	VIM-VAR ½ inch Plate	
Condition	1650F, 1 hour WQ + 1500F, 1 hour WQ + Weld + 950F, 5 hours AC	
Weld Location	Manual Stringer Bead CW-GTA Butt Welds[1] Weld	HAZ
Charpy V[1] ft-lbs		
Average	49.7	44.5
Std. Dev.	5.0	5.6

1. See Table 4.0318 for tensile properties & weld parameters

TABLE 4.03113 IMPACT ENERGY FOR GTA WELD METAL & HAZ IN VIM-VAR MELT ½ INCH PLATE

Alloy	Fe-0.16C-14Co-10Ni-2Cr-1Mo	
Source	(7) p 84	
Form	VIM-VAR 1½ inch Plate	
Condition	Electron Beam Weld	
Specimen No.	E97	E98
K_{Ic} - ksi $\sqrt{in.}$	71.1	72.5
F_{ty} - ksi	230	230

TABLE 4.03115 PLANE STRAIN FRACTURE TOUGHNESS OF ELECTRON BEAM WELDS MADE IN VIM-VAR MELT PLATE

	Fe
0.16	C
14	Co
10	Ni
2	Cr
1	Mo

AF1410

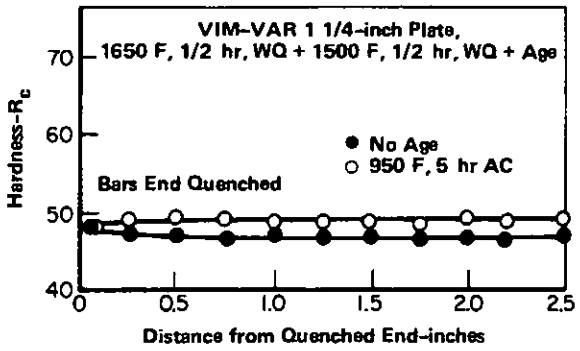


FIGURE 1.061. END QUENCH HARDENABILITY
(5) P. 18

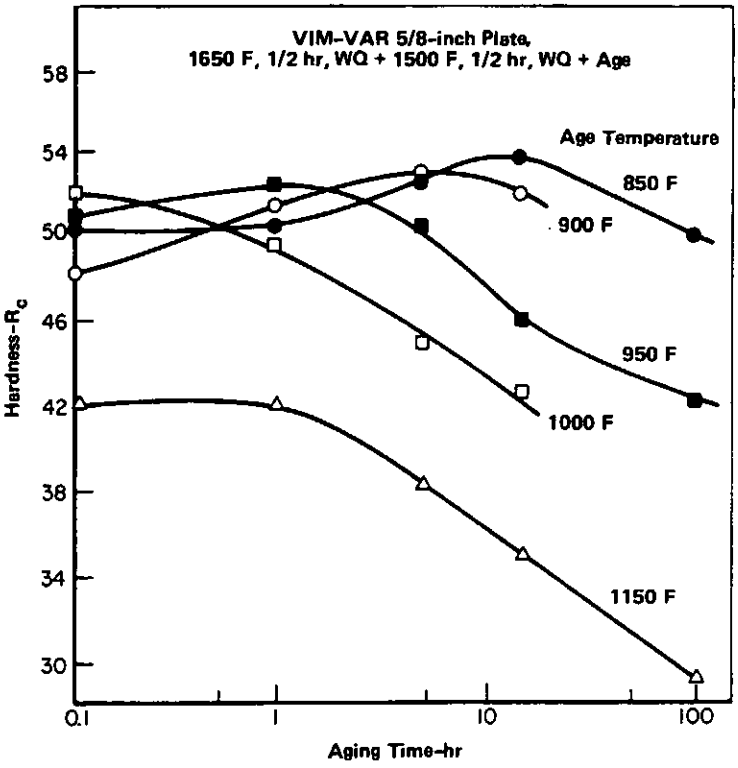


FIGURE 1.062. EFFECT OF AGING TIME AND TEMPERATURE ON HARDNESS OF VIM-VAR MELT PLATE
(7) P. 53

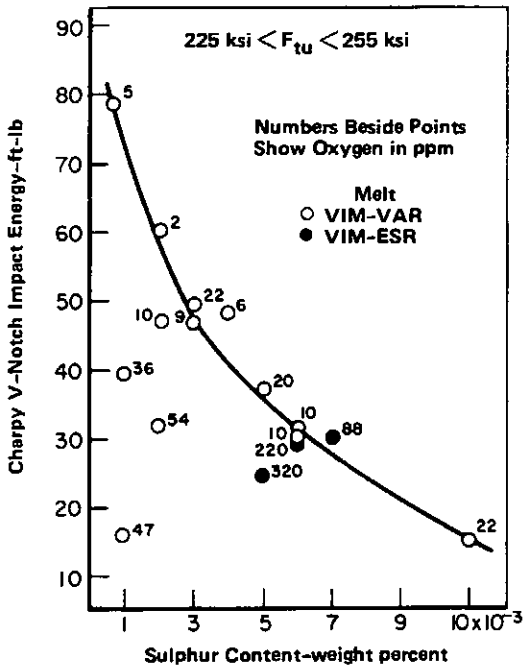


FIGURE 1.094. EFFECT OF SULPHUR AND OXYGEN CONTENT ON THE IMPACT ENERGY OF VIM-VAR AND VIM-ESR MELT ALLOY (12) P. 28

	Fe
0.16	C
14	Co
10	Ni
2	Cr
1	Mo

AF1410

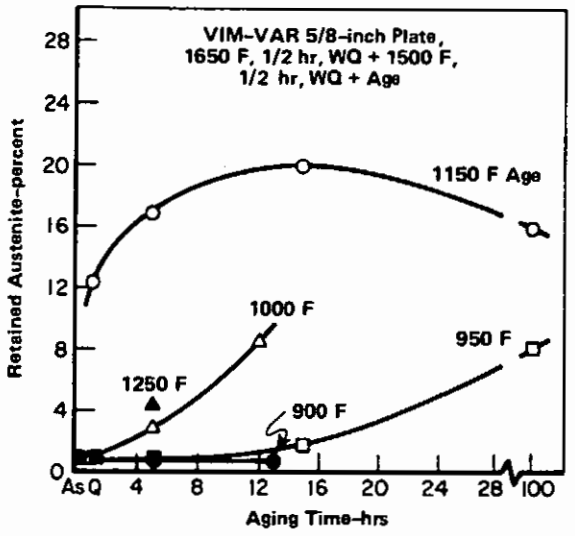


FIGURE 2.0121. EFFECT OF AGING TIME AND TEMPERATURE ON AMOUNT OF RETAINED AUSTENITE IN VIM-VAR MELT PLATE (7) P. 60

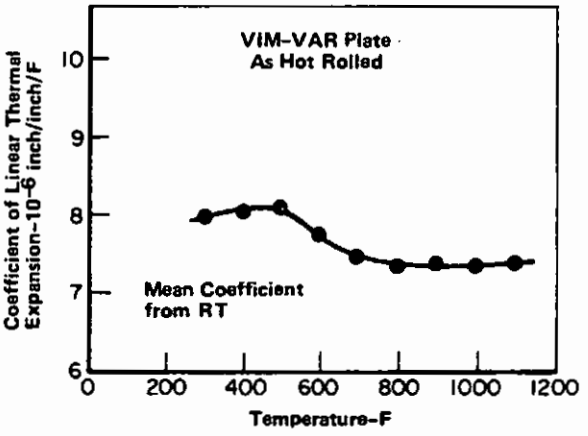


FIGURE 2.0141. MEAN COEFFICIENT OF LINEAR THERMAL EXPANSION (5) P. 17

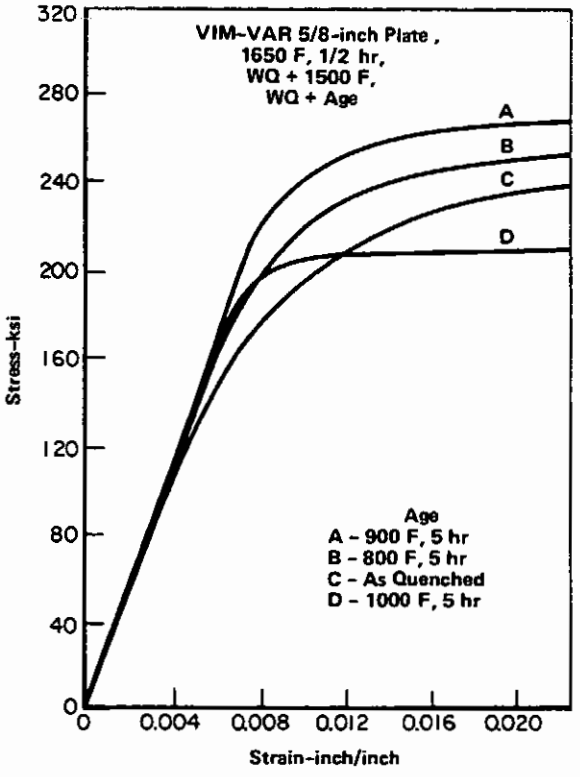


FIGURE 3.0211. EFFECT OF AGING TEMPERATURE ON TENSION STRESS STRAIN CURVES OF VIM-VAR PLATE (7) P. 94

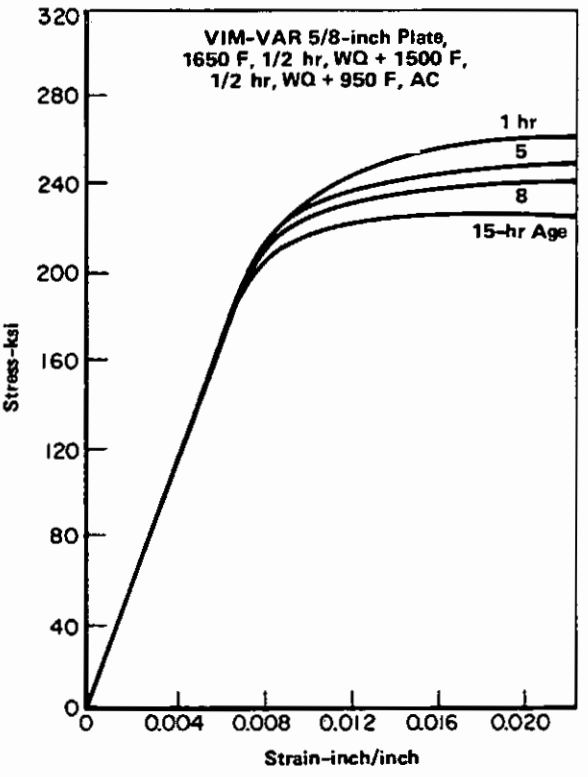


FIGURE 3.0212. EFFECT OF AGING TIME ON TENSION STRESS STRAIN CURVES FOR VIM-VAR PLATE (7) P. 42

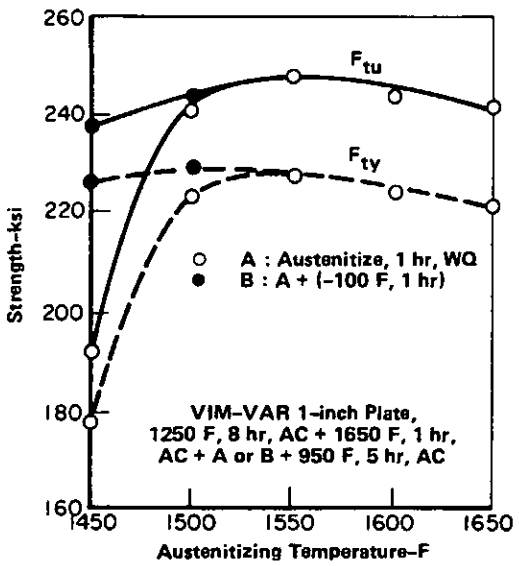


FIGURE 3.0213. EFFECT OF AUSTENITIZING TEMPERATURE AND REFRIGERATION TREATMENT ON PROPERTIES OF VIM-VAR WATER QUENCH PLATE (8) P. 189, 192

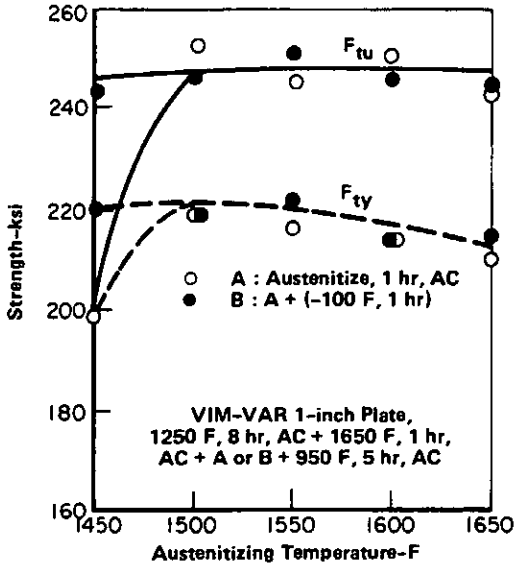


FIGURE 3.0214. EFFECT OF AUSTENITIZING TEMPERATURE AND REFRIGERATION TREATMENT ON TENSILE PROPERTIES OF AIR COOLED VIM-VAR PLATE (8) P. 187, 190

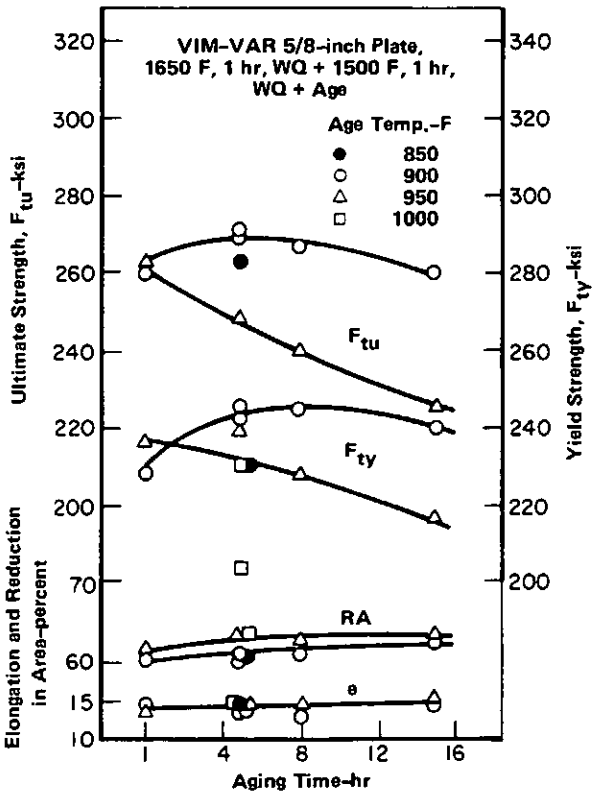


FIGURE 3.0215. EFFECT OF AGING TIME AND TEMPERATURE ON TENSILE PROPERTIES OF VIM-VAR 5/8-INCH PLATE (9) P. 40

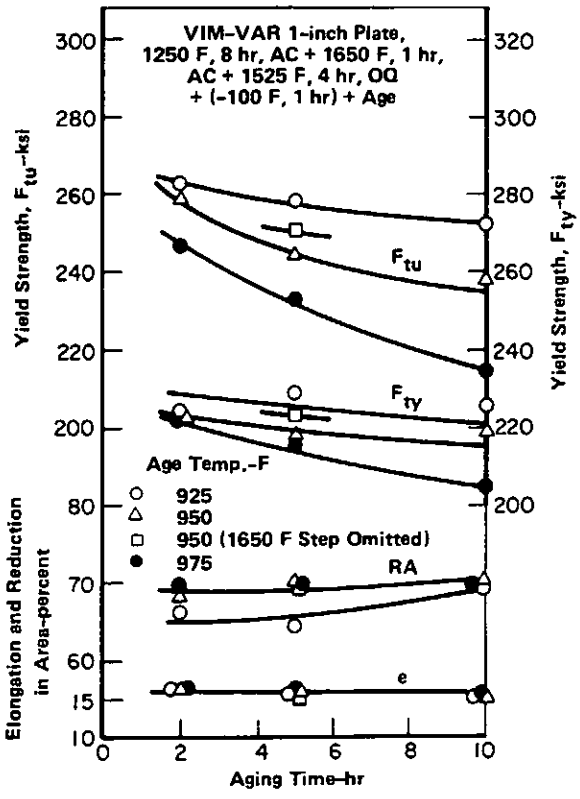


FIGURE 3.0216. EFFECT OF AGING ON TENSILE PROPERTIES OF VIM-VAR 1-INCH PLATE GIVEN A PRE-MACHINING HEAT TREATMENT (9) P. 2

	Fe
0.16	C
14	Co
10	Ni
2	Cr
1	Mo

AF1410

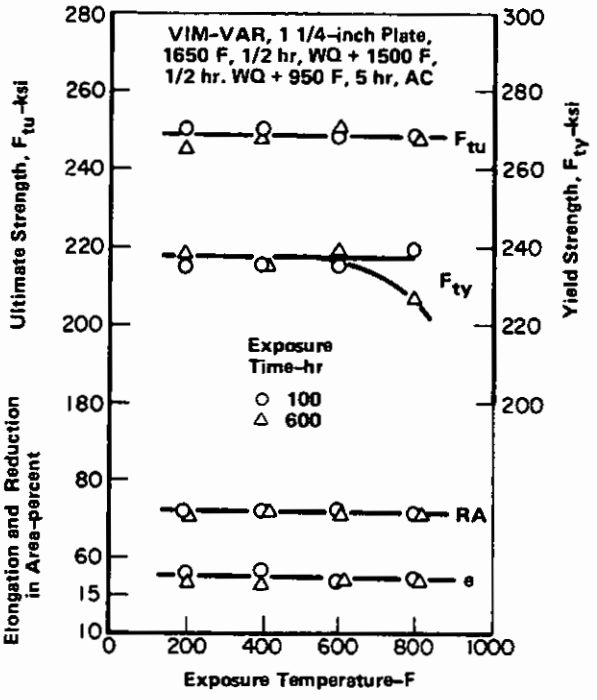
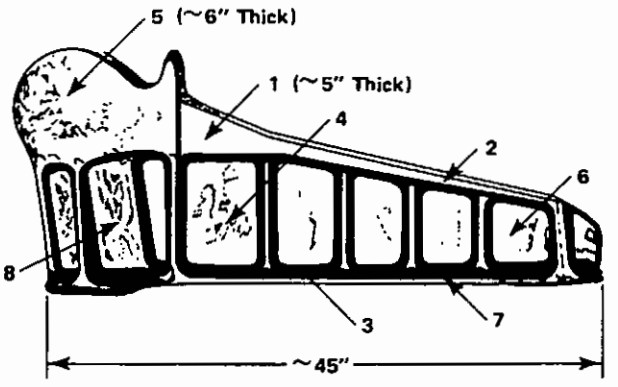


FIGURE 3.0217. EFFECT OF EXPOSURE TO ELEVATED TEMPERATURE ON ROOM TEMPERATURE TENSILE PROPERTIES (6) P. 14



Test Location	Mechanical Tests
1	Tensile, Compression, Charpy, K_{ic}
2	Tensile, Charpy
3	Tensile, Compression, Charpy
4	Tensile, Compression
5	Tensile, Charpy, K_{ic}
6	Tensile, Compression
7	Tensile
8	Tensile, Charpy

FIGURE 3.0218. WING SWEEP ACTUATOR VIM-VAR FORGING SHOWING CRITICAL TEST LOCATIONS AND MECHANICAL TEST SPECIMENS CUT FROM THESE AREAS (11) P. 15

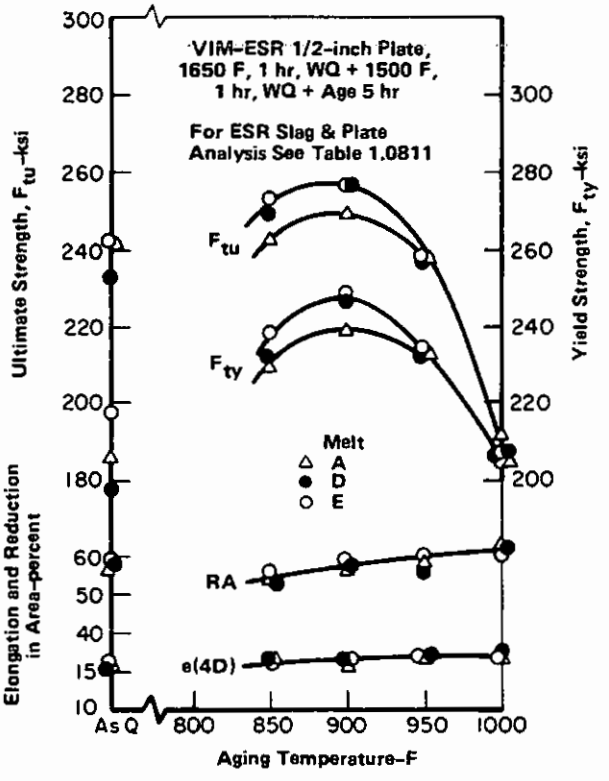


FIGURE 3.02111. EFFECT OF AGING TEMPERATURE ON THE TENSILE PROPERTIES OF THREE VIM-ESR MELTS (10) P. 20

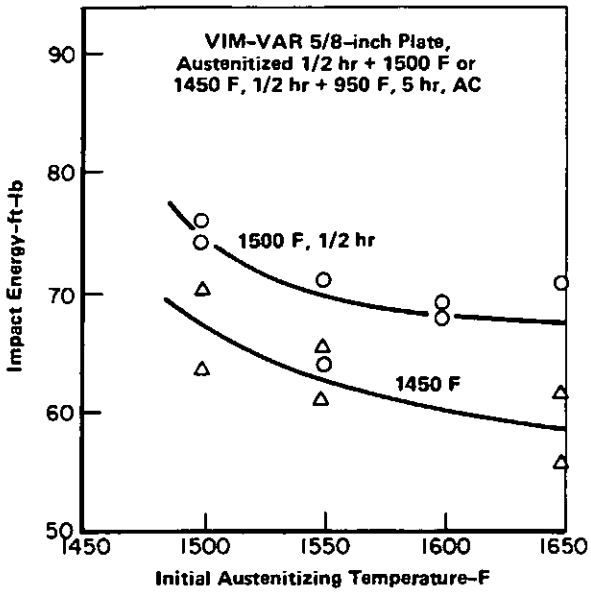


FIGURE 3.0231. EFFECT OF AUSTENITIZING TEMPERATURES ON IMPACT ENERGY OF VIM-VAR MELT PLATE (3) P. 21

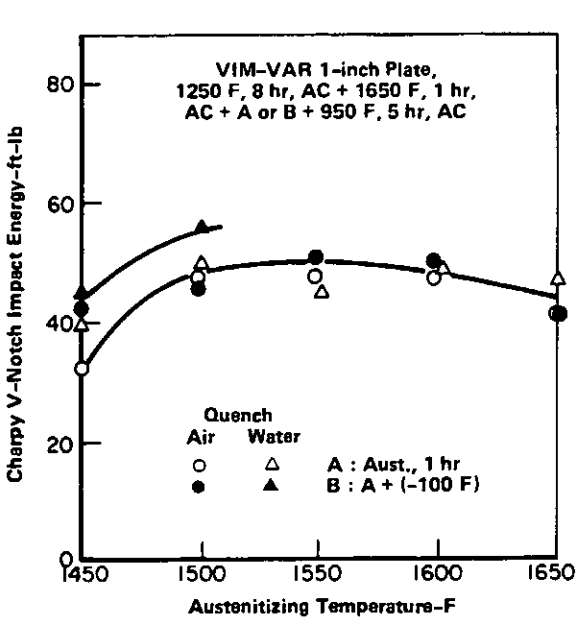


FIGURE 3.0232. EFFECT OF AUSTENITIZING TEMPERATURE AND REFRIGERATION TREATMENT ON IMPACT ENERGY OF VIM-VAR MELT PLATE AIR COOLED OR WATER QUENCHED FROM THE AUSTENITIZING TEMPERATURE (8) P. 193, 195

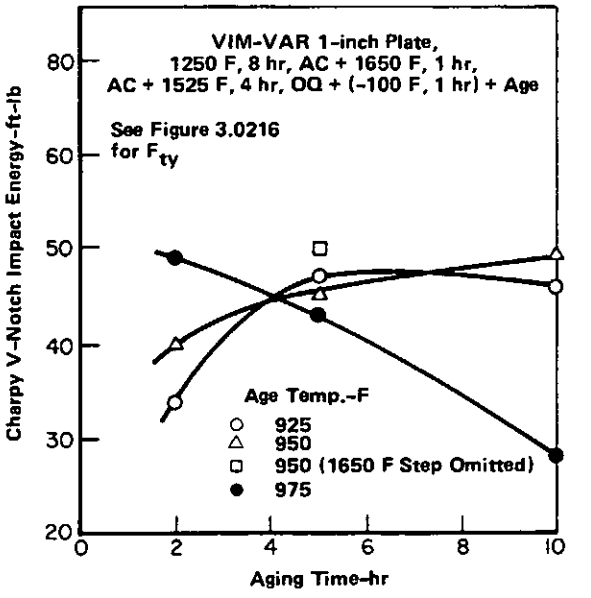


FIGURE 3.0233. EFFECT OF AGING TEMPERATURE AND TIME ON IMPACT ENERGY OF VIM-VAR MELT 1-INCH PLATE GIVEN A PRE-MACHINING HEAT TREATMENT (9) P. 2

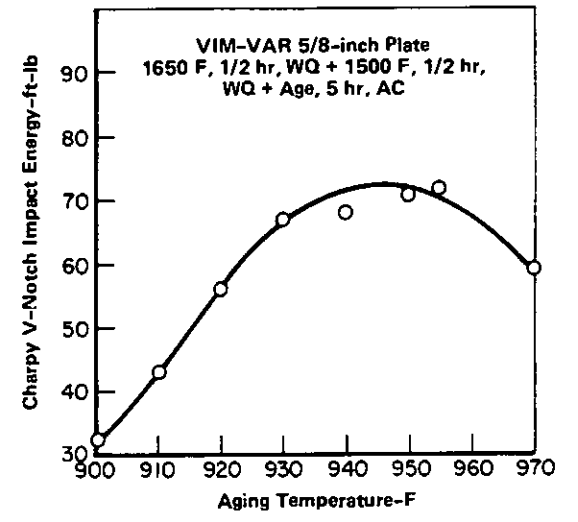


FIGURE 3.0234. EFFECT OF AGING TEMPERATURE ON IMPACT ENERGY OF VIM-VAR PLATE (2) P. 31

	Fe
0.16	C
14	Co
10	Ni
2	Cr
1	Mo

AF1410

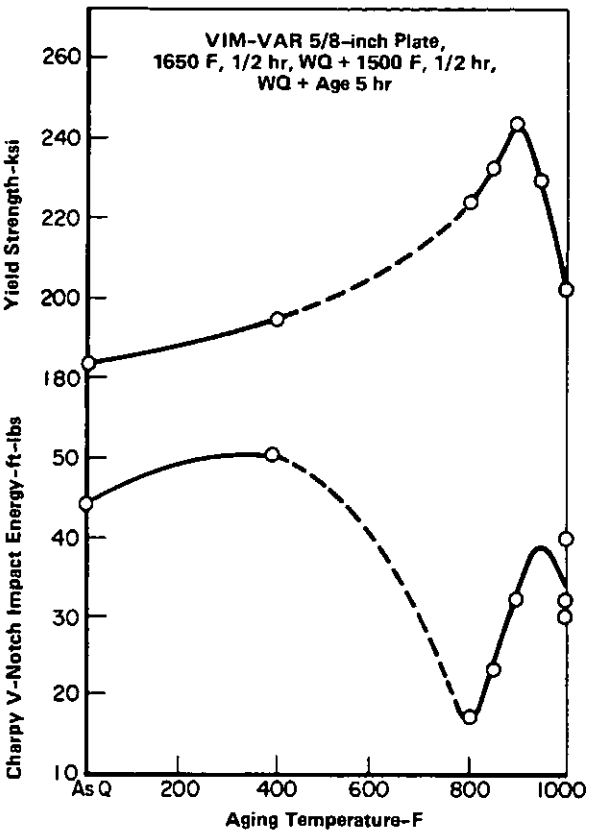


FIGURE 3.0235. EFFECT OF AGING TEMPERATURE ON IMPACT ENERGY AND YIELD STRENGTH OF VIM-VAR PLATE (7) P. 46

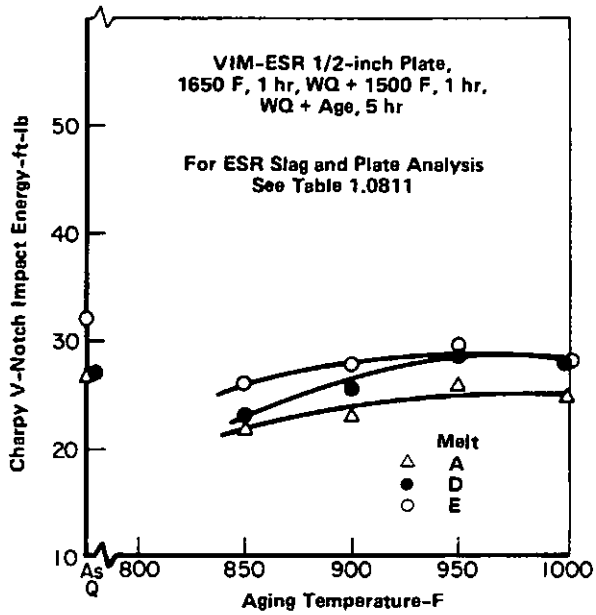


FIGURE 3.0236. EFFECT OF AGING TEMPERATURE ON IMPACT ENERGY OF THREE VIM-ESR MELTS (10) P. 20

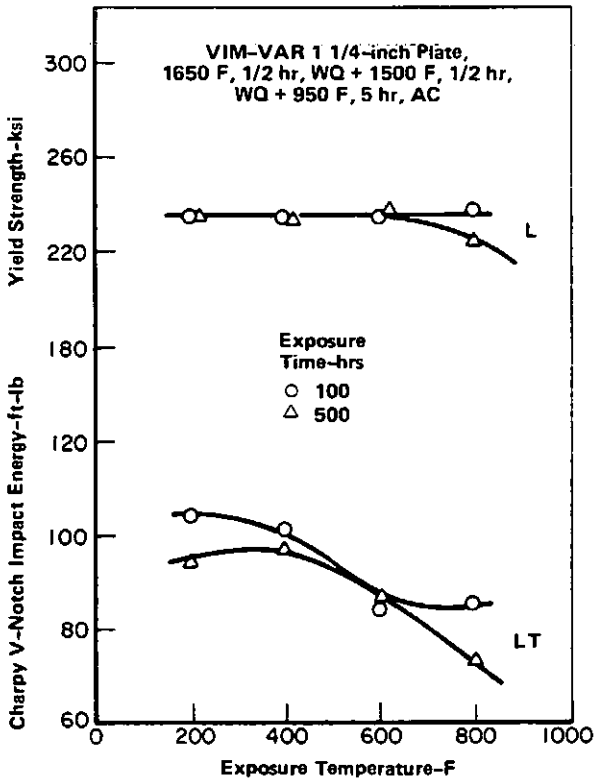


FIGURE 3.0237. EFFECT OF EXPOSURE TO ELEVATED TEMPERATURES ON ROOM TEMPERATURE-CHARPY V IMPACT ENERGY AND TENSILE YIELD STRENGTH OF VIM-VAR MELT PLATE (6) P. 13, 14

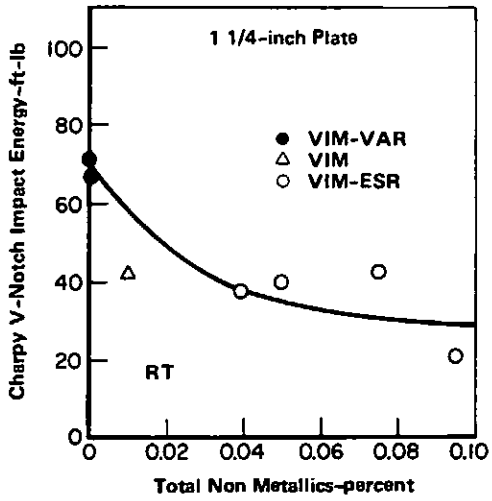
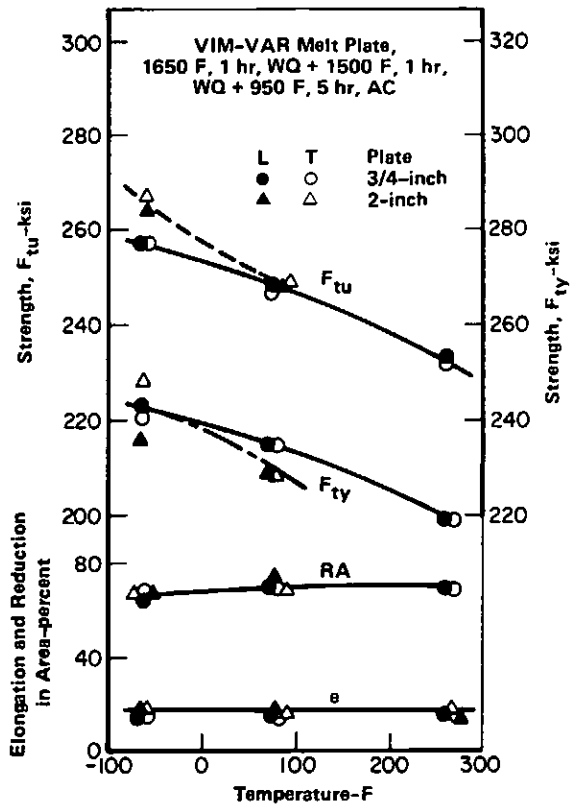


FIGURE 3.0238. CHARPY IMPACT ENERGY FOR PLATE AS FUNCTION OF TOTAL NON-METALLICS AS DETERMINED WITH QUANTITATIVE TELEVISION MICROSCOPE (2) P. 19



	Fe
0.16	C
14	Co
10	Ni
2	Cr
1	Mo

AF1410

FIGURE 3.0311. EFFECT OF TEST TEMPERATURE ON TENSILE PROPERTIES OF 3/4-INCH AND 2-INCH-VIM-VAR-MELT-PLATE (8) P. 73 & 74

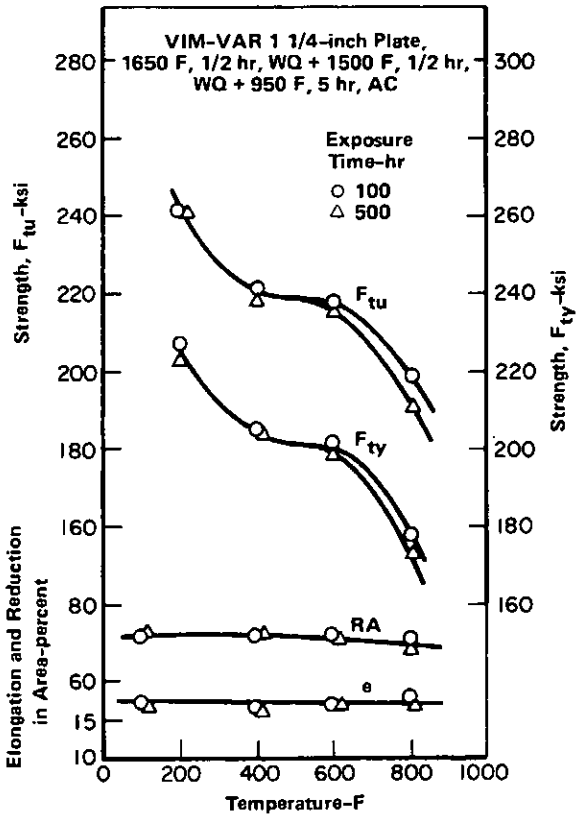


FIGURE 3.0312. EFFECT OF TEST TEMPERATURE ON TENSILE PROPERTIES OF VIM-VAR MELT PLATE EXPOSED AT THE TEST TEMPERATURE (6) P. 14

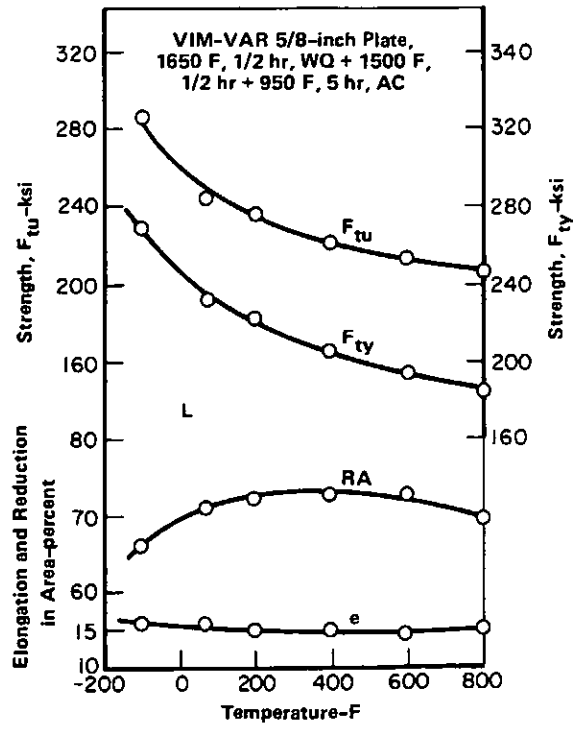


FIGURE 3.0313. EFFECT OF LOW AND ELEVATED TEMPERATURE ON TENSILE PROPERTIES OF VIM-VAR MELT PLATE (4) P. 15

	Fe
0.16	C
14	Co
10	Ni
2	Cr
1	Mo

AF1410

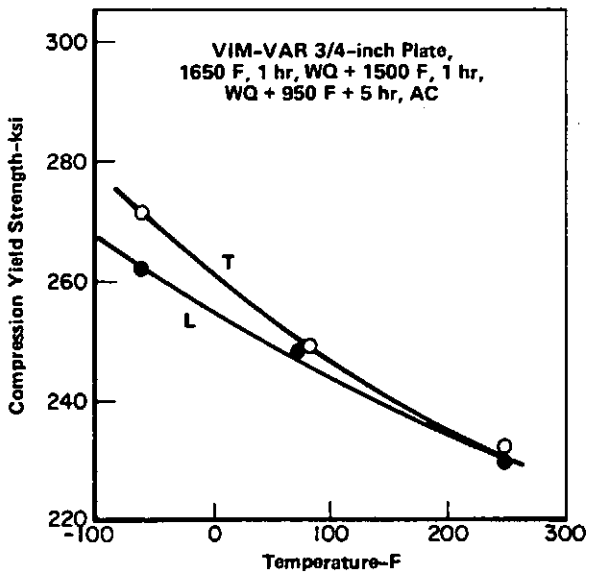


FIGURE 3.0322. EFFECT OF TEMPERATURE ON COMPRESSION YIELD STRENGTH OF VIM-VAR MELT PLATE (8) P. 75

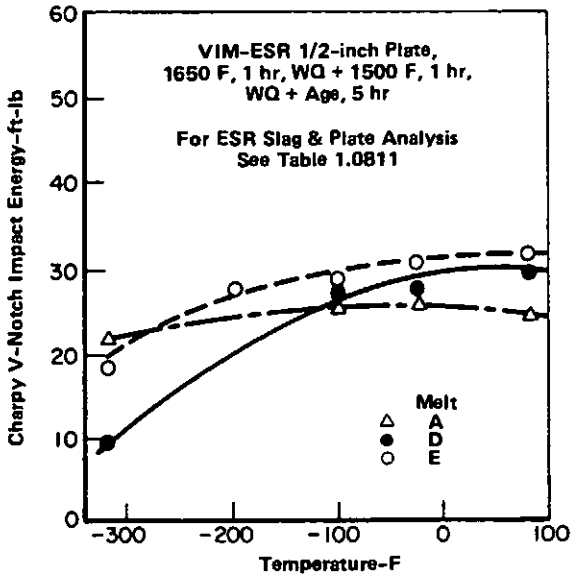


FIGURE 3.0331. EFFECT OF TEST TEMPERATURE ON IMPACT ENERGY OF THREE VIM-ESR MELTS (10) P. 22

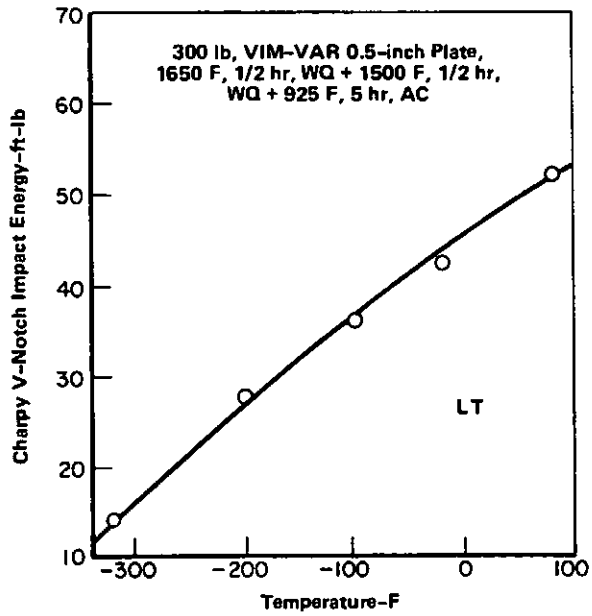


FIGURE 3.0332. EFFECT OF LOW TEST TEMPERATURES ON IMPACT ENERGY OF A 300-LB VIM-VAR MELT PLATE (7) P. 35

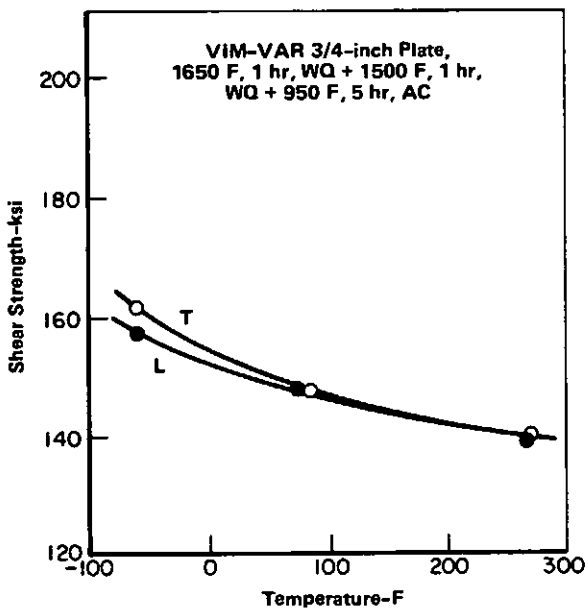


FIGURE 3.0351. EFFECT OF TEMPERATURE ON SHEAR STRENGTH OF VIM-VAR MELT PLATE (8) P. 76

	Fe
0.16	C
14	Co
10	Ni
2	Cr
1	Mo

AF1410

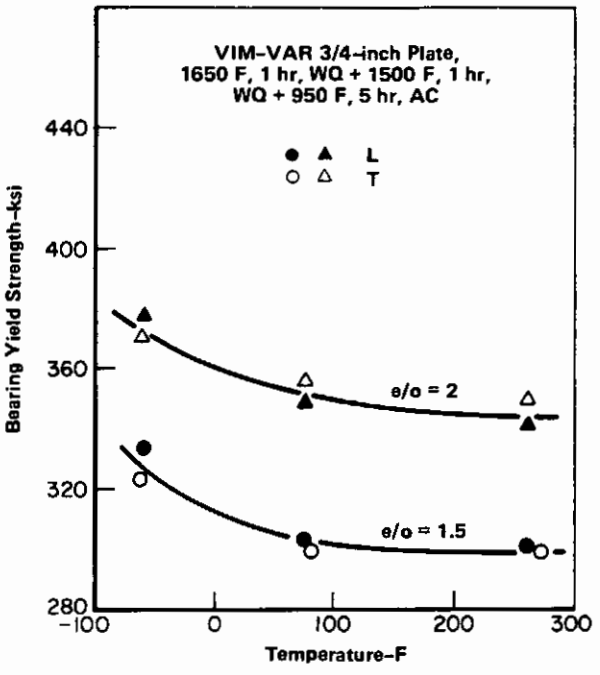


FIGURE 3.0361. EFFECT OF TEMPERATURE ON BEARING YIELD STRENGTH OF VIM-VAR MELT PLATE (8) P. 78

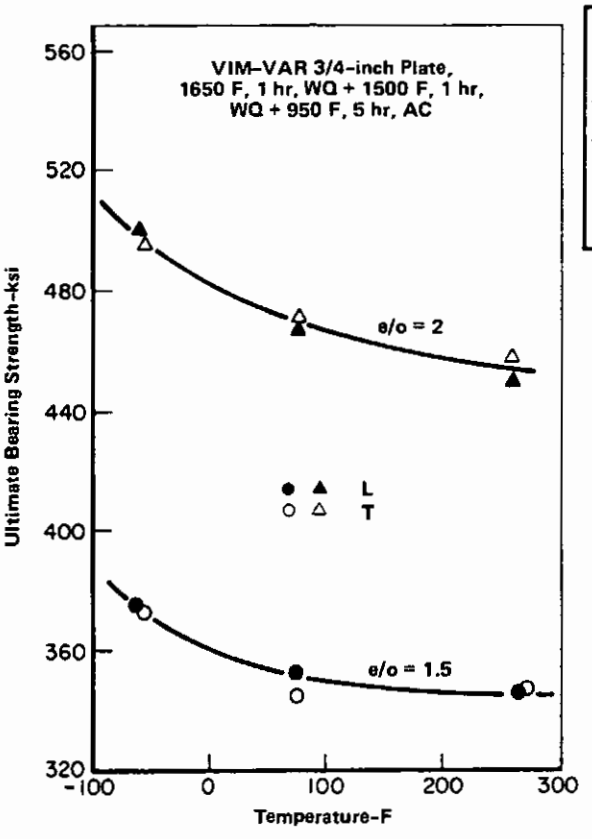


FIGURE 3.0362. EFFECT OF TEMPERATURE ON BEARING ULTIMATE STRENGTH OF VIM-VAR MELT PLATE (8) P. 78

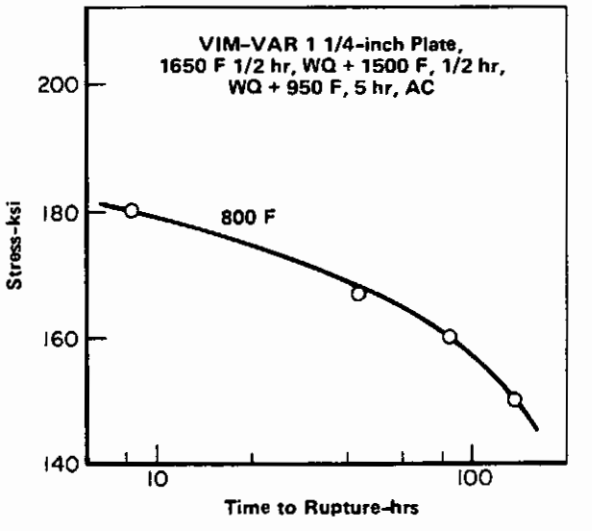


FIGURE 3.041. CREEP RUPTURE CURVE AT 800 F FOR VIM-VAR MELT PLATE (11) P. 27

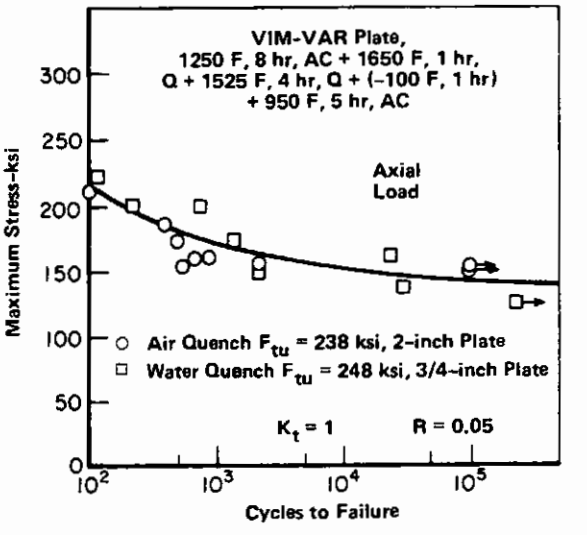


FIGURE 3.051. AXIAL LOAD S-N DATA FOR VIM-VAR MELT PLATE GIVEN A PREMACHINING HEAT TREATMENT AND THEN WATER OR AIR QUENCHED FOLLOWING AUSTENITIZING (9) P. 11

	Fe
0.16	C
14	Co
10	Ni
2	Cr
1	Mo

AF1410

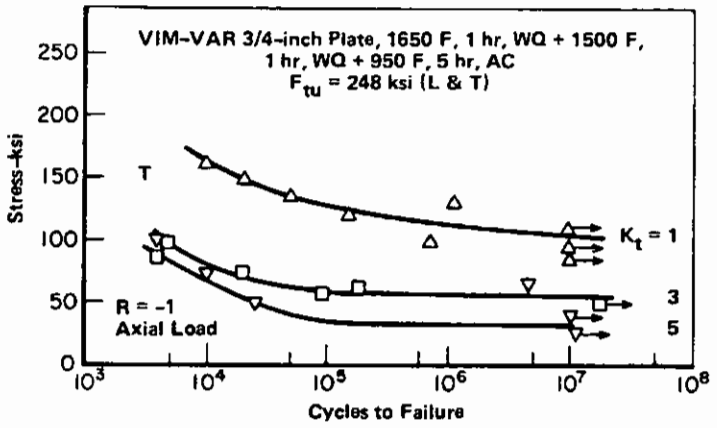


FIGURE 3.052. S-N CURVES AT ROOM TEMPERATURE FOR VIM-VAR MELT PLATE TESTED IN TRANSVERSE DIRECTION AT SEVERAL STRESS CONCENTRATIONS FOR R = - 1 (8) P. 87, 91, 95

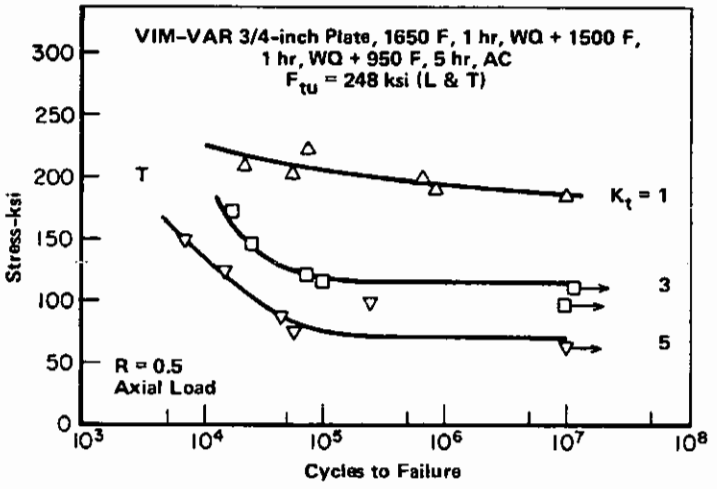


FIGURE 3.053. S-N CURVES AT ROOM TEMPERATURE FOR VIM-VAR MELT PLATE TESTED IN TRANSVERSE DIRECTION AT SEVERAL STRESS CONCENTRATION FACTORS FOR R = 0.5 (8) P. 86, 90, 94

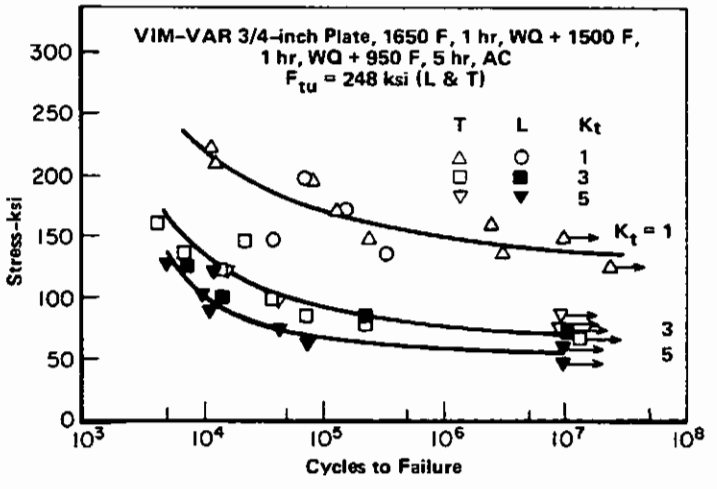


FIGURE 3.054. S-N CURVE AT ROOM TEMPERATURE FOR VIM-VAR MELT PLATE FOR SEVERAL STRESS CONCENTRATION FACTORS AT R = 0.05 (8) P. 84, 85, 88, 89, 92, 93

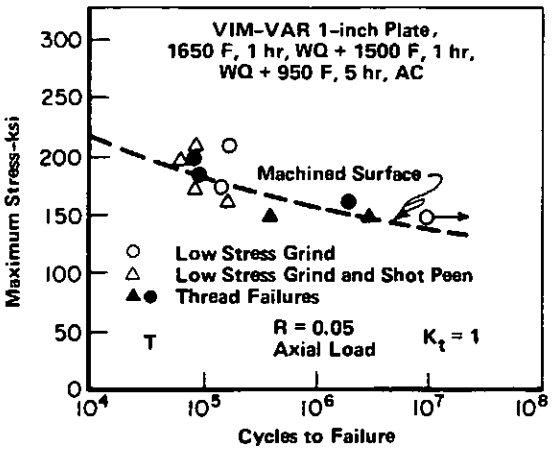


FIGURE 3.055. S-N CURVES FOR VIM-VAR MELT PLATE FOR SPECIMENS WITH GROUND OR GROUND AND SHOT PEENED SURFACES (8) P. 120

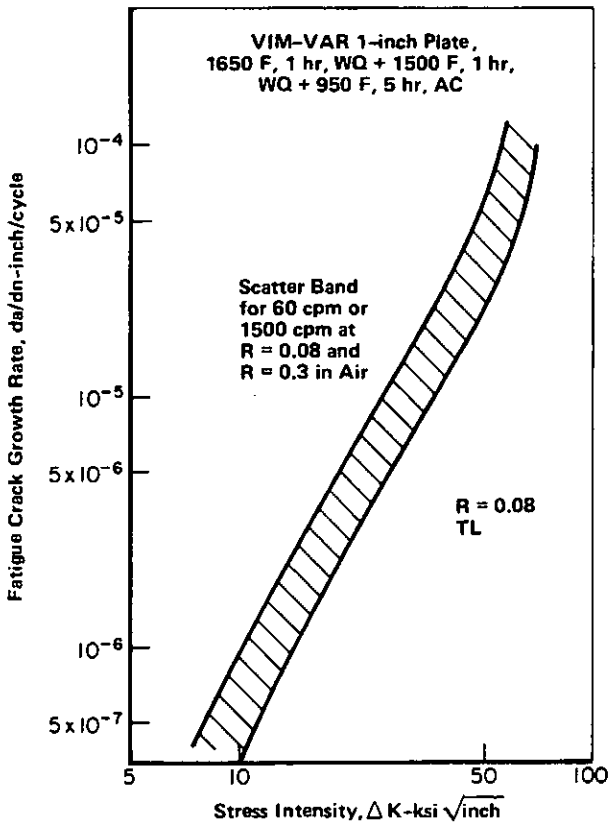
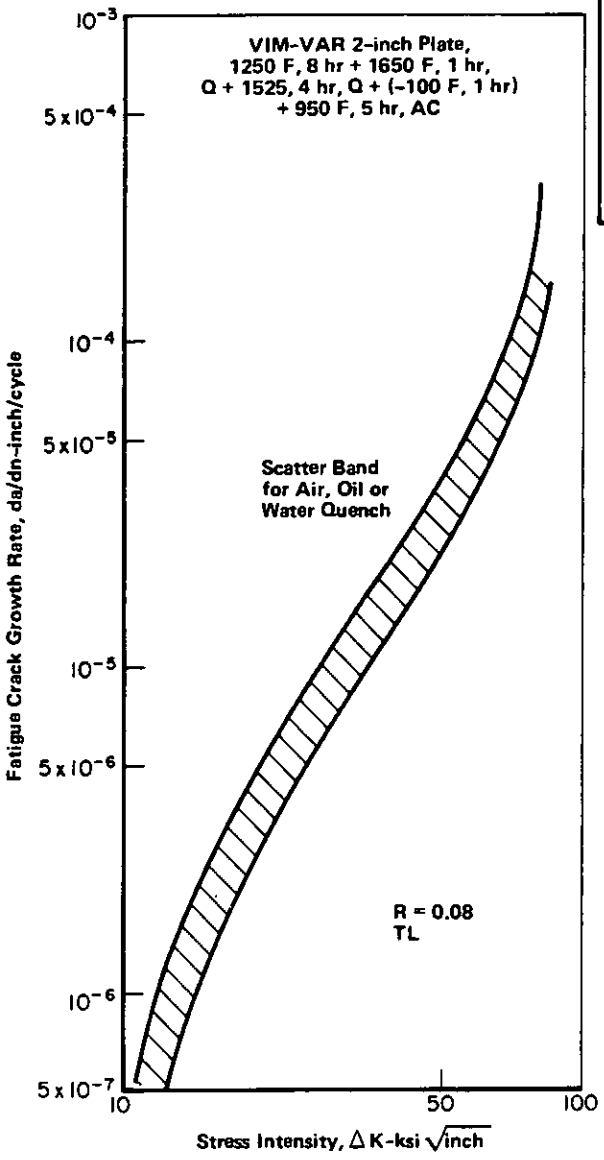


FIGURE 3.057. FATIGUE CRACK GROWTH RATE AT TWO FREQUENCIES AND TWO R RATIOS, FOR VIM-VAR PLATE AT ROOM TEMPERATURE IN LOW HUMIDITY AIR (9)



	Fe
0.16	C
14	Co
10	Ni
2	Cr
1	Mo

AF1410

FIGURE 3.056. FATIGUE CRACK GROWTH RATE FOR VIM-VAR MELT 2-INCH PLATE GIVEN A PREMACHINING HEAT TREATMENT AND THEN WATER OR AIR QUENCHED FOLLOWING AUSTENITIZING (9) P. 9

	Fe
0.16	C
14	Co
10	Ni
2	Cr
1	Mo

AF1410

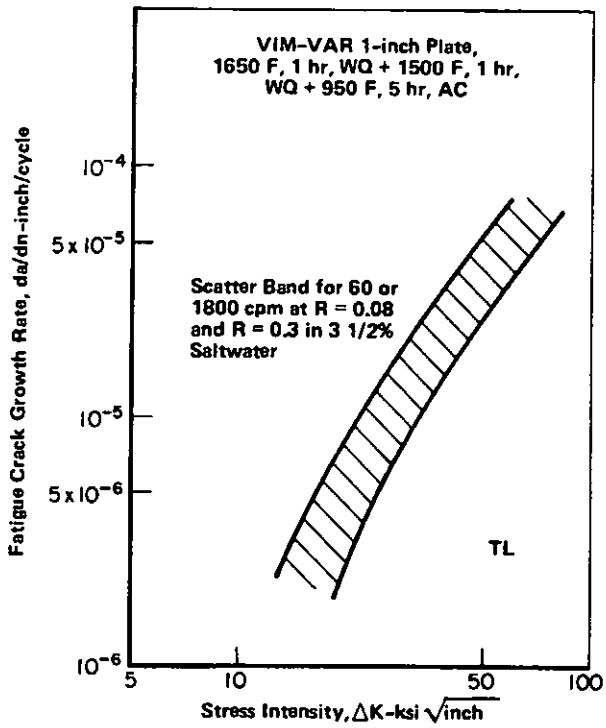


FIGURE 3.058. FATIGUE CRACK GROWTH RATE AT TWO FREQUENCIES AND TWO R RATIOS FOR VIM-VAR MELT PLATE AT ROOM TEMPERATURE IN 3 1/2% SALTWATER (8) P. 100, 111

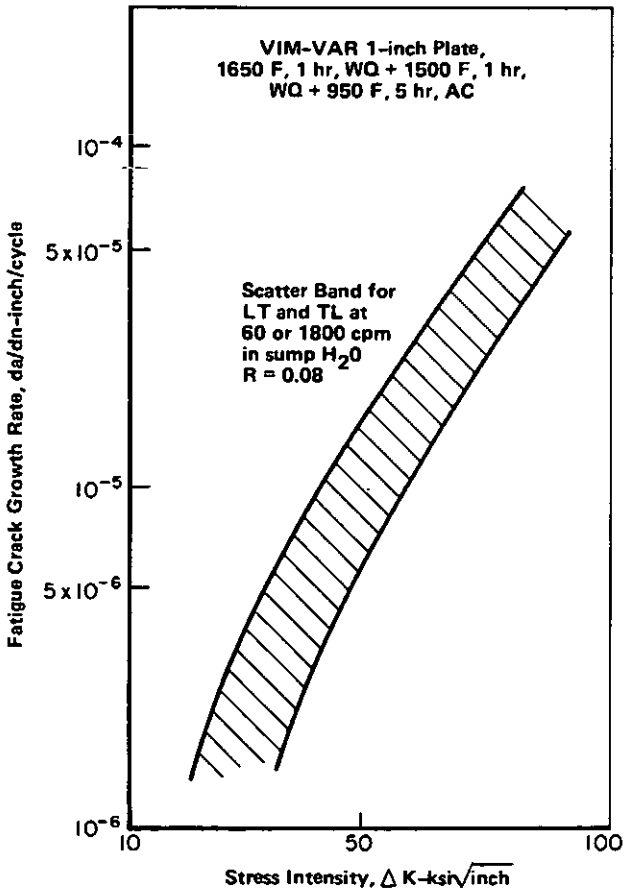


FIGURE 3.059. FATIGUE CRACK GROWTH RATE AT TWO FREQUENCIES FOR VIM-VAR MELT PLATE AT ROOM TEMPERATURE IN SUMP TANK WATER (8) P. 112

	Fe
0.16	C
14	Co
10	Ni
2	Cr
1	Mo

AF1410

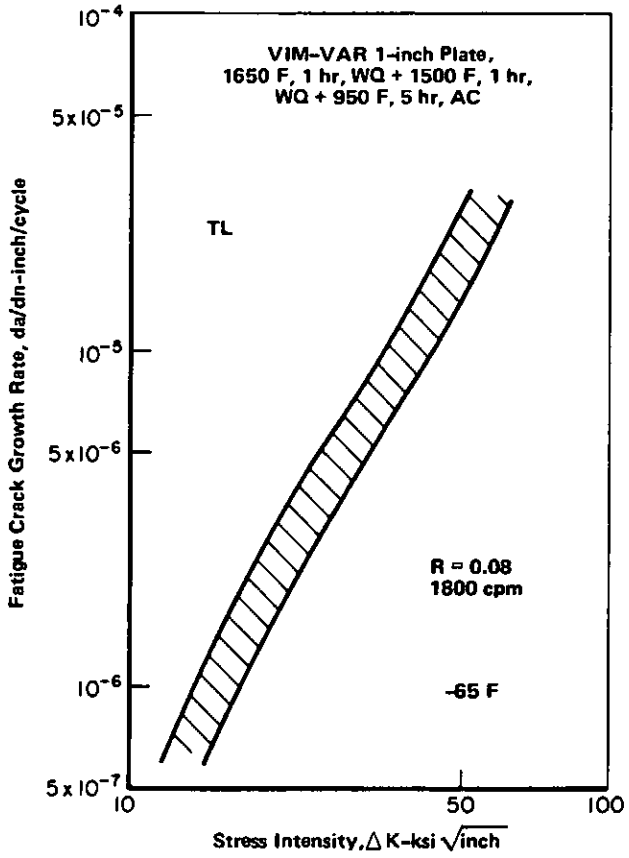


FIGURE 3.0510. FATIGUE CRACK GROWTH RATE FOR VIM-VAR PLATE AT -65F (8) P. 113

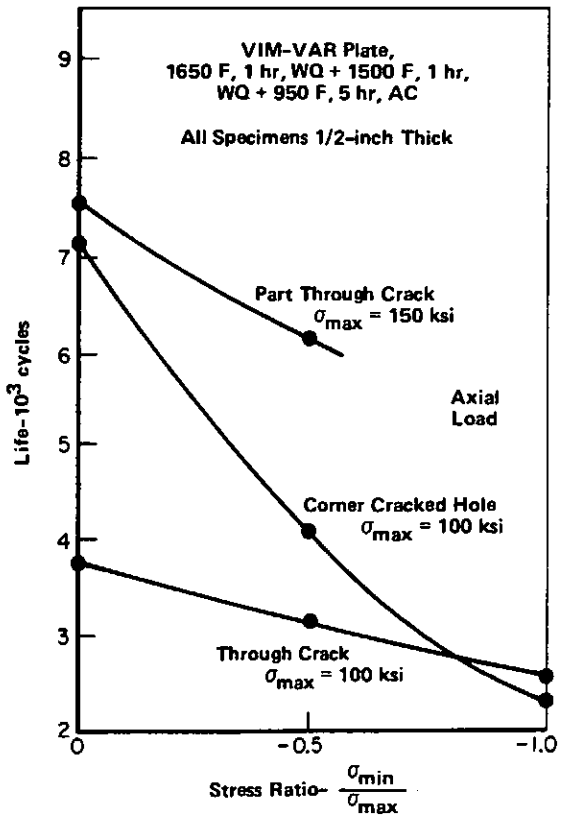


FIGURE 3.0511. EFFECT OF STRESS RATIO ON FATIGUE LIFE OF VARIOUS CRACKED SPECIMENS SUBJECTED TO CONSTANT AMPLITUDE LOADING (8) P. 178

	Fe
0.16	C
14	Co
10	Ni
2	Cr
1	Mo

AF1410

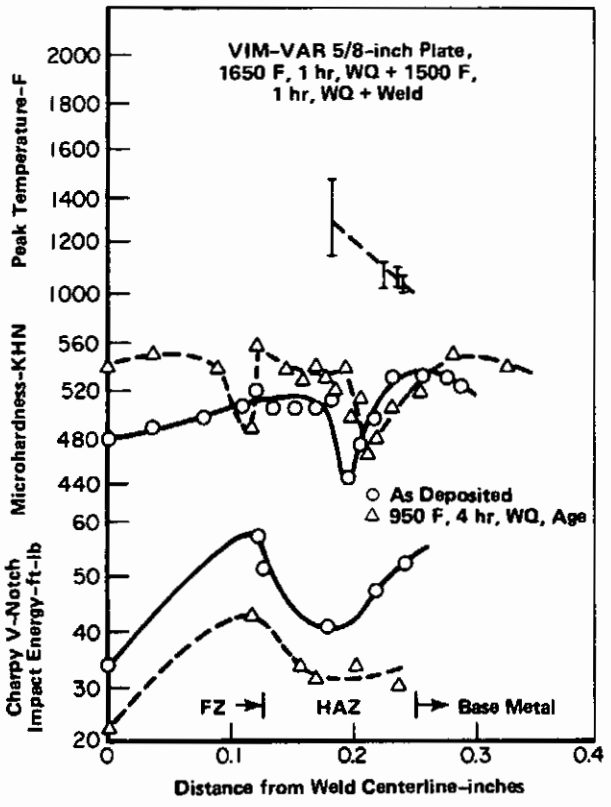


FIGURE 4.0319. HARDNESS AND IMPACT ENERGY AS A FUNCTION OF DISTANCE FROM WELD CENTERLINE FOR CW-GTA WELDS IN VIM-VAR PLATE (12) P. 69

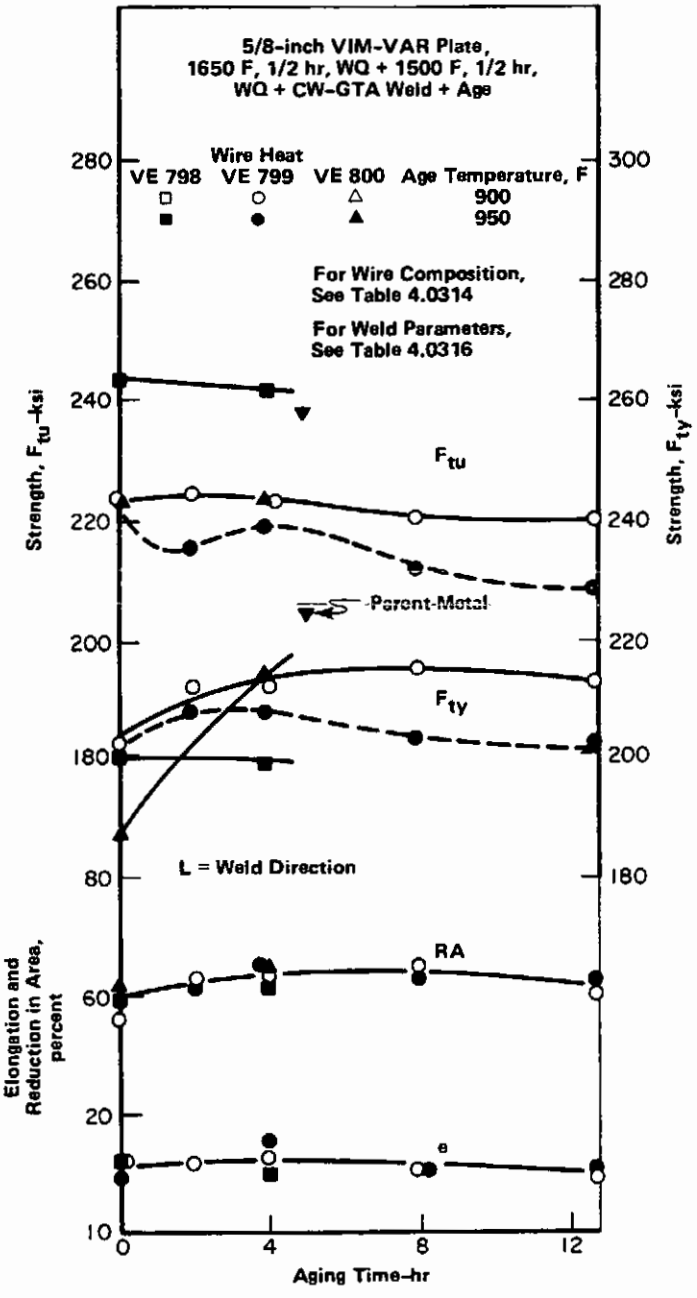


FIGURE 4.03110. FUSION ZONE TENSILE PROPERTIES OF VIM-VAR MELT PLATE CW-GTA WELDED WITH SEVERAL FILLER WIRES AND AGED FOR VARIOUS TIMES AT 900 AND 950 F (12) P. 35

	Fe
0.16	C
14	Co
10	Ni
2	Cr
1	Mo

AF1410

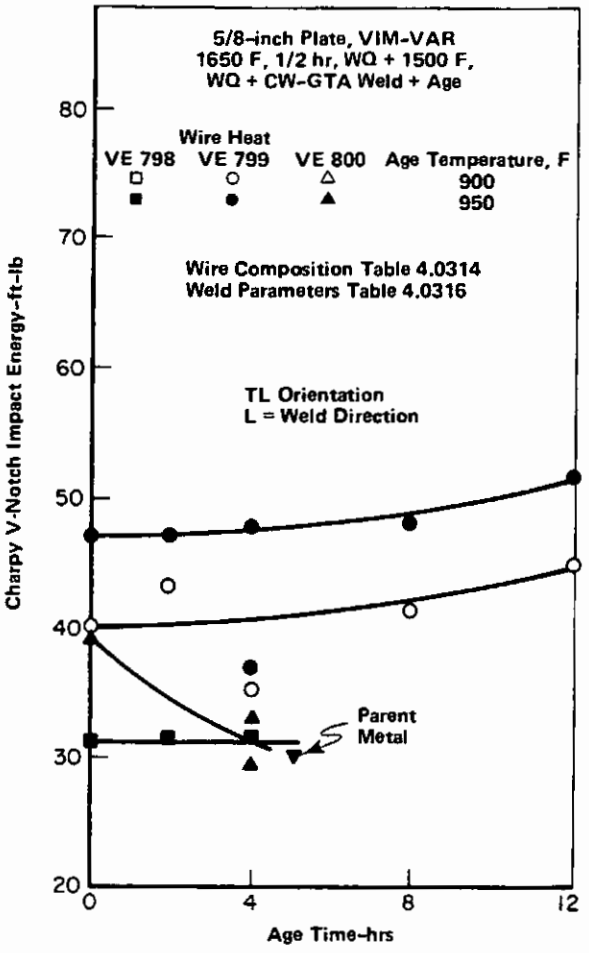


FIGURE 4.03111. FUSION ZONE CHARPY IMPACT ENERGY OF VIM-VAR MELT PLATE CW-GTA WELDED USING SEVERAL FILLER WIRES AND AGED FOR VARIOUS TIMES AT 900 AND 950 F (12) P. 38

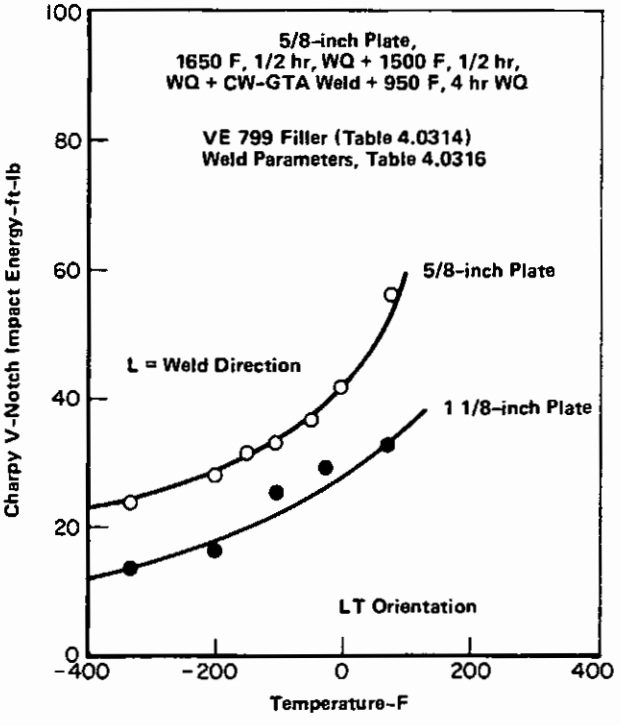


FIGURE 4.03114. EFFECT OF TEMPERATURE ON FUSION ZONE IMPACT ENERGY OF CW-GTA WELDS IN VIM-VAR PLATE (12) P. 83

	Fe
0.16	C
14	Co
10	Ni
2	Cr
1	Mo

AF1410

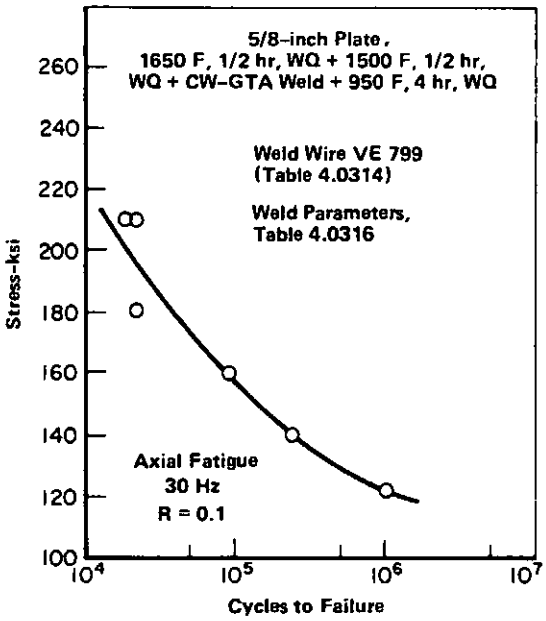


FIGURE 4.03116. FUSION ZONE FATIGUE STRENGTH OF CW-GTA WELD IN VIM-VAR MELT PLATE (12) P. 44

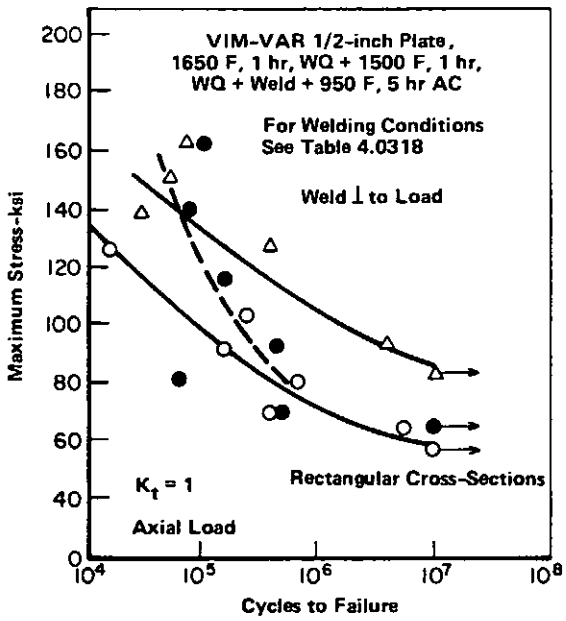


FIGURE 4.03117. S-N CURVES FOR GTA BUTT WELDS IN VIM-VAR MELT 1/2-INCH PLATE WITH WELD BEAD GROUND OFF (8) P. 145-146

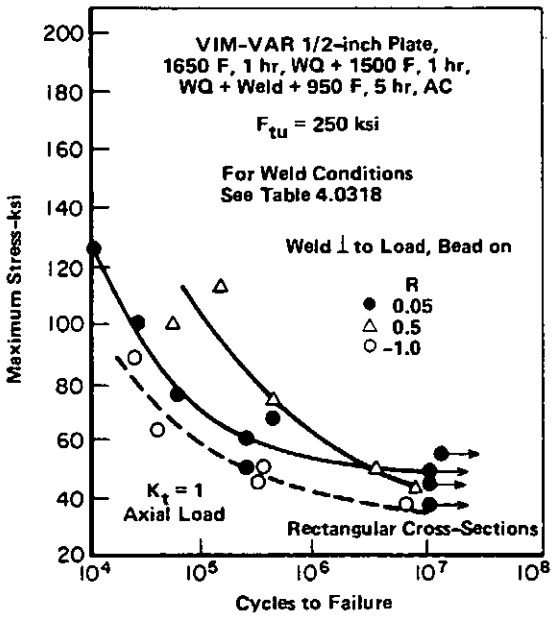


FIGURE 4.03118. S-N CURVES FOR GTA BUTT WELDS IN VIM-VAR 1/2-INCH PLATE WITH WELD BEAD ON (8) P. 135, 138, 139

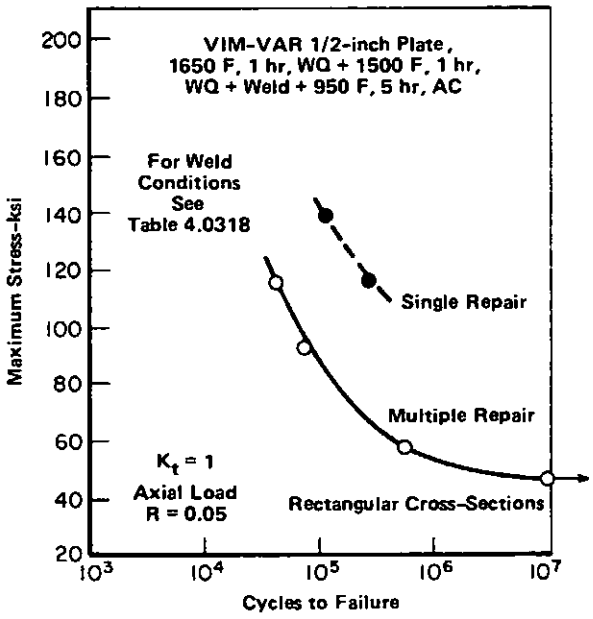


FIGURE 4.03119. S-N CURVES FOR GTA REPAIRED BUTT WELDS IN VIM-VAR 1/2-INCH PLATE WITH BEAD GROUND OFF (8) P. 144-146

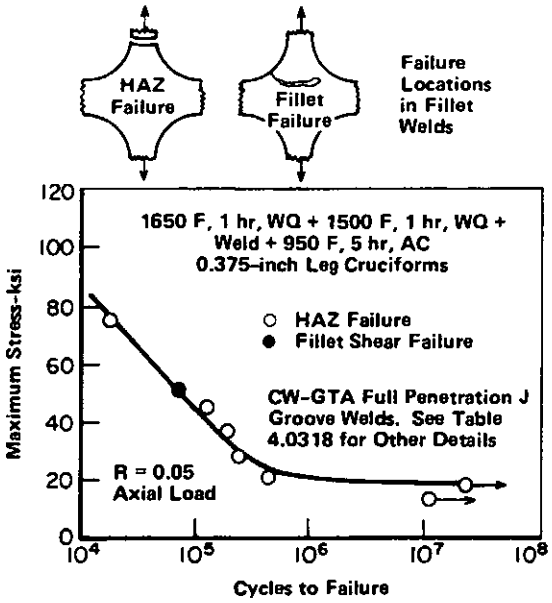
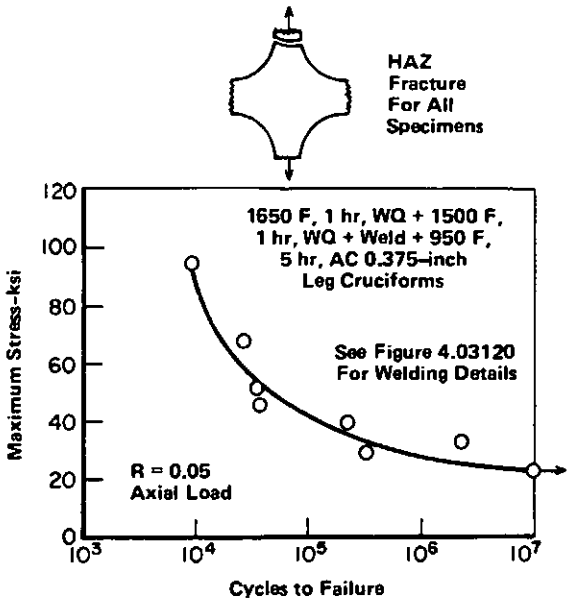


FIGURE 4.03120. S-N CURVE FOR FULL PENETRATION FILLET WELDED VIM-VAR MELT CRUCIFORMS WITH NONSYMMETRICAL JOINTS (8) P. 163



	Fe
0.16	C
14	Co
10	Ni
2	Cr
1	Mo

AF1410

FIGURE 4.03121. S-N CURVE FOR FULL PENETRATION FILLET WELDED VIM-VAR MELT CRUCIFORMS WITH SYMMETRICAL JOINTS (8) P. 161

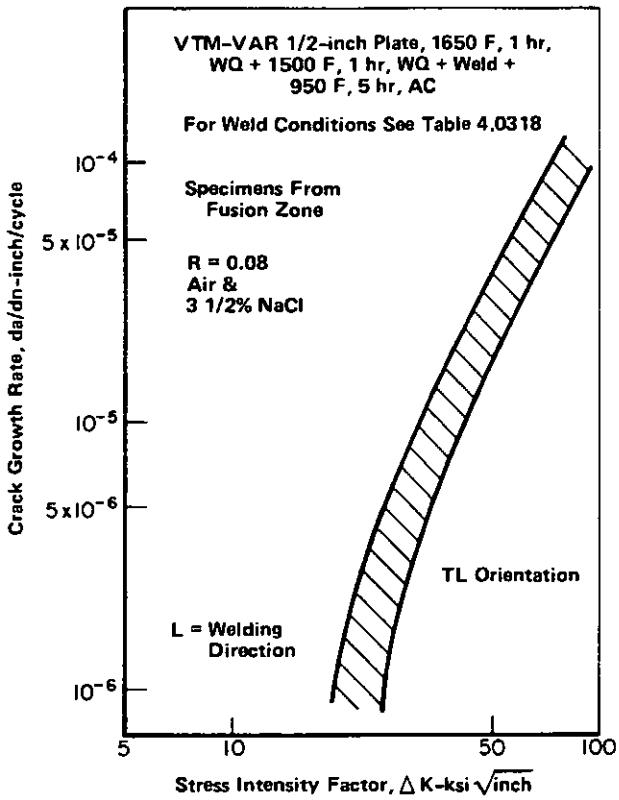


FIGURE 4.03122. FATIGUE CRACK GROWTH RATE IN AIR AND IN 3.5% SALTWATER FOR GTA WELD IN VIM-VAR 1/2-INCH PLATE (8) P. 167

	Fe
0.16	C
14	Co
10	Ni
2	Cr
1	Mo

AF1410

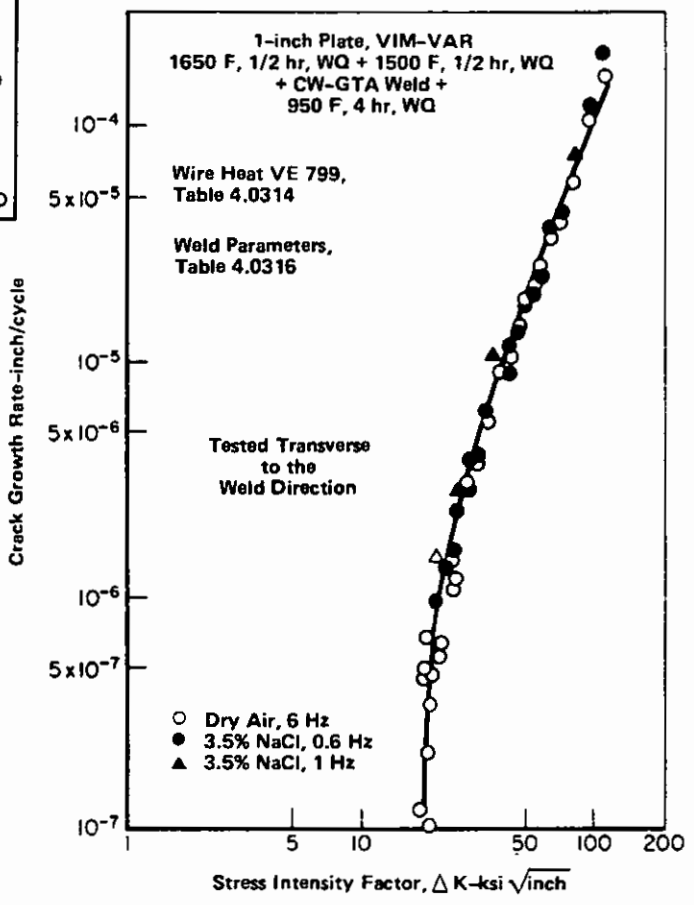


FIGURE 4.03123. FATIGUE CRACK GROWTH OF FUSION ZONE OF CW-GTA WELDS IN VIM–VAR MELT PLATE (12) P. 46 & 47

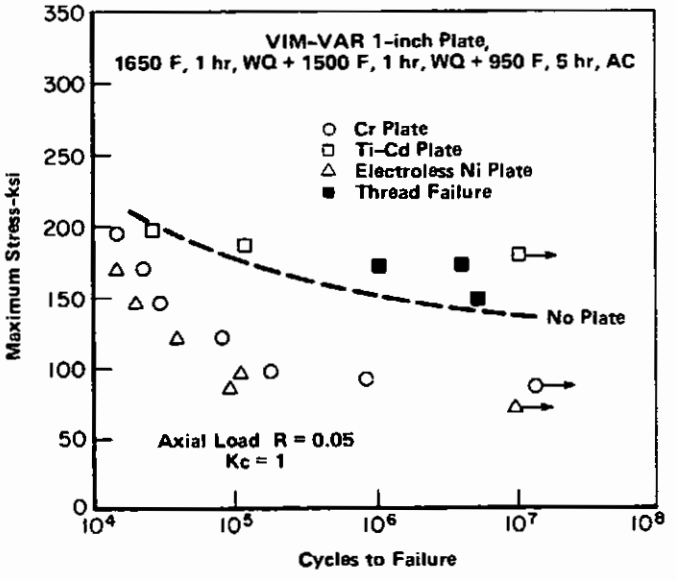


FIGURE 4.041. S-N CURVES FOR VIM-VAR MELT PLATE FOR SPECIMENS PLATED BY VARIOUS PROCESSES (8) P. 121

REVISED: MARCH 1970
AUTHOR: S. S. MANSON

FERROUS ALLOYS

1. GENERAL

AFC-77 is a martensitic stainless steel which has been modified by the addition of substantial amounts of Co and Mo. It is still under development, both in regard to heat treatment and mechanical processing. It is subject to a very strong secondary hardening reaction and tensile strengths up to 260 ksi, and yield strengths of 210 ksi can be obtained by quenching and tempering in the range of 700-1100F, depending on composition and austenitizing temperature. The Mo and Co promote high temperature strength, and yield strengths above 150 ksi at 1000F can be achieved by tempering between 1000 and 1100F. By combinations of heavy cold work and tempering, wires with tensile strengths of 500 ksi can be produced.

Unfortunately, like other martensitic stainless steels, this alloy is subject to embrittlement when tempered in the range of secondary hardening. In this case, the embrittlement is quite severe, and in terms of tempering temperature, extends from about 700F to well beyond the secondary hardening peak. For this reason the high strength conditions are not suitable for critical applications where resistance to crack propagation is a consideration. When tempered in the range between 400 and 700F, the yield strength is between 160 and 170 ksi, but the fracture toughness is greatly improved. However, alloys tempered at low temperatures are unstable and embrittle when exposed to even moderately elevated temperatures for extended times. Attempts have been made to achieve high strength without embrittlement by combinations of tempering and cold work. However, the data available on such treatments are as yet inadequate to permit judgement of their practical value.

1.01 Commercial Designation

AFC-77

1.02 Alternate Designations

1.03 Specifications

1.04 Composition

Table 1.04.

TABLE 1.04

Source	(1) (2)			
	Percent			
	Nominal	(a)	(b)	(c)
Carbon	0.15	0.173	0.164	0.147
Chromium	14.5	14.34	14.36	14.22
Cobalt	13.5	13.61	13.73	12.93
Copper	–	0.016	0.013	0.07
Manganese	-	0.01	0.02	0.10
Molybdenum	5.0	4.93	4.90	4.62
Nickel	–	0.05	0.10	0.08
Nitrogen	0.05	0.02	0.02	0.03
Phosphorus	-	0.006	0.004	0.010
Silicon	-	0.20	0.19	0.07
Sulfur	-	0.011	0.008	0.008
Tungsten	-	0.02	-	-
Vanadium	0.5	0.52	0.51	0.30
Iron	Balance			

(a) Measured (one-ton heat air-induction melted).
(b) Measured (vacuum arc-remelted heat).
(c) Measured (15-ton heat air-induction melted).

1.05 Heat Treatment

1.051 Austenitize. 1800 to 2000F, 1 hour, oil quench or air cool.

1.052 Refrigerate. -100F, 30 minutes.

1.053 Temper. 400 to 1100F, 2 + 2 hours.

1.06 Hardness

1.061 After austenitizing at 2000F, oil quenching and refrigerating at -100F for 30 minutes. Rockwell hardness is RC 48-50.

1.062 Effect of austenitizing and tempering temperature on Rockwell hardness, Figure 1.062.

1.063 Effect of refrigeration and tempering conditions on hardness of alloy austenitized at 1900F, Figure 1.063.

1.064 Effect of tempering temperature on hardness of sheet, Figure 1.064.

1.07 Forms and Conditions Available

A variety of products have been successfully produced from a 15-ton air-induction heat which included wire (to 1/8 inch diameter), bar (to 3 inch diameter), hot rolled sheet and strip (0.033 to 0.125 inch thick) and billets (7 1/2 inch square).

1.08 Melting and Casting Practice

Conventional air-arc melting and vacuum-arc remelting. The alloy has been produced in one-ton, two-ton, and fifteen-ton heats.

	Fe
0.15	C
14.5	Cr
13.5	Co
5	Mo
0.5	V
0.05	N_2

AFC-77

1.09 Special Considerations

In common with other martensitic stainless steels, this alloy is subject to a severe embrittlement when tempered above about 700F. The tempering temperature range over which this embrittlement occurs is much more extensive than in other martensitic stainless steels and extends to nearly 1400F (e.g. Figure 3.02712 and Figure 3.0331). It is interesting to note that no substantial recovery in the embrittlement is noted for 1200F tempering even though this temperature is well beyond the secondary hardening peak. Cold rolling preceding tempering in the brittle range can substantially increase the strength but also increases the embrittlement (see Figure 3.03711). The alloy is not stable during elevated temperature exposure and long time exposures to moderately elevated temperatures can substantially increase the embrittlement(see Figure 3.03714). As might be expected, the low temperature crack and notch strength are very poor for conditions tempered in the brittle range (see Figure 3.03711, 3.03713 and 3.03714).

If tempering is confined to temperatures below about 700F, the yield strength is below about 170 ksi and the room temperature fracture toughness is high (e.g. Figure 3.02712). No valid values of K_{Ic} are available for these tempered conditions. It would be expected that the low tempered conditions would not be stable during elevated temperature exposure, and that a time-temperature dependent embrittlement would develop.

Attempts have been made by Webster to improve the toughness of the high strength conditions by increasing the amount of retained austenite by austenitizing at high temperatures (about 2000F) and tempering at low temperatures where the retained austenite is stable (12). High strength is produced by introducing cold work following a low temperature temper (500F) and then re-tempering. Tensile yield strengths of about 270 ksi can be produced by moderate amounts of cold work. Unfortunately, Webster does not describe his fracture toughness tests in sufficient detail to permit judgement of the practical value of the proposed treatments. However, it would be expected that retained austenite would increase the toughness, particularly if it produced a layered structure that would cause crack branching. Such a structure might be produced by cold work following tempering at a low temperature but could be quite directional in its fracture properties.

2. PHYSICAL AND CHEMICAL PROPERTIES

2.01 Thermal Properties

2.011 Melting range.

2.012 Phase changes.

2.0121 Time-temperature-transformation diagrams.

2.013 Thermal conductivity.

2.014 Thermal expansion, Figure 2.014.

2.0141 Effect of tempering temperature on dimensional change of alloy austenitized at 2000F, Figure 2.0141.

2.015 Specific heat.

2.016 Thermal diffusivity.

	Fe
0.15	C
14.5	Cr
13.5	Co
5	Mo
0.5	V
0.05	N_2

AFC-77

2.02 Other Physical Properties
2.021 Density.
2.022 Electrical properties.
2.023 Magnetic properties.
2.024 Emissivity.
2.025 Damping capacity.

2.03 Chemical Properties

In general, the oxidation and corrosion resistance are characteristic of martensitic stainless steels. However, when tempered to its highest strength conditions, it is very susceptible to stress corrosion. This susceptibility develops in the same range of tempering temperatures as does the temper embrittlement (compare Figure 2.031 and Figure 3.02712).

2.031 Effect of tempering temperature on time to failure of statically stressed fatigue-cracked tensile specimens exposed to salt solution, Figure 2.031.

2.04 Nuclear Properties

3. MECHANICAL PROPERTIES

3.01 Specified Mechanical Properties

3.02 Mechanical Properties at Room Temperature
3.021 Tension.
3.0211 Stress-strain diagrams. (see also 3.03111 and 3.03112)
3.032111 Typical stress-strain curve at room temperature for cold-drawn fine wire, Figure 3.02111.
3.0212 Sheet.
3.02121 Effect of tempering temperature on tensile properties of sheet cold reduced 55 percent, Figure 3.02121.
3.02122 Effect of tempering temperature on tensile properties of sheet, Figure 3.02122.
3.02123 Effect of cold reduction and tempering temperature on sheet austenitized at 2000F, Figure 3.02123.
3.02124 Effect of austenitizing and tempering temperature on tensile and yield strength of sheet, Figure 3.02124.
3.0213 Bar.
3.02131 Effect of austenitizing and tempering temperature on tensile properties of bar, Figure 3.02131.
3.0214 Wire.
3.02141 Effect of cold reduction on tensile properties of wire, Figure 3.02141.
3.02142 Effect of cold reduction on tensile strength of rod, Figure 3.02142.
3.02143 Effect of exposure for 18 hours at various temperatures on tensile strength of fine wire, Figure 3.02143.
3.02144 Effect of short exposure to elevated temperatures on tensile strength of fine wire, Figure 3.02144.
3.02145 Tensile strengths achievable by combinations of cold reduction and tempering in successive stages, Figure 3.02145.

3.022 Compression.
3.0221 Stress-strain diagrams (see 3.03113 and 3.03114).
3.0222 Effect of austenitizing and tempering temperatures on compressive yield strength, Figure 3.0222.
3.023 Impact (see also 3.0331 and 3.0332).
3.0231 Effect of austenitizing temperature on Charpy impact energy of bar tempered at 500 and 700F, Figure 3.0231.

3.024 Bending.
3.025 Torsion and shear.
3.0251 Double shear strength of pins, Table 3.0251.

TABLE 3.0251

Source	(4)	
Alloy	Fe-(0.15C)-14.5Cr-13.5Co-5Mo-0.5V	
Form	(0.506 in round bar)	
Property	Double Shear Test	
Condition	1800, 1 hr, OQ+(-100F), 30 minutes, +1050F, 2 + 2 hours, AC	1900F, 1 hr, OQ + (-100F) 30 minutes, +1000F, 2 + 2 hours, AC
Double shear strength, lb	58.9	65.8
Shear stress - ksi (a)	149.9	167.5

(a) Stress calculated at twice the area corresponding to nominal diameter of shear pin, (0.3927 square inches).

3.026 Bearing.
3.027 Stress concentration.
3.0271 Notch properties.
3.02711 Effect of cold reduction on crack strength of sheet, Figure 3.02711.
3.02712 Effect of tempering temperature on yield strength, crack strength, and plane strain fracture toughness of sheet, Figure 3.02712.
3.0272 Fracture toughness.
3.02721 General. While only a very limited amount of meaningful plane strain fracture toughness data is available, tests on sharply notched or cracked specimens definitely indicate that very low fracture toughness is to be expected for tempering above about 700F, where high tensile and yield strengths can be obtained. Low tempering temperatures produce much tougher conditions, but these have relatively low strength (see also 1.09).
3.02722 Effect of tempering temperature on plane strain fracture toughness of sheet, Figure 3.02722. This figure is shown to indicate qualitatively that fracture toughness is substantially increased if tempering temperature is kept below 700F. The K_Q values (tempering temperature less than 800F) are from specimens not meeting ASTM size requirements (5).
3.028 Combined properties.

3.03 Mechanical Properties at Various Temperatures
3.031 Tension (see also 3.037).
3.0311 Stress-strain diagrams.
3.03111 Stress-strain curves in tension for sheet tempered at 700F, Figure 3.03111.
3.03112 Stress-strain curves in tension for sheet tempered at 1100F, Figure 3.03112.
3.0312 Bar.
3.03121 Effect of test temperature on tensile properties of bar after austenitizing at 2000F, Figure 3.03121.
3.03122 Tensile properties at room temperature, 900F and 1200F, Table 3.03122.

TABLE 3.03122

Source	(4)											
Alloy	AFC-77 (0.506 in round bar)											
Condition	1800F, 1 hr, OQ + (-100F), 30 min +1050F, 2 + 2 hr, AC						1900F, 1 hr, OQ + (-100F), 30 min, + 1000F, 2+2 hr, AC					
Form	0.357 inch specimen			1/2 x 20 Bolt *			0.357 inch specimen			1/2 x 20 Bolt *		
Temperature - F	RT	900	1200	RT	900	1200	RT	900	1200	RT	900	1200
F_{tu}, (avg) - ksi	259	217	101	262	222	117	285	209	101	294	246	127
F_{ty}, (avg) - ksi	213	184	94	187	153	76	208	165	93	181	176	82
e, (avg) - percent	8.2	10.6	11.4	-	-	-	13.5	8.5	10.7	-	-	-
RA, (avg) - percent	26.7	38.8	52.2	-	-	-	48.5	31.3	52.3	-	-	-
Hardness, RC												
As received	37.0	-	-	-	-	-	37	-	-	-	-	-
HT	48.5	-	-	-	-	-	52.5	-	-	-	-	-

* Stress for bolts based on Basic Pitch Diameter area of 0.1716 square inch. All bolt threads were rolled.

3.03123 Effect of test temperature on tensile properties of smooth and notched bar for alloy austenitized at 2000F and tempered at 1100F, Figure 3.03123.
3.0313 Sheet.
3.03131 Effect of test temperature on tensile properties of .010 inch sheet tempered at 700F, Figure 3.03131.
3.03132 Effect of test temperature on tensile properties of .010

	Fe
0.15	C
14.5	Cr
13.5	Co
5	Mo
0.5	V
0.05	N_2

AFC-77

inch sheet tempered at 1100F, Figure 3.03132.

3.03133 Effect of test temperature on tensile properties of .050 inch sheet tempered at various temperatures, Figure 3.03133.

3.03134 Effect of test temperature, prior exposure to stress and temperature, on yield strength of sheet in as-heat treated condition and after 10 percent cold roll, Figure 3.03134.

3.0314 Wire.

3.03141 Effect of test temperature on tensile strength of .006 inch diameter wire, Figure 3.03141.

3.03142 Effect of elevated temperatures on tensile strength of .006 inch wire thermomechanically processed to a room temperature tensile strength of 530 ksi, Figure 3.03142.

3.032 Compression.

3.0321 Stress-strain curves in compression for sheet tempered at 700F, Figure 3.0321.

3.0322 Stress-strain curves in compression for sheet tempered at 1100F, Figure 3.0322.

3.033 Impact.

3.0331 Effect of tempering temperature on Charpy-V impact properties at room temperature and 500F test temperatures, Figure 3.0331.

3.0332 Effect of tempering temperature on impact energy of subsize Charpy specimen at room and elevated temperatures, Figure 3.0332.

3.034 Bending. Specimens tempered at 1400F, 2 + 2 hours permitted. 180° bend for R/T = 4.5 at temperatures of 50, 25, 0, -25, and -50F (6, p. 132).

3.035 Torsion and shear. Average shear strength of sheet in longitudinal and transverse direction 170 ksi (6, p. 138).

3.036 Bearing.

3.037 Stress concentration.

3.0371 Notch properties.

3.03711 Effect of test temperature on tensile properties of smooth and notched sheet in as-heat treated condition and after 10 percent cold roll, Figure 3.03711.

3.03712 Effect of test temperature and prior exposure to stress and temperature on tensile properties of smooth and notched sheet tempered at 750F, Figure 3.03712.

3.03713 Effect of test temperature and prior exposure to stress and temperature on tensile strength and elongations of smooth and notched sheet in as-heat treated condition and after 10 percent cold roll, Figure 3.03713.

3.03714 Effect of test temperature on crack strength of sheet tempered at 900 and 1100F, Figure 3.03714.

3.0372 Fracture toughness.

3.03721 General. While no plane strain fracture toughness values are available at various temperatures, tests on sharply notched or cracked specimens indicate that fracture toughness would be poor at subzero temperatures (e.g. Figure 3.03711). Fracture toughness at moderately elevated temperatures is considerably improved over that at room temperature; however, the alloy is not stable for long time exposures to moderately elevated temperatures if tempered to give high strength (e.g. Figure 3.03712).

3.038 Combined properties.

3.04 Creep and Creep Rupture Properties

3.041 Bar.

3.0411 Creep rupture curves at 1000F and 1050F for smooth and notched bar tempered at 1400F, Figure 3.0411.

3.0412 Effect of austenitizing temperature on creep rupture life and ductility at 90 ksi and 1000F for smooth bar and on rupture life for notched bar, Figure 3.0412.

3.042 Sheet.

3.0421 Curves for 0.2 and 0.5 percent deformation and for rupture of sheet tempered at 1100F, Figure 3.0421.

3.043 Wire.

3.0431 Creep-rupture properties of .006 inch diameter wire drawn to room temperature tensile strength of 550 ksi and tested at temperatures from 800 to 1100F, Figure 3.0431.

3.05 Fatigue Properties

3.051 Axial fatigue of sheet tempered at 700F and tested at room and elevated temperatures, Figure 3.051.

3.052 Axial fatigue of sheet tempered at 1100F and tested at room and elevated temperatures, Figure 3.052.

3.06 Elastic Properties

3.061 Poisson's ratio.

3.062 Modulus of elasticity.

3.0621 Elastic modulus at room and elevated temperatures for sheet tempered at 700F, Figure 3.0621.

3.0622 Elastic modulus at room and elevated temperatures for sheet tempered at 1100F, Figure 3.0622.

4. FABRICATION

4.01 Formability

4.011 Although experience is limited, this alloy appears to be readily formable by conventional methods.

4.012 Forming has been accomplished by heating to temperatures from 2000 to 2300F, and forging from 2300 to 1600F minimum without difficulty. Upper limit temperature of workability determined by soaking furnace available and by the tendency of a given heat to form free ferrite. (Contents of free ferrite above 5 percent may cause cracking.) Lower limit temperature of workability is determined by the capacity of available forging or rolling equipment. The high strength of this alloy implies need of high working forces, as temperature is lowered. In general, the hot workability of this alloy may be regarded as similar to that of Type 316 Stainless Steel.

4.013 For alloy austenitized at temperatures between 2000 and 2200F and water quenched, reduction by cold rolling is limited to approximately 25 percent before reannealing becomes necessary as a result of rapid strain hardening. If alloy is austenitized between 1600 and 2000F, air cooled, and tempered at 1400F for 2 + 2 + 2 hours, reductions of 75 percent can be accomplished, although high roll separating forces are required.

4.02 Machining and Grinding

Machining is best accomplished after tempering at 1400F.

4.03 Welding

4.04 Heat Treatment

4.05 Surface Treatment

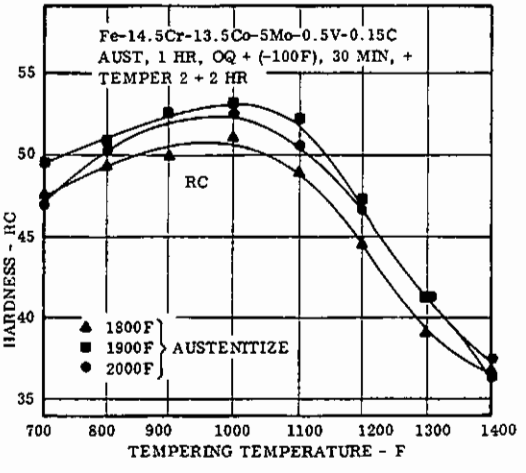


FIG. 1.062 EFFECT OF AUSTENITIZING AND TEMPERING TEMPERATURE ON ROCKWELL HARDNESS. (1, p. 112)

	Fe
0.15	C
14.5	Cr
13.5	Co
5	Mo
0.5	V
0.05	N_2

AFC-77

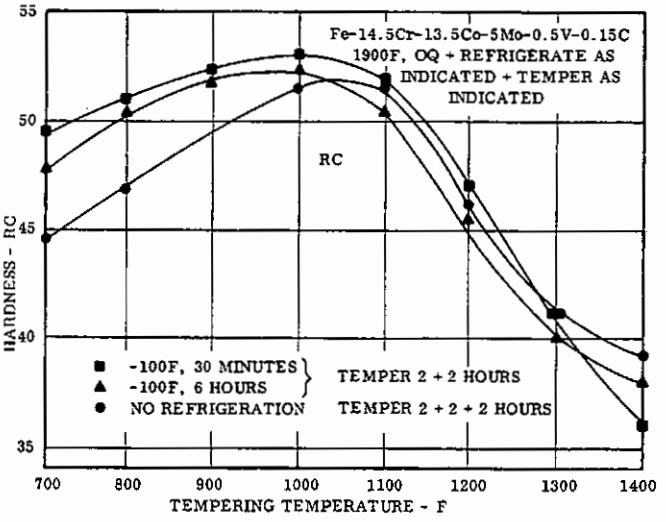


FIG. 1.063 EFFECT OF REFRIGERATION AND TEMPERING CONDITIONS ON HARDNESS OF ALLOY AUSTENITIZED AT 1900F. (1, p. 113)

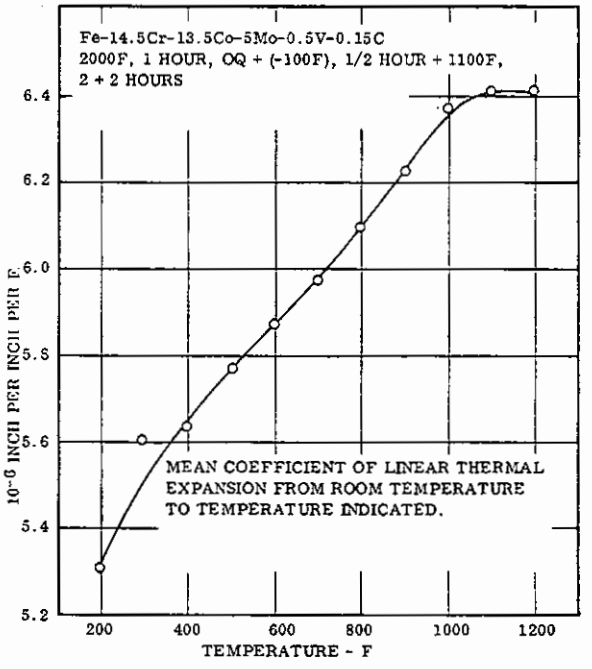


FIG. 2.014 THERMAL EXPANSION. (11, p. 37)

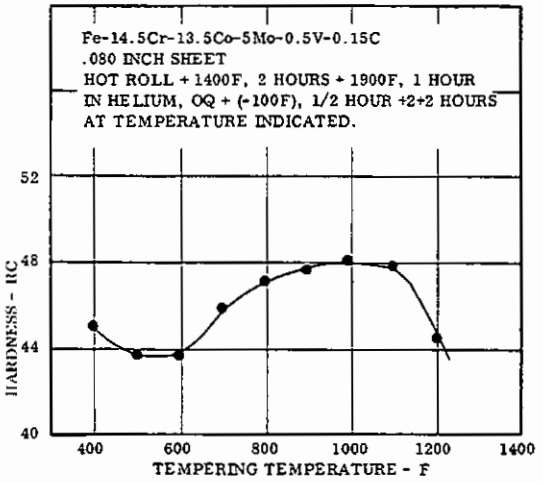


FIG. 1.064 EFFECT OF TEMPERING TEMPERATURE ON HARDNESS OF SHEET. (7, p. 77)

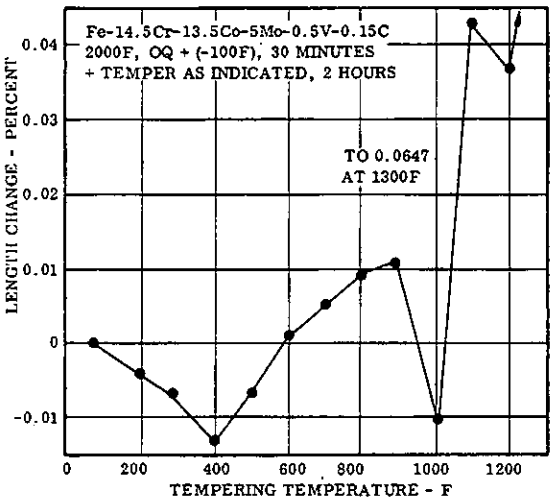
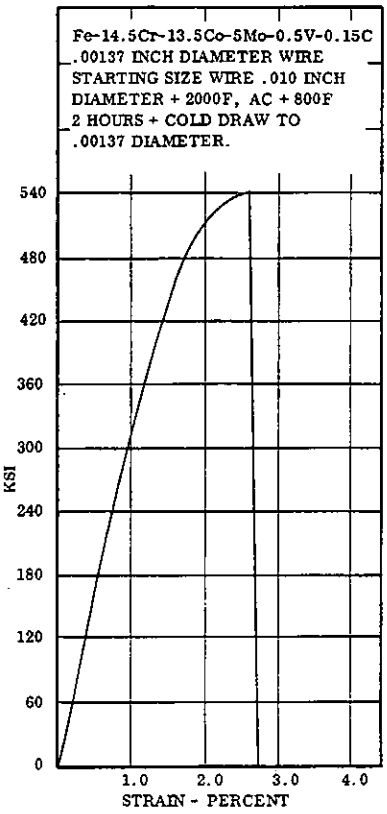


FIG. 2.0141 EFFECT OF TEMPERING TEMPERATURE ON DIMENSIONAL CHANGE OF ALLOY AUSTENITIZED AT 2000F. (1, p. 97)



	Fe
0.15	C
14.5	Cr
13.5	Co
5	Mo
0.5	V
0.05	N_2

AFC-77

FIG. 3.02111 TYPICAL STRESS-STRAIN CURVE FOR COLD-DRAWN FINE WIRE. (9, p. 33)

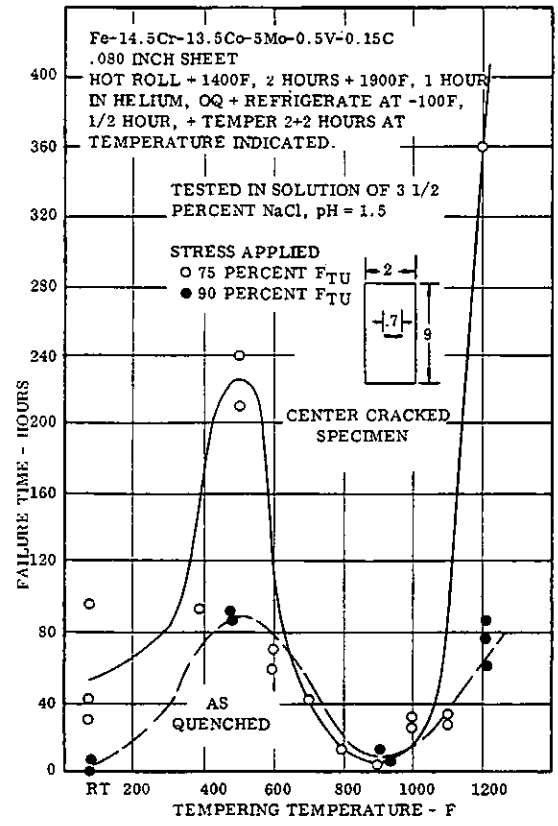


FIG. 2.031 EFFECT OF TEMPERING TEMPERATURE ON TIME TO FAILURE OF STATICALLY STRESSED FATIGUE CRACKED TENSILE SPECIMENS EXPOSED TO SALT SOLUTION. (7, p. 79)

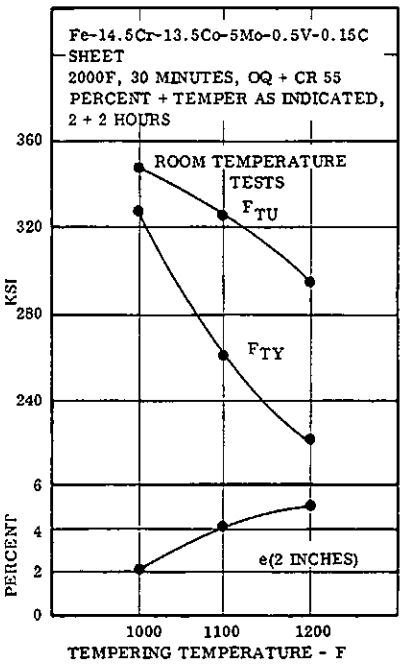


FIG. 3.02121 EFFECT OF TEMPERING TEMPERATURE ON TENSILE PROPERTIES OF SHEET COLD REDUCED 55 PERCENT. (2, p. 130)

	Fe
0.15	C
14.5	Cr
13.5	Co
5	Mo
0.5	V
0.05	N_2

AFC-77

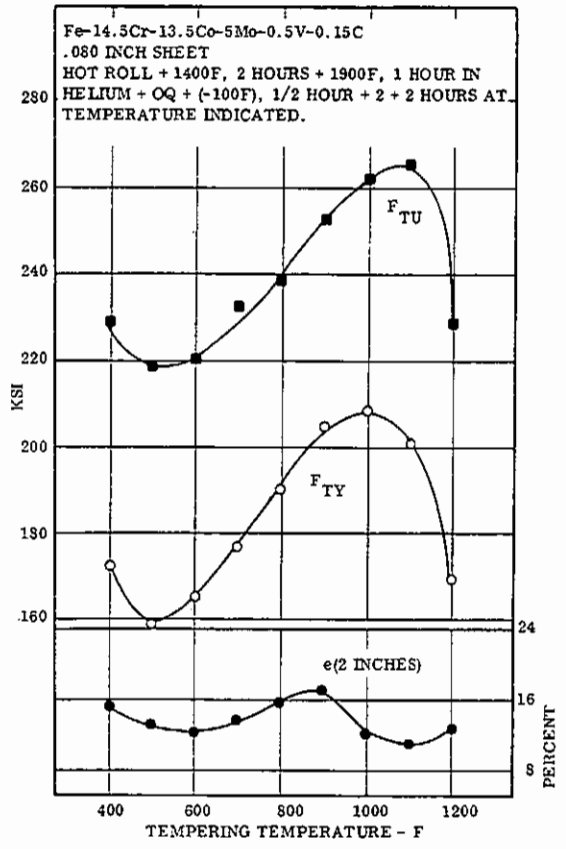


FIG. 3.02122 EFFECT OF TEMPERING TEMPERATURE ON TENSILE PROPERTIES OF SHEET. (7, p. 77)

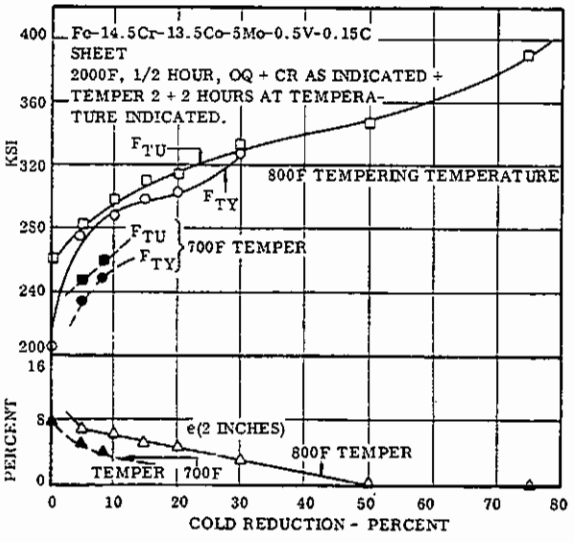


FIG. 3.02123 EFFECT OF COLD REDUCTION AND TEMPERING TEMPERATURE ON SHEET AUSTENITIZED AT 2000F. (11, p. 33)

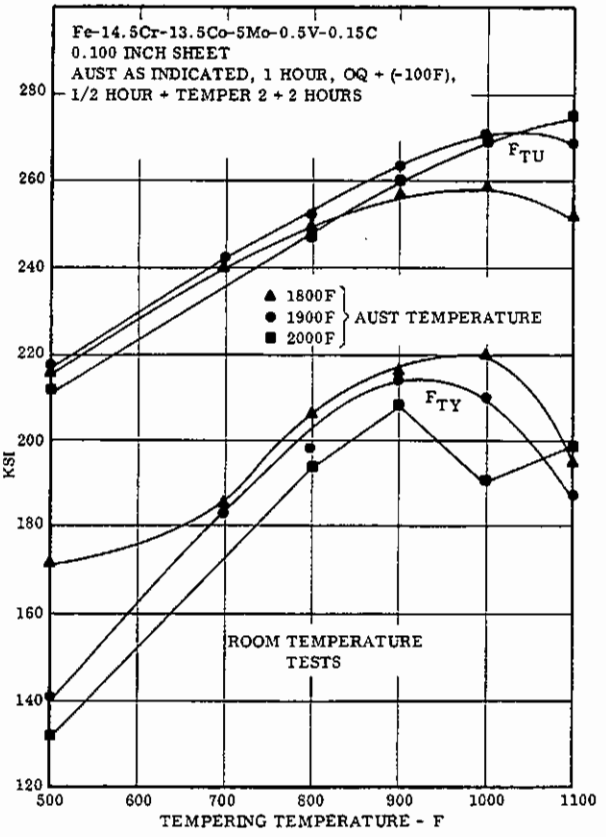


FIG. 3.02124 EFFECT OF AUSTENITIZING AND TEMPERING TEMPERATURE ON TENSILE AND YIELD STRENGTH OF SHEET AT ROOM TEMPERATURE. (1, p. 114)(11, p. 34)

	Fe
0.15	C
14.5	Cr
13.5	Co
5	Mo
0.5	V
0.05	N_2

AFC-77

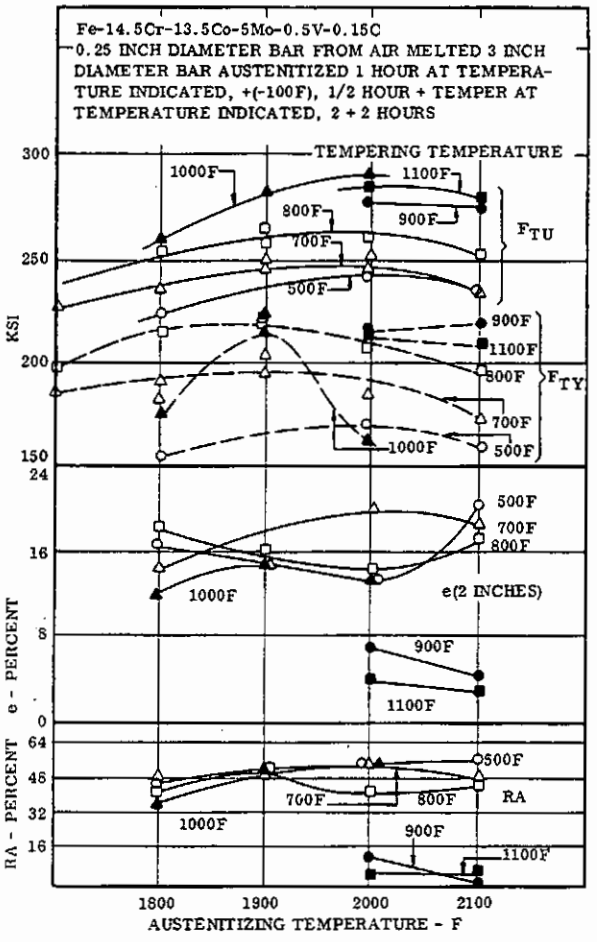


FIG. 3.02131 EFFECT OF AUSTENITIZING AND TEMPERING TEMPERATURE ON TENSILE PROPERTIES OF BAR. (12, pp. 820, 821)

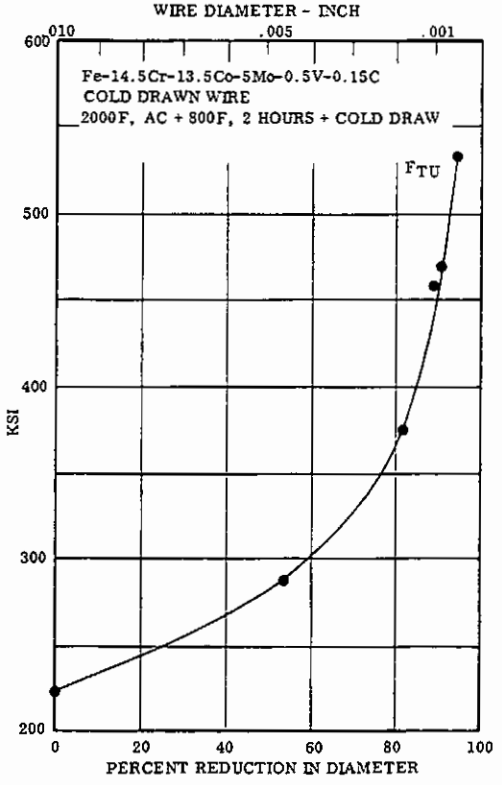


FIG. 3.02141 EFFECT OF COLD REDUCTION ON TENSILE STRENGTH OF WIRE. (9, p. 32)

	Fe
0.15	C
14.5	Cr
13.5	Co
5	Mo
0.5	V
0.05	N_2

AFC-77

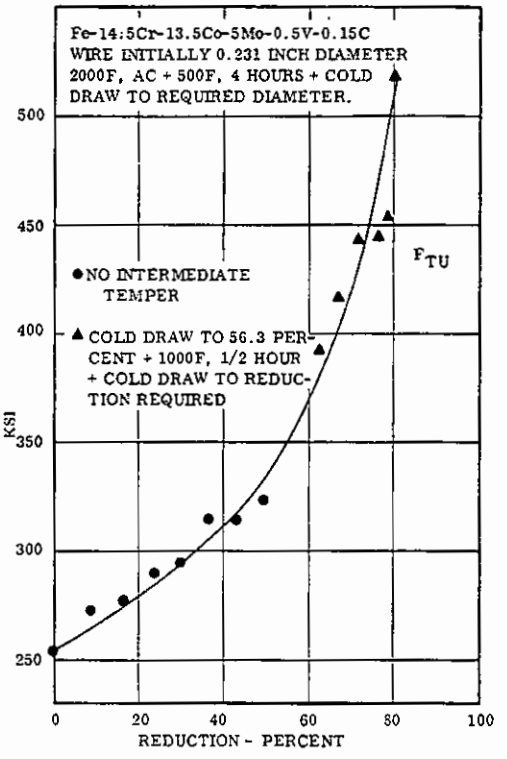


FIG. 3.02142 EFFECT OF COLD REDUCTION ON TENSILE STRENGTH OF ROD. (9, p. 37)

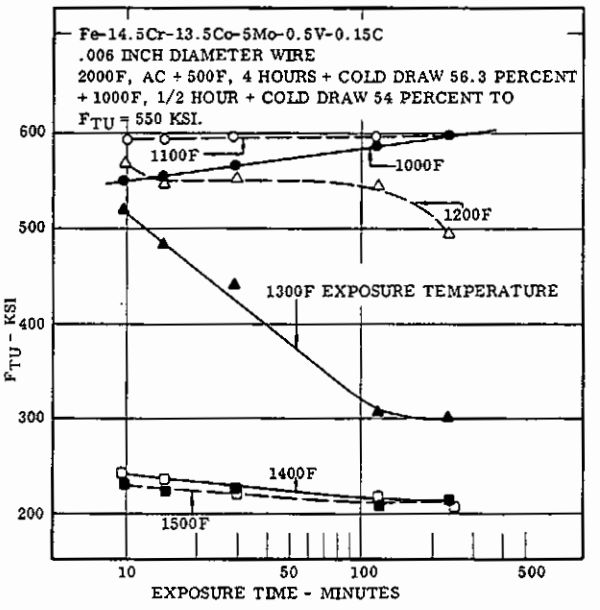


FIG. 3.02144 EFFECT OF SHORT EXPOSURE TO ELEVATED TEMPERATURES ON TENSILE STRENGTH OF FINE WIRE. (9, p. 34)

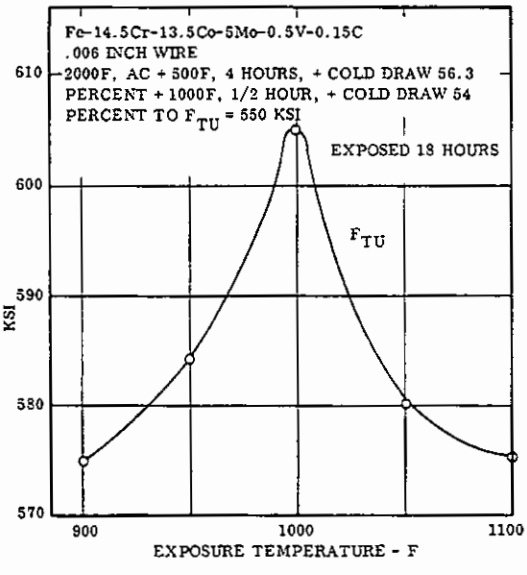


FIG. 3.02143 EFFECT OF EXPOSURE FOR 18 HOURS AT VARIOUS TEMPERATURES ON TENSILE STRENGTH OF FINE WIRE. (9, p. 23)

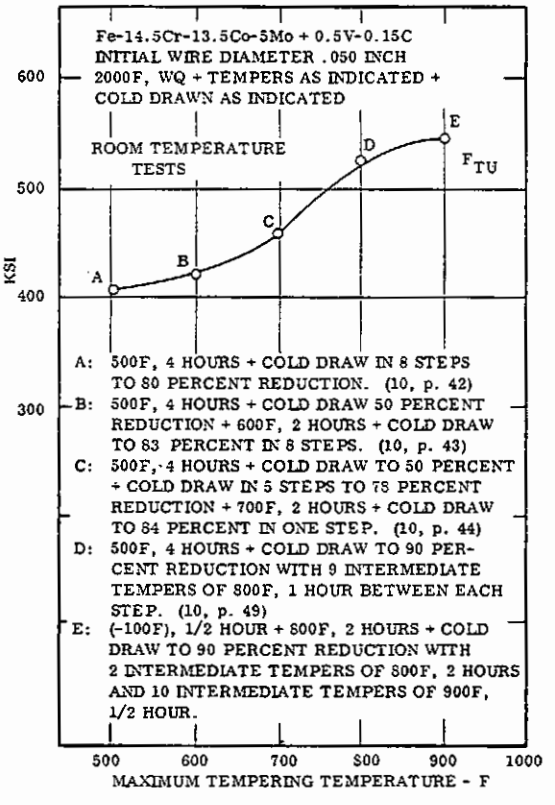


FIG. 3.02145 TENSILE STRENGTHS ACHIEVABLE BY COMBINATIONS OF COLD REDUCTION AND TEMPERING IN SUCCESSIVE STAGES. (10, pp. 42, 43, 49, 50, 56)

	Fe
0.15	C
14.5	Cr
13.5	Co
5	Mo
0.5	V
0.05	N_2

AFC-77

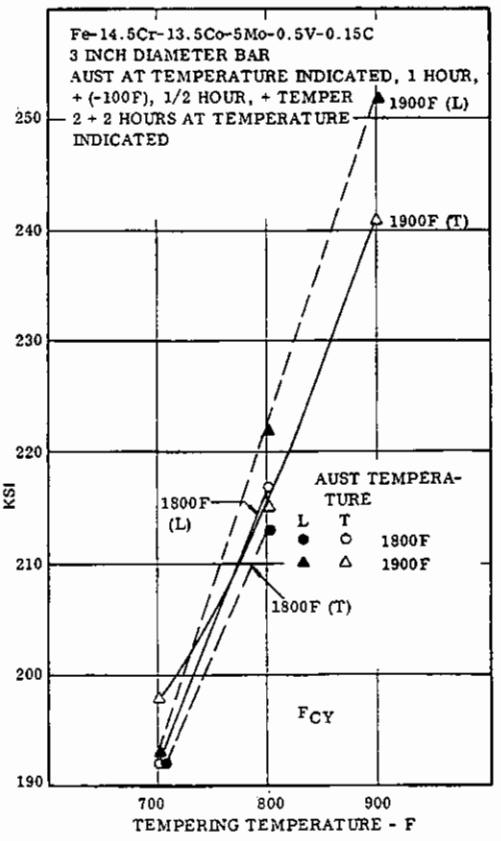


FIG. 3.0222 EFFECT OF AUSTENITIZING AND TEMPERING TEMPERATURES ON COMPRESSIVE YIELD STRENGTH. (12, p. 822)

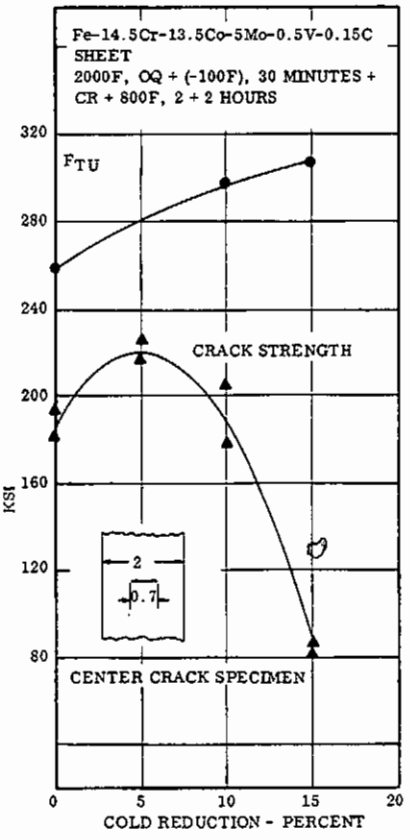


FIG. 3.02711 EFFECT OF COLD REDUCTION ON CRACK STRENGTH. (1, p. 49)

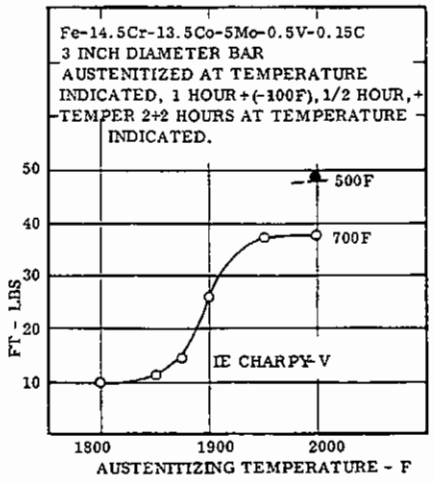


FIG. 3.0231 EFFECT OF AUSTENITIZING TEMPERATURE ON CHARPY IMPACT ENERGY OF BAR TEMPERED AT 500 AND 700F. (12, p. 819)

	Fe
0.15	C
14.5	Cr
13.5	Co
5	Mo
0.5	V
0.05	N_2

AFC-77

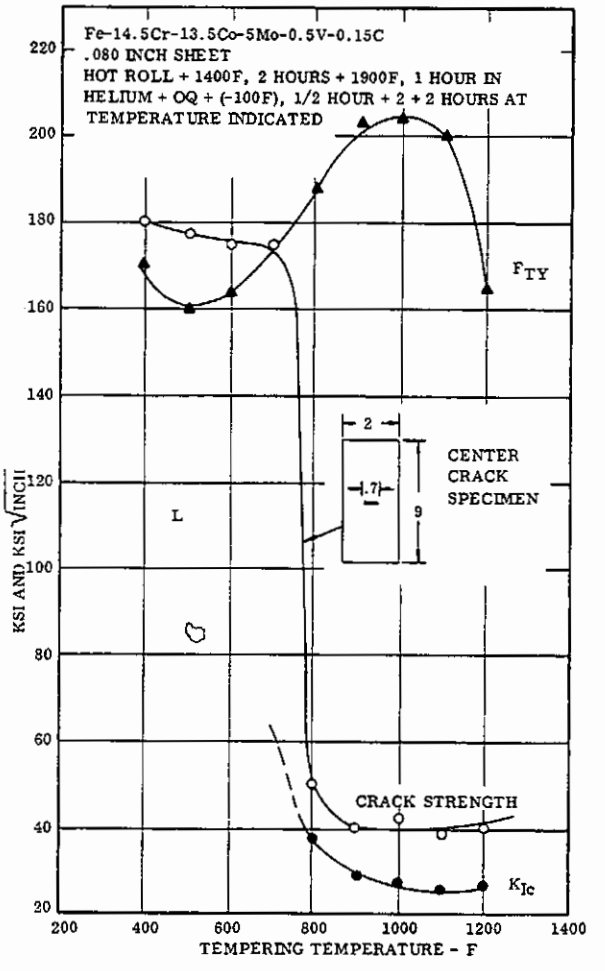


FIG. 3.02712 EFFECT OF TEMPERING TEMPERATURE ON YIELD STRENGTH, CRACK STRENGTH, AND PLANE STRAIN FRACTURE TOUGHNESS OF SHEET. (7, p. 78)

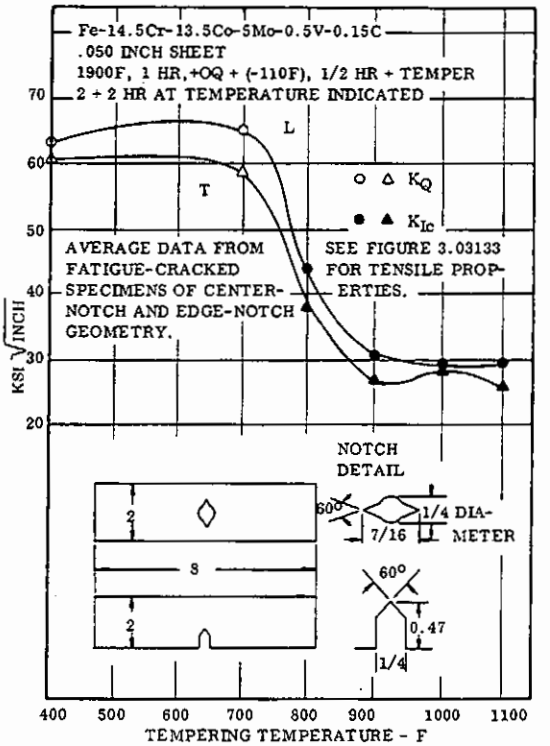


FIG. 3.02722 EFFECT OF TEMPERING TEMPERATURE ON PLANE STRAIN FRACTURE TOUGHNESS OF SHEET. (8, p. 38)

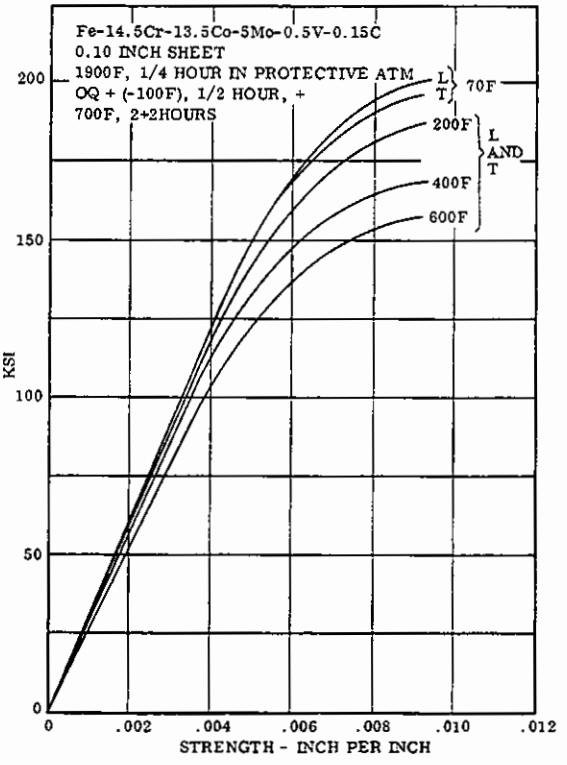


FIG. 3.03111 STRESS-STRAIN CURVES IN TENSION FOR SHEET TEMPERED AT 700F. (6, p. 145)

	Fe
0.15	C
14.5	Cr
13.5	Co
5	Mo
0.5	V
0.05	N_2

AFC-77

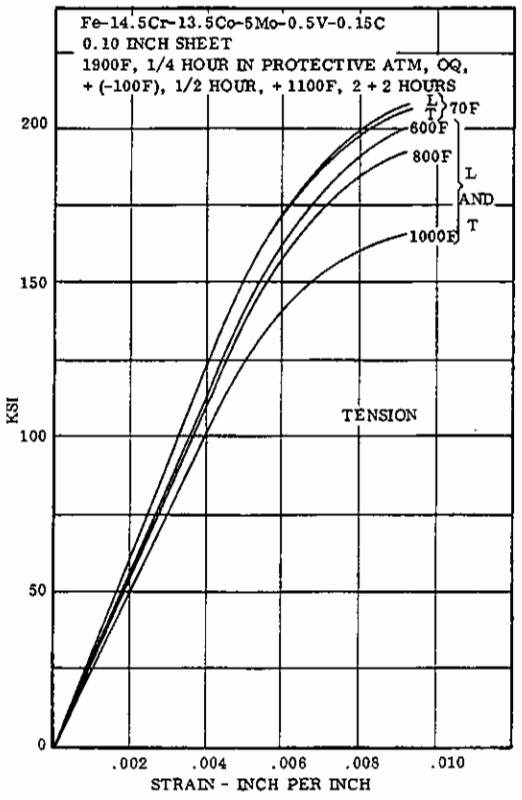


FIG. 3.03112 STRESS-STRAIN CURVES IN TENSION FOR SHEET TEMPERED AT 1100F. (61, p. 160)

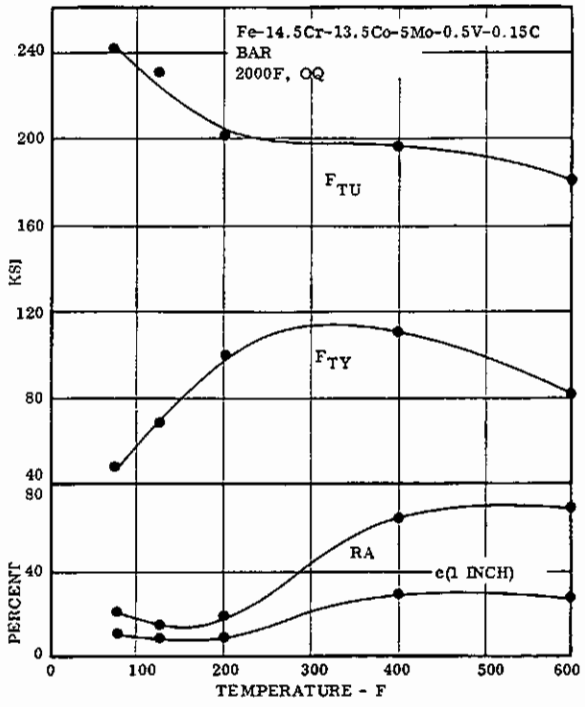


FIG. 3.03121 EFFECT OF TEST TEMPERATURE ON TENSILE PROPERTIES OF BAR AFTER AUSTENITIZING AT 2000F. (2, p. 48)

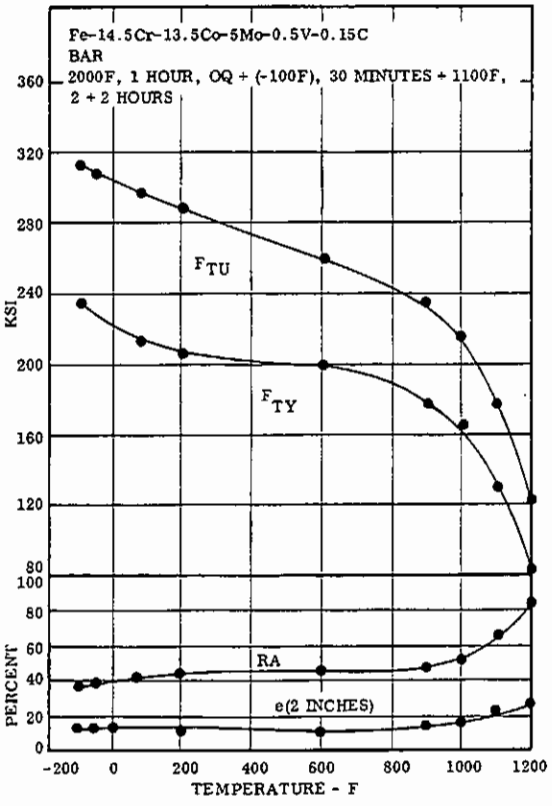


FIG. 3.03123 EFFECT OF TEST TEMPERATURE ON TENSILE PROPERTIES OF BAR FOR ALLOY AUSTENITIZED AT 2000F, AND TEMPERED AT 1100F. (1, p. 81)

	Fe
0.15	C
14.5	Cr
13.5	Co
5	Mo
0.5	V
0.05	N_2

AFC-77

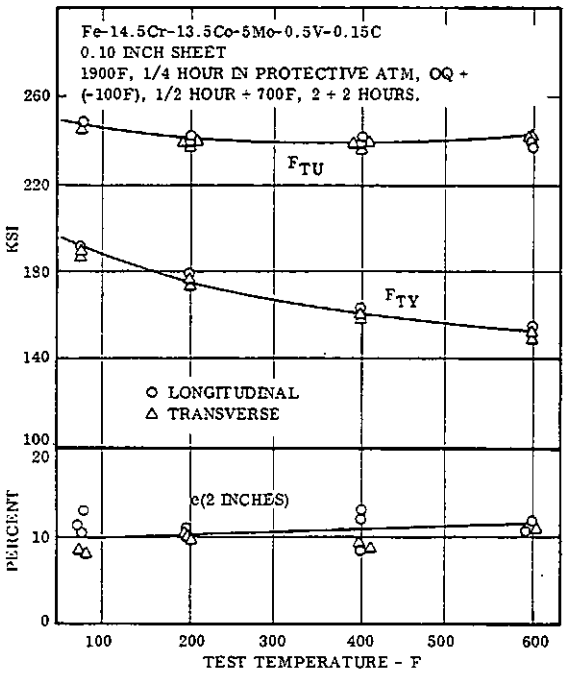


FIG. 3.03131 EFFECT OF TEST TEMPERATURE ON TENSILE PROPERTIES OF 0.10 INCH SHEET TEMPERED AT 700F. (6, p. 146)

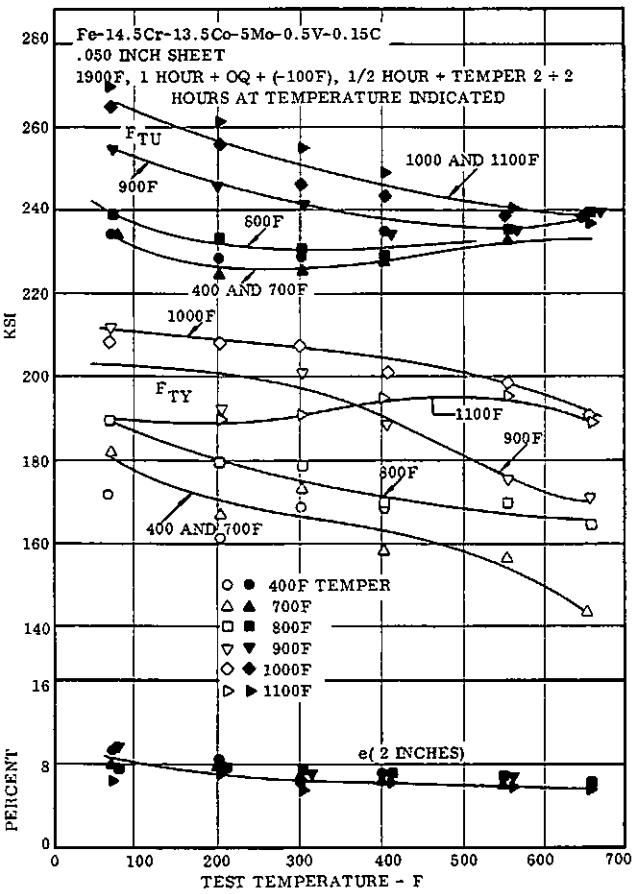


FIG. 3.03133 EFFECT OF TEST TEMPERATURE ON TENSILE PROPERTIES OF .050 INCH SHEET TEMPERED AT VARIOUS TEMPERATURES. (8, p. 22)

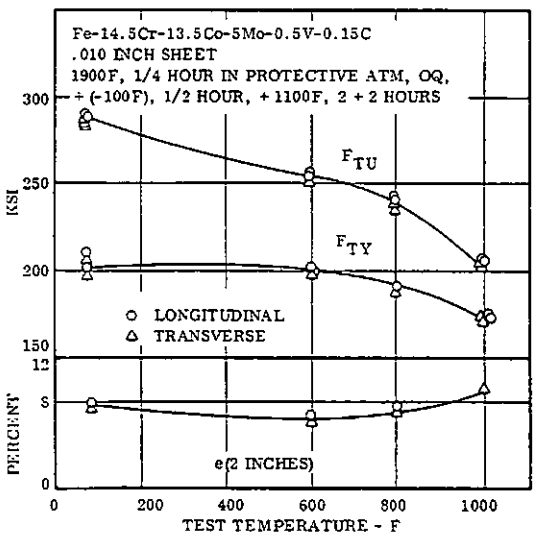
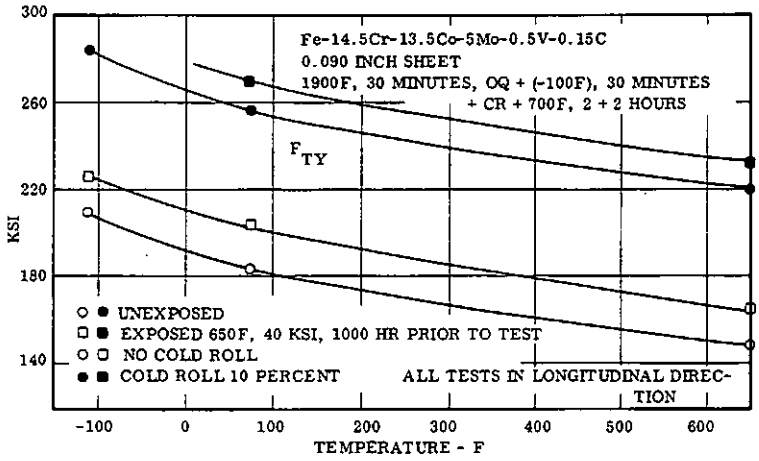


FIG. 3.03132 EFFECT OF TEST TEMPERATURE ON TENSILE PROPERTIES OF .010 INCH SHEET TEMPERED AT 1100F. (6, p. 161)



	Fe
0.15	C
14.5	Cr
13.5	Co
5	Mo
0.5	V
0.05	N_2

AFC-77

FIG. 3.03134 EFFECT OF TEST TEMPERATURE, PRIOR EXPOSURE TO STRESS AND TEMPERATURE ON YIELD STRENGTH OF SHEET IN AS-HEAT-TREATED CONDITION AND AFTER 10 PERCENT COLD ROLL. (1, p. 76)

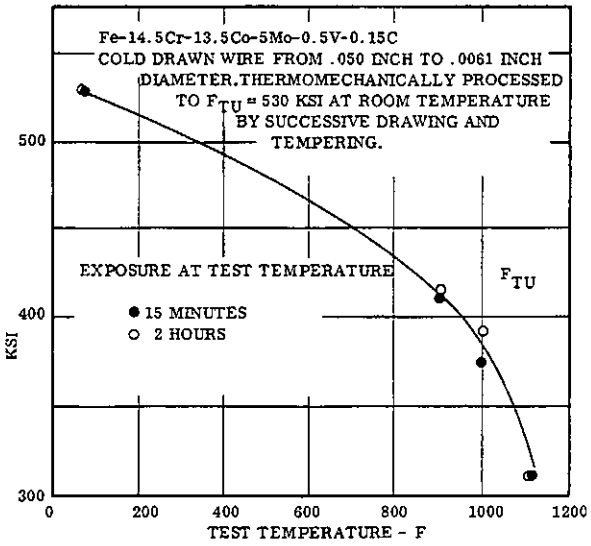


FIG. 3.03142 EFFECT OF ELEVATED TEMPERATURES ON TENSILE STRENGTH OF .006 INCH DIAMETER WIRE THERMOMECHANICALLY PROCESSED TO A ROOM TEMPERATURE TENSILE STRENGTH OF 530 KSI. (10, p. 58)

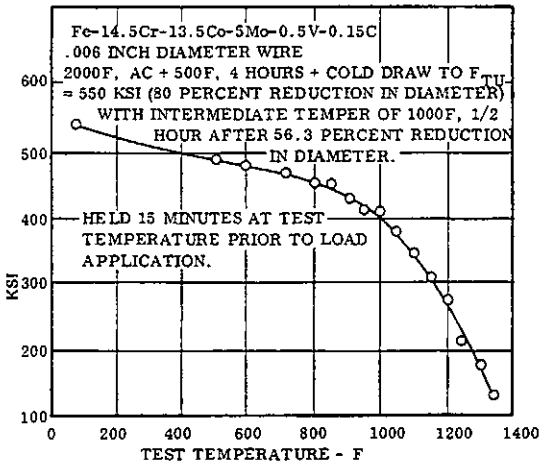


FIG. 3.03141 EFFECT OF TEST TEMPERATURE ON TENSILE STRENGTH OF .006 INCH DIAMETER WIRE. (9, p. 24)

	Fe
0.15	C
14.5	Cr
13.5	Co
5	Mo
0.5	V
0.05	N_2

AFC-77

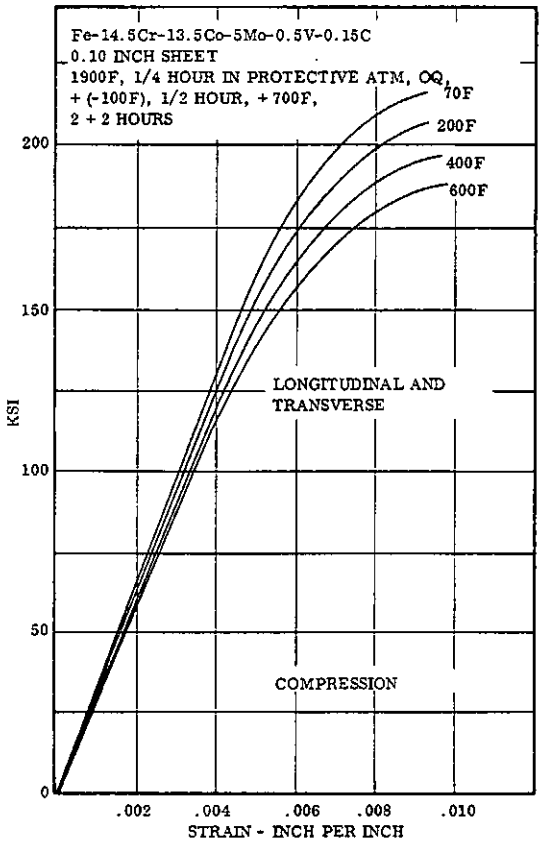


FIG. 3.0321 STRESS-STRAIN CURVES IN COMPRESSION FOR SHEET TEMPERED AT 700F. (6, p. 147)

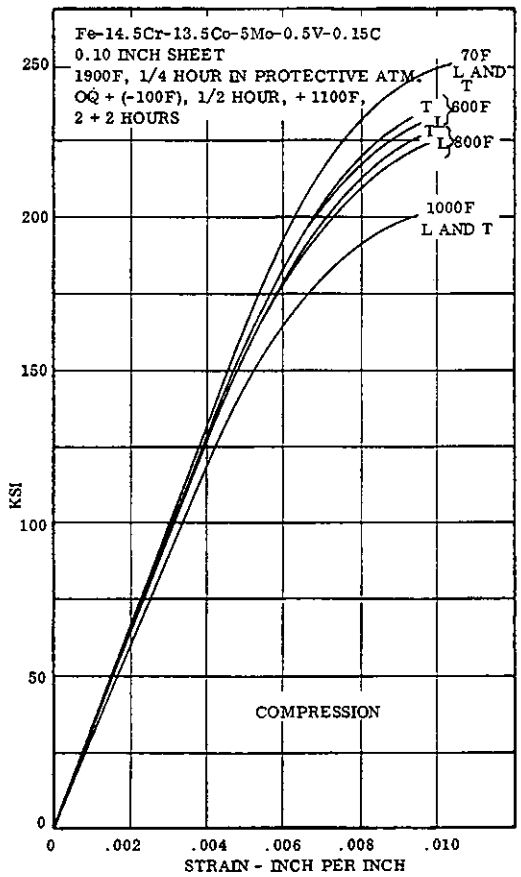


FIG. 3.0322 STRESS-STRAIN CURVES IN COMPRESSION FOR SHEET TEMPERED AT 1100F. (6, p. 162)

	Fe
0.15	C
14.5	Cr
13.5	Co
5	Mo
0.5	V
0.05	N_2

AFC-77

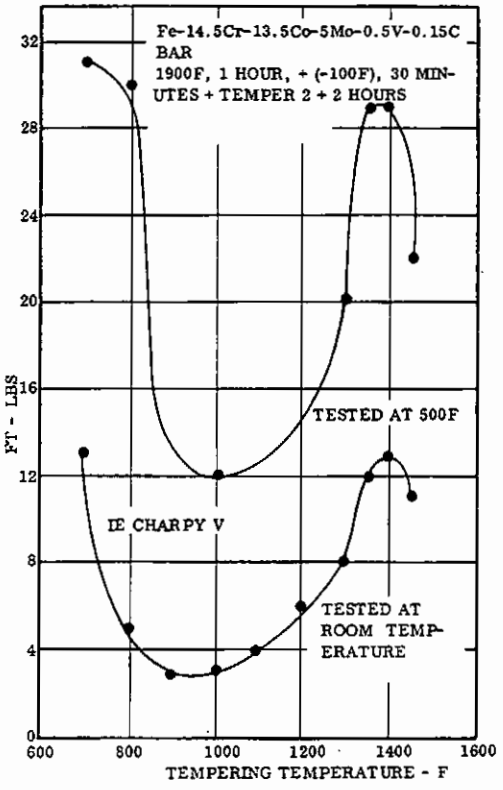


FIG. 3.0331 EFFECT OF TEMPERING TEMPERATURE ON CHARPY V IMPACT PROPERTIES AT ROOM TEMPERATURE AND 500F TEST TEMPERATURES. (1, p. 80)

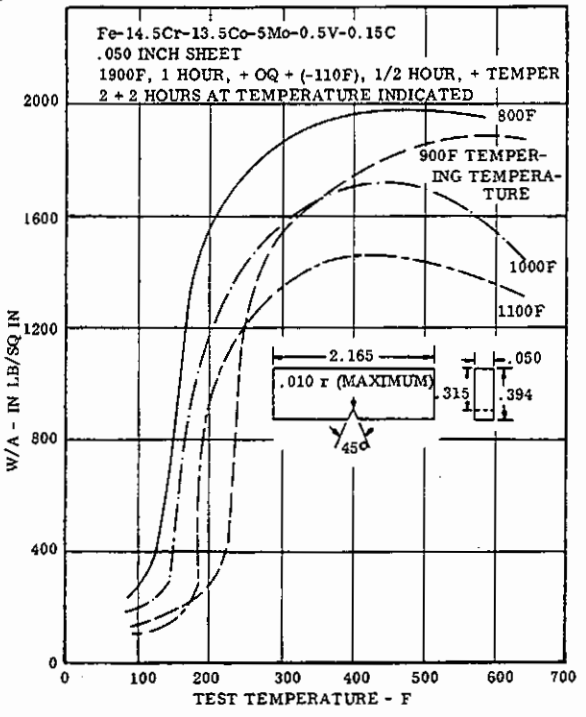


FIG. 3.0332 EFFECT OF TEMPERING TEMPERATURE ON IMPACT ENERGY OF SUBSIZE CHARPY SPECIMEN AT ROOM AND ELEVATED TEMPERATURES. (8, pp. 30, 32, 34, 36)

	Fe
0.15	C
14.5	Cr
13.5	Co
5	Mo
0.5	V
0.05	N_2

AFC-77

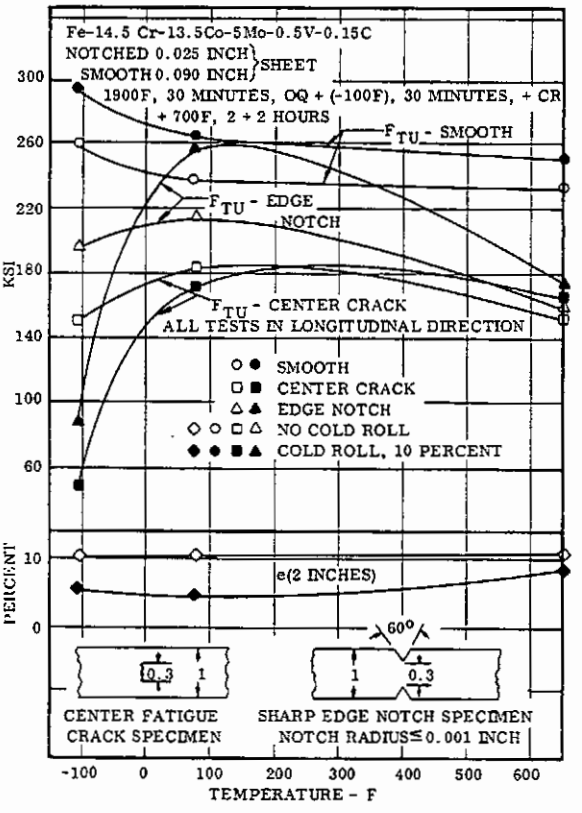


FIG. 3.03711 EFFECT OF TEST TEMPERATURE ON TENSILE PROPERTIES OF SMOOTH AND NOTCHED SHEET IN AS-HEAT-TREATED CONDITION AND AFTER 10 PERCENT COLD ROLL. (1, p. 76)

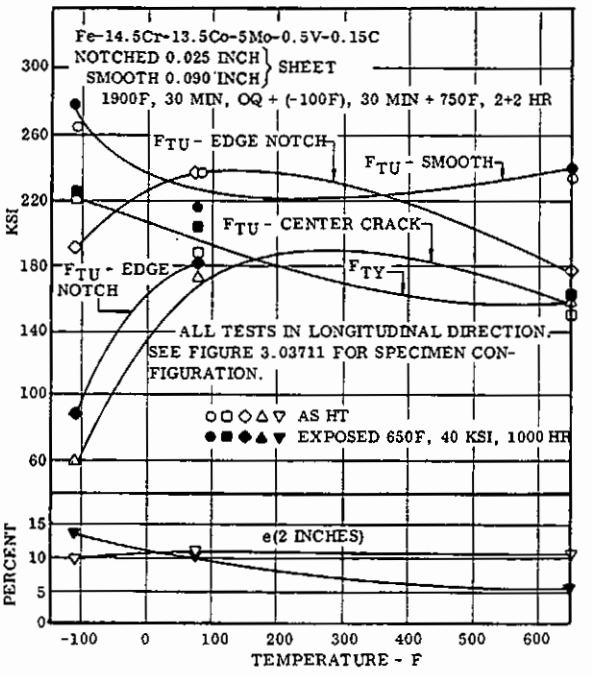


FIG. 3.03712 EFFECT OF TEST TEMPERATURE AND PRIOR EXPOSURE TO STRESS AND TEMPERATURE ON TENSILE PROPERTIES OF SMOOTH AND NOTCHED SHEET TEMPERED AT 750F. (1, p. 76)

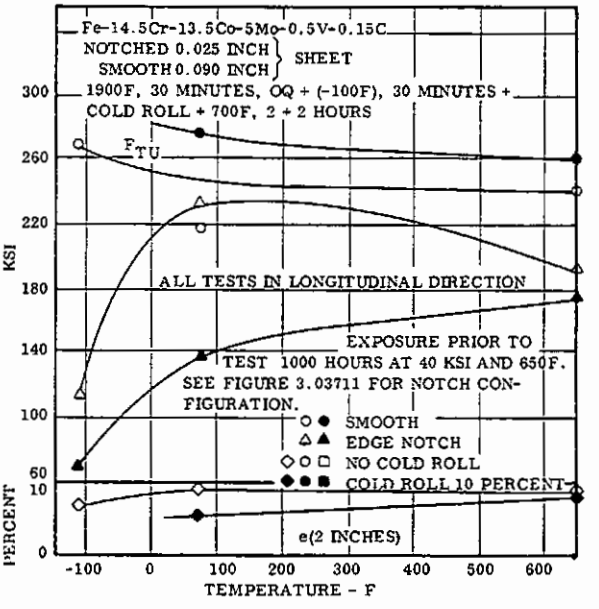


FIG. 3.03713 EFFECT OF TEST TEMPERATURE AND PRIOR EXPOSURE TO STRESS AND TEMPERATURE ON TENSILE STRENGTH AND ELONGATIONS OF SMOOTH AND NOTCHED SHEET IN AS-HEAT-TREATED CONDITION AND AFTER 10 PERCENT COLD ROLL. (1, p. 76)

	Fe
0.15	C
14.5	Cr
13.5	Co
5	Mo
0.5	V
0.05	N_2

AFC-77

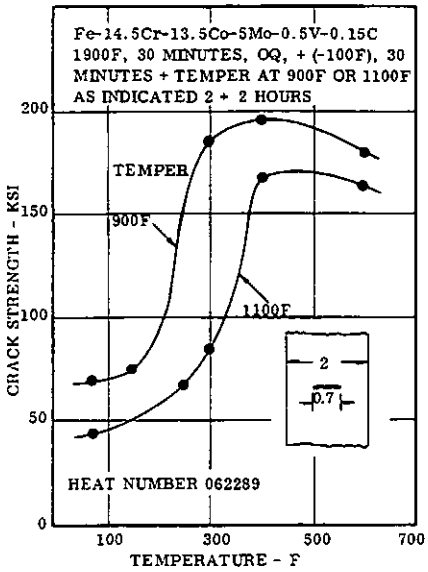


FIG. 3.03714 EFFECT OF TEST TEMPERATURE ON CRACK STRENGTH OF SHEET TEMPERED AT 900 AND 1100F. (5)

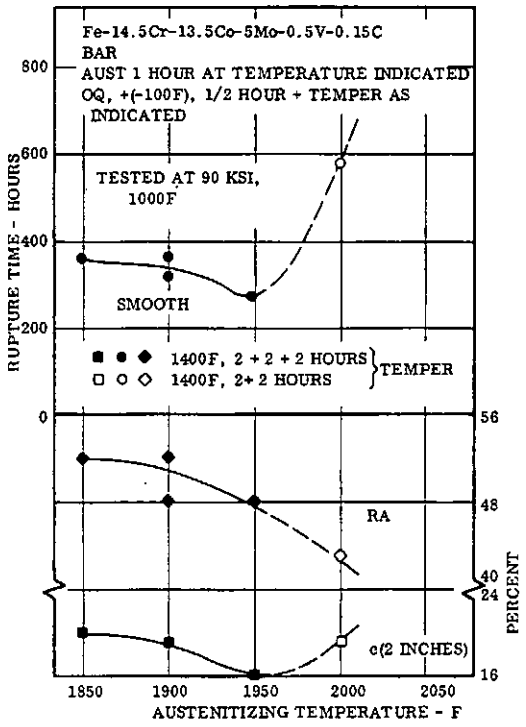


FIG. 3.0412 EFFECT OF AUSTENITIZING TEMPERATURE ON CREEP RUPTURE LIFE AND DUCTILITY AT 90 KSI AND 1000F FOR SMOOTH BAR. (11, p. 36)

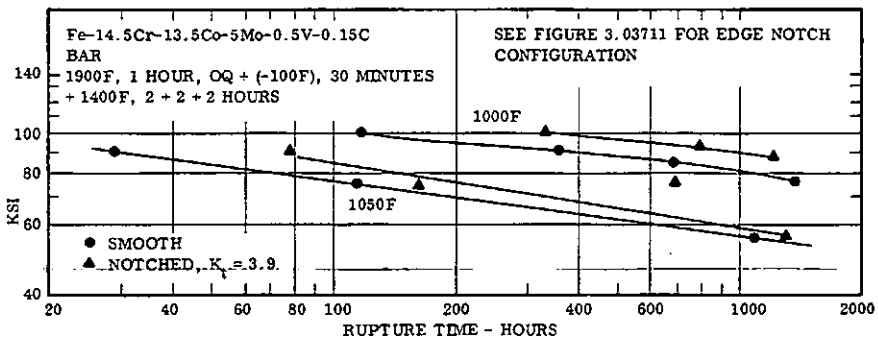


FIG. 3.0411 CREEP RUPTURE CURVES AT 1000 AND 1050F FOR SMOOTH AND NOTCHED BAR TEMPERED AT 1400F. (1, p. 52)

Fe
17 Cr
4 Ni
3 Mo

AM-350

1 GENERAL

This alloy is one of a series of age hardening steels which combines high strength at temperatures up to 800F and higher with the corrosion resistance of stainless steels. In the annealed condition, the alloy is soft and ductile, having many of the desirable forming characteristics of the austenitic stainless steels. In the hardened condition it possesses the high strength and hardness characteristic of the martensitic stainless steels. It is designed primarily for light sections, and is available in sheet, strip, bar, and wire. A companion alloy, AM 355, having slightly lower chromium and higher carbon content, is best suited for heavy sections such as forgings, billets, bars, and plate.

1.01 Commercial Designation

AM-350.

1.02 Alternate Designations

UNS S35000.

1.03 Specifications

Table 1.03.

1.04 Composition

AMS Compositions, Table 1.04.

1.05 Heat Treatment

1.051 For maximum formability and stability, anneal to Condition H.

1.0511 Heat to 1850 to 1975F, air cool or quench in oil or water at rate rapid enough to prevent precipitation of chromium carbides.

1.0512 Sheet and strip, 3/4 hour minimum per inch thickness, rapid air cool to 80F maximum.

1.0513 Forging stock, 1 hour minimum per inch thickness, oil or water quench to 80F maximum.

1.0514 Strip and sheet supplied from mill in Condition H.

1.0515 Bars and forgings should not be annealed to Condition H because of resulting lack of response to heat treatment in larger sizes.

1.052 To prepare alloy for maximum response to subsequent hardening, anneal to Condition L.

1.0521 Heat to 1685 to 1735F, air cool or quench in oil or water, rapid cooling not mandatory, but very slow cooling rates should be avoided.

1.0522 Sheet and strip, 3/4 hour minimum per inch thickness (4 minutes minimum), rapid air cool to 80F maximum.

1.0523 Bars and forgings, 1 hour minimum per inch of thickness, oil or water quench to 80F maximum.

1.053 For best machining equalize and overtemper bar 3 hours at 1425F ± 50F, cool to 80F maximum, 3 hours at 1075F ± 25F.

1.054 For material Condition L, reducing the temperature to -100F causes transformation of austenite to martensite. One method of hardening is, therefore, to reduce the temperature to -100F allowing a minimum of 3 hours to permit the transformation to be completed. Subsequent tempering for 3 hours minimum at 850 to 1050F produces good strength and ductility. This treatment of subcooling and tempering is designated SCT.

1.0541 For highest strength and good ductility use Condition SCT-850. Anneal to Condition L; subcool to -100F, 3 hours minimum; temper 825 to 875F, 3 hours minimum. Higher tempering temperatures, up to 1000F, may be used to increase room temperature impact resistance or to improve machinability. For Condition SCT-1000, age at 975 to 1025F, 3 hours minimum. Effect of aging temperature on tensile properties of sheet in SCT Condition, Fig. 1.0541.

1.055 Alternate method of hardening alloy is by double aging, DA. Starting from either Condition H or Condition L, age at 1350 to 1400F, 2 hours, air cool to 80F maximum, + 850 to 1050F, 3 hours.

1.056 Condition DADF, for improved stress corrosion resistance, consists of Condition SCT followed by subzero freeze at -100F for 3 hours minimum. See section 2.033.

1.057 Hardening may also be accomplished by cold rolling and tempering, CRT. Condition H + cold roll 20 to 45 percent, + temper 700 to 950F.

1.0571 Effect of tempering temperature, test temperature, and prior exposure on properties of sheet cold rolled 30 percent prior to tempering, Fig. 1.0571.

1.0572 Effect of tempering temperature, test temperature, prior exposure, and test direction on notch properties of sheet cold rolled 30 percent prior to tempering, Fig. 1.0572.

1.058 Dimensional changes occur during heat treatment, see section 2.017.

1.06 Hardness

1.061 Effect of test temperature on Brinell hardness of alloy in Conditions SCT and DA, Fig. 1.061.

1.062 Alloy hardness fully in large section sizes after heat treating to either Conditions SCT or DA.

1.07 Forms and Conditions Available

1.071 Alloy is available in sheet, strip, foil, bar, wire, and forgings. Companion alloy AM-355 is, however, preferred in heavy sections such as bar and forgings.

1.072 Sheet, strip, foil, forgings stock, and wire are available in Condition H. Bars and wire are also available in the equalized and tempered Conditions.

1.08 Melting Practice

Electric arc furnace melt followed by argon-oxygen-decarburizing (AOD). Consumable electrode remelt or electroslag remelt are optional.

1.09 Special Considerations

1.091 Heating to temperature above those specified for Condition H should be avoided because of excessive delta ferrite formation and loss of response to hardening.

1.092 Annealing of heavy bar and forging to Condition H may result in loss of response to heat treating.

1.093 Forging of heavy sections should be finished at about 1750F to ensure adequate response to heat treating.

Fe
17 Cr
4 Ni
3 Mo

AM-350

1.094 CRT has optimum stress corrosion resistance. SCT requires either a minimum of 10 percent delta ferrite or a 1000F temper for optimum stress corrosion resistance.

1.095 Dimensional changes during heat treatment require special consideration, see 2.017.

2 PHYSICAL AND CHEMICAL PROPERTIES

2.01 Thermal Properties

2.011 Melting range 2500 to 2550F.

2.012 Phase changes. Alloy at temperature above 1100F starts reverting to austenite. Reversion essentially completed at approximately 1600F. Upon cooling austenite transforms to martensite. On rapid cooling from 1710F, the M_s point is between 80 and 200 F. The austenite is substantially transformed to martensite by cooling to -110F. Holding 3 hours at -110F is desirable since an isothermal transformation component is present. On cooling from 1375F, as in DA treatment, the M_s point is between 250 and 400F and cooling to RT is desirable for substantial transformation to martensite. In both hardening treatments approximately 10 to 20 percent austenite is retained in the structure. This austenite is thermally stable.

2.0121 Time-temperature-transformation diagrams.

2.013 Thermal conductivity, Fig. 2.013.

2.014 Thermal expansion, Fig. 2.014.

2.015 Specific heat, 0.12 Btu per lb F.

2.016 Thermal diffusivity.

2.017 Dimensional changes during various heat treatments, Table 2.017.

2.02 Other Physical Properties

2.021 Density. Table 2.021.

2.022 Electrical properties.

2.0221 Electrical resistivity at room temperature for various conditions, Table 2.0221.

2.0222 Electrical resistivity of bar in SCT Condition, Fig. 2.0222.

2.023 Magnetic properties. Alloy is ferromagnetic. Typical magnetic properties, Table 2.023.

2.024 Emittance.

2.0241 Effect of test temperature and surface condition on total normal emittance and on spectral normal emittance at $\gamma = 0.665$, Fig. 2.0241.

2.025 Damping capacity.

2.03 Chemical Environments

2.031 Corrosion resistance.

2.0311 General corrosion resistance approaches that of austenitic stainless steels.

2.0312 Intergranular attack may occur in Condition DA.

2.032 Oxidation resistance. Comparable to that of austenitic stainless steels.

2.033 Stress corrosion resistance. Tests on 0.020 and 0.060 inch sheet, heat treated to yield strengths of 160 to 198 ksi (standard SCT, modified SCT with annealing temperature 1975F instead of 1925F, and DADF in which a subzero freeze of -100F for 3 hours was added to the SCT treatment), and tested at stress levels of 80 percent F_{ty} did not fall after 1000 hours exposure to two types of stress-corrosion tests:

a) Exposure to semi-industrial atmosphere of Seattle, Washington
b) Alternate immersion in a 3.5 percent NaCl solution. No stress-corrosion cracking was obtained on 0.060 inch welded sheet (both automatic and manual weldments) when exposed for 1000 hours at 80 percent F_{ty} (16).

2.0331 More severe stress corrosion than alternate immersion in a NaCl solution are produced by:

a) exposure to seashore air environment and
b) salt spray.

When exposed to to beach atmosphere at El Segundo, Calif., the SCT-850 alloy is susceptible to stress corrosion cracking. This tendency is detectable at 30-40 percent of F_{ty} and becomes very severe at 60-90 percent of F_{ty}. Susceptibility to stress corrosion cracking becomes even more severe when the alloy in the SCT Condition is heated for 1000 hours at 650F prior to stress corrosion testing. Stress corrosion cracking starts from surface pits with microfissures penetrating along the delta ferrite and possible prior austenite boundaries as a result of some electrochemical (or combination of electrochemical and mechanical) action. Groups of microfissures are formed in positions approximately perpendicular to the direction of tensile load. When the microfissures sufficiently penetrate into the metal they are joined together by breaking down of the bridges of metal separating them (17, p. 369, 374). Effect of several stress corrosion environments on time to failure of unnotched sheet in SCT-850 Condition, Fig. 2.0331.

The stress corrosion resistance of AM-350 SCT with an 850F temper is considerably improved if a minimum of 60 percent delta ferrite is present in the structure. Further improvement is achieved by tempering at 1000F.

2.0332 In the SCT-850 Condition, the alloy is also susceptible to corrosion fatigue at room temperature. At 110 ksi maximum stress (R = 0.2), corrosion fatigue life was 16 percent of air fatigue life. There was no significant effect of frequency (100 cpm~1800 cpm) on fatigue life either in air or in synthetic seawater environments (17, p. 369). Effect of synthetic seawater environment and cyclic frequency on axial fatigue of sheet in SCT-850 Condition, Fig. 2.0332.

2.0333 Exposure for 1000 hours at 650F and braze cycling increased susceptibility to stress corrosion cracking of SCT-850 sheet. Surface condition was also found to be important. Vapor honing and passivation reduced susceptibility to stress corrosion cracking. Welding had no effect (17, p. 11-12).

2.0334 Good resistance to stress corrosion cracking was obtained by alloy in CRT Condition. However, welded CRT alloy showed tendency to initiate stress corrosion cracks at root of pre-existing fatigue cracks. Effect of stress, precracking, and alternate immersion in synthetic seawater, on stress corrosion cracking of

AM-350 CRT subjected to prior exposure of 650F for 1000 hours, Fig. 2.0334.

2.04 Nuclear Properties

3 MECHANICAL PROPERTIES

3.01 Specified Mechanical Properties

3.011 AMS specified mechanical properties for strip, sheet, and tubing, Table 3.011.

3.012 AMS specified mechanical properties for bars and forgings, Table 3.012.

3.013 Producer's specified mechanical properties, Table 3.013.

3.02 Mechanical Properties at Room Temperature
See also 3.03.

3.021 Tension.

3.0211 Stress-strain diagrams, see 3.0311.

3.0212 Effect of exposure time and temperature on room temperature tensile properties of sheet from three heats in Condition H-1900, Fig. 3.0212.

3.0213 Effect of stretching and subsequent aging to Condition SCT-850 on tensile properties of sheet in Condition L, Fig. 3.0213.

3.0214 Effect of tempering temperature and test direction on notch strength of sheet, Fig. 3.0214.

3.0215 Effect of percent cold draw and of tempering time and temperature on tensile properties of wire, Fig. 3.0215.

3.022 Compression, see 3.032.

3.0221 Stress-strain diagrams, see 3.032.

3.023 Impact, see 3.033.

3.024 Bending.

3.025 Torsion and shear.

3.026 Bearing, see 3.036.

3.027 Stress concentration, see 3.037.

3.0271 Notch properties, see 3.0214.

3.0272 Fracture toughness.

3.028 Combined properties.

3.03 Mechanical Properties at Various Temperatures

3.031 Tension.

3.0311 Stress-strain diagrams.

3.03111 Tensile and compressive stress-strain curves for sheet in L annealed Condition at room and elevated temperatures, Fig. 3.03111.

3.03112 Stress-strain curves for sheet in SCT Condition at room and elevated temperature, Fig. 3.03112.

3.03113 Stress-strain curves for sheet in DA Condition at room and elevated temperature, Fig. 3.03113.

3.03114 Stress-strain curves for sheet in SCT Condition at low temperature, Fig. 3.03114.

3.03115 Stress-strain curves for sheet in 20 percent CRT Condition at temperatures between -110 to 650F, Fig. 3.03115.

3.03116 Stress-strain curves of sheet in 30 percent CRT Condition at temperature between -110 to 650F, Fig. 3.03116.

3.0312 Effect of test temperature and prior exposure to stress and temperature on tensile properties of sheet in L annealed Condition, Fig. 3.0312.

3.0313 Effect of test temperature on tensile properties of sheet rolled from two heats in Condition H-1900, Fig, 3.0313.

3.0314 Effect of test temperature on tensile properties of sheet in Condition DA, Fig. 3.0314.

3.0315 Effect of test temperature on tensile properties of sheet in Condition SCT, Fig. 3.0315.

3.0316 Effect of low test temperature on tensile properties of sheet in Condition SCT, Fig. 3.0316.

3.0317 Effect of test temperature on transverse tensile properties of sheet in CRT Condition, Fig. 3.0317.

3.0318 Effect of test temperature, cold reduction, and prior exposure on tensile properties of sheet in CRT Condition, Fig. 3.0318. See also Fig. 1.0571 and 1.0572.

3.032 Compression.

3.0321 Compressive stress-strain curves for sheet in L annealed Condition at room and elevated temperatures, see Fig. 3.03111.

3.0322 Stress-strain curves in compression for sheet in DA Condition at room and elevated temperatures, Fig. 3.0322.

3.0323 Stress-strain curves in compression for sheet in SCT Condition at room and elevated temperatures, Fig. 3.0323.

3.0324 Effect of test temperature on compressive yield strength of sheet in Condition H, DA, and SCT, Fig. 3.0324.

3.033 Impact.

3.0331 Effect of test temperature on Charpy V impact properties of alloy in SCT Condition, Fig. 3.0331.

3.034 Bending.

3.035 Torsion and shear.

3.0351 Effect of test temperature on shear strength of sheet in L annealed Condition, Fig. 3.0351.

3.0352 Effect of test temperature on shear strength of sheet in Condition SCT-850, Fig. 3.0352.

3.036 Bearing.

3.0361 Effect of test temperature on bearing properties of sheet in annealed Condition, Fig. 3.0361.

3.0362 Effect of test temperature on bearing properties of sheet in Condition SCT-850, Fig. 3.0362.

3.037 Stress concentration.

3.0371 Effect of low test temperature on notch strength and notch strength ratio of sheet in SCT Condition, Fig. 3.0371.

3.0372 Effect of net section area and test temperature on net section strength of sheet in DA Condition, Fig. 3.0372.

3.0373 Effect of net section area and test temperature on net section strength of sheet in CRT Condition, Fig. 3.0373.

3.0374 Effect of test temperature, cold reduction, test direction, and prior exposure on ratio of sharp notch strength to yield strength of sheet in CRT Condition, Fig. 3.0374.

3.0375 Effect of test temperature, amount of cold work, tempering conditions, and testing direction on notch tensile strength after exposure to coating of natural sea salt while under stress at high temperature, Fig. 3.0375.

3.0376 Effect of crack length fraction, method of producing crack, prior exposure, and test temperature on residual strength and net section strength of sheet in CRT Condition, Fig. 3.0376.

3.0377 Effect of test temperature on fracture toughness and residual strength ratio of three heats of sheet in Condition SCT, Fig. 3.0377.

Fe
17 Cr
4 Ni
3 Mo

AM-350

Fe
17 Cr
4 Ni
3 Mo

AM-350

3.0378 Effect of test temperature on fracture toughness and residual strength ratio of sheet in Condition CRT, Fig. 3.0378.

3.038 Combined properties.

3.04 Creep and Creep Rupture Properties

3.041 General.

3.042 Creep rupture properties.

3.0421 Creep rupture properties at 800 to 1000F of alloy in DA Condition, Fig. 3.0421.

3.0422 Creep rupture properties at 800 and 900F of sheet in SCT Condition, Fig. 3.0422.

3.043 Creep deformation.

3.0431 Minimum creep rate curves at 600, 700, and 800F for sheet in SCT Condition, Fig. 3.0431.

3.0432 Total creep curves at 800F for sheet in Condition SCT, Fig. 3.0432.

3.0433 Isochronous stress–strain curves for sheet in Condition SCT at 600 to 800F, Fig. 3.0433.

3.05 Fatigue Properties

3.051 Fatigue curves for sheet in Condition SCT, Fig. 3.051.

3.052 Fatigue properties in Condition SCT (850F) at 550F, 650F, and 800F, Fig. 3.052.

3.053 Effect of stress and test temperature on the fatigue of brazed lap joints in Condition SCT, Fig. 3.053.

3.054 Crack propagation rate as a function of the stress intensity factor for AM-350 CRT, Fig. 3.054.

3.055 Fatigue behavior of smooth and notched sheet in Condition SCT with salt coating, Table 3.055.

3.056 Effect of joining method and of stress concentration on fatigue behavior at room temperature of sheet in Condition CRT, Fig. 3.056.

3.057 Effect of test temperature and prior exposure on fatigue behavior of smooth and notched sheet in Condition CRT, Fig. 3.057.

3.058 Effect of joining method and of stress concentration on fatigue behavior at 550F of sheet in Condition CRT, Fig. 3.058.

3.059 Effect of joining method and of stress concentration on fatigue behavior at 800F of sheet in Condition CRT, Fig. 3.059.

3.06 Elastic Properties

3.061 Poisson's ratio.

3.062 Modulus of elasticity.

3.0621 Modulus of elasticity at various temperatures of alloy in Condition SCT 850 and DA, Fig. 3.0621.

3.0622 Effect of test temperature and prior exposure to stress and temperature on elastic modulus of sheet in annealed Condition, Fig. 3.0622.

3.063 Modulus of rigidity at room and elevated temperatures, Fig. 3.063.

4. FABRICATION

4.01 Forming

4.011 General. Condition H has a formability similar to that of austenitic steels except for a higher rate of strain hardening due to martensite formation. Condition L is even less stable. It strain hardens more rapidly and therefore possesses inferior forming characteristics. Alloy in Conditions H and L can be formed with advantage at 300F or higher due to absence of martensite formation and correspondingly decreased rate of strain hardening. The heat treated Condition SCT permits minor forming operations, including bending, straightening and dimpling, while Condition DA is still more difficult to form.

4.012 Bending. Bend factor for Condition SCT = 3, for Condition DA = 5.

4.013 Sheet formed in Condition H needs a subsequent full heat treatment. If it is possible to form the alloy in Condition L, subsequent aging to Condition SCT will produce about the same properties as obtained without the strain hardening due to forming.

4.014 Straightening of parts to be heat treated to Condition SCT is performed preferably after cooling to -100F to reduce the dimensional changes occurring during heat treating. Stretched parts show little dimensional changes.

4.015 Forging. Starting temperature 2100F maximum. Finishing temperature should be about 1750F to ensure adequate response to heat treating. Before heat treating, forgings should be equalized at 1375F.

4.02 Machining and Grinding

4.021 General. Machining properties of AM-350 are similar to those of austenitic stainless steels. Rigid supports, positive cuts, and adequate cooling are required.

4.022 Conditions H and L do not machine well because of their initial softness and their high rate of strain hardening. For best machining, it is recommended that the alloy be subjected to an equalizing treatment with a resulting hardness of about 35 RC (see Section 1.053).

4.023 Allowance must be made for growth on subsequent heat treatment. For extreme dimensional accuracy, finish machining should be done on material in Condition SCT or DA, which machine in a manner similar to low alloy steels of equal hardness.

4.03 Joining

4.031 Welding.

4.0311 General. AM-350 can be welded by all the conventional methods used for chromium-nickel stainless steels. Gas tungsten-arc, gas metal-arc, covered electrode, submerged arc or flash welding can be used to produce sound welds with good ductility. It is easier to weld martensitic steels because they do not require preheating or postheating to minimize cracking. As-welded AM-350 can be hardened by the DA treatment (see 1.055) without reannealing. To obtain proper response to the SCT treatment, AM-350 must be reannealed at 1675 to 1775F prior to hardening. To obtain greatest weld strength, AM-355 weld filler metal should be used. Where ductility is more important

than strength requirements, austenitic welding rods such as AISI Type 308, 309 or 310 can be used. Heat treated welds having 90 to 100 percent joint efficiency in light gage material can be obtained without filler metal. AM-350 may be electric resistance welded in either the hardened or annealed condition. Resistance welding may precede or follow hardening to obtain high strength joints. Spot welding of hardened sheet can be performed by proper selection of current and electrode size to give tension shear values equal to and tension impact and fatigue strength values higher than those of welded and subsequently hardened material.

When joining wrought AM-350 to AM-355 castings, highest strength can be obtained in the weld and heat affected zones by heating at 1375 to 1475F for 3 hrs, air cooling to 80F maximum, reannealing at 1675 to 1775F followed by rapid cooling. This is followed by the normal SCT treatment.

4.0312 The properties of AM-350 sheet welded with AM-350 or AM-355 filler metal, Table 4.0312.

4.0313 Tensile properties of sheet welded transverse to the rolling direction and given several post-weld treatments Table 4.0313.

4.0314 Elevated temperature properties of AM-350 sheet welded transverse to the rolling direction, Fig. 4.0314.

4.0315 Room temperature shear strength of spot welded AM-350 sheet, .024 in. thick, Table 4.0315.

REFERENCES

1 "Allegheny Ludlum Precipitation Hardening Stainless Steels, AM-350 and AM-355", Allegheny Ludlum Steel Corp., (1960)

2 "Latest Information on AM-350 and AM-355 as of 1959", Allegheny Ludlum Steel Corp., (1959)

3 "Engineering Properties of Precipitation Hardening Alloys, AM-350 and AM-355", Allegheny-Ludlum Steel Corp.

4 Raring, R. H., Freeman, J. W., Schultz, J. W. and Voorhees, H. R., "Progress Report of the NASA Special Committee on Materials Research for Supersonic Transports", NASA TN D-1798", (May 1963)

5 Ludwigson, D. C., "Semi-Austenitic Precipitation Hardenable Stainless Steels", DMIC Report 164", (December 5, 1961)

6 Pearl, H. A., Kappelt, G. F., King, E. J., "Mechanical Properties of Selected Alloys at Elevated Temperatures", WADC TR-59-702, Part I, (March 1960)

7 Figge, I. E., "Residual Static Strength of Several Titanium and Stainless Steel Alloys and One Superalloy at -109F, 70F and 550F", NASA TN D-2045, (December 1963)

8 Gideon, D. N., Marschall, C. W., Holden, F. C., and Hyler, W. S., "Exploration of Mechanical Cycling Fatigue Behavior of Materials for the Supersonic Transport", NASA CR-28, (April 1964)

9 Peterson, J. J., "Fatigue Behavior of AM-350 Stainless Steel and Titanium 8Al-1Mo-IV Sheet at Room Temperature, 550F and 800F", NASA CR-23, (May 1964)

10 Henning, R. G. and Brisbane, A. W., "Mechanical Properties of AM-350 Potomac A, Potamac M and Vascojet 1000 Steel Alloys in the Annealed Condition", ASD-TDR-63-116, (May 1963)

11 Favor, R. J., Grover, H. J. and Achbach, W. P., "Fatigue Data on Precipitation Hardenable Stainless Steels", DMIC Memo. 46, (March 1960)

12 Epsey, G. B. Bubsey, R. T. and Brown, W. F., Jr., "A Preliminary Report on the NASA Sheet Alloy Screening Program for Mach 3 Transport Skins", ASTM, Vol. 62, (1962)

13 "General Materials Information", Northrop Corp., Phase I, Prog. Report No. 2, (July 1 to Sept. 30, 1961)

14 "Notch Resistance and Fracture Toughness Characteristics of High Strength Metals", Douglas Aircraft Corp., ASD-TDR-63-494, (September 1963)

15 Wood, W. D., Deem, H. W. and Lucks, C. F., "Thermal Radiative Properties of Selected Materials", DMIC Report 177, Vol. 1, (November 15, 1962)

16 Dreyer, G. A. and Gallaugher, W. C., "Investigation of the Effects of Stress Corrosion on High Strength Alloy Steels", AF Material Laboratory Report, ML-TDR-64-3, (February 1965)

17 "Chloride Stress Corrosion Susceptibility of High Strength Stainless Steel, Titanium Alloy and Superalloy Sheet", Douglas Aircraft Corp., Technical Documentary Report No. ML-TDR-64-44, Vol. 1, (March 1964)

18 AMS 5745B (April 1, 1981)

19 AMS 5546 (July 16, 1979)

20 AMS 5548 F (Oct. 15, 1979)

21 NASA, (1959)

22 "Growth of AM-350 Sheet and Strip During Heat Treatment", Allegheny Ludlum Steel Corp., Data Sheet, 116-102258-350, (1959)

23 "Room and Elevated Temperature Tensile and Compressive Properties of Type AM-350", Allegheny Ludlum Steel Corp., Data Sheet 86-11457-350, (1958)

24 McGee, R. L., Campbell, J. E., Carlson, R. L. and Manning, G. K., "The Mechanical Properties of Certain Structural Metals at Very Low Temperature", WADC-TR 58-386, (June 1958)

25 "Shear and Bearing Strength of AM-350 at Room and Elevated Temperature", Allegheny Ludlum Steel Corp., Data Sheet 125-71659-350, (1957)

26 "Stainless Steel AM-350", North American Aviation Corp., Data Sheet, A. L-Z604, (1957)

27 NASA, (1959)

28 "Creep Data AM-350 and AM-355 Alloys", Allegheny Ludlum Steel Corp., Data Sheet 119-121658S, . . .

Fe
17 Cr
4 Ni
3 Mo

AM-350

Fe
17 Cr
4 Ni
3 Mo

AM-350

29 "Flexural Fatigue Strength of AM-350", Allegheny Ludlum Steel Corp., Data Sheet 115-92358-350, (1959)

30 "Elastic Constants of AM-350 and AM-355", Allegheny Ludlum Steel Corp., Data Sheet 90-1758-R, (1959)

31 AMS 5546, (July 16, 1979)

32 Alessandro L. P., Lachmann H. P. "Fatigue Evaluation of Ti-8Al-1Mo-1V and AM-350 (SCT) Stainless Steel. Air Force Mat. Lab. Report MAA 67-3 (Jan. 1967)

33 Lehr, K. R. and Liu, H. W., "Fatigue Crack Propagation and Strain Cycling Properties", Syracuse University Research Institute MET.E. 1340-0768-ITR (July 1968)

34 "The Properties of AM-350 Welds", Allegheny Ludlum Steel Corp. Data Sheet 114

35 "Engineering Properties of Precipitation Hardening Alloys AM-350 and AM-355", Allegheny Ludlum Steel Corp. (1960)

36 "The Tension Shear Strength of Spot Welded AM-350", Allegheny Ludlum Steel Corp. Data Sheet 124

37 AMS 5554 (Jan. 1, 1982)

38 AMS 5775 A (April 15, 1978)

39 AMS 5774 B (July 1, 1981)

AMS	Form	Condition
5745	Bars and Forgings	Heat treated to F_{TU} = 165 ksi min
5546	Sheet and Strip, Cold Rolled, Tempered	
5548	Sheet and Strip, High Temperature Annealed	
5554	Steel Tubing, Seamless	
5775	Welding Electrodes, Covered	
5774	Welding Wire	

TABLE 1.03. AMS SPECIFICATIONS

Alloy	Fe-17Cr-4Ni-3Mo	
	Percent	
	Min	Max
C(a)	0.07	0.11
Mn	0.50	1.25
Si	–	0.050
P	–	0.040
S	–	0.030
Cr	16.00	17.00
Ni	4.00	5.00
Mo	2.50	3.25
Ni	0.07	0.13

(a) AMS 5554 (37), AMS 5774B (38) & AMS 5775A (39) give 0.08 to 0.12 C

TABLE 1.04. AMS COMPOSITIONS (18)(19)(20)(37)(38)(39)

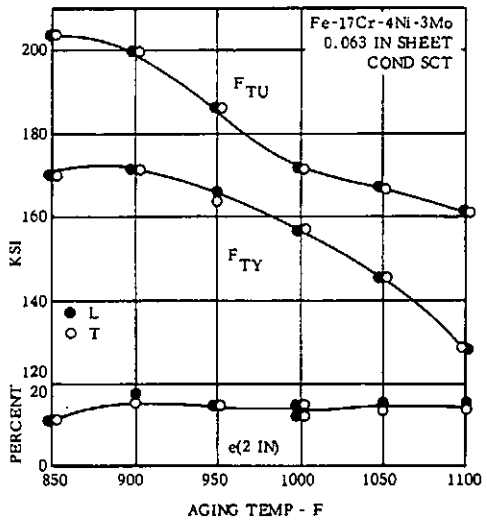


FIG. 1.0541 EFFECT OF AGING TEMPERATURE ON TENSILE PROPERTIES OF SHEET IN SCT CONDITION (21)

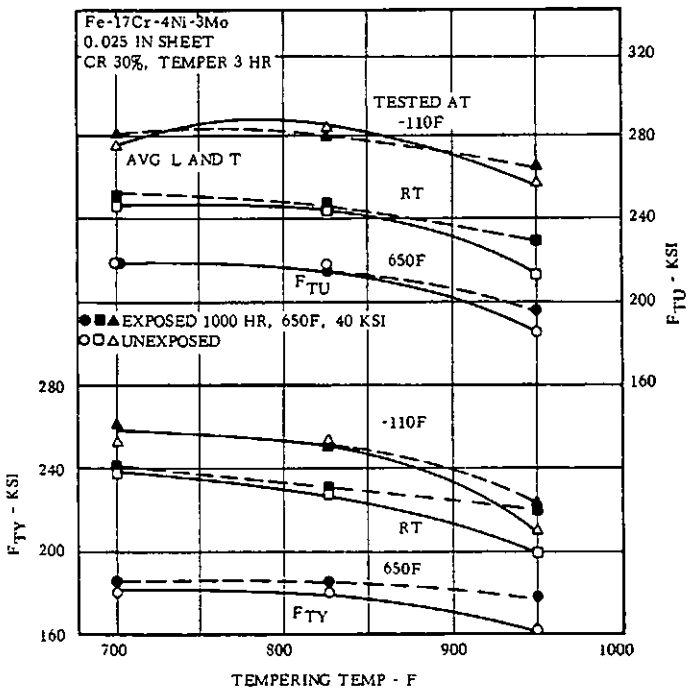


FIG. 1.0571 EFFECT OF TEMPERING TEMPERATURE, TEST TEMPERATURE AND PRIOR EXPOSURE ON TENSILE PROPERTIES OF SHEET COLD ROLLED 30 PERCENT PRIOR TO TEMPERING (12, p. 843)

Fe
17 Cr
4 Ni
3 Mo

AM-350

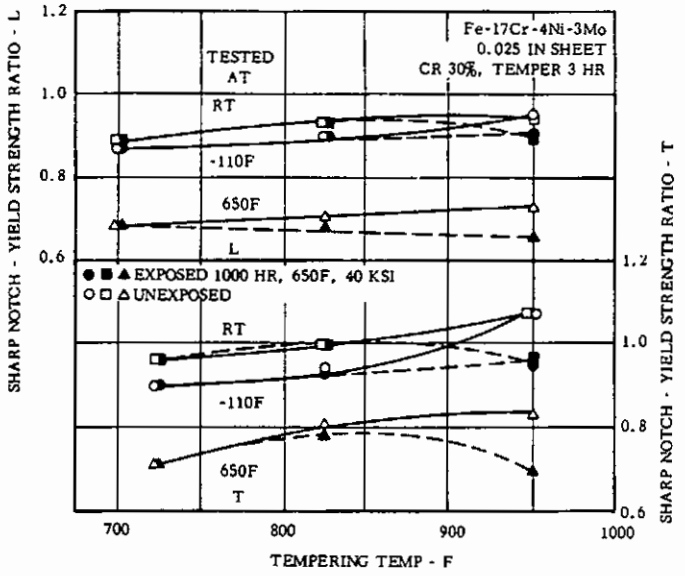


FIG. 1.0572 EFFECT OF TEMPERING TEMPERATURE, TEST TEMPERATURE PRIOR EXPOSURE AND TEST DIRECTION ON NOTCH PROPERTIES OF SHEET COLD ROLLED 30 PERCENT PRIOR TO TEMPERING (12, p. 843)

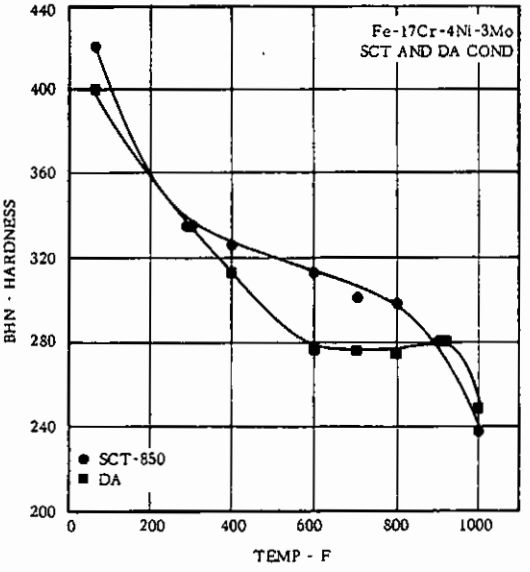


FIG. 1.061 EFFECT OF TEST TEMPERATURE ON BRINELL HARDNESS OF ALLOY IN CONDITIONS SCT AND DA (2)

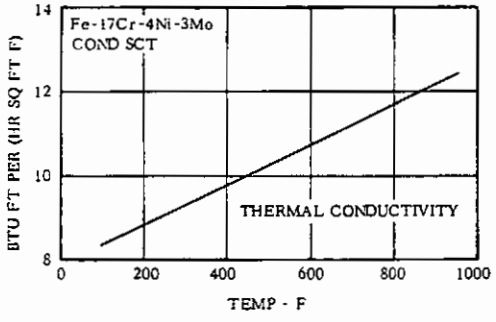


FIG. 2.013 THERMAL CONDUCTIVITY (1, p. 8)

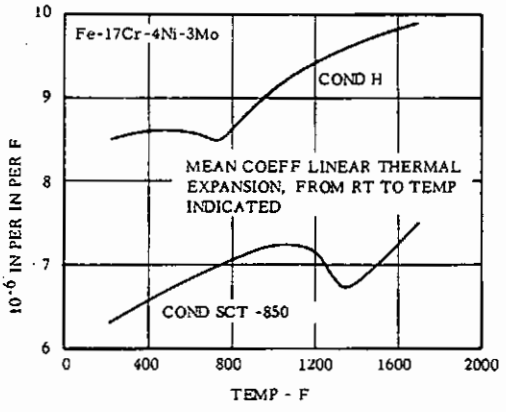


FIG. 2.014 THERMAL EXPANSION (1, p. 4)

Alloy	Fe-17Cr-4Ni-3Mo
Form	0.039 to 0.062 in. Sheet, L and T. (Average of 4 heats)
Condition or Treatment	Dimensional change in./in.
H + 1375F, 2 hr, AC	+0.0045
+ 850F, 3 hr, AC	-0.0002
H to DA	+0.0043
H to L	+0.0015
L + 1375F, 2 hr, AC	+0.0036
+ 850F, 3 hr, AC	-0.0002
L to DA	+0.0034
H to L to DA	+0.0049
L + -100F, 3 hr	+0.0034
+ 850F, 3 hr, AC	-0.0002
L to SCT	+0.0032
H to L to SCT	+0.0047

TABLE 2.017. DIMENSIONAL CHANGES DURING VARIOUS HEAT TREATMENTS (2) (22)

Fe
17 Cr
4 Ni
3 Mo

AM-350

Alloy	Fe-17Cr-4Ni-3Mo	
Condition	lb/cu in.	gr/cu cm
H	0.286	7.92
SCT-850	0.282	7.81

TABLE 2.021. DENSITY (1, p.8)

Alloy	Fe-17Cr-4Ni-3Mo
Condition	Electrical resistivity, microhm - in.
H	28.0
SCT	31.9
DA	32.7

TABLE 2.0221. ELECTRICAL RESISTIVITY AT ROOM TEMPERATURE FOR VARIOUS CONDITIONS (3, p.17)

Alloy	Fe-17Cr-4Ni-3Mo		
Condition	H	SCT	DA
Induction at 200 oersteds, gauss	1700	8600	9980
Permeability, Max	14	76	115
Permeability, Initial	12	18	18

TABLE 2.023. TYPICAL MAGNETIC PROPERTIES (2)

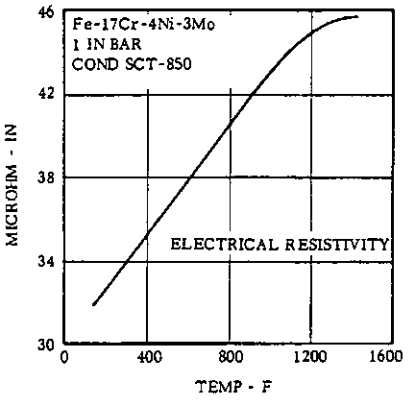


FIG. 2.0222 ELECTRICAL RESISTIVITY OF BAR IN SCT CONDITION (1, p. 8)

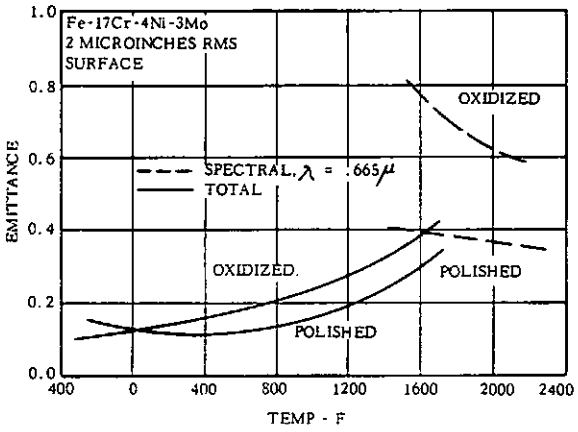


FIG. 2.0241 EFFECT OF TEST TEMPERATURE AND SURFACE CONDITION ON TOTAL NORMAL EMITTANCE AND ON SPECTRAL NORMAL EMITTANCE AT λ = 0.665 (15, p. 74, 75)

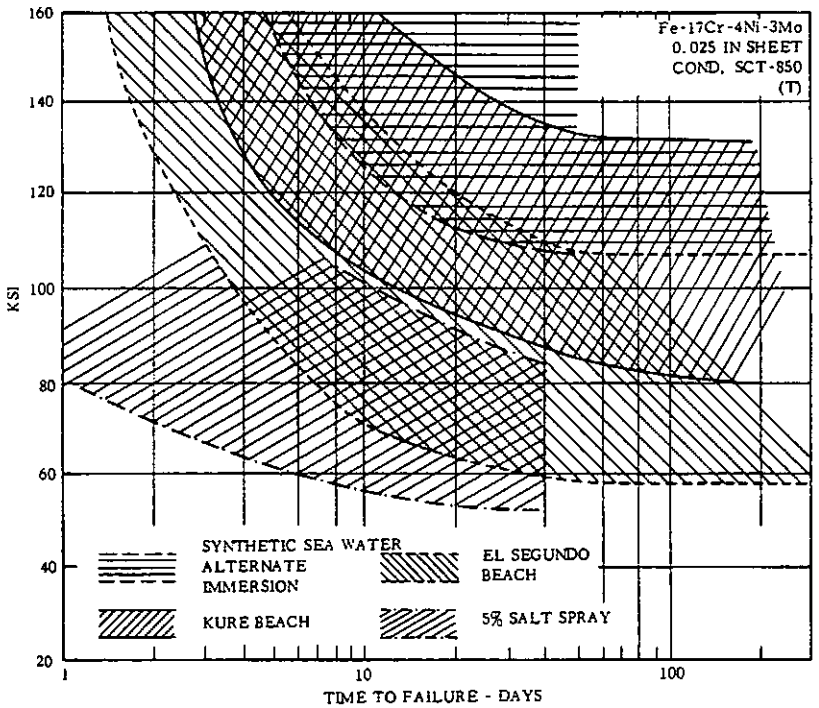


FIG. 2.0331 EFFECT OF SEVERAL STRESS CORROSION ENVIRONMENTS ON TIME TO FAILURE OF UNNOTCHED SHEET IN SCT-850 CONDITION (17, Fig. 15)

Fe
17 Cr
4 Ni
3 Mo

AM-350

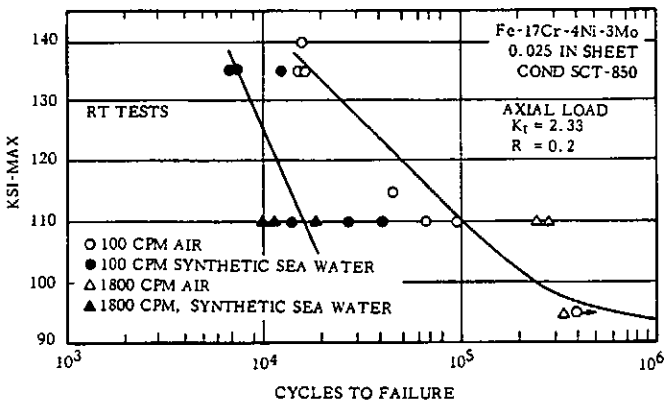


FIG. 2.0332 EFFECT OF SYNTHETIC SEA WATER ENVIRONMENT AND CYCLIC FREQUENCY ON AXIAL FATIGUE OF SHEET IN SCT-850 CONDITION (17, p. 297)

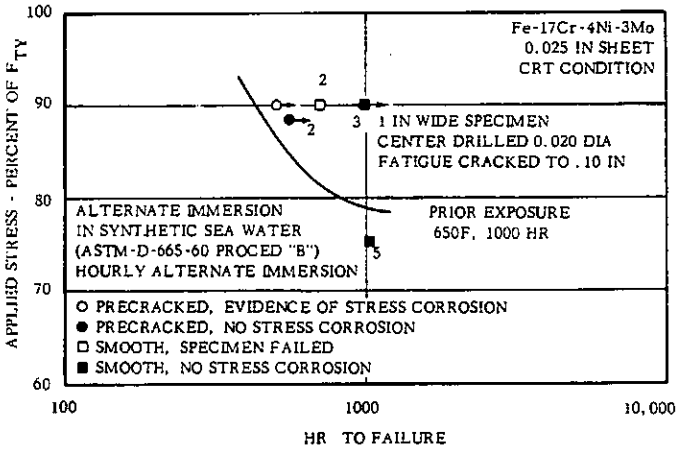


FIG. 2.0334 EFFECT OF APPLIED STRESS, PRECRACKING AND ALTERNATE IMMERSION IN SYNTHETIC SEA WATER ON RESISTANCE TO STRESS CORROSION CRACKING OF ALLOY IN CRT CONDITION SUBJECTED TO PRIOR EXPOSURE OF 650F FOR 1000 HR (17, Fig. 97)

Alloy	Fe-17Cr-4Ni-1Mo													
Form	Sheet & Strip			Sheet & Strip						Sheet & Strip					Tubing
Condition	Cold Rolled & Temper			Annealed						SCT 850					DA
Thickness - in.	<0.010	0.010 to 0.080	>0.080 to 0.125	0.0005 to 0.0015	>0.0015 to 0.002	>0.002 to 0.005	>0.005 to 0.0100	>0.0100 to 0.0200	>0.0200 to 0.1875	0.0005 to 0.0015	>0.0015 to 0.002	>0.002 to 0.0100	>0.0100 to 0.0500	>0.0500 to 0.1875	-
F_{tu}, (min)-ksi	200	200	200	200	197	194	191	188	185	185-215	185-215	185-215	185-215	185-215	165
F_{ty}, (min)-ksi	180	180	180	90	88	86	84	82	80	150	150	150	150	150	130
e, 2 in. (min)-per	6	8	10	8	9	10	12	14	20	2	4	6	8	10	10
Hardness															
RC (min)	43	43	43							42	42	42	42	42	-
RC (max)	-	-	-	25	25	25	25	25	25	48	48	48	48	48	-

TABLE 3.011. AMS SPECIFIED MECHANICAL PROPERTIES FOR STRIP, SHEET & TUBING (19)(20)(37)

Fe
17 Cr
4 Ni
3 Mo

AM-350

Alloy	Fe-17Cr-4Ni-1Mo
Form	Bars & Forgings
Condition	SCT 1000
F_{tu}, (min)-ksi	165
F_{ty}, (min)-ksi	140
e (4D) (min) percent	10
RA (min) percent	20
Hardness, RC (min)	38
(max)	48

TABLE 3.012. AMS SPECIFIED MECHANICAL PROPERTIES FOR BARS & FORGINGS (18)

Alloy	Fe-17Cr-4Ni-3Mo					
Form	Bar		Sheet			
Condition	SCT 850	DA	L*	H	SCT 850	DA
Thickness - in						
F_{tu} -min-ksi	185	165	200	185	185	165
-max-ksi	-	-	-	-	-	-
F_{ty} -min-ksi	150	135	80	75	150	135
-max-ksi	-	-	-	-	-	-
e(2in) min-percent	10	10	15	20	10	8
RA -percent	20	20	-	-	-	-
Hardness						
RA -min	-	-	-	-	-	-
-max	-	-	-	-	-	-
RC -min	34	36	-	25	-	-
-max	48	46	-	-	-	-

(*) After re-anneal of Condition H by customer at 1710 ± 25F

TABLE 3.013. PRODUCER'S SPECIFIED MECHANICAL PROPERTIES (3)

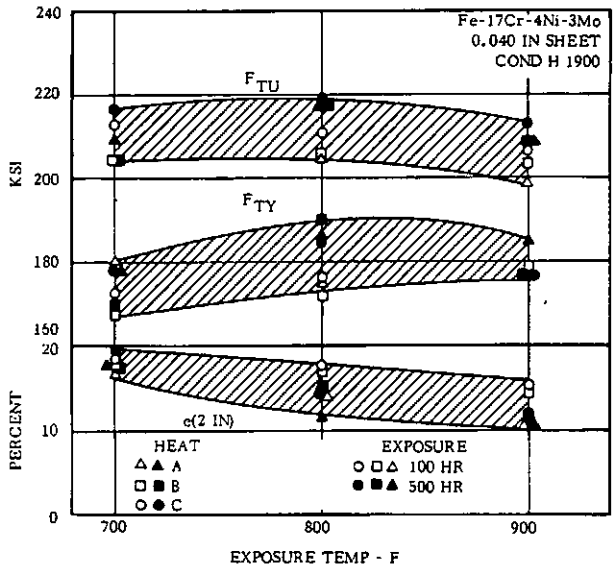


FIG. 3.0212 EFFECT OF EXPOSURE TIME AND TEMPERATURE ON ROOM TEMPERATURE TENSILE PROPERTIES OF SHEET FROM THREE HEATS IN CONDITION H-1900 (13, p. 3-4)

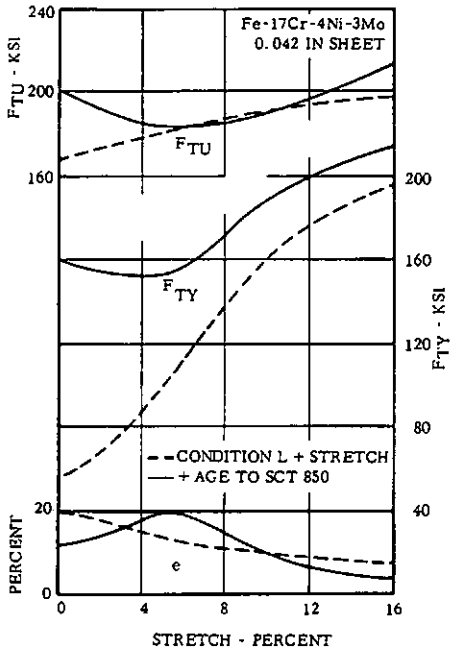


FIG. 3.0213 EFFECT OF STRETCHING AND SUBSEQUENT AGING TO CONDITION SCT 850 ON TENSILE PROPERTIES OF SHEET IN CONDITION L (1)

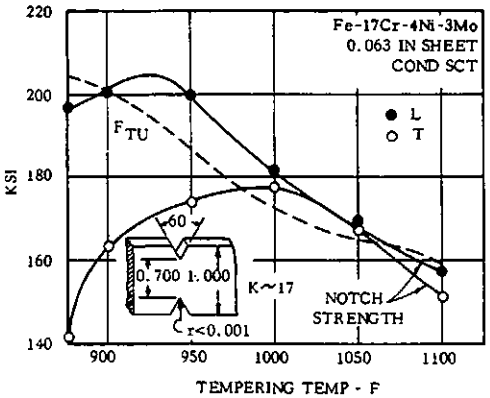


FIG. 3.0214 EFFECT OF TEMPERING TEMPERATURE AND TEST DIRECTION ON NOTCH STRENGTH OF SHEET (27)

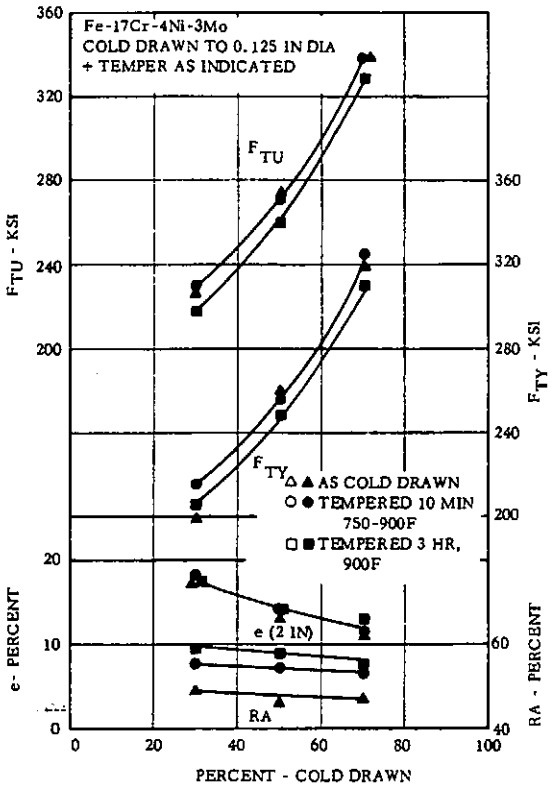


FIG. 3.0215 EFFECT OF PERCENT COLD DRAW AND OF TEMPERING TIME AND TEMPERATURE ON TENSILE PROPERTIES OF WIRE

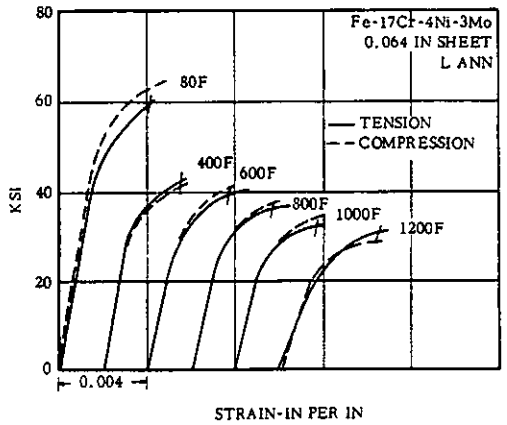


FIG. 3.03111 TENSILE AND COMPRESSIVE STRESS-STRAIN CURVES FOR SHEET IN ANNEALED CONDITION AT ROOM AND ELEVATED TEMPERATURES (10, Figs. 65, 66)

Fe
17 Cr
4 Ni
3 Mo

AM-350

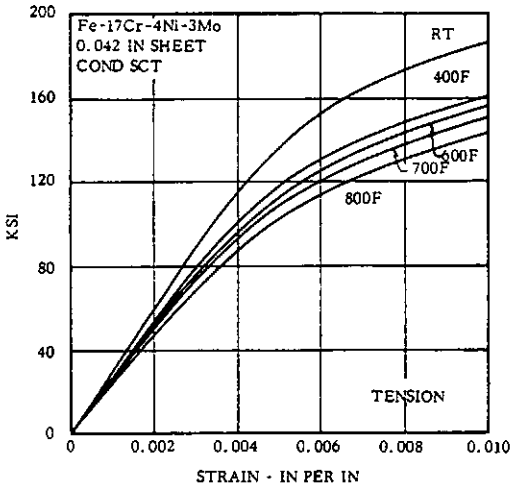


FIG. 3.03112 STRESS-STRAIN CURVES FOR SHEET IN SCT CONDITION AT ROOM AND ELEVATED TEMPERATURES (23)

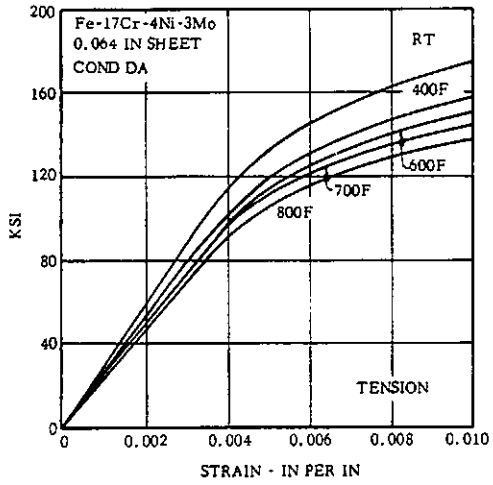


FIG. 3.03113 STRESS-STRAIN CURVES FOR SHEET IN DA CONDITION AT ROOM AND ELEVATED TEMPERATURES (23)

Fe
17 Cr
4 Ni
3 Mo

AM-350

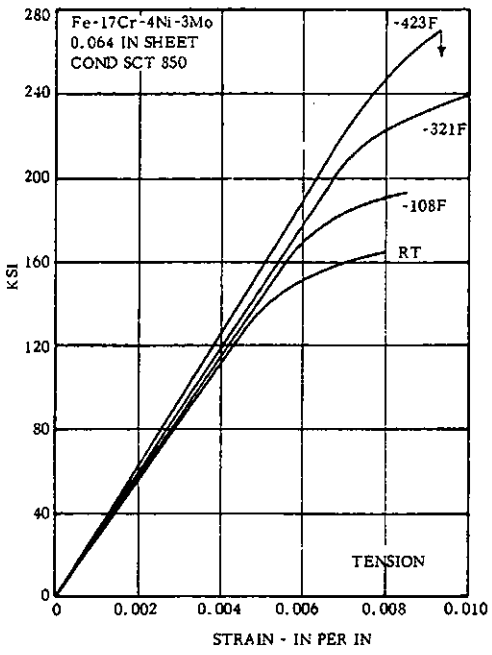


FIG. 3.03114 STRESS-STRAIN CURVES FOR SHEET IN SCT CONDITION AT LOW TEMPERATURES (24)

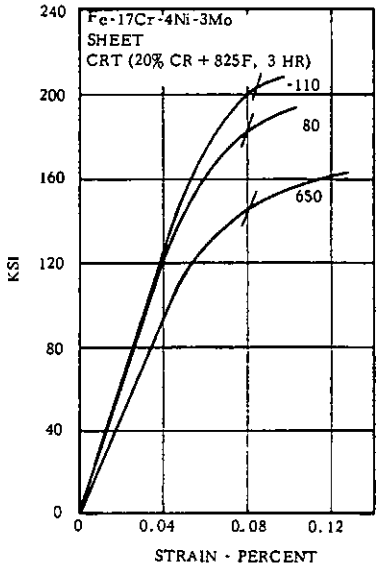


FIG. 3.03115 STRESS-STRAIN CURVES FOR SHEET IN 20 PERCENT CRT CONDITION AT TEMPERATURES BETWEEN -110 AND 650F

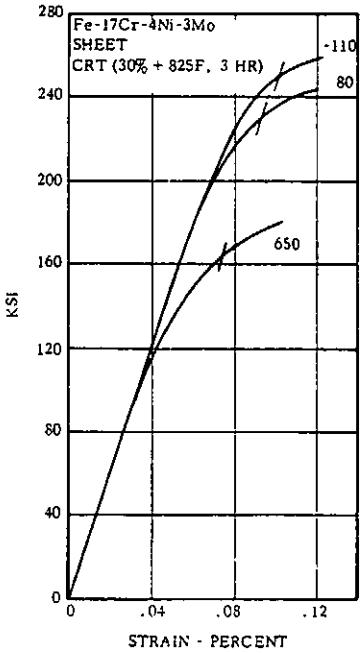


FIG. 3.03116 STRESS-STRAIN CURVES FOR SHEET IN 30 PERCENT CRT CONDITION AT TEMPERATURES BETWEEN -110 AND 650F

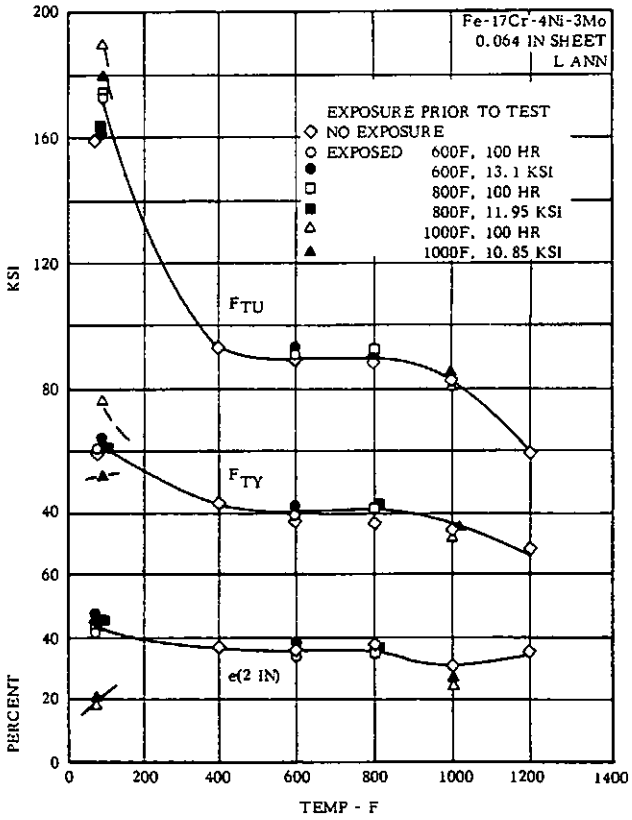


FIG. 3.0312 EFFECT OF TEST TEMPERATURE AND PRIOR EXPOSURE TO STRESS AND TEMPERATURE ON TENSILE PROPERTIES OF SHEET IN ANNEALED CONDITION (10, Fig. 22, 24, 25)

Fe
17 Cr
4 Ni
3 Mo

AM-350

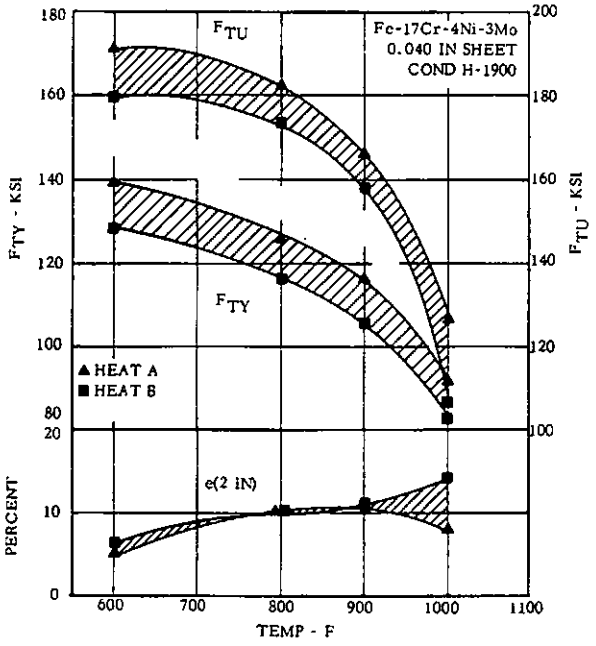


FIG. 3.0313 EFFECT OF TEST TEMPERATURE ON TENSILE PROPERTIES OF SHEET ROLLED FROM TWO HEATS IN CONDITION H-1900 (13, p. 1-2)

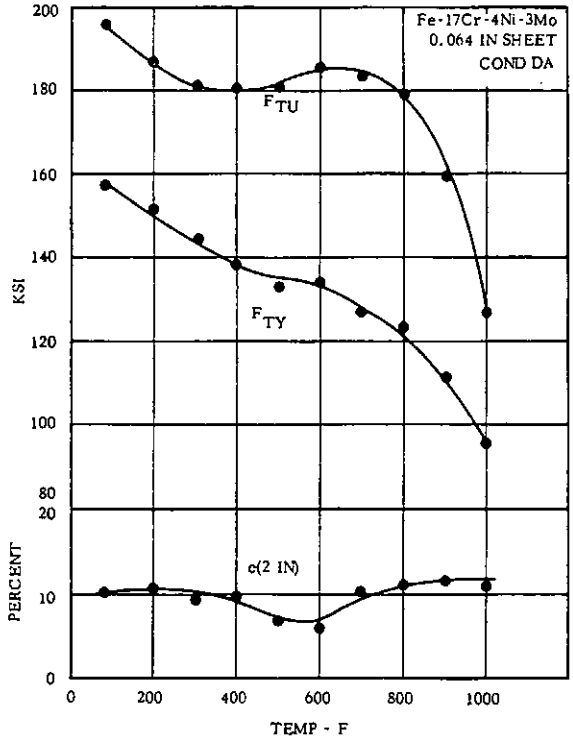


FIG. 3.0314 EFFECT OF TEST TEMPERATURE ON TENSILE PROPERTIES OF SHEET IN DA CONDITION (23)

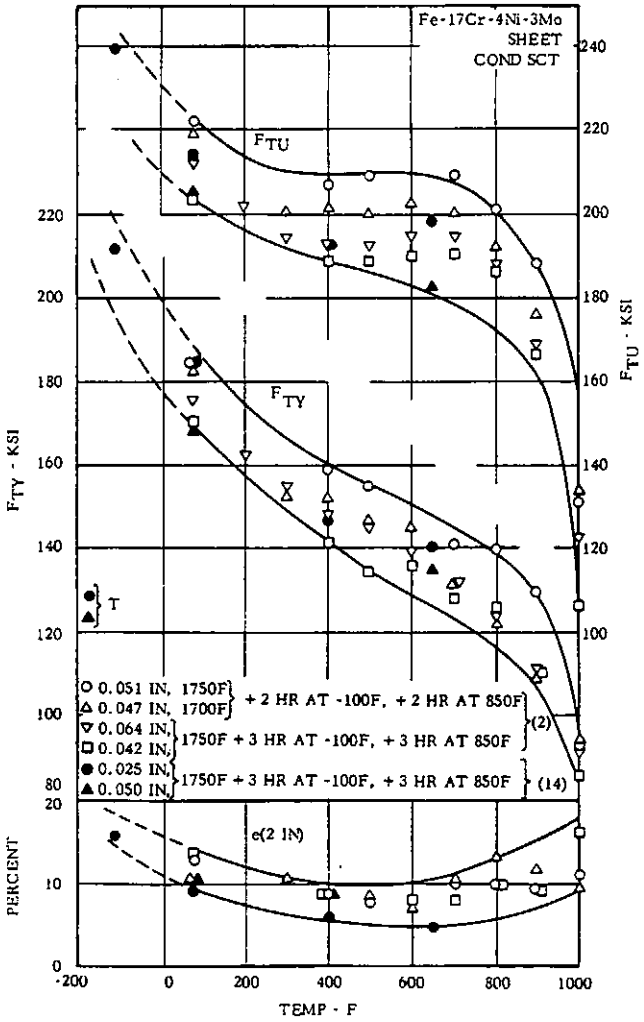


FIG. 3.0315 EFFECT OF TEST TEMPERATURE ON TENSILE PROPERTIES OF SHEET IN SCT CONDITION (2) (14, p. 36)

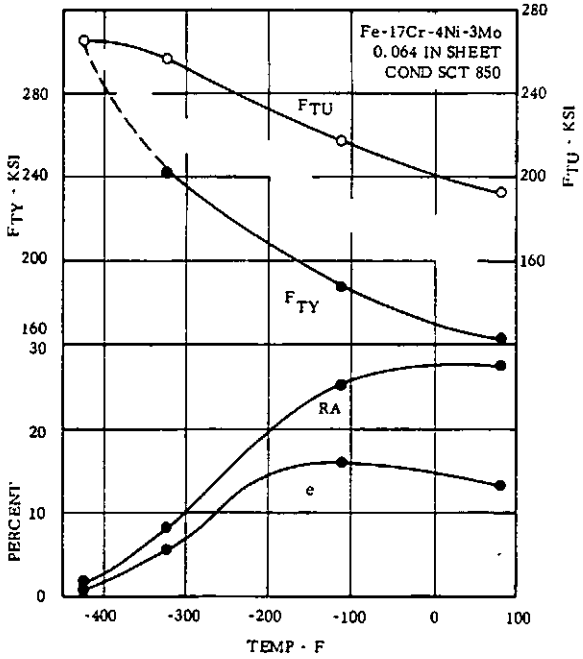


FIG. 3.0316 EFFECT OF LOW TEST TEMPERATURE ON TENSILE PROPERTIES OF SHEET IN SCT CONDITION (28)

Fe
17 Cr
4 Ni
3 Mo

AM-350

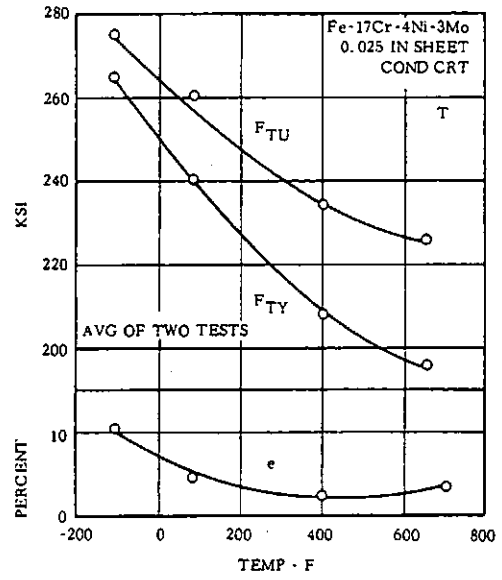


FIG. 3.0317 EFFECT OF TEST TEMPERATURE ON TRANSVERSE TENSILE PROPERTIES OF SHEET IN CRT CONDITION (14, p. 43)

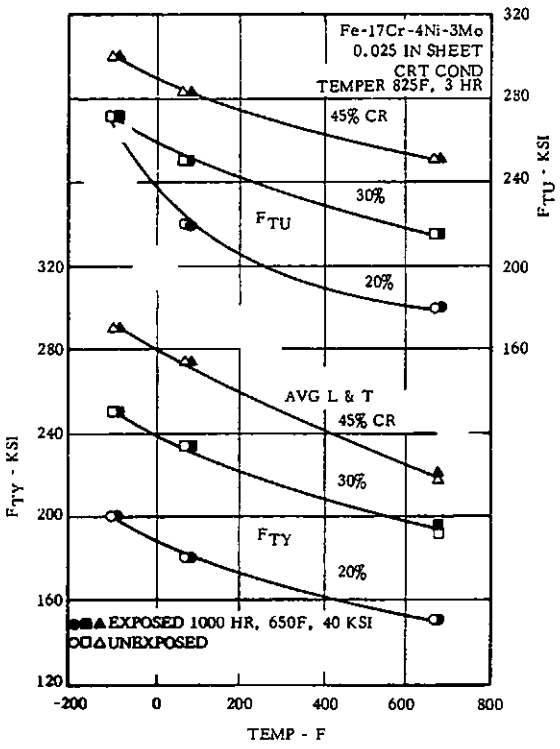


FIG. 3.0318 EFFECT OF TEST TEMPERATURE, COLD REDUCTION AND PRIOR EXPOSURE ON TENSILE PROPERTIES OF SHEET IN CRT CONDITION (12, p. 844)

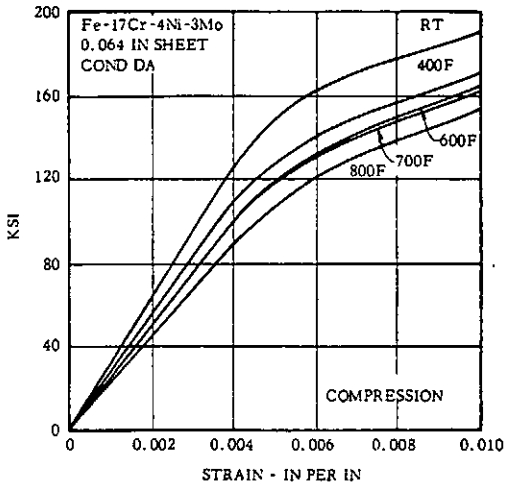


FIG. 3.0322 STRESS STRAIN CURVES IN COMPRESSION FOR SHEET IN DA CONDITION AT ROOM AND ELEVATED TEMPERATURES (23)

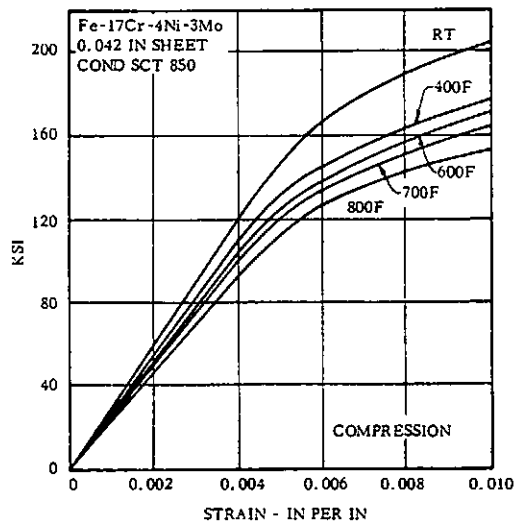


FIG. 3.0323 STRESS-STRAIN CURVES IN COMPRESSION FOR SHEET IN SCT CONDITION AT ROOM AND ELEVATED TEMPERATURES (23)

Fe
17 Cr
4 Ni
3 Mo

AM-350

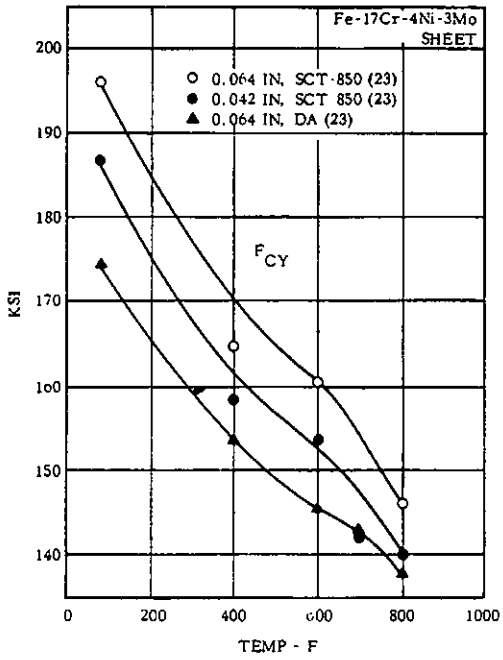


FIG. 3.0324 EFFECT OF TEST TEMPERATURE ON COMPRESSIVE YIELD STRENGTH OF SHEET IN CONDITIONS H, DA AND SCT (23)

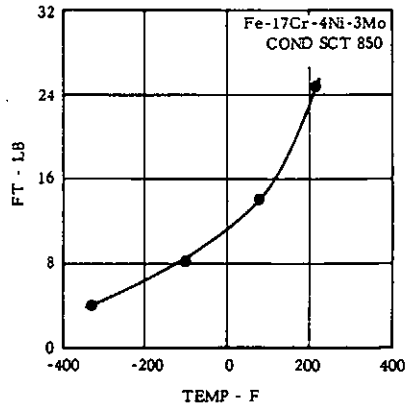


FIG. 3.0331 EFFECT OF TEST TEMPERATURE ON CHARPY V IMPACT PROPERTIES OF ALLOY IN SCT CONDITION (5, p. A-2-3)

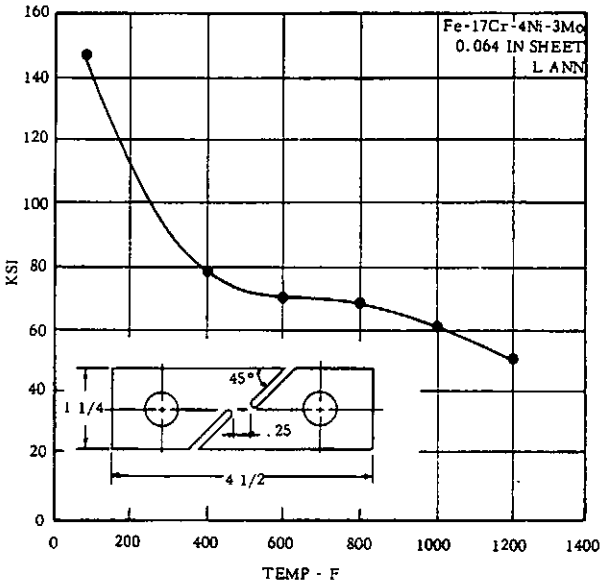


FIG. 3.0351 EFFECT OF TEST TEMPERATURE ON SHEAR STRENGTH OF SHEET IN ANNEALED CONDITION (10, Fig. 29)

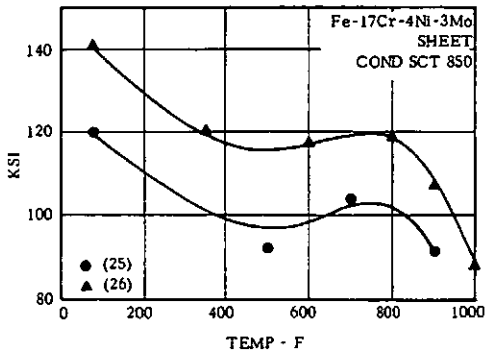


FIG. 3.0352 EFFECT OF TEST TEMPERATURE ON SHEAR STRENGTH OF SHEET IN CONDITION SCT 850 (25)(26)

Fe
17 Cr
4 Ni
3 Mo

AM-350

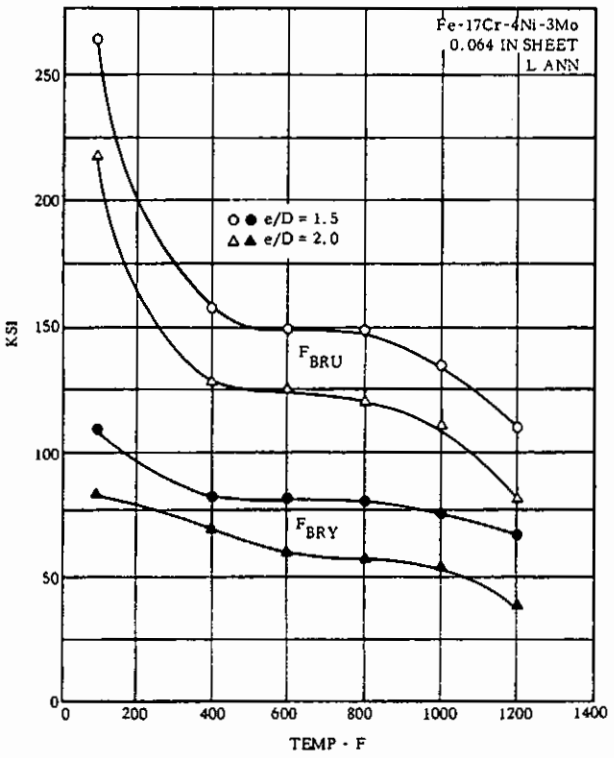


FIG. 3.0361 EFFECT OF TEST TEMPERATURE ON BEARING PROPERTIES OF SHEET IN ANNEALED CONDITION (10)

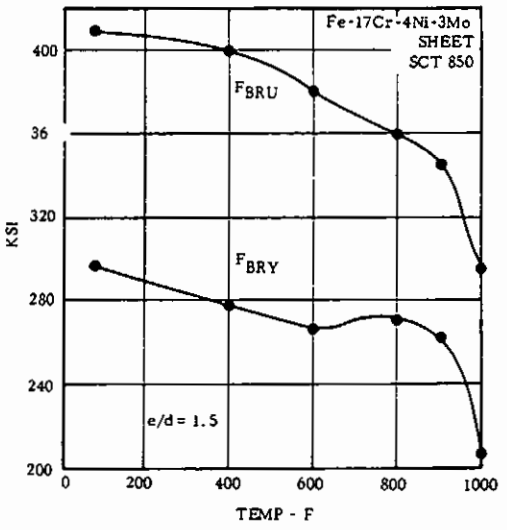


FIG. 3.0362 EFFECT OF TEST TEMPERATURE ON BEARING PROPERTIES OF SHEET IN CONDITION SCT 850 (25)

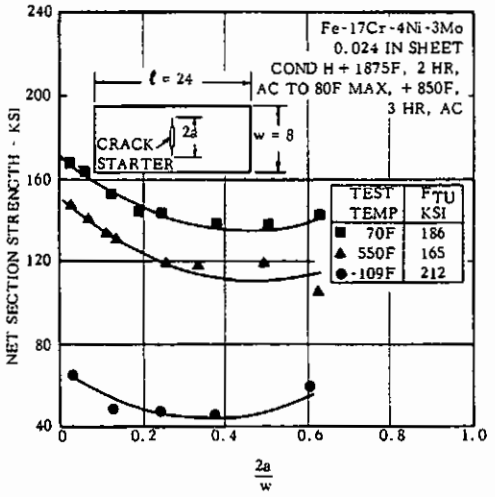


FIG. 3.0372 EFFECT OF NET SECTION AREA AND TEST TEMPERATURE ON NET SECTION STRENGTH OF SHEET IN DA CONDITION (7, Tbl. 2, 3, 5)

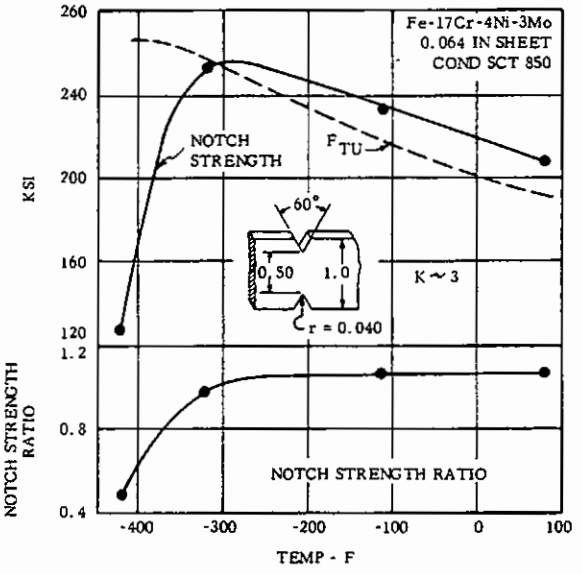


FIG. 3.0371 EFFECT OF LOW TEST TEMPERATURE ON NOTCH STRENGTH AND NOTCH STRENGTH RATIO OF SHEET IN SCT CONDITION (24)

Fe
17 Cr
4 Ni
3 Mo

AM-350

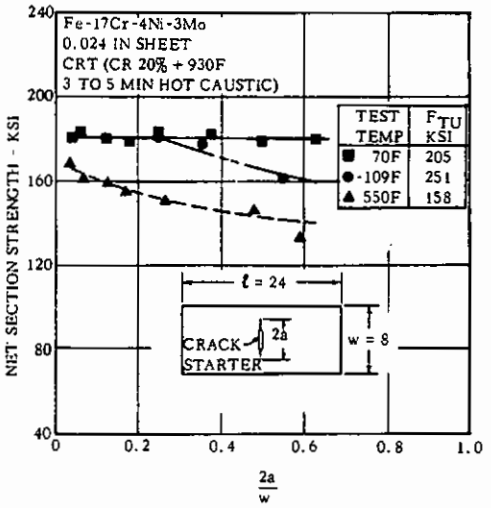


FIG. 3.0373 EFFECT OF NET SECTION AREA AND TEST TEMPERATURE ON NET SECTION STRENGTH OF SHEET IN CRT CONDITION (7, p.11-13)

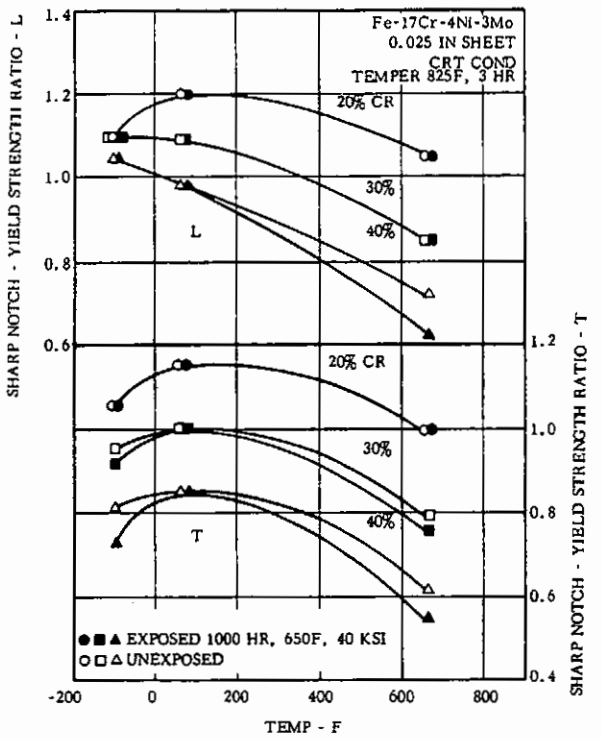


FIG. 3.0374 EFFECT OF TEST TEMPERATURE, COLD REDUCTION, TEST DIRECTION AND PRIOR EXPOSURE ON RATIO OF SHARP NOTCH STRENGTH TO YIELD STRENGTH OF SHEET IN CRT CONDITION (12, p. 844)

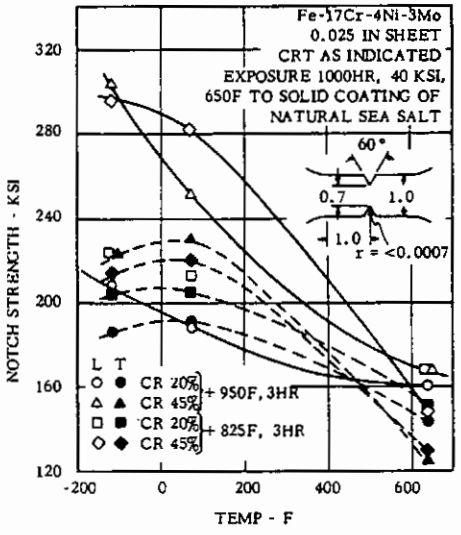


FIG. 3.0375 EFFECT OF TEST TEMPERATURE, AMOUNT OF COLD WORK, TEMPERING CONDITIONS AND TESTING DIRECTION ON NOTCH TENSILE STRENGTH AFTER EXPOSURE TO COATING OF NATURAL SEA SALT WHILE UNDER STRESS AT HIGH TEMPERATURE (4, p. 99)

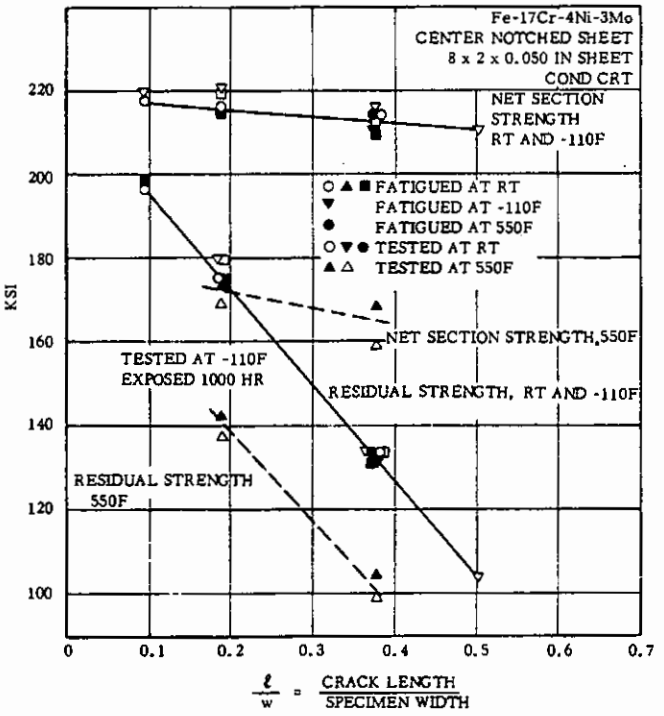


FIG. 3.0376 EFFECT OF CRACK LENGTH FRACTION, METHOD OF PRODUCING CRACK, PRIOR EXPOSURE AND TEST TEMPERATURE ON RESIDUAL STRENGTH AND NET SECTION STRENGTH OF SHEET IN CRT CONDITION (8, p. 26, 27)

Fe
17 Cr
4 Ni
3 Mo

AM-350

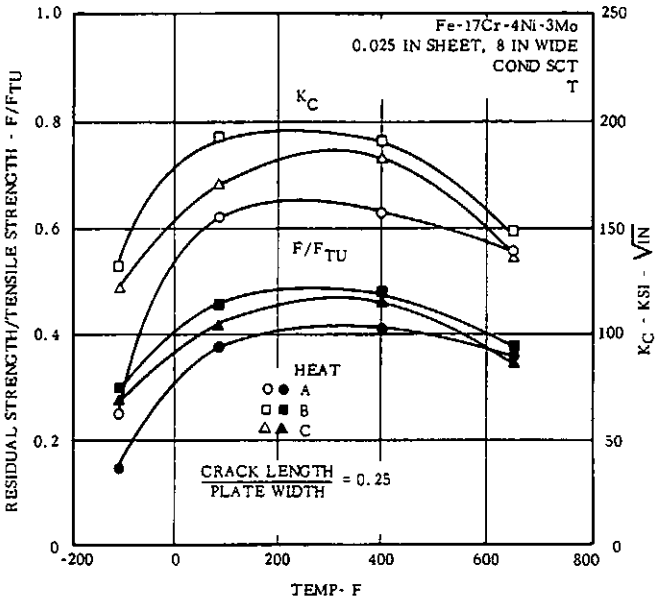


FIG. 3.0377 EFFECT OF TEST TEMPERATURE ON FRACTURE TOUGHNESS AND RESIDUAL STRENGTH RATIO OF THREE HEATS OF SHEET IN CONDITION SCT (14, p. 105)

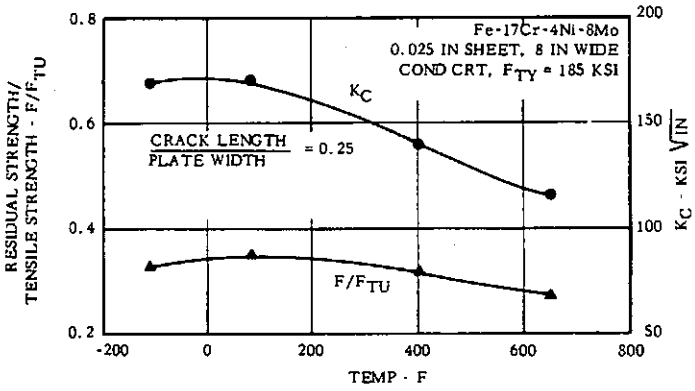


FIG. 3.0378 EFFECT OF TEST TEMPERATURE ON FRACTURE TOUGHNESS AND RESIDUAL STRENGTH RATIO OF SHEET IN CONDITION CRT (14, p. 143)

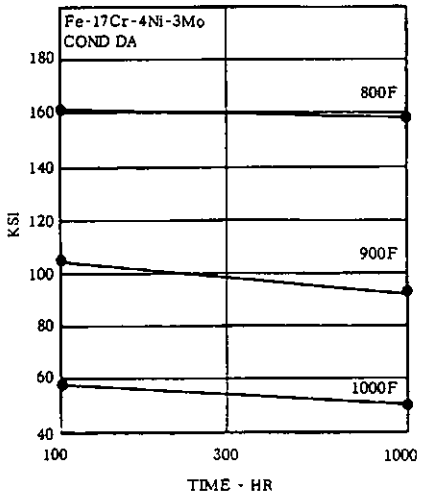


FIG. 3.0421 CREEP RUPTURE PROPERTIES AT 800 TO 1000F OF ALLOY IN DA CONDITION (5, p. A-1-2)

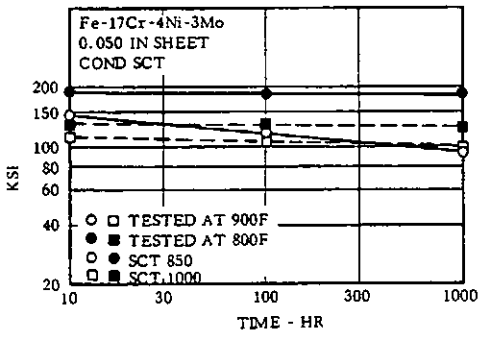


FIG. 3.0422 CREEP RUPTURE PROPERTIES AT 800 AND 900F OF SHEET IN SCT CONDITION (1, p. 7)

Fe
17 Cr
4 Ni
3 Mo

AM-350

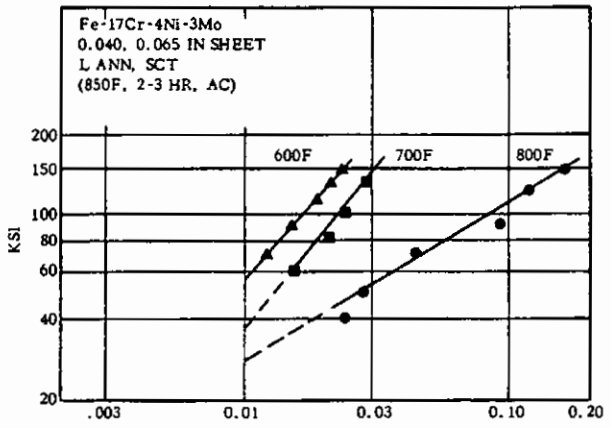


FIG. 3.0431 MINIMUM CREEP RATE CURVES AT 600, 700 AND 800F FOR SHEET IN SCT CONDITION (3, p. 48)

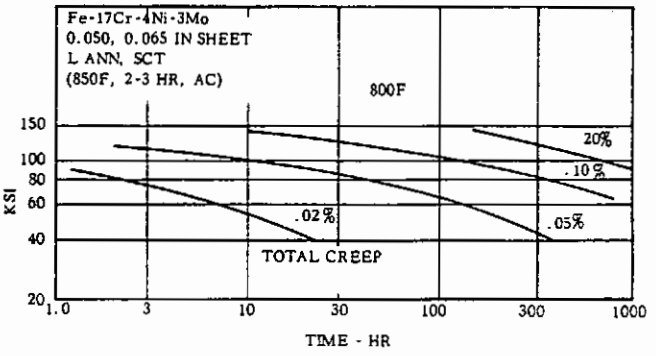


FIG. 3.0432 TOTAL CREEP CURVES AT 800F FOR SHEET IN SCT CONDITION (28)

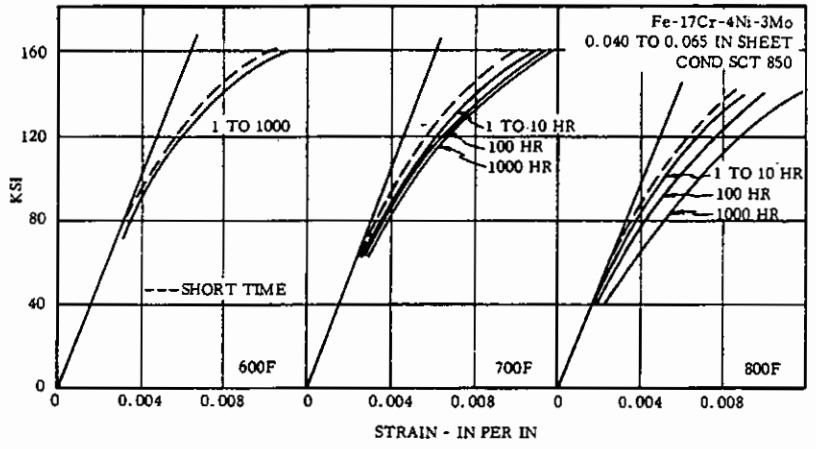


FIG. 3.0433 ISOCHRONOUS STRESS-STRAIN CURVES FOR SHEET IN CONDITION SCT AT 600 TO 800F (28)

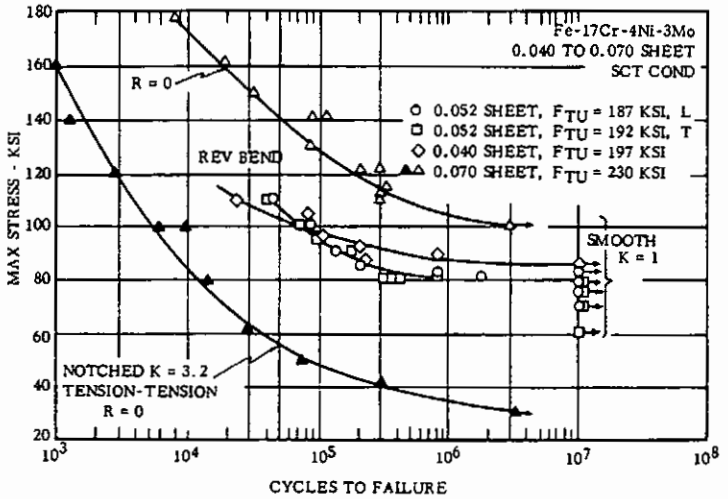


FIG. 3.051 FATIGUE CURVES FOR SHEET IN SCT CONDITION (29) (Fig. 5, 6, 7)

Fe
17 Cr
4 Ni
3 Mo

AM-350

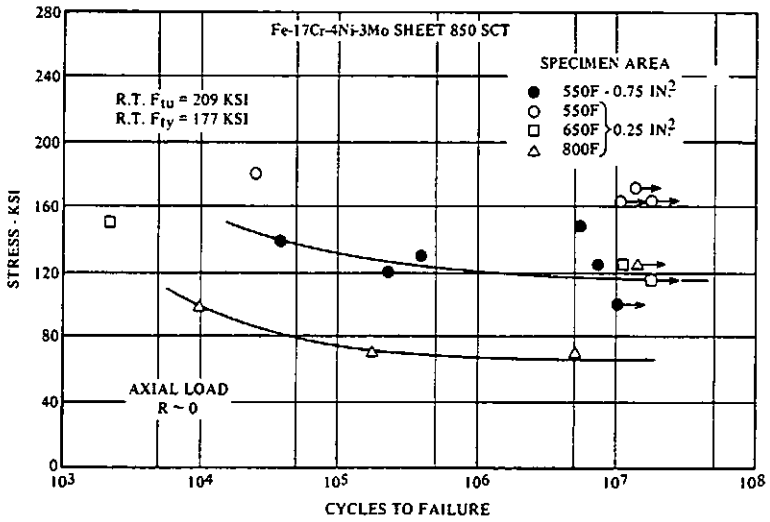


FIG. 3.052. S-N CURVE FOR SPECIMENS OF TWO SIZES HAVING RECTANGULAR CROSS SECTIONS & TESTED AT SEVERAL TEMPERATURES (23)

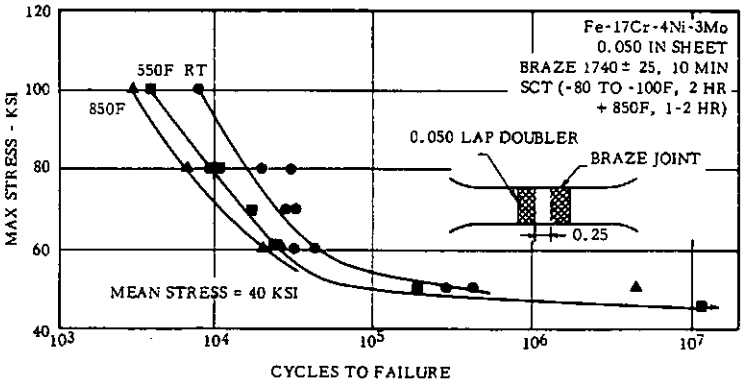


FIG. 3.053 EFFECT OF STRESS AND TEST TEMPERATURE ON FATIGUE OF BRAZED LAP JOINTS OF SHEET IN SCT CONDITION (9, p. 45)

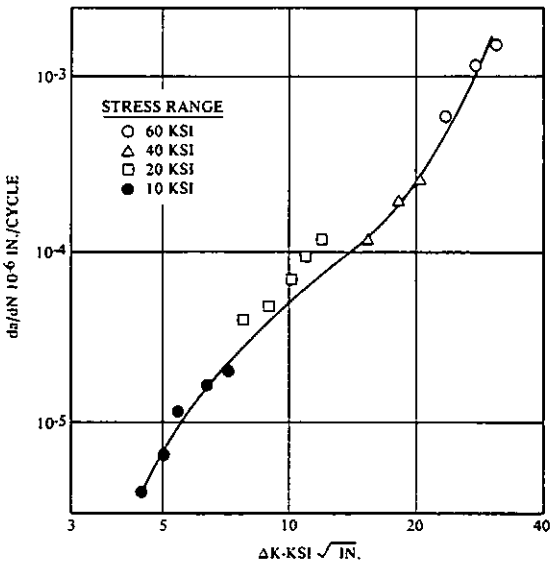


FIG. 3.054. CRACK PROPAGATION RATE AS A FUNCTION OF THE STRESS INTENSITY FACTOR RANGE FOR AM 350 CRT STAINLESS STEEL SHEET (33)

Fe
17 Cr
4 Ni
3 Mo

AM-350

Alloy	Fe-17Cr-4Ni-1Mo			
Form	0.040 in sheet, smooth and notched, notched sheet 60°V, depth 0.010 inch, radius 0.005 inch machined across flat surface			
Condition	Brazed at 1900F cooled to RT,+ SCT-850 salt coated by dripping in hot concentrated 6 parts NaCl + 1 part $MgCl_2$ and drying			
Test Method	Cantilever beam, 650F in circulating air furnace			
	Maximum stress, ksi		Fracture	Surface condition
Test Condition	Smooth	Notched	time, hours	at 4700 hours
Bare surface, continuously exposed	58.3, 59.0, 59.1	160.3, 159.4	(a)	Slight bluing
Salt coated, Continuously exposed (b)	55.9, 55, 58.1	152.8, 148.4	(a)	Gold to brown color rust spots on 20 to 50 percent of surface
Brazed and salt coated, continuously exposed	51.6, 50.8, 52.1	129.5, 186	(a)	
Salt coated - 2 weeks at 650F, + 2 weeks in humidity cabinet at 100F intermittently	57.1 57.2 57.0 56.3		3360 3290 3290 2880	Surface heavily rusted, and two specimens had cracks other than failure

(a) Unbroken at 4700 hours (b) Salt coating appeared spotty at 4700 hours

TABLE 3.055. FATIGUE BEHAVIOR OF SMOOTH & NOTCHED SHEET WITH SALT COATING (4)

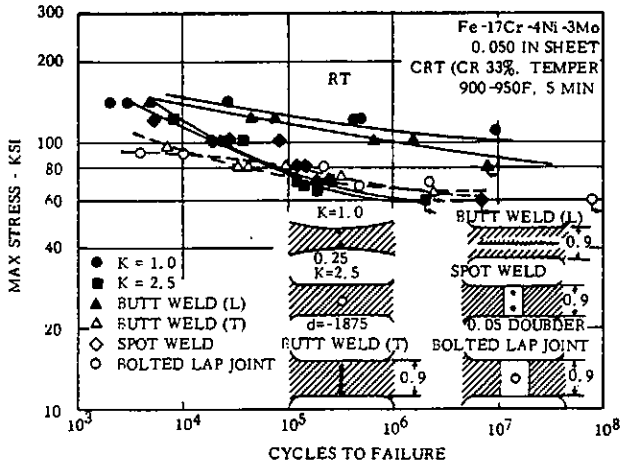


FIG. 3.056 EFFECT OF JOINING METHOD AND OF STRESS CONCENTRATION ON FATIGUE BEHAVIOR AT ROOM TEMPERATURE OF SHEET IN CONDITION CRT (9, p. 40-46)

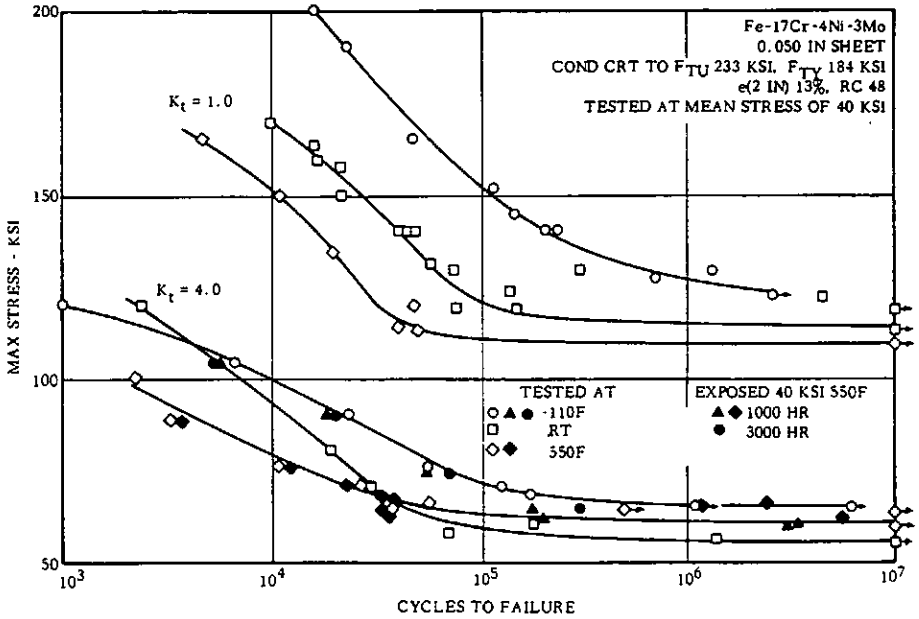


FIG. 3.057 EFFECT OF TEST TEMPERATURE AND PRIOR EXPOSURE ON FATIGUE BEHAVIOR OF SMOOTH AND NOTCHED SHEET IN CONDITION CRT (28, Fig. 16, 17, 18, 19)

Fe
17 Cr
4 Ni
3 Mo

AM-350

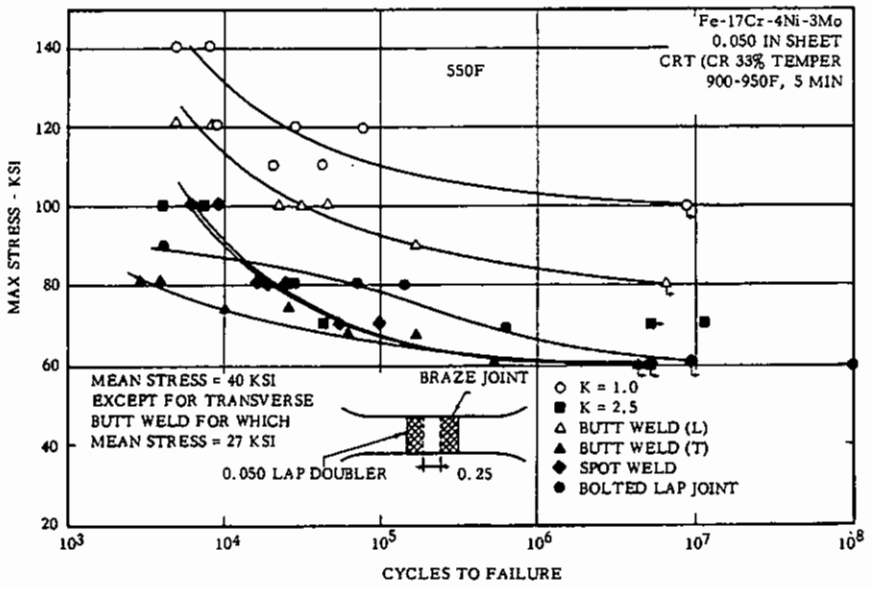


FIG. 3.058. EFFECT OF JOINING METHOD AND OF STRESS CONCENTRATION ON FATIGUE BEHAVIOR AT 550F OF SHEET IN CONDITION CRT (23, Fig. 5-9, 11)

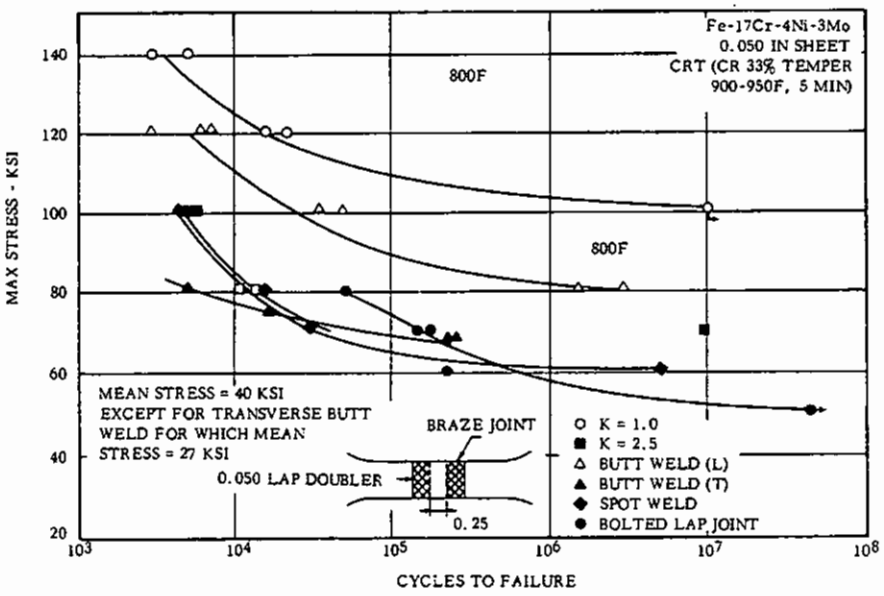


FIG. 3.059 EFFECT OF JOINING METHOD AND OF STRESS CONCENTRATION ON FATIGUE BEHAVIOR AT 800F OF SHEET IN CONDITION CRT (23, Fig. 5-9, 11)

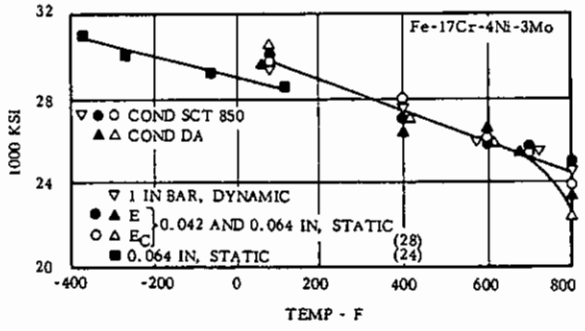


FIG. 3.0621 MODULUS OF ELASTICITY AT VARIOUS TEMPERATURES OF ALLOY IN CONDITIONS SCT 850 AND DA (24)(28)

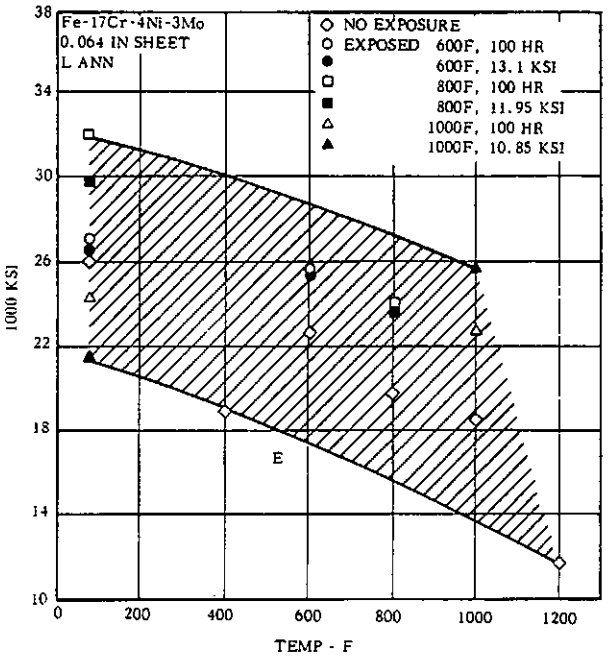


FIG. 3.0b22 EFFECT OF TEST TEMPERATURE AND PRIOR EXPOSURE TO STRESS AND TEMPERATURE ON ELASTIC MODULUS OF SHEET IN ANNEALED CONDITION (10, Tbl. 6, 10, 14)

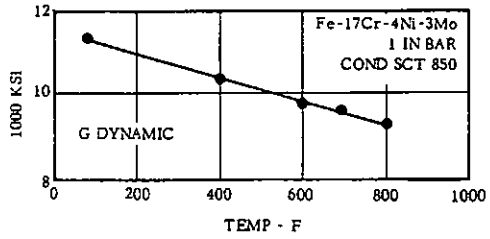


FIG. 3.063 MODULUS OF RIGIDITY AT ROOM AND ELEVATED TEMPERATURES (30)

Fe
17 Cr
4 Ni
3 Mo

AM-350

Alloy	Fe-17Cr-4Ni-3Mo				
Form	0.078-in. Sheet				
Condition	H-Annealed + GTA Weld + Heat Treatment				
Material	Heat Treatment	Yield Strength 0.2% Offset, ksi	Tensile Strength, ksi	Elong., in 2 in., %	Fracture
AM 350 with 350 Filler Metal	As Welded	83	145	6.5	in Weld
AM 350 with 355 Filler Metal	As Welded	62	136	12.0	in Weld
AM 350 with 350 Filler Metal	Welded + SCT (850 F)	87	148	6.0	in Weld
AM 350 with 355 Filler Metal	Welded + SCT (850 F)	90	153	8.0	in Weld
AM 350 with 350 Filler Metal	Welded + 1710 F + SCT (850 F)	165	191	4.0	in Weld
AM 350 with 355 Filler Metal	Welded + 1710 F + SCT (850 F)	169	199	9.0	Base Metal
AM 350 with 350 Filler Metal	Welded + DA	153	178	9.0	Base Metal
AM 350 with 355 Filler Metal	Welded + DA	157	184	8.0	Base Metal
AM 350 with 350 Filler Metal	Welded + 1710 F + DA	160	188	5.0	in Weld
AM 350 with 355 Filler Metal	Welded + 1710 F + DA	156	185	8.0	Base Metal

TABLE 4.0312. THE PROPERTIES OF AM 350 WELDED WITH AM 350 OR AM 355 FILLER METAL (34)

Alloy	Fe-17Cr-4Ni-3Mo			
Form	0.078-in. Sheet			
Condition	H-Annealed + GTA Welded with AM 350 Filler + Heat Treatment			
Post Weld Heat Treatment	Yield Strength 0.2% Offset, ksi	Tensile Strength, ksi	Elongation in 2 in., %	Elongation in 0.5 in., %
As Welded	83	145	6.5	27.0
Welded + SCT (850 F)	87	148	n.a.	n.a.
Welded + 1710 F + SCT (850 F)	165	191	4.0	19.0
Welded + 1710 F + SCT (1000 F)	145	165	11.0	n.a.
Welded + DA	153	178	9.0	7.0
Welded + 1710 + DA	160	180	n.a.	n.a.

TABLE 4.0313. TENSILE PROPERTIES OF SHEET WELDED TRANSVERSE TO ROLLING DIRECTION & GIVEN SEVERAL POST WELD TREATMENTS (35)

Fe
17 Cr
4 Ni
3 Mo

AM-350

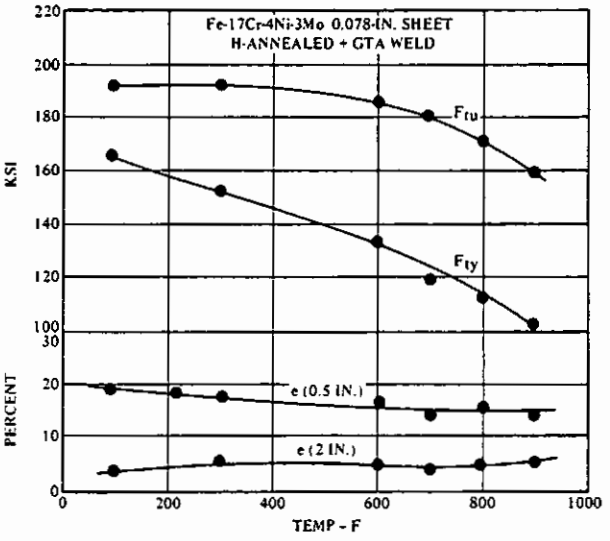


FIG. 4.0314. ELEVATED TEMPERATURE PROPERTIES OF SHEET WELDED TRANSVERSE TO THE ROLLING DIRECTION CONDITION: WELDED, 1710 F, SCT (850F) (35)

Alloy	Fe-17Cr-4Ni-3Mo					
Form	0.024-in. Sheet					
Condition	Electrode diam, in.	Electrode Force, pounds	Weld Time, cycles	Welding Current, amp	Weld diam, in.	Shear Strength, pounds
1750 F then welded	5/32	1200	10	8,500	5/32	1120
	5/32	1200	12	8,500	5/32	1090
	5/32	1200	14	8,500	5/32	1060
	5/32	1200	16	8,500	5/32	1065
	1/4	1200	24	10,500	7/32	1020
	1/4	1200	26	10,500	7/32	1000
	1/4	1200	28	10,500	7/32	1070
	1/4	1200	30	10,500	7/32	1140
1750 F, SCT (850 F) then welded	5/32	1200	12	7,500	5/32	1020
	5/32	1200	14	7,500	6/32	1000
	5/32	1200	16	7,500	6/32	1070
	5/32	1200	18	7,500	6/32	1140
	1/4	1200	12	9,500	6/32	1440
	1/4	1200	14	9,500	6/32	1445
	1/4	1200	16	9,500	7/32	1510
	1/4	1200	18	9,500	7/32	1500

TABLE 4.0315. TENSION SHEAR STRENGTH OF SPOT WELDED SHEET (36)

Fe
15.5 Cr
4.5 Ni
3 Mo

AM-355

1 GENERAL

This alloy is one of a series of age hardening steels which combines high strength, at temperatures up to 800 F and higher, with the corrosion resistance of stainless steels. In the annealed condition the alloy is austenitic. Upon forming at room temperature the alloy work hardens very rapidly because of martensite formation during working. Formation of martensite can be avoided by working at temperatures of about 300 F or higher, in which case the alloy forms in much the same manner as conventional austenitic stainless steels. AM-355 is a companion alloy to AM-350 differing from it by a slightly lower chromium content and a higher amount of carbon. Although designed primarily to meet the demand for heavier sections including plate, bar, and forgings, it is also available in sheet form which is the principal field for AM-350. While the compositions of the two alloys are very similar, the small differences account for significant changes in structure. For example, the AM-350 has 5 to 20 percent delta ferrite; AM-355 usually has little or none.

1.01 Commercial Designation

AM-355.

1.02 Alternate Designations

None.

1.03 Specifications

1.031 AMS Specifications, Table 1.031.

1.04 Composition

1.041 Composition of cast and wrought forms, Table 1.041.

1.05 Heat Treatment

1.051 AM-355 in bar or billet form can be supplied by the producers in several heat treated conditions for specific purposes. The subsequent final heat treatments made by the user in order to attain desirable mechanical properties, machinability, or resistance to stress corrosion have to correspond to a specific mill heat treatment. The relationships between the mill heat treatments and the final treatments applied by the users are shown in Table 1.0514.

1.0512 Sheet, strip, and tubing are supplied in the annealed condition: 1850 to 1900 F, 3/4 hr minimum per inch of thickness, rapid air cool.

1.0513 Plate is supplied in Condition H for maximum structural stability and formability. If not subsequently severely cold formed, it should be equalized before annealed to Condition L and aged to Condition SCT.

1.0514 Mill supplied conditions and user heat treatments for all forms according to alloy producer, Table 1.0514.

1.0515 AMS specified heat treatments for bars, forgings, plate, sheet, and strip, Table 1.0515.

1.052 Heat treatment of castings.

1.0521 Homogenize sand castings at 2000 F, 2 to 4 hours (investment castings at 1900 F, 1 hour) air cool up to 1 inch thickness, oil or water quench sections above 1 inch. For optimum structure and maximum corrosion resistance, subzero cool for 3 hours at -100 F.

1.0522 Equalize for improved machinability after homogenization and subzero cooling treatment. 1375 to 1475 F, 3 hours, air cool to 80 F maximum plus 1000 to 1150 F, 3 hours, air cool.

1.0523 Condition anneal 1750 to 1850 F, 1 hour per inch thickness, water quench plus subzero cool (-100 F) 3 hours.

1.0524 Age to Condition SCT. Same as wrought products, see 1.051.

1.0525 AMS specified heat treatments for sand and investment castings, Table 1.0525.

1.053 Subzero cool and age Condition L to Condition SCT. Cool to -100 F, hold 3 hr minimum plus 850 to 1050 F, 3 hr minimum. Effect of aging temperature on tensile properties of various forms, Figure 1.053.

1.06 Hardness

1.061 Effect of test temperature on Brinell hardness of alloy in Condition SCT, Figure 1.061.

1.062 Alloy hardens fully in large section sizes after heat treating to Condition SCT.

1.07 Forms and Condition Available

AM-355 is available as forging, billet, and bar heat treated as shown in Table 1.0514. It is also available in other forms. Sheet and strip are available in Condition H or in the cold rolled temper (CRT).

1.08 Melting Practice

Electric arc furnace melt followed by argon-oxygen-decarburizing (AOD). Consumable electrode remelt or electroslag remelt are used for billet and bar products and are optional for sheet products.

1.09 Special Considerations

1.091 Heating to temperatures above those specified for Condition H should be avoided because of grain coarsening and less of a response to hardening.

1.092 Dimensional changes on heat treating require special consideration.

1.093 AM-355, when hardened by the carbide solution subzero treatment (see 1.055), has stress corrosion resistance superior to that of AM-350 in the SCT (850) Condition and comparable to that of AM-350 in the SCT (1000) Condition.

2 PHYSICAL AND CHEMICAL PROPERTIES

2.01 Thermal Properties

2.011 Melting range. 2500 to 2550 F.

2.012 Phase changes. Transformation temperatures. On cooling from 1710 F the M_s point is about 250 F and the M_f point is slightly below room temperature on rapid cooling. On cooling from 1375 F the M_s point is between 700 and 400 F and the martensite transformation is complete at room temperature.

2.013 Thermal conductivity, Figure 2.013.

2.014 Thermal expansion, Figure 2.014.

2.015 Specific heat, 0.12 Btu per lb F.

2.016 Dimensional changes. Equalized and aged material to Condition SCT, about 0.0015 inch per inch growth. Condition CRT to Condition SCT, about 0.00275 inch per inch growth (8).

Fe
15.5 Cr
4.5 Ni
3 Mo

AM-355

2.02 **Other Physical Properties**

2.021 Density, Table 2.021.

2.022 Electrical resistivity of alloy in Condition SCT 850, Figure 2.022.

2.023 Magnetic properties, Table 2.023.

2.024 Emittance.

2.025 Damping capacity.

2.03 **Chemical Environments**

2.031 Corrosion resistance.

2.0311 General corrosion resistance of this alloy is between that of Type 410 and Type 302.

2.0312 The alloy appears to be relatively free from intergranular corrosion in the SCT (1000) Condition.

2.0313 This alloy has been shown to be susceptible to hydrogen embrittlement under laboratory conditions when heat treated to 180 ksi ultimate tensile strength. Therefore, the alloy should be considered to be sensitive to hydrogen embrittlement (41).
Testing in high-pressure (10,000 psi) hydrogen has shown degradation in mechanical properties for some stainless steels (42). Therefore, the possibility of loss in mechanical properties should be considered when using this alloy in contact with high pressure hydrogen.

2.032 Oxidation resistance up to 850 F and higher is comparable to that of austenitic stainless steels.

2.033 Stress corrosion resistance. The SCT (850) Condition should not be used when stress corrosion resistance is important. The SCT (1000) Condition has improved but erratic resistance to stress corrosion which varies with the metallurgical structure of the material. If the material contains continuous intergranular precipitated carbides, intergranular stress corrosion failures may occur. If the structure is free from intergranular carbides, the material has excellent resistance to stress corrosion when tempered at 1000 F. Consumable electrode melted material should be hardened by using the carbide solution subzero treatment (see 1.055) which will consistently produce a homogenous structure free of continuous intergranular carbides. When hardened by this heat treatment, all AM-355 wrought products, welds, and castings have excellent resistance to stress corrosion. This has been demonstrated by stress corrosion tests on all of these products, stressed to 90 percent of F_{ty} and exposed for more than 300 days in salt spray without cracking (35).

2.04 **Nuclear Environments**

3 **MECHANICAL PROPERTIES**

3.01 **Specified Mechanical Properties**

3.011 AMS specified mechanical properties for sand and investment castings, Table 3.011.

3.012 AMS specified mechanical properties for bars, forgings, plate, sheet, and strip, Table 3.012.

3.013 Producer's guaranteed mechanical properties, Table 3.013.

3.02 **Mechanical Properties at Room Temperature**

3.021 Tension.

3.0211 Stress-strain diagrams, see 3.0311.

3.0212 Effect of percent cold roll on tensile and compressive properties of sheet in CRT Condition, Figure 3.0212.

3.0213 Typical tensile properties of alloy for various heat treated conditions, Table 3.0213.

3.0214 Effect of consumable electrode melting on transverse properties of bar, Table 3.0214.

3.0215 Effect of exposure to elevated temperatures on tensile properties of bar in Conditions SCT 850 and SCT 1000, Figure 3.0215.

3.0216 Effect of exposure to elevated temperatures under load on tensile properties of sheet in Condition SCT 850, Table 3.0216.

3.0217 Effect of percent cold roll on tensile properties of alloy in Condition CRT, Figure 3.0217.

3.0218 Effect of annealing temperature and percent cold roll on longitudinal and transverse properties of CRT alloy, Figure 3.0218.

3.022 Compression. See 3.032 and 3.0212.

3.023 Impact. (See also 3.033.) Effect of exposure time and temperature on impact energy measured at room temperature for bar in SCT Condition, Figure 3.023.

3.024 Bending. Relationship between tensile yield strength and transverse bend factor, Figure 3.024.

3.025 Torsion and shear. See 3.035.

3.026 Bearing. See 3.036.

3.027 Stress concentration.

3.0271 Notch properties.

3.02711 Effect of tempering temperature on smooth and notched bar tensile properties for alloy in Condition SCT, Figure 3.02711.

3.02712 Effect of annealing temperature and percent cold roll on longitudinal and transverse notch strength and notch strength ratio of CRT alloy, Figure 3.02712.

3.02713 Effect of rate of loading on calculated stress intensity factor at failure for CRT alloy tested at room temperature in longitudinal direction, Figure 3.02713.

3.0272 Fracture toughness.

3.028 Combined properties.

3.03 **Mechanical Properties at Various Temperatures**

3.031 Tension.

3.0311 Stress-strain curves in tension at room and elevated temperatures for sheet in CRT Condition, Figure 3.0311.

3.0312 Stress-strain curves in tension at room and elevated temperatures for sheet in SCCRT Condition, Figure 3.0312.

3.0313 Stress-strain curves in tension at room and elevated temperatures for sheet in Condition XH, Figure 3.0313.

3.0314 Effect of test temperature on tensile properties of sheet in Condition SCT 850, Figure 3.0314.

3.0315 Effect of test temperature on tensile properties of bar and forged disks in Conditions SCT 850 and SCT 1000, Figure 3.0315.

3.0316 Effect of test temperature on tensile properties of bar in Condition SCT 850, Figure 3.0316.

3.0317 Effect of exposure time and temperature on tensile properties of bar in SCT 850 Condition, Figure 3.0317.

3.0318 Effect of test temperature and test direction on tensile properties of sheet in Condition CRT, Figure 3.0318.

3.0319	Effect of test temperature and test direction on tensile properties of sheet in SCCRT Condition, Figure 3.0319.
3.03110	Effect of test temperature on transverse tensile properties of sheet in Condition XH, Figure 3.03110.
3.03111	Effect of test temperature and tempering temperature on tensile properties of sand cast keel blocks, Figure 3.03111.
3.032	Compression.
3.0321	Stress–strain curves in compression at room and elevated temperatures for sheet in CRT Condition, Figure 3.0321.
3.0322	Stress–strain curves in compression at room and elevated temperatures in SCCRT Condition, Figure 3.0322.
3.0323	Effect of test temperature and test direction on compressive yield strength of sheet in Conditions SCT, CRT, and SCCRT, Figure 3.0323.
3.033	Impact.
3.0331	Effect of test temperature on impact strength for bar in SCT Conditions, Figure 3.0331.
3.0332	Effect of test temperature on impact strength for bar in various SCT Conditions, Figure 3.0332.
3.0333	The effect of special heat treatments on the impact strength in the longitudinal and transverse direction, Figure 3.0333.
	3.0333
3.034	Bending.
3.035	Torsion and shear.
3.0351	Effect of test and exposure temperature on shear strength of sheet and bar in SCT 850 Condition, Figure 3.0351.
3.0352	Effect of test temperature on stress intensity factor at failure in tear test of CRT alloy in longitudinal and transverse direction, Figure 3.0352.
3.036	Bearing.
3.0361	Effect of test temperature on bearing properties of sheet in SCT Condition, Figure 3.0361.
3.037	Stress concentration.
3.0371	Effect of test temperature on notch strength of bar in Condition SCT 850, Figure 3.0371.
3.0372	Fracture toughness of plate for various age Conditions, Figure 3.0372.
3.038	Combined properties.
3.04	**Creep and Creep Rupture Properties**
3.041	General.
3.042	Creep–rupture properties.
3.0421	Creep–rupture curves for sheet in various Conditions, Figure 3.0421.
3.0422	Creep–rupture curves for bar and castings in various Conditions, Figure 3.0422.
3.043	Creep deformation.
3.0431	Effect of stress on creep rate at 600 and 800 F for sheet in Condition SCT 850, Figure 3.0431.
3.0432	Total creep data at 700 and 800 F for alloy in Condition CRT, Figure 3.0432.
3.0433	Effect of temperature on stress to produce creep rate of 1 percent per 100,000 hours, Figure 3.0433.
3.0434	Isochronous stress–strain curves at 600 to 800 F for sheet in Condition SCT 850, Figure 3.0434.
3.05	**Fatigue Properties**
3.051	Fatigue properties of bar and sheet in SCT Conditions, Table 3.051.
3.052	Reversed bending fatigue curve for bar in Condition SCT 850, Figure 3.052.
3.053	Fatigue strength at 10^8 cycles for SCT 850 and SCT 1000 F Conditions, Table 3.053.
3.054	Combined stress diagram for AM-355 SCT (1000 F), Figure 3.054.
3.06	**Elastic Properties**
3.061	Poisson's ratio.
3.062	Modulus of elasticity.
3.0621	Modulus of elasticity for bar in Condition SCT 850 at room and elevated temperatures, Figure 3.0621.
3.0622	Effect of test temperature on tensile and compressive elastic modulus of alloy in Condition SCT, Figure 3.0622.
3.0623	Modulus of elasticity for sheet in CRT Condition at room and elevated temperatures, Figure 3.0623.
3.0624	Modulus of elasticity for sheet in Condition SCCRT at room and elevated temperatures, Figure 3.0624.
3.063	Modulus of rigidity for bar in Condition SCT 850 at room and elevated temperatures, Figure 3.063.
3.064	Tangent modulus.
3.0641	Tangent modulus in compression at 600 F for exposure times from 1/2 hour to 1000 hours for bar stock in Condition SCT 850, Figure 3.0641.
3.0642	Tangent modulus in compression at 800 F for exposure times from 1/2 hour to 1000 hours for bar stock in Condition SCT 850, Figure 3.0642.
3.0643	Tangent modulus in compression at 900 F for exposure times from 1/2 hour to 1000 hours for bar stock in Condition SCT 850, Figure 3.0643.
3.0644	Tangent modulus in compression at 1000 F for exposure times from 1/2 hour to 1000 hours for bar stock in Condition SCT 850, Figure 3.0644.

Fe
15.5 Cr
4.5 Ni
3 Mo

AM-355

4 FABRICATION

See AM-350 also. Only different and complementary information given below.

4.01 Forming

Upon forming at room temperature the alloy work hardens very rapidly because of martensite formation during working. The formation of martensite can be avoided by working at about 300 F or higher. Using this procedure, the alloy forms in a manner similar to the austenitic stainless steels.

4.02 Machining and Grinding

4.03 Welding

4.031 Bar, plate, and forgings in all Conditions are normally fusion welded with the addition of filler rod. The alloy remains ductile during cooling although its structure changes from austenite to one containing about 5 percent ferrite. Any austenitic steel filler rod or electrode may be used unless high strength in the joint is required. Welds heat treated to

Fe
15.5 Cr
4.5 Ni
3 Mo

AM-355

Condition SCT approaching 100 percent efficiency can be obtained with AM-355 welding wire or coated electrodes. Alloy is highly resistant to weld cracking. Consequently preheating, control of interpass temperature, and postheating are not required. A specially compounded submerged arc welding flux (Arcosite S-12) can be used with AM-355 wire to deposit AM-355 weld metal. The carbide solution subzero treatment is fully applicable to welded AM-355.

4.032 Fusion welding of sheet in Conditions CRT and SCCRT destroys the effects of cold rolling in any section heated above 900 F.

4.033 Resistance welding of sheet is possible in all conditions.

4.034 Typical weldment and weld metal properties for various methods, Table 4.034.

4.04 Heat Transfer

4.05 Surface Treatment

REFERENCES

1 AMS 5359B (Oct. 1, 1981)
2 AMS 5368A (Jan. 15, 1976)
3 AMS 5743E and AMS 5744B (Apr. 1, 1981)
4 AMS 5549D (Apr. 1, 1981)
5 AMS 5547D (Apr. 1, 1981)
6 AMS 5780A (Jul. 16, 1979)
7 AMS 5781A (Jan. 15, 1978)
8 Miller, J. R., "Personal Communication", Allegheny Ludlum Steel Corp., (August 19, 1959)
9 Allegheny Ludlum Steel Corp., "AM-355", (1959)
10 Allegheny Ludlum Steel Corp., "Thermal Conductivity of AM-350 and AM-355", Data Sheet 83-11557-P, (1959)
11 Allegheny Ludlum Steel Corp., "Thermal Expansion of AM-350 and AM-355", Data Sheet 46-11557-G, (1959)
12 Allegheny Ludlum Steel Corp., Data Sheet, Table IX, (1959)
13 Allegheny Ludlum Steel Corp., "Room and Elevated Temperature Tensile and Compressive Properties of SCCRT AM-355", Data Sheet 114-82158-355, (1958)
14 Allegheny Ludlum Steel Corp., "Electrical Resistivity of AM-350 and AM-355 Alloys Versus Temperature", Data Sheet 88-121657-Q, (1959)
15 Allegheny Ludlum Steel Corp., "Room and Elevated Temperature Tensile and Compressive Properties of CRT AM-355", (1959)
16 Allegheny Ludlum Steel Corp., "Creep Data AM-350 and AM-355 Alloys", Data Sheet, 119-121658-5, (1959)
17 Allegheny Ludlum Steel Corp., Data Sheet, (1959)
18 Brisbane, A. W., "Mechanical Properties of AM-350 and AM-355 Stainless Steel", WADC TR 58-672, ASTIA Doc. No. 208664, (February 1959)
19 North American Aviation, Inc., (1957)
20 Allegheny Ludlum Steel Corp., "Allegheny Ludlum Precipitation Hardening Stainless Steels, AM-350 and AM-355", (1960)
21 Allegheny Ludlum Steel Corp., "Latest Information on AM-350 and AM-355 as of 1959", (1959)
22 Allegheny Ludlum Steel Corp., "Engineering Properties of Precipitation Hardening Alloys AM-350 and AM-355, (1959)
23 Douglas Aircraft Corp., "Chloride Stress Corrosion Susceptibility of High Strength Stainless Steel, Titanium Alloy and Superalloy Sheet", Technical Documentary Report No. ML-TDR 64-44, Vol. I, (March 1964)
24 Dreyer, G. A. and Gallaugher, W. C., "Investigation of the Effects of Stress Corrosion on High Strength Alloy Steels", A. F. Materials Laboratory Report ML-TDR 64-3, (February 1964)
25 Pearl, J. A., Kappelt, G. F., and King, E. J., "Mechanical Properties of Selected Alloys at Elevated Temperatures", WADC TR 59-702, Part I, (March 1960)
26 Ludwigson, D. C., "Semi-Austenitic Precipitation Hardenable Stainless Steels, DMIC Rpt. 164, (December 6, 1961)
27 Battelle Memorial Institute, "Notch Tests-AM-355", (April 28, 1960)
28 Allegheny Ludlum Data Sheet 121-12159-355, (1959)
29 Allegheny Ludlum Data Sheet 130-10859-355, (1959)
30 Allegheny Ludlum Memorandum, "Relationship Between Tensile and Compressive Properties of AM-355 CRT, (1959)
31 Boeing Airplane Co., "Summary of Tear Tests", (May 1962)
32 Allegheny Ludlum Steel Corp., "Engineering Properties of Precipitation Hardening Alloys AM-350 and AM-355"
33 Allegheny Ludlum Steel Corp., "Stress Rupture and Creep Strength of AM-355 in CRT Condition", (June 16, 1960)
34 AMS 5594, (January 31, 1964)
35 Bergman, P. A. and Palty, A. E., "Development of Corrosion Resistance in AM-355", Transactions, Am. Soc. Metals, Vol. 56, (1963), p. 728.
36 Amateau, M. F. and Steigerwald, E. A., "Fracture Characteristics of Structural Steels", Thompson Ramo Wooldridge, Final Report ER-5937-3 to Bur. Naval Weapons, (January 1965)
37 Allegheny Ludlum Steel Corp., "AM 350/355 Precipitation Hardening Stainless Steels", (1961)
38 Private Communication. General Electric Co. Aircraft Engine Group (P. Bergman, Nov. 1981)
39 Allegheny Ludlum Steel Corp., "Engineering Properties of Precipitation Hardening Alloys AM 350 and AM 355", (1960)
40 Allegheny Ludlum Steel Corp., "The Effect of Heat Treatment on Impact Strength", Data Sheet (1963)
41 Groeneveld, T. P., Fletcher, E. E., and Elsea, A. R., "A Study of Hydrogen Embrittlement of Various Alloys", Final Report to NASA, Contract NA58-20029, (January 23, 1969)
42 Chandler, W. T. and Walters, R. J., "Testing to Determine the Effect of High-Pressure Hydrogen Environments on the Mechanical Properties of Metals", ASTM STP 543, American Society for Testing and Materials, p. 170-197 (1974)

(For Additional Bibliography See p. 22)

Fe
15.5 Cr
4.5 Ni
3 Mo

AM-355

AMS	Form	Condition
5359B	Sand Castings	Solution Treated
5368A	Investment Castings	Solution Treated
5743E	Bars and Forgings	Solution Treated Equalized and Overtempered
5744B	Bars and Forgings	Heat Treated to F_{tu} = 170 ksi
5549D	Plate	Solution Treated
5547D	Sheet and Strip	
5780A	Welding Wire	
5781A	Covered Electrodes	

TABLE 1.031. AMS SPECIFICATIONS

Source	AMS					
Form	Castings (1) (2)		Bar, Forgings, Plate, Sheet, and Strip (3) (4) (5)		Welding Wire and Covered Electrodes (6) (7)	
Composition	Min	Max	Min	Max	Min	Max
C	0.08	0.15	0.10	0.15	0.010	0.15
Mn	0.040	1.10	0.50	1.25	0.50	1.25
Si	–	0.75	–	0.05	–	0.50
P	–	0.04	–	0.040	–	0.040
S	–	0.03	–	0.030	–	0.030
Cr	14.5	15.5	15.00	16.00	15.00	16.00
Ni	3.5	4.5	4.00	5.00	4.00	5.00
Mo	2.0	2.6	2.50	3.25	2.50	3.25
N	0.05	0.13	0.07	0.13	0.07	0.13
C and Ni	0.15	0.25	–	–	–	–
Cu	–	–	–	–	–	0.050
Fe	Balance		Balance		Balance	

TABLE 1.041. COMPOSITION OF CAST AND WROUGHT PRODUCTS

Alloy	Fe-15.5Cr-4.5Ni-3Mo		
Form	All		
Mill Supplied Conditions	Heat Treatment by Mill		Purpose
Equalized and overtempered E + OT	2–4 hr at 1425 ± 50°, oil or water quench or air cool to 50 F max plus 2–4 hr at 1075 F ± 25°, air cooled		Preparation for machining
Carbide solutioned, equalized and overtempered S + (E+OT)	1–3 hr at 1900 F ± 25°, water quenched* plus 3 hr at –100 F plus equalized and overtempered		Preparation for machining with optimum microstructure for stress corrosion resistance when followed by subsequent L anneal plus SCT
Fully hardened SCT (1000 F) FH	1–3 hr at 1900 F ± 25°, water quenched* plus 3 hr at –100 F plus L anneal plus SCT (1000 F)		Heat treatment by user not required. Material has good machinability and optimum microstructure for stress corrosion resistance
H	Solution treated at 1950 F and water quenched		Preparation for reforging by user
Mill Supplied Condition Prior to User Heat Treatment	Condition Through User Treatment	Heat Treatment by User	Purpose
Any	L	1675–1775 F, rapid air cool or water quench	Preparation for hardening
Any	L + SCT	L plus subzero cool 3 hr at –100 F and temper for 3 hr at 850 or 1000 F	Hardening for highest strength 850 F, or highest toughness (1000 F)
E + OT	Carbide solution hardening treatment	1–3 hr at 1900 F ± 25°, water quenched* plus 3 hr at –100 F plus L anneal plus SCT (1000 F)	Hardened for optimum microstructure and best resistance to stress corrosion
Carbide Solutioned E + OT	Carbide solution hardening treatment + SCT	L plus SCT (1000 F)	Hardened for optimum microstructure and resistance to stress corrosion
Carbide Solutioned, + L + SCT (1000 F)		None Following user fabrication stress relieving treatment up to 1000 F maximum may be employed	Hardened for good machinability, high toughness and optimum microstructure for stress corrosion resistance
H	Forging should be controlled to finish working at a low temperature to produce fine grain size. Following forging, carbide solution hardening treatment is recommended. However, the L + SCT treatment may be used without prior carbide solutioning treatment if a microstructure free of grain boundary carbides is not essential.		

*A minimum cooling rate of 100° per minute to 1200 F must be used to avoid precipitation of grain boundary carbides.

TABLE 1.0514. MILL SUPPLIED CONDITIONS AND USER HEAT TREATMENTS FOR ALL FORMS ACCORDING TO ALLOY PRODUCER (37)

Fe
15.5 Cr
4.5 Ni
3 Mo

AM-355

Form	Bars and Forgings		Plate	Sheet and Strip
Condition	Solution Treat	Equalize and Overtemper	Solution Treat	Solution Treat
	1875-1925 F, 1 to 3 hr, WQ	ST + 1375 to 1475 F, 3 hr AC (< 80 F) + 1050 to 1100 F, 3 hr AC	1875-1925 F, 1 to 3 hr, WQ	1875-1925 F, 3/4 hr, WQ
Condition		1000 SCT ST + 1725 to 1775 F, 10 to 60 min, WQ + 3 hr at -100 F, Air Warm + 975 to 1025 F, 3 hr AC	1000 SCT ST + 2 hr at -100 F, Air Warm + 1725 to 1775 F, 10 to 60 min, WQ + 3 hr at -100 F, Air Warm + 975 to 1025 F, 3 hr AC	1000 SCT See Plate

TABLE 1.0515. AMS SPECIFIED HEAT TREATMENTS FOR BARS, FORGINGS, PLATE, SHEET, AND STRIP (3) (4) (5)

Form	Sand Castings (2)[a]	Investment Castings (2)
Condition	Solution Treat 1950-2050 F, 1 hr AC for Sections < 1 in., WQ or OQ for Sections > 1 in.	Solution Treat 1850-1975 F, 1 hr, AC for Sections < 1 in., WQ or OQ for Sections > 1 in.
Condition	Equalize or overtemper ST + 1350 F to 1450 F, 3 hr min., AC + 1025 to 1075 F, 3 hr AC	850 SCT ST 1750 to 1825 F, 1 hr, WQ + 3 hr at -100 F, Air Warm 825 to 875 F, 3 hr AC
Condition	1000 SCT ST + 1725 to 1850 F, 1 hr, WQ + 3 hr at -100 F, Air Warm + 975 to 1025 F, 3 hr AC	

(a) Separately cast specimens or specimens cut from castings.

TABLE 1.0525. AMS SPECIFIED HEAT TREATMENTS FOR SAND AND INVESTMENT CASTINGS (1) (2)

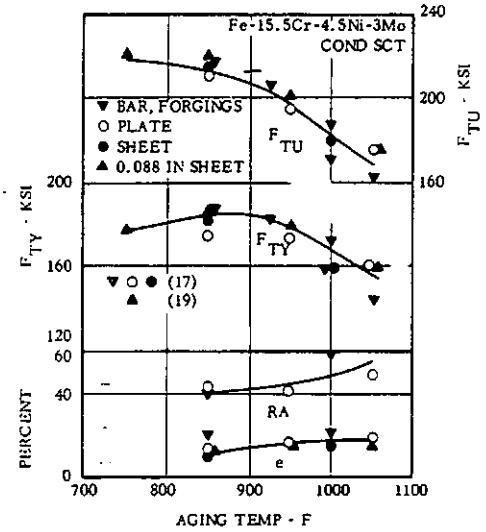


FIG. 1.053. EFFECT OF AGING TEMPERATURE ON TENSILE PROPERTIES OF VARIOUS FORMS (17) (19)

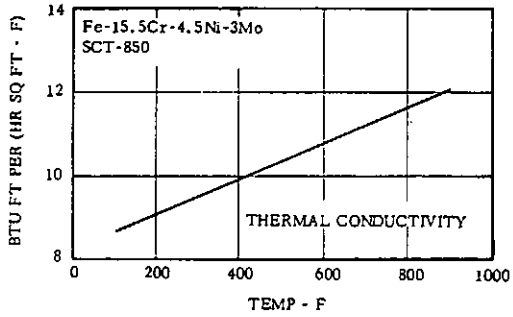


FIG. 2.013 THERMAL CONDUCTIVITY (20, p. 12)

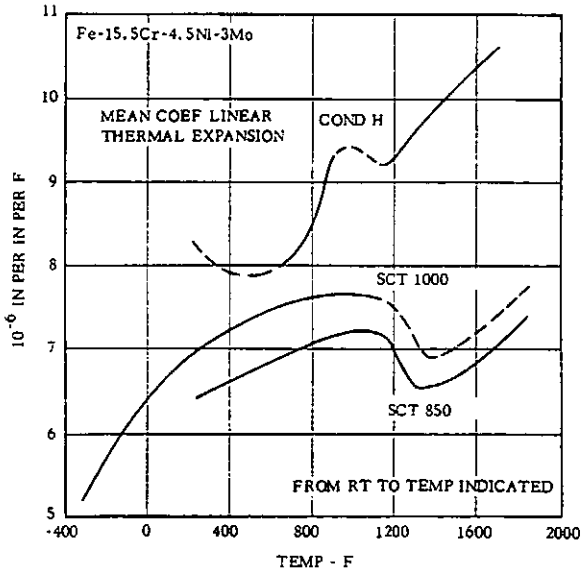


FIG. 2.014 THERMAL EXPANSION (21)

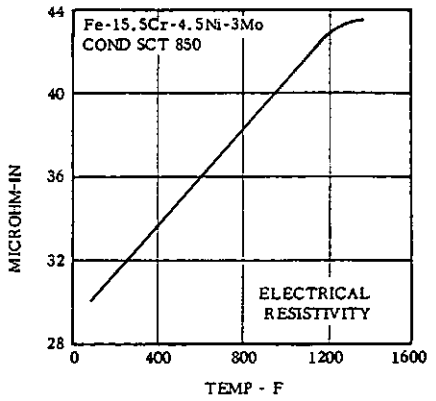


FIG. 2.022 ELECTRICAL RESISTIVITY OF ALLOY IN CONDITION SCT 850 (14)

Condition	Density lb per cu in	Density gr per cu cm
H (1875F)	0.286	7.91
Equalized and aged	0.283	7.82
SCT 850	0.281	7.79
CRT	0.284	7.86
SCCRT	0.2805	7.76

TABLE 2.021 DENSITY (8)

Condition	SCT 850	SCT 1000
Max permeability	87	150
Induction at 200 oersteds	9660	11508

TABLE 2.023 MAGNETIC PROPERTIES

Fe
15.5 Cr
4.5 Ni
3 Mo

AM-355

Source	AMS 5368(1)	AMS 5359(2)
Form	Sand Castings	Investment Castings
Condition	SCT (1000)	SCT (850)
F_{tu}, Min, ksi	165	200
F_{ty}, Min, ksi	140	150
Elongation, 4D, Min, percent	8	8(a)
Hardness, R_C, Min	37	40

(a) Elongation in 1 inch or 4D.

TABLE 3.011 AMS SPECIFIED MECHANICAL PROPERTIES FOR AM-355 SAND AND INVESTMENT CASTINGS

Source	AMS 5743(3)	AMS 5749(4)	AMS 5747(5)
Form	Bars and Forgings	Plate	Sheet and Strip
Condition	SCT (1000)	SCT (1000)	SCT (1000)
F_{tu}, Min, ksi	170	165	165
F_{ty}, 0.2% offset, Min, ksi	155	140	140
Elongation, 2 in. or 4D, Min, percent	12	12	10(a)
Reduction in Area, Min, percent	25	–	–
Hardness, R_C	37–44(b)	37–44(b)	37 (Min)

(a) Up to 0.010 inch thick inclusive, the elongation is not specified but is "as agreed upon". The elongation for sheet and strip over 0.010 to 0.1875 inch thick exclusive, is 10 percent minimum.
(b) Not to be rejected on hardness requirement if the tensile properties meet specification.

TABLE 3.012 AMS SPECIFIED MECHANICAL PROPERTIES FOR AM-355 BARS, FORGINGS, PLATE, SHEET, AND STRIP

Alloy		Fe-15.5Cr-4.5Ni-3Mo						
Form		Sheet, strip**		Plate		Bar, forgings		Castings Sand, Investment
Melt		-		Cons. elect		Cons. electrode		-
Condition		H	SCT(850)	H	SCT(1000)	SCT(850)	SCT(1000)	SCT(850)
F_{tu},	min-ksi L	-	190	-	170	200	170	200
	T	-	190	-	170	200	170	-
F_{ty},	min-ksi L	-	165	-	155	165	155	150
	T	-	165	-	155	165	155	-
e,	min-percent L	-	-	-	12	10	12	8
	T	*	*	-	12	5	-	-
RA,	min-percent L	-	-	-	-	20	25	-
	T	-	-	-	-	5	-	-
Hardness, RC								
	min	-	43	-	37	40	37	40
	max	35	53	35	43	50	44	-

* Depends on thickness
** Commercial to 0.010 in thickness, experimental to 0.1875 in thickness.

TABLE 3.013 PRODUCER'S GUARANTEED MECHANICAL PROPERTIES (17)

Fe
15.5 Cr
4.5 Ni
3 Mo

AM-355

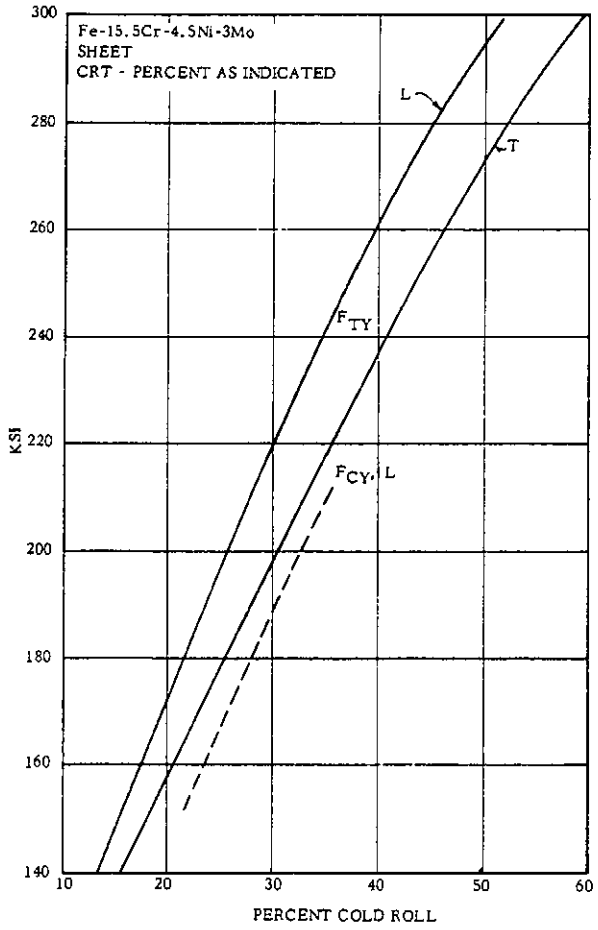


FIG. 3.0212 EFFECT OF PERCENT COLD ROLL ON TENSILE AND COMPRESSIVE PROPERTIES OF SHEET IN CRT CONDITION (30)

Form	Sheet T			Plate Avg L, T			Bar Forgings		Cast Test Bars	
Condition	H	SCT 850	SCT 1000	H	SCT 850	SCT 1000	SCT 850	SCT 1000	SCT 850	SCT 1000
F_{tu}, -ksi	186	219	178	160	210	180	216	186	218	175
F_{ty}, -ksi	55	181	160	57	174	170	182	171	173	159
e(2in) -percent	29.5	13	13	26	14	17	19	19	16	14
RA -percent	-	-	-	-	40	50	38.5	57	35	40

TABLE 3.0213 TYPICAL TENSILE PROPERTIES OF ALLOY FOR VARIOUS HEAT TREATED CONDITIONS (17)

Form	4 to 10 in sq bar		
Condition	SCT 850		SCT 1000
Melt	Air	Cons. El.	Cons. El.
F_{tu}, -ksi T	208	220	185
F_{ty}, -ksi T	168.5	185	169
RA -percent T	7.6	20.5	39.5
e(2in) -percent T	5.3	11.5	14.8
No. of tests*	14	40	40
No. of heats	2	18	25

* Specimens taken from center

TABLE 3.0214 EFFECT OF CONSUMABLE ELECTRODE MELTING ON TRANSVERSE PROPERTIES OF BAR (17)

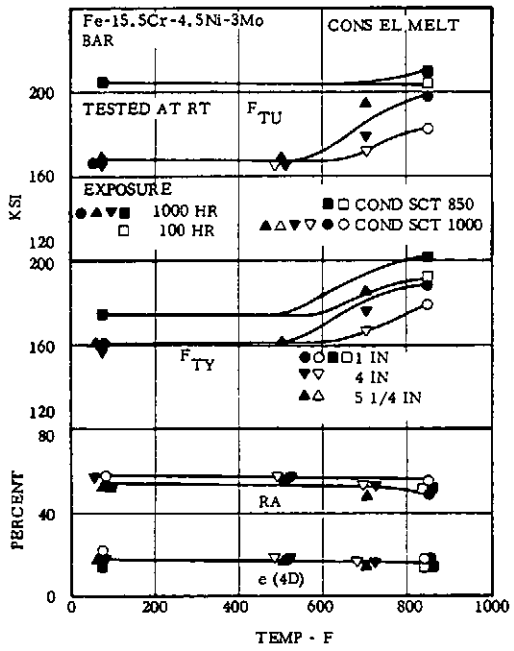


FIG. 3.0215 EFFECT OF EXPOSURE TO ELEVATED TEMPERATURES ON TENSILE PROPERTIES OF BAR IN CONDITIONS SCT 850 AND SCT 1000 (17)

Form		0.050 in sheet						
Condition		SCT 850						
Exposure	Temp-F	RT	600		700		800	
Exposure	Load-ksi	-	66	148.5	64.6	145.4	62.1	139.8
Property		-	Change from RT value, in 1000 hr Tested at RT					
F_{tu},	-ksi	211.4	+ 2	+ 2	+ 6	+ 7	+16	+16
F_{ty},	-ksi	169.4	+10	+31	+ 8	+48	+30.5	+51
e(2in),	-percent	11.5	+0.5	- 4	- 1	- 6	+ 1	-2.5

TABLE 3.0216 EFFECT OF EXPOSURE TO ELEVATED TEMPERATURES UNDER LOAD ON TENSILE PROPERTIES OF SHEET IN CONDITION SCT 850 (17)

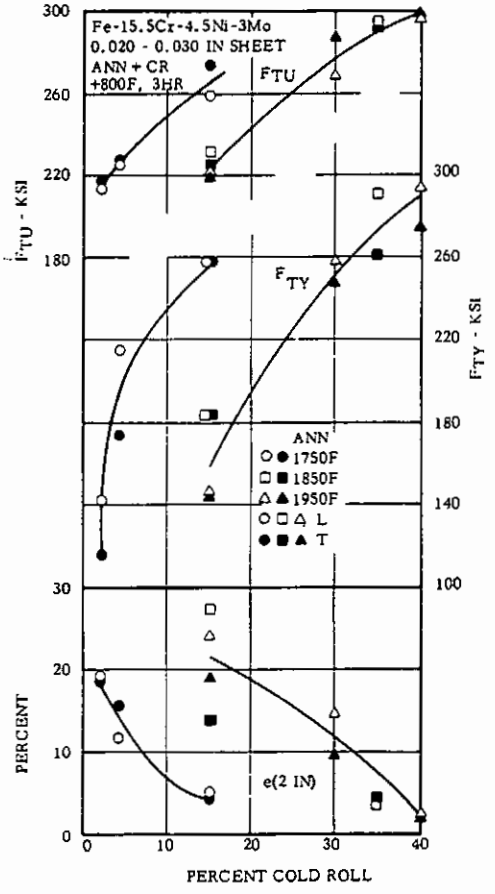


FIG. 3.0218 EFFECT OF ANNEALING TEMPERATURE AND PERCENT COLD ROLL ON LONGITUDINAL AND TRANSVERSE TENSILE PROPERTIES OF CRT ALLOY (27)

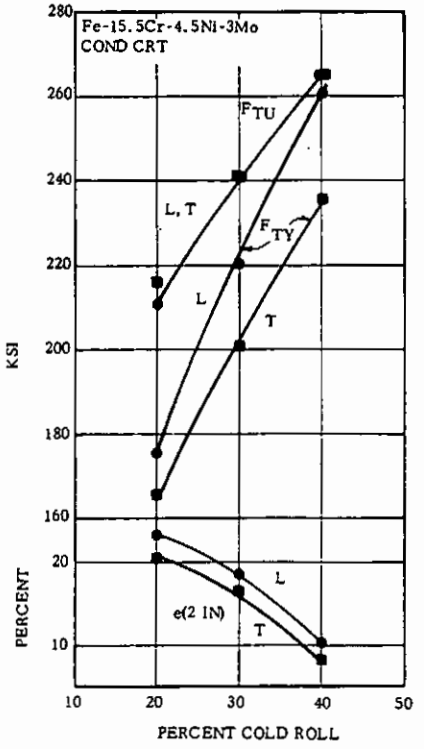


FIG. 3.0217 EFFECT OF PERCENT COLD ROLL ON TENSILE PROPERTIES OF ALLOY IN CONDITION CRT (26, p. 21)

Fe
15.5 Cr
4.5 Ni
3 Mo

AM-355

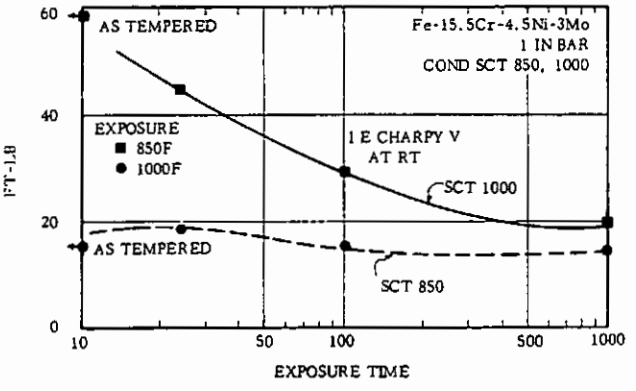


FIG. 3.023 EFFECT OF EXPOSURE TIME AND TEMPERATURE ON IMPACT ENERGY MEASURED AT ROOM TEMPERATURE FOR BAR IN SCT CONDITION (21, Table XV)

Fe
15.5 Cr
4.5 Ni
3 Mo

AM-355

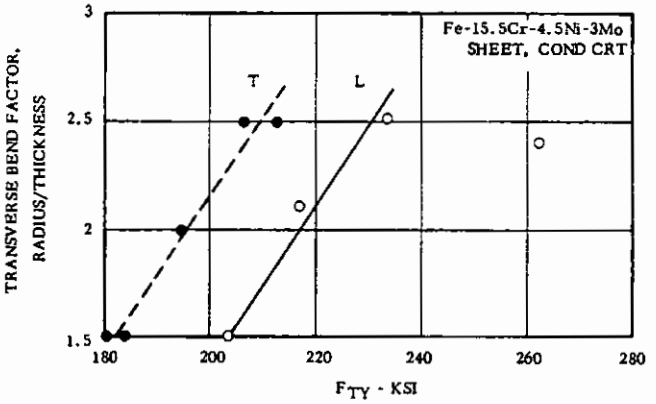


FIG. 3.024 RELATIONSHIP BETWEEN TENSILE YIELD STRENGTH AND TRANSVERSE BEND FACTOR FOR SHEET IN CONDITION CRT (30)

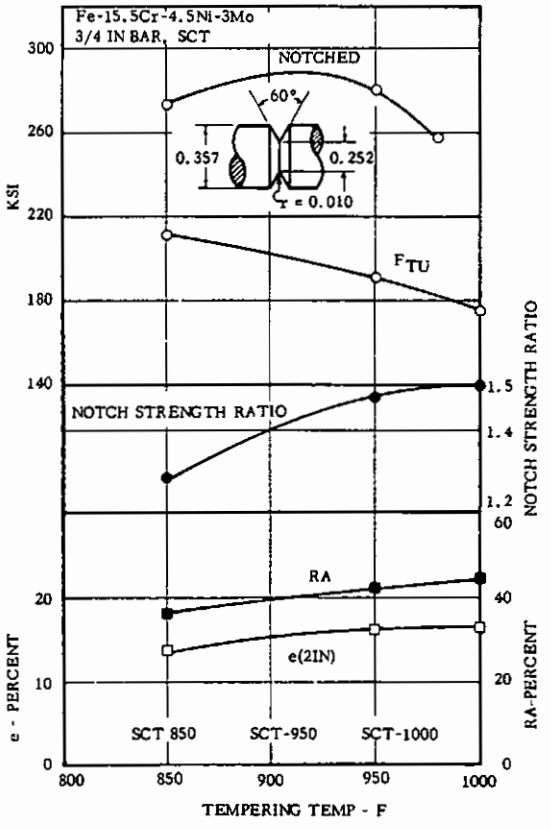


FIG. 3.02711 EFFECT OF TEMPERING TEMPERATURE ON SMOOTH AND NOTCHED BAR TENSILE PROPERTIES FOR ALLOY IN CONDITION SCT (32)

Fe
15.5 Cr
4.5 Ni
3 Mo

AM-355

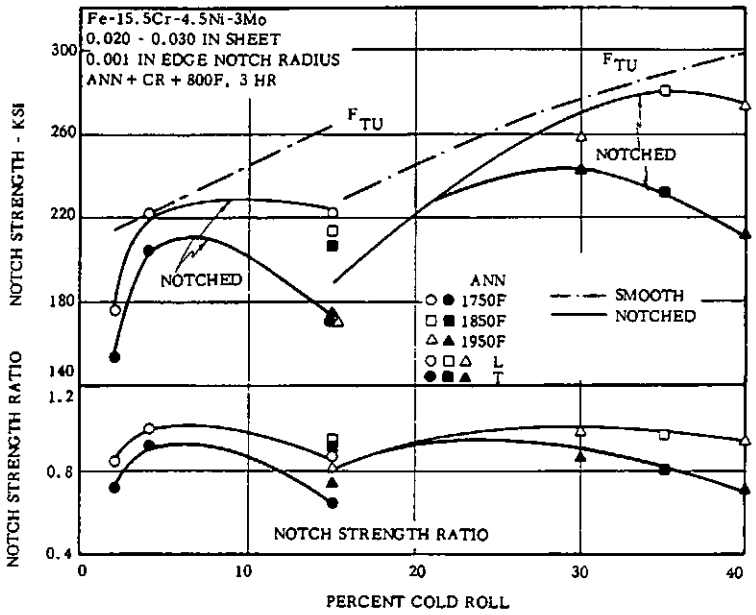


FIG. 3.02712 EFFECT OF ANNEALING TEMPERATURE AND PERCENT COLD ROLL ON LONGITUDINAL AND TRANSVERSE NOTCH STRENGTH AND NOTCH STRENGTH RATIO OF CRT ALLOY (27)

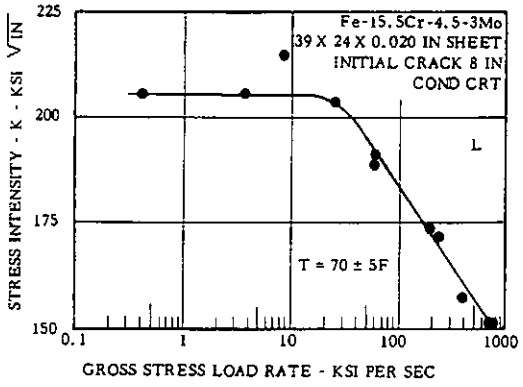


FIG. 3.02713 EFFECT OF RATE OF LOADING ON CALCULATED STRESS INTENSITY FACTOR AT FAILURE FOR CRT ALLOY TESTED AT ROOM TEMPERATURE IN LONGITUDINAL DIRECTION (31)

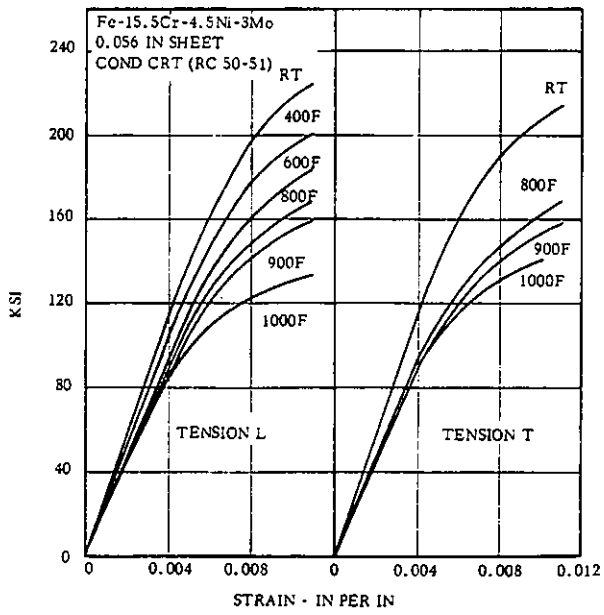


FIG. 3.0311 STRESS-STRAIN CURVES IN TENSION AT ROOM AND ELEVATED TEMPERATURES FOR SHEET IN CRT CONDITION (28)

Fe
15.5 Cr
4.5 Ni
3 Mo

AM-355

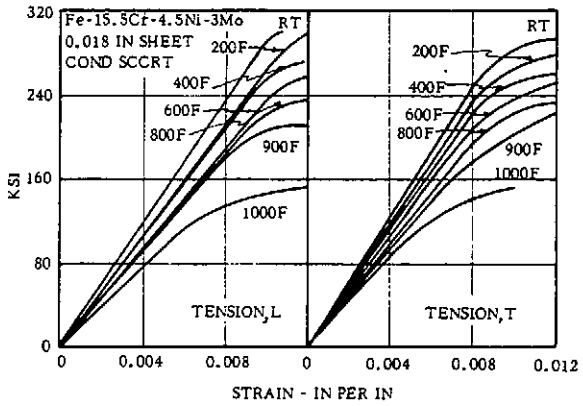


FIG. 3.0312 STRESS-STRAIN CURVES IN TENSION AT ROOM AND ELEVATED TEMPERATURES FOR SHEET IN SCCRT CONDITION (13)

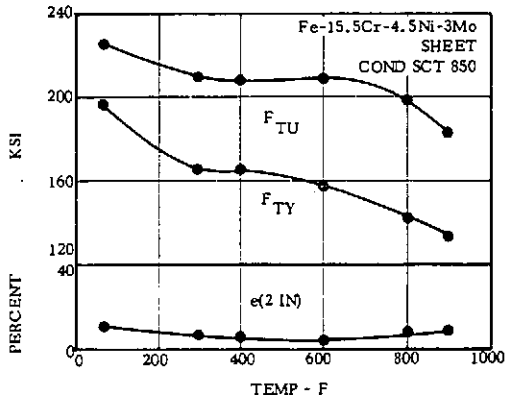


FIG. 3.0314 EFFECT OF TEST TEMPERATURE ON TENSILE PROPERTIES OF SHEET IN CONDITION SCT 850 (13)

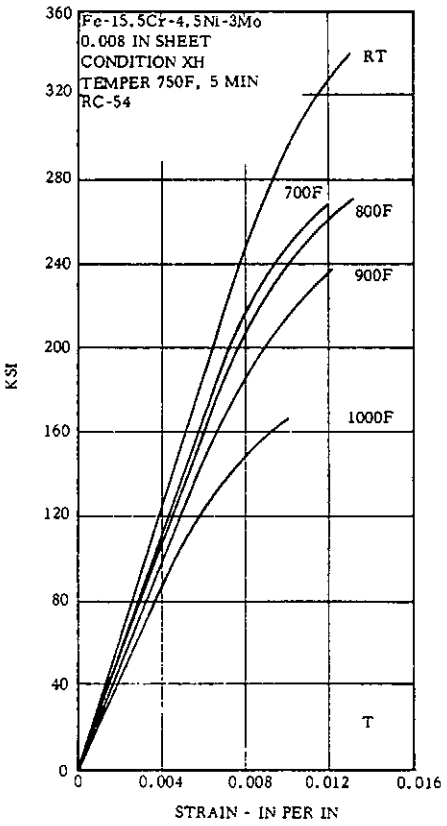


FIG. 3.0313 STRESS-STRAIN CURVES IN TENSION AT ROOM AND ELEVATED TEMPERATURES FOR SHEET IN CONDITION XH (29)

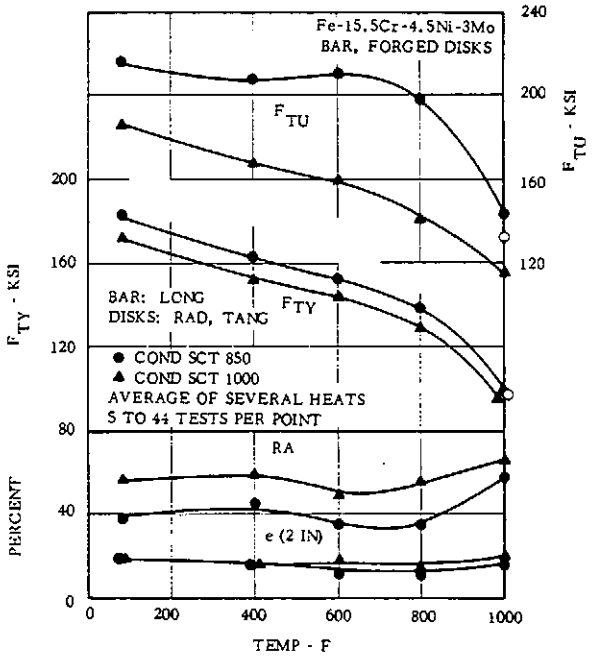


FIG. 3.0315 EFFECT OF TEST TEMPERATURE ON TENSILE PROPERTIES OF BAR AND FORGED DISKS IN CONDITIONS SCT 850 AND SCT 1000 (17)

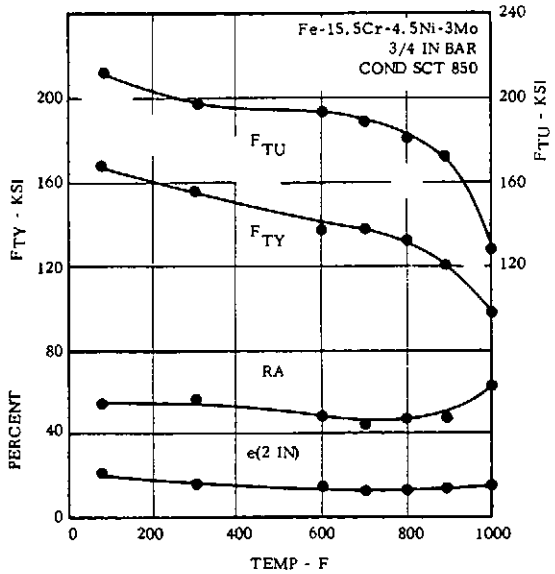


FIG. 3.0316 EFFECT OF TEST TEMPERATURE ON TENSILE PROPERTIES OF BAR IN CONDITION SCT 850 (17)

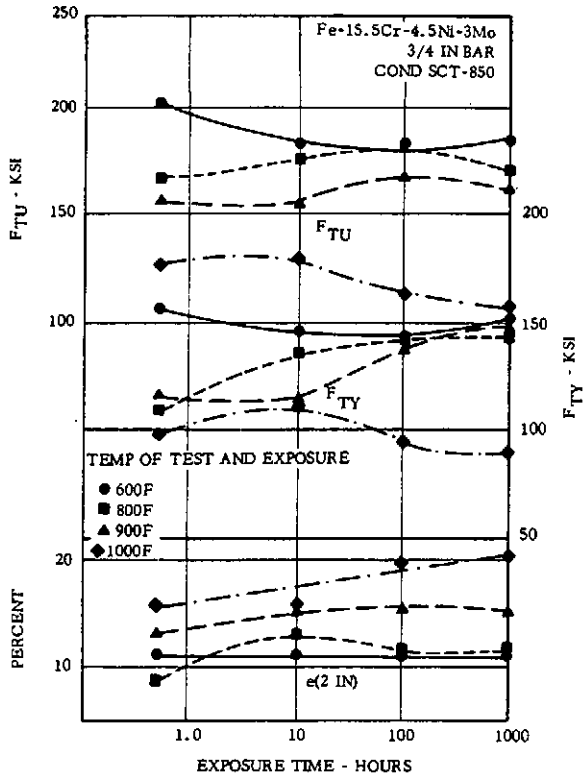
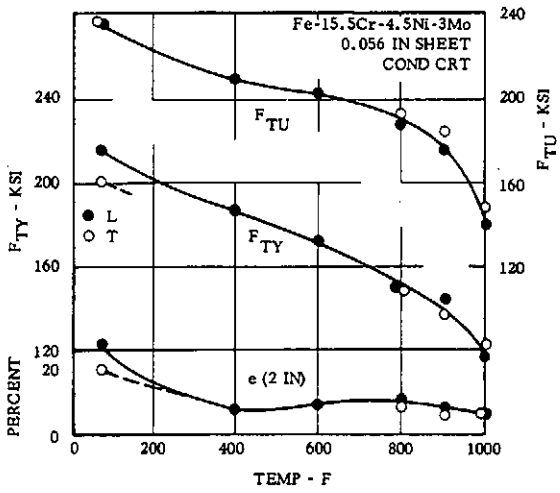


FIG. 3.0317 EFFECT OF EXPOSURE TIME AND TEMPERATURE ON TENSILE PROPERTIES OF BAR IN SCT-850 CONDITION (25, p. 87-90, 99-102, 111-114)



Fe
15.5 Cr
4.5 Ni
3 Mo
AM-355

FIG. 3.0318 EFFECT OF TEST TEMPERATURE AND TEST DIRECTION ON TENSILE PROPERTIES OF SHEET IN CONDITION CRT (15)

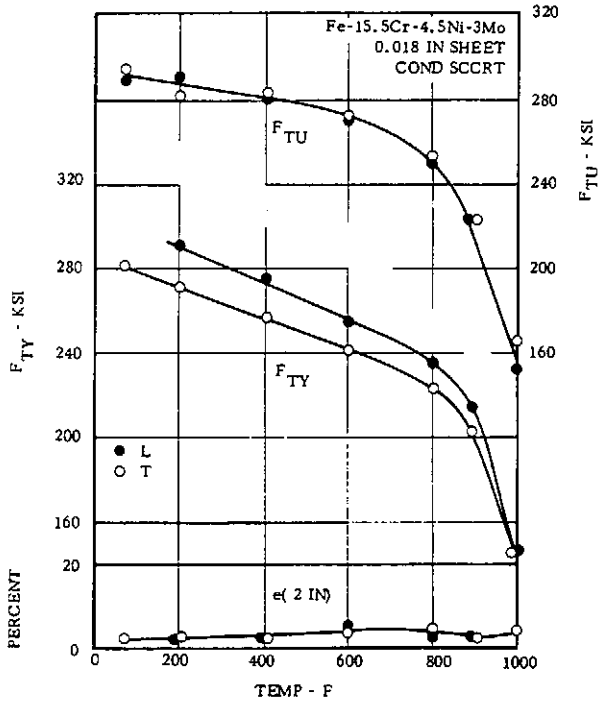


FIG. 3.0319 EFFECT OF TEST TEMPERATURE AND TEST DIRECTION ON TENSILE PROPERTIES OF SHEET IN SCCRT CONDITION (13)

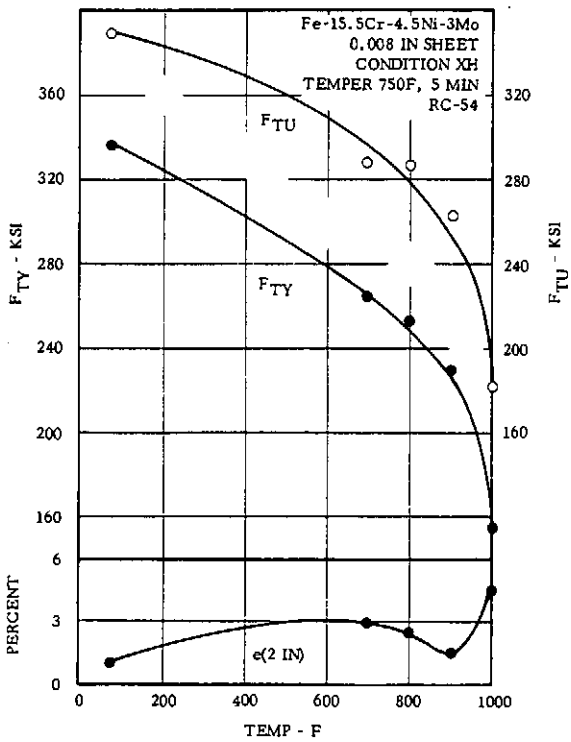


FIG. 3.03110 EFFECT OF TEST TEMPERATURE ON TRANSVERSE TENSILE PROPERTIES OF SHEET IN CONDITION XH (29)

Fe
15.5 Cr
4.5 Ni
3 Mo

AM-355

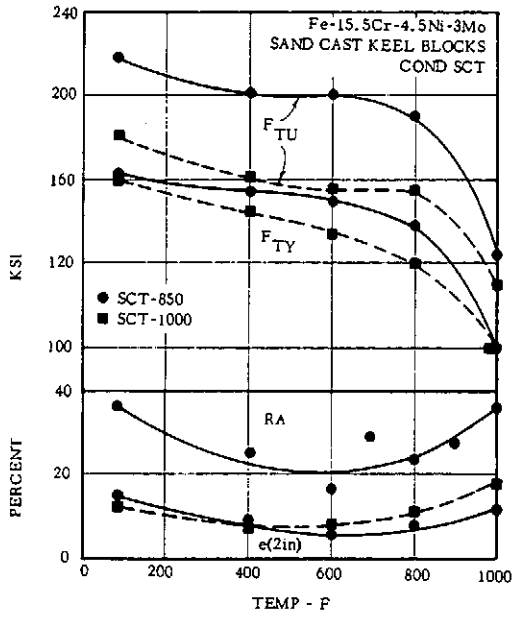


FIG. 3.03111 EFFECT OF TEST TEMPERATURE AND TEMPERING TEMPERATURE ON TENSILE PROPERTIES OF SAND CAST KEEL BLOCKS (26, p. B-2-3)(21, Table X)

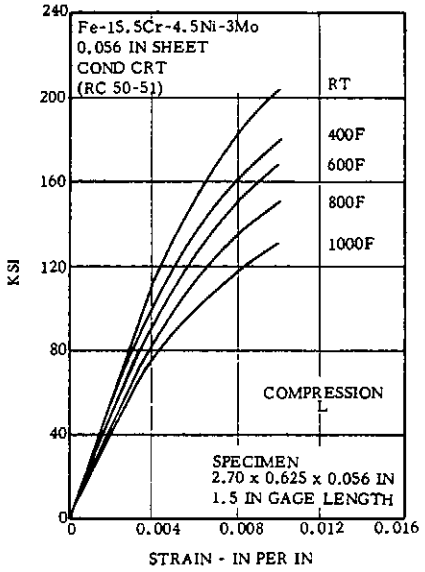


FIG. 3.0321 STRESS-STRAIN CURVES IN COMPRESSION AT ROOM AND ELEVATED TEMPERATURES FOR SHEET IN CRT CONDITION (28)

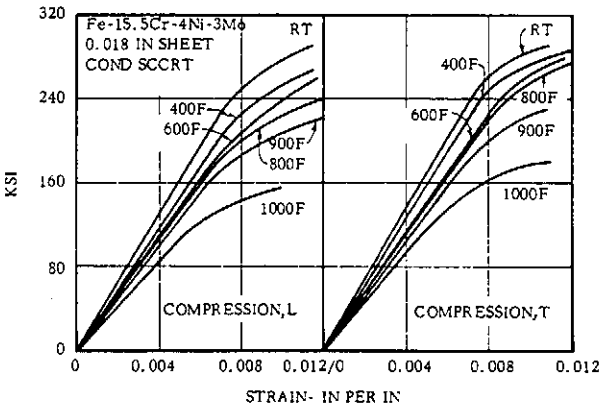


FIG. 3.0322 STRESS-STRAIN CURVES IN COMPRESSION AT ROOM AND ELEVATED TEMPERATURES FOR SHEET IN SCCRT CONDITION (13)

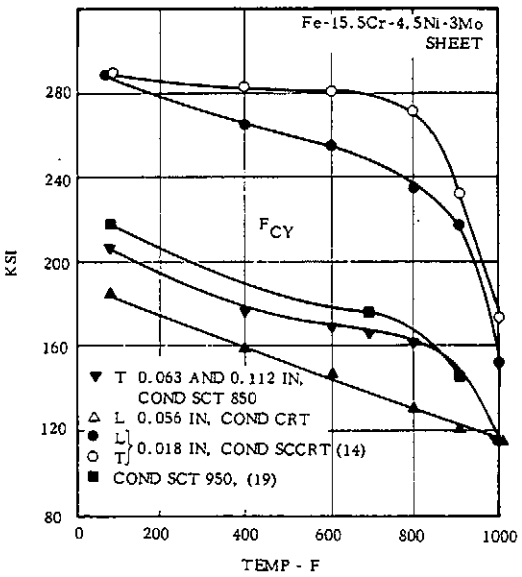


FIG. 3.0323 EFFECT OF TEST TEMPERATURE AND TEST DIRECTION ON COMPRESSIVE YIELD STRENGTH OF SHEET IN CONDITIONS SCT, CRT AND SCCRT (14)(19)

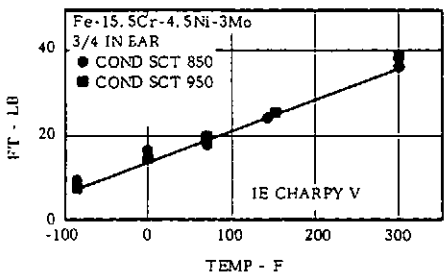


FIG. 3.0331 EFFECT OF TEST TEMPERATURE ON IMPACT STRENGTH FOR BAR IN SCT CONDITIONS (18)

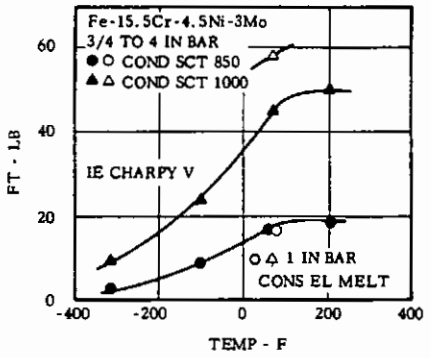


FIG. 3.0332 EFFECT OF TEST TEMPERATURE ON IMPACT STRENGTH FOR BAR IN VARIOUS SCT CONDITIONS (17)

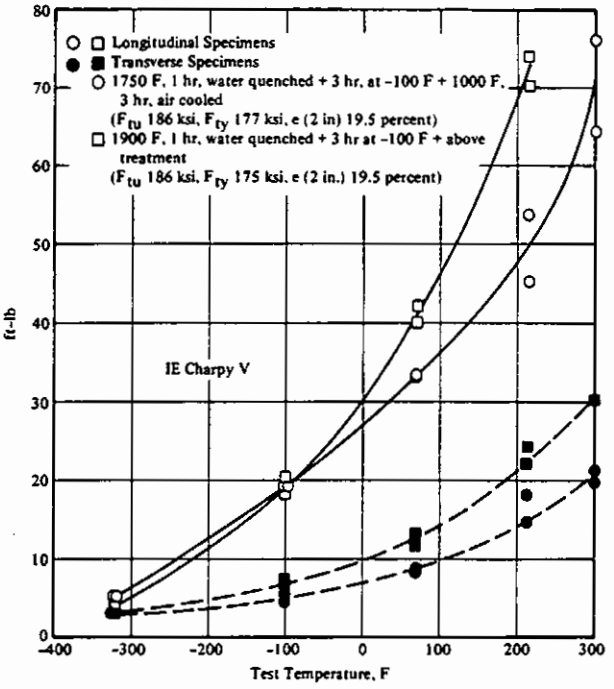


FIG. 3.0333 THE EFFECT OF SPECIAL HEAT TREATMENT ON IMPACT STRENGTH IN LONGITUDINAL AND TRANSVERSE DIRECTION (40)

Fe
15.5 Cr
4.5 Ni
3 Mo

AM-355

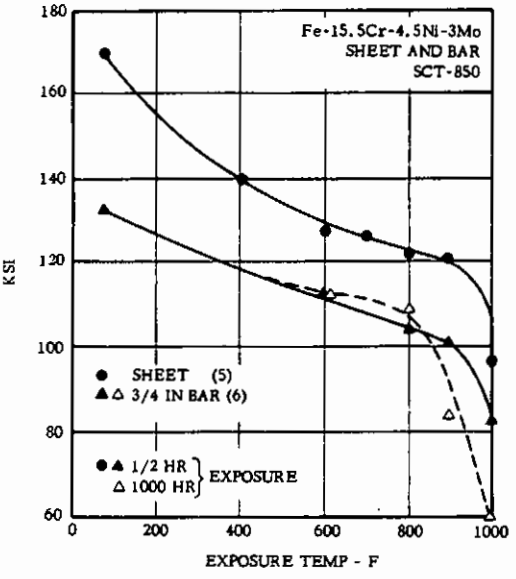


FIG. 3.0351 EFFECT OF TEST AND EXPOSURE TEMPERATURE ON SHEAR STRENGTH OF SHEET AND BAR IN SCT 850 CONDITION (25)(26)

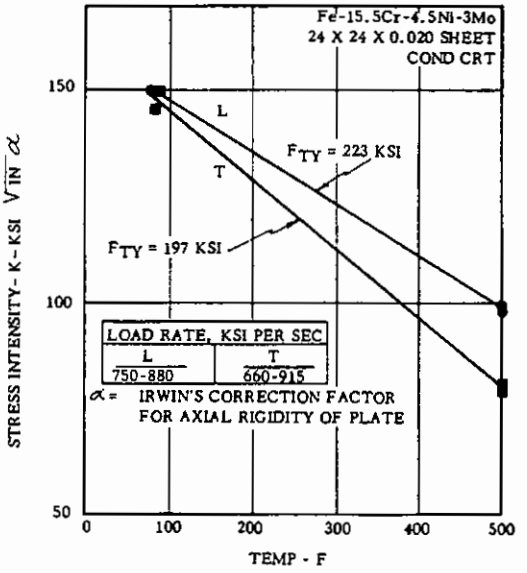


FIG. 3.0352 EFFECT OF TEST TEMPERATURE ON STRESS INTENSITY FACTOR AT FAILURE IN TEAR TEST OF CRT ALLOY IN LONGITUDINAL AND TRANSVERSE DIRECTION (31)

Fe
15.5 Cr
4.5 Ni
3 Mo

AM-355

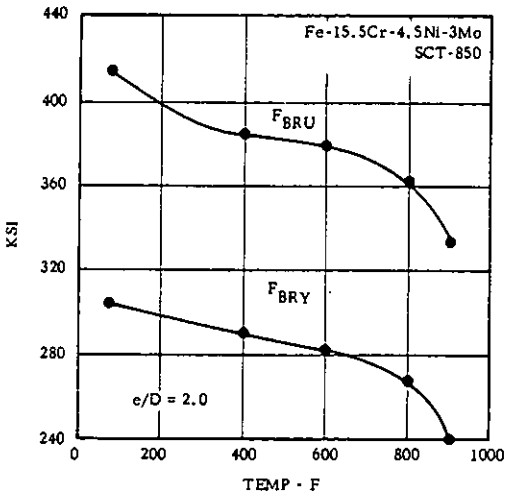


FIG. 3.0361 EFFECT OF TEST TEMPERATURE ON BEARING PROPERTIES OF SHEET IN SCT CONDITION (26, p. B-2-5)

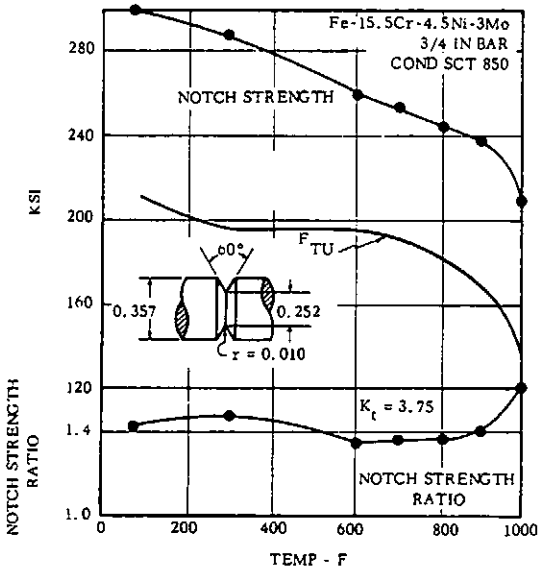


FIG. 3.0371 EFFECT OF TEST TEMPERATURE ON NOTCH STRENGTH OF BAR IN CONDITION SCT 850 (16)

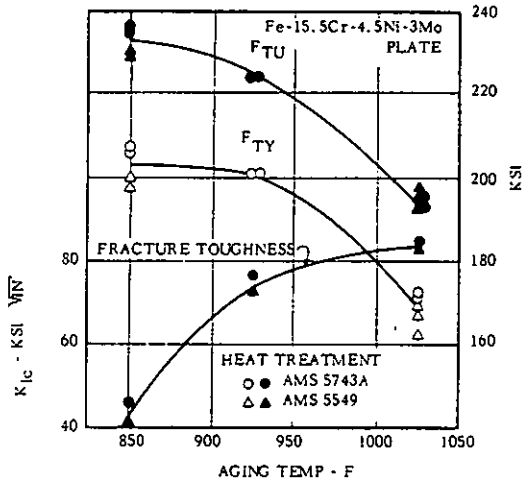


FIG. 3.0372 FRACTURE TOUGHNESS OF PLATE FOR VARIOUS AGE CONDITIONS (36)

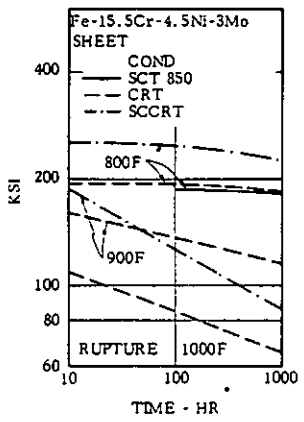


FIG. 3.0421 CREEP RUPTURE CURVES FOR SHEET IN VARIOUS CONDITIONS (14)

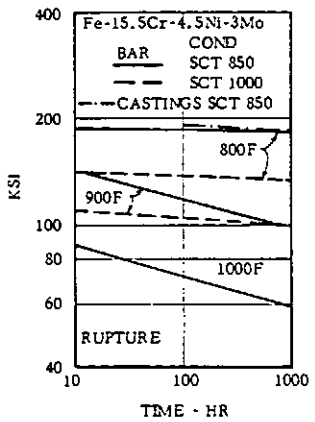


FIG. 3.0422 CREEP RUPTURE CURVES FOR BAR AND CASTINGS IN VARIOUS CONDITIONS (14)

Fe
15.5 Cr
4.5 Ni
3 Mo

AM-355

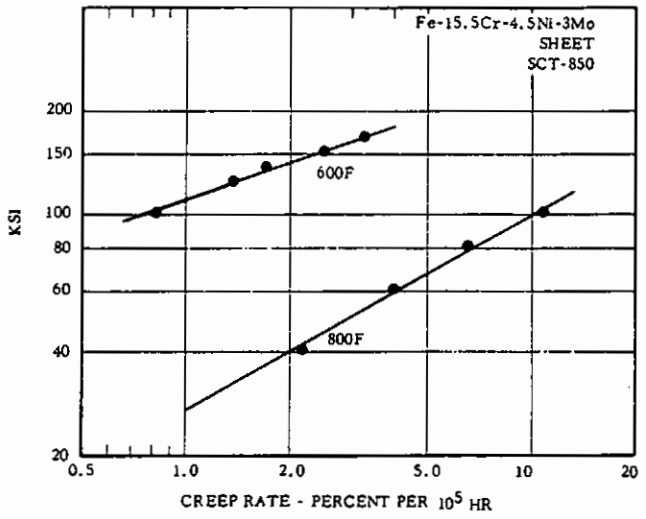


FIG. 3.0431 EFFECT OF STRESS ON CREEP RATE AT 600 AND 800F FOR SHEET IN CONDITION SCT-850 (32, p. 49)

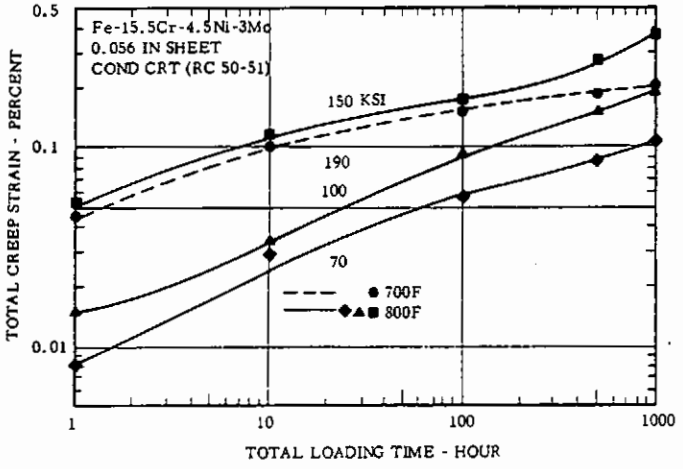


FIG. 3.0432 TOTAL CREEP DATA AT 700 AND 800F FOR ALLOY IN CONDITION CRT (33)

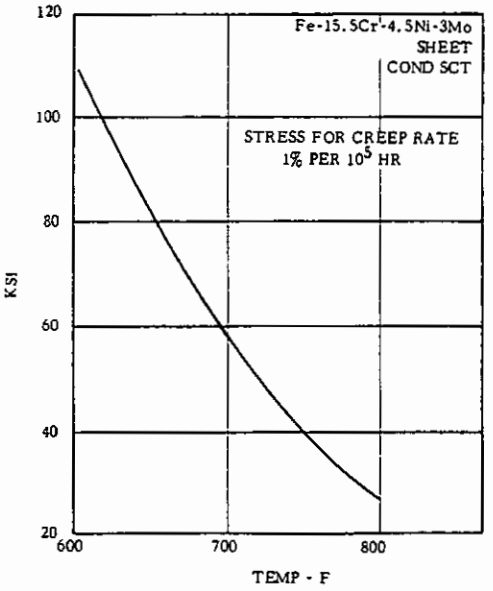


FIG. 3.0433 EFFECT OF TEMPERATURE ON STRESS TO PRODUCE CREEP RATE OF 1 PERCENT PER 10^5 HOUR (32, p. 46)

Fe
15.5 Cr
4.5 Ni
3 Mo

AM-355

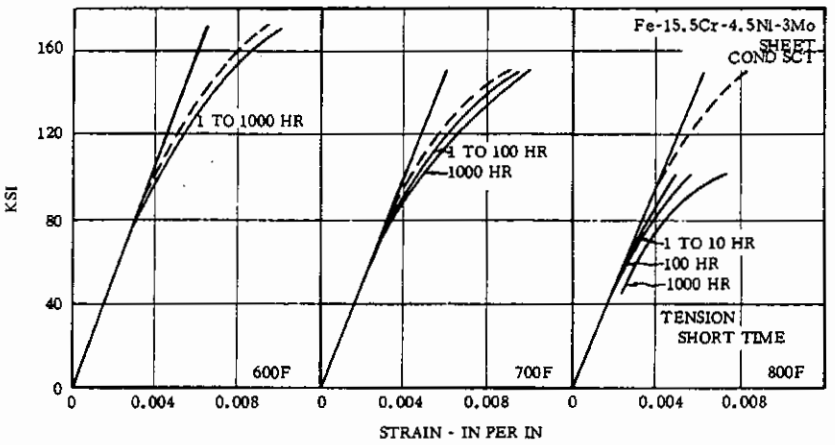


FIG. 3.0434 ISOCHRONOUS STRESS-STRAIN CURVES AT 600 TO 800F FOR SHEET IN CONDITION SCT 850 (16)

Source			A (1)		B (2)			C(3)	
Form			Bar		Bar			Sheet	
Condition			(a) SCT 850		(b) SCT 1000			(c) SCT 850	
	Stress ratio		Stress	Fatigue strength, max, ksi at cycles					
Test temp-F	A	R	Concentration	10^4	10^5	10^6	10^7	10^8
(A) RT		-1	Smooth		116	98	90	
800			K = 1			79	65	57
(B) RT		-1	K = 1		120	106	104	
(C) RT L, T		-1	K = 1		147	136	136	
RT	1	0.6	K = 3.5	91	67	55	55	

TABLE 3.051 FATIGUE PROPERTIES OF BAR AND SHEET IN SCT CONDITIONS

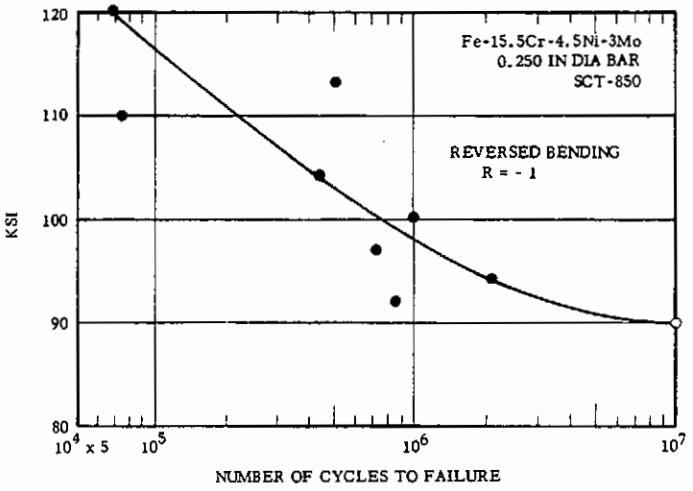


FIG. 3.052 REVERSED BENDING FATIGUE CURVE FOR BAR IN CONDITION SCT-850 (32, p. 45)

Form	0.25 in. Specimens, R = -1	
Condition	SCT 850 F	SCT 1000 F
F_{tu}, ksi	214	164
F_{ty}, ksi	176	156
Fatigue Strength at 10^8 Cycles, ksi	108	97

TABLE 3.053. FATIGUE STRENGTH AT 10^8 CYCLES FOR SCT 850 AND SCT 1000 F CONDITIONS (37)

Fe
15.5 Cr
4.5 Ni
3 Mo

AM-355

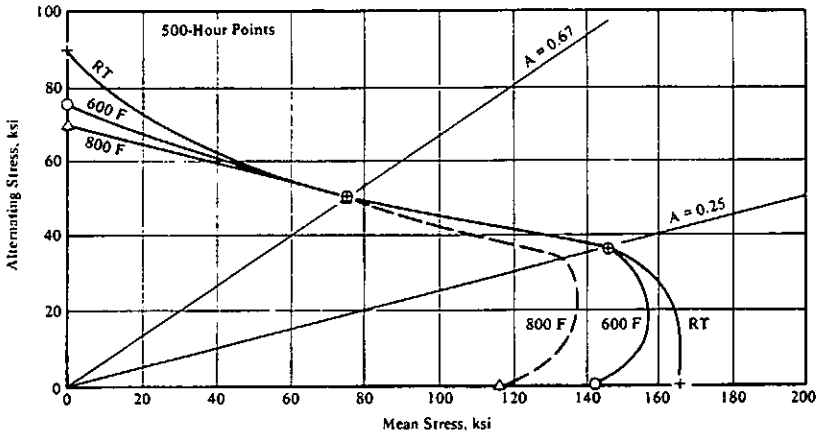


FIG. 3.054 COMBINED STRESS DIAGRAM FOR AM-355 SCT (1000 F) (38)

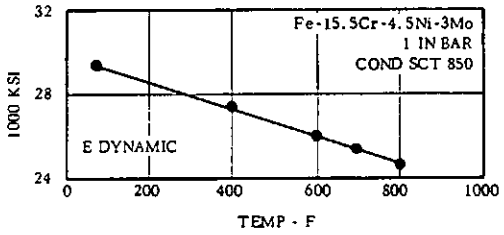


FIG. 3.0621 MODULUS OF ELASTICITY FOR BAR IN CONDITION SCT 850 AT ROOM AND ELEVATED TEMPERATURES (14)

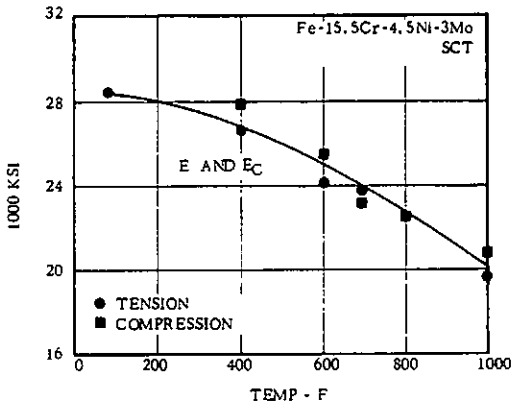


FIG. 3.0622 EFFECT OF TEST TEMPERATURE ON TENSILE AND COMPRESSIVE ELASTIC MODULUS OF ALLOY IN CONDITION SCT (26, p. B-2-4)

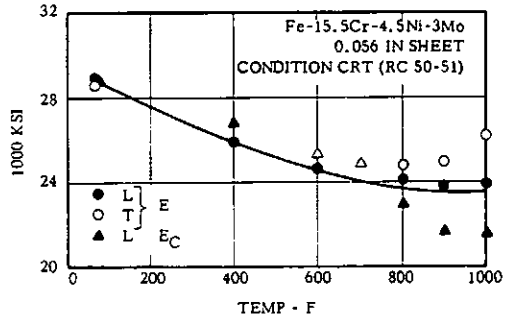


FIG. 3.0623 MODULUS OF ELASTICITY FOR SHEET IN CRT CONDITION AT ROOM AND ELEVATED TEMPERATURES (28)

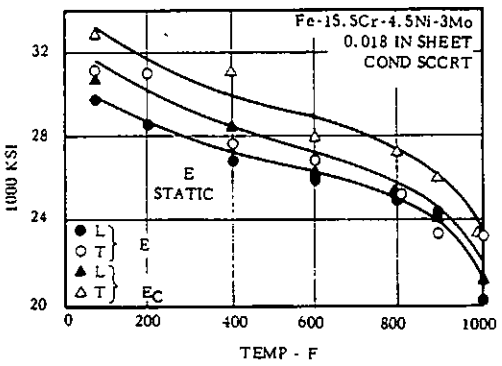


FIG. 3.0624 MODULUS OF ELASTICITY FOR SHEET IN CONDITION SCCRT AT ROOM AND ELEVATED TEMPERATURES (13)

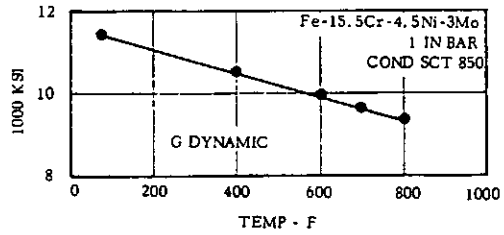


FIG. 3.063 MODULUS OF RIGIDITY FOR BAR IN CONDITION SCT 850 AT ROOM AND ELEVATED TEMPERATURES (14)

Fe
15.5 Cr
4.5 Ni
3 Mo

AM-355

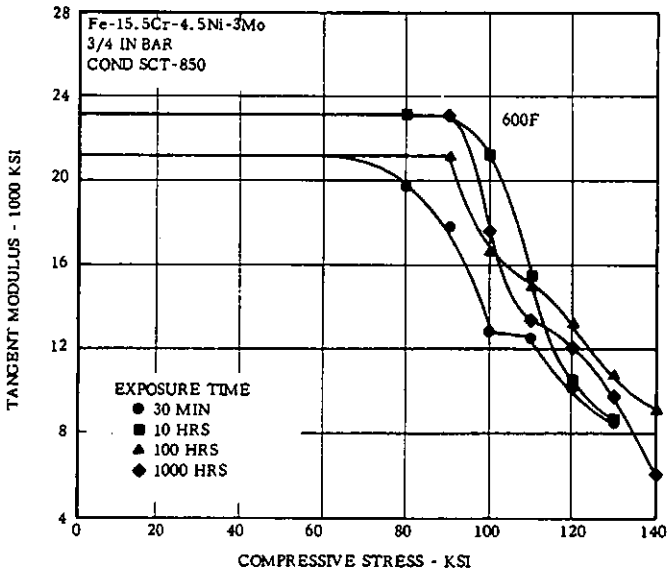


FIG. 3.0641 TANGENT MODULUS IN COMPRESSION AT 600F FOR EXPOSURE TIMES FROM 30 MINUTES TO 1000 HOURS FOR BAR STOCK IN COND SCT-850 (25, p. 138)

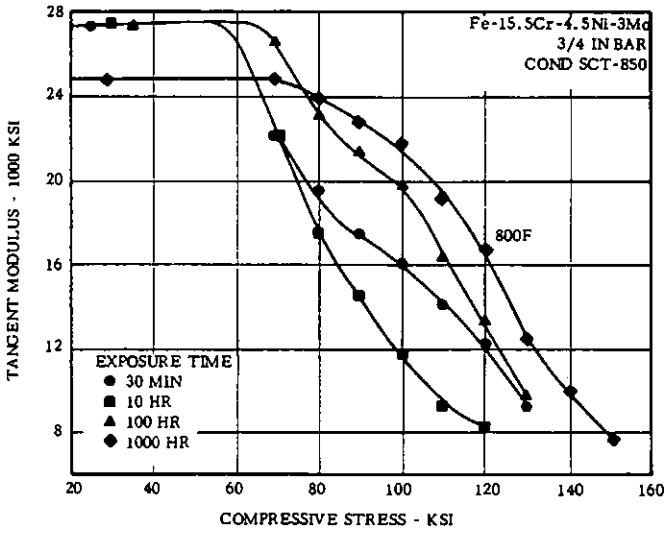


FIG. 3.0642 TANGENT MODULUS IN COMPRESSION AT 800F FOR EXPOSURE TIMES FROM 30 MIN TO 1000 HOURS FOR BAR STOCK IN COND SCT-850 (25, p. 139)

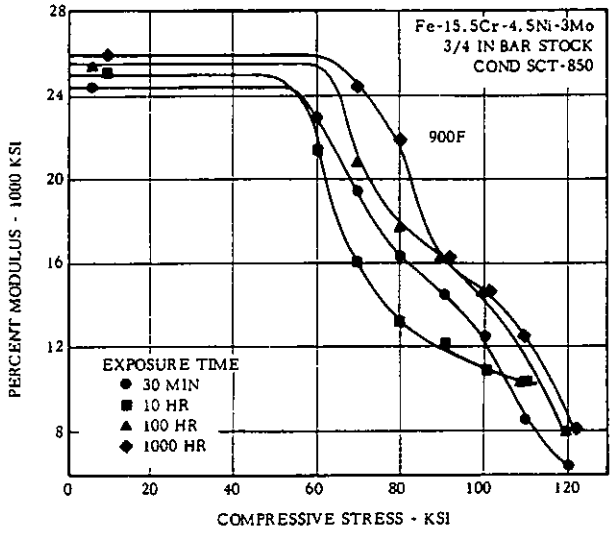


FIG. 3.0643 TANGENT MODULUS IN COMPRESSION AT 900F FOR EXPOSURE TIME FROM 30 MINUTES TO 1000 HOURS FOR BAR STOCK IN COND SCT-850 (25, p. 140)

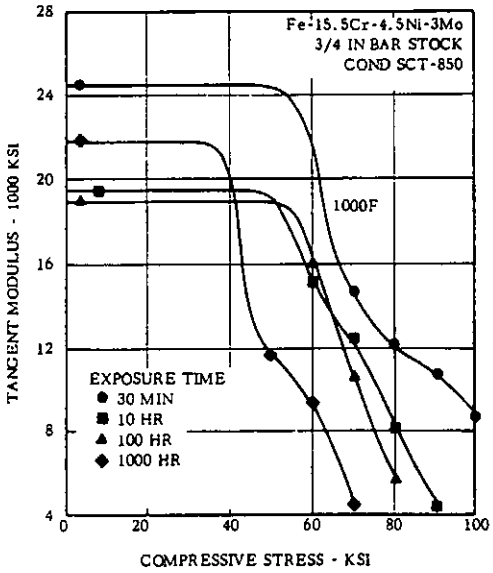


FIG. 3.0644 TANGENT MODULUS IN COMPRESSION AT 1000F FOR EXPOSURE TIMES FROM 30 MINUTES TO 1000 HOURS FOR BAR STOCK IN COND SCT-850 (25, p. 141)

Fe
15.5 Cr
4.5 Ni
3 Mo

AM-355

Welding Process	Heat Treatment[a]	Yield Strength, ksi 0.02% Offset, ksi	Yield Strength, ksi 0.2% Offset, ksi	Ultimate Tensile Strength, ksi	Elong. in 2 in., %	Red. in Area, %	Charpy V-Notch Impact, ft-lb	Hardness Rockwell C	Location of Fracture
Gas Tungsten-Arc Welding AM-355 wire Transversely welded 1/2-inch plate tensiles	1710 F + SCT (850 F)	132	173	205	4	–	–	43	Weld
	1375 F, 3 hr. AC + 1710 F + SCT (850 F)	138	176	208	7	–	–	43	Weld
Gas Metal-Arc Welding AM-355 wire All-weld-metal tensiles	1710 F + SCT (850 F)	137	180	216	6	18	–	45	
AM-355 Covered Electrodes All-weld-metal tensiles	1375 F, 3 hr. AC + 1710 F + SCT (850 F)	121	163	198	12	26	–	44	
	1375 F, 3 hr. AC + 1710 F + SCT (1000 F)	134	159	175	13	30	11	41	
Submerged Arc Welding AM-355 wire Arcosite S-12 flux All-weld-metal tensiles	1375 F, 3 hr. AC + 1710 F + SCT (850 F)	136	170	195	11	24	–	42	
	1375 F, 3 hr. AC + 1710 F + SCT (1000 F)	145	169	187	10	29	8	38	

(a) Post weld heat treatment.

TABLE 4.034. TYPICAL WELDMENT & WELD METAL PROPERTIES FOR VARIOUS WELDING METHODS (39)

Fe
15.5 Cr
4.5 Ni
3 Mo

AM-355

BIBLIOGRAPHY

Mortland, J. E., Evans, R. M., and Monroe, R. E., "Welding and Brazing of Precipitation Hardening Stainless Steels", Battelle Memorial Institute, NASA Special Report, NASW-1948 (April 30, 1970).

Olafson, C. T., Gurklis, J. A., and Boulger, F. W., "Machining and Grinding of Precipitation-Hardenable Stainless Steels", NASA Special Report, NASW-1948 (April 30, 1970).

Drennen, D. C., Hall, A. M., and Wagner, H. J., "Surface Treatments for Precipitation-Hardenable Stainless Steels", NASA Special Report, NASW-1948 (April 30, 1970).

Kura, J. G., Joyce, J. F., and McIntire, H. O., "The Casting and Powder Metallurgy Forming of Precipitation-Hardenable Stainless Steels", NASA Special Report, NASW-1948 (April 30, 1970).

Strohecker, D. E., Gerds, A. F., and Olafson, C. T., "Deformation Processing of Precipitation-Hardenable Stainless Steels", NASA Special Report, NASW-1948 (April 30, 1970).

Marschall, C. W. and Hall, A. M., "Thermal and Mechanical Treatment for Precipitation-Hardening Stainless Steels", NASA Special Report, NASW-1948 (April 30, 1970).

Steigerwald, E. A., "Plane Strain Fracture Toughness of High Strength Materials", Engineering Fracture Mechanics, Vol 1, (1969) p 473-494.

Stanley, J. K., "Stress Corrosion Cracking and Hydrogen Embrittlement of High-Strength Fasteners", Aerospace Corp., SAMSO TR-73-131 (April 1973).

"Liquid Rocket Metal Tanks and Tank Components", NASA Monograph, NASA SP-8088 (May 1974).

Devine, J. and Krause, P. C., "Ultrasonic Cold Forming of Aircraft Sheet Materials", Sonoland Corp., West Chester, Pa., Final Report to Hughes Helicopters (January 1981).

	Fe
15	Cr
7	Ni
	Ti

AM-362

1. GENERAL

This alloy combines the heat treatment advantages and low work hardening characteristics of 18 Ni maraging steels with a corrosion resistance approaching that of the stainless steels. Maximum strength levels available approach 200 Ksi. However the highest strength condition have only limited crack propagation resistance in heavy sections. The strength and toughness are strongly dependent on the titanium content, and welding of heavy sections, requires close attention to both process and wire titanium content. At the present time the highest strength conditions are used primarily in thin sections (e.g.) cold drawn pressure vessels for aircraft application). (24)

1.01 Commercial Designation
AM 362, Almar 362

1.02 Alternate Designation
None

1.03 Specifications
None

1.04 Composition
Table 1.04

TABLE 1.04

Source	(1)	
	Percent	
	Min	Max
Carbon		0.05
Chromium	14.00	15.00
Nickel	6.00	7.00
Manganese	—	0.50
Silcon	—	0.30
Phosphorus	—	0.30
Sulfur	—	0.30
Titanium	0.55	0.90

1.05 Heat Treatment

1.051 General - As in the case of the 18 Ni maraging steels this alloy is annealed (solution treated) and aged. Hardenability is not a function of section size, tensile strength and yield strength increase with annealing temperature, however, high annealing temperatures reduce the toughness. (see Figures 3.0231 and 3.02711). Material annealed at a high temperature will increase its impact strength if reannealed at a lower temperature (see Table 3.0232). Full aging is obtained at 900 F, in about 4 hours and aging times of 2 hours or longer at 1000 F, produce overaged conditions (see Figure 3.0218). Toughness as measured by impact strength and sharp notch strength increase rapidly as overaging progreses. (see Table 3.0212 and Figures 3.0233 and 3.02712). Aging produces only very small dimensional changes, approximately 0.05 percent. (14)

1.052 Anneal - 1500 F, 1 hour AC . Strip is continuously annealed.

1.053 Age - 900 F, to 1150 F, AC depending on strength level (see Figures 3.0215 and 3.0218). For maximum strength age 900 F, three to four hour AC .

1.06 Hardness

1.061 Effect of titanium content on hardness of sheet aged at several temperatures. Figure 1.061.

1.07 Forms and Conditions Available
Sheet, strip, bar, wire, tubing and forging billets.

1.08 Melting and Casting Practice
Electric furnace air melt and consumable electrode vacuum melt.

1.09 Special Considerations
This alloy like the conventional 12 Cr steels is subject to an embrittlement when held for long times at temperatures between 700 and 1000 F, (see Table 3.0234), This is also reflected in low impact strength for tempering temperatures below about 1000F, (see Figure 3.0233). The toughness of the alloy is strongly influenced by the titanium content and decreases with increasing titanium. (see Figure 3.03711).

2. PHYSICAL AND CHEMICAL PROPERTIES

2.01 Thermal Properties

2.011 Melting range.

2.012 Phase changes. (22)
A_1 - 1166F A_3 - 1490F
M_S - 510F M_f - 320F

2.0121 Time-temperature transformation diagrams.

2.013 Thermal conductivity.

2.014 Thermal expansion. Figure 2.014

2.015 Specific heat.

2.016 Thermal diffusivity.

2.02 Physical Properties

2.021 Density. 0.281 lbs per cu in, 7.78 gm per cu cm (16)

2.022 Electrical properties.

2.0221 Resistivity.

2.02211 Resistivity of aged alloy. Table 2.02211.

TABLE 2.02211

Source	(16)			
Alloy	Fe-15 Cr-7Ni-Ti			
Form	Sheet			
Anneal	1500F, 1 hr AC			
Age	None	900F, 4hr	1000F, 3hr	1125F, 2hrs
Electrical Resistivity μ-ohm-in	35.4	30.4	30.2	28.1

2.023 Magnetic properties.

2.0231 Permeability of aged alloy. Table 2.0231

2.024 Emissivity.

2.025 Damping capacity.

2.03 Chemical Properties

2.031 General - On the basis of limited data available thus far, the general corrosion resistance of this alloy is superior to that of Type 410 and in normal atmospheres equal to Type 430. Strip tempered at 900 F, and stressed in the transverse direction to 75% of the yield strengths showed no cracks, rust or pits following 250 days exposure to a 5% salt spray. (22)

TABLE 2.0231

Source	(16)			
Alloy	15Cr-7Ni-Ti			
Form	3/4 in dia Bar			
Anneal	1500F, 1hr AC			
Age	None	900F, 4 hr	1025F, 3 hr	1125F, 2 hr
Max μ (H=25 oersteds)	180	280	298	180
Saturation μ (H=200 oersteds)	67	76	75	62

	Fe
15	Cr
7	Ni
	Ti

AM-362

2.04 Nuclear Properties

3. MECHANICAL PROPERTIES

3.01 Specified Mechanical Properties

3.011 Producers minimum mechanical properties for bar, Table 3.011.

TABLE 3.011

Source	(24)		
Alloy	Fe-15 Cr-7Ni-Ti		
Form	Bar		
Condition	1500F, Anneal AC + Age		
Age	900F, 4hr	1000F, 2hr	1125F, 1hr
F_{tu}-min ksi	180	155	135
F_{ty}-min ksi	175	145	105
e (4D) min Percent	10	12	15
RA min Percent	40	45	50

3.02 Mechanical Properties at Room Temperature

3.021 Typical mechanical properties. Table 3.021.

3.0212 Tensile and impact properties of plate aged at two temperatures. Table 3.0212.

TABLE 3.0212

Source	(4)			
Alloy	Fe-15 Cr-7Ni-Ti			
Form	1/2in Plate (specimen dia=0.375 in) (0.82 Ti)			
Condition	1500F, 1hr AC + 900F, 4hr		1500F, 1hr AC + 1050F, 2hr	
Direction	L	T	L	T
F_{tu}-ksi	188	190	157	157
F_{ty}-ksi	184	184	148	153
e(4D) percent	14	12	18	16
R. A. percent	51	46	65	54
Charpy V ft-lb	6	4	40	23

3.0213 Tensile properties of bar as influenced by specimen location. Table 3.0213.

TABLE 3.0213

Source	(4)			
Alloy	Fe-15 Cr-7Ni-Ti			
Condition	1500F, 1hr AC + 900F, 8hr			As Hot Rolled
Form	2 to 2 3/4 in dia Bar (0.82 Ti)			1 in dia Bar (0.82 Ti)
Location	Mid Radius		Center	
	L	T	T	L
F_{tu}-ksi	184	188	185	135
F_{ty}-ksi	178	180	179	104
e(2in) percent	17	9	10	11.5
R. A. percent	55	28	28	45

3.0214 Effect of annealing temperature on tensile properties of bar, Figure 3.0214.

3.0215 Effect of aging temperature on tensile properties of bar. Figure 3.0215.

3.0216 Effect of cold reduction on tensile properties. Figure 3.0216.

TABLE 3.021

Alloy	Fe-15 Cr-7Ni-Ti									
Source	(3)(4)(6)(7)									
Form (1)	Strip				Plate				Bar (2)	
Condition	1600 F, + 900F, 4 hr		1600 F, + 1000F, 4 hr		1500 F, 1hr AC +900F, 4 hr		1500 F, 1hr AC 1050F, 3 hr		HR	1500 F, 1hr AC
Direction	L	T	L	T	L	T	L	T	L	L
F_{tu}-ksi	200	210	168	175	188	190	157	157	135	125
F_{ty}-ksi	199	208	160	168	184	184	148	153	104	108
e(2in) percent	5	2	9	8						
e(4 D) percent					14	12	18	16	12	16
R. A. percent					51	46	65	54	45	68

(1) All forms from same 0.82 Ti heat

(2) See also Table 3.011

3.0217 Effect of titanium on tensile properties of sheet aged at several temperatures. Figure 3.0216.

3.0218 Effect of aging time and temperature on tensile properties of continuously annealed strip. Figure 3.0217.

3.0219 Effect of aging temperature on tensile properties of continuously annealed strip. Figure 3.0219.

3.02110 Effect of sheet thickness on the tensile properties of annealed and aged alloy. Figure 3.02110.

3.02111 Effect of cold rolling and aging on tensile properties of sheet. Figure 3.02111.

3.02112 Effect of cold drawing on tensile properties of extruded tubing. Figure 3.02112.

3.02113 Effect of annealing and aging on tensile properties of extruded tubing. Table 3.02113.

TABLE 3.02113

Source				
Alloy	Fe-15 Cr-7Ni-Ti			
Form	3.226 OD x 2.500 ID Tubing (0.82 Ti)			
Condition	As Extruded	1500F, 1hr AC	1500F, 1 hr AC 900F, 8hr	1500F, 1 hr AC 1000F, 8 hr
F_{tu}-ksi	130	112	176	150
F_{ty}-ksi	111	98	171	141
e(2in) percent	11	16	16	18

3.022 Compression.
3.0221 Effect of aging on compressive yield strength of bar, Figure 3.0221.

TABLE 3.0221

Source	(4)		
Alloy	Fe-15 Cr-7Ni-Ti		
Form	1 in dia Bar (0.82Ti)		
Condition	Anneal 1500F, 1 hr AC + Age		
Age	900F, 8hr	975F, 4hr	1050F, 2hr
F_{cy}-ksi	187	168	145

3.023 Impact
3.0231 Effect of annealing temperature on impact strength of bar, Figure 3.023.
3.0232 Effect of double annealing on impact strength of aged bar, Table 3.0232.

TABLE 3.0232

Source	(20)			
Alloy	Fe-15 Cr-7 Ni-Ti			
Form	2 1/2 in Bar (0.76 Ti) T			
Condition	1400 F, 1 hr AC +1000 F, 3 hr	1500 F, 1 hr AC + 1000 F, 3 hr	1500 F, 1 hr AC + 1400 F, 1 hr AC + 1000 F, 3 hr	1650 F, 1 hr AC + 1400 F, AC + 1000 F, 3 hr
F_{tu} - ksi	159 (1)	158 (1)	-	154
F_{ty} - ksi	150	152	-	148
e (4 D) percent	-	-	-	11
R. A. percent	-	-	-	50
Charpy V ft - lbs	7	6	10	14

(1) Longitudinal values

3.0233 Effect of aging on impact properties of bar from two heats, Figure 3.0233.
3.0234 Effect of exposure to elevated temperatures on impact strength of bar, Table 3.0234.

TABLE 3.0234

Source	(10)				
Alloy	Fe-15 Cr-7Ni-Ti				
Form	1 in dia Bar (0.76 Ti)				
Condition	1500F, 1 hr AC + 1000F, 3 hr			1500F, 1 hr AC + 1150F, 1 hr	
Exposure	None	700F 1000 hr	800F 1000 hr	None	800F 1000 hr
IE Charpy V ft-lbs	32	5	3	96	11

3.0235 Drop weight (NDT). NDT = 20F for 3/4 hot rolled plate annealed 1500 F, 1 hour AC and aged at 900 F, 8 hour or 1050 F, 2 hour. (4)
3.025 Torsion and shear.
3.0251 Torsion and shear strength of aged bar, Table 3.0251

TABLE 3.0251

Source	(23)	
Alloy	Fe-15 Cr-7Ni-Ti	
Form	1/4 in dia Bar (0.88 Ti)	
Condition	1500F, 1 hr AC + 1000F, 3 hr (F_{tu}=160 ksi, F_{ty} =155 ksi)	
Test Type	Double Shear	Torsion
F_{su}-ksi	104	133

3.026 Bearing.
3.027 Stress concentration.
3.0271 Notch properties.
3.02711 Effect of annealing temperature on notch properties of bar, Figure 3.02711.

Fe
15 Cr
7 Ni
Ti
AM-362

3.02712 Effect of aging temperature on sharp notch strength of strip, Figure 3.02712.
3.02713 Effect of cold reduction on sharp notch strength of cold rolled and aged sheet, Table 3.02713.

TABLE 3.02713

Source	(17)					
Alloy	Fe-15 Cr-7Ni-Ti					
Form	0.130 in Sheet (0.76 Ti)					
Condition	CR + 900F, 72 hr					
CR percent	62		75		90	
Direction	L	T	L	T	L	T
F_{ty}	206	214	212	227	220	242
Notch strength-ksi (2)	225	195	209	174	–	137
Notch strength (1) Ratio	1.09	0.91	0.98	0.77	–	0.57

(1) Ratio of notch strength to yield strength
(2) For specimen see Figure 3.02712

3.0272 Fracture toughness.
3.028 Combined properties.

3.03 Mechanical Properties at Various Temperatures
3.031 Stress strain diagrams.
3.0311 Stress strain curves at room and elevated temperatures for aged bar, Figure 3.0311.
3.0312 Effect of test temperature on tensile properties of aged bar, Figure 3.0312.
3.032 Compression.
3.033 Impact.
3.034 Bending.
3.035 Torsion and shear.
3.036 Bearing.
3.037 Stress concentration.
3.0371 Notch properties.
3.03711 Effect of titanium content on room and low temperature sharp notch properties of sheet, Figure 3.03711.
3.0372 Fracture toughness.
3.038 Combined properties.

	Fe
15	Cr
7	Ni
	Ti

AM-362

3.04 Creep and Creep Rupture Properties

3.05 Fatigue Properties

3.051 Fatigue strength of aged bar, Table 3.051.

TABLE 3.051

Source	(12)						
Alloy	Fe-15 Cr-7Ni-Ti						
Form	1 in. dia. bar stock (1) (F_{tu} = 163 ksi)						
Condition	1500F, 1 hr AC + 1000F, 3 hr						
Method	Stress Ratio		Stress Concentration	Fatigue Strength-ksi at cycles			
	A	R		10^5	10^6	10^7	10^8
Rotating Beam	00	-1	Smooth K_t = 1	135	114	100	95

(1) Results from 0.69 and 0.85 Ti heats are essentially identical

3.06 Elastic Properties

3.061 Poisson's ratio.

3.062 Modulus of elasticity. 28,500 to 30,500 ksi.

3.063 Modulus of rigidity. 12,200 ksi.

4. FABRICATION

4.01 Formability

4.011 General - Readily hot and cold worked by practices and equipment normally used for processing austenitic stainless steels. Because of an extremely low work hardening rate (see Figure 3.0216) this alloy has excellent cold workability. In this respect it is superior to the austenitic steels and the quenched and tempered steels in all cold forming operations with the exception of stretch forming which is not possible because of the alloy's low uniform elongation. (24)

4.012 Hot working. Initial forging and hot rolling temperatures between 2000 F and 2200 F. At these temperatures hot workability is similar to Type 304. Finishing temperatures can be as low as 1400 to 1500F. (22)

4.0121 Effect of forge upset temperature on tensile properties, Figure 4.0121.

4.0122 Effect of forge upset temperature on impact strength, Figure 4.0122.

4.02 Machining and Grinding

4.021 General-Machinability in hardened condition is good. In general, at speeds and feeds approximating those for Type 410, tool life is increased (22)

4.03 Welding

4.031 General - Welding can be accomplished by processes used for austenitic stainless steels. Precautions similar to those for the maraging steels should be observed. The TIG process is preferred for maximum weld toughness.

4.0311 Thin sections - Experience is available for thicknesses between 0.020 and 0.060 inch. Filler wire if required can have parent metal composition. When the weld metal and parent metal titanium contents are approximately equal, aging after welding will produce comparable smooth and sharp notch tensile strengths in the parent metal and in the weld joint. (compare Table 4.032 with Figure 3.02717 and 3.02712).

4.0312 Heavy sections - Problems here are similar to those encountered in welding the 18 Ni maraging steels. In order to minimize segregations in the weld deposit and consequent loss in toughness the titanium content of the weld wire should be reduced as low as is consistant with obtaining the required weld joint strength. (see Table 4.033) A weld wire with 0.42% Ti is recommended for MIG and TIG welding of plate (see Table 4.033). (15)(22)(24)

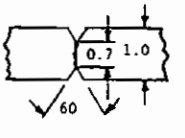
4.032 Smooth and sharp notch tensile strength characteristics of TIG welded strip given several postweld treatments, Table 4.032.

TABLE 4.032

Source	(13)							
Alloy	Fe-15 Cr-7Ni-Ti							
Condition	Annealed Strip + TIG Weld (no filler)							
Post Weld Treatment	900 F, 8 hr		1000 F, 3 hr		1500 F, 1 hr AC + 900 F, 8 hr		1500 F, 1 hr AC + 1000 F, 3 hr	
Thickness	A (1)	B	A	B	A	B	A	B
F_{tu} -ksi	193	238	172	200	189	224	161	192
F_{ty} -ksi	192	237	171	192	188	222	159	184
e (2 in) percent	2.5	1	4.5	5.0	8	1.5	5.5	4.5
Notch strength ratio (2)	0.81		1.07		0.97	0.72	1.06	0.90

(1) A - 0.031 in strip (0.70 Ti) B - 0.060 in strip. (0.99 Ti)

(2) Edge notch specimen, notch radius < 0.001 in



Notch at weld center

4.033 Effect of titanium content on tensile and impact strength of MIG welded plate, Table 4.033.

TABLE 4.033

Source	(15)											
Alloy	Fe- 15 Cr- 7 Ni-Ti											
Form	1/2 in Plate (0.85 Ti)(F_{tu} =202 ksi, F_{ty} =196ksi MIG welded											
Post Weld Treatment	As welded			Age 900 F, -8 hr			1500 F, 1 hr AC +900F, 8hr			1500 F, 1 hr AC +1000F, 8hr		
Weld Deposit Ti content %	.43	.52	.73	.43	.52	.73	.43	.52	.73	.43	.52	.73
F_{tu} - ksi (2)	126	128	126	154	169	169	–	–	168	–	–	148
F_{ty} - ksi	115	111	116	150	161	166	–	–	164	–	–	142
Impact (1) Charpy Vft-lb	34	54	60	32	8	4	51	22	4	45	28	13

(1) Notch at weld center, in weld direction and perpendicular to plate surface

(2) Smooth specimens transverse to weld

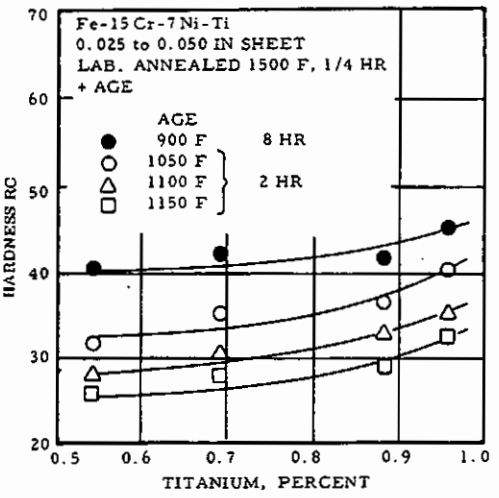


FIG. 1.061 EFFECT OF TITANIUM CONTENT ON HARDNESS OF SHEET AGED AT SEVERAL TEMPERATURES (2)

Fe
15 Cr
7 Ni
Ti

AM-362

TABLE 4.034

Source	(15)			
Alloy	Fe-15 Cr-7 Ni-Ti			
Form	1/2 in Plate (0.42 Ti)			
Condition	TIG Welded (AM 362 wire 0.40 Ti)			
Specimen Location	All Weld Metal		Transverse to Weld	
Post Weld Treatment	As Welded	900 F, 8 hr	As Welded	900 F, 8 hr
F_{tu} - ksi	122	134	113	136
F_{ty} - ksi	102	132	102	128
e (4 D) percent	18	18	15	15
R.A. percent	67	56	66	69

4.034 Tensile properties of TIG welded plate, Table 4.034

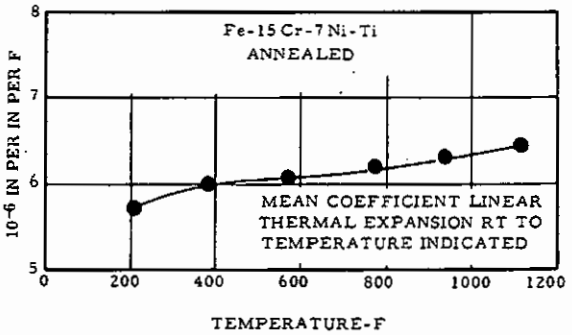


FIG. 2.014 COEFFICIENT OF EXPANSION (4)

	Fe
15	Cr
7	Ni
	Ti

AM-362

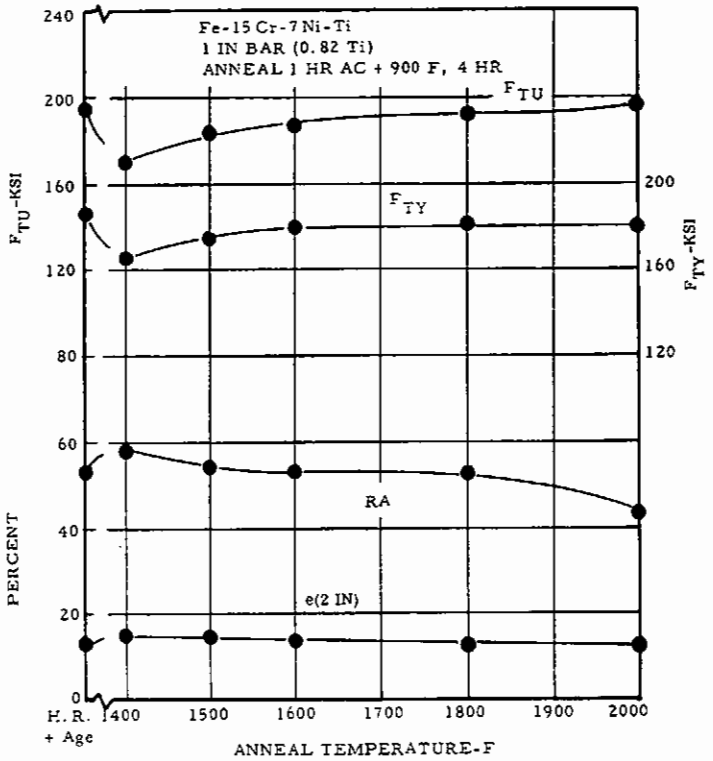


FIG. 3.0214 EFFECT OF ANNEALING TEMPERATURE ON TENSILE PROPERTIES OF BAR

(4)

	Fe
15	Cr
7	Ni
	Ti

AM-362

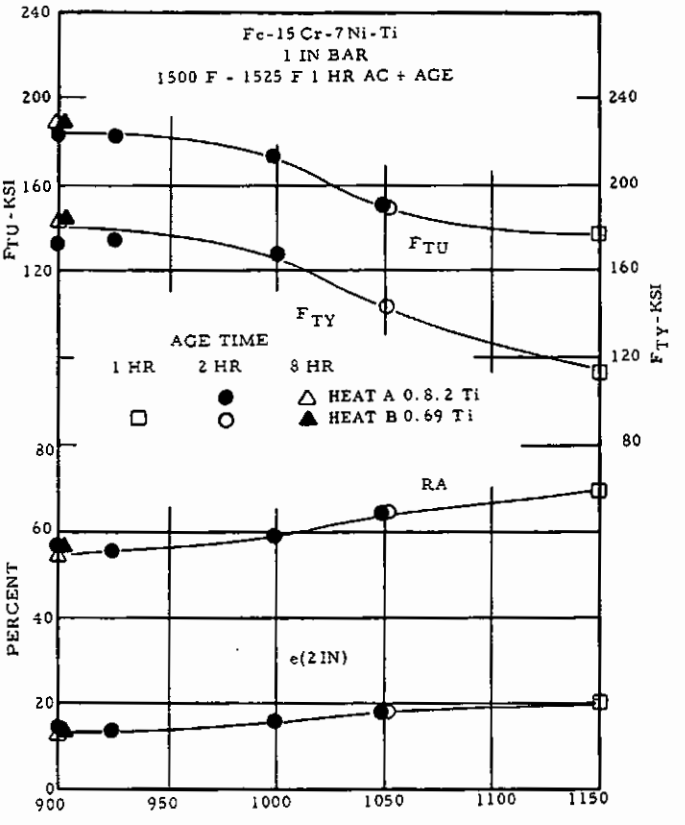


FIG. 3.0215 EFFECT OF AGING TEMPERATURE ON TENSILE PROPERTIES OF BAR

(3)(4)

	Fe
15	Cr
7	Ni
	Ti

AM-362

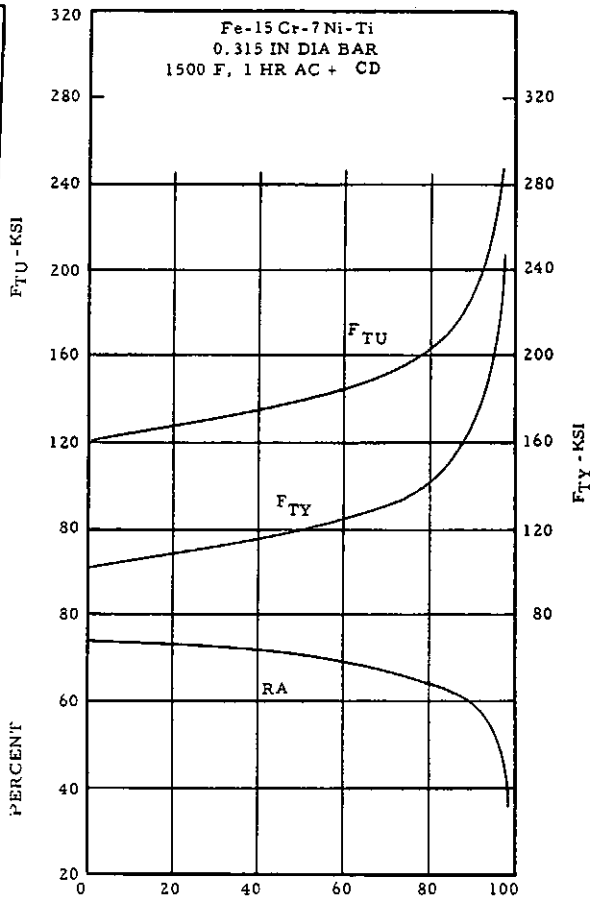


FIG. 3.0216 EFFECT OF COLD REDUCTION ON TENSILE PROPERTIES

(21)

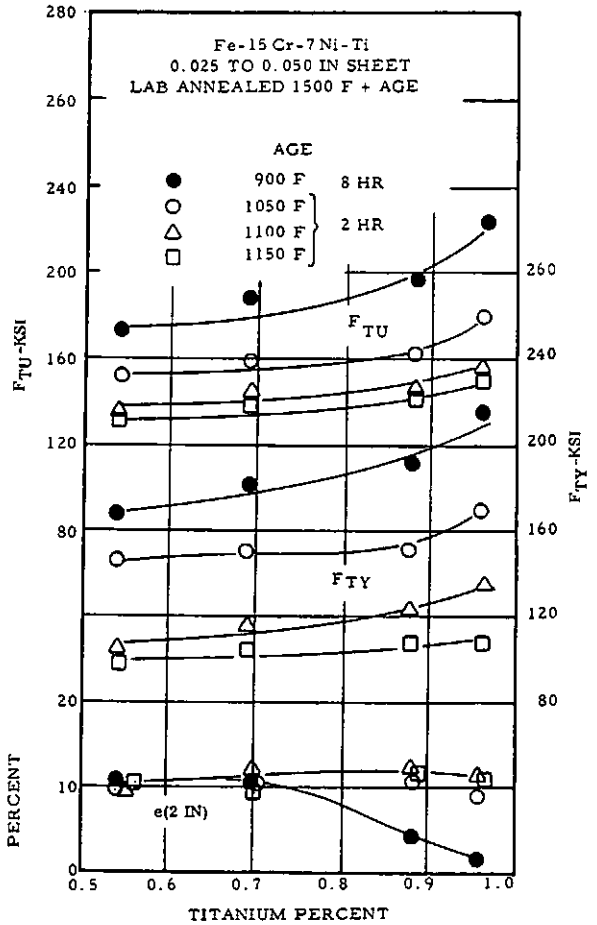


FIG. 3.0217 EFFECT OF TITANIUM ON TENSILE PROPERTIES OF SHEET AGED AT SEVERAL TEMPERATURES

(2)

	Fe
15	Cr
7	Ni
	Ti

AM-362

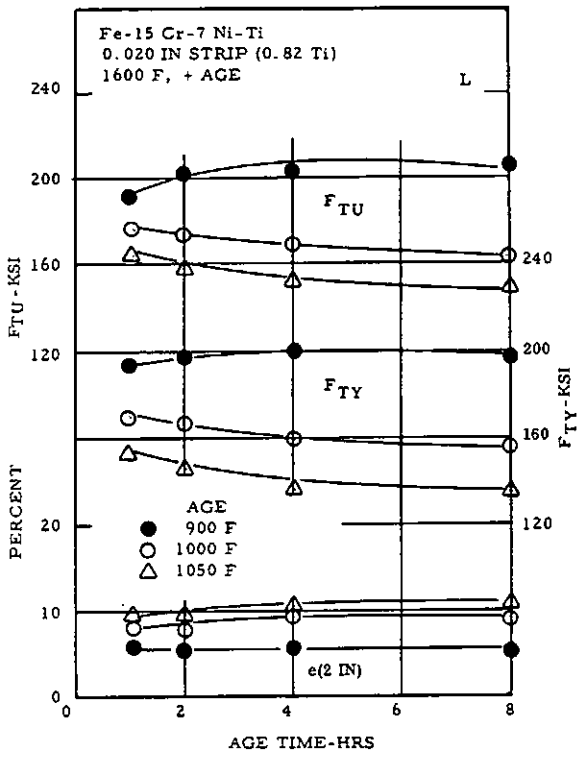


FIG. 3.0218 EFFECT OF AGING TIME AND TEMPERATURE ON TENSILE PROPERTIES OF CONTINUOUS ANNEALED STRIP

(6)

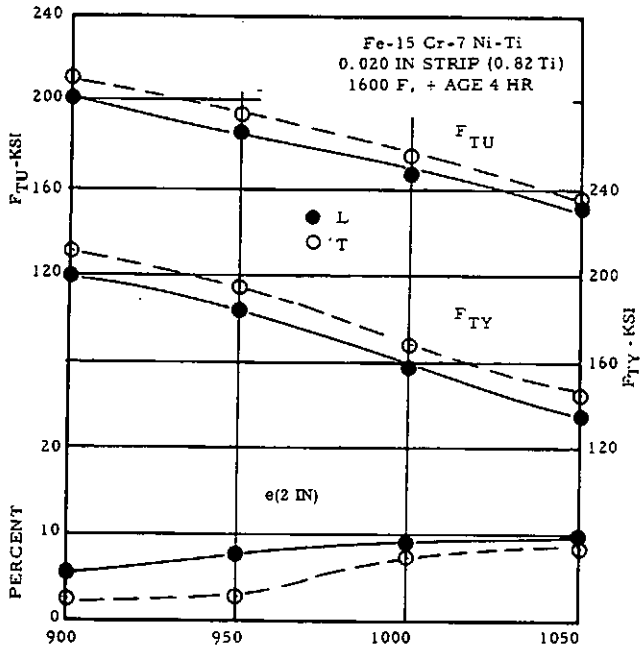


FIG. 3.0219 EFFECT OF AGING TEMPERATURE ON TENSILE PROPERTIES OF CONTINUOUS ANNEALED STRIP

(6)

	Fe
15	Cr
7	Ni
	Ti

AM-362

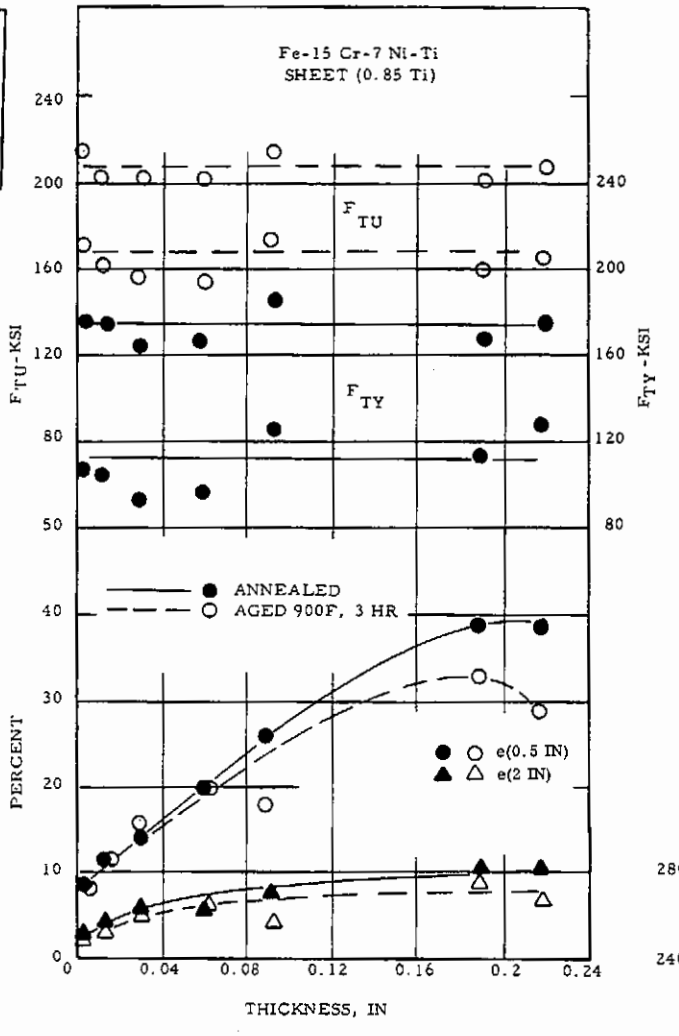


FIG. 3.02110 EFFECT OF SHEET THICKNESS ON THE TENSILE PROPERTIES OF ANNEALED & AGED ALLOY (8)

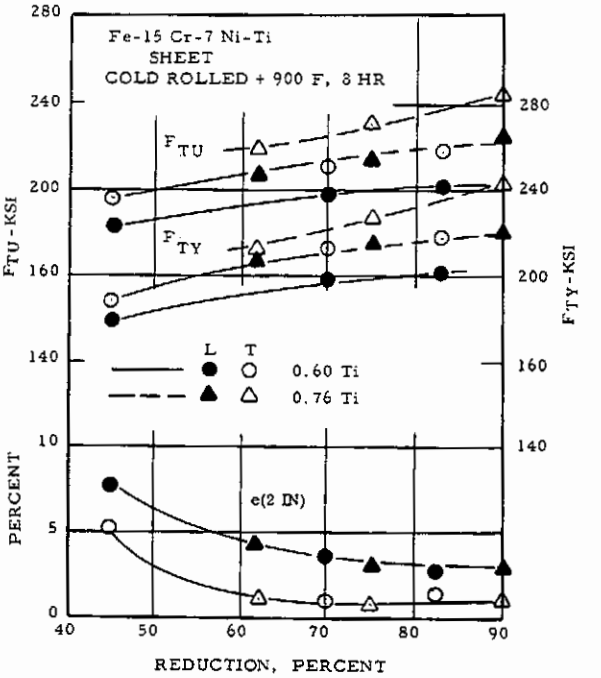


FIG. 3.02111 EFFECT OF COLD ROLLING AND AGING ON TENSILE PROPERTIES OF SHEET

(9) (17)

	Fe
15	Cr
7	Ni
	Ti

AM-362

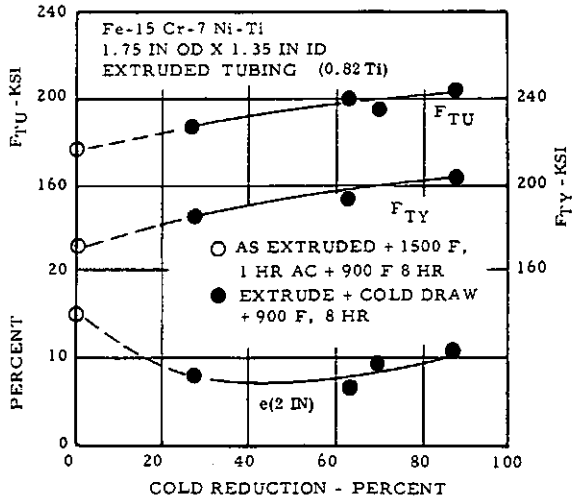


FIG. 3.02112 EFFECT OF COLD DRAWING ON TENSILE PROPERTIES OF EXTRUDED TUBING
(4)

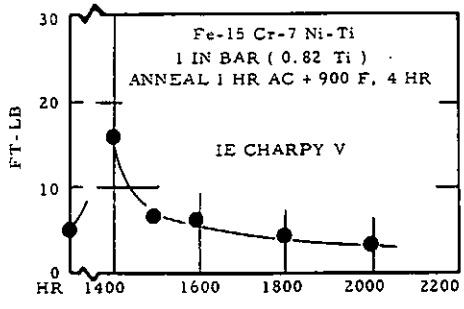


FIG. 3.0231 EFFECT OF ANNEALING TEMPERATURE ON IMPACT STRENGTH OF BAR
(4)

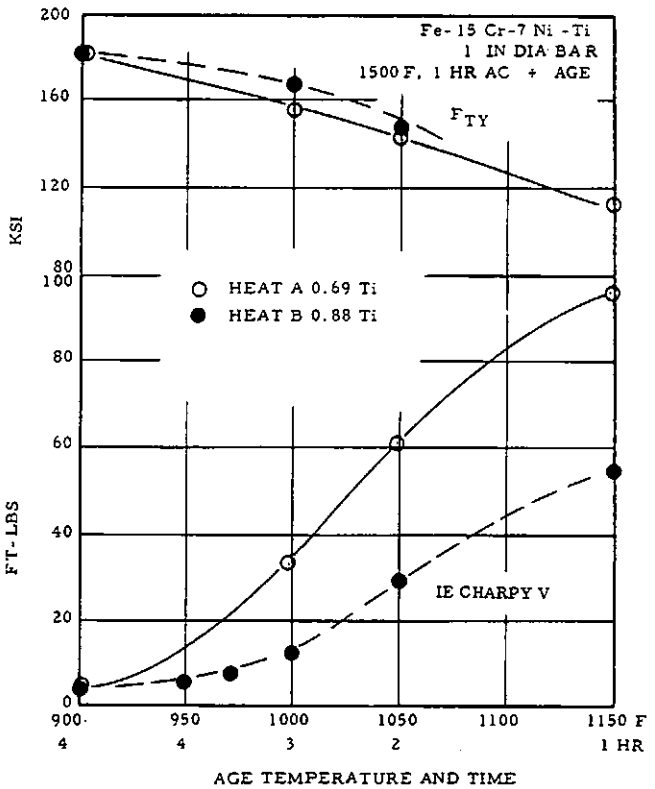


FIG. 3.0233 EFFECT OF AGING ON IMPACT PROPERTIES OF BAR FROM TWO HEATS
(5) (7)

	Fe
15	Cr
7	Ni
	Ti

AM-362

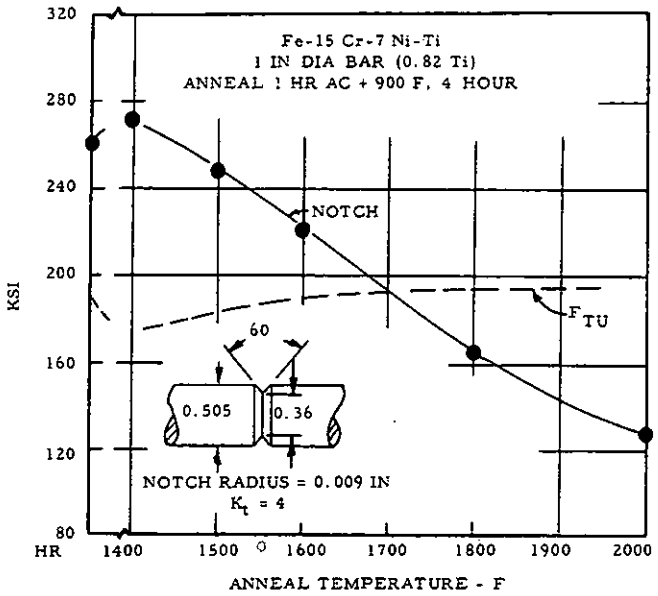


FIG. 3.02711 EFFECT OF ANNEALING TEMPERATURE ON NOTCH TENSILE PROPERTIES OF BAR
(4)

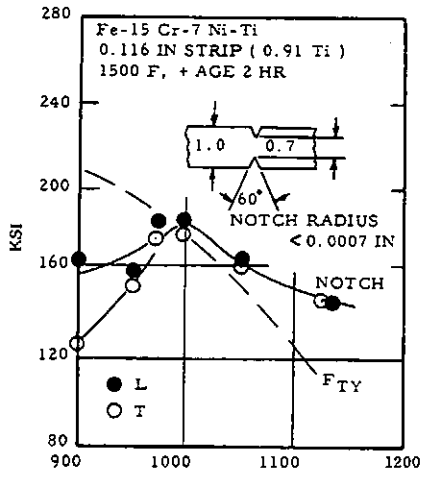


FIG. 3.02712 EFFECT OF AGING TEMPERATURE ON SHARP NOTCH STRENGTH OF STRIP
(18)

	Fe
15	Cr
7	Ni
	Ti

AM-362

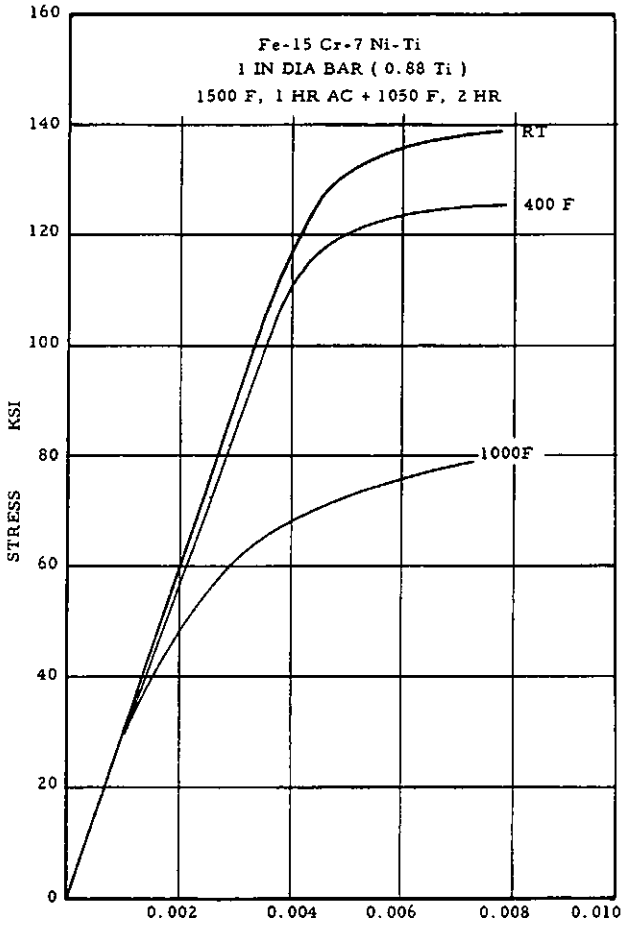


FIG. 3.0311 STRESS STRAIN CURVES AT ROOM AND ELEVATED TEMPERATURES FOR AGED BAR (11)

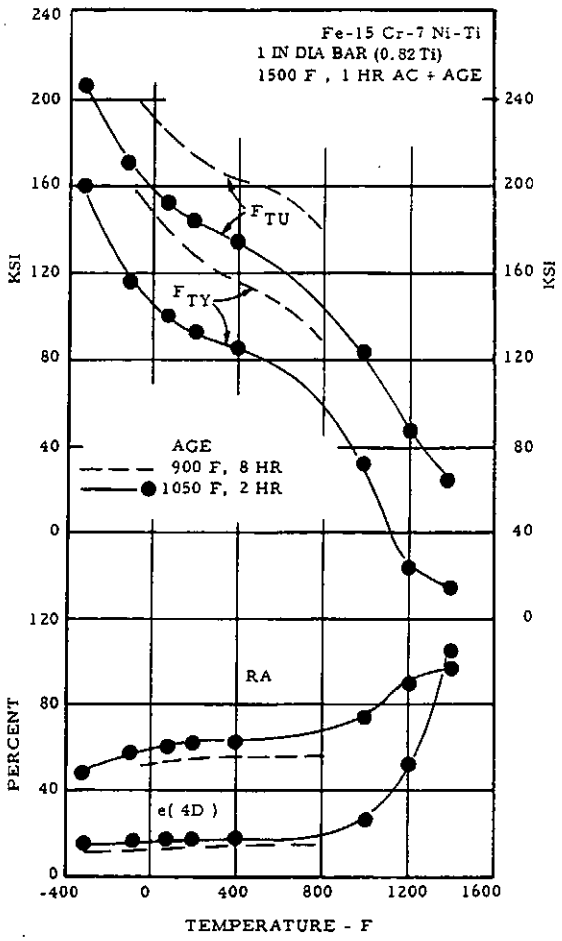


FIG. 3.0312 EFFECT OF TEST TEMPERATURE ON TENSILE PROPERTIES OF AGED BAR (4) (11)

	Fe
15	Cr
7	Ni
	Ti

AM-362

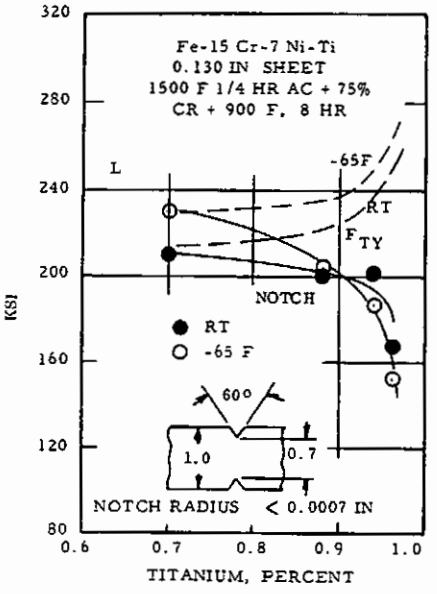


FIG. 3.03711 EFFECT OF TITANIUM CONTENT ON ROOM AND LOW TEMPERATURE SHARP NOTCH PROPERTIES OF SHEET

(19)

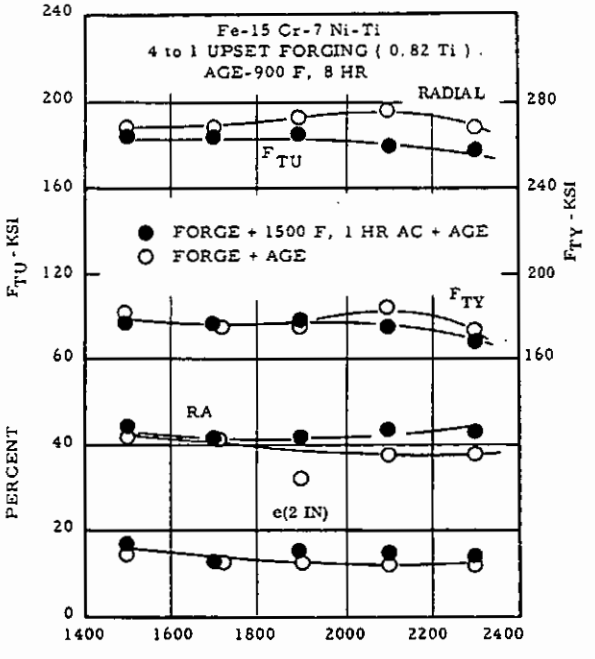


FIG. 4.0121 EFFECT OF FORGE UPSET TEMPERATURE ON TENSILE PROPERTIES

(4)

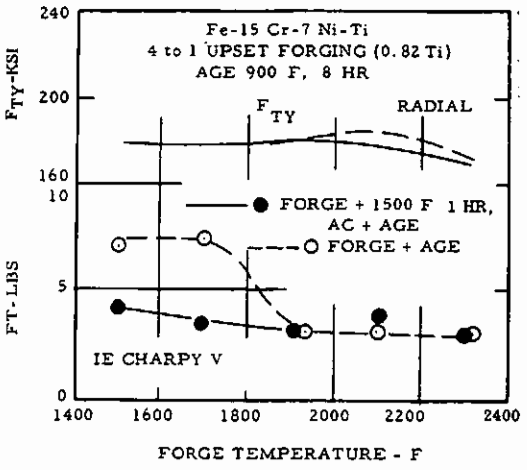


FIG. 4.0122 EFFECT OF FORGE UPSET TEMPERATURE ON IMPACT STRENGTH
(4)

	Fe
15	Cr
7	Ni
	Ti

AM-362

REFERENCES

1. Military Specification (Proposed) for Steel Bar, Hollow Bar, Wire and Forgings, Corrosion and Heat Resistant, Allegheny-Ludlum, Jan. 4, 1967.
2. Allegheny-Ludlum Steel Co. Research Data Center Sheet - 234-41565-362, "Effect of Aging Treatments on Tensile Properties of Almar 362 Sheet and Strip", April 1965.
3. Ibid: Data Sheet 205-12464-362, "Effect of Aging Temperature on Properties of AM 362 Bar", Dec 1964.
4. Ibid: Data Sheet 197-11763-362, "Properties of AM 362 Maraging Stainless Steel", November 1963.
5. Ibid: Data Sheet 209-3964-362, "Effect of Aging Temperature on Properties of AM 362 Bar", Mar 64.
6. Ibid: Data Sheet 201-12263-362, "Properties of AM 362 Strip", December 1963.
7. Ibid: Data Sheet 251-61466-362, "Impact Properties of Almar 362 Bar", June 1966.
8. Ibid: Data Sheet 258-1967-362, "Effect of Gage Length on Elongation of Almar 362", Jan 1967.
9. Ibid: Data Sheet 226-92564-362. "Tensile Properties of Cold Rolled and Aged AM 362 Sheet", Sept 1964.
10. Ibid: Data Sheet 211-41064-362, "Effect of Long Time Exposure at Elevated Temperature on Impact Properties of AM 362, April 1964.
11. Ibid: Data Sheet 197-11763-362, "Properties of AM 362 Maraging Stainless Steel", Nov. 1963.
12. Ibid: Data Sheet 239-11165-362, "Fatigue Strength of Almar 362, November 1965.
13. Ibid: Data Sheet 238-8565-362, "Properties of Almar Welded Strip", August 1965.
14. Ibid: Data Sheet 219-72164-362, "Dimensional Change of AM 362 Resulting from Aging", July 1964
15. J. E. Mosser, "Welding Almar 362", Allegheny Ludlum Steel Co., Research Center Memo 1967.
16. Allegheny-Ludlum Steel Co., Research Center Data Sheet 252-62066-362, "Magnetic Properties of Almar 362", June 1966.
17. Ibid: Data Sheet 221-83164-362, "Cold Rolled and Aged Tensile Properties of Am 362", August 1964
18. Ibid: Data Sheet 260-42667-362, "Comparative Properties, Almar 362 and AISI 4130", April 1967.
19. Ibid: Data Sheet 221-83164-362, "Cold Rolled and Aged Tensile Properties of AM 362", August 1964.
20. Ibid: Data Sheet 222-9464-362, "Annealing Treatments for AM 362 Bar", September 1964.
21. Allegheny-Ludlum Steel Co., "Technical Notes on Almar 362 Maraging Stainless Steel".
22. Technical Horizons, "Almar 362 a Maraging Stainless Steel", Allegheny-Ludlum Steel Co., Pittsburgh, Pa., 1966
23. Allegheny-Ludlum Steel Co., Research Center Data Sheet, 256-81966-362, "Shear Strength of Almar 362, August 1966.
24. A. J. Spitzner and R. H. Kaltenhauser, "Stainless Maraging Steel for Welded Pressure Vessels", To be published - Welding Journal 1967

Fe
0.04 C
11.5 Cr
4 Ni
0.3 Ti

AM-363

1. GENERAL

AM-363 is a recently developed low cost, medium strength stainless steel alloy for structural applications. Its strength levels can be compared to low alloy structural steels and 1/4 to 1/2 hard Type 201 Stainless Steel. Its corrosion resistance in the atmosphere can be compared to Type 430 Stainless Steel. This alloy is an outgrowth of an attempt to produce a maraging stainless steel. At best it may be considered a lean maraging steel. The alloy, when aged at 900 to 950F for 2 to 8 hours, will not increase in tensile strength and will increase in yield strength only slightly. This suggests that the alloy be considered as a low alloy structural steel rather than as a maraging steel. The alloy is obtainable as sheet or strip with a guaranteed yield strength of 100 ksi and a tensile strength of 120 ksi. It can be formed and joined by welding. At room temperature, the alloy's structure consists of low carbon martensite. At the annealing temperature, the structure is austenitic, (1)(2)(3)(4).

1.01 Commercial Designation
AM-363

1.02 Alternate Designations

1.03 Specifications

1.04 Composition
Table 1.04.

TABLE 1.04

Source	(5)	
	Percent	
	Min	Max
Carbon	-	0.05
Chromium	11.00	12.00
Manganese	-	0.30
Nickel	4.00	5.00
Silicon	-	0.15
Titanium	0.30	0.60
Iron	Balance	

1.05 Heat Treatment

1.051 All necessary heat treating is done in the mill. For a majority of applications subsequent heat treating is not required, (1)(2).

1.052 Solution temperature. 1600F, (1).

1.053 Annealing temperature range. 1500 to 1700F, (1).

1.054 Age at 900 to 950F for 2 to 8 hours. Aging will not increase the tensile strength but will increase the yield strength slightly to its maximum value, (2).

1.06 Hardness

1.061 At room temperature and at -50F the hardness is 26 RC.

1.07 Forms and Conditions Available

1.071 Available as sheet or strip heat treated at the mill.

1.08 Melting and Casting Practice

1.09 Special Considerations

2. PHYSICAL AND CHEMICAL PROPERTIES

2.01 Thermal Properties

2.011 Melting range. 2550 to 2650F.

2.012 Phase changes. A_3 - 1375F, A_1 - 1250F, M_s - 770F, M_f - 500F,

2.0121 Time-temperature transformation diagrams

2.013 Thermal conductivity

2.014 Thermal expansion Fig. 2.014.

2.015 Specific heat

2.016 Thermal diffusivity

2.02 Other Physical Properties

2.021 Density. 0.281 lb per cu in; 7.77 gr per cu cm, (1).

2.022 Electrical properties

2.023 Magnetic properties. The alloy is ferromagnetic, (1)

2.024 Emissivity

2.025 Damping capacity

2.026 Crystal structure:
Face centered cubic, at annealing temperature,
Body centered cubic, at room temperature, (1)

2.03 Chemical Properties

2.031 The resistance of this alloy to atmospheric corrosion is excellent. The alloy does not develop a visible oxide film or stain in the atmosphere, (1).

2.032 Exposure time for rusting to develop in the 5% neutral salt spray test for the alloy is from 72 to 100 hours, (1).

2.033 The effect of various chemical environments on the oxidizing activity of the alloy, Table 2.033.

TABLE 2.033

Source	(1)		
Alloy	Fe(0.04C)-11.5Cr-4Ni-0.3Ti		
Test medium	Boiling solution		
	25% Nitric acid	20% Phosphoric acid	60% Acetic acid
Time	5-48 hr	24 hr	24 hr
Penetration, in per Month	0.0125	0.0009	0.034

2.034 Alloy exhibits good resistance to stress corrosion cracking. Tests on two heats stressed almost to Fty showed complete resistance to stress corrosion cracking after 155 days exposure to 5% neutral salt spray, (1).

2.04 Nuclear Properties

3. MECHANICAL PROPERTIES

3.01 Specified Mechanical Properties

3.02 Mechanical Properties at Room Temperature

3.021 Tension

3.0211 Stress-strain diagrams

3.02111 Stress-strain curve at room temperature for strip, Fig. 3.02111.

3.0212 Room temperature tensile properties of sheet in various conditions, Table 3.0212.

TABLE 3.0212

Source	(5)				(1)	
Alloy	Fe(0.04C)-11.5Cr-4Ni-0.3Ti					
Form	Sheet					
Condition	As HR	Ann 1600F	Ann + age 1050F, 5Min	Ann + age 900F, 8 hr	Mill ann L	Mill ann T
F_{tu}, -ksi	138	124	123	124	123	125
F_{ty}, -ksi	131	105	117	118	106.5	112
e(2 in)-percent	11.0	8.0	11.0	11.5	12.5	11.5

3.022 Compression

3.0221 Stress-strain diagrams

3.0222 F_{cy} at room temperature, transverse direction, 122 ksi, (2).

3.023 Impact

3.024 Bending

3.025 Torsion and shear

3.026 Bearing

3.027 Stress concentration

3.0271 Notch properties

3.0272 Fracture toughness

3.028 Combined properties

3.03 Mechanical Properties at Various Temperatures

3.031 Tension

3.0311 Stress-strain diagrams

3.0312 Effect of test temperatures on tensile properties of sheet, Fig. 3.0312.

3.032 Compression

3.0321 Stress-strain diagrams

Fe
0.04 C
11.5 Cr
4 Ni
0.3 Ti

AM-363

3.033 Impact

3.0331 Effect of test temperature on impact energy of bar, Fig. 3.0331.

3.034 Bending

3.035 Torsion and shear

3.036 Bearing

3.037 Stress concentration

3.0371 Notch properties

3.03711 Effect of test temperature on notch strength of strip, Fig. 3.03711.

3.0372 Fracture toughness

3.038 Combined properties

3.04 Creep and Creep Rupture Properties

3.05 Fatigue Properties

3.051 S-N curves for smooth and notched specimens in tension, Fig. 3.051.

3.06 Elastic Properties

3.061 Poisson's ratio
Longitudinal 0.320,
Transverse 0.330, (1).

3.062 Modulus of elasticity
Longitudinal 27.9×10^3 ksi,
Transverse 27.5×10^3 ksi, (1).

3.063 Modulus of rigidity
Longitudinal 10.6×10^3 ksi,
Transverse 10.3×10^3 ksi, (1).

4. FABRICATION

4.01 Formability

4.011 Can be formed by all conventional methods. The alloy has very good deep drawing characteristics but is only limited in stretching operations, (3).

4.012 The alloy can be bent in the transverse direction 135° around a pin whose radius is 1.0 to 1.5 times the thickness of the sheet, (1).

4.02 Machining and Grinding

4.021 Alloy was tested with 1/4 inch M-1 drill using Gulf cutting oil 43A with a constant feed of 0.005 in per revolution giving a tool speed for constant wear of 135 sfpm, (1).

4.03 Welding

4.031 The alloy has been successfully butt-welded by the automatic gas tungsten-arc process to itself and to austenitic and ferritic stainless steels without the use of filler material, (1). Preparation for welding, welding parameters and welding performance are similar to the austenitic stainless steels, (2). Welded tensile tests indicate that both the welded and welded plus aged strength compare favorably with the unwelded aged material, (2).

4.032 Manual gas tungsten-arc welding with 0.035 inch diameter AM-363 welding wire produced a 1/2 inch butt-weld which compared in tensile properties to the mill-aged unwelded material, (2).

4.033 The alloy has excellent electrical resistance spot welding characteristics similar to austenitic stainless steel. Approximately the same welding conditions as used for austenitic stainless steels will produce tension-shear tests results greater than the required minimum values, (1).

4.04 Heat Treatment

4.05 Surface Treatment

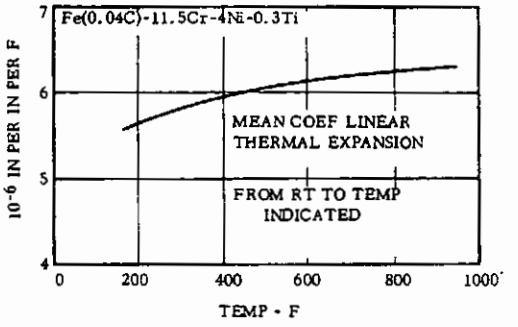


FIG. 2.014 THERMAL EXPANSION (5)

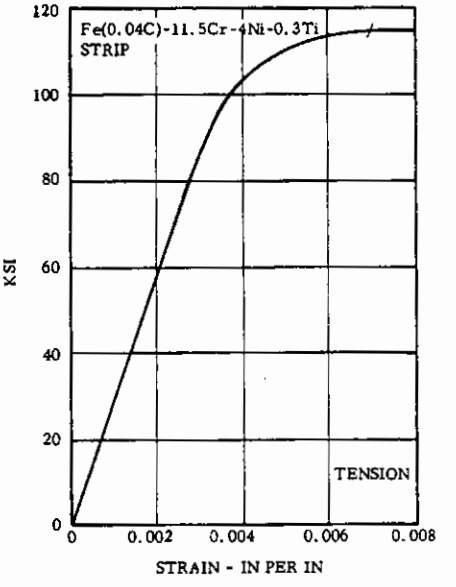


FIG. 3.02111 STRESS-STRAIN CURVE AT ROOM TEMPERATURE FOR STRIP (2)

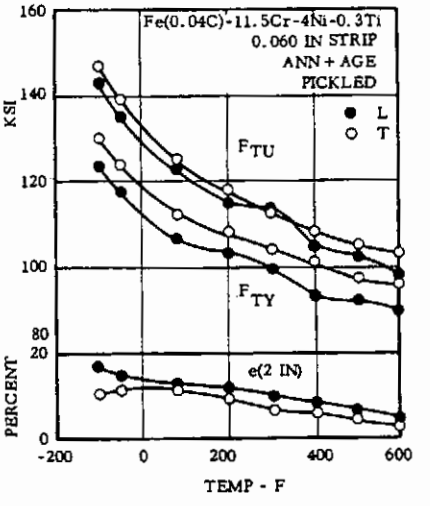


FIG. 3.0312 EFFECT OF TEST TEMPERATURE ON TENSILE PROPERTIES OF SHEET (1)

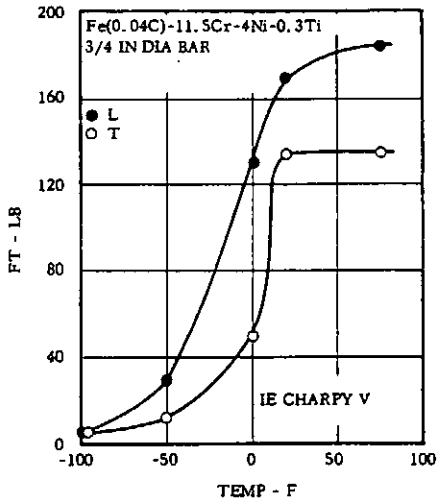
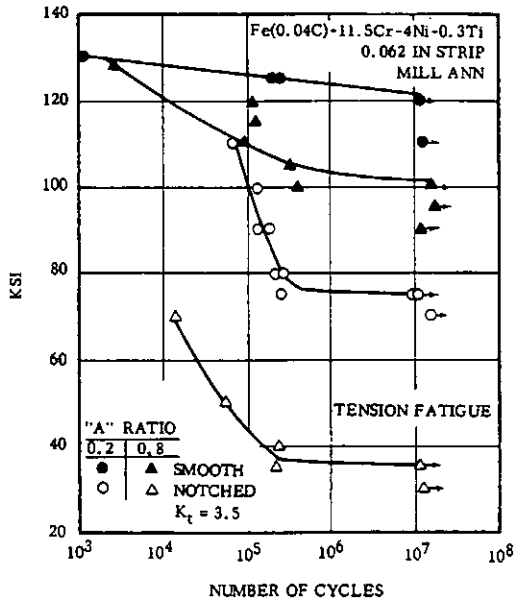


FIG. 3.0331 EFFECT OF TEST TEMPERATURE ON IMPACT ENERGY OF BAR (1)



Fe
0.04 C
11.5 Cr
4 Ni
0.3 Ti

AM-363

FIG. 3.051 S-N CURVES FOR SMOOTH AND NOTCHED SPECIMENS IN TENSION (4)

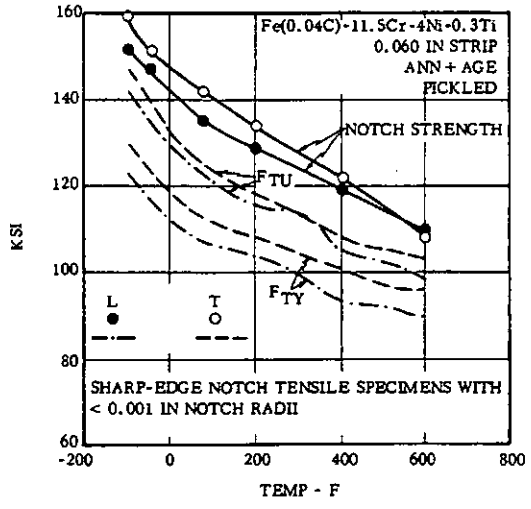


FIG. 3.03711 EFFECT OF TEST TEMPERATURE ON NOTCH STRENGTH OF STRIP (1)

REFERENCES

1 "AM-363 a Mar-Aging Stainless Steel", Preliminary Data, Allegheny Ludlum Steel Corp.

2 "AM-363 Strip for Structural Applications", Preliminary Data Sheet, Allegheny Ludlum Steel Corp. (Feb. 11, 1963)

3 "Low Alloy-Stainless Steels for Structural Applications", Allegheny Ludlum Steel Corp.

4 "Personal Communication", R. L. Cook, Allegheny Ludlum Steel Corp. with Syracuse University, (Jan. 19, 1965)

5 Roberts, D. A., "High Strength Stainless Steels", Review of Recent Developments, DMIC, (May 29, 1964)

Author **John L. Shannon, Jr.**

1. GENERAL

Fe
12 Cr
8.5 Ni
0.3 Cb+Ta
1.1 Ti
2.0 Cu
< .05 C

Custom 455 is a versatile low carbon, martensitic, age-hardening Cr-Ni stainless steel with good corrosion resistance and favorable fabrication characteristics, intended for service up to 800F. A single aging treatment in the range of 900-1050F develops high tensile and yield strengths. Fracture toughness and ductility in tensile tests decrease with increasing strength level. K_{Iscc} values in salt solution drop with decreasing aging temperature and are relatively low for the fully-aged condition. The alloy can be readily cold-formed, welded, and machined in the annealed condition.

Applications include high-strength aircraft fasteners and forgings, components for nuclear reactors, bolts, load hooks, drive pins, ball screw assemblies, springs, valve stems, gears, shafts, ring seals, retaining rings, pressure vessels, and parts for use at cryogenic temperatures to -60F.

1.1 Commercial Designation - Custom 455 stainless steel.

1.2 Alternate Designations - Carpenter Custom 455; AMS 5617; Almar 455; UNS S45500.

1.3 Specifications

1.3.1 *[Table]* Specifications.

1.4 Composition

1.4.1 *[Table]* Composition.

1.5 Heat Treatment

(See also Sections 1.9.9 and 2.1.2)

1.5.1 Anneal. Annealing is done at 1500-1650F, holding at temperature for 15 minutes to 1 hour, and rapid cooling. The preferred annealing range is 1500-1550F, and water quenching is recommended for small sections. (Ref. 105)

1.5.2 Solution Heat Treatment. Solution treating is done at 1500-1550F, holding for 5 to 30 minutes depending on section thickness and rapid cooling. The producer recommends (Ref. 106) water quenching sections less than 1.5 inches, oil quenching sections 1.5 to 6.0 inches, and air cooling sections greater than 6.0 inches. (See Section 1.9.9) Low solution temperatures result in incomplete solution. Temperatures over 1650F produce recrystallization and excessive grain growth. (Ref. 8)

1.5.2.1 Embrittlement is reported for solution treating at 1700F followed by aging in the 850-950F range (See Table 1.5.2.2 and Figure 3.2.1.8), and for 850F aging following the recommended 1500F solution treatment. (See Table 1.5.2.2 and Figure 3.2.1.10) Superior toughness is achieved by double solution treating 1250F + 1500F for product aged 850-900F; but the double solutioning offers no advantage for 950F aged product. (See Table 1.5.2.1) (Ref. 26) It appears that triple solution treating 1700F + 1250F + 1500F further improves notch strength and impact energy of product aged 950-1000F, but with some penalty in tensile strength. (See Table 1.5.2.2)

1.5.2.2 *[Table]* Effect of solution treatment on room temperature smooth and mild-notch tensile strengths, and Charpy-V impact energy of solution treated and aged bar.

1.5.3 Aging Treatment. Precipitation hardening consists of heating to a selected temperature within the range of 900-1000F, holding for 4 hours, and air cooling. The optimum combination of room temperature tensile properties is obtained by aging at 950F. Aging at 900F produces the highest strength, whereas aging at 1000F results in improved ductility with slightly lower strength.

1.5.3.1 Effect of aging treatment on dimensions. The 4-hour aging treatment results in a contraction of 0.0007 inch per inch when aged at 900F and 0.0012 inch per inch at 1000F. (Ref. 5)

1.5.4 Nitriding. (See also Section 4.4.2)

1.5.4.1 *[Table]* Nitriding depth and hardness.

1.6 Hardness

1.6.1 AMS specified hardness. (See Table 3.1.1)

1.6.2 *[Table]* Typical hardness.

1.6.3 *[Figure]* Effect of aging time at 980F on hardness of forged block.

1.6.4 *[Figure]* Effect of aging time at 995-1000F on hardness of forged block.

1.6.5 *[Table]* Effect of cold drawing on hardness of wire.

This section produced with the support of NASA-Lewis Research Center.

© 1996 by Purdue Research Foundation, West Lafayette, Indiana 47907. All Rights Reserved. U.S. Government License. This material may be used, duplicated or disclosed by United States Government agencies without the payment of any royalty.

1.6.6 Nitriding depth and hardness. (See Table 1.5.4.1)

1.7 Forms and Conditions Available

The alloy is available as forging billets, wire, bars, shapes, forgings, cold-finished rounds, hot- and cold-finished sheet, strip, and plate, and tubing, all in a wide range of commercial sizes and conditions. (Ref. 5)

1.8 Melting and Casting Practice

Double vacuum melted only (vacuum induction followed by vacuum arc remelting). (Ref. 13)

1.9 Special Considerations

1.9.1 When parts are machined in the annealed or solution treated condition, allowance should be made for a slight contraction of about 0.001 inch per inch on aging. (See Section 1.5.3.1)

1.9.2 See Section 2.3 for a thorough discussion of corrosion resistance. Pitting and crevice corrosion, galvanic corrosion, and stress corrosion cracking, or a combination of these may be a problem, particularly for product aged below 1000F. K_{Iscc} values in 3.5 percent NaCl solution decrease with increasing section size for all aging temperatures. (See Figure 2.3.4.1) Yield strength has a strong influence on K_{Iscc} in a variety of corrosive media, with resistance increasing with decreasing yield strength. (See Figure 2.3.4.10)

1.9.3 As with other high strength martensitic stainless steels, Custom 455 is susceptible to hydrogen embrittlement. (Ref. 5)

1.9.4 Solution temperature above 1600F results in substantial drop in notch strength and presumably in fracture toughness. (See Figure 3.2.1.8)

1.9.5 Material aged at 950F exhibits an increase in tensile and yield strengths when exposed for 1000 hours at 700 or 800F, coupled with decrease in Charpy-V impact energy. (See Table 3.2.1.13)

1.9.6 Plane strain fracture toughness decreases with decreasing test temperature. Values at -65F for forging aged at 1000F are about one-half those at 75F. (See Table 3.3.7.2.4)

1.9.7 The response of plane strain fracture toughness to test temperature depends on heat treated section size and on the characteristics of a given heat, so that a substantial variability in toughness values can be encountered at a particular aging temperature. (See Figure 3.3.7.2.1)

1.9.8 Available evidence indicates no K_{Ic} directionality effects for forgings. (See Table 3.3.7.2.4)

1.9.9 The more rapid the cooling from the anneal/solution temperature, the finer the martensite lattice and lesser the amount of retained austenite. Both are desirable for toughness. The alloy producer therefore recommends water quenching thin sections (< 1.5 inches). Water quenching heavy sections (> 6.0 inches) carries the risk of surface cracking from induced stresses. Air cooling is recommended for heavy sections. Oil quenching is recommended for intermediate section sizes (1.5 to 6.0 inches). An exception to these producer recommendations is that of SAE-AMS 5860D which specifies water quenching for plate exceeding 1.25 inches (as indicated in Table 3.1.1). No explanation was found for this contrary AMS recommendation.

2. Physical Properties and Environmental Effects

2.1 Thermal Properties

2.1.1 Melting Range.

2.1.2 Phase Changes. M_s and M_f temperatures, 325F and 150F, respectively. (Ref. 26) Recrystallization temperature, 1650F. (Ref. 8)

The reaction kinetics of this alloy have been studied by Widge. (Ref. 26) His conclusions are summarized in the following paragraphs.

Custom 455 transforms completely to martensite on cooling from the solution temperature. Increasing aging temperature lowers strength and hardness and raises ductility and toughness. This is explained in terms of overaging the precipitation hardening phase and/or accompanying austenite reversion.

The conventional 1500F solution treated structure contains precipitated Fe_2Ti. Pretreatment at 1250F for 4 hours enhances Fe_2Ti precipitation. Higher temperature solution treatment (e.g., 1700F) results in a coarsened martensite lath structure and no Fe_2Ti.

Age hardening occurs by the precipitation of coherent, h.c.p. Ni_3Ti. Coherency appears to persist at aging temperatures to 1050F. Beyond that, increasing aging temperature produces a precipitate of increasing coarsness; progressing from very fine spherical particles to rods, to particles that give the appearance of needles but are in fact agglomerates of many rods. Increasing solution temperature appears to reduce the rate of coarsening of the aging precipitate.

The Ni_3Ti precipitates along <111> directions of the b.c.c. alloy matrix, inhibiting slip, and making the alloy prone to lath boundary failure. Ductility of the alloy can be improved by austenite reversion at the martensite lath boundaries. (A detrimental effect on toughness would be obtained if reverted austenite were to precipitate at prior austenite grain boundaries.)

Solution treatments that precipitate Fe_2Ti promote austenite reversion at the lath boundaries (due to increased available matrix Ni), simultaneously with

Ni_3Ti matrix precipitation (even at low aging temperatures), thus improving toughness. Solution treatments that thwart austenite reversion (due to a shortage of Fe_2Ti precipitate) embrittle due to excessive Ni_3Ti aging precipitate.

Absence of Fe_2Ti, presence of excessive Ni_3Ti, and enlarged lath size of the alloy's structure all contribute to reduced toughness and notch ductility by reducing austenite reversion. But precipitation of Fe_2Ti by use of the 1250F + 1500F solution treatment restores loss in toughness related to precipitation; however, the reduction in austenite reversion related to lathe size is not restored.

The amount of reverted austenite required for significant toughness improvement is only about 3 percent. For aging at 850-900F, a double 1250F + 1500F solution treatment (compared to the standard 1500F treatment) produces satisfactory austenite reversion. It is hypothesized that following the 1250F treatment the structure contains reverted austenite and overaged precipitation hardening phase in a martensitic matrix. When this structure is solution annealed at 1500F, the overaged precipitate goes into solution but the reverted austenite laths are relatively unaffected. Upon cooling to room temperature, the reverted austenite is stable primarily due to the alloy's high nickel content, and the aging precipitate is re-precipitated in a finer morphology via final aging treatment. It is reasoned that this microstructure obtains its strength from the precipitation hardening phase and its toughness from the reverted austenite.

At higher aging temperatures, satisfactory austenite reversion occurs following the simple 1500F solution treatment.

The mechanical response, especially toughness, is thus influenced by the interplay of: (1) Fe_2Ti precipitate present in the solution treated structure; (2) coherent h.c.p. Ni_3Ti aging precipitate; (3) martensite lath (grain) size; and, (4) reverted austenite at the martensite lath boundaries.

The amount of Ti in matrix solution varies with the amount of precipitated Fe_2Ti. The more Fe_2Ti present, the more Ni available to promote austenite reversion. The less Fe_2Ti present, the more Ni_3Ti precipitated on aging. The more Ni_3Ti precipitated, the less matrix Ni available to promote austenite reversion. When 1100-1200F exposure follows high temperature solution treatment, austenite reversion is almost completely restored due to Fe_2Ti precipitation (i.e., no lath size role). This explains the observed lesser austenite reversion for 1700F + 1250F + 1500F solution treatment compared to 1250F + 1500F. Solution treating 1100F + 1500F produces no more Fe_2Ti than the standard 1500F solution treatment and consequently results in identical aging and austenite reversion.

High aging temperatures increase austenite reversion accompanied by coarser precipitation and corresponding decrease in strength. The increase in toughness for 1050F aging obtained by solution treatments that precipitate Fe_2Ti appears to be related to this decrease in strength. Results indicate that it is only worthwhile to use a 1250F + 1500F solution treatment, compared to the standard 1500F treatment, if the aging temperature is to be 850-900F. Use of the double treatment offers no benefit for aging at 950F. Higher aging temperature causes austenite reversion to occur even with the standard 1500F solution treatment. The 1250F + 1500F treatment is also effective in restoring toughness loss caused by a higher solution treatment, related to the ability of the pretreatment to precipitate Fe_2Ti.

2.1.3 *[Figure]* Thermal conductivity.

2.1.4 *[Figure]* Thermal expansion.

2.1.5 Specific Heat.

2.1.6 Thermal Diffusivity.

2.2 Other Physical Properties

2.2.1 Density. 0.280 lb per cu.in. , 7.75 gr per cu.cm. in 950F aged condition. (Refs. 5, 9)

2.2.1.1 Specific gravity. 7.7 - 7.8 in 950F aged condition. (Refs. 5, 9)

2.2.2 Electrical Properties.

2.2.2.1 *[Figure]* Electrical resistivity.

2.2.3 Magnetic Properties.

2.2.3.1 *[Figure]* DC normal induction.

2.2.4 Emittance.

2.2.5 Damping Capacity.

2.3 Chemical Environments

2.3.1 General Corrosion.

2.3.1.1 The general corrosion resistance of Custom 455 lies between that of Types 410 and 430 stainless steel. It resists staining in normal air atmospheres and shows no corrosion in fresh water. (Ref. 5) Oxidation resistance is judged to be excellent up to 1100F. (Ref. 5)

Corrosion resistance in acetic and sulfuric acids is better than Types 410 and 431 stainless steel, and slightly inferior to Type 430. Aging temperature has no significant effect on corrosion rate in acetic acid. Corrosion rate in sul-

furic acid is aging temperature dependent with lowest aging temperature resulting in highest corrosion rate. (Ref. 5)

In the more oxidizing nitric acid environment which tends to attack precipitate phases, the corrosion rate is also influenced by aging temperature with lowest aging temperature resulting in lowest corrosion rate. (Ref. 5)

2.3.1.2 *[Figure]* Corrosion rates in acetic, sulfuric, and nitric acid media.

2.3.1.3 Pitting and Crevice Corrosion. Tests in 5 percent salt spray at 95F show good resistance to pitting. (Ref. 5)

Pitting resistance is comparable to other precipitation hardening grades of reasonably similar compositions when tested by immersion in 5 w/o ferric chloride at room temperature for 10 minutes. (Ref. 5) Bolts with tape-wrapped shanks exhibited corrosion grooves at the tape edges after six-hours immersion at room temperature in 10 w/o ferric chloride solution. This result suggests likely susceptibility to crevice corrosion in fastener thread crests or wherever else a differential aeration cell is produced. (Refs. 45, 49)

Stressed (to 75 percent F_{ty}) and unstressed specimens of base and weld metal (950F and 1050F age), with and without protective coating, were immersed at approximately one-mile depth in the Atlantic (23 deg 52 min N, 76 deg 46.6 min W, identified as the Tongue of the Ocean) and Pacific (33 deg 51 min N, 120 deg 35 min W, approximately 75 miles west of Port Hueneme, California) Oceans. Unstressed Atlantic specimens exposed four years with protective coating showed no corrosion attack. Companion unstressed specimens without protective coating experienced substantial pitting and crevice corrosion attack ranging from less than 0.005 in. to 0.12 in. in depth under adhesive tape and at fixture contact areas. There were no occurrences of cracking of the Atlantic stress corrosion specimens. The performance of specimens exposed six months in the Pacific was similar to that of specimens exposed four years in the Atlantic. Crevice corrosion attack ranged from a depth of 0.07 in. to 0.10 in. The difference between the Pacific and Atlantic specimens in maximum crevice corrosion was only 0.020 in. (0.10 versus 0.12 in.), indicating that the Pacific site with its very low oxygen content initiates loss of passivity (at local crevices) much more rapidly than the higher-oxygen-content test site in the Atlantic. The results show the alloy to be highly susceptible to pitting and crevice corrosion. (Ref. 65)

2.3.1.4 Galvanic Corrosion. The alloy may come into contact with more active metals during service, for example in aerospace applications where aluminum is widely used. Not stress corrosion cracking, but rather hydrogen cracking due to hydrogen produced on the alloy which serves as the electrode, may be a problem that must be considered. In this situation, if the alloy's resistance to stress corrosion cracking is due to high toughness, then this property will be useful in resisting hydrogen cracking when in contact with active metals. On the other hand, if it owes its stress corrosion cracking resistance primarily to good corrosion and crevice corrosion resistance, then these properties are of no use in avoiding the galvanic corrosion problem and could in fact aggravate it by increasing one of the driving forces (potential difference). Toughness, potential differences, area ratios, design parameters and polarization characteristics (particularly for the active metal) may be more useful for predicting performance in some situations than are stress corrosion data.

In aircraft applications where fasteners are used in contact with aluminum, the open circuit potential (voltage) between the noble metal in the fastener and the active metal in the structure is about 0.5v in the presence of an aqueous electrolyte containing chlorides. With a potential this high, galvanic corrosion of the aluminum is inevitable. Sacrificial coating of the fastener may be employed not to protect the bolt, as with low alloy steels, but to protect the structure around the bolt. (Ref. 49)

The alloy is susceptible to electrochemical attack (galvanic crevice corrosion) in environments containing combinations of N_2O_4 and salt solution. (Ref. 28)

2.3.2 Stress Corrosion. Eight direct tension specimens aged at 950F were stressed to 90-95 percent of F_{ty} in artificial seawater; no failures occurred and tests were discontinued after 154 days. (Ref. 5) Bolts loaded to 75 percent of F_{tu} in 7075-T651 blocks were swabbed with 3.5 percent NaCl solution to examine the possibility of embrittlement cracking due to hydrogen formation by intense galvanic reaction between the bare bolt (cathode) and the aluminum block (anode). No cracking was observed in 1,800 hours and the tests were terminated. Bolt shanks notched to $K_t = 3.5$ and 6.0 and either charged or plated to produce hydrogen were then hung at sustained load at 75 percent of NTS. An acid charging solution consisting of 0.1N NaOH with 0.1N NaCN was used for charging at 1 ampere for 30 minutes. Plating was done in production cyanide cadmium or sulfamate nickel baths at normal current densities.

The alloy was only affected when acid charged, showing that it is susceptible to hydrogen embrittlement in certain circumstances. (Ref. 49)

The alloy exhibits a marked increase in saltwater K_{Iscc} as the aging temperature is increased, largely a reflection of K_{Ic} changes. Saltwater K_{Iscc} is about 85% K_{Ic} for all conditions. [Carter et al (Ref. 103) also obtained no failures at stresses up to 85% of K_{Ic}.] There appears to be an almost linear relationship between saltwater K_{Iscc} and yield strength. (Ref. 7)

Figure 2.3.2.1 shows a marked influence of product size and emphasizes the need to consider product size in the application of K_{Iscc} to design. Again, changes due to product size are largely a function of K_{Ic} changes. Grain size decreased in Figure 2.3.2.1 from ASTM 2 for the 9-inch square to ASTM 7 for the 1-1/4-inch square. All data in Figure 2.3.2.1 are for the LT orientation; TL specimens exhibited K_{Ic} and K_{Iscc} values about 10 percent lower. Caution must be exercised when using K_{Iscc} as a design criterion. Failure of Custom 450 precracked cantilever beam specimens across the cantilever plane (i.e., the plane of maximum stress), rather than the notch/crack plane, has been observed to originate at a pit formed in the crevice between the corrosion cell and the specimen. (Ref. 7) Scale left on the specimen is thought to have accelerated the attack. The same phenomenon has been observed by Brown (Ref. 104) for a precipitation hardening 13Cr-8Ni-2Mo stainless steel. Brown logically uses that type of failure as evidence that the prime function of a precrack is to serve as a crevice for local chemistry changes - more specifically a lowering of the pH to produce a potential -pH condition favorable to the formation of hydrogen. In the case of the cited aberrant failures, the crevice at the cell wall (cantilever plane) was more capable of producing corrosion and hydrogen than the one at the notch/crack bottom. The fact that a crevice existed all around the specimen at the cell wall provided a potential greater source of hydrogen. Ostensibly the stress intensity in the corrosion crack area exceeded the K_{Iscc}, or the corrosion resistance at the site was less crack resistant than K_{Iscc} would suggest. It is necessary, then, that for applications where stress corrosion is a consideration, both toughness and general corrosion resistance be considered. In this regard, it is noticed that Custom 455 has good general corrosion resistance owing to the fact that the hardening precipitate (Laves - Fe, Ti) does not deplete the matrix of large amounts of corrosion resistant elements (e.g., chromium).

2.3.2.1 *[Figure]* Effect of section size and age temperature on room temperature K_{Iscc} in 3.5 percent NaCl solution (pH 5).

2.3.2.2 *[Figure]* Delayed failure of fatigue precracked cantilever bend specimens (from billet) in 3.5 percent aqueous NaCl solution.

2.3.2.3 *[Figure]* Delayed failure of fatigue precracked cantilever bend specimens (from forging) in 3.5 percent aqueous NaCl solution.

2.3.2.4 *[Figure]* Effect of aging temperature on delayed failure characteristics of fatigue precracked cantilever beam specimens in 3.5 percent aqueous NaCl solution.

2.3.2.5 *[Table]* Effect of aging temperature on cracking time of U-bend specimens exposed to salt-water atmospheres.

2.3.2.6 0.062-in-thick C-ring specimens, annealed 1500F, 30 min, WQ + aged at 1000F, 1100F, or 1150F, 4 hr in vacuum, cooled in Argon, were stressed in the transverse direction to 50, 75, 90 and 100 percent of longitudinal F_{ty} and alternately immersed in 3.5 percent NaCl solution, 10 minutes in solution and 50 minutes out of solution, for 180 days with no evidence of cracking. (Ref. 80)

2.3.2.7 *[Table]* Effect of alternate immersion in NaCl solution, under tension stress, on room temperature strength, ductility, hardness, and elastic modulus.

2.3.2.8 *[Figure]* Delayed failure of smooth tensile specimens in alternating salt spray.

2.3.2.9 *[Table]* Delayed failure in 5 percent salt fog atmosphere of notched specimens variously plated.

2.3.2.10 Following the procedure of MIL-STD-13212, a total of thirteen bolts were loaded to 75 percent of F_{tu} and alternately immersed in 3.5 percent NaCl solution, 10 minutes in solution followed by 50 minutes of forced air drying. No failures were observed in some specimens exposed as long a 6,534 hours; three specimens failed in the shank area in 2,316 to 2,735 hours. (Refs. 40, 49)

2.3.2.11 *[Table]* Susceptibility to hydrogen sulfide stress cracking.

2.3.2.12 *[Figure]* K_{Iscc} as a function of F_{ty} in various environments containing water, aqueous chlorides, air, H_2S gas, or H_3BO_4 solution.

2.4 Nuclear Environments

2.4.1 *[Table]* Helium embrittlement at 1300F.

3. Mechanical Properties

3.1 Specified Mechanical Properties

3.1.1 *[Table]* AMS specified mechanical properties.

3.1.2 *[Table]* AMS specified mechanical properties for spring temper wire.

3.1.3 *[Table]* Producer's specified mechanical properties.

3.2 Mechanical Properties at Room Temperature

3.2.1 Tension Stress-strain Diagrams and Tensile Properties.

3.2.1.1 *[Figure]* True stress-true strain curves.

3.2.1.2 *[Table]* Typical mechanical properties for billet and bar.

3.2.1.3 *[Table]* Typical mechanical properties for plate.

3.2.1.4 *[Table]* Typical mechanical properties for sheet.

3.2.1.5 *[Table]* Typical mechanical properties for strip.

3.2.1.6 *[Table]* Typical mechanical properties for foil.

3.2.1.7 *[Table]* Typical mechanical properties for welded tubing.

3.2.1.8 *[Figure]* Effect of solution temperature on smooth and sharp-notch tensile strengths of bar aged at 950F.

3.2.1.9 *[Table]* Effect of cooling rate from the solution temperature on strength, hardness, and Charpy-V impact energy of billet aged at 950F.

3.2.1.10 *[Figure]* Effect of aging temperature on smooth and sharp-notch tensile properties of bar.

3.2.1.11 *[Figure]* Effect of aging time on smooth and sharp-notch tensile properties of bar.

3.2.1.12 *[Figure]* Smooth tensile properties of sheet aged in the 1000-1150F range.

3.2.1.13 *[Table]* Effect of 1000-hour exposure in air at elevated temperature on the room temperature smooth and sharp-notch tensile properties and Charpy-V impact energy of solution treated and aged bar.

3.2.1.14 *[Figure]* Effect of cold work on the smooth tensile properties of wire in the as-drawn and cold-drawn plus aged conditions.

3.2.1.15 *[Table]* Comparison of bolt strength to material strength.

3.2.2 Compression Stress-strain Diagrams and Compression Properties.

3.2.2.1 Stress-strain diagrams. (See Figure 3.3.2.1)

3.2.2.2 Compressive yield strength. Average F_{cy} of 261 ksi in the 900F aged condition and 265 ksi for the 950F aged condition have been reported for longitudinal specimens taken from 4-inch square billets (Ref. 8), somewhat higher than the values shown in Table 3.2.2.3.

3.2.2.3 *[Table]* Compressive yield strength and elastic modulus.

3.2.3 Impact. (See also Tables 1.5.2.2, 3.2.1.9, and 3.2.1.13)

3.2.3.1 *[Table]* Effect of aging temperature on Charpy-V impact energy of bar and billet.

3.2.3.2 *[Table]* Effect of aging temperature on tensile and Izod impact properties of bar.

3.2.3.3 *[Table]* Effect of aging temperature on Charpy-V and precracked Charpy impact energy.

3.2.3.4 *[Table]* Effect of 100-hour exposure in air at elevated temperature on room temperature precracked Charpy impact energy.

3.2.4 Bending.

3.2.5 Torsion and Shear.

3.2.5.1 Torsional yield strength. F_{sty} is approximately 50 percent of F_{tu} in the aged condition. (Ref. 5)

3.2.5.2 Shear strength. The double shear strength for 1/4-inch to 3/4-inch diameter bars in the 900F aged condition ranges from 141 to 152 ksi or approximately 56 to 60 percent of F_{tu}. (Refs. 5, 14)

3.2.5.2.1 *[Table]* Tensile and double shear strengths of bolts.

3.2.6 Bearing.

3.2.7 Stress Concentration.

3.2.7.1 Notch properties. (See also Section 3.3.7.1)

3.2.7.1.1 AMS specified mild-notch tensile strength. (See Table 3.1.1)

3.2.7.1.2 Typical sharp-notch tensile strength for billet and bar. (See Table 3.2.1.2)

3.2.7.1.3 Effect of solution treatment on sharp-notch tensile strength of solution treated and aged bar. (See Table 1.5.2.2)

3.2.7.1.4 Effect of solution temperature on sharp-notch tensile strength of bar aged at 950F. (See Figure 3.2.1.8)

3.2.7.1.5 Effect of aging temperature on sharp-notch tensile strength of bar. (See Figure 3.2.1.10)

3.2.7.1.6 Effect of aging time on sharp-notch tensile strength of bar. (See Figure 3.2.1.11)

3.2.7.1.7 Effect of 1000-hour exposure in air at elevated temperature on room temperature sharp-notch tensile strength of bar. (See Table 3.2.1.13)

3.2.7.1.8 *[Table]* Effect of notch acuity on mild-notch tensile strength.

3.2.7.2 Fracture toughness. (See also Section 3.3.7.2)

3.2.7.2.1 *[Figure]* Relationship between yield strength and plane strain fracture toughness.

3.2.8 Combined Loading.

3.3 Mechanical Properties at Various Temperatures

3.3.1 Tension Stress-strain Diagrams and Tensile Properties.

3.3.1.1 *[Figure]* Typical stress-strain curves at room and elevated temperatures for aged bar.

3.3.1.2 *[Figure]* Effect of test temperature on tensile properties of billet and bar in the 900F aged condition.

3.3.1.3 *[Figure]* Effect of test temperature on smooth tensile properties and notch strength ratio of bar in the 950F aged condition.

3.3.1.4 *[Figure]* Effect of test temperature on smooth tensile properties and notch strength ratio of bar in the 1000F aged condition.

3.3.1.5 *[Figure]* Effect of test temperature on smooth tensile properties and notch strength ratio of bar in the 1050F aged condition.

3.3.1.6 *[Figure]* Effect of cryogenic test temperature on the tensile properties of sheet in the 950F aged condition.

3.3.1.7 *[Figure]* Effect of cryogenic test temperature on the tensile properties of sheet in the 1000F aged condition.

3.3.1.8 *[Figure]* Smooth and mild-notch tensile properties at cryogenic temperatures for sheet aged at 1000F.

3.3.1.9 *[Figure]* Effect of cryogenic test temperature on the tensile properties of sheet in the 1050F aged condition.

3.3.1.10 *[Figure]* Smooth and sharp-notch tensile properties at cryogenic temperatures for sheet aged at 1100F.

3.3.1.11 *[Figure]* Smooth and sharp-notch tensile properties at cryogenic temperatures for sheet aged at 1150F.

3.3.2 Compression Stress-strain Diagrams and Compression Properties.

3.3.2.1 *[Figure]* Typical compression stress-strain and tangent modulus curves for aged bar.

3.3.2.2 *[Figure]* Effect of test temperature on compressive yield strength of bar aged at 950F.

3.3.3 Impact.

3.3.3.1 *[Table]* -70F Charpy-V impact energy for bar aged at 1050F.

3.3.3.2 *[Figure]* Effect of test temperature on the impact strength of bar in the 900-1050F aged condition.

3.3.3.3 *[Table]* Charpy-V impact energy at cryogenic temperature for bar aged in the 1000-1150F range.

3.3.4 Bending.

3.3.5 Torsion and Shear.

3.3.5.1 *[Table]* Effect of age temperature and test temperature on double restrained shear strength.

3.3.6 Bearing.

3.3.7 Stress Concentration.

3.3.7.1 Notch properties.

3.3.7.1.1 Effect of cryogenic test temperature on notch tensile strength of bar. (See Figures 3.3.1.3, 3.3.1.4, and 3.3.1.5)

3.3.7.1.2 *[Figure]* Effect of cryogenic test temperature on notch tensile strength of sheet in the longitudinal direction.

3.3.7.1.3 *[Figure]* Effect of cryogenic test temperature on notch tensile strength of sheet in the transverse direction.

3.3.7.2 Fracture Toughness.

3.3.7.2.1 *[Figure]* Effect of aging temperature on room temperature tensile properties and low temperature plane strain fracture toughness of bar in a variety of sizes and shapes from seven heats.

3.3.7.2.2 *[Table]* Symbols legend for Figure 3.3.7.2.1.

3.3.7.2.3 *[Table]* Effect of quenched section size on -65F, LS orientation plane strain fracture toughness of forged block variously heat treated to a common strength level of approximately 200 ksi.

3.3.7.2.4 *[Table]* Room temperature, -65F, and -110F smooth and mild-notch tensile strength and plane strain fracture toughness of forging.

3.3.8 Combined Properties.

3.4 Creep and Creep Rupture Properties

3.4.1 *[Table]* Plastic deformation in 100 and 1000 hours at 400-850F.

3.4.2 *[Figure]* Minimum creep rate for bar at 400F, 600F, and 850F.

3.4.3 *[Figure]* Stress-rupture and plastic deformation curves for bar at 400F, 600F, and 850F.

3.4.4 *[Figure]* Creep rupture curves at 400-900F for aged billet and bar.

3.4.5 *[Figure]* Loss of load in one hour at 400-600F during static loading of compression spring made from 0.060-inch wire.

3.5 Fatigue Properties

3.5.1 Conventional Fatigue.

3.5.1.1 *[Figure]* Effect of aging temperature on room temperature rotating beam smooth and mild-notch fatigue strength of bar.

3.5.1.2 *[Figure]* Room temperature axial-load smooth and mild-notch (K_t = 3.3) fatigue strength of billet aged at 950F.

3.5.1.3 *[Figure]* Room and elevated temperature axial-load smooth and mild-notch (K_t = 3.0) fatigue strength of bar aged at 950F.

3.5.1.4 *[Figure]* Typical axial-load smooth and mild-notch (K_t = 3.0) constant-life fatigue diagram for bar aged at 950F.

3.5.1.5 *[Figure]* Typical axial-load smooth and mild-notch (K_t = 3.0) constant-life fatigue diagram for bar aged at 1000F.

3.5.1.6 *[Figure]* Room temperature diametral-strain-controlled low-cycle fatigue life.

3.5.1.7 *[Figure]* Axial-load smooth fatigue strength at several stress ratios for specimens machined from bar after 950F age treatment.

3.5.1.8 *[Figure]* Axial-load mild-notch (K_t = 2.5) fatigue strength at several stress ratios for specimens machined from bar after 950F age treatment.

3.5.1.9 *[Figure]* Axial-load mild-notch (K_t = 4.0) fatigue strength at several stress ratios for specimens machined from bar after 950F age treatment.

3.5.1.10 *[Figure]* Haig diagram for axial-load smooth specimens machined from bar after 950F age treatment.

3.5.1.11 *[Figure]* Haig diagram for axial-load mild-notch (K_t = 2.5) specimens machined from bar after 950F age treatment.

3.5.1.12 *[Figure]* Haig diagram for axial-load mild-notch (K_t = 4.0) specimens machined from bar after 950F age treatment.

3.5.1.13 *[Figure]* Room temperature axial-load fatigue strength of sheet.

3.5.1.14 *[Figure]* Room temperature axial-load fatigue strength of two-hole (K_t = 3.0) sheet specimens.

3.5.1.15 *[Table]* Room temperature axial tension fatigue strength of bolts.

3.5.2 Fatigue Crack Propagation.

3.6 Elastic Properties

3.6.1 Poisson's Ratio. 0.30 in the 950F aged condition. (Ref. 5)

3.6.2 Modulus of Elasticity. 29 x 10^3 ksi; 200 x 10^3 MPa in the 950F aged condition. (Refs. 5, 9)

3.6.2.1 *[Figure]* Modulus of elasticity in tension (E) and compression (E_c) at temperatures ranging from -200F to 800F.

3.6.2.2 Modulus of elasticity at room temperature for sheet aged in the 1000-1150F range. See Figure 3.2.1.12)

3.6.3 Modulus of Rigidity. 11 x 10^3 ksi, 7.7 x 10^5 kg per cm^2 in the 950F aged condition. (Refs. 5, 9)

3.6.4 Tangent Modulus.

3.6.5 Secant Modulus.

4. Fabrication

4.1 Forming

4.1.1 Hot Workability. The alloy can be easily forged or rolled within the range of 2300-1650F. For optimum mechanical properties, heating prior to final hot reduction should be within the range 1900-2100F with adequate time at heat followed by hot finishing within 1500-1700F. This procedure should result in optimum grain size and properties after heat treatment. (Refs. 5, 9, 10)

4.1.2 Cold Workability. As in other low carbon martensitic, precipitation hardening steels, cold working can be readily performed in the annealed condition at the hardness level of Rockwell C 30-35. Since the elonga-

tion tends to be localized, deep drawing and similar stretching operations will require intermediate annealing. For other cold forming operations, such as cold-drawing and cold-rolling, the work-hardening rate in the annealed condition is extremely low, allowing considerable reduction without intermediate annealing. (See Figure 4.1.2.1) Cold- and warm-heading operations can also be performed easily. Cold working prior to aging increases the strength level in the heat treated condition. (See Tables 3.1.2, 3.2.1.4, and 3.2.1.6) (Refs. 5, 9, 10)

4.1.2.1 *[Figure]* Effect of cold drawing in the annealed condition on tensile strength of wire.

4.1.3 Primary and secondary deformation processes for precipitation-hardenable stainless steels are discussed in Ref. 55.

4.2 Machining and Grinding

4.2.1 Machining and grinding can be performed successfully using the same practices required for other high strength, heat-treated alloys; namely slow speeds, positive cuts, adequate use of coolants, and rigid tool and work supports. The machining characteristics are similar to those of the nickel maraging steels (Code 1220). Specific and detailed data for turning, milling, drilling, tapping, and grinding are given in Ref. 5.

4.3 Joining

4.3.1 The alloy can be successfully welded by resistance butt welding, spot welding, and the inert-gas-shielded methods. Pre-heating and post-weld annealing are not required. However, optimum ductility in the weld metal is obtained by post-weld annealing prior to aging, which also improves the resistance to corrosion. After aging, the joint efficiencies which are possible are 100 percent in small sections and 85 percent or greater in large sections. Some general recommendations for metal-gas-arc welding procedures are given in Refs. 5, 32, and 73. Other welding procedures used for the nickel maraging steels are applicable. (Refs. 5, 6, 9) Laser welding is discussed in Ref. 27.

4.3.2 Impact resistance of restraint pin welds in the post weld 950F aged condition are reported to be unacceptably low at service temperatures in the range -50F to -60F. Resolution treating after welding, prior to aging, restores impact strength to acceptable parent metal levels. (Refs. 67-71)

4.4 Surface Treating

4.4.1 Cleaning. After forging or annealing, descaling is accomplished by wet-grit blasting or acid cleaning. The latter consists of immersing for 2 to 3 minutes in 15 percent muriatic acid at 180F followed by 4 to 6 minutes in 15 percent nitric plus 3 percent hydrofluoric at room temperature (acid concentrations are in volume percent). Desmut by immersion in 20 percent nitric acid at room temperature. The heat tint from aging is removed by pickling for 5 to 10 minutes in 15 percent nitric plus 3 percent hydrofluoric followed by a water rinse. Fused-salt descaling baths that operate at 800-1000F should not be used during cleaning between intermediate anneals, since age-hardening can occur. All parts should be passivated in a 40 to 60 percent nitric solution as the final processing step. Machined parts should be degreased prior to heat treatment. (Refs. 5, 6, 9)

4.4.2 Nitriding. The surface hardness of the basic alloy is increased to improve wear resistance by nitriding, but at some sacrifice in corrosion resistance. Nitriding is performed in a cyanide salt bath or in a gas atmosphere, and aging is accomplished in the same operation. A chemically clean surface is imperative to achieve a uniform case. Nitriding at 960-1025F for 24 to 48 hours produces a case depth of 0.003-0.006 inch, a case hardness of 65-70 Rockwell C, and a core hardness of 39-45 Rockwell C. (Ref. 5)

Table 1.3.1 Specifications (Refs. 1-4, 83-87)

Alloy		Custom 455	
Form	Condition	Specification	Ref.
Welded Tubing	ST and ST + Age	AMS 5578D	1
Bar, Wire, Forging	ST and ST + Age	AMS 5617G	2
Wire	CD	AMS 5672B	3
Sheet, Strip, Plate	ST and ST + Age	AMS 5860D	4
Bar, Wire	ST and ST + Age	MIL-S-83311[a]	83
Spring Wire	CD and CD + Age	ASTM A 313	84
Bar and Shapes	ST and ST + Age	ASTM A 564/A 564M	85
Plate, Sheet, Strip	ST and ST + Age	ASTM A 693	86
Forging	ST and ST + Age	ASTM A 705/A 705M	87

[a] This specification active for replacement parts only. For new design and new purchases, use Refs. 2 and 3.

Table 1.4.1 Composition (Refs. 1-5, 83-87, 93)

Alloy	Custom 455																	
Source	Carpenter UNS		AMS 5578D		AMS 5617G		AMS 5617G		AMS 5672B		AMS 5860D		MIL-S-83311		ASTM A 313, A 693		ASTM A 564/A 564M, A 705/A 705M	
Reference	5, 93		1		2		2		3		4		83		84, 86		85, 87	
Form	All		Welded Tubing		Bar, Wire, Forging [Grade 1]		Bar, Wire, Forging [Grade 2]		Spring Temper Wire		Sheet, Strip, Plate		Bar, Wire		Plate, Sheet, Strip, Spring Wire		Bar, Shapes, Forging	
	Element (Percent)																	
	Min.	Max.	Min.	Max.	Min.	Max.	Min.	Max.	Min.	Max.	Min.	Max.	Min.	Max.	Min.	Max.	Min.	Max.
Carbon		0.05		0.05		0.03		0.010		0.05		0.05		0.05		0.05		0.03
Manganese		0.50		0.50		0.50		0.50		0.50		0.50		0.50		0.50		0.50
Silicon		0.50		0.50		0.50		0.20		0.50		0.50		0.50		0.50		0.50
Phosphorous		0.040		0.015		0.015		0.010		0.025		0.025		0.025		0.040		0.015
Sulfur		0.030		0.015		0.015		0.010		0.025		0.025		0.025		0.030		0.015
Chromium	11.00	12.50	11.00	12.50	11.00	12.50	11.00	12.50	11.00	12.50	11.00	12.50	11.00	12.50	11.00	12.50	11.00	12.50
Nickel	7.50	9.50	7.50	9.50	7.50	9.50	7.50	9.50	7.50	9.50	7.50	9.50	7.50	9.50	7.50	9.50	7.50	9.50
Columbium + Tantalum	0.10	0.50	0.10	0.50		0.50		0.50	0.10	0.50	0.10	0.50	0.10	0.50	0.10	0.50	0.10	0.50
Titanium	0.80	1.40	0.80	1.40	0.90	1.40	1.00	1.35	0.80	1.40	0.80	1.40	0.80	1.40	0.80	1.40	0.90	1.40
Copper	1.50	2.50	1.50	2.50	1.50	2.50	1.50	2.50	1.50	2.50	1.50	2.50	1.50	2.50	1.50	2.50	1.50	2.50
Molybdenum		0.50		0.50		0.50		0.50		0.50		0.50		0.50		0.50		0.50
Nitrogen						0.015		0.010		0.015								
Iron		Balance		Balance		Balance		Balance		Balance		Balance		Balance		Balance		Balance

Table 1.5.2.2 Effect of solution treatment on room temperature smooth and sharp-notch tensile strengths, and Charpy-V impact energy of solution treated and aged bar (Ref. 26)

Alloy	Custom 455						
Form	Hot Rolled 2-in. Bar						
Condition	ST + Age						
ST	Age	F_{tu} (ksi)	F_{ty} (ksi)	e (percent)	RA (percent)	NTS[a] (ksi)	IE Charpy-V (ft-lb)
1500F, 30 min, WQ	850	254.6	248.6	10.2	40.4	210	5.5
	900	252.3	245.8	10.1	49.1	257	10.0
	950	238.2	234.1	10.1	56.6	326	18.0
	1000	194.0	181.1	17.6	63.0	293	34.0
1700F, 30 min, WQ	850	252.8	249.0	thread failure		69	2.0
	900	256.5	246.5	4.6	16.7	96	2.0
	950	243.8	234.8	11.4	48.0	154	3.5
	1000	190.4	175.9	16.1	63.4	291	36.5
1100F, 4 hr, AC + 1500F, 30 min, WQ	850	255.8	248.5	10.6	45.6	198	6.0
	900	255.1	249.5	10.8	48.7	257	9.0
	950	239.5	235.3	11.7	53.5	323	17.0
	1000	194.4	181.8	18.4	62.3	291	42.5
1250F, 4 hr, AC + 1500F, 30 min, WQ	850	251.1	246.3	11.2	46.8	269	11.0
	900	247.7	243.0	10.0	45.6	303	14.0
	950	233.4	230.5	11.7	54.5	323	18.5
	1000	189.5	176.5	17.7	63.0	287	46.5
1700F, 30 min, WQ + 1250F, 4 hr, AC + 1500F, 30 min, WQ	850	248.3	242.5	11.1	41.7	200	6.5
	900	245.0	240.0	11.3	49.0	300	13.5
	950	227.0	223.0	16.4	55.6	330	23.0
	1000	183.7	170.6	16.7	63.9	282	67.0

All values average duplicate tests.

[a] Notch specimen:

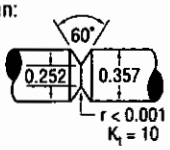


Table 1.5.4.1 Nitriding depth and hardness (Ref. 5)

Alloy			Custom 455		
Nitriding			Hardness (R_C)		Case Depth (in.)
Procedure	Temperature (F)	Time (hr)	Case	Core	
Cyanide Bath	960 - 990	24	68 - 70	42 - 44	0.003
		48	65 - 70	43 - 45	0.006
Gas Nitriding	1025	24	68	39	0.004

Table 1.6.2 Typical hardness (Ref. 5)

Alloy		Custom 455			
Form		Bar, Plate, Strip			
Condition	ST[a]	ST + Age at[b]			
		900F	950F	1000F	1050F
Hardness (R_C)	31 - 34	49 - 51	47 - 48	44 - 46	40

[a] 1500F, 30 minutes, WQ.

[b] 1500F, 30 minutes, WQ + age temperature, 4 hours, AC.

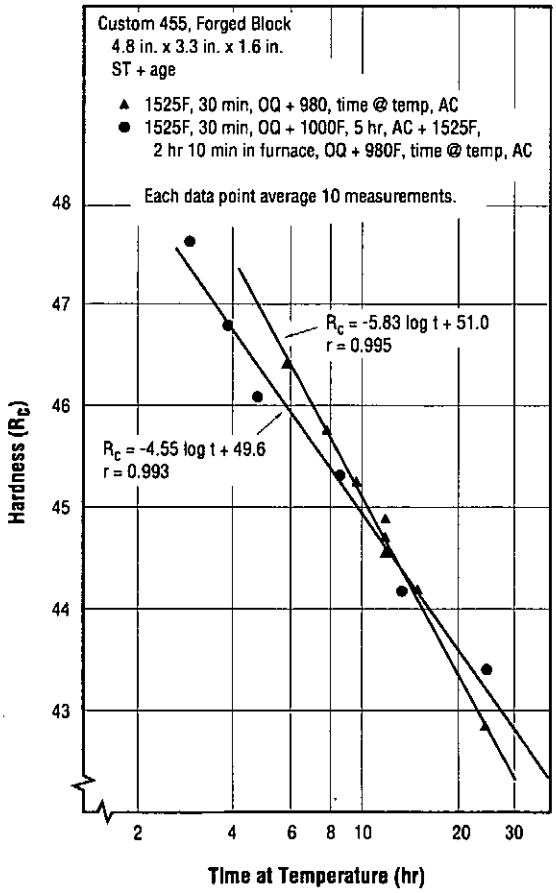


Figure 1.6.3 Effect of aging time at 980F on hardness of forged block (Ref. 98)

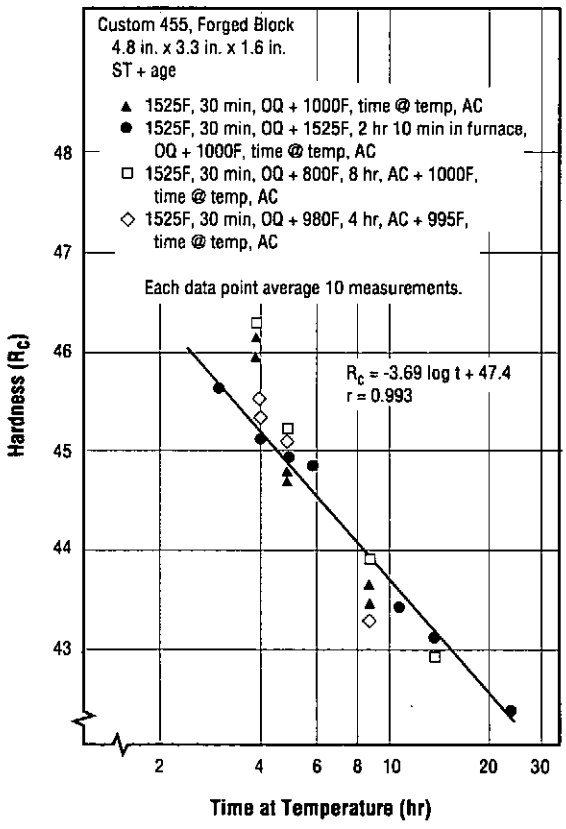


Figure 1.6.4 Effect of aging time at 995-1000F on hardness of forged block (Ref. 98)

Table 1.6.5 Effect of cold drawing on hardness of wire (Ref. 5)

Alloy	Custom 455							
Form	Wire							
Size	0.250-in. Initial Diameter							
Condition	Annealed[a] + CD				Annealed[a] + CD + Age[b]			
CD (percent)	0	20	40	60	0	20	40	60
Hardness (R_C)	31 - 32	33	35	37	49	50	52	53

[a] 1500F, 30 minutes, WQ.

[b] 900F, 4 hours, AC.

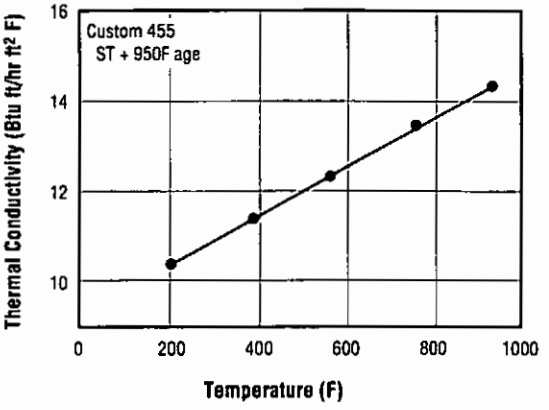


Figure 2.1.3 Thermal conductivity (Refs. 5, 9)

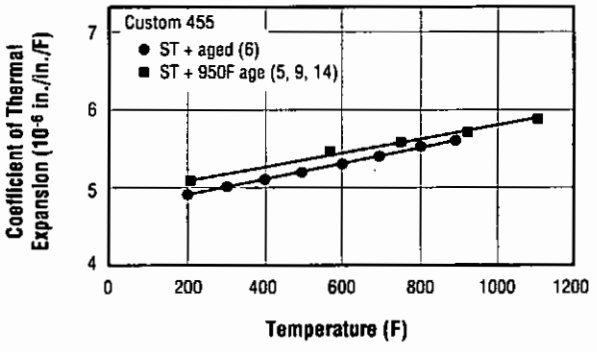


Figure 2.1.4 Thermal expansion (Refs. 5, 6, 9, 14, 54)

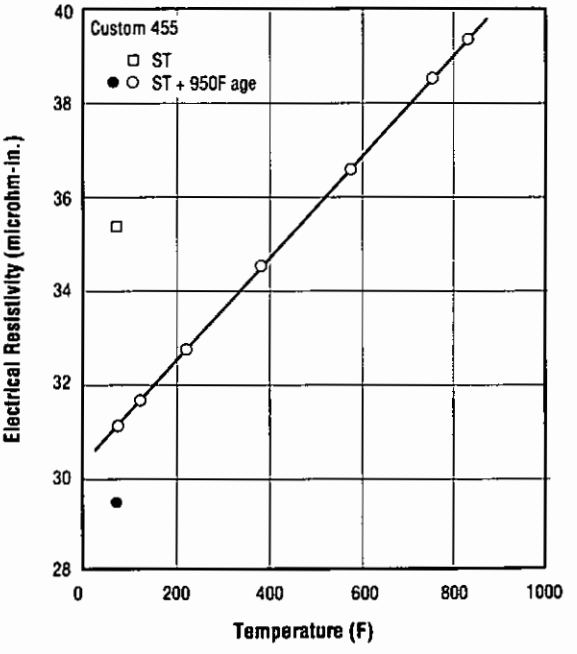


Figure 2.2.2.1 Electrical resistivity (Refs. 5, 9)

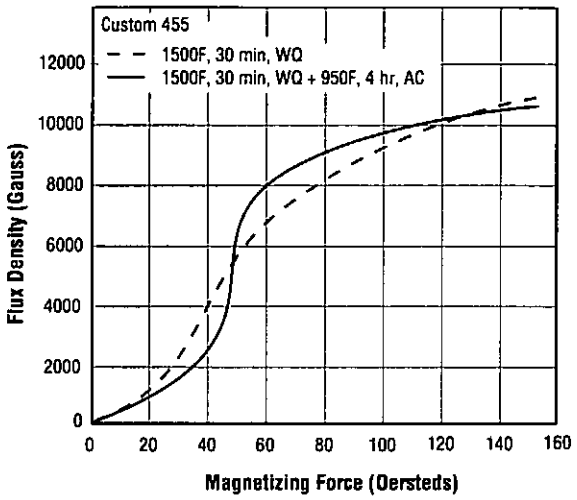


Figure 2.2.3.1 DC normal induction (Ref. 5)

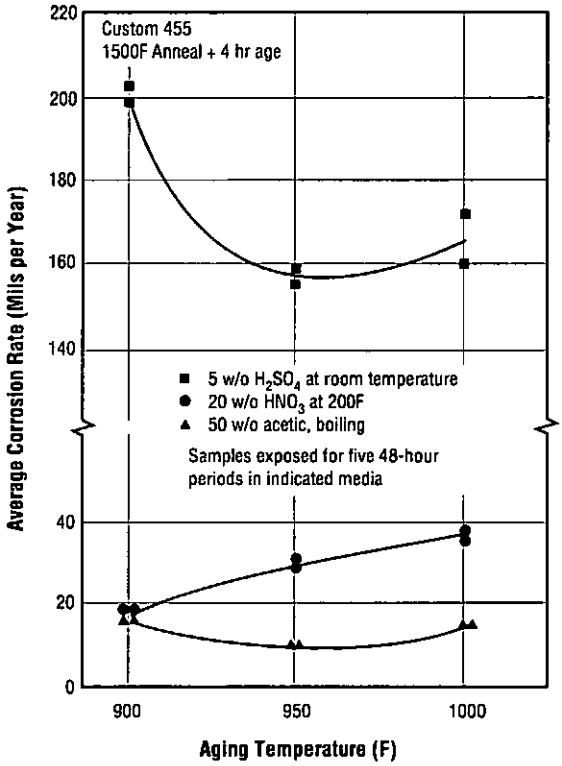


Figure 2.3.1.2 Corrosion rates in acetic, sulfuric, and nitric acid media (Ref. 5)

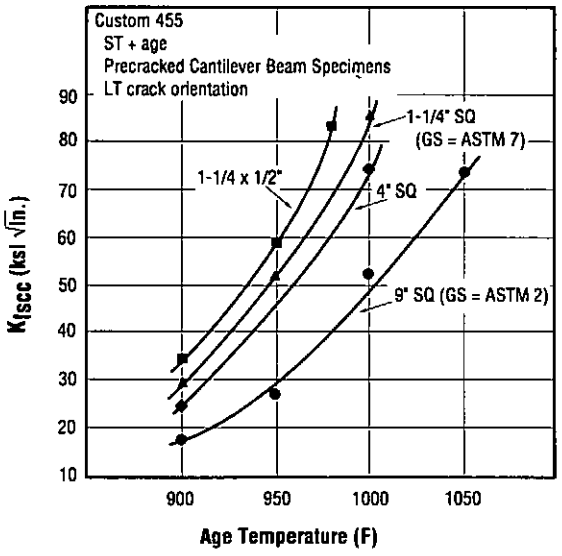


Figure 2.3.2.1 Effect of section size and age temperature on room temperature K_{Iscc} in 3.5 percent NaCl solution (pH 5) (Ref. 7)

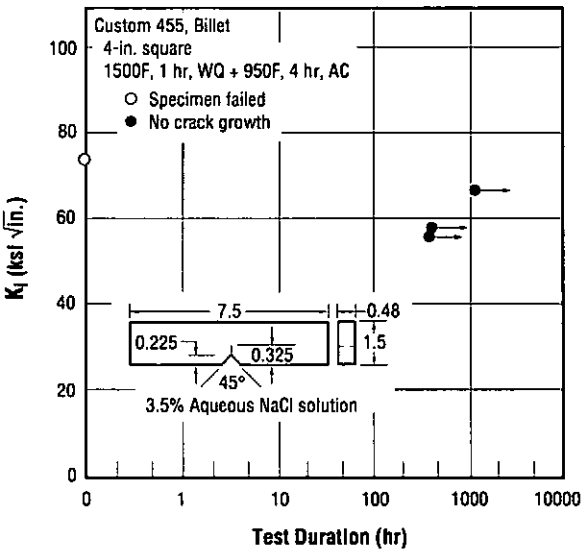


Figure 2.3.2.2 Delayed failure of fatigue precracked cantilever bend specimens (from billet) in 3.5 percent aqueous NaCl solution (Ref. 20)

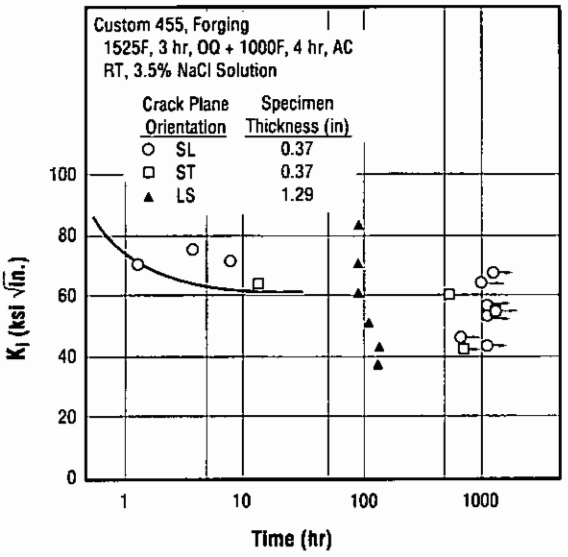


Figure 2.3.2.3 Delayed failure of fatigue precracked cantilever bend specimens (from forging) in 3.5 percent aqueous NaCl solution (Ref. 99)

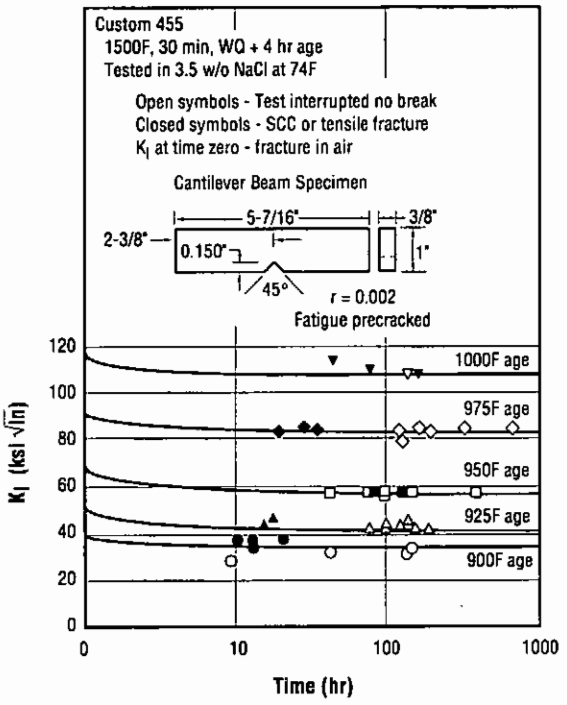


Figure 2.3.2.4 Effect of aging temperature on delayed failure characteristics of fatigue precracked, cantilever beam specimens in 3.5 percent aqueous NaCl solution (Refs. 5, 7, 11)

Table 2.3.3.5 Effect of aging temperature on cracking time of U-bend specimens exposed to saltwater atmospheres (Refs. 5, 7, 11, 13)

Alloy	Custom 455					
Specimen	U-bend: 3.88-in. x 0.38-in. x 0.105-in., 0.5-in. Bend Radius					
Exposure	20 percent Salt Spray at 95F			Marine Atmosphere at INCO Kure Beach, 80-ft. from Atlantic Ocean		
Age Temperature (F)	Number of Specimens Tested	Number of Specimens Cracked	Duration of Test	Number of Specimens Tested	Number of Specimens Cracked	Duration of Test
900	5	3	4, 141, 463, remainder uncracked after 485 days	3	3	1, 2, 3 days
950	4	1	3, remainder uncracked after 278 days			
1000	5	0	No cracks in 278 days	3	0	No cracks in 1000 days

Table 2.3.2.7 Effect of alternate immersion in NaCl solution, under tension stress, on room temperature strength, ductility, hardness, and elastic modulus (Ref. 80)

Alloy	Custom 455							
Form	0.034-in Sheet							
Condition	1500F, 30 min, WQ + Age, 4 hr in Vacuum, Argon Cool							
Age Temperature (F)	Hardness (R_C)	Exposure Time[c] (Days)	Exposure Stress[c] (Percent of F_{ty})	Properties After Exposure				Number of Specimens Tested
				F_{tu} (ksi)	F_{ty} (ksi)	e, 2-in. (percent)	E (10^3 ksi)	
Longitudinal								
Unaged	34.0	None	0	164.7	126.9	4.9	22.8	3
1000	49.0	None	0	249.9	240.6	4.8	26.4	3
		180	0	249.6	244.8	4.9	30.8	4
			75	249.7	243.9	4.3	31.0	3
			90	249.2	242.5	4.7	29.7	
			100	249.0	241.5	4.5	29.2	
1100	43.0	None	0	208.2	189.9	7.0	31.1	4
		180	0	209.0	191.9	7.8	29.3	
			75	208.9	183.4	7.2[a]	30.7	
			100	207.8	184.3	7.6	27.7	
1150	37.0	None	0	173.4	124.0	13.0	24.9	4
		180		174.4	127.4	11.9	25.0	
			75	173.9	119.6	12.9	24.0	
			100	173.6	118.2	12.8	25.0	
Transverse								
Unaged	34.0	None	0	171.2	133.2	4.5	24.0	3
1000	49.0	None	0	259.7	252.9	3.2	32.5	3
		180	0	261.1	256.4	3.0[b]	32.6	4
			75	256.2	243.0	3.5[a]	33.1	3
			90	259.6	253.0	3.2[b]	31.3	
			100	259.7	252.7	3.2	31.9	
1100	43.0	None	0	215.8	199.4	6.9	30.9	4
		180	0	215.7	200.1	7.0[a]	30.4	
			75	215.9	195.1	6.8	32.0	
			100	216.4	195.6	7.0	29.5	
1150	37.0	None	0	179.7	137.4	12.4	29.4	4
		180	0	179.7	130.8	10.8	26.5	
			75	176.1	127.4	8.8	27.4	
			100	181.4	127.4	11.5	26.8	

[a] One test.

[b] Two tests.

[c] Alternate immersion in NaCl solution: 10 minutes in; 50 minutes out.

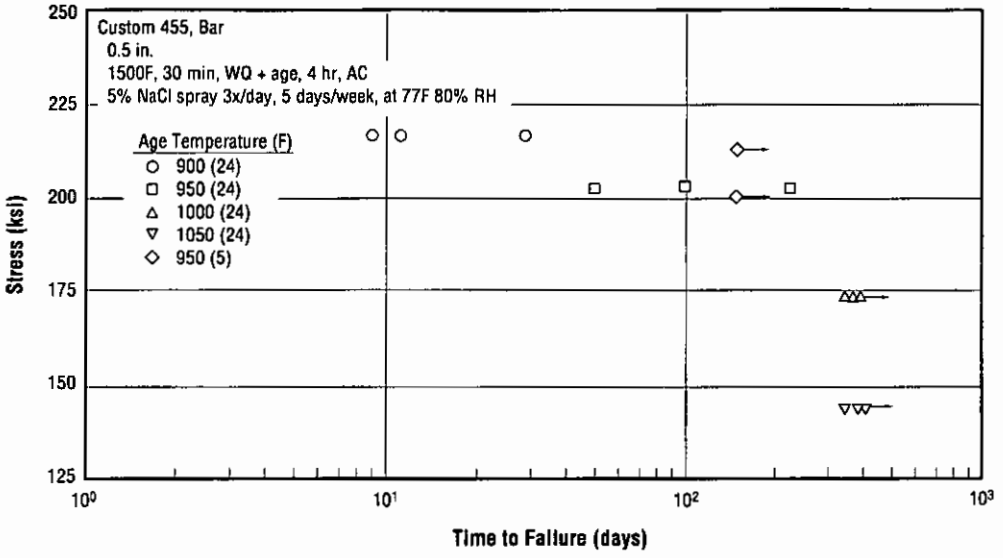
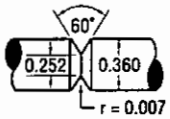


Figure 2.3.2.8 Delayed failure of smooth tensile specimens in alternating salt spray (Refs. 5, 24)

Table 2.3.2.9 Delayed failure in 5 percent salt fog atmosphere of notched specimens variously plated (Ref. 18)

Alloy	Custom 455					
Form	1-in. Bar					
Condition	Annealed + 950F, 4 hr, AC					
F_{tu} (ksi)	F_{ty} (ksi)	e, 1-in. (percent)	RA (percent)	Life in 5 percent salt fog atmosphere[a] (hr)		
				Unplated	Vacuum deposited cadmium plated[b]	Nickel-cadmium diffusion plated[c]
230.3	223.9	12.7	53.0	> 1000	95	> 1000

[a] Notched longitudinal specimens stressed to 142 ksi. All values average from triplicate tests.



[b] 0.002/0.005-inch vacuum deposited cadmium plate + chromate.

[c] 0.002/0.004-inch diffusion (630F, 30 minutes) nickel-cadmium plate.

Table 2.3.2.11 Susceptibility to hydrogen sulfide stress cracking (Ref. 47)

Alloy		Custom 455		
Form		2.5-in. Bar		
Condition		Annealed + 1050F, 4 hrs, AC		
F_{tu} (ksi)	F_{ty} (ksi)	E (10^3 ksi)	Specimen No.[a]	Failure time, t, at yield stress (days)[b, c]
199.3	186.7	32.6	1	1 < t < 4
			2	1 < t < 4
			3	< 1
			4	1 < t < 4

[a] C-ring specimen: outer fiber stress perpendicular to longitudinal grain of bar and equal to F_{ty}.

[b] Corrodent: 5 w/o NaCl solution containing 0.5 w/o acidic acid (pH = 2.84), through which nitrogen bubbled prior to the addition of gaseous H_2S. Gases were flowed daily after inspection.

[c] Cracked specimens all failed at position of maximum stress in C-ring, 90° to loading axis. All cracks were straight, with no branching, and followed prior austenite grain boundaries, suggesting hydrogen embrittlement as failure mode.

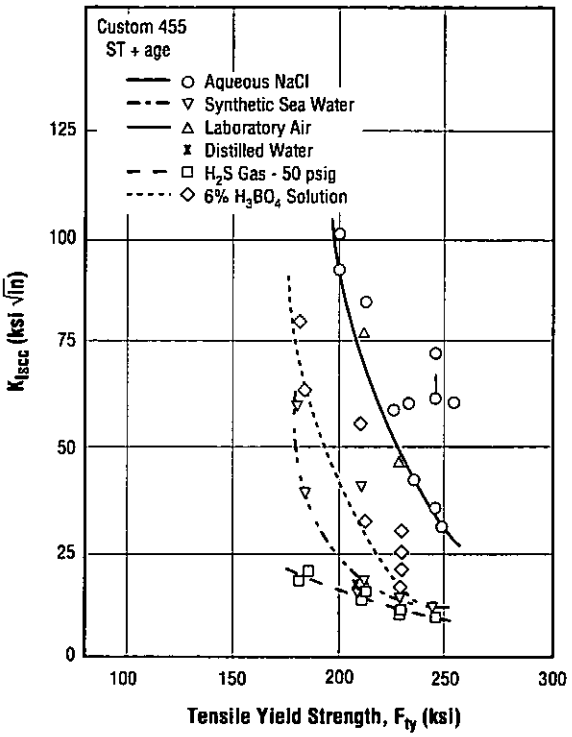


Figure 2.3.2.12 K_{Iscc} as a function of F_{ty} in various environments containing water, aqueous chlorides, air, H_2S gas, or H_3BO_4 solution (Ref. 53)

Table 2.4.1 Helium embrittlement at 1300F (Ref. 64)

Alloy	Custom 455	
Condition	1500F, 30 min, WQ + 1000F, 4 hr, AC	
Helium Concentration[a] (appm)	Uniform Elongation[b] (percent)	Total Elongation[b] (percent)
0	6	40
25	5	8

[a] Helium injected into tensile specimen using α-particle irradiation from a cyclotron, and measured with gas-source mass spectrometer. Residual hardening due to α-particle irradiation annealed out during heating to 1300F test temperature.

[b] Tensile strengths not reported since they are unaffected by presence of helium.

Table 3.1.1 AMS specified mechanical properties (Refs. 1, 2, 4)

Alloy		Custom 455															
Form		Welded Tubing (1)				Bar, Wire, Forging [Grades 1 and 2] (2)				Sheet, Strip, Plate (1)							
Condition		ST[b]	ST + 950 Age[c]			ST[d,h]	ST + 950 Age[f,h]		ST + 1000F Age[g,h]	ST[i]	ST + 950 Age[m,h]			ST + 1000 Age[n,h]			
Thickness[a] (in.)		—	< 0.020	0.020 - 0.062	> 0.062	—	≤ 4.000	4.000 - 6.000	≤ 8.000	—	≤ 0.020	> 0.020 - ≤ 0.062	> 0.062	≤ 0.020	> 0.020 - ≤ 0.062	> 0.062	
F_{tu}	max (ksi)	165				175				175							
	min (ksi)		220	220	220		225	220	220		225	225	225	200	200	200	
F_{ty}	max (ksi)									160							
	min (ksi)		205	205	205		210	205	185		210	210	210	185	185	185	
e, 2-in. or 4D, min (percent)			As agreed upon	4	3		10[j]	10[j]	10	3	2	3	4	3	4	5	
RA, min (percent)							40[j]	40[j]	40								
NTS ($K_t \geq 6$), min (ksi)							225	220	220								
Hardness (R_C)	max									35[k]							
	min		42	42	42						44[k]	44[k]	44[k]	40[k]	40[k]	40[k]	
(BHN)	max					331[e]											
	min																
Bending										l							

a Nominal diameter or distance between parallel sides.

b 1500 - 1550F, ≥ 5 minutes, WQ.

c 1500 - 1550F, ≥ 5 minutes, WQ + 940 - 960F, 3.75 - 4.24 hours, AC.

d 1500 - 1550F, ≥ 30 minutes, OQ or WQ.
Continuous-process wire: ≥1525F, time commensurate with thickness, AC.

e Bar and forging.

f 1500 - 1550F, ≥ 30 minutes, OQ or WQ + 940 - 960F, 3.75 - 4.25 hours, AC.

g 1500 - 1550F, ≥ 30 minutes, OQ or WQ + 990 - 1010F, 3.75 - 4.25 hours, AC.

h Specified properties apply equally to material re-solution heat treated, or re-solution heat treated + aged.

i For Grade 2 product ≤ 6 inches, e(4D) ≥ 5 percent and RA ≥ 20 percent.

j Plate ≤ 1.25 inch: 1500 - 1550F, 5 - 30 minutes, Rapid Quench.
Plate > 1.25 inch: 1500 - 1550F, 5 - 30 minutes, WQ.
Continuous-process wire: 1625 - 1675F, time commensurate with thickness, AC.

k Thickness ≥ 0.010 inch.

l Thickness ≤ 0.1874 inch, bend angle 90° around 2.5t diameter with bend axis parallel to rolling direction.

m 1500 - 1550F, 5 - 30 minutes, Rapid Quench (WQ for t > 1.25 inch) + 940 - 960F, 3.75 - 4.25 hours, AC.

n 1500 - 1550F, 5 - 30 minutes, Rapid Quench (WQ for t > 1.25 inch) + 990 - 1010F, 3.75 - 4.25 hours, AC.

Table 3.1.2 AMS specified mechanical properties for spring temper wire (Ref. 3)

Alloy	Custom 455			
Form	Spring Temper Wire			
Condition	CD		CD + 850F Age[a]	
Diameter (in.)	F_{tu} (ksi)		F_{ty} (ksi)	
	min	max	min	max
0.010 - 0.040	245	—	310	340
0.041 - 0.050	235	—	305	335
0.051 - 0.060	225	—	300	330
0.061 - 0.075	220	—	295	325
0.076 - 0.085	215	—	290	320
0.086 - 0.095	210	—	285	315
0.096 - 0.110	200	—	278	308
0.111 - 0.125	195	—	272	302
0.126 - 0.150	190	—	265	295
0.151 - 0.500	180	—	260	290

[a] 840 - 860F, 27 - 30 minutes, AC.

Table 3.1.3 Producer's specified mechanical properties (Ref. 5)

Alloy	Custom 455			
Form	Bar, Wire, Forging			
Condition	Annealed + 900F Age[a]	Annealed + 950F Age[b]	Annealed + 1000F Age[c]	Annealed + 1050F Age[d]
F_{tu} (ksi)	235	220	205	180
F_{ty} (ksi)	220	205	185	165
e, 2-in. or 4D (percent)	8	10	10	12
RA (percent)	30	40	40	45
Hardness (BNH)	444	415	363	352

[a] 1500 - 1550F, ≥ 30 minutes, WQ < 6-inch sections and OQ or rapid air cool > 6-inch sections + 900F, 4 hours, AC

[b] 1500 - 1550F, ≥ 30 minutes, WQ < 6-inch sections and OQ or rapid air cool > 6-inch sections + 950F, 4 hours, AC

[c] 1500 - 1550F, ≥ 30 minutes, WQ < 6-inch sections and OQ or rapid air cool > 6-inch sections + 1000F, 4 hours, AC

[d] 1500 - 1550F, ≥ 30 minutes, WQ < 6-inch sections and OQ or rapid air cool > 6-inch sections + 1050F, 4 hours, AC

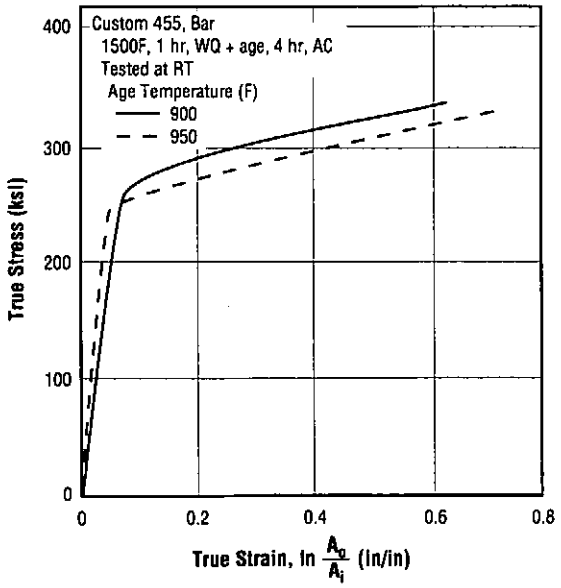


Figure 3.2.1.1 True stress-true strain curves (Ref. 13)

Table 3.2.1.2 Typical mechanical properties for billet and bar (Refs. 5, 13)

Alloy	Custom 455								
Form	4-in. x 4-in. Square Billet				1-in. Diameter Bar				
Condition	ST[a]	ST[a] + Age[b] at			ST[a]	ST[a] + Age[b] at			
		950F	1000F	1050F		900F	950F	1000F	1050F
F_{tu} (ksi)	140	230	205	190	145	250	235	210	190
F_{ty} (ksi)	115	220	195	175	115	245	225	200	175
e, 4D (percent)	12	10	12	14	14	10	12	14	15
RA (percent)	50	45	45	50	60	45	50	55	55
NTS[c] (ksi)	—	250	250	250	230	260	300	290	260
IE Charpy-V (ft-lb)	—	8	12	25	70	9	14	20	35
Hardness (R_C)	31	48	45	40	31	49	48	45	40

[a] 1525F, 30 minutes, WQ.

[b] 4 hours at temperature, AC.

[c] Longitudinal Tests.

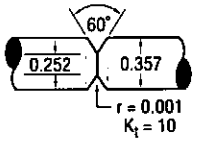


Table 3.2.1.3 Typical mechanical properties for plate (Ref. 5)

Alloy	Custom 455				
Form	0.375-in. Plate				
Condition	Test Direction	F_{tu} (ksi)	F_{ty} (ksi)	e, 2-in. (percent)	RA (percent)
1525F, 30 min, WQ	L	146	120	13	50
	T	152	128	15	60
1525F, 30 min, WQ + 900F, 4 hr, AC	L	252	248	9	33
	T	258	—	9	37
1525F, 30 min, WQ + 950F, 4 hr, AC	L	237	235	11	45
	T	240	237	9	40

Table 3.2.1.4 Typical mechanical properties for sheet (Ref. 5)

Alloy	Custom 455			
Form	0.030-in. Sheet			
Condition	Test Direction	F_{tu} (ksi)	F_{ty} (ksi)	e, 1-in. (percent)
As Rolled (50 percent)	L	174	—	3.6
	T	183		3.2
As Rolled + 950F, 4 hr, AC	L	254	252	3.5
	T	265	263	2.9

Table 3.2.1.5 Typical mechanical properties for strip (Ref. 5)

Alloy	Custom 455											
Form	0.050-in. Strip						0.160-in. Strip					
Condition	F_{tu} (ksi)	F_{ty} (ksi)	e, 1-in. (percent)	e, 2-in. (percent)	RA (percent)	Hardness (R_C)	F_{tu} (ksi)	F_{ty} (ksi)	e, 1-in. (percent)	e, 2-in. (percent)	RA (percent)	Hardness (R_C)
1525F, 30 min, WQ	160	150	10	6	—	34	160	135	18	8	54	33
1525F, 30 min, WQ + 900F, 4 hr, AC	260	250	6	3	—	51	260	250	8	3	25	51
1525F, 30 min, WQ + 950F, 4 hr, AC	250	240	8	4	—	47	250	240	10	4	40	48
1525F, 30 min, WQ + 1000F, 4 hr, AC	220	210	12	5	—	44	220	210	14	6	45	46

Table 3.2.1.6 Typical mechanical properties for foil (Ref. 5)

Alloy	Custom 455		
Form	0.001-in. Foil		
Condition	Test Direction	F_{tu} (ksi)	e, 1-in. (percent)
CR 60%	L	192	1.6
	T	200	
CR 60% + 850F, 30 min, AC	L	298	0.7
	T	287	1.0

Table 3.2.1.7 Typical mechanical properties for welded tubing (Ref. 5)

Alloy	Custom 455					
Form	Welded Tubing					
OD (in.)	Wall (in.)	Condition	Properties			
			F_{tu} (ksi)	F_{ty} (ksi)	e, 2-in. (percent)	Hardness (R_C)
1.130	0.107	Annealed	152	148	10.1	32
		900F Age	260	258	6.2	51
0.875	0.105	Annealed	138	131	14.5	32
		900F Age	254	253	3.9	50
1.000	0.083	Annealed	150	120	14.0	35
		900F Age	261	260	4.6	50
0.750	0.063	Annealed	148	139	14.0	32
		900F Age	252	250	10.0	50
0.500	0.060	Annealed	143	133	10.9	32
		900F Age	250	144	6.2	50

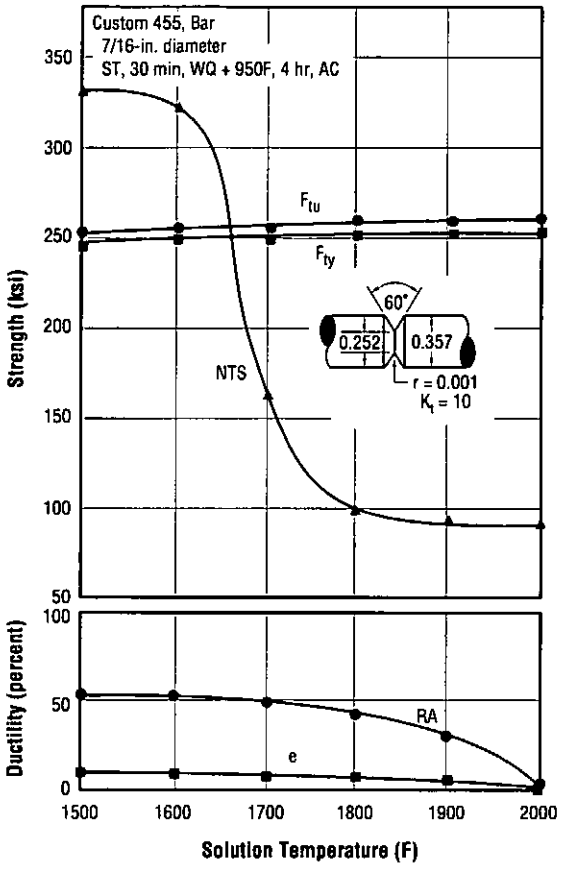


Figure 3.2.1.8 Effect of solution temperature on smooth and sharp-notch strength of bar aged at 950F (Ref. 5)

Table 3.2.1.9 Effect of cooling rate from the solution temperature on strength, hardness, and Charpy-V impact energy of billet aged at 950F (Ref. 5)

Alloy	Custom 455	
Form	4-in. Square Billet[a]	
Condition	1500F, 30 min, WQ + 950F, 4 hr, AC	1500F, 30 min, AC + 950F, 4 hr, AC
F_{tu} (ksi)[b]	220	210
F_{ty} (ksi)	210	205
e, 2-in. (percent)	9	11
RA (percent)	36	45
Hardness (R_C)	47	44
IE Charpy-V (ft-lb)	4	7

[a] Billet rolled from 9-inch square to 4-inch square at 2000F.

[b] All tests longitudinal direction.

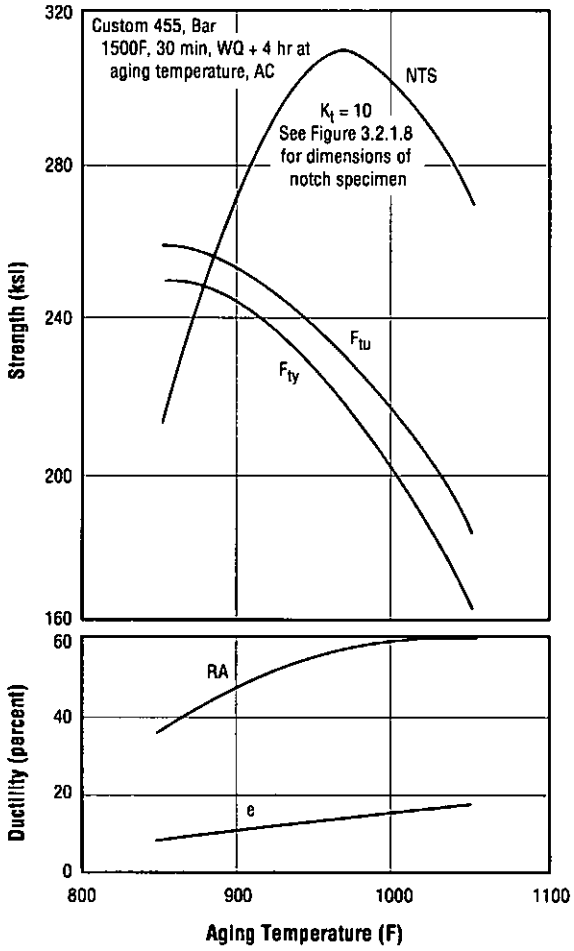


Figure 3.2.1.10 Effect of aging temperature on smooth and sharp-notch tensile properties of bar (Ref. 5)

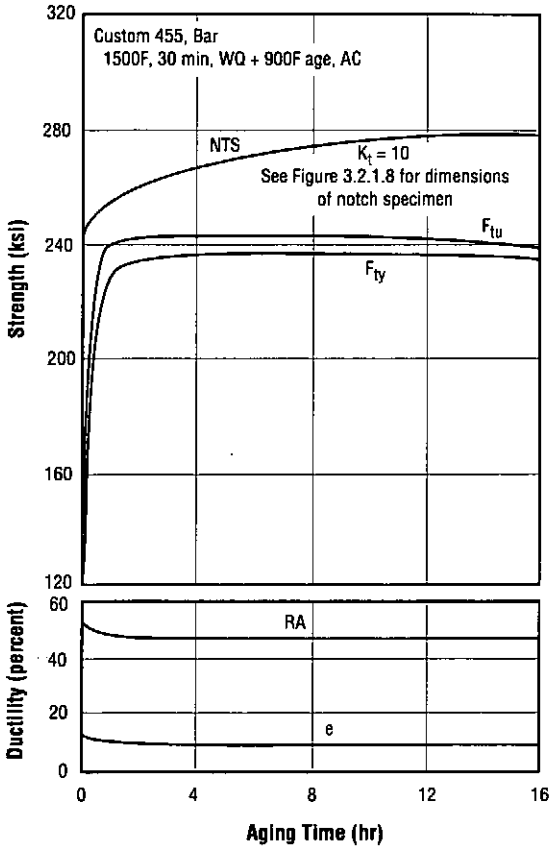


Figure 3.2.1.11 Effect of aging time on smooth and sharp-notch tensile properties of bar (Ref. 5)

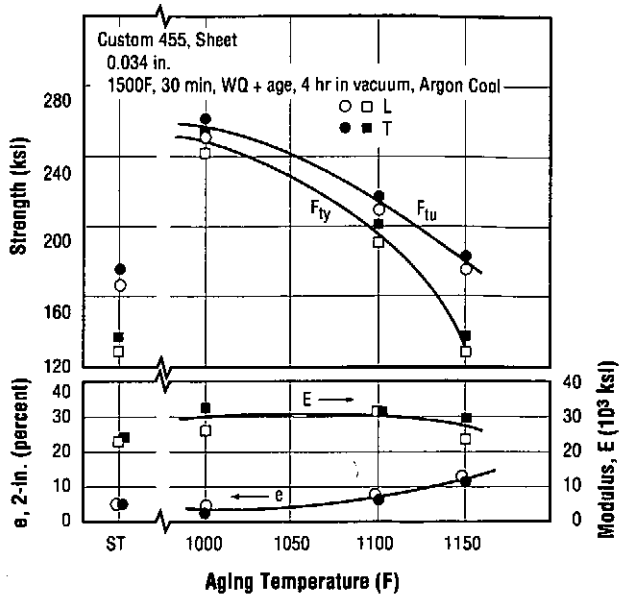


Figure 3.2.1.12 Smooth tensile properties of sheet aged in the 1000-1150F range (Ref. 80)

Table 3.2.1.13 Effect of 1000-hour exposure in air at elevated temperature on the room temperature smooth and sharp-notch tensile properties and Charpy-V impact energy of solution treated and aged bar (Ref. 5)

Alloy	Custom 455		
Form	Bar		
Condition	ST + 900F, 4 hr, AC + Exposure in Air		
Exposure in Air	None	1000 hr at 700F	1000 hr at 800F
F_{tu} (ksi)	250	272	270
F_{ty} (ksi)	240	264	262
e, 1-in. (percent)	11	10	10
RA (percent)	46	43	43
NTS (K_t = 10)[a] (ksi)	260	220	230
IE Charpy-V (ft-lb)	10	6	7

[a] See Table 3.2.1.2 for notch specimen configuration.

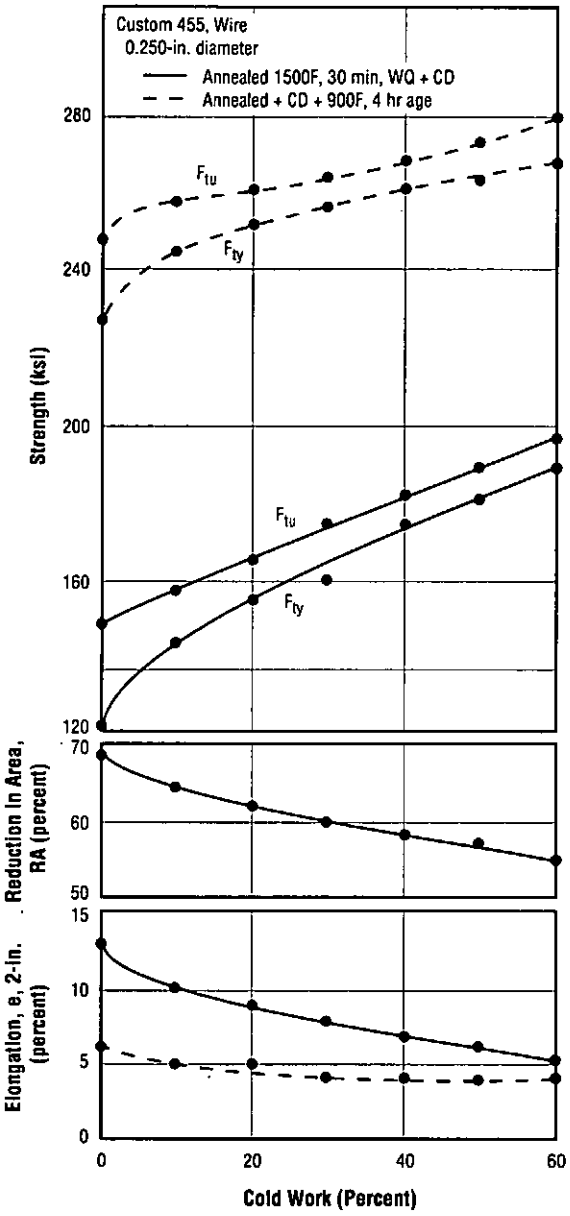


Figure 3.2.1.14 Effect of cold work on the smooth tensile properties of wire in the as-drawn and cold-drawn plus aged conditions (Refs. 5, 9)

Table 3.2.1.15 Comparison of bolt strength to material strength (Ref. 50)

Alloy		Custom 455	
Form		1/4-in. Diameter Hex Head Bolt	
Condition		Head + ST + 900F Age + Grind Shank and Thread Diameters + Roll Threads + Roll Head and Shank Fillet Radius	
Materials Properties		Bolt Properties	
F_{tu} (ksi)	NTS[a] (ksi)	F_{tu}[b] (ksi)	F_{tu}[c] (ksi)
253.6	368.3	317.8	269.8

[a] K_t = 3.0.

[b] Stress area based on maximum minor diameter of MIL-S-8879 thread.

[c] Stress area based on maximum pitch diameter of MIL-S-8879 thread.

Table 3.2.2.3 Compressive yield strength and elastic modulus (Ref. 5)

Alloy	Custom 455	
Condition	Annealed + Age, 4 hr, AC	
Age Temperature (F)	F_{cy} (ksi)	E_c (10^3 ksi)
950	246 - 251	30
1000	212 - 216	29 - 30

Table 3.2.3.1 Effect of aging temperature on Charpy-V impact energy of bar and billet (Refs. 5, 8, 12)

Alloy		Custom 455				
Form		Bar and Billet				
Condition		1525F, 30 min, WQ + Age, 4 hr, AC				
Age Temperature (F)		Unaged	900	950	1000	1050
Size, Form	Ref.	IE Charpy-V (ft-lb)				
1-in. Bar	5	70	9	14	20	35
1-1/16-in. Bar	5		10	17	27	43
4-in. Bar	5	—	—	8	12	25
1-in. Bar	12	—	—	12	23	35
Billet (size not reported)[a]	8	—	5	6	19	—

[a] 1500F, 1 hour, OQ + age, 4 hours, AC.

Table 3.2.3.2 Effect of aging temperature on tensile and Izod impact properties of bar (Ref. 24)

Alloy	Custom 455				
Form	0.5-in. Bar				
Condition	ST + Age, 4 hr, AC				
Age Temperature (F)	F_{tu} (ksi)	F_{ty} (ksi)	e ($\sqrt{A}$) (percent)	E (10^3 ksi)	IE Izod, J[a]
900	253	243	12.8	28.8	11.2
950	237	230	15.2	29.4	20.0
1000	204	194	21.0	29.1	37.5
1050	184	165	20.0	29.2	51.5

[a] Each value average six tests.

Table 3.2.3.3 Effect of aging temperature on Charpy-V and precracked Charpy impact energy (Ref. 8)

Alloy		Custom 455		
Form		Billet		
Condition		1500F, 1 hr, Rapid Cool + Age, 4 hr, AC		
Heat	Age Temperature (F)	F_{ty}[a] (ksi)	IE Charpy-V[b] (ft-lb)	IE Precracked Charpy[b] (in-lb)
A	900	251	4.82	15.2
B	950	246	6.42	37.0
B	1000	212	19.1	124.6

[a] L Direction.

[b] LT Orientation.

Table 3.2.3.4 Effect of 100-hour exposure in air at elevated temperature on room temperature precracked Charpy impact energy (Ref. 8)

Alloy	Custom 455	
Form	Billet	
Condition	1500F, 1 hr, Rapid Cool + 900F, 4 hr, AC	
F_{ty}[a] (ksi)	100 hr Air Exposure Temperature (F)	IE Precracked Charpy[b] (in-lb)
251	Unexposed	4.8
	600	15.5
	700	10.7
	800	11.5
	900	94.3

[a] L Direction.

[b] LT Orientation.

Table 3.2.5.2.1 Tensile and double shear strengths of bolts (Ref 49)

Alloy	Custom 455	
Form	12-Point External Wrenching Bolt with MIL-S-8879 Thread	
Condition	Forge + ST + 950F Age + Grind Shank and Thread Roll Diameters + Roll Threads and Head-To-Shank Fillet	
F_{tu} [a] (ksi)		F_{su} [b] (ksi)
240.1		139.1

[a] Based on basic pitch diameter.

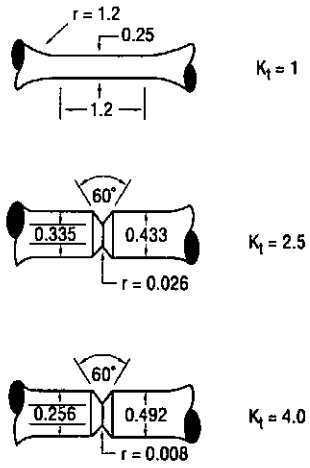
[b] Based on twice the area at nominal shank diameter.

Table 3.2.7.1.8 Effect of notch acuity on mild-notch tensile strength (Ref. 22)

Alloy	Custom 455
Form	0.787-in. Bar
Condition	ST + 950F, 4 hr, AC [a]
K_t [b]	NTS (ksi)
1.0	234
2.5	346
4.0	378

[a] F_{tu} = 234 ksi.

[b] Specimen configurations:



Specimens machined after heat treatment.

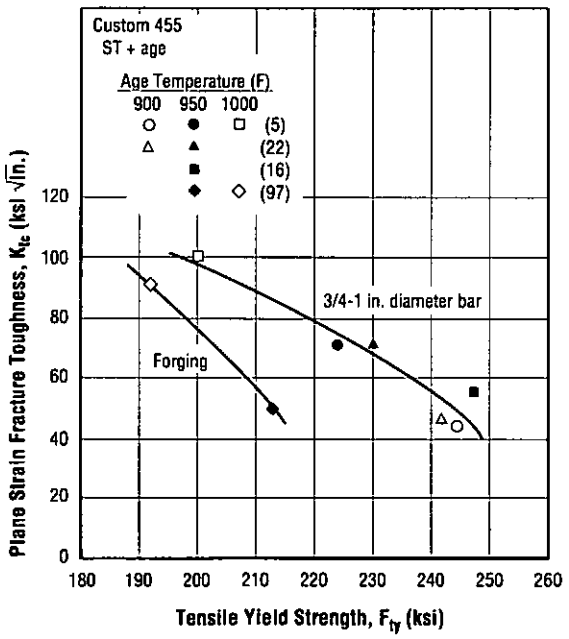


Figure 3.2.7.2.1 Relationship between yield strength and plane strain fracture toughness (Refs. 5, 16, 22, 97)

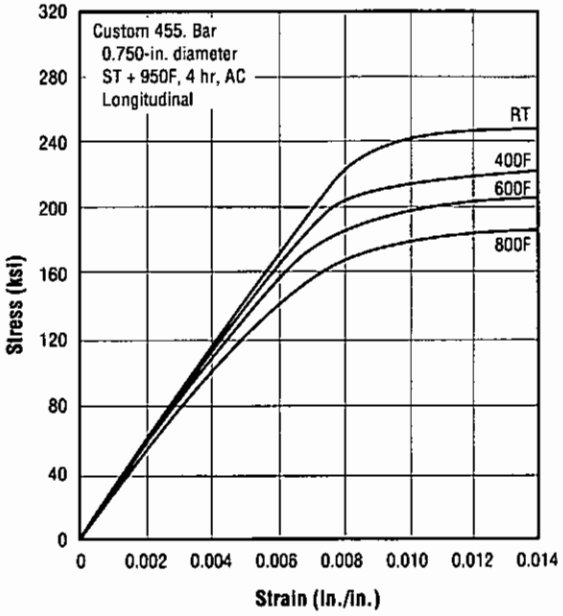


Figure 3.3.1.1 Typical stress-strain curves at room and elevated temperatures for aged bar (Ref. 16)

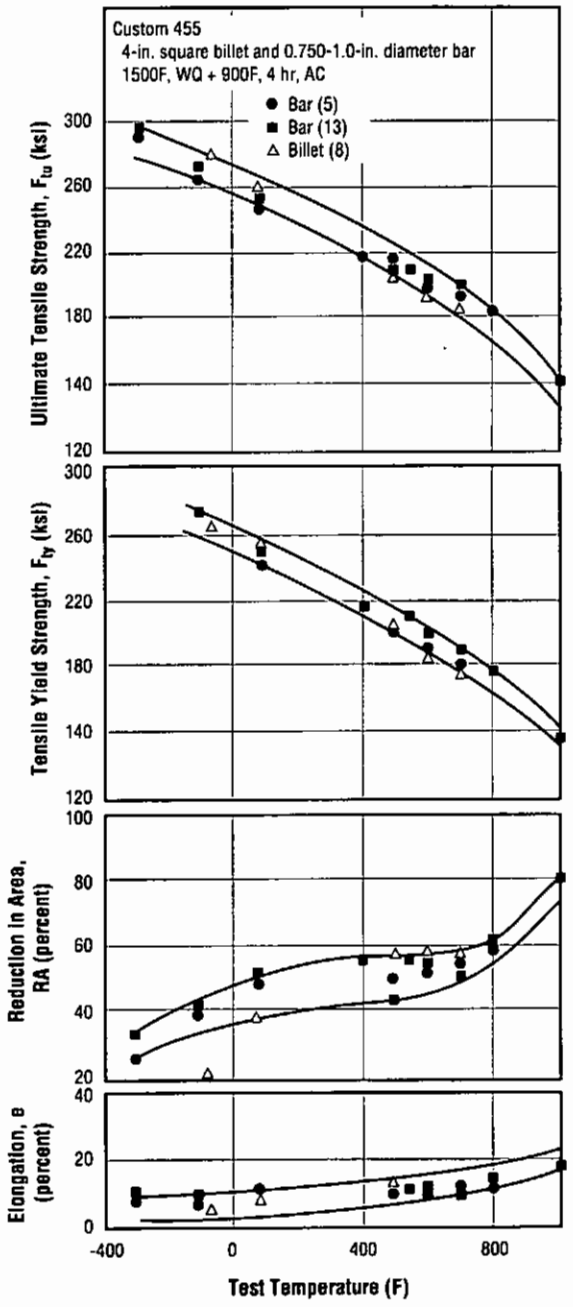


Figure 3.3.1.2 Effect of test temperature on tensile properties of billet and bar in the 900F aged condition (Refs. 5, 8, 13)

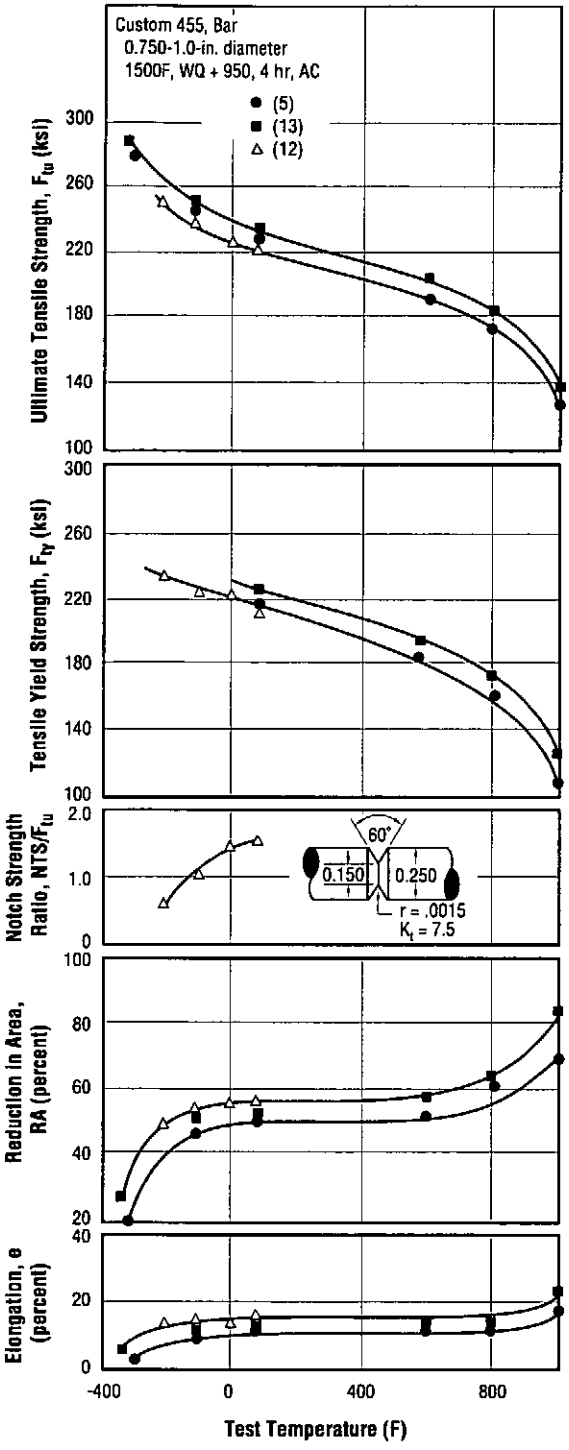


Figure 3.3.1.3 Effect of test temperature on smooth tensile properties and notch strength ratio of bar in the 950F aged condition (Refs. 5, 12, 13)

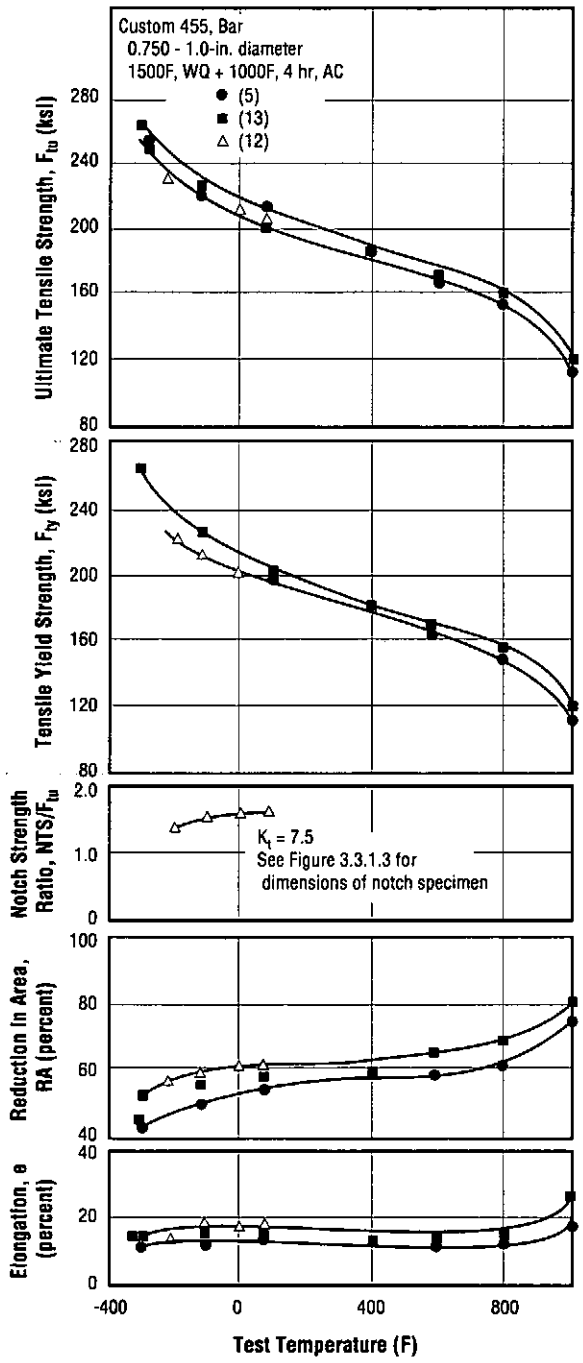


Figure 3.3.1.4 Effect of test temperature on smooth tensile properties and notch strength ratio of bar in the 1000F aged condition (Refs. 5, 12, 13)

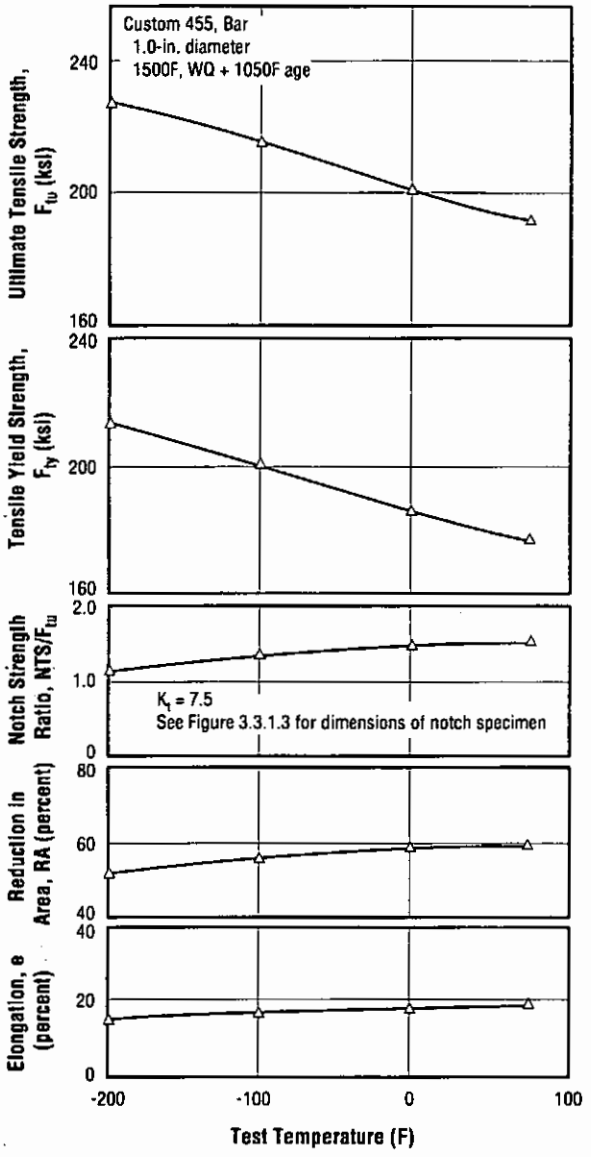


Figure 3.3.1.5 Effect of test temperature on smooth tensile properties and notch strength ratio of bar in the 1050F aged condition (Ref. 12)

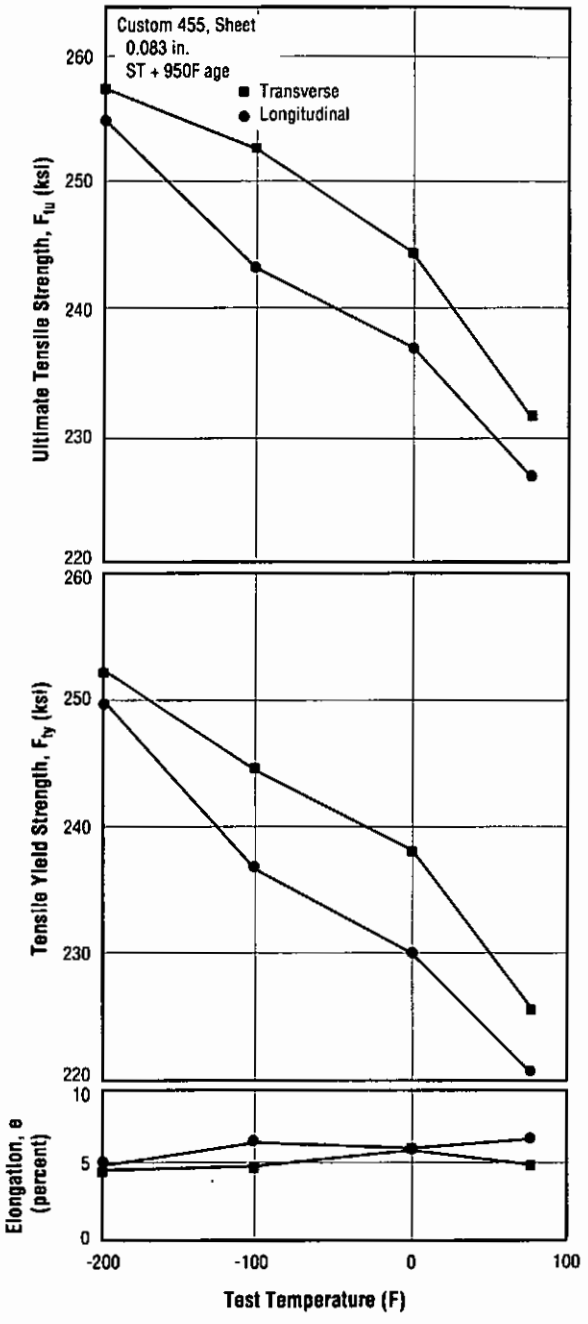


Figure 3.3.1.6 Effect of cryogenic test temperature on tensile properties of sheet in the 950F aged condition (Ref. 12)

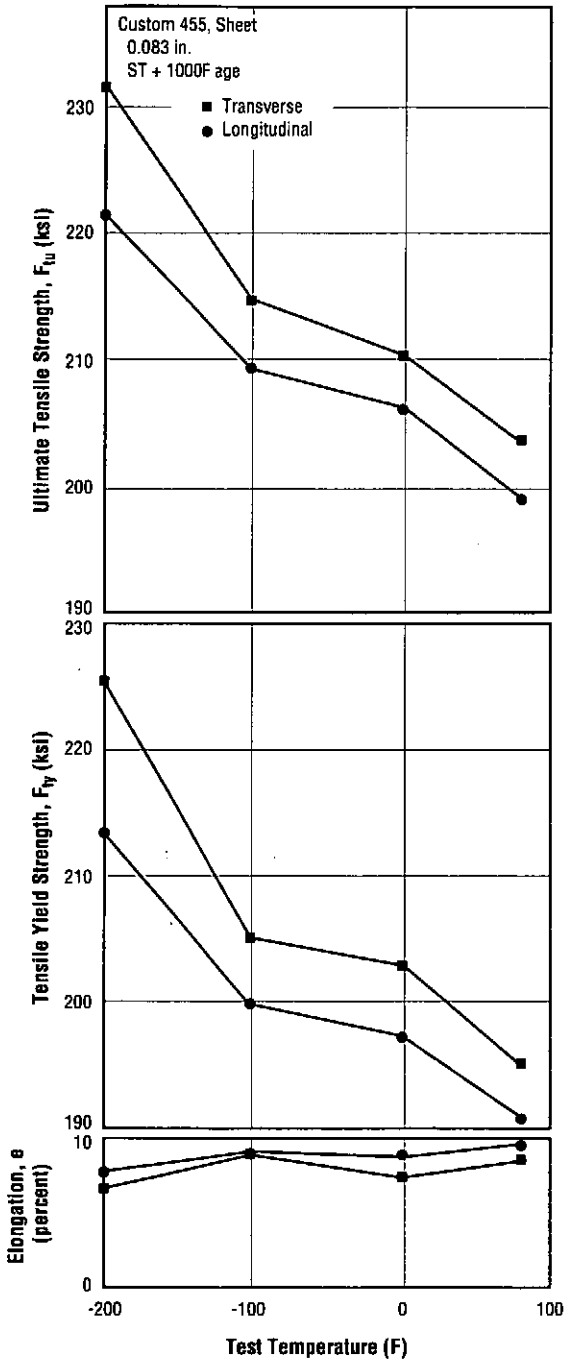


Figure 3.3.1.7 Effect of cryogenic test temperature on the tensile properties of sheet in the 1000F aged condition (Ref. 12)

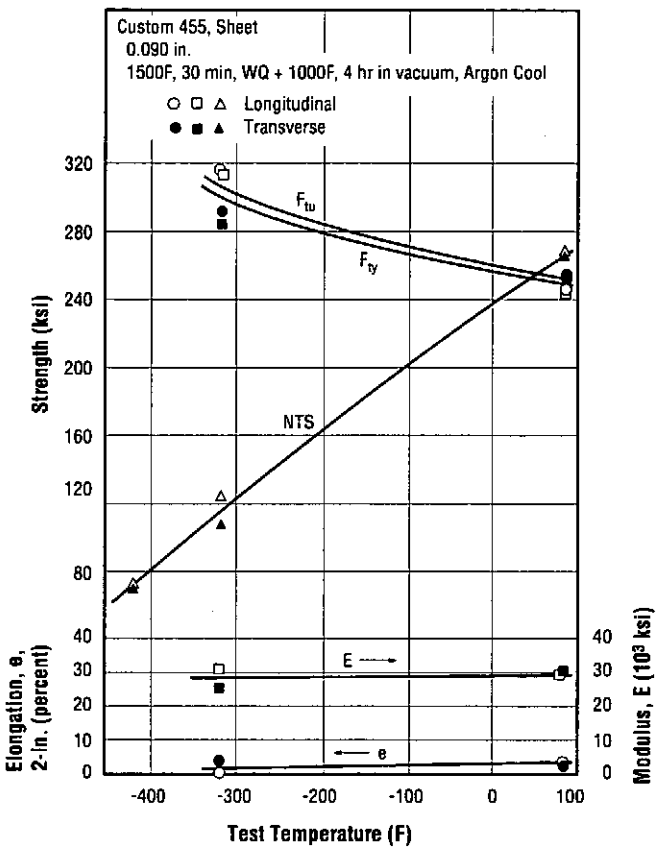


Figure 3.3.1.8 Smooth and mild-notch tensile properties at cryogenic temperatures for sheet aged at 1000F (Ref. 80)

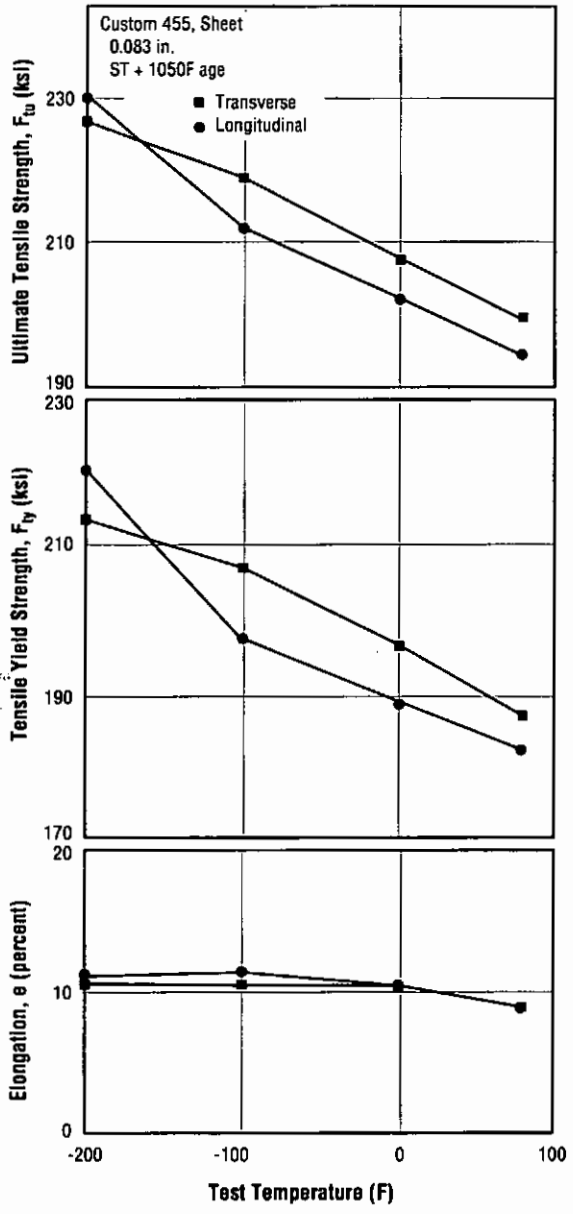


Figure 3.3.1.9 Effect of cryogenic test temperature on tensile properties of sheet in the 1050F aged condition (Ref. 12)

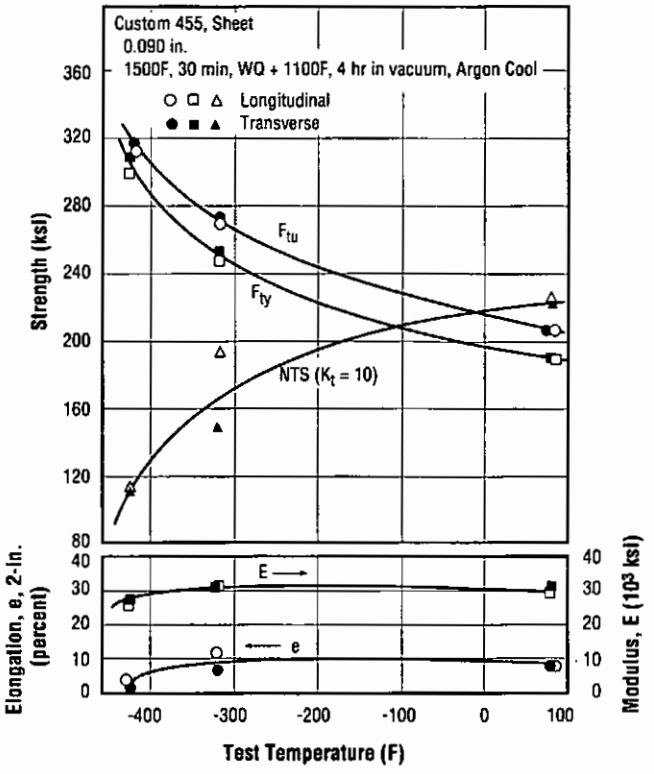


Figure 3.3.1.10 Smooth and sharp-notch tensile properties at cryogenic temperatures for sheet aged at 1100F (Ref. 80)

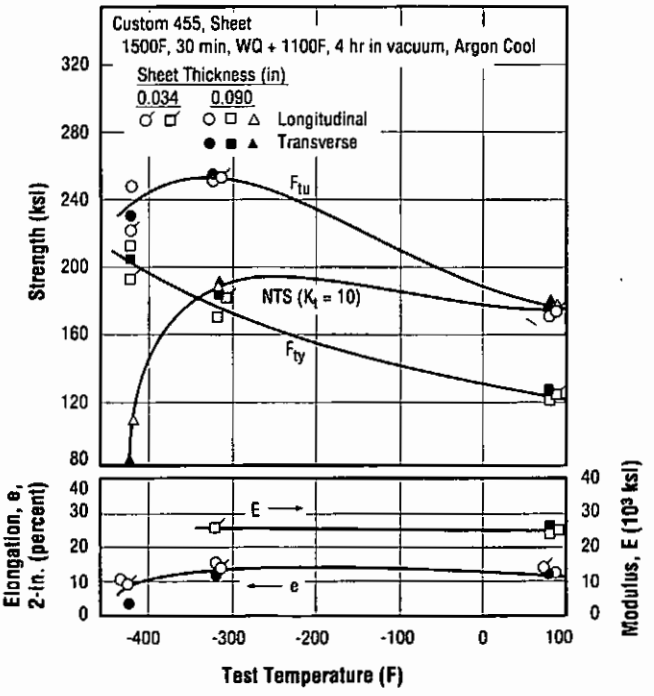


Figure 3.3.1.11 Smooth and sharp-notch tensile properties at cryogenic temperatures for sheet aged at 1150F (Ref. 80)

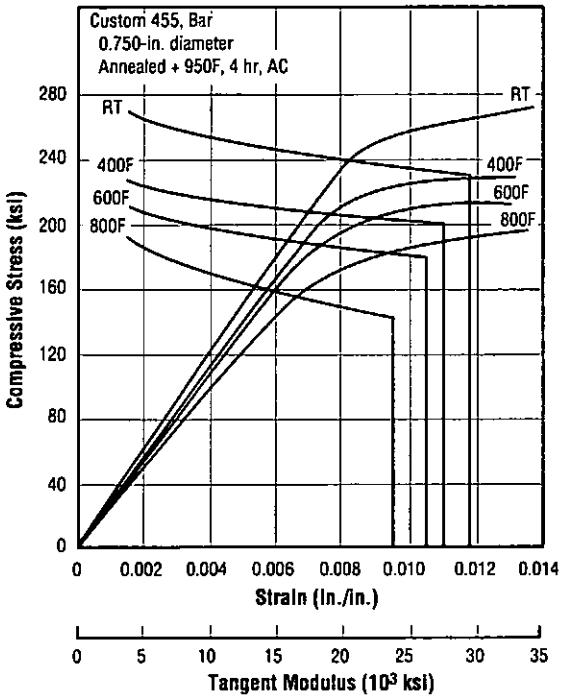


Figure 3.3.2.1 Typical compression stress-strain and tangent modulus curves for aged bar (Ref. 16)

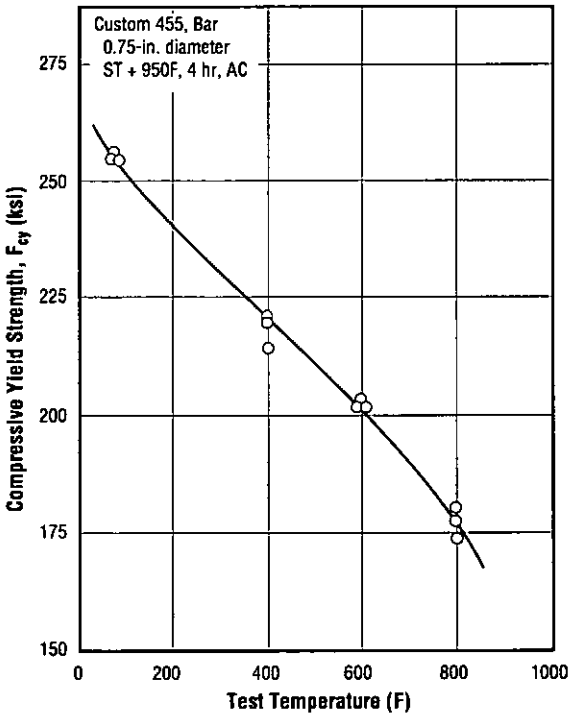


Figure 3.3.2.2 Effect of test temperature on compressive yield strength of bar aged at 950F (Ref. 16)

Table 3.3.3.1 - 70F Charpy-V impact energy for bar aged at 1050F (Ref. 47)

Alloy	Custom 455			
Form	2.5-in. Bar			
Condition	ST + 1050F, 4 hr, AC			
F_{tu} (ksi)	F_{ty} (ksi)	E (10^3 ksi)	Specimen Number	-70F IE Charpy-V (ft-lb)
199.3	186.7	32.6	1 2 3	5 4 4

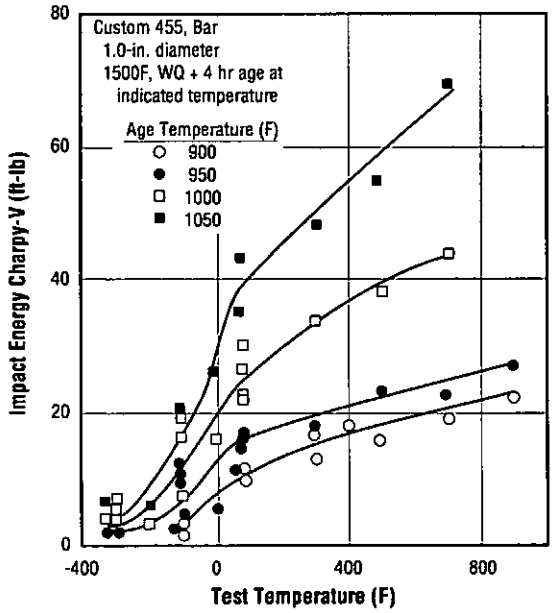


Figure 3.3.3.2 Effect of test temperature on impact energy of bar in the 900-1050F aged condition (Refs. 5, 12, 13)

Table 3.3.3.3 Charpy-V impact energy at cryogenic temperature for bar aged in 1000-1150F range (Ref. 80)

Alloy	Custom 455		
Form	13/16-in Diameter Bar		
Condition	1500F, 30 min, WQ + Age, 4 hr in Vacuum, Argon Cool		
Age Temperature (F)	Test Temperature (F)	IE Charpy-V[a] (ft-lb)	F_{ty}[b] (ksi)
1000	-80	19 20	243.7
	-320	2.5 3.0	317.1
1100	-80	43.5 45.0	189.8
	-320	6.5 8.0	247.4
1150	-80	64.0 66.8	121.0
	-320	15.5 16.0	176.8

[a] LT Orientation.

[b] Longitudinal yield strength of 0.090-inch sheet; see Figures 3.3.1.8, 3.3.1.10, and 3.3.1.11 for remainder of tensile properties.

Table 3.3.5.1 Effect of age temperature and test temperature on double restrained shear strength (Ref. 5)

Alloy	Custom 455		
Form	Annealed + Age, 4 hr, AC		
Age Temperature (F)	Test Temperature (F)	F_{tu} (ksi)	F_{su}[a] (ksi)
900	RT	248 - 256	142 - 152
950	-100	257 - 263	157 - 166
	RT	234 - 245	141 - 151
	400	202 - 214	122 - 129
	600	188 - 193	112 - 116
	800	168 - 172	102 - 105
1000	-100	222 - 235	139 - 149
	RT	201 - 214	127 - 133
	400	176 - 189	111 - 118
	600	164 - 172	100 - 107
	800	145 - 154	83 - 90

[a] Double restrained shear strength.

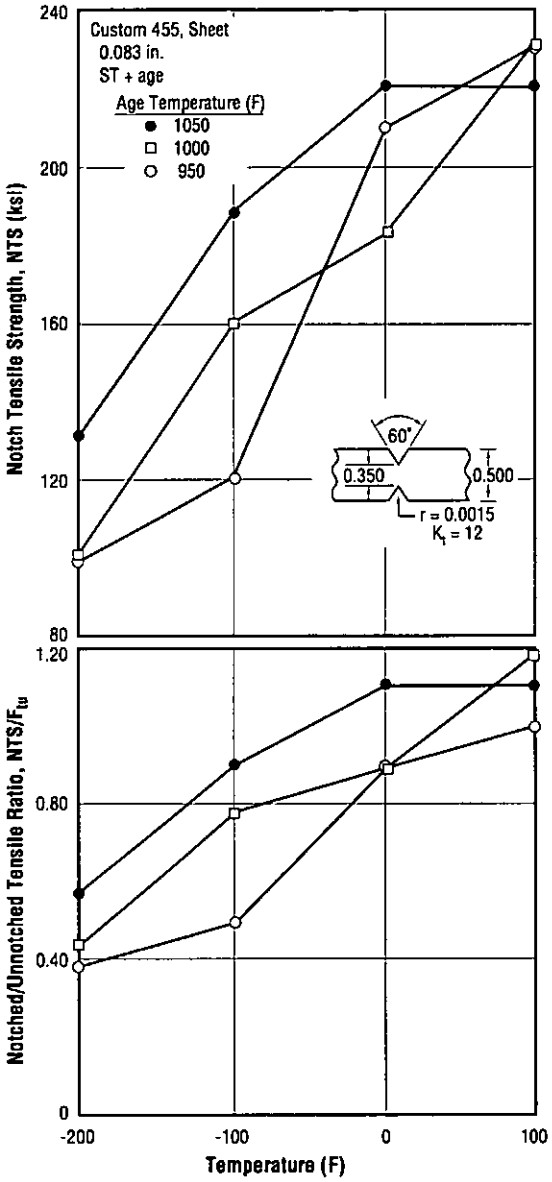


Figure 3.3.7.1.2 Effect of cryogenic test temperature on sharp-notch tensile strength and sharp-notch strength ratio of sheet in the longitudinal direction (Ref. 12)

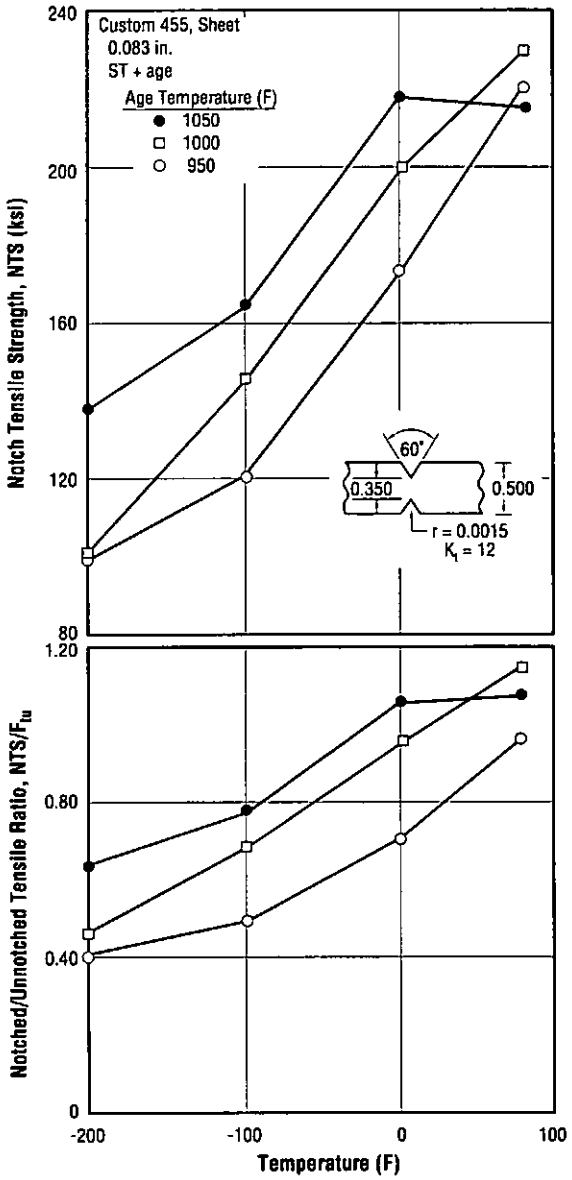


Figure 3.3.7.1.3 Effect of cryogenic test temperature on notch tensile strength of sheet in the transverse direction (Ref. 12)

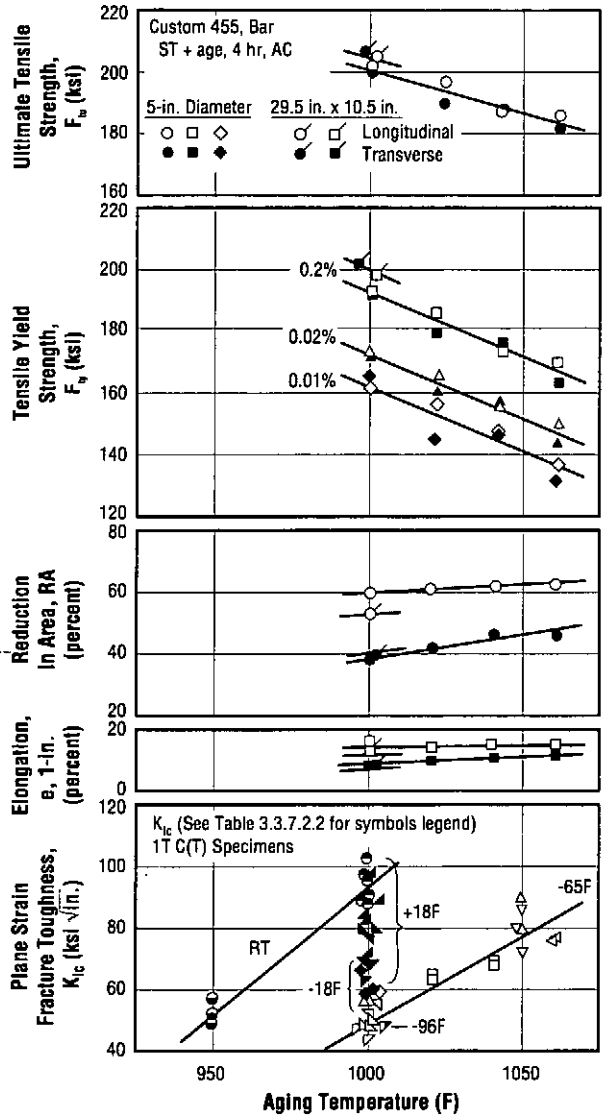


Figure 3.3.7.2.1 Effect of aging temperature on room temperature tensile properties and low temperature plane strain fracture toughness of bar in a variety of sizes and shapes from seven heats (Ref. 97)

Table 3.3.7.2.2 Symbols legend for Figure 3.3.7.2.1

Symbol	Heat Number	Bar Size (in. x in.)	Test Temperature (F)	Crack Plane Orientation
◒	85284	3.5 x 3.5	RT	LT
◓	96145	29.5 x 10.0	RT	LS
◢	88543	7.0 Diameter	+ 18	Unknown
◤	96145	29.5 x 10.0	+ 18	TL
◥	96145	29.5 x 10.0	+ 18	LS
◣	94189	5.0 Diameter	+18	LR
◆	88543	7.0 Diameter	- 18	Unknown
△	82125	3.0 Diameter	- 65	CR
◺	85137	8.75 x 4.75	- 65	TL
◇	94189	5.0 Diameter	- 65	LR
◹	96145	29.5 x 10.0	- 65	LS
◸	96145	29.5 x 10.0	- 65	TL
□	94189	5.0 Diameter	- 65	LR
△	82185	3.0 Diameter	- 65	CR
▽	86818	6.0 Diameter	- 65	CR
◁	94189	5.0 Diameter	- 65	LR
◸	94189	5.0 Diameter	- 96	LR

Table 3.3.7.2.3 Effect of quenched section size on -65F, LS orientation plane strain fracture toughness of forged block variously heat treated to a common strength level of approximately 200 ksi (Ref. 98)

Alloy		Custom 455	
Form		Forged Block	
Quenched Section Thickness (in.)	Heat Treatment	F_{tu} [a] (ksi)	K_{Ic} [b] (ksi $\sqrt{in.}$)
1.6	1525F, 30 min, OQ + 1525F, 2 hr, 10 min in furnace, OQ + 1000F, 8 hr, AC	198	68.8, 73.0, 61.8[c]
1.6	1525F, 30 min, OQ + 1525F, 2 hr, 10 min in furnace, OQ + 1000F, 5 hr, AC	204	55.8, 53.5, 50.0[c]
9 - 10	1525F, 30 min, OQ + 1000F, 5 hr, AC	203	45.5, 49.2, 47.8
9 - 10	1525F, 30 min, OQ + 980F, 12 hr, AC	201	47.8[c], 46.4[c]
9 - 10	1525F, 30 min, OQ + 980F, 4 hr, AC + 995F, 5 hr, AC	203	44.9[c], 47.1, 46.7
9 - 10	1525F, 30 min, OQ + 800F, 8 hr, AC + 1000F, 5 hr, AC	203	48.0, 46.0, 49.3

[a] Room temperature, longitudinal direction.

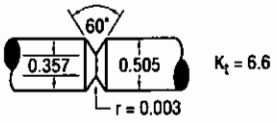
[b] -65F, LS crack plane orientation, 1T C(T) specimen.

[c] Not valid according to ASTM E 399.

Table 3.3.7.2.4 Room temperature, -65, and -110F smooth and mild-notch tensile strength and plane strain fracture toughness of forging (Ref. 99)

Alloy		Custom 455						
Form		Forging						
Condition		1525F, 3 hr, OQ + 1000F, 4 hr, AC						
Test Temperature (F)	Test Direction	F_{tu} (ksi)	F_{ty} (ksi)	e, 2-in. (percent)	RA (percent)	NTS[a] (ksi)	Crack Plane Orientation	K_{Ic}[b] (ksi $\sqrt{in.}$)
70	L	201.2	192.2	13.0	50.0	292.7	LT	95.1, 92.6 89.7
	T					298.3	TL	
	ST					261.7	LS	104.9, 93.2 96.2, 88.2
-65	L	212.2	203.0	12.2	44.6		LT	46.0, 50.7 46.4, 44.6 44.2, 45.7 49.2
	T	217.3	207.7	11.7	41.3		TL	47.7 47.0
	ST	212.5	205.5	7.0	15.5		LS	49.3, 48.1 44.1, 45.7 46.4, 44.0 51.3, 45.5
-110	L	217.0	207.5	11.5	44.0		LT	37.5, 42.5 38.0, 46.1 46.4
	T						TL	
	ST						LS	39.9, 43.0 44.7, 37.5 39.1, 38.6 38.1, 42.4

[a] Notched cylindrical specimen:



[b] CT specimen: RT tests, 1.0-inch thick, - 65F and - 110F tests, 0.5-inch thick.

Table 3.4.1 Plastic deformation in 100 and 1000 hours at 400-850F. (Refs. 14, 16)

Alloy	Custom 455		
Form	Bar		
Size	0.75-1.0-in. Diameter		
Condition	ST + 950F, 4 hr, AC		
Test Temperature (F)	400	600	850
Stress (ksi) for:			
0.2 percent plastic deformation in 100 hours	207	163	44
0.2 percent plastic deformation in 1000 hours	203	155	30

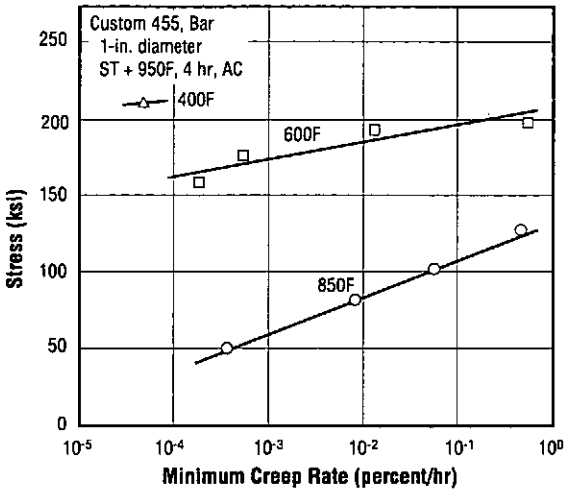


Figure 3.4.2 Minimum creep rate for bar at 400F, 600F, and 850F (Ref. 16)

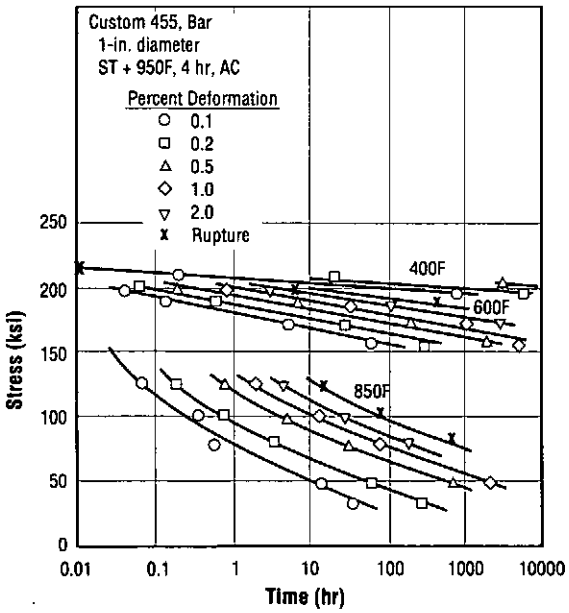


Figure 3.4.3 Stress-rupture and plastic deformation curves for bar at 400F, 600F, and 850F (Ref. 16)

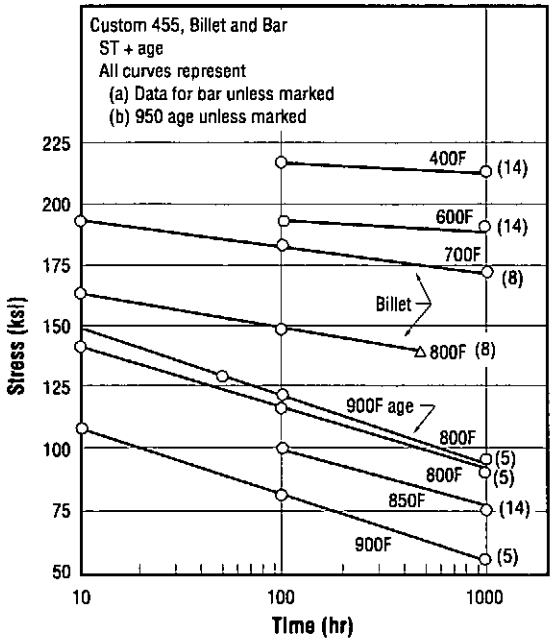


Figure 3.4.4 Creep rupture curves at 400-900F for billet and bar (Refs. 5, 8, 14)

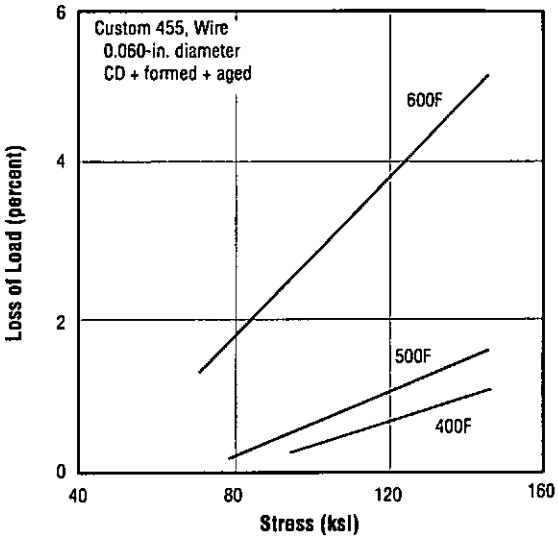


Figure 3.4.5 Loss of load in one hour at 400-600F during static loading of compression spring made from 0.060-inch wire (Ref. 5)

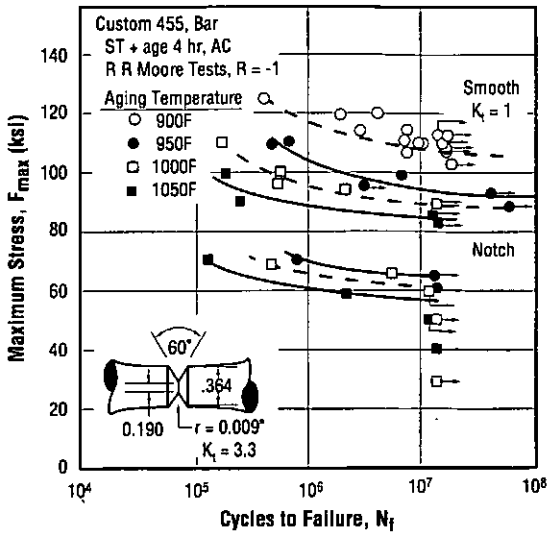


Figure 3.5.1.1 Effect of aging temperature on room temperature rotating beam smooth and mild-notch fatigue strength of bar (Refs. 5, 13)

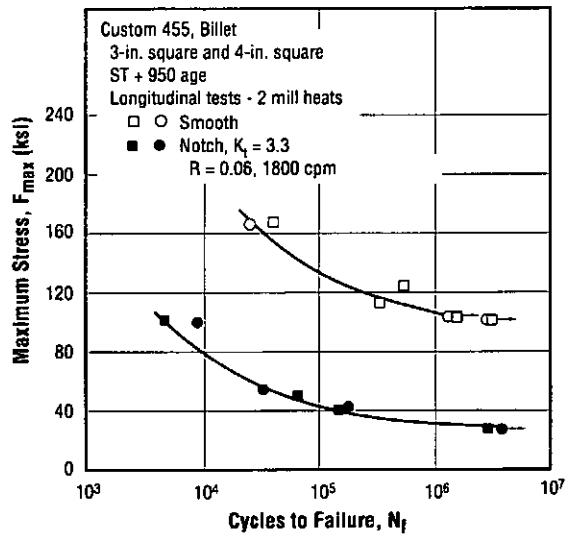


Figure 3.5.1.2 Room temperature axial-load smooth and mild-notch (K_t = 3.3) fatigue strength of billet aged at 950F (Ref. 8)

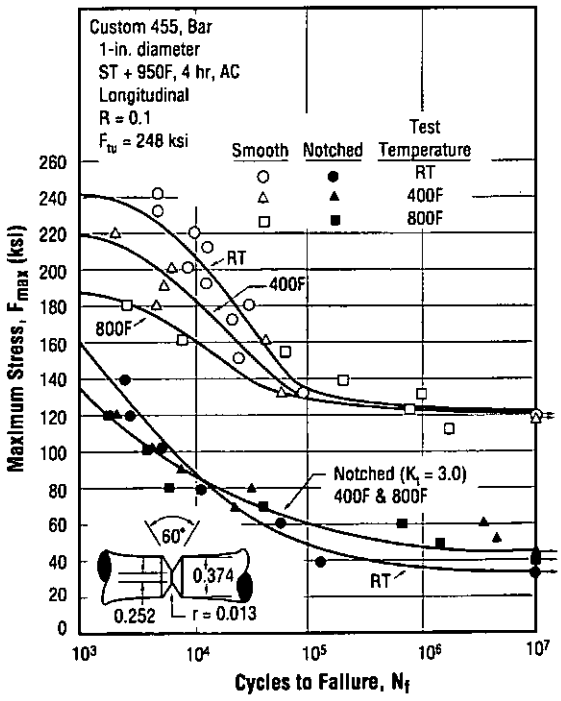


Figure 3.5.1.3 Room and elevated temperature axial-load smooth and mild-notch (K_t = 3.0) fatigue strength of bar aged at 950F (Ref. 16)

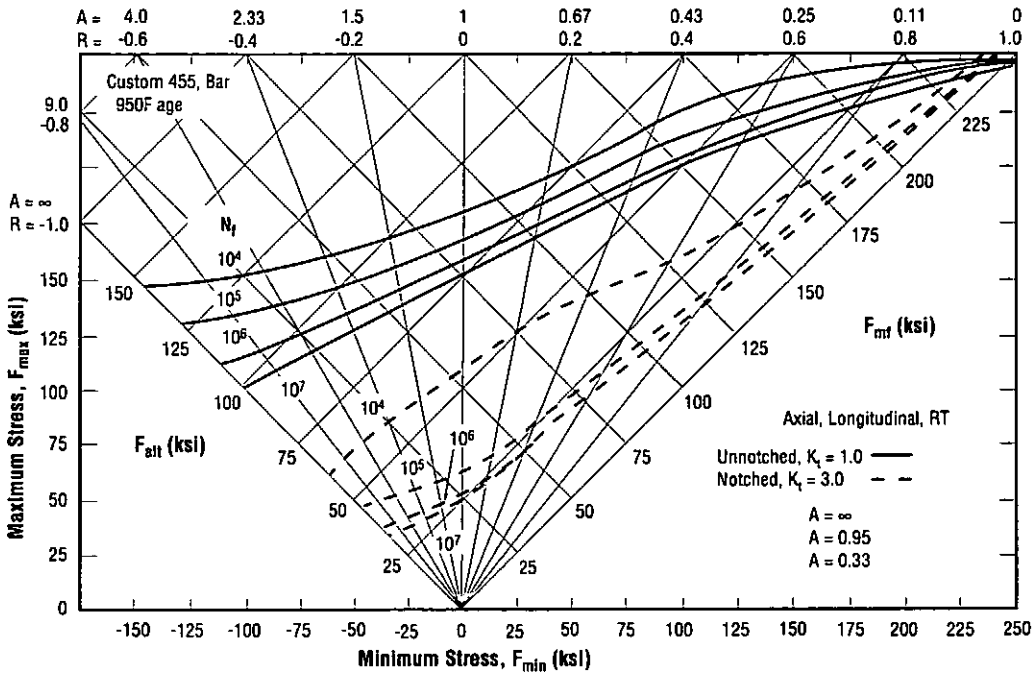


Figure 3.5.1.4 Typical axial-load smooth and mild-notch (K_t = 3.0) constant-life fatigue diagram for bar aged at 950F (Ref. 5)

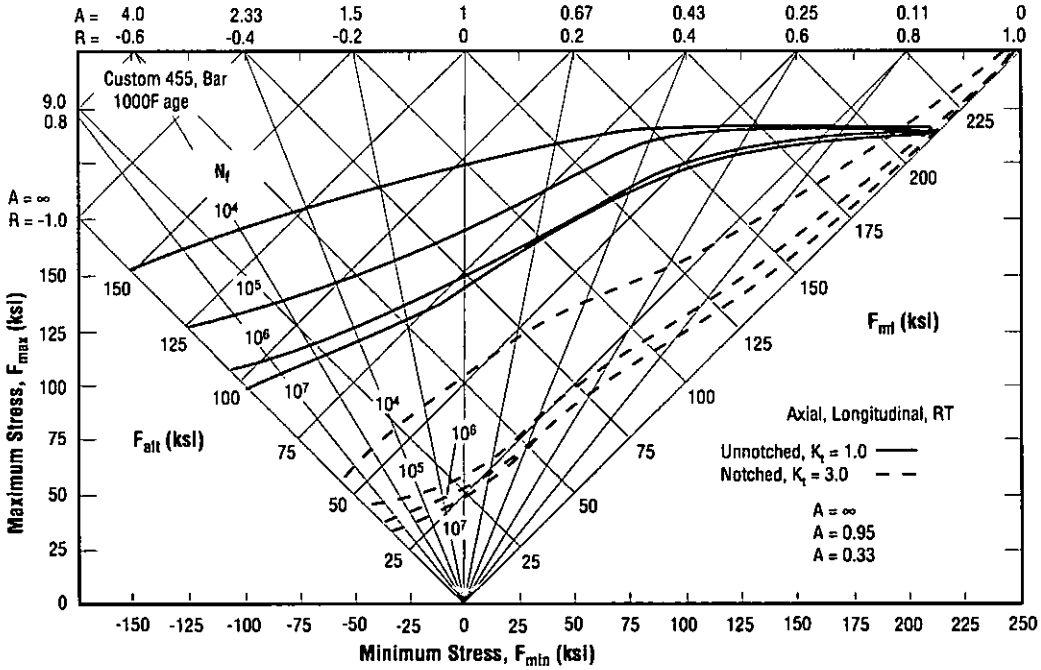


Figure 3.5.1.5 Typical axial-load smooth and mild-notch (K_t = 3.0) constant-life fatigue diagram for bar aged at 1000F (Ref. 5)

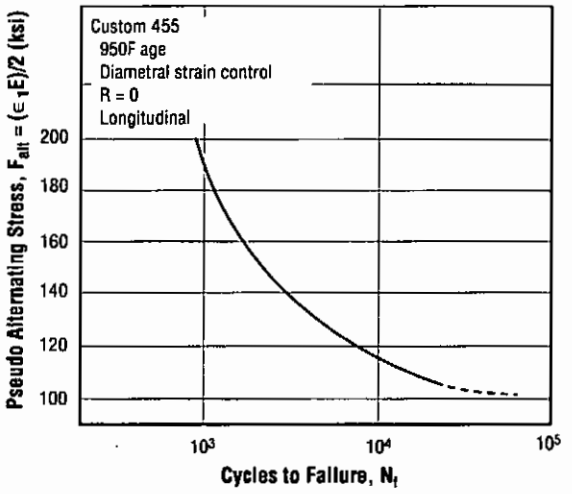


Figure 3.5.1.6 Room temperature diametral-strain-controlled low-cycle fatigue life (Ref. 5)

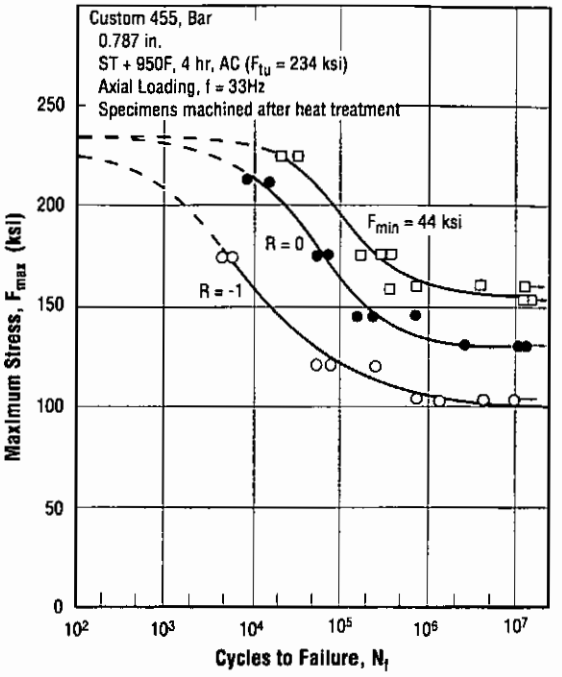


Figure 3.5.1.7 Axial-load smooth fatigue strength at several stress ratios for specimens machined from bar after 950F age treatment (Ref. 22)

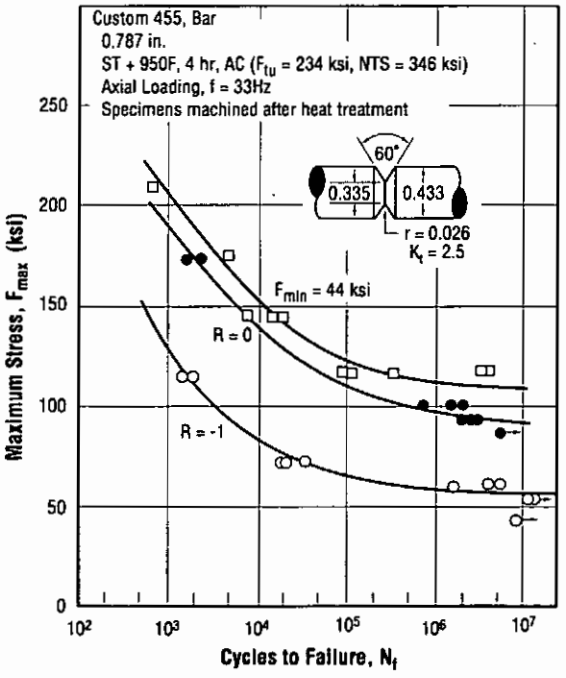


Figure 3.5.1.8 Axial-load mild-notch (K_t = 2.5) fatigue strength at several stress ratios for specimens machined from bar after 950F age treatment (Ref. 22)

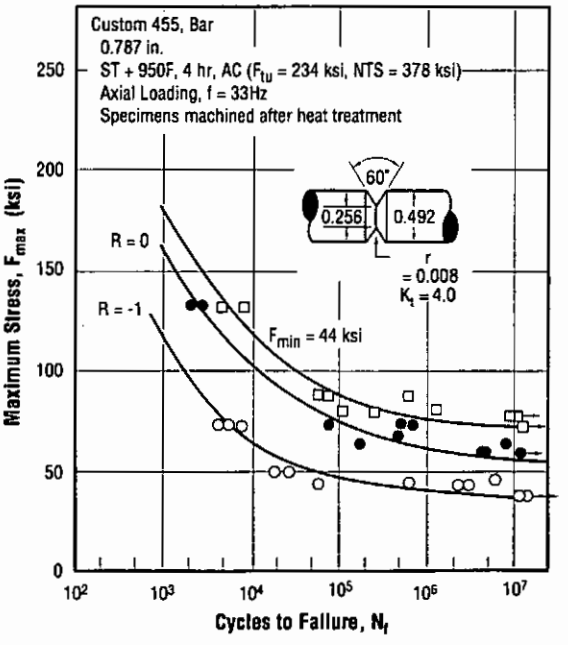


Figure 3.5.1.9 Axial-load mild-notch (K_t = 4.0) fatigue strength at several stress ratios for specimens machined from bar after 950F age treatment (Ref. 22)

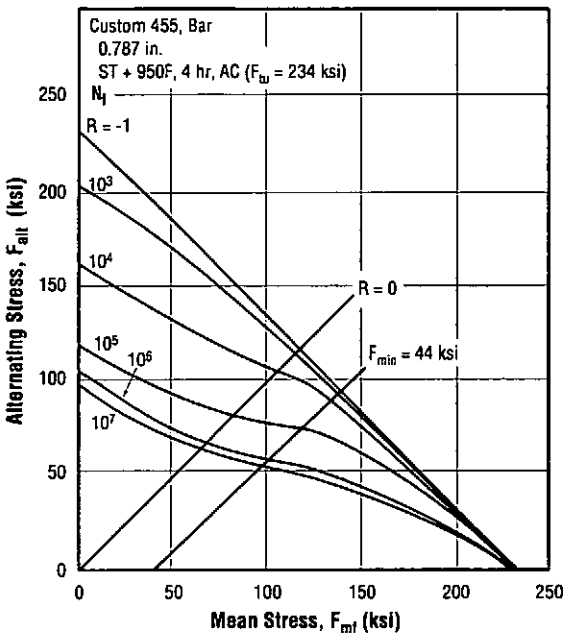


Figure 3.5.1.10 Haig diagram for axial-load smooth specimens machined from bar after 950F age treatment (Ref. 22)

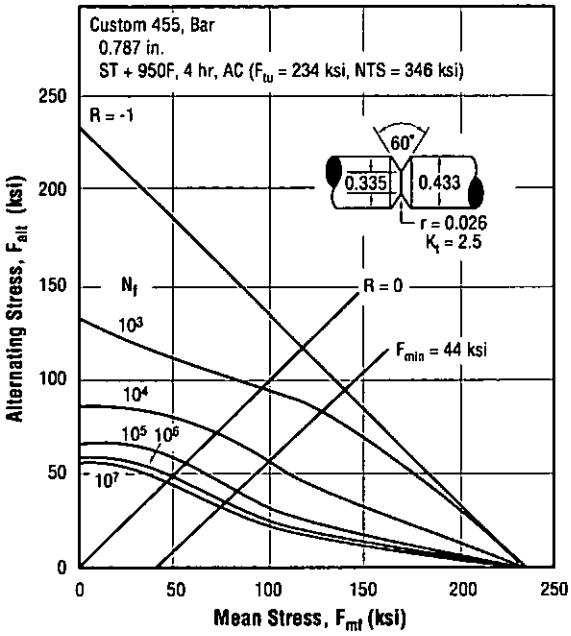


Figure 3.5.1.11 Haig diagram for axial-load mild-notch (K_t = 2.5) specimens machined from bar after 950F age treatment (Ref. 22)

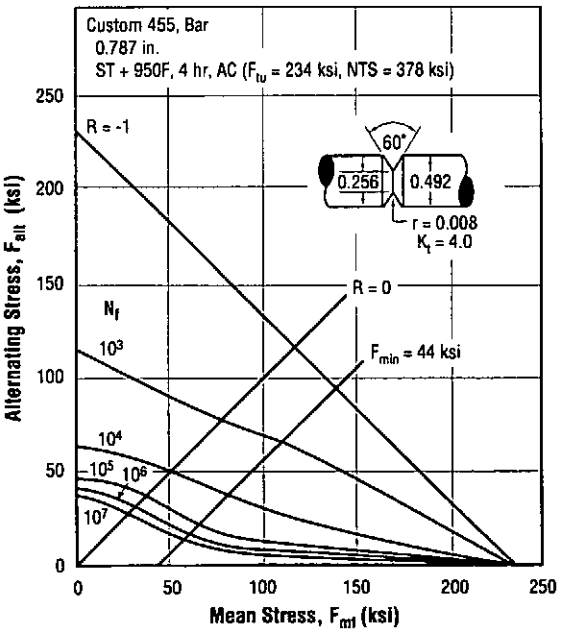


Figure 3.5.1.12 Haig diagram for axial-load mild-notch (K_t = 4.0) specimens machined from bar after 950F age treatment (Ref. 22)

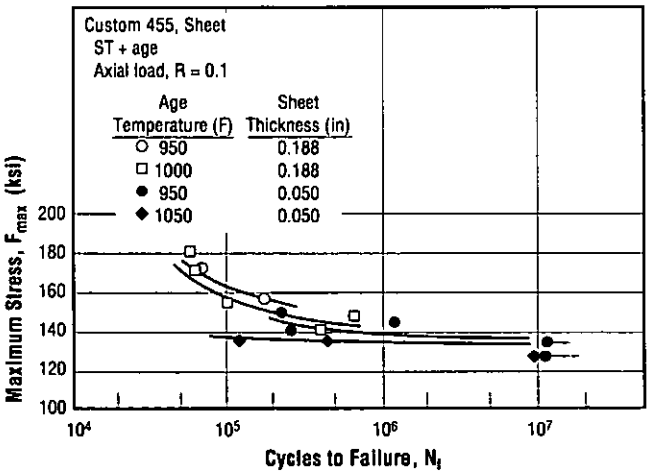


Figure 3.5.1.13 Room temperature axial-load fatigue strength of sheet (Ref. 56)

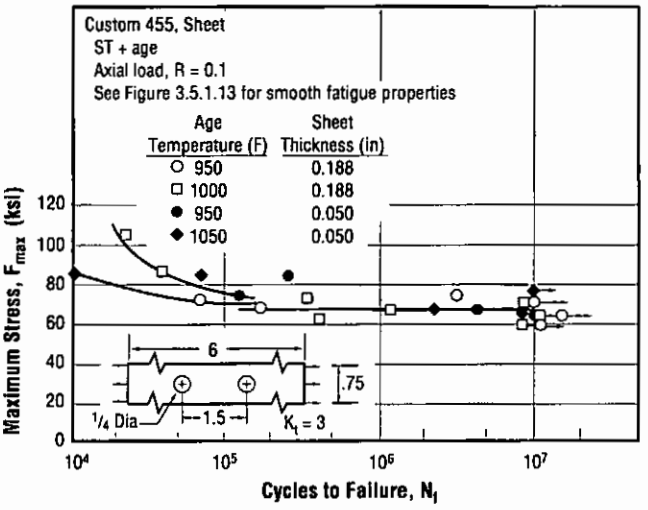


Figure 3.5.1.14 Room temperature axial-load fatigue strength of two-hole (K_t = 3.0) sheet specimens (Ref. 56)

Table 3.5.1.15 Room temperature axial tension fatigue strength of bolts (Ref. 49)

Alloy	Custom 455
Form	12-Point External Wrenching Bolt with MIL-S-8879 Thread
Condition	Forge + ST + 950F Age + Grind Shank and Thread Roll Diameters + Roll Threads and Head-To-Shank Fillet
F_{tu}[a] (ksi)	Cycles to Failure[b], N_f
240.1	500,000

[a] Based on basic pitch diameter.

[b] F_{max} = 99 ksi; R = 0.1. All failures in threads.

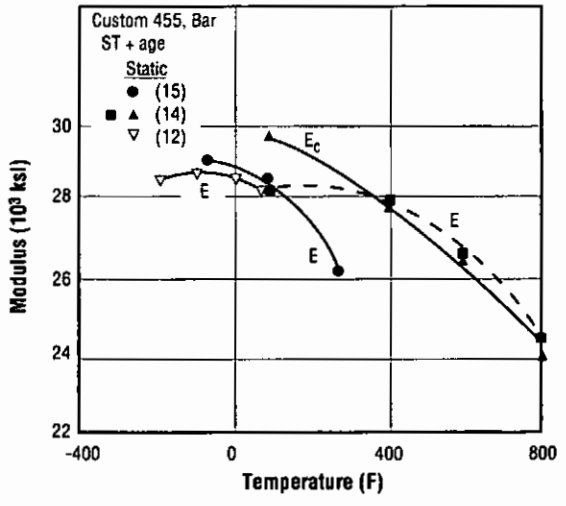


Figure 3.6.2.1 Modulus of elasticity in tension (E) and compression (E_c) at temperatures ranging from -200F to 800F (Refs. 12, 14, 15)

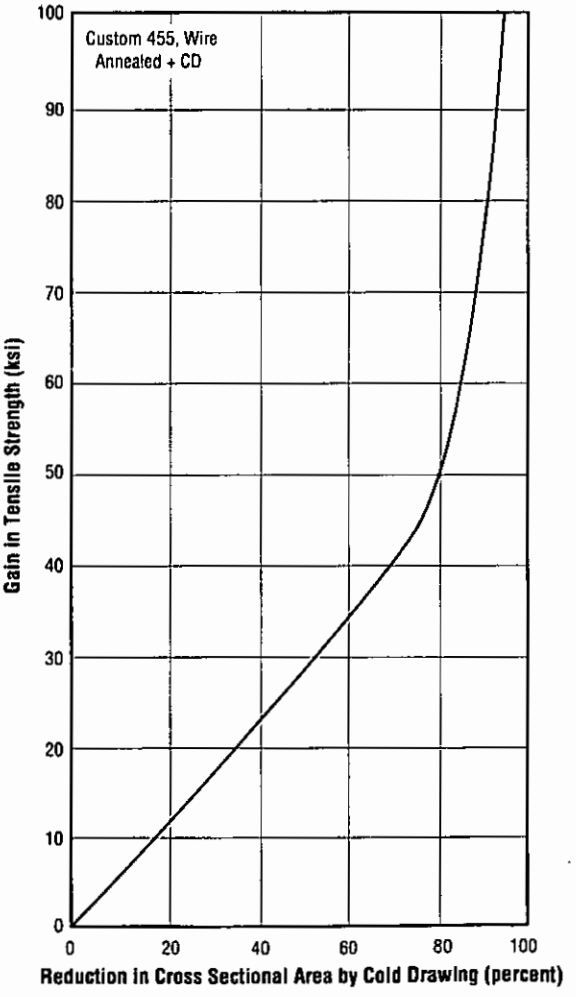


Figure 4.1.2.1 Effect of cold drawing in the annealed condition on tensile strength of wire (Ref. 5)

References

1. Aerospace Materials Specification, AMS 5578D, Society of Automotive Engineers (May 1995).
2. Aerospace Materials Specification, AMS 5617G, Society of Automotive Engineers (April 1990).
3. Aerospace Materials Specification, AMS 5672B, Society of Automotive Engineers (October 1987).
4. Aerospace Materials Specification, AMS 5860D, Society of Automotive Engineers (January 1992).
5. "Carpenter Custom 455 Stainless - High-Strength Stainless Steel," Carpenter Technology Corporation, Reading, PA (1971).
6. A.F. Hoenie and D.B. Roach, "New Developments in High-Strength Stainless Steels," DMIC Report 223, Battelle Memorial Institute, Columbus, OH (January 3, 1966).
7. M. Henthorne, "Stress-Corrosion Cracking of Martensitic, Precipitation-Hardening Stainless Steels," AGARD-CP-98, AGARD Conference Proceedings No. 98, Brussels, Belguim (October 5-6, 1971).
8. J.M. Uchida, "Evaluation of Carpenter Custom 455," Document No. D6-23928, Boeing Co., Commercial Airplane Division, Renton, WA (February 1970).
9. "Carpenter Custom 455 Technical Data," Carpenter Technology Corporation, Reading, PA (April 1969).
10. C.J. Slunder, A.F. Hoenie, and A.M. Hall, "Thermal and Mechanical Treatment for Precipitation-Hardening Stainless Steels," NASA SP-5089, AEC/NASA Technology Utilization Handbook prepared by Battelle Memorial Institute, Columbus, OH, for NASA Marshall Space Flight Center, Huntsville, AL.
11. N.B. Schmidt and M. Hentborne, "Precipitation-Hardening Stainless Steels - An Evaluation of Their Resistance to Stress-Corrosion Cracking," Carpenter Technology Corporation, Reading, PA (March 1973).
12. J.W. Montano, "A Mechanical Property and Stress Corrosion Evaluation of Custom 455 Stainless Steel Alloy," NASA TM X-64682, George C. Marshall Space Flight Center, Huntsville, AL (August 2, 1972).
13. N.B. Schmidt, private communication, unpublished data, Carpenter Technology Corporation, Reading, PA (January 8, 1974).
14. "Mechanical Property Data - Custom 455," prepared by Battelle Columbus Laboratories for Air Force Materials Laboratory, F33615-70-C-1070 (March, 1971).
15. N.B. Schmidt, unpublished data, Carpenter Technology Corporation, Reading, PA (May 1, 1972).
16. O.L. Deel and H. Mindlin, "Engineering Data on New Aerospace Structural Materials," Technical Report AFML-TR-71-249, Battelle Columbus Laboratories, Columbus, OH (December 1971)
17. G.J. Biefer, "Environmental Cracking Susceptibility of High Strength Steels," *Materials Protection* (November 1968).
18. E.A. Lauchner, "The Stress Corrosion Resistance of High Strength Steels for Bolting Applications," Nor-69-91, Northrop Corporation, Aircraft Division (July 16, 1969).
19. "New Maraging Alloy Upgrades Performance of Landing Gear Bolts," *Design Engineering* (September 1969).
20. C.S. Carter, D.G. Farwick, A.M. Ross, and J.M. Uchida, "Stress-Corrosion Properties of High-Strength Precipitation-Hardening Steels in 3.5% Aqueous Sodium Chloride Solution," D6-25219, Boeing Co., Commercial Airplane Group, Renton, WA (February 1970); *Corrosion*, Vol. 27, No. 5 (May 1971).
21. C.S. Carter, D.G. Farwick, A.M. Ross, and J.M. Uchida, "Stress Corrosion Properties of High Strength Precipitation Hardening Steels," *CORROSION*-NACE, Vol. 27, No. 5 (May 1971).
22. N. Larsson, "Fatigue Testing of Precipitating Steel 1745 (Custom 455) with Machining as the Final Process," Technical Note FFA HU—1965, The Aeronautical Research Institute of Sweden, Stockholm, Sweden (January 1979).
23. E. Turci, "Grabber Arm Mechanism for the Italian Research Interim Stage (IRIS)," 21st Aerospace Mechanisms Symposium, Houston, TX, (April 29 - May 1, 1987), NASA CP-2470 (1987).
24. T.S. Baker, "Effect of Ageing Temperature on the Mechanical and Stress Corrosion Properties of Carpenter Custom 455 Stainless Steels," Technical Memorandum Mat Str 1072, Royal Aircraft Establishment, England (November 1985).
25. E.A. Merrick, A. Rivers, J. Bickford, and T.U. Marston, "Prevention of Bolting Degradation or Failure in Pressure Boundary and Support Applications," *International Journal of Pressure Vessels and Piping*, Vol. 25, No. 1-4 (1986).
26. S.Y. Widge, "A Study of the Effects of Varying Solution Treatment on the Toughness of a Stainless Maraging Alloy," PhD Dissertation, Lehigh University (December 1984), Diss. Abstr. Int. Vol. 46, No. 3 (September 1985).
27. D.L. Wirth, "Laser Welding of Thermally Sensitive Alloys," *Lasers and Applications*, Vol. 4, No. 3 (March 1985).

28. M. Katcher, B. Schneier, and F.K. Lampson, "Galvanic Crevice Corrosion of Custom 455 Alloy in an Oxidizer and Salt Water Environment," International Symposium for Testing and Failure Analysis, Los Angeles, CA, October 27-29, 1980, published by International Society for Testing and Failure Analysis, ATFA, Inc., Lawndale, CA (1980).

29. E. Vallerani, P. Marchese, and G. Banino, "Fracture Mechanics and Fatigue Criteria in Material Selection for Space Applications," AGARD (NATO) CP-327, Aeritalia, Space Sector, Torino, Italy (March 1983).

30. A.W. Birks, and C.G. Ludlow, "Autofrettage Characteristics for High-Strength Alloy and Maraging Steels," High-Pressure Engineering and Technology for Pressure Vessels and Piping Systems, Orlando, FL, June 27 - July 2, 1982, published by American Society of Mechanical Engineers, New York, NY (1982).

31. L.P. Myers, "PH Martensitics to the Rescue - Modern Stainless Steels Provide a Wide Choice of Properties to Answer 'Distress Calls'," *Materials Engineering*, Vol. 94, No. 3 (September 1981).

32. R.S. Brown, "Welding the Specialty Stainless Steels," *Welding Design and Fabrication*, Vol. 51, No. 11 (November 1978).

33. J.E. Truman, "Stainless Steels - A Survey, Part 2: Special Grades," *The Metallurgist and Materials Technologist*, Vol. 12, No. 2 (February 1980).

34. S.W. Frost and K.T. Kamber, "Coil Spring Failures in Aerospace Hardware," *Metal Progress*, Vol. 115, No. 3 (March 1979).

35. G.E. Kerns, M.T. Wang, and R.W. Staehle, "Stress Corrosion Cracking and Hydrogen Embrittlement of Iron Base Alloys," Stress Corrosion Cracking and Hydrogen Embrittlement of Iron Base Alloys, Unieux-Firminy, France, June 12-16, 1973, published by National Association of Corrosion Engineers, Houston, TX (1977).

36. J. Koutsky and V. Pechman, "Maraging Steels - New Materials for Highly Stressed Parts of Steam Turbines," *Strojirenstvi*, Vol. 27, No. 11, (Czech) (November 1977).

37. K.H. Miska, "Precipitation Hardenable Steels Combine High Strength With Corrosion Resistance," *Materials Engineering*, Vol. 86, No. 7 (December 1977).

38. "Five PH Steels," *Manufacturing Engineering*, Vol. 79, No. 4 (October 1977).

39. G.R. Smoluk, "Stainless Alloy Cuts Cost of Aneroid Bellows," *Design News*, Vol. 33, No. 7 (April 4, 1977).

40. E. Taylor, "Stress Corrosion Cracking Evaluation of Aerospace Bolting Alloys," Stress Corrosion - New Approaches, 78th ASTM Annual Meeting, Montreal, Canada, June 22-27, 1975, published in ASTM STP 610, American Society for Testing and Materials, Philadelphia, PA (1976).

41. M.G. Fontana and R.W. Staehle, "Stress-Corrosion Cracking of Metallic Materials," AFML-TR-72-102, The Ohio State University Research Foundation, Columbus, OH (April 1975).

42. O.A. Bannykh and Y.K. Kovneristyi, "High-Strength Steels," Itogi Nauk. Tekh. Metalloved. Term, Ovrab., Vol. 10, (Russian) (1976).

43. J.B. Hughes and E.L. Hayman, "Inertia Welding Halves Torsion Tube Replacement Cost," *Metal Progress/West*, Vol. 2, No. 1 (March 1976).

44. R.S. Hodder, "Progress in Maraging Steels," *Industrial Heating*, Vol. 41, No. 5 (May 1974).

45. E. Taylor, "Compatible Coatings for Corrosion Resistant Aerospace Fasteners," Corrosion/73, National Association of Corrosion Engineers, Anaheim, CA, March 19-23, 1973, published in *Materials Performance*, Vol. 13, No. 2 (February 1974).

46. M. Kaneo and Y. Kawabe, "Current Super-High Tensile Steels and Their Fracture Toughness," *Bulletin Japan Institute of Metals*, Vol. 12, No. 5 (Japanese) (May 1973).

47. P.W. Rice, R.A. Beverly, C.E. Ivey, and B.R. Keeney, "New Alloys for Oil and Gas Hydrogen Sulfide Service," *Materials Protection and Performance*, Vol. 12, No. 10 (October 1973).

48. "Carpenter Custom 455," *Alloy Digest* (April 1967).

49. S. Patel and E. Taylor, "New High-Strength Fastener Materials Resist Corrosion," *Metal Progress*, Vol. 100, No. 3 (September 1971).

50. B.P. Zelus and P.M. Rush, "Survey of Fastener Technology," *Metals Engineering Quarterly*, Vol. 10, No. 3 (August 1970).

51. E.A. Merrick, P.V. Guthrie, J.R. Haueter, and M.N. Bressler, "High Strength Bolt Failure Analysis and Integrity Assessment-Lessons Learned," International Symposium on Contribution of Materials Investigation to the Resolution of Problems Encountered in PWR Plants, Fontevraud Chinon, France, September 3-5, 1985, published by Societe Francais d'Energie Nucleaire, 48 rue de la Procession, 75724 Paris Cedex, France (September 1985).

52. P.R. Burke and P.A. Coronato, "Evaluation of a Double Gimbal IPACS Design," NASA CR 178040, Allied Signal Bendix Aerospace, Teterboro, NJ, for NASA Langley Research Center (May 1986).

53. A. Goldberg and M.C. Juhas, "Lower-Bound K_{Iscc} Values for Bolting Materials: A Literature Study," Report No. NUREG/CR-2467 UCRL-53035, Lawrence Livermore National Laboratory, Livermore, CA (February 1982).

54. J.N. Howell, "Mechanical Fasteners for High Temperature Structure," National SAMPE Technical Conference, Seattle, WA (September 9-11, 1969).

55. D.E. Strohecker, A.F. Gerds, and F.W. Boulger, "Deformation Processing of Precipitation-Hardening Stainless Steels," NASA SP-5088, AEC-NASA Technology Utilization Handbook prepared by Battelle Memorial Institute, Columbus, OH, for NASA Marshall Space Flight Center, Huntsville, AL (May 1970).

56. G.D. Deveaux, "Static Tensile and Axial Fatigue Materials Properties Test of Custom 455 Maraging Steels," Hughes Tool Company Aircraft Division, Culver City, CA, Report 385-T-21 (October 14, 1966).

57. "Qualification of BACB30NH2OU-95 Bolt, 12-Point 220 Ksi Min. Tensile Custom 455 Material," Valley Todeco, Inc., Sylmar, CA, Report VT 1067 (October 1970).

58. "Qualification of BACB30NH14U-44 Bolt, 12-Point 220 Ksi Min. Tensile Custom 455 Material," Valley Todeco, Inc., Sylmar, CA, Report VT 1066 (1970).

59. B.P. Zelus and P.M. Rush, "High Strength Stainless Steel Fasteners," 1969 Westec Conference, Los Angeles, CA (March 10-13, 1969).

60. J.L. Everhart, "Specialty Stainless Steels," *Materials Engineering*, Vol. 74, No. 5 (October 1971).

61. J.K. Stanley, "The Current Situation on the Stress Corrosion Cracking and Hydrogen Embrittlement of High Strength Fasteners," AIAA/ASME/SAE 13th Structures, Structural Dynamics, and Materials Conference, San Antonio, TX, Report AIAA-72-385 (April 10-12, 1972).

62. J.K. Stanley, "Stress Corrosion Cracking and Hydrogen Embrittlement of High-Strength Fasteners," Air Force Report No. SAMSO-TR-73-131, Systems Engineering Operations, The Aerospace Corporation, El Segundo, CA (April 30, 1973).

63. C.E. Carlson, "Mechanical Properties of Custom 455 Steel (AMS 5617)," Hamilton Standard, Windsor Locks, CT (March 1972).

64. D. Kramer, K.R. Garr, A.G. Pard, and C.G. Rhodes, "A Survey of Helium Embrittlement of Various Alloy Types," Atomics International, North American International, Canoga Park, CA (December 8, 1972).

65. J.F. Rynewicz, "Evaluation of Paint Coatings Tested in the Deep Atlantic and Pacific Oceans," ASTM STP 558, Corrosion in Natural Environments: Proceedings of Three Symposia Presented at the Seventy-Sixth Annual Meeting, American Society for Testing and Materials, Philadelphia, PA, June 24-29, 1973 (August 1974).

66. J.W. Macedo, "Low Temperature Impact Strength of Welded Custom 455," (AMS 5617), Martin Marietta Aerospace, Orlando, FL (May 24, 1978).

67. A.C. Tribley, "Patriot Canister Restraint Pin Pendulum Shock Tests," Martin Marietta Aerospace, Orlando, FL (May 19, 1978).

68. A.C. Tribley, "Canister Restraint Pin Failure Analysis," Martin Marietta Aerospace, Orlando, FL (April 17, 1978).

69. D.S. Crowther, "Restraint Pins — Failures During Minus 50F Rail Hump Tests at Huntsville 11 Jan 78 — Metallurgical Evaluation," Martin Marietta Aerospace, Orlando, FL (February 14, 1978).

70. D.S. Crowther, "Restraint Pin: Welded and Aged. MMCO Confirmatory Tests at Minus 50F — Metallurgical Evaluation," Martin Marietta Aerospace, Orlando, FL (March 23, 1978).

71. D.S. Crowther, "Restraint Pins — MMCO Tests: Room Temperature (Post Weld Aged Only) and at Minus 57F (Post Weld Solution Annealed and Aged)," Martin Marietta Aerospace, Orlando, FL (April 17, 1978).

72. O. Deel, "Collected Engineering Data Sheets (Air Force Data Sheet Program)," AFML TR-78-179, Battelle Columbus Labs, OH (December 1978).

[Regarding Ref #72, supporting data for the individual data sheets are contained in one of the following: AFML-TR-67-418, AFML-TR-68-211, AFML-TR-70-252, AFML-TR-71-249, AFML-TR-72-196, Volumes I and II, AFML-TR-73-114, AFML-TR-75-97, or AFML-TR-77-198.]

73. C.R. Weymueller, "The PH Stainless — Simple to Weld but Touchy," *Welding Design and Fabrication*, Vol. 53, No. 5 (May, 1980).

74. N.B. Schmidt, "Mechanical Property Data — Carpenter Custom 455," Carpenter Technology Corporation, Reading, PA, perconal communication to J. Wolf, Mechanical Properties Data Center, Traverse City, MI (May 1, 1972).

75. J.E. Truman, "Stress-Corrosion Cracking of Martensitic and Ferritic Stainless Steels," *International Metals Reviews*, Vol. 26, No. 6 (1981).

76. R.S. Brown, "The Three-Way Tradeoff in Stainless-Steel Selection," *Materials Engineering*, Vol. 96, No. 5 (November 1982).

77. H.M. Ledbetter, "Physical Properties Data Compilations Relevant to Energy Storage. V: Mechanical Properties Data on Alloys for Use in Flywheels," Technical Report NSRDS-NBS 61, Part V, PB82-232919, National Bureau of Standards, Boulder, CO (January 1982).

78. J.E. Campbell, "Fracture Properties of Wrought Stainless Steels," *Application of Fracture Mechanics for Selection of Metallic Structural Materials*, Chapter 5, American Society for Metals, Metals Park, OH (1982).

79. E. Hultgren, "Current Requirements on Specifications for Corrosion Prevention," SAAB-Scania AB, Linkoeping, Sweden, from Proceedings of Workshop on Requirements for Aircraft Corrosion Control, London, England (April 10-15, 1983).

80. J.W. Montano, "Low Temperature Mechanical Properties and Ambient Temperature Stress Corrosion Properties of Custom 455 Stainless Steel Alloy," NASA TM X-53665, NASA George C. Marshall Space Flight Center, Huntsville, AL (October 20, 1967).

81. T.S. Humphries and E.E. Nelson, "Stress Corrosion Cracking Evaluation of Martensitic Precepitation Hardening Stainless Steels," NASA TM-78257, NASA George C. Marshall Space Flight Center, Huntsville, AL (January 1980).

82. Military Standard MIL-STD-1568B (USAF), "Materials and Processes for Corrosion Prevention and Control in Aerospace Weapons Systems" (October 12, 1994).

83. Military Specification MIL-S-83311 (USAF), Steel Bar, and Wire, (455) Corrosion Resistant, Precepitation Hardening (Issued February 11, 1971; Validated July 30, 1987; Deactivated February 10, 1993).

84. ASTM A 313/A 313M - 95, Standard Specification for Stainless Steel Spring Wire, 1995 Annual Book of ASTM Standards, Vol. 01.03: Steel-Plate, Sheet, Strip, Wire, American Society for Testing and Materials, Philadelphia, PA (March 1995).

85. ASTM A 564/A 564M - 95, Standard Specification for Hot-Rolled and Cold-Finished Age-Hardening Stainless Steel Bars and Shapes, 1995 Annual Book of ASTM Standards, Vol. 01.05: Steel-Bars, Forgings, Bearing, Chain, Springs, American Society for Testing and Materials, Philadelphia, PA (March 1995).

86. ASTM A 693 - 93, Standard Specification for Precipitation-Hardening Stainless and Heat-Resisting Steel Plate, Sheet, and Strip, 1995 Annual Book of ASTM Standards, Vol. 01.03: Steel-Plate, Sheet, Strip, Wire, American Society for Testing and Materials, Philadelphia, PA (September 1993).

87. ASTM A 705/A 705M - 93, Standard Specification for Age-Hardening Stainless Steel Forgings, 1995 Annual Book of ASTM Standards, Vol. 01.05: Steel-Bars, Forgings, Bearing, Chain, Springs, American Society for Testing and Materials, Philadelphia, PA (March 1995).

88. "Carpenter Precipitation Hardening Stainless Steels," Carpenter Technology, Carpenter Steel Division (1986).

89. M. Balbi, "The Welding of Stainless Steels, XV - Weldability of Precipitation Hardening Steels," Polytechnic of Milan, Acciaio Inossid, Vol. 3 (July 24 - September 29, 1988).

90. F.W. McMaan and G.N. Manair, "Stainless Steel - Upgrading the Quality of Today's Cars," *Automotive Engineering*, Vol. 96, No. 5 (May 1988).

91. G.E. Kerns, M.T. Wang, and R.W. Staehle, "Stress Corrosion Cracking and Hydrogen Embrittlement in High Strength Steels," Conference on Stress Corrosion Cracking and Hydrogen Embrittlement of Iron Base Alloys, Unieux-Firminy, France, June 12-16, 1973, published by National Association of Corrosion Engineers, Houston, TX (1977).

92. C.W. Marschall and A.M. Hall, "Thermal and Mechanical Treatment for Precipitation-Hardening Stainless Steel," NASA Special Report, prepared by Battelle Memorial Institute, Columbus, OH (April, 1970).

93. *Metals & Alloys in the Unified Numbering System*, Sixth Edition, Jointly Published by the Society of Automotive Engineers, Inc. (as SAE HS-1086 FEB93) and the American Society for Testing and Materials (as ASTM DS-56 E).

94. Military Standard MIL-STD-1312-9B (October 19, 1984).

95. Military Standard MIL-STD-1312-9A (October 19, 1984).

96. "Design Criteria for Controlling Stress Corrosion Cracking," MSFC-SPEC-522A, NASA George C. Marshall Space Flight Center, Huntsville, AL (November 18, 1977).

97. Michael L. Shor, private communication, Carpenter Technology Corporation, Carpenter Steel Division, Reading, PA (February 28, 1986).

98. "Custom 455 Material Properties Optimization," Report on Special Study P&LS 86-004, Boeing Aerospace Company on Air Force Space Division (AFSC) Inertial Upper Stage (IUS) Program Contract F04701-85-C-0101 (April 8, 1987).

99. H.G. Lenhart, "IUS ECP 2256 Materials Tests," Boeing Aerospace Company Structural Components and Materials Laboratory Test Progress Report TRP-2-5611-0-88-002 (January 26, 1988).

100. J.I. Kim and J.W. Morris, "On the Scavenging Effect of Precipitated Austenite in a Low Carbon Fe-5.5Ni Alloy," *Metallurgical Transactions A*, Vol. 11A, pp. 1401-1406 (1980).

101. B. Francis, "Increasing the Fracture Toughness of a Maraging Steel Type Alloy," *Metallurgical Transactions A*, Vol. 7A, pp. 465-486 (March 1976).

102. S. Widge, Unpublished work, 1978.

103. C.S. Carter, D.G. Farwich, A.M. Ross, and J.M. Uchida, *Corrosion*, Vol. 27, pp. 190-195 (May 1971).

104. B.F. Brown, "ARPA Coupling Program on Stress-Corrosion Cracking - Final Technical Report 7130," Navel Research Laboratories, Washington, D.C. (June 16, 1970).

105. ALLOY DATA, Custom 455 Stainless, Carpenter Technology Corporation (July 1993).

106. Private communication with Bruce Weller and James Dahl, Carpenter Technology Corporation (February 1, 1996).

	Fe
0.46	C
1.0	Cr
1.0	Mo
0.55	Ni

D6A
D6AC

GENERAL

D6AC is a quench-hardenable medium carbon low alloy steel. It is very similar to other popular grades such as Types 4340 and 4140, but has higher molybdenum content. The higher molybdenum content improves its hardenability, which is superior to that of 4340 steel. Tensile strength can be varied from about 90 to 300 ksi by changing the tempering temperature. Fracture toughness tends to decrease with increasing tensile strength but can also vary considerably at a given value of tensile strength. Fracture toughness has been found to be highly dependent on the quenching rate from the austenitizing or ausbay temperature. A high quench rate is required for high fracture toughness.

D6AC is susceptible to stress-corrosion cracking and to corrosion fatigue in moist and in aqueous environments, especially when tempered to high strength levels. The susceptibility is comparable to that of 300 M steels heat treated to similar strength levels. Weldability is good using the GTA process if proper procedures are followed. Although originally developed for hot die applications, D6AC is currently used extensively in aerospace applications requiring yield strength in the 215 ksi range combined with good fracture toughness. These applications include high performance aircraft structures, such as carry-through support structures, and the space shuttle solid rocket booster casings.

1.01 **Commercial Designations**
D6A (air melt), D6AC (consumable electrode vacuum melt).

1.02 **Alternate Designations**
UNS K24728, UNS K24729.

1.03 **Specifications**

1.031 AMS specifications, Table 1.031.

1.032 Other specifications: ASTM A579, MIL-S-8949, MIL-S-47036.

1.04 **Composition**

1.041 Composition, Table 1.041.

1.05 **Heat Treatment**

1.051 General. The heat treatment of D6AC is based on conventional quench and temper procedures in which sufficiently rapid cooling from the austenitizing (or ausbay) temperature produces a high strength martensitic structure which can be tempered to a wide range of strength levels. As commonly observed with low alloy high strength steels, the tensile strength decreases with increasing tempering temperature accompanied by an increase in the tensile ductility and in fracture toughness. However, variations in the austenitizing temperature and in the quench rate are capable of producing substantial changes in plane strain fracture toughness without appreciably affecting the tensile properties. These effects of heat treatment are discussed in Section 3.02721, which relates them to the microstructure. The achievement of a high level of tensile strength coupled with adequate fracture toughness requires special heat treating procedures and careful control, particularly for complex parts and heavy sections. Some examples are given below.

Ausbay quenching has the advantage of reducing thermal gradients and consequent distortion but increases production costs. Salt quenching from the austenitizing temperature (martempering) also reduces thermal gradients and minimizes quench cracking as compared with oil or water quenching. However, depending on section size and salt temperature, the cooling rate between about 900 F and the M_S temperature (approximately 550 F) may be insufficient to avoid the formation of intermediate products (bainites) which can reduce the fracture toughness. A complicating factor is the exothermic reaction which accompanies the martensite formation and can under some circumstances (e.g., insufficient salt-to-metal mass ratio) result in a decreased cooling rate during conversion to martensite. As pointed out in Section 3.02721, the cooling rate during martensite formation appears to be critical in establishing the fracture toughness. It is for the above reasons that sections having thicknesses or diameters greater than 1 inch are often oil quenched.

Oil quenching should not result in cracking provided that drastic changes in section size and high stress concentrations are avoided. Snap tempering is often employed and is designed to eliminate delayed cracking sometimes observed following quenching. In some cases, distortions produced by quenching may be eliminated by a sizing operation during tempering.

1.052 Anneal, 1500 to 1550 F, cool at 50 F per hour max to 1000 F (4).

1.053 Normalize, 1600 to 1750 F, air cool (29).

1.054 AMS conventional quench and temper procedures, Table 1.054.

1.055 Special quench and temper procedures. Following are two examples of heat treatment schedules which produce superior combinations of tensile strength and fracture toughness.

1.0551 Complex heavy sections. The F-111 carry-through structure is an example of a complex part involving sections of various thicknesses and requiring minimum distortion as a result of heat treatment. The procedure developed (53) is as follows: austenitize for at least 30 minutes at 1700 F; cool to 1550 F and equalize; ausbay quench at greater than 6 F/minute to 975 F and hold for 2 hours maximum; quench into 140 F oil; snap temper at 400 F for 2 hours minimum; temper at 1000 to 1025 F for 2 hours minimum, air cool; and retemper at 1015 to 1060 F for 2 hours minimum, air cool. The final tempering temperature was adjusted to produce the target properties of 220 to 240 ksi ultimate tensile strength and 90 ksi $\sqrt{\text{in.}}$ fracture toughness.

1.0552 Thin sections. The space shuttle solid rocket booster case is an example of relatively thin sections (approximately 0.30 inch) which can be resized during tempering to remove distortions

	Fe
0.46	C
1.0	Cr
1.0	Mo
0.55	Ni

D6A
D6AC

introduced during quenching. The procedure used (70) is as follows: austenitize in a protective atmosphere at 1590 to 1640 F for 2.5 hours minimum; salt quench to 325 F maximum, hold for at least 15 minutes, air cool to 175 F maximum; snap temper within 2 hours at 310 to 345 F for at least 3 hours; and double temper at 1070 to 1115 F for 6 to 7 hours and air cool to 175 F maximum. The tempering temperature is selected to produce the target properties of F_{ty} = 180 ksi minimum, F_{tu} = 195 to 225 ksi and K_{Ic} = 90 ksi $\sqrt{in.}$ minimum. Tempering temperatures are held to within ±10 F.

1.056 Stress relief, 1100 to 1200 F depending on the application.

1.057 Marstrain. Application of a small plastic strain after a relatively low temperature temper followed by a second low temperature temper can increase the tensile strength but reduces tensile ductility and crack strength (see Figures 3.02122 and 3.027112).

1.06 **Hardness**

1.061 End quench hardenability, Figure 1.061.

1.062 Effect of stress relief on hardness of cold worked sheet, Figure 1.062.

1.063 Effect of tempering temperatures on hardness, Figure 1.063.

1.064 Effect of austenitizing temperature on hardness, Figure 1.064.

1.07 **Forms and Conditions Available**

Sheet, bar, forging stock, tubing. Extrusions on special order.

1.08 **Melting and Casting Practice**

Electric furnace air melt is available but alloy is generally consumable electrode vacuum remelted or AOD/VAR melted.

1.09 **Special Considerations**

1.091 Fracture toughness is highly dependent on heat treatment conditions and can vary significantly independently of strength properties. See Sections 1.05 and 3.02721.

1.092 D6AC is subject to stress corrosion and corrosion fatigue in moist or aqueous environments. Crack-growth rates are increased by one order of magnitude or more in these environments as compared to rates in dry air or vacuum. Inhibitors such as sodium nitrite plus sodium borate effectively eliminate the environmental enhancement of crack-growth rates. Increased tempering time may also reduce susceptibility to stress corrosion. (See Section 2.032.)

1.093 Decarburizing should be avoided by use of suitable furnace atmospheres. (See 4340.)

2 PHYSICAL PROPERTIES AND ENVIRONMENTAL EFFECTS

2.01 **Thermal Properties**

2.011 Melting range, approximately 2740 F.

2.012 Phase changes.

2.0121 Time-temperature-transformation diagram, Figure 2.0121.

2.013 Thermal conductivity.

2.014 Thermal expansion, Figure 2.014.

2.015 Specific heat.

2.016 Thermal diffusivity.

2.02 **Other Physical Properties**

2.021 Density, 0.284 lb/in.^{3}, 7.87 gr/cm^3 (4).

2.022 Electrical properties.

2.023 Magnetic properties, ferromagnetic.

2.024 Emittance.

2.025 Damping capacity.

2.03 **Chemical Environments**

2.031 General corrosion.

2.0311 The potential-pH (Pourbaix) corrosion diagram for D6AC in an aqueous solution of 0.1M NaCl is shown in Figure 2.0312. General corrosion occurs at low pH values at potentials above -0.77 volt (standard calomel electrode). At lower potentials, no corrosion occurs. In the passive region, a protective film forms. This region contains two areas: an area of imperfect passivation where preexisting pits can grow, and an area of perfect passivation where these pits cannot grow (55, 56).

2.0312 Pourbaix diagram for corrosion of D6AC in 0.1M NaCl, Figure 2.0312.

2.032 Stress corrosion.

2.0321 D6AC is susceptible to stress-corrosion cracking and corrosion fatigue in moist and in aqueous environments. Variables affecting stress corrosion behavior include tempering temperature and time, specimen orientation, and the presence or absence of chemical inhibitors.

The effects of tempering temperature on the stress-corrosion crack-growth rates in distilled water and in H_2S are shown in Figure 2.0322. Lowest subcritical crack-growth rates in both water and H_2S are observed for material tempered at 1000 F. This material has the highest fracture toughness and lowest tensile strength. Conversely, the highest crack-growth rates are observed for material tempered at 400 F, which has the lowest fracture toughness and highest tensile strength. Crack propagation in H_2S is transgranular, while it is intergranular in non-sulfide aqueous environments (57).

2.0322 Effects of tempering temperature on stress-corrosion crack-growth behavior in water and in hydrogen sulfide, Figure 2.0322.

2.0323 The susceptibility of D6AC to stress-corrosion cracking is anisotropic when the microstructure is banded. Banded microstructure, characterized by alternate layers of solute-rich and solute-depleted layers, is common and results from standard fabrication and heat treatment procedures. As shown in Figure 2.0324 for material in the 2 hr/1020 F tempered condition, crack-growth rates in both distilled water and in hydrogen are about 10-fold greater for the S-L orientation than for the T-L orientation. These differences reflect the greater susceptibility of solute-rich bands (which

Fe	
0.46	C
1.0	Cr
1.0	Mo
0.55	Ni

D6A
D6AC

are more favorably oriented for corrosion in the S-L specimens) to intergranular crack growth as compared with solute-depleted bands. However, crack-growth rates can be reduced by nearly two orders of magnitude and the threshold stress intensity almost doubled by increasing the tempering time at 1020 F from 2 hours to 200 hours. This improvement, shown in Figure 2.0325, is achieved without loss in tensile strength or fracture toughness. The fracture path is also changed from intergranular to transgranular on increasing the tempering time. These improvements are attributed to increased precipitation of Mo_3P and decreased grain boundary segregation of molybdenum and phosphorus with increasing tempering time (58).

2.0324 Effects of orientation on subcritical stress-corrosion crack-growth behavior in distilled water and in hydrogen, Figure 2.0324.

2.0325 Effect of tempering time at 1020 F on subcritical stress-corrosion crack-growth behavior in distilled water, Figure 2.0325.

2.0326 The environmental enhancement of crack-growth rates under static sustained load or low cycle fatigue conditions can be minimized or eliminated through the use of chemical inhibitors. As shown in Figures 2.0327 and 2.0328, the stress-corrosion and corrosion fatigue crack-growth rates in an aqueous solution of 0.1M NaCl are significantly reduced by the addition of an inhibitor consisting of 0.1M $NaNO_2$ plus 0.1M $Na_2B_4O_7$ (59). This inhibitor system lowers crack-growth rates by one-half to one order of magnitude to rates substantially identical to those observed in ambient air (60). This inhibitor combination is equally effective in the presence or absence of sodium chloride. In the absence of inhibitors, distilled water is slightly more aggressive than sodium chloride solutions in accelerating crack-growth rates (60). Hydrazine is also effective in reducing the stress-corrosion crack-growth rate in 0.1M NaCl and nil chloride solutions. Inhibition of crack growth is related to the formation of nitride ion which prevents hydrogen evolution at the crack tip. Sodium dichromate (0.1M $Na_2Cr_2O_7$) inhibits crack growth in nil chloride solutions but is ineffective in chloride solutions (60, 61). Corrosion inhibitors also increase the value of K_{Iscc}. This is of potential practical importance since the critical flaw size varies as the square of K_{Iscc}. Increasing the critical flaw size improves the ease with which such flaws can be detected by nondestructive methods (62).

2.0327 Effects of inhibitors on stress-corrosion crack-growth behavior, Figure 2.0327.

2.0328 Effects of inhibitors on corrosion fatigue crack-growth behavior, Figure 2.0328.

2.0329 Accelerated corrosion under static or dynamic stress conditions is attributed to localized hydrogen embrittlement at propagating crack tips. Measurements of local pH at advancing crack tips indicate that the crack tips are acidified with respect to the bulk corrodent solutions (such as distilled water or aqueous NaCl solutions). Hydrogen analyses of local areas of fracture surfaces also indicate increased hydrogen contents after corrosion in aggressive environments. In contrast, the addition of an oxidizing inhibitor such as hydrazine to distilled water or a salt solution causes the pH and the potential at the crack tip to remain the same as in the bulk solution and therefore unfavorable for hydrogen evolution. Local hydrogen analyses confirm that hydrogen contents remain at a low level near the crack tip under these conditions (62).

2.03210 The apparent incubation time for subcritical crack growth under stress corrosion conditions tends to decrease with decreasing stress intensity on initial loading, as shown in Figure 2.03211. Unfortunately, the scatter in these data precludes the derivation of a definitive relationship between incubation time and applied stress intensity. It has been suggested that the incubation period may be a function of the ratio of the applied stress intensity at experimental load conditions to that employed during fatigue precracking (63). Incubation time also varies with the sensitivity of the device used to detect cracking, further complicating the understanding of its relation to other factors.

Crack arrest periods and changes in crack propagation rates have also been observed following load-shedding. The period of crack arrest and the crack-growth rate following crack arrest vary with the amount of load shed and the original applied stress intensity. The greater the amount of load shed, the longer is the crack arrest period, and the higher the original applied stress intensity, the shorter is the crack arrest period for the same amount of load shedding. The crack-growth rates following crack arrest are lower following greater increments of load shedding. However, as for incubation times following initial load application, the apparent crack arrest times and changes in crack propagation rates vary in a complex manner with prior load history. Definitive relationships have yet to be established. It does appear that prestressing retards stress-corrosion cracking and is therefore beneficial (63, 64).

2.03211 Incubation times for stress-corrosion crack-growth initiation in aqueous solutions as a function of initial stress intensity factor, Figure 2.03211.

2.033 Mercury corrosion.

2.0331 Stress-corrosion crack-growth behavior in liquid mercury and low pressure hydrogen environments, Figure 2.0331.

2.034 Hydrogen environment effects. (See Figures 2.0324, 2.0331, and 3.0516.)

3 MECHANICAL PROPERTIES

3.01 Specified Mechanical Properties

3.011 AMS specified mechanical properties, Table 3.011.

3.02 Mechanical Properties at Room Temperature

3.021 Tension – stress-strain diagrams – tension properties.

3.0211 Stress-strain diagrams.

3.02111 D6AC exhibits cyclic softening in the quenched and tempered condition, as shown in Figure 3.02112a and b. This cyclic softening results in an 18 percent decrease in yield strength under cyclic,

	Fe
0.46	C
1.0	Cr
1.0	Mo
0.55	Ni

D6A
D6AC

as compared to monotonic, conditions. This reduction in yield strength can occur during design life as a result of cyclic loading and should be considered by the designer as the performance of components can be impaired.

Cyclic softening has been related to the monotonic work hardening exponent n, with small values indicating a propensity for cyclic softening. Low n values reflect minimal work hardening and a starting microstructure which is optimally strengthened. The values of n for D6AC for the two heat treatments (Figure 3.02112a and b) are quite low, 0.03 and 0.02, respectively, and are consistent with the observed cyclic softening. Strength-differential effects between tension and compression are also exhibited by D6AC, but these effects are smaller than the cyclic softening effect. In monotonic loading, the flow stress is greater in compression than in tension, while the opposite occurs during cyclic loading (52).

3.02112 Monotonic and cyclic stress-strain curves for two different heat treatments [(a) 2-hour temper and (b) 4-hour temper], Figure 3.02112.

3.02113 Effects of tempering temperature on stress-strain curves at room temperature, Figure 3.02113.

3.0212 Tensile properties for sheet.

3.02121 Effect of tempering temperature on tensile properties of sheet, Figure 3.02121.

3.02122 Effect of marstrain on tensile properties of sheet, Figure 3.02122.

3.02123 Effect of low carbon content and various tempering temperatures on tensile properties of sheet, Figure 3.02123.

3.02124 Effect of tempering temperature on tensile properties at two austenitizing temperatures, Figure 3.02124.

3.02125 Effect of tempering temperature on tensile properties of air and vacuum melt alloy sheet, Figure 3.02125.

3.0213 Tensile properties for plate.

3.02131 Effect of tempering temperature on tensile properties of plate, Figure 3.02131.

3.02132 Range of tensile properties in plates tempered at 500 to 550 F, Table 3.02132.

3.02133 Effect of austempering temperature on tensile properties of plate, Figure 3.02133.

3.0214 Tensile properties for bar.

3.02141 Effect of tempering temperature on tensile properties of bar, Figure 3.02141.

3.02142 Effect of tempering temperature on tensile properties of strain-aged bar, Figure 3.02142.

3.0215 Tensile properties for forgings.

3.02151 Effect of tempering temperature on tensile properties of rolled ring forgings, Figure 3.02151.

3.02152 Effect of forging reduction on tensile properties of a variable-cross-section ausformed forging tempered at 500 F, Figure 3.02152.

3.02153 Effect of forging reduction on tensile properties of a variable-cross-section ausformed forging tempered at 900 F, Figure 3.02153.

3.02154 Effect of forging and tempering temperature on tensile properties of ausformed forgings, Figure 3.02154.

3.02155 Effect of shot peening and tempering temperature on tensile properties, Figure 3.02155.

3.02156 Effect of tempering temperature on tensile properties for three thermal mechanical processing treatments of forged alloy, Figure 3.02156.

3.0216 Tensile properties of extrusions.

3.02161 Tensile properties of extrusion at two tempering temperatures, Table 3.02161.

3.0217 Tensile properties of shear spun alloy.

3.02171 Effect of tempering temperature on tensile properties of shear spun alloy, Figure 3.02171.

3.02172 Effect of shear form reduction on tensile properties, Figure 3.02172.

3.022 Compression – stress-strain diagrams – compression properties.

3.0221 Compression stress-strain diagrams, see Section 3.0211.

3.023 Impact (see also Section 3.033).

3.0231 Effect of tempering temperature on impact properties, Figure 3.0231.

3.024 Bending.

3.025 Torsion and shear.

3.0251 Effect of shear form reduction on shear strength, Figure 3.0251.

3.026 Bearing.

3.027 Stress concentration.

3.0271 Notch properties. (See also Section 3.0272.)

3.02711 Notch properties for sheet.

3.027111 Effect of tempering temperature on sharp notch properties of sheet, Figure 3.027111.

3.027112 Effect of marstrain on sharp notch properties of sheet, Figure 3.027112.

3.027113 Effect of tempering temperature on sharp notch properties of air and vacuum melt sheet, Figure 3.027113.

3.027114 Effect of low carbon content and tempering temperature on sharp notch strength of sheet, Figure 3.027114.

3.027115 Effect of notch root radii on sharp notch strength of sheet, Figure 3.027115.

3.02712 Notch properties of plate.

3.027121 Effect of crack length on crack strength of three thicknesses of plate each from a different heat, Figure 3.027121.

3.027122 Effect of surface cracks on crack strength of plate at strength levels between F_{ty} = 190 and 215 ksi, Figure 3.027122.

3.02713 Notch properties for bar.

3.027131 Effect of tempering temperature on notch and smooth tensile properties of bar, Figure 3.027131.

3.027132 Effect of tempering temperature on the sharp notch strength of bar, Figure 3.027132.

3.02714 Notch properties for forgings.

3.027141 Effect of surface cracks on crack strength of forging, Figure 3.027141.

3.02715 Effect of tempering temperature on sharp notch properties of shear spun alloy, Figure 3.02715.

3.02716 Effect of surface cracks on burst strength of thin walled cylinders, Figure 3.02716.

3.0272 Fracture toughness. (See also Section 3.0372.)

3.02721 General. The fracture toughness of D6AC is highly dependent on heat treatment variables, as discussed in Section 1.05. Results from a fracture toughness study in support of the F-111 aircraft wing pivot support structure (carry-through box) are shown in Figure 3.02722 and Tables 3.02723, 3.02724, 3.02725, and 3.02726. Additional data from a separate program on heat treatment effects

	Fe
0.46	C
1.0	Cr
1.0	Mo
0.55	Ni

D6A
D6AC

are presented in Table 3.02727. These studies indicate that D6AC can be heat treated to give similar tensile properties but with fracture toughness values differing by a factor of more than 3.

An increase in toughness associated with increasing austenitizing temperature (Figure 3.02722) has also been observed in 4340 tempered at 400 F (71). In this case, the beneficial effect from increasing the austenitization temperature was attributed to increasing solution of second phase void nucleating particles (carbide particles and sulfide inclusions), which resulted in larger void spacings and consequent increased energy absorption by plastic flow during fracture.

The variation in fracture toughness associated with changes in the quenching rate are illustrated in Table 3.02727. These data relate to quenching an 0.75-inch thick section from an ausbay temperature of 970 F, but similar effects would be expected for direct quenching from the austenitizing temperature. Focusing on an austenitizing temperature of 1700 F and a tempering temperature of 1020 F, it is evident that oil quenching gives the highest toughness (94.2 ksi $\sqrt{in.}$). Salt quenching at 365 F gives a toughness of 88 ksi $\sqrt{in.}$, while salt quenching at 410 F or air cooling both give lower toughnesses. It should be noted that tensile strength properties vary insignificantly for these quenching conditions.

It has been suggested (66) that these changes in fracture toughness with quenching rate are related to the nature of the as-quenched martensite structure. High toughness values are obtained after tempering micro-twinned plate martensite, which predominates after oil quenching. Low toughness values are obtained after tempering lath-type martensite, which predominates after air cooling and is associated with a bainitic form of carbide precipitation.

3.02722 Effects of austenitizing temperature and quench medium on fracture toughness, Figure 3.02722.
3.02723 Plane strain fracture toughness of 0.8-inch thick CVM plate, Table 3.02723.
3.02724 Plane strain fracture toughness of CVM forgings, Table 3.02724.
3.02725 Plane strain fracture toughness of plate and forged parts, Table 3.02725.
3.02726 Effects of heat treatment on fracture toughness of plate, forgings, and billets at room temperature, Table 3.02726.
3.02727 Effects of heat treatment on fracture toughness of bar, Table 3.02727.
3.02728 The majority of plane strain fracture toughness data reported apply to yield strength levels below 220 ksi. However, a limited amount of information from fatigue-cracked cylindrical specimens (Figure 3.02729) indicates that the toughness drops rapidly with increasing strength level and that the highest strength conditions are relatively brittle.
3.02729 Effect of tempering temperature on sharp notch properties and fracture toughness of plate, Figure 3.02729.
3.027210 Effect of tempering temperature on fracture toughness and yield strength for three thermal-mechanical processing treatments of forged alloy, Figure 3.027210.
3.028 Combined properties.

3.03 **Mechanical Properties at Various Temperatures**
3.031 Tension – stress-strain diagrams – tension properties.
3.0311 Stress-strain curves for plate at room temperature and 250 F, Figure 3.0311.
3.0312 Effect of test temperature on tensile properties of bar at several strength levels, Figure 3.0312.
3.0313 Effect of test temperature on tensile properties of bar, Figure 3.0313.
3.0314 Effect of test temperature on tensile properties of plate, Table 3.0314.
3.0315 Effect of test temperature on tensile properties of forgings, Table 3.0315.
3.032 Compression – stress-strain diagrams – compression properties.
3.033 Impact.
3.0331 Elevated temperature Charpy V-notch impact properties, Figure 3.0331.
3.0332 Elevated temperature Charpy U-notch impact properties for various strength levels, Figure 3.0332.
3.0333 Low temperature Charpy V-notch impact properties, Figure 3.0333.
3.0334 Effect of test temperature on impact strength of a variable cross section ausformed forging, Figure 3.0334.
3.034 Bending
3.035 Torsion and shear.
3.036 Bearing.
3.037 Stress concentration.
3.0371 Notch properties.
3.0372 Fracture toughness.
3.03721 Effect of test temperature on plane strain fracture toughness of 0.8-inch thick CVM plate, Figure 3.03721.
3.03722 Effect of test temperature on plane strain fracture toughness of 1.5 to 1.8-inch thick CVM plate, Figure 3.03722.
3.03723 Effect of test temperature on plane strain fracture toughness of CVM forgings, Figure 3.03723.
3.038 Combined properties.

3.04 **Creep and Creep-Rupture Properties**
3.041 Creep-rupture curves at 900 and 1000 F, Figure 3.041.
3.042 Creep-rupture strength of smooth and notched bar at elevated temperatures, Figure 3.042.

3.05 **Fatigue Properties**
3.051 Fatigue strength of marstrained sheet, Table 3.051.
3.052 Effect of test temperature on smooth and notched fatigue properties of bar, Table 3.052.
3.053 Low cycle fatigue behavior of cracked plate specimens and tanks, Figure 3.053.
3.054 S-N curves for 220 to 240 ksi hot rolled plate, Figure 3.054.
3.055 S-N curves for 260 to 280 ksi forged bar, Figure 3.055.
3.056 Effects of humidity on fatigue behavior of keyhole notched bar at 95 F, Figure 3.056.

	Fe
0.46	C
1.0	Cr
1.0	Mo
0.55	Ni

D6A
D6AC

3.057 The fatigue crack-growth behavior for materials quenched and tempered to two different strength levels and four different fracture toughness levels is shown in Figure 3.058. In the central portions of these curves, the fatigue crack-growth rates are proportional to $\Delta K^{2.4}$ and are independent of fracture toughness for toughness values ranging from 42 to 91 ksi $\sqrt{in.}$ at essentially the same tensile strength. Variations in yield and ultimate strength have no significant effect on the rate of fatigue crack growth in the range where da/dN is proportional to $\Delta K^{2.4}$. At ΔK values greater than $0.7K_{Ic}$, void coalescence and microcleavage cause progressively accelerated crack growth as the fracture toughness is approached (68). Data from the F-111 program, shown in Figure 3.059, are in agreement with data in Figure 3.058.

3.058 Effects of quenching on fatigue crack-growth behavior in dry air at room temperature, Figure 3.058.

3.059 Fatigue crack-growth rates for high and medium toughness plate in desiccated air at room temperature, Figure 3.059.

3.0510 Figures 3.0511 through 3.0514 illustrate the fact that water, which is almost always present in service environments, constitutes an aggressive environment under conditions of cyclic loading. The rate of crack growth is not influenced by the presence of water vapor or water at a cyclic frequency of 600 cpm, as shown in Figure 3.0511a. However, when the frequency is reduced to 60 cpm, moisture clearly increases the rate of crack growth, as shown in Figure 3.0511b.

Moderate humidity, distilled water, and water-saturated JP-4 fuel environments all increase the fatigue crack-growth rate at low frequency (6 cpm), as shown in Figures 3.0512, 3.0513, and 3.0514, respectively. The change in frequency and sensitivity to moisture are also associated with a change in fracture mode from transgranular at the higher frequency to intergranular at the lower frequency (69).

3.0511 Effects of humidity and frequency on fatigue crack-growth behavior at room temperature [(a) frequency 600 cycles/minute and (b) frequency 60 cycles/minute], Figure 3.0511.

3.0512 Fatigue crack-growth rates for medium toughness plate in laboratory air (50 to 70 percent RH) at room temperature, Figure 3.0512.

3.0513 Fatigue crack-growth rates for high and medium toughness plate in distilled water at room temperature, Figure 3.0513.

3.0514 Fatigue crack-growth rates for high and medium toughness plate in water-saturated JP-4 fuel at room temperature, Figure 3.0514.

3.0515 Fatigue crack-growth rates in hydrogen are higher than those in dry air or vacuum, as shown in Figure 3.0516. The rates in hydrogen are also frequency dependent, with lowest frequencies giving the highest crack-growth rates. In contrast, the crack-growth rates in dry air or in vacuum are much less frequency dependent (over the range 3 to 60 cpm). The crack-growth rates in hydrogen are proportional to the duration of the maximum stress intensity during each loading cycle for the square wave illustrated in Figure 3.0512. For wave forms such as triangular, positive sawtooth, and negative sawtooth (ratios of loading to unloading times of 1:1, 10:1, and 1:10, respectively), the crack-growth rates are proportional to the duration of the loading portion of the cycle (65).

3.0516 Effects of cyclic frequency on fatigue crack-growth behavior in hydrogen with comparison to air and vacuum, Figure 3.0516.

3.06 **Elastic Properties**

3.061 Poisson's ratio.

3.062 Modulus of elasticity.

3.0621 Modulus of elasticity at room and elevated temperatures, Figure 3.0621.

3.063 Modulus of rigidity.

3.064 Tangent modulus.

3.065 Secant modulus.

4 FABRICATION

4.01 **Forming**

4.011 Forging. Starting temperature 2250 F maximum, finishing temperature 1800 F minimum. Slow cool after finishing. Alternately hold at 1200 F, 12 hours immediately following forging, raise temperature to 1650 F and then cool to 1200 F, hold 10 hours and air cool.

4.02 **Machining and Grinding**

Properties are similar to those of Type 4340, Code 1206.

4.03 **Joining**

4.031 General. This alloy is weldable in sheet and heavy sections. Extensive experience is available in the welding of pressure vessels having section thickness between 0.2 and 1.0 inch (5, 22), heat treated to yield strength levels between 180 and 215 ksi. For critical applications the GTA process is preferred using vacuum melted wires of lower carbon content than the parent metal and containing minimum amounts of P, S, and gases. Welds made in this manner will have a higher toughness but a somewhat lower yield strength than the parent plate. If tempering temperatures above about 1125 F are employed 17-22A (S) (AMS 6458) weld wire has been used. This substitution improves weld strength for the higher tempering temperatures (5). Using proper techniques, primary weld efficiencies after heat treatment approach 100 percent. Preheat and a postheat immediately following welding are necessary to avoid cracking (see Table 4.0311). The toughness of primary GTA welds heat treated to yield strength levels less than about 200 ksi is essentially equal to that of the parent metal (see Figure 4.0312). Weld repair following heat treatment requires special precautions (see Table 4.0311) and results in some loss in strength and toughness (see Figure 4.0312) (4, 5, 22).

4.0311 Recommended weld heat treat sequence for primary welds and weld repair after heat treatment, Table 4.0311.

4.0312 Effect of surface crack size on sharp notch strength of primary welds and weld repairs made after heat treatment, Figure 4.0312.

4.0313 Effect of welding on low temperature Charpy V impact properties, Figure 4.0313.

4.0314 Hardness survey on welded plate, Figure 4.0314.

4.09 **Surface Treating**
(See 4340, Code 1206.)

REFERENCES

1 Henning, H. J. and Boulger, F. W., "High Strength Steel Forgings", DMIC Report 143 (January 5, 1961).

2 Kaiser Fleetwings, Inc., "Final Report on the Effect of Stress Relief vs a Normalize and Temper Treatment on the Final Mechanical Properties of AMS 6434, Ladish D6A, X2 (Modified 4137)" (November 1960).

3 Kennedy, E. M., Jr., "The Status of Research and Development for High Strength Aircraft Steels", WADC TN 59-326 (July 1960).

4 Ladish Co., "Ladish D6A, High Strength Steel" (October 4, 1957) (1963).

5 Private Communication, G. R. Sipple, General Motors Allison Division with W. F. Brown, Jr. (1965).

6 Brown, W. F., Jr., Personal Communication, NASA Unpublished Data (1960).

7 Check, S. V., "Progress Report on Slow Crack Extension and Low Cycle Fatigue of Ladish D6AC at 240,000 psi Yield Strength Level", U.S. Naval Weapons Plant, Technical Memo 169 (September 1961).

8 Hanink, D. K., Personal Communication, General Motors Allison Division (November 1961).

9 David, C. K., Personal Communication, Ladish Co. (January 15, 1962).

10 Martin, C. F., Williams, A. J., and Gerberich, W. W., "Effects of Deformation of the Metastable Austenitic Condition on the Properties of High Strength Steel Forgings", Aeronutronic Division, Philco Corp., ASK-TDR 63-836, ASD Contract AF33(657)-8539 (September 1963).

11 Yount, R. E., "Determination of Engineering Properties of Marstrained Steels", General Electric, Evandale, Ohio, ASD-TDR-62-230, ASD Contract AF33(616)-7655 (August 1962).

12 Davis, S. O., "Elevated Temperature Fatigue Properties of D6AC High Strength Steel", ASD-TDR-63-645 (October 1963).

13 Carmen, C. M. and Mulherin, J. H., "Low Cycle Fatigue Characteristics of Ultra High Strength Steels", Frankford Arsenal Report R-1707 (February 1964).

14 Pratt, W. W., "Material Evaluation of D6AC Steel Extrusion Mechanical and Metallurgical Properties", General Dynamics, Fort Worth, Test Data Memo FTDM 3234, ASD Contract AF33(657)-11214 (April 15, 1964).

15 Bhat, G. K., "A Study of the Behavior of Small Pressure Vessels Under Biaxial Stress Conditions and in Presence of Surface Cracks", Mellon Institute, NRL Contract NOnr-3764(00)(X) (June 25, 1963).

16 Carmen, C. M., Armiento, D. F., and Markus, H., "Plane Strain Fracture Toughness Measurements of High Strength Steels", ASME Journal of Basic Engineering (March 1963).

17 Terry, E. L. and McClaren, S. W., "Biaxial Stress and Strain Data on High Strength Alloys for Design of Pressurized Components", Chance-Vought Corp., ASD-TDR-62-401, ASD Contract AF33(616)-7720 (July 1962).

18 Tiffany, C. F. and Lorenz, P. M., "An Investigation of Low Cycle Fatigue Failures Using Applied Fracture Mechanics", The Boeing Company, Aero-Space Division, ML-TDR 64-53, ASD Contract 33(657)-10251 (May 1964).

19 Check, S. V., "Toughness, Slow Crack Extension and Low Cycle Fatigue of Ladish D6AC at 24,000 psi, Y.S. Level", U.S. Naval Weapons Plant, Technical Memo No. 169, NRL-Project 62ROS-19A (September 26, 1961).

20 Urban, R. J., "Plane Strain Fracture Toughness of Large D6AC Steel Specimens Heat Treated to 220–240 and 260–280 ksi Strength Level", General Dynamics, Fort Worth, Test Data Memo FTDM-3178, ASD Contract AF33(657)-11214 (April 15, 1964).

21 Urban, R. J., "Plane Strain Fracture Toughness of Large D6AC Steel Specimens", General Dynamics, Fort Worth, Report FGT3064, ASD Contract AF33(657)-8260-1 (November 1, 1963).

22 Mehra, Y., "Mechanical and Fracture Toughness Properties of D6AC Post Heat Treat Weld Repair", Curtiss Wright Corp., Wright Aero Division (October 23, 1964).

23 Betner, D. C., "Effect of Section Thickness and Partial Thickness Crack Size on Gross Strength of D6AC Steel at Ultimate Strength Level of 215 ksi", Allison Materials Research Laboratory, Report 62M23 (September 21, 1962).

24 Green, R. B., "Evaluation of D6AC and 18-Ni-Co-Mo-High Strength Steel Plate for Heavy Wall Large Diameter Rocket Motor Case Applications", Allison Materials Research Laboratories, Report No. 62M34 (June 7, 1963).

25 Wessel, E. T., Hovan, R. P., and Pryle, W. H., "Preliminary Evaluation of the Fracture Characteristics of D6AC Rocket Motor Cases", Westinghouse Research Laboratories, Research Report 63-848-307-R1 (August 27, 1963).

26 Haese, W. P. and Masters, J. N., "An Evaluation of Large Diameter Solid Propellant Motor Case Materials", The Boeing Company, Report No. 02-22314M (May 22, 1963).

27 Crucible Steel Company, "Data Sheet for Crucible D6", Issue No. 2 (1965).

28 AMS 6431F (January 15, 1980).

29 AMS 6438C (July 1, 1981).

30 Excelo Developments, Inc., "Investigation and Evaluation of High Strength Steels in Heavy Gauges for Large Diameter Solid Propellant Rocket Engine Cases", Mellon Institute, AF Contract No. AF04(611)-8517 (January 1963).

31 "Evaluation of Low Carbon Ladish D6AC Steel", Aerojet General Corporation, Report No. 278, Contract No. AF33(657)-8890 (September 1962).

32 Vazquez, A. J., "Developing a Process for Ausforming Large, High Strength Steel Aircraft

	Fe
0.46	C
1.0	Cr
1.0	Mo
0.55	Ni

D6A
D6AC

	Fe
0.46	C
1.0	Cr
1.0	Mo
0.55	Ni

D6A
D6AC

Structural Components With Improved Design and Weight Reduction", Report IV, IR-8-354, Ladish Company (July 1966).

33 Jacobs, F., "Mechanical Properties of Materials Fabricated by Shear Forming", T.D.R. ASD-TDR-62-830, Contract AF33(616)-7874, Temco Electronics and Missiles Company (February 1963).

34 Weiss, V., Nash, G., and Schroder, K., "Crack Initiation in Metallic Materials", Syracuse University Research Institute, Contract NOw-64-0265-d (March 1965).

35 Smith, H. R., "Evaluation of Ladish D6AC Steel", Aerojet General Corporation, Contract AF33(657)-8890 (January 1963).

36 Davish, R. C. and Crownover, W. S., "A Comparison of the Toughness Characteristics of D6 Air and Vacuum Melt Material", Army Missile Command, DA Project LB 222901A205 AMC RA RK TR 64 11 (March 1964).

37 Amateau, M. F. and Steigerwald, E. A., "Fracture Characteristics of Structural Metals", Contract NOw-64-0186C (January 1965).

38 Albom, J. J., "Brazing of Ultra High Strength Steel", Aerojet General Corporation, Contract No. AF33(657)-8890 (January 1963).

39 Faulker, J. M., Hanna, G. L., and Peck, J. V., "Development of Welding Procedures and Filler Materials for Joining High Strength Low Alloy Steels", TRW Inc., Contract AF33(657)-11229 (September 1965).

40 Robinson, R. B. and Uzdarwin, R. J., "Investigation of Stress Corrosion Cracking of High Strength Alloys", Aerojet General Corporation, Contract DA-04-495-ORD-3069, Report 2092 (August 1961).

41 Hartbower, C. E., Gerberich, W. W., and Crimmins, P. P., "Characterization of Fatigue Crack Growth by Stress-Wave Emission", Contract NAS-1-4902, Aerojet General Corporation, Sacramento, California (June 1966).

42 Ault, R. T., McDowell, K. O., and Hendricks, P. L., "Increased Reliability of a High Strength Steel Through Thermal Mechanical Treatments", AFML-TR-66-276 (September 1966).

43 Hartbower, C. E. and Orner, G. M., "Metallurgical Variables Affecting Fracture Toughness in High Strength Sheet Alloys", ASD-TDR-62-868 (June 1963).

44 Heitzmann, R. J., "Effect of Decarburization and Surface Defects on the Notched Fatigue Strength of Steel", ADR 02-09-67, Grumman Aircraft Engineering Corp., Advanced Development Program (April 1967).

45 Feddersen, C. E., Moon, D. P., and Hyler, W. S., "Crack Behavior in D6AC Steel – An Evaluation of Fracture Mechanics Data for the F-111 Aircraft", Metals and Ceramics Information Center, MCIC-72-04 (January 1972).

46 Wei, R. P., Novak, S. R., and Williams, D. P., "Some Important Considerations in the Development of Stress Corrosion Cracking Test Methods", Materials Research and Standards, ASTM Vol. 12 (September 1972), p 25.

47 Mulherin, J. H., "Stress Corrosion Susceptibility of High Strength Steel in Relation to Fracture Toughness", *Journal of Basic Engineering*, Trans. ASME Serial D, Vol. 88 (December 1966), pp 777–782.

48 Campbell, J. E., Berry, W. E., and Feddersen, C. E., "Damage Tolerant Design Handbook", Metals and Ceramics Information Center, HB-01 (December 1972).

49 Private Communication from C. Dale Little, General Dynamics Corporation, Convair Aerospace Division, Fort Worth to W. F. Brown, Jr. (1973).

50 AMS 5027B (July 1, 1984).

51 AMS 5028A (October 15, 1980).

52 Jones, W. B. and Swearengen, J. C., "Mechanical Stability of Ultrahigh Strength Steels", *Materials Science and Engineering*, Vol. 41, No. 2 (December 1979), pp 225–235.

53 Peterman, G. L. and Jones, R. L., "Effects of Quenching Variables on Fracture Toughness of D6AC Steel Aerospace Structures", *Metals Engineering Quarterly*, Vol. 15, No. 2 (May 1975), pp 59–64.

54 Ortiz, R. T., "Heat Treating Space Shuttle Parts to Fracture Toughness Specifications", *Metal Progress*, Vol. 111, No. 3 (March 1977), pp 54–55.

55 Parrish, P. A., Chen, C. M., and Verink, E. D., Jr., "Retardation of Crack Propagation for D6AC High-Strength, Low-Alloy Steel in Aqueous Media by Addition of Oxidizing Inhibitors", Stress Corrosion – New Approaches, ASTM STP 610 (1976), pp 189–198.

56 Verink, E. D., Jr., "Use of the Experimental Pourbaix Diagram for D6AC Steel to Interpret Its Corrosion Behavior in Aqueous Media", Florida University, Gainesville, AFML TR-76-8 (February 1976).

57 Cullen, W. H., "A Study of Hydrogen Sulfide Accelerated Stress-Corrosion Cracking in D6AC Steel", Naval Research Laboratory, Washington, D.C., NRL–MR-3200 (January 1976).

58 Pollock, W. J., Ryan, N. E., and Nankivell, J. F., "Relationship Between Banding and Susceptibility to Environment-Assisted Cracking in a Quenched and Tempered Low Alloy Steel", *Corrosion Science*, Vol. 22, No. 3 (1982), pp 215–229.

59 Bhansali, K., Lynch, C. T., Vahldiek, F., and Summitt, R., "Effect of Multifunctional Inhibitors on Crack Propagation Rates of High Strength Steel in Corrosive Environments", paper presented at International Conference on Effect of Hydrogen on Behavior of Materials, Moran, Wyoming (September 7–11, 1975).

60 Lynch, C. T., Vahldiek, F. W., and Thornton, F., "Comparison of Environmentally Enhanced Crack-Growth Rates of 1410 and Other High-Strength Steels", Proceedings of the 1978 Tri-Service Conference on Corrosion, New Orleans, Louisiana (October 4–6, 1978), pp 341–369.

61 Lynch, C. T., Bhansali, K. J., and Parrish, P. A., "Inhibition of Crack Propagation of High Strength Steels Through Single and Multifunctional Inhibitors", Air Force Materials Laboratory, Wright-Patterson AFB, Ohio, AFML-TR-76-120 (August 1976).

62 Parrish, P. A., Das, K. B., Chen, C. M., and Verink, E. D., Jr., "Inhibition of Hydrogen Embrittlement of D6AC Steel in Aqueous Oxidizing Media".

paper presented at International Conference on Effect of Hydrogen on Behavior of Materials, Moran, Wyoming (September 7–11, 1975).

63 Gilbreath, W. P. and Adamson, M. J., "Aqueous Stress-Corrosion Cracking of High-Toughness D6AC Steel", Stress Corrosion – New Approaches, ASTM STP 610 (1976), pp 176–187.

64 Noronha, P. J., "Kinetic Studies of the Stress Corrosion Cracking of D6AC Steel", NASA Marshall Space Flight Center, Huntsville, Alabama, NASA TM X-64923 (March 25, 1975).

65 Lynch, S. P. and Ryan, N. E., "Mechanisms of Hydrogen Embrittlement – Crack Growth in a Low-Alloy Ultra-High-Strength Steel Under Cyclic and Sustained Stresses in Gaseous Hydrogen", Aeronautical Research Labs, Melbourne, Australia, ARL/MAT-103 (May 1978).

66 Ryan, N. E., "Relationship Between Microstructure and Fracture Toughness in D6AC Steel", Aeronautical Research Labs, Melbourne, Australia, ARL/MET-NOTE–103 (April 1974).

67 Mann, J. Y. and Kemsley, D. S., "The Effects of Very Dry and Fully Water Saturated Air Environments on the Fatigue Life of D6AC Steel Under Constant and Variable Amplitude Loading Sequences", *Corrosion*, Vol. 35, No. 10 (October 1979), pp 465–471.

68 Ryan, N. E., "Fatigue-Crack Growth in D6AC Steel Heat-Treated to Different Values of Fracture Toughness", Aeronautical Research Labs, Melbourne, Australia, ARL/MAT-110 (April 1979).

69 Ryan, N. E., "Fatigue-Crack Growth and Fracture in D6AC Steel", Aeronautical Research Labs, Melbourne, Australia, ARL/MAT-368 (September 1976).

70 Specification STW7-2608, Wasatch Division, Morton-Thiokol, Inc. (August 1, 1985).

71 Ritchie, R. O. and Horn, R. M., "Further Considerations on the Inconsistency in Toughness Evaluation of AISI 4340 Steel Austenitized at Increasing Temperatures", *Metallurgical Transactions*, Vol. 9A (March 1978), pp 331–341.

72 Gallagher, J., "Damage Tolerant Design Handbook", Metals and Ceramics Information Center, Battelle Columbus Division, Columbus, Ohio, MCIC-HB-01R (December 1983).

Fe
0.46 C
1.0 Cr
1.0 Mo
0.55 Ni

D6A
D6AC

Alloy	D6AC
AMS Specification	Product Form
6431F	Bars, Forgings, and Tubing, Premium Quality, Consumable Electrode Vacuum Melted
6438C	Sheet, Strip, Plate, Premium Aircraft Quality, Consumable Electrode Melted
5027B	Welding Wire, Vacuum Melted
5028A	Welding Wire, Vacuum Melted

TABLE 1.031. AMS SPECIFICATIONS (28, 29, 50, 51)

Alloy	D6AC					
AMS Specification	6431F, 6438C		5027B		5028A	
	Percent		Percent		Percent	
Element	Min	Max	Min	Max	Min	Max
Carbon	0.45	0.50	0.26	0.32	0.34	0.40
Chromium	0.90	1.20	0.90	1.20	0.90	1.20
Molybdenum	0.90	1.10	0.90	1.10	0.90	1.10
Nickel	0.40	0.70	0.40	0.70	0.40	0.70
Vanadium	0.08	0.15	0.05	0.10	0.05	0.10
Manganese	0.60	0.90	0.60	0.90	0.60	0.90
Silicon	0.15	0.30	0.10	0.30	0.15	0.30
Copper	–	0.35	–	0.35	–	0.35
Phosphorus	–	0.010(a)	–	0.010	–	0.008
Sulfur	–	0.010(a)	–	0.010	–	0.008
Oxygen	–	–	–	0.0025	–	0.0025
Nitrogen	–	–	–	0.0050	–	0.0050
Hydrogen	–	–	–	0.0010	–	0.0010

(a) 0.015 percent maximum for AMS 6438C.

TABLE 1.041. COMPOSITION (28, 29, 50, 51)

	Fe
0.46	C
1.0	Cr
1.0	Mo
0.55	Ni

D6A
D6AC

Alloy	D6AC			
	Procedures			
Form	Austenitize	Quench	Stress Relief(a)	Temper
Bars, Forgings, Tubing (28)	1650 – 1700 F, 40 min/in., 1 hr Min	Oil	390 – 410 F, 1 hr/in., 1 hr Min, AC	1025 – 1050 F, 2 hr/in., 4 hr Min
Sheet, Strip, Plate (29)	1600 – 1650 F ±10 F, 20 min Min	Oil	390 – 410 F, 1 hr, AC	≥1000 F, 4 hr Min, AC

(a) Snap temper.

TABLE 1.054. AMS CONVENTIONAL QUENCH AND TEMPER PROCEDURES

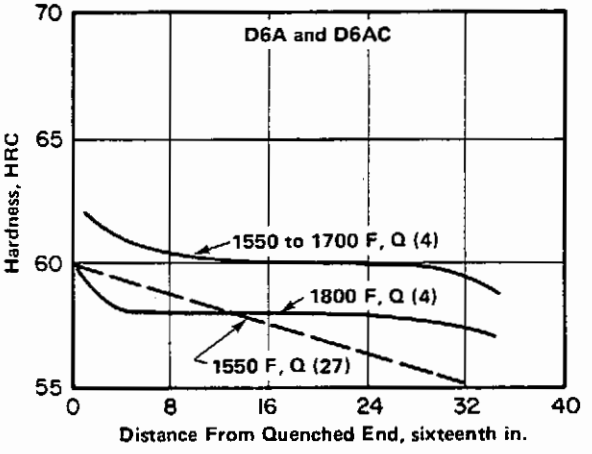


FIGURE 1.061. END QUENCH HARDENABILITY (4, 27)

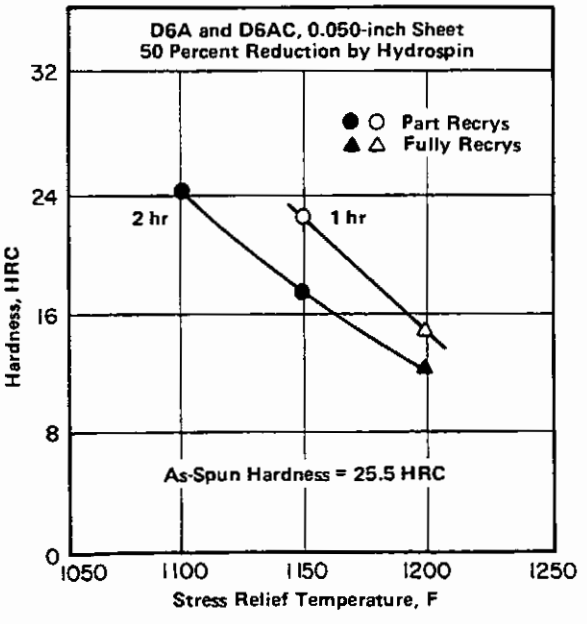


FIGURE 1.062. EFFECT OF STRESS RELIEF ON HARDNESS OF COLD WORKED SHEET (2)

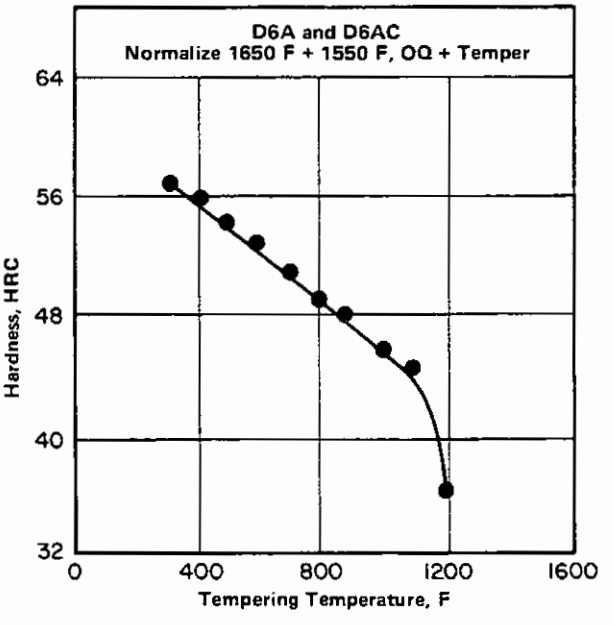


FIGURE 1.063. EFFECT OF TEMPERING TEMPERATURES ON HARDNESS (4)

	Fe
0.46	C
1.0	Cr
1.0	Mo
0.55	Ni

D6A
D6AC

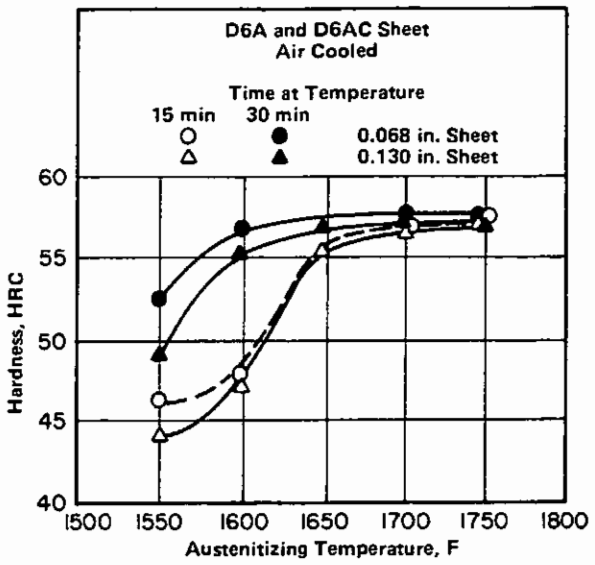


FIGURE 1.064. EFFECT OF AUSTENITIZING TEMPERATURE ON HARDNESS (43)

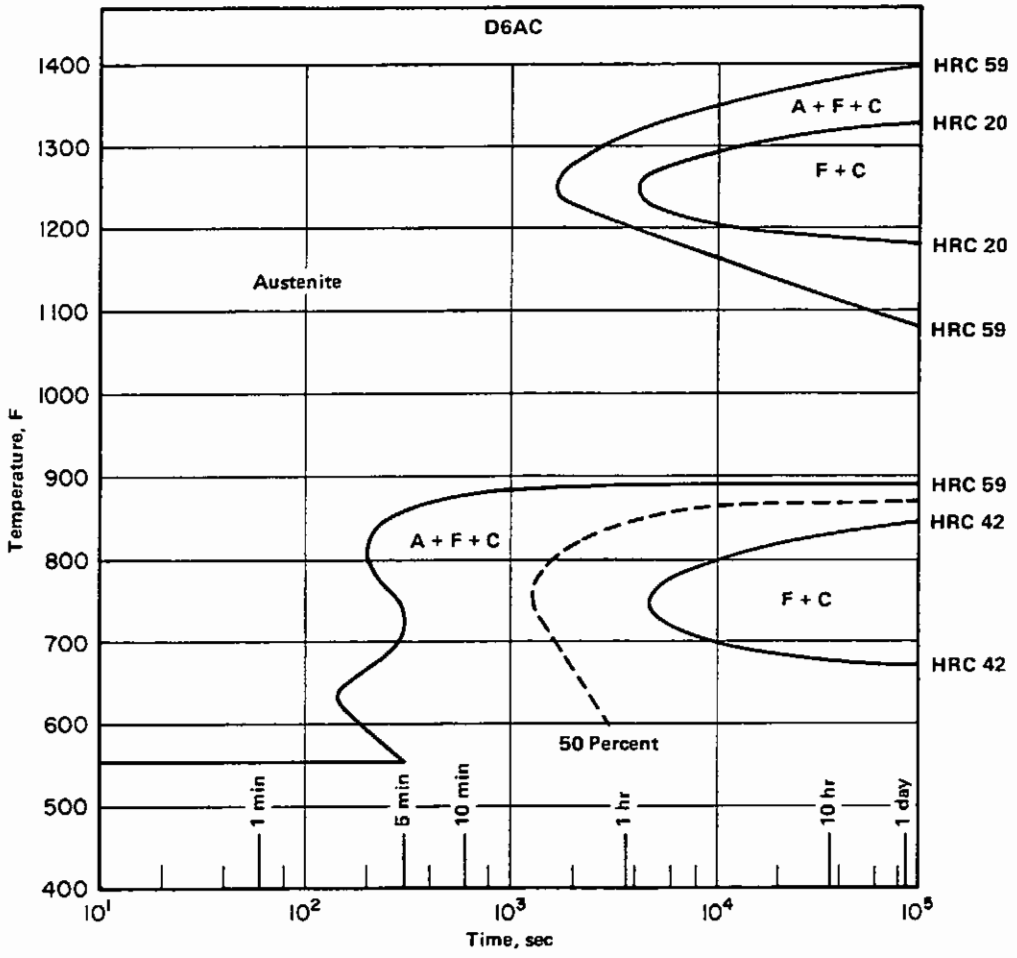


FIGURE 2.0121. TIME-TEMPERATURE-TRANSFORMATION DIAGRAM (53)

Fe
0.46 C
1.0 Cr
1.0 Mo
0.55 Ni

D6A
D6AC

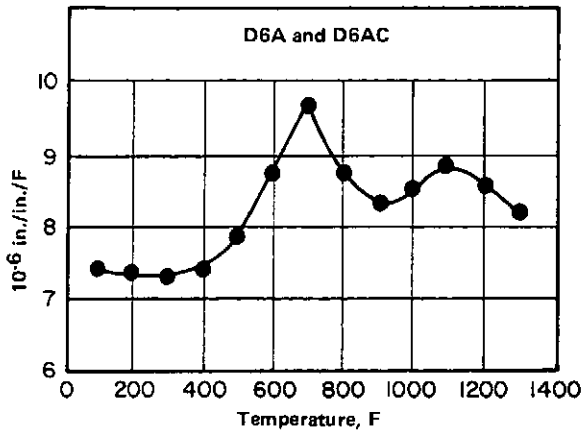


FIGURE 2.014. THERMAL EXPANSION

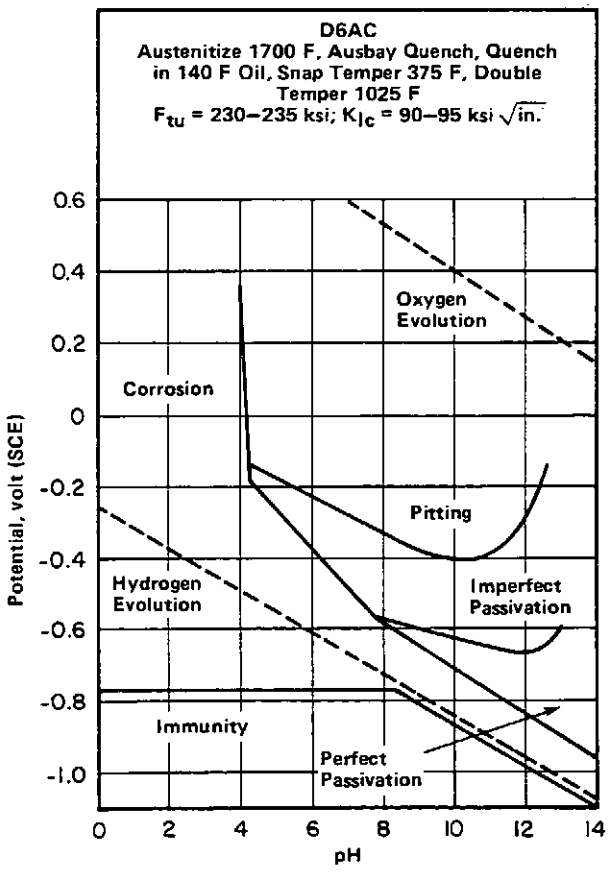


FIGURE 2.0312. POURBAIX DIAGRAM FOR CORROSION OF D6AC IN 0.1M NaCl (55)

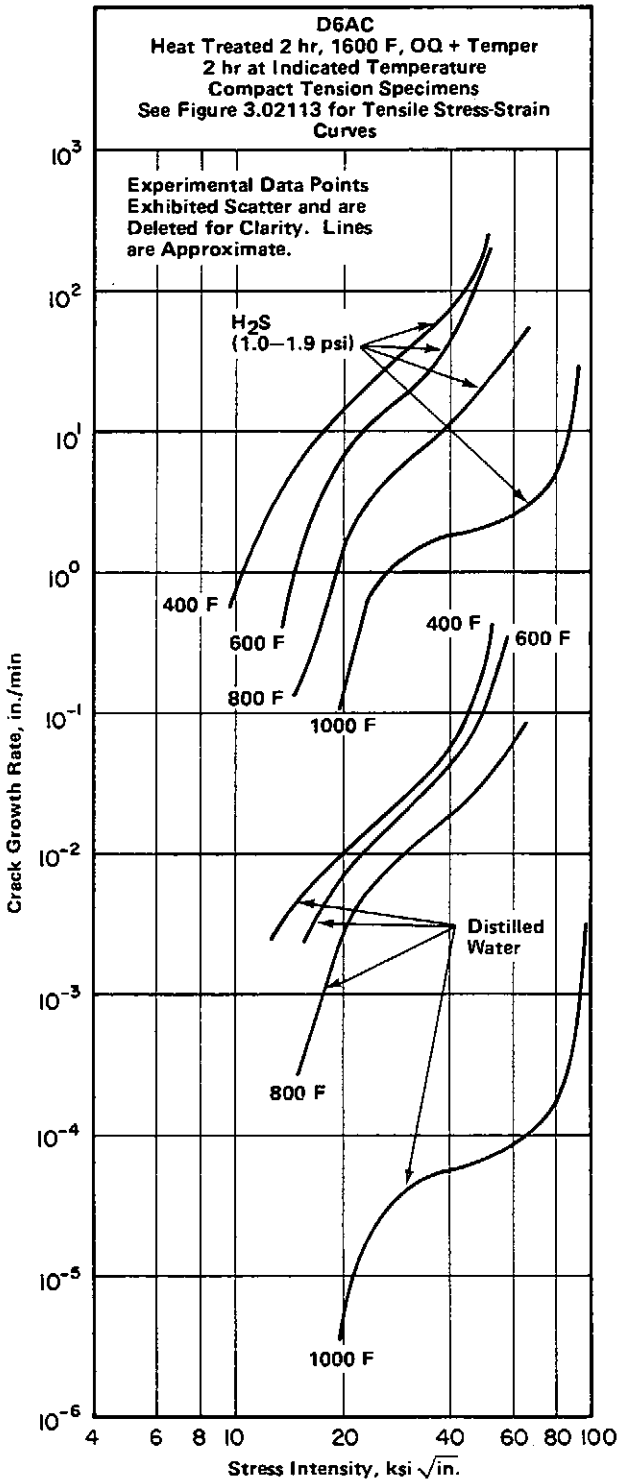


FIGURE 2.0322. EFFECTS OF TEMPERING TEMPERATURE ON STRESS-CORROSION CRACK-GROWTH BEHAVIOR IN WATER AND IN HYDROGEN SULFIDE (57)

	Fe
0.46	C
1.0	Cr
1.0	Mo
0.55	Ni

D6A
D6AC

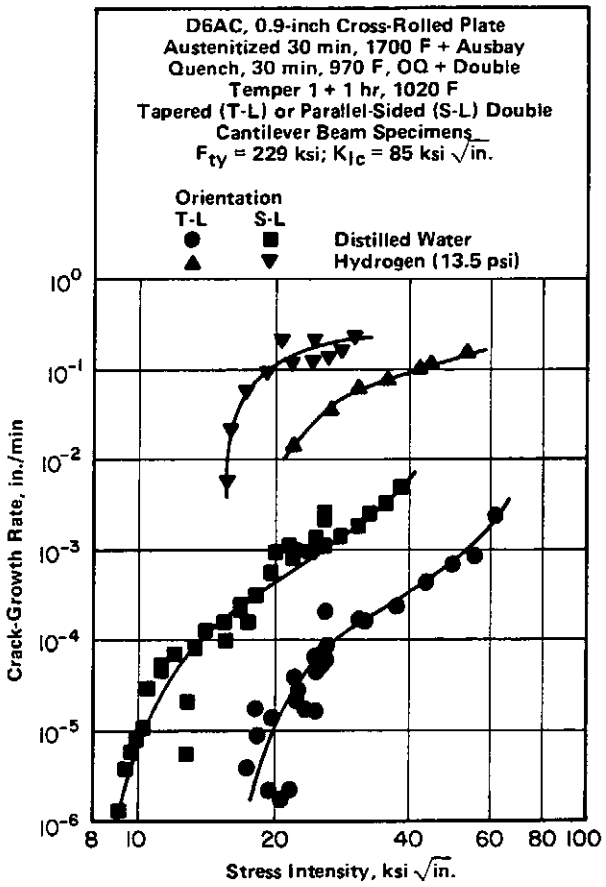


FIGURE 2.0324. EFFECTS OF ORIENTATION ON SUB-CRITICAL STRESS-CORROSION CRACK-GROWTH BEHAVIOR IN DISTILLED WATER AND IN HYDROGEN (58)

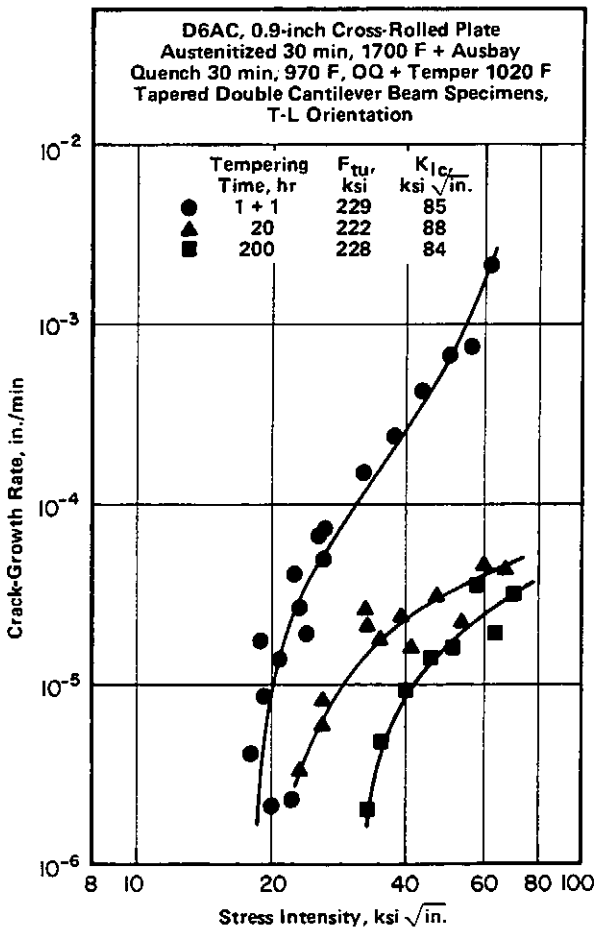


FIGURE 2.0325. EFFECT OF TEMPERING TIME AT 1020 F ON SUBCRITICAL STRESS-CORROSION CRACK-GROWTH BEHAVIOR IN DISTILLED WATER (58)

	Fe
0.46	C
1.0	Cr
1.0	Mo
0.55	Ni

D6A
D6AC

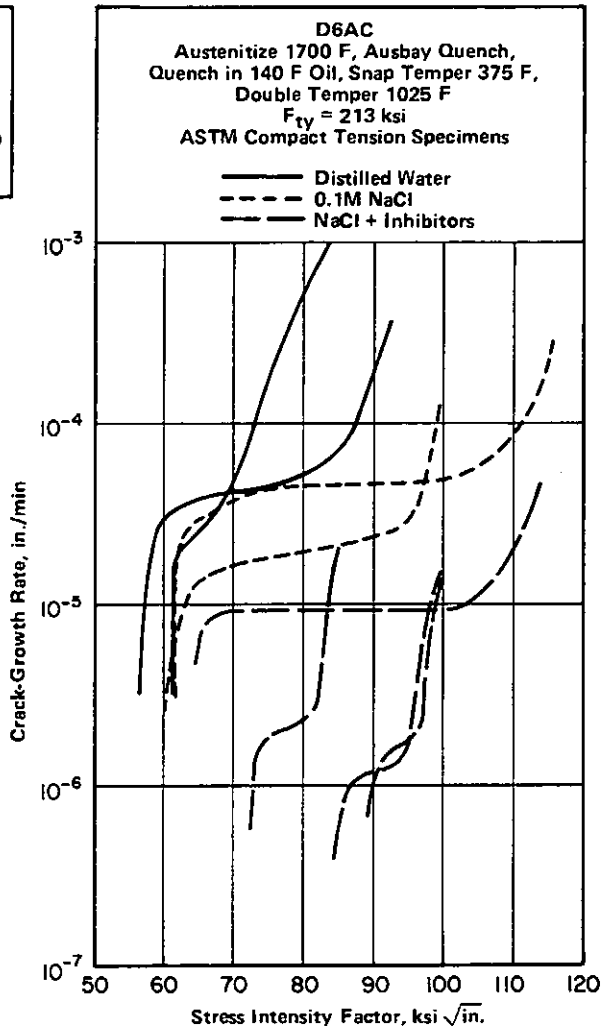


FIGURE 2.0327. EFFECTS OF INHIBITORS ON STRESS-CORROSION CRACK-GROWTH BEHAVIOR (60)

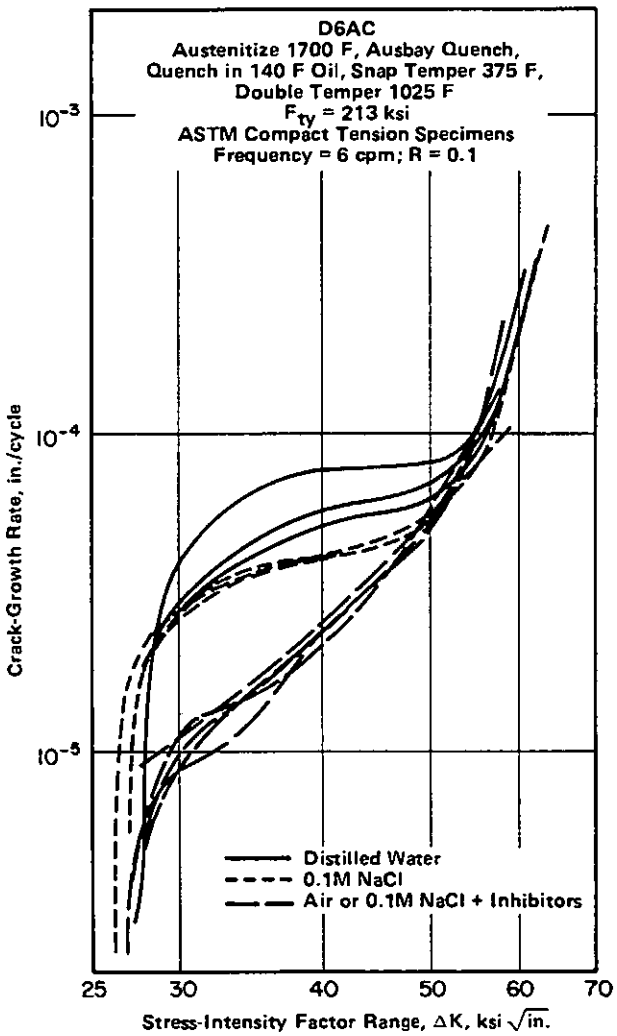


FIGURE 2.0328. EFFECTS OF INHIBITORS ON CORROSION FATIGUE CRACK-GROWTH BEHAVIOR (60)

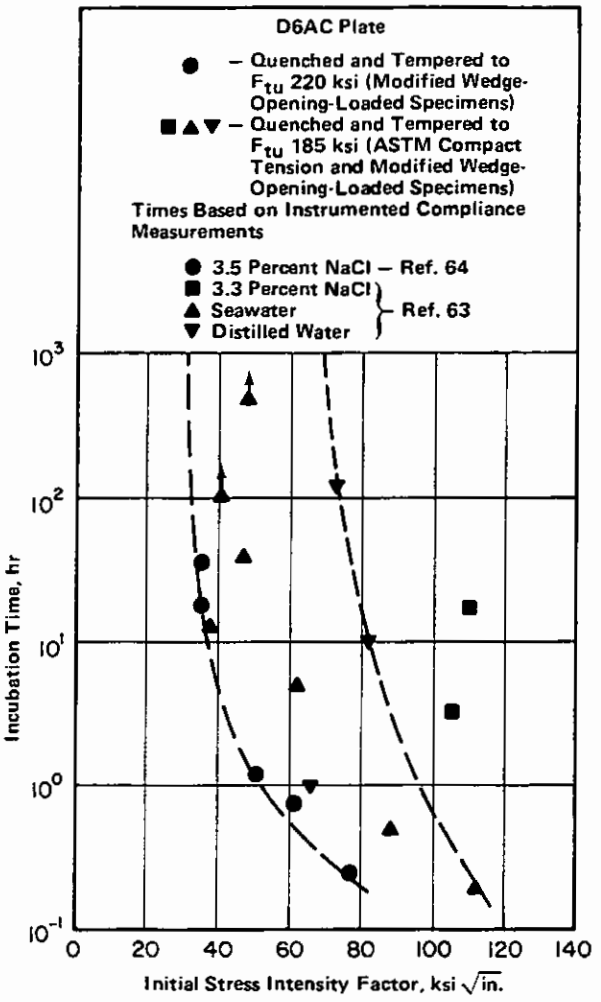


FIGURE 2.03211. INCUBATION TIMES FOR STRESS-CORROSION CRACK-GROWTH INITIATION IN AQUEOUS SOLUTIONS AS A FUNCTION OF INITIAL STRESS INTENSITY FACTOR (63, 64)

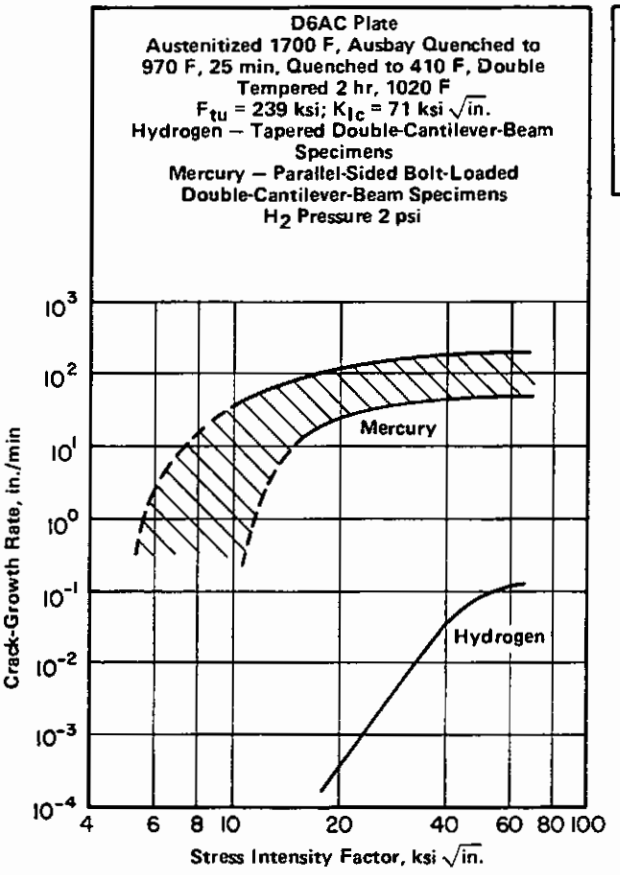


FIGURE 2.0331. STRESS-CORROSION CRACK-GROWTH BEHAVIOR IN LIQUID MERCURY AND LOW PRESSURE HYDROGEN ENVIRONMENTS (65)

Fe	
0.46	C
1.0	Cr
1.0	Mo
0.55	Ni

D6A
D6AC

Alloy	D6AC									
AMS Spec.	Product Form	Condition	Thickness, in.	F_{tu}, ksi Min	F_{tu}, ksi Max	F_{ty}, ksi Min	Elongation, %, Min	RA, %, Min	Hardness Min	Hardness Max
6431F	Bar	Cold Finished	≤0.500	–	145	–	–	–	–	–
		Hot Finished	>0.500	–	–	–	–	–	–	265 BHN
		Cold Finished	>0.500	–	–	–	–	–	–	285 BHN
	Mechanical Tubing	Cold Finished	–	–	–	–	–	–	–	25 HRC
		Hot Finished	–	–	–	–	–	–	–	285 BHN
	Bars, Forgings, Tubing	Heat Treated[a]	(Longitudinal)[b]	220	250	190	12	35	46 HRC	–
			(Transverse)[a]	220	250	190	9	30[d]	46 HRC	–
6438C	Sheet, Strip, Plate	Annealed or	–	–	–	–	–	–	–	–
		Norm. + Temp	–	–	–	–	–	–	–	30 HRC
		Spheroidize Ann.	–	–	–	–	–	–	–	100 HRB
		Heat Treated[a]	–	224	–	195	7	–	47 HRC[e]	–

Note: The original AMS document should be consulted for complete specification details.

(a) See Table 1.054 for heat treatment.
(b) Testing in longitudinal direction need not be performed on material tested in transverse direction.
(c) Tensile specimens must not be less than 2.50 in. in length.
(d) Average of all tests; any one test must be minimum of 25 percent reduction in area.
(e) Product shall not be rejected on basis of hardness if tensile properties are met.

TABLE 3.011. AMS SPECIFIED MECHANICAL PROPERTIES (28, 29)

	Fe
0.46	C
1.0	Cr
1.0	Mo
0.55	Ni

D6A
D6AC

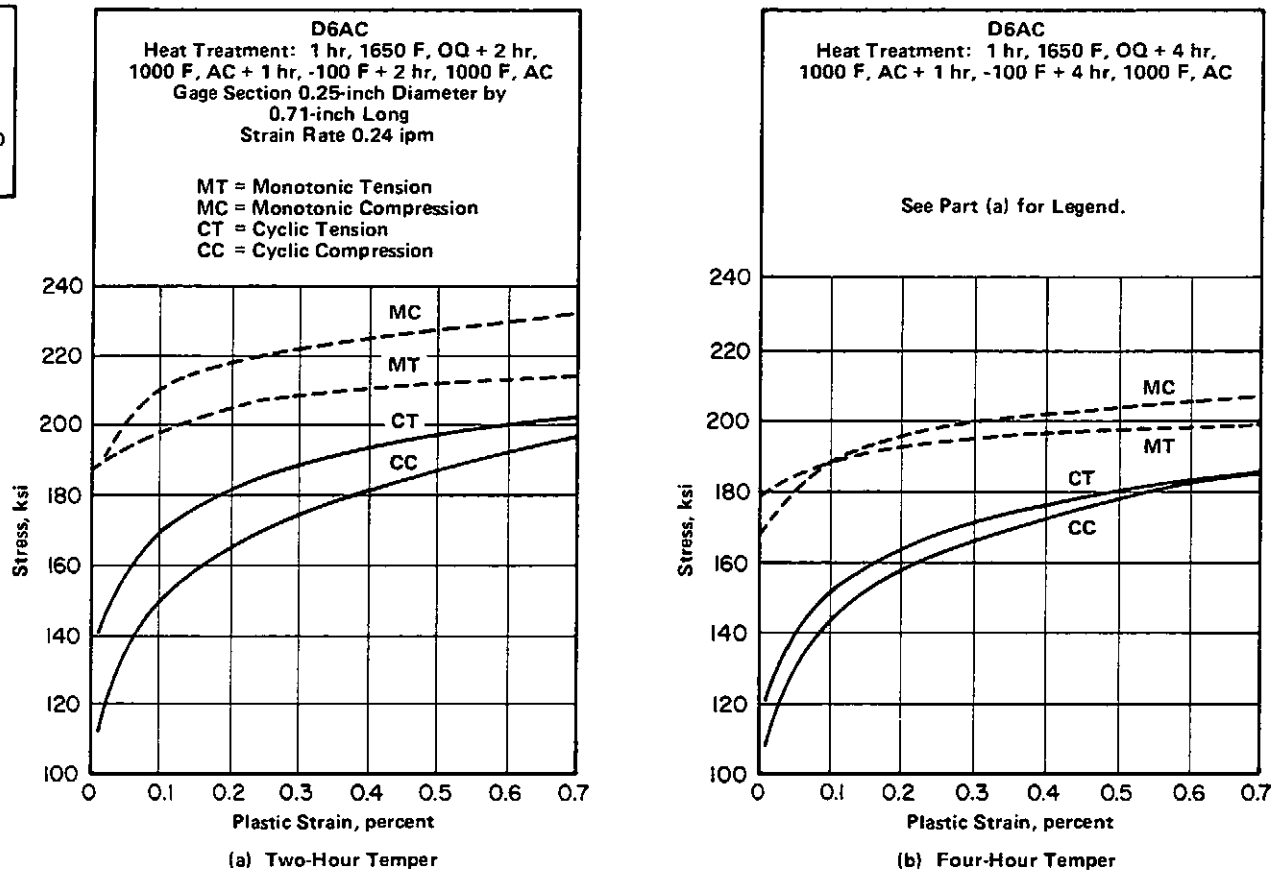


FIGURE 3.02112. MONOTONIC AND CYCLIC STRESS-STRAIN CURVES FOR TWO DIFFERENT HEAT TREATMENTS (52)

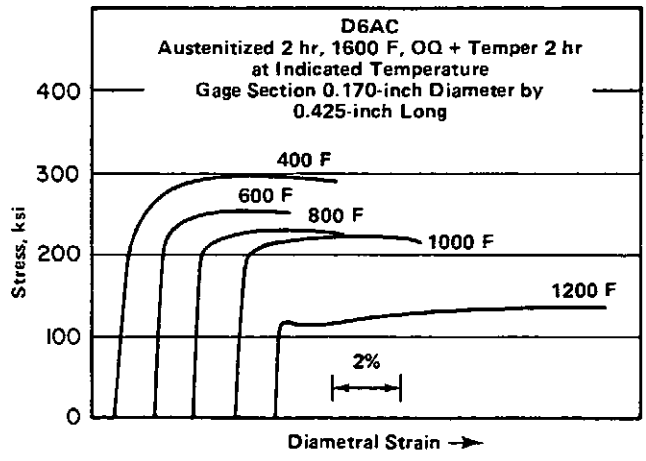


FIGURE 3.02113. EFFECTS OF TEMPERING TEMPERATURE ON STRESS-STRAIN CURVES AT ROOM TEMPERATURE (57)

	Fe
0.46	C
1.0	Cr
1.0	Mo
0.55	Ni

D6A
D6AC

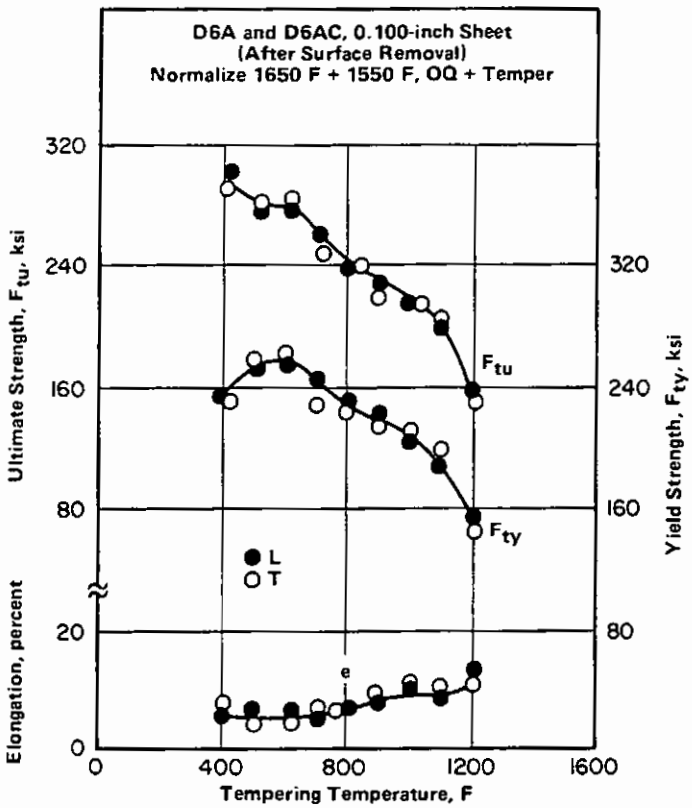


FIGURE 3.02121. EFFECT OF TEMPERING TEMPERATURE ON TENSILE PROPERTIES OF SHEET (4)

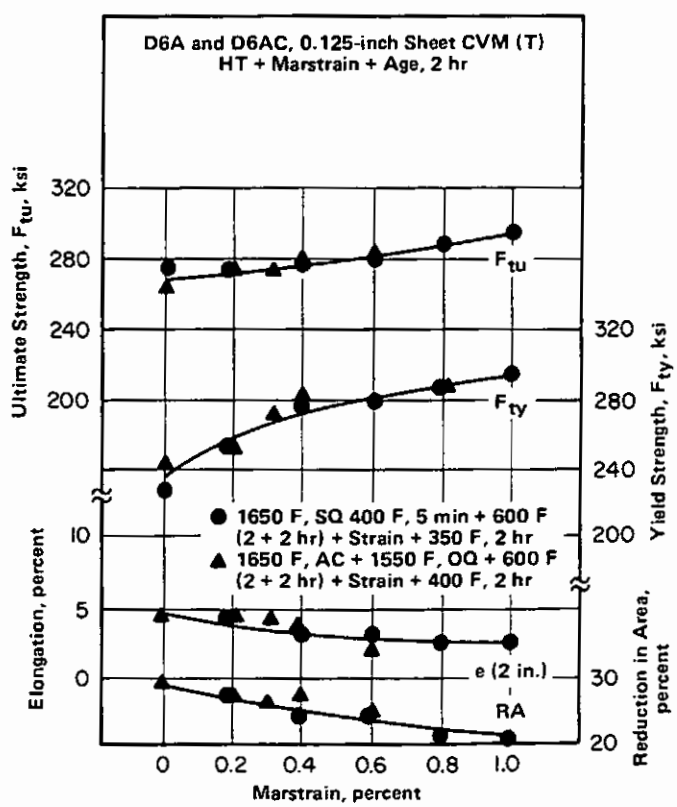


FIGURE 3.02122. EFFECT OF MARSTRAIN ON TENSILE PROPERTIES OF SHEET (11)

Fe	
0.46	C
1.0	Cr
1.0	Mo
0.55	Ni

D6A
D6AC

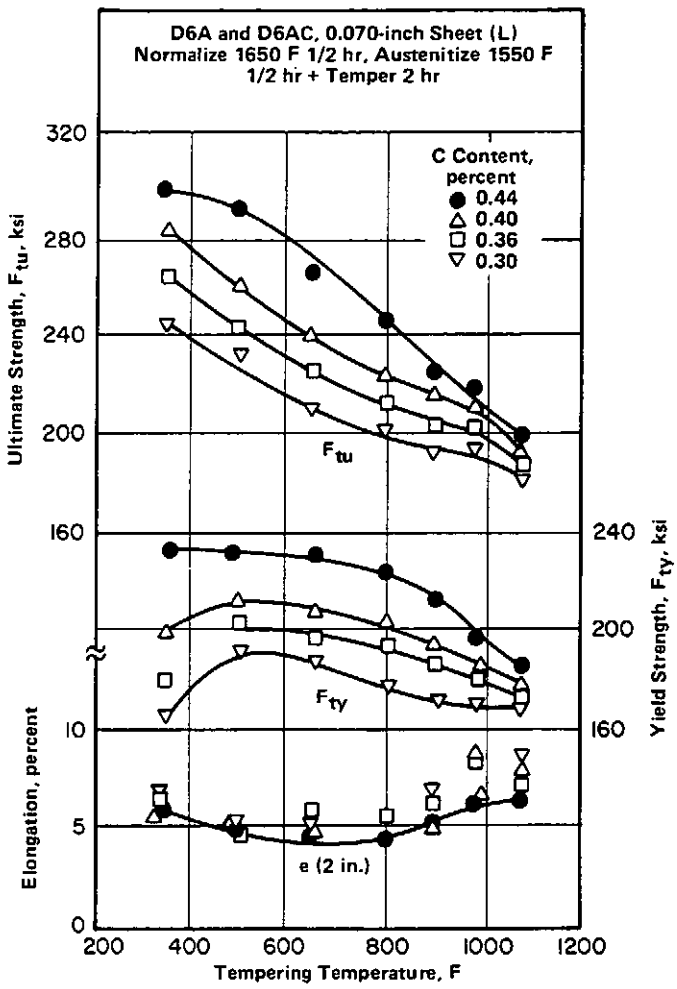


FIGURE 3.02123. EFFECT OF LOW CARBON CONTENT AND VARIOUS TEMPERING TEMPERATURES ON TENSILE PROPERTIES OF SHEET (31)

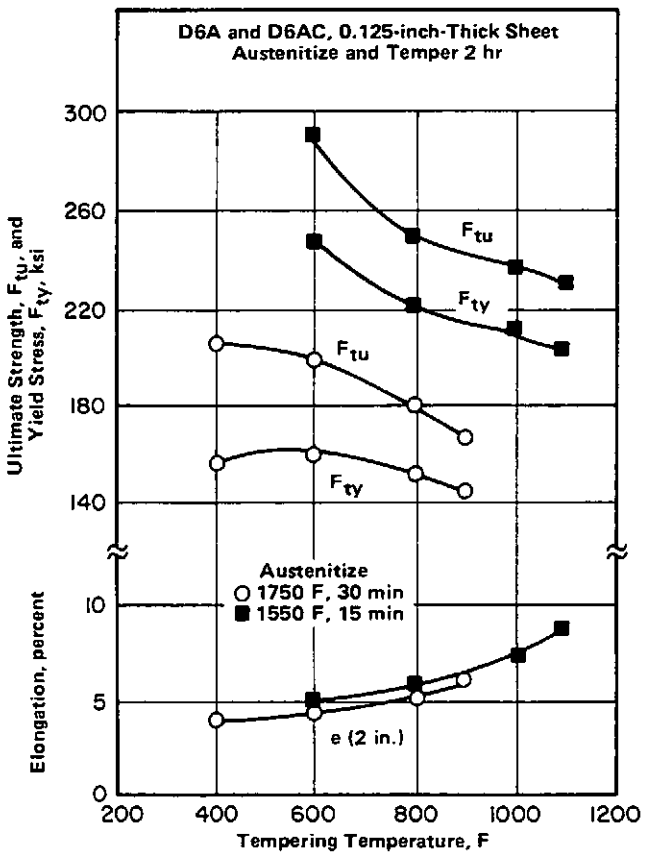


FIGURE 3.02124. EFFECT OF TEMPERING TEMPERATURE ON TENSILE PROPERTIES AT TWO AUSTENITIZING TEMPERATURES (41)

	Fe
0.46	C
1.0	Cr
1.0	Mo
0.55	Ni

D6A
D6AC

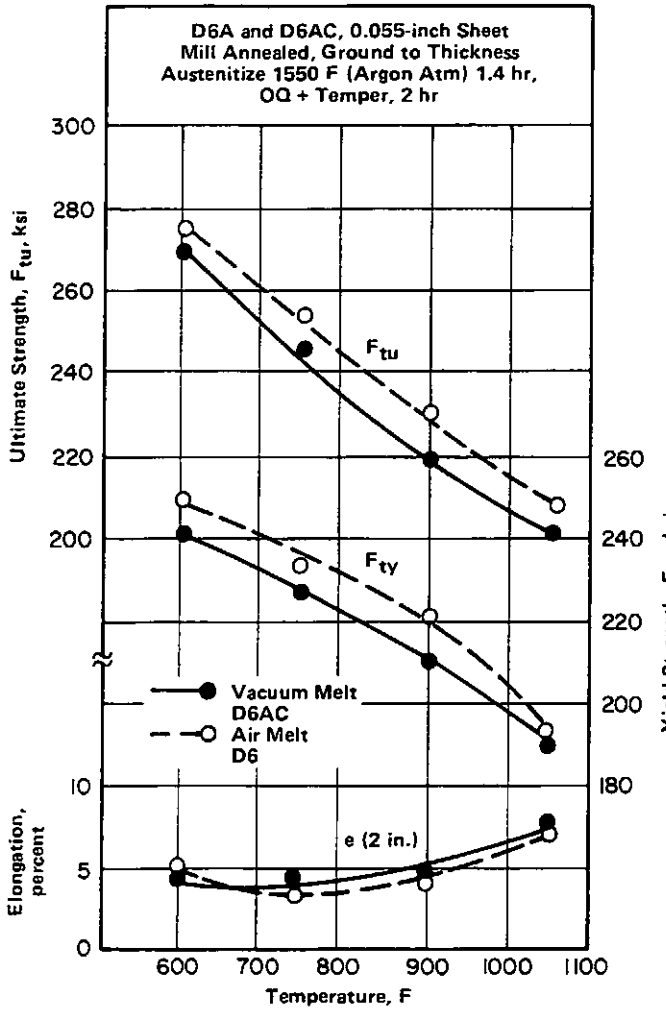


FIGURE 3.02125. EFFECT OF TEMPERING TEMPERATURE ON TENSILE PROPERTIES OF AIR AND VACUUM MELT ALLOY SHEET (36)

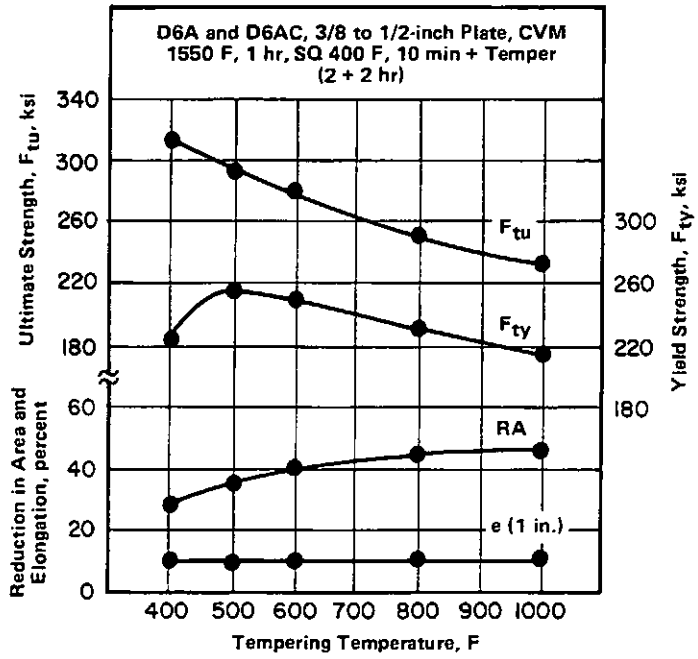


FIGURE 3.02131. EFFECT OF TEMPERING TEMPERATURE ON TENSILE PROPERTIES OF PLATE (18)

Alloy	D6A – D6AC
Form	Plate
Condition	1650 F, 1 hr OQ (140 F) + 500 to 550 F Temper
F_{tu}, ksi	275
Range	268 – 284
F_{ty}, ksi	233
Range	225 – 245

TABLE 3.02132. RANGE OF TENSILE PROPERTIES IN PLATES TEMPERED AT 500 TO 550 F (49)

	Fe
0.46	C
1.0	Cr
1.0	Mo
0.55	Ni

D6A
D6AC

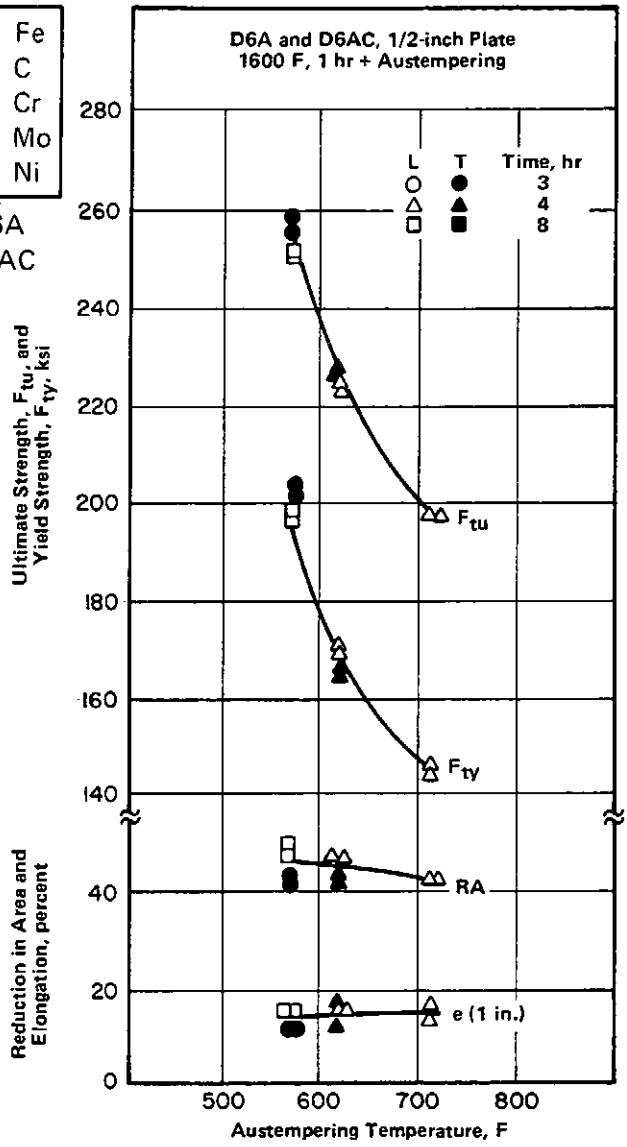


FIGURE 3.02133. EFFECT OF AUSTEMPERING TEMPERATURE ON TENSILE PROPERTIES OF PLATE (39)

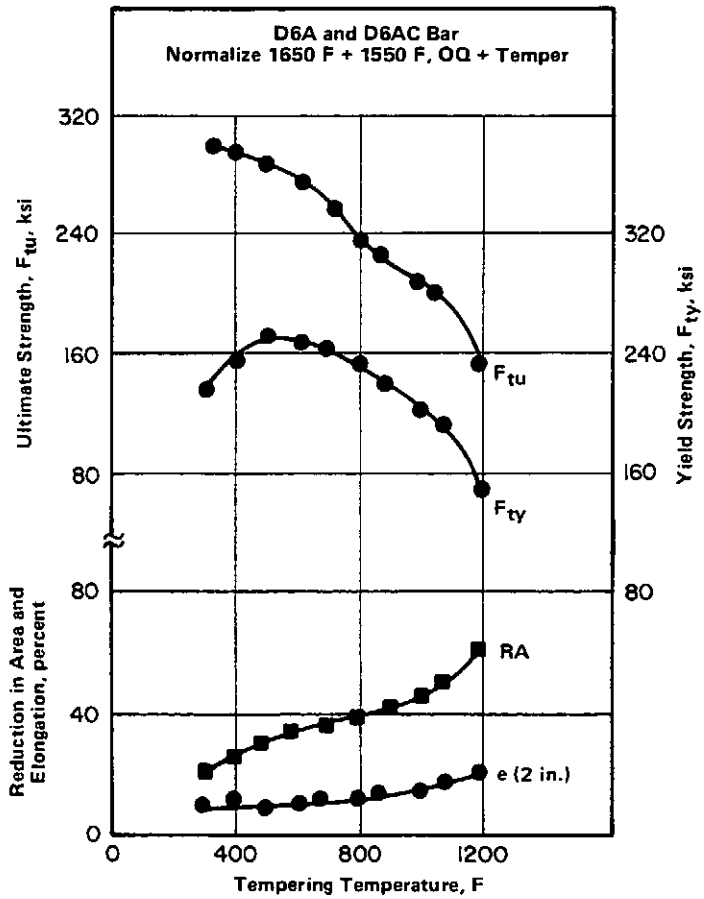


FIGURE 3.02141. EFFECT OF TEMPERING TEMPERATURE ON TENSILE PROPERTIES OF BAR (4)

	Fe
0.46	C
1.0	Cr
1.0	Mo
0.55	Ni

D6A
D6AC

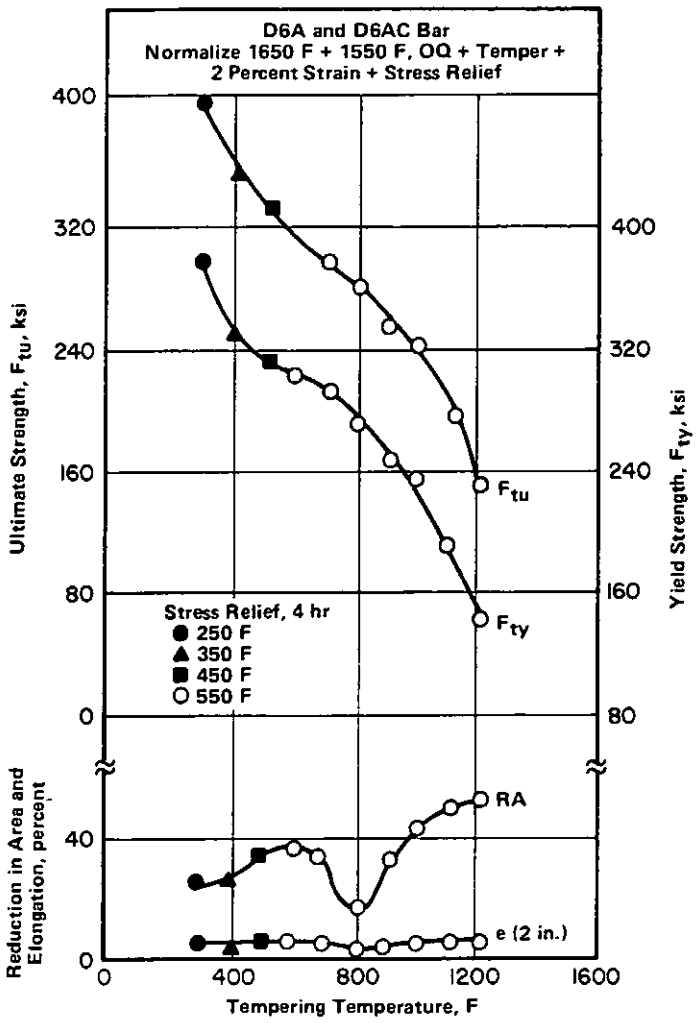


FIGURE 3.02142. EFFECT OF TEMPERING TEMPERATURE ON TENSILE PROPERTIES OF STRAIN-AGED BAR (4)

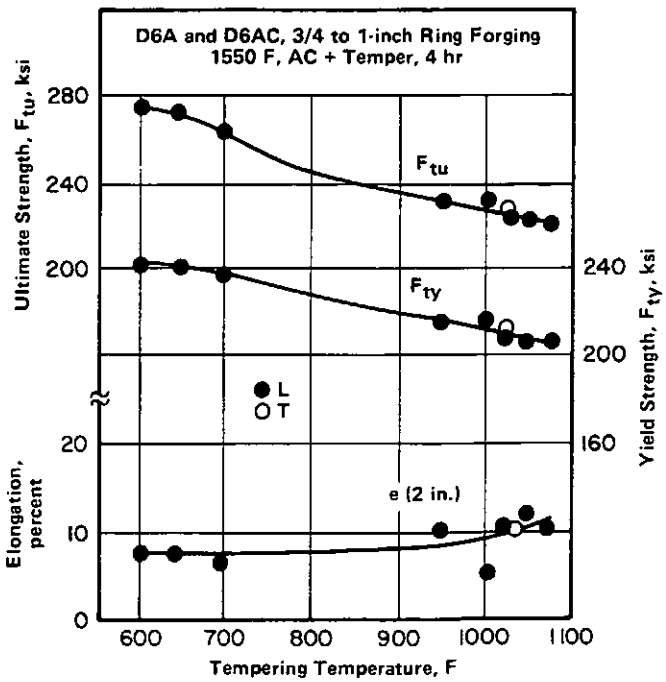


FIGURE 3.02151. EFFECT OF TEMPERING TEMPERATURE ON TENSILE PROPERTIES OF ROLLED RING FORGINGS (13)

	Fe
0.46	C
1.0	Cr
1.0	Mo
0.55	Ni

D6A
D6AC

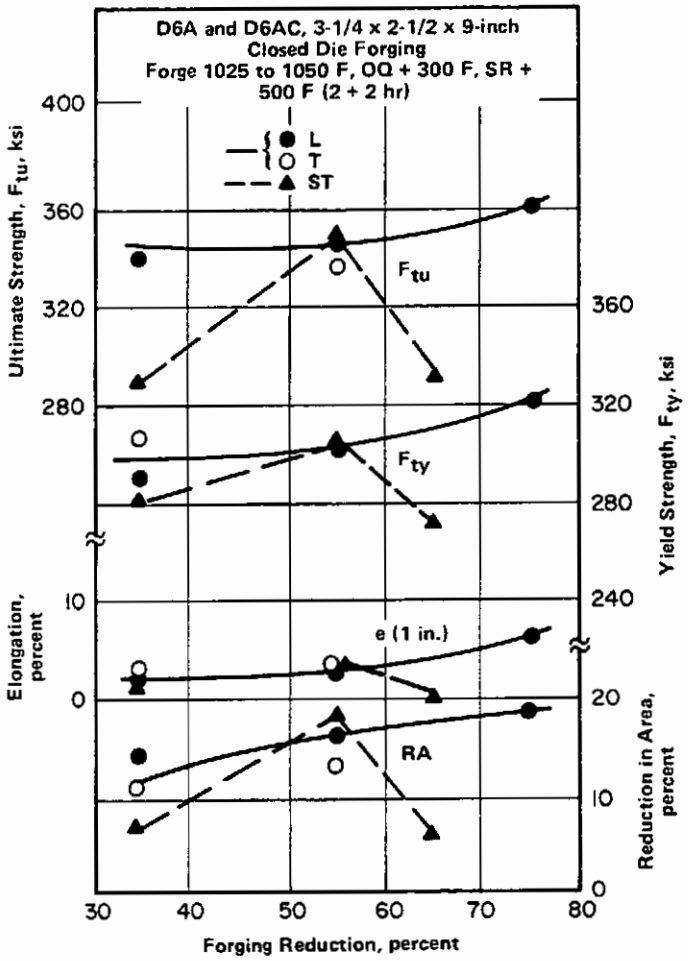


FIGURE 3.02152. EFFECT OF FORGING REDUCTION ON TENSILE PROPERTIES OF A VARIABLE-CROSS-SECTION AUSFORMED FORGING TEMPERED AT 500 F (10)

	Fe
0.46	C
1.0	Cr
1.0	Mo
0.55	Ni

D6A
D6AC

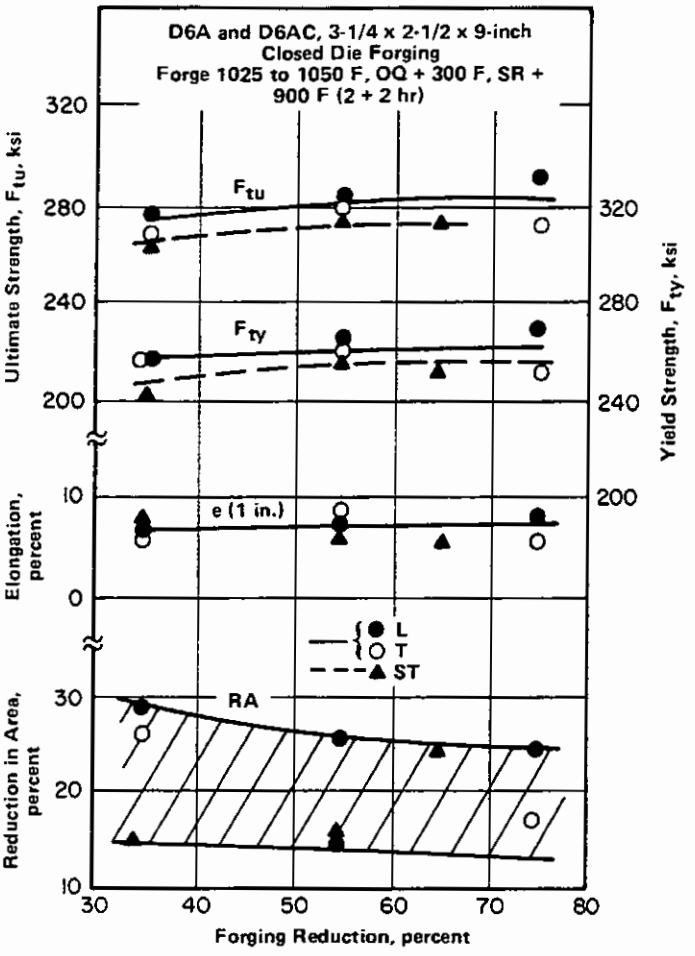


FIGURE 3.02153. EFFECT OF FORGING REDUCTION ON TENSILE PROPERTIES OF A VARIABLE-CROSS-SECTION AUSFORMED FORGING TEMPERED AT 900 F (10)

	Fe
0.46	C
1.0	Cr
1.0	Mo
0.55	Ni

D6A
D6AC

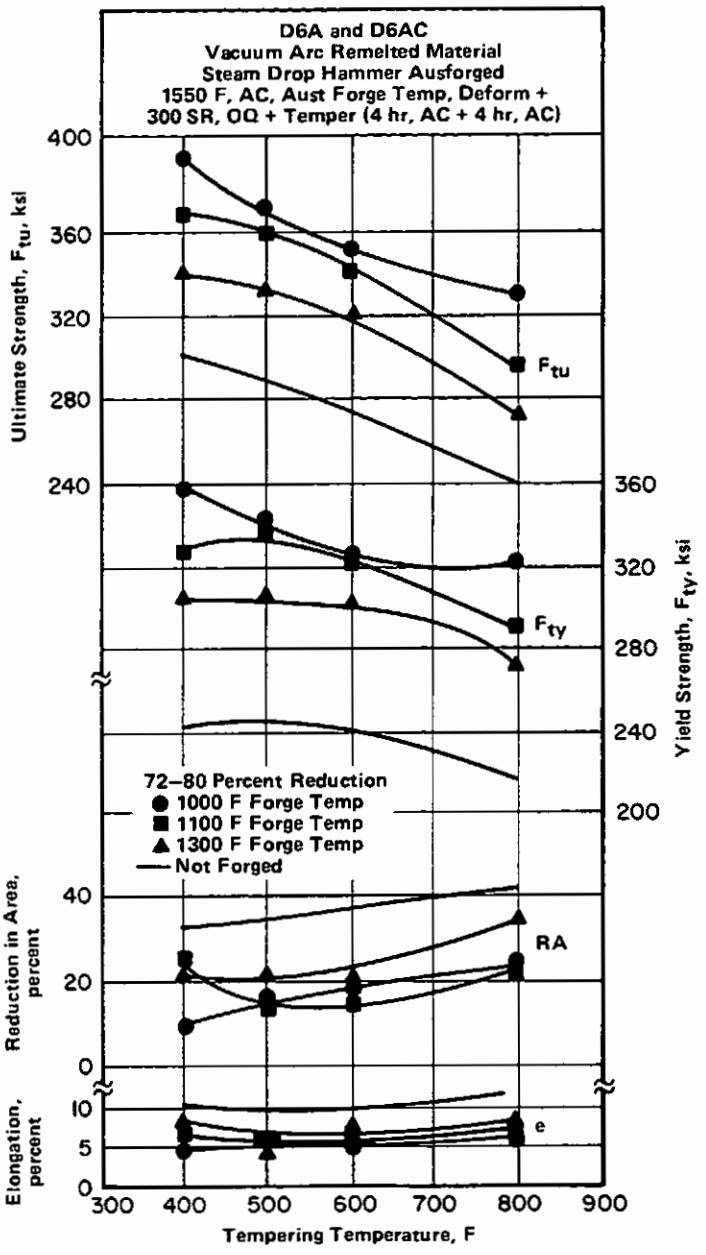


FIGURE 3.02154. EFFECT OF FORGING AND TEMPERING TEMPERATURE ON TENSILE PROPERTIES OF AUSFORMED FORGINGS (32)

	Fe
0.46	C
1.0	Cr
1.0	Mo
0.55	Ni

D6A
D6AC

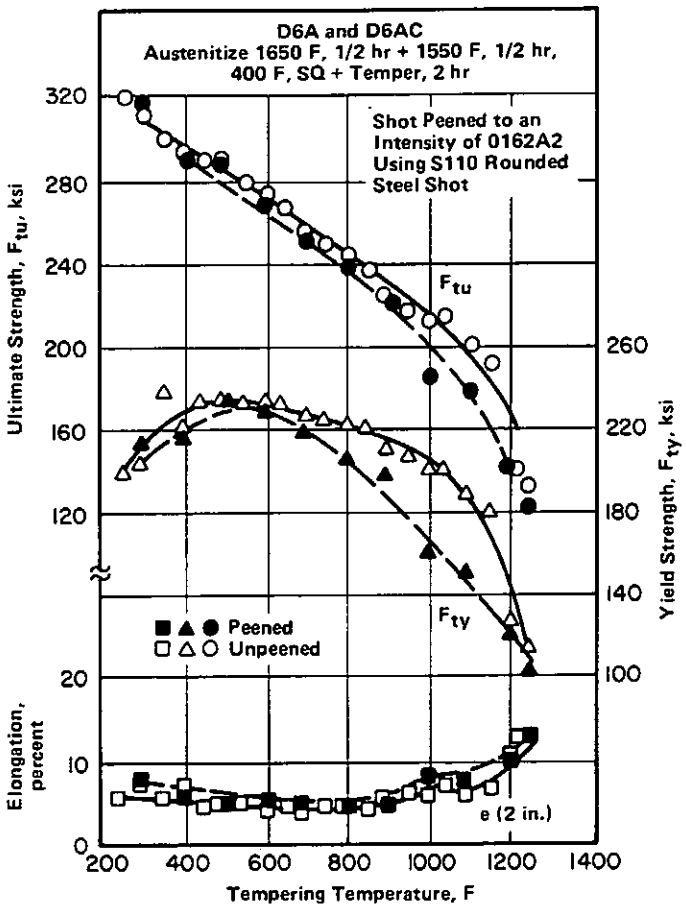


FIGURE 3.02155. EFFECT OF SHOT PEENING AND TEMPERING TEMPERATURE ON TENSILE PROPERTIES (35)

	Fe
0.46	C
1.0	Cr
1.0	Mo
0.55	Ni

D6A
D6AC

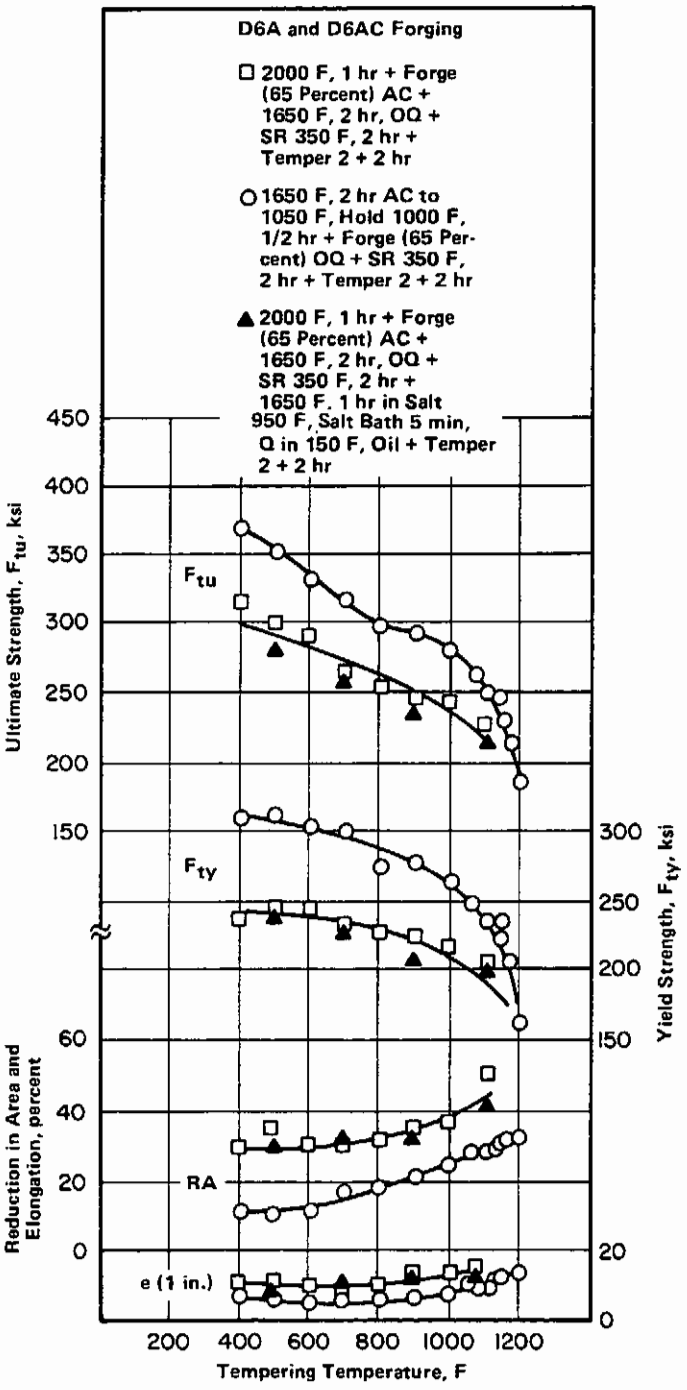


FIGURE 3.02156. EFFECT OF TEMPERING TEMPERATURE ON TENSILE PROPERTIES FOR THREE THERMAL-MECHANICAL PROCESSING TREATMENTS OF FORGED ALLOY (42)

Alloy	D6A – D6AC									
Form	T-Shaped Extrusion 4-3/4 x 4-3/8 x 72 in. (CVM) With 3/8 and 5/8 in.-Thick Legs									
Condition	1650 F, 30 min, FC + 1625 F, 30 min, 950 F, 1 hr, 400 F Salt, 15 min, AC + Temper (2 + 2 hr)									
Temper	650 F					1025 F				
Location	Center	5/8 in. Leg		3/8 in. Leg		Center	5/8 in. Leg		3/8 in. Leg	
Direction	L	L	T	L	T	L	L	T	L	T
F_{tu}, ksi	290	285	281	282	284	239	238	236	239	237
F_{ty}, ksi	255	248	254	245	250	218	218	218	220	219
e (1 in.), percent	12	11	9	12	10	15	13	12	13	12
RA, percent	40	38	34	42	35	49	30	40	52	42

	Fe
0.46	C
1.0	Cr
1.0	Mo
0.55	Ni

D6A
D6AC

TABLE 3.02161. TENSILE PROPERTIES OF EXTRUSION AT TWO TEMPERING TEMPERATURES (14)

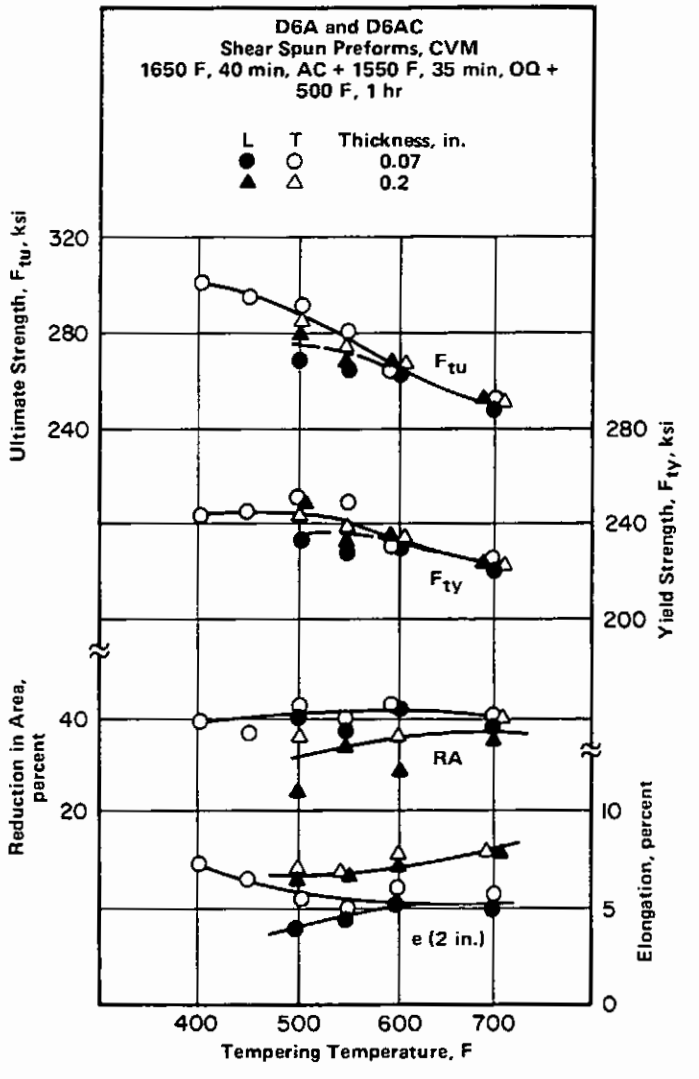


FIGURE 3.02171. EFFECT OF TEMPERING TEMPERATURE ON TENSILE PROPERTIES OF SHEAR SPUN ALLOY (19)

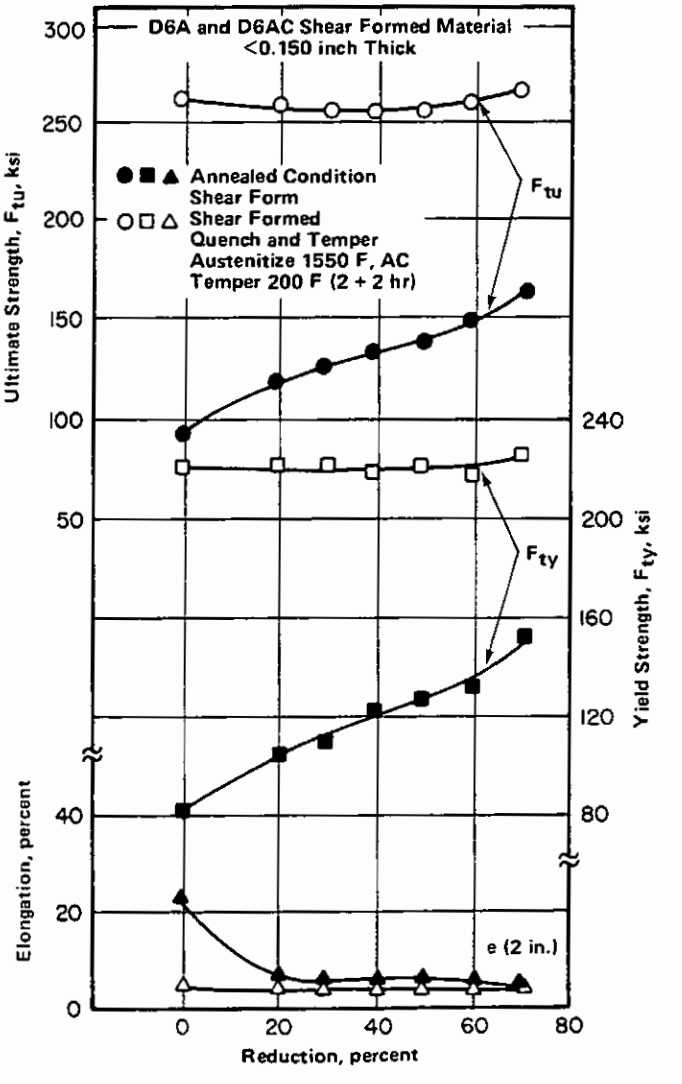


FIGURE 3.02172. EFFECT OF SHEAR FORM REDUCTION ON TENSILE PROPERTIES (33)

	Fe
0.46	C
1.0	Cr
1.0	Mo
0.55	Ni

D6A
D6AC

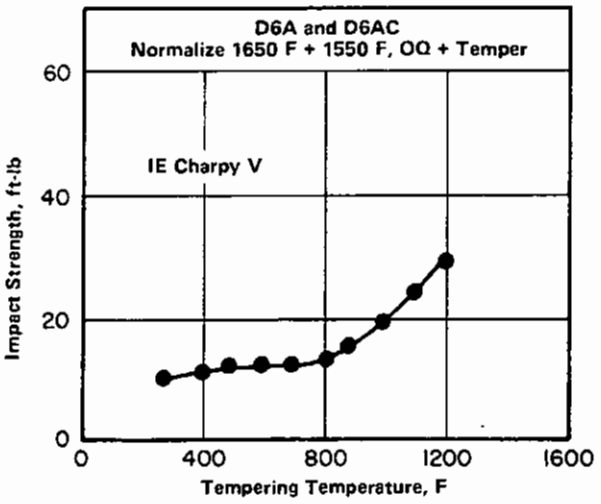


FIGURE 3.0231. EFFECT OF TEMPERING TEMPERATURE ON IMPACT PROPERTIES (4)

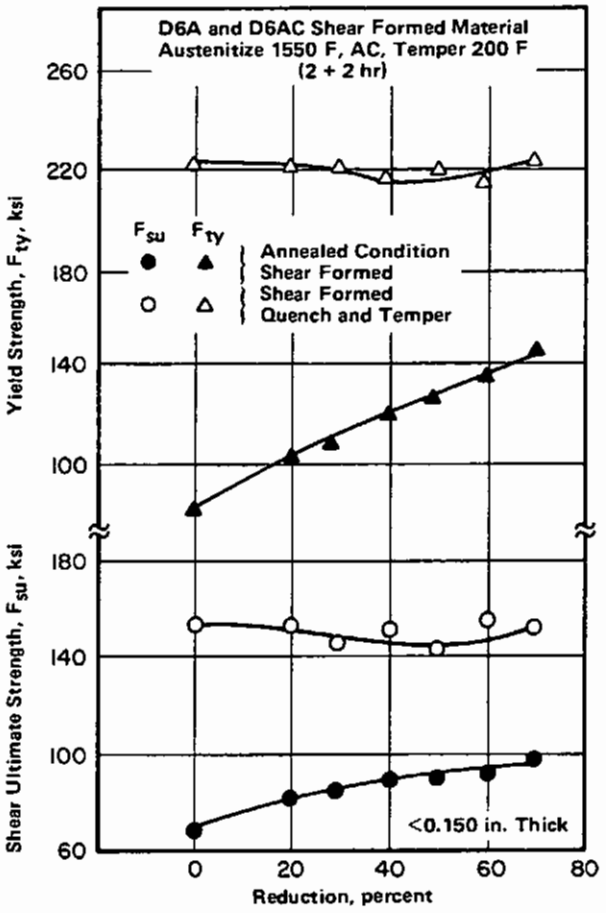


FIGURE 3.0251. EFFECT OF SHEAR FORM REDUCTION ON SHEAR STRENGTH (33)

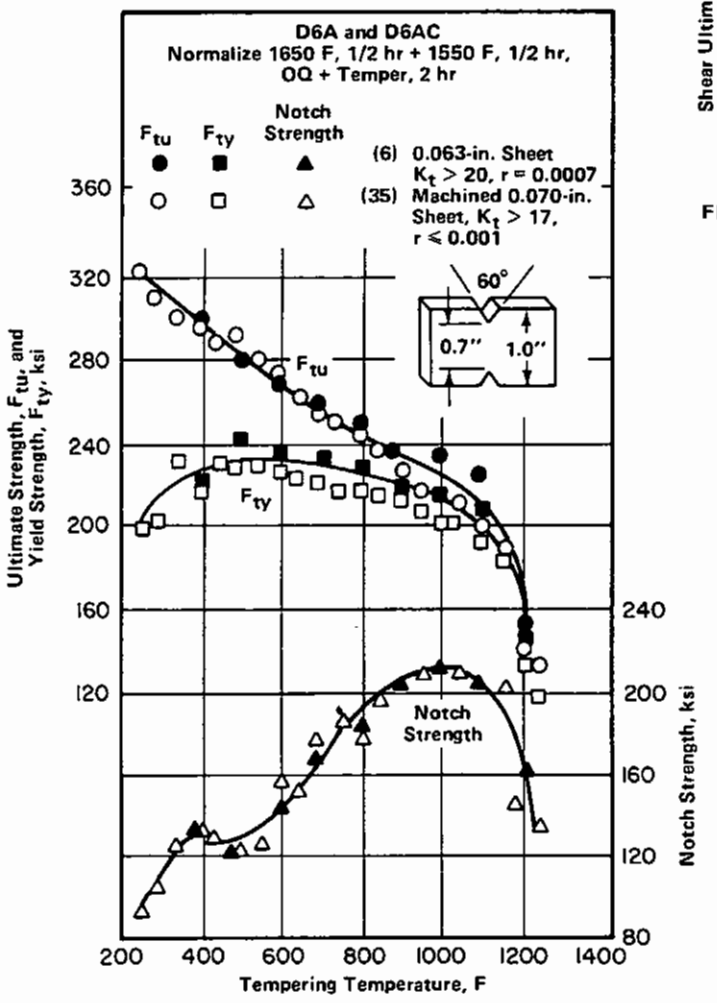


FIGURE 3.027111. EFFECT OF TEMPERING TEMPERATURE ON SHARP NOTCH PROPERTIES OF SHEET (6, 35)

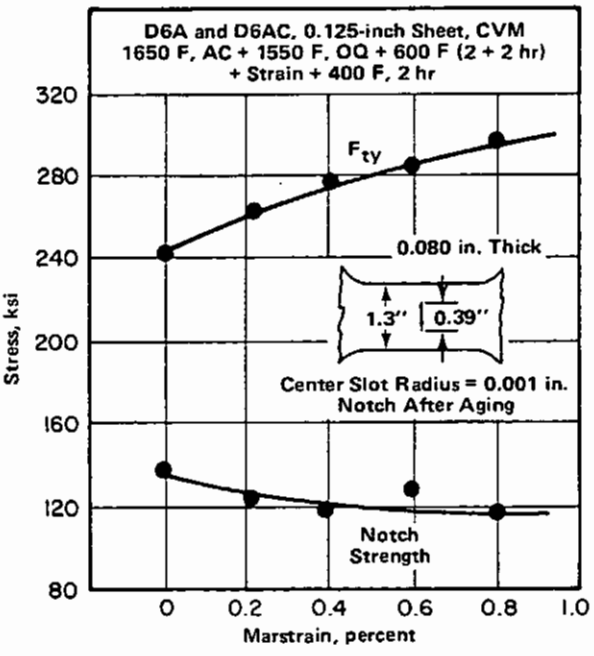


FIGURE 3.027112. EFFECT OF MARSTRAIN ON SHARP NOTCH PROPERTIES OF SHEET (11)

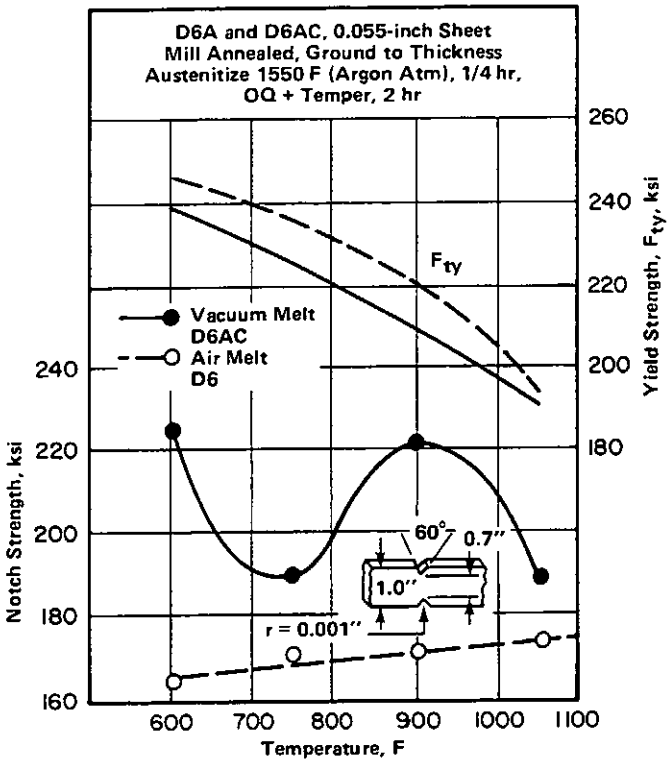
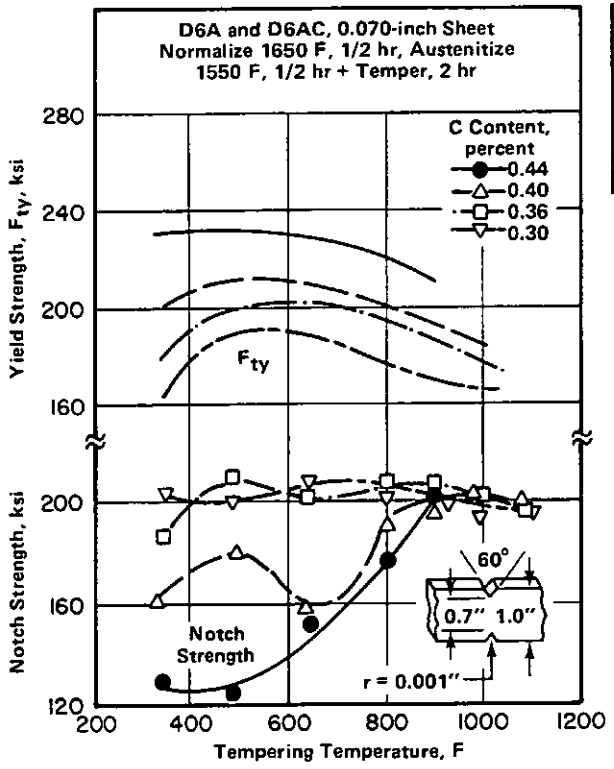


FIGURE 3.027113. EFFECT OF TEMPERING TEMPERATURE ON SHARP NOTCH PROPERTIES OF AIR AND VACUUM MELT SHEET (36)



	Fe
0.46	C
1.0	Cr
1.0	Mo
0.55	Ni

D6A
D6AC

FIGURE 3.027114. EFFECT OF LOW CARBON CONTENT AND TEMPERING TEMPERATURE ON SHARP NOTCH STRENGTH OF SHEET (31)

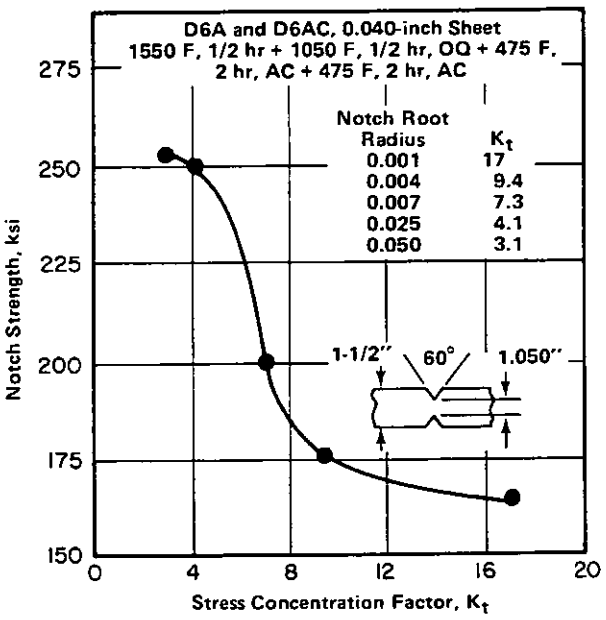


FIGURE 3.027115. EFFECT OF NOTCH ROOT RADII ON SHARP NOTCH STRENGTH OF SHEET (34)

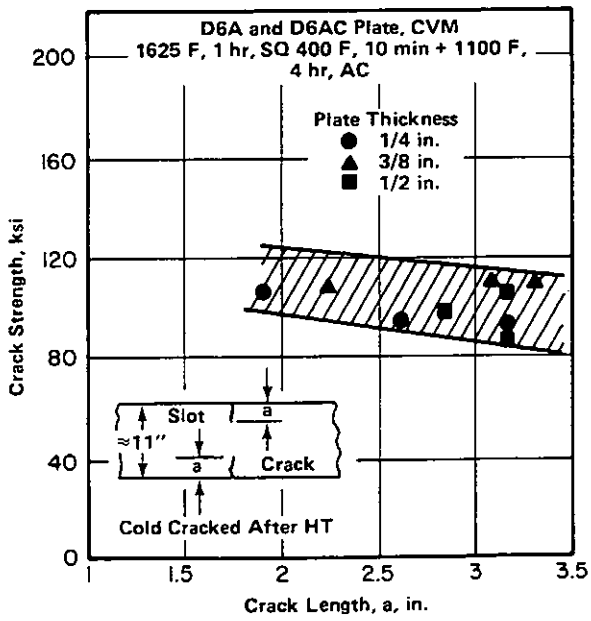


FIGURE 3.027121. EFFECT OF CRACK LENGTH ON CRACK STRENGTH OF THREE THICKNESSES OF PLATE EACH FROM DIFFERENT HEAT (24)

	Fe
0.46	C
1.0	Cr
1.0	Mo
0.55	Ni

D6A
D6AC

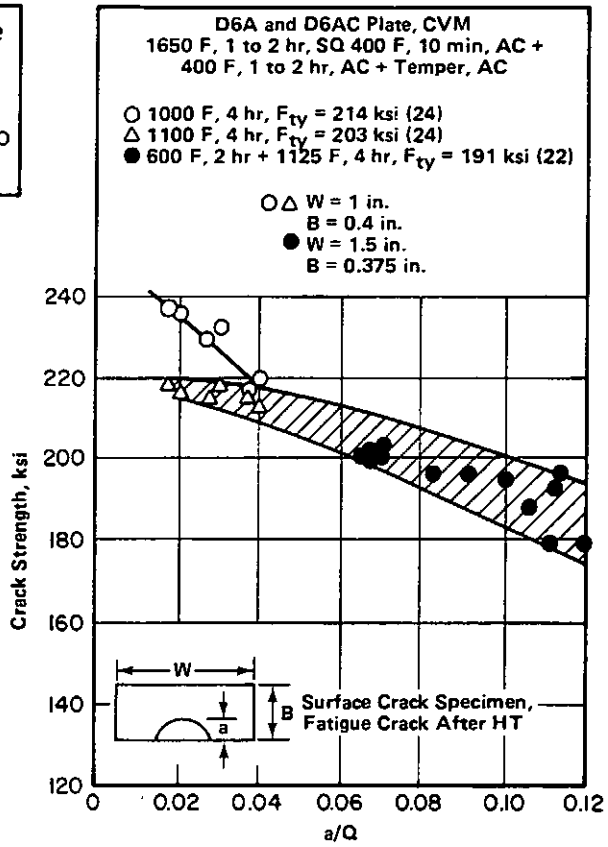


FIGURE 3.027122. EFFECT OF SURFACE CRACKS ON CRACK STRENGTH OF PLATE AT STRENGTH LEVELS BETWEEN F_{ty} = 190 AND 215 KSI (22, 24)

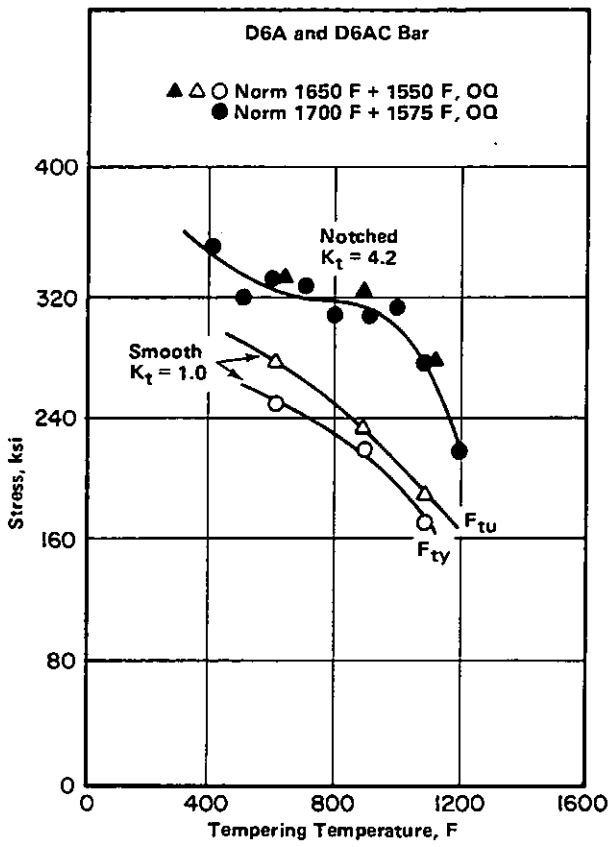


FIGURE 3.027131. EFFECT OF TEMPERING TEMPERATURE ON NOTCH AND SMOOTH TENSILE PROPERTIES OF BAR (4)

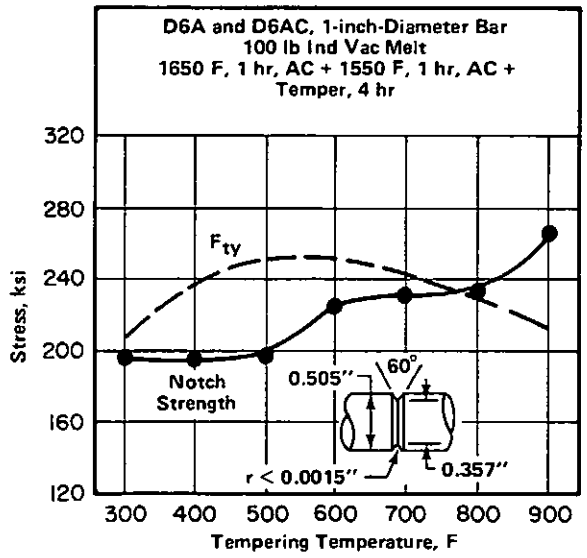


FIGURE 3.027132. EFFECT OF TEMPERING TEMPERATURE ON THE SHARP NOTCH STRENGTH OF BAR (16)

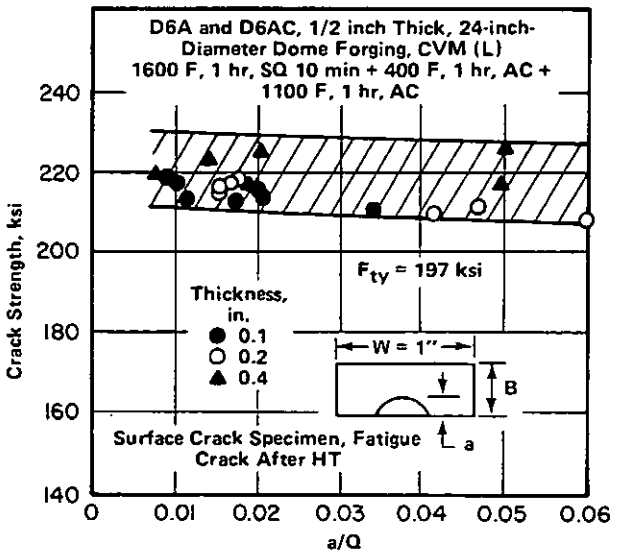


FIGURE 3.027141. EFFECT OF SURFACE CRACKS ON CRACK STRENGTH OF FORGING (23)

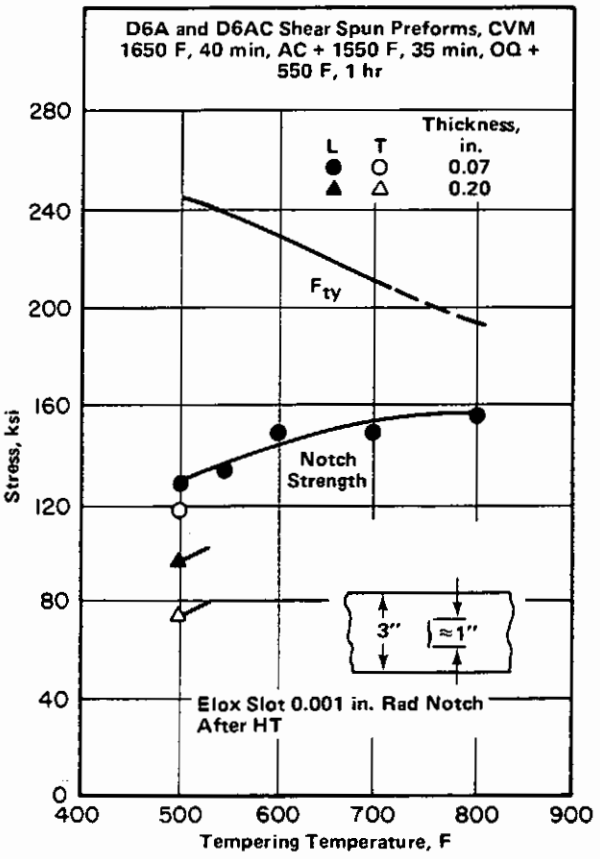


FIGURE 3.02715. EFFECT OF TEMPERING TEMPERATURE ON SHARP NOTCH PROPERTIES OF SHEAR SPUN ALLOY (19)

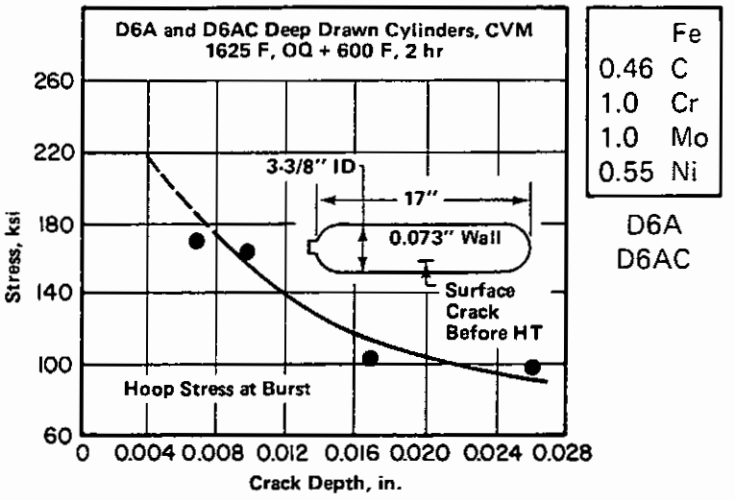


FIGURE 3.02716. EFFECT OF SURFACE CRACKS ON BURST STRENGTH OF THIN WALLED CYLINDERS (15)

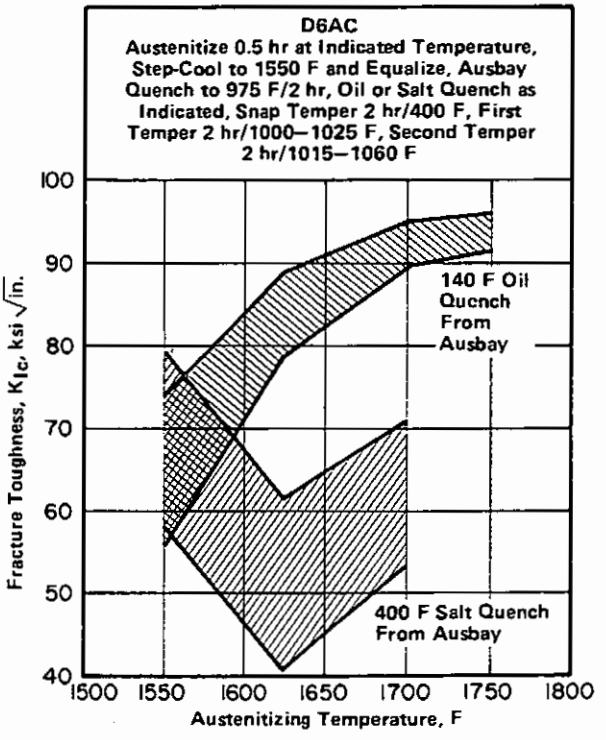


FIGURE 3.02722. EFFECTS OF AUSTENITIZING TEMPERATURE AND QUENCH MEDIUM ON FRACTURE TOUGHNESS (53)

	Fe
0.46	C
1.0	Cr
1.0	Mo
0.55	Ni

D6A
D6AC

Alloy	D6A – D6AC	
Form	0.8-in. Plate (CVM), LT (for F_{ty} see Table 3.0314)	
Condition	A	E (Slack Quench)
K_{Ic}, ksi $\sqrt{in.}$	95(a)	64(b)
Range	(83 – 102)	(44 – 91)

(a) Average of 21.
(b) Average of 82.
Condition A: 1700 F + Ausbay quench to 975 F in furnace + quench in 140 F oil + temper at 1000 F to 1025 F, 2 + 2 hr + AC.
Condition E: 1650 F + Ausbay quench to 975 F in furnace + quench in 400 F salt + temper at 1000 F to 1025 F, 2 + 2 hr + AC.

TABLE 3.02723. PLANE STRAIN FRACTURE TOUGHNESS OF 0.8-INCH-THICK CVM PLATE (45)

Alloy	D6A – D6AC	
Form	0.8 and 1.5 – 1.8 in. Forging (CVM), LT (for F_{ty} see Table 3.0315)	
Condition	A & B	E (Slack Quench)
K_{Ic}, ksi $\sqrt{in.}$	95(a)	65(b)
Range	(85 – 109)	(47 – 96)

(a) Average of 34.
(b) Average of 60.
Conditions A & B: 1700 F + Ausbay quench to 975 F in furnace + quench in 140 F oil + temper at 1000 F to 1025 F, 2 + 2 hr + AC.
Condition E: 1650 F + Ausbay quench to 975 F in furnace + quench in 400 F salt + temper at 1000 F to 1025 F, 2 + 2 hr + AC.

TABLE 3.02724. PLANE STRAIN FRACTURE TOUGHNESS OF CVM FORGINGS (45)

Alloy	D6A – D6AC	
Condition	1650 F 1 hr, OQ (140 F) + 500 – 550 F Temper	
Form	Plate	Forging (Complex Part)
Thickness	≤2 in.	≈1-1/2 in.
Slack Quench	No	Yes
F_{ty}, ksi	233	233
K_{Ic}, ksi $\sqrt{in.}$	56	52
Range	(54 – 59)	(35 – 59)

TABLE 3.02725. PLANE STRAIN FRACTURE TOUGHNESS OF PLATE AND FORGED PARTS (49)

Fe
0.46 C
1.0 Cr
1.0 Mo
0.55 Ni

D6A
D6AC

Alloy	D6AC								
Heat Treatment Temperature, F				Mechanical Properties					
					Fracture Toughness				
Austenitize	Ausbay	Quench	Temper	F_{ty}, ksi	Specimen Thickness, in.	Specimen Orientation	K_{Ic}, ksi $\sqrt{in.}$	Std. Dev., ksi $\sqrt{in.}$	No. Tests
Plate									
Heat Treated to HRC 46				206	0.70	T-L	85.8	1.8	2
1675/AC + 1575	None	OQ	2H/400 + 2H/1100	–	1.0	–	77.2	1.0	4
1675/AC + 1575	None	OQ	2H/400 + 2H/1100	–	1.0	–	53.7	1.6	4
1675/AC + 1575	None	OQ	2H/400 + 2H/500	–	1.0	–	34.5	1.2	4
Forgings									
2.25H/1615	None	325	3H/310–345 + 6–6.5/1080	199	1.0	L-S	64.7	5.5	3
	Same HT			201	1.0	T-L	78.4	15.1	6
	Same HT			187–203	1.0	S-L	83.9	14.8	52
1650	960	OQ, 180	2+2H/1025	219	0.50	–	87.7	0.7	3
Billets									
1H/1650/FC + 1H/1650	None	OQ	2+2H/1025	210	1.0	L-T	78.5	4.7	2
1H/1650	960	OQ, 150	2+2H/1000	211	1.0	L-T	80.3	0.8	2
1700	960	OQ, 150	2+2H/1000	215	1.0	L-T	80.3	4.3	3
1700	None	OQ	2+2H/1025	214–216	1.0	L-T	77.3	2.4	6
1H/1725/AC + 1H/1700	None	OQ	1H/1000 + 1H/1025	213	1.0	L-T	77.2	2.7	3
1H/1725/AC + 1H/1700	None	OQ	2+2H/1100	200–205	1.0	L-T	101.2	6.1	5
1H/1725/AC + 1H/1700	None	OQ	2+2H/1025	213–217	1.0	L-T	74.4	6.2	6
1H/1725/AC +1H/1650	960	SQ, 350	2+2H/1025	221	1.0	L-T	75.1	10.1	3

TABLE 3.02726. EFFECTS OF HEAT TREATMENT ON FRACTURE TOUGHNESS OF PLATE, FORGINGS, AND BILLETS AT ROOM TEMPERATURE (72)

D6AC, 1-inch Diameter Bar, Specimen Quench Size = 0.75-inch-Thick Blocks							
Heat Treatment Temperature, F				Mechanical Properties			
Austenitize	Ausbay	Quench	Temper	F_{ty}, ksi	F_{tu}, ksi	K_{Ic}, ksi $\sqrt{in.}$(a)	Std. Dev., ksi $\sqrt{in.}$
1700	970	OQ, 140	1025	211	233	94.2	2.7
1700	970	OQ, 140	1050	208	230	95.4	–
1700	970	OQ, 140	1075	205	229	100.6	1.8
1700	970	OQ, 140	618	217	259	54.6	1.5
1700	970	OQ, 140	550	219	278	45.0	1.0
1700	None	OQ, 140	1025	211	235	95.5	3.1
1700	970	SQ, 410	1025	210	235	77.7	2.0
1700	970	SQ, 365	1025	211	235	88.0	2.2
1700	970	AC	1025	210	239	42.2	3.3
1650	970	AC	1025	207	229	34.8	1.8

(a) Average of 2 to 6 values. Fracture toughness was measured on standard ASTM E399/72T compact tension specimens.

TABLE 3.02727. EFFECTS OF HEAT TREATMENT ON FRACTURE TOUGHNESS OF BAR (66)

Fe	
0.46	C
1.0	Cr
1.0	Mo
0.55	Ni

D6A
D6AC

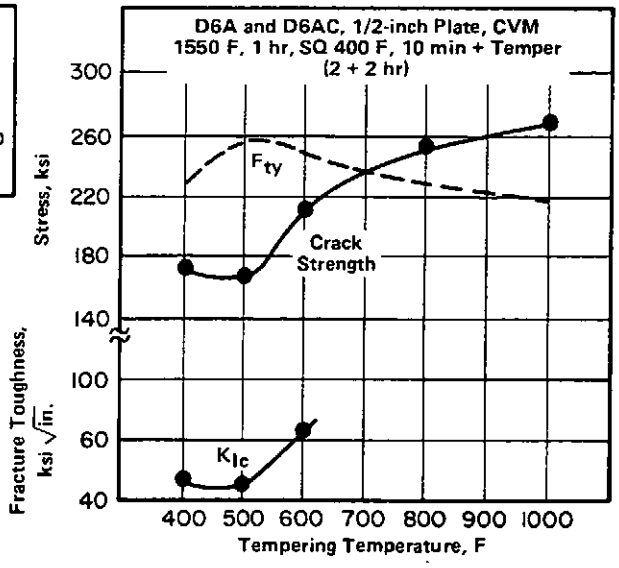


FIGURE 3.02729. EFFECT OF TEMPERING TEMPERATURE ON SHARP NOTCH PROPERTIES AND FRACTURE TOUGHNESS OF PLATE (18)

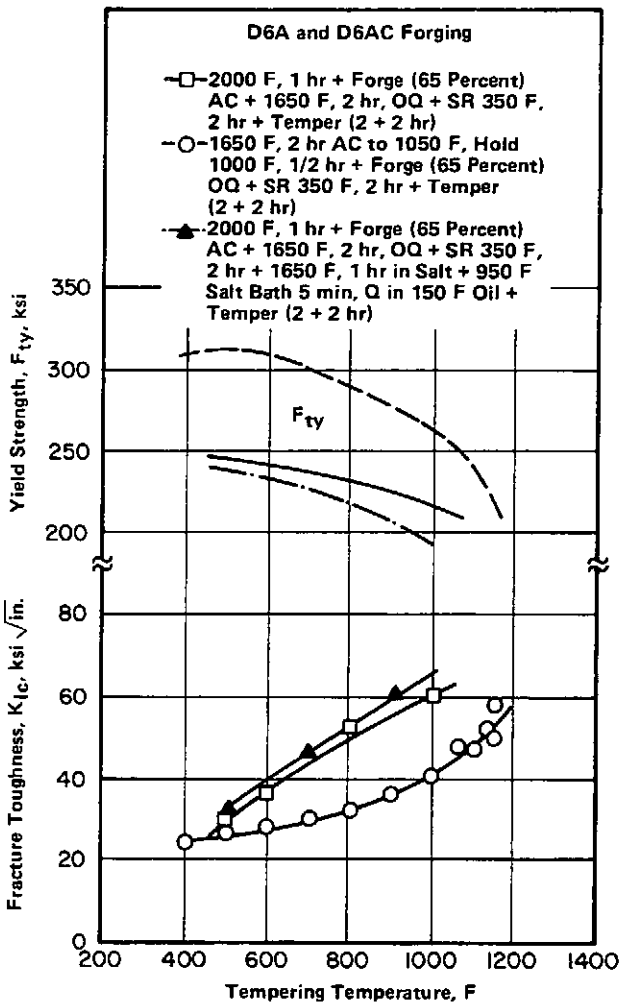


FIGURE 3.027210. EFFECT OF TEMPERING TEMPERATURE ON FRACTURE TOUGHNESS AND YIELD STRENGTH FOR THREE THERMAL-MECHANICAL PROCESSING TREATMENTS OF FORGED ALLOY (42)

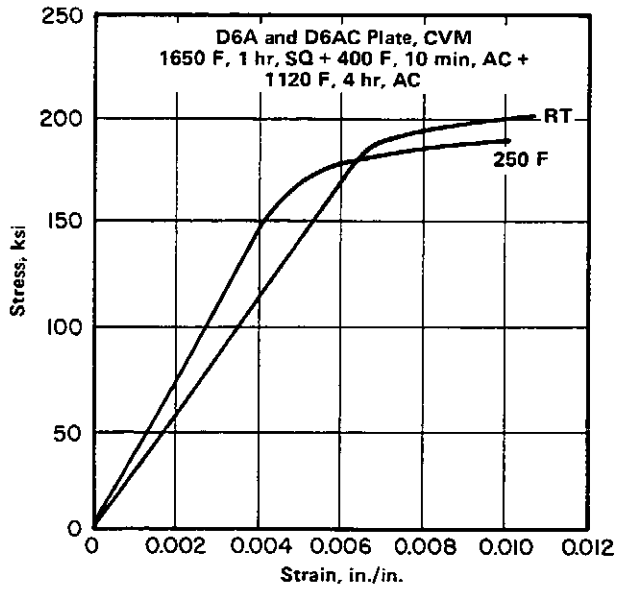


FIGURE 3.0311. STRESS-STRAIN CURVES FOR PLATE AT ROOM TEMPERATURE AND 250 F (5)

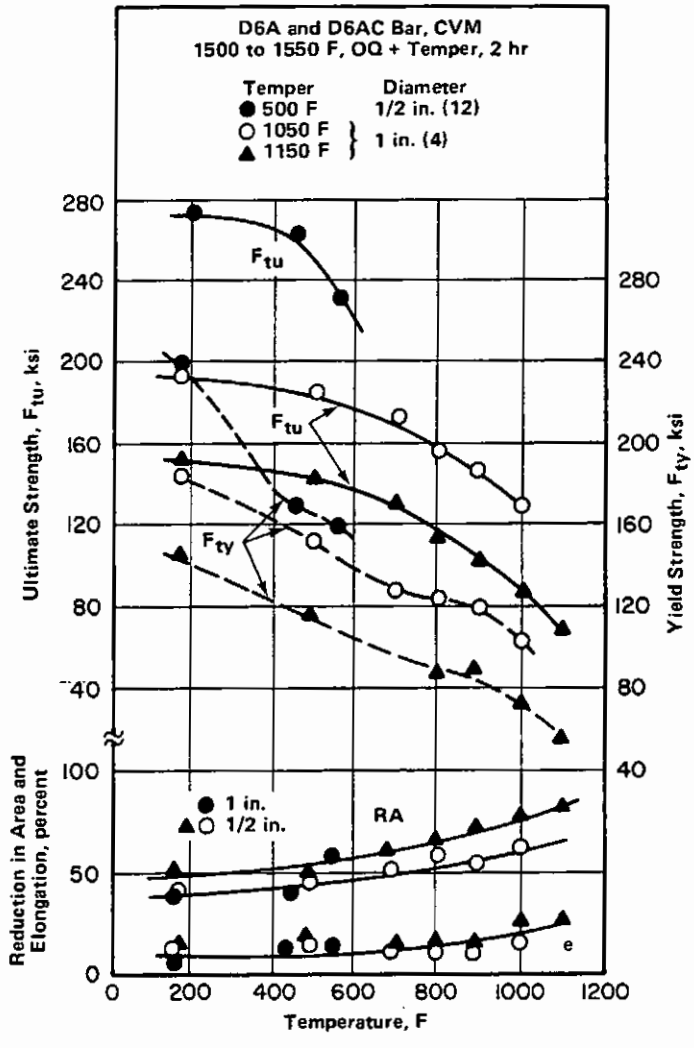


FIGURE 3.0312. EFFECT OF TEST TEMPERATURE ON TENSILE PROPERTIES OF BAR AT SEVERAL STRENGTH LEVELS (4, 12)

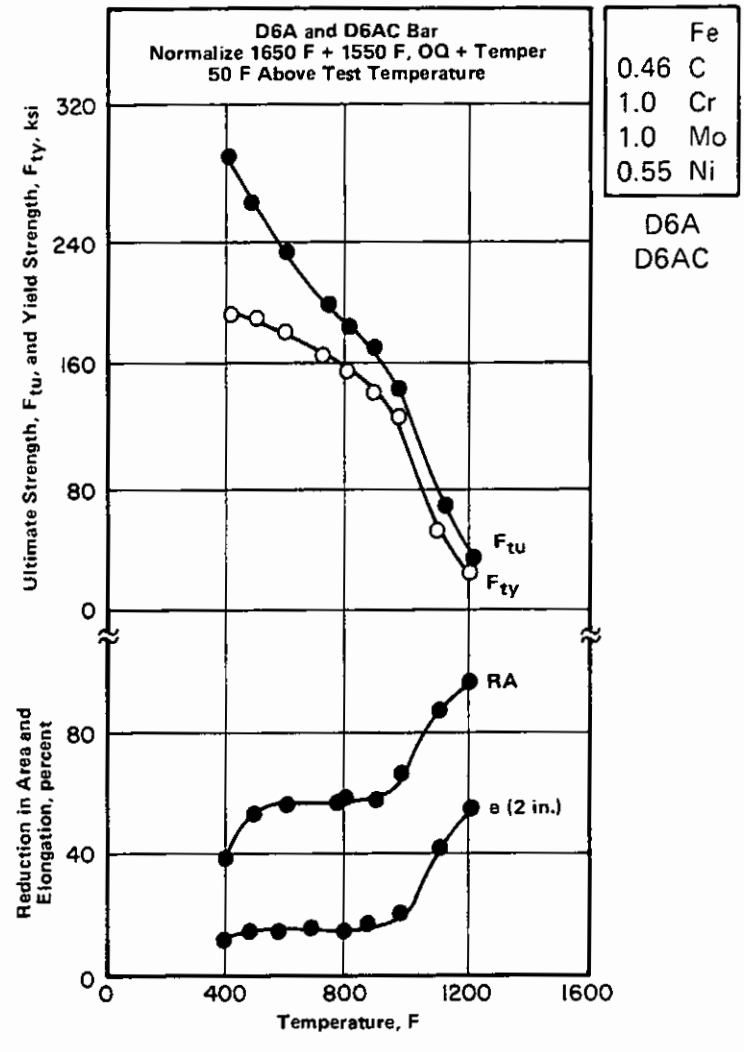


FIGURE 3.0313. EFFECT OF TEST TEMPERATURE ON TENSILE PROPERTIES OF BAR (4)

Alloy	D6A – D6AC			
Form	0.8-in. and 1.5 – 1.8-in. Plate (CVM) – L			
Condition	1650 F or 1700 F + Ausbay Quench to 975 F + Quench in Oil or Salt + Temper at 1000 F to 1025 F, 2 + 2 hr + AC			
Test Temp, F	-40	+35	+70	+175
F_{tu}, ksi	247(a)	241(c)	238(d)	231(c)
F_{ty}, ksi	229(a)	224(c)	217(d)	211(c)
e (1 or 2 in.), percent	11(b)	13(c)	13(e)	15(c)
RA, percent	41(b)	43(c)	45(f)	50(c)

(a) Average of 9.
(b) Average of 5.
(c) Average of 2.
(d) Average of 59.
(e) Average of 36.
(f) Average of 38.

TABLE 3.0314. EFFECT OF TEST TEMPERATURE ON TENSILE PROPERTIES OF PLATE (45)

	Fe
0.46	C
1.0	Cr
1.0	Mo
0.55	Ni

D6A
D6AC

Alloy	D6A – D6AC	
Form	0.8 in. and 1.5 – 1.8 in. Forgings (CVM) – L	
Condition	1650 F or 1700 F + Ausbay Quench to 975 F + Quench in Oil or Salt + Temper at 1000 F to 1025 F, 2 + 2 hr + AC	
Test Temp, F	-40	+70
F_{tu}, ksi	247(a)	233(c)
F_{ty}, ksi	229(a)	214(c)
e (1 or 2 in.), percent	11(b)	13(d)
RA, percent	41(b)	45(d)

(a) Average of 5. (c) Average of 17.
(b) Average of 2. (d) Average of 12.

TABLE 3.0315. EFFECT OF TEST TEMPERATURE ON TENSILE PROPERTIES OF FORGINGS (45)

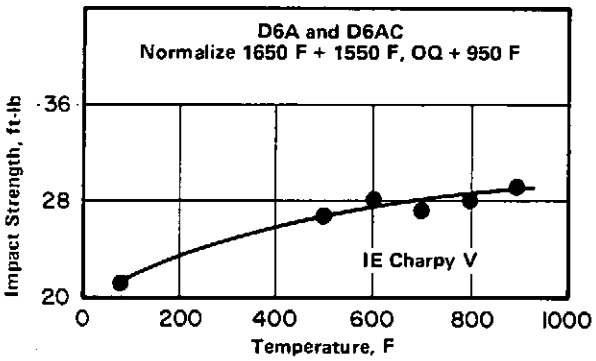


FIGURE 3.0331. ELEVATED TEMPERATURE CHARPY V-NOTCH IMPACT PROPERTIES (4)

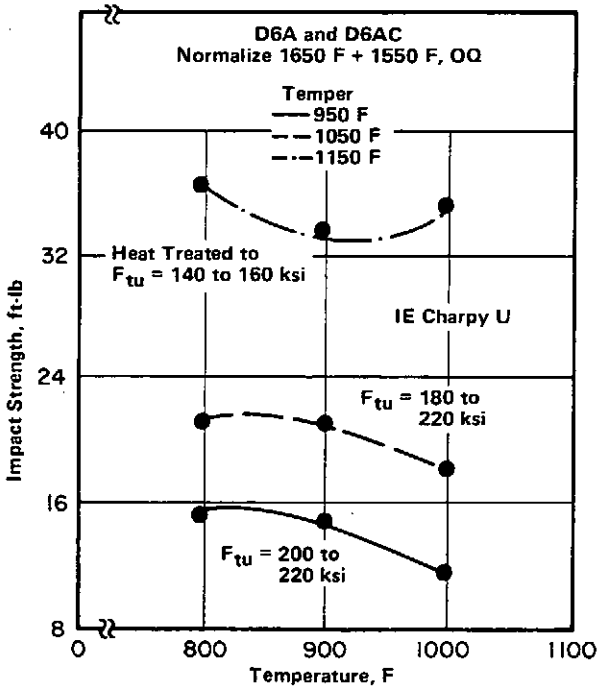


FIGURE 3.0332. ELEVATED TEMPERATURE CHARPY U-NOTCH IMPACT PROPERTIES FOR VARIOUS STRENGTH LEVELS (4)

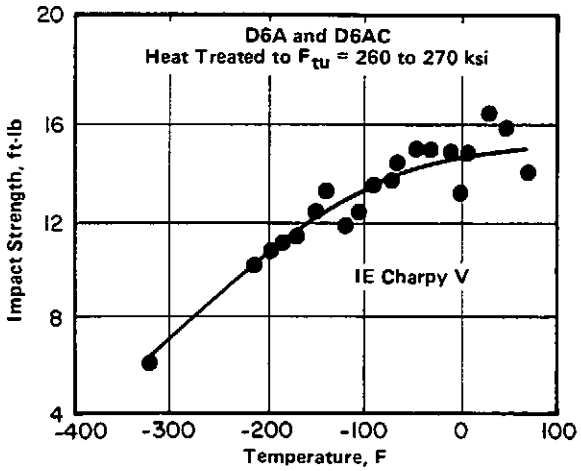


FIGURE 3.0333. LOW TEMPERATURE CHARPY V-NOTCH IMPACT PROPERTIES (4)

	Fe
0.46	C
1.0	Cr
1.0	Mo
0.55	Ni

D6A
D6AC

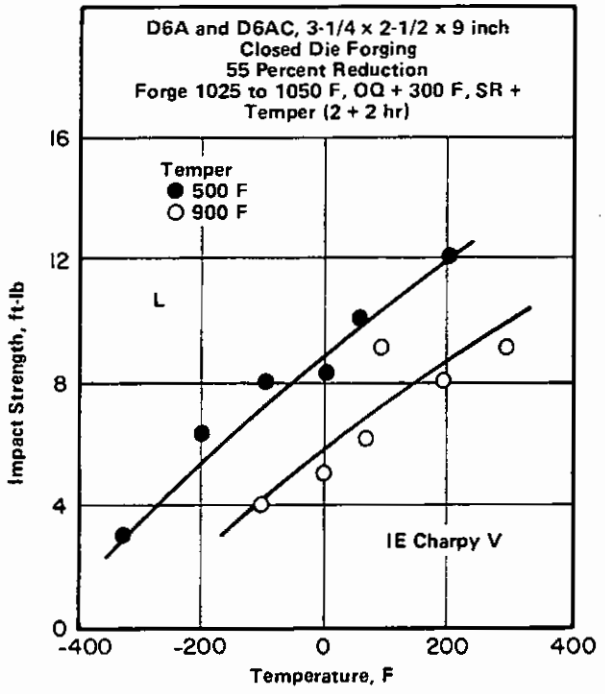


FIGURE 3.0334. EFFECT OF TEST TEMPERATURE ON IMPACT STRENGTH OF A VARIABLE CROSS SECTION AUSFORMED FORGING (10)

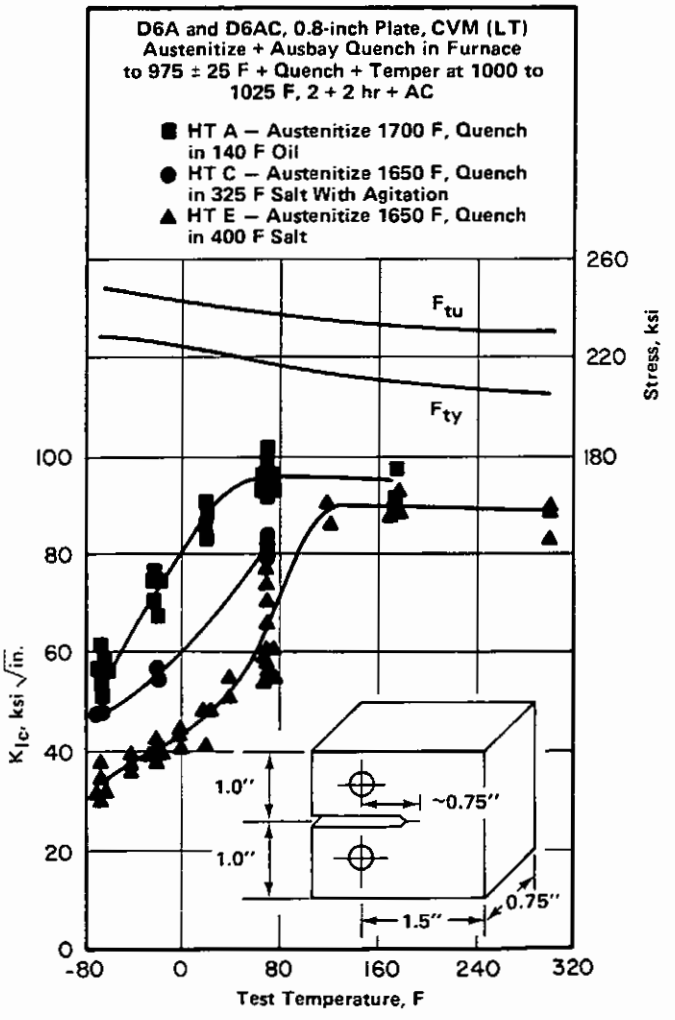


FIGURE 3.03721. EFFECT OF TEST TEMPERATURE ON PLANE STRAIN FRACTURE TOUGHNESS OF 0.8-INCH THICK CVM PLATE (45)

	Fe
0.46	C
1.0	Cr
1.0	Mo
0.55	Ni

D6A
D6AC

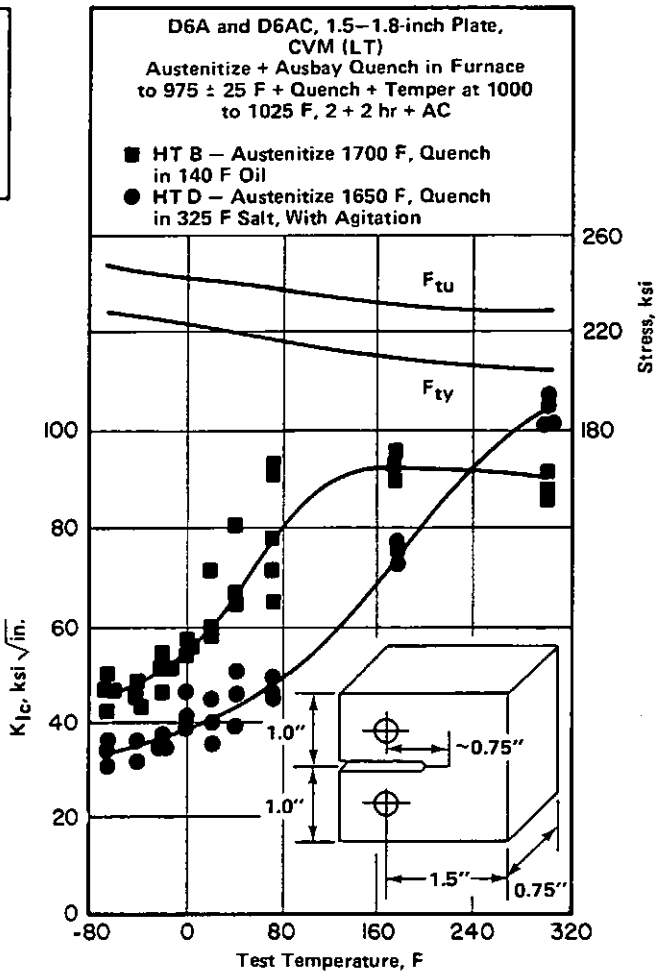


FIGURE 3.03723. EFFECT OF TEST TEMPERATURE ON PLANE STRAIN FRACTURE TOUGHNESS OF CVM FORGINGS (45)

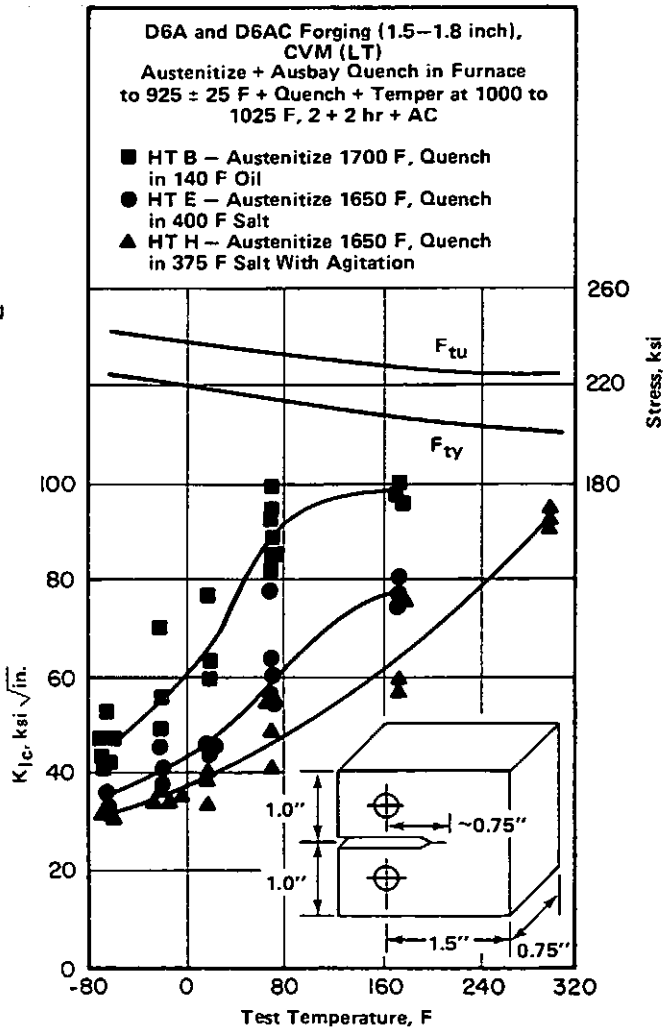


FIGURE 3.03723. EFFECT OF TEST TEMPERATURE ON PLANE STRAIN FRACTURE TOUGHNESS OF CVM FORGINGS (45)

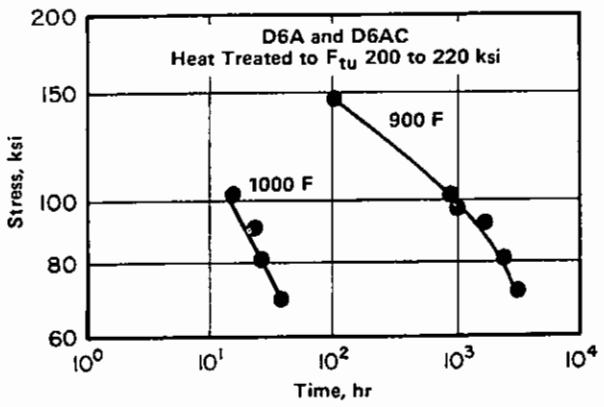


FIGURE 3.041. CREEP-RUPTURE CURVES AT 900 AND 1000 F (4)

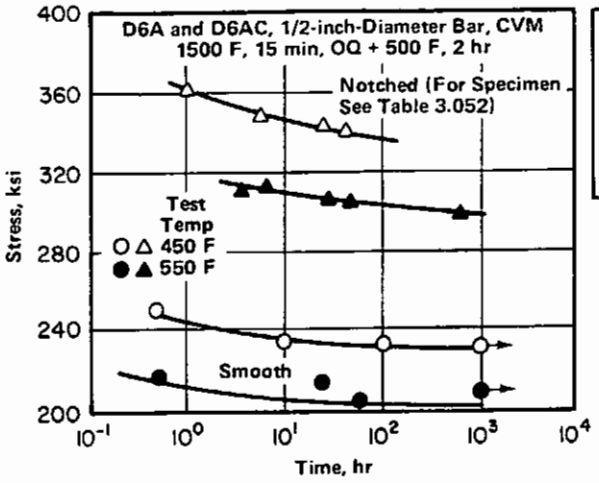


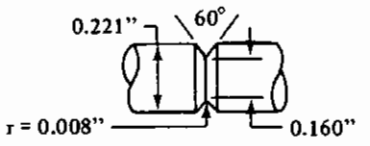
FIGURE 3.042. CREEP-RUPTURE STRENGTH OF SMOOTH AND NOTCHED BAR AT ELEVATED TEMPERATURES (12)

Alloy	D6A – D6AC								
Form	0.125-inch Sheet (CVM)								
Condition	1650 F, AC + 1550 F, OQ + 600 F (2 + 2 hr) + 0.38 percent Strain + 400 F, 2 hr								
	Stress Ratio		Stress Concen-	Fatigue Strength, ksi, at Cycles					
Method	A	R	tration	10^2	10^3	10^4	10^5	10^6	10^7
Direct Stress	1	0	Smooth	270	260	230	125	120	120

TABLE 3.051. FATIGUE STRENGTH OF MARSTRAINED SHEET (11)

Alloy	D6A – D6AC								
Form	1/2-inch Bar								
Condition	1500 F, 15 min, OQ + 500 F, 2 hr								
	Direct Stress Ratio		Stress Concen-	Fatigue Strength, ksi, at Cycles					
Test Temp, F	A	R	tration	10^2	10^3	10^4	10^5	10^6	10^7
RT	1	0	Smooth	–	270	230	170	150	150
	∞	-1		220	180	160	130	100	100
450	1	0	Smooth	–	260	220	170	150	135
	∞	-1		220	180	160	130	100	90
550	1	0	Smooth	–	240	215	170	150	130
	∞	-1		220	180	140	110	85	75
RT	1	0	Notched	300	190	120	80	80	80
	∞	-1		200	135	65	50	50	50
450	1	0	Notched	–	–	100	85	70	60
	∞	-1		–	–	–	45	40	40
550	1	0	Notched	280	140	100	80	65	55
	∞	-1		170	100	65	50	45	40

Notched Specimen



$K_t = 3.00$

TABLE 3.052. EFFECT OF TEST TEMPERATURE ON SMOOTH AND NOTCHED FATIGUE PROPERTIES OF BAR (12)

	Fe
0.46	C
1.0	Cr
1.0	Mo
0.55	Ni

D6A
D6AC

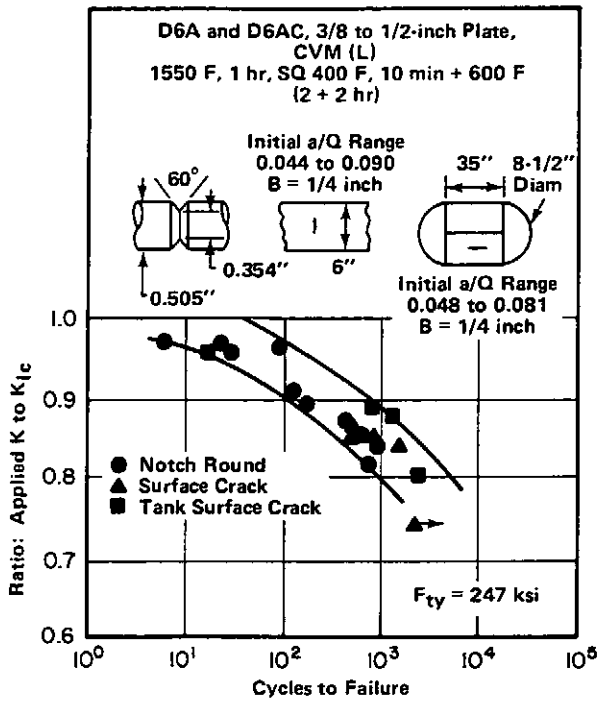


FIGURE 3.053. LOW CYCLE FATIGUE BEHAVIOR OF CRACKED PLATE SPECIMENS AND TANKS (18)

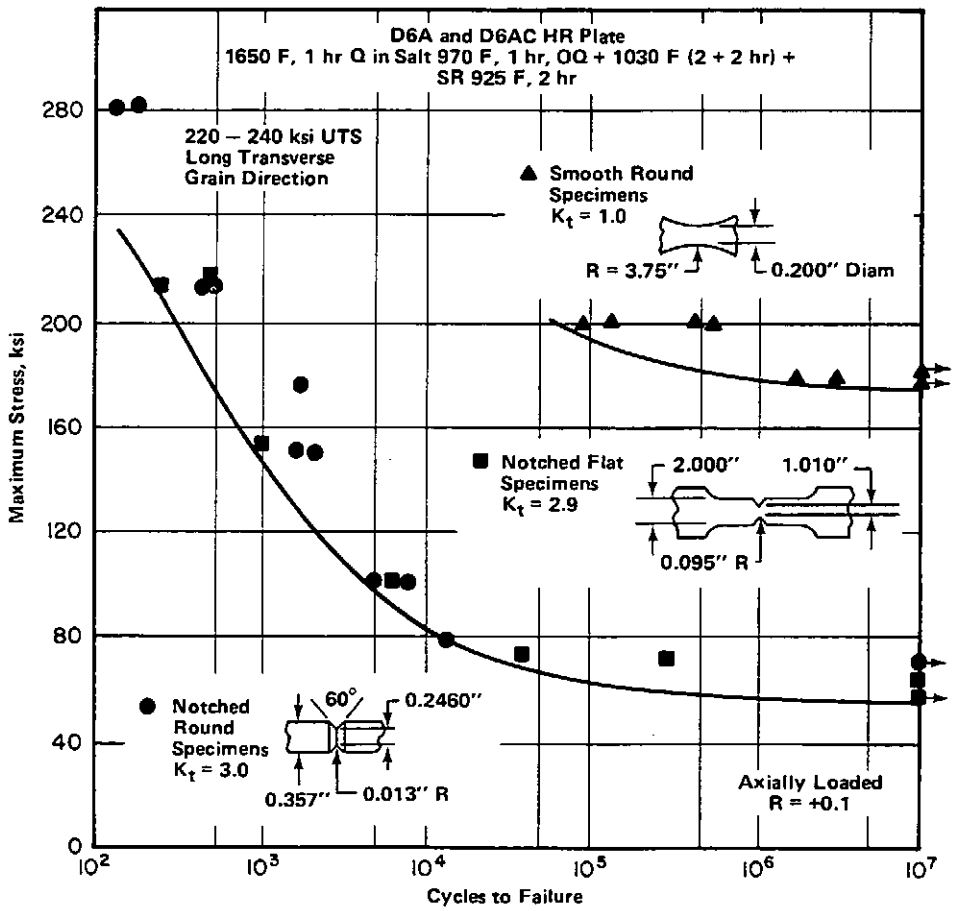


FIGURE 3.054. S-N CURVES FOR 220 TO 240 KSI HOT ROLLED PLATE (44)

	Fe
0.46	C
1.0	Cr
1.0	Mo
0.55	Ni

D6A
D6AC

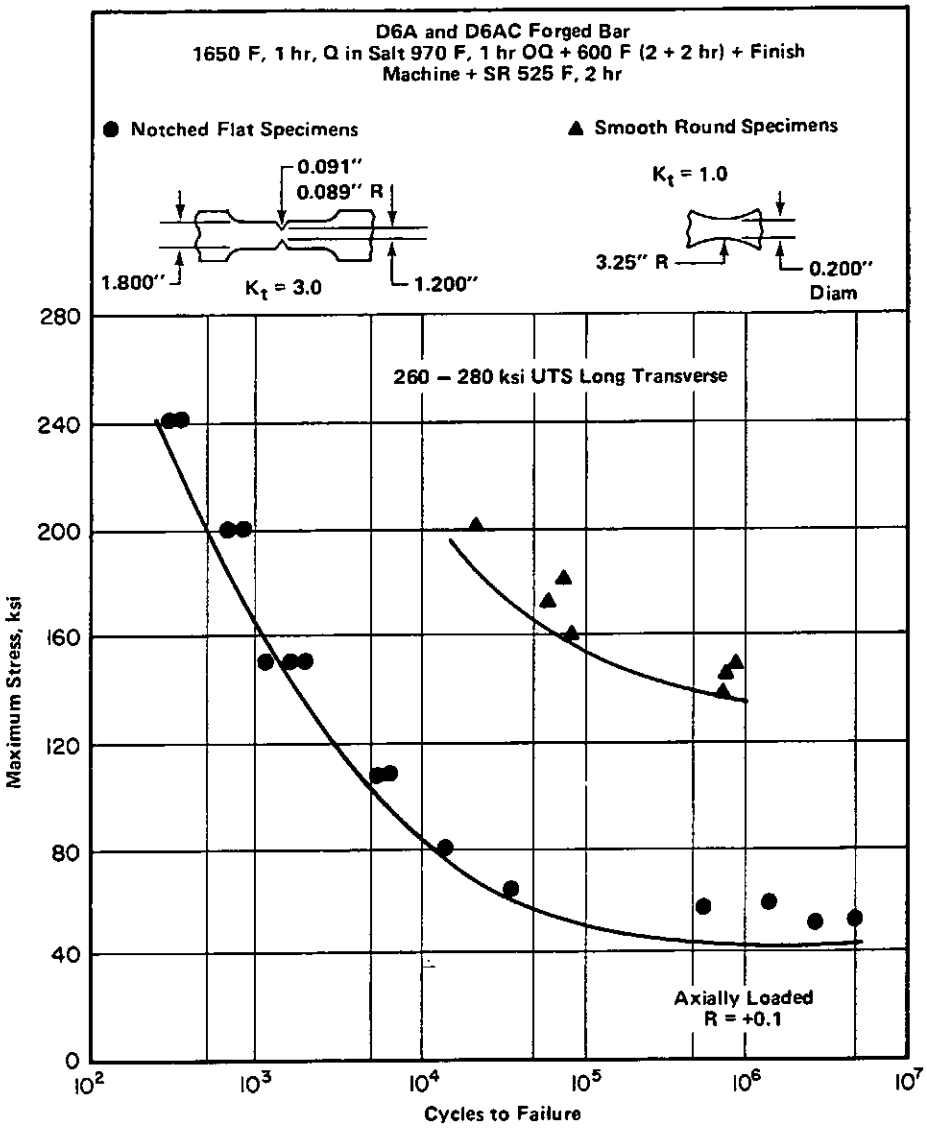


FIGURE 3.055. S-N CURVES FOR 260 TO 280 KSI FORGED BAR (44)

	Fe
0.46	C
1.0	Cr
1.0	Mo
0.55	Ni

D6A
D6AC

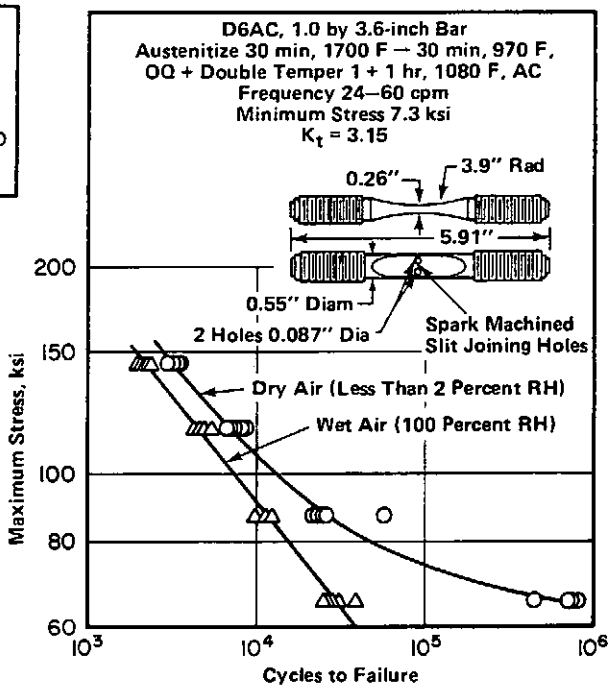


FIGURE 3.056. EFFECTS OF HUMIDITY ON FATIGUE BEHAVIOR OF KEYHOLE NOTCHED BAR AT 95 F (67)

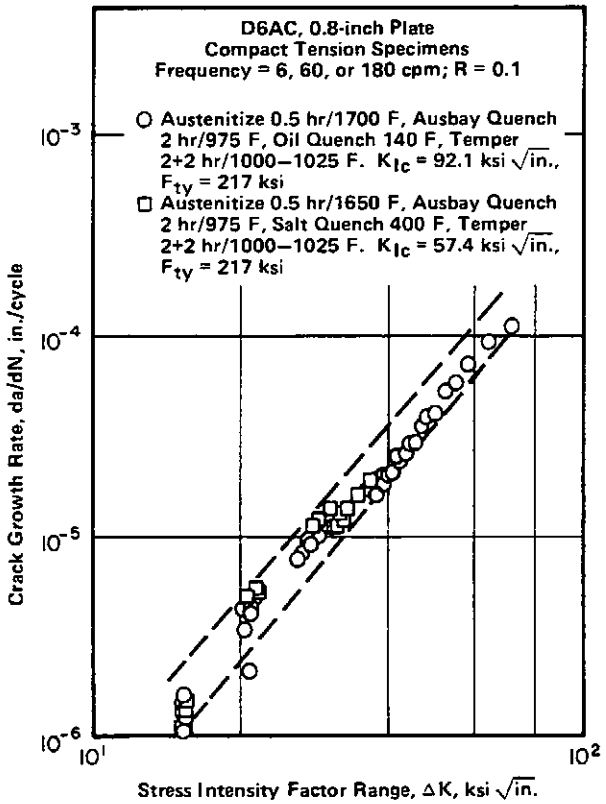


FIGURE 3.059. FATIGUE CRACK-GROWTH RATES FOR HIGH AND MEDIUM TOUGHNESS PLATE IN DESICCATED AIR AT ROOM TEMPERATURE (45)

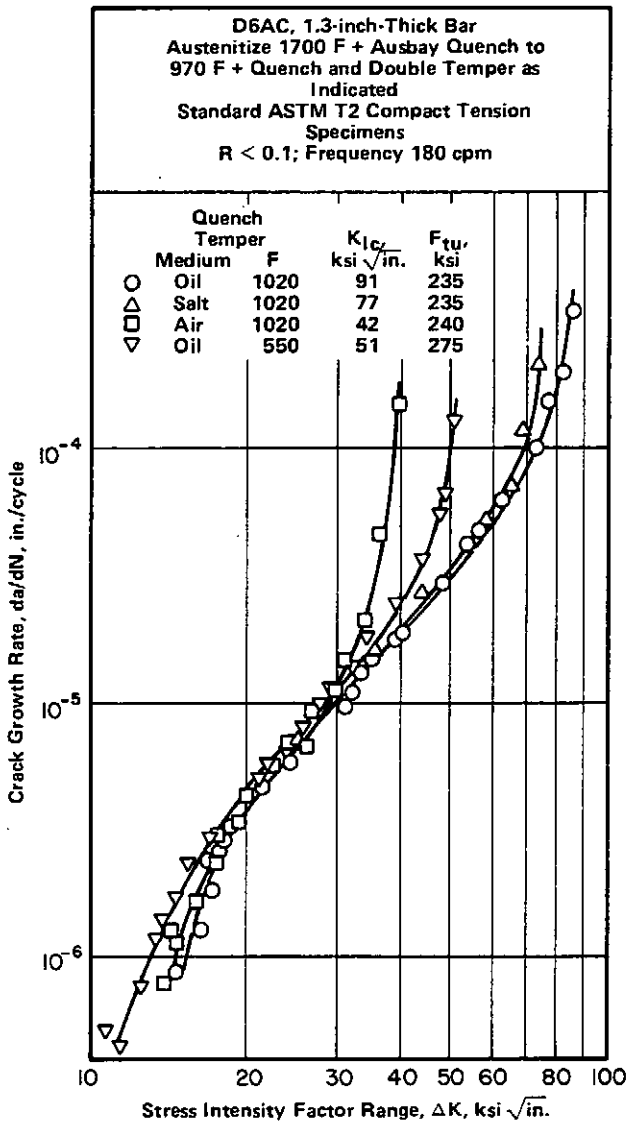
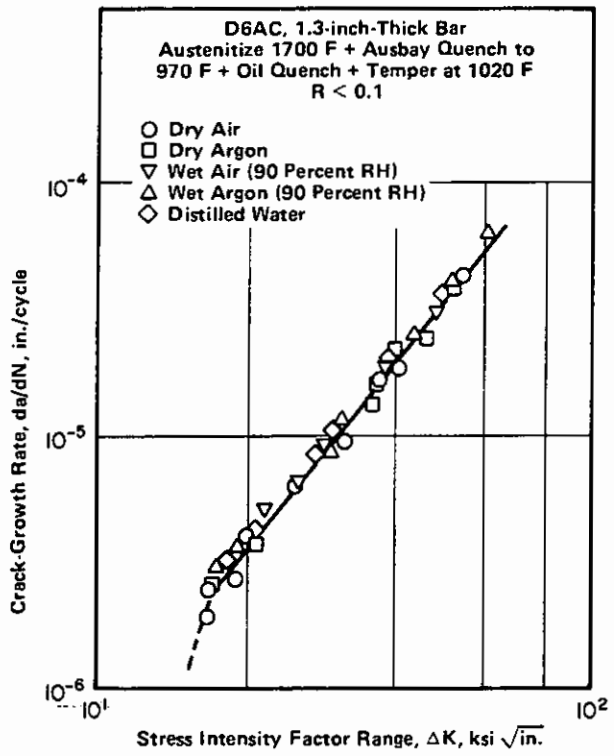
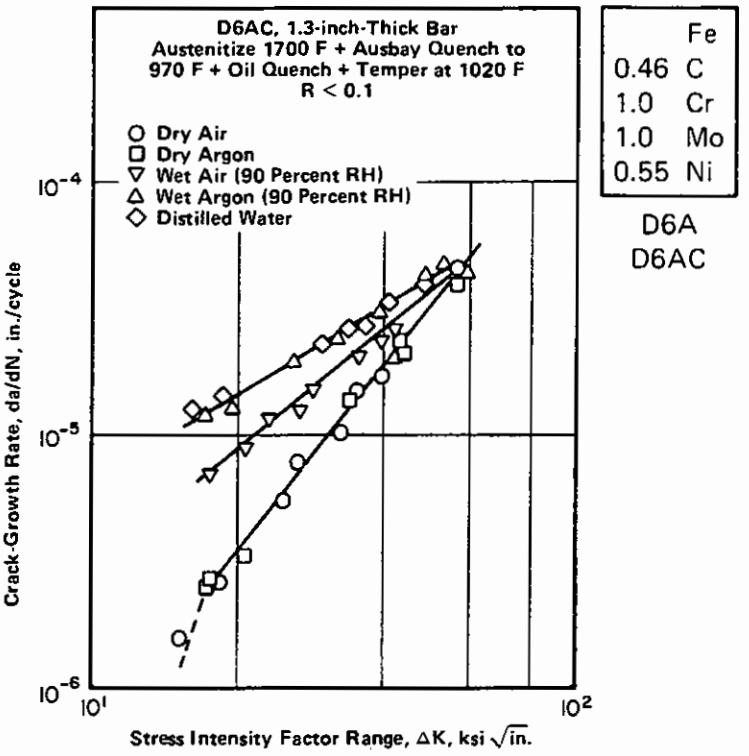


FIGURE 3.058. EFFECTS OF QUENCHING ON FATIGUE CRACK-GROWTH BEHAVIOR IN DRY AIR AT ROOM TEMPERATURE (68, 69)



(a) Frequency 600 Cycles/Minute

FIGURE 3.0511. EFFECTS OF HUMIDITY AND FREQUENCY ON FATIGUE CRACK-GROWTH BEHAVIOR AT ROOM TEMPERATURE (68, 69)



(b) Frequency 60 Cycles/Minute

FIGURE 3.0511. EFFECTS OF HUMIDITY AND FREQUENCY ON FATIGUE CRACK-GROWTH BEHAVIOR AT ROOM TEMPERATURE (68, 69)

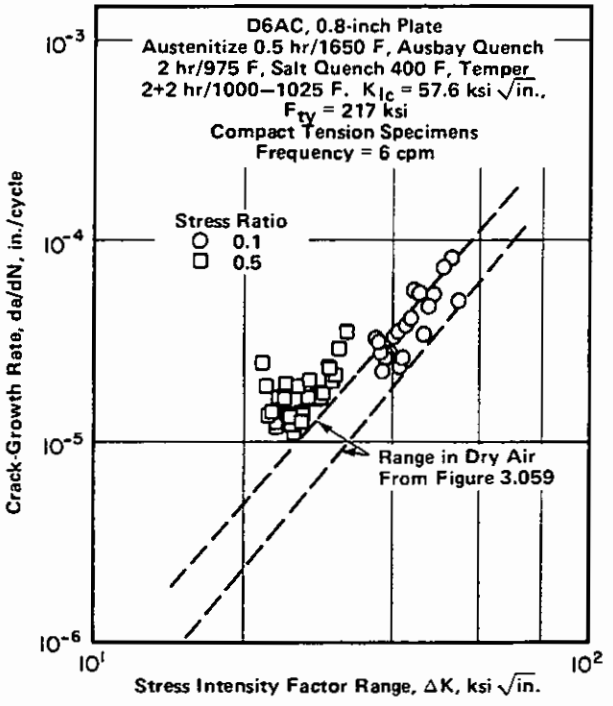


FIGURE 3.0512. FATIGUE CRACK-GROWTH RATES FOR MEDIUM TOUGHNESS PLATE IN LABORATORY AIR (50 TO 70 PERCENT RH) AT ROOM TEMPERATURE (45)

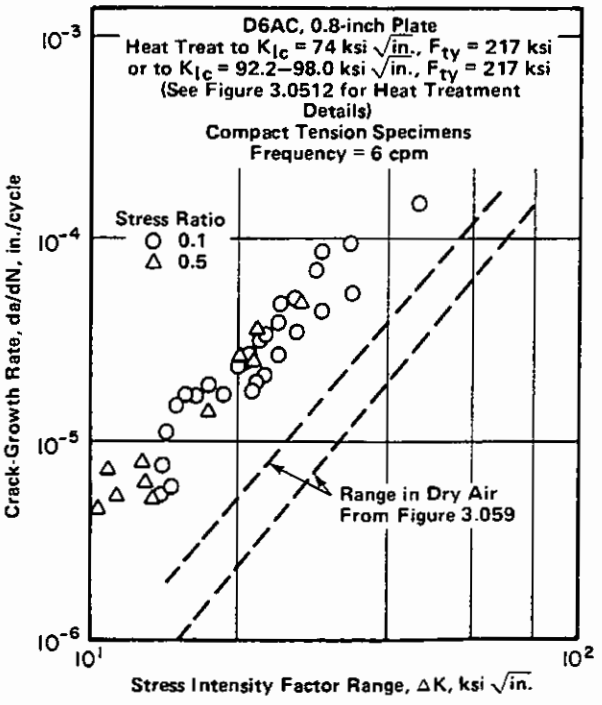


FIGURE 3.0513. FATIGUE CRACK-GROWTH RATES FOR HIGH AND MEDIUM TOUGHNESS PLATE IN DISTILLED WATER AT ROOM TEMPERATURE (45)

	Fe
0.46	C
1.0	Cr
1.0	Mo
0.55	Ni

D6A
D6AC

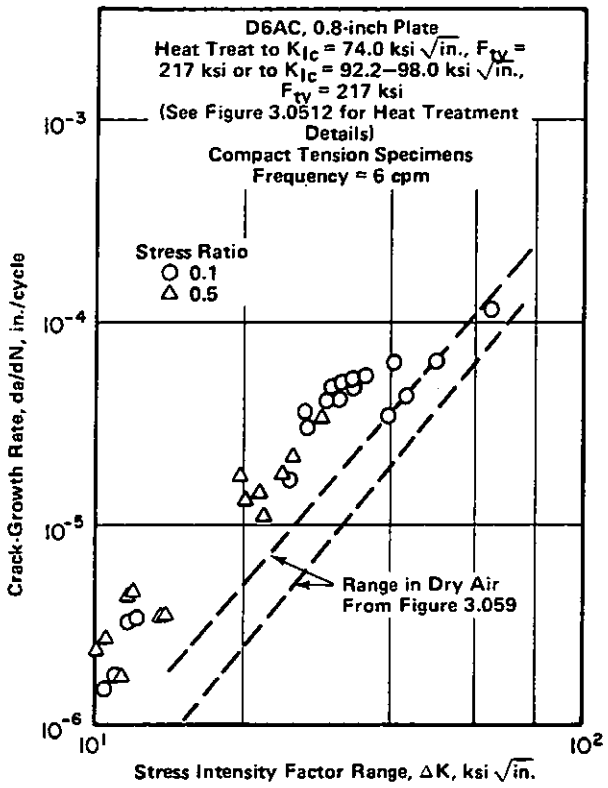


FIGURE 3.0514. FATIGUE CRACK-GROWTH RATES FOR HIGH AND MEDIUM TOUGHNESS PLATE IN WATER-SATURATED JP-4 FUEL AT ROOM TEMPERATURE (45)

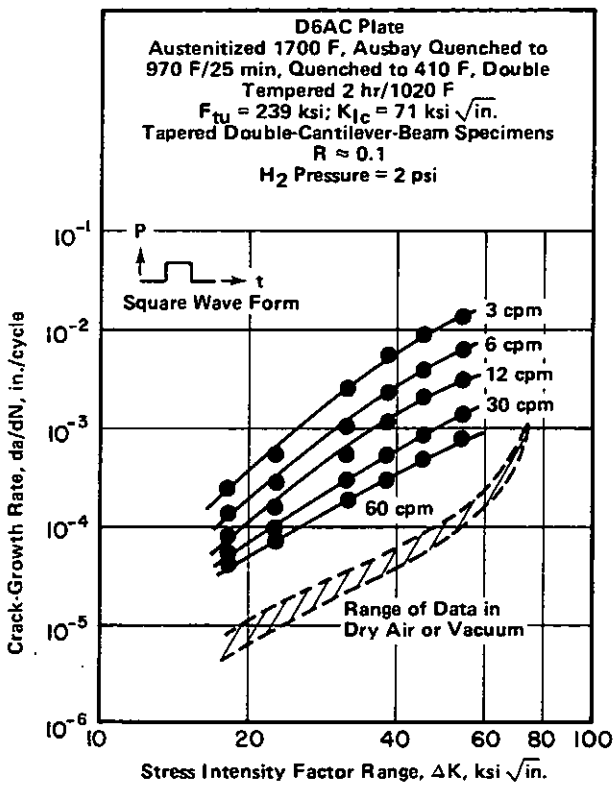


FIGURE 3.0516. EFFECTS OF CYCLIC FREQUENCY ON FATIGUE CRACK-GROWTH BEHAVIOR IN HYDROGEN WITH COMPARISON TO AIR AND VACUUM (65)

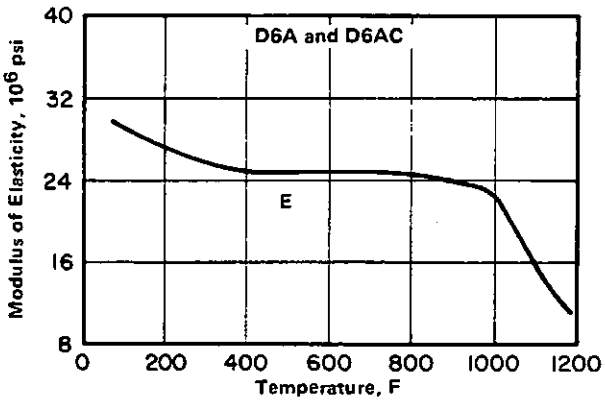


FIGURE 3.0621. MODULUS OF ELASTICITY AT ROOM AND ELEVATED TEMPERATURES (4)

Fe
0.46 C
1.0 Cr
1.0 Mo
0.55 Ni

D6A
D6AC

Alloy	D6A – D6AC	
Thickness, in.	0.1 to 0.375	
GTA Weld	Primary (5)	Weld Repair After HT (22)
Temperature Preheat and Interpass	500 to 650 F	500 to 650 F
Postheat	(a, b)	650 to 700 F, 2 hr, AC to 150 to 175 F + 650 F to 700 F, 1 hr, AC
Stress Relief	1200 to 1250 F(b)	1100 F, 1 hr, AC
Heat Treatment	1650 F, 1 hr, SQ 400 F 10 min, AC + 400 F, 1 hr AC + 1075 F, 4 hr, AC (F_{ty} = 215 ksi)	1650 F, 2 hr, FC to 1600 F 30 min, SQ 400 F, 10 min, AC + 400 F, 2 hr AC + 1125 F, 4 hr, AC (F_{ty} = 180 ksi)

(a) For highly restrained sections, Ref. 4 gives 575 to 625 F, 1.5 hr, AC to 300 F as soon after welding as possible followed by immediate stress relief.

(b) For welded tank fabrications (0.2 to 1.0-inch sections), Ref. 5, stress relief before part has cooled below interpass temperature.

TABLE 4.0311. RECOMMENDED WELD HEAT TREAT SEQUENCE FOR PRIMARY WELDS AND WELD REPAIR AFTER HEAT TREATMENT (5, 22)

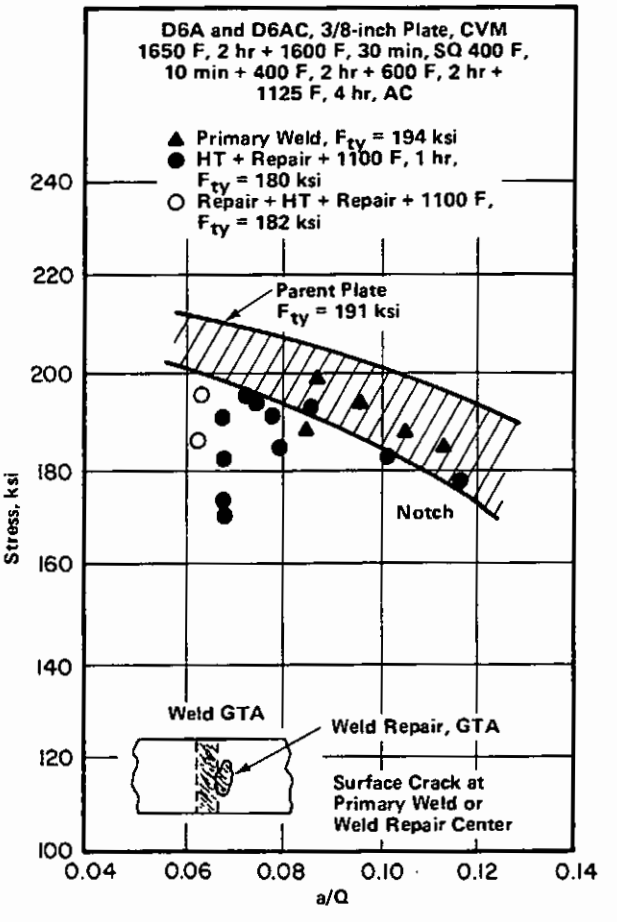


FIGURE 4.0312. EFFECT OF SURFACE CRACK SIZE ON SHARP NOTCH STRENGTH OF PRIMARY WELDS AND WELD REPAIRS MADE AFTER HEAT TREATMENT (22)

	Fe
0.46	C
1.0	Cr
1.0	Mo
0.55	Ni

D6A
D6AC

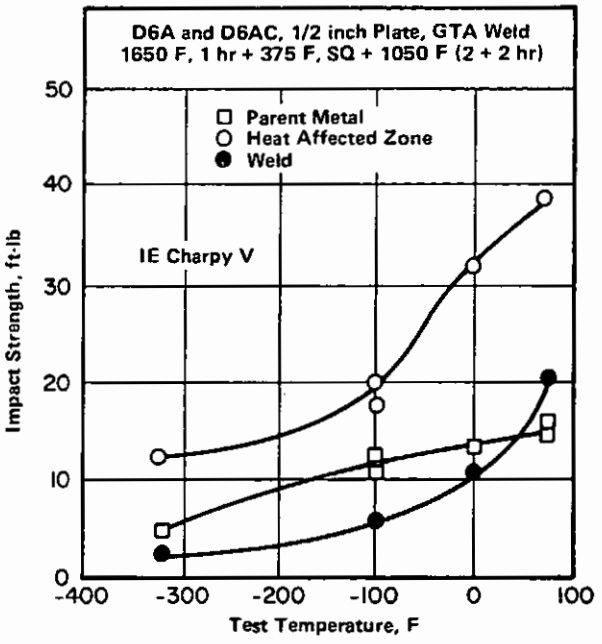


FIGURE 4.0313. EFFECT OF WELDING ON LOW TEMPERATURE CHARPY V IMPACT PROPERTIES (39)

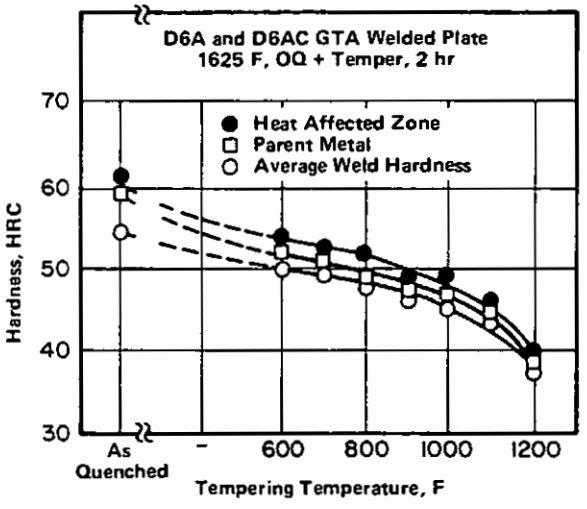


FIGURE 4.0314. HARDNESS SURVEY ON WELDED PLATE (30)

REVISED: DECEMBER 1972
AUTHOR: W. F. BROWN, JR.

FERROUS ALLOYS

1. GENERAL

T-1 steel is a low carbon quenched and tempered low alloy constructional steel with a high yield strength (90 to 100 ksi) and good toughness at room and moderately low temperatures. Its resistance to atmospheric corrosion is superior to that of the carbon steels. T-1A and T-1B are lower alloyed modifications of T-1 that are more economical but have somewhat lower toughness and hardenability. The service range of the T-1 steels should be restricted to -50F to 800F. The T-1 steels are normally supplied in the quenched and tempered condition, and unless otherwise stated the properties given in this chapter refer to that condition as defined in Section 1.05. All grades are weldable, however, the strength and toughness of the weld metal and the heat affected zone will depend on the welding conditions. These steels are not recommended for service conditions where tolerance for large plastic deformation is required under dynamic loads.

1.01 Commercial Designations

T-1, T-1 TypeA, T-1 Type B.

1.02 Alternate Designations

USS T-1, USS T-1 Type A, USS T-1 Type B.

1.03 Specifications

1.031 MIL-S-19795.

1.032 ASME SA 517, ASTM A 514-70 Types F, B and H, ASTM A 517-70a Types F, B and H.

1.04 Composition

1.041 Chemical composition of T-1, Table 1.041.

1.042 Chemical composition of T-1 Type A, Table 1.042.

1.043 Chemical composition of T-1 Type B, Table 1.043.

1.05 Heat Treatment

1.051 General. The strength and hardness of the T-1 steels are imparted by quenching and tempering. These alloys should not be used without heat treatment (2)(28).

1.052 Austenitize. 1650F to 1750F, water quench(15).

1.053 Temper. 1150F to 1275F. Quenching after tempering is desirable but not absolutely necessary (2)(8). Tempering temperature should not exceed 1275F (15).

1.054 To improve notch toughness of heavy sections over 2.5 inches, the following is recommended: 1750F, water quench, reheat to 1650F, water quench. Temper as in 1.053 (15).

1.06 Hardness

1.061 Typical hardness of heat treated plate for all types is approximately 258 BHN.

1.062 Effect of tempering temperature on hardness, Figure 1.062.

1.063 End quench hardenability bands, Figure 1.063.

1.07 Forms and Conditions Available

1.071 All types are available in the form of plates, structural shapes, bars, tubes. Non heat treated forms can be furnished under special conditions. Heat treated castings and rolled rings are available through a licensee of U.S. Steel.

1.072 Thickness ranges available for the three types under several specifications, Table 1.072.

1.08 Melting and Casting Practice

1.09 Special Considerations. (see also 2.03 and 4.03)

1.091 Blooms, billets, bars or ingots which have not been heat treated should never be gas cut. They should be sawed or hot sheared; or cold sheared if the size permits (15).

1.092 When heating to 1100F for forming, temperature should be accurately controlled.

1.093 Alloys must always be in the quenched and tempered condition before welding or gas cutting.

1.094 Alloys form an adherent scale; thus extremely high forging temperatures should be avoided.

1.095 High pressure hydrogen promotes crack growth in T-1 steel when the applied stress intensity is sufficiently high, (Table 1.095). Based on these results and on unpublished data the threshold K level for crack propagation has been estimated at 60 to 65 ksi-in$^{1/2}$ (32).

1.0951 Effect of high pressure hydrogen on crack propagation in T-1 plate, Table 1.0951.

2. PHYSICAL AND CHEMICAL PROPERTIES

2.01 Thermal Properties

2.011 Melting range.

2.012 Phase changes.

2.0121 Time-temperature transformation diagram, Figure 2.0121.

2.013 Thermal conductivity.

2.014 Thermal expansion, all types -50 to +150F = 6.5 x 10^{-6} in/in/F (1).

2.015 Specific heat.

2.016 Thermal diffusivity.

2.02 Other Physical Properties

2.021 Density. 0.284 lb per cu in. 7.85 gr per cu cm, (2).

2.022 Electrical properties.

2.0221 Resistivity 7.2 to 10.4 microhm-in.

2.023 Magnetic properties.

2.0231 Normal D-C magnetization curve for plate, Figure 2.0231.

2.024 Emissivity.

2.025 Damping capacity.

2.03 Chemical Properties

2.031 The atmospheric corrosion resistance of T-1 and T-1A are approximately four times and two times, respectively, that of structural carbon steels (15).

2.032 Weight loss in industrial, marine and semi-rural atmospheres for T-1 steel, Table 2.032.

2.033 Exposure of T-1 steel to various stress corrosion media, Table 2.033.

2.034 Results of four year exposure tests in sea water, Table 2.034.

2.035 No crack growth was observed when precracked DCB specimens of both T-1 plate metal and weld were loaded to 70% of the estimated K_{Ic} value in N_2O_4 (MIL-P-25539B) for up to 68 days at room temperature. Similar exposure of plate metals to unsymmetrical dimethylhydrazine (UDMH) (MIL-P-25604C) at 120F up to 33 days produced no crack growth (30).

2.036 In anhydrous ammonia service protection against stress corrosion can be obtained by the addition of a small amount of water (33).

2.037 Hydrogen sulfide promotes stress corrosion in the T-1 steels and for this reason they should not be used in construction of storage tanks for those oils containing detectable amounts of hydrogen sulfide (33).

2.04 Nuclear Properties

2.041 Effect of neutron irradiation on impact properties, Table 2.041.

2.042 Effect of neutron irradiation on tensile properties, Table 2.042.

3. MECHANICAL PROPERTIES

3.01 Specified Mechanical Properties

3.011 Producer's specified mechanical properties.

3.0111 Producer's specified tensile properties for T-1 plate, Table 3.0111.

3.0112 Producer's specified impact properties for T-1 plate, Table 3.0112.

3.0113 Producer's specified tensile properties for T-1 Type A plates and sheets and T-1 Type B plate, Table 3.0113.

3.0114 Producer's specified impact properties for T-1 Type A and T-1 Type B plate, Table 3.0114.

3.0115 Producer's specified tensile properties for heat treated bar, Table 3.0115.

3.0116 Producer's specified tensile properties for heat treated tubular products, Table 3.0116.

3.0117 Producer's bend test values for heat treated plate when specified, Table 3.0117.

Fe
0.15 C
0.80 Mn
0.85 Ni
0.53 Cr
0.50 Mo
0.32 Cu
0.25 Si
0.05 V
+ B

T-1

Fe
0.16 C
0.85 Mn
0.53 Cr
0.27 Si
0.20 Mo
0.05 V
0.02 Ti
+ B

T-1A

Fe
0.16 C
1.12 Mn
0.52 Cr
0.50 Ni
0.27 Si
0.25 Mo
0.05 V
+ B

T-1B

Fe
0.15 C
0.80 Mn
0.85 Ni
0.53 Cr
0.50 Mo
0.32 Cu
0.25 Si
0.05 V
+ B

T-1

Fe
0.16 C
0.85 Mn
0.53 Cr
0.27 Si
0.20 Mo
0.05 V
0.02 Ti
+ B

T-1A

Fe
0.16 C
1.12 Mn
0.52 Cr
0.50 Ni
0.27 Si
0.25 Mo
0.05 V
+ B

T-1B

3.02 Mechanical Properties at Room Temperature.

3.021 Tension (see also 3.01 and 3.031).

3.0212 Typical tensile values for wrought T-1 alloy, Table 3.0212.

3.0213 Effect of tempering temperature on tensile properties of T-1 steel, Figure 3.0213.

3.022 Compression.

3.0221 Typical compressive stress-strain diagram for T-1 steel at room temperature, Figure 3.0221.

3.023 Impact (see also 3.01 and 3.033).

3.0231 Effect of strain and strain plus aging on Charpy V ductility transition temperature, Table 3.0231.

3.024 Bending (see 3.0117).

3.025 Torsion and shear,
F_{su} = 75% of F_{tu} (approx.)
F_{sy} = 58% of F_{ty} (approx.)

3.026 Bearing

3.027 Stress concentration

3.0271 Notch properties

3.0272 Fracture toughness (See Appendix C)

3.028 Combined properties

3.03 Mechanical Properties at Various Temperatures

3.031 Tension.

3.0311 Stress-strain diagrams.

3.0312 Effect of test temperature on tensile properties for three thicknesses of T-1 plate, Figure 3.0312.

3.0313 Effect of test temperature on tensile properties for two thicknesses of T-1 Type A plate, Figure 3.0313.

3.0314 Effect of strain-rate on tensile properties of T-1 at various temperatures, Figure 3.0314.

3.0315 Effect of low temperature on the yield strength of plate, Figure 3.0315.

3.0316 Effect of test temperature on plane strain and axi-symmetric ductility of plate, Figure 3.0316.

3.032 Compression.

3.0321 Stress-strain diagrams.

3.033 Impact.

3.0331 Effect of test temperature on longitudinal Charpy V notch values of T-1 plate, Figure 3.0331.

3.0332 Effect of test temperature on transverse Charpy V notch values of T-1 plate, Figure 3.0332.

3.0333 Effect of temperature on Charpy V notch values for T-1 Type A plate, Figure 3.0333.

3.0334 Effect of test temperature on Charpy V impact and slow bend results for plate, Figure 3.0334.

3.0335 Effect of plate thickness on Charpy V-notch impact transition temperature, Figure 3.0335.

3.034 Bending (see 3.024).

3.035 Torsion and shear.

3.036 Bearing.

3.037 Stress concentration.

3.0371 Notch properties.

3.0372 Fracture toughness.

3.03721 General. The plane strain fracture toughness cannot be measured at room temperature at a thickness of two inches (25) but from the trend of the data in Figure 3.03722 and 3.03723 should be in excess of 140 ksi-$in^{1/2}$. The plane strain fracture toughness decreases with decreasing test temperature to a value of about 35 ksi-$in^{1/2}$ at -320F. The effect of increasing loading rate is to reduce the apparent plane strain fracture toughness (Figure 3.0723) and a corresponding effect is noted for the Charpy V impact values (see Figure 3.0334). See Section 4.03 for the fracture toughness of weldments.

3.03722 Effect of temperature on the plane strain fracture toughness of T-1 plate of several thicknesses, Figure 3.03722.

3.03723 Effect of temperature on the plane strain fracture toughness of 2 inch T-1 plate, Figure 3.03723.

3.03724 Effect of test temperature and strain rate on apparent plane strain fracture toughness of plate, Figure 3.03724.

3.038 Combined properties.

3.04 Creep and Creep Rupture Properties

3.041 Creep rupture strength of T-1 alloy at various temperatures, Figure 3.041.

3.05 Fatigue Properties

3.051 Stress range diagram for T-1 plate, Table 3.051.

3.06 Elastic Properties

3.061 Poisson's ratio.

3.062 Modulus of elasticity at room and elevated temperatures, Figure 3.062.

3.0621 Compressive modulus.
30×10^3 ksi (approx.) (15).

3.063 Modulus of rigidity.

3.064 Typical compression tangent modulus curve for T-1 steel, Figure 3.064.

4. FABRICATION

4.01 Formability

4.011 General. T-1 steels may be hot or cold formed, sheared, punched, gas cut and machined using conventional equipment. Wherever possible fabrication should be done in the heat treated condition. Hot working operations can alter the as heat treated properties and in these cases complete reheat treatment is necessary. Stress relief is desirable prior to surface machining (15).

4.012 Forging. Steels may be forged by usual methods at a temperature about 50F lower than that used for plain carbon steels. A blast of compressed air or steam should be used on the forging to prevent the formation of scale pits. Forgings over 16 inches square cross section should be cooled in lime, dry sand or other medium to prevent cracking. All forged pieces must be heat treated to provide adequate mechanical properties (15). (See also 1.094).

4.013 Cold forming. Steels may be readily cold formed or angle bent if sufficient power and suitable bend radii are used. Suggested minimum bend radii for plates up to 1.0 inch is 2 T, and for plates from 1.0 inch to 2.0 inch is 3 T. For brake press forming, the lower die span should be at least 16 times the plate thickness. Air bends are preferable to closed-die bends. Mutiple bits should be used where possible (15).

4.014 Hot forming. Hot forming can be employed when plate sizes are too heavy for cold forming. Forming temperature should not exceed 1100F and heating should preferably be done in a controlled atmosphere furnace. If this temperature is exceeded for severe formations (never higher than 1800F) the steel must be subsequently quenched and tempered to restore mechanical properties (15).

4.015 Punching and blanking. Steels may be satisfactorily punched in thickness to 0.5 inch.
For circle-blanking of plate, die clearances should be as close as possible.

4.016 Shearing. Steels may be sheared in thicknesses up to 1.0 inch if sufficient shear capacity and blade strength are available.

4.017 Gas cutting. T-1 steels can be readily gas cut by hand or machine. No preheating is necessary for sections up to 4 inches in thickness, but sections larger than 4 inches should be preheated 300 to 400F (not higher than 400F). Stack cutting of light plates should be avoided. The gas cut edge will be hard (about 415 Brinell) but will also be tough. The gas cut surface can be softened to facilitate machining but the softening temperature must not exceed 1100F (15).

4.02 Machining and Grinding

4.021 Carbide tools are recommended for all machining operations although high speed steel tools may also be satisfactory. Tools should be kept sharp and considerable coolant should be used. In general, machining speeds are reduced about 40 percent as compared to steels such as ASTM-A36. For drilling, two-flute drills with included point angle of 135 degrees have been successfully employed with speeds of 30-50 sfpm and feeds 15-25 percent less than those used for mild steel. Positive feed must be used to prevent glazing ahead of the drill point.

4.022 It is recommended that plates or other sections of T-1 steels be stress-relieved after heat treatment to reduce residual stresses and prevent excessive movement during machining (15).

4.03 Welding

4.031 General. The T-1 steels can be welded by the SMA, sub arc, GMA and GTA processes with 100 percent tensile joint efficiency. Oxyacetylene gas and electroslag welding are not recommended. The strength and toughness of the weld metal and HAZ are a function of the welding conditions. Satisfactory weld performance can only be obtained by following recommended procedures. These have been outlined in detail (9)(33) and the fabricator should consult these references as a guide in all welded construction using T-1 steels. If service conditions are expected to be particularly severe or highly restrained welds are unavoidable or when post weld heat treatment is required, technical assistance should be requested from the alloy developer (U.S. Steel Corp.). What follows is a brief summary of the recommended welding procedures, precautions and weld properties.

4.032 Welding procedures. Filler metals satisfactory for use with the T-1 steels are listed in Table 4.0321. It should be noted that sub arc welding with carbon steel wire and alloy flux is generally not recommended because very close control of the welding conditions are necessary to avoid composition gradients in the weld which could lead to local cracking. It is necessary to keep the moisture content of SMA electrode coating below 0.2 percent in order to avoid hydrogen embrittlement of the weld metal and heat affected zone. Likewise it is important that the total hydrogen content of bare wire electrodes not exceed 5 ppm. Recommended preheat temperatures are a function of thickness (Table 4.0322). The use of preheats less than 100F requires close control of environmentally induced moisture. No welding should be done when the ambient temperature is below 0F. The strength and toughness of the weld metal and the heat affected zone are controlled by their microstructure which is in turn a function of the cooling rate. To achieve the minimum cooling rate necessary to produce the desired microstructure it is necessary to control the heat input during welding as a function of the preheat temperature and the metal thickness. Recommendations are given in Tables 4.0323 and 4.0324. The stringer bear technique is preferred since it permits better control of the heat input. Good practice requires the use of multiple beads to take advantage of the improved toughness associated with the grain refining and tempering action of subsequent passes.

4.0321 Recommended filler metals for use in various welding processes for T-1 steels, Table 4.0321.

4.0322 Recommended preheat temperatures for several welding processes used with T-1 steels, Table 4.0322.

4.0323 Recommended maximum welding heat inputs for T-1 steel, Table 4.0323.

4.0324 Recommended maximum welding heat input for T-1A and T-1B steels, Table 4.0324.

4.033 As welded HAZ toughness. Dynamic fracture tests on the heat affected zone in T-1A weldments show reduced toughness in this zone as compared with that of the parent plate. (Table 4.0331 and Figure 4.0332). In multiple shot explosion bulge tests at 30F on SMA and sub arc welded one and two inch T-1 plate (17) and in similar tests at 0F on SMA welded T-1 plate (16), fractures were frequently observed near the weld reinforcement in the HAZ but rarely did any fracture occur on the first shot. This behavior in the explosion bulge test is characteristic of this class of steels which are not intended for service conditions characterized by dynamic loads and high plastic deformation.

In contrast to the behavior in dynamic tests, plane strain fracture toughness tests on the heat affected zone of sub arc welded T-1 plate give K_{Ic} values higher than those of the parent metal, (Figure 4.0333 and Figure 4.0334).

4.0331 Tensile properties and drop weight test data for parent plate and weldments, Table 4.0331.

4.0332 Dynamic tear values for T-1A (A517B with 0.25 Ni) parent plate and weld heat affected zone, Figure 4.0332.

4.0333 Effect of test temperature on the plane strain fracture toughness of sub arc plate welds (heat input 35 kjoules per inch). Figure 4.0333.

4.0334 Effect of test temperature on plane strain fracture toughness of sub arc plate welds (heat input 70 kjoules per inch), Figure 4.0334.

4.034 Post weld treatments. The use of post weld stress relief treatments should be avoided where possible. Application of a post weld treatment above about 900F can produce a heat affected zone microstructure which is prone to cracking during the stress relief operation (24). For example, the unexpected catastrophic failure of a large experimental T-1 pressure vessel was traced to microcracks in highly restrained stress relieved weldments (29). In addition, the application of post weld thermal treatments in the range from 900 to 1200F can impair the heat affected zone toughness (see Tables 4.0341 through 4.0344 and Figures 4.0333 and 4.0334). These problems and some remedial measures are discussed further in Reference 24.

4.0341 Results from crack starter explosion bulge tests on welded plate of T-1 and T-1A, Table 4.0341.

4.0342 Transition temperatures determined from Kinzel notch bend tests on parent plate and weldments, Figure 4.0342

4.0343 Notch bend, drop weight and explosion bulge data for T-1 plate and weldments, Table 4.0343.

4.0344 Transition temperatures determined on weldments using notch bend and drop weight tests. Table 4.0344.

4.04 Heat Treatment

4.05 Surface Treatment

4.051 Scale and rust may be removed by acid pickling, grit or shot blasting or wire brushing. If flame descaling is used, the surface of the scale should never show a red color, even in the dark (15).

4.052 T-1 Type A usually will pickle faster and cleaner than T-1 steel.

4.053 The improved corrosion resistance of T-1 steels will result in better paint life than can be obtained with structural carbon steels. Prime and finish coats should be applied in accordance with the paint manufacturers instructions. Electro-deposited coatings while not commonly used on the T-1 steels may be applied if the usual steps to avoid hydrogen embrittlement are adopted. Baking for removal of hydrogen will not affect the properties of T-1 steels. Any sprayed metal coating may be used without special practices (15).

4.054 Carburizing.

4.0541 Hardness results obtained following various pack carburizing cycles are reported by Vettraino (28). Case depths of about 0.040 in and hardnesses of 62 to 64 Rc were produced in one-half inch thick sections by carburizing at 1650F, 4 to 8 hours. Quenching from carburizing temperature and tempering at 350F reduced the case hardness to approximately 57 Rc. Quenching from carburizing followed by cold treating (-100F) plus tempering produced case hardnesses of about 62 to 63 Rc. For all treatments the core remained at 35 to 37 Rc.

Source	(1, p.1)(14) A514-70 Type F, A517-70a Type F	
Alloy	T-1	
	Percent	
	Min	Max
Carbon	0.10	0.20
Chromium	0.40	0.65
Manganese	0.60	1.00
Molybdenum	0.40	0.60
Nickel	0.70	1.00
Phosphorous	-	0.035
Sulphur	-	0.040
Vanadium	0.03	0.08
Silicon	0.15	0.35
Boron	0.002	0.006
Copper	0.15	0.50

TABLE 1.041 CHEMICAL COMPOSITION OF T-1.

Fe
0.15 C
0.80 Mn
0.85 Ni
0.53 Cr
0.50 Mo
0.32 Cu
0.25 Si
0.05 V
+ B

T-1

Fe
0.16 C
0.85 Mn
0.53 Cr
0.27 Si
0.20 Mo
0.05 V
0.02 Ti
+ B

T-1A

Fe
0.16 C
1.12 Mn
0.52 Cr
0.50 Ni
0.27 Si
0.25 Mo
0.05 V
+ B

T-1B

Fe
0.15 C
0.80 Mn
0.85 Ni
0.53 Cr
0.50 Mo
0.32 Cu
0.25 Si
0.05 V
+ B

T-1

Source	(1, p.3) A514-70 Type B, A517-70a Type B	
Alloy	T-1 Type A	
	percent	
	Min.	Max.
Carbon (a)	0.12	0.21
Chromium	0.40	0.65
Manganese	0.70	1.00
Molybdenum	0.15	0.25
Phosphorous	-	0.035
Sulphur	-	0.040
Silicon	0.20	0.35
Vanadium	0.03	0.08
Titanium	0.01	0.03
Boron	0.0005	0.005
Copper (b)	0.20	0.040

(a) Carbon 0.15 to 0.21 furnished for orders specifying ASTM A517 Grade B or ASME SA517 Grade B.
(b) Optional addition for increased corrosion resistance.

TABLE 1.042 CHEMICAL COMPOSITION OF T-1 TYPE A.

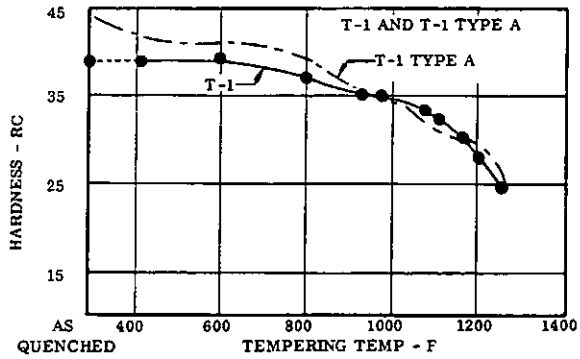


FIG 1.062 EFFECT OF TEMPERING TEMPERATURE ON HARDNESS (15)

Fe
0.16 C
0.85 Mn
0.53 Cr
0.27 Si
0.20 Mo
0.05 V
0.02 Ti
+ B

T-1A

Source	(1, p.5) A514-70 Type H, A517-70a Type H	
Alloy	T-1 Type B	
	percent	
	Min	Max
Carbon	0.12	0.21
Chromium	0.40	0.65
Manganese	0.95	1.30
Molybdenum	0.20	0.30
Nickel	0.30	0.70
Phosphorous	-	0.035
Sulphur	-	0.040
Silicon	0.20	0.35
Vanadium	0.030	0.080
Boron	0.0005	-
Copper (1)	0.20	0.40

(1) Optional addition for increased corrosion resistance.

TABLE 1.043 CHEMICAL COMPOSITION OF T-1 TYPE B.

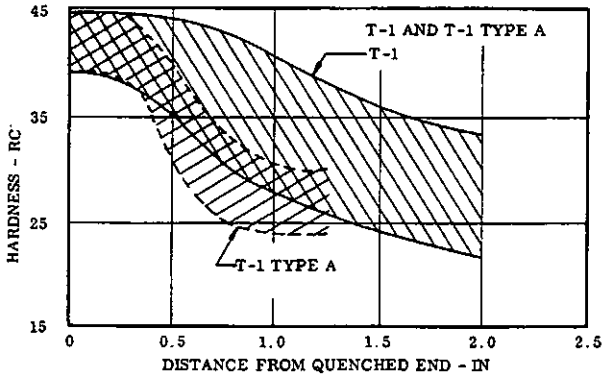


FIG 1.063 END - QUENCH HARDENABILITY BANDS (15)

Fe
0.16 C
1.12 Mn
0.52 Cr
0.50 Ni
0.27 Si
0.25 Mo
0.05 V
+ B

T-1B

Source	(1)		
Type (a)	T-1	T-1 Type A	T-1 Type B
Specification	Thickness	Thickness	Thickness
None (Structural quality)	3/16 - 7 in	-	-
ASTM A514 (Welded structure)	Grade F 4 in	Grade B 3/16 - 1-1/4 in	Grade H 3/16 - 2 in
ASTM A517 (Pressure vessel)	Grade F 3/16 - 2-1/2 in	Grade B 3/16 - 1-1/4 in	Grade H 3/16 - 2 in
Min. BHN plates			
321	3/16 - 4 in	3/16 - 1-1/4 in	3/16 - 2 in
340	3/16 - 2 in	3/16 - 1 in	3/16 - 1-1/2 in
360	3/16 - 1-1/2 in	3/16 - 1/2 in	3/16 - 1 in

(a) 200 in width max for all types.

TABLE 1.072 THICKNESS RANGES AVAILABLE FOR THE THREE TYPES UNDER SEVERAL SPECIFICATIONS.

Source	(32)			
Alloy	T-1			
Form	2 inch plate			
Condition	1660F, 1 hr WQ + 1230F, 1-1/2 hr WQ, F_{tu} = 121 ksi, F_{ty} = 110 ksi			
Exposure	10,000 psi hydrogen (electrolytic grade) 65F (a)			
Exposure time days	28	63		105
Applied K-ksi- in.	92	67	92	61
Crack extension - in.	0.448	.115	.076	0

(a) Bolt loaded WOL specimen one inch thick, 5 percent face notches.

TABLE 1.0951 EFFECT OF HIGH PRESSURE HYDROGEN ON CRACK PROPAGATION IN T-1 PLATE.

Fe
0.15 C
0.80 Mn
0.85 Ni
0.53 Cr
0.50 Mo
0.32 Cu
0.25 Si
0.05 V
+ B

T-1

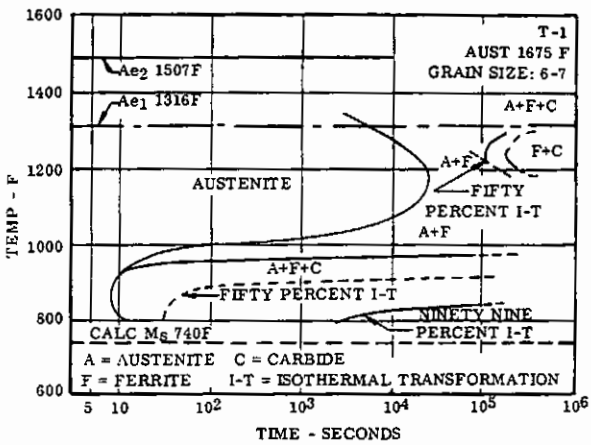


FIG. 2.0121 TIME-TEMPERATUE TRANSFORMATION DIAGRAM (15)

Source	(15)			
Alloy	T-1			
Test	Atmospheric corrosion			
Form	4 in x 6 in flat			
Atmosphere	Weight loss-grams			
	0.5 years	1.5 years	3.5 years	7.5 years
Industrial	5.0	8.2	9.4	11.3
Marine	2.8	5.9	10.4	15.4
Semi-rural	-	7.1	9.6	11.4

TABLE 2.032 WEIGHT LOSS IN INDUSTRIAL, MARINE AND SEMI-RURAL ATMOSPHERES FOR T-1 STEEL.

Fe
0.16 C
0.85 Mn
0.53 Cr
0.27 Si
0.20 Mo
0.05 V
0.02 Ti
+ B

T-1A

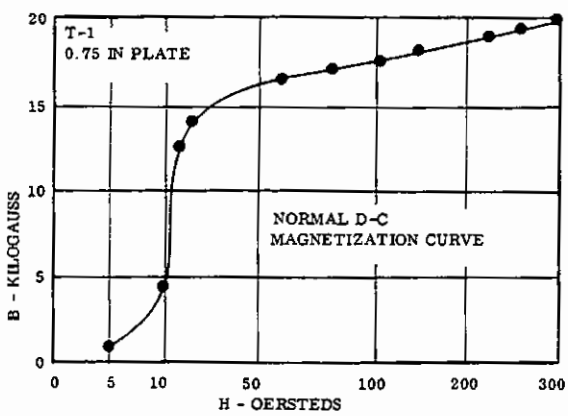


FIG. 2.0231 NORMAL D-C MAGNETIZATION CURVE FOR PLATE. (15)

Source	(15)	
Alloy	T-1	
Test	Exposure to stress-corrosion media	
	Test Medium	Susceptibility to cracking
Pickling acid, 12 percent H_2SO_4 at 160F		No
3 percent NaCl solution (aerated)		No
3 percent NaCl solution (aerated with cathodic protection at 300 amps per sq cm		No
Sea water		No
Marine atmosphere		No
Water, H_2S saturated		Yes
Molten sulfur with small amounts of H_2S		No
Molten sulfur with small amounts of H_2S and water		No
Sour crude oil (containing H_2S)		Yes
Uncontaminated ammonia		No
Agricultural ammonia, contaminated with air		Yes
Agricultural ammonia, contaminated with air and inhibited 0.2 percent water		No

TABLE 2.033 EXPOSURE OF T-1 STEEL TO VARIOUS STRESS CORROSION MEDIA.

Fe
0.16 C
1.12 Mn
0.52 Cr
0.50 Ni
0.27 Si
0.25 Mo
0.05 V
+ B

T-1B

Fe
0.15 C
0.80 Mn
0.85 Ni
0.53 Cr
0.50 Mo
0.32 Cu
0.25 Si
0.05 V
+ B

T-1

Source	(13)	
Alloy	T-1	
Form	16 ft strip	
Location in sea water (a)	Feet from top of strip	Corrosion rate mils per yr
Splash zone	1	0.9
	2	0.7
	3	1.0
Tidal zone	4	0.4
	5	-
	6	0.3
Immersed zone	7	0.9
	8	5.1
	9	4.3
	10	3.9
	11	4.6
	12	5.2
	13	4.5
	14	5.0
	15	4.5
	16	2.4

(a) Four year exposures.

TABLE 2.034 RESULTS OF FOUR YEAR EXPOSURE TESTS IN SEA WATER.

Source	(6)(11)					
Alloy	T-1					
Specimen	V-notch impact, 0.187 to 0.2 in, cantilever					
Test	Effect of irradiation on impact properties					
Irradiation Conditions			Transition Temp- F (a)		Max energy absorption in-lb (b)	
Temp- F	Exposure, nvt (c)		Control	Irradiated	Control	Irradiated
< 100	1.3×10^{21}		-165	+167	67	22
< 200	5×10^{18}		-240	- 40	48	40
< 200	7×10^{19}		-240	+150	48	23
575	5×10^{18}		-240	-115	48	48
< 200	2.3×10^{19}		-214	+ 19	86	52
< 200	3.3×10^{19}		-214	+ 68	86	52

(a) Taken from transition curve, criterion: 50 percent of maximum impact energy.
(b) Taken from transition curve.
(c) > 1 Mev

TABLE 2.041 EFFECT OF NEUTRON IRRADIATION ON IMPACT PROPERTIES.

Fe
0.16 C
0.85 Mn
0.53 Cr
0.27 Si
0.20 Mo
0.05 V
0.02 Ti
+ B

T-1A

Source	(13)										
Alloy	T-1										
Atmosphere	Industrial				Marine				Semi-rural		
Exposure Time - yrs	0.5	1.5	3.5	7.5	0.5	1.5	3.5	7.5	1.5	3.5	7.5
Weight loss gms (a)	5.0	8.2	9.4	11.3	2.8	5.9	10.4	15.4	7.1	9.6	11.4

(a) Total grams per 4 x 6 inch specimen.

TABLE 2.035 RESULTS OF LONG TIME EXPOSURES TO VARIOUS ATMOSPHERES.

Source	(6)					
Alloy	T-1 Steel					
Test	Effect of irradiation on tensile properties					
Irrad Cond		F_{tu} ksi		F_{ty} ksi		e (1 in)-percent
Temp F	Exposure nvt	Control	Irrad	Control	Irrad	Control	Irrad
<100	1.3×10^{21}	116.0	180.0	100.0(a)	180.0(a)	20.0	4.7
<200	1.7×10^{19}	129.0	171.0	120.0	170.0	14.0	4.5
<200	1.0×10^{20}	129.0	187.2	120.0	186.0	14.0	3.8
<200	2.3×10^{19}	139.7	186.4	129.3	184.0	15.0(b)	9.0(b)
<200	3.3×10^{19}	139.7	189.4	129.3	186.8	15.0(b)	8.6(b)

(a) 0.1 percent offset yield strength
(b) 0.275 inch gage length

TABLE 2.042 EFFECT OF NEUTRON IRRADIATION ON TENSILE PROPERTIES.

Fe
0.16 C
1.12 Mn
0.52 Cr
0.50 Ni
0.27 Si
0.25 Mo
0.05 V
+ B

T-1B

Source	(1)					
Alloy type	T-1					
Form	Plate					
Thickness-in	3/16 to 2-1/2		> 2-1/4 to 4 incl.		>4 to 6 incl.	
Direction (2)	L	T	L	T	L	T
F_{tu}-ksi (max)	135	135	135	135	135	135
(min)	115	115	105	105	105	105
F_{ty}-ksi (min)	100	100	90	90	90	90
e (2 in)-percent(min)(1)	18	16	17	15	16	-
R.A.-percent (min) ≤3/4 in (3)	40	35	-	-	-	-
>3/4 in >1/2 in dia spec.(4) >1-1/2 in wide	50	45	50	45	45	
Full thick spec. (3)	40	35				-

(1) Deduct 1.25 percent for each 1/32 in decrease in thickness under 5/16, not to exceed 3 percent.
(2) Transverse may be specified for any thickness up to 4 in. Transverse values shown are required by ASTM A517 Grade F (ASME SA517, Grade F).
(3) Specimens according to ASTM A370, Fig. 4.
(4) ASTM 370, Fig. 6.

TABLE 3.0111 PRODUCER'S SPECIFIED TENSILE PROPERTIES FOR T-1 PLATE.

Source	(1)	
Alloy Type	T-1	
Form	Plate	
Thickness - in	7/16 to 2-1/4 inch	
Direction	L	T
Impact (a) IE Charpy V ft-lb (min.)		
0 F or higher	30	20
<0 to -50 F	20	15
(a) Applicable to pressure vessel quality and higher.		

TABLE 3.0112 PRODUCER'S SPECIFIED IMPACT PROPERTIES FOR T-1 PLATE.

Source	(2)(15)(7)			
Alloy	T-1			T-1A
Test	Tensile			
Condition	HT			
Form	Bar(b)			
Size-in	Up thru 4.0 Flats to 2.5	4.0 thru 7.0 Flats > 2.5	7.0 thru 9.5	Up to 1.75
F_{tu} - max-ksi	140	135	135	140
min-ksi	115	105	105	115
F_{ty} - max-ksi	-	-	-	-
min-ksi	100	95	90	100
e(2in) min-percent	18	16	16	18
RA - min-percent	55(a)	45	45	55(a)
(a) Reduction of area for flats 0.75 inch and under is 45 percent.				
(b) Longitudinal properties.				

TABLE 3.0115 PRODUCER'S SPECIFIED TENSILE PROPERTIES FOR HEAT TREATED BAR.

Fe
0.15 C
0.80 Mn
0.85 Ni
0.53 Cr
0.50 Mo
0.32 Cu
0.25 Si
0.05 V
+ B

T-1

Source	(1)					
Alloy Type	T-1A				T-1B	
Form	Plates and Sheets				Plates	
Thickness-in	<3/4	0.180 to 3/4 incl.	>3/4 to 1-1/4 incl.		3/16 to 2 incl.	
Direction (a)	L	T	L	T	L	T
F_{tu}-ksi (max)	135	135	135	135	135	135
(min)	115	115	115	115	115	115
F_{ty}-ksi (min)	100	100	100	100	100	100
e (2 in) percent (min)						
Plates	18(b)	16(b)	18	16	18(b)	16(b)
Sheet or strip	10					
R.A. percent (min)						
Plates (c)	40	35	40(d)	35(d)	40 (e)	35(e)

(a) Tranverse tensile values shown are mandatory for plates to ASTM A517, Grade B (ASME SA517, Grade B).
(b) Deduct 1.25 percent for each 1/32 inch decrease in thickness under 5/16, not to exceed 3 percent.
(c) Specimens according to ASTM A370, Figure 4.
(d) For 1/2 in diameter specimen RA = 50 percent L and 45 percent T.
(e) Over 3/4 in thick: using 1/2 in diameter specimen RA = 50 percent L and 45 percent T.

TABLE 3.0113 PRODUCER'S SPECIFIED TENSILE PROPERTIES FOR T-1 TYPE A PLATES AND SHEETS AND T-1 TYPE B PLATE.

Source	(7)(15)
Alloy	T-1 and T-1 type A
Test	Tensile
Condition	HT
Form	Seamless tubing (b)
Thickness-in	(a)
F_{tu} - max-ksi	145
min-ksi	115
F_{ty} - max-ksi	-
min-ksi	100
e (2 in) - min-percent	18
RA - min-percent	-

(a) All wall thicknesses for round, square, and rectangular tubing.
(b) On strip specimens $\leq$ 0.25 inch, e is reduced accordingly.

TABLE 3.0116 PRODUCER'S SPECIFIED TENSILE PROPERTIES FOR HEAT TREATED TUBULAR PRODUCTS.

Fe
0.16 C
0.85 Mn
0.53 Cr
0.27 Si
0.20 Mo
0.05 V
0.02 Ti
+ B

T-1A

Source	(1)			
Alloy Type	T-1A		T-1B	
Form	Plate		Plate	
Thickness-in	7/16 - 1-1/4		7/16 to 2	
Direction	L	T	L	T
Impact (a) IE Charpy V ft-lbs (min.)				
-50 F	15	15	-	-
> 10 F	-	-	20	15
<10 to -50 F	-	-	15	-
(a) Applicable to pressure vessel quality and higher.				

TABLE 3.0114 PRODUCER'S SPECIFIED IMPACT PROPERTIES FOR T-1 TYPE A AND T-1 TYPE B PLATE.

Source	(7)(15)			
Alloy	T-1		T-1 type A	
Condition	HT		HT	
Form	Plate			
Test	ASTM bend test (a)			
Quality	Structural	Pressure Vessel	Structural	Pressure Vessel
Orientation	L	T	L	T
Thickness-in				
to 1.0	2t	2t	2t	2t
1.0 to 1.25	-	-	3t	3t
1.0 to 2.5	3t	3t	-	-
2.5 to 4.0	4t	4t	-	-
over 4.0	None	-	-	-
(a) 180 degree bend.				

TABLE 3.0117 PRODUCER'S BEND TEST VALUES FOR HEAT TREATED PLATE WHEN SPECIFIED.

Fe
0.16 C
1.12 Mn
0.52 Cr
0.50 Ni
0.27 Si
0.25 Mo
0.05 V
+ B

T-1B

Fe
0.15 C
0.80 Mn
0.85 Ni
0.53 Cr
0.50 Mo
0.32 Cu
0.25 Si
0.05 V
+ B

T-1

Fe
0.16 C
0.85 Mn
0.53 Cr
0.27 Si
0.20 Mo
0.05 V
0.02 Ti
+ B

T-1A

Fe
0.16 C
1.12 Mn
0.52 Cr
0.50 Ni
0.27 Si
0.25 Mo
0.05 V
+ B

T-1B

Source	(15)
Alloy	T-1
Condition	HT
F_{tu} typ-ksi	122
F_{ty} typ-ksi	111
Uniform e (2 in)-percent	8.2
Total e (2 in)-percent	18.5
RA -percent	62
Strain hardening exponent	0.07

TABLE 3.0212 TYPICAL TENSILE VALUES FOR WROUGHT T-1 ALLOY.

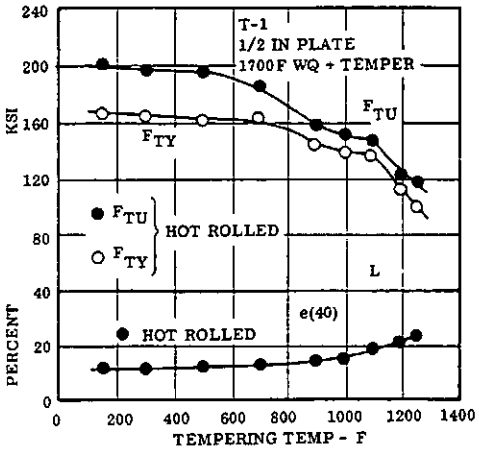


FIG. 3.0213 EFFECT OF TEMPERING TEMPERATURE ON TENSILE PROPERTIES OF T-1 PLATE. (33, fig. 1)

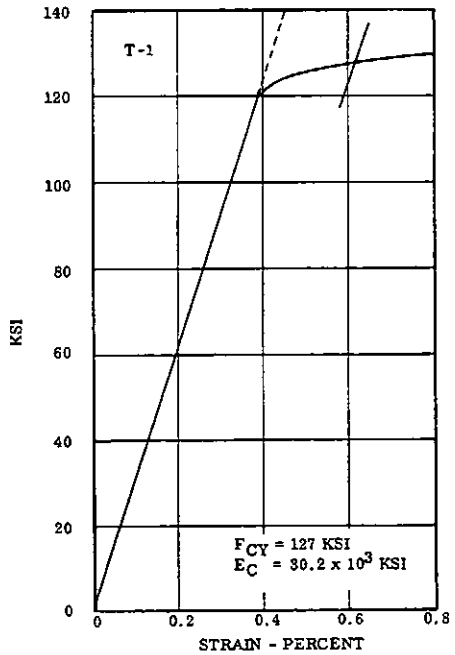


FIG 3.0221 TYPICAL COMPRESSIVE STRESS-STRAIN DIAGRAM FOR T-1 STEEL AT ROOM TEMPERATURE (15)

Source	(15)	
Test	Effect of strain and strain + age	
Specimen	Charpy V (a)	
Alloy	T-1	T-1 type A
Condition	Ductility transition temp- F(b)	
Unstrained	-225	-95
Strain 5 percent	-170	-50
Strain 5 percent + age	-150	-50
Strain 5 percent + age + stress relieve	-180	-100

(a) Longitudinal specimens
(b) 15 ft-lb

TABLE 3.0231 EFFECT OF STRAIN AND STRAIN PLUS AGING ON CHARPY V DUCTILITY TRANSITION TEMPERATURE.

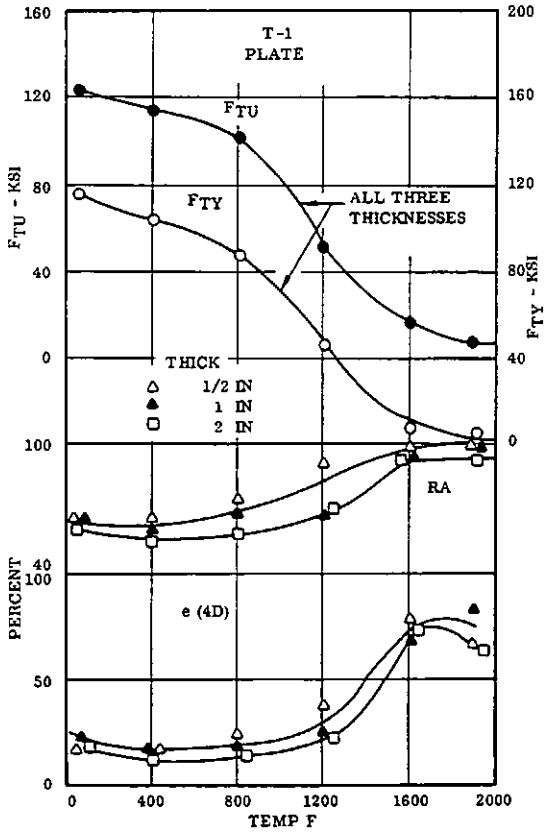


FIG 3.0312 EFFECT OF TEST TEMPERATURE ON TENSILE PROPERTIES FOR THREE THICKNESSES OF T-1 PLATE. (13)

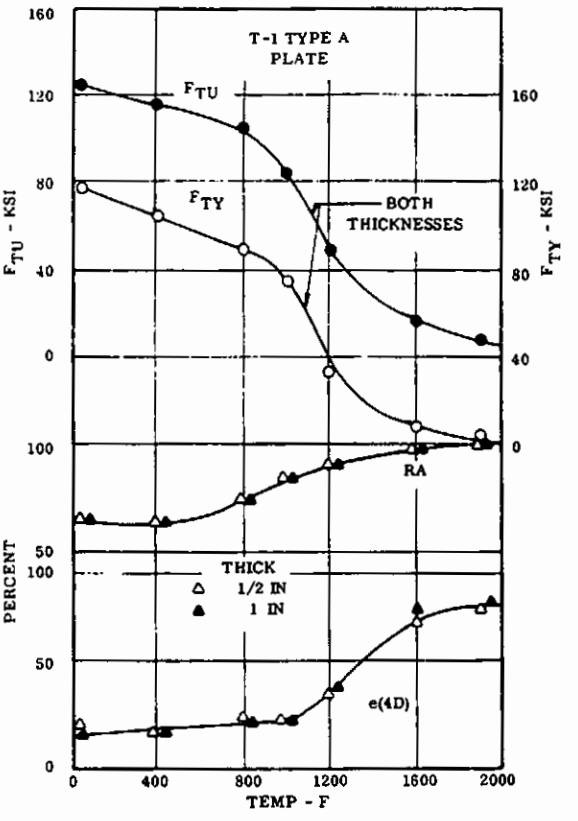


FIG 3.0313 EFFECT OF TEST TEMPERATURE ON TENSILE PROPERTIES FOR TWO THICKNESSES OF T-1 TYPE A PLATE (13)

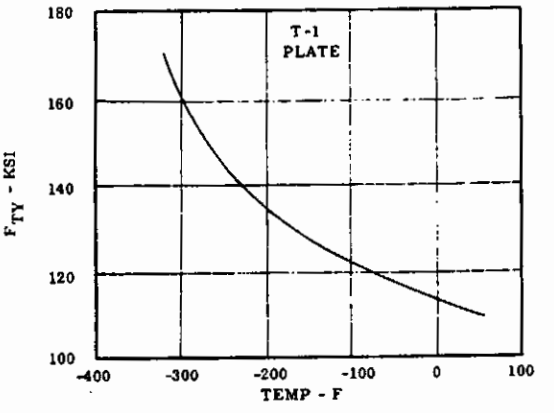


FIG 3.0315 EFFECT OF LOW TEMPERATURE ON YIELD STRENGTH OF PLATE (26) FIG 16

Fe
0.15 C
0.80 Mn
0.85 Ni
0.53 Cr
0.50 Mo
0.32 Cu
0.25 Si
0.05 V
+ B

T-1

Fe
0.16 C
0.85 Mn
0.53 Cr
0.27 Si
0.20 Mo
0.05 V
0.02 Ti
+ B

T-1A

Fe
0.16 C
1.12 Mn
0.52 Cr
0.50 Ni
0.27 Si
0.25 Mo
0.05 V
+ B

T-1B

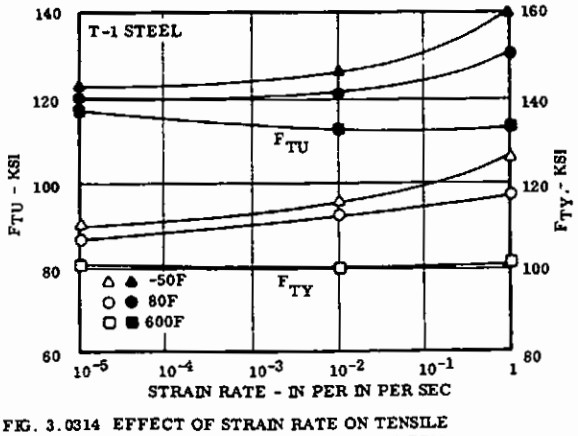


FIG. 3.0314 EFFECT OF STRAIN RATE ON TENSILE PROPERTIES OF T-1 AT VARIOUS TEMPERATURES. (15)

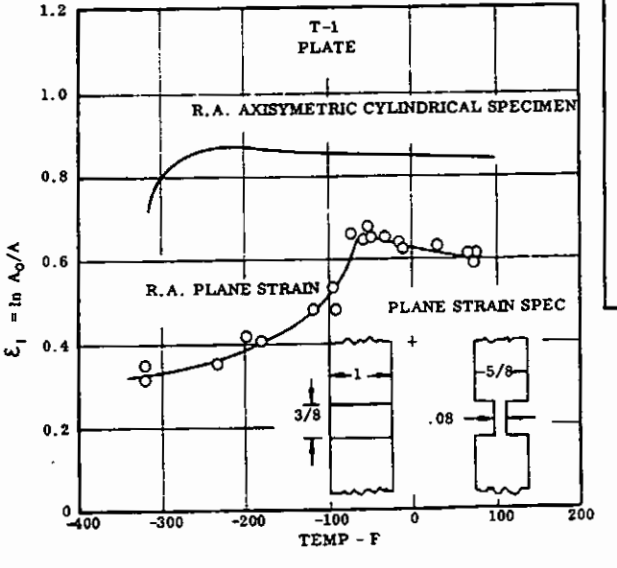


FIG 3.0316 EFFECT OF TEST TEMPERATURE ON PLANE STRAIN AND AXISYMETRIC DUCTILITY OF PLATE (26) FIG 10

Fe
0.15 C
0.80 Mn
0.85 Ni
0.53 Cr
0.50 Mo
0.32 Cu
0.25 Si
0.05 V
+ B

T-1

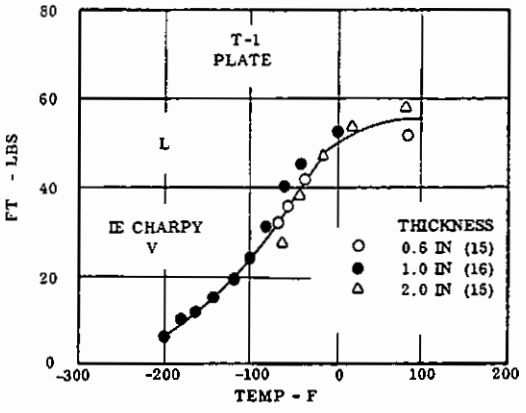


FIG. 3.0331 EFFECT OF TEST TEMPERATURE ON LONGITUDINAL CHARPY V NOTCH VALUES OF T-1 PLATE. (16, p.3)(15)

Fe
0.16 C
0.85 Mn
0.53 Cr
0.27 Si
0.20 Mo
0.05 V
0.02 Ti
+ B

T-1A

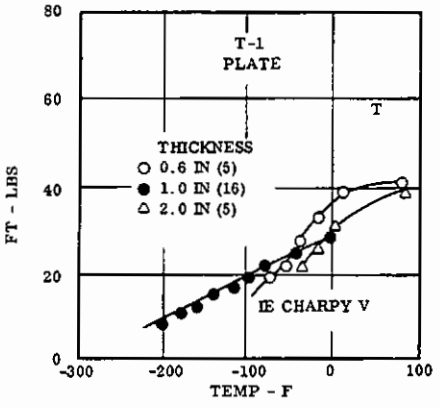


FIG. 3.0332 EFFECT OF TEST TEMPERATURE ON TRANSVERSE CHARPY V NOTCH VALUES OF T-1 PLATE (16 p.3)(15)

Fe
0.16 C
1.12 Mn
0.52 Cr
0.50 Ni
0.27 Si
0.25 Mo
0.05 V
+ B

T-1B

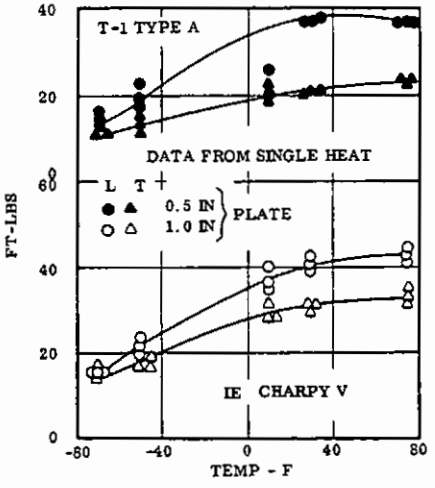


FIG 3.0333 EFFECT OF TEMPERATURE ON CHARPY V - NOTCH VALUES FOR T-1 TYPE A PLATE (15)

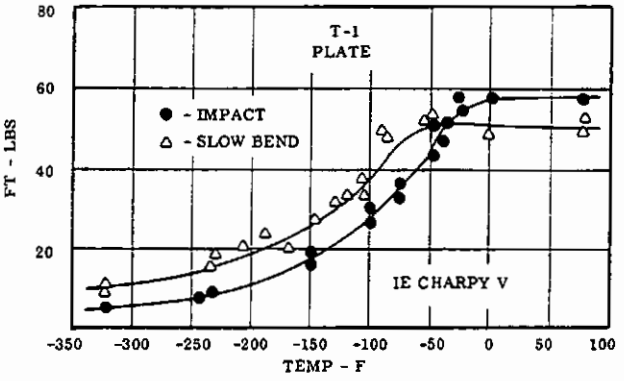


FIG 3.0334 EFFECT OF TEST TEMPERATURE ON CHARPY V IMPACT AND SLOW BEND RESULTS FOR PLATE (25, fig. 14)

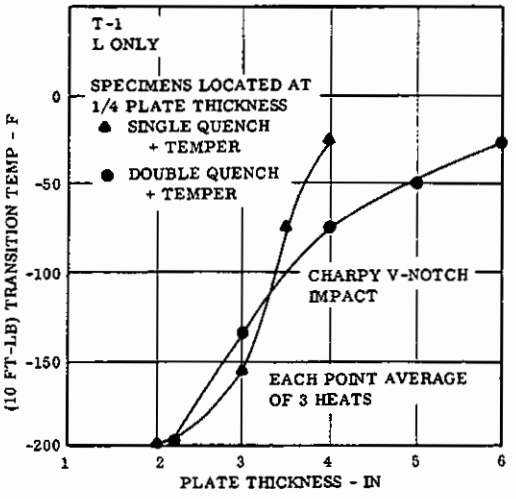


FIG. 3.0335 EFFECT OF PLATE THICKNESS ON CHARPY V-NOTCH IMPACT TRANSITION TEMPERATURE. (15)

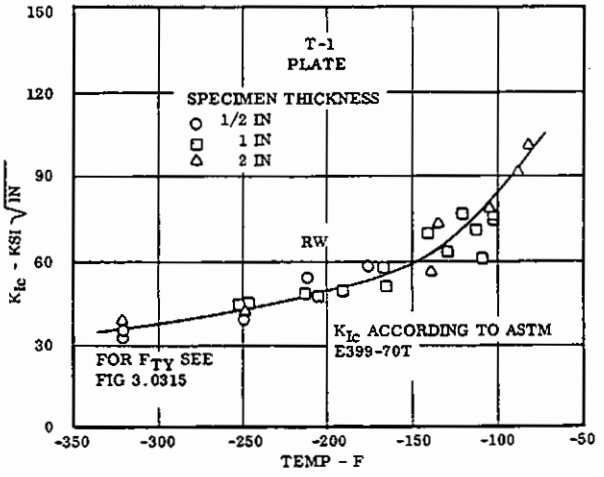


FIG 3.03722 EFFECT OF TEMPERATURE ON PLANE STRAIN FRACTURE TOUGHNESS OF PLATE OF SEVERAL THICKNESSES. (25, fig. 5)

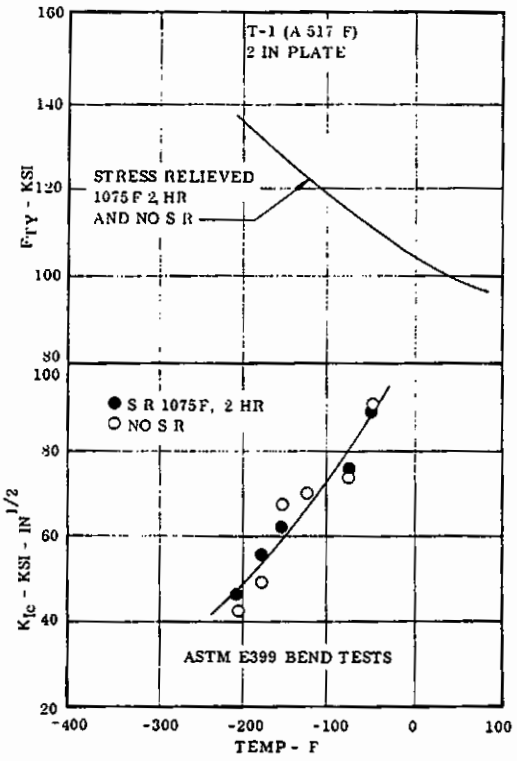


FIG. 3.03723 EFFECT OF TEMPERATURE ON PLANE STRAIN FRACTURE TOUGHNESS OF 2 IN T-1 PLATE. (31, table 2, fig. 21)

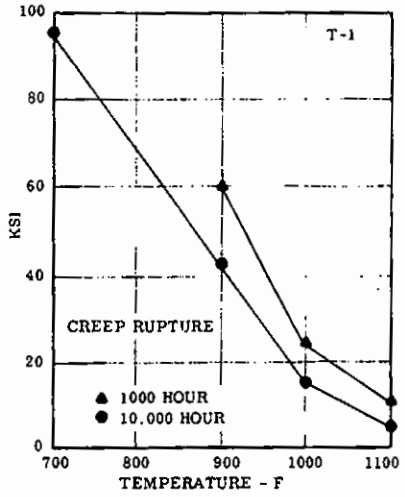


FIG. 3.041 CREEP RUPTURE STRENGTH OF T-1 STEEL AT VARIOUS TEMPERATURES. (15)

Fe
0.15 C
0.80 Mn
0.85 Ni
0.53 Cr
0.50 Mo
0.32 Cu
0.25 Si
0.05 V
+ B

T-1

Fe
0.16 C
0.85 Mn
0.53 Cr
0.27 Si
0.20 Mo
0.05 V
0.02 Ti
+ B

T-1A

Source	(5, p. 230)								
Alloy	T-1								
Form	3/4 in plate F_{tu} = 121 ksi F_{ty} = 112 ksi								
Stress Ratio	R = -1 A = ∞			R = 0 A = 1			R = 0.5 A = .33		
Cycles to Failure	10^5	$6x10^5$	$2x10^6$	10^5	$6x10^5$	$2x10^6$	10^5	$6x10^5$	$2x10^6$
F_{max} - ksi	55	35	30	90	50	40	115	80	60

TABLE 3.051 STRESS RANGE RESULTS FOR T-1 PLATE.

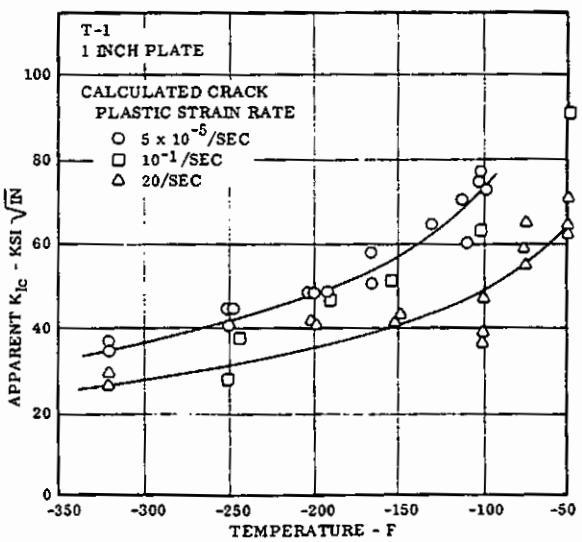


FIG. 3.03724 EFFECT OF TEST TEMPERATURE AND STRAIN RATE ON APPARENT PLANE STRAIN FRACTURE TOUGHNESS OF PLATE. (27, fig. 5)

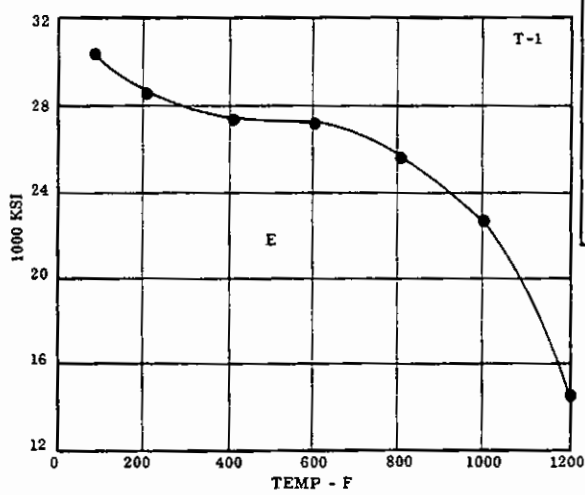


FIG. 3.062 MODULUS OF ELASTICITY AT ROOM AND ELEVATED TEMPERATURES (15)

Fe
0.16 C
1.12 Mn
0.52 Cr
0.50 Ni
0.27 Si
0.25 Mo
0.05 V
+ B

T-1B

Fe
0.15 C
0.80 Mn
0.85 Ni
0.53 Cr
0.50 Mo
0.32 Cu
0.25 Si
0.05 V
+ B

T-1

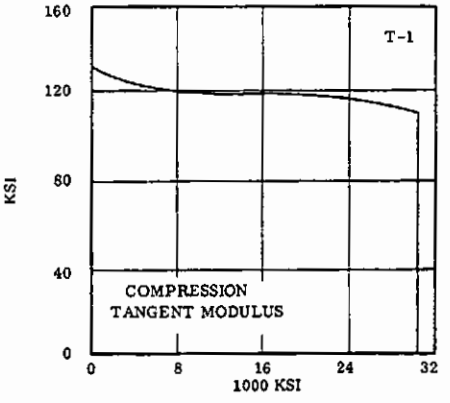


FIG 3.064 TYPICAL COMPRESSION TANGENT MODULUS CURVE FOR T-1 STEEL (15)

Source	(33) Table 4		
Alloy	T-1 (A517)		
Weld process	SMA	Sub arc	GMA
Filler metal	E11018G (a)(b)	Mn-Ni-Cr-Mo wire + neutral flux or carbon steel wire + alloy flux (c)	Mn-Ni-Cr-Mo-wire + Argon-0_2 gas

(a) Lower strength, low H_2 electrodes may be used.
(b) Higher strength electrode (e.g. E120186) may be necessary for thin plates of T-1A (A517B).
(c) Very close control of welding conditions required to avoid composition variations and cracking.

TABLE 4.0321 RECOMMENDED FILLER METALS FOR USE IN VARIOUS WELDING PROCESSES USED WITH T-1 STEELS.

Fe
0.16 C
0.85 Mn
0.53 Cr
0.27 Si
0.20 Mo
0.05 V
0.02 Ti
+ B

T-1A

Source	(33 Table 6) (a)			
Alloy	T-1, T-1A and T-1B			
Weld process	SMA	GMA	Sub Arc	Sub Arc
Plate thick (in.)				
≤ 1/2	100F	100F	100F	100F
> 1/2 to 1	100	100	100	200
> 1 to 2	150	150	150	300
> 2	200	200	200	400

TABLE 4.0322 RECOMMENDED PREHEAT TEMPERATURES FOR SEVERAL WELDING PROCESSES USED WITH T-1 STEELS.

Fe
0.16 C
1.12 Mn
0.52 Cr
0.50 Ni
0.27 Si
0.25 Mo
0.05 V
+ B

T-1B

Source	(33 Table 9)							
Alloy	T-1							
Welding condition	Max. heat input in Kjoules/in. for various thicknesses							
Thickness - in.	3/16	1/4	1/2	3/4	1	1-1/4	1-1/2	2
Preheat and interpass temp-F								
70	27	36	70	121	Any	Any	Any	Any
200	21	29	56	99	173	Any	Any	Any
300	17	24	47	82	126	175	Any	Any
400	13	19	40	65	93	127	165	Any

4.0323 RECOMMENDED MAXIMUM WELDING HEAT INPUTS FOR T-1 STEEL.

Source	(33 Table 8)							
Alloy	T-1A and T-1B							
Welding condition	Max. heat input in Kjoules/in. for various thicknesses							
Thickness - in.	3/16	1/4	3/8	1/2	5/8	3/4	1	1-1/4
Preheat and interpass temp-F								
70	17.5	23.7	35	47.4	64.5	88.6	Any	Any
150	15.3	20.9	30.7	41.9	57.4	77.4	120.0	Any
200	14	19.2	28	35.5	53.0	69.9	110.3	154.0
300	11.5	15.8	23.5	31.9	42.5	55.7	86.0	120.0
400	9.0	12.3	18.5	25.9	33.5	41.3	65.6	94.0

TABLE 4.0324 RECOMMENDED MAXIMUM WELDING HEAT INPUT FOR T-1A AND T-1B STEELS.

Source	(18, p.5) (19, p.3)			
Alloy	T-1		T-1A (0.25%Ni)	
Form	1 in. plate		1 in. plate	
Condition	Austenitize + 1150F	Austenitize + 900F	As Rec'd. Q & T	As Rec'd. + Welded (b)(c)
F_{tu} - ksi	125	153	121	-
F_{ty} - ksi	119	143	113	-
RA - percent	48	40	55	-
NDT - F(a)	-65	+10	-80	+10
DWTT at 30F ft-lbs				
TL	-	-	1478	-
LT	-	-	3633	-

(a) ASTM E208-69
(b) See Figure 4.0332 for welding conditions.
(c) NDT specimen notched in HAZ.

TABLE 4.0331 TENSILE PROPERTIES AND DROP WEIGHT TEST FOR PARENT PLATE AND WELDMENTS.

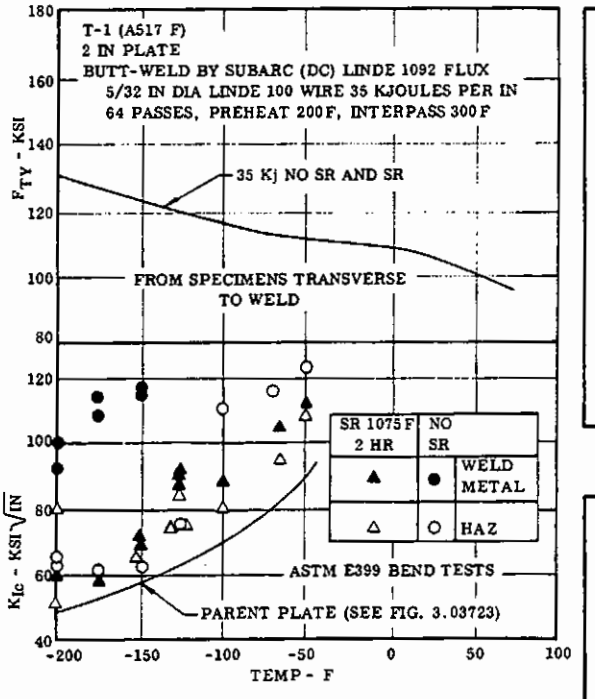


FIG. 4.0333 EFFECT OF TEST TEMPERATURE ON PLANE STRAIN FRACTURE TOUGHNESS OF SUBARC PLATE WELDS. (31, table 2)

Fe
0.15 C
0.80 Mn
0.85 Ni
0.53 Cr
0.50 Mo
0.32 Cu
0.25 Si
0.05 V
+ B

T-1

Fe
0.16 C
0.85 Mn
0.53 Cr
0.27 Si
0.20 Mo
0.05 V
0.02 Ti
+ B

T-1A

Fe
0.16 C
1.12 Mn
0.52 Cr
0.50 Ni
0.27 Si
0.25 Mo
0.05 V
+ B

T-1B

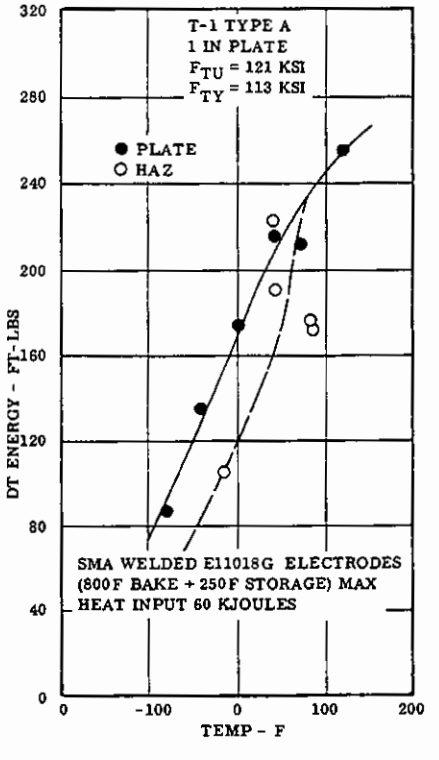


FIG. 4.0332 DYNAMIC TEAR VALUES FOR T-1A (A517B WITH 0.25 Ni) PARENT PLATE AND WELD HEAT AFFECTED ZONE. (23, table 7)

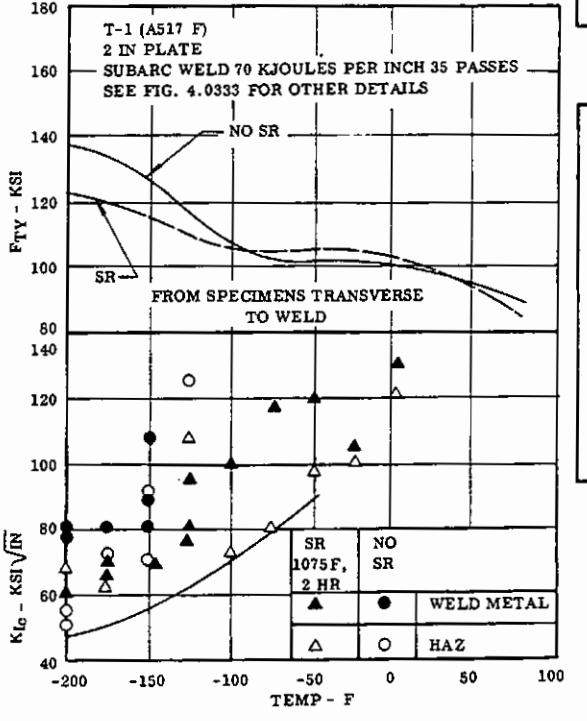


FIG. 4.0334 EFFECT OF TEST TEMPERATURE ON PLANE STRAIN FRACTURE TOUGHNESS OF SUBARC PLATE WELDS. (31, table 2, fig. 21)

Fe
0.15 C
0.80 Mn
0.85 Ni
0.53 Cr
0.50 Mo
0.32 Cu
0.25 Si
0.05 V
+ B

T-1

Source	(14)(17)							
Alloy	T-1				T-1A			
Thickness-in	1				1		1-3/8	
Condition (a)	A	SMA	SMA +SR	SA	A	SMA	A	SMA
Test temp. for transition to elastic fracture (FTE) -F	-40	-30 to -40	-10 to -30	-10 to -30	-60	-15	-10	-25

(a) A - as received Q and T; SMA - shielded metal arc SA - submerged arc; SR - stress relief 1100F, 1 hr.

TABLE 4.0341 RESULTS FROM CRACK STARTER EXPLOSION BULGE TESTS ON WELDED PLATE OF T-1 AND T-1A.

Fe
0.16 C
0.85 Mn
0.53 Cr
0.27 Si
0.20 Mo
0.05 V
0.02 Ti
+ B

T-1A

Source	(15)				
Alloy	T-1				
Form	1/2 in plate				
Type	T-1			T-1A	
Condition	A (a)	A + Weld	A + Weld + 1100F, 1 hr	A	A + Weld + 1100F, 1 hr
Ductility Transition Temp - F (b)	-68	-42	-30	-56	-40
50 percent shear transition Temp - F (b)	-67	-42	-27	-44	-12

(a) Q and T as received.
(b) Kinzel notch bend test

TABLE 4.0342 TRANSITION TEMPERATURES DETERMINED FROM KINZEL NOTCH BEND TESTS ON PARENT PLATE AND WELDMENTS.

Fe
0.16 C
1.12 Mn
0.52 Cr
0.50 Ni
0.27 Si
0.25 Mo
0.05 V
+ B

T-1B

Source	(15)(10)			
Alloy	T-1			
Form	Plate			
Thickness-in	0.5			
Test	Notch toughness			
	Specimen Orientation	Condition of Specimen	Ductility Transition Temp- F(a)	Fracture Appearance Transition Temp- F(b)
Kinzel Notch-bend	L	unwelded	-68	-67
	T	unwelded	-62	-59
	L	welded	-42	-42
	T	welded	-50	-47
	L	welded + stress rel.(c)	-30	-27
NRL drop-weight	L	welded (d)	-80	-
	T	welded (d)	-80	-
NRL bulge-explosion	-	welded (d)	-	-50 (e)

(a) Ductility transition temperature at middle of band for Kinzel notch-bend and total failure at 3 percent angle for NRL drop-weight test.
(b) Fracture appearance transition temperature selected at 50 percent shear for Kinzel notch-bend and failure across plate for NRL bulge-explosion test.
(c) Stress relieved at 1100F for 1 hour.
(d) Hard facing electrodes.
(e) Fracture-arrest transition temperature.

TABLE 4.0343 NOTCH BEND, DROP WEIGHT AND EXPLOSION BULGE DATA FOR T-1 PLATE AND WELDMENTS.

Source	(15)(10)			
Alloy	T-1 Type A			
Form	Plate			
Thickness-in	0.5			
Test	Notch Toughness			
	Specimen Orientation	Condition of Specimen	Ductility Transition Temp- F(a)	Fracture Appearance Transition Temp- F(b)
Kinzel notch-bend	L	welded	-56	-44
	L	welded + stress rel(c)	-40	-12
NRL drop-weight	L	welded (d)	-60	-

(a)(b)(c)(d) see Table 4.038

TABLE 4.0344 TRANSITION TEMPERATURES DETERMINED ON WELDMENTS USING NOTCH BEND AND DROP WEIGHT TESTS.

REFERENCES

1. Properties Card, "U.S.S. T-1 Constructional Alloy", U.S. Steel Corporation (March 1969).
2. Alloy Digest, "USS T-1 Type A", Filing Code: SA-157, Steel Alloy (November 1963).
3. Bennett, E. V., "Super-Strength Structural Steel", prepared for the Climax Molybdenum Company.
4. United States Steel Corporation, "New Steels, New Shapes, New Concepts" (1961).
5. Brockenbrough, R. L. and Johnston, B. G., "USS Steel Design Manual", USS ADUSS 27-3400-02 (November 1968).
6. Porter, L. F., "Radiation Effects in Steel", ASTM Special Technical Publication No. 276, Materials in Nuclear Applications (June 1960).
7. United States Steel Corporation, "Availabilities Guide, Qualities, Forms, Sizes and Properties, USS T-1 and T-1 Type A Steels" (May 1963).
8. Alloy Digest, "Carilloy T-1", Filing Code: SA-25, Steel Alloy (January 1955).
9. United States Steel Corporation, "How to Weld T-1 and T-1 Type A Steels", Publication No. ADUCO 01006 (latest revision).
10. Puzak, P. P. and Pellini, W. S., "Evaluation of the Significance of Charpy Tests for Quench and Tempered Steels", The Welding Journal, Vol. 35 (6), Research Suppl. 275-S to 290-S (1956).
11. Balai, N., Kettles, T. L. and Bailey, R. E., "Reactor Pressure Vessel Design for Nuclear Reactions", Symposium on Radiation Effects on Materials, Vol. 3, ASTM STP No. 233 (1958).
12. McDonnell Aircraft Corporation, "Mechanical Properties and Weldability of Cast T-1 Steel", from First Quarterly Progress Report on Unpublished Materials Research and Development Programs, Rep. No. 8743, Vol. IV, Ser. 1 (April 1962).
13. Reichold, H. M., U. S. Steel Corporation, personal communication with W. F. Brown, Jr. (February 29, 1972).
14. Doty, W. D., "Welding of Quenched and tempered Alloy Steels", Metals Engineering Quarterly (February 1969).
15. Carney, D. J., U.S. Steel Corporation, personal communication with W. F. Brown, Jr. (January 27, 1972)
16. Puzak, P. P., "Explosion Bulge Test Performance of Low Carbon Ni-Cr-Mo-B Quenched and Tempered Steel Weldments", NRL Report 4919 (May 17, 1957).
17. Doty, W. D., Benten, W. P. and Manning, R. D., "Performance Tests of a High Yield Strength Steel for Ships", The Welding Journal, Vol. 47, No. 12, Res. Supp. (1968) p. 534s.
18. Puzak, P. P. and Babecki, A. J., "Explosion Tear Test Studies of High Strength Q and T Steels", NRL Report 5836 (September 6, 1962).
19. McGeady, L. J., "Fracture Properties of Quenched and Tempered Steel Weldment Specimens", NRL Report 6602, (October 10, 1967).
20. Pellini, W. S., et al, "Review of Concepts and Status of Procedures for Fracture Safe Design of Complex Welded Structures Involving Metals of Low to Ultra High Strength Levels", NRL Report 6300 (June 1965).
21. Pellini, W. S. and Puzak, P. P., "Practical Considerations in Applying Laboratory Fracture Criteria to the Fracture Safe Design of Pressure Vessels", NRL Report 6030 (November 5, 1963).
22. Pellini, W. S., "Advances in Fracture Toughness Characterization Procedures and in Quantitative Interpretations to Fracture Safe Design for Structural Steels", NRL Report 6713 (April 3, 1968).
23. McGeady, L. J., "Procedures for the Evaluation of the Fracture Toughness of Heat Affected Zones", Welding Journal, Vol. 51, No. 12, (December 12, 1972), Res. Supp. p. 569s.
24. Doty, W. D., "Weldability of Steels and Selection of Welding Procedures", Paper presented during 37th Midyear Meeting of American Petroleum Institute's Division of Refining (May 11, 1972).
25. Barsom, J. M., "Relationship Between Plane Strain Ductility and K_{Ic} for Various Steels", Ind. Eng. for Industry (November 1971) p. 1209.
26. Barsom, J. M. and Rolfe, S. T., "K_{Ic} Transition Behavior of A517-F Steel", U. S. Steel Applied Research Lab Report No. 89.018-022 (1), Contract Nobs-94535 (FBM) (November 29, 1968).
27. Shoemaker, A. K. and Rolfe, S. T., "The Static and Dynamic Low Temperature Crack-Toughness Performance of Seven Structural Steels", Eng. Fracture Mechs. Vol. 2 (1971) p. 319.
28. Vettraino, J., "T-1 Steel Investigation", Army Tank Automotive Center, Detroit Arsenal, Report 7139, AD 477546L (November 1961).
29. Lange, E. A., Pickett, A. G. and Wylie, R. D., "Failure Analysis of PVRC Vessel No. 5. Part I, A Study of Materials Properties and Fracture Development", Welding Research Council Bulletin No. 98 (August 1964).
30. Raymond, L. and Usell, R. J. Jr., "The Effect of N_2O_4 and UDMH on Subcritical Crack Growth in Various High Toughness Low-Strength Steels", Aerospace Corporation Report No. TR-0059 (6250-10)-8 (June 15, 1971).
31. Gentilcore, V. C., Pense, A. W. and Stout, R. D., "Fracture Toughness of Pressure Vessel Steel Weldments", The Welding Journal, Vol. 49, No. 8 (August 1970), Res. Supp. p. 341s.
32. Loginow, A. W., U. S. Steel Research Laboratory, Personal Communication with W. F. Brown, Jr. (January 1972).
33. Doty, W. D., "Welding of Quenched and Tempered Alloy Steels", Metals Engineering Quarterly, ASM (February 1969).

Fe	
0.15	C
0.80	Mn
0.85	Ni
0.53	Cr
0.50	Mo
0.32	Cu
0.25	Si
0.05	V
+ B	

T-1

Fe	
0.16	C
0.85	Mn
0.53	Cr
0.27	Si
0.20	Mo
0.05	V
0.02	Ti
+ B	

T-1A

Fe	
0.16	C
1.12	Mn
0.52	Cr
0.50	Ni
0.27	Si
0.25	Mo
0.05	V
+ B	

T-1B

REVISED: MARCH 1976
AUTHOR: J. R. KATTUS

FERROUS ALLOYS

	Fe
13	Cr
3	W
2	Ni

GREEK ASCOLOY

1. GENERAL

Greek Ascoloy is a hardenable, martensitic 13 percent chromium stainless steel, in which additions of nickel and tungsten provide improved mechanical properties and heat resistance over Type 410 stainless steel. It retains corrosion and oxidation resistance up to its maximum recommended service temperature of 1100F, and its creep-rupture properties in this temperature range are equal or superior to those of the austenitic stainless steels. The alloy has good hot-working characteristics and brazability but only fair cold formability and weldability. Its good combination of creep properties and corrosion resistance accounts for its use in compressor blades and vanes and discs in the lower-temperature stages of gas turbines. Other components made from this alloy include rings for jet engines, numerous types of fasteners, and valve parts (5)(6)(7).

1.01 Commercial Designation

Greek Ascoloy

1.02 Alternate Designations

Type 418 Special, AMS 5616, AISI 615, 12-2W (Armco Steel), Unitemp 1415 NW (Universal Cyclops), 436 (Howmet Corp.), Croloy 12-3W (Babcock and Wilcox), UNS S41800.

1.03 Specifications

Table 1.03.

1.04 Composition

Table 1.04.

1.05 Heat Treatment

1.051 Full anneal: 1450F 2 to 4 hours, furnace cool to 800F, air cool to 200F, reheat to 1250F 12 hours, air cool. The resulting hardness is about 225 to 250 BHN (5)(6).

1.052 Subcritical anneal or stress relief: 1300F 4 hours, air cool. This treatment results in a hardness of about 270 to 280 BHN (5)(6).

1.053 Hardening: 1700 to 1900F, oil quench section size larger than 3 inches and air cool or oil quench sections less than 3 inches thick. Preheating at 1200 to 1400F is recommended for parts with large variations in thickness. Exothermic or endothermic furnace atmospheres are recommended to minimize scaling and decarburization (5)(6)(7).

1.054 Temper: 500 to 1250F 2 to 4 hours, air cool. A double temper is recommended for heavy sections or where maximum dimensional stability is required. For parts that are straightened after tempering, a final treatment at 50F lower than the initial tempering temperature is sometimes used to at least partially relieve residual stresses (5)(6)(7).

1.06 Hardness

1.061 Effects of tempering temperature, after two different austenitizing treatments, on room-temperature hardness, Figure 1.061.

1.062 Effects of tempering two hours at various temperatures on hardness, Figure 1.062.

1.063 Hardness range for annealed billets and bars, 240-311 BHN, 23-33 R_C (7).

1.064 Hardness of extrusions in the annealed and hardened-and-tempered conditions, Table 1.064.

1.065 Effects of elevated temperatures on hardness, Figure 1.065.

1.07 Forms and Conditions Available

Greek Ascoloy is available as billets, bars, wire, strip forgings, and investment castings. Other forms, such as extrusions and tubing, can also be produced. It can be furnished annealed, hardened and tempered, hot rolled, cold finished, or cold rolled depending upon the form desired (6)(7)(13).

1.08 Melting and Casting Practice

The alloy is generally air melted in electric-arc furnaces. For applications requiring exceptional quality, it is vacuum remelted by consumable electrode or induction techniques.

1.09 Special Considerations

1.091 Although tempering in the secondary hardening range of about 650 to 950F produces high strength, it also results in reduced notched toughness; therefore tempering in this range is generally not recommended (see Figure 3.0231).

2. PHYSICAL AND CHEMICAL PROPERTIES

2.01 Thermal Properties

2.011 Melting range, 2600 - 2700F (6).

2.012 Phase changes.

2.0121 Time-temperature-transformation diagrams.

2.0122 In the annealed condition, Greek Ascoloy consists of ferrite and carbides; in the hardened condition its structure is martensitic. At temperatures of about 1500F and above the structure is austenitic. The presence of nickel in the alloy prevents the formation of delta ferrite (5).

2.013 Thermal conductivity.

2.014 Thermal expansion, Figure 2.014.

2.015 Specific heat, 0.11 Btu per (lb-F) from 32 to 212F (5).

2.016 Thermal diffusivity.

2.02 Other Physical Properties

2.021 Density, 0.284 lb per cu in, 7.86 gr per cu cm (6)(7)(8).

2.022 Electrical properties.

2.0221 Electrical properties at various temperatures, Table 2.0221.

2.023 Magnetic properties, ferromagnetic.

2.0231 Magnetic permeability after tempering at 700 to 900F, Table 2.0231.

2.024 Emittance.

2.025 Damping capacity.

2.03 Chemical Properties

2.031 The resistance to general corrosion and to rusting of Greek Ascoloy, which is optimum in the hardened and tempered condition, is similar to that of Type 410 stainless steel and other 12 percent chromium stainlesses (see Types 403, 410, 416, Code 1401) (6)(7).

2.032 Its resistance to stress corrosion and to hydrogen embrittlement is superior to that of Type 410. Tempering in the secondary hardening range of about 650 to 950F reduces resistance to stress-corrosion cracking (5)(7).

2.033 The alloy resists oxidation up to 1500F for continuous service and to 1300F for intermittent service. It has good resistance to oxidizing acids but not to reducing acids. It also resists sulfur gases over its entire service temperature range (6)(7).

2.04 Nuclear Properties

3. MECHANICAL PROPERTIES

3.01 Specified Mechanical Properties

Table 3.01.

3.02 Mechanical Properties at Room Temperature

3.021 Tension- stress/strain diagrams-tension properties.

3.0211 Effects of tempering temperature, after two different austenitizing treatments, on tensile properties, Figure 3.0211.

3.0212 Effects of tempering temperature on tensile properties of bars of various diameters and carbon content, Figure 3.0212.

3.0213 Tensile properties of extrusions in the annealed and the hardened-and-tempered conditions, Table 3.0213.

3.0214 Ranges of tensile properties for annealed billets and bars, Table 3.0214.

3.022 Compression- stress/strain diagrams - compression properties.

Fe
13 Cr
3 W
2 Ni

GREEK ASCOLOY

3.023 Impact.
3.0231 Effects of tempering temperature, after two different austenitizing treatments, on room temperature impact properties, Figure 3.0231.
3.0232 Effect of tempering temperature on charpy keyhole impact properties, Figure 3.0232.
3.0233 Room temperature Izod impact strength of annealed bar, 50-90 ft lb (7).
3.024 Bending.
3.025 Torsion and shear.
3.026 Bearing.
3.027 Stress concentration.
3.0271 Notch properties.
3.0272 Fracture toughness.
3.028 Combined properties.

3.03 Mechanical Properties at Various Temperatures
3.031 Tension - stress/strain diagrams - tension properties.
3.0311 Effects of elevated temperatures on tensile properties of bar austenitized at two temperatures and tempered at 1050F, Figure 3.0311.
3.0312 Effects of elevated temperatures on tensile properties of bar austenitized at two temperatures and tempered at 1200F, Figure 3.0312.
3.0313 Effects of temperature on tensile properties of bar of various diameters and carbon contents, Figure 3.0313.
3.032 Compression - stress/strain diagrams - compression properties.
3.033 Impact.
3.034 Bending.
3.035 Torsion and shear.
3.036 Bearing.
3.037 Stress concentration.
3.0371 Notch properties.
3.0372 Fracture toughness.
3.038 Combined properties.

3.04 Creep and Creep Rupture Properties
3.041 Creep-rupture curves for bar with three different heat treatments, Figure 3.041.
3.042 Stresses required to produce 0.1 and 1 percent creep deformation in 100 and 150 hours at temperatures from 700 to 1100F, Figure 3.042.
3.043 Creep-rupture curves for bar at 600 to 1200F, Figure 3.043.
3.044 Creep-rupture curves for notched bar at 600 to 1200F, Figure 3.044.
3.045 Creep-rupture curves for smooth and notched sheet at 1050 to 1200F, Figure 3.045.

3.05 Fatigue Properties
3.051 Effects of temperature on the fatigue endurance limit at 10^7 cycles for bar heat treated to two hardness levels, Figure 3.051.

3.06 Elastic Properties
3.061 Poisson's ratio.
3.062 Modulus of elasticity.
3.0621 Modulus of elasticity at various temperatures, Table 3.0621.
3.063 Modulus of rigidity.

4. FABRICATION

4.01 Forming
4.011 Since Greek Ascoloy is not as soft as Type 410 stainless in the annealed condition, it requires somewhat greater pressures for cold forming. Although it does not work harden as much as 18-8 type stainless, intermediate anneals may be required, depending upon the degree and nature of the deformation. Severely cold-formed parts should be annealed or stress relieved (5)(6)(7).
4.012 The alloy can be hot worked by any of the conventional methods, such as forging, rolling, and extrusion. Hot working should be done in the range 2150 to 1700F; working below 1700F tends to cause cracking. Large sections should be heated at 1200 to 1400F prior to heating to hot-working temperatures in order to prevent strain cracking. Also to prevent strain cracking after hot work, the material should be cooled slowly in Sil-O-Cel or some other insulating material, or stress relieved at 1300F, or fully annealed, which produces optimum machinability (5)(6)(7).

4.02 Machining and Grinding
4.021 Because of its higher annealed hardness, Greek Ascoloy does not machine as easily as Type 410 stainless; however, because of its lower work-hardening it does machine better than Type 18-8 stainlesses. Based on 100 percent machinability for resulfurized B 1112 steel, annealed Greek Ascoloy is rated at 55 percent (5)(6).

4.03 Joining
4.031 Greek Ascoloy can be welded by fusion or resistance methods, but weldability is not considered good because of its susceptibility to strain cracking. Since the alloy is air hardening, preheat and interpass temperatures of 400 to 600F and postweld annealing or tempering above 1000F are recommended. Subsequently, weldments may be hardened and tempered to obtain desired properties. Optimum weld ductility is obtained with austenitic filler rods such as Type 310 stainless, but optimum strength is obtained with Greek Ascoloy filler metal (5)(6)(7).
4.032 High-strength brazed joints for elevated-temperature applications can be made in Greek Ascoloy by brazing in hydrogen at 1800 to 1850F, preferably with a filler metal of 82 Au - 18 Ni. Other acceptable filler metals are 58.5 Cu-31.5 Mn-10 Co for service temperatures up to 1000F and 54 Ag-25Pd-21Cu for service temperatures up to 800F. For optimum properties the brazed assembly should be furnace cooled to about 1700F, then rapidly cooled, and finally tempered (12).
4.033 In an evaluation of the effects of simulated service conditions on arc-welded and brazed Greek Ascoloy compressor blades and vanes and compressor discs, no deterioration in tensile properties and no corrosion in the welded and brazed joints occurred in four hours exposure to temperatures up to 800F at stresses of 90 percent of F_{ty} in a sea-salt atmosphere. The welded joints had been made by the tungsten-inert-gas method with Greek Ascoloy filler metal, and the weldments were hardened and tempered. The brazed joints were made in a hydrogen atmosphere at 1800F with an 82 Au-18Ni braze alloy and were tempered at 1050F (11).

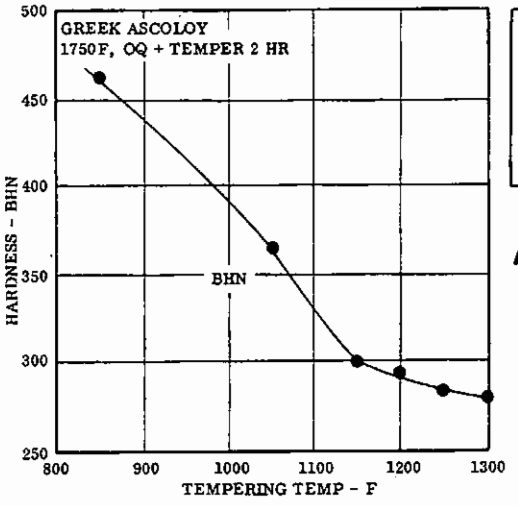
4.04 Surface Treatment
4.041 Because of its good resistance to oxidation and corrosion, protective surface treatments and coatings are not normally needed.
4.042 Preferred methods for removal of hot-work and heat-treat scales are either mechanical techniques such as sand or vapor blasting, or immersion in a molten caustic bath followed by light acid pickling. Somewhat less effective is acid pickling alone in either 10 percent nitric acid or 20 percent hydrocholoric acid at about 130F; some scrubbing of the surface may subsequently be required to complete the scale removal. After acid pickling of hardened and tempered parts, baking at 400F is recommended as a precaution against hydrogen embrittlement (5).

Alloy	Greek Ascoloy	
Source	Form	Specification
(1)	Sheet, strip, plate	AMS 5508 B
(2)	Bars, forgings, tubing	AMS 5616 E
(3)	Welding wire	AMS 5817 A
(4)	Investment castings	AMS 5354 B

TABLE 1.03 SPECIFICATIONS

Alloy	Greek Ascoloy			
Form	Wrought		Cast	
Source	AMS 5508 B (1) AMS 5616 E (2) AMS 5817 A (3)		AMS 5354 B (4)	
	Min	Max	Min	Max
Carbon	0.15	0.20	0.12	0.20
Manganese	-	0.50	-	1.0
Silicon	-	0.50	-	1.0
Phosphorus	-	0.040	-	0.04
Sulfur	-	0.030	-	0.03
Chromium	12.00	14.00	12.0	14.0
Nickel	1.80	2.20	1.8	2.2
Tungsten	2.50	3.50	2.5	3.5
Molybdenum	-	0.50	-	0.50
Aluminum	-	0.15	-	-
Copper	-	0.50	-	0.50
Tin	-	0.05	-	-
Iron	Balance		Balance	

TABLE 1.04 COMPOSITION



Fe
13 Cr
3 W
2 Ni

GREEK ASCOLOY

FIG. 1.062 EFFECT OF TEMPERING TWO HOURS AT VARIOUS TEMPERATURES ON HARDNESS. (6)

Alloy	Greek Ascoloy	
Form	0.75 in x 3-1/8 in extruded flat	
Source	(10)	
Condition		BHN
Ann. 1450F, 2 hr.		331
Ann. 1600F, FC to 1100F		290
1800F, AC + temper 700F		429

TABLE 1.064 HARDNESS OF EXTRUSIONS IN THE ANNEALED AND THE HARDENED-AND-TEMPERED CONDITIONS

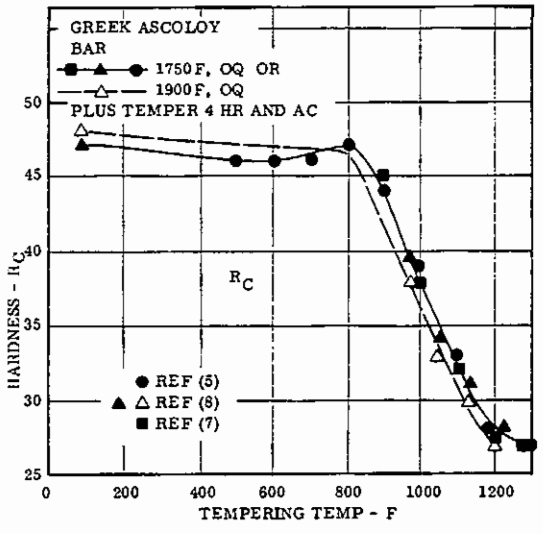


FIG. 1.061 EFFECTS OF TEMPERING TEMPERATURE, AFTER TWO DIFFERENT AUSTENITIZING TREATMENTS, ON ROOM TEMPERATURE HARDNESS. (5)(7)(8)

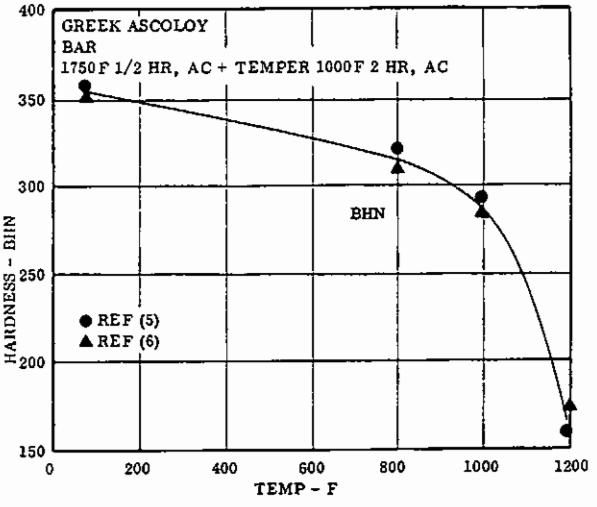


FIG. 1.065 EFFECTS OF ELEVATED TEMPERATURES ON HARDNESS. (5)(6)

Fe
13 Cr
3 W
2 Ni

GREEK ASCOLOY

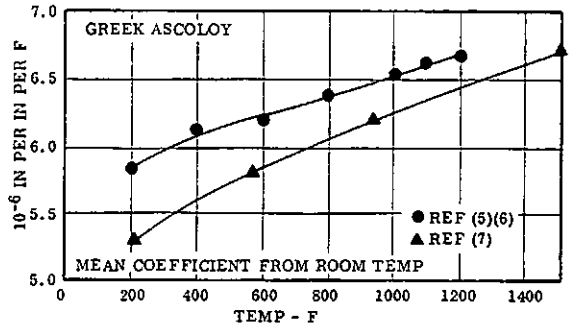


FIG. 2.014 THERMAL EXPANSION. (5)(6)(7)

Alloy	Greek Ascoloy		
Condition	Quenched and tempered		
Source	(5)		
	Electrical Conductivity		Electrical
Temp, F	Percent IACS	Megohms per in^3	Resistivity Microhm-in
77	2.12	0.0322	31.0
700	2.80	0.0411	24.3
800	2.84	0.0419	23.9
900	2.86	0.0422	23.7

TABLE 2.0221 ELECTRICAL PROPERTIES AT VARIOUS TEMPERATURES

Alloy	Greek Ascoloy	
Condition	Quenched and tempered	
Source	(5)	
Tempering	Magnetic Permeability	
Temp, F	at 100 Oersteds	Maximum
700	85	85
800	75	92
900	93	100

TABLE 2.0231 MAGNETIC PERMEABILITY AFTER TEMPERING AT 700 TO 900F

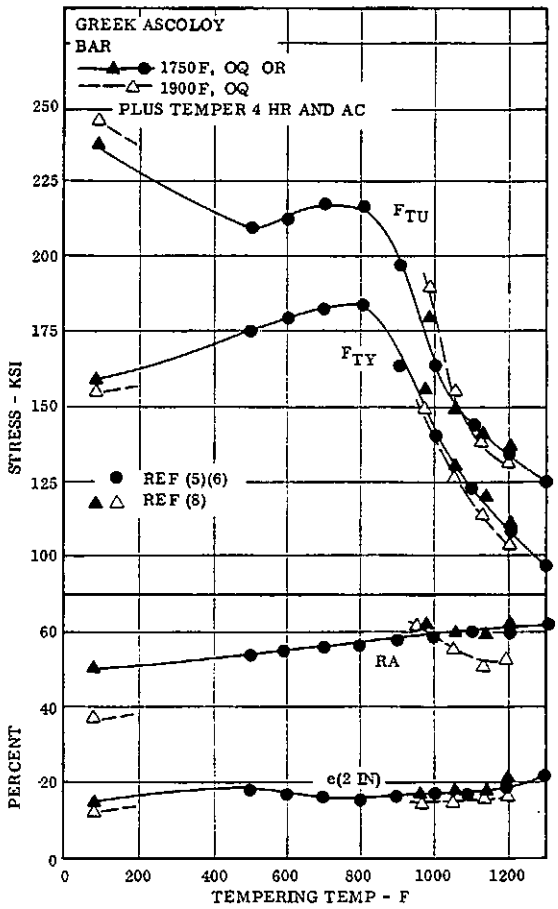


FIG. 3.0211 EFFECTS OF TEMPERING TEMPERATURE, AFTER TWO DIFFERENT AUSTENITIZING TREATMENTS, ON TENSILE PROPERTIES. (5)(6)(8)

Alloy	Greek Ascoloy							
			F_{ty} (ksi)	F_{tu} (ksi)		e (4D)	Hardness	
Source	Form	Condition	min	min	max	min	R_C (min)	BHN (max)
AMS 5508 B (1)	Sheet, strip, plate	Annealed	-	-	150	10	-	-
	Sheet, strip, plate	1800F, AC	-	-	-	-	42	-
AMS 5616 E (2)	Bars, welded rings	Annealed	-	-	-	-	-	311
	Tubing	Ann. and cold finished	-	-	-	-	-	311
	Wire	Ann. and cold finished	-	-	155	-	-	-
	Bars, tube, forgings	1750F, OQ	-	-	-	-	45	-
AMS 5817 A (3)	Weld metal deposit							
	1/4 inch thick	1800F, AC	-	-	-	-	42	-
AMS 5354 B (4)	Investment cast	1750F, AC	-	-	-	-	45	-
		1750F, AC+1300F 1 hr, AC	65	90	-	3	-	-

TABLE 3.01 SPECIFIED MECHANICAL PROPERTIES

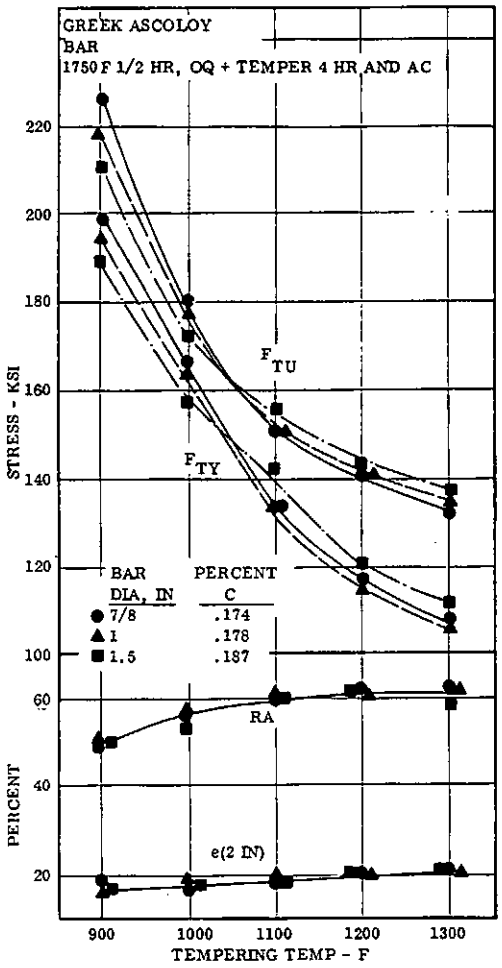


FIG. 3.0212 EFFECTS OF TEMPERING TEMPERATURE ON TENSILE PROPERTIES OF BARS OF VARIOUS DIAMETERS AND CARBON CONTENTS. (9)

Alloy	Greek Ascoloy
Condition	Annealed
Source	(7)
F_{ty} (ksi)	85 to 120
F_{tu} (ksi)	115 to 150
e (2 in) (percent)	18 to 22

TABLE 3.0214 RANGES OF TENSILE PROPERTIES FOR ANNEALED BILLETS AND BARS

	Fe
13	Cr
3	W
2	Ni

GREEK ASCOLOY

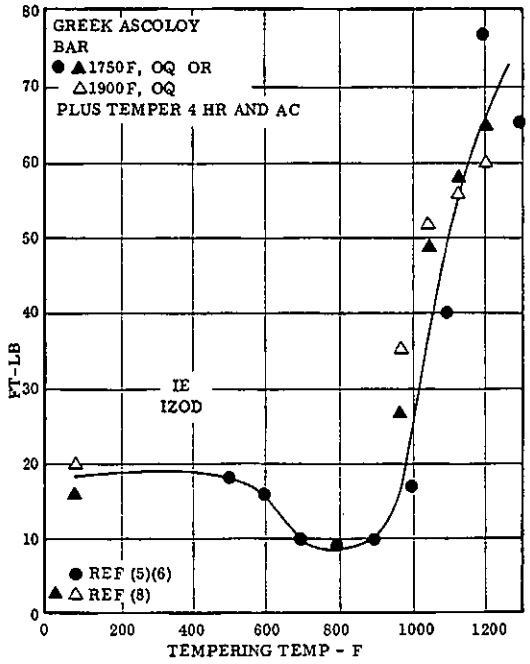


FIG. 3.0231 EFFECTS OF TEMPERING TEMPERATURE, AFTER TWO DIFFERENT AUSTENITIZING TREATMENTS, ON ROOM TEMPERATURE IMPACT PROPERTIES. (5)(6)(8)

Alloy	Greek Ascoloy					
Form	0.75 in. x 3-1/8 in extruded flat					
Source	(10)					
Condition	Orientation	ASTM Grain size	F_{ty} (ksi)	F_{tu} (ksi)	e (4D) (percent)	RA (percent)
Ann. 1450F 2 hr.	L	6-7	120	147	18	56
	T	6-7	122	147	18	44
Ann. 1600F, FC to 1100F	L	7-8	120	146	18	68
	T	7-8	120	145	11	59
1800F, AC + temper 700F	L	7-8	178	206	20	46
	T	7-8	169	203	13	31
1750F, OQ + temper 1050F 2 hr	L	7-8	128	147	21	71
	T	7-8	129	146	17	60

TABLE 3.0213 TENSILE PROPERTIES OF EXTRUSIONS IN THE ANNEALED AND THE HARDENED-AND-TEMPERED CONDITIONS

	Fe
13	Cr
3	W
2	Ni

GREEK ASCOLOY

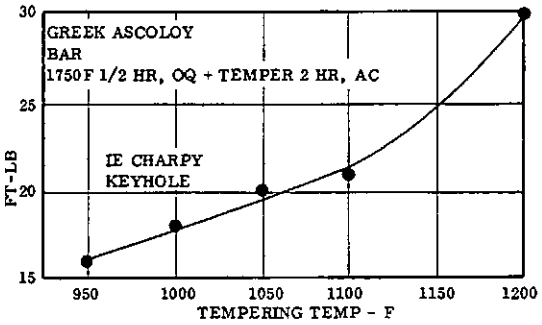


FIG. 3.0232 EFFECT OF TEMPERING TEMPERATURE ON CHARPY KEYHOLE IMPACT PROPERTIES. (5)

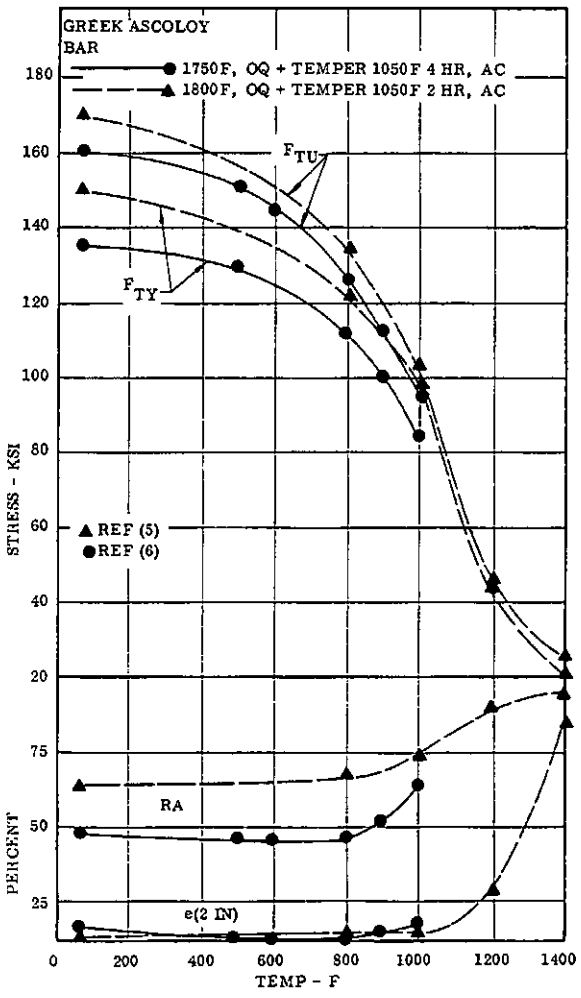


FIG. 3.0311 EFFECTS OF ELEVATED TEMPERATURES ON TENSILE PROPERTIES OF BAR AUSTENITIZED AT TWO TEMPERATURES AND TEMPERED AT 1050F. (5)(6)

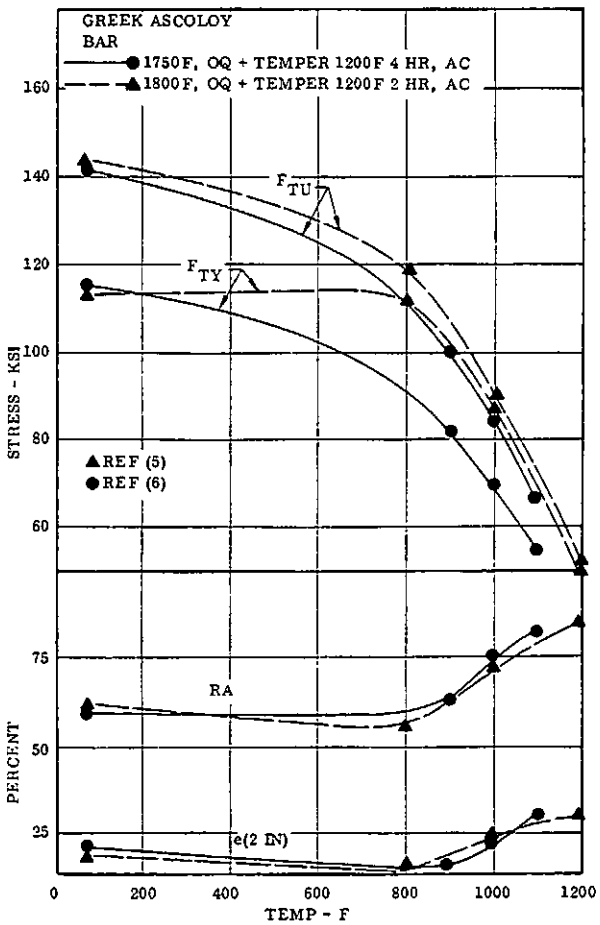


FIG. 3.0312 EFFECTS OF ELEVATED TEMPERATURES ON TENSILE PROPERTIES OF BAR AUSTENITIZED AT TWO TEMPERATURES AND TEMPERED AT 1200F. (5)(6)

	Fe
13	Cr
3	W
2	Ni

GREEK ASCOLOY

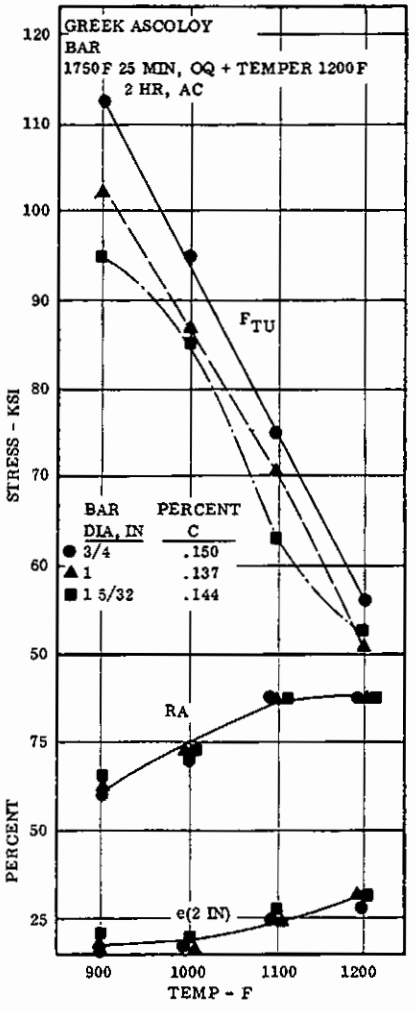


FIG. 3.0313 EFFECTS OF TEMPERATURE ON TENSILE PROPERTIES OF BAR OF VARIOUS DIAMETERS AND CARBON CONTENTS. (8)

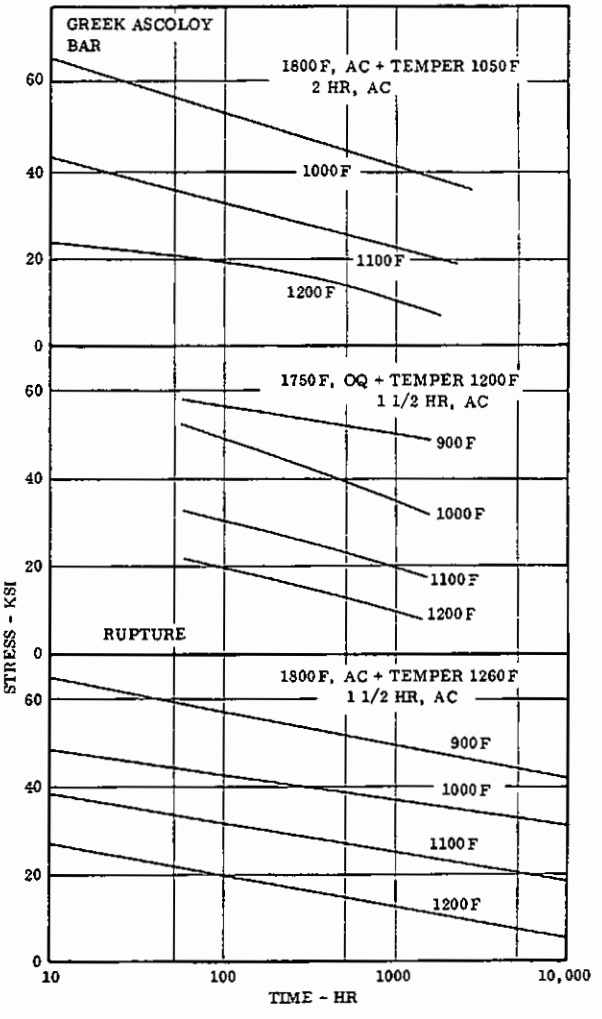


FIG. 3.041 CREEP-RUPTURE CURVES FOR BAR WITH THREE DIFFERENT HEAT TREATMENTS. (5)(6)(7)

	Fe
13	Cr
3	W
2	Ni

GREEK ASCOLOY

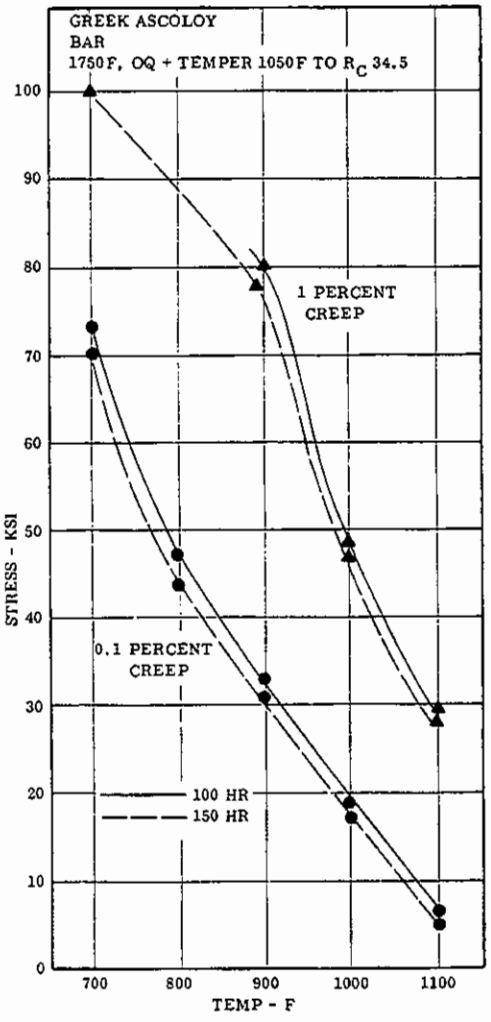


FIG. 3.042 STRESSES REQUIRED TO PRODUCE 0.1 AND 1 PERCENT CREEP DEFORMATION IN 100 AND 150 HOURS AT TEMPERATURES FROM 700 TO 1100 F. (5)

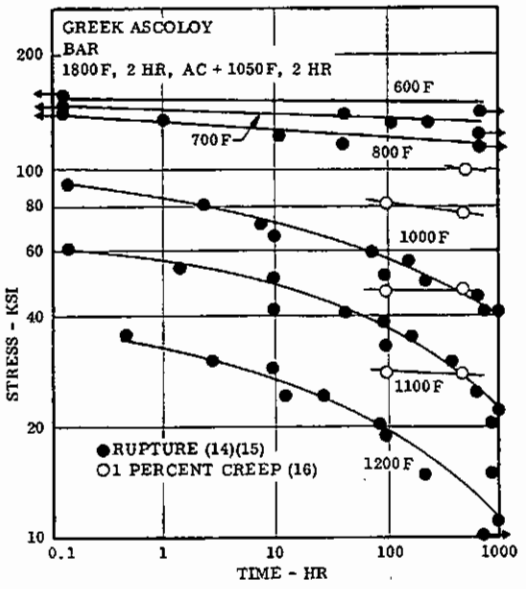


FIG. 3.043 CREEP-RUPTURE CURVES FOR BAR AT 600 TO 1200 F. (14)(15)(16)

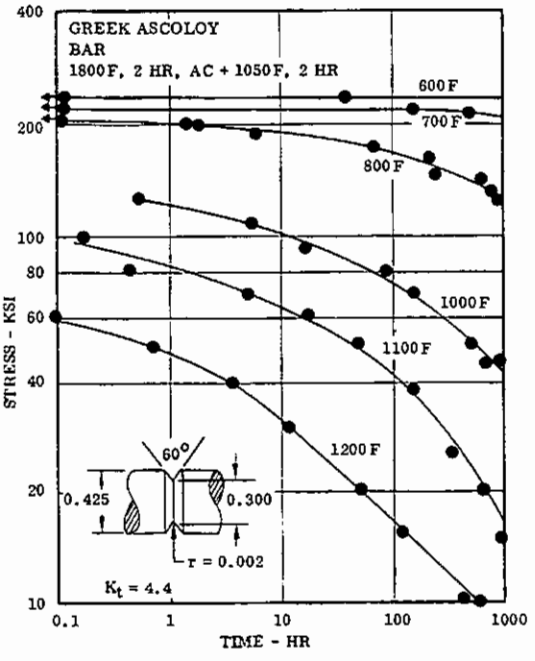


FIG. 3.044 CREEP-RUPTURE CURVES FOR NOTCHED BAR AT 600 TO 1200 F. (14)(15)

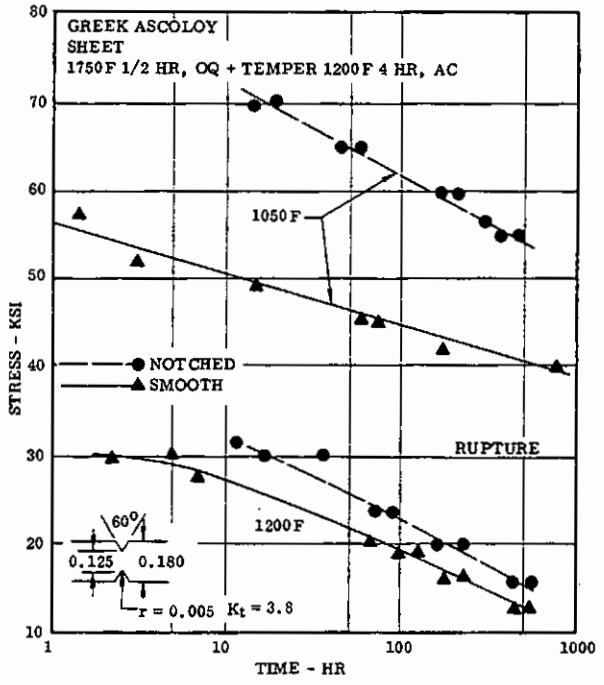


FIG. 3.045 CREEP-RUPTURE CURVES FOR SMOOTH AND NOTCHED SHEET AT 1050 AND 1200F. (17)

Alloy	Greek Ascoloy
Source	(5)
Temperature, F	E, 10^3 ksi
70	29.0
1000	21.5
1100	17.0

TABLE 3.0621 MODULUS OF ELASTICITY AT VARIOUS TEMPERATURES

	Fe
13	Cr
3	W
2	Ni

GREEK ASCOLOY

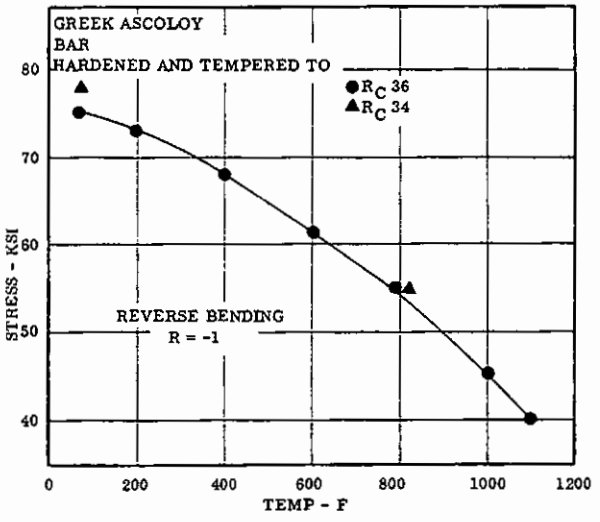


FIG. 3.051 EFFECTS OF TEMPERATURE ON THE FATIGUE ENDURANCE LIMIT AT 10^7 CYCLES FOR BAR HEAT TREATED TO TWO HARDNESS LEVELS. (5)

REFERENCES

1. AMS 5508B (May 15, 1973).
2. AMS 5616E (November 1, 1969).
3. AMS 5817A (January 15, 1963).
4. AMS 5354B (June 30, 1962).
5. Universal Cyclops Specialty Steel Division, "Unitemp 1415 NW High Temperature Metal" (1971).
6. Carpenter Technology Steel Division, "Carpenter AMS 5616" (May 1972).
7. Allegheny Ludlum Steel Corp., "Stainless Steel Type 418 Special", Blue Sheet.
8. Allegheny Ludlum Steel Corp., "Mechanical and Physical Properties of Type 418 Special", Data Sheet 131-101559-418 Sp.
9. Allegheny Ludlum Steel Corp., "Effect of Tempering Temperature on Mechanical Properties of Type 418 Special", Data Sheet 132-101359-418 Sp.
10. Fiorentino, R.J., and Subroff, A.M., "Availability and Mechanical Properties of High-Strength Steel Extrusions", DMIC Report 138 (October 26, 1960).
11. O'Connor, J.J. and Vozzella, P.A., "Evaluation of Welded and Brazed Stainless Steels and Superalloys in a Corrosive Environment", AFML TR 67-258, Pratt & Whitney Div. (October 1968).
12. Schaefer, R.P., Flynn, J.E. and Doyle, J.R., "Brazing Filler Metal Evaluation for an Aircraft Gas Turbine Engine Application", Welding Jr., Research Supplement, Vol. 50, p. 394S - 400S (September 1971)
13. Armco Steel Corp., "Armco Stainless Steels", Brochure LA-172 (1972).
14. Brown, W.F., Jr., Jones, M.H. and Newman, D.P., "Influence of Sharp Notches on the Stress Rupture Characteristics of Heat-Resisting Alloys, Part II", Proceedings ASTM, Vol. 53, p 661-676 (1953).
15. Sessler, J.G. and Brown, W.F., Jr., "Notch and Smooth Bar Stress-Rupture Characteristics of Several Heat-Resistant Alloys in the Temperature Range 600 to 1000F", Proceedings ASTM, Vol. 56, p. 738 (1956)
16. The Carpenter Steel Co., "Carpenter High-Temperature Alloys" (January 1962).
17. Alloy Digest, Filing Code SS-78, "Greek Ascoloy" (September 1958).

1 General

H-11 Mod is a martensitic hot work die steel which can be heat treated to ultimate strengths up to 300 ksi. It contains chromium, molybdenum, and vanadium to promote hardenability. The alloy is hardened by an austenitizing heat treatment followed by air cooling or oil quenching. Double or triple tempering is employed to achieve the best combinations of strength and toughness. Ultimate tensile strengths of 200 to 300 ksi are developed by appropriate tempering treatments and high strength is maintained at elevated temperatures. H-11 Mod has excellent thermal shock resistance, hot hardness, hot abrasion resistance, and good fatigue properties. The steel has good formability and machinability in the annealed condition, is readily welded, and exhibits little distortion when heat treated. However, the fracture toughness is low and at yield strength levels above 200 ksi care should be taken to avoid small defects if used in critical applications. Concern about the stress corrosion resistance of H-11 Mod fasteners has led to a decrease in use of the alloy in some critical aerospace applications. Wear resistance can be improved by surface treatments such as nitriding. H-11 Mod is widely used in industry for hot work and casting dies, in ordnance for gun barrel and related applications, and in aerospace for landing gear, arrester hooks, solid propellant rocket cases, fasteners, and structural sections.

1.1 Commercial Designation

H-11 Mod

1.2 Alternate Designations

AISI Type H11, SAE Type H11, UNS T20811, Al Tech Potomac A, Carpenter No. 882, Chromo-V, Guterl H-11, Hot Form No. 2.

1.3 Specifications

1.3.1 *[Table]* AMS Specifications.

1.4 Composition

1.4.1 *[Table]* AMS Specified Composition.

1.5 Heat Treatment

1.5.1 General. Heat treatment conditions are critical with regard to developing the desired combination of toughness and strength and preventing quench cracking in H-11 Mod. Good hardenability is conferred in H-11 Mod by the chromium, molybdenum, and vanadium additions, which enable fully or nearly fully martensitic structures to be obtained with modest cooling rates following the initial austenitizing heat treatment. The carbon content of 0.4 percent is required to provide high strength, but also causes a low M_f temperature and high austenite-to-martensite transformation strains. High internal stresses thus can develop if the quench after austenitizing is severe, especially in large sections. Air cooling with or without forced circulation is appropriate under most circumstances.

Fe
0.4 C
5.0 Cr
1.3 Mo
0.5 V

The most stable carbide in H-11 Mod is VC, which is only partially dissolved at an austenitizing temperature of 1900F. Other carbides, such as Mo_2C containing dissolved chromium and vanadium and chromium-molybdenum-rich $M_{23}C_6$, are also present. These undissolved carbides particles pin the grain boundaries and help maintain the highly desirable fine austenite grain size. As the carbides dissolve with increasing austenitizing temperature, the carbon content of the austenite increases and the subsequent martensite phase is progressively hardened. The optimum austenitizing temperature thus represents in part a balance between maintenance of a fine austenite grain size and hardness of the martensite phase.

Double tempering is required in order to develop full toughness, especially in larger sections. The first tempering treatment causes any retained austenite to transform to a ferrite-carbide aggregate such as bainite or to precipitate alloy carbides, which raises the M_f temperature so that the retained austenite transforms to martensite on cooling. This new martensite is then tempered during the second tempering treatment. At least two and in some cases three or more tempering treatments are recommended to minimize retained austenite and untempered martensite. Retained austenite is particularly undesirable as it can transform during service and cause distortion or cracking.

H-11 Mod is a "secondary hardening" steel, i.e., room temperature hardness increases with increasing tempering temperature up to the temperature of maximum secondary hardening, about 950F. Secondary hardening is associated with reprecipitation of VC in which some molybdenum is dissolved. At higher tempering temperatures, overageing occurs with coarsening of the VC and additional precipitation of $M_{23}C_6$. Increased austenitizing temperature, in addition to increasing the carbon content of the martensite, increases the extent of the secondary hardening reactions. Maintenance of properties at high operating temperatures is promoted by these secondary hardening reactions.

Alternative explanations for the reactions responsible for secondary hardening have been advanced, as discussed in Section 3.2.3.6. Also the data on relative carbide abundance after tempering, presented later in Figure 2.1.2.4, do not indicate a major role for VC, in disagreement with the reactions suggested in the previous paragraph.

Tempering at the temperature of maximum secondary hardening is not recommended due to the marked embrittlement which occurs. The optimum tempering temperature for this steel is about 1100F.

© 1992 by Purdue Research Foundation, West Lafayette, Indiana 47907.
All Rights Reserved.

1.5.2 Normalize. Generally not necessary. For effective homogenization, heat to about 1950F, soak 1 hour for each inch of thickness, and air cool. Anneal immediately after the part reaches room temperature. There is a possibility that H-11 Mod may crack during this treatment.

1.5.3 Anneal. Heat to 1550 to 1625F and hold to equalize temperature, cool slowly in the furnace to about 900F, then more rapidly to room temperature. This treatment should produce a fully spheroidized microstructure free of grain boundary carbide networks.

1.5.4 Austenitize. Preheat to 1400 to 1500F and then raise the temperature to 1850 to 1875F and hold 20 min plus 5 min for each 1 inch of thickness, air cool. For section thicknesses greater than 10 inches, austenitize at 1825-1850F and oil quench. For parts with abrupt section changes, quench in salt bath to 800F, hold for 20 to 30 minutes to equilibrate, then air cool to room temperature.

1.5.5 Temper. Heat at 950 to 1200F, depending on strength desired. Close temperature control is important, since properties change sharply with temperature. Double temper, 1 to 4 hours each, depending on thickness, and cool to room temperature between tempers. Triple tempering is more desirable, especially for critical parts. For high temperature applications, parts should be tempered at a temperature above the maximum service temperature to guard against undesirable property changes during service. Distortion during tempering is very low, not exceeding 0.001 inch per inch of cross-section.

1.5.6 Intermediate Anneal. Heat to 1200 to 1250F, 4 hours, air cool. This treatment is used to achieve greater dimensional accuracy in heat treated parts by intermediate annealing rough-machined parts, then finish machining, and finally heat treating to the desired hardness.

1.5.7 Stress Relief. Heat at 875 to 900F, 2 to 4 hours, for finished parts after grinding, machining, or straightening (Refs. 81, pp. 439-441; Refs. 82-86; Ref. 98, pp. 8-11).

1.6 Hardness

1.6.1 *[Figure]* End quench hardenability.

1.6.2 *[Figure]* Effect of austenitizing temperature and type of cooling on hardness.

1.6.3 *[Figure]* Effect of carbon content and tempering temperature on hardness of air melt and vacuum melt alloy.

1.6.4 *[Figure]* Effect of austenitizing temperature and tempering temperature on hardness for a single tempering treatment.

1.6.5 *[Figure]* Effect of austenitizing temperature and tempering temperature on hardness for a double tempering treatment.

1.6.6 *[Figure]* Effect of austenitizing temperature and tempering temperature on hardness for a triple tempering treatment.

1.6.7 *[Figure]* Effect of low temperature on hardness of sheet.

1.6.8 *[Figure]* Hot hardness of bar austenitized at 1825 or 1900F and tempered at temperatures from 1025 to 1225F.

1.6.9 *[Figure]* Hot hardness after tempering at 1050 to 1150F.

1.7 Forms and Conditions Available

1.7.1 H-11 Mod is available in the form of forgings, extrusions, billets, plate, sheet, strip, bar, rod, and wire.

1.8 Melting and Casting Practice

1.8.1 Standard practice includes electric furnace air melting, induction vacuum, and consumable electrode vacuum melting. Vacuum arc remelting, vacuum degassing, and electroslag refining are effective in producing cleaner, finer-grained, and more uniform alloy with greater freedom from segregation and harmful impurities and with improved toughness.

1.9 Special Considerations

1.9.1 Decarburization can occur during heat treatment unless special precautions are taken. Heat treatments should be conducted in a neutral atmosphere furnace or salt bath or with parts packed in a neutral packing compound.

1.9.2 Parts should be protected from hydrogen embrittlement by baking for a minimum of 24 hours at 375F or higher after plating in an acid bath or after other processing that might introduce hydrogen into the metal.

1.9.3 Sulfur adversely affects notch impact strength and should be held low, preferably below 0.005 percent.

1.9.4 Alloy has low fracture toughness after tempering at 1000F to high strength levels. However, the fracture toughness can be improved at a cost of decreased strength by increasing the tempering temperature above 1000F, the approximate temperature of maximum secondary hardening

2 Physical Properties and Chemical Environmental Effects

2.1 Thermal Properties

2.1.1 Melting Range, 2500-2600F (Ref. 23, p. 22).

2.1.2 Phase Changes.

2.1.2.1 *[Figure]* Time-temperature-transformation diagram.

2.1.2.2 The TTT diagram for transformation of austenite to pearlite exhibits the usual C curve with the nose temperature at 1330F and the bay temperature inferred to be approximately 1200F, as shown in Figure 2.1.2.1.

The rate of transformation to pearlite can be markedly accelerated by pre-deforming the austenitic alloy at 1200F. This acceleration is related to an increase in the pearlite nucleation rate per unit volume of material (Ref. 87, p. 776).

2.1.2.3 The A_{c1} transformation temperature from ferrite to austenite on heating is 1505-1580F. The A_{r1} temperature on cooling is 1490-1445F.

2.1.2.4 *[Figure]* Relative carbide intensity (abundance) as a function of tempering temperature.

2.1.3 Thermal Conductivity.

2.1.3.1 *[Figure]* Thermal Conductivity.

2.1.4 Thermal Expansion.

2.1.4.1 *[Figure]* Thermal Expansion.

2.1.5 Specific Heat, 0.11 Btu per lb F.

2.1.6 Thermal Diffusivity.

2.2 Other Physical Properties

2.2.1 Density, 0.280 lb per cu. in. 7.75 gr per cu. cm.

2.2.2 Electrical Properties.

2.2.2.1 *[Figure]* Electrical resistivity.

2.2.3 Magnetic Properties. This steel is highly ferro-magnetic, but becomes nonmagnetic at temperatures above 1400 to 1500F.

2.2.4 Emittance.

2.2.4.1 *[Figure]* Emittance.

2.2.5 Damping Capacity.

2.3 Chemical Environments

2.3.1 General Corrosion. The general corrosion resistance of this steel is low and surface protection is required.

2.3.2 Stress Corrosion.

2.3.2.1 H-11 Mod has good stress-corrosion resistance as compared to other non-stainless steels heat treated to comparable strength levels, as shown in Figure 2.3.2.2. The good stress-corrosion resistance of H-11 Mod may be due to its combination of high chromium and molybdenum contents. Higher purity vacuum melted material and material final tempered at higher temperatures have improved stress-corrosion resistance, as shown in Figures 2.3.2.3, 2.3.2.4, and 2.3.2.5. The stress-corrosion resistance in an aqueous solution of NaCl is similar to that in distilled water, as shown in Figure 2.3.2.6.

The threshold stress intensity for stress-corrosion cracking is much less than the fracture toughness when tested in seacoast environments or aqueous salt solutions (Tables 2.3.2.7 and 2.3.2.8). Similarly the crack growth rate is greatly increased in distilled water and in moist argon as compared to dry argon (Figures 2.3.2.9 and 2.3.2.10).

2.3.2.2 *[Figure]* Comparison of stress-corrosion cracking characteristics of alloy with corresponding behavior of several other martensitic steels heat treated to tensile strength levels of approximately 240 ksi.

2.3.2.3 *[Figure]* Effect of applied stress on time to stress-corrosion failure for air-melt and vacuum melt alloy.

2.3.2.4 *[Figure]* Effect of temperature of final temper on stress-corrosion resistance in 5 percent aqueous solution of NaCl.

2.3.2.5 *[Figure]* Effect of tempering temperature on stress-corrosion resistance of billet.

2.3.2.6 *[Figure]* Delayed failure of alloy at 206 ksi yield strength level when tested in distilled water and in aqueous solution containing 3 percent NaCl.

2.3.2.7 *[Table]* Plane strain fracture toughness and threshold for stress-corrosion cracking in seacoast test and in accelerated tests for alloy in three conditions.

2.3.2.8 *[Table]* Plane strain fracture toughness and threshold for stress-corrosion cracking in 3-1/2 percent NaCl aqueous solution.

2.3.2.9 *[Figure]* Sustained load crack growth rate in humid argon and in distilled water.

2.3.2.10 *[Figure]* Effect of stress intensity on crack growth rate for a wide range of relative humidity in an argon environment.

2.3.2.11 In the heat treated condition for F_{ty} = 245 ksi, alloy is susceptible to severe rusting (accompanying stress-corrosion cracking) when subjected to a moist chloride environment or a semi-industrial atmosphere (Ref. 50, p. 4).

2.3.2.12 H-11 Mod double tempered at 970 or 1100F is not subject to stress corrosion when exposed in hydraulic oil (Ref. 89, pp. 347-353).

2.3.2.13 Pitting and stress corrosion can result from use of manufacturing chemicals high in sulfur or chlorine. These chemicals include cutting fluids, penetrating fluids, solvents, lubricants and penetrants, developers, anti-seize thread compounds, steam cleaners, and machining coolants. Sulfur and chlorine contents of these fluids should be held below 5500 ppm each to minimize the possibility of stress corrosion. The addition of thermally stable corrosion inhibitors such as triethanolamine reduces the corrosivity of these chemicals (Ref. 90, pp. 59-65).

2.3.3 Hydrogen Embrittlement.

2.3.3.1 Hydrogen embrittlement may occur in material heat treated to high strength if exposed to a hydrogen-containing environment. Certain surface treatments such as acid or alkaline pickling, cathodic cleaning, or phosphatizing

may result in hydrogen embrittlement for material having F_{tu} of 200 ksi or higher. Approved plating methods should be followed by baking at temperatures ranging from 375F for 23 hours to 950F for short times (Ref. 57, p. 127).

2.3.3.2 Acid baths used in chemical milling initially embrittle alloy, but recovery of ductility occurs within one week at RT if there is no barrier to escape of hydrogen (such as plating). A recovery treatment of 48 hours at RT followed by 4 hours at 375F is recommended (Ref. 76).

2.3.3.3 *[Table]* Notch strength in helium and hydrogen at 10 ksi pressure.

2.3.3.4 The diffusivity of hydrogen in H-11 Mod at 72F is 3×10^{-8} cm^2/sec. (Ref. 91, p. 437).

2.4 Nuclear Environments

2.4.1 H-11 Mod has good resistance to swelling following high fluence neutron irradiation. As shown in Figure 2.4.2, swelling in H-11 Mod ranges from -0.3 to +0.16 percent under the indicated conditions, slightly less than observed for Type 416 martensitic stainless steel. By comparison, 20 percent cold-worked Type 316 austenitic stainless steel would be expected to swell about 30 percent at its peak swelling temperature of 1100F. H-11 Mod shows promise for fusion reactor first wall applications in terms of swelling resistance (Ref. 92, pp. 969-973).

2.4.2 *[Figure]* Effect of irradiation temperature on swelling in H-11 Mod and Type 416 Martensitic Stainless Steel.

3 Mechanical Properties

3.1 Specified Mechanical Properties

3.1.1 *[Table]* AMS specified mechanical properties.

3.2 Mechanical Properties at Room Temperature

3.2.1 Tension Stress-strain Diagrams and Tensile Properties.

3.2.1.1 Stress-strain relations.

3.2.1.1.1 *[Figure]* Stress-strain curves for bar tempered at 950 to 1300F.

3.2.1.2 Heat treatment effects. This next group of figures illustrates primarily the effects of tempering temperature on tensile properties. Of particular interest is the steepness of the decrease in tensile strength with increasing tempering temperature for tempering temperatures above 1000F (Figures 3.2.1.2.1 and 3.2.1.2.2), emphasizing the need for strict temperature control during tempering. Also of interest is the secondary hardening peak at 950F, most apparent in Figure 3.2.1.2.2. Transverse tensile properties are similar to longitudinal tensile properties (Figure 3.2.1.2.3). Increased carbon content increases the tensile strength of hardened and tempered alloy, while vacuum melting results in improved tensile ductility (Figure 3.2.1.2.4).

3.2.1.2.1 *[Figure]* Effects of tempering at 900 to 1300F on tensile properties of sheet and bar.

3.2.1.2.2 *[Figure]* Effects of tempering up to 1300F on tensile properties of bar.

3.2.1.2.3 *[Figure]* Effects of tempering at 1000 to 1100F on transverse tensile properties of bar and extrusion.

3.2.1.2.4 *[Figure]* Effects of carbon content and tempering temperature on tensile properties of air melted and vacuum melted alloy.

3.2.1.3 Exposure effects. Exposure at temperatures of -300F and lower results in increased strength and decreased ductility on subsequent room temperature testing, shown in Figure 3.2.1.3.1. This behavior may result from additional austenite-to-martensite transformation. The approximate high temperature time-temperature limits for stability of mechanical properties are shown in Figure 3.2.1.3.2.

3.2.1.3.1 *[Figure]* Effects of low temperature exposure on tensile properties of sheet.

3.2.1.3.2 *[Figure]* Maximum temperatures for stability of mechanical properties for various exposure times.

3.2.1.4 Thermomechanical processing effects. Deformation during or after heat treatment increases strength and slightly decreases ductility. The effects of warm rolling after austenitizing (ausforming) on the properties of untempered alloy are shown in Figure 3.2.1.4.1. Tempering after ausforming reduces strength and improves ductility similarly to conventional austenitized and tempered alloy but the strength improvements from ausforming are retained, as shown in Figures 3.2.1.4.2, 3.2.1.4.3, and 3.2.1.4.4. Strength increases are also effected by prestraining and aging material which has been previously austenitized and tempered, shown in Figure 3.2.1.4.5.

3.2.1.4.1 *[Figure]* Effects of rolling on tensile properties of austenitized sheet.

3.2.1.4.2 *[Figure]* Effects of forging and tempering on tensile properties of austenitized steel.

3.2.1.4.3 *[Figure]* Effects of forging and tempering on tensile properties of vacuum melted alloy.

3.2.1.4.4 *[Figure]* Effects of tempering temperature on yield strength for conventional alloy and ausformed alloy.

3.2.1.4.5 *[Figure]* Effects of pre-straining on tensile properties of austenitized and tempered sheet.

3.2.1.5 Environmental effects.

3.2.1.5.1 *[Table]* Tensile properties of bar in air at atmospheric pressure and in helium and hydrogen at 10 ksi pressure.

3.2.2 Compression Stress-strain Diagrams and Compression Properties.

3.2.2.1 *[Figure]* True stress - true strain curves in tension and compression of bar.

3.2.2.2 *[Figure]* True stress - true strain curves in tension and compression for ausformed bar.

3.2.3 Impact.

3.2.3.1 The impact energy of H-11 Mod decreases with increasing tempering temperature to a minimum at about 900F, then increases with further increases in tempering temperature, shown in Figures 3.2.3.2 - 3.2.3.5. This behavior is a further reflection of the secondary hardening reaction shown earlier to affect tensile properties. The detrimental effects of increasing carbon content and the beneficial effects of vacuum melting on impact energy are also illustrated in Figure 3.2.3.4.

3.2.3.2 *[Figure]* Effect of tempering temperature on Charpy impact energy at RT and -321F.

3.2.3.3 *[Figure]* Effects of tempering temperature on Charpy impact energy and hardness.

3.2.3.4 *[Figure]* Effect of carbon content and tempering temperature on Charpy impact strength of air melt and vacuum melt alloy.

3.2.3.5 *[Figure]* Effect of tempering temperature on tensile and yield strength and on Izod impact energy.

3.2.3.6 Several possible causes have been advanced for the secondary hardening behavior exhibited by H-11 Mod. One possible cause involves the carbide precipitation reactions discussed earlier in Section 1.5.1. A second possibility relates to alloy composition. As shown in Figure 3.2.3.7, both commercial H-11 Mod and a laboratory heat containing zero manganese showed decreased impact energy after tempering at 932 or 1022F. However, a second laboratory heat with both manganese and silicon removed did not exhibit embrittlement, suggesting that embrittlement may be associated with silicon content. A third possible cause for embrittlement is suggested by a study of the effects of both time and temperature of retempering on impact energy, the results of which are shown in Figure 3.2.3.8. Kinetic data derived from this figure, along with additional microstructural and microchemical observations (Ref. 93, p. 1182), suggest that segregation primarily of phosphorus but also of sulfur and silicon to preaustenitic grain boundaries and other interfaces may be responsible for secondary embrittlement.

3.2.3.7 *[Figure]* Effects of tempering temperature and manganese and silicon contents on Charpy impact energy.

3.2.3.8 *[Figure]* Effects of retempering time and temperature on Charpy impact energy and hardness.

3.2.4 Bending.

3.2.5 Torsion and Shear.

3.2.6 Bearing.

3.2.6.1 *[Table]* Typical bearing and shear properties.

3.2.7 Stress Concentration.

3.2.7.1 Notched properties, see also Sections 3.3.7 and 3.5.

3.2.7.1.1 Material tempered at 900 to 1050F is particularly notch-sensitive. However, the notch-sensitivity decreases with increasing tempering temperature and is essentially absent for material tempered at 1200F, as shown in Figures 3.2.7.1.2 and 3.2.7.1.3. Increasing stress concentration factor and increasing length of initial fatigue crack both sharply reduce the notch strength of material tempered at 1000 or 1060F, but less strength reduction is noted for material tempered at 1100 or 1150F (Figures 3.2.7.1.4 and 3.2.7.1.5). Increased carbon content is beneficial to notch strength. As illustrated in Figure 3.2.7.1.6, for a given original ultimate strength, the notch strength increases with increasing carbon content.

3.2.7.1.2 *[Figure]* Effects of tempering temperature on notch strength of sharply notched sheet.

3.2.7.1.3 *[Figure]* Effects of tempering temperature on sharp notch strength ratio for sheet.

3.2.7.1.4 *[Figure]* Effects of stress concentration on notch strength of heat treated sheet.

3.2.7.1.5 *[Figure]* Effects of initial crack length on net section strength for sheet heat treated to F_{tu} from 200 to 300 ksi.

3.2.7.1.6 *[Figure]* Effect of carbon content and strength on sharp edge notch tensile strength ratio of air melt and vacuum melt sheet.

3.2.7.2 Fracture toughness.

3.2.7.2.1 Increasing austenizing temperature decreases the fracture toughness for material subsequently tempered to medium strength-high toughness at 1202F but not for material tempered to high strength-lower toughness at 1022F. Also, decreasing the volume percent of microstructural inclusions by argon ladling increases the fracture toughness of the 1202F-tempered material but not of the 1022F-tempered material, as shown in Figure 3.2.7.2.2. Tempering temperature significantly affects fracture toughness. A minimum in fracture toughness is observed for a tempering temperature of 1000F, the temperature region of maximum secondary hardening, as shown in Figure 3.2.7.1.2. (Additional fracture toughness data in Tables 2.3.2.7 and 2.3.2.8 support the trends shown in Figure 3.2.7.2.3.)

3.2.7.2.2 *[Figure]* Effects of austenitizing temperature, tempering temperature, and melting practice on fracture toughness.

3.2.7.2.3 *[Figure]* Effect of tempering temperature on fracture toughness.

3.2.8 Combined Properties.

3.3 Mechanical Properties at Various Temperatures

3.3.1 Tension Stress-strain Diagrams and Tensile Properties.

3.3.1.1 *[Figure]* Stress-strain curves at room and low temperatures for sheet.

3.3.1.2 *[Figure]* Stress-strain curves at room and elevated temperatures for materials heat treated to F_{tu} = 260 ksi.

3.3.1.3 *[Figure]* Stress-strain curves at room and elevated temperatures for annealed sheet.

3.3.1.4 *[Figure]* Stress-strain curves at room and elevated temperatures for sheet heat treated to F_{tu} = 280 ksi.

3.3.1.5 *[Figure]* Stress-strain curves at room and low temperatures for bar.

3.3.1.6 *[Figure]* Effect of low test temperature on tensile properties of bar.

3.3.1.7 *[Figure]* Effect of low test temperature on tensile properties of sheet.

3.3.1.8 *[Figure]* Effect of test temperature on tensile properties for tempering temperatures of 1000F to 1150F of bar and sheet.

3.3.1.9 *[Figure]* Effects of test temperature and tempering temperature on tensile properties of bar.

3.3.1.10 *[Figure]* Effect of test temperature on tensile properties of bolts heat treated to F_{tu} = 220 ksi minimum.

3.3.1.11 *[Figure]* Effects of test temperature, holding time and strain rate on tensile properties of sheet.

3.3.1.12 *[Figure]* Effect of test temperature on tensile properties of air melt alloy tempered to F_{tu} = 260 ksi and 310 ksi.

3.3.1.13 *[Figure]* Effects of test temperature on tensile properties of ausformed and conventionally heat treated steel.

3.3.1.14 *[Figure]* Effect of test temperature on tensile properties of annealed sheet.

3.3.1.15 *[Figure]* Effect of elastic strain rate on yield stress at RT and 600F.

3.3.1.16 *[Figure]* Effect of test temperature on tensile properties of sheet heat treated to F_{tu} = 260 and 280 ksi minimum.

3.3.2 Compression Stress-strain Diagrams and Compression Properties.

3.3.2.1 *[Figure]* Stress-strain curves in compression at room and elevated temperatures for annealed sheet.

3.3.2.2 *[Figure]* Effect of test temperature on compressive yield strength of sheet.

3.3.2.3 *[Figure]* Effect of test temperature on compressive yield strength of annealed sheet.

3.3.3 Impact.

3.3.3.1 *[Figure]* Effect of temperature on Charpy impact energy of bar.

3.3.3.2 *[Figure]* Effect of carbon content and test temperature on Charpy impact strength of air melt and vacuum melt alloy.

3.3.4 Bending.

3.3.5 Torsion and Shear.

3.3.5.1 *[Figure]* Effect of test temperature on shear strength of heat treated bolts.

3.3.5.2 *[Figure]* Effect of test temperature on shear strength of annealed sheet.

3.3.6 Bearing.

3.3.6.1 *[Figure]* Effect of test temperature on bearing properties of annealed sheet.

3.3.7 Stress Concentration.

3.3.7.1 Notch properties.

3.3.7.1.1 *[Figure]* Effect of test temperature on notch strength for various stress concentration factors of sheet.

3.3.7.1.2 *[Figure]* Effect of low test temperature on notch strength of sheet.

3.3.7.1.3 *[Figure]* Effect of low test temperature on notch tensile strength for stress concentration factors from 4 to 12.5.

3.3.7.1.4 *[Figure]* Effect of low temperatures, loading rates and stress concentration factors on notch strength of sheet.

3.3.7.1.5 *[Figure]* Effects of low test temperature and tempering temperature on notch strength of bar.

3.3.7.1.6 *[Figure]* Effects of low test temperature on crack strength of sheet.

3.3.7.1.7 *[Figure]* Effects of low test temperature and tempering temperature on crack strength of bar.

3.3.7.1.8 *[Figure]* Effect of test temperature on crack strength of sheet.

3.3.7.2 Fracture toughness.

3.3.7.2.1 *[Figure]* Effect of test temperature on smooth specimen tensile properties and on fracture toughness of plate.

3.4 Creep and Creep Rupture Properties

3.4.1 *[Figure]* Creep rupture behavior at 900 to 1200F for two tempering temperatures.

3.4.2 *[Figure]* Creep rupture curves for alloy at various strength levels at 700 to 1000F.

3.4.3 *[Figure]* Creep rupture curves at 800 to 1000F for sheet heat treated to F_{tu} = 190 ksi.

3.4.4 *[Figure]* Short time creep and creep rupture curves at 1000 and 1200F for sheet heat treated to F_{tu} = 290 ksi.

3.4.5 *[Figure]* Stress to produce creep rates of 10^{-3} to 10^{-5} percent per hour at 700 to 900F.

3.5 Fatigue Properties

3.5.1 Conventional Fatigue.

3.5.1.1 *[Figure]* S-N curves for heat treated bar.

3.5.1.2 *[Figure]* Fatigue scatterband for bar specimens from eight separate heats tested in axial tension.

3.5.1.3 *[Figure]* S-N curves for notched and smooth specimens at room temperature.

3.5.1.4 *[Figure]* S-N curves for notched and smooth specimens at 800F.

3.5.1.5 *[Figure]* S-N curves for notched and smooth specimens at 1000F.

3.5.1.6 *[Table]* Fatigue properties of bar and bolts.

3.5.1.7 *[Table]* Tensile and fatigue properties at room temperature and at -320F for bolts machined from bar heat treated to 240 ksi yield strength.

3.5.1.8 *[Table]* Tensile and fatigue properties of bolts made from material heat treated to several strength levels.

3.5.1.9 *[Figure]* Low-cycle fatigue of notched (K_t = 5.0) specimens cut from large plate.

3.5.1.10 *[Figure]* Low-cycle fatigue of notched (K_t = 3.0) specimens cut from long and short transverse directions of forging.

3.5.1.11 *[Figure]* Effect of surface machining and grinding (to remove decarburized layer) on reversed bending fatigue of sheet.

3.5.1.12 *[Table]* Fatigue strength at 10^6 cycles in rotating bending for vacuum and air melted alloy in various conditions of surface treatment after exposure to elevated temperature.

3.5.1.13 *[Figure]* S-N curves in rotating beam bending for smooth specimens and for specimens subjected to glass bead peening.

3.5.1.14 *[Figure]* Cyclic strain hardening in ausformed bar as manifested by reduction in plastic strain range (increase in elastic strain range) as cycles are increased during strain cycling tests in which total strain amplitudes are maintained constant.

3.5.1.15 *[Figure]* S-N curves for ausformed and conventionally heat treated steel.

3.5.2 Fatigue Crack Propagation.

3.5.2.1 The threshold stress intensity for fatigue crack propagation is considerably less than the plane strain fracture toughness and varies inversely with stress ratio R, as seen in Figure 3.5.1.2. This behavior is observed also with other high strength martensitic steels. The exponent "m" in the relation

$$da/dn = C\Delta K^m$$

is about 3 for H-11 Mod, compared to a range of 2.3 to 3.1 for other steels such as Type 4340, Hy-Tuf, and A-286.

3.5.2.2 *[Figure]* Fatigue crack growth rates in air at room temperature.

3.5.2.3 *[Figure]* Fatigue crack growth rates in air at 650F.

3.6 Elastic Properties

3.6.1 Poisson's Ratio, 0.281.

3.6.2 Modulus of Elasticity.

3.6.2.1 *[Figure]* Modulus of elasticity at room and elevated temperature.

3.6.2.2 *[Figure]* Modulus of elasticity for alloy heat treated to various hardness levels.

3.6.2.3 *[Figure]* Modulus of elasticity in compression at room and elevated temperatures for annealed sheet.

3.6.3 Modulus of Rigidity.

3.6.4 Tangent Modulus.

3.6.4.1 *[Figure]* Tangent modulus curves at room and elevated temperatures for bar heat treated to F_{tu} = 260 ksi.

3.6.5 Secant Modulus.

4 Fabrication

4.1 Forming

4.1.1 General. This alloy, in the fully annealed condition, can be readily formed by all common methods.

4.1.2 Forging. H-11 Mod is readily forged at temperatures in the range 1950 to 2100F. Forging stock should be preheated at 1500F to insure temperature uniformity, then slowly further heated to the forging temperature. Forging should not be continued below 1700F, but parts may be reheated as often as necessary. Care must be exercised during cooling after forging to prevent stress cracking. Small simple forgings may be cooled slowly in lime or dry ashes, but larger parts should be soaked at 1450F after forging and furnace cooled. Forged parts should then be annealed as soon as possible.

4.1.3 Bending. Sheet with thickness less than 0.090 inch has a room temperature production bend factor of 2 in the annealed condition and 6 when heat treated to F_{tu} = 260 to 280 ksi.

4.1.4 Straightening can be performed either during cooling from austenitizing or during heating for tempering.

4.2 Machining and Grinding

4.2.1 H-11 Mod is readily machinable in the annealed condition. It has a machinability rating of 55-75 compared to 100 for a 1 percent carbon tool steel or about 40-50 compared to 100 for B1112. Stress corrosion may result from the use of cutting fluids or cleaning fluids high in sulfur or chlorine (see Figure 2.3.2.9). Hydrogen embrittlement may occur during chemical milling (see Section 2.3.3.2).

4.3 Joining

4.3.1 Fusion welding is accomplished using inert gas shielding or with coated electrodes. Filler metal should be of the same general composition as the base metal. Parts to be welded should be preheated to 1000F and temperature should be maintained above 600F during welding. Welded parts, especially those with heavy sections, should be cooled slowly in a furnace or in an insulating medium after welding to prevent cracking. Welded parts should then be given a full anneal as soon after welding as possible. Welding should be performed in the annealed condition. However, if welding is performed in the hardened condition, the part must be retempered after welding. Maximum strength in welded tanks may be obtained after an intermediate temper at 1050F, as shown in Figure 4.3.2. These data further show significantly lower strengths for vessels welded from material previously tempered at 950 or 1000F, suggesting that tempering temperatures of 1050F or higher are preferable for material to be welded.

4.3.2 *[Figure]* Effect of tempering temperature on strength of welded sheet and pressure vessels.

4.4 Surface Treating

4.4.1 Conditions having higher strength than 200 ksi should be cleaned by mechanical methods or by anodic pickling. Acid or alkaline pickling or cathodic cleaning can result in hydrogen embrittlement.

4.4.2 Corrosion and oxidation resistance of this steel is obtained by a variety of surface coatings. One preferred method is plating with nickel cadmium (AMS 2416). (Ref. 101) Aluminizing, chromizing, vapor deposition of metal coatings, and silicone paints are also successfully used in production. Special plating methods are used for the high strength conditions, usually followed by baking at 375F minimum, for 23 hours.

4.4.3 Chemical milling may be accomplished in either the annealed or heat treated conditions. Baking of heat treated parts after chemical milling is recommended. The mechanical properties of sheet heat treated to F_{tu} = 280 ksi minimum and milled from 0.200 to 0.100 in thickness were found to be unchanged.

4.4.4 The surface of H-11 Mod can be hardened using either conventional nitriding or ion nitriding techniques. Temperatures employed are frequently in the range 1000 to 1100F in order to obtain the best efficiency and yet avoid formation of the epsilon-prime iron nitride phase, which flakes off easily. Ion nitriding can be accomplished at temperatures as low as 300F. Nitrogen and hardness profiles for H-11 Mod ion nitrided at 480F are shown in Figure 4.4.5. The calculated diffusivity of nitrogen in H-11 Mod at this temperature is 1.74×10^{-10} cm^2/sec. (Ref. 99, p. 1495).

4.4.5 *[Figure]* Nitrogen content and hardness profiles for ion-nitrided H-11 Mod.

Table 1.3.1 AMS Specifications (Refs. 77-80)

Alloy: H-11 Mod	
AMS Specification	**Product Form**
6437D	Sheet, Strip, and Plate
6485F	Bars, Forgings, and Forging Stock
6487F	Bars, Forgings, and Forging Stock (premium quality, consumable electrode vacuum melted)
6488C	Bars, Forgings, and Forging Stock (premium quality)

Table 1.4.1 AMS Specified Composition (Refs. 77-80)

Alloy: H-11 Mod		
Element	**Percent**	
	Min	**Max**
Carbon	0.38	0.43
Chromium	4.75	5.25
Molybdenum	1.20	1.40
Vanadium	0.40	0.60
Silicon	0.80	1.00
Manganese	0.20	0.40
Copper	-	0.35
Nickel	-	0.25
Phosphorus	-	0.020 (a)
Sulfur	-	0.020 (a)
Iron	Balance	

(a) Max phosphorus and sulfur contents are 0.015 percent for AMS 6487F and AMS 6488D.

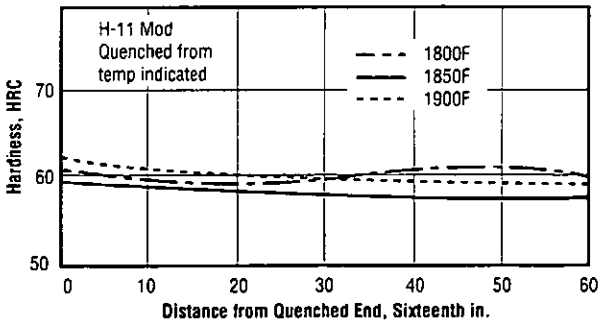


Fig. 1.6.1 End quench hardenability (Ref. 9)

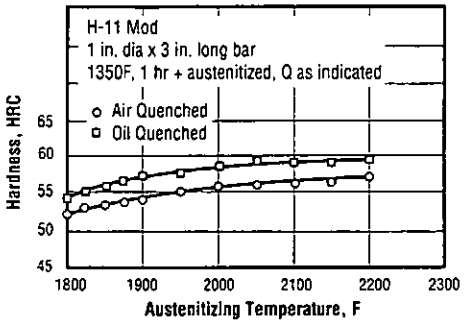


Fig. 1.6.2 Effect of austenitizing temperature and type of cooling on hardness (Ref. 82)

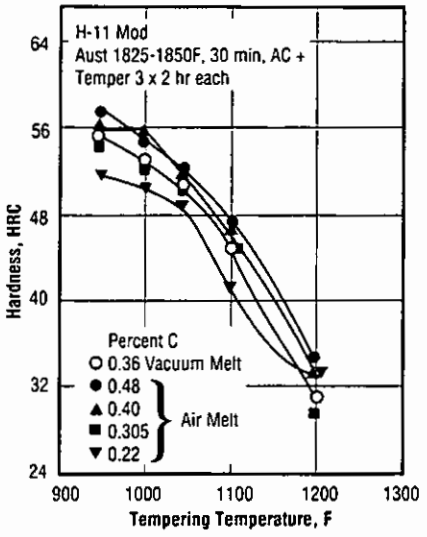


Fig. 1.6.3 Effect of carbon content and tempering temperature on hardness of air melt and vacuum melt alloy (Ref. 22)

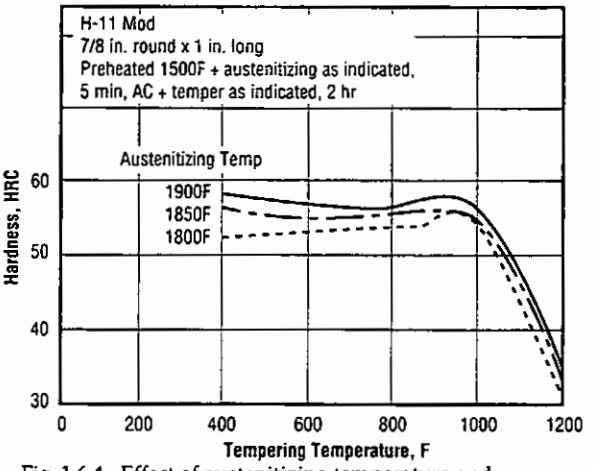


Fig. 1.6.4 Effect of austenitizing temperature and tempering temperature on hardness for a single tempering treatment (Ref. 38)

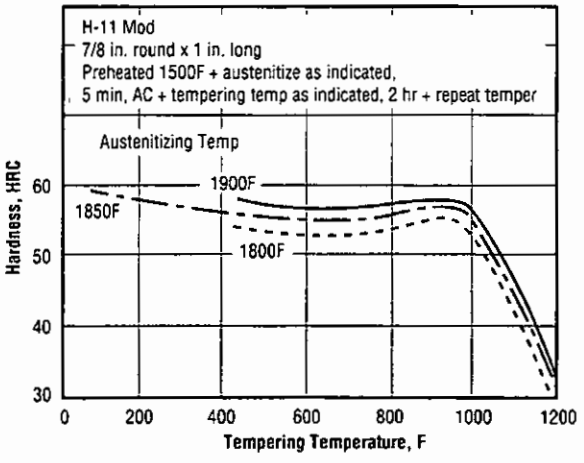


Fig. 1.6.5 Effect of austenitizng temperature and tempering temperature on hardness for a double tempering treatment (Ref. 38)

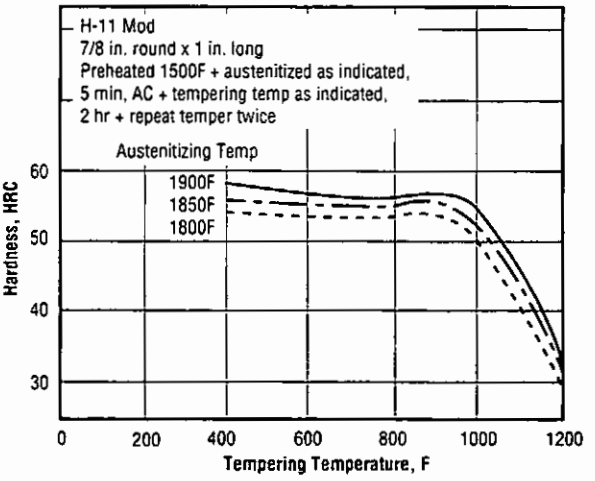


Fig. 1.6.6 Effect of austenitizing temperature and tempering temperature on hardness for a triple tempering treatment (Ref. 38)

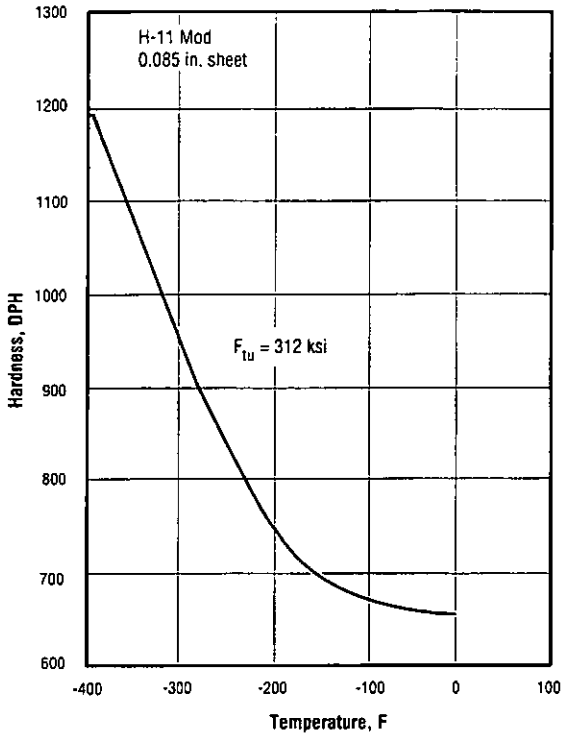


Fig. 1.6.7 Effect of low temperature on hardness of sheet (Ref. 26)

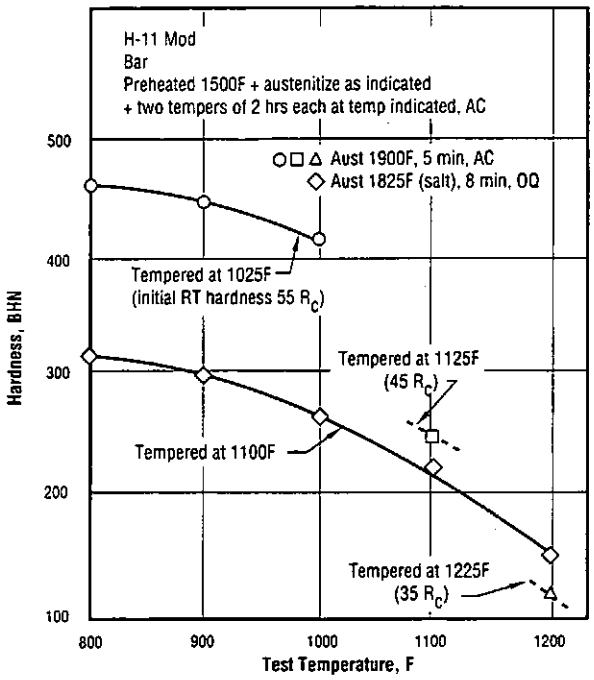


Fig. 1.6.8 Hot hardness of bar austenitized at 1825 or 1900F, and tempered at temperatures from 1025 to 1225F (Ref. 38)

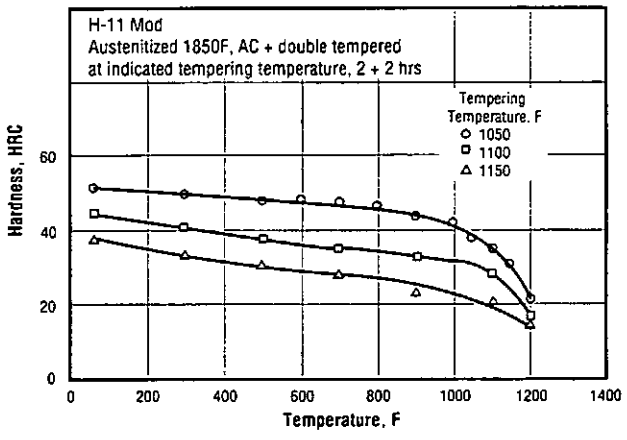


Fig. 1.6.9 Hot hardness after tempering at 1050 to 1150F (Ref. 81)

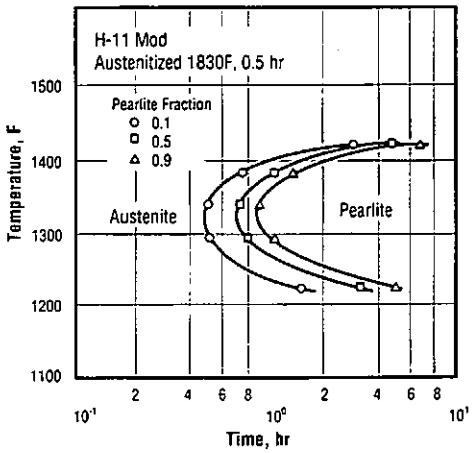


Fig. 2.1.2.1 Time-temperature-transformation diagram (Ref. 87)

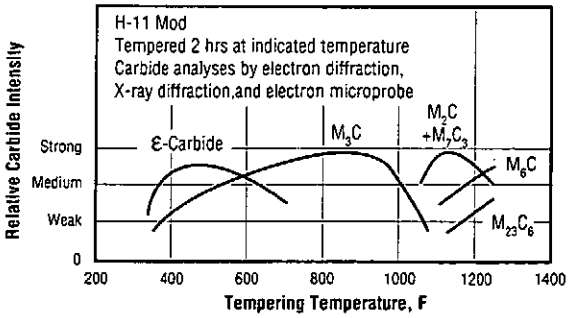


Fig. 2.1.2.4 Relative carbide intensity (abundance) as a function of tempering temperature (Ref. 88)

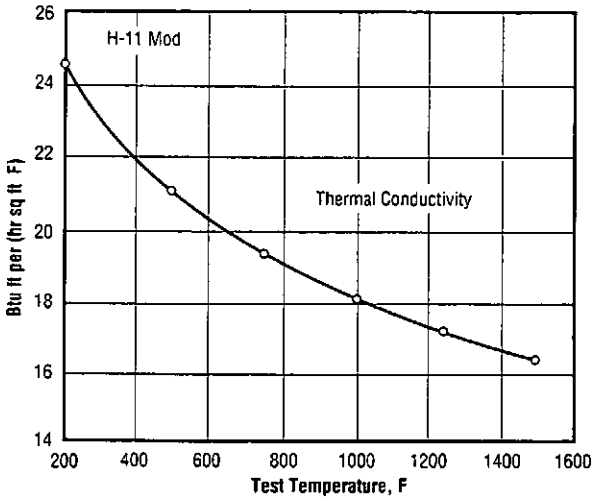


Fig. 2.1.3.1 Thermal Conductivity (Ref. 38)

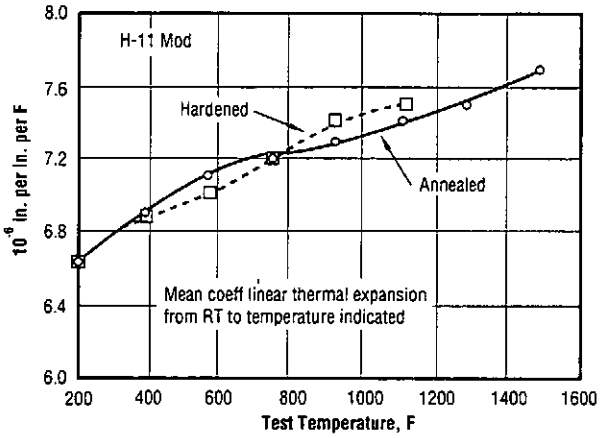


Fig. 2.1.4.1 Thermal Expansion (Ref. 38)

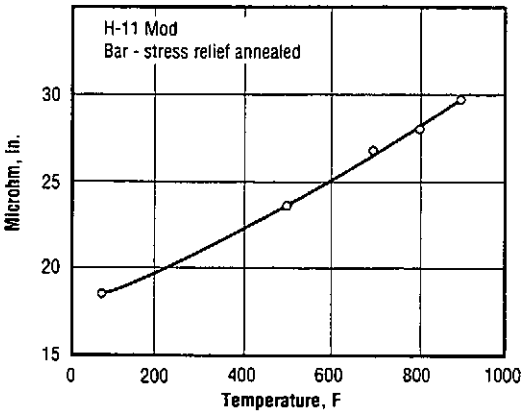


Fig. 2.2.2.1 Electrical Resistivity (Ref. 75)

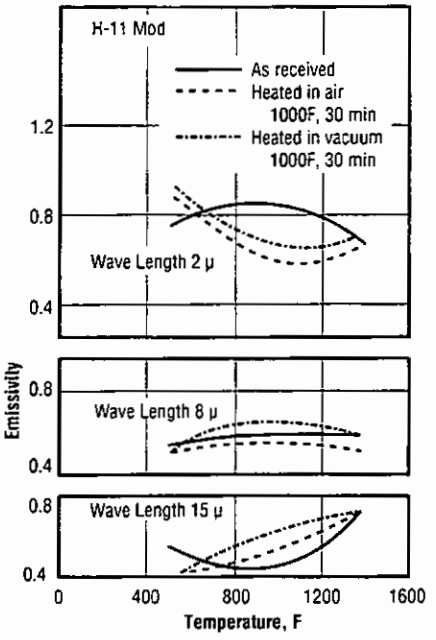


Fig. 2.2.4.1 Emittance (Ref. 25)

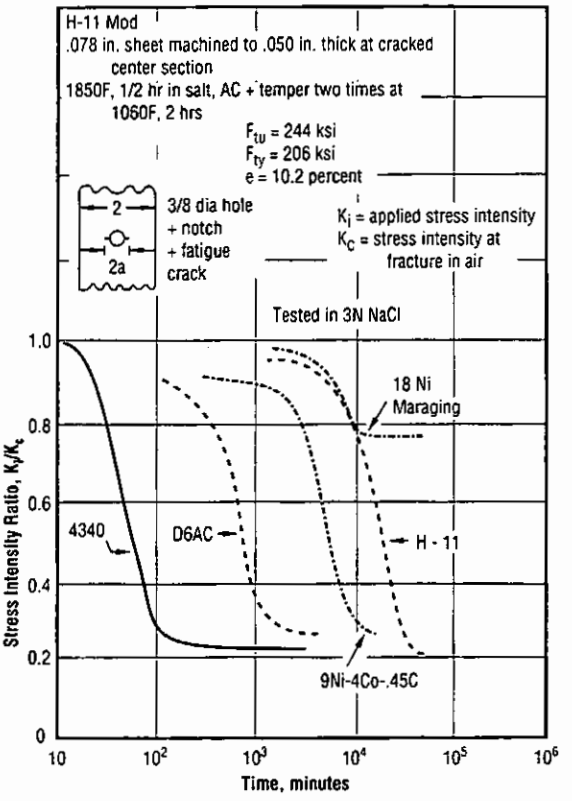


Fig. 2.3.2.2 Comparison of stress corrosion cracking characteristics of alloy with corresponding behavior of several other martenistic steels heat treated to tensile strength levels of approximately 240 ksi (Ref. 56)

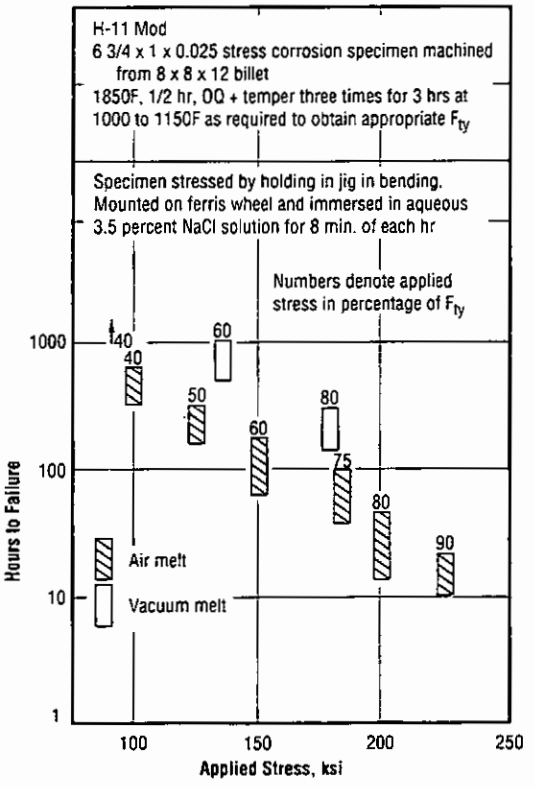


Fig. 2.3.2.3 Effect of applied stress on time to stress corrosion failure for air melt and vacuum melt alloy (Ref. 63)

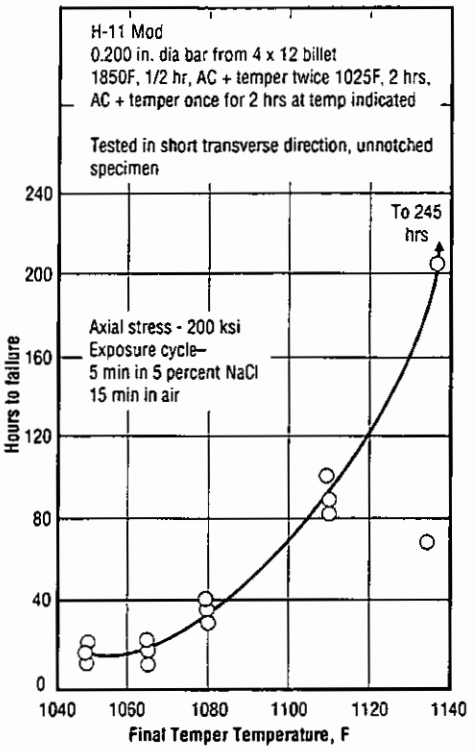


Fig. 2.3.2.4 Effect of temperature of final temper on stress-corrosion resistance in 5 percent aqueous solution of NaCl (Ref. 62)

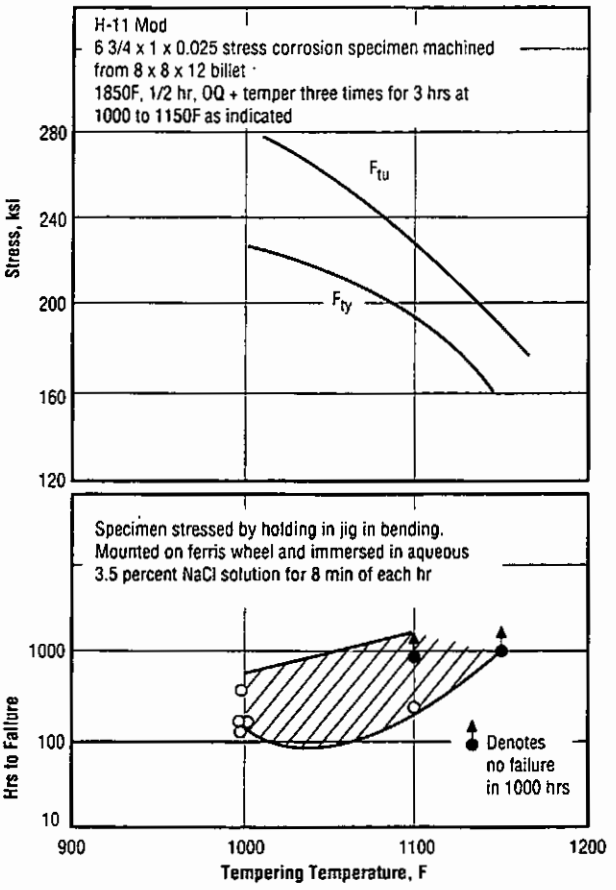


Fig. 2.3.2.5 Effect of tempering temperature on stress-corrosion resistance of billet (Ref. 63)

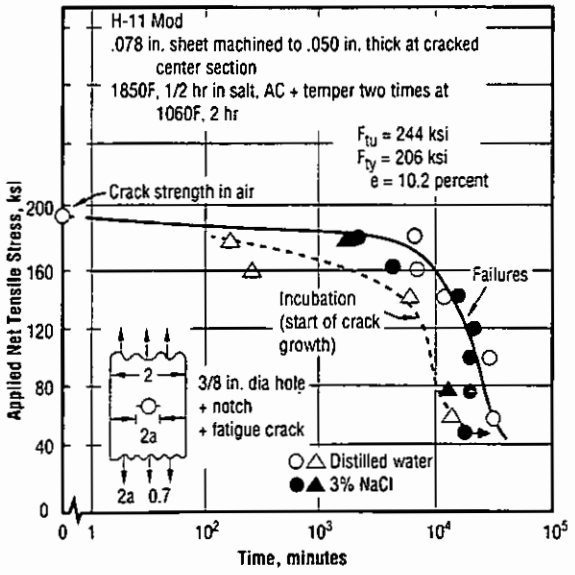
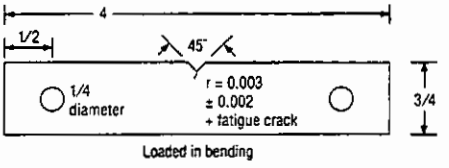


Fig. 2.3.2.6 Delayed failure of alloy at 206 ksi yield strength level when tested in distilled water and in aqueous solution containing 3 percent NaCl (Ref. 56)

Table 2.3.2.7 Plane strain fracture toughness and threshold for stress corrosion cracking in seacoast test and in accelerated tests for alloy in three conditions (Ref. 47)

Alloy: H-11 Mod			
Form	**1/4 in. sheet (a)**		
Condition	**Vac. Melt 2+2 hr @ 1000F F_{ty} 280-300 ksi**	**Air Melt 2+2 hr @ 1000F F_{ty} 280-300 ksi**	**Air Melt 2+2 hr @ 1100F F_{ty} 220-240 ksi**
K_{Ic} (ksi $\sqrt{in}$)	28.5	27.6	52.8
K_{Iscc} (ksi $\sqrt{in}$)			
Seacoast (b)	11.4 ± 5.6	16.7 ± 2.8	39.5 ± 4.4
Accelerated (c)	10.8 ± 1.9	8.6 ± 1.4	23.2 ± 0.2

(a)

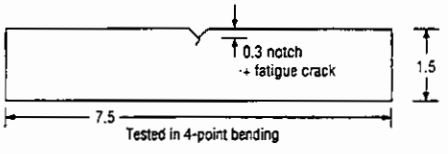


(b) One face exposed to Pacific Ocean (L.A. Dept. of Water & Power)
(c) Immersed in solution of 200g NaCl per liter distilled water.

Table 2.3.2.8 Plane strain fracture toughness and threshold for stress corrosion cracking in 3-1/2 percent NaCl aqueous solution (Ref. 52)

Alloy: H-11 Mod			
Form	**1/2 plate**		
Condition	**Quenched and tempered at 1100F**		
	F_{ty} (ksi)	**K_{Ic} (ksi $\sqrt{in}$)**	**K_{Iscc} (ksi $\sqrt{in}$)**
	188	54	30

Tested at RT in water containing 3-1/2 percent NaCl.



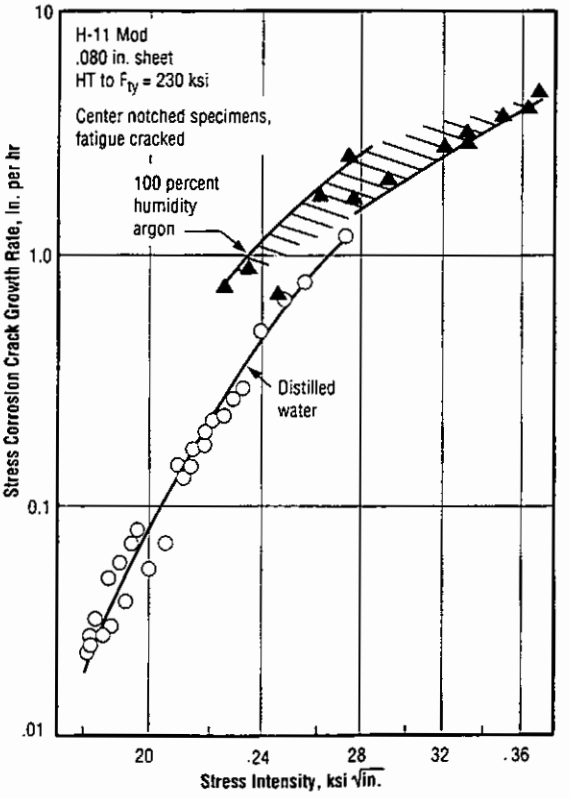


Fig. 2.3.2.9 Sustained load crack growth rate in humid argon and in distilled water (Ref. 53)

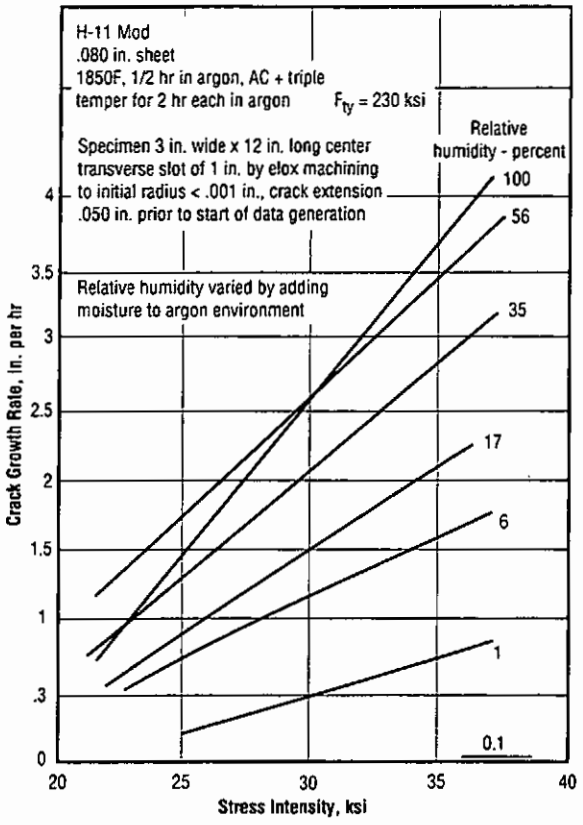
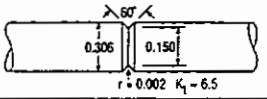


Fig. 2.3.2.10 Effect of stress intensity on crack growth rate for a wide range of relative humidity in an argon environment (Ref. 41)

Table 2.3.3.3 Notch strength in helium and hydrogen at 10 ksi pressure (Ref. 46)

Alloy: H-11 Mod		
Form (a)	1 in bar machined to notch shown 	
Condition	**1850F, 40 min. AC + triple temper 1000F, 2 hr AC**	
	Notch strength (a) (ksi)	**Ductility (RA)**
Helium	253	0
Hydrogen	62	0
Hydrogen after 1 hr hold at 50 ksi	65	0
Hydrogen after 100 hr hold at 50 ksi	103	0

(a) Average of replicate tests with small variations in geometry and strength values.

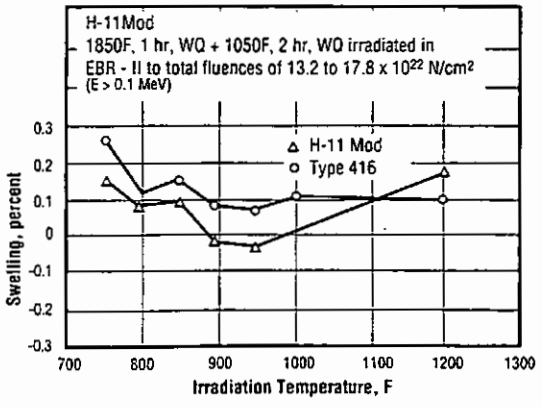


Fig. 2.4.2 Effect of irradiation temperature on swelling in H-11 Mod and Type 416 martensitic stainless steel (Ref. 92)

Table 3.1.1 AMS-Specified Mechanical Properties (Refs. 77-80)

Alloy: H-11 Mod						
AMS Specification	**6437D**	**6485F**			**6487F, 6488D**	
Form	**Sheet, Strip, and Plate**	**Bars & Forgings**			**Bars & Forgings (premium quality)**	
Heat Treatment	**Austenitize 1825-1875F, 15-25 min, AC**	**Austenitize 1825-1875F, 15-45 min, AC**				
	Triple Temper, 1000F, 2-3 Hr					
Test Temperature	**RT**	**RT**		**1000F**	**RT**	
Test Orientation	**L**	**L**	**T**	**L**	**L**	**T (c)**
Tensile Properties						
F_{tu} (ksi, min)	260	260	260	175	260	260 (d)
F_{ty} (ksi, min)	220	215	215	135	215	215
e (pct, min) (a)	5	8		10	8	6
RA (pct, min)		30		35	30	
Cross-section area (square inch)						
25 to 75			6			
75 to 100			6			
100 to 150			5			
150 to 225			4			
225 to 256						
Bend Properties						
Angle (deg, min) (b) Thickness (inch)						
up to .250	180					
.250 to .437	90					

Note: The original AMS documents should be consulted for complete specification details.
(a) 2 inches or 4 D
(b) Free bend around 3 T diameter
(c) 6488D only
(d) 280 ksi max

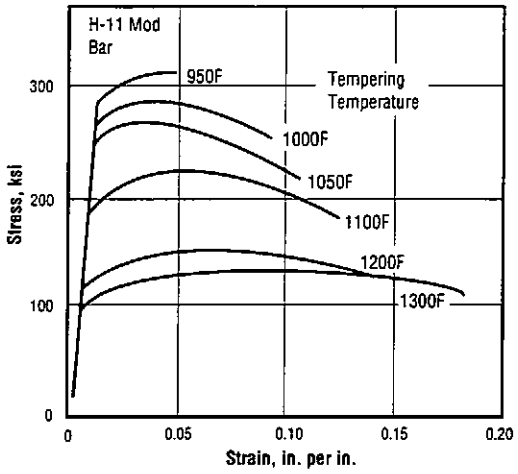


Fig. 3.2.1.1.1 Stress strain curves for bar tempered at 950 to 1300F (Ref. 9)

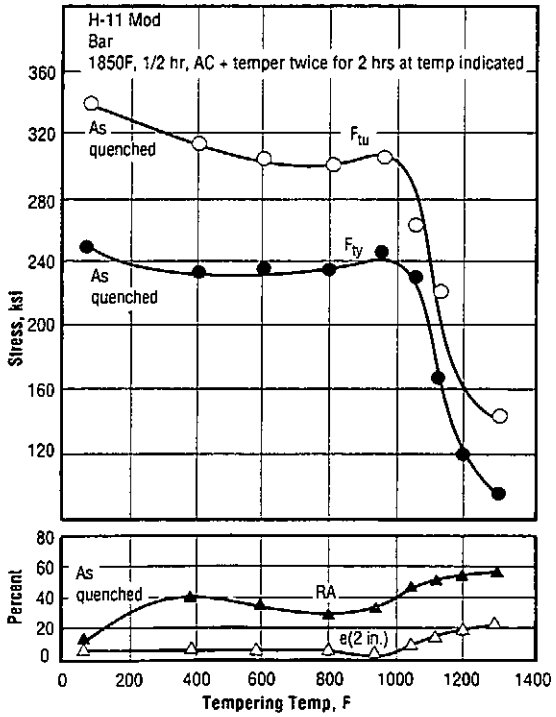


Fig. 3.2.1.2.2 Effects of tempering up to 1300F on tensile properties of bar (Ref. 40)

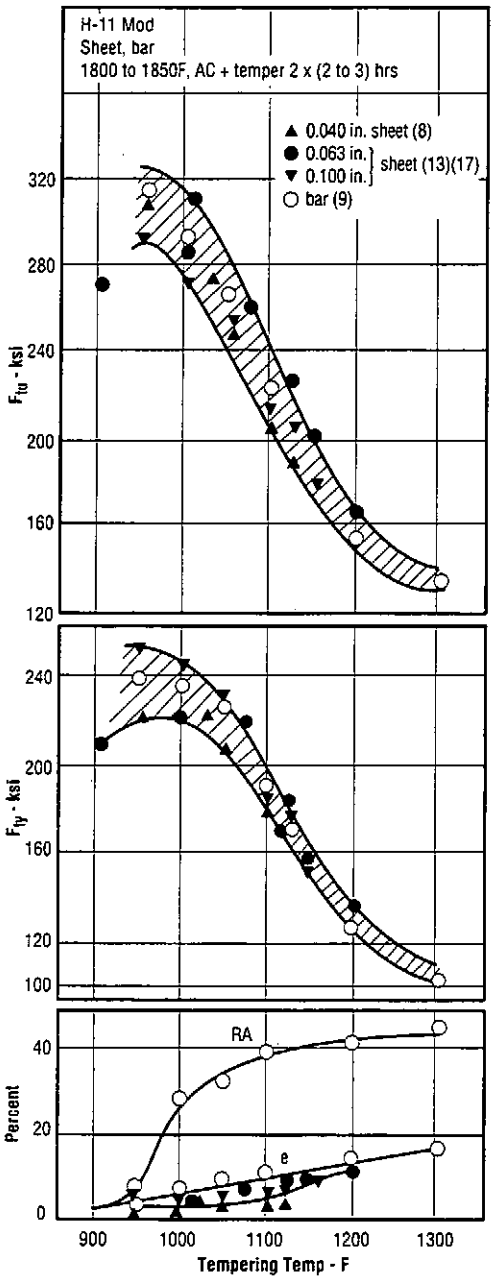


Fig. 3.2.1.2.1 Effect of tempering at 900 to 1300F on tensile properties of sheet and bar (Ref. 8, 9, 13, 17)

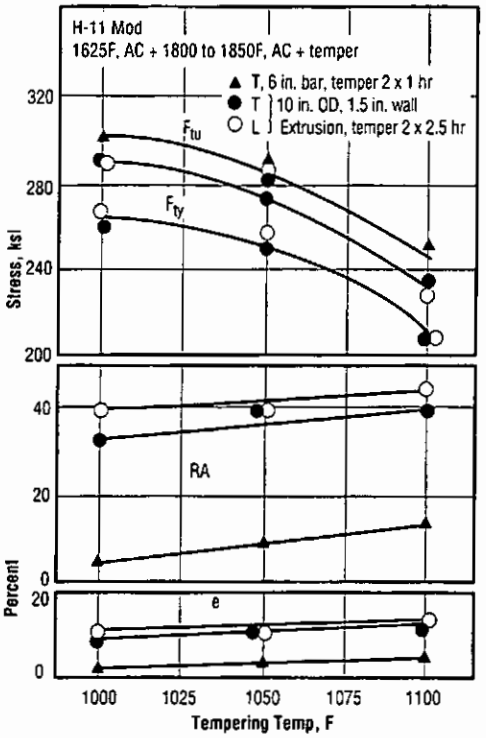


Fig. 3.2.1.2.3 Effects of tempering at 1000 to 1100F on transverse tensile properties of bar and extrusions (Ref. 16)

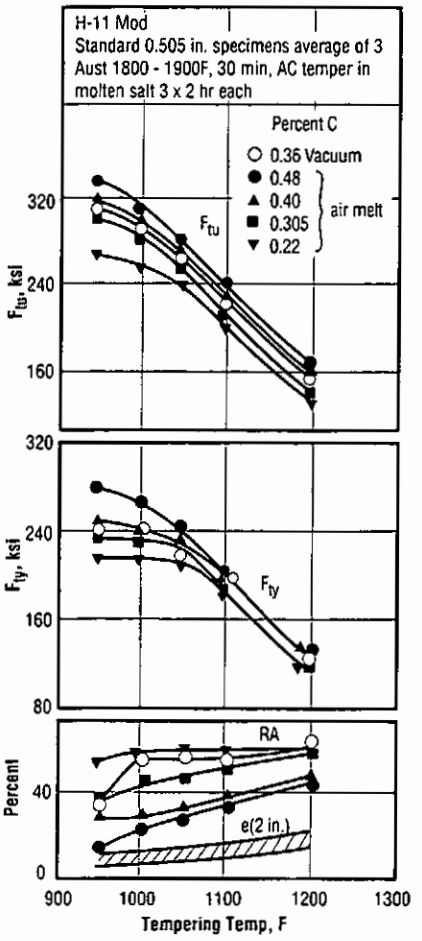


Fig. 3.2.1.2.4 Effects of carbon content and tempering temperature on tensile properties of air melted and vacuum melted alloy. (Ref. 22)

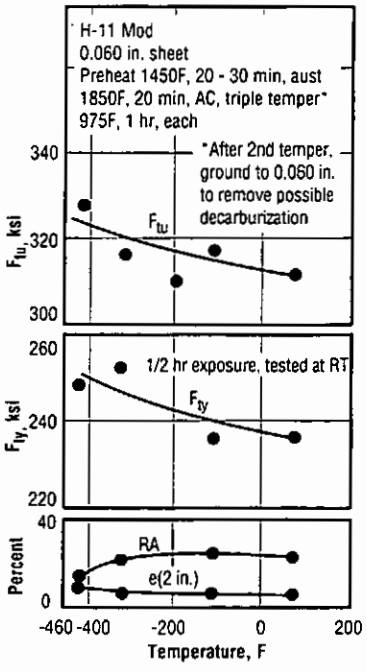


Fig. 3.2.1.3.1 Effects of low temperature exposure on tensile properties of sheet (Ref. 26)

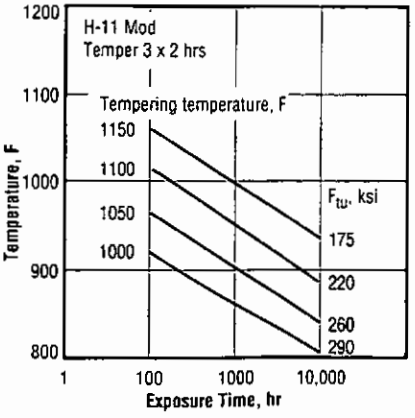


Fig. 3.2.1.3.2 Maximum temperatures for stability of mechanical properties for various exposure times (Ref. 6)

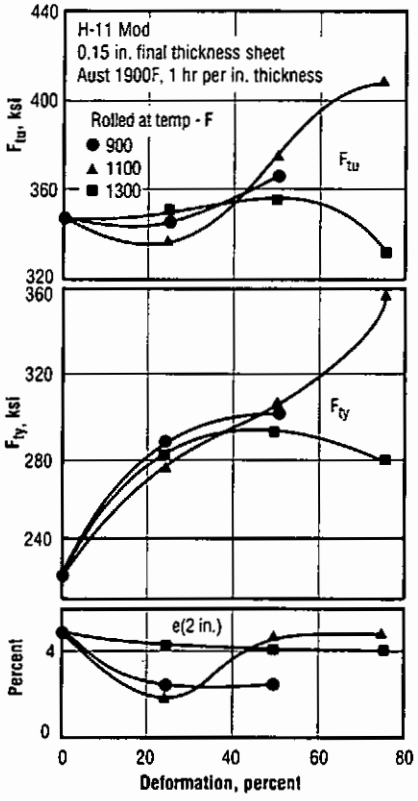


Fig. 3.2.1.4.1 Effects of rolling on tensile properties of austenitized sheet (Ref. 31)

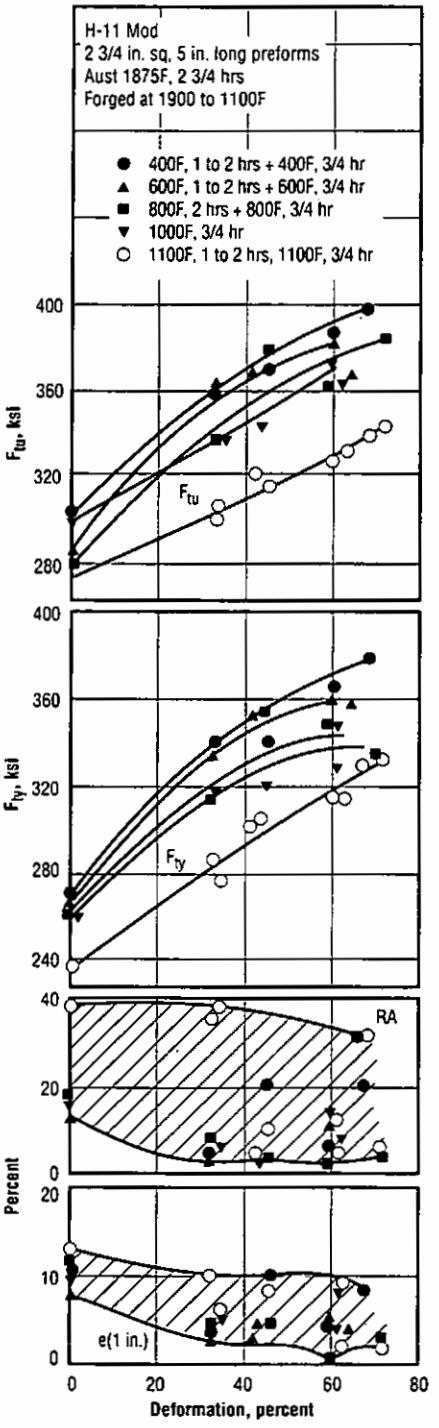


Fig. 3.2.1.4.2 Effects of forging and tempering on tensile properties of austenitized steel (Ref. 32)

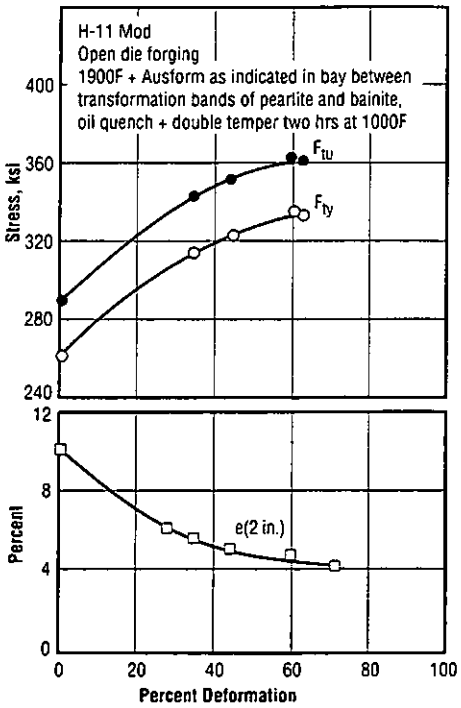


Fig. 3.2.1.4.3 Effects of forging and tempering on tensile properties of vacuum melted alloy (Ref. 69)

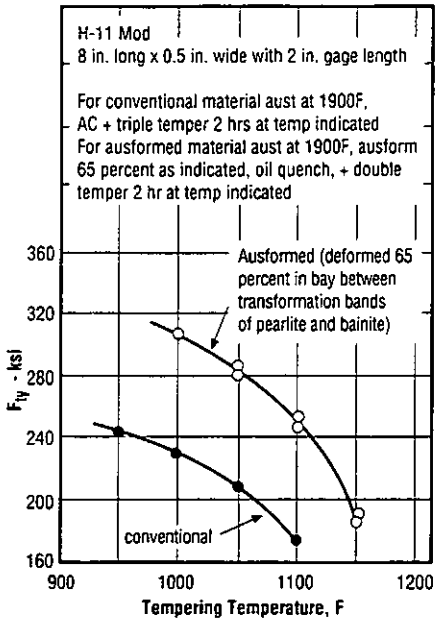


Fig. 3.2.1.4.4 Effects of tempering temperature on yield strength for conventional alloy and for ausformed alloy (Ref. 69)

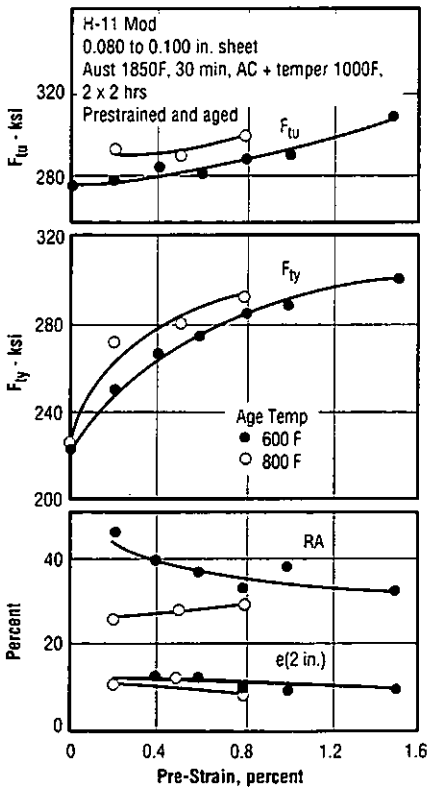


Fig. 3.2.1.4.5 Effects of pre-straining on tensile properties of austentized and tempered sheet (Ref. 36)

Table 3.2.1.5.1 Tensile properties of bar in air at atmospheric pressure and in helium and hydrogen at 10 ksi pressure (Ref. 46)

Alloy: H-11 Mod			
Form	**1 inch bar machined to tensile spec.**		
Condition	**1850F, 40 min., AC + triple temper 1000F, 2 hr, AC**		
	F_{tu} (ksi)	**e, 1 in. (pct)**	**RA (pct)**
Air at atmosphere press	293	11	30
He at 10 ksi press	299	8.8	30
He (hydrogen contaminated) at 10 ksi press	278	1.4	1.2
Hydrogen, at 10 ksi press	170	0	0
Hydrogen, after 1 hr hold at 128 ksi stress	171	0	0
Hydrogen, after 100 hr hold at 128 ksi stress	166	0	0

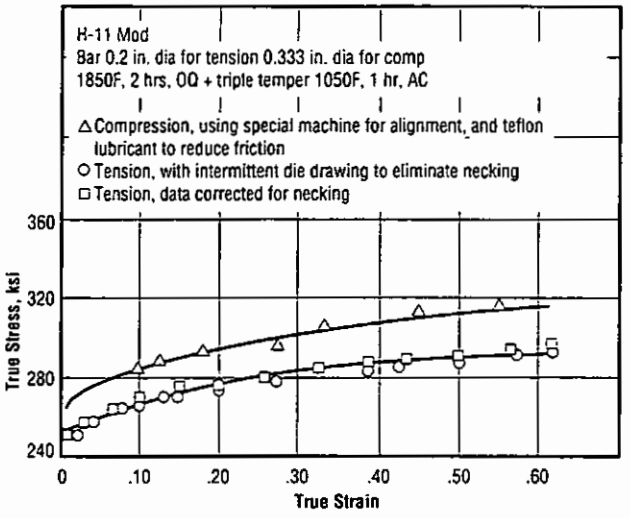


Fig. 3.2.2.1 True stress - true strain curves in tension and compression of bar (Ref. 43)

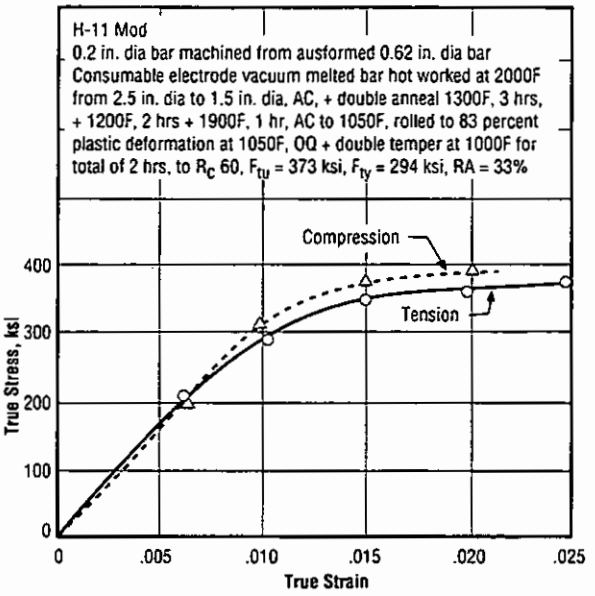


Fig. 3.2.2.2 True stress - true strain curves in tension and compression for ausformed bar (Ref. 64)

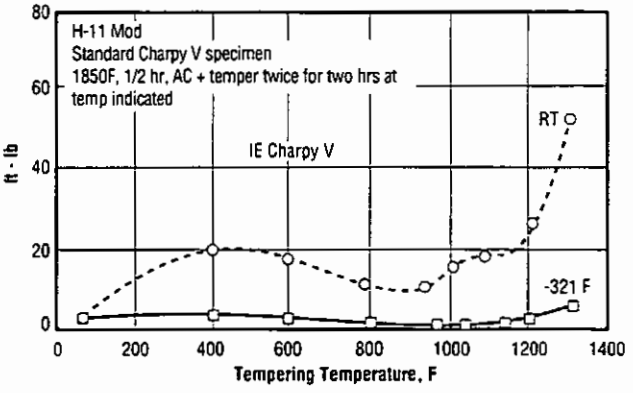


Fig. 3.2.3.2 Effect of tempering temperature on Charpy impact energy at RT and -321F (Ref. 40)

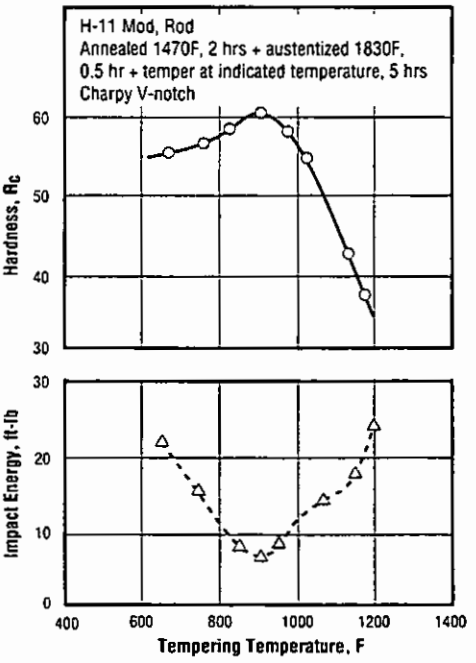


Fig. 3.2.3.3 Effects of tempering temperature on Charpy impact energy and hardness (Ref. 93,)

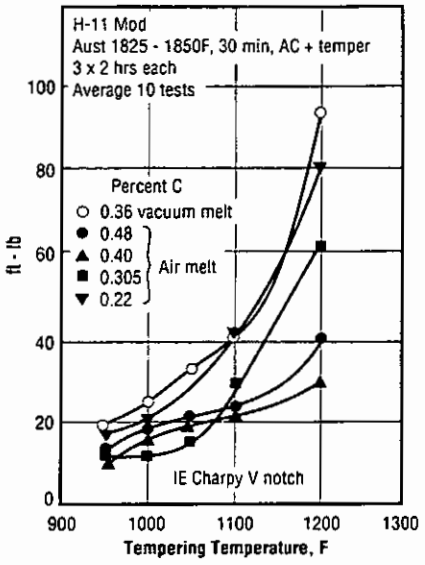


Fig. 3.2.3.4 Effect of carbon content and tempering temperature on Charpy impact strength of air melt and vacuum melt alloy (Ref. 22)

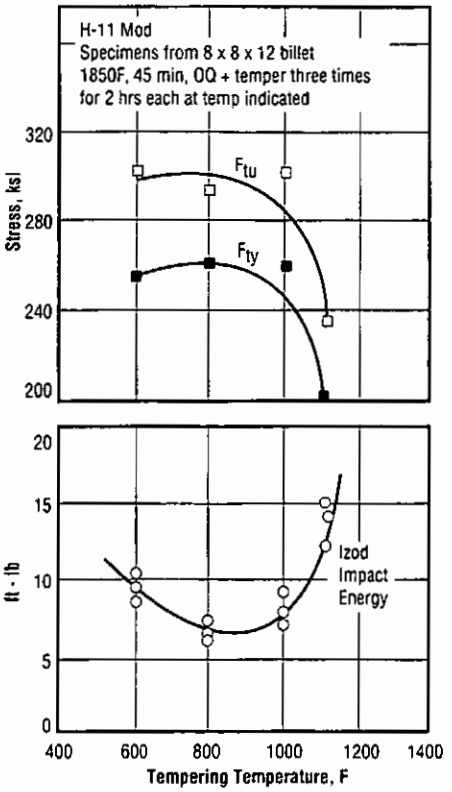


Fig. 3.2.3.5 Effect of tempering temperature on tensile and yield strength and on Izod impact energy (Ref. 63)

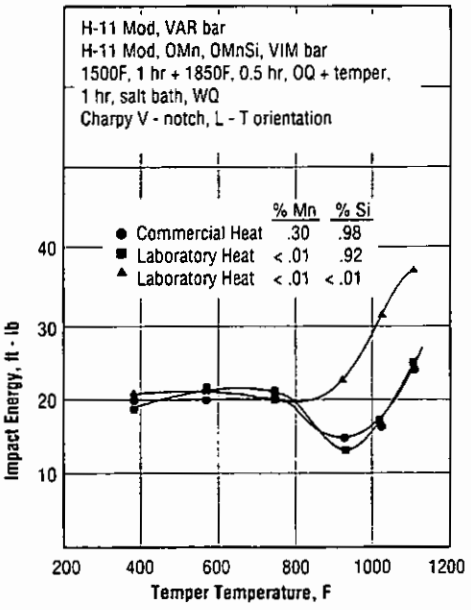


Fig. 3.2.3.7 Effects of tempering temperature and manganese and silicon contents on Charpy impact energy (Ref. 94)

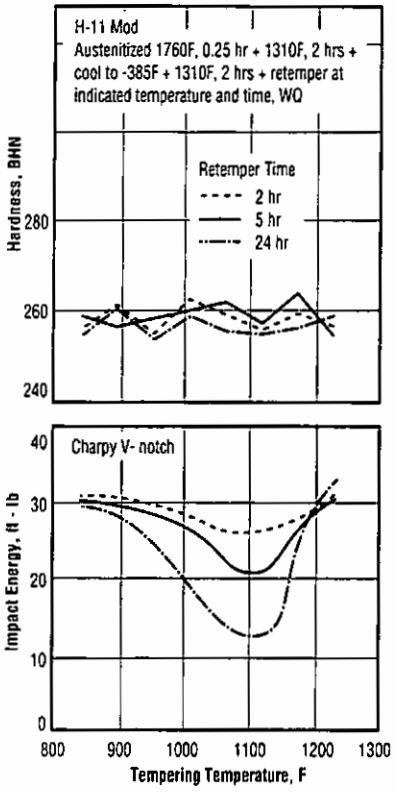


Fig. 3.2.3.8 Effects of retempering time and temperature on Charpy impact energy and hardness (Ref. 93)

Table 3.2.6.1 Typical bearing and shear properties (Ref. 4)

Alloy: H-11 Mod						
Form	**Sheet**					
Condition F_{tu} (ksi)	**260 to 280**			**280 to 300**		
Thickness (in.)	**0.063**	**0.063**	**0.078**	**0.063**	**0.063**	**0.078**
F_{bru} (ksi)						
e/D=1.5 L	-	-	378	-	-	432
e/D=2.0 L	512	477	-	547	525	-
e/D=2.0 T	509	-	-	529	-	-
F_{bry} (ksi)						
e/D=1.5 L	-	-	316	-	-	369
e/D=2.0 L	364	338	-	388	380	-
e/D=2.0 T	371	-	-	392	-	-
F_{su} (ksi) L	170	166.5	170	178	184	186
F_{su} (ksi) T	171	169	171	183	186	187.5
F_{su}/F_{tu} (avg)	0.631	0.635	0.642	0.634	0.635	0.635

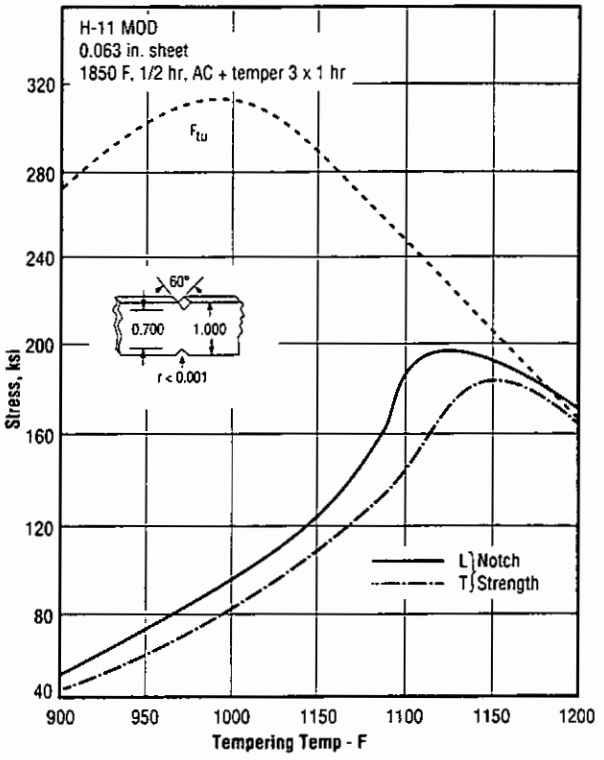


Fig. 3.2.7.1.2 Effects of tempering temperature on notch strength of sharply notched sheet. (Ref. 13)

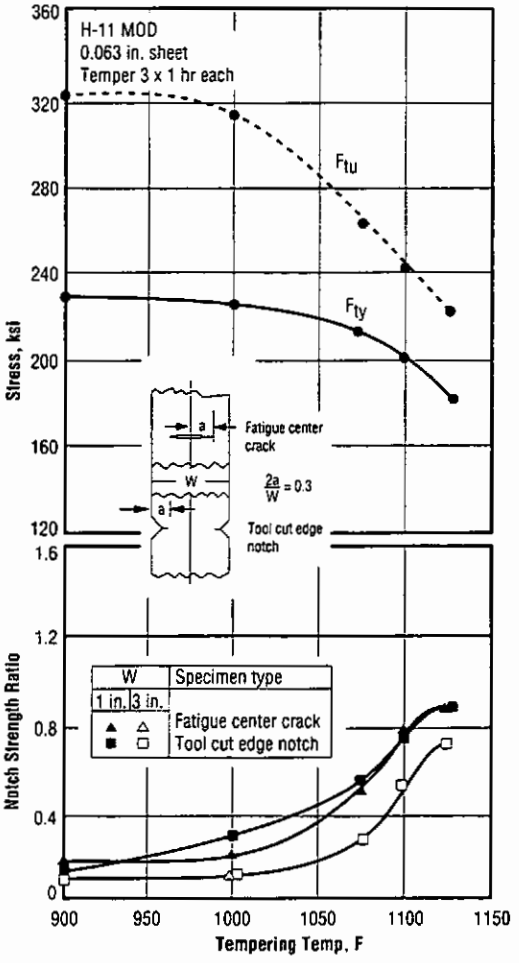


Fig. 3.2.7.1.3 Effects of tempering temperature on sharp notch strength ratio for sheet. (Ref. 27)

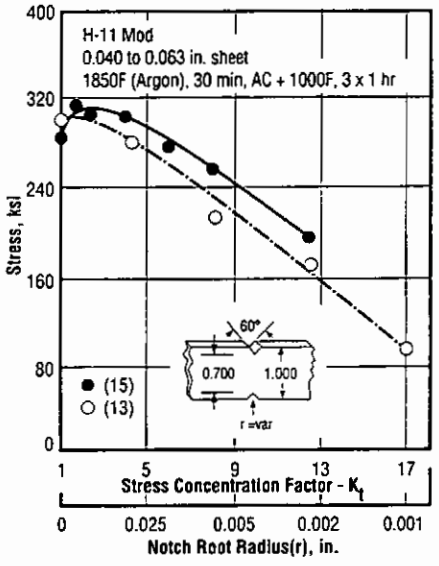


Fig. 3.2.7.1.4 Effects of stress concentration on notch strength of heat treated sheet. (Refs. 13, 15)

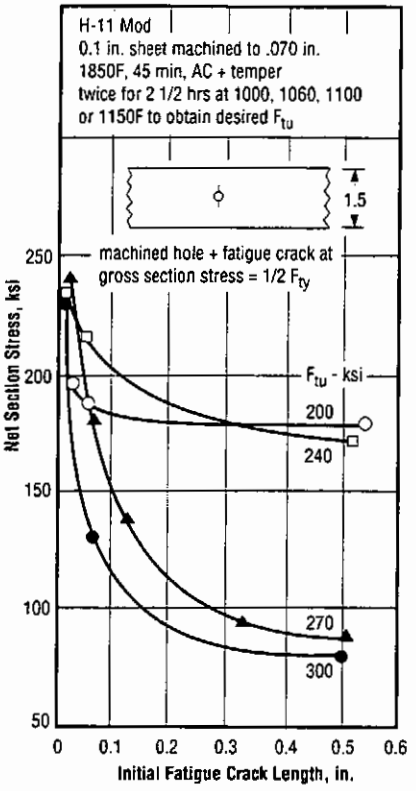


Fig. 3.2.7.1.5 Effects of initial crack length on net section strength for sheet heat treated to F_{tu} from 200 to 300 ksi (Ref. 58)

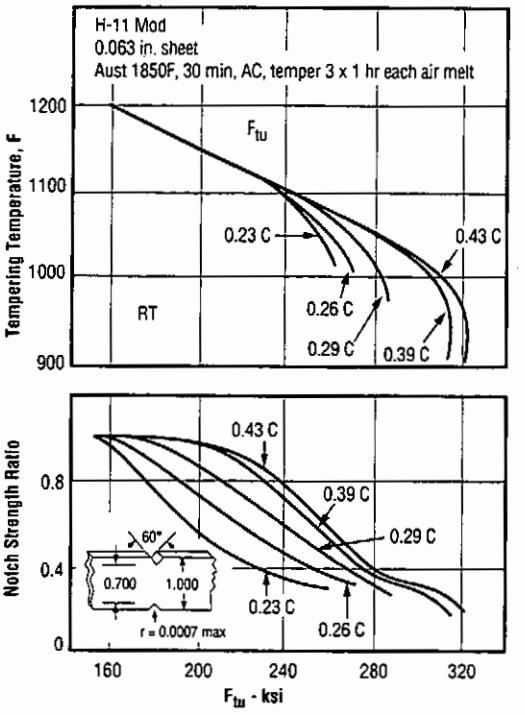


Fig. 3.2.7.1.6 Effect of carbon content and strength on sharp edge notch tensile strength ratio of air melt and vacuum melt sheet (Ref. 17)

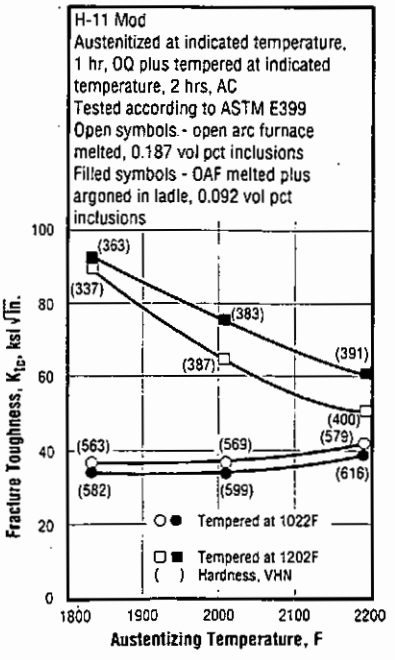


Fig. 3.2.7.2.2 Effects of austenitizing temperature, tempering temperature, and melting practice on fracture toughness (Ref. 95)

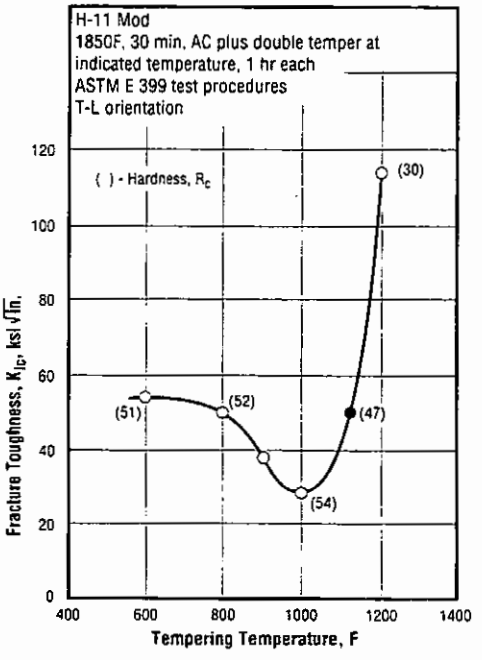


Fig. 3.2.7.2.3 Effect of tempering temperature on fracture toughness (Ref. 96)

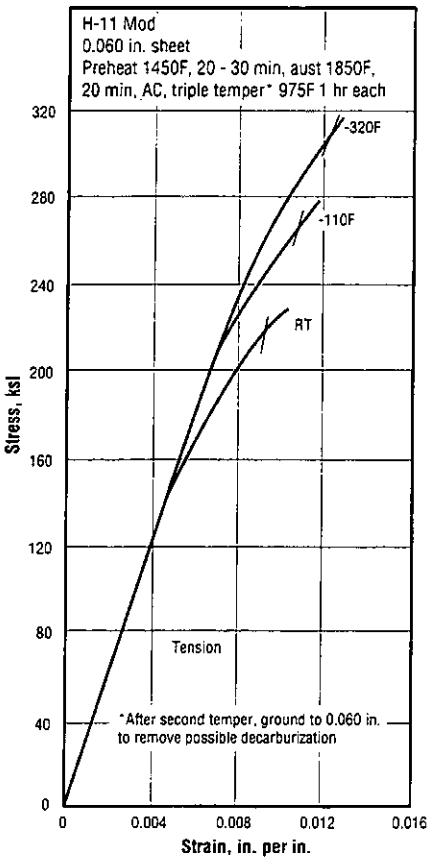


Fig. 3.3.1.1 Stress-strain curves at room and low temperatures for sheet (Ref. 26)

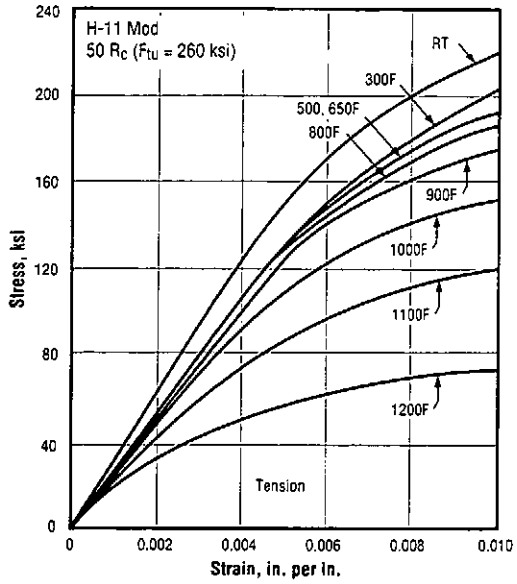


Fig. 3.3.1.2 Stress-strain curves at room and elevated temperatures for material heat treated to F_{tu} = 260 ksi (Ref. 9)

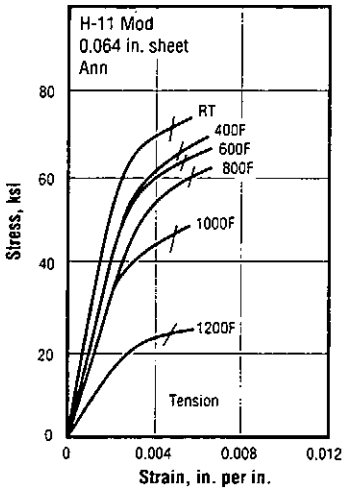


Fig. 3.3.1.3 Stress - strain curves at room and elevated temperatures for annealed sheet (Ref. 34)

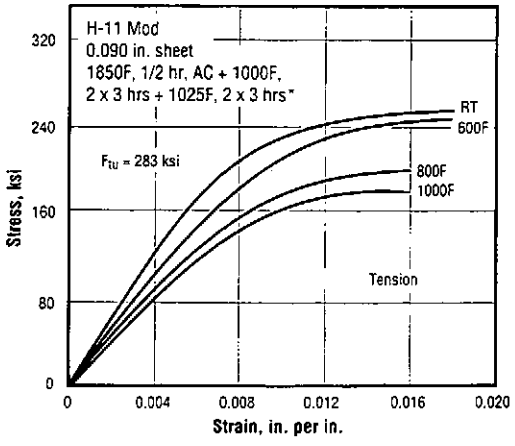


Fig. 3.3.1.4 Stress-strain curves at room and elevated temperatures for sheet heat treated to F_{tu} = 280 ksi (Ref. 7)

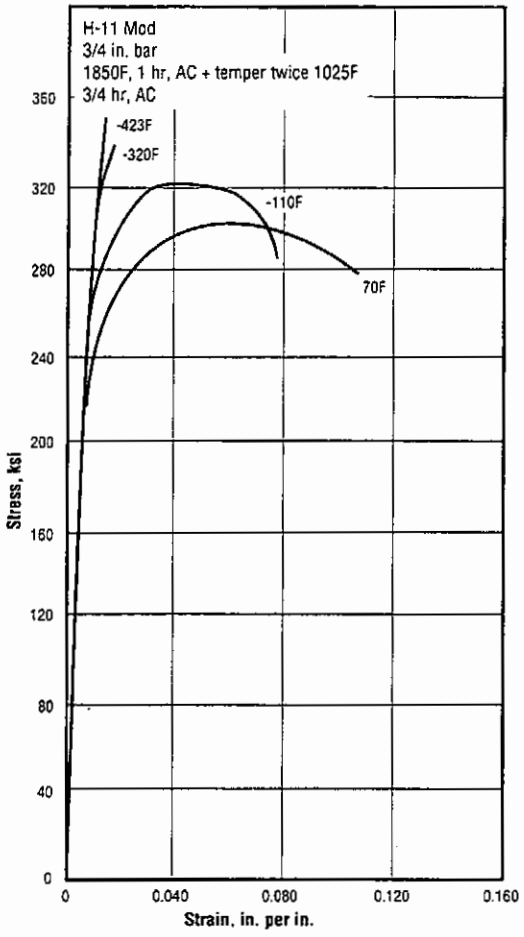


Fig. 3.3.1.5 Stress-strain curves at room and low temperatures for bar (Ref. 67)

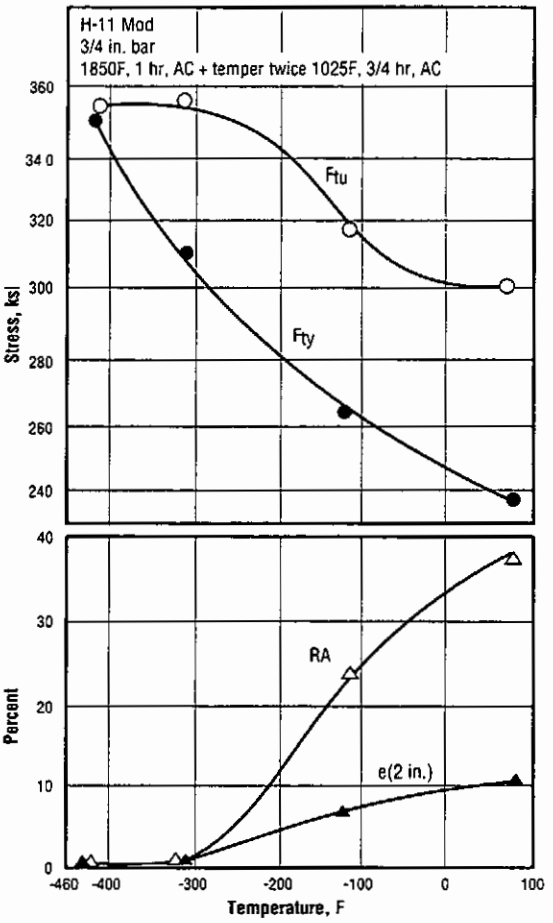


Fig. 3.3.1.6 Effect of low test temperature on tensile properties of bar. (Ref. 67)

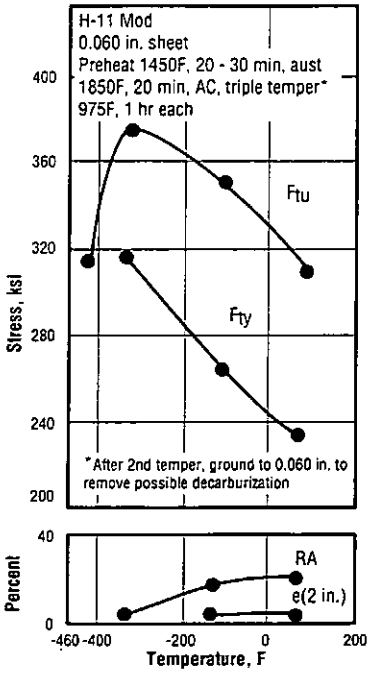


Fig. 3.3.1.7 Effect of low test temperature on tensile properties of sheet (Ref. 26)

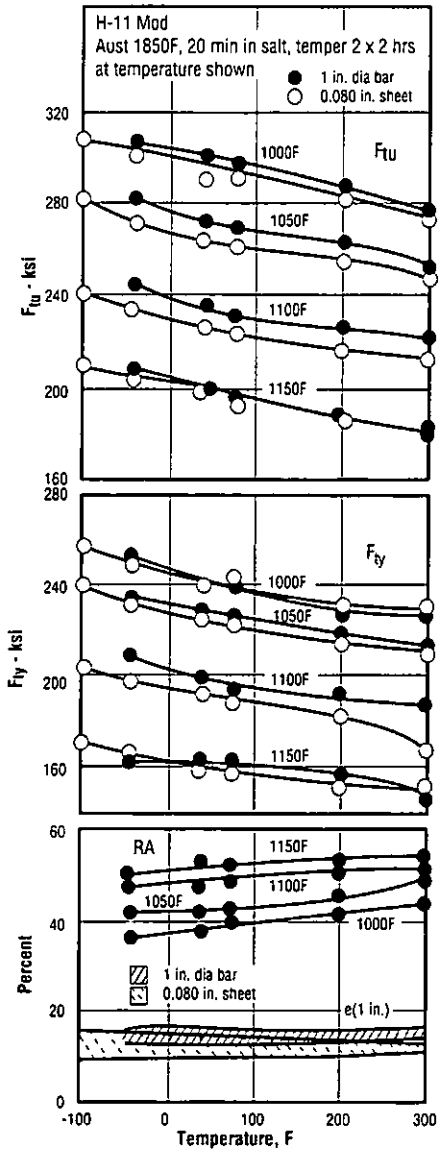


Fig. 3.3.1.8 Effect of test temperature on tensile properties for tempering temperatures of 1000 to 1150F of bar and sheet (Ref. 30)

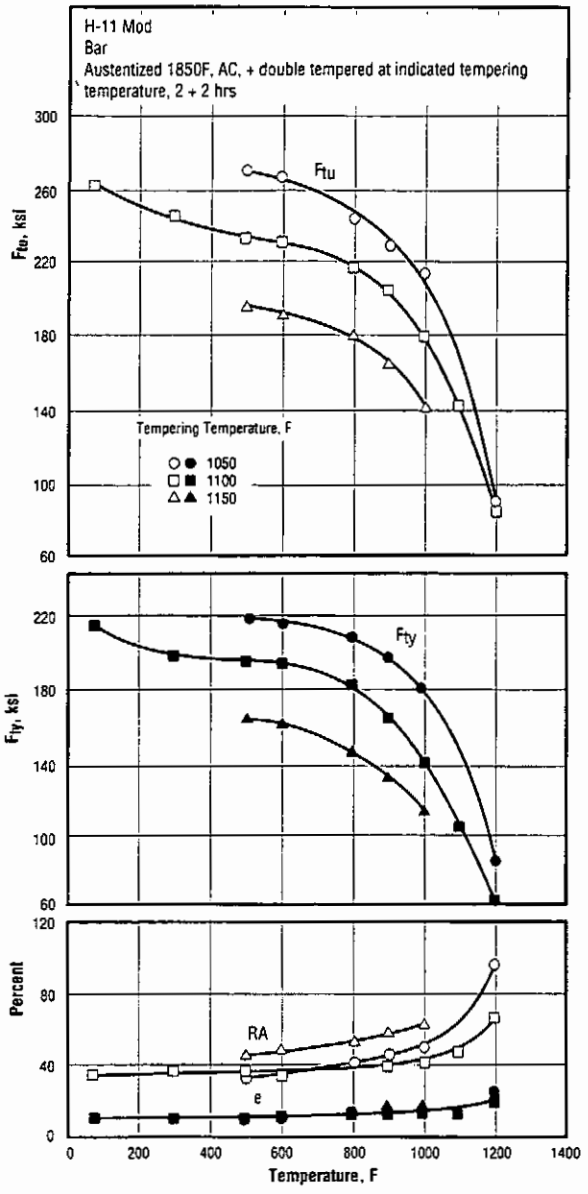


Fig. 3.3.1.9 Effects of test temperature and tempering temperature on tensile properties of bar (Ref. 81)

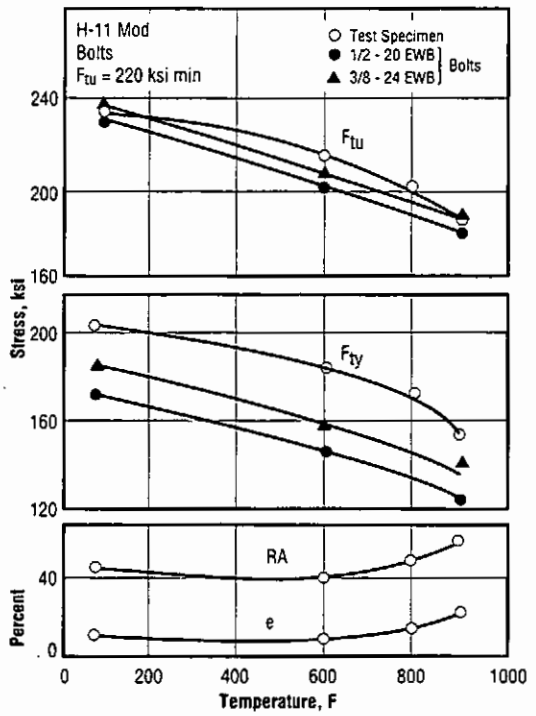


Fig. 3.3.1.10 Effect of test temperature on tensile properties of bolts heat treated to F_{tu} = 220 ksi minimum (Ref. 10)

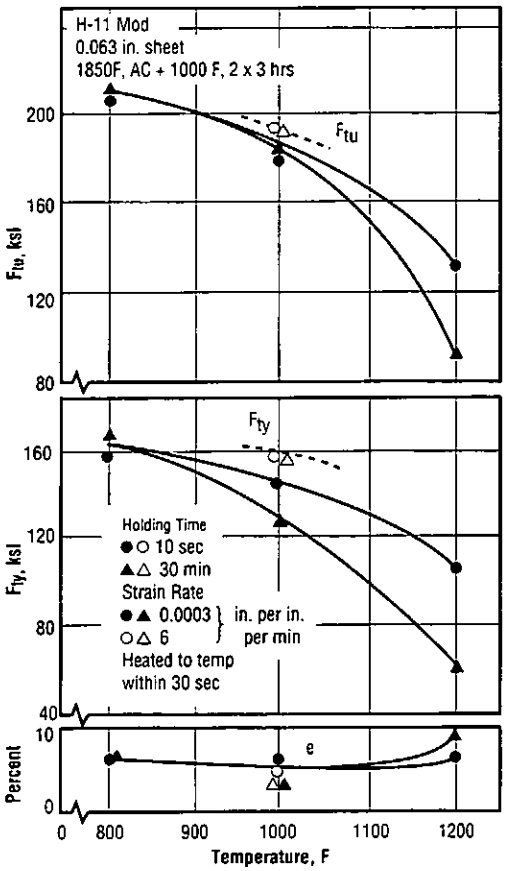


Fig. 3.3.1.11 Effects of test temperature, holding time and strain rate on tensile properties of sheet (Ref. 20)

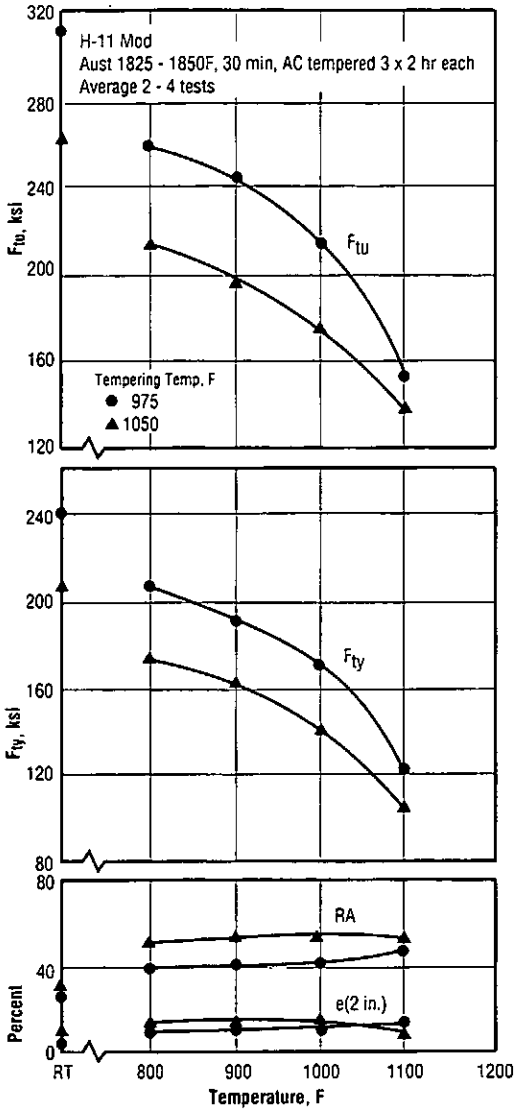


Fig. 3.3.1.12 Effect of test temperature on tensile properties of air melt alloy tempered to F_{tu} = 260 ksi and 310 ksi (Ref. 22)

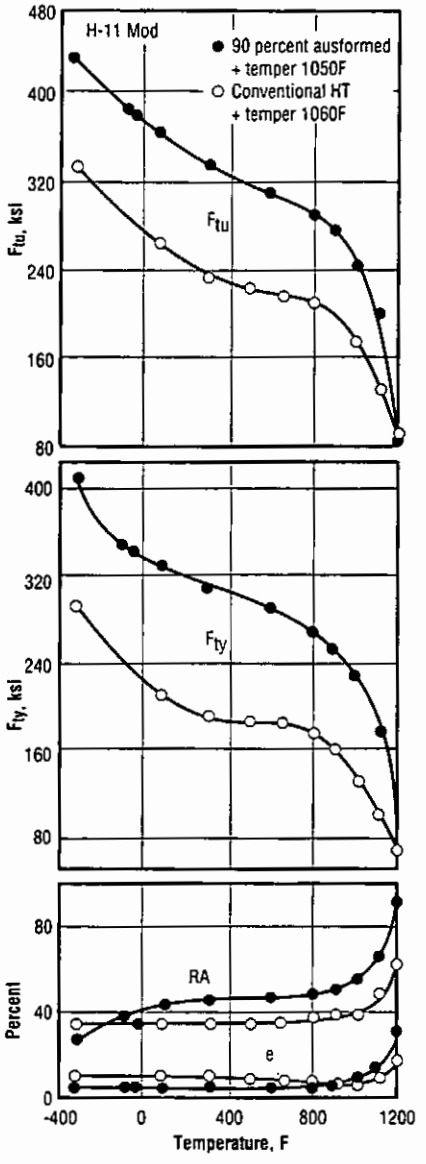


Fig. 3.3.1.13 Effect of test temperature on tensile properties of ausformed and conventionally heat treated steel (Ref. 37)

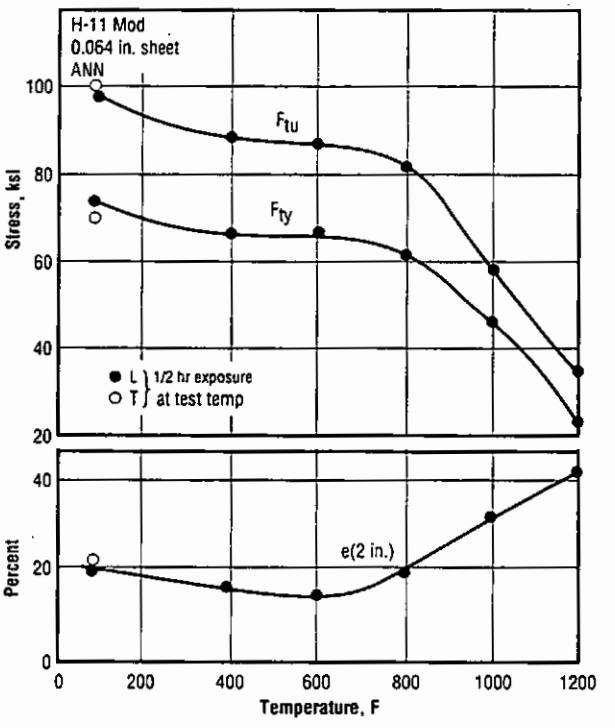


Fig. 3.3.1.14 Effect of test temperature on tensile properties of annealed sheet (Ref. 34)

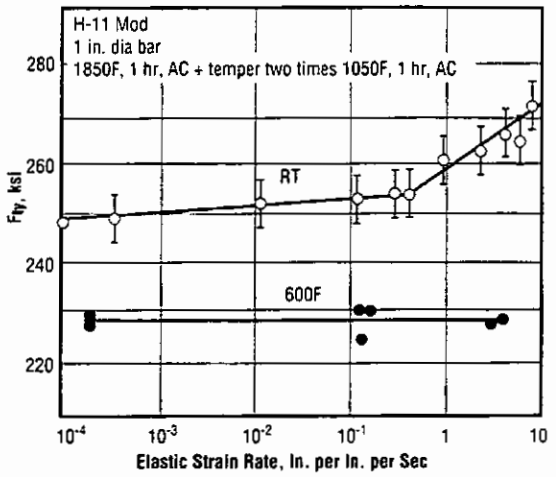


Fig. 3.3.1.15 Effect of elastic strain rate on yield stress at RT and 600F (Refs. 65, 66)

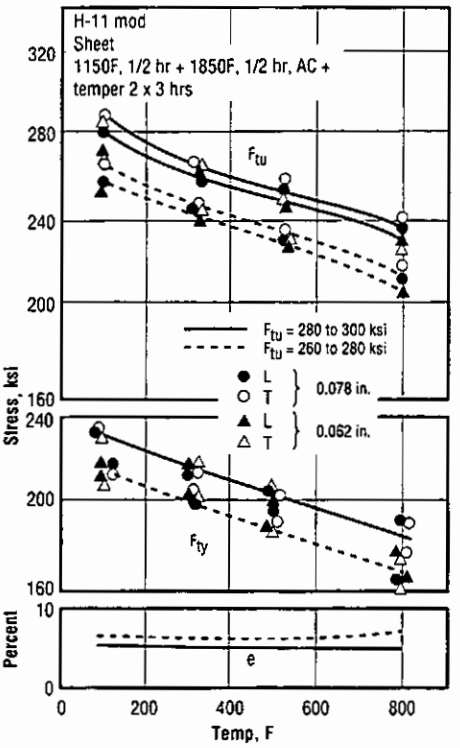


Fig. 3.3.1.16 Effect of test temperature on tensile properties of sheet heat treated to F_{tu} = 260 and 280 ksi minimum (Refs. 4, 5)

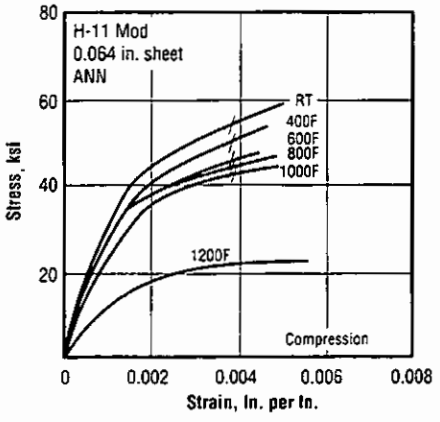


Fig. 3.3.2.1 Stress-strain curves in compression at room and elevated temperatures for annealed sheet (Ref. 34)

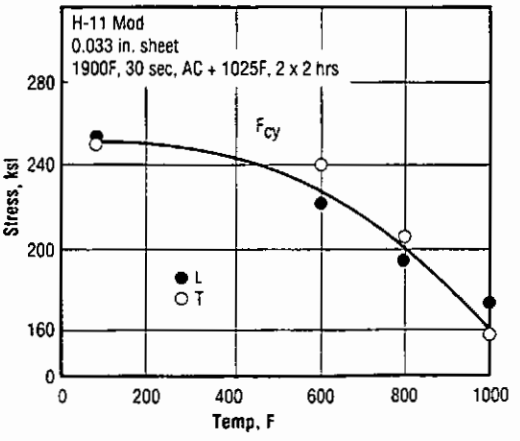


Fig. 3.3.2.2 Effect of test temperature on compressive yield strength of sheet (Ref. 7)

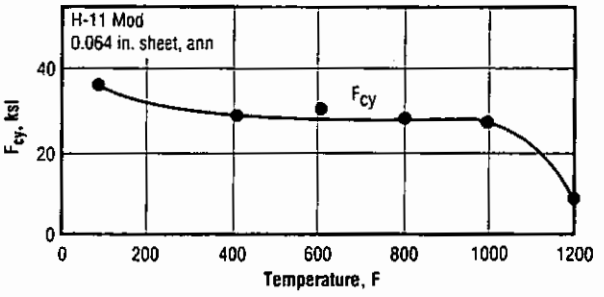


Fig. 3.3.2.3 Effect of test temperature on compressive yield strength of annealed sheet (Ref. 34)

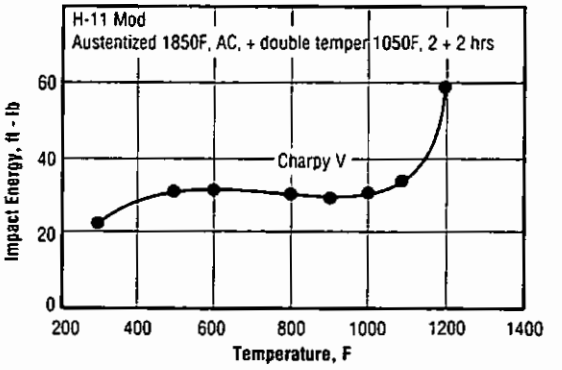


Fig. 3.3.3.1 Effect of temperature on Charpy impact energy of bar (Ref. 81)

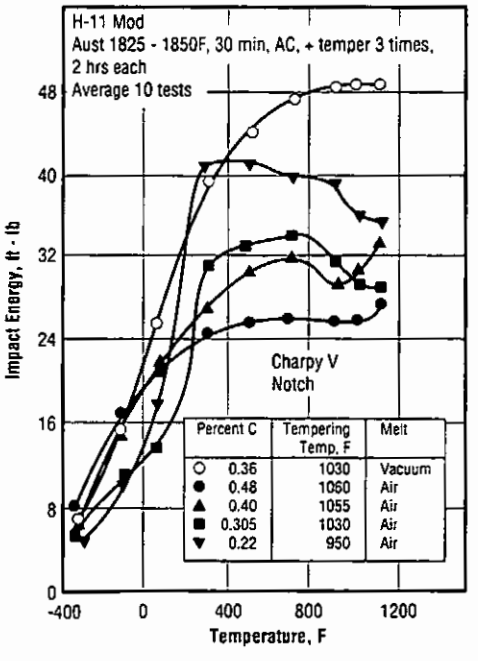


Fig. 3.3.3.2 Effect of carbon content and test temperature on Charpy impact strength of air melt and vacuum melt alloy (Ref. 22)

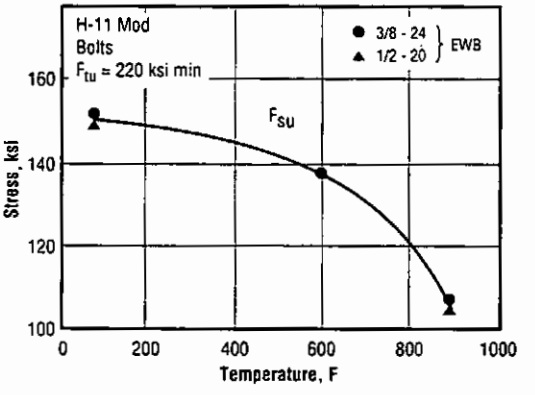


Fig. 3.3.5.1 Effect of test temperature on shear strength of heat treated bolts (Ref. 10)

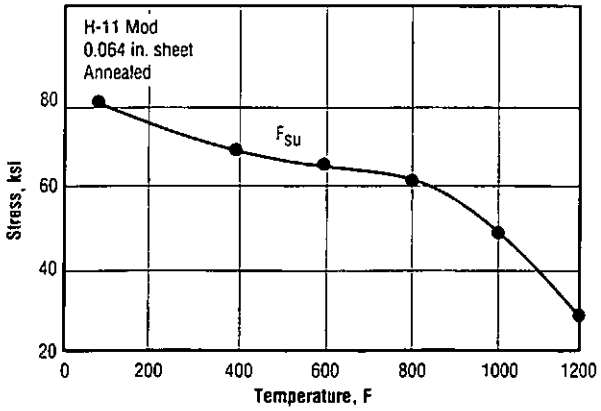


Fig. 3.3.5.2 Effect of test temperature on shear strength of annealed sheet (Ref. 34)

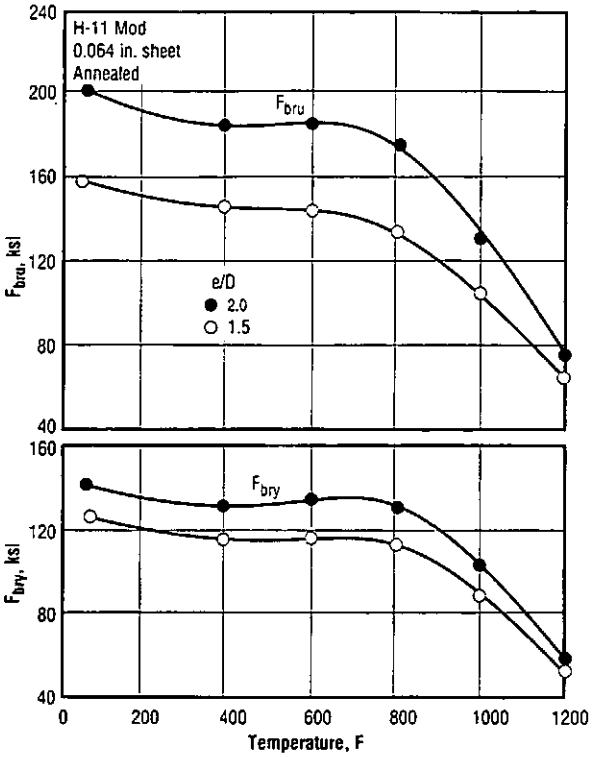


Fig. 3.3.6.1 Effect of test temperature on bearing properties of annealed sheet (Ref. 34)

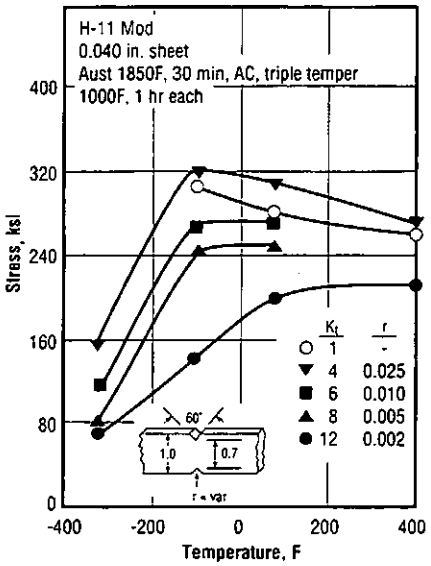


Fig. 3.3.7.1.1 Effect of test temperature on notch strength for various stress concentration factors of sheet (Ref. 15)

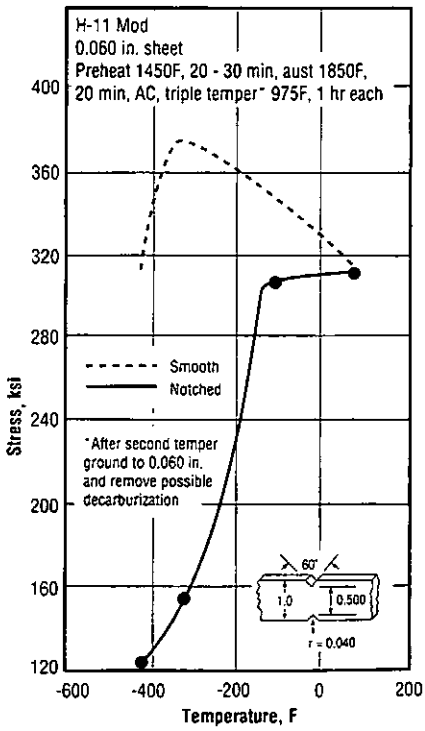


Fig. 3.3.7.1.2 Effect of low test temperature on notch strength of sheet (Ref. 26)

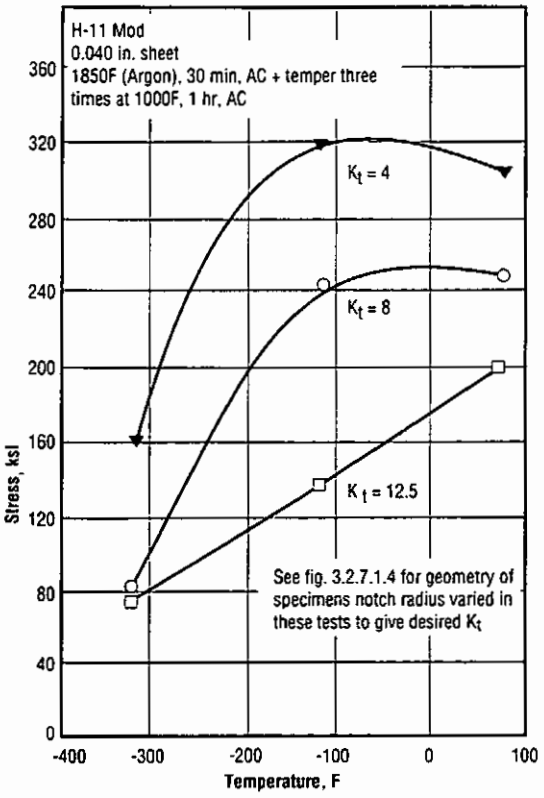


Fig. 3.3.7.1.3 Effect of low test temperature on notch tensile strength for stress concentration factors from 4 to 12.5 (Ref. 15)

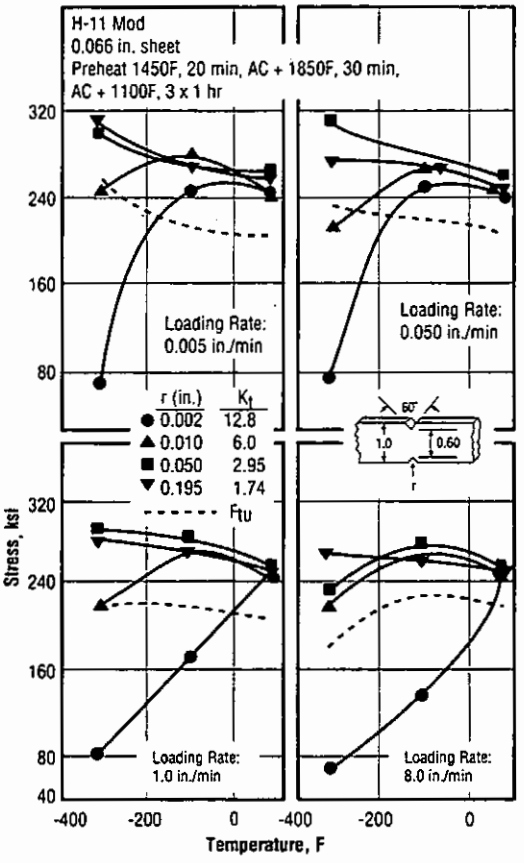


Fig. 3.3.7.1.4 Effect of low temperatures, loading rates and stress concentration factors on notch strength of sheet (Ref. 29)

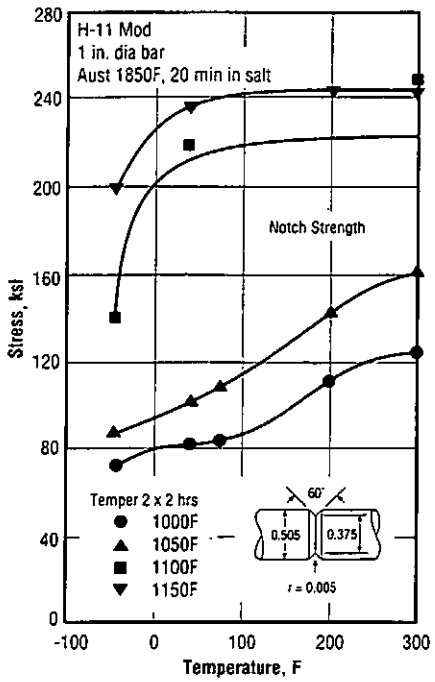


Fig. 3.3.7.1.5 Effect of low test temperature and tempering temperature on notch strength of bar (Ref. 30)

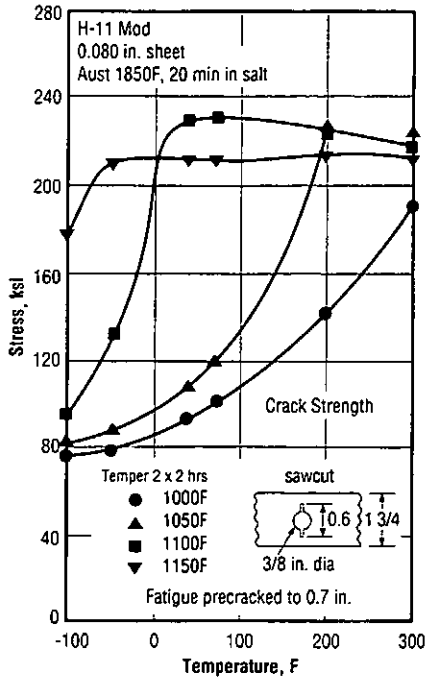


Fig. 3.3.7.1.6 Effect of low test temperature on crack strength of sheet (Ref. 30)

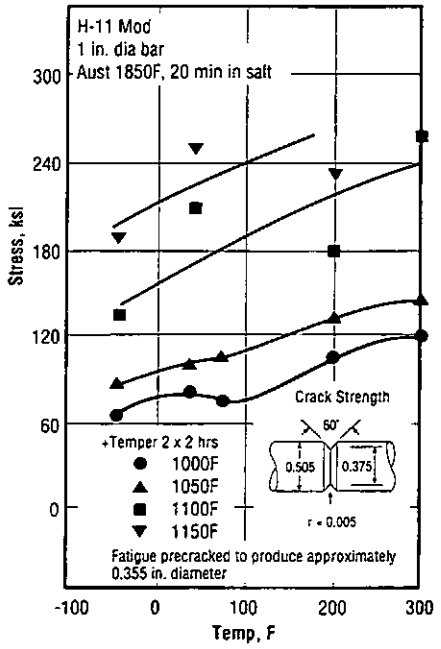


Fig. 3.3.7.1.7 Effect of low test temperature and tempering temperature on crack strength of bar (Ref. 30)

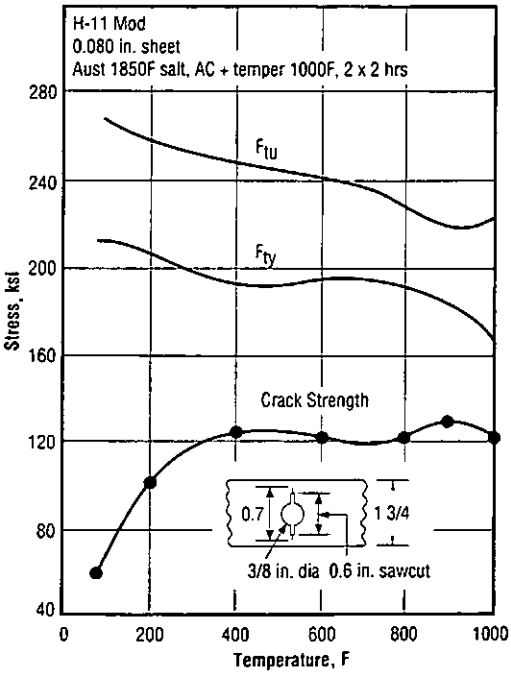


Fig. 3.3.7.1.8 Effect of test temperature on crack strength of sheet (Ref. 35)

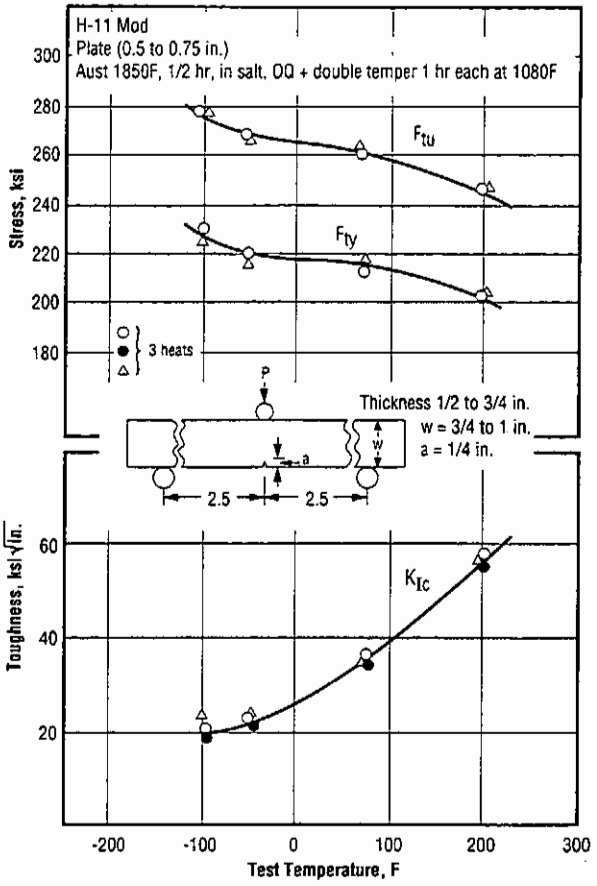


Fig. 3.3.7.2.1 Effect of test temperature on smooth specimen tensile properties and on fracture toughness of plate (Ref. 42)

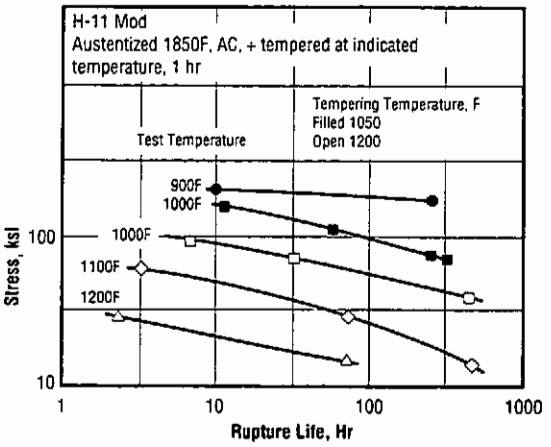


Fig. 3.4.1 Creep rupture behavior at 900 to 1200F for two tempering temperatures (Ref. 81)

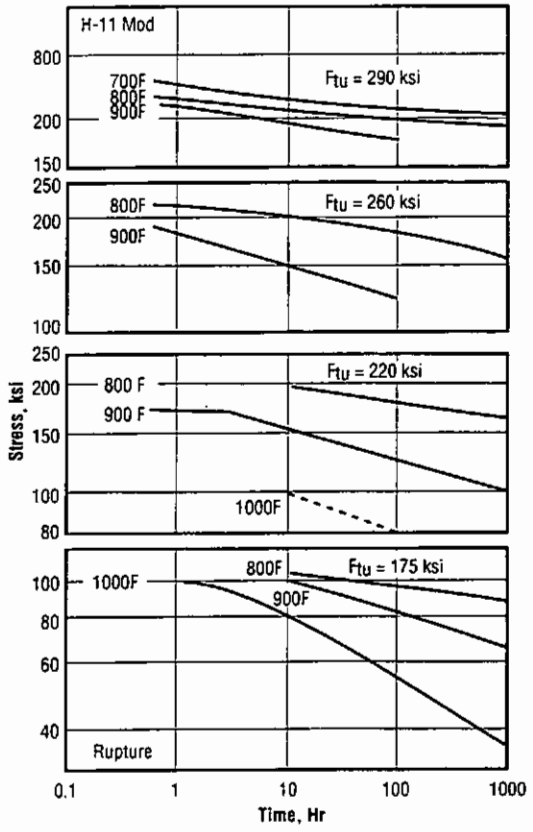


Fig. 3.4.2 Creep rupture curves for alloy at various strength levels at 700 to 1000F (Ref. 8)

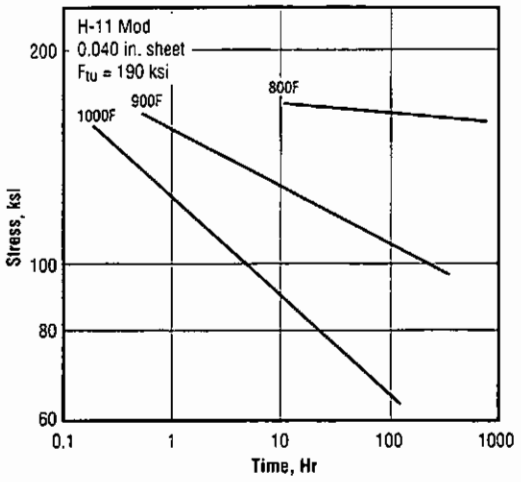


Fig. 3.4.3 Creep rupture curves at 800 to 1000F for sheet heat treated to F_{tu} = 190 ksi (Ref. 8)

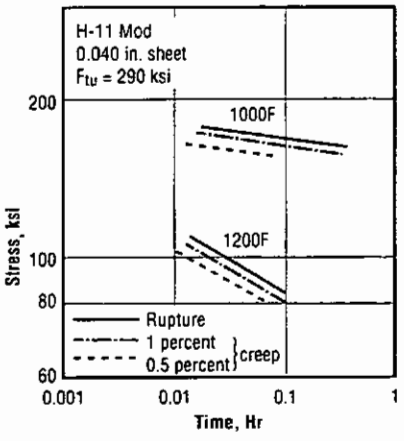


Fig. 3.4.4 Short time creep and creep rupture curves at 1000 and 1200F for sheet heat treated to F_{tu} = 290 ksi (Ref. 20)

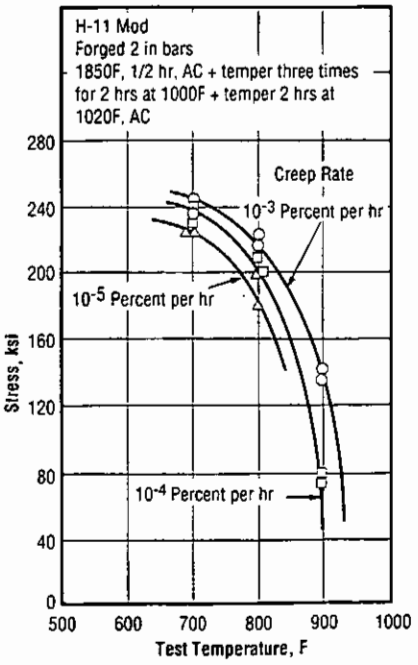


Fig. 3.4.5 Stress to produce creep rates of 10^{-3} to 10^{-5} percent per hr at 700 to 900F (Ref. 44)

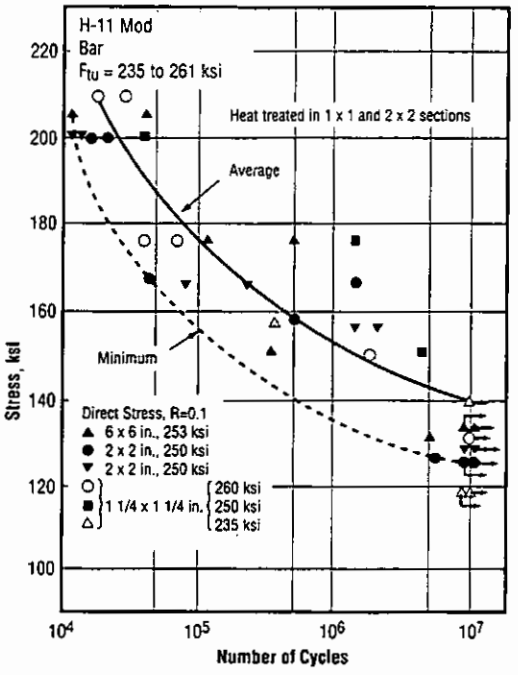


Fig. 3.5.1.1 S-N curves for heat treated bar (Ref. 12)

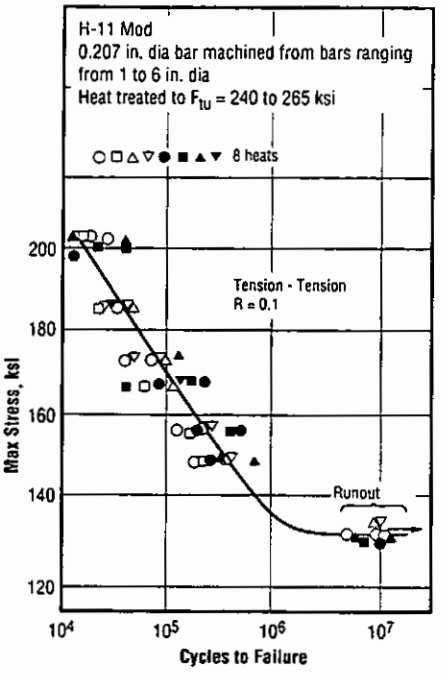


Fig. 3.5.1.2 Fatigue scatter band for bar specimens from eight separate heats tested in axial tension (Ref. 61)

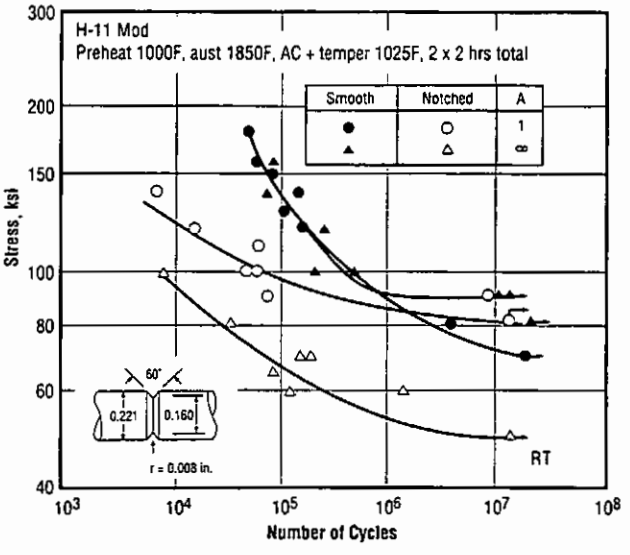


Fig. 3.5.1.3 S-N curves for notched and smooth specimens at room temperature (Ref. 28)

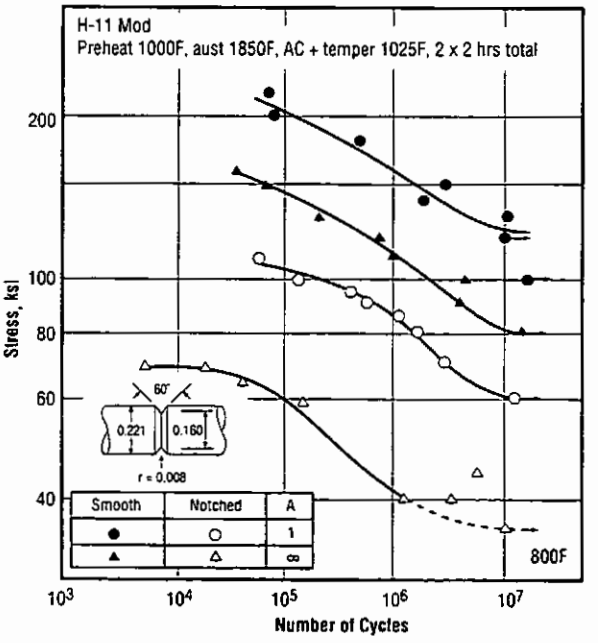


Fig. 3.5.1.4 S-N curves for notched and smooth specimens at 800F (Ref. 28)

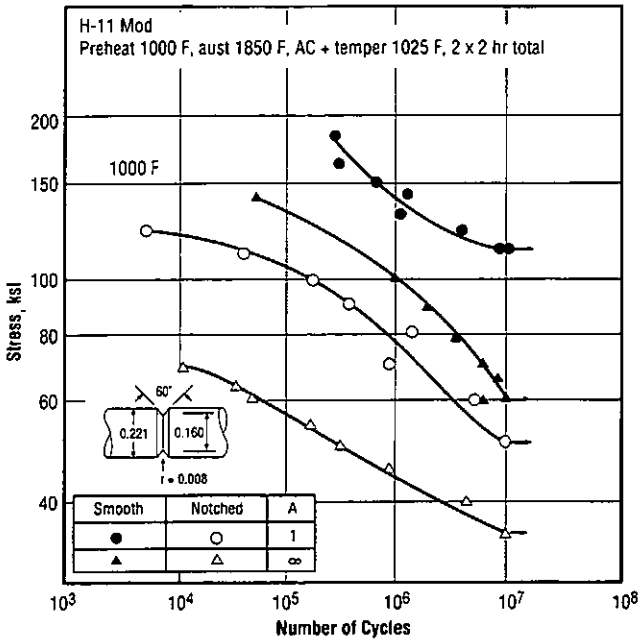


Fig. 3.5.1.5 S - N curves for notched and smooth specimens at 1000 F (Ref. 28)

Table 3.5.1.6 Fatigue properties of bar and bolts (Refs. 6-10, 12)

Alloy: H-11 Mod									
Form	**Bar**								
Condition	**Heat treated to F_{tu} = 260 ksi**								
Temp (F)	**Source**	**Method**	**Stress Ratio**		**Stress Concentration**	**Fatigue Strength (ksi) at Cycles**			
			A	**R**		**10^5**	**10^6**	**10^7**	**10^8**
RT	(7)	Rot bend	∞	-1	Smooth K_t=1	155	135	130	130
RT	(6)	Direct stress	0.82	0.1		155	135	130	130
	(10)					173	150	140	-
900	(6)					95	82	80	-
RT (a)	(6)					100	60	53	-
Form	**Threaded bolts**								
Condition	**Heat treated to F_{tu} = 260 ksi**								
Temp (F)	**Dia (in.) (b)**	**Method**	**Stress Ratio**		**Stress Concentration**	**Fatigue Strength (ksi) at Cycles**			
			A	**R**		**10^5**	**10^6**	**10^7**	**10^8**
RT	3/8	Direct stress	0.82	0.1		112	84	80	-
	1/2					118	94	90	-
900	3/8					91	81	80	-
RT (a)	3/8					95	60	55	-

(a) Tested at RT after exposure at 900F, 100 hr.
(b) Bolt types 3/8 in., 24 EWB: 1/2 in., 20 EWB.

Table 3.5.1.7 Tensile and fatigue properties at room temperature and at -320F for bolts machined from bar heat treated to 240 ksi yield strength (Ref. 60)

Alloy: H-11 Mod		
Form	**Smooth bar and 1/2 x 20 aircraft bolt**	
Condition	**Unspecified heat treatment to obtain tensile properties shown**	
Test temp.	**70F**	**-320F**
Material F_{tu} (ksi)	279	302
Material F_{ty} (ksi)	240	263
e, 4D (percent)	11.5	10.2
RA (percent)	42	39
Charpy impact (a) (ft lbs)	5	1.5
Bolt F_{tu} (ksi)	280	297
Bolt, fatigue cycles at 135 ksi max. stress, R = 0	100,000	65,000

(a) Subsize specimen per ASTM E 23, Type W.

Table 3.5.1.8 Tensile and fatigue properties of bolts made from material heat treated to several strength levels (Ref. 60)

Alloy: H-11 Mod			
Form	**Smooth bar and 1/2 x 20 aircraft bolt**		
Condition	**Unspecified heat treatments to obtain tensile properties shown**		
	A	**B**	**C**
Material F_{tu} (ksi)	197.7	236.8	288
Material F_{ty} (ksi)	158.2	199.4	243.7
e, 4D (percent)	15.5	13.5	12.1
RA (percent)	47.7	48.3	41.4
Notch ratio at K_t = 6	1.4	1.3	1.1
Bolt F_{tu} (ksi)	198	239	288.4
Fatigue cycles at max. stress approx. 1/2 F_{tu} (a), R = 0	321,100	417,600	700,000

(a) 93 ksi for A, 115 ksi for B, 135 ksi for C.

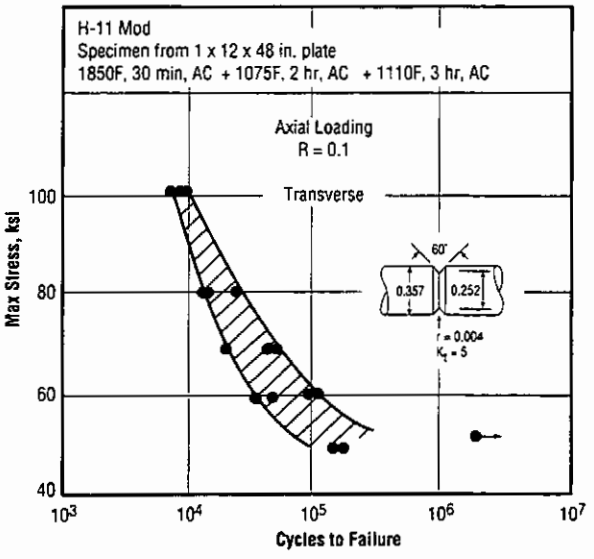


Fig. 3.5.1.9 Low cycle fatigue of notched (K_t = 5.0) specimens cut from large place. (Ref. 70)

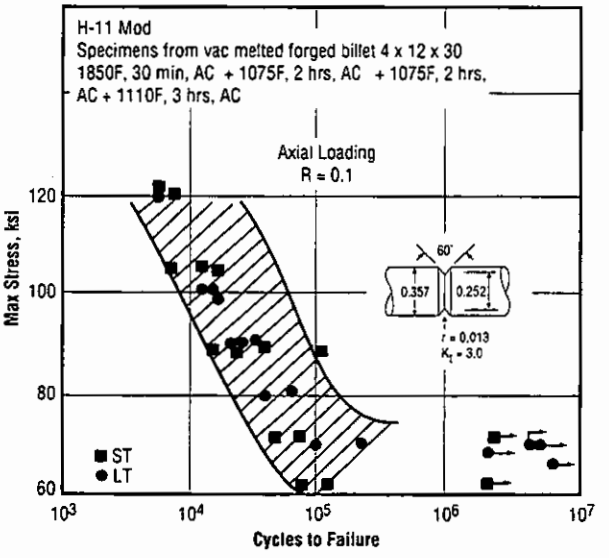


Fig. 3.5.1.10 Low-cycle fatigue of notched (K_t = 3.0) specimens cut from long and short transverse directions of forging (Ref. 70)

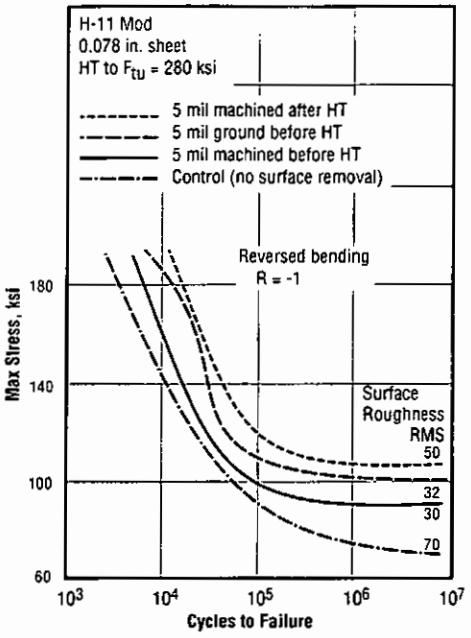


Fig. 3.5.1.11 Effect of surface machining and grinding (to remove decarburized layer) on reversed bending fatigue of sheet (Ref. 72)

Table 3.5.1.12 Fatigue strength at 10^6 cycles in rotating bending for vacuum and air melted alloy in various conditions of surface treatment after exposure to elevated temperature (Ref. 39)

Alloy: H-11 Mod							
Form	**Rot. beam spec. from 6 in. square air melt or CVM billet**						
Condition (a)	**CVM: F_{tu} = 272 ksi, F_{ty} = 228 ksi, e = 7 percent Air Melt: F_{tu} = 264 ksi, F_{ty} = 222 ksi, e = 7 percent**						
	10^6 cycle. Endurance limits (ksi) at 75F after 4 hr exposure at temperature indicated						
		75F	**375F**	**500F**	**750F**	**1000F**	**1250F**
Polished	Air	91	91	88	85	81	64
	Vac	94	93	90	90	90	80
Cr plated (0.002 in.)	Air	54	-	-	74	80	-
	Vac	56	60	63	80	87	-
Peened (b)	Air	90	87	-	-	82	66
	Vac	96	94	90	89	89	80
Plated & Peened	Air	89	88	87	83	76	72
	Vac	96	94	90	89	88	80
Peened & Plated	Vac	96	-	-	-	87	-

(a) 1850F, 45 min, AC, + double temper 1050F, 2 hr, AC.
(b) .009 to .010A (on Almen Scale, refers to height of arc of standard strip specimen after being subjected to similar peening on one side only).

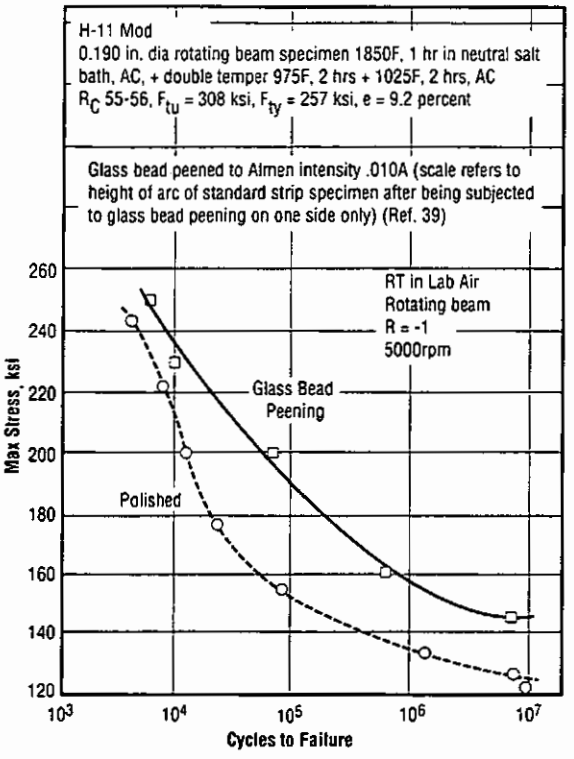


Fig. 3.5.1.13 S-N curves in rotating beam bending for smooth specimens and for specimens subjected to glass bead peening (Ref. 39)

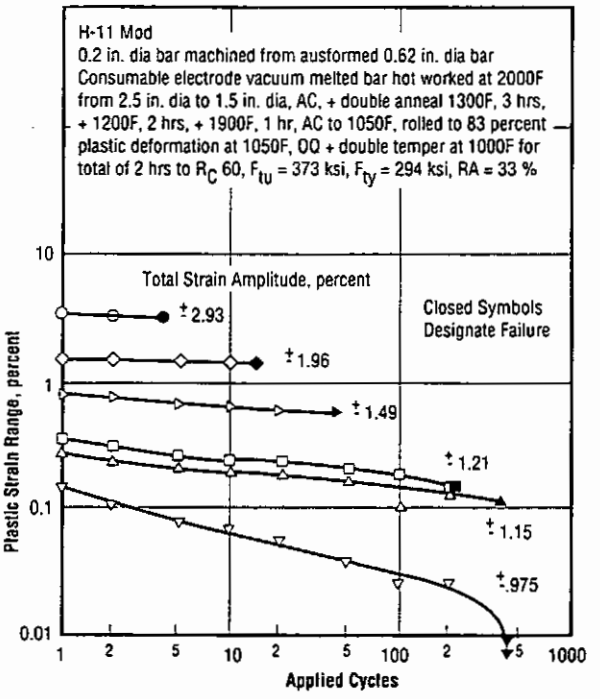


Fig. 3.5.1.14 Cyclic strain hardening in ausformed bar as manifested by reduction in plastic strain range (increase in elastic strain range) as cycles are increased during strain cycling tests in which total strain amplitudes are maintained constant (Ref. 64)

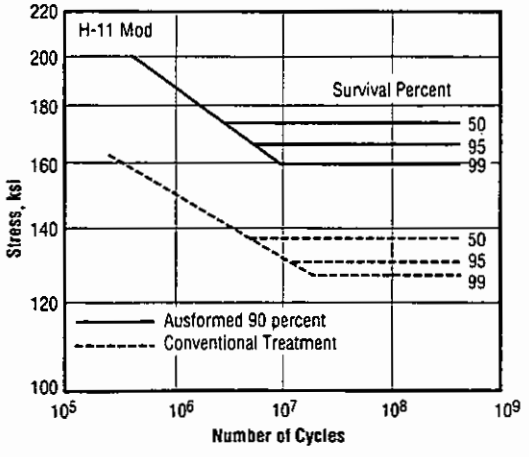


Fig. 3.5.1.15 S-N curves for ausformed and conventionally heat treated steel (Ref. 37)

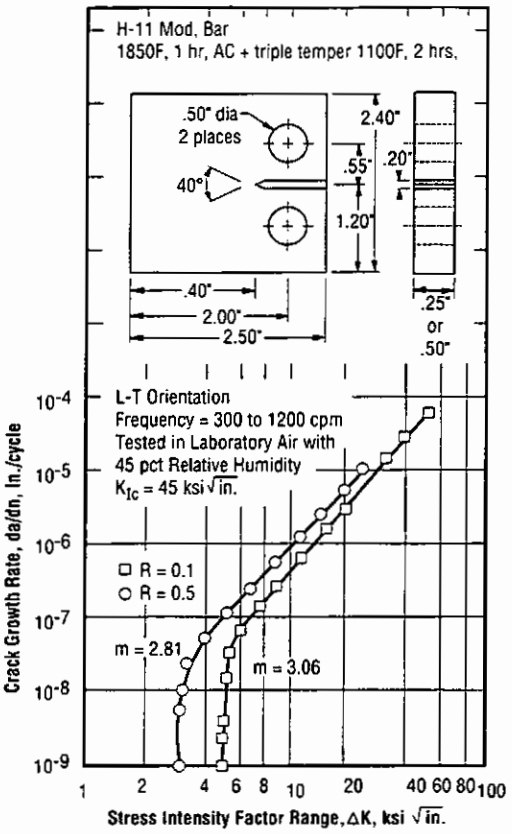


Fig. 3.5.2.2 Fatigue crack growth rates in air at room temperature (Ref. 97)

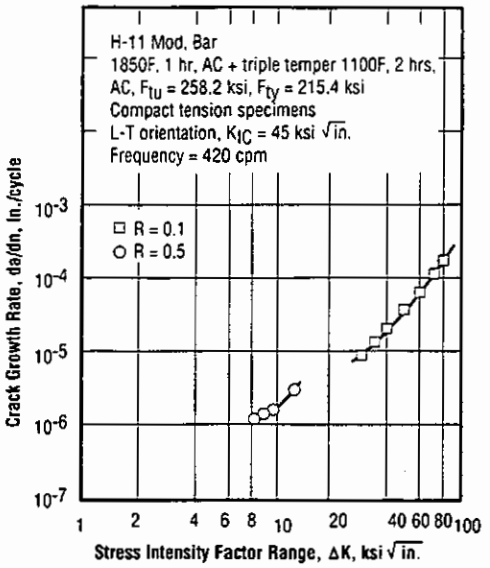


Fig. 3.5.2.3 Fatigue crack growth rates in air at 650F (Ref. 100)

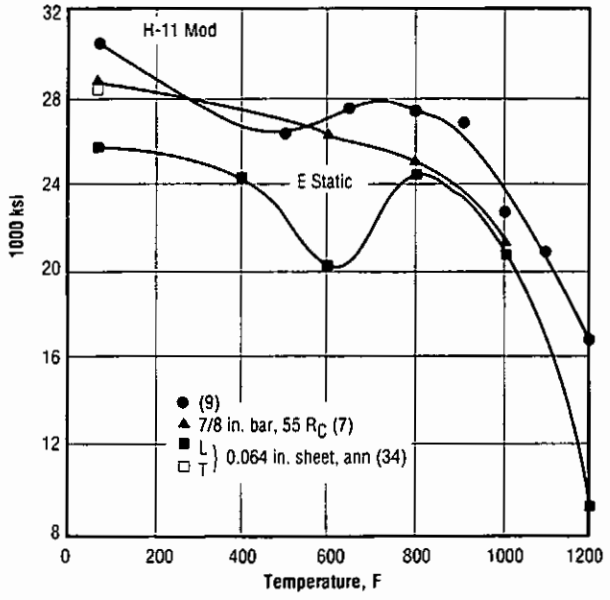


Fig. 3.6.2.1 Modulus of elasticity at room and elevated temperatures (Refs. 7, 9, 34)

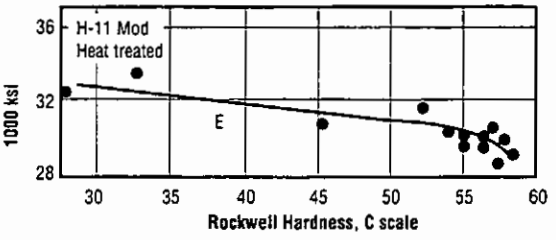


Fig. 3.6.2.2 Modulus of elasticity for alloy heat treated to various hardness levels (Ref. 9)

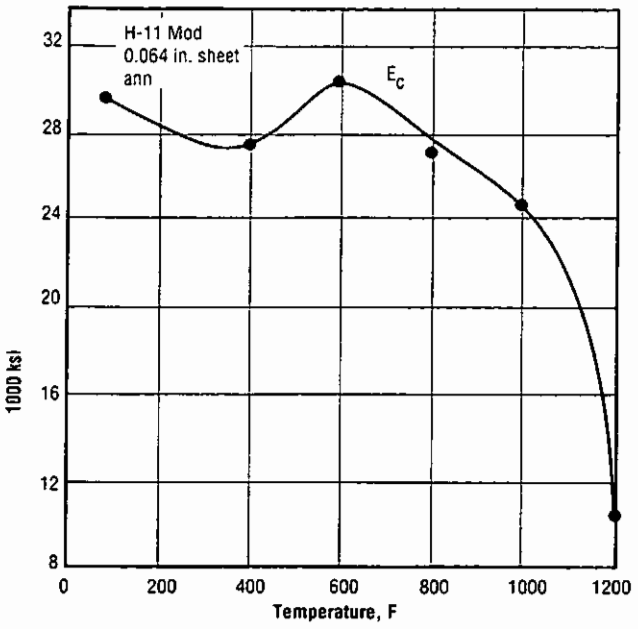


Fig. 3.6.2.3 Modulus of elasticity in compression at room and elevated temperatures for annealed sheet (Ref. 34)

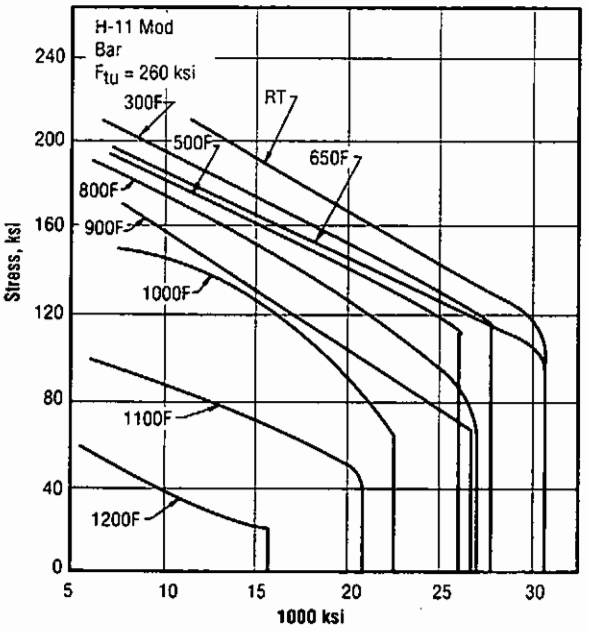


Fig. 3.6.4.1 Tangent modulus curves at room and elevated temperatures for bar heat treated to F_{tu} = 260 ksi (Ref. 11)

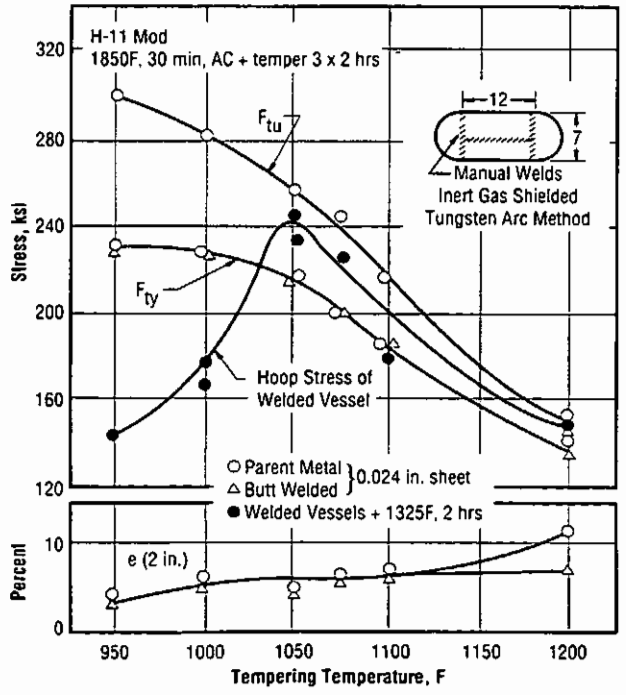


Fig. 4.3.2 Effect of tempering temperature on strength of welded sheet and pressure vessels (Ref. 21)

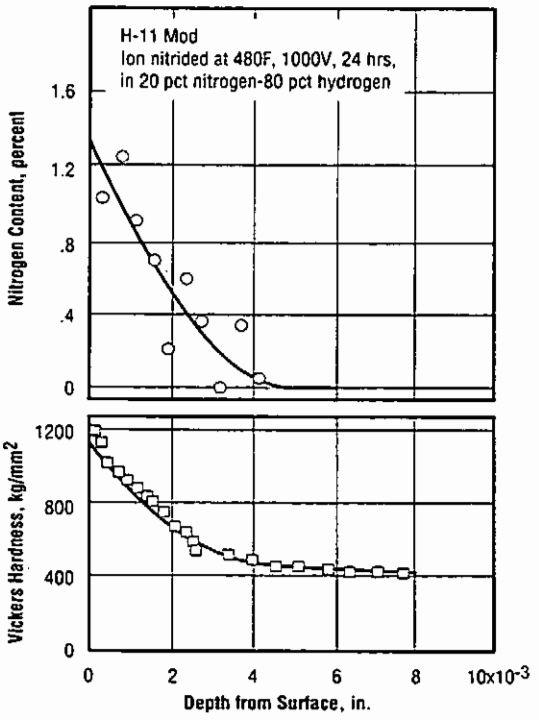


Fig. 4.4.5 Nitrogen content and hardness profiles for ion-nitrided H-11 Mod (Ref. 99)

References

1. AMS 6437A (January 31, 1964; replaced by Ref. 77).
2. AMS 6485B (May 1, 1969; replaced by Ref. 78).
3. AMS 6487C (May 1, 1968; replaced by Ref. 79).
4. North American Aviation, Inc., Columbus Div., "Thermold A, Thermold J and Vascojet 1000 Steel Sheet Evalution," Rep. No. NA 58H-302 (July 22, 1958).
5. North American Aviation, Inc., Columbus Div., "Thermold J and Vascojet 1000 Bar and Billet Evalution," Rep. No. NA 58 H-416 (October 9, 1958).
6. Vanadium Alloys Steel Co., "Inspection Results on Vascojet 1000 Billets for North American Aviation," Data Sheet (September 1959).
7. Allegheny Ludlum Steel Corp., "AISI H 11 or Potomac A," Data Sheet (September 1959).
8. Crucible Steel Co. of America, "Crucible 218, Martensitic Type High Temperature Steel" (May 1958).
9. Vanadium Alloys Steel Co., "Vascojet 1000 for Ultra High Strength Structural Requirements" (1959).
10. Baumgartner, T., Standard Pressed Steel Co., Rep. No. 86 (May 1957).
11. Vanadium Alloys Steel Co., "Mechanical and Physical Properties of Vascojet 1000," Data Sheet (November 4, 1958).
12. Boder, N., and Simkovich, E. A., "Tension-Tension Fatigue Properties of 5Cr-Mo-V Steel Bar Heat Treated to the 220 - 270 ksi Ultimate Tensile Strength Range," Republic Aviation Corp., ERMR 387G (May 19, 1958).
13. Espey, G. B.; Jones, M. H.; and Brown, W. F., Jr., "The Sharp Edge Notch Tensile Strengths of Several High-Strength Steel Sheet Alloys," *Proceedings* of the ASTM, Vol. 59 (1959).
14. Srawley, J. E., and Beachem, C. D., "Crack Propagation Tests of Some High Strength Sheet Steels," NRL Rep. 5263 (January 10, 1959).
15. Sachs, G., and Sessler, J. G., "Effect of Stress Concentration on Tensile Strength of Titanium and Steel Alloy Sheet at Various Temperatures," ASTM, STP No. 287 (1960).
16. Cameron Iron Works, Inc., Houston, TX, "Report on Evaluation of the Forgeability and Mechanical Properties of Vascojet 1000 Alloy," Project ZAX-14, ZCLR-154 (1958).
17. Shannon, J. L., Jr.; Espey, G. B.; Repko, A. J.; and Brown, W. F., Jr., "Effect of Carbon Content and Melting Practice on Room Temperature Sharp Edge Notch Tensile Characteristics of H-11 Modified and 300M Sheet Steels," *Proceedings* of the ASTM, Vol. 60 (1960).
18. AiResearch (1958).
19. Cleveland Pneumatic Tool Co. (1958).
20. International Nickel Co. (1958).
21. Baloga, M., "Effect of Heat Treatment Variations on the Bursting Strength of Thin Walled Pressure Vessels Fabricated from Vascojet 1000 Steel," Martin Co., Rep. No. ER-10121-5 (September 1958).
22. Hamaker, J. E., Jr., and Vater, E. J., "Carbon Strength Relationships on 5 Percent Chromium Ultra High Strength Steels," *Proceedings* of the ASTM, Vol. 60 (1960).
23. American Iron and Steel Institute, "High Temperature High Strength Alloys" (February 1963).
24. Crucible Steel Company, "Halcomb 218 Hot Work Steel," Data Sheet No. 4 (October 1962).
25. Adams, J. G., "The Determination of Spectral Emissivities Reflectivities and Absorptivities of Materials and Coatings," Northrop Corporation Report No. Nor. 61-189 (August 3, 1961).
26. Rice, L. P.; Cambell, J. E.; and Simmons, W. F., "Evaluation of the Effects of Very Low Temperature on Properties of Aircraft and Missile Metals," WADD TR 60-214 (February 1960).
27. "Fracture Testing of High Strength Sheet Materials," 3rd Report of a Special ASTM Committee Materials Research and Standards, Vol. 1 (November 1961).
28. Brodrick, R. F., "Fatigue and Dynamic Creep of High Strength Steels," ASD TDR-62-480 (August 1962).
29. Brisbane, A. W., "The Investigation of the Effects of Loading Rate and Stress Concentration Factors on the Notch Properties of Three Sheet Alloys at Subzero Temperatures," ASD TDR-62-930 (March 1963).
30. Hanna, G. L., and Steigerwald, E. A., "Fracture Characteristics of Structural Metals," Final Summary Technical Report ER-5426, TAPCO Division Thompson Ramo Wooldridge, Inc. (June 30, 1963).
31. Martin, C. F.; Gerberich, W. W.; McCamont, J. M.; and Harmon, K. L., "Research in the Mechanism of Strengthening in Ausformed Steel," ASD TDR-62-692 (February 1963).
32. Semka, R. P.; Heise, R. E.; and Ross, S. T., "Ausform Processing of Steel by Forging," ASD TR-61-428 (March 1962).
33. Banerjee, B. R., and Hauser, J. J., "Research and Application Engineering to Determine the Effect of Processing Variables in Crack Propagation of High-Strength Steels and Titanium," ASD TDR-62-1034, Part 1 (April 1963).
34. Henning, R. G., and Brisbane, A. W., "Mechanical Properties of AM 350, Potomac A, Potomac M, and Vasco Jet-1000 Steel Alloys in the Annealed Condition," ASD TDR-63-116 (May 1963).
35. Steigerwald, E. A., and Hanna, G. L., "Strain Aging and Delayed Failure in High-Strength Steels," ASD TDR-62-968 (November 1962).
36. Yount, R. E., "Determination of Engineering Propertiesof Mar-Strained Steels," ASD TDR-62-230 (August 1962).

37. Justusson, W. M., and Zackay, V. W., "Engineering Properties of Ausformed Steel," *Metal Progress*, Vol. 82, No. 6 (December 1962).

38. Allegheny Ludlum Steel Corp., "Potomac A, Hot Work and Structural Steel AISI Type H-11" (1972).

39. Campbell, J. E., "Shot Peening for Improved Fatigue Properties and Stress-Corrosion Resistance," MCIC Report 71-02 (December 1971).

40. Bucher, J. H.; Powell, G. W.; and Spretnak, J. W., "A Micrographic Analysis of Fracture Surfaces in Some Ultra-High-Strength Steels," in *Application of Fracture Toughness Parameters to Structural Metals*, H. D. Greenberg, ed., AIME Metallurgical Soc. Conf., Vol. 31 (1966).

41. Johnson, H. H., and Willner, A. M., "Moisture and Stable Crack Growth in a High Strength Steel," *Applied Materials Research*, pp. 34-40 (January 1965).

42. Steigerwald, E. A., "Plane Strain Fracture Toughness for Handbook Presentation," AFML-TR-67-187 (July 1967).

43. Chait, R., "Factors Influencing the Strength Differential in High Strength Steels," *Met. Trans.*, Vol. 3, pp. 365-371 (February 1972).

44. VanEcho, J. A., and Simmons, W. F., "Supplemental Report on the Elevated Temperature Properties of Chromium-Molybdenum Steels," ASTM Data Series Publication No. DS 6S1 (June 1966).

45. Carman, C. M., and Katlin, J. M., "Low Cycle Fatigue Crack Propagation Characteristics of High Strength Steels," *Trans. ASME Jour. Basic Eng.*, Paper No. 66-Met 3 (1966).

46. Walter, R. J., and Chandler, W. T., "Effects of High-Pressure Hydrogen on Metals at Ambient Temperature," Final Report to NASA on Contract NAS8-19, Rocketdyne Report R-7780-2 (February 28, 1969).

47. Freedman, A. H., "An Accelerated Stress Corrosion Test for High Strength Ferrous Alloys," *Jour. of Materials*, Vol. 5, No. 2, pp. 431-166 (June 1970).

48. Beck, W., and Jankowsky, E. J., "Delayed Brittle Failure in Cadmium Plated Steels," *Metal Progress*, pp. 92-95 (August 1963).

49. Kalish, D.; Kulen, S. A.; and Cohn, M., "Thermomechanical Treatments Applied to Ultra High Strength Bainites," *Structure and Properties of Ultra High Strength Steels*, ASTM STP 370, pp. 172-207 (March 1965).

50. Humphries, T. S., and Nelson, E. E., "Stress Corrosion Cracking Evaluation of Several Ferrous and Nickel Alloys," NASA TMX-64511 (April 2, 1970).

51. Amateau, M. F., and Steigerwald, E. A., "Fracture Mechanics of Structural Metals," Final Report to U.S. Navy Bureau of Naval Weapons Contract NOw-64-0186 C Report No. ER 5937-3 (January 22, 1965).

52. Carter, C. S., "Stress Corrosion Crack Branching in High Strength Steels," *Engineering Fracture Mechanics*, Vol. 3, No. 1, pp. 1-14 (July 1971).

53. Wei, R. P., and Landes, J. D., "Correlation Between Sustained-Load and Fatigue Crack Growth in High-Strength Steels," ASTM MRS Vol. 9, No. 7, pp. 25-28 (July 1969).

54. Miller, G. A., "The Dependence of Fatigue Crack Growth Rate on Stress Intensity Factor and the Mechanical Properties of Some High-Strength Steels," *Trans. ASM*, Vol. 61, pp. 442-447 (1968).

55. Bert, C. W.; Mills, E. J.; and Hyler, W. J., "Mechanical Properties of Aerospace Structural Alloys Under Biaxial Conditions," AFML TR 66-229 (August 1966).

56. Benjamin, W. D., and Steigerwald, E. A., "Environmentally Induced Delayed Failures in Martensitic High Strength Steels," AFML-TR-68-80 (April 1968).

57. Groenveld, T. P.; Fletcher, E. E.; and Elsea, A. R., "A Study of Hydrogen Embrittlement of Various Alloys," Final Report of NASA, G. C. Marshall Space Flight Center, Contract NAS8-20029 (1969).

58. Manning, G. K., "Effect of Small Crack on the Load Carrying Ability of High Strength Steel," in "Evaluation of Metallic Materials in Design for Low-Temperature Service," ASTM STP 302, pp. 49-68 (1961).

59. Schaeffer, G. T., and Weiss, V., "Effect of Section Size on Notch Tensile Strength," Interim Tech. Report No. 2, University of Syracuse to Army Research Office Durham, Contract DA-31-124-ARO (D)-106 (June 1964).

60. Hood, A. C., and Sproat, R. L., "Ultra High Strength Steel Fasteners," ASTM STP 370, pp. 208-221 (1965).

61. Simkovich, E. A., and Loria, E. A., "Effect of Decarburization and Grinding Conditions on Fatigue Strength of 5 Percent Cr-Mo-V Sheet Steel," ASM Preprint No. 185 (October 17-21, 1960).

62. Jones, R. L., and Nordquist, F. C., "An Evaluation of High Strength Steel Forgings," RTD-TDR-63-4050 (May 1964).

63. Dreyer, G. A., and Gallaugher, W. C., "Investigation of the Effects of Stress Corrosion on High Strength Steel Alloys," A. F. Mat. Lab., ML-TDR-64-3 (February 1964).

64. Matheny, J. E., Jr., "Low Cycle Fatigue Properties of the Ausformed Steel," University of Illinois, T & A. M. Report No. 308 (February 1968).

65. Kendall, D. P., and Davidson, T. E., "The Effect of Strain Rate on Yielding of High Strength Steels," Watervliet Arsenal Report WVT 6618 (May 1966).

66. Kendall, D. P., "The Effect of Strain Rate and Temperature on Yielding in Steels," Watervliet Arsenal Report WVT 7061 (November 1970).

67. Warren, K. A., and Reed, R. P., "Tensile and Impact Properties of Selected Materials From 20 to 300°K," NBS Monograph 63 (June 28, 1963).

68. Hamaker, J. C., Jr., and Vater, E. J., "Carbon: Strength Relationships in 5 Percent Chromium Ultra-High Strength Steels," Preprint 800, ASTM (1960).

69. Gerberich, W. W.; Williams, A. J.; Martin, C. F.; and Heise, R. E., "Ausform Fabrication and Properties of High Strength Alloy Steel," ASTM STP 370, pp. 154-171 (1965).

70. Pratt, W. M., "Material Evaluation of H-11 High Strength Steel for F-111," General Dynamics, Fort Worth, Report N64-20060 (April 15, 1964).

71. Hanna, G. L., and Steigerwald, E. A., "Influence of Environment on Crack Propagation and Delayed Failures in High Strength Steels," A. F. Mat. Lab. Report No. RTD-TDR-63-4225 (January 1964).

72. Ruff, P. E., "Hot Work Tool Steel for Aircraft," *Metal Progress*, Vol. 75, pp. 103-107 (March 1959).

73. AMS 6488A (May 15, 1971) [See Ref. 80].

74. Banerjee, B. R., "Fracture Micromechanics in High Strength Steels," ASTM STP 370, pp. 94-120 (March 1965).

75. Kueser, P. E., "Magnetic Materials Topical Report," NASA CR 54091, Westinghouse WAED 6452E (September 1964).

76. Ketcham, S. J., "Chemical Milling of Alloy Steels," Report No. NAEC-AML-2418, U.S. Naval Air Engineering Center (March 1966).

77. AMS 6437D, Society of Automotive Engineers (Oct. 1985).

78. AMS 6485F, Society of Automotive Engineers (July 1, 1989).

79. AMS 6487F, Society of Automotive Engineers (January 1, 1990).

80. AMS 6488D, Society of Automotive Engineers (January 1, 1985).

81. Philip, T. V., and McCaffrey, T. J., "Ultrahigh-Strength Steels," 1990 Metals Handbook, 10th Ed., Vol. 1, ASM Int'l. Materials Park, OH, *Properties and Selection: Iron, Steels, and High-Performance Alloys*, pp. 430-448.

82. "Chromo-V," *Alloy Digest*, Filing Code TS-313 (February 1977).

83. "Carpenter No. 882," *Alloy Digest*, Filing Code TS-339 (October 1978).

84. "Hotform No. 2," *Alloy Digest*, Filing Code TS-394 (February 1982).

85. "Guterl H-11," *Alloy Digest*, Filing Code TS-412 (March 1983).

86. "AL Tech Potomac A," *Alloy Digest*, Filing Code TS-478 (July 1987).

87. Umemoto, M.; Ohtsuka, H.; and Tamura, I., "Transformation to Pearlite from Work-Hardened Austenite," Transactions of the Iron and Steel Institute of Japan, Vol. 23:9 (Sept. 83).

88. Kerns, G. E.; Wang, M. T.; and Staehle, R. W., "Stress Corrosion Cracking and Hydrogen Embrittlement in High Strength Steels," *Proceedings* of an Int'l. Corrosion Conference in France, pp. 700-735 (June 12-16, 1973).

89. Kroupa, K. M.; Venkatesan, P. S.; and Wood, J. D., "Fracture Toughness of H-11 Steel and Its Susceptibility to Stress Corrosion Cracking," *Engineering Fracture Mechanics*, Vol. 8, pp. 547-553 (1976).

90. Saia, R. J., and Gould, G. C., "Evaluating the Corrosivity of Manufacturing Chemicals," presented at ASME Conference on Improved Technology for Critical Bolting Applications, Chicago, IL (July 20-24, 1986).

91. Namboodhiri, T. K. G., "Measurement of Hydrogen in Metals," *Transactions of The Indian Institute of Metals*, Vol. 31, No. 6, pp. 435-438 (December 1978).

92. Powell, R. W.; Peterson, D. T.; Zimmerschied, M. K.; and Bates, J. F., "Swelling of Several Commercial Alloys Following High Fluence Neutron Irradiation," *Journal of Nuclear Materials*, Vol. 104, No. 1-3, pp. 969-973 (1981).

93. Ule, B.; Vodopivec, F.; Pristavec, M.; and Gresovnik, F., "Temper Embrittlement of Hot Work Die Steel," *Materials Science and Technology*, Vol. 6, No. 12, pp. 1181-1185 (December 1990).

94. Garrison, W. M., Jr., "Influence of Silicon on Strength and Toughness of 5 wt. Percent Chromium Secondary Hardening Steel," *Materials Science and Technology*, Vol. 3, No. 4, pp. 256-259 (April 1987).

95. Pacyna, J., "Effect of Non-Metallic Inclusions on Fracture Toughness of Tool Steels," *Steel Research*, Vol. 57, No. 11, pp. 586-592 (1986).

96. Place, T. A.; Howarth, R. A.; and Smith, N. L., "Microstructural Analysis of Toughness Anomalies in H-11 Steel," presented at ISTFA Conference on Testing and Failure Analysis, San Jose, CA (October 25-27, 1982).

97. Mackay, T. L.; Alperin, B. J.; and Bhatt, D. D., "Near-Threshold Fatigue Crack Propagation of Several High Strength Steels," *Engineering Fracture Mechanics*, Vol. 18, No. 2, pp. 403-416 (1983).

98. Pickering, F. B., "The Properties of Tool Steels for Mold and Die Applications," presented at Conference on Tool Materials for Molds and Dies: Application and Performance, St. Charles, IL (September 30-October 2, 1987).

99. Trejo-Luna, R.; Zironi, E. P.; Rickards, J.; and Romero, G., "Some Features of Low-Temperature Ion Nitriding of Steels," *Scripta Metallurgica*, Vol. 23, pp. 1493-1496 (1989).

100. Gallagher, J., "Damage Tolerant Design Handbook," Metals and Ceramics Information Center, Battelle-Columbus Laboratories, pp. 6.13-1 - 6.13-12, distributed by CINDAS/Purdue (1983).

101. AMS 2416G, "Plating, Nickel-Cadmium, Diffused," Society of Automotive Engineers (Oct. 1990).

This page is blank.

REVISED MARCH 1963

FERROUS ALLOYS

	Fe
0.3	C
18.5	Cr
9.5	Ni
3.5	Mn

HNM

1. GENERAL
HNM is a precipitation hardening austenitic steel, specifically developed for high stress rupture and creep properties in the range of 1000 to 1400 F and is not prone to overaging in this temperature range. It has very low magnetic permeability, and is normally supplied in the solution treated condition, to a hardness of Brinell 201 maximum. Typical applications include, transformer parts, nonmagnetic balls, aircraft structural and engine components, shafts and gears, (1, p.1, 2).

1.01 Commercial Designation. Crucible HNM.

1.02 Alternate Designation. None.

1.03 Specifications. MIL-S-17759-D (ships).

1.04 Composition. Table 1.04.

TABLE 1.04

Source	Crucible (1, p. 1)
	Percent Nominal
Carbon	0.30
Chromium	18.5
Manganese	3.5
Nickel	9.5
Phosphorus	0.25
Silicon	0.50
Sulfur	0.025
Iron	Balance

1.05 Heat Treatment
1.051 Anneal. 2000 to 2150 F, 30 min, water quench. Sections < 5/8 in thick may be air cooled. The optimum solution treatment for best properties after aging is approximately 2050 F. (1, p.1).
1.052 Age. 1300 F, 16 hr, air cool.

1.06 Hardenability
1.061 The alloy is hardenable by precipitation treatment, see 1.052, (1, p. 2).

1.07 Forms and Conditions Available
1.071 The alloy is available in the form of bar, sheet and strip in the solution treated condition (BHN 201 maximum), (1, p.1).

1.08 Melting and Casting Practice

1.09 Special Considerations

2. PHYSICAL AND CHEMICAL PROPERTIES

2.01 Thermal Properties
2.011 Melting range
2.012 Phase changes. None.
2.013 Thermal conductivity
2.014 Thermal expansion, Fig. 2.014.
2.015 Specific heat

2.02 Other Physical Properties
2.021 Density. 0.284 lb per cu in. 7.85 gr per cu cm.
2.022 Electrical resistivity, Fig. 2.022, (1, p.1).
2.023 Magnetic properties
2.0231 Magnetic permeability, Table 2.0231.

TABLE 2.0231

Source	(1, p.3)	
Alloy	Fe-(0.3C)-18.5Cr-9.5Ni-3.5Mn	
Condition	ST + age	
Induction, oersteds	H = 200	H = 500
Maximum permeability	1.003	1.003

2.03 Chemical Properties
2.031 Corrosion resistance. This alloy satisfactorily resists rusting and pitting under normal atmospheric conditions. It is, however, inferior to the regular 18Cr-8Ni stainless steel types, but superior to the straight chromium stainless steel types, (1, p. 3).
2.032 Oxidation resistance. See 2.031.

2.04 Nuclear Properties

3. MECHANICAL PROPERTIES

3.01 Specified Mechanical Properties

3.02 Mechanical Properties at Room Temperature. See 1.05.
3.021 Producer's typical mechanical properties for bar and sheet, Table 3.021.

TABLE 3.021

Source	(1, p. 4)			
Alloy	Fe-(0.3C)-18.5Cr-9.5Ni-3.5Mn			
Form	Bar		Sheet	
Condition	ST 2050 F, 30 MIN OQ	ST 2050 F, WQ + age 1300 F, 16 hr	ST 2050 F, 15 MIN AC	ST 2050 F, AC + age 1300 F, 16 hr
F_{tu}, - ksi	116	145	106	133.5
F_{ty}, - ksi	56	92	55	90.4
e (2 in)- percent	57.5	23	48	11
RA, - percent	60	38	-	-
Hardness,				
BHN	192	302	-	-
RB	-	-	67.5	-
RC	-	-	-	33

3.022 Effect of solution temperature on room temperature tensile properties of aged alloy, Fig. 3.022.
3.023 Effect of solution temperature on room temperature impact properties of aged alloy, Fig. 3.023.
3.024 Effect of aging temperature and time on room temperature tensile properties, Fig. 3.024.

3.03 Mechanical Properties at Various Temperatures
3.031 Short time tension properties
3.0311 Effect of test temperature on tensile properties, Fig. 3.0311.
3.032 Short time properties other than tension
3.0321 Effect of low and elevated temperatures on impact strength, Fig. 3.0321.
3.033 Static stress concentration effects

3.04 Creep and Creep Rupture Properties
3.041 Creep rupture curves at 1000 to 1500 F, Fig. 3.041.
3.042 Isochronous stress strain curves at 900 and 1200 F for sheet, Fig. 3.042.

3.05 Fatigue Properties
3.051 S-N curves for bar, Fig. 3.051.

3.06 Elastic Properties
3.061 Modulus of elasticity at room temperature. 29×10^3 ksi, (1, p. 3).
3.062 Modulus of rigidity at room temperature. 12.3×10^3 ksi, (1, p. 5).

4. FABRICATION

4.01 Forming and Casting
4.011 Forging. Starting temperature 1850 to 1950 F, finishing temperature 1700 F, minimum, (1, p.1).
4.012 Since the alloy is very susceptible to work hardening resolution treatment should precede and follow each drastic forming operation, (1, p.1).

4.02 Machining
4.021 Similar to the 18-8 types of austenitic steel requiring, heavy positive feed, rigid equipment and sharp tools, (1, p. 2).

	Fe
0.3	C
18.5	Cr
9.5	Ni
3.5	Mn

HNM

4.03 Welding

4.031 General. The alloy is difficult to weld and is not recommended where welding is required. Heats with lower phosphorus content are slightly more weldable and the use of ferritic weld metal reduces the extent of weld cracking, (1, p. 2).

4.032 Brazing. HNM can be successfully brazed by oxyacetylene torch and furnace methods using an alloy conforming to AMS-Specification 4775. Furnace brazing and solution treating can be performed simultaneously at 2150 F, 30 min in argon gas. The tensile strength of the brazed joint is 74 ksi at 1300 F, (1, p. 3).

4.04 Heating and Heat Treating

4.05 Surface Treating

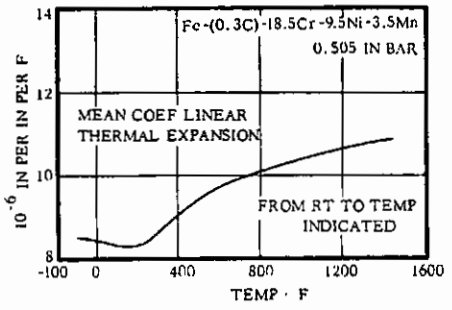


FIG. 2.014 THERMAL EXPANSION (1, p. 3)

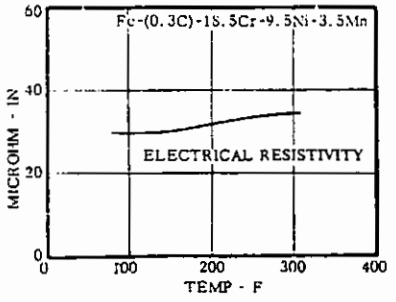


FIG. 2.022 ELECTRICAL RESISTIVITY (1, p. 3)

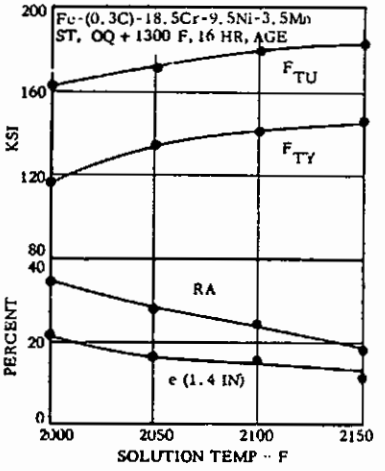


FIG. 3.022 EFFECT OF SOLUTION TEMPERATURE ON ROOM TEMPERATURE TENSILE PROPERTIES OF AGED ALLOY (2, p. 3)

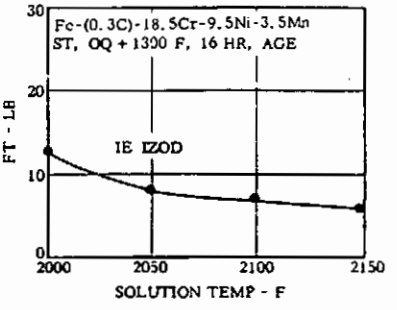


FIG. 3.023 EFFECT OF SOLUTION TEMPERATURE ON ROOM TEMPERATURE IMPACT PROPERTIES OF AGED ALLOY (2, p. 3)

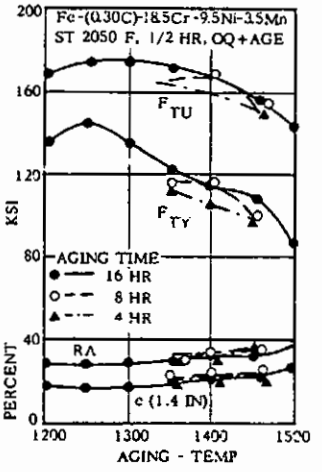


FIG. 3.024 EFFECT OF AGING TEMPERATURE AND TIME ON ROOM TEMPERATURE TENSILE PROPERTIES (2, p. 4)

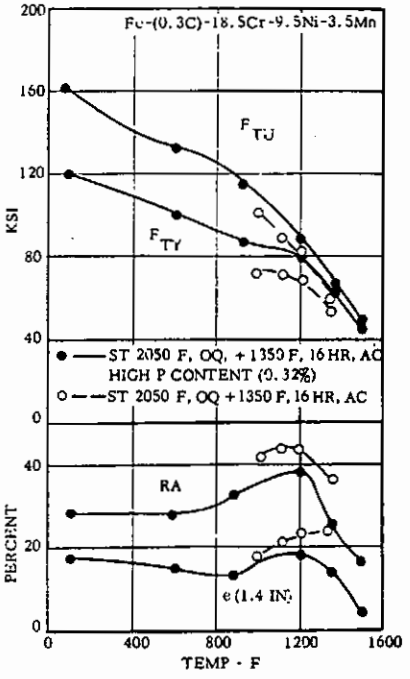
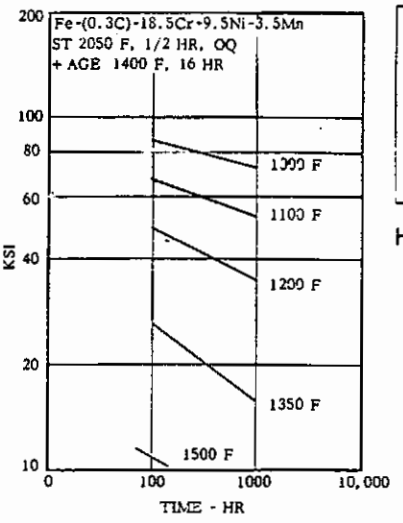


FIG. 3.0311 EFFECT OF TEST TEMPERATURE ON TENSILE PROPERTIES

(1, p. 5, 6)



	Fe
0.3	C
18.5	Cr
9.5	Ni
3.5	Mn

HNM

FIG. 3.041 CREEP RUPTURE CURVES AT 1000 TO 1500 F

(1, p. 6)

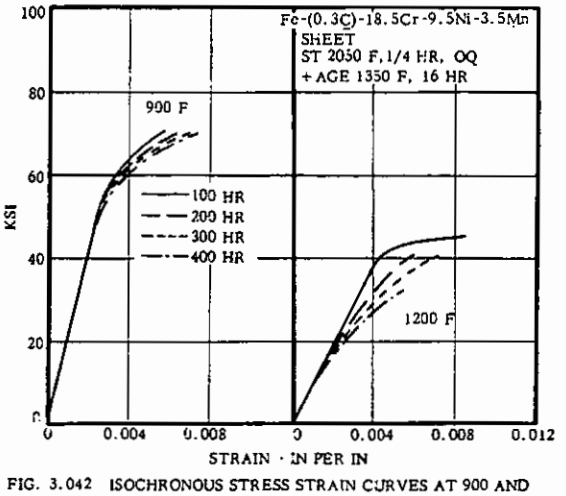


FIG. 3.042 ISOCHRONOUS STRESS STRAIN CURVES AT 900 AND 1200 F FOR SHEET

(1, Fig. 3, 4)

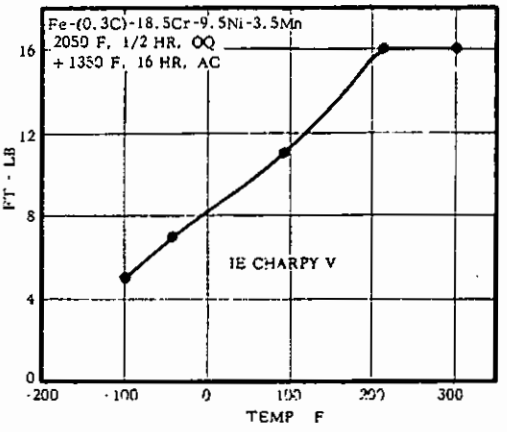


FIG. 3.0321 EFFECT OF LOW AND ELEVATED TEMPERATURES ON IMPACT STRENGTH

(2, p. 5)

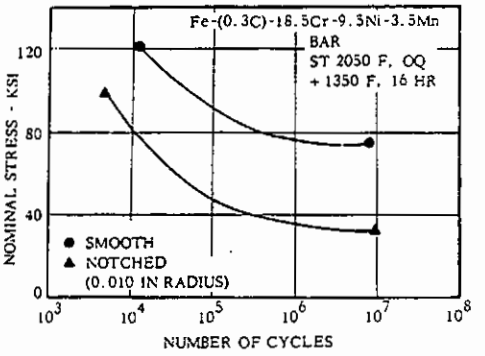


FIG. 3.051 S-N CURVES FOR BAR

(1, Fig. 2)

REFERENCES

1 "Crucible HNM", Preliminary Data Sheet, Crucible Steel Co., Issue # 2, (June 1960)

2 "Crucible HNM (Hardenable Non-Magnetic Steel)", Tentative Data Sheet, Crucible Steel Co., (Aug. 31, 1954)

	Fe
0.25	C
1.8	Ni
1.5	Si
1.3	Mn
0.4	Mo

HY-TUF

1 **GENERAL**

Hy-Tuf is a low alloy ultrahigh strength steel. It is one of the first developed to exceed a strength of 200 ksi. The alloy is used in the range of 220 to 240 ksi ultimate tensile strength. In this range it combines relatively high impact strength and low notch sensitivity with good ductility.

1.01 **Commercial Designation**

Hy-Tuf.

1.02 **Alternate Designations**

UNS K32550.

1.03 **Specifications**

1.031 Specification, Table 1.031.

1.04 **Composition**

1.041 Composition, Table 1.041.

1.05 **Heat Treatment**

1.051 Normalize, 1690 to 1710 F, air cool.

1.052 Subcritical anneal for shearing and sawing: 1200 F, 15 to 20 hours. Resulting hardness should be about 260 BHN.

1.053 Isothermal anneal for best machinability: 1360 to 1380 F, cool at 50 F per hour maximum to 1100 F, then air cool + 1175 to 1225 F, 15 to 20 hours. Resulting hardness should be about 230 BHN. Alternatively anneal 1360 to 1380 F, place in furnace and hold at 1175 to 1225 F, 24 hours.

1.054 Heat treat for regular machining. Normalize or austenitize + 1200 F (1250 maximum), 15 to 20 hours. Resulting hardness should be 229 to 248 BHN.

1.055 Austenitize, 1575 to 1625 F, oil quench. AMS gives 1565 to 1585 F.

1.056 Temper, 400 to 600 F, preferably 550 F. Tempering outside of this range is not recommended.

1.06 **Hardness**

1.061 End quench hardenability, Figure 1.061.

1.07 **Forms and Conditions Available**

1.071 Alloy is available in the full commercial range of sizes for sheet, plate, bar and forgings.

1.072 Alloy is available in the annealed or hot rolled conditions.

1.08 **Melting and Casting Practice**

Electric furnace air melt. Induction and consumable electrode vacuum melts.

1.09 **Special Considerations**

1.091 Tempering on either side of the 400 to 600 F range is not recommended.

1.092 Center soundness is not guaranteed in sizes over 100 square inch cross-sectional area for rolled bar or in sizes over 196 square inch for forged products.

2 **PHYSICAL PROPERTIES AND ENVIRONMENTAL EFFECTS**

Nearly the same as those of other low alloy steels (see 4340), except for the data given below.

2.01 **Thermal Properties**

2.011 Melting range.

2.012 Phase changes, transformation from austenite to ferrite. Critical temperatures, A_c1 = 1300 F, A_c3 = 1550 F.

2.0121 Time-temperature-transformation curve for alloy, Figure 2.0121.

2.013 Thermal conductivity.

2.014 Thermal expansion.

2.015 Specific heat.

2.016 Thermal diffusivity.

2.02 **Other Physical Properties**

2.021 Density, 0.281 lb/in.^{3}, 7.77 gr/cm^3.

2.022 Electrical properties.

2.023 Magnetic properties.

2.024 Emittance.

2.025 Damping capacity.

2.03 **Chemical Environments**

2.031 Stress corrosion.

2.0311 The resistance to stress corrosion is improved by cadmium plating. This was determined on material which was quenched and tempered to an ultimate strength of 243 ksi. Notched (K_t = 7.7) specimens were stressed to 142 ksi and exposed in a 5 percent salt fog atmosphere at room temperature. Bare specimens failed in less than one day under these conditions. Additional specimens were plated with low hydrogen porous cadmium, 0.0002 to 0.0005 inch thick, and given a supplementary chromate treatment. These specimens failed only after 12 to 19 days' exposure under similar conditions, indicating substantial improvement in stress corrosion resistance from the plating (9).

2.032 Hydrogen embrittlement.

2.0321 Hy-Tuf is moderately susceptible to hydrogen embrittlement. It is more susceptible than Type 18Ni Maraging (250 grade) and the 9Ni-4Co fully bainitic steels but less susceptible than Type 4340 and the 9Ni-4Co martensitic and mixed bainitic steels. These comparisons are based on stressed exposures (210 or 240 ksi applied stress) of up to 30 days at room temperature after cadmium plating to induce hydrogen embrittlement (10).

2.04 **Nuclear Environments**

3 **MECHANICAL PROPERTIES**

3.01 **Specified Mechanical Properties**

3.011 AMS specified mechanical properties, Table 3.011.

3.02 **Mechanical Properties at Room Temperature**

3.021 Tension – stress-strain diagrams – tension properties.

3.0211 Stress-strain curves in tension for heat treated tubing, Figure 3.0211.

3.0212 Typical mechanical properties, Table 3.0212.

3.0213 Effect of tempering temperature from 400 to 550 F on tensile properties of bar, Figure 3.0213.

3.0214 Effect of tempering temperature from 400 to 1000 F on tensile properties of bar, Figure 3.0214.

3.0215 Effect of as-quenched section size on tensile properties of heat treated bar, Figure 3.0215.

3.022 Compression – stress-strain diagrams – compression properties.

	Fe
0.25	C
1.8	Ni
1.5	Si
1.3	Mn
0.4	Mo

HY-TUF

3.023 Impact.
3.0231 Izod V-notch impact energy at room temperature as a function of tempering temperature, Figure 3.0231.
3.024 Bending.
3.0241 Effect of wall thickness on modulus of rupture in bending for heat treated tubing, Figure 3.0241.
3.025 Torsion and shear.
3.0251 Typical torsion strength of heat treated bar, F_{st} = 193.5 ksi.
3.026 Bearing.
3.027 Stress concentration.
3.0271 Notch properties.
3.02711 Effects of specimen size, test direction, and stress concentration factor on notch strength ratio for bar, Figure 3.02711.
3.0272 Fracture toughness.
3.02721 Fracture toughness at room temperature, Table 3.02721.
3.028 Combined properties.

3.03 **Mechanical Properties at Various Temperatures**
3.031 Tension – stress-strain diagrams – tension properties.
3.0311 Stress-strain curves for plate at room and elevated temperatures, Figure 3.0311.
3.0312 Effect of test temperature on tensile and yield strength of plate, Figure 3.0312.
3.032 Compression – stress-strain diagrams – compression properties.
3.0321 Stress-strain curves in compression for plate at room and elevated temperatures, Figure 3.0321.
3.0322 Effect of test temperature on compressive yield strength of plate, Figure 3.0322.
3.033 Impact.
3.0331 Effect of test temperature from -320 to +212 F on impact strength of bar, Figure 3.0331.
3.0332 Effect of test temperature from -100 to +380 F on impact strength of bar, Figure 3.0332.
3.0333 Effect of tempering temperature on impact strength of bar at -100 F, Figure 3.0333.
3.034 Bending.
3.035 Torsion and shear.
3.036 Bearing.
3.037 Stress concentration.
3.0371 Notch properties.
3.03711 Effect of low test temperature on notch strength of bar, Table 3.03711.
3.0372 Fracture toughness.
3.038 Combined properties.

3.04 **Creep and Creep-Rupture Properties**

3.05 **Fatigue Properties**
3.051 Fatigue strength of smooth and notched bar, Table 3.051.
3.052 Axial fatigue of smooth and notched material at room temperature [(a) smooth, R = 0.2, (b) smooth, R = -1.0, (c) notched (K_t = 3.0), R = 0.2, and (d) notched (K_t = 3.0), R = -1.0], Figure 3.052.
3.053 Rotating beam fatigue behavior at room temperature, Figure 3.053.
3.054 Near-threshold fatigue crack propagation rates, Figure 3.054.

3.06 **Elastic Properties**
3.061 Poisson's ratio.
3.062 Modulus of elasticity.
3.0621 Modulus of elasticity at room and elevated temperatures, Figure 3.0621.
3.063 Modulus of rigidity.
3.064 Tangent modulus.
3.0641 Tangent modulus curves in compression at room and elevated temperatures, Figure 3.0641.
3.065 Secant modulus.
3.0651 Secant modulus curves in compression at room and elevated temperatures, Figure 3.0651.

4 FABRICATION

See 4330 Mod. also.

4.01 **Forming**
4.011 Forging. Starting temperature between 2100 and 2175 F, finishing temperature 1650 F minimum. When closed die forgings are made, temperature should be maintained on the high side.

4.02 **Machining and Grinding**
4.021 Machinability is comparable to other alloy steels of similar microstructure and hardness. Annealed conditions are preferred (see Section 1.05). Machining of heat treated material having a hardness of 48 to 50 RC is possible with heavy and rigid tool supports.

4.03 **Joining**
4.031 Alloy is easily welded by conventional methods using low hydrogen electrodes of similar composition. Joint efficiencies are 92 to 95 percent.

4.04 **Surface Treating**
4.041 Carburizing. At 1600 F, 8 hour, produces carburizing to a depth of 0.015 inch. Carburizing is followed by oil quench and tempering at 400 to 600 F.

REFERENCES

1 AMS 6418F (October 1, 1984).
2 Crucible Steel Company of America, "Hy-Tuf Alloy Steel", Data Sheet (November 1957).
3 Muvdi, B. B., Sachs, G., and Klier, E. P., "Design Properties of High Strength in the Presence of Stress Concentrations", WADC TR 56-395, Pt. 1 (December 1956).
4 Sachs, G., "Survey of Low-Alloy Aircraft Steels Heat Treated to High-Strength Levels", WADC TR 53-254, Pt. 4 (December 1953).
5 Hughes, P. J., Inge, J. E., and Prosser, S. B., "Tensile and Compressive Stress-Strain Properties of Some High-Strength Sheet Alloys at Elevated Temperatures", NACA TN 3315 (November 1954).
6 Muvdi, B. B., Klier, E. P., and Sachs, G., "Design Properties of High-Strength Steels in the Presence of Stress-Concentrations and Hydrogen Embrittlement", WADC TR 55-103, Supp. 1 (January 1956).
7 The Cleveland Pneumatic Tool Co., "Stress-Strain Curves for High-Strength Alloy Steel", Rep. No. 732 (February 25, 1955).
8 Crucible Steel Company of America, "Data Sheet", Rev. No. 2 (November 1957).

9 Lauchner, E. A., "The Stress Corrosion Resistance of High-Strength Steels for Bolting Applications", Norair Division, Northrup Corporation, Hawthorne, California, NOR-69-91 (July 16, 1969).

10 Thrash, C. V., "Evaluation of High-Strength Steels for Heavy Section Applications", Douglas Aircraft Division, McDonnell Douglas Corporation, Long Beach, California, DAC-LB-32437 (November 29, 1965).

11 Barrett, G. N., Jr., and Lindow, A., "Investigation of 'Hy-Tuf' Steel", Cleveland Pneumatic Company, Cleveland, Ohio, MPDC-66727 (1970).

12 Hauser, J. J., "Data on Vacuum-Arc-Remelted (VAR) Hy-Tuf, a High-Strength Steel of Excellent Toughness", Crucible Materials Research Center, Colt Industries, Incorporated, Pittsburgh, Pennsylvania, private communication to J. E. Campbell, Metals and Ceramics Information Center, Columbus, Ohio (December 3, 1974).

13 Mackay, T. L., Alperin, B. J., and Bhatt, D. D., "Near-Threshold Fatigue Crack Propagation of Several High-Strength Steels", *Engineering Fracture Mechanics*, Vol. 18, No. 2 (1983), pp 403–416.

Fe	
0.25	C
1.8	Ni
1.5	Si
1.3	Mn
0.4	Mo

HY-TUF

Alloy	Hy-Tuf	
AMS	Form	Military
6418 F	Bar, Forgings, and Mechanical Tubing	MIL-S-7108

TABLE 1.031. SPECIFICATION

Alloy	Hy-Tuf	
	Percent	
Element	Min	Max
Carbon	0.23	0.28
Nickel	1.65	2.00
Silicon	1.30	1.70
Manganese	1.20	1.50
Molybdenum	0.35	0.45
Chromium	0.20	0.40
Copper	–	0.35
Phosphorus	–	0.025
Sulfur	–	0.025

TABLE 1.041. COMPOSITION (1)

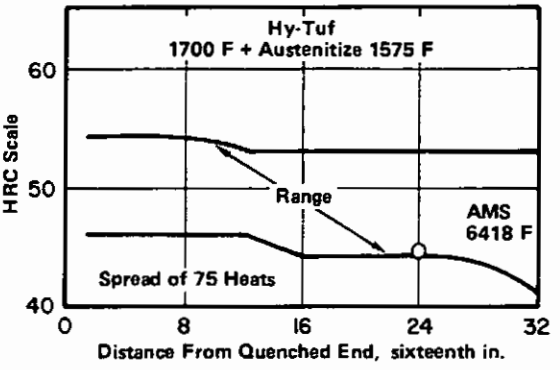


FIGURE 1.061. END QUENCH HARDENABILITY (2)

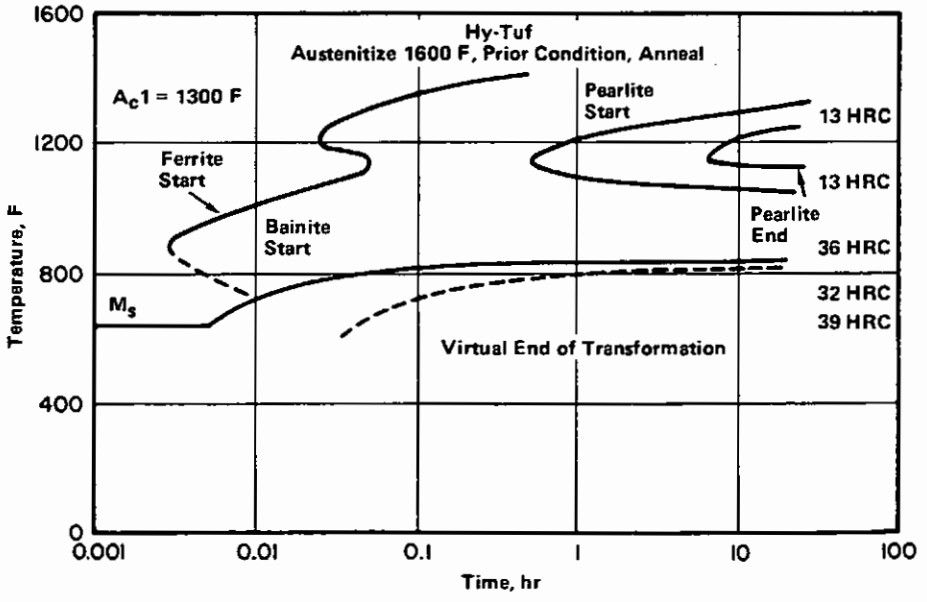


FIGURE 2.0121. TIME-TEMPERATURE-TRANSFORMATION CURVE FOR ALLOY (4)

	Fe
0.25	C
1.8	Ni
1.5	Si
1.3	Mn
0.4	Mo

HY-TUF

Alloy	Hy-Tuf	
Normalize 1 hr, 1725 F, AC + Austenitize 1 hr, 1600 F, OQ + Temper 2–3 hr, 550 F, AC		
Property	Min	Max
F_{tu}, ksi	220	245
F_{ty}, 0.2 Percent Offset, ksi	185	–
Elongation (4D), percent	5	–
Reduction in Area, percent		
Average	20	–
Individual	15	–

Note: The original AMS document should be consulted for complete specification details.

TABLE 3.011. AMS SPECIFIED MECHANICAL PROPERTIES (1)

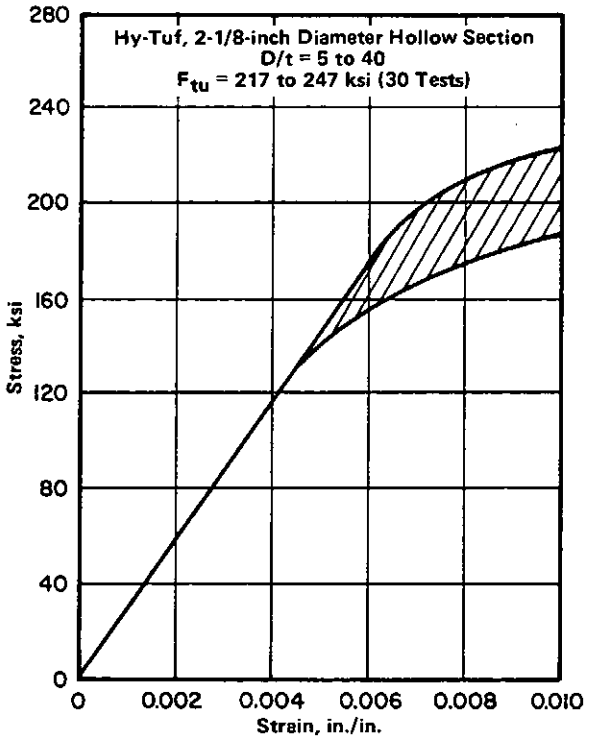


FIGURE 3.0211. STRESS-STRAIN CURVES IN TENSION FOR HEAT TREATED TUBING (7)

Alloy	Hy-Tuf			
Form	1-inch Bar			
Condition	1600 F, OQ + Temper			
Temper Temp, F	400	500	550	600
F_{tu}, ksi	239	235	234	230
F_{ty}, ksi	183	191	193	194
e (2 in.), percent	14.3	13.9	13.1	14.0
RA, percent	46.6	49.7	49.7	51.7
HRC	48	47	46.5	46
IE, Izod, ft-lb				
-40 F	29	27	25	26
RT	33	33	31	29

TABLE 3.0212. TYPICAL MECHANICAL PROPERTIES (2)

	Fe
0.25	C
1.8	Ni
1.5	Si
1.3	Mn
0.4	Mo

HY-TUF

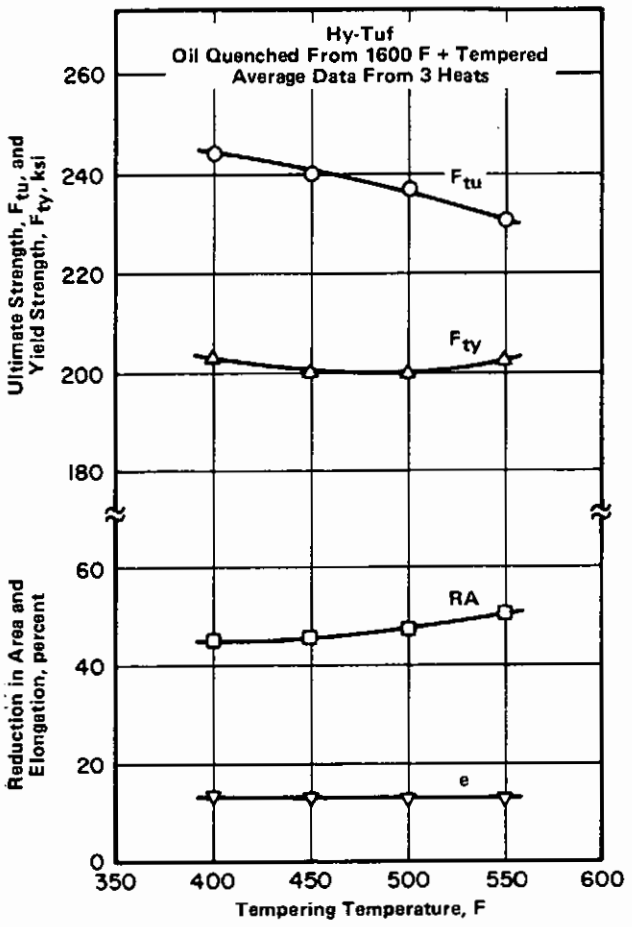


FIGURE 3.0213. EFFECT OF TEMPERING TEMPERATURE FROM 400 TO 550 F ON TENSILE PROPERTIES OF BAR (11)

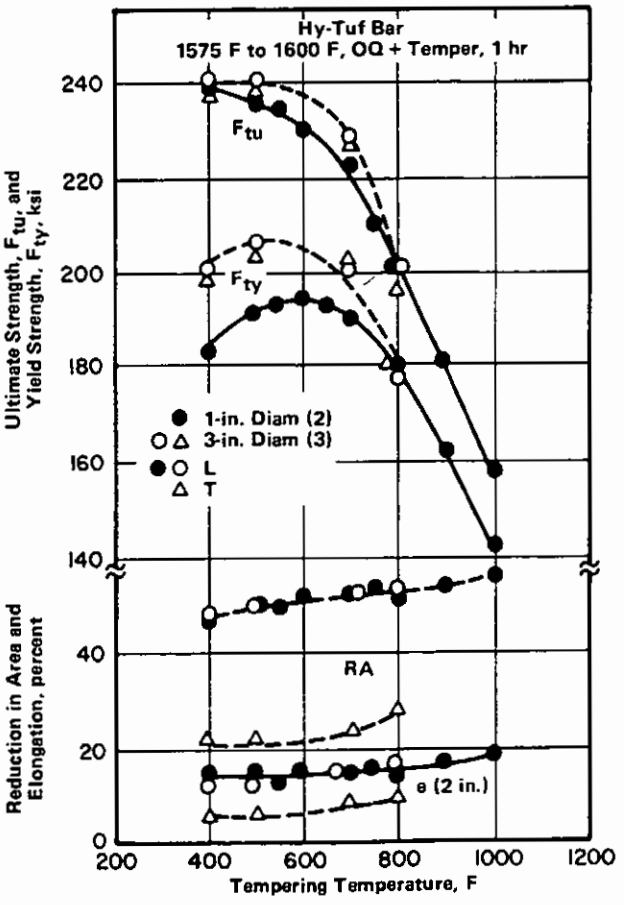


FIGURE 3.0214. EFFECT OF TEMPERING TEMPERATURE FROM 400 TO 1000 F ON TENSILE PROPERTIES OF BAR (2, 3)

	Fe
0.25	C
1.8	Ni
1.5	Si
1.3	Mn
0.4	Mo

HY-TUF

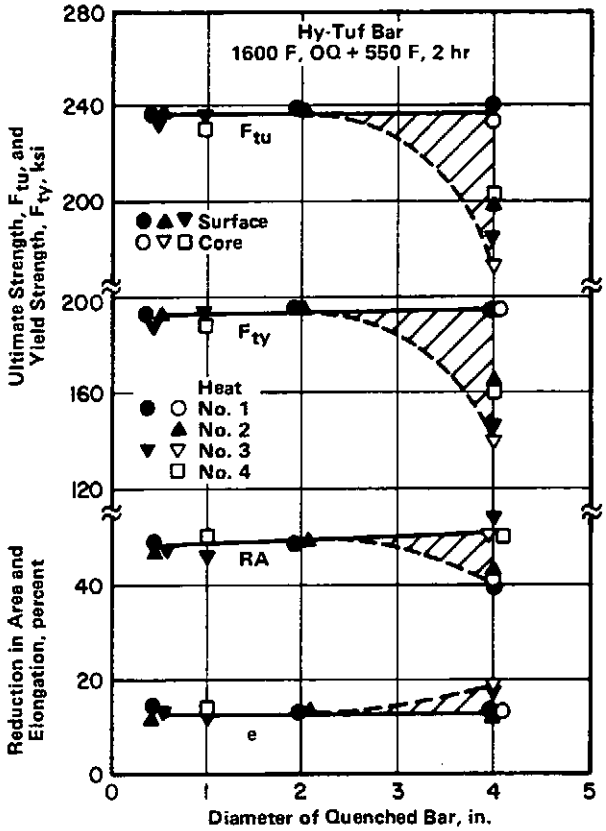


FIGURE 3.0215. EFFECT OF AS-QUENCHED SECTION SIZE ON TENSILE PROPERTIES OF HEAT TREATED BAR (4)

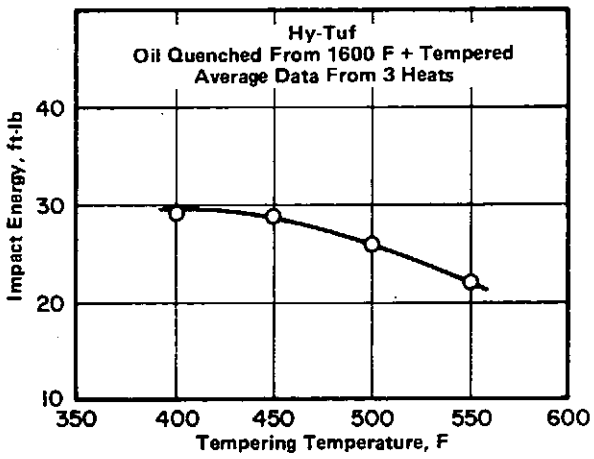


FIGURE 3.0231. IZOD V-NOTCH IMPACT ENERGY AT ROOM TEMPERATURE AS A FUNCTION OF TEMPERING TEMPERATURE (11)

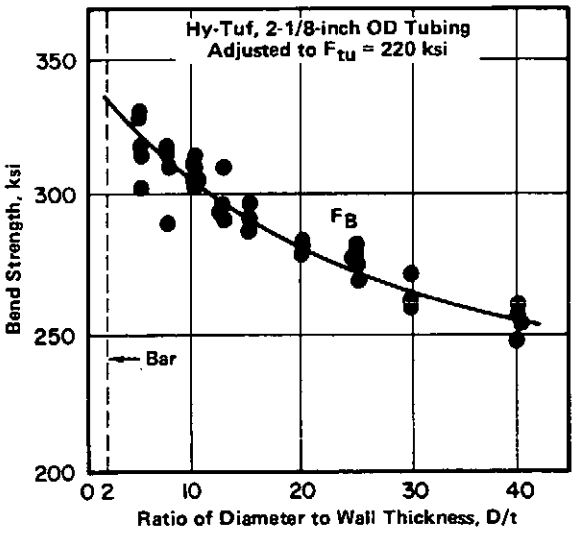


FIGURE 3.0241. EFFECT OF WALL THICKNESS ON MODULUS OF RUPTURE IN BENDING FOR HEAT TREATED TUBING (7)

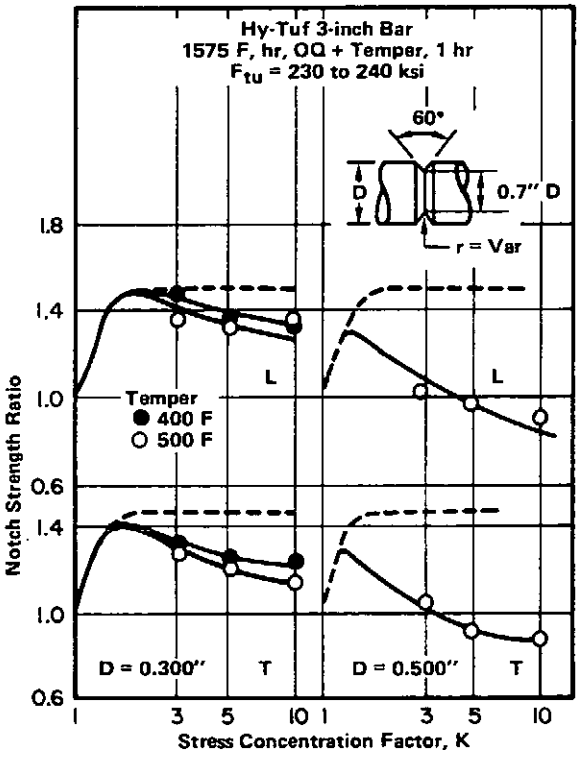


FIGURE 3.02711. EFFECTS OF SPECIMEN SIZE, TEST DIRECTION, AND STRESS CONCENTRATION FACTOR ON NOTCH STRENGTH RATIO FOR BAR (6)

Alloy	Hy-Tuf				
	Tensile Properties		Fracture Toughness		
Condition	F_{ty}, ksi	F_{tu}, ksi	Orientation	K_{Ic}, ksi $\sqrt{in.}$	Reference
Air Melted: Heat Treated	197	231	L	81	10, p 88
			T	80	
Vacuum Arc Remelted: 1 hr, 1700 F, AC + 1 hr, 1600 F, OQ + 2 hr, 550 F	198	242	L-T	116.1	12
			T-L	111.5	
Vacuum Arc Remelted: 1 hr, 1700 F, AC + 1 hr, 1600 F → 20 min, 1000 F, OQ + 2 hr, 550 F	199	243	L-T	120.3	12
			T-L	113.3	
Vacuum Arc Remelted: 1 hr, 1600 F, OQ + 1 hr, 525 F	197	242	L-T	109	13, p 404

	Fe
0.25	C
1.8	Ni
1.5	Si
1.3	Mn
0.4	Mo

HY-TUF

TABLE 3.02721. FRACTURE TOUGHNESS AT ROOM TEMPERATURE

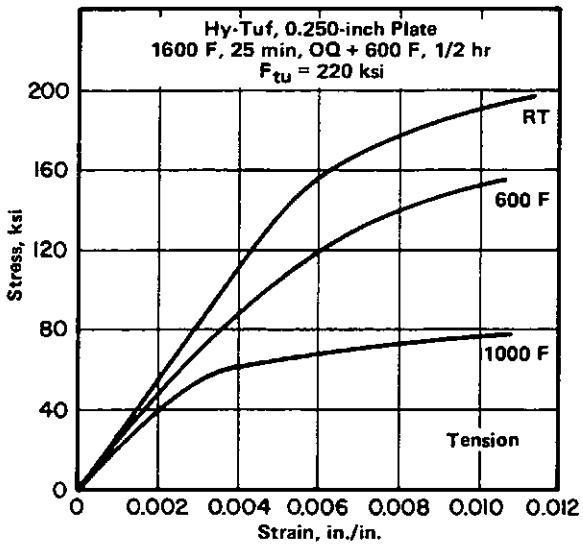


FIGURE 3.0311. STRESS-STRAIN CURVES FOR PLATE AT ROOM AND ELEVATED TEMPERATURES (5)

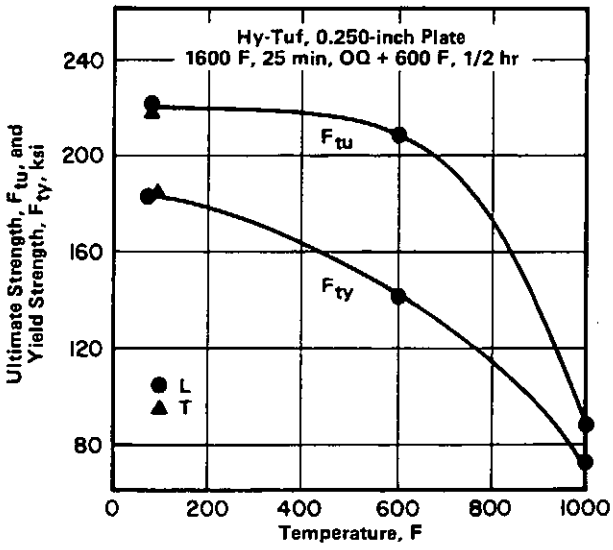


FIGURE 3.0312. EFFECT OF TEST TEMPERATURE ON TENSILE AND YIELD STRENGTH OF PLATE (5)

	Fe
0.25	C
1.8	Ni
1.5	Si
1.3	Mn
0.4	Mo

HY-TUF

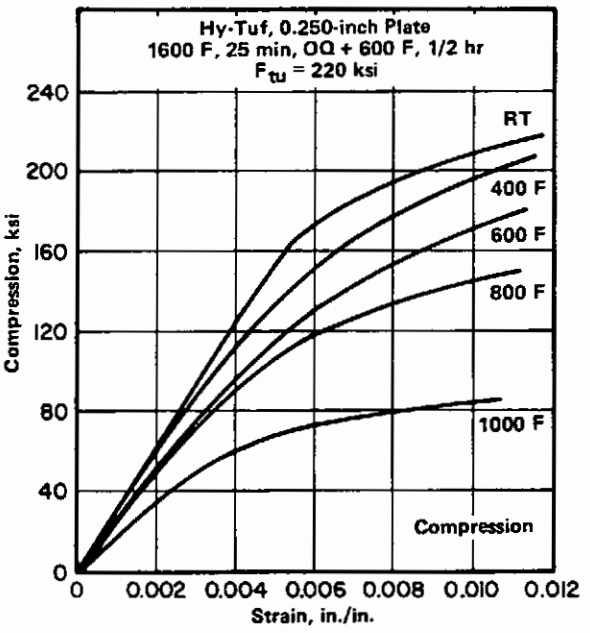


FIGURE 3.0321. STRESS-STRAIN CURVES IN COMPRESSION FOR PLATE AT ROOM AND ELEVATED TEMPERATURES (5)

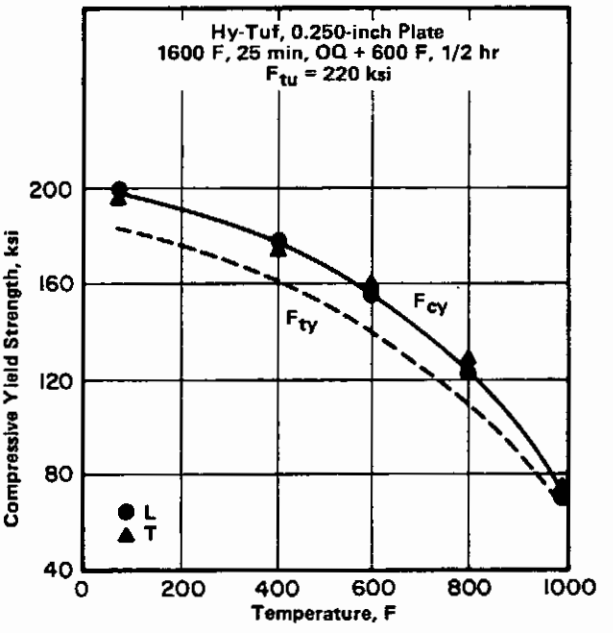


FIGURE 3.0322. EFFECT OF TEST TEMPERATURE ON COMPRESSIVE YIELD STRENGTH OF PLATE (5)

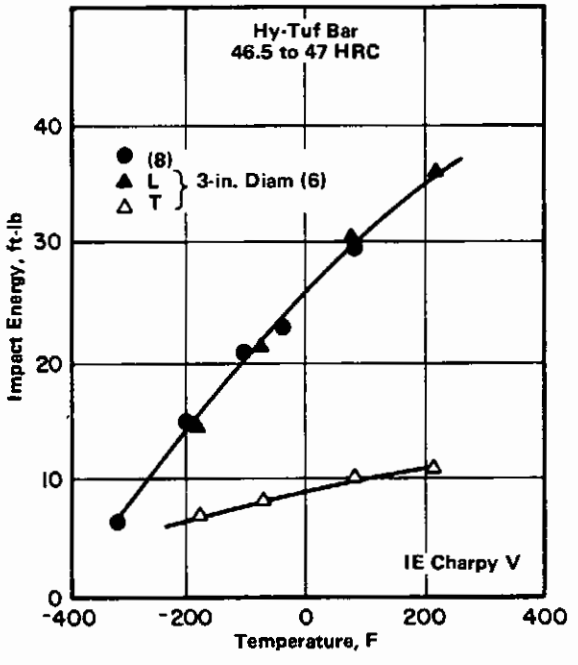


FIGURE 3.0331. EFFECT OF TEST TEMPERATURE FROM -320 TO +212 F ON IMPACT STRENGTH OF BAR (6, 8)

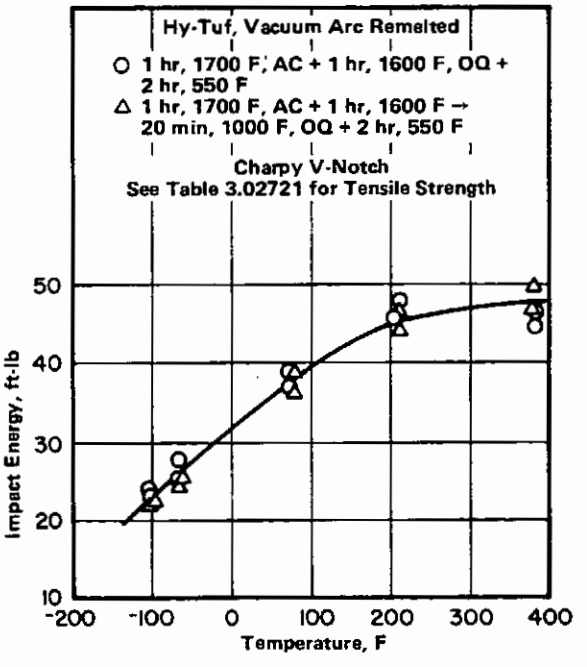


FIGURE 3.0332. EFFECT OF TEST TEMPERATURE FROM -100 TO +380 F ON IMPACT STRENGTH OF BAR (12)

	Fe
0.25	C
1.8	Ni
1.5	Si
1.3	Mn
0.4	Mo

HY-TUF

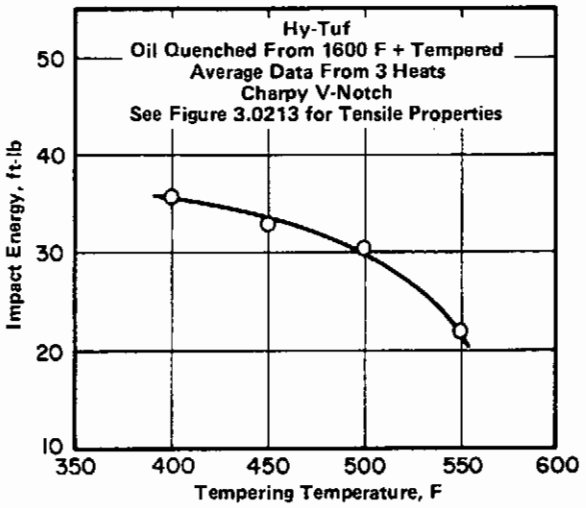


FIGURE 3.0333. EFFECT OF TEMPERING TEMPERATURE ON IMPACT STRENGTH OF BAR AT -100 F (11)

Alloy	Hy-Tuf					
Form	1/2-inch Bar					
Test Temperature, F	RT			-40		
F_{tu}, Smooth, ksi	210	220	230	210	220	230
Notch Strength, ksi K = 9.5	285	296	305	280	296	310
Notch Strength Ratio	1.36	1.34	1.32	–	–	–

TABLE 3.03711. EFFECT OF LOW TEST TEMPERATURE ON NOTCH STRENGTH OF BAR (2)

Alloy	Hy-Tuf							
Form	Bar							
Condition	F_{tu} = 230 ksi							
Temperature, F	Method	Stress Ratio A	Stress Ratio R	Stress Concentration	Fatigue Strength, ksi, at Cycles 10^4	10^5	10^6	10^7
RT	Rot Beam	∞	-1	Smooth	190	132	103	88
				Notched	140	55	50	46
-320				K = 2.5	90	75	60	47

TABLE 3.051. FATIGUE STRENGTH OF SMOOTH AND NOTCHED BAR (2)

	Fe
0.25	C
1.8	Ni
1.5	Si
1.3	Mn
0.4	Mo

HY-TUF

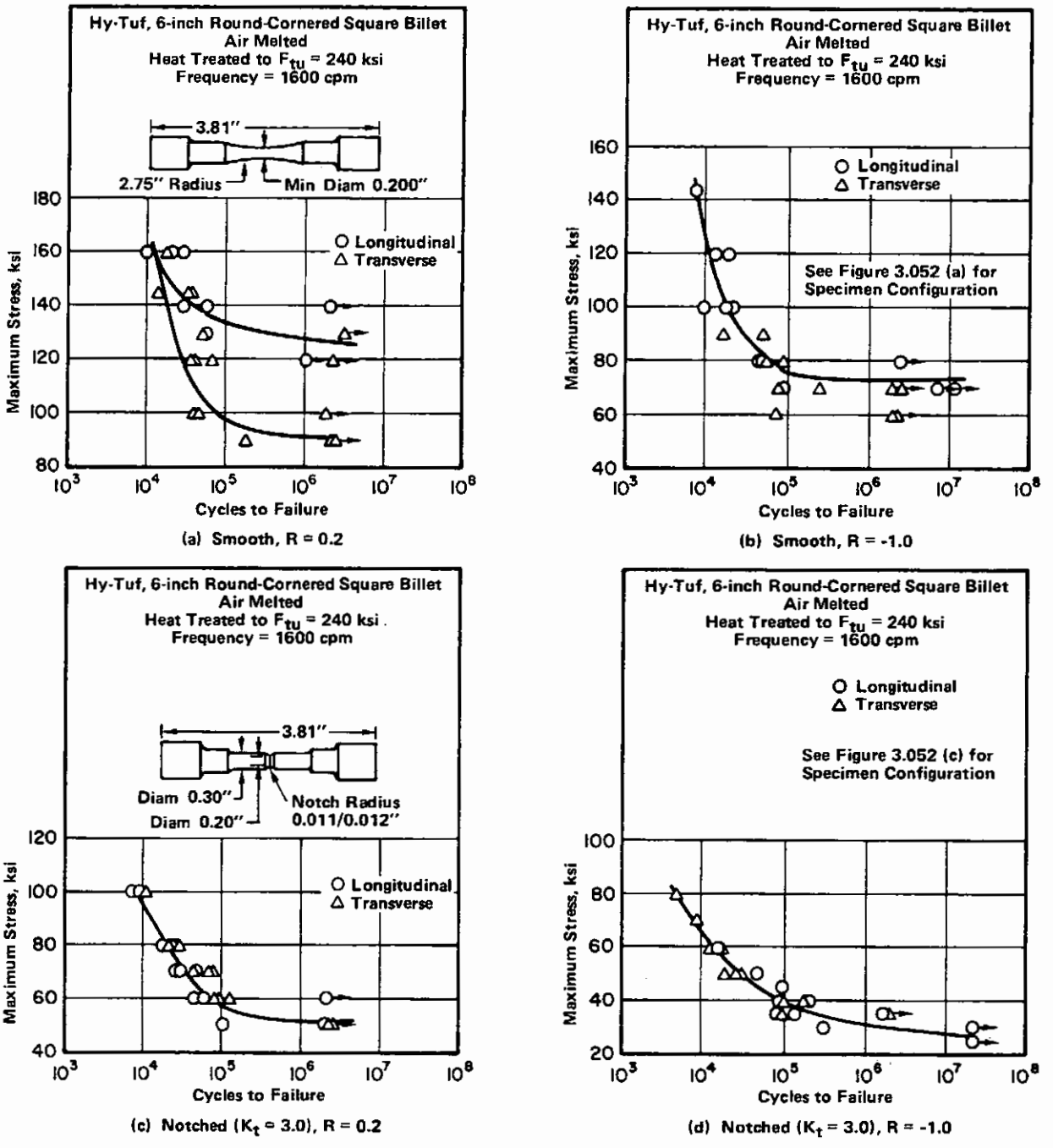


FIGURE 3.052. AXIAL FATIGUE OF SMOOTH AND NOTCHED MATERIAL AT ROOM TEMPERATURE (10)

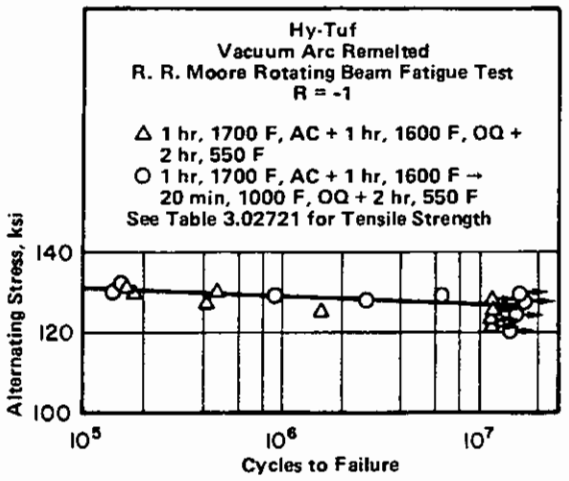


FIGURE 3.053. ROTATING BEAM FATIGUE BEHAVIOR AT ROOM TEMPERATURE (12)

	Fe
0.25	C
1.8	Ni
1.5	Si
1.3	Mn
0.4	Mo

HY-TUF

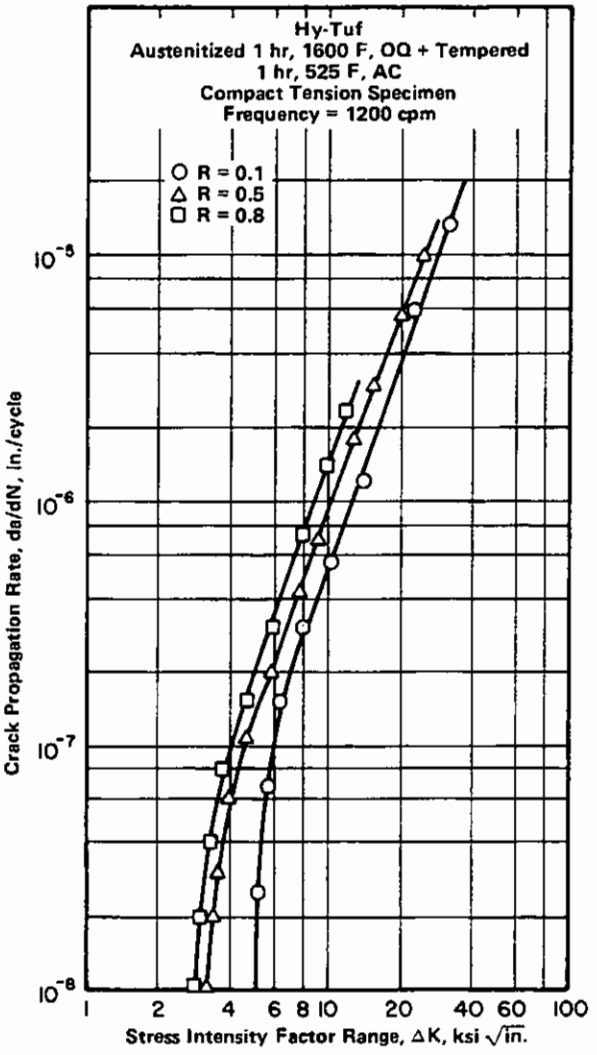


FIGURE 3.054. NEAR-THRESHOLD FATIGUE CRACK PROPAGATION RATES (13)

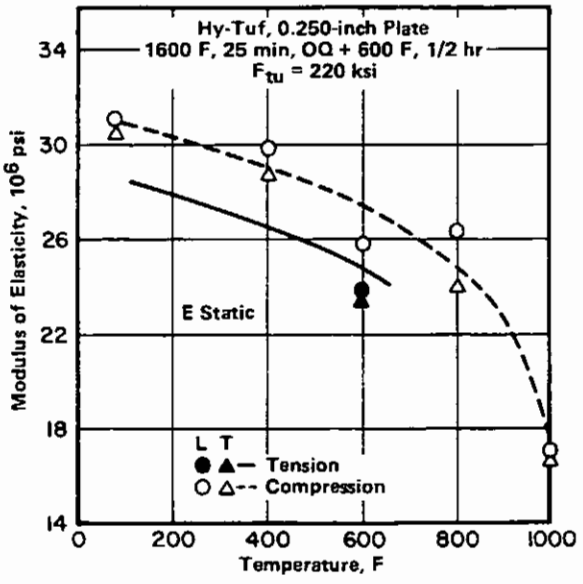


FIGURE 3.0621. MODULUS OF ELASTICITY AT ROOM AND ELEVATED TEMPERATURES (5)

	Fe
0.25	C
1.8	Ni
1.5	Si
1.3	Mn
0.4	Mo

HY-TUF

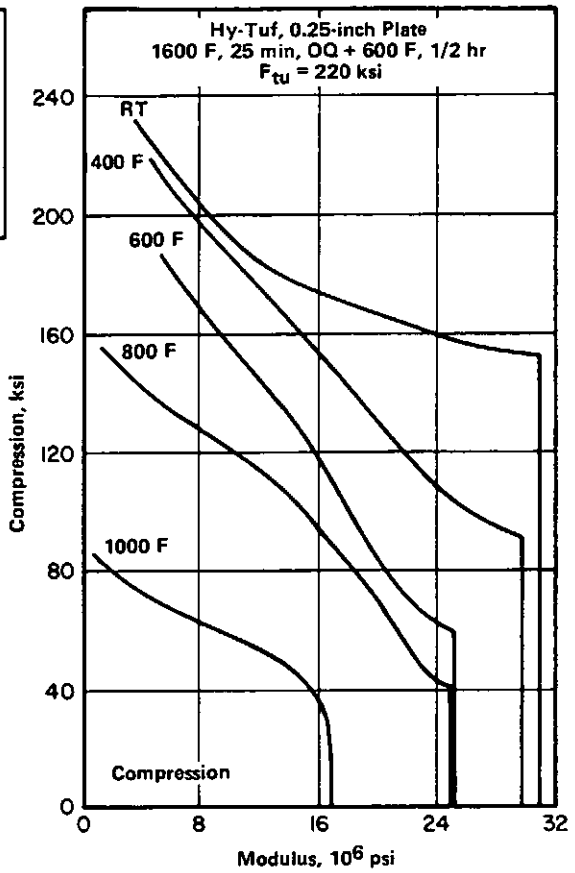


FIGURE 3.0641. TANGENT MODULUS CURVES IN COMPRESSION AT ROOM AND ELEVATED TEMPERATURES (5)

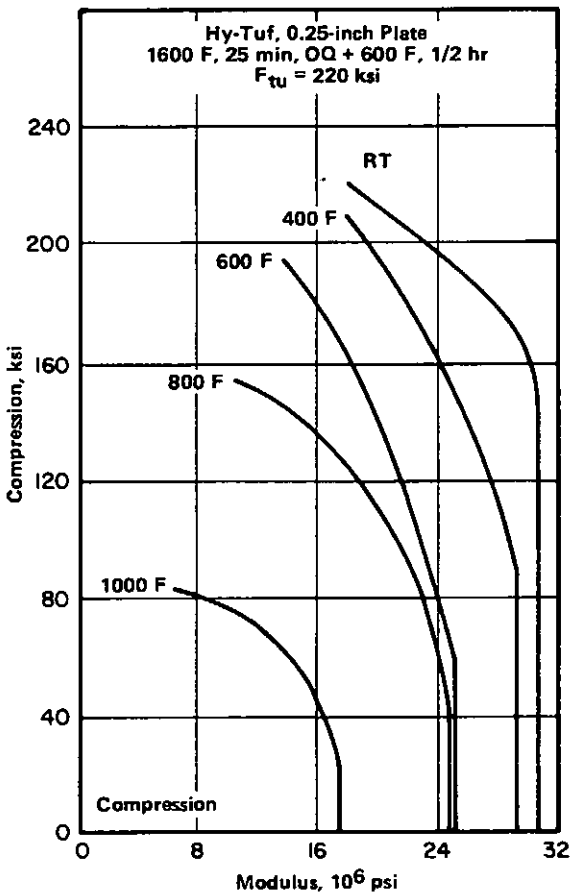


FIGURE 3.0651. SECANT MODULUS CURVES IN COMPRESSION AT ROOM AND ELEVATED TEMPERATURES (5)

	Fe
32	Ni
21	Cr
0.75	Mn
0.05	C

Incoloy Alloy 800H

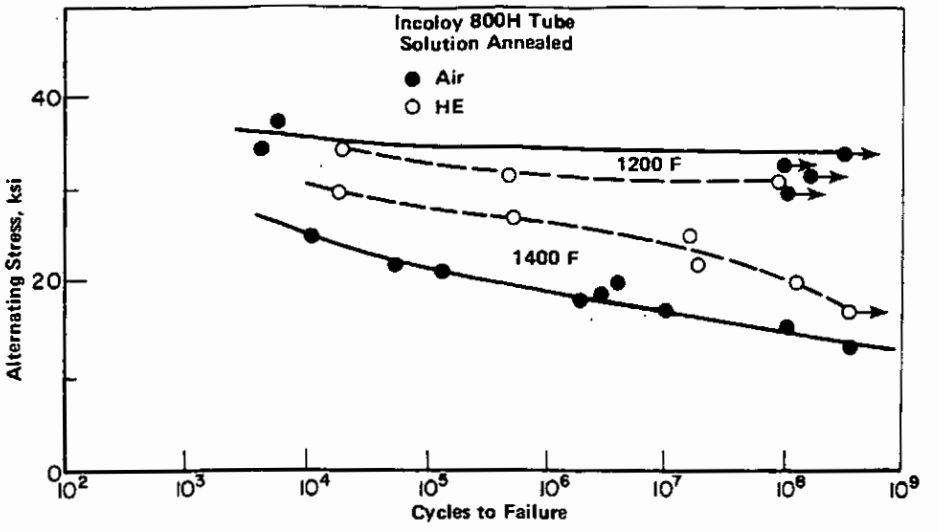


FIGURE 3.0551. HIGH-CYCLE FATIGUE AT 1200 F AND 1400 F IN AIR AND HELIUM (16, p K 23)

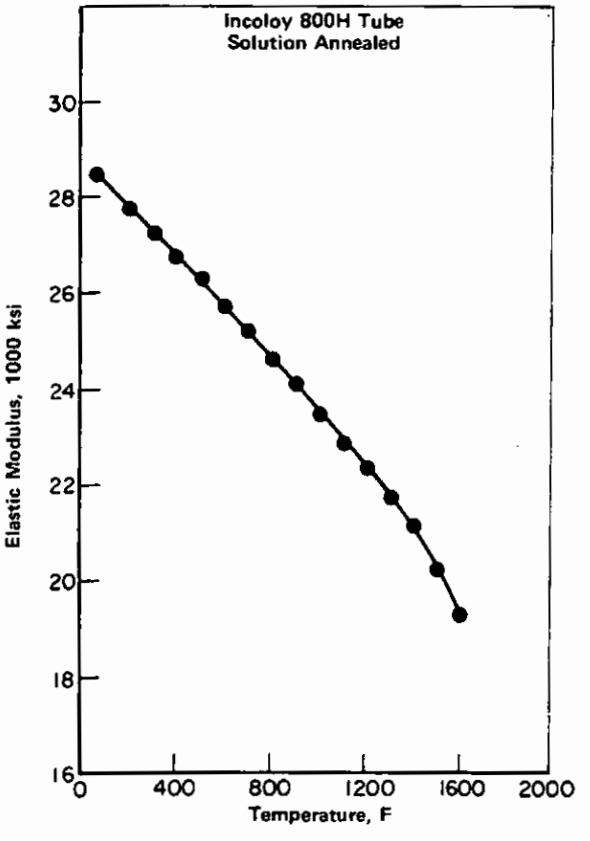


FIGURE 3.061. ELASTIC MODULUS (11, p 379)

Author **W. F. Brown, Jr.**

Introduction

This section introduces the reader to the general objective, contents, and format of this handbook. Definitions of the physical and mechanical properties are presented as well as pertinent comments on the selected data.

The general objective is to provide an unbiased characterization of alloys of interest to the aerospace designer so that alloy selection for a particular application may be made with a knowledge not only of typical physical and mechanical properties, but especially of those factors which limit the load carrying capacity, whether associated with the service conditions or with the metallurgical history of the alloy.

This handbook contains typical data as contrasted to statistically derived design data presented in MIL-HDBK-5 (Ref. 1). However, specified mechanical properties are frequently presented as derived from AMS, federal, and industrial sources and specifications. Caution should be used when comparing data from different sources because mechanical properties are sensitive to processing history and testing techniques. Data in this handbook are characterized as to source, product form and size, and all pertinent details of thermal-mechanical processing and testing history.

An attempt is made to provide an organized record of important mechanical and selected physical properties. However, it should be realized that a vast amount of information relating to mechanical and physical properties of alloys used in the aerospace and related industries has been and is still being generated. Some of this is confined to specific pieces of hardware and/or applications and has limited general usefulness (e.g., flight spectrum fatigue loading behavior). This type of information is not generally included in this handbook. Also in the case of alloys such as 4340 steel, Ti-6Al-4V, and 2024Al which have been widely used for many years and where design allowables are well established, it is not practical to make a comprehensive record here. Extensive data bases for such alloys exist in industrial and government organizations. For such well characterized alloys this handbook presents an overview with emphasis on those factors limiting load carrying capacity.

With respect to chapter revision and deletion, all chapters are identified by their date of preparation. While it has always been the desire of the editors to update chapters on some regular basis, limited funds have forced concentration on new materials and have restricted revisions to alloys whose characterization is substantially changed by new information. Chapters are deleted when the alloy has had limited use and is no longer in production.

A special problem exists in determining what data to delete when a chapter is revised. A decision is easy to make when there has been a clear change in the composition or the processing practice. On the other hand, some alloys have a rather wide range of accepted compositions and are processed in several ways which have evolved over a period of years. Under these circumstances data are not deleted during a chapter revision unless evidence has been presented that it was, for some reason, obtained from faulty test or analysis procedures. Comments on the significance of data are made on the basis of the most recent information in a particular chapter.

Alloy Classification

The chapters are classified according to specific alloy categories and each category is assigned a code number. Chapters are then numbered serially under their respective codes as they are added to the handbook. The chapter code numbers appear at the bottom of each page along with the page number. An outline of the categories and their numbers is given below.

Ferrous Alloys

Category	Code Series
Carbon and Low Alloy Steels (FeC)	1100
Ultra High Strength Steels (FeUH)	1200
Austenitic Stainless Steels (FeA)	1300
Martensitic Stainless Steels (FeM)	1400
Age Hardening Steels (FeAH)	1500
Nickel Chromium Steels (FeNC)	1600

Non-Ferrous Alloys

Category	Code Series
Aluminum Alloys; Cast (AlC)	3100
Aluminum Alloys; Wrought, Heat Treatable (AlWT)	3200
Aluminum Alloys; Wrought, Not Heat Treatable (AlWN)	3300
Magnesium Alloys; Cast (MgC)	3400
Magnesium Alloys; Wrought, Heat Treatable (MgWT)	3500
Magnesium Alloys; Wrought, Not Heat Treatable (MgWN)	3600
Titanium Alloys (TiW)	3700
Titanium Alloys Cast (TiC)	3800
Nickel Base Alloys (<5% Co) (Ni)	4100
Nickel Base Alloys (>5% Co) (NiCo)	4200
Cobalt Base Alloys (Co)	4300
Beryllium Alloys (Be)	5100
Columbium (Niobium) Alloys (Cb)	5200
Molybdenum Alloys (Mo)	5300
Tantalum Alloys (Ta)	5400
Tungsten Alloys (W)	5500
Vanadium Alloys (V)	5600
Zirconium Alloys (Zr)	5700

Alloy Identification

Alloys are identified by their chemical composition. The major elements are listed in decreasing order of their percentage by weight followed by the minor elements listed in the same way. When two or more elements are present in equal quantities they are listed alphabetically. Minor elements are given only when they are intentionally added to yield special mechanical properties. Impurities are neglected. The only

© 1992 by Purdue Research Foundation, West Lafayette, Indiana 47907.
All Rights Reserved.

exception to this practice is for ferritic steels; when carbon is the element having the predominate influence on the mechanical properties, it is listed immediately after iron.

In addition to the above described system of identification, the most commonly used designations (e.g., AISI Code) are given along with the number from the SAE/ASTM Unified Number System (Ref. 2). To facilitate the location of a particular alloy an index is provided in Volume 5 which gives cross-references for alloy category codes and commonly used designations.

Measurement System

The data presented in this handbook are obtained from sources in various countries. The original units of data measurement vary depending on the source. Where practical, mechanical property data are presented in English units (inch, pounds force, seconds, Fahrenheit) which are customarily used by the aerospace industry. Physical property data are generally given in the units used by the source. To assist in converting SI and other units to the customary units a conversion table is presented in Appendix D.

Data Organization

The data for each alloy are presented according to a property code system designed for this handbook. The numbers of the tables and figures that follow each section correspond to their respective paragraphs in the text. An outline of this code follows. (Please note also that the numbering system used in the earlier handbooks has been altered. For example, 1.01 is now 1.1, 2.011 is 2.1.1, and so forth.)

1 General

1.1 Commercial Designation
1.2 Alternate Designations
1.3 Specifications
1.4 Composition
1.5 Heat Treatment
1.6 Hardness (formerly Hardenability)
1.7 Forms and Conditions Available
1.8 Melting and Casting Practice
1.9 Special Considerations

2 Physical Properties and Environmental Effects (formerly Physical and Chemical Properties)

2.1 Thermal Properties
2.1.1 Melting Range
2.1.2 Phase Changes
2.1.2.1 Time-temperature-transformation diagrams
2.1.3 Thermal Conductivity
2.1.4 Thermal Expansion
2.1.5 Specific Heat
2.1.6 Thermal Diffusivity
2.2 Other Physical Properties
2.2.1 Density
2.2.2 Electrical Properties
2.2.3 Magnetic Properties
2.2.4 Emittance
2.2.5 Damping Capacity
2.3 Chemical Environments
2.3.1 General Corrosion
2.3.2 Stress Corrosion
2.4 Nuclear Environments

3 Mechanical Properties

3.1 Specified Mechanical Properties
3.2 Mechanical Properties at Room Temperature
3.2.1 Tension Stress-strain Diagrams and Tensile Properties
3.2.2 Compression Stress-strain Diagrams and Compression Properties
3.2.3 Impact
3.2.4 Bending
3.2.5 Torsion and Shear
3.2.6 Bearing
3.2.7 Stress Concentration
3.2.7.1 Notch properties
3.2.7.2 Fracture toughness
3.2.8 Combined Loading (formerly Combined Properties)
3.3 Mechanical Properties at Various Temperatures
3.3.1 Tension Stress-strain Diagrams and Tensile Properties
3.3.2 Compression Stress-strain Diagrams and Compression Properties
3.3.3 Impact
3.3.4 Bending
3.3.5 Torsion and Shear
3.3.6 Bearing
3.3.7 Stress Concentration
3.3.7.1 Notch properties
3.3.7.2 Fracture toughness
3.3.8 Combined Loading
3.4 Creep and Creep Rupture Properties
3.5 Fatigue Properties
3.5.1 Conventional High-Cycle Fatigue
3.5.2 Low-Cycle Fatigue
3.5.3 Fatigue Crack Propagation
3.6 Elastic Properties
3.6.1 Poisson's Ratio
3.6.2 Modulus of Elasticity
3.6.3 Modulus of Rigidity
3.6.4 Tangent Modulus
3.6.5 Secant Modulus

4 Fabrication

4.1 Forming
4.2 Machining and Grinding
4.3 Joining
4.4 Surface Treating

Data Presentation

Data points are generally shown for physical and mechanical properties. Multiple data points for a particular value of the independent variable are averaged to establish the trend curves. Where large data scatter is encountered or where a very large number of data points are reported (e.g., fatigue crack propagation data) a scatter band is shown to represent the upper and lower bounds of the data. However, such bands should not be used to represent lower bound properties for design purposes.

The mechanical properties and, to a lesser extent, the physical properties of metallic alloys are strongly dependent on the processing history of the test material. Where possible the most important features of processing are identified and reported in the data representations. Melting practice, product form, heat treatment, cold work, joining conditions, and related information (such as the testing direction and the specimen location with respect to the surfaces of the part from which they were removed) are included. Unfortunately, such complete characterizations are not available in many cases and, occasionally, so little information of this type is available that the data in question are excluded.

1 General

This section contains a brief general description of the selected alloy including a listing of any different grades, special features of interest to the structural designer relating to the alloy's advantages and limitations, and its typical applications.

1.1 Commercial Designation

The most commonly used designation is given first. This may originate with the alloy producer or from widely used specifications such as the Society of Automotive Engineers - Aerospace Materials Specifications (SAE-AMS). Trade names are generally not used, but in a few cases no other satisfactory designation is available. The reader should be aware of the rules governing the use of trade names.

1.2 Alternate Designations

The alternate designations include proprietary names and others encountered in the literature. No attempt is made to be complete here. A list of alloy names used in the handbook is given in the Index. For further information, see Ref. 3.

1.3 Specifications

This section provides a listing of specifications along with a description of the product forms and related metallurgical conditions. The primary sources are the Aerospace Material Specifications (AMS) issued by the SAE and the ASTM. Military and federal specifications may also be given. In some cases the alloy user may develop a specification for a particular application that also may be reported if it assists in the proper characterization of the data.

1.4 Composition

The SAE-AMS specifications are the primary source of reported chemical composition limits. In cases where an AMS specification has not been published the composition limits given by the producer are reported. It should be realized that for some materials a relatively small variation in composition limits for certain elements may have a substantial influence on the properties. These effects may be discovered as application experience is accumulated. Important compositional influences are discussed in Section 1.9, Special Considerations.

1.5 Heat Treatment

This section defines and discusses the thermal and/or deformation process applied to the alloy to achieve desired properties. A given heat treatment may be designated by either the process or the result. Because a clear understanding of heat treating terms is necessary to properly use material presented in this section, a Glossary of Heat Treating Terms is given in Appendix B.

1.6 Hardness

Hardness, as used herein, refers to an alloy's resistance to permanent deformation by indentation. Several indentation methods of measuring hardness have been standardized by the ASTM, namely Brinell E 10 (Ref. 4), Rockwell E 18 (Ref. 5), Vickers E 92 (Ref. 6) and Microhardness E 384 (Ref. 7). Hardness values reported in this handbook relate to one of these standardized procedures. In general, the hardness is related to the alloy tensile strength; hence, hardness values are often used to delineate the response of an alloy to heat treatment or cold work. This section reports the effect of various variables on the hardness. The depth to which an alloy will harden as a result of heat treatment is an important consideration in structural applications. The load carrying capacity of a component will be reduced if the desired hardness cannot be achieved throughout the cross section. The property that relates to the depth of hardening is called the hardenability. It is strongly dependent on the composition and, to a lesser extent, on the details of heat treatment. In the case of titanium alloys and steels, the higher the hardenability the less rapid the cooling rate from the solution or austenitizing temperature that is required to produce a given hardness level at the center of the cross section. In steels, insufficient hardenability or too slow a quenching rate can produce undesirable transformation products in the microstructure which may embrittle the steel. Hardenability is measured in several different ways. For steels the end quench hardenability test is frequently employed. This test, ASTM Standard A 255 (Ref. 8), consists of water quenching one end face of a steel cylinder and then determining the distribution of

hardness along the axis of the cylinder. More complete information is obtained by quenching cylinders of various diameters and measuring the hardness distribution on a diameter. In some cases the depth of hardening is judged by abstracting tensile specimens from different positions in the cross section or from cross sections of different sizes.

1.7 Forms and Conditions Available

The availability of a particular form will change with the market conditions. Current information on availability of forms and conditions should be obtained from the alloy producer.

1.8 Melting and Casting Practice

Melting practice can have a strong influence on the mechanical properties when these are sensitive to impurities. In such cases the details of melting practice are given in this section. Many of the alloys included in this handbook can be cast. However, only a limited number have cast properties which are of interest to the aerospace and related industries. The production of high quality castings requires very careful control of pouring and gating techniques as well as cooling rates in various portions of the cast structure. This section will contain detailed information on such casting techniques for those alloys where high quality castings are of interest to the designer.

1.9 Special Considerations

This section summarizes problems which may be encountered in the production of alloys as well as in their application. Emphasis is placed on those factors which limit the load carrying capacity in intended applications. Included are such factors as hydrogen embrittlement introduced by plating or cleaning processes or resulting from exposure to high pressure hydrogen gas. Where appropriate this section may reference other sections for further information. In addition, this section may include comments on particular advantages possessed by an alloy.

2 Physical Properties and Environmental Effects

A concise presentation of those physical properties of importance to the designer is given rather than a comprehensive compilation. When values of physical properties are reported without a specified test temperature, the values are for room temperature only. In some cases, the determination of the property requires measurements at two or more temperatures (e.g., thermal expansion). These temperatures, unless otherwise indicated, are in the range from room temperature to 212F. Usually the difference in property values for any two temperatures in this range is less than the uncertainty in the values themselves. Frequently the source material does not give the form and the condition of the alloy for which the physical property determination was made. The influence of form and condition may explain some of the differences between published values for the same alloy. For detailed information on physical properties (excluding magnetic properties) the reader is referred to CINDAS/Purdue University, West Lafayette, Indiana 47906.

Environmental effects include the influence of various chemical agents on the mechanical properties and on the general corrosion behavior. The influence of nuclear environments is also covered here. Particular attention is given to the environmental factors that affect the crack propagation characteristics of an alloy.

2.1 Thermal Properties

Thermal properties include the melting range, phase changes, thermal conductivity, thermal expansion, specific heat, and, where available, thermal diffusivity and dimensional changes on heat treating.

2.1.1 Melting Range. The melting range is bound by the solidus temperature on the low end and the liquidus temperature on the high end. These two temperatures are influenced by compositional variations within specified limits. The range reported is generally established by experience with the solidus being set low enough to avoid incipient melting during hot working which could damage the alloy.

2.1.2 Phase Changes. A phase is any physically discrete homogeneous portion of an alloy system. In some cases a phase change refers to a change in the crystal structure of the major alloying element. This can be observed in low alloy steels where face centered cubic austenite transforms to a body centered cubic structure on cooling below a certain critical temperature. However, precipitations of intermetallic compounds from solid solution also constitute phase changes. Phase changes may be caused or accelerated by cold work. Phase changes may be beneficial or detrimental with respect to the load carrying capacity of a part. For example, creep resistance may be increased by precipitations occurring during heat treatment or during the creep process. On the other hand, when quenching steels from the austenitizing temperature, too slow a cooling rate (slack quenching) may produce embrittling constituents in the microstructure. In welded components, phase changes may result in dimensional changes which can give rise to residual stresses. A detailed discussion of phase changes and transformation structures may be found in Ref. 9.

2.1.2.1 Time-temperature transformation diagrams. These are also referred to as isothermal transformation diagrams or T-T-T diagrams and enable the user to estimate how an alloy will respond to cooling through a range of temperatures where phase transformations take place. Where appropriate, continuous cooling transformation diagrams are shown.

2.1.3 Thermal Conductivity. This quantity, more properly called the coefficient of thermal conductivity K, proportions the heat flow rate H over a conducting distance x to the area of the conductor A and the temperature difference ΔT over the conducting distance. K is given by the following expression:

$$K = \frac{Hx}{A\Delta T}$$

A variety of units is used to report the thermal conductivity in the literature. This handbook uses Btu-ft per (hr sq ft F). The Btu is defined in several different ways; however, for the present purposes, the difference in thermal conductivity depending on the definition is negligible.

2.1.4 Thermal Expansion. This section reports the mean coefficient of linear expansion defined as

$$\alpha = \frac{\Delta L}{L_o}\frac{1}{\Delta T}$$

where α is the coefficient and ΔL the change in original length L due to a temperature $\Delta T = T - T_o$. In this handbook room temperature is used as the reference temperature T_o. Units for the coefficient are in. per in. per F.

2.1.5 Specific Heat. The specific heat at a specified temperature is the amount of heat necessary to raise a unit mass of a substance one degree in temperature divided by that necessary to raise a unit mass of water one degree at the same temperature. For engineering purposes the specific heat of metallic alloys may be taken equal to their heat capacity. The heat capacity of alloys will vary with temperature. Unless the reference temperature is specified the values of specific heat given in this handbook refer to room temperature.

2.1.6 Thermal Diffusivity. This quantity is the thermal conductivity divided by the density and the heat capacity at constant pressure. The units used here are sq ft per hr.

2.2 Other Physical Properties

2.2.1 Density. The weight density is reported as either lbs per cu. in. or as gms per cu. cm.

2.2.2 Electrical Properties. This section reports the electrical resistivity on a volume basis (sometimes referred to as the "volume resistivity"), which proportions the electrical resistance to the dimensions of the conductor according to the expression

$$R = \frac{\rho l}{A}$$

where R is the resistance, ρ the resistivity, l the length, and A the cross sectional area of the conductor. A variety of units is used for the volume resistivity, the most common being microhm-inch. Conversion factors for several units are given in Appendix D.

2.2.3 Magnetic Properties. Materials are classified as paramagnetic, ferromagnetic, or diamagnetic. Bars of paramagnetic and ferromagnetic materials align their long dimensions in the flux direction in a magnetic field, while diamagnetic materials align their long dimensions normal to the field. For the purposes of electrical engineering, ferromagnetic materials are of the greatest interest. A number of magnetic properties for ferromagnetic materials can be derived from the normal induction curve or from the normal hysteresis loop. Standard methods for determining these curves are given in ASTM A 34 (Ref. 10).

In non-magnetic media any change in the magnetizing force H measured in oersteds is accompanied by an equal change in magnetic induction B measured in gauss. However, in ferromagnetic materials the relation between H and B is non-linear and a plot of B vs H is known as the normal induction curve. This is illustrated by the heavy line in Figure 2.2.3.1. Increasing H beyond a certain value produces only a small further increase in B. The limiting value of B is designated as the saturation induction B_s. The ratio of B to H at any point on the normal induction curve is known as the normal permeability μ.

The units of permeability are gauss per oersted. However, it is usual to report a dimensionless quantity which is the ratio of the normal permeability described above to that of a vacuum which is unity in the cgs system but $4\pi \times 10^{-7}$ in the SI system. This number is known as the relative permeability μ_r. The normal permeability has a maximum value μ_m near the knee of the induction curve and is represented by the slope of a line passing through the origin and tangent to the induction curve. The slope of the induction curve at the origin is known as the initial permeability μ_o. Other values of permeability are sometimes reported being representative of the B/H ratio at some particular value of the magnetizing force. It should be noted that the permeability of paramagnetic materials is slightly greater than unity, essentially independent of the magnetizing force, and that diamagnetic materials have permeabilities slightly less than unity. For diamagnetic materials it is common to report the susceptibility K. The relation between μ and K in the cgs system is

$$\mu = 1 + 4\pi K$$

Referring to Figure 2.2.3.1, if the value of H is reduced from any point on the induction curve, hysteresis is evident and it is necessary to reverse the magnetizing force to produce a condition of zero induction. The result is a hysteresis loop. There are two quantities of special interest that can be derived from the hysteresis loop, namely, the residual induction B_r remaining after H has been reduced to zero and H_c which is the negative value of H necessary to reduce B to zero. If the

normal hysteresis loop is representative of a condition where the peak magnetizing force was sufficiently high to produce saturation induction (as in Figure 2.2.3.1), the B_r is designated as the retentivity B_{rs} and H_c is designated as the coercivity H_{cs}. The details of magnetic measurements are discussed in Refs. 11 and 12.

2.2.3.1 *[Figure]* Normal induction curve and hysteresis loop for ferromagnetic materials.

2.2.4 Emittance. The hemispherical emittance is the ratio of the radiance of a body to the radiance of a black body at the same temperature. The radiance is the rate of radiant energy emission from a unit area of the source in all radial directions of the overspreading hemisphere. If measurements are made normal to the surface, the quantity determined is called the normal emittance. When the measurements are made at a specific wave length, the result is designated as spectral emittance. Emittance is a dimensionless quantity with values less than unity. For further information the reader is referred to Ref. 13.

2.2.5 Damping Capacity. If the excitation is removed from a metal specimen subjected to torsional or bending vibrations the amplitude will decay due to internal friction which results in the dissipation of energy. The higher the damping the larger the rate of amplitude decay. Various measures have been proposed for damping and these are reviewed in Ref. 14. One that is frequently used in engineering is the damping capacity or specific damping energy measured as energy dissipated per unit volume per cycle.

2.3 Chemical Environments

This section includes information concerning the resistance of an alloy to various environments which can degrade its load carrying capacity by chemical reaction with its surface or interior. While a large number of corrosion tests have been standardized none of these give information which can directly be related to the degradation in load carrying capacity of a structural component. However, valuable comparative information can be obtained by selecting tests which represent the service environment. Corrosion tests can be divided into two generally recognized categories, namely, general corrosion and stress corrosion. This distinction is somewhat blurred by the influence of residual stresses which can affect the results of a general corrosion test. When corrosion data are reported, reference is made to an applicable ASTM or other standard for the test method and data evaluation. However, as pointed out in ASTM G 31 (Ref. 15), it is not possible to rigorously standardize corrosion testing because of the great variety of factors, many of which can not be well controlled.

2.3.1 General Corrosion. Smooth specimens are exposed to a variety of environments for various lengths of time. For example, specimens may be exposed to a seacoast or an industrial atmosphere, to a salt spray, to continuous immersion, or to alternate immersion in a salt solution (e.g., 3.5% NaCl). Tests of this type are commonly applied to aluminum and magnesium alloys and to high strength steels. The specimen surface is periodically examined for evidence of pitting and/or exfoliation and the observed surface conditions may be graded according to photographs contained in appropriate standards. In some cases, weight loss is determined and the result expressed as a time rate, or the result is converted to a dimensional loss rate (e.g., mils per year). Aluminum and magnesium alloys are quite susceptible to increased corrosion when electrically coupled in a corrosive media to a more noble alloy (e.g., Mg to steel in a salt solution). This galvanic corrosion is dependent on many variables and is not treated in this handbook. Some guidelines on predicting the behavior of galvanic coupled metals are given in ASTM G 82 (Ref. 16).

Some alloys (e.g., stainless steels and Ni-rich Cr-bearing high temperature alloys) when improperly heat treated are susceptible to intergranular corrosion. Accelerated test methods for evaluating the susceptibility of such alloys have been developed. The results may be expressed in terms of weight change or by bending the specimen and examining the tension surface for cracks related to intergranular attack.

2.3.2 Stress Corrosion. Most alloys are rendered more susceptible to corrosive attack if subjected to a stress in the aggressive environment. Stress corrosion tests are designed to measure the resistance to this type of behavior. A large number of tests have been standardized which make use of smooth specimens generally subjected to some fraction of the yield strength (e.g., tension specimens ASTM G 49 [Ref. 17] and C ring specimens ASTM G 38 [Ref. 18]). Specimens may be continuously exposed or alternately exposed to the environment and then to air. After an incubation time, cracks frequently form due to the adsorption of and diffusion of hydrogen generated by the corrosion reaction. Specimens are examined periodically to determine the presence of stress corrosion cracks. In tests using tension loading, specimens often fracture completely after crack initiation. Failure in tests using bending loads must be established by careful examination of the surface. The results of stress corrosion tests exhibit large scatter due to the difficulty of establishing the time to first cracking, premature fracture resulting from loss of load carrying area associated with general corrosion, and the fact that the cracks represent the behavior of a very localized region of the specimen. Frequently specimens subjected to tensile loading are removed from the aggressive environment and fractured to determine the retained load carrying capacity. This type of data has qualitative value in establishing the degeneration of load carrying capacity due to the aggressive environment.

To establish the structural load carrying capacity of a material, fracture mechanics tests can be used to obtain a measure of the effect of an aggressive environment. Sustained load tests on cracked specimens are used to establish a value of applied stress intensity factor K below which cracks will not grow in a particular aggressive environment. This value is known as K_{Iscc} and may be well below K_{Ic}. (K and K_{Ic} are defined in ASTM E 399 [Ref. 19].) At present there are no standardized tests for K_{Iscc}; when such values are reported herein the test conditions are described. If the application involves alternating loads, the K threshold below which cracks will not grow in an aggressive environment may be below K_{Iscc}.

2.4 Nuclear Environments

This section includes information concerning the resistance of metallic alloys to neutron radiation such as may be encountered in power generating reactors. Neutron radiation can result in large changes in mechanical properties and it is these changes that are emphasized in this section. The mechanical properties are represented as a function of the integrated neutron flux multiplied by the exposure time. This product is called the fluence, often designated as nvt. The neutron energy is also reported in millions of electron volts (Mev).

3 Mechanical Properties

The properties treated in these sections include those conventionally used in design as well as properties derived from special tests such as those from notch or precracked specimens. Information on mechanical properties is given concerning the effects of composition, heat treatment, and processing methods. Emphasis is on commercial practice. However, results obtained from experimental procedures are reported where these contribute to a better understanding of the effects of the variables influencing the mechanical properties.

While it is general practice to put all mechanical properties under these sections, where appropriate, mechanical properties may also be located in Section 1.5 on Heat Treatment, Section 1.9 on Special Considerations, and in Section 4 on Fabrication.

3.1 Specified Mechanical Properties

The specified mechanical properties reported in this section should not be taken as design values. Design values are given in MIL-HDBK-5 and the reader should obtain that handbook as a companion volume. It should be remembered that specifications are sometimes subject to frequent change, especially in the case of new alloys.

Room temperature mechanical properties form the core of most specifications. However, for heat resistant alloys, elevated temperature mechanical properties are sometimes specified. Specifications generally give minimum values of strength and ductility properties although occasionally maximum values are given. Forming limits in terms of minimum bend radii are specified in certain cases but this type of information is usually not included in the handbook.

3.2 Mechanical Properties at Room Temperature

This section includes data on conventional mechanical properties determined at room temperature with the exception of creep, fatigue, and elastic properties which are covered in separate sections. Used in the present sense, room temperature is a common but loose way of defining a test temperature. In this handbook it refers to the temperature range between 60 and 90F. In this range there is negligible time dependent flow (creep) for the great majority of structural alloys. Room temperature data will also be found in Section 3.3 where it appears as one of a series of values at various temperatures.

3.2.1 Tension Stress-strain Diagrams and Tensile Properties. Unless otherwise stated, stress is based on the original cross-section area. Elongation and reduction of area refer to percent changes from an original dimension. Occasionally, true stress and true strain are reported where the stress and strains are related to instantaneous values. Stress-strain curves generally encompass the range between zero and one percent strain. Such curves are useful in determining the static modulus and the yield strength. The tensile strength F_{tu} is the stress at maximum load. The yield strength F_{ty}, sometimes called proof stress, is the stress at a specified amount of plastic strain. In the United States this is generally 0.2 percent. The deformation values, elongation e and the reduction of area RA, are also reported. A standard method for measuring these strength and deformation values at room temperature is given in ASTM E 8 (Ref. 20). The tensile strength of brittle materials is influenced by any bending stresses introduced by the loading and gripping devices. These bending stresses may vary from test to test and result in substantial scatter of the strength values (ASTM E 1012, Ref. 21). It should be appreciated that the elongation of an alloy exhibiting necking before fracture may vary with the gage length. Neither elongation nor reduction of area are satisfactory predictors of fracture toughness (Ref. 22).

3.2.2 Compression Stress-strain Diagrams and Compression Properties. As in tension the stress and strain refer to the original dimension of the specimen and the compression yield strength F_{cy} is analogous to the tensile yield strength. Compression loads are influenced by friction at the interface between the anvils of the test machine and the specimen ends. Various means have been used to overcome these effects (e.g., large length to diameter ratios and/or lubrication; see ASTM E 9, Ref. 23). Unfortunately, information on specimen di-

mensions and means to minimize friction are seldom reported with compression data. In the absence of frictional effects the compression yield strength for most materials is essentially equal to the tensile yield strength.

3.2.3 Impact, see Section 3.3.3.

3.2.4 Bending. This section reports data from slow (as distinct from impact) bend tests on smooth specimens. These types of tests are sometimes used to evaluate the ability of welds to resist cracking at high deformations (ASTM E 290, Ref. 24). They are also used to determine the modulus of elasticity and yield strength in bending (ASTM E 855, Ref. 25). The yield strength so determined may not be equal to the yield strength in pure tension. The strength and deformation capacity of very brittle materials are frequently evaluated in three point bend tests commonly called modulus of rupture tests (ASTM B 406, Ref. 26). These tests have limited application in evaluation of aerospace alloys.

3.2.5 Torsion and Shear. The property reported here is the ultimate strength in shear (F_{su}) as determined from a torsion test or from one of a number of special shear tests.

3.2.6 Bearing. Bearing tests measure the yield (F_{bry}) and ultimate strength (F_{bru}) of a material when subjected to bearing loads. In a pinned or riveted joint the effective bearing area is the product of the hole diameter and the thickness of the bearing member. Specimen geometry must be considered when evaluating the results from these tests. Pin type bearing tests of metallic materials have been standardized and are described in ASTM E 238 (Ref. 27).

3.2.7 Stress Concentration, see Section 3.3.7.

3.2.7.1 Notch properties, see Section 3.3.7.1.

3.2.7.2 Fracture toughness, see Section 3.3.7.2.

3.2.8 Combined Loading (formerly Combined Properties). This section reports data from tests involving combinations of static loads such as combined bending and tension or multiaxial stress tests. Tests of this nature have not been standardized and only a limited amount of data from such tests is reported in this handbook.

3.3 Mechanical Properties at Various Temperatures (see also Section 3.2).

This section includes only the so-called short-time properties determined in conventional tests. The rate of deformation can influence the strength values at temperatures where time dependent flow occurs. At sufficiently high temperatures the time necessary to stabilize the specimen temperature may be sufficiently long to cause metallurgical changes in the material. For these reasons the scatter observed in elevated temperature mechanical properties is sometimes considerably larger than in the room or low temperature properties. At cryogenic temperatures some alloys become quite brittle and may break before the yield strength is reached. Under such circumstances the ultimate strength values may exhibit considerable scatter.

3.3.1 Tension Stress-strain Diagrams and Tensile Properties, see also Section 3.2.1. Methods recommended for conducting high temperature tensile tests are described in ASTM E21 (Ref. 28). This recommended practice emphasizes the importance of loading rate effects which depend on the testing techniques used.

3.3.2 Compression Stress-strain Diagrams and Compression Properties, see also Section 3.2.2. Compression properties, like tension properties, are sensitive to loading and heating rate effects at sufficiently high temperatures. ASTM E 209 (Ref. 29) gives recommended practices for conducting compression tests at elevated temperatures for conventional or rapid heating rates and strain rates.

3.3.3 Impact. Impact tests provide a measure of toughness in terms of an alloy's resistance to fracture when the load is applied at relatively high rates. Such tests do not directly provide a result that can be used in determining structural load carrying capacity. However, they are useful for ranking alloys in terms of their resistance to impact loading and in some cases may provide safe temperature limits for avoiding brittle fracture. Various types of impact tests have been described in the literature and several have been standardized. This handbook will report data only from standard test methods (Refs. 30, 31, 32, 33). These methods are listed in Table 3.3.3 which identifies the test method, the specimen type, and the indices of toughness reported. The standardized impact tests fall into two general classes, namely, those employing small specimens (Charpy and Izod) and those employing large specimens (NDT, Drop Weight Tear, and Dynamic Tear). The Charpy and Izod tests have been used for many years in the evaluation of a variety of alloys. The most widely used Charpy specimen has a V notch with a 0.01 in. radius. Charpy specimens without a notch and those with mild notches (Keyhole and U) have limited applications to special situations where the relatively sharp V notch is considered undesirable. The large specimens are designed to bring the test conditions more in line with structural applications. In general, the larger the specimen and the sharper the notch the greater is the sensitivity to factors producing brittle behavior. Consequently, the results of impact tests from different types of specimens should not be co-mingled. The trend of the impact energy with test temperature is strongly dependent on crystallographic structure, composition, and heat treatment. Body center cubic structures are particularly sensitive to temperature. Ferritic steels and beta titanium alloys generally show a marked decrease in impact energy within a relatively narrow temperature range. The center temperature of this range is the transition temperature. At temperatures outside this

range the impact energy tends to level out. At temperatures above the transition range the nearly level value of impact energy is known as the upper shelf value and has been given special significance in defining tough behavior. At sufficiently high temperatures the impact energy will decrease due to loss of strength. At subtransition temperatures the impact energy may fall to a few ft-lbs indicating very brittle behavior. Heat treated high strength steels do not exhibit strong transitional behavior and the impact energy is a less useful quantity than for the ferritic steels. The impact energy values may be supplemented by measurement of the lateral expansion and/or percent shear. Lateral expansion refers to a measurement of the maximum thickness increase after fracture which results from the development of shear lips. The percent shear refers to percentage of the fracture projected area consumed by shear lips. This measurement procedure is necessarily arbitrary because the shear zone generally varies as the crack progresses through the specimen. Fracture appearance measurements are likely to be more easily determined from large specimens. Both lateral expansion and percent shear generally follow the same temperature trend as the impact energy with the brittle conditions exhibiting very low values. The NDT and Drop Weight Tear tests do not require measurement of an energy value. The NDT test is designed to determine the highest temperature where a specimen breaks when subjected to a small deflection (approximating yield point loading) in the presence of cleavage crack originating in a brittle weld bead. This temperature is defined as the nil ductility temperature. The Drop Weight Tear test is designed to determine the fracture appearance in terms of percent shear as a function of test temperature for impact values at least sufficient to completely fracture the specimen.

3.3.3.1 *[Table]* Summary of ASTM selected standard impact texts.

3.3.4 Bending, see Section 3.2.4.

3.3.5 Torsion and Shear, see Section 3.2.5.

3.3.6 Bearing, see Section 3.2.6.

3.3.7 Stress Concentration. This section is concerned with the effects of stress concentrations on the static strength of alloys. Stress concentrations are of special concern when high strength alloys are being used in severe service. In these circumstances large losses in load carrying capacity can accompany the presence of high stress concentrations. The majority of tests used to investigate the effect of stress concentrations may be classified either as notch tests or crack tests. Detailed discussion of both types of these tests may be found in Appendix C: Fracture Properties (under revision). The effect of stress concentrations on the static strength can be strongly influenced by the metallurgical structure as determined by the fabrication history and heat treatment, as well as by the external environment.

3.3.7.1 Notch properties. The results from notch tests are generally presented in terms of the notch strength computed from the maximum load and the original dimensions of the notched section (e.g., ASTM E 602, Ref. 34). Occasionally the strength reported is based on the unnotched section dimensions and in such cases the strength value is referred to as the residual strength. Strength values determined from notched specimens are dependent on the geometry of the notch and specimen size. For this reason it is not possible to compare data from different sources unless the specimen geometry and sizes are identical. Results from notch specimen tests reported in this handbook are accompanied by information concerning the notch geometry and pertinent specimen dimensions.

3.3.7.2 Fracture toughness. Fracture toughness in this context is concerned with the influence of cracks on the strength of alloys. Evaluation of fracture toughness requires the use of specimens containing so called "natural cracks." These are generally produced by fatigue loading of specimens provided with sharp notch crack starters. Results from such tests may be reported as crack strength, analogous to the notch strength, or as an index of fracture toughness which can be used to give an indication of structural load carrying capacity in the presence of cracks or crack-like flaws. Various indices have been developed and test methods for defining several of them have been standardized, namely, K_{Ic} (ASTM E 399, Ref. 19), J_{Ic} (ASTM E 813, Ref. 35), and CTOD (ASTM E 1290, Ref. 36). These methods are primarily concerned with determining critical values corresponding to crack initiation under static loading. Each method contains certain criteria which must be met to qualify the test result as a valid value. Invalid results are frequently published as indicators of toughness trends (e.g., changes in toughness with tempering temperature). Such values have dubious value for this purpose (Ref. 22) and should be used with caution. The plane strain fracture toughness K_{Ic} is considered to be a lower bound of fracture toughness where crack initation is primarily controlled by the linear elastic stress field at the crack tip. It has special significance for predicting the fracture behavior of high strength materials under highly constrained loading (e.g., thick sections). The J_{Ic} and CTOD indices of fracture toughness are designed to characterize materials where crack initiation is accompanied by an amount of plastic flow sufficient to invalidate

the determination of K_{Ic}. CTOD tests have proven useful in cases where bursts of cleavage crack extension are observed in the test records. This type of behavior is commonly observed in ferritic steels. Under dynamic loads the fracture toughness may be well below the value determined from the static tests. This effect of rapid loading is most pronounced in ferritic steels but has also been observed in heat treated low alloy steels (Ref. 37). There appears to be a limiting value of the stress intensity factor below which increases in loading rate produce no further decrease in toughness. Thus, a fast running crack would arrest if the K level falls below this value. The arrest value K_{Ia} is determined according to ASTM E 1221 (Ref. 38) which relates specifically to ferritic steels.

Stable crack growth resistance under static loads following initiation can be determined in terms of K (ASTM E 561, Ref. 39) or in terms of J (ASTM E 1152, Ref. 40). The resistance is expressed as a curve relating K or J to crack extension. The K resistance curves are dependent on material thickness and criteria are provided to ensure that the uncracked ligament is always predominantly elastic. The J resistance curves are presumably independent of thickness if the validity criteria of the method are met. Resistance curves can be used to estimate the amount of stable crack growth (tearing) which precedes unstable fracture in very ductile alloys.

Other types of tests have been proposed to measure fracture toughness either directly or by correlations with valid values from K_{Ic}, J_{Ic}, or CTOD tests. The chevron notch specimen (ASTM E 1304, Ref. 41) measures a plane strain toughness quantity K_{Iv} which may be equal to K_{Ic} for materials of low toughness but will overestimate K_{Ic} for materials having a rising crack growth resistance curve (e.g., most aluminum alloys, Ref. 42). Fracture toughness values from Chevron notch specimens are reported only when valid K_{Ic} or J_{Ic} values are not available. An equivalent energy method (ASTM E 992, Ref. 43) yields a K-EE value from invalid ASTM E 399 tests. However, the equivalent energy method does not transform invalid K_{Ic} values to valid values. K-EE values are useful only in restricted circumstances and are not reported in this handbook.

Many attempts have been made to correlate Charpy V impact test results with K_{Ic}. A review of these (Ref. 44) indicates that there is no general relation which can be applied to a wide range of alloys. An example of this lack of generality is shown in Ref. 22 for a variety of steels where valid K_{Ic} values were available. The difficulty of establishing general relationships is not surprising considering the differences in strain rate and notch acuity in the two types of tests. The slow bend precracked Charpy test (ASTM E 812, Ref. 45) has been used to establish correlations between K_{Ic} and the crack strength of the Charpy specimens. These correlations are limited by plastic yielding in the small Charpy specimen (Ref. 46) and should never be extrapolated.

3.3.8 Combined Loading (formerly Combined Properties), see Section 3.2.8.

3.4 Creep and Creep Rupture Properties

In most cases, creep tests are performed in tension with temperature and the applied load held constant. Stress values generally are based on the original area of the specimen. In creep rupture tests the deformation is not reported and the data are represented as stress vs time to failure (rupture). ASTM E 139 (Ref. 47) gives recommended practices for creep and creep-rupture tests which are followed by most investigators. A wide variety of specimen sizes are employed and, except for very brittle materials or for tests on notched specimens, the size has little effect on the results. On the other hand, the atmosphere in contact with the specimen can have a substantial influence on the results depending on the surface reactions which may occur. Since most tests are carried out in air, caution should be used in applying such data to situations where the environment may be more or less aggressive.

Creep data are reported in terms of either total strain or as only the plastic component of the strain. The basic data are represented as strain as a function of time for various applied stress levels at a constant temperature. Creep deformation curves of this type usually give more information than is needed for practical applications and the data are often replotted in different ways using the normal stress as an independent variable but plotting it on the ordinate: (a) stress vs time with strain and temperature held constant, (b) stress vs minimum creep rate at a constant temperature, (c) stress for a specified creep strain as a function of temperature with time constant, and (d) isochronous stress vs strain curves at constant temperature. To obtain an isochronous curve the total creep strain or the plastic portion of the strain is plotted as the abscissa with the stress necessary to obtain that strain as an ordinate. Time is then the parameter. The plastic portion of the creep strain is obtained by subtracting the elastic part from the total strain. This procedure is somewhat indefinite because of the uncertainty regarding the modulus of elasticity which is indicated by the tangent at the origin of the isochronous curve. In graphical representation of creep data, logarithmic stress

and time scales are generally used although no special physical significance is attributed to the trends of the data on log-log representations. If the data are very limited or cover only a small range of the variables, tabular representations may be employed. The creep rupture strength of notched specimens is sensitive to the time-temperature dependent embrittlement that develops in many high temperature alloys. These embrittlements are frequently associated with microstructural changes, some of which enhance the smooth creep strength. Generally, the sensitivity to embrittling reactions increases with increasing notch sharpness. For this reason creep tests using very sharp notches or cracks have special significance in the selection of materials for use in critical components which operate at elevated temperatures for extended periods of time (e.g., steam and gas turbines). The notch rupture strength is calculated on the basis of the initial area of the notched section and, to be a useful indicator of embrittlement, must be compared with the smooth strength at the corresponding rupture time.

For some applications (e.g., steam and gas turbine components) it is desired to characterize alloy behavior for service times of many years. Very long time creep or creep rupture tests are very expensive and subject to interruptions due to power failure or equipment breakdown. It has been recognized for many years that it would be advantageous to substitute temperature for time in such a way that the long time behavior could be predicted from time-temperature parameters. One of the first and simplest proposed is the Larson-Miller parameter (Ref. 48). Many others followed having increased complexity. It is not yet clear which, if any, have general applicability and none have been standardized. This handbook prefers to present creep and rupture directly and will report data in terms of a time-temperature parameter only if no direct data is available. Time-temperature parameters should be used with caution particularly when extrapolation outside the data range is attempted.

3.5 Fatigue Properties

This section presents the effects of repeated loading on the strength and deformation properties. In some cases the temperature may vary as well as the load. For the purposes of this discussion the information on fatigue properties may be divided into (1) conventional high-cycle fatigue, (2) low-cycle fatigue, and (3) fatigue crack propagation. In conventional fatigue the strains throughout the test are predominantly elastic and consequently the stresses are relatively low and the number of cycles to failure large. In low-cycle fatigue the plastic component of the total strain is larger than the elastic component, the stresses are relatively high, and the cycles to failure relatively short. Both conventional high-cycle and low-cycle fatigue tests are concerned with total life including the crack initiation and propagation phases, and in some cases data are reported for each phase. Fatigue-crack growth is most commonly obtained from specimens with pre-existing cracks.

3.5.1 Conventional High-cycle Fatigue. The basic types of tests used are (1) rotating beam where a specimen of circular cross-section rotates under an applied bending moment, (2) reverse bending where a specimen generally of rectangular crossection is subjected to alternating bending, and (3) axial load in which the alternating load is parallel to the specimen axis. Both smooth and notched specimens are employed in these tests. Generally the load is allowed to fluctuate between two definite limits although random load spectrum tests are frequently employed in the design of a particular component. Random load test data have limited application and are not reported in this handbook. The stresses are calculated by conventional elastic formulae. The maximum stress is referred to as F_{max} and the minimum stress as F_{min}. The stress ratio R is defined as follows:

$$R = F_{min}/F_{max}$$

Another definition of the stress relationship is the A ratio defined as follows:

$$A = F_{alt}/F_{mf}$$

where $F_{alt} = \frac{1}{2}(F_{max} - F_{min})$ is the alternating stress and where $F_{mf} = \frac{1}{2}(F_{max} + F_{min})$ is the mean stress. The stress range is $2F_{alt}$. Where only one stress ratio is involved, it is common to report this ratio and plot the fatigue strength as a function of the number of cycles to failure. Where more than one stress ratio is used the data may be presented in the form of a stress range diagram. Each curve in this diagram gives the alternating stress as a function of the mean stress for a given number of cycles to failure. The fatigue strength is derived from these diagrams by the following relation:

$$F_{max} = F_{mf} + F_{alt}$$

When reporting the results of notch fatigue tests an attempt is made to give the dimensions of the notch specimen as well as the stress concentration factor K_t. It should be noted that the fatigue strength of a notched specimen will, in some cases, be dependent on the absolute size of the specimen while the elastic stress concentration factor will be independent of size providing the proportions remain unchanged. For both smooth and notched specimens, the fatigue properties will be dependent on the type of loading, specimen type, stress ratio and, in many cases, the surface condition of the specimen.

Two types of behavior are noted in high-cycle fatigue tests at room temperature. In one case a definite fatigue or endurance limit exists. Stresses below this limit produce no failure in an extreme number of cycles.

This behavior is most clearly noted in ferritic steels and is less pronounced in heat treated low alloy steels. In the other case no definite limit is observed. This type of behavior characterizes aluminum alloys and other face center cubic materials. In this case the fatigue limit is arbitrarily assigned, usually at 10^6 or 10^7 cycles.

3.5.2 Low-cycle Fatigue. The most commonly used low-cycle fatigue tests employ cylindrical specimens subjected to axial loads. Attention is focused primarily on the strain and strain range rather than on the stress and stress range. Tests are generally carried out between fixed strain limits. It is important to recognize that under these conditions the alloy may either cyclically harden or soften. When hardening occurs, progressively higher stresses are produced under a constant strain range. If strain softening occurs, the stresses will progressively decrease under a constant strain range. In order to simplify the material characterization it is common to express the strain range in terms of the stress range developed at the half-life (half the cycles to failure) point. Such a plot of strain vs stress at a given number of cycles is called the cyclic stress-strain curve. For cyclically strain hardening materials, the cyclic stress-strain curve is above the monotonic curve; for cyclically softening materials it is below the conventional stress-strain curve. Cyclic stress-strain curves are more useful in design against low-cycle fatigue than are the conventional monotonic curves. A simple criterion for establishing whether the material is cyclically strain hardening or softening (Ref. 49) is the ratio F_{tu}/F_{ty}. When this ratio is greater than 1.4 the material is likely to be cyclically strain hardening; if less than 1.2, the material is likely to be strain softening. Ratios between 1.2 and 1.4 do not clearly identify either strain hardening or strain softening. A more complex and somewhat more accurate criterion for determining whether softening or hardening takes place under cyclic loading is given in Ref. 50. The basic relation between fatigue life and plastic strain in the absence of creep, first formulated by Manson (Ref. 51) and Coffin (Ref. 52), is

$$\Delta\varepsilon_p = MN_f^z$$

where ε_p is the plastic component of the cyclic strain, N_f is the number of cyles to failure, and M and z are material constants. Thus, the low-cycle fatigue behavior of a material is often characterized by a plot of plastic strain vs cyclic life on log-log coordinates. According to the Manson-Coffin relation such a plot should be a straight line; however, curvature is sometimes noted in the high-cycle range.

General relationships. The fatigue limit generally increases with tensile strength and sometimes is estimated as one-half the tensile strength. However, at best, this relationship is a very rough approximation. Steels heat treated to hardness above about 40 RC can not be characterized by such a simple relation (Ref. 53), probably because at high hardness levels steels become very sensitive to crack initiation at surface irregularities and/or inclusions. Much more useful estimates of fatigue lives from tensile properties have been made by developing relationships based on the total strain (elastic plus plastic). The following relation has been proposed (Ref. 54) for estimating the fatigue life in terms of the total strain and the tensile properties.

$$\Delta\varepsilon = (N_f/D)^{-0.6} + 3.5(F_{tu}/E)N_f^{-0.12}$$

where D is the true diametrical strain = ln(1 - RA), where RA is the reduction in area at fracture and N_f is the fatigue life at a total strain range of $\Delta\varepsilon$. For most materials this relation gives useful results in the range between 10 and 10^7 cycles.

At elevated temperatures creep may be superimposed on fatigue and the interpretation of the data becomes rather complicated. Frequency of cycling is an important variable under these circumstances. If temperature and mean stress are sufficiently high, creep rupture becomes the primary mode of failure and the times to failure are often reported rather than the number of cycles to failure. For much of the elevated temperature fatigue test data, it is not possible to clearly classify the information as conventional high-cycle or as low-cycle fatigue.

3.5.3 Fatigue Crack Propagation. This section contains information on propagation of so-called natural cracks under cyclic loading. With few exceptions these cracks are produced from a starter notch by fatigue cycling at stress intensity levels well below K_{Ic}. ASTM E 647 (Ref. 59) gives details concerning the preparation of specimens, testing methods, and validity criteria. Logarithmic coordinates are most frequently used to plot crack propagation rates (da/dN) as a function of the stress intensity range ΔK. Such plots often define two major regions of interest: (1) region where the rate is a nearly linear function of the stress intensity range and (2) a value of the stress intensity range, designated as ΔK_{th}, below which fatigue crack propagation presumably will not occur under the test conditions. It is important to realize that the crack propagation rates and the K_{th} value will be a function of the test environment and the mean value of the stress intensity range. In come cases the value of K_{th} will be below K_{Iscc}. At elevated temperatures and in the presence of aggressive environments, the test results can be a function of the cyclic load frequency. Appendix C (under revision) gives further details.

3.6 Elastic Properties

This section includes not only the classical elastic constants but also the tangent and secant moduli which extend into the plastic region. A high degree of sensitivity and precision in strain measurements is required in determining the elastic constants. Values reported

in the literature often exhibit considerable scatter due to poor testing techniques. Some annealed alloys have no true proportional limit at room temperature, and at sufficiently high temperature no alloy has a well defined proportional limit. Under these circumstances truly elastic properties do not exist and attempts to determine the elastic constants will result in values which depend strongly on the testing technique.

3.6.1 Poisson's Ratio. Poisson's ratio is the absolute value of the ratio of the transverse strain to the corresponding axial strain resulting from uniformly distributed axial stress below the proportional limit of the material. Poisson's ratio is related to the elastic modulus E and shear modulus G as follows:

$$\mu = \frac{E}{2G} - 1$$

ASTM D 132 (Ref. 55) is a standard method for determination of Poisson's ratio at room temperature.

3.6.2 Modulus of Elasticity. For the purposes of this handbook the modulus of elasticity refers to Young's modulus. The static modulus of elasticity is the ratio of the normal stress to the corresponding strain measured at stresses below the proportional limit of the material. The determination may be made in either tension or compression (ASTM E 111, Ref. 56). The tension modulus E is theoretically equal to the compression modulus E_c; however, residual stresses may produce some difference in these values. The modulus may also be determined by resonance methods (Ref. 57) and when so determined is generally referred to as the dynamic modulus. At temperatures where time dependent deformation is absent the static and dynamic moduli are essentially equal with the dynamic value in some materials being slightly lower than the static value. At temperatures where time dependent deformation would occur in static tests the dynamic modulus is useful where vibratory loads accompany creep deformation. The modulus of elasticity decreases with increasing temperature and is much less sensitive to the metallurgical structure than is the flow stress. However, the modulus will depend on the testing direction in cases where a bulk crystallographic anisotropy is present.

3.6.3 Modulus of Rigidity. The modulus of rigidity or the shear modulus is the ratio of the shear stress to the corresponding shear strain for shear stresses below the proportional limit in shear of the material. The modulus of rigidity is related to Young's modulus and Poisson's ratio as follows:

$$G = \frac{E}{2(1+\mu)}$$

ASTM E 143 (Ref. 58) gives a standard method for determining the shear modulus.

3.6.4 Tangent Modulus. The tangent modulus is the slope of the stress strain curve at each stress value considered. Reported values are subject to considerable variation because of the basic difficulty in determining the slope of any curve. The tangent modulus may be determined in either tension or compression.

3.6.5 Secant Modulus. The secant modulus is the slope of a line from the origin to the stress values considered. The secant modulus may be determined in either tension or compression.

4 Fabrication

The term fabrication is used here to mean all of the processes, except heat treatment, which may normally be employed in the manufacture of components from material supplied by the alloy producers. These processes include forming (forging, rolling, drawing, etc.), metal removal (machining, chem milling, etc.), joining (welding, soldering, brazing, etc.), and post fabrication treatments that may be required (cleaning and other surface treatments). In many cases the fabrication process may profoundly alter the mechanical properties of the material through the effect on the microstructure by the introduction of residual stresses or the production of crack like defects. This handbook can devote only a limited amount of space to the very large amount of information that exists on the so-called fabricability of an alloy or the details of recommended fabrication procedures. Emphasis is placed on the effect of fabrication processes which can adversely affect the load carrying capacity in service. In this connection particular attention is given to welding and other joining processes.

4.1 Forming

The information presented in this section relates primarily to the effects of various forming processes on the mechanical properties. Forming includes the processes of permanent metal deformation (e.g., forging, rolling, drawing, etc.). Forging temperatures are reported as the maximum starting and the minimum finishing temperature. These apply to closed die or blacksmith forgings in the weight range from 5 to 1000 lbs. Forging temperatures for small parts are approximately the same; however, for small forgings a great deal of care must be exercised to avoid critical strains which can induce grain growth on reheating for a subsequent operation or during heat treating.

4.2 Machining and Grinding

Only a very limited amount of information on these subjects is presented. The reader is referred to the Machinability Data Center, Metcut Research Associates, Cincinnati, Ohio, for detailed information on the machinability of the alloys in this handbook.

4.3 Joining

The joining processes of welding and brazing and, to a lesser extent, soldering can produce damaged regions in a fabricated component which may severely limit its load carrying capacity. Thus, the deposited filler metal or heat affected zone of the parent metal may contain embrittled regions or cracks. Special attention is given to the effects of welding and brazing parameters on the fracture properties and to recommended procedures which will produce sound joints.

4.4 Surface Treating

Attention here is focused on cleaning procedures or special surface treatments (e.g., case hardening) that could influence the mechanical properties.

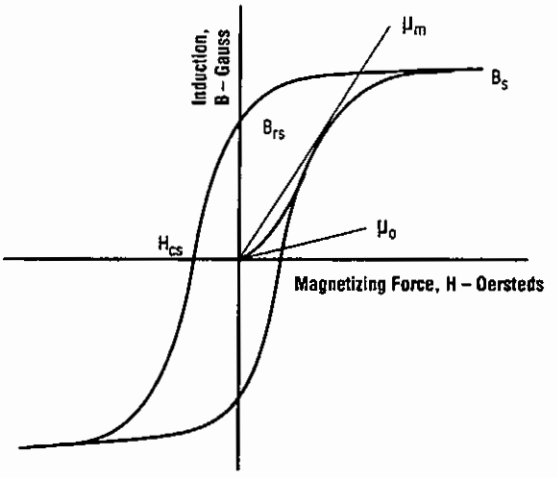


Fig. 2.2.3.1 Normal induction curve and hysteresis loop for ferromagnetic materials

Table 3.3.3 Summary of ASTM selected standard impact tests

Name	Specimen	Notch	Index of Toughness	Reference
Charpy and Izod	Simple Beam	None	Absorbed Energy	ASTM E 23 Ref. 30
Charpy and Izod	Notched Beam 10x10 mm (a)	V, Keyhole or U	Absorbed Energy Lateral Expansion Transition Temp. Fracture Appearance	ASTM E 23 Ref. 30
NDT	Surface Crack Plate	Brittle Weld Crack Starter	Nil Ductility Transition Temp.	ASTM E 208 Ref. 31
Drop Weight Tear	Edge Notch Plate 3x12 in. full thickness	Pressed V R < 0.001 in.	Fracture Appearance	ASTM E 436 Ref. 32
Dynamic Tear	Edge Notch Plate 7x1.6 in. 3/16<t<5/8 in.	Pressed V R < 0.001 in.	Absorbed Energy Fracture Appearance	ASTM E 604 Ref. 33

(a) Subsized Charpy specimens permitted

References

1. MIL-HDBK-5, *Metallic Materials and Elements for Aerospace Vehicle Structures*, Department of Defense and Federal Aviation Administration, Naval Publication and Forms.
2. ASTM E 527, "Standard Practice for Numbering Metals and Alloys (UNS)," *ASTM Annual Book of Standards*.
3. Woldman, N. E., *Engineering Alloys*, ASM Int'l., Materials Park, OH.
4. ASTM E 10, "Standard Test Method for Brinell Hardness of Metallic Materials," *ASTM Annual Book of Standards*.
5. ASTM E 18, "Standard Test Methods for Rockwell Hardness and Rockwell Superficial Hardness of Metallic Materials," ibid.
6. ASTM E 92, "Standard Test Method for Vickers Hardness of Metallic Materials," ibid.
7. ASTM E 384, "Standard Test Method for Microhardness of Materials," ibid.
8. ASTM A 255, "Standard Method for End Quench Hardenability of Steel," ibid.
9. "Transformation Structures," *Metals Handbook*, ASM Vol. 8 (1973), p. 175.
10. ASTM A 34, "Standard Practice for Procurement Testing and Sampling of Magnetic Materials," *ASTM Annual Book of Standards*.
11. "Direct - Current Magnetic Measurements for Soft Magnetic Materials," ASTM STP 371 S1 (1970).
12. "Direct - Current Magnetic Hysteresigraphs," ASTM STP 523 (1973).
13. Wood, W. D.; Dean, H. W.; and Lucks, C. F., "Thermal Radiative Properties of Selected Materials," DMIC Report 177 (November 15, 1962).
14. McClintock, F. A., and Argon, A. S. (editors), *Mechanical Behavior of Materials*, Addison-Wesley Publishing Co., Reading, MA (1966).
15. ASTM G 31, "Recommended Practice for Laboratory Immersion Corrosion Testing of Metals," *ASTM Annual Book of Standards*.
16. ASTM G 82, "Guide for Development and Use of a Galvanic Series for Predicting Galvanic Corrosion Performance," ibid.
17. ASTM G 49, "Recommended Practice for Preparation and Use of Direct Tension Stress Corrosion Test Specimens," ibid.
18. ASTM G 38, "Standard Practices for Making and Using C-Ring Stress Corrosion Cracking Test Specimens," ibid.
19. ASTM E 399, "Standard Test Method for Plane-Strain Fracture Toughness of Metallic Materials," ibid.
20. ASTM E 8, "Standard Test Methods for Tension Testing of Metallic Materials," ibid.
21. ASTM E 1012, "Standard Practice for Verification of Specimen Alignment Under Tensile Loading," ibid.
22. Brown, Jr., W. F., and Strawley, J. E., "Commentary on Present Practice," ASTM STP 463 (1970), p. 216.
23. ASTM E 9, "Standard Test Methods of Compression Testing of Metallic Materials at Room Temperature," *ASTM Annual Book of Standards*.
24. ASTM E 290, "Standard Test Method for Semi-Guided Bend Test for Ductility of Metallic Materials," ibid.
25. ASTM E 855, "Standard Test Methods for Bend Testing of Metallic Flat Materials for Spring Applications Involving Static Loading," ibid.
26. ASTM B 406, "Standard Test Method for Transverse Rupture Strength of Cemented Carbides," ibid.
27. ASTM E 238, "Standard Test Method for Pin-Type Bearing Test of Metallic Materials," ibid.
28. ASTM E 21, "Standard Practice for Elevated Temperature Tests of Metallic Materials," ibid.
29. ASTM E 209, "Standard Practice for Compression Tests of Metallic Materials at Elevated Temperatures with Conventional or Rapid Heating Rates and Strain Rates," ibid.
30. ASTM E 23, "Standard Test Methods for Notched Bar Impact Testing of Metallic Materials," ibid.
31. ASTM E 208, "Standard Test Method for Conducting Drop-Weight Test to Determine Nil-Ductility Transition Temperature of Ferritic Steels," ibid.
32. ASTM E 436, "Standard Method for Drop-Weight Tear Tests of Ferritic Steels," ibid.
33. ASTM E 604, "Standard Test Method for Dynamic Tear Testing of Metallic Materials," ibid.
34. ASTM E 602, "Standard Method for Sharp-Notch Tension Testing with Cylindrical Specimens," ibid.
35. ASTM E 813, "Standard Test Method for J_{Ic}, A Measure of Fracture Toughness," ibid.
36. ASTM E 1290, "Standard Test Method for Crack-Tip Opening Displacement (CTOD) Fracture Toughness Measurement," ibid.
37. Ripling, E. J.; Mulherin, J. H.; and Crosley, P. B., "Crack Arrest Toughness of Two High Strength Steels (AISI 4140 and AISI 4340)," *Met. Trans.*, Vol. 13A, April 1982, p. 657.
38. ASTM E 1221, "Standard Test Method for Determining Plane-Strain Crack-Arrest Fracture Toughness, K_{Ia}, of Ferritic Steels," *ASTM Annual Book of Standards*.

39. ASTM E 561, "Standard Practice for R-Curve Determination," ibid.

40. ASTM E 1152, "Standard Test Method for Determining J-R Curves," ibid.

41. ASTM E 1304, "Standard Test Method for Plane-Strain (Chevron-Notch) Fracture Toughness of Metallic Materials," ibid.

42. Munz, D., "Determination of Fracture Toughness of High Strength Aluminum Alloys with Chevron Notched Short Bar and Short Rod Specimens," *Eng. Fracture Mechanics*, Vol. 15, Nos. 1-2 (1981), p. 231.

43. ASTM E 992, "Standard Practice for Determination of Fracture Toughness of Steels Using Equivalent Energy Methodology," ibid.

44. Roberts, R., and Newton, C., "Interpretive Report on Small-Scale Correlations with K_{Ia} Data," *Welding Research Bulletin*, No. 265, February 1981.

45. ASTM E 812, "Standard Test Method for Crack Strength of Slow-Bend Precracked Charpy Specimens of High-Strength Metallic Materials," *ASTM Annual Book of Standards.*

46. Succop, G., and Brown, W. F., Jr., "Estimation of K_{Ic} from Slow Bend Precracked Charpy Specimen Strength Rations," ASTM STP 632 (1977), p. 179.

47. ASTM E 139, "Standard Practice for Conducting Creep, Creep-Rupture, and Stress-Rupture Tests of Metallic materials," *ASTM Annual Book of Standards.*

48. Larson, F. R., and Miller, J., "A Time-Temperature Relation for Rupture and Creep Stresses," *Trans. Am. Soc. Mech. Engs.*, Vol. 74 (1952), p. 765.

49. Smith, R. W.; Hirschberg, M. H.; and Manson, S. S., "Fatigue Behavior of Materials Under Strain Cycling in the Low and Intermediate Life Range," NASA TN D-1574 (April 1963).

50. Manson, S. S., "Interfaces Between Fatigue, Creep and Fracture," *International Journal of Fracture Mechanics*, Vol. 2 (1966), p. 327.

51. Manson, S. S., "Behavior of Materials Under Conditions of Thermal Stress," Heat Transfer Symposium, University of Michigan Research Institute (1953), p. 9.

52. Coffin, L. F., "A Study of Cyclic Thermal Stresses in a Ductile Metal," *Trans. ASME*, Vol. 76 (1954), p. 931.

53. "Properties and Selection of Metals," *Metals Handbook*, 8th edition, Vol. 1 (1961), p. 217.

54. Manson, S. S., "Fatigue, a Complex Subject - Some Simple Approximations," The William M. Murray Lecture 1964, *Experimental Mechanics* (July 1965).

55. ASTM E 132, "Standard Test Method for Poisson's Ratio at Room Temperature," *ASTM Annual Book of Standards.*

56. ASTM E 111, "Standard Test Method for Young's Modulus, Tangent Modulus, and Chord Modulus," ibid.

57. Schrieber, E.; Anderson, O. L.; and Soga, N., *Elastic Constants and Their Measurement*, McGraw-Hill (1973), p. 17-122.

58. ASTM E 143, "Standard Test Method for Shear Modulus at Room Temperature," *ASTM Annual Book of Standards.*

59. ASTM E 647, "Standard Test Method for Measurement of Fatigue Crack Growth Rates," *ASTM Annual Book of Standards.*

	Fe
0.8	C
4	Cr
4	Mo
1	V
0.2	Si

M50

1 GENERAL

AISI M50 is one of a class of semi-high-speed steels which have greater abrasion resistance than plain carbon steels but lower red hardness than the high-speed cutting steels. M50 is one of the leaner alloys of its class. High austenitizing temperatures are required to produce full hardness after tempering. The relatively low content of carbide phase results in rapid grain coarsening at the austenitizing temperature and for that reason close control of austenitizing temperature and time are required to produce a fine grain structure. The steel exhibits secondary hardening and is normally tempered near or at the peak of secondary hardness. Retained austenite can be reduced to negligible amounts by multiple tempering. The fully hardened steel is quite brittle and small cracks can result in catastrophic failure of components stressed well below the yield strength.

M50 is used in woodworking tools, hydraulic pump assemblies, pump pistons, pump vanes, in rolling element bearings operating at elevated temperatures, and in heavy duty gearing. M50 is widely used in aircraft gas turbine engine bearings and for this application high cleanliness and close composition control is obtained by vacuum induction melting (VIM) followed by consumable electrode melting (VAR). The low toughness of M50 is a limiting factor on the speed of large jet engine bearings and investigations are presently under way to produce bearings having races with a very hard surface but a relatively soft and tough core (28).

1.01 Commercial Designation

AISI M50, VASCO M-50, LATROBE MV-1, ALLEGHENY-LUDLUM HTB-2.

1.02 Alternate Designations

None

1.03 Specifications

1.031 AMS specifications, Table 1.031.

1.032 Inclusion ratings specified by AMS 6490 C and 6491, Table 1.032.

1.04 Composition

1.041 AMS composition limits, Table 1.041.

1.05 Heat Treatment

1.051 General. The general requirements for heat treating steels of this type are given in Reference 17 and the complex carbide changes during annealing, hardening, and tempering are discussed in detail in Reference 1. Relatively high austenitizing temperatures are necessary to ensure satisfactory carbide solution. Short exposure times at the austenitizing temperature are desirable in order to minimize grain size. Generally, hold times are no longer than to produce temperature equalization throughout the part (Table 1.058). Special attention should be given to avoid decarburization during annealing or austenitizing through the use of neutral salt baths or atmosphere furnaces. The steel exhibits secondary hardening in the tempering temperature range between 800 and 1100 F (Figure 1.0513). The as-quenched alloy contains substantial amounts of retained austenite (Figure 1.059) which is stable at tempering temperatures up to about 800 F. The transformation of the retained austenite occurs concurrently with the secondary hardening (Figure 1.059). The retained austenite content is well below 1 percent for tempering temperatures above about 1000 F for multiple tempered alloy. A cold treatment following the first of three tempers did not result in a decrease in the content of retained austenite (Figure 1.0510).

1.052 Normalizing. Not recommended (5).

1.053 Annealing. Heat slowly 1525 to 1650 F, 1 hr, FC at 35 F/hr maximum. Decarburization may be avoided by using controlled atmosphere or pack annealing with cast iron chips (5)(10). Hardness of the annealed condition is about 200 BHN (10).

1.054 Austenitizing. Preheat slowly 1500 to 1650 F. Harden at 2000 to 2050 F, only enough to equalize, preferably in neutral salt, AC or OQ. To minimize the possibility of cracking or distorting complex shapes, a salt quench at 1100 to 1150 F, 2 min., and AC from the hardening temperature is recommended (2)(6).

1.055 Cold treatment. To minimize retained austenite, a -100 F treatment immediately following quenching is recommended by one producer (4).

1.056 Tempering, 900 to 1200 F, AC. The maximum hardness will generally be obtained by tempering 1000 to 1025 F. Multiple tempers (cooling to room temperature between each temper) are generally used to minimize retained austenite. Triple tempering (2 + 2 + 2 hr) is sometimes used and there is evidence that the 2-hr temper repeated 5 times may increase the fracture toughness (see 3.0272). Multiple tempers have little effect on hardness (Figure 1.0513).

1.057 Stress relief. Stress relief following machining may be carried out at the tempering temperature.

1.058 AMS specified heat treatments, Table 1.058.

1.059 Effect of tempering temperature on retained austenite and hardness of CVM bar, Figure 1.059.

1.0510 Effect of tempering temperature on retained austenite in VIM + VAR bar, Figure 1.0510.

1.0511 Effect of austenitizing temperature on hardness and grain size of oil quenched or air cooled CVM bar, Figure 1.0511.

1.0512 Effect of tempering time on hardness of air induction melted bar, Figure 1.0512.

1.0513 Effect of multiple tempering on the hardness of CVM alloy, Figure 1.0513.

1.0514 The effect of tempering temperature on the hardness of VIM + VAR bar, Figure 1.0514.

1.0515 Effect of tempering temperature on the hardness of VIM + VAR bar austenitized at several temperatures, Figure 1.0515.

	Fe
0.8	C
4	Cr
4	Mo
1	V
0.2	Si

M50

1.06 **Hardness**

1.061 General. A high initial hardness following tempering and the stability of this hardness for long times at elevated temperatures are necessary to minimize spalling and pitting of bearings during service. A minimum hardness of 58 R_C has been suggested for critical bearing applications such as would be encountered in gas turbines (18)(19). The steel is deep hardening and hardness levels of 60 to 64 R_C should be obtainable at the center of 4-inch thick sections.

The available hardness data support the conclusion that for steel having a room temperature hardness greater than 60 R_C the hardness at 600 F will be greater than 58 R_C. The stability of the initial as heat treated room temperature hardness to long time exposure at elevated temperature depends on the initial hardness level (Figure 1.064). Data concerning the effects of exposure at the test temperature to the hardness at this temperature (Figure 1.065) indicate that 1000 hr exposure to 600 F will reduce the 600 F hardness from 59 R_C to about 57 R_C for a steel with an initial as heat treated hardness of 64 R_C. According to Figure 1.066 the steel with an initial room temperature hardness of about 62 R_C had an 800 F hardness of about 58 R_C after 750 hr exposure at 800 F. Stability effects would be expected to depend on both the initial hardness and the composition limits with the higher hardness levels being somewhat less stable after exposure at elevated temperatures for extended times.

1.062 Effect of test temperature on the hardness of CVM bar, Figure 1.062.

1.063 Effect of test temperature on the hardness of CVM forging tempered at 950 or 1075 F, Figure 1.063.

1.064 Stability temperature of room temperature hardness for various exposure times, Figure 1.064.

1.065 Effect of exposure temperature and test temperature on hardness of air induction melted bar, Figure 1.065.

1.066 Effect of exposure to 600 and 800 F for various times on hardness at the exposure temperature and at room temperature after long exposure, Figure 1.066.

1.067 Effect of test temperature on Vickers hardness of CVM alloy, Figure 1.067.

1.068 Effect of high test temperature on hardness of VIM-VAR bar, Figure 1.068.

1.069 Effect of test temperature on hardness of CVM bar, Figure 1.069.

1.07 **Forms and Conditions Available**

1.071 Bars, forgings, and tubing in as formed or annealed condition.

1.08 **Melting and Casting Practice**

1.081 Applications in high-speed bearings and in gearing require material of closely controlled composition, low content of tramp elements, and generally high cleanliness. Consumable electrode melting (CVM) or vacuum induction melting followed by consumable electrode melting (VIM-VAR) is necessary to meet these requirements. The preferred method for highest quality is VIM-VAR (Table 1.082). The details of this melting practice are discussed in References 7 and 16, with particular reference to improved aircraft bearing performance.

1.082 Gas content and inclusion ratings for various melting practices, Table 1.082.

1.09 **Special Considerations**

1.091 Cleanliness and microstructure must be closely controlled for critical bearing applications. Double vacuum melting (VIM-VAR) coupled with careful control of the heat treatment are necessary to achieve low inclusion content, a small grain size, and uniform carbide distribution (see 1.05 and 1.08).

1.092 Like other tool steels, the high hardness conditions of this alloy have low fracture toughness and this has become a cause for concern as the speed of the large bore rolling element bearings has increased. The combination of the large bore and the high speed results in high centrifugal stresses which can cause catastrophic race failure in the presence of small cracks originating from spalls (see 3.0272).

1.093 Dimensional change following 1000 hr exposure to elevated temperatures, Table 1.093.

2 PHYSICAL PROPERTIES AND ENVIRONMENTAL EFFECTS

2.01 **Thermal Properties**

2.011 Melting range.

2.012 Phase changes, A_C 1490 to 1555 F, A_r 1385 to 1345 F.

2.0121 Time-temperature-transformation diagrams.

2.01211 Isothermal transformation diagram, Figure 2.01211.

2.013 Thermal conductivity.

2.0131 Thermal conductivity of CVM forging, Table 2.0131.

2.014 Thermal expansion.

2.0141 Coefficient of thermal expansion, Figure 2.0141.

2.015 Specific heat.

2.016 Thermal diffusivity.

2.02 **Other Physical Properties**

2.021 Density, 0.288 lb per cu in. [7.97 gm per cc] (12).

2.022 Electrical properties.

2.023 Magnetic properties. Alloy is ferromagnetic.

2.024 Emittance.

2.025 Damping capacity.

2.03 **Chemical Environment**

2.031 General. The alloy is subject to oxidation in normal air if not protected. From experience with other tempered martensitic steels it might be expected that crack propagation would be influenced by the service environment. However, no information on such effects was available at the time this chapter was prepared.

2.032 Oxidation of CVM alloy exposed in air for 50 and 150 hr at the tempering temperature, Table 2.032.

2.04 **Nuclear Environment**

	Fe
0.8	C
4	Cr
4	Mo
1	V
0.2	Si

M50

3 MECHANICAL PROPERTIES

3.01 Specified Mechanical Properties

3.011 AMS specified mechanical properties, Table 3.011.

3.02 Mechanical Properties at Room Temperature

3.021 Tension properties. Tension – Stress/strain diagrams.

3.0211 Effect of tempering temperature on the tensile properties of VIM-VAR bar, Figure 3.0211.

3.022 Compression properties. Compression – Stress/strain diagrams (see 3.032).

3.023 Impact.

3.0231 Effect of tempering temperature on the unnotched Izod impact energy of CVM bar austenized at 2000 or 2050 F, Figure 3.0231.

3.0232 Effect of tempering temperature on the unnotched Izod impact energy of VIM-VAR bar austenitized at several temperatures, Figure 3.0232.

3.024 Bending.

3.025 Torsion and shear.

3.026 Bearing.

3.027 Stress concentration.

3.0271 Notch properties.

3.0272 Fracture toughness.

3.02721 General. When this steel is heat treated to the high hardness levels used in high-speed bearings and in gearing, it exhibits low plane strain fracture toughness. Tempering at temperatures beyond those corresponding to the secondary hardening peak results in rising fracture toughness with only small losses in tensile strength hardness (compare Figure 3.02722 with Figures 3.0211 and 1.0514). However, data are insufficient to define the extent of increased toughness and decreased strength and hardness associated with overtempering. It has recently been reported that the plane strain fracture toughness of the same material as represented by the data in Figure 3.02722 can be increased to 21 ksi-$\sqrt{\text{in.}}$ by tempering five times at 1000 F (20). This multiple tempering cycle did not change the hardness and would not be expected to change the tensile strength.

3.02722 Effect of tempering temperature on the plane strain fracture toughness of bar, Figure 3.02722.

3.028 Combined properties.

3.03 Mechanical Properties at Various Temperatures

3.031 Tension properties. Tension – Stress/strain diagrams.

3.0311 Effect of elevated temperatures on the tensile properties of CVM bar, Figure 3.0311.

3.032 Compression properties. Compression – Stress/strain diagrams.

3.0321 Effect of test temperature on compression yield strength of air induction melted bar, Figure 3.0321.

3.033 Impact.

3.034 Bending.

3.035 Torsion and shear.

3.036 Bearing.

3.037 Stress concentration.

3.0371 Notch properties.

3.0372 Fracture and fracture toughness.

3.038 Combined properties.

3.04 Creep and Creep-Rupture Properties

3.05 Fatigue Properties

3.051 General. There is considerable information on the performance of this steel under conditions representing service in high-speed bearings (22)(23)(25)(26). M50 steel is considerably superior to SAE 52100 for bearing applications above about 350 F. It has been further demonstrated that VIM-VAR melting of M50 increases bearing life compared to air plus VAR melting (Table 3.052).

3.052 Comparative performance of AM + VAR and VIM + VAR material in a rolling contact fatigue test, Table 3.052.

3.053 S-N curves for VIM bar at room temperature and 500 F, Figure 3.053.

3.054 Crack propagation rate as a function of stress intensity factor range for VIM-VAR bar, Figure 3.054.

3.06 Elastic Properties

3.061 Poisson's ratio.

3.062 Modulus of elasticity.

3.0621 Effect of test temperature on modulus of elasticity, Figure 3.0621.

3.063 Modulus of rigidity, 12,000 ksi (11).

3.064 Tangent modulus.

3.065 Secant modulus.

4 FABRICATION

4.01 Forming

4.011 Forging. Preheat 1400 to 1500 F to equalize and then heat to a maximum forging temperature of 2050 F (4)(6)(10)(11). Minimum forging temperature is given as 1800 F (4), 1700 F (6)(11), and 1600 F(10). Forgings should be furnaced cooled or very slowly cooled in an insulating material.

4.012 Ausforging. Ausforging of this steel may be carried out between about 850 and 1100 F. This process is particularly effective in producing a structure with small and uniformly distributed carbides. Studies conducted in bearing test rigs, actual bearing tests, and in gear tests indicate superior performance for ausforged CVM material as compared with that conventionally forged (21)(22)(23)(27). However, large reductions [80 percent] are necessary to obtain substantial improvements and it becomes increasingly difficult and costly to produce sound forgings as the size increases. Because of these difficulties and because the advent of VIM-VAR melting has substantially increased performance, ausforging has not gained commercial acceptance.

4.013 Effect of high test temperature on tensile impact energy of VIM-VAR as-forged billet, Figure 4.013.

4.02 Machining and Grinding

4.021 General. The machinability is rated between 55 and 65 percent of a 1 percent carbon water

	Fe
0.8	C
4	Cr
4	Mo
1	V
0.2	Si

M50

hardening tool steel, or about 45 to 55 percent of AISI B1112. Approximate turning speeds of 70 to 90 surface feet per minute are recommended when using high speed cutting tools (5)(6).

4.03 **Joining**

4.031 Welding or brazing is not recommended (12).

4.04 **Surface Treating**

REFERENCES

1 Bridge, J. Edwin, Jr., Maniak, G. N., and Philip, T. V., "Carbides in M-50 High Speed Steel", Met. Trans. Vol. 2 (August 1971) p 2209.

2 AMS 6490 C (December 15, 1974).

3 AMS 6491 (January 15, 1976).

4 Berger, E. J., Carpenter Technology Corp., Technical Data on M-50 Steel (June 4, 1981).

5 Bhat, G. K. and Nehrenberg, A. E., "A Study of the Metallurgical Properties of Bearing Materials at Temperatures in the Range from Room Temperature to 1000 F for Aircraft Service", Crucible Steel Corp. AFML Contract AF 33(616)-3318 WADC Report 57-343 (April 1957).

6 Latrobe Steel Corp. Data Sheet, Lescalloy M50 VIM-VAR (June 1977).

7 Schlatter, R. and Stroup, J. P., "Improved M-50 Aircraft Bearing Steel Through Advanced Vacuum Melting Processes", J. Vac. Sci. Tech. Vol. 9 No. 6 (December 1972) p 1326.

8 Latrobe Steel Co., "Metallurgical Report Hot Hardness Characteristics of Speciality Bearing Steels" (July 1965).

9 High Temperature High Strength Alloys, Am. Iron and Steel Institute (February 1968).

10 Allegheny-Ludlum Steel Corp., Pittsburgh, PA M-50 Data Sheets.

11 Vanadium Alloys Steel Co., Vasco M-50 Data Sheets (1974).

12 General Electric, Materials Handbook, Section 2 Iron Base Alloy M-50 (September 12, 1973).

13 Rescalvo, J. A. and Auerbach, B. L., "Fracture & Fatigue in M-50 & 18-4-1 High Speed Steels", Met. Trans. Vol. 10A (September 1979) p 1265.

14 Chevalier, J. I., Dietrich, M. W., and Zaretsky, E. V., "Hot Hardness Characteristics of Ausformed AISI M-50, Matrix II, WD-65, Modified 440C and Super Nitralloy", NASA TN D 7244 (May 1973).

15 Latrobe Steel Corp. Electrite MV-1 (1964).

16 Schlatter, R., "Double Vacuum Melting of High Performance Bearing Steels", Industrial Heating (September 1974) p 40.

17 Roberts, G. A., Hamaker, J. C., and Johnson, A. R., Tool Steels, 3rd Edition, ASM (1962).

18 Bamberger, E. N. and Harris, T., "Life Adjustment Factors for Ball and Roller Bearings – An Engineering Design Guide", ASME New York, NY (1971).

19 Schlict, H. and Zwirlein, O., "Varying Heat Treatment Parameters to Optimize Material and Roller Contact Fatigue Strength", Journal of Heat Treating, Vol. No. 3 (June 1980) p 73.

20 Private communication with E. N. Bamberger, General Electric Aircraft Engine Group. Project Manager on AF Contract 33615-80-C-2018 reporting data obtained by B. L. Auerbach on this contract (1982).

21 Bamberger, E. N., "The Effect of Ausforming on the Rolling Contact Fatigue Life of a Typical Bearing Steel", Journal of Lubrication Technology, Trans. ASME (January 1967) p 63.

22 Bamberger, E. N., "Materials for Rolling Element Bearings", Bearing Design – Historical Aspects, Present Technology, and Future Problems, International Conference on Bearing Design, W. J. Anderson, Editor ASME (August 1980).

23 Parker, R. J. and Zaretsky, E. V., "Rolling-Element Fatigue Life of Ausformed M-50 Steel Balls", NASA TN D 4954 (December 1968).

24 Bamberger, E. N., "Thermomechanical Working of Electroslag Melted M 50 Bearing Steel", General Electric Co. AF33615-70-C-1234, AFML TR 72-183 (July 1972).

25 Morrison, F. R., McCool, J. I., and Ninos, N. J., "M 50 Steel Bearing Material Factors for Rolling Element Life Calculations", SKF Technology Services, AVRADCOM Technical Report TR 79-35 (April 1979).

26 Parker, R. J. and Zaretsky, E. V., "Rolling Element Fatigue Bearing Life of AISI M-50 18-4-1 Balls", NASA Technical Paper 1202 (April 1978).

27 Townsend, D. P., Bamberger, E. N., and Zaretsky, E. V., "A Life Study of Ausforged, Standard Forged and Standard Machined AISI M-50 Spur Gears", Journal of Lubrication Technology, Trans. ASME (July 1976) p 418.

28 AF Contract 33615-80-C-2018, General Electric Aircraft Engine Group, E. N. Bamberger, Manager.

Alloy	Fe-0.80C-4.0Cr-4.2Mo-1V	
AMS	Form	Condition
6491	Bars, Forgings, and Tubing	Consumable Vacuum Melt
6490 C	Bars, Forgings, and Tubing	Double Vacuum Melt (VIM-VAR)

TABLE 1.031. AMS SPECIFICATIONS

	Fe
0.8	C
4	Cr
4	Mo
1	V
0.2	Si

M50

Alloy	Fe-0.80C-4.0Cr-4.2Mo-1V							
Form	Bars, Forgings, and Tubing							
Source	AMS 6490 C[a]				AMS 6491[b]			
Condition	CVM				VIM + VAR			
Inclusion Type[c][d] Worst Field	A	B	C	D	A	B	C	D
Thin	2.0	1.5	1.5	1.5	1.5	1.0	1.0	1.5
Heavy	1.0	1.0	1.0	1.0	1.0	1.0	1.0	1.0

(a) Radial specimens 0.28 $in.^2$ surface area, fully heat treated, and examined on face parallel to rolling direction.
(b) Radial specimens 0.28 $in.^2$ surface area taken midway between center and surface of hardened fracture samples (>55 R_C), examined on face parallel to rolling direction.
(c) Rating by ASTM E45 method D Plate III.
(d) A - Sulphides, B - Alumina, C - Silicates, and D - Globular Oxides.

TABLE 1.032. INCLUSION RATINGS SPECIFIED BY AMS 6490 C AND 6491

Alloy	Fe-0.80C-4.0Cr-4.2Mo-1V			
Form	Bars, Forgings, and Tubing			
Source	AMS 6491 (3)		AMS 6490 C (2)	
	Percent		Percent	
Composition	Min	Max	Min	Max
C	0.80	0.85	0.77	0.85
Mn	0.15	0.35	–	0.35
Si	–	0.25	–	0.25
P	–	0.015	–	0.015
S	–	0.008	–	0.015
Cr	4.00	4.25	3.75	4.25
Mo	4.00	4.50	4.00	4.50
V	0.90	1.10	0.90	1.10
Ni	–	0.15	–	0.15
Co	–	0.25	–	0.25
W	–	0.25	–	0.25
Cu	–	0.10	–	0.10

TABLE 1.041. AMS COMPOSITION LIMITS

Alloy	Fe-0.80C-4.0Cr-4.2Mo-1V	
Form	Bars, Forgings, and Tubing	
Source	AMS 6490 C	AMS 6491
Condition	CVM	VIM-VAR
Preheat	1500 - 1600 F	–
Austenitize	2025 - 2050 F	2025 - 2050 F
Time	To Equalize	To Equalize
Salt Quench	1100 - 1150 F	1100 - 1150 F[a]
Time	> 2 min, AC	108 to 132 sec
Temper	1000 - 1025 F	1000 - 1025 F
	2 hr AC	1.75 to 2.25 hr AC
Hardness R_C	60-64	60 (Min)

(a) This step may be omitted and austenitized specimens may be air cooled before tempering.

TABLE 1.058. AMS SPECIFIED HEAT TREATMENTS

	Fe
0.8	C
4	Cr
4	Mo
1	V
0.2	Si

M50

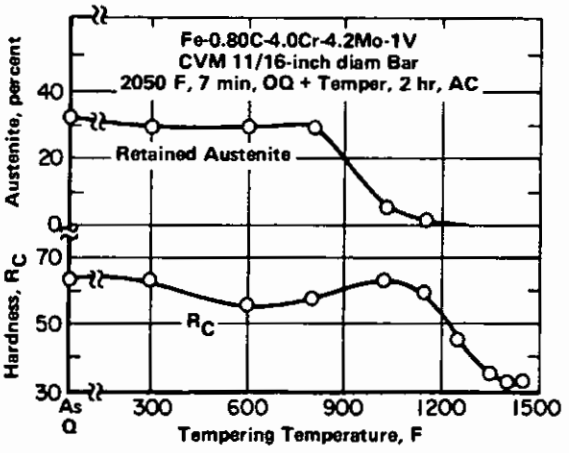


FIGURE 1.059. EFFECT OF TEMPERING TEMPERATURE ON RETAINED AUSTENITE AND HARDNESS OF CVM BAR (1, FIGURE 2)

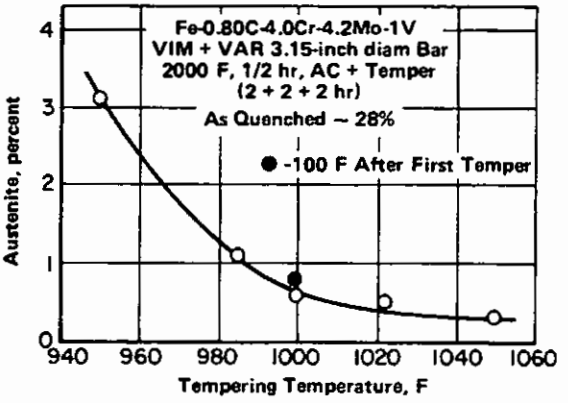


FIGURE 1.0510. EFFECT OF TEMPERING TEMPERATURE ON RETAINED AUSTENITE IN VIM + VAR BAR (13, TABLE 5)

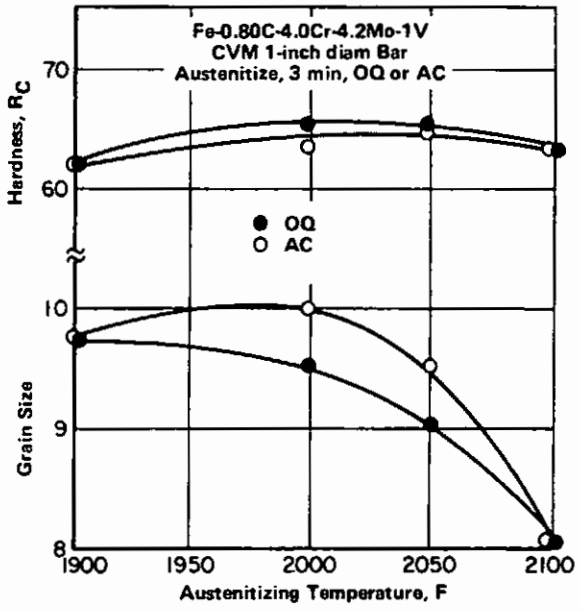


FIGURE 1.0511. EFFECT OF AUSTENITIZING TEMPERATURE ON HARDNESS AND GRAIN SIZE OF OIL QUENCHED OR AIR COOLED CVM BAR (10)

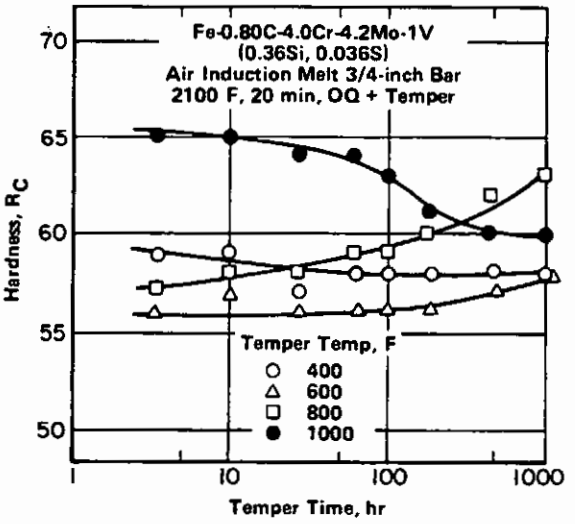


FIGURE 1.0512. EFFECT OF TEMPERING TIME ON HARDNESS OF AIR INDUCTION MELTED BAR (5, TABLE 3)

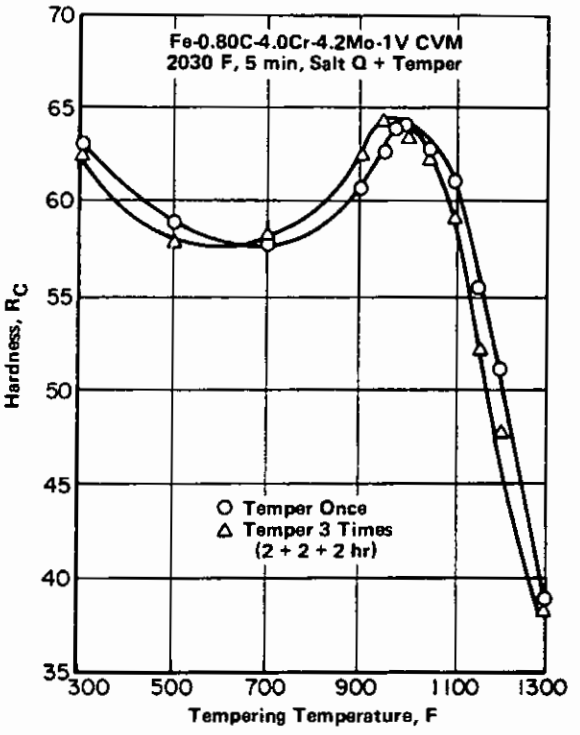


FIGURE 1.0513. EFFECT OF MULTIPLE TEMPERING ON THE HARDNESS OF CVM ALLOY (11)

	Fe
0.8	C
4	Cr
4	Mo
1	V
0.2	Si

M50

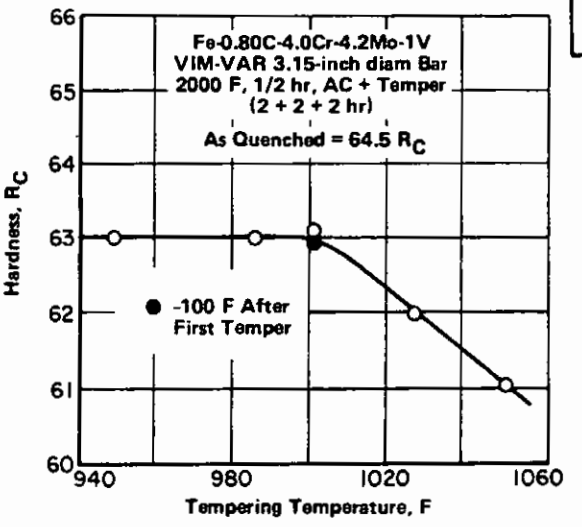


FIGURE 1.0514. EFFECT OF TEMPERING TEMPERATURE ON THE HARDNESS OF VIM-VAR BAR (13, FIGURE 1)

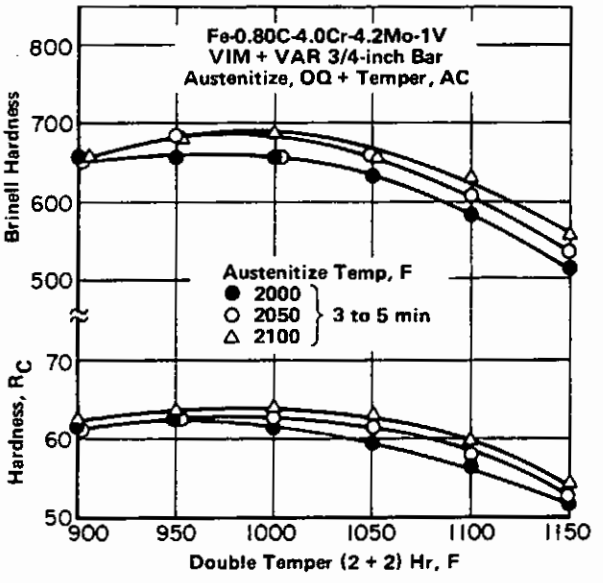


FIGURE 1.0515. EFFECT OF TEMPERING TEMPERATURE ON THE HARDNESS OF VIM + VAR BAR AUSTENITIZED AT SEVERAL TEMPERATURES (4)

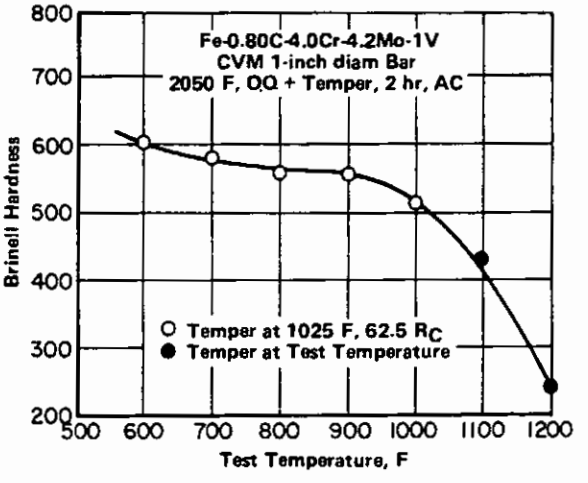


FIGURE 1.062. EFFECT OF TEST TEMPERATURE ON THE HARDNESS OF CVM BAR (10)

	Fe
0.8	C
4	Cr
4	Mo
1	V
0.2	Si

M50

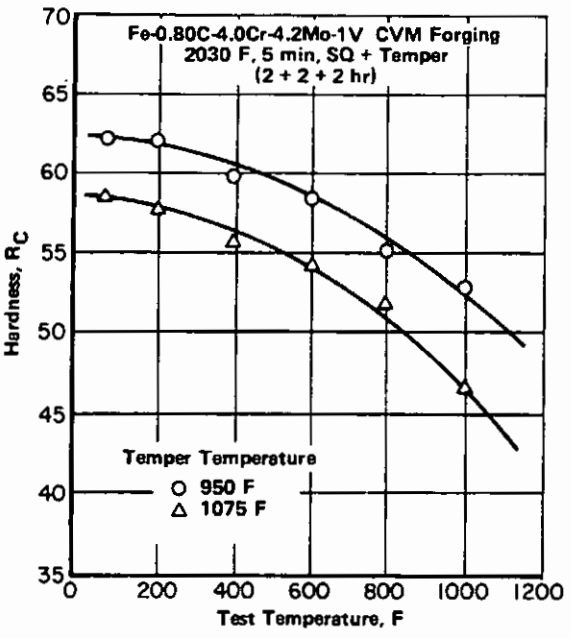


FIGURE 1.063. EFFECT OF TEST TEMPERATURE ON HARDNESS OF CVM FORGING TEMPERED AT 950 OR 1075 F (11)

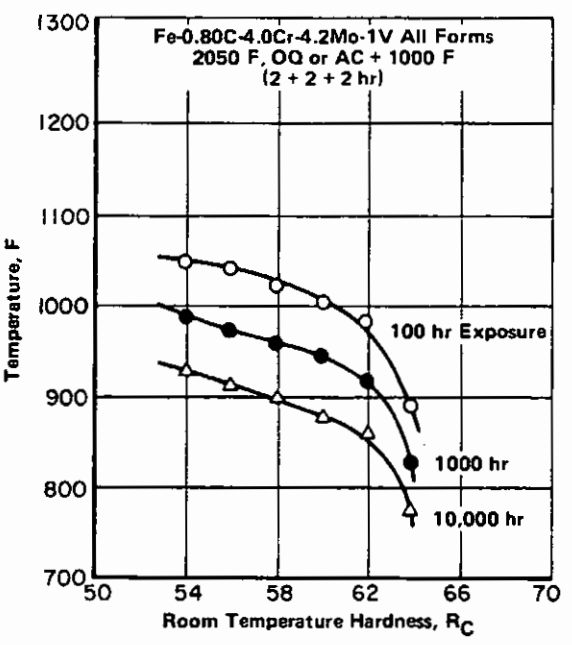


FIGURE 1.064. STABILITY TEMPERATURE OF ROOM TEMPERATURE HARDNESS FOR VARIOUS EXPOSURE TIMES (11)

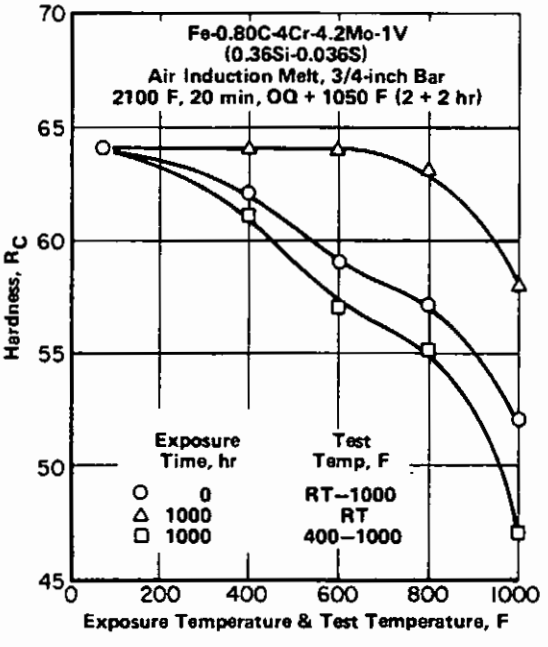


FIGURE 1.065. EFFECT OF EXPOSURE TEMPERATURE AND TEST TEMPERATURE ON HARDNESS OF AIR INDUCTION MELTED BAR (5, TABLE 4)

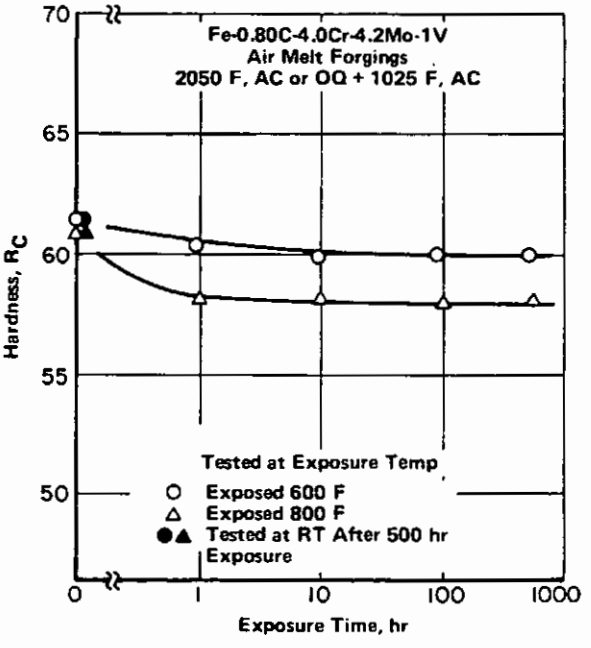


FIGURE 1.066. EFFECT OF EXPOSURE TO 600 AND 800 F FOR VARIOUS TIMES ON HARDNESS AT THE EXPOSURE TEMPERATURE AND AT ROOM TEMPERATURE AFTER LONG EXPOSURE (8, TABLES 2 AND 3)

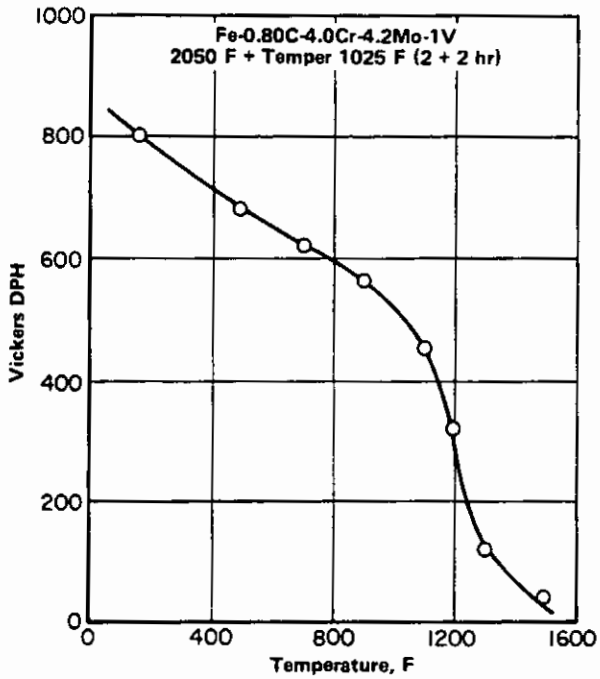


FIGURE 1.067. EFFECT OF TEST TEMPERATURE ON VICKERS HARDNESS OF CVM ALLOY (11)

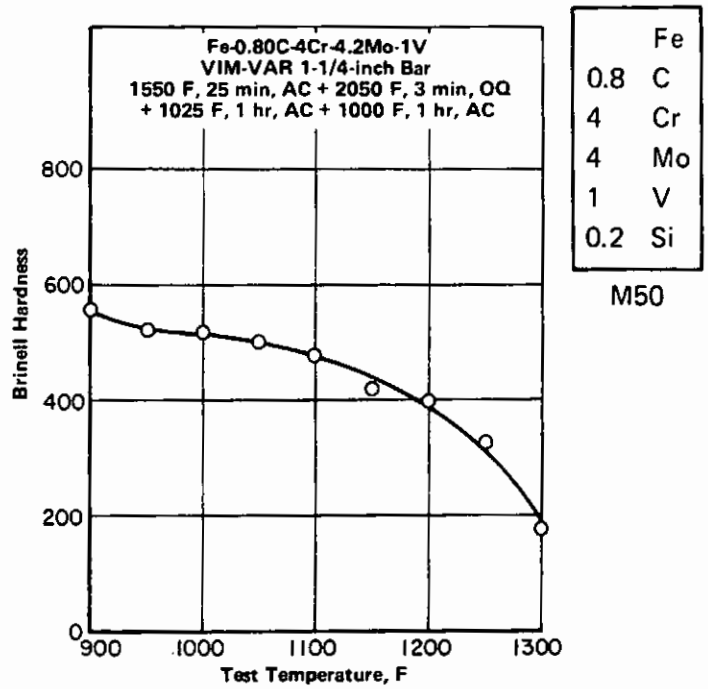


FIGURE 1.068. EFFECT OF HIGH TEST TEMPERATURE ON HARDNESS OF VIM-VAR BAR (4, FIGURE 1)

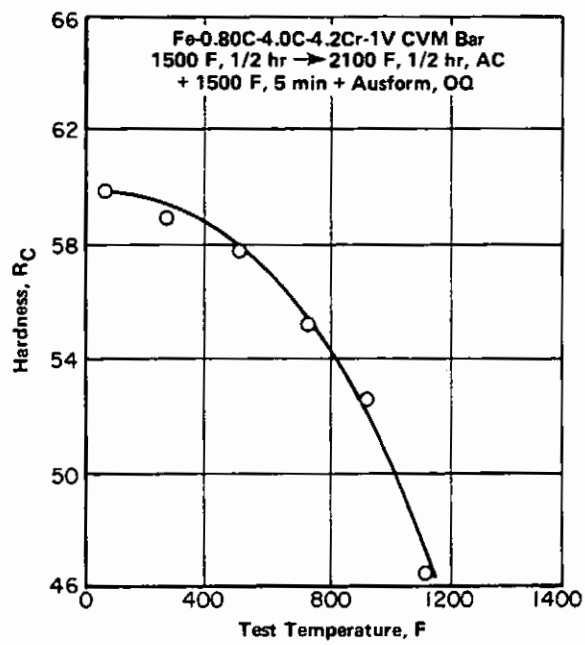


FIGURE 1.069. EFFECT OF TEST TEMPERATURE ON HARDNESS OF CVM BAR (14, FIGURE 3)

	Fe
0.8	C
4	Cr
4	Mo
1	V
0.2	Si

M50

Alloy	Fe-0.80C-4.0Cr-4.2Mo-1V						
Form	0.4-inch diam Bar						
Condition	1550 F, 6 min → 2050 F (Salt), 3 min, Salt Q, 1050 F, AC + 1050 F (2 + 2 hr), AC + 1050 - 1070 F, AC to give 61.5 to 62 R_C						
Melt[a] Practice	AM	AM + VG	AM + VAR	AM + 2 VAR	AM + 3 VAR	VIM	VIM + VAR
Gas Content, ppm							
H_2	4.8	3.2	1.8	<1.0	<1.0	<1.0	<1.0
N_2	150	120	80	60	50	85	60
O_2	67	46	37	9	5	21	6
Inclusion Rating[b] Worst Field							
A Thin	–	–	1/2	–	–	–	1/2
A Heavy	–	–	0	–	–	–	0
B Thin	–	–	1/2-1	–	–	–	1/2-1
B Heavy	–	–	0	–	–	–	0
C Thin	–	–	0	–	–	–	0
C Heavy	–	–	0	–	–	–	0
D Thin	–	–	1	–	–	–	1
D Heavy	–	–	0	–	–	–	0

(a) AM – Air Melt, VG – Vacuum Degass, VAR – Consumable Vacuum Arc Remelt, and VIM – Vacuum Induction Melt.
(b) Rating by ASTM E145 (100X).

TABLE 1.082. GAS CONTENT AND INCLUSION RATINGS FOR VARIOUS MELTING PRACTICES (7p, 1329)

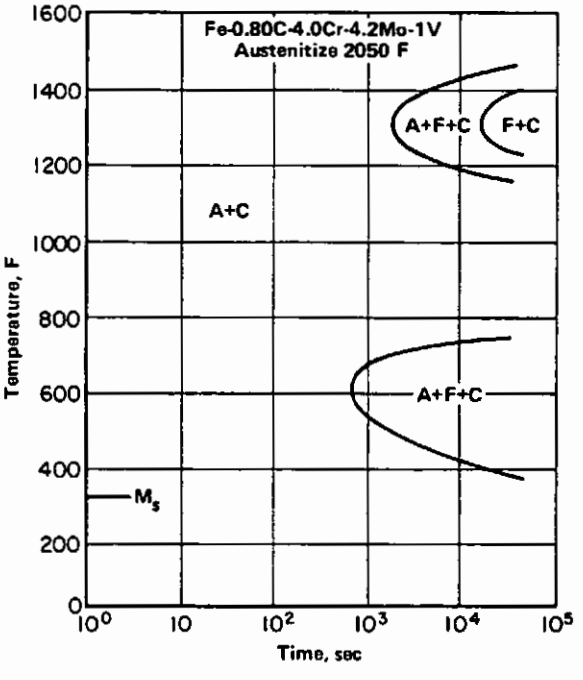


FIGURE 2.01211. ISOTHERMAL TRANSFORMATION DIAGRAM (4)

Alloy	Fe-0.80C-4.0Cr-4.2Mo-1V (0.036S-0.365Si)
Form	Air Induction Melt, 3/8-inch Bar
Condition	2100 F, 20 min, OQ + 1050 F (2 +2 hr), AC
1000 hr Exposure Temp, F	Length Change, percent[a]
400	0.0022
600	0.0012
800	0.0027
1000	0.0050

(a) Specimen 4.000±0.001-inch long. Estimated precision of measurement 0.001 percent.

TABLE 1.093. DIMENSIONAL CHANGE FOLLOWING 1000 HR EXPOSURE TO ELEVATED TEMPERATURES (5, TABLE 5)

Alloy	Fe-0.80C-4.0Cr-4.2Mo-1V		
Form	CVM Forging		
Condition	Annealed or Heat Treated		
Temp, F	212	572	932
Thermal Conductivity, Btu ft/(hr ft^2 F)	21.4	20.2	19.7

TABLE 2.0131. THERMAL CONDUCTIVITY OF CVM FORGING (15)

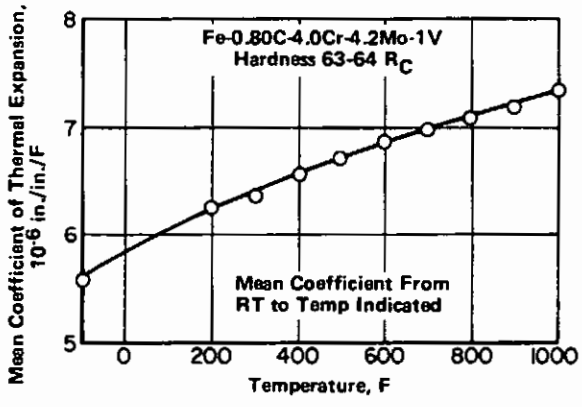


FIGURE 2.0141. COEFFICIENT OF THERMAL EXPANSION (6, 15)

Alloy	Fe-0.80C-4.0Cr-42.Mo-1V			
Form	CVM 1/4-inch Thick			
Condition	1500 F → 2050 F, OQ + Temper 2 hr			
Exposure Time in Air	50 hr		150 hr	
Temper Temp, F	1000	1100	1000	1100
Exposure Temp, F	1000	1100	1000	1100
Weight Gain, mg/cm^2	0.281	1.81	0.481	2.36

	Fe
0.8	C
4	Cr
4	Mo
1	V
0.2	Si

M50

TABLE 2.032. OXIDATION OF CVM ALLOY EXPOSED IN AIR FOR 50 AND 150 HR AT THE TEMPERING TEMPERATURE (10)

Alloy	Fe-0.80C-4.0Cr-4.2Mo-1V				
AMS	6491 and 6490 C				
Form	Bars Diam ≤ 0.500 inch	Bars Diam > 0.500 inch		Mechanical Tubing	
Condition[a]	Cold Finish[b]	Hot Finish	Cold Finish	Cold Finish	Hot Finish
F_{tu}, ksi (Min)	120[c]	–	–	–	–
Hardness, BHN (Min)	–	229[b]	248[b]	–	–
Hardness, R_C or RB (Min)	–	–	–	25 R_C	99 R_B

(a) Fully heat treated: AMS 6491 gives 60 R_C (minimum), AMS 6490 C gives 60 to 64 R_C.
(b) AMS 6490 C specifies sphereodize anneal following hot or cold finish.
(c) AMS 6490 C gives 125 ksi (maximum).

TABLE 3.011. AMS SPECIFIED MECHANICAL PROPERTIES

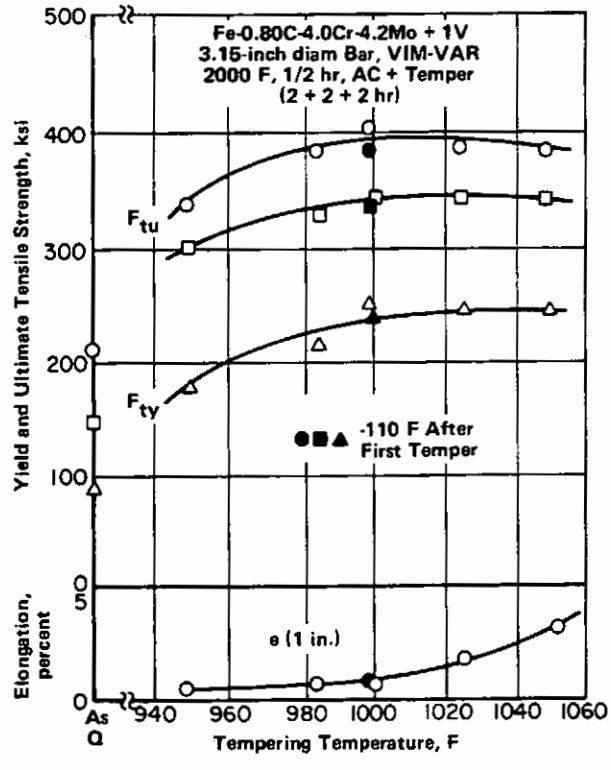


FIGURE 3.0211. EFFECT OF TEMPERING TEMPERATURE ON TENSILE PROPERTIES OF VIM-VAR BAR (13, FIGURES 5 AND 7)

	Fe
0.8	C
4	Cr
4	Mo
1	V
0.2	Si

M50

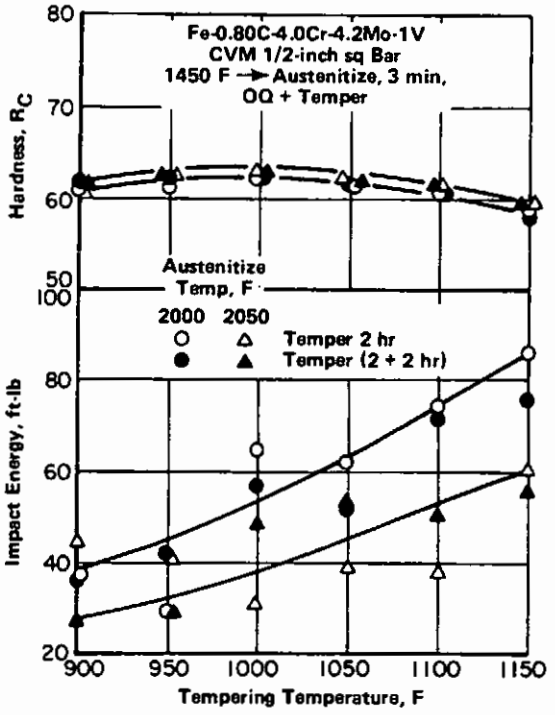


FIGURE 3.0231. EFFECT OF TEMPERING TEMPERATURE ON THE UNNOTCHED IZOD IMPACT ENERGY OF CVM BAR AUSTENITIZED AT 2000 OR 2050 F (6)

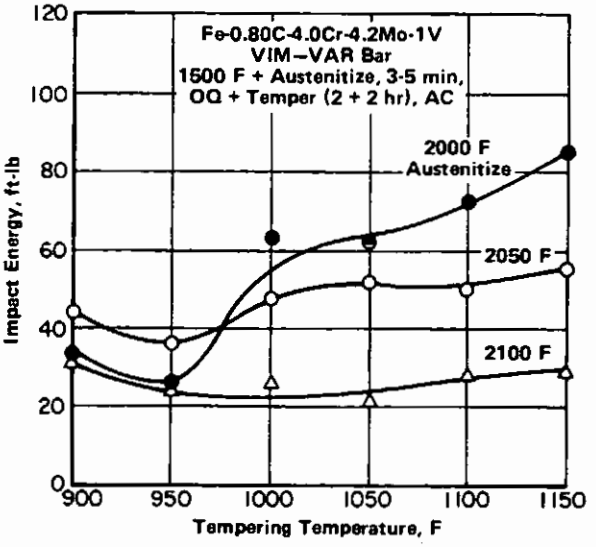


FIGURE 3.0232. EFFECT OF TEMPERING TEMPERATURE ON THE UNNOTCHED IZOD IMPACT ENERGY OF VIM-VAR BAR AUSTENITIZED AT SEVERAL TEMPERATURES (4)

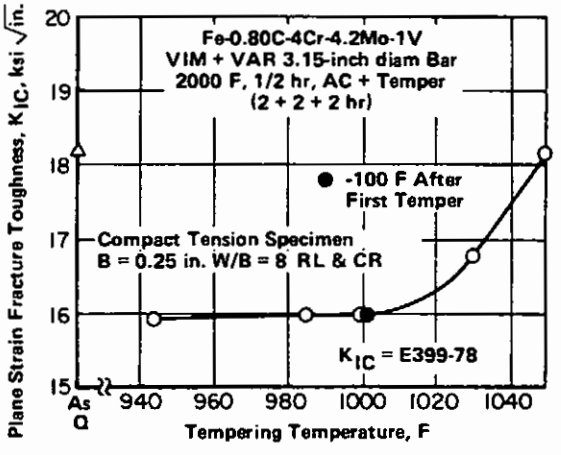


FIGURE 3.02722. EFFECT OF TEMPERING TEMPERATURE ON PLANE STRAIN FRACTURE TOUGHNESS OF BAR (13, FIGURE 11)

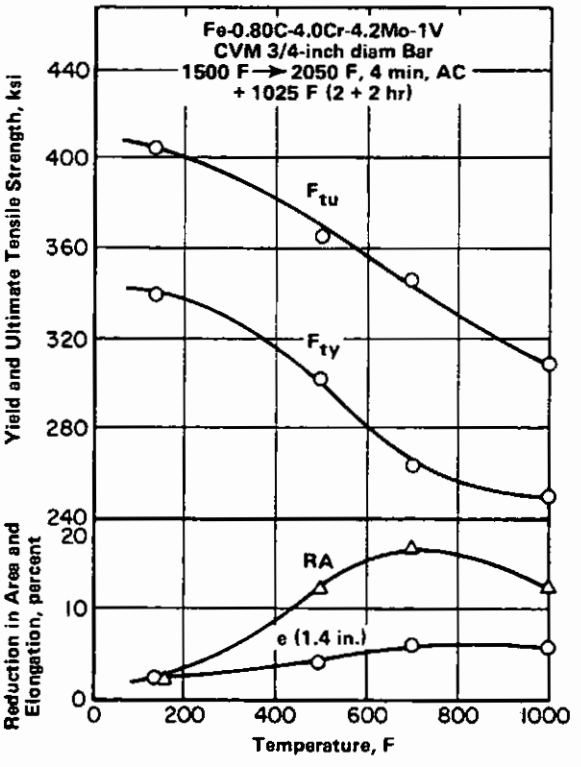


FIGURE 3.0311. EFFECT OF ELEVATED TEMPERATURES ON THE TENSILE PROPERTIES OF CVM BAR (10)

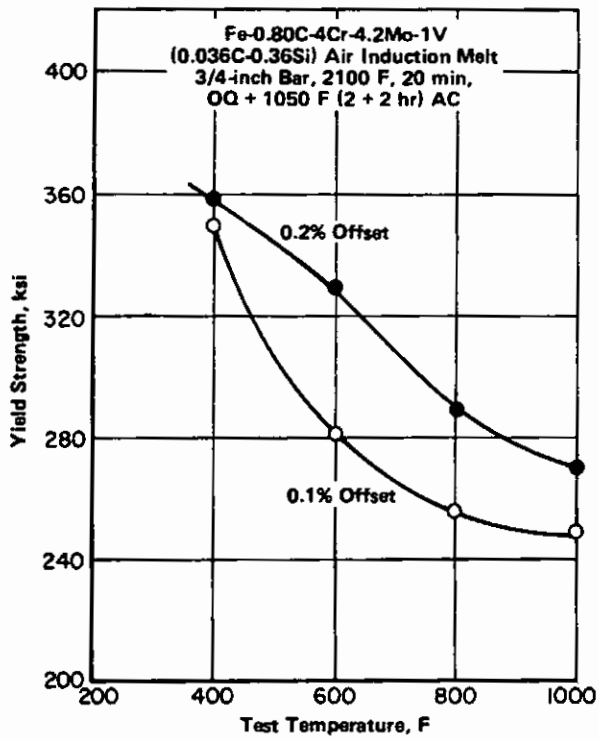


FIGURE 3.0321. EFFECT OF TEST TEMPERATURE ON COMPRESSION YIELD STRENGTH OF AIR INDUCTION MELTED BAR (5, TABLE 6)

Alloy	Fe-0.80C-4.0Cr-4.2Mo-1V	
Form	0.375-inch diam Cylinders	
Condition	8-10 μin. Finish See Table 1.082	
Rolling Contact Fatigue	700,000 Max Hertz Pressure, 20,000 Cycles/min, Lubricant MIL-L-7808, Wheel Finish 8-10 μin. Ground	
Melt Practice	AM + VAR	VIM + VAR
B_{10}, 10^6 Cycles(a)	2.03	4.18
B_{50}, 10^6 Cycles	4.25	7.19
B_1, 10^6 Cycles(b)	0.81	2.13
Weibull Slope	2.52	3.48
Correlation Coefficient	0.93	0.96

(a) B_1, B_{10}, and B_{50} – The number of cycles below which 1%, 10%, and 50%, respectively, of small type failures will occur.
(b) Extrapolated.

TABLE 3.052. COMPARATIVE PERFORMANCE OF AM+VAR AND VIM+VAR MATERIAL IN A ROLLING CONTACT FATIGUE TEST (7p, 1330)

	Fe
0.8	C
4	Cr
4	Mo
1	V
0.2	Si

M50

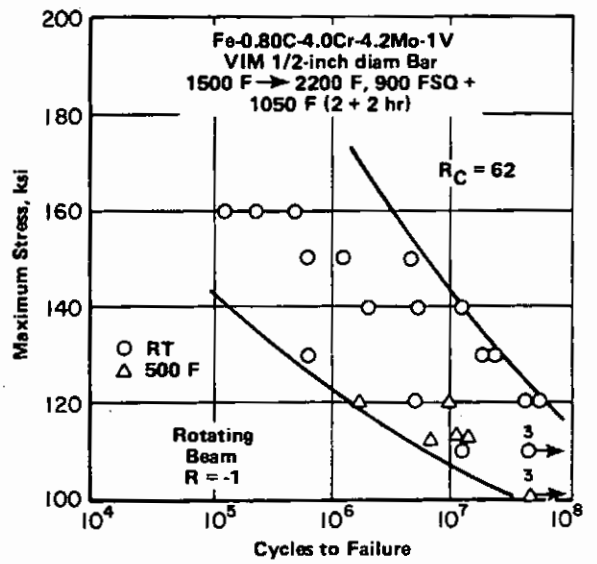


FIGURE 3.053. S-N CURVES FOR VIM BAR AT ROOM TEMPERATURE AND 500 F

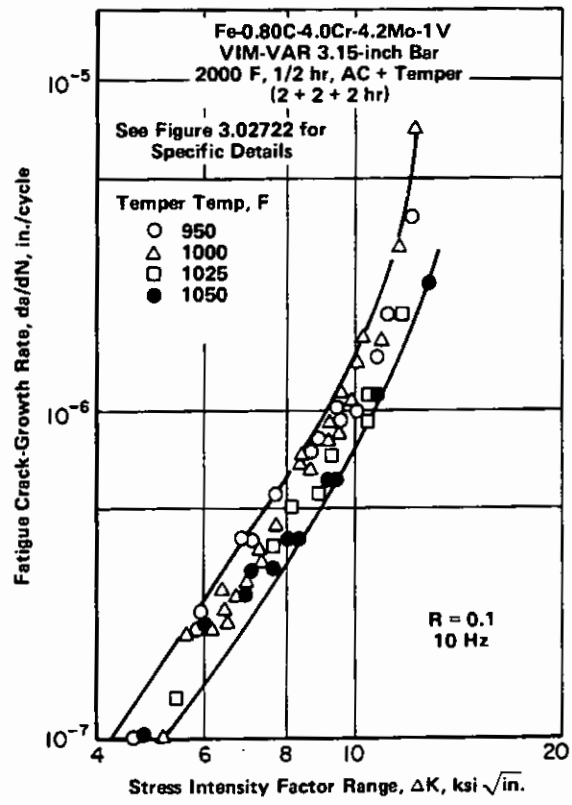


FIGURE 3.054. CRACK PROPAGATION RATE AS FUNCTION OF STRESS INTENSITY FACTOR RANGE FOR VIM-VAR BAR (13, FIGURE 15)

	Fe
0.8	C
4	Cr
4	Mo
1	V
0.2	Si

M50

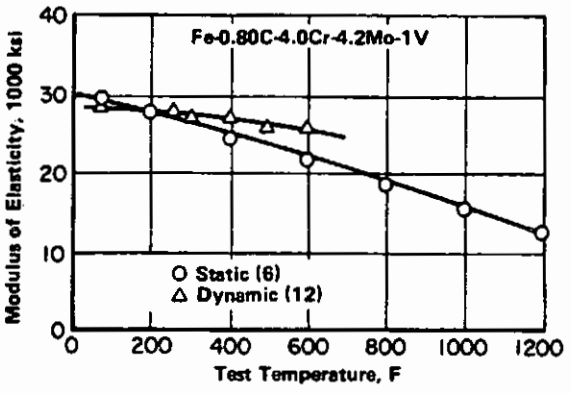


FIGURE 3.0621. EFFECT OF TEST TEMPERATURE ON MODULUS OF ELASTICITY (6, 12)

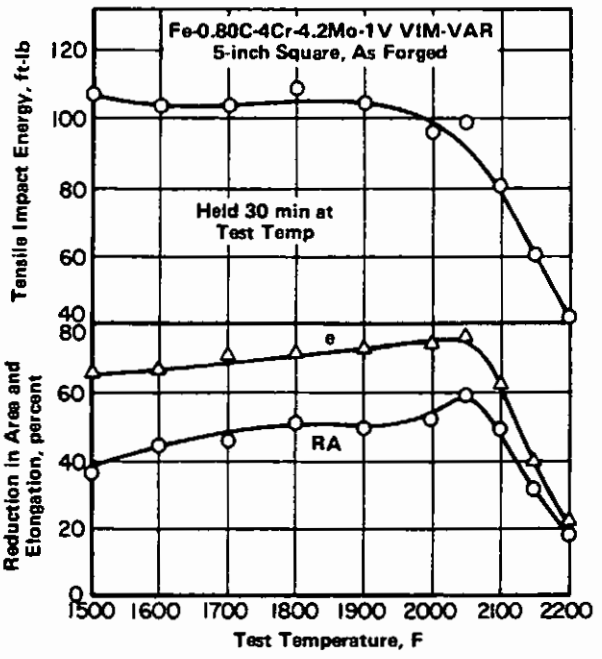


FIGURE 4.013. EFFECT OF HIGH TEST TEMPERATURE ON TENSILE IMPACT ENERGY OF VIM-VAR AS FORGED BILLET (4)

	Fe
0.4	C
1.6	Cr
1.1	Al
0.6	Mn
0.35	Mo

Nitralloy 135 Mod.

1 GENERAL

The composition of this steel, in particular the aluminum and chromium contents, is optimized for maximum case hardening by nitriding. The steel can also be strengthened by standard quench and temper procedures, allowing the production of parts with a high strength core and a hardened surface. Applications for nitrided Nitralloy 135 modified steel are widespread and its behavior has been characterized through many years of commercial use. Specific applications include weapons components, roller shafts, crankshafts, and transmission spur gears. Parts are normally final machined and heat treated before nitriding, which results in minimal dimensional change. The nitrided surface provides improved fatigue resistance, wear resistance, corrosion resistance, and resistance to softening at temperatures to 1200 F (1–4, 8–10).

1.01 Commercial Designation

Nitralloy 135 modified.

1.02 Alternate Designations

Nitralloy Type G modified, AMS 6470 Nitriding Steel, SAE 7140, UNS K24065.

1.03 Specifications

1.031 Specifications, Table 1.031.

1.04 Composition

1.041 Composition, Table 1.041.

1.05 Heat Treatment

1.051 Anneal, 1450 F, 6 hours, furnace cool (3).

1.052 Normalize, slowly heat to 1790 to 1810 F, air cool (3, 4).

1.053 Austenitize, 1700 to 1750 F (3).

1.054 Quench, less than 2 inch diameter or thickness, oil quench. Larger than 2 inch diameter or thickness, water quench (3).

1.055 Temper, 1000 to 1300 F, 1 hour minimum per inch of thickness. Temper 50 F minimum above nitriding temperatures (2).

1.056 Nitriding, 930 to 1050 F (1–3).

1.06 Hardness

1.061 End quench hardenability, Figure 1.061.

1.0611 AMS 6470 E specifies J50 = 8 and J45 = 12 minimum. AMS 6471B specifies J50 = 12 and J46 = 16 minimum.

1.062 Effect of tempering temperature on hardness of bar, Figure 1.062.

1.063 Hot hardness of nitrided alloy, Figure 1.063.

1.07 Forms and Conditions Available

1.071 This steel is available in most wrought forms such as rods, bars, plates, tubing, and forgings (1).

1.08 Melting and Casting Practice

1.09 Special Considerations

1.091 Part surfaces must be thoroughly cleaned before nitriding.

1.092 White layer is hard, brittle, and tends to crack. If greater than 0.0005 inch thick after nitriding, it should be removed to prevent flaking and surface roughening.

2 PHYSICAL PROPERTIES AND ENVIRONMENTAL EFFECTS

2.01 Thermal Properties

2.011 Melting range.

2.012 Phase changes. Critical temperature, A_{c1} = 1435 F (3).

2.0121 Time-temperature-transformation diagrams.

2.013 Thermal conductivity, 30.0 Btu ft/hr ft^2 F at 212 F (1).

2.014 Thermal expansion, Figure 2.014.

2.015 Specific heat, 0.11 to 0.12 Btu/lb F (1).

2.016 Thermal diffusivity.

2.02 Other Physical Properties

2.021 Density, 0.283 lb/$in.^3$. 7.83 gr/cm^3 (1).

2.022 Electrical properties.

2.0221 Electrical resistivity, 10.6 to 11.4 microhm-in. (1).

2.023 Magnetic properties. Steel is ferromagnetic.

2.024 Emittance.

2.025 Damping capacity.

2.03 Chemical Environments

2.031 The presence of the outer skin or white layer of the nitrided alloy increases its corrosion resistance compared with conventionally heat treated low alloy steels. However, the case is corroded by mineral acids (1, 2).

2.04 Nuclear Environments

3 MECHANICAL PROPERTIES

3.01 Specified Mechanical Properties

3.011 AMS specified mechanical properties, Table 3.011.

3.012 Typical producer's specified properties, Table 3.012.

3.02 Mechanical Properties at Room Temperature

3.021 Tension – stress-strain diagrams – tension properties.

3.0211 Effect of tempering temperature on room temperature tensile properties of bar, Figure 3.0211.

3.0212 Effect of tempering temperature on room temperature tensile properties of as-tempered and nitrided alloy, Figure 3.0212.

3.022 Compression – stress-strain diagrams – compression properties.

3.023 Impact.

3.0231 Effect of tempering temperature on room temperature impact properties of as-tempered and nitrided alloy, Figure 3.0231.

3.024 Bending.

3.025 Torsion and shear.

3.026 Bearing.

3.027 Stress concentration.

3.0271 Notch properties.

3.0272 Fracture toughness.

3.028 Combined properties.

	Fe
0.4	C
1.6	Cr
1.1	Al
0.6	Mn
0.35	Mo

Nitralloy 135 Mod.

3.03 **Mechanical Properties at Various Temperatures**

3.031 Tension – stress-strain diagrams – tension properties.

3.032 Compression – stress-strain diagrams – compression properties.

3.033 Impact.

3.034 Bending.

3.035 Torsion and shear.

3.036 Bearing.

3.037 Stress concentration.

3.0371 Notch properties.

3.0372 Fracture toughness.

3.038 Combined properties.

3.04 **Creep and Creep-Rupture Properties**

3.041 Nitrided Nitralloy tested at 1000 F at 10 ksi stress creeps 0.2 percent in 4000 hour with no further extension during an additional 5000 hour (2).

3.05 **Fatigue Properties**

3.051 Endurance limits of as tempered and nitrided steel, Table 3.051.

3.052 Fatigue behavior at room temperature, Figure 3.052.

3.06 **Elastic Properties**

3.061 Poisson's ratio.

3.062 Modulus of elasticity.

3.0621 Modulus of elasticity in tension at room temperature 29-30 x 10^3 ksi (1).

3.063 Modulus of rigidity.

3.064 Tangent modulus.

3.065 Secant modulus.

4 FABRICATION

4.01 **Forming**

4.011 Forging, starting temperature 1950 to 2200 F, finishing temperature 1650 F, minimum (3).

4.02 **Machining and Grinding**

4.021 Rough machining prior to heat treatment is recommended particularly for large parts. If large amounts of stock must be removed, normalizing or annealing should precede machining. Residual stresses should be avoided as these may cause warping during nitriding. For this reason heat treated material must be machined with light cuts and be stress relieved after machining at a temperature not less than 100 F above the nitriding temperature. In any case sufficient material must be removed to eliminate any decarburized surface (2, 7).

4.03 **Joining**

4.031 The major problem is to avoid loss in chromium and aluminum in the weld area which would prevent subsequent nitriding. The most successful method employs 2.5 percent Cr, medium carbon rods with the atomic hydrogen process. If the weld area does not require nitriding, conventional welding methods may be employed. Welded parts should be heat treated before any machining (1, 2).

4.04 **Surface Treating**

4.041 Nitriding.

4.0411 Three nitriding processes are of commercial importance. These are conventional single-stage nitriding, two-stage Floe process nitriding, and ion nitriding. The first two processes employ anhydrous ammonia as the nitrogen source. At the nitriding temperatures of 975 F for single-stage nitriding and 975 to 1050 F for two-stage nitriding, the ammonia dissociates into atomic nitrogen and hydrogen, which react at the hot surface being nitrided. Ion nitriding has become industrially important more recently. In this process, the work piece is heated by arc discharge in a low pressure (about 0.15 psi) atmosphere of $80N_2$–$20H_2$. The current density is adjusted to maintain a work piece temperature of 975 to 1050 F. Processing times vary with the case thickness desired but generally range from 20 to 80 hours (2, 3, 9). Typical hardness-depth curves for single stage nitriding at 975 F are shown in Figure 4.0412, while case depths for various treatment times using the Floe process are given in Table 4.0413.

4.0412 Depth-hardness for several nitriding times, Figure 4.0412.

4.0413 Case depth using the Floe process on Nitralloy 135 modified, Table 4.0413.

4.0414 The mechanism of nitriding involves the initial formation of a layer of Fe_4N (white layer) at the work surface. This layer provides a constant surface concentration of nitrogen. As nitriding proceeds, nitrogen diffuses into the alloy, forming a nitrogen solution with the matrix and nitride precipitates with strong nitride-forming alloying elements such as chromium and aluminum. The thickness of the white layer and of the nitride case increase parabolically with time, as shown in Figure 4.0415, reflecting the diffusion-controlled nature of the reaction. Aluminum in Nitralloy 135 modified is nitrided easily and provides a sharp front to the nitrided case layer. The chromium-nitrogen reaction is weaker and stable precipitate nuclei do not form until relatively large supersaturations are achieved (10).

4.0415 Diffusion case and white layer thickness as a function of ion nitriding time at 970 F, Figure 4.0415.

4.0416 The ion nitriding process possesses several advantages over the single-stage and two-stage (Floe) nitriding processes. These advantages include (1) shorter processing time to achieve the same case thickness, and (2) thinner residual white layer on the surface. Case thicknesses for various treatment times are shown for the three processes in Figure 4.0417 and illustrate the shorter processing time for ion nitriding. This shorter processing time is attributed to cleaning of the work piece by sputtering, which removes adsorbed gases and films which might inhibit nitriding. The rapid cleaning during ion nitriding allows earlier formation of the Fe_4N surface layer than occurs with conventional ammonia nitriding. Although the white layer forms earlier during ion nitriding, it remains thinner because of sputtering. The thinner white layer is advantageous because white layer is normally considered detrimental and must be removed by mechanical or chemical means if greater than about 0.0005 inch in thickness (9).

4.0417 Case thickness as a function of treatment time for ion nitrided, conventional nitrided, and Floe process nitrided alloy, Figure 4.0417.

4.0418 Parts to be nitrided must be cleaned of surface contaminants such as oil, grease, machining lubricants, oxides, copper, lead, and so forth. Vapor degreasing will remove organic compounds, but the remaining contaminants must be removed by buffing, glass shot blasting, or chemical stripping. Mechanical masking is the preferred method of preventing ion nitriding of selected areas. The mechanical mask is fabricated from low carbon steel and fits the workpiece with a clearance of 0.010 to 0.025 inch. Copper or nickel electroplates are unacceptable for masking during ion nitriding because of sputtering and redeposition elsewhere (copper) or diffusional contamination of the substrate (nickel) (9). During conventional nitriding with ammonia, areas of parts that do not require nitriding may be protected by tin, bronze or copper plating (2).

4.0419 Size increase due to nitriding is approximately 0.001 to 0.002 inch depending on the time and temperature of nitriding. Dimensions may be restored by careful grinding or lapping (3).

REFERENCES

Alloy Digest, "Nitralloy 135 Modified," Filing Code: SA-24, Steel-Alloy (December 1954).
Homerberg, V. O., and Floe, C. F., "Nitralloy and Nitriding Including the New Floe Process," The Nitralloy Corp. (1954).
Crucible Steel Co. of America, "Nitriding Steel #135 Modified," Data Sheet, Issue (July 1949).
AMS 6470H (April 1, 1982).
"Alloy Steel Bars for Nitriding," ASTM Designation: A 355-57 T, Class A, Pt. 1 (1961).
AMS 6471B (October 15, 1979).
AMS 6472B (October 1, 1984).
Spencer, R. M., "Nitriding Long, Heavy Parts in Pit-Type Furnaces," Metal Progress, Vol. 103, No. 2 (February 1973), pp 92-94.
Busch, R. D., "Ionitriding of Weapon Components," General Thomas J. Rodman Laboratory, Rock Island Arsenal, Illinois, RIA-R-TR-74-002 (January 1974).
Robino, C. V., and Inal, O. T., "Ion Nitriding Behavior of Several Low Alloy Steels," Materials Science and Engineering, Vol. 59, No. 1 (May 1983), pp 79-90.
Chase, J. J., and Crump, D. N., "A Study and Evaluation of the Effects of Various New Surface Diffusion Treatments," TRW, Incorporated, Cleveland, Ohio, AMSWE-RE 71-50 (August 1971).

Fe	
0.4	C
1.6	Cr
1.1	Al
0.6	Mn
0.35	Mo

Nitralloy 135 Mod.

Nitralloy 135 Modified	
AMS Specification	Product Form
6470H	Bars, Forgings, Tubing
6471B	Bars, Forgings, Tubing
6472B	Bars, Forgings

TABLE 1.031. SPECIFICATIONS (4, 6, 7)

Nitralloy 135 Modified				
AMS Specifications	6470H, 6472B		6471B	
	Percent		Percent	
Element	Min	Max	Min	Max
Carbon	0.38	0.43	0.38	0.43
Chromium	1.40	1.80	1.40	1.80
Aluminum	0.95	1.30	0.95	1.30
Manganese	0.50	0.80	0.50	0.80
Molybdenum	0.30	0.40	0.30	0.40
Silicon	0.20	0.40	0.15	0.40
Copper	–	0.35	–	0.35
Nickel	–	0.25	–	0.25
Phosphorus	–	0.025	–	0.015
Sulfur	–	0.025	–	0.015

TABLE 1.041. COMPOSITION (4, 6, 7)

	Fe
0.4	C
1.6	Cr
1.1	Al
0.6	Mn
0.35	Mo

Nitralloy 135 Mod.

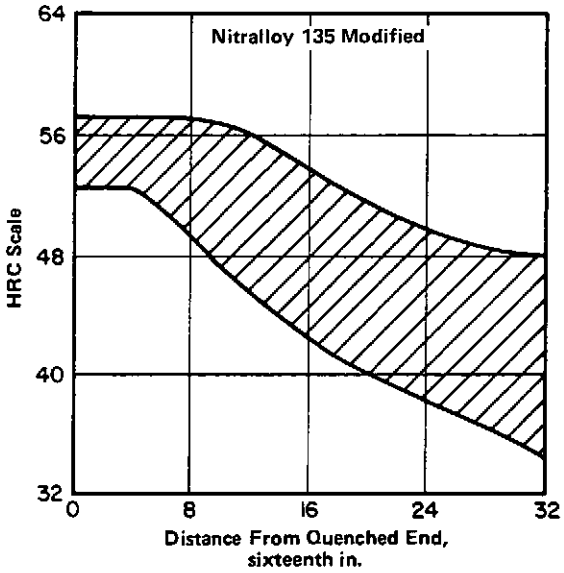


FIGURE 1.061. END QUENCH HARDENABILITY (2)

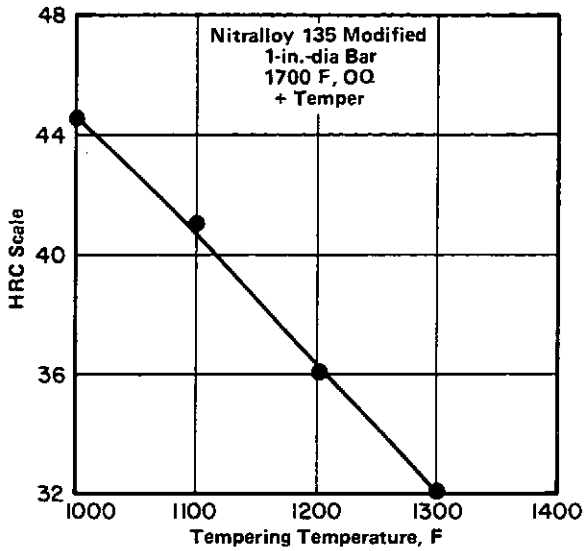


FIGURE 1.062. EFFECT OF TEMPERING TEMPERATURE ON HARDNESS OF BAR (1)

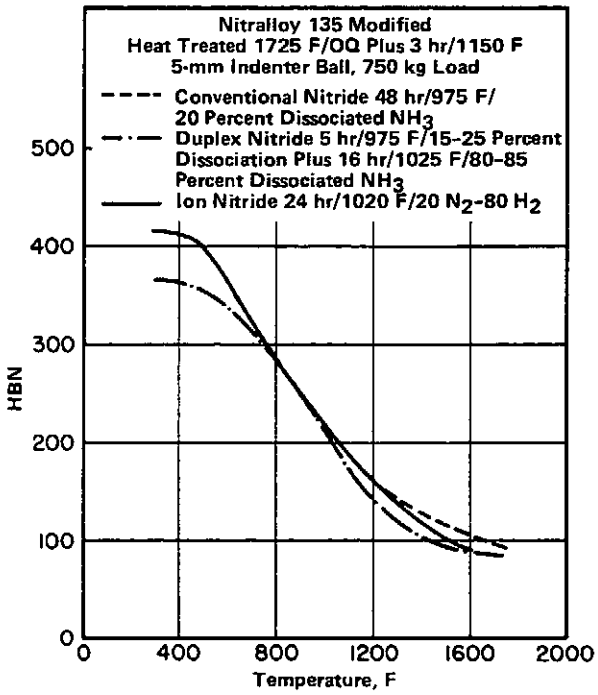


FIGURE 1.063. HOT HARDNESS OF NITRIDED ALLOY (11)

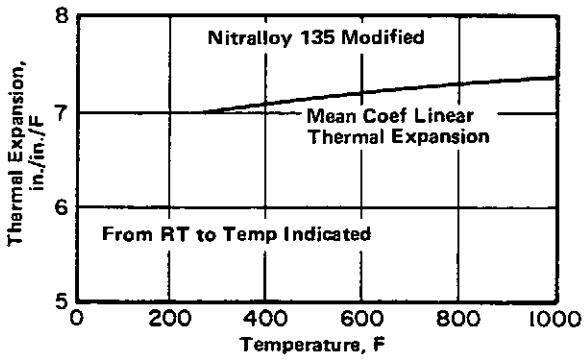


FIGURE 2.014. THERMAL EXPANSION (3)

Nitralloy 135 Modified										
AMS Spec	Product Form	Condition	Thickness, in.	F_{tu}, ksi Min	F_{tu}, ksi Max	F_{ty}, ksi, Min	Elongation, %, Min	RA, pct, Min	Hardness Min	Hardness Max
6470H, 6471B	Bar	Cold Finished	≤0.500	–	135	–	–	–	–	–
	Bar	Cold Finished	>0.500	–	–	–	–	–	–	269 HB
	Bar	Hot Finished	>0.500	–	–	–	–	–	–	229 HB
	Tubing	Cold Finished	–	–	–	–	–	–	–	25 HRC
	Tubing	Hot Finished Plus Annealed	–	–	–	–	–	–	–	99 HRB
6472B	Bars, Forgings	Quenched, Tempered[a]	–	112	–	90	16	50	–	–
	Bars, Forgings	Quenched, Tempered[a]	≤3.125	–	–	–	–	–	241 HB	285 HB
	Bars, Forgings	Quenched, Tempered[a]	>3.125; ≤6.000	–	–	–	–	–	229 HB	285 HB

Fe	
0.4	C
1.6	Cr
1.1	Al
0.6	Mn
0.35	Mo

Nitralloy 135 Mod.

Note: The original AMS documents should be consulted for complete specification details.
(a) Quenched from 1700 F and hardened to meet tensile property requirements of AMS 6472B.

TABLE 3.011. AMS SPECIFIED MECHANICAL PROPERTIES (4, 6, 7)

Alloy	Nitralloy 135 Modified		
Form	Bar[a]		
Condition	1725 F, OQ < 3 in WQ > 3 in Temper 1200 F (Min) 5 hr		
Size, dia	<1-1/2	>1-1/2 to 3	>3 to 5
F_{tu}, Min, ksi	135	125	110
F_{ty}, Min, ksi	100	90	85
e (2 in.) Min, percent	16	15	15
RA, Min, percent	50	40	40
BHN			
Min	280	269	240
Max	340	321	300

(a) Specimen taken at 1/2 radius.

TABLE 3.012. TYPICAL PRODUCER'S SPECIFIED PROPERTIES (2)

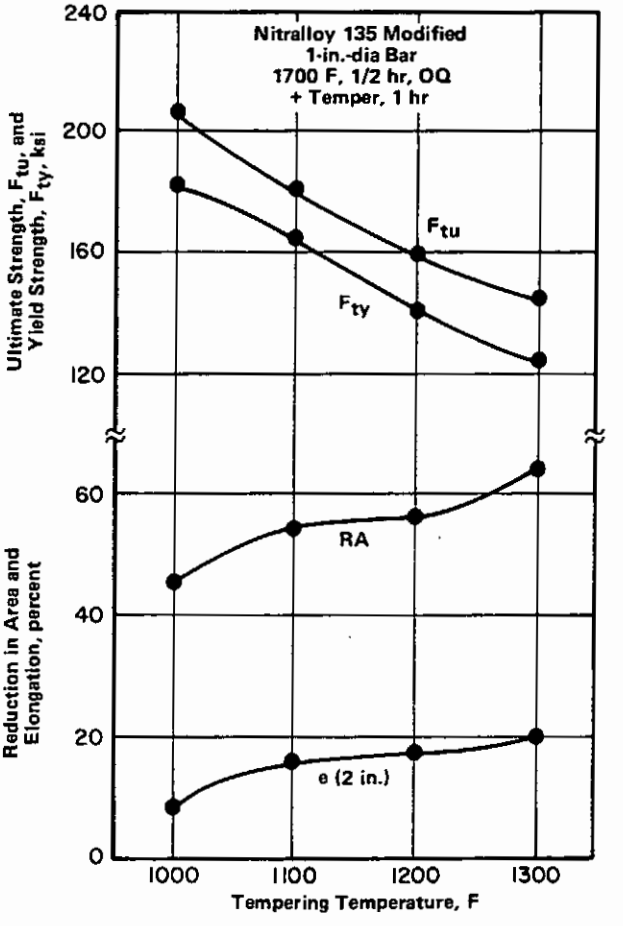


FIGURE 3.0211. EFFECT OF TEMPERING TEMPERATURE ON ROOM TEMPERATURE TENSILE PROPERTIES OF BAR (1, 2)

	Fe
0.4	C
1.6	Cr
1.1	Al
0.6	Mn
0.35	Mo

Nitralloy 135 Mod.

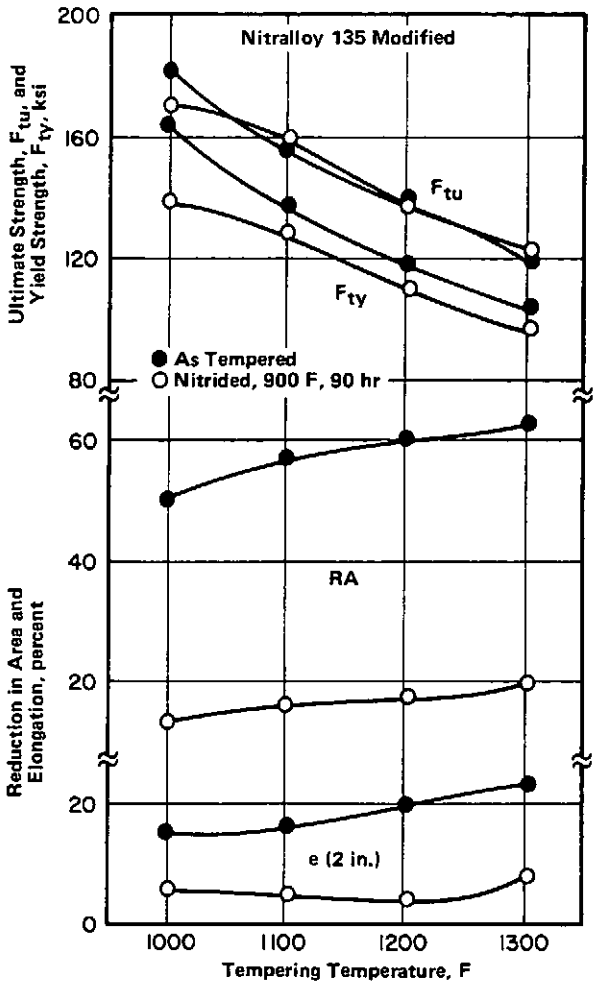


FIGURE 3.0212. EFFECT OF TEMPERING TEMPERATURE ON ROOM TEMPERATURE TENSILE PROPERTIES OF AS-TEMPERED AND NITRIDED ALLOY (1)

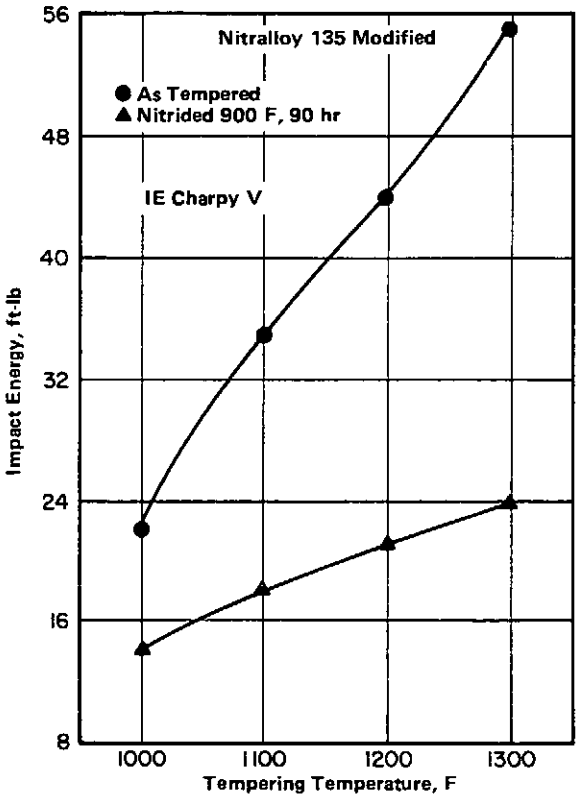


FIGURE 3.0231. EFFECT OF TEMPERING TEMPERATURE ON ROOM TEMPERATURE IMPACT PROPERTIES OF AS-TEMPERED AND NITRIDED ALLOY (1)

Alloy	Nitralloy 135 Modified		
Form	Bar		
Condition	HT and Nitrided 975 F, 40 hr		
Reverse Bending (Rayflex)		Endurance Limit, ksi As Tempered to BHN 269	Nitrided
Smooth	K = 1.0	45	90
Notched	K = 3.3	24	80

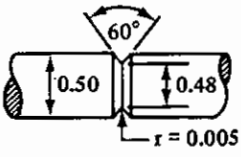


TABLE 3.051. ENDURANCE LIMITS OF AS-TEMPERED AND NITRIDED STEEL (2)

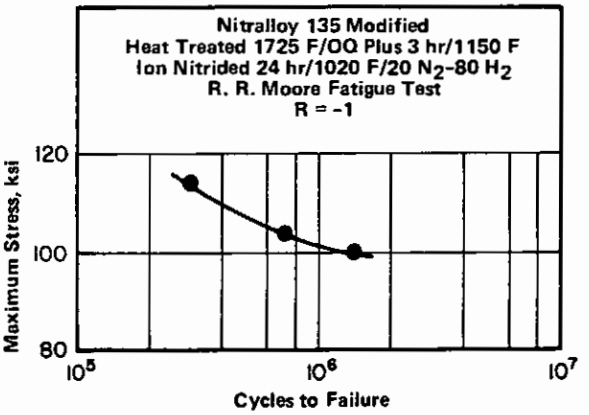


FIGURE 3.052. FATIGUE BEHAVIOR AT ROOM TEMPERATURE (11)

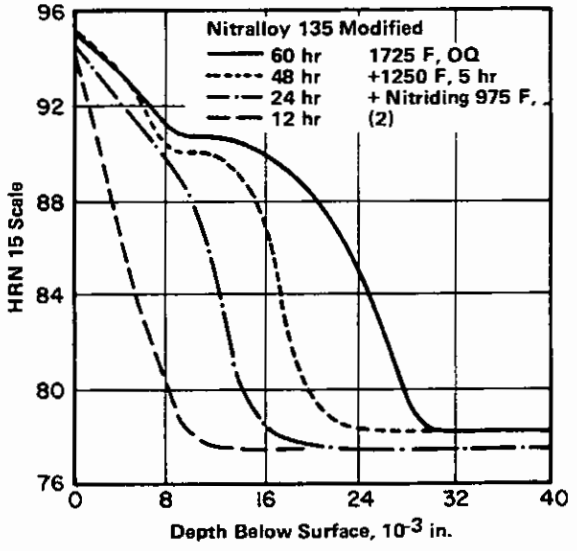


FIGURE 4.0412. DEPTH-HARDNESS FOR SEVERAL NITRIDING TIMES (2)

Alloy	Nitralloy 135 Modified	
Stage	First	Second
Temperature	975 F	1050 F
Percent Ammonia Dissociation	15–25	83–86
Case Depth, in.	Time, hr	Time, hr
0.005–0.008	5	0
0.008–0.012	5	5
0.011–0.015	5	20
0.013–0.018	6	26
0.017–0.022	8	42

TABLE 4.0413. CASE DEPTH USING THE FLOE PROCESS ON NITRALLOY 135 MODIFIED (2)

	Fe
0.4	C
1.6	Cr
1.1	Al
0.6	Mn
0.35	Mo

Nitralloy 135 Mod.

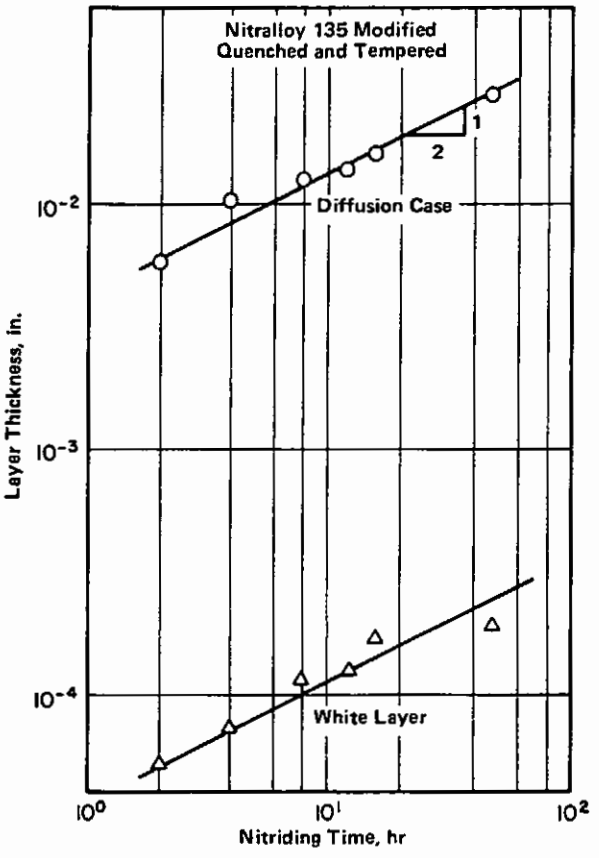


FIGURE 4.0415. DIFFUSION CASE AND WHITE LAYER THICKNESS AS A FUNCTION OF ION NITRIDING TIME AT 970 F (10)

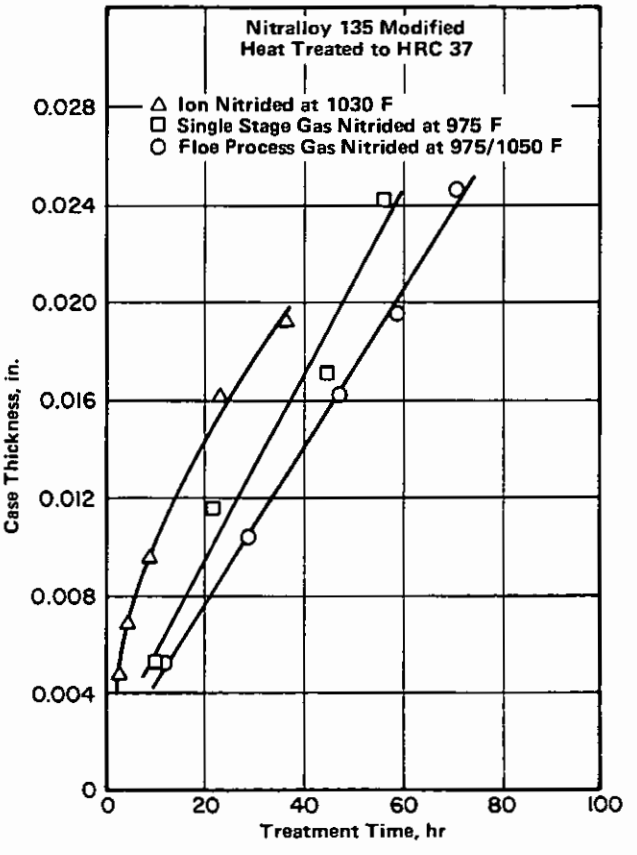


FIGURE 4.0417. CASE THICKNESS AS A FUNCTION OF TREATMENT TIME FOR ION NITRIDED, CONVENTIONAL NITRIDED, AND FLOE PROCESS NITRIDED ALLOY (9)

Fe
13 Cr
8 Ni
2 Mo

PH13-8Mo

1 GENERAL

This alloy is a precipitation-hardenable martensitic stainless steel combining excellent corrosion resistance with exceptionally high strength and hardness. PH13-8Mo was developed during the 1960's. It is normally made by vacuum-induction melting plus consumable-electrode vacuum-arc remelting. It was developed specifically for use in large cross-section parts which require yield strength up to about 220 ksi and good ductility properties irrespective of grain orientation. Toughness in the transverse direction is achieved by compositional control to prevent formation of delta ferrites, by lower carbon content to minimize grain-boundary carbide precipitation, and by double vacuum melting to reduce alloy segregation. The M_S temperature is near room temperature. It has good fabrication properties. Heat treatment consists of a solution treatment followed by aging. Cooling rates from the solution temperature are not critical, allowing heavy sections to be air cooled. Strengthening is effected both by transformation to martensite during cooling from the solution temperature and by precipitation of NiAl intermetallic phase during aging. Long-time exposure at moderately elevated temperatures causes microstructural instability which results in decreased fracture toughness. The alloy has good resistance to general corrosion and to stress corrosion.

PH13-8Mo is generally supplied in the solution-treated condition, ready for fabrication and subsequent age hardening by the user. It can also be supplied in the hardened and the overaged conditions for cold heading or forging if desired. Applications include forgings, cold-headed and machined fasteners, aircraft parts, shuttle rocket-engine mounts, launch-structure parts, nuclear-reactor components, landing-gear parts, pins and lock washers, high-performance shafting, and petrochemical components requiring stress-corrosion resistance combined with high strength. PH13-8Mo is an alloy designation of Armco Steel Corporation.

1.01 **Commercial Designation**

PH13-8Mo stainless steel.

1.02 **Alternate Designation**

UNS 13800.

1.03 **Specifications**

1.031 AMS specifications, Table 1.031.

1.04 **Composition**

1.041 Specified composition, Table 1.041.

1.05 **Heat Treatment**

1.051 The alloy is supplied from the mill in Condition A and can be heat treated at any one of several temperatures to develop a wide range of properties. In Condition A the alloy can be joined to PH14-8Mo, PH15-7Mo or 17-7PH and the entire assembly hardened by three-step heat treatments compatible with the latter grades. For brazed assemblies the steel can be heat treated to satisfactory strength levels using the braze-cycle heat treatment as defined in 1.055. After hot working, brazing, welding, or other treatments that change the metallurgical structure, PH13-8Mo should be reheat-treated to get full design properties (20).

1.052 Condition A. Solution treated 1685 to 1715 F, oil quenched or air cooled below 60 F. Solution treating time should be long enough to assure that the steel is heated thoroughly through the section. Bar and wire items can be effectively heat treated in continuous furnaces. In batch-type furnaces, it is recommended that parts be held at the solution temperature 15 to 30 minutes to assure uniformity.

1.053 Aging treatments, Table 1.053.

1.054 Additional heat-treated conditions (see Table 3.0215).

1.055 Braze-cycle heat treatment (BCHT) condition: 1700 F, 1 hour, cool to 1000 F in 1 hour plus 8 hours at -110 F plus age.

1.056 PH13-8Mo can be satisfactorily heat treated in air-atmosphere furnaces. Inert atmospheres such as argon are often used for aging heat treatment or braze-cycle heat treatments. Controlled reducing atmospheres, such as cracked ammonia, may cause nitriding and are not recommended. In practice, parts are usually fabricated from material in Condition A and only a low-temperature aging treatment in air is required thereafter (22). Solution treatment (1700 F) in molten salt is not recommended because of the danger of carburization and/or intergranular penetration.

1.06 **Hardness**

1.061 Typical hardness of bar in various heat-treated conditions, Table 1.061.

1.062 Effect of solution temperature on the hardness of solution treated-and-aged bar, Figure 1.062.

1.063 Maximum hardening and strengthening are obtained in PH13-8Mo by aging at about 980 F after solution treating at 1650 or 2010 F, as shown in Figures 1.064 and 3.0212. (The standard solution-treating temperature is 1700 F.) In the solution treated-and-quenched condition, the alloy is completely martensitic. Subsequent aging of this martensitic structure in the temperature range 840 to 1070 F leads to finely distributed spherical particles of NiAl precipitate, identified by X-ray diffraction. The lattice mismatch ratio between the matrix and precipitate is very low (less than 0.002). The NiAl precipitate particles, which have a mean radius of 50 Å after aging for 4 hours at 980 F, remain fully coherent with the matrix even after considerable coarsening. Small quantities also of fine cuboidal austenite phase form by reversion on aging at temperatures above 930 F. At aging temperatures higher than 980 F, the amount of austenite phase becomes significant and the austenite particles coarsen rapidly. A major fraction of the observed increase in the flow stress of the aged alloy over that of the solution-treated alloy arises from the presence of the NiAl precipitate. The mechanisms involved include coherency hardening associated with lattice mismatch strains between the matrix and the NiAl precipitate

Fe
13 Cr
8 Ni
2 Mo

PH13-8Mo

particles, modulus hardening resulting from the difference in shear moduli between the matrix and precipitate, and order hardening due to the ordered nature of the precipitate. In addition, the fine austenite particles which form in the martensite matrix contribute significantly toward strengthening the aged alloy (24).

1.064 Effects of aging for 1 or 4 hours on hardness of solution-treated bar, Figure 1.064.

1.065 Effects of aging for 2 hours on hardness of solution-treated bar, Figure 1.065.

1.066 Cold work is seen in Figure 1.067 to first increase and then decrease the hardness of solution-annealed bar. In contrast, the bar data in Table 1.068 indicate constant hardness with increasing cold work after an initial hardness increase. The reason for these differences is not known.

1.067 Effects of cold work on hardness, Figure 1.067.

1.068 Effect of cold work on hardness of bar in various conditions, Table 1.068.

1.069 Effect of aging temperature and time on hardness of cold-worked bar, Table 1.069.

1.07 **Forms and Conditions Available**
Bar, wire, plate, and forging billets in Condition A in hardened conditions, or in an overaged condition.

1.08 **Melting and Casting Practice**
Vacuum-induction melting plus consumable-electrode vacuum-arc remelting (designated VIM + VAR) (3).

1.09 **Special Considerations**

1.091 The fracture toughness of this alloy is good in heavy sections at room temperature and above but decreases rapidly at temperatures below 0 F (see crack strength, Figures 3.03713 and 3.03714). Heavy sections exhibit negligible directionality of tensile properties (see Tables 2.0313, 2.0314, 3.0215, and Figure 3.0218). Fracture toughness also is essentially independent of orientation (see Tables 3.02721 and 3.03722). In common with other alloys of this class, the impact-energy and fracture toughness decrease as a result of long-time exposure to moderately elevated temperature (see Figure 3.0333).

1.092 The resistance to general corrosion of PH13-8Mo exceeds that of Types 410 and 431, and is approximately equal to 17-4PH. Like other precipitation-hardening stainless steels, its level of general corrosion resistance is greatest in the fully hardened condition and decreases slightly as the aging temperature is increased (3). The alloy is the most stress-corrosion resistant of the PH stainless steels (3). See also 2.03.

1.093 Fatigue properties for smooth and notched specimens are independent of orientation (see Figures 3.053, 3.054, and 3.055).

1.094 The highest strength levels in this alloy are obtained by cold working prior to precipitation hardening.

2 PHYSICAL PROPERTIES AND ENVIRONMENTAL EFFECTS

2.01 **Thermal Properties**

2.011 Melting range, 2560 to 2680 F.

2.012 Phase changes. Austenite above about 1500 F, M_S is approximately 250 F but will vary some with composition and can be below room temperature. However, in most cases the martensite transformation is practically complete below 70 F. Aging precipitates intermetallic compounds.

2.0121 Time-temperature transformation diagrams.

2.013 Thermal conductivity, Table 2.013.

2.014 Thermal expansion.

2.0141 Thermal expansion, Figure 2.0141.

2.0142 Dilatometer curve indicating dimensional changes and transformation temperatures for Condition A, Figure 2.0142.

2.015 Specific heat, 0.11 Btu/lb F.

2.016 Thermal diffusivity.

2.02 **Other Physical Properties**

2.021 Density, Table 2.021.

2.022 Electrical properties.

2.0221 Electrical resistivity, Table 2.0221.

2.023 Magnetic properties.

2.0231 Magnetic permeability, Table 2.0231.

2.024 Emittance.

2.025 Damping capacity.

2.03 **Chemical Environments**

2.031 The resistance to general corrosion of PH13-8Mo approaches that of 17-4PH. This is indicated by laboratory immersion tests in both strongly oxidizing and reducing media, as well as by atmospheric exposure. In all heat-treated conditions the alloy exhibits very little rusting after 500 hours exposure to 5 percent salt fog at 95 F. Like other precipitation-hardening stainless steels, its level of general corrosion resistance is greatest in the fully hardened condition and decreases slightly as the aging temperature is increased. PH13-8Mo is the most stress-corrosion resistant of the hardenable stainless steels. It offers higher useful mechanical properties than any other ferrous-base material under extreme environmental conditions (3). Its resistance to stress-corrosion cracking increases as a function of increased aging temperature (see Tables 2.0311 and 2.0317).

2.0311 Stress-corrosion cracking in marine atmosphere, Table 2.0311.

2.0312 Stress-corrosion cracking at Kure Beach in marine atmosphere, Table 2.0312.

2.0313 Stress-corrosion behavior in salt spray and marine atmosphere, Table 2.0313.

2.0314 Stress-corrosion cracking in an NaCl solution, Table 2.0314.

2.0315 Fracture toughness and stress-corrosion values in a 3.5 percent NaCl solution, Table 2.0315.

2.0316 Axial fatigue behavior in seawater and in air, Figure 2.0316.

2.0317 Stress-corrosion cracking in an NaCl-acetic acid-H_2S solution, Table 2.0317.

2.0318 Effects of heat treatment and hardness on stress-corrosion behavior in an NaCl-acetic acid-H_2S solution, Figure 2.0318.

2.0319 Effect of hydrogen charging time on tensile properties, Figure 2.0319.

2.03110 Delayed-failure behavior while being charged with hydrogen, Figure 2.03110.

2.03111	The notched tensile strength is greatly reduced by hydrogen charging. Bar specimens indicated a notched-to-unnotched tensile strength ratio of 1.34, consistent with the high toughness of this alloy. However, after electrolytically charging for 1 hour in 1N H_2SO_4 saturated with CS_2, the tensile-strength ratio for notched charged-to-notched uncharged materials was reduced to 0.39. These results indicate that a considerable reduction in toughness is effected by hydrogen charging. The bar was heat treated to Condition H 950; notched specimens had K_t = 15, 60° circumferential notch, 1.5-mil notch root radius (30).
2.04	**Nuclear Environments**
3	**MECHANICAL PROPERTIES**
3.01	**Specific Mechanical Properties**
3.011	AMS-specified mechanical properties, Table 3.011.
3.012	Producers' guaranteed mechanical properties, Table 3.012.
3.02	**Mechanical Properties at Room Temperature**
3.021	Tension – stress-strain diagrams – tension properties.
3.0211	Stress-strain curves for bar in various aged conditions, Figure 3.0211.
3.0212	True stress-true strain curves for solution-treated and solution treated-and-aged alloy, Figure 3.0212.
3.0213	Typical tensile properties for bar in various heat-treated conditions, Table 3.0213.
3.0214	Effect of solution-treating temperature on the tensile properties of forgings aged at two temperatures, Figure 3.0214.
3.0215	Mechanical properties for various aged conditions, Table 3.0215.
3.0216	Effect of aging and solution-treating temperature on the tensile properties of forgings, Figure 3.0216.
3.0217	Effect of aging temperature on the short transverse tensile properties of forgings, Figure 3.0217.
3.0218	Effect of testing direction on tensile properties of solution treated-and-aged forgings, Figure 3.0218.
3.0219	Effects of cold work on tensile properties, Figure 3.0219.
3.022	Compression – stress-strain diagrams – compression properties.
3.0221	Stress-strain curve in compression for Condition H 1000, Figure 3.0221.
3.0222	Typical compressive yield strengths for bar in various aged conditions, Table 3.0222.
3.023	Impact (see also Tables 3.0215 and 4.0131).
3.0231	Typical impact properties for various heat-treated conditions, Table 3.0231.
3.0232	Effect of solution-treating temperature on the short-transverse impact properties, Figure 3.0232.
3.0233	Effect of aging and solution-treating temperature on impact properties, Figure 3.0233.
3.0234	Effect of solution-treating temperature on the short-transverse impact energy before and after elevated-temperature exposure, Figure 3.0234.
3.024	Bending.
3.025	Torsion and shear.
3.0251	Torsion and shear properties, Table 3.0251.
3.026	Bearing.
3.0261	Bearing properties of sheet in Condition H 1000, Table 3.0261.
3.027	Stress concentration.
3.0271	Notch properties.
3.02711	Effect of surface cracks on crack strength, Figure 3.02711.
3.0272	Fracture toughness.
3.02721	Plane-strain fracture toughness for Condition H 1000, Table 3.02721.
3.02722	Plane-strain fracture toughness in a 3.5 percent NaCl solution (see Table 2.0315).
3.028	Combined properties.
3.03	**Mechanical Properties at Various Temperatures**
3.031	Tension – stress-strain diagrams – tension properties.
3.0311	Stress-strain curves at elevated temperatures for bar in Condition H 1000, Figure 3.0311.
3.0312	Stress-strain curves at room and low temperatures for bar in Condition H 1000, Figure 3.0312.
3.0313	Effect of test temperature on tensile properties of a forging, Figure 3.0313.
3.0314	Effect of test temperature and orientation on the tensile properties of various-size forgings, Table 3.0314.
3.0315	Tensile properties of bar at cryogenic and elevated temperatures, Figure 3.0315.
3.032	Compression – stress-strain diagrams – compression properties.
3.0321	Stress-strain curves for a forging in compression at elevated temperatures, Figure 3.0321.
3.0322	Effect of temperature on compressive yield strength, Figure 3.0322.
3.033	Impact.
3.0331	Typical low-temperature impact energies of bar in various aged conditions, Table 3.0331.
3.0332	Effect of test temperature on impact properties of a forging, Figure 3.0332.
3.0333	Effect of test temperature and exposure temperature on the impact energy of forgings, Figure 3.0333.
3.034	Bending.
3.035	Torsion and shear.
3.036	Bearing.
3.037	Stress concentration.
3.0371	Notch properties.
3.03711	Effect of test temperature on sharp-notch strength of a forging, Figure 3.03711.
3.03712	Effect of stress-concentration factor on tensile and notch properties of bar at room and low temperature, Table 3.03712.
3.03713	Effect of thickness on crack strength of a forging, Figure 3.03713.
3.03714	Effect of test temperature on crack strength of a forging, Figure 3.03714.
3.0372	Fracture toughness.
3.03721	Plane-strain fracture toughness of a forging at low temperature, Table 3.03721.
3.03722	Fracture toughness of various wrought forms at room and cryogenic temperatures, Table 3.03722.
3.038	Combined properties.
3.04	**Creep and Creep-Rupture Properties**
3.041	Time to 0.2 percent creep deformation for bar at elevated temperatures, Figure 3.041.

Fe
13 Cr
8 Ni
2 Mo

PH13-8Mo

Fe
13 Cr
8 Ni
2 Mo

PH13-8Mo

3.042 Time to rupture for bar at elevated temperatures, Figure 3.042.

3.05 **Fatigue Properties** (see also Section 2.0316).

3.051 Effect of stress concentrations on fatigue strength of a forging, Figure 3.051.

3.052 S-N curve for smooth and notched specimens of bar, Figure 3.052.

3.053 S-N curves for longitudinal and transverse smooth and notched specimens from bar at a stress ratio of R = 0.1, Figure 3.053.

3.054 S-N curves for longitudinal and transverse smooth and notched specimens from bar at a stress ratio of R = 0.5, Figure 3.054.

3.055 S-N curves for longitudinal and transverse smooth and notched specimens from bar at a stress ratio of R = -1.0, Figure 3.055.

3.056 S-N curves at elevated temperature for longitudinal smooth and notched specimens from a forging at a stress ratio of R = 0.1, Figure 3.056.

3.057 Fatigue crack-growth rate at room temperature for plate, Figure 3.057.

3.058 Extensive studies of the fatigue-crack-growth behavior of PH13-8Mo (Condition H 1000) were conducted as part of the B-1 bomber design program. The trends observed in these studies with respect to several variables are summarized as follows:

Cyclic frequency – There was no consistently significant effect on varying the frequency from 60 to 360 cpm in low-humidity air or from 6 to 60 cpm in artificial fuel-tank sump residue (water containing 0.12 percent mixed metal chlorides).

Test temperature – Results were inconsistent but suggested that crack-growth rates may be higher at room temperature than at -65 F (see Figure 3.059).

Specimen thickness – There was no consistent difference in crack-growth behavior between 0.5- and 1.0-inch-thick specimens.

R factor – Results ranged from inconsistent effect to significant acceleration when R was increased from 0.08 to 0.3.

Environment – Crack-growth rates were greater in fuel-tank sump residue water (see Figure 3.0510) and in shop cleaning fluid (a trisodium phosphate-type cleaning solution) than in low-humidity air at stress-intensity-factor ranges greater than about 20 ksi $\sqrt{in.}$

Test direction – In general, fatigue-crack-growth rates are slightly greater in the LT direction than in the TL direction. However, in low-humidity air at -65 F, the reverse was observed, as seen by comparison of the data in Figures 3.059 (a) and (b).

Product form – In low-humidity air, no significant differences in crack-growth-rate behavior were observed among forged bar, rolled bar, extrusions, and upset forgings.

The curves shown in Figures 3.059 and 3.0510 are representative of the data observed in PH13-8Mo (31).

3.059 Fatigue crack-growth rate in low-humidity air at low temperatures, (a) LT orientation, and (b) TL orientation, Figure 3.059.

3.0510 Fatigue crack-growth rate in fuel-tank sump water and in air at room temperature, Figure 3.0510.

3.06 **Elastic Properties**

3.061 Poisson's ratio, $\mu = 0.278$.

3.062 Modulus of elasticity.

3.0621 Tensile moduli of bar in various aged conditions, Table 3.0621.

3.0622 Elastic moduli of forged bar in tension and compression at room and elevated temperatures, Figure 3.0622.

3.063 Modulus of rigidity, $G = 11.1 \times 10^3$ ksi (Condition H 950); $G = 10.9 \times 10^3$ ksi (Condition H 1000).

3.064 Tangent modulus.

3.065 Secant modulus.

4 FABRICATION

4.01 **Forming**

4.011 In fabricating PH13-8Mo it is important to keep in mind the low temperature at which the start of transformation to martensite (M_s) and the finish of the martensite transformation (M_f) occur. These temperatures are approximately 250 and 70 F, respectively, but they both vary with composition. Therefore, it is necessary to cool parts in process below 60 F prior to subsequent heat treatments in order to assure grain refinement and good ductility. The following are examples of situations where cooling below 60 F is an important step: (a) cool below 60 F after solution treating prior to applying any of the precipitation-hardening treatments, (b) cool forged parts below 90 F after final forging before solution treating, and (c) cool any weldment below 90 F prior to solution treating (3).

4.012 Forging is the recommended method for forming intricate shapes of this alloy. Forging blanks should be heated uniformly to 2150 to 2200 F and held at temperature for at least 15 minutes before forging. On reheating, they should be soaked thoroughly. After forging, sections should be cooled to below 90 F as stated in Section 4.011. Then, to assure the best condition for the hardening operations, the parts must be re-solution treated to Condition A. In heating for forgings, as in the heat treatment of the alloy, endothermic atmospheres (or other atmospheres that may cause carburization or decarburization) should not be used (3).

4.013 The heat treatment lends itself to a braze cycle (see Section 1.055) which permits brazing heavy sections of this alloy to lighter sections of PH13-8Mo or similar sheet alloys.

4.0131 Tensile and impact properties of forgings subjected to a braze-cycle heat treatment, Table 4.0131.

4.02 **Machining and Grinding**

4.021 General. In Condition A good tool life and surface finish are obtained when machined at speeds 20 to 30 percent lower than those used for 17-4PH

at similar hardness levels. Cutting procedures commonly used for standard chromium-nickel stainless steels are generally satisfactory for PH13-8Mo (3).

4.03 **Joining**

4.031 General. Composition of the alloy is balanced for optimum performance in welding. Low carbon content restricts the hardness of rapidly cooled material and avoids the formation of cracks in weld deposits and heat-affected zones of the base metal, eliminating the need for preheating. It possesses sufficient ductility to prevent stress cracking, thus permitting welding in Condition A or in any heat-treated condition (3).

4.032 Welding process. The weld process most widely used for joining PH13-8Mo is gas tungsten arc (GTA) and the preferred shielding gas is helium. Other processes which can be used include plasma arc and electron beam either with or without the addition of a filler, plus gas metal arc and shielded metal arc where chromium-nickel or nickel-base fillers are to be used (3).

4.033 Filler metal. Choice of weld metal to join the alloy depends on properties required in the weld. When properties comparable to the base metal are required, weld metal of PH13-8Mo can be used. The weld metal can be produced by simple fusion of the base metal, but deposition of WPH13-8Mo filler wire is preferred in order to insure good weld ductility in the hardened condition. The only difference in composition between the base metal and the WPH weld wire is that the latter has a lower aluminum maximum. Austenitic chromium-nickel stainless steel weld metal may be used for joining the alloy when toughness and ductility are the major criteria. When PH13-8Mo is to be joined to a dissimilar material, dilution must be considered. In joining the alloy to a plain-carbon or low-alloy steel, Type 309 stainless should be used. In other dissimilar metal joints when similar thermal-expansion characteristics are needed, the use of a nickel-base alloy weld should be employed (3).

4.034 Effect of heat treatment on the mechanical properties of weldments as a function of plate thickness. Table 4.034.

4.035 The microstructure of PH13-8Mo weld metal at room temperature consists of a small amount of delta ferrite in a martensite-like matrix. The delta ferrite helps maintain high immunity to hot cracking and provides good ductility in the hardened condition (35).

4.036 Fracture-toughness values in butt-weld joints and in weld overlays tested at room temperature range from 79 to 98 ksi $\sqrt{in.}$, as shown in Table 4.037. These values are equal to or greater than 90 percent of the average fracture-toughness values of the parent metal. Differences in fracture-toughness values for HAZ (heat-affected zone) versus weld bead in weld joints, as-welded versus stress-relieved (2 hours, 950 F) weld overlays, and weld overlays versus weld joints were all within replicate scatter ranges (31).

4.037 Fracture toughness of welded material at room and cryogenic temperatures. Table 4.037.

4.04 **Surface Treating**

4.041 The discoloration developed in the final heat treatment can be removed by dipping in a 10 percent HNO_3-2 percent HF pickle solution for 3 minutes maximum. All parts should be passivated in 40 to 60 percent HNO_3 after final cleaning (22).

Fe
13 Cr
8 Ni
2 Mo

PH13-8Mo

REFERENCES

1 AMS 5629C (January 1, 1985).

2 AMS 5840A (July 16, 1979).

3 Armco Steel Corporation, Product Data Bulletin, Armco PH13-8Mo, S-33C (August 1972).

4 Clarke, W. C., Jr., and Garvin, H. W., "Effect of Composition and Section Size on Mechanical Properties of Some Precipitation Hardening Stainless Steels", American Society for Testing Materials, Special Technical Publication No. 369, "Advances in the Technology of Stainless Steels and Related Alloys" (1965).

5 Crossley, F. A., "Research on the Basic Nature of Stress Corrosion for Various Structural Alloys at Room and Elevated Temperature", IIT Research Institute, Air Force Contract AF33(657)-10971 (May 1964).

6 Garvin, H. W., Armco Steel Corporation, Baltimore, Maryland, personal communication with W. F. Brown, Jr. (1964).

7 Alloy Digest, Armco PH13-8Mo (May 1969).

8 Hoenie, A. F., and Roach, D. B., "New Developments in High-Strength Stainless Steels", DMIC Report 223 (January 3, 1966).

9 Humphries, T. S., and Nelson, E. E., "Stress Corrosion Cracking Evaluation of Several Precipitation Hardening Stainless Steels", NASA Technical Memorandum Report No. 53910, Marshall Space Flight Center (September 12, 1969).

10 Carter, C. S., et al., "Stress-Corrosion Properties of High Strength Precipitation-Hardening Stainless Steels in 3.5 Percent Aqueous Sodium Chloride Solution", Boeing Commercial Airplane Group, D6-25219 (February 1970).

11 Garvin, H. W., Armco Steel Corporation, Baltimore, Maryland, personal communication with W. F. Brown, Jr. (1964).

12 "Thick Section Fracture Toughness", ML-TDR 64-236, Boeing North American, Air Force Contract AF 33(657)-11461 (October 1964).

13 Johnson, P. W., Jr., Armco Steel Corporation, Baltimore, Maryland, personal communication with C. F. Hickey, Jr. (February 1973).

14 Bubsey, R. T., and Brown, W. F., Jr., "Crack Toughness Characteristics of Several Alloys for Use in Heavy Sections of High Speed Aircraft", NASA TN D-4998, Lewis Research Center (January 1969).

15 Takas, E. G., Armco Steel Corporation, Baltimore, Maryland, personal communication with C. F. Hickey, Jr. (February 1973).

16 Uchida, J. M., "Evaluation of Armco PH13-8Mo", Boeing Company, Renton, Washington, AD 700 762 (November 19, 1969).

17 Deel, O. L., and Mindlin, H., "Engineering Data on New Aerospace Structural Materials", AFML-TR-72-196, Vol 2 (September 1972).

Fe
13 Cr
8 Ni
2 Mo

PH13-8Mo

18 Shahinian, P., et al., "Fatigue Crack Growth in Selected Alloys for Reactor Applications", *Journal of Materials*, Vol 7, No. 4 (December 1972).

19 AMS 5864 (April 15, 1980).

20 Anonymous, "Good Steels for Tough Weldments", *Welding Design and Fabrication*, Vol 49, No. 2 (February 1976), pp 52–56.

21 "The Effect of Composition and Section Size on Transverse Properties of Precipitation-Hardening Stainless Steels – Part III: PH13-8Mo Stainless Steels", Armco Steel Corporation, Middletown, Ohio, trade literature (1981), 3 pp.

22 "Armco PH13-8Mo", Alloy Digest, Filing Code: SS-224 (May 1969).

23 "Armco Precipitation-Hardening Stainless Steels", Armco Steel Corporation, Baltimore, Maryland, trade literature (1978), 21 pp.

24 Seetharaman, V., Sundararaman, M., and Krisknan, R., "Precipitation Hardening in a PH13-8Mo Stainless Steel", *Materials Science and Engineering*, Vol 47, No. 1 (January 1981), pp 1–11.

25 Asayama, Y., "Precipitation Processes and Notch Tensile Strengths of Precipitation Hardening Stainless Steels", *Journal of the Japan Institute of Metals*, Vol 45, No. 7 (July 1981), pp 731–739.

26 Humphries, T. S., and Nelson, E. E., "Stress Corrosion Cracking Evaluation of Martensitic Precipitation Hardening Stainless Steels", NASA-TM-78257 (January 1980), 34 pp.

27 Tipton, D. G., "Corrosion Fatigue of High Strength Fastener Materials in Seawater", NASA CR-174677 (December 1983), 26 pp.

28 Gaugh, R. R., "Sulfide Stress Cracking of Precipitation Hardening Stainless Steels", *Materials Performance*, Vol 16, No. 9 (September 1977), pp 24–29.

29 Murray, G. T., Honegger, H. H., and Mousel, T., "Hydrogen Embrittlement of PH13-8Mo Stainless Steel – The Effect of Surface Condition", *Corrosion*, Vol 40, No. 4 (April 1984), pp 146–151.

30 Thompson, A. W., "Hydrogen Effects on Fracture of PH13-8Mo Steel", Proceedings of the Fourth International Conference on Fracture", University of Waterloo, Ontario, Canada (June 1977), 6 pp.

31 Ferguson, R. R., and Berryman, R. C., "Fracture Mechanics Evaluation of B-1 Materials. Volume I. Text", AFML TR-76-137-Vol-1 (October 1976).

32 Deel, O., "Collected Enginering Data Sheets (Air Force Data Sheet Program)", AFML TR-78-179 (December 1978).

33 Ferguson, R. R., and Berryman, R. C., "Fracture Mechanics Evaluation of B-1 Materials. Volume II. Fatigue Crack Growth Data", AFML TR-76-137-Vol-2 (October 1976).

34 "Armco PH13-8Mo – Precipitation-Hardening Stainless Steel Bar, Wire, Plate and Forging Billets", Armco Steel Corporation, Baltimore, Maryland, Product Data Bulletin S-33b (May 1970).

35 Espy, H., "Welding the PH Grades", Armco Steel Corporation, Middletown, Ohio, trade literature (1978).

Alloy	PH13-8Mo
AMS Specification	Product Form
5629C	Bars, forgings, rings, extrusions
5840A	Welding wire
5864	Plate

TABLE 1.031. AMS SPECIFICATIONS (1,2,19)

Alloy	PH13-8Mo			
AMS Specification	5629C 5864		5840A	
	Percent		Percent	
Element	Min	Max	Min	Max
Chromium	12.25	13.25	12.25	13.25
Nickel	7.50	8.50	7.50	8.50
Molybdenum	2.00	2.50	2.00	2.50
Aluminum	0.90	1.35	0.90	1.35
Manganese	–	0.10	–	0.10
Silicon	–	0.10	–	0.10
Carbon	–	0.05	–	0.05
Nitrogen	–	0.010	–	0.01
Phosphorus	–	0.010	–	0.008
Sulfur	–	0.008	–	0.010
Oxygen	–	–	–	0.005
Hydrogen	–	–	–	0.0025

TABLE 1.041. SPECIFIED COMPOSITION (1,2,19)

Alloy	PH13-8Mo	
Condition	Aging Temperature, F	Aging Time, hr, Plus AC
RH 950	950(a)	4
H 950	950	4
H 1000	1000	4
H 1025	1025	4
H 1050	1050	4
H 1100	1100	4
H 1150	1150	4
H 1150-M	1400	2
	Followed by	
	1150	4

(a) Refrigerate 2 hours at -100 F within 24 hours after solution annealing and prior to aging.

TABLE 1.053. AGING TREATMENTS (21)

Alloy	PH13-8Mo
Form	1 to 3-inch Bar
Condition	Hardness, HRC
A	33
RH 950	48
H 950	47
H 1000	45
H 1050	43
H 1100	35
H 1150	33
H 1150-M	32

TABLE 1.061. TYPICAL HARDNESS OF BAR IN VARIOUS HEAT-TREATED CONDITIONS (23)

Fe
13 Cr
8 Ni
2 Mo

PH13-8Mo

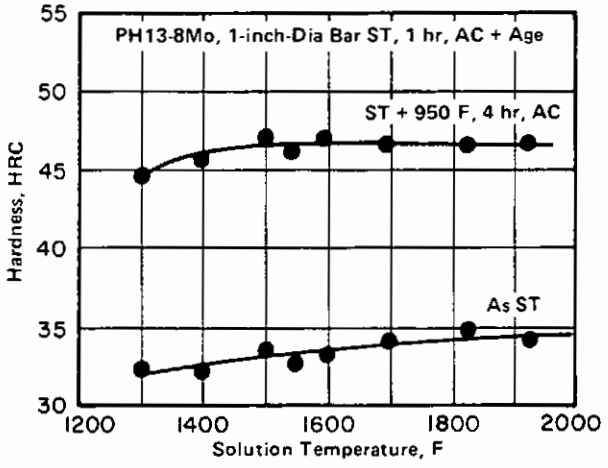


FIGURE 1.062. EFFECT OF SOLUTION TEMPERATURE ON THE HARDNESS OF SOLUTION TREATED-AND-AGED BAR (6)

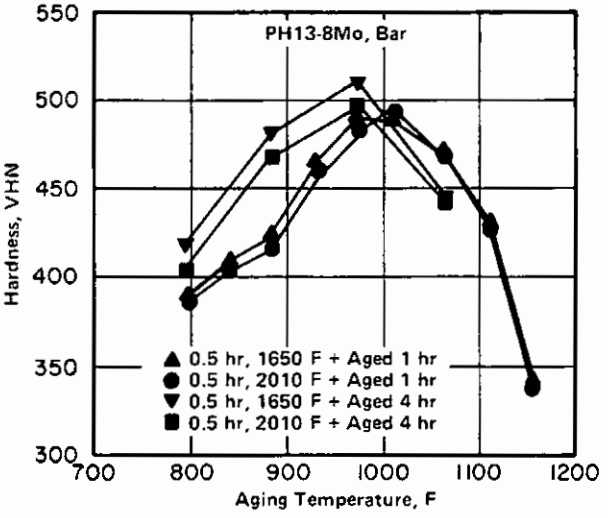


FIGURE 1.064. EFFECTS OF AGING FOR 1 OR 4 HOURS ON HARDNESS OF SOLUTION-TREATED BAR (24)

Fe
13 Cr
8 Ni
2 Mo
PH13-8Mo

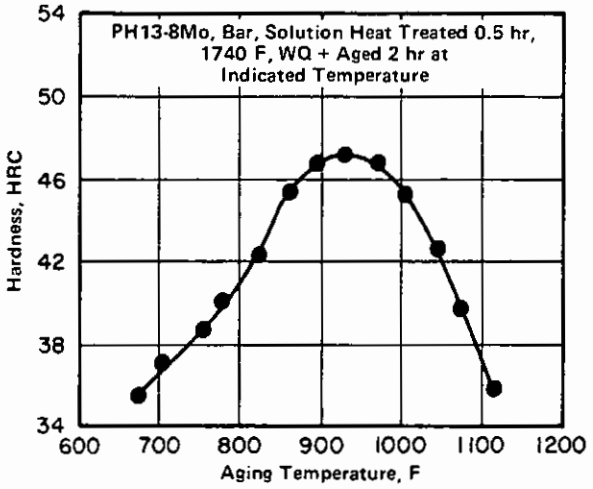


FIGURE 1.065. EFFECTS OF AGING FOR 2 HOURS ON HARDNESS OF SOLUTION-TREATED BAR (25)

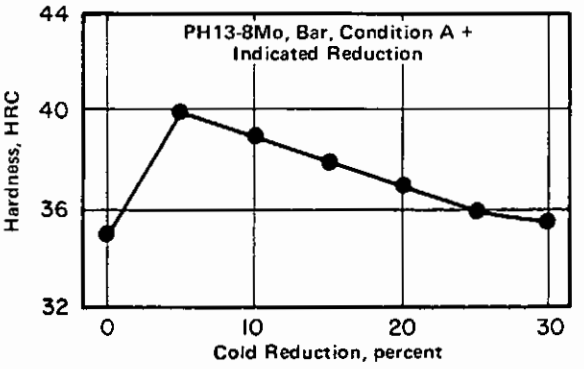


FIGURE 1.067. EFFECTS OF COLD WORK ON HARDNESS (22)

Alloy	13PH-8Mo		
Condition	A	H 900[a]	H 950[a]
Reduction in Diameter (by forging), percent	Hardness, HRC		
0	35	46	45
5	40	48	46
10	40	48	46
15	40	48	46
20	40	47	46
25	40	–	–
30	40	–	–

(a) Fabrication sequence – A + CW + age 4 hours.

TABLE 1.068. EFFECT OF COLD WORK ON HARDNESS OF BAR IN VARIOUS CONDITIONS (3)

Alloy	13PH-8Mo			
Form	0.750-inch-Diameter Bar (Final Diameter)			
Condition	Cold Reduced 10 percent + H 900		Cold Reduced 10 percent + H 1000	
Aging Time, hr	Hardness		Hardness	
1	47	46	47	46
4	48	47	46	46
8	49	48	45	44
16	49	48	44	43

TABLE 1.069. EFFECT OF AGING TEMPERATURE AND TIME ON HARDNESS OF COLD-WORKED BAR (3)

Alloy	PH13-8Mo
Condition	A
Temperature, F	Thermal Conductivity, Btu·ft/hr·ft^2·F
212	8.1
392	9.1
599	10.3
797	11.8
1004	12.7
1112	13.1

Fe
13 Cr
8 Ni
2 Mo
PH13-8Mo

TABLE 2.013. THERMAL CONDUCTIVITY (3)

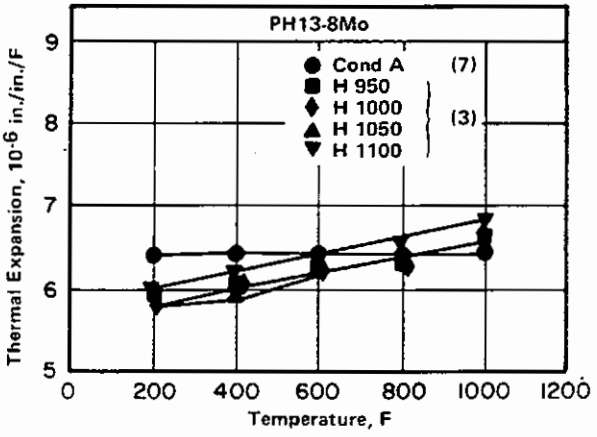


FIGURE 2.0141. THERMAL EXPANSION (3,7)

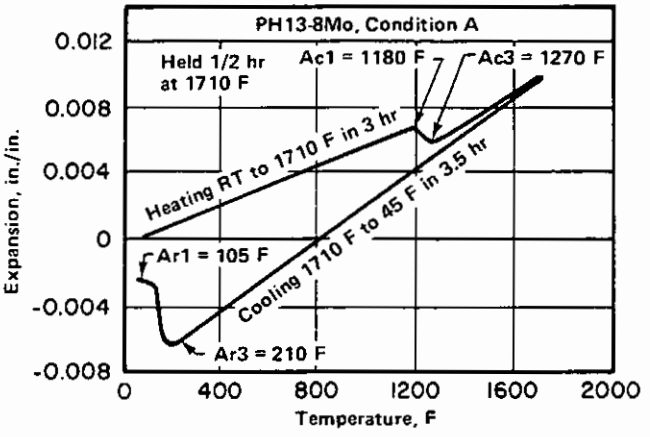


FIGURE 2.0142. DILATOMETER CURVE INDICATING DIMENSIONAL CHANGES AND TRANSFORMATION TEMPERATURES FOR CONDITION A (3)

Alloy	PH13-8Mo	
Condition	A	H 1000
lb/in.^{3}	0.279	0.279
gr/cm^3	7.74	7.76

TABLE 2.021. DENSITY (3)

Alloy	PH13-8Mo
Condition	A
Temperature, F	Electrical Resistivity, μohm-in.
212	40.1
392	41.2
599	41.8
797	42.6
1004	43.0
1112	43.2

TABLE 2.0221. ELECTRICAL RESISTIVITY (3)

Fe
13 Cr
8 Ni
2 Mo
PH13-8Mo

Alloy	PH13-8Mo					
Condition	H 950					
Field Strength, oersteds	10.5	54.7	110.5	164.5	217	264
Permeability	52	127	85	65	53	46

TABLE 2.0231. MAGNETIC PERMEABILITY (15)

Alloy	PH13-8Mo	
Form	0.062-inch Strip	
Condition	Applied Stress[a], ksi	Days to Failure[b] (80-ft lot, Kure Beach)
H 950[c]	204	1 sample failed after 353 days; 1 after 1077 days; 1 NF
	184	1 sample failed after 51 days; 2 NF
	153	1 sample failed after 1077 days; 2 NF
H 1000[c]	199	3 NF
	179	3 NF
	149	3 NF
H 1050[c]	172	3 NF
	155	3 NF
	149	3 NF
Solution treated, welded, aged at 1000 F for 4 hours	195	3 samples failed after 43 days
	176	3 samples failed after 43 days
	146	1 sample failed after 43 days; 1 after 100 days
Solution treated, welded, solution treated and aged at 1000 F for 4 hours	195	3 NF
	176	3 NF
	146	3 NF

(a) Applied stresses were 100, 90, and 75 percent of the 0.2 percent yield strength, using smooth, bent beam specimens tested in the longitudinal direction.
(b) NF indicates no failure in 1405 days' exposure.
(c) Heat treatment includes solution treatment at 1700 F for 15 minutes.

TABLE 2.0311. STRESS-CORROSION CRACKING IN MARINE ATMOSPHERE (3)

Alloy	PH13-8Mo			
Form	0.050-inch Sheet			
Condition	BCHT-900			
	Original Properties		Applied Stress 90 Percent F_{ty}	
Orientation	F_{tu}, ksi	F_{ty}, ksi	Stress, ksi	Days to Failure, (80-ft lot)
Longitudinal	235	215	193	396
Transverse	248	223	201	487

TABLE 2.0312. STRESS-CORROSION CRACKING AT KURE BEACH IN MARINE ATMOSPHERE (8)

Fe
13 Cr
8 Ni
2 Mo
PH13-8Mo

Alloy		PH13-8Mo				
Form		Bar[a]				
		Original Tensile Properties		Applied Tensile Stress, Percent F_{ty}	Ratio of Failures to Number Exposed	
Condition	Orientation	F_{tu}, ksi	F_{ty}, ksi		Salt Spray[b]	Seacoast[c]
H 950	Longitudinal	222	206	75	0/3	–
				100	0/3	–
	Transverse	221	203	75	3/9	1/5
				100	5/12	3/5
H 1000	Longitudinal	205	194	25	–	0/3
				50	0/3	0/3
				75	0/3	–
				100	2/3	–
	Transverse	206	200	25	0/6	0/22
				50	7/45	10/50
				75	12/54	8/34
				100	11/39	0/30
H 1050	Longitudinal	183	172	25	–	0/3
				50	1/3	0/3
				75	1/3	–
	Transverse	183	177	25	0/3	0/17
				50	5/33	0/37
				75	5/33	0/27
				100	2/20	1/19

(a) Average data from seven heats.
(b) 6-month exposure.
(c) 14-month exposure.

TABLE 2.0313. STRESS-CORROSION BEHAVIOR IN SALT SPRAY AND MARINE ATMOSPHERE (26)

Alloy		PH13-8Mo				
Form		10-inch-Diameter Bar				
Test Environment		3.5 percent NaCl				
		Original Properties		Applied Stress		Days to Failure[a]
Condition	Orientation	F_{tu}, ksi	F_{ty}, ksi	ksi	Percent F_{ty}	
H 950	Longitudinal	231	217	163	75	NF
		231	217	196	90	NF
	Transverse	226	211	158	75	NF
		226	211	190	90	NF
H 1000	Longitudinal	222	212	159	75	NF
		222	212	191	90	NF
	Transverse	219	210	158	75	NF
		219	210	190	90	NF

(a) NF denotes no failure after 6 months.

TABLE 2.0314. STRESS-CORROSION CRACKING IN AN NaCl SOLUTION (9)

Fe
13 Cr
8 Ni
2 Mo

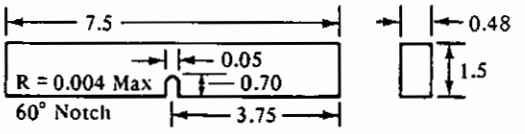
PH13-8Mo

Alloy	PH13-8Mo			
Form	4-inch-Square Billet			
Condition	F_{tu}[a], ksi	F_{ty}[a], ksi	Plane-Strain Fracture Toughness[b], K_{Ic}, ksi $\sqrt{in.}$	Plane-Strain Stress-Corrosion Threshold[c], K_{Iscc}, ksi $\sqrt{in.}$
H 950	225	208	73.9	73.9[d,e]

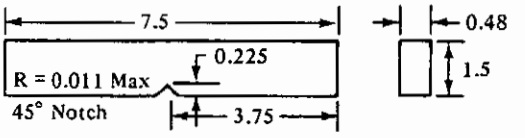
Note: Data average of two longitudinal tests. Specimens heat treated in blank form. Notch specimens were fatigue cracked after heat treatment to produce a precrack approximately 0.1 inch long at the notch root.

(a) 0.25-inch-diameter tension specimen.

(b)



(c)



(d) Test environment 3.5 percent NaCl.

(e) No stress-corrosion crack growth at stress-intensity levels exceeding approximately 85 percent K_{Ic}. No crack growth after 1000 hours.

TABLE 2.0315. FRACTURE-TOUGHNESS AND STRESS-CORROSION VALUES IN A 3.5 PERCENT NaCl SOLUTION (10)

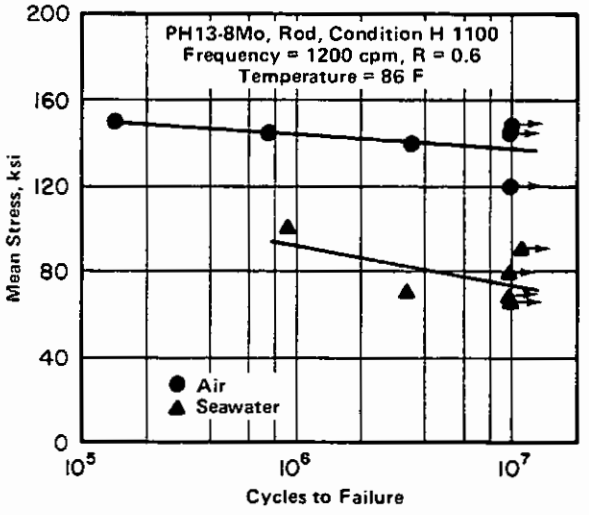


FIGURE 2.0316. AXIAL FATIGUE BEHAVIOR IN SEA-WATER AND IN AIR (27)

Fe
13 Cr
8 Ni
2 Mo
PH13-8Mo

Alloy	PH13-8Mo		
Form	0.250-inch Bar		
Test Environment	6 percent Sodium Chloride Plus 1/2 percent Acetic Acid, Saturated With Hydrogen Sulfide		
Condition	Original F_{ty}, ksi	Applied Stress, ksi	Time to Failure, hr
H 1000	205	100	2.6
		75	3.7
		50	7.4
		25	75.0
H 1100	150	100	8.0
		75	24.0
		50	170.0
		25	>1000

TABLE 2.0317. STRESS-CORROSION CRACKING IN AN NaCl-ACETIC ACID-H_2S SOLUTION (3)

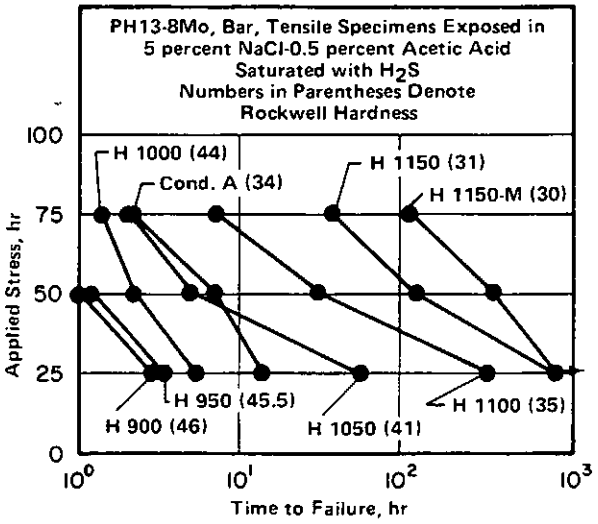


FIGURE 2.0318. EFFECTS OF HEAT TREATMENT AND HARDNESS ON STRESS-CORROSION BEHAVIOR IN AN NaCl-ACETIC ACID-H_2S SOLUTION (28)

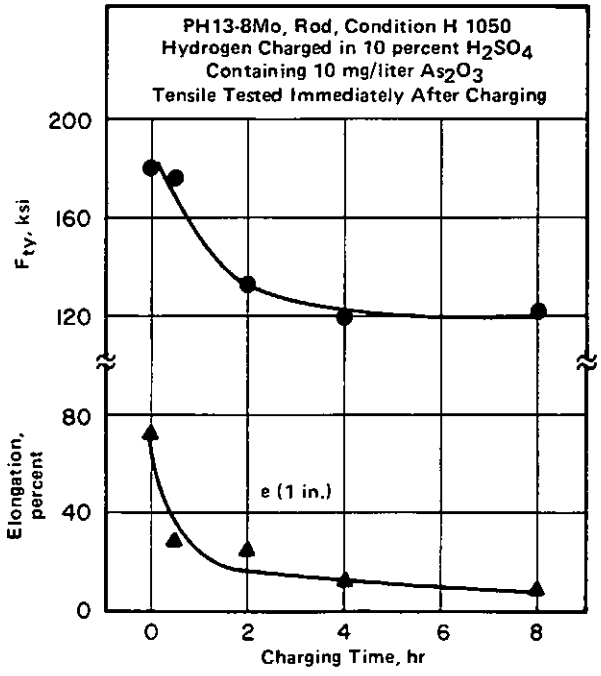


FIGURE 2.0319. EFFECT OF HYDROGEN CHARGING TIME ON TENSILE PROPERTIES (29)

Fe
13 Cr
8 Ni
2 Mo

PH13-8Mo

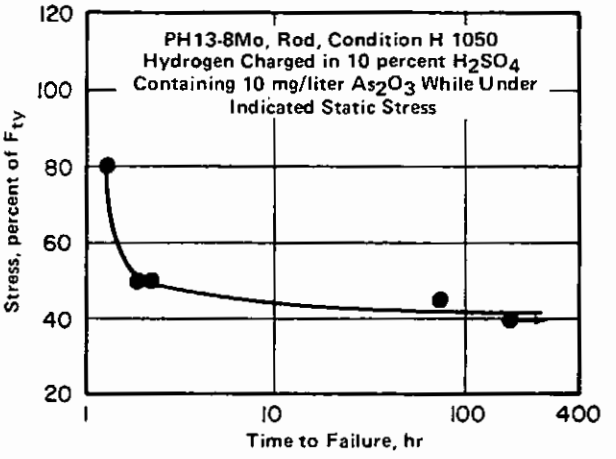


FIGURE 2.03110. DELAYED FAILURE BEHAVIOR WHILE BEING CHARGED WITH HYDROGEN (29)

Alloy	PH13-8Mo								
			Tensile Properties						
AMS Specification	Condition	Specimen Orientation	F_{tu}, ksi Min	F_{tu}, ksi Max	F_{ty}, ksi (Min)	e, percent (Min)(a)	RA, percent (Min)	Hardness Min(b)	Hardness Max
5629C	A	–	–	175(c)	–	–	–	–	363 HB
	H 950	Long.	220	–	205	10	45	45 HRC	–
		Trans.	220	–	205	10	35	45 HRC	–
	H 1000	Long.	205	–	190	10	50	43 HRC	–
		Trans.	205	–	190	10	40	43 HRC	–
	H 1025	Long.	185	–	175	11	50	41 HRC	–
		Trans.	185	–	175	11	45	41 HRC	–
	H 1050	Long.	175	–	165	12	50	40 HRC	–
		Trans.	175	–	165	12	45	40 HRC	–
	H 1100	Long.	150	–	135	14	50	34 HRC	–
		Trans.	150	–	135	14	50	34 HRC	–
	H 1150	Long.	135	–	90	14	50	30 HRC	–
		Trans.	135	–	90	14	50	30 HRC	–
5864	A	–	–	–	–	–	–	–	38 HRC
	H 950	Long.	220	–	205	10	45	45 HRC	–
		Short trans.	220	–	205	10	35	45 HRC	–
	H 1000	Long.	205	–	190	10	50	43 HRC	–
		Short trans.	205	–	190	10	40	43 HRC	–
	H 1025	Long.	185	–	175	11	50	41 HRC	–
		Short trans.	185	–	175	11	45	41 HRC	–
	H 1050	Long.	175	–	165	12	50	40 HRC	–
		Short trans.	175	–	165	12	45	40 HRC	–
	H 1100	Long.	150	–	135	14	50	34 HRC	–
		Short trans.	150	–	135	14	50	34 HRC	–
	H 1150	Long.	135	–	90	14	50	30 HRC	–
		Short trans.	135	–	90	14	50	30 HRC	–

Note: The original AMS documents should be consulted for complete specification details.

(a) 2 inches or 4D.
(b) Not required if tensile-property requirements are met.
(c) Wire only.

TABLE 3.011. AMS-SPECIFIED MECHANICAL PROPERTIES (1,19)

Alloy	PH-13-8Mo (Up to 12-inch Section Size)															
Condition	RH 950		H 950		H 1000		H 1025		H 1050		H 1100		H 1150		H 1150-M	
Orientation	Long.	Trans.	Long.	Trans.	Long.	Trans.	Long.	Trans.	Long.	Trans.	Long.	Trans.	Long.	Trans.	Long.	Trans.
F_{tu}, Min, ksi	220	220	220	220	205	205	185	185	175	175	150	150	135	135	125	125
F_{ty}, Min, ksi	205	205	205	205	190	190	175	175	165	165	135	135	90	90	85	85
e (2 in.), Min, percent	10	10	10	10	10	10	11	11	12	12	14	14	14	14	16	16
RA, Min, percent	45	35	45	35	50	40	50	45	50	45	50	50	50	50	55	55
Hardness, HRC, Min	45	45	45	45	43	43	41	41	40	40	34	34	30	30	26	26
Hardness, BHN, Min	430	430	430	430	400	400	–	–	372	372	313	313	283	283	–	–

Fe
13 Cr
8 Ni
2 Mo
PH13-8Mo

TABLE 3.012. PRODUCERS' GUARANTEED MECHANICAL PROPERTIES (23)

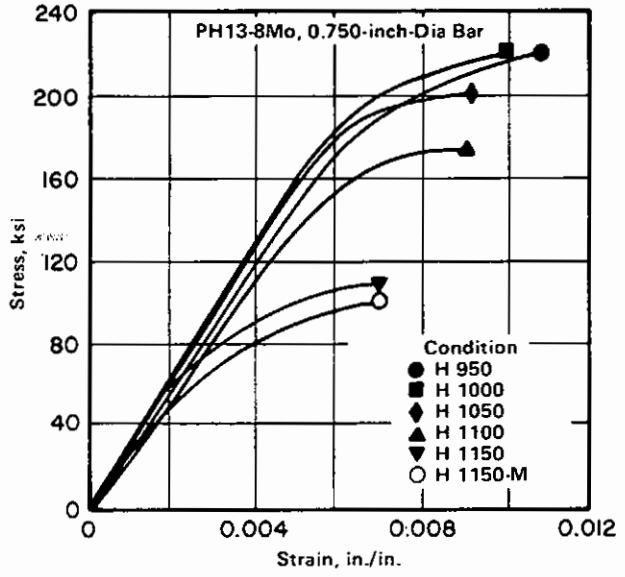


FIGURE 3.0211. STRESS-STRAIN CURVES FOR BAR IN VARIOUS AGED CONDITIONS (13)

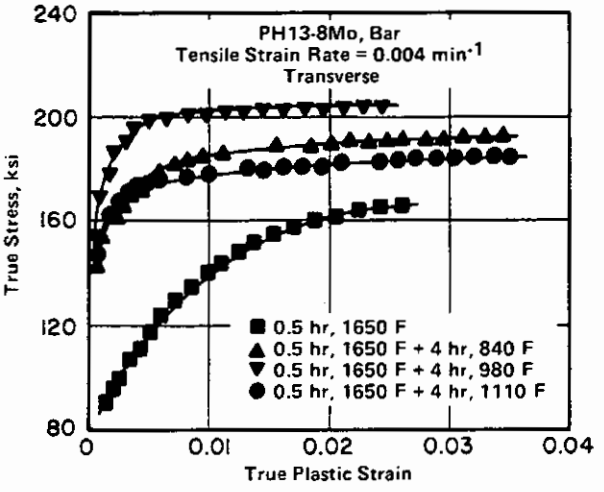


FIGURE 3.0212. TRUE STRESS-TRUE STRAIN CURVES FOR SOLUTION TREATED AND SOLUTION TREATED-AND-AGED ALLOY (24)

Alloy	PH13-8Mo															
Form	1 to 3-inch Bar															
Condition	A		RH 950		H 950		H 1000		H 1050		H 1100		H 1150		H 1150-M	
Orientation	Long.	Trans.	Long.	Trans.	Long.	Trans.	Long.	Trans.	Long.	Trans.	Long.	Trans.	Long.	Trans.	Long.	Trans.
F_{tu}, ksi	160	160	235	235	225	225	215	215	190	190	160	160	145	145	130	130
F_{ty}, ksi	120	120	215	215	210	210	205	205	180	180	150	150	105	105	85	85
e (2 in.), percent	17	17	12	12	12	12	13	13	15	15	18	18	20	20	22	22
RA, percent	65	65	45	35	50	40	55	50	55	55	60	60	63	63	70	70

TABLE 3.0213. TYPICAL TENSILE PROPERTIES FOR BAR IN VARIOUS HEAT-TREATED CONDITIONS (23)

Fe
13 Cr
8 Ni
2 Mo

PH13-8Mo

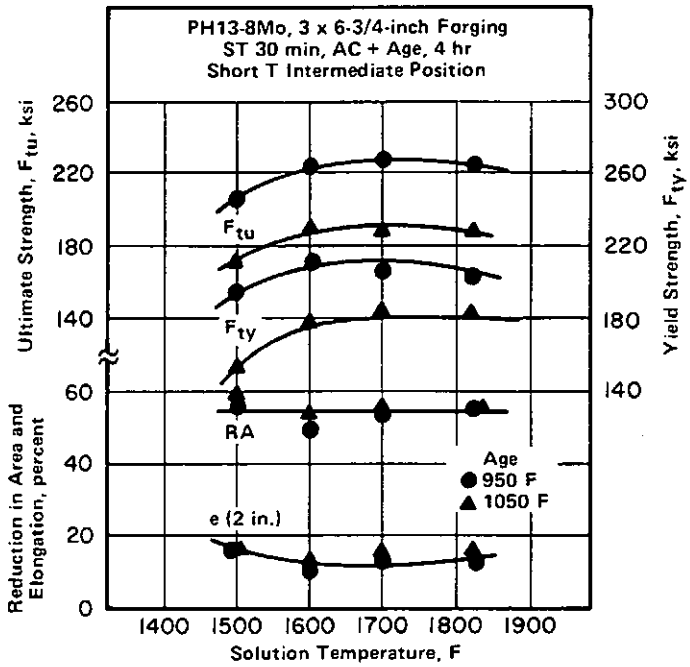


FIGURE 3.0214. EFFECT OF SOLUTION-TREATING TEMPERATURE ON THE TENSILE PROPERTIES OF FORGINGS AGED AT TWO TEMPERATURES (3)

Alloy	PH13-8Mo						
Section Size, in.	Condition[a]	Direction and Location[b]	F_{ty}, ksi	F_{tu}, ksi	e (4 x D), percent	RA, percent	IE Charpy V, ft-lb
9 by 9	A 950	LI	196	218	14	37	–
		TI	201	220	13	31	–
		TC	190	213	14	33	–
3 by 8	A 950	LI	188	214	16	66	18
		LCT	198	220	14	63	–
		STC	193	218	14	53	–
3 by 8	A 1000	LI	188	217	16	66	50
	A 1050	LI	187	195	15	69	111
	A 1100	LI	162	173	18	72	149
	ORH 950	LI	204	225	14	66	28
		STC	200	223	13	61	–

Note: 1825 F is not the recommended solution temperature; data are included for comparison purposes only.

(a) A 950 – 1825 F, 1/2 hr, AC + 950 F, 1 hr, AC
A 1000 – 1825 F, 1/2 hr, AC + 1000 F, 1 hr, AC
A 1050 – 1825 F, 1/2 hr, AC + 1050 F, 1 hr, AC
A 1100 – 1825 F, 1/2 hr, AC + 1100 F, 1 hr, AC
ORH 950 – 1150 F, 4 hr, AC + 1700 F, 1 hr, AC + -100 F, 8 hr + 950 F, 1 hr, AC.
(b) LI = longitudinal intermediate; TC = transverse center; STC = short transverse center.

TABLE 3.0215. MECHANICAL PROPERTIES FOR VARIOUS AGED CONDITIONS (4)

Fe
13 Cr
8 Ni
2 Mo

PH13-8Mo

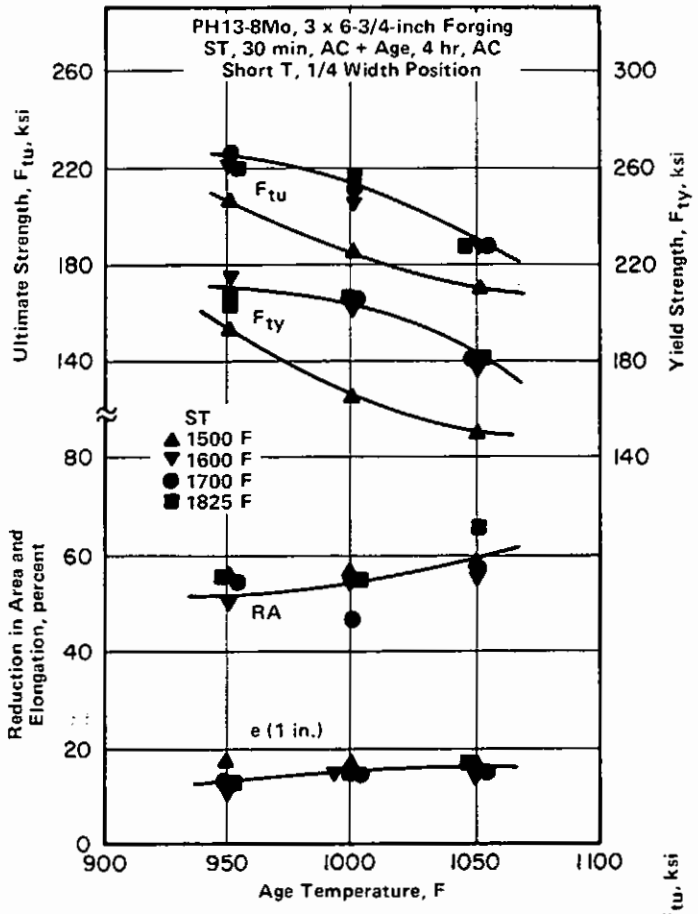


FIGURE 3.0216. EFFECT OF AGING AND SOLUTION-TREATING TEMPERATURE ON THE TENSILE PROPERTIES OF FORGINGS (11)

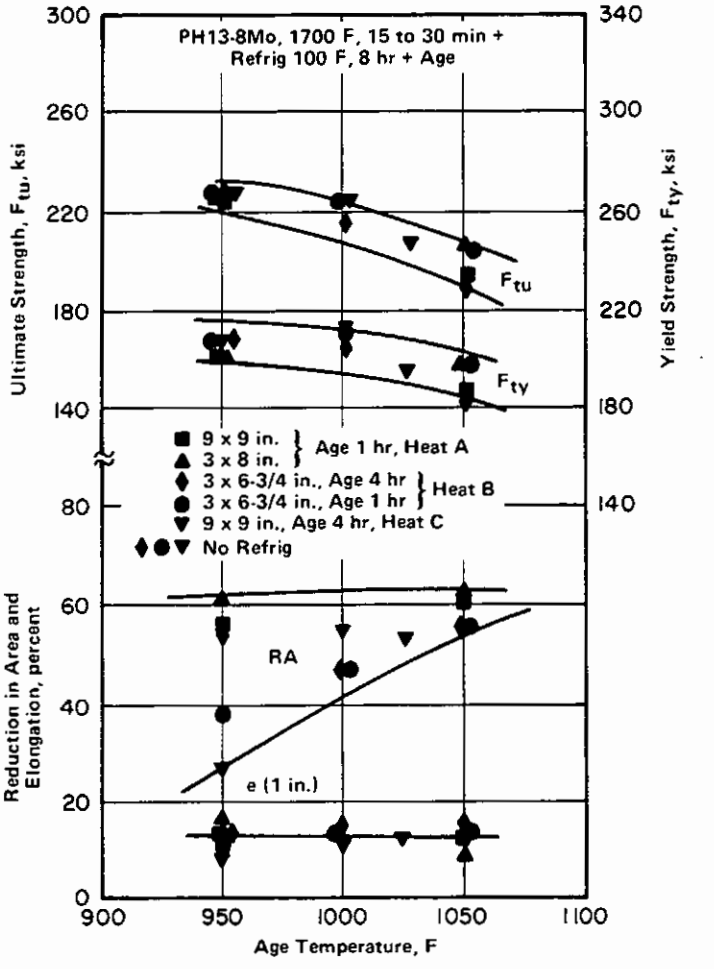


FIGURE 3.0217. EFFECT OF AGING TEMPERATURE ON THE SHORT TRANSVERSE TENSILE PROPERTIES OF FORGINGS (11,12)

Fe
13 Cr
8 Ni
2 Mo

PH13-8Mo

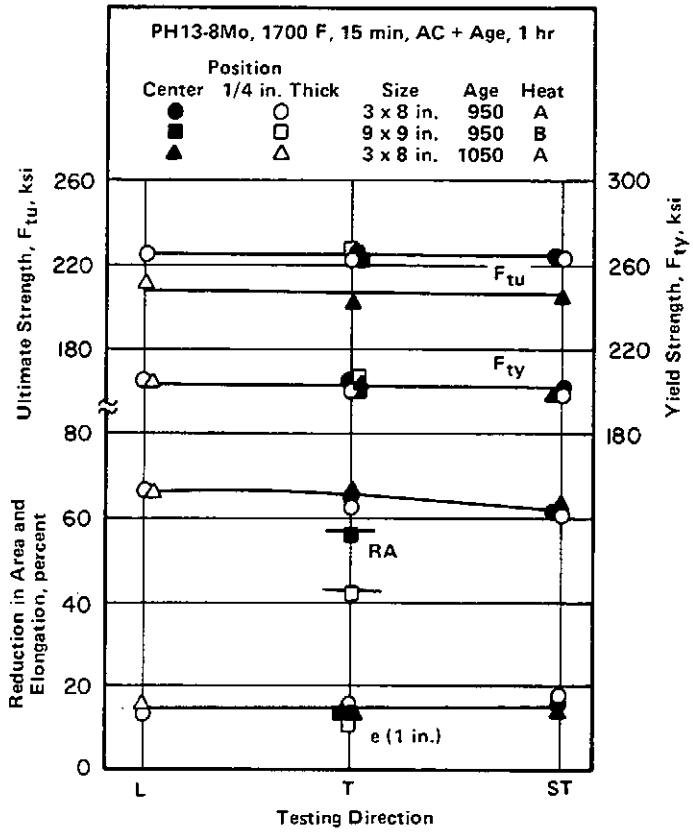


FIGURE 3.0218. EFFECT OF TESTING DIRECTION ON TENSILE PROPERTIES OF SOLUTION TREATED-AND-AGED FORGINGS (11)

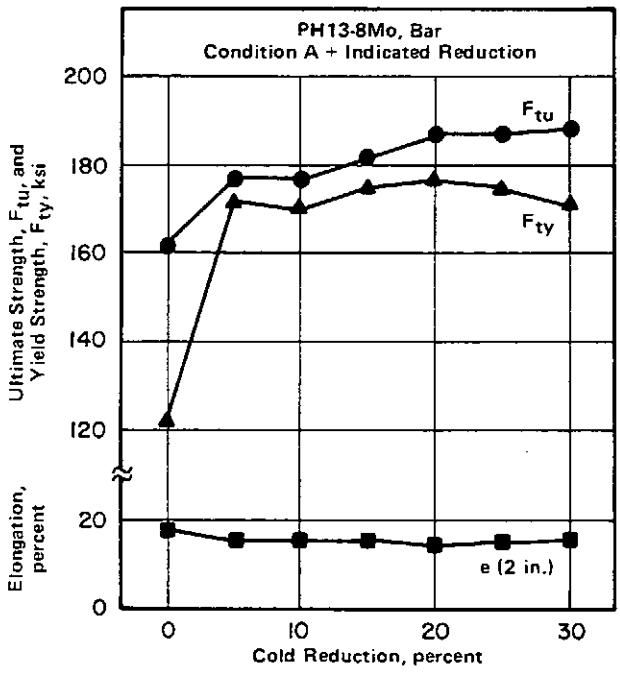


FIGURE 3.0219. EFFECTS OF COLD WORK ON TENSILE PROPERTIES (22)

Fe
13 Cr
8 Ni
2 Mo

PH13-8Mo

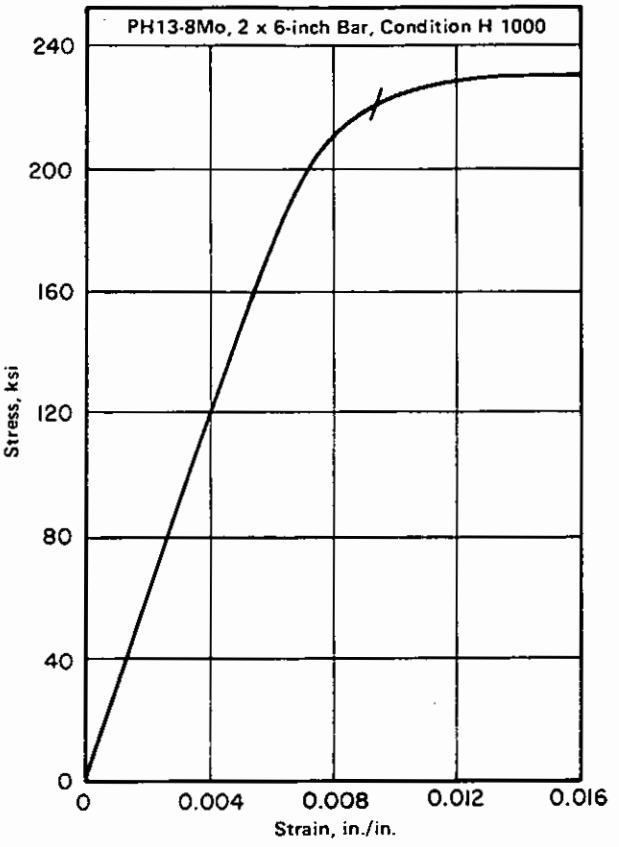


FIGURE 3.0221. STRESS-STRAIN CURVE IN COMPRESSION FOR CONDITION H 1000 (13)

Alloy	PH13-8Mo		
Form	7/8-inch-Diameter Bar		
Condition	H 950	H 1000	H 1050
F_{cy}, ksi			
0.2 percent	220	224	198
0.02 percent	181	196	174

TABLE 3.0222. TYPICAL COMPRESSIVE YIELD STRENGTHS FOR BAR IN VARIOUS AGED CONDITIONS (3)

Alloy	PH13-8Mo	
Form	1 to 3-inch Bar	
	Impact Energy, ft-lb[a]	
Condition	Longitudinal	Transverse
A	60	40
RH 950	20	10
H 950	20	15
H 1000	30	20
H 1050	50	30
H 1100	60	40
H 1150	80	60
H 1150-M	120	80

(a) Charpy V-notch.

TABLE 3.0231. TYPICAL IMPACT PROPERTIES FOR VARIOUS HEAT-TREATED CONDITIONS (23)

Fe
13 Cr
8 Ni
2 Mo

PH13-8Mo

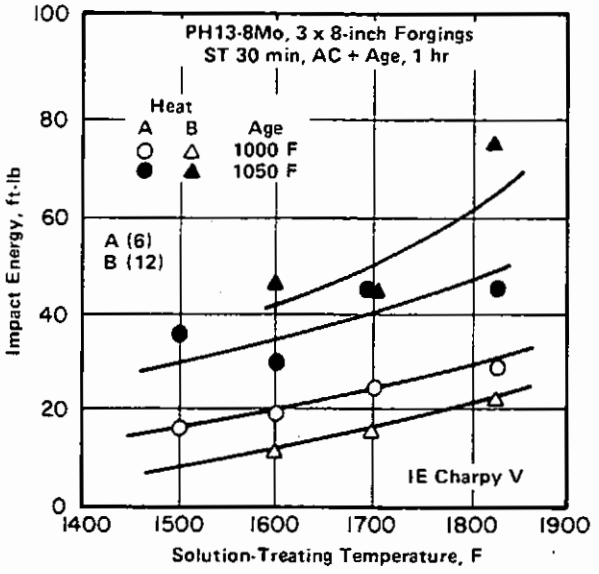


FIGURE 3.0232. EFFECT OF SOLUTION-TREATING TEMPERATURE ON SHORT-TRANSVERSE IMPACT PROPERTIES (6,12)

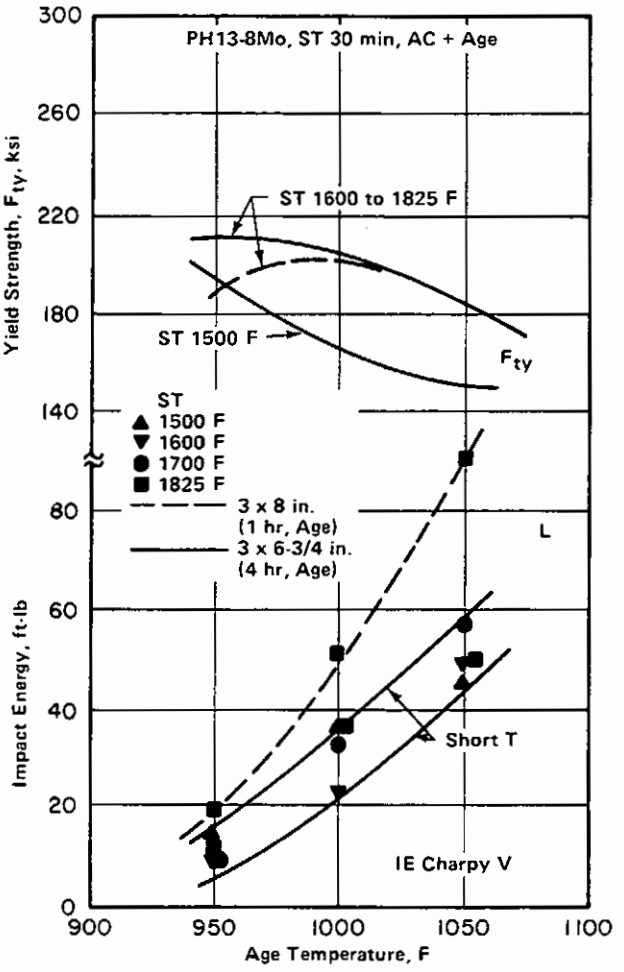


FIGURE 3.0233. EFFECT OF AGING AND SOLUTION-TREATING TEMPERATURE ON IMPACT PROPERTIES (6)

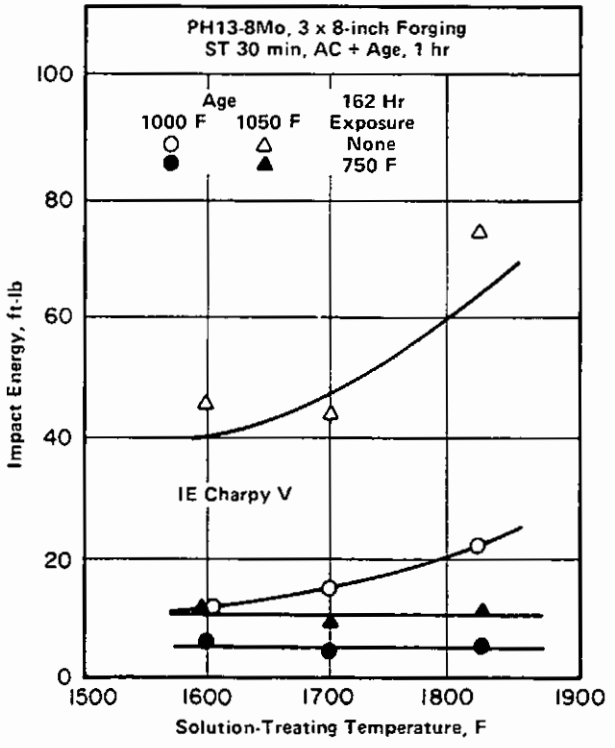


FIGURE 3.0234. EFFECT OF SOLUTION-TREATING TEMPERATURE ON SHORT-TRANSVERSE IMPACT ENERGY BEFORE AND AFTER ELEVATED-TEMPERATURE EXPOSURE (6)

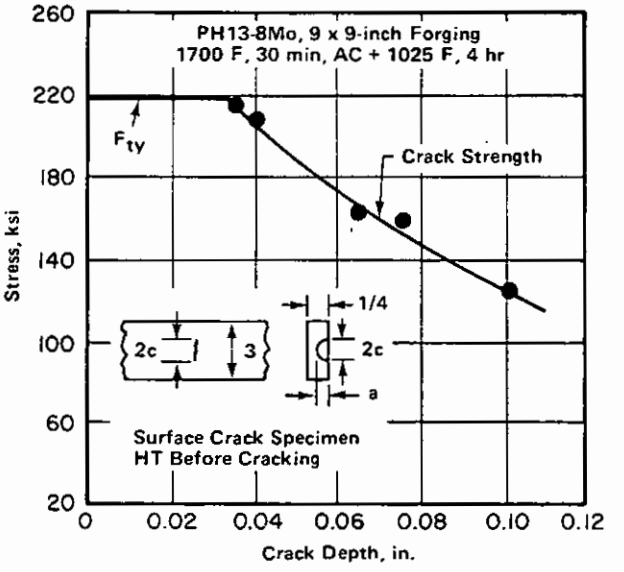


FIGURE 3.02711. EFFECT OF SURFACE CRACKS ON CRACK STRENGTH (12)

Alloy	PH13-8Mo	
Form	Bar	
Condition	H 950	H 1000
F_{sy}[a], ksi	137.1	134.0
F_{sty}, ksi	148.0	143.2
G, ksi	11.1×10^3	10.9×10^3
F_{st}, ksi	184.4	171.9

(a) Shear yield strength.

TABLE 3.0251. TORSION AND SHEAR PROPERTIES (3)

Alloy	PH13-8Mo			
Form	0.1-inch Sheet			
Condition	Test Direction	e/D	F_{bry}, ksi	F_{bru}, ksi
H 1000	L	1.5	290	330
		2.0	375	448
	T	1.5	300	340
		2.0	380	442

TABLE 3.0261. BEARING PROPERTIES OF SHEET IN CONDITION H 1000 (13)

Fe
13 Cr
8 Ni
2 Mo

PH13-8Mo

Alloy	PH13-8Mo	
Condition	H 1000	
	Forging Cross-Section Size, inch	
Form	6 x 21	5 x 24
Orientation	Plane Strain Fracture Toughness, K_{Ic}, ksi $\sqrt{in.}$	
TL	108	116
LT	–	115
		75[a]

Note: Testing procedure and data conform to ASTM E 399; data average of two or more tests; compact tension specimen; thickness, B, 1 inch.

(a) Test temperature – 65 F.

TABLE 3.02721. PLANE-STRAIN FRACTURE TOUGHNESS FOR CONDITION H 1000 (15)

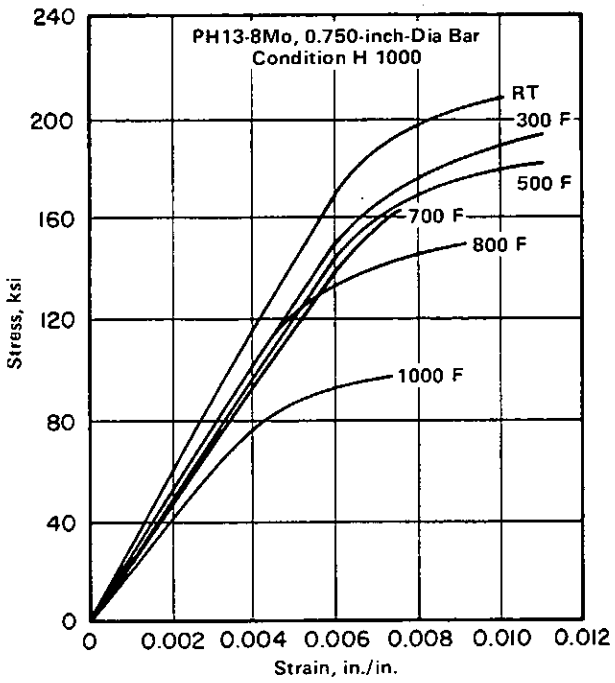


FIGURE 3.0311. STRESS-STRAIN CURVES AT ELEVATED TEMPERATURES FOR BAR IN CONDITION H 1000 (13)

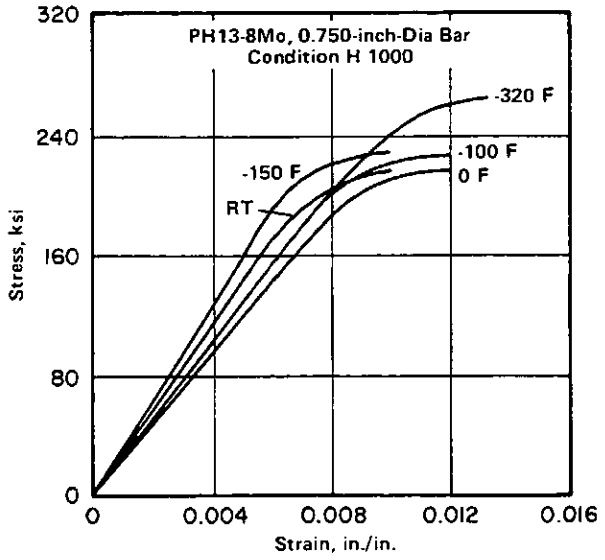


FIGURE 3.0312. STRESS-STRAIN CURVES AT ROOM AND LOW TEMPERATURE FOR BAR IN CONDITION H 1000 (13)

Fe
13 Cr
8 Ni
2 Mo

PH13-8Mo

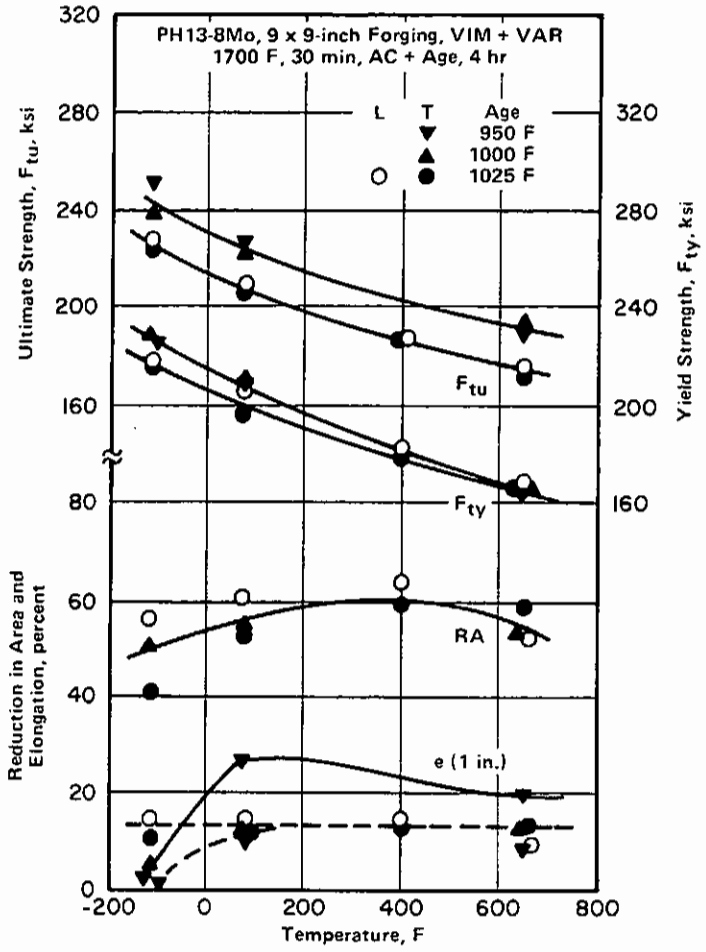


FIGURE 3.0313. EFFECT OF TEST TEMPERATURE ON TENSILE PROPERTIES OF A FORGING (12)

Alloy	PH13-8Mo					
Condition	H 1000					
Form	Forging					
Cross-Sectional Size, in.	Test Temp., F	Orientation	F_{tu}, ksi	F_{ty}, ksi	e (1 in.), percent	RA, percent
13 x 13	RT	L	212	205	14	60
		T	210	204	14	58
		ST	205	200	14	58
	-110	L	234	224	15	56
		T	230	218	16	51
		ST	230	216	15	50
4-1/2 x 4-1/2	RT	L	214	206	14	55
		T	218	210	14	55
	-110	L	235	229	14	53
		T	234	227	13	47
1-1/2 x 13	RT	L	208	202	14	60
		T	212	204	16	61
	-110	L	227	219	16	58
		T	234	226	14	58

Note: Data average of two tests.

TABLE 3.0314. EFFECT OF TEST TEMPERATURE AND ORIENTATION ON THE TENSILE PROPERTIES OF VARIOUS-SIZE FORGINGS (14)

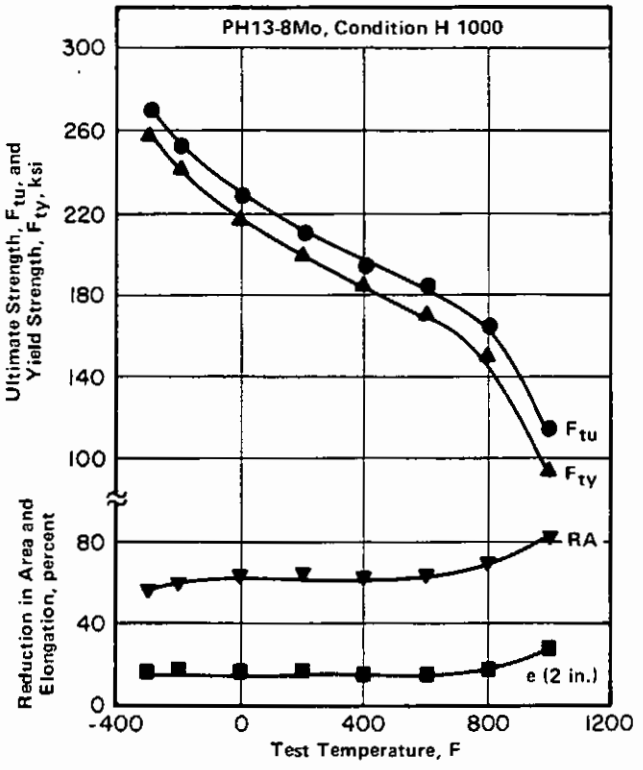


FIGURE 3.0315. TENSILE PROPERTIES OF BAR AT CRYOGENIC AND ELEVATED TEMPERATURES (22)

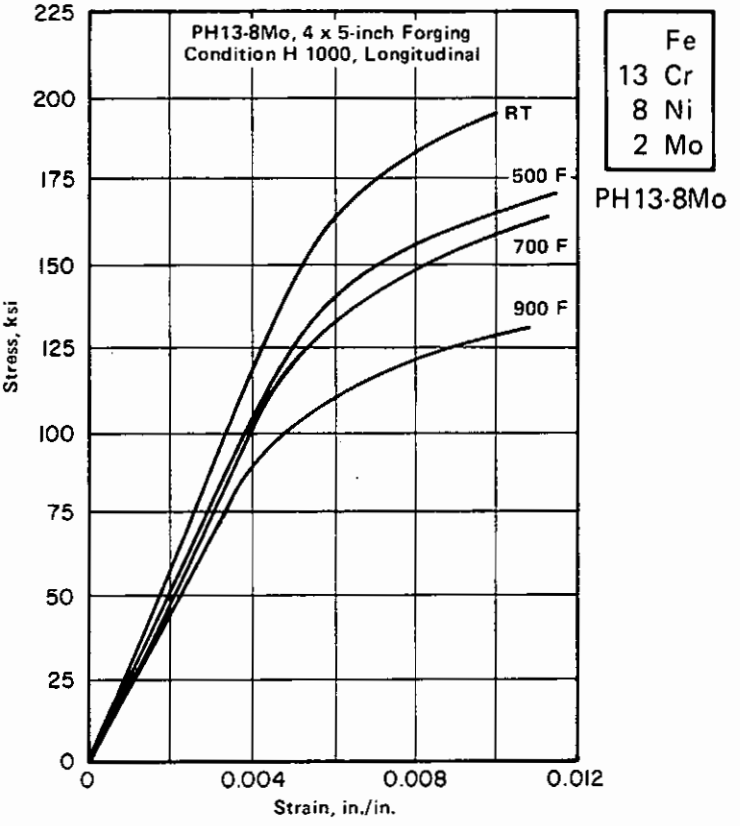


FIGURE 3.0321. STRESS-STRAIN CURVES FOR A FORGING IN COMPRESSION AT ELEVATED TEMPERATURES (17)

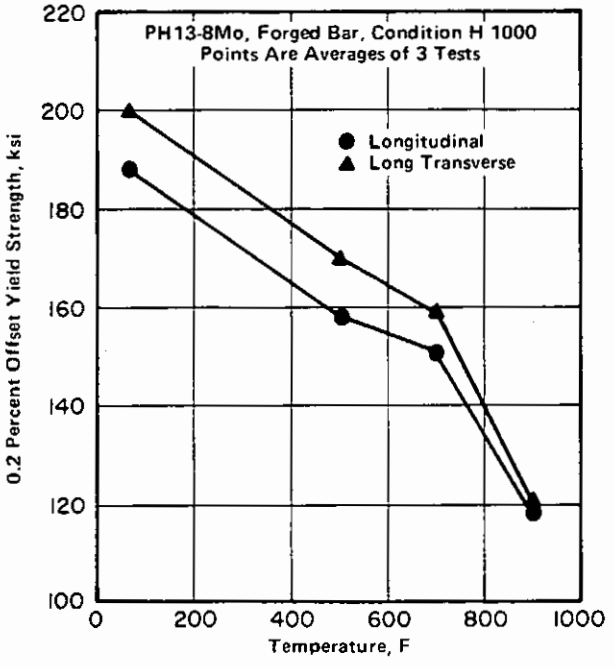


FIGURE 3.0322. EFFECT OF TEMPERATURE ON COMPRESSIVE YIELD STRENGTH (17)

Fe
13 Cr
8 Ni
2 Mo

PH13-8Mo

Alloy	PH13-8Mo				
Form	1-inch-Diameter Bar				
Condition	H 950	H 1000	H 1050	H 1100	H 1150-M
Test Temp., F	IE Charpy V, ft-lb				
RT	24	30	40	50	–
-32	11	20	35	46	–
-65	7	12	22	38	–
-110	5	8	13	32	88
-175	3	6	–	–	71
-220	2	5	6	14	–
-320	2	4	4	5	30

TABLE 3.0331. TYPICAL LOW-TEMPERATURE IMPACT ENERGIES OF BAR IN VARIOUS AGED CONDITIONS (3)

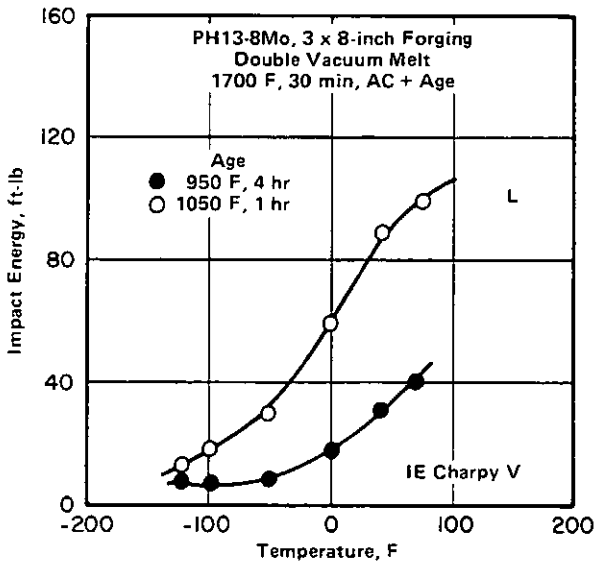


FIGURE 3.0332. EFFECT OF TEST TEMPERATURE ON IMPACT PROPERTIES OF A FORGING (6)

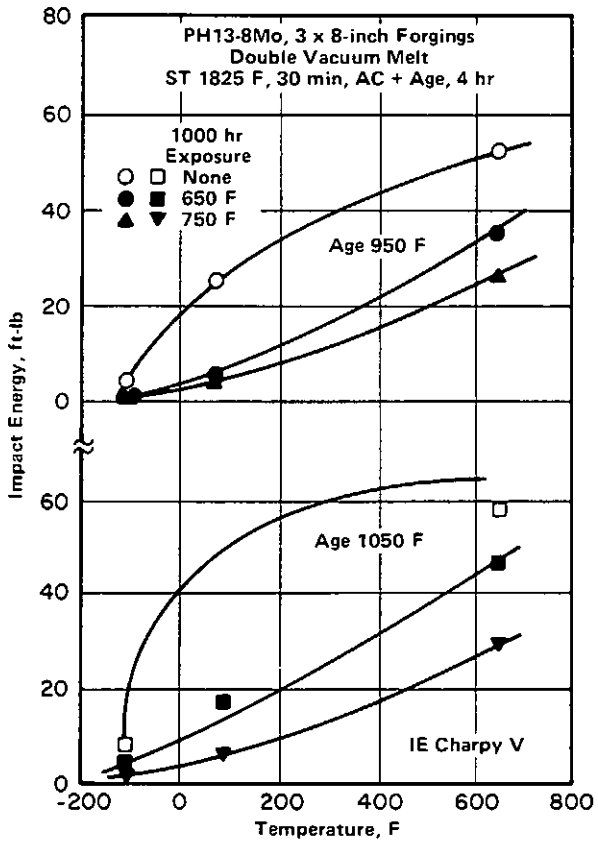


FIGURE 3.0333. EFFECT OF TEST TEMPERATURE AND EXPOSURE TEMPERATURE ON THE IMPACT ENERGY OF FORGINGS (6)

Fe
13 Cr
8 Ni
2 Mo

PH13-8Mo

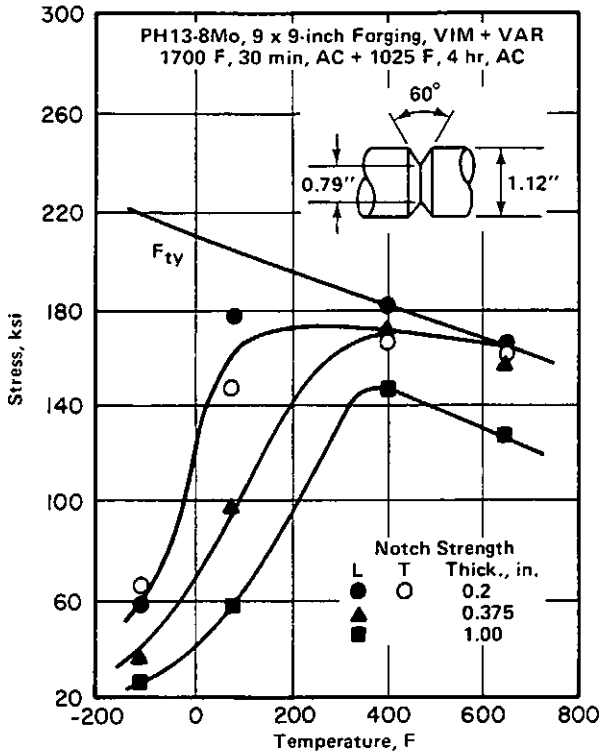


FIGURE 3.03711. EFFECT OF TEST TEMPERATURE ON SHARP NOTCH STRENGTH OF A FORGING (12)

Alloy	PH13-8Mo				
Form	0.75-inch-Diameter Bar				
Condition	H 1000				
Test Temp., F	Stress Concentration Factor, K_t	F_{ty}, ksi	F_{tu}, ksi	NTS, ksi	NTS/F_{tu}
80	3.8	212	220	355	1.61
	5.25	212	220	347	1.57
-110	3.8	–	235	384	1.64
	5.25	–	235	373	1.59

Notched Round Bar

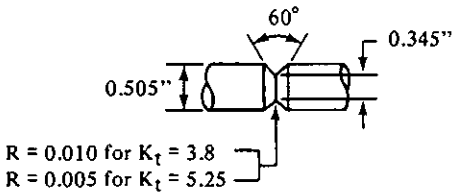


TABLE 3.03712. EFFECT OF STRESS-CONCENTRATION FACTOR ON TENSILE AND NOTCH PROPERTIES OF BAR AT ROOM AND LOW TEMPERATURE (3)

Fe
13 Cr
8 Ni
2 Mo
PH13-8Mo

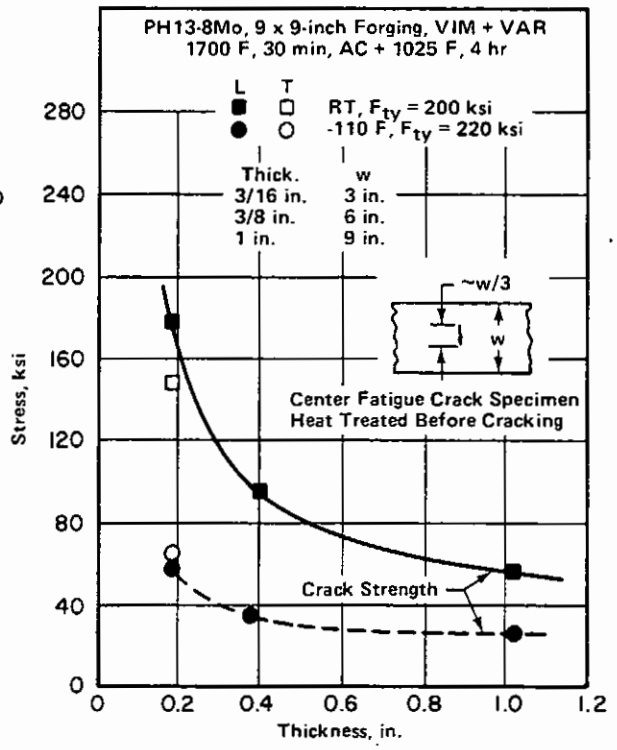


FIGURE 3.03713. EFFECT OF THICKNESS ON CRACK STRENGTH OF A FORGING AT ROOM AND LOW TEMPERATURE (12)

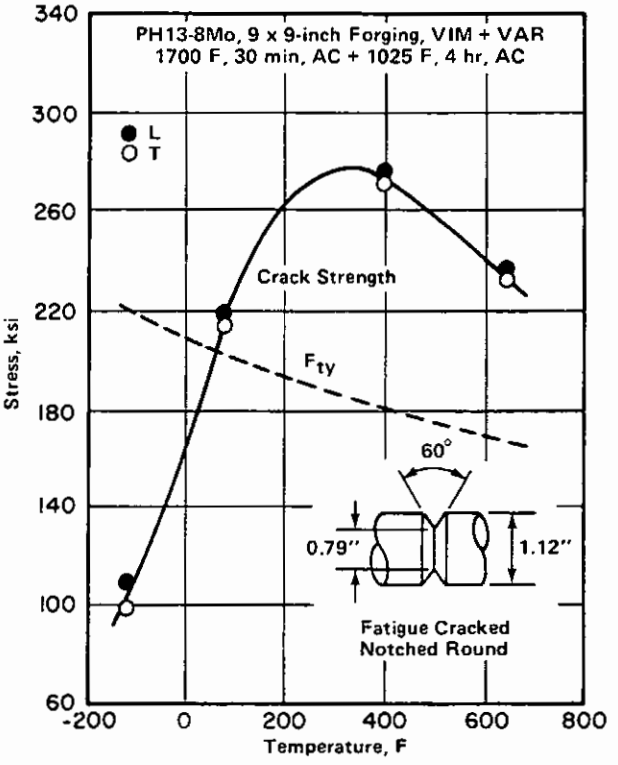


FIGURE 3.03714. EFFECT OF TEST TEMPERATURE ON CRACK STRENGTH OF A FORGING (12)

Alloy	PH13-8Mo		
Condition	H 1000		
Test Temp.	-110 F		
Form	Forging Cross-Sectional Size, inch		
	13 x 13	4-1/2 x 4-1/2	1-1/2 x 13
Orientation	Plant Strain Fracture Toughness, K_{Ic}, ksi $\sqrt{in.}$		
LT	53	43	47
TL	56	41	47

Note: Testing procedure and data conform to ASTM E 399. Data average of two or more tests. Single-edge crack specimen: thickness, B, 0.5 inch.

TABLE 3.03721. PLANE-STRAIN FRACTURE TOUGHNESS OF A FORGING AT LOW TEMPERATURE (14)

Fe
13 Cr
8 Ni
2 Mo
PH13-8Mo

Alloy	PH13-8Mo			
Form	Condition	Test Temperature, F	Specimen Orientation	Fracture Toughness[a], K_{Ic}, ksi $\sqrt{in.}$
Upset forging	H 1000	70	TL	82 (1)
			ST	86 (1)
		-65	LT	53 (2)
Forged bar	H 1000	70	LT	98 (5)
			TL	91 (3)
		-65	TL	55 (2)
Extruded bar	Re-solution + H 1000	70	LT	74 (3)
Rolled bar	H 1000	70	LT	89 (4)
			TL	75 (2)
		-65	LT	50 (4)
	RH 950	70	LS	60 (4)
	RH 975	70	LS	70 (3)
	RH 1000	70	LS	95 (1)

(a) Values averaged from number of specimens in parentheses.

TABLE 3.03722. FRACTURE TOUGHNESS OF VARIOUS WROUGHT FORMS AT ROOM AND CRYOGENIC TEMPERATURES (31)

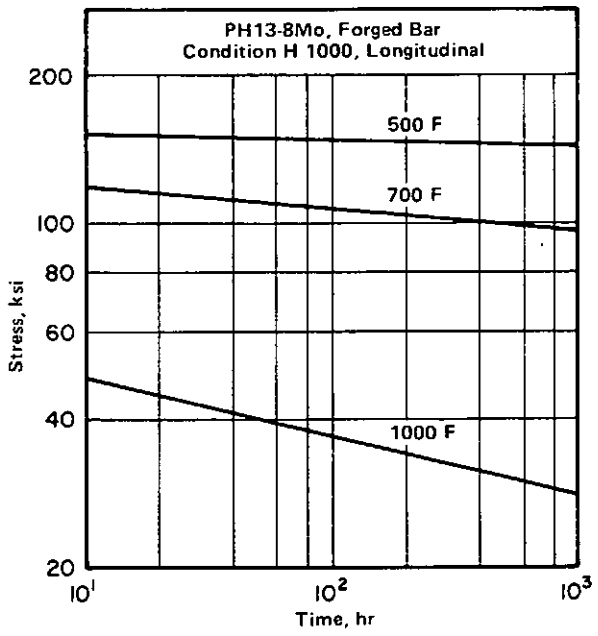


FIGURE 3.041. TIME TO 0.2 PERCENT CREEP DEFORMATION FOR BAR AT ELEVATED TEMPERATURES (32)

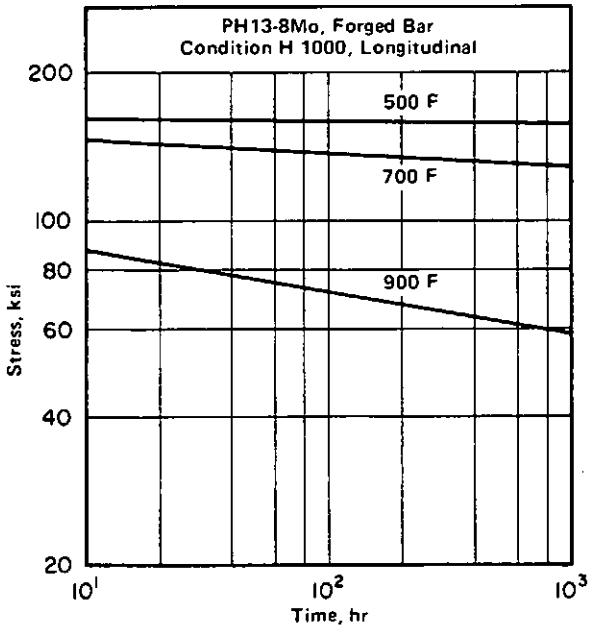


FIGURE 3.042. TIME TO RUPTURE FOR BAR AT ELEVATED TEMPERATURES (32)

Fe
13 Cr
8 Ni
2 Mo

PH13-8Mo

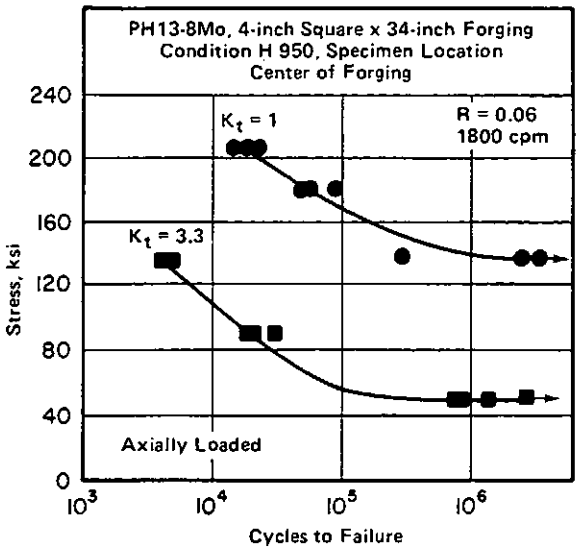


FIGURE 3.051. EFFECT OF STRESS CONCENTRATIONS ON FATIGUE STRENGTH OF A FORGING (16)

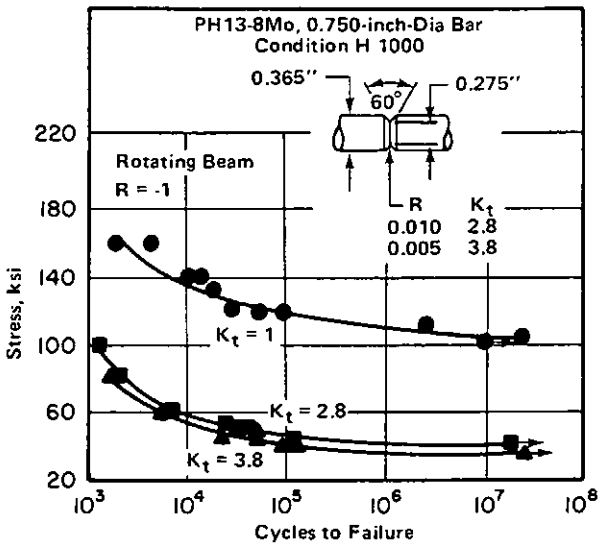


FIGURE 3.052. S-N CURVES FOR SMOOTH AND NOTCHED SPECIMENS OF BAR (3)

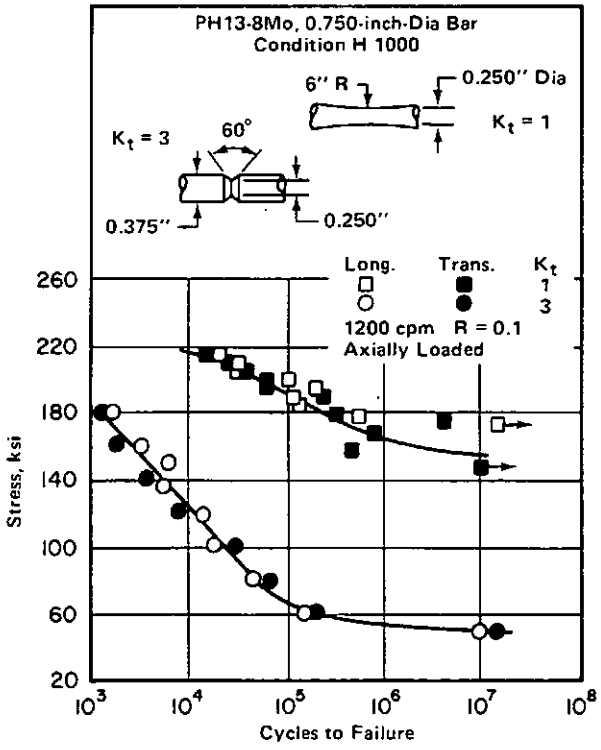


FIGURE 3.053. S-N CURVES FOR LONGITUDINAL AND TRANSVERSE SMOOTH AND NOTCHED SPECIMENS FROM BAR AT A STRESS RATIO OF R = 0.1 (3)

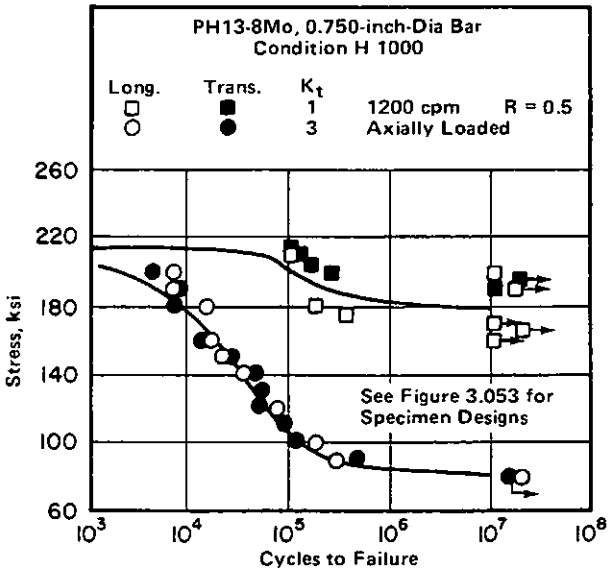


FIGURE 3.054. S-N CURVES FOR LONGITUDINAL AND TRANSVERSE SMOOTH AND NOTCHED SPECIMENS FROM BAR AT A STRESS RATIO OF R = 0.5 (3)

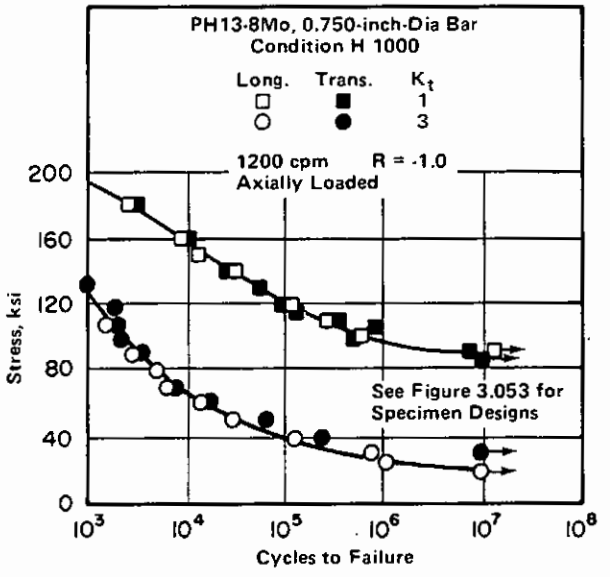
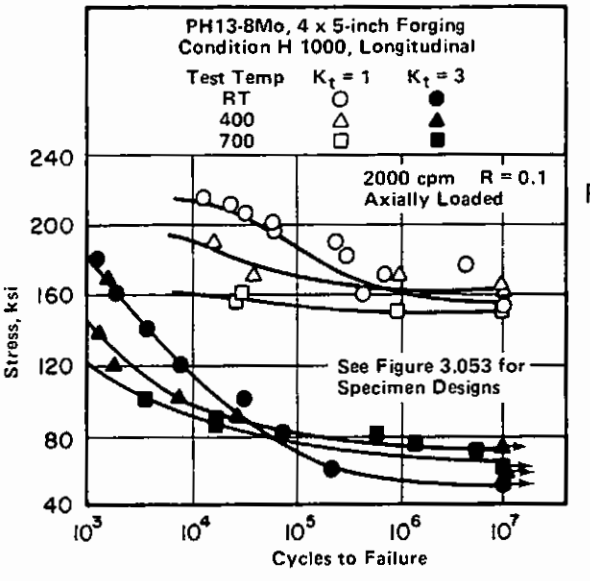


FIGURE 3.055. S-N CURVES FOR LONGITUDINAL AND TRANSVERSE SMOOTH AND NOTCHED SPECIMENS FROM BAR AT A STRESS RATIO OF R = -1.0 (3)



Fe
13 Cr
8 Ni
2 Mo

PH13-8Mo

FIGURE 3.056. S-N CURVES AT ELEVATED TEMPERATURES FOR LONGITUDINAL SMOOTH AND NOTCHED SPECIMENS FROM A FORGING AT A STRESS RATIO OF R = 0.1 (17)

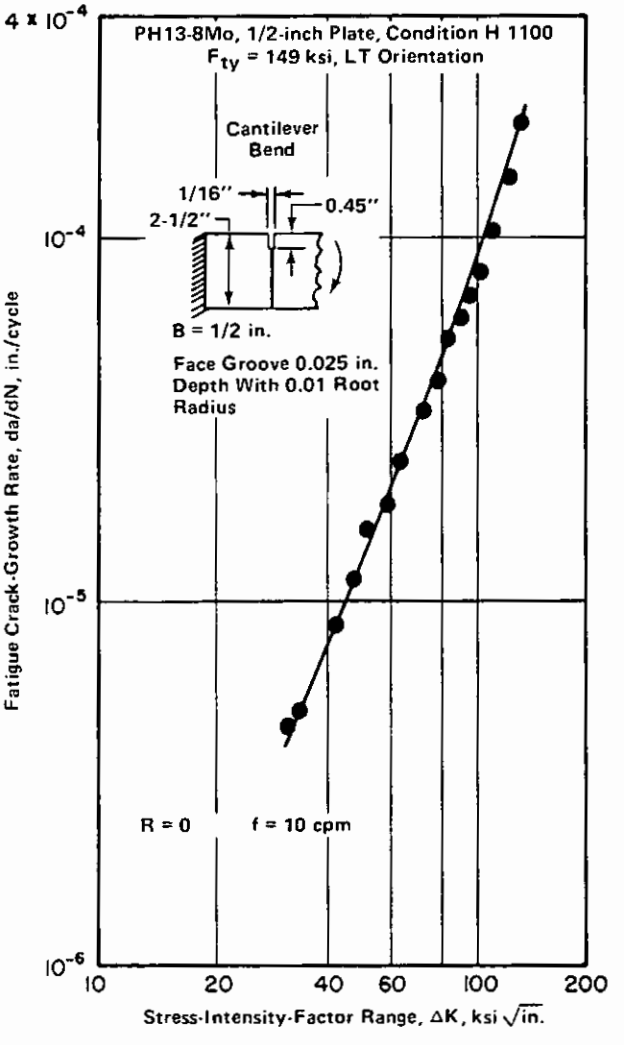
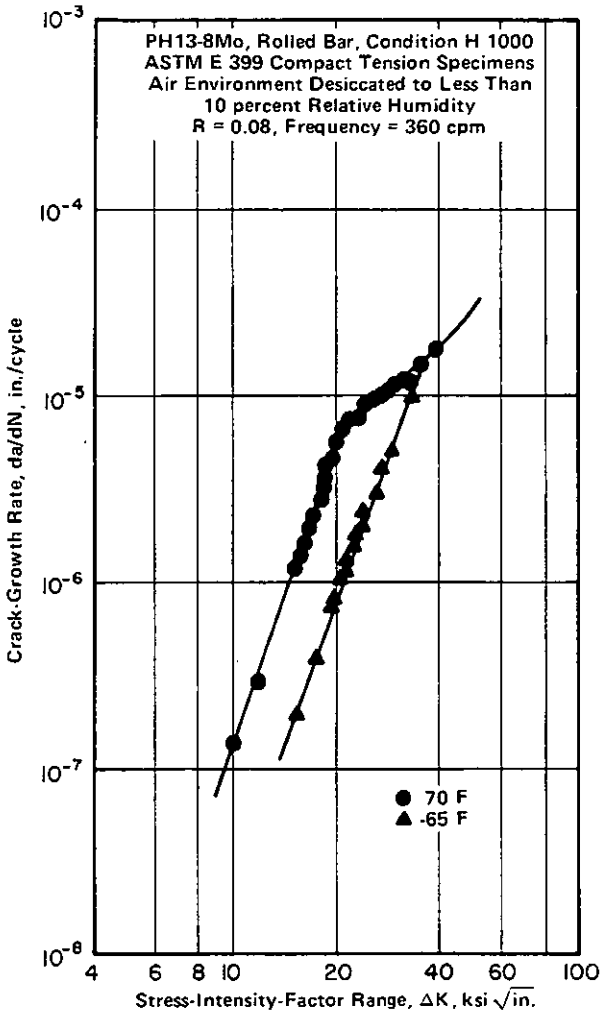


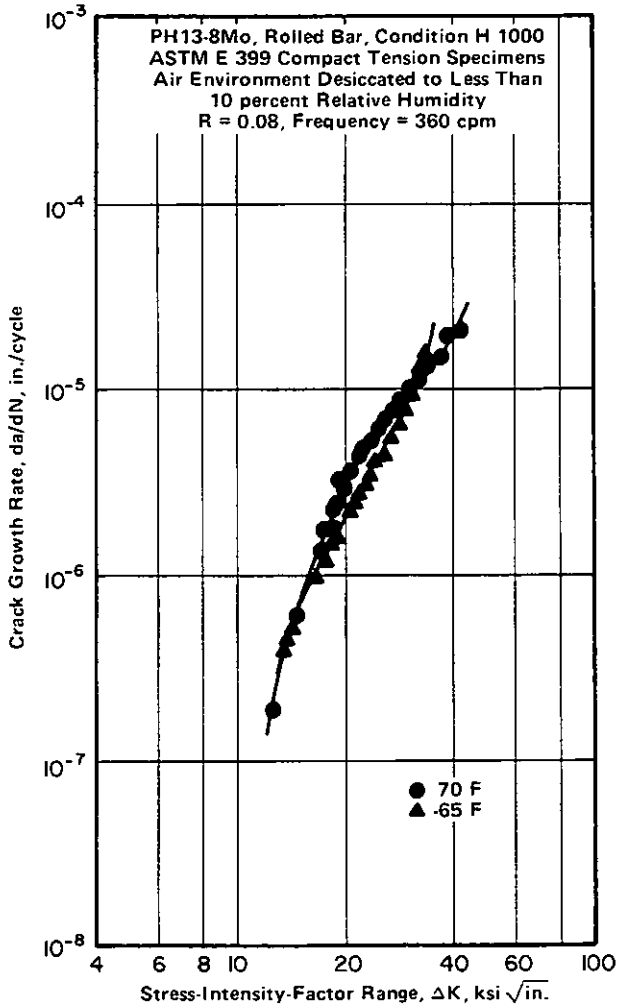
FIGURE 3.057. FATIGUE CRACK-GROWTH RATE AT ROOM TEMPERATURE FOR PLATE (18)

Fe
13 Cr
8 Ni
2 Mo

PH13-8Mo



(a) LT Orientation



(b) TL Orientation

FIGURE 3.059. FATIGUE CRACK-GROWTH RATE IN LOW-HUMIDITY AIR AT LOW TEMPERATURES (31,33)

Fe
13 Cr
8 Ni
2 Mo
PH13-8Mo

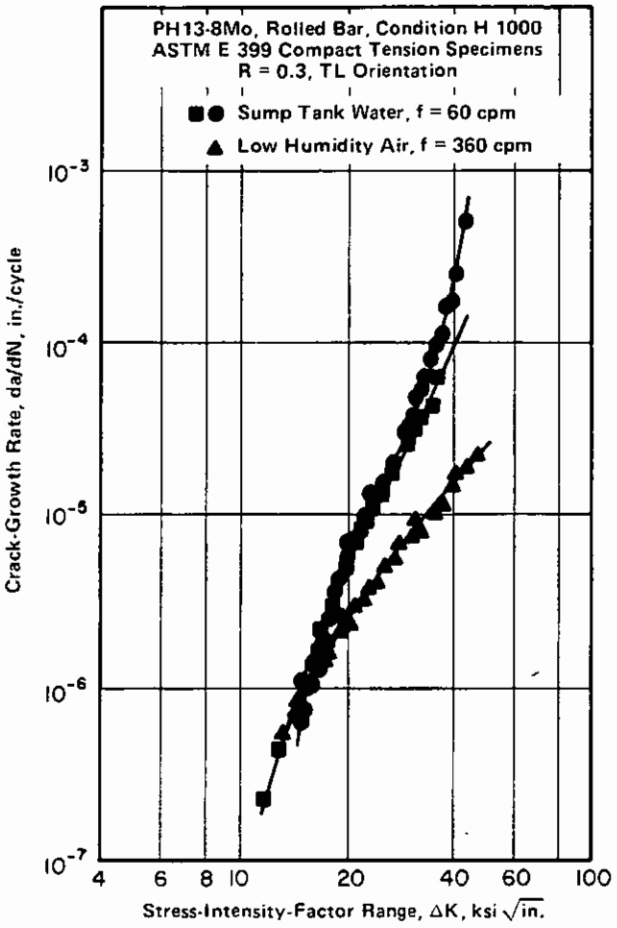


FIGURE 3.0510. FATIGUE CRACK-GROWTH RATE IN FUEL-TANK SUMP WATER AND IN AIR AT ROOM TEMPERATURE (31,33)

Alloy	PH13-8Mo			
Form	0.750-inch-Diameter Bar			
Condition	H 950	H 1000	H 1050	H 1100
E, ksi x 10^3	28.6	32.0	30.8	28.6

TABLE 3.0621. TENSILE MODULUS OF BAR IN VARIOUS AGED CONDITIONS (13)

Fe
13 Cr
8 Ni
2 Mo

PH13-8Mo

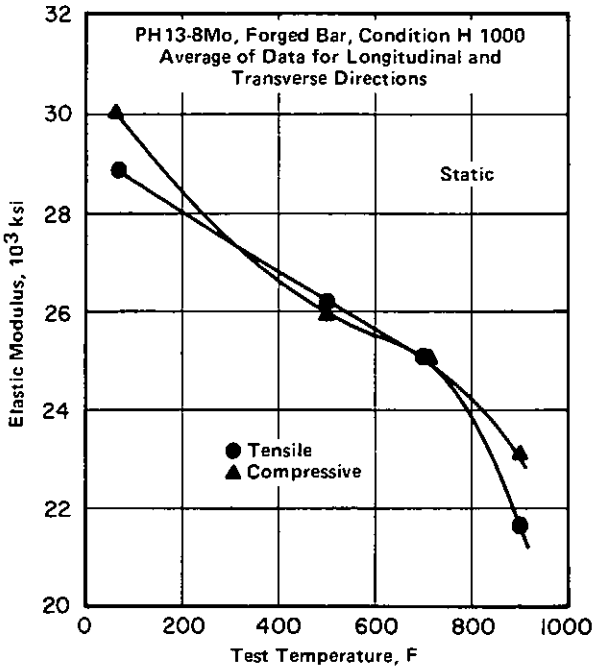


FIGURE 3.0622. ELASTIC MODULI OF FORGED BAR IN TENSION AND COMPRESSION AT ROOM AND ELEVATED TEMPERATURES (32)

Alloy	PH13-8Mo		
Form	3 x 3-inch Forging		
Condition	BCHT 950(a)		
Direction	L	T	ST
F_{tu}, ksi	226	223	224
F_{ty}, ksi	207	200	199
e (1 in.), percent	13	15	17
RA, percent	66	63	61
Charpy V, ft-lb	22	–	–
Hardness, HRC	47	–	–

(a) Specimen blanks were cut and then heat treated.

TABLE 4.0131. TENSILE AND IMPACT PROPERTIES OF FORGINGS SUBJECTED TO A BRAZE-CYCLE HEAT TREATMENT (5)

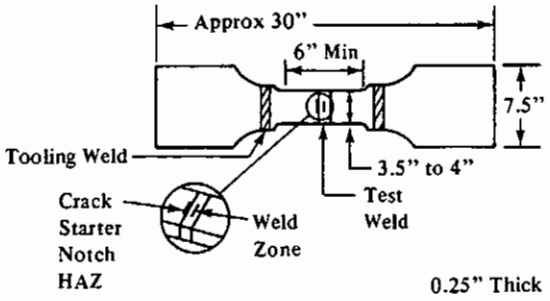
Alloy	PH13-8Mo											
Form	Plate											
	Tensile Properties at Indicated Plate Thickness, inch											
	F_{tu}, ksi			F_{ty}, ksi			e, percent			RA, percent		
Condition(a)	0.187	0.50	0.75	0.187	0.50	0.75	0.187	0.50	0.75	0.187	0.50	0.75
Unwelded base plate + H 950	220	232	225	204	214	208	12	17	16	–	63	62
Weld + H 950	215	207	195	203	173	160	10	14	13	–	51	47
Weld + Condition A + H 950	216	217	213	203	203	195	10	9	18	–	26	20
Unwelded base plate + H 1000	214	216	160	200	210	132	13	17	22	–	65	71
Weld + H 950	204	200	152	199	163	94	11	14	20	–	61	70
Weld + Condition A + H 1000	201	210	147	197	205	96	11	9	20	–	37	60
Unwelded base plate + H 1100	–	173	–	–	163	–	–	22	–	–	71	–
Weld + H 1100	–	165	–	–	124	–	–	18	–	–	71	–
Weld + Condition A + H 1100	–	162	–	–	158	–	–	8(b)	–	–	29(b)	–

(a) Welding conditions: GTA (gas tungsten arc) weld process; base plate welded in Condition A; filler metal was WPH13-8Mo.
(b) Low-ductility values resulted from incomplete weld penetration.

TABLE 4.034. EFFECT OF HEAT TREATMENT ON THE MECHANICAL PROPERTIES OF WELDMENTS AS A FUNCTION OF PLATE THICKNESS (3,34)

Fe
13 Cr
8 Ni
2 Mo
PH13-8Mo

Alloy	PH13-8Mo			
Weld Type	Postweld Stress Relief	Notch Location	Test Temperature, F	Fracture Toughness[a], K_{Ic}, ksi $\sqrt{in.}$
Butt weld	2 hr, 950 F	HAZ	70	88 (4)
			-65	95 (2)
		Weld	70	83 (1)
			-65	98 (1)
	4 hr, 1000 F	HAZ	70	93 (2)
Weld overlay	None	Weld	70	83 (1)
	2 hr, 950 F	Weld	70	79 (1)



(a) Value averaged from number of specimens in parentheses. These are conditional values based on data from part-through-cracked specimens.

TABLE 4.037. FRACTURE TOUGHNESS OF WELDED MATERIAL AT ROOM AND CRYOGENIC TEMPERATURES (31)

REVISED: MARCH 1971
AUTHOR: C. F. HICKEY, JR.

FERROUS ALLOYS

	Fe
14	Cr
8	Ni
2.5	Mo
	Al

PH14-8Mo

1. GENERAL

This sheet alloy is a precipitation hardening semi-austenitic stainless steel similar to 17-7PH in its general characteristics but having somewhat higher strength and better fracture toughness. The highest toughness and least directionality are obtained by vacuum melting. The alloy possesses good weldability by the GTA or electron beam processes; however, for critical applications welding should be confined to vacuum melted sheet using vacuum melted wire of a special composition. The alloy is unstable at moderately elevated temperatures and for long time exposures above about 500 F, this instability can produce significant loss in fracture toughness. Fracture toughness decreases at subzero temperatures and the alloy should not be used at cryogenic temperatures.

1.01 Commercial Designation
PH14-8Mo precipitation hardening stainless steel.

1.02 Alternate Designations
None.

1.03 Specifications
None.

1.04 Composition
Table 1.04.

TABLE 1.04

Source	ARMCO (1)			
Alloy	Fe-14Cr-8Ni-2.5Mo-Al			
Grade	Air Melt		Vacuum Melt	
	Percent		Percent	
Element	Minimum	Maximum	Minimum	Maximum
Aluminum	0.75	1.50	0.90	1.35
Carbon	-	0.05	-	0.05
Chromium	13.75	15.00	14.75	15.50
Manganese	-	1.00	-	0.10
Molybdenum	2.00	3.00	2.00	2.50
Nickel	7.50	8.75	8.00	8.75
Phosphorus	-	0.015	-	0.010
Silicon	-	1.00	-	0.10
Sulfur	-	0.010	-	0.008
Nitrogen	-	-	-	0.01
Iron	Balance		Balance	

1.05 Heat Treatment

1.051 Anneal to Condition A, 1800 to 1850 F, 30 minutes, air cool (1) (see Figure 3.02141 for effect of solution temperature).

1.052 Age Condition A to SRH conditions 1685 to 1715 F, 1 hour, air cool to room temperature (Condition A 1700) and within one hour cool to -100 F, 8 hours (Condition SR100) + age 1 hour, air cool. Aging at 940 to 960 F (Condition SRH 950) or 1040 to 1060 F (Condition SRH 1050) is generally used, with the higher temperature giving somewhat lower strength but better toughness (see Figures 3.02142 and 3.02143 for effect of aging temperature).

1.053 Aging of cold worked alloy (Condition C) 890 to 910 F (Condition CH 900) 940 to 960 F (Condition CH 950) and 1040 to 1060 F (Condition CH 1050) 1 hour, air cool (1).

1.06 Hardness

1.061 Typical hardness of sheet and strip for various conditions, Table 1.061.

TABLE 1.061

Source	(1, pp. 8, 24)
Alloy	Fe-14Cr-8Ni-2.5Mo-Al
Condition	Rockwell Hardness C
A (a)	88 (c)
SRH950 (a)	49
SRH1050(a)	46
A(b)	88 (c)
SRH950 (b)	48
SRH1050 (b)	45
C (a)	42 (d)
CH950 (a)	52 (d)
CH1050 (a)	51 (d)

(a) Air melted.
(b) Vacuum induction melted.
(c) R_b
(d) Applies to material 0.010 inch and thicker

1.062 Effect of cold rolling and cold rolling plus aging on the hardness of sheet, Figure 1.062.

1.063 Effect of cold working on tensile properties and hardness for Condition CH 950 (see 3.02144).

1.07 Forms and Conditions Available

1.071 Forms. Sheet and strip.

1.072 Condition. Annealed (Condition A) and cold worked (Condition C).

1.08 Melting and Casting Practice.
Conventional stainless steel melting and casting practices. Electric arc and vacuum induction melts. Vacuum induction melting allows the full potential of the alloy to be realized because of the close control of quality and composition that is possible (1). For example, vacuum melting results in higher toughness properties and a reduction in the directionality of fracture toughness.

1.09 Special Considerations

1.091 When PH14-8Mo is fabricated in Condition A, and subsequently heat treated, an allowance should be made for the dimensional change (an overall expansion of approximately 0.004 inches per inch) that occurs during heat treatment (1).

1.092 Thorough cleaning prior to thermal treatments is recommended in order to avoid carburization and to minimize difficulties when descaling.

1.093 Embrittlement. As might be expected for martensitic stainless steels, this alloy exhibits a metallurgical instability which is manifest as an increase in the tensile yield strength and a decrease in the static crack propagation resistance when cracked or sharply notched specimens are exposed for long periods of time at moderately elevated temperatures and then tested at the exposure temperature or at lower temperatures (e.g. Figures 3.02151 thorugh 3.02156, Figures 3.0313 and 3.03141 and Table 3.02713). These instability effects are not reduced by vacuum melting (see Figures 3.03713 and 3.03714) and appear to be larger the higher the strength level of the material (e.g. Table 3.02712). There is insufficient data to establish the time-temperature relation for the effect of the instability on the mechanical properties; however, it would appear that exposure at temperatures below about 400 F produces negligible embrittlement. In general, the longitudinal direction of sheet has a higher toughness than the transverse direction. However, this directionality is reduced by vacuum melting (see Figure 3.03712). The alloy has poor fracture toughness below about -200 F and should not be used at cryogenic temperatures (see Figure 3.03711).

2. PHYSICAL AND CHEMICAL PROPERTIES

2.01 Thermal Properties

2.011 Melting range. 2580 to 2640 F.

	Fe
14	Cr
8	Ni
2.5	Mo
	Al

PH14-8Mo

2.012 Phase changes.

2.0121 Phases.

Condition A	92 percent austenite
	8 percent ferrite
Condition SRH	77 percent martensite
	15 percent austenite
	8 percent ferrite (1).

2.013 Time-temperature-transformation diagrams.

2.014 Thermal conductivity, comparable to PH15-7Mo (3).

2.015 Thermal expansion, Figure 2.015.

2.0151 Dimensional changes on heat treating (see 1.091).

2.016 Specific heat.

2.017 Thermal diffusivity.

2.02 Other Physical Properties

2.021 Density, Table 2.021.

TABLE 2.021

Source	(1, p. 29)		
Condition	A	SR-100	SRH950
lb per cu in	0.283	0.278	0.278
gr per cu in	7.82	7.69	7.71

2.022 Electrical resistivity.

2.023 Magnetic properties.

2.024 Emissivity.

2.025 Damping capacity.

2.03 Chemical Properties

2.031 General corrosion resistance of the alloy in the hardened condition is comparable or superior to that of 17-7PH and PH15-7Mo (1)(3).

2.032 Stress corrosion cracking. Results of stress-cracking exposure tests on air melted sheet in various conditions at Kure Beach, Table 2.032.

TABLE 2.032

Source	(1, p. 32)						
Alloy	Fe-14Cr-8Ni-2.5Mo-Al						
Form	0.050 inch Sheet - Air Melt						
		Original Properties		Stressed 80 percent F_{ty}		Stressed 50 percent F_{ty}	
Condition	Direction	F_{tu} ksi	F_{ty} ksi	Stress ksi	Days to Failure 80 ft lot	Stress ksi	Days to Failure 80 ft lot
SRH 950	L	232	213	171	NF	107	NF
SRH 950 + 1000 hr at 650F	L	250	232	186	449 (1 of 5) (b)	116	NF
SRH 1050	L	213	205	164	NF	103	NF
SRH 1050 + 1000 hr at 650F	L	232	221	176	NF	110	NF
BCHT 1050(a)	L	220	212	170	NF	106	NF
BCHT 1050 + 1000 hr at 650F	L	236	226	181	NF	113	NF
SRH 950	T	241	225	180	NF	112	NF
SRH 950 + 1000 hr at 650F	T	261	236	189	159.2	118	NF
SRH 1050	T	221	213	170	NF	106	NF
SRH 1050 + 1000 hr at 650F	T	242	230	184	292 (3 of 5) (b)	115	NF
BCHT 1050	T	220	211	169	NF	105	NF
BCHT 1050 + 1000 hr at 650F	T	240	226	181	175.6	113	NF
CH 900	L	268	266	212	NF	133	NF
CH 900 + 1000 hr at 650F	L	294	291	233	NF	146	NF
CH 1050	L	238	233	186	NF	116	NF
CH 1050 + 1000 hr at 650F	L	258	254	203	NF	127	NF
CH 900	T	279	275	220	272(4/5)(b)	137	NF
CH 900 + 1000 hr at 650F	T	294	290	232	142.6	145	231.2
CH 1050	T	255	250	200	NF	125	NF
CH 1050 + 1000 hr at 650F	T	266	264	211	NF	132	NF

(a) Braze-cycle heat treatment.
(b) Indicates number of specimens that failed at average time shown; remainder did not fail in 908 days.
NF denotes no failure after 908 days.

2.04 Nuclear Properties

3. MECHANICAL PROPERTIES

3.01 Specific Mechanical Properties

Mechanical properties acceptable for material specifications for sheet and strip, Table 3.01.

TABLE 3.01

Source	(1, p. 3)		
Alloy	Fe-14Cr-8Ni-2.5Mo-Al		
Form	Sheet and Strip		
Condition	A	SRH950	SRH1050
F_{tu}			
maximum - ksi	150	-	-
minimum - ksi	-	220	200
F_{ty}			
maximum - ksi	65	-	-
minimum - ksi	-	190	180
e(2 in) min-percent			
Thickness - inch			
0.1874-0.020	20	4	4
0.0199-0.010	20	3	3
0.0099-0.005	20	2	2
Hardness, R_c	100*max	45-51	38-45

* R_b
Properties apply to both air and vacuum induction melts.
Transverse data.
All values minimum unless otherwise noted.

3.02 Mechanical Properties at Room Temperature

3.021 Tension.

3.0211 Stress-strain curves for sheet in Condition SRH 1050, Figure 3.0211.

3.0212 Producers mechanical properties for sheet and strip for annealed and SRH conditions, Table 3.0212.

TABLE 3.0212

Source	(1, p. 8)				
Alloy	Fe-14Cr-8Ni-2.5Mo-Al				
Form	Sheet and Strip				
Condition	F_{tu} ksi	F_{ty} ksi	e(2 in) percent	Hardness R_c	Toughness W/A(a) in-lb/in^2
Air Melted					
A	125	55	25	88 (b)	-
SRH950	235	220	5	49	850
SRH1050	215	205	5	46	1000
Vacuum Induction Melted					
A	125	55	25	88 (b)	-
SRH950	230	215	6	48	1800
SRH1050	210	200	6	45	2200

(a) Precracked sheet Charpy specimen: Same as ASTM E23-64, Figure 4A, except thickness of specimen is sheet thickness and specimen is precracked by fatigue to a depth of 0.030-0.060in
(b) R_b
Transverse data.

3.0213 Producers typical mechanical properties for sheet and strip for cold rolled conditions, Table 3.0213.

TABLE 3.0213

Source	(1, p. 24)		
Alloy	Fe-14Cr-8Ni-2.5Mo-Al		
Form	Sheet and Strip		
Condition	C (a)	CH900	CH950
F_{tu} - ksi	210	280	270
F_{ty} - ksi	180	270	260
e(2 in) - percent	5	1.5	1.5
Hardness RC (b)	42	52	51

(a) Condition C represents 60 percent cold reduction.
(b) Applies to material 0.010 inch and thicker.
Transverse data.

	Fe
14	Cr
8	Ni
2.5	Mo
	Al

PH14-8Mo

3.0214 Effect of heat treatment and cold work on mechanical properties.

3.02141 Effect of solution temperature on the tensile properties of air melt sheet in Conditions A and SRH 950, Figure 3.02141.

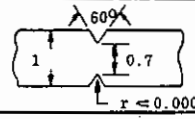
3.02142 Effect of aging temperature on the tensile properties of high purity air melt sheet (SRH conditions), Figure 3.02142.

3.02143 Effect of aging temperature and time on the tensile and precracked Charpy impact properties of sheet (SRH conditions), Figure 3.02143.

3.02144 Effect of cold work on mechanical properties of air and vacuum melted sheet in Condition CH 950, Table 3.02144

TABLE 3.02144

Source	(1, p. 25)							
Alloy	Fe-14Cr-8Ni-2.5Mo-Al							
Form	0.025 inch Sheet							
Condition	CH 950							
Grade	Air Melted				Vacuum Induction Melted			
Cold Reduction percent	40		60		40		60	
Direction	L	T	L	T	L	T	L	T
F_{tu} - ksi	259	270	278	298	240	261	264	279
F_{ty} - ksi	254	260	273	289	235	256	258	269
e(2 in) percent	2.0	1.5	2.0	1.5	1.5	1.5	1.5	1.5
NTS - ksi*	253	206	237	154	241	241	249	237
Sharp notch to yield strength ratio	1.0	0.79	0.86	0.53	1.03	0.94	0.97	0.88
Hardness, R_c	51	51	52	52	50	50	50	50

* 

3.02145 Effect of cold rolling on the tensile properties of as rolled and rolled and aged air melted sheet, Figure 3.02145.

3.0215 Effect of exposure on tensile properties.

3.02151 Effect of exposure temperature and time on the tensile properties of air melted sheet in SRH 950 Condition, Figure 3.02151.

3.02152 Effect of exposure temperature and time on the tensile properties of air melted sheet in SRH 1050 condition, Figure 3.02152.

3.02153 Effect of exposure temperature and time on the tensile and precracked Charpy impact properties of vacuum melted sheet in SRH 950 condition, Figure 3.02153.

3.02154 Effect of exposure temperature and time on the tensile and precracked Charpy impact properties of vacuum melted sheet in SRH 1050 condition, Figure 3.02154.

3.02155 Effect of exposure temperature and time on the tensile properties of air melted sheet in CH 900 condition, Figure 3.02155.

3.02156 Effect of exposure temperature and time on the tensile properties of air melted sheet in CH 1050 condition, Figure 3.02156.

3.02157 Effect of high temperature exposure temperature on the tensile properties of air melt sheet (SRH conditions), Figure 3.02157.

3.022 Compression. Compressive yield strength (0.2 percent) data indicate higher values in the transverse direction. Typical longitudinal and transverse values (average of 3 tests) are 214.5 and 220.1 ksi, respectively (4).

3.0221 Stress-strain diagrams.

3.023 Impact.

3.0231 General. Due to thickness limitations, impact values measured by the standard techniques (Charpy notch or Keyhole, Izod, tension impact, or drop weight tests) are not available. However, a limited amount of precracked Charpy impact data does exist for sheet material. Typical values are shown in Figures 3.02143, 3.02153, and 3.02154 which indicate the impact energy for Condition SRH 1050 is superior to that for Condition SRH 950. The precracked Charpy values are improved by vacuum melting (see Table 3.0212).

3.024 Bending. Comparable in bend quality to 17-7PH.

3.025 Torsion and shear. Ultimate shear strength data indicates slighly higher values in the longitudinal direction. Typical longitudinal and transverse values (average of 3 tests) are 133.3 and 131.4 ksi, respectively (4).

3.026 Bearing.

3.0261 Bearing properties of sheet in Condition SRH 1050, Table 3.0261.

TABLE 3.0261

Source	(4)		
Alloy	Fe-14Cr-8Ni-2.5Mo-Al		
Form	0.050 inch Sheet		
Condition	SRH1050		
Test Direction	e/D	F_{bry} - ksi	F_{bru} - ksi
L	1.5	289.3	330.9
T	1.5	290.9	332.2
L	2.0	350.9	441.0
T	2.0	353.5	441.3

Each value represents the average of three tests.

3.027 Stress concentration.

3.0271 Notch properties.

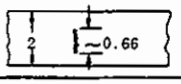
3.02711 Effect of aging temperature on the sharp notch properties of high purity air melt sheet in SRH condition, Figure 3.02711.

3.02712 Tensile yield strength and crack strength for SRH 950, SRH 1050 and BCHT conditions before and after elevated temperature exposure, Table 3.02712.

TABLE 3.02712

Source	(3, p. 8)																	
Alloy	Fe-14Cr-8Ni-2.5Mo-Al																	
Form	0.050 inch Sheet, Air Melt																	
Condition	SRH 950						SRH 1050						BCHT 1050*					
Exposure	None		500F 1000 hr		650F 1000 hr		None		500F 1000 hr		650F 1000 hr		None		500F 1000 hr		650F 1000 hr	
Direction	L	T	L	T	L	T	L	T	L	T	L	T	L	T	L	T	L	T
F_{ty} - ksi	215	216	223	221	240	232	207	204	210	211	221	220	206	206	211	207	230	225
Crack strength ksi	202	163	205	169	197	147	202	175	206	182	209	175	189	167	199	171	200	155
Crack to yield strength ratio	0.94	0.75	0.92	0.76	0.82	0.63	0.98	0.86	0.98	0.86	0.94	0.79	0.92	0.81	0.94	0.82	0.87	0.69

* Simulated braze cycle: 1675F, 15 min→1000F in 30 min, AC + 100F, 8 hr + 1050F, 8 hr, AC.



Center fatigue crack, aged before cracking.

Fe
14 Cr
8 Ni
2.5 Mo
Al

PH14-8Mo

3.02713 Tensile yield strength and crack strength for CH 900 and CH 1050 conditions before and after elevated temperature exposure, Table 3.02713.

TABLE 3.02713

Source	(1, p. 28)															
Alloy	Fe-14Cr-8Ni-2.5Mo-Al															
Form	0.050 inch Sheet, Air Melt															
Condition	CH 900								CH 1050							
Exposure	None		500F 1000 hr		650F 1000 hr		500F 10,000 hr		None		500F 1000 hr		650F 1000 hr		500F 10,000 hr	
Direction	L	T	L	T	L	T	L	T	L	T	L	T	L	T	L	T
F_{ty} - ksi	267	271	270	273	290	294	278	286	249	254	251	258	284	270	247	264
Crack strength ksi	233	142	243	135	227	119	192	111	223	159	229	169	236	153	190	119
Crack to yield strength ratio	0.86	0.52	0.90	0.50	0.78	0.41	0.69	0.39	0.89	0.62	0.91	0.65	0.83	0.57	0.77	0.45

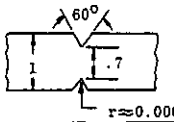
See Table 3.02712 for specimen design.

3.02714 Sharp notch properties for air and vacuum melted sheets as a function of cold working in the CH 950 condition (see Table 3.02144).

3.03142 Effect of test temperature on tensile and sharp notch properties of air melt sheet (SRH 950 condition) before and after elevated temperature stress exposure, Table 3.03142.

TABLE 3.03142

Source	(6, p. 38)															
Alloy	Fe-14Cr-8Ni-2.5Mo-Al															
Form	0.050 inch Sheet Air Melt															
Condition	SRH 950															
Exposure	None				550F, 2,400 hr				550F, 7,000 hr				550F, 10,000 hr			
Test Temp - F	80		-110		80		-110		80		-110		80		-110	
Direction	L	T	L	T	L	T	L	T	L	T	L	T	L	T	L	T
F_{ty} - ksi	183	184	210	206	186	186	203	197	191	201	214	222	193	189	210	221
F_{tu} - ksi	225	227	261	256	227	235	266	267	231	233	270	280	229	226	268	270
e(2 in) - percent	12	10	14	-	13	8	11	11	12	7	14	11	11	10	15	-
NTS - ksi	211	189	227	185	204	-	232	-	207	185	229	198	213	171	220	191
Sharp notch to yield strength ratio	1.2	1.0	1.1	.90	1.1	-	1.1	-	1.1	.92	1.1	.89	1.1	.90	1.1	.86



Notched before exposure

3.0272 Fracture toughness.

3.02721 General. Valid plane strain fracture toughness values (K_{Ic}) are not available for this alloy and probably could not be obtained in sheet gages except at cryogenic temperatures. However, a measure of the mixed mode fracture toughness can be obtained from tests on sharply notched or cracked specimens. Tests of these types indicate the toughness decreases with an increase in the yield strength. Thus, the SRH 1050 condition is slightly tougher than the SRH 950 condition (e.g. Figure 3.03711) and the CH 900 and CH 1050 conditions are considerably less tough than the corresponding SRH conditions (compare Table 3.02712 and Table 3.02713). As discussed in 1.09, long time exposure at moderately elevated temperatures can reduce the fracture toughness of this alloy in all commercial conditions of temper. The toughness is generally lower in the transverse than in the longitudinal direction although this directionality is reduced by vacuum melting (see Figure 3.03712). Fracture toughness at cryogenic temperatures is very poor (see Figure 3.03711).

3.03 Mechanical Properties at Various Temperatures

3.031 Tension.

3.0311 Stress-strain diagrams.

3.0312 Effect of test temperature on the tensile properties of normal and high purity air melt sheet (SRH 950 condition), Figure 3.0312.

3.0313 Effect of test temperature on the tensile properties of high purity air melt sheet (SRH 1050 condition), Figure 3.0313.

3.0314 Effect of exposure on tensile properties at elevated temperatures.

3.03141 Effect of test temperature on tensile properties of air melt sheet (SRH 950 condition) before and after elevated temperature stress exposure, Figure 3.03141.

3.03143 Effect of test temperature on tensile properties of vacuum melt sheet (SRH 950 condition) before and after elevated temperature stressed exposure, Figure 3.03143

3.03144 Effect of test temperature on tensile properties of vacuum melt sheet (SRH 1050 condition) before and after elevated temperature stressed exposure, Figure 3.03144.

3.032 Compression.

3.033 Impact(see also 3.0231). Limited data available indicates a large difference in (W/A) values for the SRH conditions. Typical values obtained at -300F for vacuum melted SRH 950 and SRH 1050 conditions are 800 and 1676 in-lbs/in^2, respectively (1, p. 13). Air melted data for Condition SRH 1050 is much lower - 814 in-lbs/in^2 (1, p. 13).

3.034 Bending.

3.035 Torsion and shear.

3.036 Bearing.

3.037 Stress concentration.

3.0371 Notch properties.

3.03711 Effect of test temperature on the sharp notch properties of high purity air melt sheet in SRH 950 and SRH 1050 conditions, Figure 3.03711.

3.03712 Effect of test temperature on longitudinal and transverse sharp notch properties of air and vacuum melted sheet (SRH 950 condition), Figure 3.03712.

3.03713 Effect of test temperature on the longitudinal and transverse sharp notch properties of air and vacuum melted sheet (SRH 950 condition) after elevated temperature stress exposure, Figure 3.03713.

3.03714 Effect of test temperature on the transverse sharp notch properties of air and vacuum melted sheet (SRH 950 condition) before and after elevated temperature stressed exposure, Figure 3.03714.

	Fe
14	Cr
8	Ni
2.5	Mo
	Al

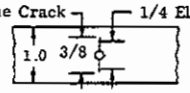
PH14-8Mo

3.03715 Effect of test temperature on tensile and sharp notch properties of air melt sheet (SRH 950 condition) before and after elevated temperature stress exposure (see Table 3.03142).

3.03716 Effect of test temperature on the crack strength of sheet (SRH 1050 condition) before and after elevated temperature creep exposure (cracked after exposure), Table 3.03716.

TABLE 3.03716

Source	(7, pp. 179, 195)											
Alloy	Fe-14Cr-8Ni-2.5Mo-Al											
Form	0.025 inch Sheet											
Condition	SRH 1050											
Exposure	None		550F 754 hr		550F 1000 hr		550F 6000 hr		550F 25,060 hr		550F 25,800 hr	
Test Temp	RT	-65F	RT	-65F	RT	-65F	RT	-65F	RT	-65F	RT	-65F
Crack Strength ksi	199	243	227	255	229	249	235	253	232	244	237	252
Crack to Yield Strength Ratio	0.91	1.08	1.03	1.11	1.02	1.08	1.08	1.12	1.04	1.05	1.06	1.08



Specimen Cracked After Exposure

Longitudinal data, average of 4 or more tests.

3.0372 Fracture toughness, (see 3.0272).

3.038 Combined properties.

3.04 Creep and Creep Rupture Properties

3.041 Effect of stress level on smooth creep properties for sheet in Condition SRH 1050, Figure 3.041.

3.042 Effect of exposure (time and temperature) and creep stress on room temperature and elevated temperature tensile properties for sheet in Condition SRH 1050, Table 3.042.

TABLE 3.042

Source	(7, pp. 155-157)				
Alloy	Fe-14Cr-8Ni-2.5Mo-Al				
Form	0.025 inch Sheet				
Condition	SRH 1050				
Creep Stress Level - ksi	Exposure Temp-F	Exposure Time-hr	Static Test Temp-F	F_{ty}(a) ksi	F_{tu} (a) ksi
-	-	-	RT	199(b)	216(b)
-	-	-	550	174(b)	190(b)
Heat soaked only	550	754	RT	209	220
			550	178	192
		1,000	RT	209	222
			550	177	194
		6,000	RT	200	218
			550	180	194
		25,060	RT	210	221
			550	175	195
103	550(c)	754	RT	194	219
			550	189	202
120		1,000	RT	195	224
			550	189	200
85		6,000	RT	192	224
			550	180	196
67		25,060	RT	205	221
			550	175	195
Heat soaked only	550(d)	25,800	RT	209	223
			550	181	195
67			RT	203	220
			550	176	197

(a) Average of 3 or more tests.
(b) Data supplied by Armco Steel Corporation.
(c) Intermittent heating and loading.
(d) Creep applied during steady state heating.

3.05 Fatigue Properties

3.051 S-N curves for smooth sheet as a function of stress ratio in Condition SRH 1050, Figure 3.051.

3.052 S-N curves for notched sheet as a function of stress ratio in Condition SRH 1050, Figure 3.052.

3.053 Fatigue-crack propagation curves as a function of test temperature and alternating stress amplitude for sheet in Condition SRH 950, Figure 3.053.

3.054 Fatigue-crack propagation rate at three temperatures for sheet in Condition SRH 950, Figure 3.054.

3.06 Elastic Properties

3.061 Poisson's ratio.

3.062 Modulus of elasticity.

3.0621 Young's modulus, E. Static E:

Condition	Temperature - F	Direction	E - 10^6 psi
SRH 950	550	L	23.3
		T	-
	RT	L	28.3
		T	29.4
	-109	L	29.4
		T	-

3.063 Modulus of rigidity.

4. FABRICATION

4.01 Formability
(see 17-7PH and PH15-7Mo)

4.02 Machining and Grinding
(see 17-7PH)

4.03 Welding

4.031 General. The general welding characteristics of this alloy are similar to those of 17-7PH and PH15-7Mo. GTA or electron beam welds in the annealed sheet followed by SRH treatment possess essentially 100 percent tensile strength joint efficiency (see Tables 4.035, 4.036 4.038, and 4.039). Welding wire composition may be similar to that of the parent metal. However, where good weld toughness is required a special vacuum melted wire composition should be used (Table 4.032). Based on precracked Charpy test specimen results, welds in air melted material are likely to have low toughness even when the special wire is used (see Table 4.033). However, welds in vacuum melted sheet using the special filler have W/A values somewhat higher than those obtained for the parent metal (compare Table 4.034 and Table 3.0212). Heat treatment may be adapted to either high or low temperature brazing cycles. However, brazing temperatures higher than 1975F may cause grain growth and intergranular penetration which will adversely effect the final heat treated properties. The alloy is readily brazed in Condition A, then transformed and aged. However, variations in brazing cycle and heat treating sequence are possible. A series of brazing cycle heat treatments is shown in Table 4.0311. Care should be taken to see that parts are not under tension while the brazing alloy is liquid or intergranular cracking may occur. Parts should be thoroughly cleaned before and after brazing in order to obtain best brazing results.

Fe
14 Cr
8 Ni
2.5 Mo
Al

PH14-8Mo

4.032 Composition of precipitation-hardening weld wire available for use as filler wire, Table 4.032.

TABLE 4.032

Source	(1, p. 41)	
Alloy	Fe-14Cr-8Ni-2.5Mo-Al	
Form	Sheet and Strip	
	Composition Range - Percent	
Element	Weld Wire WPH14-8Mo(a)	Weld Wire WPH13-8Mo(b)
C	0.02-0.05	0.05 max
Mn	1.00 max	1.00 max
P	0.015 max	0.015 max
S	0.010 max	0.010 max
Si	1.00 max	1.00 max
Cr	13.50-15.50	12.00-14.00
Ni	7.50-9.50	7.00-9.00
Mo	2.00-3.00	2.00-3.00
Al	0.75-1.50	0.75-1.50

(a) Air melted, similar in composition to PH14-8Mo base material and is satisfactory filler in many applications.
(b) Vacuum melted, recommended for joining vacuum melted materials or where maximum strength, ductility, and toughness are required.

4.033 Mechanical properties of GTA welded joints for air melted sheet in SRH conditions, Table 4.033.

TABLE 4.033

Source	(1, p. 43)				
Alloy	Fe-14Cr-8Ni-2.5Mo-Al				
Form	0.050 inch Sheet, Air Melted				
Condition		Annealed + Welded + SRH 950		Annealed + Welded + SRH 1050	
Filler		Heat A	Heat B	Heat A	Heat B
(a)	F_{ty} - ksi	204	195	196	191
(b)		216	208	199	194
(a)	F_{tu} - ksi	217(c)	211(c)	201(d)	195(c)
(b)		227(c)	224(c)	207(d)	204(c)
(a)	e(2 in) - percent	1.2	3.0	2.7	2.0
(b)		2.3	2.3	4.3	4.6
(a)	W/A - in lbs/in^2 (e)	227	97	168	142
(b)		253	370	-	550

(a) WPH14-8Mo
(b) WPH13-8Mo
(c) Fracture in weld metal
(d) Fracture in base metal
(e) See Table 3.0212.

4.034 Mechanical properties of GTA welded joints for vacuum melted sheet in SRH conditions, Table 4.034.

TABLE 4.034

Source	(1, p. 44)		
Alloy	Fe-14Cr-8Ni-2.5Mo-Al		
Form	0.050 inch Sheet, Vacuum Melted		
Condition		Annealed + Welded + SRH950	Annealed + Welded + SRH 1050
Filler			
(a)	F_{ty} - ksi	209	199
(b)		216	206
(a)	F_{tu} - ksi	215	200
(b)		230	210
(a)	e(2 in) - percent	1.5	1.7
(b)		2.5	2.8
(a)	W/A - in lbs/in^2 (c)	2217	2667
(b)		2443	2760

(a) None.
(b) WPH 13-8Mo
(c) See Table 3.0212.
All Tensile fractures occurred in weld metal.

4.035 Tensile properties of air and vacuum melted electron beam welded sheet in the SRH conditions, Table 4.035.

TABLE 4.035

Source	(1, p. 45)			
Alloy	Fe-14Cr-8Ni-2.5Mo-Al			
Form	0.050 inch Sheet			
Condition	Vacuum Melted		Air Melted	
	EB + SRH950	EB + SRH1050	EB + SRH950	EB + SRH1050
F_{ty} - ksi	218	208	214	203
F_{tu} - ksi	229(a)	209(a)	224(b)	206(c)
e(2 in) percent	3.5	2	3.5	3

(a) Fracture in heat affected zone.
(b) Fracture in fusion line.
(c) Fracture at junction of fusion line and base metal.

4.036 Effect of test temperature on the tensile properties of air melted, GTA welded sheet in the SRH 950 condition, Table 4.036.

TABLE 4.036

Source	(1, p. 45)		
Alloy	Fe-14Cr-8Ni-2.5Mo-Al		
Form	0.025 in Sheet, Air Melted		
Condition	GTA Welded + SRH 950		
Test Temperature	650F	RT	-100F
F_{ty} - ksi	176	189	-
F_{tu} - ksi (a)	198	224	246
e(2 in) - percent	2.8	2.3	0.5

(a) All fractures in weld metal.

4.037 Sharp notch properties at low and elevated temperatures for welded sheet in the SRH 1050 condition, Table 4.037.

TABLE 4.037

Source	(1)			
Alloy	Fe-14Cr-8Ni-2.5Mo-Al			
Form	0.050 in Sheet, Air Melted			
Condition	GTA Weld + SRH 1050			
Crack Location	Parent Metal		Weld	HAZ
Direction	L	T		
Notch Strength ksi (a)				
-100F	-	-	96	217
RT	202	175	170	193
650F	-	-	142	146

(a) For specimen see Table 3.02712.

	Fe
14	Cr
8	Ni
2.5	Mo
	Al

PH14-8Mo

4.038 Effect of exposure time and temperature on the tensile properties of air melted welded sheet in SRH conditions, Table 4.038.

TABLE 4.038

Source	(1, p. 46)				
Alloy	Fe-14Cr-8Ni-2.5Mo-Al				
Form	0.050 inch Sheet, Air Melted				
Condition	Exposure	F_{ty} ksi	F_{tu} ksi	e(2 in) percent	Fracture Location
SRH950	None	216	227	8	-
EB + SRH950		214	224	3.5	FL
SRH950	1270 hrs -650F	230	243	9	-
EB + SRH950		227	239	4	FL/BM
SRH950	1060 hrs -750F	246	258	6	-
EB + SRH950		245	253	2.5	WM/FL
SRH1050	None	202	207	6.5	-
EB + SRH1050		203	206	3	FL/BM
SRH1050	1270 hrs-650F	217	223	5.5	-
EB + SRH1050		213	217	3.5	WM/FL
SRH1050	1060 hrs -750F	235	236	5	-
EB + SRH1050		230	234	2	FL

FL - Fusion Line
BM - Base Metal
WM - Weld Metal

4.039 Effect of exposure time and temperature on the tensile properties of vacuum melted welded sheet in SRH conditions, Table 4.039.

TABLE 4.039

Source	(1, p. 47)				
Alloy	Fe-14Cr-8Ni-2.5Mo-Al				
Form	0.050 inch Sheet, Vacuum Melted				
Condition	Exposure	F_{ty} ksi	F_{tu} ksi	e(2 in) percent	Fracture Location
SRH950	None	221	235	6	-
EB + SRH950		218	230	3.5	HAZ
GTA + SRH950		224	235	2	WM
SRH950	1270 hrs -650F	236	251	6	-
EB + SRH950		233	247	3	HAZ/BM
GTA + SRH950		242	245	2	WM
SRH950	1060 hrs -750F	247	266	3.5	-
EB + SRH950		247	262	3.5	HAZ/BM
GTA + SRH950		235	260	1	WM
SRH1050	None	209	212	4	-
EB + SRH1050		208	209	2	HAZ
GTA + SRH1050		210	210	1.5	WM
SRH1050	1270 hrs -650F	224	228	4	-
EB + SRH1050		224	227	2.5	HAZ/W
GTA + SRH1050		224	224	1.5	WM
SRH1050	1060 hrs -750F	239	245	4.5	-
EB + SRH1050		240	244	2.5	WM
GTA + SRH1050		244	245	2.5	WM

HAZ - Heat Affected Zone
WM - Weld Metal
BM - Base Metal

4.0310 Tensile and hardness properties of sheet produced by various brazing cycle heat treatments, Table 4.0310.

TABLE 4.0310

Source	(1, p. 40)				
Alloy	Fe-14Cr-8Ni-2.5Mo-Al				
Form	Sheet				
Brazing Cycle		F_{ty} ksi	F_{tu} ksi	e(2 in) percent	Hardness R_c
A	Air Melted	201	221	7	48.5
B		208	223	5.5	49
C		221	238	8	49.5
D		217	234	8	49
E		212	228	5	48
F		217	226	4	46.5
G		211	219	4	46
H		210	217	4	45.5
J		208	215	4.5	45.5
K		209	217	4.5	45.5
L		212	227	4.5	47.5
F	Vacuum Melted	212	-	5	45
G		208	-	6	44
H		205	-	6	44
J		200	-	7	43
K		198	-	7	44
L		209	-	5.5	46

A - 1950F, 10 min; Cool to 1700F in 5/10 min, Hold 30 min; Cool to 100F in 20 min; Cool to 75F; Cool to -100F, hold 8 hrs; 950F, 30 hrs.
B - 1950F, 10 min; Cool to 1000F in 20 min; Cool to 75F; 1700F 30 min; Cool to 1000F in 20 min; Cool to 75F; Cool to -100F, hold 8 hrs; 950F, 3 hrs.
C - 1740F, 15 min; Cool to 1000F in 17 min; Cool to 75F; Cool to -100F, hold for 8 hrs; 950F, 1 hr.
D - Same as cycle C except cooling time to 1000F was 120 min.
E - Same as cycle C except cooling time to 1000F was 165 min.
F - Heat to 1600F in 8 hrs; heat to 1685F in 30 min; hold 15 min; Cool to 1525F in 30 min; hold 2 hrs; cool to 1000F in 1 hr; Cool to 300F in 4 hrs; air cool to 75F; Cool to -160F in 5 hrs, hold 8 hrs; Warm to 30F in 10 hrs; Air warm to 75F; Harden at 1050F, 1 hr.
G - Same as cycle F except cool to -100F in 3 hrs, hold 8 hrs; warm to 30F in 9 hrs.
H - Same as cycle F except cool to -100F in 5 hrs; hold 4 hrs; warm to 30F in 11 hrs.
J - Same as cycle F except cool to -50F in 2 hrs, hold 8 hrs; warm to 30F in 7 hrs.
K - Same as cycle F except cool to -50F in 2 hrs, hold 8 hrs; warm to 30F in 7 hrs.
L - Heat to 1600F in 8 hrs; Heat to 1685F in 45 min; Hold 15 min; Cool to 1000F in 50 min; Cool to 300F in 4 hrs; air cool to 75F; Cool to -140F in 4 hrs, hold 8 hrs; warm to 30F in 10 hrs; Air warm to 75F; Harden at 1050F, 1 hr; air cool.

	Fe
14	Cr
8	Ni
2.5	Mo
	Al

PH14-8Mo

4.0311 Effect of test temperature on tensile properties of vacuum melt sheet given simulated braze cycle and tested before and after elevated temperature stressed exposure, Figure 4.0311.

4.0312 Effect of test temperature on the sharp notch properties of vacuum melted sheet given simulated braze cycle and tested before and after elevated temperature exposure, Figure 4.0312.

4.0313 Effect of exposure time and temperature on the tensile properties of vacuum melted sheet in various simulated braze cycle conditions, Table 4.0313.

TABLE 4.0313

Source	(1, p. 47)				
Alloy	Fe-14Cr-8Ni-2.5Mo-Al				
Form	0.050 inch Sheet, Vacuum Melted				
Condition	Exposure	F_{ty} ksi	F_{tu} ksi	e(2 in) percent	Fracture Location
BCHT 950	None	222	233	4.5	-
EB + BCHT 950		228	237	3	WM/BM
TIG + BCHT950		216	216	2	WM
BCHT 950 + EB		157	157	1.5	FL/WM
BCHT 950	1270 hr -650F	242	256	4	-
EB + BCHT 950		243	249	2	WM/HAZ
TIG + BCHT950		240	239	1.5	WM
BCHT 950 + EB		173	190	1	FL/W
BCHT 950	1060hr -750F	261	272	3	-
EB + BCHT950		257	268	2	WM
TIG + BCHT950		251	251	1	WM
BCHT 950 + EB		200	209	1	WM
BCHT 1050	None	211	215	6	-
EB + BCHT1050		210	213	2.5	WM
TIG+BCHT1050		206	206	4	WM
BCHT 1050	1270 hr -650F	224	227	3.5	-
EB+BCHT1050		232	226	2	HAZ
TIG+BCHT1050		207	207	1.5	WM
BCHT 1050	1060 hr -750F	240	246	3.5	-
EB + BCHT1050		243	247	1.5	WM
TIG + BCHT1050		231	231	1.5	WM

See Tables 4.038 and 4.039 for definition of fracture locations.

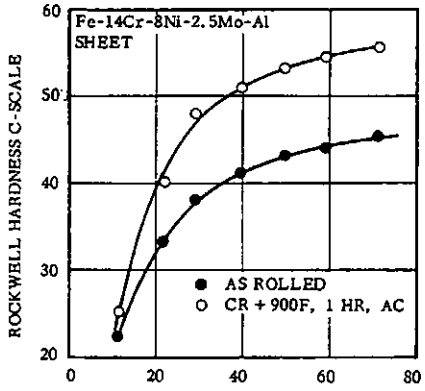


FIG. 1.062 EFFECT OF COLD ROLLING AND COLD ROLLING PLUS AGING ON THE HARDENSS OF SHEET (1)

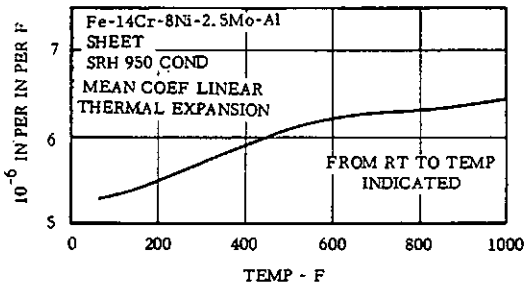


FIG. 2.015 THERMAL EXPANSION (1)

4.04 Heat Treatment
(see also 17-7PH, 4.043 and 4.044)

4.041 Air is a satisfactory furnace atmosphere for annealing or heat treating. Electric furnaces or full-muffle fuel-fired furnaces to protect the material from combustion products and flame impingement are best suited for heat treatment. Dry hydrogen, argon, helium, or vacuum atmospheres may be used for annealing if quench rates approaching air cooling can be attained. Controlled atmospheres such as dissociated ammonia are not recommended because of the hazard of nitriding. Molten salts should not be used because of the danger of carburization or intergranular attack (3). For complete freedom from scale or heat discoloration, a vacuum furnace is required.

4.05 Surface Treating
(see also 17-7PH, 4.051 and 4.052)

4.051 Some degree of intergranular penetration usually occurs during any pickling operation. However, in Conditions A and CH 900, the penetration resulting from acid pickling is usually slight (1).

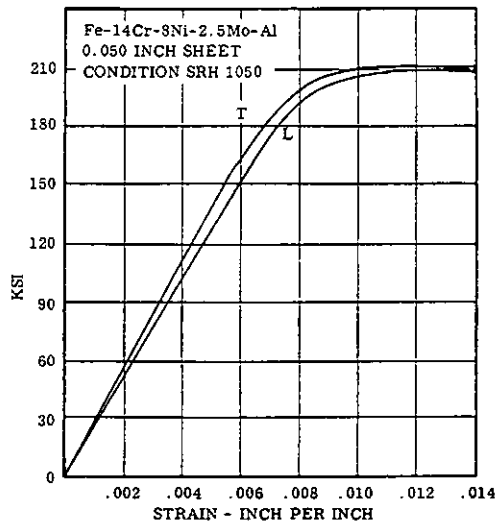


FIG. 3.0211 STRESS-STRAIN CURVES FOR SHEET IN CONDITION SRH 1050. (4)

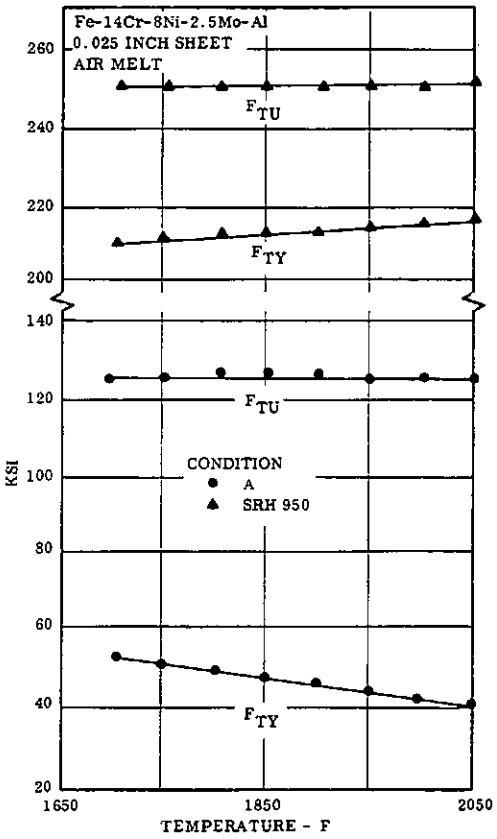


FIG. 3.02141 EFFECT OF SOLUTION TEMPERATURE ON THE TENSILE PROPERTIES OF AIR MELTED SHEET IN CONDITIONS A AND SRH 950. (1, p. 21)

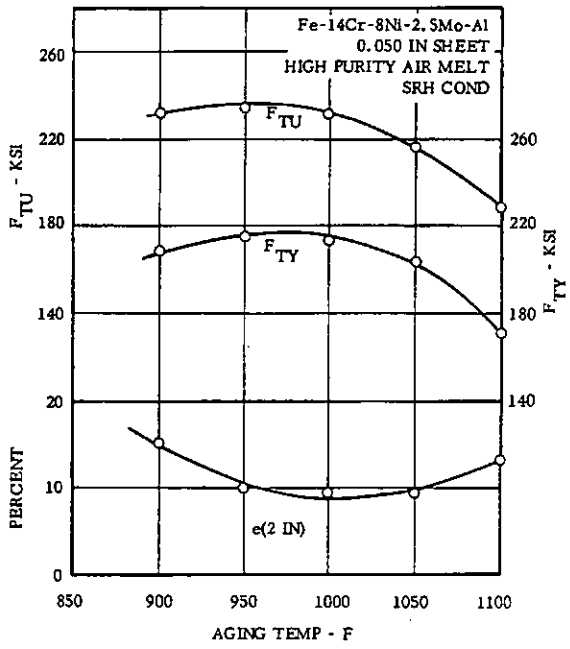


FIG. 3.02142 EFFECT OF AGING TEMPERATURE ON THE TENSILE PROPERTIES OF HIGH PURITY AIR MELT SHEET (SRH CONDITIONS) (5)

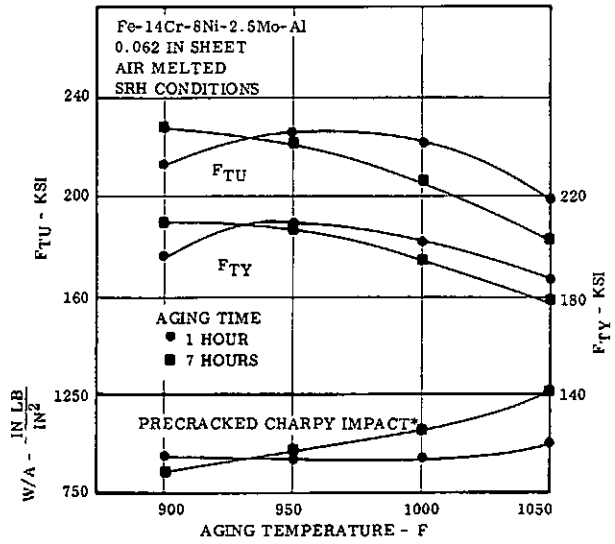


FIG. 3.02143 EFFECT OF AGING TEMPERATURE ON THE TENSILE AND PRECRACKED CHARPY IMPACT PROPERTIES OF SHEET (SRH CONDITIONS). (1, p. 23)

* see Table 3.0212

	Fe
14	Cr
8	Ni
2.5	Mo
	Al

PH14-8Mo

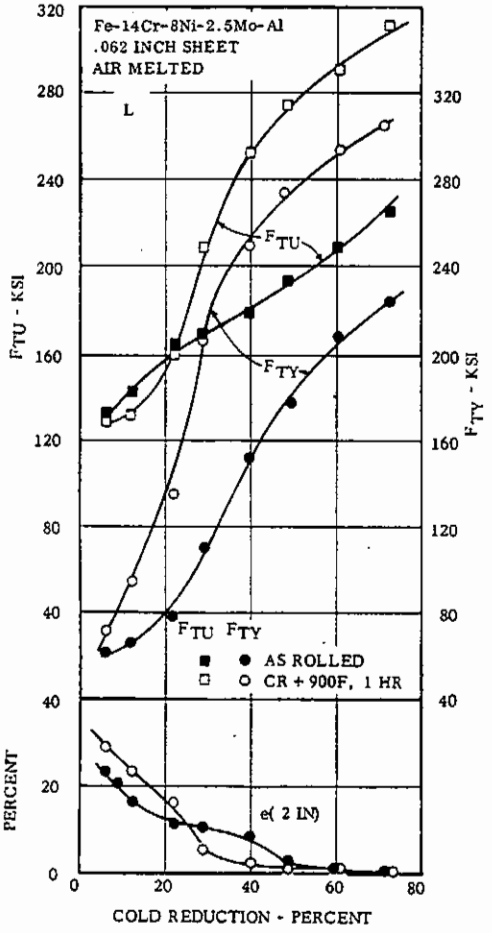


FIG. 3.02145 EFFECT OF COLD ROLLING ON THE TENSILE PROPERTIES OF AS ROLLED AND ROLLED AND AGED AIR MELTED SHEET. (1, p. 24)

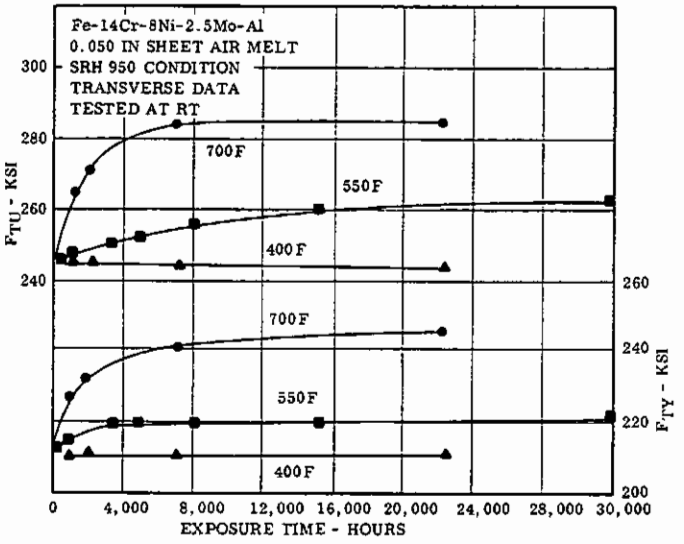


FIG. 3.02151 EFFECT OF EXPOSURE TEMPERATURE AND TIME ON THE TENSILE PROPERTIES OF AIR MELTED SHEET IN SRH 950 CONDITION. (1, p. 14)

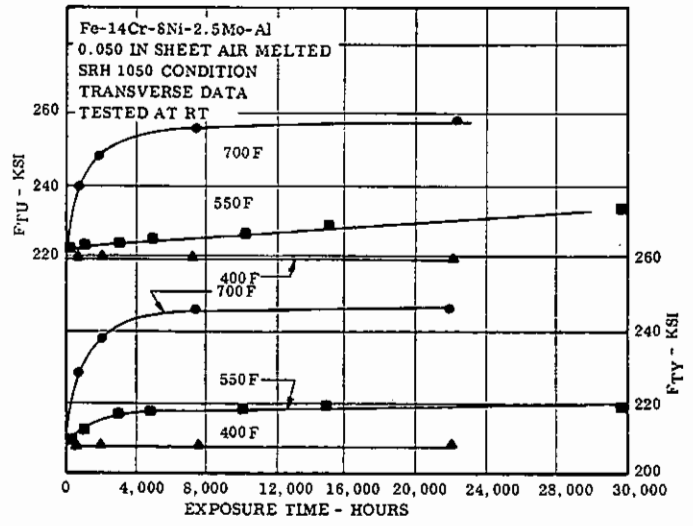


FIG. 3.02152 EFFECT OF EXPOSURE TEMPERATURE AND TIME ON THE TENSILE PROPERTIES OF AIR MELTED SHEET IN SRH 1050 CONDITION. (1, p. 14)

© 1971, Belfour Stulen, Inc.

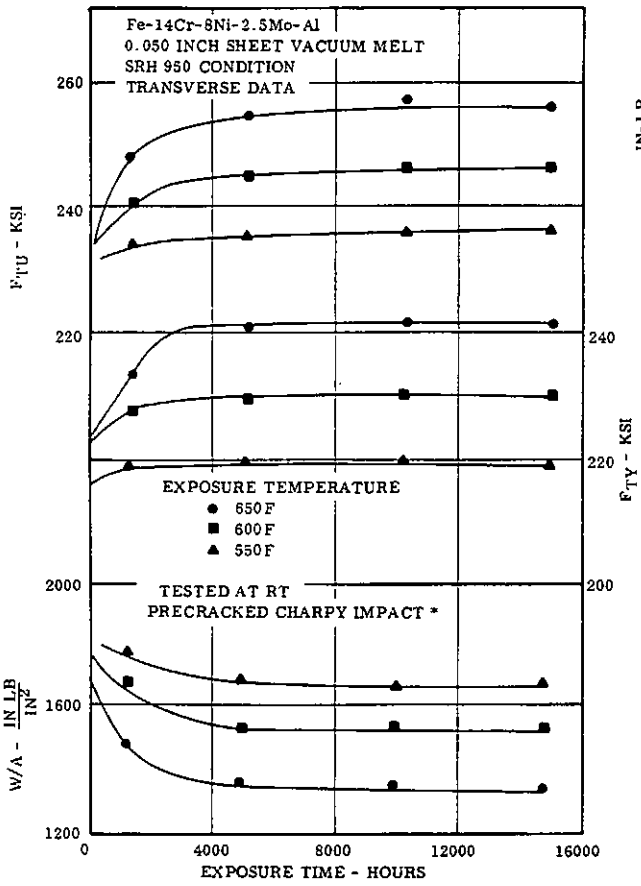


FIG. 3.02153 EFFECT OF EXPOSURE TEMPERATURE ON TIME ON THE TENSILE AND PRECRACKED CHARPY IMPACT PROPERTIES OF VACUUM MELTED SHEET IN SRH 950 CONDITION. (1, p. 19)

* See Table 3.0212.

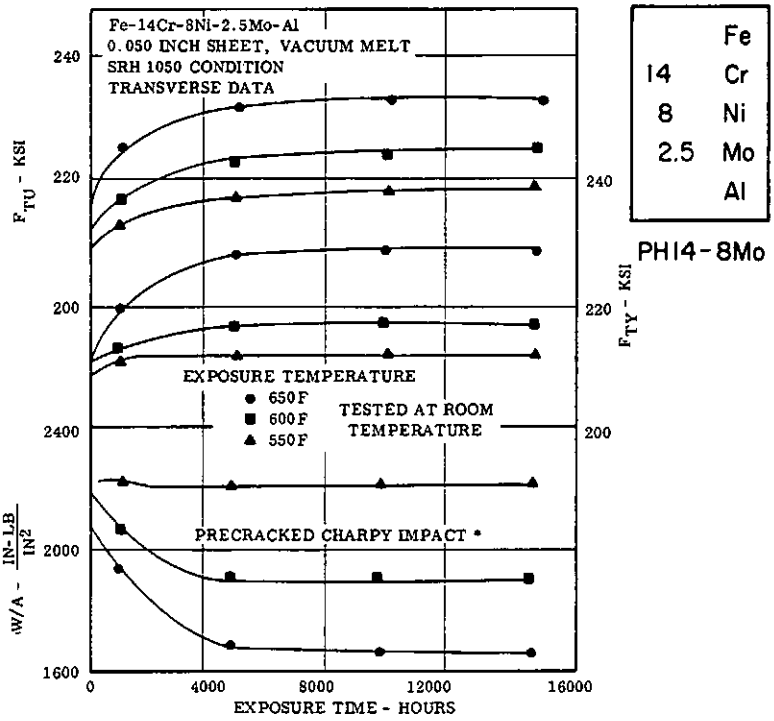


FIG. 3.02154 EFFECT OF EXPOSURE TEMPERATURE AND TIME ON THE TENSILE AND PRECRACKED CHARPY IMPACT PROPERTIES OF VACUUM MELTED SHEET IN SRH 1050 CONDITION. (1, p. 20)

*See Table 3.0212.

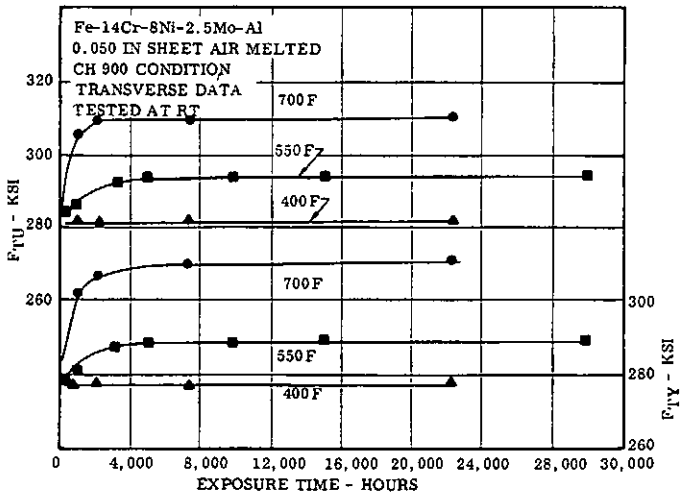


FIG. 3.02155 EFFECT OF EXPOSURE TEMPERATURE AND TIME ON THE TENSILE PROPERTIES OF AIR MELTED SHEET IN CH 900 CONDITION. (1, p. 26)

	Fe
14	Cr
8	Ni
2.5	Mo
	Al

PH14-8Mo

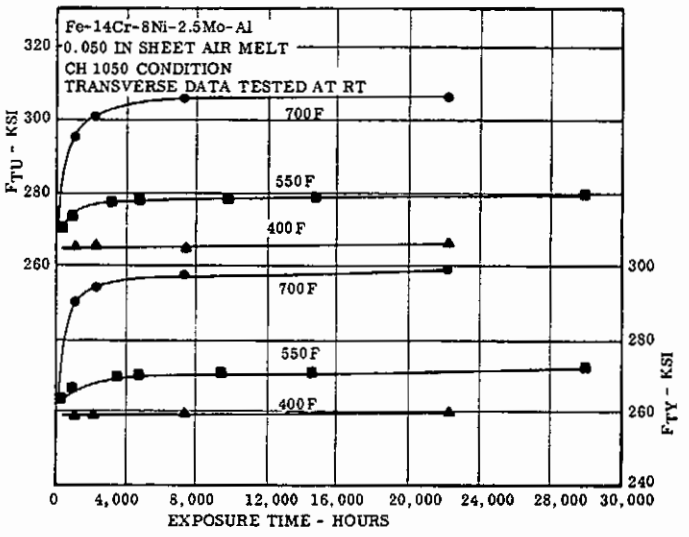


FIG. 3.02156 EFFECT OF EXPOSURE TEMPERATURE AND TIME ON THE TENSILE PROPERTIES OF AIR MELTED SHEET IN CONDITION CH 1050. (1, p. 27)

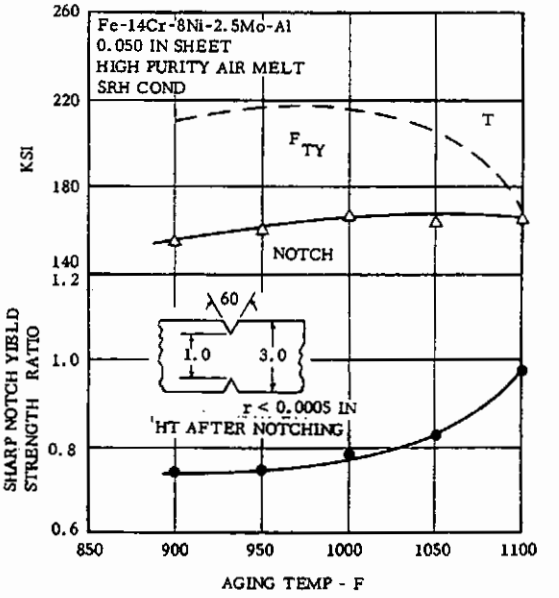


FIG. 3.02711 EFFECT OF AGING TEMPERATURE ON THE SHARP NOTCH PROPERTIES OF HIGH PURITY AIR MELT SHEET IN SRH CONDITION (5)

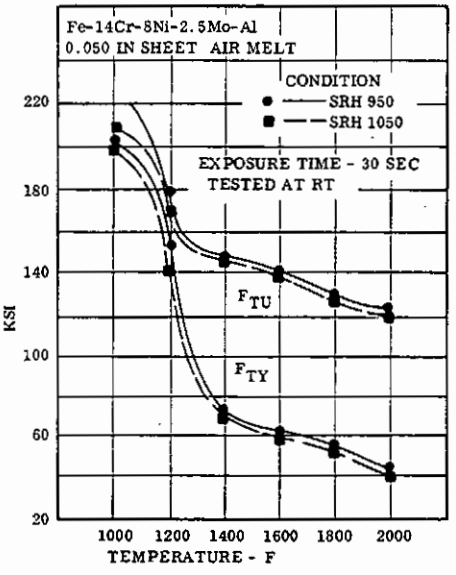


FIG. 3.02157 EFFECT OF HIGH TEMPERATURE EXPOSURE TEMPERATURE ON THE TENSILE PROPERTIES OF AIR MELT SHEET (SRH CONDITIONS). (1, p. 11)

	Fe
14	Cr
8	Ni
2.5	Mo
	Al

PH14-8Mo

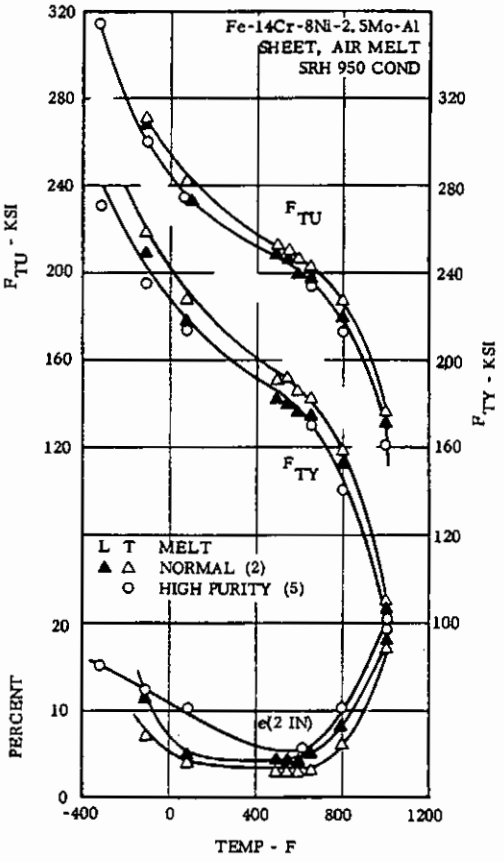


FIG. 3.0312 EFFECT OF TEST TEMPERATURE ON THE TENSILE PROPERTIES OF NORMAL AND HIGH PURITY AIR MELT SHEET (SRH 950) (2)(5)

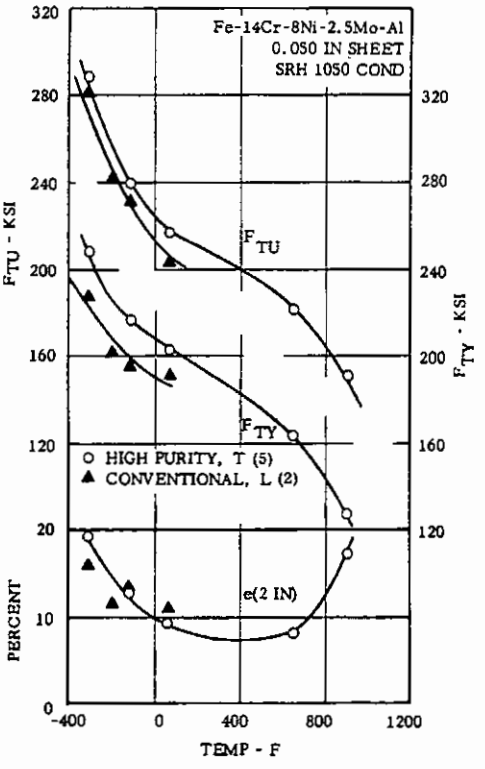


FIG. 3.0313 EFFECT OF TEST TEMPERATURE ON THE TENSILE PROPERTIES OF HIGH PURITY AIR MELT SHEET (SRH 1050) (2)(5)

	Fe
14	Cr
8	Ni
2.5	Mo
	Al

PH14-8Mo

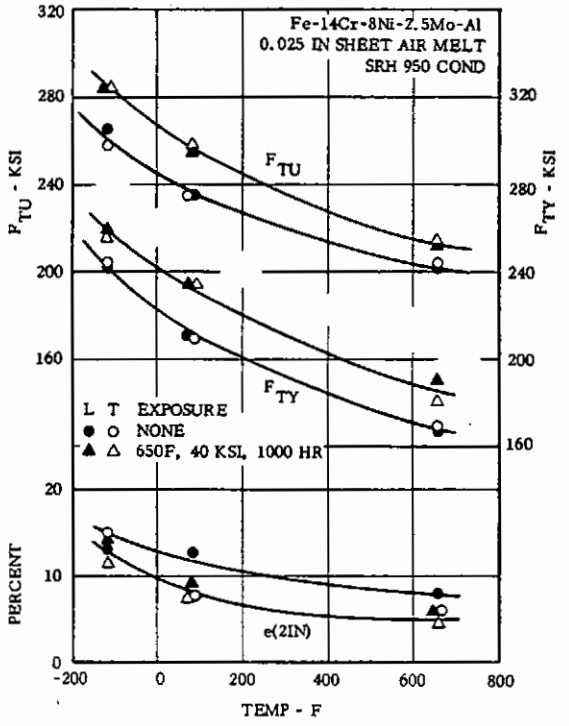


FIG. 3.03141 EFFECT OF TEST TEMPERATURE ON TENSILE PROPERTIES OF AIR MELT SHEET (SRH 950) BEFORE AND AFTER ELEVATED TEMPERATURE STRESSED EXPOSURE (5)

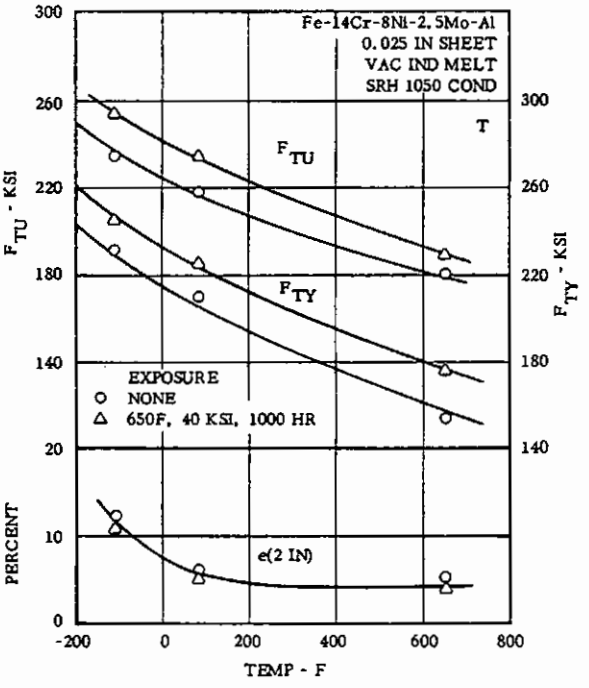


FIG. 3.03144 EFFECT OF TEST TEMPERATURE ON TENSILE PROPERTIES OF VACUUM MELT SHEET (SRH 1050) BEFORE AND AFTER ELEVATED TEMPERATURE STRESSED EXPOSURE (5)

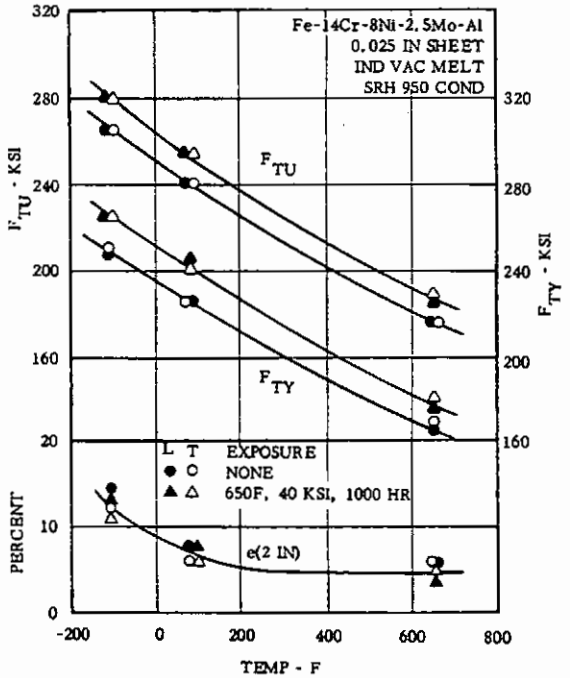


FIG. 3.03143 EFFECT OF TEST TEMPERATURE ON TENSILE PROPERTIES OF VACUUM MELT SHEET (SRH 950) BEFORE AND AFTER ELEVATED TEMPERATURE STRESSED EXPOSURE (5)

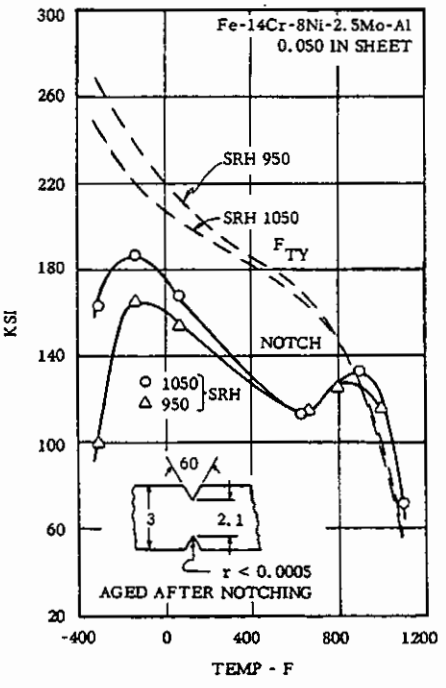


FIG. 3.03711 EFFECT OF TEST TEMPERATURE ON THE SHARP NOTCH PROPERTIES OF HIGH PURITY AIR MELT SHEET IN SRH 950 AND SRH 1050 CONDITIONS (5)

	Fe
14	Cr
8	Ni
2.5	Mo
	Al

PH14-8Mo

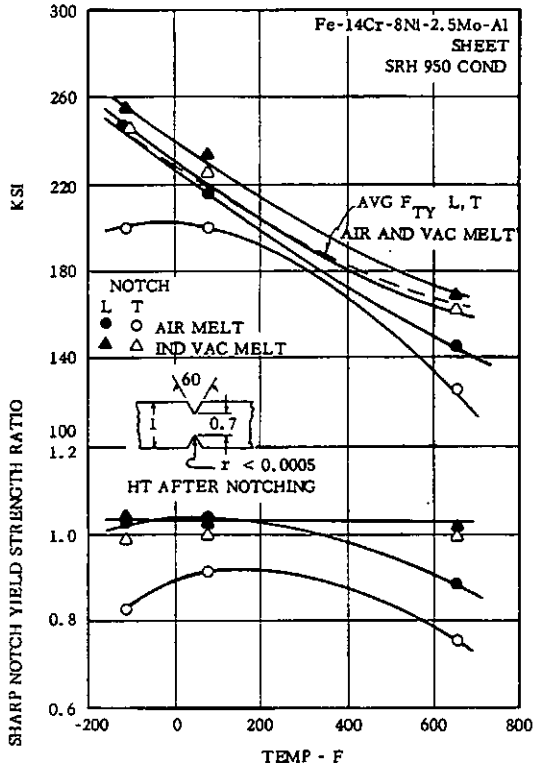


FIG. 3.03712 EFFECT OF TEST TEMPERATURE ON LONGITUDINAL AND TRANSVERSE SHARP NOTCH PROPERTIES OF AIR AND VACUUM MELTED SHEET (SRH 950) (5)

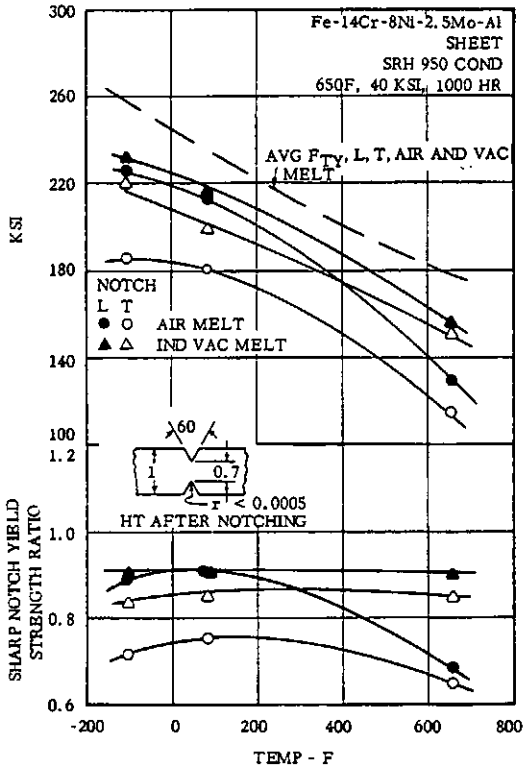


FIG. 3.03713 EFFECT OF TEST TEMPERATURE ON THE LONGITUDINAL AND TRANSVERSE SHARP NOTCH PROPERTIES OF AIR AND VACUUM MELTED SHEET (SRH 950) AFTER ELEVATED TEMPERATURE STRESS EXPOSURE (5)

	Fe
14	Cr
8	Ni
2.5	Mo
	Al

PH14-8Mo

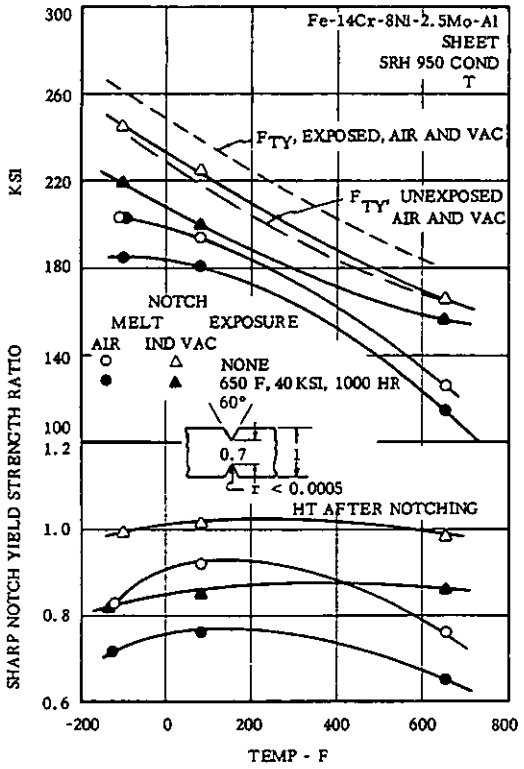


FIG. 3.03714 EFFECT OF TEST TEMPERATURE ON THE TRANSVERSE SHARP NOTCH PROPERTIES OF AIR AND VACUUM MELTED SHEET (SRH 950) BEFORE AND AFTER ELEVATED TEMPERATURE STRESSED EXPOSURE (5)

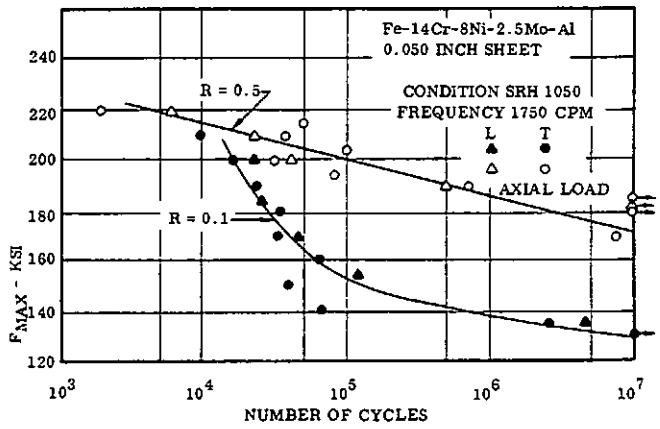


FIG. 3.051 S-N CURVES FOR SMOOTH SHEET AS A FUNCTION OF STRESS RATIO IN CONDITION SRH 1050. (4)

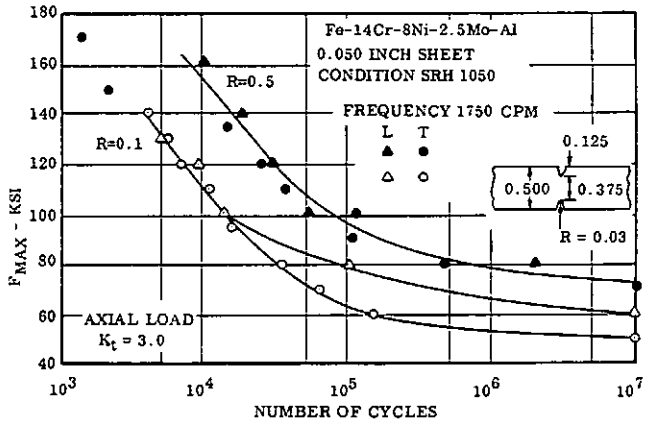


FIG. 3.052 S-N CURVES FOR NOTCHED SHEET AS A FUNCTION OF STRESS RATIO IN CONDITION SRH 1050. (4)

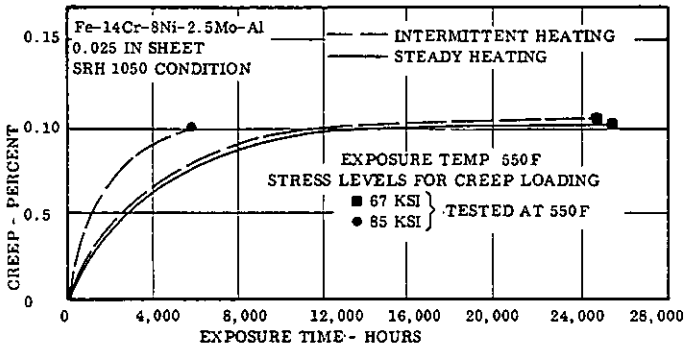


FIG. 3.041 EFFECT OF STRESS LEVEL ON SMOOTH CREEP PROPERTIES FOR SHEET IN CONDITION SRH 1050. (7, p. 47)

NOTE: Data represents total creep, elastic strain not included, and none of the creep is recoverable.

	Fe
14	Cr
8	Ni
2.5	Mo
	Al

PH14-8Mo

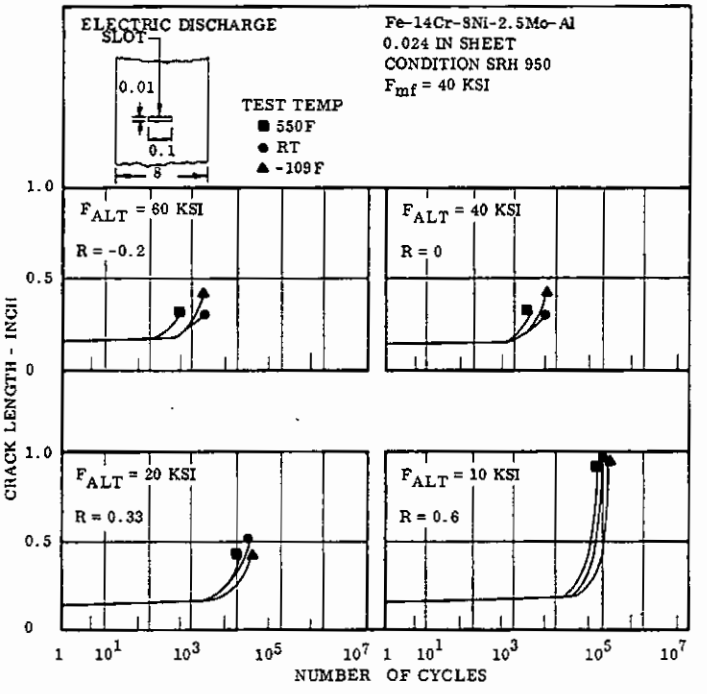


FIG. 3.053 FATIGUE CRACK PROPAGATION CURVES AS A FUNCTION OF TEST TEMPERATURE AND ALTERNATING STRESS AMPLITUDE FOR SHEET IN CONDITION SRH 950. (9, p. 13)

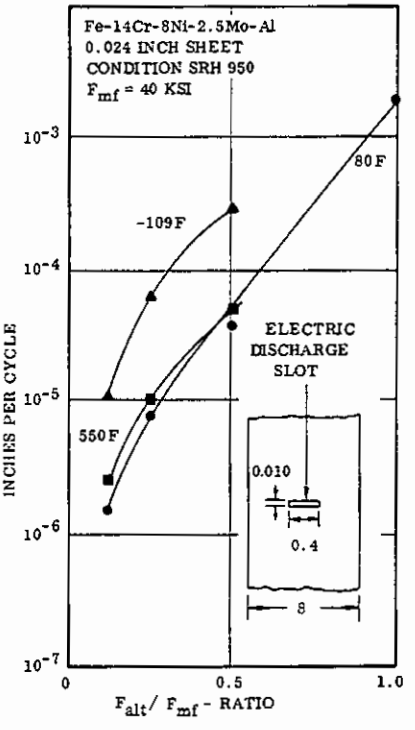


FIG. 3.054 FATIGUE CRACK PROPAGATION RATE AT THREE TEMPERATURES FOR SHEET IN CONDITION SRH 950. (9, pp. 18, 19, 20)

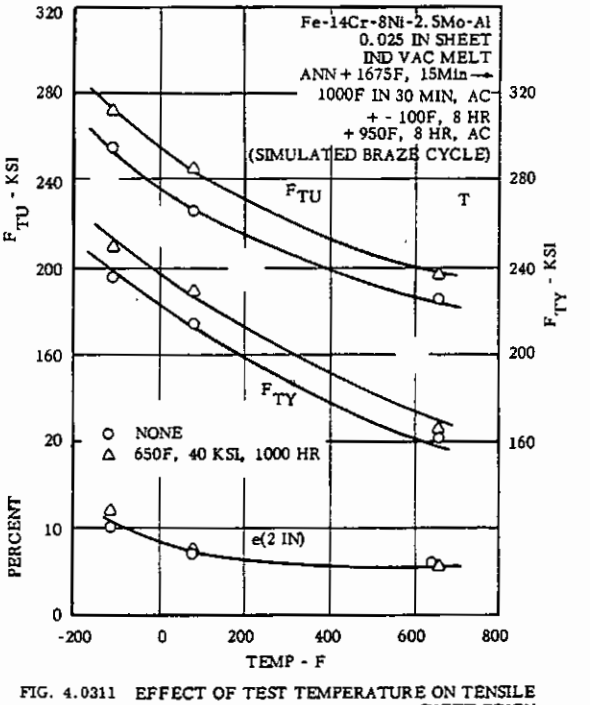


FIG. 4.0311 EFFECT OF TEST TEMPERATURE ON TENSILE PROPERTIES OF VACUUM MELT SHEET GIVEN SIMULATED BRAZE CYCLE AND TESTED BEFORE AND AFTER ELEVATED TEMPERATURE STRESSED EXPOSURE (5)

	Fe
14	Cr
8	Ni
2.5	Mo
	Al

PH14-8Mo

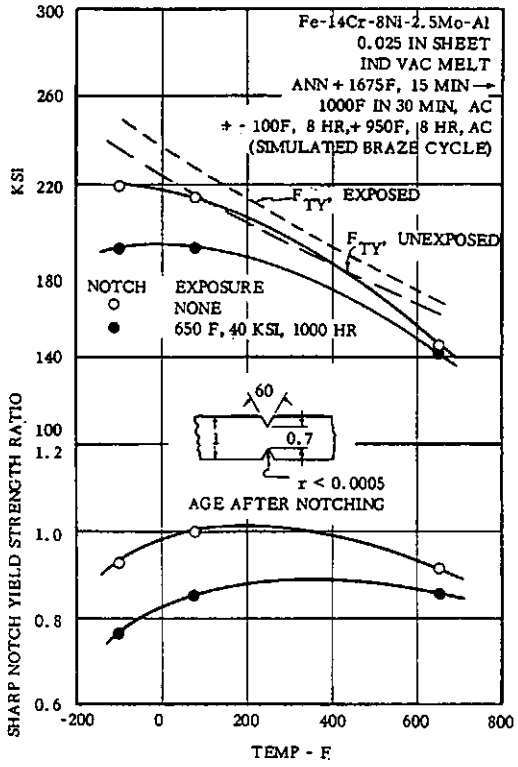


FIG. 4.0312 EFFECT OF TEST TEMPERATURE ON THE SHARP NOTCH PROPERTIES OF VACUUM MELTED SHEET GIVEN SIMULATED BRAZE CYCLE AND TESTED BEFORE AND AFTER ELEVATED TEMPERATURE EXPOSURE. (5)

REFERENCES

1. "Armco PH14-8Mo Stainless Steel Sheet and Strip," Armco Steel Corporation (November 1966).
2. Perry, D. C., "Stainless, PH14-8Mo, Flat Rolled Compilation of Data for Technical Data Manual," Armco Steel Corporation Research Center (September 6, 1963).
3. Hoenie, A. F. and Roach, D. B., "New Developments in High-Strength Stainless Steels," DMIC Report 223 (January 3, 1966).
4. "Fatigue Evaluation of PH14-8Mo (SRH 1050) Alloy," Armco Steel Corporation, Advanced Materials Division (September 17, 1969).
5. Espey, G. B. and Bubsey, R. T., NASA Lewis Research Center Data, Unpublished.
6. Heimerl, G. F., Baucom, R. M., Manning, C. R., and Braski, D. N., "Stability of Four Titanium-Alloys and Four Stainless-Steel Sheet Materials After Exposure Up to 22,000 Hours at 550F," NASA, Langley Research Center, TN D-2607 (February 1965).
7. Thompson, O. N. and Jones, R. L., "Intermittent Creep and Stability of Materials for SST Applications," General Dynamics Corporation, Fort Worth Division, AFML - TR-66-407 (January 1967).
8. "Recommended Practice for Plane-Strain Fracture Toughness Testing of High Strength Metallic Materials Using a Fatigue Cracked Bend Specimen," ASTM Book of Standards, Part 31 (1968).
9. Hudson, C. M., "Fatigue-Crack Propagation in Several Titanium and Stainless-Steel Alloys and One Superalloy," Langley Research Center, NASA TN D-2331 (October 1964).

REVISED: JUNE 1970
AUTHOR: C. F. HICKEY JR.

FERROUS ALLOYS

	Fe
15	Cr
7	Ni
2.5	Mo

PH15-7Mo

1. GENERAL

This alloy is a semi-austenite precipitation-hardening stainless steel. It is a modified 17-7PH alloy in which 2 to 3 percent molybdenum is substituted for an equivalent percentage of chromium, thus higher strengths can be obtained both at room and elevated temperatures in the various heat treated conditions (16). The alloy can be considered for utilization at temperatures up to 1000F. PH 15-7Mo is essentially austenitic at room temperature in the annealed or solution-treated condition, but can be transformed to martensite by a series of thermal treatments or by cold working. The alloy can then be further hardened by thermal treatment to strengths in excess of 200 ksi at room temperature (9). The alloy is available in sheet, strip, plate, bar and wire form. It can be formed readily in the annealed condition and is easily welded by various methods. Its heat treatment is identical with that of 17-7PH and much of the information available for the latter alloy also applies to PH 15-7Mo (9).

1.01 Commercial Designation
PH 15-7Mo

1.02 Alternate Designation
AISI No. 632

1.03 Specifications
Table 1.03

TABLE 1.03

AMS	ASTM	Form	Military
5520A	-	Sheet, Strip, Plate	MIL-A-8955 (ASG)
5657	A461, A564	Bars and Forgings	-
5812B	-	Welding Wire	-
5813A	-	Welding Wire	-

1.04 Composition
1.041 Specification composition, Table 1.041.

TABLE 1.041

Source	AMS (1)(2) ASTM (5)(6) MIL (7)		AMS (3)(4) (b)	
Element	Percent		Percent	
	Min	Max	Min	Max
Aluminum	0.75	1.50	0.75	1.25
Carbon	-	0.09	-	0.09
Chromium	14.00	16.00	14.00	15.25
Manganese	-	1.00	-	1.00
Molybdenum	2.00	3.00	2.00	2.75
Nickel	6.50	7.75	6.50	7.75
Phosphorus	-	0.04	-	0.025(c)
Silicon	-	1.00	-	0.50
Sulfur	-	0.03(a)	-	0.025
Iron	Balance		Balance	

(a) 0.040 for ASTM A461(5) and MIL-S-8955 (ASG)(7)
(b) Maximum 50 ppm oxygen and 25 ppm hydrogen for AMS 5812B (3)
(c) 0.010 for AMS 5812B (3)

1.042 Typical producer composition, Table 1.042.

TABLE 1.042

Source	(8, p. 571)
Alloy	Fe-15Cr-7Ni-2.5Mo
Element	Composition
Aluminum	1.26
Carbon	.07
Chromium	15.05
Manganese	.69
Molybdenum	2.30
Nickel	7.16
Phosphorus	.019
Silicon	.20
Sulfur	.017
Iron	Balance

1.05 Heat Treatment
1.051 Solution treat to Condition A.
1.0511 Sheet and strip. 1925 to 1975F, 3 minutes per 0.1 inch thickness, air cool (1)(9).
1.0512 Bar and forging. 1925 to 1975F, water quench (2)(5)(7); 1875 to 1925, water quench (6).
1.052 Age condition A to Condition TH 1050. 1375 to 1425F, 1 1/2 hr (austenite conditioning), air cool to 50 to 60F within 1 hr, hold at 50 to 60F, 1/2 hr (Condition T) + 1040 to 1060F, 1 1/2 hr, air cool (1)(2)(5)(6)(7).
1.053 Age Condition A to Condition RH 950. 1735 to 1765F, 10 minutes (austenite conditioning), air cool (Condition A 1750) + -90 to -110F, 8 hr (Condition R-100) + 940 to 960F, 1 hr, air cool (2)(5)(6)(7).
1.054 Age Condition C of sheet (cold rolled) or wire (cold drawn) to Condition CH 900. 890 to 910F, 1 hr, air cool (7)(9).
1.055 TH and RH conditions are also used with different final age hardening temperatures, e.g., TH 1150, RH 1050, etc. Effect of aging temperature on tensile properties of sheet in various RH conditions, Figures 1.055 and 1.0551.

1.06 Hardness
1.061 Typical hardness of sheet for various conditions, Table 1.061.

TABLE 1.061

Source	(9, p. 2, 14) (a)	(11, p. 66)
Alloy	Fe-15Cr-7Ni-2.5Mo	
Condition	Rockwell Hardness C	
A	100(b)(c)	90(b)
T	28	28
TH 1050	40	45
A1750	85(b)	85(b)
R 100	40	40
RH 950	45	48
C	41	45
CH 900	46	50

(a) Applies to material .010 inch and thicker.
(b) RB
(c) maximum

1.062 Effect of aging temperature on hardness in Condition RH 950 (see 3.0214).
1.063 Effect of cold work in Condition A on hardness in Condition TH 1050, Table 1.063.

TABLE 1.063

Source	(9, p. 70)
Alloy	Fe-15Cr-7Ni-2.5Mo
Condition	A + CR + TH 1050
Percent Reduction in Thickness (by rolling)	Hardness, RC
0	44.5
20	43.0
30	42.5

1.0631 Effect of modified TH 1050 heat treatment on cold worked properties (see Special Considerations, section 1.095).
1.064. Relationship between hardness and strength for heat treated conditions, Figure 1.064.

1.07 Forms and Conditions Available
1.071 Alloy is available in the full commercial range of sizes for sheet, strip, plate, bar, wire and welded tubing (12).
1.072 Alloy is available in the Condition A for the full range of products. Strip up to 0.050 inch thick and wire up to 0.050 inch diameter are also available in Condition C (13).

1.08 Melting and Casting Practice
Conventional stainless steel melting and casting practices are used. Induction and consumable electrode vacuum melts are also available.

	Fe
15	Cr
7	Ni
2.5	Mo

PH15-7Mo

1.09 Special Considerations

1.091 Alloy is available in numerous forms (see 1.071), but the primary usage is in the sheet and strip form (13).

1.092 In common with the general class of precipitation hardening stainless steels, this alloy is unstable during exposure to temperatures exceeding about 500F. This instability is reflected in an increase in the yield strength and a decrease in fracture toughness. The transverse direction has lower toughness than the longitudinal direction.

1.093 Dimensional changes during heat treating to Conditions TH 1050 or RH 950 need consideration and special provisions must be made for machining and tooling.

1.094 Thorough cleaning prior to thermal treatments is recommended in order to avoid carburization and to minimize difficulties when descaling.

1.095 A modified TH 1050 heat treatment has been developed to compensate for cold working in Condition A when TH 1050 properties are desired (9,p.70). The treatment is as follows:

Austenite Condition	Air Cool & Refrigerate
1550F ± 25F 90 min	0F ± 10F 4 hrs

Precipitation Harden
1050F ± 10F 90 min

2. PHYSICAL AND CHEMICAL PROPERTIES

2.01 Thermal Properties

2.011 Melting range. 2580 to 2640F.

2.012 Phase changes. Similar to those in 17-7PH.

2.0121 Time-temperature-transformation diagrams.

2.013 Thermal conductivity, Figure 2.013.

2.014 Thermal expansion, Figure 2.014.

2.015 Specific heat, 0.11 Btu per lb F.

2.016 Thermal diffusivity

2.017- Dilatometer curve indicating dimensional changes during heat treatment from Condition A to Condition RH 950, Figure 2.017.

2.02 Other Physical Properties

2.021 Density, Table 2.021.

TABLE 2.021

Source	(9, p. 76)			
Alloy	Fe-15Cr-7Ni-2.5Mo			
Condition	A	TH 1050	RH 950	CH 900
lb per cu in	0.282	0.277	0.277	0.277
gr per cu cm	7.804	7.685	7.680	7.67

2.022 Electrical resistivity, Table 2.022.

TABLE 2.022

Source	(9, p. 76)			
Alloy	Fe-15Cr-7Ni-2.5Mo			
Condition	A	TH 1050	RH 950	CH 900
Microhm - inches	31.5	32.3	32.7	33.1

2.023 Magnetic properties. Permeability, Table 2.023.

TABLE 2.023

Source	(9, p. 76)			
Alloy	Fe-15Cr-7Ni-2.5Mo			
	Permeability			
Field Strength Oersteds	Condition A	Condition TH 1050	Condition RH 950	Condition CH 900
25	5.1	142	65	-
50	5.2	147	118	-
100	5.1	94	87	70
200	4.7	55	53	44
maximum	5.3	150	119	125

2.024 Emittance, Figure 2.024.

2.025 Damping capacity.

2.03 Chemical Properties

2.031 Corrosion resistance (see also 17-7PH).

2.0311 General corrosion resistance of PH 15-7Mo in Condition TH1050 and RH 950 is superior to standard hardenable types of stainless steels such as Types 410, 420, and 431, but is not quite as good as Type 304 (9).

2.0312 Corrosion rate in several corrosive media, Table 2.0312.

TABLE 2.0312

Source	(9, p. 86)	
Alloy	Fe-15Cr-7Ni-2.5Mo	
Form	0.050 Inch Sheet	
Condition	TH 1050 MPY*	RH 950 MPY*
H_2SO_4, 95F		
1 percent	273	0.5
2 percent	78	0.7
5 percent	453	482
H_2SO_4, 176F		
1 percent	560(3)	690(2)
2 percent	1300(2)	1440(1)
HCl, 95F		
0.5 percent	31	0.3
1 percent	280	152
HNO_3, Boil		
25 percent	119	36
50 percent	512	128
65 percent	748	210
Formic Acid, 176F		
5 percent	161	7.3
10 percent	123	74
Acetic Acid, Boil		
33 percent	3.0	7.6
60 percent	33	6.8
H_3PO_4, Boil		
20 percent	15.4	22.2
50 percent	97	52
70 percent	600(3)	277
NaOH, 176F		
30 percent	43	3.3
NaOH, Boil		
30 percent	142	139

MPY = Mils Per Year
Rates were determined by total immersion for five 48-hour periods. Specimens were activated by brief exposure to DC current for the last three test periods except in the 65 percent nitric acid or where brackets indicate total number of immersion periods.

2.0313 Stress corrosion cracking. Results of stress-cracking exposure tests on sheet in various conditions at Kure Beach, Table 2.0313.

TABLE 2.0313

Source	(9, p. 88)							
Alloy	Fe-15Cr-7Ni-2.5Mo							
Form	Sheet							
	Original Properties		Stressed 60 Percent F_{ty}			Stressed 40 Percent F_{ty}		
	F_{tu}	F_{ty}	Stress	Days to Failure		Stress	Days to Failure	
Condition	ksi	ksi	ksi	80ft lot	800ft lot	ksi	80ft lot	800ft lot
TH 1050	222	212	127	182	NF	85	NF	NF
	217	209	125	73(4)	NF	84	NF	NF
	215	206	124	71(2)	NF	82	NF	NF
RH 950	243	218	131	28.2	179(4)	87	92(3)	346(1)
	243	220	132	22.2	126(4)	88	74(4)	NF
	239	218	131	19	164(4)	87	82(1)	NF
RH 1050	227	219	131	14(4)	NF	88	NF	NF
	222	215	129	21.2(2)	NF	86	NF	NF

NF denotes no failures after 400 days.
( ) Denotes number of specimens failed at average time shown.
Remainder of 5 specimens not failed after 400 days.

2.03131 Salt coated specimens of this alloy in Condition 1050 exhibit excellent resistance to stress corrosion cracking at 550F for exposure times to 10,000 hours; however, it does show susceptibility to pitting (15).

	Fe
15	Cr
7	Ni
2.5	Mo

PH15-7Mo

2.0314 Intergranular corrosion may occur during acid pickling, except in Conditions A and CH 900.

2.0315 Hydrogen embrittlement may occur during plating and recommended procedures for preventing same must be followed (12).

2.032 Oxidation resistance (see 17-7PH).

2.04 Nuclear Properties

3. MECHANICAL PROPERTIES

3.01 Specific Mechanical Properties

3.011 AMS and MIL specified mechanical properties for sheet, strip, and plate, Table 3.011.

TABLE 3.011

Source	AMS (1) MIL (7)				
Alloy	Fe-15Cr-7Ni-2.5Mo				
Form	Sheet, Strip, Plate				
Condition	A (1) (7)	TH 1050 (1) (7)	RH 950 (1) (7)	C (7)	CH 900 (7)
F_{tu} - max - ksi	150	-	-	-	-
min - ksi	-	190	225	200	240
F_{ty} - max - ksi	65	-	-	-	-
min - ksi	-	170	200	175	230
e(2 in) min - percent					
Thickness - inch					
0.0015 - 0.500	25	-	-	1	1
0.0015 - 0.004	-	2(a)	1(a)	-	-
0.005 - 0.009	-	3	2	-	-
0.010 - 0.019	-	4	3	-	-
0.020 - 0.187	-	5	4	-	-
0.188 - 0.500	-	6	5	-	-
Hardness					
RB, max	100(a)	-	-	-	-
RC, min	-	40 (a)(b)	40 (a)(b)	-	-

(a) AMS only
(b) For thicknesses greater than 0.010

3.012 AMS and ASTM specified mechanical properties for bar, Table 3.012.

TABLE 3.012

Source	AMS (2), ASTM (5)			
Alloy	Fe-15Cr-7Ni-2.5Mo			
Form	Bar			
Condition	TH 1050			RH 950
Thickness-Inches	6 inch diameter and under or distance between parallel sides (2)	0.250 to 0.625 (5)	0.625 to 6 (5)	6 inch diameter and under or distance between parallel sides (2) (5)
F_{tu}, min - ksi	180	185	180	200
F_{ty}, min - ksi	160	160	160	175
e(4D), minimum-percent	8	10	8	7
RA, min-percent	25	30	25	25
Hardness, BHN, minimum	375	371	375	415*

* ASTM gives 418.

3.013 Producers' guaranteed mechanical properties for sheet, strip, and plate, Table 3.013.

TABLE 3.013

Source	(9, p. 2)						
Alloy	Fe-15Cr-7Ni-2.5Mo						
Form	Sheet, Strip, Plate						
Condition	A	TH 1050		RH 950		C	CH 900
Thickness - Inch	All	0.0015 to 0.1874	0.1875 to 0.6250	0.0015 to 0.1874	0.1875 to 0.6250	0.0015 to 0.050	0.0015 to 0.050
F_{tu}, minimum ksi	-	190	190	225	225	200	240
maximum ksi	150	-	-	-	-	-	-
F_{ty}, minimum ksi	-	170	170	200	200	175	230
maximum ksi	65	-	-	-	-	-	-
e(2 in), min-percent							
0.0015-0.0049	25	2	-	1	-	1	1
0.005 - 0.0099	25	3	-	2	-	1	1
0.010 - 0.0199	25	4	-	3	-	1	1
0.020 - 0.0369	25	5	-	4	-	1	1
0.036 - 0.1874	25	5	-	4	-	1	1
0.1875 - 0.6250	25	-	4	-	4	-	-
>0.6250	25	-	-	-	-	-	-
RA, min - percent	-	-	20	-	20	-	-
Hardness							
RB, maximum	100	-	-	-	-	-	-
RC, minimum	-	40	40	46	45	41	46
BHN maximum	-	-	372	-	426	-	-
Transverse tensile data							

3.02 Mechanical Properties at Room Temperature

3.021 Tension (see also 1.055)

3.0211 Stress-strain diagrams.

3.0212 Typical tensile properties for various conditions of sheet, strip, and plate, Table 3.0212.

TABLE 3.0212

Source	(9, p. 14)(16, p. 5)							
Alloy	Fe-15Cr-7Ni-2.5Mo							
Form	Sheet, Strip, Plate							
Condition	A (9) (16)	T (9) (16)	C (16)	TH 1050 (9)(16)	A 1750 (9)(16)	R 100 (9)(16)	RH 950 (9)(16)	CH 900 (16)
F_{tu} - ksi	130	145	220	210	150	180	240	265
F_{ty} - ksi	55	90	190	200	55	125	225	260
e(2 in) - percent	35	7	5	7	12	7	6	2

3.0213 Effect of solution temperature on tensile properties in Conditions A, TH 1050, and RH 950, Figure 3.0213.

3.0214 Effect of aging temperature on tensile properties and hardness in Condition RH 950, Figure 3.0214.

3.0215 Effect of exposure to elevated temperatures on tensile properties of sheet in Conditions RH 950 and TH 1050, Figure 3.0215.

3.0216 Effect of exposure time to elevated temperatures on strength properties in Condition RH 1075, Figure 3.0216.

3.0217 Effect of exposure time, elevated temperatures, and load on tensile properties of sheet in Condition RH 950, Table 3.0217.

TABLE 3.0217

Source	(2)		
Form	0.050 Inch Sheet		
Condition	RH 950		
1000 hours exposure	Properties After Exposure		
Temperature F	Load ksi	Room Temp F_{tu} - ksi	e (2 in) percent, T
RT	-	248	6.5
600	90	252	6.5
	200	283	3.5
700	40	276.2	4.25
	190	302.1	2.25
800	40	282.4	4.5
	170	308.3	1.75
900	20	249.8	5.5
	70	262.4	4.0

Fe
15 Cr
7 Ni
2.5 Mo

PH15-7Mo

3.0218 Effect of thickness on tensile properties of sheet, Figure 3.0218.

3.0219 Effect of reduction by shear forming on tensile properties of sheet, Figure 3.0219.

3.02111 Effect of reduction by cold working in Condition A on tensile properties in Condition TH 1050, Table 3.02111.

TABLE 3.02111

Source	(9, p. 70)		
Alloy	Fe-15Cr-7Ni-2.5Mo		
Form	0.050 Inch Sheet (Initial Thickness)		
Condition	TH 1050		
Percent Reduction in Thickness (by rolling) Condition A	F_{ty} - ksi (0.2 percent)	F_{tu} ksi	e(2 in) percent
0	188	199	9.5
20	163	191	10.8
30	150	189	11.4

(a) Longitudinal data
(b) Cold working PH15-7Mo in Condition A produces no deleterious effect on mechanical properties in Condition RH 950 (9, p. 71).

3.02112 Effect of percent cold reduction and cold reduction temperature on yield strength, Figure 3.02112.

3.022 Compression.

3.0221 Stress-strain diagrams (see Figure 3.0321).

3.023 Impact.

3.024 Bending.

3.025 Torsion and shear.

3.0251 Effect of reduction by shear forming on shear strength of sheet, Figure 3.0251.

3.026 Bearing.

3.0261 Bearing properties of sheet in Conditions TH 1050 and RH 950, Table 3.0261.

TABLE 3.0261

Source	(9, p. 44)				
Alloy	Fe-15Cr-7Ni-2.5Mo				
Form	Sheet				
Condition	Sheet Thickness inch	Test Direction	e/D	F_{bry} ksi	F_{bru} ksi
TH 1050	0.064	L	1.5	339	402
			2.0	345	497
		T	1.5	325	410
			2.0	378	463
	0.050	L	1.5	316	418
			2.0	342	501
		T	1.5	343	427
			2.0	342	504
RH 950	0.064	L	1.5	350	455
			2.0	390	543
		T	1.5	366	471
			2.0	372	507
	0.050	L	1.5	344	470
			2.0	405	564
		T	1.5	346	476
			2.0	349	487

Each value represents the average of three tests.

3.027 Stress concentration.

3.0271 Notch properties.

3.02711 Effect of aging temperature on sharp notch strength of sheet in various RH conditions, Figure 3.02711.

3.02712 The effect of crack length on percent of tensile strength of sheet, Figure 3.02712.

3.0272 Fracture toughness.

Condition	K_Q (plain strain)
TH 1050	63 ksi$\sqrt{in}$
RH 950	52 ksi$\sqrt{in}$

Valid plain strain fracture toughness, K_{Ic}, data which have been derived from tests that conform in all aspects to the ASTM Recommended Practice appears to be lacking for this material (22). However, data reported by Steigerwald can be presented as K_Q and used as a qualitative measure of fracture toughness (23). For example, the above data indicates a strong dependence on heat treat condition (this also applies to 17-7PH) (23). Due to the relatively low fracture toughness which exists for PH 15-7Mo and 17-7PH in Condition RH 950, the PH 14-8Mo alloy should be used when a combination of high strength and high fracture toughness is required (9, p. 14).

3.028 Combined properties.

3.03 Mechanical Properties at Various Temperatures

3.031 Tension.

3.0311 Stress-strain diagrams.

3.03111 Stress-strain curves for sheet in Conditions TH 1050 and RH 950 at elevated temperatures, Figure 3.03111.

3.03112 Stress-strain curves at room and low temperature for sheet in Condition RH 950, Figure 3.03112.

3.03113 Stress-strain curves in tension for sheet in Condition TH 1050 at elevated temperatures and for various exposure times, Figure 3.03113.

3.03114 Stress-strain curves in tension for sheet in Condition RH 950 for various exposure times at elevated temperatures, Figure 3.03114.

3.0312 Tension properties for Condition TH.

3.03121 Effect of test temperature on tensile properties of sheet in Conditions TH 1050 and RH 950, Figure 3.03121.

3.03122 Effect of exposure and test temperature on tensile properties of sheet in Condition TH 1050, Figure 3.03122.

3.0313 Tension properties for Condition RH.

3.03131 Effect of test temperature on tensile properties of sheet in Condition RH 950 (see 3.03121).

3.03132 Effect of test temperature on tensile properties of exposed and unexposed sheet in Condition RH 1050, Figure 3.03132.

3.03133 Effect of test temperatures on tensile properties of exposed and unexposed sheet in Condition RH 1100, Figure 3.03133.

3.03134 Effect of low test temperature on tensile properties of sheet in Condition RH 950, Figure 3.03134.

3.0314 Tension properties for Condition CH.

3.03141 Effect of test temperature on tensile properties of exposed and unexposed sheet in Condition CH 900, Figure 3.03141.

3.03142 Effect of test temperature on tensile properties of sheet in Condition CH 900, Figure 3.03142.

3.0315 Tension properties for various conditions.

3.03151 Effect of exposure temperature on tensile properties of sheet in Conditions TH 1050 and RH 950, Figure 3.03151.

3.03152 Effect of low test temperature up to 200F on tensile properties of sheet in Conditions RH 950 and CH 1100, Figure 3.03152.

3.03153 Effect of test temperature on tensile properties of plate in Condition TH 1050, Figure 3.03153.

3.03154 Effect of test temperature on tensile properties of plate in Condition RH 950, Figure 3.03154.

3.032 Compression.

3.0321 Stress-strain curves in compression at elevated temperatures for sheet in Conditions TH 1050 and RH 950, Figure 3.0321.

3.0322 Effect of test temperature on compressive yield strength of sheet in Conditions TH 1050, RH 950 and CH 900, Figure 3.0322.

3.0323 Effect of exposure time and test temperature on compressive yield strength of sheet in Condition TH 1050, Figure 3.0323.

3.033 Impact.

3.0331 Effect of low test temperature on impact strength of alloy in Condition TH 1050 and RH 950, Figure 3.0331.

3.034 Bending.

3.035 Torsion and shear.

3.0351 Effect of test temperature on shear strength of sheet in Condition TH 1050 and RH 950, Figure 3.0351.

3.0352 Effect of exposure time and test temperature on shear strength of sheet in Condition TH 1050, Figure 3.0352.

3.036 Bearing.

3.0361 Effect of exposure time and test temperature on bearing properties of sheet in Condition TH 1050, Figure 3.0361.

3.0362 Effect of exposure time and test temperature on bearing properties of sheet in Condition TH 1050, Figure 3.0362.

3.037 Stress concentration.

3.0371 Notch properties.

3.03711 Effect of test temperature on notch and crack strength of sheet in Condition CH 900, Figure 3.03711.

3.03712 Effect of test temperature on notch and crack strength

	Fe
15	Cr
7	Ni
2.5	Mo

PH15-7Mo

of sheet in Condition RH 1050, Figure 3.03712.

3.03713 Effect of test temperature on the sharp notch strength ratio and crack strength ratio for sheet in RH 1050 Condition, Figure 3.03713.

3.03714 Effect of test temperature on notch and crack strength of sheet in Condition RH 1100, Figure 3.03714.

3.03715 Effect of exposure and test temperature on notch strength of sheet in Condition TH 1050, Figure 3.03715.

3.03716 Effect of low test temperature on notch strength of sheet in Condition RH 950, Figure 3.03716.

3.03717 Effect of stress concentration factor on notch strength ratio at room temperature and -320F for sheet in Conditions CH 900 and RH 1100, Figure 3.03717.

3.0372 Fracture toughness.

3.038 Combined properties.

3.04 Creep and Creep Rupture Properties

3.041 Creep properties for sheet, strip and plate in Condition RH 950 at 600 to 900F, Table 3.041.

TABLE 3.041

Source	(9, p. 37)	
Alloy	Fe-15Cr-7Ni-2.5Mo	
Form	0.050 Inch Sheet	
Condition	RH 950	
Time - hours	1000	
Creep - percent	0.1	0.2
Temperature - F	Stress - ksi	
600	132	150
700	121	142
800	95	109
900	36	41

3.042 Creep rupture properties for sheet in Condition TH 1050 and RH 950 at various temperatures, Table 3.042.

TABLE 3.042

Source	(14, F-1-3, F-2-3)					
Alloy	Fe-15Cr-7Ni-2.5Mo					
Form	0.050 Inch Sheet					
Condition	TH 1050			RH 950		
Time - hours	10	100	1000	10	100	1000
Temperature - F	Creep Rupture Strength - ksi					
600	-	179	178	-	202	200
700	177	161	159	200	193	191
800	159	139	137	190	174	171
900	132	108	98	168	125	108

3.043 Isochronous stress-strain curves for sheet in Condition RH 950 at 600 to 900F, Figure 3.043.

3.044 Creep and creep rupture curves for alloy in Condition RH 950, Figure 3.044.

3.045 Creep rupture curves for alloy at 1000F in Condition RH 950, Figure 3.045.

3.05 Fatigue properties

3.051 S-N curve for sheet in Condition RH 950, Figure 3.051.

3.052 S-N curve for notched sheet in Condition RH 950, Figure 3.052.

3.053 S-N curves for notched and smooth sheet as a function of temperature in Condition TH 1050, Figure 3.053.

3.054 S-N curves for notched and unnotched sheet as a function of temperature in Condition TH 1050, Figure 3.054.

3.055 S-N curves for notched and unnotched sheet as a function of temperature in Condition TH 1050, Figure 3.055.

3.056 Fatigue-crack propagation rate for two test temperatures for sheet in Condition TH 1050, Figure 3.056.

3.057 Fatigue-crack propagation curves as a function of initial net section stress for sheet in Condition TH 1050, Figure 3.057.

3.058 Fatigue-crack propagation curves as a function of initial net section stress for sheet in Condition TH 1050 at R = -1, Figure 3.058.

3.06 Elastic Properties

3.061 Poisson's ratio. Condition RH 950, 0.28.

3.062 Modulus of elasticity.

3.0621 Modulus of elasticity at room and elevated temperatures, Figure 3.0621.

3.0622 Modulus of elasticity in compression at room and elevated temperatures, Figure 3.0622.

3.0623 Effect of exposure time and test temperature on modulus of elasticity in compression of sheet in Condition TH 1050, Figure 3.0623.

3.063 Modulus of rigidity.

3.0631 Modulus of rigidity at room and elevated temperatures, Figure 3.0631.

3.064 Tangent modulus.

3.0641 Tangent modulus curves in compression for sheet in Condition TH 1050 at elevated temperatures and for various exposure time, Figure 3.0641.

3.0642 Secant modulus curves in compression at elevated temperatures for sheet in Conditions TH 1050 and RH 950, Figure 3.0642.

4. FABRICATION

4.01 Formability
(see also 17-7PH)

4.011 Hydroforming and marforming operations can readily be performed on this alloy and 17-7PH in Condition A. Parts including formers, flanges, hat sections, and frames which have been processed by these methods are used by aircraft manufacturers (9).

4.012 Spinning characteristics of this alloy are similar to 17-7PH and Type 301. The strength developed during cold working is primarily dependent upon the amount of cold-work and the temperature at which it is done (see 3.0219, 3.02112, and 3.0251) (9).

4.02 Machining and Grinding
(see also 17-7PH)

4.021 Grinding. Material appears to offer no major problems in grinding; however, Conditions TH 1050 and RH 950 are easier to grind than Condition A material (9). Conventional grinding wheels at conventional speeds and feeds appear satisfactory. Grinding characteristics of 17-7PH are comparable to those of this alloy (9).

4.03 Welding
(see also 17-7PH)

4.031 Inert gas tungsten arc fusion welding of annealed and subsequently heat treated metal yields a weld efficiency of 80 to 100 percent.

4.032 Most welding is performed with the inert gas tungsten arc process or the resistance spot and seam welding processes. Resistance flash butt welding is not recommended for joints to be placed in high strength conditions (11, p. 65).

4.033 The molybdenum addition in this alloy causes larger amounts of delta ferrite or free ferrite to form in weld deposits upon solidification. The amounts of ferrite requires some control in order to maintain good ductility in the highest strength conditions. The control is effected through the use of filler metal of appropriate chemical composition or through heat treatment (11, p. 65).

	Fe
15	Cr
7	Ni
2.5	Mo

PH15-7Mo

4.034 To avoid problems with weld metal cracking or lowered ductility a specific composition of hardenable weld wire, designated as W PH 15-7Mo, is recommended for use as electrode or filler rod, Table 4.034.

TABLE 4.034

Source	(9, p. 116)
Alloy	Fe-15Cr-7Ni-2.5Mo
Form	Sheet and Strip
Element	Composition Range, Percent Weld Wire WPH15-7Mo
Carbon	0.09 - maximum
Manganese	1.00 - maximum
Phosphorus	0.025 - maximum
Sulfur	0.025 - maximum
Silicon	0.50 - maximum
Chromium	14.00 - 15.25
Nickel	6.50 - 7.75
Aluminum	0.75 - 1.25
Molybdenum	2.00 - 2.75

WPH15-7Mo serves satisfactorily for most welded articles which are heat treated to the lower levels of strength and hardness; that is any treatment involving a final hardening temperature of 1100F or higher.

4.035 Strength of spot welded joints, Table 4.035.

TABLE 4.035

Source	(9, p. 119)		
Form	0.049 Inch Sheet		
Condition in which welded	Condition in which tested	Shear Breaking Load lbs/weld (a)	Tension Breaking Load lbs/weld (a)
A	TH 1050	3103	580
T	TH 1050	3438	1648
TH 1050	TH 1050	2896	2015
A	RH 950	2853	520
A 1750	RH 950	3426	-
R 100	RH 950	3335	1232
RH 950	RH 950	2630	2170

(a) Average of twenty (20) tests.

4.04 Heat Treatment
(see 17-7PH)

4.05 Surface Treatment
(see 17-7PH)

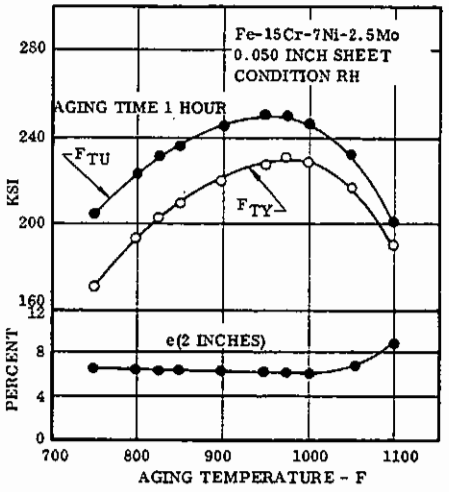


FIG. 1.055 EFFECT OF AGING TEMPERATURE ON TENSILE PROPERTIES OF SHEET IN VARIOUS RH CONDITIONS. (9, p. 68)

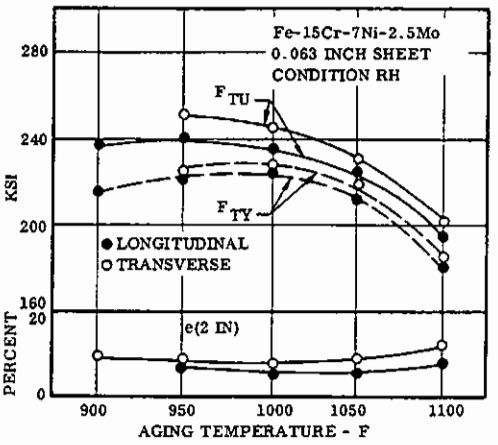


FIG. 1.0551 EFFECT OF AGING TEMPERATURE ON TENSILE PROPERTIES OF SHEET IN VARIOUS RH CONDITIONS. (10, p. 864)

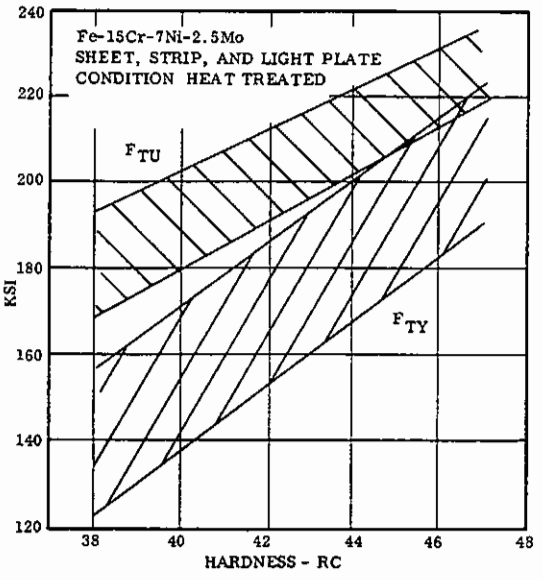


FIG. 1.064 RELATIONSHIP BETWEEN HARDNESS AND STRENGTH FOR HEAT TREATED CONDITIONS (SPREAD IN STRENGTH PROPERTIES DUE PRIMARILY TO VARIATIONS IN CHEMICAL COMPOSITION.) (9, p. 67)

	Fe
15	Cr
7	Ni
2.5	Mo

PH15-7Mo

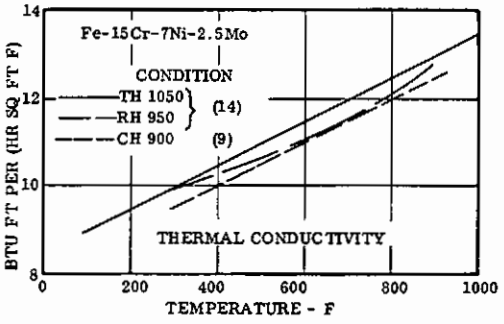


FIG. 2.013 THERMAL CONDUCTIVITY. (9, p. 76)
(14, p. F-1-1, F-2-1)

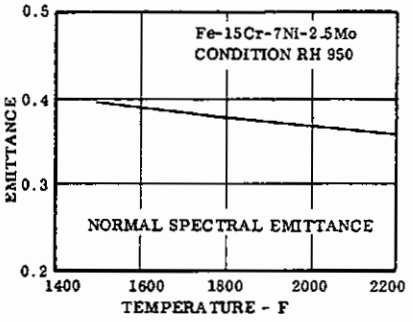


FIG. 2.024 EMITTANCE (9, p. 81; 14, p. F-2-1)

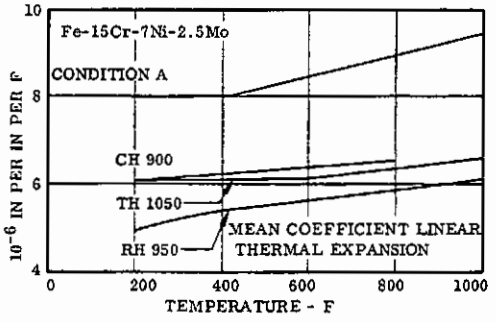


FIG. 2.014 THERMAL EXPANSION. (9, p. 76)

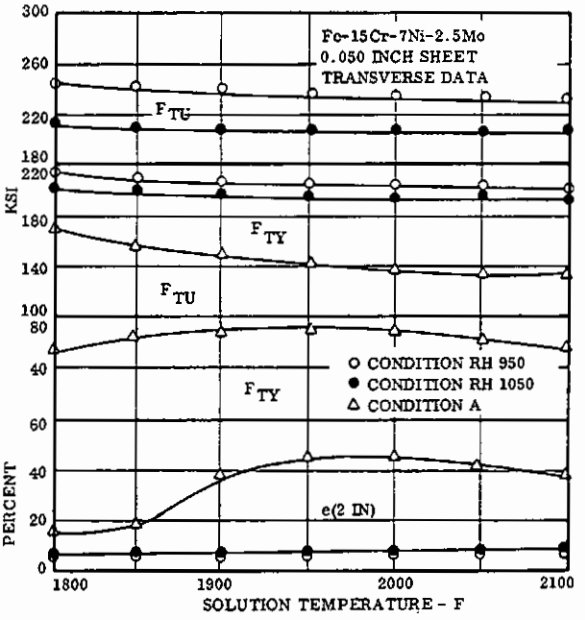


FIG. 3.0213 EFFECT OF SOLUTION TEMPERATURES ON TENSILE PROPERTIES IN CONDITIONS A, TH 1050, AND RH 950.
(9, p. 58, 59)

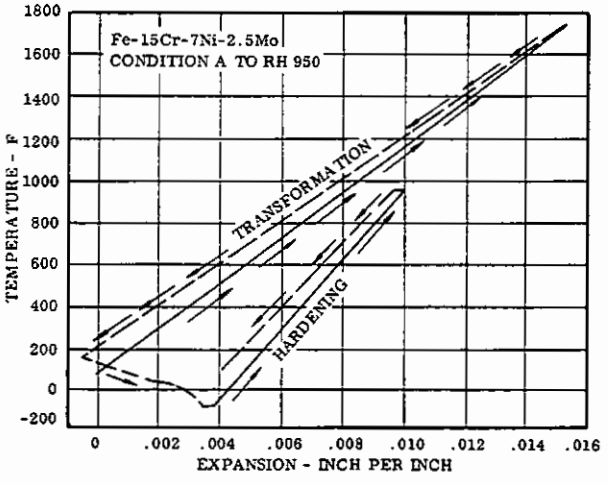


FIG. 2.017 DILATOMETER CURVE INDICATING DIMENSIONAL CHANGES DURING HEAT TREATMENT FROM CONDITION A TO CONDITION RH 950. (9, p. 78)

	Fe
15	Cr
7	Ni
2.5	Mo

PH15-7Mo

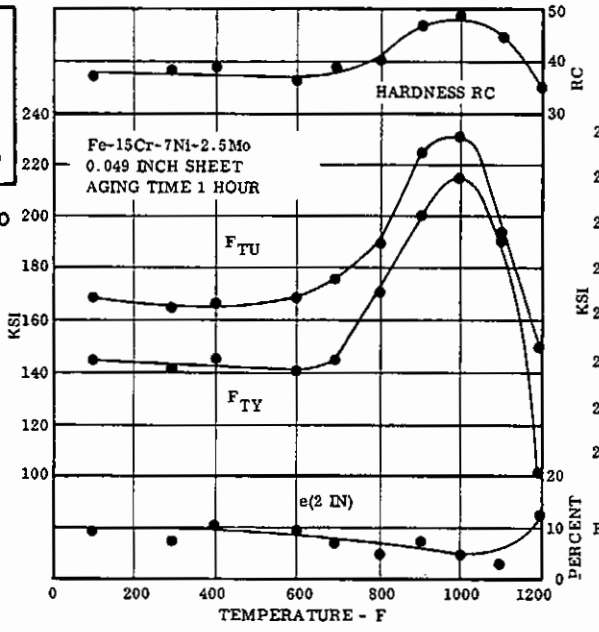


FIG. 3.0214 EFFECT OF AGING TEMPERATURE ON TENSILE PROPERTIES AND HARDNESS IN CONDITION RH 950. (17, p. 113)

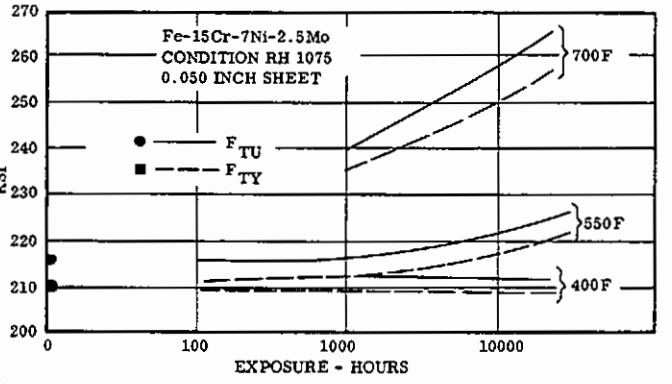


FIG. 3.0216 EFFECT OF EXPOSURE TIME TO ELEVATED TEMPERATURES ON STRENGTH PROPERTIES IN CONDITION RH 1075. (9, p. 57)

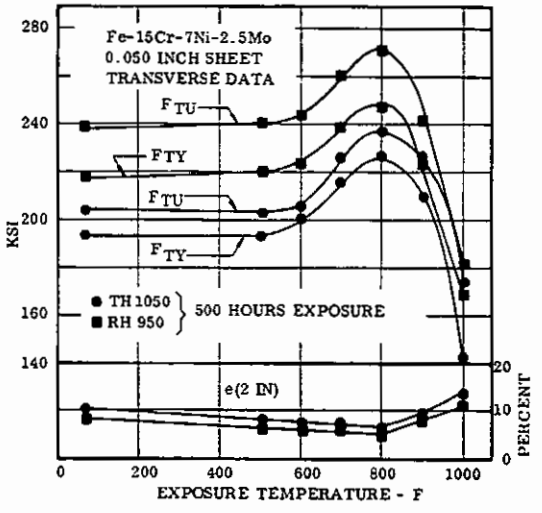


FIG. 3.0215 EFFECT OF EXPOSURE TO ELEVATED TEMPERATURES ON TENSILE PROPERTIES OF SHEET IN CONDITIONS RH 950 AND TH 1050. (9, p. 55)

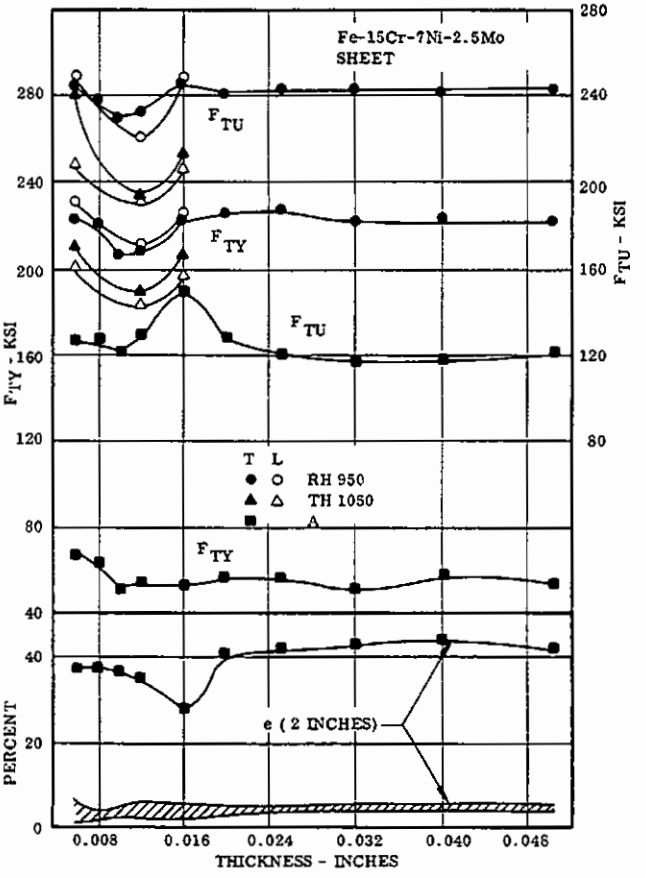
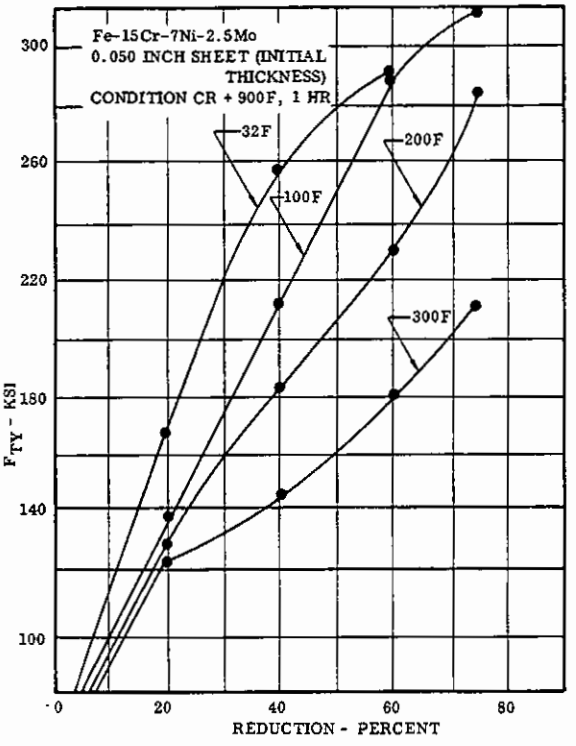


FIG. 3.0218 EFFECT OF THICKNESS ON TENSILE PROPERTIES OF SHEET. (18, p. 164, 167-169)



	Fe
15	Cr
7	Ni
2.5	Mo

PH15-7Mo

FIG. 3.02112 EFFECT OF PERCENT COLD REDUCTION AND COLD REDUCTION TEMPERATURE ON YIELD STRENGTH. (9, p. 103)

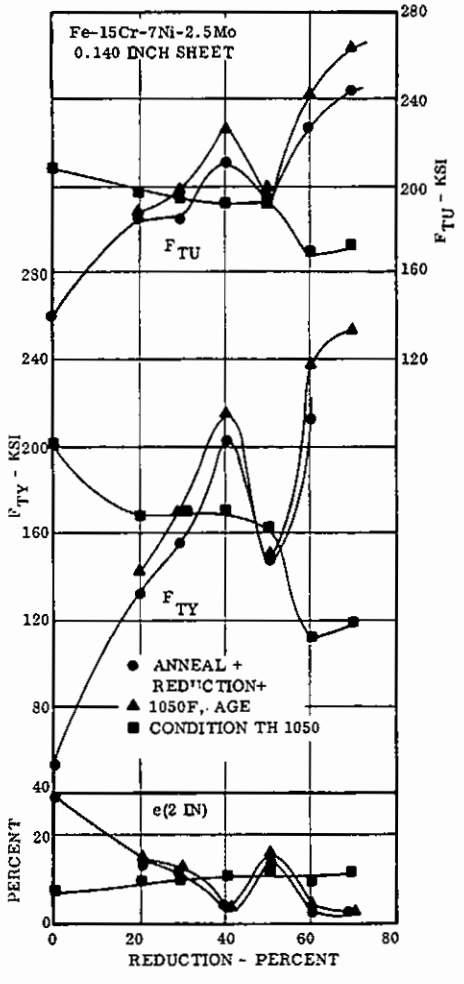


FIG. 3.0219 EFFECT OF REDUCTION BY SHEAR FORMING ON TENSILE PROPERTIES OF SHEET. (19, p. 188-192)

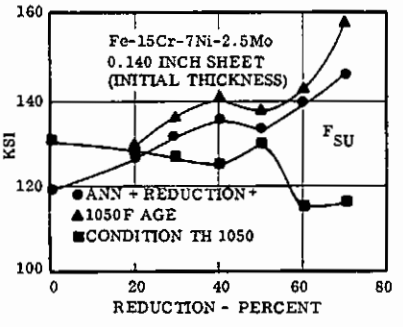


FIG. 3.0251 EFFECT OF REDUCTION BY SHEAR FORMING ON SHEAR STRENGTH OF SHEET. (19, p. 274-277)

	Fe
15	Cr
7	Ni
2.5	Mo

PH15-7Mo

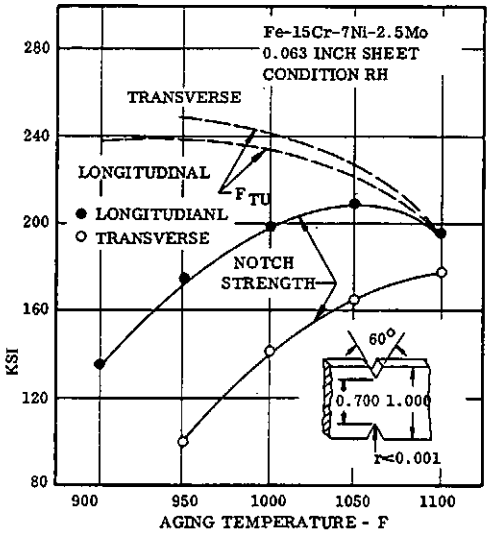


FIG. 3.02711 EFFECT OF AGING TEMPERATURE ON SHARP NOTCH STRENGTH OF SHEET IN VARIOUS RH CONDITIONS. (20, p. 854)

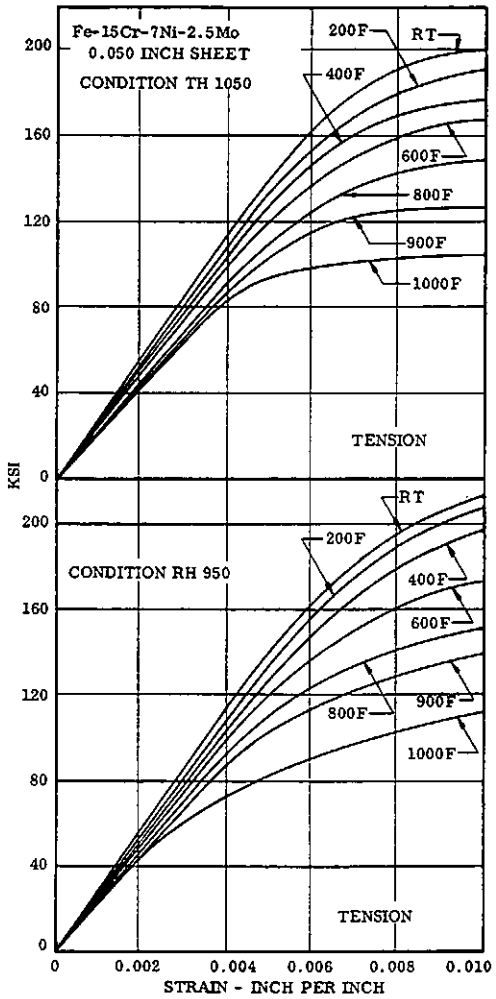


FIG. 3.03111 STRESS-STRAIN CURVES FOR SHEET IN CONDITIONS TH 1050 AND RH 950 AT ELEVATED TEMPERATURES. (12)

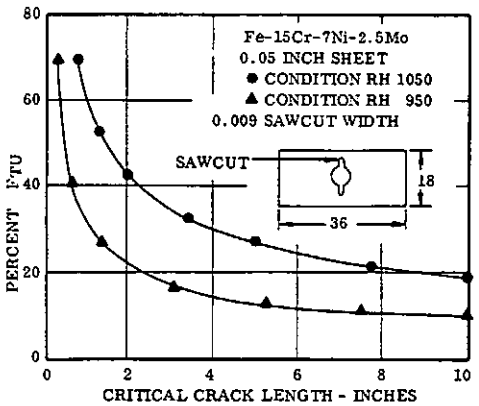


FIG. 3.02712 EFFECT OF CRACK LENGTH ON PERCENT OF TENSILE STRENGTH OF SHEET. (21, p. 325)

	Fe
15	Cr
7	Ni
2.5	Mo

PH15-7Mo

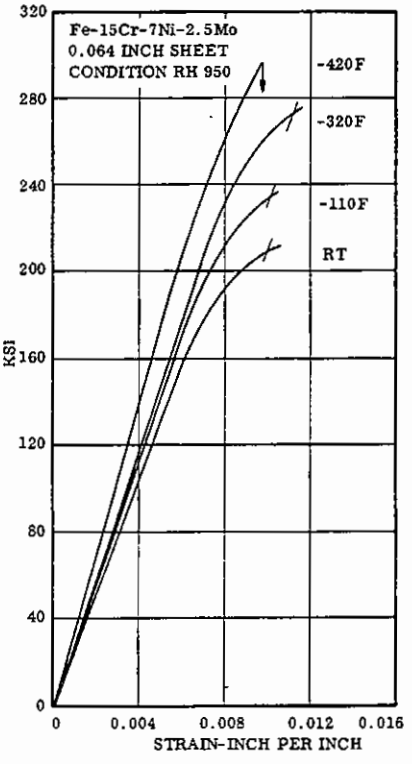


FIG. 3.03112 STRESS-STRAIN CURVES AT ROOM AND LOW TEMPERATURES FOR SHEET IN CONDITION RH 950.
(24, p. 40)

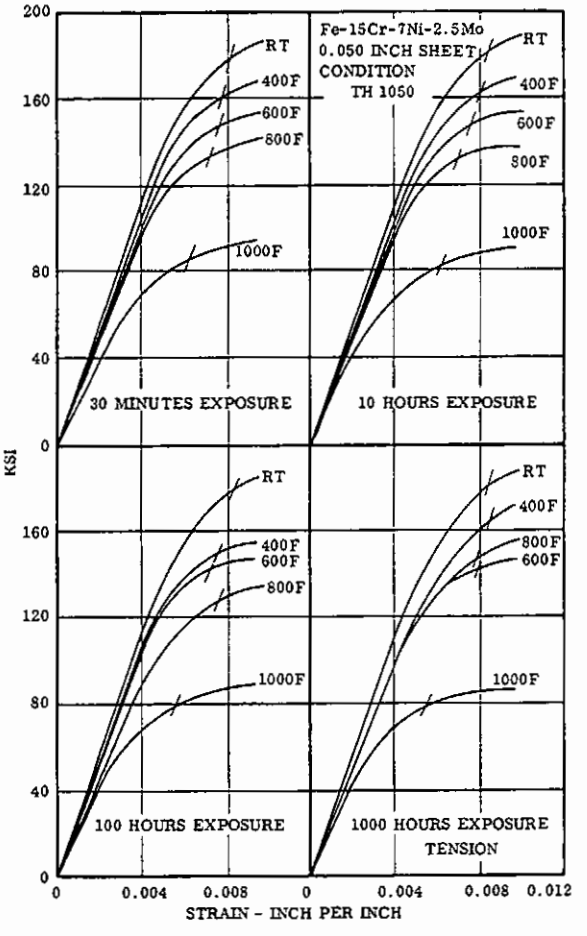


FIG. 3.03113 STRESS-STRAIN CURVES IN TENSION FOR SHEET IN CONDITION TH 1050 AT ELEVATED TEMPERATURES AND FOR VARIOUS EXPOSURE TIMES.
(25, p. 194-197)

	Fe
15	Cr
7	Ni
2.5	Mo

PH15-7Mo

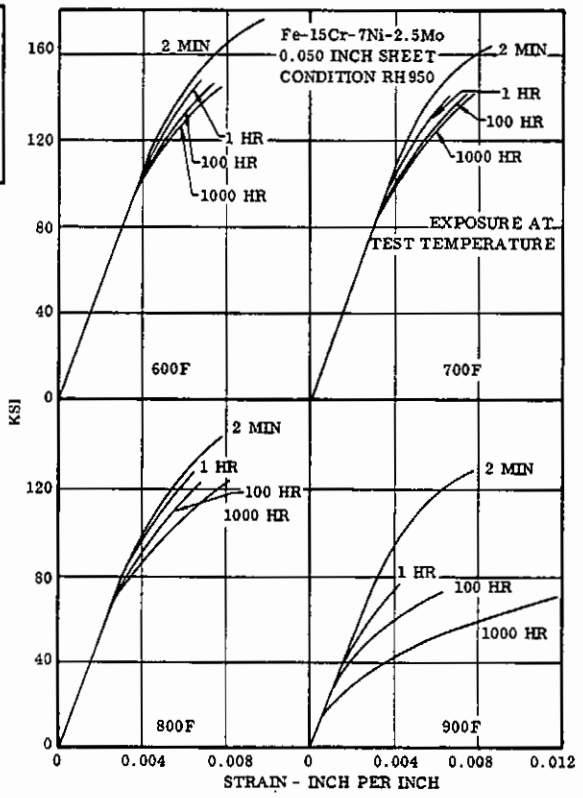


FIG. 3.03114 STRESS-STRAIN CURVES IN TENSION FOR SHEET IN CONDITION RH 950 FOR VARIOUS EXPOSURE TIMES AT ELEVATED TEMPERATURES. (9, p. 37)

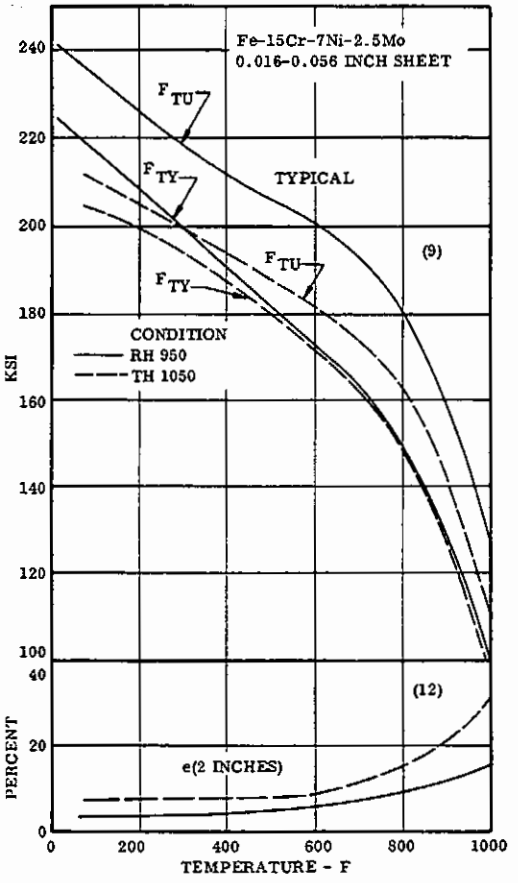


FIG. 3.03121 EFFECT OF TEST TEMPERATURE ON TENSILE PROPERTIES OF SHEET IN CONDITIONS TH 1050 AND RH 950. (9, p. 17, 12)

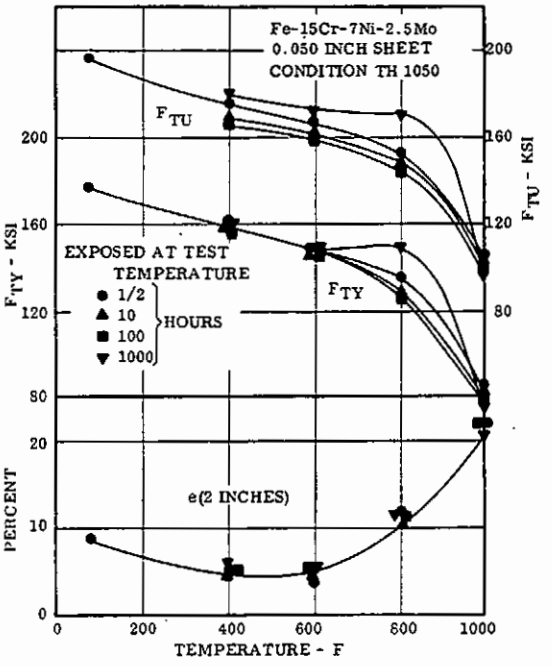


FIG. 3.03122 EFFECT OF EXPOSURE AND TEST TEMPERATURE ON TENSILE PROPERTIES OF SHEET IN CONDITION TH 1050. (25, p. 41-44)

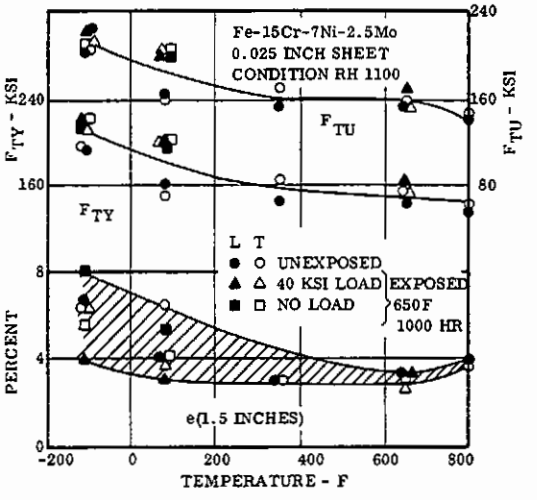


FIG. 3.03133 EFFECT OF TEST TEMPERATURE ON TENSILE PROPERTIES OF EXPOSED AND UNEXPOSED SHEET IN CONDITION RH 1100. (20)

	Fe
15	Cr
7	Ni
2.5	Mo

PH15-7Mo

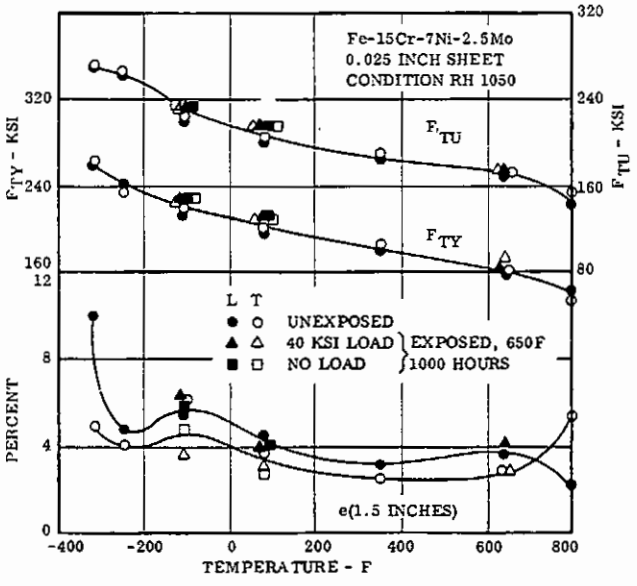


FIG. 3.03132 EFFECT OF TEST TEMPERATURE ON TENSILE PROPERTIES OF EXPOSED AND UNEXPOSED SHEET IN CONDITION RH 1050. (20)

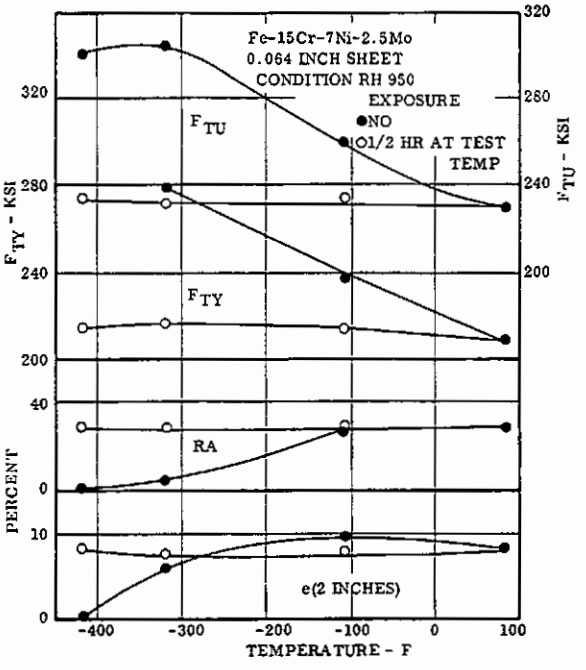


FIG. 3.03134 EFFECT OF LOW TEST TEMPERATURE ON TENSILE PROPERTIES OF SHEET IN CONDITION RH 950. (24, p. 22)

	Fe
15	Cr
7	Ni
2.5	Mo

PH15-7Mo

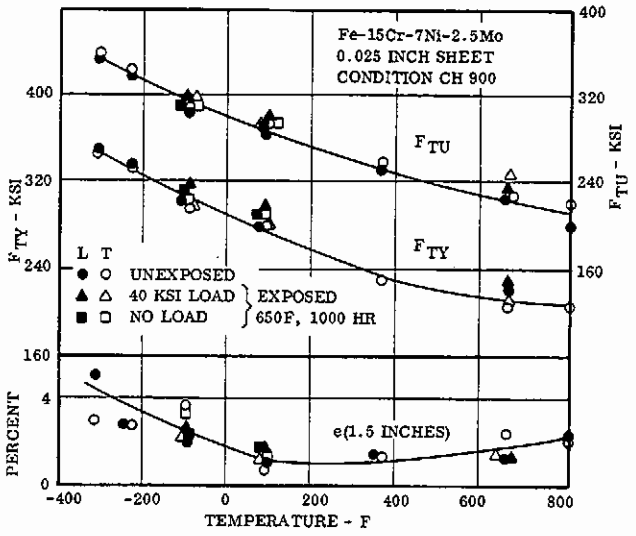


FIG. 3.03141 EFFECT OF TEST TEMPERATURE ON TENSILE PROPERTIES OF EXPOSED AND UNEXPOSED SHEET IN CONDITION CH 900. (20)

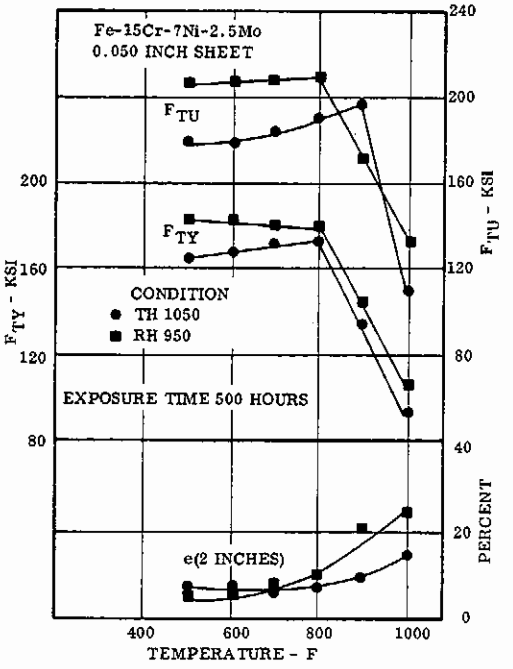


FIG. 3.03151 EFFECT OF EXPOSURE TEMPERATURE ON TENSILE PROPERTIES OF SHEET IN CONDITIONS TH 1050 AND RH 950. (9, p. 55)

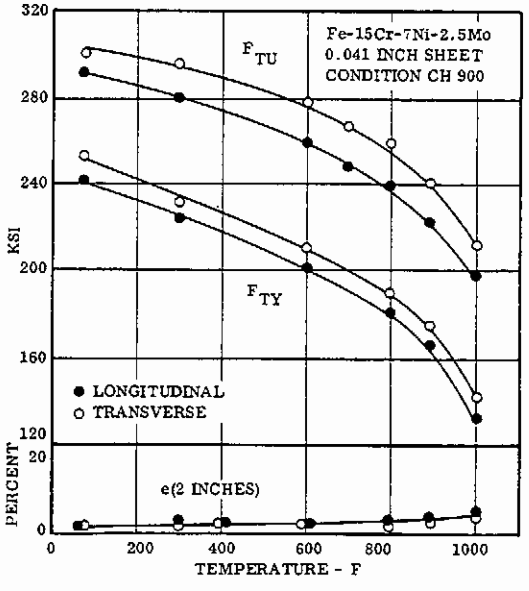


FIG. 3.03142 EFFECT OF TEST TEMPERATURE ON TENSILE PROPERTIES OF SHEET IN CONDITION CH 900. (26, p. 4)

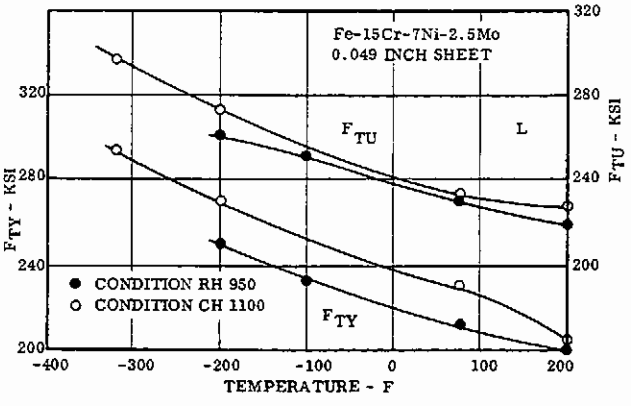
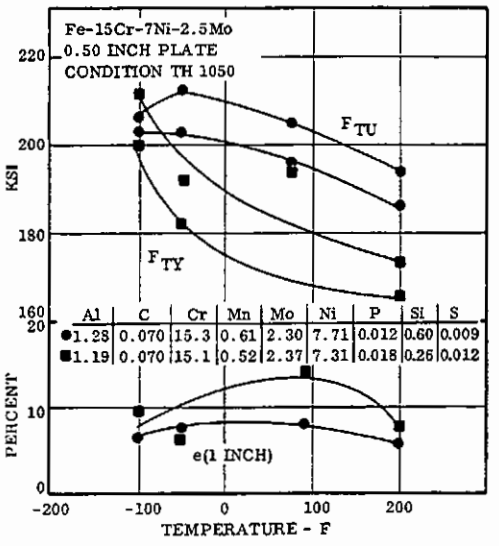
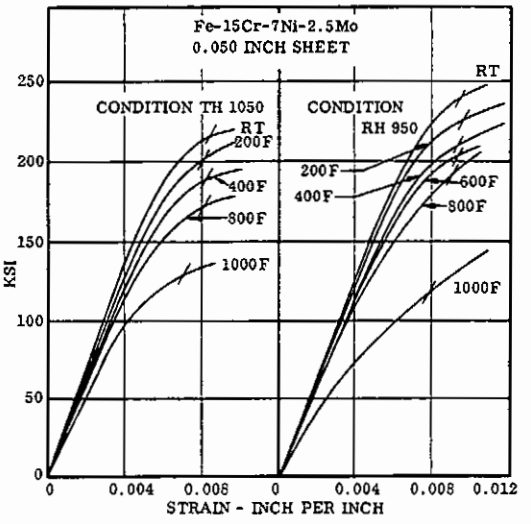


FIG. 3.03152 EFFECT OF LOW TEST TEMPERATURE ON TENSILE PROPERTIES OF SHEET IN CONDITION RH 950 AND CH 1100. (27, p. 57)



	Al	C	Cr	Mn	Mo	Ni	P	Si	S
●	1.28	0.070	15.3	0.61	2.30	7.71	0.012	0.60	0.009
■	1.19	0.070	15.1	0.52	2.37	7.31	0.018	0.26	0.012

FIG. 3.03153 EFFECT OF TEST TEMPERATURE ON TENSILE PROPERTIES OF PLATE IN CONDITION TH 1050. (23, p. 73)



	Fe
15	Cr
7	Ni
2.5	Mo

PH15-7Mo

FIG. 3.0321 STRESS-STRAIN CURVES IN COMPRESSION AT ELEVATED TEMPERATURES FOR SHEET IN CONDITIONS TH 1050 AND RH 950. (9, p. 29)

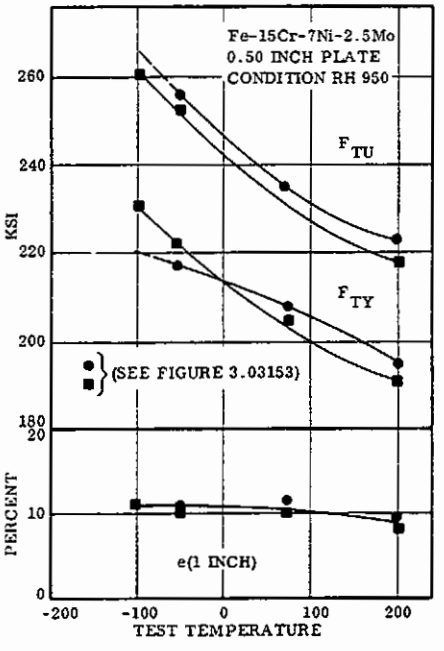


FIG. 3.03154 EFFECT OF TEST TEMPERATURE ON TENSILE PROPERTIES OF PLATE IN CONDITION RH 950. (23, p. 75)

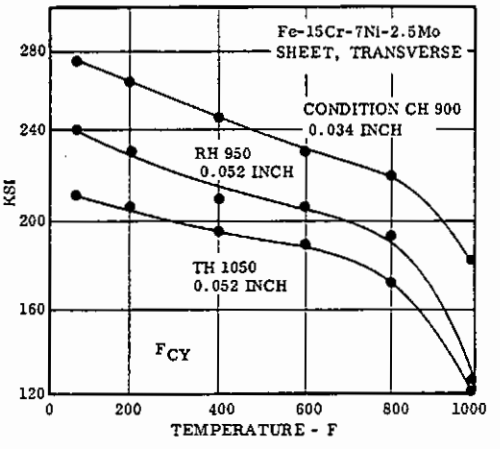


FIG. 3.0322 EFFECT OF TEST TEMPERATURE ON COMPRESSIVE YIELD STRENGTH OF SHEET IN CONDITIONS TH 1050, RH 950, AND CH 900. (12)

	Fe
15	Cr
7	Ni
2.5	Mo

PH15-7Mo

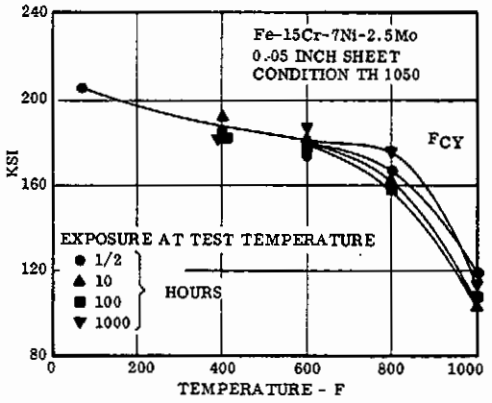


FIG. 3.0323 EFFECT OF EXPOSURE TIME AND TEST TEMPERATURE ON COMPRESSIVE YIELD STRESS OF SHEET IN CONDITION TH 1050. (25, p. 51-53)

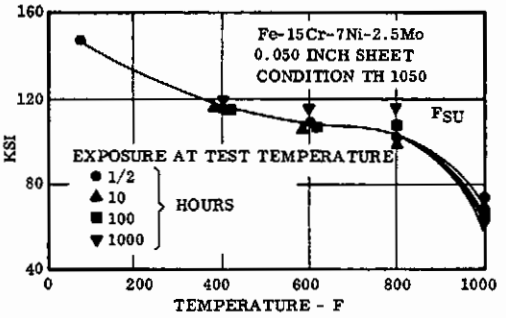


FIG. 3.0352 EFFECT OF EXPOSURE TIME AND TEST TEMPERATURE ON SHEAR STRENGTH OF SHEET IN CONDITION TH 1050. (25, p. 60-62)

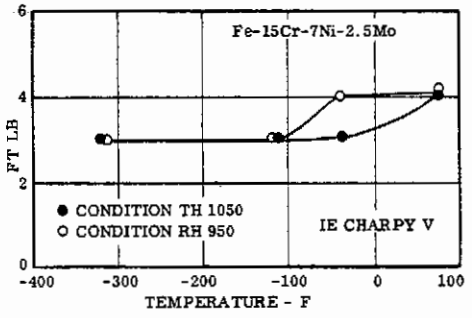


FIG. 3.0331 EFFECT OF LOW TEST TEMPERATURE ON IMPACT STRENGTH OF ALLOY IN CONDITION TH 1050 AND RH 950. (14, p. F-1-3, F-2-4)

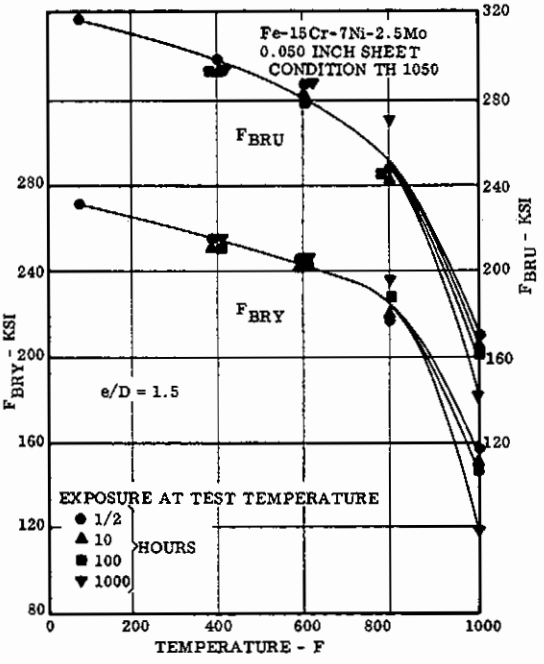


FIG. 3.0361 EFFECT OF EXPOSURE TIME AND TEST TEMPERATURE ON BEARING PROPERTIES OF SHEET IN CONDITION TH 1050. (25, p. 54-56)

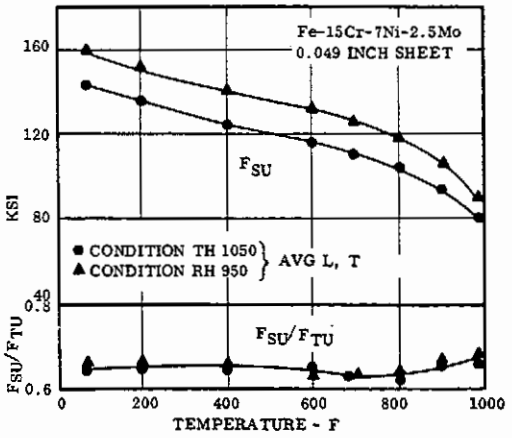


FIG. 3.0351 EFFECT OF TEST TEMPERATURE ON SHEAR STRENGTH OF SHEET IN CONDITIONS TH 1050 AND RH 950. (12, 2A-9-1)

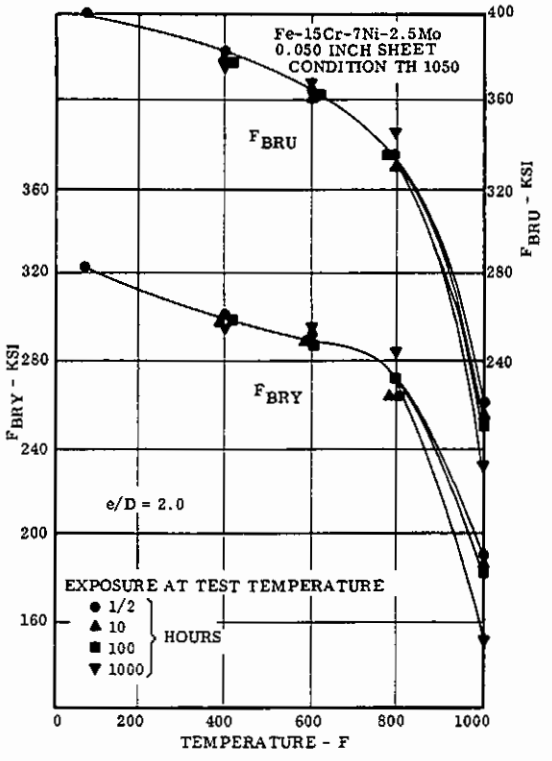


FIG. 3.0362 EFFECT OF EXPOSURE AND TEST TEMPERATURE ON BEARING PROPERTIES OF SHEET IN CONDITION TH 1050.
(25, p. 57-59)

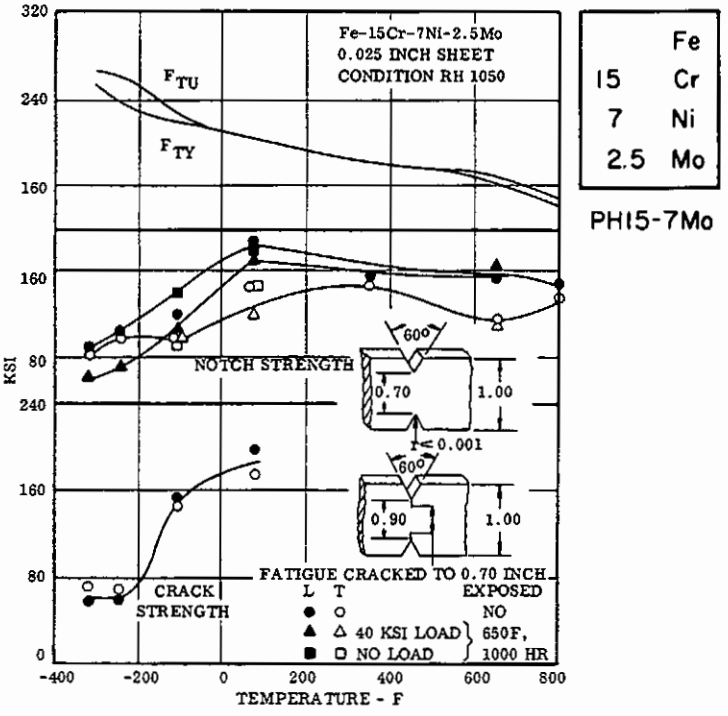


FIG. 3.03712 EFFECT OF TEST TEMPERATURE ON NOTCH AND CRACK STRENGTH OF SHEET IN CONDITION RH 1050.
(20)

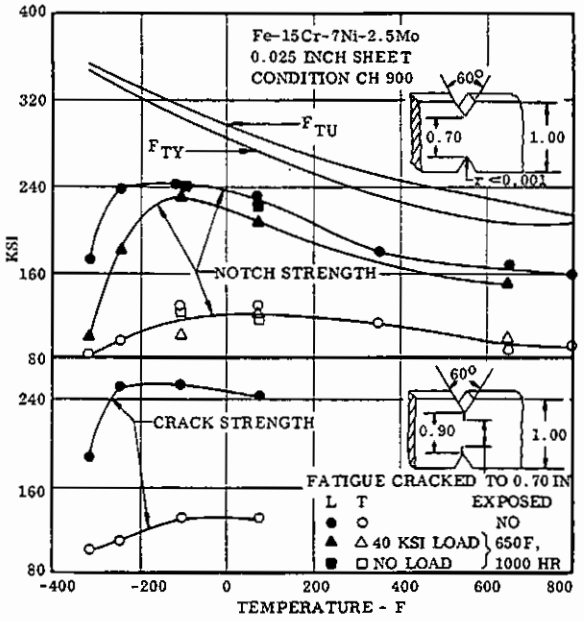


FIG. 3.03711 EFFECT OF TEST TEMPERATURE ON NOTCH AND CRACK STRENGTH OF SHEET IN CONDITION CH 900
(20)

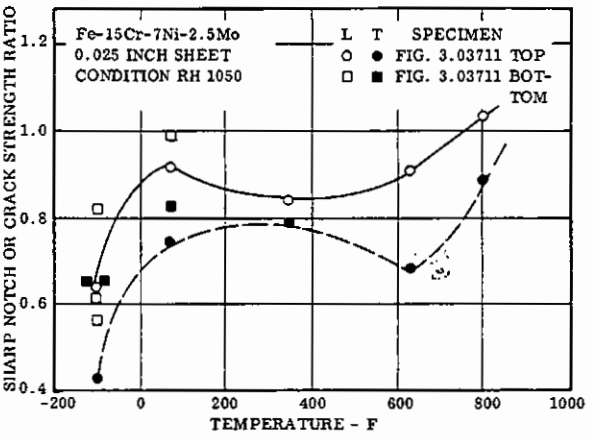


FIG. 3.03713 EFFECT OF TEST TEMPERATURE ON THE SHARP NOTCH TENSILE STRENGTH RATIO AND CRACK STRENGTH RATIO FOR SHEET IN CONDITION RH 1050.
(28, p. 867)

	Fe
15	Cr
7	Ni
2.5	Mo

PH15-7Mo

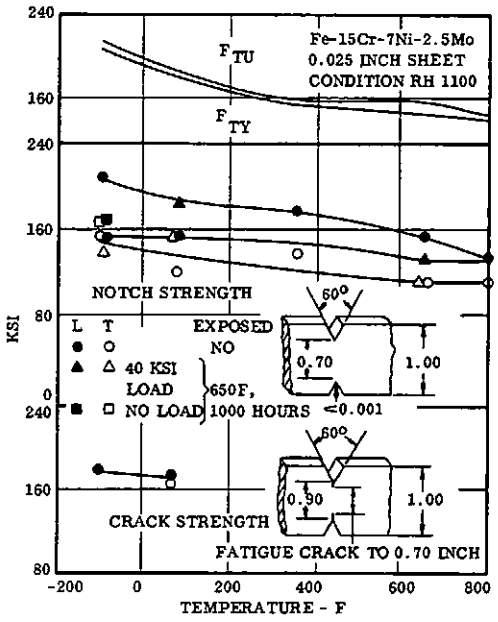


FIG. 3.03714 EFFECT OF TEST TEMPERATURE ON NOTCH AND CRACK STRENGTH OF SHEET IN CONDITION RH 1100. (20)

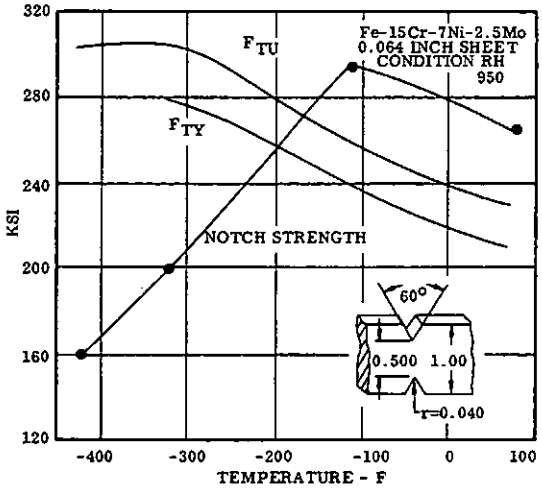


FIG. 3.03716 EFFECT OF LOW TEST TEMPERATURE ON NOTCH STRENGTH OF SHEET IN CONDITION RH 950. (24, p. 23)

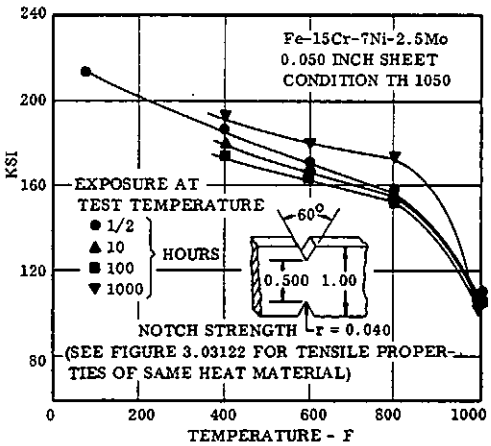


FIG. 3.03715 EFFECT OF EXPOSURE AND TEST TEMPERATURE ON NOTCH STRENGTH OF SHEET IN CONDITION TH 1050. (25, p. 45-47)

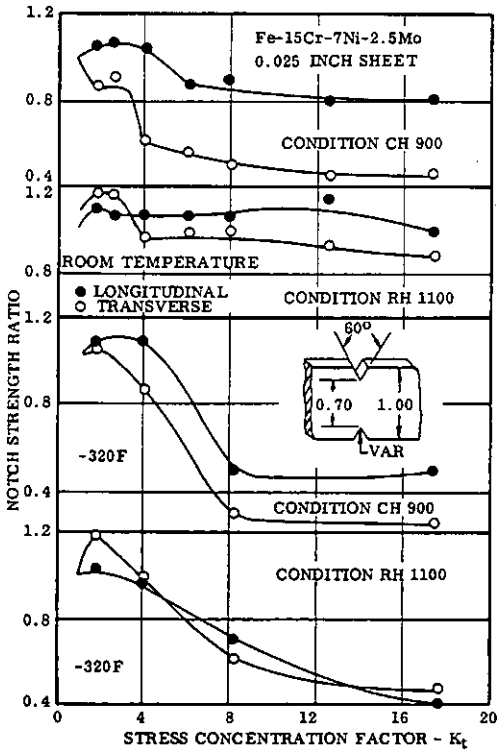


FIG. 3.03717 EFFECT OF STRESS CONCENTRATION FACTOR ON NOTCH STRENGTH RATIO AT ROOM TEMPERATURE AND -320F FOR SHEET IN CONDITIONS CH 900 AND RH 1100. (20, p. 34, 35)

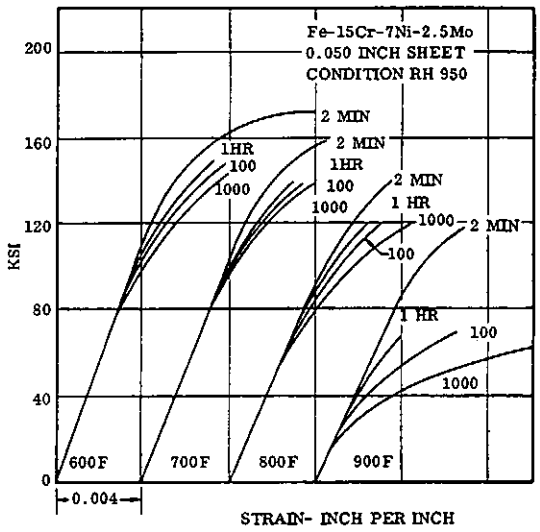


FIG. 3.043 ISOCHRONOUS STRESS-STRAIN CURVES FOR SHEET IN CONDITION RH 950 AT 600 TO 900F. (9, p. 37)

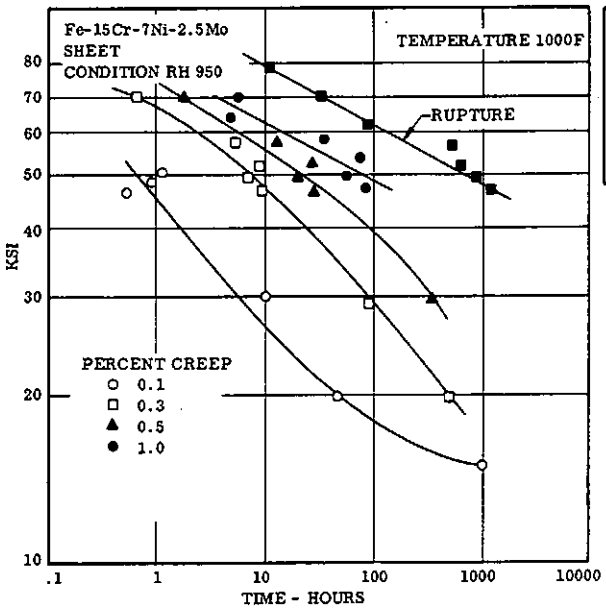


FIG. 3.045 CREEP RUPTURE CURVES FOR ALLOY AT 1000 F IN CONDITION RH 950. (8, p. 663)

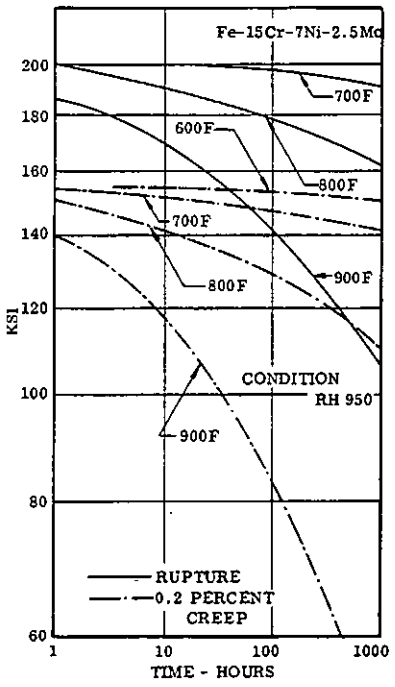


FIG. 3.044 CREEP AND CREEP RUPTURE CURVES FOR ALLOY IN CONDITION RH 950. (29, p. 345)

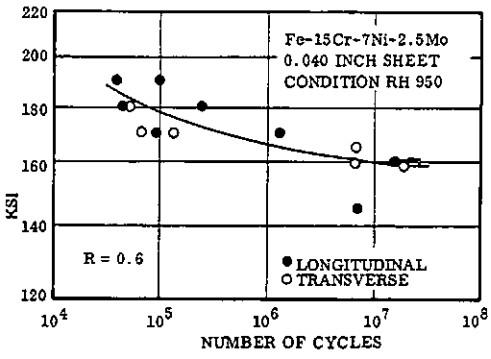


FIG. 3.051 S-N CURVE FOR SHEET IN CONDITION RH 950. (14, p. F-2-4)

	Fe
15	Cr
7	Ni
2.5	Mo

PH15-7Mo

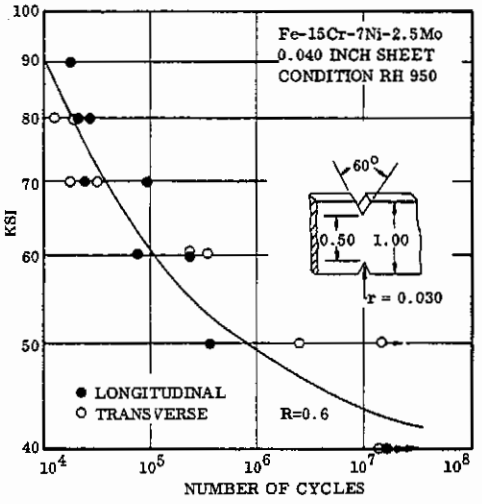


FIG. 3.052 S-N CURVE FOR NOTCHED SHEET IN CONDITION RH 950. (30, p. 12)

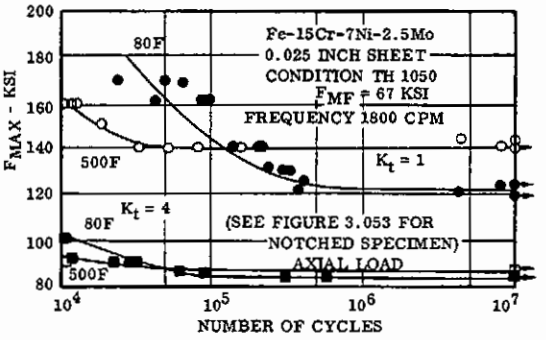


FIG. 3.055 S-N CURVES FOR NOTCHED AND SMOOTH SHEET AS A FUNCTION OF TEMPERATURE IN CONDITION TH 1050. (31, p. 21-23)

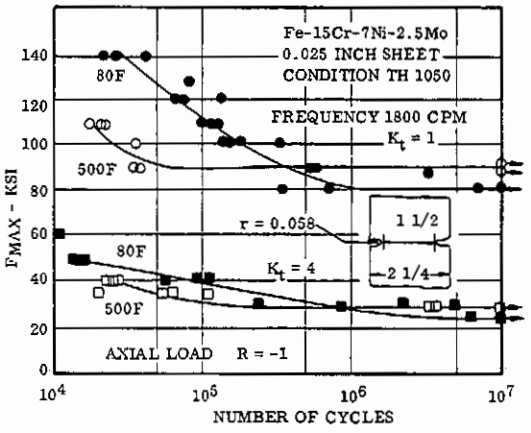


FIG. 3.053 S-N CURVES FOR NOTCHED AND SMOOTH SHEET AS A FUNCTION OF TEMPERATURE IN CONDITION TH 1050. (31, p. 21-23)

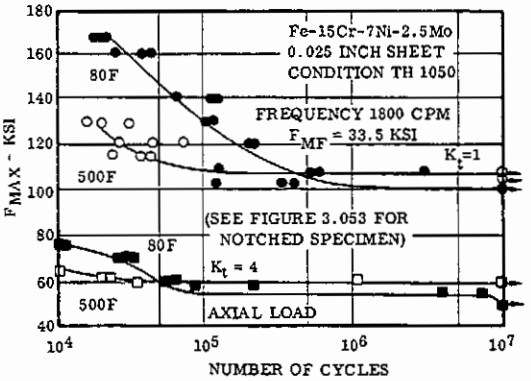


FIG. 3.054 S-N CURVES FOR NOTCHED AND SMOOTH SHEET AS A FUNCTION OF TEMPERATURE IN CONDITION TH 1050. (31, p. 21-23)

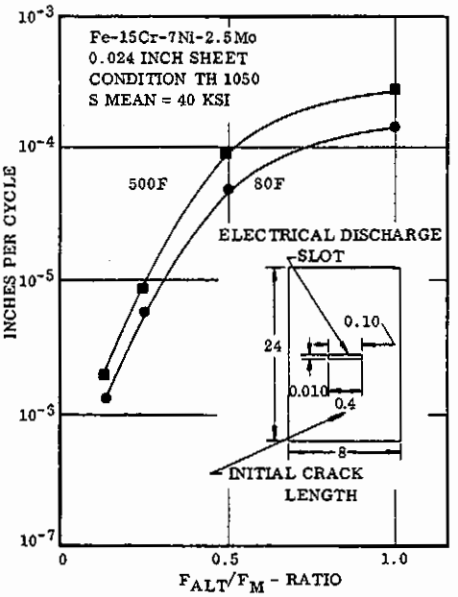


FIG. 3.056 FATIGUE-CRACK PROPAGATION RATE FOR TWO TEST TEMPERATURES FOR SHEET IN CONDITION TH 1050. (32, p. 18, 19)

	Fe
15	Cr
7	Ni
2.5	Mo

PH15-7Mo

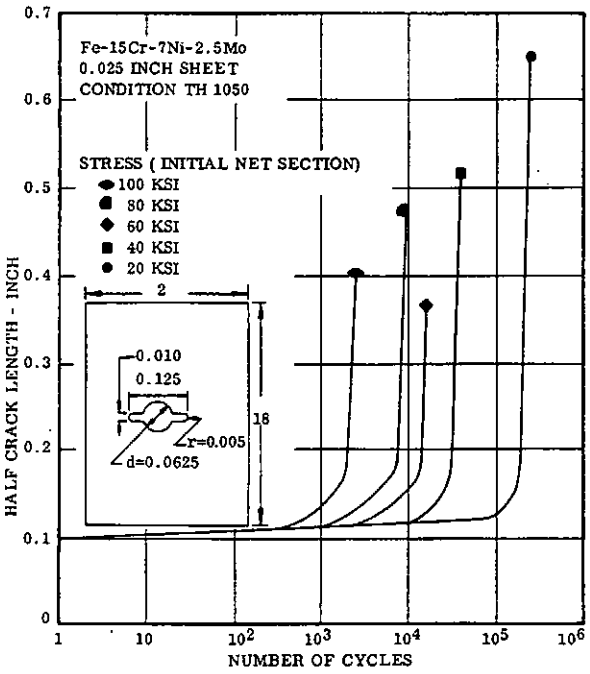


FIG. 3.057 FATIGUE-CRACK PROPAGATION CURVES AS A FUNCTION OF INITIAL NET SECTION STRESS FOR SHEET IN CONDITION TH 1050. (33, p. 21)

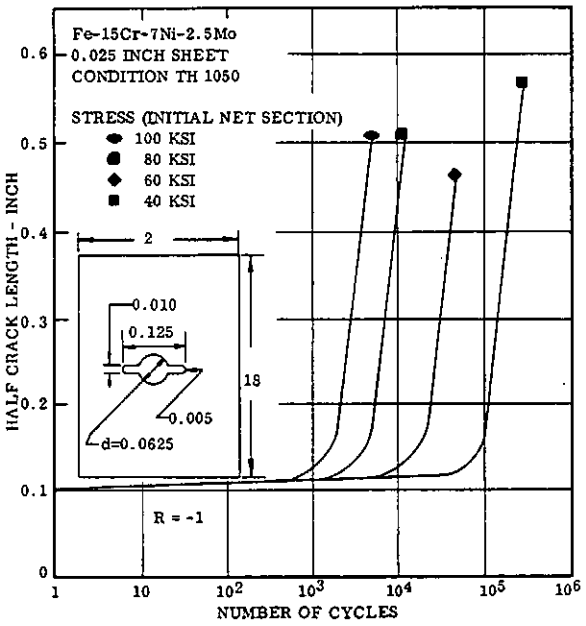


FIG. 3.058 FATIGUE-CRACK PROPAGATION CURVES AS A FUNCTION OF INITIAL NET SECTION STRESS FOR SHEET IN CONDITION TH 1050. (33, p. 22)

	Fe
15	Cr
7	Ni
2.5	Mo

PH15-7Mo

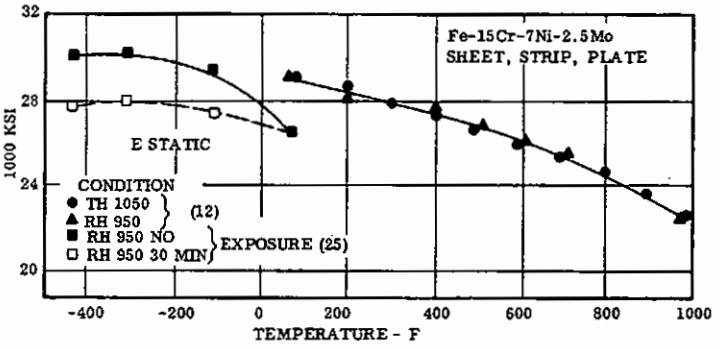


FIG. 3.0621 MODULUS OF ELASTICITY AT ROOM AND ELEVATED TEMPERATURES.
(12, p. 2B-4-1)(25, p. 22)

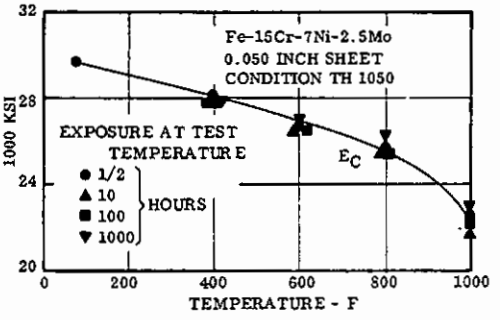


FIG. 3.0623 EFFECT OF EXPOSURE AND TEST TEMPERATURE ON MODULUS OF ELASTICITY IN COMPRESSION OF SHEET IN CONDITION TH 1050. (25, p. 51-53)

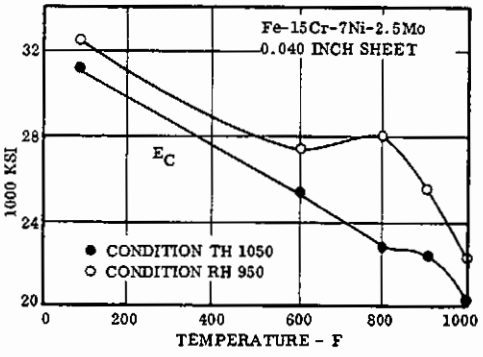


FIG. 3.0622 MODULUS OF ELASTICITY IN COMPRESSION AT ROOM AND ELEVATED TEMPERATURES.
(34, p. 31, 46, 47)

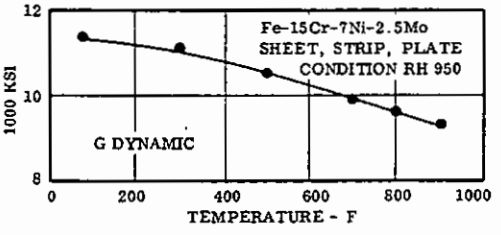


FIG. 3.0631 MODULUS OF RIGIDITY AT ROOM AND ELEVATED TEMPERATURES.
(12, p. 2A-4-1)

	Fe
15	Cr
7	Ni
2.5	Mo

PH15-7Mo

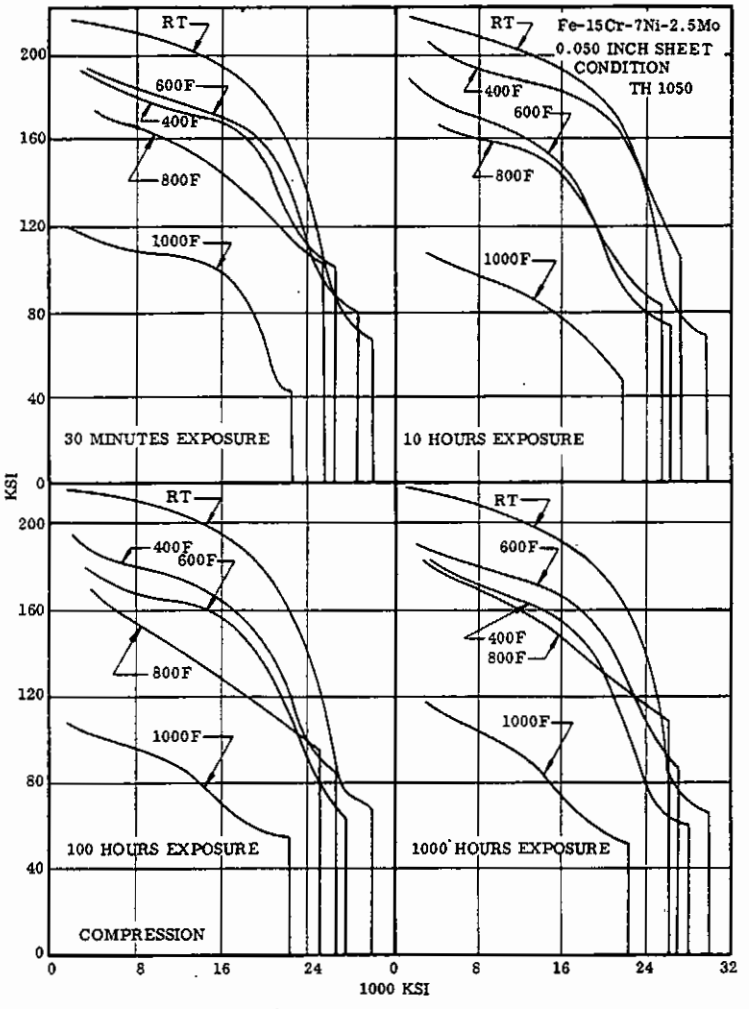


FIG. 3.0641 TANGENT MODULUS CURVES IN COMPRESSION FOR SHEET IN CONDITION TH 1050 AT ELEVATED TEMPERATURES AND FOR VARIOUS EXPOSURE TIMES. (25, p. 202-205)

	Fe
15	Cr
7	Ni
2.5	Mo

PH15-7Mo

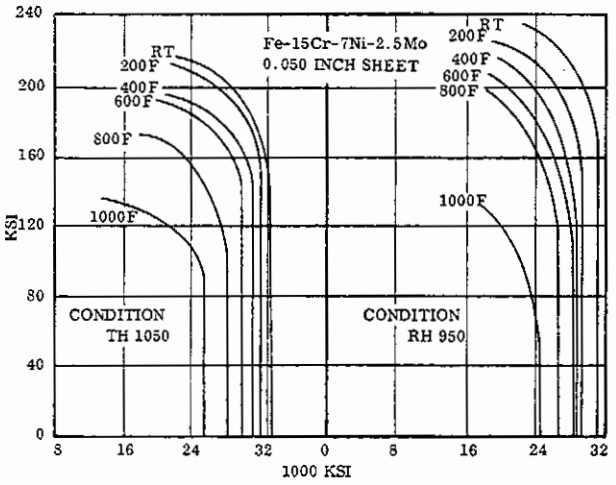


FIG. 3.0642 SECANT MODULUS CURVES IN COMPRESSION AT ELEVATED TEMPERATURES FOR SHEET IN CONDITIONS TH 1050 AND RH 950. (9, p. 30)

REFERENCES

1. AMS 5520 A (Nov. 1, 1958).
2. AMS 5657 (June 30, 1960).
3. AMS 5812 B (Jan. 15, 1963).
4. AMS 5813 A (Jan. 15, 1963).
5. ASTM A461 (Aug. 31, 1965).
6. ASTM A564 (Sept. 7, 1966).
7. MIL-S-8955(ASG) (Oct. 25, 1965).
8. "Compilation of Tensile and Creep Rupture Data of Several Al, Mg, Ti, and Steel Alloys, and Ni Superalloys," AFML-TR-67-259 (April 1968).
9. Armco Steel Corporation, Armco 17-7PH and PH 15-7Mo (July 1968).
10. Espey, G.B., Jones, M. H., and Brown, Jr., W. F., "The Sharp Edge Notch Tensile Strength of Several High Strength Steel Sheet Alloys," American Society of Test Materials, Proceedings Volume 59 (1959).
11. AISI, "High Temperature High Strength Alloys" (Feb. 1963).
12. Armco Steel Corporation, "Armco Precipitation Hardening Stainless Steels Technical Manual" (March 1, 1958).
13. Private communication with R. I. Psyck, Metallurgist, Armco Steel Corporation, Baltimore, Maryland.
14. Ludgigson, D. C.,"Semiaustenitic Precipitation-Hardenable Stainless Steels," DMIC Report 164 (Dec. 6, 1961).
15. Braski, D. N.,."The Susceptibility of Six Stainless Steels to Stress Corrosion at Ambient and Elevated Temperatures," NASA TN D-2499 (Dec. 1964).
16. Favor, R. J., Deel, O. C., and Achbach, W. P., "Design Information on PH 15-7Mo Stainless Steel for Aircraft and Missiles," DMIC Report 135 (Aug. 22, 1960).
17. "Fracture Micromechanics in High-Strength Steels and Titanium," ML-TDR-64-182 (July 1964).
18. Chance Vought Corporation, "Mechanical Properties of Some Engineering Materials-Unpublished Data from Company Sponsored Programs" (March 15, 1962).
19. Jacobs, F., "Mechanical Properties of Materials by Shear Forming," ASD TDR-62-830 (Feb. 1963).
20. Roy, A., Chave, C., and Weiss, V., "Materials Evaluation for a Mach III Transport Plane," Quart. Rep. No. 4A, Syracuse University (April 1963).
21. Spalding, L. P., "The Use of Precipitation Hardening Stainless Steels in Supersonic Aircrafts," Materials Science and Technology for Advanced Science, Prentice Hall, Inc. (1962).
22. "Recommended Practice for Plain-Strain Fracture Toughness Testing of High Strength Metallic Materials Using a Fatigue Cracked Bend Specimen," ASTM Book of Standards. Part 31 (1968).
23. Steigerwald, E. A., "Plane Strain Fracture Toughness for Handbook Presentation," AFML-TR-67-187 (July 1967).
24. Rice, L. P., Campbell, J. E. and Simmons, W. F., "The Evaluation of the Effects of Very Low Temperatures on the Properties of Aircraft and Missile Metals," WADD TR 60-254 (Feb. 1960).
25. Lemcoe, M. M., Trevino, Jr., A., "Determination of the Effect of Elevated Temperature Materials Properties of Several High Temperature Alloys," ASD TDR-61-529 (June 1962).
26. Armco (Feb. 1959).
27. Banerjee, B. R. and Hauser, J. J., "Research and Application Engineering to Determine the Effect of Processing Variables on Crack Propagation of High-Strength Steels and Titanium," ASD-TDR-62-1034, Part 1 (April 1963).
28. Epsey, G. B., Bubsey, R. T., and Brown, Jr., W. F., "A Preliminary Report on the NASA Sheet Alloy Screening Program for Mach III Transport Skins," American Society of Test Materials, Proceedings Volume 62 (1962).
29. Denke, P. H., "Materials for the Supersonic Transport," Materials Science & Technology of Advanced Application,Prentice Hall, Inc. (1962).
30. Titanium Metals Corporation of America, "Fatigue Properties of High Strength Titanium and Stainless Steel Sheet Alloys," TMCA (Jan. 1960).
31. Illg. W., and Castle, C. B., "Axial-Load Fatigue Properties of PH 15-7Mo Stainless Steel in Condition TH 1050 at Ambient Temperature and 500F," Langley Research Center, NASA TN D-2358 (July 1964).
32. Hudson, C. M., "Fatigue-Crack Propagation in Several Titanium and Stainless-Steel Alloys and One Superalloy," Langley Research Center, NASA TN D-2331 (Oct. 1964).
33. Hudson, C. M., "Fatigue-Crack Propagation and Residual Static Strength of PH 15-7Mo (TH 1050) Stainless Steel," Langley Research Center, NASA TN D-3151 (Dec. 1965).
34. Northrop Corporation, "General Materials Information-Phase I Progress Report No. 2" (Sept. 30, 1961).

Fe
18 Cr
8 Ni

Type 301
Type 302

1.061 Substantial hardening can be produced in metastable austenitic steels such as Types 301 and 302 by deformation below the M_d temperature (highest temperature for deformation-induced martensitic transformation) to produce alpha-prime martensite. Type 301 is less stable than Type 302 and produces more martensite and greater hardening, as shown in Figures 1.062 and 1.063. Essentially no martensite is produced in either steel on deformation at 330 F, but martensite is produced in both steels by deformation at or below room temperature. Cooling to liquid-nitrogen temperature (-320 F) without deformation produces about 12 percent alpha-prime martensite in Type 301 and 4 percent in Type 302. For a given degree of deformation applied at various temperatures, the hardness is linearly related to the content of strain-induced alpha-prime martensite, as shown in Figure 1.064. Short-time (2 minute) annealing at elevated temperatures causes reductions in both amount of martensite and hardness, as shown in Figures 1.065 and 1.066. It is concluded from these data that the A_{c1} temperature for both steels is in the range 1020 to 1110 F. The A_{c3} temperature for Type 301 is 1380 to 1470 F and for Type 302 is 1290 to 1380 F (55).

1.062 Hardness and martensite contents of Type 301 after rolling to various reductions at 330 F to -320 F, Figure 1.062.

1.063 Hardness and martensite contents of Type 302 after rolling to various reductions at 330 F to -320 F, Figure 1.063.

1.064 Effect of strain-induced martensite content on hardness, Figure 1.064.

1.065 Hardness and martensite contents of Type 301 after cold rolling followed by heat treatment at 1020 to 1560 F, Figure 1.065.

1.066 Hardness and martensite contents of Type 302 after rolling followed by heat treatment at 1020 to 1560 F, Figure 1.066.

1.067 Effect of extrusion temperature on hardness, Figure 1.067.

1.068 AISI typical values for hardness, Table 1.068.

1.069 Effect of low test temperature on hardness of extra-hard cold-rolled sheet, Figure 1.069.

1.0610 Effect of aging temperature on hardness of 67 percent cold-rolled sheet, Figure 1.0610.

1.0611 Effect of hydrogen environment at elevated temperature on surface hardness of half-hard sheet, Figure 1.0611.

1.07 **Forms and Conditions Available**

1.071 Alloy is available in the full commercial range of sizes and conditions for various forms as follows:

1.0711 Type 301 sheet with strip, annealed, 1/4 H, 1/2 H, 3/4 H, full H, extra H, and stress-relieved tempers.

1.0712 Type 302 bar, annealed and two standard tempers.

1.0713 Type 302 wire, annealed and three standard tempers.

1.08 **Melting and Casting Practice**

Electric furnace air melt. Induction and consumable-electrode vacuum melts and remelts are also available. Vacuum-arc and electroslag consumable-electrode remelting are used where high cleanliness and low gas content are required (57).

1.09 **Special Considerations**

1.091 Types 301 and 302 become subject to severe intergranular corrosion after heating in the temperature range 800 to 1500 F. This sensitization, which also occurs after welding, is attributed to precipitation of chromium carbide at the grain boundaries which causes depletion of chromium from the matrix in the intergranular regions. Corrosion resistance can be restored by annealing to re-solution the chromium carbides. See 2.032.

1.092 Improved strength properties can be obtained by cold working at cryogenic temperatures rather than at room temperature. (See Section 3.0217.)

1.093 Increased tensile ductility and drawing properties can be achieved in Type 301 by deforming at 130 to 140 F, just below the M_d temperature. The improved ductility is related to the strain-induced martensitic transformation, which increases work hardening and resistance to necking. (See Section 3.03154.)

1.094 Although these steels are generally considered to have good resistance to hydrogen embrittlement, the notch strength of Type 301 is decreased considerably in hydrogen as compared to air. Further, high contents of dissolved hydrogen in Type 301, such as obtainable by electrolytic charging, can cause crack growth under constant load. (See Section 2.034.)

1.095 The 300-grade stainless steels, including Types 301 and 302, are subject to salt-water corrosion in crevices or under deposits. Corrosion is reduced or eliminated in turbulent seawater or when cathodic protection is present. (See Section 2.0312.)

2 PHYSICAL AND CHEMICAL PROPERTIES

2.01 **Thermal Properties**

2.011 Melting ranges are 2250 to 2590 F for Type 301 and 2550 to 2590 F for Type 302 (51).

2.012 Phase changes.

2.0121 Time-temperature-transformation diagrams.

2.0122 Transformation temperatures, Table 2.0122.

2.013 Thermal conductivity, Figure 2.013.

2.014 Thermal expansion: (a) Type 301, (b) Type 302, Figure 2.014.

2.015 Specific heat, Figure 2.015.

2.016 Thermal diffusivity, Figure 2.016.

2.02 **Other Physical Properties**

2.021 Density, Figure 2.021.

2.022 Electrical properties.

2.0221 Electrical resistivity, Figure 2.0221.

2.023 Magnetic properties.

2.0231 These alloys are nonmagnetic in the annealed (fully austenitic) condition. However, the alloys become magnetic on cold working due to the deformation-induced transformation from nonmagnetic austenite to magnetic alpha-prime martensite. The extent of magnetization on cold working decreases with increasing nickel content in Series 300 stainless steels, as shown in Figure

Fe
18 Cr
8 Ni

Type 301
Type 302

2.0232. This is a result of nickel stabilization of the austenite phase.

2.0232 Effect of composition and reduction on magnetic permeability and tensile strength of 300 series sheet, Figure 2.0232.

2.024 Emittance, Figure 2.024.

2.025 Damping capacity.

2.03 **Chemical Environments**

2.031 General corrosion.

2.0311 General corrosion resistance of Type 301, like that of all austenitic stainless steels, is very high, but it is at the lower end of the corrosion scale for 18-8 steels; Type 302 is slightly superior to Type 301.

2.0312 The 300 series stainless steels can undergo deep localized crevice corrosion in mechanical crevices or under deposits in quiescent seawater. The differences in performance of the various grades of 300 stainless steels under these conditions are not of practical significance. Cathodic protection can be effectively accomplished with iron, zinc, aluminum, or magnesium anodes or by an impressed electrical current system. Multi-component assemblies containing different alloys frequently offer built-in cathodic protection. Turbulent seawater with sufficient agitation to keep austenitic stainless steels free of deposits, either biological or inorganic, permits stainless steel to remain passive and corrosion-free. Chloride stress-corrosion cracking is not a problem in ambient-temperature seawater (64).

2.0313 Corrosion in tropical environments for times up to 16 years, Table 2.0313.

2.0314 Based on galvanic current data and corrosion rates, Type 301 is considered compatible with graphite-epoxy composite materials in aerated neutral 3.5 percent NaCl solution at room temperature (66).

2.032 Intergranular corrosion.

2.0321 A potentially serious problem against which precautions should be taken is intergranular corrosion of "sensitized" alloy. Sensitization occurs when these steels are heated in the temperature range 800 to 1500 F. The sensitization time depends primarily on temperature but is also influenced by the chemical and metallurgical characteristics of the alloy, such as carbon content and grain size. Sensitization is most generally attributed to depletion of chromium from regions adjacent to the grain boundaries because of precipitation of chromium-rich $(Fe,Cr)_{23}C_6$ carbides. During welding, the heat-affected zone reaches the critical temperature range for a short time, promoting nucleation of chromium-rich carbides at the grain boundaries. If a welded component operates below the temperature range for normal sensitization (for example, 600 to 800 F), the previously nucleated carbides grow, but the low temperature prevents further nucleation and restricts chromium diffusion from the grain interiors. However, after extended time periods, such as 10 years, low-temperature sensitization occurs and increases the probability of intergranular stress-corrosion cracking. If material has been sensitized either by welding or by exposure, it should be fully annealed to re-solution the precipitated chromium-rich carbides. This anneal will restore the original corrosion resistance. Self-healing and restoration of corrosion resistance can also occur on heating for very long times in the sensitization temperature range. Self-healing occurs by diffusion of chromium from the grain interiors into the depleted zones. The time-temperature conditions for sensitization of Type 302 are shown in Figure 2.0322 (67).

2.0322 Effects of heat treatment on susceptibility to intergranular stress-corrosion cracking in polythionic acid and in acid copper sulfate, Figure 2.0322.

2.0323 Effect of prior exposure temperature and time on average corrosion rate in boiling nitric acid of cold-rolled sheet, Figure 2.0323.

2.033 Stress-corrosion cracking.

2.0331 Stress cracking may be pronounced in these steels in the formed condition, if high residual stresses are present. The tendency to stress cracking depends primarily on the value of tensile strength developed. Severely formed parts, particularly in the harder tempers of Type 301, should be immediately annealed or stress relieved to prevent cracking.

The susceptibility of cold-worked material to stress corrosion cracking may be related in part to the presence of deformation-induced martensite. The hcp epsilon martensite phase corrodes more rapidly than the matrix austenite phase (69,70).

2.0332 Stress-corrosion cracking may occur in certain media, primarily in hot chlorides, if residual stresses are present. Under normal atmospheric conditions no stress corrosion is observed, even in extra hard sheet. Stress-corrosion cracking can result, for example, from surface contamination with zinc chloride from solder flux (71,72).

2.0333 Effects of cold reduction on yield stress in air and on threshold corrosion stress in boiling 0.5N NaCl + 0.1N $NaNO_2$ aqueous solution, Figure 2.0333.

2.034 Hydrogen embrittlement.

2.0341 Although austenitic stainless steels are generally considered to have good resistance to hydrogen embrittlement, the notch tensile strength of Type 301 is reduced considerably when tested in hydrogen rather than in air. The detrimental effect is lessened when oxygen is present as an impurity in the hydrogen atmosphere, as shown in Figure 2.0342. Oxygen reacts with surface adsorption sites and, if in sufficient quantity, will completely inhibit the adsorption of hydrogen and thus prevent embrittlement (74).

2.0342 Effects of oxygen impurity in hydrogen on notch strength of Type 301, Figure 2.0342.

2.0343 Sustained-load crack growth is observed in material charged to 13 wt ppm hydrogen or more, as shown in Figure 2.0344. The crack-growth rate at a given stress intensity factor increases strongly with increasing hydrogen content. The fracture surface of material which has failed by slow crack growth exhibits brittle transgranular cleavage. Material containing less than 3 wt ppm hydrogen exhibits ductile fracture upon reaching a critical load and

Fe
18 Cr
8 Ni

Type 301
Type 302

does not exhibit slow crack growth. Although the levels of dissolved hydrogen which cause sustained-load crack growth are higher than would normally be encountered in service, it is evident that some reduction of ductility in Type 301 can be affected by hydrogen (73).

2.0344 Sustained-load crack-growth rate of hydrogen-charged Type 301, Figure 2.0344.

2.035 Oxidation.

2.0351 Air oxidation of Type 302 is slight at 1202 and 1292 F, as shown in Figure 2.0352. There is no subsurface oxide penetration at these temperatures. At 1382 F oxide penetration occurs but the surface oxide is still quite protective. Oxidation begins to increase sharply with temperature above 1472 F and the time dependence on an arithmetic basis approaches linearity at 1562 F, indicating a nonprotective scale. Type 302 is considered suitable for continuous service at temperatures up to 1600 F and for intermittent service up to 1700 F (75).

2.0352 Time dependence of oxidation of Type 302 in air at elevated temperatures, Figure 2.0352.

2.04 **Nuclear Environments**

2.041 Effect of irradiation exposure on tensile properties and hardness of alloy, Table 2.041.

3 **MECHANICAL PROPERTIES**

3.01 **Specified Mechanical Properties**

3.011 AMS-specified mechanical properties, Table 3.011.

3.02 **Mechanical Properties at Room Temperature**

3.021 Tension – stress-strain diagrams – tension properties.

3.0211 Stress-strain curves for sheet and strip cold rolled to different temper, Figure 3.0211.

3.0212 Stress-strain curves for sheet and strip cold rolled to full-hard and extra-hard tempers, Figure 3.0212.

3.0213 Percentage cold reduction and corresponding tensile strength for various tempers of Type 301 and Type 302, Table 3.0213.

3.0214 Effect of rolling reduction and composition on tensile properties of 300 series steels, Figure 3.0214.

3.0215 Effect of cold reduction on tensile properties of Type 301, Figure 3.0215.

3.0216 Effects of cold work on tensile properties of Type 302, Figure 3.0216.

3.0217 Cold working at cryogenic temperatures increases the tensile strength to a greater degree than equivalent working at room temperature. The ductility of material cryogenically rolled to a given strength is higher than that of material rolled at room temperature to the same strength, as shown in Figures 3.0218 and 3.0219. The effects of cold rolling on tensile properties are primarily through the amount of martensite produced. The amount of cold work introduced into the matrix has an additional strengthening effect, as shown in Figures 3.02110 and 3.02111. Heat treating cold-worked material at 550 F further increases the yield strength, as shown in Figures 3.02112 and 3.02113.

3.0218 Effect of cold reduction at room and cryogenic temperatures on tensile properties of Type 301, Figure 3.0218.

3.0219 Effect of cold reduction at room and cryogenic temperatures on tensile properties of Type 302, Figure 3.0219.

3.02110 Relationship between tensile properties and martensite content for Type 301, Figure 3.02110.

3.02111 Relationship between tensile properties and martensite content for Type 302, Figure 3.02111.

3.02112 Effect of cold reduction at room and cryogenic temperatures plus heat treatment on tensile properties of Type 301, Figure 3.02112.

3.02113 Effect of cold reduction at room and cryogenic temperatures plus heat treatment on tensile properties of Type 302, Figure 3.02113.

3.02114 Effect of stress-relief temperature on tensile properties of 60 percent reduced sheet, Figure 3.02114.

3.02115 Effect of cyclic exposure stress on room-temperature tensile properties of 60 percent reduced sheet exposed at 600 and 900 F, Figure 3.02115.

3.02116 Effect of exposure at low temperature on room-temperature tensile properties of extra-hard cold-rolled sheet, Figure 3.02116.

3.02117 Effects of extrusion temperature on longitudinal tensile properties of Type 301, Figure 3.02117.

3.02118 Effects of extrusion temperature on longitudinal tensile properties of Type 302, Figure 3.02118.

3.02119 Effect of stretching on tensile yield strength of Type 302, Figure 3.02119.

3.022 Compression – stress-strain curves – compression properties.

3.0221 Effect of stretching on compressive yield strength of Type 302, Figure 3.0221.

3.023 Impact.

3.0231 Impact properties at room temperature, Table 3.0231.

3.0232 Relation between impact energy and tensile strength for cold-rolled Type 302, Figure 3.0232.

3.0233 Effects of exposure time in air at elevated temperatures on impact energy, Figure 3.0233.

3.024 Bending.

3.025 Torsion and shear.

3.026 Bearing.

3.027 Stress concentration.

3.0271 Notch properties.

3.02711 Effect of cold rolling and test direction on notch strength of sheet, Figure 3.02711.

3.02712 Effect of exposure at low temperature on room-temperature notch strength of extra-hard cold-rolled sheet, Figure 3.02712.

3.02713 Effect of test direction in relation to rolling direction on tensile properties and notch strength of 60 percent cold-reduced sheet, Figure 3.02713.

3.0272 Fracture toughness.

3.028 Combined properties.

3.03 **Mechanical Properties at Various Temperatures**

3.031 Tension – stress-strain curves – tension properties.

3.0311 Stress-strain curves.

3.03111 The stress-strain curves for Types 301 and 302 are influenced by the deformation-induced transformation of austenite to martensite. The work-hardening rate (slope of the stress-strain curve) for Type 302

Fe
18 Cr
8 Ni

Type 301
Type 302

at -112 F is compared to that of the structurally stable Type 310 alloy in Figure 3.03112. Type 302 is metastable at this temperature and exhibits an increase in work-hardening rate between about 4 and 20 percent strain due to the martensitic transformation. The Type 310 alloy shows a continuous decrease in work-hardening rate with increasing strain. Stress-strain curves for annealed Types 301 and 302 at temperatures near and below M_d are shown in Figures 3.03113 and 3.03114, respectively. Both stable (continuously decreasing work-hardening rate) and metastable (decreasing and increasing work-hardening rate) curves are seen, depending on test temperature. Type 301 shows increasing work hardening due to martensite formation at 68 F and lower, while Type 302 exhibits martensitic hardening up to at least 77 F (77,78).

3.03112 Tensile work-hardening rates for Types 302 and 310 at -112 F, Figure 3.03112.

3.03113 Stress-strain curves for annealed Type 301, Figure 3.03113.

3.03114 True stress-strain curves for annealed Type 302 at room and cryogenic temperatures, Figure 3.03114.

3.03115 Stress-strain curves for Type 301 full-hard and full-hard stress-relieved sheet at room and elevated temperatures, Figure 3.03115.

3.03116 Stress-strain curves in tension for various temperatures and exposure times for 60 percent cold-reduced sheet, Figure 3.03116.

3.03117 Stress-strain curves in tension at low temperatures of extra-hard cold-rolled sheet, Figure 3.03117.

3.03118 Stress-strain curves for Type 301 extra-hard and extra-hard stress-relieved sheet at room and elevated temperatures, Figure 3.03118.

3.0312 Rolling effects on tension properties.

3.03121 Effect of cold rolling on tensile properties of Type 301 sheet at room temperature and -320 F, Figure 3.03121.

3.03122 Effect of percent reduction on tensile properties of sheet tested at room temperature and -423 F, Figure 3.03122.

3.03123 Effect of low temperature and percent cold reduction on tensile properties of sheet, Figure 3.03123.

3.03124 Effect of low rolling temperature on tensile properties at room temperature and -320 F of reduced sheet, Figure 3.03124.

3.03125 Effect of low rolling temperature on tensile properties at room temperature and -423 F of 10 percent reduced sheet, Figure 3.03125.

3.03126 Effect of rolling temperature on tensile properties at room temperature and -423 F of 65 percent reduced sheet, Figure 3.03126.

3.03127 Effect of test direction on tensile strength of cold-rolled sheet at room and cryogenic temperatures, Figure 3.03127.

3.0313 Prior exposure and strain-rate effects on tension properties.

3.03131 Tensile ductility of Types 301 and 302 is affected by strain rate, temperature, and phase stability, as well as microstructure. For constant microstructure, Type 302 exhibits a minimum in elongation at room temperature at a strain rate of about 200 min^{-1}. A similar but less pronounced minimum is noted for uniform reduction in area, as shown in Figure 3.03132. The ductility at all strain rates from 0.02 to 19,000 min^{-1} is good, ranging from 40 to 80 percent elongation. Similar behavior is exhibited at liquid-nitrogen temperature, with the ductility values being slightly less than those at room temperature, as shown in Figure 3.03133. Type 301 is less stable than Type 302 with respect to martensite formation during deformation and has slightly less ductility at room temperature, as shown in Figure 3.03134 (80).

3.03132 Effects of strain rate on tensile ductility of Type 302 at room temperature, Figure 3.03132.

3.03133 Effects of strain rate on tensile ductility of Type 302 at -321 F, Figure 3.03133.

3.03134 Effects of strain rate on tensile ductility of Type 301 at room temperature, Figure 3.03134.

3.03135 Effect of test temperature, strain rate, and holding time on tensile properties of Type 301 1/2-hard sheet, Figure 3.03135.

3.03136 Effect of test temperature, strain rate, and holding time on tensile properties of Type 301 3/4-hard sheet, Figure 3.03136.

3.03137 Effect of test temperature, strain rate, and holding time on tensile properties of 45 percent reduced sheet, Figure 3.03137.

3.03138 Effect of test temperature, strain rate, and holding time on tensile properties of 60 percent reduced sheet, Figure 3.03138.

3.03139 Effect of test temperature and exposure time on tensile properties of 60 percent cold-reduced sheet, Figure 3.03139.

3.031310 Effect of test temperature and prior exposure on tensile properties of 34 percent cold-reduced sheet, Figure 3.031310.

3.031311 Effect of test temperature and prior exposure on tensile properties of 51 percent cold-reduced sheet, Figure 3.031311.

3.031312 Effect of test temperature and prior exposure on tensile properties of 60 percent cold-reduced sheet, Figure 3.031312.

3.0314 Stress-relief effects on tension properties.

3.03141 Effect of test temperature, test direction, and stress relief on tensile properties of Type 301 full-hard sheet, Figure 3.03141.

3.03142 Effect of test temperature, test direction, and stress relief on tensile properties of Type 301 extra-hard sheet, Figure 3.03142.

3.03143 Effect of stress relief and test temperature on tensile properties of cold-rolled sheet, Figure 3.03143.

3.0315 Elevated-test-temperature effects on tension properties.

3.03151 Effect of test temperature on tensile strength of annealed Type 302 sheet, Figure 3.03151.

3.03152 Effect of test temperature on tensile properties of Type 301 1/2-hard sheet, Figure 3.03152.

3.03153 Effect of test temperature on tensile properties of 60 percent reduced sheet, Figure 3.03153.

3.03154 Type 301 shows a tensile elongation peak at about 130 F, as shown in Figure 3.03155. The maximum elongation is slightly greater for small-grain-size material and slower deformation rate, but the temperature effect remains unchanged. As shown in Figure 3.03156, the temperature for maximum

Fe
18 Cr
8 Ni

Type 301
Type 302

elongation appears to be slightly higher in biaxial straining as compared to uniaxial straining. The elongation peak is related to the strain-induced transformation of austenite to cubic alpha-martensite, which occurs through an intermediate hexagonal epsilon-martensite phase. The volume fraction of epsilon compared to alpha is negligible above about 15 percent strain. The strain-induced martensitic transformation increases the rate of work hardening so that the material is better able to resist necking during straining. The occurrence of a sharp elongation peak at a temperature just below M_d apparently indicates that the distribution of strain-induced martensite is most uniform at this temperature. The temperature dependence of martensite content for Type 301 is shown in Figure 3.03157. The strain dependence of martensite content for Types 301 and 302 is sigmoidal, as shown in Figures 3.03158 and 3.03159. The amount of martensite formed, for example, at 32 F is much greater for Type 301 than for Type 302, reflecting the lower phase stability of Type 301.

3.03155 Effects of grain size, strain rate, and temperature on tensile elongation of Type 301, Figure 3.03155

3.03156 Effects of temperature on failure strain for several types of deformation, Figure 3.03156.

3.03157 Effects of grain size, strain rate, and temperature on martensite content of fractured tensile specimens of Type 301, Figure 3.03157.

3.03158 Effects of grain size, test temperature, and tensile strain on martensite content of Type 301, Figure 3.03158.

3.03159 Effects of test temperature and true tensile strain on martensite content of Type 302, Figure 3.03159.

3.031510 Effects of temperature on tensile properties of cast Type 302, Figure 3.031510.

3.0316 Effects of cryogenic temperatures on tensile properties.

3.03161 Effect of cryogenic temperatures on nominal tensile properties of annealed Type 301 sheet, strip, plate, and bar, Figure 3.03161.

3.03162 Effect of cryogenic temperatures on nominal tensile properties of annealed Type 302 sheet, strip, plate, and bar, Figure 3.03162.

3.03163 Effect of cryogenic temperatures on the tensile properties of annealed bar, Figure 3.03163.

3.03164 Effect of cryogenic temperatures on tensile properties of 40 percent reduced sheet, Figure 3.03164.

3.03165 Effect of cryogenic temperatures on tensile properties of 50 percent reduced sheet, Figure 3.03165.

3.03166 Effect of cryogenic temperatures on tensile properties of 40 and 60 percent reduced sheet, Figure 3.03166.

3.03167 Effect of cryogenic temperatures on tensile properties of 60 percent cold-reduced sheet, Figure 3.03167.

3.03168 Effects of cryogenic temperatures and thickness on tensile properties of 60 percent reduced sheet, Figure 3.03168.

3.03169 Effect of cryogenic temperatures on tensile properties of extra-hard cold-rolled sheet, Figure 3.03169.

3.031610 Effects of cryogenic temperatures and melt method on tensile properties of 70 percent reduced sheet, Figure 3.031610.

3.032 Compression – stress-strain diagrams – compression properties.

3.0321 Stress-strain diagrams.

3.03211 Stress-strain curves in compression for Type 301 annealed sheet at elevated temperatures, Figure 3.03211.

3.03212 Stress-strain curves in compression for Type 301 full-hard and full-hard stress-relieved sheet at room and elevated temperatures, Figure 3.03212.

3.03213 Stress-strain curves in compression for Type 301 extra-hard and extra-hard stress-relieved sheet at room and elevated temperatures, Figure 3.03213.

3.0322 Effect of test temperature on compressive yield strength of Type 301 annealed sheet, Figure 3.0322.

3.0323 Effect of test temperature and test direction on compressive yield strength of Type 301 1/2-hard sheet, Figure 3.0323.

3.0324 Effect of test temperature on compressive yield strength of 45 and 60 percent reduced sheet, Figure 3.0324.

3.0325 Effect of test temperature and exposure time on compressive yield strength of 60 percent cold-reduced sheet, Figure 3.0325.

3.0326 Effect of test temperature, test direction, and stress relief on compressive yield strength of Type 301 full-hard and extra-hard sheet, Figure 3.0326.

3.0327 Effect of test temperature on compressive strength of annealed Type 302 sheet, Figure 3.0327.

3.033 Impact.

3.0331 Impact energy of Type 301 plate at room and cryogenic temperatures, Figure 3.0331.

3.0332 Impact energy of Type 301 bar at room and cryogenic temperatures, Figure 3.0332.

3.0333 The impact energy of heat-treated cast Type 302 (CF-20) decreases with decreasing test temperature, as shown in Figure 3.0334. Carbide precipitation, caused by heat treating in the sensitizing temperature range, lowers the impact energy at cryogenic temperatures (83).

3.0334 Effect of sensitizing heat treatments on the impact energy of cast Type 302 at cryogenic temperatures, Figure 3.0334.

3.034 Bending.

3.035 Torsion and shear.

3.0351 Effect of test temperature on shear strength of Types 301 and 302, Figure 3.0351.

3.0352 Effect of test temperature and exposure time on shear strength of 60 percent cold-reduced sheet, Figure 3.0352.

3.036 Bearing.

3.0361 Effect of test temperature on bearing properties of Types 301 and 302 sheet, Figure 3.0361.

3.0362 Effect of test temperature and exposure time on bearing properties of 60 percent cold-reduced sheet, Figure 3.0362.

3.037 Stress concentration.

3.0371 Notch properties.

3.03711 Rolling effects on notch properties.

3.037111 Effect of rolling temperature on notch strength at room temperature and -423 F of 10 percent reduced sheet, Figure 3.037111.

Fe
18 Cr
8 Ni

Type 301
Type 302

3.037112 Effect of low rolling temperature on notch strength at room temperature and -423 F of 10 percent reduced sheet, Figure 3.037112.

3.037113 Effect of low temperature and percent cold reduction on notch strength of sheet, Figure 3.037113.

3.037114 Effect of low temperature and percent cold reduction on notch strength of various percent reduced sheet, Figure 3.037114.

3.037115 Effect of percent cold reduction on notch strength of sheet tested at room temperature and -320 F, Figure 3.037115.

3.037116 Effect of percent cold reduction on notch strength of sheet tested at room temperature and -423 F, Figure 3.037116.

3.03712 Prior exposure and rate of loading effects on notch strength.

3.037121 Effect of test temperature and prior exposure on notch properties of 60 percent cold-reduced sheet, Figure 3.037121.

3.037122 Effect of test temperature and exposure time on notch strength of 60 percent cold-reduced sheet, Figure 3.037122.

3.037123 Effect of test temperature and prior exposure on notch properties of 34 percent cold-reduced sheet, Figure 3.037123.

3.037124 Effect of stress concentration factor, temperature, and loading rate on notch strength of extra-hard cold-rolled sheet, Figure 3.037124.

3.03713 Stress-relief effects on notch strength.

3.037131 Effect of stress relief and low test temperature on notch strength of Type 301 sheet, Figure 3.037131.

3.03714 Crack effects on notch strength.

3.037141 Effect of test temperature on net fracture stress of full-hard sheet, Figure 3.037141.

3.037142 Effect of percent cold reduction on edge-cracked properties of sheet at room temperature and -110 F, Figure 3.037142.

3.03715 Low-test-temperature effects on notch strength.

3.037151 Effect of low test temperature on notch strength of 60 percent cold-reduced sheet, Figure 3.037151.

3.037152 Effect of low temperature on notch strength of extra-hard cold-rolled sheet, Figure 3.037152.

3.037153 Effect of low test temperature on notch strength of 40 and 60 percent reduced Type 302 sheet, Figure 3.037153.

3.037154 Effect of low test temperature on notch strength of 50 percent reduced sheet, Figure 3.037154.

3.037155 Effect of low test temperature on notch strength of 40 percent reduced sheet, Figure 3.037155.

3.037156 Effect of low test temperature and thickness on notch strength of 60 percent reduced sheet, Figure 3.037156.

3.037157 Effect of low test temperature on notch strength of 70 percent reduced vacuum-melt sheet, Figure 3.037157.

3.037158 Effect of low test temperature on notch strength of 70 percent reduced air-melt sheet, Figure 3.037158.

3.0372 Fracture toughness.

3.03721 Effect of low test temperature on fracture toughness of 60 percent cold-reduced sheet, Figure 3.03721.

3.03722 Effect of initial notch length on fracture toughness of 60 percent cold-reduced sheet at room temperature, -320, and -423 F, Figure 3.03722.

3.03723 The crack strength of Type 302 sheet is significantly affected by orientation with respect to the rolling direction, as shown in Figure 3.03724. At an angle of 90 degrees to the rolling direction, or transverse, the crack strength is about 10 percent less at room temperature and 34 percent less at -320 and -423 F than at 0 degrees to the rolling direction. However, the crack strength at an angle of 11 degrees to the rolling direction is not degraded. The 11-degree angle equals the helix angle at which some liquid-propellant rocket tanks have been spiral welded (79).

3.03724 Effects of center crack and test direction on tensile strength of cold-rolled sheet at room and cryogenic temperatures, Figure 3.03724.

3.04 **Creep and Creep Rupture Properties**

3.041 Creep curves for Type 302 annealed sheet at 1200 to 1600 F, Figure 3.041.

3.042 Short-time total strain curves for annealed Type 302 at 1200 to 1800 F, Figure 3.042.

3.043 Creep and creep-rupture curves for Type 301 1/2-hard sheet at 1200 to 1500 F, Figure 3.043.

3.044 Creep-rupture curves for Type 301 full-hard and stress-relieved sheet at 800 to 1200 F, Figure 3.044.

3.045 Creep-rupture curves for Type 301 extra-hard and stress-relieved sheet at 800 to 1200 F, Figure 3.045.

3.046 Creep curves for Type 301 60 percent reduced sheet under cyclic load at 600 and 900 F, Figure 3.046.

3.047 Creep and creep rupture curves for Type 301 60 percent reduced sheet at 600 and 900 F, Figure 3.047.

3.048 Creep and creep-rupture curves for 80 percent cold-reduced sheet at 1000, 1200, and 1400 F, Figure 3.048.

3.049 Creep-rupture properties of cast Type 302, Figure 3.049.

3.0410 Stress relaxation at room and slightly elevated temperatures, Figure 3.0410.

3.05 **Fatigue Properties**

3.051 Cyclic stress-strain curves for annealed Type 301 at temperatures between M_S and M_d, Figure 3.051.

3.052 Strain-controlled fatigue behavior of annealed rod at room temperature, Figure 3.052.

3.053 Bending fatigue behavior of cold-worked and of annealed sheet at room temperature, Figure 3.053.

3.054 S-N curves in flexure for extra-full-hard sheet at low temperatures, Figure 3.054.

3.055 Axial tension fatigue behavior of smooth and notched sheet at room and cryogenic temperatures, Figure 3.055.

3.056 Aging for up to 26,300 hours at 550 F has little effect on the room-temperature fatigue behavior of smooth or notched Type 301, as seen by comparison of Figures 3.057 and 3.058 (89,90).

3.057 Effects of notches on fatigue behavior of sheet, Figure 3.057.

3.058 Fatigue behavior of smooth and notched sheet at room temperature after aging for 26,300 hours at 550 F, Figure 3.058.

3.059 Low cycle S-N curves for complex welded joints of 60 percent cold-rolled sheet, Figure 3.059.

Fe
18 Cr
8 Ni

Type 301
Type 302

3.0510 S-N curves for uniaxial and biaxial sheet for R = 0.50, Figure 3.0510.

3.0511 S-N curves for uniaxial and biaxial sheet for R = 0.10, Figure 3.0511.

3.0512 Effects of fusion and spot welding on fatigue behavior of sheet, Figure 3.0512.

3.0513 Fatigue behavior of welded sheet at room temperature after aging for 26,300 hours at 550 F, Figure 3.0513.

3.0514 Type 301 alloy is unstable under stress, with the austenite phase transforming martensitically to alpha-prime to a much greater extent than the more stable Type 302 alloy. This stress-induced martensitic phase transformation can lead to remarkable work hardening. The effect of martensite formation on the fatigue crack-growth rate (FCGR) is shown in Figure 3.0515. For annealed material cycled to a maximum stress of 10.9 ksi, the FCGR of Type 301 is only about one-half that of Type 302. However, at a higher maximum stress of 21.5 ksi or in the 19 percent cold-worked condition (shown in Figure 3.0516), the two alloys have similar FCGR's. The difference in FCGR's for the annealed materials at low stress is related to alloy stability. The less stable Type 301 alloy forms more martensite during loading, resulting in greater work hardening and a lower FCGR. Cold rolling of annealed strip from 0.060 in. thick to reductions of 20, 27, and 40 percent resulted in formation of 10, 20, and 30 vol percent alpha-prime martensite in Type 301 and 0.5 to 2.5 vol percent in Type 302, as determined by magnetic measurements (59).

3.0515 Fatigue crack-growth behavior at room temperature for Types 301 and 302 annealed sheet tested at two different stress levels, Figure 3.0515.

3.0516 Fatigue crack-growth behavior at room temperature for Types 301 and 302 cold-rolled sheet tested at two different stress levels, Figure 3.0516.

3.0517 Fatigue crack-growth rates in hydrogen are more rapid than those in argon or in air. The enhancement is greater in Type 301 than in Type 302 because of hydrogen embrittlement of the alpha-prime martensite phase, which forms to a greater extent in Type 301. At a maximum stress of 18.3 ksi, the FCGR for Type 301 is higher by a factor of about six in hydrogen as compared to air, while the factor for the more stable Type 302 alloy is about three. At a slightly higher maximum stress of 19.8 ksi, rates for the two alloys are almost identical in argon but Type 301 is inferior to Type 302 in hydrogen, as shown in Figures 3.0518 and 3.0519. The FCGR's are decreased by cold work in both argon and hydrogen, but cold-worked alloys are more degraded by hydrogen than annealed alloys (90). The FCGR in hydrogen is thought to be controlled by the rate of supply of hydrogen to the highly stressed region ahead of the crack. Hydrogen permeability has been shown to be greater in Type 301 than Type 302 in the temperature range 400 to 600 F. Also, the permeability of hydrogen is increased under stress for Type 302. These factors are consistent with the above observation on enhancement of FCGR's by hydrogen (91,92).

3.0518 Fatigue crack-growth behavior at room temperature for Types 301 and 302 annealed sheet tested in dry hydrogen, dry argon, and air, Figure 3.0518.

3.0519 Fatigue crack-growth behavior at room temperature for annealed and cold-worked sheet tested in argon and in hydrogen, Figure 3.0519.

3.06 **Elastic Properties**

3.061 Poisson's ratio.

3.062 Modulus of elasticity.

3.0621 Modulus of elasticity for Type 301 1/2-hard sheet at room and elevated temperatures, Figure 3.0621.

3.0622 Modulus of elasticity in tension for Type 301 full-hard and extra-hard sheet, Figure 3.0622.

3.0623 Effect of low test temperature on modulus of elasticity for 60 percent reduced sheet, Figure 3.0623.

3.0624 Effect of test temperature, strain rate, and holding time on modulus of elasticity in tension of 45 and 60 percent reduced sheet, Figure 3.0624.

3.0625 Effect of temper on modulus of elasticity in tension and compression for Type 301 sheet, Figure 3.0625.

3.0626 Modulus of elasticity in compression for Type 301 full-hard and extra-hard sheet, Figure 3.0626.

3.0627 Effect of test temperature on modulus of elasticity in compression of 45 and 60 percent reduced sheet, Figure 3.0627.

3.063 Modulus of rigidity.

3.0631 Modulus of rigidity, Figure 3.0631.

3.0632 Effects of cold reduction and temperature on modulus of rigidity, Figure 3.0632.

3.064 Tangent modulus.

3.0641 Tangent modulus curves in compression for Type 301 sheet in various conditions, Figure 3.0641.

3.0642 Tangent modulus curves for 60 percent cold-reduced sheet for various exposure times and temperatures, Figure 3.0642.

4 **FABRICATION**

4.01 **Forming**

4.011 General. Although Types 301 and 302 in annealed condition possess a tensile strength relatively high compared to that of other ductile metals, they are readily formable because of their low yield strength. In fact, the high elongation of Type 301 permits particularly severe forming in certain operations, such as bending, stretch forming, and deep drawing. On the other hand, their high rate of strain hardening leads to a large springback which increases with increasing temper conditions, to a pronounced tendency to buckle and wrinkle under compressive strains, and to considerable difficulties in removing distortions. These characteristics call for forming techniques which differ slightly from those used for other metals. The forming of sheet becomes necessarily more difficult with increasing temper; 1/4-hard sheet can still be fabricated readily by many forming techniques, while the forming of 3/4-hard and full-hard sheet is restricted primarily to straight bending.

Stress cracking of deep drawn and spun sheet parts occurs if the resulting local hardening and residual

stresses are high. Such parts require immediate stress relief by full annealing.

4.012 Bending and stretching.

4.0121 Practical bend factors for sheet, Table 4.0121.

4.0122 For effect of stretching on yield strength, see Figures 3.02119 and 3.0221.

4.013 Forging. Starting temperature 2300 F maximum, finishing temperature 1500 F, minimum.

4.014 Deep drawing is enhanced under thermal conditions depressing the amount of strain-induced martensite formed (see Figure 3.03156).

4.015 Extrusion. For effect of extrusion temperature on tensile properties, see Figures 3.02117 and 3.02118.

4.02 **Machining and Grinding**

Because of their high rate of strain hardening, 18-8 stainless steels require maximum feed at relatively low sulface speeds during machining operations. Their high strength necessitates the use of rigid supports of both the tools and the work and very sharp tools. Their turning speeds are approximately 50 percent of those for mild carbon steels. A highly concentrated sulfur-base oil in ample quantity should be used as a coolant.

4.03 **Joining**

4.031 These steels can be readily welded by all techniques, but the weld and heat-affected zone becomes susceptible to intergranular corrosion, unless annealed after welding. For fusion welding, Type 308 electrodes or filler rod are generally used.

4.032 Hard tempers of Type 301 sheet are generally unsuitable for fusion welding and brazing. However, spot welding is possible in hard tempers. Cracking in spot welds can be greatly reduced by the introduction of nickel foil between the faying surfaces. The effect of nickel is to reduce martensite formation in the spot-weld region.

4.05 **Surface Treatment**

4.051 Cleaning. These steels exhibit maximum corrosion resistance only when thoroughly clean, as the corrosion resistance depends on maintaining a thin dense film of chromium oxide. Both preventive measures and removal of all foreign matter from the surfaces by conventional cleaning methods prior to any heating are particularly important.

4.052 Descaling is generally done in a solution of nitric and hydrofluoric acids. Molten caustic soda baths are also widely used for descaling. For removing heavy scale, sand or vapor blasting should precede pickling.

REFERENCES

1 AMS 5515H (April 1, 1985).
2 AMS 5516J (April 1, 1985).
3 AMS 5517G (July 1, 1984).
4 AMS 5518F (July 1, 1984).
5 AMS 5519H (October 1, 1984).
6 AMS 5536C (October 1, 1981).
7 AMS 5637D (October 1, 1981).
8 AMS 5688G (January 15, 1981).
9 AMS 5358 (January 1, 1984).
10 American Iron and Steel Institute, "Stainless and Heat Resisting Steels", Steel Products Manual, pp 22–23 (June 1957).
11 Allegheny Ludlum Steel Corporation, "High Strength Cold Rolled Stainless Steels", Data Sheet (1958).
12 North American Aviation, Inc., "Stainless Steel – Type 301", Data Sheet AL-2604 (1957).
13 American Casting Institute, "Corrosion Resistant Type CF-20", Data Sheet (June 1954).
14 Lucks, C. F., and Deem, H. W., "Thermal Properties of Thirteen Metals", ASTM STP No. 227 (February 1958).
15 Favor, R. J., Achbach, W. P., and Hyler, W. S., "Materials – Property – Design Criteria for Metals, The Conventional Short-Time Elevated-Temperature Properties of Selected Stainless Steels and Super Alloys", WADC TR 55-150, Pt. 5, ASTIA Doc. No. AD 142069 (October 1957).
16 Miller, J., Smith, L. W., and Porter, P. K., "Utilization of Low Alloy Materials for High Temperature Service Applications", AF TR No. 5929 (June 1959).
17 Roe, W. P., and Kattus, J. R., "Tensile Properties of Aircraft Structural Metals at Various Rates of Loading After Rapid Heating", WADC TR 55-199, Pt. III, ASTIA Doc. No. AD 142003 (September 1957).
18 NASA, E-502 (1959).
19 Miller, D. E., "Determination of the Tensile, Compressive and Bearing Properties of Ferrous and Non-Ferrous Structural Sheet Materials at Elevated Temperatures", Armour Research Foundation, AF TR No. 6517, Pt. V (December 1957).
20 Watter, M., and Lincoln, R. A., "Strength of Stainless Steel Structural Members as Function of Design", Allegheny Ludlum Steel Corporation (1950).
21 Goldsmith, A., Hirschhorn, H. J., and Waterman, T. E., "Thermophysical Properties of Solid Materials", Vol II – Alloys, WADC TR 58-476 (November 1960).
22 International Nickel Co. (1949).
23 "Compilation of Materials Research Data", MRG-307, General Dynamics Astronautics (April 4, 1962).
24 "Compilation of Materials Research Data", MRG-244, General Dynamics Astronautics (February 12, 1962).
25 "Compilation of Materials Research Data", MRG-298, General Dynamics Astronautics (March 12, 1962).
26 "Compilation of Materials Research Data", MRG-247, General Dynamics Astronautics (August 14, 1961).
27 "Compilation of Materials Research Data", MRG-269, General Dynamics Astronautics (October 31, 1961).
28 "USS 301: A Standard AISI Type Stainless Steel Cold-Reduced to Higher Properties for Aircraft and Missiles", United States Steel Corp. (June 1959).
29 Steir, H., Turner, H. C., and Sutherland, W. M., "Material – Aluminum, Columbium, Magnesium, Nickel Base, Stainless Steel and Titanium Alloys – Effect of Hydrogen Environment at 400 to

Fe
18 Cr
8 Ni

Type 301
Type 302

Fe
18 Cr
8 Ni

Type 301
Type 302

2400 F", General Dynamics, Report No. 8926-010 (January 23, 1961).

30 Morrison, J. D., and Kattus, J. R., "An Investigation of Methods for Determining the Crack Propagation Resistance of High Strength Alloys", Southern Research Institute (January 1961).

31 Watson, J. R., and Christian, J. L., "Low-Temperature Properties of Cold-Rolled AISI Types 301, 302", presented at ASTM Annual Meeting, Atlantic City (June 1960).

32 Rue, L. P., Campbell, J. E., and Simmons, W. F., "The Evaluation and the Effects of Very Low Temperatures on the Properties of Aircraft and Missile Metals", WADD-TR-60-254 (February 1960).

33 DiSisto, T. S., and Carr. F. L., "Low Temperature Mechanical Properties of 300 Series Stainless Steels and Titanium", Watertown Arsenal Laboratories (December 1961).

34 Hanson, M. P., "Smooth and Sharp-Notch Tensile Properties of Cold-Reduced AISI 301 and 304L Stainless Steel Sheet at 75°, -320° and -423°F", NASA TN D-592 (February 1961).

35 Shober, F. R., "The Effect of Nuclear Radiation on Structural Metals", DMIC Report 166 (September 15, 1961).

36 Christian, J. L., "Physical and Mechanical Properties of Pressure Vessel Materials for Application in a Cryogenic Environment", ASD-TDR-62-258 (March 1962).

37 Christian, J. L., and Hurlich, A., "Physical and Mechanical Properties of Pressure Vessel Materials for Application in a Cryogenic Environment", ASD-TDR 62-258, Part II (April 1963).

38 Lemcoe, M. M., and Trevim, A., Jr., "Determination of the Effects of Elevated Temperature Materials Properties of Several High Temperature Alloys", ASD-TDR-61-529 (June 1962).

39 Favor, R. J., et al., "Investigation of Fatigue Behavior of Certain Alloys in the Temperature Range Room Temperature to -423 F", WADD TR 61-132 (June 1961).

40 Wood, W. D., Deem, H. W., and Lucks, C. F., "The Emittance of Stainless Steels", DMIC Memo 111 (June 12, 1961).

41 Slunder, C. J., "Stress Corrosion Cracking of High-Strength Stainless Steels in Atmospheric Environment", DMIC Report 158 (September 15, 1961).

42 Gideon, D. N., Favor, R. J., Koppenhofer, A., Grover, H. J., and McClure, G. M., "Investigation of Notch Behavior of Certain Alloys in the Temperature Range of Room Temperature to -423 F", ASD-TDR-62-351 (August 1962).

43 Banerjee, B. R., and Hauser, J. J., "Research and Application Engineering to Determine the Effect of Processing Variables on Crack Propagation of High-Strength Steels and Titanium", ASD-TDR-62-1034, Part I (1962).

44 Brisbane, A. W., "The Investigation of the Effects of Cooling Rate and Stress Concentration Factors on the Notch Properties of Three Sheet Alloys at Subzero Temperatures", ASD-TDR-62-930 (1962).

45 Raring, R. H., Freeman, J. W., Schultz, J. W., and Voorhees, H. C., "Progress Report of the NASA Special Committee on Materials Research for Supersonic Transports", NASA TR D-1798 (May 1963).

46 McClaren, S. W., and Best, J. H., "Low Cycle Fatigue Design Data on Materials in Multi-Axial Stress Field", RTD-TDR-63-4094 (November 1963).

47 Kattus, J. R., and McDonell, D. W., Jr., "Strength of Structural Alloys Under Rapid Heating and Loading", Proceedings from American Society for Testing Materials, Vol 60, p 928 (1960).

48 Christian, J. L., "Effects of Chemistry and Processing on the Mechanical Properties of Engineering Alloys at Cryogenic Temperatures", Metals Engineering Quarterly of ASM, Vol 4, No. 3 (August 1964).

49 Personal Communication, B. Wasil with R. L. Cook of Allegheny Ludlum Steel Corporation Research Center (October 15, 1964).

50 "Metals Handbook", Vol 1, Properties and Selection of Metals, Am. Soc. Metals, 8th Edition (1961).

51 Anonymous, "Typical Properties of Wrought Stainless Steel", *Metal Progress*, Vol 92, No. 2 (August 1967), pp 106–109, 112–115.

52 AMS 5500B (July 16, 1979).

53 AMS 5600B (October 1, 1981).

54 AMS 5693 (July 1, 1982).

55 Laptev, D. V., and West, D.R.F., "Structure and Strength of Certain Austenitic Stainless Steels After Plastic Deformation and Subsequent Annealing", *Metals Technology*, Vol 4, No. 3 (March 1977), pp 128–135.

56 McCallum, R., and Cockcroft, M. G., "The Structure and Properties of Warm Extruded Austenitic Stainless Steels", National Engineering Laboratory, East Kilbride, Scotland, NEL 517 (June 1972).

57 Bishop, H. L., Jr., "Melting and Refining Specialty Steels at Allegheny Ludlum Industries", *Metal Progress*, Vol 106, No. 3 (August 1974), pp 53–59.

58 Pineau, A. G., Van Swam, L. F., and Pelloux, R. M., "Cyclic Stress-Strain Curves of a Stainless Austenitic Steel in the M_S-M_d Range", Scripta Metallurgica, Vol 7, No. 6 (June 1973), pp 657–660.

59 Schuster, G., and Altstetter, C., "Fatigue of Annealed and Cold Worked Stable and Unstable Stainless Steels", *Metallurgical Transactions*, Vol 14A, No. 10 (October 1983), pp 2077–2084.

60 Papadakis, E. P., "Tabulation of the Coefficients of a Quadratic Function for the Thermal Expansion of Various Alloys and Other Engineering Materials", *Materials Science and Engineering*, Vol 10 (1972), pp 195–203.

61 Williams, L. R., Young, J. D., and Schmidt, E. H., "Design and Development Engineering Handbook of Thermal Expansion Properties of Aerospace Materials at Cryogenic and Elevated Temperatures", NAS 8-19 (March 30, 1967).

62 International Nickel Company, Inc., "Mechanical and Physical Properties of the Austenitic Chromium-Nickel Stainless Steels at Elevated Temperatures", Trade Literature (March 1964).

63 Clark, A. F., Childs, G. E., and Wallace, G. H., "Electrical Resistivity of Some Engineering Alloys at Low Temperatures", *Cryogenics*, Vol 10, No. 4 (August 1970), pp 295–305.

64 Moller, G. E., "The Successful Use of Austenitic Stainless Steels in Sea Water", *Society of Petroleum Engineers Journal*, Vol 17, No. 2 (April 1977), pp 101–110.

65 Southwell, C. R., and Bultman, J. D., "Corrosion of Metals in Tropical Environments: Part 10 – Final Report of Sixteen-Year Exposures", NRL-7834 (January 2, 1975).

66 Miller, B. A., and Lee, S. G., "The Effect of Graphite-Epoxy Composites on the Galvanic Corrosion of Aerospace Alloys", AFML-TR-76-121 (September 1976).

67 Sinigaglia, D., Fassina, P., Wenger, D., and Re, G., "Experimental Evaluation of a Metallurgical Model for Austenitic Stainless Steels Sensitization", *Corrosion*, Vol 38, No. 2 (February 1982), pp 92–97.

68 Cowan, R. L., II, and Gordon, G. M., "Intergranular Stress Corrosion Cracking and Grain Boundary Composition of Fe-Ni-Cr Alloys", Proceedings, International Corrosion Conference, Stress Corrosion Cracking and Hydrogen Embrittlement of Iron Base Alloys, held at Unieux-Firminy, France (June 12–16, 1973).

69 Vermilyea, D. A., "Susceptibility of Iron- and Nickel-Base Alloys to SCC in pH 2.5 H_2SO_4 at 289 C", *Corrosion*, Vol 31, No. 12 (December 1975), pp 421–424.

70 De, P. K., and Elayaperumal, K., "Preferential Corrosion of Epsilon-Martensite in Austenitic Stainless Steel", *Transactions of the Indian Institute of Metals*, Vol 28, No. 5 (October 1975), pp 380–384 and 451.

71 Truman, J. E., and Pirk, K. R., "A Note on the Corrosion Produced Under Deposits of Chlorides on Austenitic Stainless Steel", *Corrosion Science*, Vol 17, No. 1 (1977), pp 71–74.

72 Logan, H. L., and McBee, M. J., "Stress-Corrosion Cracking of Cold-Reduced Austenitic Stainless Steels", *Materials Research and Standards*, Vol 7, No. 4 (April 1967), pp 137–145.

73 Singh, S., and Altstetter, C., "Effects of Hydrogen Concentration on Slow Crack Growth in Stainless Steels", *Metallurgical Transactions*, Vol 13A, No. 10 (October 1982), pp 1799–1808.

74 Kesterson, R. L., "Effects of Irradiation and Oxygen on Hydrogen Environment Embrittlement of Selected Alloys", Paper presented at the 75th Annual Meeting of the American Society for Testing Materials, Los Angeles, California (June 25–30, 1972).

75 Edwards, A. M., and Nicholson, A., "Some Effects of Reheating Stainless Steels", *Journal of the Iron and Steel Institute*, Vol 207, No. 8 (August 1969), pp 1067–1081.

76 The International Nickel Company, Inc., "Mechanical and Physical Properties of Austenitic Chromium-Nickel Stainless Steels at Ambient Temperatures", trade literature (October 1966).

77 Rosen, A., Jago, R., and Kjer, T., "Tensile Properties of Metastable Stainless Steels", *Journal of Materials Science*, Vol 7 (1972), pp 870–876.

78 Monteiro, S. N., and Fonseca, H., "The Effect of Phase Transformation on the Tensile Fracture of Austenitic Stainless Steel", Proceedings of the Fourth International Conference on Fracture, University of Waterloo, Ontario, Canada (June 1977), pp 135–140.

79 Calfo, F. D., "Cryogenic Fracture Properties of Thin AISI 301 60-Percent Cold-Reduced Sheet at Various Angles to the Rolling Direction", NASA TN D-5413 (September 1969).

80 Neff, D. V., Mitchell, T. E., and Troiano, A. R., "The Influence of Temperature, Transformation, and Strain Rate on the Ductility Properties of Austenitic Stainless Steels", *ASM Transactions Quarterly*, Vol 62, No. 4 (December 1969), pp 858–868.

81 Livitsanos, C. P., and Thomson, P. F., "The Effect of Temperature and Deformation Rate on Transformation-Dependent Ductility of a Metastable Austenitic Stainless Steel", *Materials Science and Engineering*, Vol 30, No. 2 (October 1977), pp 93–98.

82 Muraca, R. F., and Whittick, J. S., "Materials Data Handbook – Stainless Steel Type 301 (Second Edition)", NASA CR-123780 (April 1972).

83 The International Nickel Company, Inc., "Cast Stainless Steels", trade literature (July 1964).

84 Fox, A., "Stress Relaxation in Bending of AISI 301 Type Corrosion-Resistant Steel Strip", Proceedings of ASTM Symposium on Stress Relaxation Testing held in Kansas City, Missouri (May 24–25, 1978), pp 78–88.

85 Hennessy, D., Steckel, G., and Altstetter, C., "Phase Transformation of Stainless Steel During Fatigue", *Metallurgical Transactions*, Vol 7A, No. 3 (March 1976), pp 415–424.

86 Wright, R. N., "The High Cycle Fatigue Strength of Commercial Stainless Steel Strip", *Materials Science and Engineering*, Vol 22, No. 3 (March 1976), pp 223–230.

87 Nachtigall, A. J., Klima, S. J., and Freche, J. C., "Fatigue of Liquid Rocket Engine Metals at Cryogenic Temperatures to -452 F (4 K)", NASA TN D-4274 (December 1967).

88 Illg, W., and Imig, L. A., "Fatigue of Four Stainless Steels, Four Titanium Alloys, and Two Aluminum Alloys Before and After Exposure to Elevated Temperatures for Up to Three Years", NASA TN D-6145 (April 1971).

89 Illg, W., and Castle, C. B., "Fatigue of Four Stainless Steels and Three Titanium Alloys Before and After Exposure to 550 F (561 K) Up to 8800 Hours", NASA TN D-2899 (July 1965).

90 Schuster, G., and Altstetter, C., "Fatigue of Stainless Steel in Hydrogen", *Metallurgical Transactions*, Vol 14A, No. 10 (October 1983), pp 2085–2090.

91 Perng, T. P., and Altstetter, C. J., "Hydrogen Permeation and Diffusion in Cryoformed AISI 301 Stainless Steel", *Scripta Metallurgica*, Vol 18, No. 1 (January 1984), pp 67–70.

Fe
18 Cr
8 Ni

Type 301
Type 302

Fe
18 Cr
8 Ni

Type 301
Type 302

92 Studebaker, P., Altstetter, C., and Conley, W., "Hydrogen Permeation of Stainless Steel Under Stress", Proceedings of 3rd International Conference on Effect of Hydrogen on Behavior of Materials, Hydrogen Effects in Metals held in Moran, Wyoming (August 26–31, 1980), pp 169–175.

93 Mikesell, R. P., and Reed, R. P., "Magnetic Transformation and the Influence of Plastic Strain on the Shear Modulus of Fe-Cr-Ni Alloys", *Journal of Research*, Vol 70C, No. 3 (July–September 1966), pp 207–210.

Alloy Type	AMS Specification	Form
301	5517G	Sheet, strip, 125 ksi
	5518F	Sheet, strip, 150 ksi
	5519H	Sheet, strip, 185 ksi
302	5358B	Investment castings
	5500B	Sheet, laminated
	5515H	Sheet, strip, plate, ST
	5516J	Sheet, strip, plate, ST
	5600B	Sheet, laminated
	5636C	Bar, 100 ksi
	5637D	Bar, 125 ksi
	5688G	Wire, spring temper
	5693	Wire, cryogenically drawn

TABLE 1.03. SPECIFICATIONS (1–9, 52–54)

Alloy	Type 301				Type 302					
AMS Specification	5517G		5518F, 5519H		5358B		5500B, 5516J, 5600B, 5636C, 5637D, 5688G, 5693		5515H	
	Percent		Percent		Percent		Percent		Percent	
Element	Min	Max	Min	Max	Min	Max	Min	Max	Min	Max
Chromium	17.00	–	16.00	18.00	17.00	19.00	17.00	19.00	17.00	19.00
Nickel	7.00	–	6.00	8.00	8.00	10.00	8.00	10.00	7.00	10.00
Manganese	–	2.00	–	2.00	–	1.50	–	2.00	–	2.00
Silicon	–	1.00	–	1.00	–	2.00	–	1.00	–	1.00
Carbon	–	0.15	–	0.15	–	0.25	–	0.15	0.08	0.15
Molybdenum	–	0.75	–	0.75	–	0.75	–	0.75(a)	–	0.75
Copper	–	0.75	–	0.75	–	0.75	–	0.75(a)	–	0.75
Phosphorus	–	0.040	–	0.040	–	0.04	–	0.040	–	0.040
Sulfur	–	0.030	–	0.030	–	0.03	–	0.030	–	0.030

(a) AMS 5500B specifies 0.50 max molybdenum and 0.50 max copper.

TABLE 1.04. COMPOSITION (1–9, 52–54)

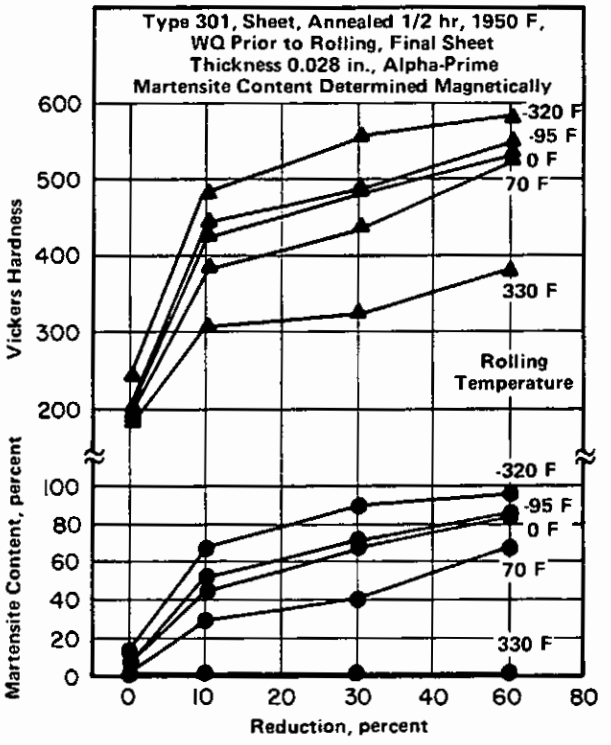


FIGURE 1.062. HARDNESS AND MARTENSITE CONTENTS OF TYPE 301 AFTER ROLLING TO VARIOUS REDUCTIONS AT 330 F TO -320 F (55)

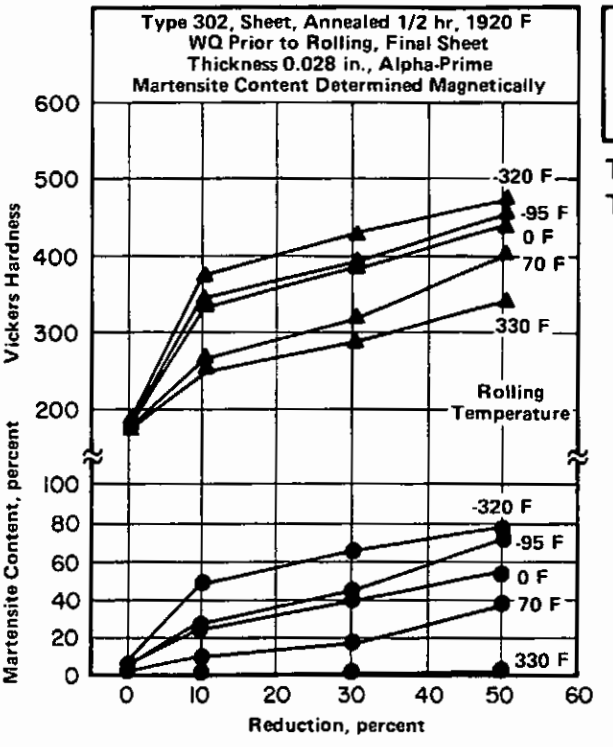


FIGURE 1.063. HARDNESS AND MARTENSITE CONTENTS OF TYPE 302 AFTER ROLLING TO VARIOUS REDUCTIONS AT 330 F TO -320 F (55)

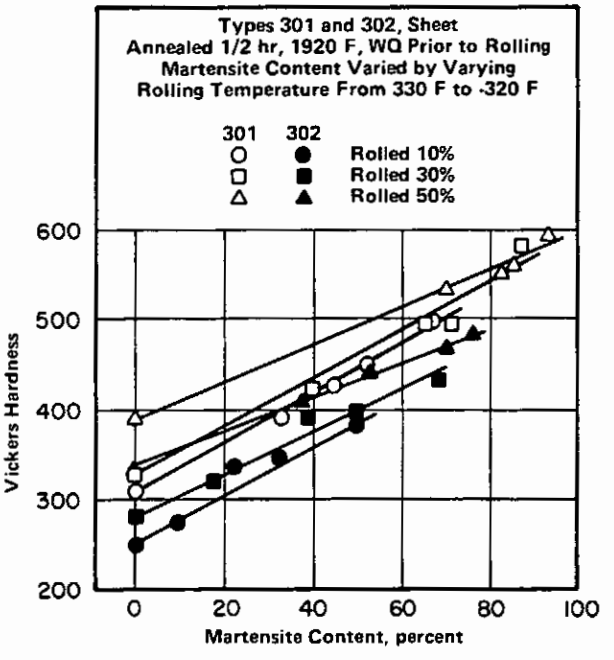


FIGURE 1.064. EFFECT OF STRAIN-INDUCED MARTENSITE CONTENT ON HARDNESS (55)

Fe
18 Cr
8 Ni

Type 301
Type 302

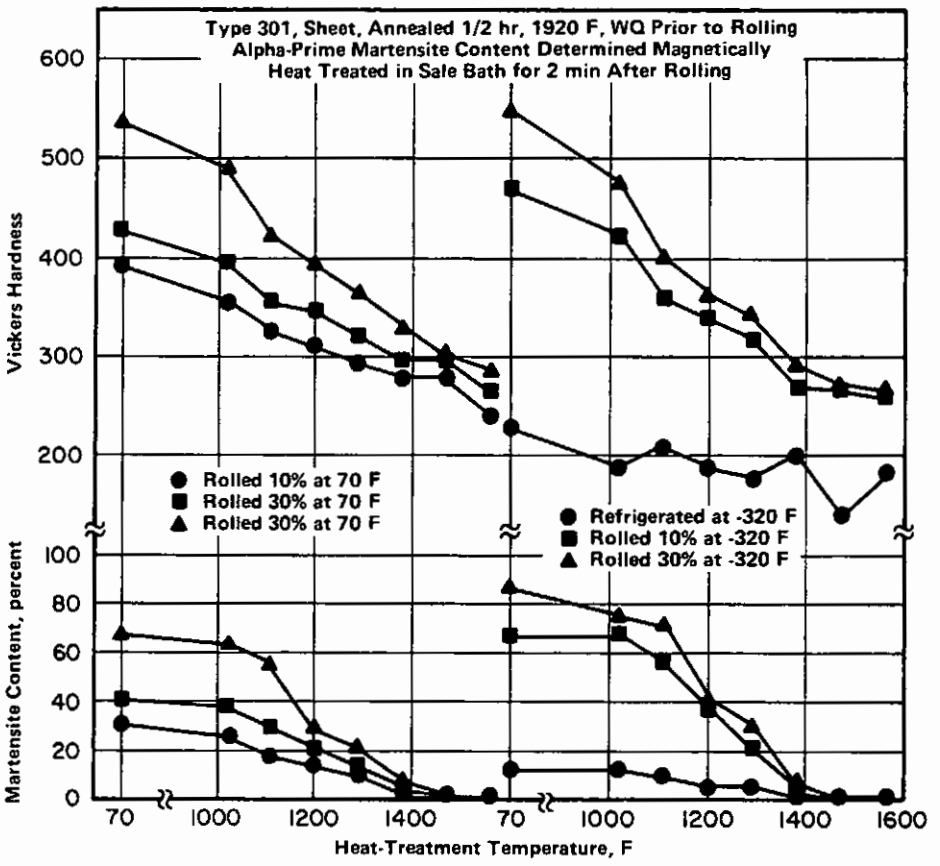


FIGURE 1.065. HARDNESS AND MARTENSITE CONTENTS OF TYPE 301 AFTER COLD ROLLING FOLLOWED BY HEAT TREATMENT AT 1020 TO 1560 F (55)

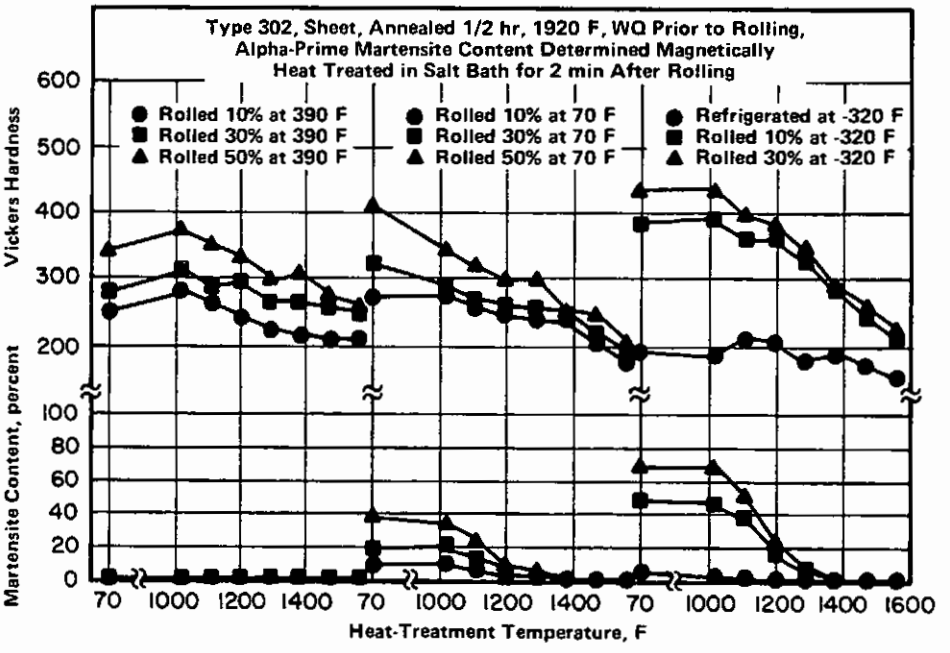


FIGURE 1.066. HARDNESS AND MARTENSITE CONTENTS OF TYPE 302 AFTER ROLLING FOLLOWED BY HEAT TREATMENT AT 1020 TO 1560 F (55)

Fe
18 Cr
8 Ni

Type 301
Type 302

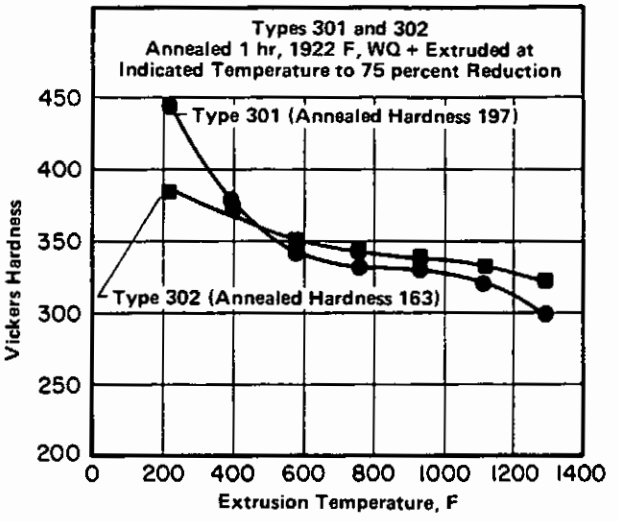


FIGURE 1.067. EFFECT OF EXTRUSION TEMPERATURE ON HARDNESS (56)

Form	Sheet, Strip					Plate
Condition	Anneal	1/4 H	1/2 H	3/4 H	Full H	Anneal
Hardness						
Type 301	85 RB	25 RC	32 RC	37 RC	41 RC	165 BHN
Type 302	85 RB	25 RC	–	–	–	80 RB
Form	Bar			Wire		
Condition	Anneal	CD	High Tension	Anneal	Soft	Hard
Hardness						
Type 301	–	–	–	–	–	–
Type 302	150 BHN	212 BHN	240–277 BHN	83 RB	95 RB	33 RC

TABLE 1.068. AISI TYPICAL VALUES FOR HARDNESS (10)

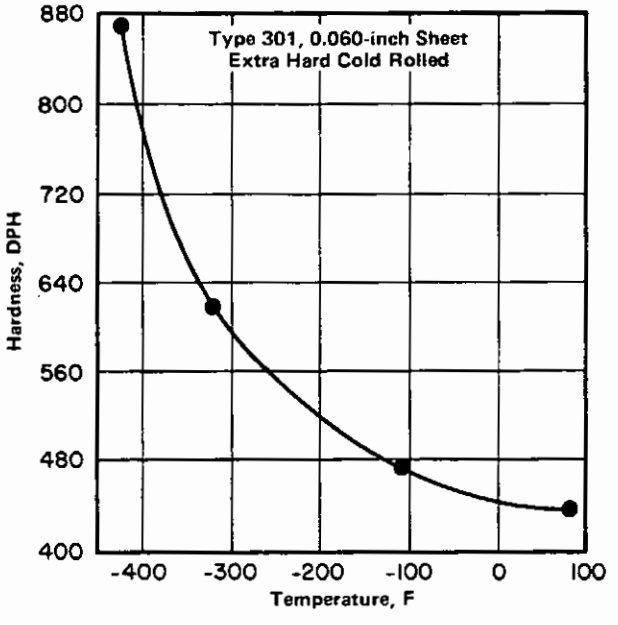


FIGURE 1.069. EFFECT OF LOW TEST TEMPERATURE ON HARDNESS OF EXTRA-HARD COLD-ROLLED SHEET (32)

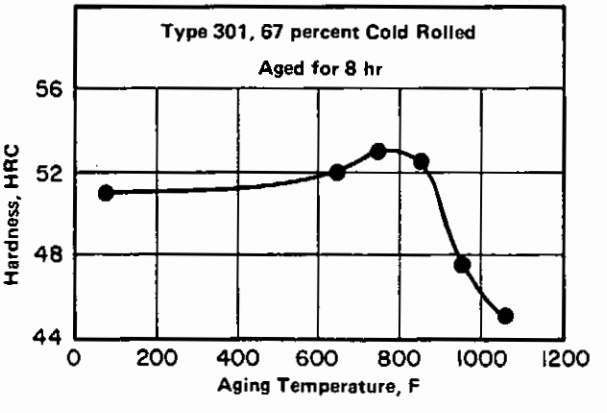


FIGURE 1.0610. EFFECT OF AGING TEMPERATURE ON HARDNESS OF 67 PERCENT COLD-ROLLED SHEET (43)

Fe
18 Cr
8 Ni

Type 301
Type 302

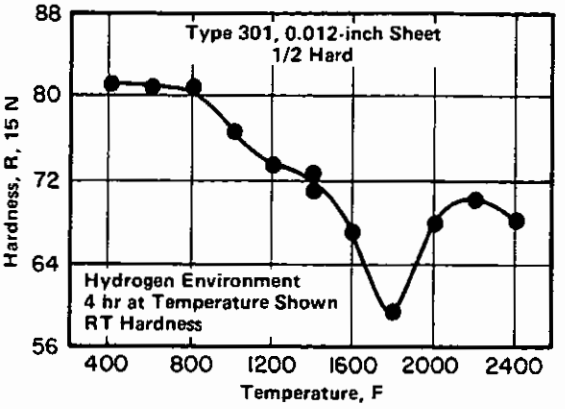


FIGURE 1.0611. EFFECT OF HYDROGEN ENVIRONMENT AT ELEVATED TEMPERATURE ON SURFACE HARDNESS OF HALF-HARD SHEET (29)

Phase Change	Temperature, F	
	Type 301	Type 302
M_s	-35 to -112	-251
M_d	135 to 194	-8
A_{c1}	1020 to 1110	1020 to 1110
A_{c3}	1380 to 1470	1290 to 1380

TABLE 2.0122. TRANSFORMATION TEMPERATURES (55,58,59)

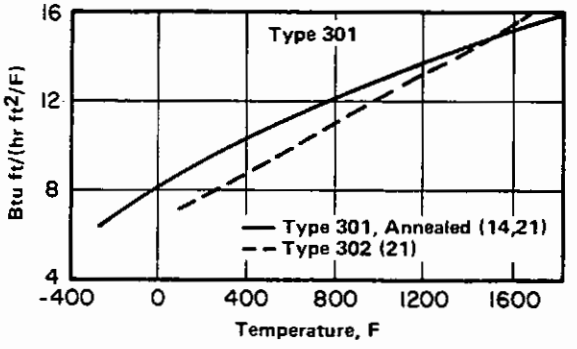
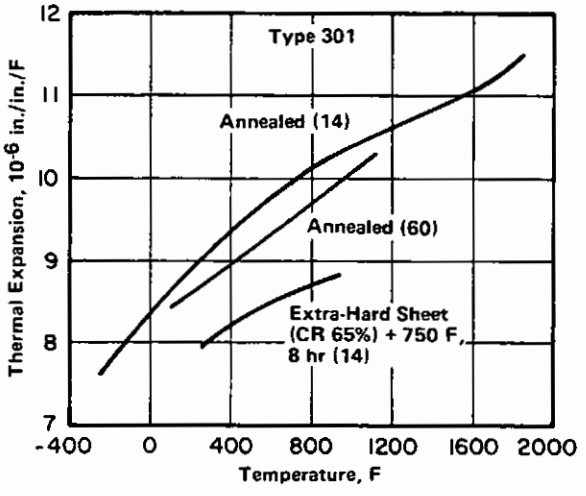
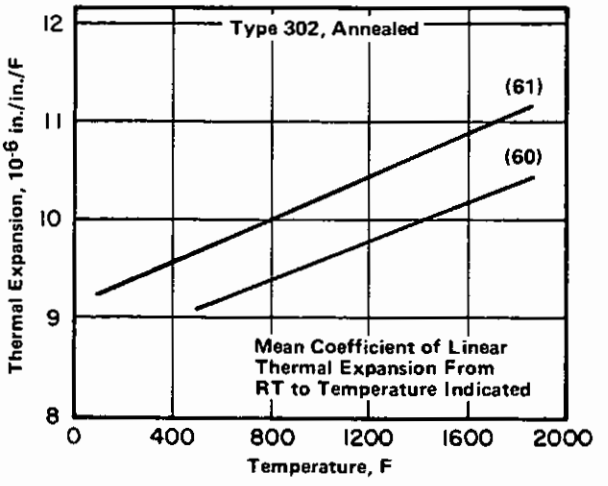


FIGURE 2.013. THERMAL CONDUCTIVITY (14,21)



(a) Type 301



(b) Type 302

FIGURE 2.014. THERMAL EXPANSION (60,61)

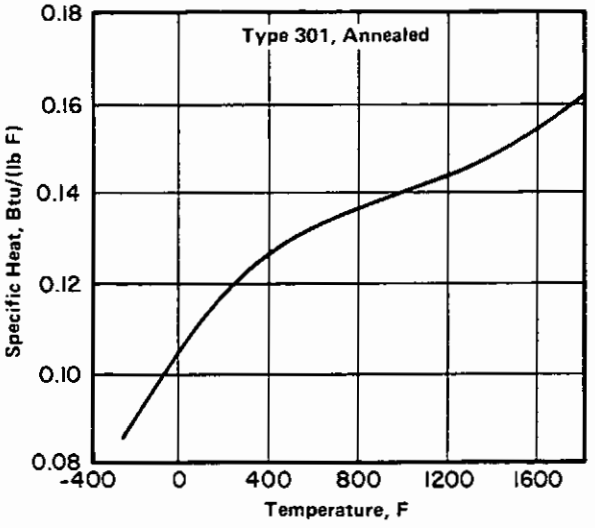
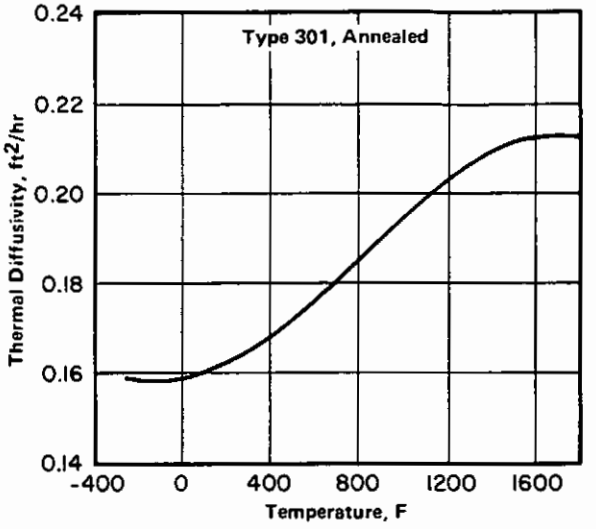


FIGURE 2.015. SPECIFIC HEAT (14)



Fe
18 Cr
8 Ni

Type 301
Type 302

FIGURE 2.016. THERMAL DIFFUSIVITY (14)

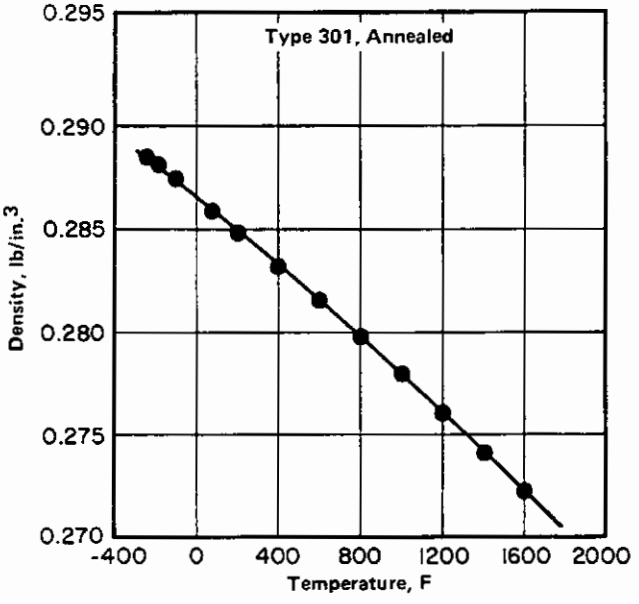


FIGURE 2.021. DENSITY (62)

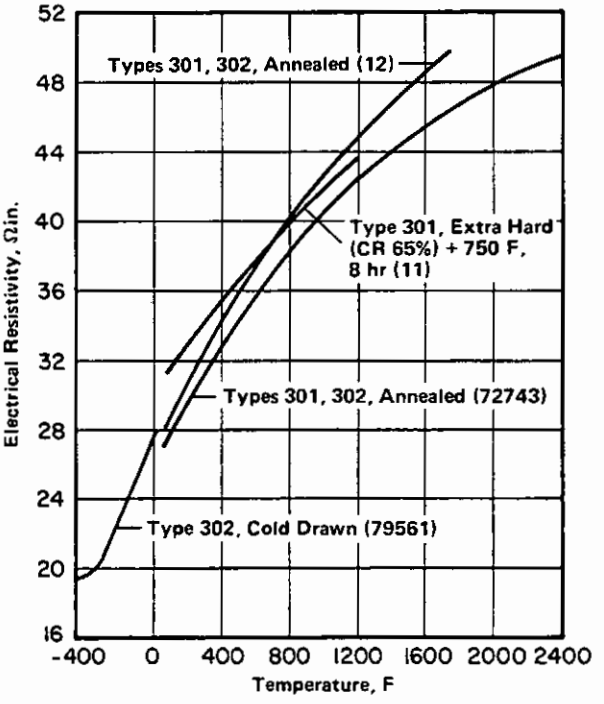


FIGURE 2.0221. ELECTRICAL RESISTIVITY (63)

Fe
18 Cr
8 Ni

Type 301
Type 302

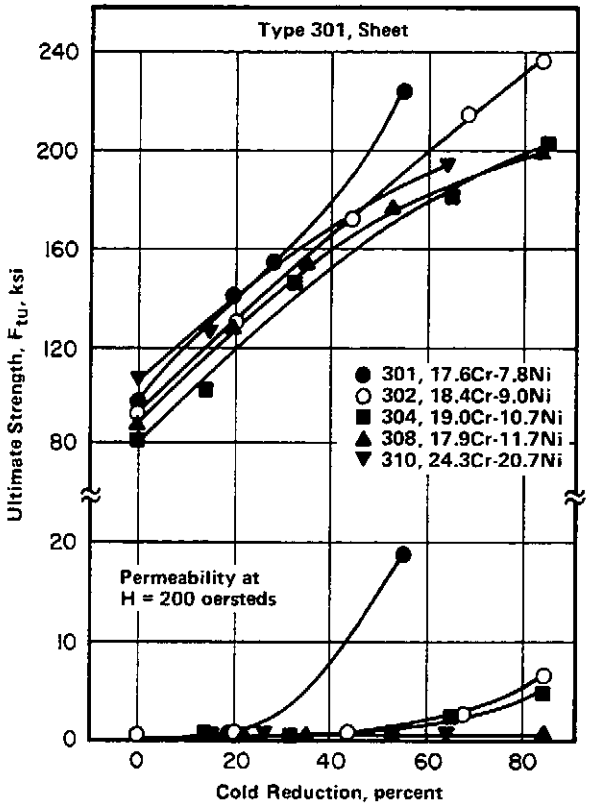


FIGURE 2.0232. EFFECT OF COMPOSITION AND REDUCTION ON MAGNETIC PERMEABILITY AND TENSILE STRENGTH OF 300 SERIES SHEET (22)

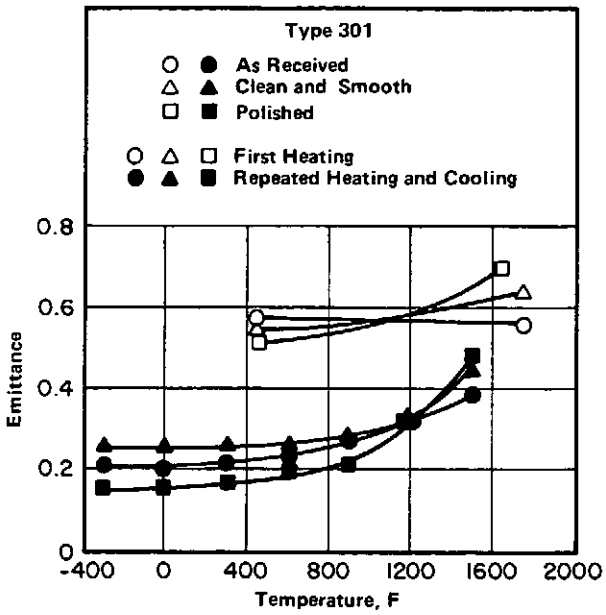


FIGURE 2.024. EMITTANCE (40)

Alloy Type	Exposure[a]	General Corrosion: Weight Loss, g/dm² 1 Yr	8 Yr	16 Yr	General Corrosion: Average Penetration, mils 1 Yr	8 Yr	16 Yr	Steady State Rate, mpy	Pitting Penetration, mils[c] 1 Yr	8 Yr	16 Yr
302	S	2.9	11.0	18.7	1.51	5.51	9.51	(b)	70 (P)	140	151 (P)
	M	0.4	1.8	3.3	0.2	0.9	1.6	(b)	6	58	50 (110)
	L	0.0	0.0	0.0	0.0	0.0	0.0	0.0	<5	<5	<5 (<5)
301	A	0.01	0.01	0.03	0.01	0.01	0.02	0.01	<5	<5	<5 (<5)
	B	0.00	0.01	0.00	0.00	0.00	0.00	0.00	<5	<5	<5 (<5)

(a) S – seawater immersion
M – seawater at mean tide level for intermittent immersion
L – freshwater immersion
A – tropical marine atmospheric exposure
B – tropical inland atmospheric exposure
Panels for aqueous exposures measured 9 x 9 x 0.25 inch; those for atmospheric exposures measured 4 x 8 x 0.063 inch.

(b) Deep local pitting; average penetration not appropriate.

(c) Twenty pit average as determined from the five deepest pits on each surface of duplicate panels. The deepest pit during the 16-year exposure is shown in parentheses. Perforation is shown by a "P".

TABLE 2.0313. CORROSION IN TROPICAL ENVIRONMENTS FOR TIMES UP TO 16 YEARS (65)

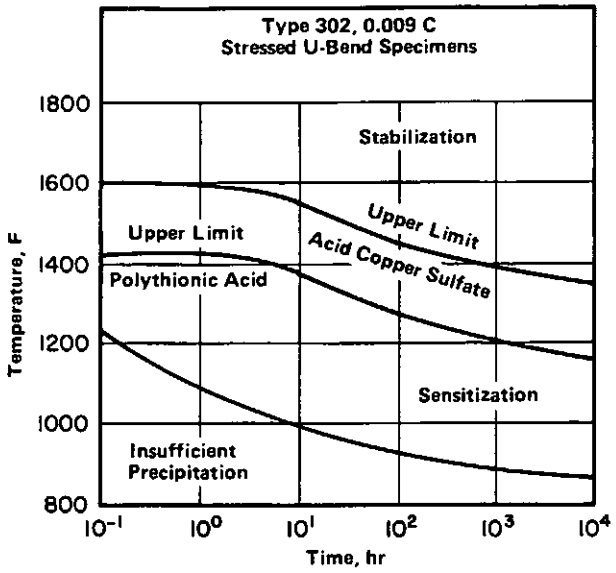
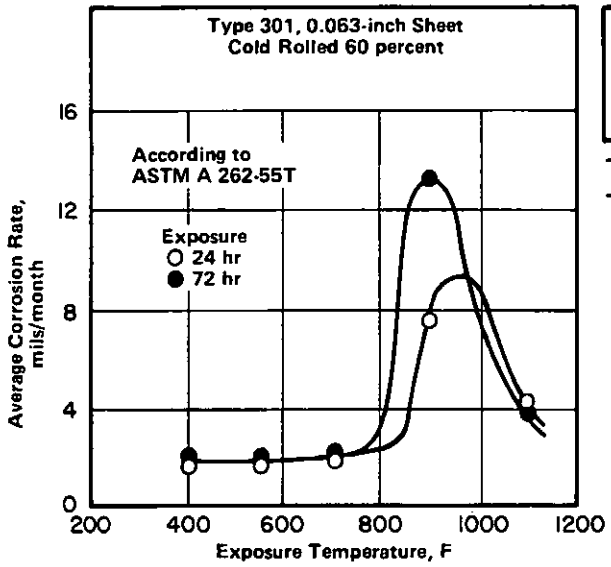


FIGURE 2.0322. EFFECTS OF HEAT TREATMENT ON SUSCEPTIBILITY TO INTERGRANULAR STRESS CORROSION CRACKING IN POLYTHIONIC ACID AND IN ACID COPPER SULFATE (68)



Fe
18 Cr
8 Ni

Type 301
Type 302

FIGURE 2.0323. EFFECT OF PRIOR EXPOSURE TEMPERATURE AND TIME ON AVERAGE CORROSION RATE IN BOILING NITRIC ACID OF COLD-ROLLED SHEET (18)

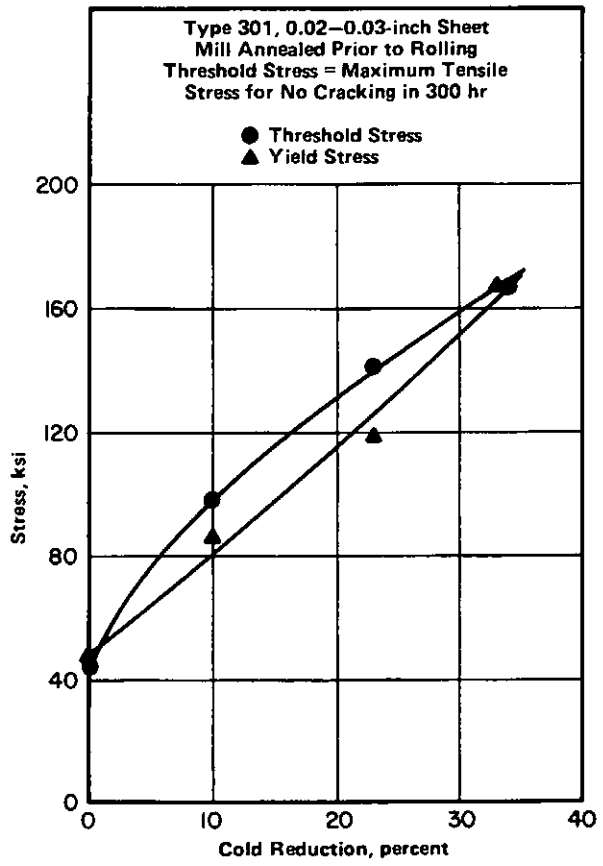


FIGURE 2.0333. EFFECTS OF COLD REDUCTION ON YIELD STRESS IN AIR AND ON THRESHOLD CORROSION STRESS IN BOILING 0.5N NaCl + 0.1N $NaNO_2$ AQUEOUS SOLUTION (72)

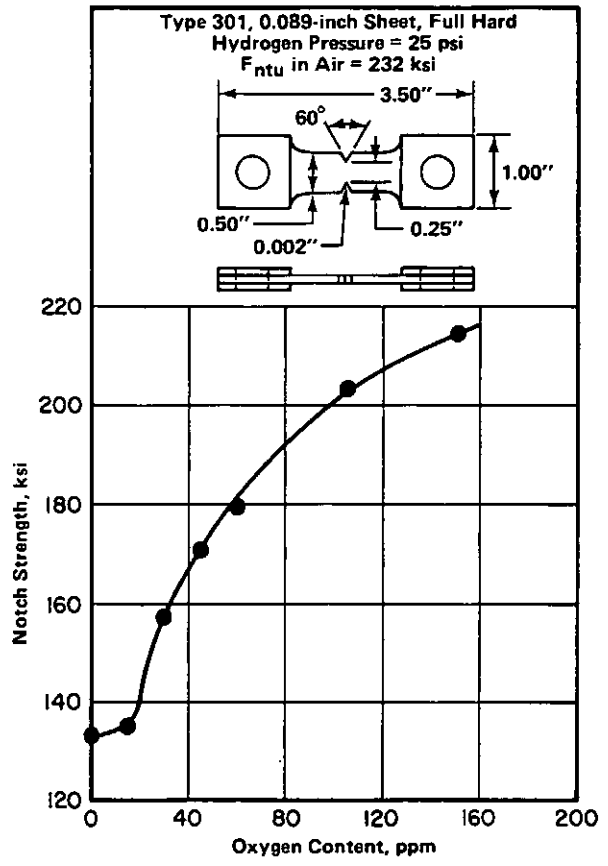


FIGURE 2.0342. EFFECTS OF OXYGEN IMPURITY IN HYDROGEN ON NOTCH STRENGTH OF TYPE 301 (74)

Fe
18 Cr
8 Ni

Type 301
Type 302

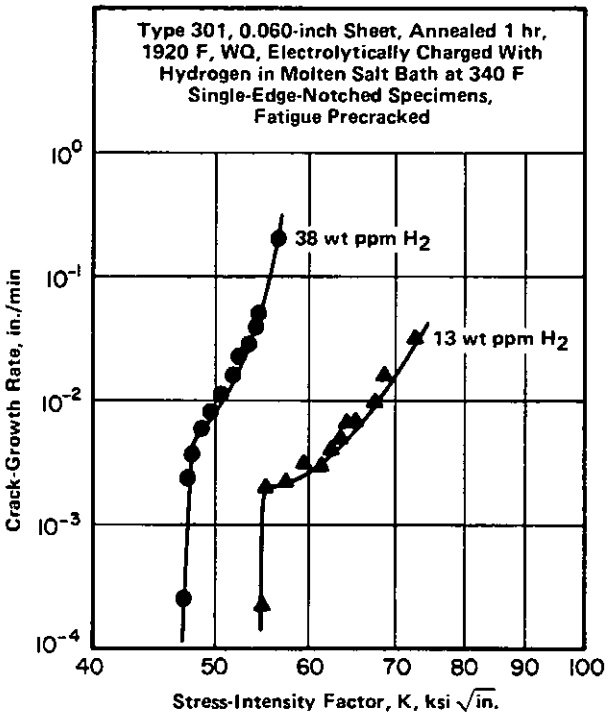


FIGURE 2.0344. SUSTAINED-LOAD CRACK-GROWTH RATE OF HYDROGEN-CHARGED TYPE 301 (73)

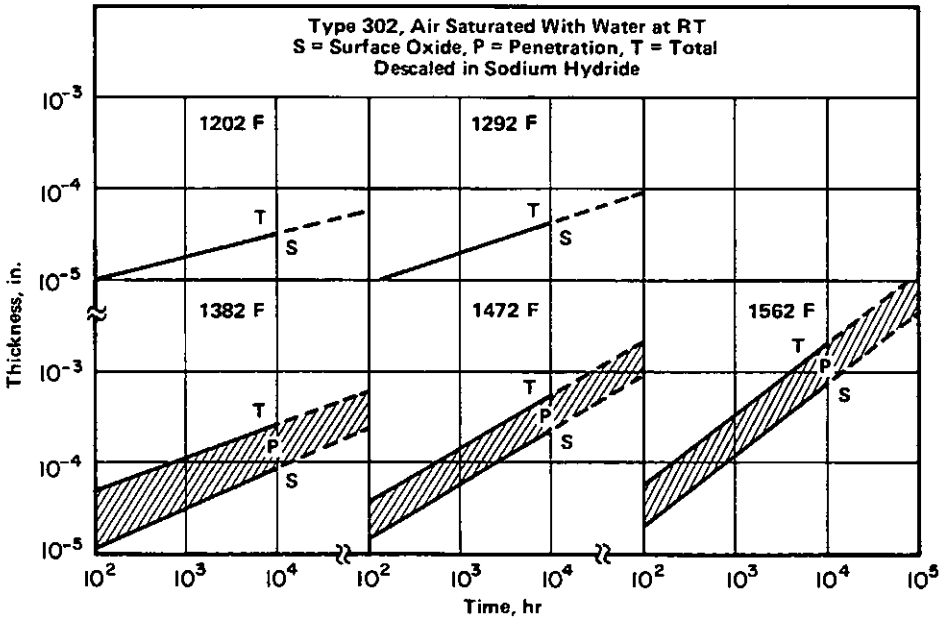


FIGURE 2.0352. TIME DEPENDENCE OF OXIDATION OF TYPE 302 IN AIR AT ELEVATED TEMPERATURES (75)

Fe
18 Cr
8 Ni

Type 301
Type 302

Alloy	Type 301				Type 302	
Condition	Annealed		60% (Cold Worked)		Annealed	
Irradiation Temperature, F	200	–	-416	–	200	–
Irradiation Exposure, n(m^{-2})	3.9×10^9	Control	2.0×10^{17}	Control	3.9×10^9	Control
Test Temperature, F	RT		-423		RT	
F_{tu}, ksi	113.2	98.7	284	391	111.3	95.5
F_{ty}, ksi	87.0	38.4	284	300	84.0	33.8
e, percent	50.0	56.0	8	13	–	–
RA, percent	81.0	83.0	–	–	–	–
Hardness, HRB	94	94	–	–	–	–

TABLE 2.041. EFFECT OF IRRADIATION EXPOSURE ON TENSILE PROPERTIES AND HARDNESS OF ALLOY (35)

Alloy	Types 301 and 302									
AMS Spec	Product Form	Condition(d)	Thickness, in.	F_{tu}, ksi Min	F_{tu}, ksi Max	F_{ty}, ksi Min	F_{ty}, ksi Max	El., percent, Min	RA, percent, Min	Hardness, Max
3517G	Sheet, strip	CR, 125 ksi	–	125	150	75	–	25	–	–
5518F	Sheet, strip	CR, 150 ksi	⩽0.015	150	–	110	–	15	–	–
			>0.015	150	–	110	–	18	–	–
5519H	Sheet, strip	CR, 185 ksi	⩽0.015	185	–	140	–	8	–	–
			>0.015	185	–	140	–	9	–	–
5358B	Investment cast	SHT	–	–	–	–	–	–	–	174 HB
5515H	Sheet, strip, plate	SHT	<0.025	–	120	–	–	50	–	–
			⩾0.025	–	120	–	–	55	–	–
5516J	Sheet, strip, plate	SHT	0.002 ⩽ 0.003	75	110	36	60	30	–	–
			>0.003 ⩽ 0.004	75	105	36	60	35	–	–
			>0.004 ⩽ 0.176	75	100	36	60	40	–	–
			>0.176	75	100	–	–	40	–	–
5636C	Bar	CD, 100 ksi	–	100	–	60	–	32	50	–
5637D	Bar	CD, 125 ksi	–	125	–	100	–	17	45	–
5688G	Wire	Spring temper	0.009–0.394(a)	142	355	–	–	–	–	–
5693	Wire	Cryogenically drawn	0.050–0.148(b)	275	310	–	–	–	–	–
			0.050–0.148(c)	245	280	–	–	–	–	–
		SR	0.050–0.148(b)	290	340	–	–	–	–	–
			0.050–0.148(c)	260	310	–	–	–	–	–

Note: The original AMS documents should be consulted for complete specification details.
(a) Tensile strengths specified for numerous diameters and thicknesses in range 0.009–0.394 inch.
(b) Round wire.
(c) Square or rectangular wire.
(d) CR = cold rolled; SHT = solution heat treated; CD = cold drawn; SR = stress relieved.

TABLE 3.011. AMS SPECIFIED MECHANICAL PROPERTIES (1–9, 54)

Fe
18 Cr
8 Ni

Type 301
Type 302

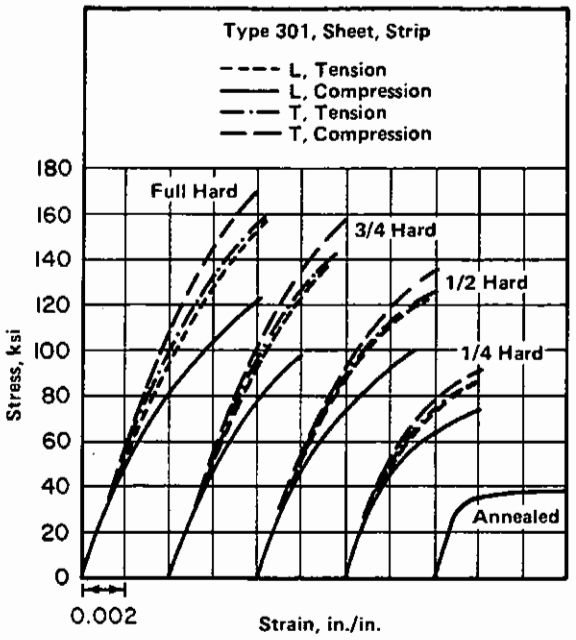


FIGURE 3.0211. STRESS-STRAIN CURVES FOR SHEET AND STRIP COLD ROLLED TO DIFFERENT TEMPER (20)

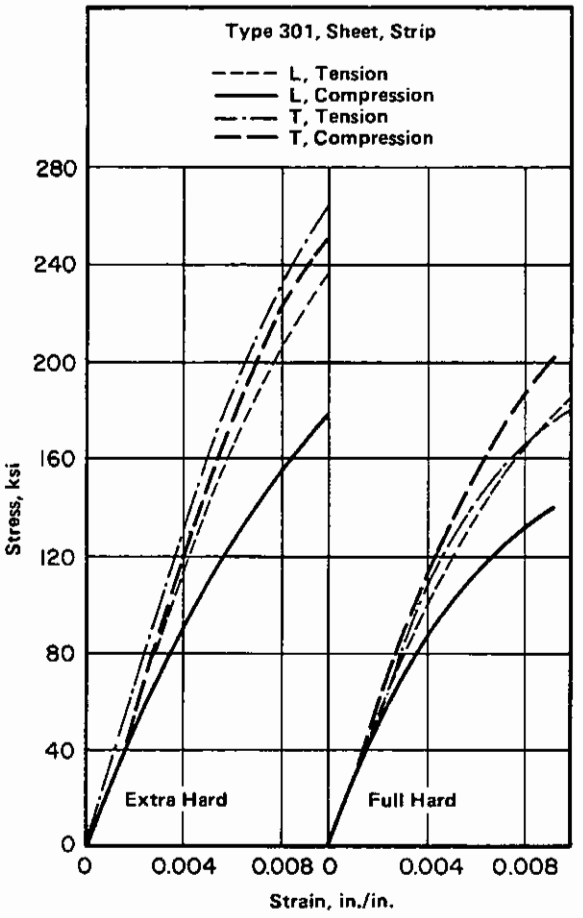


FIGURE 3.0212. STRESS-STRAIN CURVES FOR SHEET AND STRIP COLD ROLLED TO FULL-HARD AND EXTRA-HARD TEMPERS (11)

Alloy	Type 301		Type 302	
Temper	Percent Cold Reduction – Range	F_{tu} – Range, ksi	Percent Cold Reduction – Range	F_{tu} – Range, ksi
1/4 Hard	7–11	125–155	20–22	125–150
1/2 Hard	18–21	150–180	30–33	150–170
3/4 Hard	29–32	175–195	40	170–190
Full Hard	40	190–220	50	185–200
Extra Full Hard	65	240–275	–	–

TABLE 3.0213. PERCENTAGE COLD REDUCTION AND CORRESPONDING TENSILE STRENGTH FOR VARIOUS TEMPERS OF TYPES 301 AND 302 (49)

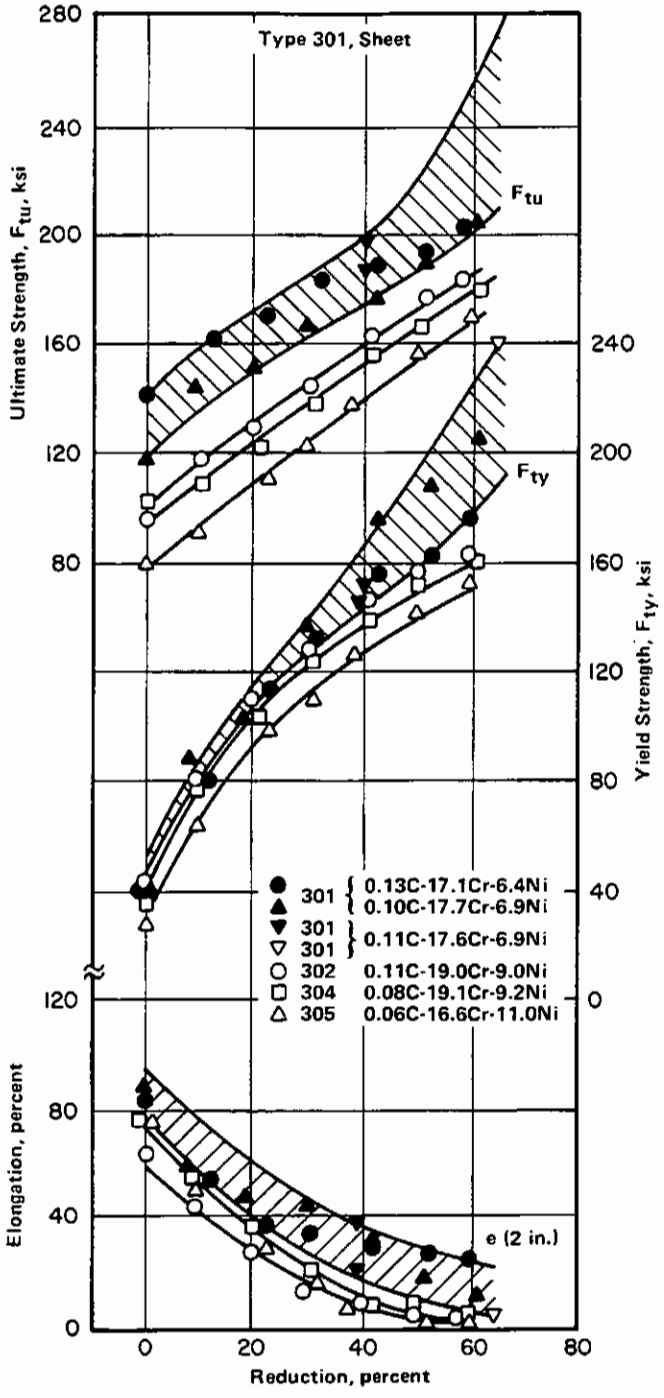


FIGURE 3.0214. EFFECT OF ROLLING REDUCTION AND COMPOSITION ON TENSILE PROPERTIES OF 300 SERIES STEELS (11)

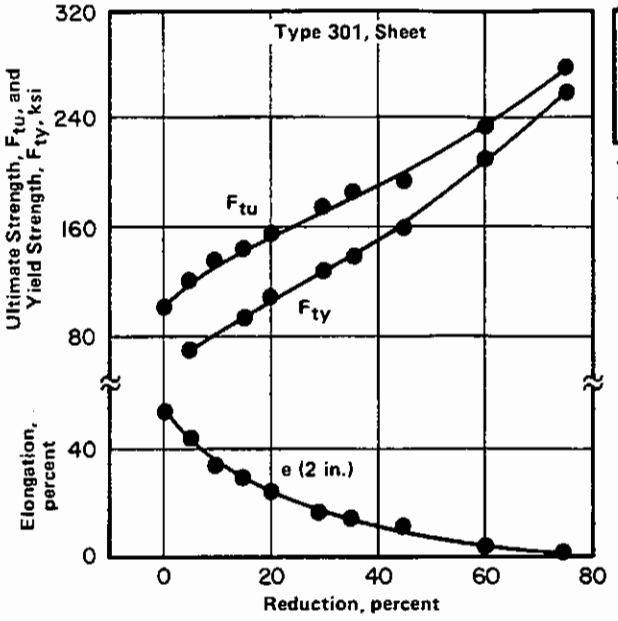


FIGURE 3.0215. EFFECT OF COLD REDUCTION ON TENSILE PROPERTIES OF TYPE 301 (28)

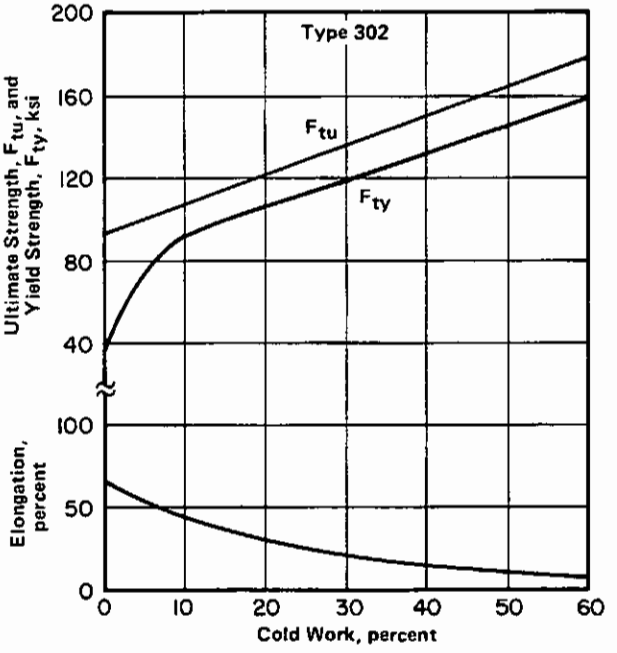


FIGURE 3.0216. EFFECTS OF COLD WORK ON TENSILE PROPERTIES OF TYPE 302 (76)

Fe
18 Cr
8 Ni

Type 301
Type 302

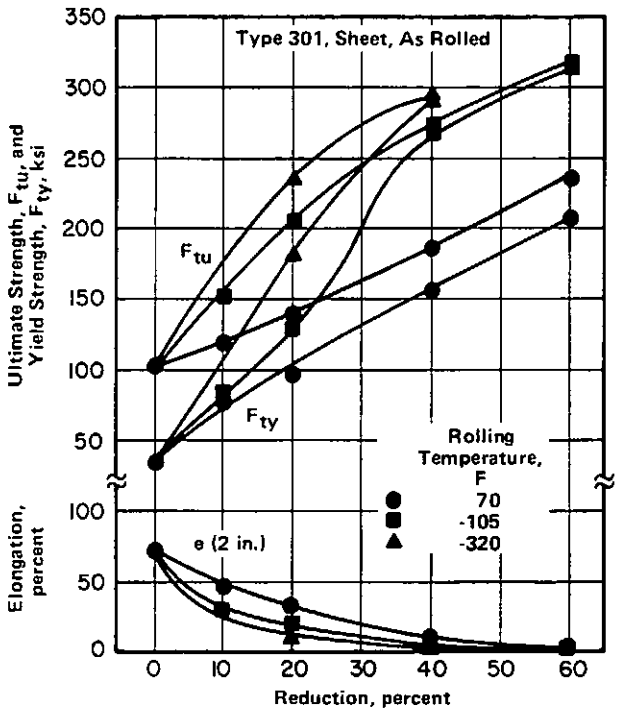


FIGURE 3.0218. EFFECT OF COLD REDUCTION AT ROOM AND CRYOGENIC TEMPERATURES ON TENSILE PROPERTIES OF TYPE 301 (76)

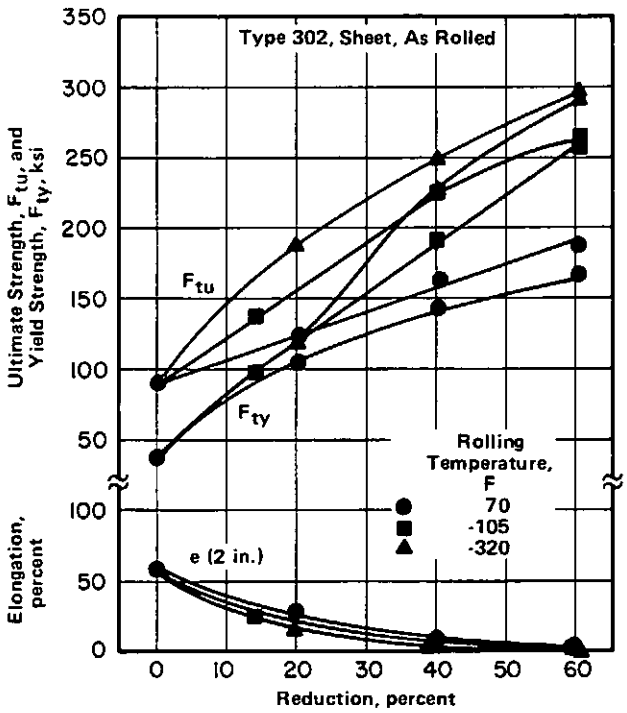


FIGURE 3.0219. EFFECT OF COLD REDUCTION AT ROOM AND CRYOGENIC TEMPERATURES ON TENSILE PROPERTIES OF TYPE 302 (76)

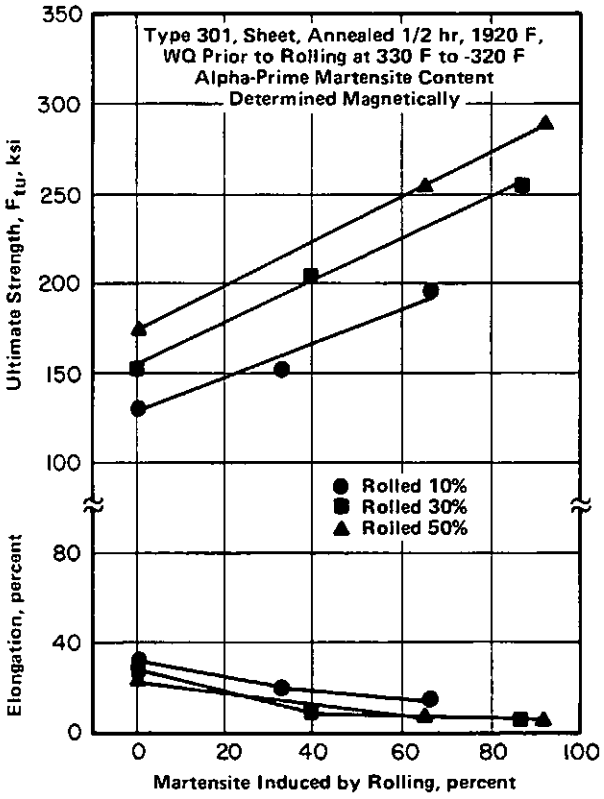


FIGURE 3.02110. RELATIONSHIP BETWEEN TENSILE PROPERTIES AND MARTENSITE CONTENT FOR TYPE 301 (55)

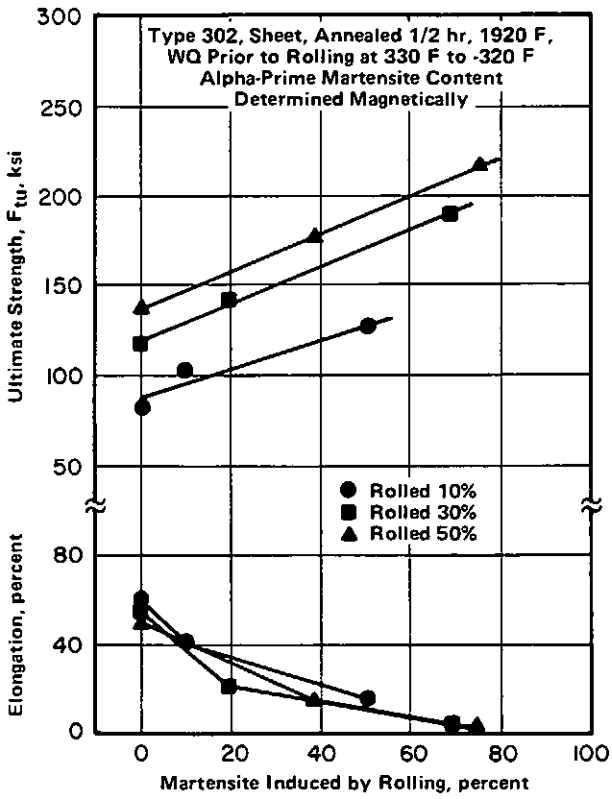


FIGURE 3.02111. RELATIONSHIP BETWEEN TENSILE PROPERTIES AND MARTENSITE CONTENT FOR TYPE 302 (55)

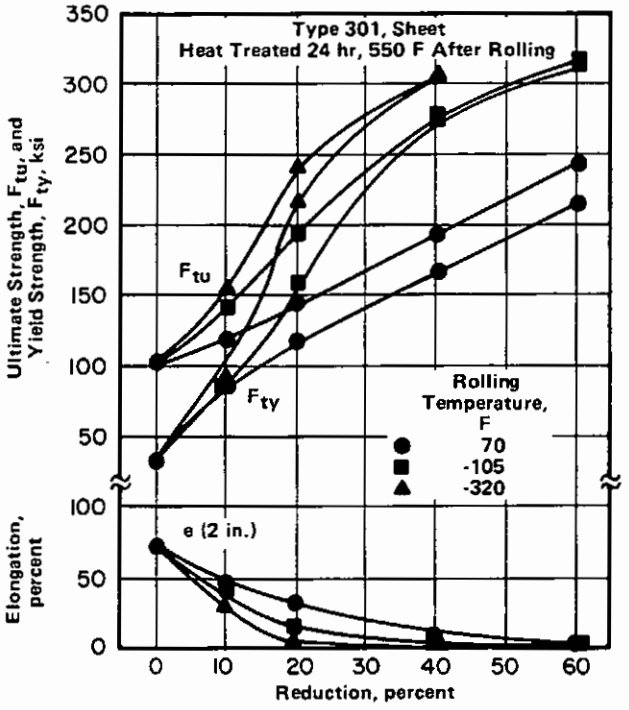


FIGURE 3.02112. EFFECT OF COLD REDUCTION AT ROOM AND CRYOGENIC TEMPERATURES PLUS HEAT TREATMENT ON TENSILE PROPERTIES OF TYPE 301 (76)

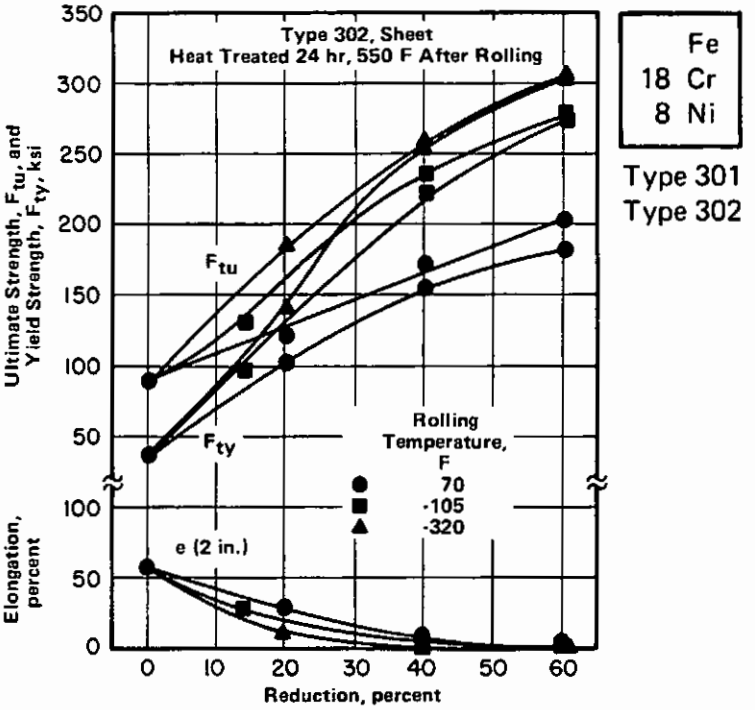


FIGURE 3.02113. EFFECT OF COLD REDUCTION AT ROOM AND CRYOGENIC TEMPERATURES PLUS HEAT TREATMENT ON TENSILE PROPERTIES OF TYPE 302 (76)

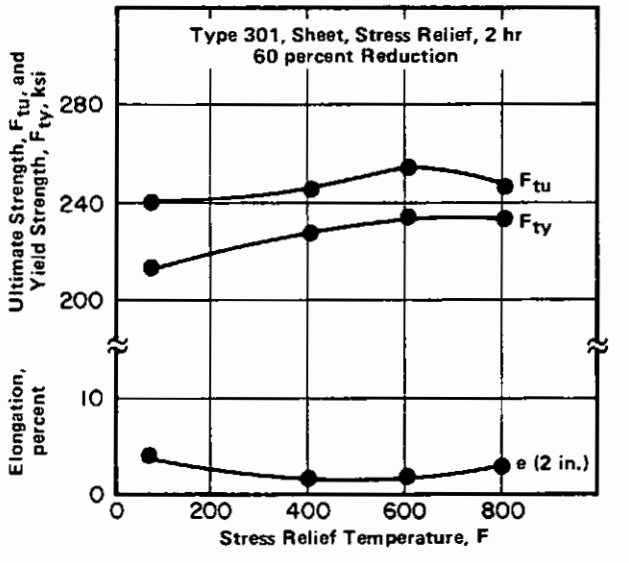


FIGURE 3.02114. EFFECT OF STRESS-RELIEF TEMPERATURE ON TENSILE PROPERTIES OF 60 PERCENT REDUCED SHEET (28)

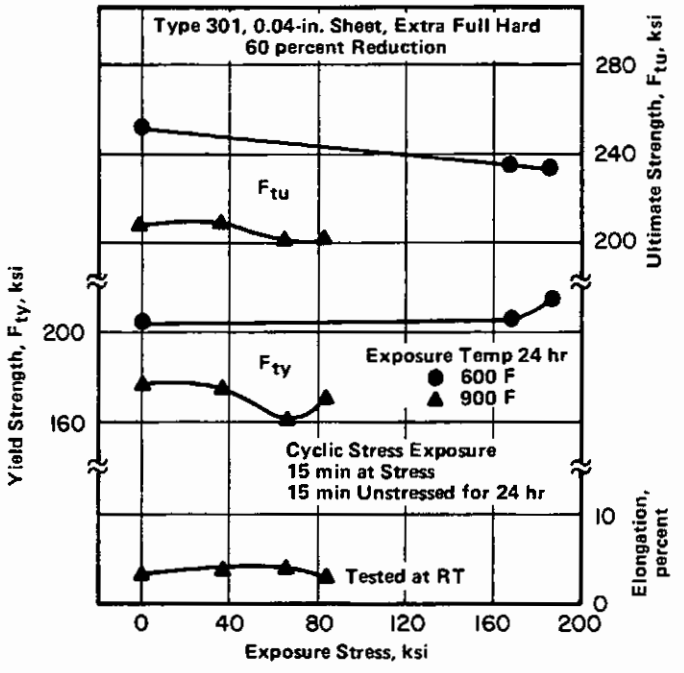


FIGURE 3.02115. EFFECT OF CYCLIC EXPOSURE STRESS ON ROOM-TEMPERATURE TENSILE PROPERTIES OF 60 PERCENT REDUCED SHEET EXPOSED AT 600 AND 900 F (27)

Fe
18 Cr
8 Ni

Type 301
Type 302

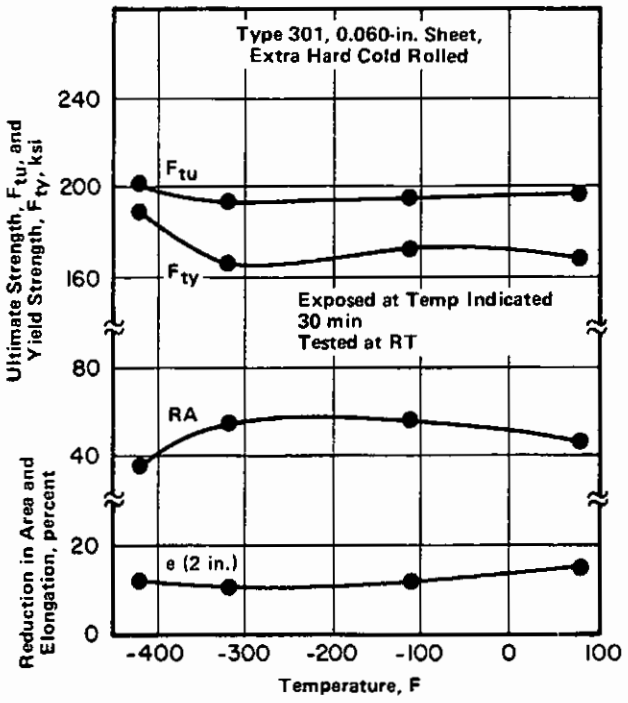


FIGURE 3.02116. EFFECT OF EXPOSURE AT LOW TEMPERATURE ON ROOM-TEMPERATURE TENSILE PROPERTIES OF EXTRA-HARD COLD-ROLLED SHEET (32)

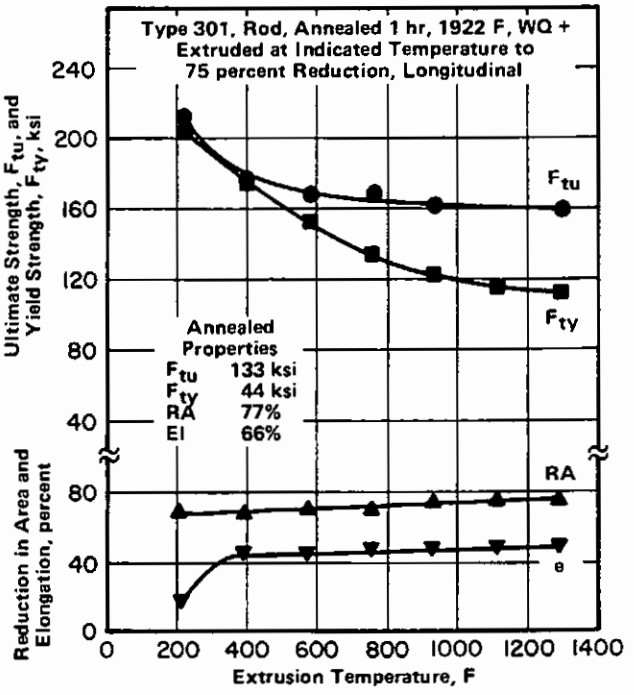


FIGURE 3.02117. EFFECTS OF EXTRUSION TEMPERATURE ON LONGITUDINAL TENSILE PROPERTIES OF TYPE 301 (56)

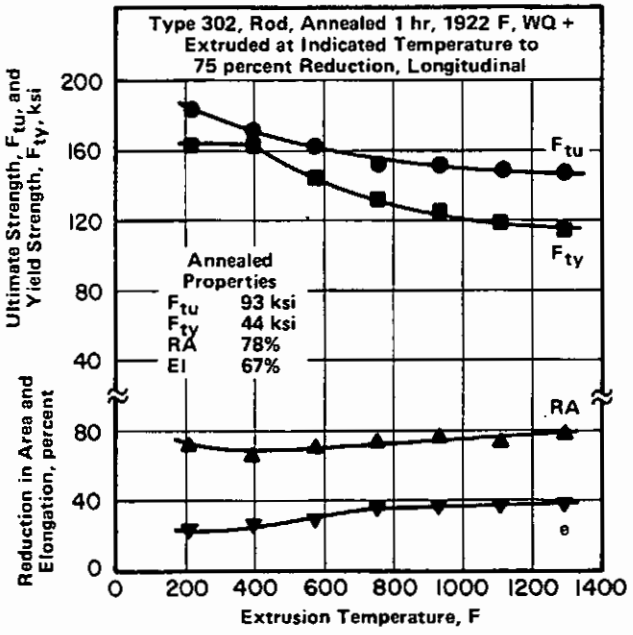


FIGURE 3.02118. EFFECTS OF EXTRUSION TEMPERATURE ON LONGITUDINAL TENSILE PROPERTIES OF TYPE 302 (56)

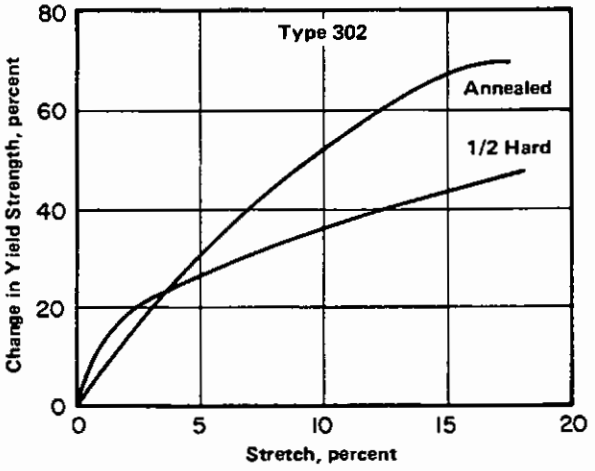


FIGURE 3.02119. EFFECT OF STRETCHING ON TENSILE YIELD STRENGTH OF TYPE 302 (76)

Fe
18 Cr
8 Ni

Type 301
Type 302

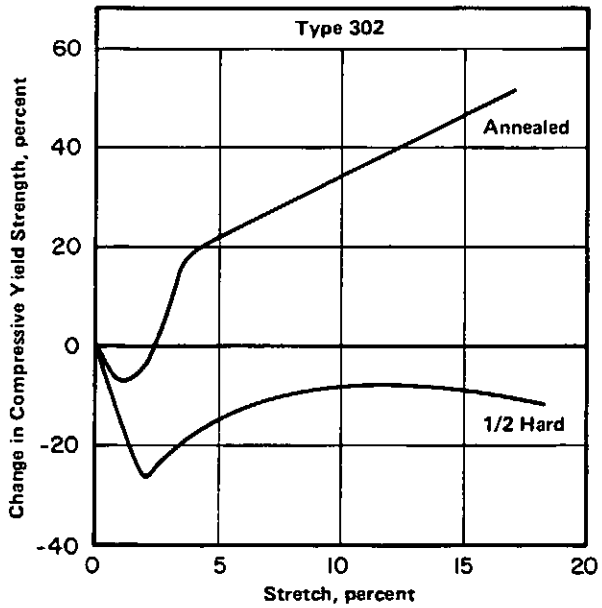


FIGURE 3.0221. EFFECT OF STRETCHING ON COMPRESSIVE YIELD STRENGTH OF TYPE 302 (76)

Type	Impact Energy, ft-lb		
	Izod	Charpy Keyhole Notch	Charpy V Notch
301(a)	70–120	90	110
302(a)	70–120	68–92	–
302B(a)	70–90	–	–
CF-20(b)	–	60	–

(a) Annealed.
(b) Heat treated at 2000 F plus water quench.

TABLE 3.0231. IMPACT PROPERTIES AT ROOM TEMPERATURE (76)

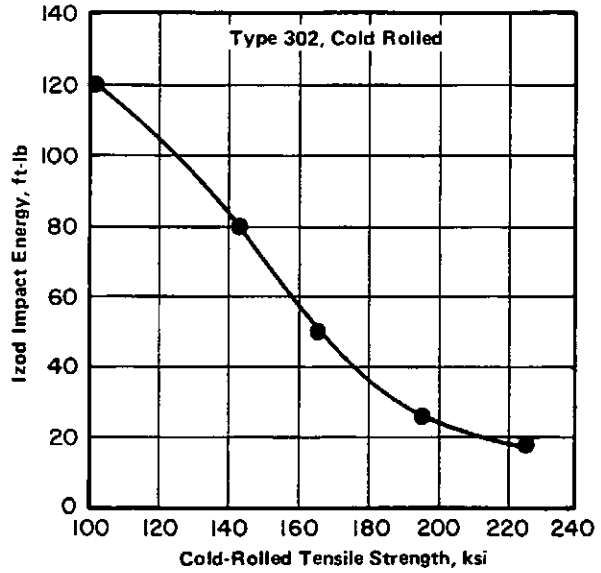


FIGURE 3.0232. RELATION BETWEEN IMPACT ENERGY AND TENSILE STRENGTH FOR COLD-ROLLED TYPE 302 (76)

Fe
18 Cr
8 Ni

Type 301
Type 302

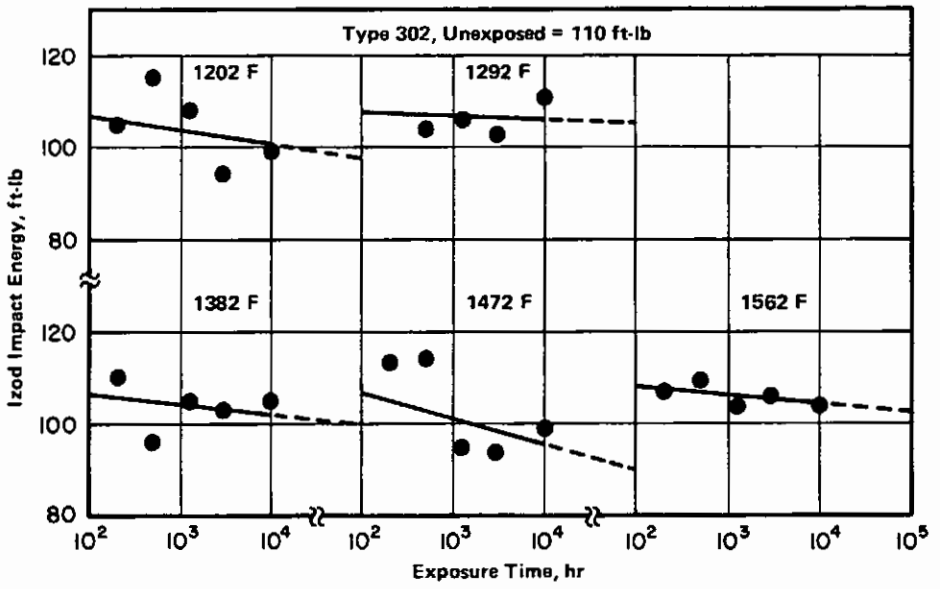


FIGURE 3.0233. EFFECTS OF EXPOSURE TIME IN AIR AT ELEVATED TEMPERATURES ON IMPACT ENERGY (75)

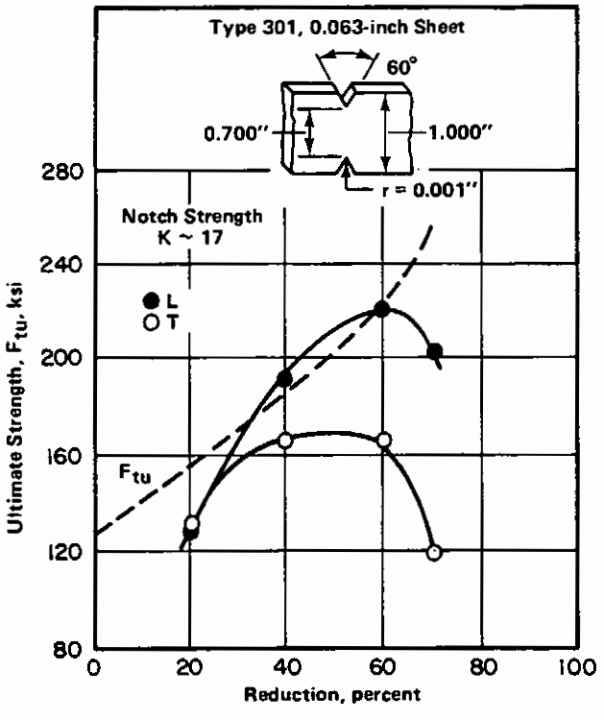


FIGURE 3.02711. EFFECT OF COLD ROLLING AND TEST DIRECTION ON NOTCH STRENGTH OF SHEET

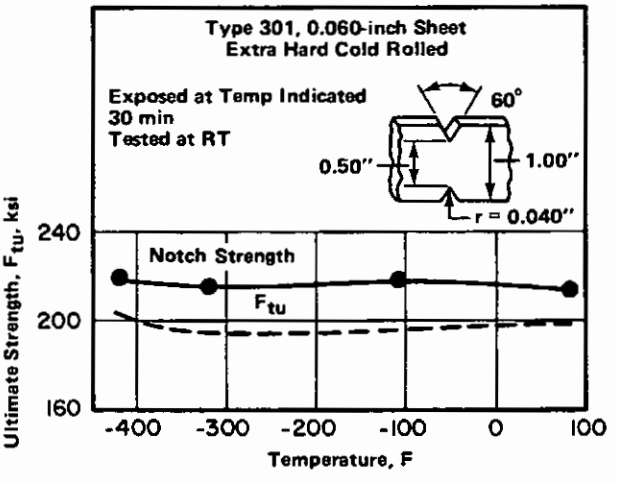


FIGURE 3.02712. EFFECT OF EXPOSURE AT LOW TEMPERATURE ON ROOM-TEMPERATURE NOTCH STRENGTH OF EXTRA-HARD COLD-ROLLED SHEET (32)

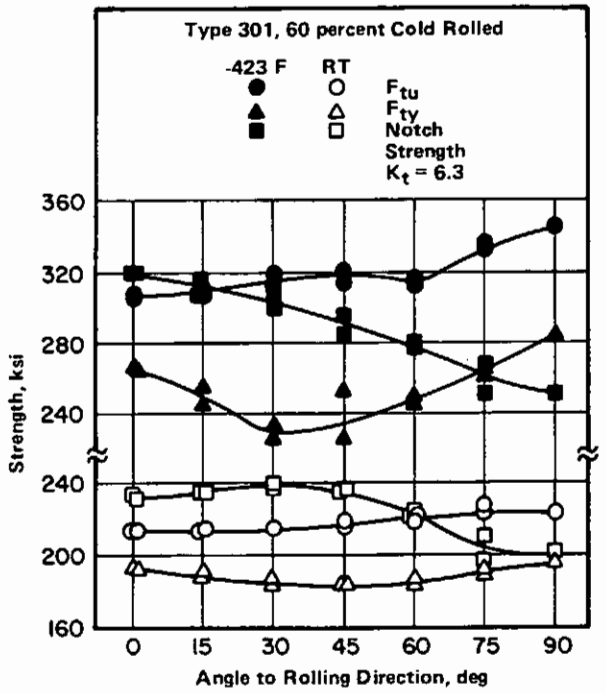
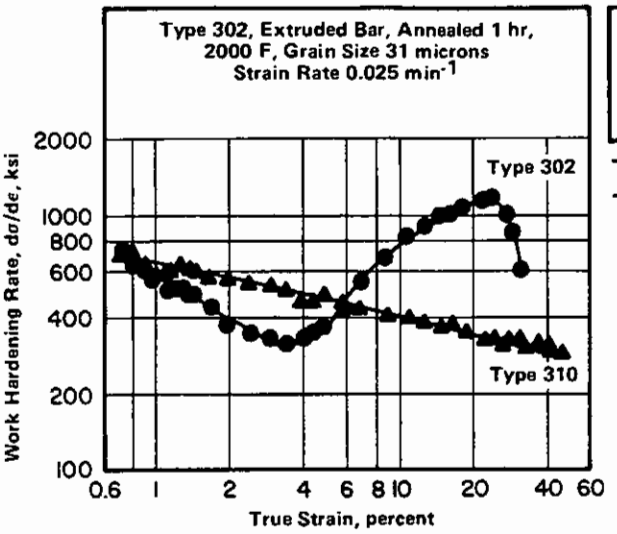


FIGURE 3.02713. EFFECT OF TEST DIRECTION IN RELATION TO ROLLING DIRECTION ON TENSILE PROPERTIES AND NOTCH STRENGTH OF 60 PERCENT COLD-REDUCED SHEET (48)



Fe
18 Cr
8 Ni

Type 301
Type 302

FIGURE 3.03112. TENSILE WORK-HARDENING RATES FOR TYPES 302 AND 310 AT -112 F (78)

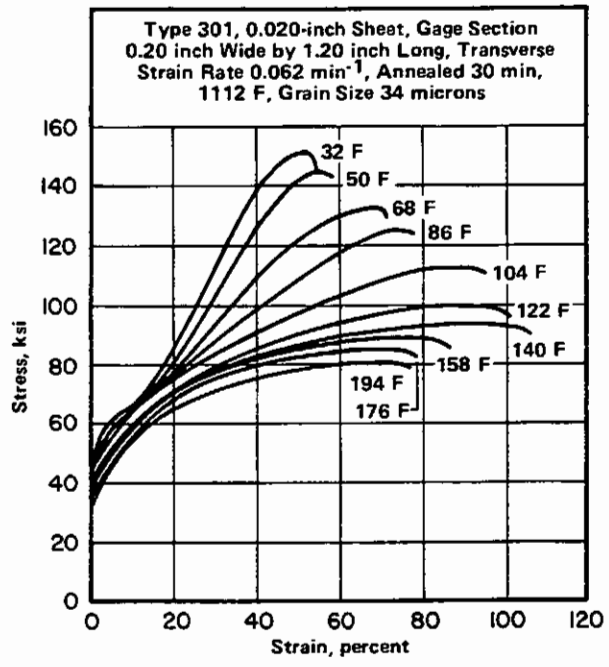


FIGURE 3.03113. STRESS-STRAIN CURVES FOR ANNEALED TYPE 301 (77)

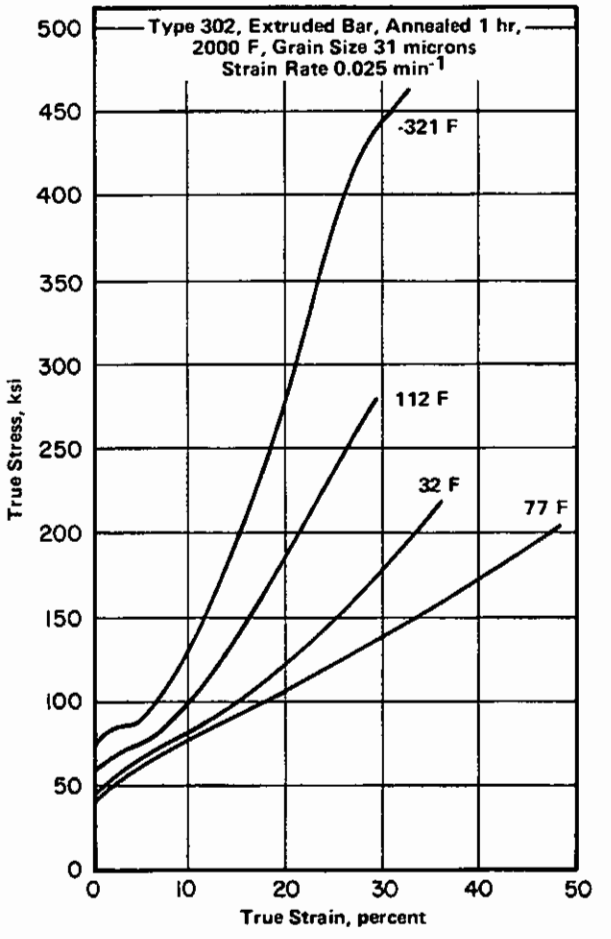


FIGURE 3.03114. TRUE STRESS-STRAIN CURVES FOR ANNEALED TYPE 302 AT ROOM AND CRYOGENIC TEMPERATURES (78)

Fe
18 Cr
8 Ni

Type 301
Type 302

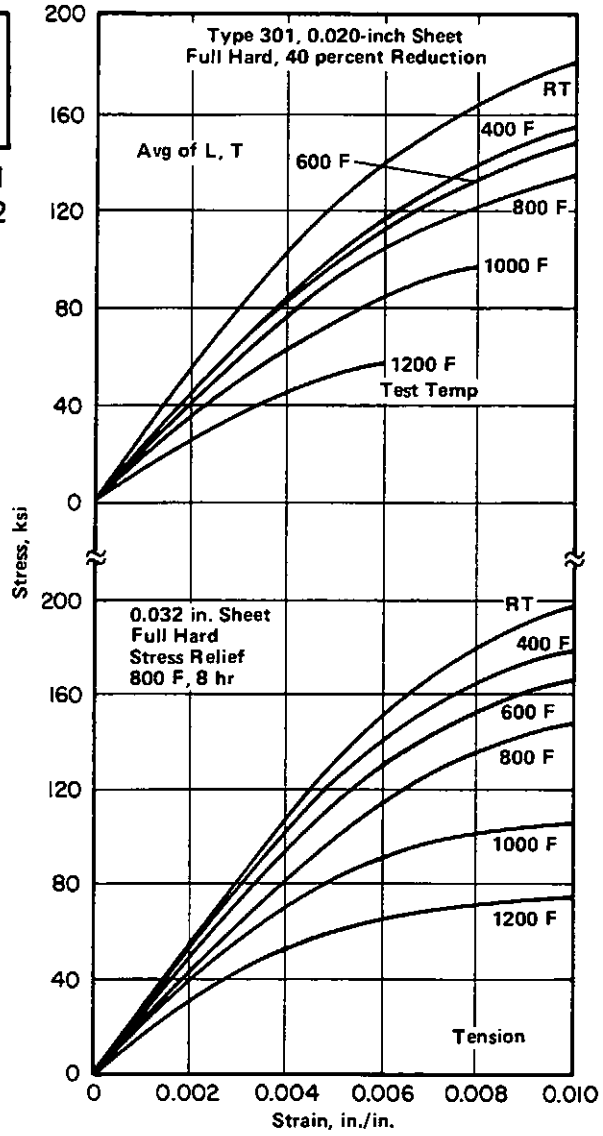


FIGURE 3.03115. STRESS-STRAIN CURVES FOR TYPE 301 FULL-HARD AND FULL-HARD STRESS-RELIEVED SHEET AT ROOM AND ELEVATED TEMPERATURES (11)

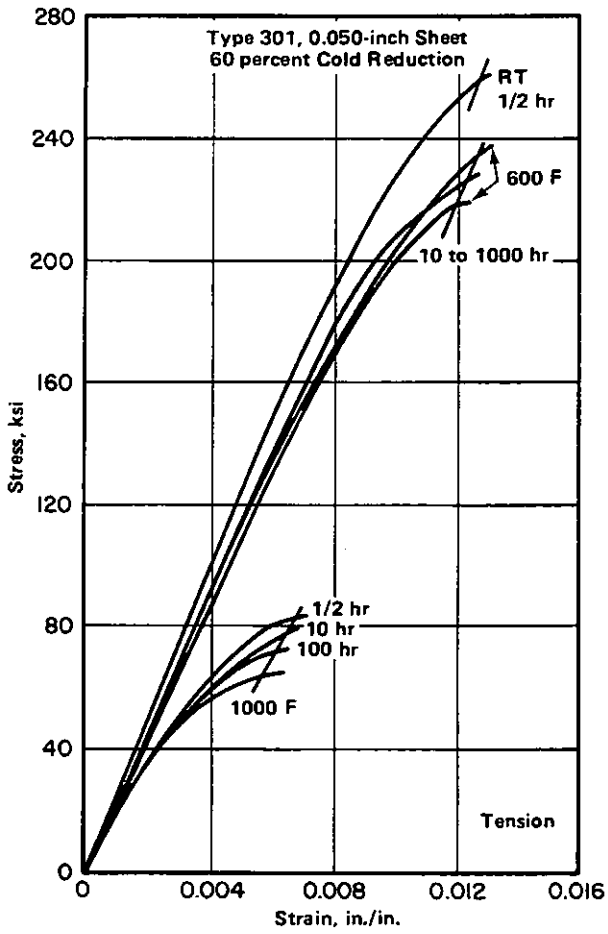


FIGURE 3.03116. STRESS-STRAIN CURVES IN TENSION FOR VARIOUS TEMPERATURES AND EXPOSURE TIMES FOR 60 PERCENT COLD-REDUCED SHEET (38)

Fe
18 Cr
8 Ni

Type 301
Type 302

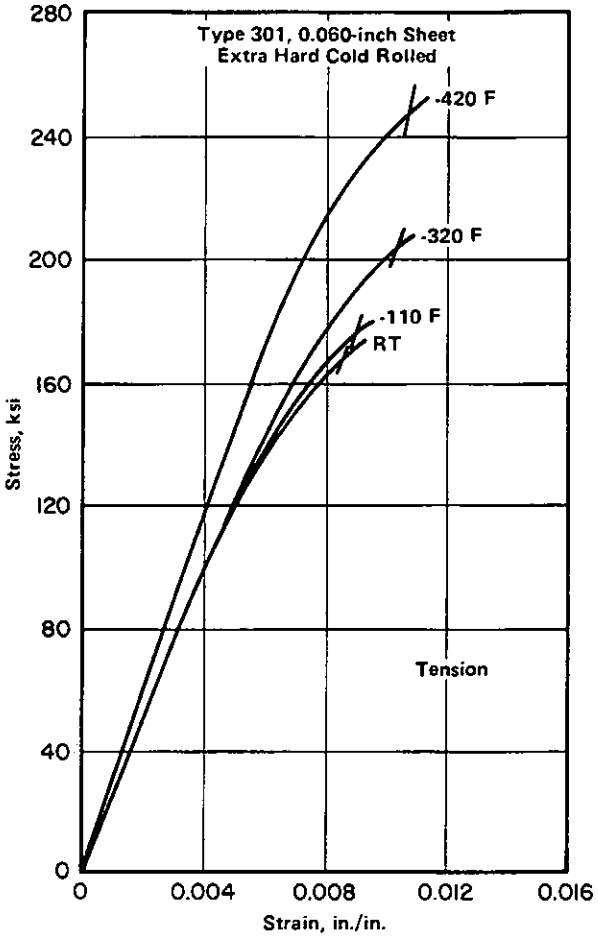


FIGURE 3.03117. STRESS-STRAIN CURVES IN TENSION AT LOW TEMPERATURES OF EXTRA-HARD COLD-ROLLED SHEET (32)

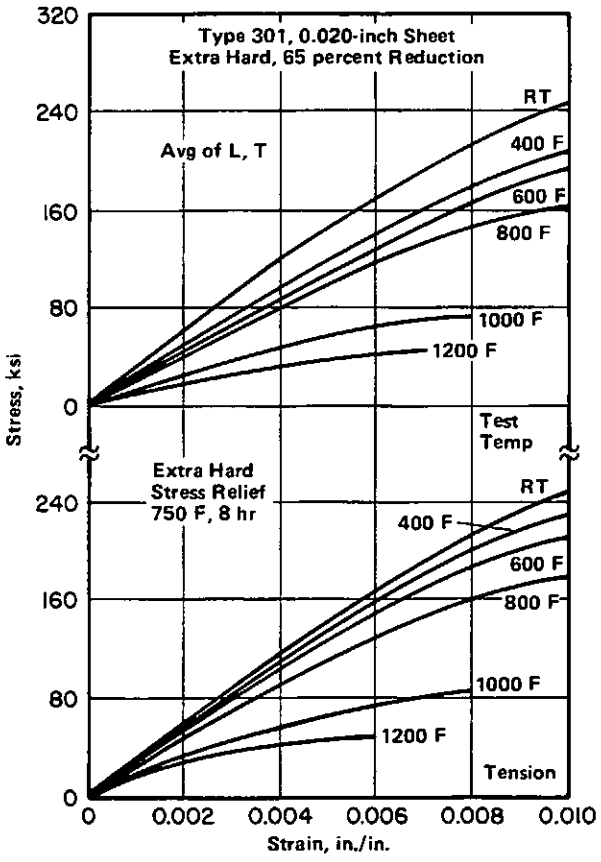


FIGURE 3.03118. STRESS-STRAIN CURVES FOR TYPE 301 EXTRA-HARD AND EXTRA-HARD STRESS-RELIEVED SHEET AT ROOM AND ELEVATED TEMPERATURES (11)

Fe
18 Cr
8 Ni

Type 301
Type 302

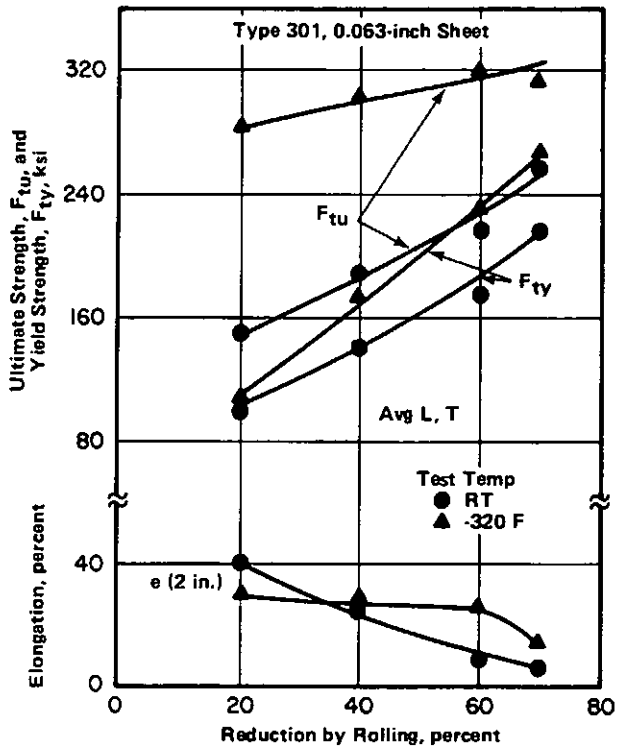


FIGURE 3.03121. EFFECT OF COLD ROLLING ON TENSILE PROPERTIES OF TYPE 301 SHEET AT ROOM TEMPERATURE AND -320 F (18)

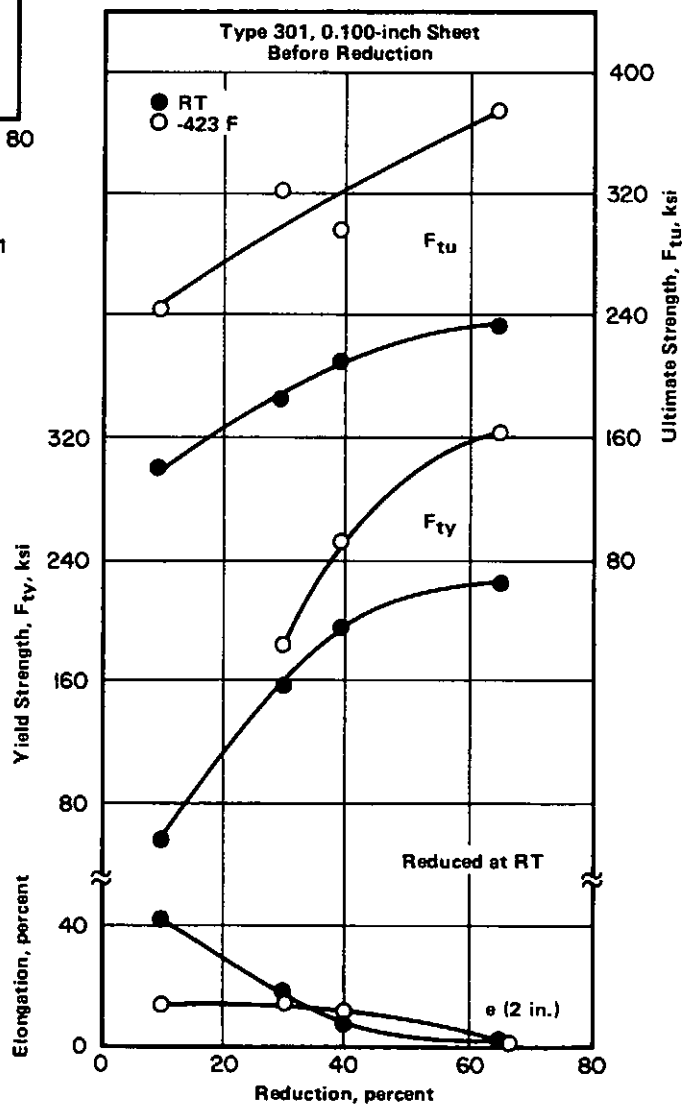


FIGURE 3.03122. EFFECT OF PERCENT REDUCTION ON TENSILE PROPERTIES OF SHEET TESTED AT ROOM TEMPERATURE AND -423 F (24)

Fe
18 Cr
8 Ni

Type 301
Type 302

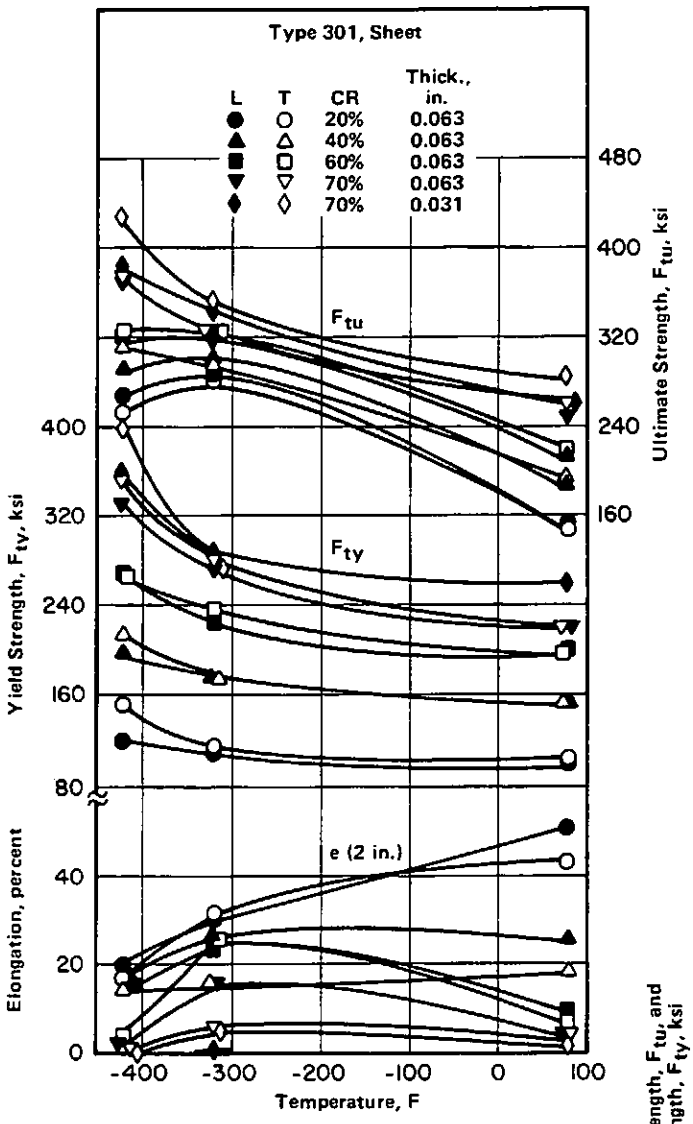


FIGURE 3.03123. EFFECT OF LOW TEMPERATURE AND PERCENT COLD REDUCTION ON TENSILE PROPERTIES OF SHEET (34)

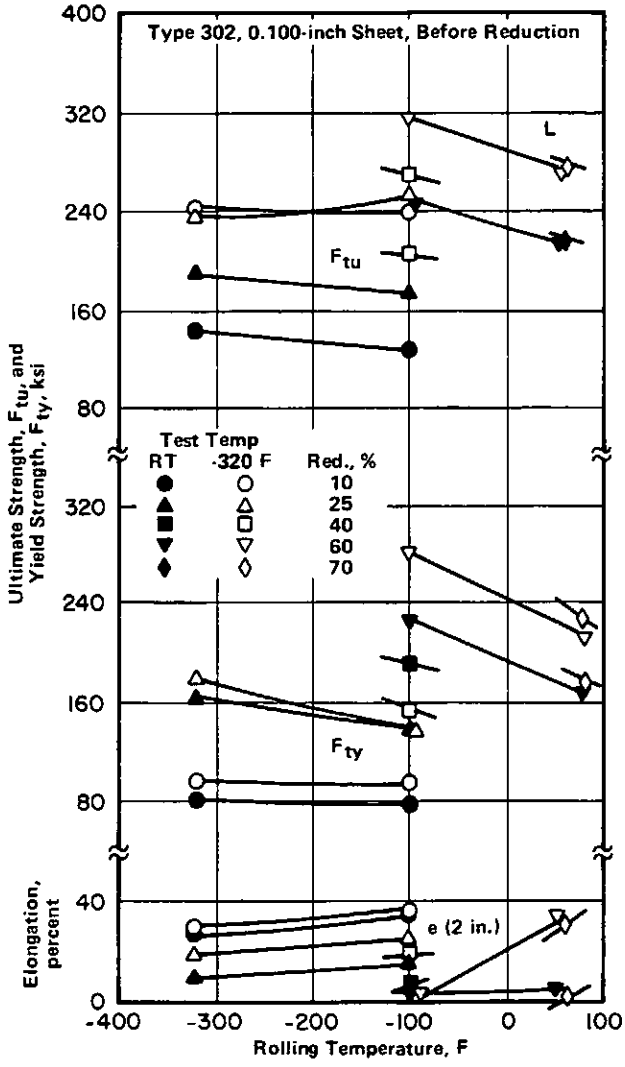


FIGURE 3.03124. EFFECT OF LOW ROLLING TEMPERATURE ON TENSILE PROPERTIES AT ROOM TEMPERATURE AND -320 F OF REDUCED SHEET (24)

Fe
18 Cr
8 Ni

Type 301
Type 302

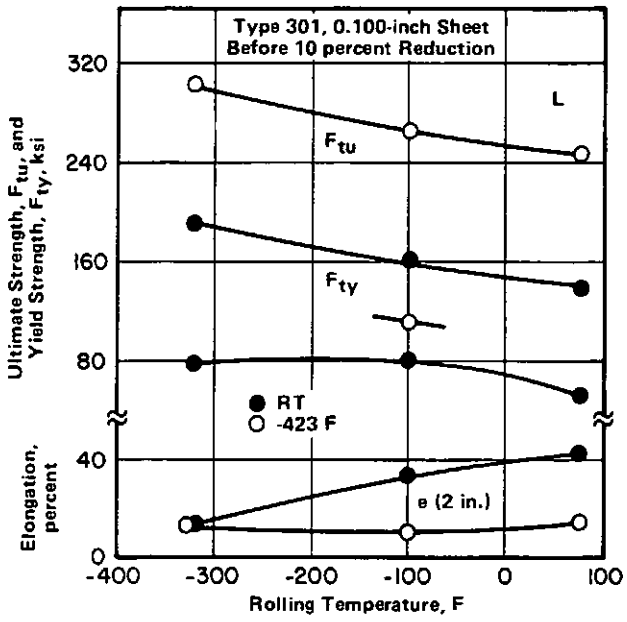


FIGURE 3.03125. EFFECT OF LOW ROLLING TEMPERATURE ON TENSILE PROPERTIES AT ROOM TEMPERATURE AND -423 F OF 10 PERCENT REDUCED SHEET (24)

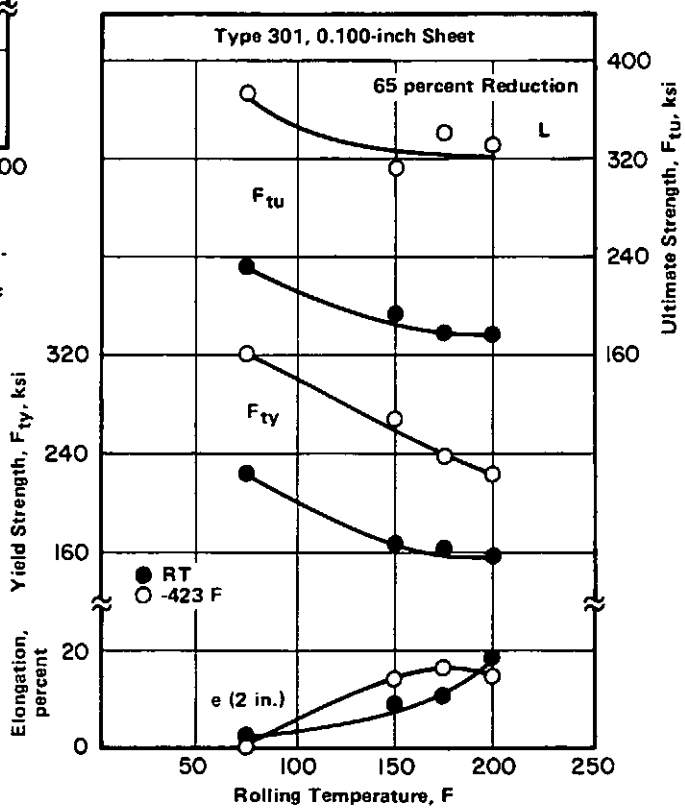


FIGURE 3.03126. EFFECT OF ROLLING TEMPERATURE ON TENSILE PROPERTIES AT ROOM TEMPERATURE AND -423 F OF 65 PERCENT REDUCED SHEET (24)

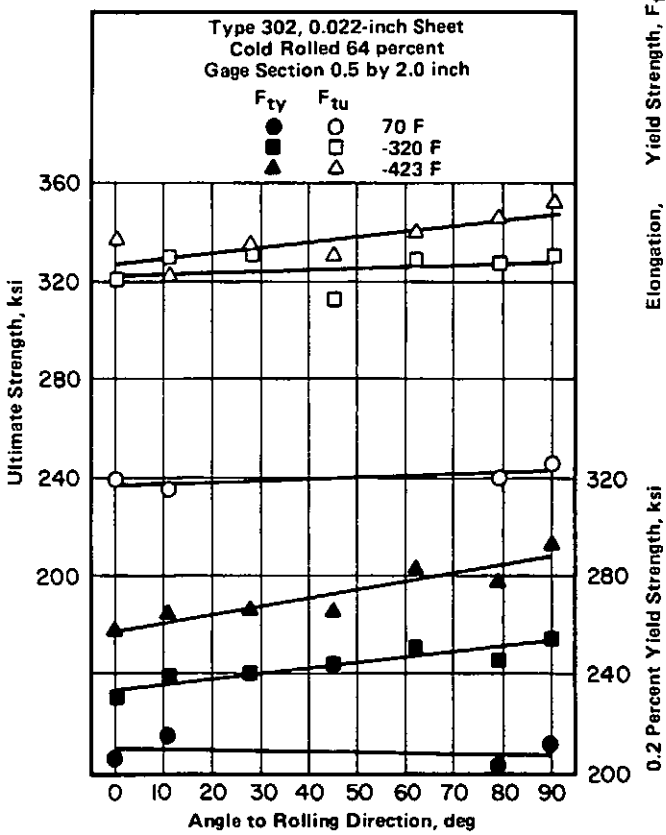


FIGURE 3.03127. EFFECT OF TEST DIRECTION ON TENSILE STRENGTH OF COLD-ROLLED SHEET AT ROOM AND CRYOGENIC TEMPERATURES (79)

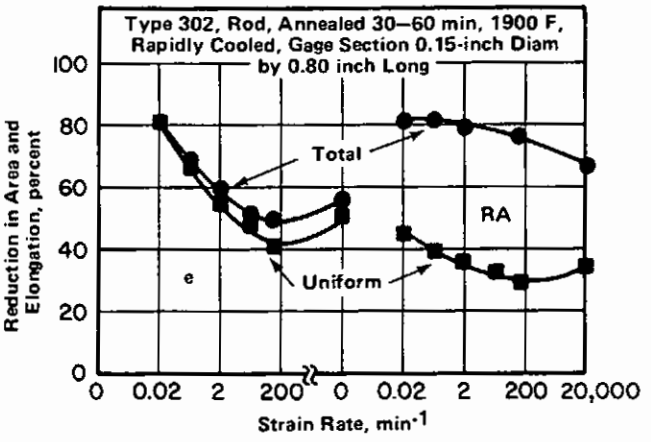


FIGURE 3.03132. EFFECTS OF STRAIN RATE ON TENSILE DUCTILITY OF TYPE 302 AT ROOM TEMPERATURE (80)

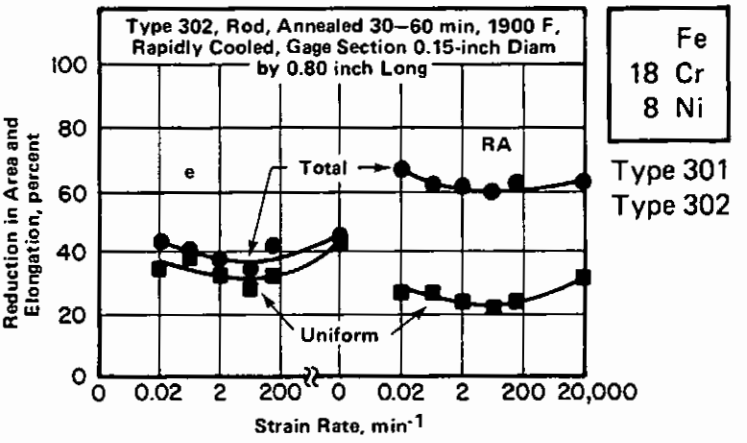


FIGURE 3.03133. EFFECTS OF STRAIN RATE ON TENSILE DUCTILITY OF TYPE 302 AT -321 F (80)

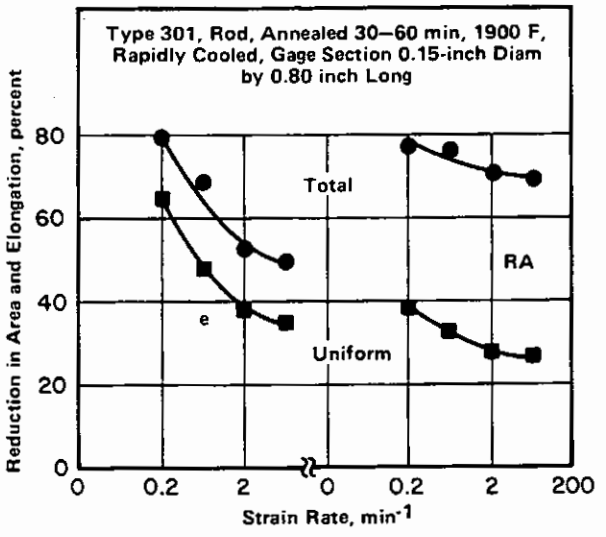


FIGURE 3.03134. EFFECTS OF STRAIN RATE ON TENSILE DUCTILITY OF TYPE 301 AT ROOM TEMPERATURE (80)

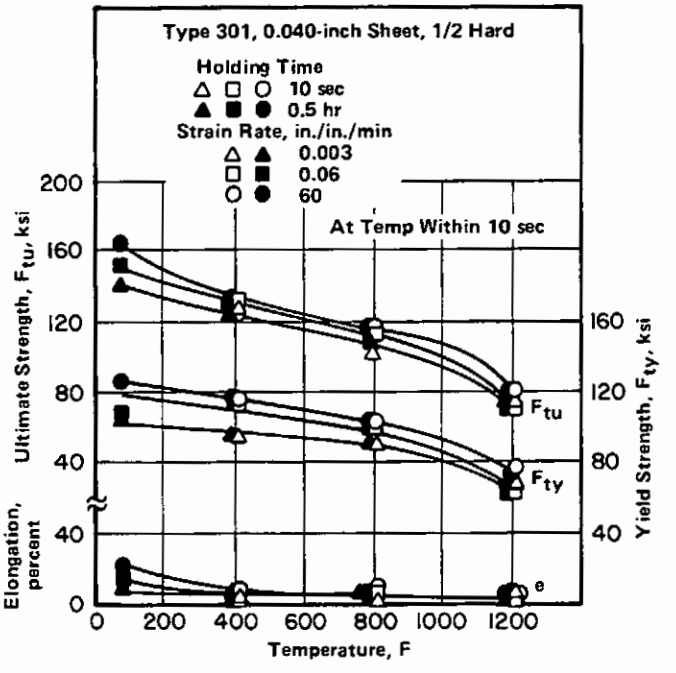


FIGURE 3.03135. EFFECT OF TEST TEMPERATURE, STRAIN RATE, AND HOLDING TIME ON TENSILE PROPERTIES OF TYPE 301 1/2-HARD SHEET (17)

Fe
18 Cr
8 Ni

Type 301
Type 302

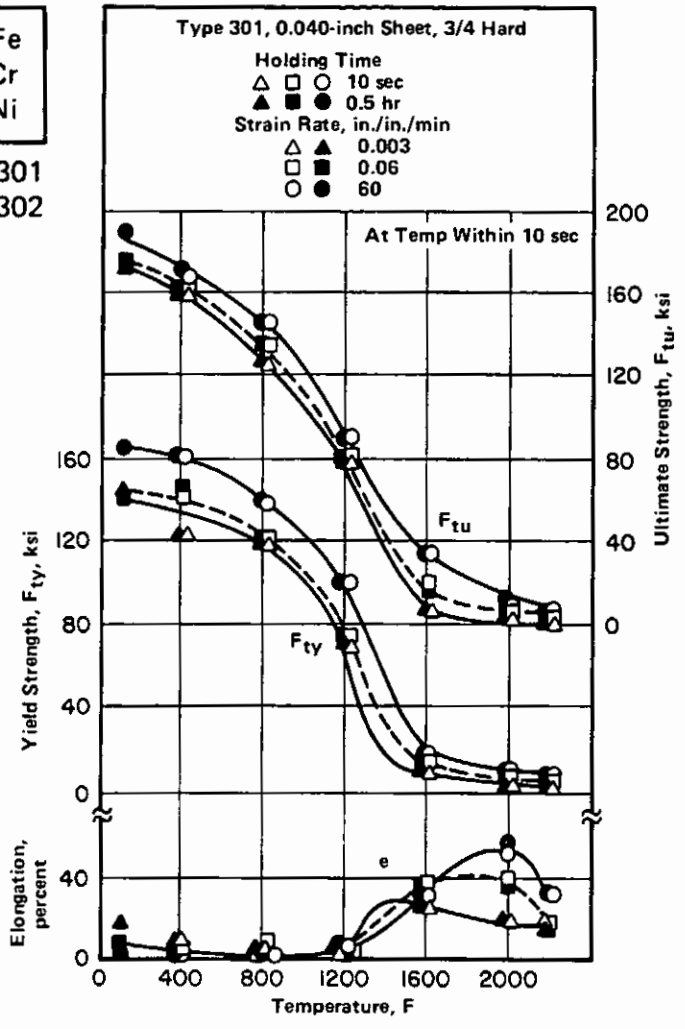


FIGURE 3.03136. EFFECT OF TEST TEMPERATURE, STRAIN RATE, AND HOLDING TIME ON TENSILE PROPERTIES OF TYPE 301 3/4-HARD SHEET (17)

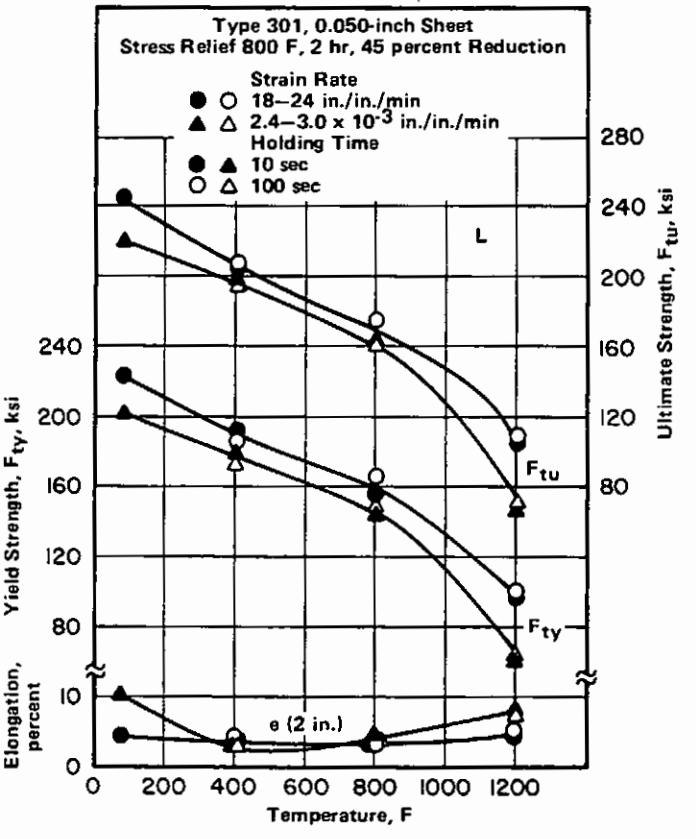


FIGURE 3.03137. EFFECT OF TEST TEMPERATURE, STRAIN RATE, AND HOLDING TIME ON TENSILE PROPERTIES OF 45 PERCENT REDUCED SHEET (28)

Fe
18 Cr
8 Ni

Type 301
Type 302

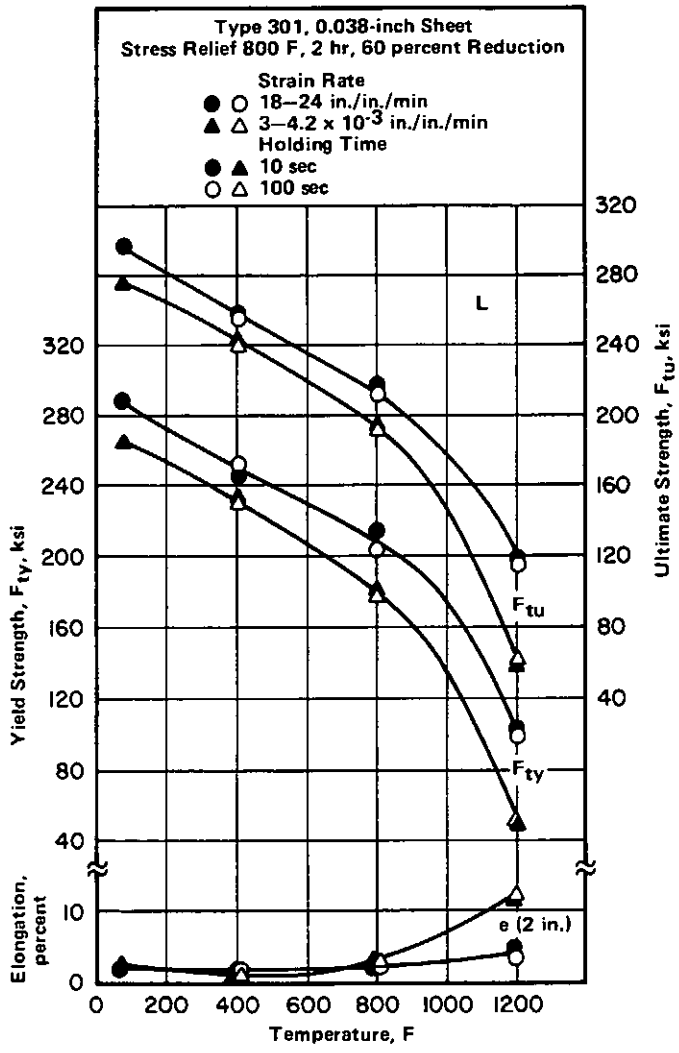


FIGURE 3.03138. EFFECT OF TEST TEMPERATURE, STRAIN RATE, AND HOLDING TIME ON TENSILE PROPERTIES OF 60 PERCENT REDUCED SHEET (28)

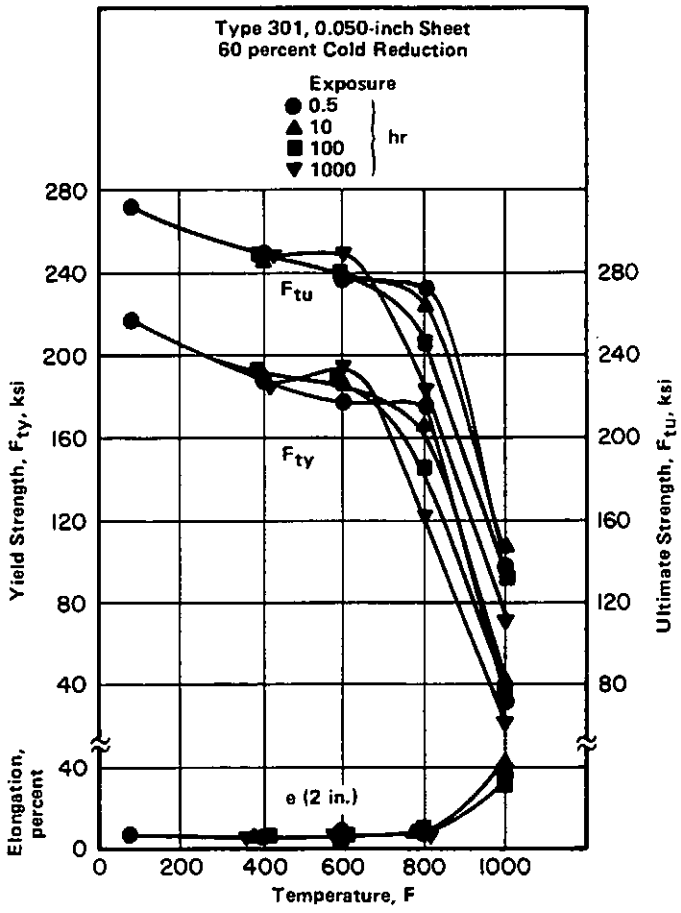


FIGURE 3.03139. EFFECT OF TEST TEMPERATURE AND EXPOSURE TIME ON TENSILE PROPERTIES OF 60 PERCENT COLD-REDUCED SHEET (38)

Fe
18 Cr
8 Ni

Type 301
Type 302

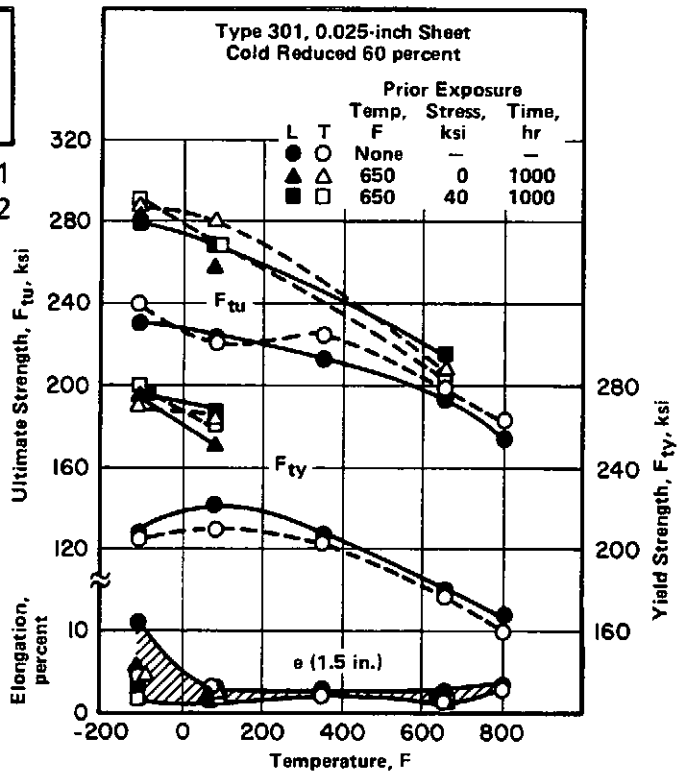


FIGURE 3.031312. EFFECT OF TEST TEMPERATURE AND PRIOR EXPOSURE ON TENSILE PROPERTIES OF 60 PERCENT COLD-REDUCED SHEET (45)

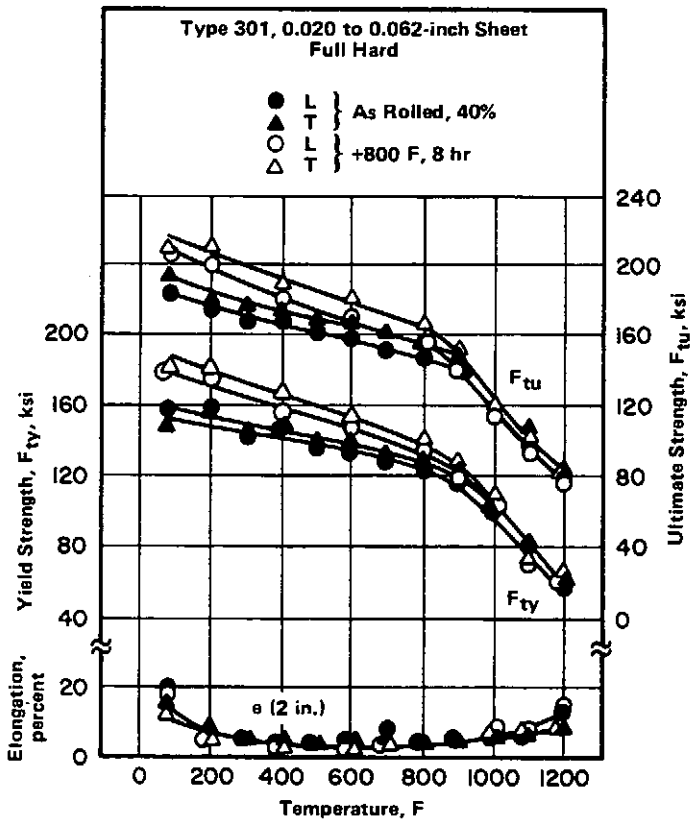


FIGURE 3.03141. EFFECT OF TEST TEMPERATURE, TEST DIRECTION, AND STRESS RELIEF ON TENSILE PROPERTIES OF TYPE 301 FULL-HARD SHEET (11)

Fe
18 Cr
8 Ni

Type 301
Type 302

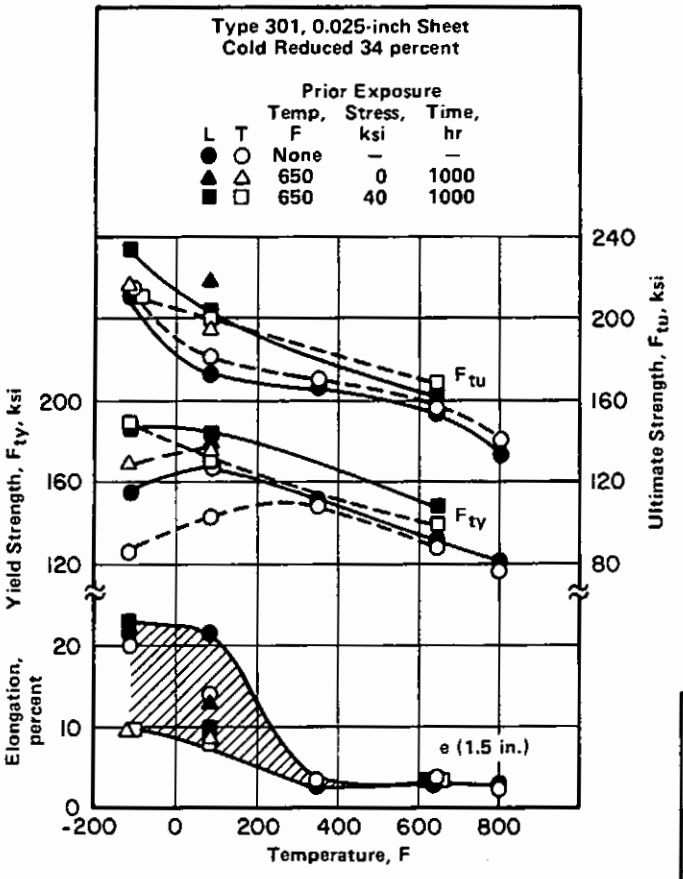


FIGURE 3.031310. EFFECT OF TEST TEMPERATURE AND PRIOR EXPOSURE ON TENSILE PROPERTIES OF 34 PERCENT COLD-REDUCED SHEET (45)

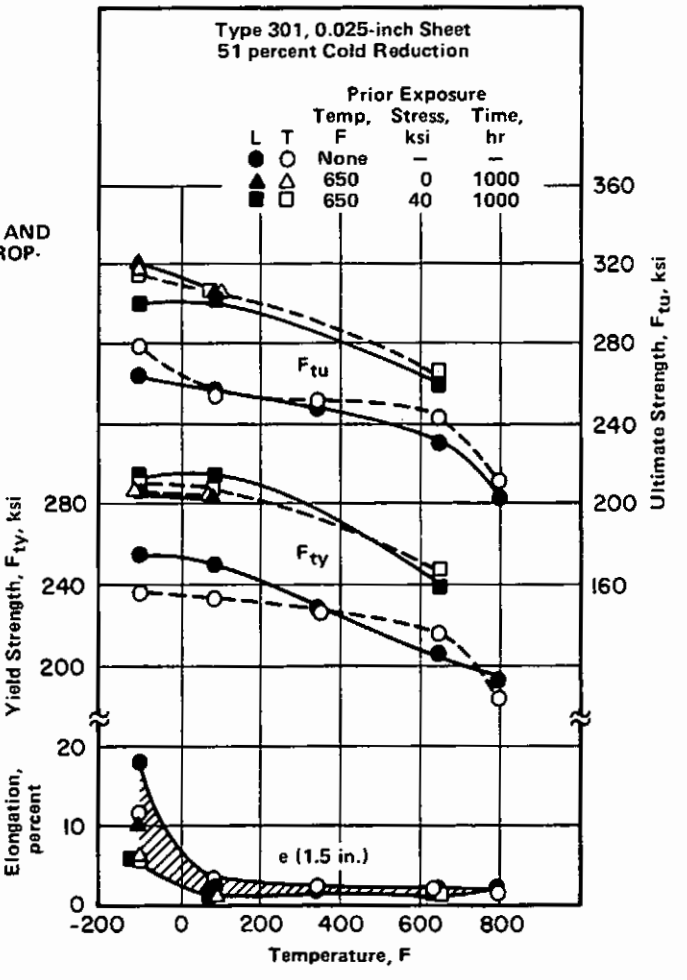


FIGURE 3.031311. EFFECT OF TEST TEMPERATURE AND PRIOR EXPOSURE ON TENSILE PROPERTIES OF 51 PERCENT COLD-REDUCED SHEET (45)

Fe
18 Cr
8 Ni

Type 301
Type 302

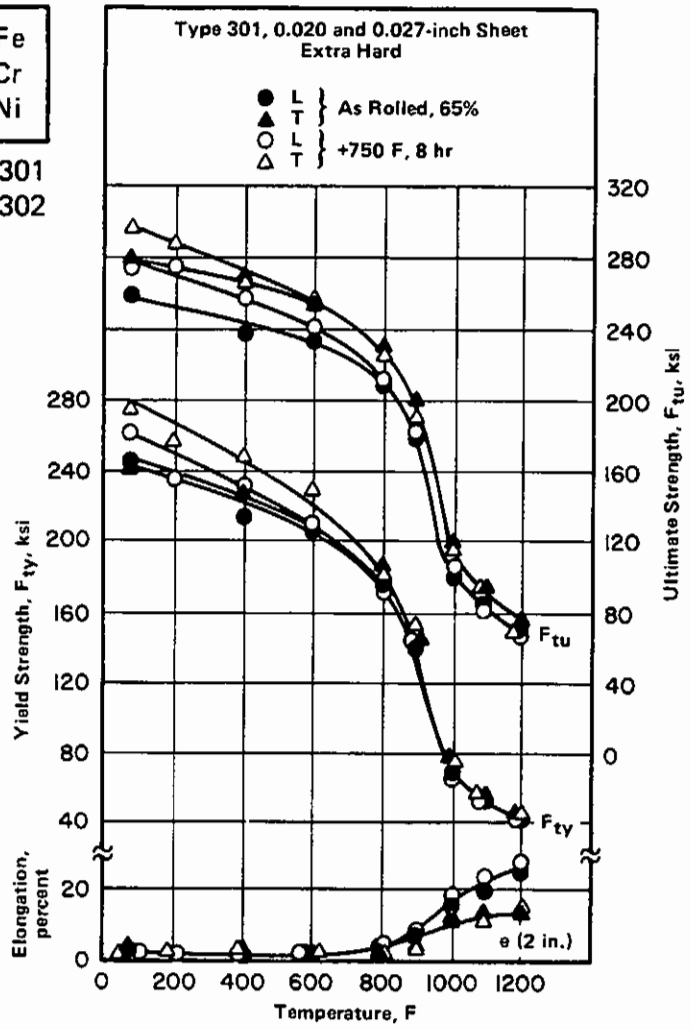


FIGURE 3.03142. EFFECT OF TEST TEMPERATURE, TEST DIRECTION, AND STRESS RELIEF ON TENSILE PROPERTIES OF TYPE 301 EXTRA-HARD SHEET (11)

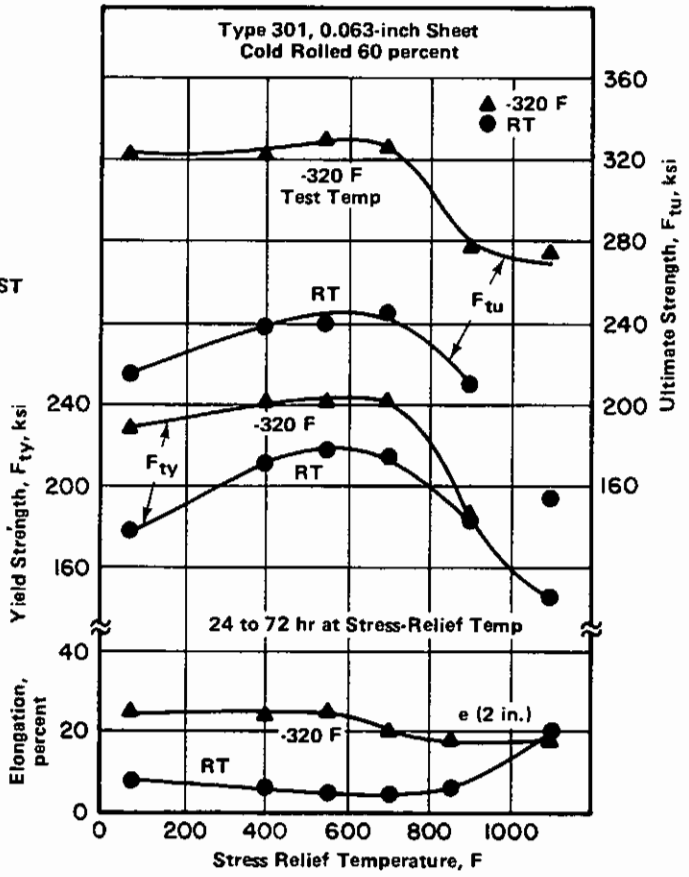


FIGURE 3.03143. EFFECT OF STRESS RELIEF AND TEST TEMPERATURE ON TENSILE PROPERTIES OF COLD-ROLLED SHEET (18)

Fe
18 Cr
8 Ni

Type 301
Type 302

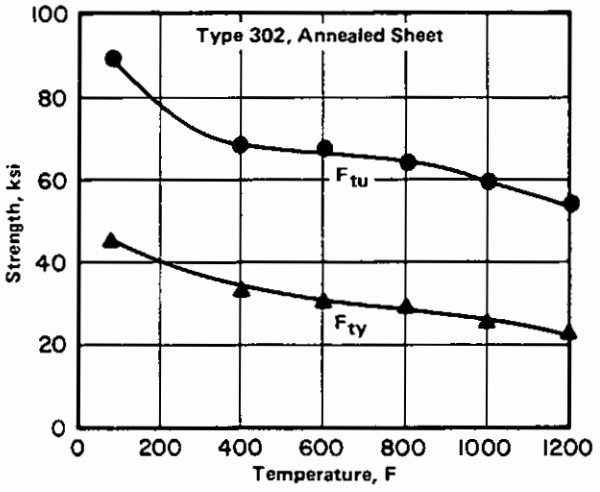


FIGURE 3.03151. EFFECT OF TEST TEMPERATURE ON TENSILE STRENGTH OF ANNEALED TYPE 302 SHEET (62)

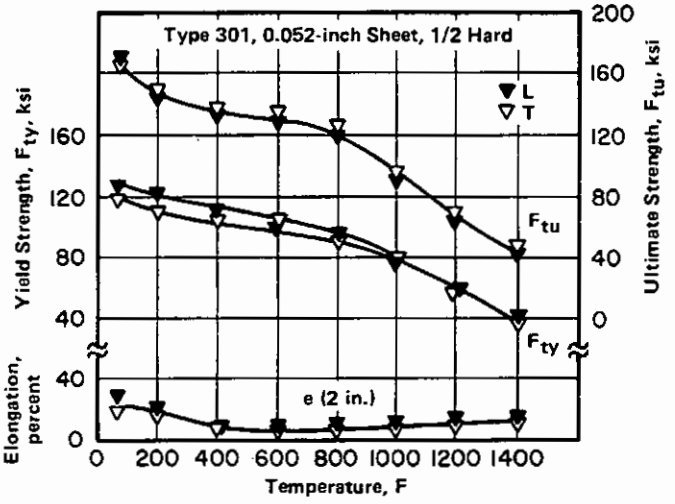


FIGURE 3.03152. EFFECT OF TEST TEMPERATURE ON TENSILE PROPERTIES OF TYPE 301, 1/2 HARD SHEET (11)

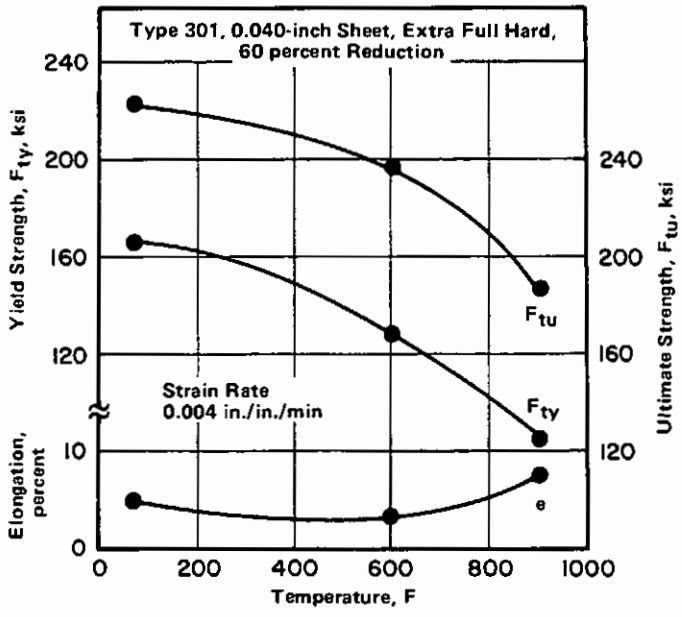


FIGURE 3.03153. EFFECT OF TEST TEMPERATURE ON TENSILE PROPERTIES OF 60 PERCENT REDUCED SHEET (26)

Fe
18 Cr
8 Ni

Type 301
Type 302

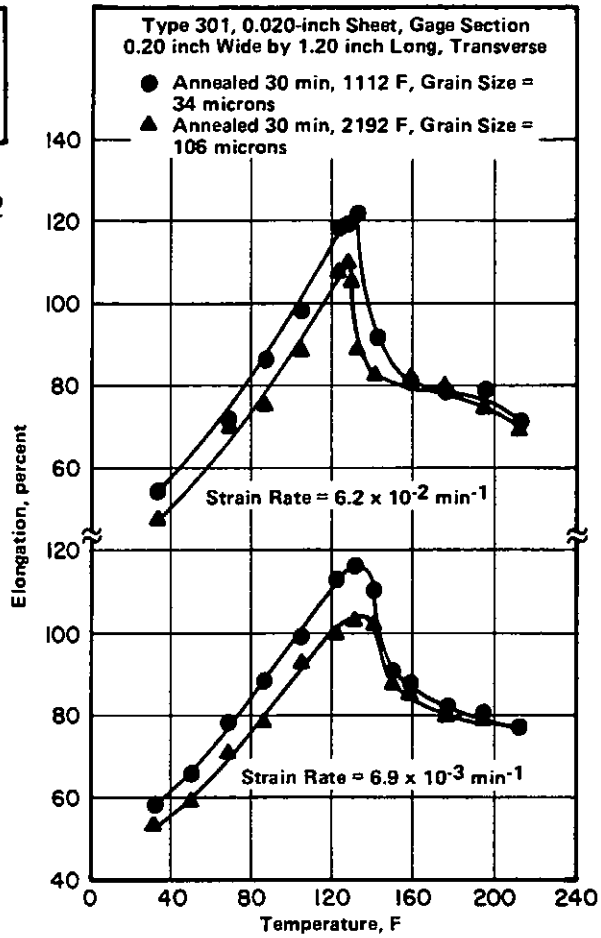


FIGURE 3.03155. EFFECTS OF GRAIN SIZE, STRAIN RATE, AND TEMPERATURE ON TENSILE ELONGATION OF TYPE 301 (77)

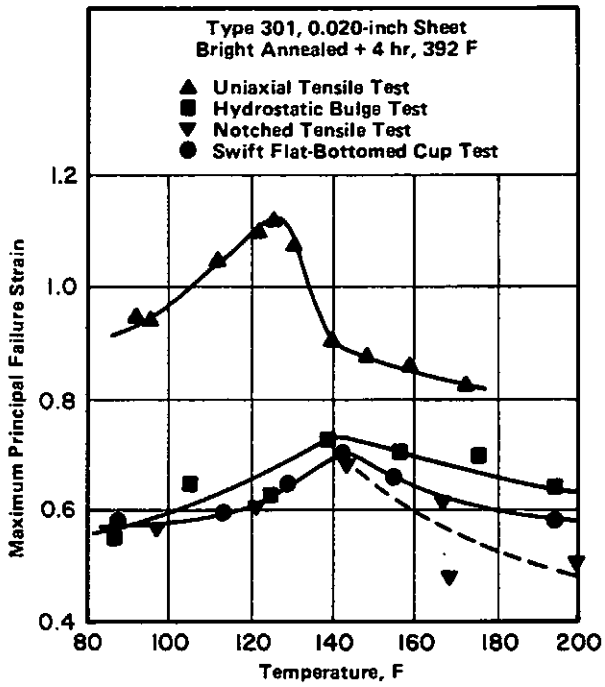


FIGURE 3.03156. EFFECTS OF TEMPERATURE ON FAILURE STRAIN FOR SEVERAL TYPES OF DEFORMATION (81)

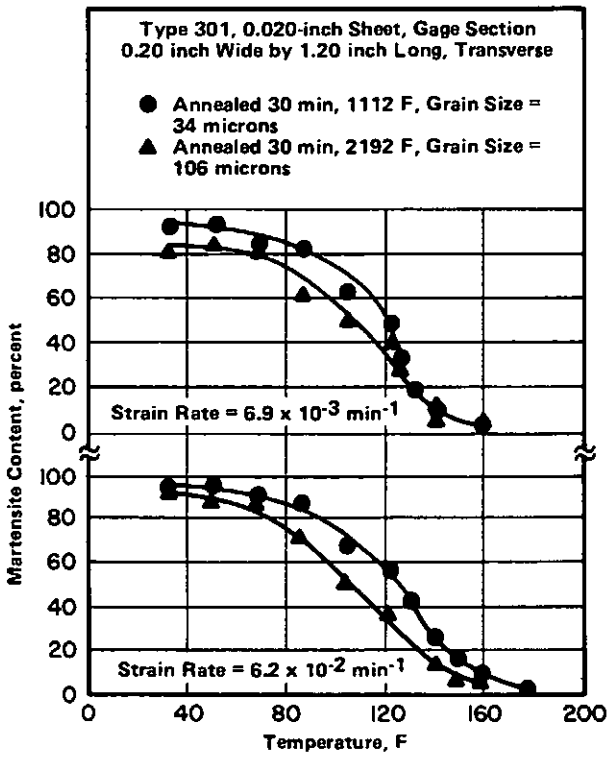


FIGURE 3.03157. EFFECTS OF GRAIN SIZE, STRAIN RATE, AND TEMPERATURE ON MARTENSITE CONTENT OF FRACTURED TENSILE SPECIMENS OF TYPE 301 (77)

Fe
18 Cr
8 Ni

Type 301
Type 302

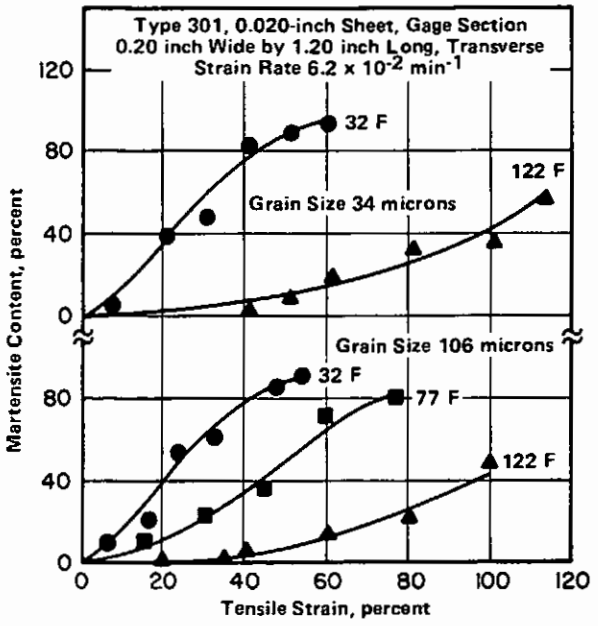


FIGURE 3.03158. EFFECTS OF GRAIN SIZE, TEST TEMPERATURE, AND TENSILE STRAIN ON MARTENSITE CONTENT OF TYPE 301 (77)

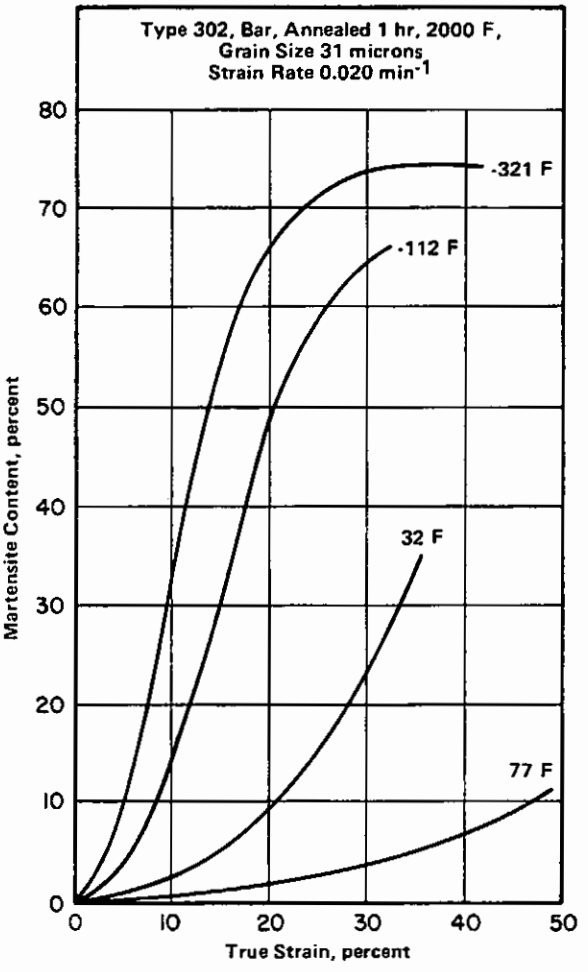


FIGURE 3.03159. EFFECTS OF TEST TEMPERATURE AND TRUE TENSILE STRAIN ON MARTENSITE CONTENT OF TYPE 302 (78)

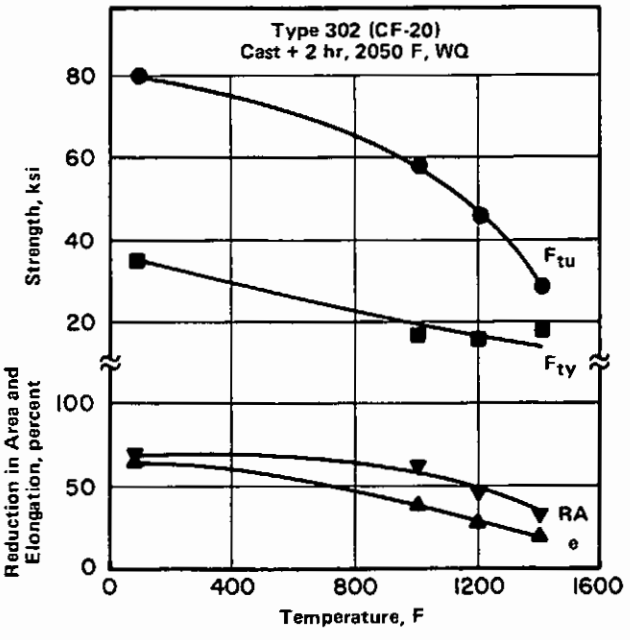


FIGURE 3.031510. EFFECTS OF TEMPERATURE ON TENSILE PROPERTIES OF CAST TYPE 302 (62)

Fe
18 Cr
8 Ni

Type 301
Type 302

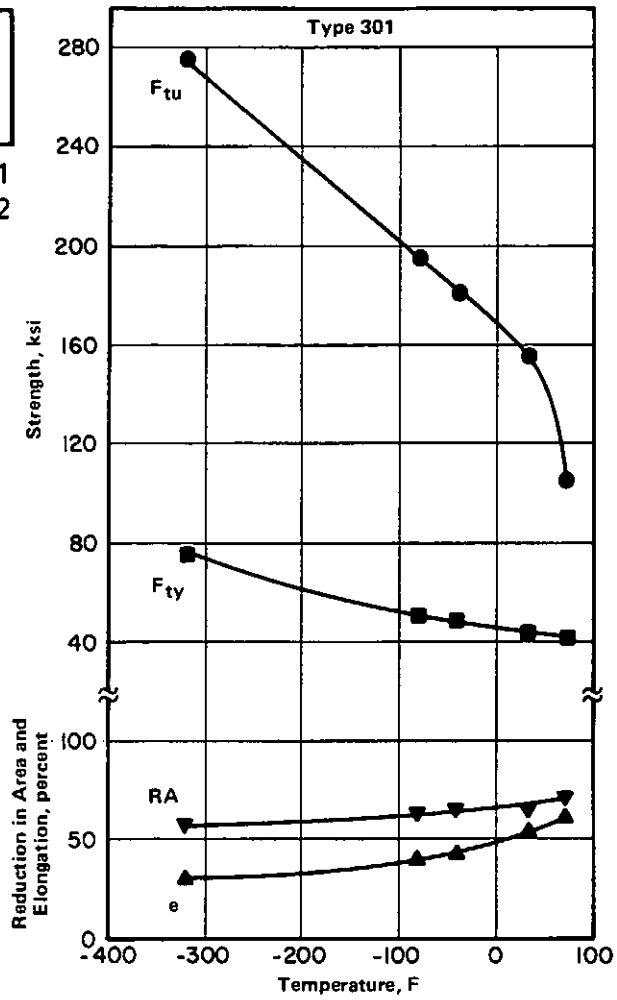


FIGURE 3.03161. EFFECT OF CRYOGENIC TEMPERATURES ON NOMINAL TENSILE PROPERTIES OF ANNEALED TYPE 301 SHEET, STRIP, PLATE, AND BAR (51)

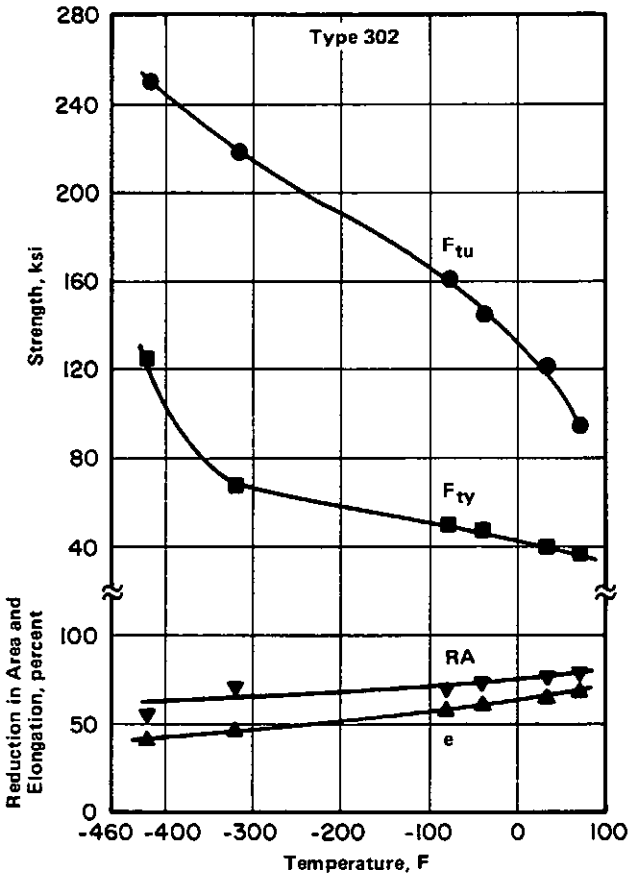


FIGURE 3.03162. EFFECT OF CRYOGENIC TEMPERATURES ON NOMINAL TENSILE PROPERTIES OF ANNEALED TYPE 302 SHEET, STRIP, PLATE, AND BAR (51)

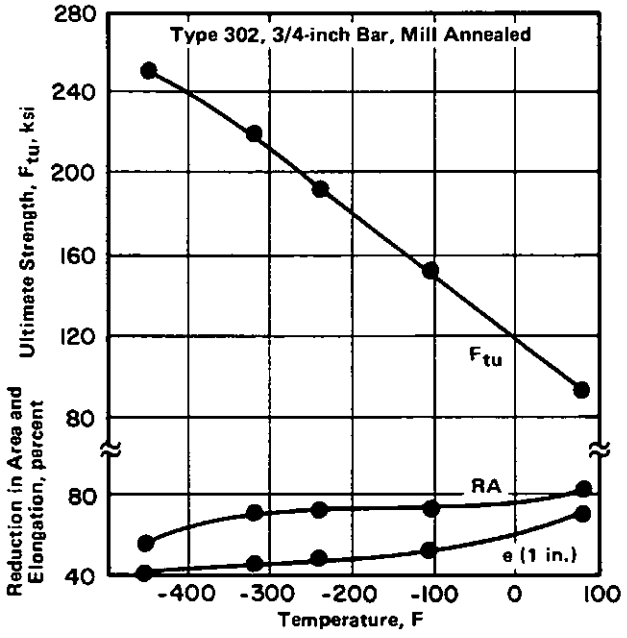


FIGURE 3.03163. EFFECT OF CRYOGENIC TEMPERATURES ON THE TENSILE PROPERTIES OF ANNEALED BAR (33)

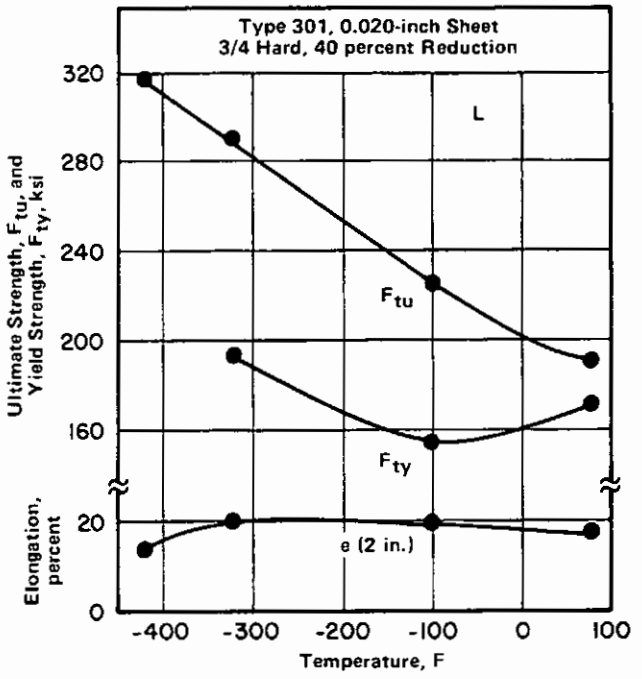


FIGURE 3.03164. EFFECT OF CRYOGENIC TEMPERATURES ON TENSILE PROPERTIES OF 40 PERCENT REDUCED SHEET (31)

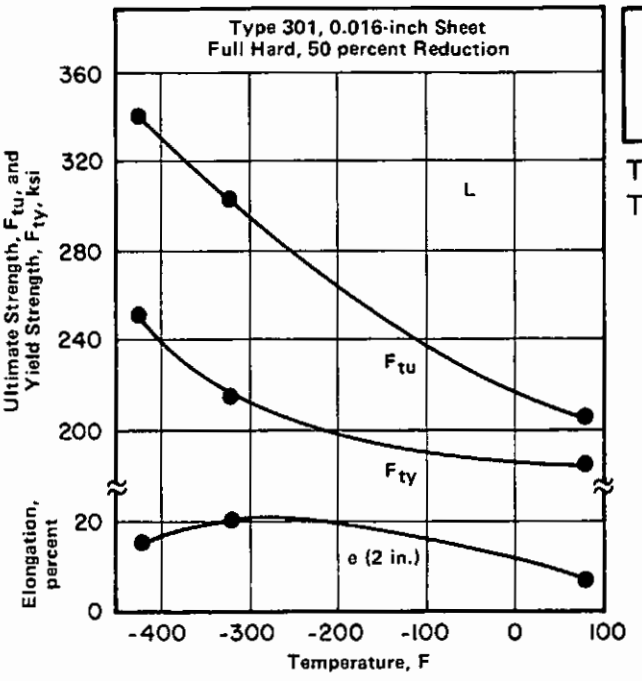


FIGURE 3.03165. EFFECT OF CRYOGENIC TEMPERATURES ON TENSILE PROPERTIES OF 50 PERCENT REDUCED SHEET (31)

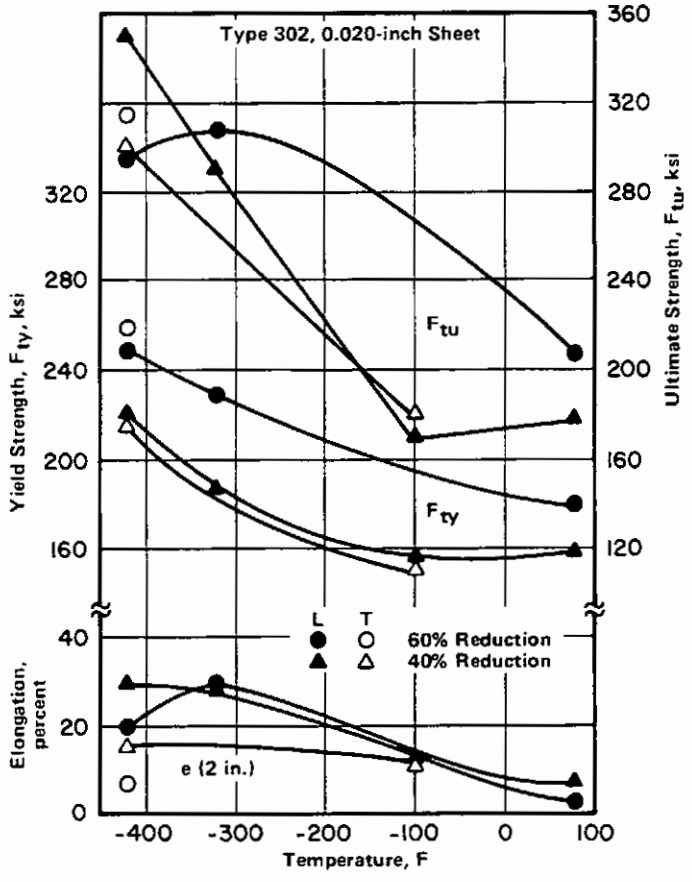


FIGURE 3.03166. EFFECT OF CRYOGENIC TEMPERATURES ON TENSILE PROPERTIES OF 40 AND 60 PERCENT REDUCED SHEET (31)

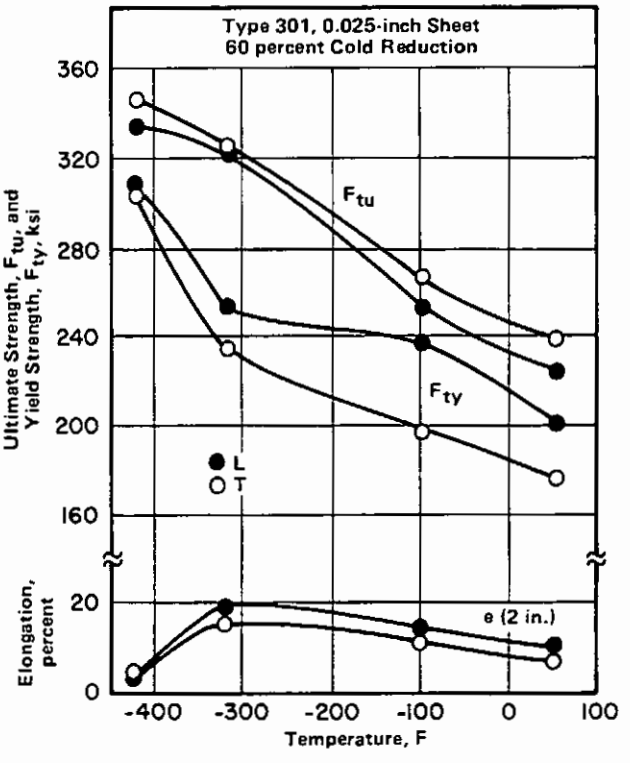


FIGURE 3.03167. EFFECT OF CRYOGENIC TEMPERATURES ON TENSILE PROPERTIES OF 60 PERCENT COLD-REDUCED SHEET (36)

Fe
18 Cr
8 Ni

Type 301
Type 302

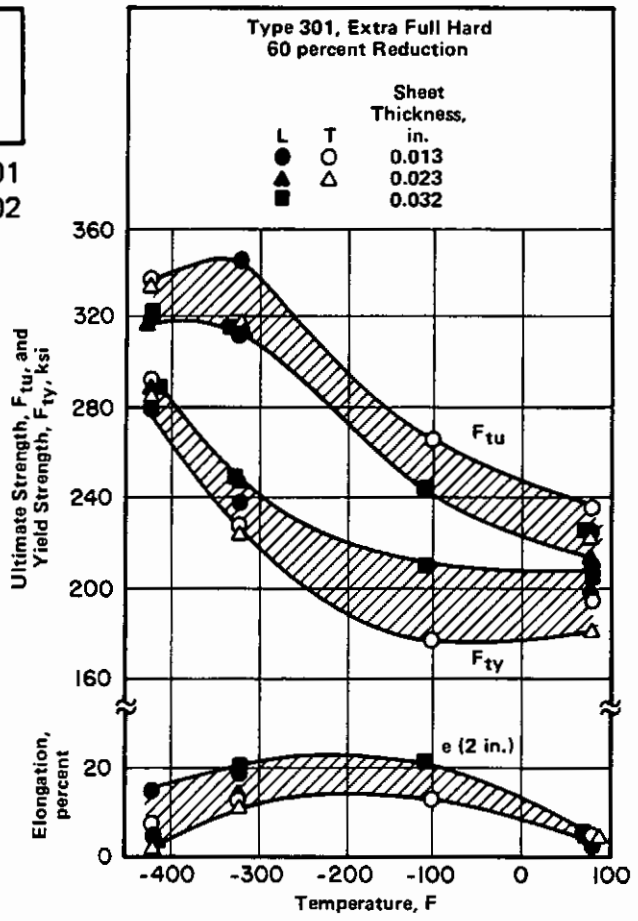


FIGURE 3.03168. EFFECTS OF CRYOGENIC TEMPERATURES AND THICKNESS ON TENSILE PROPERTIES OF 60 PERCENT REDUCED SHEET (31)

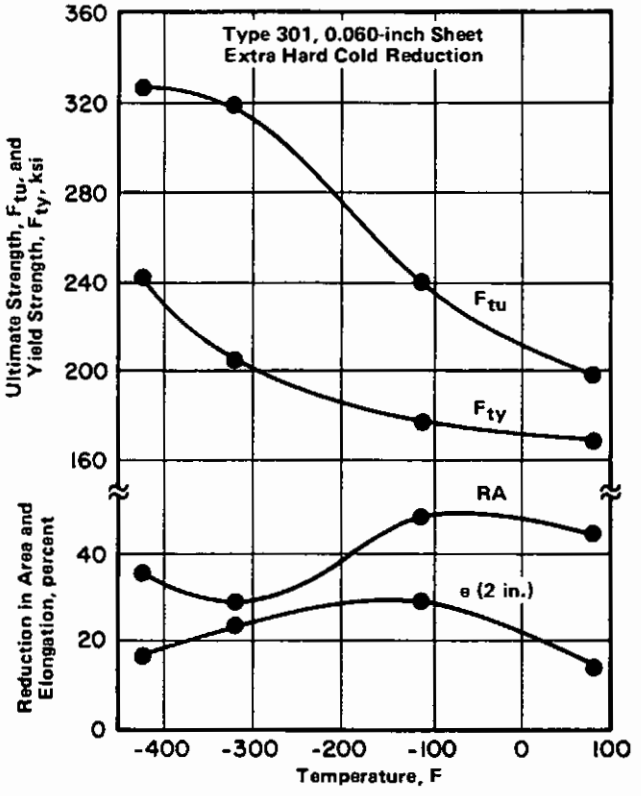


FIGURE 3.03169. EFFECT OF CRYOGENIC TEMPERATURES ON TENSILE PROPERTIES OF EXTRA-HARD COLD-ROLLED SHEET (32)

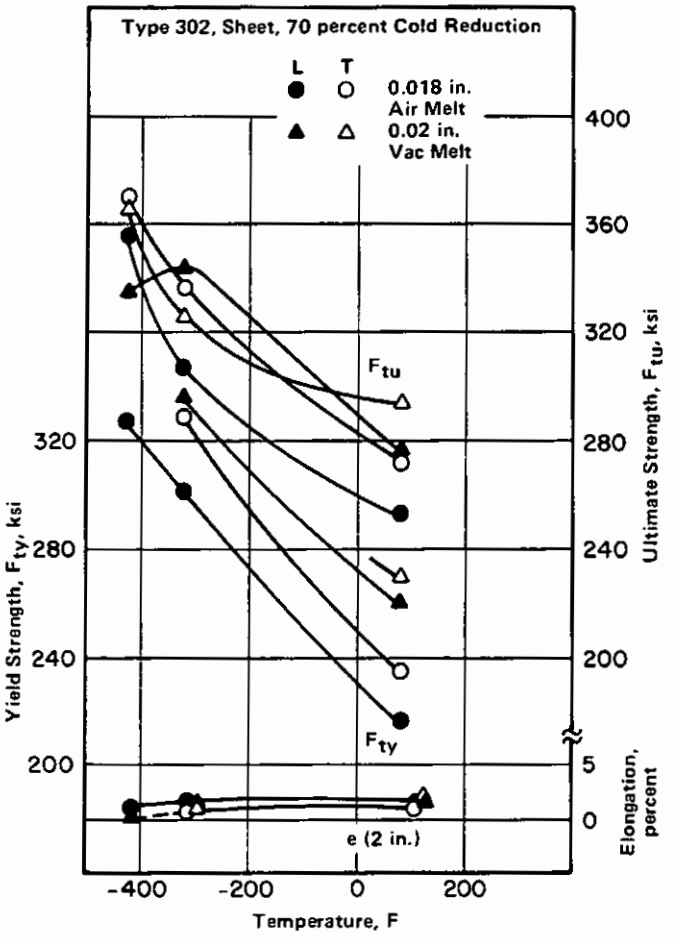
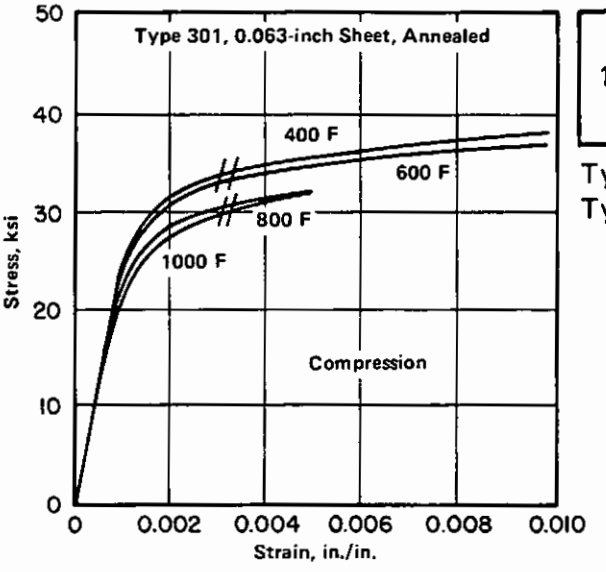


FIGURE 3.031610. EFFECTS OF CRYOGENIC TEMPERATURES AND MELT METHOD ON TENSILE PROPERTIES OF 70 PERCENT REDUCED SHEET (23)



Fe
18 Cr
8 Ni

Type 301
Type 302

FIGURE 3.03211. STRESS-STRAIN CURVES IN COMPRESSION FOR TYPE 301 ANNEALED SHEET AT ELEVATED TEMPERATURES (19)

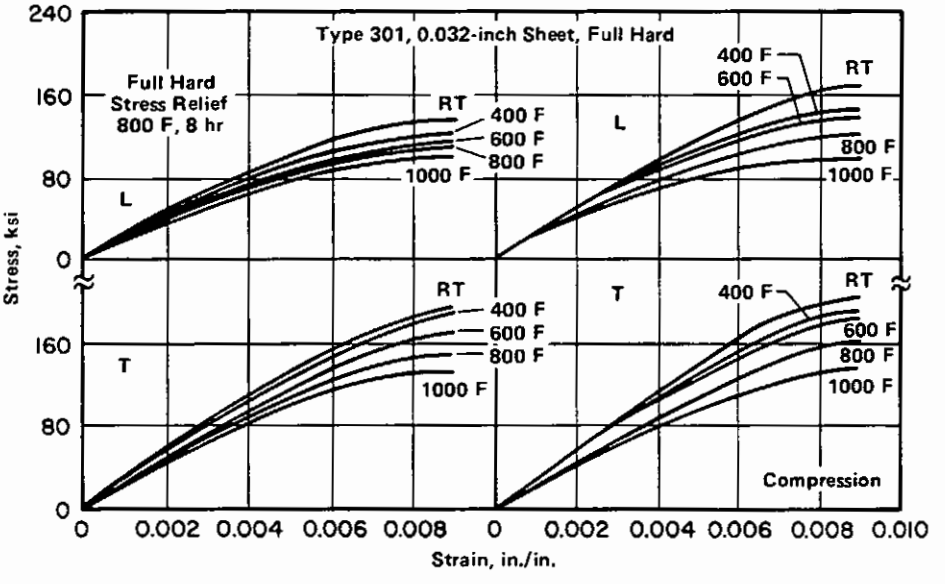


FIGURE 3.03212. STRESS-STRAIN CURVES IN COMPRESSION FOR TYPE 301 FULL-HARD AND FULL-HARD STRESS-RELIEVED SHEET AT ROOM AND ELEVATED TEMPERATURES (11)

Fe
18 Cr
8 Ni

Type 301
Type 302

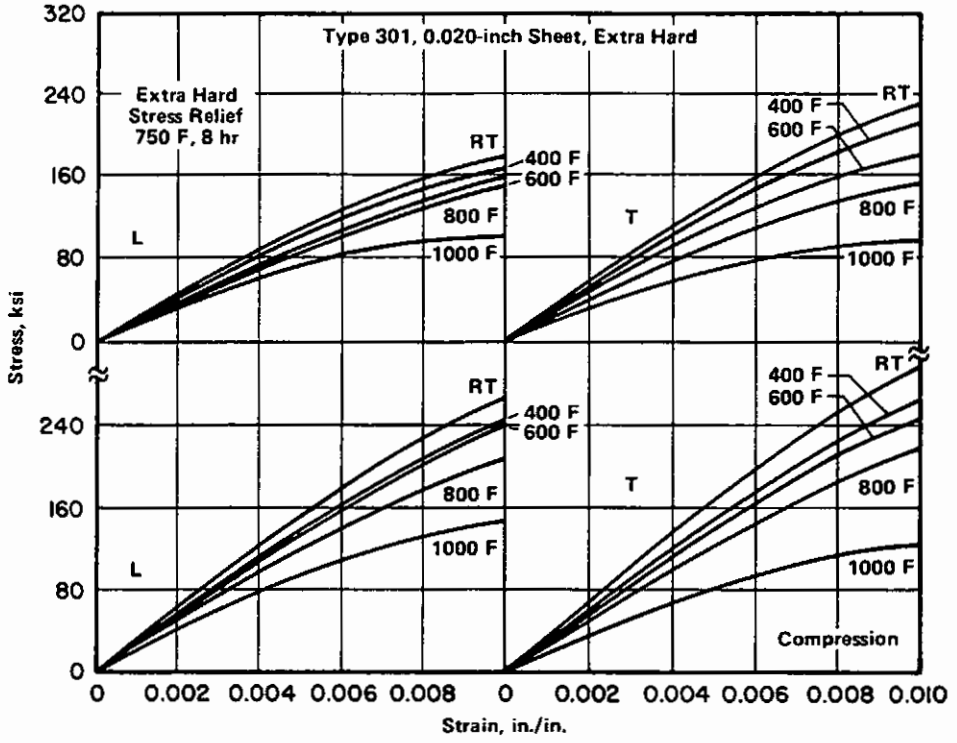


FIGURE 3.03213. STRESS-STRAIN CURVES IN COMPRESSION FOR TYPE 301 EXTRA-HARD AND EXTRA-HARD STRESS-RELIEVED SHEET AT ROOM AND ELEVATED TEMPERATURES (11)

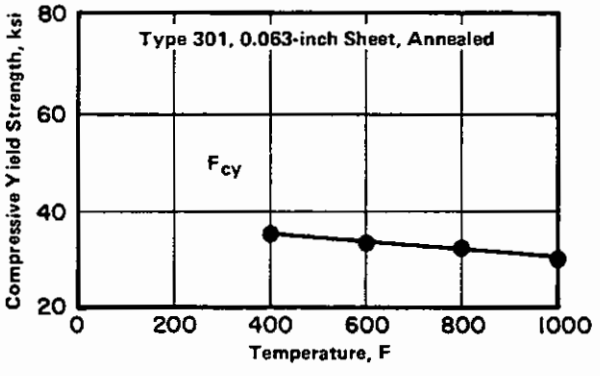


FIGURE 3.0322. EFFECT OF TEST TEMPERATURE ON COMPRESSIVE YIELD STRENGTH OF TYPE 301 ANNEALED SHEET (19)

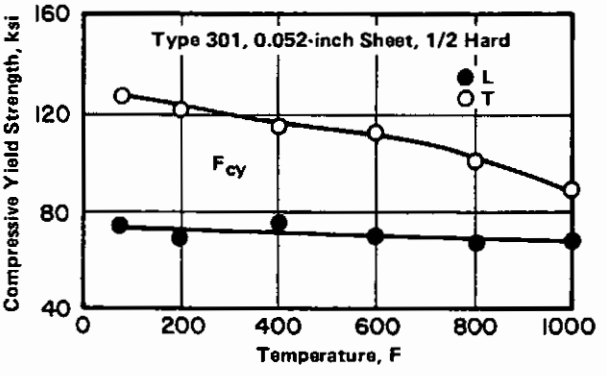


FIGURE 3.0323. EFFECT OF TEST TEMPERATURE AND TEST DIRECTION ON COMPRESSIVE YIELD STRENGTH OF TYPE 301 1/2-HARD SHEET (11)

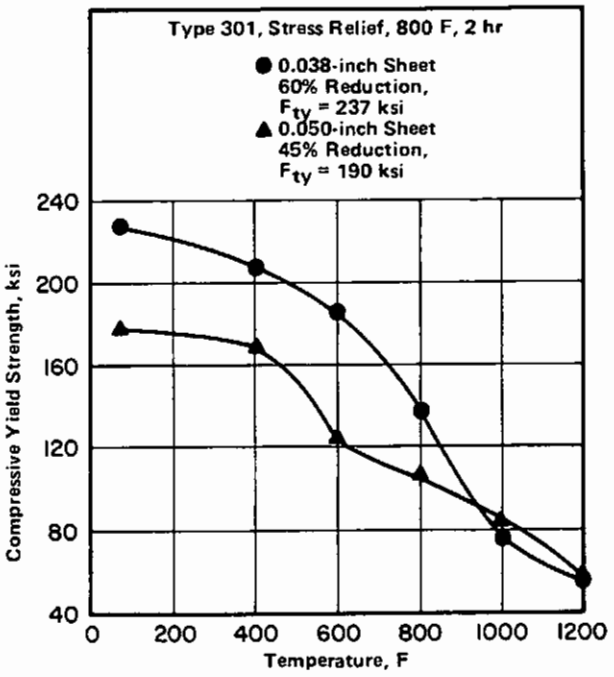
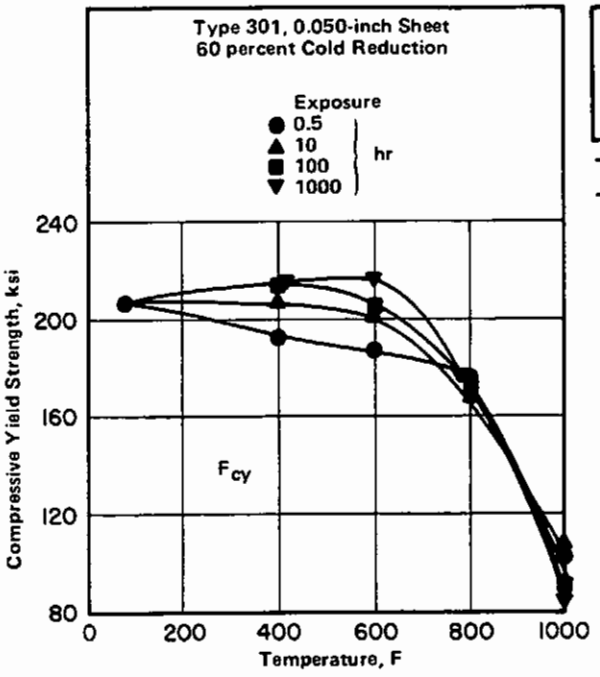


FIGURE 3.0324. EFFECT OF TEST TEMPERATURE ON COMPRESSIVE YIELD STRENGTH OF 45 AND 60 PERCENT REDUCED SHEET (28)



Fe
18 Cr
8 Ni

Type 301
Type 302

FIGURE 3.0325. EFFECT OF TEST TEMPERATURE AND EXPOSURE TIME ON COMPRESSIVE YIELD STRENGTH OF 60 PERCENT COLD-REDUCED SHEET (38)

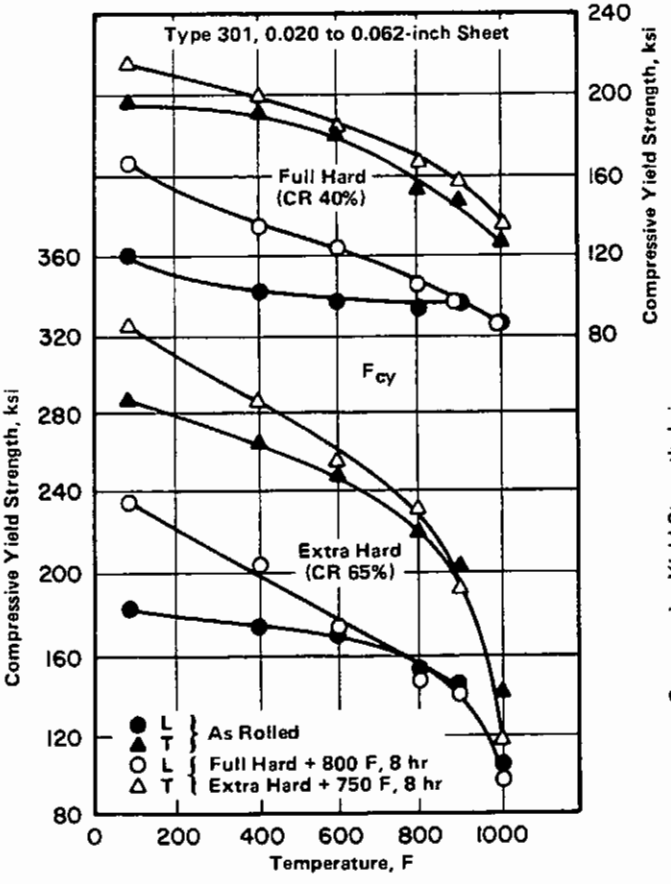


FIGURE 3.0326. EFFECT OF TEST TEMPERATURE, TEST DIRECTION, AND STRESS RELIEF ON COMPRESSIVE YIELD STRENGTH OF TYPE 301 FULL-HARD AND EXTRA-HARD SHEET (11)

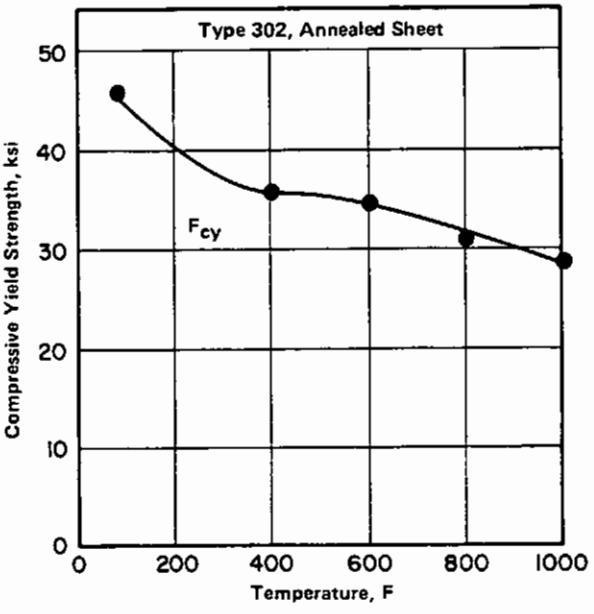


FIGURE 3.0327. EFFECT OF TEST TEMPERATURE ON COMPRESSIVE STRENGTH OF ANNEALED TYPE 302 SHEET (62)

Fe
18 Cr
8 Ni

Type 301
Type 302

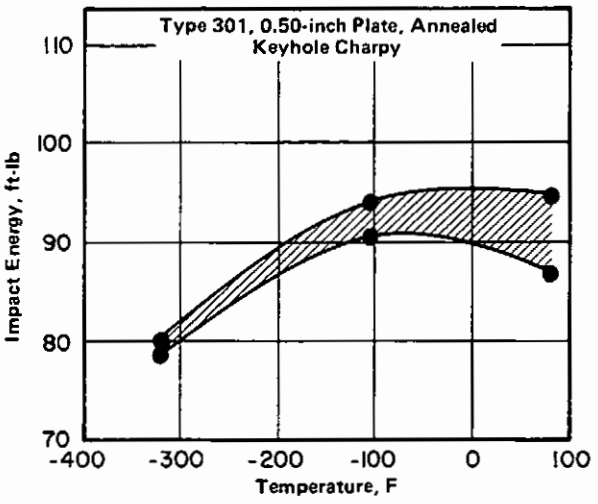


FIGURE 3.0331. IMPACT ENERGY OF TYPE 301 PLATE AT ROOM AND CRYOGENIC TEMPERATURES (82)

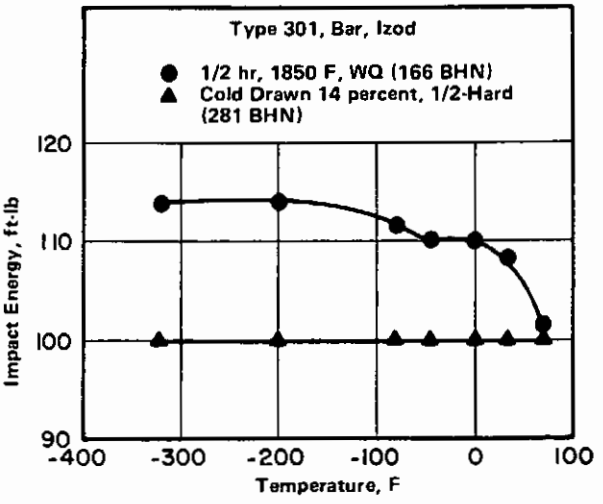


FIGURE 3.0332. IMPACT ENERGY OF TYPE 301 BAR AT ROOM AND CRYOGENIC TEMPERATURES (82)

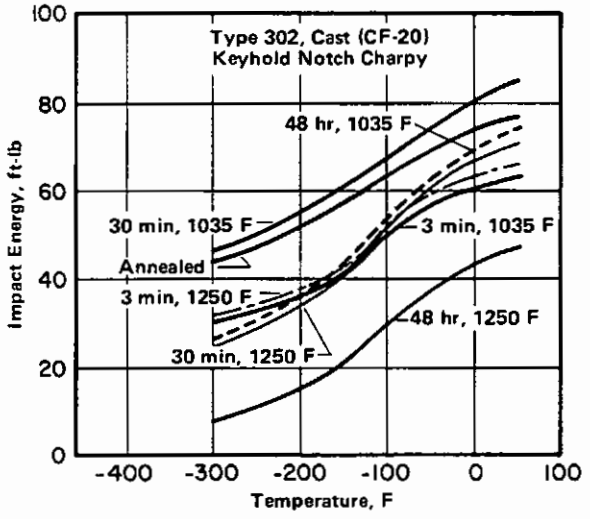


FIGURE 3.0334. EFFECT OF SENSITIZING HEAT TREATMENTS ON THE IMPACT ENERGY OF CAST TYPE 302 AT CRYOGENIC TEMPERATURES (83)

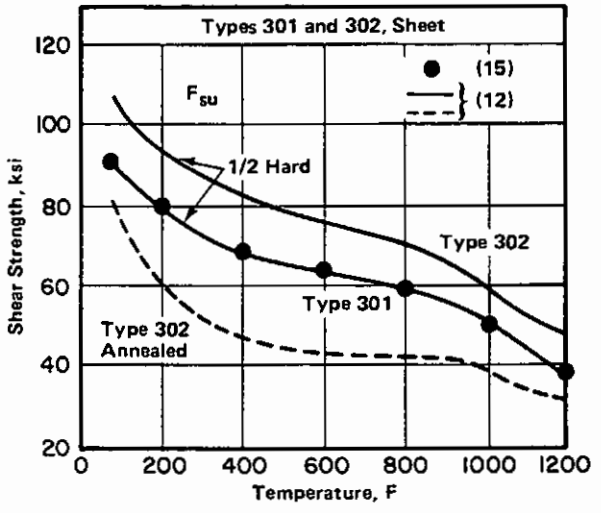


FIGURE 3.0351. EFFECT OF TEST TEMPERATURE ON SHEAR STRENGTH OF TYPES 301 AND 302 (12,15)

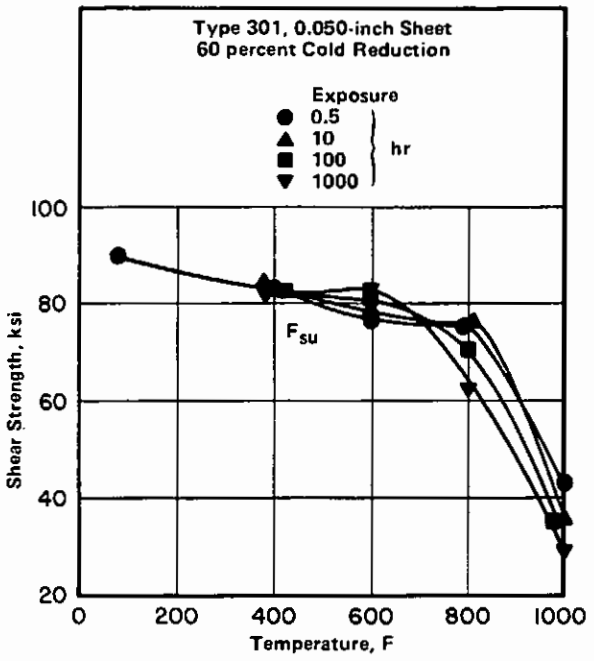
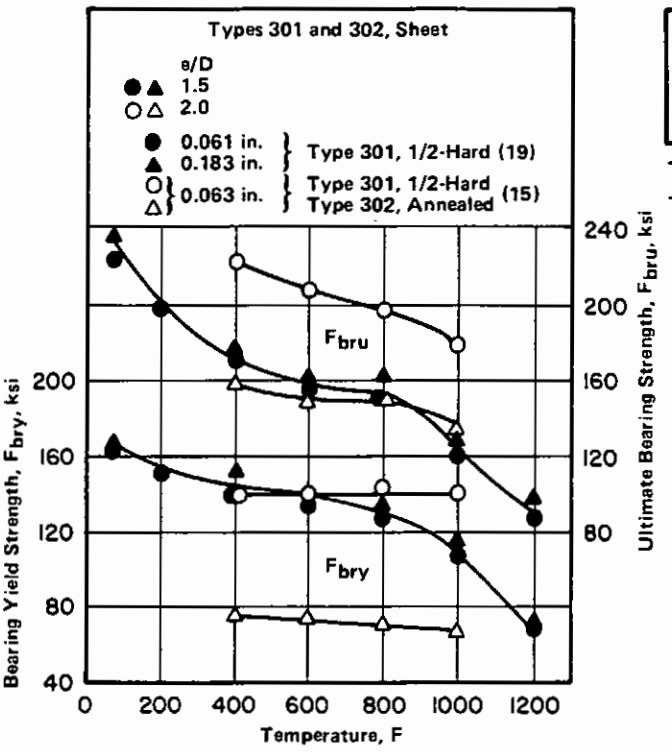


FIGURE 3.0352. EFFECT OF TEST TEMPERATURE AND EXPOSURE TIME ON SHEAR STRENGTH OF 60 PERCENT COLD-REDUCED SHEET (38)



Fe
18 Cr
8 Ni

Type 301
Type 302

FIGURE 3.0361. EFFECT OF TEST TEMPERATURE ON BEARING PROPERTIES OF TYPES 301 AND 302 SHEET (15,19)

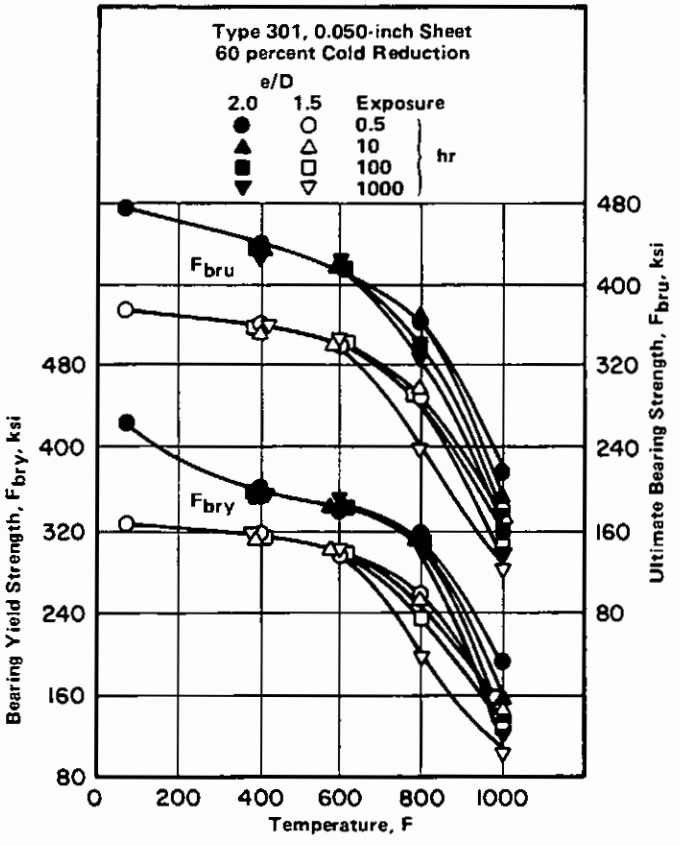


FIGURE 3.0362. EFFECT OF TEST TEMPERATURE AND EXPOSURE TIME ON BEARING PROPERTIES OF 60 PERCENT COLD-REDUCED SHEET (38)

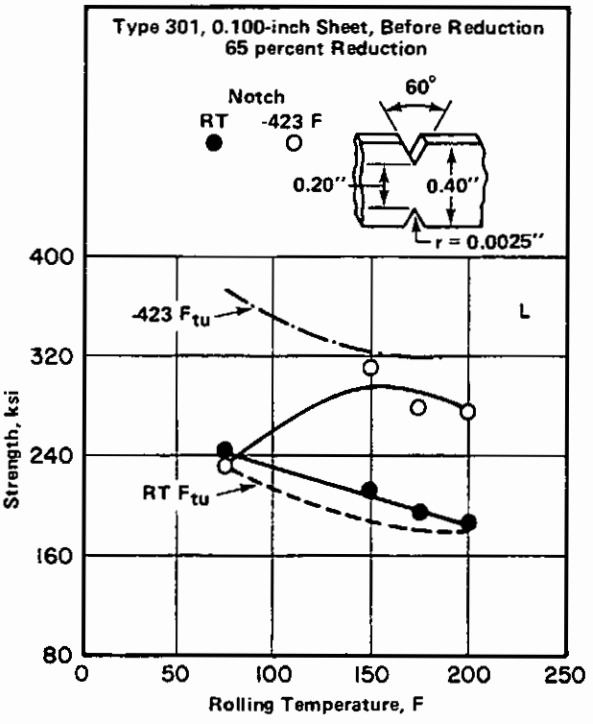


FIGURE 3.03711. EFFECT OF ROLLING TEMPERATURE ON NOTCH STRENGTH AT ROOM TEMPERATURE AND -423 F OF 65 PERCENT REDUCED SHEET (24)

Fe
18 Cr
8 Ni

Type 301
Type 302

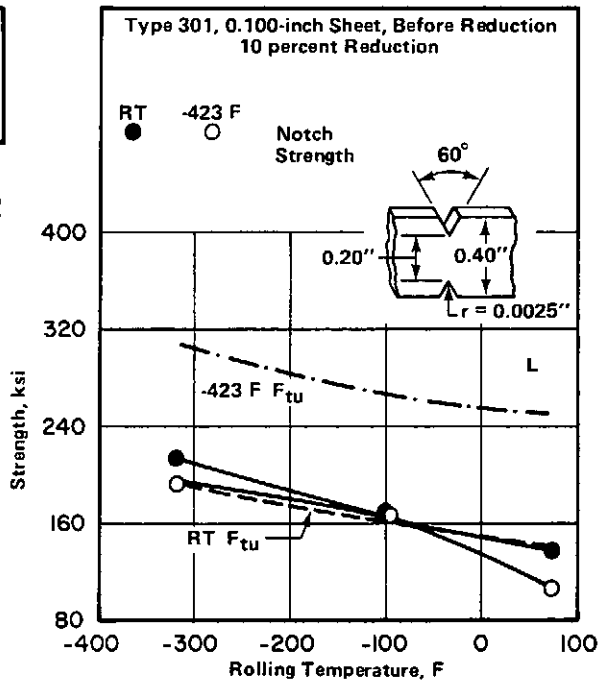


FIGURE 3.037112. EFFECT OF LOW ROLLING TEMPERATURE ON NOTCH STRENGTH AT ROOM TEMPERATURE AND -423 F OF 10 PERCENT REDUCED SHEET (24)

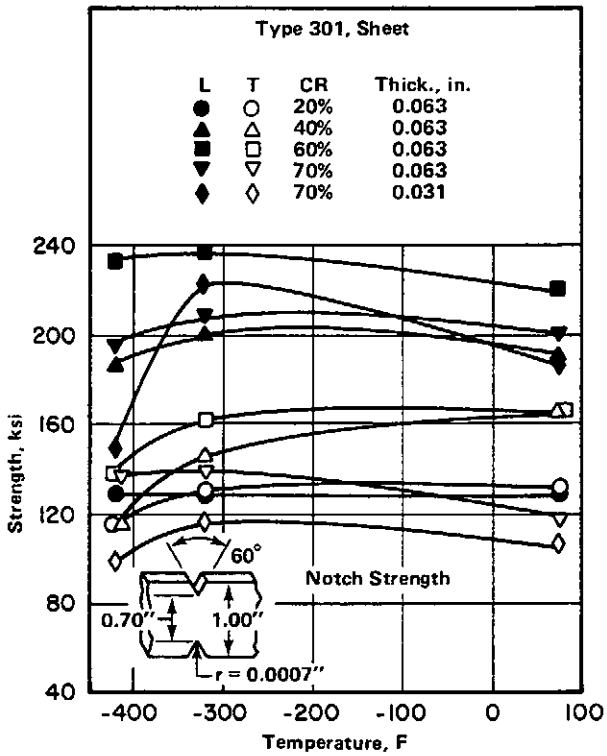


FIGURE 3.037113. EFFECT OF LOW TEMPERATURE AND PERCENT COLD REDUCTION ON NOTCH STRENGTH OF SHEET (34)

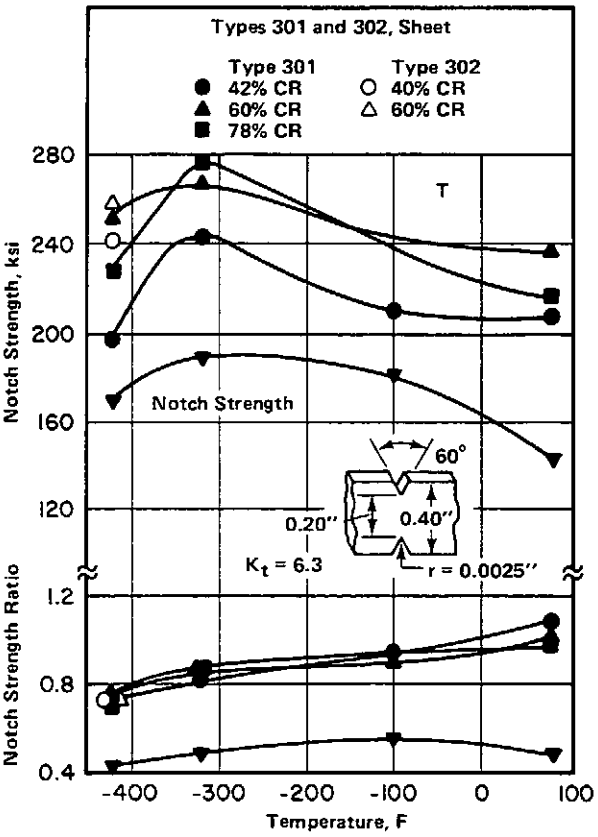


FIGURE 3.037114. EFFECT OF LOW TEMPERATURE AND PERCENT COLD REDUCTION ON NOTCH STRENGTH OF VARIOUS PERCENT REDUCED SHEET (25)

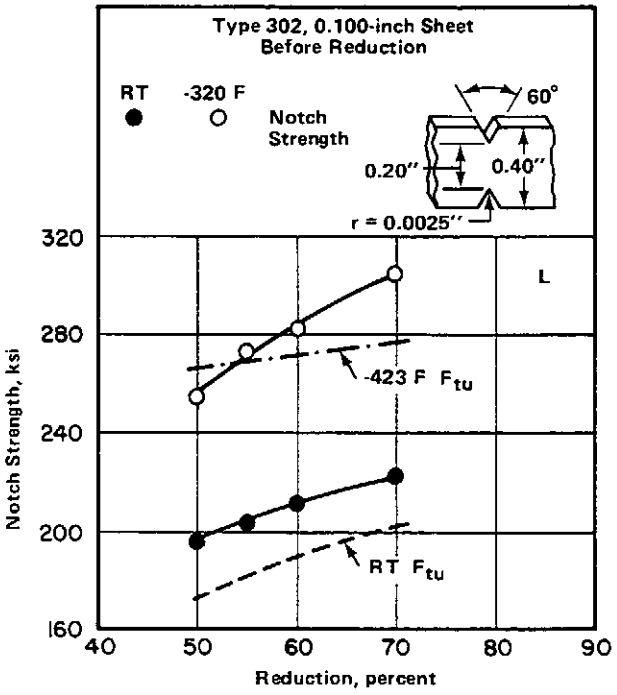


FIGURE 3.037115. EFFECT OF PERCENT COLD REDUCTION ON NOTCH STRENGTH OF SHEET TESTED AT ROOM TEMPERATURE AND -320 F (24)

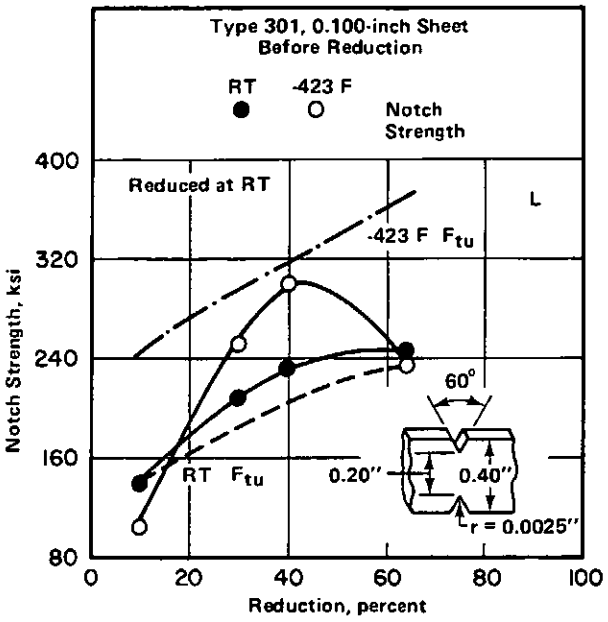


FIGURE 3.037116. EFFECT OF PERCENT COLD REDUCTION ON NOTCH STRENGTH OF SHEET TESTED AT ROOM TEMPERATURE AND -423 F (24)

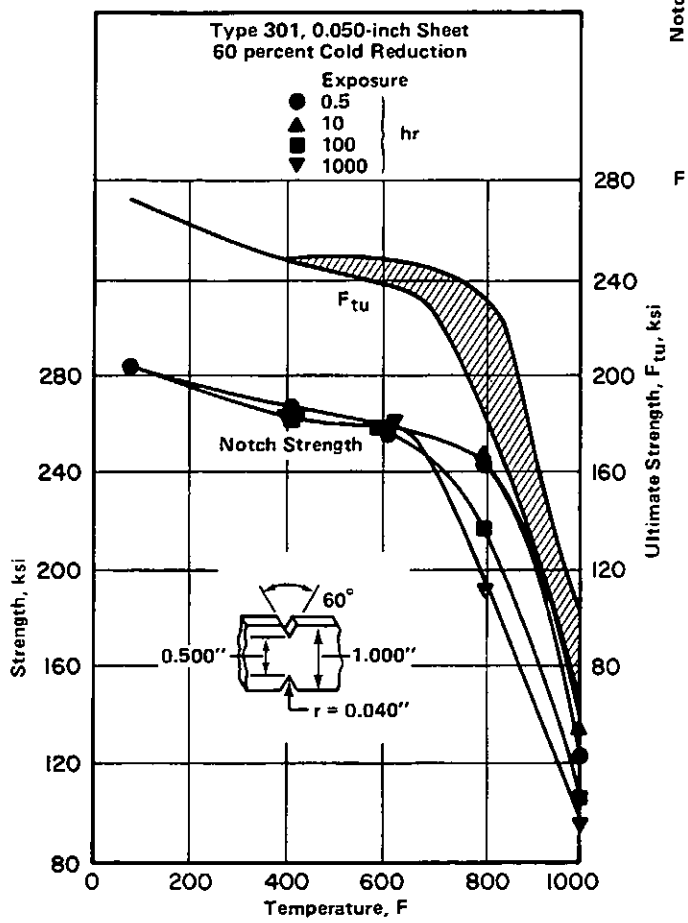


FIGURE 3.037122. EFFECT OF TEST TEMPERATURE AND EXPOSURE TIME ON NOTCH STRENGTH OF 60 PERCENT COLD-REDUCED SHEET (38)

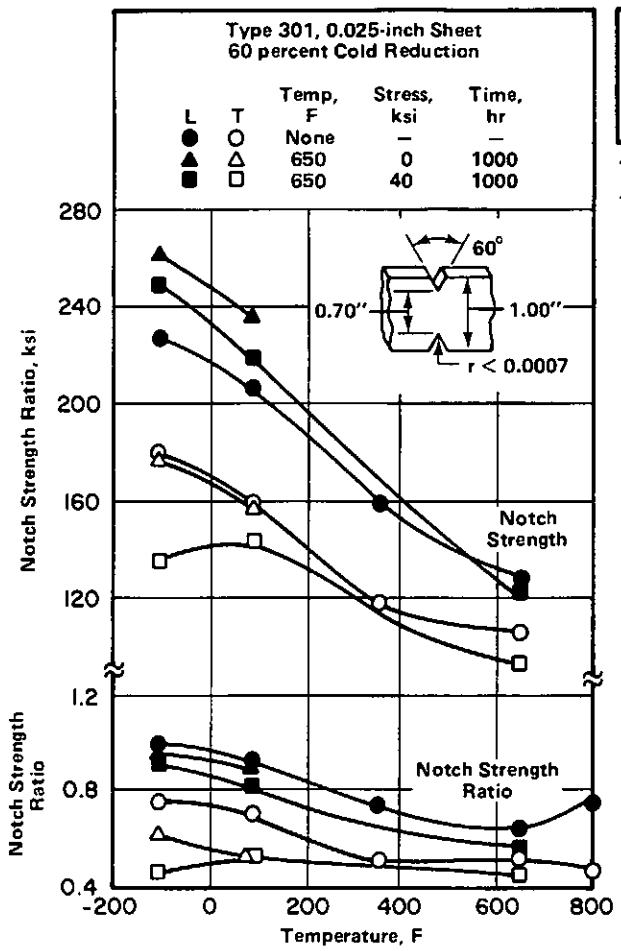


FIGURE 3.037121. EFFECT OF TEST TEMPERATURE AND PRIOR EXPOSURE ON NOTCH PROPERTIES OF 60 PERCENT COLD-REDUCED SHEET (45)

Fe
18 Cr
8 Ni

Type 301
Type 302

Fe
18 Cr
8 Ni

Type 301
Type 302

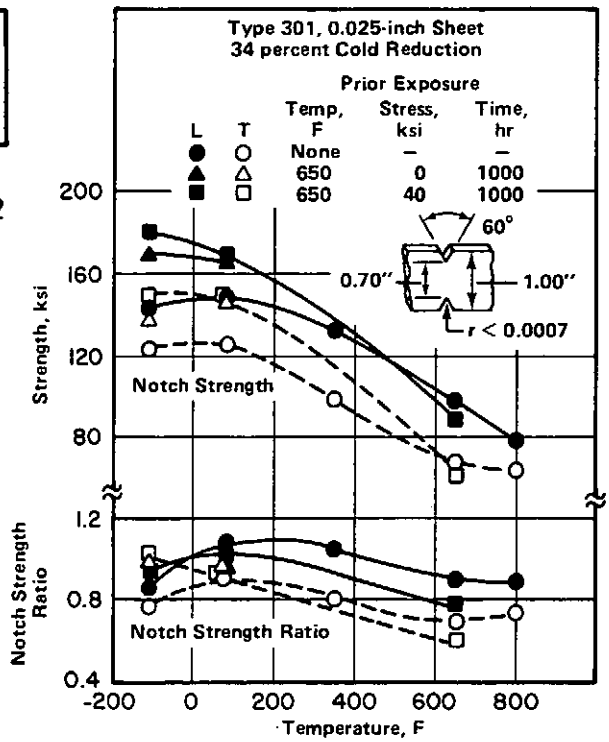


FIGURE 3.037123. EFFECT OF TEST TEMPERATURE AND PRIOR EXPOSURE ON NOTCH PROPERTIES OF 34 PERCENT COLD-REDUCED SHEET (45)

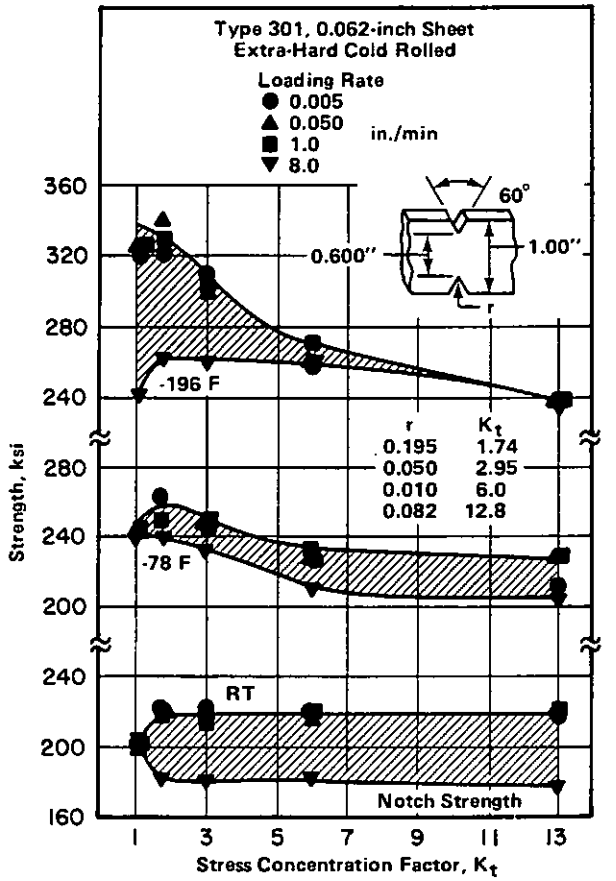


FIGURE 3.037124. EFFECT OF STRESS CONCENTRATION FACTOR, TEMPERATURE, AND LOADING RATE ON NOTCH STRENGTH OF EXTRA-HARD COLD-ROLLED SHEET (44)

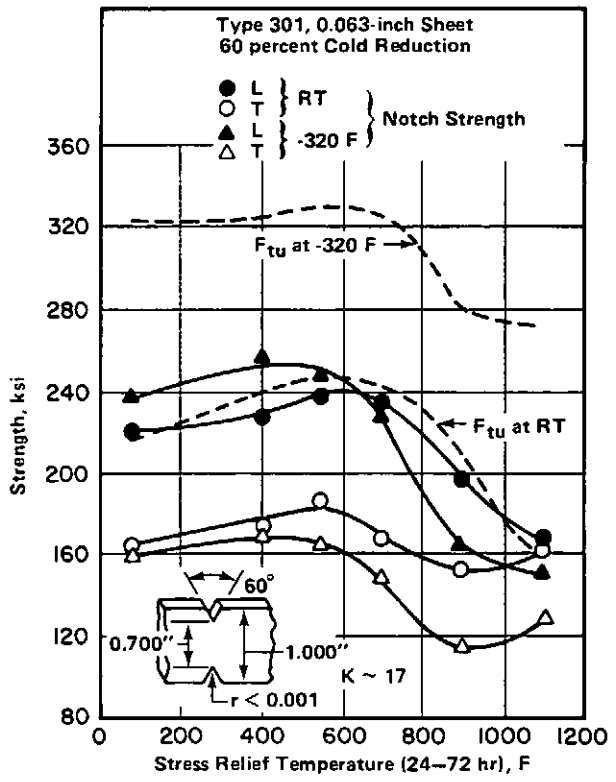


FIGURE 3.037131. EFFECT OF STRESS RELIEF AND LOW TEST TEMPERATURE ON NOTCH STRENGTH OF TYPE 301 SHEET (18)

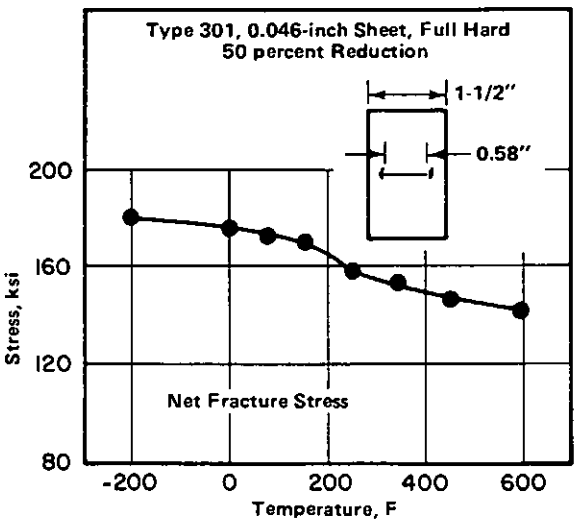


FIGURE 3.037141. EFFECT OF TEST TEMPERATURE ON NET FRACTURE STRESS OF FULL-HARD SHEET (30)

Fe
18 Cr
8 Ni

Type 301
Type 302

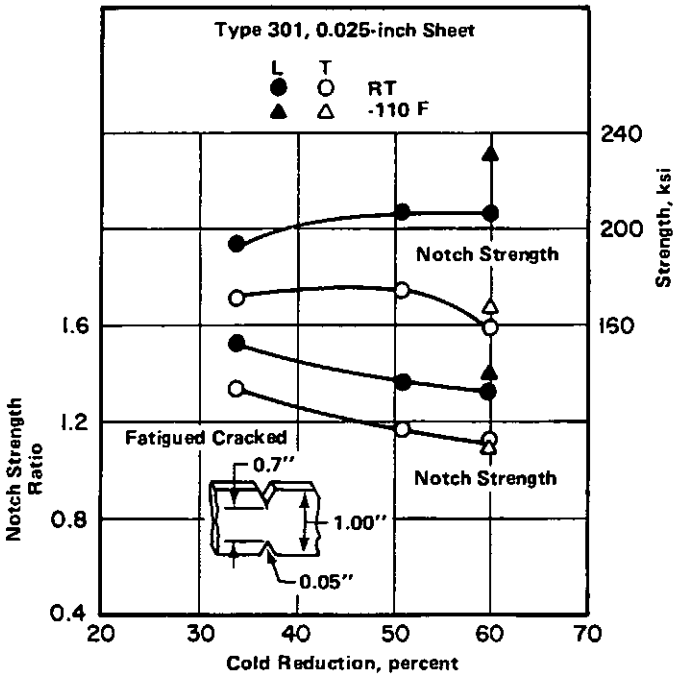


FIGURE 3.037142. EFFECT OF PERCENT COLD REDUCTION ON EDGE-CRACKED PROPERTIES OF SHEET AT ROOM TEMPERATURE AND -110 F (45)

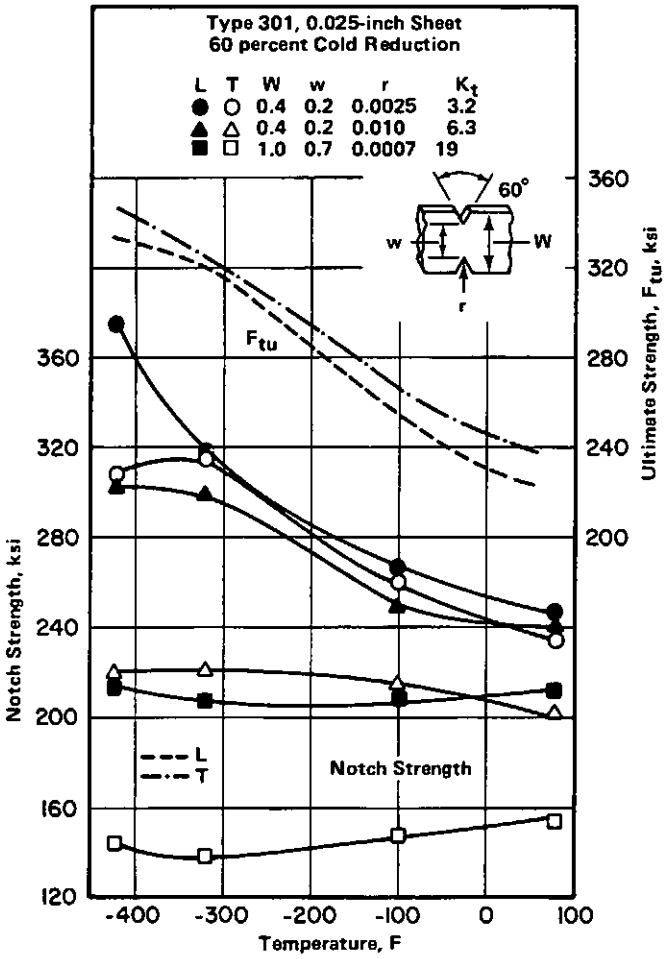


FIGURE 3.037151. EFFECT OF LOW TEST TEMPERATURE ON NOTCH STRENGTH OF 60 PERCENT COLD-REDUCED SHEET (36)

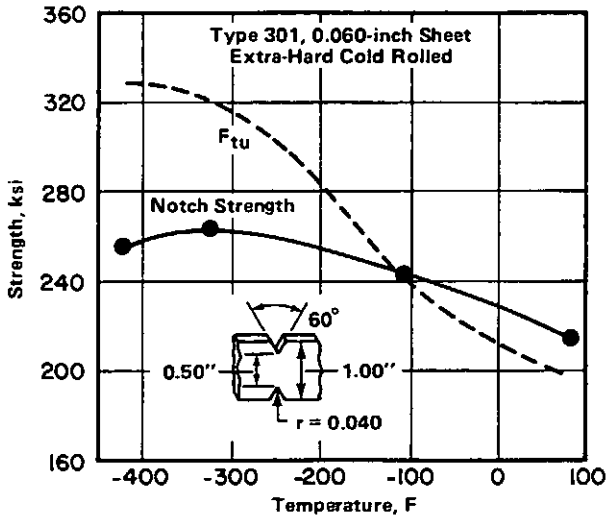


FIGURE 3.037152. EFFECT OF LOW TEMPERATURE ON NOTCH STRENGTH OF EXTRA-HARD COLD-ROLLED SHEET (32)

Fe
18 Cr
8 Ni

Type 301
Type 302

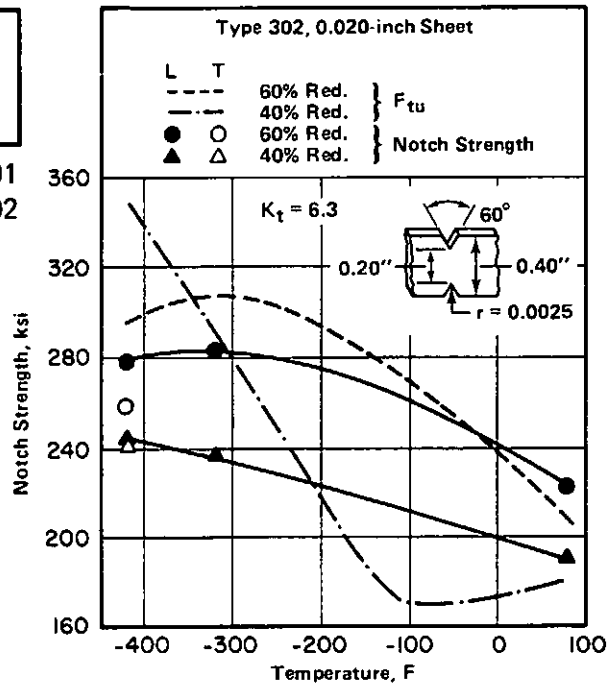


FIGURE 3.037153. EFFECT OF LOW TEST TEMPERATURE ON NOTCH STRENGTH OF 40 AND 60 PERCENT REDUCED TYPE 302 SHEET (31)

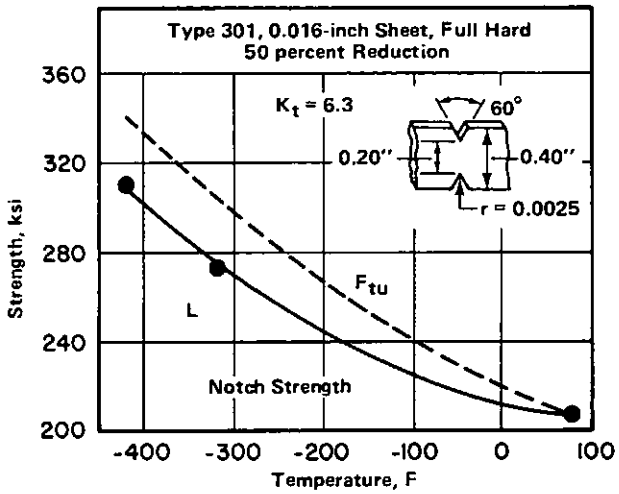


FIGURE 3.037154. EFFECT OF LOW TEST TEMPERATURE ON NOTCH STRENGTH OF 50 PERCENT REDUCED SHEET (31)

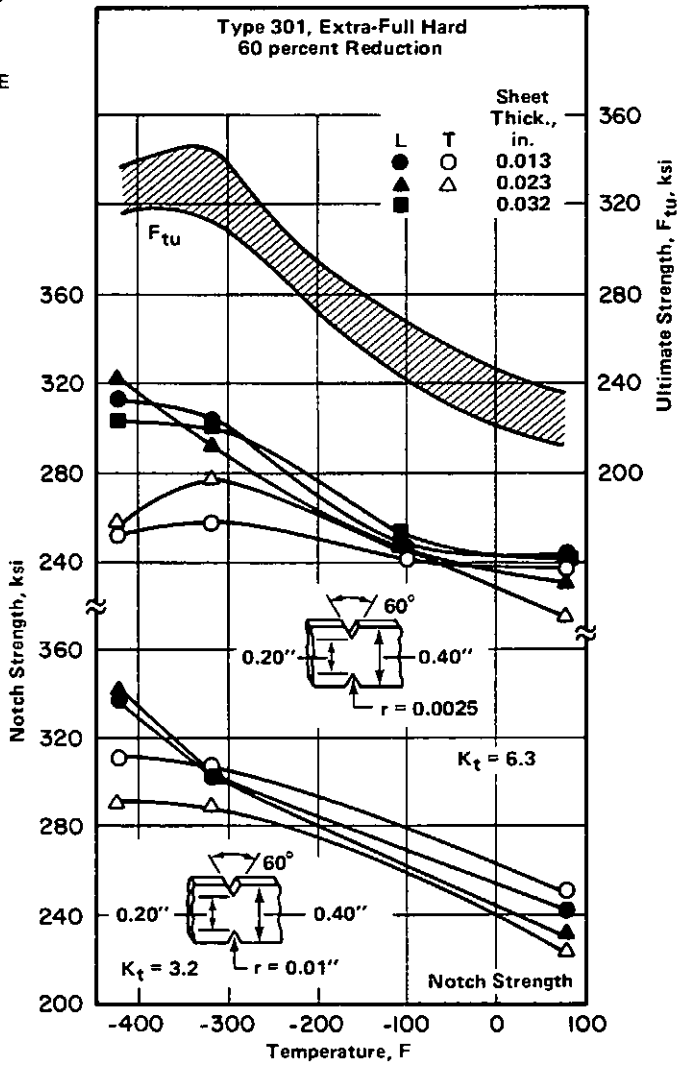


FIGURE 3.037156. EFFECT OF LOW TEST TEMPERATURE AND THICKNESS OF NOTCH STRENGTH OF 60 PERCENT REDUCED SHEET (31)

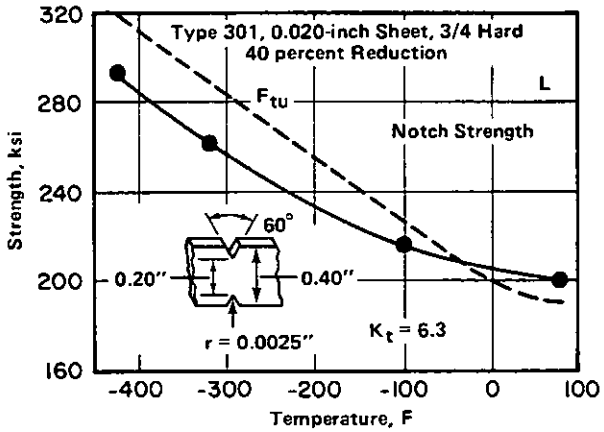


FIGURE 3.037155. EFFECT OF LOW TEST TEMPERATURE ON NOTCH STRENGTH OF 40 PERCENT REDUCED SHEET (31)

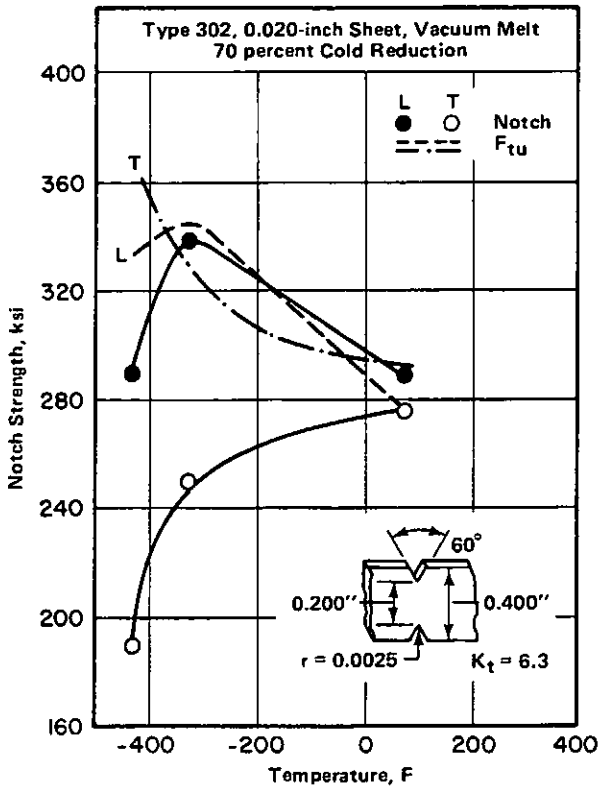
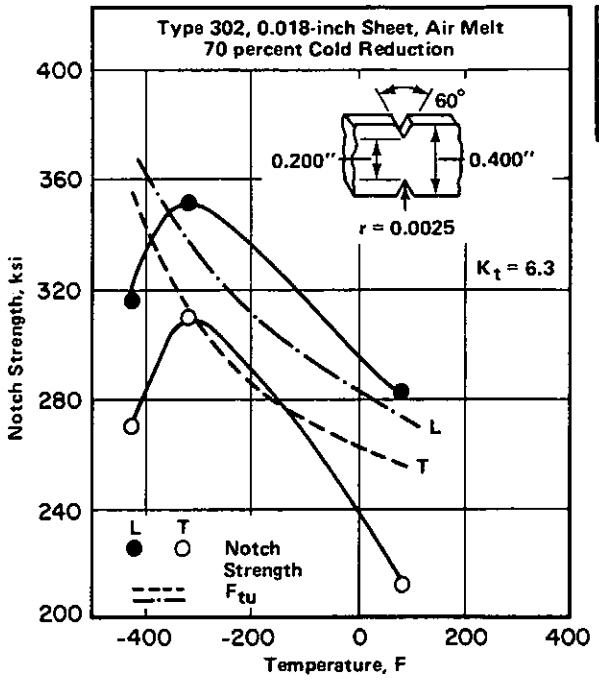


FIGURE 3.037157. EFFECT OF LOW TEST TEMPERATURE ON NOTCH STRENGTH OF 70 PERCENT REDUCED VACUUM-MELT SHEET (23)



Fe
18 Cr
8 Ni

Type 301
Type 302

FIGURE 3.037158. EFFECT OF LOW TEST TEMPERATURE ON NOTCH STRENGTH OF 70 PERCENT REDUCED AIR-MELT SHEET (23)

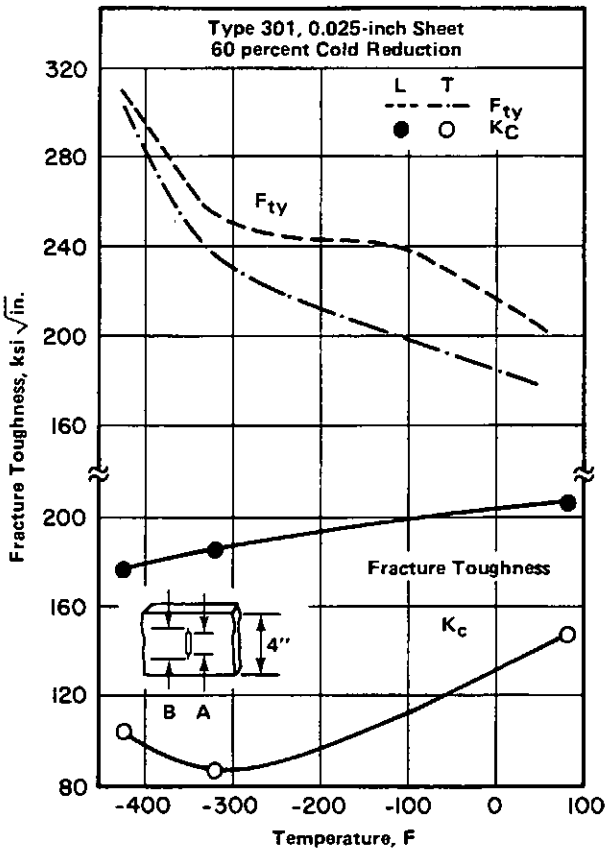


FIGURE 3.03721. EFFECT OF LOW TEST TEMPERATURE ON FRACTURE TOUGHNESS OF 60 PERCENT COLD-REDUCED SHEET (37)

A. Notch length 1.22 ± 0.03.
B. Critical crack length 1.19 to 2.02. Critical crack length telescopically measured.

Fe
18 Cr
8 Ni

Type 301
Type 302

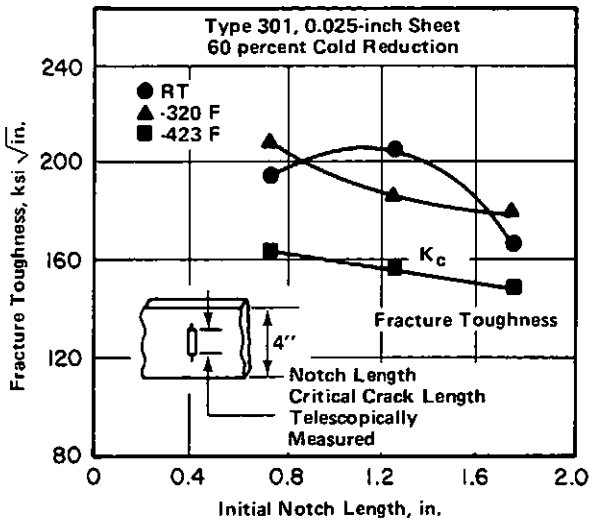


FIGURE 3.03722. EFFECT OF INITIAL NOTCH LENGTH ON FRACTURE TOUGHNESS OF 60 PERCENT COLD-REDUCED SHEET AT ROOM TEMPERATURE, -320, AND -423 F (37)

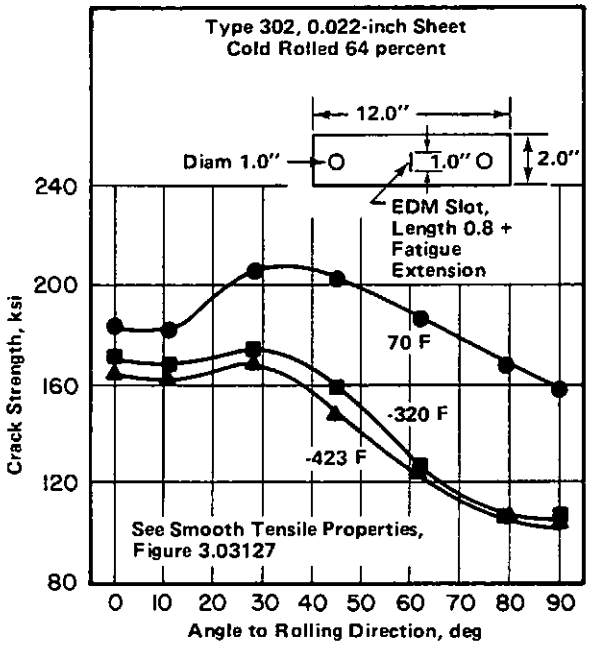


FIGURE 3.03724. EFFECTS OF CENTER CRACK AND TEST DIRECTION ON TENSILE STRENGTH OF COLD-ROLLED SHEET AT ROOM AND CRYOGENIC TEMPERATURES (79)

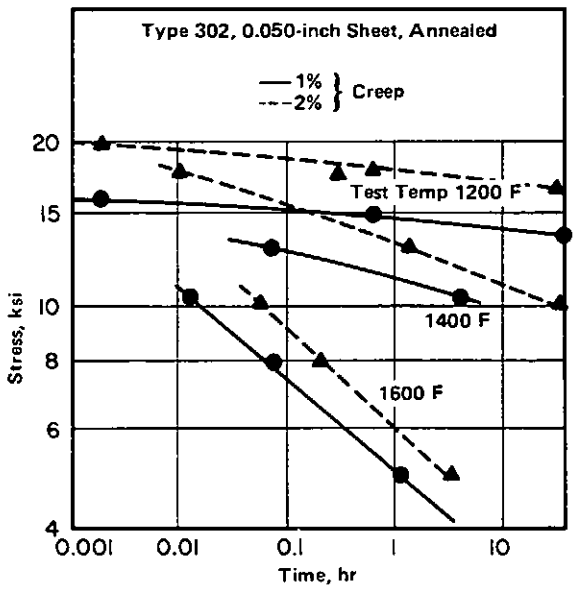


FIGURE 3.041. CREEP CURVES FOR TYPE 302 ANNEALED SHEET AT 1200 TO 1600 F (16)

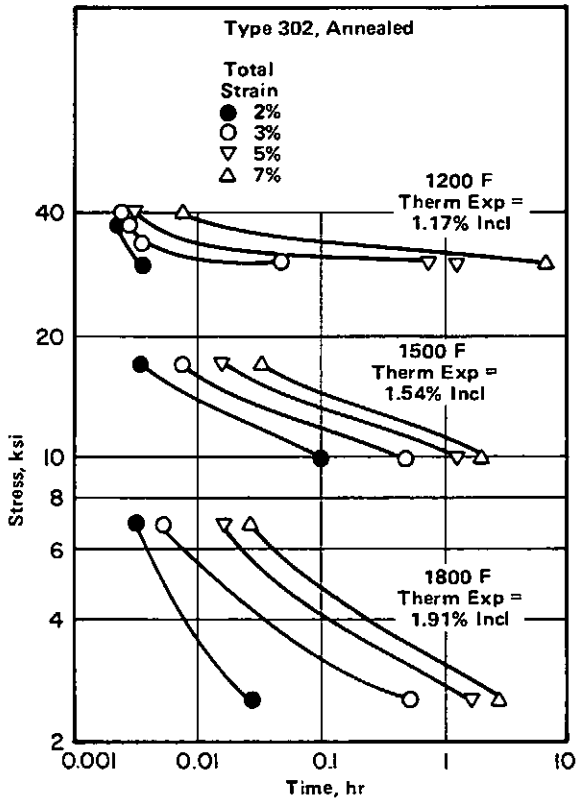


FIGURE 3.042. SHORT-TIME TOTAL STRAIN CURVES FOR ANNEALED TYPE 302 AT 1200 TO 1800 F (12)

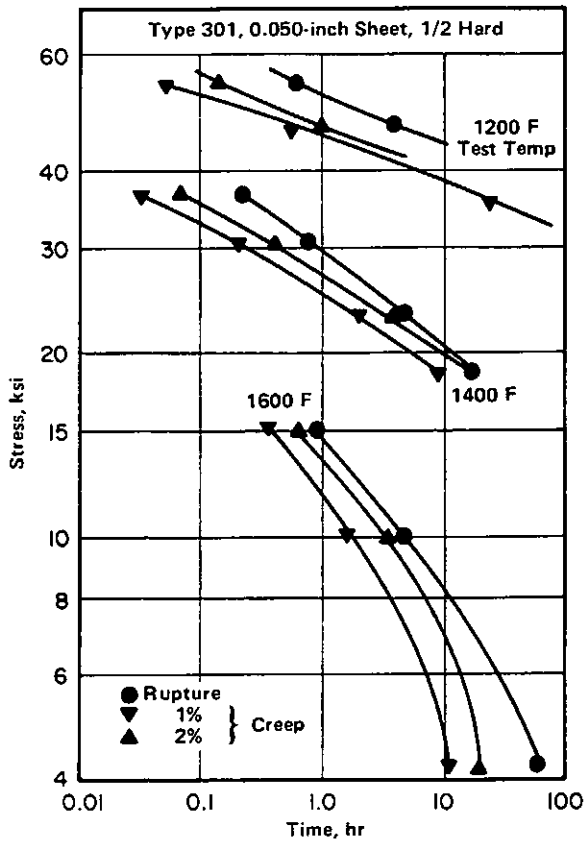
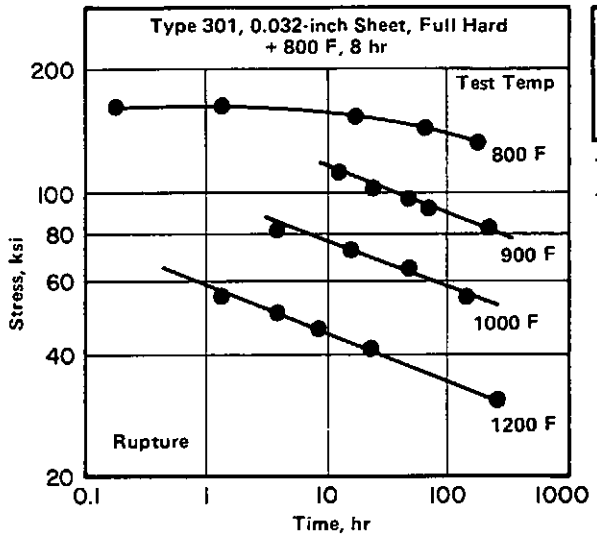


FIGURE 3.043. CREEP AND CREEP-RUPTURE CURVES FOR TYPE 301 1/2-HARD SHEET AT 1200 TO 1500 F (16)



Fe
18 Cr
8 Ni

Type 301
Type 302

FIGURE 3.044. CREEP-RUPTURE CURVES FOR TYPE 301 FULL-HARD AND STRESS-RELIEVED SHEET AT 800 TO 1200 F (11)

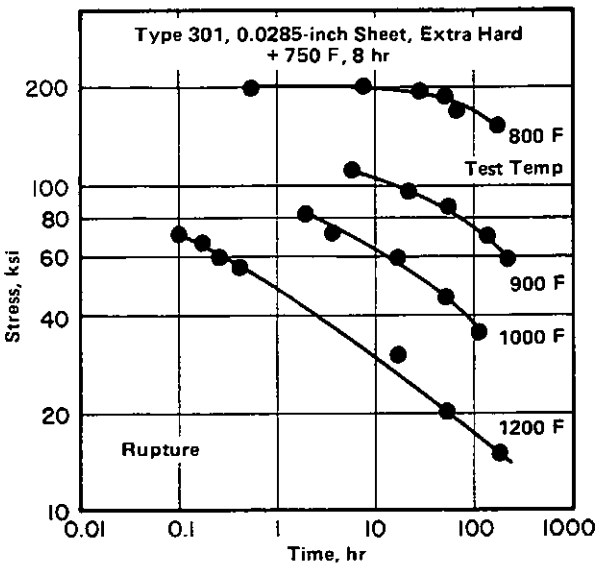


FIGURE 3.045. CREEP-RUPTURE CURVES FOR TYPE 301 EXTRA-HARD AND STRESS-RELIEVED SHEET AT 800 TO 1200 F (11)

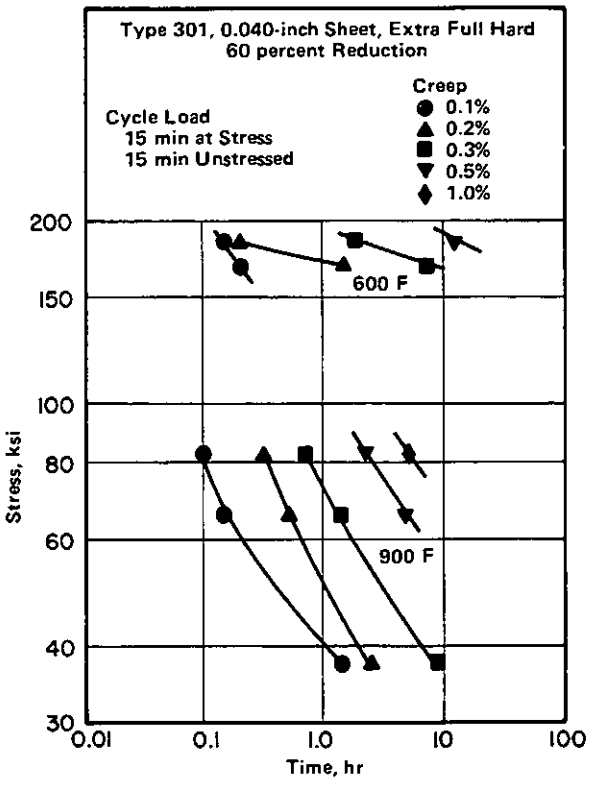


FIGURE 3.046. CREEP CURVES FOR TYPE 301 60 PER-CENT REDUCED SHEET UNDER CYCLIC LOAD AT 600 AND 900 F (27)

Fe
18 Cr
8 Ni

Type 301
Type 302

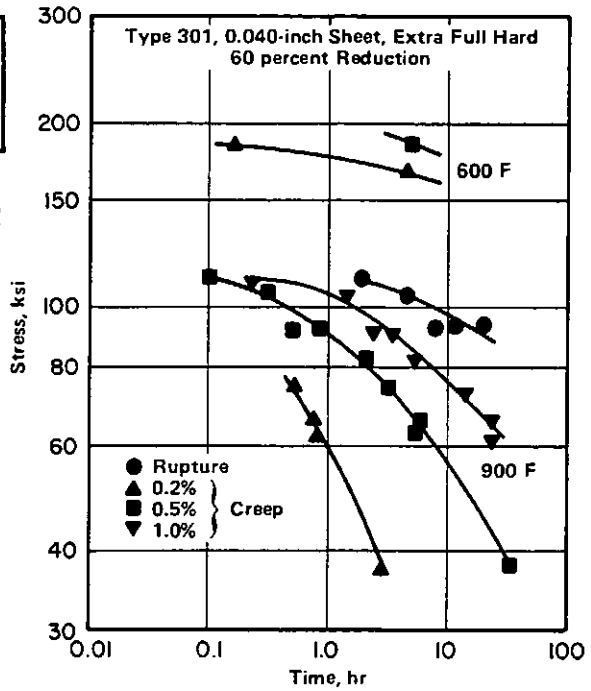


FIGURE 3.047. CREEP AND CREEP-RUPTURE CURVES FOR TYPE 301 60 PERCENT REDUCED SHEET AT 600 AND 900 F (26)

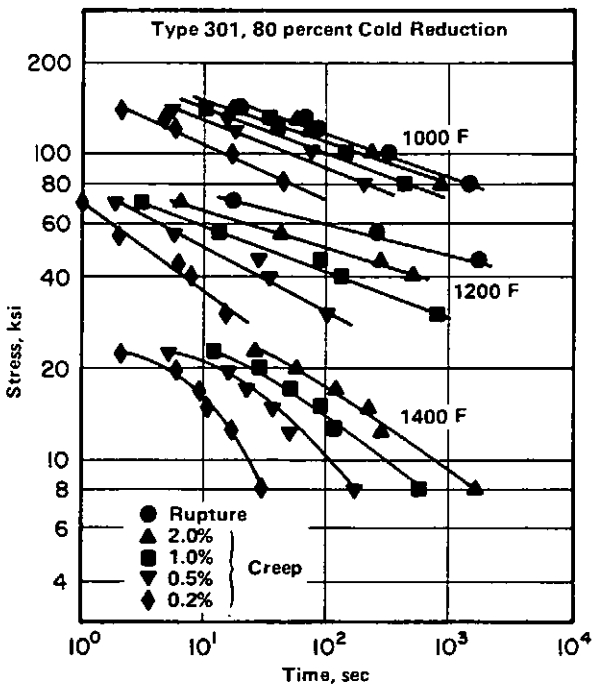


FIGURE 3.048. CREEP AND CREEP-RUPTURE CURVES FOR 80 PERCENT COLD-REDUCED SHEET AT 1000, 1200, AND 1400 F (47)

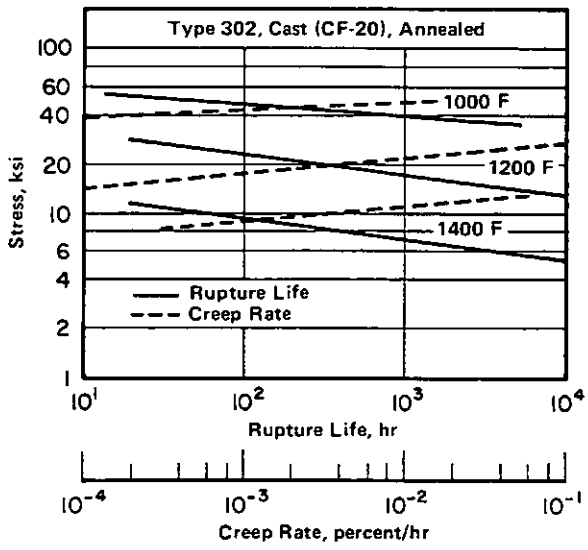


FIGURE 3.049. CREEP-RUPTURE PROPERTIES OF CAST TYPE 302 (62)

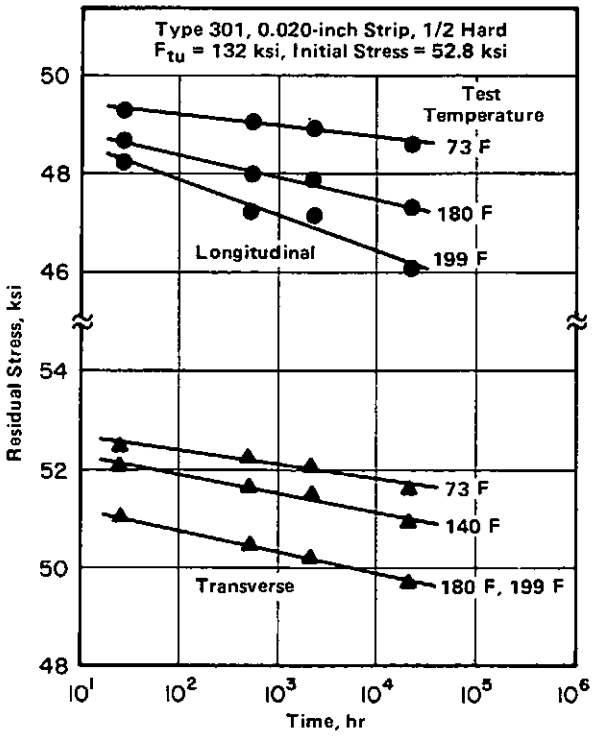


FIGURE 3.0410. STRESS RELAXATION AT ROOM AND SLIGHTLY ELEVATED TEMPERATURES (84)

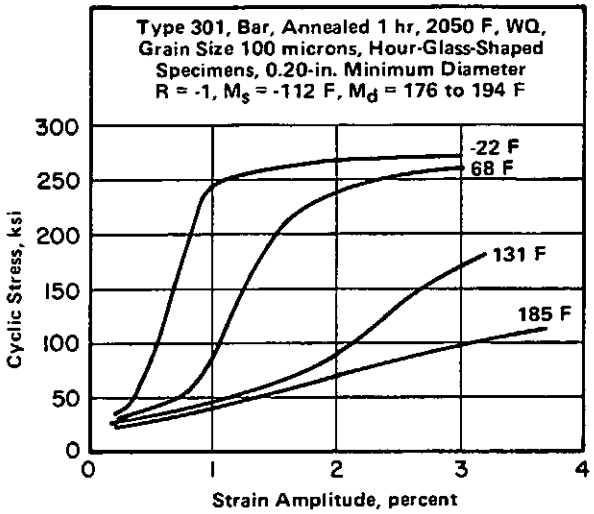
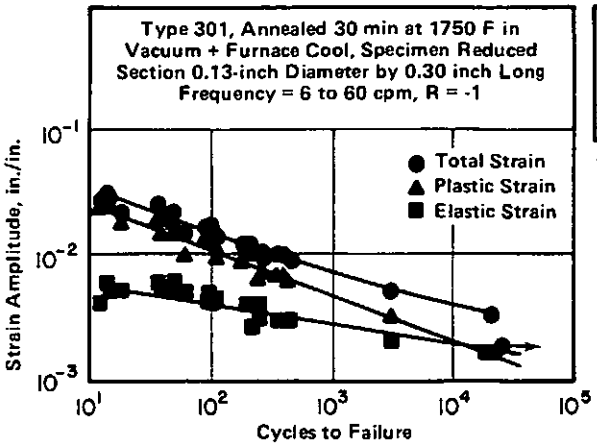


FIGURE 3.051. CYCLIC STRESS-STRAIN CURVES FOR ANNEALED TYPE 301 AT TEMPERATURES BETWEEN M_s AND M_d (58)



Fe
18 Cr
8 Ni

Type 301
Type 302

FIGURE 3.052. STRAIN-CONTROLLED FATIGUE BEHAVIOR OF ANNEALED ROD AT ROOM TEMPERATURE (85)

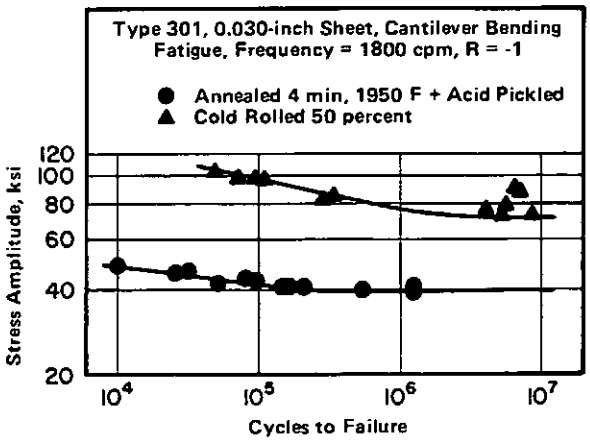


FIGURE 3.053. BENDING FATIGUE BEHAVIOR OF COLD-WORKED AND OF ANNEALED SHEET AT ROOM TEMPERATURE (86)

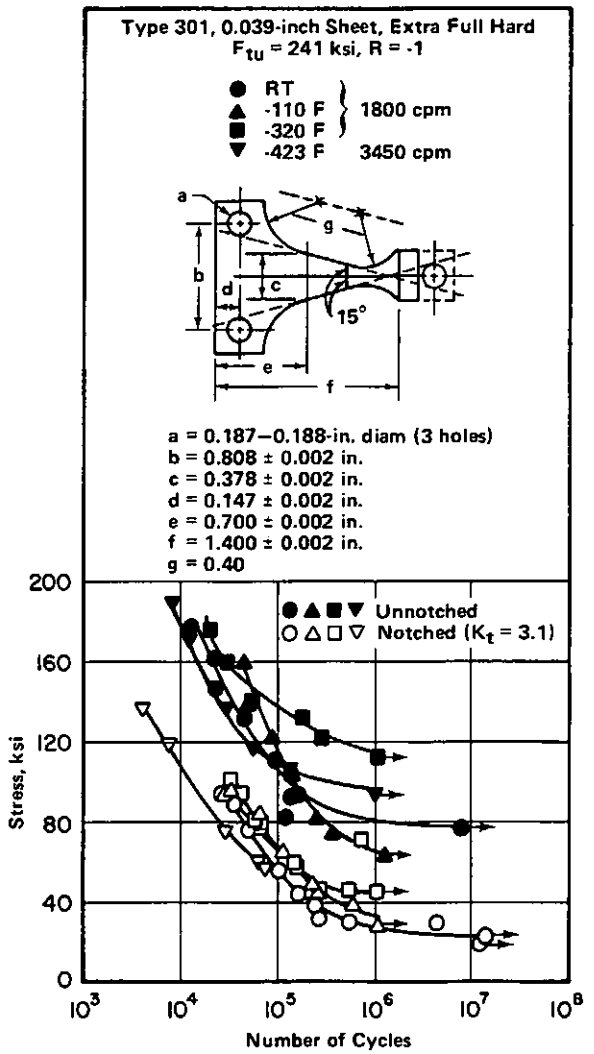


FIGURE 3.054. S-N CURVES IN FLEXURE FOR EXTRA-FULL-HARD SHEET AT LOW TEMPERATURES (39,42)

Fe
18 Cr
8 Ni

Type 301
Type 302

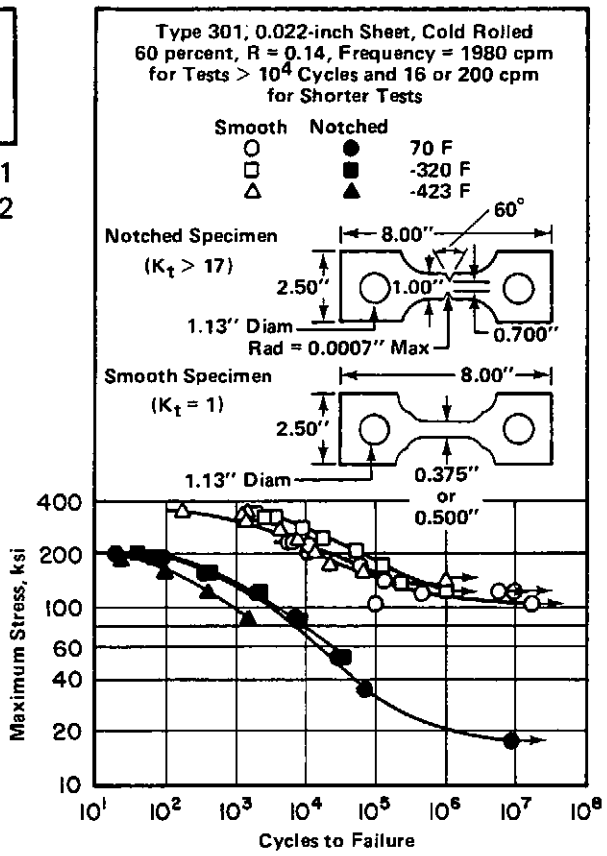


FIGURE 3.055. AXIAL TENSION FATIGUE BEHAVIOR OF SMOOTH AND NOTCHED SHEET AT ROOM AND CRYOGENIC TEMPERATURES (87)

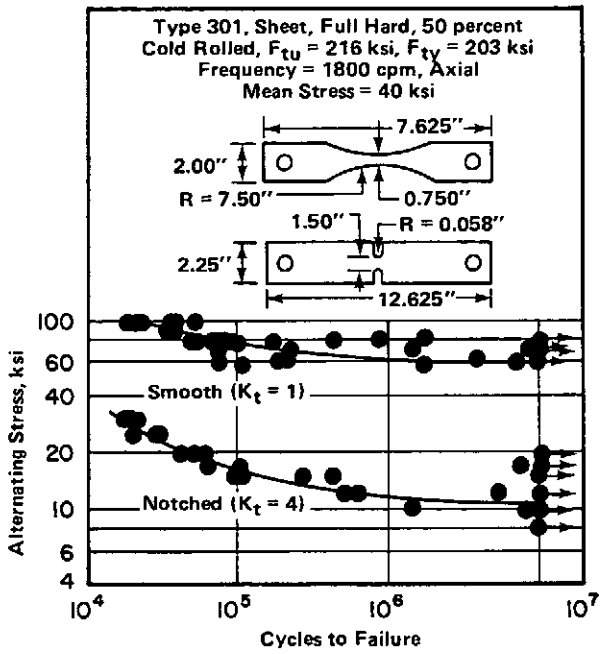


FIGURE 3.057. EFFECTS OF NOTCHES ON FATIGUE BEHAVIOR OF SHEET (89)

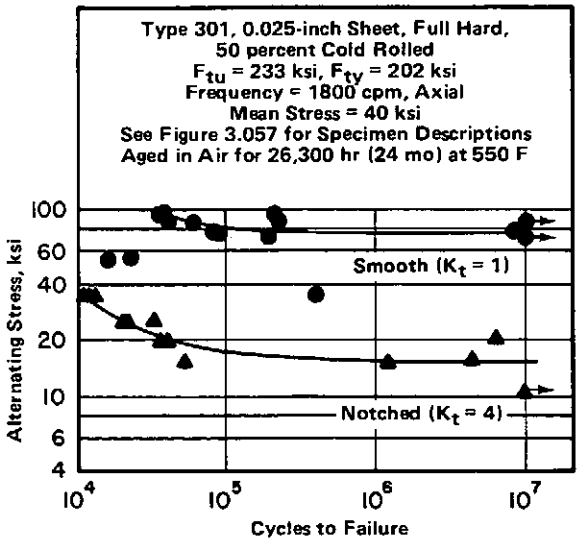


FIGURE 3.058. FATIGUE BEHAVIOR OF SMOOTH AND NOTCHED SHEET AT ROOM TEMPERATURE AFTER AGING FOR 26,300 HOURS AT 550 F (88)

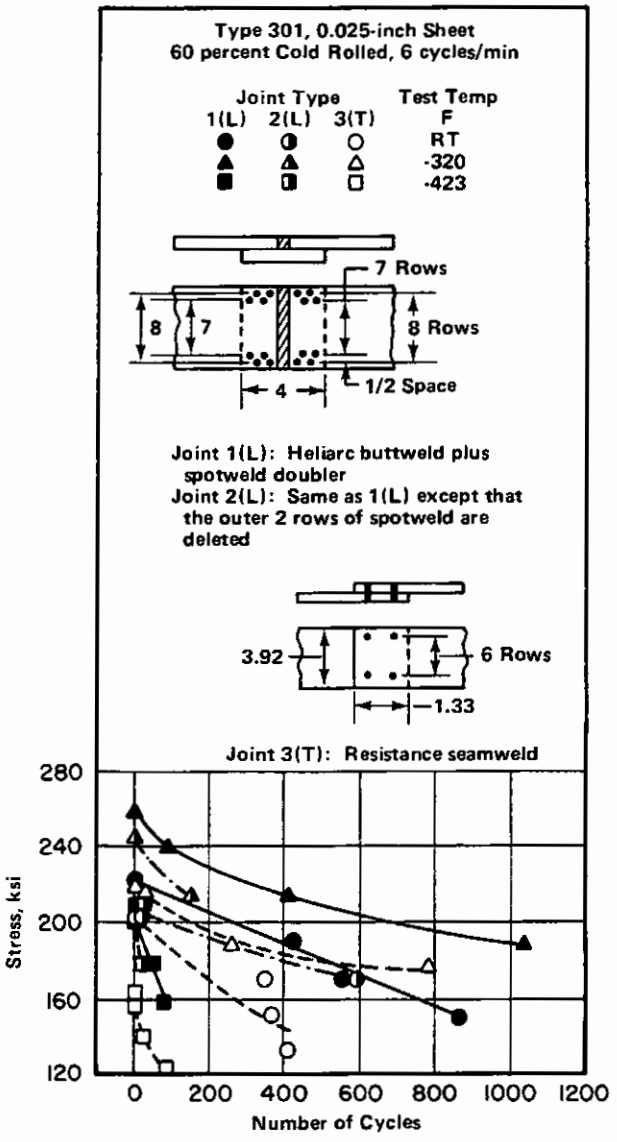
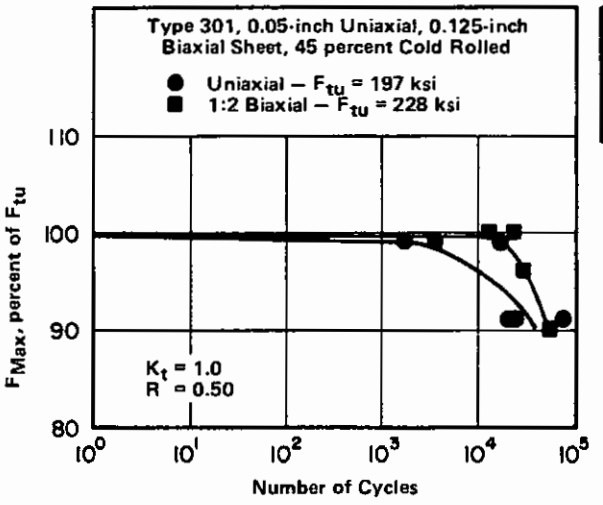


FIGURE 3.059. LOW-CYCLE S-N CURVES FOR COMPLEX WELDED JOINTS OF 60 PERCENT COLD-ROLLED SHEET (36)



Fe
18 Cr
8 Ni

Type 301
Type 302

FIGURE 3.0510. S-N CURVES FOR UNIAXIAL AND BIAXIAL SHEET FOR R = 0.50 (46)

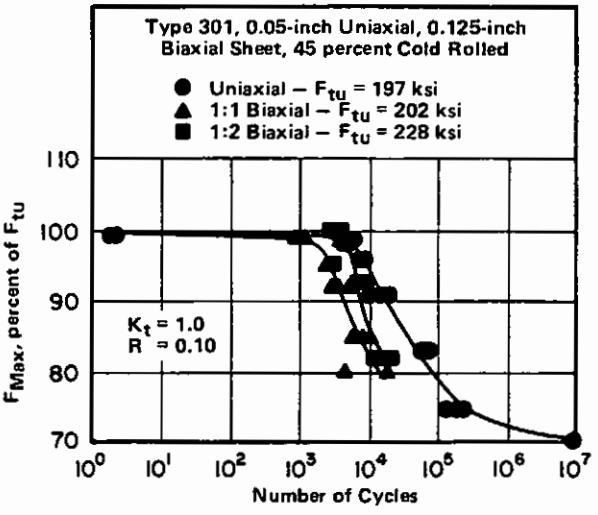


FIGURE 3.0511. S-N CURVES FOR UNIAXIAL AND BIAXIAL SHEET FOR R = 0.10 (46)

Fe
18 Cr
8 Ni

Type 301
Type 302

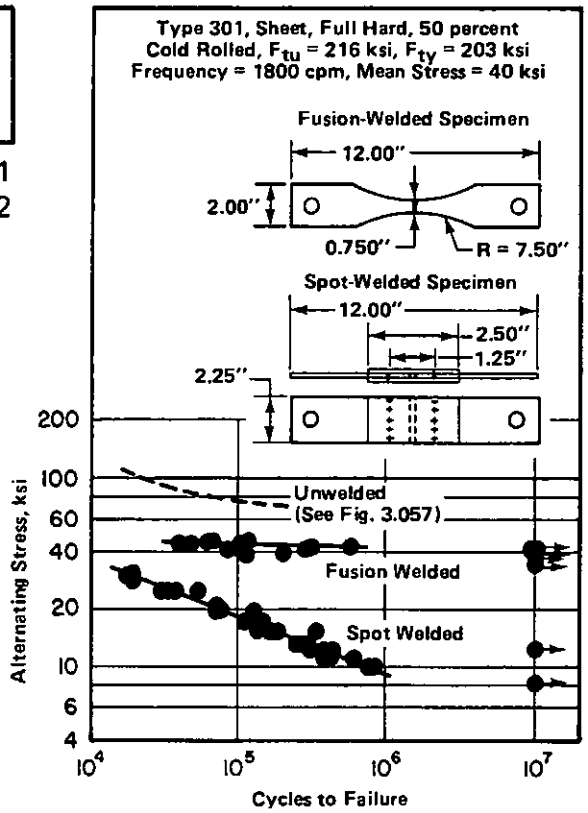


FIGURE 3.0512. EFFECTS OF FUSION AND SPOT WELDING ON FATIGUE BEHAVIOR OF SHEET (89)

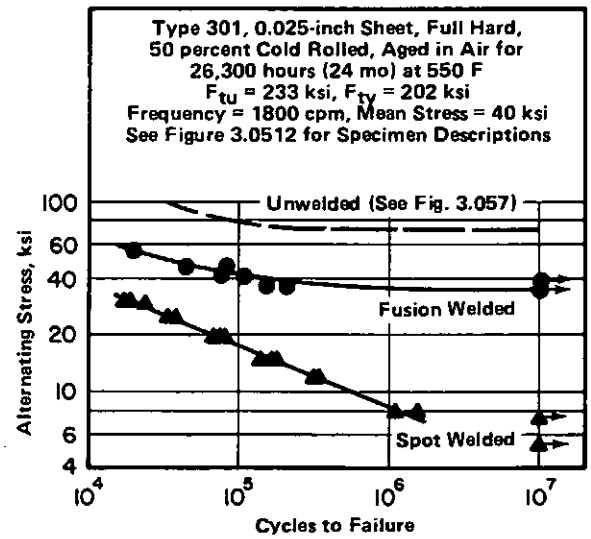


FIGURE 3.0513. FATIGUE BEHAVIOR OF WELDED SHEET AT ROOM TEMPERATURE AFTER AGING FOR 26,300 HOURS AT 550 F (88)

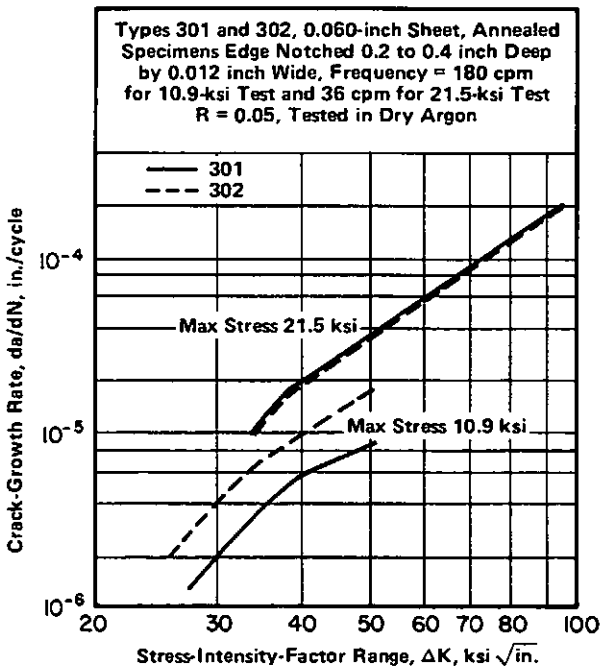


FIGURE 3.0515. FATIGUE CRACK-GROWTH BEHAVIOR AT ROOM TEMPERATURE FOR TYPES 301 AND 302 ANNEALED SHEET TESTED AT TWO DIFFERENT STRESS LEVELS (59)

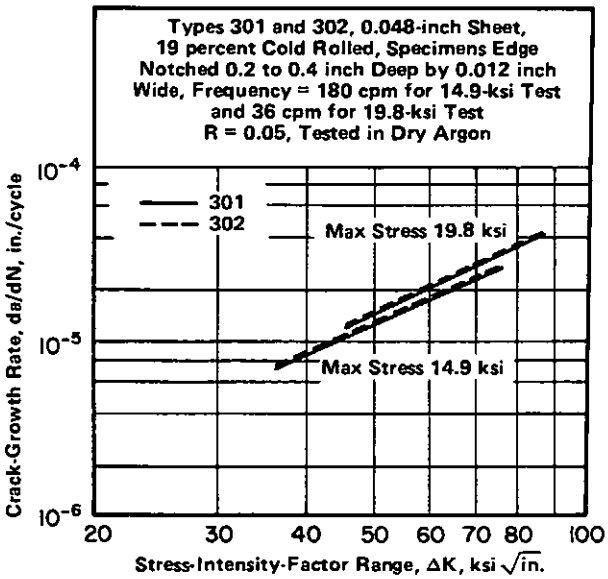


FIGURE 3.0516. FATIGUE CRACK-GROWTH BEHAVIOR AT ROOM TEMPERATURE FOR TYPES 301 AND 302 COLD-ROLLED SHEET TESTED AT TWO DIFFERENT STRESS LEVELS (59)

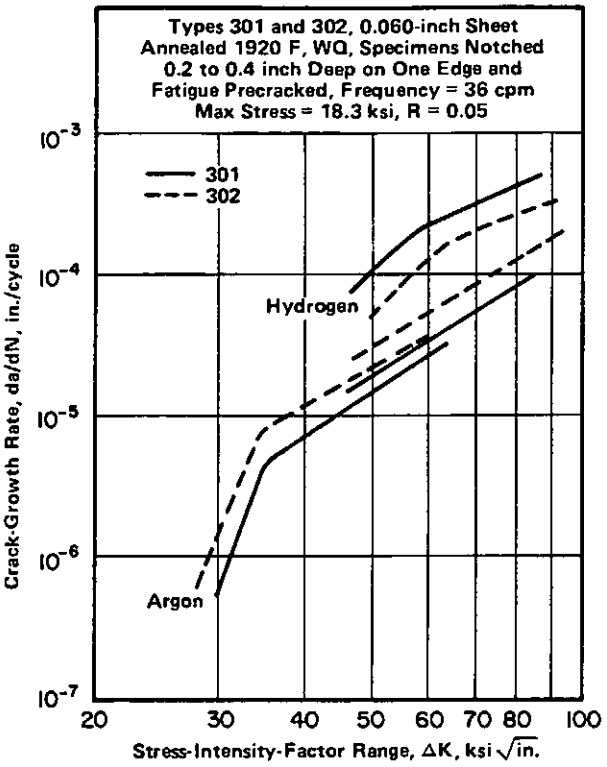
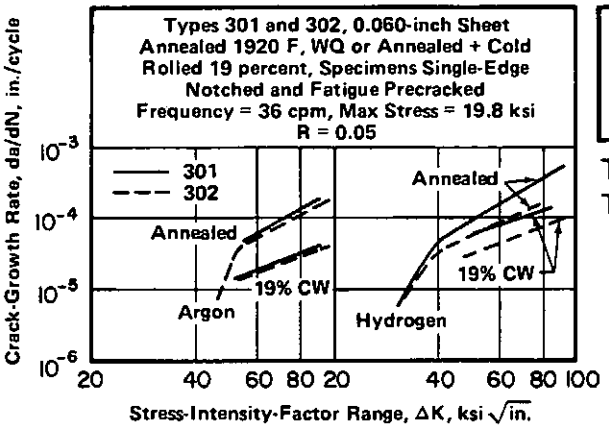


FIGURE 3.0518. FATIGUE CRACK-GROWTH BEHAVIOR AT ROOM TEMPERATURE FOR TYPES 301 AND 302 ANNEALED SHEET TESTED IN DRY HYDROGEN, DRY ARGON, AND AIR (90)



Fe
18 Cr
8 Ni

Type 301
Type 302

FIGURE 3.0519. FATIGUE CRACK-GROWTH BEHAVIOR AT ROOM TEMPERATURE FOR ANNEALED AND COLD-WORKED SHEET TESTED IN ARGON AND HYDROGEN (90)

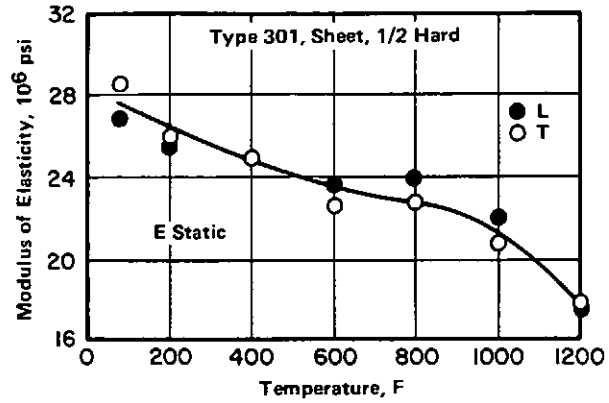


FIGURE 3.0621. MODULUS OF ELASTICITY FOR TYPE 301 1/2-HARD SHEET AT ROOM AND ELEVATED TEMPERATURES (11)

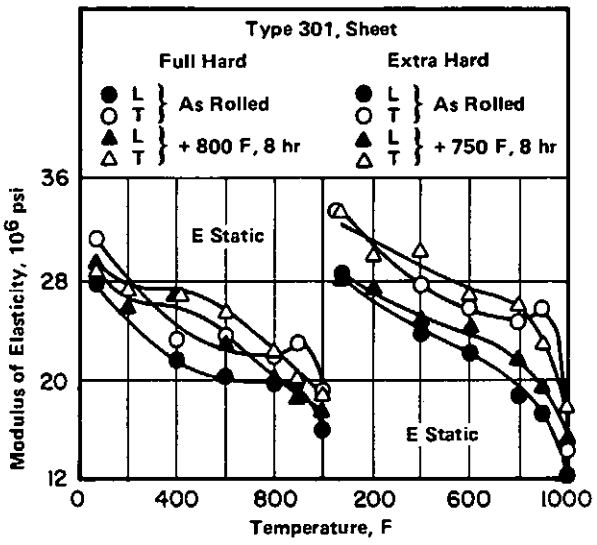


FIGURE 3.0622. MODULUS OF ELASTICITY IN TENSION FOR TYPE 301 FULL-HARD AND EXTRA-HARD SHEET (11)

Fe
18 Cr
8 Ni

Type 301
Type 302

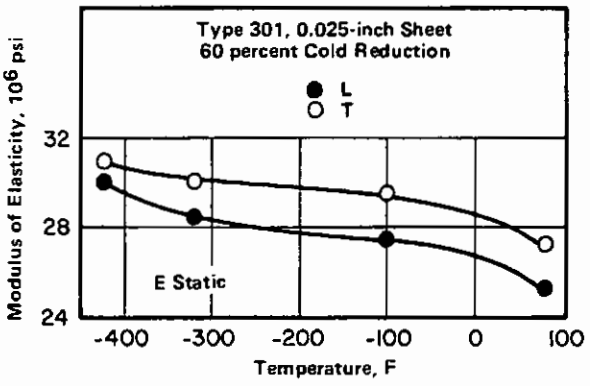


FIGURE 3.0623. EFFECT OF LOW TEST TEMPERATURE ON MODULUS OF ELASTICITY FOR 60 PERCENT REDUCED SHEET (36)

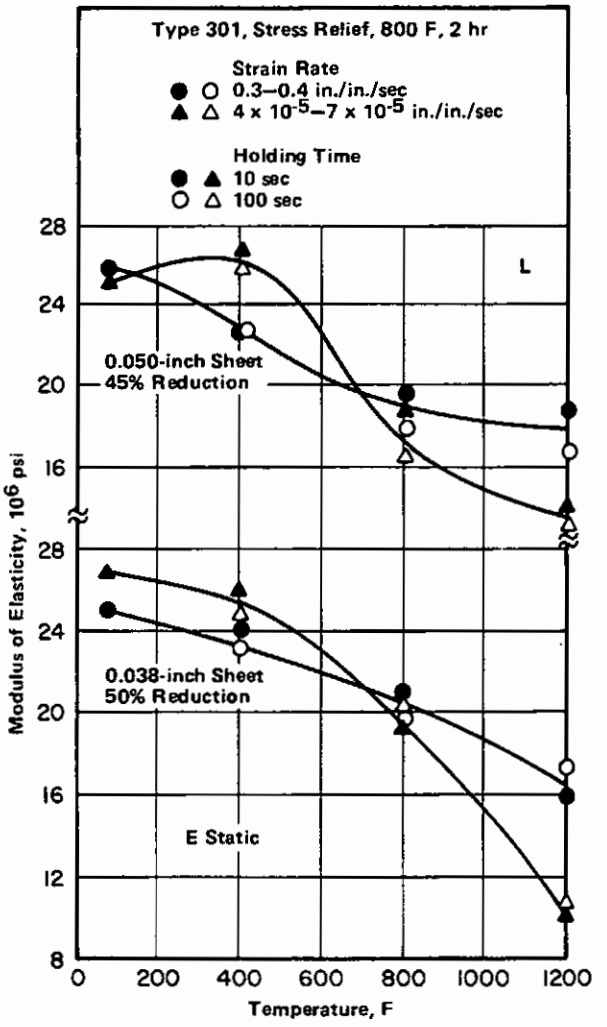


FIGURE 3.0624. EFFECT OF TEST TEMPERATURE, STRAIN RATE, AND HOLDING TIME ON MODULUS OF ELASTICITY IN TENSION OF 45 AND 60 PERCENT REDUCED SHEET (28)

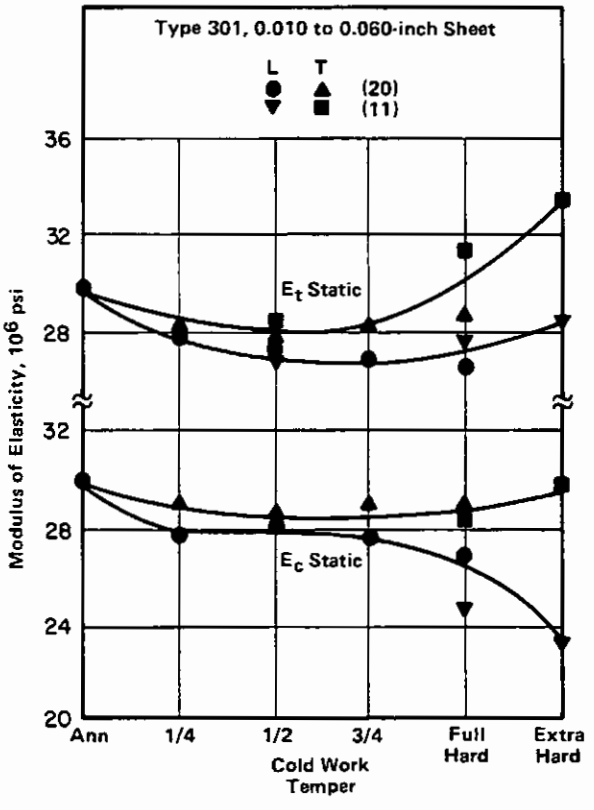


FIGURE 3.0625. EFFECT OF TEMPER ON STATIC MODULUS OF ELASTICITY IN TENSION AND COMPRESSION FOR TYPE 301 SHEET (11,20)

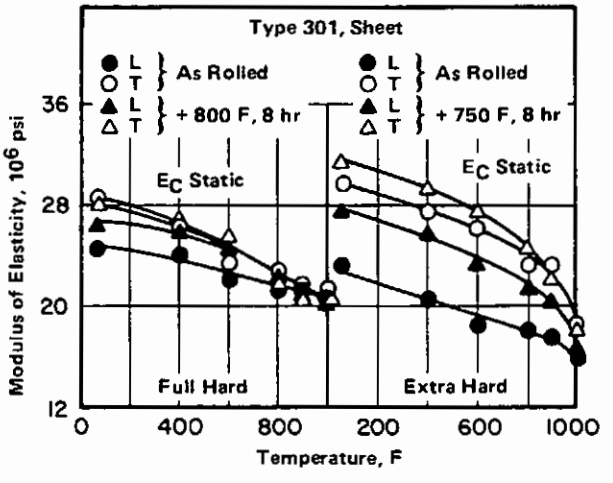


FIGURE 3.0626. MODULUS OF ELASTICITY IN COMPRESSION FOR TYPE 301 FULL-HARD AND EXTRA-HARD SHEET (11)

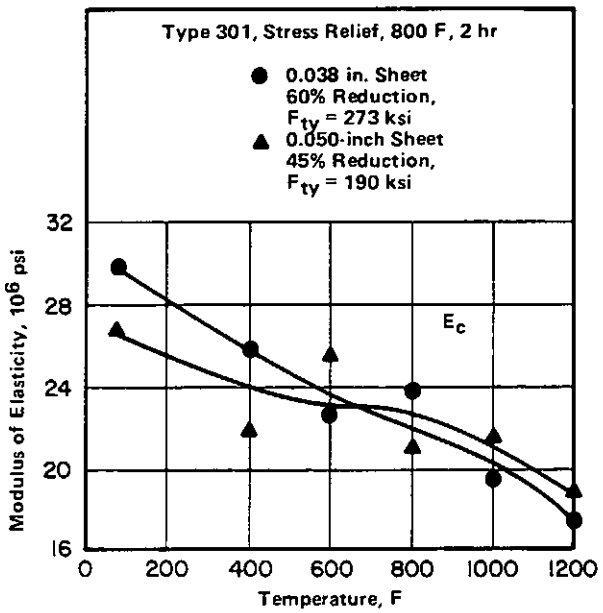


FIGURE 3.0627. EFFECT OF TEST TEMPERATURE ON MODULUS OF ELASTICITY IN COMPRESSION OF 45 AND 60 PERCENT REDUCED SHEET (28)

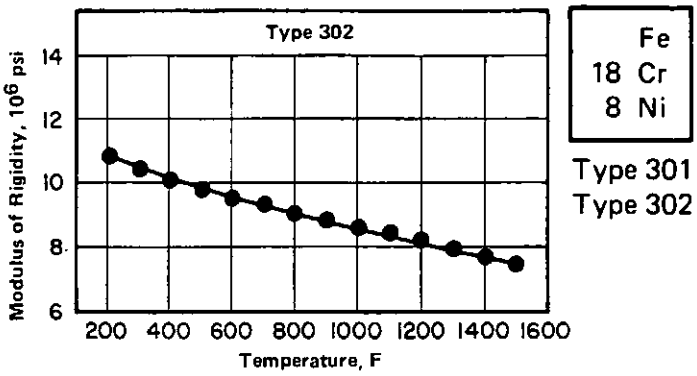


FIGURE 3.0631. MODULUS OF RIGIDITY (62)

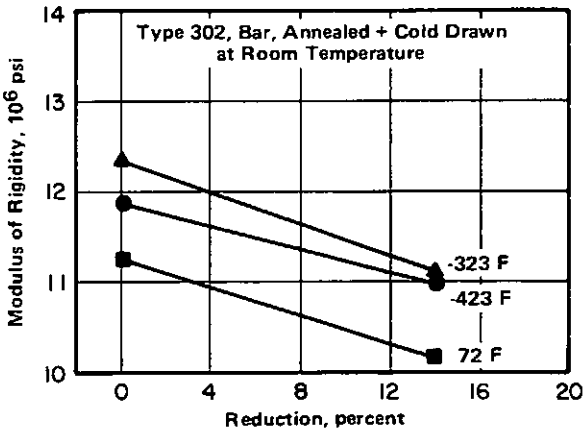


FIGURE 3.0632. EFFECTS OF COLD REDUCTION AND TEMPERATURE ON MODULUS OF RIGIDITY (93)

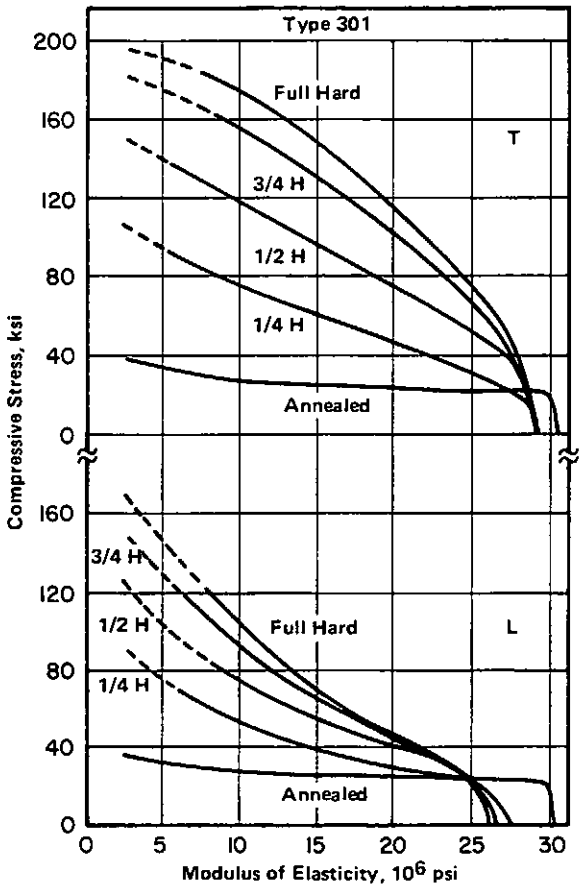


FIGURE 3.0641. COMPRESSIVE TANGENT MODULUS CURVES FOR TYPE 301 SHEET IN VARIOUS CONDITIONS (20)

Fe
18 Cr
8 Ni

Type 301
Type 302

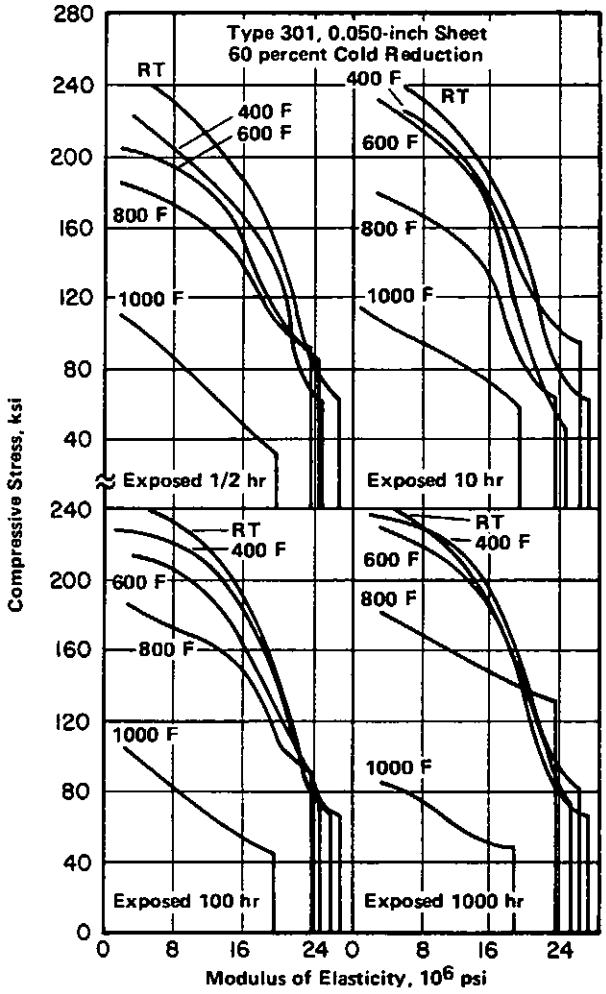


FIGURE 3.0642. COMPRESSIVE TANGENT MODULUS CURVES FOR 60 PERCENT COLD-REDUCED SHEET FOR VARIOUS EXPOSURE TIMES AND TEMPERATURES (38)

Temper	Anneal	1/4 H	1/2 H	3/4 H	Full H
Bend Factor, t	1/2 to 1-1/4	1 to 2-1/4	2-1/2 to 4	3 to 4	4 to 6

TABLE 4.0121. PRACTICAL BEND FACTORS FOR SHEET

	Fe
17	Cr
7	Ni
+	Ti

Stainless W

1. GENERAL

This alloy is one of the first precipitation-hardening, semi-austenitic stainless steels. Precipitation hardening after solution annealing is primarily due to the presence of titanium and also influenced by the balance of other elements. The alloy can be aged to strengths up to about 220 ksi and possesses good oxidation and corrosion resistance. It can be machined and formed in its annealed condition and is available in most wrought forms, (6). After fabrication this alloy may be converted into a wide range of high strength conditions by a simple single heat treatment for a short period at moderate temperatures with a minimum of surface oxidation distortion and dimensional changes. The alloy has had usages such as knives in paper pulp refining machinery, pump shafts, valve parts, springs, bearing plate on bridges, rollers and locks for dams, flexible nozzle walls of supersonic wind tunnels and flak panels on bombers, (10).

1.01 Commercial Designation
Stainless "W".

1.02 Alternate Designations
USS "W", AISI 635.

1.03 Specification
None.

1.04 Composition
Table 1.04.

TABLE 1.04

Source	DMIC (1)		US STEEL (6)		AISI (10)
Aluminum	Percent		Percent		Percent
	Min	Max	Min	Max	Typical
Aluminum	-	1.00	-	1.00	0.20
Carbon	-	0.12	-	0.10	0.06
Chromium	16.0	18.0	16.0	18.0	17.0
Manganese	-	1.00	-	1.00	0.55
Nickel	6.00	8.00	6.00	8.00	7.00
Silicon	-	1.00	-	1.50	0.60
Titanium	-	1.00	-	1.20	0.80
Nitrogen	-	0.2	-	-	-
Phosphorus	-	-	-	0.045	-
Sulfur	-	-	-	0.030	-
Iron	Balance		Balance		Balance

1.05 Heat Treatment
1.051 Solution anneal. 1850 to 1950F, 15 to 30 minutes, air cool, (3).
1.0511 Effect of solution annealing temperature on room temperature tensile properties of aged sheet, Fig. 1.0511.
1.052 Age. 950 to 1150F, 30 minutes, air cool. Exact treatment depends on properties desired, see 1.062 and 3.0211. Most widely used age treatment, 1000F, 30 minutes, air cool or quench, (10).

1.06 Hardness
1.061 Transformation to martensite after air cooling from solution anneal temperature requires 2 to 4 hours. Resulting hardness RC 22 to 28, (6).
1.062 Effect of aging temperature and time on hardness, Fig. 1.062.
1.063 Effect of low temperature on hardness of aged alloy, Fig. 1.063.

1.07 Forms and Conditions Available
The alloy is available in the form of strip, sheet, plate, bar, variety of forged shapes, forging billets, extrusions and wire, (6).

1.08 Melting and Casting Practice
Conventional arc or induction electric furnace practices employed for producing standard stainless steels can be used. However, attention must be given to holding the aluminum, titanium and nitrogen within specifications to avoid entrapment of aluminum and titanium oxide inclusions, (7).

1.09 Special Considerations
None.

2. PHYSICAL AND CHEMICAL PROPERTIES

2.01 Thermal Properties
2.011 Melting range
2.012 Phase changes. Ac3 approx. 1050F, Ar3 approx. 250F.
2.013 Thermal conductivity, Fig. 2.013.
2.014 Thermal expansion, Fig. 2.014.
2.015 Specific heat
2.016 Thermal diffusivity

2.02 Other Physical Properties
2.021 Density. 0.28 lb per cu in. 7.65 gr per cu cm, (7).
2.022 Electrical resistivity. 39.37 microhm-in, annealed, (6), 33.46 microhm-in, aged, (2).
2.023 Magnetic properties
2.0231 Magnetic permeability. At H = 100 oersteds: Annealed = 81; Aged = 101.(6).
2.024 Emissivity
2.025 Damping capacity

2.03 Chemical Properties
2.031 Corrosion resistance. This steel is not susceptible to intergranular corrosion and satisfactorily resists corrosion when subjected to salt spray or sea water immersion tests. Resistance to corrosion from boiling nitric acid is inferior to other stainless steels, especially in the precipitation hardened condition. Resistance to atmospheric corrosion and corrosion resistance to hydrogen sulphide gas, sulfur dioxide gas and hot milk are equivalent to 18-8 stainless steel, (8).
2.0311 Effect of stress level on atmospheric stress corrosion of solution annealed and aged sheet, Fig. 2.0311.
2.0312 Tests performed at Monroeville, Pa., of atmospheric stress corrosion on solution annealed and aged sheet of a stress level of 75 percent of F_{ty} = 210 ksi, had 7 specimens which were exposed 520 days without failure, (11).
2.032 Oxidation resistance
2.0321 Effect of rate of oxidation in air on exposure temperature of alloy, Fig. 2.0321.

2.04 Nuclear Properties
2.041 Effect of irradiation on tensile yield stress of alloy, Table 2.041.

TABLE 2.041

Source	(12, p. 36, 37)	
Alloy	Fe-17Cr-7Ni-+Ti	
Temp-F	RT	
Irradiation	5.1×10^{20} n per sq cm at RT	
	Irradiated	Control
F_{tu}, -ksi	134	113

3. MECHANICAL PROPERTIES

3.01 Specified Mechanical Properties

3.02 Mechanical Properties at Room Temperature
3.021 Tension
3.0211 Stress-strain diagrams
3.02111 Stress-strain curves for different aging temperatures of sheet, Fig. 3.02111.

Fe
17 Cr
7 Ni
+ Ti
Stainless W

3.0212 Effect of aging temperature on room temperature tensile properties, Table 3.0212.

TABLE 3.0212

Source	(6)(10)							
Alloy	Fe-17Cr-7Ni+Ti							
Form	Sheet, strip					Bar, plate		
Thickness-in			≤0.030	>0.030 <0.060	>0.060	≤1/2	>1/2	
Heat treatment	F_{tu} -ksi	F_{ty} -ksi	e(2 in) percent minimum for thickness indicated					RC
SA(1)	135	95	3	4	5	8	10	26
SA(1)+aged at 950F 30 minutes, AC	210	200	3	4	5	8	10	44
SA(1)+aged at 1000F 30 minutes, AC	200	190	3	4	5	8	10	42
SA(1)+aged at 1050F 30 minutes, AC	190	170	4	5	7	8	10	39
SA(2)	135		5	6	7	10	12	26
SA(2)+aged at 950F, 30 minutes, AC	170	155	5	6	7	10	12	38
SA(2)+aged at1000F 30 minutes, AC	160	145	5	6	7	10	12	37
SA(2)+aged at1050F 30 minutes, AC	150	130	5	6	8	10	12	34

SA(1) 1850F to 1950F, air cool
SA(2) 1850F to 1950F, air cool
+ 1300F, air cool

3.0213 Effect of exposure time and temperature on room temperature tensile properties of solution annealed sheet, Fig. 3.0213.

3.0214 Effect of exposure time and temperature on room temperature tensile properties of aged sheet, Fig. 3.0214.

3.022 Compression

3.0221 Stress-train diagrams

3.023 Impact

3.0231 Effect of exposure time and temperature on room temperature impact strength of solution annealed and aged alloy, Fig. 3.0231.

3.024 Bending

3.025 Torsion and shear

3.026 Bearing

3.027 Stress concentration

3.0271 Notch properties

3.0272 Fracture toughness

3.028 Combined properties

3.03 Mechanical Properties at Various Temperatures

3.031 Tension

3.0311 Stress-strain diagrams

3.03111 Stress-strain curves in tension at room and elevated temperatures for sheet, Fig. 3.03111.

3.0312 Effect of test temperature on tensile property of aged, forged bar, Fig. 3.0312.

3.0313 Effect of test temperature on tensile properties of solution annealed and aged sheet, Fig. 3.0313.

3.0314 Effect of low temperature on tensile properties of solution annealed and aged alloy, Fig. 3.0314.

3.032 Compression

3.0321 Stress-strain diagrams

3.03211 Stress-strain curves in compression at room and elevated temperatures for sheet, Fig. 3.03211.

3.0322 Effect of test temperature on the compressive yield strength of solution annealed and aged sheet, Fig. 3.0322.

3.033 Impact

3.0331 Effect of test temperature on impact energy of alloy, Fig. 3.0331.

3.0332 Effect of low test temperature on impact energy of solution annealed and aged alloy, Fig. 3.0332.

3.034 Bending

3.035 Torsion and shear

3.036 Bearing

3.037 Stress concentration

3.0371 Notch properties

3.0372 Fracture toughness

3.038 Combined properties

3.04 Creep and Creep Rupture Properties

3.041 Creep and creep rupture properties of aged bar, Table 3.041.

TABLE 3.041

Source	(8, p. 24-25)			
Alloy	Fe-17Cr-7Ni+Ti			
Condition	SA, 1650F, 40 min + 1000F, 1 hr			
Form	Bar			
Thickness - in	1			
Test temp - F	600	800	1000	1200
Stress for 0.2% plastic deformation in 500 hr, ksi	125	40	-	-
Rupture stress ksi, in 100 hr	-	-	32	12.5

3.05 Fatigue Properties

3.051 S-N curves for smooth and notched specimen of aged bar stock, Fig. 3.051.

3.052 Torsional endurance limit (20,000,000 cycles) solution treated 1950F, air cool and aged 925F, 2 hours, 58 ksi, (8).

3.053 Fatigue limit for thin sheet as received and ground and polished, Table 3.053.

TABLE 3.053

Source	(10, p. 87)					
Alloy	Fe-17Cr-7Ni +Ti					
Condition	SA 1950F +Age 925F, 30 Min					SA 1600F + 925F, 30 min
Form	Sheet					
Surface	As received				Ground*	As received
Thickness-in	0.018		0.050		0.050	0.018
Direction	L	T	L	T	L	L
F_{tu}, -ksi	183.5	168.6	196.5	201.0	-	168.4
Fatigue limit - ksi	56.0	54.0	54.0	54.0	70.0	50.0

* and polished

3.054 Effect of low temperature on the fatigue strength of alloy, Fig. 3.054.

3.06 Elastic Properties

3.061 Poisson's ratio at variuos temperatures, Fig. 3.061.

3.062 Modulus of elasticity

3.0621 Modulus of elasticity at various temperatures, Fig. 3.0621.

3.0622 Compression modulus at various temperatures, Fig. 3.0622.

3.063 Modulus of rigidity at various temperatures, Fig. 3.063.

4. FABRICATION

4.01 Formability

4.011 May be hot rolled, cold rolled or extruded by conventional process. Maximum formability is obtained in the solution annealed or overaged condition. However, the rather low elongations limit the amount of deformation during forming, (3)(7). The alloy in the softest solution annealed condition has cold formability approximating that of 1/2 hard AISI Type No. 302. When more than moderate forming is required, it is necessary to do the forming in one or more draws with intermediate annealing between draws. Intermediate annealing at 1200 to 1300F provides optimum ductility, (10).

4.012 Forging and hot working characteristics of the alloy are similar to those of AISI Type No. 321 stainless steel. Forging may be performed over a wide range of temperatures. Best practice dictates the use of temperature no higher than is necessary to accomplish the required deformations and to avoid excessive holding times at forging or rolling temperatures, particularly at temperatures above 2100F. Initial forging temperatures of 2100 to 2150F and finishing temperatures above 1700F are suggested, (10).

4.02 Machining and Grinding

4.021 The alloy may be machined in either annealed or the precipitation hardened conditions with about the same tooling and machining set ups as used for the austenitic stainless steels. The use of high speed steel or carbide tools, sturdy machines, slow feeds and speeds are important.

Ordinarily rough machining is performed on the alloy in the solution annealed condition and light finish machining done subsequently on the part after it has been aged when the part is to be used in the hardened condition. Machining of the hardened alloy leaves a good finish, removes the heat tint resulting from the aging treatment and also removes any minor distortion or dimension changes, (10).

4.03 Welding

4.031 Stainless W can be welded in either the solution annealed or aged condition by using techniques conventional for austenitic stainless steels. When welded in the solution treated condition, 100 percent joint efficiency is obtained. Aged material welded and reheat treated, exhibits about 90 percent joint efficiency. Specially coated electrodes having composition similar to that of the parent metal are recommended, (8).

4.032 Bend test of sheet welded with direct current with argon as the shielding gas, Table 4.032.

TABLE 4.032

Source	(10, p. 83)							
Alloy	Fe-17Cr-7Ni +Ti							
Form	Sheet							
Condition	weld, 1000F, 1/2hr		SA 1900F+ weld, SA 1870F+ 1000F, 1/2hr		1000F, 1/2hr weld		1000F,1/2hr, weld, 1000F,1/2hr	
Direction bend to weld	L	T	L	T	L	T	L	T
Angle of bend to failure	180	90	140	90	180*	135	110	90

*No failure

4.04 Heat Treatment

4.041 Close temperature control is necessary during aging due to the rapid response to precipitation hardening.

4.05 Surface Treatment

4.051 Cleaning methods for this alloy are similar to Type 302 stainless steel.

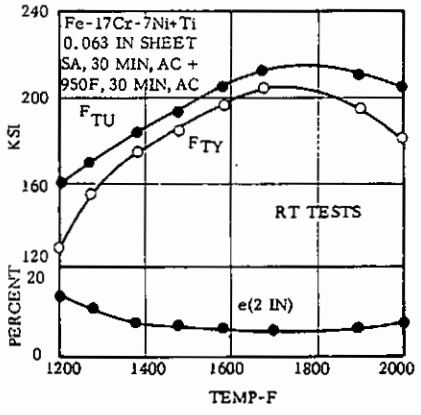


FIG. 1.0511 EFFECT OF SOLUTION ANNEALING TEMPERATURE ON ROOM TEMPERATURE TENSILE PROPERTIES OF AGED SHEET (6, p. 8)

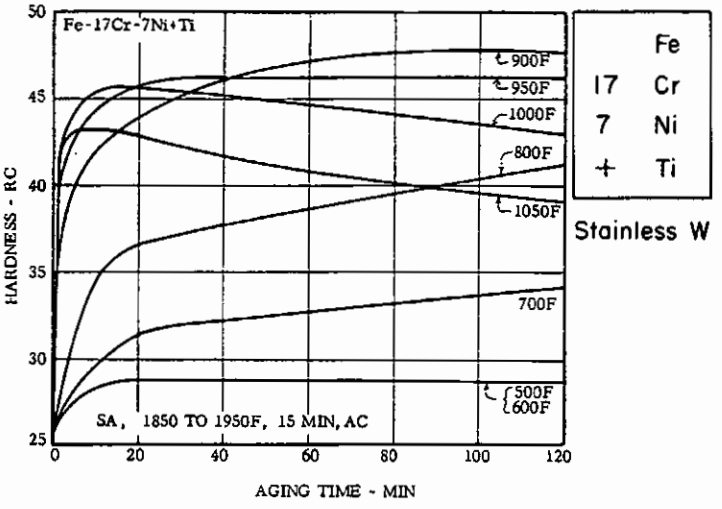


FIG. 1.062 EFFECT OF AGING TEMPERATURE AND TIME ON HARDNESS (6, p. 8-9)

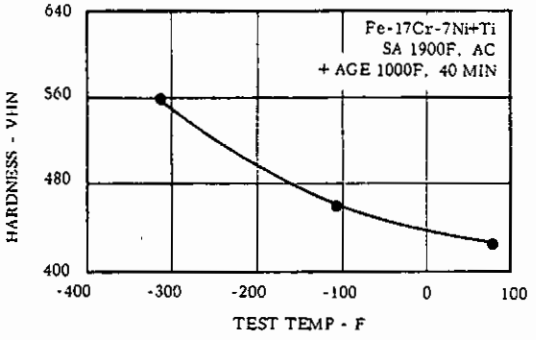


FIG. 1.063 EFFECT OF LOW TEMPERATURE ON HARDNESS OF AGED ALLOY (10, p. 88)

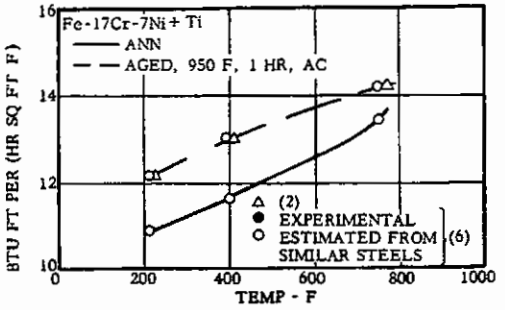


FIG. 2.013 THERMAL CONDUCTIVITY (2, p. 8) (6, p. 15)

	Fe
17	Cr
7	Ni
+	Ti

Stainless W

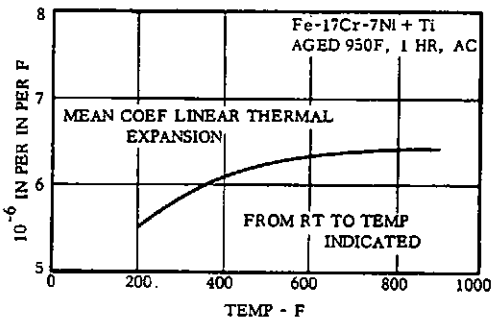


FIG. 2.014 THERMAL EXPANSION

(2, p. 8)

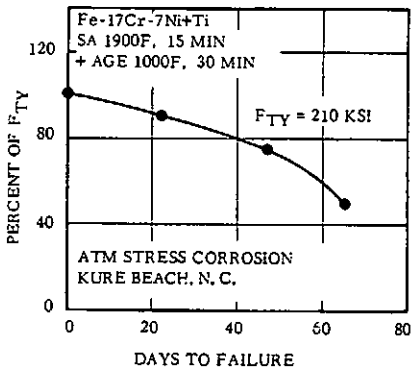


FIG. 2.0311 EFFECT OF STRESS LEVEL ON ATMOSPHERIC STRESS CORROSION OF SOLUTION ANNEALED AND AGED SHEET (11, p. 48, 51)

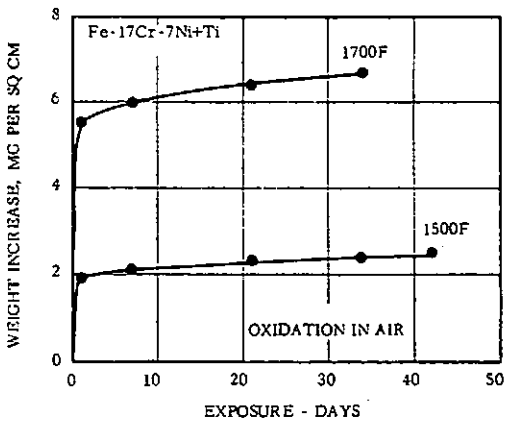


FIG. 2.0321 EFFECT OF RATE OF OXIDATION IN AIR ON EXPOSURE TEMPERATURE OF ALLOY

(10, p. 89)

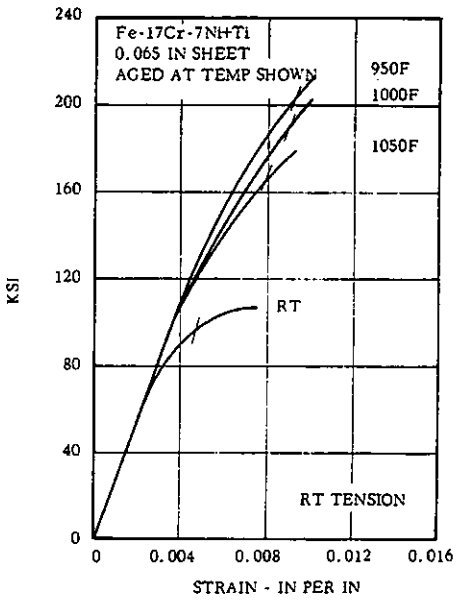


FIG. 3.02111 STRESS-STRAIN CURVES IN TENSION FOR DIFFERENT AGING TEMPERATURES OF SHEET (10, p. 88)

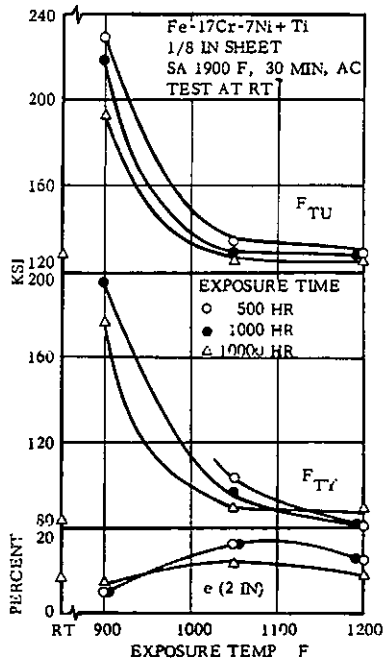


FIG. 3.0213 EFFECT OF EXPOSURE TIME AND TEMPERATURE ON ROOM TEMPERATURE TENSILE PROPERTIES OF SOLUTION ANNEALED SHEET

(6, p. 13)

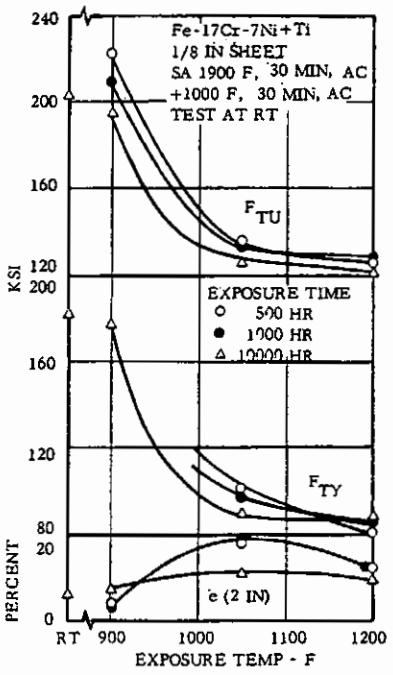


FIG. 3.0214 EFFECT OF EXPOSURE TIME AND TEMPERATURE ON ROOM TEMPERATURE TENSILE PROPERTIES OF AGED SHEET

(6, p. 13)

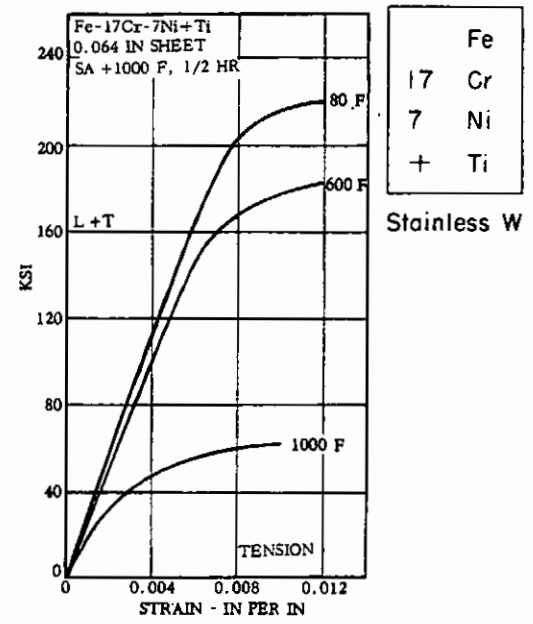


FIG. 3.03111 STRESS STRAIN CURVES IN TENSION AT ROOM AND ELEVATED TEMPERATURES FOR SHEET

(9, p. 19)

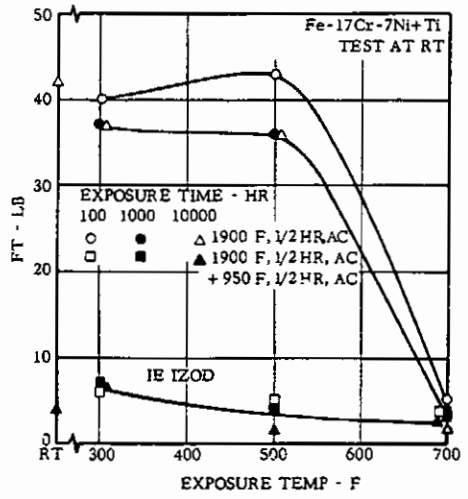


FIG. 3.0231 EFFECT OF EXPOSURE TIME AND TEMPERATURE ON ROOM TEMPERATURE IMPACT STRENGTH OF SOLUTION ANNEALED AND AGED ALLOY

(6, p. 12)

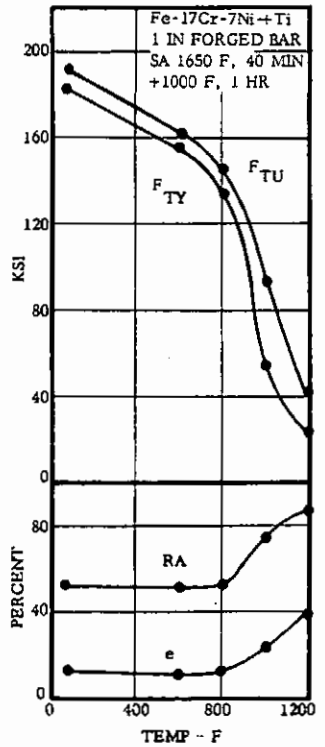


FIG. 3.0312 EFFECT OF TEST TEMPERATURE ON TENSILE PROPERTIES OF AGED, FORGED BAR

(8 p. 29)

	Fe
17	Cr
7	Ni
+	Ti

Stainless W

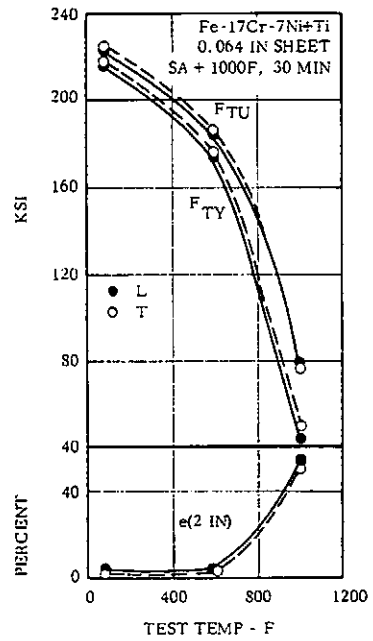


FIG. 3.0313 EFFECT OF TEST TEMPERATURE ON TENSILE PROPERTIES OF SOLUTION ANNEALED AND AGED SHEET (10, p. 88)

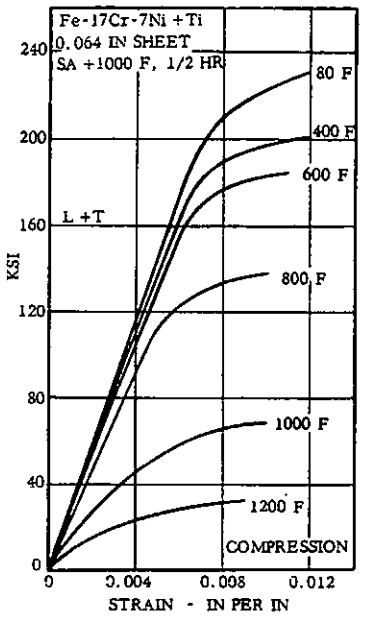


FIG. 3.03211 STRESS-STRAIN CURVES IN COMPRESSION AT ROOM AND ELEVATED TEMPERATURES FOR SHEET (9, p. 20)

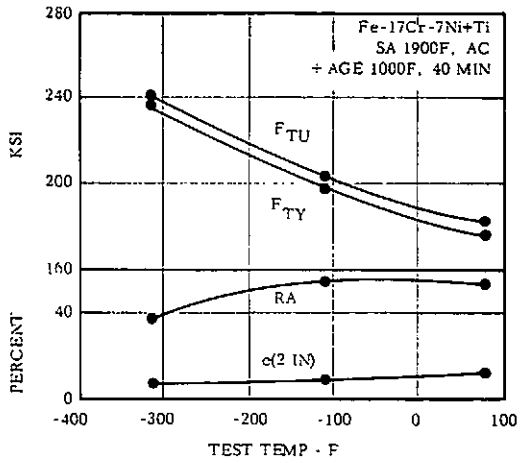


FIG. 3.0314 EFFECT OF LOW TEMPERATURES ON TENSILE PROPERTIES OF SOLUTION ANNEALED AND AGED ALLOY (10, p. 88)

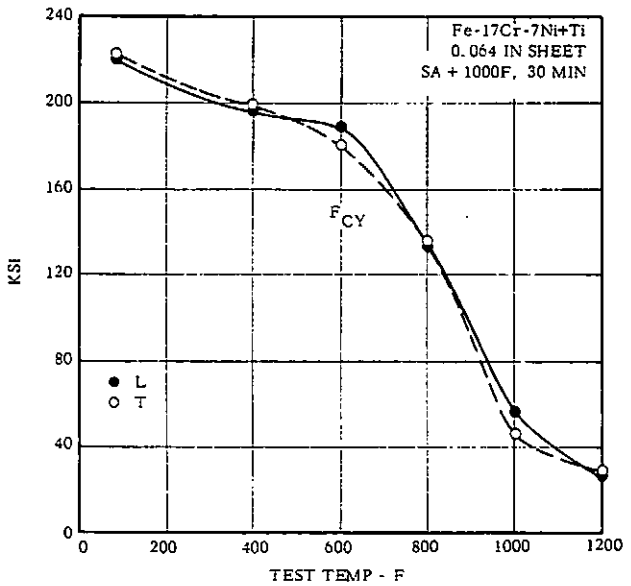


FIG. 3.0322 EFFECT OF TEST TEMPERATURE ON THE COMPRESSIVE YIELD STRENGTH OF SOLUTION ANNEALED AND AGED SHEET (10, p. 88)

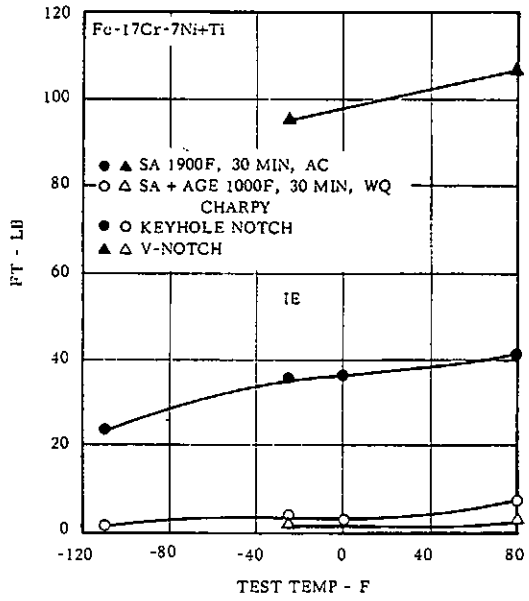


FIG. 3.0331 EFFECT OF TEST TEMPERATURE ON IMPACT ENERGY OF ALLOY (10, p. 88)

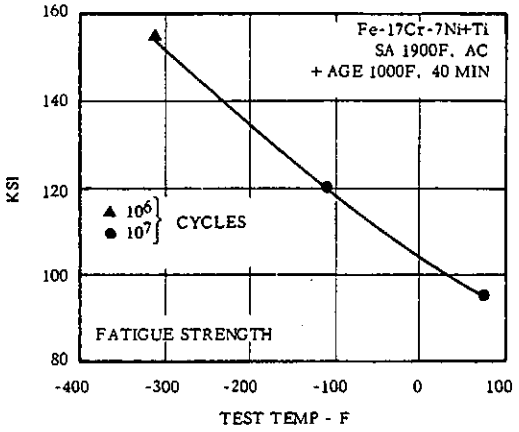


FIG. 3.054 EFFECT OF LOW TEMPERATURES ON THE FATIGUE STRENGTH OF ALLOY (10, p. 88)

	Fe
17	Cr
7	Ni
+	Ti

Stainless W

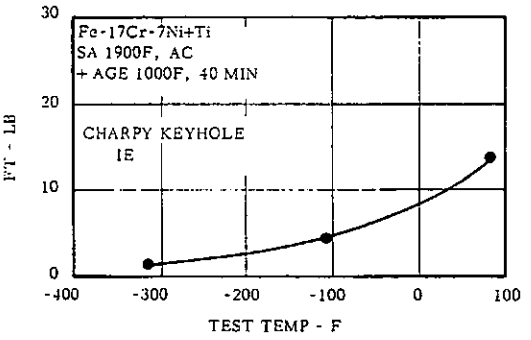


FIG. 3.0332 EFFECT OF LOW TEST TEMPERATURES ON IMPACT ENERGY OF SOLUTION ANNEALED AND AGED ALLOY (10, p. 88)

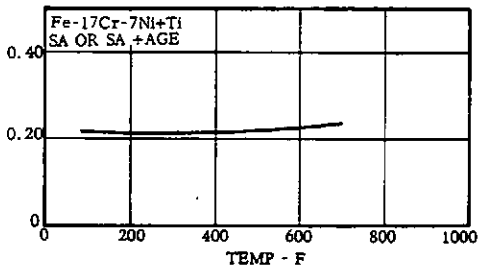


FIG. 3.061 POISSON'S RATIO AT VARIOUS TEMPERATURES (6, p. 16)

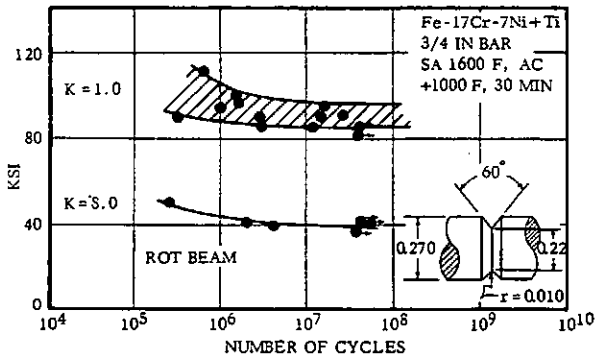


FIG. 3.051 S-N CURVES FOR SMOOTH AND NOTCHED SPECIMEN OF AGED BAR STOCK (8, p. 22)

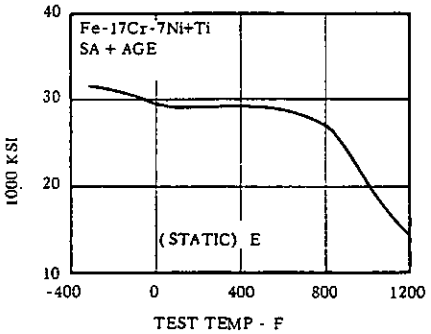


FIG. 3.0621 MODULUS OF ELASTICITY AT VARIOUS TEMPERATURES (6, p. 10), (7, A-6), (10, p. 88)

	Fe
17	Cr
7	Ni
+	Ti

Stainless W

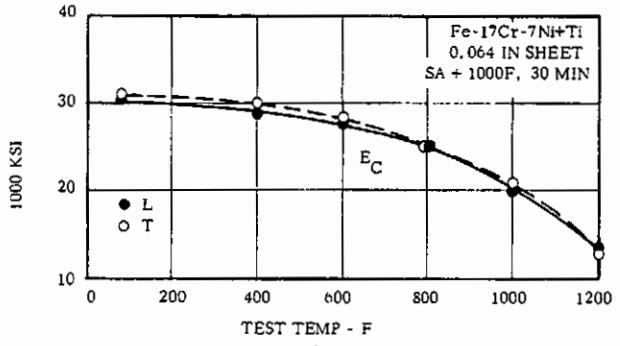


FIG. 3.0622 COMPRESSION MODULUS AT VARIOUS TEMPERATURES (10, p. 88)

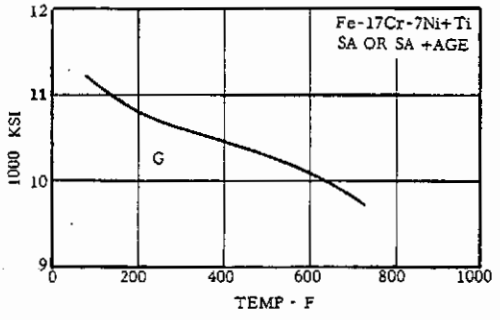


FIG. 3.063 MODULUS OF RIGIDITY AT VARIOUS TEMPERATURES (6, p. 16)

REFERENCES

1 Fiorentino, R.J., Roach, D.B. and Hall, A.M., "Heat Treatment of High-Strength Steels for Airframe Applications", DMIC Rep. 119, (Nov. 27, 1959)

2 Roberts, D.A., Roach, D.B. and Hall, A.M., "Physical and Mechanical Properties of Nine Commercial Precipitation-Hardenable Stainless Steels", DMIC Rep. 112, (May 1, 1959)

3 Ludwigson, D.C. and Hall, A.M., "The Physical Metallurgy of Precipitation-Hardenable Stainless Steels", DMIC Rep. 111, (Apr. 20, 1959)

4 Favor, R.J., Achbach, W.P. and Hyler, W.S., "Materials-Property-Design Criteria for Metals", WADC TR 55-150, Pt. 5, (Oct. 1957)

5 Lena, A.J. and Reynolds, E.E., "High Strength Steels for Aircraft Applications", Preprint AISI Meeting New York (May 21, 1958)

6 United States Steel Corp., "USS Stainless W", (May 1958)

7 Roach, D.B. and Hall, A.M., "The Engineering Properties of Precipitation-Hardenable Stainless Steels", TML Rep. No. 48, (July 20, 1956)

8 Smith, R., Wyche, E.H. and Gove, W., "A New Precipitation Hardening Stainless Steel", Metals Technology T.P. 2006, (Feb. 1946)

9 Hughes, P.J., Inge, J.E. and Prosser, S.B., "Tensile and Compressive Stress-Strain Properties of Some High-Strength Sheet Alloys at Elevated Temperatures", NACA TN 3315, (Nov. 1954)

10 "Contributions to the Metallurgy of Steel: High Temperature High Strength Alloys", AISI, (Feb. 1963)

11 Phelps, E.H. and Loginow, A.W., "Stress Corrosion of Steels for Aircraft and Missiles", Symposium on High-Strength Steels for the Missile Industry, (Feb. 1960)

12 Shober, F.R., "The Effect of Nuclear Radiation on Structural Metals", DMIC Rep. 166, (Sept. 15, 1961)

Fe
18 Ni
3 Mo
Ti
Al

T-250
Maraging

1 **GENERAL**

T-250 (MS 250) is a maraging steel which contains no cobalt. Cobalt has been considered as a strategic element because of uncertain supply coupled with a high and volatile price. The strength of the cobalt-free alloy is essentially equal to that of the conventional cobalt-containing 250 grade maraging steel. This equivalent strength has been obtained by a substantial increase in the titanium content and the alloy properties are significantly influenced by variations in titanium within the specified composition limits. T-250 maintains many of the desirable characteristics of the cobalt-containing alloy including excellent hot- and cold-formability, simple heat treatment with very small dimensional change, high fracture toughness, and good weldability.

Applications to date have been primarily in the production of relatively small rocket motor cases by high-cold-reduction shear forming. Demonstration projects have shown that very large cases (e.g., solid rocket motor case segments for the Space Shuttle) can be successfully produced by the same processes.

1.01 **Commercial Designations**

Maraging T-250 and Maraging MS 250.

1.02 **Alternate Designations**

Maraging Free-Co.

1.03 **Specifications**

MIS 36275 Steel Bar, billet and forgings; AMS 6518 and AMS 6591A.

1.04 **Composition**

1.041 Composition, Table 1.04.

1.05 **Heat Treatment**

1.051 Homogenize: 1800 F to 2000 F. Used under special circumstances to control retained austenite and dissolve precipitated phases (e.g., see 4.03).

1.052 Solution treat (solution anneal or anneal). This treatment is designed to take into solution the strengthening phases which precipitate on aging. It also produces a soft structure and for that reason has been called solution anneal or anneal. Normally 1475 to 1525 F, 1 hr per inch with 1/2 hr minimum. Higher annealing temperatures may be used but can result in large grain sizes (see also Code 1220).

1.053 Aging: 800 F to 1000 F, depending on the strength level desired. Normally 875 to 925 F, 3 to 4 hrs, which gives the highest strengths. (See also Code 1220.)

1.06 **Hardness**

1.061 Hardness of 3 inch diameter bars in the annealed condition and after aging, Table 1.061.

1.062 Effect of aging temperature on hardness of bar of two titanium contents, Figure 1.062.

1.07 **Forms and Conditions Available**

Bar, billet, plate, sheet, forgings and wire.

1.08 **Melting and Casting Practice**

Close control of raw material is required to insure low carbon and residual element content. Electric furnace melting plus argon/oxygen decarbonization (AOD) followed by double vacuum melting (VIM/VAR) is recommended.

1.09 **Special Considerations**

1.091 Effect of composition. The tensile and yield strength are significantly influenced by variations in the titanium content within the ranges given in the AMS Specifications. Increased titanium raises these strength properties (see Figure 3.0212) and reduces the fracture toughness (see Figure 3.02722). A discussion of the effects of the alloying elements is given in (3).

1.092 Hydrogen embrittlement. The alloy is very susceptible to hydrogen embrittlement. Hydrogen embrittlement studies (8) show that tensile samples with hydrogen contents of about 18 ppm exhibit large reductions in strength and negligible ductility. A high degree of embrittlement is also observed when tested in 10 ksi hydrogen gas (8). Hydrogen is rapidly absorbed into the lattice structure and the alloy should not be used under cathodic conditions. (See also 4.03.)

1.093 Stress corrosion in salt solutions appears to be accerelated by tempering at 850 F and below (8).

2 **PHYSICAL PROPERTIES AND ENVIRONMENTAL EFFECTS**

2.01 **Thermal Properties**

2.011 Melting range: 2615 to 2740 F (20).

2.012 Phase changes. There is considerable hysteresis in the thermal expansion on heating and cooling. The exact nature of this behavior will depend on variations in composition within the specified limits. On cooling from a completely austenitic condition, martensite transformation starts at about 400 F and is complete at about 250 F. This martensite is a heavily dislocated lath structure. Aging primarily produces very fine Ni_3Ti needle-like particles which are coherent with the matrix. Increasing the aging temperature increases the size of these particles. Aging at 900 F results in a uniform distribution of particles which form a Widmanstatten pattern (19).

Reheating the aged material results in austenite reversion starting at about 1000 F. Complete solution of the Ni_3Ti is normally complete at about 1500 F.

A uniform shrinkage of about 0.001 in./in. occurs on solution annealing and on aging (2).

2.012 Linear expansion curves showing the MS and start of austenite reversion, Figure 2.0121.

2.0121 Time-temperature transformation diagram.

2.013 Thermal conductivity.

2.014 Thermal expansion.

2.0141 Mean coefficient of linear thermal expansion, Figure 2.0141.

2.015 Specific heat.

2.016 Thermal diffusivity.

Fe
18 Ni
3 Mo
Ti
Al

T-250
Maraging

2.02 **Other Physical Properties**
2.021 Density: 0.286 lb/in.^{3} (19).
2.022 Electrical properties.
2.023 Magnetic properties.
2.024 Emittance.
2.025 Damping capacity.

2.03 **Chemical Environments**
2.031 General corrosion. Limited general corrosion information indicates the alloy is superior to 4340 but may be somewhat inferior to the cobalt-containing grade in long-term exposures in salt atmospheres.

2.0311 General corrosion resistance for several alloys, Table 2.0311.

2.032 Stress corrosion. The tendency for stress corrosion cracking has been measured using a variety of test methods (e.g., ASTM G30 for U-bend specimens, ASTM G38 for C-ring specimens and ASTM G 49 for direct-tension specimens). While these types of tests are useful in comparing the general response of various alloys to a given environment, the results are difficult to use in structural life prediction or in fracture control programs. Preferably, the stress corrosion resistance should be measured using a fracture mechanics approach, which can yield both crack growth rates in a corrosive environment as well as a K_{Iscc} value below which cracks should be stable in this environment. This type of information should be emphasized in evaluation of high strength alloys. Unfortunately, there is, as yet, no ASTM standard method for determining K_{Iscc} and various procedures have been used to determine this value. The information that follows is derived from test methods which are generally acceptable.

T-250 steel, like other high strength steels, is susceptible to stress corrosion cracking in chloride solutions and in high humidity air. The crack growth rates of these steels will increase and the K_{Iscc} values decrease with increasing strength level and with increasing cathodic potential.

K_{Iscc} values have been reported for both plate and for large ring forgings of T-250 steel. From the limited data available (Table 2.0321), an estimate of K_{Iscc} is between 18 to 21 ksi $\sqrt{in.}$ at a yield-strength level of 250 ksi for alternate immersion in 3.5% NaCl or in 100% R.H. air. This range is somewhat lower than the 29 ksi $\sqrt{in.}$ reported for the cobalt-containing grade at the same yield-strength level. It should be noted that the interpretation of these values is complicated by the lack of information on the free corrosion potentials in the media used.

The influence of cathodic potential on the K_{Iscc} of T-250 at several strength levels is shown in Table 2.0323. As expected, the K_{Iscc} decreases with the strength level at a constant applied potential. However, it should be noted that the potential of -1.2 volts is a very severe condition unlikely to be encountered during service. Reducing the negative potential to -0.8 volts results in a large increase in the measured values of K_{Iscc}. To apply data of this type to structural life prediction it would be necessary to know the service potential.

2.0321 K_{Iscc} results for plate and forging exposed to artificial seawater and to 100% R.H. air, Table 2.0321.

2.0322 Crack-growth data for T-250 ring forging in artificial seawater and in 100% R.H. air, Figure 2.0322.

2.0323 K_{Iscc} data showing the effects of applied potential in a 3.5% NaCl solution using a small, step-loaded slow bend test, Table 2.0323.

2.04 **Nuclear Environments**

3 **MECHANICAL PROPERTIES**

3.01 **Specified Mechanical Properties**
AMS and MIS Specified Mechanical Properties, Table 3.01.

3.02 **Mechanical Properties at Room Temperature**
3.021 Tension – stress-strain diagrams – tension properties.
3.0211 Stress strain curve for aged bar, Figure 3.0211.
3.0212 Effect of titanium content on tensile yield strength, Figure 3.0212.
3.0213 Tensile properties and hardness of annealed alloy from various sources, Table 3.0213.
3.0214 Mechanical properties of various forms in the aged condition, Table 3.0214.
3.0215 Effect of solution temperature and resolution treatment on tensile properties of bar, Figure 3.0215.
3.0216 Effect of aging temperature on tensile properties of bar of two titanium contents, Figure 3.0216.
3.0217 Tensile strength properties of bar aged for 3 or 12 hours at various temperatures, Figure 3.0217.
3.0218 Effect of aging temperature on tensile properties of bar, showing effects of inclusions on ductility, Figure 3.0218.
3.0219 Effect of cold reduction on the tensile properties of unaged 1.26 percent titanium alloy, Figure 3.0219.
3.02110 Effect of cold reduction on tensile properties of aged 1.26 percent titanium alloy, Figure 3.02110.
3.02111 Effect of cold reduction on tensile properties of unaged 1.43 percent titanium alloy, Figure 3.02111.
3.02112 Effects of cold reduction on tensile properties of aged 1.43 percent titanium alloy, Figure 3.02112.
3.02113 Tensile properties at various stages of fabrication of a small solid propellant rocket motor case, Table 3.02113.
3.02114 Tensile properties of a large shear-formed cylinder from a demonstration project, Table 3.02114.
3.02115 Statistical summary of tensile properties derived from tests on 59 heats, Table 3.02115.
3.022 Compression – stress-strain diagrams – compression properties.
3.023 Impact.
3.0231 Effect of solution temperature and resolution treatment on impact energy for bar, Figure 3.0231.
3.0232 Effect of aging temperature on impact energy of bar given a double solution treatment, Figure 3.0232.
3.0233 Effect of test temperature and exposure temperature on the impact energy for bar, Figure 3.0233.
3.024 Bending.
3.025 Torsion and shear.
3.026 Bearing.

3.027 Stress concentration.
3.0271 Effect of stress concentration on the ultimate tensile strength of bar, Figure 3.0271.
3.0272 Fracture toughness.
3.02721 Plane strain fracture toughness of various forms in the aged condition from several commercial heats, Table 3.02721.
3.02722 Effect of aging temperature on plane strain fracture toughness of bar of two titanium contents, Figure 3.02722.
3.028 Combined properties.

3.03 **Mechanical Properties at Various Temperatures**
3..031 Tension – stress-strain diagrams – tensile properties.
3.0311 Stress strain curves at elevated temperatures for heavily cold worked and aged alloy, Figure 3.0311.
3.0312 Effect of test temperature on tensile properties of bar, Figure 3.0312.
3.0313 Effect of test temperature and exposure temperature on tensile properties of solution treated and aged bar, Figure 3.0313.
3.033 Compression – stress-strain diagrams – tensile properties.
3.034 Bending.
3.035 Torsion and shear.
3.036 Bearing.
3.037 Stress concentration.
3.0371 Fracture toughness.
3.038 Combined properties.

3.04 **Creep and Creep Rupture Properties**

3.05 **Fatigue Properties**
3.051 Rotating beam fatigue strength for aged bar given several solution treatments, Figure 3.051.
3.052 Fatigue crack growth rate for plate, Figure 3.052.

3.06 **Elastic Properties**
3.061 Poisson's ratio.
3.062 Modulus of elasticity: 27.64 x 10^6 psi (20).
3.063 Modulus of rigidity.
3.064 Tangent modulus.
3.065 Secant modulus.

4 **FABRICATION**

4.01 **Formability**
4.011 Hot working. The alloy has excellent hot workability as evidenced by the tensile data at temperatures above 1400 F (Figure 4.0111). Titanium and molybdenum have a tendency to segregate (banding) and for this reason proper homogenization is required before forging or welding. The required homogenization is normally applied by the alloy producer using proprietary processes. Hot forging and pressing are usually done in the temperature range between 2000 and 2150 F, finishing at 1500 to 1750 F. Finishing above 1750 F can result in undesirably large prior austenite grain size.
4.0111 Effect of test temperature on the tensile strength and ductility of bar, Figure 4.0111.
4.012 Cold forming. In the solution annealed condition very large cold reductions can readily be obtained without cracking (e.g., cold rolling up to 80 reduction without intermediate anneals) (4). Similar results have been obtained in shear forming of large cylinders (see Table 3.02114). Aging of cold-formed material can give tensile strengths above 300 ksi (see Figures 3.02110 and 3.02112).

4.02 **Machining and Grinding**
In the solution-annealed condition, the machinability is comparable to 4340 at the same hardness level. Dimensional stability is such that machining prior to aging is possible in most applications.

4.03 **Joining**
4.031 General. Present information indicates the alloy is readily weldable using the electron beam or GTA processes. No preheat should be employed beyond that necessary to avoid condensation of moisture and interpass temperatures must be held below the MS with 200 to 250 F being recommended. The alloy is very susceptible to hydrogen embrittlement and care should be taken to employ low-hydrogen filler wire (4 to 5 ppm) and to take suitable precautions to avoid hydrogen contamination from other sources. Weldability studies have not been completed and the information in this chapter should be supplemented by reference to the alloy supplier and/or INCO.
4.032 Electron beam welding. Large thin-walled shear-formed cylinders (Table 4.0321) have been successfully electron-beam welded with the welds exhibiting 96 percent joint efficiency (compare Table 4.0321 with Table 3.02114). Investigations (5,6,7) of electron beam welding of 3/4 inch thick plate have suggested several practically useful conclusions, some of which require further study. Microfissuring in the HAZ appears to be related to banding in the parent metal and to be associated with dark etching bands in the aged weld HAZ microstructure of plate welded in the 1500 F solution annealed condition (5). The effects of the microfissuring on the tensile properties and fracture toughness of weldments has not been clearly established. However, microfissuring cannot be considered an innocuous condition. Homogenization (preweld treatment) of a banded plate (1.44 percent titanium) at 2000 F resulted in a coarse prior austenite grain size but eliminated the microfissures. However, it produced relatively low impact energies in the HAZ for post-weld solution annealing at 1500 F plus aging, or post-weld aging alone (Table 4.0324). The low impact energies appeared to be associated with precipitations due to the weld thermal cycle. These precipitations were located at prior austenite grain boundaries and were thought to be associated with the coarse grained austenite (5). Postweld homogenization at 2000 F resulted in HAZ impact values essentially equal to those of the weld and increased tensile strength and ductility (see Table 4.0324). A preweld homogenization at 1800 F appeared to be effective in producing satisfactory HAZ impact values and resulted in a much finer grain size than the 2000 F treatment (Table 4.0325).
4.0321 Tensile properties of transverse weld specimens taken from EB-welded large shear-formed cylinders, Table 4.0321.
4.0322 Welding conditions and specimen orientation for electron-beam plate welds, Figure 4.0322.

Fe
18 Ni
3 Mo
Ti
Al

T-250
Maraging

Fe
18 Ni
3 Mo
Ti
Al

T-250
Maraging

4.0323 Hardness variations across electron-beam welded plate after several postweld heat treatments (see Figure 4.0322 for welding conditions), Figure 4.0323.

4.0324 Transverse tensile and impact properties of electron-beam welded plate showing the effects of pre- and postweld heat treatments, Table 4.0324.

4.0325 Tensile and impact properties of electron-beam welded plate showing the effects of preweld heat treatments on grain size and HAZ toughness, Table 4.0325.

4.0326 Plane strain fracture toughness of electron beam welds, Table 4.0326.

4.033 GTA welding. The alloy may be readily joined by GTA welding in the solution-annealed or in the aged condition. Filler wire of T-250 composition (Table 4.0331) was used to make GTA welds in solution-annealed 7/8 inch thick plate given a post-weld treatment of 1500 F 1/2 hr plus a 900 F, 4 hr age (Table 4.0332). Joint efficiencies of approximately 86 percent were obtained. A post-weld homogenization of 2000 F or 1800 F (Table 4.0332) resulted in joint efficiencies of approximately 98 percent. Solution treated and aged or aged weld-metal tensile strengths are well below those of the parent metal (Table 4.0332). These low weld-metal strength values are probably associated with retained austenite. Development of high joint efficiencies in GTA welds made in conventionally solution-annealed and aged plate will require the development of a higher strength filler wire.

4.0331 Welding conditions for GTA welds in 7/8 inch plate, Table 4.0331.

4.0332 Transverse and all weld-metal tensile properties of GTA welds in 1.36 percent titanium plate showing the effects of pre- and postweld heat treatments, Table 4.0332.

4.04 Surface Treating

4.041 Nitriding. Preliminary information indicates that nitriding should be carried out at 900 F for 10 to 20 hr. This is below the industry standard of 975 F but reflects the overaging of maraging steels which can occur at this temperature for long time exposures (23).

4.042 Corrosion resistant coatings are required for long time exposures in normal atmospheres.

REFERENCES

1 Henery, R. J., "New Concepts in Maraging Steels", Teledyne Vasco, Latrobe, PA (1982).

2 VascoMax T-250 Data Sheet, ibid. (1985).

3 Floreen, S., and Bayer, A. W., "Development and Characterization of Cobalt Free Maraging Steels", AIME Met. Trans., to be published (1990).

4 Coffee, L. G., and Smith, D. F., "Processing, Metallurgical and Physical Property Characteristics of INCO Alloy MS 250", Laboratory Report, INCO Alloys International, Huntington, WV (May 12, 1988).

5 O'Donnell, D. B., and Bishel, B. A., "Electron Beam Weld Fracture Toughness and Weldability Progress Report on INCO Alloy MS 250", Laboratory Report, INCO Alloys International, Huntington, WV (May 12, 1988).

6 O'Donnell, D. B., and Bishel, B. A., "Gas Tungsten Welding of INCO MS 250 With Matching Filler Metal", ibid. (December 17, 1987).

7 O'Donnell, D. B., "Fusion Welding of MS 250 Using Elevated Post Weld Anneals for Strength Improvements", ibid. (May 27, 1988).

8 Hibner, E. L., and Crum, J. R., "INCO Alloy MS 250 Corrosion Testing", ibid. (May 1, 1988).

9 Hickey, C. S., "Mechanical Property Characterization of Vascomax T-250 Maraging Steels: Recent Developments and Applications", R. K. Wilson, Editor, Minerals, Metals and Materials Society (1988), p 73.

10 Personal communication from Louie Coffee, INCO, Huntington, WV to W. F. Brown, Jr. (1989).

11 Aerospace Materials Specification, AMS 6519A (April 4, 1987).

12 Aerospace Materials Specification, AMS 6518 (June 1, 1986).

13 Military Specification: Steel Bar, Billet and Forgings, Cobalt Free Maraging Steel, MIS 36275 (June 17, 1983).

14 Personal communication from A. M. Bayer, Teledyne Vasco to W. F. Brown, Jr. (1989).

15 Lampson, F. K., "Free-CO Cobalt Free Maraging Steel Stinger Motor Case Fabrication Development", The Marquart Company, U.S. Army Missile Command, TR RK-CR-83-12 (1983).

16 Lampson, F. K., "Manufacturing Methods Interim Report for Cobalt-Free (Free-CO) Maraging Steel Rocket Motor Components", The Marquart Co., U.S. Army Missile Command, TR RK-CR-83-14 (1983).

17 Burnette, T. D., and Lampson, F. K., "Fabrication and Delivery of Cobalt Free (Free-CO) Maraging Steel Rocket Motor Components", The Marquart Co., U.S. Army Missile Command, TR RK-CR-84-5 (1984).

18 Lampson, F. K., and Wood, J. L., ibid., TR RK-CR-83-12 (1982).

19 Siebein, K. N., "Microstructural Characterization of a Cobalt Free Maraging Steel, Vascomax T-250", U.S. Army Materials Technology Laboratory, Report MTL-TR-87-12 (1987).

20 INCO Alloy MS 250, INCO Alloys International, Huntington, WV (1986).

21 VascoMax T-200/T-250/T-300, Data Sheets, Teledyne Vasco, Latrobe, PA (1985).

22 Personal communication from W. B. Austin, Hercules Inc., McGregor, TX (November 14, 1989).

23 Martin, J. M., "Nitriding INCO Alloy MS 250", INCO International Inc., Huntington, WV (September 1, 1986).

24 Scanlon, J. F., and Hickey, C. F., "Stress Corrosion Cracking of Maraging Steels", U.S. Army Materials Technology Laboratory, Watertown, MA; presented at 1989 Tri-Service Corrosion Conference.

25 Emanuelson, R. H., "Stress Corrosion Cracking Characteristics and Constant Extension Rate Tests on T-250 Maraging Steel and D6AC Low Alloy Steel", projects sponsored by Thiokol Corp., Wasatch Operations, at Babcock & Wilcox, Alliance Research Center (1988).

26 LRA Laboratories, Irvine, CA, "Reports on Stress Corrosion Cracking of T-250 Maraging Steel and D6AC Steel", prepared for Thiokol Corp., Wasatch Operations (1988).

27 Personal communication from Eldon Bott, Thiokol Corp., Brigham City, UT, to W. F. Brown, Jr., January 1990.

28 Raymond, L., and Crumly, W. R., "Accelerated Low Cost Test Method for Measuring the Susceptibility of HY-Steels to Hydrogen Embrittlement", p 477, Proceedings of the First International Conference on Current Solutions to Hydrogen Problems in Steels, ASM, Washington, DC (November, 1982).

Fe
18 Ni
3 Mo
Ti
Al

T-250 Maraging

Alloy	T-250 Maraging			
Composition	Weight, percent			
Form	Bars, Forgings, Tubing and Rings		Sheet, Strip and and Plate(a)	
	Min	Max	Min	Max
Carbon	–	0.03	–	0.03
Manganese	–	0.10	–	0.10
Silicon	–	0.10	–	0.10
Phosphorous	–	0.010	–	0.010
Sulphur	–	0.010	–	0.010
Nickel	18.00	20.00	18.00	20.00
Molybdenum	2.75	3.25	2.75	3.25
Titanium	1.30	1.45	1.20	1.60
Aluminum	0.05	0.15	0.05	0.15
Chromium	–	0.50	–	0.50
Cobalt	–	0.50	–	0.50
Copper	–	0.50	–	0.50

(a) Same as MIS 36275 (13) for bar, billet and forgings except no copper is specified in MIS 36275.

TABLE 1.04. AMS AND MIS SPECIFICATIONS FOR VARIOUS FORMS (11,12)

Alloy	T-250 Maraging	
Form	3-inch Diameter Bar	
Number of Bars	6	6
Heat Treatment	1500 F, 1 hr, AC	1500 F, 1 hr, AC 900 F, 3 hr
Hardness, HRC		
Mean	29.4	49.5
Std Dev	0.71	0.45

TABLE 1.061. HARDNESS OF 3 INCH DIAMETER BARS IN ANNEALED CONDITION AND AFTER AGING (16, TABLE 3)

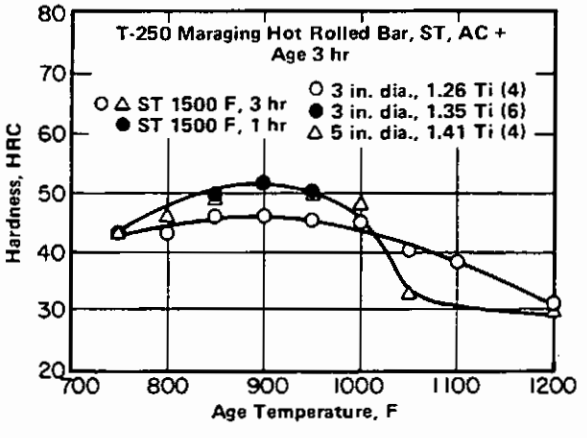


FIGURE 1.062. EFFECT OF AGING TEMPERATURE ON HARDNESS OF BAR OF TWO TITANIUM CONTENTS (4, TABLE 3), (9, TABLE 2)

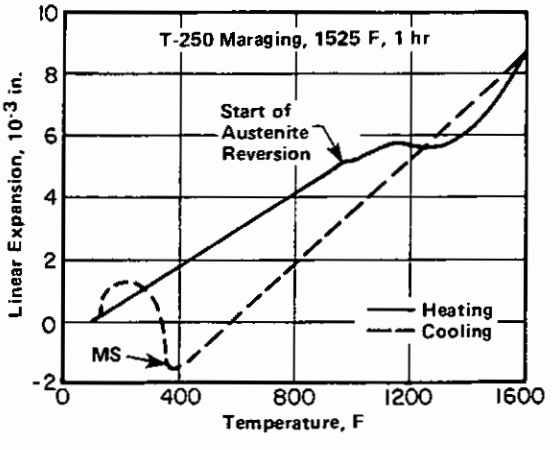


FIGURE 2.0121. LINEAR EXPANSION CURVES SHOWING THE MS AND START OF AUSTENITE REVERSION (4, FIGURE 4)

Fe
18 Ni
3 Mo
Ti
Al

T-250
Maraging

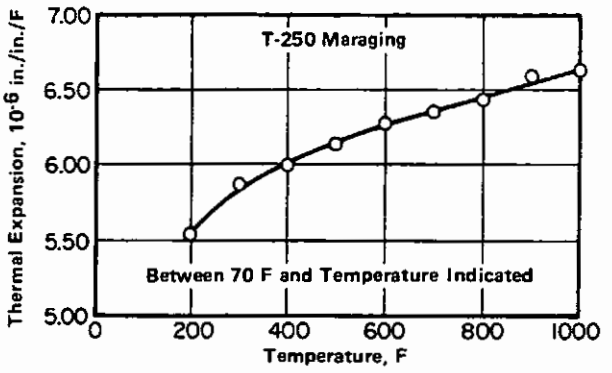


FIGURE 2.0141. MEAN COEFFICIENT OF LINEAR THERMAL EXPANSION (20, TABLE 3)

Form	1/16 inch Sheet								
Environment	3.5 percent NaCl, 75 F, for 500 hr			Sea Water-Splash/Spray for 150 Days			Kurie Beach (25 meters) for 153 Days		
Alloy[a]	T-250	18Ni 300	4340	T-250	18Ni 300	4340	T-250	18Ni 300	4340
Corrosion Rate, mils/yr	1.11	1.29	1.58	0.62	0.38	1.41	0.99	0.47	1.77

TABLE 2.0311. GENERAL CORROSION RESISTANCE FOR SEVERAL ALLOYS (8, TABLES 2 AND 3)

Alloy	T-250		C-250[a]	
Source	(24)	(25)	(25)	(24)
Form	3/4 inch Plate	Ring Forging 156 in. OD x 2-1/2 in. Wall	Ring Forging 156 in. OD x 2-1/2 in. Wall	5/8 inch Plate
Heat Treat	1500 F, 1 hr, AC + 900 F, 4 hr	1500 F, 1 hr, AC + 910 F, 6 hr	1500 F, 1 hr, AC + 910 F, 6 hr	1500 F, 1 hr, AC + 900 F, 3 hr
Specimen Thickness, in.	1/2	0.8	0.8	1/2
F_{tu}, ksi	–	267	267	–
F_{ty}, ksi	249	250	250	250
Method	CB[b]	CT Load Shedding[c]	CT Load Shedding[c]	CB[b]
Environment	3.5% NaCl	Alt. Immersion 10 min Seawater 50 min Air[d]	100% R.H.	3.5% NaCl
Duration, hr	1000	–	–	1000
K_{Iscc}, ksi $\sqrt{in.}$	21	18 to 20[e]	Approx. 20[e]	29

(a) Cobalt containing maraging steel.
(b) Cantilever bend constant load.
(c) Compact tension; computer load control.
(d) Artificial Seawater: 41.953 gm/liter of ASTM D1141-52 artificial sea salt.
(e) See also Figure 2.0322.

TABLE 2.0321. K_{Iscc} RESULTS FOR PLATE AND FORGING EXPOSED TO ARTIFICIAL SEAWATER AND TO 100% R.H. AIR (24,25)

Fe
18 Ni
3 Mo
Ti
Al

T-250
Maraging

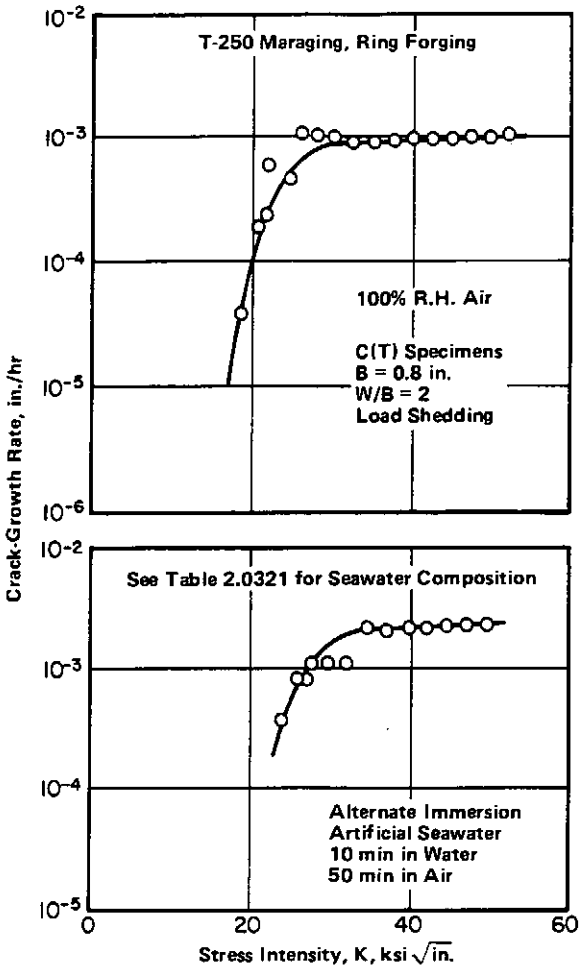


FIGURE 2.0322. CRACK-GROWTH DATA FOR T-250 RING FORGING IN ARTIFICIAL SEAWATER AND IN 100% R.H. AIR (25)

Alloy	T-250 Maraging					
Test Method	Step Load Slow Bend[a]					
Test Environment	3.5% NaCl					
Form	1/2 and 1 inch Plate (T)					Ring Forging (T) (See Table 2.0321)
Solution Treat	1500 F, 1 hr, AC + Age					
Age	3 hr, 1200 F + 900 F, 3 hr	1000 F, 3 hr	950 F, 3 hr	900 F, 3 hr	910 F, 6 hr	910 F, 6 hr
F_{ty}, ksi	192	234	242	242	264	264
Applied Potential, volts	-1.2	-1.2	-1.2	-0.8	-1.2	-0.8
K_{Iscc}, ksi $\sqrt{in.}$	30	14	12	33	10	22

(a) Charpy-size specimen with sharp notch and deep side grooves (see Ref. 28).

TABLE 2.0323. K_{Iscc} DATA SHOWING THE EFFECTS OF APPLIED POTENTIALS IN A 3.5% NaCl SOLUTION USING A SMALL STEP LOADED SLOW BEND TEST (26)

Fe
18 Ni
3 Mo
Ti
Al

T-250
Maraging

Alloy	T-250 Maraging				
Source	AMS 6591A (11)				AMS 6518 (12)
Condition	1475–1725 F, 1–2 hr, AC + 890–910 F, 4–6 hr				1475–1525 F, AC + 890–910 F, 4–6 hr
Form	Bars, Forgings, Tubing and Rings				Sheet, Strip and Plate
Thickness, in.	<4		4–10 inc.(c)		<0.03–>0.375
Direction	L	T	L	T	Not specified
F_{tu}, ksi	255	255	250	250	255
F_{ty}, ksi	245	245	240	240	245
RA, percent	45	35	30	20	Not specified
e, percent	6	4	5	3	(a)
F_{tu}, ksi, Annealed	160 (Max)(b)				–
Hardness, Aged	48 HRC (Min)				Not specified)
Hardness, Annealed	321 HBN(b)				34 HRC max

(a) Specified elongation varies widely with thickness and gage length; see Specification for details.
(b) Thickness 0.5 inch or greater.
(c) Same as MIS 36275 (13) except MIS gives e = 6 percent for L and does not specify RA.

TABLE 3.01. AMS AND MIS SPECIFIED MECHANICAL PROPERTIES

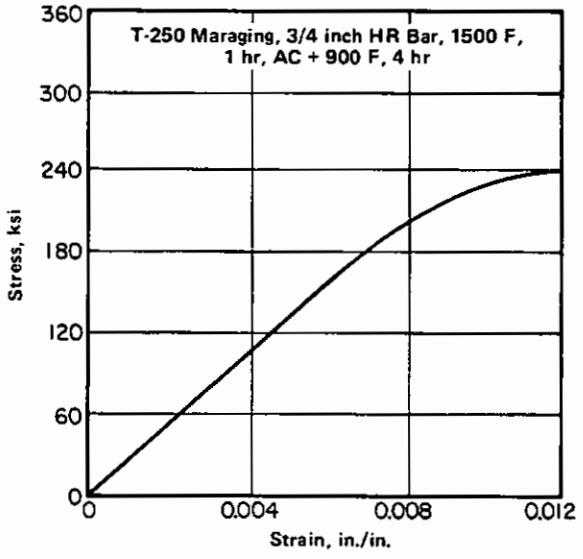


FIGURE 3.0211. STRESS STRAIN CURVE FOR AGED BAR (14)

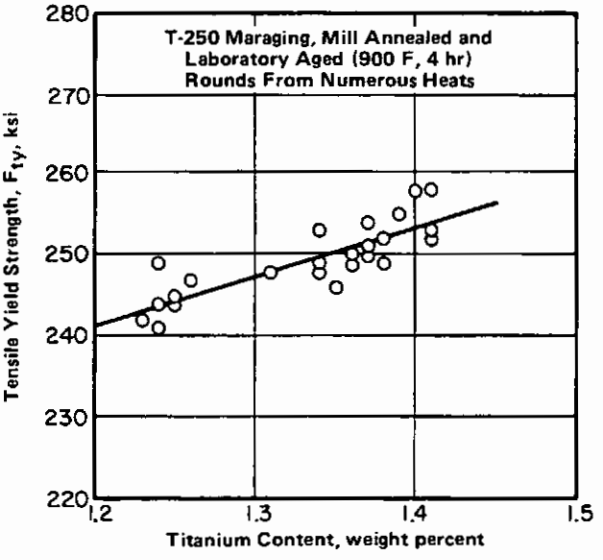


FIGURE 3.0212. EFFECT OF TITANIUM CONTENT ON TENSILE YIELD STRENGTH (4, FIGURE 3)

Fe
18 Ni
3 Mo
Ti
Al

T-250
Maraging

Alloy	T-250 Maraging		
Form	All		
Condition	Solution Anneal (1500 F)		
Reference	(2)	(21)	(20)
Hardness, HRC	27/29	30/32	32
F_{tu}, ksi	140	140	155
F_{ty}, ksi	100	95	110
e, percent	21	16	16
RA, percent	92	70	71

TABLE 3.0213. TENSILE PROPERTIES AND HARDNESS OF ANNEALED ALLOY FROM VARIOUS SOURCES

Alloy	T-250 Maraging						
Condition	Solution Annealed + 900 F, 3 hr						
Form	5/8 in. Rd.	2 in. Rd.	3 in. Rd.	6 in. Sq.	6 in. Sq.	0.2 in. Sheet	0.25 in. Sheet
Direction	Long.	Long.	Long.	Long.	Trans.	Trans.	Long.
Hardness, HRC	51	51	50	51	50	50	51
F_{tu}, ksi	266	259	266	260	260	262	260
F_{ty}, ksi	258	253	260	254	254	254	252
e, percent	12	11	10	11	9	7	8
RA, percent	59	58	52	56	46	54	62

TABLE 3.0214. MECHANICAL PROPERTIES OF VARIOUS FORMS IN THE AGED CONDITION (21)

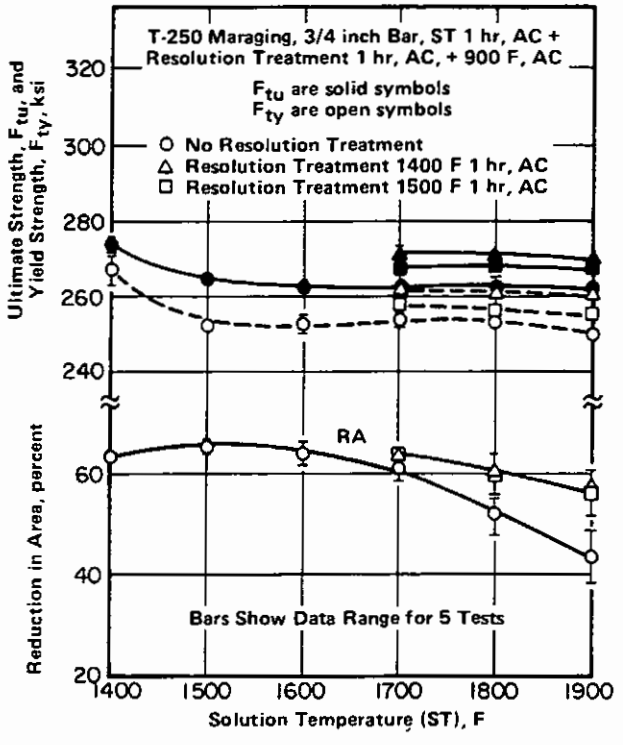


FIGURE 3.0215. EFFECT OF SOLUTION TEMPERATURE AND RESOLUTION TREATMENT ON TENSILE PROPERTIES OF BAR (1, APP. 4 AND 5)

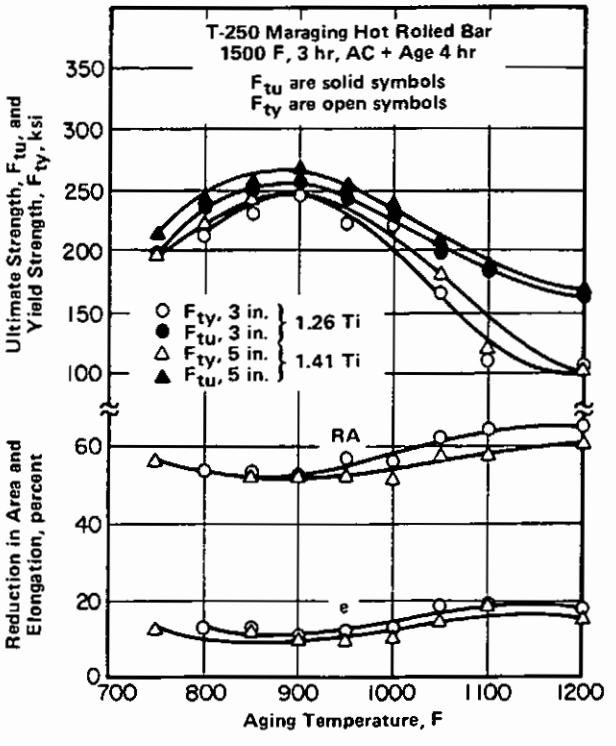


FIGURE 3.0216. EFFECT OF AGING TEMPERATURE ON TENSILE PROPERTIES OF BAR OF TWO TITANIUM CONTENTS (4, TABLE 3)

Fe
18 Ni
3 Mo
Ti
Al

T-250
Maraging

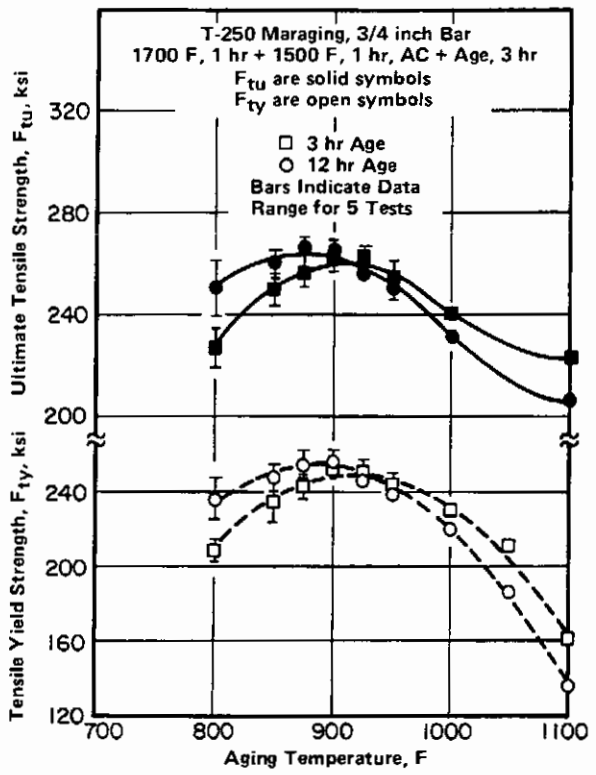


FIGURE 3.0217. TENSILE STRENGTH PROPERTIES OF BAR AGED FOR 3 OR 12 HOURS AT VARIOUS TEMPERATURES (1, APP. 1)

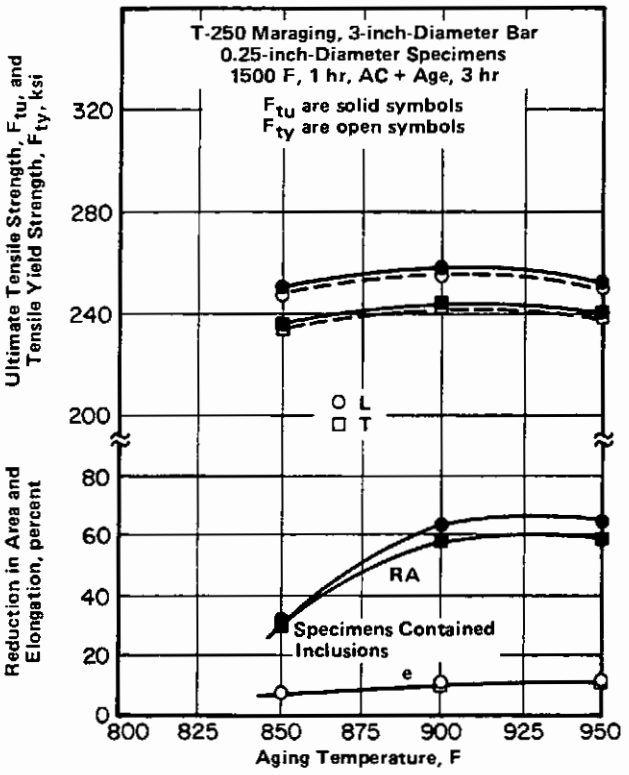


FIGURE 3.0218. EFFECT OF AGING TEMPERATURE ON TENSILE PROPERTIES OF BAR, SHOWING EFFECTS OF INCLUSIONS ON DUCTILITY (9, TABLE 6)

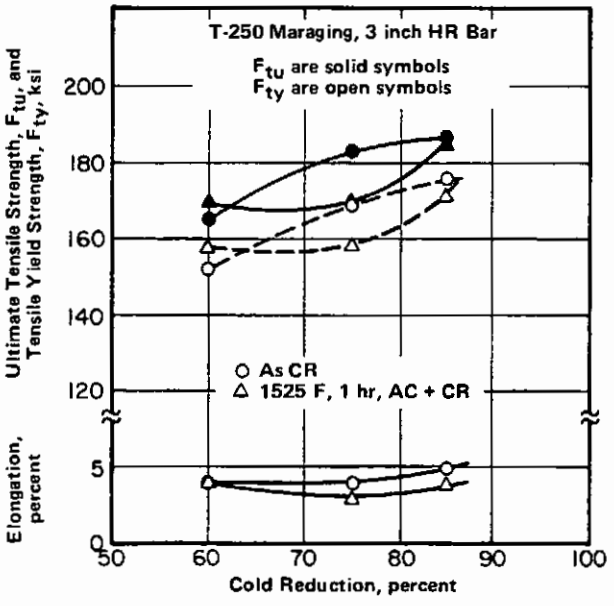


FIGURE 3.0219. EFFECT OF COLD REDUCTION ON TENSILE PROPERTIES OF UNAGED 1.26 PERCENT TITANIUM ALLOY (10)

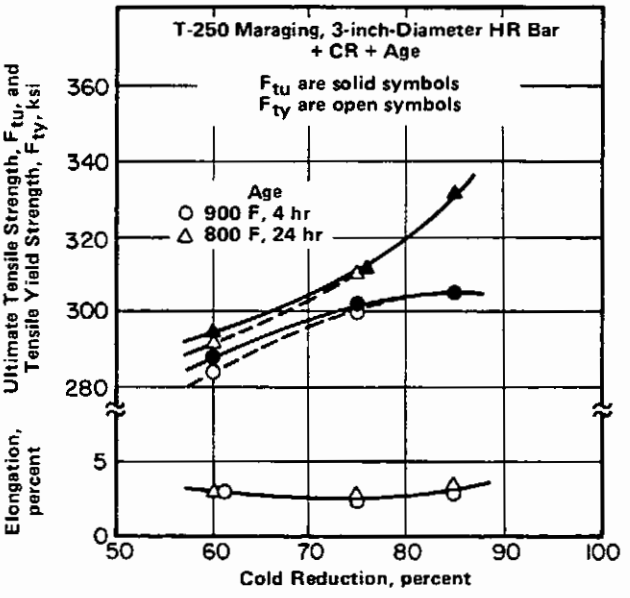


FIGURE 3.02110. EFFECT OF COLD REDUCTION ON TENSILE PROPERTIES OF AGED 1.26 PERCENT TITANIUM ALLOY (10)

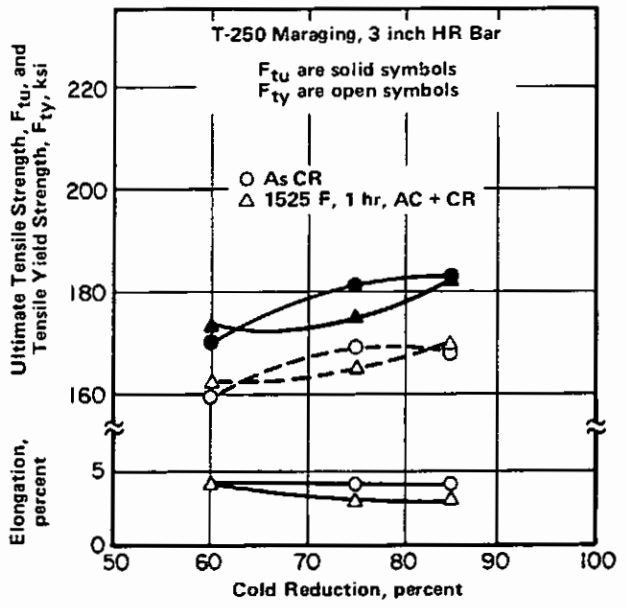
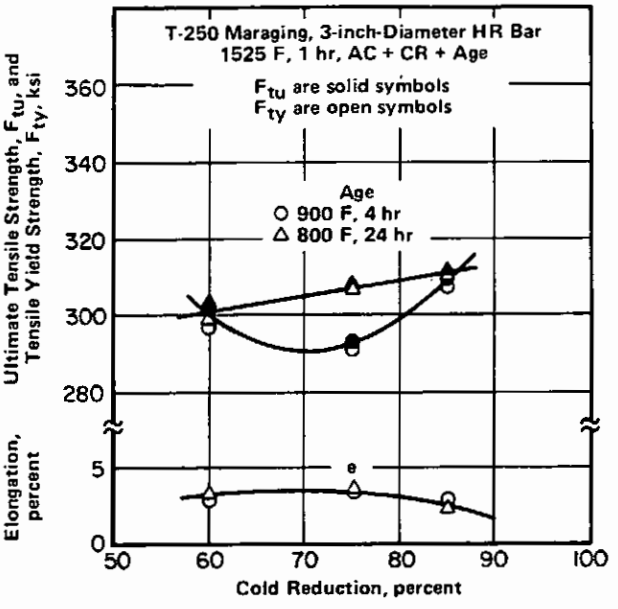


FIGURE 3.02111. EFFECT OF COLD REDUCTION ON TENSILE PROPERTIES OF UNAGED 1.43 PERCENT TITANIUM ALLOY (10)



Fe
18 Ni
3 Mo
Ti
Al

T-250 Maraging

FIGURE 3.02112. EFFECTS OF COLD REDUCTION ON TENSILE PROPERTIES OF AGED 1.43 PERCENT TITANIUM ALLOY (10)

Alloy	T-250 Maraging			
Form	As Received	Forged	2nd Shear Form(b)	Final Shear Form
Thickness, in.(a)	2 in. Dia Bar	0.65	0.175	0.023
Heat Treat(c)	ST + 900 F, 4 hr	ST	52% Reduction ST	75% Reduction 900 F, 4 hr
F_{ty}, ksi				
No. of Tests	4	2	1	7
Mean	253	122	124	296
Std Dev	2.39	–	–	7.27
F_{tu}, ksi				
No. of Tests	4	2	2	–
Mean	261	154	174	–
Std Dev	2.12	–	–	–
e, percent				
No. of Tests	4	–	2	5
Mean	11.4	18	15	2.2
Std Dev	0.48	–	–	0.45
RA, percent				
No. of Tests	4	2	2	–
Mean	56	55	55	–
Std Dev	1.97	–	–	–

(a) Except as indicated, thickness refers to cylindrical wall of motor case.
(b) Shear preform had 0.36 inch wall.
(c) ST = solution treat 1500 F, 1 hr, AC.

TABLE 3.02113. TENSILE PROPERTIES AT VARIOUS STAGES OF FABRICATION OF A SMALL SOLID PROPELLANT ROCKET MOTOR CASE (12, FIGURE 10 AND TABLE 5)

Fe
18 Ni
3 Mo
Ti
Al

T-250 Maraging

Alloy	T-250 Maraging			
Form	Shear-Formed Cylinders			
Fabrication	8 inch RCS Forged and Punched at 2150 F + Ring Rolled (16 inch OD x 1/8 inch ID x 14 inch Long) Finish at 1750 F + 1650 F, 1 hr, AC, Machine Shear Preform With 0.45 inch Wall + Spin to 22–33 inch Long With Thickness Indicated. Specimens Longitudinal.			
Thickness, in.	0.100	0.119	0.137	0.143
Shear Form Reduction, percent	76	74	77	68
Heat Treatment After Shear Form	1500 F, 1 hr, AC, + 900 F, 4 hr	900 F, 4 hr	1500 F, 1 hr, AC, 900 F, 4 hr	900 F, 4 hr
F_{ty}, ksi				
Mean[a]	259	268	259	266
Std Dev	1.6	3 Tests	1.9	0.8
F_{tu}, ksi				
Mean	268	275	269	273
Std Dev	2.1	1.3	0.96	0.5
e, percent				
Mean	6	4.3	7.8	6
Std Dev	0	0.5	0.5	0

(a) Four tests unless indicated.

TABLE 3.02114. TENSILE PROPERTIES OF A LARGE SHEAR-FORMED CYLINDER FROM A DEMONSTRATION PROJECT (18, TABLE 12)

Alloy	T-250 Maraging			
Form	3 inch Diameter Rounds			
Heat Treatment	1500 F, 1 hr, AC + 900 F, 3 hr			
No. of Heats	59			
	Avg	s[a]	Min	Max
F_{tu}, ksi	257.8	4.6	250	265.8
F_{ty}, ksi	251.0	4.6	232.8	260.2
Elongation, percent	11.2	0.7	10	13.0
Reduction of Area, percent	56.9	2.0	52	61.0

(a) S: sample standard deviation.

TABLE 3.02115. STATISTICAL SUMMARY OF TENSILE PROPERTIES DERIVED FROM TESTS ON 59 HEATS (27)

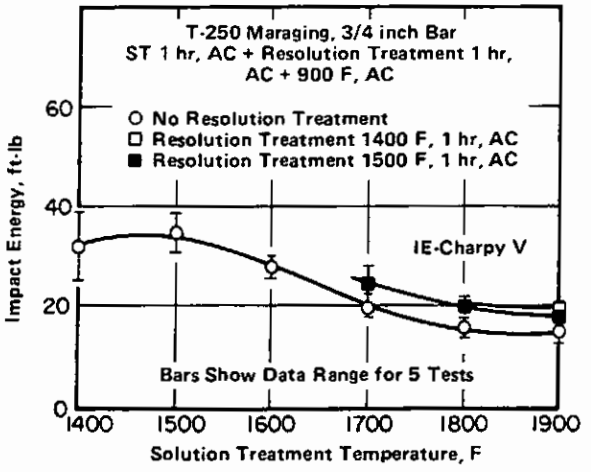


FIGURE 3.0231. EFFECT OF SOLUTION TREATMENT TEMPERATURE AND RESOLUTION TREATMENT ON IMPACT ENERGY FOR BAR (1, APP. 4 AND 5)

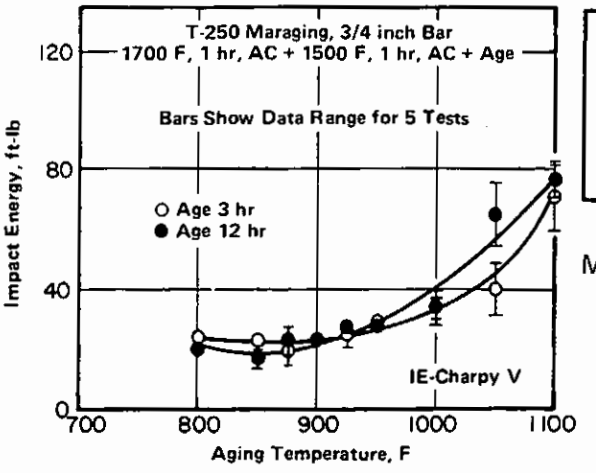


FIGURE 3.0232. EFFECT OF AGING TEMPERATURE ON IMPACT ENERGY OF BAR GIVEN A DOUBLE SOLUTION TREATMENT (1, APP. 1 AND 3)

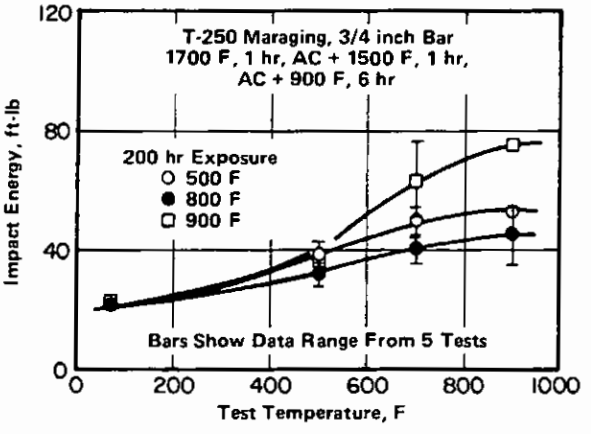


FIGURE 3.0233. EFFECT OF TEST TEMPERATURE AND EXPOSURE TEMPERATURE ON IMPACT ENERGY FOR BAR (1, APP. 6)

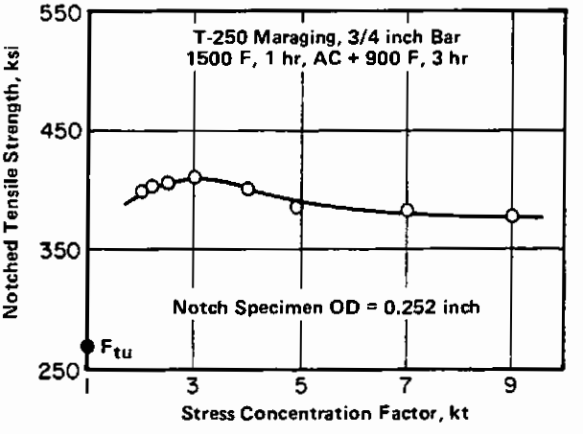


FIGURE 3.0271. EFFECT OF STRESS CONCENTRATION ON THE ULTIMATE TENSILE STRENGTH OF BAR (21, FIGURE 2)

Alloy	T-250 Maraging				
Condition	Bend Specimens; 1500 F, 1 hr, AC + 900 F, 3 hr				
Form	0.25 in. Sheet	0.5 in. Plate	2 in. Round	3 in. Round	8 in. Square
K_{Ic}, ksi $\sqrt{in.}$	89	99	112	98	95

TABLE 3.02721. PLANE STRAIN FRACTURE TOUGHNESS OF VARIOUS FORMS IN THE AGED CONDITION FROM SEVERAL COMMERCIAL HEATS (21, FIGURE 7)

Fe
18 Ni
3 Mo
Ti
Al

T-250
Maraging

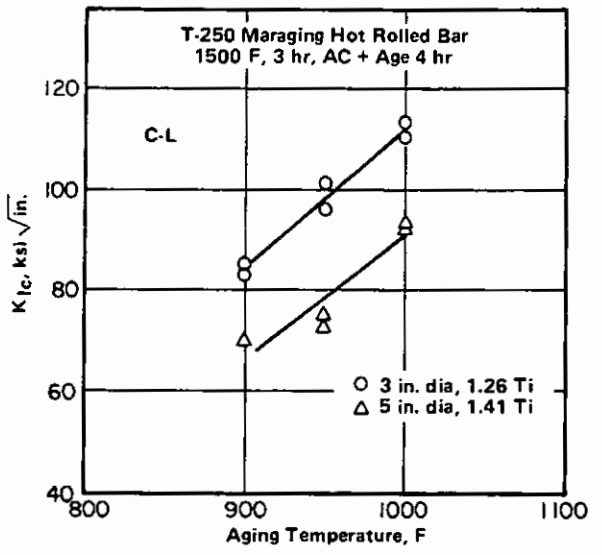


FIGURE 3.02722. EFFECT OF AGING TEMPERATURE ON PLANE STRAIN FRACTURE TOUGHNESS OF BAR OF TWO TITANIUM CONTENTS (4, TABLE 3)

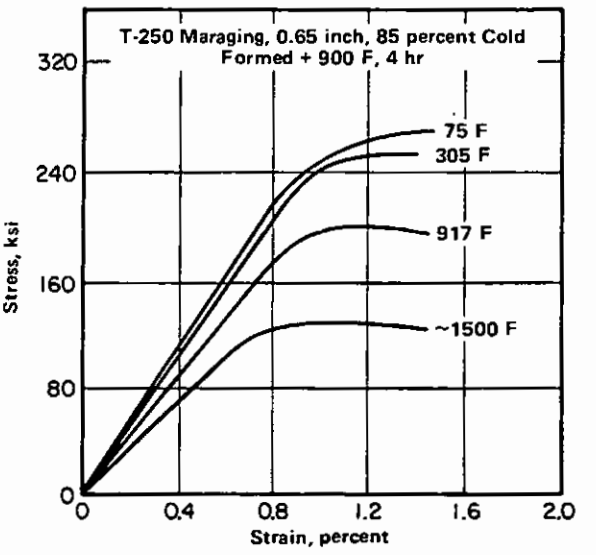


FIGURE 3.0311. STRESS-STRAIN CURVES AT ELEVATED TEMPERATURES FOR HEAVILY COLD WORKED AND AGED ALLOY (22)

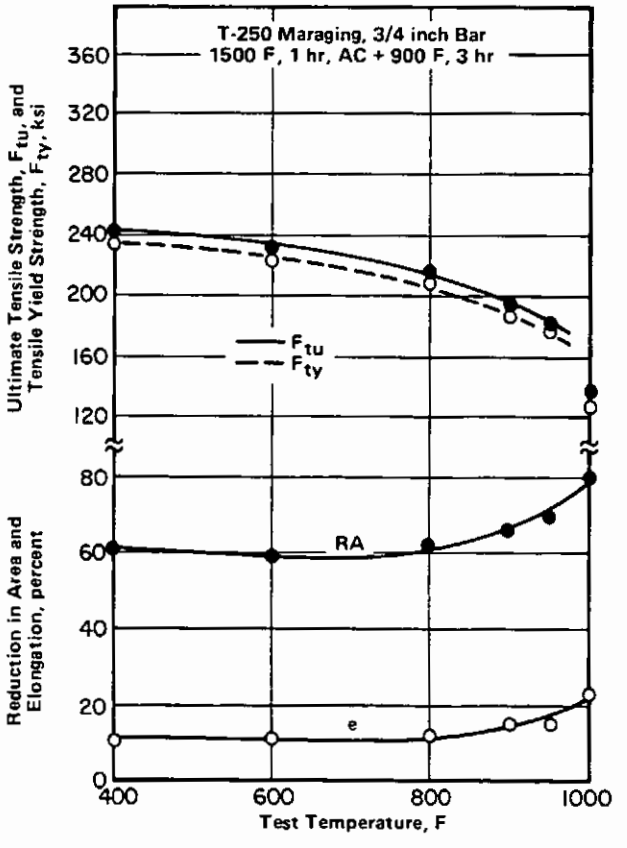


FIGURE 3.0312. EFFECT OF TEST TEMPERATURE ON TENSILE PROPERTIES OF BAR (21, FIGURE 1)

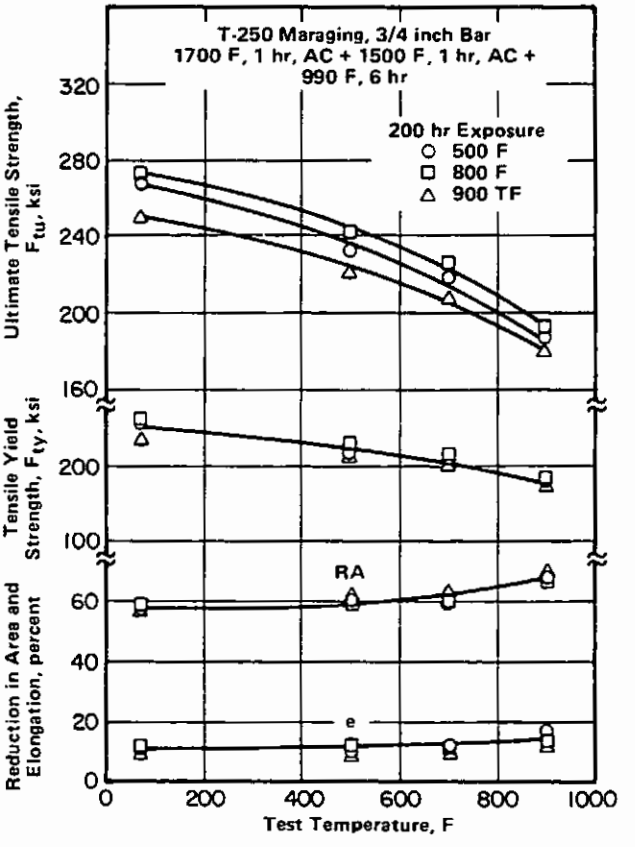


FIGURE 3.0313. EFFECT OF TEST TEMPERATURE AND EXPOSURE TEMPERATURE ON TENSILE PROPERTIES OF SOLUTION TREATED AND AGED BAR (1, APP. 6)

Fe
18 Ni
3 Mo
Ti
Al

T-250
Maraging

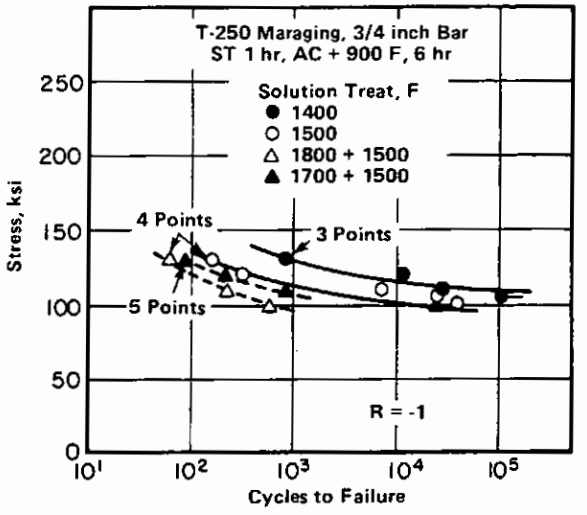


FIGURE 3.051. ROTATING BEAM FATIGUE STRENGTH FOR AGED BAR GIVEN SEVERAL SOLUTION TREATMENTS (14)

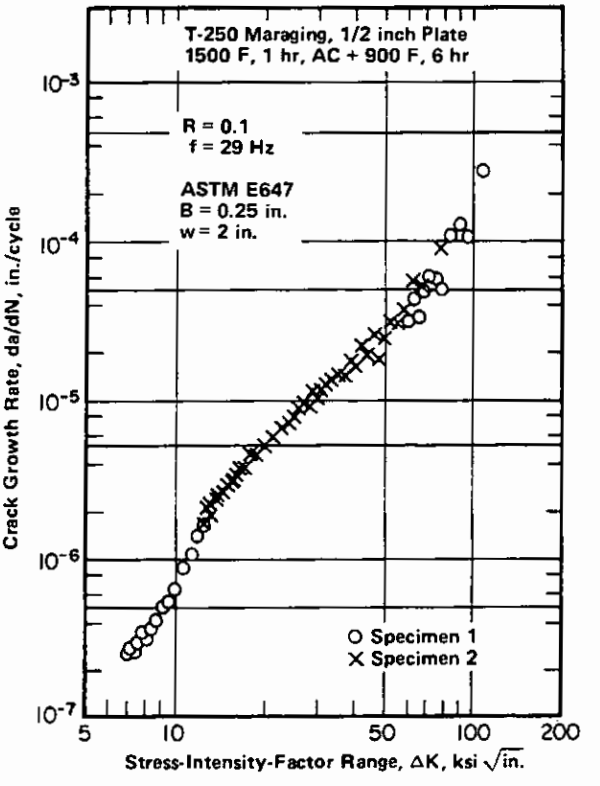


FIGURE 3.052. FATIGUE CRACK GROWTH RATE FOR PLATE (27)

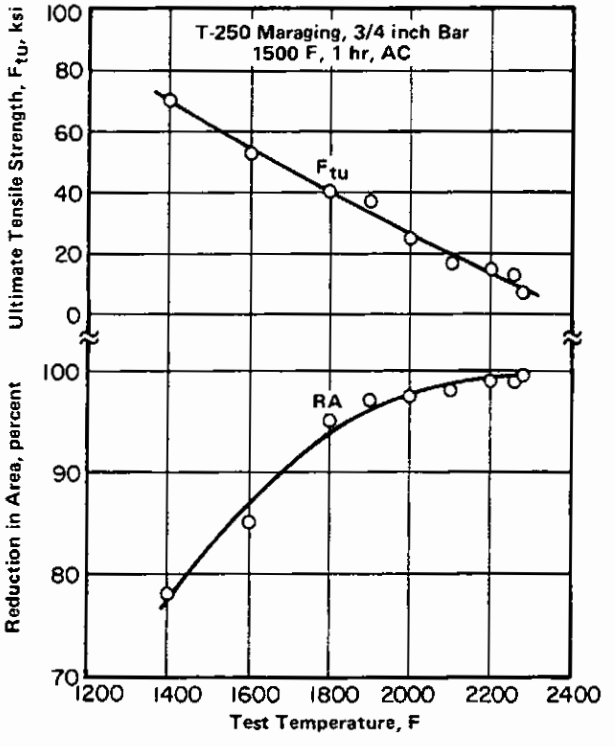


FIGURE 4.0111. EFFECT OF TEST TEMPERATURE ON THE TENSILE STRENGTH AND DUCTILITY OF BAR (4, FIGURE 1)

Fe
18 Ni
3 Mo
Ti
Al

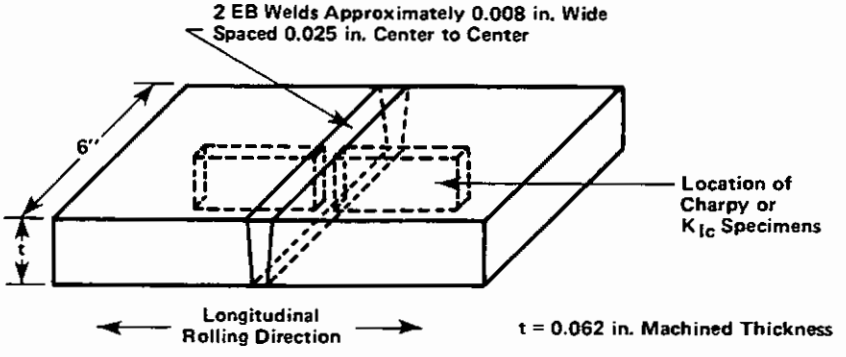
T-250
Maraging

Alloy	T-250 Maraging			
Form	Transverse EB Weld Specimens From Shear Formed Cylinders			
Fabrication	See Table 3.02114 for Fabrication and Parent Metal Properties			
Shear Forming Reduction, percent	76	74	77	68
Thickness, in.	0.100	0.119	0.137	0.149
Heat Treat After Weld	1500 F, 1 hr, AC, 900 F, 4 hr	900 F, 4 hr	1500 F, 1 hr, AC, 900 F, 4 hr	900 F, 4 hr
Failure Location	Weld area	–	Weld area	Weld area
F_{ty}, ksi				
Mean[a]	249	259	249	257
Std Dev	0.8	2.4	0.5	1.4
F_{tu}, ksi				
Mean	268	263	257	261
Std Dev	2.1	2.4	0.5	1.7
e, percent				
Mean	6	2	1.8	2.2
Std Dev	0	0	0.5	0.5

(a) Four tests per condition.

TABLE 4.0321. TENSILE PROPERTIES OF TRANSVERSE WELD SPECIMENS TAKEN FROM EB-WELDED LARGE SHEAR-FORMED CYLINDERS (18, TABLE 12)

T-250 Maraging, 3/4 inch Plate Welded in Annealed or Aged Condition



Welding Conditions

Acceleration, volts	Beam Current	Feed, in./min	Focus, in. from gun	Gun to Work, in.	Beam Deflection	Worst Vacuum
150 EV	50 mA	26	6	5.5	0.028 in. circular	10^{-3} μm

FIGURE 4.0322. WELDING CONDITIONS AND SPECIMEN ORIENTATION FOR ELECTRON-BEAM PLATE WELDS (5)

Fe
18 Ni
3 Mo
Ti
Al

T-250
Maraging

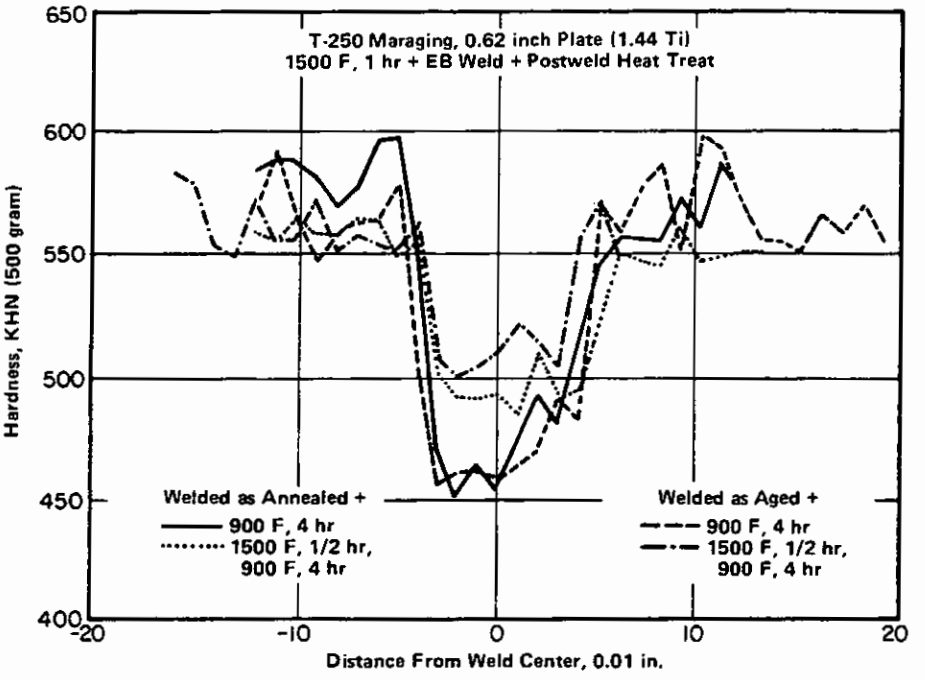


FIGURE 4.0323. HARDNESS VARIATION ACROSS EB WELDED PLATE AFTER SEVERAL POSTWELD HEAT TREATMENTS (SEE FIGURE 4.0322 FOR WELDING CONDITIONS) (5)

Alloy	T-250 Maraging									
Form	3/4 inch Plate With Double Electron Beam Welds									
1.44 Ti Parent Metal	Heat Treated: 1500 F, 1/2 hr + 900 F, 4 to 8 hr									
Tensile Properties	F_{tu} = 271 ksi, F_{ty} = 258 ksi, e = 12 percent, RA = 56 percent									
Welding Conditions	See Figure 4.0322									
Preweld Heat Treat	2000 F, 1 hr, AC[a]								1500 F, 1/2 hr, AC[b]	
Postweld Heat Treat	1500 F, 1/2 hr, AC + 900 F, 4 hr		900 F, 4 hr		2000 F, 1 hr, AC + 900 F, 4 hr		2000 F, 1 hr, AC, 1500 F, 1/2 hr, AC, 900 F, 4 hr		1500 F, 1/2 hr, AC + 900 F, 4 hr	
Location	Weld	HAZ	Weld	HAZ	Weld	HAZ	Weld	HAZ	Weld	HAZ
Charpy V, ft-lb[c,d]	16	10	15	8	13	14	15	15	15	16
	19	7	15	9	14	14	15	17	16	17
F_{tu}, ksi[e]	238		232		268		271		250	
F_{ty}, ksi	228		224		251		258		241	
e, percent	6		6		10		10		6	
RA, percent	37		36		50		48		36	

(a) Prior austenite G.S. approximately 2.5.
(b) Prior austenite G.S. approximately 8.
(c) Charpy values from 1.36 percent Ti heat.
(d) For Charpy specimen orientation see Figure 4.0322.
(e) Tensile values from 1.47 percent Ti heat.

TABLE 4.0324. TRANSVERSE TENSILE AND IMPACT PROPERTIES OF ELECTRON-BEAM WELDED PLATE SHOWING THE EFFECTS OF PRE- AND POSTWELD HEAT TREATMENTS (5, TABLES 3 AND 4)

Fe
18 Ni
3 Mo
Ti
Al

T-250 Maraging

Alloy	T-250 Maraging					
Form	3/4 inch Plate With Double Electron Beam Welds					
Welding Conditions	See Figure 4.0322					
Preweld Heat Treat	1500 F, 1/2 hr, AC		2000 F, 1 hr, AC		1800 F, 1 hr, AC	
Approx. Prior Austenite G.S.	8		2.5		4–5	
Postweld Heat Treat	1500 F, 1/2 hr, AC, 900 F, 4 hr		1500 F, 1/2 hr, AC, 900 F, 4 hr		1500 F, 1 hr, AC, 900 F, 4 hr	
Location	Weld	HAZ	Weld	HAZ	Weld	HAZ
Charpy V, ft-lb[b,c]	15 16	16 17	16 19	10 7	13.7[a]	18.5[a]
F_{tu}, ksi[d,e]	250		238			
F_{ty}, ksi	241		228			
e, percent	6		6			
RA, percent	36		37			

(a) Average of three test results.
(b) Charpy values from a 1.36 percent Ti heat.
(c) For Charpy specimen orientation, see Figure 4.0322.
(d) Tensile values from a 1.44 percent Ti heat.
(e) For base metal properties, see Table 4.0324.

TABLE 4.0325. TENSILE AND IMPACT PROPERTIES OF ELECTRON-BEAM WELDED PLATE SHOWING THE EFFECTS OF PREWELD HEAT TREATMENTS ON GRAIN SIZE AND HAZ TOUGHNESS (7, TABLE 3)

Alloy	T-250 Maraging							
Form	Electron Beam Welds in 0.62 inch 1.44 percent Ti Plate							
Welding Conditions and Specimen Orientation	See Figure 4.0322							
Preweld Heat Treat	1500 F, 1/2 hr, AC							
Postweld Heat Treat	900 F, 4 hr		1500 F, 1/2 hr, AC + 900 F, 4 hr		1000 F, 4 hr		1500 F, 1/2 hr, AC + 1000 F, 4 hr	
	Weld	HAZ	Weld	HAZ	Weld	HAZ	Weld	HAZ
F_{ty}, ksi	235	–	241	–	–	–	–	–
K_{Ic}, ksi $\sqrt{in.}$	90 76	83 72	67 73	68 66	(a) (a)	79 88	(a) (a)	86 82

(a) Toughness too high for specimen thickness.

TABLE 4.0326. PLANE STRAIN FRACTURE TOUGHNESS OF ELECTRON BEAM WELDS (5, TABLES 3 AND 5)

Fe
18 Ni
3 Mo
Ti
Al

T-250
Maraging

Alloy	T-250 Maraging
Filler Wire Composition, weight percent	C-0.01, Ti-1.44, Mo-3.03 (Hydrogen-13 ppm)
Polarity	Straight
Electrode	1/8 inch Tungsten 1 percent Thoriated
Current, amps	180–210
Filler Metal	0.093 inch diameter MS 250
Shielding Gas	Argon (30 ft^3/hr)
Arc Length, V	13–16
Maximum Interpass Temp	220–250 F

TABLE 4.0331. WELDING CONDITIONS FOR GTA WELDS IN 7/8 INCH PLATE (6, TABLE 4)

Alloy	T-250 Maraging				
Form	7/8 inch Plate, GTA Welds				
1.36% Ti Parent Metal	Heat Treated: 1500 F, 1/2 hr + 900 F, 4 hr				
Tensile Properties	F_{tu} = 276 ksi, F_{ty} = 265 ksi, e = 7.5 percent, RA = 38 percent				
Welding Conditions	See Table 4.0331				
Specimen Type	Transverse to Weld Unless Noted				
Preweld Heat Treat	1500 F, 1 hr, AC				
Postweld Heat Treat	None	900 F, 4 hr	1500 F, 1/2 hr, AC + 900 F, 4 hr	2000 F, 1 hr, AC + 900 F, 4 hr	1800 F, 1 hr, AC + 900 F, 4 hr
F_{tu}, ksi	163	237	233	272	267
F_{ty}, ksi	143	226	226	255	253
e, percent	5	7	2(a)	7.5	7.5
RA, percent	52	36	12	–	–
Preweld Heat Treat	900 F, 4 hr				
F_{tu}, ksi	203	234	234		
F_{ty}, ksi	169	221	226		
e, percent	7.5	7.5	7		
RA, percent	34	36	38		
Specimen Type	All Weld Metal				
F_{tu}, ksi	193	228	234		
F_{ty}, ksi	121	198	213		
e, percent	9.5	13	11		
RA, percent	26	49	45		

(a) Small defect on fracture surface.

TABLE 4.0332. TRANSVERSE AND ALL WELD METAL TENSILE PROPERTIES OF GTA WELDS IN 1.36 PERCENT TITANIUM PLATE SHOWING THE EFFECTS OF PRE- AND POSTWELD HEAT TREATMENTS (6, TABLE 2)

	Fe
5	Ni
0.55	Cr
0.47	Mo
0.075	V

5 Ni Cr Mo V

1. GENERAL

This alloy is one of a series of quenched and tempered steels developed under contract by the Naval Ships Systems Command (44) (45) (46) (47). It has very high resistance to crack propagation in heavy sections at temperatures down to about -80 F. The steel exhibits secondary hardening with the degree depending primarily on the Mo content. There is little change in yield strength in the tempering temperature range between 900 and 1100 F. Yield strength levels between 130 and 150 ksi can be obtained by tempering at temperatures somewhat higher than that at the secondary hardening peak. In this tempering range the toughness is high and increases rapidly with increasing tempering temperature. Specifications have been developed for both plate and forgings. Hardenability is sufficient to obtain 140 ksi yield strength at the center of 4-inch-thick plates.

Cold formability in the quenched and tempered condition is quite good and adequate for all normal fabrication operations. The steel is easily welded by inert gas and covered electrode processes. Detailed techniques and specifications have been worked out for GMA and SMA processes. The latter requires special care to avoid hydrogen embrittlement. Stress relief of heavy weldments is not recommended due to temper embrittlement. Resistance to general corrosion in marine atmospheres and seawater is substantially equivalent to that of HY 80 steel. However, crack growth rates of HY 130 base plate and weldments are enhanced by seawater to a greater extent than those of HY 80 steel. Conventional fatigue strength of HY 130 is deleteriously affected by seawater and salt solutions.

Applications of HY 130 include pressure vessels where light weight is not a prime factor, such as large solid propellant rocket motor cases, high pressure gas storage vessels, and submersibles.

1.01 Commercial Designation:
HY 130, 5 Ni-Cr-Mo-V Steel

1.02 Alternate Designation
UNS K51255

1.03 Specifications
Table 1.03

1.04 Composition
Table 1.04

1.05 Heat Treatment

1.051 General. The austenitizing and tempering procedure will depend on the composition and quenched section size. In general, compositions having Mo, Cr, and C at the lower composition limits will require lower tempering temperatures to achieve a given yield strength within the range of 130 to 150 ksi. Bainite will be present in water quenched plates over about 2 in. thick (see Table 1.057) and consequently with increasing thickness above 2 in. the tempering temperature should be reduced.

1.052 Austenitize. Plates and all other forms < 2 inches thick should be austenitized at 1475 to 1525 F, 1 hour per inch and water quenched. Plates ⩾ 2 inches thick should be double austenitized: 1625 to 1675 F, 1 hour per inch and water quenched plus 1475 to 1525 F, 1 hour per inch and water quenched (1).

1.053 Tempering. Within the specified composition range and for thicknesses up to about 4 in. the required tempering temperature can vary from 1050 to 1160 F. Temper one hour per inch of thickness and water quench.

1.054 Stress relief. Not recommended. However, experimental low manganese compositions have been developed which reduce the tendency to embrittlement on long-time stress relief (see 1.09). These compositions are not available as production items.

1.055 Safety treatments for castings. To eliminate hydrogen flaking, cool in mold to 400 F. Then heat to 1600 F, hold 6 hours, furnace cool to 1100 F, hold 6 hours, furnace cool to <600 F. This treatment is not completely effective in sections greater than 4 inches thick (1).

1.056 Rapid heat treatment. Substantial gains in yield strength may be obtained by applying several cycles of an experimental heat treatment consisting of a preheat followed by induction heating (e.g., 2.5 to 16 F per second) to about 1430 F followed by water quenching (see Figure 3.0217). Some loss in impact strength accompanies these treatments, giving the greatest increase in yield strength (Figure 3.03317). The increase in strength is associated with a decrease in austenitic grain size. The effectiveness of the process will decrease with increasing plate thickness due to heating rate limitations which have yet to be established (17). This treatment is covered by U.S. Patent 3,178,324 but is not yet a production process.

1.057 Mechanical properties and microstructure for plate of various thicknesses illustrating variations in heat treatments producing mechanical properties within the range of 136 to 145 ksi. Table 1.057.

1.06 Hardness
(see also 1.05)

1.061 Effect of tempering temperature on hardness of stress relievable plate, Figure 1.061.

1.07 Forms and Conditions Available
Plate (to 6 inches), forging stock, castings and structural shapes.

1.08 Melting and Casting Practice
Electric furnace air melt, air melt + vacuum degas, air melt + vacuum AVC remelt and vaccum induction melt.

1.09 Special Considerations

1.091 Temper embrittlement. Like all commercial quenched and tempered alloy steels, this steel is subject to temper embrittlement. Stress relief treatments can result in temper embrittlement if the dwell time in the temperature range between 900 and 1100 F is sufficiently long.

	Fe
5	Ni
0.55	Cr
0.47	Mo
0.075	V

5 Ni Cr Mo V

This embrittlement can substantially reduce the impact energy particularly at low temperatures without appreciably affecting the tensile strength (e.g., see Fig. 3.0339). Cold deformation prior to stress relief appears to increase the embrittlement (see Fig. 3.0338).

A statistical study by L. F. Porter, G. C. Carter, and S. J. Manganello (41) of the role of Mn, Mo and Ni indicated that increasing Mo and Mn contents played a major role in increasing embrittlement. In addition, Mo interacts with Cr so that both elements together produce embrittlement. However, major modifications in Cr and Mo content cannot be made without unfavorably affecting the hardenability and tempering characteristics of the steel.

As a result of these studies a stress relievable composition was developed (61) having the following nominal composition: 0.10 C-0.25 Mn-5.75 Ni-0.75 Cr-0.35 Mo-0.07 V. The tensile and impact properties of this composition (Steel A) were compared with one having the normal HY 130 composition (Steel B) (61). Both these heats contained a very low content of tramp elements (As, Sb, and Sn) which are known to contribute to temper embrittlement. When air cooled from the austenitizing and from the tempering temperature, both heats exhibited a minimum in impact energy when tempered in the range from about 800 to 1100 F (see Fig. 3.03310). Under these conditions of heat treatment the low Mn composition (Steel A) had only slightly superior impact energy to the conventional composition and identical tensile yield strength. If water quenched from the austenitizing and from the tempering temperature (see Fig. 3.03310) the impact energy minimum disappears and the stress relievable composition (Steel A) exhibits superior impact energy over the range of tempering temperatures investigated. Again no difference was observed in the tensile yield strength of the two compositions. Further tests on the normal and low Mn composition (see Fig. 3.03311) were made to investigate the effect of stress relief treatments given following water quenching from both the austenitizing and the tempering temperature. These tests revealed essentially no change in room temperature or 0 F impact energy for the low Mn composition for times of stress relief up to 25 hours. In contrast, large losses in impact energy are observed for the normal composition. The stress relief treatments had no effect on the tensile yield strength of either composition. An 80 ton heat of the stress relievable composition behaved equally well following a typical commercial stress relief treatment (see Fig. 3.03314).

Using laboratory heats of the stress relievable composition, studies were made of the influence of V, P, N, Al, and O. Of these elements only P (see Fig. 3.0335) was found to contribute significantly to the temper embrittlement as measured by the Charpy V impact test (5) (41).

There has apparently been no commercial production of the stress relievable composition. Problems with voids were encountered in the previously mentioned 80 ton heat (61). These were attributed to hot shortness resulting from the combination of reduced C and Mn. It is possible that vacuum melting would eliminate the internal voids. If HY 130 is to find applications in welded structures subjected to fatigue loading a stress relievable composition would be desirable.

1.092 Embrittling Effects of Carbon, Oxygen and Sulphur. As might be expected the Charpy impact energy decreases with an increase in the content of these elements (see Figs. 3.0333, 3.0334, and 3.0336). It appears that castings of a low Mn composition may be more sensitive to the effects of sulphur than the normal Mn steel (see Table 3.03318). Apparently vacuum melting can improve the impact properties of steels with low sulphur contents presumably by a reduction in the oxygen content (see Fig. 3.0336).

1.093 Hydrogen Embrittlement. Fatigue crack growth rates are substantially increased by the presence of relatively low pressure dry hydrogen as compared with those observed for tests in laboratory air (see Fig. 1.0931). Based on very limited data (see Table 1.0932) it appears that sustained load crack growth will occur in high pressure hydrogen gas. However, the data are not sufficient to establish a threshold K_I value for this environment.

1.0931 Effect of low pressure dry hydrogen gas (-76 F dew point) on fatigue crack growth rates of plate. Fig. 1.0931.

1.0932 Effect of exposure to high pressure hydrogen gas on crack propagation of fatigue cracked sustained load specimens. Table 1.0932.

1.094 Non-metallic segregation. Low short transverse RA values in thick plate, reported by Rosenstein and Gross (10), found to be associated with nonmetallic segregation in an air-melted heat (see Table 3.0214). The producer claims (49) that these low values are not typical of air-melted heats and that e(2 In) = 13 percent and RA = 40 percent would better represent present practice. Vacuum melted alloy did not exhibit such segregation and had high RA values in the short transverse direction (see Table 3.0214).

1.095 Castings. Castings from Si-Al-Ti deoxidized heats were found to be considerably lower in Charpy impact strength than castings from Si-Al deoxidized heats (7). Hydrogen flaking in heavy sections of castings can not be completely eliminated by a safety treatment (see 1.05).

2.0 PHYSICAL PROPERTIES AND ENVIRONMENTAL EFFECTS

2.01 Thermal Properties

2.011 Melting range.

2.012 Phase changes

A_{c1} = 1210 F

A_{c3} = 1415 F

M_s = 715 F.

2.0121	Isothermal transformation diagram, Fig. 2.0121.
2.013	Thermal conductivity, Fig. 2.013.
2.014	Thermal expansion, 7.3 x 10^{-6} in. per in. per F.
2.015	Specific heat, Fig. 2.015.
2.016	Thermal diffusivity.
2.02	Other Physical Properties
2.021	Density, 0.285 lb per $in.^3$ (7.89 gm per cc).
2.022	Electrical properties.
2.0221	Electrical resistivity, Fig. 2.0221.
2.023	Magnetic properties Saturation induction B_S = 20,500 gauss at 2200 oersteds Retentivity B_{rs} = 11,000 gauss Coercivity H_{cs} = 11 oersteds Permeability μm = 630.
2.024	Emissivity.
2.025	Damping capacity.
2.03	Chemical Environments (see also 4.03).
2.031	General. The general corrosion rates of plates and plate weldments in marine environments are low with the largest effects being observed for flowing seawater. Under these conditions the weld metal appears to be poorer than the HAZ or the parent metal (see Fig. 2.032 and Table 4.0351). Conventional U bend specimens strained 16 percent of plate and plate welds showed no cracking after 37 months in the environments listed in Fig. 2.032 or after equal time at 2500 ft depth (14). In smooth low cycle fatigue tests the life of plate specimens is reduced somewhat by the presence of artificial seawater (see Fig. 3.0512). However, similar tests on welds do not reveal a clear influence of this environment (see Fig. 4.0362). Notched plate specimens exhibit a loss in life when subjected to low cycle fatigue tests in brackish river water (see Fig. 3.0513). Rotating beam high cycle fatigue tests of plate with both smooth and notched specimens (see Fig. 3.0514) show large reductions in life (cycles to failure) and in endurance limit when tested in brackish river water as compared to similar tests in air. Similar deleterious effects are noted for sheet when tested in ASTM seawater (see Fig. 3.0511). Environmental sustained load tests made with fatigue cracked and side grooved cantilever bend specimens in most all cases did not furnish valid K_{Iscc} values because of insufficient specimen size (i.e., specimen loads required to produce crack growth resulted in large scale yielding at the crack tip). However, results from these tests are valuable in defining the influence of variables on the sensitivity to environmental controlled crack growth under static load. For plate tested in artificial seawater this sensitivity is small (Figs. 2.033 and 2.034) but is increased by small amounts of cold work (Fig. 2.033). As shown in Fig. 2.034 cathodic polarization also increases the sensitivity. The results of fatigue crack growth rate studies indicate that the crack growth rate is increased (with respect to that in air) by 3.5 percent NaCl in the range where the gross strains are primarily elastic, but is about the same as that in air where the gross strains are primarily plastic (Fig. 2.035).
2.032	General corrosion of plate in marine environments, Fig. 2.032.
2.033	Sustained load crack failure behavior of plate in artificial seawater as influenced by plastic strain, Fig. 2.033.
2.034	Sustained load crack failure behavior of plate in artificial seawater and subjected to cathodic polarization, Fig. 2.034.
2.035	Crack growth rate scatter bands for plate subjected to reversed bending in air and in 3.5 percent NaCl, Fig. 2.035.
2.04	Nuclear Environments
3.	MECHANICAL PROPERTIES
3.01	Specified Mechanical Properties
3.011	Transverse properties for quenched and tempered plate specified by the Navy (Ships), Table 3.011.
3.012	Longitudinal and transverse properties for quenched and tempered forgings specified by the Navy (Ships), Table 3.012.
3.013	Longitudinal tensile and impact properties specified by ASTM, Table 3.013.
3.014	Producers specification for minimum mechanical properties for plate and forgings, Table 3.014.
3.015	Specifications for weldments (see 4.03).
3.02	Mechanical Properties at Room Temperature
3.021	Tension (see also 3.03).
3.0211	Stress-strain curve for plate, Fig. 3.0211.
3.0212	Effect of tempering temperature on tensile properties of casting, Fig. 3.0212.
3.0213	Effect of plate thickness on tensile properties, Fig. 3.0213.
3.0214	Effect of testing direction on tensile properties of air and vacuum melted plate, Table 3.0214.
3.0215	Effect of tempering temperatures on tensile properties of plate from several heats, Fig. 3.0215.
3.0216	Effect of tempering temperature on tensile properties of stress relievable plate, Fig. 3.0216.
3.0217	Effect of rapid austenitizing on tensile properties of plate, Fig. 3.0217.
3.022	Compression.
3.0221	Stress-strain diagrams.
3.0222	Effect of tempering temperature on the longitudinal compressive yield strength of stress relievable plate, Fig. 3.0222.
3.023	Impact, see 3.033.
3.024	Bending.
3.025	Torsion and shear.
3.026	Bearing.
3.027	Stress concentration.
3.0271	Notch properties.
3.0272	Fracture toughness (see also 3.0372).
3.02721	General. This alloy is extremely tough at room temperature and valid K_{Ic} values were not obtained using 4-inch-thick specimens of plate having a yield strength of 149 ksi (40). The producer estimates a room temperature K_{Ic} = 250 ksi $\sqrt{in.}$ This seems reasonable based on extrapolation of valid data obtained at lower temperatures (see Fig. 3.03722). Apparently there can be significant spread in the low temperature K_{Ic} values and this may also be reflected in the room temperature toughness.

	Fe
5	Ni
0.55	Cr
0.47	Mo
0.075	V

5 Ni Cr Mo V

	Fe
5	Ni
0.55	Cr
0.47	Mo
0.075	V

5 Ni Cr Mo V

Experimental tanks with 1-inch-thick walls, 35 inches in diameter with two longitudinal welds and hemispherical ends were tested by C. F. Tiffany, J. N. Masters and R. E. Regan (38). A surface crack (about 2.25 in. long, 0.8 in. deep) was introduced into the longitudinal weld of two tanks. One tank was subjected to 225 cycles (the last 25 with 3 percent NaCl solution in the crack) at membrane stresses about 70 percent of the parent metal yield. The pressure was then increased to 8800 psig at which point the tank leaked at the crack. The membrane stress at failure was 143 ksi as compared with a reported weld F_{ty} = 150 ksi and a parent metal F_{ty} = 137 ksi. The second tank was subjected to fewer cycles and pressurized to burst at 8950 psig. This tank after failure showed considerable evidence of gross plastic deformation.

3.02722 Surface crack strength of plate in air and in salt solution, Table 3.02722.

3.02723 R curves for plate, Fig. 3.02723.

3.028 Combined properties.

3.03 Mechanical Properties at Various Temperatures

3.031 Tension (see also 3.02).

3.0311 Stress-strain diagrams.

3.0312 Effect of test temperature on tensile properties of plate, Fig. 3.0312.

3.032 Compression.

3.033 Impact.

3.0331 Effect of tempering temperature on zero degree F impact strength of castings, Fig. 3.0331.

3.0332 Effect of tempering temperature on zero degree F impact strength of forging for several testing directions, Table 3.0332.

3.0333 Effect of carbon content on zero degree F impact strength of plate, Fig. 3.0333.

3.0334 Effect of oxygen on -80 F impact strength of low manganese plate as tempered and after stress relief, Fig. 3.0334.

3.0335 Effect of phosphorous on the -80 F impact strength of low manganese plate as tempered and after stress relief, Fig. 3.0335.

3.0336 Effect of sulphur content on low temperature impact strength of plate from laboratory heats, Fig. 3.0336.

3.0337 Effect of low test temperature on the impact strength of plate, Fig. 3.0337.

3.0338 Effect of cold deformation (bending) and stress relief on -80 F impact properties of plate, Fig. 3.0338.

3.0339 Effect of various stress relief treatments on low temperature impact energy of plate, Fig. 3.0339.

3.03310 Effect of tempering temperature on low temperature impact energy of laboratory heats of HY 130 (steel B) and a stress relievable composition (steel A) air cooled or water quenched after austenitizing or tempering, Fig. 3.03310.

3.03311 Effect of stress relief time on room temperature and 0 F impact energy of a stress relievable composition (steel A) and HY 130 (steel B) when slowly cooled following stress relief, Fig.3.03311.

3.03312 Effect of stress relief on low temperature impact strength of normal and low manganese laboratory heats of various thickness plates, Table 3.03312.

3.03313 Effect of tempering temperature on impact strength of stress relievable plate from production heat, Fig. 3.03313.

3.03314 Effect of low test temperature on impact energy of plate of a stress relievable composition given two stress relief treatments, Fig. 3.03314.

3.03315 Effect of tempering temperature on zero degree F impact strength of several heats of plate, Fig. 3.03315.

3.03316 Effect of plastic deformation on stress relief embrittlement, Table 3.03316.

3.03317 Effect of rapid austenitizing on grain size of zero degree F impact strength of plate, Fig. 3.03317.

3.03318 Effect of mold cooling rate on zero degree F impact strength of plate castings with normal and low manganese content and with normal and high sulphur content, Table 3.03318.

3.03319 Special impact tests.
NDT (1 inch plate) -120 F typical.
DWTT (1 inch plate) 5000 ft-lbs typical.

3.034 Bending.

3.035 Torsion and shear.

3.036 Bearing.

3.037 Stress concentration.

3.0371 Notch properties.

3.0372 Fracture toughness.

3.03721 General. No valid K_{Ic} data has been reported at temperatures above -100 F. At lower temperatures the toughness decreases and quite low values would be expected for cryogenic temperatures. The rate of decrease in toughness with decreasing temperature as well as the toughness reached at very low temperatures can vary from heat to heat for as yet unknown reasons (see Fig. 3.03722).

3.03722 Effect of low test temperature on the plane strain fracture toughness of plate from two heats, Fig. 3.03722.

3.03723 Effect of low test temperature and calculated crack tip strain rate on plane strain fracture toughness of plate, Fig. 3.03723.

3.04 Creep and Creep Rupture Properties

3.041 Minimum creep rate for plate, Fig. 3.041.

3.042 Creep rupture strength of plate, Fig. 3.042.

3.05 Fatigue Properties

3.051 Conventional properties.

3.0511 Effect of ASTM synthetic seawater on smooth and notched fatigue strength of sheet, Fig. 3.0511.

3.0512 Low cycle fatigue properties of plate in air and synthetic seawater, Fig. 3.0512.

3.0513 Effect of stress concentrations and brackish river water on low cycle fatigue characteristics of plate, Fig. 3.0513.

3.0514 Effect of stress concentration and brackish river water on fatigue strength of plate, Fig. 3.0514.

3.052 Fatigue crack propagation.

3.0521 Fatigue crack propagation rates for 0.9 inch plate, Fig. 3.0521.

3.0522 Fatigue crack propagation rates for 1 and 2 in. plates, Fig. 3.0522.

3.0523 Effect of R ratio on fatigue crack growth of 0.5 in. plate in air, Fig. 3.0523.

3.0524 Fatigue crack propagation rates for surface crack specimens at several R ratios, Fig. 3.0524.

3.0525 Fatigue crack propagation rates for as heat treated and stress relieved specimens of various thicknesses showing total scatterband and regression lines, Fig. 3.0525.

3.0526 Fatigue crack propagation rates for plate in air and ASTM seawater, Fig. 3.0526.

3.0527 Effect of loading frequency on fatigue crack growth rate in 3.5 percent NaCl, Fig. 3.0527.

3.06 Elastic Properties

3.061 Poisson's ratio.

3.062 Modulus of elasticity, 29,500 ksi (37).

3.063 Modulus of rigidity.

3.064 Tangent modulus.

3.0641 Range of tangent and secant tension moduli for plate of several thicknesses, Fig. 3.0641.

3.0642 Range of tangent and secant compression moduli for plate of several thicknesses, Fig. 3.0642.

3.065 Secant modulus (see 3.0641).

4. FABRICATION

4.01 Forming

4.011 General. The alloy may be either hot or cold formed by conventional processes. Cold forming may be carried out in the quenched and tempered condition and typical bend radii are 2T for 180 degrees. Cold forming will result in some loss in impact strength (see Fig. 3.0338) and large plastic strains (in excess of about 10 percent) should be avoided.

4.012 Rolling. Cross rolling ratios should approach 1:1 in order to eliminate mechanical anisotropy.

4.0121 Effect of specimen orientation on impact strength of plates given different rolling ratios (ratio of thickness reduction in final longitudinal direction to prior thickness reduction in the transverse direction), Fig. 4.0121.

4.013 Forging. Readily forgeable in the temperature range between 1700-2250 F, maximum forging temperature 2300 F.

4.02 Machining and Grinding

About the same as for quenched and tempered SAE 4140 steel at 36 RC (37).

4.03 Joining

4.031 Welding.

4.0311 General. A large amount of work has been done to define production welding techniques with particular emphasis on high deposition rate processes. Specifications have been developed semi-automatic and automatic GMA (spray and pulsed spray arc), automatic GTA and for SMA processes (57) (58) (65) (66) (70) (71). In addition, some work has been done to develop suitable techniques for hot wire GTA and sub-arc welding (31). GMA and SMA electrode and GTA wire compositions are available for producing an overmatching weldment in terms of yield strength with excellent toughness at low temperatures (see Tables 4.0311, 4.03111, 4.03113, 4.03117, and 4.03119). In addition, electrode compositions are available which produce weld metal yield strengths between 70 and 120 ksi which can be used to weld HY 130 to HY 130 or to other steels (see Tables 4.03112, 4.03114, 4.03115, 4.03118, 4.031110 and 4.031111). Weld metal yield strengths between 120 and 150 ksi are produced using Mn-Ni-Cr-Mo electrode compositions while the lower yield strength welds are produced with Mn-Ni-Mo electrodes. Heavy walled pressure vessels (1-inch-thick wall) simulating solid rocket motor cases have been made successfully using GTA welding with wire of the parent metal (HY 130) composition (see 3.02721). Such welds have high toughness as measured by the Charpy V impact test but somewhat lower yield strength than can be obtained with the Mn-Ni-Cr-Mo compositions (see Table 4.03131).

	Fe
5	Ni
0.55	Cr
0.47	Mo
0.075	V

5 Ni Cr Mo V

4.03111 Composition by weight of bare wire electrodes for GTA or GMA welding of HY 130 to HY 130, Table 4.03111.

4.03112 Composition by weight of bare wire electrodes for welding HY 130 to HY 130 or to other steels with less than 0.30 C, Table 4.03112.

4.03113 Composition by weight of weld metal deposited by SMA process specified for all position welding HY 130 to HY 130, Table 4.03113.

4.03114 Composition by weight of bare wire electrodes for flat or horizontal spray GMA welding of HY 130 to other steels with less than 0.30 C, Table 4.03114.

4.03115 Composition by weight of weld metal deposited by SMA process specified for welding HY 130 to HY 130 or to other steels with less than 0.30 C, Table 4.03115.

4.03116 Composition by weight of weld metal deposited by SMA process specified for producing horizontal fillets and flat weldments of HY 130 which are to be heat treated. Table 4.03116.

4.03117 Wire compositions by weight for welds used in producers weldment development studies, Table 4.03117.

4.03118 Minimum mechanical properties of deposited GTA and GMA weld metal for joining HY 130 to HY 130 or to other lower strength steels with less than 0.30 C, Table 3.03119.

4.03119 Minimum mechanical properties of deposited GTA and GMA weld metal for joining HY 130 to HY 130 or to other steels with less than 0.30 C, Table 3.03119.

4.031110 Minimum mechanical properties of deposited SMA weld metal specified for joining HY 130 to HY 130, Table 4.031110.

4.031111 Minimum mechanical properties of deposited GMA weld metal for electrode composition specified for joining HY 130 to other lower strength steels with less than 0.30 C, Table 4.031111.

4.031112 Minimum mechanical properties of deposited SMA weld metal specified for welding HY 130 to HY 130 or to other lower strength steels with less than 0.30 C, Table 4.031112.

4.031113 Minimum mechanical properties of deposited SMA weld metal after reheat treatment of HY 130 weldment. Table 4.031113.

4.0312 Welding Conditions. Recommended welding conditions for GMA and SMA plate welding are listed in Table 4.0312. Particular attention should be given to the elimination of moisture during welding which can result in hydrogen embrittlement (64). High strength SMA electrodes should be maintained on the job site in containers heated between 225 and 300 F and used immediately after removal from these containers. High strength wires for the GTA or GMA processes should be stored in a dry environment on the job and if not to be used within 24 hours should be stored in sealed containers with a desiccant not in direct contact with the wire. High strength SMA welds made with the E14018

	Fe
5	Ni
0.55	Cr
0.47	Mo
0.075	V

5 Ni Cr Mo V

electrode (see Table 4.03113) should be subjected to hydrogen removal baking treatments which vary with thickness and with types of repair welding (see Table 4.03121). Preheat and interpass temperatures and maximum specified heat input are a function of metal thickness (see Tables 4.03122 and 4.03123). For a given heat input the impact energy will increase with the number of passes used to complete the weld (see Fig. 4.03124).

Electrode compositions and welding procedures have been developed for SMA and GMA weldments that are to be completely reheat treated (see Table 4.03133). Specifications have been issued for heat treatable SMA weldments which use a high nickel wire (see Table 4.03116). The reheated SMA weldments are specified to have the same mechanical properties as those produced with the E14018 electrode (compare Table 4.031113 with Table 4.031110). Specified preheat and interpass temperatures, heat input and details of reheat treatment are given in Table 4.03123. It should be noted that a minimum post weld soak of 350 F for 12 hours minimum is recommended for SMA weldments made with the high nickel electrodes. Specifications have not been developed for reheatable GMA weldments. However, experimental GMA reheatable weldments have been produced using a high nickel wire which have satisfactory mechanical properties following complete reheat treatment (see Table 4.03133). These weldments were also subjected to an extended post-weld soak.

4.03123 Specified preheat and interpass temperatures and welding heat inputs for SMA weldments to be heat treated. Table 4.03123.

4.03124 Impact energy of GTA and GMA welds as influenced by the number of beads. Fig. 4.03124.

4.0313 Weld Embrittlement. Embrittlement may result from high temperature thermal treatments, stress relief or from hydrogen contamination. High temperature heat treatments such as might be associated with hot forming can result in considerable reduction in the low temperature impact energy (see Tables 4.03131 and 4.03132). This effect may be somewhat less pronounced in GTA and GMA welds made with wire of parent metal composition than with the conventional Mn-Ni-Cr-Mo wires.

Stress relief treatments can result in temper embrittlement associated with long dwell times in the temperature range between 900 and 1000 F (see also 1.09). The degree of embrittlement will vary with both the holding time and the temperature of stress relief (see Fig. 4.03134) and is sufficiently severe that stress relief of HY 130 weldments is not recommended for use in critical applications (56) (1). It appears that use of an electrode of parent metal (HY130) composition in GMA welding results in less stress relief embrittlement than would be obtained using the Mn-Ni-Cr-Mo compositions (see Fig. 4.03135). Attempts to recover the properties of stress relieved weldments by a 1150 F heat treatment followed by water quenching were not successful for GMA welds made with a Mn-Ni-Cr-Mo wire (see Fig. 4.03134) but were successful for both the parent metal and GMA welds made with HY 130 wire (see Table 4.03136).

Hydrogen embrittlement commonly results from moisture contained within the coating of SMA electrodes (see 4.0312). The potent effects of hydrogen in causing weld metal grain boundary cracks which propagate into the HAZ is illustrated by the results of strain augmented cracking tests on high strength SMA weldments (see Table 4.03137).

4.03131 Effects of reheat treatment on the mechanical properties of GMA and GTA welds made with different wires, Table 4.03131.

4.03132 Influence of high temperature heat treatments on the mechanical properties of GMA welds, Table 4.03132.

4.03133 Tensile and low temperature impact energy of heat-treatable SMA and GMA weld metal, Table 4.03133.

4.03134 Effect of stress relief on impact energy of GMA Mn-Ni-Cr-Mo weldments, Fig. 4.03134.

4.03135 Effect of stress relief treatments on impact energy of GMA weldments made with two electrode compositions, Fig. 4.03135.

4.03136 Effect of stress relief and a stress relief recovery treatment on the mechanical properties of GMA welds made with an HY 130 composition wire, Table 4.03136.

4.03137 Results of strain augmented cracking tests for several SMA electrode conditions and applied strains following welding, Table 4.03137.

4.032 Influence of welding process. The mechanical properties resulting from welding are complex functions of a large number of variables. However, in general for a particular heat input and wire composition the impact strength of the weld metal will increase with the number of passes necessary to complete the weld.

4.0321 Impact strength of welds made by several processes as influenced by the number of beads, Fig. 4.03124.

4.033 Stress relief. Temper embrittlement is produced by stress relief treatments that involve long holding times or very slow cooling through the temperature range between 900 and 1100 F (see 1.091). The degree of embrittlement will vary with both the holding time and the temperature of stress relief (Fig. 4.03134) and is sufficiently severe in terms of loss in Charpy impact properties that stress relief is not recommended for weldments in critical applications (1). It appears that a 5Ni-Cr-Mo-V wire gives less stress relief embrittlement in the GMA processes than does a Mn-Ni-Cr-Mo wire (Fig. 4.03135). Attempts to recover the properties of stress relieved weldments by a 1150 F heat treatment followed by water quench were not successful for GMA welds made with Mn-Ni-Cr-Mo wire (Fig. 4.03134) but were successful for both parent metal and GMA welds made with 5Ni-Cr-Mo-V wire (Table 4.03136). Work is under way to develop a wire composition which will exhibit less stress relief embrittlement than those now available.

4.0333 Effect of GMA welding on tensile properties of plate, Table 4.03136.

4.034 Crack strength. Surface crack tests of GTA (5Ni-Cr-Mo-V) wire weldments reveal very high toughness in both the weld metal and HAZ (Table 4.0341, see also 3.02721).

4.0341 Surface crack strength of GTA weldments tested in air in 3.5 percent NaCl, Table 4.0341.

4.035 Corrosion. General corrosion in seawater environment is somewhat higher for weld metal than for parent metal and somewhat lower in the HAZ than in parent metal (Table 4.0351). Stress corrosion behavior of weldments has been investigated using fatigue cracked cantilever beam specimens subjected to sustained loads and an environment of 3 percent NaCl solution. These specimens failed at K_Q values above the K_{Ic} measuring capacity of the specimen. However the results are still useful for comparative purposes. Both GMA and SMA weldments made with Mn-Ni-Cr-Mo wire show delayed failure in the salt solution. The rate at which the exposure time to failure increases with K_Q and the stress intensity level below which no failures are observed varies with the welding technique and the crack oreintation (Figs. 4.0352 and 4.0353). Unfortunately, it is not possible to make a good comparison between parent metal and weld metal in this test since the available data does not apply to the same size specimens in both cases.

The fatigue crack propagation rate is increased in salt solutions. The effect observed depends on the frequency of loading and on the stress intensity level (see Figs. 3.0526 and 3.0527). For frequencies between 0.1 and 10 Hz negligible effects are observed at K_{max} less than about 15 ksi $\sqrt{in}$ (see Fig. 3.0527). At K_{max} levels above 30 ksi $\sqrt{in}$. substantial effects of frequency appear with growth rate in salt solution becoming increasingly higher than that in air as the frequency of loading decreases.

4.0351 General corrosion of parent metal, weld metal and HAZ in seawater, Table 4.0351.

4.0352 Sustained load crack failure behavior in 3 percent NaCl solution for plate welded by several processes, Fig. 4.0352.

4.0353 Sustained load crack failure behavior in 3 percent NaCl solution for two orientations in SMA welds, Fig. 4.0353.

4.036 Fatigue of welds. When tested in air the low cycle fatigue resistance of GMA welds is superior to that of SMA welds. This behavior is observed for tests in air (see Fig. 4.0361) and for tests in ASTM artificial seawater (see Fig. 4.0362). There appears to be no significant difference between the low cycle fatigue resistance of GMA welds tested in air or in ASTM seawater (see Fig. 4.0362). For tests in air or seawater the low cycle fatigue resistance of the parent metal appears to be superior to that of the GMA welds.

4.0361 Low cycle fatigue behavior in air of SMA and GMA heat treatable weld metal, Fig. 4.0361.

4.0362 Low cycle fatigue behavior of GMA welds in air and ASTM seawater and SMA welds in air, Fig. 4.0362.

REFERENCES

1. L. F. Porter et al, "The Development of an HY 130(T) Steel Weldment", U.S. Steel Applied Research Laboratory, Report 39.018-001, NOBS 88540 (July 1, 1966)
2. "Interim Specification for HY 130 and HY 140 Steel Plates", U.S. Steel Applied Research Laboratory (March 16, 1966)
3. S. J. Manganello, L. F. Porter, and R. J. Sitko, "Effect of Sulphur on Mechanical Properties of 5Ni-Cr-Mo Steel", Ibid Report No. 39.018-001 (45), NOBS 88540 (July 1, 1965)
4. S. J. Manganello and L. F. Porter, "Effect of Rolling Ratio on the Anisotrophy of 5Ni-Cr-Mo Steel Plates", Ibid Report No. 40.018-001 (36), NOBS 88540 (December 1, 1964)
5. S. J. Manganello, L. F. Porter, and R. J. Sitko, "Effect of Variations in Phosphorus, Vanadium, Nitrogen, Aluminum, and Oxygen on the Mechanical Properties of 5Ni-Cr-Mo Steel", Ibid Report No. 39.018-013 (1), NOBS 94535 (FBM) (January 1, 1967)
6. Ibid, "Suitability of 5 Ni-Cr-Mo Steels as Forgings", U.S. Steel Applied Research Laboratory, Report No. 39.018-001 (53) (January 1, 1966)
7. S. J. Manganello, L. F. Porter, F. W. Simpson, and R. W. Zabelsky, Ibid Report No. 39.018-001 (57) (January 1, 1966)
8. T. L. Boblenz, J. M. Fisher, and S. T. Rolfe, "Secant and Tangent Moduli Values for 5Ni-Cr-Mo-V Steel", Ibid Report No. 39.018-001 (54) (January 1, 1966)
9. S. R. Novak, J. A. Kozub, and S. T. Rolfe, "Short Time Cryogenic and Elevated Temperature Tensile Properties of HY 80, 5 Ni-Cr-Mo and 2 1/4 Cr-1Mo Steels", Ibid Report No. 39.018-001 (50) (November 1, 1965)
10. A. H. Rosenstein and M. R. Gross, "Properties of HY 130, 5 Ni-Cr-Mo-V Steel", Summary, Naval Ship Research and Development Center, Marine Engineering Laboratory, Report 2448 (September, 1967)
11. T. L. Boblenz and S. T. Rolfe, "Effect of Cold Forming on Charpy V-Notch Impact Properties of 5Ni-Cr-Mo-V Steel", U.S. Steel Applied Research Laboratory Report No. 39.018-001 (46), NOBS 88540 (July 1, 1965)
12. Ibid, "Effect of Cold Forming on Tensile and Compressive Properties of 5Ni-Cr-Mo-V Steel", U.S. Steel Applied Research Laboratory, Report No. 39.018-001 (55), NOBS 88540 (January 1, 1966)
13. Ibid, "Corrosion Fatigue Characteristics of HY 80, 5Ni-Cr-Mo-V, 12Ni-5Cr-3Mo and 18Ni-8Co-3Mo Steels", Ibid Report No. 39.018-002 (37), NOBS 88540 (January 1, 1966)
14. A. W. Loginow, "Corrosion and Stress Corrosion of HY 130(T) and HY 80 Steel in Marine Environments", Ibid Report No. 39.001-100 (2) (July 15, 1967)
15. L. P. Connor, L. F. Porter, S. T. Rolfe, "Second Progress Report: Extended Investigation of HY 130/150 Weldments", U.S. Steel Applied Research Laboratory, Report No. 39.018-016 (4), NOBS 94535 (FBM) (August 1, 1967)

	Fe
5	Ni
0.55	Cr
0.47	Mo
0.075	V

5 Ni Cr Mo V

	Fe
5	Ni
0.55	Cr
0.47	Mo
0.075	V

5 Ni Cr Mo V

16. L. F. Porter et al, "Eighth Progress Report Development of an HY 130/150 Weldment", U.S. Steel Applied Research Laboratory, Report No. 39.018-001 (58), NOBS 88540 (January 1, 1966)
17. D. S. Dabkowski and L. F. Porter, "Effect of Rapid Heat Treating Parameters on the Mechanical Properties of 5Ni-Cr-Mo-V Steel", U.S. Steel Applied Research Laboratory, NOBS 94535 (FBM), Report No. 39.018-007 (13) (August 1, 1967)
18. R. C. Schwab and M. R. Gross, "Fatigue Properties of 5 Ni-Cr-Mo-V, HY 130/150 Steel, "Marine Engineering Laboratory (MEL), Report 365/65 (October 1965)
19. W. H. Asche and M. R. Gross, "Effect of Tempering on the Strength, Hardness, and Notch Toughness of HY 130/150, 5Ni-Cr-Mo-V Steel", Marine Engineering Laboratory (MEL), Report 72/66 (March, 1966)
20. G. C. Carter, T. L. Boblenz, and L. F. Porter, "Effect of Cold Deformation and Stress Relief Treatments on the Mechanical Properties of Standard and Low Manganese HY 130(T) Steel", U.S. Steel Applied Research Laboratory, Report No. 39.018-013 (4), NOBS 94535 (FBM) (August 1, 1967)
21. A. K. Shoemaker and S. T. Rolfe, "Static and Dynamic Low-Temperature K_{Ic} Behavior of Steels", Ibid Report No. 39.018-007 (16), NOBS 94535 (FBM) (December 29, 1967)
22. D. P. Clausing, "Effect of Stress Relief Treatments on Dimensional Stability of HY 130(T) Steel Components", Ibid (August 1, 1967)
23. W. F. Domis, "Creep and Creep Rupture Properties of HY 80 and HY 130(T) Steels", U.S. Steel Applied Research Laboratory, Report No. 39.012-006 (1) (July 15, 1968)
24. H. P. Leckie and A. W. Loginow, "A Comparison of the Stress Corrosion Behavior of Some High Strength Steels", U.S. Steel Applied Research Laboratory, Report No. 39.001-001 (2), NOBS 94535 (FBM) (July 15, 1968)
25. S. R. Novak, "Effect of Plastic Strain on the K_{Iscc} of HY 80, HY 130(T) and 12Ni-5Cr-3Mo Steels", Ibid Report Nol 39.018-007 (20) (January 1, 1968)
26. T. L. Boblenz and S. T. Rolfe, "Low Cycle Fatigue Characteristics of HY 130(T) Weldments", Ibid Report No. 39.018-006 (6), Ibid (June 1, 1967)
27. R. M. Orehoski, J. P. Paulina, and A. M. Rathbone, "Effects of Heat Treatment on the Mechanical Properties of HY 130(T) Steel Weld Metals", Ibid Report No. 39.018-014 (1) (January 1, 1967)
28. L. F. Porter, A. M. Rathbone, and S. T. Rolfe, "First Progress Report, Extended Investigation of HY 130/150 Weldments", Ibid Report No. 39.018-016 (1) (January 1, 1967)
29. P. J. Konkol, "Stress Relief Embrittlement of HY 130(T) Weld Metals", Ibid Report No. 39.018-013 (2) (August 1, 1967)
30. L. P. Connor, L. F. Porter, and S. T. Rolfe, "Third Progress Report, Extended Investigation of HY 130/150 Weldments", Ibid Report No. 39.018-016 (8) (January, 1968)
31. Ibid, "Fourth Progress Report, Extended Investigation of HY 130/150 Weldments", Ibid Report No. 39.018-016 (9) (July 1, 1968)
32. J. J. Pepe, "Preliminary Study of the Hot Wire GTA Welding Process", Ibid Report No. 39.018-017 (1) (January 1, 1968)
33. C. F. Tiffany, J. N. Masters, and R. E. Regen, "A Study of Weldments and Pressure Vessels Made of HY 150 Steel Plates", The Boeing Company, NASA CR. 72155 (January 1967)
34. J. H. Smith and S. J. Rolfe, "Effects of Welding Position and Progress on the K_{Iscc} of HY 130(T) Weld Metals", U.S. Steel Applied Research Laboratory, Report No. 39.018-016 (7), NOBS 94535 (FBM) (January 1, 1968)
35. J. H. Smith and S. T. Rolfe, 'Effect of Notch Orientation on K_{Iscc} of Weld Metal", Ibid Report No. 37.018-016 (5) (December 29, 1967)
36. J. P. Paulina and L. F. Porter, "Microstructures in HY 130(T) Steel Plates", Ibid Report No. 39.018-006 (7) (July 1, 1968)
37. Interim Technical Data, HY 130(T) and HY 140(T), U.S. Steel, Pittsburgh, Pennsylvania
38. ASTM A579-67 Alloy 12, ASTM Standards Pt4, (January 1968) page 890
39. "Large Motor Case Technology Evaluation", First Year Summary Progress Report, The Boeing Company, AF Contract AF33(615)-1623 (June, 1965)
40. S. T. Rolfe, "Cooperative Program on Testing of Medium Strength High Toughness Materials", Letter to J. M. Kraft, Chairman, ASTM E-24, Sub III (September 27, 1968)
41. L. F. Porter, G. C. Carter, and S. J. Manganello, "A Study of Temper Embrittlement During Stress Relieving of 5Ni-Cr-Mo-V Steels", ASTM STP 407 page 20
42. S. T. Rolfe, "Formability of Thick 5Ni-Cr-Mo-V Steel Plates", U.S. Steel Applied Research Laboratory Report No. 39.018-001 (40) (March 1, 1965)
43. T. W. Crooker and E. H. Lange, "Corrosion Fatigue Crack Propagation in Modern High Performance Structural Steels", Trans ASM Volume 60, 1967, p. 198
44. S. J. Manganello et al, "Development of a High Toughness Alloy Plate Steel with a Minimum Yield Strength of 140 ksi", Welding Journal (November 1964) page 1
45. A. M. Rathbone, L. P. Connor, and J. H. Gross, "Weldability of a High Toughness Alloy Plate Steel with a Minimum Yield Strength of 140 ksi", Ibid (December 1964) page 8
46. K. E. Dorschu and A. Lesnewich, "Development of a Filler Metal for a High Toughness Alloy Plate with a Minimum Yield Strength of 140 ksi", Ibid (December 1964) page 21
47. S. T. Rolfe, R. P. Haak, and J. H. Gross, "Structural Suitability of a High Toughness Alloy Plate Weldment with a Minimum Yield Strength of 140 ksi", Ibid (January 1965) page 34
48. Materials Development and Application Office, NAVSEC Code 61010, Washington, D.C.
49. L. F. Porter, U.S. Steel, Personal Communication with W. F. Brown Jr. (1968 and 1980)
50. A. M. Sullivan and T. W. Crooker, "The Effects of Specimen Thickness and Stress Relief on Fatigue Crack Growth Rate in Nickel-Chromium-Molybdenum-Vanadium Steel", J. of Testing and Evaluation, ASTM, Vol. 5, No. 2, 1977, p. 96

51. A. M. Sullivan and T. W. Crooker, "Analysis of Fatigue Crack Growth in a High Strength Steel – Part I: Stress Level and Stress Ratio Effects at Constant Amplitude", J. of Pressure Vessel Tech., Vol. 98, May 1976, p. 179
52. J. M. Barsom, E. J. Imhof, and S. T. Rolfe, "Fatigue Crack Propagation in High-Yield Strength Steels", Engineering Fracture Mechanics, Vol. 2, No. 4, 1971, p. 301
53. D. E. McCabe and J. D. Landes, "Elastic-Plastic R-Curves", Trans. ASME, Vol. 100, July 1978, p. 258
54. D. D. Miller, "Hydrofoil Material Evaluation – Base Metal (& Coated Metal) Fatigue and Fracture Studies", Report No. D 180-15197-3, The Boeing Co., November 1974
55. Oldrich Vosokovsky, "Frequency, Stress Ratio and Potential Effects on Fatigue Crack Growth of HY 130 Steel in Salt Water, J. of Testing and Evaluation, ASTM, Vol. 5, May 1978, p. 175
56. P. M. Palermo, Naval Sea Systems Command, Personal Communication with W. F. Brown, Jr., 1980
57. MIL-E-24355A (SHIPS) Military Specification, Electrodes, Welding, Bare, Solid, Nickel-Manganese, Chromium-Molybdenum Alloy Steel for Producing HY 130 Weldments for As Welded Applications, Oct. 24, 1975
58. MIL-E-22200/9A (SHIPS), Military Specification, Electrodes, Welding, Mineral Covered, Low Hydrogen, or Iron Powder, Low Hydrogen, Nickel-Manganese-Chromium-Molybdenum Steel for Producing HY 130 Weldments for As-Welded Applications, June 13, 1975
59. A. W. Loginow, "Crack Propagation Behavior of Steels in High Pressure Hydrogen Gas II", U.S. Steel Research Laboratory Report, Project No. 43.001-003 (2), December 15, 1971
60. A. H. Rosenstein, "Phenomenological Investigations of Stress Relief Embrittlement", Welding Research Supp., March 1970, p. 122s
61. D. S. Dabkowski and L. F. Porter, "Evaluation of a Stress Relievable HY 130 Steel", U.S. Steel Applied Research Laboratory, Project No. 39.018-013 (6), NOBS-94535 (FBM), June 30, 1969
62. L. P. Connor, "Development of a Heat-Treatable HY 130 Weld Metal", U.S. Steel Applied Research Laboratory, Project No. 39.018-014 (4), NOBS-94535 (FBM), January 28, 1971
63. P. J. Konkol and L. P. Connor, "Weldability of Stress-Relievable HY 130 Steel", Ibid, Project No. 39.018-013 (5), Ibid, January 2, 1969
64. W. F. Savage, E. F. Nippes, and T. Tokunaga, "Hydrogen Induced Cracking in HY 130 Steel Weldments", Welding Research Supplement, April 1978, p. 118
65. MIL-E-23765/2A (SHIPS) Military Specification, Electrodes and Rods-Welding, Bare, Solid, Low Alloy Steel, May 19, 1973
66. MIL-E-19822A (SHIPS), Military Specification, Electrodes, Welding, Bare, High Yield Steel, March 1, 1961
67. MIL-S-24371A (SHIPS), Military Specification, Steel Plate, Alloy Structural, High Yield Strength (HY 130), October 16, 1975
68. MIL-S-24512 (SHIPS), Military Specification, Steel Forgings, Alloy, Structural, High Yield Strength (HY 130), September 4, 1975
69. ANSI/ASTM A579-77, Standard Specification for Superstrength Alloy Steel Forgings, ASTM Annual book of Standards, Pt. 5
70. MIL-E-22200/1 (SHIPS), Military Specification, Electrodes, Welding, Mineral Covered, Iron-Powder, Low Hydrogen Medium and High Tensile Steel, As Welded or Stress-Relieved Application, October 3, 1973
71. MIL-E-0022200/10 (SHIPS) Military Specification, Electrodes, Welding, Mineral Covered, Low Hydrogen, Iron Powder for Producing HY 100 Steel Weldments for As Welded Applications, May 12, 1972.
72. W. G. Clark, Jr., "The Effect of Hydrogen Gas on the Fatigue Crack Growth Rate of HY 80 and HY 130 Steels", Hydrogen in Metals, American Society for Metals, Cleveland, Ohio, 1974
73. E. G. Hamburg, "Physical Properties of Ultra-service Steels", U.S. Steel Applied Research Laboratory, Project No. 39.018-007 (44), February 3, 1971.
74. MIL-E-22200/11 (SHIPS) Military Specification, "Electrodes, Welding, Mineral Covered, Iron-Powder, Low Hydrogen, 8 Nickel-Chromium-Molybdenum-Vanadium Alloy Steel for Producing HY 130 Weldments to be Heat-Treated", October 10, 1975

	Fe
5	Ni
0.55	Cr
0.47	Mo
0.075	V

5 Ni Cr Mo V

Alloy	Fe-0.11C-5Ni-0.55Cr-0.47Mo-0.07V	
Form	Plate	Forgings
	MIL-S-24371A (Ships) Aug. 21, 1975 Amendment - 1 Oct. 16, 1975	ANSI - ASTM A579-77 MIL-S-24512 (Ships) Sept. 4, 1975

TABLE 1.03. SPECIFICATIONS FOR PLATE AND FORGINGS (67) (68) (69)

Alloy	Fe-0.11C-5Ni-0.55Cr-0.47Mo-0.07V			
Composition	Weight Percent			
Form	Plate (67)		Forgings (68) (69)	
	Min	Max	Min	Max
C	–	0.12	–	0.12
Mn	0.60	0.90	0.60	0.90
P	–	0.010	–	0.010
S	–	0.010	–	0.010
Si	0.15	0.35	0.20	0.35
Ni	4.75	5.25	4.75	5.25
Cr	0.40	0.70	0.40	0.70
Mo	0.30	0.65	0.30	0.65
V	0.05	0.10	0.05	0.10
Ti(a)	–	0.02	–	0.02
Cu(a)	–	0.25	–	0.25

(a) Residual elements

TABLE 1.04. COMPOSITION OF PLATE AND FORGINGS (67) (68) (69)

	Fe
5	Ni
0.55	Cr
0.47	Mo
0.075	V

5 Ni Cr Mo V

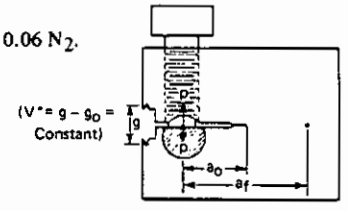
Alloy	Fe-0.11C-5Ni-0.55Cr-0.47Mo-0.07V					
Form	Plate (4 Heats)					
Thickness, inches	1/2	1	2	3	4	6
Condition(b)	1500 F, 1 hr + 1160 F, 3/4 hour	1500 F, 1½ hr + 1160 F, 1½ hour	1500 F, 2 hr + 1500 F, 2 hour + 1160 F, 23 hour	1650 F, 3 hr + 1500 F, 3 hour + 1100 F, 2 hr	1650 F, 3 hr + 1500 F, 3 hour + 1075 F, 2 hr	1600 F, 4 hr + 1050 F, 3 hour
F_{tu}, ksi(a)	152	152	148	145	153	151
F_{ty}, ksi	139	144	138	136	145	137
RA, Percent	63	65	62	65	64	67
IE Charpy-V(a) (0 F), ft-lb	87	85	97	73	78	85
Percent Martensite at Mid Thickness	100	100	100	80	75	65
ASTM Grain Size at Mid Thickness	8.5	6.5	8.0	7.3	7.0	3.5 – 5.5 (Duplex)

(a) Longitudinal at 1/4 thickness, 1-6 plate, mid thickness, 1/2-inch plate.
(b) WQ following austenitizing and tempering.

TABLE 1.057. MECHANICAL PROPERTIES AND MICROSTRUCTURE FOR PLATE OF VARIOUS THICKNESS ILLUSTRATING VARIATIONS IN HEAT TREATMENT PRODUCING MECHANICAL PROPERTIES (F_{ty}) WITHIN THE RANGE OF 136–145 KSI [(36) TABLE 4]

Alloy	Fe-0.11C-5Ni-0.55Cr-0.47Mo-0.07V		
Form	1-inch Plate		
Condition	1500 F, 1½ hour, WQ + 1160 F, 1½ hour, WQ, F_{ty} = 135 ksi		
Initial (a) Applied K_Q, ksi $\sqrt{in.}$	101	71	
Exposure Time to 10 ksi H_2, weeks	15	15	15
Crack Extension, a_f, inch	1.41	1.29	1.21

(a) K_Q in air = 168 ksi $\sqrt{in.}$ based on a_o.
(b) Hydrogen composition (vol. percent): 0.001 O_2, 0.06 N_2.



BOLT LOADED SPECIMEN

TABLE 1.0932. EFFECT OF EXPOSURE TO HIGH PRESSURE HYDROGEN GAS ON CRACK PROPAGATION OF FATIGUE CRACKED SPECIMENS [(59) TABLE 8]

Alloy	Fe-0.11C-5Ni-0.55Cr-0.47Mo-0.07V		
Form	Plate		
Condition	Quenched and Tempered		
Thickness t, inch	3/16 to 3/4	>3/4	1/2 to 4
F_{ty}, ksi	130 – 150	130 – 145	
e (2 inch), percent (Min)(a)	14	15	
RA, percent (Min)	–	50	
Charpy-V at (c)(d) 0 F, ft-lb (Min)			60(b)

(a) 3/16-inch < t < 1/4-inch, e = 11 percent (Min); 1/4-inch < t < 3/8-inch, e = 12 percent (Min).
(b) Average of 3 tests with no test value < 55 ft-lbs.
(c) 3 tests at 70 F (Min) also required with their average not more than 15 ft-lb greater than average of 0 F tests.
(d) As alternative to Charpy-V, 0 F dynamic tear minimum: 5/8-inch specimen = 500 ft-lbs; 1-inch specimen = 4000 ft-lbs.

TABLE 3.011. TRANSVERSE PROPERTIES FOR QUENCHED AND TEMPERED PLATE SPECIFIED BY THE NAVY (SHIPS)(67)

Alloy	Fe-0.11C-5Ni-0.55Cr-0.47Mo-0.07V	
Form	Forging	
Condition	Quenched and Tempered	
Source	SHIPS	ASTM
F_{tu}, ksi (Min)	–	150
F_{ty}, ksi (Min)	130 – 145	140
e, percent (Min)	15	13
RA, percent (Min)	50	40
Charpy-V(c)		
at 0 F, ft-lb (Min)	55(a)	
75 F, ft-lb (Min)	See Note(b)	50

(a) Average L + T for plate and cylindrical shapes or tangential + longitudinal in ring forgings with no value > 40 ft-lbs.
(b) L + T tests at 70 F (Min) also required with their average not more than 15 ft-lbs greater than the average of 0 F tests.
(c) Dynamic tear tests as alternative to Charpy-V (See Table 3.011).

TABLE 3.012. LONGITUDINAL AND TRANSVERSE PROPERTIES FOR QUENCHED AND TEMPERED FORGINGS SPECIFIED BY THE NAVY (SHIPS) (68) AND ASTM (69)

	Fe
5	Ni
0.55	Cr
0.47	Mo
0.075	V

5 Ni Cr Mo V

Alloy	Fe-0.11C-5Ni-0.55Cr-0.47Mo-0.07V
Form	Forgings < 4-inch Cross Section(a)
Condition	Quenched and Tempered
F_{tu}, ksi (Min)(b)	150
F_{ty}, ksi (Min)	140
e, percent (Min)	13
RA, percent (Min)	40
Charpy-V, RT (Min)	50

(a) ASTM A579 Grade 12.
(b) Tensile and impact properties at 1/4 thickness.

TABLE 3.013. LONGITUDINAL TENSILE AND IMPACT PROPERTIES SPECIFIED BY ASTM (69)

Alloy	Fe-0.11C-5Ni-0.55Cr-0.47Mo-0.07V					
Direction	L & T					
Form	Plate				Forgings	
Thickness, inch	≤5/8		>5/8 to 4		≤4	
Condition	Hy 130	Hy 140	Hy 130	Hy 140	Hy 130	Hy 140
F_{ty}, ksi	130 to 150	140 to 160	130 to 145	140 to 155	130 to 145	140 (Min)
e (2 inch), percent (Min)	14	14	15	15	15	15
RA, percent (Min)	–	–	55L 50T	55L 50T	50	50
Charpy-V, ft-lb at 0 F (Min)	60	50	60	50	60	50

(a) For forgings properties are longitudinal for plate types and tangential for ring types.

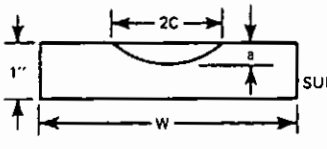
TABLE 3.014. PRODUCERS SPECIFICATION FOR MINIMUM MECHANICAL PROPERTIES FOR PLATE AND FORGINGS (49)

Alloy	Fe-0.11C-5Ni-0.55Cr-0.47Mo-0.07V			
Condition	1500 F, 2 hour, WQ + 1075 F, 2 hour, WQ			
Form	Air Melt 2-inch Plate			Vac. Induction Melt 2-inch Plate
Direction	L	T	ST	ST
F_{tu}, ksi	149	149	147	149
F_{ty}, ksi	142	142	141	140
e (1 inch), percent	–	–	7	17
e (2 inch), percent	20	20	–	–
RA, percent	65	59	23	61

TABLE 3.0214. EFFECT OF TESTING DIRECTION ON TENSILE PROPERTIES OF AIR AND VACUUM MELTED PLATE [(10) TABLE 3]

Alloy	Fe-0.11C-5Ni-0.55Cr-0.47Mo-0.07V		
Form	1-inch Plate		
Condition	Quenched and Tempered to F_{ty} = 143 ksi		
Environment	Air		3-1/2 percent NaCl(a)
Flaw Size			
a, inch	0.401	0.495	0.500
2C, inch	1.04	2.13	2.11
a/ϕ^2	0.21	0.36	0.34
W, inch	3	5	5
Notch, Yield Strength Ratio	1.05	1.09	1.08

(a) Specimen held 1 hour net stress of 130 ksi with no crack growth.



SURFACE CRACK SPECIMEN

TABLE 3.02722. SURFACE CRACK STRENGTH OF PLATE IN AIR AND IN SALT SOLUTION [(39) TABLE 12]

	Fe
5	Ni
0.55	Cr
0.47	Mo
0.075	V

5 Ni Cr Mo V

Alloy	Fe-0.11C-5Ni-0.55Cr-0.47Mo-0.07V											
Form	1/2-inch Plate (300 lb Lab Heats)[b]											
Condition	1500 F, 1 hour, [a] + 1100 F [a]											
Composition	Normal (See Table 1.04)						Modified 0.25Mn, 5.76Ni, 0.76Cr					
Stress Relief	None		1025 F, 25 hour; Cool 200 F/hour				None			1025 F, 25 hour; Cool 200 F/hour		
Simulated[a] Thickness, inch	1/2	4 1/2	6	1/2	4 1/2	6	1/2	4 1/2	6	1/2	4 1/2	6
F_{ty}, ksi	142	120	103	139	130	115	138	126	113	135	122	119
Charpy-V, ft-lbs												
+80 F	79	88	84	50	70	82	98	82	83	106	94	100
0 F	76	84	60	32	43	53	99	84	79	99	93	95

(a) Simulated by controlled cooling rate.
(b) Both heats low in temper embrittling elements (0.003As, 0.001Sb, 0.002Sn).

TABLE 3.03312. EFFECT OF STRESS RELIEF ON LOW TEMPERATURE IMPACT STRENGTH OF NORMAL AND LOW MANGANESE LABORATORY HEATS OF VARIOUS THICKNESS PLATES [(30) TABLE 13]

Alloy	Fe-0.11C-5Ni-0.55Cr-0.47Mo-0.07V			
Form	2-inch Plate, F_{ty} = 141 ksi L			
Condition	A[a] As Rec'd	B A + 1.5% Strain	C A + 1025 F 24 hr, FC	D B + C
Charpy-V 0 F, ft-lb	90	80	37	20

(a) 1510 F, 2 hour, WQ + 1050 F, 2 hour, WQ.

TABLE 3.03316. EFFECT OF PLASTIC DEFORMATION ON STRESS RELIEF EMBRITTLEMENT [(60) Figure 17]

Alloy	Fe-0.11C-5Ni-0.55Cr-0.47Mo-0.07V				
Form	Air Melt 4 x 12 x 12-inch Plate Casting				
Condition	1700 F, 7 hour, WQ + 1500 F, 2 hour, WQ + 1080 F, 2 hour, WQ				
Composition	Normal Mn & Al		Low Mn (0.22 to 0.25 Percent)		
	0.07S[c] 0.022Al	0.015S 0.020Al	0.002S 0.005Al	0.002S 0.027Al	0.015S 0.017Al
Cooling Rate[a]	Normal	Slow	Slow	Slow	Slow
F_{tu}, ksi	155	145 to 156	141 to 156	143 to 158	–
F_{ty}, ksi	143 to 146	136 to 149	133 to 147	139 to 149	–
Charpy-V at[d], ft-lb	42 to 58	25 to 40	40 to 75	29 to 69	5 to 24

(a) Normal, cooled in mold.
(b) Slow, cooled in mold insulated with Vermiculite.
(c) 1 x 6 x 6-inch plate casting.
(d) Zero degrees F.

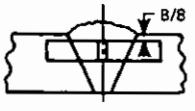
TABLE 3.03318. EFFECT OF MOLD COOLING RATE ON ZERO DEGREES F IMPACT STRENGTH OF PLATE CASTINGS WITH NORMAL AND LOW MANGANESE CONTENT AND WITH NORMAL AND HIGH SULPHUR CONTENT [(7) TABLE 3]

Alloy	Fe-0.11C-5Ni-0.55Cr-0.47Mo-0.07V		
Form	Ring Forging 41-inch OD, 6-inch Wall, 40-inch Longitudinal (Vacuum Degas)		
Condition	1490 F, 3 hour WQ + 500 F, 6 hour + 1050 F, 6 hour, WQ		
Location	Longitudinal	Radial	Tangential
F_{tu}, ksi	152	149	152
F_{ty}, ksi	143	137	145
e (2 inch), percent	17	16	18
RA, percent	61	47	63
Charpy-V at 0 F, ft-lb	48	43	55

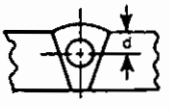
TABLE 3.0332. EFFECT OF TEMPERING TEMPERATURE ON ZERO DEGREES F IMPACT STRENGTH OF FORGING FOR SEVERAL TESTING DIRECTIONS [(6) TABLE 3]

Alloy	Fe-0.11C-5Ni-0.55Cr-0.47Mo-0.07V	
Condition	GMA Weld (For Conditions See Tables 4.0312 and 4.03116)	SMA (Covered Electrode) Weld (For Conditions See Tables 4.0312 and 4.03116)
Form	1-inch Plate	1/2 & 1-inch Plate[a]
F_{ty}, min, ksi	135	135
e (2 inch), percent (Min)	14	14
Charpy-V ft-lb (Min)		
+30 F	50	40
−60 F	20	20

(a) 5/32 and 3/16 diameter electrodes for 1-inch plate
1/8-inch diameter electrodes for 1/2-inch plate.



IMPACT SPECIMEN LOCATION



TENSILE SPECIMEN LOCATION
d = 3/8 for 1-inch Plate and 1/4 for 1/2-inch Plate

TABLE 4.0311. MINIMUM MECHANICAL PROPERTIES FOR GMA AND SMA WELDMENTS [(1) PP 34-73]

Alloy	Fe-0.11C-5Ni-0.55Cr-0.47Mo-0.07V	
Form	GTA or GMA Base Electrode[a]	
Wire Composition	Weight Percent	
	Min	Max
C	–	0.12
Mn	1.50	2.0
P	–	0.010
S	–	0.010
Si	0.30	0.50
Cw	–	0.15
Ni	1.95	3.10
Cr	0.65	1.05
Mo	0.40	1.00
V	–	0.04
Ti	–	0.04
Zr	–	0.04
Al	–	0.04
H_2	–	<3 ppm

(a) MIL-1405, GMA automatic or semi-automatic welding. All position welding with pulsed arc. Flat or horizontal with pulsed and spray arc.

TABLE 4.03111. COMPOSITION BY WEIGHT OF BASE WIRE ELECTRODES FOR GTA OR GMA WELDING OF HY130 TO HY130 (57)

Alloy	Fe-0.11C-5Ni-0.55Cr-0.47Mo-0.07V			
Form	GTA or GMA Bare Electrode[a]			
Type	MIL 100S-1		MIL 120S-1	
Composition	Weight Percent			
	Min	Max	Min	Max
C	–	0.08	–	0.10
Mn	1.25	1.80	1.40	1.80
Si	0.20	0.55	0.25	0.60
P	–	0.01	–	0.01
S	–	0.01	–	0.01
Ni	1.40	2.10	2.00	2.80
Mo	0.25	0.55	0.30	0.65
Cr	–	0.30	–	0.60
V	–	0.05	–	0.03
Al	–	0.10	–	0.10
Ti	–	0.10	–	0.10
Zr	–	0.10	–	0.10

(a) For welding Hy130 to HY130 see footnote (a) on Table 4.03111. All positions for HY130 to other steels.

TABLE 4.03112. COMPOSITION BY WEIGHT OF BARE WIRE ELECTRODES FOR WELDING HY130 TO HY130 OR TO OTHER STEELS WITH LESS THAN 0.30C (65)

Fe
5 Ni
0.55 Cr
0.47 Mo
0.075 V

5 Ni Cr Mo V

Alloy	Fe-0.11C-5Ni-0.55Cr-0.47Mo-0.07V	
Form	MIL14018 SMA Covered Electrode[a]	
Deposited Weld Metal Composition	Weight Percent	
	Min	Max
C	–	0.10
Mn	0.75	1.35
P	–	0.13
S	–	0.10
Si	–	0.65
Ni	3.10	3.90
Cr	0.35	1.20
Mo	0.30	1.10
V	–	0.09

(a) Water content of coating <0.10% by weight total. Iron content of coating including combined iron <15%.

TABLE 4.03113. COMPOSITION BY WEIGHT OF WELD METAL DEPOSITED BY SMA PROCESS SPECIFIED FOR ALL POSITION WELDING OF HY130 TO HY130 (58)

Alloy	Fe-0.11C-5Ni-0.55Cr-0.47Mo-0.07V	
Form	MIL-B88, GMA Bare Electrode	
Wire Composition	Weight Percent	
	Min	Max
C	–	0.08
Mn	1.15	1.55
P	–	0.025
S	–	0.025
Si	0.35	0.65
Ni	1.15	1.55
Mo	0.30	0.60
V	0.10	0.20

TABLE 4.03114. COMPOSITION BY WEIGHT OF BARE WIRE ELECTRODES FOR FLAT OR HORIZONTAL SPRAY GMA WELDING OF HY130 TO LOW STRENGTH STEELS WITH LESS THAN 0.30C (66)

Alloy	Fe-0.11C-5Ni-0.55Cr-0.47Mo-0.07V					
Form	SMA Covered Electrode					
Type	MIL 9018 (70)		MIL 11018 (70)		MIL 12018 (71)	
Deposited Weld Metal Composition	Weight Percent					
	Min	Max	Min	Max	Min	Max
C	–	0.10	–	0.10	–	0.10
Mn	0.60	1.25	1.30	1.80	0.80	1.60
Si	–	0.80	–	0.60	–	0.65
P	–	0.030	–	0.030	–	0.015
S	–	0.030	–	0.030	–	0.010
Cr	–	0.15	–	0.40	0.50	0.65
M	1.40	1.80	1.25	2.50	3.00	3.80
Mo	–	0.35	0.25	0.50	0.30	0.90
V	–	0.05	–	0.05	–	0.05

TABLE 4.03115. COMPOSITION BY WEIGHT OF WELD METAL DEPOSITED BY SMA PROCESS SPECIFIED FOR WELDING HY130 TO HY130 OR TO OTHER STEELS WITH LESS THAN 0.30C (70) (71)

	Fe
5	Ni
0.55	Cr
0.47	Mo
0.075	V

5 Ni Cr Mo V

Alloy	Fe-0.11C-5Ni-0.55Cr-0.47Mo-0.07V	
Form	SMA Covered Electrode	
Type	MIL 14018Ht Class 2	
Deposited Weld Metal Composition	Weight Percent	
	Min	Max
C	0	0.10
Mn	0.40	0.80
P	–	0.013
S	–	0.010
Si	–	0.50
Ni	7.00	9.00
Cr	0.05	0.60
Mo	0.40	0.70
V	0.04	0.10

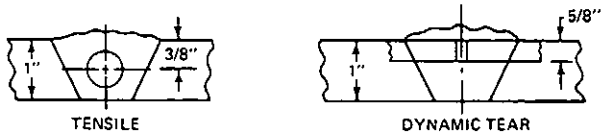
TABLE 4.03116. COMPOSITION BY WEIGHT OF WELD METAL DEPOSITED BY SMA PROCESS SPECIFIED FOR PRODUCING HORIZONTAL FILLETS AND FLAT WELDMENTS OF HY130 WHICH ARE TO BE HEAT TREATED (74)

Alloy	Fe-0.11C-5Ni-0.55Cr-0.47Mo-0.07V					
Welding Process	Gas Metal Arc (1)(4)(5)				SMA (2)(3)	
Wire Composition	Weight Percent					
	Min	Max	Min	Max	Min	Max
C	–	0.12	–	0.12	–	0.10
Mn	1.65	2.00	1.50	1.50	1.50	2.00
P	–	0.010	–	0.010	–	0.010
S	–	0.010	–	0.010	–	0.010
Si	0.30	0.50	0.30	0.50	–	0.50
Cu	–	0.15	–	0.15	–	–
Ni	1.80	2.20	2.50	2.90	2.00	2.75
Cr	0.80	1.05	0.50	0.70	0.50	1.00
Mo	0.40	0.60	0.75	0.95	0.30	0.60
V	–	0.04	–	0.04	–	0.05
Ti	–	0.04	–	0.04	–	–
Zr	–	0.04	–	0.04	–	–
Al	–	0.04	–	0.04	–	–
H	–	0.0003	–	0.0003	–	–

(1) Wire composition.
(2) Composition of weld deposit (welded with coated electrode).
(3) Coating <0.10 percent H_2O, total metallics >15 percent.
(4) Gas 1 to 2 percent O_2 + Argon.
(5) Two compositions shown are used interchangeable.

TABLE 4.03117. WIRE COMPOSITIONS BY WEIGHT FOR WELDS USED IN PRODUCERS WELDMENT DEVELOPMENT STUDIES [(1) P. 37, 51 & 56]

Alloy	Fe-0.11C-5Ni-0.55Cr-0.47Mo-0.07V
Form	Weld Metal Deposited by Automatic GTA or Semi-automatic & Automatic GMA with Spray or Pulsed Spray Arc See Table 4.03111.
	Minimum Mechanical Properties
F_{ty}, ksi	135 to 150
e (2 inch), percent	14
5/8-inch Dynamic Tear at 30 F, ft-lb (ASTM E604)	500



Specimen Locations in 45° Butt Welds

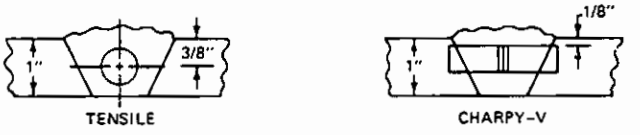
TABLE 4.03118. MINIMUM MECHANICAL PROPERTIES OF DEPOSITED GTA & GMA WELD METAL FOR JOINING HY 130 TO HY 130 OR TO OTHER STEELS WITH LESS THAN 0.3 C (57)

Alloy	Fe-0.11C-5Ni-0.55Cr-0.47Mo-0.07V	
Form	Weld Metal Deposited by Automatic or Semi-automatic GMA Spray or Pulsed Spray Arc (See Table 4.03112)	
	Minimum Mechanical Properties[a]	
Electrode Type	100S-1	120S-1
F_{ty}, ksi	88 – 102	105 – 122
e (2 inch), percent (Min)	16	14
Charpy-V at -60 F, ft-lbs	50	50
5/8-inch Dynamic Tear at -60 F, ft-lb	--	450

(a) MIL-E-23765/2A

Fe
5 Ni
0.55 Cr
0.47 Mo
0.075 V

5 Ni Cr Mo V



Specimen Locations in 45° Butt Welds
Dynamic Tear Specimen in Charpy Location

TABLE 4.03119. MINIMUM MECHANICAL PROPERTIES OF DEPOSITED GTA & GMA WELD METAL FOR ELECTRODE. COMPOSITIONS SPECIFIED FOR FILLET WELDING OF HY130 TO HY130 AND FOR ALL WELDED JOINTS BETWEEN HY130 AND LOWER STRENGTH STEELS WITH LESS THAN 0.30C (65)

Alloy	Fe-0.11C-5Ni-0.55Cr-0.47Mo-0.07V
Form	SMA Weld Metal[a] (See Table 4.03113)
	Minimum Mechanical Properties
F_{ty}, ksi	135 – 150
e (2 inch), percent	14
5/8-inch Dynamic Tear at -60 F, ft-lb	475

(a) See Table 4.03118 for specimen location.

TABLE 4.031110. MINIMUM MECHANICAL PROPERTIES OF DEPOSITED SMA WELD METAL SPECIFIED FOR JOINING HY130 TO HY130 (58)

Alloy	Fe-0.11C-5Ni-0.55Cr-0.47Mo-0.07V		
Form	SMA Weld Metal (See Table 4.03115)		
	Minimum Mechanical Properties[a]		
Type	MIL 9018	MIL 11018	MIL 12018-MI
F_{tu}, ksi	90	110	--
F_{ty}, ksi	78 – 90	95 – 107	108 – 120
Charpy-V, ft-lbs			
at -60 F	20	20	--
at 0 F	--	--	50
at RT	--	--	75

(a) For specimen location see Table 4.03119.

TABLE 4.031112. MINIMUM MECHANICAL PROPERTIES OF DEPOSITED SMA WELD METAL FOR ELECTRODE COMPOSITIONS SPECIFIED FOR FILLET WELDING HY130 to HY130 AND FOR WELDING HY130 TO LOWER STRENGTH STEELS WITH LESS THAN 0.30 C (70) (71)

Alloy	Fe-0.11C-5Ni-0.55Cr-0.47Mo-0.07V
Form	Weld Metal Deposited by GMA Semi-automatic & Automatic Spray Process (See Table 4.03114)
	Minimum Mechanical Properties
Hardness, VPN, 10 kg	260 – 300
F_{ty}, ksi	88
e, percent	14
Charpy-V at 30 F, ft-lb	20

(a) For specimen location see Table 4.03119.

TABLE 4.031111. MINIMUM MECHANICAL PROPERTIES OF DEPOSITED GMA WELD METAL FOR ELECTRODE COMPOSITION SPECIFIED FOR JOINING HY130 TO LOWER STRENGTH STEELS WITH LESS THAN 0.30 C (66)

Alloy	Fe-0.11C-5Ni-0.55Cr-0.47Mo-0.07V
Form	Weld Metal Deposited by SMA Process and Heat Treatment[a]
	Minimum Mechanical Properties
F_{ty}, ksi	135 – 150
e (1.4 or 2 in.)	14
5/8 in. Dynamic[b] Tear at 30 F, ft-lb	475

(a) See Table 4.03116 for electrode composition and Table 4.03123 for welding conditions.
(b) See Figure 4.03118 for location of dynamic tear specimen.

TABLE 4.031113. MINIMUM MECHANICAL PROPERTIES OF DEPOSITED SMA WELD METAL AFTER REHEAT TREATMENT OF HY130 WELDMENT (74)

	Fe
5	Ni
0.55	Cr
0.47	Mo
0.075	V

5 Ni Cr Mo V

Alloy	Fe-0.11C-5Ni-0.55Cr-0.47Mo-0.07V	
Weld Process	GMA D.C. Reverse Polarity	SMA Covered Electrode D.C. Reverse Polarity(b)
Form(a)	1-inch Plate	1/2 and 1-inch
Equipment	Manual or Automatic	
Wire Composition	See Table 4.03117	See Table 4.03117
Preheat and Interpass Temp, F	200 to 225	125 to 175 (1/8-inch Electrode) 225 to 275 (5/32 & 3/16 Electrode)
Maximum Heat Input, J/inch	45,000	40,000
Position	Flat	Flat

(a) For details of welding procedure for other plate thickness see (1).
(b) 750 F to 800 F baking required, see (1)

TABLE 4.0312. RECOMMENDED WELDING CONDITIONS FOR GMA AND SMA PLATE WELDING (1)

Alloy	Fe-0.11C-5Ni-0.55Cr-0.47Mo-0.07V							
Form	SMA Welds with E14018 Electrode (See Table 4.03113)							
Category	Weld Thickness, inch	Repair Depth, inch	Min Excavation Soak		Min Interweld(b) Soak		Min Post Weld(a) Soak	
			Temp, F	Time, hr	Temp, F	Time, hr	Temp, F	Time, hr
Original Welds	≤1/2	–	–	–	–	–	250	4
	>1/2	–	–	–	250	10	350	12
Repairs For Cracks	≤1/2	All	250	4	–	–	250	4
	>1/2	≤1/2	250	4	–	–	350	8
		>1/2	350	6	250	10	350	12
Repairs Other Than Cracks	All	≤1/2	None	–	None	–	250	4
		>1/2	None	–	250	10	350	12
Interruption of Preheat	≤1/2	–	–	–	–	–	250	4
	>1/2	–	–	–	–	–	350	12

(a) No post weld soak required if interweld soak is used.
(b) Soak for each 1/2-inch or less of weld deposited on any one side of joint.

TABLE 4.03121. SMA WELD HYDROGEN REMOVAL TREATMENTS (56)

Alloy	Fe-0.11C-5Ni-0.55Cr-0.47Mo-0.07V							
Weld Process	GMA Automatic or Semi-automatic				SMA			
Thickness, inch	≤5/8		>5/8		≤5/8		>5/8	
Preheat & Interpass Temp, F	150 – 200		150 – 300		150 – 200		200 – 300	
Weld Process	GMA & SMA(a)							
Thickness, t, inch	1/2 < t < 3/4		3/4 < t < 1-1/4		t > 1-1/4		Unequal(b)	
Heat Input, kJ/inch	Min	Max	Min	Max	Min	Max	Min	Max
	30	40	30	40	30	50	30	45

(a) For welding to austenitic stainless or non ferrous alloys 45 kJ/inch (Max) for t < 1/2-inch.
55 kJ/inch (Max) for t > 1/2-inch.
(b) Only if t of one member > 1-1/4-inch.

TABLE 4.03122. SPECIFIED PREHEAT AND INTERPASS TEMPERATURES AND WELDING HEAT INPUTS FOR GMA AND SMA PROCESSES (56)

Alloy	Fe-0.11C-5Ni-0.55Cr-0.47Mo-0.07V
Weld Process	SMA (See Table 4.03116 for Electrode Composition)
Thickness	All
Preheat & Interpass Temp, F (a)	250 - 275
Heat Input, kJ/in.	38 to 42
Heat Treatment(b)	1675 -1725 F, 1 hr/in., WQ + 1475 - 1525 F, 1 hr/in., WQ + 1075 - 1125 F, 1 hr/in., WQ

(a) Interrupted welding must be followed immediately by soaking 250-275 F, 4 hr minimum for welds 1/2 in. thick or less and 350-375 F, 12 hr minimum for thicker welds.
(b) Welds should not be cooled below interpass temperature before heat treatment.

TABLE 4.03123. SPECIFIED PREHEAT, INTERPASS TEMPERATURES, AND WELDING HEAT INPUTS FOR SMA WELDMENTS TO BE HEAT TREATED (74)

	Fe
5	Ni
0.55	Cr
0.47	Mo
0.075	V

5 Ni Cr Mo V

Alloy	Fe-0.11C-5Ni-0.55Cr-0.47Mo-0.07V				
Form	2-inch Plate	1-inch Plate			
Weld	GMA	GTA	GMA	GMA	GMA
Process and Wire	Mn-Ni-Cr-Mo(1)	Mn-Ni-Cr-Mo	5Ni-Cr-Mo-V(2)	Mn-Ni-Cr-Mo	5Ni-Cr-Mo-V
Post Weld	None	None	None	1700 F, 1 hr WQ + 1550 F, 1 hr WQ + 1100 F, 1 hr WQ	1750 F, 1 hr WQ + 1500 F, 1 hr WQ + 1100 F, WQ
F_{tu}, ksi	163	163	156	155	150
F_{ty}, ksi	143	144	136	145	142
RA, percent	46	29(3)	55	64	63
Charpy-V ft-lbs, 80 F	–	72	–	30	62
30 F	46	–	59	14	–
-60 F	23	40	53	–	23

(1) Composition Table 4.03117 (0.31Cu).
(2) Composition Table 1.04.
(3) Porosity.

TABLE 4.03131. EFFECTS OF REHEAT-TREATMENT ON THE MECHANICAL PROPERTIES OF GMA AND GTA WELDS MADE WITH DIFFERENT WIRES [(27) TABLES 5 AND 6]

Alloy	Fe-0.11C-5Ni-0.55Cr-0.47Mo-0.07V			
Form	1-inch Plate			
Condition	GMA Weld(1) 5Ni, Cr, Mo, V Wire (See Table 1.04)			
Post Weld Treatment	None	1750 F, 1 hr WQ + 1500 F, 1 hr WQ + 1125 F, 1 hr WQ	2200 F, 1 hr WQ + 1500 F, 1 hr WQ + 1125 F, 1 hr WQ	2300 F, 1 hr WQ + 1650 F, 1 hr WQ + 1500 F, 1 hr WQ
F_{tu}, ksi	156	148	143	147
F_{ty}, ksi	136	140	136	139
RA, percent	55	61	64	58
Charpy-V at 30 F	59	67	39	35
-60 F	53	24	12	25

(1) For specimen location see Table 4.03119.

TABLE 4.03132. INFLUENCE OF HIGH TEMPERATURE HEAT-TREATMENTS ON THE MECHANICAL PROPERTIES OF GMA WELDS [(27) TABLES 5 AND 6]

Alloy	Fe-0.11C-5Ni-0.55Cr-0.47Mo-0.07V			
Form	Heat Treated Weld Metal - 1700 F, 2 hr WQ + 1500 F, 2 hr WQ + 1100 F, 2 hr WQ			
Welding Conditions	60° Double V Butt Welds in 2-inch Plate Preheat & Interpass 325 – 350 F + Holding Completed Weldment 325 F, 16 hour Min			
	SMA(a) 230 Amps, 24 V 8-11 inch/min 35-40 kJ/inch		GMA(b) 350 Amps, 30 V 11-12 inch/min 50-55 kJ/inch A + 2% O_2	
Specimen Location	Surface	Center	Surface	Center
F_{tu}, ksi	154	152	153	151
F_{ty}, ksi	145	142	142	141
Charpy-V, ft-lbs + 30 F	57	50	55	48
-60 F	50	39	46	46

(a) SMA 0.8C, 0.62Mn, 0.07P, 0.008S, 0.40Si, 7.97Ni, 0.58Cr, 0.53Mo, 0.007V.
(b) GMA 0.11C, 0.52Mn, 0.001P, 0.010S, 0.29 Si, 8.08Ni, 0.50Cr, 0.41Mo, 0.069V.

TABLE 4.03133. TENSILE AND LOW TEMPERATURE IMPACT ENERGY OF HEAT TREATABLE SMA AND GMA WELD METAL [(62) TABLE 14]

	Fe
5	Ni
0.55	Cr
0.47	Mo
0.075	V

5 Ni Cr Mo V

Alloy	Fe-0.11C-5Ni-0.55Cr-0.47Mo-0.07V					
Form	1-inch Plate					
Condition	GMA Weld 5Ni-Cr-Mo-V Wire			Parent Metal		
	As Weld	Weld + S.R.(1)	Weld + S.R. + 1150 F, WQ	No S.R.	S.R. (1)	S.R. + 1150 F, WQ
F_{tu}, ksi	150	133	131	142	139	134
F_{ty}, ksi	131	122	120	134	131	129
RA, percent	59	63	65	70	66	68
Charpy-V at 0 F, ft-lb(2)	77	9	81	86	39	88

(1) S.R. = stress relief 1025 F, 16 hour, cool 200 F/hour.
(2) For specimen location, see Table 4.03119.

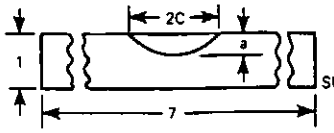
TABLE 4.03136. EFFECT OF STRESS RELIEF AND A STRESS RELIEF RECOVERY TREATMENT ON MECHANICAL PROPERTIES OF GMA WELDS MADE WITH HY130 COMPOSITION WIRE [(29) TABLES 7 AND 8]

Alloy	Fe-0.11C-5Ni-0.55Cr-0.47Mo-0.07V								
Form	2-inch Plate F_{ty} = 139 ksi T								
Specimen Details	2-inch Long x 1/2-inch Wide x t Strained Cracking Tests Weld Parallel to Plate Rolling Direction and Along the 2-inch Plate Center Plane. Following Welding Specimens Were Loaded 24 hours in Bending Jig of Fixed Radius								
Welding Conditions	SMA E14018 Electrode 165 Amps, 22V, 7.5-inch/min, 29 kJ/inch								
Condition of Electrodes(b)	A			B			C		
Specimen Thickness, t, inch(c)	0.2	0.14	0.08	0.2	0.14	0.08	0.2	0.14	0.08
Cracks in Weld Metal(a)	Many	Many	2	Many	2	0	0	0	0
Cracks in HAZ	Deep	0.2	0	Deep	0	0	0	0	0

(a) Cracks originated in weld metal grain boundaries and propagated into HAZ.
(b) A - Fully wet B - Long time air exposure C - Baked 750 F, 1 hour.
For electrode composition see Table 4.03117.
(c) Strain at outer fibers, $\Sigma = 0.01$ for $5 = 0.2$, $\Sigma = 0.0035$ for t = 0.14, $\Sigma = 0.001$ for t = 0.08-inch.

TABLE 4.03137. RESULTS OF STRAIN AUGMENTED CRACKING TESTS FOR SEVERAL SMA ELECTRODE CONDITIONS AND APPLIED STRAINS FOLLOWING WELDING [(64) TABLE 2]

Alloy	Fe-0.11C-5Ni-0.55Cr-0.47Mo-0.07V			
Form	1-inch Plate (F_{ty} = 137 ksi)			
Condition	1500 F, 1 hr WQ + 1140 F, 1 hr WQ + GTA Weld 0.062-inch Diameter, 5Ni-Cr-Mo-V Wire, 40 Passes, 200 F Preheat, F_{ty} = 150 ksi			
Type of Test	Static		Sustained Load Gross Stress = 109 ksi	
Environment	Air		3.5 percent NaCl	
Flaw Location	Weld Centerline	HAZ	Weld Centerline	HAZ
Flaw Size, 2C, inch	2.25	2.28	2.22	7.37
a, inch	0.65	0.62	0.67	0.65
Failure Time, hr	–	–	20.2	24.1
Net Fracture Strength, ksi	145	145	134	151



SURFACE CRACK SPECIMEN

TABLE 4.0341. SURFACE CRACK STRENGTH OF GTA WELDMENTS TESTED IN AIR IN 3.5 PERCENT NaCl [(33) TABLE 17]

Alloy	Fe-0.11C-5Ni-0.55Cr-0.47Mo-0.07V											
Form	1/2-inch Plate											
Condition	1500 F, 1 hour WQ + 1120 F, 1 hour WQ + GMA Weld											
Environment	Flowing Water			Tide Zone			Total Immersion			Marine(2) Atmosphere		
Location(3)	P	HAZ	W	P	HAZ	W	P	HAZ	W	P	HAZ	W
Average Metal Loss in 2 Years, mil	15	10	22	3	2	9	7.5	3	5	1	1	1

(1) Tested as 4 x 12-inch specimens.
(2) Kure beach 80 ft lot.
(3) P - parent metal, HAZ - heat affected zone, W - weld metal.

TABLE 4.0351. GENERAL CORROSION OF PARENT METAL, WELD METAL AND HAZ IN SEA WATER [(14) FIGURES 9, 10 AND 11]

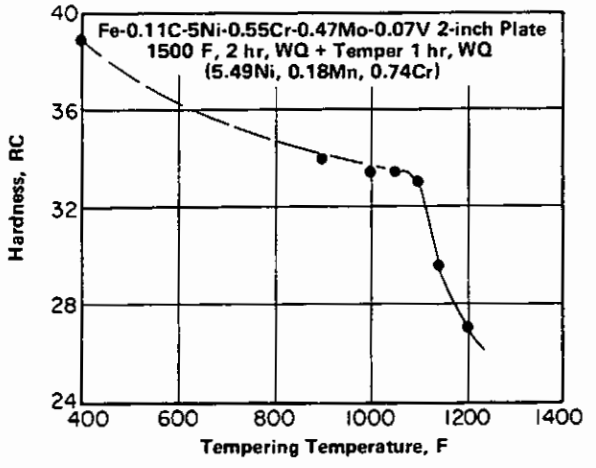


FIGURE 1.061. EFFECT OF TEMPERING TEMPERATURE ON HARDNESS OF STRESS RELIEVABLE PLATE [(31) TABLE 13]

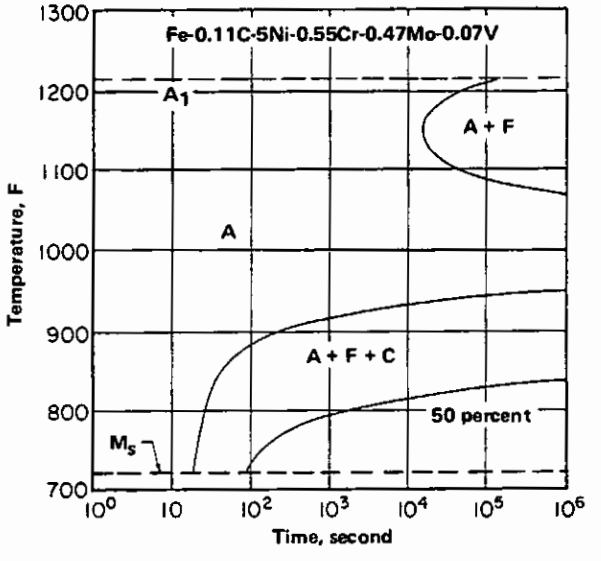


FIGURE 2.0121. ISOTHERMAL TRANSFORMATION DIAGRAM [(1) FIG. 25]

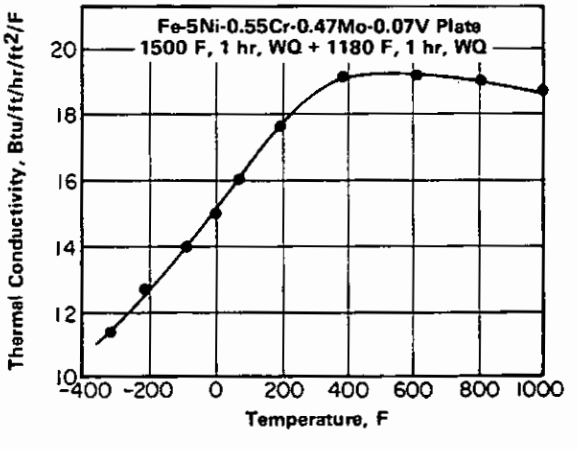
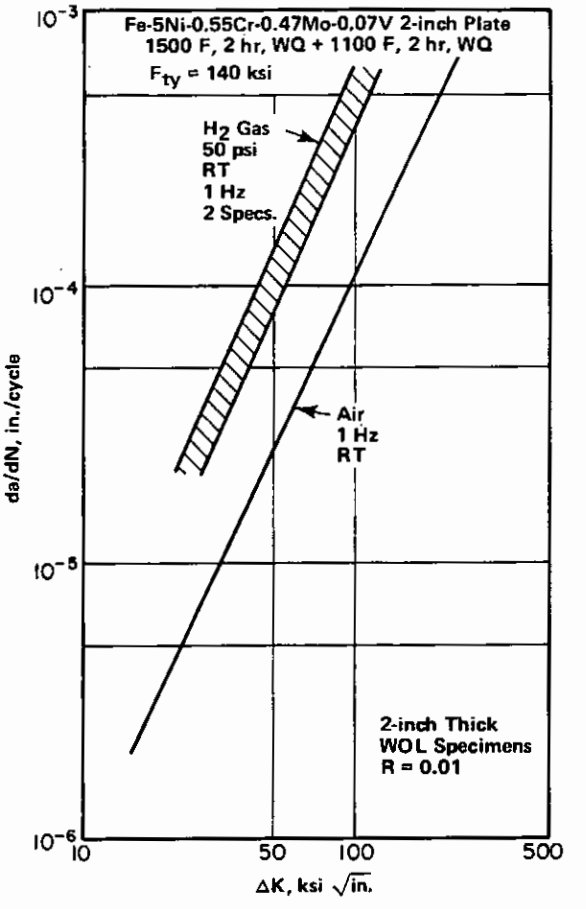


FIGURE 2.013. THERMAL CONDUCTIVITY [(73) TABLE 21]



	Fe
5	Ni
0.55	Cr
0.47	Mo
0.075	V

5 Ni Cr Mo V

FIGURE 1.0931. EFFECT OF LOW PRESSURE DRY HYDROGEN (-76 F DEW POINT) ON FATIGUE CRACK GROWTH RATES OF PLATE [(72) P 158]

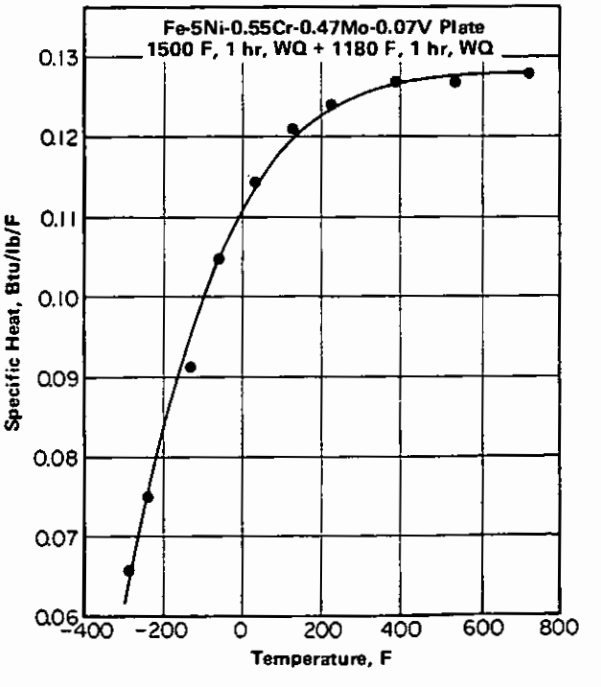


FIGURE 2.015. SPECIFIC HEAT [(73) TABLE 4]

	Fe
5	Ni
0.55	Cr
0.47	Mo
0.075	V

5 Ni Cr Mo V

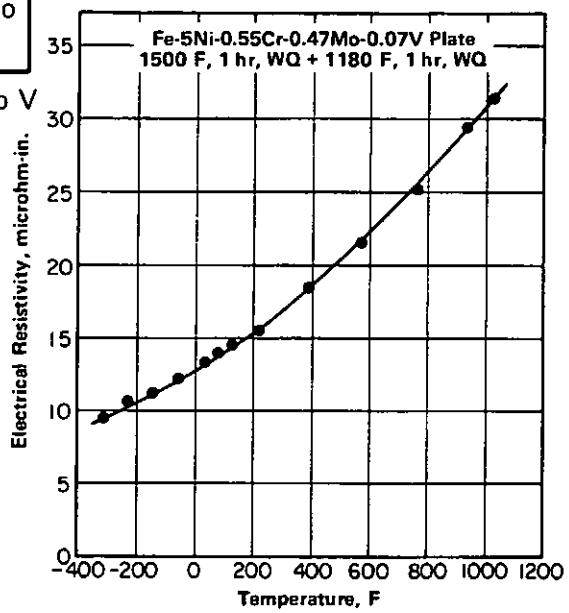


FIGURE 2.0221. ELECTRICAL RESISTIVITY [(73) TABLE 2B]

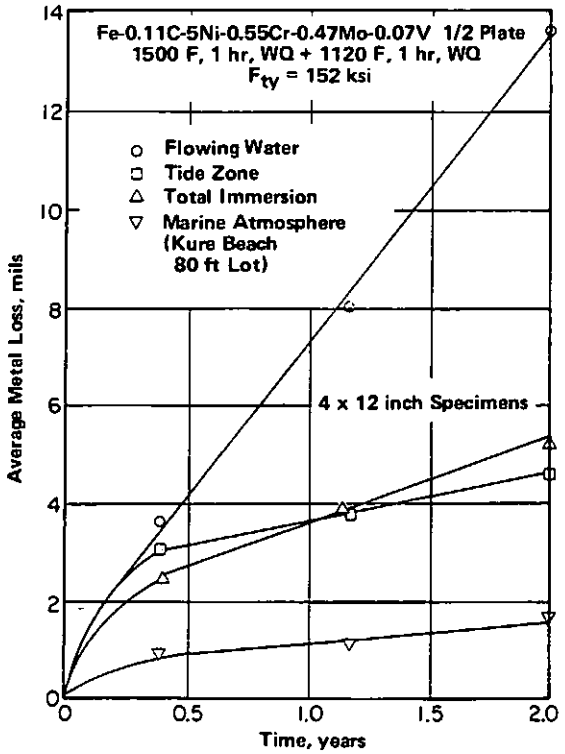


FIGURE 2.032. GENERAL CORROSION OF PLATE IN MARINE ENVIRONMENTS [(14) FIG. 8]

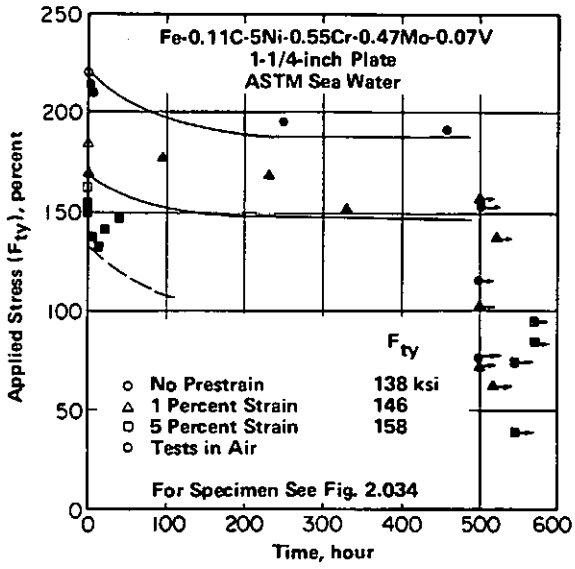


FIGURE 2.033. SUSTAINED LOAD CRACK FAILURE BEHAVIOR OF PLATE IN ARTIFICIAL SEA WATER AS INFLUENCED BY PLASTIC STRAIN [(25) TABLES A6 - A8]

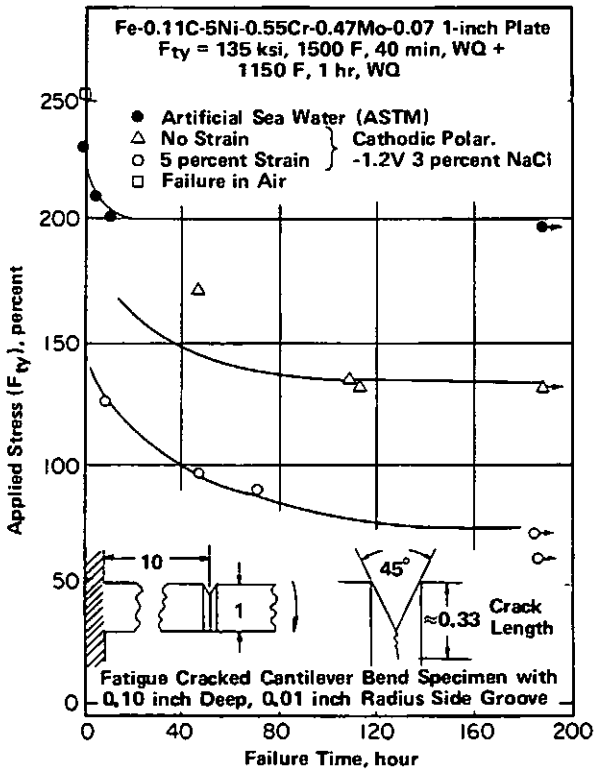


FIGURE 2.034. SUSTAINED LOAD CRACK FAILURE BEHAVIOR OF PLATE IN ARTIFICIAL SEA WATER AND SUBJECTED TO CATHODIC POLARIZATION [(24) FIG. 6]

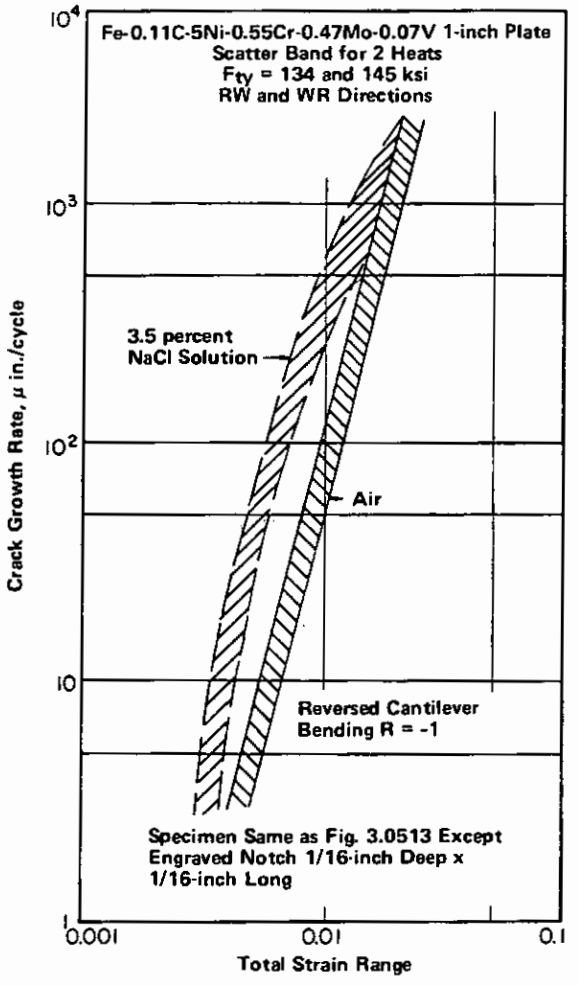


FIGURE 2.035. CRACK GROWTH RATE SCATTER BANDS FOR PLATE SUBJECTED TO REVERSED BENDING IN AIR AND 3.5 PERCENT NaCl [(43) FIG. 4]

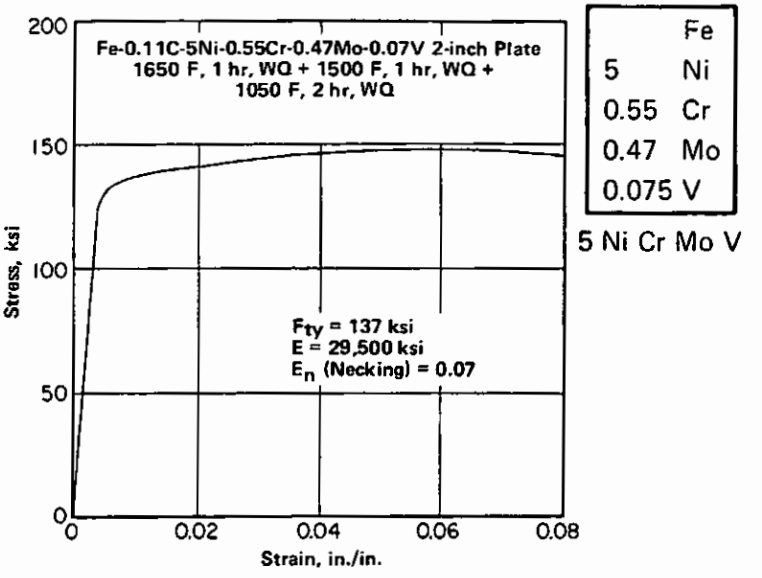


FIGURE 3.0211. STRESS-STRAIN CURVE FOR PLATE [(1) FIG. 11]

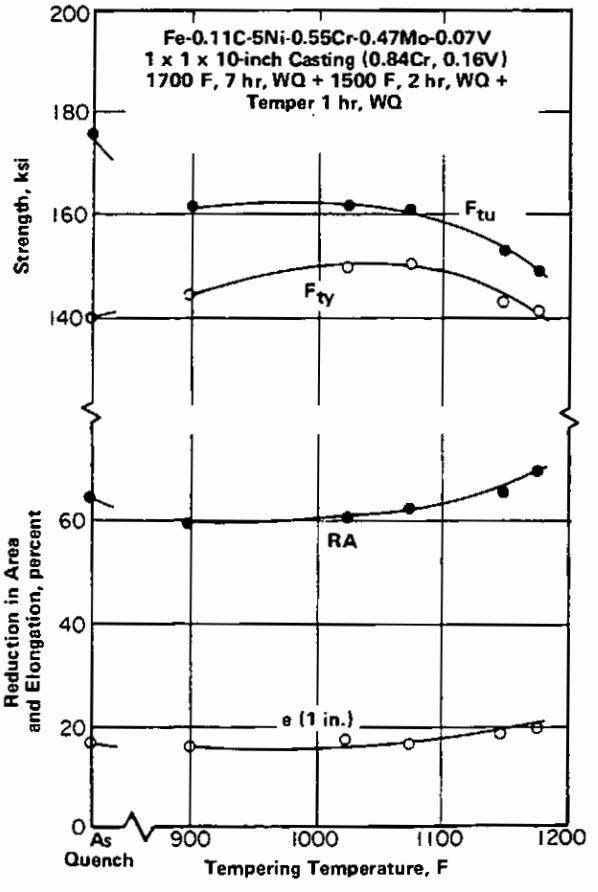


FIGURE 3.0212. EFFECT OF TEMPERING TEMPERATURE ON TENSILE PROPERTIES OF CASTING [(16) TABLE 7]

	Fe
5	Ni
0.55	Cr
0.47	Mo
0.075	V

5 Ni Cr Mo V

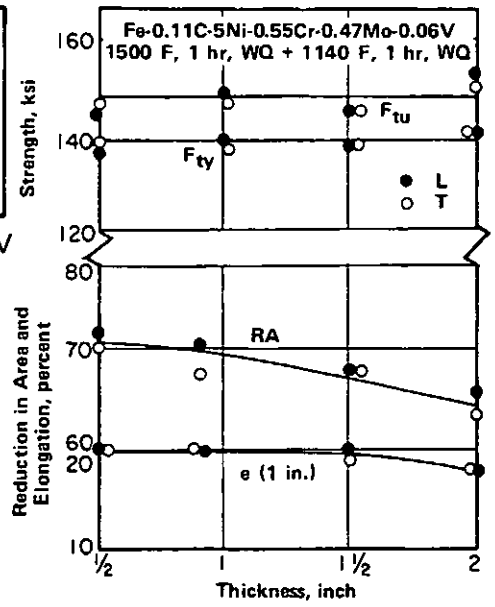


FIGURE 3.0213. EFFECT OF PLATE THICKNESS ON THE TENSILE PROPERTIES [(1) TABLE 14]

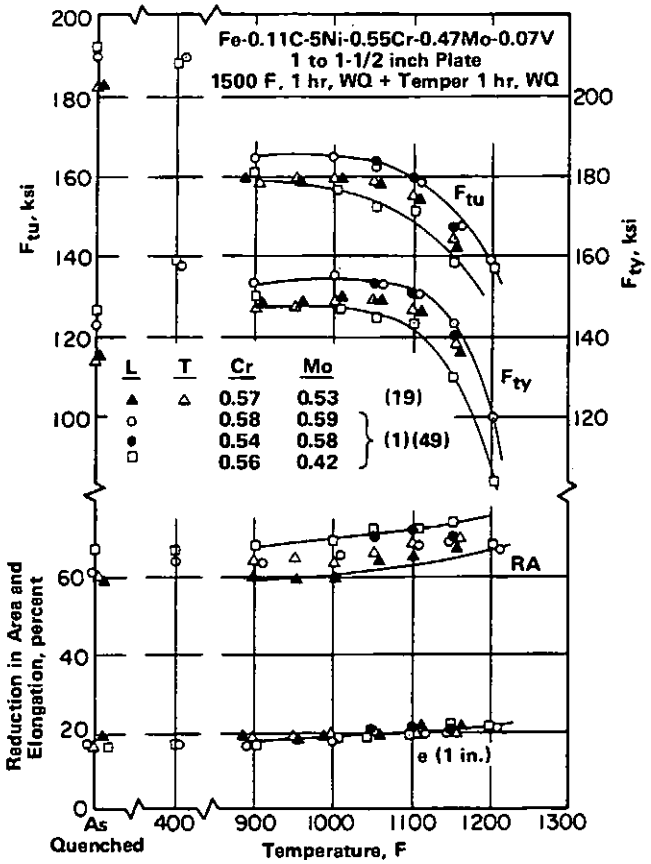


FIGURE 3.0215. EFFECT OF TEMPERING TEMPERATURE ON TENSILE PROPERTIES OF PLATE FROM SEVERAL HEATS (49)(19)

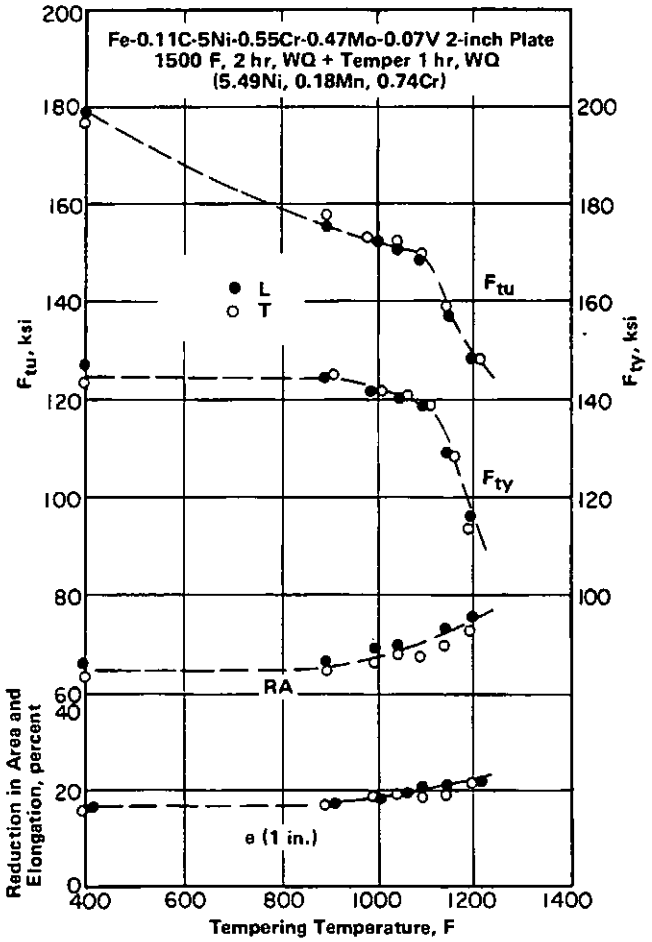


FIGURE 3.0216. EFFECT OF TEMPERING TEMPERATURE ON TENSILE PROPERTIES OF STRESS RELIEVABLE PLATE [(31) TABLE 3]

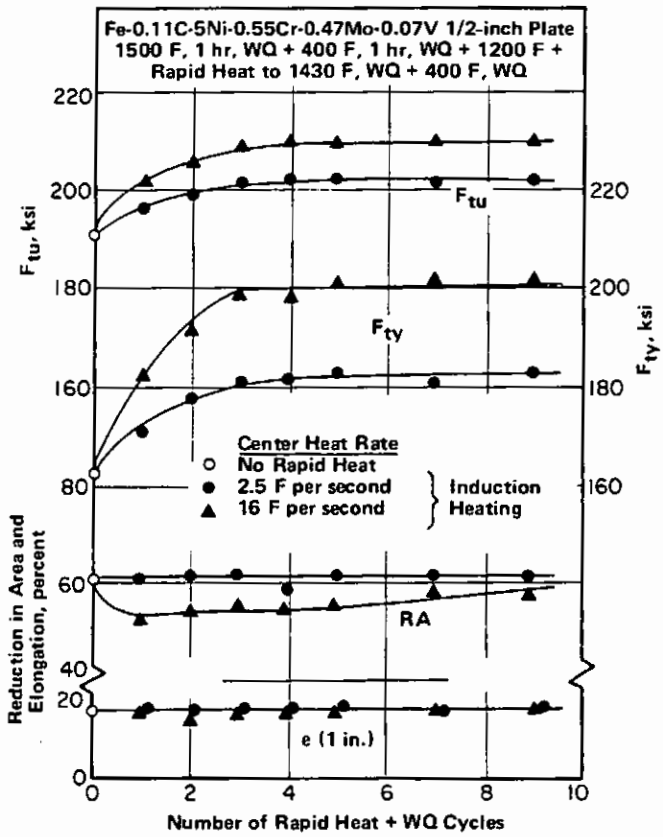


FIGURE 3.0217. EFFECT OF RAPID AUSTENITIZING ON TRANSVERSE TENSILE PROPERTIES OF PLATE [(17) TABLE 3]

	Fe
5	Ni
0.55	Cr
0.47	Mo
0.075	V

5 Ni Cr Mo V

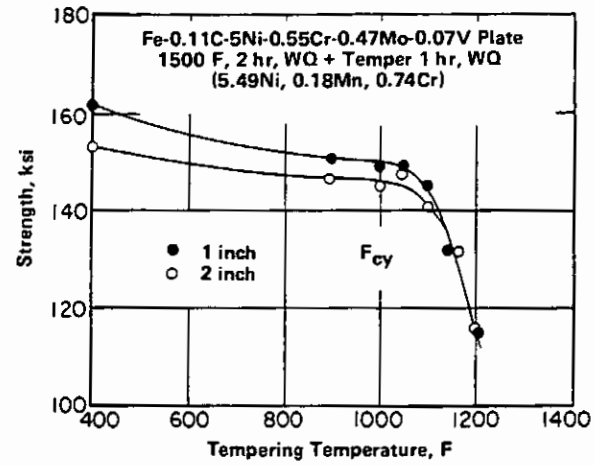


FIGURE 3.0222. EFFECT OF TEMPERING TEMPERATURE ON LONGITUDINAL COMPRESSIVE YIELD STRENGTH OF STRESS RELIEVABLE PLATE [(31) TABLE 13]

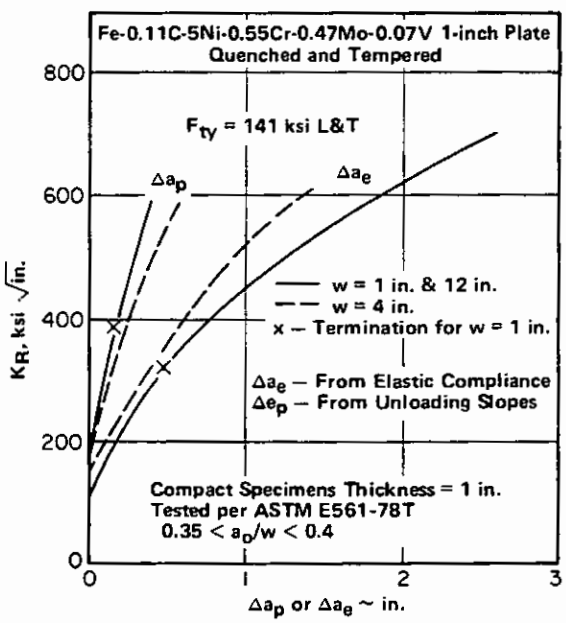


FIGURE 3.02723. R CURVES FOR PLATE [(53) FIGURES 7, 8, AND 10]

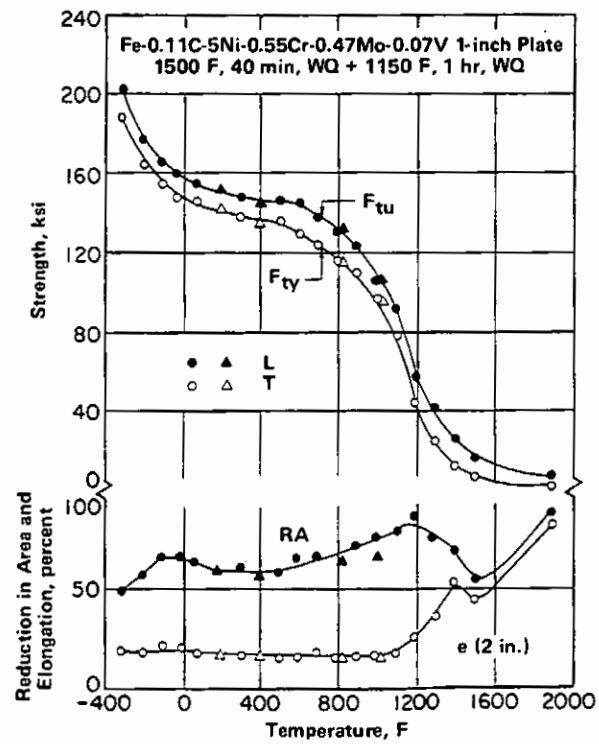


FIGURE 3.0312. EFFECT OF TEST TEMPERATURE ON TENSILE PROPERTIES OF PLATE [(9) TABLES 5 AND 6]

	Fe
5	Ni
0.55	Cr
0.47	Mo
0.075	V

5 Ni Cr Mo V

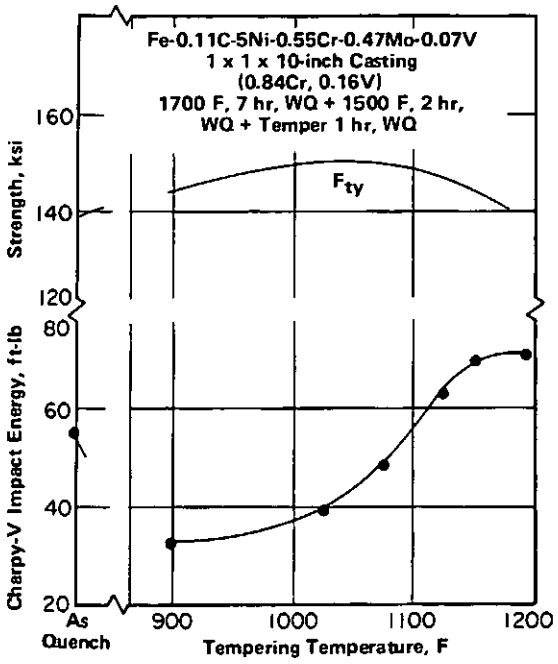


FIGURE 3.0331. EFFECT OF TEMPERING TEMPERATURE ON THE ZERO DEGREES F IMPACT STRENGTH OF CASTINGS [(16) TABLE 7]

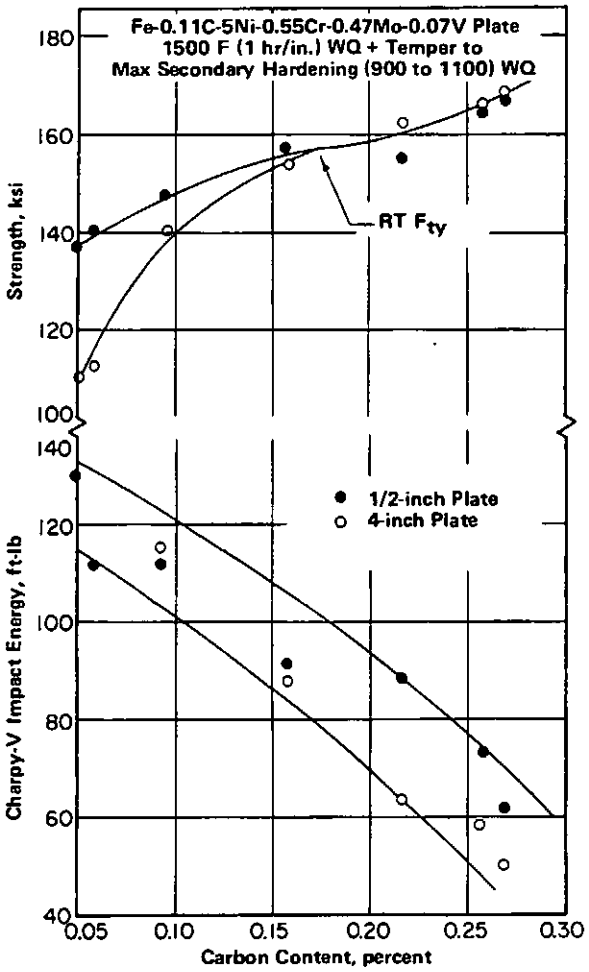


FIGURE 3.0333. EFFECT OF CARBON CONTENT ON ZERO DEGREES F IMPACT STRENGTH OF PLATE [(1) FIGURE 4]

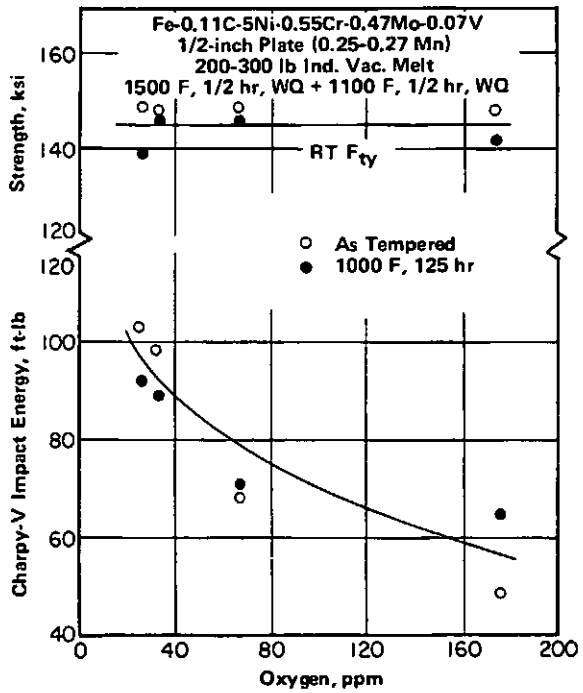


FIGURE 3.0334. EFFECT OF OXYGEN ON -80 F IMPACT STRENGTH OF LOW MANGANESE PLATE AS TEMPERED AND AFTER STRESS RELIEF [(5) TABLE 3]

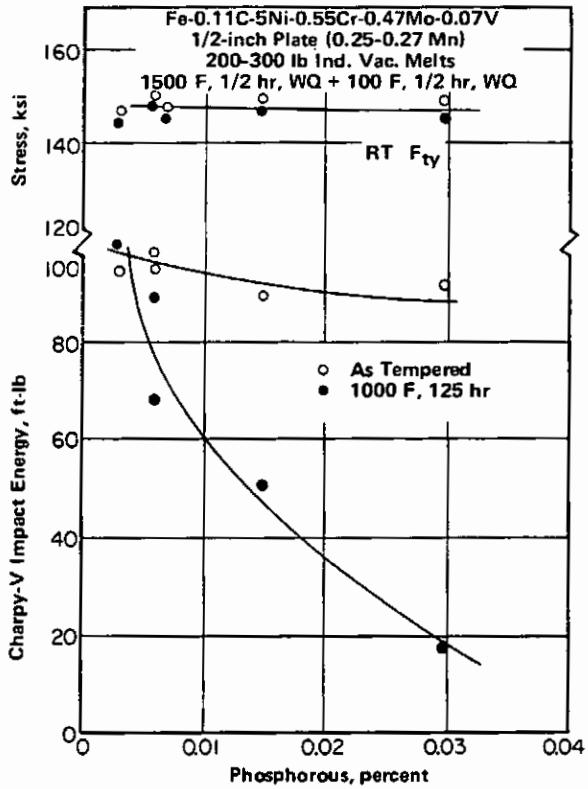


FIGURE 3.0335. EFFECT OF PHOSPHOROUS ON THE -80 F IMPACT STRENGTH OF LOW MANGANESE PLATE AS TEMPERED AND AFTER STRESS RELIEF [(5) TABLE 3]

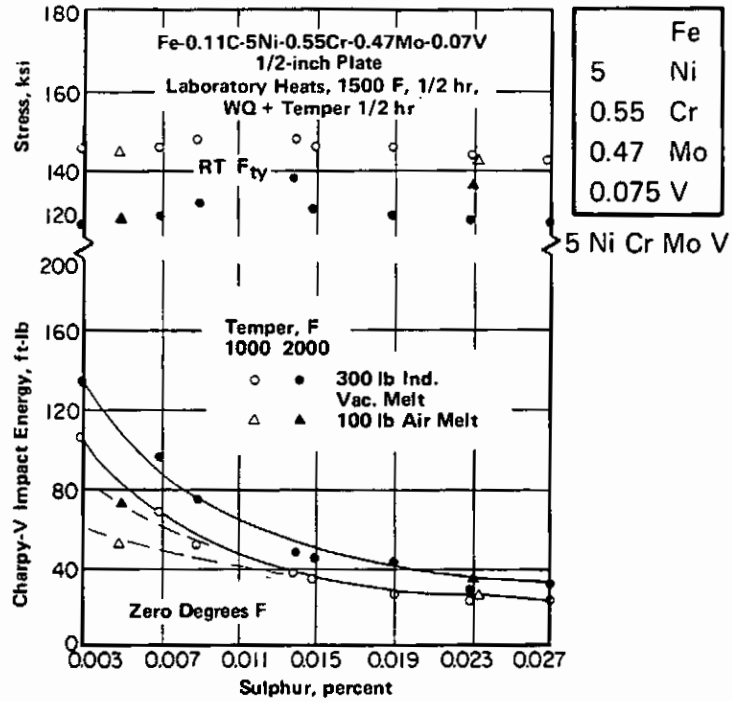


FIGURE 3.0336. EFFECT OF SULPHUR CONTENT ON LOW TEMPERATURE IMPACT STRENGTH OF PLATE FROM LABORATORY HEATS [(3) TABLE 2]

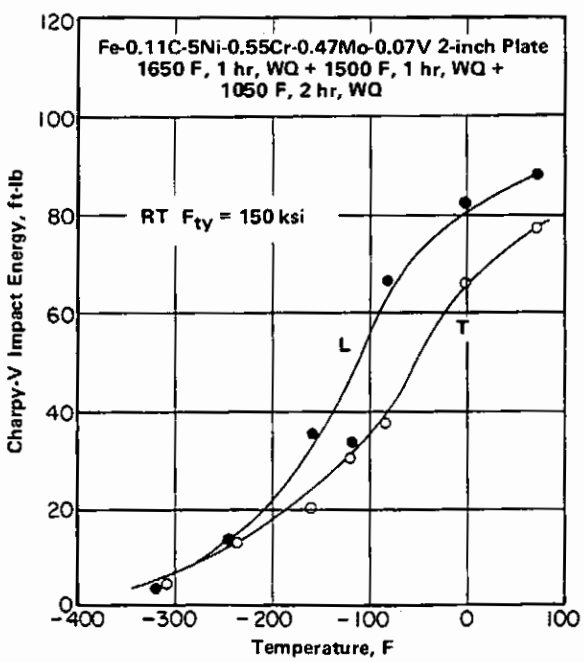


FIGURE 3.0337. EFFECT OF LOW TEST TEMPERATURE ON THE IMPACT STRENGTH OF PLATE [(11) TABLE A5]

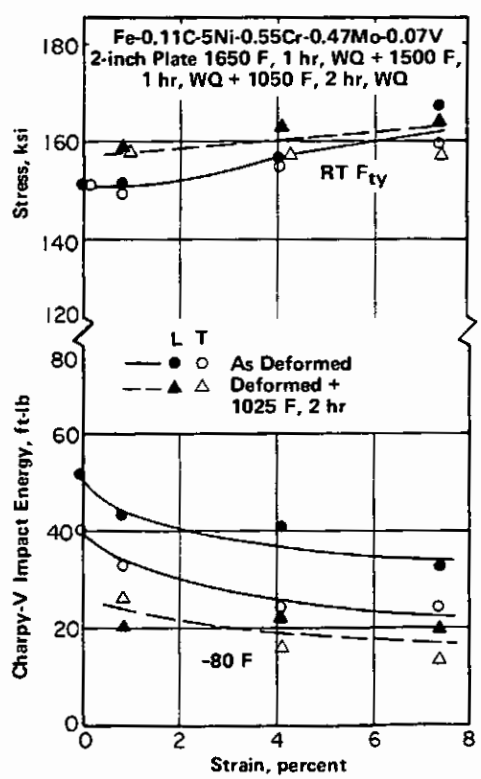


FIGURE 3.0338. EFFECT OF COLD DEFORMATION (BENDING) AND STRESS RELIEF ON LOW TEMPERATURE IMPACT PROPERTIES OF PLATE [(11) TABLES A2-A11, (12) TABLES 2 AND 3]

	Fe
5	Ni
0.55	Cr
0.47	Mo
0.075	V

5 Ni Cr Mo V

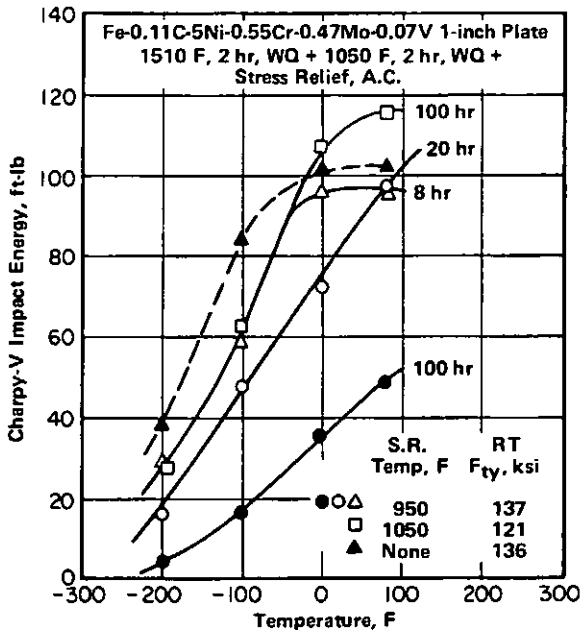


FIGURE 3.0339. EFFECT OF VARIOUS STRESS RELIEF TREATMENTS ON LOW TEMPERATURE IMPACT ENERGY OF PLATE [(60) TABLE 2]

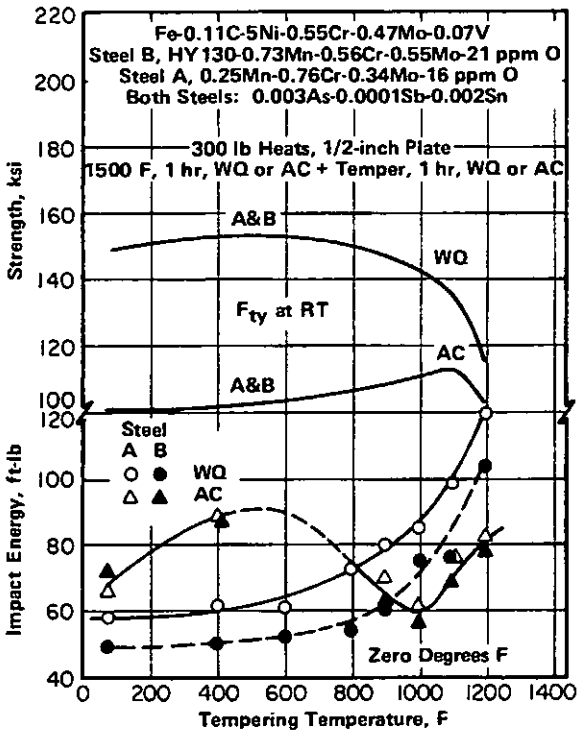


FIGURE 3.03310. EFFECT OF TEMPERING TEMPERATURE ON LOW TEMPERATURE IMPACT ENERGY OF LABORATORY HEATS OF HY130 (STEEL B) AND A STRESS-RELIEVABLE COMPOSITION (STEEL A) AIR COOLED OR WATER QUENCHED AFTER AUSTENITIZING OR TEMPERING [(61) TABLES 2 AND 3]

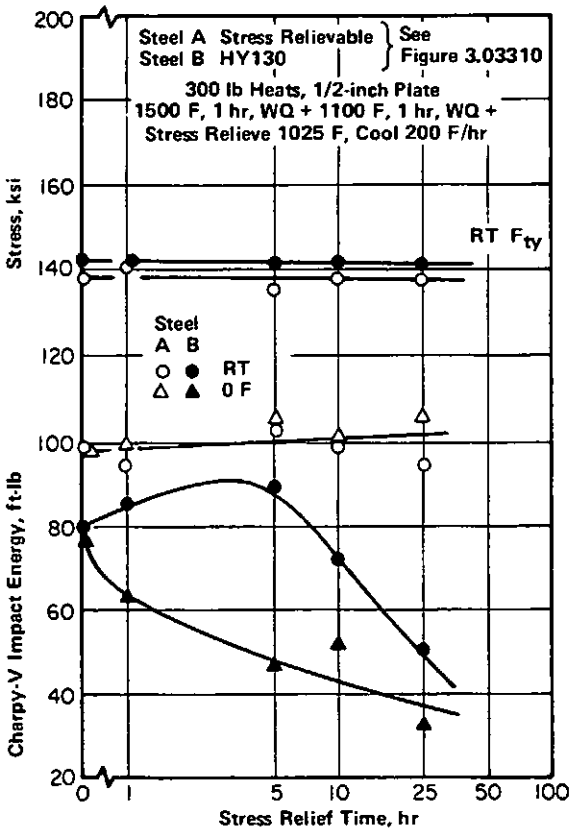


FIGURE 3.03311. EFFECT OF STRESS RELIEF TIME ON ROOM TEMPERATURE AND OF IMPACT ENERGY OF A STRESS RELIEVABLE COMPOSITION (STEEL A) AND HY130 (STEEL B) WHEN SLOWLY COOLED FOLLOWING STRESS RELIEF [(61) TABLE 4]

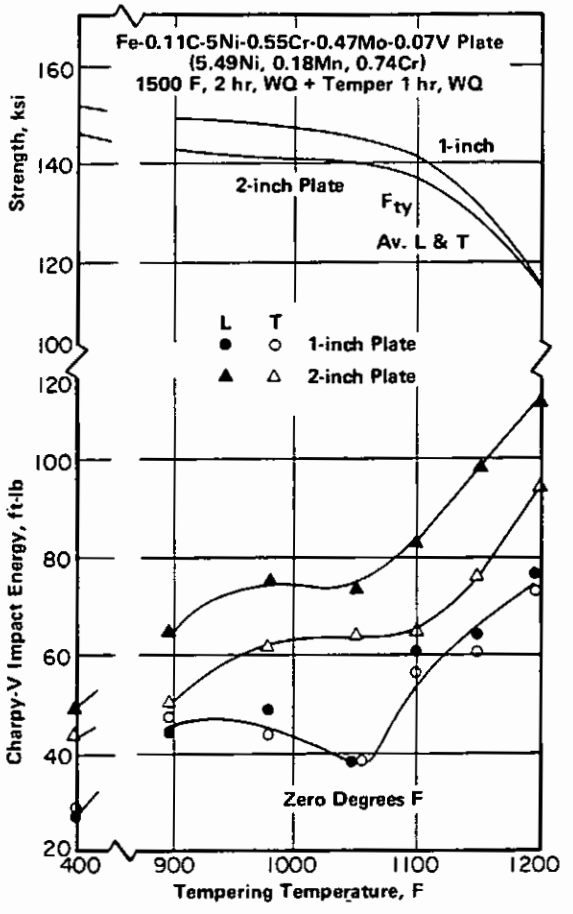
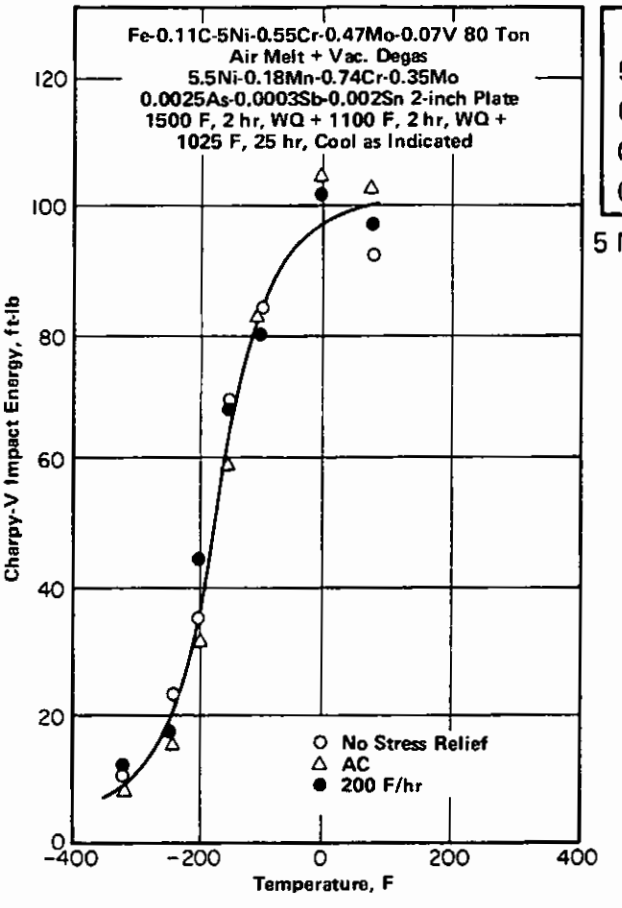


FIGURE 3.03313. EFFECT OF TEMPERING TEMPERATURE ON IMPACT STRENGTH OF STRESS RELIEVABLE PLATE FROM PRODUCTION HEAT [(31) TABLE 13]



	Fe
5	Ni
0.55	Cr
0.47	Mo
0.075	V

5 Ni Cr Mo V

FIGURE 3.03314. EFFECT OF LOW TEST TEMPERATURE ON IMPACT ENERGY OF PLATE OF A STRESS RELIEVABLE COMPOSITION GIVEN TWO STRESS RELIEF TREATMENTS [(61) FIGURE 10]

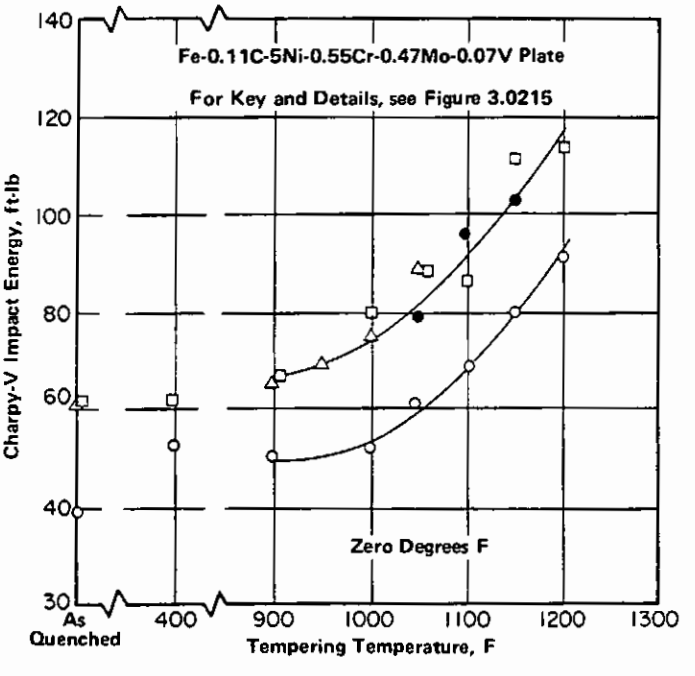


FIGURE 3.03315. EFFECT OF TEMPERING TEMPERATURE ON ZERO DEGREE F IMPACT STRENGTH OF SEVERAL HEATS OF PLATE [(49)(19) TABLE 2]

	Fe
5	Ni
0.55	Cr
0.47	Mo
0.075	V

5 Ni Cr Mo V

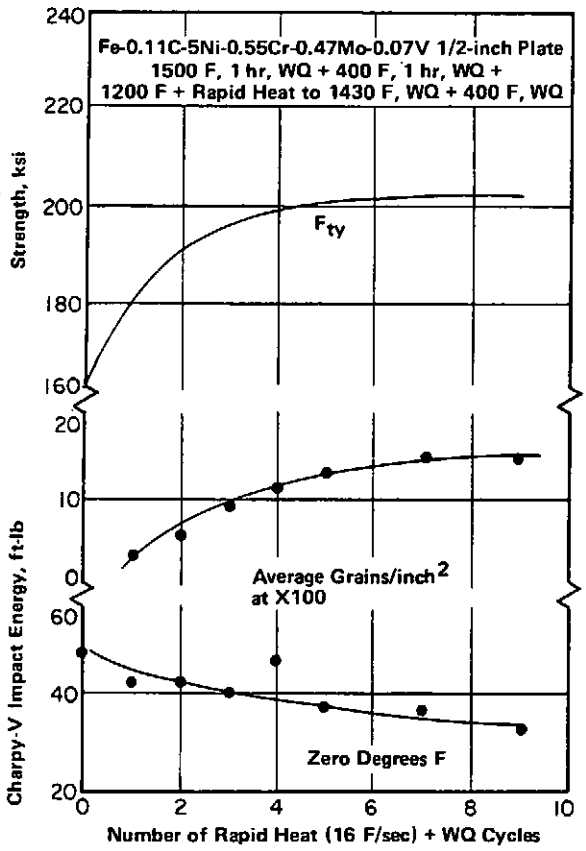


FIGURE 3.03317. EFFECT OF RAPID AUSTENITIZING ON GRAIN SIZE AND ZERO DEGREE F TRANSVERSE IMPACT STRENGTH OF PLATE [(17) TABLE 3]

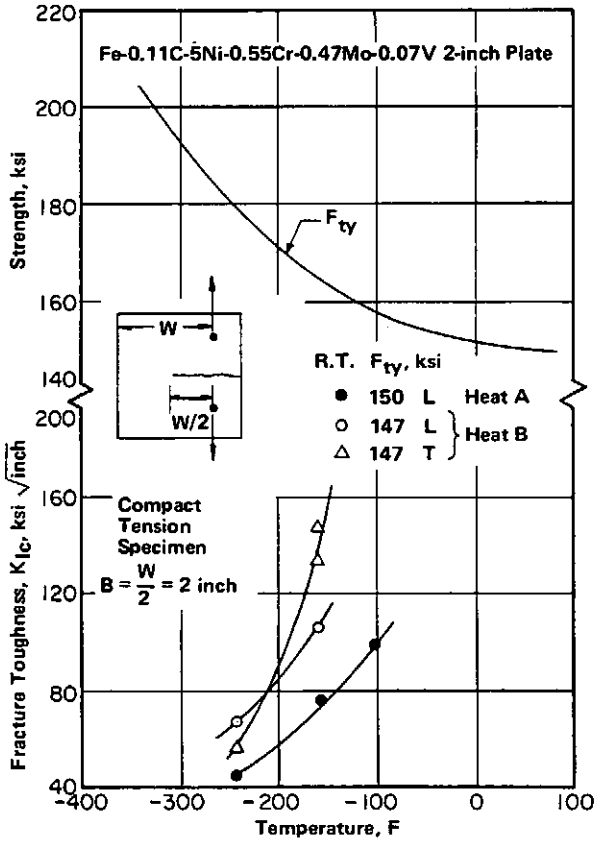


FIGURE 3.03722. EFFECT OF LOW TEST TEMPERATURE ON PLANE STRAIN FRACTURE TOUGHNESS OF PLATE FROM TWO HEATS (40)

	Fe
5	Ni
0.55	Cr
0.47	Mo
0.075	V

5 Ni Cr Mo V

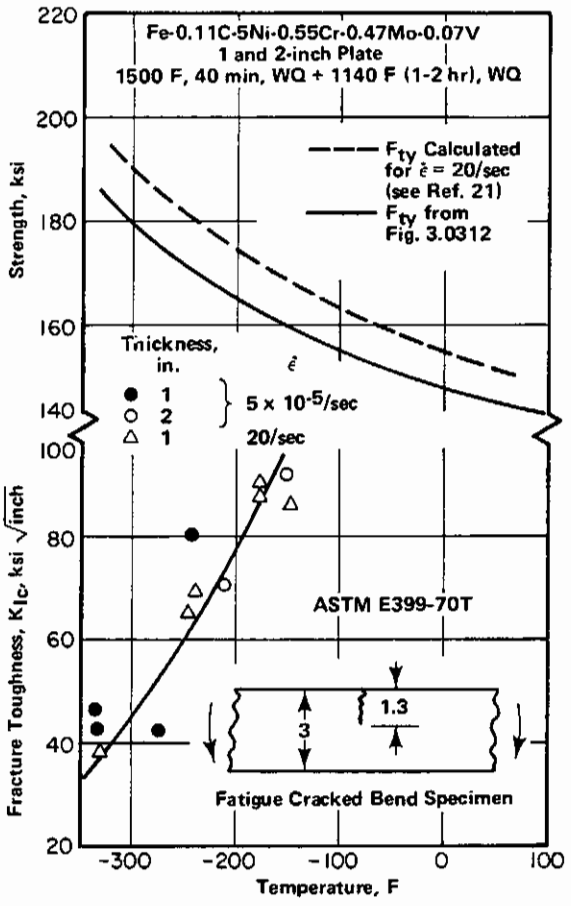


FIGURE 3.03723. EFFECT OF LOW TEST TEMPERATURE AND CALCULATED CRACK TIP STRAIN RATE ON PLANE STRAIN FRACTURE TOUGHNESS OF PLATE [(21) FIGURE 5, (52) FIGURE 6]

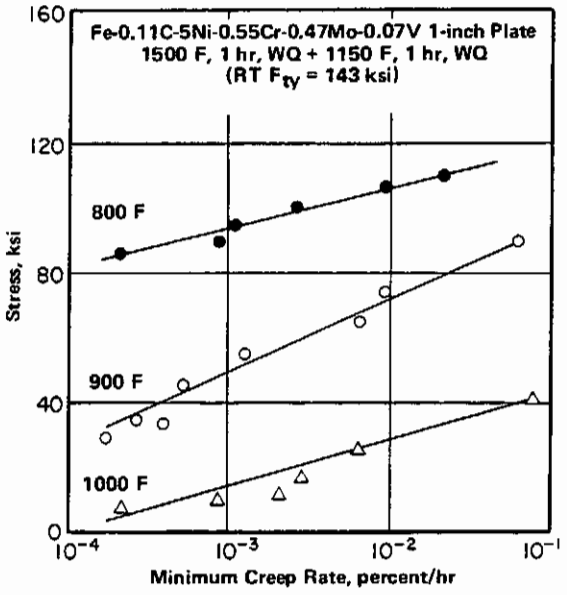


FIGURE 3.041. MINIMUM CREEP RATE FOR PLATE [(23) TABLE 4]

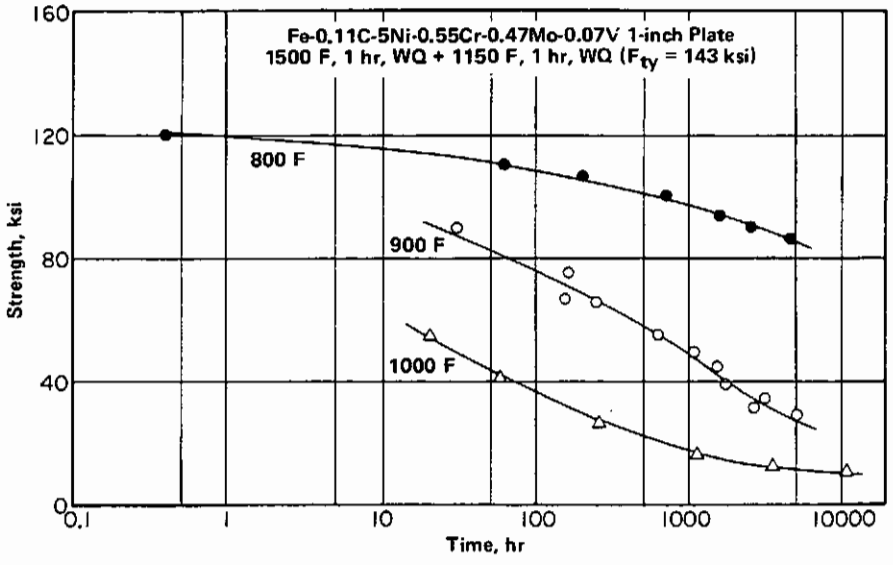


FIGURE 3.042. CREEP RUPTURE STRENGTH OF PLATE [(23) TABLE 4]

	Fe
5	Ni
0.55	Cr
0.47	Mo
0.075	V

5 Ni Cr Mo V

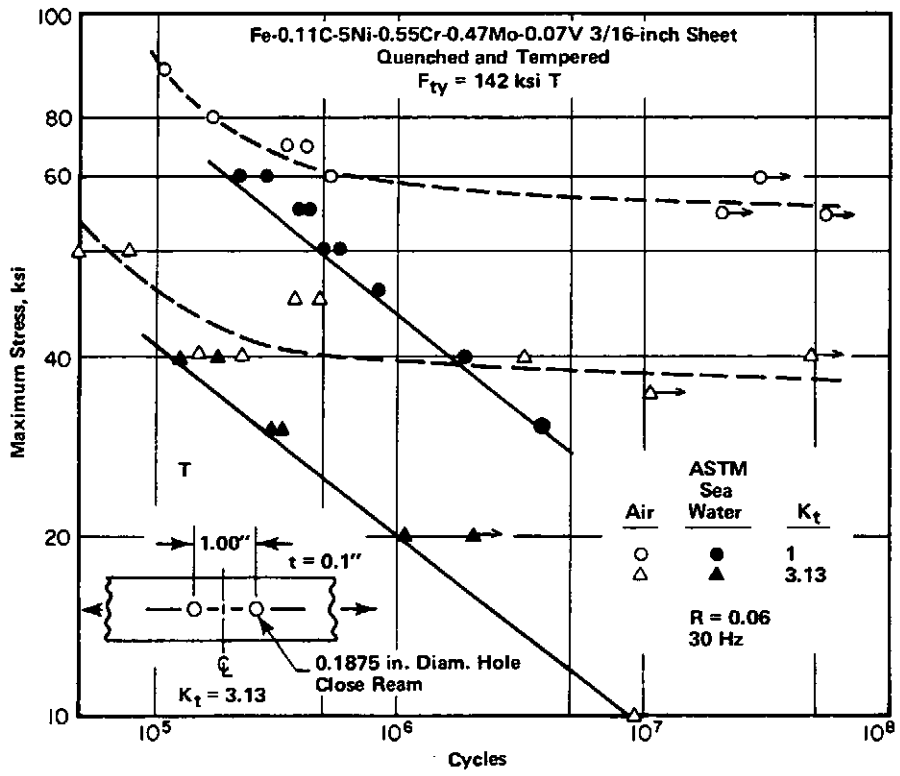


FIGURE 3.0511. EFFECT OF ASTM SYNTHETIC SEAWATER ON SMOOTH AND NOTCHED FATIGUE STRENGTH OF SHEET [(54) FIGURE 11]

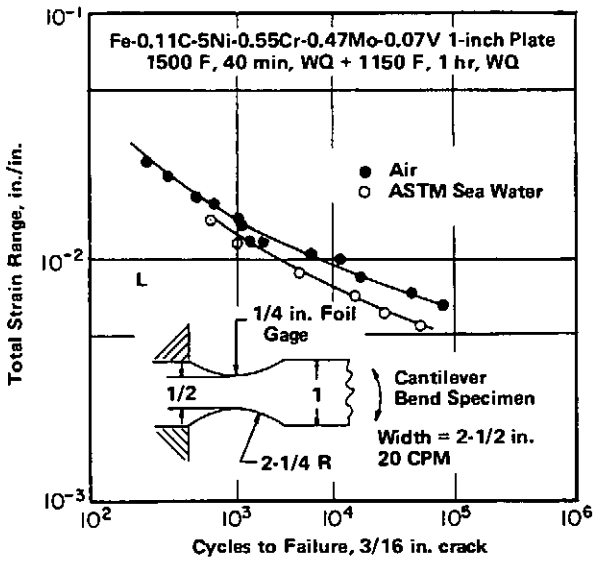


FIGURE 3.0512. LOW CYCLE FATIGUE PROPERTIES OF PLATE IN AIR AND SYNTHETIC SEA WATER [(13) PP 15-16]

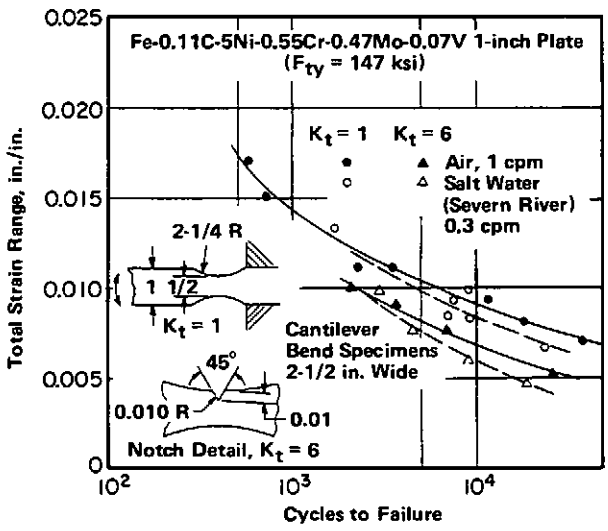


FIGURE 3.0513. EFFECT OF STRESS CONCENTRATIONS AND BRACKISH RIVER WATER ON LOW CYCLE FATIGUE CHARACTERISTICS OF PLATE [(18) APPENDIX A]

	Fe
5	Ni
0.55	Cr
0.47	Mo
0.075	V

5 Ni Cr Mo V

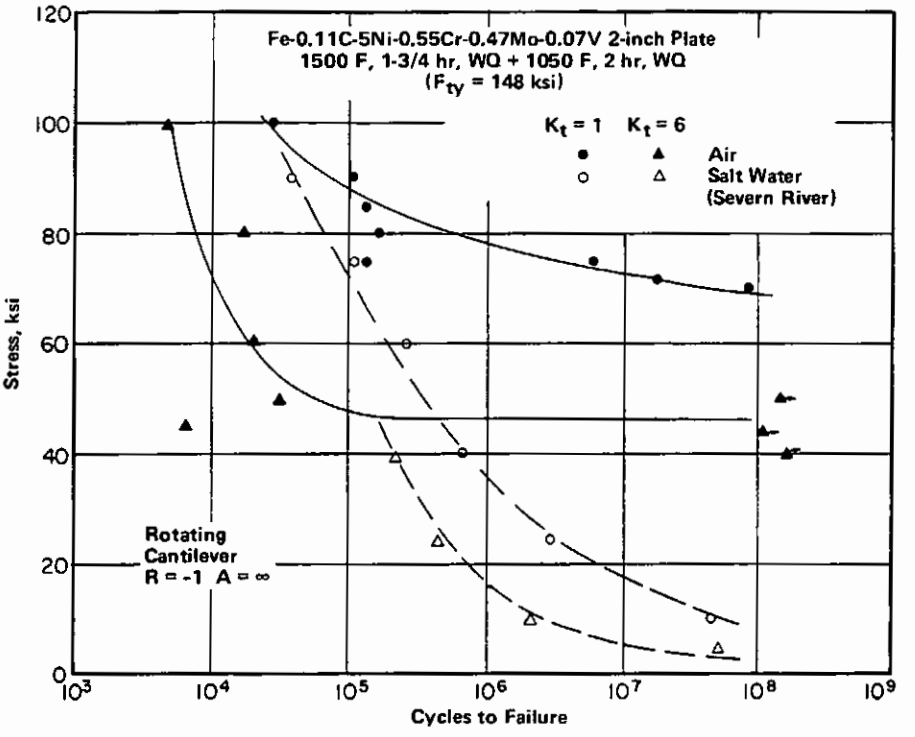


FIGURE 3.0514. EFFECT OF STRESS CONCENTRATIONS AND BRACKISH RIVER WATER ON FATIGUE STRENGTH OF PLATE [(18) APPENDIX A]

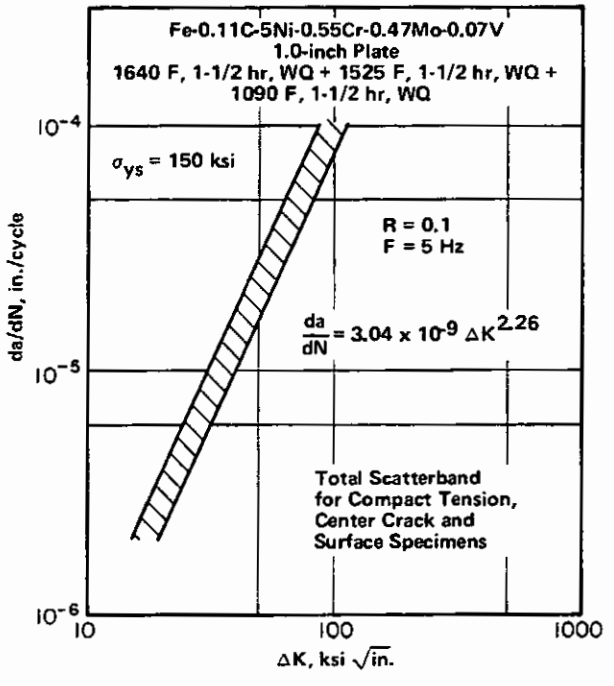


FIGURE 3.0521. FATIGUE CRACK PROPAGATION RATES FOR 0.9-INCH PLATE [(50) FIGURE 3]

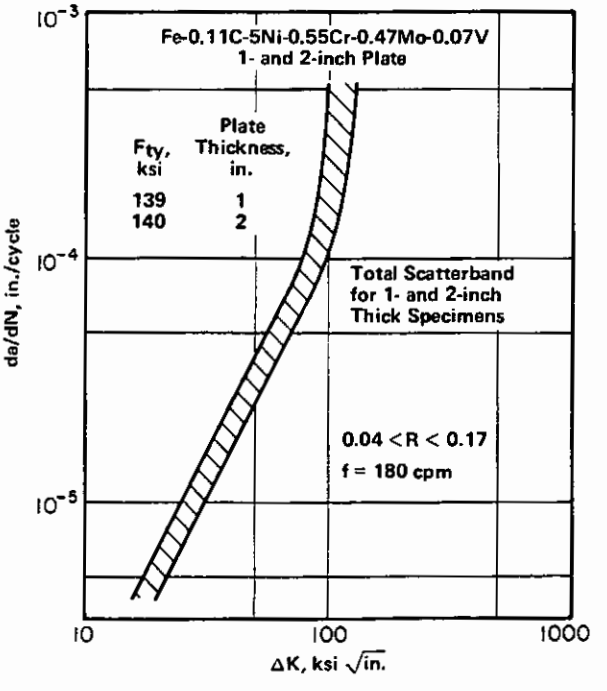


FIGURE 3.0522. FATIGUE CRACK PROPAGATION RATES FOR 1- AND 2-INCH PLATE [(52) FIGURE 8]

	Fe
5	Ni
0.55	Cr
0.47	Mo
0.075	V

5 Ni Cr Mo V

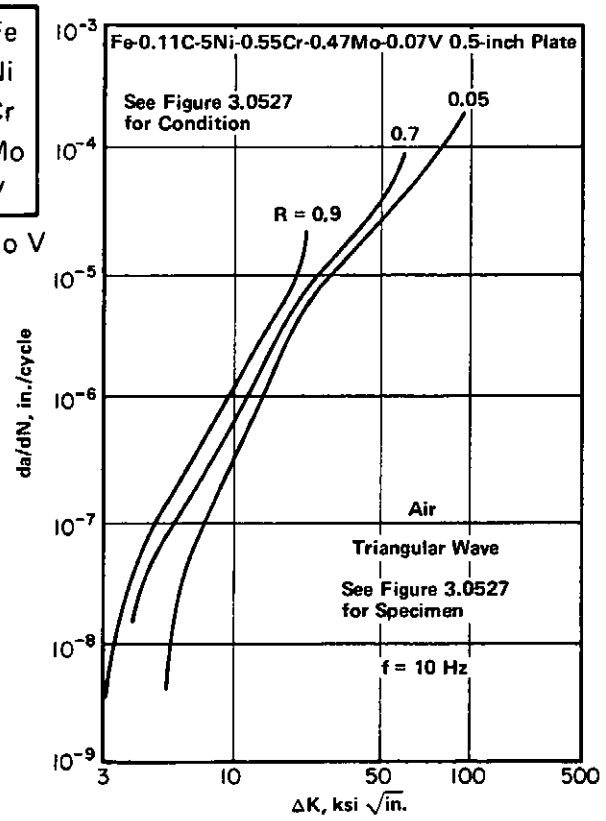


FIGURE 3.0523. EFFECT OF R RATIO ON FATIGUE CRACK GROWTH OF 0.5-INCH PLATE IN AIR [(55) FIGURE 1]

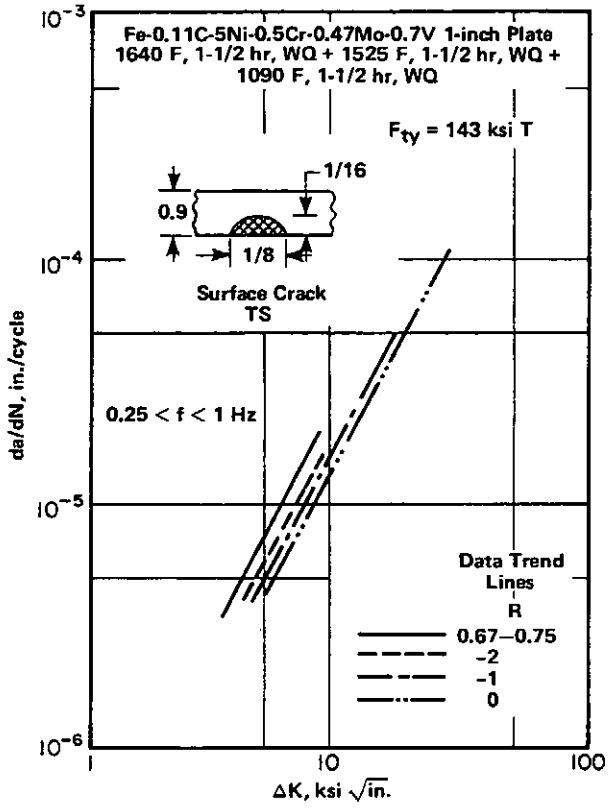


FIGURE 3.0524. FATIGUE CRACK PROPAGATION RATES FOR SURFACE CRACK SPECIMENS AT SEVERAL R RATIOS (51)

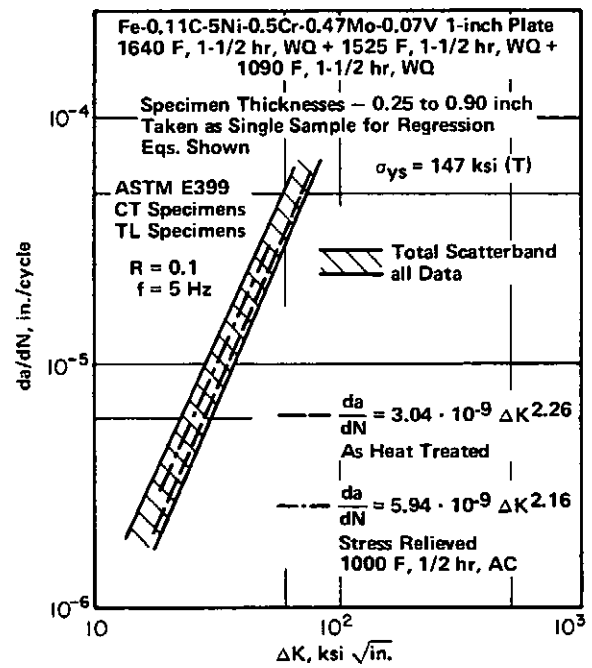


FIGURE 3.0525. FATIGUE CRACK PROPAGATION RATES FOR AS HEAT TREATED AND STRESS RELIEVED SPECIMENS OF VARIOUS THICKNESSES SHOWING TOTAL SCATTERBAND AND REGRESSION LINES [(50) FIGURE 2]

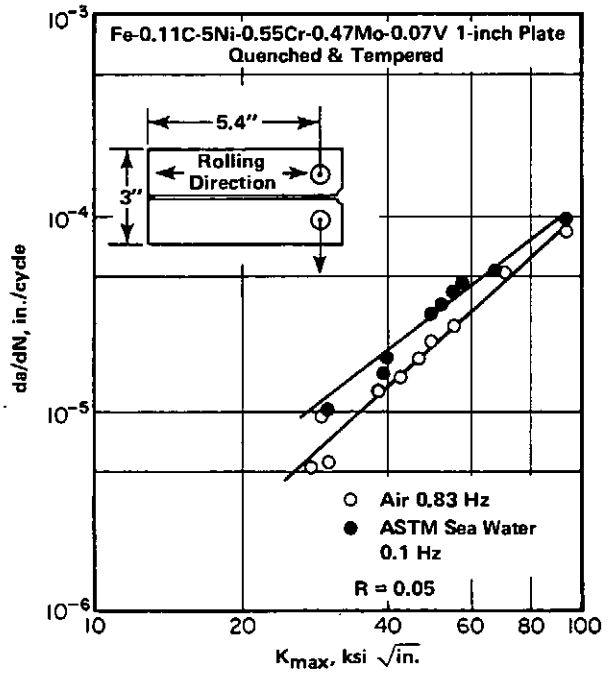


FIGURE 3.0526. FATIGUE CRACK PROPAGATION RATES FOR PLATE IN AIR AND ASTM SEA WATER [(54) FIGURE 17]

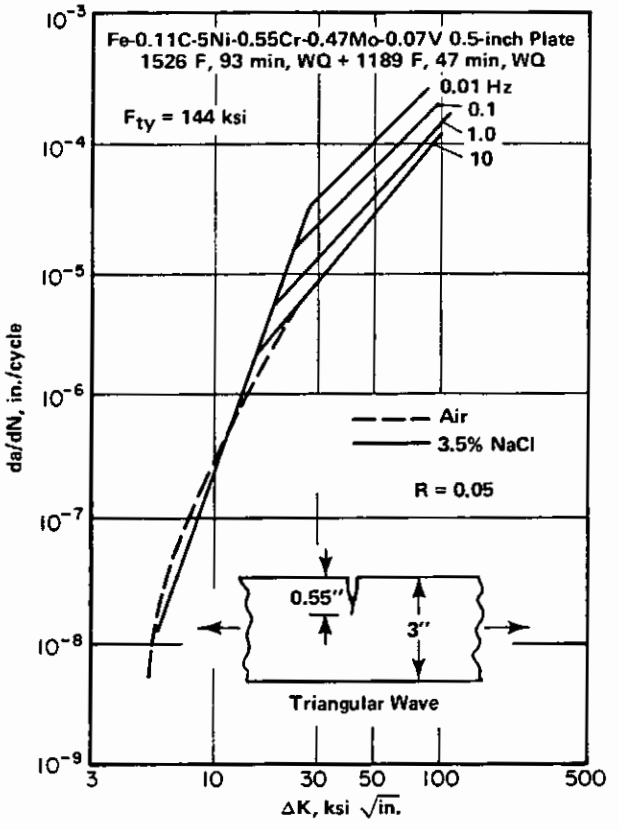
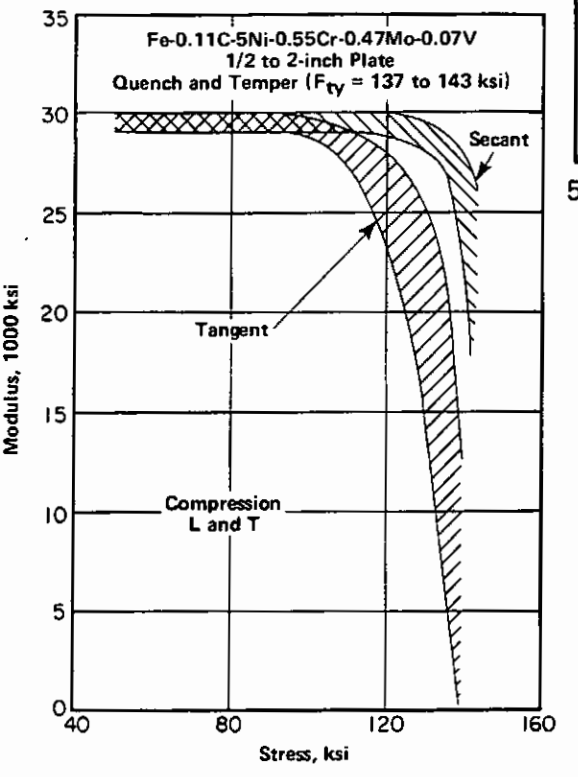


FIGURE 3.0527. EFFECT OF LOADING FREQUENCY ON FATIGUE CRACK GROWTH RATE IN 3.5 PERCENT NaCl [(55) FIGURE 2]



	Fe
5	Ni
0.55	Cr
0.47	Mo
0.075	V

5 Ni Cr Mo V

FIGURE 3.0641. RANGE OF TANGENT AND SECANT TENSION MODULI FOR PLATE OF SEVERAL THICKNESSES (8)

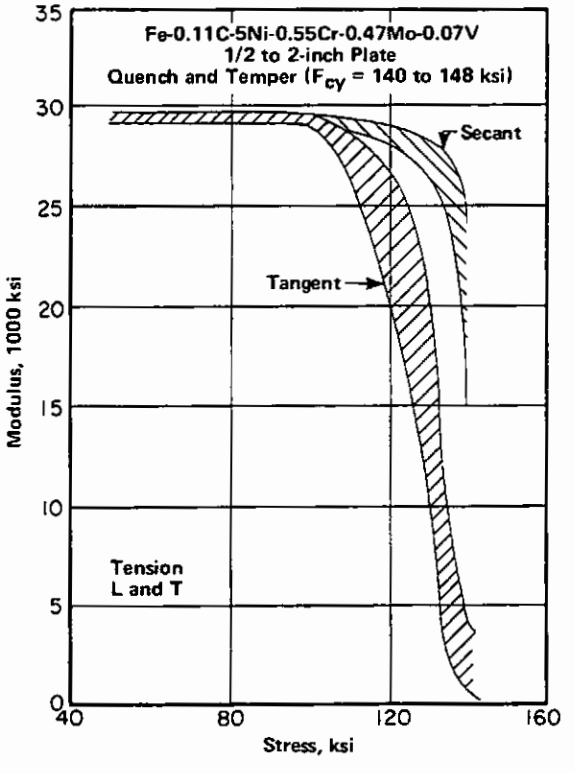


FIGURE 3.0642. RANGE OF TANGENT AND SECANT COMPRESSION MODULI FOR PLATE OF SEVERAL THICKNESSES (8)

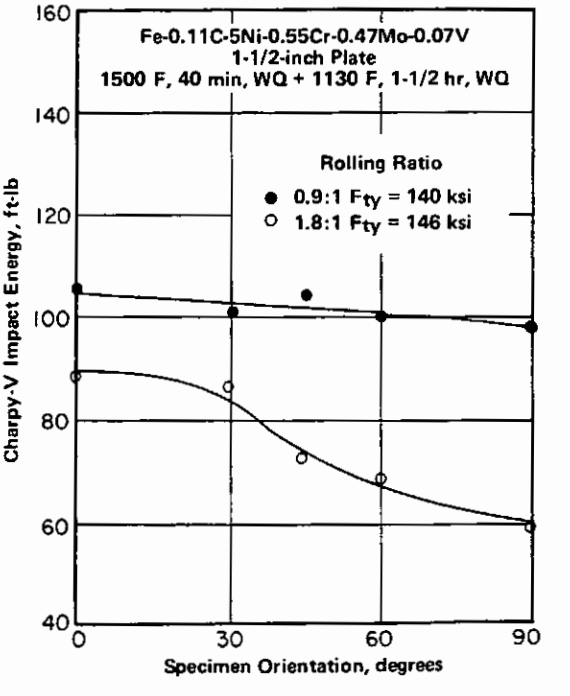


FIGURE 4.0121. EFFECT OF SPECIMEN ORIENTATION ON ZERO DEGREES F IMPACT STRENGTH OF PLATES GIVEN DIFFERENT ROLLING RATIOS (RATIO OF THICKNESS REDUCTION – FINAL LONGITUDINAL TO PRIOR TRANSVERSE) (1) (4)

	Fe
5	Ni
0.55	Cr
0.47	Mo
0.075	V

5 Ni Cr Mo V

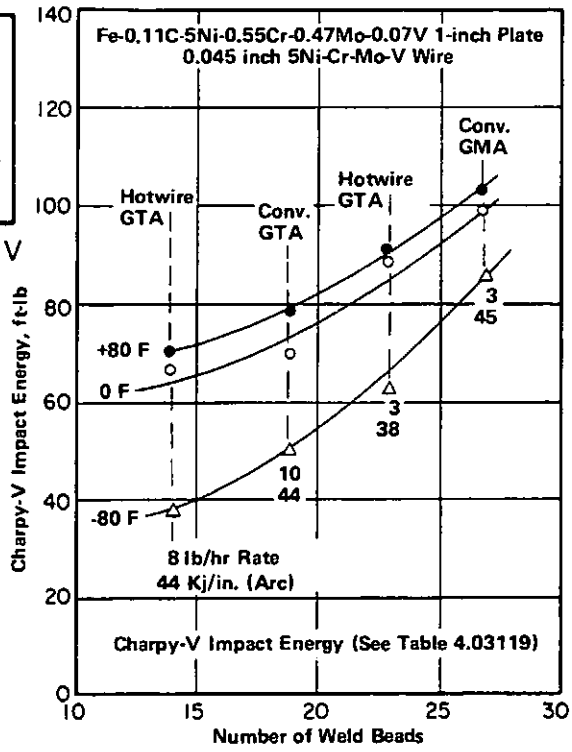


FIGURE 4.03124. IMPACT ENERGY OF WELDS MADE BY SEVERAL PROCESSES AS INFLUENCED BY THE NUMBER OF BEADS [(32) FIGURE 4]

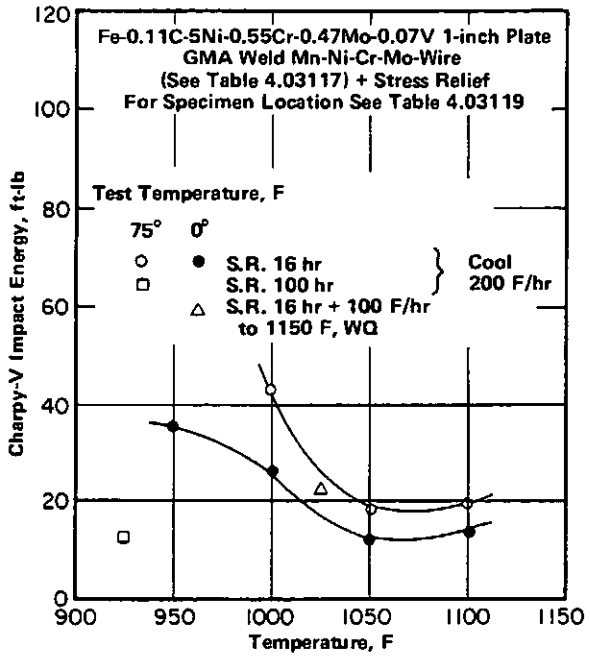


FIGURE 4.03134. EFFECT OF STRESS RELIEF ON IMPACT ENERGY OF GMA Mn-Ni-Cr-Mo WELDMENTS [(29) TABLES 3, 4 AND 6]

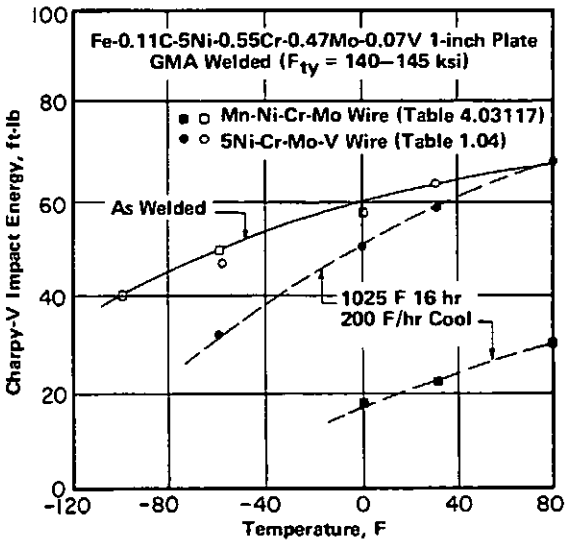


FIGURE 4.03135. EFFECT OF STRESS RELIEF TREATMENTS ON IMPACT ENERGY OF GMA WELDMENTS WITH TWO ELECTRODE COMPOSITIONS [(28) FIGURE 8]

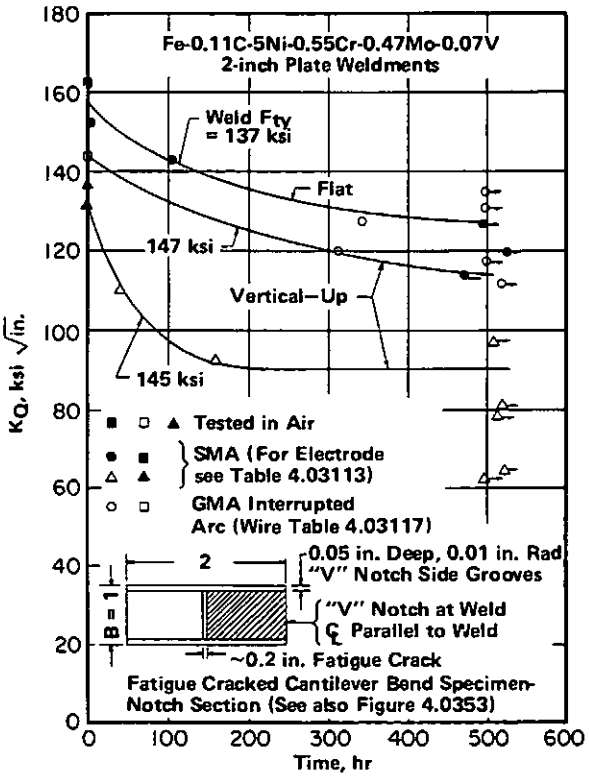


FIGURE 4.0352. SUSTAINED LOAD CRACK FAILURE BEHAVIOR IN 3 PERCENT NaCl FOR PLATE WELDED BY SEVERAL PROCESSES [(34) TABLES A-1 TO A-3]

	Fe
5	Ni
0.55	Cr
0.47	Mo
0.075	V

5 Ni Cr Mo V

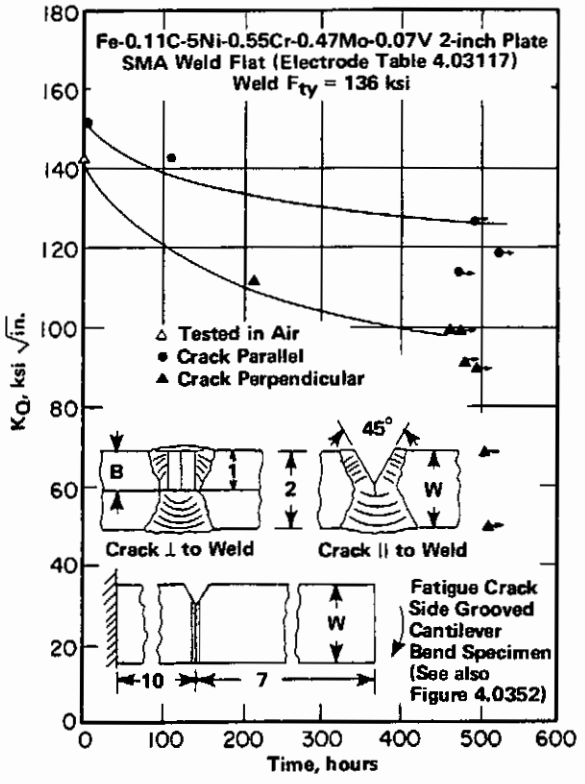


FIGURE 4.0353. SUSTAINED LOAD CRACK FAILURE BEHAVIOR IN 3 PERCENT NaCl FOR TWO ORIENTATIONS IN SMA WELDS [(35) TABLES A AND 5]

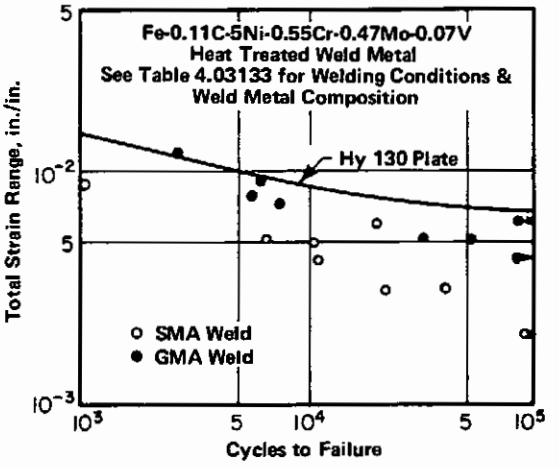


FIGURE 4.0361. LOW CYCLE FATIGUE BEHAVIOR IN AIR OF SMA & GMA HEAT TREATABLE WELD METAL [(62) FIGURE 9]

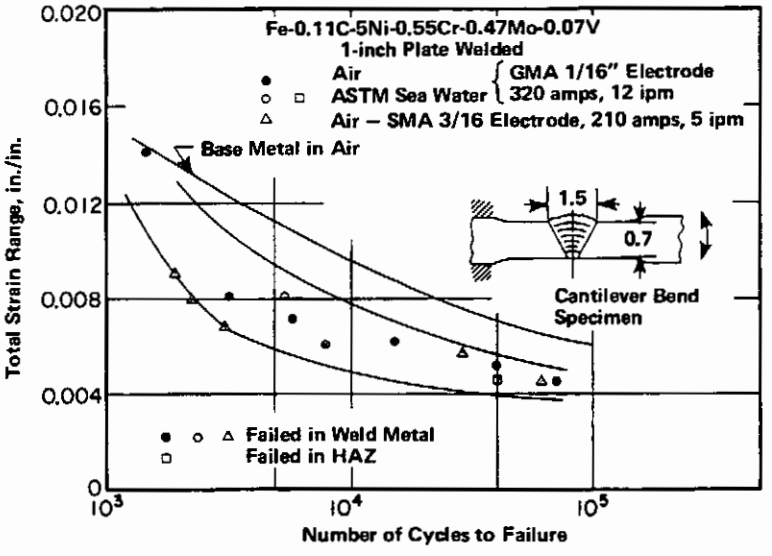


FIGURE 4.0362. LOW CYCLE FATIGUE BEHAVIOR OF GMA WELDS IN AIR AND ASTM SEA WATER AND SMA WELDS IN AIR [(26) PP 14 AND 25]

AUTHOR: W. F. BROWN, JR.

	Fe
0.13 max	C
8.5–9.5	Ni
0.9	Mn
0.15–0.30	Si

9 Ni Steel

1 GENERAL

This steel was designed specifically for use at cryogenic temperatures. Heat treatments have been developed which produce Charpy-V, impact energies well in excess of 25 ft lb at -320 F. Room temperature tensile strength varies from about 90 to 120 ksi depending on the carbon content and the heat treatment. Unless special attention is given to reducing the content of tramp elements temper embrittlement may be encountered during slow cooling or prolonged heating in the temperature range 500 to 1000 F.

Welding practices have been developed using high-nickel electrodes that produce welds having cryogenic impact values in excess of those of the parent metal. Recently efforts have been made to develop ferritic electrodes which are capable of producing welds with high cryogenic impact values but at a lower cost than characteristic of those made with the high-nickel electrodes.

The steel is widely used in various cryogenic storage vessels with the major application being in transportation and storage of liquified natural gas and other liquid gases. ASME Code permits the use in these applications without stress relief. In the aerospace field, applications include structural members and compressor disks of low temperature (high Reynolds number) wind tunnels.

1.01 Commercial Designation

9 Ni Steel

1.02 Alternate Designations

1.03 Specifications

Table 1.03

1.04 Composition

Table 1.04

1.05 Heat Treatment

1.051 General. The commercial heat treatments have been developed to provide an optimum combination of room temperature tensile strength and toughness at cryogenic temperatures. When quenched from above the Ae_3 in section sizes less than about 2 inches, the alloy is fully martensitic with a small amount of retained austenite. Reheating at temperatures above about 900 F will result in the formation of austenite which is retained after cooling from the tempering temperature. The amount of retained austenite is time-temperature dependent (see Fig. 1.055). At a given tempering temperature the amount of retained austenite passes through a maximum with increasing tempering time and this maximum shifts to lower times as the tempering temperature is increased. Tempering temperatures above about 1000 F are necessary to produce significant amounts of austenite in practical time periods. The stability of the austenite at cryogenic temperatures depends on the alloy composition and the temperature at which the austenite is formed. Lower tempering temperatures tend to produce more stable austenites but require longer times to produce a given amount. Generally, the commercially heat treated alloy will contain from 4 to 10 percent austenite.

The alloy's high toughness at cryogenic temperatures is associated with the presence of retained austenite as can be seen by comparing Fig. 1.055 with 1.056 and by reference to Fig. 1.0513. The minimum in the -320 F impact energy for material tempered at 950 and 1000 F is associated with an embrittlement reaction discussed later (see 1.09). Tempering at temperatures above 1000 F followed by cooling to -320 F will result in some of the retained austenite transforming to martensite. This is illustrated in Fig. 1.055 which shows the reduction in austenite content for samples cooled to -320 F after tempering. Since this transformation will also occur during cryogenic service, tempering temperatures in excess of 1100 F are not generally used.

Various mechanisms have been suggested to explain the beneficial effect of the retained austenite on the cryogenic toughness. The most likely mechanisms are the scavenging of detrimental impurities from solid solution thereby increasing the toughness of the martensite and/or crack blunting at the martensite-austenite boundaries through crack branching (16) (28).

If cooling above the Ae_3 is sufficiently slow, bainites will be produced and these structures will have reduced yield strengths and toughnesses compared with the martensitic structure (see Fig. 1.057). Large amounts of bainite are found in heavy sections which have been air cooled from the austenitizing temperature (e.g., Table 1.0514).

From the foregoing it is evident that considerable variation in mechanical properties could be encountered due to variations in composition within specification limits, as well as variations in tempering treatments and cooling rates from above the Ae_3 (e.g., Table 1.058). However, with proper care in heat treatment there is no difficulty in meeting the current specifications for tensile strengths and -320 F Charpy-V impact energies in plate less than 1 inch thick (e.g., see Table 3.012) and even very heavy sections can be produced with excellent cryogenic toughness by using special melting practices (e.g., see Tables 1.0922 and 1.0923).

1.052 Quench and temper. Austenitize 1450 to 1500 F, 1 hour per inch but not less than ¼ hour, W.Q. + 1050 to 1125 F, 1 hour per inch but not less than ¼ hour, W.Q. or A.C. at minimum rate of 300 F per hour (14) (15) (30) (31).

	Fe
0.13 max	C
8.5-9.5	Ni
0.9	Mn
0.15-0.30	Si

9 Ni Steel

1.053 Double normalize and temper. 1625 to 1675 F, 1 hour per inch but not less than ¼ hour, A.C. + 1425 to 1475 F, 1 hour per inch but not less than ¼ hour, A.C. + 1050 to 1125 F, 1 hour per inch but not less than ¼ hour, W.Q. or A.C. at minimum rate of 300 F per hour (13) (15) (30) (31).

1.054 Stress relief. 1025 to 1085 F, 2 hour for thicknesses up to 1 inch + 1 hour per inch for greater thicknesses, cool at a minimum rate of 300 F per hour (15) see also 1.09.

1.055 Effect of tempering temperature and time on austenite retention at R.T. and -320 F. Fig. 1.055.

1.056 Impact energy at -320 F as a function of tempering time for several tempering temperatures. Fig. 1.056.

1.057 Tensile and impact properties at cryogenic temperatures as a function of percent bainite. Fig. 1.057.

1.058 Variation in mechanical properties of commercially heat treated plate. Table 1.058.

1.059 Tensile and -320 F impact properties of a double quenched and tempered 5 inch thick slab before and after stress relief. Table 1.059.

1.0510 Effect of cold work and subsequent stress relief on -320 F Charpy-V impact energy of plate, Table 1.0510.

1.0511 Effect of grain refining heat treatment on cryogenic tensile and impact properties of plate. Table 1.0511.

1.0512 Effect of low test temperatures on impact energy of plate tempered for various times. Fig. 1.0512.

1.0513 Charpy-V and drop weight tear impact energies at -320 F as a function of percent austenite. Fig. 1.0513.

1.0514 Effect of cooling rates from austenitizing and from the tempering temperature on formation of bainite. Table 1.0514.

1.06 Hardness

1.061 Effect of test temperature on hardness of quenched and tempered plate. Fig. 1.061.

1.062 End quench hardenability. Fig. 1.062.

1.07 Forms and Conditions Available. Sheet, plate, forgings, tubing, seamless pipe in hot formed or heat treated conditions.

1.08 Melting and Casting Practice

1.081 General. The melting and casting practice is designed to minimize inclusion content and to reduce the content of tramp elements. Electric furnace or converter air melting is generally employed with a double slag process. DH vacuum or vacuum stream degassing is used to reduce the hydrogen and oxygen content. DH vacuum degassed ingots are sometimes bottom poured with the metal stream being protected by an inert gas. Continuous casting is employed in some United States steel plants.

1.09 Special Considerations

1.091 Embrittlement. The metallurgical changes occurring in this steel during heat treatment are complex and can have a profound effect on the toughness. The optimum structure appears to consist of a low carbon martensite with about 5 to 10 percent retained austenite. Variations from this structure which contribute to embrittlement are associated with over or under tempering and excessively slow cooling rates from the austenitizing or tempering (or stress relieving) temperature. Over tempering can result in a decreased austenite stability and the consequent formation of untempered martensite. Under tempering can result in temper embrittlement. These deleterious effects can be overcome by proper control of the tempering process. However, the damaging effects of excessively slow cooling rates may be difficult to avoid if the section sizes are sufficiently large.

1.0911 Effects of Cooling Rates. Problems arise from two sources: (1) mixed structures which are produced by too slowly cooling from the austenitizing temperature and (2) temper embrittlement which can be encountered by too long a dwell time in the range between 500 and 1000 F. It is possible to encounter both phenomena during a given heat treat cycle. Fortunately, recent advances in composition and processing control can minimize the temper embrittlement.

Appreciable amounts of bainite (mixed structures) will be produced in sections over about 3 inches thick even though the alloy is quenched. These structures have reduced toughness at cryogenic temperature as compared with the tempered martensites (see Fig. 1.057). The effect of cooling rates from the austenitizing temperature are illustrated in Table 1.0914 which gives results for tests on two heavy sections oil quenched or air cooled from the austenitizing temperature. Note that substantial losses in impact energy at -320 F are associated with air cooling.

Temper embrittlement in this steel is a time-temperature dependent phenomenon with the largest effects being noted between about 700 and 900 F (see Figs. 1.0915, 1.0916, and 1.0917). The effect of very slow cooling from a normal tempering temperature is shown in Table 1.0919. The temper embrittlement is reversible and the toughness may be recovered by retempering at a temperature above about 1050 F (Table 1.0920) but such recovery treatments are not possible if the original embrittlement was associated with heavy sections.

	Fe
0.13 max	C
8.5-9.5	Ni
0.9	Mn
0.15-0.30	Si

9 Ni Steel

When heat treating sufficiently thick sections, the effects of temper embrittlement are superimposed on those associated with mixed structures. For example, Table 1.0921 gives results for simulated cooling rates of a plate 27.5 inches thick subjected to water quenching or air cooling from both the austenitizing and tempering temperature. Note that low impact values at -320 F characterize both cooling conditions but that the room temperature tensile strength is not subtantially changed. Apparently very little information is available concerning the influence of temper embrittlement on valid K_{Ic} values of this alloy. Data obtained from tests on a large forged billet (see Table 3.03722) indicate that substantial reductions in plane strain fracture toughness can accompany stress relief of very heavy sections.

From the foregoing it is evident that stress relief may pose a problem if the cooling rates are sufficiently slow. It is for this reason that ASTM A522 specifies a relatively rapid cooling rate (300 F per hour minimum) from the stress relief temperature. The effect of cooling rate will depend on the alloy composition.

1.0912 Effects of Alloy Composition: Temper brittleness is associated with grain boundary segregation of certain tramp elements. The worst of these are P, Sb, Sn, and As. The effect of these elements can be altered to some extent by modification of the composition. For example, Cr and Si appear to strengthen the embrittling effect of P while the addition of Mo in minor amounts appears to reduce the embrittling effect of the tramp elements. (17) (18) (19).

Special studies and composition control have been employed (20) (21) to minimize temper embrittlement associated with slow cooling from the stress relief temperature. The beneficial effects of reduced Si and increased Mo contents are illustrated in Table 1.0922 for small vacuum melted heats containing low residuals. The improvements are obtained with no sacrifice in tensile strength. Tests of specimens cut from a very large forged cylinder, Table 1.0923, containing very low content of tramp elements, show only a small loss in Charpy-V impact energy associated with very slow cooling (18 F per hour) from the stress relief temperature. In addition, plane strain fracture toughness tests on specimens cut from a very large stress relieved forged disk (see Table 3.03723) show high K_{Ic} values at both the rim and disk bore.

On the basis of the above results it appears that by suitable composition control temper embrittlement can be practically eliminated during stress relief of heavy sections.

1.0913 Other Factors Influencing Toughness. As might be expected impact energy at cryogenic temperatures decreases with an increase in inclusion content (see Fig. 1.0927) and the transverse impact energy (see Fig. 1.0928) decreases with an increase in the cross rolling ratio. Hot or cold worked material should be completely heat treated rather than simply tempered, in order to develop good toughness at cryogenic temperatures (see Table 1.0929).

1.0914 Effect of section size and cooling rate from the austenitizing temperature on the room temperature tensile strength and the -320 F Charpy impact energy of forgings. Table 1.0914.

1.0915 Effect of tempering temperature on hardness and -320 F impact energy of bar. Fig. 1.0915.

1.0916 Iso-embrittlement diagram for plate. Fig. 1.0916.

1.0917 Effect of retempering time and temperature on -320 F impact energy of bar. Fig. 1.0917.

1.0918 Effect of test temperature on impact energy of bar after retempering at 600 F and 800 F. Fig. 1.0918.

1.0919 Influence of cooling rate from tempering temperature on the room temperature tensile strength and the -320 F impact energy of cast bar. Table 1.0919.

1.0920 Impact results illustrating the reversibility of temper embrittlement. Table 1.0920.

1.0921 Effect of cooling rate from austenitizing and tempering temperature on the room temperatrue tensile strength and the -320 F impact energy of a 2-inch thick plate cooled at a rate to simulate that of a 27.5-inch thick plate. Table 1.0921.

1.0922 Average values of room temperature tensile strength and -320 F impact properties of specimens from two heats illustrating the influence of composition on temper embrittlement. Table 1.0922.

1.0923 Influence of stress relief heat treatments on the average values of tensile strength and -320 F impact energy of specimens from a quenched and tempered, thick-walled cylinder. Table 1.0923.

1.0924 Effect of test temperature and stress relief on low temperature impact energy of a large forged billet. Table 1.0924.

1.0925 Tensile properties of a very large quenched and tempered and stress relieved disk forgings. Table 1.0925.

1.0926 Charpy-V impact energies at cryogenic temperatures for a very large quenched and tempered and stress relieved disk forging. Table 1.0926.

1.0927 Transverse impact energy at -320 F as function of inclusions. Fig. 1.0927.

1.0928 Influence of cross rolling ratio on transverse impact energy of plate. Fig. 1.0928.

1.0929 Effect of several heat treatments on the tensile and impact properties of hot worked and cold worked pipe. Table 1.0929.

2 PHYSICAL PROPERTIES AND ENVIRONMENTAL EFFECTS

2.01 Thermal Properties

2.011 Melting range. 2700 to 2900 F.

2.012 Phase changes (see Fig. 2.01211).

2.0121 Time-temperature-transformation diagrams.

	Fe
0.13 max	C
8.5-9.5	Ni
0.9	Mn
0.15-0.30	Si

9 Ni Steel

2.01211 Isothermal transformation diagram. Fig. 2.01211.
2.013 Thermal conductivity. Fig. 2.013.
2.014 Thermal expansion.
2.0141 Coefficient of linear thermal expansion. Fig. 2.0141.
2.015 Specific heat. Table 2.015.
2.016 Thermal diffusivity.

2.02 Other Physical Properties
2.021 Density, 0.28 lb/in^3
2.022 Electrical properties.
2.023 Magnetic properties.
2.0231 Magnetic properties of double normalized alloy. Table 2.0231.

2.03 Chemical Environments
2.031 Corrosion. The corrosion rate of fully descaled U-bend and panel specimens exposed for periods up to 3.8 years at Harbor Island, in warm sea water (constant immersion depth) was 0.004 inch per year. At the 800 ft station at Kure Beach, N.C. the average corrosion rate after two years of exposure was 0.003 inch per year. U-bend specimens gave no indications of stress corrosion. In general the corrosion behavior is similar to other low alloy steels (3).

2.04 Nuclear Environments

3 MECHANICAL PROPERTIES

3.01 Specified Mechanical Properties
3.011 Specified mechanical properties for various product forms. Table 3.011.
3.012 Producers tensile and -320 F Charpy-V impact properties obtained by tests on many 3/8-inch thick plates. Table 3.012.

3.02 Mechanical Properties at Room Temperature. (see 3.03)
3.021 Tension, stress-strain diagrams–tension properties.
3.022 Compression, stress-strain–compression properties.
3.023 Impact.
3.024 Bending.
3.025 Torsion and shear.
3.026 Bearing.
3.027 Stress concentration.
3.0271 Notch properties.
3.0272 Fracture toughness.
3.028 Combined properties.

3.03 Mechanical Properties at Various Temperatures
3.031 Tension, stress-strain diagrams–tension properties.
3.0311 Effect of elevated temperatures on tensile properties of quenched and tempered and of double normalized plate. Fig. 3.0311.
3.0312 Range of tensile strengths for double normalized and tempered plate of various thicknesses, Fig. 3.0312.
3.0313 Range of tensile strengths for quenched and tempered plate of various thicknesses. Fig. 3.0313.
3.0314 Effect of low test temperatures on tensile properties of double normalized and of quenched and tempered plate. Fig. 3.0314.
3.0315 Effect of low test temperatures on the tensile properties of quenched and tempered plate. Fig. 3.0315.
3.0316 Effect of low test temperatures on the tensile properties of quenched and tempered 1½ inch plate. Fig. 3.0316.
3.032 Compression-stress/strain diagrams–compression properties.
3.033 Impact.
3.0331 Effect of low test temperatures on the Charpy keyhole impact energy of double normalized and tempered 0.5 inch plate. Fig. 3.0331.
3.0332 Effect of low test temperatures on the Charpy-keyhole impact energy of quenched and tempered 0.5-inch plate. Fig. 3.0332.
3.0333 Effect of low test temperatures on ¾ width Charpy-V energy for double normalized and for tempered and quenched 3/8-inch plate. Fig. 3.0333.
3.0334 Effect of low test temperatures on the Charpy-V impact energy of double normalized 0.5-inch plate. Fig. 3.0334.
3.0335 Effect of low test temperatures on Charpy-V impact energy of quenched and tempered 0.5-inch plate. Fig. 3.0335.
3.0336 Effect of low test temperatures on Charpy-V impact energies of three thicknesses of double normalized and tempered plate. Fig. 3.0336.
3.0337 Effect of low test temperatures on Charpy-V impact energies of three thicknesses of quenched and tempered plate. Fig. 3.0337.
3.0338 Effect of low test temperatures on the Charpy-V impact energies of plate from a 100-ton, air-melt heat. Fig. 3.0338.
3.0339 Drop-Weight-Tear and Charpy-V energies at -320 F for double normalized and for quenched and tempered plates of two thicknesses. Table 3.0339.
3.035 Torsion and shear.
3.036 Bearing.
3.037 Stress concentration.
3.0371 Notch properties.
3.0372 Fracture toughness.
3.03721 Plane strain fracture toughness of plate at cryogenic temperatures. Table 3.03721.
3.0722 Effect of test temperature and stress relief on room temperature and -320 F tensile properties and plane strain fracture toughness of a large forged billet. Table 3.03722.
3.03723 Tensile properties and plane strain fracture toughness of a very large, quenched and tempered and stress relieved disk forging. Table 3.03723.
3.038 Combined properties.

3.04 Creep and Creep Rupture Properties

3.05 Fatigue Properties
3.051 Conventional fatigue properties.
3.0511 S-N Curves for double normalized and tempered, 0.75-inch diameter bar at room and cryogenic temperatures. Fig. 3.0511.

	Fe
0.13 max	C
8.5–9.5	Ni
0.9	Mn
0.15–0.30	Si

9 Ni Steel

3.0512 S-N Curves for 0.75-inch, quenched and tempered plate. Fig. 3.0512.
3.0513 Rotating-beam fatigue strength for 0.25-inch, quenched and tempered plate at -270 F. Table 3.0513.
3.0514 S-N Curves for smooth and cracked specimens from quenched and tempered plate tested at room temperature and -320 F. Fig. 3.0514.
3.0515 Plastic strain range vs cycles to failure for quenched and tempered plate. Fig. 3.0515.
3.052 Fatigue crack propagation.
3.0521 Fatigue crack propagation rates at room temperature for double normalized and tempered, 1.3-inch plate. Fig. 3.0521.
3.0522 Fatigue crack propagation rate scatterband for quenched and tempered, 0.34-inch plate at room temperature. Fig. 3.0522.
3.0523 Fatigue crack propagation rate scatterband for quenched and tempered, 0.34-inch plate at -260 F. Fig. 3.0523.
3.0524 Fatigue crack propagation rates at room and cryogenic temperatures for quenched and tempered 1.25-inch plate. Fig. 3.0524.

3.06 Elastic Properties
3.061 Poisson's ratio.
3.062 Modulus of elasticity.
3.0621 Static modulus at room temperature and -320 F. Table 3.0621.

4 FABRICATION

4.01 Forming
4.011 General. There are no difficult problems with the hot or cold forming of this alloy and with few exceptions practices commonly employed for other low alloy steels should be satisfactory.
4.012 Forging. Starting 2250 F, finishing 1600 F.
4.013 Rolling. Relatively high soaking temperatures and substantial amounts of cross rolling result in improved impact proeprties (see Fig. 4.014). Air cooling following rolling tends to avoid the precipitation of AlN and MnS along austenite grain boundaries. Soaking temperatures below about 2012 F tend to produce a nickel enriched scale at the metal surface that is associated with grain boundary oxidation. In some cases slabs are covered on the face and back with thin steel sheets to reduce surface oxidation during rolling (35).
4.014 Effect of rolling ratio and soaking temperature on room temperature Charpy-V energy. Fig. 4.014.

4.02 Machining and Grinding.

4.03 Joining
4.031 Welding. General comments: Welding is generally done on stock in the fully heat treated condition. In so far as the steel is concerned, the only special precaution necessary is the avoidance of induced magnetism which can result in arc instability using DC processes. Remnant fields should be below 50 Oersted or AC electrodes (see Table 4.0315) should be used. Welding research and development has concentrated on those problems associated with the fabrication of large cryogenic storage vessels both for use in sea shipment of liquified gases and for ground storage. In production of these vessels post weld heat treatments are generally not possible nor have they been proven necessary (e.g., Table 4.03136). Weldments are required to have room temperature strengths, tensile and yield, close to those of the parent metal combined with very high toughness at cryogenic temperatures. The general practice is to use relatively low-carbon, high-nickel electrodes and filler wires (see Table 4.0315 and 4.0316). In some compositions the Ni content is reduced and the Mo or Cr content increased.

These high Ni wires and electrodes are expensive and considerable care is necessary in both the design of the weld joint and in control of the weld process to avoid hot cracking. Attempts have been made to use austenitic stainless steel electrodes but thin layers of hard martensite were formed at the fusion line which resulted in clevage fractures at the weld metal boundary (41). More recently considerable effort has been directed to the development of relatively low cost ferritic fillers. However, as yet no substantial production has been undertaken with these compositions.

Various welding processes are used in the fabrication of 9Ni Steel structures (e.g., Table 4.0317). Submerged metal arc (SMA) welding is generally used on the vertical joints and overhead. Automatic gas tungsten arc (GTA) welding in the vertical position is under development and has been used in the production of LNG (Liquified Natural Gas) storage tanks (37). Subarc and GMA welding is frequently used in the horizontal position. An excellent review of welding practices published in 1973 (27) gives valuable information concerning the various techniques and precautions that characterize the successful welding of 9Ni Steel. The following sections will not duplicate this detailed information but will concentrate on the mechanical properties of weld metal and weldments.

4.0311 Submerged Metal Arc Welding: This process when used with the high nickel electrodes is capable of producing very high -320 F Charpy-V values in the weld metal, in the fusion zone and in the heat affected zone (HAZ) (see Tables 4.0318 to 4.03111). Tensile ultimate and yield strengths for SMA deposited weld metal are generally lower than those of the parent metal with the largest difference being observed in the yield strength (compare Table 4.03112 with Tables 3.011 and 2.012). Special electrode compositions have been developed to produce a weld metal with room temperature tensile and yield strength matching that of the parent metal (e.g., Table 4.03113). However, such high strength weld metal will have lower -320 F Charpy-V energies than that produced by the more commonly used electrodes (e.g., compare Tables 4.0319 and 4.03110). Stress relief does

	Fe
0.13 max	C
8.5-9.5	Ni
0.9	Mn
0.15-0.30	Si

9 Ni Steel

not reduce the Charpy values of the commonly used high nickel weld metals (see Tables 4.03110 and 4.03111). The influence of stress relief on the HAZ is more difficult to define due to the non-uniform properties within this zone and the varability that exists from one weldment to another. This variation introduces considerable scatter into the Charpy data. However, on the basis of averages there appears to be no substantial reduction in -320 F Charpy energies in the HAZ associated with stress relief (see Tables 4.0318 to 4.0311). Room temperature tensile properties of SMA high nickel weld metal do not appear to be influenced by stress relief (see Tables 4.03113 and 4.03114).

The results of wide center-crack plate tests on high nickel SMA weldments reveal crack strengths at -320 F in the HAZ well below those of the parent metal (see Figs. 4.03115 and 4.03116). Crack propagation tests on wide panels with cracks in the high nickel weld metal or in the fusion zone reveal da/dN values to be essentially equal to those of the parent metal at ΔK values above about 50 ksi $\sqrt{\text{inch}}$. However, at lower values of ΔK the crack propagation rates of the weld metal and the fusion zone appear to be lower than those of the parent metal (compare Figs. 4.03117 and 4.03118 with 3.0523). At -260 F the crack propagation rates in the fusion zone appear to be somewhat lower than at room temperature (see Fig. 4.03118).

Attempts have been made to develop ferritic electrodes (11 percent Ni) for the SMA process. However, the weld metal Charpy impact energies at -320 F have been considerably below those produced by the high nickel electrodes (see Table 4.03120) and at present no commercial applications appear to exist for the SMA process with ferritic electrodes.

4.0312 Gas Metal Arc Welding. Two modifications of this process, pulsed spray and short arc are adapted to automation and can be used in the vertical and overhead positions (37). With low carbon high nickel fillers, the -320 F weld metal Charpy-V and tensile properties of GMA welds are essentially the same as produced by the SMA process using similar high nickel electrodes (see Table 4.03121).

Investigation of ferritic fillers for the GMA process have defined an optimum nickel content in the wire of about 11 percent (see Fig. 4.03124). Using ferritic wire with the spray or short arc process, weld metal -320 F Charpy-V values in excess of 45 ft lbs were obtained in the vertical position and in excess of 65 ft.-lbs. were obtained in the horizontal position (see Fig. 4.03125). However, GMA welding using ferritic fillers has not been used in commercial production but rather emphasis has shifted to development of the more flexible GTA process (36).

4.0313 Gas Tungsten Arc Welding. The GTA process permits control of heat input and wire feed rates over a wide range. In addition, elements such as boron which can not be transferred in a metal arc can be added to GTA filler wire and the GTA process is adapted to reheating of final weld passes or to smoothing weld toes. Recently a highly automated GTA apparatus has been developed which permits welding in the vertical and overhead positions (37).

Using high nickel fillers based on the Hastalloy composition, very high -320 F Charpy-V energies characterize weld metal deposited by the automatic GTA technique (see Table 4.03126). Room temperature tensile properties are essentially equal to those produced by other processes using the high nickel wires or electrodes.

Because of the inherent flexibility of the GTA process, considerable attention has been given to its use with ferritic fillers (36) (37) (38). Using a low carbon ferritic filler containing about 11 percent Ni, Charpy-V values in excess of 60 ft lbs can be obtained at -320 F for weld metal providing the oxygen and nitrogen content of the weld metal is below about 50 ppm (see Fig. 4.03127). It appears that boron additions up to about 0.002 percent are necessary to control intergranular fracture at cryogenic temperatures (38). The Charpy-V energies in ferritic GTA weld metal and in the parent plate HAZ decrease rapidly with heat inputs above about 100 kJ/inch (see Figure 4.03128). A decrease in the weld metal tensile strength properties is also observed with increasing heat input (see Fig. 4.03129). The impact energies of the weld metal and the HAZ obtained with ferritic fillers will be a function of the amount of weld metal deposited on each pass. Small amounts deposited at relatively low heat inputs result in the best properties due to the auto-tempering of the previously deposited metal. To assist in this process, remelting of the finishing passes may be employed (see Tables 4.03130 and 4.03131). Using this reheating process high -320 F Charpy energies are obtained in the weld metal throughout the plate thickness (see Table 4.03132) and in the fusion zone and HAZ (see Table 4.03133). It is not clear from the published information to what extent reheating would be necessary during commercial welding nor how this process could be controlled effectively in the field. Presumably it would be increasingly necessary as the parent plate thickness decreased. While laboratory tests indicate considerable promise for use of ferritic fillers in the GTA, process no commercial applications have been reported.

4.0314 Sub-arc Welding. Automatic sub-arc welding is frequently used in the horizontal seams of large cryogenic fluid storage tanks. With the use of nickel filler wire with basic fluxes high deposition rates are possible that result in welds having -320 F Charpy-V impact energies essen-

	Fe
0.13 max	C
8.5–9.5	Ni
0.9	Mn
0.15–0.30	Si

9 Ni Steel

tially equal to those produced by the SMA process. The room temperature tensile strength and the cryogenic impact energy will depend on the filler wire composition with the higher carbon contents giving lower impact values but higher tensile strengths. Typical results using a 0.12 C high nickel filler are shown in Table 4.03135. Attempts to use ferritic fillers (11 percent Ni) with the submerged arc process employing a flux cored wire have resulted in -320 F Charpy-V impact energies less than about 30 ft lb for the weld metal (26). Apparently there is presently no intensive development of ferritic fillers for the sub-arc process.

4.0315 Typical compositions of welding wire for coated electrodes. Table 4.0315.

4.0316 Typical compositions of welding wire for filler metal. Table 4.0316.

4.0317 Examples of electrodes used in various welding processes for fabrication of LNG tanks of 9Ni Steel. Table 4.0317.

4.0318 Charpy-V impact energies at room and -320 F at several positions with respect to the weld in SMA welded double normalized and tempered plate. Table 4.0318.

4.0319 Impact energies at -320 F at various locations in an SMA Weldment. Table 4.0319.

4.03110 Impact energies at -320 F at various locations in an SMA butt welded plate before and after stress relief. Table 4.03110.

4.03111 Effect of stress relief on -320 F Charpy impact values of SMA weld metal. Table 4.03111.

4.03112 Examples of weld processes, electrodes and fillers used in the United States along with typical mechanical properties of weld metal. Table 4.03112.

4.03113 Tensile properties of SMA weldments made on pieces cut from a large ring forging. Table 3.03113.

4.03114 Room temperature tensile properties of SMA weld metal in manually welded double normalized and tempered plate. Table 4.03114.

4.03115 Effect of low test temperatures on crack strength of the HAZ in a manual weldment of quenched and tempered plate. Fig. 4.03115.

4.03116 Effect of low test temperatures on crack strength of parent and of weld metal in a manual weldment of quenched and tempered plate. Fig. 4.03116.

4.03117 Fatigue crack propagation rates at room temperature for quenched and tempered SMA welded plate. Fig. 4.03117.

4.03118 Fatigue crack propagation rates at room temperature and -260 F for quenched and tempered SMA welded plate. Fig. 4.03118.

4.03119 Welding conditions for test results represented in Figs. 4.03115 to 4.03118. Table 4.03119.

4.03120 Shielded metal arc weld metal properties for a high and low nickel-coated electrode composition. Table 4.03120.

4.03121 Impact energies for SMA and GMA welds made in 0.5-inch plate and not stress relieved. Table 4.03121.

4.03122 Impact energies at -270 F for pulsed GMA and SMA welded plate. Table 4.03122.

4.03123 Rotating beam fatigue strength at cryogenic temperatures for base metal GMA and SMA welds. Table 4.03123.

4.03124 Impact energy of GMA weld metal at -320 F as function of nickel content of wire. Fig. 4.03124.

4.03125 Effect of low temperatures on impact energy of 11 percent Ni GMA weld metal. Fig. 4.03125.

4.03126 Room temperature tensile properties and -320 F impact energy of automatic GTA weld metal for various welding positions. Table 4.03126.

4.03127 Effect of nitrogen or oxygen content on -320 F impact energy of ferritic weld metal deposited by automatic GTA process. Fig. 4.03127.

4.03128 Effect of heat input on -320 F impact energy of weld metal and HAZ produced by automatic GTA process using a ferritic filler. Fig. 4.03128.

4.03129 Effect of heat input on tensile properties of ferritic weld metal produced by automatic GTA process. Fig. 4.03129.

4.03130 Effect of surface reheat on -320 F Charpy-V impact energies of GTA weldments made with a ferritic filler. Table 4.03130.

4.03131 Low temperature tensile and impact properties of ferritic weld metal deposited by automatic GTA. Table 4.03131.

4.03132 Impact energy at -320 F for ferritic weld metal deposited by automatic GTA as function of notch distance from plate surface. Fig. 4.0313.

4.03133 Impact energy at -320 F for ferritic weld metal deposited by automatic GTA as function of distance from weld center. Fig. 4.03133.

4.03134 Welding conditions with ferritic filler and resulting weld metal -320 F Charpy impact values. Table 4.03134.

4.03135 Example of sub-arc welding conditions and resulting weld properties. Table 4.03135.

4.03136 Results of cryogenic burst tests on as-welded test cylinders. Table 4.03136.

REFERENCES

1 Zick, L.P., Crossett, J.W., and Langford, W.T. Jr., "Destructive Tests of 9 Percent Nickel Steel Vessels at -320 F", ASME paper 62-WA-273 (1962).

2 Hardwick, D., "Properties of 9% Nickel Steel, Metallurgical Developments in High Alloy Steels" Special Report No. 86 Iron and Steel Institute, p. 49, (1964).

3 "9% Nickel Steel for Low Temperature Service", International Nickel Co. One New York Plaza, N.Y., N.Y. 10004 (1975).

4 Pense, A. W., Lehigh University, personal communication with W.F. Brown Jr., (1978).

5 Haynes, A.G., Firth, K., Holloy, G.E., and Buchan, J., "Strength and Toughness of Nickel Containing Steels" Properties of Metals for Liquified Gas Tankage, ASTM STP 579, p. 228 (1975).

6 Porter, L.F., U.S. Steel Corp. personal communication with W.F. Brown Jr. (1978).

	Fe
0.13 max	C
8.5-9.5	Ni
0.9	Mn
0.15-0.30	Si

9 Ni Steel

7 Properties of a 9 Percent Nickel Steel Heat-Treated to Simulate a 27½ Inch Thick Plate", Research Bulletin, U.S. Steel Corporation (October 24, 1975).

8 Sarno, D.A., McCabe, D.E. Jr., and Heberling, T.G., "Fatigue and Fracture Toughness Properties of 9 Percent Nickel Steel at LNG Temperatures", J. of Engineering for Industry, Trans. ASME, p. 1069 (Nov. 1973).

9 Tenge, P., and Solli, O., "Fracture Mechanics in Design of Large Spherical Tanks for Ship Transport of LNG", Norwegian Maritime Research, Vol. 1 and 2, p. 1 (1973).

10 Zambrow, J.L., and Fontana, M.G., "Mechanical Properties Including Fatigue of Aircraft Alloys at Very Low Temperatures", Trans. ASM, Vol. 41, p. 480 (1949).

11 "Final Results from Operations Cryogenics–9% Nickel Steel Vessels Impact and Burst Tests", The International Nickel Co., Chicago Bridge and Iron Co., and United States Steel Corporation (1961).

12 Tobler, R.L., Mikesell, R.P., and Reed, R.P., "Cryogenic Effects on the Fracture Mechanics Parameters of Ferritic Nickel Alloy Steels", Preliminary Data from Cryogenics Division NBS, Boulder, Colorado (Sept. 1977).

13 "Standard Specification for Pressure Vessel Plates. Alloy Steel, 9 Percent Nickel Double Normalized and Tempered", ASTM A 353-74.

14 Ibid. "Alloy Steel Quenched and Tempered 8 and 9 Percent Nickel", ASTM A 553-74.

15 "Standard Specification for Forged or Rolled 8 and 9 Percent Nickel Alloy Steel Flanges, Fittings, Vavles and Parts for Low Temperature Service", ASTM A 522-76.

16 Marschall, C.W., Hehemann, R.F., and Toriano, A.R., "The Characteristics of 9% Ni Low Carbon Steel", Trans. ASM, Vol. 55, p. 135 (1962).

17 McMahon, R.J., Cianelli, A.K., and Feng, H.C., "The Influence of Mo on P- Induced Temper Embrittlement in Ni-Cr Steel", Met. Trans. Vol 8A, p. 1055 (July 1977).

18 Cianelli, A.K., Feng, H.C., Ucisik, A.H., and McMahon, C.J., Jr., "Temper Embrittlement of Ni-Cr Steel by Sn", Ibid, p. 1059.

19 McMahon, C.J. Jr., "Temper Brittleness–An Interpretative Review", Temper Embrittlement in Steel, ASTM STP 407, p. 127 (1968).

20 "Report of Progress of the Investigation for Heavy Section 9% Ni Steel", Section 3 Ref. PL 76-12-326, Japan Steel Research Laboratory, Hokkaido, Japan (Dec. 4, 1976).

21 Ibid: Section 2 Ref. PL 77-3-352 and Section 3 Ref. PL 77-3-353, Japan Steel Research Laboratory, Muroran Plant, Hokkaido, Japan (April 15, 1977).

22 Nisbett, E.G., National Forge Co., personal communication with W.F. Brown Jr. (1978).

23 Unpublished dat, W.F. Brown Jr., NASA-Lewis, 1978.

24 Armstrong, T.N., Gross, J.H., and Brien, R.E., "Properties Affecting the Stability of 9 Percent Ni Steel for Low Temperature Service", Welding Res. Supplement, p. 575 (Feb. 1959).

25 Pense, A.W., and Stout, R.D., "Fracture Toughness and Related Characteristics of the Cryogenic Nickel Steels", WRC Bulletin No. 205 (May 1975).

26 "Note on the Low Temperature 9 Percent Ni Steel Plate and Its Welding", Sumitomo Metals, Report 74-E-02 (in Japanese) (1974).

27 Tharby, R.H., Heath, D.J., and Flannery, J.W., "Welding 9% Nickel Steel–A Review of Current Practices", proc. Conf. on Welding Low Temperature Containment Plant, Welding Inst. (1973).

28 Kim, K.J., and Schwartz, L.H., "On the Effects of Intercritical Tempering on the Impact Energy of Fe-9Ni-0.1C", Materials Science and Engineering, Vol. 33, p. 5 (1978).

29 Syn, C.K., Jin, S., and Morris, J.W.,: "Cryogenic Fracture Toughness of 9 Ni Steel Enhanced Through Grain Refinement", Met. Trans. A Vol. 7A, p. 1827 (December 1976).

30 Scott, R., "Directionality of Mechanical Properties in Hot Rolled Steel Plates", Metals Technology, p. 71 (February 1976).

31 "Standard Specification for Seamless Welded Carbon and Alloy Steel Tubes for Low Temperature Service", ASTM A 334-77.

32 "Standard Specification for Seamless Welded Steel Pipe for Low Temperature Service", ASTM A 333-77.

33 Data from Japan Steel furnished to W.F. Brown Jr. (1979).

34 W.F. Brown Jr. Unpublished data, NASA-Lewis (1979).

35 Joining: Huntington Alloys (1978).

36 Mariyama, K., Yoshinaga, J., Kishida, T., Sakai, K., Yamamoto, M., and Ootani, H., "Production of 9 Ni Steel Plate for Tank of Ultra Low Temperature Service", Sumitomo Serach, No. 18 (November 1977).

37 Mahin, K.W., Morris, J.W. Jr., and Watanabe, I., "Review of the Development of Ferritic Consumables for the Welding of 9% Nickel: Research in the U.S. and Japan", Cryogenic Engineering Conference (August 21-24, 1979).

38 Arikawa, M., Ohi, A., Sugiyama, T., Hashimoto, C., and Nishikawa, Y., "High Quality All-Position Welding of 9 Ni Steels", Proc. 2nd International Symposium of Japan Welding Society on Advanced Welding Technology, Paper No. 2-2-(12) (August 1975).

39 Godia, T., Sugiyama, T., Nishikawa, Y., Ikeda, K., Aoki, M., and Kiuchi, A., "Fracture Characteristics and Mechanical Properties of 9% Nickel Steel Welded with Ferritic Filler", Welding Research International, Vol. 8, No. 5, p. 379 (1978).

40 Tokushige, H., "5th Report of the Study of 230 mm Thick 9% Nickel Steel Forged Ring-Weldability and Mechanical Properties of SMAW Butt Welds", Ref. No. PL 77-8-386, Japan Steel Research Laboratory, Muroran Plant (August 15, 1977).

41 Rosa, G.F., and Bove, O., "Automatic Welding of 9 Ni Steel Plate for Large LNG Storage Tanks", Weld. and Metal Fab., Vol. 41, p. 62 (1973).

	Fe
0.13 max	C
8.5-9.5	Ni
0.9	Mn
0.15-0.30	Si

9 Ni Steel

Alloy	Fe-9Ni			
Form	Plate	Forgings	Tubing	Pipe
ASTM	A353-74 A553-74	A522-76	A334-77	A333-77
ASME	SA 353 SA 553	SA 522	SA 334	SA 333
SAE-ASTM Unified Number	K81340	K81340	K81340	K81340

TABLE 1.03. SPECIFICATIONS

Alloy	Fe-9Ni				
Form	Plate		Forgings	Tubing	Pipe
Source	(13)(14)		(15)	(30)	(31)
Composition, percent	Min	Max	Min	Max	
Carbon	--	0.13	--	0.13	
Manganese	--	0.90	--	0.90	
Phosphorous	--	0.035	--	0.040	
Sulphur	--	0.040	--	0.040	
Silicon	0.15	0.30	0.15	0.30	
Nickel	8.50	9.50	8.50	9.50	

TABLE 1.04. CHEMICAL COMPOSITION BY HEAT ANALYSIS (13)(14)(15)(30)(31)

Alloy	Fe-9Ni			
Form	0.38 to 3-inch Plate(a)			
Condition	Double Normalized and Tempered		Quenched and Tempered	
Test Temp, F	RT	-320	RT	-320 F
No. of Tests	16	10	58	26
F_{tu}, ksi				
Average	111	171	112	162
Std Dev	6.9	5.9	4.1	10.1
F_{ty}, ksi				
Average	93	135	103	130
Std Dev	8.4	10.5	6.1	17.9
No. of Tests	--	7	--	15
Charpy-V, ft lb (at -320 F)				
Average	--	39	--	50
Std Dev	--	5.6	--	17.5

(a) The data base was insufficient to distinguish an effect of thickness.

TABLE 1.058. VARIATION IN MECHANICAL PROPERTIES OF COMMERCIALLY HEAT TREATED PLATE [(25), TABLES 12 AND 14]

Alloy	Fe-9Ni							
Form	5-inch Slab							
Condition	1553 F, 2 hr, WQ + 1481 F, 2 hr, WQ + 1103 F, 2 hr, AC							
Stress Relieve	No				1050 F, 15 hr, AC			
Location	¼ Thick		Center		¼ Thick		Center	
Direction	L	T	L	T	L	T	L	T
F_{tu}, ksi	100	100	–	–	96	95	–	–
F_{ty}, ksi	89	89	–	–	87	86	–	–
Charpy-V, ft lb (at -320 F)	71	55	55	58	42	49	47	46

TABLE 1.059. TENSILE AND -320 F IMPACT PROPERTIES OF A DOUBLE QUENCHED AND TEMPERED 5-INCH THICK SLAB BEFORE AND AFTER STRESS RELIEF (6)

Alloy	Fe-9Ni											
Form	½-inch Plate											
Condition	1475 F, ½ hr, WQ + 1100 F, 2 hr, WQ						1650 F, ½ hr, AC + 1450 F, ½ hr, AC + 1100 F, 2 hr, WQ					
Stress Relief after Plastic Strain	1050 F 2 hr, AC			None			1050 F 2 hr, AC			None		
Plastic Strain, percent	0	5	10	0	5	10	0	5	10	0	5	10
Charpy-V, ft lb (at -320 F)	–	42	40	33	21	18	–	39	40	32	12	10

TABLE 1.0510. EFFECT OF COLD WORK AND SUBSEQUENT STRESS RELIEF ON CHARPY-V IMPACT ENERGY OF PLATE [(3), FIGURE 9]

	Fe
0.13 max	C
8.5–9.5	Ni
0.9	Mn
0.15–0.30	Si

9 Ni Steel

Alloy	Fe-9Ni							
Form	0.94-inch Plate							
Condition	1625 F, 1 hr, WQ + 1454, 1 hr, WQ + 1067 F, 1 hr, WQ(a)		1625 F, 2 hr, WQ + 1346 F, 1 hr, WQ + 1202 F, 1 hr, WQ + 1346 F, 1 hr, WQ + 1202 F, 1 hr, WQ + Temper 1 hr(b) at					
			1022 F, WQ		1067 F, WQ		1112 F, WQ	
Test Temp, F	-320	-452	-321	-452	-320	-452	-320	-452
F_{tu}, ksi	163	204	–	–	163	223	–	–
F_{ty}, ksi	145	189	–	–	146	191	–	–
e, percent	34	25	–	–	–	–	–	–
RA, percent	72	65	–	–	–	–	–	–
Charpy-V, ft lb	125	75	137	128	–	–	107	106

(a) Grain size ~ 10μm. (b) Grain size after tempering ~ 1-4μm.

TABLE 1.0511. EFFECT OF GRAIN REFINING HEAT TREATMENT ON CRYOGENIC TENSILE AND IMPACT PROPERTIES OF PLATE [(29), P. 1830]

Alloy	Fe-9Ni				
Form	1.2-inch Plate				
Condition	1475 F, 1 hr, Cool at Rates A, B, C, D, or E Between 1292 and 572 F + 1075 F, 1 hr, Cool at Rates A, B, C, D, or E Between 1292 and 572 F				
Cooling Rate(a)	A	B	C	D	E
Plate Thickness For Equivalent Cooling Rate in					
Air, inches	0.08	0.67	0.91	1.4	11(b)
Water, inches	1.2	4.3	5.5	7.0	–
Bainite, percent	0	10	25	60	95

(a) Rates in F/min between 1292 and 572 F: A = 882, B = 94, C = 67, D = 41, E = 4.5.
(b) Cooled in Vermiculite.

TABLE 1.0514. EFFECT OF COOLING RATES FROM AUSTENITIZING AND FROM TEMPERING TEMPERATURES ON FORMATION OF BAINITE [(5), TABLE 5]

Alloy	Fe-9Ni			
Composition	0.11 C, 0.21 Si, 0.59 Mn,, 0.007 S, 0.013 P			
Section Size	4¾-inch Sq Billet		9-inch Dia Forging	
Heat Treatment(a)	1454 F, AC + 1063 F, AC	1454 F, OQ + 1063 F, AC	1454 F, AC + 1058 F, AC	1454 F, OQ + 1058 F, AC
RT F_{tu}, ksi(b)	98	98(c)	120	110
RT F_{ty}, ksi(b)	72	88(c)	74	88
Charpy-V, ft lb(b) (at -320 F)	30	62	5	22

(a) Austenitizing was preceded by 1652 F normalize with quench medium as for austenitize.
(b) All tests represent center positions in the billets or forgings except as indicated.
(c) Mid radius position.

TABLE 1.0914. EFFECT OF SECTION SIZE AND COOLING RATE FROM THE AUSTENITIZING TEMPERATURE ON THE ROOM TEMPERATURE TENSILE STRENGTH AND THE -320 F CHARPY IMPACT ENERGY OF FORGINGS [(2), TABLE 7]

Alloy	Fe-9Ni	
Composition	0.10 C, 0.40 Si, 0.50 Mn, 0.008 S, 0.006 P, 0.010 Sn, 0.003 Sb, 0.035 As	
Form	Cast 5/8-inch Bar From 28 lb Heats	
Heat Treatment	1652 F, AC + 1050 F, 4 hr, WQ	1562 F, AC + 1050 F, 4 hr, Cool 18 F/hr
RT F_{tu}, ksi	114	114
RT F_{ty}, ksi	103	103
Charpy-V, ft lb (at -320 F)	50	8

TABLE 1.0919. INFLUENCE OF COOLING RATE FROM THE TEMPERING TEMPERATURE ON THE ROOM TEMPERATURE TENSILE STRENGTH AND THE -320 F IMPACT ENERGY OF CAST BAR [(2), FIGURES 7, 8, 9, AND TABLE 8]

	Fe
0.13 max	C
8.5–9.5	Ni
0.9	Mn
0.15–0.30	Si

9 Ni Steel

Alloy	Fe-9Ni					
Form	¾-inch Bar					
Condition	1450 F, ½ hr, WQ + 1050 F, 20 hr, WQ + A, B or C					
	A = 800 F, 6 days, WQ		B = A + 1050 F, 2 hr, WQ		C = B + A	
Test Temp, F	RT	-320 F	RT	-320 F	RT	-320 F
Charpy-V, ft lb	127	23	141	60	132	23

TABLE 1.0920. IMPACT RESULTS ILLUSTRATING THE REVERSIBILITY OF TEMPER EMBRITTLEMENT [(16), P. 143]

Alloy	Fe-9Ni			
Composition	0.09 C, 0.42 Mn, 0.012 S, 0.012 P, 0.25 Si, 0.01 Mo, 0.02 Cr			
Form	2-inch Plate			
Heat Treatment	1650 F, 2 hr, FC + 1100 F, 2 hr, FC FC at Rate to Simulate Cooling of a WQ, 27½-inch Thick Plate		1650 F, 2 hr, FC + 1100 F, 2 hr, FC FC at Rate to Simulate Cooling of a AC, 27½-inch Thick Plate	
Specimen Position in 27½-inch Plate	Mid Thickness	¼ Thickness	Mid Thickness	¼ Thickness
RT F_{tu}, ksi	118	115	115	118
RT F_{ty}, ksi	94	90	81	84
Charpy-V, ft lb (at -320 F)	13	14	4	9

TABLE 1.0921. EFFECT OF COOLING RATE FROM THE AUSTENITIZING AND TEMPERING TEMPERATURE ON THE ROOM TEMPERATURE TENSILE STRENGTH AND THE -320 F IMPACT ENERGY OF A 2-INCH THICK PLATE COOLED AT A RATE TO SIMULATE THAT OF A 27½-INCH THICK PLATE (7)

Alloy	Fe-9Ni					
Composition	0.10 C, 0.27 Si, 0.01 Mo, 0.14 Cr[a]			0.10 C, 0.14 Si, 0.15 Mo, 0.16 Cr[b]		
Heat Treatment[c]	Quench and Temper	Stress Relieved	Very Slow Cool	Quench and Temper	Stress Relieved	Very Slow Cool
RT F_{tu}, ksi	114	110	–	115	114	–
RT F_{ty}, ksi	82	85	–	101	101	–
Charpy-V, ft lb (at -320 F)	52	18	7	68	66	53
Lateral Expansion, mils	29	9	3	43	47	34

(a) Heat V-8 residuals: 0.012 P, 0.005 S, 0.010 As, 0.019 Sn, 0.0031 Sb.
(b) Heat V-3 residuals: 0.010 P, 0.006 S, 0.008 As, 0.021 Sn, 0.0025 Sb.
(c) Quench and temper: 1472 F, 3 hrs, cool 36 F/min. + 1061 F, 8 hrs, WQ.
Stress relieved: Quench and temper + 1049 F, 15 hrs, cool 299 F/hr.
Very slow cool: Quench and temper + 1049 F, 1 hr, cool 18 F/hr.

TABLE 1.0922. AVERAGE VALUES OF ROOM TEMPERATURE TENSILE STRENGTH AND -320 F IMPACT PROPERTIES OF SPECIMENS FROM TWO HEATS ILLUSTRATING THE INFLUENCE OF COMPOSITION ON TEMPER EMBRITTLEMENT [(21), SECTION 3, TABLES 1, 3, 4, 5, 6 AND 7]

	Fe
0.13 max	C
8.5–9.5	Ni
0.9	Mn
0.15–0.30	Si

9 Ni Steel

Alloy	Fe-9Ni					
Composition	0.08 C, 0.18 Si, 0.54 Mn, 0.005 S, 0.005 P, 0.02 Mo, 0.006 As, 0.008 Sn, 0.0013 Sb					
Form	50-inches OD x 31.5-inches ID x 28-inches High Forged Cylinder					
Specimen Location	4½ inches From Quenched End at Mid Thickness (½T)					
Heat Treatment	Quench and Temper[a]		Stress Relieved[b]		Very Slow Cool[c]	
Test Direction	Tangential	Axial	Tangential	Axial	Tangential	Axial
RT F_{tu}, ksi	99	–	99	–	99	–
RT F_{tu}, ksi	78	–	77	–	79	–
Charpy-V, ft lb (at -320 F)	58	50	52	47	43	44
Lateral Expansion, mils	37	33	33	29	29	32

(a) Quench and Temper: 1492 F, 9 hr, WQ + 1076 F, 8 hr, WQ.
(b) Stress Relieved: Quench and Temper + 1058 F, 8 hr, cool 299 F/hr.
(c) Very Slow Cool: Quench and Temper + 1058 F, 16 hr, cool 18 F/hr.

TABLE 1.0923. INFLUENCE OF STRESS RELIEF HEAT TREATMENTS ON THE AVERAGE VALUES OF TENSILE STRENGTH AND -320 F IMPACT ENERGY OF SPECIMENS FROM A QUENCHED AND TEMPERED THICK WALLED CYLINDER [(21), SECTION 2, TABLES 1 AND 2]

Alloy	Fe-9Ni							
Form	9 x 20 x 34-inches, Forged Billet[a] [e]							
Condition	1650 F, 9 hr, WQ + 1475 F, 9 hr, WQ + 1080 F, 9 hr, WQ + Stress Relief							
Test Temp, F	-150				-320			
Test Direction[f]	LT		TL		LT		TL	
Stress Relief[b]	Yes	No	Yes	No	Yes	No	Yes	No
Charpy-V, ft lb[c] (at -320 F)	95	67	–	–	50	49	–	30

(a) Composition: 0.11 C, 0.59 Mn, 0.010 S, 0.009 P, 0.26 Si, 8.58 Ni, 0.28 Cr, 0.08 Mo, 0.10 Cu.
(b) Stress Relief: 1055 F, 20 hr, cool 300 F max/hr.
(c) Specimens at center of 9-inch dimension.
(e) RT $F_{tu}(L)$ = 124 ksi, RT $F_{tu}(T)$ = 121, RT $F_{tu}(L)$ = 118 ksi after stress relief.
(f) See ASTM E399-78.

TABLE 1.0924. EFFECT OF TEST TEMPERATURE AND STRESS RELIEF ON LOW TEMPERATURE IMPACT ENERGY OF A LARGE FORGED BILLET(22)

Alloy	Fe-9Ni			
Form	11-inches Thick x 162-inches dia Forged Disk[a] Electric Furnace Air Melt, Al Deoxidation in Ladel, Vacuum Stream Degassed			
Condition	1652 F, 16 hrs, AC + 1112 F, 16 hr, AC + 1472 F, 12 hr, WQ + 1076 F, 18 hr, AC + 1022 F, 15 hr, AC + 842 F, 4 hrs, Cool 54 F/hr, to RT			
Specimen Position in Reference to Disk Faces	Surface		Center	
Specimen Radial Position	Rim	Bore	Rim	Bore
Test Direction	Radial	Radial	Tangential	Tangential
F_{tu}, ksi	116	118	115	117
F_{ty}, ksi	104	106	104	105
e (2-inches), percent	26	27	27	27
RA, percent	78	69	75	73

(a) Composition: 0.12 C, 0.15 Si, 0.64 Mn, 0.006 P, 0.010 S, 9.17 Ni, 0.20 Mo, 0.013 Al, 0.10 Cr, 0.05 Cu, 0.007 Sn, 0.0015 Sb, 0.0073 N, 11 ppm H, 15 ppm O.

TABLE 1.0925. TENSILE PROPERTIES OF VERY LARGE QUENCHED AND TEMPERED AND STRESS RELIEVED DISK FORGING (32)

Alloy	Fe-9Ni			
Form	11-inches Thick x 162-inches Dia Disks[a]			
Condition	See Table 1.0925			
Specimen Position Respect to Disk Faces	Surface		Center	
Specimen Radial Position	Rim	Bore	Rim	Bore
Notch Orientation[b]	RC	RC	CR	CR
Charpy-V, ft lb				
at -275 F	93	95	–	–
at -320 F	79	78	85	82

(a) For Composition see Table 1.0925. (b) See ASTM E399-78.

	Fe
0.13 max	C
8.5-9.5	Ni
0.9	Mn
0.15-0.30	Si

9 Ni Steel

TABLE 1.0926. CHARPY-V IMPACT ENERGIES AT CRYOGENIC TEMPERATURES FOR A VERY LARGE QUENCHED AND TEMPERED AND STRESS RELIEVED DISK FORGING (32)

Alloy	Fe-9Ni					
Form	Hot Worked Pipe 6¼-inches ID x 2 23/32-inches Wall Thickness			Cold Worked Pipe 6-inches ID x 3/8-inch Wall Thickness		
Condition	Double Normalize[a] + Temper	Quench[b] + Temper	As Rec'd[c] + Temper	Double Normalize + Temper	Quench + Temper	As Rec'd + Temper
F_{tu}, ksi	100	101	–	103	105	98
F_{ty}, ksi	84	93	–	90	88	92
e, percent	34	33	–	36	36	34
RA, %	76	79	–	80	80	79
Charpy-V, ft lb						
RT	155	166	131	133	142	122
-320 F	51	135	9	71	59	38

(a) 1650 F, AC + 1450 F, AC + 1060 F, 2 hr, AC. (b) 1450 F, WQ + 1060 F, 2 hr, WQ.
(c) As received + 1060 F, 2 hr, AC.

TABLE 1.0929. EFFECT OF SEVERAL HEAT TREATMENTS ON THE TENSILE AND IMPACT PROPERTIES OF HOT WORKED AND COLD WORKED PIPE [(2), TABLE 3]

Alloy	Fe-9Ni			
Condition	1650 F, AC + 1450 F, AC + 1100 F, AC			
Temp, F	-320 to 80	80 to 700	80 to 1000	700 to 1000
Mean Btu/lb/F	0.0878	0.119	0.131	0.156

TABLE 2.015. SPECIFIC HEAT [(3), TABLE 12]

Alloy	Fe-9Ni			
Form	Plate	Forgings	Tubing	Pipe
Source	(13)(14)	(15)	(30)	(31)
F_{tu}, ksi	100-120	100 (min)	100 (min)	100 (min)
F_{ty}, ksi	85 (min)	75 (min)	75 (min)	75 (min)
e (2-inches), %	20 (min)	--	(b)	(b)
RA, percent	--	45 (min)	--	--
Charpy-V, ft lb[a] (at -320 F)				
L	25 (min)	--	--	--
T	20 (min)	--	--	--

(a) Average of three tests with not more than one value below the minimum and no value < 20 ft lb.

(b) See ASTM A334 (tubing) or ASTM A333 (pipe) for elongation minimum values for various specimen types and wall thicknesses.

TABLE 3.011. SPECIFIED MECHANICAL PROPERTIES FOR VARIOUS PRODUCT FORMS

Alloy	Fe-9Ni
Condition	1650 F, AC + 1450 F, AC + 1100 F, AC
Temp, F	Saturation Induction - Gauss at 16,700 Oersteds
-320	21,360
-148	20,830
32	20,300
68	20,210
212	19,850
316	19,250
572	18,500
752	17,570
932	16,290

TABLE 2.0231. MAGNETIC PROPERTIES OF DOUBLE NORMALIZED ALLOY [(3), TABLE 13]

	Fe
0.13 max	C
8.5-9.5	Ni
0.9	Mn
0.15-0.30	Si

9 Ni Steel

Alloy	Fe-9Ni			
Form	3/8-inch Plate			
Condition	1475 F, ½ hr, WQ + 1100 F, 2 hr, WQ		1650 F, ½ hr, AC + 1450 F, ½ hr, AC + 1100 F, 2 hr, WQ	
	9 Plates		6 Plates	
	Avg	Std Dev	Avg	Std Dev
F_{tu}, ksi	108.9	2.7	105.4	3.5
F_{ty}, ksi	101.8	3.4	83.4	1.8
Charpy-V, ft lb (at -320 F)	30.6	2.5	29.1	3.1

TABLE 3.012. PRODUCERS TENSILE AND -320 F CHARPY-V IMPACT PROPERTIES OBTAINED BY TESTS ON MANY 3/8-INCH PLATES [(11), P. 13]

Alloy	Fe-9Ni							
Form	Plate							
Condition	Double Normalize and Temper per ASTM A553				Quench and Temper per ASTM A353			
Thickness, inches	0.63		0.75		0.63		0.75	
RT F_{tu}, ksi	111	115	113	118	112	117	111	119
RT F_{ty}, ksi	91	94	83	104	103	110	94	115
Drop Weight, ft lb (at -320 F)	1379	800	649	800	2094	991	2334	2534
Charpy-V, ft lb (at -320 F)	36	39	33	27	50	29	54	35

TABLE 3.0339. DROP WEIGHT TEAR AND CHARPY-V ENERGIES AT -320 F FOR DOUBLE NORMALIZED AND FOR QUENCHED AND TEMPERED PLATES OF TWO THICKNESSES [(25), TABLE 13]

Alloy	Fe-9Ni			
Form	3-inch Plate[a]		1¼-inch Plate[b]	
Condition	As Rolled		1455 F, 1½ hr, WQ 1119 F, 1¼ hr, AC	
Test Temp, F	-170	-320	-320	-423
F_{ty}, ksi	–	–	149	174
K_{Ic}, ksi-inch^{½}	45	63	153[c]	83

(a) Ref 4 (b) Ref 12, Table 4 (c) Converted from J_{Ic}

TABLE 3.03721. PLANE STRAIN FRACTURE TOUGHNESS OF PLATE AT CRYOGENIC TEMPERATURES (4) (12)

Alloy	Fe-9Ni			
Form	9 x 20 x 34-inches Forged Billet[a]			
Direction[b]	SL			
Condition[c]	A		B	C
Test Temp, F	RT	-320	-320	-320
F_{tu}, ksi	124	177	178	178
F_{ty}, ksi	118	163	161	149
RA, percent	50	15	14	24
K_{Ic}, ksi-inch^{½}	–	91	85	132
Charpy-V, ft lb	–	22	–	–

(a) For Composition see Table 1.0911.
(b) See ASTM E399-78.
(c) Condition A - 1650 F, 9 hr, AC + 1050 F, 9 hr, AC + 1470 F, 9 hr, WQ + 1050 F, 9 hr, AC + Stress Relief 1025 F, 9 hr, AC to 800 F, 4 hr, FC 18 F/hr.
Condition B - Condition A + 1050 F, 3 hr, FC 150 F/hr, specimen blanks heat treated.
Condition C - Condition A + 1050 F, 3 hr, WQ, specimen blanks heat treated.

TABLE 3.03722. EFFECT OF TEST TEMPERATURE AND STRESS RELIEF ON ROOM TEMPERATURE AND -320 F TENSILE PROPERTIES AND PLANE STRAIN FRACTURE TOUGHNESS OF A LARGE FORGED BILLET (33)

	Fe
0.13 max	C
8.5-9.5	Ni
0.9	Mn
0.15-0.30	Si

9 Ni Steel

Alloy	Fe-9Ni		
Form	11-inches Thick x 162-inches Dia Forged Disk		
Condition	See Table 1.0925 For Condition and Composition		
Specimen Position With Respect to Disk Faces	Center		
Specimen Radial Position	Rim		Bore
Test Direction(b)	RL	LR	RL
F_{tu}, ksi (RT)	116	115	114
F_{ty}, ksi (RT)	105	105	102
RA, percent (RT)	72	73	66
F_{tu}, ksi (-320 F)	178	178	179
F_{ty}, ksi (-320 F)	146	147	141
RA, percent (-320 F)	54	42	60
K_{Ic}, ksi-inch$^{1/2}$(a) (-320 F)	193	193	182

(a) Converted from J_{Ic} (E at -320 F = 29000 ksi) (b) See ASTM E399-78

TABLE 3.03723. TENSILE PROPERTIES AND PLANE STRAIN FRACTURE TOUGHNESS OF A VERY LARGE QUENCHED AND TEMPERED AND STRESS RELIEVED DISK FORGING (33)

Alloy	Fe-9Ni			
Form	¼-inch Plate From Air Melt 100 Ton Heat			
Condition(a)	1475 F, ¼ hr, WQ + 1120 F, ½ hr, AC			
Method	Rotating Beam R = 1 F = 10,000 rpm			
	Fatigue Strength at -270 F, ksi at Cycles			
	10^4	10^5	10^6	10^7
Stress Conc.				
K_t = 1	–	(135)	100	98
K_t = 2.7	(110)(b)	65	48	40

(a) -270 F, F_{tu} = 152 ksi.
(b) Numbers in ( ) extrapolated.

TABLE 3.0513. ROTATING BEAM FATIGUE STRENGTH AT -270 F FOR ¼-INCH QUENCHED AND TEMPERED PLATE [(8), FIGURE 6]

Alloy	Fe-9Ni	
Form	11-inches, Thick x 162-inches Dia Forged Disk	
Condition	See Table 1.0912	
Temp	RT	-320 F
E, 1000 ksi	29.5	28.6

TABLE 3.0621. STATIC ELASTIC MODULUS AT ROOM TEMPERATURE AND -320 F (33)

Alloy	Fe-9Ni						
Form	Welding Wire - Coated Electrodes						
Designation	Inco Weld A	Inco(c) Weld B	Inco 182	Nyloid-2(c)	Cryotherm 60	ERNo Cv-6	Inco(a) 113
Element, percent							
C	0.03	0.10	0.05	0.08	0.17	0.12	0.05
Ni	70.0	70.0	67.0	65.0	51	66(b)	62.5
Cr	15.0	15.0	14.0	13.0	10	5	21.5
Mo	15.0	2.0	–	6.0	2.5	24	9.0
Mn	2.0	2.0	7.8	3.0	2.7	1.0	1.0
Fe	9.0	9.0	7.5	Bal	Bal	5.5	2.5
Cb + Ta	1.8	2.5	1.8	1.2	1.3	–	2.8
Ti	–	–	0.4	–	–	–	–
S	0.008	0.008	0.008	–	–	0.03	0.01
Cu	0.006	0.06	0.1	–	–	–	0.2
Si	0.3	0.3	0.5	–	–	1.0	0.4
W	–	–	–	1.2	–	–	–
V	–	–	–	–	–	–	0.60

(a) Supercedes Inco 112. (b) Includes 2.5% Co. (c) For use with AC.

TABLE 4.0315. TYPICAL COMPOSITIONS OF WELDING WIRE FOR COATED ELECTRODES [(27), TABLE 5; (34), P. 59]

	Fe
0.13 max	C
8.5-9.5	Ni
0.9	Mn
0.15-0.30	Si

9 Ni Steel

Alloy	Fe-9Ni				
Form	Welding Wire - Filler Metal				
Designation	Inconel 92	Inconel 82	Inconel 625	Chromenar	ERNo Cv-3
Element, percent					
C	0.03	0.02	0.05	0.04	0.10
Ni	71.0	72.0	61.0	67.0	67.0
Cr	16.4	20.0	21.5	–	20.0
Mo	–	–	9.0	–	–
Mn	2.3	3.0	0.2	3.0	3.0
Fe	6.6	1.0	2.5	1.0	3.0
Cb + Ta	–	2.5	3.6	2.5	2.5
Ti	3.2	0.6	0.2	0.5	0.75
S	0.007	0.007	0.008	–	0.015
Cu	0.04	0.04	–	–	0.50
Si	0.1	0.2	0.2	–	0.50
Al	–	–	0.2	–	–

TABLE 4.0316. TYPICAL COMPOSITIONS OF WELDING WIRE FOR FILLER METAL [(27), TABLE 6; (34), P. 58 AND 59]

Alloy	Fe-9Ni			
Welding Process	SMA	Subarc	GMA	GTA
Electrodes and/or Fluxes	See Table 4.0311 Hastelloy C	Wires: AWS ERNiCr-3 Inco 92 Inco 82 Fluxes Inco 4 Lincoln 880 Nittetsu-10	Inco 625 Inco 92 Inco 82	NGS 709W(a)

(a) 0.025 C, 0.16 Si, 0.23 Mn, 14.6 Cr, 13.7 Mo, 2.8 W, 5.6 Fe, Bal Ni.

TABLE 4.0317. EXAMPLES OF ELECTRODES USED IN VARIOUS WELDING PROCESSES FOR FABRICATION OF LNG TANKS OF 9NI STEEL

Alloy	Fe-9Ni									
Form	1.02-inch Plate									
Condition	Double Normalized and Tempered per ASTM A353-722 + Weld									
Welding Conditions	SMA, 0.16-inch Dia Electrode(a), 120-130 Amps, 27 V, 5.9-inches/min, 34,300 J/inch									
Stress Relief	None					1058 F, 1 hr, AC				
Specimen Location	A	B	C	D	E	A	B	C	D	E
Charpy-V, ft lb(b)										
RT	79	65	123	101	108	79	65	123	101	108
-320 F	78	65	80	40	42	75	65	80	40	30

(a) For composition of electrode see Table 4.0319.
(b) See Table 4.03114 for weld tensile strengths.

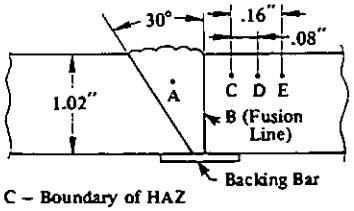


TABLE 4.0318. CHARPY-V IMPACT ENERGIES AT ROOM AND -320 F AT SEVERAL POSITIONS WITH RESPECT TO THE WELD IN SMA WELDED DOUBLE NORMALIZED AND TEMPERED PLATE [(26), P. 47, 48, 50-54]

	Fe
0.13 max	C
8.5–9.5	Ni
0.9	Mn
0.15–0.30	Si

9 Ni Steel

Alloy	Fe-9Ni									
Form	1.97-inch Plate									
Condition	Quenched and Tempered per ASTM 553-72a + Weld									
Welding Conditions	SMA, 0.16-inch Dia Electrode[a], 140 Amps, 25 V, 5.9-inches/min 35,600 J/inch									
Stress Relief	None					1058 F, 2 hr, AC				
Specimen Location[b]	A	B	C	D	E	A	B	C	D	E
Charpy-V, ft lb[c]										
RT	65	51	170	126	130	65	66	170	126	130
-320 F	60	51	66	52	46	70	61	79	64	46

(a) 0.04 C, 0.35 Si, 1.76 Mn, 0.004 P, 0.004 S, 71 Ni, 15.8 Cr, 0.87 Mo, 2.29 Cb (Essentially Inco Weld A).
(b) For specimen location see Table 4.0318.
(c) For weld tensile strengths see Table 4.03114.

TABLE 4.0319. IMPACT ENERGIES AT -320 F AT VARIOUS LOCATIONS IN AN SMA WELDMENT [(26), P. 60-64]

Alloy	Fe-9Ni						
Form	See Table 4.03113						
Composition	See Table 4.03113						
Welding Conditions	High Strength Electrode (See Table 4.03113)						
Specimen[a] Location	Weld Metal	Fusion Line	HAZ Center	HAZ Boundary	Distance From HAZ Boundary 0.08-inch	0.20-inch	Base Metal
Charpy-V, ft lb (at -320 F)							
As Welded	40	39	70	53	43	45	45
After Stress Relief[b]	40	30	56	56	47	40	34

(a) Notch at ¾ thickness position. (b) Stress relief, 1058 F, 16 hrs.

TABLE 4.03110. IMPACT ENERGIES AT -320 F AT VARIOUS LOCATIONS IN A SMA BUTT WELDED PLATE BEFORE AND AFTER STRESS RELIEF [(39), TABLE 8]

Alloy	Fe-9Ni							
Form	0.98-inch Plate							
Conditions	Quenched and Tempered Per ASTM 553-72a 3 SMA Weld + SR							
Welding Condition	Double V SMA Weld[a], 150 Amps, 25 V, 5.5 inches/min, 41,000 J/inch Interpass Temp < 212 F							
Test Location	Weld Metal				HAZ			
Stress Relief 1 hr, AC	None	1000	1058	1112	None	1000	1058	1112
F_{tu}, ksi[b]	107	106	103	106	–	–	–	–
Charpy-V, ft lb (at -320 F)	65	65	65	65	72	76	79	90

(a) Electrode Composition: 0.03 C, 70 Ni, 15 Cr, 2 Mo, 9 Mn, 3 W, 0.03 Fe.
(b) Tensile strength of transverse weld joint.

TABLE 4.03111. EFFECT OF STRESS RELIEF ON -320 F CHARPY IMPACT VALUES OF SMA WELD METAL [(26), P. 112]

	Fe
0.13 max	C
8.5-9.5	Ni
0.9	Mn
0.15-0.30	Si

9 Ni Steel

Alloy	Fe-9Ni				
Form	Weld Metal				
Weld Process	SMA DC	SMA AC	Subarc		GMA
Filler Wire or Electrode	Inco 113 ACRO Alloy Ni-9 Nylord-2	Inco Weld B	Inco 82 Inco 92	Lincoln Flux 880	Inco 625 Inco 92 Inco 82 ERNiCr-3
F_{tu}, ksi	100	108	98		100-120
F_{ty}, ksi	60	68	55		65-80
Charpy-V, ft lb (at -320 F)	47	44	80		50-100

TABLE 4.03112. EXAMPLES OF WELD PROCESSES, ELECTRODES AND FILLERS USED IN THE UNITED STATES ALONG WITH TYPICAL MECHANICAL PROPERTIES OF WELD METAL (3) (27)

Alloy	Fe-9Ni			
Form	1.18-inch Plate Cut Tangentially From Mid Thickness of 50-inch OD x 31.5 ID x 28-inch High Forged Cylinder			
Composition	See Table 1.0923 (Parent Metal)			
Welding Conditions	42 Pass SMA Butt Welds With Inconel Electrode 112, 100-130 A Direct Current, Reverse Polarity, 25-26 V, 7 to 7.5 inches/min			
Specimen	Transverse Butt Weld[a]			
	As Welded	Weld + 1058 F, 16 hr	All Weld Metal As Deposited	Parent[b] Metal
F_{tu}, ksi	102	100	111	102
F_{ty}, ksi	72	74	80	78
e(2-inch), %	31	38	38	33
RA, percent	71	70	--	72

(a) All specimens failed in base metal. (b) Quenched and tempered per ASTM 553-72a.

TABLE 4.03113. TENSILE PROPERTIES OF SMA WELDMENTS MADE ON PIECES CUT FROM A LARGE RING FORGING [(39), TABLE 5]

Alloy	Fe-9Ni			
Form	Plate			
Condition	Double Normalized and Tempered per ASTM A353-72a + Weld		Quenched and Tempered per ASTM A553-72a + Weld	
Thickness, inches	1.02		1.97	
Welding Conditions	60° Double V, SMA Butt Weld 0.16-inch Dia Electrode[c] 120-130 Amps 27 V 5.91 inches/min 34,300 J/inch		60° Double V, SMA Butt Weld 0.16-inch Dia Electrode[c] 130 Amps 24 V 5.91 inches/min 31,800 J/inch	
Stress Relief	None[a]	1058 F, 1 hr, AC	None[b]	1058 F, 1 hr, AC
F_{tu}, ksi	101	103	102	100
F_{ty}, ksi	87	91	92	94

(a) Parent Metal F_{tu} = 106 ksi, F_{ty} = 90 ksi. (b) Parent Metal F_{tu} = 107 ksi, F_{ty} = 98 ksi.
(c) For composition see Table 4.0319.

TABLE 4.03114. ROOM TEMPERATURE TENSILE PROPERTIES OF SMA WELD METAL IN MANUALLY WELDED DOUBLE NORMALIZED AND TEMPERED PLATE [(26), P. 45-46]

	Fe
0.13 max	C
8.5-9.5	Ni
0.9	Mn
0.15-0.30	Si

9 Ni Steel

Alloy	Fe-9Ni	
Form	Plate	
Condition	Quench and Temper per ASTM 553-72a + Weld	
Thickness, inches	0.63	0.98
Weld Type	Manual SMA	Manual SMA
Electrode(a)	Hastalloy C	Hastalloy C
Current, Amps	600	650
Voltage	35	35
Speed, inch/min	16.5	15.4
Heat Input, J/inch	76,200	88,900

(a) Composition: 0.08 C, 1.0 Si, 1.0 Mn, 15 Cr, 16 Mo, 3.75 W, 5.5 Fe, 0.35 V + remainder of Ni + Co.

TABLE 4.03119. WELDING CONDITIONS FOR TEST RESULTS REPRESENTED IN FIGURES 4.03115 TO 4.03118 [(26), P. 68]

Alloy	Fe-9Ni	
Form	0.55-inch Plate	
Condition	Plate Condition Not Specified + SMA V Groove Weld	
Welding Condition	To Specification JIS Z 3211	
Weld Electrode	N-9-70(a)	N-9-12(b)
F_{tu}, ksi	96	85
F_{ty}, ksi	56	61
Charpy-V, ft lb		
at RT	116	104
at -320 F	51	30

(a) 0.04 C, 0.35 Si, 1.76 Mn, 0.004 P, 0.004 S, 15.8 Cr, 71 Ni, 0.87 Mo.
(b) 0.12 C, 0.34 Si, 7.04 Mn, 0.024 P, 0.008 S, 16.33 Cr, 11.46 Ni, 0.06 Mo.

TABLE 4.03120. SHIELDED METAL ARC WELD METAL PROPERTIES FOR A HIGH AND LOW NICKEL COATED ELECTRODE COMPOSITION [(26), P. 118]

Alloy	Fe-9Ni			
Form	½-inch Plate			
Condition	1650 F, ½ hr, AC + 1450 F, ½ hr, AC + 1050 F, 2 hr, AC + Weld			
Welding(a)	SMA(b)		GMA(c)	
Notch Location	Weld	HAZ	Weld Metal	HAZ
Charpy-V, ft lb				
at RT	68-80	119-127	104-114	76-104
at -320 F	60-71	68-82	96-101	43-60

(a) Welding Conditions: 80° V, Cu backing bar, no preheat or post heat, Interpass < 200 F; SMA - 3/16-inch dia Inco-weld A, 140-150 amp rev polarity, 5 passes + root seal; GMA - 1/16-inch dia Inconel filler 92, 300-310 amp reverse polarity, 75 ft^3/hr Argon, 4 passes + root seal.
(b) RT Transverse Tensile: F_{tu} = 97 ksi, F_{ty} = 63 ksi, e = 19 percent.
(c) RT Transverse Tensile: F_{tu} = 101 ksi, F_{ty} = 66 ksi, e = 17 percent.

TABLE 4.03121. IMPACT ENERGIES FOR SMA AND GMA WELDS MADE IN ½-INCH PLATE AND NOT STRESS RELIEVED [(24), TABLE 9]

	Fe
0.13 max	C
8.5-9.5	Ni
0.9	Mn
0.15-0.30	Si

9 Ni Steel

Alloy	Fe-9Ni									
Form	¼-inch Plate From Air Melt 100 Ton Heat									
Condition[d]	1475 F, ¼ hr, WQ + 1120 F, ½ hr, AC + Single V Weld									
Weld[b][c]	Pulsed GMA Filler Inconel 92, 75% He + 25% A 4 to 6 Passes, Interpass 150 F max, 8.2 to 12.5 inches/min, 9.6 to 20.4 KJ/inch					SMA - Inco Weld B 3 to 4 Passes, Interpass 150 F max, 2.8 to 5.0 inches/min, 23.6 to 44.4 KJ/inch				
Specimen Location	Weld Metal	Fusion Line	Fusion Line + 1 mm	Fusion Line + 3 mm	Fusion Line + 5 mm	Weld Metal	Fusion Line	Fusion Line + 1 mm	Fusion Line + 3 mm	Fusion Line + 5 mm
Charpy-V, ft lb[a] at -270 F	34	31	26	30	54	19	22	22	29	37

(a) 2/3 specimen size for pulsed GMA, ½ specimen size for SMA notch plane parallel to weld direction and normal to plate surface.
(b) Welded in rolling direction.
(c) Weld Tensile Properties: Pulsed GMA, RT F_{tu} = 103 ksi, -320 F F_{tu} = 128 ksi; SMA RT F_{tu} = 104 ksi, -320 F F_{tu} = 133 ksi.
(d) For plate properties see Figure 3.031.

TABLE 4.03122. IMPACT ENERGIES AT -270 F FOR PULSED GMA AND SMA WELDED PLATE [(8), TABLES 2 AND 3]

Alloy	Fe-9Ni						
Form	¼-inch Plate From Air Melt 100 Ton Heat						
Condition	1475 F, ¼ hr, WQ + 1120 F, ½ hr, AC						
Method	Rotating Beam R = -1, F = 10,000 rpm						
	Test Temp, F	Stress Conc	Fatigue Strength, ksi at cycles 10^4	10^5	10^6	10^7	10^8
Base Metal	-320	K_t = 2.7	(95)[b]	65	42	30	27
Pulsed GMA[a] Weld	-320	K_t = 2.7	(85)	58	42	35	34
SMA Weld[a]	-320	K_t = 2.7	(85)	58	42	35	34
Base Metal	-270	K_t = 1	–	(135)	100	100	–

(a) For welding conditions and tensile properties see Table 4.03122.
(b) Numbers in ( ) extrapolated.

TABLE 4.03123. ROTATING BEAM FATIGUE STRENGTH AT CRYOGENIC TEMPERATURES FOR BASE METAL, GMA AND SMA WELDS [(8), FIGURES 6 AND 7]

Alloy	Fe-9Ni				
Form	Weld Metal in 0.9-inch Plate				
Weld Process	Automatic GTA Filler Composition 0.025 C, 0.16 Si, 0.23 Mn, 14.6 Cr, 13.7 Mn, 2.8 W, 5.6 Fe, < 50 ppm O_2, Bal Ni				
Weld Position	Flat	45° Vertical	Vertical	45° Overhead	Overhead
F_{tu}, ksi	100	99	102	101	100
F_{ty}, ksi	60	56	60	60	60
e, percent	38	38	36	44	37
Charpy-V, ft lb at -320 F	86	82	81	87	102

TABLE 4.03126. ROOM TEMPERATURE TENSILE PROPERTIES AND -320 F IMPACT ENERGY OF AUTOMATIC GTA WELD METAL FOR VARIOUS WELDING POSITIONS [(37), TABLE 2]

	Fe
0.13 max	C
8.5–9.5	Ni
0.9	Mn
0.15–0.30	Si

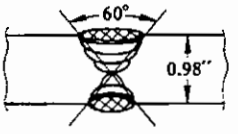
9 Ni Steel

Alloy	Fe-9Ni													
Form	0.47-inch Plate													
Wire Composition	0.04 C, 0.01 Si, 0.39 Mn, 11 Ni													
Specimen Location	GTA Weld Metal							Fusion Zone						
Weld Heat Input, KJ/inch	43		66			84		43		66			84	
Surface Reheat, KJ/inch	0	25	0	25	43	0	25	0	25	0	25	43	0	25
Charpy-V, ft lb (at -320 F)	56	59	39	52	60	30	48	52	81	22	41	66	22	44

TABLE 4.03130. EFFECT OF SURFACE REHEAT ON -320 F CHARPY-V IMPACT ENERGIES OF GTA WELDMENTS MADE WITH A FERRITIC FILLER (36)

Alloy	Fe-9Ni			
Form	Ferritic Weld Metal Deposited by Automatic GTA			
Composition	0.034 C, 0.36 Mn, 0.03 Si, 0.003 P, 0.005 S, 11.22 Ni, 0.36 Co 0.018 Al, 0.008 Ti, 0.001 B, 5 ppm N			
Welding Conditions	Verticle, 230-280 A, 10.5-11.5 V, 1.7-2.4 inches/min 84 KJ - 119 KJ/inch, Shield Argon, Interpass < 300 F GTA Surface Remelt (See Below)			
Test Temp, F	32	-148	-302	-320
F_{tu}, ksi[a]	120	137	148	169
F_{ty}, ksi	106	119	132	153
e, percent	22	22	24	25
RA, percent				
Charpy-V, ft lb[a]	166	155	140	111

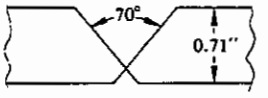
(a) Specimens at plate center.



GTA Remelt – 200 A, 10 V
2.1 inches per minute

TABLE 4.03131. LOW TEMPERATURE TENSILE AND IMPACT PROPERTIES OF FERRITIC WELD METAL DEPOSITED BY AUTOMATIC GTA [(38), TABLE 4 AND FIGURE 25]

Alloy	Fe-9Ni			
Form	0.71-inch Plate			
Wire Compositions	0.04 C, 0.01 Si, 0.39 Mn, 11 Ni			
Welding Conditions	Semi-Automatic GTA, 230 Amps, 1.6 to 3.5 inches/min			
Argon Flow Rate, ft^3/min	0.35	0.44	0.53	1.06
O_2 in Weld, ppm	31	27	33	30
Charpy-V, ft lb at -320 F	57	122	127	100



Joint Geometry

TABLE 4.03134. WELDING CONDITIONS WITH FERRITIC FILLER AND RESULTING WELD METAL -320 F CHARPY IMPACT VALUES [(36), TABLE 1]

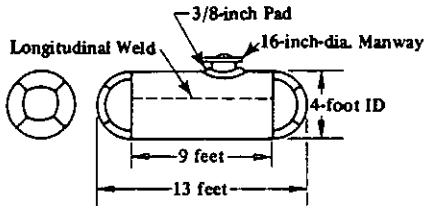
	Fe
0.13 max	C
8.5–9.5	Ni
0.9	Mn
0.15–0.30	Si

9 Ni Steel

Alloy	Fe-9Ni	
Form	0.39 to 0.59-inch Plate	
Condition	Automatic Subarc Weld	
Welding Conditions	ERNiCr-3[a] Filler With Basic Flux, 240-270 A, 28-30 V, Speed 10 inches/min to 28 inches/min, Interpass Temp < 100 F, 7 Passes/Joint	
Location	Weld Metal	HAZ
F_{tu}, ksi	101	–
Charpy-V, ft lb (at -320 F)	72	50

(a) See Table 4.0316.

TABLE 4.03135. EXAMPLE OF SUBARC WELDING CONDITIONS AND RESULTING WELD PROPERTIES (40)



Alloy	Fe-9Ni			
Form	Welded Test Vessel 3/8-inch Wall			
Condition[a]	Double Normalize + Temper F_{tu} = 105 ksi		Quench and Temper F_{tu} = 109 ksi	
	As Welded[b]	SR[c]	As Welded[b]	SR[c]
Burst Temp, F	-310	-320	-302	-311
Burst Stress, ksi	136	93	133	130

(a) For material heat treatment see Table 3.021.
(b) SMA Type 310 stainless steel coated electrodes.
(c) Stress relief 1050 F, 2 hr, cool 300 F/hr to 600 F, AC.

TABLE 4.03136. RESULTS OF CRYOGENIC BURST TESTS ON AS-WELDED TEST CYLINDERS [(1), TABLE 5]

	Fe
0.13 max	C
8.5-9.5	Ni
0.9	Mn
0.15-0.30	Si

9 Ni Steel

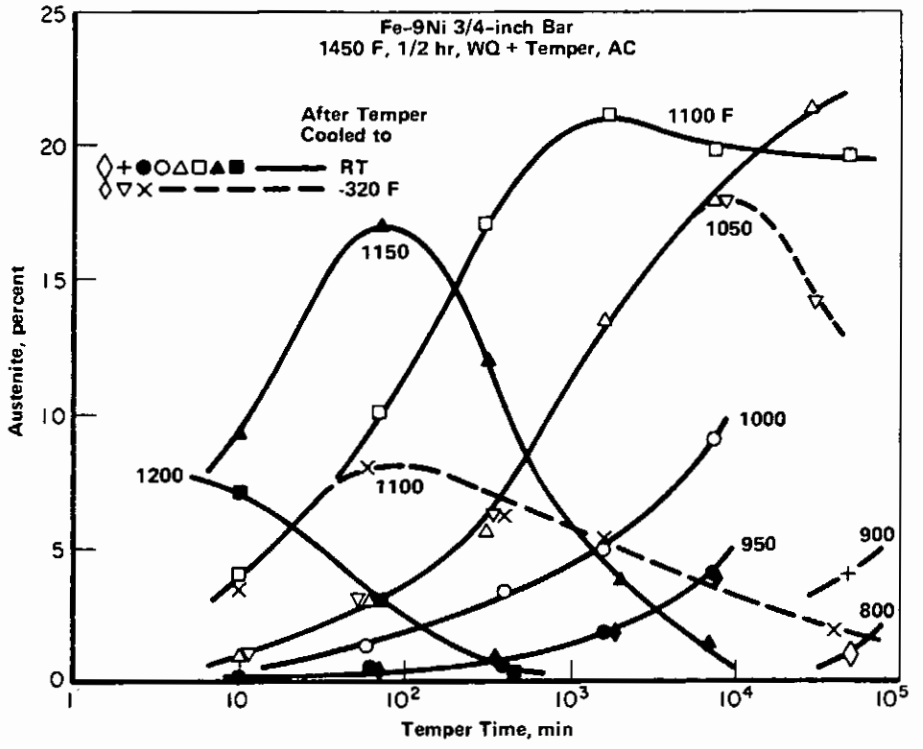


FIGURE 1.055. EFFECT OF TEMPERING TEMPERATURE AND TIME ON AUSTENITE RETENTION AT RT AND -320 F, [(16) FIGURE 3]

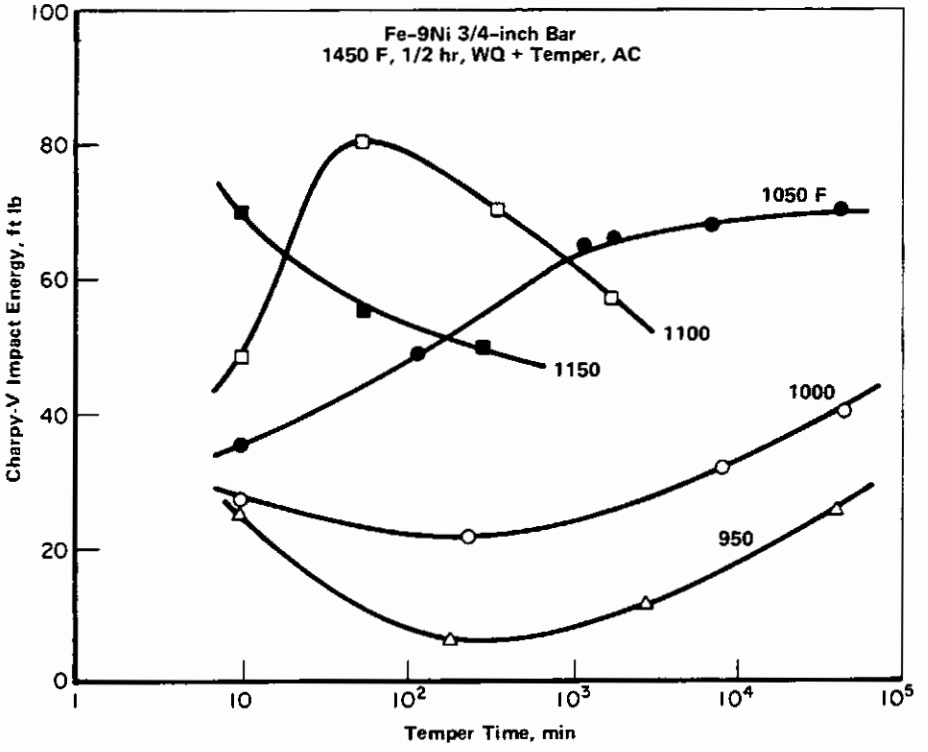


FIGURE 1.056. IMPACT ENERGY AT -320 F AS A FUNCTION OF TEMPERING TIME FOR SEVERAL TEMPERING TEMPERATURES [(16) FIGURE 6]

	Fe
0.13 max	C
8.5–9.5	Ni
0.9	Mn
0.15–0.30	Si

9 Ni Steel

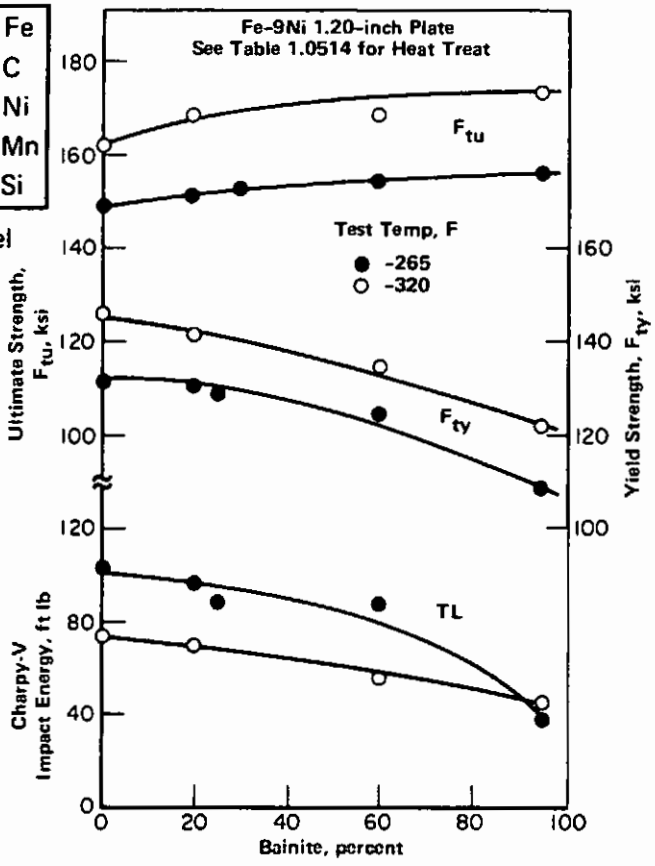


FIGURE 1.057. TENSILE AND IMPACT PROPERTIES AT CRYOGENIC TEMPERATURES AS FUNCTION OF PERCENT BAINITE [(5) TABLE 3]

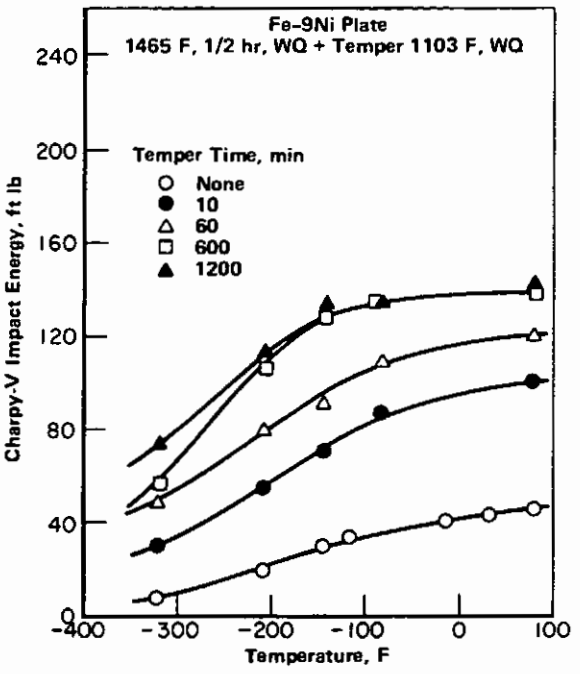


FIGURE 1.0512. EFFECT OF LOW TEST TEMPERATURES ON IMPACT ENERGY OF PLATE TEMPERED FOR VARIOUS TIMES [(28) FIGURE 8]

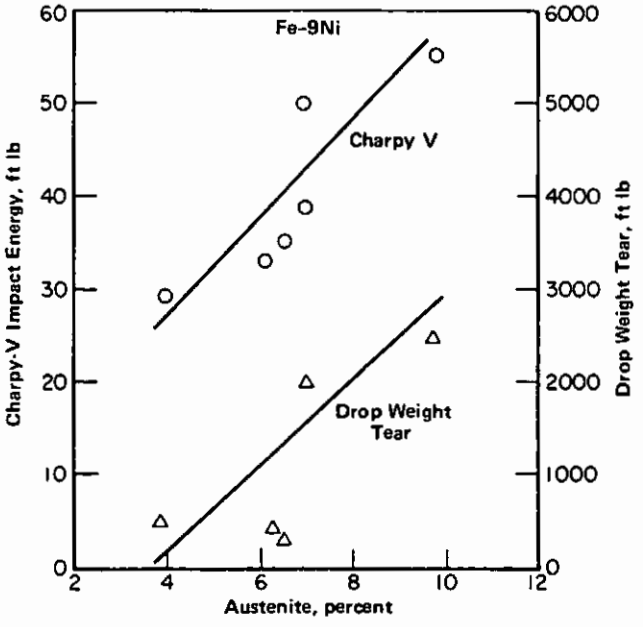


FIGURE 1.0513. CHARPY V AND DROP WEIGHT TEAR IMPACT ENERGIES AT -320 F AS FUNCTION OF PERCENT AUSTENITE [(25) FIGURE 25]

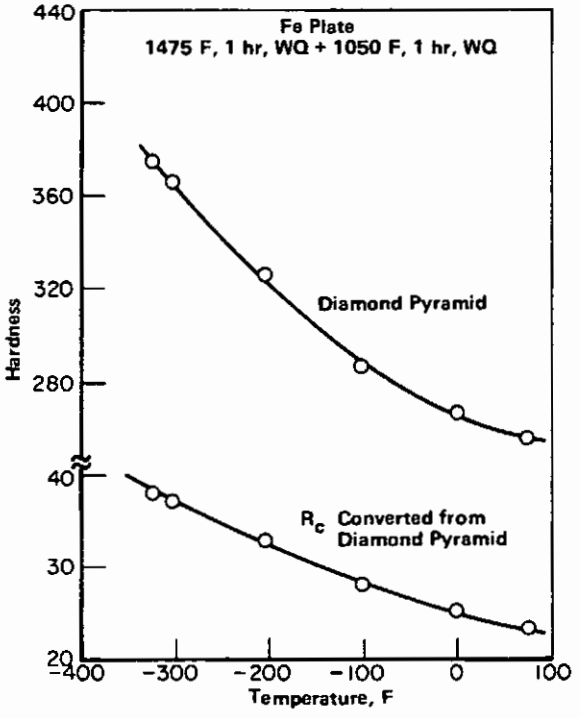


FIGURE 1.061. EFFECT OF TEST TEMPERATURE ON HARDNESS OF QUENCHED AND TEMPERED PLATE [(3) TABLE 5]

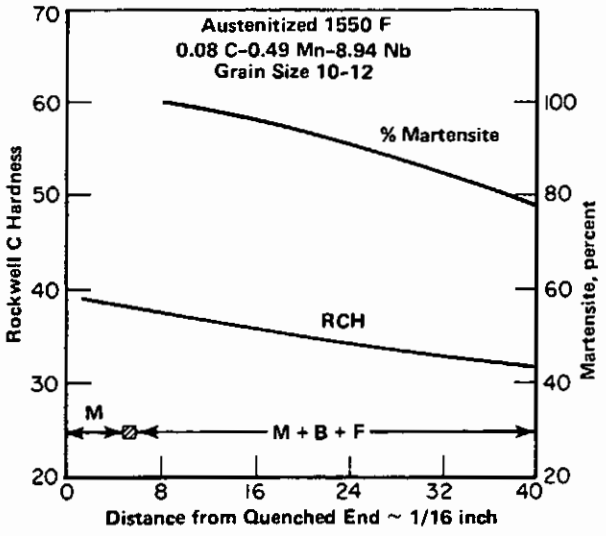


FIGURE 1.062. END QUENCHED HARDENABILITY [(3) FIGURE 4]

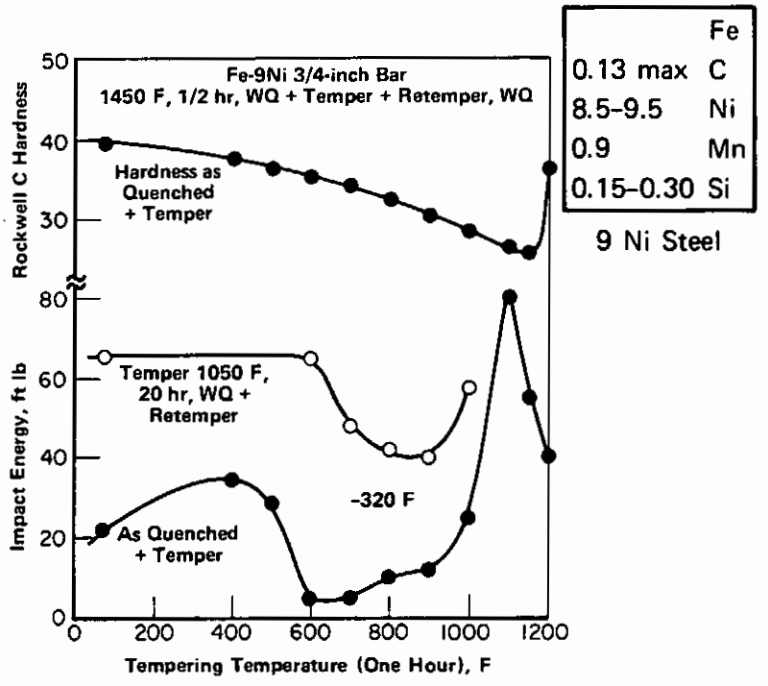


FIGURE 1.0915. EFFECT OF TEMPERING TEMPERATURE ON HARDNESS AND -320 F IMPACT ENERGY OF BAR [(16) FIGURES 5 AND 9]

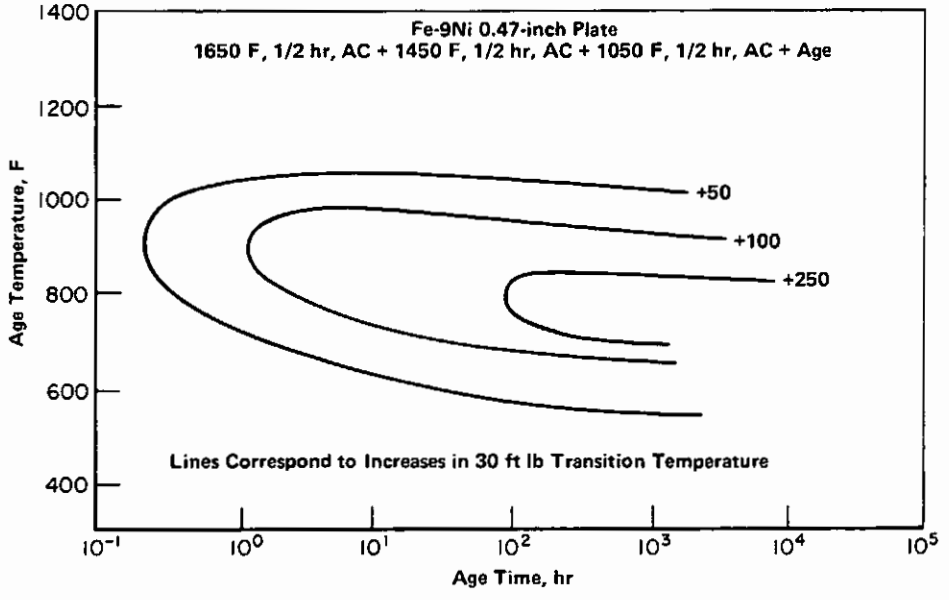


FIGURE 1.0916. ISO-EMBRITTLEMENT DIAGRAM FOR PLATE (4)

	Fe
0.13 max	C
8.5–9.5	Ni
0.9	Mn
0.15–0.30	Si

9 Ni Steel

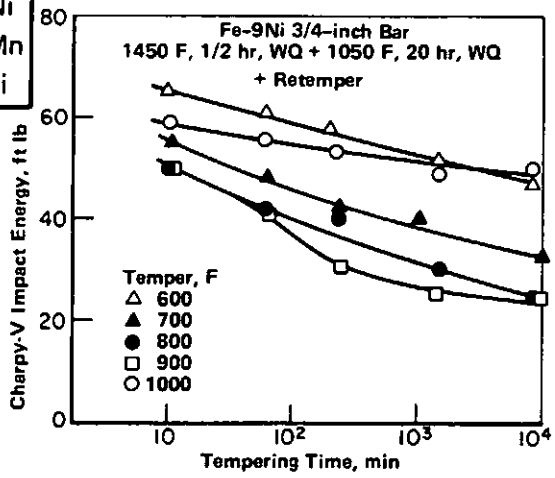


FIGURE 1.0917. EFFECT OF RETEMPERING TIME AND TEMPERATURE ON -320 F IMPACT ENERGY OF BAR [(16) FIGURE 10]

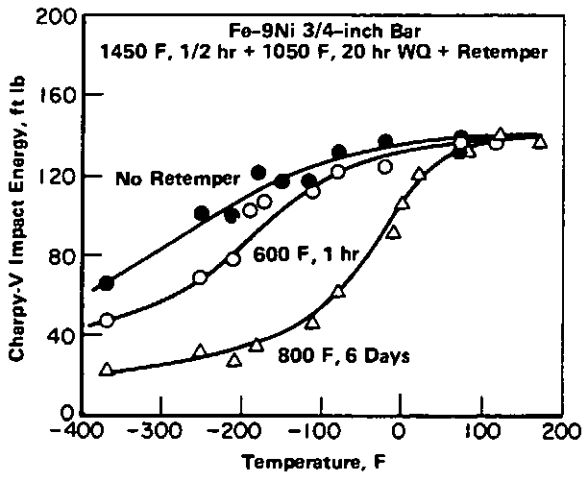


FIGURE 1.0918. EFFECT OF TEST TEMPERATURE ON IMPACT ENERGY OF BAR AFTER RETEMPERING AT 600 F AND 800 F [(16) FIGURE 11]

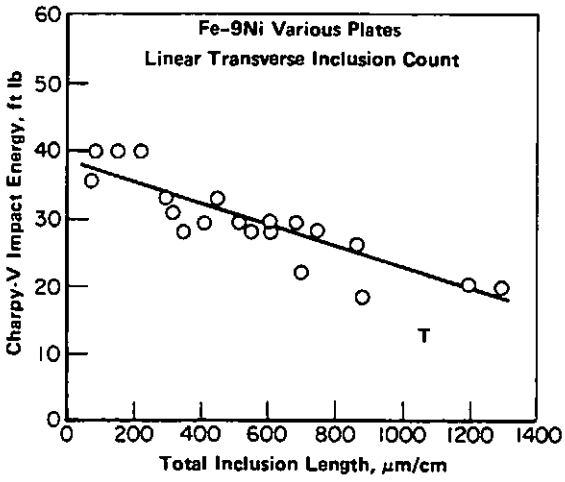


FIGURE 1.0927. TRANSVERSE IMPACT ENERGY AT -320 F AS FUNCTION OF INCLUSIONS [(29) FIGURE 2]

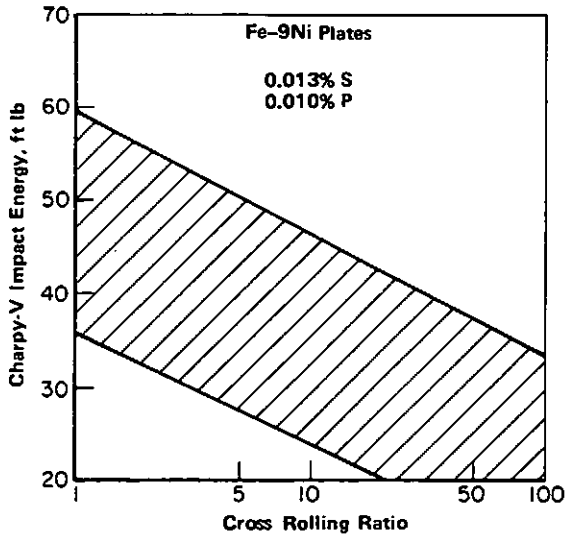


FIGURE 1.0928. INFLUENCE OF CROSS ROLLING RATIO ON TRANSVERSE IMPACT ENERGY OF PLATE [(29) FIGURE 4]

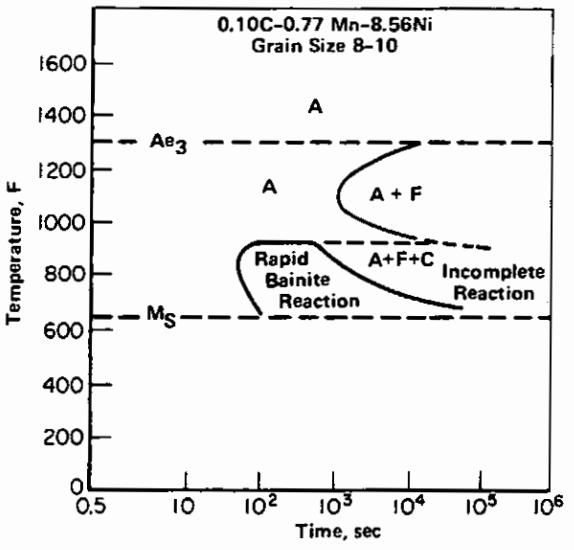


FIGURE 2.01211. ISOTHERMAL TRANSFORMATION DIAGRAM [(3) FIGURE 5]

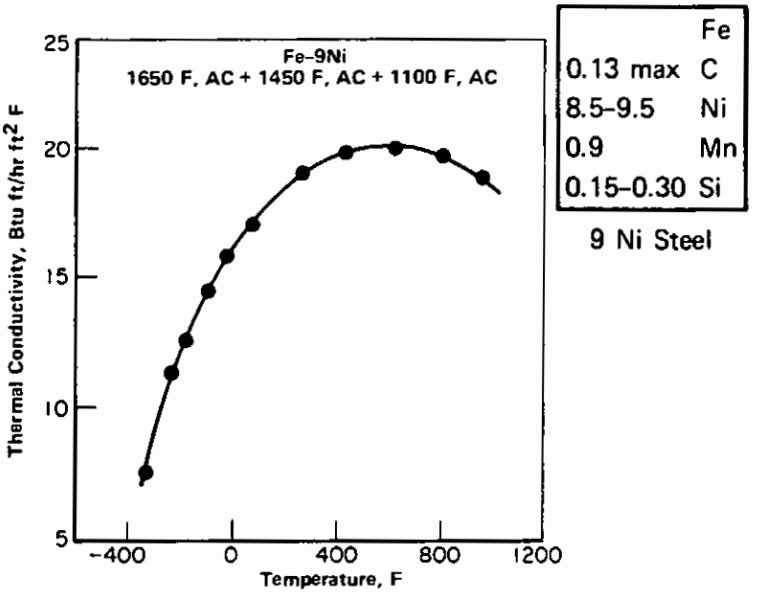


FIGURE 2.013. THERMAL CONDUCTIVITY [(3) TABLE 11]

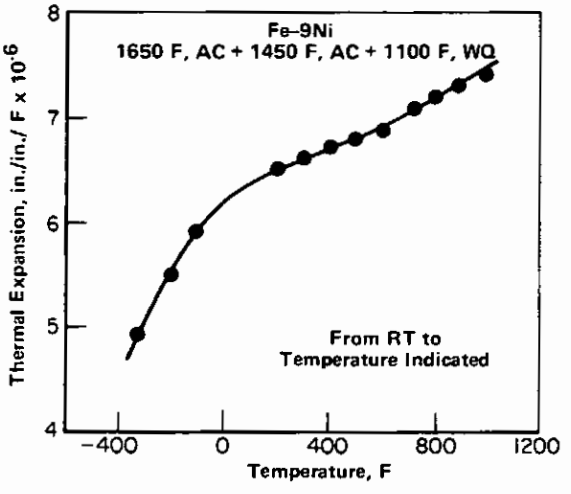


FIGURE 2.0141. COEFFICIENT OF LINEAR THERMAL EXPANSION [(3) TABLE 10]

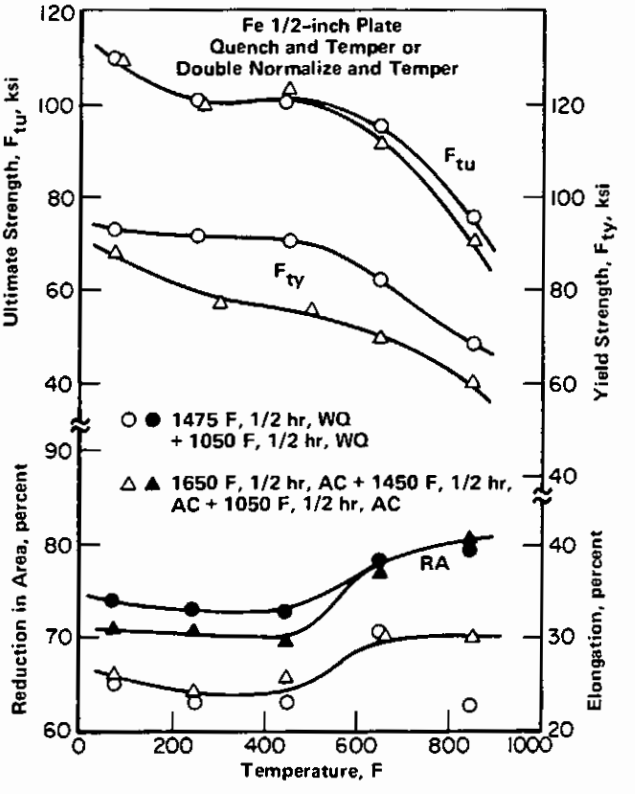


FIGURE 3.0311. EFFECT OF ELEVATED TEMPERATURES ON TENSILE PROPERTIES OF QUENCHED AND TEMPERED OR DOUBLE NORMALIZED 1/2-INCH PLATE [(3) TABLE 9]

	Fe
0.13 max	C
8.5-9.5	Ni
0.9	Mn
0.15-0.30	Si

9 Ni Steel

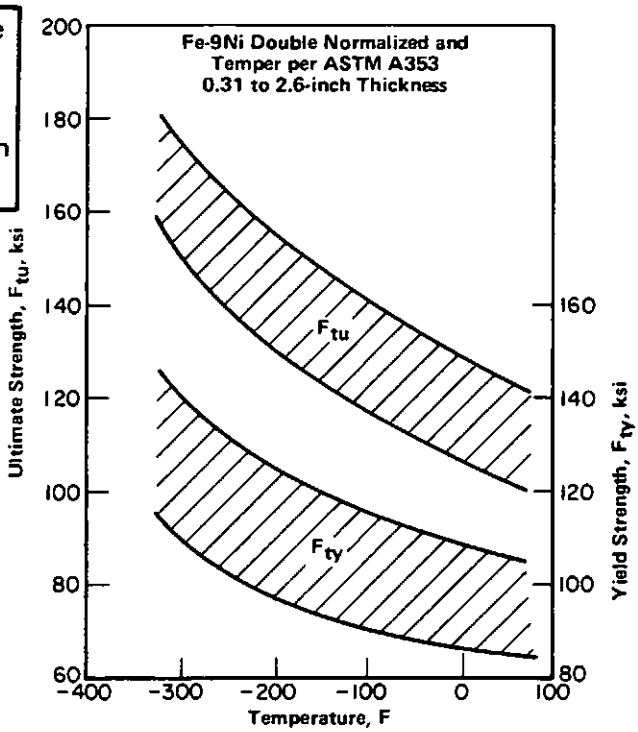


FIGURE 3.0312. RANGES OF TENSILE AND YIELD STRENGTHS FOR DOUBLE NORMALIZED AND TEMPERED PLATE OF VARIOUS THICKNESSES [(25) FIGURE 20]

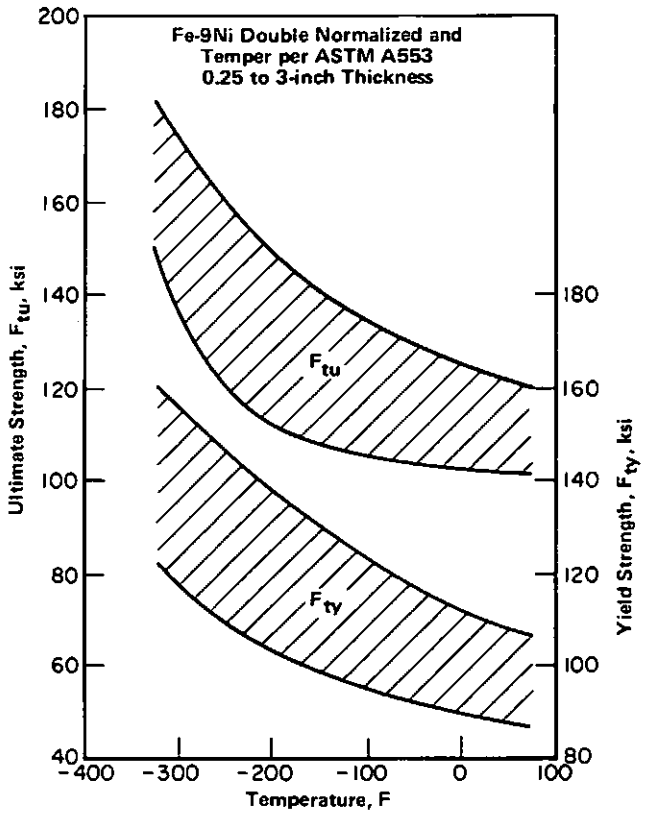


FIGURE 3.0313. RANGES OF TENSILE AND YIELD STRENGTHS FOR QUENCHED AND TEMPERED PLATE OF VARIOUS THICKNESSES [(25) FIGURE 21]

	Fe
0.13 max	C
8.5–9.5	Ni
0.9	Mn
0.15–0.30	Si

9 Ni Steel

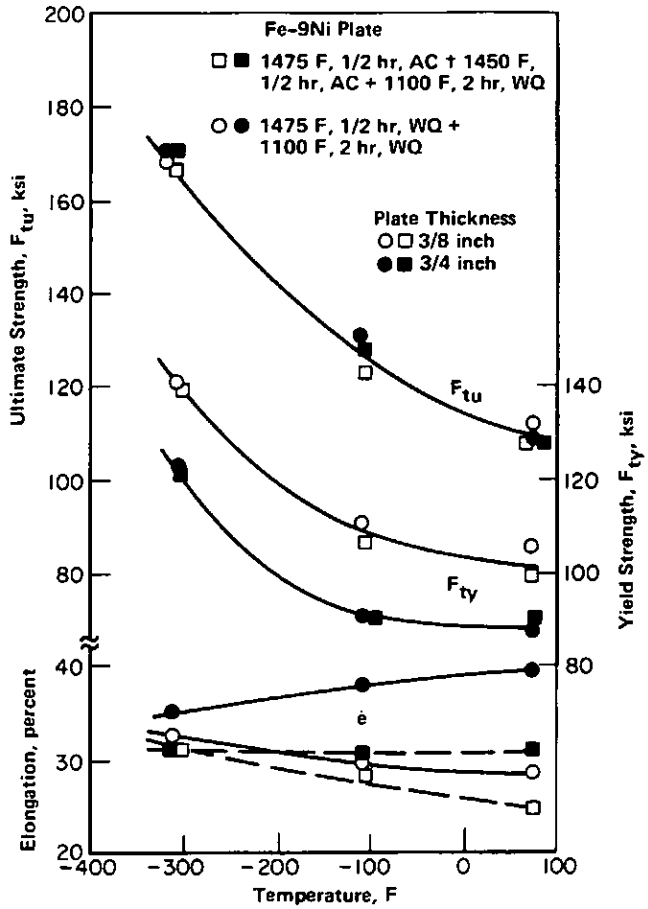


FIGURE 3.0314. EFFECT OF LOW TEST TEMPERATURES ON TENSILE PROPERTIES OF DOUBLE NORMALIZED AND TEMPERED AND QUENCHED AND TEMPERED PLATE [(11) P. 15]

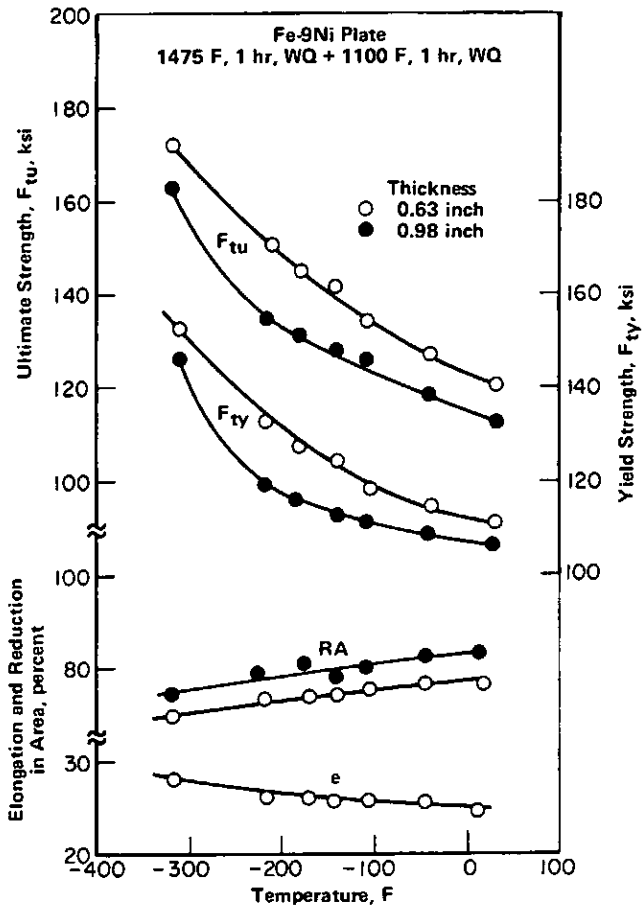


FIGURE 3.0315. EFFECTS OF LOW TEST TEMPERATURES ON THE TENSILE PROPERTIES OF QUENCHED AND TEMPERED PLATE [(26) P. 37]

	Fe
0.13 max	C
8.5-9.5	Ni
0.9	Mn
0.15-0.30	Si

9 Ni Steel

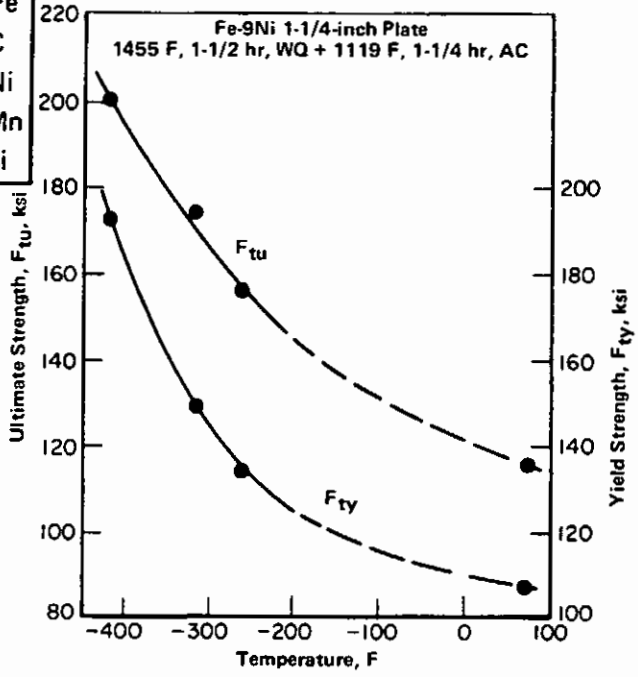


FIGURE 3.0316. EFFECT OF LOW TEST TEMPERATURES ON TENSILE PROPERTIES OF QUENCHED AND TEMPERED 1-1/2 INCH THICK PLATE [(12) TABLE 2]

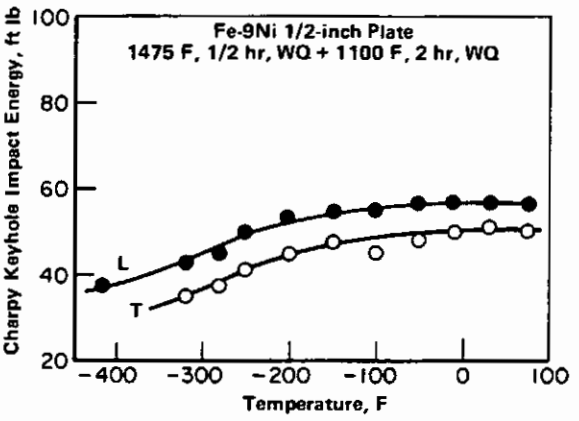


FIGURE 3.0331. EFFECT OF LOW TEST TEMPERATURES ON THE CHARPY KEYHOLE IMPACT ENERGY OF DOUBLE NORMALIZED AND TEMPERED 1/2-INCH PLATE [(11) P. 17]

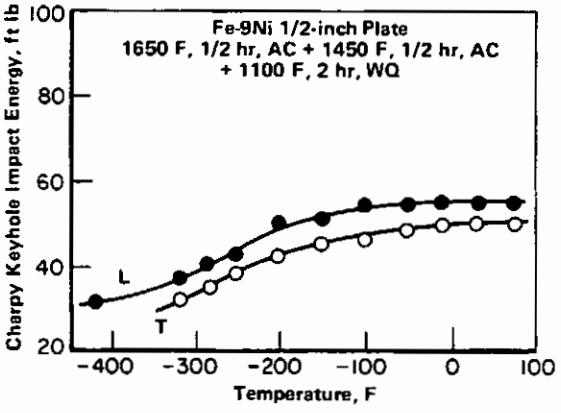


FIGURE 3.0332. EFFECT OF LOW TEST TEMPERATURES ON THE CHARPY KEYHOLE IMPACT ENERGY OF QUENCHED AND TEMPERED 1/2-INCH PLATE [(11) P. 17]

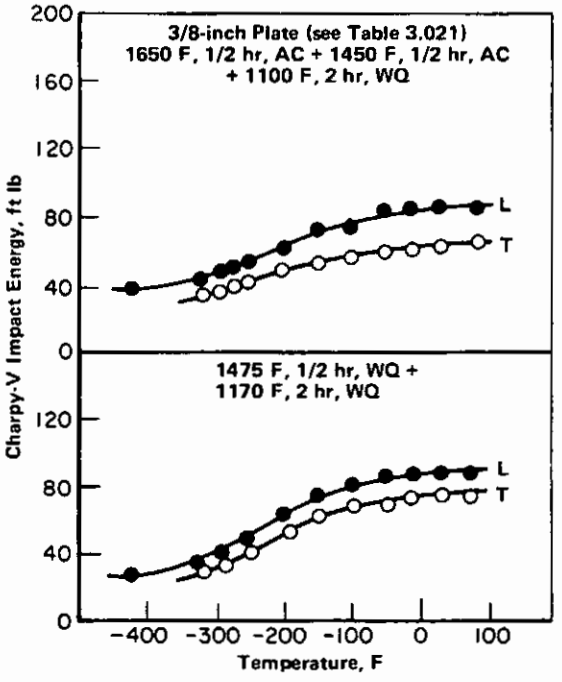


FIGURE 3.0333. EFFECT OF LOW TEST TEMPERATURES ON 3/4 WIDTH CHARPY V ENERGY FOR DOUBLE NORMALIZED AND FOR QUENCHED AND TEMPERED 3/8-INCH PLATE [(1) FIGURE 2]

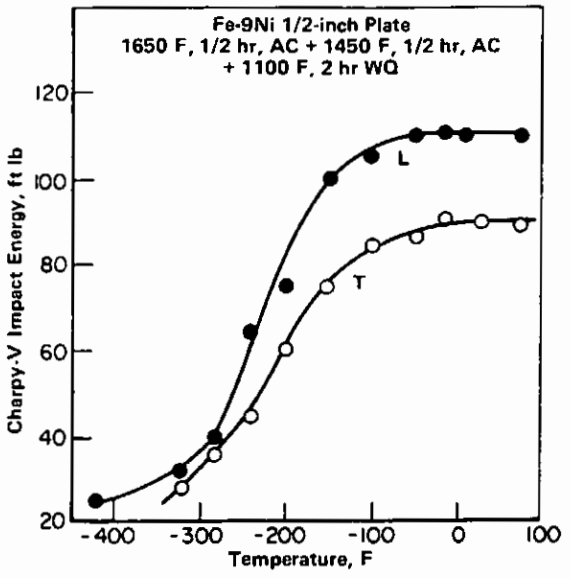
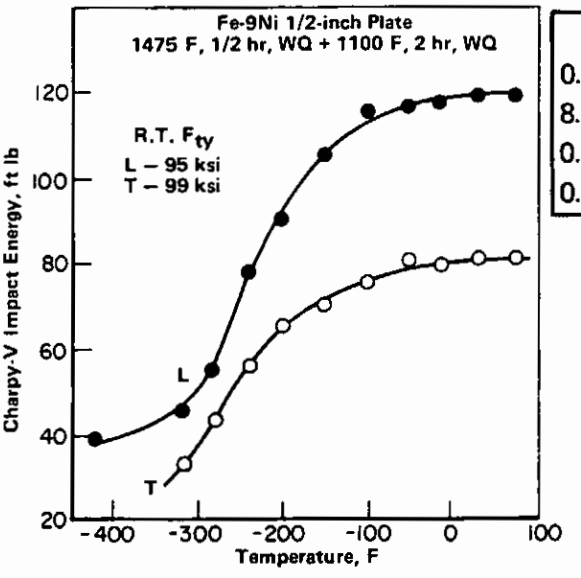


FIGURE 3.0334. EFFECT OF LOW TEST TEMPERATURES ON THE CHARPY V IMPACT ENERGY OF DOUBLE NORMALIZED 1/2 IN. PLATE [(11) P. 16]



	Fe
0.13 max	C
8.5–9.5	Ni
0.9	Mn
0.15–0.30	Si

9 Ni Steel

FIGURE 3.0335. EFFECT OF LOW TEST TEMPERATURES ON CHARPY V IMPACT ENERGY OF QUENCHED AND TEMPERED 1/2 IN. PLATE [(11) P. 16]

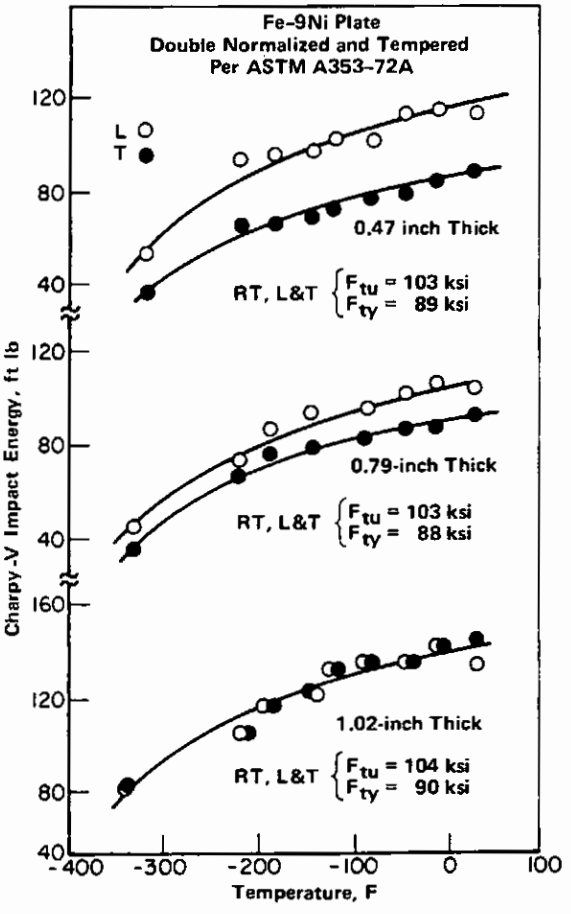


FIGURE 3.0336. EFFECT OF LOW TEST TEMPERATURES ON CHARPY V IMPACT ENERGIES OF THREE THICKNESSES OF DOUBLE NORMALIZED AND TEMPERED PLATE [(26), P. 15-17]

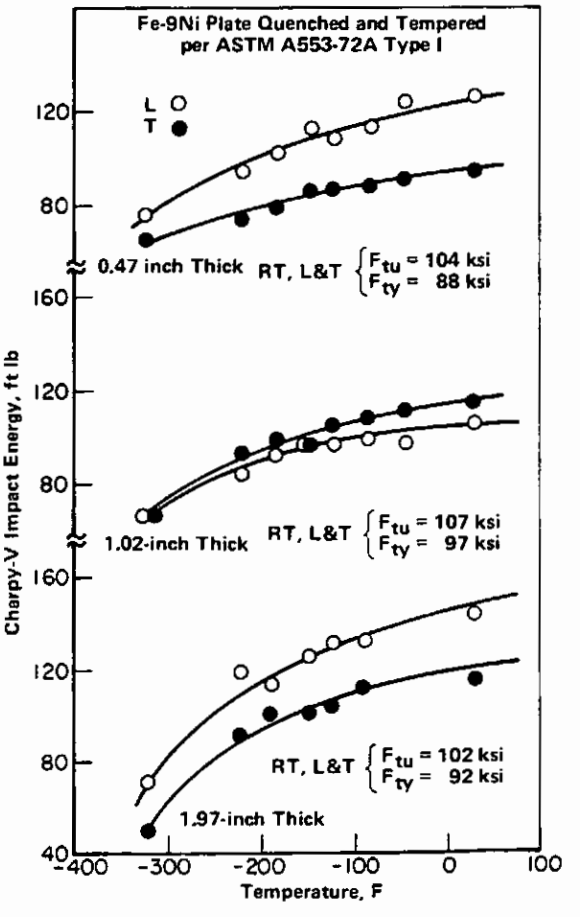


FIGURE 3.0337. EFFECT OF LOW TEST TEMPERATURES ON CHARPY V IMPACT ENERGIES OF THREE THICKNESSES OF QUENCHED AND TEMPERED PLATE [(26), P. 19-22]

	Fe
0.13 max	C
8.5-9.5	Ni
0.9	Mn
0.15-0.30	Si

9 Ni Steel

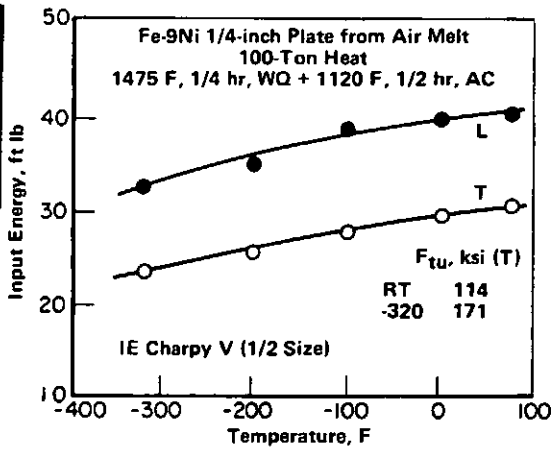


FIGURE 3.0338. EFFECT OF LOW TEST TEMPERATURES ON CHARPY V IMPACT ENERGIES OF PLATE FROM A 100-TON AIR MELT HEAT [(8) TABLE 1]

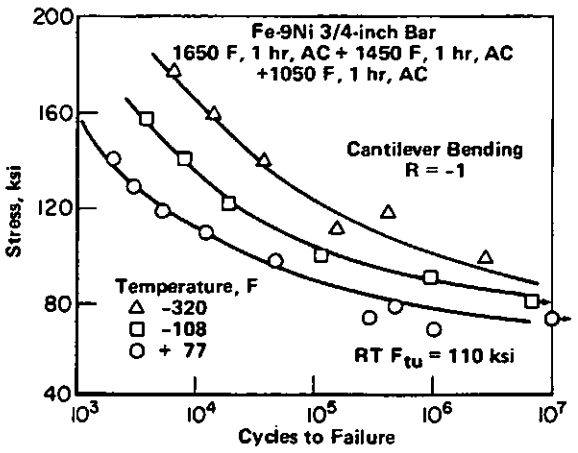


FIGURE 3.0511. S-N CURVES FOR DOUBLE NORMALALIZED AND TEMPERED 3/4-INCH-DIA. BAR AT ROOM AND CRYOGENIC TEMPERATURES [(10) FIGURE 17]

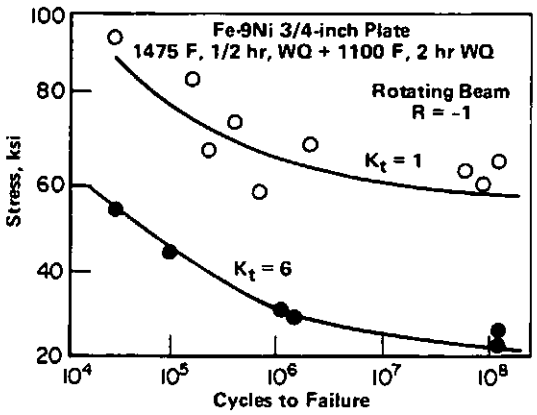


FIGURE 3.0512. S-N CURVES FOR 3/4-INCH QUENCHED AND TEMPERED PLATE [(11) P. 15]

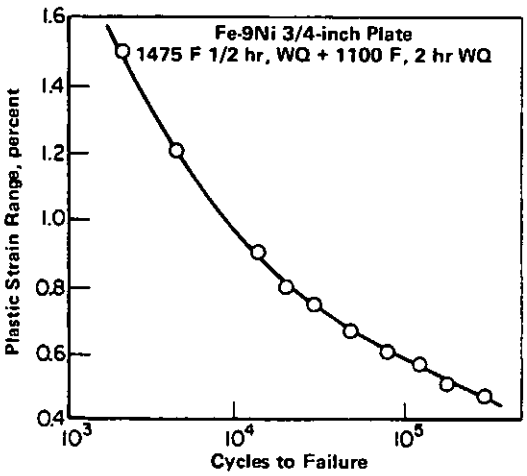


FIGURE 3.0515. PLASTIC STRAIN RANGE VS CYCLES TO FAILURE FOR QUENCHED AND TEMPERED PLATE [(11) P. 15]

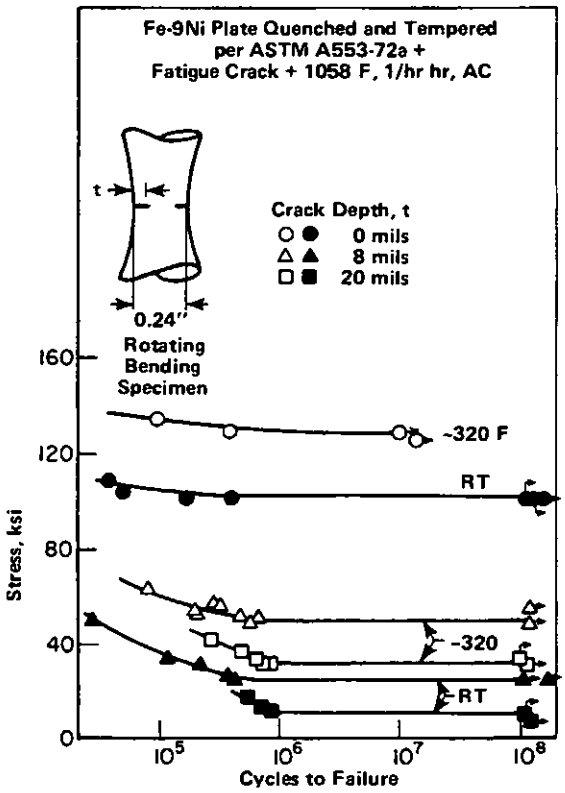


FIGURE 3.0514. S-N CURVES FOR SMOOTH AND CRACKED SPECIMENS FROM QUENCHED AND TEMPERED PLATE TESTED AT RT AND -320 F [(26) P. 91]

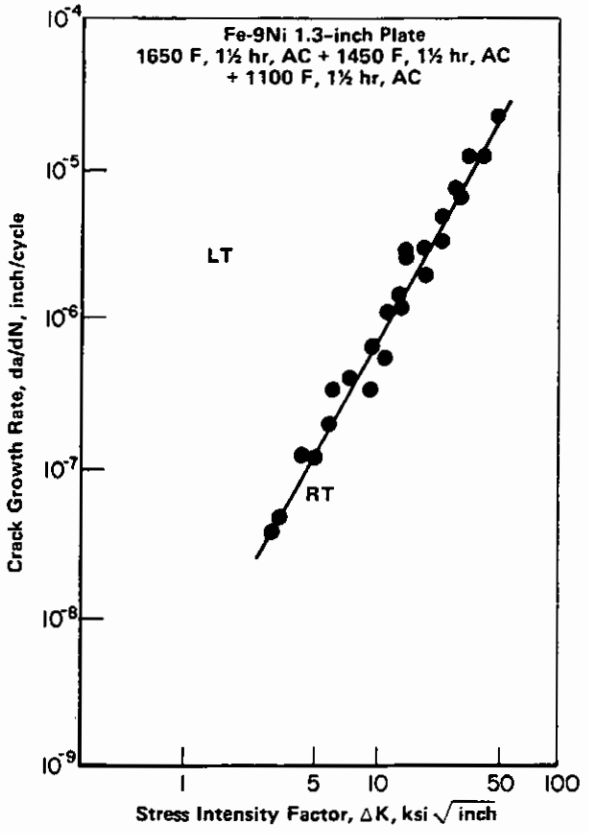


FIGURE 3.0521. FATIGUE CRACK PROPAGATION RATES AT ROOM TEMPERATURE FOR DOUBLE NORMALIZED AND TEMPERED 1.3-INCH PLATE [(9) FIGURE 8]

	Fe
0.13 max	C
8.5–9.5	Ni
0.9	Mn
0.15–0.30	Si

9 Ni Steel

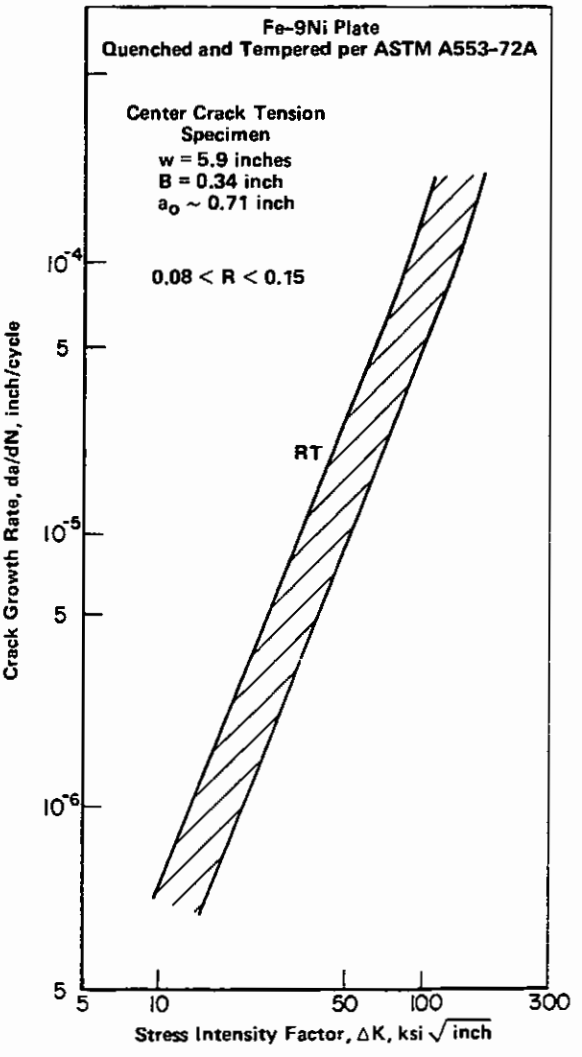


FIGURE 3.0522. FATIGUE CRACK PROPAGATION RATE SCATTERBAND FOR QUENCHED AND TEMPERED 0.34-INCH PLATE AT ROOM TEMPERATURE [(26) P. 83]

	Fe
0.13 max	C
8.5-9.5	Ni
0.9	Mn
0.15-0.30	Si

9 Ni Steel

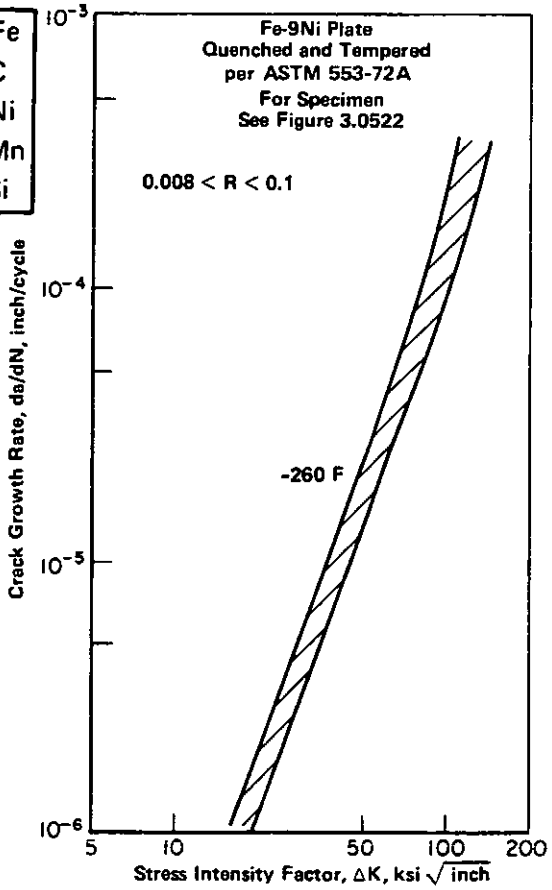


FIGURE 3.0523. FATIGUE CRACK PROPAGATION RATE SCATTERBAND FOR QUENCHED AND TEMPERED 0.34-INCH PLATE AT -260 F [(26) P. 84]

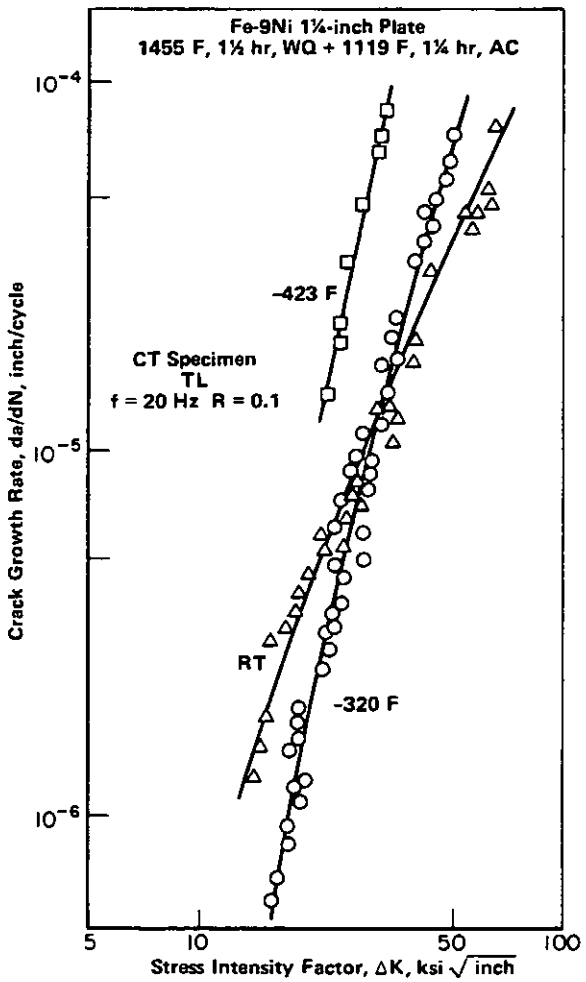


FIGURE 3.0524. FATIGUE CRACK PROPAGATION RATES AT ROOM AND CRYOGENIC TEMPERATURES FOR QUENCHED AND TEMPERED 1-1/4 INCH PLATE [(13) FIG. 9]

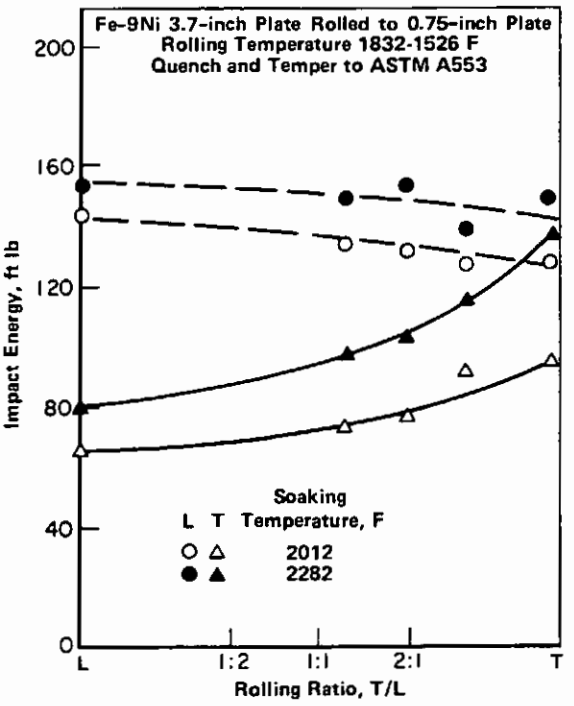
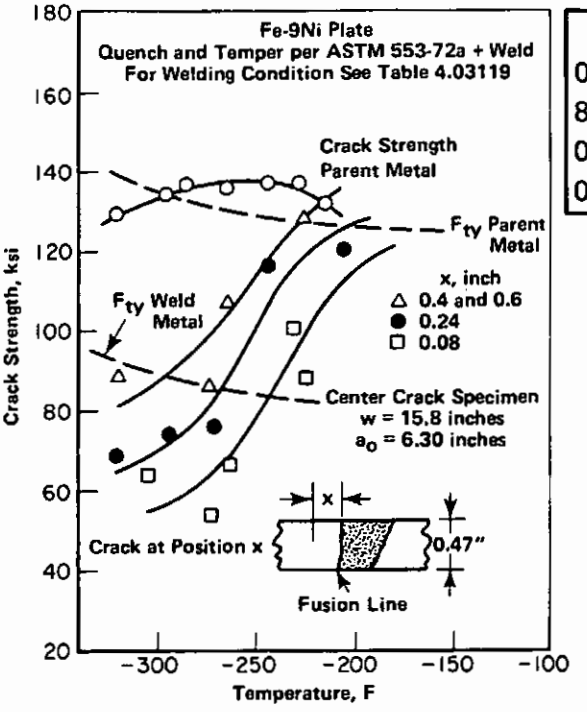


FIGURE 4.014. EFFECT OF ROLLING RATIO AND SOAKING TEMPERATURE ON ROOM TEMPERATURE CHARPY-V ENERGY [(35) FIGURE 5]



	Fe
0.13 max	C
8.5–9.5	Ni
0.9	Mn
0.15–0.30	Si

9 Ni Steel

FIGURE 4.03115. EFFECT OF LOW TEST TEMPERATURES ON CRACK STRENGTH OF THE HAZ IN A MANUAL WELDMENT OF QUENCHED AND TEMPERED PLATE [(26) P. 72]

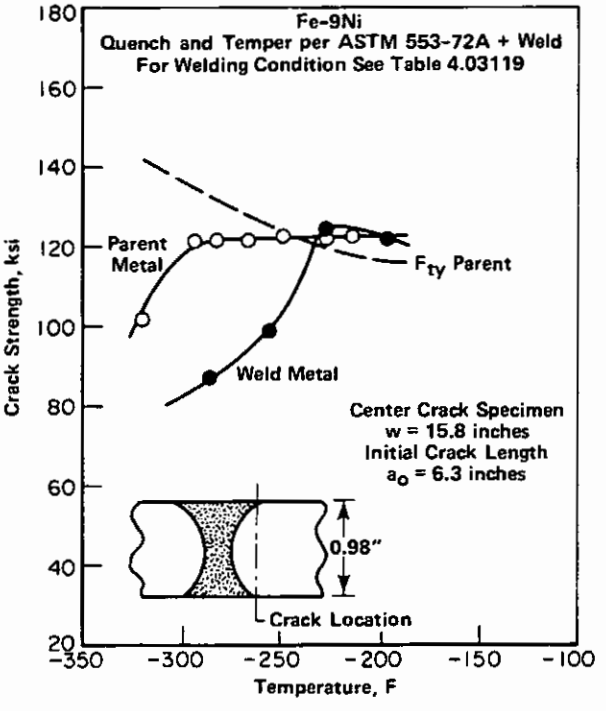


FIGURE 4.03116. EFFECT OF LOW TEST TEMPERATURES ON CRACK STRENGTH OF PARENT AND OF WELD METAL IN A MANUAL WELDMENT OF QUENCHED AND TEMPERED PLATE [(26) P. 73]

	Fe
0.13 max	C
8.5-9.5	Ni
0.9	Mn
0.15-0.30	Si

9 Ni Steel

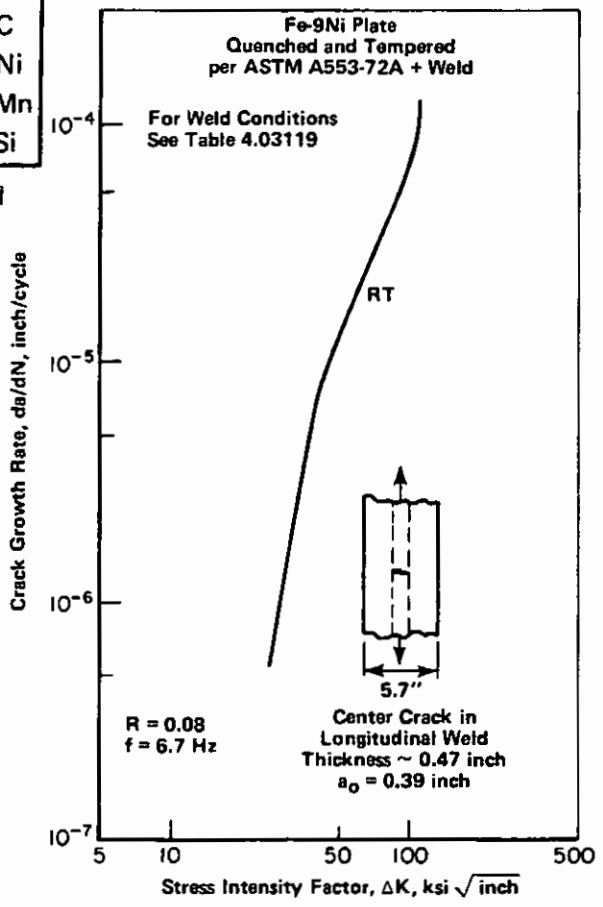


FIGURE 4.03117. FATIGUE CRACK PROPAGATION RATES AT ROOM TEMPERATURE FOR QUENCHED AND TEMPERED SMA WELDED PLATE [(26) P. 86]

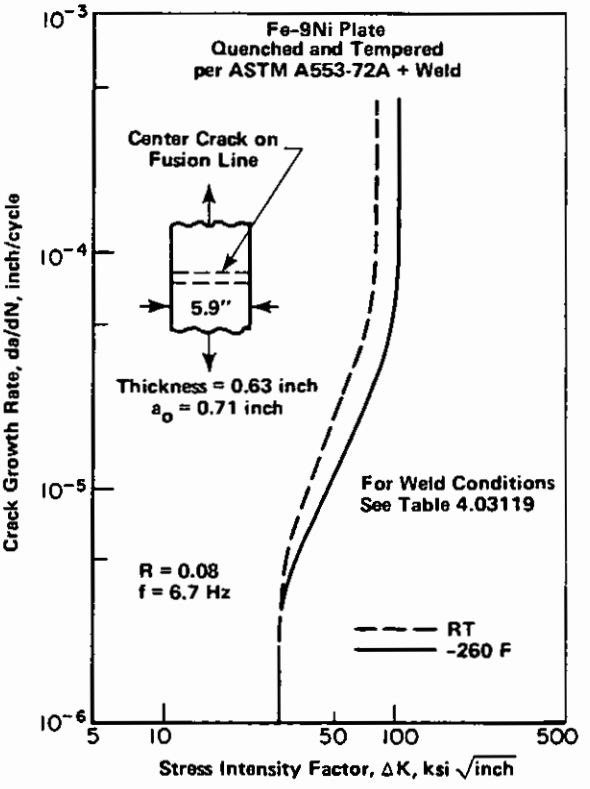


FIGURE 4.03118. FATIGUE CRACK PROPAGATION RATES AT RT AND FOR QUENCHED AND TEMPERED SMA WELDED PLATE [(26) P. 85]

	Fe
0.13 max	C
8.5–9.5	Ni
0.9	Mn
0.15–0.30	Si

9 Ni Steel

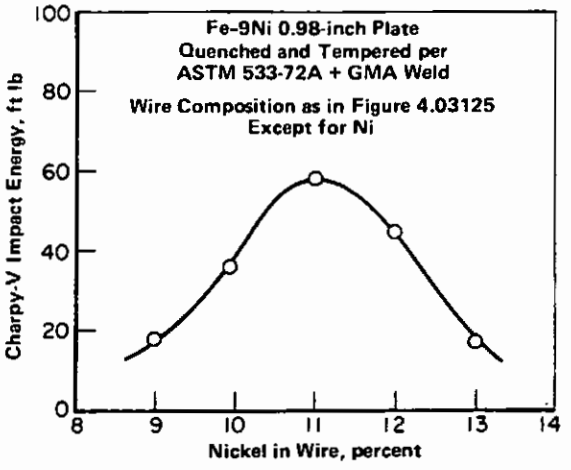


FIGURE 4.03124. IMPACT ENERGY OF GMA WELD METAL AT -320 F FUNCTION OF WIRE Ni CONTENT [(26) P. 129]

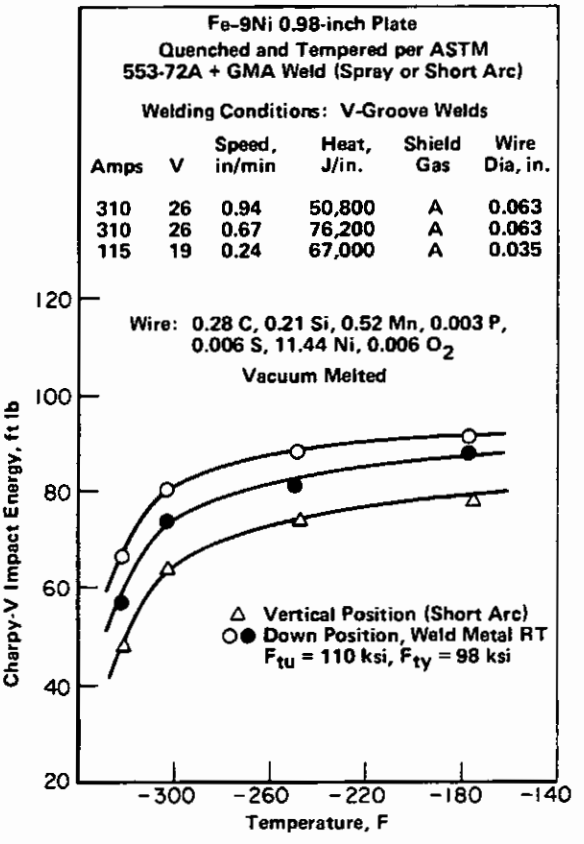


FIGURE 4.03125. EFFECT OF LOW TEMPERATURES ON IMPACT ENERGY OF 11 PERCENT Ni GMA WELD METAL [(26) P. 125-127]

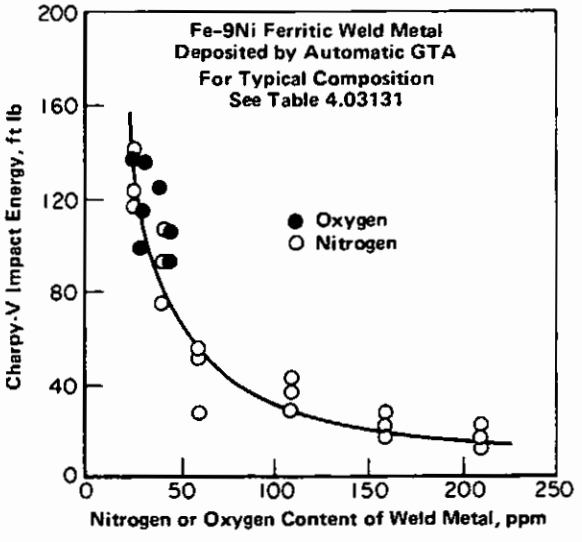


FIGURE 4.03127. EFFECT OF NITROGEN OR OXYGEN CONTENT ON -320 F IMPACT ENERGY OF FERRITIC WELD METAL DEPOSITED BY AUTOMATIC GTA PROCESS [(38) FIGURE 2 AND 3]

	Fe
0.13 max	C
8.5-9.5	Ni
0.9	Mn
0.15-0.30	Si

9 Ni Steel

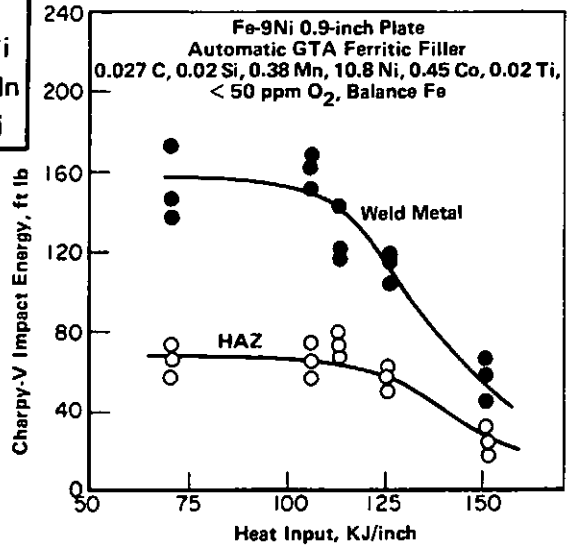


FIGURE 4.03128 EFFECT OF HEAT INPUT ON -320 F IMPACT ENERGY OF WELD METAL AND HAZ PRODUCED BY AUTOMATIC GTA PROCESS USING A FERRITIC FILLER [(37) FIG. 3]

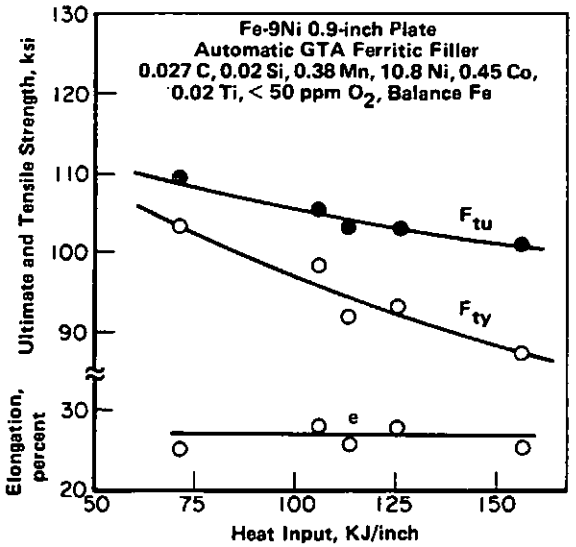


FIGURE 4.03129 EFFECT OF HEAT INPUT ON TENSILE PROPERTIES OF FERRITIC WELD METAL PRODUCED BY AUTOMATIC GTA PROCESS [(37) FIG. 4]

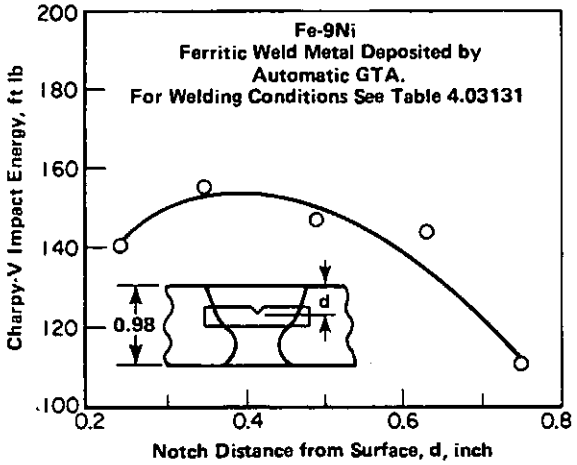


FIGURE 4.03132. IMPACT ENERGY AT -320 F FOR FERRITIC WELD METAL DEPOSITED BY AUTOMATIC GTA AS FUNCTION OF NOTCH DISTANCE FROM PLATE SURFACE [(38) FIG. 26]

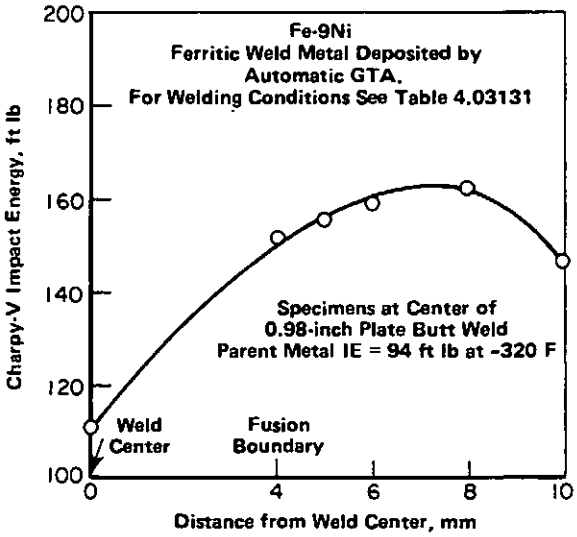


FIGURE 4.03133. IMPACT ENERGY AT -320 F FOR FERRITIC WELD METAL DEPOSITED BY AUTOMATIC GTA AS FUNCTION OF DISTANCE FROM WELD CENTER [(38) FIG. 24]

Fe
9 Ni
4 Co
Cr
Mo
V

9Ni-4Co

GENERAL

This steel was developed by Republic Steel Corporation (now LTV Steel Corporation) in the 1960s and combines high hardenability with good fracture toughness. Its proprietary composition is protected under U.S. Patent No. 3,365,471. Originally it was available in four grades, designated 0.20, 0.25, 0.30, and 0.45 carbon respectively, but is now available only in the 0.20 and 0.30 carbon grades. The 0.20 carbon grade provides tensile strengths in the range 195 to 215 ksi with good weldability and temper resistance. It can be welded in the fully heat treated condition and achieve essentially 100 percent joint efficiency without preheat or postheat treatment. Its weldments may be stress relieved without significant loss in Charpy V impact energy or tensile properties providing the recommended composition filler wire is used with the GTA process. The 0.30 carbon grade is intended for applications requiring tensile strength levels between 220 and 240 ksi with good resistance to strength loss at moderately elevated temperatures. There is very little experience in welding this higher carbon grade, as it is intended primarily for use in forged parts not requiring welding. The alloy was originally produced by the CEVM (C-deox) process (see Section 1.08), and is now produced by the EF-AOD, CEVM process (see again Section 1.08). This current processing provides improved microcleanliness (particularly inclusions) with consequent improved fracture toughness. CEVM (C-deox) processed material is so designated throughout the chapter. When no processing is identified, EF-AOD, CEVM processing is implied. The primary market for this steel is the aerospace industry.

1.01 **Commercial Designation**
9Ni-4Co.

1.02 **Alternate Designations**
HP-9-4-20, HP-9-4-30, and UNS K91283.

1.03 **Specifications**
Table 1.03.

1.04 **Composition**
Composition, Table 1.04.

1.041 This alloy contains the secondary hardening elements Cr and Mo in proportions which encourage the formation of alloy carbides and allow the use of high tempering temperatures. The Ni and Co contents are so balanced that high hardenability together with toughness is produced, while retained austenite is minimized. Mn and Si levels are kept low: since Mn does not contribute to the toughness of this alloy, no more than 0.35 to 0.40 weight percent is present; because this steel is produced by EF-AOD/CEVM practice (see Section 1.08), the Si level is also kept quite low, not exceeding 0.10 to 0.20 weight percent. A small amount of vanadium is present as a grain refiner.

The selection of alloying elements was dictated primarily by their effects on toughness (29). Detailed discussion of alloying effects can be found in References (38) and (39). Only the more significant alloying aspects are discussed in the sections which follow.

1.042 Carbon. In common with all tempered martensitic steels, carbon is the principal strengthening element. While strength increases with increasing carbon level, toughness predictability decreases (Figures 1.0421 through 1.0423). As discussed in 4.032, when an optimum combination of toughness and weldability is required, carbon content should be kept as low as is consistent with strength requirements.

1.0421 Effect of carbon content on tensile properties of forgings, Figure 1.0421.

1.0422 Effect of carbon content in the range of 0.20C grade on the room temperature tensile and 0 F Charpy V impact properties of plate, Figure 1.0422.

1.0423 Effect of tempering temperature on the room temperature tensile and 0 F Charpy V impact properties of plate at three carbon levels, Figure 1.0423.

1.043 Nickel. This element contributes substantially to solid solution strengthening and increased toughness. It also promotes the retention of austenite, which effect limits its constituent level.

1.044 Cobalt. Cobalt increases the austenite-to-martensite M_S transformation temperature, thereby minimizing the retention of austenite promoted by the high nickel content. The rise in M_S temperature enhances the self-tempering characteristics of the alloy. It also contributes to strengthening by solid solution hardening.

1.045 Chromium and molybdenum. These carbide forming elements impart resistance to overtempering at higher tempering temperatures. Such tempering temperatures improve notch toughness substantially without loss in strength, and reduce residual stresses.

1.046 Manganese. This element is similar to nickel in its effects on transformation characteristics. However, its presence in substantial amounts does not contribute to toughness; therefore its level is limited to 0.40 weight percent, with most production heats not exceeding 0.30 weight percent.

1.047 Silicon. This element is not considered to be an alloying element and commercial production practices result in low levels of its content. In significant amount this element can reduce notch toughness and promote "500 F" embrittlement.

1.048 Vanadium. In the small amounts in which this element is present in this alloy, it prolongs the reaction times of both the pearlite and bainite transformations. Its major function, however, is as a grain refiner.

1.05 **Heat Treatment**

1.051 General. Both grades develop their strength by quenching and tempering, producing thereby a tempered martensitic structure. Because of the high nickel content of this alloy, the transformation of austenite to pearlite does not normally occur, and the transformation to bainite is suppressed considerably. Because of the fairly high M_S temperature, self tempering can occur during cooling. This is beneficial as it improves the

Fe
9 Ni
4 Co
Cr
Mo
V

9Ni-4Co

properties of the heat-affected zone of weldments made from this alloy.

1.052 Recommended heat treatment, Table 1.052.

1.053 Results (24) have shown that rapidly solidified 0.20C grade exhibits a high resistance to austenitic grain coarsening for 1-hour holding at temperatures ranging from 1450 to 2200 F compared to conventionally processed material. For example, at 2200 F where the conventionally processed material coarsens to a grain size of several hundred microns, the rapidly solidified material retains a grain size of approximately 20 microns. However, long time treatments of the rapidly solidified material at 2000 to 2200 F eventually leads to discontinuous coarsening, but yet an order of magnitude less than conventionally processed stock. It is speculated (24) that high austenitizing treatment of rapidly solidified 9Ni-4Co will improve plane strain fracture toughness (which is already quite high); exploitation of this processing, however, would require an extreme level of cleanliness in powder processing.

1.054 Austenite grain size as a function of 1-hour austenitizing temperature for 0.20C grade, Figure 1.054.

1.055 Isothermal austenite grain growth characteristics for 0.20C grade, Figure 1.055.

1.056 Stress relief characteristics of several steels, including 0.20C grade 9Ni-4Co steel, and steel weldments, Figure 1.056.

1.06 **Hardness**

1.061 Typical Jominy end quench hardenability established from six AOD-processed heats of 0.20C grade, Figure 1.061.

1.062 Typical Jominy end quench hardenability established from five AOD-processed heats of 0.30C grade, Figure 1.062.

1.063 Additional 0.20C grade hardness data, Table 1.063.

1.064 Additional 0.30C grade hardness data, Table 1.064.

1.07 **Forms and Conditions Available**

Plate, billet, bar, rod, and welding wire, mill annealed.

1.08 **Melting and Casting Practice**

Original production of this alloy was by basic electric furnace melting of an unkilled heat having excess carbon and very low silicon and aluminum. Remelting by the consumable electrode vacuum process (CEVM) using a cold wall crucible resulted in carbon deoxidation. The process was designated CEVM (C-deox). The advantage of the process (compared to air melting) was the elimination of inclusions associated with silicon and aluminum normally added to kill air melted steel. More recently the alloy is electric furnace (90 ton capacity) melted with a modified aluminum deoxidation practice, followed by processing through an argon/oxygen decarburization vessel. It is poured into electrode ingot molds for subsequent consumable electrode vacuum remelting. This latter process is designated EF-AOD/CEVM. There is no difference in the resulting chemistry of either melting process. However, the EF-AOD/CEVM process produces improved microcleanliness (particularly inclusions) with consequent improved fracture toughness. Ninety percent of the alloy production is melted by the patent holder, LTV Steel Corporation; the balance by Latrobe and Allegheny Steel Corporations under license from LTV. LTV's patent on the alloy expired in 1985.

Data for material produced by the earlier CEVM (C-deox) process is so identified throughout the chapter. EF-AOD/CEVM processing is otherwise implied.

1.09 **Special Considerations**

(See also 1.05, 1.08, 2.03, and 4.03.)

1.091 Section size and directionality. This alloy has very high hardenability as evidenced by the small gradient in strength and ductility through the thickness of heavy forgings and plate (see Figure 3.02113 and Tables 3.02115 and 3.02117). The directionality of smooth strength properties is negligible. However, the fracture properties as measured by the Charpy V impact energy decreases with increasing section size (Figure 3.0236) and can exhibit directionality with the transverse directions having considerably lower impact and dynamic tear energies than the longitudinal direction (see Table 3.0232 and Figures 3.0234, 3.0331, and 3.03314).

1.092 Embrittlement. The impact energy and plane strain fracture toughness of both grades increases with increasing tempering temperature, and rises substantially above 1000 F (see Figures 3.0234, 3.0239, 3.02727, and 3.0338).

The plane strain fracture toughness of either grade could drop from room temperature to -65 F, or remain unchanged (see Tables 3.03721 and 3.03722). Fracture toughness data at lower test temperatures is unavailable. Charpy V impact energy and dynamic tear energy, as expected, decrease with decreasing test temperature, and this effect can be substantial (see Section 3.033).

Elevated temperature exposure can produce an increase in tensile strength and a decrease in ductility (see Figure 3.03110). While the effects shown are not large, their magnitude may depend on rather minor variations in alloy chemistry and may be associated with an increase in crack sensitivity.

Large reductions in tensile ductility and notch strength can be expected when the alloy is tested in high pressure hydrogen (see Table 2.0331).

1.093 Strain rate. High rates of loading can raise the ultimate strength of this alloy, but at no cost in ductility (see Figure 3.0317).

1.094 Fracture toughness. The plane strain fracture toughness of this alloy is variable. Data for 0.20C grade (Tables 3.02721, 3.02723, and 3.02724), however, indicate a reliable toughness of

100 ksi (in.)$^{1/2}$ at a yield strength of 185 ksi. Likewise, data for 0.30C grade (Table 3.02116 and Figure 3.02727) indicate a reliable toughness of 80 ksi (in.)$^{1/2}$ at a yield strength of 215 ksi.

2 PHYSICAL PROPERTIES AND ENVIRONMENTAL EFFECTS

2.01 Thermal Properties

2.011 Melting range. 0.20C grade, 2620 to 2699 F (13).

2.012 Phase changes.

2.01201 0.20C grade. Upon heating, transformation from martensite or bainite to austenite begins in the range 1130 to 1310 F (A_{c_1}) and is completed in the range 1380 to 1567 F (A_{c_3}) (13, 17, 25, 28, 32). On cooling from the austenitic condition at rates exceeding about 600 F/minute, the transformation to martensite begins in the range 635 to 448 F (M_s) and is completed in the range 246 to 120 F (M_f) (13, 17, 25, 28, 32). At slower cooling rates, the transformation to bainite begins at 675 F (B_s) and is completed at 625 F (B_f) (28). Typical of either grade of this alloy, no pearlitic decomposition products are formed within 36 hours.

2.01202 0.30C grade. Upon heating, transformation from martensite or bainite to austenite begins in the range 1180 to 1231 F (A_{c_1}) and is completed in the range 1375 to 1546 F (A_{c_3}) (14, 25). On cooling from the austenitic condition at rates exceeding about 60 F/minute, the transformation to martensite begins in the range 475 to 550 F (M_s) (14, 25), and is completed at about 120 F (M_f) (14). At slower cooling rates, the transformation to bainite begins at 725 F (B_s) and is completed at 565 F (B_f) (14).

2.0121 Time-temperature-transformation diagrams.

2.01211 Time-temperature-transformation diagram for 0.20C grade, Figure 2.01211.

2.01212 Time-temperature-transformation diagram for 0.30C grade, Figure 2.01212.

2.0122 Continuous-cooling-transformation diagrams.

2.01221 Continuous-cooling-transformation diagram for 0.20C grade, Figure 2.01221.

2.01222 Continuous-cooling-transformation diagram for 0.30C grade, Figure 2.01222.

2.013 Thermal conductivity, Table 2.013.

2.014 Thermal expansion.

2.0141 Mean coefficient of linear thermal expansion for 0.20C and 0.30C grades, Table 2.0141.

2.0142 Linear thermal expansion curve for 0.20C grade at heating rate of 10 F/minute, Figure 2.0142.

2.0143 Linear thermal expansion curve for 0.20C grade at heating rate of 36 F/minute, Figure 2.0143.

2.0144 Mean coefficients of linear thermal expansion for 0.20C grade at two heating rates, Table 2.0144.

2.015 Specific heat.

2.0151 Specific heat of 0.20C grade as a function of temperature, Figure 2.0151.

2.0152 Specific heat of 0.20C grade liquid alloy, 0.196 Btu/lb F (17).

2.016 Thermal diffusivity.

2.0161 Thermal diffusivity of 0.20C grade as a function of temperature, Figure 2.0161.

2.017 Enthalpy.

2.0171 Enthalpy, $H_T - H_{RT}$, as a function of temperature for 0.20C grade, Figure 2.0171.

2.0172 Heat of fusion, 0.20C grade, 99 Btu/lb (17).

2.0173 Heat of the α to γ transition, estimated at 7.0 Btu/lb (17).

2.02 Other Physical Properties

2.021 Density, 0.283 lb/in.^{3}.

2.0211 Specific gravity, 7.84.

2.022 Electrical properties.

2.0221 Electrical resistivity, Table 2.0221.

2.023 Magnetic properties.

2.024 Emittance.

2.0241 Normal spectral emittance, 0.20C grade, at $\lambda = 25.6 \times 10^{-6}$ inch = 0.40 ± 0.05 between 1610 F and the solidus temperature (2620 F) (17).

2.025 Damping capacity.

2.03 Chemical Environments

(See also 3.05.)

2.031 General. The general corrosion and oxidation resistance of this alloy is superior to AISI 4340; however, coatings are necessary to protect it from atmospheric attack. A considerable amount of stress corrosion data has been generated to characterize the delayed failure and fatigue crack growth behavior of the alloy. In some instances the results are inconsistent, and of course not all situations have been addressed. For corrosion-critical applications the alloy should be evaluated by specially designed stress corrosion tests which simulate the service environments and stresses.

The influence of certain fabrication variables such as grinding, drilling, shot peening, etc., and protective coatings have been studied by Turley and Avery (62) and by Dreyer and Gallagher (82).

2.032 Smooth specimen stress corrosion tests – liquid environment. Results from stress corrosion tests using smooth specimens are sparse. Seven 0.050-inch thick x 0.5-inch wide specimens from the 0.20C grade forged bar whose tensile properties are displayed in Figure 3.0316 were stressed to 80 percent of the yield strength in four-point bending and alternately immersed (10 minutes in, 50 minutes out) in 3.5 percent NaCl solution at room temperature (20, 21). No cracks were observed in 1000 hours total test time. Similar results were obtained for 0.30C grade smooth tension specimens alternately immersed under stress in both 3.5 percent NaCl solution and synthetic seawater (Table 2.0321). In the absence of results for 0.20C grade for test times beyond 1000 hours, it is not possible to say which grade is more stress corrosion resistant in 3.5 percent NaCl solutions. Bulloch, et al (61) report that the stress corrosion resistance of 0.30C grade at yield strengths less than 210 ksi is significantly less susceptible to delayed failure than 4330 V-Modified and H-11 steels.

Potentiodynamic-polarization test results (59) on 0.20C grade plate EB and GTA weldments in buffered solutions that varied in chloride ion concentration and pH are presented in Figures 2.0322 through 2.0327. Figure 2.0322 shows that, in the absence of chloride ions, only the most strongly acidic solution does not have a plateau indicative of a passive region in the anodic portion of the

Fe
9 Ni
4 Co
Cr
Mo
V

9Ni-4Co

Fe
9 Ni
4 Co
Cr
Mo
V

9Ni-4Co

curve. When the chloride ion concentration is low, as in the 0.01 molar NaCl solution (Figure 3.0323), the passive anodic region disappears for all but the most basic solution (highest pH). When the chloride ion content is 0.1 mole/liter, none of the curves show passive anodic regions (Figure 3.0324).

The attack observed in the potentiodynamic-polarization tests was in all cases uniform pitting corrosion. Effects of chloride ion content on the pitting behavior is illustrated in Figures 2.0325 through 2.0327 for pH values of 4 to 12.7. The "no-chloride" curves have a broad, passive region at all levels of acidity. In contrast, the 0.1M solution appears most aggressive, as indicated by the more negative "open circuit potential" (earlier onset of anodic behavior; i.e., current goes to zero) and the greater current density for the solutions with the higher chloride ion content.

The attack that resulted from the potentiodynamic tests indicates that more pitting occurs at high chloride ion concentrations and low pH values. The curves in Figures 2.0322 through 2.0327 also indicate that the 0.1 molar NaCl solution with a pH of 5 was the most corrosive in that study. Metallographic examination showed uniform pitting (no preferential attack on weld metal or weld heat affected zone) for either weld method (i.e., electron beam or GTA).

Time to failure in the most corrosive solution (0.1M NaCl solution buffered to a pH of 5) as a function of stress level is shown in Figure 2.0328, comparing the stress-corrosion cracking susceptibility of the base metal and weldments. There are insufficient results to establish statistically that the welded and unwelded specimens are of the same population, but the curves show a close similarity in the time to failure, which were longer at a given stress level for the unbuffered 3.5 percent NaCl exposures at a pH of 7, emphasizing the accelerating effect of a lower pH on the attack rate. No stress-corrosion cracking failures were observed; specimens failed in every case from a reduction in area by dissolution-type corrosion in acidic chloride-containing solutions. All were ductile failure.

2.0321 Results of alternate immersion stress corrosion tests on 0.30C grade plate and forged billet using smooth specimens, Table 2.0321.

2.0322 Potentiodynamic-polarization corrosion curves for 0.20C grade plate welds in solutions containing chloride ions at various pH values, Figure 2.0322.

2.0323 Potentiodynamic-polarization corrosion curves for 0.20C grade plate welds in 0.1 molar sodium chloride solutions at various pH values, Figure 2.0323.

2.0324 Potentiodynamic-polarization corrosion curves for 0.20C grade plate welds in 0.1 molar sodium chloride solutions at various pH values, Figure 2.0324.

2.0325 Potentiodynamic-polarization corrosion curves for 0.20C grade plate welds in solutions at a pH of 4 to 4.1 and at various chloride ion concentrations, Figure 2.0325.

2.0326 Potentiodynamic-polarization corrosion curves for 0.20C grade plate welds in solutions at a pH of 9 to 9.6 and at various chloride ion concentrations, Figure 2.0326.

2.0327 Potentiodynamic-polarization corrosion curves for 0.20C grade plate welds in solutions at a pH of 12.5 to 12.7 and at various chloride ion concentrations, Figure 2.0327.

2.0328 Sustained-load stress corrosion life of 0.20C grade plate base metal and weld in buffered (pH 5 and 6.6) sodium chloride solutions at two chloride ion concentrations, Figure 2.0328.

2.033 Smooth and sharp-notch stress corrosion tests – gaseous environment.

2.0331 Effect of testing in high pressure hydrogen on the smooth and sharp notch tensile properties of 0.20C grade rod, Table 2.0331.

2.034 Cracked specimen delayed failure tests – liquid environment. Cracked or sharply notched specimens of this alloy exhibit delayed failure when subjected to stress in the presence of distilled water or saltwater solutions (see, for example, Figure 2.0341). The data from cracked specimens are frequently reported in terms of the initial applied K_I value, and that value below which failure is not observed for very long exposure times is designated as the K_{Iscc} value. Stress corrosion tests of 0.20C grade crack arrest specimens for maximum 1500 hours exposures in saltwater have given threshold K_{Iscc} values for base metal of 92 to 110 ksi $(in.)^{1/2}$ for the LT and TL orientations, and 75 to 81 ksi $(in.)^{1/2}$ for the ST orientation (80). Other tests of the same grade using constant load-type specimens (Figure 2.0342) suggest a K_{Iscc} of about 110 ksi $(in.)^{1/2}$ for exposures approaching 2000 hours. One source (81) indicates that for extremely long (>10,000 hours) exposures in saltwater under stress, K_{Iscc} may actually be much lower than indicated above.

2.5-inch thick plate and a 4-inch x 18-inch x 36-inch forging of 0.20C grade heat treated to the 190 ksi yield strength level (1650 F, 1–1.5 hours, AC + 1525 F, 1–1.5 hours, AC or OQ + -100 F, 1–1.5 hours + 1025–1075 F, 4 hours, AC) were stress corrosion cracking tested in fuel tank sump residue water (a 0.12 percent metal chloride solution consisting of 11 different chlorides in distilled water) and shop cleaning solvent (aliphatic naptha) using 1-inch thick bolt-loaded double cantilever specimens (47). All specimens in the LT and TL orientations were able to sustain stress intensity of 104 ksi $(in.)^{1/2}$ for 60 days without failure, at which time all tests were discontinued. Crack extension ranged from 0.04 to 0.29 inch. LT oriented specimens in shop cleaning solvent sustained 122 ksi $(in.)^{1/2}$ stress intensity without failure in 1000 hours. ST oriented specimens in fuel tank sump residue water sustained 80 ksi $(in.)^{1/2}$ stress intensity without failure in 60 days, with crack extensions ranging to 0.31 inch.

The same products, in the same heat treated condition, welded and postweld stress relieved at 950 F for 2 hours, were fashioned into 0.25- and 0.50-inch

thick double-cantilever specimens and tested in fuel tank sump residue water and an aqueous trisodium phosphate field cleaning solution. Weld specimens sustained 79 ksi $(in.)^{1/2}$ stress intensity without failure in 1000 hours; the heat affected zone specimens sustained 62 ksi $(in.)^{1/2}$ without failure in the same time. No failure was observed for heat-affected zone specimens at 77 ksi $(in.)^{1/2}$ for 1000 hours in the field cleaning solution.

The effectiveness of oxidizing inhibitors in controlling hydrogen embrittlement and consequent stress-corrosion cracking of 0.30C grade plate in NaCl solutions was studied by Verink and Das (60). Three inhibitors were identified as effective in controlling crack tip electrode potential and pH so that hydrogen evolution in the crack is prevented and a passive oxide film is formed. Analysis for hydrogen on failed specimens showed that inhibitors to essentially halve the hydrogen remaining on the fracture surface (from 3.50 ppm to between 1.17 and 1.60 ppm). As shown in Figure 2.0343, all three inhibitors increased K_{Iscc} and reduced crack-growth rate substantially compared to uninhibited NaCl solutions.

2.0341 Delayed failure of 0.20C grade plate in seawater, Figure 2.0341.

2.0342 Stress corrosion cracking behavior of 0.20C grade plate in seawater, Figure 2.0342.

2.0343 Sustained-load crack growth rates for 0.30C grade plate in uninhibited and inhibited NaCl solutions, Figure 2.0343.

2.035 Fatigue crack-growth rate tests – humid air and liquid environments. The fatigue crack-growth rate of 0.20C grade forged bar is slightly greater in 100 percent humidity air than in low humidity air, the magnitude decreasing with increasing R-ratio until at R = 0.5 the difference in rates is negligible except at the lower range of ΔKs where rates in the more moist environment are higher (Figures 2.0351 through 2.0353). In 100 percent humidity air, growth rates are the same at R = 0.08 and 0.3, and slightly higher at R = 0.5, but only at lower ΔK (Figure 2.0354). Growth rates in shop cleaning solvent and fuel tank sump residue water are about the same as in low humidity air at intermediate ΔKs, and slightly greater at higher ΔKs (Figure 2.0355). No influence of specimen orientation (LT versus TL) on the crack growth rates displayed in Figures 2.0351 through 2.0355 was observed; therefore only one test direction is treated in each figure. Crack growth rates in saltwater solutions are either no different or only slightly greater than in air (Figures 2.0356 through 2.0358). Surprisingly, weld metal crack-growth rates in fuel tank sump residue water are no different than in low humidity air (Figure 2.03510) but lower in distilled water compared to low humidity air at low ΔKs (Figure 2.03511), and rates in 100 percent humidity air are shown to be either the same or lower than in low humidity air in Figure 2.03512. Weld repair by weld overlay, compared to grindout reweld, exhibits substantially higher fatigue crack-growth rates in distilled water, be they stress relieved or not (Figures 2.03513 and 2.03514).

The fatigue crack-growth rate of 0.30C grade in 3.5 percent NaCl solution is no different than that in air over the range shown in Figure 2.03515. Likewise there is no difference in rates for fuel tank sump residue water as the environment compared to low humidity air above about ΔK = 15 ksi $(in.)^{1/2}$, but differ at lower ΔKs in an inconsistent manner (Figures 2.03516 through 2.03518). Specimen thickness over the narrow range 0.75 inch to 1.0 inch has, expectedly, no influence of crack-growth rate of this grade in fuel tank sump residue water (Figure 2.03519), and loading wave shape has no influence on rate in NaCl solution at 10 Hz (Figure 2.03520). The data in Figures 2.03521 and 2.03522 show a small influence of cyclic load frequency in substitute seawater in the "Paris Law" region, but considerable difference in apparent threshold stress intensity factor range. R-ratio effects are as expected for the lower range of ΔK in fuel tank sump residue water (Figure 2.03525), but mixed for 3.5 percent NaCl solution environment (Figure 2.03526). A substantial effect of R-ratio is shown for cyclic loading during alternate immersion in synthetic seawater in Figure 2.03527.

Fe
9 Ni
4 Co
Cr
Mo
V

9Ni-4Co

2.0351 Effect of moisture on crack-growth rate at R = 0.08 of 0.20C grade forged bar, Figure 2.0351.

2.0352 Effect of moisture on crack-growth rate at R = 0.3 of 0.20C grade forged bar, Figure 2.0352.

2.0353 Effect of moisture on crack-growth rate at R = 0.5 of 0.20C grade forged bar, Figure 2.0353.

2.0354 Effect of R-ratio on fatigue crack-growth rate in 100 percent humidity air of 0.20C grade forged bar, Figure 2.0354.

2.0355 Effect of environment on fatigue crack-growth rate of 0.20C grade forged bar, Figure 2.0355.

2.0356 Fatigue crack-growth characteristics of 0.20C grade plate in air and 3.5 percent NaCl saltwater, Figure 2.0356.

2.0357 Fatigue crack-growth rate of 0.20C grade plate in air and 3.5 percent NaCl solution, Figure 2.0357.

2.0358 Fatigue crack-growth rate of 0.20C grade plate in air and seawater, Figure 2.0358.

2.0359 Effect of specimen thickness on fatigue crack-growth rate in distilled water of 0.20C grade plate GTA manual weld heat affected zone, Figure 2.0359.

2.03510 Effect of environment on fatigue crack-growth rate of 0.20C grade plate GTA manual weld heat affected zone, Figure 2.03510.

2.03511 Effect of environment on fatigue crack-growth rate of 0.20C grade forged billet GTA manual weld heat affected zone, Figure 2.03511.

2.03512 Effect of environment on fatigue crack-growth rate of 0.20C grade plate GTA machine welds, Figure 2.03512.

2.03513 Fatigue crack-growth rates in distilled water of 0.20C grade repaired and unstress-relieved GTA manual welds, Figure 3.03513.

2.03514 Fatigue crack-growth rates in distilled water of 0.20C grade repaired and stress relieved plate GTA manual welds, Figure 2.03513.

2.03515 Fatigue crack-growth rate of 0.30C grade forged rectangular bar in air and 3.5 percent NaCl solution, Figure 2.03515.

Fe
9 Ni
4 Co
Cr
Mo
V

9Ni-4Co

2.03516 Effect of environment on fatigue crack-growth rate at R = 0.08 of 0.30C grade forged bar, Figure 2.03516.

2.03517 Effect of environment on fatigue crack-growth rate at R = 0.3 of 0.30C grade forged bar, Figure 2.03517.

2.03518 Effect of environment on fatigue crack-growth rate at R = 0.5 of 0.30C grade forged bar, Figure 2.03518.

2.03519 Effect of specimen thickness on fatigue crack-growth rate in fuel tank sump residue water (12 percent metal chloride solution of 11 different chlorides in distilled water) of 0.30C grade forged bar, Figure 2.03519.

2.03520 Effect of loading wave shape and environment on fatigue crack-growth rate of 0.30C grade hand forged billet, Figure 2.03520.

2.03521 Effect of loading frequency (sinusoidal) on fatigue crack-growth rate in synthetic seawater of 0.30C grade hand forged billet, Figure 2.03521.

2.03522 Effect of loading frequency (trapezoidal) on fatigue crack-growth rate in synthetic seawater of 0.30C grade hand forged billet, Figure 2.03522.

2.03523 Effect of loading frequency (sinusoidal) on fatigue crack-growth rate in 3.5 percent NaCl solution of 0.30C grade hand forged billet, Figure 2.03523.

2.03524 Effect of loading frequency (trapezoidal) on fatigue crack-growth rate in 3.5 percent NaCl solution of 0.30C grade hand forged billet, Figure 2.03524.

2.03525 Effect of R-ratio on fatigue crack-growth rate in fuel tank sump residue water (12 percent metal chloride solution of 11 different chlorides in distilled water) of 0.30C grade forged bar, Figure 2.03525.

2.03526 Effect of R-ratio on fatigue crack-growth rate in 3.5 percent NaCl solution of 0.30C grade hand forged billet, Figure 2.03526.

2.03527 Effect of R-ratio on fatigue crack-growth rate of 0.30C grade hand forged billet in synthetic seawater, Figure 2.03527.

2.036 Fatigue crack-growth rate tests – gaseous environment. Fatigue crack-growth rates for 0.20C grade forgings in gaseous hydrogen are substantially higher than in vacuum (Figure 2.0361), and are uniquely related to the crack propagation path (i.e., intergranular versus transgranular) (Figure 2.0362). This influence of gaseous hydrogen on fatigue crack growth is most pronounced at room temperature (Figure 2.0363). Gaseous hydrogen is the most aggressive of the gaseous environments portrayed in Figure 2.0364.

2.0361 Fatigue crack-growth rate of 0.20C grade forging at 32 F in hydrogen and in vacuum, Figure 2.0361.

2.0362 Dependence of hydrogen-accelerated fatigue crack-growth rate on stress intensity factor for 0.20C grade forging, Figure 2.0362.

2.0363 Temperature dependence of fatigue crack-growth rate of 0.20C grade forging in hydrogen and vacuum, Figure 2.0363.

2.0364 Fatigue crack-growth rate of 0.20C grade forging at 32 F in various gaseous environments, Figure 2.0364.

2.04 **Nuclear Environments**

2.041 Effect of 550 F irradiation on strength of 0.20C grade plate and weldments, Table 2.041.

2.042 Effect of 550 F irradiation on up-shelf Charpy V impact energy and temperature of 0.20C grade plate and weldments, Table 2.042.

2.043 Permeability of annealed 0.20C grade to deuterium, Figure 2.043.

3 MECHANICAL PROPERTIES

3.01 Specified Mechanical Properties

3.011 SAE-AMS specified room temperature mechanical properties for 0.20C grade, Table 3.011.

3.012 Producer's typical room temperature mechanical properties for 0.20C grade, Table 3.012.

3.013 Producer's guaranteed minimum room temperature mechanical properties for 0.20C grade, Table 3.013.

3.014 Users' specified room temperature mechanical properties for 0.20C grade, Table 3.014.

3.015 SAE-AMS specified room temperature mechanical properties for 0.30C grade, Table 3.015.

3.016 ASTM specified room temperature mechanical properties for 0.30C grade, Table 3.016.

3.017 Producer's typical room temperature mechanical properties for 0.30C grade, Table 3.017.

3.018 Producer's guaranteed minimum room temperature mechanical properties for 0.30C grade, Table 3.018.

3.019 Users' specified room temperature mechanical properties for 0.30C grade, Table 3.019.

3.02 Mechanical Properties at Room Temperature

3.021 Tension – stress-strain diagrams – tension properties (see also 1.04, 3.031, and 4.03).

3.0211 True stress-true strain characteristics of 0.20C grade plate variously heat treated, Table 3.0211.

3.0212 Stress-strain curves for reheat treated 0.20C grade plate, Figure 3.0212.

3.0213 Effect of quench media on the tensile properties of 0.20C grade plate, Table 3.0213.

3.0214 Effect of cooling rate from the austenitizing temperature on the room temperature tensile properties and Charpy V impact energy of 0.20C grade, Figure 3.0214.

3.0215 Effect of isothermal transformation treatment on room temperature tensile properties of 0.20C grade, Table 3.0215.

3.0216 Effect of bainite transformation temperature on room temperature tensile properties and 0 F Charpy V impact energy of 0.20C grade with and without subsequent tempering, Figure 3.0216.

3.0217 Effect of martensite tempering temperature on room temperature tensile properties and 0 F Charpy V impact energy of 0.20C grade, Figure 3.0217.

3.0218 Effect of tempering temperature on the room temperature tensile properties, Charpy V impact energy and hardness of 0.20C grade quenched within the martensitic range and tempered, Figure 3.0218.

3.0219 Effect of tempering temperature on tensile properties of 0.20C grade plate, Figure 3.0219.

3.02110 Effect of tempering temperature on tensile properties of 0.20C grade plate, Figure 3.02110.

3.02111 Effect of tempering temperature on tensile properties and hardness of reheat treated 0.20C grade plate, Figure 3.02111.

3.02112	Effect of stress relief treatment on room temperature tensile properties and hardness of 0.20C grade plate, Table 3.02112.
3.02113	Effect of plate thickness on tensile properties of 0.20C grade plate from one heat, Figure 3.02113.
3.02114	Range of room temperature tensile properties and Charpy V impact energy for 29 billets from 26 heats of 0.20C grade, Table 3.02114.
3.02115	Mean values and standard deviations for tensile properties of 0.20C grade plate tempered at several temperatures, Table 3.02115.
3.02116	Room temperature tensile properties, elastic modulus, and plane strain fracture toughness of 0.20C grade forged round bar, Table 3.02116.
3.02117	Tensile and Charpy V impact properties for several large forgings of 0.20C grade, Table 3.02117.
3.02118	Effect of cooling rate from the austenitizing temperature on the room temperature tensile properties and Charpy V impact energy of 0.30C grade, Figure 3.02118.
3.02119	Effect of tempering temperature on room temperature tensile properties of 0.30C grade plate variously quenched from the austenitizing temperature, Figure 3.02119.
3.02120	Effect of tempering temperature on the room temperature tensile properties, Charpy V impact energy, and hardness of 0.30C grade quenched within the martensitic range and tempered, Figure 3.02120.
3.02121	Effect of tempering temperature on tensile properties of 0.30C grade forged billet, Figure 3.02121.
3.02122	Room temperature tensile properties, elastic modulus, and plane strain fracture toughness of 0.30C grade forged rectangular bar, Table 3.02122.
3.02123	Room temperature tensile properties and plane strain fracture toughness of 0.30C grade plate variously heat treated, Table 3.02123.
3.02124	Range of room temperature tensile properties, Charpy V impact energy, and plane strain fracture toughness of 33 billets from 25 heats of 0.30C grade, Table 3.02124.
3.02125	Effect of elevated temperature exposure under stress on subsequent room temperature strength, Table 3.02125.
3.022	Compression – stress-strain diagrams – compression properties (see 3.032).
3.023	Impact. (See also 3.033 and 4.03.)
3.0231	Range of room temperature tensile properties and Charpy V impact energy for 29 billets from 26 heats of 0.20C grade, see Table 3.02114.
3.0232	Room temperature Charpy V impact energy for 0.20C grade forged bar, Table 3.0232.
3.0233	Effect of cooling rate from the austenitizing temperature on the room temperature tensile properties and Charpy V impact energy of 0.20C grade, see Figure 3.0214.
3.0234	Effect of tempering temperature on Charpy V impact energy of 0.20C grade plate, Figure 3.0234.
3.0235	Effect of tempering temperature on the room temperature tensile properties, Charpy V impact energy, and hardness of 0.20C grade quenched within the martensitic range and tempered, see Figure 3.0218.
3.0236	Effect of plate thickness on Charpy V impact energy of 0.20C grade plate from one heat, Figure 3.0236.
3.0237	Range of room temperature tensile properties, Charpy V impact energy, and plane strain fracture toughness of 33 billets from 25 heats of 0.30C grade, see Table 3.02124.
3.0238	Effect of cooling rate from the austenitizing temperature on the room temperature tensile properties and Charpy V impact energy of 0.30C grade, see Figure 3.02118.
3.0239	Effect of tempering temperature on Charpy V impact energy of 0.30C grade plate variously quenched from the austenitizing temperature, Figure 3.0239.
3.02310	Effect of tempering temperature on the room temperature tensile properties, Charpy V impact energy, and hardness of 0.30C grade quenched within the martensitic range and tempered, see Figure 3.02120.
3.024	Bending.
3.025	Torsion and shear. (See also 3.035.)
3.0251	Room temperature shear strength of 0.20C grade forged bar, Table 3.0251.
3.026	Bearing. (See also 3.036.)
3.027	Stress concentration.
3.0271	Notch properties. (See also 3.0371.)
3.02711	Effect of testing in high pressure hydrogen on the smooth and sharp notch tensile properties of 0.20C grade rod, see Table 2.0331.
3.0272	Fracture toughness. (See also 3.0372.)
3.02721	The plane strain fracture toughness of this alloy varies widely and unpredictably. Additional data is available in the Damage Tolerant Design Handbook (79), and that data also scatters through the same range as the data presented in this section and in Section 3.0372. Data not satisfying all of the requirements of ASTM Method of Test E-399 have been excluded from presentation.
3.02722	Room temperature tensile properties, elastic modulus, and plane strain fracture toughness of 0.20C grade forged round bar, see Table 3.02116.
3.02723	Plane strain fracture toughness of 0.20C grade forged billet, Table 3.02723.
3.02724	Effect of final forging temperature on room temperature plane strain fracture toughness of 0.20C grade hand forgings, Table 3.02724.
3.02725	Room temperature tensile properties, elastic modulus, and plane strain fracture toughness of 0.30C grade forged rectangular bar, see Table 3.02122.
3.02726	Room temperature tensile properties and plane strain fracture toughness of 0.30C grade plate variously heat treated, see Table 3.02123.
3.02727	Effect of tempering temperature on plane strain fracture toughness of 0.30C grade plate and forged billet, Figure 3.02727.
3.02728	Range of room temperature tensile properties, Charpy V impact energy, and plane strain fracture toughness of 33 billets from 25 heats of 0.30C grade, see Table 3.02124.
3.02729	One and one-half-inch thick compact specimens were determined (47) to be insufficiently thick to measure K_{Ic} of manual GTA welds with or without 950 F, 2 hours postweld stress relief. K_I at maximum load for 1/4- to 3/4-inch thick specimens with part-through cracks located in the heat-affected zone ranged from 90 to 118 ksi $(in.)^{1/2}$ at room temperature, and 82 ksi $(in.)^{1/2}$ single result at -65 F.

Fe
9 Ni
4 Co
Cr
Mo
V

9Ni-4Co

Fe
9 Ni
4 Co
Cr
Mo
V
9Ni-4Co

3.028 Combined properties.

3.03 **Mechanical Properties at Various Temperatures**

3.031 Tension – stress-strain diagrams – tension properties.

3.0311 Typical longitudinal tension stress-strain curves at room temperature and elevated temperature for 0.20C grade forged bar, Figure 3.0311.

3.0312 Typical transverse tension stress-strain curves at room temperature and elevated temperature for 0.20C grade forged bar, Figure 3.0312.

3.0313 Tensile stress-strain curves at various temperatures for 0.30C grade forged billet, Figure 3.0313.

3.0314 Effect of test temperature on tensile properties and plane strain fracture toughness of 0.20C grade plate, Figure 3.0314.

3.0315 Elevated temperature tensile properties of 0.20C grade plate, Figure 3.0315.

3.0316 Effect of test temperature on tensile properties of 0.20C grade forged bar, Figure 3.0316.

3.0317 Effect of test temperature on tensile properties of 0.20C grade rolled plate measured at conventional and high strain rates, Figure 3.0317.

3.0318 Effect of test temperature on tensile properties of 0.30C grade forged billet, Figure 3.0318.

3.0319 Effect of test temperature on tensile properties of 0.30C grade billet, Figure 3.0319.

3.03110 Effect of test temperature and elevated temperature exposure under stress on tensile properties of 0.30C grade plate, Figure 3.03110.

3.032 Compression – stress-strain diagrams – compression properties.

3.0321 Typical longitudinal compressive stress-strain curves at room and elevated temperatures for 0.20C grade forged bars, Figure 3.0321.

3.0322 Typical transverse compressive stress-strain curves at room and elevated temperatures for 0.20C grade forged bars, Figure 3.0322.

3.0323 Compressive stress-strain curves at various temperatures for 0.30C grade forged billet, Figure 3.0323.

3.0324 Effect of test temperature on compressive yield strength of 0.20C grade forged bar, Figure 3.0324.

3.0325 Effect of test temperature on compressive yield strength of 0.30C grade forged billet, Figure 3.0325.

3.033 Impact. (See also 4.03.)

3.0331 Effect of test temperature on Charpy V impact energy of 0.20C grade plate, Figure 3.0331.

3.0332 Range of Charpy V impact energy as function of test temperature for three plates from two heats of 0.20C grade with closely matching compositions, Figure 3.0332.

3.0333 Tensile and Charpy V impact properties for several large forgings of 0.20C grade, see Table 3.02117.

3.0334 Charpy V impact energy at various temperatures for 0.20C grade plate quenched and tempered with and without prior normalizing, Table 3.0334.

3.0335 Effect of test temperature on Charpy V impact energy for 0.20C grade after cooling within the bainitic range from the austenitizing treatment, Figure 3.0335.

3.0336 Effect of test temperature on Charpy V impact energy of 0.20C grade plate variously quenched from the austenitizing temperature, Figure 3.0336.

3.0337 Effect of test temperature on the Charpy V impact energy of 0.20C grade plate quenched in various media, Figure 3.0337.

3.0338 Effect of test temperature on the Charpy V impact energy of 0.20C grade plate tempered at various temperatures, Figure 3.0338.

3.0339 Effect of martensite tempering temperature on room temperature tensile properties and 0 F Charpy V impact energy of 0.20C grade, see Figure 3.0217.

3.03310 Effect of bainite transformation temperature on room temperature tensile properties and 0 F Charpy V impact energy of 0.20C grade with and without subsequent tempering, see Figure 3.0216.

3.03311 Effect of test temperature on the Charpy V impact energy of 0.20C grade plate variously stress relieved, Figure 3.03311.

3.03312 Effect of test temperature on Charpy V impact energy and lateral expansion of 0.20C grade plate with and without stress relief treatment, Figure 3.03312.

3.03313 Effect of test temperature on dynamic tear test energy of 0.20C grade cross rolled plate, Figure 3.03313.

3.03314 Effect of test temperature on dynamic tear energy of 0.20C grade rolled plate, Figure 3.03314.

3.03315 Effect of test temperature on Charpy V impact energy for 0.30C grade after cooling within the bainitic range from the austenitizing treatment, Figure 3.03315.

3.034 Bending.

3.035 Torsion and shear.

3.0351 Effect of test temperature on shear strength of 0.30C grade forged billet, Figure 3.0351.

3.036 Bearing.

3.0361 Effect of test temperature on bearing strength of 0.30C grade forged billet, Figure 3.0361.

3.037 Stress concentration.

3.0371 Notch properties.

3.03711 Mild notch strength of 0.30C grade forged billet at room temperature and -110 F, Table 3.03711.

3.0372 Fracture toughness.

3.03721 Plane strain fracture toughness at room temperature and -65 F for 0.20C grade in a variety of product forms, each from a separate heat and variously heat treated, Table 3.03721.

3.03722 Plane strain fracture toughness at room temperature and -65 F of 0.30C grade forged blocks variously heat treated, Table 3.03722.

3.038 Combined properties.

3.04 **Creep and Creep-Rupture Properties**

3.041 Creep-rupture curves for 0.20C grade plate, Figure 3.041.

3.042 Creep and stress-rupture properties of 0.20C grade forged bar at 500, 700, and 900 F, Figure 3.042.

3.05 **Fatigue Properties**
(See also 2.035 and 2.036.)

3.051 Rotating beam smooth and mild-notch fatigue strength of 0.20C grade plate, Figure 3.051.

3.052 Rotating beam smooth and mild-notch fatigue strength of 0.20C grade plate, Figure 3.052.

3.053 Axial load mild-notch fatigue strength of 0.20C grade forged round bar, Figure 3.053.

3.054	Axial load smooth fatigue strength at room temperature, 500 F, and 700 F for 0.20C grade forged bar, Figure 3.054.
3.055	Axial load mild-notch fatigue strength at room temperature, 500 F, and 700 F for 0.20C grade forged bar, Figure 3.055.
3.056	High and low cycle smooth and mild-notch fatigue strength of 0.20C grade plate in air and salt-water, Figure 3.056.
3.057	Effect of cyclic frequency on fatigue crack-growth rate in low humidity air of 0.20C grade forged bar, Figure 3.057.
3.058	Effect of cyclic frequency on fatigue crack-growth rate in low humidity air of 0.20C grade forged bar, Figure 3.058.
3.059	Effect of test temperature on the LT fatigue crack-growth rate in low humidity air of 0.20C grade rolled plate, Figure 3.059.
3.0510	Effect of test temperature on the TL fatigue crack-growth rate in low humidity air of 0.20C grade rolled plate, Figure 3.0510.
3.0511	Effect of test temperature on fatigue crack-growth rate in low humidity air of 0.20C grade forged bar, Figure 3.0511.
3.0512	Effect of specimen thickness on fatigue crack-growth rate in low humidity air of 0.20C grade rolled plate, Figure 3.0512.
3.0513	Effect of specimen thickness on fatigue crack-growth rate in low humidity air of 0.20C grade forged bar, Figure 3.0513.
3.0514	Effect of R-ratio on fatigue crack-growth rate in low humidity air of 0.20C grade forged bar, Figure 3.0514.
3.0515	Comparison of the room temperature fatigue crack propagation of 0.20C grade to other high strength steels, all in commercial heat treated condition, Figure 3.0515.
3.0516	Influence of retained austenite on room temperature fatigue crack propagation in 0.20C grade forging, see Figure 4.0365.
3.0517	A study on 0.20C grade of fatigue crack-growth and fracture of surface flaws and of part-through and straight-through cracks originating at fastener holes under constant-amplitude cyclic load, periodic overload, and spectrum load is described in Reference 54. Surface flaw test variables included loading mode (tension bending, and combined tension and bending), cyclic stress ratio ($R = 0.1$, 0.3, and 0.5), initial flaw shape ($0.15 < a/2c < 0.45$), and initial flaw depth ($0.2 < a/t < 0.8$). Fastener hole flaw test variables included hole condition (conventional reamed and cold worked), fastener type (close tolerance and Taper-lok), and initial crack shape (uniform through-thickness and quarter-circular part-through). All tests were performed in air having a relative humidity of about 10 percent. The reader is referred to Reference 54 for results.
3.0518	Effect of cyclic frequency on fatigue crack-growth rate in low humidity air of 0.20C grade plate GTA machine welds, Figure 3.0518.
3.0519	Effect of test temperature on fatigue crack-growth rate in low humidity air of 0.20C grade forged billet GTA manual weld heat-affected zone, Figure 3.0519.
3.0520	Effect of specimen thickness on fatigue crack-growth rate in low humidity air of 0.20C grade plate GTA manual weld heat-affected zone, Figure 3.0520.
3.0521	Effect of R-ratio on fatigue crack-growth rate in low humidity air of 0.20C grade plate GTA machine welds, Figure 3.0521.
3.0522	Base metal and heat-affected zone fatigue crack-growth rates in low humidity air of 0.20C grade plate GTA manual welds, Figure 3.0522.
3.0523	Fatigue crack-growth rates in low humidity air of 0.20C grade plate and forged bar GTA manual weld heat-affected zone, Figure 3.0523.
3.0524	Rotating beam smooth fatigue strength of 0.30C grade plate, Figure 3.0524.
3.0525	Axial load mild-notch fatigue strength of 0.30C grade forgings, Figure 3.0525.
3.0526	Axial load constant life diagram for mild-notch specimens of 0.30C grade forgings, Figure 3.0526.
3.0527	Axial load mild-notch fatigue strength of 0.30C grade forged rectangular bar, Figure 3.0527.
3.0528	Axial load mild-notch fatigue strength of 0.30C grade forged billet, Table 3.0528.
3.0529	Effect of cyclic frequency on fatigue crack-growth rate in low humidity air of 0.30C grade forged bar, Figure 3.0529.
3.0530	Effect of R-ratio on fatigue crack-growth rate in low humidity air of 0.30C grade forged bar, Figure 3.0530.
3.0531	Effect of R-ratio on fatigue crack-growth rate of 0.30C grade hand forged billet in low humidity air (<10 percent relative humidity), Figure 3.0531.
3.0532	Effect of R-ratio on fatigue crack-growth rate of 0.30C grade hand forged billet in low humidity air (<10 percent relative humidity), plotted as a function of K_{max}, Figure 3.0532.
3.0533	Fatigue crack propagation rates at room temperature for 0.30C grade mill annealed rolled plate, Figure 3.0533.
3.0534	Fatigue crack propagation rates at room temperature for 0.30 grade rolled plate quenched and tempered to 179 ksi yield strength, Figure 3.0534.
3.0535	Fatigue crack propagation rates at room temperature for 0.30C grade rolled plate quenched and tempered to 203 ksi yield strength, Figure 3.0535.
3.0536	Effect of test temperature on fatigue crack growth in low humidity air of 0.30C grade forged bar, Figure 3.0536.
3.0537	Fatigue crack propagation rates at room temperature, 500, and 650 F, and two cyclic frequencies for 0.30C grade rolled plate, Figure 3.0537.
3.0538	For a constant stress intensity range (ΔK) the crack-growth rate for 0.30C grade plate increases with increasing strength and decreasing toughness (see constant amplitude data in Table 3.0539). Overload cycles retard crack propagation with relationship to the toughness and strength; that is, the retardation increases as the toughness increases and the strength decreases. It is not certain which property controls the crack propagation or its retardation due to overload.
3.0539	Retardation effect of overload sequence on room temperature fatigue crack propagation for 0.30C grade plate in three heat treated (strength level) conditions, Table 3.0539.

Fe
9 Ni
4 Co
Cr
Mo
V

9Ni-4Co

Fe
9 Ni
4 Co
Cr
Mo
V

9Ni-4Co

3.06 **Elastic Properties**

3.061 Poisson's ratio, $\mu = 0.296$ (static at room temperature) (64), 0.299 (dynamic at room temperature).

3.062 Modulus of elasticity.

3.0621 Dynamic modulus of elasticity in tension, $E = 28.9 \times 10^3$ ksi (13).

3.0622 Room temperature tensile properties, elastic modulus, and plane strain fracture toughness of 0.20C grade forged round bar, Table 3.02116.

3.0623 Effect of test temperature on tensile modulus of elasticity for 0.20C grade, Figure 3.0623.

3.0624 Effect of test temperature on tensile properties of 0.20C grade rolled plate measured at conventional and high strain rates, see Figure 3.0317.

3.0625 Effect of test temperature on compressive modulus of elasticity for 0.20C grade forged bar, Figure 3.0625.

3.0626 Dynamic modulus of elasticity of 0.30C grade bar, Figure 3.0626.

3.0627 Room temperature tensile properties, elastic modulus, and plane strain fracture toughness of 0.30C grade forged rectangular bar, see Table 3.02122.

3.0628 Precision tensile moduli of 0.30C grade at room temperature (according to ASTM E-111), Table 3.0628.

3.0629 Effect of temperature on modulus of elasticity in tension and compression for 0.30C grade forged billet, Figure 3.0629.

3.063 Modulus of rigidity, $G = 11.1 \times 10^3$ ksi (static at room temperature) (13), 10.9×10^3 ksi (dynamic at room temperature).

3.064 Tangent modulus.

3.0641 Typical compressive tangent-modulus curves at room and elevated temperatures for 0.20C grade forged bars, Figure 3.0641.

3.0642 Typical compressive tangent-modulus curves at room and elevated temperatures for 0.20C grade forged bars, Figure 3.0642.

3.065 Secant modulus.

4 FABRICATION

4.01 Forming

4.011 General. A considerable amount of data on the influence of hot working conditions on the mechanical properties of plate and forgings is available in Republic Steel Corporation reports originating from Air Force Contract AF 33(657)-11277 (38–42). This information is summarized in Reference 43. The reader should refer to these and to the alloy producer for information concerning particulars of forming. In general, hot working will be somewhat more difficult than AISI-4340 due to the high cobalt content, and the absence of aluminum will result in rapid grain growth at temperatures above 2050 F.

4.012 0.20C grade. This grade is forged easily by open die or closed die forging techniques. The recommended (44) hot-forging or hot-rolling temperature is 2050 F maximum. The alloy can be formed in the annealed or quenched and tempered conditions by any cold-forming technique (44).

4.013 0.30C grade. Like the 0.20C grade, this grade can be easily forged by open die or closed die forging techniques, and the recommended (45) forging temperature is 2050 F maximum. It can be formed in the annealed condition by any normal cold-forming technique, such as bending, rolling, or shear spinning (45).

4.02 Machining and Grinding

The machinability of 0.30C grade was assessed as a function of heat treated condition by a series of turning and drilling tests. The results are given in Table 4.0131 and Figure 4.0132. Results of the turning tests indicate that the relative machinability of the normalized and tempered conditions are essentially equivalent, and superior to the annealed condition. Drilling tests results indicate the normalized and single tempered condition has the best relative machinability. With regard to the other heat treated conditions, at cutting speeds greater than 45 feet per minute, the annealed condition drills more easily; at lesser speeds, the reverse is true.

Specific guidance on machining operations for both grades can be found in the *Machining Data Handbook*, Machinability Data Center, Metcut Research Associates, Inc., publisher, Cincinnati, Ohio.

4.03 Joining

4.031 General. The 0.20 carbon grade can be readily welded in the fully heat treated condition and achieve essentially 100 percent joint efficiency without preheat or postheat treatment. Its weldments may be stress relieved without loss in Charpy V impact energy or tensile properties providing the AMS specified filler wire is used. On the basis of information available, the cold wire GTA process with argon shielding is preferred (see Table 4.0311). Care should be taken to keep oxide away from the weld area and adjacent surfaces by suitable interpass cleaning because the parent metal has insufficient silicon to block carbon oxidation and consequent weld porosity. High heat input should be avoided since it can result in low tensile strength welds having reduced toughness, as well as an increased tendency toward porosity and cracking. With the cold wire GTA process, the tensile and impact properties of 2-1/4 inch plate are shown in Table 4.0312 to be independent of heat input between 30 and 70 kilojoules/inch. Normal precautions should be taken to avoid hydrogen embrittlement. Specific information on weld filler wire composition, recommended weld parameters, and potential embrittling effects of stress relief treatment are discussed below.

4.0311 Room temperature tensile properties and 0 F Charpy V impact energy of 0.20C grade plate welds produced by the cold wire and hot wire GTA processes, Table 4.0311.

4.0312 Effect of heat input on room temperature tensile properties and low temperature Charpy V impact energy of as-deposited 2-1/4-inch-thick plate GTA welds, Table 4.0312.

4.032 Filler wire composition. Weld filler wire composition has been studied by Ries and Poole (29) and by Savas, et al (19) with the aim of developing a

commercially usable, 180 to 200 ksi yield strength, 50 foot-pound minimum 30 F Charpy V impact energy, GTA filler metal whose strength and toughness is retained after postweld stress relieving. The individual and combined influences of constituent elements on the target properties were examined. The result was the successful development of a stress relievable composition which meets the aforementioned requirements, and this wire has become an AMS standard. The following discussion of compositional influences on weldability and weld properties is based on that work of Ries and Poole (29) and of Savas, et al (19).

Since the weld structure in this alloy is predominately martensite, a strong carbon influence is to be expected. Increasing carbon produces a general decrease in Charpy V impact energy and corresponding increase in yield strength, as seen in Figure 4.0321. The scatter in these data suggest that elements other than carbon are also active in controlling the as-deposited weld properties. The average curve through the Charpy V data suggests carbon levels be kept below 0.17 weight percent to achieve 50 foot-pound at 30 F. To ensure as-deposited yield strength of 180 ksi minimum, the data of Figure 4.0321 as well as results of Ries and Poole (29) indicate that the carbon level should not be lower than about 0.14 weight percent. Carbon does not appear to independently contribute to property changes associated with stress relieving.

Manganese in the filler metal increases the fluidity and decreases the surface tension of the weld puddle, thereby promoting good fusion of the weld puddle with the base plate. However, it has a moderately detrimental effect on all mechanical properties in the as-deposited or stress-relieved conditions when it is considered separately from all the other elements. Its influence on stress-relief embrittlement increases markedly when it is associated with substantial levels of silicon and phosphorus.

Sound, dense welds require a deoxidizer such as silicon to block carbon-oxygen reaction in the weld puddle (which would produce carbon monoxide gas to be trapped in the solidified weld metal) due to extraneous oxygen contamination from, say, the shielding gas or oxide scale. Silicon has a beneficial influence on strength and toughness in the as-deposited condition. After stress relief, however, silicon lowers the toughness drastically, particularly in association with manganese. The data in Figure 4.0322 shows the lower bound total of manganese plus silicon at 0.6 for zero change in Charpy V energy following stress relief. Silicon in amounts sufficient to effect deoxidation (between 0.15 and 0.25 weight percent) is essential in producing weldments free of porosity. Therefore, silicon at a nominal content of 0.2 weight percent, and manganese at twice that amount are indicated by the existing data, and are quoted at these levels in the nonembrittling composition of the AMS specified wire.

Nickel lowers as-deposited yield strength with no corresponding increase in toughness. It increases the stress-relieved yield strength slightly and is very beneficial to the stress-relieved toughness. Cobalt imparts a small degree of strengthening to the as-deposited metal, but has no effect on the stress-relieved strength. In contrast to nickel, cobalt is detrimental to stress-relief embrittlement as well as to as-deposited toughness. Cobalt is necessary in this alloy to minimize the presence of retained austenite. The location of the M_S temperature is influenced by the cobalt content in that this temperature has been raised sufficiently to confer some self-tempering effects. This effect is considered to be of particular benefit in improving the properties of the heat-affected zone. The cobalt and nickel contents are designed to promote resistance to embrittlement and to enable the steel to undergo repeated weld thermal cycles without significant impairment of strength or toughness.

Fe
9 Ni
4 Co
Cr
Mo
V

9Ni-4Co

Chromium has no appreciable influence on as-deposited weld mechanical properties, but slightly lowers the yield strength and imparts embrittlement resistance to stress-relieved weldments. In contrast, molybdenum increases yield strength in both the as-deposited and stress-relieved conditions, and decreases the toughness in both conditions. The chromium:molybdenum proportion should be kept high to benefit embrittlement resistance, but enough molybdenum must be included to achieve desired strength levels by thermal treatment. Figure 4.0323 shows the synergistic influence of chromium and molybdenum on the stress-relieved strength and toughness in terms of the factor: Mo(Cr + Mo)/Cr. In order to obtain a yield strength of 180 ksi and an impact toughness of 50 foot-pounds at 30 F as minimum properties values, the weld metal composition must have a chromium:molybdenum factor between 0.7 and 0.9, which corresponds to about 0.50 weight percent molybdenum and 1.0 weight percent chromium.

Vanadium is included in this alloy's composition as a grain refiner. It is a strengthening constituent, and in the quantity specified is not harmful to stress-relief embrittlement resistance. At levels greater than 0.15 weight percent, it would be deleterious.

Phosphorus increases susceptibility to stress-relief embrittlement. Because it is present in low levels, its effect on embrittlement is modest, and the control of embrittlement resistance is accomplished by regulating the manganese and silicon levels. Sulfur is also kept low in this alloy, and at its specified level has no noticeable effect on mechanical properties in either the as-deposited or stress-relieved conditions.

Based on the above guidelines, a special nonembrittling GTA weld filler wire composition has been developed and is specified as AMS-6468A (30).

4.0321 Effect of weld metal carbon content on as-deposited room temperature yield strength and

Fe
9 Ni
4 Co
Cr
Mo
V

9Ni-4Co

30 F Charpy V impact energy of GTA welds, Figure 4.0321.

4.0322 Effect of total (Mn + Si) content on change in 30 F Charpy V impact energy due to stress relieving of 0.20C grade plate GTA welds produced using various weld filler wires, Figure 4.0322.

4.0323 Effect of Cr:Mo ratio on room temperature yield strength and 30 F Charpy V impact energy of stress relieved 0.20C grade plate GTA welds produced using various weld filler wires, Figure 4.0323.

4.0324 AMS specified GTA weld filler wire composition, Table 4.0324.

4.033 Welding parameters. Room temperature yield strength of 180 ksi minimum and -80 F Charpy V impact energy of 50 ft-lb minimum can be obtained using 0.063-inch diameter filler wire of the composition specified in Table 4.0324 and the welding parameters given in Table 4.0332. Typical properties are presented in Table 4.0331 which demonstrate 1-inch and 2-inch-thick welds to be fully equivalent to base plate. A transverse tensile specimen from the welded 2-inch plate failed in the base metal remote from the weld and heat affected zone at F_{tu} = 198.0 ksi, F_{ty} = 187.9 ksi, and RA = 56.6 percent.

The producer's recommended welding parameters are given in Table 4.0332. No preheat or postheat is recommended and the maximum interpass temperature should be 200 F.

4.0331 Typical tensile and Charpy V impact properties at room and cryogenic temperatures for as-deposited GTA welds of 1-inch and 2-inch plate, Table 4.0331.

4.0332 Producer's recommended GTA welding parameters, Table 4.0332.

4.034 Stress relief. A study by Rosenstein, et al (32) indicates that a stress relief treatment of 1000 F for 24 hours followed by furnace cooling will produce an 80 percent reduction in weld residual stress. As reported by Ries and Poole (29), the exposure of some filler metal compositions to such a stress-relief treatment can produce a severe loss in toughness, even though the as-deposited weld properties may be excellent. This is illustrated by the results of Savas, et al, in Figure 4.0341. Use of the AMS specified weld filler wire (30), however, results in welds that are completely resistant to stress relief embrittlement at 30 and 70 F, but exhibit some embrittlement at -80 F, as shown by the data of Figure 4.0342 and Table 4.0343. Stress-relief treatment produces no damage to the base material (Table 4.0344) nor the weld heat affected zone (Figure 4.0345).

During repair welding, a weldment may be subjected to repeated thermal cycles. Table 4.0344 shows multiple thermal cycles at 975 F (50 F below the tempering temperature) have no effect on mechanical properties.

4.0341 Effect of stress relief at various temperatures and times on room temperature tensile yield strength and 30 F Charpy V impact energy of 0.20C grade plate GTA welds produced with various embrittling weld filler wires, Figure 4.0341.

4.0342 Effect of 1000 F stress relief time on room temperature tensile yield strength and 30 F Charpy V impact energy of 0.20C grade plate GTA welds produced using AMS specified weld filler wire and producer's recommended welding parameters, Figure 4.0342.

4.0343 Effect of stress-relief treatment on room temperature tensile and low temperature Charpy V impact properties of 1-inch and 2-inch-thick 0.20C grade plate GTA welds, Table 4.0343.

4.0344 Effect of stress-relief treatment and of multiple thermal cycles on room temperature tensile and low temperature Charpy V impact properties for 0.20C grade plate in two thicknesses, Table 4.0344.

4.0345 Effect of stress-relief treatment on low temperature Charpy V impact energy for simulated heat-affected zone microstructures of 0.20C grade plate, Figure 4.0345.

4.035 Weld heat-affected zone embrittlement. A simulated weld thermal cycle study to investigate heat-affected zone embrittlement (Figure 4.0351) showed that in the peak temperature region between 1300 and 2400 F, where reaustenitizing occurs on heating, the hardness increased to between 45 and 48 R_C and the Charpy V impact energy at 0 F decreased (by nearly a factor of 2) to between 31 and 41 ft-lb, values typical of as-quenched martensite at this carbon level. Post-weld tempering could probably restore some of the toughness in this region by tempering the martensite (31).

4.0351 Hardness and 0 F Charpy V impact energy as functions of peak temperature produced by simulated welding cycle, Figure 4.0351.

4.036 Weld metal retained austenite. As-quenched martensitic structures of 0.20C grade base metal generally contains less than 3 percent retained austenite, which is readily removed by refrigeration prior to tempering. Industrial weldments of the alloy, on the other hand, contain as much as 10 percent austenite in their stress-relieved weld and heat-affected zone areas, which is only partially removed by subsequent refrigeration (see Table 4.0361). This larger volume of austenite is thought to be associated with thermal cycling during welding through the intercritical range (1180 to 1375 F), where the steel is in the ($\gamma + \alpha$) two-phase region, and from austenite reversion during subsequent stress relieving above 930 F.

Ritchie, et al (18) have studied the influence of such retained austenite in tempered (0.20C grade) structures on mechanical properties of commercially heat treated stock (containing less than 3 percent austenite) and of intercritically heat treated and tempered material (containing approximately 14 percent austenite – refer to Figure 4.0362), the latter representative of the weld microstructure. The increased proportion of austenite in the intercritically heat treated and tempered material (simulated weld material) lowers the strength and raises the ductility and work hardening capacity in comparison to the commercially heat treat (base metal) stock, as shown in Table 4.0363. These properties are consistent with the strain-induced transformation of the

austenite on loading, as indicated by magnetic saturation measurements of austenite stability during tensile tests in Table 4.0364. The small percentage (<3 percent) of retained austenite in the commercially heat treated material is mechanically unstable and transforms completely during loading to merely 0.002 strain. Austenite retained in the intercritically heat treated and tempered material (simulating a weldment), however, continues to transform with increasing strain beyond yield, which results in greater work hardening and hence in improved uniform elongation.

Fatigue crack propagation rates in the range 4×10^{-10} to 4×10^{-4} inch/cycle were measured for the same two structures in an environment of moist, room temperature air. These results are given in Figure 4.0365. For the intermediate range of growth rates, represented by the linear portion of the growth rate curves from 4×10^{-8} to 4×10^{-5} inch/cycle, an increased proportion of retained austenite appears to have little effect on crack propagation rate. In this range, mechanisms of fatigue failure in both structures were primarily ductile striation growth consistent with the lack of any microstructural influence on cracking behavior. At higher growth rates exceeding 4×10^{-5} inch/cycle, the fracture morphology of both structures included increasing amounts of microvoid coalescence in addition to striation growth, characteristic of fatigue crack propagation in high toughness steels at high stress intensities. Extensive secondary cracking was evident at all growth rates in the simulated weld material, but not the base metal. At low, near-threshold growth rates less than 4×10^{-8} inch/cycle, the simulated weld material containing 14 percent austenite showed somewhat superior resistance to crack propagation, the threshold stress intensity factor for crack growth being over 20 percent higher than in the base material. Macroanalysis of fracture surfaces for both structures showed distinct rust deposits where growth rates were less than about 2×10^{-8} inch/cycle, suggesting a significant corrosion effect in moist air at near-threshold growth rates in this steel. Microscopically, near-threshold failures in the base material were characterized by a fine-scale ductile transgranular mechanism with isolated facets of intergranular cracking typical of near-threshold crack propagation of high strength steels in moist air. The proportion of such facets reached a maximum of 15 percent at $\Delta K = 5.0$ ksi $(in.)^{1/2}$ and then gradually decreased with increasing ΔK to 0 percent at $\Delta K = 10$ ksi $(in.)^{1/2}$. No intergranular fracture was observed in the simulated weld material. It is concluded that significant proportions of retained austenite are not detrimental to fatigue crack propagation resistance in the 0.20C grade material, and may indeed have a beneficial effect at very low, near-threshold growth rates by increasing resistance to environmentally-assisted cracking.

4.0361 Volume fraction of austenite in industrial multipass GTA weldments of 0.20C grade plate, Table 4.0361.

4.0362 Variation of volume fraction of retained austenite with intercritical reheating time at 1325 F, before and after tempering at 1025 F for 4 hours, for 0.20C grade forging, Figure 4.0362.

4.0363 Room temperature tensile properties of base and simulated weld material from 0.20C grade forging showing effect of retained austenite, Table 4.0363.

4.0364 Mechanical stability of austenite in base and simulated weld material from 0.20C grade forging, Table 4.0364.

4.0365 Influence of retained austenite on room temperature fatigue crack propagation in 0.20C grade forging, Figure 4.0365.

4.037 Weld metal stress corrosion cracking. Plate weldments exhibit delayed failure when fatigue cracked (at weld center) and subjected to a sustained load in seawater (Figures 4.0371 and 4.0372). As might be expected for steels of this class, substantial loss in strength is observed and the weld metal is more susceptible than the parent material. The as-deposited metal K_{Iscc} appears to be about 60 ksi $(in.)^{1/2}$. The data of Figure 4.0372 can be interpreted to indicate a beneficial effect of stress relieving.

4.0371 Delayed failure of 0.20C grade plate GTA weld in seawater, Figure 4.0371.

4.0372 Stress corrosion cracking behavior of 0.20C grade welds in seawater, Figure 4.0372.

4.04 **Surface Treating**

4.041 Carburizing. The carburizing response of 0.20C grade was studied by Kronbach (46). Three carburizing potentials (0.60, 0.70, and 0.80 percent C) were employed in conjunction with three postcarburizing heat treatments: direct quench from the 1700 F carburizing treatment, furnace cool to 1500 F and then quenched, and a reheat treatment to 1500 F; each with and without refrigeration at -100 F. His results are presented in Figures and Tables 4.042 through 4.0410.

Reheat treatment with or without refrigeration prior to tempering produces the best core properties (Table 4.042). Carburizing at a relatively low carbon potential (0.60 percent) followed by the same reheat treatment produces the highest unnotched Charpy impact toughness (Table 4.045). Nearly equivalent carburized unnotched impact toughness (Table 4.045), with some sacrifice in core yield strength (Table 4.042), is produced with the 0.70 and 0.80 percent C potential cycles with a direct quench and no refrigeration prior to tempering. Refrigeration after the direct quench and before tempering reduces retained austenite, and decreases the carburized (0.70 and 0.80 percent C potential) impact toughness significantly while slightly increasing the case surface hardness (Table 4.045). With the same carburizing cycle (0.70 and 0.80 percent C potential), reheat treatment prior to refrigeration and tempering produces an increase in case hardness (Table 4.045) with increased core yield strength (Table 4.042) and reduced carburized unnotched Charpy impact toughness (Table 4.045) compared to the condition of refrigeration and tempering directly after carburizing.

When carburized with the 0.80 percent C potential and with a reheat treatment, AISI-9310 alloy is

Fe
9 Ni
4 Co
Cr
Mo
V

9Ni-4Co

Fe
9 Ni
4 Co
Cr
Mo
V

9Ni-4Co

capable of producing higher hardness in the case (Figure 4.048) and greater core toughness (Table 4.047) than can be attained in the 0.20C grade of 9Ni-4Co similarly carburized and heat treated. However, the 9Ni-4Co 0.20C grade provides significantly higher core and case hardenability.

4.042 Pseudocarburized core properties of stock used in carburizing studies reported upon in Figures and Tables 4.043 through 4.046, Table 4.042.

4.043 Microhardness profile of 0.20C grade rounds carburized to 0.050-inch depth, Table 4.043.

4.044 Carbon gradient achieved for 0.20C grade carburized at three carbon potentials, Figure 4.044.

4.045 Room temperature impact energy and surface hardness of carburized 0.20C grade unnotched Charpy specimens, Table 4.045.

4.046 Influence of a refrigeration cycle on the case hardness of carburized 0.20C grade bars, Table 4.046.

4.047 Room temperature surface and core hardness and core Charpy V impact energy for carburized 0.20C grade and AISI-9310 rounds used in carburizing studies reported upon in Figures and Tables 4.048 through 4.0410, Table 4.047.

4.048 Case hardness profile of carburized 0.20C grade and AISI-9310, Figure 4.048.

4.049 Carbon profile for carburized 0.20C grade and AISI-9310 rounds, Figure 4.049.

4.0410 Effect of refrigeration on the retained austenite levels of 0.20C grade and AISI-9310 carburized rounds, Table 4.0410.

4.0411 Scale formed during hot working is dense and tough with decarburization deeper than observed for AISI-4340 (39); otherwise, similar to AISI-4340.

REFERENCES

1 Aerospace Material Specification, AMS-6523B (October 15, 1979).

2 Aerospace Material Specification, AMS-6525 (January 15, 1976).

3 Boeing Material Specification, BMS-7-182B (August 7, 1974).

4 McDonnell Douglas Material Specification, MMS-2101 (Revision A) (October 9, 1978).

5 Northrop Material Specification, NAI-1374 (March 2, 1973).

6 Rockwell International Material Specification, ST0160LB0002 (Revision F) (August 30, 1976).

7 Aerospace Material Specification, AMS-6524B (April 1, 1985).

8 Aerospace Material Specification, AMS-6526B (July 1, 1981).

9 American Society for Testing and Materials Specification A 579-77 (June 24, 1977).

10 McDonnell Douglas Material Specification, MMS-2102 (Revision B) (February 7, 1978).

11 Northrop Material Specification, NAI-1373 (March 2, 1973).

12 Rockwell International Material Specification, ST0160LB0004 (Revision B) (September 1, 1982).

13 Materkowski, J. P., "Properties of Republic HP 9-4-20 Steel: A Summary Report", Republic Steel Research Center Report PR-12,049-82-3 (November 1982).

14 Materkowski, J. P., "Properties of Republic HP 9-4-30 Steel: A Summary Report", Republic Steel Research Center Report PR-12,049-82-2 (July 1982).

15 Lynch, J. M. and Sommer, A. W., "Developing the Heat Treatment: HP-9-4-.20 Steel", *Journal of the Society for the Advancement of Material and Process Engineering (SAMPE)*, Vol. 10, No. 1 (January/February 1974) pp 10–13.

16 Ault, R. T., LTV Steel Research Center, Cleveland, Ohio, private communication (1985).

17 Stephens, H. P., "The Enthalpy and Specific Heat of a Nickel-Cobalt Steel to 2000 K", *High Temperature Science*, Vol. 10 (1978) pp 95–107.

18 Ritchie, R. O., Chang, V. A., and Paton, N. E., "Influence of Retained Austenite on Fatigue Crack Propagation in HP 9-4-20 High Strength Alloy Steel", Fatigue of Engineering Materials and Structures (1979) pp 107–121.

19 Savas, J., Becker, P. C., and Matas, S. J., "Development of a 180 ksi Yield Strength Stress Relievable 9Ni-4Co Filler Metal Composition", *Welding Journal*, Welding Research Supplement (November 1969) pp 479-s–492-s.

20 Deel, O. L. and Mindlin, H., "Engineering Data on New Aerospace Structural Materials", AFML-TR-72-196, Vol. II (September 1972).

21 Deel, O., "Collected Engineering Data Sheets (Air Force Data Sheet Program)", AFML-TR-78-179 (December 1978).

22 Moss, M., "Filament-Reinforced Cylindrical Pressure Vessels: Analysis and Numerical Evaluation", SAND-77-0403, Sandia Laboratories.

23 McHenry, H. I. and Pense, A. W., "Fatigue Crack Propagation in Steel Alloys at Elevated Temperatures", *Fatigue at Elevated Temperatures*, ASTM STP 520, American Society for Testing and Materials (1973) pp 345–354.

24 Suga, M., Goss, J. L., Olson, G. B., and Vander Sande, J. B., "Austenitic Grain Growth Characteristics in Rapidly Solidified Martensitic Steels", Proceedings of the 2nd Conference on Rapid Solidification Processing Principles and Technologies, Reston, Virginia (March 23–26, 1980).

25 Magnee, A., Drapier, J. M., Dumont, J., Coutsouradis, D., and Habraken, L., "Cobalt-Containing High-Strength Steels: A Critical Review of the Physical Metallurgy of Cobalt-Containing High-Strength Steels, and a Survey of Their Processing, Properties and Uses", Centre D'Information Du Cobalt, Brussels (1974).

26 Petrak, G. J. and Gallagher, J. P., "Predictions of the Effect of Yield Strength on Fatigue Crack Growth Retardation in HP-9Ni-4Co-30C Steel", Transactions of the ASME, *Journal of Engineering Materials and Technology* (July 1975) pp 206–213.

27 Petrak, G. J., USAF Flight Dynamics Laboratory, Wright Patterson Air Force Base, Ohio, private communication (1985).

28 Ault, R. T., "HP 9-4-20 Steel Data", TR 12018-132, Project 12018, Republic Steel Research Center, Cleveland, Ohio (March 11, 1968).

29 Ries, G. D. and Poole, S. W., "Welding of Quenched and Tempered 9Ni-4Co Steels", *Welding Journal*, Vol. 45, No. 10, Research Supplement (1966) pp 465-s–476-s.

30 Aerospace Material Specification, AMS-6468A (October 1, 1983).

31 Dabkowski, D. S., Konkol, P. J., Novak, S. R., and Porter, L. F., "Evaluation of the HP9-4-20 Steel Weldment System", U.S. Steel Report on Project No. 39.018-007(30), U.S. Navy Contract NObs-94535(FBM)SF020-01-01, Task 854 B-61209-1, Contract Item 6 (January 2, 1969).

32 Rosenstein, A. H., Gross, M. R., Schreitz, W. G., and Wacker, G. A., "Metallurgical Investigation of 9Ni-4Co-.2C Steel", Naval Research and Development Report 2678 (July 1968).

33 Rosenstein, A. H. and Asche, W. H., "Stress-Relief Embrittlement of High-Strength Quenched and Tempered Alloy Steels", *ASTM STP 407*, Temper Embrittlement in Steel (1968).

34 Benson, L. E. and Watson, S. J., "Low Temperature Stress Relieving of Mild Steel Welded Structures", Transaction of the Institute of Welding (August 1953) pp 90–95.

35 Crooker, T. W. and Lange, E. A., "Corrosion-Fatigue Crack Propagation Studies of Some New High-Strength Structural Steels", NRL Report 6870 (April 3, 1969).

36 Rosenstein, A. H. and Spaanderman, J. J., "Effects of Stress-Relief Heat Treatments on High-Strength Steels: A Summary Report", Naval Ship Research and Development Center Report 3216 (June 1970).

37 Petrak, G. J., "Strength Level Effects on Fatigue Crack Growth and Retardation", *Engineering Fracture Mechanics*, Vol. 6 (1974) pp 725–733.

38 Republic Steel Corporation, "Manufacturing Process Development for High Strnegth Steel – Sheet and Plate Survey of 18Ni-CoMo Maraging and 9Ni-4Co Quench and Temper High Strength Steels", Interim Engineering Progress Report IR-8-157 (II) (November 1963).

39 Republic Steel Corporation, "Manufacturing Process Development for High Strength Steel – Forging Survey of 18Ni-CoMo Maraging and 9Ni-4Co Quench and Temper High Strength Steels", Interim Engineering Progress Report IR-8-157 (I) (September 1963).

40 Republic Steel Corporation, "Manufacturing Process Development for High Strength Steels: Phase II Process Development", Interim Engineering Progress Report IR-8-157 (V), AF Contract 33(657)-11277 (October 1964).

41 Ibid., IR-8-157 (VII) (May 1965).

42 Ibid., IR-8-157 (VIII) (August 1965).

43 "Manufacturing Process Development for High Strength Steels", AFML TR 66-340 (December 1966).

44 "Republic HP 9-4-20", Alloy Digest, Filing Code SA-270 (December 1971).

45 "Republic HP 9-4-30", Alloy Digest, Filing Code SA-278 (July 1972).

46 Kronbach, G. E., "Carburizing Response of HP 9-4-20 Steel", Republic Steel Corporation, Report PR 12036-77-1 (April 1977).

47 Ferguson, R. R. and Barryman, R. C., "Fracture Mechanics Evaluation of B-1 Materials", Rockwell International, Air Force Contract F33657-70-C-0800, AFML-TR-76-137, Vol. I (October 1976).

48 Ibid., Vol. II.

49 Saff, C. R., "Environment-Load Interaction Effects on Crack Growth in Landing Gear Steels", McDonnell Aircraft Company, Report No. NADC-79095-60, December 1980, on Naval Air Development Center Contract N62269-79-C-0275.

50 Dill, H. D. and Saff, C. R., "Environment-Load Interaction Effects on Crack Growth", McDonnell Aircraft Company, Air Force Flight Dynamics Laboratory Contract F33615-76-C-3133, AFFDL-TR-78-137 (November 1978).

51 Private communication with H. D. Dill, McDonnell Douglas Corporation, McDonnell Aircraft Company (June 1985).

52 Prado, M. E. and Cordill, C. A., "Static, Dynamic Toughness, and High Strain Rate Properties of Maraging 259, HY-180, and HP-9-4-20 Steels", Lawrence Livermore Laboratory, University of California/Livermore, Report UCRL-52017 (February 11, 1976).

53 Frandsen, J. D. and Marcus, H. L., "Environmentally Assisted Fatigue Crack Propagation in Steel", Metallurgical Transactions A, Vol. 8A (February 1977) pp 265–272.

54 Hall, L. R., Shah, R. C., and Engstrom, W. L., "Fracture and Fatigue Crack Growth of Surface Flaws and Flaws Originating at Fastener Holes", Boeing Aerospace Company on Air Force Flight Dynamics Laboratory Contract F33615-72-C-1740, AFFDL-TR-74-47, Vol. I – IV (May 1974).

55 Dill, H. D., "Evaluation of Steel Alloys 300M, HP-9Ni-4Co-.20, HP-9Ni-4Co-.30, and PH 13-8Mo", McDonnell Aircraft Company Report No. MDC A2639 (December 21, 1973).

56 Hawthorne, J. R. and Watson, H. E., "Strength and Notch Ductility of Selected Structural Alloys After High-Fluence, 550 F (288 C) Irradiation", NRL Report 7813 (December 2, 1974).

57 Louthan, Jr., M. R., Derrick, R. G., Donovan, J. A., and Caskey, Jr., G. R., "Hydrogen Transport in Iron and Steel", *Effect of Hydrogen on Behavior of Materials*, American Institute of Mining, Metallurgical and Petroleum Engineers, New York, (1976) pp 337–347.

58 Pohlman, S. L., "Prevention of Galvanic Corrosion and Electrochemical Behavior of Selected Structural Materials", Sandia Labs., Albuquerque, N.M., presented at the International Corrosion Forum devoted exclusively to the Protection and Performance of Materials, Houston (March 22, 1976).

59 Dobbins, A. G., Koger, J. W., and Mustaleski, Jr., T. M., "Corrosion Testing Type HP 9-4-20 Steel", Union Carbide Oak Ridge Y-12 Plant under DOE Contract W-7405 eng 26 (February 20, 1979).

60 Verink, Jr., E. D. and Das, K. B., "Research on Inhibition for Corrosion Fatigue of High Strength Alloys", AFML-TR-78-178 (December 15, 1978).

61 Bulloch, D. F., Eichenberger, T. W., and Guthrie, J. L., "Evaluation of the Mechanical Properties of 9Ni-4Co Steel Forgings", The Boeing Company on AFML Contract AF 33615-67-C-1724, AFML TR 68-57 (March 1968).

62 Turley, R. V., Avery, C. H., and Sinclaire, M., "The Effect of Processing Variables on Stress Corrosion Cracking in 9Ni-4Co Alloy", Third Quarterly Progress Report, Douglas Aircraft Company, Long

Fe
9 Ni
4 Co
Cr
Mo
V

9Ni-4Co

Fe
9 Ni
4 Co
Cr
Mo
V

9Ni-4Co

Beach, California, Air Force Contract AF33(615)-2849 (January 1966).

63 Pascover, J. S., "Properties of Production Product of HP 9-4-30 (Cr, Mo), Report IV", Republic Steel Research Center, Report TR 12018-94 (December 8, 1965).

64 "HP 9-4-20 Steel: Its Development, Production, and Properties", a presentation prepared for Rockwell International, B-1 Division, Los Angeles, California, Republic Steel Research Center Report (June 30, 1977).

65 Ault, R. T., private communication with W. F. Brown, Jr. (October 30, 1969).

66 Abraham, J. K., "Fatigue Properties of HP 9Ni-4Co Steels", Republic Steel Research Center, Report TR-12018-134 (December 30, 1968).

67 Marcus, H. L., "Gaseous Environmental Effects on Fatigue Crack Growth", in Environmental Degradation of Engineering Materials; Proceedings of the Conference, Virginia Polytechnic Institute and State University, Blackburg, VA (1978) pp 41–54.

68 Walter, R. J. and Chandler, W. T., "Effects of High Pressure Hydrogen on Metals at Ambient Temperature", Rocketdyne Research Division on NASA Contract NAS8-19, Final Report R7780-1 (February 28, 1969).

69 Ibid., Final Report R7780-2 (February 28, 1969).

70 Ault, R. T., Republic Steel Research Center, private communication with W. F. Brown, Jr. (1970).

71 Matas, S. J., Republic Steel Research Center, private communication with W. F. Brown, Jr. (1963).

72 Shimmin, J. T., "Development of Notch Property Data for Heat Treated 9Ni-4CoVM, 4340 AM, 4340VM and 18Ni-7Co-5MoVM Steels by General Dynamics Corporation, Dallas, Texas", Republic Steel Laboratory Report No. 637 (October 26, 1962).

73 Rinebolt, J. A., "Evaluation of Mechanical Properties of the 9Ni-4Co Alloy Sheet Composition in Various Section Sized From Vacuum Melt Heats", TR 693, Republic Steel Corporation (November 1962).

74 Miner, R. E., "Elastic Modulii of Various High Strength Steels", Republic Steel Research Center, TR 12037-23 (August 22, 1966).

75 Clark, Jr., W. G. and Wessel, E. T., "Influence of a Synthetic Seawater Environment on the Fracture Behavior of HP 9-4-25 and HP 9-4-20 Alloy Steels", ASTM STP 445 Materials Performance and the Deep Sea (1969) p 63.

76 Puzak, P. P. and Lange, E. A., "Fracture Toughness Characteristics of the New Weldable Steels of 180 to 210 ksi Yield Strengths", NRL Report 6951 (September 18, 1969).

77 Ault, R. T., "Effect of Carbon Level on the Mechanical Properties of HP 9-4-20 Steel", TM-12, 018-136, Republic Steel Research Center (November 20, 1968).

78 Vishnevsky, C. and Steigerwald, E. A., "Plane Strain Fracture Toughness of Some Cryogenic Materials at Room and Subzero Temperatures", ASTM STP 496 (1971) pp 3–26.

79 Damage Tolerant Design Handbook, Metals and Ceramics Information Center Publication MCIC-HB-01R, Battelle Columbus Laboratories, 505 King Avenue, Columbus, Ohio 43201.

80 Dawson, D. B., "Comparison of 9Ni-4Co-0.20C Steel and Titanium Alloy Properties for Weight-Critical Structural Applications", Sandia Laboratories Report SAND75-8301, citing private communication with R. Furguson, B-1 Division, Rockwell International (1975).

81 Judy, Jr., R. W. and Goode, R. J., "Stress-Corrosion Cracking of High-Strength Steels and Titanium Alloys", NRL Report No. 7371, Naval Research Laboratory (March 1972).

82 Dreyer, G. A. and Gallagher, W. G., "Investigation of the Effect of Stress Corrosion on High Strength Steel Alloys", ML-TDR-64-3, Boeing Company, Air Force Contract AF33(657)-8705 (February 1964).

ADDITIONAL REFERENCES

Salzbrenner, R. J., "Some Preliminary Studies on RSP 9Ni-4Co Steels".

Murphy, J. L. and Turner, P. W., "Wire Feeder and Positioner for Narrow Groove Electron Beam Welding", *Welding Journal*, Vol. 55 (March 1976), pp 181–190.

Ault, R. T., "Effect of Carbon Level on the Mechanical Properties of HP 9-4-20 Steel", TM-12,018-136, Republic Steel Research Center (November 20, 1968).

Crooker, T. W. and Lange, E. A., "Failure of Structural Alloys by Slow Crack Growth", NRL Report 6944 (October 14, 1969).

Puzak, P. P. and Lange, E. A., "Fracture Toughness Characteristics of the New Weldable Steels of 180- to 210-ksi Yield Strengths", NRL Report 6951 (September 18, 1969).

Brewer, D. H., "Predicting Stress Corrosion Cracking in Welded Steel Based on Residual Stress Measurements", Bendix, Kansas City Division, U.S. Department of Energy Contract DE-AC04-76-DP00613 (February 1979).

Sippel, K. O. and Weisgerber, D., "Flight by Flight Crack Propagation Test Results With Several Load Spectra and Comparison With Calculation According to Different Models", Messerschmitt-Bolkow-Blohm GMBH, Ottobrunn bei Munchen, presented at ICAF Symposium, Darmstadt, FR (West) Germany (May 12, 1977).

Bhat, G. K., "Evaluation of the Mechanical Properties of Electroslag Refined Iron Alloys", Carnegie-Mellon Institute of Research, NASA-Lewis Research Center Contract NAS3-18929, NASA Contract Report CR-135044 (December 1976).

Hall, L. R., "Fatigue Crack-Growth Behavior of Fastener Hole Flaws", in Advances in Joining Technology: Proceedings of the Fourth Army Materials Technology Conference, Boston, Massachusetts (September 16–19, 1975).

Lynch, C. T., Vahldiek, F. W., and Thorton, F., , "Comparison of Environmentally Enhanced Crack-Growth Rates of 1410 and Other High-Strength Steels", 1978 Tri-Service Conference on Corrosion, New Orleans, LA (October 4–6, 1978), Published by Metals and Ceramics Information Center, Battelle's Columbus Laboratories, Columbus. OH (1979).
Dawson, D. B., "Comparison of 9Ni-4Co-0.20C Steel and Titanium Alloy Properties for Weight-Critical Structural Applications", Sandia Laboratories Report SAND75-8301 (January 1976).
Katcher, M., "Crack-Growth Retardation Under Aircraft Spectrum Loads", Engineering Fracture Mechanics, Vol. 5 (1973) pp 793–818.
Carden, J. J., "AF1410 Steel in the F/A-18A", Metal Progress (March 1981) pp 61–64.
Shah, R. C., "Exploratory Investigation of Rapid Crack Propagation and Crack Arrest", Boeing Aerospace Company on Air Force Contract AF33615-72-C-1063, Report No. D180-17529-1 (August 1973).
Young, J. D. and Kumar, A., "Use of Laboratory Failure Simulation Exemplars to Study Intergranular Fracture Modes in 9Ni-4Co-0.20C Steel", in Fractrography in Failure Analysis; Proceedings of the Symposium, ASTM STP 645 (1978) pp 32–48.
Waid, G. M., "Elevated Temperature Properties of HP 9-4-30 Alloy Steel", Republic Steel Corporation, IOC (August 19, 1977).
Suga, M., Goss, J. L., Olson, G. B., and Vandersande, J. B., "Austenitic Grain Growth Characteristics in Rapidly Solidified Martensitic Steels, TLSP Technical Report (October 1978 to January 1980), Massachusetts Institute of Technology, Cambridge, Massachusetts, Presented at 2nd International Conference on Rapid Solidification Processing Principals and Technologies, Reston, Virginia (March 23–26, 1980).
Engle, R. J., Jr., "Aspect Ratio Variability in Part-Through Crack Life Analysis", in Part-Through Crack Fatigue Life Prediction, ASTM STP-687 (1979) pp 74–88.
Vroman, G. A., "Life Prediction Analysis of Part-Through Cracks, Ibid., pp 89–95.
Bates, R. C., "Correlations of Microvoid Formation, Fatigue Crack-Growth Rates, and Fracture Toughness", Proceedings of the 2nd Symposium on Mechanical Behavior of Materials, Society of Materials Science, Japan, Kyoto, Japan, Vol. 1 (1974) pp 163–177.
Christopher, J. D. and Wuebbling, G. J., "Turning and Drilling 9Ni-4Co Steel", Report 1469-31064-1, Metcut Research Associates, Inc. (April 1981).

Fe
9 Ni
4 Co
Cr
Mo
V

9Ni-4Co

Alloy		9Ni-4Co	
Source	Specification	Grade	Form
(1)	AMS-6523B	0.20C	Sheet, Strip, and Plate
(2)	AMS-6525	0.20C	Bars, Forgings, Tubing, and Rings
(3)	BMS-7-182B	0.20C, 0.30C	Forged or Rolled Bar, Forging Stock, Forged Block, and Mechanical Tubing
(4)	MMS-2101	0.20C	Forgings
(5)	NAI-1374	0.20C	Forgings
(6)	ST0160LB0002	0.20C	Bars, Forgings, and Reforging Stock
(7)	AMS-6524B	0.30C	Sheet, Strip, and Plate
(8)	AMS-6526B	0.30C	Bars, Forgings, Tubing, and Rings
(9)	ASTM A 579-77	0.30C	Forgings
(10)	MMS-2102	0.30C	Bars and Forgings
(11)	NAI-1373	0.30C	Forgings
(12)	ST0160LB0004	0.30C	Bars, Forgings, and Reforging Stock
(30)	AMS-6468A	0.20C	Weld Filler Wire

Unified Numbering System Designation, K91283

TABLE 1.03. SPECIFICATIONS

Fe
9 Ni
4 Co
Cr
Mo
V

9Ni-4Co

Alloy	9Ni-4Co							
Grade	0.20C		0.30C					
Source	(1–6)		(7, 8, 10, 11)		(12)		(9)*	
	Composition, weight percent							
Element	Min	Max	Min	Max	Min	Max	Min	Max
Carbon	0.17	0.23	0.29	0.34	0.29	0.34	0.28	0.34
Chromium	0.65	0.85	0.90	1.10	0.90	1.10	0.90	1.10
Cobalt	4.25	4.75	4.25	4.75	4.25	5.00	4.0	5.0
Manganese	0.20	0.40	0.10	0.35	0.10	0.35	0.10	0.35
Molybdenum	0.90	1.10	0.90	1.10	0.90	1.10	0.90	1.10
Nickel	8.50	9.50	7.00	8.00	7.00	8.00	7.0	8.5
Phosphorus	–	0.010	–	0.010	–	0.010	–	0.010
Silicon	–	0.20	–	0.20	–	0.10	–	0.10
Sulphur	–	0.010	–	0.010	–	0.010	–	0.010
Vanadium	0.06	0.12	0.06	0.12	0.06	0.12	0.06	0.12
Copper	–	0.35	–	0.35	–	0.35	Not specified	
Iron	Balance		Balance		Balance		Balance	

*0.06 calcium, 0.003 boron, and 0.02 zirconium added.

TABLE 1.04. SPECIFIED COMPOSITION

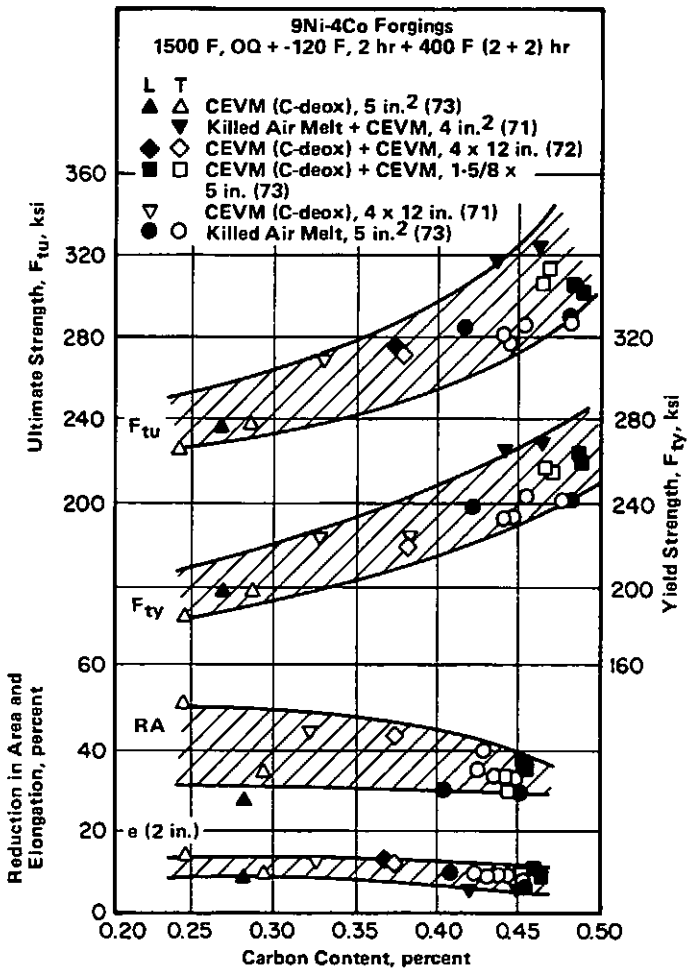


FIGURE 1.0421. EFFECT OF CARBON CONTENT ON TENSILE PROPERTIES OF FORGINGS (71–73)

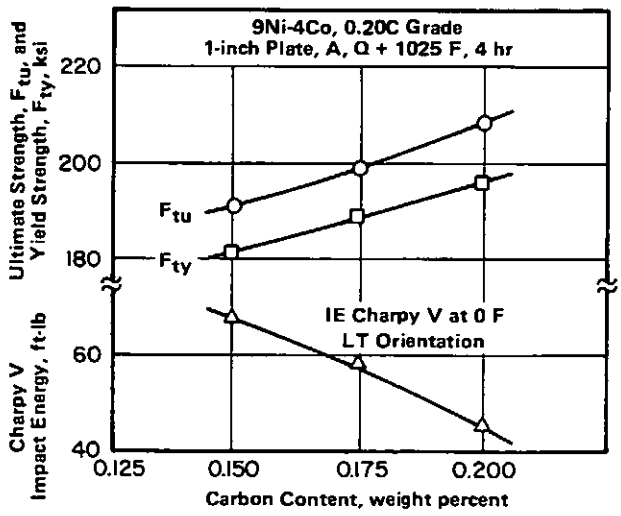


FIGURE 1.0422. EFFECT OF CARBON CONTENT IN THE RANGE OF 0.20C GRADE ON THE ROOM TEMPERATURE TENSILE AND 0 F CHARPY V IMPACT PROPERTIES OF PLATE (77)

Fe
9 Ni
4 Co
Cr
Mo
V

9Ni-4Co

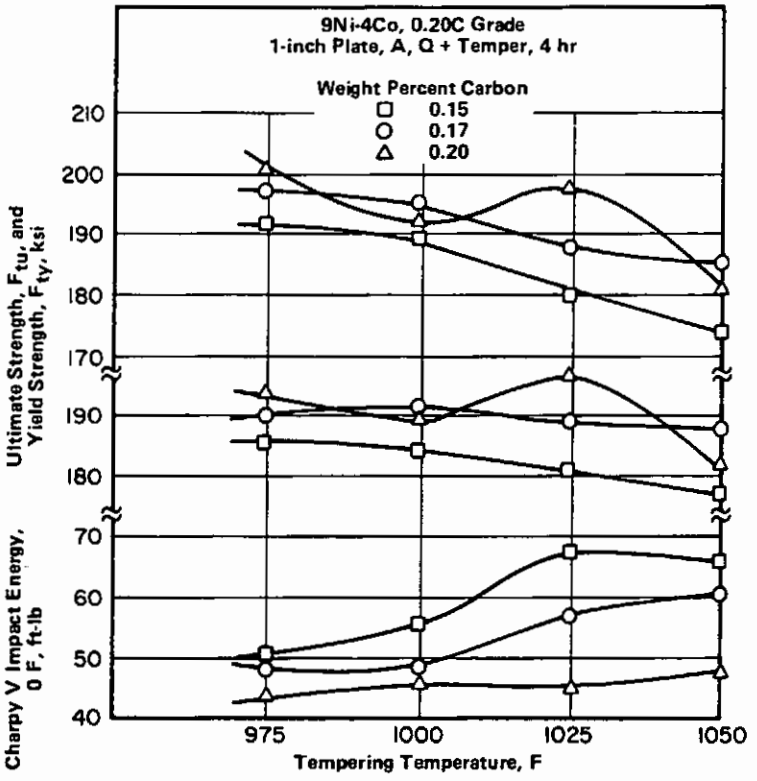


FIGURE 1.0423. EFFECT OF TEMPERING TEMPERATURE ON THE ROOM TEMPERATURE TENSILE AND 0 F CHARPY V IMPACT PROPERTIES OF PLATE AT THREE CARBON LEVELS (77)

Alloy	9Ni-4Co	
	Grade	
Heat Treatment	0.20C	0.30C
Normalize	1650 ± 25 F, 1 hr/in. (1-hr Min), AC	1650 ± 50 F, 1 hr/in. (1-hr Min), AC
Preheat	1150 ± 25 F, 1/2-hr Min Before Transferring to Austenitizing Furnace (Optional)	1150 ± 25 F, 1/2-hr Min Before Transferring to Austenitizing Furnace
Austenitize	1550 ± 25 F, 1 hr/in. (1-hr Min), OQ or WQ, or AC*	1550 ± 25 F, 1 hr/in. (1-hr Min), OQ or WQ
Refrigerate	-100 ± 25 F, 1-hr Min	-100 ± 25 F, 1-hr Min
Temper	400–1100 F, 4–8 hr, AC (1025–1075 F, 4–8 hr for Min Guaranteed Properties)	400–1100 F (2 + 2) hr Min, AC (1000–1075 F (2 + 2) hr Min for Min Guaranteed Properties)
Anneal	1250 ± 25 F, 4 hr, AC + 1150 ± 25 F, 4–12 hr, AC or 1150 ± 25 F, 8–24 hr, AC	1250 ± 25 F, 4 hr, AC + 1150 ± 25 F, 4–12 hr, AC or 1150 ± 25 F, 8–24 hr, AC

*For distortion considerations, but only for sections < 2 inches.

TABLE 1.052. RECOMMENDED HEAT TREATMENT (4–6, 8, 10, 11, 16)

Fe
9 Ni
4 Co
Cr
Mo
V

9Ni-4Co

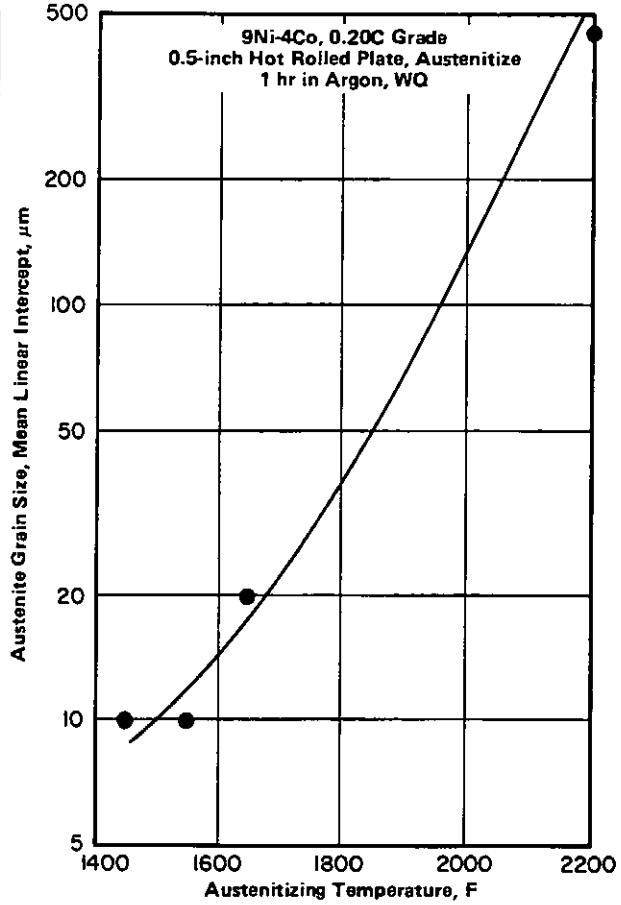


FIGURE 1.054. AUSTENITE GRAIN SIZE AS A FUNCTION OF 1-HOUR AUSTENITIZING TEMPERATURE FOR 0.20C GRADE (24)

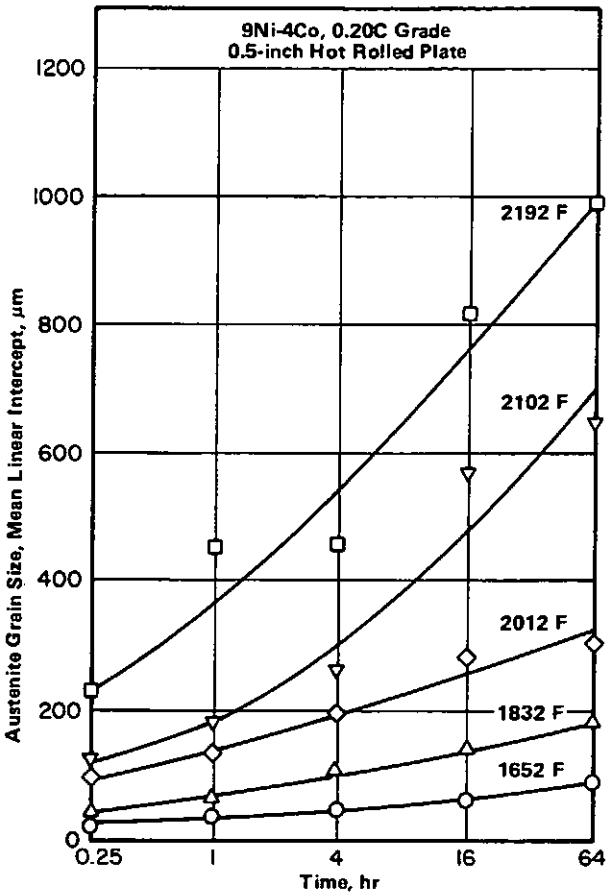


FIGURE 1.055. ISOTHERMAL AUSTENITE GRAIN GROWTH CHARACTERISTICS FOR 0.20C GRADE (24)

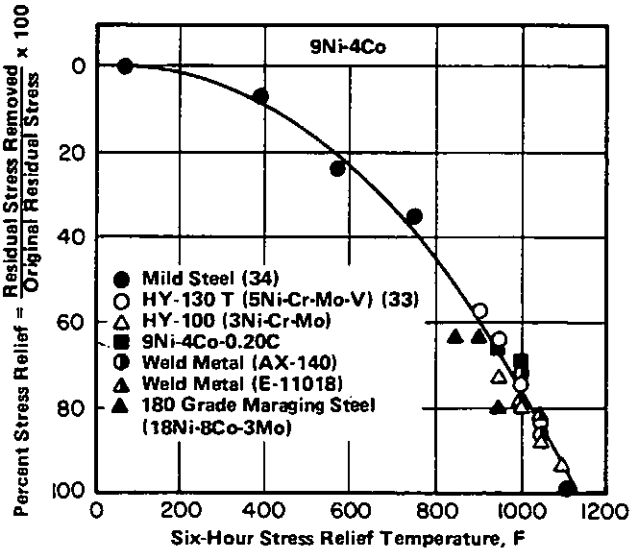


FIGURE 1.056. STRESS RELIEF CHARACTERISTICS OF SEVERAL STEELS, INCLUDING 0.20C GRADE 9Ni-4Co STEEL, AND STEEL WELDMENTS, DETERMINED BY STRESS-RELAXATION TESTS (32)

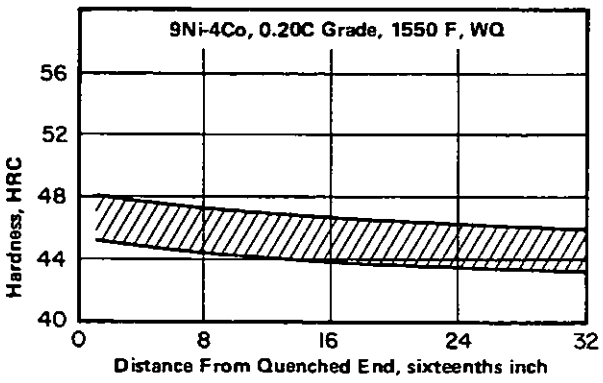


FIGURE 1.061. TYPICAL JOMINY END QUENCH HARDENABILITY ESTABLISHED FROM SIX AOD-PROCESSED HEATS OF 0.20C GRADE (13)

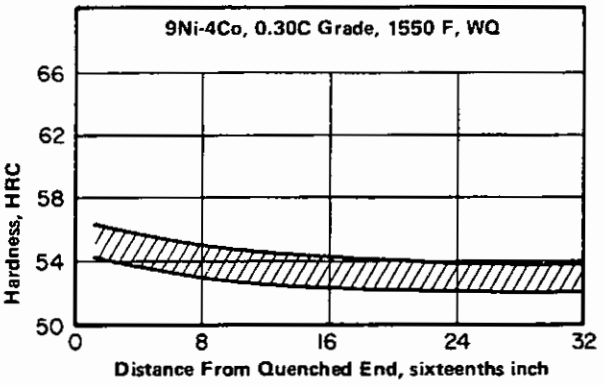


FIGURE 1.062. TYPICAL JOMINY END QUENCH HARDENABILITY ESTABLISHED FROM FIVE AOD-PROCESSED HEATS OF 0.30C GRADE (14)

Alloy	9Ni-4Co
Grade	0.20C
Figures	Tables
2.01221	3.011
3.0218	3.012
3.02111	3.014
4.0351	3.02112
	4.042
	4.043
	4.045
	4.046
	4.047
	4.048

TABLE 1.063. ADDITIONAL 0.20C GRADE HARDNESS DATA

Fe
9 Ni
4 Co
Cr
Mo
V

9Ni-4Co

Alloy	9Ni-4Co
Grade	0.30C
Figures	Tables
2.01222	3.015
3.02120	3.017
	3.019

TABLE 1.064. ADDITIONAL 0.30C GRADE HARDNESS DATA

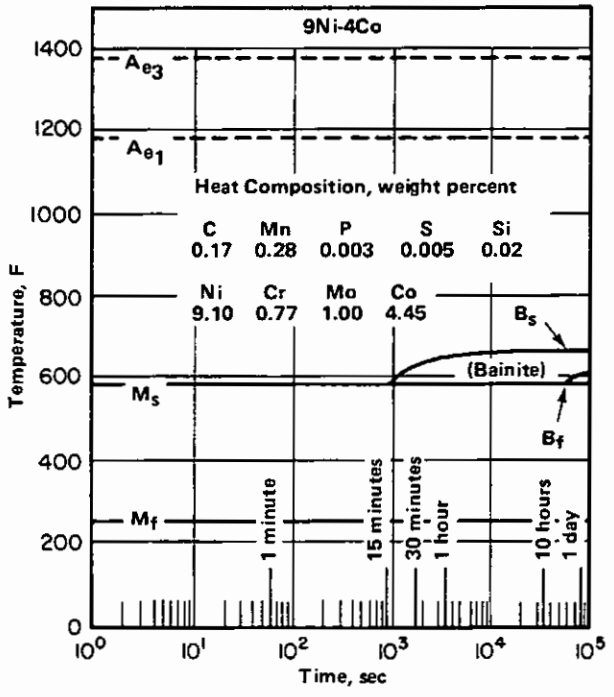


FIGURE 2.01211. TIME-TEMPERATURE-TRANSFORMATION DIAGRAM FOR 0.20C GRADE (13, 25, 28)

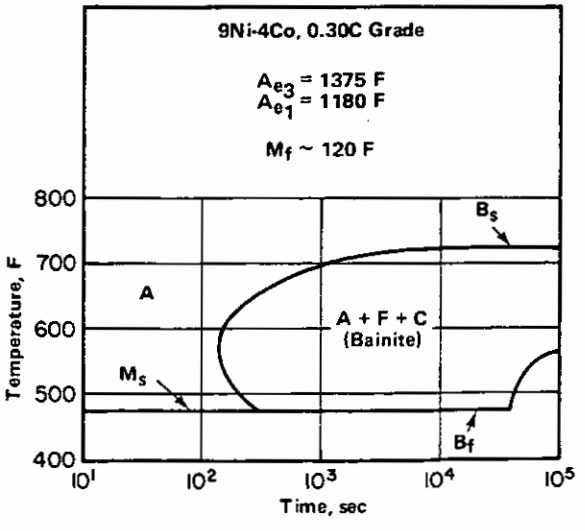


FIGURE 2.01212. TIME-TEMPERATURE-TRANSFORMATION DIAGRAM FOR 0.30C GRADE (14)

Fe
9 Ni
4 Co
Cr
Mo
V

9Ni-4Co

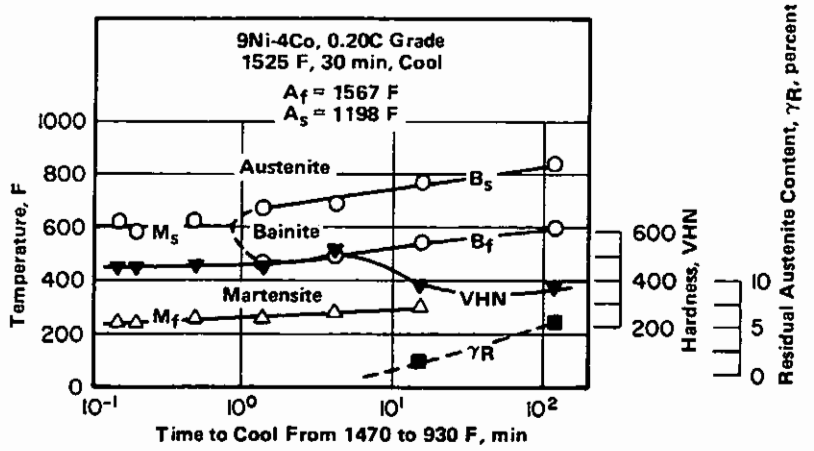


FIGURE 2.01221. CONTINUOUS-COOLING-TRANSFORMATION DIAGRAM FOR 0.20C GRADE (25)

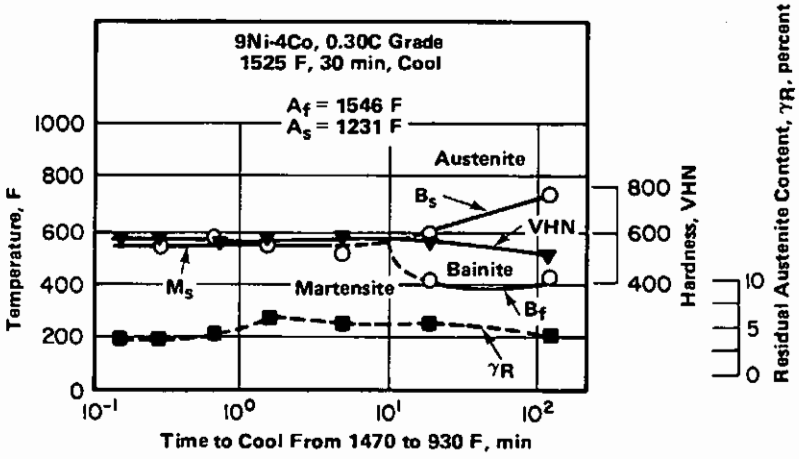


FIGURE 2.01222. CONTINUOUS-COOLING-TRANSFORMATION DIAGRAM FOR 0.30C GRADE (25)

Alloy	9Ni-4Co			
Grade	0.20C		0.30C	
Condition	A, Q + 1025 F, 4 hr	A, Q + 1025 F, 4 hr + 1150 F Anneal	A, Q + -110 F, 2 hr + 950 F (2 + 2) hr	A, Q + -110 F, 2 hr + 950 F (2 + 2) hr + 1150 F Anneal
Thermal Conductivity, Btu ft/(hr ft^2 F)	14.1	14.1	13.3	15.0

TABLE 2.013. THERMAL CONDUCTIVITY (70)

Alloy	9Ni-4Co	
Grade	0.20C	0.30C
Condition	A, Q + 1025 F, 4 hr	A, Q + -110 F, 2 hr + 950 F (2 + 2) hr
Mean Coefficient of Linear Thermal Expansion (RT to 200 F), 10^{-6} in./in./F	6.4	6.3

Fe
9 Ni
4 Co
Cr
Mo
V

9Ni-4Co

TABLE 2.0141. MEAN COEFFICIENT OF LINEAR THERMAL EXPANSION FOR 0.20C AND 0.30C GRADES (70)

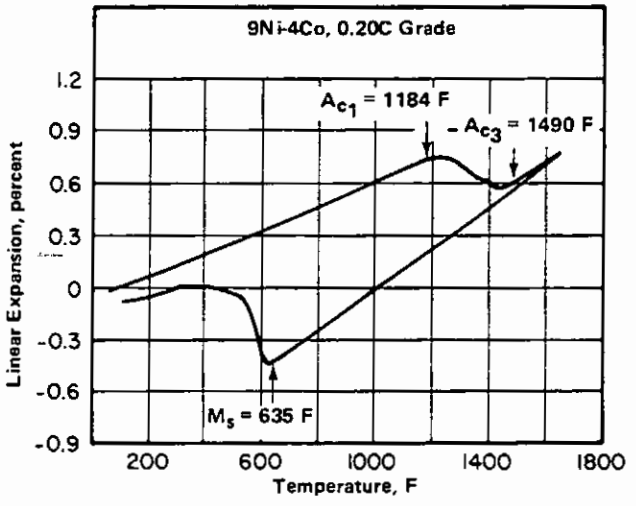


FIGURE 2.0142. LINEAR THERMAL EXPANSION CURVE FOR 0.20C GRADE AT HEATING RATE OF 10 F/MIN (13)

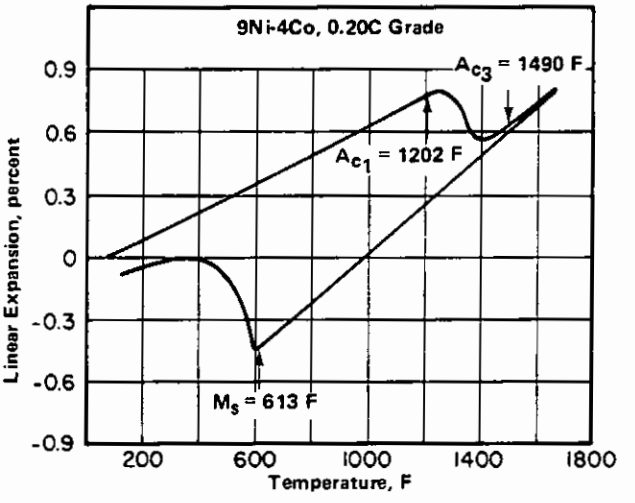


FIGURE 2.0143. LINEAR THERMAL EXPANSION CURVE FOR 0.20C GRADE AT HEATING RATE OF 36 F/MIN (13)

Alloy	9Ni-4Co	
Grade	0.20C	
Heating Rate, F/min	10	36
Temperature Interval, F	Mean Coefficient of Linear Thermal Expansion, 10^{-6} in./in./F	
68 to 212	6.0	5.8
68 to 392	6.1	6.1
68 to 572	6.2	6.4
68 to 752	6.4	6.5
68 to 932	6.7	6.7
68 to 1112	6.8	6.8
68 to 1292	6.0	6.3
68 to 1472	4.2	4.2
68 to 1652	4.9	5.1

TABLE 2.0144. MEAN COEFFICIENTS OF LINEAR THERMAL EXPANSION FOR 0.20C GRADE AT TWO HEATING RATES (13)

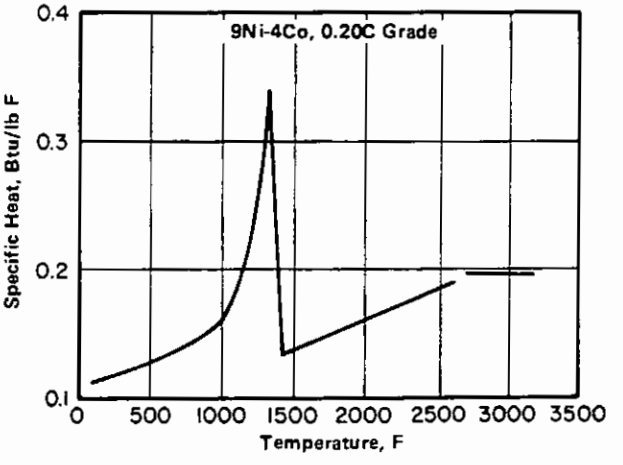


FIGURE 2.0151. SPECIFIC HEAT OF 0.20C GRADE AS A FUNCTION OF TEMPERATURE (17)

Fe
9 Ni
4 Co
Cr
Mo
V
9Ni-4Co

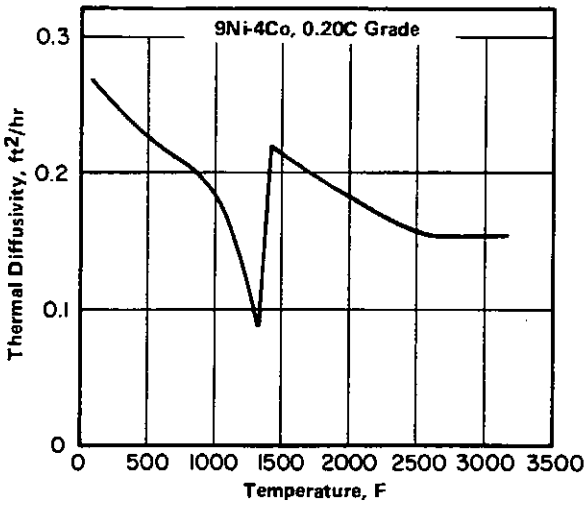


FIGURE 2.0161. THERMAL DIFFUSIVITY OF 0.20C GRADE AS A FUNCTION OF TEMPERATURE (17)

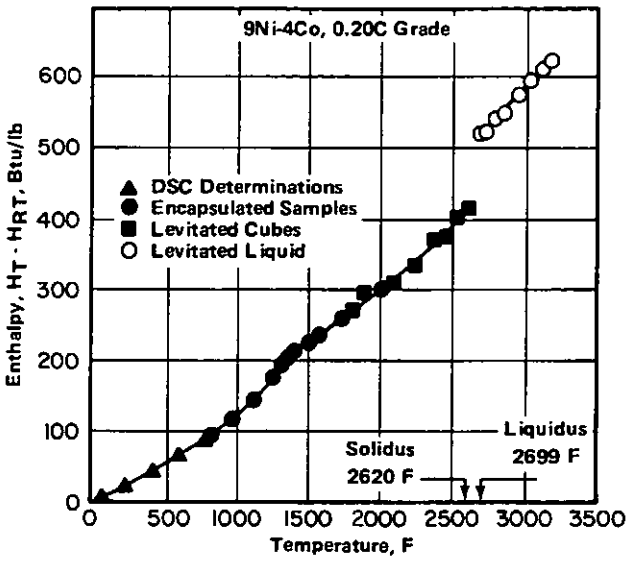


FIGURE 2.0171. ENTHALPY, $H_T - H_{RT}$, AS A FUNCTION OF TEMPERATURE FOR 0.20C GRADE (17)

Alloy	9Ni-4Co			
Grade	0.20C		0.30C	
Condition	A, Q + 1025 F, 4 hr	A, Q + 1025 F, 4 hr + 1150 F Anneal	A, Q + -110 F, 2 hr + 950 F (2 + 2) hr	A, Q + -110 F, 2 hr + 950 F (2 + 2) hr + 1150 F Anneal
Electrical Resistivity, microhm-in.	14.4	14.5	14.6	12.9

TABLE 2.0221. ELECTRICAL RESISTIVITY (70)

Alloy	9Ni-4Co	
Grade	0.30C, CEVM (C-deox)	
Form	Plate	3-in. x 9-in. x 24-in. Forged Billet
Condition	Q & T	1600–1700 F, 1 hr, AC + 1150 ± 25 F, 1/2 hr Minimum + 1550 ± 25 F, 1 hr, OQ + -100 F, 2 hr + 950 ± 25 F (2 + 2) hr, AC
	F_{tu} = 220 to 240 ksi F_{ty} = 210 ksi	F_{tu} = 230 ksi F_{ty} = 195 ksi
Specimen	1/8-in. x 1/2-in. Tension	1/4-in. x 1-in. Bend
Direction	T	T
Exposure Stress, ksi	0.85 F_{ty}	0.80 F_{ty}
Environment	Synthetic Seawater, pH = 7.8–8.2	3.5 percent NaCl Solution
Exposure	10 min Salt + 50 min Air	8 min Salt + 52 min Air
Results	No Failures in 1000 hr	Failures in 1032 to 1488 hr

TABLE 2.0321. RESULTS OF ALTERNATE IMMERSION STRESS CORROSION TESTS ON 0.30C GRADE PLATE AND FORGED BILLET USING SMOOTH SPECIMENS (61, 62)

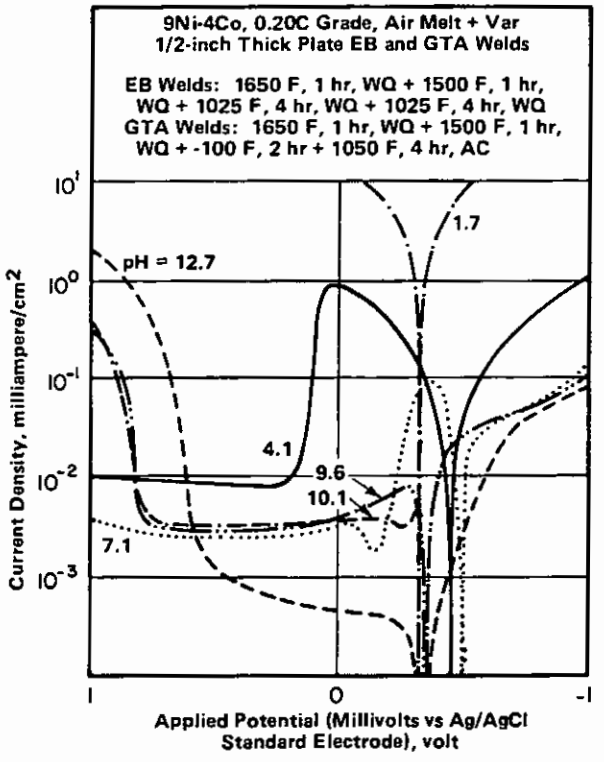
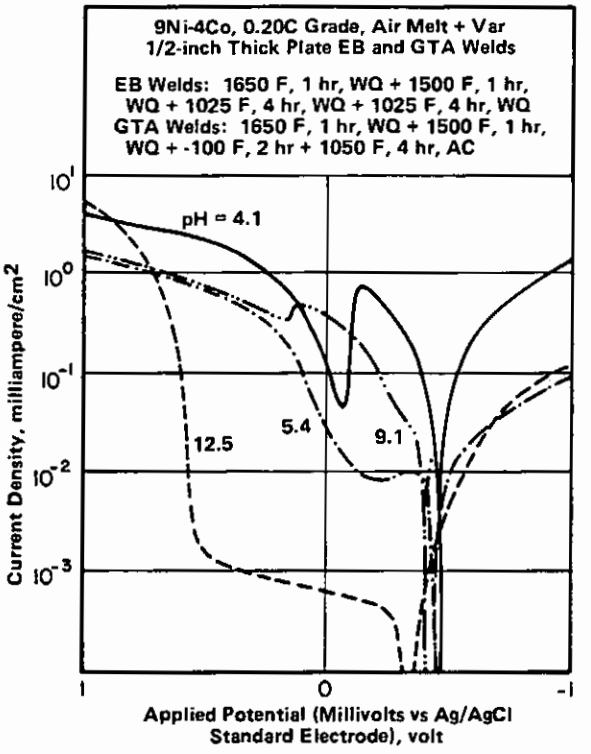


FIGURE 2.0322. POTENTIODYNAMIC-POLARIZATION CORROSION CURVES FOR 0.20C GRADE PLATE WELDS IN SOLUTIONS CONTAINING NO CHLORIDE IONS AT VARIOUS pH VALUES (59)



Fe
9 Ni
4 Co
Cr
Mo
V

9Ni-4Co

FIGURE 2.0323. POTENTIODYNAMIC-POLARIZATION CORROSION CURVES FOR 0.20C GRADE PLATE WELDS IN 0.01 MOLAR SODIUM CHLORIDE SOLUTIONS AT VARIOUS pH VALUES (59)

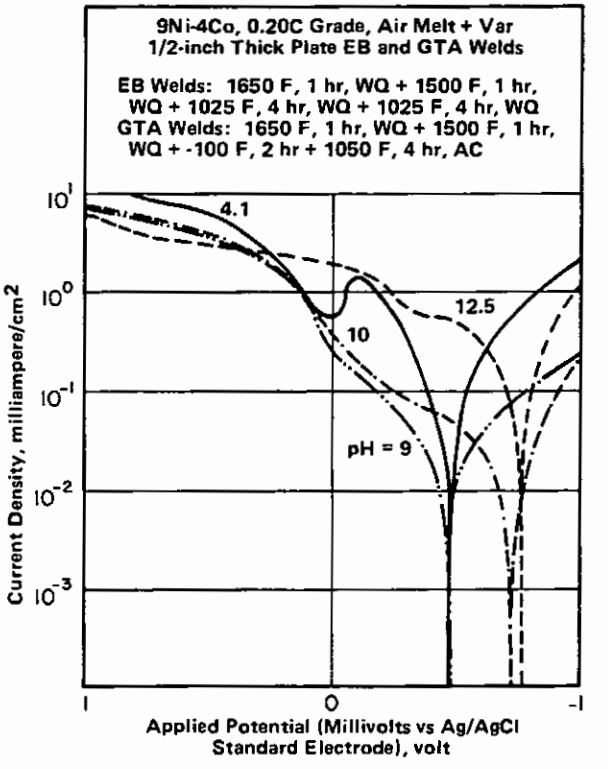


FIGURE 2.0324. POTENTIODYNAMIC-POLARIZATION CORROSION CURVES FOR 0.20C GRADE PLATE WELDS IN 0.1 MOLAR SODIUM CHLORIDE SOLUTIONS AT VARIOUS pH VALUES (59)

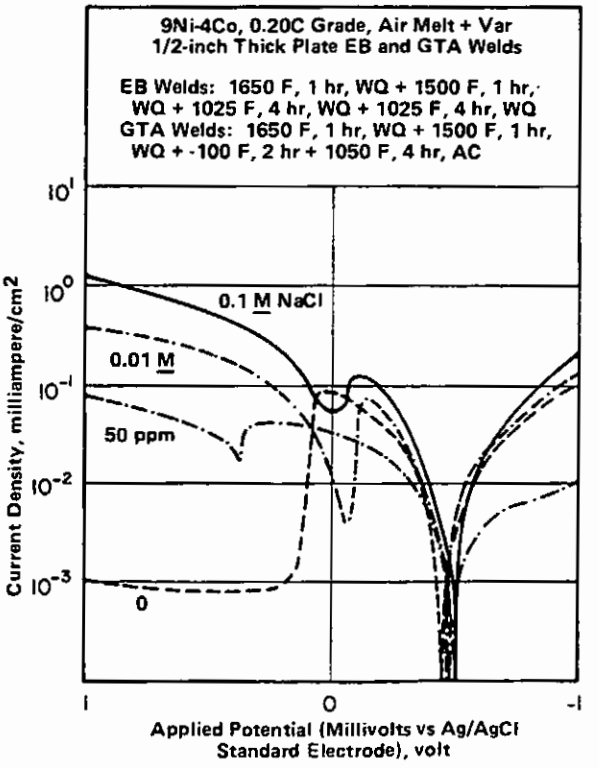


FIGURE 2.0325. POTENTIODYNAMIC-POLARIZATION CORROSION CURVES FOR 0.20C GRADE PLATE WELDS IN SOLUTIONS AT A pH OF 4 TO 4.1 AND AT VARIOUS CHLORIDE ION CONCENTRATIONS (59)

Fe
9 Ni
4 Co
Cr
Mo
V

9Ni-4Co

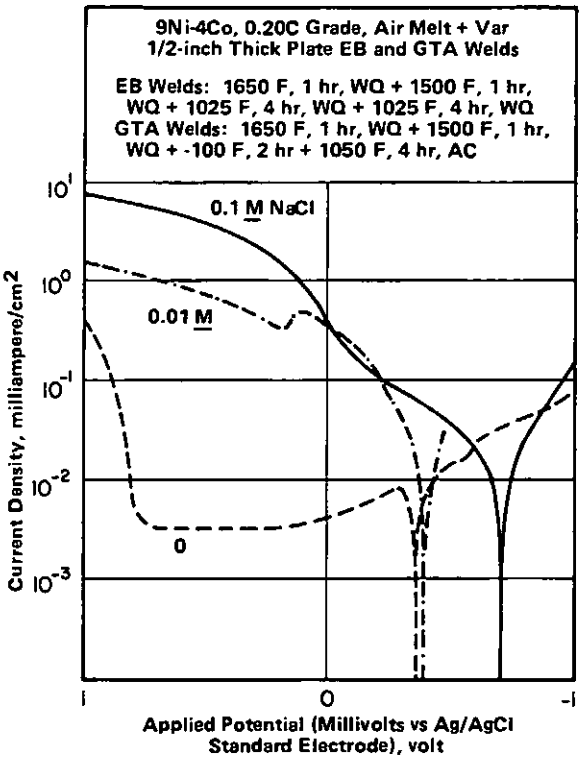


FIGURE 2.0326. POTENTIODYNAMIC-POLARIZATION CORROSION CURVES FOR 0.20C GRADE PLATE WELDS IN SOLUTIONS AT A pH OF 9 TO 9.6 AND AT VARIOUS CHLORIDE ION CONCENTRATIONS (59)

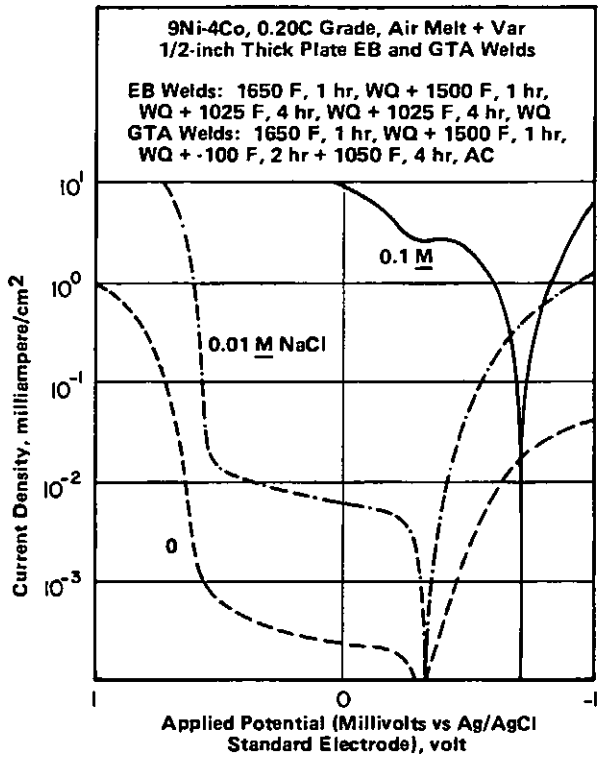


FIGURE 2.0327. POTENTIODYNAMIC-POLARIZATION CORROSION CURVES FOR 0.20C GRADE PLATE WELDS IN SOLUTIONS AT A pH OF 12.5 TO 12.7 AND AT VARIOUS CHLORIDE ION CONCENTRATIONS (59)

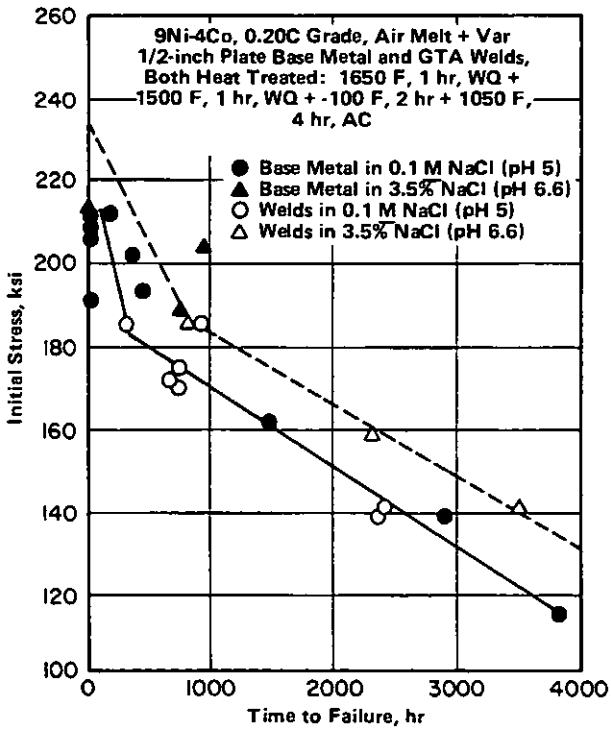


FIGURE 2.0328. SUSTAINED-LOAD STRESS CORROSION LIFE OF 0.20C GRADE PLATE BASE METAL AND WELDS IN BUFFERED (pH 5 AND 6.6) SODIUM CHLORIDE SOLUTIONS AT TWO CHLORIDE ION CONCENTRATIONS (59)

Alloy	9Ni-4Co		
Grade	0.20C, CEVM (C-deox)		
Form	7/16-inch Diameter Rod		
Condition	1550 F, 1 hr, OQ + 1000 F (2 + 2) hr, AC		
Environment	Air	Helium	Hydrogen
Pressure, psig	0	10,000	10,000
F_{tu}, ksi	208	199	175
F_{ty}, ksi	202	187	143
e (1-1/4-in.), percent	15	15	1.0
RA, percent	65	67	15
NTS[a], ksi	373	368	86

(a) Sharp notch tensile specimen:

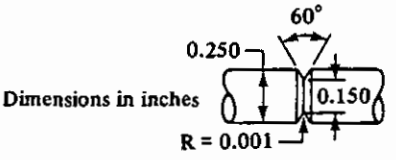


TABLE 2.0331. EFFECT OF TESTING IN HIGH PRESSURE HYDROGEN ON THE SMOOTH AND SHARP NOTCH TENSILE PROPERTIES OF) 0.20C GRADE ROD (68, 69)

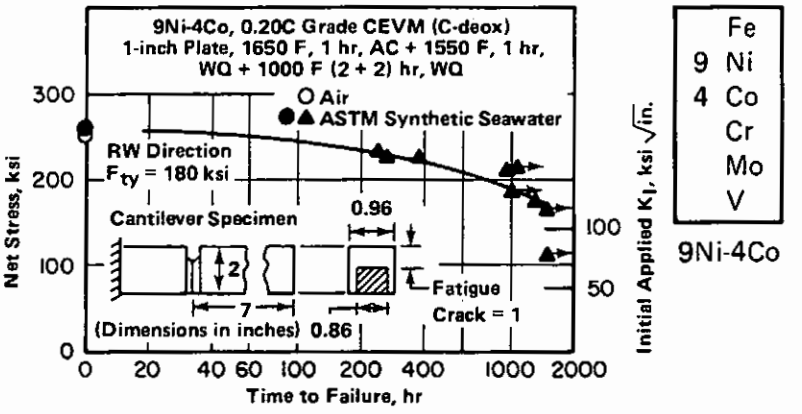


FIGURE 2.0341. DELAYED FAILURE OF 0.20C GRADE PLATE IN SEAWATER (31)

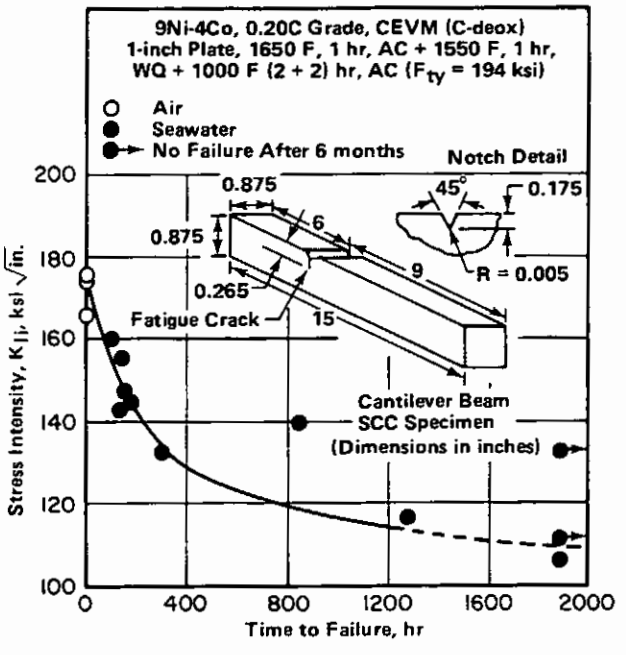


FIGURE 2.0342. STRESS CORROSION CRACKING BEHAVIOR OF 0.20C GRADE PLATE IN SEAWATER (32)

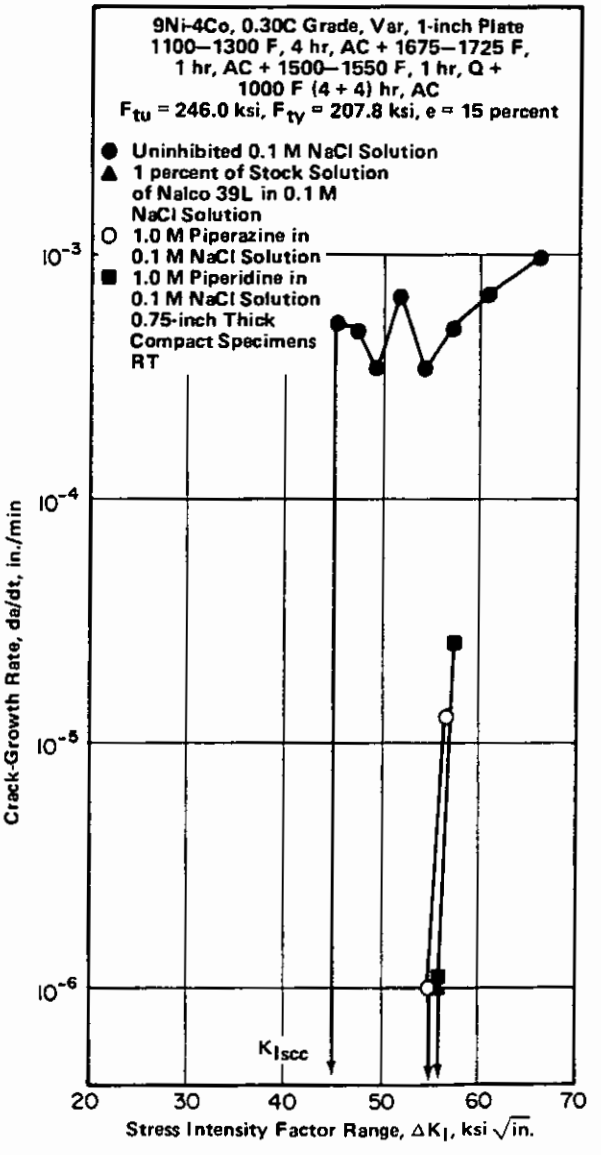


FIGURE 2.0343. SUSTAINED-LOAD CRACK-GROWTH RATES FOR 0.30C GRADE PLATE IN UNINHIBITED AND INHIBITED NaCl SOLUTIONS (60)

Fe
9 Ni
4 Co
Cr
Mo
V

9Ni-4Co

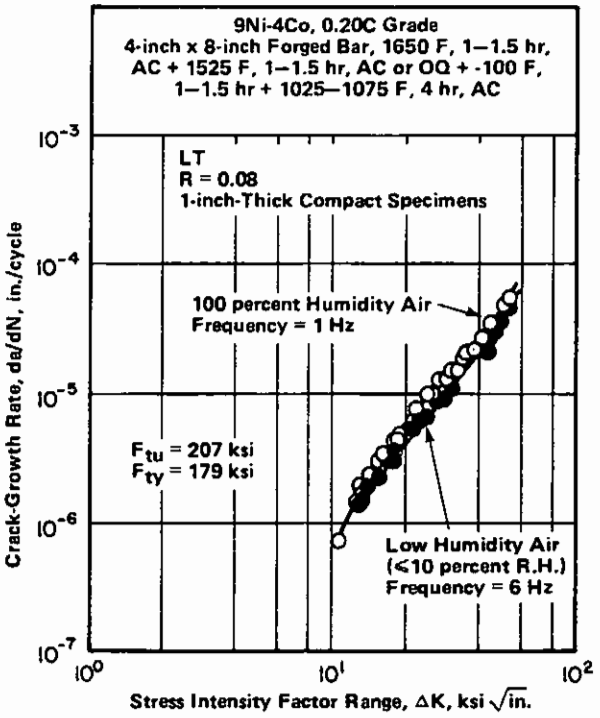


FIGURE 2.0351. EFFECT OF MOISTURE ON CRACK-GROWTH RATE AT R = 0.08 OF 0.20C GRADE FORGED BAR (47, 48)

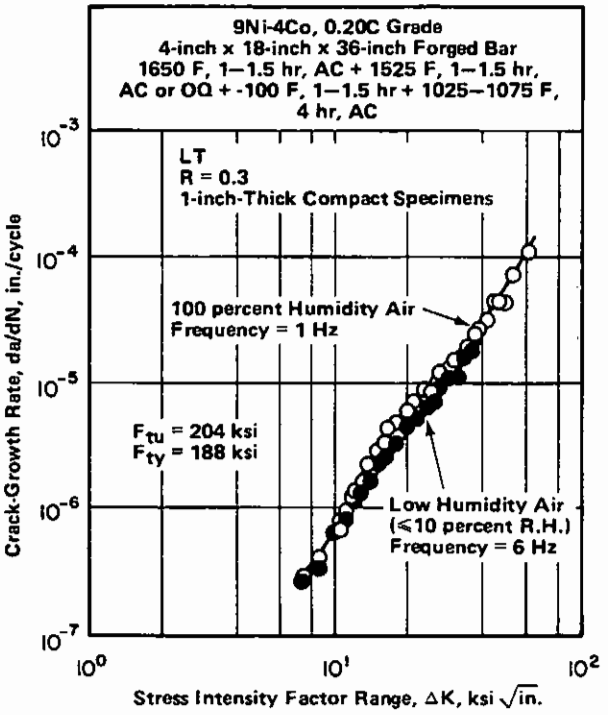


FIGURE 2.0352. EFFECT OF MOISTURE ON CRACK-GROWTH RATE AT R = 0.3 OF 0.20C GRADE FORGED BAR (47, 48)

	Fe
9	Ni
4	Co
	Cr
	Mo
	V

9Ni-4Co

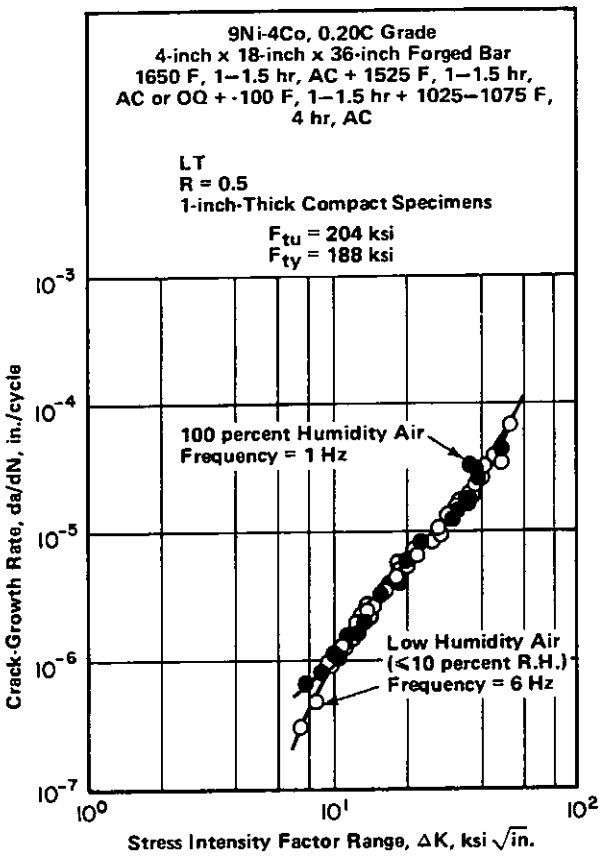


FIGURE 2.0353. EFFECT OF MOISTURE ON CRACK-GROWTH RATE AT R = 0.5 OF 0.20C GRADE FORGED BAR (47, 48)

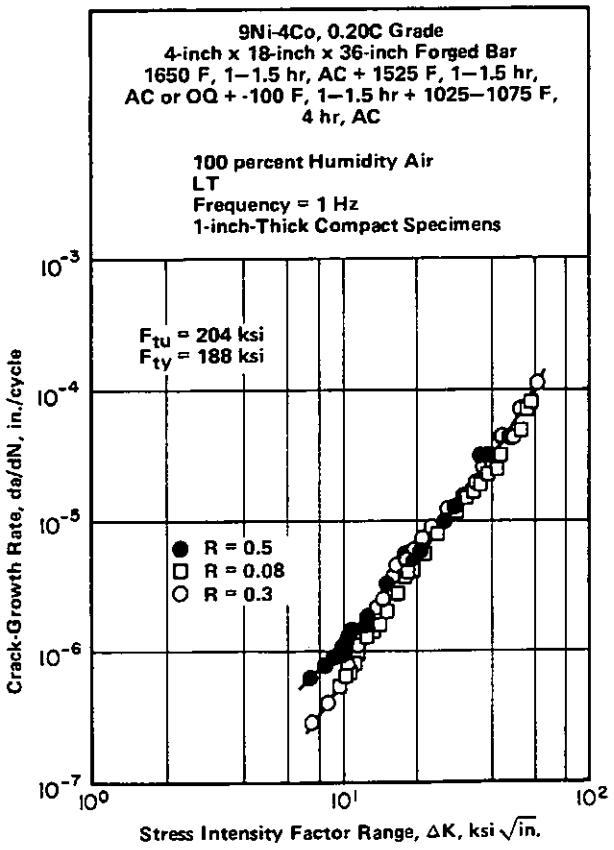


FIGURE 2.0354. EFFECT OF R-RATIO ON FATIGUE CRACK-GROWTH RATE IN 100 PERCENT HUMIDITY AIR OF 0.20C GRADE FORGED BAR (47, 48)

Fe
9 Ni
4 Co
Cr
Mo
V

9Ni-4Co

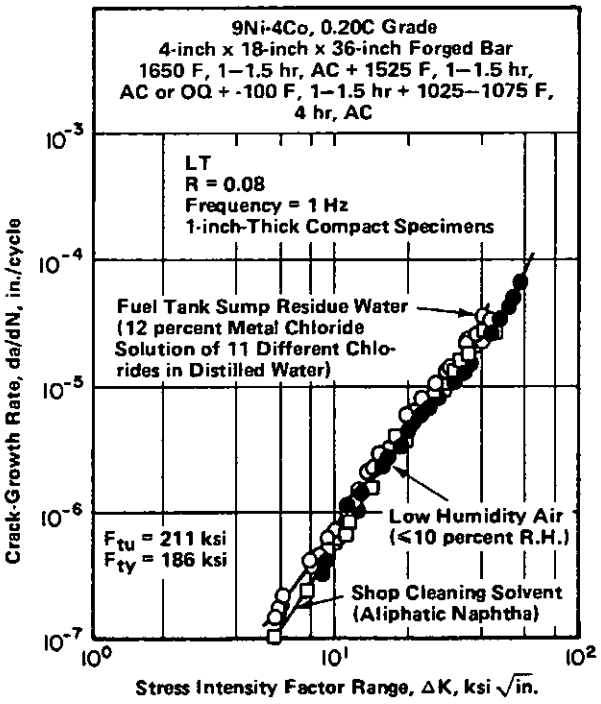


FIGURE 2.0355. EFFECT OF ENVIRONMENT ON FATIGUE CRACK-GROWTH RATE OF 0.20C GRADE FORGED BAR (47, 48)

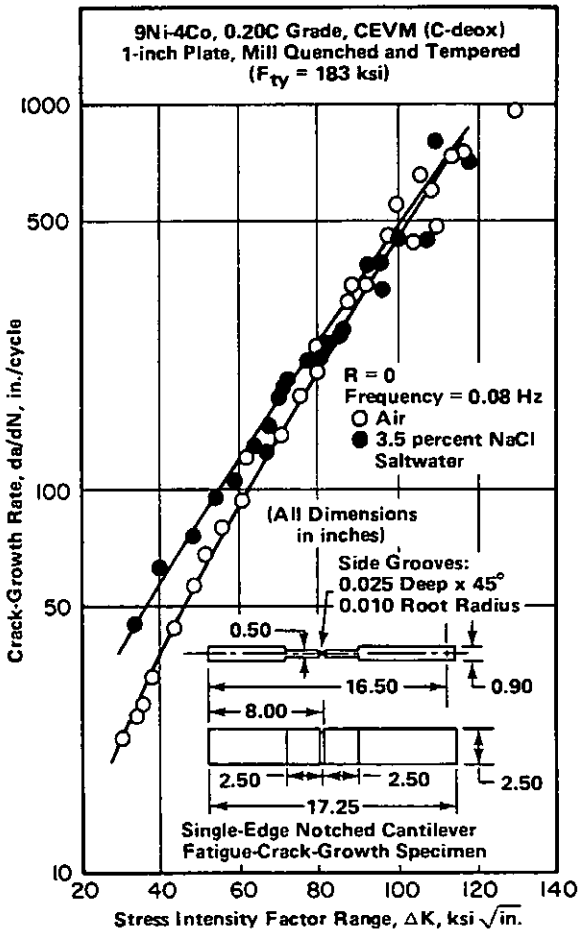


FIGURE 2.0356. FATIGUE CRACK-GROWTH CHARACTERISTICS OF 0.20C GRADE PLATE IN AIR AND 3.5 PERCENT NaCl SALTWATER (35)

Fe
9 Ni
4 Co
Cr
Mo
V
9Ni-4Co

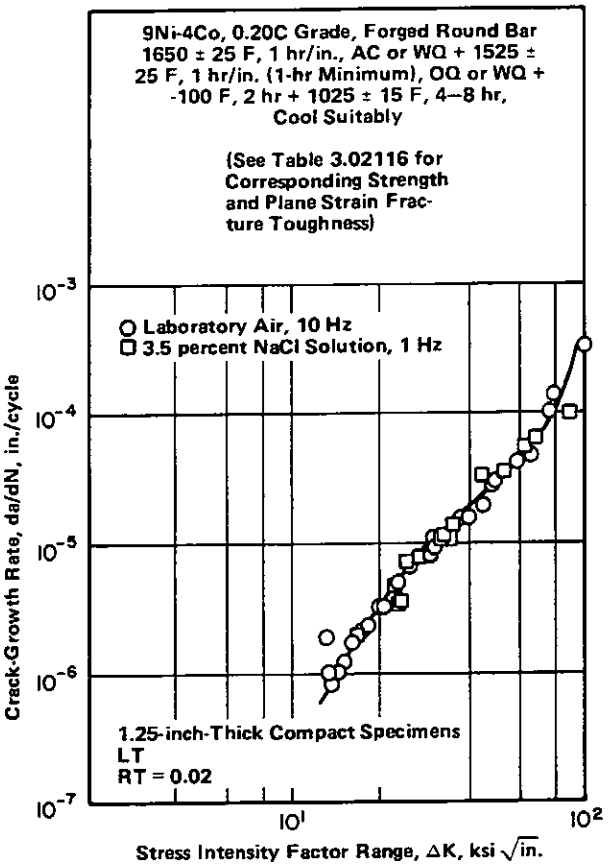


FIGURE 2.0357. FATIGUE CRACK-GROWTH RATE OF 0.20C GRADE FORGED ROUND BAR IN AIR AND 3.5 PERCENT NaCl SOLUTION (55)

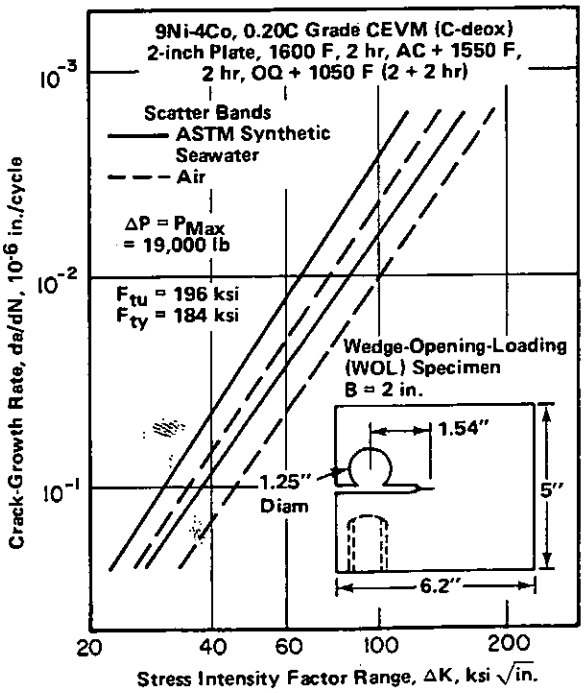


FIGURE 2.0358. FATIGUE CRACK-GROWTH RATE OF 0.20C GRADE PLATE IN AIR AND SEAWATER (75)

Fe
9 Ni
4 Co
Cr
Mo
V

9Ni-4Co

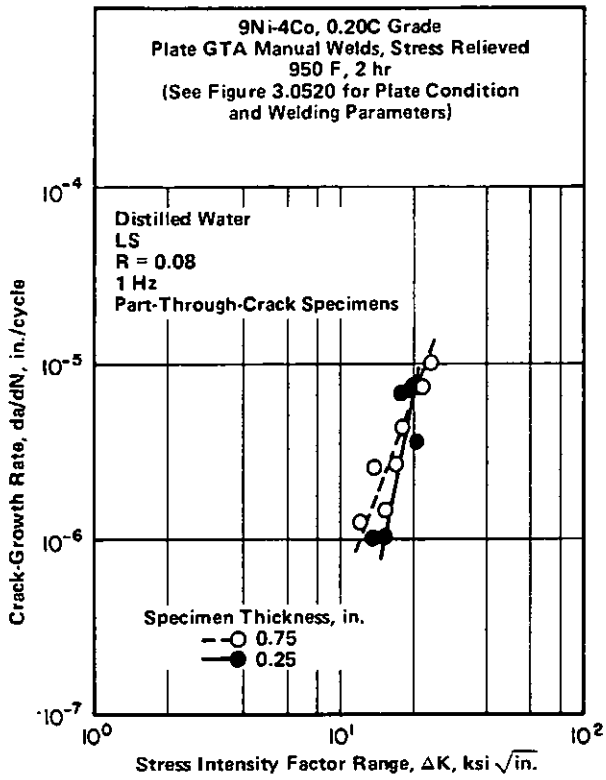


FIGURE 2.0359. EFFECT OF SPECIMEN THICKNESS ON FATIGUE CRACK-GROWTH RATE IN DISTILLED WATER OF 0.20C GRADE PLATE GTA MANUAL WELD HEAT AFFECTED ZONE (47, 48)

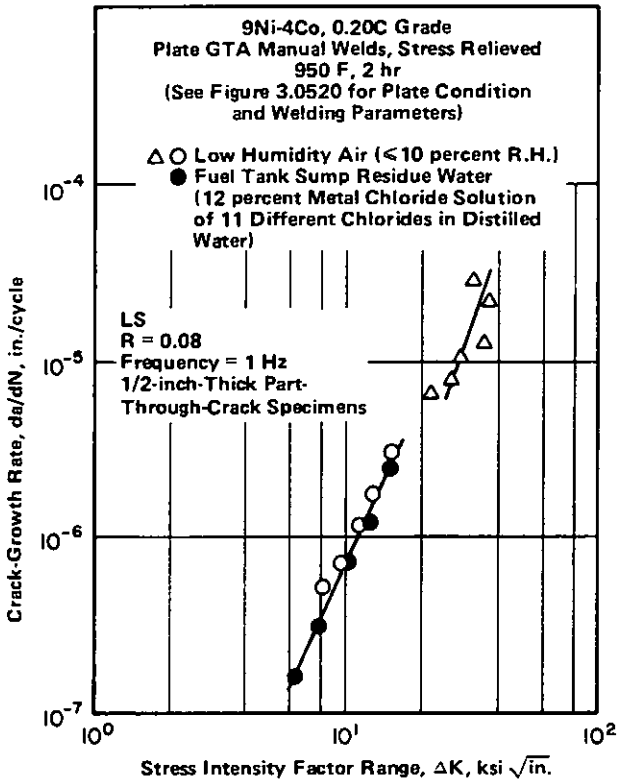


FIGURE 2.03510. EFFECT OF ENVIRONMENT ON FATIGUE CRACK-GROWTH RATE OF 0.20C GRADE PLATE GTA MANUAL WELD HEAT AFFECTED ZONE (47, 48)

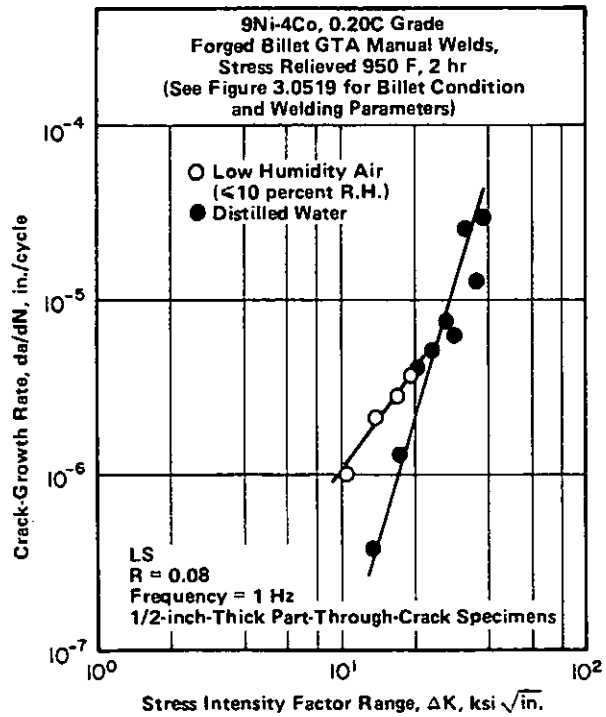


FIGURE 2.03511. EFFECT OF ENVIRONMENT ON FATIGUE CRACK-GROWTH RATE OF 0.20C GRADE FORGED BILLET GTA MANUAL WELD HEAT AFFECTED ZONE (47, 48)

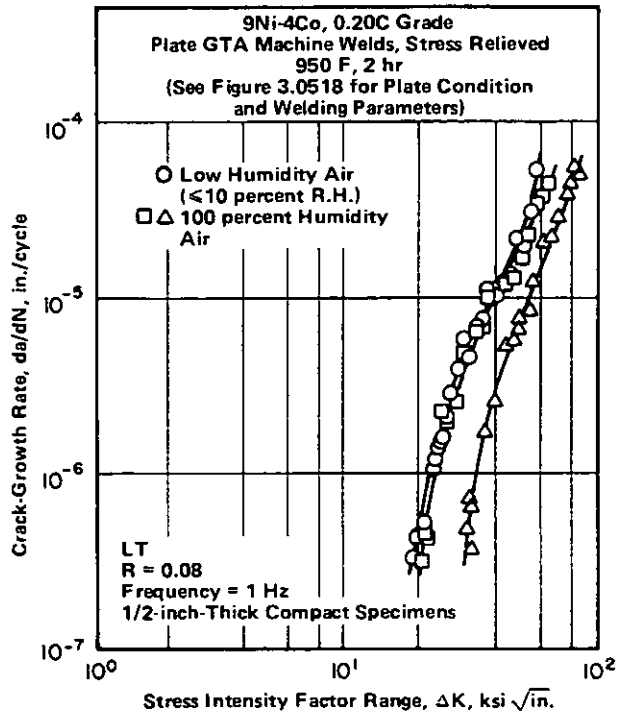


FIGURE 2.03512. EFFECT OF ENVIRONMENT ON FATIGUE CRACK-GROWTH RATE OF 0.20C GRADE PLATE GTA MACHINE WELDS (47, 48)

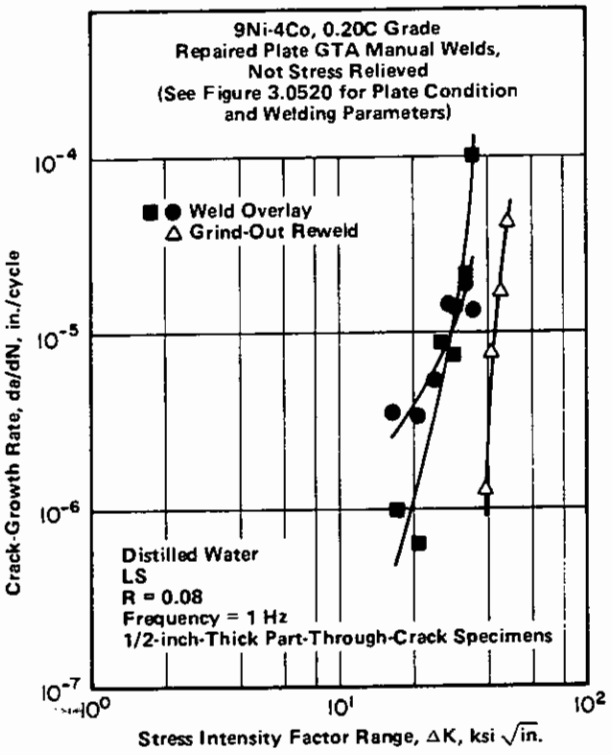
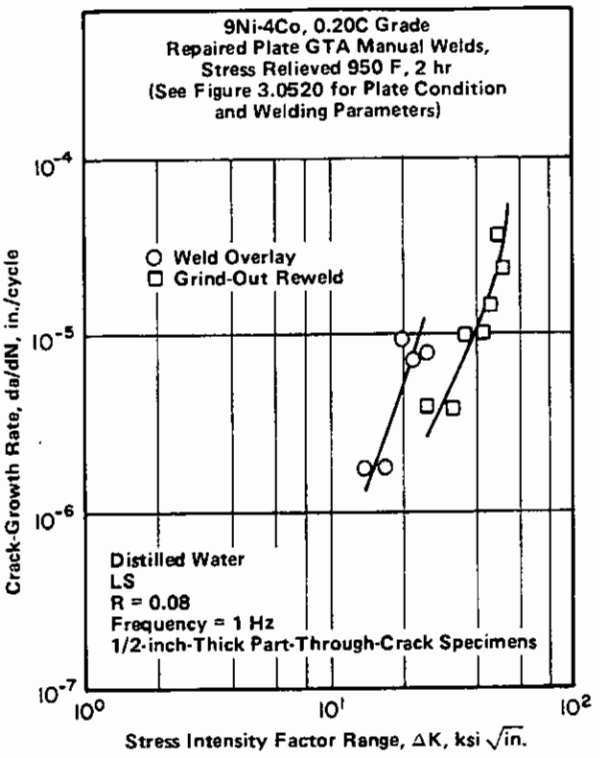


FIGURE 2.03513. FATIGUE CRACK-GROWTH RATES IN DISTILLED WATER OF 0.20C GRADE REPAIRED AND UNSTRESS-RELIEVED GTA MANUAL WELDS (47, 48)



Fe
9 Ni
4 Co
Cr
Mo
V

9Ni-4Co

FIGURE 2.03514. FATIGUE CRACK-GROWTH RATES IN DISTILLED WATER OF 0.20C GRADE REPAIRED AND STRESS-RELIEVED PLATE GTA MANUAL WELDS (47, 48)

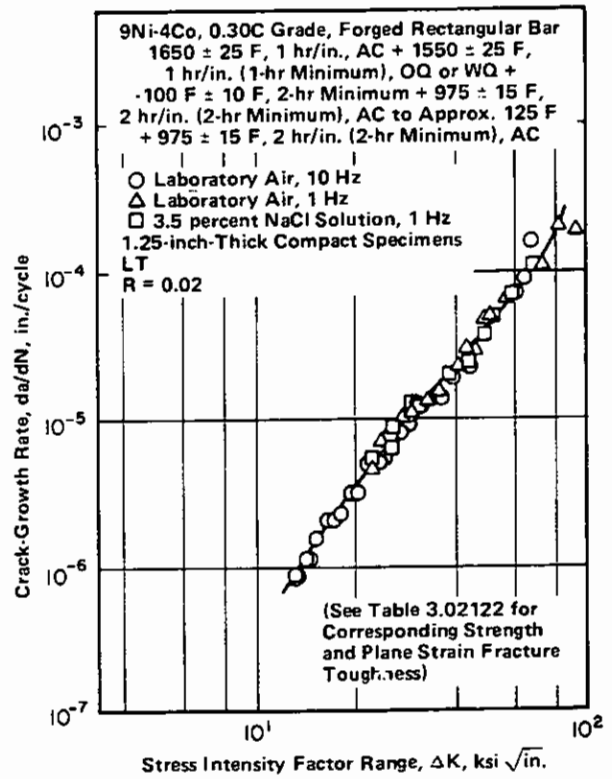


FIGURE 2.03515. FATIGUE CRACK-GROWTH RATE OF 0.30C GRADE FORGED RECTANGULAR BAR IN AIR AND 3.5 PERCENT NaCl SOLUTION (55)

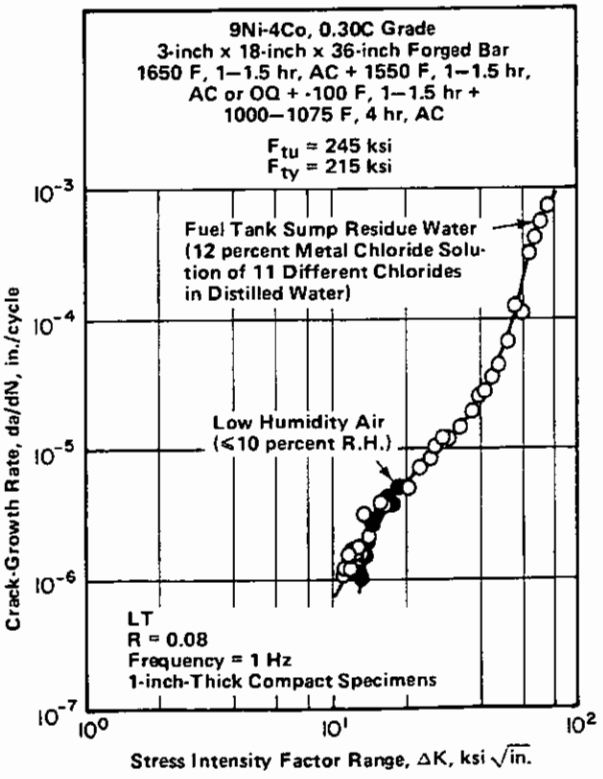


FIGURE 2.03516. EFFECT OF ENVIRONMENT ON FATIGUE CRACK-GROWTH RATE AT R = 0.08 OF 0.30C GRADE FORGED BAR (47, 48)

Fe
9 Ni
4 Co
Cr
Mo
V

9Ni-4Co

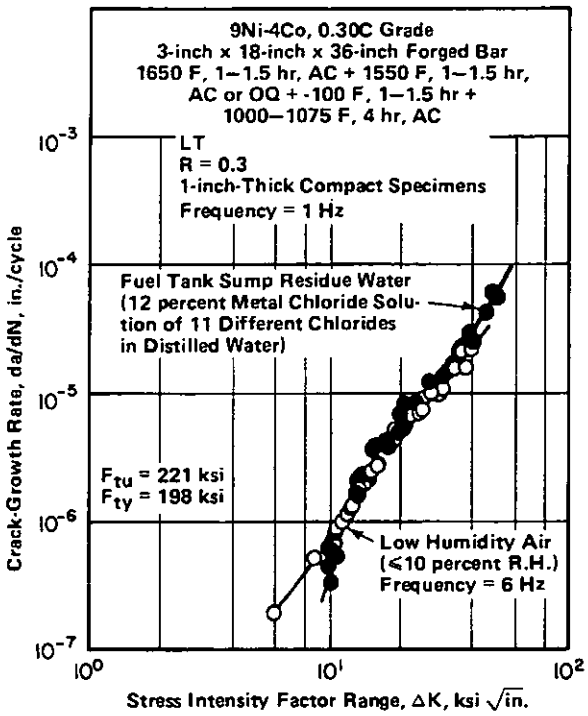


FIGURE 2.03517. EFFECT OF ENVIRONMENT ON FATIGUE CRACK-GROWTH RATE AT R = 0.3 OF 0.30C GRADE FORGED BAR (47, 48)

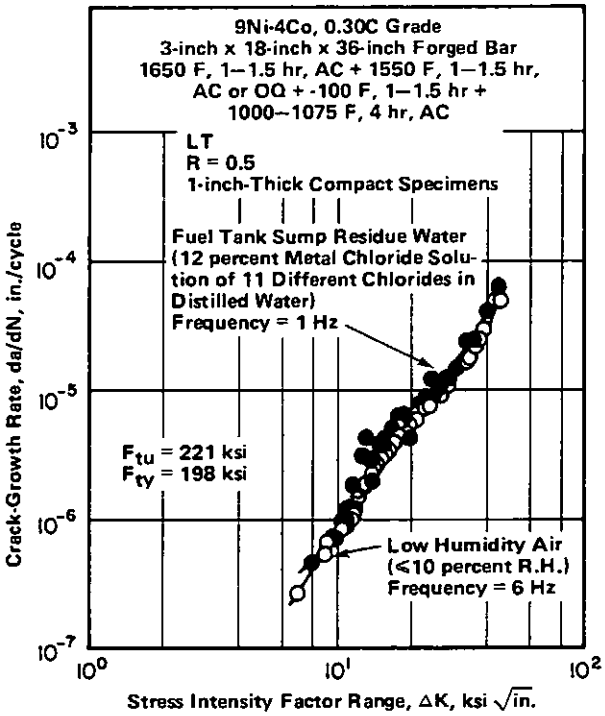


FIGURE 2.03518. EFFECT OF ENVIRONMENT ON FATIGUE CRACK-GROWTH RATE AT R = 0.5 OF 0.30C GRADE FORGED BAR (47, 48)

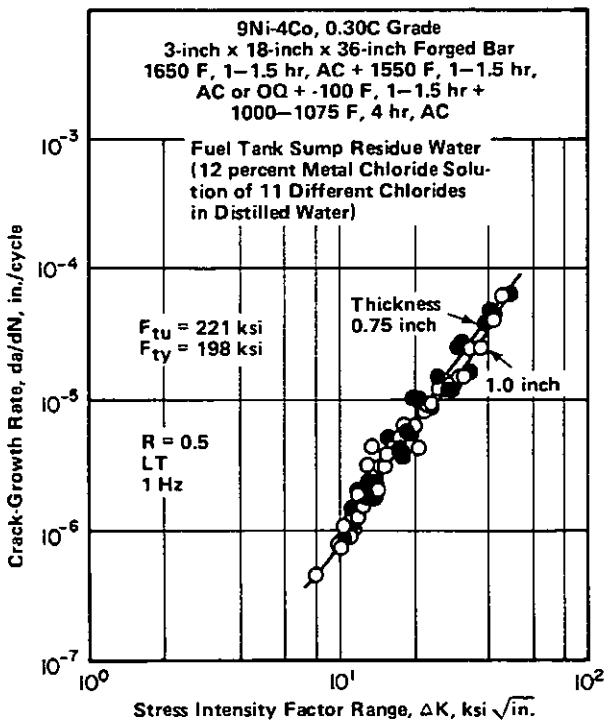


FIGURE 2.03519. EFFECT OF SPECIMEN THICKNESS ON FATIGUE CRACK-GROWTH RATE IN FUEL TANK SUMP RESIDUE WATER (12 PERCENT METAL CHLORIDE SOLUTION OF 11 DIFFERENT CHLORIDES IN DISTILLED WATER) OF 0.30C GRADE FORGED BAR (47, 48)

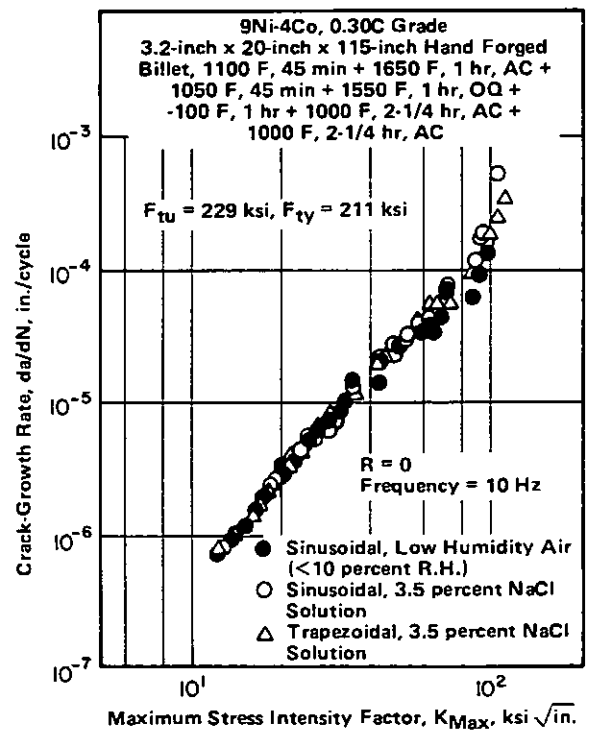


FIGURE 2.03520. EFFECT OF LOADING WAVE SHAPE AND ENVIRONMENT ON FATIGUE CRACK-GROWTH RATE OF 0.30C GRADE HAND FORGED BILLET (50, 51)

	Fe
9	Ni
4	Co
	Cr
	Mo
	V

9Ni-4Co

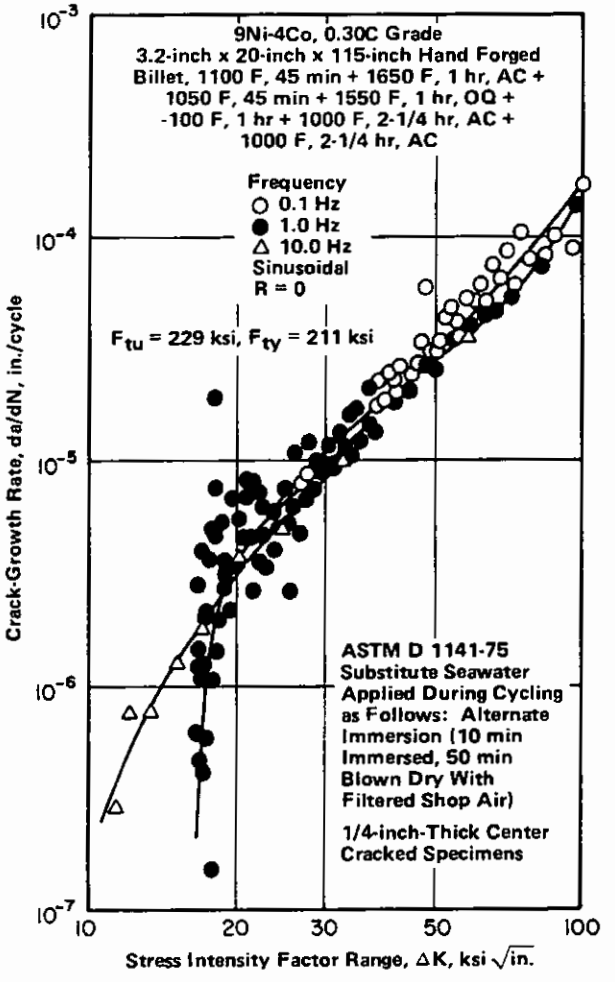


FIGURE 2.03521. EFFECT OF LOADING FREQUENCY (SINUSOIDAL) ON FATIGUE CRACK-GROWTH RATE IN SYNTHETIC SEA-WATER OF 0.30C GRADE HAND FORGED BILLET (49, 51)

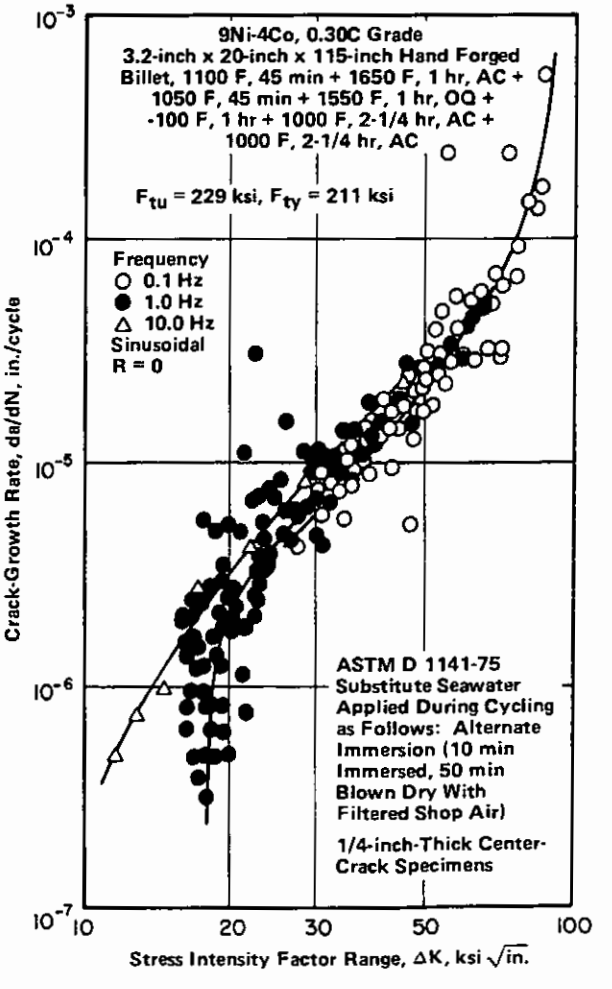


FIGURE 2.03522. EFFECT OF LOADING FREQUENCY (TRAPEZOIDAL) ON FATIGUE CRACK-GROWTH RATE IN SYNTHETIC SEAWATER OF 0.30C GRADE HAND FORGED BILLET (49, 51)

Fe
9 Ni
4 Co
Cr
Mo
V

9Ni-4Co

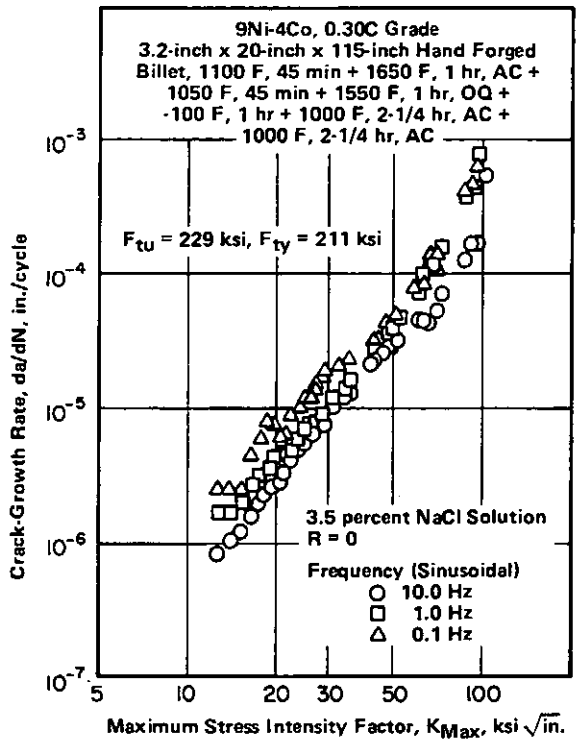


FIGURE 2.03523. EFFECT OF LOADING FREQUENCY (SINUSOIDAL) ON FATIGUE CRACK-GROWTH RATE IN 3.5 PERCENT NaCl SOLUTION OF 0.30C GRADE HAND FORGED BILLET (50, 51)

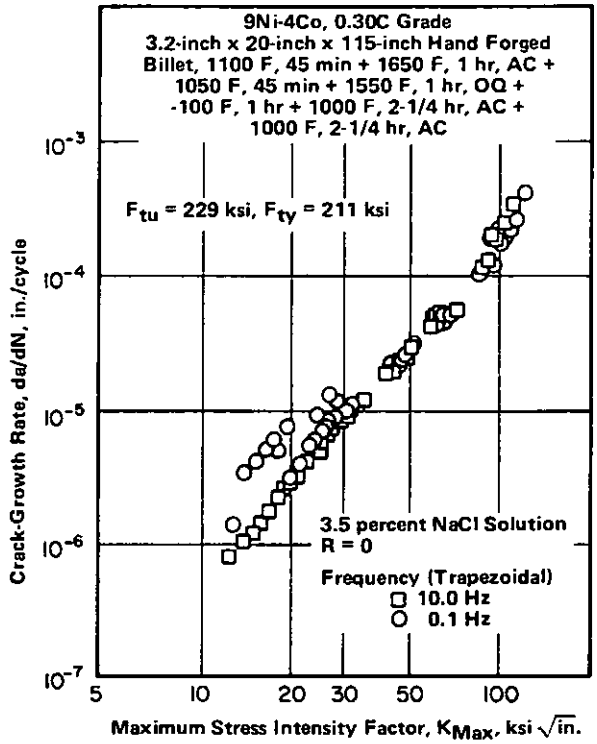


FIGURE 2.03524. EFFECT OF LOADING FREQUENCY (TRAPEZOIDAL) ON FATIGUE CRACK-GROWTH RATE IN 3.5 PERCENT NaCl SOLUTION OF 0.30C GRADE HAND FORGED BILLET (50, 51)

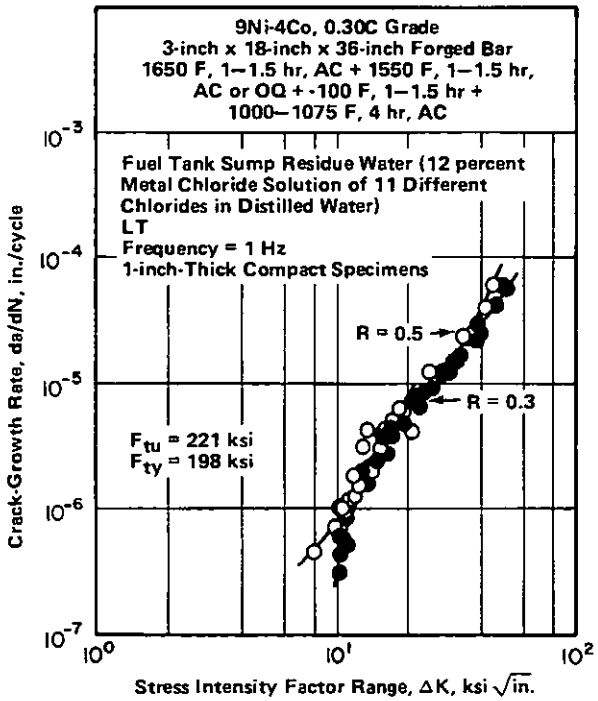


FIGURE 2.03525. EFFECT OF R-RATIO ON FATIGUE CRACK-GROWTH RATE IN FUEL TANK SUMP RESIDUE WATER (12 PERCENT METAL CHLORIDE SOLUTION OF 11 DIFFERENT CHLORIDES IN DISTILLED WATER) OF 0.30C GRADE FORGED BAR (47, 48)

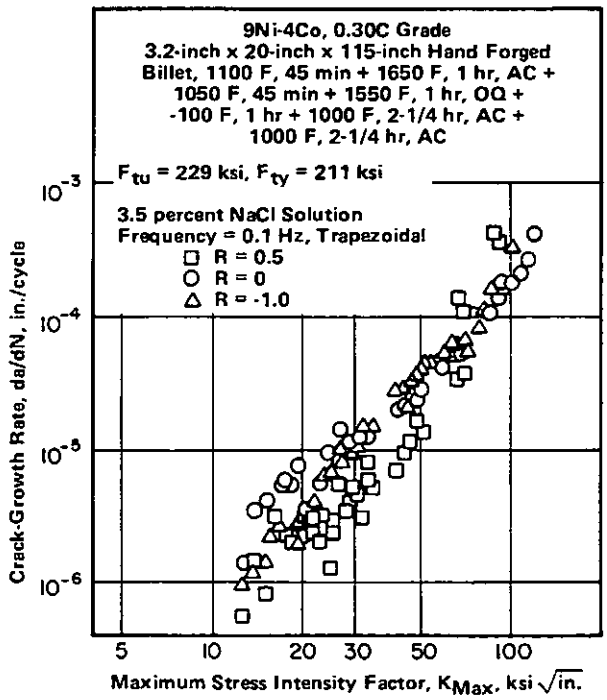


FIGURE 2.03526. EFFECT OF R-RATIO ON FATIGUE CRACK-GROWTH RATE IN 3.5 PERCENT NaCl SOLUTION OF 0.30C GRADE HAND FORGED BILLET (50, 51)

Fe
9 Ni
4 Co
Cr
Mo
V
9Ni-4Co

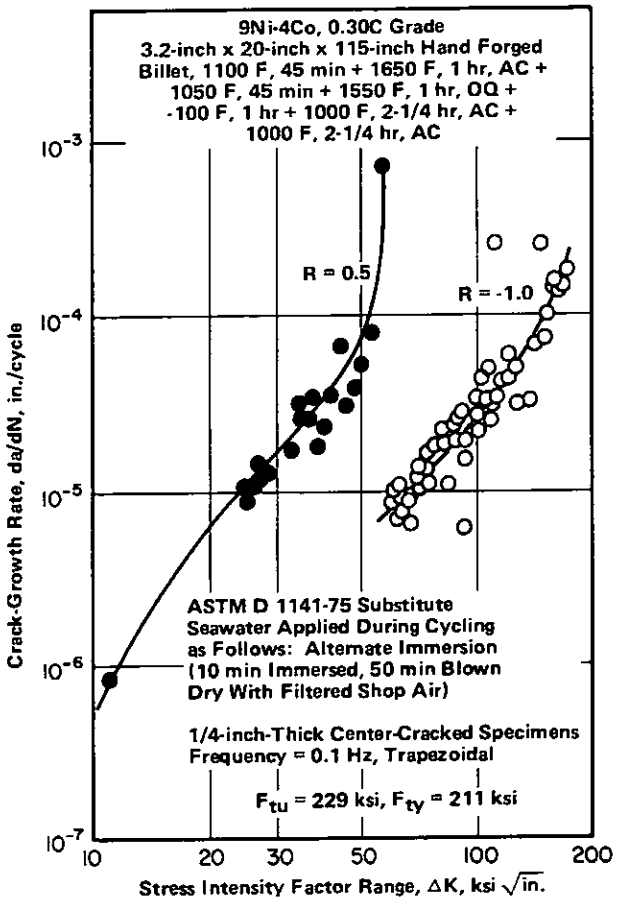


FIGURE 2.03527. EFFECT OF R-RATIO ON FATIGUE CRACK-GROWTH RATE OF 0.30C GRADE HAND FORGED BILLET IN SYNTHETIC SEAWATER (49, 51)

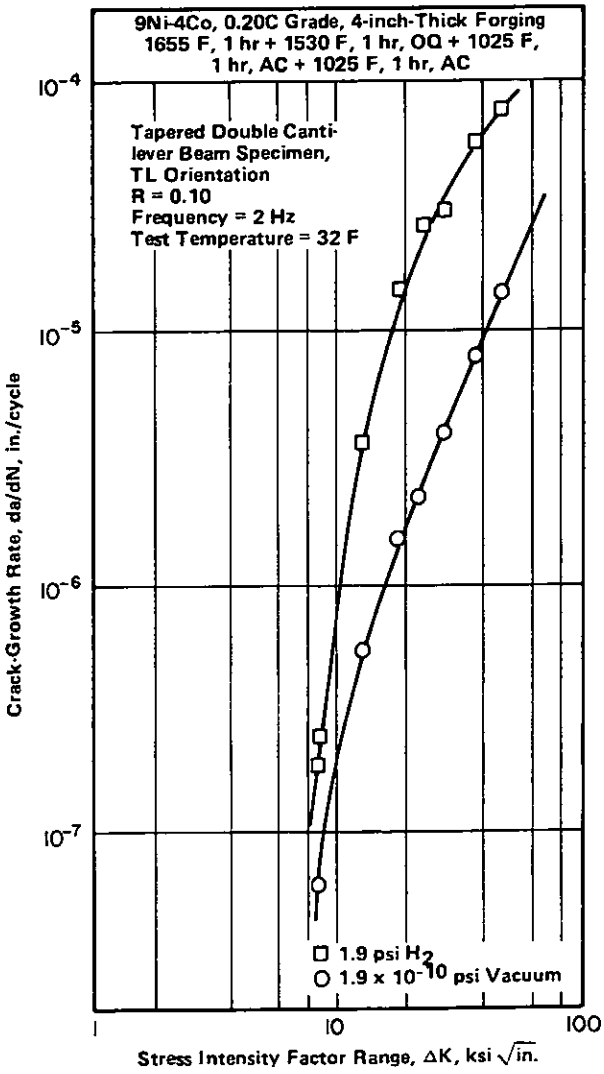


FIGURE 2.0361. FATIGUE CRACK-GROWTH RATE OF 0.20C GRADE FORGING AT 32 F IN HYDROGEN AND IN VACUUM (53)

Fe
9 Ni
4 Co
Cr
Mo
V

9Ni-4Co

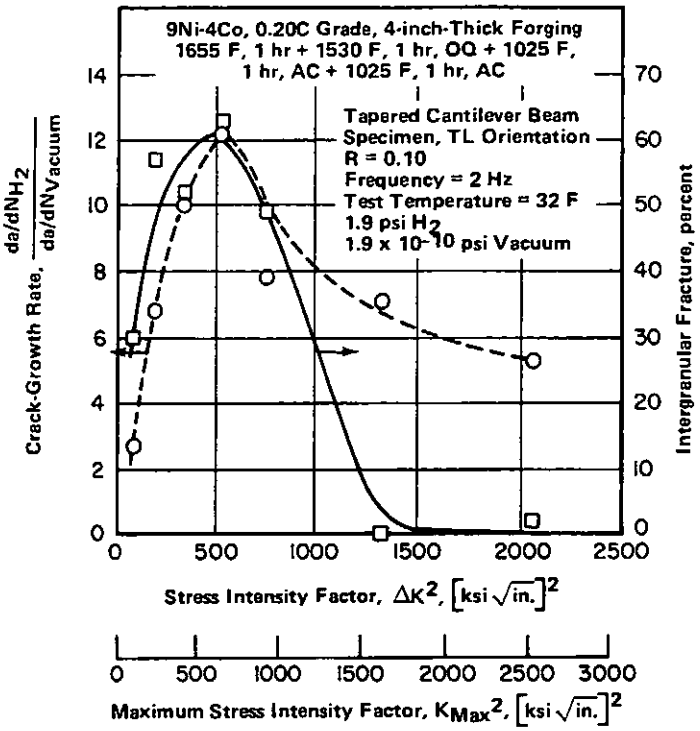


FIGURE 2.0362. DEPENDENCE OF HYDROGEN-ACCELERATED FATIGUE CRACK-GROWTH RATE ON STRESS INTENSITY FACTOR FOR 0.20C GRADE FORGING (53, 67)

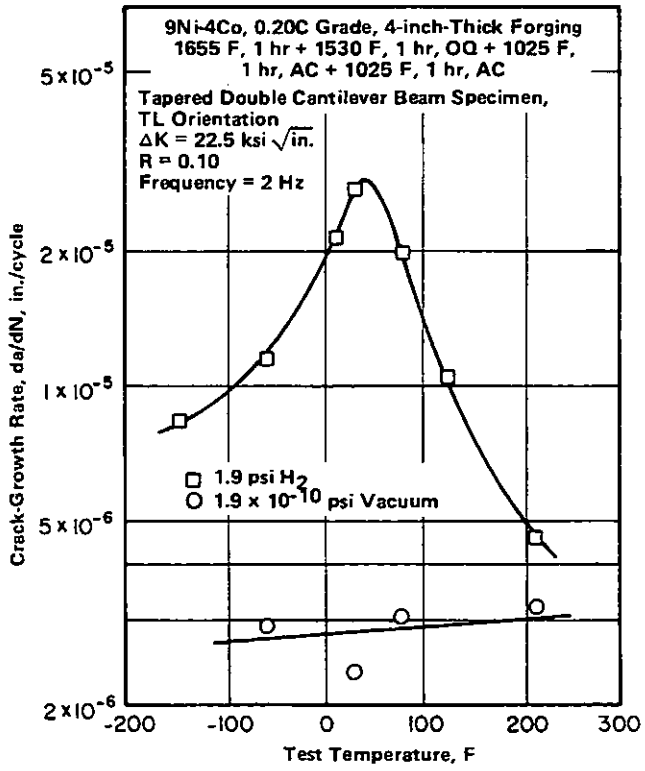


FIGURE 2.0363. TEMPERATURE DEPENDENCE OF FATIGUE CRACK-GROWTH RATE OF 0.20C GRADE FORGING IN HYDROGEN AND VACUUM (53, 67)

Fe
9 Ni
4 Co
Cr
Mo
V
9Ni-4Co

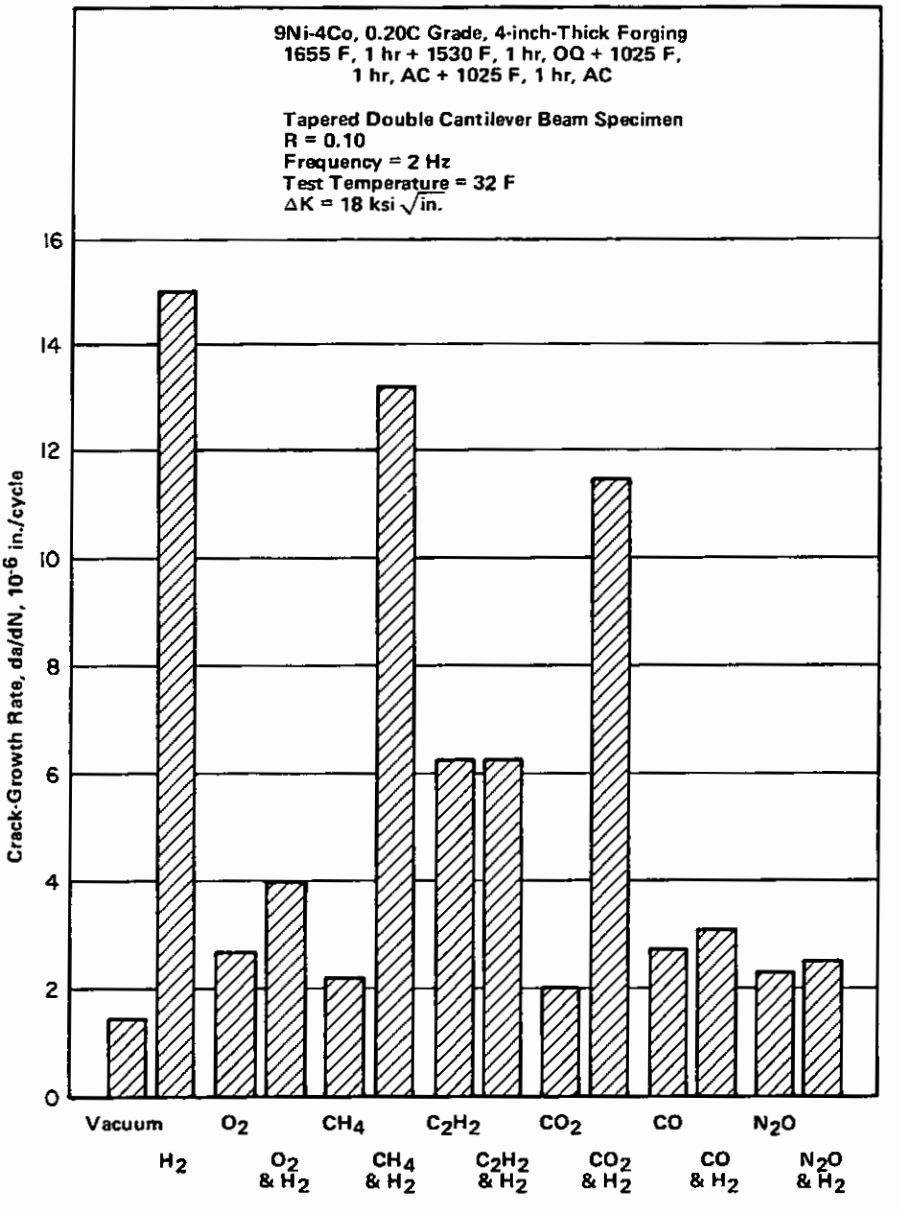


FIGURE 2.0364. FATIGUE CRACK-GROWTH RATE OF 0.20C GRADE FORGINGS AT 32 F IN VARIOUS GASEOUS ENVIRONMENTS (53)

Fe
9 Ni
4 Co
Cr
Mo
V

9Ni-4Co

Alloy	9Ni-4Co					
Grade	0.20C					
Form	Condition	Fluence[a] ($\times 10^{20}$ n/cm^2 > 1 MeV) (Φ^{cs})	(Φ^{fs})	Test Temp, F	F_{ty}, ksi	F_{tu}, ksi
2-in.-Thick Plate	1650 F, 2 hr, WQ + 1550 F, 2 hr, WQ + 1025 F, 4 hr, AC + 975 F, 6 hr, FC at 100 F/hr Maximum	0	0	75	189.6[b]	206.2[b]
		0	0	75	188.5[c]	200.9[c]
		0	0	75	188.0[d]	201.9[d]
		0	0	550	165.8[c]	180.5[c]
		0	0	550	159.6[c]	172.3[c]
		1.9	2.0	400	197.0[c]	200.0[c]
		1.9	2.0	500	192.0[c]	197.7[c]
2-in.-Thick Plate, GTA Welds	Plate: 1650 F, 2 hr, WQ + 1550 F, 2 hr, WQ + 1025 F, 4 hr, AC + 975 F, 6 hr, FC at 100 F/hr Maximum Weld: 975 F, 6 hr, FC at 100 F/hr Maximum	0	0	75	205.4[b]	217.6[b]
		1.9	2.0	500	218.1[b]	220.1[b]
		1.9	2.0	500	217.1[b]	217.1[b]

(a) Φ^{fs} = neutron energy spectrum fluence (n/cm^2 > 1.0 MeV) based on analysis of iron neutron dosimeter wires included in each irradiated specimen group assuming a fission spectrum.
Φ^{cs} = neutron energy spectrum fluence (n/cm^2 > 1.0 MeV) derived from Φ^{fs} using known nuclear relationships and claimed by the investigator to more closely represent the irradiation of the test specimens.
Calculated neutron energy spectrum fluence (Φ^{cs}) greater than 0.1 MeV may be obtained by multiplying the Φ^{cs} fluence greater than 1.0 MeV by 2.15.
(b) As fabricated.
(c) Thermally conditioned at 550 F out of reactor for 800 hours.
(d) Thermally conditioned at 700 F for 1000 hours.

TABLE 2.041. EFFECT OF 550 F IRRADIATION ON STRENGTH OF 0.20C GRADE PLATE AND WELDMENTS (56)

Alloy	9Ni-4Co				
Grade	0.20C				
Form	Condition	Fluence[a] ($\times 10^{20}$ n/cm^2 > 1 MeV) (Φ^{cs})	(Φ^{fs})	Upper-Shelf IE, Charpy V, ft-lb	Upper-Shelf Temp (Approx), F
2-in.-Thick Plate	1650 F, 2 hr, WQ + 1550 F, 2 hr, WQ + 1025 F, 4 hr, AC + 975 F, 6 hr, FC at 100 F/hr Maximum	0	0	76[b]	500
		2.0	2.1	55	<400[c]
2-in.-Thick Plate, GTA Welds	Plate: 1650 F, 2 hr, WQ + 1550 F, 2 hr, WQ + 1025 F, 4 hr, AC + 975 F, 6 hr, FC at 100 F/hr Maximum	0	0	>80[d]	>250
	Weld: 975 F, 6 hr, FC at 100 F/hr Maximum	1.9	2.0	46	>500[e]

(a) Φ^{fs} = neutron energy spectrum fluence (n/cm^2 > 1 MeV) based on analysis of iron neutron dosimeter wires included in each irradiated specimen group assuming a fission spectrum.
Φ^{cs} = neutron energy spectrum fluence (n/cm^2 > 1.0 MeV) derived from Φ^{fs} using known nuclear relationships and claimed by the investigator to more closely represent the irradiation of the test specimens.
Calculated neutron energy spectrum fluence (Φ^{cs}) greater than 0.1 MeV may be obtained by multiplying the Φ^{cs} fluence greater than 1.0 MeV by 2.15.
(b) Upper-shelf level at 500 F; upper-shelf level to 300 F was 62 ft-lb.
(c) Postirradiation tests performed in temperature range 140–500 F.
(d) Weld deposit exhibited 80 ft-lb at 250 F and rising.
(e) Tests made only at 500 F.

TABLE 2.042. EFFECT OF 550 F IRRADIATION ON UPPER-SHELF CHARPY V IMPACT ENERGY AND TEMPERATURE OF 0.20C GRADE PLATE AND WELDMENTS (56)

Fe
9 Ni
4 Co
Cr
Mo
V
9Ni-4Co

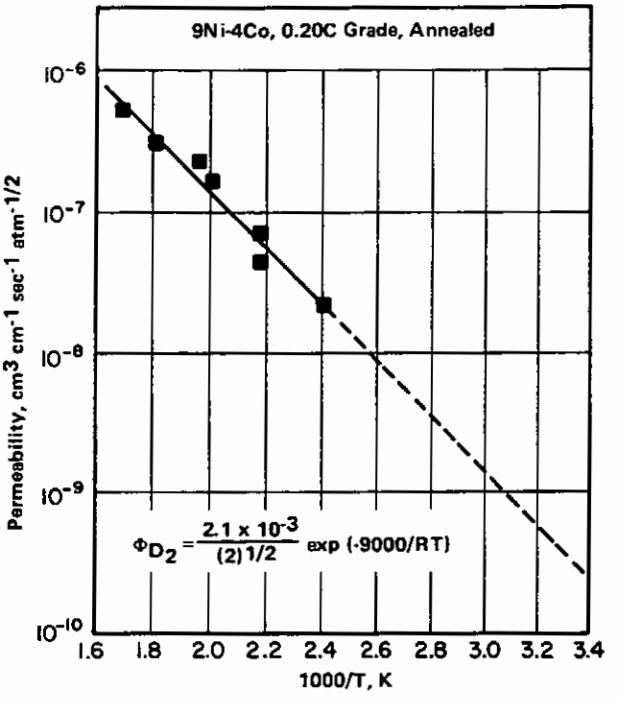


FIGURE 2.043. PERMEABILITY OF ANNEALED 0.20C GRADE TO DEUTERIUM (57)

Alloy	9Ni-4Co		
Grade	0.20C		
Form	Sheet, Strip, and Plate[a]		Bars, Forgings, Tubing, and Rings[a]
Condition	1650 ± 25 F, 1 hr/in., AC or WQ + 1525 ± 25 F, 1 hr/in. (1 hr Min), OQ or WQ + [See Footnote (b)] 1025 ± 15 F, 4–8 hr, Cool Suitably		1650 ± 25 F, 1 hr/in., AC + 1525 ± 25 F, 1 hr/in. (1 hr Min), OQ at 60–150 F + (Within 2 hr After OQ) -100 ± 25 F, 1 hr Min + 1025–1075 F, 4 hr Min, AC
Direction	(c)		(e)
Thickness, in.	<0.250	≥0.250	All[f]
F_{tu}, Min, ksi	190		190
F_{ty}, Min, ksi	175		180
e (2-in. of 4D), Min, percent	5	10	12
RA, Min, percent	45		45
Hardness, Min, HRC	41[d]		Not specified

(a) Fracture toughness testing may be specified with method and standards agreed upon by purchaser and vendor: ASTM E-338 suggested for sheet; ASTM E-399 suggested for plate and for bars, forgings, tubing, and rings with section thickness of 1.50 inch and over.

(b) Yield strength may be increased approximately 5–10 ksi by adding a refrigeration treatment of -100 F, 2 hours, at this point in the heat treat schedule, as done for bars, forgings, tubing, and rings.

(c) T direction tensile specimens for product width ≥9 inch; L direction for product width <9 inch.

(d) Product shall not be rejected on basis of hardness if tensile property requirements are met.

(e) T direction specimens from product from which a specimen ≥2.50 inch long can be obtained; otherwise L direction.

(f) Properties apply to product having cross sectional area ≤100 $\sqrt{\text{in.}}$; for product having cross sectional area >100 $\sqrt{\text{in.}}$, properties shall be agreed upon by purchaser and vendor.

TABLE 3.011. SAE-AMS SPECIFIED ROOM TEMPERATURE MECHANICAL PROPERTIES FOR 0.20C GRADE (1, 2)

Fe
9 Ni
4 Co
Cr
Mo
V

9Ni-4Co

Alloy	9Ni-4Co
Grade	0.20C
Form	Plate and Forgings
Condition	1650 ± 25 F, 1 hr/in. (1 hr Min), AC + 1550 ± 25 F, 1 hr/in. (1 hr Min), OQ or WQ + -100 ± 25 F, 1 hr Min + 1025 ± 25 F, 4–8 hr, AC
F_{tu}, ksi	195/215
F_{ty}, ksi	180/195
RA, percent	45/60
e (2-in. or 4D), percent	12/16
Hardness, HRC	39/44
IE Charpy V, ft-lb	45/60
K_{Ic}, ksi $\sqrt{in.}$	120/135

TABLE 3.012. PRODUCER'S TYPICAL ROOM TEMPERATURE MECHANICAL PROPERTIES FOR 0.20C GRADE (13, 16)

Alloy	9Ni-4Co	
Grade	0.20C	
Condition	1650 ± 25 F, 1 hr/in. (1 hr Min), AC + 1550 ± 25 F, 1 hr/in. (1 hr Min), OQ or WQ + -100 ± 25 F, 1 hr Min + 1025–1075 F, 4–8 hr, AC	
Form	Plate and Bar ≤3 in.	Billet ≤25 in.[2] Reforge
F_{tu}, ksi	190	
F_{ty}, ksi	180	
RA, percent	35	
e, percent	10	14

TABLE 3.013. PRODUCER'S GUARANTEED MINIMUM ROOM TEMPERATURE MECHANICAL PROPERTIES FOR 0.20C GRADE (13, 16)

Fe
9 Ni
4 Co
Cr
Mo
V

9Ni-4Co

Alloy	9Ni-4Co					
Grade	0.20C					
Form	Forged or Rolled Bar, Forging Stock, Forged Block, and Mechanical Tubing				Forgings	
Condition	1650 ± 25 F, 1 hr/in., AC + 1500 ± 25 F, 1 hr/in., OQ at 60–150 F + (Within 2 hr After OQ) -100 ± 10 F, 2 hr + 1025–1075 F, 2 hr, AC + 1025–1075 F, 2 hr, AC				1625–1675 F, 1 hr/in., AC + 1500–1550 F, 1 hr/in., OQ at 70–140 F + (Within 1 hr After OQ) -100 ± 25 F, 1 hr Min + 1040 ± 10 F, Twice for 2 hr Min Each, but Not Exceeding 8 hr Total, AC	
Direction	T[a,b]				L or LT & ST	T & ST or TL & SL
Cross Section, in.^{2}	<100	100–196	197–225	>225	≤100[c]	
F_{tu}, Min, ksi	190				190	
F_{ty}, Min, ksi	180				180	
e (2 in. or 4D), Min, percent	Not specified				12	10
RA, Min, percent	40	35	30	25	45	40
Hardness, HRC	Not specified				41–45	
K_{Ic}, Min, ksi $\sqrt{in.}$	Not specified				120[d]	110[d]

Form	Forgings		Bars, Forgings, and Reforging Stock
Condition	1650 ± 25 F, 1 hr/in., AC + 1525 ± 25 F, 1 hr/in., OQ at 140 F Max, + -100 F, 2 hr + 1025–1075 ± 10 F, 4–8 hr, AC + 1025–1075 ± 10 F, 4–8 hr, AC		1650 ± 25 F, 1 hr/in., AC + 1525 ± 25 F, 1 hr/in., OQ at 60–150 F + (Within 2 hr After OQ) -100 ± 25 F, 1 hr Min + 1025–1075 ± 10 F, 4 hr, AC
Direction	L[e]	T & ST or TL[e]	All[g]
Cross Section, in.^{2}	All		≤100[c]
F_{tu}, Min, ksi	190		190–210
F_{ty}, Min, ksi	180		180–200
e (2 in. or 4D), Min, percent	12	10	12
RA, Min, percent	45	40	45
Hardness, HRC	Not specified		Not specified
K_{Ic}, Min, ksi $\sqrt{in.}$		120[f]	120

(a) Specified properties are for billet or bar stock. Stock with minimum dimension less than 5 inches shall be tested in size not less than 5 inches; that with minimum dimension greater than 5 inches shall first be open frame hammered, pressed, or rolled to size commensurate with maximum size of the forging to be made from the billet or bar.

(b) Center location, T direction; however, ST for rectangular sections and L for bar less than 3 inches in diameter.

(c) Properties for cross sectional areas greater than 100 in.^{2} shall be negotiated.

(d) To be determined in accordance with ASTM E-399 using compact specimens with B = 1.5 inch and W = 2B = 3.0 inches.

(e) K_{Ic} specimens shall be taken from location as close as possible to longitudinal centerline of forging or prolongation. Tensile specimens shall be taken from the areas of both least and most reduction, and location as close as possible to mid thickness.

(f) In accordance with ASTM E-399.

(g) For rolled, drawn, and forged bar, tensile specimens shall be taken from central location in L, T, and ST directions, size permitting. K_{Ic} specimens shall be taken centrally from each bar item in LT, TL, and SL orientations.
For forged shapes, tensile specimens shall be taken as specified on forging drawing, or otherwise from central location on prolongation in L, T, and ST directions, size permitting. K_{Ic} specimens shall be taken as shown on forging drawing, otherwise in LT orientation from prolongation.
For VAR ingot qualifications, K_{Ic} specimens shall be taken centrally in LT orientation from both top and bottom of ingot forged at 1825 ± 25 F with 2:1 reduction to a final as-forged thickness of approximately 2-1/2 inches.

TABLE 3.014. USERS' SPECIFIED ROOM TEMPERATURE MECHANICAL PROPERTIES FOR 0.20C GRADE (3–6)

Fe
9 Ni
4 Co
Cr
Mo
V

9Ni-4Co

Alloy	9Ni-4Co		
Grade	0.30C		
Form	Sheet, Strip, and Plate[a]		Bars, Forgings, Tubing, and Rings[a]
Condition	1650 ± 25 F, 1 hr/in., AC + 1550 ± 25 F, 1 hr/in. (1 hr Min), OQ or WQ + -100 ± 10 F, 2 hr Min + 975 ± 15 F, 2 hr/in. (2 hr Min), AC to Approx 125 F + 975 ± 15 F, 2 hr/in. (2 hr Min), AC		1650 ± 50 F, 1 hr/in. Min, AC + 1550 ± 15 F, 1 hr/in. (1 hr Min), Q[d] + -100 ± 10 F, 2 hr Min + 1000 ± 10 F, 2 hr Min, Cool Suitably to below 125 F + 1000 ± 10 F, 2 hr Min, AC
Direction	[b]		L
Thickness, inch	<0.250	≥0.250	All
F_{tu}, Min, ksi	220		220
F_{ty}, Min, ksi	185	190	190
e (2 inch or 4D), Min, percent	6	10	10
RA, Min, percent	–	35	40
Hardness, Min, HRC	46[b]		Not specified
IE Charpy V, Min, ft-lb	Not specified		20

(a) Fracture toughness testing may be specified with method and standards agreed upon by purchaser and vendor: ASTM E-338 suggested for sheet; ASTM E-399 suggested for plate and for bars, forgings, tubing, and rings with section thickness of 0.50 inch and over.
(b) T direction tensile specimens for product width ≥9 inch; L direction for product width <9 inch.
(c) Product shall not be rejected on basis of hardness if tensile property requirements are met.
(d) Sections ≤4 inch, OQ or WQ; Sections >4 inch, OQ.

TABLE 3.015. SAE-AMS SPECIFIED ROOM TEMPERATURE MECHANICAL PROPERTIES FOR 0.30C GRADE (7, 8)

Alloy	9Ni-4Co
Grade	0.30C
Form	Forgings
Condition	Quench and Tempered (Bainitic)
Direction	L[a]
Thickness, in.	All
F_{tu}, Min, ksi	210
F_{ty}, Min, ksi	200
e, Min, percent	10
RA, Min, percent	30
IE Charpy V, Min, ft-lb	20

(a) Specimens to be taken from mid-thickness of forging or forging prelongation.
Charpy V impact energy transition temperature curve, fracture toughness, cryogenic and elevated temperature mechanical properties, and hardenability all may be specified with methods and standards to be agreed upon by purchaser and vendor.

TABLE 3.016. ASTM SPECIFIED ROOM TEMPERATURE MECHANICAL PROPERTIES FOR 0.30C GRADE (9)

Fe
9 Ni
4 Co
Cr
Mo
V

9Ni-4Co

Alloy	9Ni-4Co
Grade	0.30C
Form	Billets and Forgings
Condition	1650 ± 50 F, 1 hr/in. (1 hr Min), AC + 1150 ± 25 F, 1/2 hr Min + 1550 ± 25 F, 1 hr/in. (1 hr Min), OQ or WQ + -100 ± 25 F, 1 hr Min + 1025 ± 25 F (2 + 2) hr Min, AC
F_{tu}, ksi	220/240
F_{ty}, ksi	190/200
RA, percent	35/50
e (2-in. or 4D), percent	12/16
Hardness, HRC	44/48
IE Charpy V, ft-lb	18/25
K_{Ic}, ksi $\sqrt{in.}$	90/105

TABLE 3.017. PRODUCER'S TYPICAL ROOM TEMPERATURE MECHANICAL PROPERTIES FOR 0.30C GRADE (14, 16)

Alloy	9Ni-4Co
Grade	0.30C
Form	Billets and Forgings ≤3 in. and/or 25 $in.^2$ Reforge
Condition	1650 ± 50 F, 1 hr/in. (1 hr Min), AC + 1150 ± 25 F, 1/2 hr Min + 1550 ± 25 F, 1 hr/in. (1 hr Min), OQ or WQ + -100 ± 25 F, 1 hr Min + 1000 F (2 + 2) hr Min, AC
F_{tu}, ksi	220
F_{ty}, ksi	190
RA, percent	35
e (2-in. or 4D), percent	10

TABLE 3.018. PRODUCER'S GUARANTEED MINIMUM ROOM TEMPERATURE MECHANICAL PROPERTIES FOR 0.30C GRADE (14, 16)

Fe
9 Ni
4 Co
Cr
Mo
V

9Ni-4Co

Alloy	9Ni-4Co					
Grade	0.30C					
Form	Forged or Rolled Bar, Forging Stock, Forged Block, and Mechanical Tubing				Bars and Forgings	
Condition	1700 ± 25 F, 1 hr/in., AC + 1525 ± 25 F, 1 hr/in., OQ at 60–150 F + (Within 2 hr After OQ) -100 ± 10 F, 2 hr + 1025–1075 F, 2 hr, AC + 1025–1075 F, 2 hr, AC				1625–1675 F, 1 hr/in., AC to Below 125 F + 1150 ± 25 F, 8–24 hr Commensurate With Section Thickness, AC[c] + 1550 ± 25 F, 1 hr/in. (1 hr Min), OQ at 70–140 F + (Within 1 hr After OQ) -100 F, 1 hr Min + 1000–1075 F ± 15 F, Twice for 2 hr Min Each, but Not Exceeding 8 hr Total, AC	
Direction	T[a,b]				L or LT[d,f]	T and ST[e,f]
Cross Section, in.^{2}	<100	100–196	197–225	>225	All	
F_{tu}, ksi	220 min				220 min	
F_{ty} ksi	190 min				190 min	
e (2 in. or 4D), Min, percent	Not specified				10	8
RA, Min, percent	35	30	25	20	40	30
Hardness, HRC	Not specified				44–49	
K_{Ic}, Min, ksi $\sqrt{in.}$	Not specified				90[g]	

Form	Forgings		Bars, Forgings, and Reforging Stock	
Condition	1650 ± 25 F, 1 hr/in. or Fraction Thereof, AC to Below 125 F + 1550 ± 25 F, 1 hr/in. or Fraction Thereof, OQ at 140 F Max + -100 F, 2 hr + 1000–1075 ± 10 F, 2 hr Min, AC to Below 125 F + 1000–1075 ± 10 F, 2 hr Min, AC		1650 ± 25 F, 1 hr/in., AC + 1550 ± 25 F, 1 hr/in., OQ at 60–150 F + (Within 2 hr -100 ± 10 F, 1 hr Min + 1000 ± 10 F, 2 hr, AC	
Direction	L	T and ST or TL	L or LT[i]	S and ST or TL and SL[i]
Cross Section, in.^{2}	All		≤100[j]	
F_{tu}, ksi	220 min		220–240	
F_{ty}, ksi	190 min		190–210	
e (2 in. or 4D), Min, percent	12	10	10	
RA, Min, percent	40	35	40	35
Hardness, HRC	Not specified		Not specified	
K_{Ic}, Min, ksi $\sqrt{in.}$		90[h]	90	

(a) Specified properties are for billet or bar stock. Stock with minimum dimension less than 5 inches shall be tested in size not less than 5 inches; that with minimum dimension greater than 5 inches shall first be open frame hammered, pressed, or rolled to size commensurate with maximum size of the forging to be made from the billet or bar.

(b) Center location, T direction; however, ST for rectangular sections and L for bar less than 3 inches in diameter.

(c) Alternate to 1150 F, 8–24 hours treatment: 1250 ± 25 F, 4 hours, AC + 1150 ± 25 F, 4 hours, AC.

(d) K_{Ic} for the other orientations to be negotiated between purchaser and vendor.

(e) Size permitting.

(f) Specimens to be taken from central locations.

(g) To be determined in accordance with ASTM E-399 using compact specimens with B = 1.25 inch.

(h) K_{Ic} specimens shall be taken from location as close as possible to longitudinal centerline of forging or prolongation. Tensile specimens shall be taken from the areas of both least and most reduction, and location as close as possible to mid thickness.

(i) For rolled or drawn bar, tensile specimens shall be taken from central location in L, T, and ST directions, size permitting. K_{Ic} specimens shall be taken centrally from each bar item in LT, TL, and SL orientations.
For forgings, tensile specimens shall be taken per forging drawing, otherwise from thickest section in the forging in L, T, and ST directions. K_{Ic} specimens shall be taken in LT, TL, and SL orientations from prolongation on forged items ≥0.75 inch.
For VAR ingot qualification, K_{Ic} specimen shall be taken centrally in LT orientation from both top and bottom of ingot forged to final thickness at 4:1 or less reduction.

(j) Properties for cross sectional areas greater than 100 in.^{2} shall be negotiated.

TABLE 3.019. USERS' SPECIFIED ROOM TEMPERATURE MECHANICAL PROPERTIES FOR 0.30C GRADE (3, 10–12)

Fe
9 Ni
4 Co
Cr
Mo
V

9Ni-4Co

Alloy	9Ni-4Co		
Grade	0.20C, CEVM (C-deox)		
Form	1-inch Plate		
Condition	1675 F, 1 hr, AC + 1550 F, 1 hr, Q + T (2 + 2) hr, AC		
Quench Media	Tempering Temperature, F	$\sigma = K\epsilon^n$ K	n
Oil	No temper	305,600	0.096
	1000	277,000	0.100
	1050	262,100	0.096
	1100	241,300	0.081
Water	1000	281,800	0.092
Air	No temper	281,000	0.087

TABLE 3.0211. TRUE STRESS, TRUE STRAIN CHARACTERISTICS OF 0.20C GRADE PLATE VARIOUSLY HEAT TREATED (32)

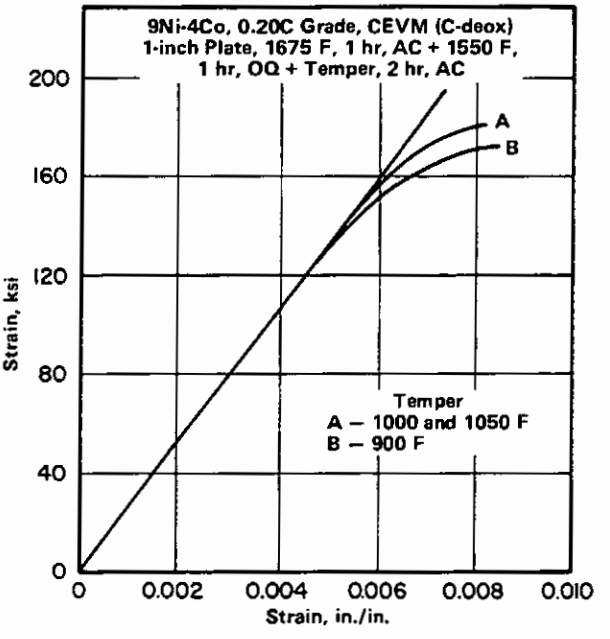


FIGURE 3.0212. STRESS-STRAIN CURVES FOR REHEAT TREATED 0.20C GRADE PLATE (32)

Alloy	9Ni-4Co		
Grade	0.20C Grade, CEVM (C-deox)		
Form	2 inch Plate		
Condition	1700 F, 2 hr, AC + 1525 F, Q + 1025 F, 4 hr		
Quench Media	Water(b)	Oil(b)	Air(c)
F_{tu}, ksi(a)	194	197	205
F_{ty}, ksi	183	176	172
e (4D), percent	18	17	17
RA, percent	64	65	66

(a) All tests longitudinal.
(b) 0.18C, 0.75Cr.
(c) 0.17C, 0.77Cr.

TABLE 3.0213. EFFECT OF QUENCH MEDIA ON THE TENSILE PROPERTIES OF 0.20C GRADE PLATE (28)

Fe
9 Ni
4 Co
Cr
Mo
V

9Ni-4Co

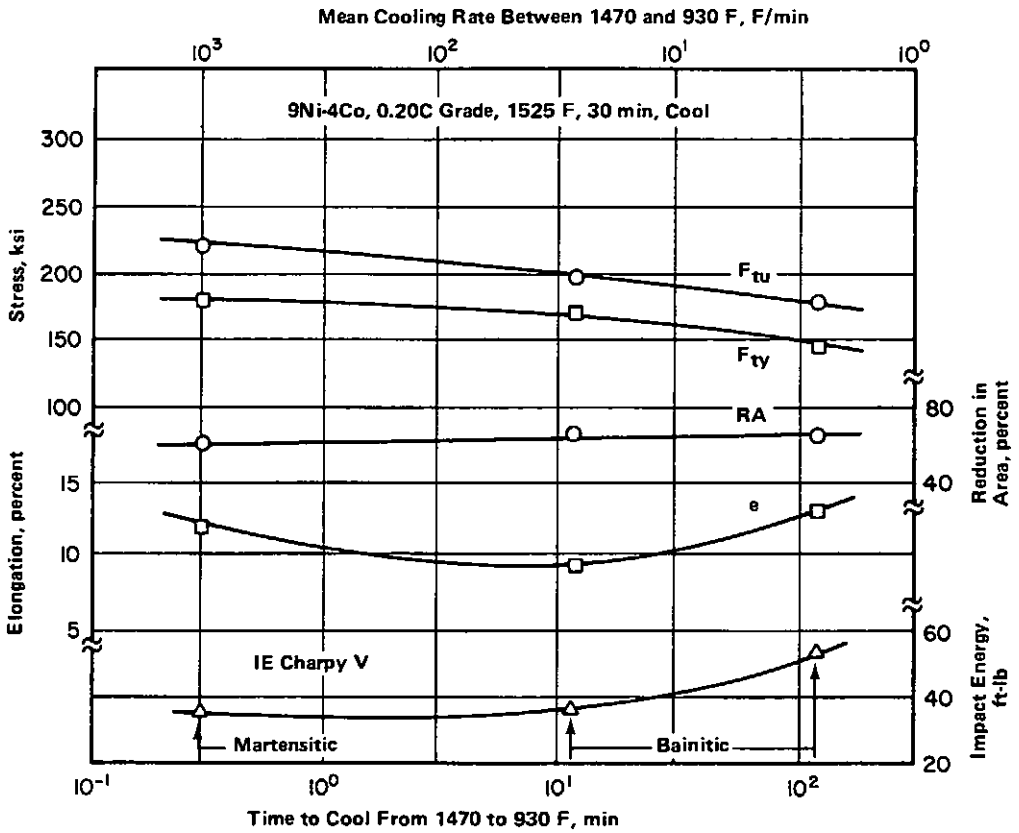


FIGURE 3.0214. EFFECT OF COOLING RATE FROM THE AUSTENITIZING TEMPERATURE ON THE ROOM TEMPERATURE TENSILE PROPERTIES AND CHARPY V IMPACT ENERGY OF 0.20C GRADE (25)

Alloy	9Ni-4Co			
Grade	0.20C			
Condition	1650 F, 1 hr, AC + 1525 F, 1 hr, Cool to Transformation Temperature, Hold, and Quench + 1000 F, 4 hr, AC			
Transformation Treatment	F_{tu}, ksi	F_{ty}, ksi	e, percent	RA, percent
1150 F, 24 hr, OQ	214.2	189.9	16.5	57.4
1150 F, 24 hr, OQ	213.0	191.7	16.0	58.4
1150 F, 24 hr, OQ	214.2	191.4	15.0	56.4
650 F, 10 hr, OQ	214.2	192.3	16.5	59.8
650 F, 10 hr, OQ	214.5	192.0	16.5	60.1
650 F, 10 hr, OQ	215.4	191.7	15.5	61.4
450 F, 8 hr, AC	221.4	183.3	15.5	58.7
450 F, 8 hr, AC	220.5	187.5	15.5	59.8
450 F, 8 hr, AC	220.8	183.0	15.0	58.4

TABLE 3.0215. EFFECT OF ISOTHERMAL TRANSFORMATION TREATMENT ON ROOM TEMPERATURE TENSILE PROPERTIES OF 0.20C GRADE (15)

Fe
9 Ni
4 Co
Cr
Mo
V

9Ni-4Co

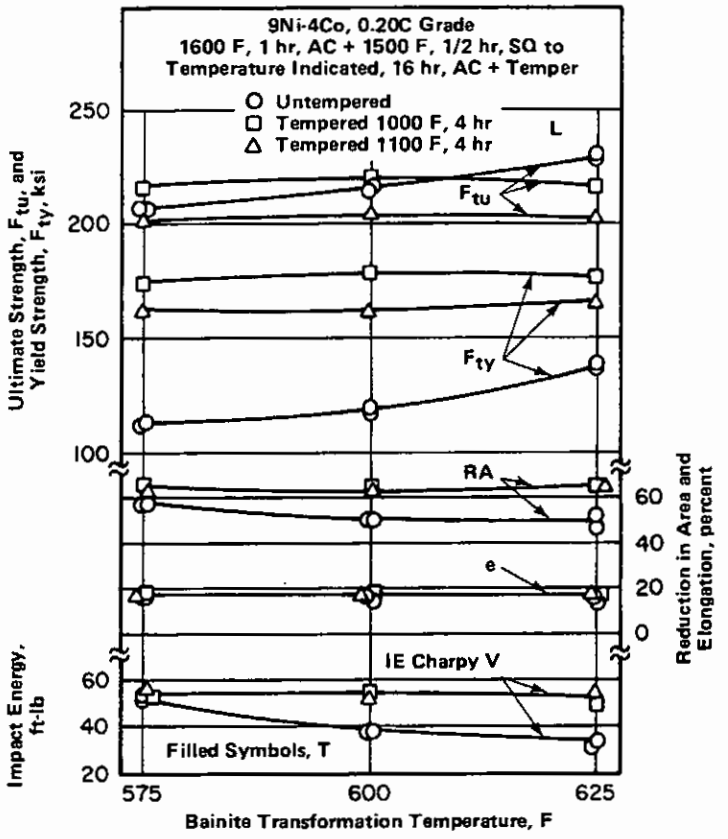


FIGURE 3.0216. EFFECT OF BAINITE TRANSFORMATION TEMPERATURE ON ROOM TEMPERATURE TENSILE PROPERTIES AND 0 F CHARPY V IMPACT ENERGY OF 0.20C GRADE WITH AND WITHOUT SUBSEQUENT TEMPERING (15)

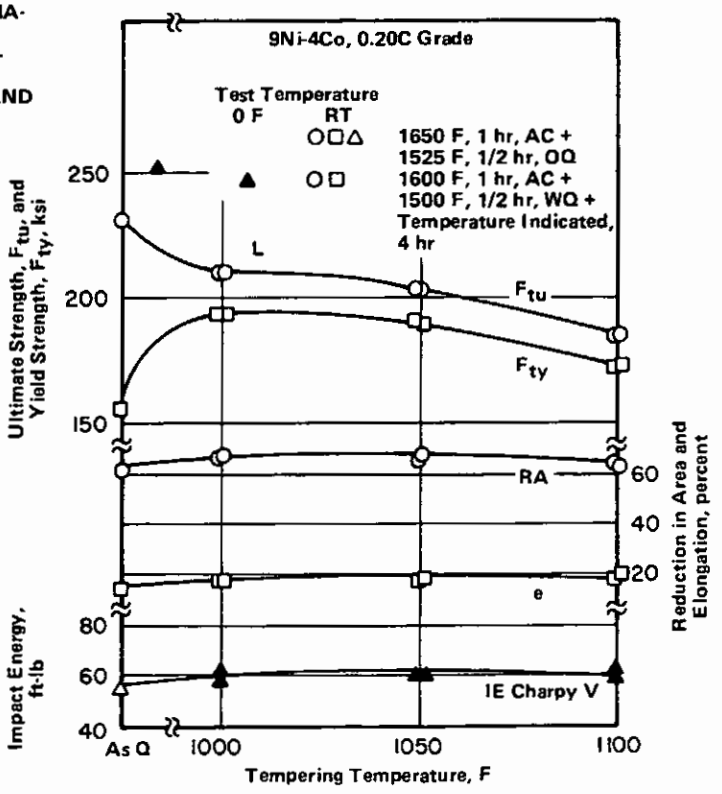


FIGURE 3.0217. EFFECT OF MARTENSITE TEMPERING TEMPERATURE ON ROOM TEMPERATURE TENSILE PROPERTIES AND OF CHARPY V IMPACT ENERGY OF 0.20C GRADE (15)

Fe
9 Ni
4 Co
Cr
Mo
V

9Ni-4Co

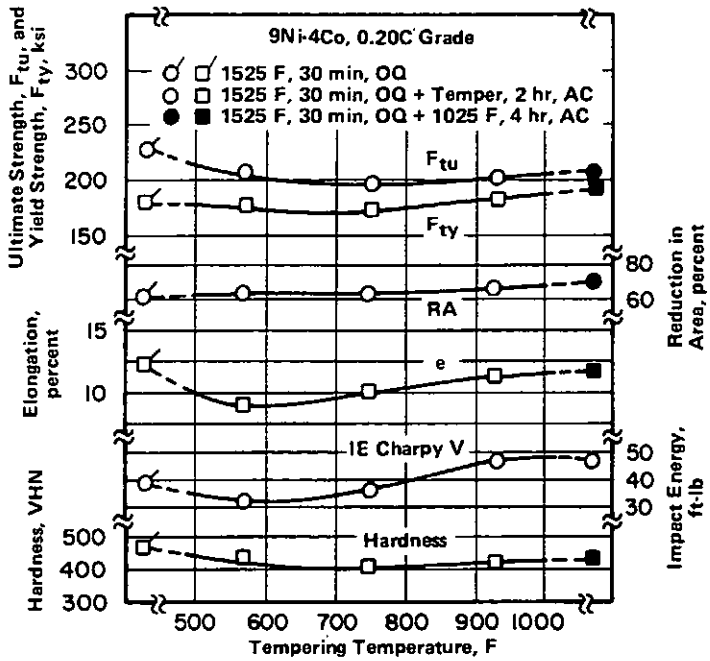


FIGURE 3.0218. EFFECT OF TEMPERING TEMPERATURE ON THE ROOM TEMPERATURE TENSILE PROPERTIES, CHARPY V IMPACT ENERGY AND HARDNESS OF 0.20C GRADE QUENCHED WITHIN THE MARTENSITIC RANGE AND TEMPERED (25)

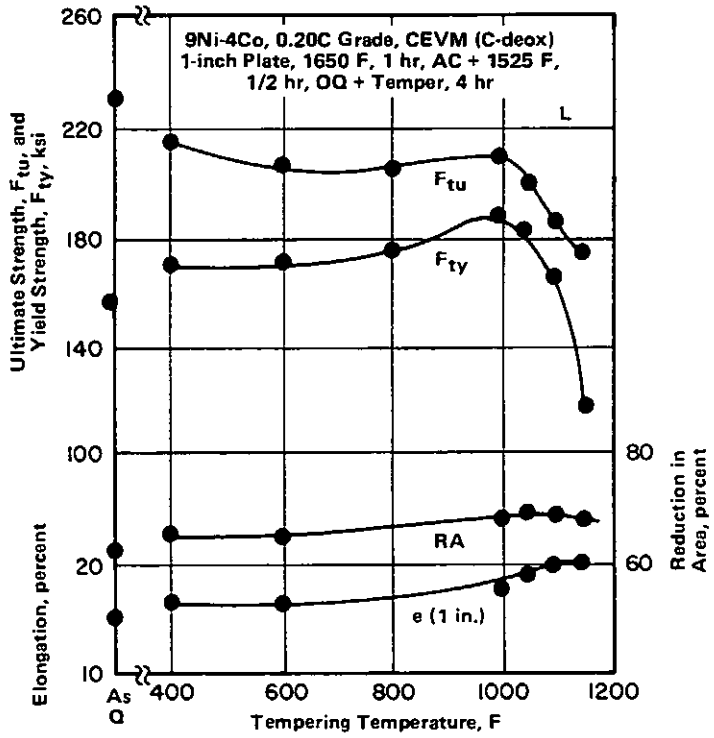


FIGURE 3.0219. EFFECT OF TEMPERING TEMPERATURE ON TENSILE PROPERTIES OF 0.20C GRADE PLATE (28)

Fe
9 Ni
4 Co
Cr
Mo
V
9Ni-4Co

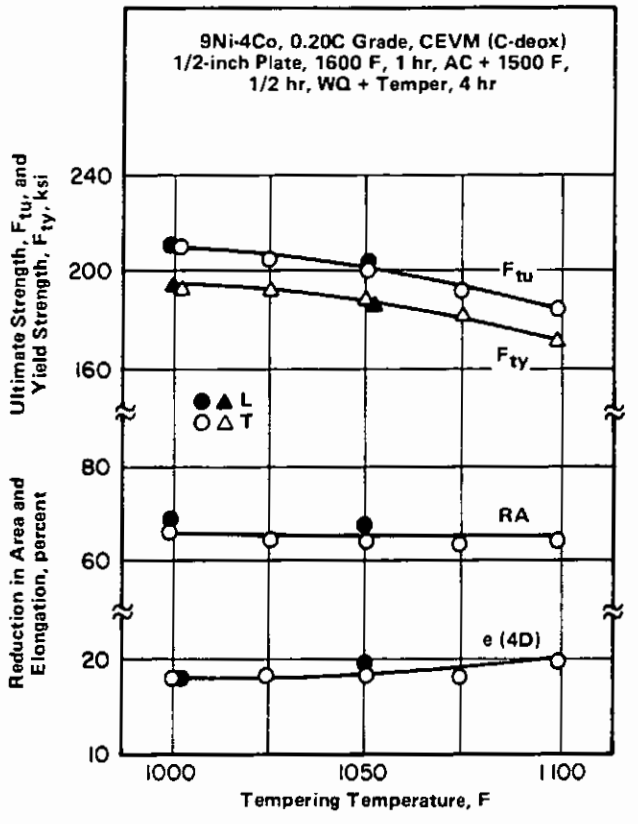


FIGURE 3.02110. EFFECT OF TEMPERING TEMPERATURE ON TENSILE PROPERTIES OF 0.20C GRADE PLATE (28)

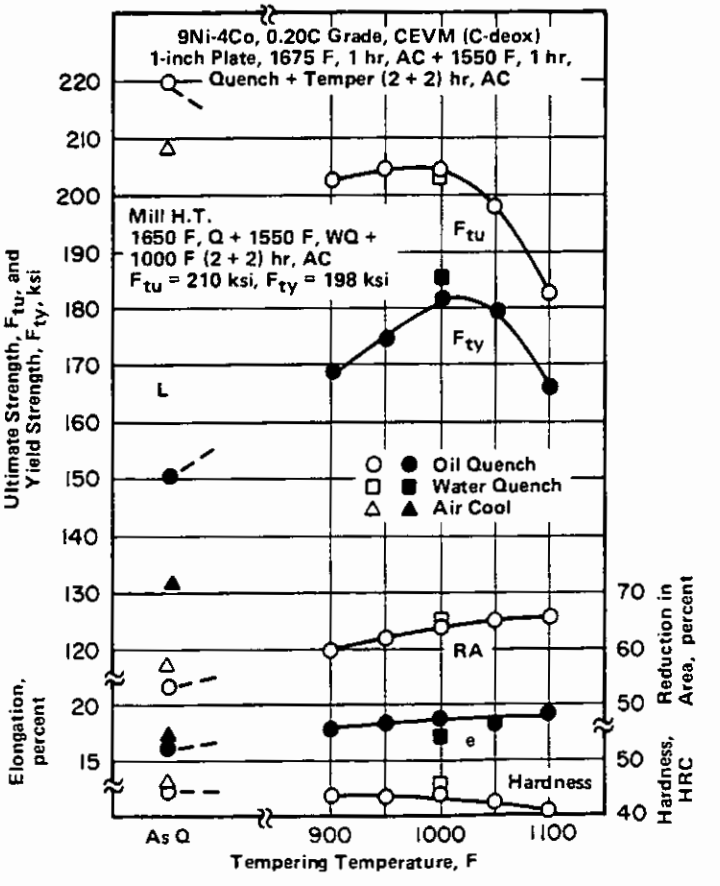


FIGURE 3.02111. EFFECT OF TEMPERING TEMPERATURE ON TENSILE PROPERTIES AND HARDNESS OF REHEAT TREATED 0.20C GRADE PLATE (32)

Fe
9 Ni
4 Co
Cr
Mo
V

9Ni-4Co

Alloy	9Ni-4Co				
Grade	0.20C, CEVM (C-deox)				
Form	Plate				
Condition	1650 F, 1 hr, AC + 1550 F, 1 hr, WQ + 1000 F (2 + 2) hr, AC				
24 hr Stress Relief Temperature, F	F_{tu}, ksi	F_{ty}, ksi	e (2 in.), percent	RA, percent	Hardness, HRC
900	202	187	19	66	42–43
950	202	192	18	63	43–44
1000	195	186	19	64	42–43

TABLE 3.02112. EFFECT OF STRESS RELIEF TREATMENT ON ROOM TEMPERATURE TENSILE PROPERTIES AND HARDNESS OF 0.20C GRADE PLATE (32)

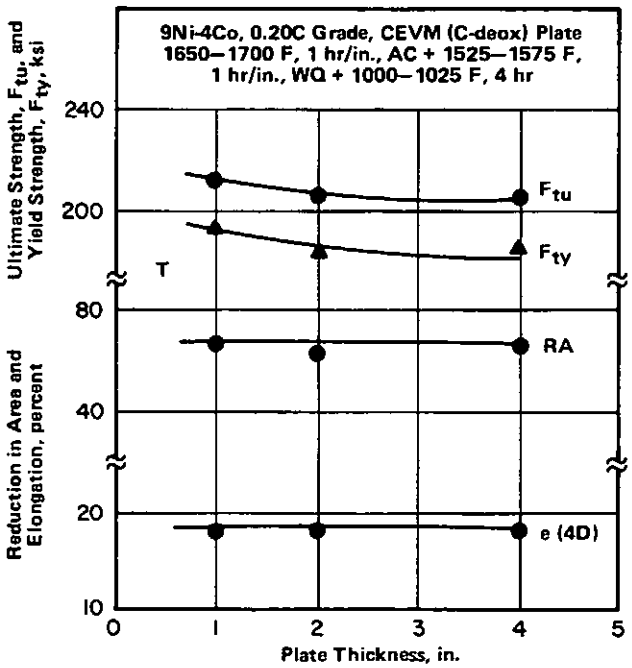


FIGURE 3.02113. EFFECT OF PLATE THICKNESS ON TENSILE PROPERTIES OF 0.20C GRADE PLATE FROM ONE HEAT (28)

Fe
9 Ni
4 Co
Cr
Mo
V
9Ni-4Co

Alloy	9Ni-4Co			
Grade	0.20C			
Form	Billet[a]			
Condition	A, Q + 1025 F Temper			
Test Specimen Direction/Orientation				
	T		TL	LT
F_{tu}, ksi	F_{ty}, ksi	RA, percent	IE Charpy V, ft-lb	
190–212	180–201	64–73	75–103	59–108

(a) Twenty-nine billets from 26 heats: billet sizes ranged from 1-7/16 inch round to 16 inch square.

TABLE 3.02114. RANGE OF ROOM TEMPERATURE TENSILE PROPERTIES AND CHARPY V IMPACT ENERGY FOR TWENTY-NINE BILLETS FROM TWENTY-SIX HEATS OF 0.20C GRADE (13)

Alloy	9Ni-4Co			
Grade	0.20C Grade, CEVM (C-deox)			
Condition	1550 F, 1 hr/in., WQ + Temper, 4 hr			
Thickness, in.	1/2 and 1 in.			2 in.
Tempering Temperature, F	1000	1025	1050	1000 to 1025
Number Tests[a]	24	8	16	8
F_{tu}, Mean, ksi	208	207	205	201
F_{tu}, Std Dev, ksi	6.9	5.5	2.5	6.6
F_{ty}, Mean, ksi	185	189	185	185
F_{ty}, Std Dev, ksi	4.2	3.7	2.2	4.7
e (4D), Mean, percent	18	17	18	17
e (4D), Std Dev, percent	0.7	0.9	0.6	1.5
RA, Mean, percent	66	67	66	66
RA, Std Dev, percent	2.6	2.9	1.5	3.0

(a) Transverse tests.

TABLE 3.02115. MEAN VALUES AND STANDARD DEVIATIONS FOR TENSILE PROPERTIES OF 0.20C GRADE PLATE TEMPERED AT SEVERAL TEMPERATURES (28)

Alloy	9Ni-4Co
Grade	0.20C
Form	Forged Round Bar
Condition	1650 ± 25 F, 1 hr/in., AC or WQ + 1525 ± F, 1 hr/in. (1 hr Minimum), OQ or WQ = -100 F, 2 hr + 1025 ± 15 F, 4–8 hr, Cool Suitably
F_{tu}, ksi	201.0
F_{ty}, ksi	185.5
e, percent	16.0
RA, percent	63.3
E, 10^3 ksi	28.0
K_{Ic}, ksi $\sqrt{in.}$[a]	94.4

(a) Determined with 1-1/4-inch-thick compact specimens.

TABLE 3.02116. ROOM TEMPERATURE TENSILE PROPERTIES, ELASTIC MODULUS, AND PLANE STRAIN FRACTURE TOUGHNESS OF 0.20C GRADE FORGED ROUND BAR (55)

Fe
9 Ni
4 Co
Cr
Mo
V

9Ni-4Co

Alloy	9Ni-4Co			
Grade	0.20C Grade, CEVM (C-deox)			
Condition	1650 F, 1 hr/in. AC + 1550 F, 1 hr/in. WQ + 1000 F, 6 hr, AC			
Form	8-1/2 in. Diam x 13 in.	9 x 9 in. x 11 in.		5 x 5 in. x 16 in.
Location[a]	Center	Center	Mid Rad	Center
F_{tu}, ksi	207	195	198	200
F_{ty}, ksi	180	177	181	180
e (4D), percent	17	17	17	17
RA, percent	56	68	67	65
Charpy V				
70 F	38	58	56	56
0 F	–	49	–	56

(a) All tests transverse.

TABLE 3.02117. TENSILE AND CHARPY V IMPACT PROPERTIES FOR SEVERAL LARGE FORGINGS OF 0.20C GRADE (28)

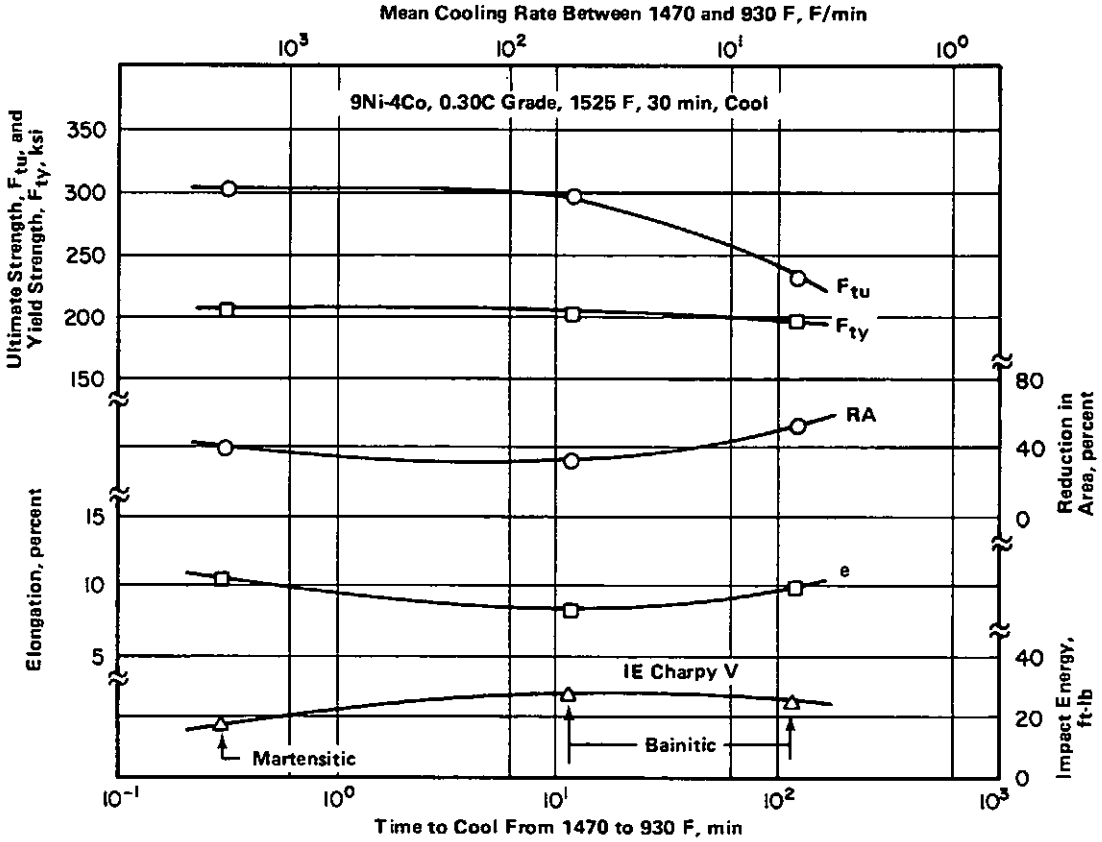


FIGURE 3.02118. EFFECT OF COOLING RATE FROM THE AUSTENITIZING TEMPERTURE ON THE ROOM TEMPERATURE TENSILE PROPERTIES AND CHARPY V IMPACT ENERGY OF 0.30C GRADE (25)

Fe
9 Ni
4 Co
Cr
Mo
V

9Ni-4Co

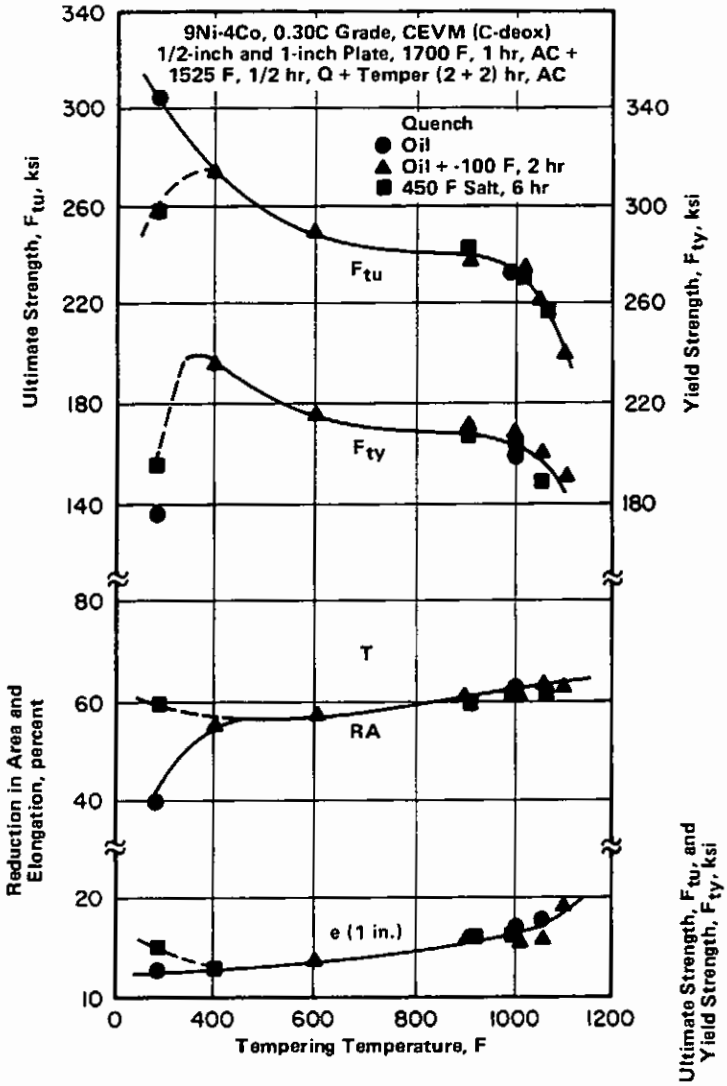


FIGURE 3.02119. EFFECT OF TEMPERING TEMPERATURE ON ROOM TEMPERATURE TENSILE PROPERTIES OF 0.30C GRADE PLATE VARIOUSLY QUENCHED FROM THE AUSTENITIZING TEMPERATURE (63)

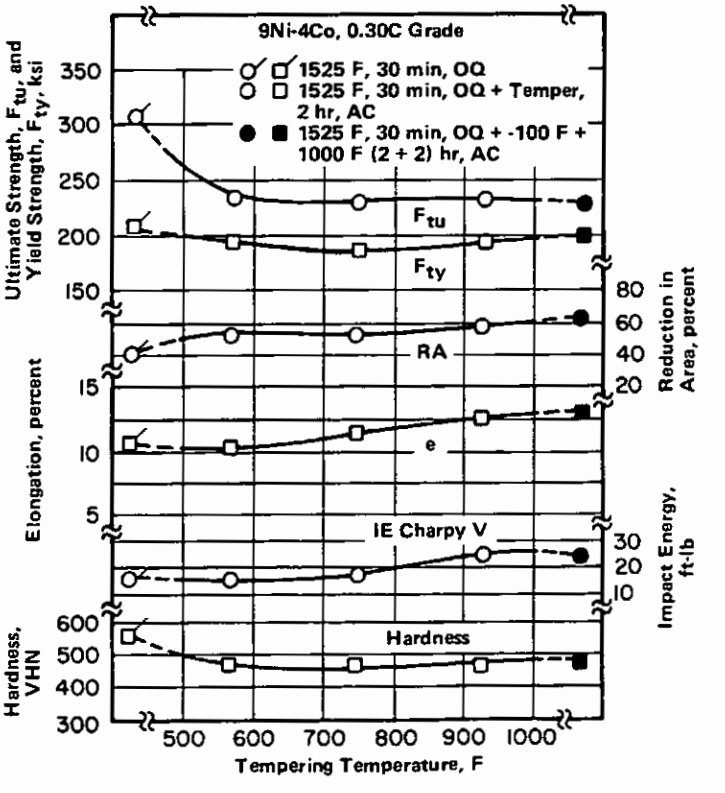


FIGURE 3.02120. EFFECT OF TEMPERING TEMPERATURE ON THE ROOM TEMPERATURE TENSILE PROPERTIES, CHARPY V IMPACT ENERGY, AND HARDNESS OF 0.30C GRADE QUENCHED WITHIN THE MARTENSITIC RANGE AND TEMPERED (25)

Fe
9 Ni
4 Co
Cr
Mo
V

9Ni-4Co

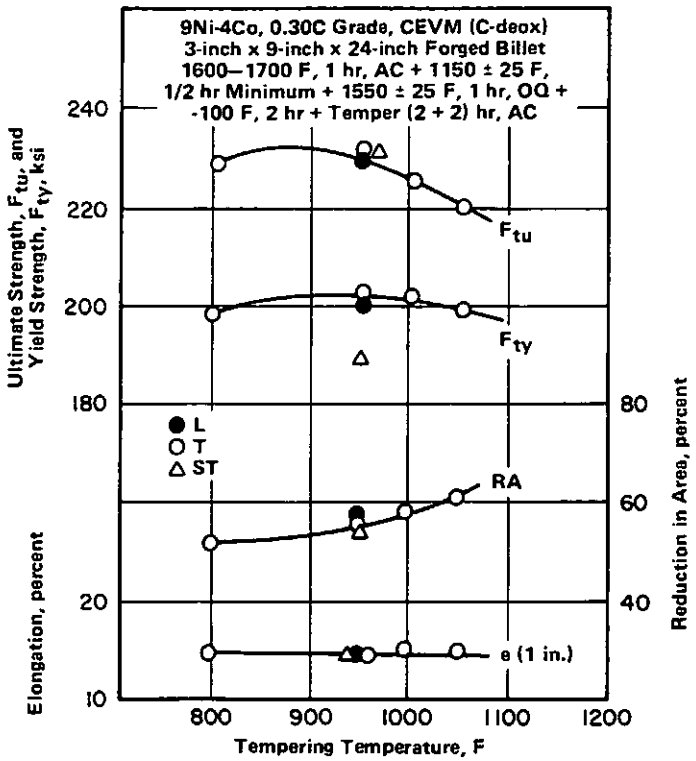


FIGURE 3.02121. EFFECT OF TEMPERING TEMPERATURE ON TENSILE PROPERTIES OF 0.30C GRADE FORGED BILLET (61)

Alloy	9Ni-4Co
Grade	0.30C
Form	Forged Rectangular Bar
Condition	1650 ± 25 F, 1 hr/in., AC + 1550 ± 25 F, 1 hr/in. (1 hr Minimum), OQ or WQ + -100 ± 10 F, 2 hr Minimum + 975 ± 15 F, 2 hr/in. (2 hr Minimum), AC to Approx 125 F + 975 ± 15 F, 2 hr/in. (2 hr Minimum), AC
F_{tu}, ksi	228.0
F_{ty}, ksi	192.5
e, percent	15.0
RA, percent	54.5
E, 10^3 ksi	27.3
K_{Ic}, ksi $\sqrt{in.}$(a)	82.0

(a) Determined with 2.0-inch-thick compact specimens.

TABLE 3.02122. ROOM TEMPERATURE TENSILE PROPERTIES, ELASTIC MODULUS, AND PLANE STRAIN FRACTURE TOUGHNESS OF 0.30C GRADE FORGED RECTANGULAR BAR (55)

Alloy	9Ni-4Co		
Grade	0.30C		
Form	1-inch Hot Rolled Plate		
Condition	Mill Annealed	1650 F, 1 hr, AC + 1550 F, 1 hr, OQ + 1100 F, 6 hr, AC	1650 F, 1 hr, AC + 1550 F, 1 hr, OQ + 950 F, 6 hr, AC
F_{tu}, ksi	162.4	209.5	241.1
F_{ty}, ksi	97.9	179.2	203.1
RA, percent	42	58	50
e, percent	15	15	13
K_{Ic}, ksi $\sqrt{in.}$	(a)	(a)	91

(a) Could not be measured with 1-inch-thick specimen.

TABLE 3.02123. ROOM TEMPERATURE TENSILE PROPERTIES AND PLANE STRAIN FRACTURE TOUGHNESS OF 0.30C GRADE PLATE VARIOUSLY HEAT TREATED (26, 27)

Fe
9 Ni
4 Co
Cr
Mo
V
9Ni-4Co

Alloy	9Ni-4Co					
Grade	0.30C					
Form	Billet[a]					
Condition	Q & T					
Test Specimen Direction/Orientation						
T				TL	TL	LT
F_{tu}, ksi	F_{ty}, ksi	e, percent	RA, percent	IE Charpy V, ft-lb	K_{Ic}, ksi $\sqrt{in.}$	
223–238	190–212	11–17	45–59	19–37	89–129	92–119

(a) Thirty-three billets from 25 heats: billet size ranged from 2-3/4 inch round to 10-1/2 inch square.

TABLE 3.02124. RANGE OF ROOM TEMPERATURE TENSILE PROPERTIES, CHARPY V IMPACT ENERGY, AND PLANE STRAIN FRACTURE TOUGHNESS OF THIRTY-THREE BILLETS FROM TWENTY-FIVE HEATS OF 0.30C GRADE (14)

Alloy	9Ni-4Co	
Grade	0.30C, CEVM (C-deox)	
Form	3-inch x 9-inch x 24-inch Forged Billet	
Condition	1600–1700 F, 1 hr, AC + 1150 ± 25 F, 1/2 hr Minimum + 1550 ± 25 F, 1 hr, OQ + -100 F, 2 hr + 950 ± 25 F (2 + 2) hr, AC	
Strength, ksi[a]	Unexposed	After Exposure[b]
F_{tu}	232	231
F_{ty}	201	201

(a) Transverse direction.
(b) 5,000 hours, 450 F, 40 ksi.

TABLE 3.02125. EFFECT OF ELEVATED TEMPERATURE EXPOSURE UNDER STRESS ON SUBSEQUENT ROOM TEMPERATURE STRENGTH (61)

Alloy	9Ni-4Co
Grade	0.20C
Form	2-1/4-inch x 6-inch x 84-inch Forged Bar
Condition	1650 F, 1 hr, AC + 1500 F, 1 hr, OQ + 1025 F, 6 hr, AC
Test Direction	IE Charpy V, ft-lb
L	73
L	37
L	62
L	63
L	77
T	50
T	54
T	52
T	56
T	54

TABLE 3.0232. ROOM TEMPERATURE CHARPY V IMPACT ENERGY FOR 0.20C GRADE FORGED BAR (20, 21)

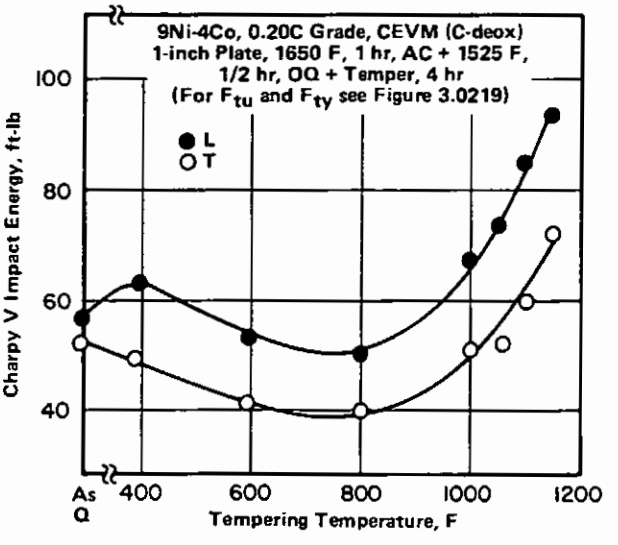


FIGURE 3.0234. EFFECT OF TEMPERING TEMPERATURE ON CHARPY-V IMPACT ENERGY OF 0.20C GRADE PLATE (28, 65)

Fe
9 Ni
4 Co
Cr
Mo
V

9Ni-4Co

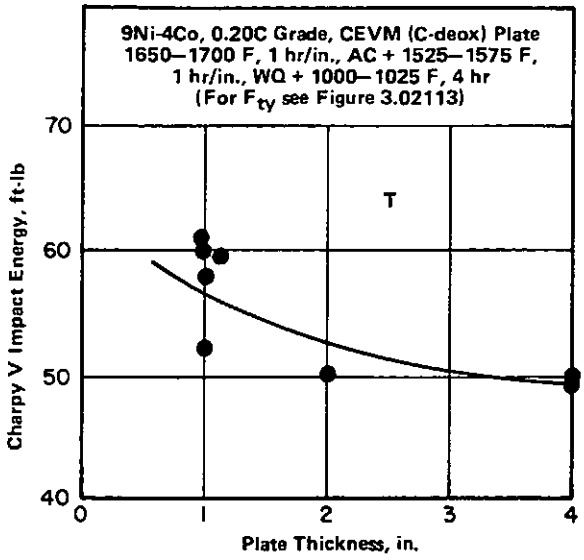


FIGURE 3.0236. EFFECT OF PLATE THICKNESS ON CHARPY V IMPACT ENERGY OF 0.20C GRADE PLATE FROM ONE HEAT (28)

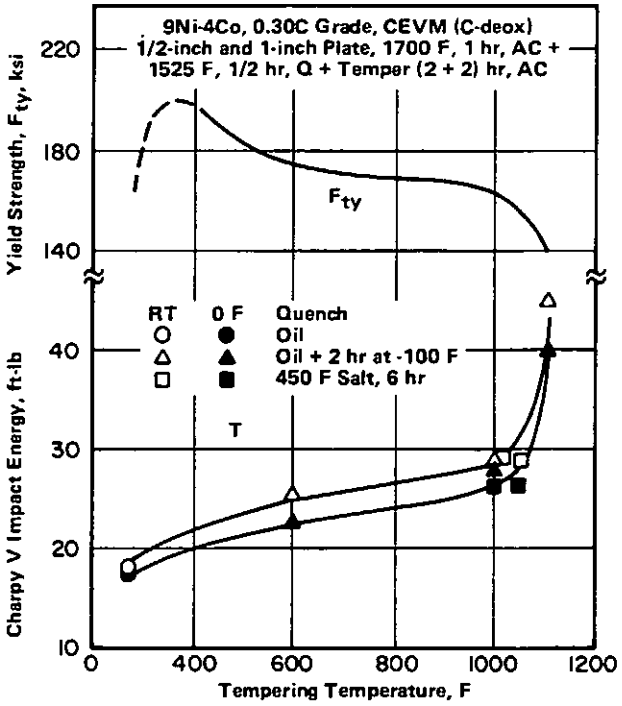


FIGURE 3.0239. EFFECT OF TEMPERING TEMPERATURE ON CHARPY V IMPACT ENERGY OF 0.30C GRADE PLATE VARIOUSLY QUENCHED FROM THE AUSTENITIZING TEMPERATURE (63)

Alloy	9Ni-4Co
Grade	0.20C
Form	2-1/4-inch x 6-inch x 84-inch Forged Bar
Condition	1650 F, 1 hr, AC + 1500 F, 1 hr, OQ + 1025 F, 6 hr, AC
Test Direction	F_{su}, ksi
L	123
L	124
L	124
T	120
T	124
T	123

TABLE 3.0251. ROOM TEMPERATURE SHEAR STRENGTH OF 0.20C GRADE FORGED BAR (20, 21)

Alloy	9Ni-4Co	
Grade	0.20C	
Form	7-inch x 2-inch Forged Billet	
Condition	A, Q + 1025 F Temper	
Heat	F_{ty}, ksi	K_{Ic}, ksi $\sqrt{in.}$(a)
A	184	168
A	183	164
B	188	172
C	185	164
D	192	171

(a) TL orientation.

TABLE 3.02723. PLANE STRAIN FRACTURE TOUGHNESS OF 0.20C GRADE FORGED BILLET (13)

Fe
9 Ni
4 Co
Cr
Mo
V

9Ni-4Co

Alloy	9Ni-4Co				
Grade	0.20C				
Form	5-inch x 8-inch x 8-inch Hand Forging (Procurement Specification: LB0160-180)				
Condition	1650 F, 2 hr, AC + 1525 F, 2 hr, OQ + 2 hr at -100 F + 1025 F, 4 hr, AC				
Final Forging Temperature, F	Compact Specimen Dimensions, inch B	W	Specimen Orientation	F_{ty}, ksi	K_{Ic}, ksi $\sqrt{in.}$
1700	2.0	5.0	LT	198	121, 130
1800	2.0	5.0	LT	198	115
1900	2.0	5.0	LT	198	123, 126

TABLE 3.02724. EFFECT OF FINAL FORGING TEMPERATURE ON ROOM TEMPERATURE PLANE STRAIN FRACTURE TOUGHNESS OF 0.20C GRADE HAND FORGINGS (47)

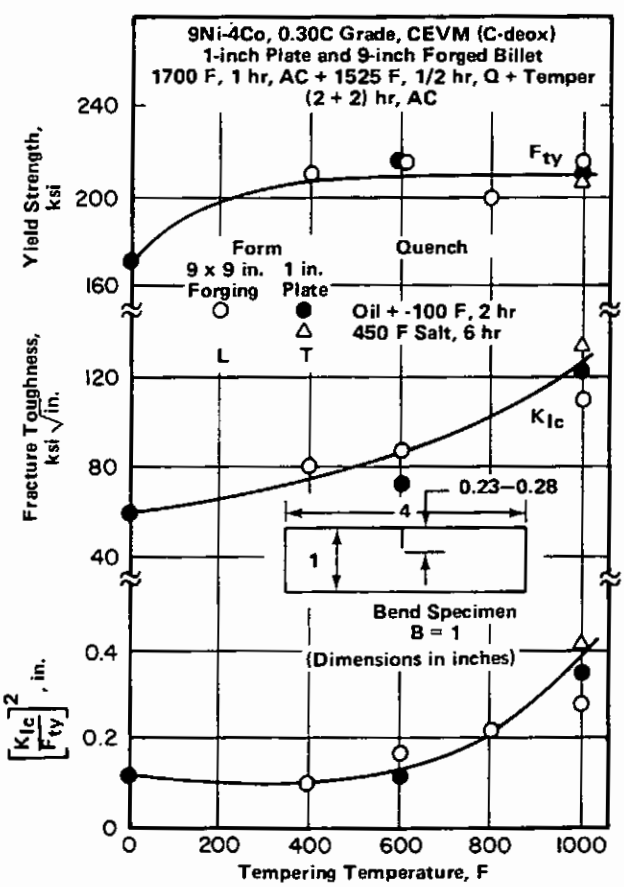


FIGURE 3.02727. EFFECT OF TEMPERING TEMPERATURE ON PLANE STRAIN FRACTURE TOUGHNESS OF 0.30C GRADE PLATE AND FORGED BILLET (63)

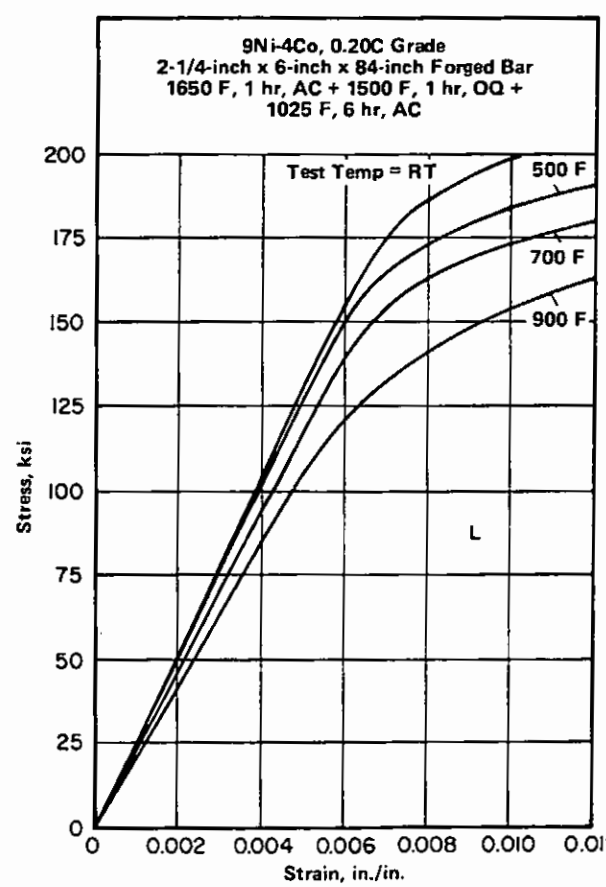


FIGURE 3.0311. TYPICAL LONGITUDINAL TENSION STRESS/STRAIN CURVES AT ROOM AND ELEVATED TEMPERATURES FOR 0.20C GRADE FORGED BAR (20, 21)

Fe
9 Ni
4 Co
Cr
Mo
V

9Ni-4Co

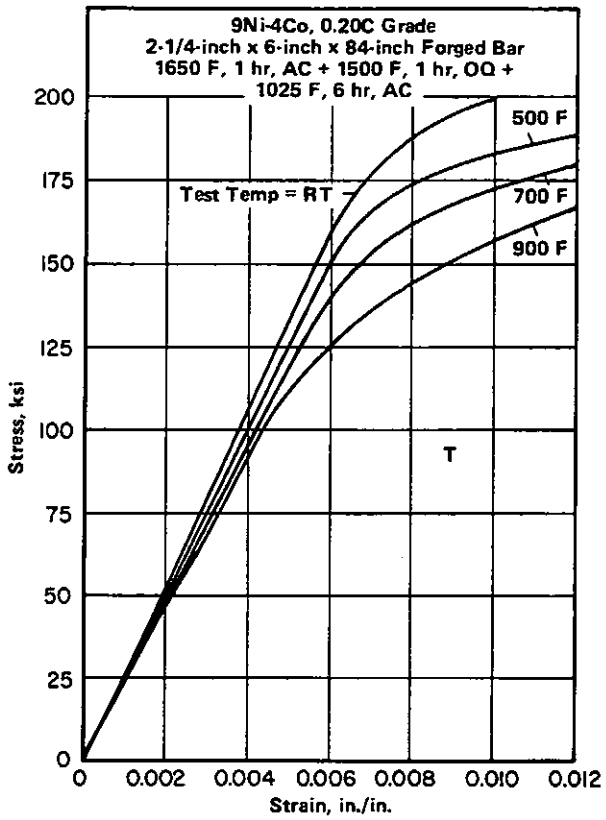


FIGURE 3.0312. TYPICAL TRANSVERSE TENSION STRESS/STRAIN CURVES AT ROOM AND ELEVATED TEMPERATURES FOR 0.20C GRADE FORGED BAR (20, 21)

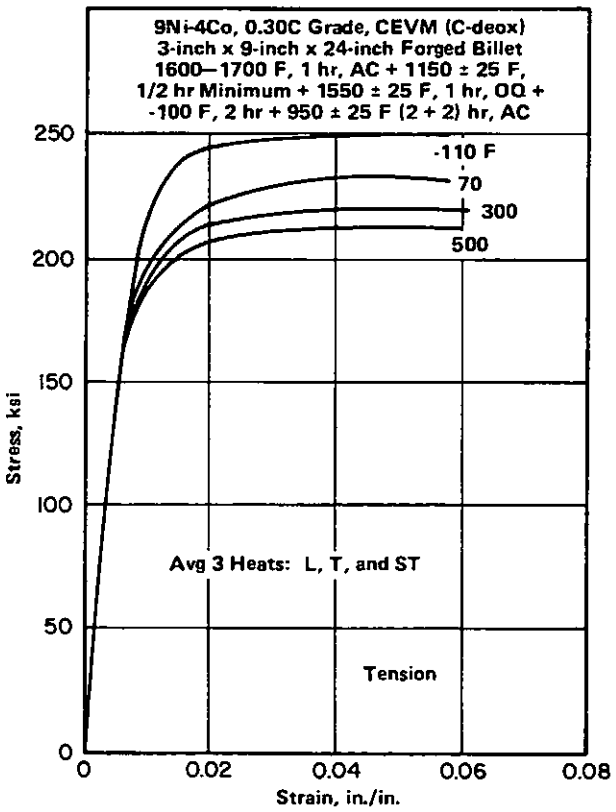


FIGURE 3.0313. TENSILE STRESS/STRAIN CURVES AT VARIOUS TEMPERATURES FOR 0.30C GRADE FORGED BILLET (61)

Fe
9 Ni
4 Co
Cr
Mo
V

9Ni-4Co

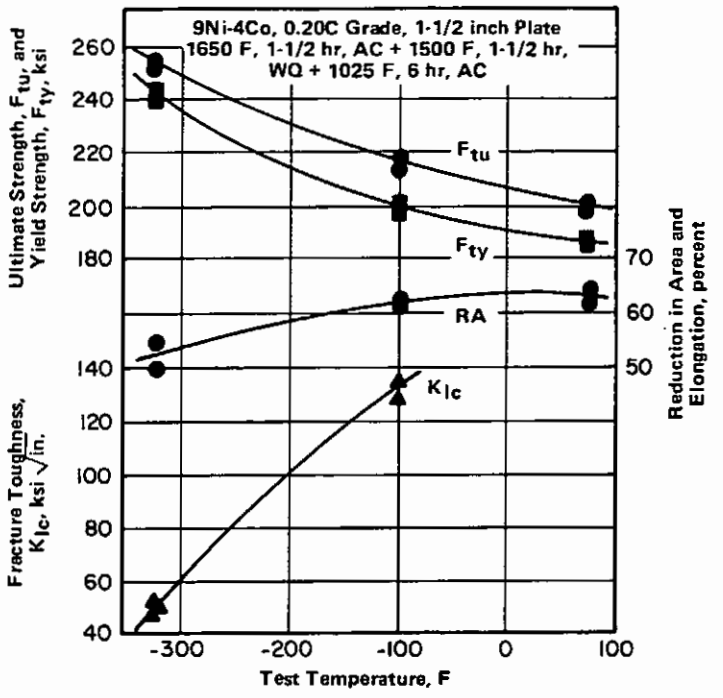


FIGURE 3.0314. EFFECT OF TEST TEMPERATURE ON TENSILE PROPERTIES AND PLANE STRAIN FRACTURE TOUGHNESS OF 0.20C GRADE PLATE (78)

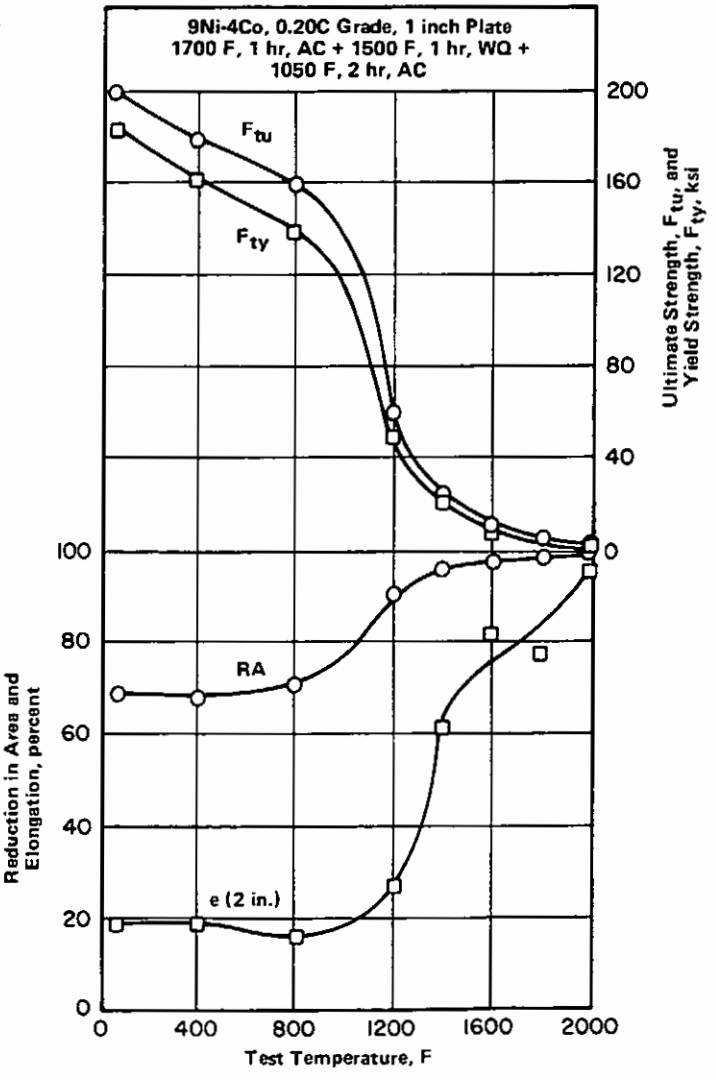


FIGURE 3.0315. ELEVATED TEMPERATURE TENSILE PROPERTIES OF 0.20C GRADE PLATE (28)

Fe
9 Ni
4 Co
Cr
Mo
V
9Ni-4Co

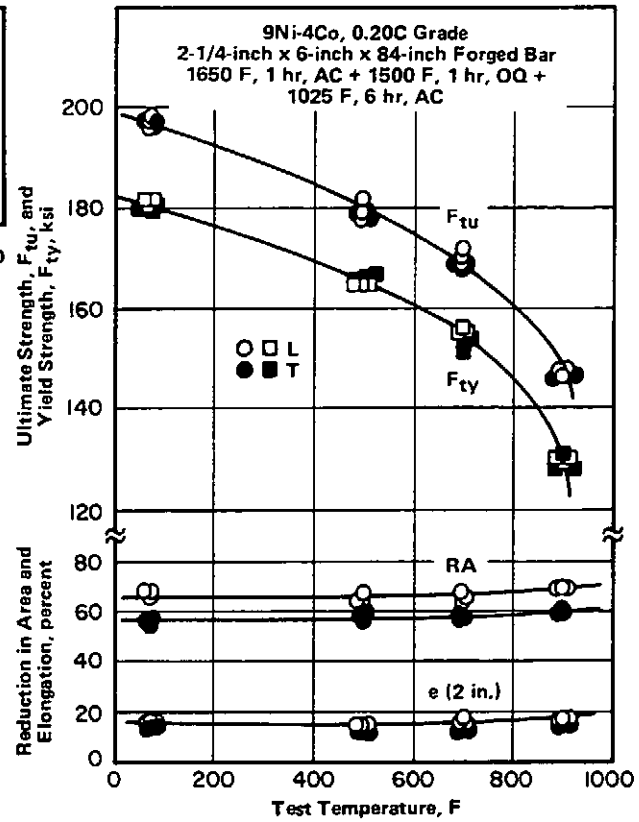


FIGURE 3.0316. EFFECT OF TEST TEMPERATURE ON TENSILE PROPERTIES OF 0.20C GRADE FORGED BAR (20, 21)

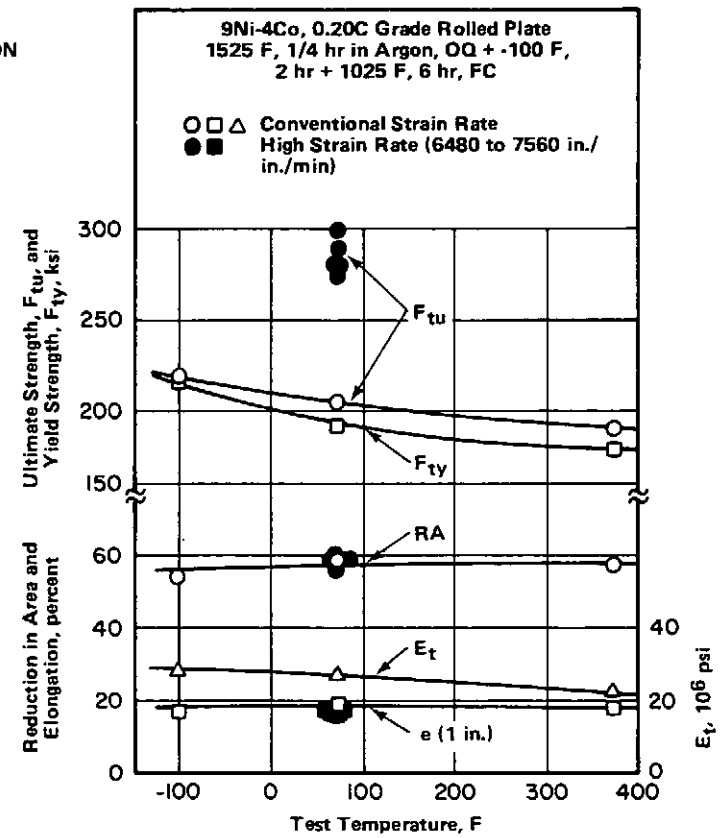


FIGURE 3.0317. EFFECT OF TEST TEMPERATURE ON TENSILE PROPERTIES OF 0.20C GRADE ROLLED PLATE MEASURED AT CONVENTIONAL AND HIGH STRAIN RATES (52)

Fe
9 Ni
4 Co
Cr
Mo
V

9Ni-4Co

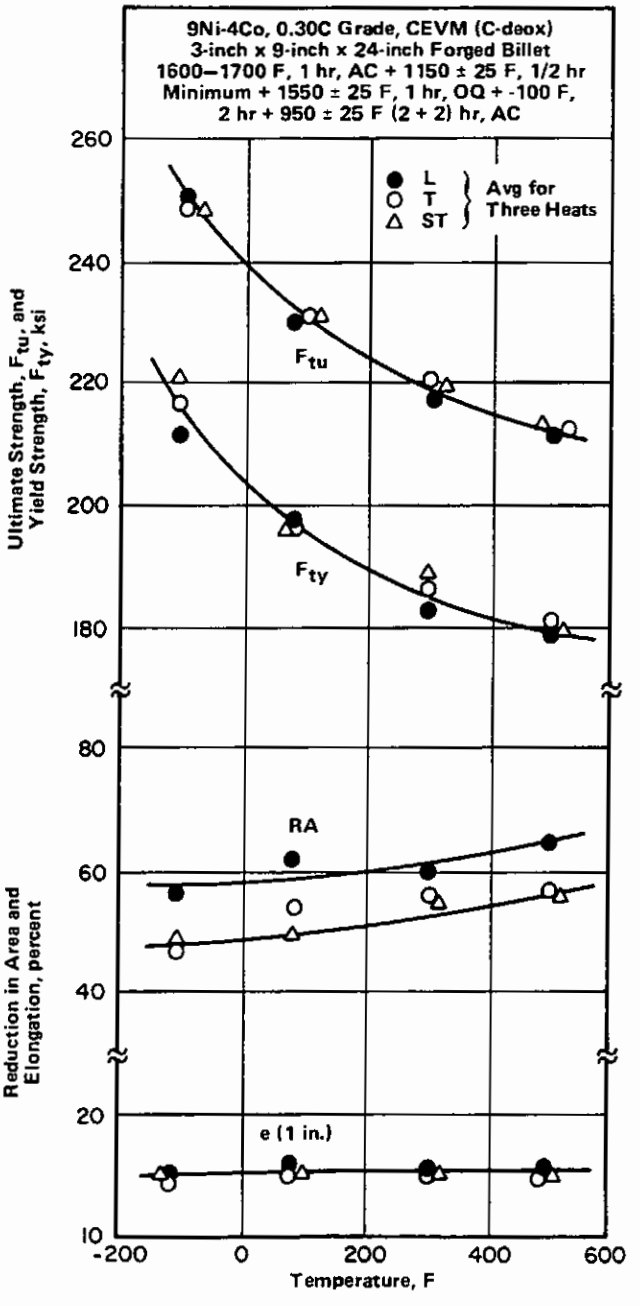


FIGURE 3.0318. EFFECT OF TEST TEMPERATURE ON TENSILE PROPERTIES OF 0.30C GRADE FORGED BILLET (61)

Fe
9 Ni
4 Co
Cr
Mo
V

9Ni-4Co

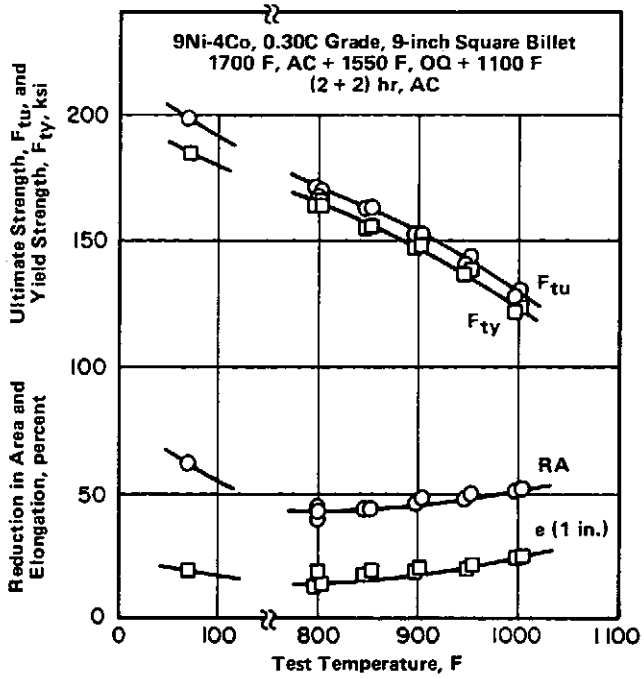


FIGURE 3.0319. EFFECT OF TEST TEMPERATURE ON TENSILE PROPERTIES OF 0.30C GRADE BILLET (14)

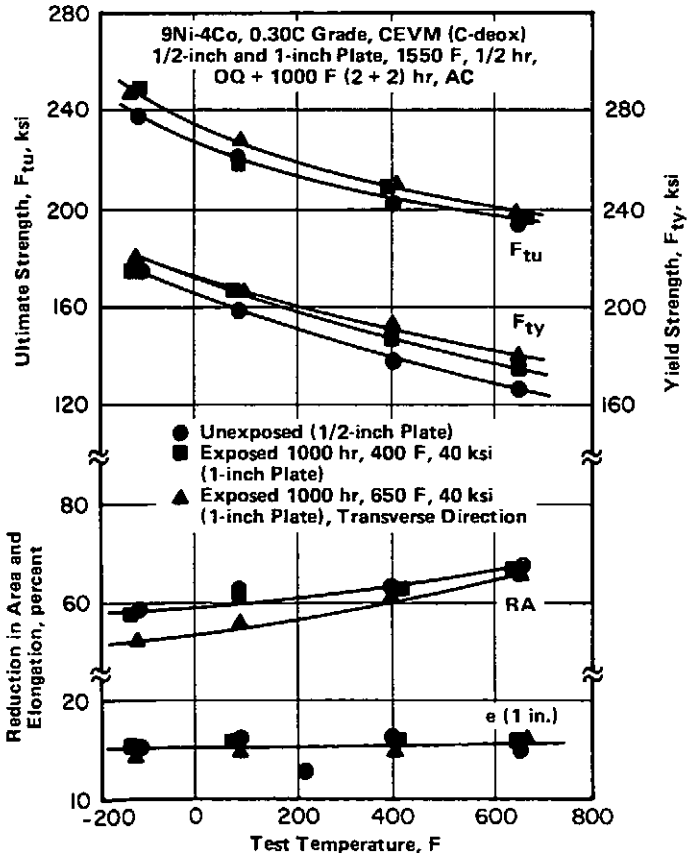


FIGURE 3.03110. EFFECT OF TEST TEMPERATURE AND ELEVATED TEMPERATURE EXPOSURE UNDER STRESS ON TENSILE PROPERTIES OF 0.30C GRADE PLATE (63)

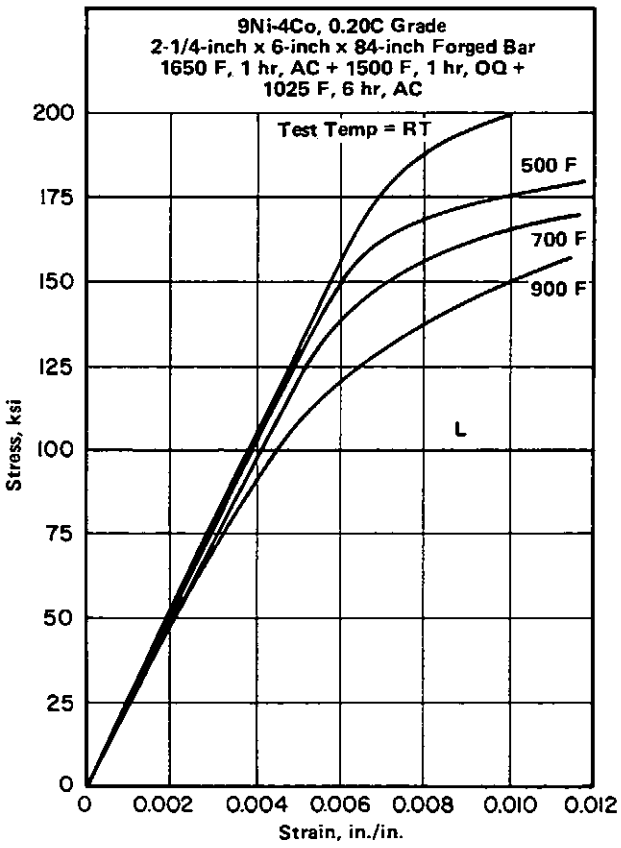


FIGURE 3.0321. TYPICAL LONGITUDINAL COMPRESSIVE STRESS/STRAIN CURVES AT ROOM AND ELEVATED TEMPERATURES FOR 0.20C GRADE FORGED BARS (20, 21)

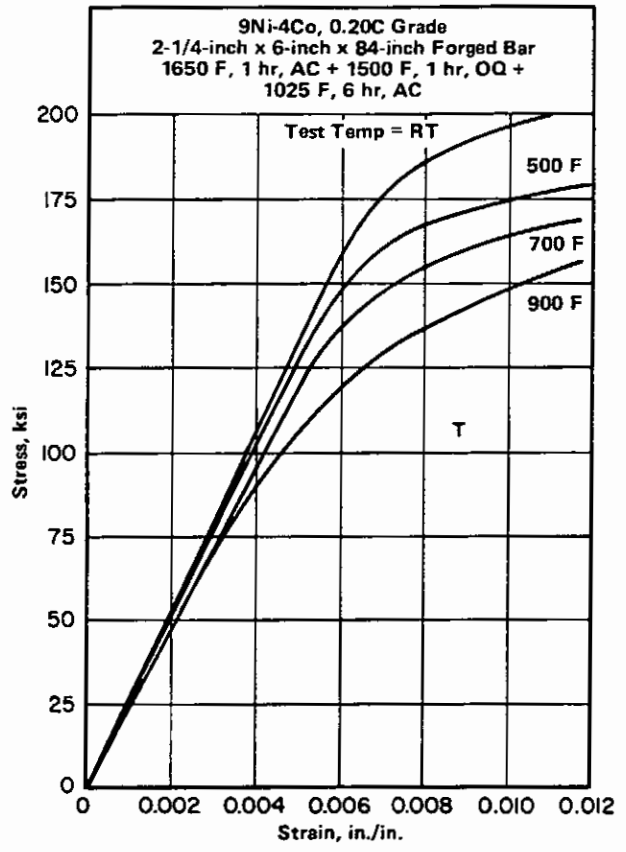


FIGURE 3.0322. TYPICAL TRANSVERSE COMPRESSIVE STRESS/STRAIN CURVES AT ROOM AND ELEVATED TEMPERATURES FOR 0.20C GRADE FORGED BARS (20, 21)

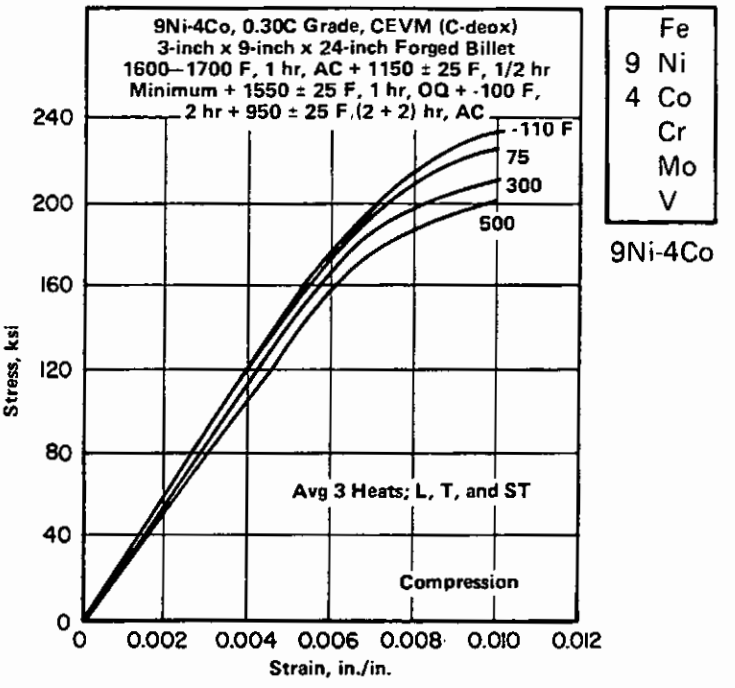


FIGURE 3.0323. COMPRESSIVE STRESS/STRAIN CURVES AT VARIOUS TEMPERATURES FOR 0.30C GRADE FORGED BILLET (61)

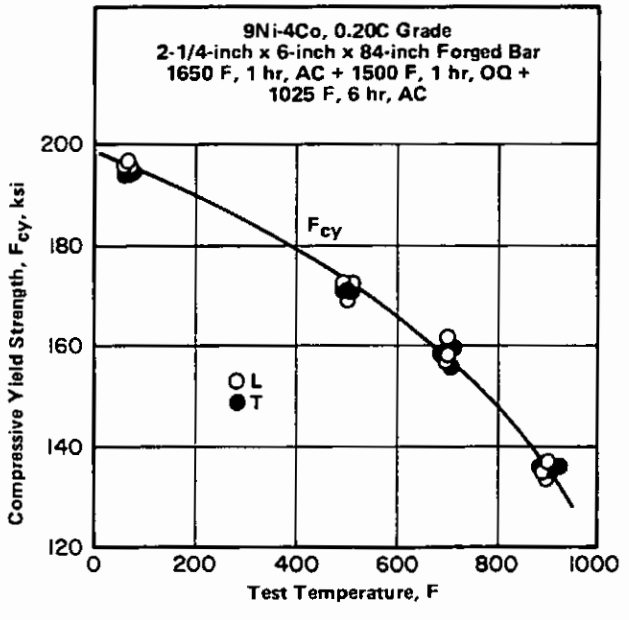


FIGURE 3.0324. EFFECT OF TEST TEMPERATURE ON COMPRESSIVE YIELD STRENGTH OF 0.20C GRADE FORGED BAR (20, 21)

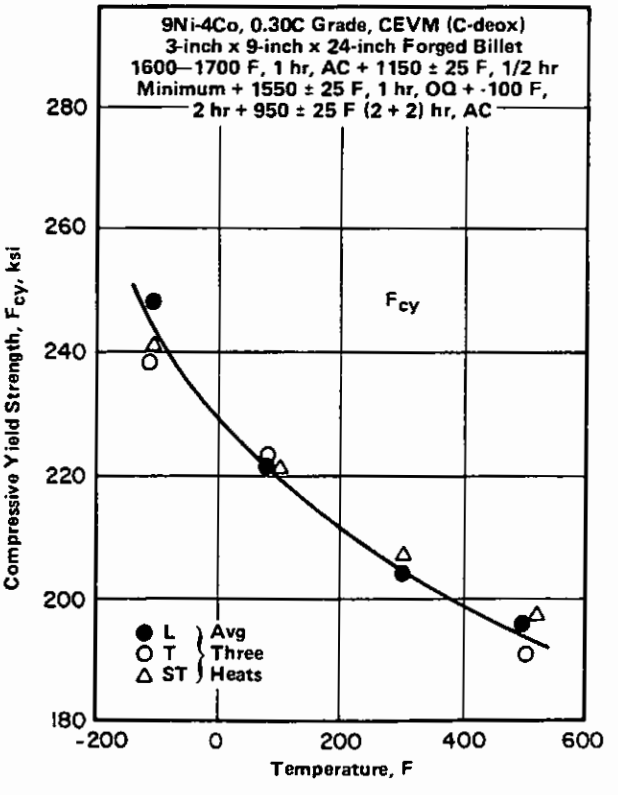


FIGURE 3.0325. EFFECT OF TEST TEMPERATURE ON COMPRESSIVE YIELD STRENGTH OF 0.30C GRADE FORGED BILLET (61)

Fe
9 Ni
4 Co
Cr
Mo
V
9Ni-4Co

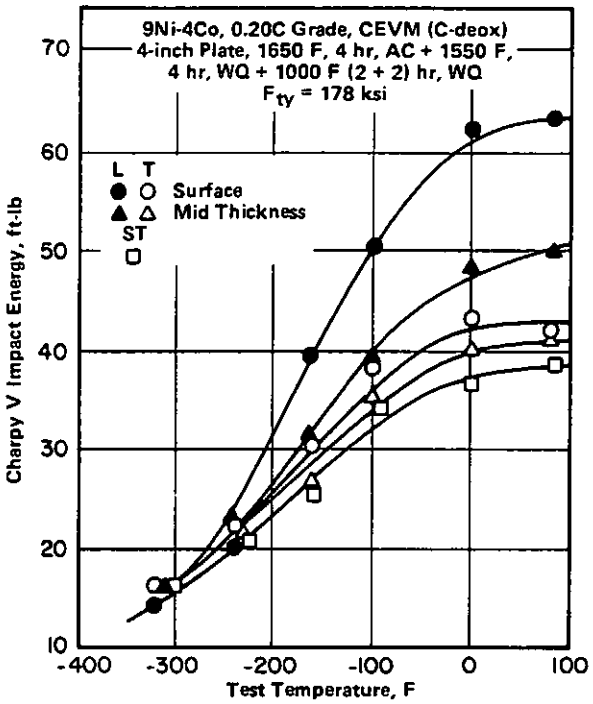


FIGURE 3.0331. EFFECT OF TEST TEMPERATURE ON CHARPY V IMPACT ENERGY OF 0.20C GRADE PLATE (31)

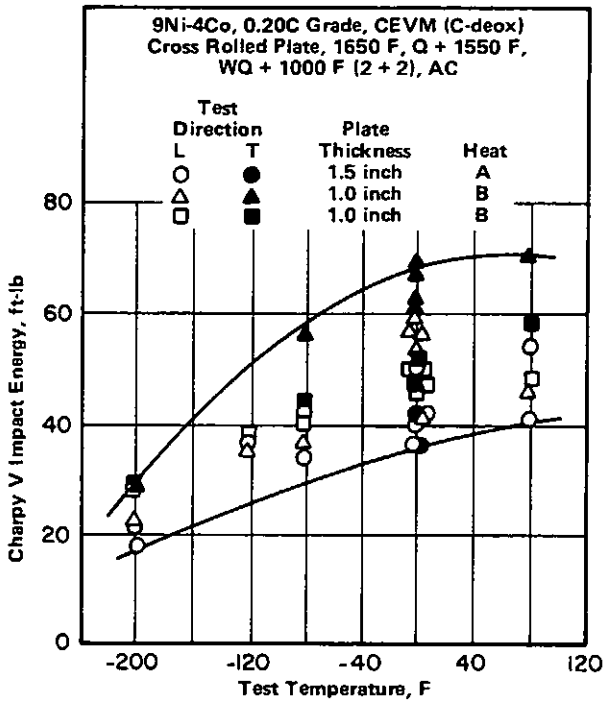


FIGURE 3.0332. RANGE OF CHARPY V IMPACT ENERGY AS FUNCTION OF TEST TEMPERATURE FOR THREE PLATES FROM TWO HEATS OF 0.20C GRADE WITH CLOSELY MATCHING COMPOSITIONS (32)

Alloy	9Ni-4Co			
Grade	0.20C, CEVM (C-deox)			
Form	1-inch Plate			
Condition	1700 F, 1 hr, AC + 1500 F, 1 hr, WQ + 1000 F (2 + 2) hr		1500 F, 1 hr, WQ + 1000 F (2 + 2) hr	
Direction	L	T	L	T
Charpy V, ft-lb				
80 F	56	55	53	52
0 F	54	54	49	47
-80 F	45	43	40	40

TABLE 3.0334. CHARPY V IMPACT ENERGY AT VARIOUS TEMPERATURES FOR 0.20C GRADE PLATE QUENCHED AND TEMPERED WITH AND WITHOUT PRIOR NORMALIZING (28)

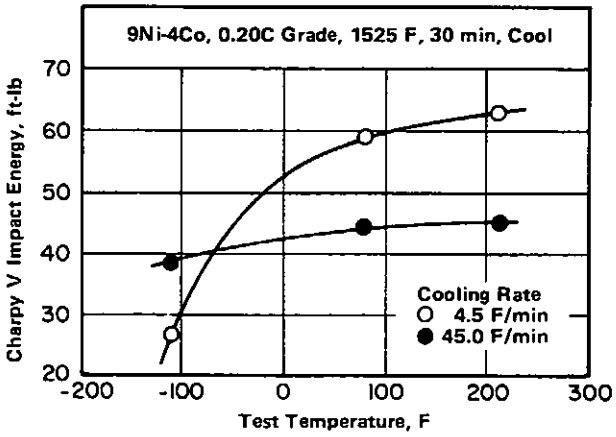


FIGURE 3.0335. EFFECT OF TEST TEMPERATURE ON CHARPY V IMPACT ENERGY FOR 0.20C GRADE AFTER COOLING WITHIN THE BAINITIC RANGE FROM THE AUSTENITIZING TREATMENT (25)

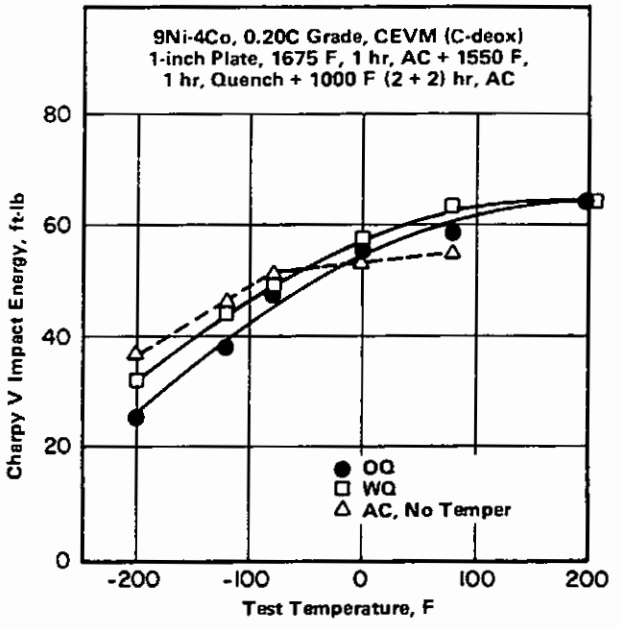


FIGURE 3.0336. EFFECT OF TEST TEMPERATURE ON CHARPY V IMPACT ENERGY OF 0.20C GRADE PLATE VARIOUSLY QUENCHED FROM THE AUSTENITIZING TEMPERATURE (32)

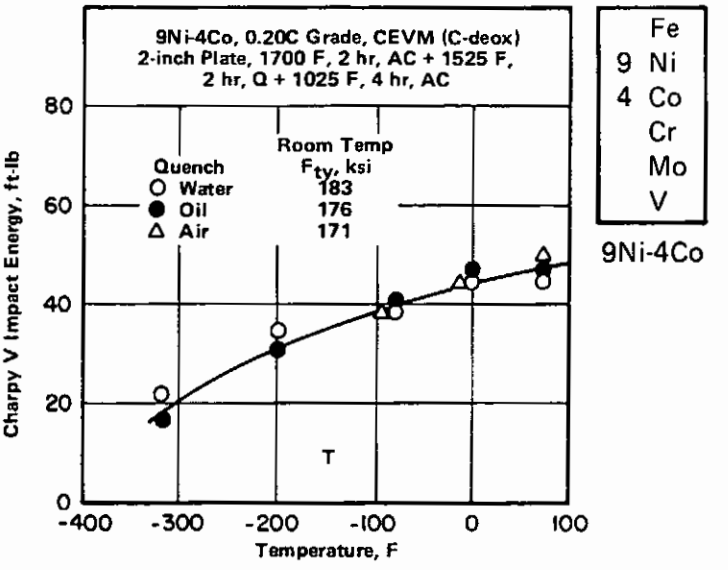


FIGURE 3.0337. EFFECT OF TEST TEMPERATURE ON CHARPY V IMPACT ENERGY OF 0.20C GRADE PLATE QUENCHED IN VARIOUS MEDIA (28)

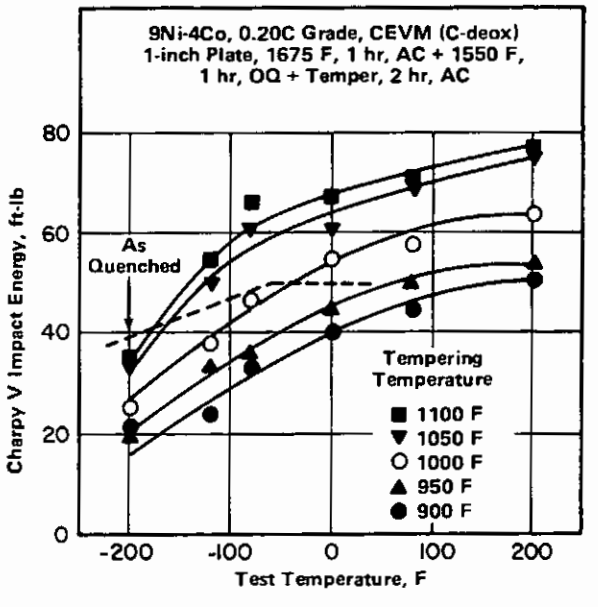


FIGURE 3.0338. EFFECT OF TEST TEMPERATURE ON THE CHARPY V IMPACT ENERGY OF 0.20C GRADE PLATE TEMPERED AT VARIOUS TEMPERATURES (32)

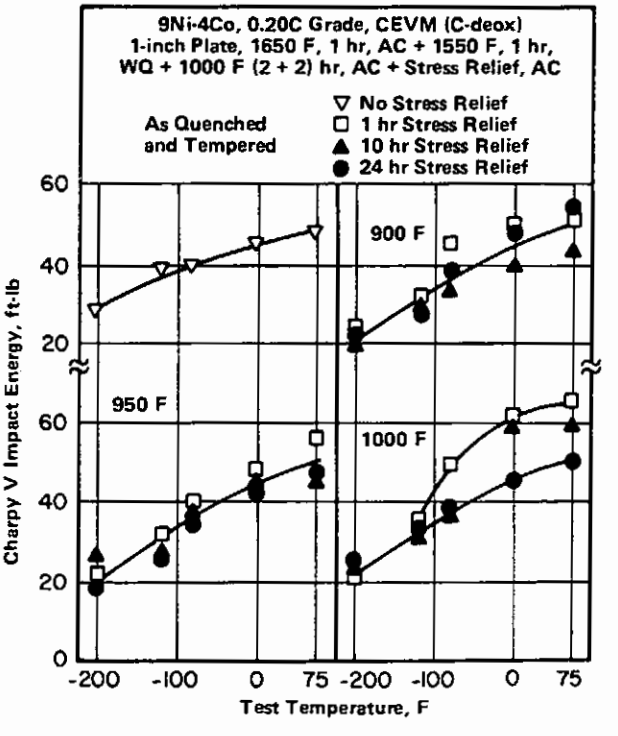


FIGURE 3.03311. EFFECT OF TEST TEMPERATURE ON THE CHARPY V IMPACT ENERGY OF 0.20C GRADE PLATE VARIOUSLY STRESS RELIEVED (36)

Fe
9 Ni
4 Co
Cr
Mo
V
9Ni-4Co

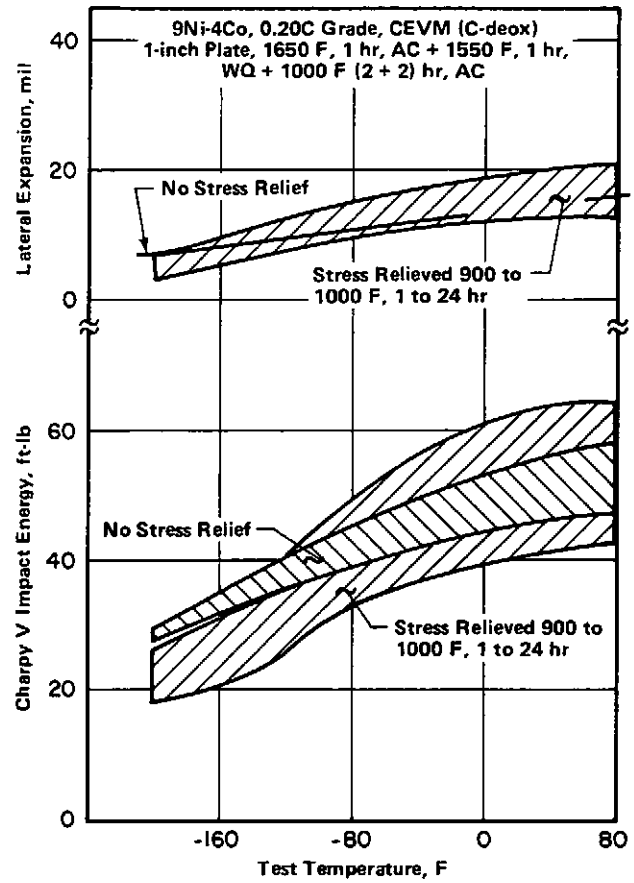


FIGURE 3.03312. EFFECT OF TEST TEMPERATURE ON CHARPY V IMPACT ENERGY AND LATERAL EXPANSION OF 0.20C GRADE PLATE WITH AND WITHOUT STRESS RELIEF TREATMENT (32)

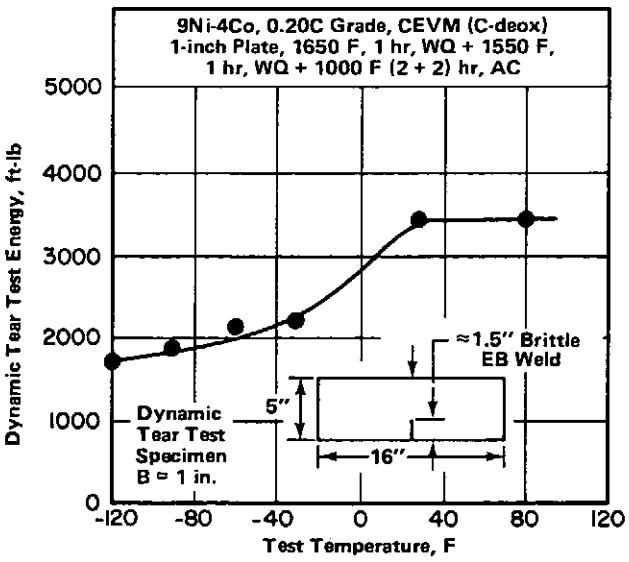


FIGURE 3.03313. EFFECT OF TEST TEMPERATURE ON DYNAMIC TEAR TEST ENERGY OF 0.20C GRADE CROSS ROLLED PLATE (76)

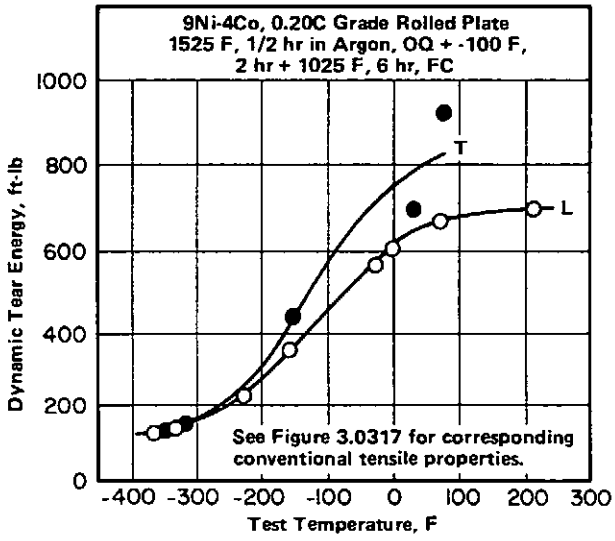


FIGURE 3.03314. EFFECT OF TEST TEMPERATURE ON DYNAMIC TEAR ENERGY OF 0.20C GRADE ROLLED PLATE (52)

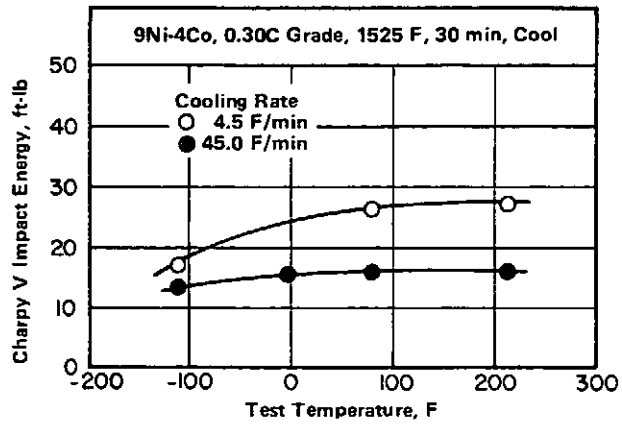


FIGURE 3.03315. EFFECT OF TEST TEMPERATURE ON CHARPY V IMPACT ENERGY FOR 0.30C GRADE AFTER COOLING WITHIN THE BAINITIC RANGE FROM THE AUSTENITIZING TREATMENT (25)

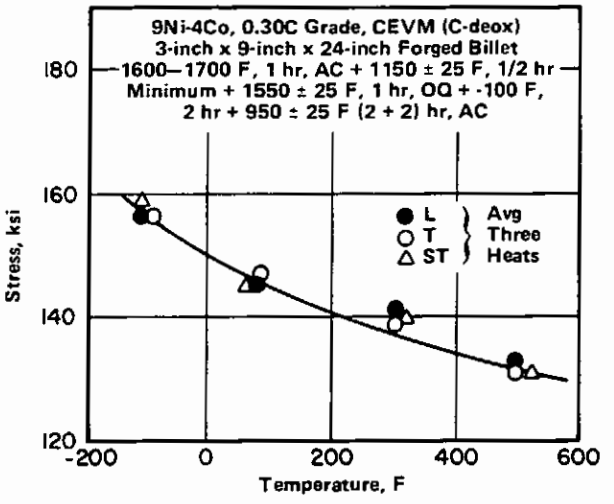
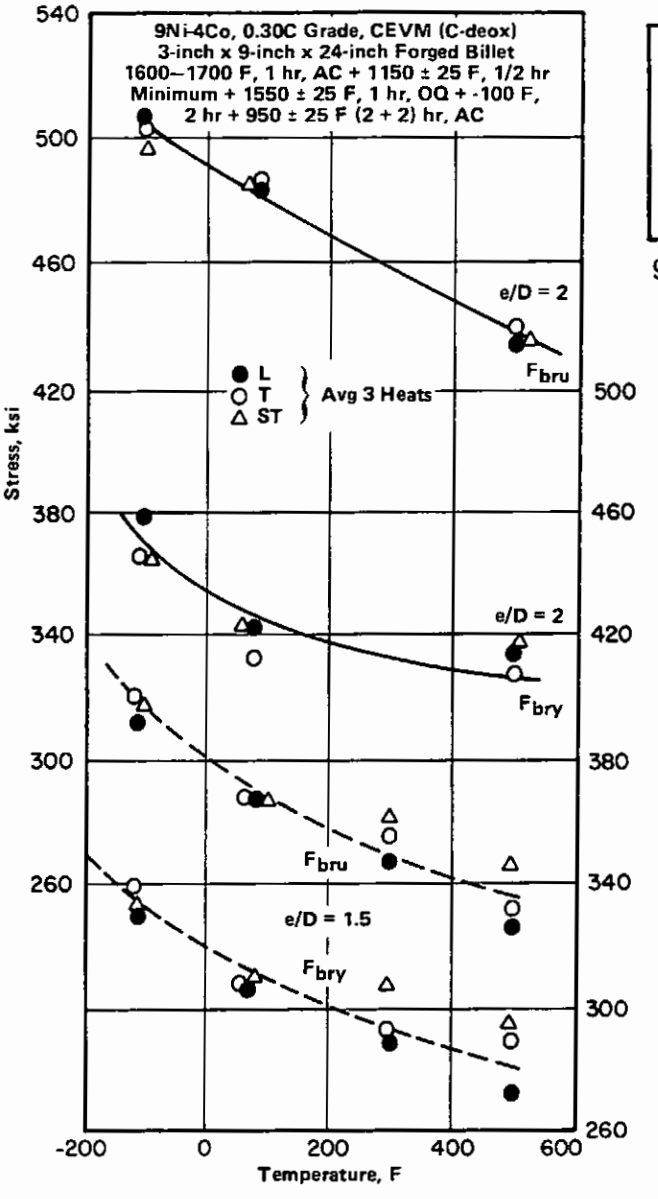


FIGURE 3.0351. EFFECT OF TEST TEMPERATURE ON SHEAR STRENGTH OF 0.30C GRADE FORGED BILLET (61)



Fe
9 Ni
4 Co
Cr
Mo
V
9Ni-4Co

FIGURE 3.0361. EFFECT OF TEST TEMPERATURE ON BEARING STRENGTH OF 0.30C GRADE FORGED BILLET (61)

Alloy	9Ni-4Co		
Grade	0.30C, CEVM (C-deox)		
Form	3-inch x 9-inch x 24-inch Forged Billet		
Condition	1600–1700 F, 1 hr, AC + 1150 ± 25 F, 1/2 hr Minimum + 1550 ± 25 F, 1 hr, OQ + -100 F, 2 hr + 950 ± 25 F (2 + 2) hr, AC		
Test Temperature, F	K_t	NTS, ksi(a)	F_{tu}, ksi(a)
RT	3	353	231
RT	3	355	231
RT	5	338	231
-110	5	358	245
-110	5	351	245

(a) Transverse direction.

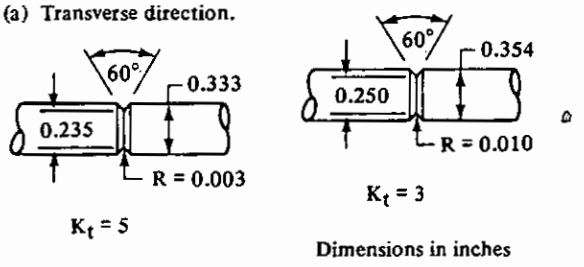


TABLE 3.03711. MILD NOTCH STRENGTH OF 0.30C GRADE FORGED BILLET AT ROOM TEMPERATURE AND -110 F (61)

Fe
9 Ni
4 Co
Cr
Mo
V

9Ni-4Co

Alloy	9Ni-4Co						
Grade	0.20C						
Form (Procurement Specification)	Condition	Compact Specimen Dimensions, inch B	Compact Specimen Dimensions, inch W	Test Temperature, F	Specimen Orientation	F_{ty}, ksi	K_{Ic}, ksi $\sqrt{in.}$
3-inch x 10-inch x 36-inch Forged Billet (AMD-65-CD)	1650–1700 F, 1–2 hr, AC + 1500–1550 F, 1–2 hr, OQ or WQ + -100 F, 2 hr + 1000 F, 4–5 hr, AC	2.0	6.0	RT	LT	180	132, 133, 139
		2.0	5.7	RT	TL	180	102
	1650–1700 F, 1–2 hr, AC + 1500–1550 F, 1–2 hr, WQ + Overnight Delay + 1025 F, 6 hr, AC	2.0	6.0	RT	LT	183	160
	1650–1700 F, 1–2 hr, AC + 1500–1550 F, 1–2 hr, WQ + -100 F, 2 hr + 1025 F, 6 hr, AC	2.0	6.0	RT	LT	185	159
	1650–1700 F, 1–2 hr, AC + 1500–1550 F, 1–2 hr, WQ + Overnight Delay + 1050 F, 4 hr, AC	2.0	6.0	RT	LT	180	165
	1650–1700 F, 1–2 hr, AC + 1500–1550 F, 1–2 hr, OQ + -100 F, 2 hr + 1050 F, 4 hr, AC	2.0	6.0	RT	LT	182	155
4-inch x 18-inch x 36-inch Forged Billet (AMD-65-CD)	1650 F, 1–2 hr, AC + 1525 F, 1–2 hr, OQ + -100 F, 1–2 hr + 1025 F, 4–6 hr, AC	2.0	6.0	RT	LT	188	151, 158, 164
		2.0	6.0	RT	TL	188	144, 146, 146
	1650 F, 1–2 hr, AC + 1525 F, 1–2 hr, AC + -100 F, 1–2 hr + 1025 F, 6 hr, AC	2.0	6.0	RT	LT	195	133
2.5-inch Rolled Plate (ST0160LB0001)	1650 F, 1–2 hr, AC + 1525 F, 1–2 hr, OQ + -100 F, 2 hr + 1025 F, 5 hr, AC	2.0	6.0	RT	LT	189	101, 142
		2.0	6.0	-65 F	LT	200	90, 91, 105
		2.0	6.0	-65 F	TL	200	92, 96, 104
	1650 F, 1–2 hr, AC + 1525 F, 1–2 hr, AC + -100 F, 1-1/2 hr + 1025 F, 4 hr, AC + 1060 F, 6 hr, AC	2.0	6.0	RT	LT	189	115, 132
		2.0	6.0	RT	TL	189	128
	1650 F, 1–2 hr, AC + 1525 F, 1–2 hr, AC + -130 F, 1-1/2 hr + 1025–1075 F, 4 hr, AC	2.0	6.0	RT	TL	186	116
Spindle Forging Core (ST0160LB0002)	1650 F, 2 hr, AC + 1525 F, 2 hr, OQ + -100 F, 2 hr + 1025 F, 4 hr, AC	1.5–1.6	4.0	RT	LT	194	135, 141, 142
		1.5	4.0	RT	TL	190	126
4-inch x 18-inch x 36-inch Forged Billet (ST0160LB0002)	1650 F, 2 hr, AC + 1525 F, 2 hr, OQ + -100 F, 2 hr + 1025 F, 4 hr, AC	2.0	6.0	RT	LT	186	136, 136, 138, 138, 140, 143
		1.6	8.0	RT	LT	186	144, 144
		2.0	6.0	RT	TL	186	121, 126, 127, 127, 127
		1.6	3.0	RT	ST	189	114, 116

TABLE 3.03721. PLANE STRAIN FRACTURE TOUGHNESS AT ROOM TEMPERATURE AND -65 F FOR 0.20C GRADE IN A VARIETY OF PRODUCT FORMS, EACH FROM A SEPARATE HEAT AND VARIOUSLY HEAT TREATED (47)

Fe
9 Ni
4 Co
Cr
Mo
V
9Ni-4Co

Alloy	9Ni-4Co						
Grade	0.20C						
Form (Procurement Specification)	Condition	Compact Specimen Dimensions, inch B	Compact Specimen Dimensions, inch W	Test Temperature, F	Specimen Orientation	F_{ty}, ksi	K_{Ic}, ksi $\sqrt{in.}$
3.7-inch x 7.7-inch x 96-inch Forged Billet (ST0160LB0002)	1650 F, 2 hr, AC + 1525 F, 2 hr, OQ + -100 F, 2 hr + 1025 F, 4 hr, AC	2.0	6.0	RT	LT	179	135
		2.0	6.0	RT	TL	179	120, 121, 133
		1.5	6.0	-65 F	LT	188	127
	1650 F, 2 hr, AC + 1525 F, 2 hr, AC + -100 F, 2 hr + 1025 F, 4 hr, AC	2.0	6.0	RT	TL	176	152
		2.0	6.0	-65 F	LT	185	163
		2.0	6.0	-65 F	TL	185	132
4-inch x 18-inch x 36-inch Forged Billet (ST0160LB0002)	1650 F, 1-1/2 hr, AC + 1525 F, 1-1/2 hr, AC + -100 F, 1-1/2 hr + 1025 F, 4 hr, AC	1.75	6.0	RT	LT	180	121, 122
		1.75	6.0	RT	TL	180	107, 108
	1650 F, 1-1/2 hr, AC + 1525 F, 1-1/2 hr, OQ + -100 F, 1-1/2 hr + 1025 F, 4 hr, AC	1.75	6.0	RT	LT	187	121, 131
		1.75	6.0	RT	TL	187	114
	1650 F, 1-1/2 hr, AC + 1525 F, 1-1/2 hr, OQ + -100 F, 1-1/2 hr + 1025 F, 12 hr, AC	1.6	6.0	RT	LT	185	123, 128
	1700 F, 4-1/2 hr, AC + 1700 F, 1-1/2 hr, AC + -100 F, 1-1/2 hr + 1025 F, 4 hr, AC	1.6	6.0	RT	LT	186	140, 141
	1650 F, 4-1/2 hr, AC to 900 F, 1/2 hr, AC + -100 F, 1-1/2 hr + 1025 F, 8 hr, Ausbay Quench	1.6	6.0	RT	LT	185	128, 129
Spindle Forging (ST0160LB0002)	1650 F, 2 hr, AC + 1525 F, 2 hr, AC + -100 F, 2 hr + 1025 F, 4 hr, AC	2.0	6.0	RT	LT	182	141, 143, 147
		2.0	6.0	RT	TL	182	116
1-1/2-inch Rolled Plate (ST0160LB0001)	1650 F, 2 hr, AC + 1525 F, 2 hr, AC + -100 F, 2 hr + 1025 F, 4 hr, AC	1.5	6.0	RT	LT	185	132
	1650 F, 2 hr, AC + 1525 F, 2 hr, OQ + -100 F, 2 hr + 1025 F, 4 hr, AC	1.5	6.0	RT	LT	185	99

TABLE 3.03721. (CONTINUED)

Fe
9 Ni
4 Co
Cr
Mo
V

9Ni-4Co

Alloy	9Ni-4Co						
Grade	0.30C						
Form (Procurement Specification)	Condition	Compact Specimen Dimensions, inch B	Compact Specimen Dimensions, inch W	Test Temperature, F	Specimen Orientation	F_{ty}, ksi	K_{Ic}, ksi $\sqrt{in.}$
3-inch x 18-inch x 36-inch Forged Block (AMD-65-CE)	1650–1700 F, 1–2 hr, AC + 1525 F, 1–2 hr, OQ + -100 F, 2 hr + 1000 F, 4–5 hr, AC	1.0 1.0 1.0	3.0 3.0 3.0	RT RT -65 F	LT TL LT	215 215 –	81, 81, 83 85, 89, 92 66, 67
	1650–1700 F, 1–2 hr, AC + 1525 F, 1–2 hr, OQ + -100 F, 2 hr + 1025 F, 6 hr, AC	1.0 1.0	3.0 3.0	RT RT	LT TL	215 215	91, 92, 92 83, 84, 86
	1650–1700 F, 1–2 hr, AC + 1525 F, 1–2 hr, OQ + -100 F, 2 hr + 1050 F, 4 hr, AC	1.0 1.0	3.0 3.0	RT RT	LT TL	197 197	87, 94, 96 81, 87, 88
3-inch x 18-inch x 36-inch Forged Block (AMD-65-CE)	1650 F, 1–2 hr, AC + 1525–1550 F, 1–2 hr, AC + -100 F, 1–3 hr + 1000 F, 4 hr, AC	1.0 1.0	3.0 3.0	RT RT	LT TL	206 206	105, 107 86
	1650 F, 1–2 hr, AC + 1525–1550 F, 1–2 hr, OQ + -100 F, 1–3 hr + 1025 F (2 + 2) hr, AC	1.0 1.0	3.0 3.0	RT RT	LT TL	205 205	116 93, 94
	1650 F, 1–2 hr, AC + 1525–1550 F, 1–2 hr, AC + -100 F, 1–3 hr + 1050 F, 4 hr, AC	1.0 1.0	3.0 3.0	RT RT	LT TL	197 197	123, 124 102

TABLE 3.03722. PLANE STRAIN FRACTURE TOUGHNESS AT ROOM TEMPERATURE AND -65 F OF 0.30C GRADE FORGED BLOCKS VARIOUSLY HEAT TREATED (47)

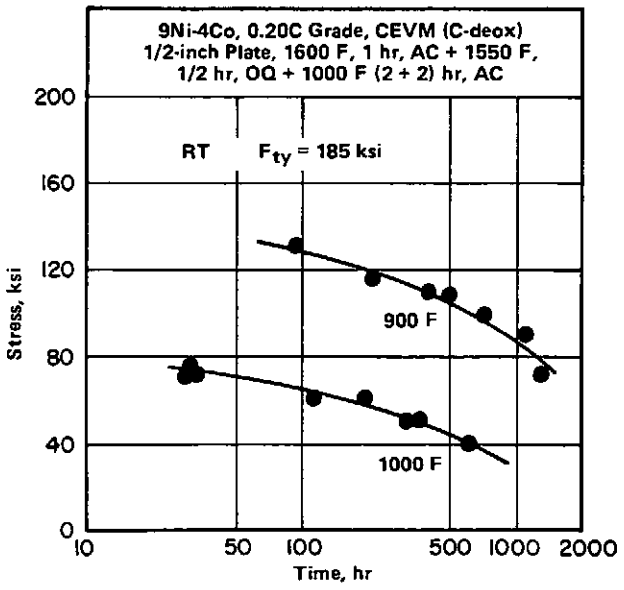


FIGURE 3.041. CREEP RUPTURE CURVES FOR 0.20C GRADE PLATE (28)

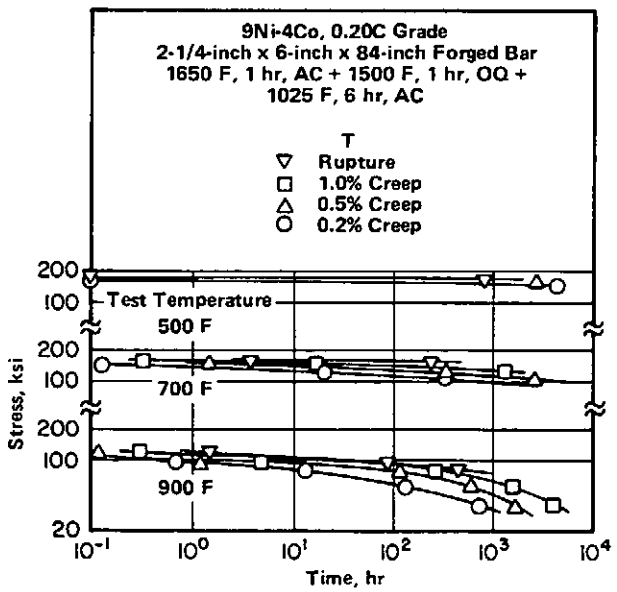


FIGURE 3.042. CREEP AND STRESS RUPTURE PROPERTIES OF 0.20C GRADE FORGED BAR AT 500, 700, AND 900 F (20, 21)

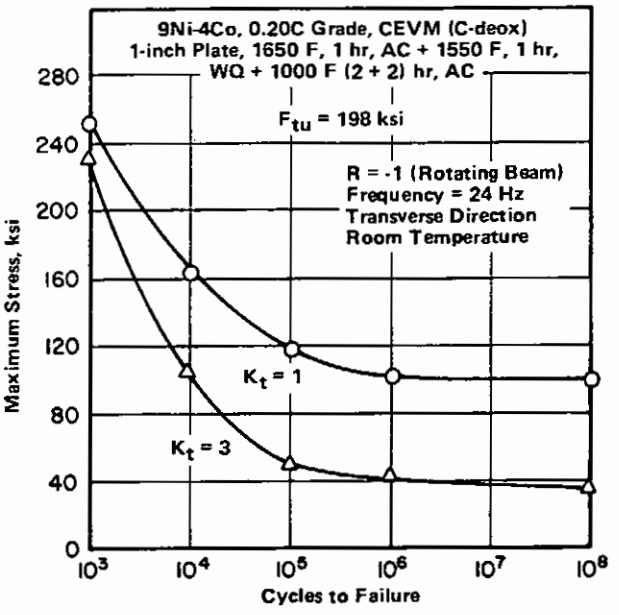


FIGURE 3.051. ROTATING BEAM SMOOTH AND MILD-NOTCH FATIGUE STRENGTH OF 0.20C GRADE PLATE (66)

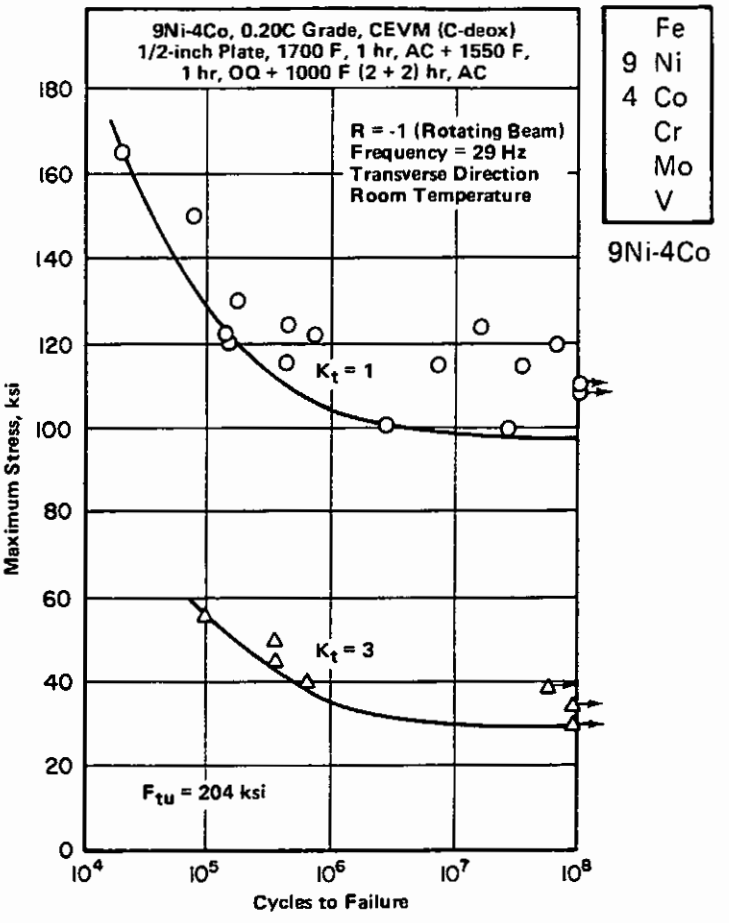


FIGURE 3.052. ROTATING BEAM SMOOTH AND MILD-NOTCH FATIGUE STRENGTH OF 0.20C GRADE PLATE (66)

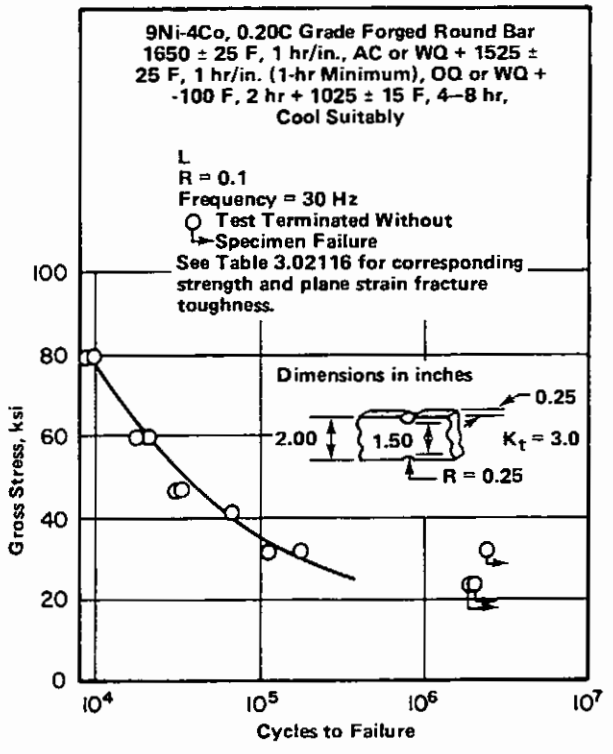


FIGURE 3.053. AXIAL LOAD MILD-NOTCH FATIGUE STRENGTH OF 0.20C GRADE FORGED ROUND BAR (55)

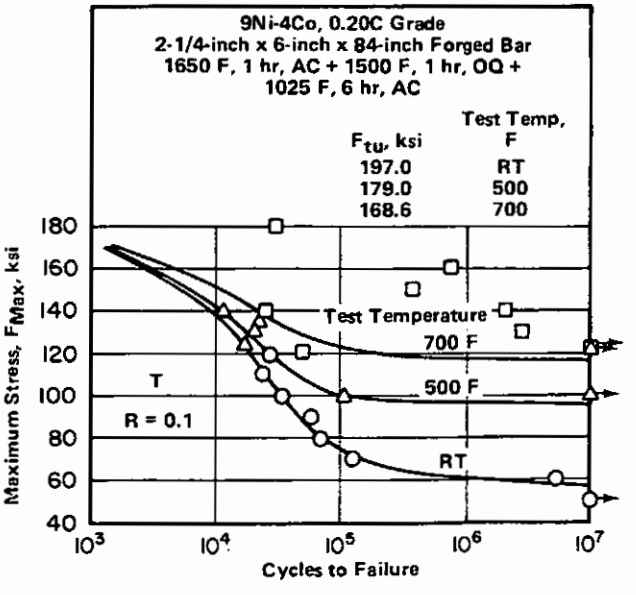


FIGURE 3.054. AXIAL LOAD SMOOTH FATIGUE STRENGTH AT ROOM TEMPERATURE, 500 F, AND 700 F FOR 0.20C GRADE FORGED BAR (20, 21)

Fe
9 Ni
4 Co
Cr
Mo
V

9Ni-4Co

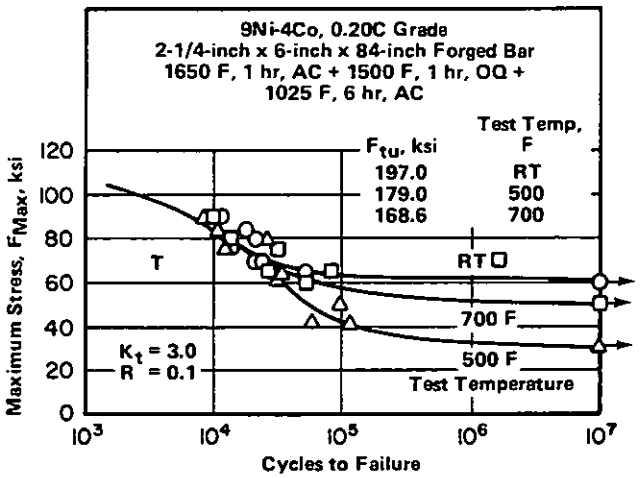


FIGURE 3.055. AXIAL LOAD MILD-NOTCH FATIGUE STRENGTH AT ROOM TEMPERATURE, 500 F, AND 700 F FOR 0.20C GRADE FORGED BAR (20, 21)

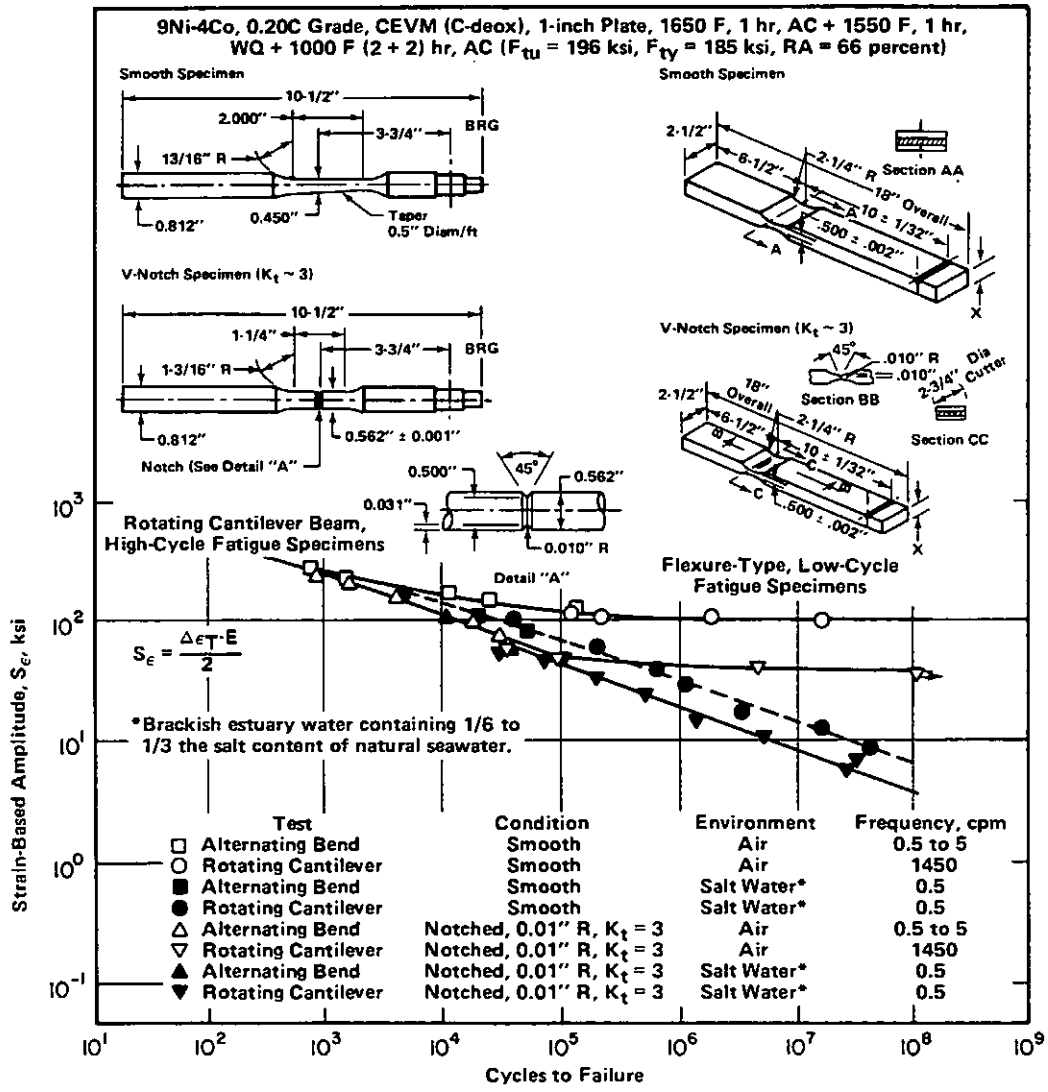


FIGURE 3.056. HIGH AND LOW CYCLE SMOOTH AND MILD-NOTCH FATIGUE STRENGTH OF 0.20C GRADE PLATE IN AIR AND SALTWATER (32)

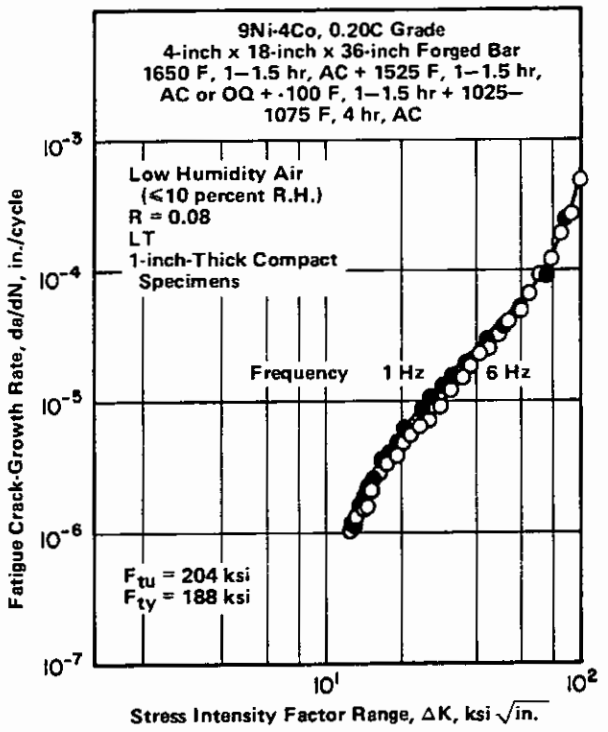
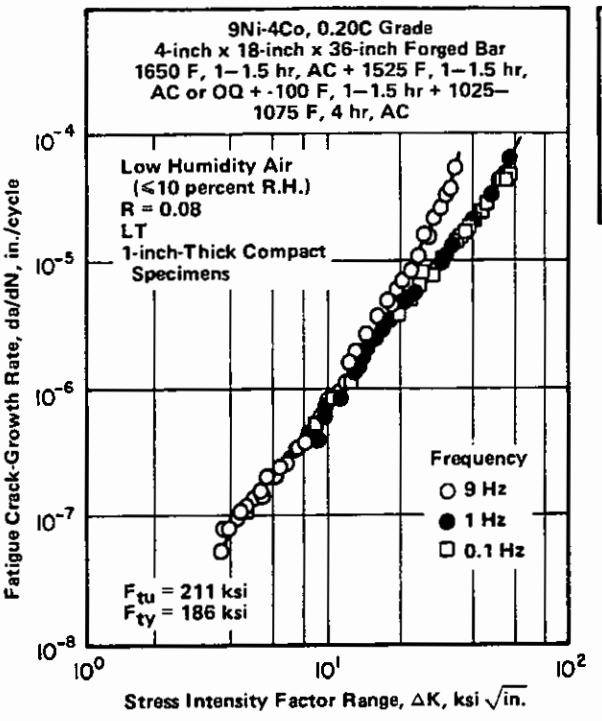


FIGURE 3.057. EFFECT OF CYCLIC FREQUENCY ON FATIGUE CRACK-GROWTH RATE IN LOW HUMIDITY AIR OF 0.20C GRADE FORGED BAR (47, 48)



Fe
9 Ni
4 Co
Cr
Mo
V

9Ni-4Co

FIGURE 3.058. EFFECT OF CYCLIC FREQUENCY ON FATIGUE CRACK-GROWTH RATE IN LOW HUMIDITY AIR OF 0.20C GRADE FORGED BAR (47, 48)

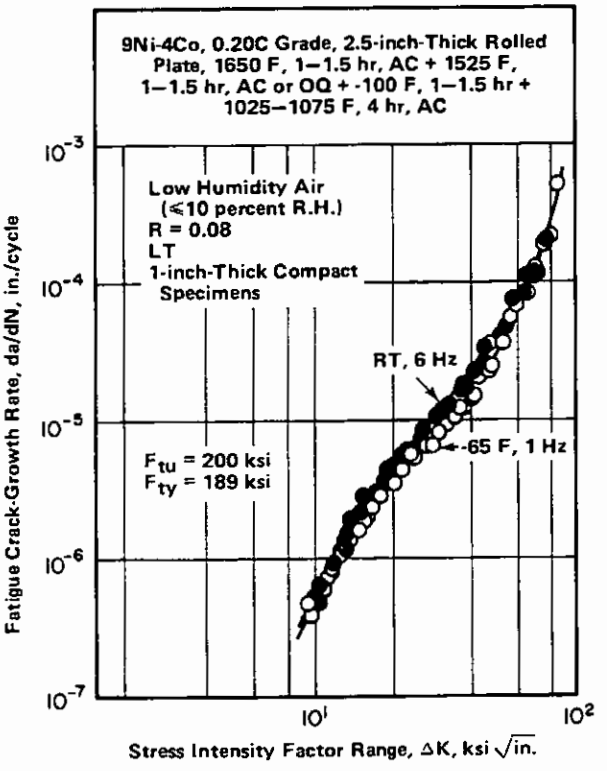


FIGURE 3.059. EFFECT OF TEST TEMPERATURE ON FATIGUE CRACK-GROWTH RATE IN LOW HUMIDITY AIR OF 0.20C GRADE ROLLED PLATE (47, 48)

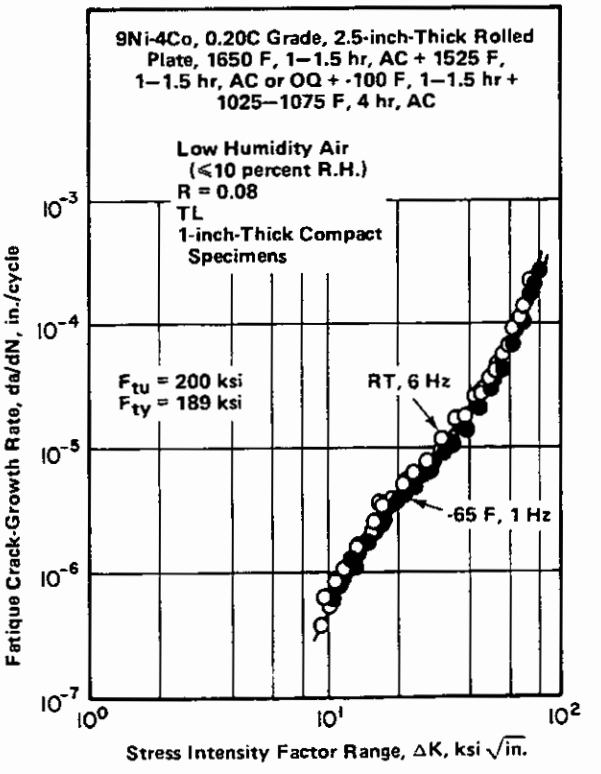


FIGURE 3.0510. EFFECT OF TEST TEMPERATURE ON FATIGUE CRACK-GROWTH RATE IN LOW HUMIDITY AIR OF 0.20C GRADE ROLLED PLATE (47, 48)

Fe
9 Ni
4 Co
Cr
Mo
V

9Ni-4Co

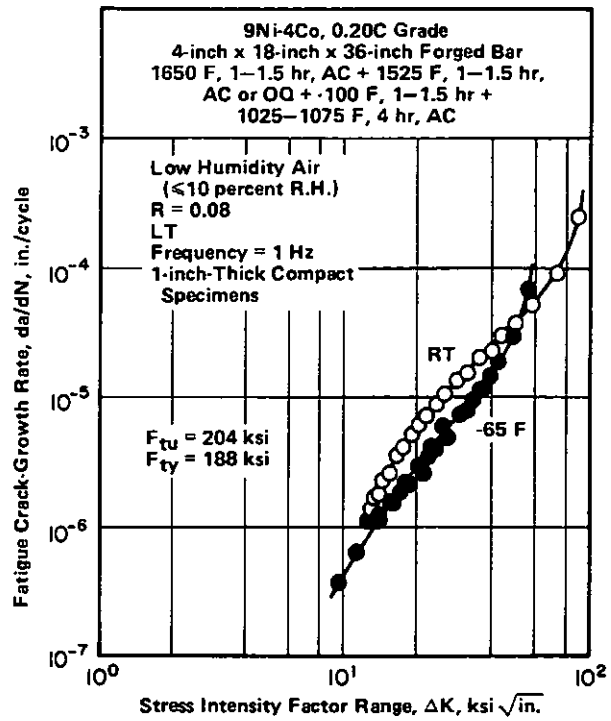


FIGURE 3.0511. EFFECT OF TEST TEMPERATURE ON FATIGUE CRACK-GROWTH RATE IN LOW HUMIDITY AIR OF 0.20C GRADE FORGED BAR (47, 48)

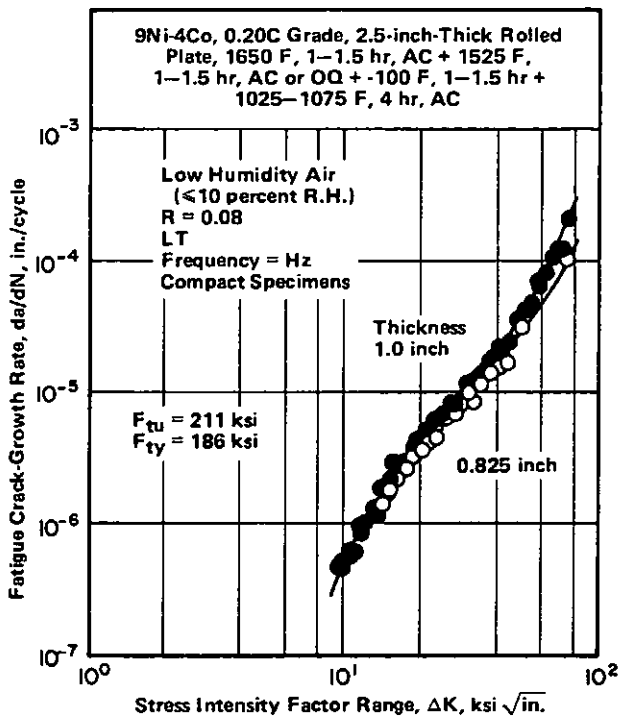


FIGURE 3.0512. EFFECT OF SPECIMEN THICKNESS ON FATIGUE CRACK-GROWTH RATE IN LOW HUMIDITY AIR OF 0.20C GRADE ROLLED PLATE (47, 48)

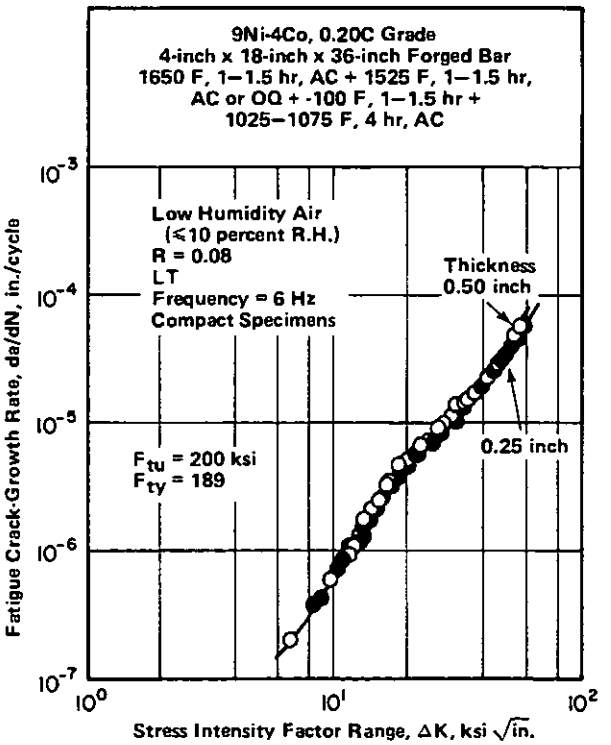


FIGURE 3.0513. EFFECT OF SPECIMEN THICKNESS ON FATIGUE CRACK-GROWTH RATE IN LOW HUMIDITY AIR OF 0.20C GRADE FORGED BAR (47, 48)

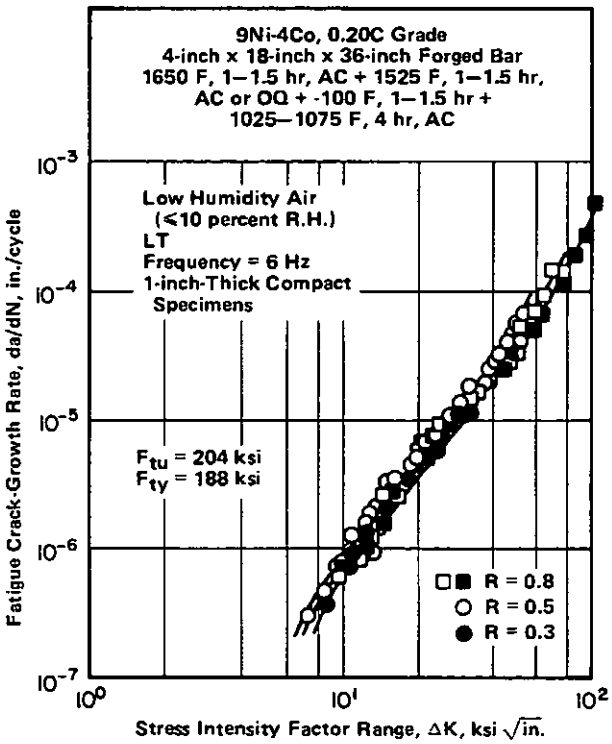


FIGURE 3.0514. EFFECT OF R-RATIO ON FATIGUE CRACK-GROWTH RATE IN LOW HUMIDITY AIR OF 0.20C GRADE FORGED BAR (47, 48)

Fe
9 Ni
4 Co
Cr
Mo
V
9Ni-4Co

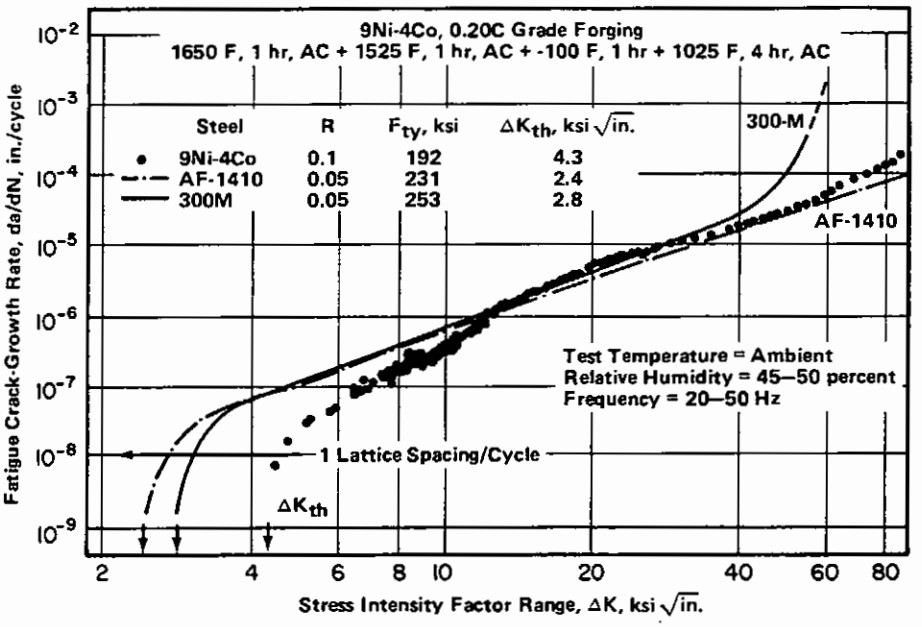


FIGURE 3.0515. COMPARISON OF ROOM TEMPERATURE FATIGUE CRACK PROPAGATION OF 0.20C GRADE TO OTHER HIGH STRENGTH STEELS, ALL IN COMMERCIAL HEAT TREATED CONDITION (18)

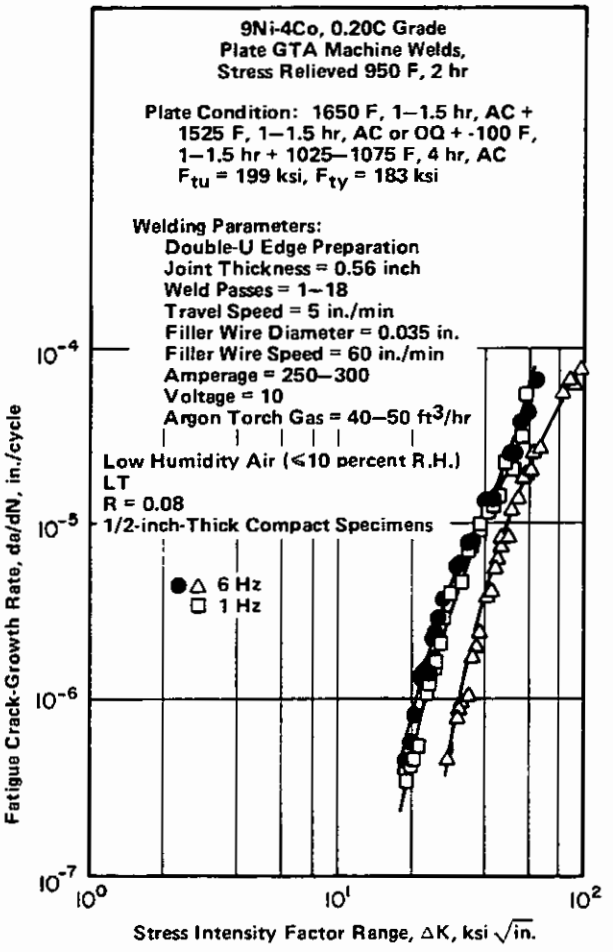


FIGURE 3.0518. EFFECT OF CYCLIC FREQUENCY ON FATIGUE CRACK-GROWTH RATE IN LOW HUMIDITY AIR OF 0.20C GRADE PLATE GTA MACHINE WELDS (47, 48)

Fe
9 Ni
4 Co
Cr
Mo
V

9Ni-4Co

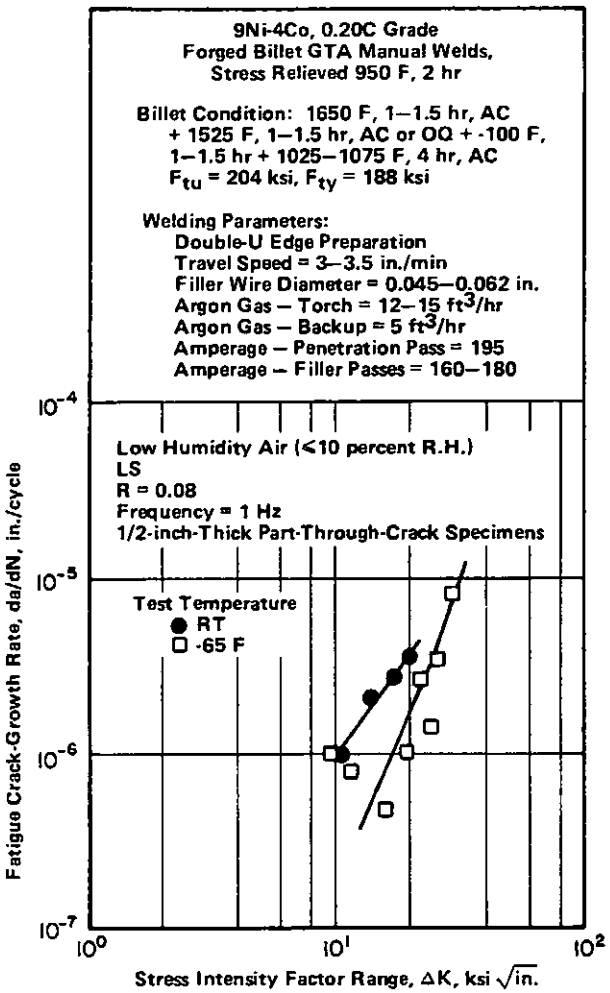


FIGURE 3.0519. EFFECT OF TEST TEMPERATURE ON FATIGUE CRACK-GROWTH RATE IN LOW HUMIDITY AIR OF 0.20C GRADE FORGED BILLET GTA MANUAL WELD HEAT AFFECTED ZONE (47, 48)

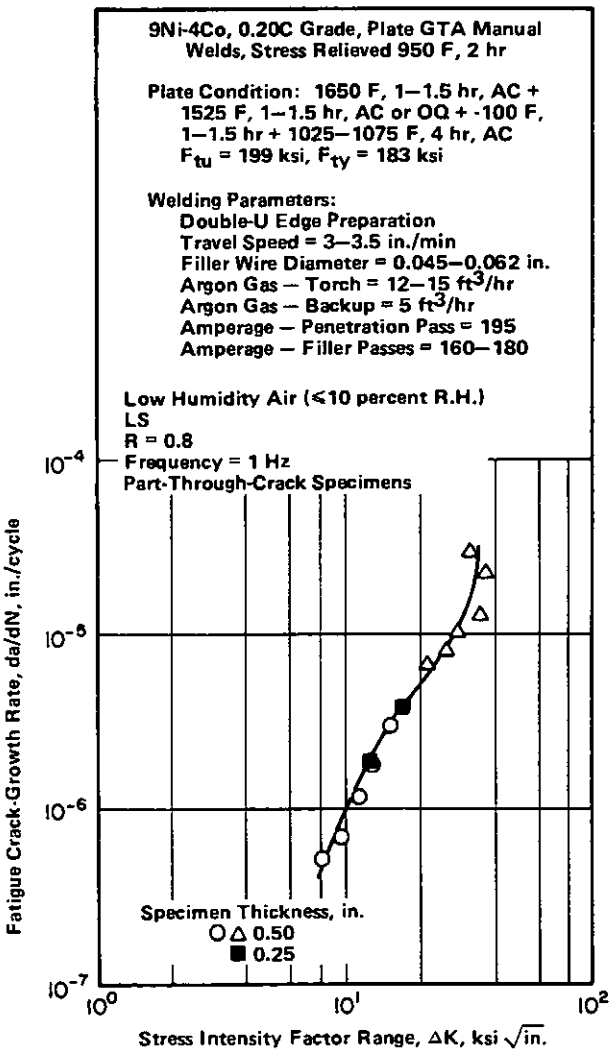


FIGURE 3.0520. EFFECT OF SPECIMEN THICKNESS ON FATIGUE CRACK-GROWTH RATE IN LOW HUMIDITY AIR OF 0.20C GRADE PLATE GTA MANUAL WELD HEAT AFFECTED ZONE (47, 48)

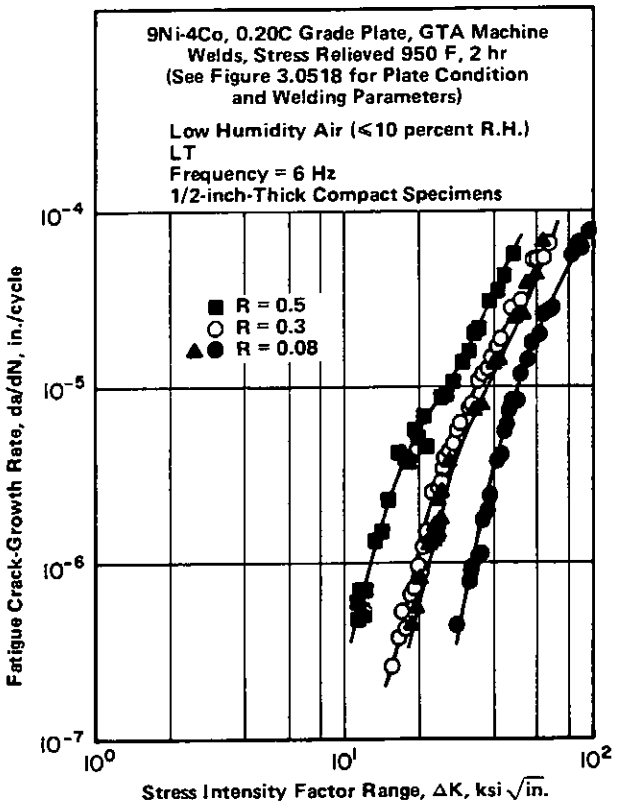
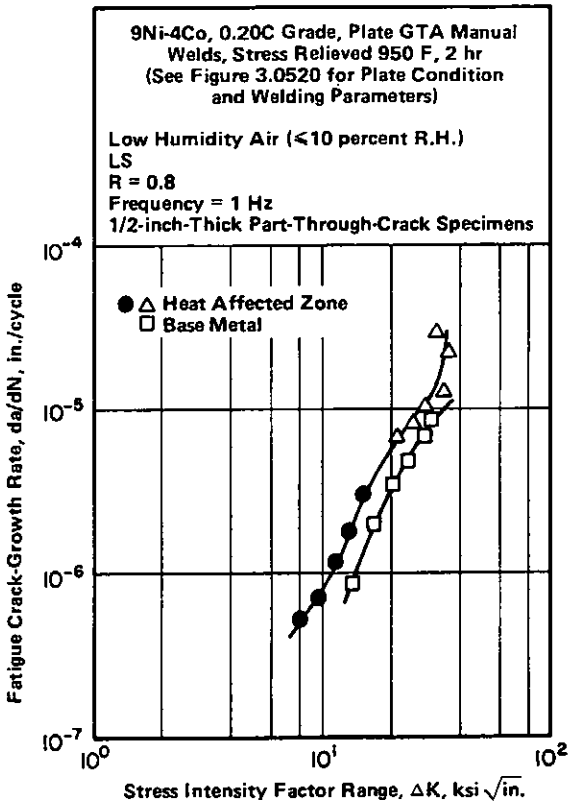


FIGURE 3.0521. EFFECT OF R-RATIO ON FATIGUE CRACK-GROWTH RATE IN LOW HUMIDITY AIR OF 0.20C GRADE PLATE GTA MACHINE WELDS (47, 48)



Fe
9 Ni
4 Co
Cr
Mo
V
9Ni-4Co

FIGURE 3.0522. BASE METAL AND HEAT AFFECTED ZONE FATIGUE CRACK-GROWTH RATES IN LOW HUMIDITY AIR OF 0.20C GRADE PLATE GTA MANUAL WELDS (47, 48)

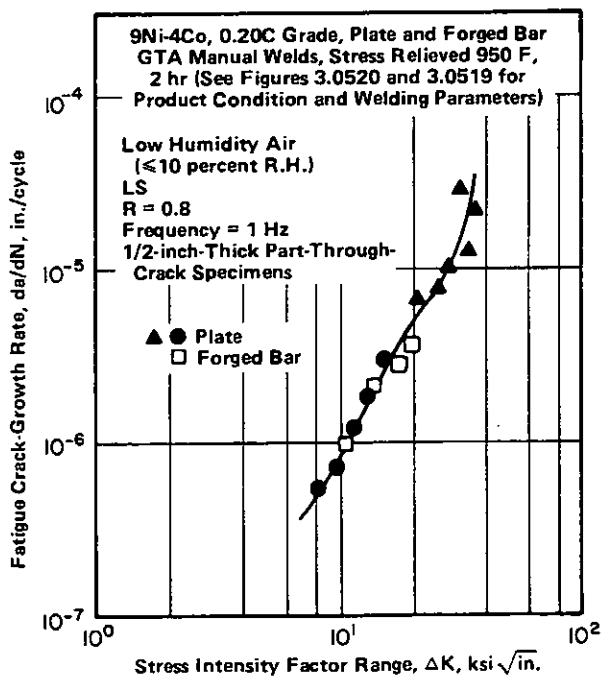


FIGURE 3.0523. FATIGUE CRACK-GROWTH RATES IN LOW HUMIDITY AIR OF 0.20C GRADE PLATE AND FORGED BAR GTA MANUAL WELD HEAT AFFECTED ZONE (47, 48)

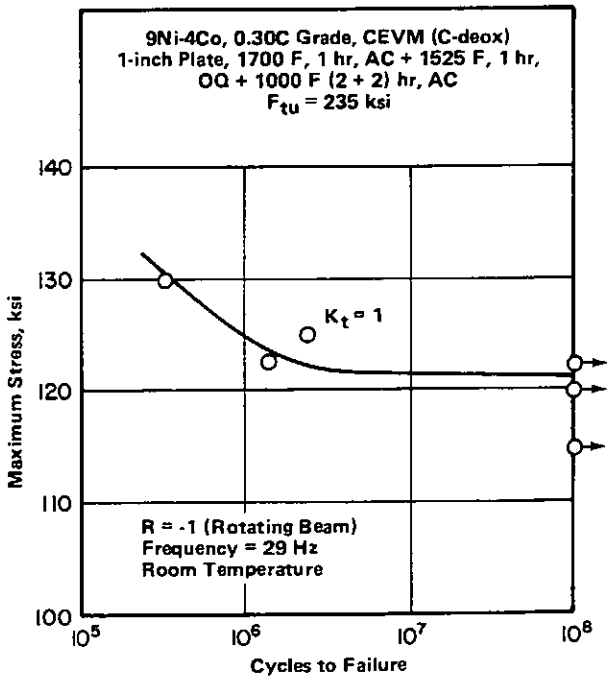


FIGURE 3.0524. ROTATING BEAM SMOOTH FATIGUE STRENGTH OF 0.30C GRADE PLATE (66)

Fe
9 Ni
4 Co
Cr
Mo
V

9Ni-4Co

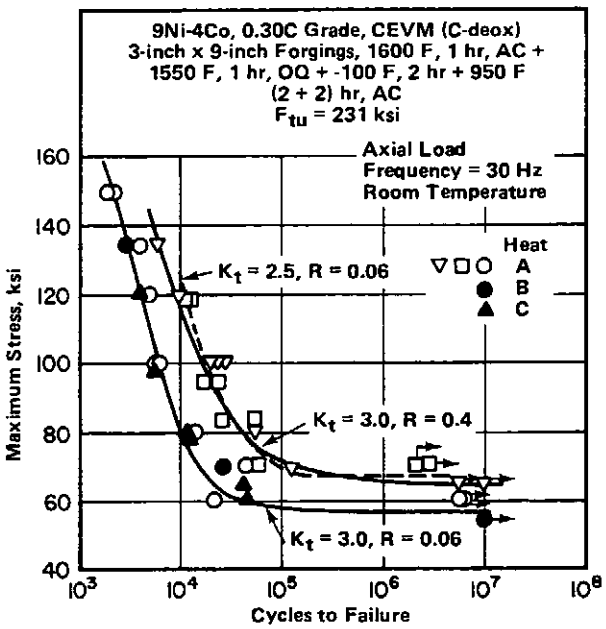


FIGURE 3.0525. AXIAL LOAD MILD-NOTCH FATIGUE STRENGTH OF 0.30C GRADE FORGINGS (66)

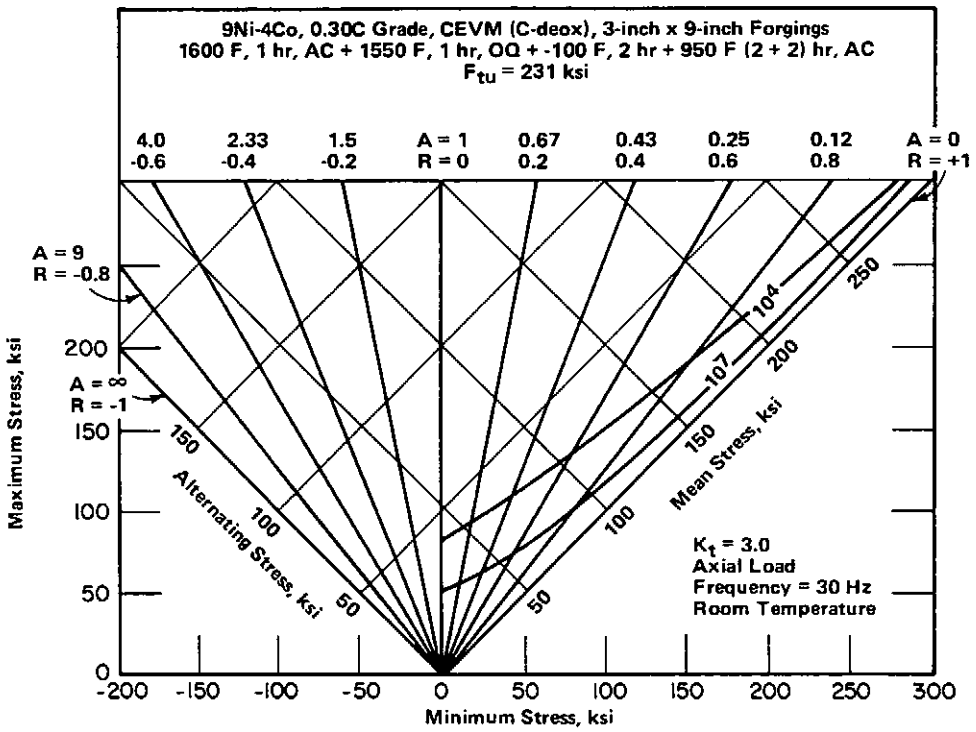


FIGURE 3.0526. AXIAL LOAD CONSTANT LIFE DIAGRAM FOR MILD-NOTCH SPECIMENS OF 0.30C GRADE FORGINGS (66)

Fe
9 Ni
4 Co
Cr
Mo
V
9Ni-4Co

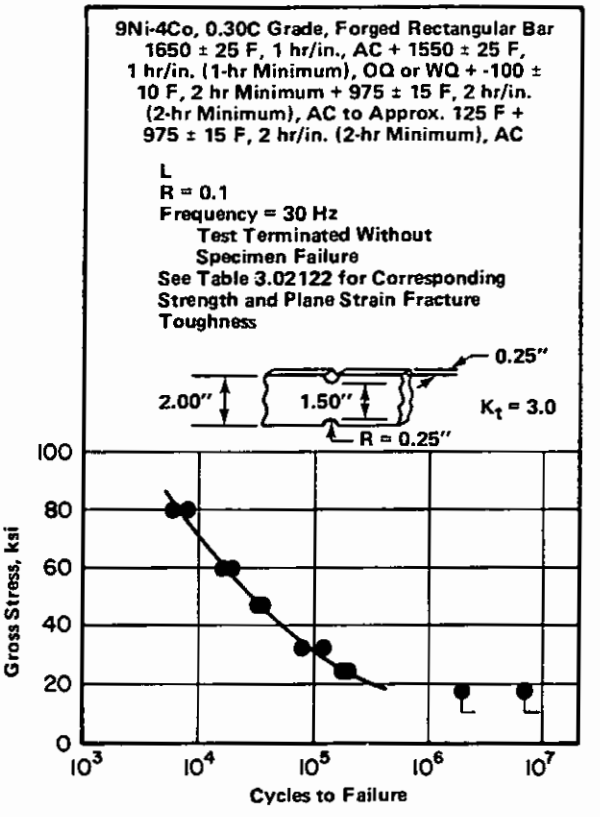


FIGURE 3.0527. AXIAL LOAD MILD-NOTCH FATIGUE STRENGTH OF 0.30C GRADE FORGED RECTANGULAR BAR (55)

Alloy		9Ni-4Co					
Grade		0.30C, CEVM (C-deox)					
Form		3-inch x 9-inch x 24-inch Forged Billet					
Condition		1600–1700 F, 1 hr, AC + 1150 ± 25 F, 1/2 hr Minimum + 1150 ± 25 F, 1 hr, OQ + -100 F, 2 hr + 950 ± 25 F (2 + 2) hr, AC (F_{ty} = 191 to 205 ksi)					
Stress Ratio			Fatigue Strength[a], ksi at cycles				
A	R	Specimen	30×10^3	10^4	10^5	10^6	10^7
0.89	0.06	Flat with hole K_t = 2.5	–	120	70	60	60
0.43	0.40	Cylindrical notched K_t = 3.0	160	120	70	62	62
0.89	0.06		130	85	60	55	55

(a) Transverse direction. Frequency = 30 Hz.

TABLE 3.0528. AXIAL LOAD MILD-NOTCH FATIGUE STRENGTH OF 0.30C GRADE FORGED BILLET (61)

Fe
9 Ni
4 Co
Cr
Mo
V

9Ni-4Co

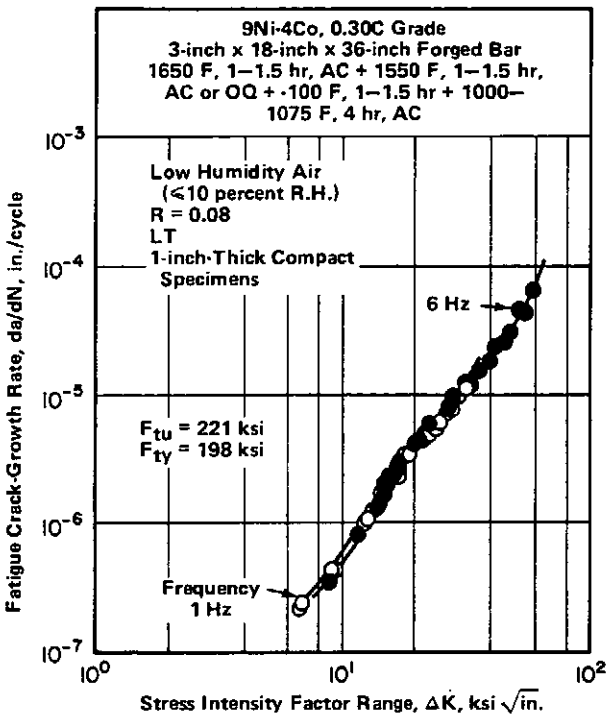


FIGURE 3.0529. EFFECT OF CYCLIC FREQUENCY ON FATIGUE CRACK-GROWTH RATE IN LOW HUMIDITY AIR OF 0.30C GRADE FORGED BAR (47, 48)

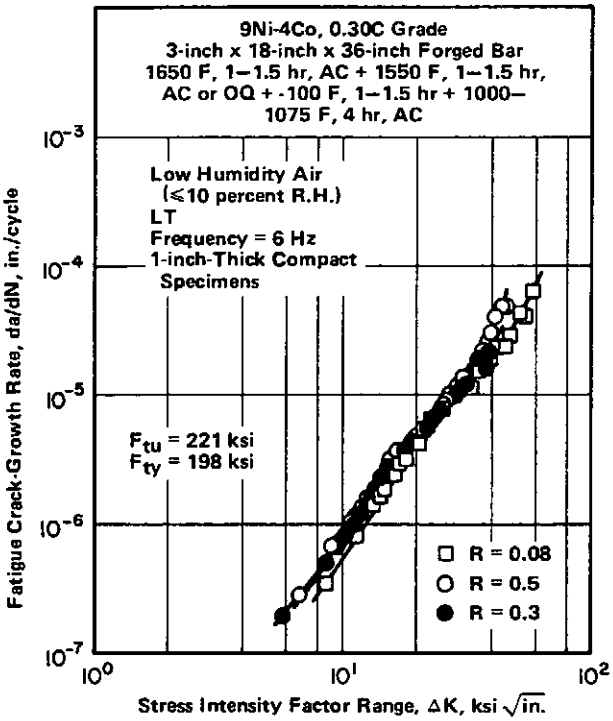


FIGURE 3.0530. EFFECT OF R-RATIO ON FATIGUE CRACK-GROWTH RATE IN LOW HUMIDITY AIR OF 0.30C GRADE FORGED BAR (47, 48)

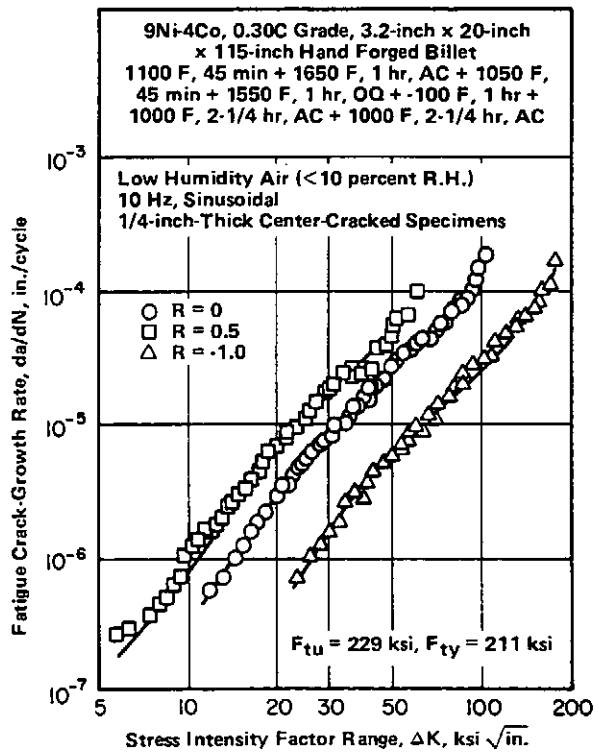


FIGURE 3.0531. EFFECT OF R-RATIO ON FATIGUE CRACK-GROWTH RATE OF 0.30C GRADE HAND FORGED BILLET IN LOW HUMIDITY AIR (<10 PERCENT RELATIVE HUMIDITY) (49, 51)

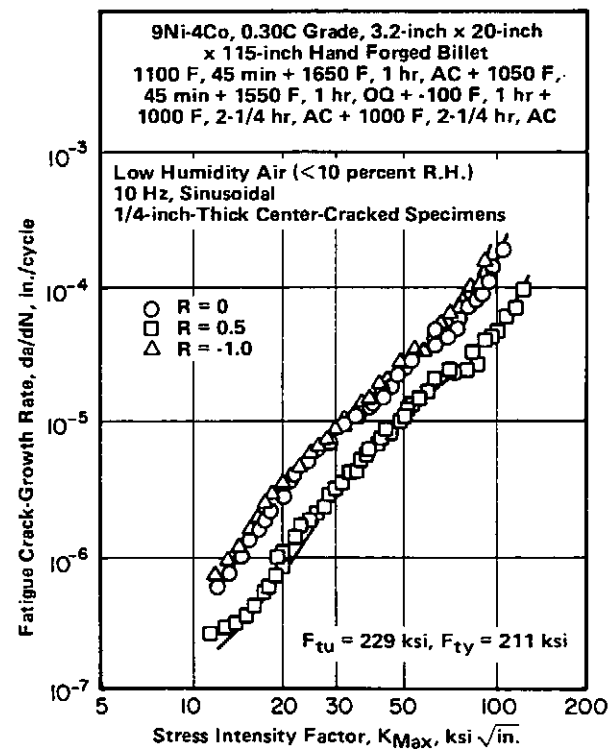


FIGURE 3.0532. EFFECT OF R-RATIO ON FATIGUE CRACK-GROWTH RATE OF 0.30C GRADE HAND FORGED BILLET IN LOW HUMIDITY AIR (<10 PERCENT RELATIVE HUMIDITY), PLOTTED AS A FUNCTION OF K_{MAX} (49, 51)

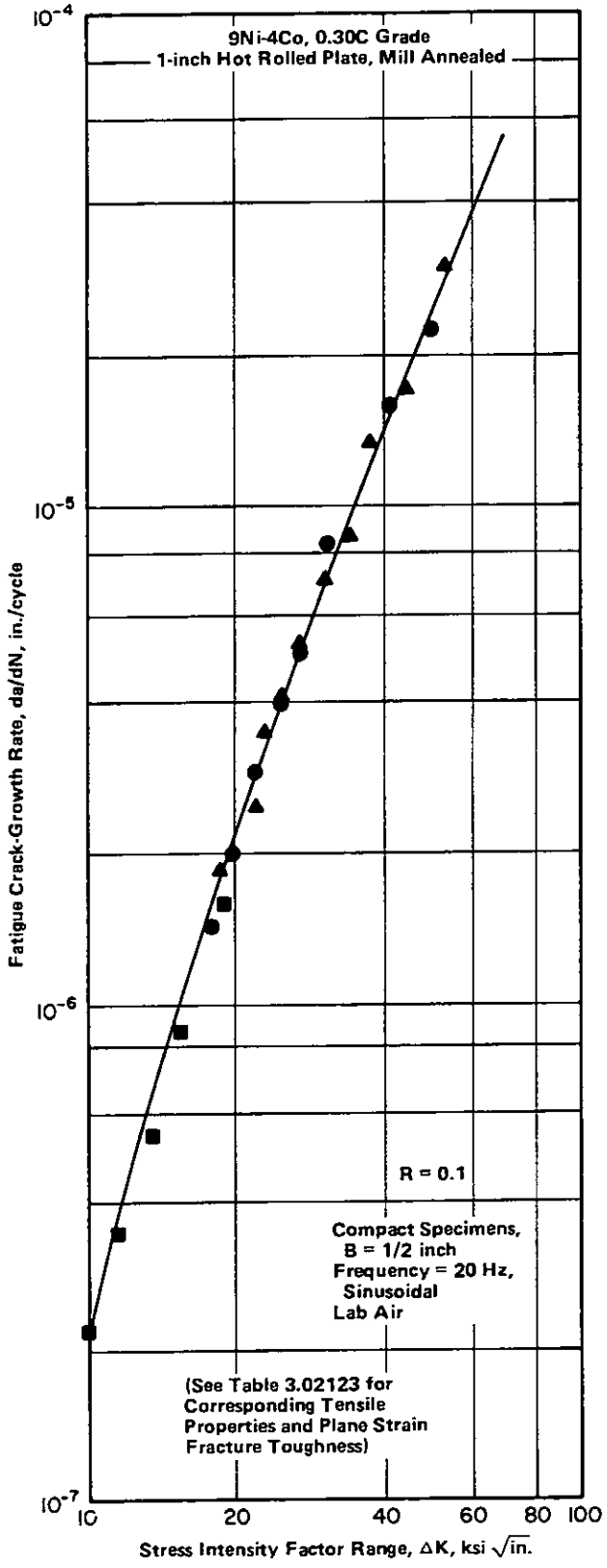


FIGURE 3.0533. FATIGUE CRACK PROPAGATION RATES AT ROOM TEMPERATURE FOR 0.30C GRADE MILL ANNEALED ROLLED PLATE (26, 27, 37)

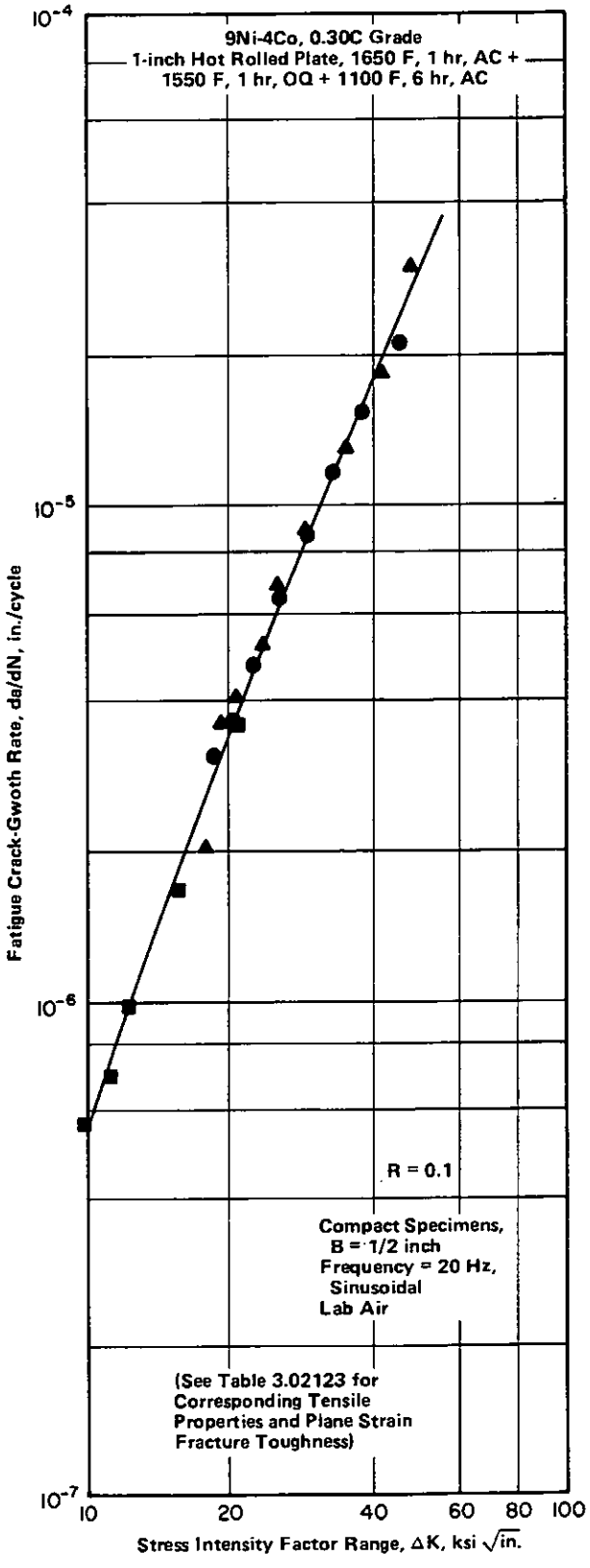


FIGURE 3.0534. FATIGUE CRACK PROPAGATION RATES AT ROOM TEMPERATURE FOR 0.30C GRADE ROLLED PLATE QUENCHED AND TEMPERED TO 179 KSI YIELD STRENGTH (26, 27, 37)

Fe
9 Ni
4 Co
Cr
Mo
V

9Ni-4Co

Fe
9 Ni
4 Co
Cr
Mo
V

9Ni-4Co

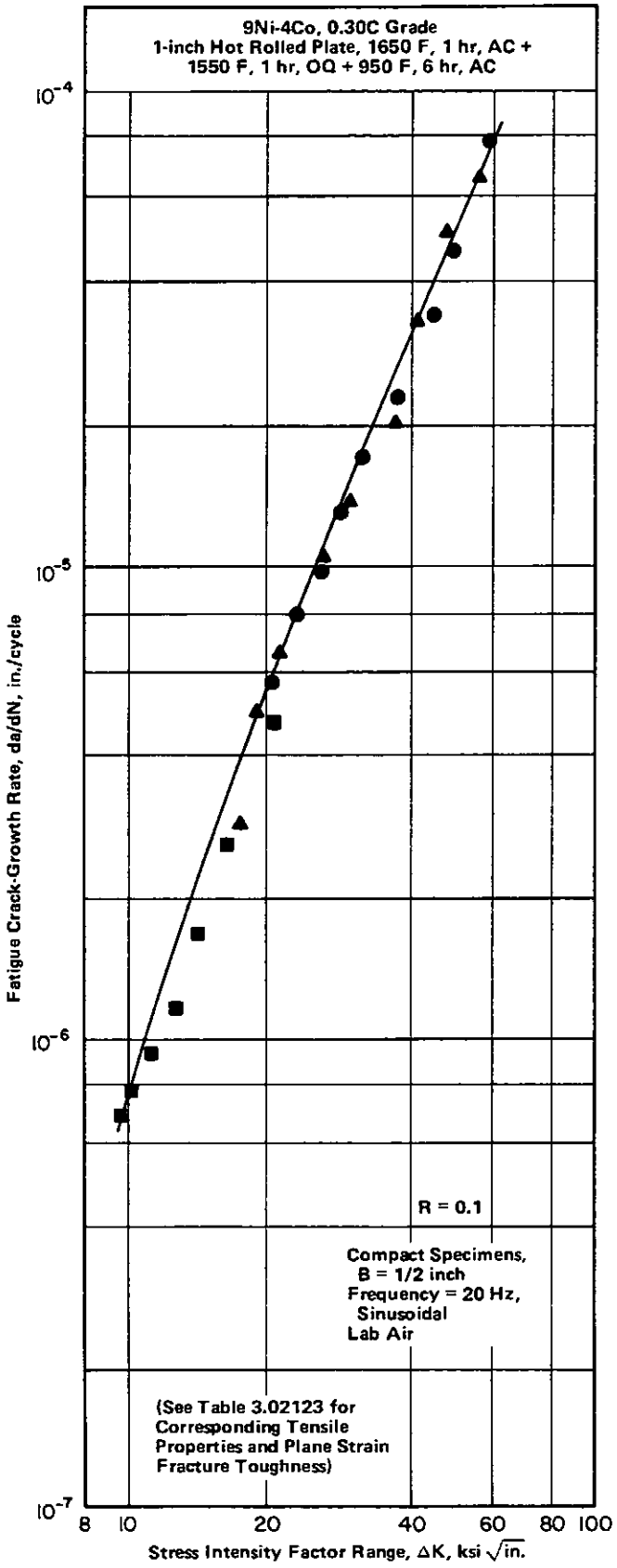


FIGURE 3.0535. FATIGUE CRACK PROPAGATION RATES AT ROOM TEMPERATURE FOR 0.30C GRADE ROLLED PLATE QUENCHED AND TEMPERED TO 203 KSI YIELD STRENGTH (26, 27, 37)

Fe
9 Ni
4 Co
Cr
Mo
V

9Ni-4Co

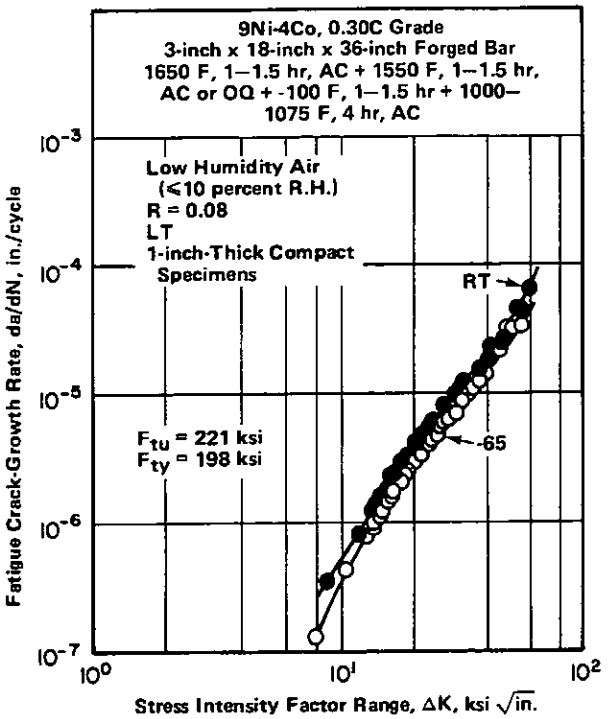


FIGURE 3.0536. EFFECT OF TEST TEMPERATURE ON FATIGUE CRACK GROWTH IN LOW HUMIDITY AIR OF 0.30C GRADE FORGED BAR (47, 48)

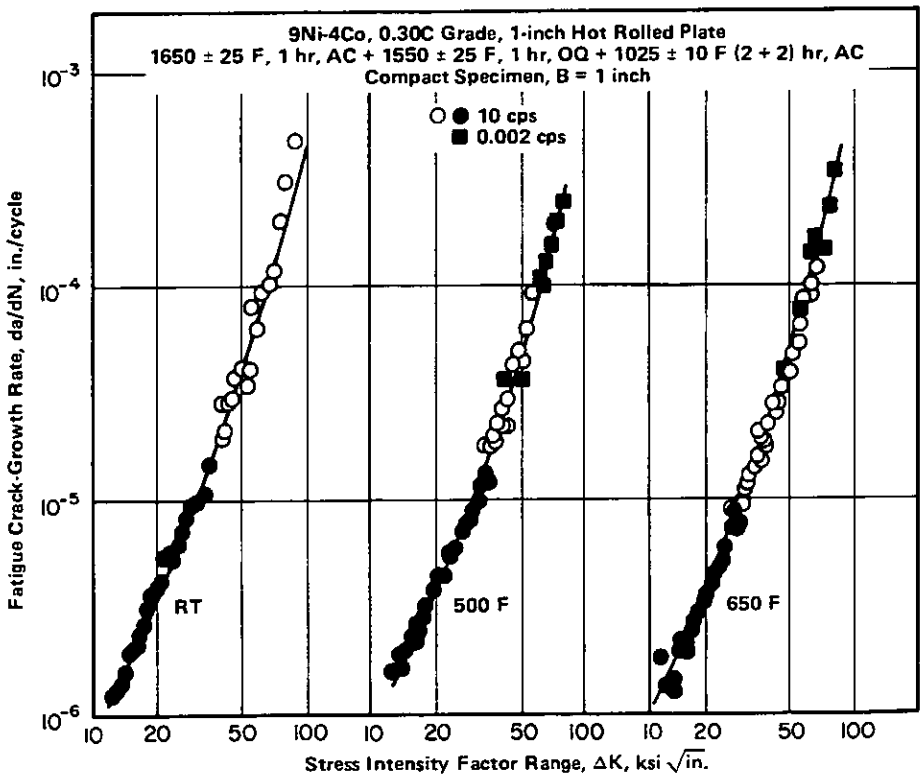


FIGURE 3.0537. FATIGUE CRACK PROPAGATION RATES AT ROOM TEMPERATURE, 500 F, AND 650 F, AND TWO CYCLIC FREQUENCIES FOR 0.30C GRADE ROLLED PLATE (23)

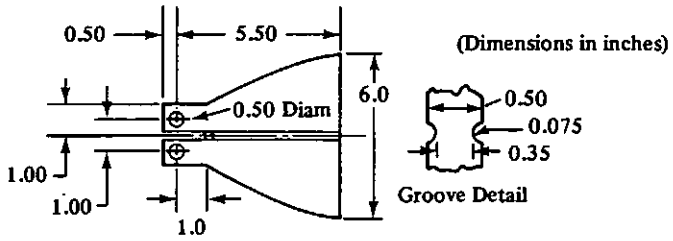
(For All Temperatures: $da/dN = 1.2 \times 10^{-15} \Delta K^{2.2}$, for $da/dN < 10^{-5}$ in./cycle, and $da/dN = 4.5 \times 10^{-20} \Delta K^{3.2}$ for $da/dN > 10^{-5}$ in./cycle.)

Fe
9 Ni
4 Co
Cr
Mo
V

9Ni-4Co

Alloy	9Ni-4Co		
Grade	0.30C		
Form	1-inch Hot Rolled Plate		
Condition[a]	Mill Annealed	1650 F, 1 hr, AC + 1550 F, 1 hr, OQ + 1100 F, 6 hr, AC	1650 F, 1 hr, AC + 1550 F, 1 hr, OQ + 950 F, 6 hr, AC
Constant Amplitude, da/dN (inch/cycle), for ΔK = 22.5 ksi $\sqrt{in}$.	3.3×10^{-6}	5.2×10^{-6}	7.3×10^{-6}
da/dN (inch/cycle), at ΔK = 22.5 ksi $\sqrt{in}$. Following Single Overload to ΔK = 45.0 ksi $\sqrt{in}$.[b]	5.0×10^{-7}	4.6×10^{-6}	6.5×10^{-6}

(a) See Table 3.02123 for corresponding tensile properties and plane strain fracture toughness.
(b) Same result for 17 such overload sequences.



Tapered Double Cantilever Beam Specimen

TABLE 3.0539. RETARDATION EFFECT OF OVERLOAD SEQUENCE ON ROOM TEMPERATURE FATIGUE CRACK PROPAGATION FOR 0.30C GRADE PLATE IN THREE HEAT TREATED (STRENGTH LEVEL) CONDITIONS (37)

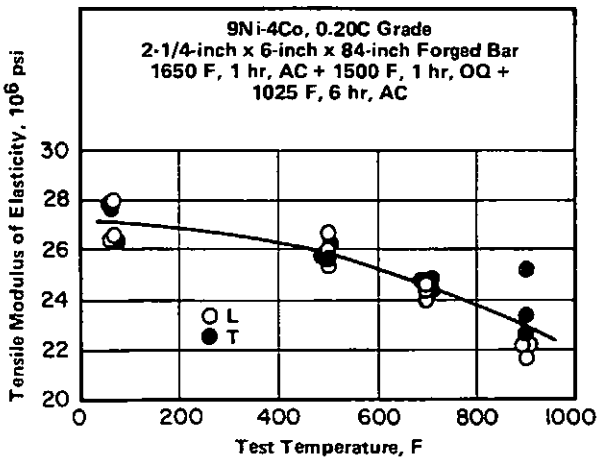


FIGURE 3.0623. EFFECT OF TEST TEMPERATURE ON TENSILE MODULUS OF ELASTICITY FOR 0.20C GRADE (20, 21)

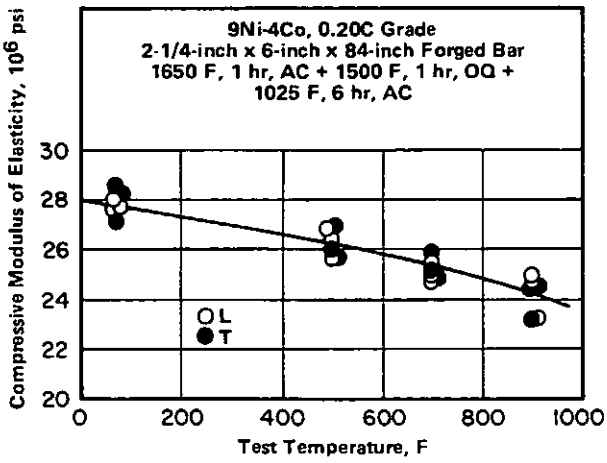


FIGURE 3.0625. EFFECT OF TEST TEMPERATURE ON COMPRESSIVE MODULUS OF ELASTICITY FOR 0.20C GRADE FORGED BAR (20, 21)

Fe
9 Ni
4 Co
Cr
Mo
V

9Ni-4Co

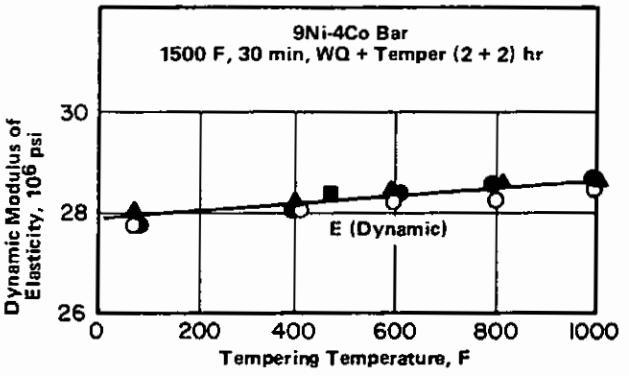


FIGURE 3.0626. EFFECT OF TEMPERING TEMPERATURE ON DYNAMIC MODULUS OF ELASTICITY OF 0.30C GRADE BAR (74)

Alloy	9Ni-4Co		
Grade	0.30C, CEVM (C-deox)		
Form	3-inch x 9-inch x 24-inch Forged Billet		
Condition	1600–1700 F, 1 hr, AC + 1150 ± 25 F, 1/2 hr Minimum + 1550 ± 25 F, 1 hr, OQ + -100 F, 2 hr + 950 ± 25 F (2 + 2) hr, AC		
Test Direction			
L		T	
Stress Interval, ksi	E (Chord Modulus), 10^3 ksi	Stress Interval, ksi	E (Chord Modulus), 10^3 ksi
25.0– 50.1	28.41	26.8– 53.6	29.45
50.1– 75.0	28.45	53.6– 80.2	28.70
75.0– 99.6	28.10	80.2–106.4	28.29
99.6–123.1	27.32	106.4–131.6	27.85
50.1– 99.6	28.28	53.6–106.4	28.47
75.0–123.1	27.71	80.2–131.6	28.08
25.0–123.1	28.06	26.8–131.6	28.48

TABLE 3.0628. PRECISION TENSILE MODULI OF 0.30C GRADE AT ROOM TEMPERATURE (ACCORDING TO ASTM E-111) (61)

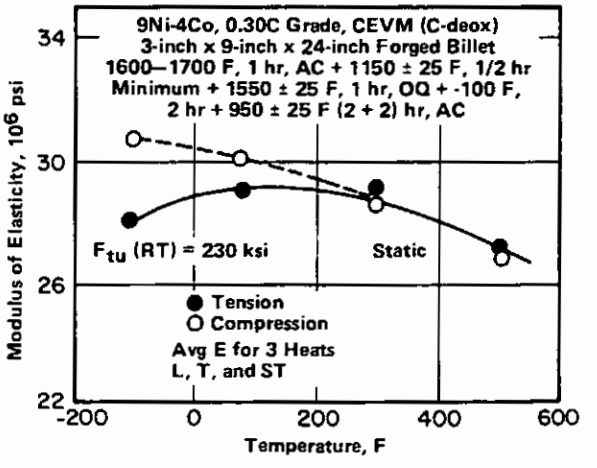


FIGURE 3.0629. EFFECT OF TEMPERATURE ON MODULUS OF ELASTICITY IN TENSION AND COMPRESSION FOR 0.30C GRADE FORGED BILLET (61)

Fe
9 Ni
4 Co
Cr
Mo
V

9Ni-4Co

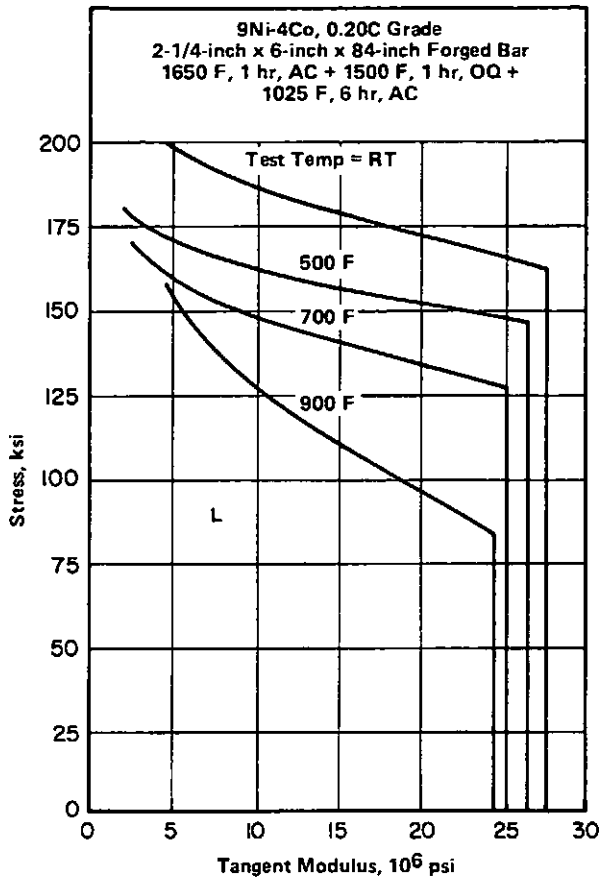


FIGURE 3.0641. TYPICAL COMPRESSIVE TANGENT-MODULUS CURVES AT ROOM AND ELEVATED TEMPERATURES FOR 0.20C GRADE FORGED BARS (20, 21)

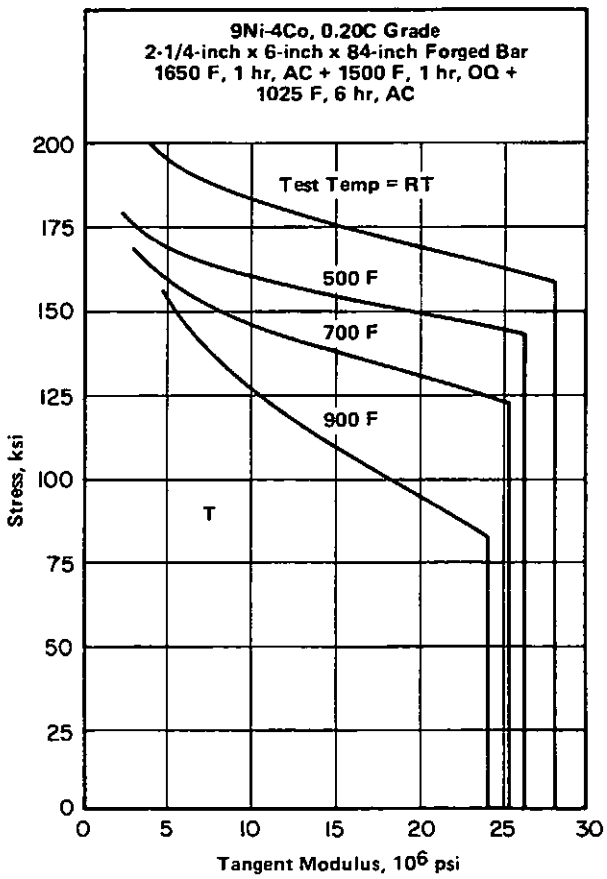


FIGURE 3.0642. TYPICAL COMPRESSIVE TANGENT-MODULUS CURVES AT ROOM AND ELEVATED TEMPERATURES FOR 0.20C GRADE FORGED BARS (20, 21)

Fe
9 Ni
4 Co
Cr
Mo
V

9Ni-4Co

Alloy	9Ni-4Co		
Grade	0.30C		
Cutting Tool	SNG-432 Carboloy 370 Carbide Insert		
Tool Geometry	Back Rake Angle: -5°	End Cutting Edge Angle: 15°	
	Side Rake Angle: -5°	Side & End Relief Angle: 5°	
	Side Cutting Edge Angle: 15°	Nose Radius: 0.030 inch	
Machining Conditions Held Constant	Feed: 0.010 inch/Revolution Depth of Cut: 0.100 inch Tool Life End Point: 0.015 inch Uniform Wear		
Alloy Condition	Annealed: 1150 F, 24 hr	Normalized: 1650 F, 1 hr/in., AC Temper: 1150 F, 24 hr, AC	Normalized: 1650 F, 1 hr/in., AC Temper: 1250 F, 4 hr, AC Retemper: 1150 F, 4 hr, AC
Cutting Speed	Tool Life, min		
300 ft/min	31.4	–	–
400 ft/min	6.6	30.0	30.0
500 ft/min	3.5	10.3	7.3
600 ft/min	–	2.4	1.3

TABLE 4.0131. CUTTING TOOL LIFE AS INFLUENCED BY HEAT TREAT CONDITION FOR TURNING 0.30C GRADE (14)

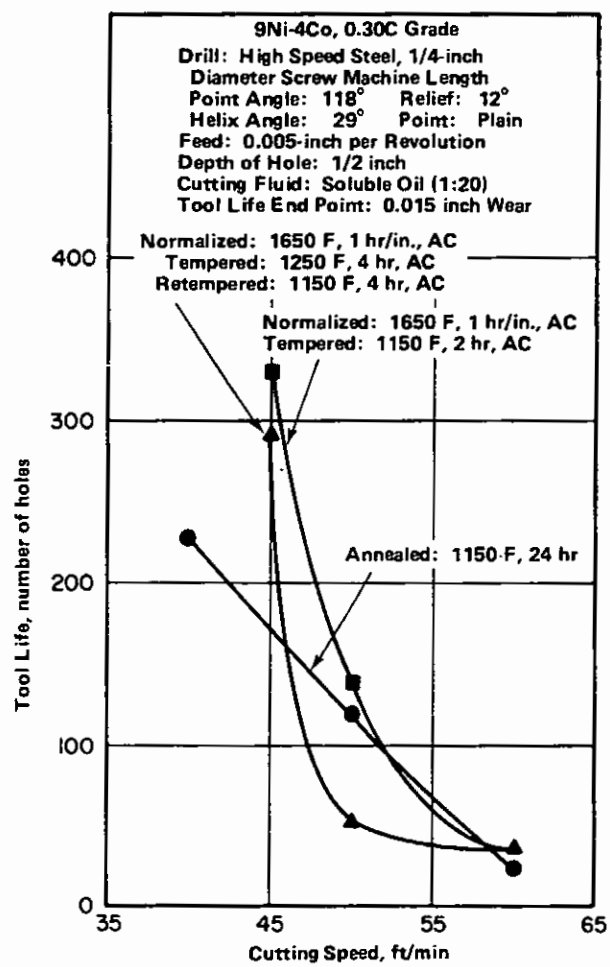
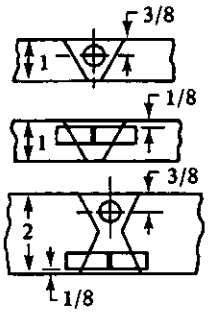


FIGURE 4.0132. CUTTING TOOL LIFE AS INFLUENCED BY HEAT TREAT CONDITION FOR DRILLING 0.30C GRADE (14)

Fe
9 Ni
4 Co
Cr
Mo
V

9Ni-4Co

Alloy	9Ni-4Co		
Grade	0.20C		
Form	As-Deposited Plate GTA Welds		
Plate Condition	1650 F, 1 hr/in., WQ + 1550 F, 1 hr/in., WQ + 1000 F (2 + 2) hr, WQ		
GTA Weld[a] Conditions	Cold Wire, 200 amps, 15 volts, 1.36 lb/hr		Hot Wire, 200 amps, 15 volts, 1950 watts Hot Wire Power, 8 lb/hr
Thickness, in.	1	2	1
Joint Design	30° Single U	30° Double U	30° Single U
F_{tu}, ksi	214	211	198
F_{ty}, ksi	193	197	172
e (2 in.), percent	18	17	6
RA, percent	59	60	14
Charpy V, 0 F, ft-lb	50	49	24



Specimen Locations
0.505-inch-Diam Tensile

Charpy V

(Dimensions in inches)

(a) 1/16-inch-diameter wire: 0.16C, 0.73Mn, 0.25Si, 0.002N, <1 ppm H, 200 F maximum preheat and interpass temperature, 75He + 25A shield.

TABLE 4.0311. ROOM TEMPERATURE TENSILE PROPERTIES AND 0 F CHARPY V IMPACT ENERGY OF 0.20C GRADE PLATE WELDS PRODUCED BY THE COLD WIRE AND HOT WIRE GTA PROCESSES (31)

Alloy		9Ni-4Co							
Grade		0.20C							
Form		As-Deposited 2-1/4-inch Plate GTA Welds[a]							
Plate Condition		1700 F, 2 hr, WQ + 1550 F, 2 hr, OQ + 1025 F (2 + 2) hr, AC							
Heat Input, K, joules/hr	Current, ampere	Voltage, volt	Travel, in./min	F_{ty}, ksi	F_{tu}, ksi	e (1 in.), percent	RA, percent	IE Charpy V, RT	IE Charpy V, -80 F
68.3	320	16.0	4.5	191.3	206.3	18.0	51.0	64	53
47.5	300	14.5	5.5	199.6	211.1	16.0	55.0	65	57
30.7	300	14.5	8.5	196.8	210.5	18.0	63.0	63	53

(a) 0.045-inch-diameter filler wire.

TABLE 4.0312. EFFECT OF HEAT INPUT ON ROOM TEMPERATURE TENSILE PROPERTIES AND LOW TEMPERATURE CHARPY V IMPACT ENERGY OF AS-DEPOSITED 2-1/4-INCH-THICK PLATE GTA WELDS (29)

	Fe
9	Ni
4	Co
	Cr
	Mo
	V

9Ni-4Co

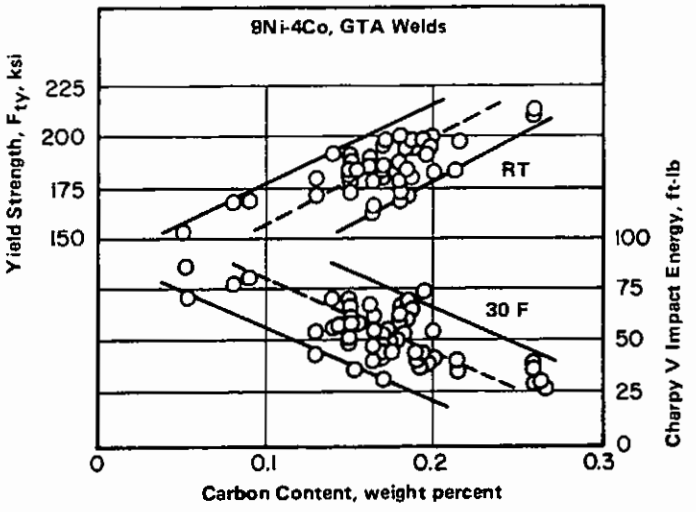


FIGURE 4.0321. EFFECT OF WELD METAL CARBON CONTENT ON AS-DEPOSITED ROOM TEMPERATURE YIELD STRENGTH AND 30 F CHARPY V IMPACT ENERGY OF GTA WELDS (19)

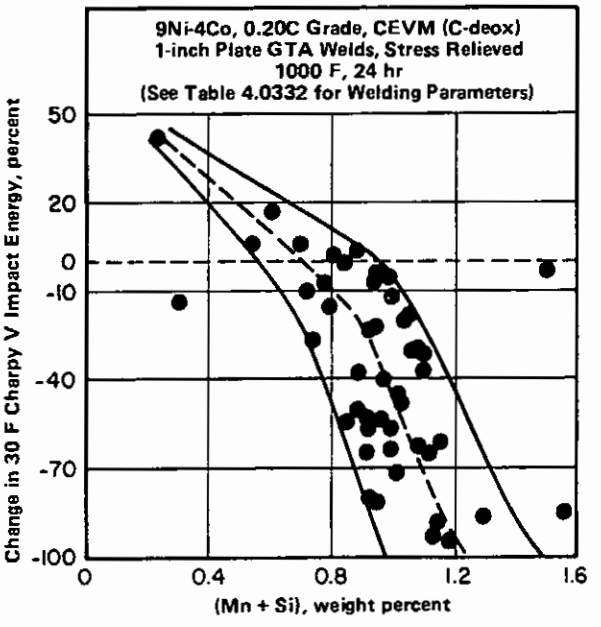


FIGURE 4.0322. EFFECT OF TOTAL (Mn + Si) CONTENT ON CHANGE IN 30 F CHARPY V IMPACT ENERGY DUE TO STRESS RELIEVING OF 0.20C GRADE PLATE GTA WELDS PRODUCED USING VARIOUS WELD FILLER WIRES (19)

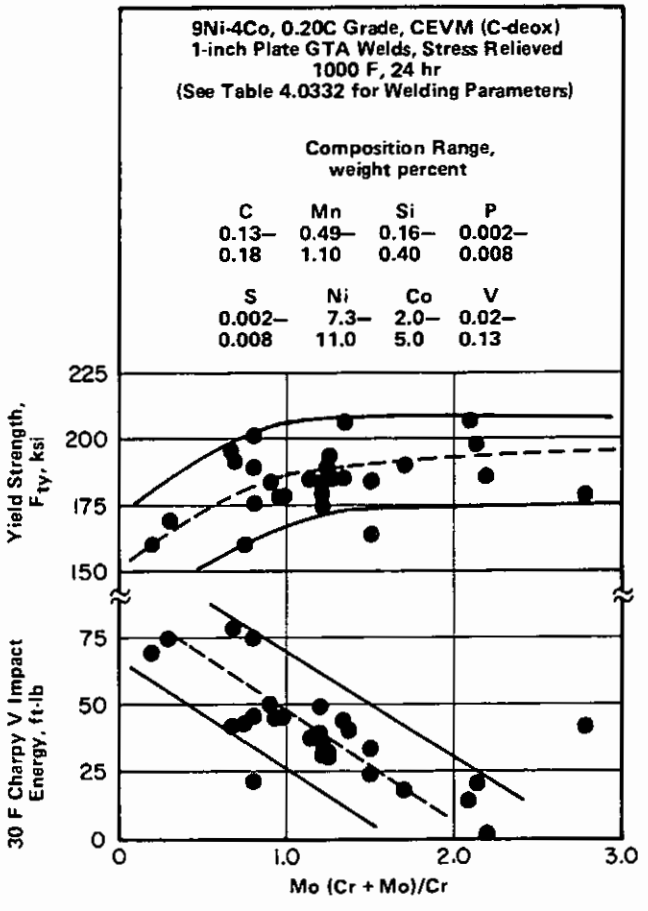


FIGURE 4.0323. EFFECT OF Cr:Mo FACTOR ON ROOM TEMPERATURE YIELD STRENGTH AND 30 F CHARPY V IMPACT ENERGY OF STRESS RELIEVED 0.20C GRADE PLATE GTA WELDS PRODUCED USING VARIOUS WELD FILLER WIRES (19)

Fe
9 Ni
4 Co
Cr
Mo
V

9Ni-4Co

Alloy	9Ni-4Co	
Grade	0.20C	
Form	GTA Weld Filler Wire	
	Composition, weight percent	
Element	Min	Max
Carbon	0.14	0.17
Manganese	0.40	0.55
Silicon	0.15	0.25
Phosphorus	–	0.008
Sulfur	–	0.008
Chromium	0.90	1.05
Nickel	9.75	10.25
Cobalt	3.50	4.00
Molybdenum	0.40	0.50
Vanadium	0.06	0.10
Copper	–	0.10
Oxygen	–	0.0050
Nitrogen	–	0.0080
Hydrogen	–	0.0010
Iron	Balance	

TABLE 4.0324. AMS SPECIFIED GTA WELD FILLER WIRE COMPOSITION (30)

Alloy	9Ni-4Co				
Grade	0.20C				
Form	Plate GTA Welds[a]				
Condition	As-Deposited				
Plate Thickness, in.	1			2	
Test Temperature, F	-80	30	70	-80	70
F_{tu} ksi[b]			211, 207	209	209
F_{ty}, ksi			203, 207	203	200
e (1 in.), percent			20, 17	19	18
RA, percent			65, 59	62	58
IE Charpy V, ft-lb	55, 50	63	64, 63	57, 58	58, 60

(a) U-joint welds; 0.062-inch diameter, AMS 6468A filler wire (Table 4.0324); producer's recommended welding parameters (Table 4.0332).
(b) Specimen locations and orientations given in Table 4.0311.

TABLE 4.0331. TYPICAL TENSILE AND CHARPY V IMPACT PROPERTIES AT ROOM AND CRYOGENIC TEMPERATURES FOR AS-DEPOSITED GTA WELDS OF 1-INCH AND 2-INCH-THICK PLATE (28)

Alloy	9Ni-4Co
Grade	0.20C
Form	GTA Welds
Current	300–350 ampere
Voltage	10–12 volts
Wire Diameter	0.063 inch
Wire Feed	20–30 inch/minute
Travel	5–10 inch/minute
Maximum Interpass Temperature	200 F
Shielding	25–35 ft^3/hr, Pure Argon
Interpass Cleaning	Power Wire Brushing

TABLE 4.0332. PRODUCER'S RECOMMENDED GTA WELDING PARAMETERS (28)

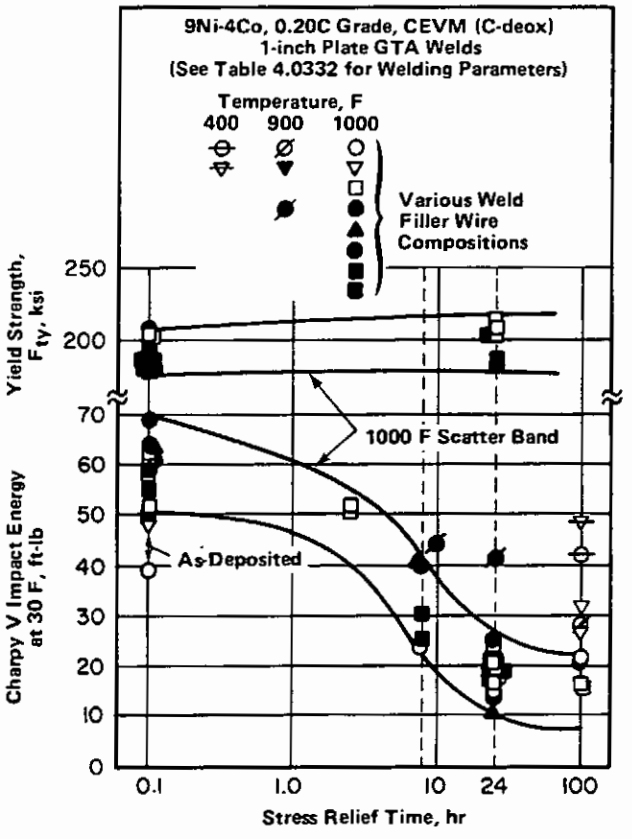


FIGURE 4.0341. EFFECT OF STRESS RELIEF AT VARIOUS TEMPERATURES AND TIMES ON ROOM TEMPERATURE TENSILE YIELD STRENGTH AND 30 F CHARPY V IMPACT ENERGY OF 0.20C GRADE PLATE GTA WELDS PRODUCED WITH VARIOUS EMBRITTLING WELD FILLER WIRES (19)

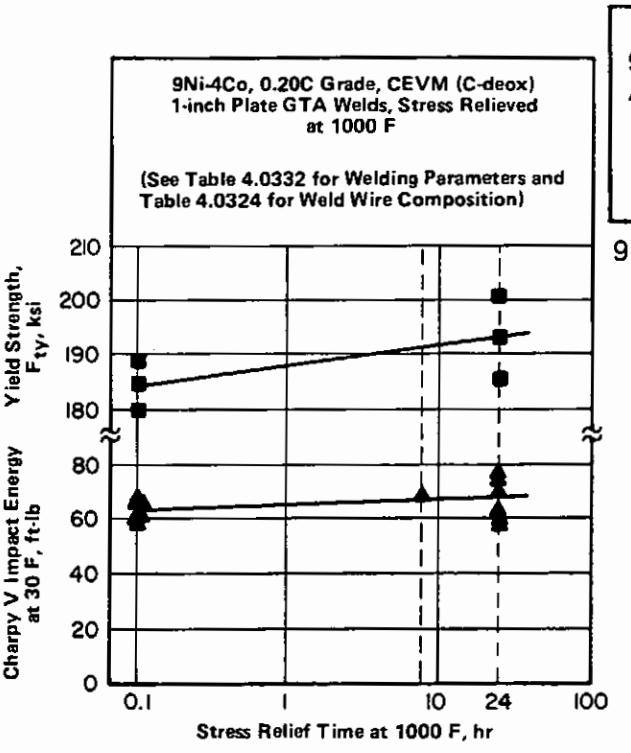


FIGURE 4.0342. EFFECT OF 1000 F STRESS RELIEF TIME ON ROOM TEMPERATURE TENSILE YIELD STRENGTH AND 30 F CHARPY V IMPACT ENERGY OF 0.20C GRADE PLATE GTA WELDS PRODUCED USING AMS SPECIFIED WELD FILLER WIRE AND PRODUCER'S RECOMMENDED WELDING PARAMETERS (19)

Alloy			9Ni-4Co						
Grade			0.20C, CEVM (C-deox)						
Form			Plate GTA Welds(a)						
Plate Thickness, inch	Weld Condition	Specimen Location	F_{tu}, ksi	F_{ty}, ksi	e (1 in.), percent	RA, percent	IE Charpy V, ft-lb		
							-80 F	30 F	70 F
1	As-Deposited	Face	208.4	181.3	19	66	–	67, 66	69
1	Stress Relieved(b)	Face	188.7	186.7	17	65	–	74, 65	70
2	As-Deposited	Top	210.8	189.0	20	65	58, 62	68, 68	67, 70
2	As-Deposited	Center	213.2	196.8	21	65	54, 60	64, 60	61, 61
2	Stress Relieved(c)	Top	206.4	201.4	19	65	45, 45	57, 54	58, 63
2	Stress Relieved(c)	Center	207.6	206.3	19	65	44, 45	61, 53	58, 50
2	Stress Relieved(c)	Bottom	204.8	200.8	19	64	–	–	–

(a) U-joint welds: 0.062-inch diameter, AMS 6468A filler wire (Table 4.0324); producer's recommended welding parameters (Table 4.0332).
(b) Stress relieved as specimen blanks at 1000 F, 24 hours, FC.
(c) Stress relieved as 2-inch x 30-inch x 48-inch plate at 1000 F, six 4-hour cycles, FC after each cycle.

TABLE 4.0343. EFFECT OF STRESS RELIEF TREATMENT ON ROOM TEMPERATURE TENSILE AND LOW TEMPERATURE CHARPY V IMPACT PROPERTIES OF 1-INCH AND 2-INCH THICK 0.20C GRADE PLATE GTA WELDS (19)

Fe
9 Ni
4 Co
Cr
Mo
V

9Ni-4Co

Alloy	9Ni-4Co							
Grade	0.20C, CEVM (C-deox)							
Form	Plate[a]							
Condition	1650 F, 2 hr, AC + 1500 F, 2 hr + 1025 F, 4 hr, WQ + Stress Relieve							
Stress Relief Treatment	Plate Thickness, inch	F_{tu}, ksi	F_{ty}, ksi	e (1 in.), percent	RA, percent	IE Charpy V, ft-lb		
						-200 F	0 F	80 F
None	1/2	201	183	17	66	–	50	52
None	2	200	184	17[b]	67	28	46	51
975 F, 4 hr, FC	1/2	202	183	17	66	–	51	52
1000 F, 4 hr, FC	1/2	201	182	17	66	–	50	52
1025 F, 4 hr, FC	1/2	200	183	17	66	–	49	54
1025 F, 4 hr, FC	1/2	201	179	19	65	–	51	54
1025 F, 20 hr, FC	1/2	205	180	18	64	–	51	53
1075 F, 4 hr, FC	1/2	193	167	19	68	–	58	62
975 F, 6 hr, FC + 975 F, 6 hr, FC + 975 F, 6 hr, FC + 975 F, 6 hr, FC	2	201	183	17[b]	66	28	40	50

(a) Transverse direction.
(b) Two-inch gage length.

TABLE 4.0344. EFFECT OF STRESS RELIEF TREATMENT AND OF MULTIPLE THERMAL CYCLES ON ROOM TEMPERATURE TENSILE AND LOW TEMPERATURE CHARPY V IMPACT PROPERTIES FOR 0.20C GRADE PLATE IN TWO THICKNESSES (19)

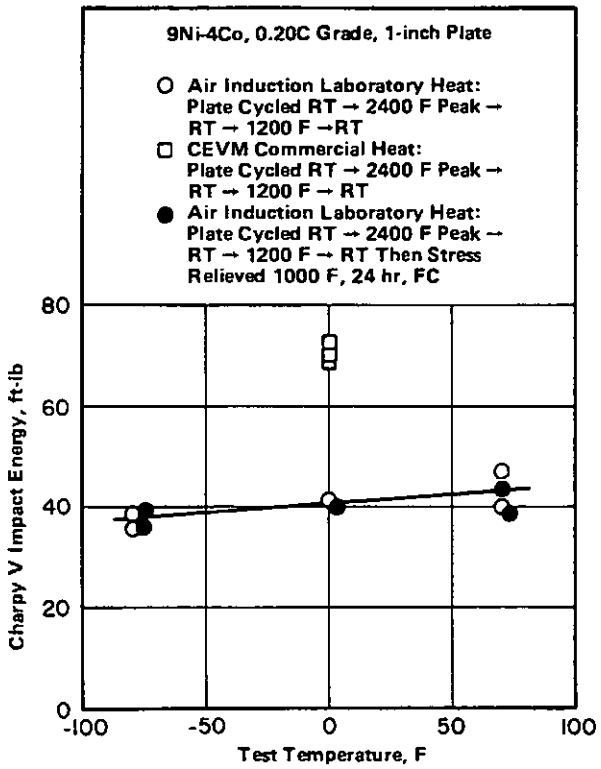


FIGURE 4.0345. EFFECT OF STRESS RELIEF TREATMENT ON LOW TEMPERATURE CHARPY V IMPACT ENERGY FOR SIMULATED HEAT-AFFECTED ZONE MICROSTRUCTURES OF 0.20C GRADE PLATE (19)

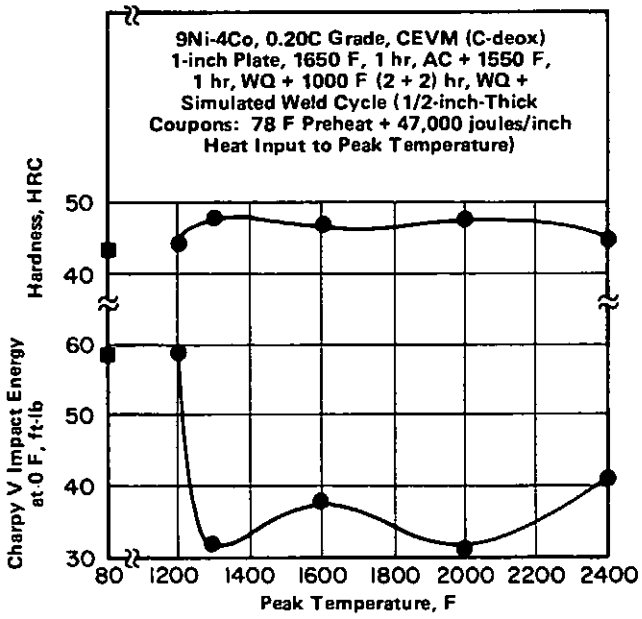


FIGURE 4.0351. HARDNESS AND 0 F CHARPY V IMPACT ENERGY AS FUNCTIONS OF PEAK TEMPERATURE PRODUCED BY SIMULATED WELDING CYCLE (31)

Fe
9 Ni
4 Co
Cr
Mo
V

9Ni-4Co

Alloy		9Ni-4Co		
Grade		0.20C		
Form		Industrial Multipass GTA Welds		
Plate Condition		1650 F, 1 hr, AC + 1525 F, 1 hr, AC + -100 F, 1 hr + 1025 F, 4 hr, AC		
		Volume Fraction of Austenite, percent[a]		
Sample	Location	After 950 F, 2 hr Stress Relief	After -100 F, 2 hr Refrigeration	After -320 F, 2 hr Refrigeration
1	Base Metal	2	0	0
1	Haz	9	5	5
1	Weld	7	5	4.5
2	Weld	8	7.5	7

(a) Determined using X-rays.

TABLE 4.0361. VOLUME FRACTION OF AUSTENITE IN INDUSTRIAL MULTIPASS GTA WELDMENTS OF 0.20C GRADE PLATE (18)

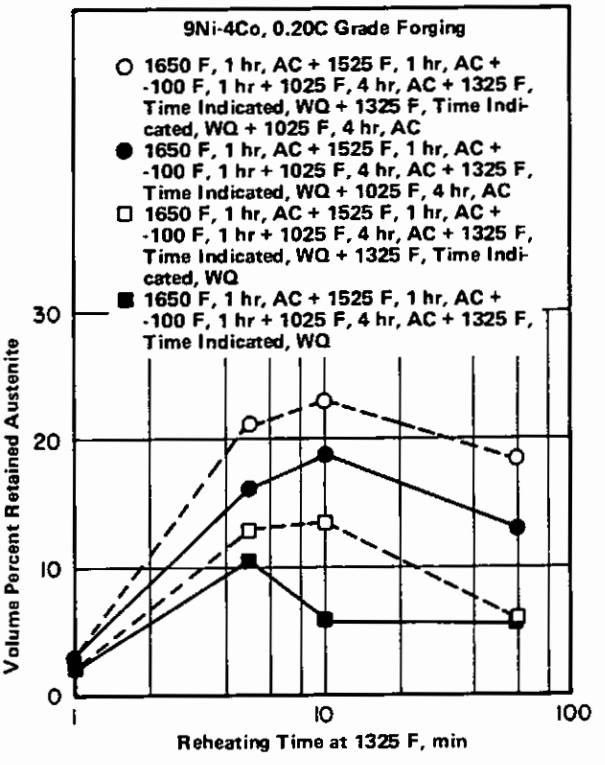


FIGURE 4.0362. VARIATION OF VOLUME FRACTION OF RETAINED AUSTENITE WITH INTERCRITICAL REHEATING CYCLES AT 1325 F, BEFORE AND AFTER TEMPERING AT 1025 F FOR 4 HOURS, FOR 0.20C GRADE FORGING (18)

Fe
9 Ni
4 Co
Cr
Mo
V

9Ni-4Co

Alloy	9Ni-4Co				
Grade	0.20C				
Form	Forging				
Condition	Volume Fraction of Retained Austenite, percent	F_{tu}, ksi	F_{ty}, ksi	e (1 in.), percent	Work Hardening Exponent[a]
1650 F, 1 hr, AC + 1525 F, 1 hr, AC + -100 F, 1 hr + 1025 F, 4 hr, AC	3.0	209	189	8.1	0.03
1650 F, 1 hr, AC + 1525 F, 1 hr, AC + -100 F, 1 hr + 1025 F, 4 hr, AC + 1325 F, 1 hr, WQ + 1025 F, 4 hr, AC	14.0	177	129	11.5	0.07

(a) Computed from true strain at maximum load.

TABLE 4.0363. ROOM TEMPERATURE TENSILE PROPERTIES OF BASE AND SIMULATED WELD MATERIAL FROM 0.20C GRADE FORGING SHOWING EFFECT OF RETAINED AUSTENITE (18)

Alloy	9Ni-4Co					
Grade	0.20C					
Form	Forging					
	Volume Fraction of Austenite, percent[a]					
Condition	ϵ = 0[b]	ϵ = 0	ϵ = 0.002	ϵ = 0.02	ϵ = 0.04	ϵ = 0.06
1650 F, 1 hr, AC + 1525 F, 1 hr, AC + -100 F, 1 hr + 1025 F, 4 hr, AC	2.8[c]	1.0	0	0	0	0
1650 F, 1 hr, AC + 1525 F, 1 hr, AC + -100 F, 1 hr + 1025 F, 4 hr, AC + 1325 F, 1 hr, WQ + 1025 F, 4 hr, AC	13.0[c]	14.9	12.6	8.1	6.7	6.2

(a) Measured using magnetic saturation technique, except where otherwise noted.
(b) ϵ refers to longitudinal true strain in a tensile specimen of 1-inch gage length.
(c) Measured using X-ray technique.

TABLE 4.0364. MECHANICAL STABILITY OF AUSTENITE IN BASE AND SIMULATED WELD MATERIAL FROM 0.20C GRADE FORGING (18)

Fe
9 Ni
4 Co
Cr
Mo
V
9Ni-4Co

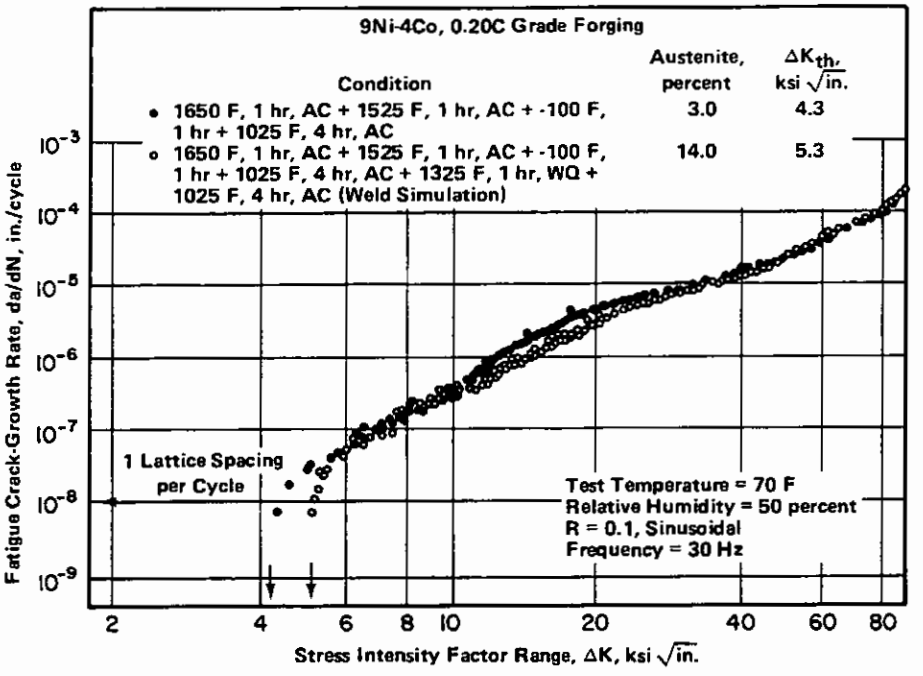


FIGURE 4.0365. INFLUENCE OF RETAINED AUSTENITE ON ROOM TEMPERATURE FATIGUE CRACK PROPAGATION IN 0.20C GRADE FORGING (18)

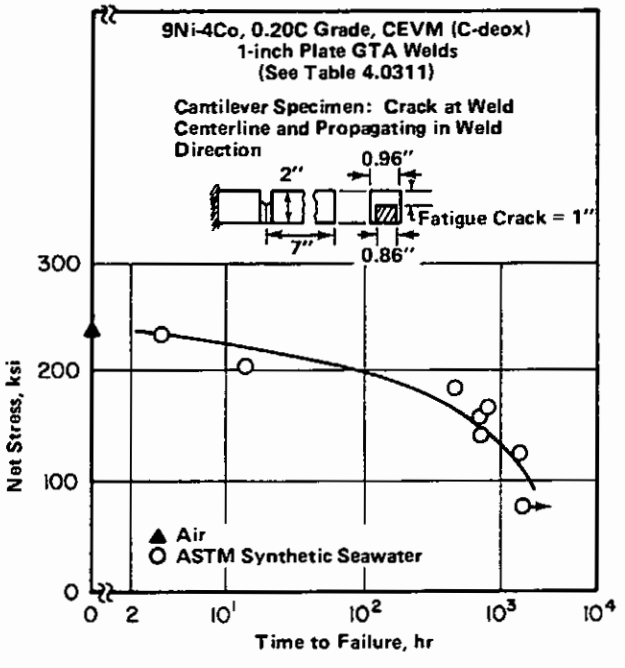


FIGURE 4.0371. DELAYED FAILURE OF 0.20C GRADE PLATE GTA WELD IN SEAWATER (31)

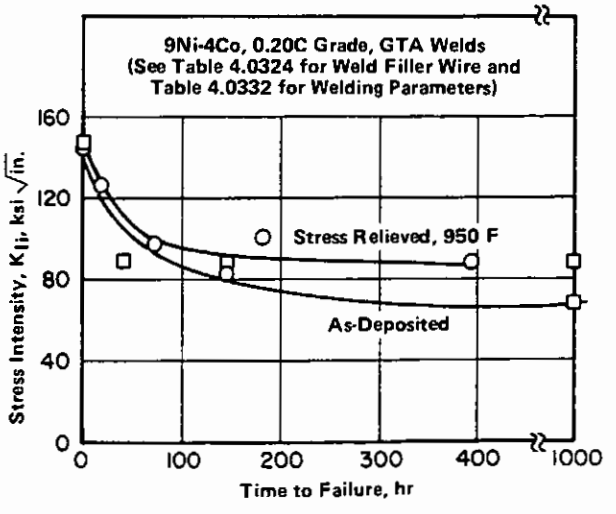


FIGURE 4.0372. STRESS CORROSION CRACKING BEHAVIOR OF 0.20C GRADE WELDS IN SEAWATER (13)

Fe
9 Ni
4 Co
Cr
Mo
V

9Ni-4Co

Alloy	9Ni-4Co					
Grade	0.20C					
Form	3/4-inch Plate					
Condition	F_{tu}, ksi	F_{ty}, ksi	e, percent	RA, percent	IE Charpy V, ft-lb	Hardness, HRC
Pseudocarburize 1700 F, 6 hr, OQ + Temper 325 F, 2 hr	217.2	157.7	16.5	62.9	67	45
Pseudocarburize 1700 F, 6 hr, OQ + Refrigerate -100 F + Temper 325 F, 2 hr	220.0	166.8	16.0	63.6	57	45
Pseudocarburize 1700 F 6 hr, FC to 1500 F, OQ + Temper 325 F, 2 hr	216.4	162.6	17.0	64.0	78	43
Pseudocarburize 1700 F, 6 hr, FC to 1500 F OQ + Refrigerate -100 F + Temper 325 F, 2 hr	217.6	168.1	17.5	65.3	77	44
Pseudocarburize 1700 F, 6 hr, AC + Reheat to 1500 F, 1 hr, OQ + Temper 325 F, 2 hr	226.9	176.6	17.0	66.0	75	43
Pseudocarburize 1700 F, 6 hr, AC + Reheat to 1500 F, 1 hr, OQ + Refrigerate -100 F + Temper 325 F, 2 hr	217.0	174.1	17.0	67.0	72	44

TABLE 4.042. PSEUDOCARBURIZED CORE PROPERTIES OF STOCK USED IN CARBURIZING STUDIES REPORTED UPON IN FIGURES AND TABLES 4.043 THROUGH 4.046 (46)

Alloy	9Ni-4Co								
Grade	0.20C								
Form	3/4-inch-Diameter Rounds From 3/4-inch Plate								
Carbon Potential	0.60 C			0.70 C			0.80 C		
Condition	(a)	(b)	(c)	(a)	(b)	(c)	(a)	(b)	(c)
Distance From Surface, inch	Hardness, HRC(d)								
0.001	50	51	49	49	52	53	45	52	51
0.002	50	51	53	49	56	55	53	53	54
0.004	53	56	54	54	55	56	57	55	56
0.006	53	55	56	54	55	57	56	53	57
0.008	53	54	53	54	56	58	53	56	57
0.012	53	53	55	54	55	56	54	55	56
0.016	53	53	53	–	54	55	55	55	56
0.020	53	52	53	53	54	53	54	53	54
0.030	52	52	52	51	53	48	53	51	53
0.040	49	50	52	49	50	48	49	49	49
0.050	45	48	48	48	48	49	47	47	49
0.060	46	46	48	48	46	49	47	46	46
0.070	45	44	46	47	45	47	46	47	47
0.080	45	45	45	46	45	45	46	45	45
Core Center	45	45	46	46	45	46	45	44	45

(a) Carburized at 1700 F for 6 hours, direct oil quench at 120 F + tempered 325 F, 2 hours.
(b) Carburized at 1700 F for 6 hours, furnace cool to 1500 F, oil quench at 120 F + temper 325 F, 2 hours.
(c) Carburized at 1700 F for 6 hours, oil quench at 120 F + reheat to 1500 F, 1 hour, oil quench at 120 F + temper 325 F, 2 hours.
(d) 500 gm Knoop converted to Rockwell C.

TABLE 4.043. MICROHARDNESS PROFILE OF 0.20C GRADE ROUNDS CARBURIZED TO 0.050-INCH DEPTH (46)

Fe
9 Ni
4 Co
Cr
Mo
V
9Ni-4Co

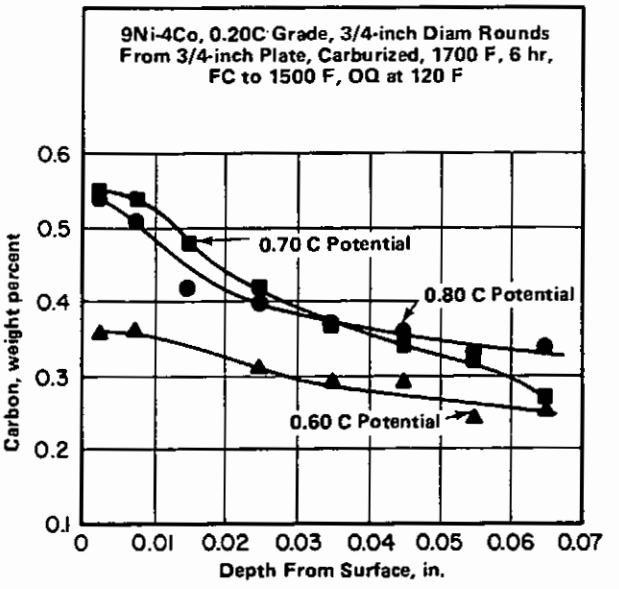


FIGURE 4.044. CARBON GRADIENT ACHIEVED FOR 0.20C GRADE CARBURIZED AT THREE CARBON POTENTIALS (46)

Alloy	9Ni-4Co											
Grade	0.20C											
Form	Unnotched Charpy Impact Specimens From 3/4-inch Plate											
Carbon Potential	0.60 C				0.70 C				0.80 C			
Condition	IE, Unnotched Charpy, ft-lb	Hardness, HRC			IE, Unnotched Charpy, ft-lb	Hardness, HRC			IE, Unnotched Charpy, ft-lb	Hardness, HRC		
		After OQ	After Refrig.	After Temper		After OQ	After Refrig.	After Temper		After OQ	After Refrig.	After Temper
Carburize at 1700 F for 6 hr, OQ + Temper 325 F, 2 hr	98	–	X	55	133	–	X	54	122	–	X	54
Carburize at 1700 F for 6 hr, OQ + Refrigerate -100 F + Temper 325 F, 2 hr	71	–	–	58	77	–	–	57	78	–	–	56
Carburize at 1700 F for 6 hr, FC to 1500 F, OQ + Temper 325 F, 2 hr	90	59	X	54	86	60	X	55	86	60	X	56
Carburize at 1700 F for 6 hr, FC to 1500 F, OQ + Refrigerate -100 F + Temper 325 F, 2 hr	64	60	61	56	64	60	63	59	64	61	62	57
Carburize at 1700 F for 6 hr, AC + Reheat to 1500 F, 1 hr, OQ + Temper 325 F, 2 hr	141	58	X	54	70	61	X	56	82	59	X	55
Carburize at 1700 F for 6 hr, AC + Reheat to 1500 F, 1 hr, OQ + Refrigerate -100 F,+ Temper 325 F, 2 hr	152	59	60	56	42	61	63	59	65	60	63	59

Note: See Table 4.042 for corresponding core properties.

TABLE 4.045. ROOM TEMPERATURE IMPACT ENERGY AND SURFACE HARDNESS OF CARBURIZED 0.20C GRADE UNNOTCHED CHARPY SPECIMENS (46)

Fe
9 Ni
4 Co
Cr
Mo
V

9Ni-4Co

Alloy	9Ni-4Co											
Grade	0.20C											
Form	0.394-inch Square (Unnotched Charpy) Bars From 3/4-inch Plate											
Carbon Potential	0.60 C				0.70 C				0.80 C			
Condition	(a)	(b)	(c)	(d)	(a)	(b)	(c)	(d)	(a)	(b)	(c)	(d)
Distance From Surface, inch	Hardness, HRC[e]											
0.001	46	49	52	47	48	49	52	55	53	50	55	52
0.002	49	50	55	51	52	52	53	55	54	52	57	55
0.004	55	54	56	53	55	53	56	–	56	55	58	58
0.006	54	55	56	54	54	54	56	58	57	55	57	57
0.008	54	53	57	55	53	54	55	58	54	55	56	58
0.010	53	54	56	54	53	54	55	58	54	54	55	57
0.012	54	55	56	53	53	53	55	58	53	54	52	56
0.016	53	54	54	53	51	54	54	56	51	53	55	55
0.020	54	54	54	52	52	53	54	55	52	53	54	55
0.030	54	22	51	50	50	52	51	53	–	53	52	54
0.040	51	50	49	49	48	50	48	51	49	50	49	52
0.050	48	49	47	49	47	48	47	49	48	48	48	49
0.060	47	49	46	48	47	48	47	47	48	47	47	48
0.070	46	49	46	47	46	47	46	47	46	47	47	46
0.080	46	48	47	46	45	46	44	47	46	46	46	47
Core Center	45	47	45	46	44	46	45	47	45	45	45	46

(a) Carburize at 1700 F for 6 hours, OQ at 120 F + temper 325 F, 2 hours.
(b) Carburize at 1700 F for 6 hours + reheat to 1500 F, 1 hour, OQ at 120 F + temper 325 F, 2 hours.
(c) Carburize at 1700 F for 6 hours, OQ at 120 F + refrigerate -100 F + temper 325 F, 2 hours.
(d) Carburize at 1700 F for 6 hours + reheat to 1500 F, 1 hour, OQ at 120 F + refrigerate -100 F + temper 325 F, 2 hours.
(e) 500 gm Knoop converted to Rockwell C.

TABLE 4.046. INFLUENCE OF A REFRIGERATION CYCLE ON THE CASE HARDNESS OF CARBURIZED 0.20C GRADE BARS (46)

Form			1-1/2-inch-Diameter Rounds From 2-inch Plate												
		IE,	Hardness at 1/8-inch Increments, HRC[a]												
		Charpy V,	Surface				Center								Surface
Alloy	Condition	ft-lb	0	1	2	3	4	5	6	7	8	9	10	11	12
9Ni-4Co 0.20C Grade	(b)	49	55	45	45	45	45	45	45	45	45	45	45	45	56
9Ni-4Co 0.20C Grade	(c)	48	58	45	45	45	45	45	45	45	45	45	45	45	59
AISI-9310	(d)	98	58	37	37	38	39	38	39	39	40	39	39	39	59
AISI-9310	(e)	93	59	38	38	38	39	39	39	40	40	40	39	42	60

(a) 500 gm Knoop converted to Rockwell C.
(b) Carburize at 1700 F for 6 hours (0.80 C potential), oil quench at 120 F + reheat to 1500 F, 1-1/2 hours, oil quench at 120 F + temper 325 F, 2 hours.
(c) Carburize at 1700 F for 6 hours (0.80 C potential), oil quench at 120 F + reheat to 1500 F, 1-1/2 hours, oil quench at 120 F + refrigerate -100 F, 1 hour + temper 325 F, 2 hours.
(d) Carburize at 1700 F for 6 hours (0.80 C potential), oil quench at 120 F + reheat to 1525 F, 1-1/2 hours, oil quench at 120 F + temper 325 F, 2 hours.
(e) Carburize at 1700 F for 6 hours (0.80 C potential), oil quench at 120 F + reheat to 1525 F, 1-1/2 hours, oil quench at 120 F + refrigerate -100 F, 1 hour + temper 325 F, 2 hours.

TABLE 4.047. ROOM TEMPERATURE SURFACE AND CORE HARDNESS AND CORE CHARPY V IMPACT ENERGY FOR CARBURIZED 0.20C GRADE AND AISI-9310 ROUNDS USED IN CARBURIZING STUDIES REPORTED UPON IN FIGURES AND TABLES 4.048 THROUGH 4.0410 (46)

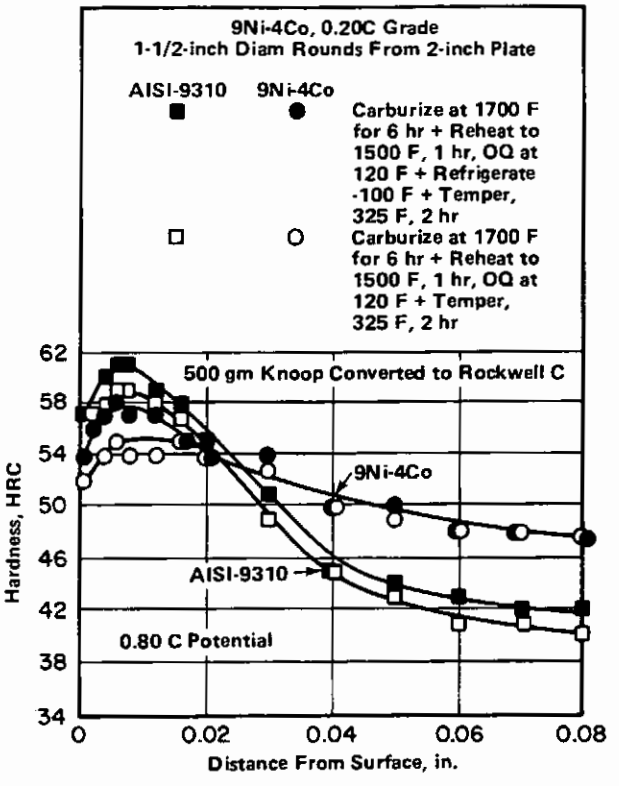


FIGURE 4.048. CASE HARDNESS PROFILE OF CARBURIZED 0.20C GRADE AND AISI-9310 (46)

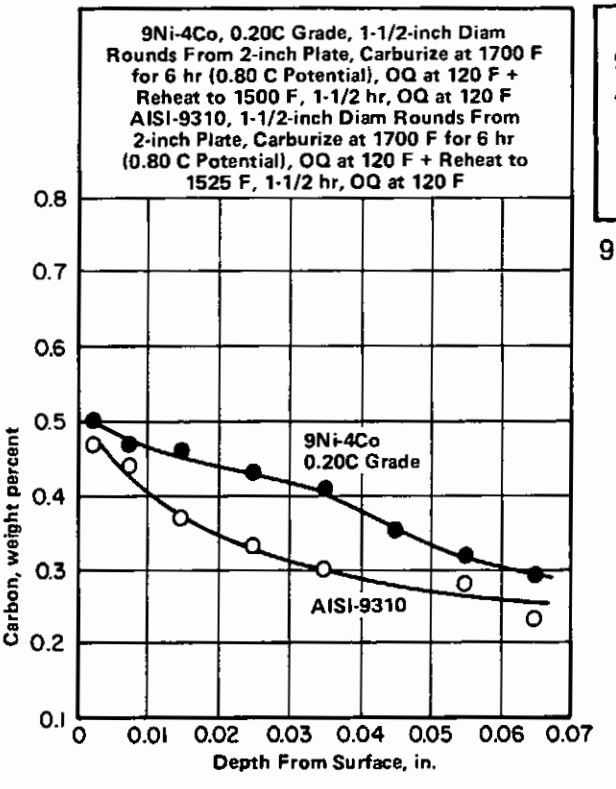


FIGURE 4.049. CARBON PROFILE FOR CARBURIZED 0.20C GRADE AND AISI-9310 ROUNDS (46)

Fe
9 Ni
4 Co
Cr
Mo
V

9Ni-4Co

Form		1-1/2-inch Diameter Rounds From 2-inch Plate	
		Percent Retained Austenite	
Alloy	Condition	Case	Core
9Ni-4Co 0.20C Grade	(a)	5.5	3.9
9Ni-4Co 0.20C Grade	(b)	9.4	4.6
AISI-9310	(c)	3.1	2.1
AISI-9310	(d)	4.6	2.9

(a) Carburize at 1700 F for 6 hours (0.80 C potential), oil quench at 120 F + reheat to 1500 F, 1-1/2 hours, oil quench at 120 F + refrigerate -100 F, 1 hour + temper 325 F, 2 hours.

(b) Carburize at 1700 F for 6 hours (0.80 C potential), oil quench at 120 F + reheat to 1500 F, 1-1/2 hours, oil quench at 120 F + temper 325 F, 2 hours.

(c) Carburize at 1700 F for 6 hours (0.80 C potential), oil quench at 120 F + refrigerate -100 F, 1 hour + temper 325 F, 2 hours.

(d) Carburize at 1700 F for 6 hours (0.80 C potential), oil quench at 120 F + reheat to 1525 F, 1-1/2 hours, oil quench at 120 F + temper 325 F, 2 hours.

TABLE 4.0410. EFFECT OF REFRIGERATION ON THE RETAINED AUSTENITE LEVELS OF 0.20C GRADE AND AISI-9310 CARBURIZED ROUNDS (46)